

INTRODUCTION

1. Overview

The *Review of Particle Physics* and the abbreviated version, the *Particle Physics Booklet*, are reviews of the field of Particle Physics. This complete *Review* includes a compilation/evaluation of data on particle properties, called the "Particle Listings." These Listings include 2000 new measurements from 610 papers, in addition to the 16,800 measurements from 4850 papers that first appeared in previous editions.

Both books include Summary Tables with our best values and limits for particle properties such as masses, widths or lifetimes, and branching fractions, as well as an extensive summary of searches for hypothetical particles. In addition, we give a long section of "Reviews, Tables, and Plots" on a wide variety of theoretical and experimental topics, a quick reference for the practicing particle physicist.

The *Review* and the *Booklet* are published in even-numbered years. This edition is an updating through December 1999 (and, in some areas, well into 2000). As described in the section "Using Particle Physics Databases" following this introduction, the content of this *Review* is available on the World-Wide Web, and is updated between printed editions (<http://pdg.lbl.gov/>).

The Summary Tables give our best values of the properties of the particles we consider to be well established, a summary of search limits for hypothetical particles, and a summary of experimental tests of conservation laws.

The Particle Listings contain all the data used to get the values given in the Summary Tables. Other measurements considered recent enough or important enough to mention, but which for one reason or another are not used to get the best values, appear separately just beneath the data we do use for the Summary Tables. The Particle Listings also give information on unconfirmed particles and on particle searches, as well as short "reviews" on subjects of particular interest or controversy.

The Particle Listings were once an archive of all published data on particle properties. This is no longer possible because of the large quantity of data. We refer interested readers to earlier editions for data now considered to be obsolete.

We organize the particles into six categories:

Gauge and Higgs bosons

Leptons

Quarks

Mesons

Baryons

Searches for monopoles,

supersymmetry, compositeness, *etc.*

The last category only includes searches for particles that do not belong to the previous groups; searches for heavy charged leptons and massive neutrinos, by contrast, are with the leptons.

In Sec. 2 of this Introduction, we list the main areas of responsibility of the authors, and also list our large number of consultants, without whom we would not have been able to produce this *Review*. In Sec. 3, we mention briefly the naming scheme for hadrons. In Sec. 4, we discuss our procedures for choosing among measurements of particle

properties and for obtaining best values of the properties from the measurements.

The accuracy and usefulness of this *Review* depend in large part on interaction between its users and the authors. We appreciate comments, criticisms, and suggestions for improvements of any kind. Please send them to the appropriate author, according to the list of responsibilities in Sec. 2 below, or to the LBNL addresses below.

To order a copy of the *Review* or the *Particle Physics Booklet* from North and South America, Australia, and the Far East, write to

Particle Data Group, MS 50-308
Lawrence Berkeley National Laboratory
Berkeley, CA 94720, USA
or send e-mail to PDG@LBL.GOV.

To order more than one copy of the *Review* or booklet, write to

c/o Anne Fleming
Technical Information Division, MS 50B-4206
Lawrence Berkeley National Laboratory
Berkeley, CA 94720, USA
or send e-mail to ASFLEMING@LBL.GOV.

From all other areas, write to

CERN Scientific Information Service
CH-1211 Geneva 23
Switzerland
or send e-mail to LIBDESK@CERN.CH.
or via the WWW from CERN
(<http://www.cern.ch/library>)
Publications

2. Authors and consultants

The authors' main areas of responsibility are shown below:

* Asterisk indicates the person to contact with questions or comments

Gauge and Higgs bosons

γ	D.E. Groom*
Gluons	R.M. Barnett,* A.V. Manohar
Graviton	D.E. Groom*
W, Z	C. Caso,* A. Gurtu*
Higgs bosons	K. Hikasa, M.L. Mangano*
Heavy bosons	C. Kolda,* M. Tanabashi, T.G. Trippe*
Axions	M.L. Mangano,* H. Murayama, K.A. Olive

Leptons

Neutrinos	M. Goodman, D.E. Groom,* K. Nakamura, K.A. Olive, A. Piepke, P. Vogel
e, μ	C. Grab, D.E. Groom*
ν_τ, τ	D.E. Groom, K.G. Hayes, K. Mönig*

Quarks

Quarks	R.M. Barnett,* A.V. Manohar
Top quark	J.L. Feng, K. Hagiwara, T.G. Trippe*
b'	J.L. Feng, K. Hagiwara, T.G. Trippe*
Free quark	D.E. Groom*

Mesons

π, η	C. Grab, D.E. Groom,* C.G. Wohl
Unstable mesons	M. Aguilar-Benitez, C. Amsler, M. Doser,* S. Eidelman, J.J. Hernández, A. Masoni, S. Navas, M. Roos, N.A. Törnqvist
K (stable)	G. Conforto, T.G. Trippe*
D (stable)	P.R. Burchat, C.G. Wohl*
B (stable)	L. Gibbons, K. Honscheid, W.-M. Yao*

Baryons

Stable baryons	C. Grab, C.G. Wohl*
Unstable baryons	C.G. Wohl,* R.L. Workman
Charmed baryons	P.R. Burchat, C.G. Wohl*
Bottom baryons	L. Gibbons, K. Honscheid, W.-M. Yao*

Miscellaneous searches

Monopole	D.E. Groom*
Supersymmetry	M.L. Mangano,* H. Murayama, K.A. Olive, L. Pape
Technicolor	C. Kolda,* T.G. Trippe*
Compositeness	C.D. Carone, M. Tanabashi, T.G. Trippe*
WIMPs and Other	J.L. Feng, K. Hikasa, K.A. Olive, T.G. Trippe*

Reviews, tables, figures, and formulae

R.M. Barnett, D.E. Groom,* T.G. Trippe, C.G. Wohl,
W.-M. Yao

Technical support

B. Armstrong,* J.L. Casas Serradilla, B.B. Filimonov,
P.S. Gee, S.B. Lugovsky, S. Mankov

The Particle Data Group benefits greatly from the assistance of some 700 physicists who are asked to verify every piece of data entered into this *Review*. Of special value is the advice of the PDG Advisory Committee which meets annually and thoroughly reviews all aspects of our operation. The members of the 1999 committee were:

P. Bloch (CERN), Chair
A. Ali (DESY)
T. Kondo (KEK)
P. Kreitz (SLAC)
Z. Kunszt (ETH Zurich)
J. LoSecco (Notre Dame)

We have especially relied on the expertise of the following people for advice on particular topics:

- S. Bethke (CERN)
- I.I. Bigi (Notre Dame University)
- S. Bilenky (Joint Inst. for Nuclear Research, Dubna)
- M. Billing (Cornell University)
- E. Blucher (University of Chicago)
- R.A. Briere (Harvard University)
- D. Bryman (TRIUMF)
- A. Buras (Tech. University of Munich)
- S.V. Burdin (Budker Inst. of Nuclear Physics)
- M. Carena (Fermilab)
- S. Catani (CERN)
- D. Chakraborty (SUNY, Stony Brook)
- M. Chanowitz (LBNL)
- M. Chertok (Texas A&M University)
- R. Clare (MIT)
- E.D. Commins (University of California, Berkeley)
- J. Conway (Rutgers University)
- G. Cowan (University of Siegen)
- P. Coyle (CPP, Marseille)
- R.L. Crawford (Glasgow)
- R.H. Dalitz (Oxford University)
- S.E. Deustua (LBNL)
- L. Di Ciaccio (Rome University)
- S. Dittmaier (CERN)
- J. Donoghue (University of Massachusetts, Amherst)
- R.K. Ellis (Fermilab)
- J. Ellison (University of California, Riverside)
- A. Falk (Johns Hopkins University)
- A. Favara (California Institute of Technology)
- T. Feldmann (RWTH Aachen)
- T. Ferbel (Rochester University)
- R. Fleischer (DESY)
- G. Fogli (University of Bari)
- S.J. Freedman (LBNL)
- H. Fritzsche (University of Munich)
- F. Gabbiani (Duke University)
- J.-F. Genat (LPHNE, Paris)
- A. Goldhaber (Stony Brook)
- A. Goussiou (SUNY, Stony Brook)
- H. Greenlee (Fermilab)
- J.-F. Grivax (INPNP, University of Paris, Sud)
- E.M. Gullikson (LBNL)
- R. Hagstrom (ANL)
- L. Hall (LBNL)
- F. Halzen (University of Wisconsin)
- D.L. Hartill (Cornell University)
- R. Harris (Fermilab)
- W.C. Haxton (University of Washington)
- J. Hewett (SLAC)
- J. Huston (Michigan State University)
- J. Imazato (KEK)
- G. Isidori (INFN, Frascati)
- P.M. Ivanov (Budker Inst. of Nuclear Physics)
- Yu.M. Ivanov (Petersburg Nuclear Physics Inst.)
- F. James (CERN)
- P. Janot (CERN)
- T. Junk (Carleton University)
- J.A. Kadyk (LBNL)
- R.W. Kenney (LBNL)
- B. Klima (Fermilab)
- I. Koop (Budker Inst. of Nuclear Physics)
- L. Addis (SLAC)
- S.I. Alekhin (COMPAS Group, IHEP, Serpukhov)
- A. Ali (DESY)
- J. Annala (Fermilab)
- T. Appelquist (Yale University)
- M. Artuso (Syracuse University)
- R. Bailey (CERN)
- A.R. Barker (University of Colorado)
- T. Barnes (University of Tennessee)
- J.-L. Basdevant (University of Paris)
- M. Battaylia (University of Helsinki)
- M. Berg (University of Texas)
- E. Berger (ANL)

- P.P. Krokovny (Budker Inst. of Nuclear Physics)
- S. Kurokawa (KEK)
- M. Lancaster (Bristol University)
- G. Landsberg (Brown University)
- K. Lane (Boston University)
- P. Lefevre (CERN)
- S. Loucatos (Saclay)
- J. Lykken (FNAL)
- G.R. Lynch (LBNL)
- W.C. Martin (NIST)
- P. Meyers (Princeton University)
- A. Milsztajn (DAPNIA, Saclay)
- P.J. Mohr (NIST)
- D. Morgan (Rutherford Appleton Lab)
- H.-G. Moser (Max-Planck-Inst. für Physik, München)
- H.N. Nelson (University of California at Santa Barbara)
- Y. Nir (Weizmann Institute)
- H. O'Connell (SLAC)
- F. Paige (Brookhaven National Lab)
- V. Parkhomchuk (Budker Inst. of Nuclear Physics)
- F. Parodi (University of Genova)
- R. Partridge (Brown University)
- M. Paulini (LBNL)
- R. Peccei (University of California, Los Angeles)
- M.R. Pennington (University of Durham)
- E. Perevedentsev (Budker Inst. of Nuclear Physics)
- N. Phinney (SLAC)
- B.V.P. Polishchuk (COMPAS Group, IHEP, Serpukhov)
- H.B. Prosper (Florida State University)
- I. Protopopov (Budker Inst. of Nuclear Physics)
- J. Qian (Michigan University)
- A. Quadt (CERN)
- J. Richman (University of California, Santa Barbara)
- T. Rizzo (SLAC)
- B.L. Roberts (Boston University)
- R.G.H. Robertson (University of Washington)
- B.P. Roe (University of Michigan)
- R. Roser (Fermilab)
- J.L. Rosner (University of Chicago)
- P. Roudeau (LAL, Orsay)
- G. Rudolph (University of Innsbruck)
- V. Ruhlmann-Kleider (DAPNIA, CEA-Saclay)
- O. Schneider (CERN)
- J. Seeman (SLAC)
- Yu. Shatunov (Budker Inst. of Nuclear Physics)
- C. Shepherd-Themistocleous (Carleton University)
- M. Shochet (University of Chicago)
- A. Sirlin (New York University)
- T. Stelzer (University of Illinois, Urbana)
- S.L. Stone (Syracuse University)
- S.I. Striganov (COMPAS Group, IHEP, Serpukhov)
- Yu. G. Stroganov (COMPAS Group, IHEP, Serpukhov)
- M. Strovink (LBNL)
- C.W. Stubbs (University of Washington)
- M. Swartz (Johns Hopkins University)
- B.N. Taylor (NIST)
- K.A. Ter-Martirosian (Moscow, ITEP)
- J.L. Tonry (University of Hawaii)
- W. Venus (RAL)
- G. Vignola (Frascati)
- C. Wagner (CERN)

- H. Wahl (CERN)
- A. Warburton (Cornell University)
- C. Weiser (CERN)
- M. Whalley (University of Durham)
- M. White (Harvard University)
- C.M. Will (Washington U., St. Louis)
- F. Willeke (DESY)
- G. Wilson (DESY)
- C. Woody (Brookhaven National Lab)
- M.P. Worah (LBNL)
- M. Zeller (Yale University)
- P. Zerwas (DESY)
- C. Zhang (IHEP, Beijing)

3. Naming scheme for hadrons

We introduced in the 1986 edition [2] a new naming scheme for the hadrons. Changes from older terminology affected mainly the heavier mesons made of u , d , and s quarks. Otherwise, the only important change to known hadrons was that the F^\pm became the D_s^\pm . None of the lightest pseudoscalar or vector mesons changed names, nor did the $c\bar{c}$ or $b\bar{b}$ mesons (we do, however, now use χ_c for the $c\bar{c}$ χ states), nor did any of the established baryons. The Summary Tables give both the new and old names whenever a change has occurred.

The scheme is described in “Naming Scheme for Hadrons” (p. 84) of this *Review*.

We give here our conventions on type-setting style. Particle symbols are italic (or slanted) characters: e^- , p , A , π^0 , K_L , D_s^+ , b . Charge is indicated by a superscript: B^- , Δ^{++} . Charge is not normally indicated for p , n , or the quarks, and is optional for neutral isosinglets: η or η^0 . Antiparticles and particles are distinguished by charge for charged leptons and mesons: τ^+ , K^- . Otherwise, distinct antiparticles are indicated by a bar (overline): $\bar{\nu}_\mu$, \bar{t} , \bar{p} , \bar{K}^0 , and $\bar{\Sigma}^+$ (the antiparticle of the Σ^-).

4. Procedures

4.1. Selection and treatment of data: The Particle Listings contain all relevant data known to us that are published in journals. With very few exceptions, we do not include results from preprints or conference reports. Nor do we include data that are of historical importance only (the Listings are not an archival record). We search every volume of 20 journals through our cutoff date for relevant data. We also include later published papers that are sent to us by the authors (or others).

In the Particle Listings, we clearly separate measurements that are used to calculate or estimate values given in the Summary Tables from measurements that are not used. We give explanatory comments in many such cases. Among the reasons a measurement might be excluded are the following:

- It is superseded by or included in later results.
- No error is given.
- It involves assumptions we question.
- It has a poor signal-to-noise ratio, low statistical significance, or is otherwise of poorer quality than other data available.
- It is clearly inconsistent with other results that appear to be more reliable. Usually we then state the criterion,

which sometimes is quite subjective, for selecting “more reliable” data for averaging. See Sec. 4.

- It is not independent of other results.
- It is not the best limit (see below).
- It is quoted from a preprint or a conference report.

In some cases, *none* of the measurements is entirely reliable and no average is calculated. For example, the masses of many of the baryon resonances, obtained from partial-wave analyses, are quoted as estimated ranges thought to probably include the true values, rather than as averages with errors. This is discussed in the Baryon Particle Listings.

For upper limits, we normally quote in the Summary Tables the strongest limit. We do not average or combine upper limits except in a very few cases where they may be re-expressed as measured numbers with Gaussian errors.

As is customary, we assume that particle and antiparticle share the same spin, mass, and mean life. The Tests of Conservation Laws table, following the Summary Tables, lists tests of *CPT* as well as other conservation laws.

We use the following indicators in the Particle Listings to tell how we get values from the tabulated measurements:

- OUR AVERAGE—From a weighted average of selected data.
- OUR FIT—From a constrained or overdetermined multi-parameter fit of selected data.
- OUR EVALUATION—Not from a direct measurement, but evaluated from measurements of related quantities.
- OUR ESTIMATE—Based on the observed range of the data. Not from a formal statistical procedure.
- OUR LIMIT—For special cases where the limit is evaluated by us from measured ratios or other data. Not from a direct measurement.

An experimentalist who sees indications of a particle will of course want to know what has been seen in that region in the past. Hence we include in the Particle Listings all reported states that, in our opinion, have sufficient statistical merit and that have not been disproved by more reliable data. However, we promote to the Summary Tables only those states that we feel are well established. This judgment is, of course, somewhat subjective and no precise criteria can be given. For more detailed discussions, see the minireviews in the Particle Listings.

4.2. Averages and fits: We divide this discussion on obtaining averages and errors into three sections: (1) treatment of errors; (2) unconstrained averaging; (3) constrained fits.

4.2.1. Treatment of errors: In what follows, the “error” δx means that the range $x \pm \delta x$ is intended to be a 68.3% confidence interval about the central value x . We treat this error as if it were Gaussian. Thus when the error is Gaussian, δx is the usual one standard deviation (1σ). Many experimenters now give statistical and systematic errors separately, in which case we usually quote both errors, with the statistical error first. For averages and fits, we then add the two errors in quadrature and use this combined error for δx .

When experimenters quote asymmetric errors $(\delta x)^+$ and $(\delta x)^-$ for a measurement x , the error that we use for that measurement in making an average or a fit with

other measurements is a continuous function of these three quantities. When the resultant average or fit \bar{x} is less than $x - (\delta x)^-$, we use $(\delta x)^-$; when it is greater than $x + (\delta x)^+$, we use $(\delta x)^+$. In between, the error we use is a linear function of x . Since the errors we use are functions of the result, we iterate to get the final result. Asymmetric output errors are determined from the input errors assuming a linear relation between the input and output quantities.

In fitting or averaging, we usually do not include correlations between different measurements, but we try to select data in such a way as to reduce correlations. Correlated errors are, however, treated explicitly when there are a number of results of the form $A_i \pm \sigma_i \pm \Delta$ that have identical systematic errors Δ . In this case, one can first average the $A_i \pm \sigma_i$ and then combine the resulting statistical error with Δ . One obtains, however, the same result by averaging $A_i \pm (\sigma_i^2 + \Delta_i^2)^{1/2}$, where $\Delta_i = \sigma_i \Delta [\sum (1/\sigma_j^2)]^{1/2}$. This procedure has the advantage that, with the modified systematic errors Δ_i , each measurement may be treated as independent and averaged in the usual way with other data. Therefore, when appropriate, we adopt this procedure. We tabulate Δ and invoke an automated procedure that computes Δ_i before averaging and we include a note saying that there are common systematic errors.

Another common case of correlated errors occurs when experimenters measure two quantities and then quote the two and their difference, *e.g.*, m_1 , m_2 , and $\Delta = m_2 - m_1$. We cannot enter all of m_1 , m_2 and Δ into a constrained fit because they are not independent. In some cases, it is a good approximation to ignore the quantity with the largest error and put the other two into the fit. However, in some cases correlations are such that the errors on m_1 , m_2 and Δ are comparable and none of the three values can be ignored. In this case, we put all three values into the fit and invoke an automated procedure to increase the errors prior to fitting such that the three quantities can be treated as independent measurements in the constrained fit. We include a note saying that this has been done.

4.2.2. Unconstrained averaging: To average data, we use a standard weighted least-squares procedure and in some cases, discussed below, increase the errors with a “scale factor.” We begin by assuming that measurements of a given quantity are uncorrelated, and calculate a weighted average and error as

$$\bar{x} \pm \delta \bar{x} = \frac{\sum_i w_i x_i}{\sum_i w_i} \pm (\sum_i w_i)^{-1/2}, \quad (1)$$

where

$$w_i = 1/(\delta x_i)^2.$$

Here x_i and δx_i are the value and error reported by the i th experiment, and the sums run over the N experiments. We then calculate $\chi^2 = \sum w_i (\bar{x} - x_i)^2$ and compare it with $N - 1$, which is the expectation value of χ^2 if the measurements are from a Gaussian distribution.

If $\chi^2/(N - 1)$ is less than or equal to 1, and there are no known problems with the data, we accept the results.

If $\chi^2/(N - 1)$ is very large, we may choose not to use the average at all. Alternatively, we may quote the calculated average, but then make an educated guess of the error, a conservative estimate designed to take into account known problems with the data.

Finally, if $\chi^2/(N-1)$ is greater than 1, but not greatly so, we still average the data, but then also do the following:

(a) We increase our quoted error, $\delta\bar{x}$ in Eq. (1), by a scale factor S defined as

$$S = [\chi^2/(N-1)]^{1/2}. \quad (2)$$

Our reasoning is as follows. The large value of the χ^2 is likely to be due to underestimation of errors in at least one of the experiments. Not knowing which of the errors are underestimated, we assume they are all underestimated by the same factor S . If we scale up all the input errors by this factor, the χ^2 becomes $N-1$, and of course the output error $\delta\bar{x}$ scales up by the same factor. See Ref. 3.

When combining data with widely varying errors, we modify this procedure slightly. We evaluate S using only the experiments with smaller errors. Our cutoff or ceiling on δx_i is arbitrarily chosen to be

$$\delta_0 = 3N^{1/2} \delta\bar{x},$$

where $\delta\bar{x}$ is the unscaled error of the mean of all the experiments. Our reasoning is that although the low-precision experiments have little influence on the values \bar{x} and $\delta\bar{x}$, they can make significant contributions to the χ^2 , and the contribution of the high-precision experiments thus tends to be obscured. Note that if each experiment has the same error δx_i , then $\delta\bar{x}$ is $\delta x_i/N^{1/2}$, so each δx_i is well below the cutoff. (More often, however, we simply exclude measurements with relatively large errors from averages and fits: new, precise data chase out old, imprecise data.)

Our scaling procedure has the property that if there are two values with comparable errors separated by much more than their stated errors (with or without a number of other values of lower accuracy), the scaled-up error $\delta\bar{x}$ is approximately half the interval between the two discrepant values.

We emphasize that our scaling procedure for *errors* in no way affects central values. And if you wish to recover the unscaled error $\delta\bar{x}$, simply divide the quoted error by S .

(b) If the number M of experiments with an error smaller than δ_0 is at least three, and if $\chi^2/(M-1)$ is greater than 1.25, we show in the Particle Listings an ideogram of the data. Figure 1 is an example. Sometimes one or two data points lie apart from the main body; other times the data split into two or more groups. We extract no numbers from these ideograms; they are simply visual aids, which the reader may use as he or she sees fit.

Each measurement in an ideogram is represented by a Gaussian with a central value x_i , error δx_i , and area proportional to $1/\delta x_i$. The choice of $1/\delta x_i$ for the area is somewhat arbitrary. With this choice, the center of gravity of the ideogram corresponds to an average that uses weights $1/\delta x_i$, rather than the $(1/\delta x_i)^2$ actually used in the averages. This may be appropriate when some of the experiments have seriously underestimated systematic errors. However, since for this choice of area the height of the Gaussian for each measurement is proportional to $(1/\delta x_i)^2$, the peak position of the ideogram will often favor the high-precision measurements at least as much as does the least-squares average. See our 1986 edition [2] for a detailed discussion of the use of ideograms.

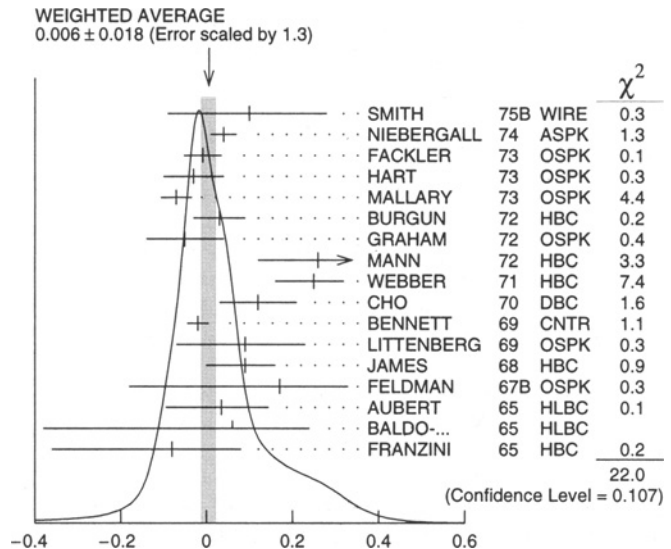


Figure 1: A typical ideogram. The arrow at the top shows the position of the weighted average, while the width of the shaded pattern shows the error in the average after scaling by the factor S . The column on the right gives the χ^2 contribution of each of the experiments. Note that the next-to-last experiment, denoted by the incomplete error flag (\perp), is not used in the calculation of S (see the text).

4.2.3. Constrained fits: Except for trivial cases, all branching ratios and rate measurements are analyzed by making a simultaneous least-squares fit to all the data and extracting the partial decay fractions P_i , the partial widths Γ_i , the full width Γ (or mean life), and the associated error matrix.

Assume, for example, that a state has m partial decay fractions P_i , where $\sum P_i = 1$. These have been measured in N_r different ratios R_r , where, e.g., $R_1 = P_1/P_2$, $R_2 = P_1/P_3$, etc. [We can handle any ratio R of the form $\sum \alpha_i P_i / \sum \beta_i P_i$, where α_i and β_i are constants, usually 1 or 0. The forms $R = P_i P_j$ and $R = (P_i P_j)^{1/2}$ are also allowed.] Further assume that *each* ratio R has been measured by N_k experiments (we designate each experiment with a subscript k , e.g., R_{1k}). We then find the best values of the fractions P_i by minimizing the χ^2 as a function of the $m-1$ independent parameters:

$$\chi^2 = \sum_{r=1}^{N_r} \sum_{k=1}^{N_k} \left(\frac{R_{rk} - R_r}{\delta R_{rk}} \right)^2, \quad (3)$$

where the R_{rk} are the measured values and R_r are the fitted values of the branching ratios.

In addition to the fitted values \bar{P}_i , we calculate an error matrix $\langle \delta \bar{P}_i \delta \bar{P}_j \rangle$. We tabulate the diagonal elements of $\delta \bar{P}_i = \langle \delta \bar{P}_i \delta \bar{P}_i \rangle^{1/2}$ (except that some errors are scaled as discussed below). In the Particle Listings, we give the complete correlation matrix; we also calculate the fitted value of each ratio, for comparison with the input data, and list it above the relevant input, along with a simple unconstrained average of the same input.

Three comments on the example above:

(1) There was no connection assumed between measurements of the full width and the branching ratios. But

often we also have information on partial widths Γ_i as well as the total width Γ . In this case we must introduce Γ as a parameter in the fit, along with the P_i , and we give correlation matrices for the widths in the Particle Listings.

(2) We do *not* allow for correlations between input data. We *do* try to pick those ratios and widths that are as independent and as close to the original data as possible. When one experiment measures all the branching fractions and constrains their sum to be one, we leave one of them (usually the least well-determined one) out of the fit to make the set of input data more nearly independent.

(3) We calculate scale factors for both the R_r and P_i when the measurements for any R give a larger-than-expected contribution to the χ^2 . According to Eq. (3), the double sum for χ^2 is first summed over experiments $k = 1$ to N_k , leaving a single sum over ratios $\chi^2 = \sum \chi_r^2$. One is tempted to define a scale factor for the ratio r as $S_r^2 = \chi_r^2 / \langle \chi_r^2 \rangle$. However, since $\langle \chi_r^2 \rangle$ is not a fixed quantity (it is somewhere between N_k and N_{k-1}), we do not know how to evaluate this expression. Instead we define

$$S_r^2 = \frac{1}{N_k} \sum_{k=1}^{N_k} \frac{(R_{rk} - \bar{R}_r)^2}{(\delta R_{rk})^2 - (\delta \bar{R}_r)^2}, \quad (4)$$

where $\delta \bar{R}_r$ is the fitted error for ratio r . With this definition the expected value of S_r^2 is one.

The fit is redone using errors for the branching ratios that are scaled by the larger of S_r and unity, from which new and often larger errors $\delta \bar{P}_i'$ are obtained. The scale factors we finally list in such cases are defined by $S_i = \delta \bar{P}_i' / \delta \bar{P}_i$. However, in line with our policy of not letting S affect the central values, we give the values of \bar{P}_i obtained from the original (unscaled) fit.

There is one special case in which the errors that are obtained by the preceding procedure may be changed. When a fitted branching ratio (or rate) \bar{P}_i turns out to be less than three standard deviations ($\delta \bar{P}_i'$) from zero, a new smaller error $(\delta \bar{P}_i'')^-$ is calculated on the low side by requiring the area under the Gaussian between $\bar{P}_i - (\delta \bar{P}_i'')^-$ and \bar{P}_i to be 68.3% of the area between zero and \bar{P}_i . A similar correction is made for branching fractions that are within three standard deviations of one. This keeps the quoted errors from overlapping the boundary of the physical region.

4.3. Discussion: The problem of averaging data containing discrepant values is nicely discussed by Taylor in Ref. 4. He considers a number of algorithms that attempt to incorporate inconsistent data into a meaningful average. However, it is difficult to develop a procedure that handles simultaneously in a reasonable way two basic types of situations: (a) data that lie apart from the main body of the data are incorrect (contain unreported errors); and (b) the opposite—it is the main body of data that is incorrect. Unfortunately, as Taylor shows, case (b) is not infrequent. He concludes that the choice of procedure is less significant than the initial choice of data to include or exclude.

We place much emphasis on this choice of data. Often we solicit the help of outside experts (consultants). Sometimes, however, it is simply impossible to determine which of a set of discrepant measurements are correct. Our scale-factor technique is an attempt to address this ignorance by increasing the error. In effect, we are saying that present experiments do not allow a precise determination of this

quantity because of unresolvable discrepancies, and one must await further measurements. The reader is warned of this situation by the size of the scale factor, and if he or she desires can go back to the literature (via the Particle Listings) and redo the average with a different choice of data.

Our situation is less severe than most of the cases Taylor considers, such as estimates of the fundamental constants like \hbar , etc. Most of the errors in his case are dominated by systematic effects. For our data, statistical errors are often at least as large as systematic errors, and statistical errors are usually easier to estimate. A notable exception occurs in partial-wave analyses, where different techniques applied to the same data yield different results. In this case, as stated earlier, we often do not make an average but just quote a range of values.

A brief history of early Particle Data Group averages is given in Ref. 3. Figure 2 shows some histories of our values of a few particle properties. Sometimes large changes occur. These usually reflect the introduction of significant new data or the discarding of older data. Older data are discarded in favor of newer data when it is felt that the newer data have smaller systematic errors, or have more checks on systematic errors, or have made corrections unknown at the time of the older experiments, or simply have much smaller errors. Sometimes, the scale factor becomes large near the time at which a large jump takes place, reflecting the uncertainty introduced by the new and inconsistent data. By and large, however, a full scan of our history plots shows a dull progression toward greater precision at central values quite consistent with the first data points shown.

We conclude that the reliability of the combination of experimental data and our averaging procedures is usually good, but it is important to be aware that fluctuations outside of the quoted errors can and do occur.

ACKNOWLEDGMENTS

The publication of the *Review of Particle Physics* is supported by the Director, Office of Science, Office of High Energy and Nuclear Physics, the Division of High Energy Physics of the U.S. Department of Energy under Contract No. DE-AC03-76SF00098; by the U.S. National Science Foundation under Agreement No. PHY-9703140; by the European Laboratory for Particle Physics (CERN); by an implementing arrangement between the governments of Japan (Monbusho) and the United States (DOE) on cooperative research and development; and by the Italian National Institute of Nuclear Physics (INFN).

We thank all those who have assisted in the many phases of preparing this *Review*. We particularly thank the many who have responded to our requests for verification of data entered in the Listings, and those who have made suggestions or pointed out errors.

REFERENCES

1. The previous edition was Particle Data Group: C. Caso *et al.*, Eur. Phys. J. **C3**, 1 (1998).
2. Particle Data Group: M. Aguilar-Benitez *et al.*, Phys. Lett. **170B** (1986).
3. A.H. Rosenfeld, Ann. Rev. Nucl. Sci. **25**, 555 (1975).
4. B.N. Taylor, "Numerical Comparisons of Several Algorithms for Treating Inconsistent Data in a Least-Squares Adjustment of the Fundamental Constants," U.S. National Bureau of Standards NBSIR 81-2426 (1982).

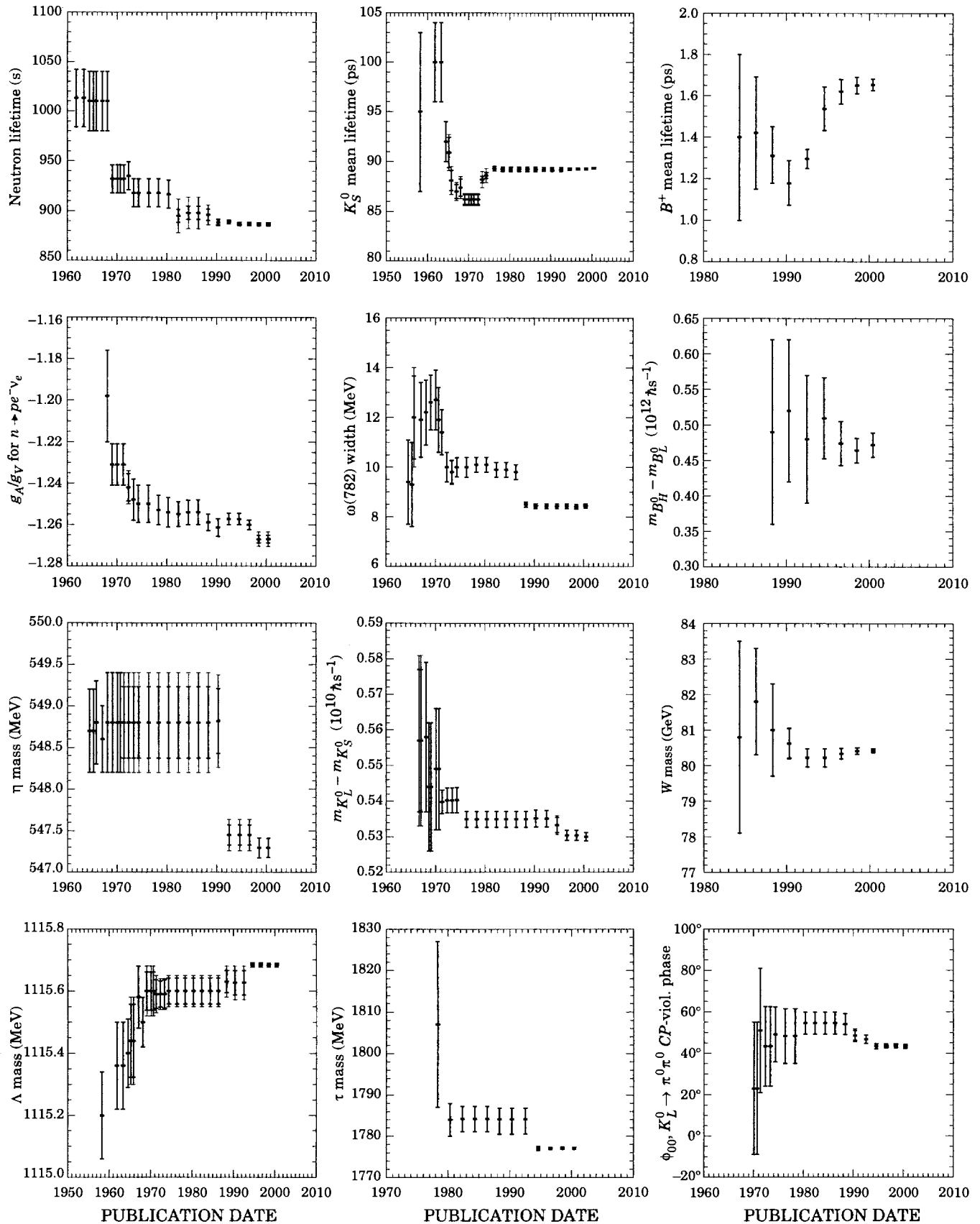


Figure 2: An historical perspective of values of a few particle properties tabulated in this *Review* as a function of date of publication of the *Review*. A full error bar indicates the quoted error; a thick-lined portion indicates the same but without the “scale factor.”

ONLINE PARTICLE PHYSICS INFORMATION

Revised April 2000 by P. Kreitz (SLAC).

The purpose of this list is to organize a broad set of online catalogs, databases, directories, World-Wide Web (WWW) pages, etc., that are of value to the particle physics community. This compilation is prescreened and highly selective. It attempts to describe the scope, size, and organization of the resources so that efficient choices can be made amongst many sites which may appear similar. Because this list must be fixed in print, it is important to consult the updated version of this compilation which includes newly added resources and hypertext links to more complete information at:

<http://www.slac.stanford.edu/library/pdg/>

In this edition, a resource is excluded if it provides information primarily of interest to one institution. In the case where there are multiple resources covering similar material, an attempt has been made in the annotation to identify the particular strength of each source. Databases and resources focusing primarily on accelerator physics have been excluded in deference to the excellent compilation at the World Wide Web Virtual Library of Beam Physics and Accelerator Technology:

<http://www.slac.stanford.edu/grp/arb/dhw/dpb/w3v1/w3.html>

My thanks to Betty Armstrong, Particle Data Group, Molly Moss, SLAC Library, Rich Dominiak, SLAC Library, and the many particle physics Web site and database maintainers who have all given me their generous assistance. Please send suggestions, additions, changes, ideas for category groupings, exclusions, etc., by e-mail to pkreitz@slac.stanford.edu.

1. Particles & Properties Data:

- **REVIEW OF PARTICLE PHYSICS (RPP):** A biennial comprehensive review summarizing much of the known data about the field of Particle Physics produced by the international Particle Data Group (PDG). Includes a compilation/evaluation of data on particle properties, summary tables with best values and limits for particle properties, extensive summaries of searches for hypothetical particles, and a long section of reviews, tables, and plots on a wide variety of theoretical and experimental topics of interest to particle and astrophysicists. The linked table of contents provides access to particle listings, reviews, summary tables, errata, indices, etc. The current printed version is Eur. Phys. J. C15, 1 (2000). Maintained at:
<http://pdg.lbl.gov/>
- **PARTICLE PHYSICS BOOKLET:** A pocket-sized booklet containing the Summary Tables and abbreviated versions of some of the other sections of the full *Review of Particle Physics*. This is extracted from the most recent edition of the full RPP. Contains images in an easy-to-read print useful for classroom studies. The last edition was July 1998 and the next edition will be August 2000. Until the new edition is published and available via the Web, students, teachers, and researchers should use the full RPP:
<http://pdg.lbl.gov/>
- **COMPUTER-READABLE FILES:** Currently available from the PDG: Tables of masses, widths, and PDG Monte Carlo particle numbers and cross-section data, including hadronic total and elastic cross sections vs laboratory momenta, and total center-of-mass energy. Check out the Palm Pilot version of the table of masses, widths, and PDG Monte Carlo particle numbers. This version will be updated in the Summer of even-numbered years coinciding with the production of the *Review of Particle Properties*:
http://pdg.lbl.gov/computer_read.html
- **PARTICLE PHYSICS DATA SYSTEM:** Contains an indexed bibliography of experimental particle physics (1895 - 1995) and computerized numerical data extracted from publications. The Web interfaces permitting simple searching for numerical data on observables in reactions and for compilations of integrated cross-section data are still under construction. Maintained by the COMPAS group at IHEP:
<http://pdg.lbl.gov/ppds>

- **HEPDATA:** Reaction Data Database: A part of the HEPDATA databases at University of Durham/RAL, this database is compiled by the Durham Database Group (UK) with help from the COMPAS Group (Russia) for the PDG. Contains numerical values of HEP reaction data such as total and differential cross sections, fragmentation functions, structure functions, and polarization measurements from a wide range of experiments. Updated at regular intervals and contains links to precompiled reviewed data such as 'Structure Functions in DIS', 'Single Photon Production in Hadronic Interactions', and 'Drell-Yan Cross-Sections':
<http://durpdg.dur.ac.uk/HEPDATA/REAC>

- **NIST Physics Laboratory:** This unit of the National Institute of Standards and Technology provides measurement services and research for electronic, optical, and radiation technologies. Two sub-pages, one on Physical Reference Data and another on Constants, Units & Uncertainty are extremely useful. Additional links to other physical properties and data of tangential interest to particle physics are also available from this page:
<http://physics.nist.gov/>

2. Collaborations & Experiments:

- **EXPERIMENTS Database:** Contains more than 2,000 experiments in elementary particle physics covering past, current, and proposed experiments in both accelerator and non-accelerator physics. Simple searches by: participant; title; experiment number; institution; date approved; accelerator; or detector; return a result that fully describes the experiment, including a complete list of authors, title, description of the experiment's goals and methods, a list of resulting journal articles, and a link to the experiment's Web page if available:
<http://www.slac.stanford.edu/spires/experiments/>
- **EXPERIMENTS ONLINE:** Current Experiments in Particle Physics: A list of almost 500 current experiments with active home pages. This list is abstracted from the EXPERIMENTS Database and links back to it for more complete information. Accelerator experiments are organized by institution, machine, and experiment name. Non-accelerator experiments are alphabetical by name:
http://www.slac.stanford.edu/spires/experiments/online_exp.html
- **HIGH ENERGY PHYSICS EXPERIMENTS:** A HEPiC page providing links to collaboration Web pages. Collaborations are arranged alphabetically by name or number under 15 major laboratories or in a catch-all group labeled 'Other':
http://www.hep.net/experiments/all_sites.html

3. Conferences:

- **CONFERENCES:** Contains conferences, schools, and meetings of interest to high-energy physics and related fields. Searchable SPIRES database produced by the SLAC, DESY, CERN, and KEK libraries with 9,000 listings covering 1973 to 2002+. Search or browse by title, acronym, date, location. Includes information about published proceedings, links to submitted papers from the SPIRES-HEP database, and links to the conference website when available. New feature permits searches by day, month, quarter, or year:
<http://www.slac.stanford.edu/spires/conferences.html>
- **CONFERENCES AND CONFERENCES:** (Subtitled: There Are Too Many Conferences!): Lists over a hundred current and future meetings in many fields of physics. This Web page provides a complete list of all conferences in ASCII or specialized lists arranged by topic: particle, quantum, condensed matter, classical, mathematical or interdisciplinary physics are provided. Includes links to the conference Web page and the contact:
<http://www.physics.umd.edu/robot/confer/confmenu.html>

- **CONFERENCES, WORKSHOPS AND SCHOOLS:** Maintained by the PhysicsWeb, this site contains several hundred entries for current national and regional physics meetings worldwide. Searchable by sub-discipline or by free text words. Provides a Web form and email address for adding a conference. Automatically uploads new entries to the EPS EurophysNet meeting list:

<http://physicsweb.org/TIPTOP/FORUM/CONF/>

- **EUROPHYSICS MEETINGS LIST:** Maintained by the European Physical Society, this international list of links to other conference lists is organized alphabetically by name of the organization, institution or other group providing a particular list of conferences. Useful for searching by organization and for providing access to meetings and conferences that are of peripheral interest:

<http://epswww.epfl.ch/conf/urls.html>

- **HEP Events:** A list maintained by CERN of approximately 100 upcoming conferences, schools, workshops, seminars, and symposia of interest to high-energy physics. Usefully organized by type of meeting, e.g.: school, workshop:

<http://www.cern.ch/Physics/Events>

4. Current Notices & Announcement Services:

- **SUBMIT EVENTS:** PhysicsWeb Calendar: Maintained by The Internet Pilot to Physics. Provides a Web form for adding a conference and automatically uploads new entries to the EPS EurophysNet meeting list. Directions on the top-level page enable you to sign up to receive weekly email notification of new conferences and deadlines:

<http://physicsweb.org/events/newconfentry.phtml>

- **CONFNEWS & WEBNEWS:** Provides a system for broadcasting a conference or job opening to "a large number of physicists worldwide." For further information, e-mail: yskim@physics.umd.edu

- **E-PRINT ARCHIVES LISTSERV NOTICES:** The LANL-based E-Print Archives provides daily notices of preprints in the fields of physics, mathematics, nonlinear sciences, and computer sciences which have been submitted to the archives as full text electronic documents. Use the Web-accessible listings:

<http://xxx.lanl.gov/>

or subscribe:

<http://xxx.lanl.gov/help/subscribe>

- **NEW EXPERIMENTS Announcement:** Submit information about a new particle physics experiment to the SPIRES EXPERIMENTS Database or modify an older entry using the form at:

<http://www.slac.stanford.edu/spires/experiments/submit.html>

- **SPIRES NEW CONFERENCES IN PARTICLE PHYSICS:** Use this form, or send email or a fax to submit information about a conference of value to the field of particle physics:

http://www.slac.stanford.edu/spires/conferences/add_conference.html

Note: Use the library pages in Section 5.3 below to find additional announcement lists for recently received preprints, books, and proceedings. Use the online journal links in Section 7 below for journal table of contents.

5. Directories:

5.1. Directories—Research Institutions:

- **CERN RESEARCH INSTITUTES:** Contains HEP Institutes used in the CERN Library catalog. Provides almost a thousand addresses, and, where available, the following: phone and fax numbers; e-mail addresses; active Web links; and information about the institution's physics program. Provides free text searching and result sorting by organization, country, or town:

<http://weblib.cern.ch/Home/HEPInstitutes/>

- **HEP INSTITUTIONS ONLINE:** Active links to the home pages of more than 800 HEP-related institutions with Web servers. Maintained by SLAC. Listed by country, and then alphabetically by institution:

http://www.slac.stanford.edu/spires/institutions/online_institutions.html

- **INSTITUTIONS:** Database of over 6,000 high-energy physics institutes, laboratories, and university departments in which some research on particle physics is performed. Covers six continents and almost one hundred countries. Searchable by name, acronym, location, etc. Provides address, phone and fax numbers, e-mail address, and Web links where available. Has pointers to the recent HEP papers from that institution. Maintained by SLAC and DESY libraries:

<http://www.slac.stanford.edu/spires/institutions/>

- **PHYSICSWEB LINKS: SEARCH DEPARTMENTS:** A useful database of web links to the home pages of physics departments worldwide. Searchable by field of research, country, or by a combination of both. Results vary since information is dependent upon submission by the institutions or by individual departments from a university:

<http://physicsweb.org/resources/dsearch.phtml>

- **WWW VIRTUAL LIBRARY—HIGH ENERGY PHYSICS WEB SITES:** An alphabetical listing of particle physics web sites maintained at CERN. Provides links to the institution's Web pages. Somewhat difficult to use because entries are listed by institutional acronym or by short name:

<http://www.cern.ch/Physics/HEP.html>

5.2. Directories—People:

- **HEPNAMES:** Searchable worldwide database of 37,000 e-mail addresses of people associated with particle physics, synchrotron radiation, and related fields:

<http://www.slac.stanford.edu/spires/hepnames/>

- **HEP VIRTUAL PHONEBOOK:** A list of links to phonebooks and directories of high-energy physics sites and collaborations around the world. Very useful if you know the place or group and are trying to find a particular individual. Maintained by HEPIC:

<http://www.hep.net/sites/directories.html>

- **US-HEPFOLK:** A searchable database of almost 3,500 physicists from 155 U.S. institutions based on a survey conducted in 1997. Searchable by first or last name, by affiliation, and/or by email address. Also provides some interesting demographic plots of the survey data:

<http://pdg.lbl.gov/us-hepfolk/index.html>

5.3. Directories—Libraries:

- Argonne National Lab Library:
<http://www.library.anl.gov/library/services.html>
- Berkeley Lab (LBNL) Library:
<http://www-library.lbl.gov/>
- Brookhaven National Lab Library:
<http://inform.bnl.gov/RESLIB/reslib.html>
- (CERN) European Organization for Nuclear Research Library:
<http://library.cern.ch/>
- Deutsches Elektronen-Synchrotron (DESY) Library:
<http://www-library.desy.de/>
- Fermilab Library:
<http://fnalpubs.fnal.gov/>
- Jefferson Lab Library:
http://www.jlab.org/div_dept/admin/library/
- (KEK) National Laboratory for High Energy Physics Library:
<http://www-lib.kek.jp/publib.html>
- Lawrence Livermore National Laboratory Library:
<http://www.llnl.gov/tid/Library.html>
- Los Alamos National Laboratory Library:
<http://lib-www.lanl.gov/>
- Oak Ridge National Laboratory Library:
<http://www.ornl.gov/Library/library-home.html>
- Sandia National Laboratory Library:
<http://www.sandia.gov/library.htm>
- Stanford Linear Accelerator Center Library:
<http://www.slac.stanford.edu/library>

5.4. Directories—Publishers:

- COMPANIES/PUBLISHERS: Contains 50 links to institutions, societies, or companies involved in supplying physics-related information:
<http://physicsweb.org/TIPTOP/paw/paw.phtml?k=Companies/Publishers&t=k&f=1>
- DIRECTORY OF PUBLISHERS AND VENDORS: Outstanding and comprehensive directory of web links to publishers. Additional lists include publishers' email addresses and a directory of science book reviews on the web. Publisher and vendor lists are searchable alphabetically or by subject areas: Science, Mathematics, and Technology Publishers; Biomedical Publishers; Computer Publishers; Engineering Publishers; General Publishers; Natural History Publishers, and University Presses:
<http://www.library.vanderbilt.edu/law/acqs/pubr.html>

5.5. Directories—Scholarly Societies:

- American Association for the Advancement of Science:
<http://www.aaas.org/>
- American Association of Physics Teachers:
<http://www.aapt.org/>
- American Astronomical Society:
<http://www.aas.org>
- American Institute of Physics:
<http://www.aip.org/>
- American Mathematical Society:
<http://www.ams.org/>
- American Physical Society:
<http://www.aps.org>
- European Physical Society:
<http://epswww.epfl.ch/>
- IEEE Nuclear and Plasma Sciences Society:
<http://hibp7.ecse.rpi.edu/~connor/ieee/npps.html>
- Institute of Physics:
<http://www.iop.org/>
- PHYSICSWEB LINKS: SOCIETIES/PHYSICAL: Contains 141 links to societies involved in the physical sciences. Organized by country with some entries containing a small annotation describing the society's focus:
<http://physicsweb.org/resources/paw.phtml?k=Societies/Physical&o=country&t=k&f=1>
- RESOURCES OF SCHOLARLY SOCIETIES—PHYSICS: Alphabetical list of several hundred scholarly societies with links to their websites. Includes acronyms and indicates when a website contains both its native language and an English-language version. Maintained by the University of Waterloo:
http://www.lib.uwaterloo.ca/society/physics_soc.html

6. E-Prints/Pre-Prints, Papers, & Reports:

- CERN ARTICLES & PREPRINTS: The CERN Library's database which contains records of more than 200,000 (CERN and non-CERN) articles, preprints, theses, CERN Yellow reports, technical notes, Grey Books, and official committee documents held by the Library or the Archives. Provides access to full text of the document and to the references when available:
<http://weblib.cern.ch/Home/Library/Catalogue/Articles.and.Preprints/>
- HEP DATABASE (SPIRES): Contains over 415,000 bibliographic summaries for particle physics e-prints, journal articles, preprints, reports, conference papers, and theses, *etc.* Covers 1974 to the present with substantial older materials added. Updated daily with links to electronic texts (*e.g.* from LANL, CERN, KEK, and other HEP servers). Searchable by all authors and authors' affiliations, title, topic, report number, citation (footnotes), e-print archive number, date, journal, *etc.* A joint project of the SLAC and DESY libraries with the collaboration of Fermilab, Durham (UK), KEK, Kyoto, and many other research institutions and scholarly societies such as the APS:
<http://www.slac.stanford.edu/spires/hep/>

- KISS (KEK Information Service System) for Preprints: KEK Library preprint and technical report database. Contains bibliographic records of preprints and technical reports held in the KEK library with links to the full text images of more than 100,000 papers scanned from their worldwide collection of preprints:
http://www-lib.kek.jp/KISS/kiss_prepri.html
 - arXiv.org E-PRINT ARCHIVE: An automated electronic repository of physics, mathematics, computer, and nonlinear science preprints. Used heavily by the sub-disciplines of high-energy physics. Began with a core set of archives in 1991. Provides access to the full text of the electronic versions of these preprints. Permits searching by author, title, and keyword in abstract. Allows limiting by subfield archive or by date. Has over 15 mirror sites around the world. Papers are sent electronically to the archives by authors:
<http://xxx.lanl.gov>
 - PARTICLE PHYSICS DATA SYSTEM—PPDS: A search interface to the bibliography of the print publication *A Guide to Experimental Elementary Particle Physics Literature* (LBL-90). This bibliography covers the published literature of theoretical and experimental particle physics from 1895 to 1995:
<http://pdg.lbl.gov/ppds>
 - PPF: PREPRINTS IN PARTICLES AND FIELDS: A weekly listing averaging 250 new preprints in particle physics and related fields. Contains bibliographic listings for and, in the Web version, full text links to, the new preprints received by and cataloged into the SPIRES High-Energy Physics (HEP) database. Includes that week's titles from the LANL e-print archives as well as preprints and articles received from other sources. Directions for subscribing to an email version can be found on the page listing the most recent week's preprints:
<http://www.slac.stanford.edu/library/documents/newppf.html>
- ## 7. Particle Physics Journals & Reviews:
- ### 7.1. Online Journals and Tables of Contents:
- Please note, some of these journals, publishers, and reviews may limit access to subscribers. If you encounter access problems, check with your institution's library.
- Advances in Theoretical and Mathematical Physics: Bimonthly electronic and hard copy publication. Table of contents has links to LANL E-Print Archives where papers for this journal are submitted:
<http://www.intlpress.com/journals/ATMP/>
 - American Journal of Physics: A monthly publication of the American Association of Physics Teachers on instructional and cultural aspects of physical science:
<http://ojps.aip.org/ajp>
 - Applied Physics Letters: Weekly publication of short (3 pages maximum) articles:
<http://ojps.aip.org/aplo/>
 - Astrophysical Journal: Published three times a month by the American Astronomical Society. See also AAS entry under Journal Publishers (below):
<http://www.journals.uchicago.edu/APJ/>
 - Classical and Quantum Gravity: Published 24 times a year by IOP:
<http://www.iop.org/Journals/cq>
 - European Physical Journal A: Hadrons and Nuclei: This monthly journal merges *Il Nuovo Cimento A* and *Zeitschrift fur Physik A*:
<http://link.springer.de/link/service/journals/10050/index.htm>
 - European Physical Journal C: Particles and Fields: This twice monthly journal is the successor to *Zeitschrift fur Physik C*:
<http://link.springer.de/link/service/journals/10052/index.htm>
 - Journal of High Energy Physics: Electronic and print available. Like *ATMP*, this is an electronically-run journal. It accepts email submission notices and 'fetches' the submitted paper from the LANL E-print archives:
<http://jhep.sissa.it/>
 - Journal of Physics G: Nuclear and Particle Physics: Monthly, published by IOP:
<http://www.iop.org/Journals/jg>
 - Journal of the Physical Society of Japan: JPSJ Online: Monthly, online since 1993:
<http://wwwsoc.nacsis.ac.jp/jps/jpsj/index.html>
 - Modern Physics Letters A: Published 40 times a year, this contains research papers in gravitation, cosmology, nuclear physics, and particles and fields. *Brief Review* section for short reports on new findings and developments:
<http://www.wspc.com.sg/journals/mpla/mpla.html>
 - Modern Physics Letters B: Published 40 times a year, this contains research papers in condensed matter physics, statistical physics, applied physics and High Tc Superconductivity. *Brief Review* section for short reports on new findings and developments:
<http://www.wspc.com.sg/journals/mplb/mplb.html>
 - New Journal of Physics: Funded by article charges from authors of published papers, *NJP* is available in a free, electronic form:
<http://www.njp.org/>
 - Nuclear Instruments and Methods in Physics Research A: Accelerators, Spectrometers, Detectors, and Associated Equipment: Published approximately 36 times per year, this journal focuses on instrumentation and large scale facilities:
<http://www.elsevier.nl/locate/nima>
 - Nuclear Physics A: Nuclear and Hadronic Physics:
<http://www.elsevier.nl/inca/publications/store/5/0/5/7/1/5/>
 - Nuclear Physics B: Particle Physics, Field Theory, Statistical Systems, and Mathematical Physics:
<http://www.elsevier.nl/inca/publications/store/5/0/5/7/1/6/>
 - Nuclear Physics B: Proceedings Supplement: Publishes proceedings of international conferences and topical meetings in high-energy physics and related areas:
<http://www.elsevier.nl/inca/publications/store/5/0/5/7/1/7/>
 - Physical Review D: Particles, Fields, Gravitation, and Cosmology: Published 24 times a year:
<http://prd.aps.org/>
 - Physical Review Special Topics – Accelerators and Beams: A peer-reviewed electronic journal freely available from the APS:
<http://prst-ab.aps.org/>
 - Physics Letters B: Nuclear and Particle Physics: Published weekly:
<http://www.elsevier.nl/locate/plb>
 - Physics—Uspekhi: English edition of *Uspekhi Fizicheskikh Nauk*:
<http://ufn.ioc.ac.ru/>
 - Progress in Particle and Nuclear Physics: Published four times a year. Many, but not all, articles are at a level suitable for the general nuclear and particle physicist:
<http://www.elsevier.nl/locate/ppartnuclphys>

7.2. Journals – Directories:

- DESY Library Electronic Journals: Use this Web page for up-to-date links to electronic journals of interest to particle physics. Contains a broader list than is included in this compilation:
<http://www-library.desy.de/eljnl.html>
- Electronic Journals: A directory of over 900 science, technology, and engineering journals online compiled by the University of Buffalo's Science and Engineering Library:
<http://ublib.buffalo.edu/libraries/units/sel/collections/ejournal2.html>

7.3. Journals – Publishers & Repositories:

- AAS: NASA Astrophysics Data System: Provides free electronic access to back issues of the *Astrophysical Journal*, *Astrophysical Journal Letters*, and the *Astrophysical Journal Supplement Series* through the end of 1996. The NASA ADS is in the process of scanning more back issues and will eventually make the complete *ApJ* available:
<http://adswww.harvard.edu/>
- AIP JOURNAL CENTER: The American Institute of Physics' top-level page for their electronic journals may be found at:
<http://www.aip.org/ojs/service.html>
- AMERICAN PHYSICAL SOCIETY: The top-level page for the APS research journals is:
<http://publish.aps.org/>
- ELSEVIER SCIENCE: This website enables browsing Elsevier-published journals by subject field. Selecting 'physics' and publication type 'journals' returns an intermediate page with links organized by the first letter of the name of the journal. Thus one must select "A" to retrieve a list of all of Elsevier's physics-related journals beginning with that letter. A somewhat inefficient way to search what Elsevier offers:
<http://www.elsevier.nl/homepage/>
- EUROPEAN PHYSICAL SOCIETY: Their journals are handled by various publishers but may be reached from this top-level page:
<http://epswww.epfl.ch/pub/index.html>
- INSTITUTE OF PHYSICS: Journals: Information: A list of the IOP journals organized by subject. A page organized by title is also available linked to this page:
<http://www.iop.org/Journals/jnlsubj>
- SPRINGER PUBLISHING: Physics: This link provides a list of Springer journals covering topics of interest to physicists. Small bullets containing the letter 'E' beside each title indicate which journals are electronic:
<http://link.springer.de/ol/pol/all.htm>

7.4. Review Publications:

- Net Advance of Physics: A free electronic service providing review articles and tutorials in an encyclopedic format. Covers all areas of physics. Includes e-prints, book announcements, full text of electronic books, and other resources with hypertext links when available. Welcomes contributions of original review articles:
<http://web.mit.edu/afs/athena.mit.edu/user/r/e/redingtn/www/netadv/welcome.html>
- Physics Reports: A review section for *Physics Letters A* and *Physics Letters B*. Each report deals with one subject. The reviews are specialized in nature, more extensive than a literature survey but normally less than book length:
<http://www.elsevier.nl/locate/physrep>
- Reviews of Modern Physics: Published quarterly. Includes traditional scholarly reviews and shorter colloquium papers intended

to describe recent research of interest to a broad audience of physicists:

<http://www.phys.washington.edu/~rmp/Welcome.html>

8. Particle Physics Education Sites:

8.1. Particle Physics Education: General Sites:

- Argonne National Laboratory Gee Whiz!: Includes links to other interesting and publically-accessible information such as the Rube Goldberg Machine Contest; Arts in Science; and the parts of the movie 'Chain Reaction' that were filmed at Argonne:
<http://www.anl.gov/OPA/geewhiz.htm>
- Brookhaven National Laboratory: Science Museum Programs:
http://www.pubaf.bnl.gov/bnl_museum.htm
- Contemporary Physics Education Project (CPEP): Provides charts, brochures, Web links, and classroom activities. Online interactive courses include: Particle Adventure; Fusion – Physics of a Fundamental Energy Source; and Nuclear Science ABC's:
<http://www.cpepweb.org/>
- Center for Particle Astrophysics in Berkeley: Excellent source for online demos aimed at middle school students (modifiable for other levels). Online demonstrations include: Air-Powered Rockets; Desktop Stars; Lunar Topography, Ping Pong Ball Launcher; Potato Power; Solar System; and more to come. Each includes an introduction, teacher and student worksheets, and a list of materials needed:
<http://cfpa.berkeley.edu/Education/DEMOS/DEMOS.html>
- Fermilab: Education and Outreach Resources for Particle Physicists: Outstanding collection of resources from the 'grandmother' of all physics lab educational programs. Sections are organized for students and educators by grade level and for general visitors:
http://www-ed.fnal.gov/trc/phys_resc.html_resc.html
- Stanford Linear Accelerator Center: This Virtual Visitor's Center website explains basic particle physics, linear and synchrotron accelerators, and the experiments conducted at SLAC. Aimed at the general public, as well as at students and teachers:
<http://www2.slac.stanford.edu/vvc/home.html>

8.2. Particle Physics Education: Meta-Sites:

- ESTEEM: The Department of Energy's exciting and visually appealing meta-site for Education in Science, Technology, Energy, Engineering, and Math. Organized both textually and graphically as a 'city'. Users can explore resources by source (energy and science museums), by subject (windmills, 'playground', virtual experiments, computers), or by targeted audience (university, middle, or elementary students). Provides excellent links to many other sites:
<http://www.sandia.gov/ESTEEM/home.html>
- Physical Science: Educational Hotlists: Created by the outstanding Franklin Institute Science Museum, these hotlists contain a prescreened list of resources for science educators, students, and enthusiasts. The criteria for inclusion is that a site stimulates creative thinking and learning about science. The excellent Physical Science list contains useful links for physics, physicists, optics, material science, applied design and engineering, sites for museums, 'doing science,' and inventors and engineers:
<http://sln.fi.edu/tfi/hotlists/hotlists.html>
- PhysicsEd: Physics Education Resources: From a group renowned for doing research on physics education. Provides links to courses and topics; curriculum development; resources for demonstrations; software; research and projects in physics education; textbooks; journals and newsletters; email discussion groups; reference resources; organizations and companies; FAQ's; and links to much more:
<http://www-hpcc.astro.washington.edu/scied/physics.html>

8.3. Particle Physics Education: Ask-a-Scientist Sites:

- Ask A Scientist: Questions are answered by volunteer scientists throughout the world. Service provided by the Newton BBS through Argonne National Lab. Submission form permits very specific age information to be included with the question so that the answer can be targeted to the questioner's level of knowledge:
<http://newton.dep.anl.gov/aasquest.htm>
- How Things Work: The author of the popular *How Things Work: the Physics of Everyday Life* has created a site that functions as a virtual 'radio call-in program'. Submit questions about how something works or consult the 60 pages of most recent questions which are searchable by date, topic, or keyword:
<http://howthingswork.virginia.edu>
- Mad Scientist's Network: Ask A Question: Responds to hundreds of questions a week. Be sure to check out their extensive archive of answered questions:
<http://www.madsci.org/submit.html>
- The Science Club: An excellent compilation of places to ask science questions. Organized by 'general' sites and then by sites that specialize in specific subjects or professions:
<http://www.halcyon.com/sciclub/kidquest.html>

8.4. Particle Physics Education: Experiments, Demos, & Fun

- Albert Einstein Online: A meta-Einstein site with links to dozens of resources by and about this scientist. Organized into Overviews; Moments (recollections of Einstein by others); Physics; Writings; Quotes; Pictures; and Miscellaneous:
<http://www.westegg.com/einstein/>
- Deep Space: Remote Access Astronomy Project: This project (RAAP) was developed as a supplement for high school, college or advanced placement physics courses to enable students to combine theory with observation by working with satellite imaging data and a Remotely Operated Telescope. The labs are available as PostScript and .doc files. Classes should also obtain the 180 page curriculum and image processing manual available for \$15.00 plus shipping:
<http://www.deepspace.ucsb.edu/rot.htm>
- The Edible/Inedible Experiments Archive of the Mad Scientist Network: Astronomy, Mathematics, and Physics are included in the scientific fields covered. Each experiment uses common materials and identifies whether the experiment is edible, inedible, or 'partially drinkable', or 'not all that edible' (!?) categories:
<http://www.madsci.org/experiments/>
- Pages of Light: From Fermi National Accelerator Laboratory, a delightful collection of pages explaining light at the advanced placement high school level or above:
<http://www.fnal.gov/pub/light/>
- The Particle Adventure: An interactive tour of particle physics and the inner workings of the atom for the general public, students and teachers. Available in five languages:
<http://ParticleAdventure.org/>
- Physics Around the World's Educational Section: Contains several useful links to collections of resources particularly the sections covering: Hands-On Experiments; Exercises and Problems; and Demonstrations. Targeted to the university level:
<http://physicsweb.org/TIPTOP/paw/>

- Science for the Millennium: Expo Web: Aimed at diverse audiences, this site focuses chiefly on astronomy, astrophysics, advanced computation, and virtual environments to showcase recent advances in these fields. The content is deep and the site is well-designed, permitting hierarchical and serendipitous use. Maintained by NCSA with significant help from the Electronic Visualization Laboratory:

<http://www.ncsa.uiuc.edu/Cyberia/Expo/information-pavilion.html>

- The Virtual Laboratory: Physics Applets: Maintained by the University of Oregon's Physics Department. A series of experiments using Java applets that are targeted to non-majors physics classes which have no physical lab sections. The experiments provide conceptual interfaces to the equations of physics and represent interaction with data that simulates a real physics experiment. Includes: Astrophysics applets; Energy and Environment applets; Mechanics applets; Thermodynamics applets; and the beginnings of some general tools such as a whiteboard to create a gif image of a particular applet's output for submitting as a homework assignment:

<http://jersey.uoregon.edu/vlab/index.html>

9. Software Directories:

- CERNLIB: CERN PROGRAM LIBRARY: A large collection of general purpose libraries and modules offered in both source code and object code forms from the CERN central computing division. Provides programs applicable to a wide range of physics research problems such as general mathematics, data analysis, detectors simulation, data-handling, etc. Also includes links to commercial, free, and other software:
<http://wwwinfo.cern.ch/asd/index.html>
- FREEHEP: A collection of software and information about software useful in high-energy physics. Searching can be done by title, subject, date acquired, date updated, or by browsing an alphabetical list of all packages:
<http://www.slac.stanford.edu/find/fhmain.html>
- FERMILAB Software Tools Program: Software repository of Fermilab-developed software packages of value to the HEP community. Permits searching for packages by title or subject, by browsing FTP site, and by recent acquisitions:
<http://www.fnal.gov/fermitools/>
- HEPIC: Software & Tools Used in HEP Research: A meta-level site with links to other sites of HEP-related software and computing tools:
<http://www.hep.net/resources/software.html>
- INTERNET PILOT TO PHYSICS: COMPUTING: The section on computing contains links to separate Web listings of: software archives; hands-on experiments; graphics & visualization; parallel computing; Java applets; and computing centers:
<http://physicsweb.org/TIPTOP/paw/>
- LIFECYCLE GLOBAL HYPERTEXT: Originally developed for managing ALEPH's massive programming code, this is a Web-based template system that publishes all documents from the software lifecycle including diagrams and code and automatically cross references the information. It can be configured to present Web output and to integrate both internal and external links. Excellent system for accessing massive amounts of complex code:
<http://light.cern.ch/>

10. Specialized Subject Pages:

10.1. *Subject Pages—Applied*

- Nanotechnology: A selective set of links providing recent news, introductory-level explanations, web videos, bibliographies of books and articles, conferences, events, and an excellent list of links to other sites:

<http://www.zyvex.com/nano/>

- Sean Morgan's Nanotechnology Pages: A large compilation that must be browsed to discover all its gems. Includes News; Molecular Nanotechnology, Scanning Probe Microscopy; Molecular Modeling; Nanoelectronics and Micromachining; Nanotechnology Mailing Lists; Electronic Magazines and Journals on MNT; and a Nanotechnology Timeline. Each list includes articles, books, conferences, and more:

<http://www.lucifer.com/~sean/Nano.html>

10.2. *Subject Pages—Concepts & Theories*

- The Official String Theory Web Site: Outstanding compilation of information about string theory includes: an introductory section on theory; cosmology; links to other sites; experiments testing string theory; black holes; a directory of people working on string theory; and a discussion forum. Many of the explanations are very accessible to an advanced high school level:

<http://superstringtheory.com/>

- Relativity: Bookmarks: Presents an almost overwhelming number of worldwide links. Topical divisions include: university sites; experimental gravitation projects; relativity-related journals and databases; historical relativity; popular relativity; visualization; relativistic raytracing; elementary, intermediate, and advanced relativity; workshops; courses and seminars; astrophysical and black hole relativity; computational; symbolic; quantum; applied; and philosophical:

<http://physics.syr.edu/research/relativity/RELATIVITY.html>

- Relativity on the World Wide Web: An excellent set of pages offering links and written information about relativity. Organized into: popular science sites; visualization sites; web tutorials; observational and experimental evidence and rebuttals; course work (divided into undergraduate and graduate levels); software; research frontiers; and further reading:

<http://www.math.washington.edu/~hillman/relativity.html>

10.3. *Subject Pages—Particles*

- Neutrino Website: John Bahcall has compiled links to: technical and popular articles books; Hubble Space Telescope and other images; models; viewgraphs; cross-section data; software; and more. The place to begin researching neutrinos at a graduate student level and beyond:

<http://www.sns.ias.edu/~jnb/>

Gauge & Higgs Boson Summary Table

SUMMARY TABLES OF PARTICLE PROPERTIES

Extracted from the Particle Listings of the
Review of Particle Physics

D.E. Groom *et al.*, Eur. Phys. Jour. **C15**, 1 (2000)
Available at <http://pdg.lbl.gov>

Particle Data Group Authors:

D.E. Groom, M. Aguilar-Benitez, C. Amsler, R.M. Barnett, P.R. Burchat,
C.D. Carone, C. Caso, G. Conforto, O. Dahl, M. Doser, S. Eidelman,
J.L. Feng, L. Gibbons, M. Goodman, C. Grab, A. Gurtu, K. Hagiwara,
K.G. Hayes, J.J. Hernández, K. Hikasa, K. Honscheid, C. Kolda,
M.L. Mangano, A.V. Manohar, A. Masoni, K. Mönig, H. Murayama,
K. Nakamura, S. Navas, K.A. Olive, L. Pape, A. Piepke, M. Roos,
M. Tanabashi, N.A. Törnqvist, T.G. Trippe, P. Vogel, C.G. Wohl,
R.L. Workman, W.-M. Yao

Technical Associates: B. Armstrong, J.L. Casas Serradilla,
B.B. Filimonov, P.S. Gee, S.B. Lugovsky, F. Nicholson

Other Authors who have made substantial contributions
to reviews since the 1996 edition:

K.S. Babu, D. Besson, O. Biebel, P. Bloch, R.N. Cahn, A. Cattai,
R.S. Chivukula, R.D. Cousins, T. Damour, K. Desler, R.J. Donahue,
D.A. Edwards, J. Erler, V.V. Ezhela, A. Fassò, W. Fetscher,
D. Froidevaux, M. Fukugita, T.K. Gaisser, L. Garren, S. Geer,
H.-J. Gerber, F.J. Gilman, H.E. Haber, C. Hagmann, I. Hinchliffe,
C.J. Hogan, G. Höhler, P. Igo-Kemenes, J.D. Jackson, K.F. Johnson,
D. Karlen, B. Kayser, S.R. Klein, K. Kleinknecht, I.G. Knowles,
E.W. Kolb, P. Kreitz, R. Landua, P. Langacker, L. Littenberg,
D.M. Manley, J. March-Russell, T. Nakada, H.R. Quinn, G. Raffelt,
B. Renk, L. Rolandi, M.T. Ronan, L.J. Rosenberg, H.F.W. Sadrozinski,
A.I. Sanda, M. Schmitt, O. Schneider, D. Scott, W.G. Seligman,
M.H. Shaevitz, T. Sjöstrand, G.F. Smoot, S. Spanier, H. Spieler,
M. Srednicki, A. Stahl, T. Stanev, M. Suzuki, N.P. Tkachenko,
M.S. Turner, G. Valencia, K. van Bibber, R. Voss, D. Ward,
L. Wolfenstein, J. Womersley

©Regents of the University of California

(Approximate closing date for data: January 1, 2000)

GAUGE AND HIGGS BOSONS

γ

$$I(J^{PC}) = 0,1(1^{- -})$$

Mass $m < 2 \times 10^{-16}$ eV
Charge $q < 5 \times 10^{-30}$ e
Mean life $\tau = \text{Stable}$

**g
or gluon**

$$I(J^P) = 0(1^-)$$

Mass $m = 0$ [a]
SU(3) color octet

W

$$J = 1$$

Charge = ± 1 e
Mass $m = 80.419 \pm 0.056$ GeV
 $m_Z - m_W = 10.76 \pm 0.05$ GeV
 $m_{W^+} - m_{W^-} = -0.2 \pm 0.6$ GeV
Full width $\Gamma = 2.12 \pm 0.05$ GeV
 $\langle N_{\text{charged}} \rangle = 19.3 \pm 0.4$

W^- modes are charge conjugates of the modes below.

W^+ DECAY MODES	Fraction (Γ_i/Γ)	Confidence level	ρ (MeV/c)
$\ell^+ \nu$	[b] (10.56 \pm 0.14) %		–
$e^+ \nu$	(10.66 \pm 0.20) %		40205
$\mu^+ \nu$	(10.49 \pm 0.29) %		40205
$\tau^+ \nu$	(10.4 \pm 0.4) %		40185
hadrons	(68.5 \pm 0.6) %		–

$\pi^+ \gamma$	< 7	$\times 10^{-5}$	95%	40205
$D_s^+ \gamma$	< 1.3	$\times 10^{-3}$	95%	–
cX	(35 \pm 4) %			–
$c\bar{s}$	(32 $^{+13}_{-11}$) %			–
invisible	[c] (1.4 \pm 2.8) %			–

Z

$$J = 1$$

Charge = 0

Mass $m = 91.1882 \pm 0.0022$ GeV [d]

Full width $\Gamma = 2.4952 \pm 0.0026$ GeV

$\Gamma(\ell^+ \ell^-) = 84.057 \pm 0.099$ MeV [b]

$\Gamma(\text{invisible}) = 499.4 \pm 1.7$ MeV [e]

$\Gamma(\text{hadrons}) = 1743.8 \pm 2.2$ MeV

$\Gamma(\mu^+ \mu^-)/\Gamma(e^+ e^-) = 0.9999 \pm 0.0032$

$\Gamma(\tau^+ \tau^-)/\Gamma(e^+ e^-) = 1.0012 \pm 0.0036$ [f]

Average charged multiplicity

$$\langle N_{\text{charged}} \rangle = 21.07 \pm 0.11$$

Couplings to leptons

$$g_V^f = -0.03795 \pm 0.00071$$

$$g_A^f = -0.50145 \pm 0.00030$$

$$g^{V_e} = 0.53 \pm 0.09$$

$$g^{V_\mu} = 0.502 \pm 0.017$$

Asymmetry parameters [g]

$$A_e = 0.152 \pm 0.004 \quad (S = 1.2)$$

$$A_\mu = 0.102 \pm 0.034$$

$$A_\tau = 0.141 \pm 0.006$$

$$A_c = 0.66 \pm 0.11$$

$$A_b = 0.91 \pm 0.05$$

Charge asymmetry (%) at Z pole

$$A_{FB}^{(\ell)} = 1.82 \pm 0.11$$

$$A_{FB}^{(0)} = 4 \pm 7$$

$$A_{FB}^{(s)} = 9.8 \pm 1.1$$

$$A_{FB}^{(c)} = 7.01 \pm 0.45$$

$$A_{FB}^{(b)} = 10.03 \pm 0.22$$

Z DECAY MODES	Fraction (Γ_i/Γ)	Scale factor/ Confidence level	ρ (MeV/c)
$e^+ e^-$	(3.367 \pm 0.005) %		45594
$\mu^+ \mu^-$	(3.367 \pm 0.008) %		45593
$\tau^+ \tau^-$	(3.371 \pm 0.009) %		45559
$\ell^+ \ell^-$	[b] (3.3688 \pm 0.0026) %		–
invisible	(20.02 \pm 0.06) %		–
hadrons	(69.89 \pm 0.07) %		–
$(u\bar{u} + c\bar{c})/2$	(10.1 \pm 1.1) %		–
$(d\bar{d} + s\bar{s} + b\bar{b})/3$	(16.6 \pm 0.6) %		–
$c\bar{c}$	(11.68 \pm 0.34) %		–
$b\bar{b}$	(15.13 \pm 0.05) %		–
$b\bar{b}b\bar{b}$	(4.2 \pm 1.6) $\times 10^{-4}$		–
$g\bar{g}g$	< 1.1 %	CL=95%	–
$\pi^0 \gamma$	< 5.2	$\times 10^{-5}$ CL=95%	45593
$\eta \gamma$	< 5.1	$\times 10^{-5}$ CL=95%	45592
$\omega \gamma$	< 6.5	$\times 10^{-4}$ CL=95%	45590
$\eta'(958) \gamma$	< 4.2	$\times 10^{-5}$ CL=95%	45588
$\gamma \gamma$	< 5.2	$\times 10^{-5}$ CL=95%	45594
$\gamma \gamma \gamma$	< 1.0	$\times 10^{-5}$ CL=95%	45594
$\pi^\pm W^\mp$	[h] < 7	$\times 10^{-5}$ CL=95%	10139
$\rho^\pm W^\mp$	[h] < 8.3	$\times 10^{-5}$ CL=95%	10114
$J/\psi(1S) X$	(3.51 $^{+0.23}_{-0.25}$) $\times 10^{-3}$	5=1.1	–
$\psi(2S) X$	(1.60 \pm 0.29) $\times 10^{-3}$		–
$\chi_{c1}(1P) X$	(2.9 \pm 0.7) $\times 10^{-3}$		–
$\chi_{c2}(1P) X$	< 3.2	$\times 10^{-3}$ CL=90%	–
$T(1S) X + T(2S) X$	(1.0 \pm 0.5) $\times 10^{-4}$		–
$+ T(3S) X$			
$T(1S) X$	< 4.4	$\times 10^{-5}$ CL=95%	–
$T(2S) X$	< 1.39	$\times 10^{-4}$ CL=95%	–
$T(3S) X$	< 9.4	$\times 10^{-5}$ CL=95%	–
$(D^0/\bar{D}^0) X$	(20.7 \pm 2.0) %		–

Gauge & Higgs Boson Summary Table

$D^\pm X$		(12.2 ± 1.7) %	—
$D^*(2010)^\pm X$	[h]	(11.4 ± 1.3) %	—
$B_s^0 X$		seen	—
$B_c^{+\pm} X$		searched for	—
anomalous $\gamma +$ hadrons	[i]	< 3.2	$\times 10^{-3}$ CL=95% —
$e^+ e^- \gamma$	[f]	< 5.2	$\times 10^{-4}$ CL=95% 45594
$\mu^+ \mu^- \gamma$	[f]	< 5.6	$\times 10^{-4}$ CL=95% 45593
$\tau^+ \tau^- \gamma$	[f]	< 7.3	$\times 10^{-4}$ CL=95% 45559
$\ell^+ \ell^- \gamma \gamma$	[f]	< 6.8	$\times 10^{-6}$ CL=95% —
$q\bar{q}\gamma\gamma$	[f]	< 5.5	$\times 10^{-6}$ CL=95% —
$\nu\bar{\nu}\gamma\gamma$	[f]	< 3.1	$\times 10^{-6}$ CL=95% 45594
$e^\pm \mu^\mp$	LF	[h] < 1.7	$\times 10^{-6}$ CL=95% 45593
$e^\pm \tau^\mp$	LF	[h] < 9.8	$\times 10^{-6}$ CL=95% 45576
$\mu^\pm \tau^\mp$	LF	[h] < 1.2	$\times 10^{-5}$ CL=95% 45576
$p e$	L,B	< 1.8	$\times 10^{-6}$ CL=95% —
$p \mu$	L,B	< 1.8	$\times 10^{-6}$ CL=95% —

Higgs Bosons — H^0 and H^\pm , Searches for

H^0 Mass $m > 95.3$ GeV, CL = 95%

H^\pm in Supersymmetric Models ($m_{H^\pm} < m_{H^0}$)

Mass $m > 82.6$ GeV, CL = 95%

A^0 Pseudoscalar Higgs Boson in Supersymmetric Models [k]

Mass $m > 84.1$ GeV, CL = 95% $\tan\beta > 1$

H^\pm Mass $m > 69.0$ GeV, CL = 95%

See the Particle Listings for a Note giving details of Higgs Bosons.

Heavy Bosons Other Than Higgs Bosons, Searches for

Additional W Bosons

W_R — right-handed W

Mass $m > 715$ GeV, CL = 90% (electroweak fit)

W' with standard couplings decaying to $e\nu, \mu\nu$

Mass $m > 720$ GeV, CL = 95%

Additional Z Bosons

Z'_{SM} with standard couplings

Mass $m > 690$ GeV, CL = 95% ($p\bar{p}$ direct search)

Mass $m > 898$ GeV, CL = 95% (electroweak fit)

Z_{LR} of $SU(2)_L \times SU(2)_R \times U(1)$

(with $g_L = g_R$)

Mass $m > 630$ GeV, CL = 95% ($p\bar{p}$ direct search)

Mass $m > 564$ GeV, CL = 95% (electroweak fit)

Z_χ of $SO(10) \rightarrow SU(5) \times U(1)_\chi$ (with $g_\chi = e/\cos\theta_W$)

Mass $m > 595$ GeV, CL = 95% ($p\bar{p}$ direct search)

Mass $m > 545$ GeV, CL = 95% (electroweak fit)

Z_ψ of $E_6 \rightarrow SO(10) \times U(1)_\psi$ (with $g_\psi = e/\cos\theta_W$)

Mass $m > 590$ GeV, CL = 95% ($p\bar{p}$ direct search)

Mass $m > 294$ GeV, CL = 95% (electroweak fit)

Z_η of $E_6 \rightarrow SU(3) \times SU(2) \times U(1) \times U(1)_\eta$ (with $g_\eta = e/\cos\theta_W$)

Mass $m > 620$ GeV, CL = 95% ($p\bar{p}$ direct search)

Mass $m > 365$ GeV, CL = 95% (electroweak fit)

Scalar Leptoquarks

Mass $m > 225$ GeV, CL = 95% (1st generation, pair prod.)

Mass $m > 200$ GeV, CL = 95% (1st gener., single prod.)

Mass $m > 202$ GeV, CL = 95% (2nd gener., pair prod.)

Mass $m > 73$ GeV, CL = 95% (2nd gener., single prod.)

Mass $m > 99$ GeV, CL = 95% (3rd gener., pair prod.)

(See the Particle Listings for assumptions on leptoquark quantum numbers and branching fractions.)

Axions (A^0) and Other Very Light Bosons, Searches for

The standard Peccei-Quinn axion is ruled out. Variants with reduced couplings or much smaller masses are constrained by various data. The Particle Listings in the full Review contain a Note discussing axion searches.

The best limit for the half-life of neutrinoless double beta decay with Majoron emission is $> 7.2 \times 10^{24}$ years (CL = 90%).

NOTES

In this Summary Table:

When a quantity has “(S = ...)” to its right, the error on the quantity has been enlarged by the “scale factor” S, defined as $S = \sqrt{\chi^2/(N-1)}$, where N is the number of measurements used in calculating the quantity. We do this when $S > 1$, which often indicates that the measurements are inconsistent. When $S > 1.25$, we also show in the Particle Listings an ideogram of the measurements. For more about S, see the Introduction.

A decay momentum p is given for each decay mode. For a 2-body decay, p is the momentum of each decay product in the rest frame of the decaying particle. For a 3-or-more-body decay, p is the largest momentum any of the products can have in this frame.

[a] Theoretical value. A mass as large as a few MeV may not be precluded.

[b] ℓ indicates each type of lepton ($e, \mu,$ and τ), not sum over them.

[c] This represents the width for the decay of the W boson into a charged particle with momentum below detectability, $p < 200$ MeV.

[d] The Z -boson mass listed here corresponds to a Breit-Wigner resonance parameter. It lies approximately 34 MeV above the real part of the position of the pole (in the energy-squared plane) in the Z -boson propagator.

[e] This partial width takes into account Z decays into $\nu\bar{\nu}$ and any other possible undetected modes.

[f] This ratio has not been corrected for the τ mass.

[g] Here $A \equiv 2g_V g_A / (g_V^2 + g_A^2)$.

[h] The value is for the sum of the charge states or particle/antiparticle states indicated.

[i] See the Z Particle Listings for the γ energy range used in this measurement.

[j] For $m_{\gamma\gamma} = (60 \pm 5)$ GeV.

[k] The limits assume no invisible decays.

LEPTONS

e

$$J = \frac{1}{2}$$

Mass $m = 0.510998902 \pm 0.000000021$ MeV
 $= (5.485799110 \pm 0.000000012) \times 10^{-4}$ u
 $(m_{e^+} - m_{e^-})/m < 8 \times 10^{-9}$, CL = 90%
 $|q_{e^+} + q_{e^-}|/e < 4 \times 10^{-8}$
Magnetic moment $\mu = 1.001159652187 \pm 0.000000000004 \mu_B$
 $(g_{e^+} - g_{e^-}) / g_{\text{average}} = (-0.5 \pm 2.1) \times 10^{-12}$
Electric dipole moment $d = (0.18 \pm 0.16) \times 10^{-26}$ e cm
Mean life $\tau > 4.2 \times 10^{24}$ yr, CL = 68% [a]

 μ

$$J = \frac{1}{2}$$

Mass $m = 105.658357 \pm 0.000005$ MeV
 $= 0.1134289168 \pm 0.0000000034$ u
Mean life $\tau = (2.19703 \pm 0.00004) \times 10^{-6}$ s
 $\tau_{\mu^+/\tau_{\mu^-}} = 1.00002 \pm 0.00008$
 $c\tau = 658.654$ m
Magnetic moment $\mu = 1.0011659160 \pm 0.0000000006 e\hbar/2m_\mu$
 $(g_{\mu^+} - g_{\mu^-}) / g_{\text{average}} = (-2.6 \pm 1.6) \times 10^{-8}$
Electric dipole moment $d = (3.7 \pm 3.4) \times 10^{-19}$ e cm

Decay parameters [b]

$\rho = 0.7518 \pm 0.0026$
 $\eta = -0.007 \pm 0.013$
 $\delta = 0.749 \pm 0.004$
 $\xi P_\mu = 1.003 \pm 0.008$ [c]
 $\xi P_\mu \delta / \rho > 0.99682$, CL = 90% [c]
 $\xi' = 1.00 \pm 0.04$
 $\xi'' = 0.7 \pm 0.4$
 $\alpha/A = (0 \pm 4) \times 10^{-3}$
 $\alpha'/A = (0 \pm 4) \times 10^{-3}$
 $\beta/A = (4 \pm 6) \times 10^{-3}$
 $\beta'/A = (2 \pm 6) \times 10^{-3}$
 $\bar{\eta} = 0.02 \pm 0.08$

μ^+ modes are charge conjugates of the modes below.

μ^- DECAY MODES	Fraction (Γ_i/Γ)	Confidence level	ρ (MeV/c)
$e^- \bar{\nu}_e \nu_\mu$	$\approx 100\%$		53
$e^- \bar{\nu}_e \nu_\mu \gamma$	[d] $(1.4 \pm 0.4)\%$		53
$e^- \bar{\nu}_e \nu_\mu e^+ e^-$	[e] $(3.4 \pm 0.4) \times 10^{-5}$		53
Lepton Family number (LF) violating modes			
$e^- \nu_e \bar{\nu}_\mu$	LF [f] < 1.2 %	90%	53
$e^- \gamma$	LF < 1.2 $\times 10^{-11}$	90%	53
$e^- e^+ e^-$	LF < 1.0 $\times 10^{-12}$	90%	53
$e^- 2\gamma$	LF < 7.2 $\times 10^{-11}$	90%	53

 τ

$$J = \frac{1}{2}$$

Mass $m = 1777.03^{+0.30}_{-0.26}$ MeV
Mean life $\tau = (290.6 \pm 1.1) \times 10^{-15}$ s
 $c\tau = 87.11$ μm
Magnetic moment anomaly > -0.052 and < 0.058 , CL = 95%
Electric dipole moment $d > -3.1$ and $< 3.1 \times 10^{-16}$ e cm, CL = 95%

Weak dipole moment

$\text{Re}(d_\tau^W) < 0.56 \times 10^{-17}$ e cm, CL = 95%
 $\text{Im}(d_\tau^W) < 1.5 \times 10^{-17}$ e cm, CL = 95%

Weak anomalous magnetic dipole moment

$\text{Re}(\alpha_\tau^W) < 4.5 \times 10^{-3}$, CL = 90%
 $\text{Im}(\alpha_\tau^W) < 9.9 \times 10^{-3}$, CL = 90%

Decay parameters

See the τ Particle Listings for a note concerning τ -decay parameters.

$\rho^\tau(e \text{ or } \mu) = 0.747 \pm 0.009$
 $\rho^\tau(e) = 0.749 \pm 0.011$
 $\rho^\tau(\mu) = 0.752 \pm 0.021$
 $\xi^\tau(e \text{ or } \mu) = 0.997 \pm 0.032$
 $\xi^\tau(e) = 0.996 \pm 0.044$
 $\xi^\tau(\mu) = 1.046 \pm 0.065$
 $\eta^\tau(e \text{ or } \mu) = 0.011 \pm 0.031$
 $\eta^\tau(\mu) = -0.013 \pm 0.097$
 $(\delta\xi)^\tau(e \text{ or } \mu) = 0.746 \pm 0.023$
 $(\delta\xi)^\tau(e) = 0.735 \pm 0.030$
 $(\delta\xi)^\tau(\mu) = 0.774 \pm 0.043$
 $\xi^\tau(\pi) = 0.992 \pm 0.046$
 $\xi^\tau(\rho) = 0.998 \pm 0.010$
 $\xi^\tau(a_1) = 0.998 \pm 0.077$
 $\xi^\tau(\text{all hadronic modes}) = 1.000 \pm 0.008$

τ^+ modes are charge conjugates of the modes below. " h^\pm " stands for π^\pm or K^\pm . " e " stands for e or μ . "Neutral" means neutral hadron whose decay products include γ 's and/or π^0 's.

τ^- DECAY MODES	Fraction (Γ_i/Γ)	Scale factor/ Confidence level	ρ (MeV/c)
Modes with one charged particle			
particle $^- \geq 0$ neutrals $\geq 0 K_L^0 \nu_\tau$ ("1-prong")	$(84.71 \pm 0.13)\%$	S=1.2	-
particle $^- \geq 0$ neutrals $\geq 0 K^0 \nu_\tau$	$(85.32 \pm 0.13)\%$	S=1.2	-
$\mu^- \bar{\nu}_\mu \nu_\tau$	[g] $(17.37 \pm 0.07)\%$		885
$\mu^- \bar{\nu}_\mu \nu_\tau \gamma$	[e] $(3.6 \pm 0.4) \times 10^{-3}$		-
$e^- \bar{\nu}_e \nu_\tau$	[g] $(17.83 \pm 0.06)\%$		889
$e^- \bar{\nu}_e \nu_\tau \gamma$	[e] $(1.75 \pm 0.18)\%$		-
$h^- \geq 0$ neutrals $\geq 0 K_L^0 \nu_\tau$	$(49.51 \pm 0.15)\%$	S=1.2	-
$h^- \geq 0 K_L^0 \nu_\tau$	$(12.35 \pm 0.12)\%$	S=1.4	-
$h^- \nu_\tau$	$(11.79 \pm 0.12)\%$	S=1.4	-
$\pi^- \nu_\tau$	[g] $(11.09 \pm 0.12)\%$	S=1.4	883
$K^- \nu_\tau$	[g] $(6.99 \pm 0.27) \times 10^{-3}$		820
$h^- \geq 1$ neutrals ν_τ	$(36.88 \pm 0.17)\%$	S=1.2	-
$h^- \pi^0 \nu_\tau$	$(25.86 \pm 0.14)\%$	S=1.1	-
$\pi^- \pi^0 \nu_\tau$	[g] $(25.40 \pm 0.14)\%$	S=1.1	878
$\pi^- \pi^0 \text{non-}\rho(770) \nu_\tau$	$(3.0 \pm 3.2) \times 10^{-3}$		878
$K^- \pi^0 \nu_\tau$	[g] $(4.54 \pm 0.33) \times 10^{-3}$		814
$h^- \geq 2\pi^0 \nu_\tau$	$(10.73 \pm 0.16)\%$	S=1.2	-
$h^- 2\pi^0 \nu_\tau$	$(9.36 \pm 0.14)\%$	S=1.2	-
$h^- 2\pi^0 \nu_\tau (\text{ex. } K^0)$	$(9.19 \pm 0.14)\%$	S=1.2	-
$\pi^- 2\pi^0 \nu_\tau (\text{ex. } K^0)$	[g] $(9.13 \pm 0.14)\%$	S=1.2	862
$\pi^- 2\pi^0 \nu_\tau (\text{ex. } K^0)$, scalar	< 9 $\times 10^{-3}$	CL=95%	-
$\pi^- 2\pi^0 \nu_\tau (\text{ex. } K^0)$, vector	< 7 $\times 10^{-3}$	CL=95%	-
$K^- 2\pi^0 \nu_\tau (\text{ex. } K^0)$	[g] $(6.0 \pm 2.4) \times 10^{-4}$		796
$h^- \geq 3\pi^0 \nu_\tau$	$(1.37 \pm 0.11)\%$	S=1.1	-
$h^- 3\pi^0 \nu_\tau$	$(1.21 \pm 0.10)\%$	S=1.1	-
$\pi^- 3\pi^0 \nu_\tau (\text{ex. } K^0)$	[g] $(1.08 \pm 0.10)\%$	S=1.1	836
$K^- 3\pi^0 \nu_\tau (\text{ex. } K^0)$, η	[g] $(3.9 \pm 2.3) \times 10^{-4}$		766
$h^- 4\pi^0 \nu_\tau (\text{ex. } K^0)$	$(1.6 \pm 0.6) \times 10^{-3}$		-
$h^- 4\pi^0 \nu_\tau (\text{ex. } K^0, \eta)$	[g] $(1.0 \pm 0.6) \times 10^{-3}$		-
$K^- \geq 0\pi^0 \geq 0 K^0 \nu_\tau$	$(1.58 \pm 0.06)\%$		-
$K^- \geq 1(\pi^0 \text{ or } K^0) \nu_\tau$	$(8.8 \pm 0.5) \times 10^{-3}$		-

Lepton Summary Table

Modes with K^0 's				Modes with five charged particles				
$K^0(\text{particles})^- \nu_\tau$	(1.71±0.06) %	S=1.1	—	$3h^- 2h^+ \geq 0$ neutrals ν_τ	(9.9±0.7) × 10 ⁻⁴	—	—	
$h^- \bar{K}^0 \geq 0$ neutrals $\geq 0 K_L^0 \nu_\tau$	(1.67±0.06) %	S=1.1	—	(ex. $K_S^0 \rightarrow \pi^- \pi^+$)	—	—	—	
$h^- \bar{K}^0 \nu_\tau$	(1.06±0.05) %	S=1.2	—	("5-prong")	—	—	—	
$\pi^- \bar{K}^0 \nu_\tau$	[g] (9.0±0.4) × 10 ⁻³	S=1.1	812	$3h^- 2h^+ \nu_\tau$ (ex. K^0)	[g] (7.8±0.6) × 10 ⁻⁴	—	—	
$\pi^- \bar{K}^0 \nu_\tau$	< 1.7 × 10 ⁻³	CL=95%	812	$3h^- 2h^+ \pi^0 \nu_\tau$ (ex. K^0)	[g] (2.2±0.5) × 10 ⁻⁴	—	—	
(non- $K^*(892)^-$) ν_τ	—	—	—	$3h^- 2h^+ 2\pi^0 \nu_\tau$	< 1.1 × 10 ⁻⁴	CL=90%	—	
$K^- K^0 \nu_\tau$	[g] (1.55±0.17) × 10 ⁻³	—	737	Miscellaneous other allowed modes				
$K^- \bar{K}^0 \geq 0 \pi^0 \nu_\tau$	(3.12±0.25) × 10 ⁻³	—	—	$(5\pi)^- \nu_\tau$	(7.9±0.7) × 10 ⁻³	—	—	
$h^- \bar{K}^0 \pi^0 \nu_\tau$	(5.3±0.4) × 10 ⁻³	—	—	$4h^- 3h^+ \geq 0$ neutrals ν_τ	< 2.4 × 10 ⁻⁶	CL=90%	—	
$\pi^- \bar{K}^0 \pi^0 \nu_\tau$	[g] (3.8±0.4) × 10 ⁻³	—	794	("7-prong")	—	—	—	
$\bar{K}^0 \rho^- \nu_\tau$	(2.2±0.5) × 10 ⁻³	—	—	$X^-(S=-1) \nu_\tau$	(2.89±0.09) %	S=1.1	—	
$K^- K^0 \pi^0 \nu_\tau$	[g] (1.57±0.21) × 10 ⁻³	—	685	$K^*(892)^- \geq 0(h^0 \neq K_S^0) \nu_\tau$	(1.94±0.31) %	—	—	
$\pi^- \bar{K}^0 \geq 1\pi^0 \nu_\tau$	(3.2±1.0) × 10 ⁻³	—	—	$K^*(892)^- \geq 0$ neutrals ν_τ	(1.33±0.13) %	—	—	
$\pi^- \bar{K}^0 \pi^0 \nu_\tau$	(2.6±2.4) × 10 ⁻⁴	—	—	$K^*(892)^- \nu_\tau$	(1.29±0.05) %	—	665	
$K^- K^0 \pi^0 \nu_\tau$	< 1.6 × 10 ⁻⁴	CL=95%	—	$K^*(892)^0 K^- \geq 0$ neutrals ν_τ	(3.2±1.4) × 10 ⁻³	—	—	
$\pi^- K^0 \bar{K}^0 \nu_\tau$	[g] (1.19±0.20) × 10 ⁻³	S=1.2	682	$K^*(892)^0 K^- \nu_\tau$	(2.1±0.4) × 10 ⁻³	—	539	
$\pi^- K^0 K^0 \nu_\tau$	(3.0±0.5) × 10 ⁻⁴	S=1.2	—	$\bar{K}^*(892)^0 \pi^- \geq 0$ neutrals ν_τ	(3.8±1.7) × 10 ⁻³	—	—	
$\pi^- K^0 K_S^0 \nu_\tau$	(6.0±1.0) × 10 ⁻⁴	S=1.2	—	$\bar{K}^*(892)^0 \pi^- \nu_\tau$	(2.2±0.5) × 10 ⁻³	—	653	
$\pi^- K^0 K_L^0 \nu_\tau$	(3.1±2.3) × 10 ⁻⁴	—	—	$(\bar{K}^*(892) \pi)^- \nu_\tau \rightarrow$	(1.0±0.4) × 10 ⁻³	—	—	
$\pi^- K^0 \bar{K}^0 \pi^0 \nu_\tau$	< 2.0 × 10 ⁻⁴	CL=95%	—	$\pi^- \bar{K}^0 \pi^0 \nu_\tau$	—	—	—	
$\pi^- K_S^0 K_L^0 \pi^0 \nu_\tau$	(3.1±1.2) × 10 ⁻⁴	—	—	$K_1(1270)^- \nu_\tau$	(4.7±1.1) × 10 ⁻³	—	433	
$\pi^- K_S^0 K_S^0 \pi^0 \nu_\tau$	< 2.0 × 10 ⁻⁴	CL=95%	—	$K_1(1400)^- \nu_\tau$	(1.7±2.6) × 10 ⁻³	S=1.7	335	
$K^0 h^+ h^- \geq 0$ neutrals ν_τ	< 1.7 × 10 ⁻³	CL=95%	—	$K^*(1410)^- \nu_\tau$	(1.5 ^{+1.4} _{-1.0}) × 10 ⁻³	—	—	
$K^0 h^+ h^- h^- \nu_\tau$	(2.3±2.0) × 10 ⁻⁴	—	—	$K_0^*(1430)^- \nu_\tau$	< 5 × 10 ⁻⁴	CL=95%	—	
Modes with three charged particles				$K_2^*(1430)^- \nu_\tau$	< 3 × 10 ⁻³	CL=95%	317	
$h^- h^- h^+ \geq 0$ neutrals ν_τ ("3-prong")	(15.18±0.13) %	S=1.2	—	$\eta \pi^- \nu_\tau$	< 1.4 × 10 ⁻⁴	CL=95%	798	
$h^- h^- h^+ \geq 0$ neutrals ν_τ	(14.58±0.13) %	S=1.2	—	$\eta \pi^- \pi^0 \nu_\tau$	[g] (1.74±0.24) × 10 ⁻³	—	778	
(ex. $K_S^0 \rightarrow \pi^+ \pi^-$)	—	—	—	$\eta \pi^- \pi^0 \pi^0 \nu_\tau$	(1.4±0.7) × 10 ⁻⁴	—	746	
$\pi^- \pi^+ \pi^- \geq 0$ neutrals ν_τ	(14.49±0.14) %	—	—	$\eta K^- \nu_\tau$	[g] (2.7±0.6) × 10 ⁻⁴	—	720	
$h^- h^- h^+ \nu_\tau$	(9.97±0.10) %	S=1.1	—	$\eta K^*(892)^- \nu_\tau$	(2.9±0.9) × 10 ⁻⁴	—	—	
$h^- h^- h^+ \nu_\tau$ (ex. K^0)	(9.61±0.10) %	S=1.1	—	$\eta K^- \pi^0 \nu_\tau$	(1.8±0.9) × 10 ⁻⁴	—	—	
$h^- h^- h^+ \nu_\tau$ (ex. K^0, ω)	(9.56±0.10) %	S=1.1	—	$\eta \bar{K}^0 \pi^- \nu_\tau$	(2.2±0.7) × 10 ⁻⁴	—	—	
$\pi^- \pi^+ \pi^- \nu_\tau$	(9.49±0.11) %	S=1.1	—	$\eta \pi^+ \pi^- \pi^- \geq 0$ neutrals ν_τ	< 3 × 10 ⁻³	CL=90%	—	
$\pi^- \pi^+ \pi^- \nu_\tau$ (ex. K^0)	(9.18±0.11) %	S=1.1	—	$\eta \pi^- \pi^+ \pi^- \nu_\tau$	(3.4±0.8) × 10 ⁻⁴	—	—	
$\pi^- \pi^+ \pi^- \nu_\tau$ (ex. K^0), non-axial vector	< 2.4 %	CL=95%	—	$\eta a_1(1260)^- \nu_\tau \rightarrow \eta \pi^- \rho^0 \nu_\tau$	< 3.9 × 10 ⁻⁴	CL=90%	—	
$\pi^- \pi^+ \pi^- \nu_\tau$ (ex. K^0, ω)	[g] (9.13±0.11) %	S=1.1	—	$\eta \eta \pi^- \nu_\tau$	< 1.1 × 10 ⁻⁴	CL=95%	—	
$h^- h^- h^+ \geq 1$ neutrals ν_τ	(5.17±0.11) %	S=1.2	—	$\eta \eta \pi^- \pi^0 \nu_\tau$	< 2.0 × 10 ⁻⁴	CL=95%	559	
$h^- h^- h^+ \geq 1$ neutrals ν_τ (ex. $K_S^0 \rightarrow \pi^+ \pi^-$)	(4.97±0.11) %	S=1.2	—	$\eta' (958) \pi^- \nu_\tau$	< 7.4 × 10 ⁻⁵	CL=90%	—	
$h^- h^- h^+ \pi^0 \nu_\tau$	(4.49±0.08) %	—	—	$\eta' (958) \pi^- \pi^0 \nu_\tau$	< 8.0 × 10 ⁻⁵	CL=90%	—	
$h^- h^- h^+ \pi^0 \nu_\tau$ (ex. K^0)	(4.30±0.08) %	—	—	$\phi \pi^- \nu_\tau$	< 2.0 × 10 ⁻⁴	CL=90%	585	
$h^- h^- h^+ \pi^0 \nu_\tau$ (ex. K^0, ω)	(2.58±0.08) %	—	—	$\phi K^- \nu_\tau$	< 6.7 × 10 ⁻⁵	CL=90%	—	
$\pi^- \pi^+ \pi^- \pi^0 \nu_\tau$	(4.32±0.08) %	—	—	$f_1(1285) \pi^- \nu_\tau$	(5.8±2.3) × 10 ⁻⁴	—	—	
$\pi^- \pi^+ \pi^- \pi^0 \nu_\tau$ (ex. K^0)	(4.20±0.08) %	—	—	$f_1(1285) \pi^- \nu_\tau \rightarrow$	(1.9±0.7) × 10 ⁻⁴	—	—	
$\pi^- \pi^+ \pi^- \pi^0 \nu_\tau$ (ex. K^0, ω)	[g] (2.47±0.08) %	—	—	$\eta \pi^- \pi^+ \pi^- \nu_\tau$	—	—	—	
$h^- h^- h^+ 2\pi^0 \nu_\tau$	(5.4±0.4) × 10 ⁻³	—	—	$\pi(1300)^- \nu_\tau \rightarrow (\rho \pi)^- \nu_\tau \rightarrow$	< 1.0 × 10 ⁻⁴	CL=90%	—	
$h^- h^- h^+ 2\pi^0 \nu_\tau$ (ex. K^0)	(5.3±0.4) × 10 ⁻³	—	—	$(3\pi)^- \nu_\tau$	—	—	—	
$h^- h^- h^+ 2\pi^0 \nu_\tau$ (ex. K^0, ω, η)	[g] (1.1±0.4) × 10 ⁻³	—	—	$\pi(1300)^- \nu_\tau \rightarrow$	< 1.9 × 10 ⁻⁴	CL=90%	—	
$h^- h^- h^+ \geq 3\pi^0 \nu_\tau$	[g] (1.3 ^{+0.8} _{-0.7}) × 10 ⁻³	S=1.3	—	$((\pi \pi)_{S\text{-wave}} \pi)^- \nu_\tau \rightarrow$	—	—	—	
$h^- h^- h^+ 3\pi^0 \nu_\tau$	(2.9±0.8) × 10 ⁻⁴	—	—	$(3\pi)^- \nu_\tau$	—	—	—	
$K^- h^+ h^- \geq 0$ neutrals ν_τ	(6.5±0.5) × 10 ⁻³	S=1.4	—	$h^- \omega \geq 0$ neutrals ν_τ	(2.36±0.08) %	—	—	
$K^- h^+ \pi^- \nu_\tau$ (ex. K^0)	(4.3±0.5) × 10 ⁻³	S=1.5	—	$h^- \omega \nu_\tau$	[g] (1.93±0.06) %	—	—	
$K^- h^+ \pi^- \pi^0 \nu_\tau$ (ex. K^0)	(1.07±0.22) × 10 ⁻³	—	—	$h^- \omega \pi^0 \nu_\tau$	[g] (4.3±0.5) × 10 ⁻³	—	—	
$K^- \pi^+ \pi^- \geq 0$ neutrals ν_τ	(4.4±0.5) × 10 ⁻³	S=1.4	—	$h^- \omega 2\pi^0 \nu_\tau$	(1.9±0.8) × 10 ⁻⁴	—	—	
$K^- \pi^+ \pi^- \geq 0\pi^0 \nu_\tau$ (ex. K^0)	(3.4±0.5) × 10 ⁻³	S=1.4	—	Lepton Family number (LF), Lepton number (L), or Baryon number (B) violating modes				
$K^- \pi^+ \pi^- \nu_\tau$ (ex. K^0)	(3.2±0.5) × 10 ⁻³	S=1.5	—	(In the modes below, ℓ means a sum over e and μ modes)				
$K^- \pi^+ \pi^- \nu_\tau$ (ex. K^0)	[g] (2.7±0.5) × 10 ⁻³	S=1.5	—	L means lepton number violation (e.g. $\tau^- \rightarrow e^+ \pi^- \pi^-$). Following common usage, LF means lepton family violation and not lepton number violation (e.g. $\tau^- \rightarrow e^- \pi^+ \pi^-$). B means baryon number violation.				
$K^- \pi^+ \pi^- \pi^0 \nu_\tau$	(1.20±0.25) × 10 ⁻³	—	—	$e^- \gamma$	LF	< 2.7 × 10 ⁻⁶	CL=90%	888
$K^- \pi^+ \pi^- \pi^0 \nu_\tau$ (ex. K^0)	(6.7±2.4) × 10 ⁻⁴	—	—	$\mu^- \gamma$	LF	< 1.1 × 10 ⁻⁶	CL=90%	885
$K^- \pi^+ \pi^- \pi^0 \nu_\tau$ (ex. K^0, η)	[g] (6.0±2.4) × 10 ⁻⁴	—	—	$e^- \pi^0$	LF	< 3.7 × 10 ⁻⁶	CL=90%	883
$K^- \pi^+ K^- \geq 0$ neut. ν_τ	< 9 × 10 ⁻⁴	CL=95%	—	$\mu^- \pi^0$	LF	< 4.0 × 10 ⁻⁶	CL=90%	880
$K^- K^+ \pi^- \geq 0$ neut. ν_τ	(2.01±0.23) × 10 ⁻³	—	—	$e^- K^0$	LF	< 1.3 × 10 ⁻³	CL=90%	819
$K^- K^+ \pi^- \nu_\tau$	[g] (1.61±0.18) × 10 ⁻³	—	685	$\mu^- K^0$	LF	< 1.0 × 10 ⁻³	CL=90%	815
$K^- K^+ \pi^- \pi^0 \nu_\tau$	[g] (4.0±1.6) × 10 ⁻⁴	—	—	$e^- \eta$	LF	< 8.2 × 10 ⁻⁶	CL=90%	804
$K^- K^+ K^- \geq 0$ neut. ν_τ	< 2.1 × 10 ⁻³	CL=95%	—	$\mu^- \eta$	LF	< 9.6 × 10 ⁻⁶	CL=90%	800
$K^- K^+ K^- \nu_\tau$	< 1.9 × 10 ⁻⁴	CL=90%	—	$e^- \rho^0$	LF	< 2.0 × 10 ⁻⁶	CL=90%	722
$\pi^- K^+ \pi^- \geq 0$ neut. ν_τ	< 2.5 × 10 ⁻³	CL=95%	—	$\mu^- \rho^0$	LF	< 6.3 × 10 ⁻⁶	CL=90%	718
$e^- e^- e^+ \bar{\nu}_e \nu_\tau$	(2.8±1.5) × 10 ⁻⁵	—	889	$e^- K^*(892)^0$	LF	< 5.1 × 10 ⁻⁶	CL=90%	663
$\mu^- e^- e^+ \bar{\nu}_\mu \nu_\tau$	< 3.6 × 10 ⁻⁵	CL=90%	885	$\mu^- K^*(892)^0$	LF	< 7.5 × 10 ⁻⁶	CL=90%	657
				$e^- \bar{K}^*(892)^0$	LF	< 7.4 × 10 ⁻⁶	CL=90%	663
				$\mu^- \bar{K}^*(892)^0$	LF	< 7.5 × 10 ⁻⁶	CL=90%	657
				$e^- \phi$	LF	< 6.9 × 10 ⁻⁶	CL=90%	596
				$\mu^- \phi$	LF	< 7.0 × 10 ⁻⁶	CL=90%	590
				$\pi^- \gamma$	L	< 2.8 × 10 ⁻⁴	CL=90%	883

Lepton Summary Table

$\pi^- \pi^0$	L	< 3.7	$\times 10^{-4}$	CL=90%	878
$e^- e^+ e^-$	LF	< 2.9	$\times 10^{-6}$	CL=90%	888
$e^- \mu^+ \mu^-$	LF	< 1.8	$\times 10^{-6}$	CL=90%	882
$e^+ \mu^- \mu^-$	LF	< 1.5	$\times 10^{-6}$	CL=90%	882
$\mu^- e^+ e^-$	LF	< 1.7	$\times 10^{-6}$	CL=90%	885
$\mu^+ e^- e^-$	LF	< 1.5	$\times 10^{-6}$	CL=90%	885
$\mu^- \mu^+ \mu^-$	LF	< 1.9	$\times 10^{-6}$	CL=90%	873
$e^- \pi^+ \pi^-$	LF	< 2.2	$\times 10^{-6}$	CL=90%	877
$e^+ \pi^- \pi^-$	L	< 1.9	$\times 10^{-6}$	CL=90%	877
$\mu^- \pi^+ \pi^-$	LF	< 8.2	$\times 10^{-6}$	CL=90%	866
$\mu^+ \pi^- \pi^-$	L	< 3.4	$\times 10^{-6}$	CL=90%	866
$e^- \pi^+ K^-$	LF	< 6.4	$\times 10^{-6}$	CL=90%	814
$e^- \pi^- K^+$	LF	< 3.8	$\times 10^{-6}$	CL=90%	814
$e^+ \pi^- K^-$	L	< 2.1	$\times 10^{-6}$	CL=90%	814
$e^- K^+ K^-$	LF	< 6.0	$\times 10^{-6}$	CL=90%	739
$e^+ K^- K^-$	L	< 3.8	$\times 10^{-6}$	CL=90%	739
$\mu^- \pi^+ K^-$	LF	< 7.5	$\times 10^{-6}$	CL=90%	800
$\mu^- \pi^- K^+$	LF	< 7.4	$\times 10^{-6}$	CL=90%	800
$\mu^+ \pi^- K^-$	L	< 7.0	$\times 10^{-6}$	CL=90%	800
$\mu^- K^+ K^-$	LF	< 1.5	$\times 10^{-5}$	CL=90%	699
$\mu^+ K^- K^-$	L	< 6.0	$\times 10^{-6}$	CL=90%	699
$e^- \pi^0 \pi^0$	LF	< 6.5	$\times 10^{-6}$	CL=90%	878
$\mu^- \pi^0 \pi^0$	LF	< 1.4	$\times 10^{-5}$	CL=90%	867
$e^- \eta \eta$	LF	< 3.5	$\times 10^{-5}$	CL=90%	700
$\mu^- \eta \eta$	LF	< 6.0	$\times 10^{-5}$	CL=90%	654
$e^- \pi^0 \eta$	LF	< 2.4	$\times 10^{-5}$	CL=90%	798
$\mu^- \pi^0 \eta$	LF	< 2.2	$\times 10^{-5}$	CL=90%	784
$\bar{p} \gamma$	L,B	< 3.5	$\times 10^{-6}$	CL=90%	641
$\bar{p} \pi^0$	L,B	< 1.5	$\times 10^{-5}$	CL=90%	632
$\bar{p} 2\pi^0$	L,B	< 3.3	$\times 10^{-5}$	CL=90%	-
$\bar{p} \eta$	L,B	< 8.9	$\times 10^{-6}$	CL=90%	476
$\bar{p} \pi^0 \eta$	L,B	< 2.7	$\times 10^{-5}$	CL=90%	-
$e^- \text{light boson}$	LF	< 2.7	$\times 10^{-3}$	CL=95%	-
$\mu^- \text{light boson}$	LF	< 5	$\times 10^{-3}$	CL=95%	-

Heavy Charged Lepton Searches

 L^\pm – charged leptonMass $m > 92.4$ GeV, CL = 95% ^[h] $m_\nu \approx 0$ L^\pm – stable charged heavy leptonMass $m > 93.5$ GeV, CL = 95%

Neutrinos

See the Particle Listings for a Note "Neutrino Mass" giving details of neutrinos, masses, mixing, and the status of experimental searches.

 ν_e

$$J = \frac{1}{2}$$

Mass $m < 3$ eV Interpretation of tritium beta decay experiments is complicated by anomalies near the endpoint, and the limits are not without ambiguity.Mean life/mass, $\tau/m_{\nu_e} > 7 \times 10^9$ s/eV (solar)Mean life/mass, $\tau/m_{\nu_e} > 300$ s/eV, CL = 90% (reactor)Magnetic moment $\mu < 1.5 \times 10^{-10} \mu_B$, CL = 90% ν_μ

$$J = \frac{1}{2}$$

Mass $m < 0.19$ MeV, CL = 90% ^[f]Mean life/mass, $\tau/m_{\nu_\mu} > 15.4$ s/eV, CL = 90%Magnetic moment $\mu < 7.4 \times 10^{-10} \mu_B$, CL = 90% ν_τ

$$J = \frac{1}{2}$$

Mass $m < 18.2$ MeV, CL = 95% ^[j]Magnetic moment $\mu < 5.4 \times 10^{-7} \mu_B$, CL = 90%Electric dipole moment $d < 5.2 \times 10^{-17}$ e cm, CL = 95%

Number of Light Neutrino Types

(including ν_e , ν_μ , and ν_τ)Number $N = 2.994 \pm 0.012$ (Standard Model fits to LEP data)Number $N = 3.00 \pm 0.06$ (Direct measurement of invisible Z width)

Massive Neutrinos and Lepton Mixing, Searches for

For excited leptons, see Compositeness Limits below.

See the Particle Listings for a Note "Neutrino Mass" giving details of neutrinos, masses, mixing, and the status of experimental searches.

There is now rather convincing evidence that neutrinos have nonzero mass from the apparent observation of neutrino oscillations, where the neutrinos come from π (or K) $\rightarrow \mu \rightarrow e$ decays in the atmosphere; the mesons are produced in cosmic-ray cascades.

Stable Neutral Heavy Lepton Mass Limits

Mass $m > 45.0$ GeV, CL = 95% (Dirac)Mass $m > 39.5$ GeV, CL = 95% (Majorana)

Neutral Heavy Lepton Mass Limits

Mass $m > 83.3$ GeV, CL = 95%(Dirac ν_L coupling to e, μ, τ ; conservative case(τ))Mass $m > 73.5$ GeV, CL = 95%(Majorana ν_L coupling to e, μ, τ ; conservative case(τ))

Solar Neutrinos

Detectors using gallium ($E_\nu \gtrsim 0.2$ MeV), chlorine ($E_\nu \gtrsim 0.8$ MeV), and Čerenkov effect in water ($E_\nu \gtrsim 7$ MeV) measure significantly lower neutrino rates than are predicted from solar models. The deficit in the solar neutrino flux compared with solar model calculations could be explained by oscillations with $\Delta m^2 \leq 10^{-5}$ eV² causing the disappearance of ν_e .

Atmospheric Neutrinos

Underground detectors observing neutrinos produced by cosmic rays in the atmosphere have measured a ν_μ/ν_e ratio much less than expected and also a deficiency of upward going ν_μ compared to downward. This could be explained by oscillations leading to the disappearance of ν_μ with $\Delta m^2 \approx 10^{-3}$ to 0.1 eV². This is presently the best evidence for neutrino mass. ν oscillation: $\bar{\nu}_e \leftrightarrow \bar{\nu}_e$ (θ = mixing angle) $\Delta m^2 < 7 \times 10^{-4}$ eV², CL = 90% (if $\sin^2 2\theta = 1$) $\sin^2 2\theta < 0.02$, CL = 90% (if $\Delta(m^2)$ is large) ν oscillation: $\nu_\mu (\bar{\nu}_\mu) \rightarrow \nu_e (\bar{\nu}_e)$ (any combination) $\Delta m^2 < 0.075$ eV², CL = 90% (if $\sin^2 2\theta = 1$) $\sin^2 2\theta < 1.8 \times 10^{-3}$, CL = 90% (if $\Delta(m^2)$ is large)

NOTES

In this Summary Table:

When a quantity has "(S = ...)" to its right, the error on the quantity has been enlarged by the "scale factor" S, defined as $S = \sqrt{\chi^2/(N-1)}$, where N is the number of measurements used in calculating the quantity. We do this when $S > 1$, which often indicates that the measurements are inconsistent. When $S > 1.25$, we also show in the Particle Listings an ideogram of the measurements. For more about S, see the Introduction.

A decay momentum p is given for each decay mode. For a 2-body decay, p is the momentum of each decay product in the rest frame of the decaying particle. For a 3-or-more-body decay, p is the largest momentum any of the products can have in this frame.

[a] This is the best "electron disappearance" limit. The best limit for the mode $e^- \rightarrow \nu \gamma$ is $> 2.35 \times 10^{25}$ yr (CL=68%).[b] See the "Note on Muon Decay Parameters" in the μ Particle Listings for definitions and details.[c] P_μ is the longitudinal polarization of the muon from pion decay. In standard V-A theory, $P_\mu = 1$ and $\rho = \delta = 3/4$.[d] This only includes events with the γ energy > 10 MeV. Since the $e^- \bar{\nu}_e \nu_\mu$ and $e^- \bar{\nu}_e \nu_\mu \gamma$ modes cannot be clearly separated, we regard the latter mode as a subset of the former.

[e] See the relevant Particle Listings for the energy limits used in this measurement.

[f] A test of additive vs. multiplicative lepton family number conservation.

[g] Basis mode for the τ .[h] L^\pm mass limit depends on decay assumptions; see the Full Listings.[i] Assumes ν_2 is the dominant mass eigenstate.[j] Assumes ν_3 is the dominant mass eigenstate.

Quark Summary Table

QUARKS

The u -, d -, and s -quark masses are estimates of so-called "current-quark masses," in a mass-independent subtraction scheme such as $\overline{\text{MS}}$ at a scale $\mu \approx 2$ GeV. The c - and b -quark masses are estimated from charmonium, bottomonium, D , and B masses. They are the "running" masses in the $\overline{\text{MS}}$ scheme. These can be different from the heavy quark masses obtained in potential models.

u	$I(J^P) = \frac{1}{2}(\frac{1}{2}^+)$
Mass $m = 1$ to 5 MeV [a] $m_u/m_d = 0.2$ to 0.8	Charge = $\frac{2}{3} e$ $I_z = +\frac{1}{2}$
d	$I(J^P) = \frac{1}{2}(\frac{1}{2}^+)$
Mass $m = 3$ to 9 MeV [a] $m_s/m_d = 17$ to 25 $\bar{m} = (m_u + m_d)/2 = 2.5$ to 6 MeV	Charge = $-\frac{1}{3} e$ $I_z = -\frac{1}{2}$
s	$I(J^P) = 0(\frac{1}{2}^+)$
Mass $m = 75$ to 170 MeV [a] $(m_s - (m_u + m_d)/2)/(m_d - m_u) = 34$ to 51	Charge = $-\frac{1}{3} e$ Strangeness = -1
c	$I(J^P) = 0(\frac{1}{2}^+)$
Mass $m = 1.15$ to 1.35 GeV	Charge = $\frac{2}{3} e$ Charm = $+1$
b	$I(J^P) = 0(\frac{1}{2}^+)$
Mass $m = 4.0$ to 4.4 GeV	Charge = $-\frac{1}{3} e$ Bottom = -1

t

$I(J^P) = 0(\frac{1}{2}^+)$

Charge = $\frac{2}{3} e$ Top = $+1$

Mass $m = 174.3 \pm 5.1$ GeV (direct observation of top events)
 Mass $m = 168.2^{+9.6}_{-7.4}$ GeV (Standard Model electroweak fit)

t DECAY MODES	Fraction (Γ_i/Γ)	Confidence level	ρ (MeV/c)
Wb			—
$\ell\nu_\ell$ anything	[b,c] (9.4 ± 2.4) %		—
$\tau\nu_\tau b$			—
$\gamma q (q=u,c)$	[d] < 3.2 %	95%	—
$\Delta T = 1$ weak neutral current (TI) modes			
$Zq (q=u,c)$	T1 [e] < 33 %	95%	—

t' (4th Generation) Quark, Searches for

Mass $m > 199$ GeV, CL = 95% ($\rho\bar{\rho}$, neutral-current decays)
 Mass $m > 128$ GeV, CL = 95% ($\rho\bar{\rho}$, charged-current decays)
 Mass $m > 46.0$ GeV, CL = 95% (e^+e^- , all decays)

Free Quark Searches

All searches since 1977 have had negative results.

NOTES

- [a] The ratios m_u/m_d and m_s/m_d are extracted from pion and kaon masses using chiral symmetry. The estimates of u and d masses are not without controversy and remain under active investigation. Within the literature there are even suggestions that the u quark could be essentially massless. The s -quark mass is estimated from SU(3) splittings in hadron masses.
- [b] ℓ means e or μ decay mode, not the sum over them.
- [c] Assumes lepton universality and W -decay acceptance.
- [d] This limit is for $\Gamma(t \rightarrow \gamma q)/\Gamma(t \rightarrow Wb)$.
- [e] This limit is for $\Gamma(t \rightarrow Zq)/\Gamma(t \rightarrow Wb)$.

Meson Summary Table

LIGHT UNFLAVORED MESONS ($S = C = B = 0$)

For $l = 1$ (π, ρ, ω): $u\bar{d}, (u\bar{u}-d\bar{d})/\sqrt{2}, d\bar{u}$;
for $l = 0$ ($\eta, \eta', h, h', \omega, \phi, f, f'$): $c_1(u\bar{u} + d\bar{d}) + c_2(s\bar{s})$

 π^\pm

$$I^G(J^{PC}) = 1^-(0^-)$$

Mass $m = 139.57018 \pm 0.00035$ MeV ($S = 1.2$)
Mean life $\tau = (2.6033 \pm 0.0005) \times 10^{-8}$ s ($S = 1.2$)
 $c\tau = 7.8045$ m

$\pi^\pm \rightarrow \ell^\pm \nu \gamma$ form factors [a]

$F_V = 0.017 \pm 0.008$
 $F_A = 0.0116 \pm 0.0016$ ($S = 1.3$)
 $R = 0.059^{+0.009}_{-0.008}$

π^- modes are charge conjugates of the modes below.

π^\pm DECAY MODES	Fraction (Γ_i/Γ)	Confidence level	p (MeV/c)
$\mu^+ \nu_\mu$	[b] (99.96770 \pm 0.00004) %		30
$\mu^+ \nu_\mu \gamma$	[c] (2.00 \pm 0.25) $\times 10^{-4}$		30
$e^+ \nu_e$	[b] (1.230 \pm 0.004) $\times 10^{-4}$		70
$e^+ \nu_e \gamma$	[c] (1.61 \pm 0.23) $\times 10^{-7}$		70
$e^+ \nu_e \pi^0$	(1.025 \pm 0.034) $\times 10^{-8}$		4
$e^+ \nu_e e^+ e^-$	(3.2 \pm 0.5) $\times 10^{-9}$		70
$e^+ \nu_e \nu \bar{\nu}$	< 5 $\times 10^{-6}$	90%	70
Lepton Family number (LF) or Lepton number (L) violating modes			
$\mu^+ \bar{\nu}_e$	L [d] < 1.5 $\times 10^{-3}$	90%	30
$\mu^+ \nu_e$	LF [d] < 8.0 $\times 10^{-3}$	90%	30
$\mu^- e^+ e^+ \nu$	LF < 1.6 $\times 10^{-6}$	90%	30

 π^0

$$I^G(J^{PC}) = 1^-(0^{++})$$

Mass $m = 134.9766 \pm 0.0006$ MeV ($S = 1.1$)
 $m_{\pi^\pm} - m_{\pi^0} = 4.5936 \pm 0.0005$ MeV
Mean life $\tau = (8.4 \pm 0.6) \times 10^{-17}$ s ($S = 3.0$)
 $c\tau = 25.1$ nm

π^0 DECAY MODES	Fraction (Γ_i/Γ)	Scale factor/ Confidence level	p (MeV/c)
2γ	(98.798 \pm 0.032) %	S=1.1	67
$e^+ e^- \gamma$	(1.198 \pm 0.032) %	S=1.1	67
γ positronium	(1.82 \pm 0.29) $\times 10^{-9}$		67
$e^+ e^+ e^- e^-$	(3.14 \pm 0.30) $\times 10^{-5}$		67
$e^+ e^-$	(6.2 \pm 0.5) $\times 10^{-8}$		67
4γ	< 2 $\times 10^{-8}$	CL=90%	67
$\nu \bar{\nu}$	[e] < 8.3 $\times 10^{-7}$	CL=90%	67
$\nu_e \bar{\nu}_e$	< 1.7 $\times 10^{-6}$	CL=90%	67
$\nu_\mu \bar{\nu}_\mu$	< 3.1 $\times 10^{-6}$	CL=90%	67
$\nu_\tau \bar{\nu}_\tau$	< 2.1 $\times 10^{-6}$	CL=90%	67
Charge conjugation (C) or Lepton Family number (LF) violating modes			
3γ	C < 3.1 $\times 10^{-8}$	CL=90%	67
$\mu^+ e^- + e^- \mu^+$	LF < 1.72 $\times 10^{-8}$	CL=90%	26

 η

$$I^G(J^{PC}) = 0^+(0^{-+})$$

Mass $m = 547.30 \pm 0.12$ MeV
Full width $\Gamma = 1.18 \pm 0.11$ keV [f] ($S = 1.8$)

C-nonconserving decay parameters

$\pi^+ \pi^- \pi^0$ Left-right asymmetry = $(0.09 \pm 0.17) \times 10^{-2}$
 $\pi^+ \pi^- \pi^0$ Sextant asymmetry = $(0.18 \pm 0.16) \times 10^{-2}$
 $\pi^+ \pi^- \pi^0$ Quadrant asymmetry = $(-0.17 \pm 0.17) \times 10^{-2}$
 $\pi^+ \pi^- \gamma$ Left-right asymmetry = $(0.9 \pm 0.4) \times 10^{-2}$
 $\pi^+ \pi^- \gamma$ β (D-wave) = 0.05 ± 0.06 ($S = 1.5$)

Dalitz plot parameter

$\pi^0 \pi^0 \pi^0$ $\alpha = -0.039 \pm 0.015$

η DECAY MODES	Fraction (Γ_i/Γ)	Scale factor/ Confidence level	p (MeV/c)
Neutral modes			
neutral modes	(71.6 \pm 0.4) %	S=1.2	—
2γ	[f] (39.33 \pm 0.25) %	S=1.1	274
$3\pi^0$	(32.24 \pm 0.29) %	S=1.2	178
$\pi^0 2\gamma$	(7.1 \pm 1.4) $\times 10^{-4}$		257
other neutral modes	< 2.8 %	CL=90%	—
Charged modes			
charged modes	(28.3 \pm 0.4) %	S=1.2	—
$\pi^+ \pi^- \pi^0$	(23.0 \pm 0.4) %	S=1.2	173
$\pi^+ \pi^- \gamma$	(4.75 \pm 0.11) %	S=1.1	235
$e^+ e^- \gamma$	(4.9 \pm 1.1) $\times 10^{-3}$		274
$\mu^+ \mu^- \gamma$	(3.1 \pm 0.4) $\times 10^{-4}$		252
$e^+ e^-$	< 7.7 $\times 10^{-5}$	CL=90%	274
$\mu^+ \mu^-$	(5.8 \pm 0.8) $\times 10^{-6}$		252
$\pi^+ \pi^- e^+ e^-$	(1.3 $^{+1.2}_{-0.8}$) $\times 10^{-3}$		235
$\pi^+ \pi^- 2\gamma$	< 2.1 $\times 10^{-3}$		235
$\pi^+ \pi^- \pi^0 \gamma$	< 6 $\times 10^{-4}$	CL=90%	173
$\pi^0 \mu^+ \mu^- \gamma$	< 3 $\times 10^{-6}$	CL=90%	210

**Charge conjugation (C), Parity (P),
Charge conjugation \times Parity (CP), or
Lepton Family number (LF) violating modes**

$\pi^+ \pi^-$	P, CP < 3.3 $\times 10^{-4}$	CL=90%	235
$\pi^0 \pi^0$	P, CP < 4.3 $\times 10^{-4}$	CL=90%	—
3γ	C < 5 $\times 10^{-4}$	CL=95%	274
$\pi^0 e^+ e^-$	C [g] < 4 $\times 10^{-5}$	CL=90%	257
$\pi^0 \mu^+ \mu^-$	C [g] < 5 $\times 10^{-6}$	CL=90%	210
$\mu^+ e^- + \mu^- e^+$	LF < 6 $\times 10^{-6}$	CL=90%	263

$f_0(400-1200)$ [h]
or σ

$$I^G(J^{PC}) = 0^+(0^{++})$$

Mass $m = (400-1200)$ MeV
Full width $\Gamma = (600-1000)$ MeV

$f_0(400-1200)$ DECAY MODES	Fraction (Γ_i/Γ)	p (MeV/c)
$\pi \pi$	dominant	—
$\gamma \gamma$	seen	—

Meson Summary Table

$\rho(770)^{[1]}$		$I^G(J^{PC}) = 1^+(1^{--})$	
Mass $m = 769.3 \pm 0.8$ MeV ($S = 2.1$)			
Full width $\Gamma = 150.2 \pm 0.8$ MeV			
$\Gamma_{ee} = 6.77 \pm 0.32$ keV			
$\rho(770)$ DECAY MODES	Fraction (Γ_i/Γ)	Scale factor/ Confidence level	ρ (MeV/c)
$\pi\pi$	~ 100	%	358
$\rho(770)^\pm$ decays			
$\pi^\pm\gamma$	$(4.5 \pm 0.5) \times 10^{-4}$	$S=2.2$	372
$\pi^\pm\eta$	< 6	$\times 10^{-3}$ CL=84%	146
$\pi^\pm\pi^+\pi^-\pi^0$	< 2.0	$\times 10^{-3}$ CL=84%	249
$\rho(770)^0$ decays			
$\pi^+\pi^-\gamma$	$(9.9 \pm 1.6) \times 10^{-3}$		358
$\pi^0\gamma$	$(6.8 \pm 1.7) \times 10^{-4}$		372
$\eta\gamma$	$(2.4^{+0.8}_{-0.9}) \times 10^{-4}$	$S=1.6$	189
$\mu^+\mu^-$	$[j] (4.60 \pm 0.28) \times 10^{-5}$		369
e^+e^-	$[j] (4.49 \pm 0.22) \times 10^{-5}$		384
$\pi^+\pi^-\pi^0$	< 1.2	$\times 10^{-4}$ CL=90%	319
$\pi^+\pi^-\pi^+\pi^-$	$(1.8 \pm 0.9) \times 10^{-5}$		246
$\pi^+\pi^-\pi^0\pi^0$	< 4	$\times 10^{-5}$ CL=90%	252

$\omega(782)$		$I^G(J^{PC}) = 0^-(1^{--})$	
Mass $m = 782.57 \pm 0.12$ MeV ($S = 1.8$)			
Full width $\Gamma = 8.44 \pm 0.09$ MeV			
$\Gamma_{ee} = 0.60 \pm 0.02$ keV			
$\omega(782)$ DECAY MODES	Fraction (Γ_i/Γ)	Scale factor/ Confidence level	ρ (MeV/c)
$\pi^+\pi^-\pi^0$	$(88.8 \pm 0.7) \%$		327
$\pi^0\gamma$	$(8.5 \pm 0.5) \%$		379
$\pi^+\pi^-$	$(2.21 \pm 0.30) \%$		365
neutrals (excluding $\pi^0\gamma$)	$(5.3^{+8.7}_{-3.5}) \times 10^{-3}$		–
$\eta\gamma$	$(6.5 \pm 1.0) \times 10^{-4}$		199
$\pi^0 e^+ e^-$	$(5.9 \pm 1.9) \times 10^{-4}$		379
$\pi^0 \mu^+ \mu^-$	$(9.6 \pm 2.3) \times 10^{-5}$		349
$e^+ e^-$	$(7.07 \pm 0.19) \times 10^{-5}$	$S=1.1$	391
$\pi^+\pi^-\pi^0\pi^0$	< 2	% CL=90%	261
$\pi^+\pi^-\gamma$	< 3.6	$\times 10^{-3}$ CL=95%	365
$\pi^+\pi^-\pi^+\pi^-$	< 1	$\times 10^{-3}$ CL=90%	256
$\pi^0\pi^0\gamma$	$(7.2 \pm 2.5) \times 10^{-5}$		367
$\mu^+\mu^-$	< 1.8	$\times 10^{-4}$ CL=90%	376
3γ	< 1.9	$\times 10^{-4}$ CL=95%	391
Charge conjugation (C) violating modes			
$\eta\pi^0$	C < 1	$\times 10^{-3}$ CL=90%	162
$3\pi^0$	C < 3	$\times 10^{-4}$ CL=90%	329

$\eta'(958)$		$I^G(J^{PC}) = 0^+(0^{-+})$	
Mass $m = 957.78 \pm 0.14$ MeV			
Full width $\Gamma = 0.202 \pm 0.016$ MeV ($S = 1.3$)			
$\eta'(958)$ DECAY MODES	Fraction (Γ_i/Γ)	Scale factor/ Confidence level	ρ (MeV/c)
$\pi^+\pi^-\eta$	$(44.3 \pm 1.5) \%$	$S=1.2$	232
$\rho^0\gamma$ (including non-resonant $\pi^+\pi^-\gamma$)	$(29.5 \pm 1.0) \%$	$S=1.2$	169
$\pi^0\pi^0\eta$	$(20.9 \pm 1.2) \%$	$S=1.2$	239
$\omega\gamma$	$(3.03 \pm 0.31) \%$		160
$\gamma\gamma$	$(2.12 \pm 0.14) \%$	$S=1.3$	479
$3\pi^0$	$(1.56 \pm 0.26) \times 10^{-3}$		430
$\mu^+\mu^-\gamma$	$(1.04 \pm 0.26) \times 10^{-4}$		467
$\pi^+\pi^-\pi^0$	< 5	% CL=90%	427
$\pi^0\rho^0$	< 4	% CL=90%	118
$\pi^+\pi^+\pi^-\pi^-$	< 1	% CL=90%	372
$\pi^+\pi^+\pi^-\pi^-\pi^0$	< 1	% CL=95%	–
$\pi^+\pi^+\pi^-\pi^-\pi^0$	< 1	% CL=90%	298
6π	< 1	% CL=90%	189
$\pi^+\pi^-\pi^0 e^+ e^-$	< 6	$\times 10^{-3}$ CL=90%	458
$\pi^0\gamma\gamma$	< 8	$\times 10^{-4}$ CL=90%	469
$4\pi^0$	< 5	$\times 10^{-4}$ CL=90%	379
$e^+ e^-$	< 2.1	$\times 10^{-7}$ CL=90%	479

Charge conjugation (C), Parity (P), Lepton family number (LF) violating modes			
$\pi^+\pi^-$	P, CP	< 2	% CL=90% 458
$\pi^0\pi^0$	P, CP	< 9	$\times 10^{-4}$ CL=90% 459
$\gamma e^+ e^-$	C	< 9	$\times 10^{-4}$ CL=90% –
$\pi^0 e^+ e^-$	C	$[g] < 1.4$	$\times 10^{-3}$ CL=90% 469
$\eta e^+ e^-$	C	$[g] < 2.4$	$\times 10^{-3}$ CL=90% 322
3γ	C	< 1.0	$\times 10^{-4}$ CL=90% 479
$\mu^+\mu^-\pi^0$	C	$[g] < 6.0$	$\times 10^{-5}$ CL=90% 445
$\mu^+\mu^-\eta$	C	$[g] < 1.5$	$\times 10^{-5}$ CL=90% 274
$e\mu$	LF	< 4.7	$\times 10^{-4}$ CL=90% –

$f_0(980)^{[K]}$		$I^G(J^{PC}) = 0^+(0^{++})$	
Mass $m = 980 \pm 10$ MeV			
Full width $\Gamma = 40$ to 100 MeV			
$f_0(980)$ DECAY MODES	Fraction (Γ_i/Γ)	ρ (MeV/c)	
$\pi\pi$	dominant	470	
$K\bar{K}$	seen	–	

$a_0(980)^{[K]}$		$I^G(J^{PC}) = 1^-(0^{++})$	
Mass $m = 984.8 \pm 1.4$ MeV ($S = 1.7$)			
Full width $\Gamma = 50$ to 100 MeV			
$a_0(980)$ DECAY MODES	Fraction (Γ_i/Γ)	ρ (MeV/c)	
$\eta\pi$	dominant	321	
$K\bar{K}$	seen	–	
$\gamma\gamma$	seen	492	

$\phi(1020)$		$I^G(J^{PC}) = 0^-(1^{--})$	
Mass $m = 1019.417 \pm 0.014$ MeV ($S = 1.8$)			
Full width $\Gamma = 4.458 \pm 0.032$ MeV			
$\phi(1020)$ DECAY MODES	Fraction (Γ_i/Γ)	Scale factor/ Confidence level	ρ (MeV/c)
K^+K^-	$(49.2 \pm 0.7) \%$	$S=1.2$	127
$K_L^0 K_S^0$	$(33.8 \pm 0.6) \%$	$S=1.2$	110
$\rho\pi + \pi^+\pi^-\pi^0$	$(15.5 \pm 0.6) \%$	$S=1.4$	–
$\eta\gamma$	$(1.297 \pm 0.033) \%$	$S=1.2$	363
$\pi^0\gamma$	$(1.26 \pm 0.10) \times 10^{-3}$		501
e^+e^-	$(2.91 \pm 0.07) \times 10^{-4}$	$S=1.2$	510
$\mu^+\mu^-$	$(3.7 \pm 0.5) \times 10^{-4}$		499
$\eta e^+ e^-$	$(1.3^{+0.8}_{-0.6}) \times 10^{-4}$		363
$\pi^+\pi^-$	$(7.5 \pm 1.4) \times 10^{-5}$		490
$\omega\pi^0$	$(4.8 \pm 2.0) \times 10^{-5}$		–
$\omega\gamma$	< 5	% CL=84%	210
$\rho\gamma$	< 1.2	$\times 10^{-5}$ CL=90%	219
$\pi^+\pi^-\gamma$	$(4.1 \pm 1.3) \times 10^{-5}$		490
$f_0(980)\gamma$	$(3.4 \pm 0.4) \times 10^{-4}$		39
$\pi^0\pi^0\gamma$	$(1.08 \pm 0.19) \times 10^{-4}$		492
$\pi^+\pi^-\pi^+\pi^-$	< 8.7	$\times 10^{-4}$ CL=90%	410
$\pi^+\pi^+\pi^-\pi^-\pi^0$	< 1.5	$\times 10^{-4}$ CL=95%	341
$\pi^0 e^+ e^-$	< 1.2	$\times 10^{-4}$ CL=90%	501
$\pi^0\eta\gamma$	$(8.6 \pm 1.8) \times 10^{-5}$		346
$a_0(980)\gamma$	< 5	$\times 10^{-3}$ CL=90%	36
$\eta'(958)\gamma$	$(6.7^{+3.5}_{-3.1}) \times 10^{-5}$		–
$\eta\pi^0\pi^0\gamma$	< 2	$\times 10^{-5}$ CL=90%	–
$\mu^+\mu^-\gamma$	$(1.4 \pm 0.5) \times 10^{-5}$		–
$\rho\gamma\gamma$	< 5	$\times 10^{-4}$ CL=90%	–
$\eta\pi^+\pi^-$	< 3	$\times 10^{-4}$ CL=90%	–

$h_1(1170)$		$I^G(J^{PC}) = 0^-(1^{+-})$	
Mass $m = 1170 \pm 20$ MeV			
Full width $\Gamma = 360 \pm 40$ MeV			
$h_1(1170)$ DECAY MODES	Fraction (Γ_i/Γ)	ρ (MeV/c)	
$\rho\pi$	seen	310	

Meson Summary Table

$b_1(1235)$		$I^G(J^{PC}) = 1^+(1^{+-})$	
Mass $m = 1229.5 \pm 3.2$ MeV ($S = 1.6$)			
Full width $\Gamma = 142 \pm 9$ MeV ($S = 1.2$)			
$b_1(1235)$ DECAY MODES	Fraction (Γ_i/Γ)	Confidence level	ρ (MeV/c)
$\omega\pi$	dominant		348
[D/S amplitude ratio = 0.29 ± 0.04]			
$\pi^\pm\gamma$	$(1.6 \pm 0.4) \times 10^{-3}$		608
$\eta\rho$	seen		—
$\pi^+\pi^+\pi^-\pi^0$	< 50 %	84%	536
$(K\bar{K})^\pm\pi^0$	< 8 %	90%	248
$K_S^0 K_S^0 \pi^\pm$	< 6 %	90%	238
$K_S^0 K_S^0 \pi^\pm$	< 2 %	90%	238
$\phi\pi$	< 1.5 %	84%	146

$a_1(1260)$ [l]		$I^G(J^{PC}) = 1^-(1^{++})$	
Mass $m = 1230 \pm 40$ MeV [m]			
Full width $\Gamma = 250$ to 600 MeV			
$a_1(1260)$ DECAY MODES	Fraction (Γ_i/Γ)		ρ (MeV/c)
$(\rho\pi)_{S\text{-wave}}$	seen		—
$(\rho\pi)_{D\text{-wave}}$	seen		—
$(\rho(1450)\pi)_{S\text{-wave}}$	seen		—
$(\rho(1450)\pi)_{D\text{-wave}}$	seen		—
$\sigma\pi$	seen		—
$f_0(980)\pi$	not seen		—
$f_0(1370)\pi$	seen		—
$f_2(1270)\pi$	seen		—
$K\bar{K}^*(892) + c.c.$	seen		—
$\pi(1300)\pi$	not seen		—
$\pi\gamma$	seen		607

$f_2(1270)$		$I^G(J^{PC}) = 0^+(2^{++})$	
Mass $m = 1275.4 \pm 1.2$ MeV			
Full width $\Gamma = 185.1^{+3.4}_{-2.6}$ MeV ($S = 1.5$)			
$f_2(1270)$ DECAY MODES	Fraction (Γ_i/Γ)	Scale factor/ Confidence level	ρ (MeV/c)
$\pi\pi$	$(84.7^{+2.4}_{-1.3})\%$	$S=1.3$	622
$\pi^+\pi^-2\pi^0$	$(7.1^{+1.5}_{-2.6})\%$	$S=1.3$	562
$K\bar{K}$	$(4.6 \pm 0.5)\%$	$S=2.8$	403
$2\pi^+2\pi^-$	$(2.8 \pm 0.4)\%$	$S=1.2$	559
$\eta\eta$	$(4.5 \pm 1.0) \times 10^{-3}$	$S=2.4$	327
$4\pi^0$	$(3.0 \pm 1.0) \times 10^{-3}$		564
$\gamma\gamma$	$(1.41 \pm 0.13) \times 10^{-5}$		637
$\eta\pi\pi$	< 8 %	$\times 10^{-3}$	475
$K_S^0 K_S^0 \pi^+ + c.c.$	< 3.4 %	$\times 10^{-3}$	293
e^+e^-	< 9 %	$\times 10^{-9}$	637

$f_1(1285)$		$I^G(J^{PC}) = 0^+(1^{++})$	
Mass $m = 1281.9 \pm 0.6$ MeV ($S = 1.7$)			
Full width $\Gamma = 24.0 \pm 1.2$ MeV ($S = 1.4$)			
$f_1(1285)$ DECAY MODES	Fraction (Γ_i/Γ)	Scale factor/ Confidence level	ρ (MeV/c)
4π	$(33.1^{+2.1}_{-1.8})\%$	$S=1.3$	563
$\pi^0\pi^0\pi^+\pi^-$	$(22.0^{+1.4}_{-1.2})\%$	$S=1.3$	566
$2\pi^+2\pi^-$	$(11.0^{+0.7}_{-0.6})\%$	$S=1.3$	563
$\rho^0\pi^+\pi^-$	$(11.0^{+0.7}_{-0.6})\%$	$S=1.3$	340
$4\pi^0$	< 7 %	$\times 10^{-4}$	568
$\eta\pi\pi$	$(52 \pm 16)\%$	$CL=90\%$	479
$a_0(980)\pi$ [ignoring $a_0(980) \rightarrow K\bar{K}$]	$(36 \pm 7)\%$		234
$\eta\pi\pi$ [excluding $a_0(980)\pi$]	$(16 \pm 7)\%$		—
$K\bar{K}\pi$	$(9.0 \pm 0.4)\%$	$S=1.1$	308
$K\bar{K}^*(892)$	not seen		—
$\gamma\rho^0$	$(5.5 \pm 1.3)\%$	$S=2.8$	410
$\phi\gamma$	$(7.4 \pm 2.6) \times 10^{-4}$		236

$\eta(1295)$		$I^G(J^{PC}) = 0^+(0^{-+})$	
Mass $m = 1297.0 \pm 2.8$ MeV			
Full width $\Gamma = 53 \pm 6$ MeV			
$\eta(1295)$ DECAY MODES	Fraction (Γ_i/Γ)		ρ (MeV/c)
$\eta\pi^+\pi^-$	seen		488
$a_0(980)\pi$	seen		245
$\eta\pi^0\pi^0$	seen		—
$\eta(\pi\pi)_{S\text{-wave}}$	seen		—

$\pi(1300)$		$I^G(J^{PC}) = 1^-(0^{-+})$	
Mass $m = 1300 \pm 100$ MeV [m]			
Full width $\Gamma = 200$ to 600 MeV			
$\pi(1300)$ DECAY MODES	Fraction (Γ_i/Γ)		ρ (MeV/c)
$\rho\pi$	seen		406
$\pi(\pi\pi)_{S\text{-wave}}$	seen		—

$a_2(1320)$		$I^G(J^{PC}) = 1^-(2^{++})$	
Mass $m = 1318.0 \pm 0.6$ MeV ($S = 1.1$)			
Full width $\Gamma = 107 \pm 5$ MeV [m]			
$a_2(1320)$ DECAY MODES	Fraction (Γ_i/Γ)	Scale factor/ Confidence level	ρ (MeV/c)
$\rho\pi$	$(70.1 \pm 2.7)\%$	$S=1.2$	419
$\eta\pi$	$(14.5 \pm 1.2)\%$		535
$\omega\pi\pi$	$(10.6 \pm 3.2)\%$	$S=1.3$	362
$K\bar{K}$	$(4.9 \pm 0.8)\%$		437
$\eta'(958)\pi$	$(5.3 \pm 0.9) \times 10^{-3}$		287
$\pi^\pm\gamma$	$(2.8 \pm 0.6) \times 10^{-3}$		652
$\gamma\gamma$	$(9.4 \pm 0.7) \times 10^{-6}$		659
$\pi^+\pi^-\pi^-$	< 8 %	$CL=90\%$	621
e^+e^-	< 2.3 %	$\times 10^{-7}$	$CL=90\%$ 659

$f_0(1370)$ [k]		$I^G(J^{PC}) = 0^+(0^{++})$	
Mass $m = 1200$ to 1500 MeV			
Full width $\Gamma = 200$ to 500 MeV			
$f_0(1370)$ DECAY MODES	Fraction (Γ_i/Γ)		ρ (MeV/c)
$\pi\pi$	seen		—
4π	seen		—
$4\pi^0$	seen		—
$2\pi^+2\pi^-$	seen		—
$\pi^+\pi^-2\pi^0$	seen		—
$2(\pi\pi)_{S\text{-wave}}$	seen		—
$\eta\eta$	seen		—
$K\bar{K}$	seen		—
$\gamma\gamma$	seen		—
e^+e^-	not seen		—

$f_1(1420)$ [n]		$I^G(J^{PC}) = 0^+(1^{++})$	
Mass $m = 1426.3 \pm 1.1$ MeV ($S = 1.3$)			
Full width $\Gamma = 55.5 \pm 2.9$ MeV			
$f_1(1420)$ DECAY MODES	Fraction (Γ_i/Γ)		ρ (MeV/c)
$K\bar{K}\pi$	dominant		439
$K\bar{K}^*(892) + c.c.$	dominant		155
$\eta\pi\pi$	possibly seen		571
$\phi\gamma$	seen		—

$\omega(1420)$ [o]		$I^G(J^{PC}) = 0^-(1^{--})$	
Mass $m = 1419 \pm 31$ MeV			
Full width $\Gamma = 174 \pm 60$ MeV			
$\omega(1420)$ DECAY MODES	Fraction (Γ_i/Γ)		ρ (MeV/c)
$\rho\pi$	dominant		488

Meson Summary Table

$\eta(1440)$ [ρ]		$I^G(J^{PC}) = 0^+(0^{-+})$	
Mass $m = 1400 - 1470$ MeV [m] Full width $\Gamma = 50 - 80$ MeV [m]			
$\eta(1440)$ DECAY MODES	Fraction (Γ_i/Γ)	ρ (MeV/c)	
$K\bar{K}\pi$	seen	-	
$K\bar{K}^*(892) + c.c.$	seen	-	
$\eta\pi\pi$	seen	-	
$a_0(980)\pi$	seen	-	
$\eta(\pi\pi)_{s\text{-wave}}$	seen	-	
$f_0(980)\eta$	seen	-	
4π	seen	-	

$a_0(1450)$		$I^G(J^{PC}) = 1^-(0^{++})$	
Mass $m = 1474 \pm 19$ MeV Full width $\Gamma = 265 \pm 13$ MeV			
$a_0(1450)$ DECAY MODES	Fraction (Γ_i/Γ)	ρ (MeV/c)	
$\pi\eta$	seen	613	
$\pi\eta'(958)$	seen	392	
$K\bar{K}$	seen	530	

$\rho(1450)$ [q]		$I^G(J^{PC}) = 1^+(1^{--})$	
Mass $m = 1465 \pm 25$ MeV [m] Full width $\Gamma = 310 \pm 60$ MeV [m]			
$\rho(1450)$ DECAY MODES	Fraction (Γ_i/Γ)	Confidence level	ρ (MeV/c)
$\pi\pi$	seen		719
4π	seen		665
$\omega\pi$	<2.0 %	95%	512
e^+e^-	seen		732
$\eta\rho$	<4 %		317
$a_2(1320)\pi$	not seen		-
$\phi\pi$	<1 %		358
$K\bar{K}$	< 1.6×10^{-3}	95%	541

$f_0(1500)$ [l]		$I^G(J^{PC}) = 0^+(0^{++})$	
Mass $m = 1500 \pm 10$ MeV ($S = 1.3$) Full width $\Gamma = 112 \pm 10$ MeV			
$f_0(1500)$ DECAY MODES	Fraction (Γ_i/Γ)	ρ (MeV/c)	
$\eta\eta'(958)$	seen	-	
$\eta\eta$	seen	513	
4π	seen	-	
$4\pi^0$	seen	690	
$2\pi^+2\pi^-$	seen	686	
$\pi\pi$	seen	-	
$\pi^+\pi^-$	seen	737	
$2\pi^0$	seen	738	
$K\bar{K}$	seen	563	

$f_2'(1525)$		$I^G(J^{PC}) = 0^+(2^{++})$	
Mass $m = 1525 \pm 5$ MeV [m] Full width $\Gamma = 76 \pm 10$ MeV [m]			
$f_2'(1525)$ DECAY MODES	Fraction (Γ_i/Γ)	ρ (MeV/c)	
$K\bar{K}$	(88.8 ± 3.1) %	581	
$\eta\eta$	(10.3 ± 3.1) %	531	
$\pi\pi$	(8.2 ± 1.5) $\times 10^{-3}$	750	
$\gamma\gamma$	(1.32 ± 0.21) $\times 10^{-6}$	763	

$\omega(1650)$ [s] was $\omega(1600)$		$I^G(J^{PC}) = 0^-(1^{--})$	
Mass $m = 1649 \pm 24$ MeV ($S = 2.3$) Full width $\Gamma = 220 \pm 35$ MeV ($S = 1.6$)			
$\omega(1650)$ DECAY MODES	Fraction (Γ_i/Γ)	ρ (MeV/c)	
$\rho\pi$	seen	637	
$\omega\pi\pi$	seen	601	
e^+e^-	seen	824	

$\omega_3(1670)$		$I^G(J^{PC}) = 0^-(3^{--})$	
Mass $m = 1667 \pm 4$ MeV Full width $\Gamma = 168 \pm 10$ MeV [m]			
$\omega_3(1670)$ DECAY MODES	Fraction (Γ_i/Γ)	ρ (MeV/c)	
$\rho\pi$	seen	647	
$\omega\pi\pi$	seen	614	
$b_1(1235)\pi$	possibly seen	359	

$\pi_2(1670)$		$I^G(J^{PC}) = 1^-(2^{-+})$	
Mass $m = 1670 \pm 20$ MeV [m] Full width $\Gamma = 259 \pm 11$ MeV [m] ($S = 1.5$)			
$\pi_2(1670)$ DECAY MODES	Fraction (Γ_i/Γ)	Confidence level	ρ (MeV/c)
3π	(95.8 ± 1.4) %		806
$f_2(1270)\pi$	(56.2 ± 3.2) %		325
$\rho\pi$	(31 ± 4) %		649
$\sigma\pi$	(13 ± 6) %		-
$f_0(1370)\pi$	(8.7 ± 3.4) %		-
$K\bar{K}^*(892) + c.c.$	(4.2 ± 1.4) %		453
$\omega\rho$	(2.7 ± 1.1) %		-
$\rho(1450)\pi$	< 3.6 $\times 10^{-3}$	97.7%	-
$b_1(1235)\pi$	< 1.9 $\times 10^{-3}$	97.7%	-

$\phi(1680)$		$I^G(J^{PC}) = 0^-(1^{--})$	
Mass $m = 1680 \pm 20$ MeV [m] Full width $\Gamma = 150 \pm 50$ MeV [m]			
$\phi(1680)$ DECAY MODES	Fraction (Γ_i/Γ)	ρ (MeV/c)	
$K\bar{K}^*(892) + c.c.$	dominant	463	
$K_S^0 K\pi$	seen	620	
$K\bar{K}$	seen	681	
e^+e^-	seen	840	
$\omega\pi\pi$	not seen	622	

$\rho_3(1690)$		$I^G(J^{PC}) = 1^+(3^{--})$	
Mass $m = 1691 \pm 5$ MeV [m] Full width $\Gamma = 161 \pm 10$ MeV [m] ($S = 1.5$)			
$\rho_3(1690)$ DECAY MODES	Fraction (Γ_i/Γ)	Scale factor	ρ (MeV/c)
4π	(71.1 ± 1.9) %		788
$\pi^\pm\pi^+\pi^-\pi^0$	(67 ± 22) %		788
$\omega\pi$	(16 ± 6) %		656
$\pi\pi$	(23.6 ± 1.3) %		834
$K\bar{K}\pi$	(3.8 ± 1.2) %		628
$K\bar{K}$	(1.58 ± 0.26) %	1.2	686
$\eta\pi^+\pi^-$	seen		728
$\rho(770)\eta$	seen		-

Meson Summary Table

 $\rho(1700)$ [q]

$${}^1G(J^{PC}) = 1^+(1^{--})$$

Mass $m = 1700 \pm 20$ MeV [m] ($\eta\rho^0$ and $\pi^+\pi^-$ modes)
 Full width $\Gamma = 240 \pm 60$ MeV [m] ($\eta\rho^0$ and $\pi^+\pi^-$ modes)

$\rho(1700)$ DECAY MODES	Fraction (Γ_i/Γ)	ρ (MeV/c)
$\rho\pi\pi$	dominant	640
$\rho^0\pi^+\pi^-$	large	640
$\rho^\pm\pi^\mp\pi^0$	large	642
$2(\pi^+\pi^-)$	large	792
$\pi^+\pi^-$	seen	838
$\pi^-\pi^0$	seen	839
$K\bar{K}^*(892)+$ c.c.	seen	479
$\eta\rho$	seen	533
$a_2(1320)\pi$	not seen	-
$K\bar{K}$	seen	692
e^+e^-	seen	850
$\pi^0\omega$	seen	662

 $f_0(1710)$ [t]

$${}^1G(J^{PC}) = 0^+(0^{++})$$

Mass $m = 1715 \pm 7$ MeV ($S = 1.1$)
 Full width $\Gamma = 125 \pm 12$ MeV

$f_0(1710)$ DECAY MODES	Fraction (Γ_i/Γ)	ρ (MeV/c)
$K\bar{K}$	seen	690
$\eta\eta$	seen	648
$\pi\pi$	seen	837

 $\pi(1800)$

$${}^1G(J^{PC}) = 1^-(0^{-+})$$

Mass $m = 1801 \pm 13$ MeV ($S = 1.9$)
 Full width $\Gamma = 210 \pm 15$ MeV

$\pi(1800)$ DECAY MODES	Fraction (Γ_i/Γ)	ρ (MeV/c)
$\pi^+\pi^-\pi^-$	seen	-
$f_0(980)\pi^-$	seen	623
$f_0(1370)\pi^-$	seen	-
$\rho\pi^-$	not seen	728
$\eta\eta\pi^-$	seen	-
$a_0(980)\eta$	seen	459
$f_0(1500)\pi^-$	seen	240
$\eta\eta'(958)\pi^-$	seen	-
$K_0^*(1430)K^-$	seen	-
$K^*(892)K^-$	not seen	560

 $\phi_3(1850)$

$${}^1G(J^{PC}) = 0^-(3^{--})$$

Mass $m = 1854 \pm 7$ MeV
 Full width $\Gamma = 87^{+28}_{-23}$ MeV ($S = 1.2$)

$\phi_3(1850)$ DECAY MODES	Fraction (Γ_i/Γ)	ρ (MeV/c)
$K\bar{K}$	seen	785
$K\bar{K}^*(892)+$ c.c.	seen	602

 $f_2(2010)$

$${}^1G(J^{PC}) = 0^+(2^{++})$$

Mass $m = 2011^{+60}_{-80}$ MeV
 Full width $\Gamma = 202 \pm 60$ MeV

$f_2(2010)$ DECAY MODES	Fraction (Γ_i/Γ)	ρ (MeV/c)
$\phi\phi$	seen	-

 $a_4(2040)$

$${}^1G(J^{PC}) = 1^-(4^{++})$$

Mass $m = 2014 \pm 15$ MeV
 Full width $\Gamma = 361 \pm 50$ MeV

$a_4(2040)$ DECAY MODES	Fraction (Γ_i/Γ)	ρ (MeV/c)
$K\bar{K}$	seen	892
$\pi^+\pi^-\pi^0$	seen	-
$\eta\pi^0$	seen	941

 $f_4(2050)$

$${}^1G(J^{PC}) = 0^+(4^{++})$$

Mass $m = 2034 \pm 11$ MeV ($S = 1.6$)
 Full width $\Gamma = 222 \pm 19$ MeV ($S = 1.8$)

$f_4(2050)$ DECAY MODES	Fraction (Γ_i/Γ)	ρ (MeV/c)
$\omega\omega$	(26 ± 6) %	658
$\pi\pi$	(17.0 ± 1.5) %	1012
$K\bar{K}$	(6.8 ^{+3.4} _{-1.8}) × 10 ⁻³	895
$\eta\eta$	(2.1 ± 0.8) × 10 ⁻³	863
$4\pi^0$	< 1.2 %	977
$a_2(1320)\pi$	seen	-

 $f_2(2300)$

$${}^1G(J^{PC}) = 0^+(2^{++})$$

Mass $m = 2297 \pm 28$ MeV
 Full width $\Gamma = 149 \pm 40$ MeV

$f_2(2300)$ DECAY MODES	Fraction (Γ_i/Γ)	ρ (MeV/c)
$\phi\phi$	seen	529

 $f_2(2340)$

$${}^1G(J^{PC}) = 0^+(2^{++})$$

Mass $m = 2339 \pm 60$ MeV
 Full width $\Gamma = 319^{+80}_{-70}$ MeV

$f_2(2340)$ DECAY MODES	Fraction (Γ_i/Γ)	ρ (MeV/c)
$\phi\phi$	seen	573

Meson Summary Table

STRANGE MESONS ($S = \pm 1, C = B = 0$)

$K^+ = u\bar{s}, K^0 = d\bar{s}, \bar{K}^0 = \bar{d}s, K^- = \bar{u}s$, similarly for K^{*+} 's

K^\pm

$$I(J^P) = \frac{1}{2}(0^-)$$

Mass $m = 493.677 \pm 0.016$ MeV [u] ($S = 2.8$)
 Mean life $\tau = (1.2386 \pm 0.0024) \times 10^{-8}$ s ($S = 2.0$)
 $c\tau = 3.713$ m

Slope parameter g [v]

(See Particle Listings for quadratic coefficients)

$$K^+ \rightarrow \pi^+ \pi^+ \pi^- = -0.2154 \pm 0.0035 \quad (S = 1.4)$$

$$K^- \rightarrow \pi^- \pi^- \pi^+ = -0.217 \pm 0.007 \quad (S = 2.5)$$

$$K^\pm \rightarrow \pi^\pm \pi^0 \pi^0 = 0.652 \pm 0.031 \quad (S = 2.7)$$

K^\pm decay form factors [a, w]

$$K_{e3}^+ \lambda_+ = 0.0276 \pm 0.0021$$

$$K_{\mu 3}^+ \lambda_+ = 0.031 \pm 0.008 \quad (S = 1.6)$$

$$K_{\mu 3}^+ \lambda_0 = 0.006 \pm 0.007 \quad (S = 1.6)$$

$$K_{e3}^+ |f_S/f_+| = 0.084 \pm 0.023 \quad (S = 1.2)$$

$$K_{e3}^+ |f_T/f_+| = 0.38 \pm 0.11 \quad (S = 1.1)$$

$$K_{\mu 3}^+ |f_T/f_+| = 0.02 \pm 0.12$$

$$K^+ \rightarrow e^+ \nu_e \gamma \quad |F_A + F_V| = 0.148 \pm 0.010$$

$$K^+ \rightarrow \mu^+ \nu_\mu \gamma \quad |F_A + F_V| < 0.23, \text{ CL} = 90\%$$

$$K^+ \rightarrow e^+ \nu_e \gamma \quad |F_A - F_V| < 0.49$$

$$K^+ \rightarrow \mu^+ \nu_\mu \gamma \quad |F_A - F_V| = -2.2 \text{ to } 0.3$$

K^- modes are charge conjugates of the modes below.

K^+ DECAY MODES	Fraction (Γ_i/Γ)	Scale factor/ Confidence level	ρ (MeV/c)
$\mu^+ \nu_\mu$	(63.51 ± 0.18) %	S=1.3	236
$e^+ \nu_e$	(1.55 ± 0.07) × 10 ⁻⁵		247
$\pi^+ \pi^0$	(21.16 ± 0.14) %	S=1.1	205
$\pi^+ \pi^+ \pi^-$	(5.59 ± 0.05) %	S=1.8	125
$\pi^+ \pi^0 \pi^0$	(1.73 ± 0.04) %	S=1.2	133
$\pi^0 \mu^+ \nu_\mu$	(3.18 ± 0.08) %	S=1.5	215
Called $K_{\mu 3}^+$			
$\pi^0 e^+ \nu_e$	(4.82 ± 0.06) %	S=1.3	228
Called K_{e3}^+			
$\pi^0 \pi^0 e^+ \nu_e$	(2.1 ± 0.4) × 10 ⁻⁵		206
$\pi^+ \pi^- e^+ \nu_e$	(3.91 ± 0.17) × 10 ⁻⁵		203
$\pi^+ \pi^- \mu^+ \nu_\mu$	(1.4 ± 0.9) × 10 ⁻⁵		151
$\pi^0 \pi^0 \pi^0 e^+ \nu_e$	< 3.5 × 10 ⁻⁶	CL=90%	135
$\mu^+ \nu_\mu \nu_\nu$	< 6.0 × 10 ⁻⁶	CL=90%	236
$e^+ \nu_e \nu_\nu$	< 6 × 10 ⁻⁵	CL=90%	247
$\mu^+ \nu_\mu e^+ e^-$	(1.3 ± 0.4) × 10 ⁻⁷		236
$e^+ \nu_e e^+ e^-$	(3.0 $\begin{smallmatrix} +3.0 \\ -1.5 \end{smallmatrix}$) × 10 ⁻⁸		247
$e^+ \nu_e \mu^+ \mu^-$	< 5 × 10 ⁻⁷	CL=90%	-
$\mu^+ \nu_\mu \mu^+ \mu^-$	< 4.1 × 10 ⁻⁷	CL=90%	185
$\mu^+ \nu_\mu \gamma$	[x,y] (5.50 ± 0.28) × 10 ⁻³		236
$\pi^+ \pi^0 \gamma$	[x,y] (2.75 ± 0.15) × 10 ⁻⁴		205
$\pi^+ \pi^0 \gamma$ (DE)	[y,z] (1.8 ± 0.4) × 10 ⁻⁵		205
$\pi^+ \pi^+ \pi^- \gamma$	[x,y] (1.04 ± 0.31) × 10 ⁻⁴		125
$\pi^+ \pi^0 \pi^0 \gamma$	[x,y] (7.5 $\begin{smallmatrix} +5.5 \\ -3.0 \end{smallmatrix}$) × 10 ⁻⁶		133
$\pi^0 \mu^+ \nu_\mu \gamma$	[x,y] < 6.1 × 10 ⁻⁵	CL=90%	215
$\pi^0 e^+ \nu_e \gamma$	[x,y] (2.62 ± 0.20) × 10 ⁻⁴		228
$\pi^0 e^+ \nu_e \gamma$ (SD)	[aa] < 5.3 × 10 ⁻⁵	CL=90%	228
$\pi^0 \pi^0 e^+ \nu_e \gamma$	< 5 × 10 ⁻⁶	CL=90%	206
$\pi^+ \gamma \gamma$	[y] (1.10 ± 0.32) × 10 ⁻⁶		227
$\pi^+ 3\gamma$	[y] < 1.0 × 10 ⁻⁴	CL=90%	227

Lepton Family number (LF), Lepton number (L), $\Delta S = \Delta Q$ (SQ)
 violating modes, or $\Delta S = 1$ weak neutral current (SI) modes

$\pi^+ \pi^+ e^- \bar{\nu}_e$	SQ	< 1.2 × 10 ⁻⁸	CL=90%	203
$\pi^+ \pi^+ \mu^- \bar{\nu}_\mu$	SQ	< 3.0 × 10 ⁻⁶	CL=95%	151
$\pi^+ e^+ e^-$	SI	(2.88 ± 0.13) × 10 ⁻⁷		227
$\pi^+ \mu^+ \mu^-$	SI	(7.6 ± 2.1) × 10 ⁻⁸	S=3.4	172
$\pi^+ \nu_\nu$	SI	(1.5 $\begin{smallmatrix} +3.4 \\ -1.2 \end{smallmatrix}$) × 10 ⁻¹⁰		227
$\mu^- \nu e^+ e^+$	LF	< 2.0 × 10 ⁻⁸	CL=90%	236
$\mu^+ \nu_e$	LF [d]	< 4 × 10 ⁻³	CL=90%	236
$\pi^+ \mu^+ e^-$	LF	< 2.1 × 10 ⁻¹⁰	CL=90%	214
$\pi^+ \mu^- e^+$	LF	< 7 × 10 ⁻⁹	CL=90%	214
$\pi^- \mu^+ e^+$	L	< 7 × 10 ⁻⁹	CL=90%	214
$\pi^- e^+ e^+$	L	< 1.0 × 10 ⁻⁸	CL=90%	227
$\pi^- \mu^+ \mu^+$	L [d]	< 1.5 × 10 ⁻⁴	CL=90%	172
$\mu^+ \bar{\nu}_e$	L [d]	< 3.3 × 10 ⁻³	CL=90%	236
$\pi^0 e^+ \bar{\nu}_e$	L	< 3 × 10 ⁻³	CL=90%	228

K^0

$$I(J^P) = \frac{1}{2}(0^-)$$

50% K_S , 50% K_L

Mass $m = 497.672 \pm 0.031$ MeV

$$m_{K^0} - m_{K^\pm} = 3.995 \pm 0.034 \text{ MeV} \quad (S = 1.1)$$

$$|m_{K^0} - m_{\bar{K}^0}| / m_{\text{average}} < 10^{-18} \text{ [bb]}$$

T-violation parameters in K^0 - \bar{K}^0 mixing [w]

$$\text{Asymmetry } A_T \text{ in } K^0\text{-}\bar{K}^0 \text{ mixing} = (6.6 \pm 1.6) \times 10^{-3}$$

CPT-violation parameters in K^0 - \bar{K}^0 mixing [w]

$$\text{Re } \Delta = (2.9 \pm 2.7) \times 10^{-4}$$

$$\text{Im } \Delta = (-0.8 \pm 3.1) \times 10^{-3}$$

K_S^0

$$I(J^P) = \frac{1}{2}(0^-)$$

Mean life $\tau = (0.8935 \pm 0.0008) \times 10^{-10}$ s

$$c\tau = 2.6786 \text{ cm}$$

CP-violation parameters [cc]

$$\text{Im}(\eta_{+-0}) = -0.002 \pm 0.009$$

$$\text{Im}(\eta_{000}) = -0.05 \pm 0.13$$

K_S^0 DECAY MODES

K_S^0 DECAY MODES	Fraction (Γ_i/Γ)	Scale factor/ Confidence level	ρ (MeV/c)
$\pi^+ \pi^-$	(68.61 ± 0.28) %	S=1.2	206
$\pi^0 \pi^0$	(31.39 ± 0.28) %	S=1.2	209
$\pi^+ \pi^- \gamma$	[x,dd] (1.78 ± 0.05) × 10 ⁻³		206
$\gamma \gamma$	(2.4 ± 0.9) × 10 ⁻⁶		249
$\pi^+ \pi^- \pi^0$	(3.2 $\begin{smallmatrix} +1.2 \\ -1.0 \end{smallmatrix}$) × 10 ⁻⁷		133
$3\pi^0$	< 1.4 × 10 ⁻⁵	CL=90%	139
$\pi^\pm e^\mp \nu_e$	[ee] (7.2 ± 1.4) × 10 ⁻⁴		229

$\Delta S = 1$ weak neutral current (SI) modes

$\mu^+ \mu^-$	SI	< 3.2 × 10 ⁻⁷	CL=90%	225
$e^+ e^-$	SI	< 1.4 × 10 ⁻⁷	CL=90%	249
$\pi^0 e^+ e^-$	SI	< 1.1 × 10 ⁻⁶	CL=90%	231

K_L^0

$$I(J^P) = \frac{1}{2}(0^-)$$

$$m_{K_L} - m_{K_S} = (0.5300 \pm 0.0012) \times 10^{10} \text{ } \hbar \text{ s}^{-1}$$

$$= (3.489 \pm 0.008) \times 10^{-12} \text{ MeV}$$

$$\text{Mean life } \tau = (5.17 \pm 0.04) \times 10^{-8} \text{ s} \quad (S = 1.1)$$

$$c\tau = 15.51 \text{ m}$$

Slope parameter g [v]

(See Particle Listings for quadratic coefficients)

$$K_L^0 \rightarrow \pi^+ \pi^- \pi^0 = 0.678 \pm 0.008 \quad (S = 1.5)$$

Meson Summary Table

 K_L decay form factors [w]

K_{e3}^0	$\lambda_+ = 0.0288 \pm 0.0015$ (S = 1.3)
$K_{\mu 3}^0$	$\lambda_+ = 0.034 \pm 0.005$ (S = 2.3)
$K_{\mu 3}^0$	$\lambda_0 = 0.025 \pm 0.006$ (S = 2.3)
K_{e3}^0	$ f_S/f_+ < 0.04$, CL = 68%
K_{e3}^0	$ f_T/f_+ < 0.23$, CL = 68%
$K_{\mu 3}^0$	$ f_T/f_+ = 0.12 \pm 0.12$
$K_L \rightarrow e^+ e^- \gamma$	$\alpha_{K^*} = -0.33 \pm 0.05$

CP-violation parameters [cc]

$\delta = (0.327 \pm 0.012)\%$
$ \eta_{00} = (2.262 \pm 0.017) \times 10^{-3}$
$ \eta_{+-} = (2.276 \pm 0.017) \times 10^{-3}$
$ \eta_{00}/\eta_{+-} = 0.9936 \pm 0.0014$ [m] (S = 1.6)
$\epsilon'/\epsilon = (2.1 \pm 0.5) \times 10^{-3}$ [m] (S = 1.6)
$\phi_{+-} = (43.3 \pm 0.5)^\circ$
$\phi_{00} = (43.2 \pm 1.0)^\circ$
$\phi_{00} - \phi_{+-} = (-0.1 \pm 0.8)^\circ$
CP asymmetry A in $K_L^0 \rightarrow \pi^+ \pi^- e^+ e^- = (13.6 \pm 2.8)\%$
j for $K_L^0 \rightarrow \pi^+ \pi^- \pi^0 = 0.0011 \pm 0.0008$
f for $K_L^0 \rightarrow \pi^+ \pi^- \pi^0 = 0.004 \pm 0.006$
$ \eta_{+-\gamma} = (2.35 \pm 0.07) \times 10^{-3}$
$\phi_{+-\gamma} = (44 \pm 4)^\circ$
$ \epsilon'_{+-\gamma} /\epsilon < 0.3$, CL = 90%

 $\Delta S = -\Delta Q$ in K_{23}^0 decay

Re $x = -0.002 \pm 0.006$
Im $x = 0.0012 \pm 0.0019$

K_L^0 DECAY MODES	Fraction (Γ_i/Γ)	Scale factor/ Confidence level	ρ (MeV/c)
$3\pi^0$	(21.13 \pm 0.27) %	S=1.1	139
$\pi^+ \pi^- \pi^0$	(12.55 \pm 0.20) %	S=1.7	133
$\pi^\pm \mu^\mp \nu_\mu$	[ee] (27.18 \pm 0.25) %	S=1.1	216
Called $K_{\mu 3}^0$.			
$\pi^\pm e^\mp \nu_e$	[ee] (38.78 \pm 0.28) %	S=1.1	229
Called $K_{e 3}^0$.			
2γ	(5.86 \pm 0.15) $\times 10^{-4}$		249
3γ	< 2.4 $\times 10^{-7}$	CL=90%	249
$\pi^0 2\gamma$	[gg] (1.68 \pm 0.10) $\times 10^{-6}$		231
$\pi^0 \pi^\pm e^\mp \nu$	[ee] (5.18 \pm 0.29) $\times 10^{-5}$		207
($\pi \mu$ atom) ν	(1.06 \pm 0.11) $\times 10^{-7}$		-
$\pi^\pm e^\mp \nu_e \gamma$	[x, ee, gg] (3.62 \pm 0.26 \pm 0.21) $\times 10^{-3}$		229
$\pi^\pm \mu^\mp \nu_\mu \gamma$	(5.7 \pm 0.6 \pm 0.7) $\times 10^{-4}$		-
$\pi^+ \pi^- \gamma$	[x, gg] (4.61 \pm 0.14) $\times 10^{-5}$		206
$\pi^0 \pi^0 \gamma$	< 5.6 $\times 10^{-6}$		209
$\mu^+ \mu^- \gamma$	(3.25 \pm 0.28) $\times 10^{-7}$		225
$e^+ e^- \gamma$	(10.0 \pm 0.5) $\times 10^{-6}$	S=1.5	249
$e^+ e^- \gamma \gamma$	[gg] (6.9 \pm 1.0) $\times 10^{-7}$		249
$\pi^0 \gamma e^+ e^-$	< 7.1 $\times 10^{-7}$	CL=90%	-

Charge conjugation \times Parity (CP, CPV) or Lepton Family number (LF) violating modes, or $\Delta S = 1$ weak neutral current (SI) modes

$\pi^+ \pi^-$	CPV	(2.056 \pm 0.033) $\times 10^{-3}$	206
$\pi^0 \pi^0$	CPV	(9.27 \pm 0.19) $\times 10^{-4}$	209
$\mu^+ \mu^-$	SI	(7.15 \pm 0.16) $\times 10^{-9}$	225
$e^+ e^-$	SI	(9 \pm 4) $\times 10^{-12}$	249
$\pi^+ \pi^- e^+ e^-$	SI [gg]	(3.5 \pm 0.6) $\times 10^{-7}$	206
$\mu^+ \mu^- e^+ e^-$	SI	(2.9 \pm 6.7 \pm 2.4) $\times 10^{-9}$	225
$e^+ e^- e^+ e^-$	SI	(4.1 \pm 0.8) $\times 10^{-8}$	S=1.2 249
$\pi^0 \mu^+ \mu^-$	CP, SI [hh]	< 5.1 $\times 10^{-9}$	CL=90% 177
$\pi^0 e^+ e^-$	CP, SI [hh]	< 4.3 $\times 10^{-9}$	CL=90% 231
$\pi^0 \nu \bar{\nu}$	CP, SI [ll]	< 5.9 $\times 10^{-7}$	CL=90% 231
$e^\pm \mu^\mp$	LF [ee]	< 4.7 $\times 10^{-12}$	CL=90% 238
$e^\pm e^\pm \mu^\mp \mu^\mp$	LF [ee]	< 6.1 $\times 10^{-9}$	CL=90% -
$\pi^0 \mu^\pm e^\mp$	LF [ee]	< 6.2 $\times 10^{-9}$	CL=90% -

 $K^*(892)$

$$I(J^P) = \frac{1}{2}(1^-)$$

$K^*(892)^\pm$	mass $m = 891.66 \pm 0.26$ MeV
$K^*(892)^0$	mass $m = 896.10 \pm 0.27$ MeV (S = 1.4)
$K^*(892)^\pm$	full width $\Gamma = 50.8 \pm 0.9$ MeV
$K^*(892)^0$	full width $\Gamma = 50.7 \pm 0.6$ MeV (S = 1.1)

$K^*(892)$ DECAY MODES	Fraction (Γ_i/Γ)	Confidence level	ρ (MeV/c)
$K\pi$	~ 100 %		291
$K^0 \gamma$	(2.30 \pm 0.20) $\times 10^{-3}$		310
$K^\pm \gamma$	(9.9 \pm 0.9) $\times 10^{-4}$		309
$K\pi\pi$	< 7 $\times 10^{-4}$	95%	224

 $K_1(1270)$

$$I(J^P) = \frac{1}{2}(1^+)$$

Mass $m = 1273 \pm 7$ MeV [m]
Full width $\Gamma = 90 \pm 20$ MeV [m]

$K_1(1270)$ DECAY MODES	Fraction (Γ_i/Γ)	ρ (MeV/c)
$K\rho$	(42 \pm 6) %	76
$K_0^*(1430)\pi$	(28 \pm 4) %	-
$K^*(892)\pi$	(16 \pm 5) %	301
$K\omega$	(11.0 \pm 2.0) %	-
$K f_0(1370)$	(3.0 \pm 2.0) %	-

 $K_1(1400)$

$$I(J^P) = \frac{1}{2}(1^+)$$

Mass $m = 1402 \pm 7$ MeV
Full width $\Gamma = 174 \pm 13$ MeV (S = 1.6)

$K_1(1400)$ DECAY MODES	Fraction (Γ_i/Γ)	ρ (MeV/c)
$K^*(892)\pi$	(94 \pm 6) %	401
$K\rho$	(3.0 \pm 3.0) %	298
$K f_0(1370)$	(2.0 \pm 2.0) %	-
$K\omega$	(1.0 \pm 1.0) %	285
$K_0^*(1430)\pi$	not seen	-

 $K^*(1410)$

$$I(J^P) = \frac{1}{2}(1^-)$$

Mass $m = 1414 \pm 15$ MeV (S = 1.3)
Full width $\Gamma = 232 \pm 21$ MeV (S = 1.1)

$K^*(1410)$ DECAY MODES	Fraction (Γ_i/Γ)	Confidence level	ρ (MeV/c)
$K^*(892)\pi$	> 40 %	95%	408
$K\pi$	(6.6 \pm 1.3) %		611
$K\rho$	< 7 %	95%	309

 $K_0^*(1430)$ [ll]

$$I(J^P) = \frac{1}{2}(0^+)$$

Mass $m = 1412 \pm 6$ MeV
Full width $\Gamma = 294 \pm 23$ MeV

$K_0^*(1430)$ DECAY MODES	Fraction (Γ_i/Γ)	ρ (MeV/c)
$K\pi$	(93 \pm 10) %	621

 $K_2^*(1430)$

$$I(J^P) = \frac{1}{2}(2^+)$$

$K_2^*(1430)^\pm$	mass $m = 1425.6 \pm 1.5$ MeV (S = 1.1)
$K_2^*(1430)^0$	mass $m = 1432.4 \pm 1.3$ MeV
$K_2^*(1430)^\pm$	full width $\Gamma = 98.5 \pm 2.7$ MeV (S = 1.1)
$K_2^*(1430)^0$	full width $\Gamma = 109 \pm 5$ MeV (S = 1.9)

$K_2^*(1430)$ DECAY MODES	Fraction (Γ_i/Γ)	Scale factor/ Confidence level	ρ (MeV/c)
$K\pi$	(49.9 \pm 1.2) %		622
$K^*(892)\pi$	(24.7 \pm 1.5) %		423
$K^*(892)\pi\pi$	(13.4 \pm 2.2) %		375
$K\rho$	(8.7 \pm 0.8) %	S=1.2	331

Meson Summary Table

$K\omega$	(2.9±0.8) %		319
$K^+\gamma$	(2.4±0.5) × 10 ⁻³	S=1.1	627
$K\eta$	(1.5 ^{+3.4} _{-1.0}) × 10 ⁻³	S=1.3	492
$K\omega\pi$	< 7.2 × 10 ⁻⁴	CL=95%	110
$K^0\gamma$	< 9 × 10 ⁻⁴	CL=90%	631

$$K^*(1680) \quad I(J^P) = \frac{1}{2}(1^-)$$

Mass $m = 1717 \pm 27$ MeV (S = 1.4)
Full width $\Gamma = 322 \pm 110$ MeV (S = 4.2)

$K^*(1680)$ DECAY MODES	Fraction (Γ_i/Γ)	ρ (MeV/c)
$K\pi$	(38.7±2.5) %	779
$K\rho$	(31.4 ^{+4.7} _{-2.1}) %	571
$K^*(892)\pi$	(29.9 ^{+2.2} _{-4.7}) %	615

$$K_2(1770) [K^*] \quad I(J^P) = \frac{1}{2}(2^-)$$

Mass $m = 1773 \pm 8$ MeV
Full width $\Gamma = 186 \pm 14$ MeV

$K_2(1770)$ DECAY MODES	Fraction (Γ_i/Γ)	ρ (MeV/c)
$K\pi\pi$		-
$K_2^*(1430)\pi$	dominant	287
$K^*(892)\pi$	seen	653
$Kf_2(1270)$	seen	-
$K\phi$	seen	441
$K\omega$	seen	608

$$K_3^*(1780) \quad I(J^P) = \frac{1}{2}(3^-)$$

Mass $m = 1776 \pm 7$ MeV (S = 1.1)
Full width $\Gamma = 159 \pm 21$ MeV (S = 1.3)

$K_3^*(1780)$ DECAY MODES	Fraction (Γ_i/Γ)	Confidence level	ρ (MeV/c)
$K\rho$	(31 ± 9) %		612
$K^*(892)\pi$	(20 ± 5) %		651
$K\pi$	(18.8 ± 1.0) %		810
$K\eta$	(30 ± 13) %		715
$K_2^*(1430)\pi$	< 16 %	95%	284

$$K_2(1820) [K^*] \quad I(J^P) = \frac{1}{2}(2^-)$$

Mass $m = 1816 \pm 13$ MeV
Full width $\Gamma = 276 \pm 35$ MeV

$K_2(1820)$ DECAY MODES	Fraction (Γ_i/Γ)	ρ (MeV/c)
$K_2^*(1430)\pi$	seen	325
$K^*(892)\pi$	seen	680
$Kf_2(1270)$	seen	186
$K\omega$	seen	638

$$K_4^*(2045) \quad I(J^P) = \frac{1}{2}(4^+)$$

Mass $m = 2045 \pm 9$ MeV (S = 1.1)
Full width $\Gamma = 198 \pm 30$ MeV

$K_4^*(2045)$ DECAY MODES	Fraction (Γ_i/Γ)	ρ (MeV/c)
$K\pi$	(9.9±1.2) %	958
$K^*(892)\pi\pi$	(9 ± 5) %	800
$K^*(892)\pi\pi\pi$	(7 ± 5) %	764
$\rho K\pi$	(5.7±3.2) %	742
$\omega K\pi$	(5.0±3.0) %	736
$\phi K\pi$	(2.8±1.4) %	591
$\phi K^*(892)$	(1.4±0.7) %	363

CHARMED MESONS (C = ±1)

$$D^+ = c\bar{d}, D^0 = c\bar{u}, \bar{D}^0 = \bar{c}u, D^- = \bar{c}d, \text{ similarly for } D^{*'}s$$

$$D^\pm$$

$$I(J^P) = \frac{1}{2}(0^-)$$

Mass $m = 1869.3 \pm 0.5$ MeV (S = 1.1)
Mean life $\tau = (1.051 \pm 0.013) \times 10^{-12}$ s
 $c\tau = 315 \mu\text{m}$

c-quark decays

$$\Gamma(c \rightarrow \ell^+ \text{ anything}) / \Gamma(c \rightarrow \text{ anything}) = 0.095 \pm 0.009 [mm]$$

CP-violation decay-rate asymmetries

$$A_{CP}(K^+ K^- \pi^\pm) = -0.017 \pm 0.027$$

$$A_{CP}(K^\pm K^{*0}) = -0.02 \pm 0.05$$

$$A_{CP}(\phi \pi^\pm) = -0.014 \pm 0.033$$

$$A_{CP}(\pi^+ \pi^- \pi^\pm) = -0.02 \pm 0.04$$

$D^+ \rightarrow \bar{K}^*(892)^0 \ell^+ \nu_\ell$ form factors

$$r_\nu = 1.82 \pm 0.09$$

$$r_2 = 0.78 \pm 0.07$$

$$r_3 = 0.0 \pm 0.4$$

$$\Gamma_L/\Gamma_T = 1.14 \pm 0.08$$

$$\Gamma_+/\Gamma_- = 0.21 \pm 0.04 \quad (S = 1.3)$$

D^- modes are charge conjugates of the modes below.

D^+ DECAY MODES	Fraction (Γ_i/Γ)	Scale factor/ Confidence level	ρ (MeV/c)
Inclusive modes			
e^+ anything	(17.2 ± 1.9) %		-
K^- anything	(24.2 ± 2.8) %	S=1.4	-
\bar{K}^0 anything + K^0 anything	(59 ± 7) %		-
K^+ anything	(5.8 ± 1.4) %		-
η anything	[$n\eta$] < 13 %	CL=90%	-
Leptonic and semileptonic modes			
$\mu^+ \nu_\mu$	(8 ⁺¹⁷ ₋₅) × 10 ⁻⁴		932
$\bar{K}^0 \ell^+ \nu_\ell$	[oo] (6.8 ± 0.8) %		-
$\bar{K}^0 e^+ \nu_e$	(6.7 ± 0.9) %		868
$\bar{K}^0 \mu^+ \nu_\mu$	(7.0 ^{+3.0} _{-2.0}) %		865
$K^- \pi^+ e^+ \nu_e$	(4.1 ^{+0.9} _{-0.7}) %		863
$\bar{K}^*(892)^0 e^+ \nu_e$ × B($\bar{K}^{*0} \rightarrow K^- \pi^+$)	(3.2 ± 0.33) %		720
$K^- \pi^+ e^+ \nu_e$ nonresonant	< 7 × 10 ⁻³	CL=90%	863
$K^- \pi^+ \mu^+ \nu_\mu$	(3.2 ± 0.4) %	S=1.1	851
$\bar{K}^*(892)^0 \mu^+ \nu_\mu$ × B($\bar{K}^{*0} \rightarrow K^- \pi^+$)	(2.9 ± 0.4) %		715
$K^- \pi^+ \mu^+ \nu_\mu$ nonresonant	(2.7 ± 1.1) × 10 ⁻³		851
($\bar{K}^*(892)\pi$) ⁰ $e^+ \nu_e$	< 1.2 %	CL=90%	714
($\bar{K}\pi\pi$) ⁰ $e^+ \nu_e$ non- $\bar{K}^*(892)$	< 9 × 10 ⁻³	CL=90%	846
$K^- \pi^+ \pi^0 \mu^+ \nu_\mu$	< 1.4 × 10 ⁻³	CL=90%	825
$\pi^0 \ell^+ \nu_\ell$	[pp] (3.1 ± 1.5) × 10 ⁻³		930

Fractions of some of the following modes with resonances have already appeared above as submodes of particular charged-particle modes.

$\bar{K}^*(892)^0 \ell^+ \nu_\ell$	[oo] (4.7 ± 0.4) %		-
$\bar{K}^*(892)^0 e^+ \nu_e$	(4.8 ± 0.5) %		720
$\bar{K}^*(892)^0 \mu^+ \nu_\mu$	(4.4 ± 0.6) %	S=1.1	715
$\bar{K}_1(1270)^0 \mu^+ \nu_\mu$	< 3.5 %	CL=95%	493
$\bar{K}^*(1410)^0 \mu^+ \nu_\mu$	< 2.7 %	CL=95%	389
$\bar{K}_2^*(1430)^0 \mu^+ \nu_\mu$	< 8 × 10 ⁻³	CL=95%	374
$\rho^0 e^+ \nu_e$	(2.2 ± 0.8) × 10 ⁻³		776
$\rho^0 \mu^+ \nu_\mu$	(2.7 ± 0.7) × 10 ⁻³		772
$\phi e^+ \nu_e$	< 2.09 %	CL=90%	657
$\phi \mu^+ \nu_\mu$	< 3.72 %	CL=90%	651
$\eta \ell^+ \nu_\ell$	< 5 × 10 ⁻³	CL=90%	-
$\eta'(958) \mu^+ \nu_\mu$	< 9 × 10 ⁻³	CL=90%	684

Meson Summary Table

Hadronic modes with a \bar{K} or $\bar{K}K\bar{K}$			
$\bar{K}^0\pi^+$	(2.89 ± 0.26) %	S=1.1	862
$K^-\pi^+\pi^+$	[qq] (9.0 ± 0.6) %		845
$\bar{K}^*(892)^0\pi^+$	(1.27 ± 0.13) %		712
$\times B(\bar{K}^{*0} \rightarrow K^-\pi^+)$			
$\bar{K}_0^*(1430)^0\pi^+$	(2.3 ± 0.3) %		368
$\times B(\bar{K}_0^{*0}(1430)^0 \rightarrow K^-\pi^+)$			
$\bar{K}^*(1680)^0\pi^+$	(3.7 ± 0.8) × 10 ⁻³		65
$\times B(\bar{K}^*(1680)^0 \rightarrow K^-\pi^+)$			
$K^-\pi^+\pi^+$ nonresonant	(8.5 ± 0.8) %		845
$\bar{K}^0\pi^+\pi^0$	[qq] (9.7 ± 3.0) %	S=1.1	845
$\bar{K}^0\rho^+$	(6.6 ± 2.5) %		680
$\bar{K}^*(892)^0\pi^+$	(6.3 ± 0.4) × 10 ⁻³		712
$\times B(\bar{K}^{*0} \rightarrow \bar{K}^0\pi^0)$			
$\bar{K}^0\pi^+\pi^0$ nonresonant	(1.3 ± 1.1) %		845
$K^-\pi^+\pi^+\pi^0$	[qq] (6.4 ± 1.1) %		816
$\bar{K}^*(892)^0\rho^+$ total	(1.4 ± 0.9) %		423
$\times B(\bar{K}^{*0} \rightarrow K^-\pi^+)$			
$\bar{K}_1(1400)^0\pi^+$	(2.2 ± 0.6) %		390
$\times B(\bar{K}_1(1400)^0 \rightarrow K^-\pi^+\pi^0)$			
$K^-\rho^+\pi^+$ total	(3.1 ± 1.1) %		616
$K^-\rho^+\pi^+$ 3-body	(1.1 ± 0.4) %		616
$\bar{K}^*(892)^0\pi^+\pi^0$ total	(4.5 ± 0.9) %		687
$\times B(\bar{K}^{*0} \rightarrow K^-\pi^+)$			
$\bar{K}^*(892)^0\pi^+\pi^0$ 3-body	(2.8 ± 0.9) %		687
$\times B(\bar{K}^{*0} \rightarrow K^-\pi^+)$			
$K^*(892)^-\pi^+\pi^+$ 3-body	(7 ± 3) × 10 ⁻³		688
$\times B(K^{*-} \rightarrow K^-\pi^0)$			
$K^-\pi^+\pi^+\pi^0$ nonresonant	[rr] (1.2 ± 0.6) %		816
$\bar{K}^0\pi^+\pi^+\pi^-$	[qq] (7.0 ± 0.9) %		814
$\bar{K}^0a_1(1260)^+$	(4.0 ± 0.9) %		328
$\times B(a_1(1260)^+ \rightarrow \pi^+\pi^+\pi^-)$			
$\bar{K}_1(1400)^0\pi^+$	(2.2 ± 0.6) %		390
$\times B(\bar{K}_1(1400)^0 \rightarrow \bar{K}^0\pi^+\pi^-)$			
$K^*(892)^-\pi^+\pi^+$ 3-body	(1.4 ± 0.6) %		688
$\times B(K^{*-} \rightarrow \bar{K}^0\pi^-)$			
$\bar{K}^0\rho^0\pi^+$ total	(4.2 ± 0.9) %		614
$\bar{K}^0\rho^0\pi^+$ 3-body	(5 ± 5) × 10 ⁻³		614
$\bar{K}^0\pi^+\pi^+\pi^-$ nonresonant	(8 ± 4) × 10 ⁻³		814
$K^-\pi^+\pi^+\pi^+\pi^-$	[qq] (7.2 ± 1.0) × 10 ⁻³		772
$\bar{K}^*(892)^0\pi^+\pi^+\pi^-$	(5.4 ± 2.3) × 10 ⁻³		642
$\times B(\bar{K}^{*0} \rightarrow K^-\pi^+)$			
$\bar{K}^*(892)^0\rho^0\pi^+$	(1.9 ± 1.1) × 10 ⁻³		242
$\times B(\bar{K}^{*0} \rightarrow K^-\pi^+)$			
$\bar{K}^*(892)^0\pi^+\pi^+\pi^-$ no- ρ	(2.9 ± 1.1) × 10 ⁻³		642
$\times B(\bar{K}^{*0} \rightarrow K^-\pi^+)$			
$K^-\rho^0\pi^+\pi^+$	(3.1 ± 0.9) × 10 ⁻³		529
$K^-\pi^+\pi^+\pi^+\pi^-$ nonresonant	< 2.3 × 10 ⁻³	CL=90%	772
$K^-\pi^+\pi^+\pi^0\pi^0$	(2.2 ± 5.0 / 0.9) %		775
$\bar{K}^0\pi^+\pi^+\pi^-\pi^0$	(5.4 ± 3.0 / 1.4) %		773
$\bar{K}^0\pi^+\pi^+\pi^+\pi^-\pi^-$	(8 ± 7) × 10 ⁻⁴		714
$K^-\pi^+\pi^+\pi^+\pi^-\pi^0$	(2.0 ± 1.8) × 10 ⁻³		718
$\bar{K}^0\bar{K}^0K^+$	(1.8 ± 0.8) %		545
Fractions of some of the following modes with resonances have already appeared above as submodes of particular charged-particle modes.			
$\bar{K}^0\rho^+$	(6.6 ± 2.5) %		680
$\bar{K}^0a_1(1260)^+$	(8.0 ± 1.7) %		328
$\bar{K}^0a_2(1320)^+$	< 3 × 10 ⁻³	CL=90%	199
$\bar{K}^*(892)^0\pi^+$	(1.90 ± 0.19) %		712
$\bar{K}^*(892)^0\rho^+$ total	[rr] (2.1 ± 1.3) %		423
$\bar{K}^*(892)^0\rho^+$ S-wave	[rr] (1.6 ± 1.6) %		423
$\bar{K}^*(892)^0\rho^+$ P-wave	< 1 × 10 ⁻³	CL=90%	423
$\bar{K}^*(892)^0\rho^+$ D-wave	(10 ± 7) × 10 ⁻³		423
$\bar{K}^*(892)^0\rho^+$ D-wave longitudinal	< 7 × 10 ⁻³	CL=90%	423
$\bar{K}_1(1270)^0\pi^+$	< 7 × 10 ⁻³	CL=90%	487
$\bar{K}_1(1400)^0\pi^+$	(4.9 ± 1.2) %		390
$\bar{K}^*(1410)^0\pi^+$	< 7 × 10 ⁻³	CL=90%	382
$\bar{K}_0^*(1430)^0\pi^+$	(3.7 ± 0.4) %		368
$\bar{K}^*(1680)^0\pi^+$	(1.43 ± 0.30) %		65
$\bar{K}^*(892)^0\pi^+\pi^0$ total	(6.7 ± 1.4) %		687
$\bar{K}^*(892)^0\pi^+\pi^0$ 3-body	[rr] (4.2 ± 1.4) %		687
$K^*(892)^-\pi^+\pi^+$ 3-body	(2.0 ± 0.9) %		688
$K^-\rho^+\pi^+$ total	(3.1 ± 1.1) %		616
$K^-\rho^+\pi^+$ 3-body	(1.1 ± 0.4) %		616
$\bar{K}^0\rho^0\pi^+$ total	(4.2 ± 0.9) %	CL=90%	614
$\bar{K}^0\rho^0\pi^+$ 3-body	(5 ± 5) × 10 ⁻³		614
$\bar{K}^0f_0(980)\pi^+$	< 5 × 10 ⁻³	CL=90%	461
$\bar{K}^*(892)^0\pi^+\pi^+\pi^-$	(8.1 ± 3.4) × 10 ⁻³	S=1.7	642
$\bar{K}^*(892)^0\rho^0\pi^+$	(2.9 ± 1.7 / 1.5) × 10 ⁻³	S=1.8	242
$\bar{K}^*(892)^0\pi^+\pi^+\pi^-$ no- ρ	(4.3 ± 1.7) × 10 ⁻³		642
$K^-\rho^0\pi^+\pi^+$	(3.1 ± 0.9) × 10 ⁻³		529
Pionic modes			
$\pi^+\pi^0$	(2.5 ± 0.7) × 10 ⁻³		925
$\pi^+\pi^+\pi^-$	(3.6 ± 0.4) × 10 ⁻³		908
$\rho^0\pi^+$	(1.05 ± 0.31) × 10 ⁻³		769
$\pi^+\pi^+\pi^-$ nonresonant	(2.2 ± 0.4) × 10 ⁻³		908
$\pi^+\pi^+\pi^-\pi^0$	(1.9 ± 1.5 / 1.2) %		882
$\eta\pi^+ \times B(\eta \rightarrow \pi^+\pi^-\pi^0)$	(6.9 ± 1.4) × 10 ⁻⁴		848
$\omega\pi^+ \times B(\omega \rightarrow \pi^+\pi^-\pi^0)$	< 6 × 10 ⁻³	CL=90%	764
$\pi^+\pi^+\pi^+\pi^-\pi^-$	(2.1 ± 0.4) × 10 ⁻³		845
$\pi^+\pi^+\pi^+\pi^-\pi^-\pi^0$	(2.9 ± 2.9 / 2.0) × 10 ⁻³		799
Fractions of some of the following modes with resonances have already appeared above as submodes of particular charged-particle modes.			
$\eta\pi^+$	(3.0 ± 0.6) × 10 ⁻³		848
$\rho^0\pi^+$	(1.05 ± 0.31) × 10 ⁻³		769
$\omega\pi^+$	< 7 × 10 ⁻³	CL=90%	764
$\eta\rho^+$	< 7 × 10 ⁻³	CL=90%	658
$\eta'(958)\pi^+$	(5.0 ± 1.0) × 10 ⁻³		680
$\eta'(958)\rho^+$	< 5 × 10 ⁻³	CL=90%	355
Hadronic modes with a $K\bar{K}$ pair			
$K^+\bar{K}^0$	(7.4 ± 1.0) × 10 ⁻³		792
$K^+K^-\pi^+$	[qq] (8.7 ± 0.7) × 10 ⁻³		744
$\phi\pi^+ \times B(\phi \rightarrow K^+K^-)$	(3.0 ± 0.3) × 10 ⁻³		647
$K^+\bar{K}^*(892)^0$	(2.8 ± 0.4) × 10 ⁻³		610
$\times B(\bar{K}^{*0} \rightarrow K^-\pi^+)$			
$K^+K^-\pi^+$ nonresonant	(4.5 ± 0.9) × 10 ⁻³		744
$K^0\bar{K}^0\pi^+$	—		741
$K^*(892)^+\bar{K}^0$	(2.1 ± 1.0) %		611
$\times B(K^{*+} \rightarrow K^0\pi^+)$			
$K^+K^-\pi^+\pi^0$	—		682
$\phi\pi^+\pi^0 \times B(\phi \rightarrow K^+K^-)$	(1.1 ± 0.5) %		619
$\phi\rho^+ \times B(\phi \rightarrow K^+K^-)$	< 7 × 10 ⁻³	CL=90%	268
$K^+K^-\pi^+\pi^0$ non- ϕ	(1.5 ± 0.7 / 0.6) %		682
$K^+\bar{K}^0\pi^+\pi^-$	< 2 %	CL=90%	678
$K^0K^-\pi^+\pi^+$	(1.0 ± 0.6) %		678
$K^*(892)^+\bar{K}^*(892)^0$	(1.2 ± 0.5) %		273
$\times B^2(K^{*+} \rightarrow K^0\pi^+)$			
$K^0K^-\pi^+\pi^+$ non- $K^{*+}\bar{K}^{*0}$	< 7.9 × 10 ⁻³	CL=90%	678
$K^+K^-\pi^+\pi^+\pi^-$	—		600
$\phi\pi^+\pi^+\pi^-$	< 1 × 10 ⁻³	CL=90%	565
$\times B(\phi \rightarrow K^+K^-)$			
$K^+K^-\pi^+\pi^+\pi^-$ nonresonant	< 3 %	CL=90%	600
Fractions of the following modes with resonances have already appeared above as submodes of particular charged-particle modes.			
$\phi\pi^+$	(6.1 ± 0.6) × 10 ⁻³		647
$\phi\pi^+\pi^0$	(2.3 ± 1.0) %		619
$\phi\rho^+$	< 1.4 %	CL=90%	268
$\phi\pi^+\pi^+\pi^-$	< 2 × 10 ⁻³	CL=90%	565
$K^+\bar{K}^*(892)^0$	(4.2 ± 0.5) × 10 ⁻³		610
$K^*(892)^+\bar{K}^0$	(3.2 ± 1.5) %		611
$K^*(892)^+\bar{K}^*(892)^0$	(2.6 ± 1.1) %		273

Meson Summary Table

Doubly Cabibbo suppressed (DC) modes, $\Delta C = 1$ weak neutral current (CI) modes, or Lepton Family number (LF) or Lepton number (L) violating modes			
$K^+ \pi^+ \pi^-$	DC	$(6.8 \pm 1.5) \times 10^{-4}$	845
$K^+ \rho^0$	DC	$(2.5 \pm 1.2) \times 10^{-4}$	681
$K^*(892)^0 \pi^+$	DC	$(3.6 \pm 1.6) \times 10^{-4}$	712
$K^+ \pi^+ \pi^-$ nonresonant	DC	$(2.4 \pm 1.2) \times 10^{-4}$	845
$K^+ K^+ K^-$	DC	$< 1.4 \times 10^{-4}$	CL=90% 550
ϕK^+	DC	$< 1.3 \times 10^{-4}$	CL=90% 527
$\pi^+ e^+ e^-$	CI	$< 5.2 \times 10^{-5}$	CL=90% 929
$\pi^+ \mu^+ \mu^-$	CI	$< 1.5 \times 10^{-5}$	CL=90% 917
$\rho^+ \mu^+ \mu^-$	CI	$< 5.6 \times 10^{-4}$	CL=90% 759
$K^+ e^+ e^-$	[ss]	$< 2.0 \times 10^{-4}$	CL=90% 869
$K^+ \mu^+ \mu^-$	[ss]	$< 4.4 \times 10^{-5}$	CL=90% 856
$\pi^+ e^\pm \mu^\mp$	LF [ee]	$< 3.4 \times 10^{-5}$	CL=90% 926
$K^+ e^\pm \mu^\mp$	LF [ee]	$< 6.8 \times 10^{-5}$	CL=90% 866
$\pi^- e^+ e^+$	L	$< 9.6 \times 10^{-5}$	CL=90% 929
$\pi^- \mu^+ \mu^+$	L	$< 1.7 \times 10^{-5}$	CL=90% 917
$\pi^- e^+ \mu^+$	L	$< 5.0 \times 10^{-5}$	CL=90% 926
$\rho^- \mu^+ \mu^+$	L	$< 5.6 \times 10^{-4}$	CL=90% 759
$K^- e^+ e^+$	L	$< 1.2 \times 10^{-4}$	CL=90% 869
$K^- \mu^+ \mu^+$	L	$< 1.2 \times 10^{-4}$	CL=90% 856
$K^- e^+ \mu^+$	L	$< 1.3 \times 10^{-4}$	CL=90% 866
$K^*(892)^- \mu^+ \mu^+$	L	$< 8.5 \times 10^{-4}$	CL=90% 703

D⁰

$$I(J^P) = \frac{1}{2}(0^-)$$

Mass $m = 1864.5 \pm 0.5$ MeV ($S = 1.1$)
 $m_{D^\pm} - m_{D^0} = 4.79 \pm 0.10$ MeV ($S = 1.1$)
 Mean life $\tau = (0.4126 \pm 0.0028) \times 10^{-12}$ s
 $c\tau = 123.7$ μ m
 $|m_{D_1^0} - m_{D_2^0}| < 7 \times 10^{10} \hbar s^{-1}$, CL = 95% [tt]
 $(\Gamma_{D_1^0} - \Gamma_{D_2^0})/\Gamma_{D^0}: -0.116 < \Delta\Gamma/\Gamma < 0.020$, CL = 95% [tt]
 $\Gamma(K^+ \ell^- \bar{\nu}_\ell \text{ (via } \bar{D}^0))/\Gamma(K^- \ell^+ \nu_\ell) < 0.005$, CL = 90%
 $\Gamma(K^+ \pi^- \text{ (via } \bar{D}^0))/\Gamma(K^- \pi^+) < 4.1 \times 10^{-4}$, CL = 95%

CP-violation decay-rate asymmetries

$A_{CP}(K^+ K^-) = 0.026 \pm 0.035$
 $A_{CP}(\pi^+ \pi^-) = -0.05 \pm 0.08$
 $A_{CP}(K_S^0 \phi) = -0.03 \pm 0.09$
 $A_{CP}(K_S^0 \pi^0) = -0.018 \pm 0.030$
 $A_{CP}(K^\pm \pi^\mp) = 0.02 \pm 0.20$

 \bar{D}^0 modes are charge conjugates of the modes below.

D ⁰ DECAY MODES	Fraction (Γ_i/Γ)	Scale factor/ Confidence level	ρ (MeV/c)
Inclusive modes			
e^+ anything	$(6.75 \pm 0.29) \%$	—	—
μ^+ anything	$(6.6 \pm 0.8) \%$	—	—
K^- anything	$(53 \pm 4) \%$	S=1.3	—
\bar{K}^0 anything + K^0 anything	$(42 \pm 5) \%$	—	—
K^+ anything	$(3.4^{+0.6}_{-0.4}) \%$	—	—
η anything	[nn] < 13 %	CL=90%	—
Semileptonic modes			
$K^- \ell^+ \nu_\ell$	[oo] $(3.47 \pm 0.17) \%$	S=1.3	867
$K^- e^+ \nu_e$	$(3.64 \pm 0.18) \%$	—	867
$K^- \mu^+ \nu_\mu$	$(3.22 \pm 0.17) \%$	—	863
$K^- \pi^0 e^+ \nu_e$	$(1.6^{+1.3}_{-0.5}) \%$	—	861
$\bar{K}^0 \pi^- e^+ \nu_e$	$(2.8^{+1.7}_{-0.9}) \%$	—	860
$\bar{K}^*(892)^- e^+ \nu_e$	$(1.35 \pm 0.22) \%$	—	719
$\times B(K^{*-} \rightarrow \bar{K}^0 \pi^-)$	—	—	—
$K^- \pi^+ \pi^- \mu^+ \nu_\mu$	< 1.2 $\times 10^{-3}$	CL=90%	821
$(\bar{K}^*(892) \pi^-)^- \mu^+ \nu_\mu$	< 1.4 $\times 10^{-3}$	CL=90%	693
$\pi^- e^+ \nu_e$	$(3.7 \pm 0.6) \times 10^{-3}$	—	927
A fraction of the following resonance mode has already appeared above as a submode of a charged-particle mode.			
$K^*(892)^- e^+ \nu_e$	$(2.02 \pm 0.33) \%$	—	719

Hadronic modes with a \bar{K} or $\bar{K}K\bar{K}$			
$K^- \pi^+$		$(3.83 \pm 0.09) \%$	861
$\bar{K}^0 \pi^0$		$(2.11 \pm 0.21) \%$	S=1.1 860
$\bar{K}^0 \pi^+ \pi^-$	[qq]	$(5.4 \pm 0.4) \%$	S=1.2 842
$\bar{K}^0 \rho^0$		$(1.21 \pm 0.17) \%$	676
$\bar{K}^0 f_0(980)$		$(3.0 \pm 0.8) \times 10^{-3}$	549
$\times B(f_0 \rightarrow \pi^+ \pi^-)$		—	—
$\bar{K}^0 f_2(1270)$		$(2.4 \pm 0.9) \times 10^{-3}$	263
$\times B(f_2 \rightarrow \pi^+ \pi^-)$		—	—
$\bar{K}^0 f_0(1370)$		$(4.3 \pm 1.3) \times 10^{-3}$	—
$\times B(f_0 \rightarrow \pi^+ \pi^-)$		—	—
$K^*(892)^- \pi^+$		$(3.4 \pm 0.3) \%$	711
$\times B(K^{*-} \rightarrow \bar{K}^0 \pi^-)$		—	—
$K_S^0(1430)^- \pi^+$		$(6.4 \pm 1.6) \times 10^{-3}$	364
$\times B(K_S^0(1430)^- \rightarrow \bar{K}^0 \pi^-)$		—	—
$\bar{K}^0 \pi^+ \pi^-$ nonresonant		$(1.47 \pm 0.24) \%$	842
$K^- \pi^+ \pi^0$	[qq]	$(13.9 \pm 0.9) \%$	S=1.3 844
$K^- \rho^+$		$(10.8 \pm 1.0) \%$	678
$K^*(892)^- \pi^+$		$(1.7 \pm 0.2) \%$	711
$\times B(K^{*-} \rightarrow K^- \pi^0)$		—	—
$\bar{K}^*(892)^0 \pi^0$		$(2.1 \pm 0.3) \%$	709
$\times B(\bar{K}^{*0} \rightarrow K^- \pi^+)$		—	—
$K^- \pi^+ \pi^0$ nonresonant		$(6.9 \pm 2.5) \times 10^{-3}$	844
$\bar{K}^0 \pi^0 \pi^0$		—	843
$\bar{K}^*(892)^0 \pi^0$		$(1.1 \pm 0.2) \%$	709
$\times B(\bar{K}^{*0} \rightarrow \bar{K}^0 \pi^0)$		—	—
$\bar{K}^0 \pi^0 \pi^0$ nonresonant		$(7.8 \pm 2.0) \times 10^{-3}$	843
$K^- \pi^+ \pi^+ \pi^-$	[qq]	$(7.49 \pm 0.31) \%$	812
$K^- \pi^+ \rho^0$ total		$(6.3 \pm 0.4) \%$	612
$K^- \pi^+ \rho^0$ 3-body		$(4.7 \pm 2.1) \times 10^{-3}$	612
$\bar{K}^*(892)^0 \rho^0$		$(9.8 \pm 2.2) \times 10^{-3}$	418
$\times B(\bar{K}^{*0} \rightarrow K^- \pi^+)$		—	—
$K^- a_1(1260)^+$		$(3.6 \pm 0.6) \%$	327
$\times B(a_1(1260)^+ \rightarrow \pi^+ \pi^+ \pi^-)$		—	—
$\bar{K}^*(892)^0 \pi^+ \pi^-$ total		$(1.5 \pm 0.4) \%$	683
$\times B(\bar{K}^{*0} \rightarrow K^- \pi^+)$		—	—
$\bar{K}^*(892)^0 \pi^+ \pi^-$ 3-body		$(9.5 \pm 2.1) \times 10^{-3}$	683
$\times B(\bar{K}^{*0} \rightarrow K^- \pi^+)$		—	—
$K_1(1270)^- \pi^+$	[rr]	$(3.6 \pm 1.0) \times 10^{-3}$	483
$\times B(K_1(1270)^- \rightarrow K^- \pi^+ \pi^-)$		—	—
$K^- \pi^+ \pi^+ \pi^-$ nonresonant		$(1.74 \pm 0.25) \%$	812
$\bar{K}^0 \pi^+ \pi^- \pi^0$	[qq]	$(10.0 \pm 1.2) \%$	812
$\bar{K}^0 \eta \times B(\eta \rightarrow \pi^+ \pi^- \pi^0)$		$(1.6 \pm 0.3) \times 10^{-3}$	772
$\bar{K}^0 \omega \times B(\omega \rightarrow \pi^+ \pi^- \pi^0)$		$(1.9 \pm 0.4) \%$	670
$K^*(892)^- \rho^+$		$(4.1 \pm 1.6) \%$	422
$\times B(K^{*0} \rightarrow \bar{K}^0 \pi^-)$		—	—
$\bar{K}^*(892)^0 \rho^0$		$(4.9 \pm 1.1) \times 10^{-3}$	418
$\times B(\bar{K}^{*0} \rightarrow \bar{K}^0 \pi^0)$		—	—
$K_1(1270)^- \pi^+$	[rr]	$(5.1 \pm 1.4) \times 10^{-3}$	483
$\times B(K_1(1270)^- \rightarrow \bar{K}^0 \pi^- \pi^0)$		—	—
$\bar{K}^*(892)^0 \pi^+ \pi^-$ 3-body		$(4.8 \pm 1.1) \times 10^{-3}$	683
$\times B(\bar{K}^{*0} \rightarrow \bar{K}^0 \pi^0)$		—	—
$\bar{K}^0 \pi^+ \pi^- \pi^0$ nonresonant		$(2.1 \pm 2.1) \%$	812
$K^- \pi^+ \pi^0 \pi^0$		$(15 \pm 5) \%$	815
$K^- \pi^+ \pi^+ \pi^- \pi^0$		$(4.0 \pm 0.4) \%$	771
$\bar{K}^*(892)^0 \pi^+ \pi^- \pi^0$		$(1.2 \pm 0.6) \%$	641
$\times B(\bar{K}^{*0} \rightarrow K^- \pi^+)$		—	—
$\bar{K}^*(892)^0 \eta$		$(2.9 \pm 0.8) \times 10^{-3}$	580
$\times B(\bar{K}^{*0} \rightarrow K^- \pi^+)$		—	—
$\times B(\eta \rightarrow \pi^+ \pi^- \pi^0)$		—	—
$K^- \pi^+ \omega \times B(\omega \rightarrow \pi^+ \pi^- \pi^0)$		$(2.7 \pm 0.5) \%$	605
$\bar{K}^*(892)^0 \omega$		$(7 \pm 3) \times 10^{-3}$	406
$\times B(\bar{K}^{*0} \rightarrow K^- \pi^+)$		—	—
$\times B(\omega \rightarrow \pi^+ \pi^- \pi^0)$		—	—
$\bar{K}^0 \pi^+ \pi^+ \pi^- \pi^-$		$(5.8 \pm 1.6) \times 10^{-3}$	768
$\bar{K}^0 \pi^+ \pi^- \pi^0 \pi^0 (\pi^0)$		$(10.6^{+7.3}_{-3.0}) \%$	771
$\bar{K}^0 K^+ K^-$		$(9.4 \pm 1.0) \times 10^{-3}$	544
$\bar{K}^0 \phi \times B(\phi \rightarrow K^+ K^-)$		$(4.3 \pm 0.5) \times 10^{-3}$	520
$\bar{K}^0 K^+ K^-$ non- ϕ		$(5.1 \pm 0.8) \times 10^{-3}$	544
$K_S^0 K_S^0 K_S^0$		$(8.3 \pm 1.5) \times 10^{-4}$	538
$K^+ K^- K^- \pi^+$		$(2.1 \pm 0.5) \times 10^{-4}$	434
$K^+ K^- \bar{K}^0 \pi^0$		$(7.2^{+4.8}_{-3.5}) \times 10^{-3}$	435

Meson Summary Table

Fractions of many of the following modes with resonances have already appeared above as submodes of particular charged-particle modes. (Modes for which there are only upper limits and $\bar{K}^*(892)\rho$ submodes only appear below.)

$\bar{K}^0\eta$	$(7.0 \pm 1.0) \times 10^{-3}$		772
$\bar{K}^0\rho^0$	$(1.21 \pm 0.17) \%$		676
$K^-\rho^+$	$(10.8 \pm 0.9) \%$	S=1.2	678
$\bar{K}^0\omega$	$(2.1 \pm 0.4) \%$		670
$\bar{K}^0\eta'(958)$	$(1.71 \pm 0.26) \%$		565
$\bar{K}^0 f_0(980)$	$(5.7 \pm 1.6) \times 10^{-3}$		549
$\bar{K}^0\phi$	$(8.6 \pm 1.0) \times 10^{-3}$		520
$K^- a_1(1260)^+$	$(7.3 \pm 1.1) \%$		327
$\bar{K}^0 a_1(1260)^0$	< 1.9 %	CL=90%	322
$\bar{K}^0 f_2(1270)$	$(4.1 \pm 1.5) \times 10^{-3}$		263
$K^- a_2(1320)^+$	< 2 $\times 10^{-3}$	CL=90%	197
$\bar{K}^0 f_0(1370)$	$(6.9 \pm 2.1) \times 10^{-3}$		—
$K^*(892)^-\pi^+$	$(5.0 \pm 0.4) \%$	S=1.2	711
$\bar{K}^*(892)^0\pi^0$	$(3.1 \pm 0.4) \%$		709
$\bar{K}^*(892)^0\pi^+\pi^-$ total	$(2.2 \pm 0.5) \%$		683
$\bar{K}^*(892)^0\pi^+\pi^-$ 3-body	$(1.42 \pm 0.32) \%$		683
$K^-\pi^+\rho^0$ total	$(6.3 \pm 0.4) \%$		612
$K^-\pi^+\rho^0$ 3-body	$(4.7 \pm 2.1) \times 10^{-3}$		612
$\bar{K}^*(892)^0\rho^0$	$(1.46 \pm 0.32) \%$		418
$\bar{K}^*(892)^0\rho^0$ transverse	$(1.5 \pm 0.5) \%$		418
$\bar{K}^*(892)^0\rho^0$ S-wave	$(2.8 \pm 0.6) \%$		418
$\bar{K}^*(892)^0\rho^0$ S-wave long.	< 3 $\times 10^{-3}$	CL=90%	418
$\bar{K}^*(892)^0\rho^0$ P-wave	< 3 $\times 10^{-3}$	CL=90%	418
$\bar{K}^*(892)^0\rho^0$ D-wave	$(1.9 \pm 0.6) \%$		418
$K^*(892)^-\rho^+$	$(6.1 \pm 2.4) \%$		422
$K^*(892)^-\rho^+$ longitudinal	$(2.9 \pm 1.2) \%$		422
$K^*(892)^-\rho^+$ transverse	$(3.2 \pm 1.8) \%$		422
$K^*(892)^-\rho^+$ P-wave	< 1.5 %	CL=90%	422
$K^-\pi^+ f_0(980)$	< 1.1 %	CL=90%	459
$\bar{K}^*(892)^0 f_0(980)$	< 7 $\times 10^{-3}$	CL=90%	—
$K_1(1270)^-\pi^+$	[rr] $(1.06 \pm 0.29) \%$		483
$K_1(1400)^-\pi^+$	< 1.2 %	CL=90%	386
$\bar{K}_1(1400)^0\pi^0$	< 3.7 %	CL=90%	387
$K^*(1410)^-\pi^+$	< 1.2 %	CL=90%	378
$K_0^*(1430)^-\pi^+$	$(1.04 \pm 0.26) \%$		364
$K_2^*(1430)^-\pi^+$	< 8 $\times 10^{-3}$	CL=90%	367
$\bar{K}_2^*(1430)^0\pi^0$	< 4 $\times 10^{-3}$	CL=90%	363
$\bar{K}^*(892)^0\pi^+\pi^-\pi^0$	$(1.8 \pm 0.9) \%$		641
$\bar{K}^*(892)^0\eta$	$(1.9 \pm 0.5) \%$		580
$K^-\pi^+\omega$	$(3.0 \pm 0.6) \%$		605
$\bar{K}^*(892)^0\omega$	$(1.1 \pm 0.4) \%$		406
$K^-\pi^+\eta'(958)$	$(7.0 \pm 1.8) \times 10^{-3}$		479
$\bar{K}^*(892)^0\eta'(958)$	< 1.0 $\times 10^{-3}$	CL=90%	99
Plonic modes			
$\pi^+\pi^-$	$(1.52 \pm 0.09) \times 10^{-3}$		922
$\pi^0\pi^0$	$(8.4 \pm 2.2) \times 10^{-4}$		922
$\pi^+\pi^-\pi^0$	$(1.6 \pm 1.1) \%$	S=2.7	907
$\pi^+\pi^+\pi^-\pi^-$	$(7.3 \pm 0.5) \times 10^{-3}$		879
$\pi^+\pi^+\pi^-\pi^-\pi^0$	$(1.9 \pm 0.4) \%$		844
$\pi^+\pi^+\pi^+\pi^-\pi^-\pi^-$	$(4.0 \pm 3.0) \times 10^{-4}$		795
Hadronic modes with a $K\bar{K}$ pair			
K^+K^-	$(4.25 \pm 0.16) \times 10^{-3}$		791
$K^0\bar{K}^0$	$(6.5 \pm 1.8) \times 10^{-4}$	S=1.2	788
$K^0K^-\pi^+$	$(6.4 \pm 1.0) \times 10^{-3}$	S=1.1	739
$\bar{K}^*(892)^0K^0$	< 1.1 $\times 10^{-3}$	CL=90%	605
$\times B(\bar{K}^{*0} \rightarrow K^-\pi^+)$			
$K^*(892)^+K^-$	$(2.3 \pm 0.5) \times 10^{-3}$		610
$\times B(K^{*+} \rightarrow K^0\pi^+)$			
$K^0K^-\pi^+$ nonresonant	$(2.3 \pm 2.3) \times 10^{-3}$		739
$\bar{K}^0K^+\pi^-$	$(5.0 \pm 1.0) \times 10^{-3}$		739
$K^*(892)^0\bar{K}^0$	< 5 $\times 10^{-4}$	CL=90%	605
$\times B(K^{*0} \rightarrow K^+\pi^-)$			
$K^*(892)^-K^+$	$(1.2 \pm 0.7) \times 10^{-3}$		610
$\times B(K^{*-} \rightarrow \bar{K}^0\pi^-)$			
$\bar{K}^0K^+\pi^-$ nonresonant	$(3.8 \pm 2.3 \pm 1.9) \times 10^{-3}$		739
$K^+K^-\pi^0$	$(1.3 \pm 0.4) \times 10^{-3}$		742

$K_S^0 K_S^0 \pi^0$	< 5.9 $\times 10^{-4}$		739
$K^+K^-\pi^+\pi^-$	[uu] $(2.50 \pm 0.23) \times 10^{-3}$		676
$\phi\pi^+\pi^- \times B(\phi \rightarrow K^+K^-)$	$(5.3 \pm 1.4) \times 10^{-4}$		614
$\phi\rho^0 \times B(\phi \rightarrow K^+K^-)$	$(3.0 \pm 1.6) \times 10^{-4}$		260
$K^+K^-\rho^0$ 3-body	$(9.0 \pm 2.3) \times 10^{-4}$		309
$K^*(892)^0K^-\pi^+$ +c.c.	[vv] < 5 $\times 10^{-4}$		528
$\times B(K^{*0} \rightarrow K^+\pi^-)$			
$K^*(892)^0\bar{K}^*(892)^0$	$(6 \pm 2) \times 10^{-4}$		257
$\times B^2(K^{*0} \rightarrow K^+\pi^-)$			
$K^+K^-\pi^+\pi^-$ non- ϕ	—		676
$K^+K^-\pi^+\pi^-$ nonresonant	< 8 $\times 10^{-4}$	CL=90%	676
$K^0\bar{K}^0\pi^+\pi^-$	$(6.8 \pm 2.7) \times 10^{-3}$		673
$K^+K^-\pi^+\pi^-\pi^0$	$(3.1 \pm 2.0) \times 10^{-3}$		600

Fractions of most of the following modes with resonances have already appeared above as submodes of particular charged-particle modes.

$\bar{K}^*(892)^0K^0$	< 1.6 $\times 10^{-3}$	CL=90%	605
$K^*(892)^+K^-$	$(3.5 \pm 0.8) \times 10^{-3}$		610
$K^*(892)^0\bar{K}^0$	< 8 $\times 10^{-4}$	CL=90%	605
$K^*(892)^-K^+$	$(1.8 \pm 1.0) \times 10^{-3}$		610
$\phi\pi^0$	< 1.4 $\times 10^{-3}$	CL=90%	644
$\phi\eta$	< 2.8 $\times 10^{-3}$	CL=90%	489
$\phi\omega$	< 2.1 $\times 10^{-3}$	CL=90%	239
$\phi\pi^+\pi^-$	$(1.07 \pm 0.28) \times 10^{-3}$		614
$\phi\rho^0$	$(6 \pm 3) \times 10^{-4}$		260
$\phi\pi^+\pi^-$ 3-body	$(7 \pm 5) \times 10^{-4}$		614
$K^*(892)^0K^-\pi^+$ + c.c.	[vv] < 7 $\times 10^{-4}$	CL=90%	—
$K^*(892)^0\bar{K}^*(892)^0$	$(1.4 \pm 0.5) \times 10^{-3}$		257

Radiative modes

$\rho^0\gamma$	< 2.4 $\times 10^{-4}$	CL=90%	773
$\omega\gamma$	< 2.4 $\times 10^{-4}$	CL=90%	768
$\phi\gamma$	< 1.9 $\times 10^{-4}$	CL=90%	654
$\bar{K}^*(892)^0\gamma$	< 7.6 $\times 10^{-4}$	CL=90%	717

Doubly Cabibbo suppressed (DC) modes, $\Delta C = 2$ forbidden via mixing (C2M) modes, $\Delta C = 1$ weak neutral current (C1) modes, or Lepton Family number (LF) violating modes

$K^+\ell^-\bar{\nu}_\ell$ (via \bar{D}^0)	C2M < 1.7 $\times 10^{-4}$	CL=90%	—
$K^+\pi^-$	DC < $(1.46 \pm 0.30) \times 10^{-4}$		861
$K^+\pi^-$ (via \bar{D}^0)	C2M < 1.6 $\times 10^{-5}$	CL=95%	861
$K^+\pi^-\pi^+\pi^-$	DC < $(1.9 \pm 2.6) \times 10^{-4}$		812
$K^+\pi^-\pi^+\pi^-$ (via \bar{D}^0)	C2M < 4 $\times 10^{-4}$	CL=90%	812
$K^+\pi^-$ or $K^+\pi^-\pi^+\pi^-$ (via \bar{D}^0)	< 1.0 $\times 10^{-3}$	CL=90%	—
μ^- anything (via \bar{D}^0)	C2M < 4 $\times 10^{-4}$	CL=90%	—
e^+e^-	C1 < 6.2 $\times 10^{-6}$	CL=90%	932
$\mu^+\mu^-$	C1 < 4.1 $\times 10^{-6}$	CL=90%	926
$\pi^0e^+e^-$	C1 < 4.5 $\times 10^{-5}$	CL=90%	927
$\pi^0\mu^+\mu^-$	C1 < 1.8 $\times 10^{-4}$	CL=90%	915
ηe^+e^-	C1 < 1.1 $\times 10^{-4}$	CL=90%	852
$\eta\mu^+\mu^-$	C1 < 5.3 $\times 10^{-4}$	CL=90%	838
$\rho^0e^+e^-$	C1 < 1.0 $\times 10^{-4}$	CL=90%	773
$\rho^0\mu^+\mu^-$	C1 < 2.3 $\times 10^{-4}$	CL=90%	756
ωe^+e^-	C1 < 1.8 $\times 10^{-4}$	CL=90%	768
$\omega\mu^+\mu^-$	C1 < 8.3 $\times 10^{-4}$	CL=90%	751
ϕe^+e^-	C1 < 5.2 $\times 10^{-5}$	CL=90%	654
$\phi\mu^+\mu^-$	C1 < 4.1 $\times 10^{-4}$	CL=90%	631
$\bar{K}^0e^+e^-$	[ss] < 1.1 $\times 10^{-4}$	CL=90%	866
$\bar{K}^0\mu^+\mu^-$	[ss] < 2.6 $\times 10^{-4}$	CL=90%	852
$\bar{K}^*(892)^0e^+e^-$	[ss] < 1.4 $\times 10^{-4}$	CL=90%	717
$\bar{K}^*(892)^0\mu^+\mu^-$	[ss] < 1.18 $\times 10^{-3}$	CL=90%	698
$\pi^+\pi^-\pi^0\mu^+\mu^-$	C1 < 8.1 $\times 10^{-4}$	CL=90%	863
$\mu^\pm e^\mp$	LF [ee] < 8.1 $\times 10^{-6}$	CL=90%	929
$\pi^0e^\pm\mu^\mp$	LF [ee] < 8.6 $\times 10^{-5}$	CL=90%	924
$\eta e^\pm\mu^\mp$	LF [ee] < 1.0 $\times 10^{-4}$	CL=90%	848
$\rho^0e^\pm\mu^\mp$	LF [ee] < 4.9 $\times 10^{-5}$	CL=90%	769
$\omega e^\pm\mu^\mp$	LF [ee] < 1.2 $\times 10^{-4}$	CL=90%	764
$\phi e^\pm\mu^\mp$	LF [ee] < 3.4 $\times 10^{-5}$	CL=90%	648
$\bar{K}^0e^\pm\mu^\mp$	LF [ee] < 1.0 $\times 10^{-4}$	CL=90%	862
$\bar{K}^*(892)^0e^\pm\mu^\mp$	LF [ee] < 1.0 $\times 10^{-4}$	CL=90%	712

Meson Summary Table

$D^*(2007)^0$	$I(J^P) = \frac{1}{2}(1^-)$ <i>I, J, P need confirmation.</i>	
Mass $m = 2006.7 \pm 0.5$ MeV ($S = 1.1$)		
$m_{D^{*0}} - m_{D^0} = 142.12 \pm 0.07$ MeV		
Full width $\Gamma < 2.1$ MeV, CL = 90%		
$\bar{D}^*(2007)^0$ modes are charge conjugates of modes below.		
$D^*(2007)^0$ DECAY MODES	Fraction (Γ_i/Γ)	ρ (MeV/c)
$D^0 \pi^0$	(61.9 ± 2.9) %	43
$D^0 \gamma$	(38.1 ± 2.9) %	137

$D^*(2010)^\pm$	$I(J^P) = \frac{1}{2}(1^-)$ <i>I, J, P need confirmation.</i>	
Mass $m = 2010.0 \pm 0.5$ MeV ($S = 1.1$)		
$m_{D^{*(2010)+}} - m_{D^+} = 140.64 \pm 0.10$ MeV ($S = 1.1$)		
$m_{D^{*(2010)+}} - m_{D^0} = 145.436 \pm 0.016$ MeV		
Full width $\Gamma < 0.131$ MeV, CL = 90%		
$D^*(2010)^-$ modes are charge conjugates of the modes below.		
$D^*(2010)^\pm$ DECAY MODES	Fraction (Γ_i/Γ)	ρ (MeV/c)
$D^0 \pi^+$	(67.7 ± 0.5) %	39
$D^+ \pi^0$	(30.7 ± 0.5) %	38
$D^+ \gamma$	(1.6 ± 0.4) %	136

$D_1(2420)^0$	$I(J^P) = \frac{1}{2}(1^+)$ <i>I, J, P need confirmation.</i>	
Mass $m = 2422.2 \pm 1.8$ MeV ($S = 1.2$)		
Full width $\Gamma = 18.9_{-3.5}^{+4.6}$ MeV		
$\bar{D}_1(2420)^0$ modes are charge conjugates of modes below.		
$D_1(2420)^0$ DECAY MODES	Fraction (Γ_i/Γ)	ρ (MeV/c)
$D^*(2010)^+ \pi^-$	seen	355
$D^+ \pi^-$	not seen	474

$D_2^*(2460)^0$	$I(J^P) = \frac{1}{2}(2^+)$	
$J^P = 2^+$ assignment strongly favored (ALBRECHT 89B).		
Mass $m = 2458.9 \pm 2.0$ MeV ($S = 1.2$)		
Full width $\Gamma = 23 \pm 5$ MeV		
$\bar{D}_2^*(2460)^0$ modes are charge conjugates of modes below.		
$D_2^*(2460)^0$ DECAY MODES	Fraction (Γ_i/Γ)	ρ (MeV/c)
$D^+ \pi^-$	seen	503
$D^*(2010)^+ \pi^-$	seen	387

$D_2^*(2460)^\pm$	$I(J^P) = \frac{1}{2}(2^+)$	
$J^P = 2^+$ assignment strongly favored (ALBRECHT 89B).		
Mass $m = 2459 \pm 4$ MeV ($S = 1.7$)		
$m_{D_2^*(2460)^\pm} - m_{D_2^*(2460)^0} = 0.9 \pm 3.3$ MeV ($S = 1.1$)		
Full width $\Gamma = 25_{-7}^{+8}$ MeV		
$D_2^*(2460)^-$ modes are charge conjugates of modes below.		
$D_2^*(2460)^\pm$ DECAY MODES	Fraction (Γ_i/Γ)	ρ (MeV/c)
$D^0 \pi^+$	seen	508
$D^{*0} \pi^+$	seen	390

CHARMED, STRANGE MESONS

($C = S = \pm 1$)

$$D_s^+ = c\bar{s}, D_s^- = \bar{c}s, \text{ similarly for } D_s^{* \pm}$$

D_s^\pm
was F^\pm

$$I(J^P) = 0(0^-)$$

$$\text{Mass } m = 1968.6 \pm 0.6 \text{ MeV } (S = 1.1)$$

$$m_{D_s^\pm} - m_{D^\pm} = 99.2 \pm 0.5 \text{ MeV } (S = 1.1)$$

$$\text{Mean life } \tau = (0.496_{-0.009}^{+0.010}) \times 10^{-12} \text{ s}$$

$$c\tau = 148.6 \mu\text{m}$$

D_s^+ form factors

$$r_2 = 1.60 \pm 0.24$$

$$r_V = 1.92 \pm 0.32$$

$$\Gamma_L/\Gamma_T = 0.72 \pm 0.18$$

Branching fractions for modes with a resonance in the final state include all the decay modes of the resonance. D_s^- modes are charge conjugates of the modes below.

D_s^+ DECAY MODES	Fraction (Γ_i/Γ)	Scale factor/ Confidence level	ρ (MeV/c)
Inclusive modes			
K^- anything	(13 $_{-12}^{+14}$) %		—
\bar{K}^0 anything + K^0 anything	(39 $_{\pm 28}$) %		—
K^+ anything	(20 $_{-14}^{+18}$) %		—
non- $K\bar{K}$ anything	(64 $_{\pm 17}$) %		—
e^+ anything	(8 $_{-5}^{+6}$) %		—
ϕ anything	(18 $_{-10}^{+15}$) %		—
Leptonic and semileptonic modes			
$\mu^+ \nu_\mu$	(4.6 \pm 1.9) $\times 10^{-3}$	S=1.3	981
$\tau^+ \nu_\tau$	(7 \pm 4) %		182
$\phi \ell^+ \nu_\ell$	[ww] (2.0 \pm 0.5) %		—
$\eta \ell^+ \nu_\ell + \eta'(958) \ell^+ \nu_\ell$	[ww] (3.5 \pm 1.0) %		—
$\eta \ell^+ \nu_\ell$	(2.6 \pm 0.7) %		—
$\eta'(958) \ell^+ \nu_\ell$	(8.9 \pm 3.4) $\times 10^{-3}$		—
Hadronic modes with a $K\bar{K}$ pair (including from a ϕ)			
$K^+ \bar{K}^0$	(3.6 \pm 1.1) %		850
$K^+ K^- \pi^+$	[qq] (4.4 \pm 1.2) %	S=1.1	805
$\phi \pi^+$	[xx] (3.6 \pm 0.9) %		712
$K^+ \bar{K}^*(892)^0$	[xx] (3.3 \pm 0.9) %		682
$f_0(980) \pi^+$	[xx] (1.8 \pm 0.8) %	S=1.3	732
$K^+ \bar{K}_0^*(1430)^0$	[xx] (7 \pm 4) $\times 10^{-3}$		186
$f_0(1710) \pi^+ \rightarrow K^+ K^- \pi^+$	[yy] (1.5 \pm 1.9) $\times 10^{-3}$		204
$K^+ K^- \pi^+$ nonresonant	(9 \pm 4) $\times 10^{-3}$		805
$K^0 \bar{K}^0 \pi^+$	—		802
$K^*(892)^+ \bar{K}^0$	[xx] (4.3 \pm 1.4) %		683
$K^+ K^- \pi^+ \pi^0$	—		748
$\phi \pi^+ \pi^0$	[xx] (9 \pm 5) %		687
$\phi \rho^+$	[xx] (6.7 \pm 2.3) %		407
$\phi \pi^+ \pi^0$ 3-body	[xx] < 2.6 %	CL=90%	687
$K^+ K^- \pi^+ \pi^0$ non- ϕ	< 9 %	CL=90%	748
$K^+ \bar{K}^0 \pi^+ \pi^-$	< 2.8 %	CL=90%	744
$K^0 K^- \pi^+ \pi^+$	(4.3 \pm 1.5) %		744
$K^*(892)^+ \bar{K}^*(892)^0$	[xx] (5.8 \pm 2.5) %		412
$K^0 K^- \pi^+ \pi^+$ non- $K^* + \bar{K}^{*0}$	< 2.9 %	CL=90%	744
$K^+ K^- \pi^+ \pi^+ \pi^-$	(8.3 \pm 3.3) $\times 10^{-3}$		673
$\phi \pi^+ \pi^+ \pi^-$	[xx] (1.18 \pm 0.35) %		640
$K^+ K^- \pi^+ \pi^+ \pi^-$ non- ϕ	(3.0 $_{-2.0}^{+3.0}$) $\times 10^{-3}$		673
Hadronic modes without K^*'s			
$\pi^+ \pi^+ \pi^-$	(1.0 \pm 0.4) %	S=1.2	959
$\rho^0 \pi^+$	< 8 $\times 10^{-4}$	CL=90%	827
$f_0(980) \pi^+$	[xx] (1.8 \pm 0.8) %	S=1.7	732
$f_2(1270) \pi^+$	[xx] (2.3 \pm 1.3) $\times 10^{-3}$		559
$f_0(1500) \pi^+ \rightarrow \pi^+ \pi^- \pi^+$	[zz] (2.8 \pm 1.6) $\times 10^{-3}$		391
$\pi^+ \pi^+ \pi^-$ nonresonant	< 2.8 $\times 10^{-3}$	CL=90%	959
$\pi^+ \pi^+ \pi^- \pi^0$	< 12 %	CL=90%	935
$\eta \pi^+$	[xx] (1.7 \pm 0.5) %		902
$\omega \pi^+$	[xx] (2.8 \pm 1.1) $\times 10^{-3}$		822

Meson Summary Table

$\pi^+\pi^+\pi^+\pi^-\pi^-$	$(6.9 \pm 3.0) \times 10^{-3}$	899
$\pi^+\pi^+\pi^-\pi^0\pi^0$	—	902
$\eta\rho^+$	[xx] $(10.8 \pm 3.1) \%$	727
$\eta\pi^+\pi^0$ 3-body	[xx] $< 4 \%$	CL=90% 886
$\pi^+\pi^+\pi^+\pi^-\pi^-$	$(4.9 \pm 3.2) \%$	856
$\eta'(958)\pi^+$	[xx] $(3.9 \pm 1.0) \%$	743
$\pi^+\pi^+\pi^+\pi^-\pi^-$	—	803
$\eta'(958)\rho^+$	[xx] $(10.1 \pm 2.8) \%$	470
$\eta'(958)\pi^+\pi^0$ 3-body	[xx] $< 1.4 \%$	CL=90% 720

Modes with one or three K's

$K^0\pi^+$	$< 8 \times 10^{-3}$	CL=90% 916
$K^+\pi^+\pi^-$	$(1.0 \pm 0.4) \%$	900
$K^+\rho^0$	$< 2.9 \times 10^{-3}$	CL=90% 747
$K^*(892)^0\pi^+$	[xx] $(6.5 \pm 2.8) \times 10^{-3}$	773
$K^+K^+K^-$	$< 6 \times 10^{-4}$	CL=90% 628
ϕK^+	[xx] $< 5 \times 10^{-4}$	CL=90% 607

 $\Delta C = 1$ weak neutral current (CI) modes, or Lepton number (L) violating modes

$\pi^+e^+e^-$	[ss] $< 2.7 \times 10^{-4}$	CL=90% 979
$\pi^+\mu^+\mu^-$	[ss] $< 1.4 \times 10^{-4}$	CL=90% 968
$K^+e^+e^-$	CI $< 1.6 \times 10^{-3}$	CL=90% 922
$K^+\mu^+\mu^-$	CI $< 1.4 \times 10^{-4}$	CL=90% 909
$K^*(892)^+\mu^+\mu^-$	CI $< 1.4 \times 10^{-3}$	CL=90% 765
$\pi^+e^\pm\mu^\mp$	LF [ee] $< 6.1 \times 10^{-4}$	CL=90% 976
$K^+e^\pm\mu^\mp$	LF [ee] $< 6.3 \times 10^{-4}$	CL=90% 919
$\pi^-e^+e^+$	L $< 6.9 \times 10^{-4}$	CL=90% 979
$\pi^-\mu^+\mu^+$	L $< 8.2 \times 10^{-5}$	CL=90% 968
$\pi^-e^+\mu^+$	L $< 7.3 \times 10^{-4}$	CL=90% 976
$K^-e^+e^+$	L $< 6.3 \times 10^{-4}$	CL=90% 922
$K^-\mu^+\mu^+$	L $< 1.8 \times 10^{-4}$	CL=90% 909
$K^-e^+\mu^+$	L $< 6.8 \times 10^{-4}$	CL=90% 919
$K^*(892)^-\mu^+\mu^+$	L $< 1.4 \times 10^{-3}$	CL=90% 765

 $D_s^{*\pm}$

$$I(J^P) = 0(?^?)$$

J^P is natural, width and decay modes consistent with 1^- .

Mass $m = 2112.4 \pm 0.7$ MeV ($S = 1.1$)

$m_{D_s^{*\pm}} - m_{D_s^\pm} = 143.8 \pm 0.4$ MeV

Full width $\Gamma < 1.9$ MeV, CL = 90%

D_s^{*-} modes are charge conjugates of the modes below.

D_s^{*+} DECAY MODES	Fraction (Γ_i/Γ)	p (MeV/c)
$D_s^+\gamma$	$(94.2 \pm 2.5) \%$	139
$D_s^+\pi^0$	$(5.8 \pm 2.5) \%$	48

 $D_{s1}(2536)^\pm$

$$I(J^P) = 0(1^+)$$

J, P need confirmation.

Mass $m = 2535.35 \pm 0.34 \pm 0.5$ MeV

Full width $\Gamma < 2.3$ MeV, CL = 90%

$D_{s1}(2536)^-$ modes are charge conjugates of the modes below.

$D_{s1}(2536)^+$ DECAY MODES	Fraction (Γ_i/Γ)	p (MeV/c)
$D^*(2010)^+K^0$	seen	150
$D^*(2007)^0K^+$	seen	169
D^+K^0	not seen	382
D^0K^+	not seen	392
$D_s^{*+}\gamma$	possibly seen	389

 $D_{sJ}(2573)^\pm$

$$I(J^P) = 0(?^?)$$

J^P is natural, width and decay modes consistent with 2^+ .

Mass $m = 2573.5 \pm 1.7$ MeV

Full width $\Gamma = 15^{+5}_{-4}$ MeV

$D_{sJ}(2573)^-$ modes are charge conjugates of the modes below.

$D_{sJ}(2573)^+$ DECAY MODES	Fraction (Γ_i/Γ)	p (MeV/c)
D^0K^+	seen	436
$D^*(2007)^0K^+$	not seen	245

BOTTOM MESONS

$$(B = \pm 1)$$

$$B^+ = u\bar{b}, B^0 = d\bar{b}, \bar{B}^0 = \bar{d}b, B^- = \bar{u}b, \text{ similarly for } B^{*'}\text{'s}$$

B-particle organization

Many measurements of B decays involve admixtures of B hadrons. Previously we arbitrarily included such admixtures in the B^\pm section, but because of their importance we have created two new sections: " B^\pm/B^0 Admixture" for $\mathcal{T}(4S)$ results and " $B^\pm/B^0/B_s^0/b$ -baryon Admixture" for results at higher energies. Most inclusive decay branching fractions are found in the Admixture sections. B^0 - \bar{B}^0 mixing data are found in the B^0 section, while B_s^0 - \bar{B}_s^0 mixing data and B - \bar{B} mixing data for a B^0/B_s^0 admixture are found in the B_s^0 section. CP -violation data are found in the B^0 section. b -baryons are found near the end of the Baryon section.

The organization of the B sections is now as follows, where bullets indicate particle sections and brackets indicate reviews.

• B^\pm

mass, mean life
branching fractions

• B^0

mass, mean life
branching fractions
polarization in B^0 decay
 B^0 - \bar{B}^0 mixing
 CP violation

• B^\pm/B^0 Admixtures

branching fractions

• $B^\pm/B^0/B_s^0/b$ -baryon Admixtures

mean life
production fractions
branching fractions

• B^*

mass

• B_s^0

mass, mean life
branching fractions
polarization in B_s^0 decay
 B_s^0 - \bar{B}_s^0 mixing
 B - \bar{B} mixing (admixture of B^0, B_s^0)

• B_c^\pm

mass, mean life
branching fractions

At end of Baryon Listings:

• Λ_b

mass, mean life
branching fractions

• b -baryon Admixture

mean life
branching fractions

Meson Summary Table

 B^\pm

$$I(J^P) = \frac{1}{2}(0^-)$$

I, J, P need confirmation. Quantum numbers shown are quark-model predictions.

$$\text{Mass } m_{B^\pm} = 5279.0 \pm 0.5 \text{ MeV}$$

$$\text{Mean life } \tau_{B^\pm} = (1.653 \pm 0.028) \times 10^{-12} \text{ s}$$

$$c\tau = 496 \text{ } \mu\text{m}$$

B^- modes are charge conjugates of the modes below. Modes which do not identify the charge state of the B are listed in the B^\pm/B^0 ADMIXTURE section.

The branching fractions listed below assume 50% $B^0\bar{B}^0$ and 50% B^+B^- production at the $T(4S)$. We have attempted to bring older measurements up to date by rescaling their assumed $T(4S)$ production ratio to 50:50 and their assumed D, D_s, D^* , and ψ branching ratios to current values whenever this would affect our averages and best limits significantly.

Indentation is used to indicate a subchannel of a previous reaction. All resonant subchannels have been corrected for resonance branching fractions to the final state so the sum of the subchannel branching fractions can exceed that of the final state.

B^\pm DECAY MODES	Fraction (Γ_i/Γ)	Scale factor/ Confidence level	ρ (MeV/c)
Semileptonic and leptonic modes			
$\ell^+ \nu_\ell$ anything	[pp] (10.2 ± 0.9) %	—	—
$\bar{D}^0 \ell^+ \nu_\ell$	[pp] (2.15 ± 0.22) %	—	—
$\bar{D}^{*0}(2007)^0 \ell^+ \nu_\ell$	[pp] (5.3 ± 0.8) %	—	—
$\bar{D}_1(2420)^0 \ell^+ \nu_\ell$	(5.6 ± 1.6) × 10 ⁻³	—	—
$\bar{D}_2^*(2460)^0 \ell^+ \nu_\ell$	< 8 × 10 ⁻³	CL=90%	—
$\pi^0 e^+ \nu_e$	< 2.2 × 10 ⁻³	CL=90%	2638
$\omega \ell^+ \nu_\ell$	[pp] < 2.1 × 10 ⁻⁴	CL=90%	—
$\rho^0 \ell^+ \nu_\ell$	[pp] < 2.1 × 10 ⁻⁴	CL=90%	—
$e^+ \nu_e$	< 1.5 × 10 ⁻⁵	CL=90%	2639
$\mu^+ \nu_\mu$	< 2.1 × 10 ⁻⁵	CL=90%	2638
$\tau^+ \nu_\tau$	< 5.7 × 10 ⁻⁴	CL=90%	2340
$e^+ \nu_e \gamma$	< 2.0 × 10 ⁻⁴	CL=90%	—
$\mu^+ \nu_\mu \gamma$	< 5.2 × 10 ⁻⁵	CL=90%	—
D, D^*, or D_s modes			
$\bar{D}^0 \pi^+$	(5.3 ± 0.5) × 10 ⁻³	—	2308
$\bar{D}^0 \rho^+$	(1.34 ± 0.18) %	—	2238
$\bar{D}^0 K^+$	(2.9 ± 0.8) × 10 ⁻⁴	—	—
$\bar{D}^0 \pi^+ \pi^+ \pi^-$	(1.1 ± 0.4) %	—	2289
$\bar{D}^0 \pi^+ \pi^+ \pi^-$ nonresonant	(5 ± 4) × 10 ⁻³	—	2289
$\bar{D}^0 \pi^+ \rho^0$	(4.2 ± 3.0) × 10 ⁻³	—	2209
$\bar{D}^0 a_1(1260)^+$	(5 ± 4) × 10 ⁻³	—	2123
$D^*(2010)^- \pi^+ \pi^+$	(2.1 ± 0.6) × 10 ⁻³	—	2247
$D^- \pi^+ \pi^+$	< 1.4 × 10 ⁻³	CL=90%	2299
$\bar{D}^*(2007)^0 \pi^+$	(4.6 ± 0.4) × 10 ⁻³	—	2256
$D^*(2010)^+ \pi^0$	< 1.7 × 10 ⁻⁴	CL=90%	2254
$\bar{D}^*(2007)^0 \rho^+$	(1.55 ± 0.31) %	—	2183
$\bar{D}^*(2007)^0 \pi^+ \pi^+ \pi^-$	(9.4 ± 2.6) × 10 ⁻³	—	2236
$\bar{D}^*(2007)^0 a_1(1260)^+$	(1.9 ± 0.5) %	—	2062
$D^*(2010)^- \pi^+ \pi^+ \pi^0$	(1.5 ± 0.7) %	—	2235
$D^*(2010)^- \pi^+ \pi^+ \pi^+ \pi^-$	< 1 %	CL=90%	2217
$\bar{D}_1^*(2420)^0 \pi^+$	(1.5 ± 0.6) × 10 ⁻³	S=1.3	2081
$\bar{D}_1^*(2420)^0 \rho^+$	< 1.4 × 10 ⁻³	CL=90%	1997
$\bar{D}_2^*(2460)^0 \pi^+$	< 1.3 × 10 ⁻³	CL=90%	2064
$\bar{D}_2^*(2460)^0 \rho^+$	< 4.7 × 10 ⁻³	CL=90%	1979
$\bar{D}^0 D_s^+$	(1.3 ± 0.4) %	—	1815
$\bar{D}^0 D_s^{*+}$	(9 ± 4) × 10 ⁻³	—	1734
$\bar{D}^*(2007)^0 D_s^+$	(1.2 ± 0.5) %	—	1737
$\bar{D}^*(2007)^0 D_s^{*+}$	(2.7 ± 1.0) %	—	1650
$\bar{D}^*(2007)^0 D^*(2010)^+$	< 1.1 %	CL=90%	—
$\bar{D}^0 D^*(2010)^+ + \bar{D}^*(2007)^0 D^+$	< 1.3 %	CL=90%	—
$\bar{D}^0 D^+$	< 6.7 × 10 ⁻³	CL=90%	—
$D_s^+ \pi^0$	< 2.0 × 10 ⁻⁴	CL=90%	2270

$D_s^{*+} \pi^0$	< 3.3 × 10 ⁻⁴	CL=90%	2214
$D_s^+ \eta$	< 5 × 10 ⁻⁴	CL=90%	2235
$D_s^{*+} \eta$	< 8 × 10 ⁻⁴	CL=90%	2177
$D_s^+ \rho^0$	< 4 × 10 ⁻⁴	CL=90%	2198
$D_s^{*+} \rho^0$	< 5 × 10 ⁻⁴	CL=90%	2139
$D_s^+ \omega$	< 5 × 10 ⁻⁴	CL=90%	2195
$D_s^{*+} \omega$	< 7 × 10 ⁻⁴	CL=90%	2136
$D_s^+ a_1(1260)^0$	< 2.2 × 10 ⁻³	CL=90%	2079
$D_s^{*+} a_1(1260)^0$	< 1.6 × 10 ⁻³	CL=90%	2014
$D_s^+ \phi$	< 3.2 × 10 ⁻⁴	CL=90%	2141
$D_s^{*+} \phi$	< 4 × 10 ⁻⁴	CL=90%	2079
$D_s^+ \bar{K}^0$	< 1.1 × 10 ⁻³	CL=90%	2241
$D_s^{*+} \bar{K}^0$	< 1.1 × 10 ⁻³	CL=90%	2184
$D_s^+ \bar{K}^*(892)^0$	< 5 × 10 ⁻⁴	CL=90%	2171
$D_s^{*+} \bar{K}^*(892)^0$	< 4 × 10 ⁻⁴	CL=90%	2110
$D_s^+ \pi^+ K^+$	< 8 × 10 ⁻⁴	CL=90%	2222
$D_s^{*+} \pi^+ K^+$	< 1.2 × 10 ⁻³	CL=90%	2164
$D_s^- \pi^+ K^*(892)^+$	< 6 × 10 ⁻³	CL=90%	2137
$D_s^{*-} \pi^+ K^*(892)^+$	< 8 × 10 ⁻³	CL=90%	2075

Charmonium modes			
$J/\psi(1S) K^+$	(10.0 ± 1.0) × 10 ⁻⁴		1683
$J/\psi(1S) K^+ \pi^+ \pi^-$	(1.4 ± 0.6) × 10 ⁻³		1612
$J/\psi(1S) K^*(892)^+$	(1.48 ± 0.27) × 10 ⁻³		1571
$J/\psi(1S) \pi^+$	(5.1 ± 1.5) × 10 ⁻⁵		1727
$J/\psi(1S) \rho^+$	< 7.7 × 10 ⁻⁴	CL=90%	1613
$J/\psi(1S) a_1(1260)^+$	< 1.2 × 10 ⁻³	CL=90%	1414
$\psi(2S) K^+$	(5.8 ± 1.0) × 10 ⁻⁴		1284
$\psi(2S) K^*(892)^+$	< 3.0 × 10 ⁻³	CL=90%	1115
$\psi(2S) K^+ \pi^+ \pi^-$	(1.9 ± 1.2) × 10 ⁻³		909
$\chi_{c1}(1P) K^+$	(1.0 ± 0.4) × 10 ⁻³		1411
$\chi_{c1}(1P) K^*(892)^+$	< 2.1 × 10 ⁻³	CL=90%	1265
K or K* modes			
$K^0 \pi^+$	(2.3 ± 1.1) × 10 ⁻⁵		2614
$K^+ \pi^0$	< 1.6 × 10 ⁻⁵	CL=90%	2615
$\eta' K^+$	(6.5 ± 1.7) × 10 ⁻⁵		2528
$\eta' K^*(892)^+$	< 1.3 × 10 ⁻⁴	CL=90%	2472
ηK^+	< 1.4 × 10 ⁻⁵	CL=90%	2587
$\eta K^*(892)^+$	< 3.0 × 10 ⁻⁵	CL=90%	2534
ωK^+	(1.5 ± 0.7 -0.6) × 10 ⁻⁵		—
$\omega K^*(892)^+$	< 8.7 × 10 ⁻⁵	CL=90%	—
$K^*(892)^0 \pi^+$	< 4.1 × 10 ⁻⁵	CL=90%	2561
$K^*(892)^+ \pi^0$	< 9.9 × 10 ⁻⁵	CL=90%	2562
$K^+ \pi^- \pi^+$ nonresonant	< 2.8 × 10 ⁻⁵	CL=90%	2609
$K^- \pi^+ \pi^+$ nonresonant	< 5.6 × 10 ⁻⁵	CL=90%	—
$K_1(1400)^0 \pi^+$	< 2.6 × 10 ⁻³	CL=90%	2451
$K_2^*(1430)^0 \pi^+$	< 6.8 × 10 ⁻⁴	CL=90%	2443
$K^+ \rho^0$	< 1.9 × 10 ⁻⁵	CL=90%	2559
$K^0 \rho^+$	< 4.8 × 10 ⁻⁵	CL=90%	2559
$K^*(892)^+ \pi^+ \pi^-$	< 1.1 × 10 ⁻³	CL=90%	2556
$K^*(892)^+ \rho^0$	< 9.0 × 10 ⁻⁴	CL=90%	2505
$K_1(1400)^+ \rho^0$	< 7.8 × 10 ⁻⁴	CL=90%	2389
$K_2^*(1430)^+ \rho^0$	< 1.5 × 10 ⁻³	CL=90%	2382
$K^+ \bar{K}^0$	< 2.1 × 10 ⁻⁵	CL=90%	2592
$K^+ K^- \pi^+$ nonresonant	< 7.5 × 10 ⁻⁵	CL=90%	—
$K^+ K^+ \pi^-$ nonresonant	< 8.79 × 10 ⁻⁵	CL=90%	—
$K^+ K^*(892)^0$	< 1.29 × 10 ⁻⁴	CL=90%	—
$K^+ K^- K^+$	< 2.0 × 10 ⁻⁴	CL=90%	2522
$K^+ \phi$	< 5 × 10 ⁻⁶	CL=90%	2516
$K^+ K^- K^+$ nonresonant	< 3.8 × 10 ⁻⁵	CL=90%	2516
$K^*(892)^+ K^+ K^-$	< 1.6 × 10 ⁻³	CL=90%	2466
$K^*(892)^+ \phi$	< 4.1 × 10 ⁻⁵	CL=90%	2460
$K_1(1400)^+ \phi$	< 1.1 × 10 ⁻³	CL=90%	2339
$K_2^*(1430)^+ \phi$	< 3.4 × 10 ⁻³	CL=90%	2332
$K^+ f_0(980)$	< 8 × 10 ⁻⁵	CL=90%	2524
$K^*(892)^+ \gamma$	(5.7 ± 3.3) × 10 ⁻⁵		2564

Meson Summary Table

$K_1(1270)^+\gamma$	< 7.3	$\times 10^{-3}$	CL=90%	2486
$K_1(1400)^+\gamma$	< 2.2	$\times 10^{-3}$	CL=90%	2453
$K_2^*(1430)^+\gamma$	< 1.4	$\times 10^{-3}$	CL=90%	2447
$K^*(1680)^+\gamma$	< 1.9	$\times 10^{-3}$	CL=90%	2361
$K_3^*(1780)^+\gamma$	< 5.5	$\times 10^{-3}$	CL=90%	2343
$K_4^*(2045)^+\gamma$	< 9.9	$\times 10^{-3}$	CL=90%	2243

Light unflavored meson modes

$\pi^+\pi^0$	< 2.0	$\times 10^{-5}$	CL=90%	2636
$\pi^+\pi^+\pi^-$	< 1.3	$\times 10^{-4}$	CL=90%	2630
$\rho^0\pi^+$	< 4.3	$\times 10^{-5}$	CL=90%	2582
$\pi^+f_0(980)$	< 1.4	$\times 10^{-4}$	CL=90%	2547
$\pi^+f_2(1270)$	< 2.4	$\times 10^{-4}$	CL=90%	2483
$\pi^+\pi^-\pi^+$ nonresonant	< 4.1	$\times 10^{-5}$	CL=90%	—
$\pi^+\pi^0\pi^0$	< 8.9	$\times 10^{-4}$	CL=90%	2631
$\rho^+\pi^0$	< 7.7	$\times 10^{-5}$	CL=90%	2582
$\pi^+\pi^-\pi^+\pi^0$	< 4.0	$\times 10^{-3}$	CL=90%	2621
$\rho^+\rho^0$	< 1.0	$\times 10^{-3}$	CL=90%	2525
$a_1(1260)^+\pi^0$	< 1.7	$\times 10^{-3}$	CL=90%	2494
$a_1(1260)^0\pi^+$	< 9.0	$\times 10^{-4}$	CL=90%	2494
$\omega\pi^+$	< 2.3	$\times 10^{-5}$	CL=90%	2580
$\omega\rho^+$	< 6.1	$\times 10^{-5}$	CL=90%	—
$\eta\pi^+$	< 1.5	$\times 10^{-5}$	CL=90%	2609
$\eta'\pi^+$	< 3.1	$\times 10^{-5}$	CL=90%	2550
$\eta'\rho^+$	< 4.7	$\times 10^{-5}$	CL=90%	2493
$\eta\rho^+$	< 3.2	$\times 10^{-5}$	CL=90%	2554
$\phi\pi^+$	< 5	$\times 10^{-6}$	CL=90%	—
$\phi\rho^+$	< 1.6	$\times 10^{-5}$	CL=90%	—
$\pi^+\pi^+\pi^+\pi^-\pi^-$	< 8.6	$\times 10^{-4}$	CL=90%	2608
$\rho^0 a_1(1260)^+$	< 6.2	$\times 10^{-4}$	CL=90%	2434
$\rho^0 a_2(1320)^+$	< 7.2	$\times 10^{-4}$	CL=90%	2411
$\pi^+\pi^+\pi^+\pi^-\pi^-\pi^0$	< 6.3	$\times 10^{-3}$	CL=90%	2592
$a_1(1260)^+ a_1(1260)^0$	< 1.3	%	CL=90%	2335

Charged particle (h^\pm) modes

$$h^\pm = K^\pm \text{ or } \pi^\pm$$

$h^+\pi^0$	$(1.6^{+0.7}_{-0.6}) \times 10^{-5}$			—
ωh^+	2.50	$\times 10^{-5}$		—

Baryon modes

$p\bar{p}\pi^+$	< 1.6	$\times 10^{-4}$	CL=90%	2439
$p\bar{p}\pi^+$ nonresonant	< 5.3	$\times 10^{-5}$	CL=90%	—
$p\bar{p}\pi^+\pi^+\pi^-$	< 5.2	$\times 10^{-4}$	CL=90%	2369
$p\bar{p}K^+$ nonresonant	< 8.9	$\times 10^{-5}$	CL=90%	—
$\rho\bar{\Lambda}$	< 2.6	$\times 10^{-6}$	CL=90%	2430
$\rho\bar{\Lambda}\pi^+\pi^-$	< 2.0	$\times 10^{-4}$	CL=90%	2367
$\Delta^0\rho$	< 3.8	$\times 10^{-4}$	CL=90%	2402
$\Delta^+\bar{\rho}$	< 1.5	$\times 10^{-4}$	CL=90%	2402
$\bar{\Lambda}_c^-\rho\pi^+$	$(6.2 \pm 2.7) \times 10^{-4}$			—
$\bar{\Lambda}_c^-\rho\pi^+\pi^0$	< 3.12	$\times 10^{-3}$	CL=90%	—
$\bar{\Lambda}_c^-\rho\pi^+\pi^+\pi^-$	< 1.46	$\times 10^{-3}$	CL=90%	—
$\bar{\Lambda}_c^-\rho\pi^+\pi^+\pi^-\pi^0$	< 1.34	%	CL=90%	—

Lepton Family number (LF) or Lepton number (L) violating modes, or $\Delta B = 1$ weak neutral current (BI) modes

$\pi^+e^+e^-$	BI	< 3.9	$\times 10^{-3}$	CL=90%	2638
$\pi^+\mu^+\mu^-$	BI	< 9.1	$\times 10^{-3}$	CL=90%	2633
$K^+e^+e^-$	BI	< 6	$\times 10^{-5}$	CL=90%	2616
$K^+\mu^+\mu^-$	BI	< 5.2	$\times 10^{-6}$	CL=90%	2612
$K^*(892)^+e^+e^-$	BI	< 6.9	$\times 10^{-4}$	CL=90%	2564
$K^*(892)^+\mu^+\mu^-$	BI	< 1.2	$\times 10^{-3}$	CL=90%	2560
$\pi^+e^+\mu^-$	LF	< 6.4	$\times 10^{-3}$	CL=90%	2637
$\pi^+e^+\mu^-$	LF	< 6.4	$\times 10^{-3}$	CL=90%	2637
$K^+e^+\mu^-$	LF	< 6.4	$\times 10^{-3}$	CL=90%	2615
$K^+e^+\mu^-$	LF	< 6.4	$\times 10^{-3}$	CL=90%	2615
$\pi^-e^+e^+$	L	< 3.9	$\times 10^{-3}$	CL=90%	2638
$\pi^-\mu^+\mu^+$	L	< 9.1	$\times 10^{-3}$	CL=90%	2633
$\pi^-e^+\mu^+$	LF	< 6.4	$\times 10^{-3}$	CL=90%	2637
$K^-e^+e^+$	L	< 3.9	$\times 10^{-3}$	CL=90%	2616
$K^-\mu^+\mu^+$	L	< 9.1	$\times 10^{-3}$	CL=90%	2612
$K^-e^+\mu^+$	LF	< 6.4	$\times 10^{-3}$	CL=90%	2615

B⁰

$$I(J^P) = \frac{1}{2}(0^-)$$

I, J, P need confirmation. Quantum numbers shown are quark-model predictions.

$$\text{Mass } m_{B^0} = 5279.4 \pm 0.5 \text{ MeV}$$

$$m_{B^0} - m_{B^\pm} = 0.33 \pm 0.28 \text{ MeV} \quad (S = 1.1)$$

$$\text{Mean life } \tau_{B^0} = (1.548 \pm 0.032) \times 10^{-12} \text{ s}$$

$$c\tau = 464 \text{ } \mu\text{m}$$

$$\tau_{B^+}/\tau_{B^0} = 1.060 \pm 0.029 \quad (\text{average of direct and inferred})$$

$$\tau_{B^+}/\tau_{B^0} = 1.062 \pm 0.029 \quad (\text{direct measurements})$$

$$\tau_{B^+}/\tau_{B^0} = 0.95^{+0.15}_{-0.12} \quad (\text{inferred from branching fractions})$$

B⁰-B⁰ mixing parameters

$$\chi_d = 0.174 \pm 0.009$$

$$\Delta m_{B^0} = m_{B_H^0} - m_{B_L^0} = (0.472 \pm 0.017) \times 10^{12} \text{ } \hbar \text{ s}^{-1}$$

$$\times_d = \Delta m_{B^0}/\Gamma_{B^0} = 0.730 \pm 0.029$$

CP violation parameters

$$\text{Re}(\epsilon_{B^0})/(1+|\epsilon_{B^0}|^2) = 0.002 \pm 0.007$$

$$\sin(2\beta) = 0.9 \pm 0.4$$

\bar{B}^0 modes are charge conjugates of the modes below. Reactions indicate the weak decay vertex and do not include mixing. Modes which do not identify the charge state of the B are listed in the B^\pm/B^0 ADMIXTURE section.

The branching fractions listed below assume 50% $B^0\bar{B}^0$ and 50% B^+B^- production at the $T(4S)$. We have attempted to bring older measurements up to date by rescaling their assumed $T(4S)$ production ratio to 50:50 and their assumed D, D_s, D^* , and ψ branching ratios to current values whenever this would affect our averages and best limits significantly.

Indentation is used to indicate a subchannel of a previous reaction. All resonant subchannels have been corrected for resonance branching fractions to the final state so the sum of the subchannel branching fractions can exceed that of the final state.

B⁰ DECAY MODES

	Fraction (Γ_i/Γ)	Scale factor/ Confidence level	ρ (MeV/c)
$\ell^+ \nu_\ell$ anything	[pp] (10.5 \pm 0.8) %		—
$D^- \ell^+ \nu_\ell$	[pp] (2.10 \pm 0.19) %		—
$D^*(2010)^- \ell^+ \nu_\ell$	[pp] (4.60 \pm 0.27) %		—
$\rho^- \ell^+ \nu_\ell$	[pp] (2.6 $^{+0.6}_{-0.7}$) $\times 10^{-4}$		—
$\pi^- \ell^+ \nu_\ell$	(1.8 \pm 0.6) $\times 10^{-4}$		—
Inclusive modes			
K^+ anything	(78 \pm 8) %		—
D, D*, or D_s modes			
$D^- \pi^+$	(3.0 \pm 0.4) $\times 10^{-3}$		2306
$D^- \rho^+$	(7.9 \pm 1.4) $\times 10^{-3}$		2236
$\bar{D}^0 \pi^+ \pi^-$	< 1.6 $\times 10^{-3}$	CL=90%	2301
$D^*(2010)^- \pi^+$	(2.76 \pm 0.21) $\times 10^{-3}$		2254
$D^- \pi^+ \pi^+ \pi^-$	(8.0 \pm 2.5) $\times 10^{-3}$		2287
$(D^- \pi^+ \pi^+ \pi^-)$ nonresonant	(3.9 \pm 1.9) $\times 10^{-3}$		2287
$D^- \pi^+ \rho^0$	(1.1 \pm 1.0) $\times 10^{-3}$		2207
$D^- a_1(1260)^+$	(6.0 \pm 3.3) $\times 10^{-3}$		2121
$D^*(2010)^- \pi^+ \pi^0$	(1.5 \pm 0.5) %		2247
$D^*(2010)^- \rho^+$	(6.8 \pm 3.4) $\times 10^{-3}$		2181
$D^*(2010)^- \pi^+ \pi^+ \pi^-$	(7.6 \pm 1.8) $\times 10^{-3}$	S=1.4	2235
$(D^*(2010)^- \pi^+ \pi^+ \pi^-)$ non-resonant	(0.0 \pm 2.5) $\times 10^{-3}$		2235
$D^*(2010)^- \pi^+ \rho^0$	(5.7 \pm 3.2) $\times 10^{-3}$		2151
$D^*(2010)^- a_1(1260)^+$	(1.30 \pm 0.27) %		2061
$D^*(2010)^- \pi^+ \pi^+ \pi^- \pi^0$	(3.5 \pm 1.8) %		2218
$\bar{D}_s^-(2460)^- \pi^+$	< 2.2 $\times 10^{-3}$	CL=90%	2064
$\bar{D}_s^-(2460)^- \rho^+$	< 4.9 $\times 10^{-3}$	CL=90%	1979
$D^- D^+$	< 1.2 $\times 10^{-3}$	CL=90%	—
$D^- D_s^+$	(8.0 \pm 3.0) $\times 10^{-3}$		1812
$D^*(2010)^- D_s^+$	(9.6 \pm 3.4) $\times 10^{-3}$		1735
$D^- D_s^{*+}$	(1.0 \pm 0.5) %		1731
$D^*(2010)^- D_s^{*+}$	(2.0 \pm 0.7) %		1649
$D_s^+ \pi^-$	< 2.8 $\times 10^{-4}$	CL=90%	2270
$D_s^{*+} \pi^-$	< 5 $\times 10^{-4}$	CL=90%	2214
$D_s^+ \rho^-$	< 7 $\times 10^{-4}$	CL=90%	2198
$D_s^{*+} \rho^-$	< 8 $\times 10^{-4}$	CL=90%	2139

Meson Summary Table

$D_s^+ a_1(1260)^-$	< 2.6	$\times 10^{-3}$	CL=90%	2079	$K_1(1270)^0 \gamma$	< 7.0	$\times 10^{-3}$	CL=90%	2486
$D_s^{*+} a_1(1260)^-$	< 2.2	$\times 10^{-3}$	CL=90%	2014	$K_1(1400)^0 \gamma$	< 4.3	$\times 10^{-3}$	CL=90%	2453
$D_s^- K^+$	< 2.4	$\times 10^{-4}$	CL=90%	2242	$K_2^*(1430)^0 \gamma$	< 4.0	$\times 10^{-4}$	CL=90%	2445
$D_s^{*-} K^+$	< 1.7	$\times 10^{-4}$	CL=90%	2185	$K^*(1680)^0 \gamma$	< 2.0	$\times 10^{-3}$	CL=90%	2361
$D_s^- K^*(892)^+$	< 9.9	$\times 10^{-4}$	CL=90%	2172	$K_3^*(1780)^0 \gamma$	< 1.0	%	CL=90%	2343
$D_s^{*-} K^*(892)^+$	< 1.1	$\times 10^{-3}$	CL=90%	2112	$K_4^*(2045)^0 \gamma$	< 4.3	$\times 10^{-3}$	CL=90%	2244
$D_s^- \pi^+ K^0$	< 5	$\times 10^{-3}$	CL=90%	2221	Light unflavored meson modes				
$D_s^{*-} \pi^+ K^0$	< 3.1	$\times 10^{-3}$	CL=90%	2164	$\pi^+ \pi^-$	< 1.5	$\times 10^{-5}$	CL=90%	2636
$D_s^- \pi^+ K^*(892)^0$	< 4	$\times 10^{-3}$	CL=90%	2136	$\pi^0 \pi^0$	< 9.3	$\times 10^{-6}$	CL=90%	2636
$D_s^{*-} \pi^+ K^*(892)^0$	< 2.0	$\times 10^{-3}$	CL=90%	2074	$\eta \pi^0$	< 8	$\times 10^{-6}$	CL=90%	2609
$\bar{D}^0 \pi^0$	< 1.2	$\times 10^{-4}$	CL=90%	2308	$\eta \eta$	< 1.8	$\times 10^{-5}$	CL=90%	2582
$\bar{D}^0 \rho^0$	< 3.9	$\times 10^{-4}$	CL=90%	2238	$\eta' \pi^0$	< 1.1	$\times 10^{-5}$	CL=90%	2551
$\bar{D}^0 \eta$	< 1.3	$\times 10^{-4}$	CL=90%	2274	$\eta' \eta'$	< 4.7	$\times 10^{-5}$	CL=90%	2460
$\bar{D}^0 \eta'$	< 9.4	$\times 10^{-4}$	CL=90%	2198	$\eta' \eta$	< 2.7	$\times 10^{-5}$	CL=90%	2522
$\bar{D}^0 \omega$	< 5.1	$\times 10^{-4}$	CL=90%	2235	$\eta' \rho^0$	< 2.3	$\times 10^{-5}$	CL=90%	2493
$\bar{D}^*(2007)^0 \pi^0$	< 4.4	$\times 10^{-4}$	CL=90%	2256	$\eta \rho^0$	< 1.3	$\times 10^{-5}$	CL=90%	2554
$\bar{D}^*(2007)^0 \rho^0$	< 5.6	$\times 10^{-4}$	CL=90%	2183	$\omega \eta$	< 1.2	$\times 10^{-5}$	CL=90%	—
$\bar{D}^*(2007)^0 \eta$	< 2.6	$\times 10^{-4}$	CL=90%	2220	$\omega \eta'$	< 6.0	$\times 10^{-5}$	CL=90%	—
$\bar{D}^*(2007)^0 \eta'$	< 1.4	$\times 10^{-3}$	CL=90%	2141	$\omega \rho^0$	< 1.1	$\times 10^{-5}$	CL=90%	—
$\bar{D}^*(2007)^0 \omega$	< 7.4	$\times 10^{-4}$	CL=90%	2180	$\omega \omega$	< 1.9	$\times 10^{-5}$	CL=90%	—
$D^*(2010)^+ D^*(2010)^-$	(6.2 \pm 4.1 \pm 3.1)	$\times 10^{-4}$		1711	$\phi \pi^0$	< 5	$\times 10^{-6}$	CL=90%	—
$D^*(2010)^+ D^-$	< 1.8	$\times 10^{-3}$	CL=90%	1790	$\phi \eta$	< 9	$\times 10^{-6}$	CL=90%	—
$D(*)^0 \bar{D}(*^0)$	< 2.7	%	CL=90%	—	$\phi \eta'$	< 3.1	$\times 10^{-5}$	CL=90%	—
Charmonium modes					$\phi \rho^0$	< 1.3	$\times 10^{-5}$	CL=90%	—
$J/\psi(1S) K^0$	(8.9 \pm 1.2)	$\times 10^{-4}$		1683	$\phi \omega$	< 2.1	$\times 10^{-5}$	CL=90%	—
$J/\psi(1S) K^+ \pi^-$	(1.2 \pm 0.6)	$\times 10^{-3}$		1652	$\phi \phi$	< 1.2	$\times 10^{-5}$	CL=90%	2435
$J/\psi(1S) K^*(892)^0$	(1.50 \pm 0.17)	$\times 10^{-3}$		1570	$\pi^+ \pi^- \pi^0$	< 7.2	$\times 10^{-4}$	CL=90%	2631
$J/\psi(1S) \pi^0$	< 5.8	$\times 10^{-5}$	CL=90%	1728	$\rho^0 \pi^0$	< 2.4	$\times 10^{-5}$	CL=90%	2582
$J/\psi(1S) \eta$	< 1.2	$\times 10^{-3}$	CL=90%	1672	$\rho^\mp \pi^\pm$	[ee] < 8.8	$\times 10^{-5}$	CL=90%	2582
$J/\psi(1S) \rho^0$	< 2.5	$\times 10^{-4}$	CL=90%	1614	$\pi^+ \pi^- \pi^+ \pi^-$	< 2.3	$\times 10^{-4}$	CL=90%	2621
$J/\psi(1S) \omega$	< 2.7	$\times 10^{-4}$	CL=90%	1609	$\rho^0 \rho^0$	< 2.8	$\times 10^{-4}$	CL=90%	2525
$\psi(2S) K^0$	< 8	$\times 10^{-4}$	CL=90%	1283	$a_1(1260)^\mp \pi^\pm$	[ee] < 4.9	$\times 10^{-4}$	CL=90%	2494
$\psi(2S) K^+ \pi^-$	< 1	$\times 10^{-3}$	CL=90%	1238	$a_2(1320)^\mp \pi^\pm$	[ee] < 3.0	$\times 10^{-4}$	CL=90%	2473
$\psi(2S) K^*(892)^0$	(9.3 \pm 2.3)	$\times 10^{-4}$		1113	$\pi^+ \pi^- \pi^0 \pi^0$	< 3.1	$\times 10^{-3}$	CL=90%	2622
$\chi_{c1}(1P) K^0$	< 2.7	$\times 10^{-3}$	CL=90%	1411	$\rho^+ \rho^-$	< 2.2	$\times 10^{-3}$	CL=90%	2525
$\chi_{c1}(1P) K^*(892)^0$	< 2.1	$\times 10^{-3}$	CL=90%	1263	$a_1(1260)^0 \pi^0$	< 1.1	$\times 10^{-3}$	CL=90%	2494
K or K* modes					$\omega \pi^0$	< 1.4	$\times 10^{-5}$	CL=90%	2580
$K^+ \pi^-$	(1.5 \pm 0.5 \pm 0.4)	$\times 10^{-5}$		2615	$\pi^+ \pi^+ \pi^- \pi^- \pi^0$	< 9.0	$\times 10^{-3}$	CL=90%	2609
$K^0 \pi^0$	< 4.1	$\times 10^{-5}$	CL=90%	2614	$a_1(1260)^+ \rho^-$	< 3.4	$\times 10^{-3}$	CL=90%	2434
$\eta' K^0$	(4.7 \pm 2.8 \pm 2.2)	$\times 10^{-5}$		2528	$a_1(1260)^0 \rho^0$	< 2.4	$\times 10^{-3}$	CL=90%	2434
$\eta' K^*(892)^0$	< 3.9	$\times 10^{-5}$	CL=90%	2472	$\pi^+ \pi^+ \pi^+ \pi^- \pi^- \pi^-$	< 3.0	$\times 10^{-3}$	CL=90%	2592
$\eta K^*(892)^0$	< 3.0	$\times 10^{-5}$	CL=90%	2534	$a_1(1260)^+ a_1(1260)^-$	< 2.8	$\times 10^{-3}$	CL=90%	2336
ηK^0	< 3.3	$\times 10^{-5}$	CL=90%	2593	$\pi^+ \pi^+ \pi^+ \pi^- \pi^- \pi^- \pi^0$	< 1.1	%	CL=90%	2572
ωK^0	< 5.7	$\times 10^{-5}$	CL=90%	—	Baryon modes				
$\omega K^*(892)^0$	< 2.3	$\times 10^{-5}$	CL=90%	—	$p \bar{p}$	< 7.0	$\times 10^{-6}$	CL=90%	2467
$K^+ K^-$	< 4.3	$\times 10^{-6}$	CL=90%	2593	$p \bar{p} \pi^+ \pi^-$	< 2.5	$\times 10^{-4}$	CL=90%	2406
$K^0 \bar{K}^0$	< 1.7	$\times 10^{-5}$	CL=90%	2592	$p \Lambda \pi^-$	< 1.3	$\times 10^{-5}$	CL=90%	2401
$K^+ \rho^-$	< 3.5	$\times 10^{-5}$	CL=90%	2559	$\bar{\Lambda} \Lambda$	< 3.9	$\times 10^{-6}$	CL=90%	—
$K^0 \rho^0$	< 3.9	$\times 10^{-5}$	CL=90%	2559	$\Delta^0 \bar{\Delta}^0$	< 1.5	$\times 10^{-3}$	CL=90%	2334
$K^0 f_0(980)$	< 3.6	$\times 10^{-4}$	CL=90%	2523	$\Delta^{++} \Delta^{--}$	< 1.1	$\times 10^{-4}$	CL=90%	2334
$K^*(892)^+ \pi^-$	< 7.2	$\times 10^{-5}$	CL=90%	2562	$\bar{\Sigma}^- \Delta^{++}$	< 1.0	$\times 10^{-3}$	CL=90%	1839
$K^*(892)^0 \pi^0$	< 2.8	$\times 10^{-5}$	CL=90%	2562	$\bar{\Lambda}_c^- \rho \pi^+ \pi^-$	(1.3 \pm 0.6)	$\times 10^{-3}$		—
$K_2^*(1430)^+ \pi^-$	< 2.6	$\times 10^{-3}$	CL=90%	2445	$\bar{\Lambda}_c^- \rho$	< 2.1	$\times 10^{-4}$	CL=90%	2021
$K^0 K^+ K^-$	< 1.3	$\times 10^{-3}$	CL=90%	2522	$\bar{\Lambda}_c^- \rho \pi^0$	< 5.9	$\times 10^{-4}$	CL=90%	—
$K^0 \phi$	< 3.1	$\times 10^{-5}$	CL=90%	2516	$\bar{\Lambda}_c^- \rho \pi^+ \pi^- \pi^0$	< 5.07	$\times 10^{-3}$	CL=90%	—
$K^- \pi^+ \pi^+ \pi^-$	[aa] < 2.3	$\times 10^{-4}$	CL=90%	2600	$\bar{\Lambda}_c^- \rho \pi^+ \pi^- \pi^+ \pi^-$	< 2.74	$\times 10^{-3}$	CL=90%	—
$K^*(892)^0 \pi^+ \pi^-$	< 1.4	$\times 10^{-3}$	CL=90%	2556	Lepton Family number (LF) violating modes, or $\Delta B = 1$ weak neutral current (BI) modes				
$K^*(892)^0 \rho^0$	< 4.6	$\times 10^{-4}$	CL=90%	2504	$\gamma \gamma$	< 3.9	$\times 10^{-5}$	CL=90%	2640
$K^*(892)^0 f_0(980)$	< 1.7	$\times 10^{-4}$	CL=90%	2467	$e^+ e^-$	BI < 5.9	$\times 10^{-6}$	CL=90%	2640
$K_1(1400)^+ \pi^-$	< 1.1	$\times 10^{-3}$	CL=90%	2451	$\mu^+ \mu^-$	BI < 6.8	$\times 10^{-7}$	CL=90%	2637
$K^- a_1(1260)^+$	[aa] < 2.3	$\times 10^{-4}$	CL=90%	2471	$K^0 e^+ e^-$	BI < 3.0	$\times 10^{-4}$	CL=90%	2616
$K^*(892)^0 K^+ K^-$	< 6.1	$\times 10^{-4}$	CL=90%	2466	$K^0 \mu^+ \mu^-$	BI < 3.6	$\times 10^{-4}$	CL=90%	2612
$K^*(892)^0 \phi$	< 2.1	$\times 10^{-5}$	CL=90%	2459	$K^*(892)^0 e^+ e^-$	BI < 2.9	$\times 10^{-4}$	CL=90%	2564
$K_1(1400)^0 \rho^0$	< 3.0	$\times 10^{-3}$	CL=90%	2389	$K^*(892)^0 \mu^+ \mu^-$	BI < 4.0	$\times 10^{-6}$	CL=90%	2559
$K_1(1400)^0 \phi$	< 5.0	$\times 10^{-3}$	CL=90%	2339	$K^*(892)^0 \nu \bar{\nu}$	BI < 1.0	$\times 10^{-3}$	CL=90%	2244
$K_2^*(1430)^0 \rho^0$	< 1.1	$\times 10^{-3}$	CL=90%	2380	$e^\pm \mu^\mp$	LF [ee] < 3.5	$\times 10^{-6}$	CL=90%	2639
$K_2^*(1430)^0 \phi$	< 1.4	$\times 10^{-3}$	CL=90%	2330	$e^\pm \tau^\mp$	LF [ee] < 5.3	$\times 10^{-4}$	CL=90%	2341
$K^*(892)^0 \gamma$	(4.0 \pm 1.9)	$\times 10^{-5}$		2564	$\mu^\pm \tau^\mp$	LF [ee] < 8.3	$\times 10^{-4}$	CL=90%	2339

Meson Summary Table

 B^\pm/B^0 ADMIXTURE

The branching fraction measurements are for an admixture of B mesons at the $\Upsilon(4S)$. The values quoted assume that $B(\Upsilon(4S) \rightarrow B\bar{B}) = 100\%$.

For inclusive branching fractions, e.g., $B \rightarrow D^\pm$ anything, the treatment of multiple D 's in the final state must be defined. One possibility would be to count the number of events with one-or-more D 's and divide by the total number of B 's. Another possibility would be to count the total number of D 's and divide by the total number of B 's, which is the definition of average multiplicity. The two definitions are identical when only one of the specified particles is allowed in the final state. Even though the "one-or-more" definition seems sensible, for practical reasons inclusive branching fractions are almost always measured using the multiplicity definition. For heavy final state particles, authors call their results inclusive branching fractions while for light particles some authors call their results multiplicities. In the B sections, we list all results as inclusive branching fractions, adopting a multiplicity definition. This means that inclusive branching fractions can exceed 100% and that inclusive partial widths can exceed total widths, just as inclusive cross sections can exceed total cross sections.

\bar{B} modes are charge conjugates of the modes below. Reactions indicate the weak decay vertex and do not include mixing.

B DECAY MODES	Fraction (Γ_i/Γ)	Scale factor/ Confidence level	p (MeV/c)	
Semileptonic and leptonic modes				
$B \rightarrow e^+ \nu_e$ anything	[bbb] (10.41 ± 0.29) %	S=1.2	-	-
$B \rightarrow \bar{p} e^+ \nu_e$ anything	< 1.6 × 10 ⁻³	CL=90%	-	-
$B \rightarrow \mu^+ \nu_\mu$ anything	[bbb] (10.3 ± 0.5) %	-	-	-
$B \rightarrow \ell^+ \nu_\ell$ anything	[pp,bbb] (10.45 ± 0.21) %	-	-	-
$B \rightarrow D^- \ell^+ \nu_\ell$ anything	[pp] (2.7 ± 0.8) %	-	-	-
$B \rightarrow \bar{D}^0 \ell^+ \nu_\ell$ anything	[pp] (7.0 ± 1.4) %	-	-	-
$B \rightarrow \bar{D}^{*+} \ell^+ \nu_\ell$	[pp,ccc] (2.7 ± 0.7) %	-	-	-
$B \rightarrow \bar{D}_1(2420) \ell^+ \nu_\ell$ anything	(7.4 ± 1.6) × 10 ⁻³	-	-	-
$B \rightarrow D \pi \ell^+ \nu_\ell$ anything + $D^* \pi \ell^+ \nu_\ell$ anything	(2.3 ± 0.4) %	-	-	-
$B \rightarrow \bar{D}_2^*(2460) \ell^+ \nu_\ell$ anything	< 6.5 × 10 ⁻³	CL=95%	-	-
$B \rightarrow D^{*-} \pi^+ \ell^+ \nu_\ell$ anything	(1.00 ± 0.34) %	-	-	-
$B \rightarrow D_s^- \ell^+ \nu_\ell$ anything	[pp] < 9 × 10 ⁻³	CL=90%	-	-
$B \rightarrow D_s^- \ell^+ \nu_\ell K^+$ anything	[pp] < 6 × 10 ⁻³	CL=90%	-	-
$B \rightarrow D_s^- \ell^+ \nu_\ell K^0$ anything	[pp] < 9 × 10 ⁻³	CL=90%	-	-
$B \rightarrow K^+ \ell^+ \nu_\ell$ anything	[pp] (6.0 ± 0.5) %	-	-	-
$B \rightarrow K^- \ell^+ \nu_\ell$ anything	[pp] (10 ± 4) × 10 ⁻³	-	-	-
$B \rightarrow K^0 / \bar{K}^0 \ell^+ \nu_\ell$ anything	[pp] (4.4 ± 0.5) %	-	-	-
D, D^*, or D_s modes				
$B \rightarrow D^\pm$ anything	(24.1 ± 1.9) %	S=1.1	-	-
$B \rightarrow D^0 / \bar{D}^0$ anything	(63.5 ± 2.9) %	-	-	-
$B \rightarrow D^*(2010)^\pm$ anything	(22.7 ± 1.6) %	-	-	-
$B \rightarrow D^*(2007)^0$ anything	(26.0 ± 2.7) %	-	-	-
$B \rightarrow D_s^\pm$ anything	[ee] (10.0 ± 2.5) %	-	-	-
$B \rightarrow D^{(*)} \bar{D}^{(*)} K^0 + D^{(*)} \bar{D}^{(*)} K^\pm$	[ee,ddd] (7.1 ^{+2.7} _{-1.7}) %	-	-	-
$b \rightarrow c \bar{c} s$	(22 ± 4) %	-	-	-
$B \rightarrow D_s^{(*)} \bar{D}^{(*)}$	[ee,ddd] (4.9 ± 1.3) %	-	-	-
$B \rightarrow D^* D^*(2010)^\pm$	[ee] < 5.9 × 10 ⁻³	CL=90%	-	-
$B \rightarrow DD^*(2010)^\pm + D^* D^\pm$	[ee] < 5.5 × 10 ⁻³	CL=90%	-	-
$B \rightarrow DD^\pm$	[ee] < 3.1 × 10 ⁻³	CL=90%	-	-
$B \rightarrow D_s^{(*)} \pm \bar{D}^{(*)} X (n\pi^\pm)$	[ee,ddd] (9 ⁺⁵ ₋₄) %	-	-	-
$B \rightarrow D^*(2010) \gamma$	< 1.1 × 10 ⁻³	CL=90%	-	-
$B \rightarrow D_s^+ \pi^-, D_s^{*+} \pi^-, D_s^+ \rho^-, D_s^{*+} \rho^-, D_s^+ \pi^0, D_s^{*+} \pi^0, D_s^+ \eta, D_s^{*+} \eta, D_s^+ \rho^0, D_s^{*+} \rho^0, D_s^+ \omega, D_s^{*+} \omega$	[ee] < 5 × 10 ⁻⁴	CL=90%	-	-
$B \rightarrow D_{s1}(2536)^+$ anything	< 9.5 × 10 ⁻³	CL=90%	-	-

Charmonium modes

$B \rightarrow J/\psi(1S)$ anything	(1.15 ± 0.06) %	-	-
$B \rightarrow J/\psi(1S)$ (direct) anything	(8.0 ± 0.8) × 10 ⁻³	-	-
$B \rightarrow \psi(2S)$ anything	(3.5 ± 0.5) × 10 ⁻³	-	-
$B \rightarrow \chi_{c1}(1P)$ anything	(4.2 ± 0.7) × 10 ⁻³	-	-
$B \rightarrow \chi_{c1}(1P)$ (direct) anything	(3.7 ± 0.7) × 10 ⁻³	-	-
$B \rightarrow \chi_{c2}(1P)$ anything	< 3.8 × 10 ⁻³	CL=90%	-
$B \rightarrow \eta_c(1S)$ anything	< 9 × 10 ⁻³	CL=90%	-

K or K* modes

$B \rightarrow K^\pm$ anything	[ee] (78.9 ± 2.5) %	-	-
$B \rightarrow K^+$ anything	(66 ± 5) %	-	-
$B \rightarrow K^-$ anything	(13 ± 4) %	-	-
$B \rightarrow K^0 / \bar{K}^0$ anything	[ee] (64 ± 4) %	-	-
$B \rightarrow K^*(892)^\pm$ anything	(18 ± 6) %	-	-
$B \rightarrow K^*(892)^0 / \bar{K}^*(892)^0$ anything	[ee] (14.6 ± 2.6) %	-	-
$B \rightarrow K_1(1400) \gamma$	< 4.1 × 10 ⁻⁴	CL=90%	-
$B \rightarrow K_2^*(1430) \gamma$	< 8.3 × 10 ⁻⁴	CL=90%	-
$B \rightarrow K_2(1770) \gamma$	< 1.2 × 10 ⁻³	CL=90%	-
$B \rightarrow K_3^*(1780) \gamma$	< 3.0 × 10 ⁻³	CL=90%	-
$B \rightarrow K_4^*(2045) \gamma$	< 1.0 × 10 ⁻³	CL=90%	-
$B \rightarrow \bar{b} \rightarrow \bar{s} \gamma$	(2.3 ± 0.7) × 10 ⁻⁴	-	-
$B \rightarrow \bar{b} \rightarrow \bar{s} \text{gluon}$	< 6.8 %	CL=90%	-
$B \rightarrow \eta$ anything	< 4.4 × 10 ⁻⁴	CL=90%	-
$B \rightarrow \eta'$ anything	(6.2 ^{+2.1} _{-2.6}) × 10 ⁻⁴	-	-

Light unflavored meson modes

$B \rightarrow \pi^\pm$ anything	[ee,eee] (358 ± 7) %	-	-
$B \rightarrow \eta$ anything	(17.6 ± 1.6) %	-	-
$B \rightarrow \rho^0$ anything	(21 ± 5) %	-	-
$B \rightarrow \omega$ anything	< 81 %	CL=90%	-
$B \rightarrow \phi$ anything	(3.5 ± 0.7) %	S=1.8	-
$B \rightarrow \phi K^*(892)$	< 2.2 × 10 ⁻⁵	CL=90%	-

Baryon modes

$B \rightarrow \Lambda_c^\pm$ anything	(6.4 ± 1.1) %	-	-
$B \rightarrow \bar{\Lambda}_c^- e^+$ anything	< 3.2 × 10 ⁻³	CL=90%	-
$B \rightarrow \bar{\Lambda}_c^- p$ anything	(3.6 ± 0.7) %	-	-
$B \rightarrow \bar{\Lambda}_c^- p e^+ \nu_e$	< 1.5 × 10 ⁻³	CL=90%	-
$B \rightarrow \bar{\Sigma}_c^{--}$ anything	(4.2 ± 2.4) × 10 ⁻³	-	-
$B \rightarrow \bar{\Sigma}_c^-$ anything	< 9.6 × 10 ⁻³	CL=90%	-
$B \rightarrow \bar{\Sigma}_c^0$ anything	(4.6 ± 2.4) × 10 ⁻³	-	-
$B \rightarrow \bar{\Sigma}_c^0 N (N = p \text{ or } n)$	< 1.5 × 10 ⁻³	CL=90%	-
$B \rightarrow \Xi_c^0$ anything	(1.4 ± 0.5) × 10 ⁻⁴	-	-
$\times B(\Xi_c^0 \rightarrow \Xi^- \pi^+)$			
$B \rightarrow \Xi_c^+$ anything	(4.5 ^{+1.3} _{-1.2}) × 10 ⁻⁴	-	-
$\times B(\Xi_c^+ \rightarrow \Xi^- \pi^+ \pi^+)$			
$B \rightarrow p / \bar{p}$ anything	[ee] (8.0 ± 0.4) %	-	-
$B \rightarrow p / \bar{p}$ (direct) anything	[ee] (5.5 ± 0.5) %	-	-
$B \rightarrow \Lambda / \bar{\Lambda}$ anything	[ee] (4.0 ± 0.5) %	-	-
$B \rightarrow \Xi^- / \bar{\Xi}^+$ anything	[ee] (2.7 ± 0.6) × 10 ⁻³	-	-
$B \rightarrow$ baryons anything	(6.8 ± 0.6) %	-	-
$B \rightarrow p \bar{p}$ anything	(2.47 ± 0.23) %	-	-
$B \rightarrow \Lambda \bar{p} / \bar{\Lambda} p$ anything	[ee] (2.5 ± 0.4) %	-	-
$B \rightarrow \Lambda \bar{\Lambda}$ anything	< 5 × 10 ⁻³	CL=90%	-

Lepton Family number (LF) violating modes or **$\Delta B = 1$ weak neutral current ($B1$) modes**

$B \rightarrow e^+ e^- s$	$B1$ < 5.7 × 10 ⁻⁵	CL=90%	-
$B \rightarrow \mu^+ \mu^- s$	$B1$ < 5.8 × 10 ⁻⁵	CL=90%	-
$B \rightarrow e^\pm \mu^\mp s$	LF < 2.2 × 10 ⁻⁵	CL=90%	-

Meson Summary Table

 $B^\pm/B^0/B_s^0/b$ -baryon ADMIXTURE

These measurements are for an admixture of bottom particles at high energy (LEP, Tevatron, $S\bar{p}\bar{p}S$).

$$\text{Mean life } \tau = (1.564 \pm 0.014) \times 10^{-12} \text{ s}$$

$$\text{Mean life } \tau = (1.72 \pm 0.10) \times 10^{-12} \text{ s} \quad \text{Charged } b\text{-hadron admixture}$$

$$\text{Mean life } \tau = (1.58 \pm 0.14) \times 10^{-12} \text{ s} \quad \text{Neutral } b\text{-hadron admixture}$$

$$\tau^{\text{charged } b\text{-hadron}}/\tau^{\text{neutral } b\text{-hadron}} = 1.09 \pm 0.13$$

$$|\Delta\tau_b|/\tau_{b,\bar{b}} = -0.001 \pm 0.014$$

The branching fraction measurements are for an admixture of B mesons and baryons at energies above the $\Upsilon(4S)$. Only the highest energy results (LEP, Tevatron, $S\bar{p}\bar{p}S$) are used in the branching fraction averages. In the following, we assume that the production fractions are the same at the LEP and at the Tevatron.

For inclusive branching fractions, e.g., $B \rightarrow D^\pm$ anything, the treatment of multiple D 's in the final state must be defined. One possibility would be to count the number of events with one-or-more D 's and divide by the total number of B 's. Another possibility would be to count the total number of D 's and divide by the total number of B 's, which is the definition of average multiplicity. The two definitions are identical when only one of the specified particles is allowed in the final state. Even though the "one-or-more" definition seems sensible, for practical reasons inclusive branching fractions are almost always measured using the multiplicity definition. For heavy final state particles, authors call their results inclusive branching fractions while for light particles some authors call their results multiplicities. In the B sections, we list all results as inclusive branching fractions, adopting a multiplicity definition. This means that inclusive branching fractions can exceed 100% and that inclusive partial widths can exceed total widths, just as inclusive cross sections can exceed total cross sections.

The modes below are listed for a \bar{b} initial state. b modes are their charge conjugates. Reactions indicate the weak decay vertex and do not include mixing.

\bar{b} DECAY MODES	Fraction (Γ_i/Γ)	Scale factor/ Confidence level	ρ (MeV/c)
-----------------------	--------------------------------	-----------------------------------	-------------------

PRODUCTION FRACTIONS

The production fractions for weakly decaying b -hadrons at high energy have been calculated from the best values of mean lives, mixing parameters, and branching fractions in this edition by the LEP B Oscillation Working Group as described in the note "Production and Decay of b -Flavored Hadrons" in the B^\pm Particle Listings. Values assume

$$B(\bar{b} \rightarrow B^+) = B(\bar{b} \rightarrow B^0)$$

$$B(\bar{b} \rightarrow B^+) + B(\bar{b} \rightarrow B^0) + B(\bar{b} \rightarrow B_s^0) + B(b \rightarrow b\text{-baryon}) = 100\%$$

The notation for production fractions varies in the literature (f_d , d_{B^0} , $f(b \rightarrow \bar{B}^0)$, $B(b \rightarrow \bar{B}^0)$). We use our own branching fraction notation here, $B(\bar{b} \rightarrow B^0)$.

B^+	(38.9 \pm 1.3) %	—
B^0	(38.9 \pm 1.3) %	—
B_s^0	(10.7 \pm 1.4) %	—
b -baryon	(11.6 \pm 2.0) %	—
B_c	—	—

DECAY MODES**Semileptonic and leptonic modes**

ν anything	(23.1 \pm 1.5) %	—
$\ell^+ \nu_\ell$ anything	[pp] (10.73 \pm 0.18) %	S=1.1
$e^+ \nu_e$ anything	(10.86 \pm 0.35) %	—
$\mu^+ \nu_\mu$ anything	(10.95 \pm 0.29 / 0.25) %	—
$D^- \ell^+ \nu_\ell$ anything	[pp] (2.02 \pm 0.29) %	—
$\bar{D}^0 \ell^+ \nu_\ell$ anything	[pp] (6.6 \pm 0.6) %	—
$D^{*-} \ell^+ \nu_\ell$ anything	[pp] (2.76 \pm 0.29) %	—
$\bar{D}_j^0 \ell^+ \nu_\ell$ anything	{pp,ff} seen	—
$D_j^- \ell^+ \nu_\ell$ anything	{pp,ff} seen	—
$\bar{D}_2^*(2460)^0 \ell^+ \nu_\ell$ anything	seen	—
$D_2^*(2460)^- \ell^+ \nu_\ell$ anything	seen	—
charmless $\ell \bar{\nu}_\ell$	[pp] (1.7 \pm 0.6) $\times 10^{-3}$	—
$\tau^+ \nu_\tau$ anything	(2.6 \pm 0.4) %	—
$\bar{c} \rightarrow \ell^- \bar{\nu}_\ell$ anything	[pp] (8.3 \pm 0.4) %	—

Charmed meson and baryon modes

\bar{D}^0 anything	(60.5 \pm 3.2) %	—
$D^0 D_s^\pm$ anything	[ee] (9.1 \pm 3.9 / 2.8) %	—
$D^\mp D_s^\pm$ anything	[ee] (4.0 \pm 2.3 / 1.8) %	—
$\bar{D}^0 D^0$ anything	[ee] (5.1 \pm 2.0 / 1.8) %	—
$D^0 D^\pm$ anything	[ee] (2.7 \pm 1.8 / 1.6) %	—
$D^\pm D^\mp$ anything	[ee] < 9 $\times 10^{-3}$ CL=90%	—
D^- anything	(23.7 \pm 2.3) %	—
$D^*(2010)^+$ anything	(17.3 \pm 2.0) %	—
$D_1(2420)^0$ anything	(5.0 \pm 1.5) %	—
$D^*(2010)^\mp D_s^\pm$ anything	[ee] (3.3 \pm 1.6 / 1.3) %	—
$D^0 D^*(2010)^\pm$ anything	[ee] (3.0 \pm 1.1 / 0.9) %	—
$D^*(2010)^\pm D^\mp$ anything	[ee] (2.5 \pm 1.2 / 1.0) %	—
$D^*(2010)^\pm D^*(2010)^\mp$ anything	[ee] (1.2 \pm 0.4) %	—
$D_2^*(2460)^0$ anything	(4.7 \pm 2.7) %	—
\bar{D}_s anything	(18 \pm 5) %	—
Λ_c anything	(9.7 \pm 2.9) %	—
\bar{c}/c anything	[eee] (117 \pm 4) %	—

Charmonium modes

$J/\psi(1S)$ anything	(1.16 \pm 0.10) %	—
$\psi(2S)$ anything	(4.8 \pm 2.4) $\times 10^{-3}$	—
$\chi_{c1}(1P)$ anything	(1.8 \pm 0.5) %	—

K or K^* modes

$\bar{s}\gamma$	(3.1 \pm 1.1) $\times 10^{-4}$	—
K^\pm anything	(74 \pm 6) %	—
K_S^0 anything	(29.0 \pm 2.9) %	—

Pion modes

π^\pm anything	(397 \pm 21) %	—
π^0 anything	[eee] (278 \pm 60) %	—

Baryon modes

p/\bar{p} anything	(13.1 \pm 1.1) %	—
----------------------	----------------------	---

Other modes

charged anything	[eee] (497 \pm 7) %	—
hadron $^+$ hadron $^-$	(1.7 \pm 1.0 / 0.7) $\times 10^{-5}$	—
charmless	(7 \pm 21) $\times 10^{-3}$	—

Baryon modes

$\Lambda/\bar{\Lambda}$ anything	(5.9 \pm 0.6) %	—
b -baryon anything	(10.2 \pm 2.8) %	—

 $\Delta B = 1$ weak neutral current ($B1$) modes

$\mu^+ \mu^-$ anything	$B1$ < 3.2 $\times 10^{-4}$ CL=90%	—
------------------------	------------------------------------	---

 B^*

$$J(P) = \frac{1}{2}(1^-)$$

I, J, P need confirmation. Quantum numbers shown are quark-model predictions.

$$\text{Mass } m_{B^*} = 5325.0 \pm 0.6 \text{ MeV}$$

$$m_{B^*} - m_B = 45.78 \pm 0.35 \text{ MeV}$$

B^* DECAY MODES	Fraction (Γ_i/Γ)	ρ (MeV/c)
$B\gamma$	dominant	46

Meson Summary Table

BOTTOM, STRANGE MESONS ($B = \pm 1, S = \mp 1$)

$$B_s^0 = s\bar{d}, \bar{B}_s^0 = \bar{s}d, \text{ similarly for } B_s^{\pm}$$

 B_s^0

$$I(J^P) = 0(0^-)$$

I, J, P need confirmation. Quantum numbers shown are quark-model predictions.

$$\text{Mass } m_{B_s^0} = 5369.6 \pm 2.4 \text{ MeV}$$

$$\text{Mean life } \tau = (1.493 \pm 0.062) \times 10^{-12} \text{ s}$$

$$c\tau = 448 \text{ } \mu\text{m}$$

B_s^0 - \bar{B}_s^0 mixing parameters

$$\chi_B \text{ at high energy} = f_d \chi_d + f_s \chi_s = 0.118 \pm 0.005$$

$$\Delta m_{B_s^0} = m_{B_s^0} - m_{\bar{B}_s^0} > 10.6 \times 10^{12} \text{ } \hbar \text{ s}^{-1}, \text{ CL} = 95\%$$

$$\chi_s = \Delta m_{B_s^0} / \Gamma_{B_s^0} > 15.7, \text{ CL} = 95\%$$

$$\chi_s > 0.4980, \text{ CL} = 95\%$$

These branching fractions all scale with $B(\bar{b} \rightarrow B_s^0)$, the LEP B_s^0 production fraction. The first four were evaluated using $B(\bar{b} \rightarrow B_s^0) = (10.7 \pm 1.4)\%$ and the rest assume $B(\bar{b} \rightarrow B_s^0) = 12\%$.

The branching fraction $B(B_s^0 \rightarrow D_s^- \ell^+ \nu_\ell \text{ anything})$ is not a pure measurement since the measured product branching fraction $B(\bar{b} \rightarrow B_s^0) \times B(B_s^0 \rightarrow D_s^- \ell^+ \nu_\ell \text{ anything})$ was used to determine $B(\bar{b} \rightarrow B_s^0)$, as described in the note on "Production and Decay of b -Flavored Hadrons."

B_s^0 DECAY MODES	Fraction (Γ_i/Γ)	Confidence level	P (MeV/c)
D_s^- anything	(92 \pm 31) %		—
$D_s^- \ell^+ \nu_\ell$ anything	[ggg] (8.1 \pm 2.4) %		—
$D_s^- \pi^+$	< 13 %		2321
$D_s^-(*) + D_s^-(*)^-$	< 21.8 %	90%	—
$J/\psi(1S)\phi$	(9.3 \pm 3.3) $\times 10^{-4}$		1590
$J/\psi(1S)\pi^0$	< 1.2 $\times 10^{-3}$	90%	1788
$J/\psi(1S)\eta$	< 3.8 $\times 10^{-3}$	90%	1735
$\psi(2S)\phi$	seen		1122
$\pi^+ \pi^-$	< 1.7 $\times 10^{-4}$	90%	1122
$\pi^0 \pi^0$	< 2.1 $\times 10^{-4}$	90%	2861
$\eta \pi^0$	< 1.0 $\times 10^{-3}$	90%	2655
$\eta \eta$	< 1.5 $\times 10^{-3}$	90%	2628
$\pi^+ K^-$	< 2.1 $\times 10^{-4}$	90%	2660
$K^+ K^-$	< 5.9 $\times 10^{-5}$	90%	2639
$\rho \bar{\rho}$	< 5.9 $\times 10^{-5}$	90%	2515
$\gamma \gamma$	< 1.48 $\times 10^{-4}$	90%	2685
$\phi \gamma$	< 7 $\times 10^{-4}$	90%	2588

Lepton Family number (LF) violating modes or $\Delta B = 1$ weak neutral current (B1) modes

$\mu^+ \mu^-$	B1	< 2.0 $\times 10^{-6}$	90%	2682
$e^+ e^-$	B1	< 5.4 $\times 10^{-5}$	90%	2864
$e^\pm \mu^\mp$	LF [ee]	< 6.1 $\times 10^{-6}$	90%	2864
$\phi \nu \bar{\nu}$	B1	< 5.4 $\times 10^{-3}$	90%	—

BOTTOM, CHARMED MESONS ($B = C = \pm 1$)

$$B_c^+ = c\bar{b}, B_c^- = \bar{c}b, \text{ similarly for } B_c^{*s}$$

 B_c^\pm

$$I(J^P) = 0(0^-)$$

I, J, P need confirmation.

Quantum numbers shown are quark-model predictions.

$$\text{Mass } m = 6.4 \pm 0.4 \text{ GeV}$$

$$\text{Mean life } \tau = (0.46^{+0.18}_{-0.16}) \times 10^{-12} \text{ s}$$

B_c^- modes are charge conjugates of the modes below.

B_c^\pm DECAY MODES	Fraction (Γ_i/Γ)	Confidence level	P (MeV/c)
$J/\psi(1S)\ell^+ \nu_\ell$ anything	[hhh] (5.2 $^{+2.4}_{-2.1}$) $\times 10^{-5}$		—
$J/\psi(1S)\pi^+$	[hhh] < 8.2 $\times 10^{-5}$	90%	—
$J/\psi(1S)\pi^+ \pi^+ \pi^-$	[hhh] < 5.7 $\times 10^{-4}$	90%	—
$J/\psi(1S)a_1(1260)$	[hhh] < 1.2 $\times 10^{-3}$	90%	—
$D^*(2010)^+ \bar{D}^0$	[hhh] < 6.2 $\times 10^{-3}$	90%	—

Meson Summary Table

 $c\bar{c}$ MESONS **$\eta_c(1S)$**

$$I^G(J^{PC}) = 0^+(0^{-+})$$

Mass $m = 2979.8 \pm 1.8$ MeV ($S = 1.9$)Full width $\Gamma = 13.2_{-3.2}^{+3.8}$ MeV

$\eta_c(1S)$ DECAY MODES	Fraction (Γ_i/Γ)	Confidence level	ρ (MeV/c)
Decays involving hadronic resonances			
$\eta'(958)\pi\pi$	$(4.1 \pm 1.7)\%$		1319
$\rho\rho$	$(2.6 \pm 0.9)\%$		1275
$K^*(892)^0 K^- \pi^+ + c.c.$	$(2.0 \pm 0.7)\%$		1273
$K^*(892)^0 \bar{K}^*(892)$	$(8.5 \pm 3.1) \times 10^{-3}$		1193
$\phi\phi$	$(7.1 \pm 2.8) \times 10^{-3}$		1086
$a_0(980)\pi$	< 2	90%	1323
$a_2(1320)\pi$	< 2	90%	1193
$K^*(892)\bar{K} + c.c.$	< 1.28	90%	1307
$f_2(1270)\eta$	< 1.1	90%	1142
$\omega\omega$	$< 3.1 \times 10^{-3}$	90%	1268
Decays into stable hadrons			
$K\bar{K}\pi$	$(5.5 \pm 1.7)\%$		1378
$\eta\pi\pi$	$(4.9 \pm 1.8)\%$		1425
$\pi^+\pi^-K^+K^-$	$(2.0_{-0.6}^{+0.7})\%$		1342
$2(K^+K^-)$	$(2.1 \pm 1.2)\%$		1053
$2(\pi^+\pi^-)$	$(1.2 \pm 0.4)\%$		1457
$\rho\bar{\rho}$	$(1.2 \pm 0.4) \times 10^{-3}$		1157
$K\bar{K}\eta$	< 3.1	90%	1262
$\pi^+\pi^-\rho\bar{\rho}$	< 1.2	90%	1023
$\Lambda\bar{\Lambda}$	$< 2 \times 10^{-3}$	90%	987
Radiative decays			
$\gamma\gamma$	$(3.0 \pm 1.2) \times 10^{-4}$		1489

 $J/\psi(1S)$

$$I^G(J^{PC}) = 0^-(1^{--})$$

Mass $m = 3096.87 \pm 0.04$ MeVFull width $\Gamma = 87 \pm 5$ keV $\Gamma_{ee} = 5.26 \pm 0.37$ keV

$J/\psi(1S)$ DECAY MODES	Fraction (Γ_i/Γ)	Scale factor/ Confidence level	ρ (MeV/c)
hadrons	$(87.7 \pm 0.5)\%$		-
virtual $\gamma \rightarrow$ hadrons	$(17.0 \pm 2.0)\%$		-
e^+e^-	$(5.93 \pm 0.10)\%$		1548
$\mu^+\mu^-$	$(5.88 \pm 0.10)\%$		1545
Decays involving hadronic resonances			
$\rho\pi$	$(1.27 \pm 0.09)\%$		1449
$\rho^0\pi^0$	$(4.2 \pm 0.5) \times 10^{-3}$		1449
$a_2(1320)\rho$	$(1.09 \pm 0.22)\%$		1125
$\omega\pi^+\pi^-\pi^+\pi^-$	$(8.5 \pm 3.4) \times 10^{-3}$		1392
$\omega\pi^+\pi^-$	$(7.2 \pm 1.0) \times 10^{-3}$		1435
$\omega f_2(1270)$	$(4.3 \pm 0.6) \times 10^{-3}$		1143
$K^*(892)^0 \bar{K}_2^*(1430)^0 + c.c.$	$(6.7 \pm 2.6) \times 10^{-3}$		1005
$\omega K^*(892)\bar{K} + c.c.$	$(5.3 \pm 2.0) \times 10^{-3}$		1098
$K^+\bar{K}^*(892)^- + c.c.$	$(5.0 \pm 0.4) \times 10^{-3}$		1373
$K^0\bar{K}^*(892)^0 + c.c.$	$(4.2 \pm 0.4) \times 10^{-3}$		1371
$K_1(1400)^\pm K^\mp$	$(3.8 \pm 1.4) \times 10^{-3}$		-
$\omega\pi^0\pi^0$	$(3.4 \pm 0.8) \times 10^{-3}$		1436
$b_1(1235)^\pm \pi^\mp$	[ee] $(3.0 \pm 0.5) \times 10^{-3}$		1299
$\omega K^\pm K_S^0 \pi^\mp$	[ee] $(2.9 \pm 0.7) \times 10^{-3}$		1210
$b_1(1235)^0 \pi^0$	$(2.3 \pm 0.6) \times 10^{-3}$		1299
$\phi K^*(892)\bar{K} + c.c.$	$(2.04 \pm 0.28) \times 10^{-3}$		969
$\omega K\bar{K}$	$(1.9 \pm 0.4) \times 10^{-3}$		1268
$\omega f_0(1710) \rightarrow \omega K\bar{K}$	$(4.8 \pm 1.1) \times 10^{-4}$		878
$\phi 2(\pi^+\pi^-)$	$(1.60 \pm 0.32) \times 10^{-3}$		1318
$\Delta(1232)^{++} \bar{\rho}\pi^-$	$(1.6 \pm 0.5) \times 10^{-3}$		1030
$\omega\eta$	$(1.58 \pm 0.16) \times 10^{-3}$		1394
$\phi K\bar{K}$	$(1.48 \pm 0.22) \times 10^{-3}$		1179
$\phi f_0(1710) \rightarrow \phi K\bar{K}$	$(3.6 \pm 0.6) \times 10^{-4}$		875
$\rho\bar{\rho}\omega$	$(1.30 \pm 0.25) \times 10^{-3}$	S=1.3	769
$\Delta(1232)^{++} \bar{\Delta}(1232)^{--}$	$(1.10 \pm 0.29) \times 10^{-3}$		938
$\Sigma(1385)^- \bar{\Sigma}(1385)^+$ (or c.c.)	[ee] $(1.03 \pm 0.13) \times 10^{-3}$		692
$\rho\bar{\rho}\eta(958)$	$(9 \pm 4) \times 10^{-4}$	S=1.7	596
$\phi f_2'(1525)$	$(8 \pm 4) \times 10^{-4}$	S=2.7	871

$\phi\pi^+\pi^-$	$(8.0 \pm 1.2) \times 10^{-4}$		1365
$\phi K^\pm K_S^0 \pi^\mp$	[ee] $(7.2 \pm 0.9) \times 10^{-4}$		1114
$\omega f_1(1420)$	$(6.8 \pm 2.4) \times 10^{-4}$		1062
$\phi\eta$	$(6.5 \pm 0.7) \times 10^{-4}$		1320
$\Xi(1530)^0 \Xi^+$	$(5.9 \pm 1.5) \times 10^{-4}$		597
$\rho K^- \bar{\Sigma}(1385)^0$	$(5.1 \pm 3.2) \times 10^{-4}$		645
$\omega\pi^0$	$(4.2 \pm 0.6) \times 10^{-4}$	S=1.4	1447
$\phi\eta'(958)$	$(3.3 \pm 0.4) \times 10^{-4}$		1192
$\phi f_0(980)$	$(3.2 \pm 0.9) \times 10^{-4}$	S=1.9	1182
$\Xi(1530)^0 \Xi^0$	$(3.2 \pm 1.4) \times 10^{-4}$		608
$\Sigma(1385)^- \bar{\Sigma}^+$ (or c.c.)	[ee] $(3.1 \pm 0.5) \times 10^{-4}$		857
$\phi f_1(1285)$	$(2.6 \pm 0.5) \times 10^{-4}$	S=1.1	1032
$\rho\eta$	$(1.93 \pm 0.23) \times 10^{-4}$		1398
$\omega\eta'(958)$	$(1.67 \pm 0.25) \times 10^{-4}$		1279
$\omega f_0(980)$	$(1.4 \pm 0.5) \times 10^{-4}$		1271
$\rho\eta'(958)$	$(1.05 \pm 0.18) \times 10^{-4}$		1283
$\rho\bar{\rho}\phi$	$(4.5 \pm 1.5) \times 10^{-5}$		527
$a_2(1320)^\pm \pi^\mp$	[ee] $< 4.3 \times 10^{-3}$	CL=90%	1263
$K\bar{K}_2^*(1430) + c.c.$	$< 4.0 \times 10^{-3}$	CL=90%	1159
$K_1(1270)^\pm K^\mp$	$< 3.0 \times 10^{-3}$	CL=90%	-
$K_2^*(1430)^0 \bar{K}_2^*(1430)^0$	$< 2.9 \times 10^{-3}$	CL=90%	588
$K^*(892)^0 \bar{K}^*(892)^0$	$< 5 \times 10^{-4}$	CL=90%	1263
$\phi f_2(1270)$	$< 3.7 \times 10^{-4}$	CL=90%	1036
$\rho\bar{\rho}\rho$	$< 3.1 \times 10^{-4}$	CL=90%	779
$\phi\eta(1440) \rightarrow \phi\eta\pi\pi$	$< 2.5 \times 10^{-4}$	CL=90%	946
$\omega f_2'(1525)$	$< 2.2 \times 10^{-4}$	CL=90%	1003
$\Sigma(1385)^0 \bar{\Lambda}$	$< 2 \times 10^{-4}$	CL=90%	911
$\Delta(1232)^+ \bar{\rho}$	$< 1 \times 10^{-4}$	CL=90%	1100
$\Sigma^0 \bar{\Lambda}$	$< 9 \times 10^{-5}$	CL=90%	1032
$\phi\pi^0$	$< 6.8 \times 10^{-6}$	CL=90%	1377

Decays into stable hadrons

$2(\pi^+\pi^-)\pi^0$	$(3.37 \pm 0.26)\%$		1496
$3(\pi^+\pi^-)\pi^0$	$(2.9 \pm 0.6)\%$		1433
$\pi^+\pi^-\pi^0$	$(1.50 \pm 0.20)\%$		1533
$\pi^+\pi^-\pi^0 K^+K^-$	$(1.20 \pm 0.30)\%$		1368
$4(\pi^+\pi^-)\pi^0$	$(9.0 \pm 3.0) \times 10^{-3}$		1345
$\pi^+\pi^-K^+K^-$	$(7.2 \pm 2.3) \times 10^{-3}$		1407
$K\bar{K}\pi$	$(6.1 \pm 1.0) \times 10^{-3}$		1440
$\rho\bar{\rho}\pi^+\pi^-$	$(6.0 \pm 0.5) \times 10^{-3}$	S=1.3	1107
$2(\pi^+\pi^-)$	$(4.0 \pm 1.0) \times 10^{-3}$		1517
$3(\pi^+\pi^-)$	$(4.0 \pm 2.0) \times 10^{-3}$		1466
$n\bar{n}\pi^+\pi^-$	$(4 \pm 4) \times 10^{-3}$		1106
$\Sigma^0 \bar{\Sigma}^0$	$(1.27 \pm 0.17) \times 10^{-3}$		992
$2(\pi^+\pi^-)K^+K^-$	$(3.1 \pm 1.3) \times 10^{-3}$		1320
$\rho\bar{\rho}\pi^+\pi^-\pi^0$	[iii] $(2.3 \pm 0.9) \times 10^{-3}$	S=1.9	1033
$\rho\bar{\rho}$	$(2.12 \pm 0.10) \times 10^{-3}$		1232
$\rho\bar{\rho}\eta$	$(2.09 \pm 0.18) \times 10^{-3}$		948
$\rho\bar{\rho}\pi^-$	$(2.00 \pm 0.10) \times 10^{-3}$		1174
$n\bar{n}$	$(2.2 \pm 0.4) \times 10^{-3}$		1231
$\Xi\Xi$	$(1.8 \pm 0.4) \times 10^{-3}$	S=1.8	818
$\Lambda\bar{\Lambda}$	$(1.30 \pm 0.12) \times 10^{-3}$	S=1.1	1074
$\rho\bar{\rho}\pi^0$	$(1.09 \pm 0.09) \times 10^{-3}$		1176
$\Lambda\bar{\Sigma}^- \pi^+$ (or c.c.)	[ee] $(1.06 \pm 0.12) \times 10^{-3}$		945
$\rho K^- \bar{\Lambda}$	$(8.9 \pm 1.6) \times 10^{-4}$		876
$2(K^+K^-)$	$(7.0 \pm 3.0) \times 10^{-4}$		1131
$\rho K^- \bar{\Sigma}^0$	$(2.9 \pm 0.8) \times 10^{-4}$		820
K^+K^-	$(2.37 \pm 0.31) \times 10^{-4}$		1468
$\Lambda\bar{\Lambda}\pi^0$	$(2.2 \pm 0.6) \times 10^{-4}$		998
$\pi^+\pi^-$	$(1.47 \pm 0.23) \times 10^{-4}$		1542
$K_S^0 K_L^0$	$(1.08 \pm 0.14) \times 10^{-4}$		1466
$\Lambda\bar{\Sigma} + c.c.$	$< 1.5 \times 10^{-4}$	CL=90%	1032
$K_S^0 K_S^0$	$< 5.2 \times 10^{-6}$	CL=90%	1466

Radiative decays

$\gamma\eta_c(1S)$	$(1.3 \pm 0.4)\%$		116
$\gamma\pi^+\pi^-2\pi^0$	$(8.3 \pm 3.1) \times 10^{-3}$		1518
$\gamma\eta\pi\pi$	$(6.1 \pm 1.0) \times 10^{-3}$		1487
$\gamma\eta(1440) \rightarrow \gamma K\bar{K}\pi$	[p] $(9.1 \pm 1.8) \times 10^{-4}$		1223
$\gamma\eta(1440) \rightarrow \gamma\gamma\rho^0$	$(6.4 \pm 1.4) \times 10^{-5}$		1223
$\gamma\eta(1440) \rightarrow \gamma\eta\pi^+\pi^-$	$(3.0 \pm 0.5) \times 10^{-4}$		-
$\gamma\rho\rho$	$(4.5 \pm 0.8) \times 10^{-3}$		1343
$\gamma\eta_2(1870) \rightarrow \gamma\pi^+\pi^-$	$(6.2 \pm 2.4) \times 10^{-4}$		-
$\gamma\eta'(958)$	$(4.31 \pm 0.30) \times 10^{-3}$		1400
$\gamma 2\pi^+ 2\pi^-$	$(2.8 \pm 0.5) \times 10^{-3}$	S=1.9	1517
$\gamma K^+ K^- \pi^+ \pi^-$	$(2.1 \pm 0.6) \times 10^{-3}$		-
$\gamma f_4(2050)$	$(2.7 \pm 0.7) \times 10^{-3}$		874
$\gamma\omega\omega$	$(1.59 \pm 0.33) \times 10^{-3}$		1337

Meson Summary Table

$\gamma\eta(1440) \rightarrow \gamma\rho^0\rho^0$	$(1.7 \pm 0.4) \times 10^{-3}$	S=1.3	1223
$\gamma f_2(1270)$	$(1.38 \pm 0.14) \times 10^{-3}$		1286
$\gamma f_0(1710) \rightarrow \gamma K\bar{K}$	$(8.5_{-0.9}^{+1.2}) \times 10^{-4}$	S=1.2	1075
$\gamma\eta$	$(8.6 \pm 0.8) \times 10^{-4}$		1500
$\gamma f_1(1420) \rightarrow \gamma K\bar{K}\pi$	$(8.3 \pm 1.5) \times 10^{-4}$		1220
$\gamma f_1(1285)$	$(6.1 \pm 0.9) \times 10^{-4}$		1283
$\gamma f_1(1510) \rightarrow \gamma\eta\pi^+\pi^-$	$(4.5 \pm 1.2) \times 10^{-4}$		-
$\gamma f_2'(1525)$	$(4.7_{-0.5}^{+0.7}) \times 10^{-4}$		1173
$\gamma f_2(1950) \rightarrow \gamma K^*(892)\bar{K}^*(892)$	$(7.0 \pm 2.2) \times 10^{-4}$		-
$\gamma K^*(892)\bar{K}^*(892)$	$(4.0 \pm 1.3) \times 10^{-3}$		-
$\gamma\phi\phi$	$(4.0 \pm 1.2) \times 10^{-4}$	S=2.1	1166
$\gamma\rho\bar{\rho}$	$(3.8 \pm 1.0) \times 10^{-4}$		1232
$\gamma\eta(2225)$	$(2.9 \pm 0.6) \times 10^{-4}$		834
$\gamma\eta(1760) \rightarrow \gamma\rho^0\rho^0$	$(1.3 \pm 0.9) \times 10^{-4}$		1048
$\gamma\pi^0$	$(3.9 \pm 1.3) \times 10^{-5}$		1546
$\gamma\rho\bar{\rho}\pi^+\pi^-$	$< 7.9 \times 10^{-4}$	CL=90%	1107
$\gamma\gamma$	$< 5 \times 10^{-4}$	CL=90%	1548
$\gamma\Lambda\bar{\Lambda}$	$< 1.3 \times 10^{-4}$	CL=90%	1074
3γ	$< 5.5 \times 10^{-5}$	CL=90%	1548
$\gamma f_2(2220)$	$> 2.50 \times 10^{-3}$	CL=99%	-
$\gamma f_2(2220) \rightarrow \gamma\pi\pi$	$(8 \pm 4) \times 10^{-5}$		-
$\gamma f_2(2220) \rightarrow \gamma K\bar{K}$	$(8.1 \pm 3.0) \times 10^{-5}$		-
$\gamma f_2(2220) \rightarrow \gamma\rho\bar{\rho}$	$(1.5 \pm 0.8) \times 10^{-5}$		-
$\gamma f_0(1500)$	$< (5.7 \pm 0.8) \times 10^{-4}$		1184
γe^+e^-	$(8.8 \pm 1.4) \times 10^{-3}$		-

 $\chi_{c0}(1P)$

$$I^G(J^{PC}) = 0^+(0^{++})$$

Mass $m = 3415.0 \pm 0.8$ MeVFull width $\Gamma = 14.9_{-2.3}^{+2.6}$ MeV

$\chi_{c0}(1P)$ DECAY MODES	Fraction (Γ_i/Γ)	Scale factor/ Confidence level	ρ (MeV/c)
Hadronic decays			
$2(\pi^+\pi^-)$	$(2.0 \pm 0.9) \%$	S=2.7	1679
$\pi^+\pi^-K^+K^-$	$(1.8 \pm 0.6) \%$	S=1.9	1580
$\rho^0\pi^+\pi^-$	$(1.6 \pm 0.5) \%$		1608
$3(\pi^+\pi^-)$	$(1.24 \pm 0.22) \%$		1633
$K^+\bar{K}^*(892)^0\pi^- + c.c.$	$(1.2 \pm 0.4) \%$		1522
$\pi^+\pi^-$	$(5.0 \pm 0.7) \times 10^{-3}$		1702
K^+K^-	$(5.9 \pm 0.9) \times 10^{-3}$		1635
$\pi^+\pi^-\rho\bar{\rho}$	$(1.8 \pm 0.9) \times 10^{-3}$	S=1.6	1320
$K^+K^-K^+K^-$	$(2.1 \pm 0.5) \times 10^{-3}$		-
$K_S^0K_S^0$	$(2.0 \pm 0.6) \times 10^{-3}$		-
$\phi\phi$	$(9 \pm 5) \times 10^{-4}$		-
$K_S^0K^+\pi^- + c.c.$	$< 7.1 \times 10^{-4}$	CL=90%	-
$\rho\bar{\rho}$	$(2.2 \pm 1.3) \times 10^{-4}$	S=2.1	1427
Radiative decays			
$\gamma J/\psi(1S)$	$(6.6 \pm 1.8) \times 10^{-3}$		303
$\gamma\gamma$	$(2.7 \pm 1.9) \times 10^{-4}$		1708

 $\chi_{c1}(1P)$

$$I^G(J^{PC}) = 0^+(1^{++})$$

Mass $m = 3510.51 \pm 0.12$ MeVFull width $\Gamma = 0.88 \pm 0.14$ MeV

$\chi_{c1}(1P)$ DECAY MODES	Fraction (Γ_i/Γ)	Scale factor	ρ (MeV/c)
Hadronic decays			
$3(\pi^+\pi^-)$	$(6.3 \pm 1.4) \times 10^{-3}$		1683
$2(\pi^+\pi^-)$	$(5.6 \pm 2.6) \times 10^{-3}$	2.2	1727
$\pi^+\pi^-K^+K^-$	$(4.9 \pm 1.2) \times 10^{-3}$	1.1	1632
$\rho^0\pi^+\pi^-$	$(3.9 \pm 3.5) \times 10^{-3}$		1659
$K^+\bar{K}^*(892)^0\pi^- + c.c.$	$(3.2 \pm 2.1) \times 10^{-3}$		1576
$K_S^0K^+\pi^-$	$(2.5 \pm 0.8) \times 10^{-3}$		-
$\pi^+\pi^-\rho\bar{\rho}$	$(5.4 \pm 2.1) \times 10^{-4}$		1381
$K^+K^-K^+K^-$	$(4.2 \pm 1.9) \times 10^{-4}$		-
$\rho\bar{\rho}$	$(8.2 \pm 1.3) \times 10^{-5}$	1.2	1483
$\pi^+\pi^- + K^+K^-$	$< 2.1 \times 10^{-3}$		-
Radiative decays			
$\gamma J/\psi(1S)$	$(27.3 \pm 1.6) \%$		389

 $\chi_{c2}(1P)$

$$I^G(J^{PC}) = 0^+(2^{++})$$

Mass $m = 3556.18 \pm 0.13$ MeVFull width $\Gamma = 2.00 \pm 0.18$ MeV

$\chi_{c2}(1P)$ DECAY MODES	Fraction (Γ_i/Γ)	Scale factor/ Confidence level	ρ (MeV/c)
Hadronic decays			
$2(\pi^+\pi^-)$	$(1.2 \pm 0.5) \%$	S=2.2	1751
$\pi^+\pi^-K^+K^-$	$(10 \pm 4) \times 10^{-3}$	S=2.0	1656
$3(\pi^+\pi^-)$	$(9.2 \pm 2.2) \times 10^{-3}$		1707
$\rho^0\pi^+\pi^-$	$(7 \pm 4) \times 10^{-3}$		1683
$K^+\bar{K}^*(892)^0\pi^- + c.c.$	$(4.8 \pm 2.8) \times 10^{-3}$		1601
$\pi^+\pi^-\rho\bar{\rho}$	$(1.4 \pm 0.6) \times 10^{-3}$	S=1.5	1410
$\phi\phi$	$(2.0 \pm 0.8) \times 10^{-3}$		-
$\pi^+\pi^-$	$(1.52 \pm 0.25) \times 10^{-3}$		1773
K^+K^-	$(8.1 \pm 1.9) \times 10^{-4}$		1708
$K^+K^-K^+K^-$	$(1.5 \pm 0.4) \times 10^{-3}$		-
$K_S^0K_S^0$	$(6.1 \pm 2.3) \times 10^{-4}$		-
$\rho\bar{\rho}$	$(9.8 \pm 1.0) \times 10^{-5}$		1510
$J/\psi(1S)\pi^+\pi^-\pi^0$	$< 1.5 \%$	CL=90%	185
$K_S^0K^+\pi^- + c.c.$	$< 1.06 \times 10^{-3}$	CL=90%	-
Radiative decays			
$\gamma J/\psi(1S)$	$(13.5 \pm 1.1) \%$		430
$\gamma\gamma$	$(1.6 \pm 0.5) \times 10^{-4}$		1778

 $\psi(2S)$

$$I^G(J^{PC}) = 0^-(1^{--})$$

Mass $m = 3685.96 \pm 0.09$ MeVFull width $\Gamma = 277 \pm 31$ keV (S = 1.1) $\Gamma_{ee} = 2.12 \pm 0.18$ keV

$\psi(2S)$ DECAY MODES	Fraction (Γ_i/Γ)	Scale factor/ Confidence level	ρ (MeV/c)
hadrons	$(98.10 \pm 0.30) \%$		-
virtual $\gamma \rightarrow$ hadrons	$(2.9 \pm 0.4) \%$		-
e^+e^-	$(8.8 \pm 1.3) \times 10^{-3}$		1843
$\mu^+\mu^-$	$(1.03 \pm 0.35) \%$		1840
Decays into $J/\psi(1S)$ and anything			
$J/\psi(1S)$ anything	$(55 \pm 5) \%$		-
$J/\psi(1S)$ neutrals	$(23.1 \pm 2.3) \%$		-
$J/\psi(1S)\pi^+\pi^-$	$(31.0 \pm 2.8) \%$		477
$J/\psi(1S)\pi^0\pi^0$	$(18.2 \pm 2.3) \%$		481
$J/\psi(1S)\eta$	$(2.7 \pm 0.4) \%$	S=1.6	200
$J/\psi(1S)\pi^0$	$(9.7 \pm 2.1) \times 10^{-4}$		527
Hadronic decays			
$3(\pi^+\pi^-)\pi^0$	$(3.5 \pm 1.6) \times 10^{-3}$		1746
$2(\pi^+\pi^-)\pi^0$	$(3.0 \pm 0.8) \times 10^{-3}$		1799
$\omega f_2(1270)$	$< 1.7 \times 10^{-4}$	CL=90%	-
$\rho a_2(1320)$	$< 2.3 \times 10^{-4}$	CL=90%	-
$\pi^+\pi^-K^+K^-$	$(1.6 \pm 0.4) \times 10^{-3}$		1726
$K^*(892)\bar{K}_2^*(1430)^0$	$< 1.2 \times 10^{-4}$	CL=90%	-
$K_1(1270)^\pm K_1^\mp$	$(1.00 \pm 0.28) \times 10^{-3}$		-
$\pi^+\pi^-\rho\bar{\rho}$	$(8.0 \pm 2.0) \times 10^{-4}$		1491
$K^+\bar{K}^*(892)^0\pi^- + c.c.$	$(6.7 \pm 2.5) \times 10^{-4}$		1673
$b_1^\pm \pi^\mp$	$(5.2 \pm 1.3) \times 10^{-4}$		-
$2(\pi^+\pi^-)$	$(4.5 \pm 1.0) \times 10^{-4}$		1817
$\rho^0\pi^+\pi^-$	$(4.2 \pm 1.5) \times 10^{-4}$		1751
$\bar{\rho}\rho$	$(1.9 \pm 0.5) \times 10^{-4}$		1586
$3(\pi^+\pi^-)$	$(1.5 \pm 1.0) \times 10^{-4}$		1774
$\bar{\rho}\rho\pi^0$	$(1.4 \pm 0.5) \times 10^{-4}$		1543
K^+K^-	$(1.0 \pm 0.7) \times 10^{-4}$		1776
$\pi^+\pi^-\pi^0$	$(8 \pm 5) \times 10^{-5}$		1830
$\rho\pi$	$< 8.3 \times 10^{-5}$	CL=90%	1760
$\pi^+\pi^-$	$(8 \pm 5) \times 10^{-5}$		1838
$\Lambda\bar{\Lambda}$	$< 4 \times 10^{-4}$	CL=90%	1467
$K_1(1400)^\pm K_1^\mp$	$< 3.1 \times 10^{-4}$	CL=90%	-
$\Xi^- \Xi^+$	$< 2 \times 10^{-4}$	CL=90%	1285
$K^+K^-\pi^0$	$< 2.96 \times 10^{-5}$	CL=90%	1754
$K^+\bar{K}^*(892)^- + c.c.$	$< 5.4 \times 10^{-5}$	CL=90%	1698
$\phi f_2'(1525)$	$< 4.5 \times 10^{-5}$	CL=90%	-

Meson Summary Table

Radiative decays		
$\gamma X_{c0}(1P)$	(9.3 ± 0.9) %	261
$\gamma X_{c1}(1P)$	(8.7 ± 0.8) %	171
$\gamma X_{c2}(1P)$	(7.8 ± 0.8) %	127
$\gamma \eta_c(1S)$	(2.8 ± 0.6) × 10 ⁻³	639
$\gamma \eta'(958)$	(1.5 ± 0.4) × 10 ⁻⁴	1719
$\gamma \eta$	< 9 × 10 ⁻⁵	CL=90% 1802
$\gamma \gamma$	< 1.6 × 10 ⁻⁴	CL=90% 1843
$\gamma \eta(1440) \rightarrow \gamma K \bar{K} \pi$	< 1.2 × 10 ⁻⁴	CL=90% 1569

 $\psi(3770)$

$$I^G(J^{PC}) = 0^-(1^{--})$$

Mass $m = 3769.9 \pm 2.5$ MeV ($S = 1.8$)
 Full width $\Gamma = 23.6 \pm 2.7$ MeV ($S = 1.1$)
 $\Gamma_{ee} = 0.26 \pm 0.04$ keV ($S = 1.2$)

$\psi(3770)$ DECAY MODES	Fraction (Γ_i/Γ)	Scale factor	p (MeV/c)
$D \bar{D}$	dominant		242
$e^+ e^-$	(1.12 ± 0.17) × 10 ⁻⁵	1.2	1885

 $\psi(4040)$ [iii]

$$I^G(J^{PC}) = 0^-(1^{--})$$

Mass $m = 4040 \pm 10$ MeV
 Full width $\Gamma = 52 \pm 10$ MeV
 $\Gamma_{ee} = 0.75 \pm 0.15$ keV

$\psi(4040)$ DECAY MODES	Fraction (Γ_i/Γ)	p (MeV/c)
$e^+ e^-$	(1.4 ± 0.4) × 10 ⁻⁵	2020
$D^0 \bar{D}^0$	seen	777
$D^*(2007)^0 \bar{D}^0 + c.c.$	seen	578
$D^*(2007)^0 \bar{D}^*(2007)^0$	seen	232

 $\psi(4160)$ [iii]

$$I^G(J^{PC}) = 0^-(1^{--})$$

Mass $m = 4159 \pm 20$ MeV
 Full width $\Gamma = 78 \pm 20$ MeV
 $\Gamma_{ee} = 0.77 \pm 0.23$ keV

$\psi(4160)$ DECAY MODES	Fraction (Γ_i/Γ)	p (MeV/c)
$e^+ e^-$	(10 ± 4) × 10 ⁻⁶	2079

 $\psi(4415)$ [iii]

$$I^G(J^{PC}) = 0^-(1^{--})$$

Mass $m = 4415 \pm 6$ MeV
 Full width $\Gamma = 43 \pm 15$ MeV ($S = 1.8$)
 $\Gamma_{ee} = 0.47 \pm 0.10$ keV

$\psi(4415)$ DECAY MODES	Fraction (Γ_i/Γ)	p (MeV/c)
hadrons	dominant	-
$e^+ e^-$	(1.1 ± 0.4) × 10 ⁻⁵	2207

 $b\bar{b}$ MESONS **$\Upsilon(1S)$**

$$I^G(J^{PC}) = 0^-(1^{--})$$

Mass $m = 9460.30 \pm 0.26$ MeV ($S = 3.3$)
 Full width $\Gamma = 52.5 \pm 1.8$ keV
 $\Gamma_{ee} = 1.32 \pm 0.05$ keV

 $\Upsilon(1S)$ DECAY MODES

DECAY MODES	Fraction (Γ_i/Γ)	Confidence level	p (MeV/c)
$\tau^+ \tau^-$	(2.67 ^{+0.14} _{-0.16}) %		4384
$e^+ e^-$	(2.38 ± 0.11) %		4730
$\mu^+ \mu^-$	(2.48 ± 0.06) %		4729

Hadronic decays

DECAY MODES	Fraction (Γ_i/Γ)	Confidence level	p (MeV/c)
$J/\psi(1S)$ anything	(1.1 ± 0.4) × 10 ⁻³		4223
$\rho \pi$	< 2 × 10 ⁻⁴	90%	4698
$\pi^+ \pi^-$	< 5 × 10 ⁻⁴	90%	4728
$K^+ K^-$	< 5 × 10 ⁻⁴	90%	4704
$\rho \bar{\rho}$	< 5 × 10 ⁻⁴	90%	4636
$\pi^0 \pi^+ \pi^-$	< 1.84 × 10 ⁻⁵	90%	-

Radiative decays

DECAY MODES	Fraction (Γ_i/Γ)	Confidence level	p (MeV/c)
$\gamma \pi^+ \pi^-$	(6.3 ± 1.8) × 10 ⁻⁵		-
$\gamma \pi^0 \pi^0$	(1.7 ± 0.7) × 10 ⁻⁵		-
$\gamma 2h^+ 2h^-$	(7.0 ± 1.5) × 10 ⁻⁴		4720
$\gamma 3h^+ 3h^-$	(5.4 ± 2.0) × 10 ⁻⁴		4703
$\gamma 4h^+ 4h^-$	(7.4 ± 3.5) × 10 ⁻⁴		4679
$\gamma \pi^+ \pi^- K^+ K^-$	(2.9 ± 0.9) × 10 ⁻⁴		4686
$\gamma 2\pi^+ 2\pi^-$	(2.5 ± 0.9) × 10 ⁻⁴		4720
$\gamma 3\pi^+ 3\pi^-$	(2.5 ± 1.2) × 10 ⁻⁴		4703
$\gamma 2\pi^+ 2\pi^- K^+ K^-$	(2.4 ± 1.2) × 10 ⁻⁴		4658
$\gamma \pi^+ \pi^- \rho \bar{\rho}$	(1.5 ± 0.6) × 10 ⁻⁴		4604
$\gamma 2\pi^+ 2\pi^- \rho \bar{\rho}$	(4 ± 6) × 10 ⁻⁵		4563
$\gamma 2K^+ 2K^-$	(2.0 ± 2.0) × 10 ⁻⁵		4601
$\gamma \eta'(958)$	< 1.3 × 10 ⁻³	90%	4682
$\gamma \eta$	< 3.5 × 10 ⁻⁴	90%	4714
$\gamma f_2'(1525)$	< 1.4 × 10 ⁻⁴	90%	4607
$\gamma f_2(1270)$	(8 ± 4) × 10 ⁻⁵		4644
$\gamma \eta(1440)$	< 8.2 × 10 ⁻⁵	90%	4624
$\gamma f_0(1710) \rightarrow \gamma K \bar{K}$	< 2.6 × 10 ⁻⁴	90%	4576
$\gamma f_0(2200) \rightarrow \gamma K^+ K^-$	< 2 × 10 ⁻⁴	90%	4475
$\gamma f_j(2220) \rightarrow \gamma K^+ K^-$	< 1.5 × 10 ⁻⁵	90%	4469
$\gamma \eta(2225) \rightarrow \gamma \phi \phi$	< 3 × 10 ⁻³	90%	4469
γX	< 3 × 10 ⁻⁵	90%	-
$X = \text{pseudoscalar with } m < 7.2 \text{ GeV}$			
$\gamma X \bar{X}$	< 1 × 10 ⁻³	90%	-
$X \bar{X} = \text{vectors with } m < 3.1 \text{ GeV}$			

 $\chi_{b0}(1P)$ [kkk]

$$I^G(J^{PC}) = 0^+(0^{++})$$

 J needs confirmation.Mass $m = 9859.9 \pm 1.0$ MeV

$\chi_{b0}(1P)$ DECAY MODES	Fraction (Γ_i/Γ)	Confidence level	p (MeV/c)
$\gamma \Upsilon(1S)$	< 6 %	90%	391

 $\chi_{b1}(1P)$ [kkk]

$$I^G(J^{PC}) = 0^+(1^{++})$$

 J needs confirmation.Mass $m = 9892.7 \pm 0.6$ MeV ($S = 1.1$)

$\chi_{b1}(1P)$ DECAY MODES	Fraction (Γ_i/Γ)	p (MeV/c)
$\gamma \Upsilon(1S)$	(35 ± 8) %	422

 $\chi_{b2}(1P)$ [kkk]

$$I^G(J^{PC}) = 0^+(2^{++})$$

 J needs confirmation.Mass $m = 9912.6 \pm 0.5$ MeV ($S = 1.1$)

$\chi_{b2}(1P)$ DECAY MODES	Fraction (Γ_i/Γ)	p (MeV/c)
$\gamma \Upsilon(1S)$	(22 ± 4) %	443

Meson Summary Table

T(2S)		$I^G(J^{PC}) = 0^-(1^{--})$	
Mass $m = 10.02326 \pm 0.00031$ GeV			
Full width $\Gamma = 44 \pm 7$ keV			
$\Gamma_{ee} = 0.520 \pm 0.032$ keV			
T(2S) DECAY MODES	Fraction (Γ_i/Γ)	Confidence level	p (MeV/c)
$T(1S)\pi^+\pi^-$	(18.8 \pm 0.6) %		475
$T(1S)\pi^0\pi^0$	(9.0 \pm 0.8) %		480
$\tau^+\tau^-$	(1.7 \pm 1.6) %		4686
$\mu^+\mu^-$	(1.31 \pm 0.21) %		5011
e^+e^-	(1.18 \pm 0.20) %		5012
$T(1S)\pi^0$	< 1.1	$\times 10^{-3}$	90% 531
$T(1S)\eta$	< 2	$\times 10^{-3}$	90% 127
$J/\psi(1S)$ anything	< 6	$\times 10^{-3}$	90% 4533
Radiative decays			
$\gamma X_{b1}(1P)$	(6.8 \pm 0.7) %		131
$\gamma X_{b2}(1P)$	(7.0 \pm 0.6) %		110
$\gamma X_{b0}(1P)$	(3.8 \pm 0.6) %		162
$\gamma f_0(1710)$	< 5.9	$\times 10^{-4}$	90% 4866
$\gamma f_2'(1525)$	< 5.3	$\times 10^{-4}$	90% 4896
$\gamma f_2(1270)$	< 2.41	$\times 10^{-4}$	90% 4931

X_{b0}(2P) [hkk]		$I^G(J^{PC}) = 0^+(0^{++})$	
J needs confirmation.			
Mass $m = 10.2321 \pm 0.0006$ GeV			
X_{b0}(2P) DECAY MODES	Fraction (Γ_i/Γ)	p (MeV/c)	
$\gamma T(2S)$	(4.6 \pm 2.1) %	210	
$\gamma T(1S)$	(9 \pm 6) $\times 10^{-3}$	746	

X_{b1}(2P) [hkk]		$I^G(J^{PC}) = 0^+(1^{++})$	
J needs confirmation.			
Mass $m = 10.2552 \pm 0.0005$ GeV			
$m_{X_{b1}(2P)} - m_{X_{b0}(2P)} = 23.5 \pm 1.0$ MeV			
X_{b1}(2P) DECAY MODES	Fraction (Γ_i/Γ)	Scale factor	p (MeV/c)
$\gamma T(2S)$	(21 \pm 4) %	1.5	229
$\gamma T(1S)$	(8.5 \pm 1.3) %	1.3	764

X_{b2}(2P) [hkk]		$I^G(J^{PC}) = 0^+(2^{++})$	
J needs confirmation.			
Mass $m = 10.2685 \pm 0.0004$ GeV			
$m_{X_{b2}(2P)} - m_{X_{b1}(2P)} = 13.5 \pm 0.6$ MeV			
X_{b2}(2P) DECAY MODES	Fraction (Γ_i/Γ)	p (MeV/c)	
$\gamma T(2S)$	(16.2 \pm 2.4) %	242	
$\gamma T(1S)$	(7.1 \pm 1.0) %	776	

T(3S)		$I^G(J^{PC}) = 0^-(1^{--})$	
Mass $m = 10.3552 \pm 0.0005$ GeV			
Full width $\Gamma = 26.3 \pm 3.5$ keV			
T(3S) DECAY MODES	Fraction (Γ_i/Γ)	Scale factor/ Confidence level	p (MeV/c)
$T(2S)$ anything	(10.6 \pm 0.8) %		296
$T(2S)\pi^+\pi^-$	(2.8 \pm 0.6) %	S=2.2	177
$T(2S)\pi^0\pi^0$	(2.00 \pm 0.32) %		190
$T(2S)\gamma\gamma$	(5.0 \pm 0.7) %		327
$T(1S)\pi^+\pi^-$	(4.48 \pm 0.21) %		814
$T(1S)\pi^0\pi^0$	(2.06 \pm 0.28) %		816
$T(1S)\eta$	< 2.2	$\times 10^{-3}$ CL=90%	-
$\mu^+\mu^-$	(1.81 \pm 0.17) %		5177
e^+e^-	seen		5177

Radiative decays			
$\gamma X_{b2}(2P)$	(11.4 \pm 0.8) %	S=1.3	87
$\gamma X_{b1}(2P)$	(11.3 \pm 0.6) %		100
$\gamma X_{b0}(2P)$	(5.4 \pm 0.6) %	S=1.1	123

T(4S) or T(10580)		$I^G(J^{PC}) = 0^-(1^{--})$	
Mass $m = 10.5800 \pm 0.0035$ GeV			
Full width $\Gamma = 14 \pm 5$ MeV (S = 1.7)			
$\Gamma_{ee} = 0.248 \pm 0.031$ keV (S = 1.3)			
T(4S) DECAY MODES	Fraction (Γ_i/Γ)	Confidence level	p (MeV/c)
$B\bar{B}$	> 96 %	95%	-
non- $B\bar{B}$	< 4 %	95%	-
e^+e^-	(2.8 \pm 0.7) $\times 10^{-5}$		5290
$J/\psi(3097)$ anything	(2.2 \pm 0.7) $\times 10^{-3}$		-
D^{*+} anything + c.c.	< 7.4 %	90%	5099
ϕ anything	< 2.3 $\times 10^{-3}$	90%	5240
$T(1S)$ anything	< 4 $\times 10^{-3}$	90%	1053
$T(1S)\pi^+\pi^-$	< 1.2 $\times 10^{-4}$	90%	-
$T(2S)\pi^+\pi^-$	< 3.9 $\times 10^{-4}$	90%	-

T(10860)		$I^G(J^{PC}) = 0^-(1^{--})$	
Mass $m = 10.865 \pm 0.008$ GeV (S = 1.1)			
Full width $\Gamma = 110 \pm 13$ MeV			
$\Gamma_{ee} = 0.31 \pm 0.07$ keV (S = 1.3)			
T(10860) DECAY MODES	Fraction (Γ_i/Γ)	p (MeV/c)	
e^+e^-	(2.8 \pm 0.7) $\times 10^{-6}$	5432	

T(11020)		$I^G(J^{PC}) = 0^-(1^{--})$	
Mass $m = 11.019 \pm 0.008$ GeV			
Full width $\Gamma = 79 \pm 16$ MeV			
$\Gamma_{ee} = 0.130 \pm 0.030$ keV			
T(11020) DECAY MODES	Fraction (Γ_i/Γ)	p (MeV/c)	
e^+e^-	(1.6 \pm 0.5) $\times 10^{-6}$	5509	

NOTES

In this Summary Table:

When a quantity has "(S = ...)" to its right, the error on the quantity has been enlarged by the "scale factor" S, defined as $S = \sqrt{\chi^2/(N-1)}$, where N is the number of measurements used in calculating the quantity. We do this when $S > 1$, which often indicates that the measurements are inconsistent. When $S > 1.25$, we also show in the Particle Listings an ideogram of the measurements. For more about S, see the Introduction.

A decay momentum p is given for each decay mode. For a 2-body decay, p is the momentum of each decay product in the rest frame of the decaying particle. For a 3-or-more-body decay, p is the largest momentum any of the products can have in this frame.

[a] See the "Note on $\pi^\pm \rightarrow \ell^\pm \nu \gamma$ and $K^\pm \rightarrow \ell^\pm \nu \gamma$ Form Factors" in the π^\pm Particle Listings for definitions and details.

[b] Measurements of $\Gamma(e^+ \nu_e)/\Gamma(\mu^+ \nu_\mu)$ always include decays with γ 's, and measurements of $\Gamma(e^+ \nu_e \gamma)$ and $\Gamma(\mu^+ \nu_\mu \gamma)$ never include low-energy γ 's. Therefore, since no clean separation is possible, we consider the modes with γ 's to be subreactions of the modes without them, and let $[\Gamma(e^+ \nu_e) + \Gamma(\mu^+ \nu_\mu)]/\Gamma_{\text{total}} = 100\%$.

[c] See the π^\pm Particle Listings for the energy limits used in this measurement; low-energy γ 's are not included.

Meson Summary Table

- [d] Derived from an analysis of neutrino-oscillation experiments.
- [e] Astrophysical and cosmological arguments give limits of order 10^{-13} ; see the π^0 Particle Listings.
- [f] See the "Note on the Decay Width $\Gamma(\eta \rightarrow \gamma\gamma)$ " in our 1994 edition, Phys. Rev. **D50**, 1 August 1994, Part I, p. 1451.
- [g] C parity forbids this to occur as a single-photon process.
- [h] See the "Note on scalar mesons" in the $f_0(1370)$ Particle Listings. The interpretation of this entry as a particle is controversial.
- [i] See the "Note on $\rho(770)$ " in the $\rho(770)$ Particle Listings.
- [j] The e^+e^- branching fraction is from $e^+e^- \rightarrow \pi^+\pi^-$ experiments only. The $\omega\rho$ interference is then due to $\omega\rho$ mixing only, and is expected to be small. If $e\mu$ universality holds, $\Gamma(\rho^0 \rightarrow \mu^+\mu^-) = \Gamma(\rho^0 \rightarrow e^+e^-) \times 0.99785$.
- [k] See the "Note on scalar mesons" in the $f_0(1370)$ Particle Listings.
- [l] See the "Note on $a_1(1260)$ " in the $a_1(1260)$ Particle Listings.
- [m] This is only an educated guess; the error given is larger than the error on the average of the published values. See the Particle Listings for details.
- [n] See the "Note on the $\eta_1(1420)$ " in the $\eta(1440)$ Particle Listings.
- [o] See also the $\omega(1650)$ Particle Listings.
- [p] See the "Note on the $\eta(1440)$ " in the $\eta(1440)$ Particle Listings.
- [q] See the "Note on the $\rho(1450)$ and the $\rho(1700)$ " in the $\rho(1700)$ Particle Listings.
- [r] See the "Note on non- $q\bar{q}$ mesons" in the Particle Listings (see the index for the page number).
- [s] See also the $\omega(1420)$ Particle Listings.
- [t] See the "Note on $f_0(1710)$ " in the $f_0(1710)$ Particle Listings.
- [u] See the note in the K^\pm Particle Listings.
- [v] The definition of the slope parameter g of the $K \rightarrow 3\pi$ Dalitz plot is as follows (see also "Note on Dalitz Plot Parameters for $K \rightarrow 3\pi$ Decays" in the K^\pm Particle Listings):

$$|M|^2 = 1 + g(s_3 - s_0)/m_{\pi^+}^2 + \dots$$

- [w] For more details and definitions of parameters see the Particle Listings.
- [x] Most of this radiative mode, the low-momentum γ part, is also included in the parent mode listed without γ 's.
- [y] See the K^\pm Particle Listings for the energy limits used in this measurement.
- [z] Direct-emission branching fraction.
- [aa] Structure-dependent part.
- [bb] Derived from measured values of ϕ_{+-} , ϕ_{00} , $|\eta|$, $|m_{K_L^0} - m_{K_S^0}|$, and $\tau_{K_S^0}$, as described in the introduction to "Tests of Conservation Laws."
- [cc] The CP -violation parameters are defined as follows (see also "Note on CP Violation in $K_S \rightarrow 3\pi$ " and "Note on CP Violation in K_L^0 Decay" in the Particle Listings):

$$\eta_{+-} = |\eta_{+-}|e^{i\phi_{+-}} = \frac{A(K_L^0 \rightarrow \pi^+\pi^-)}{A(K_S^0 \rightarrow \pi^+\pi^-)} = \epsilon + \epsilon'$$

$$\eta_{00} = |\eta_{00}|e^{i\phi_{00}} = \frac{A(K_L^0 \rightarrow \pi^0\pi^0)}{A(K_S^0 \rightarrow \pi^0\pi^0)} = \epsilon - 2\epsilon'$$

$$\delta = \frac{\Gamma(K_L^0 \rightarrow \pi^-\ell^+\nu) - \Gamma(K_L^0 \rightarrow \pi^+\ell^-\nu)}{\Gamma(K_L^0 \rightarrow \pi^-\ell^+\nu) + \Gamma(K_L^0 \rightarrow \pi^+\ell^-\nu)}$$

$$\text{Im}(\eta_{+-0})^2 = \frac{\Gamma(K_S^0 \rightarrow \pi^+\pi^-\pi^0)^{CP \text{ viol.}}}{\Gamma(K_L^0 \rightarrow \pi^+\pi^-\pi^0)}$$

$$\text{Im}(\eta_{000})^2 = \frac{\Gamma(K_S^0 \rightarrow \pi^0\pi^0\pi^0)}{\Gamma(K_L^0 \rightarrow \pi^0\pi^0\pi^0)}$$

where for the last two relations CPT is assumed valid, i.e., $\text{Re}(\eta_{+-0}) \simeq 0$ and $\text{Re}(\eta_{000}) \simeq 0$.

- [dd] See the K_S^0 Particle Listings for the energy limits used in this measurement.
- [ee] The value is for the sum of the charge states or particle/antiparticle states indicated.

[ff] ϵ'/ϵ is derived from $|\eta_{00}/\eta_{+-}|$ measurements using theoretical input on phases.

[gg] See the K_L^0 Particle Listings for the energy limits used in this measurement.

[hh] Allowed by higher-order electroweak interactions.

[ii] Violates CP in leading order. Test of direct CP violation since the indirect CP -violating and CP -conserving contributions are expected to be suppressed.

[jj] See the "Note on $f_0(1370)$ " in the $f_0(1370)$ Particle Listings and in the 1994 edition.

[kk] See the note in the $L(1770)$ Particle Listings in Reviews of Modern Physics **56** No. 2 Pt. II (1984), p. S200. See also the "Note on $K_2(1770)$ and the $K_2(1820)$ " in the $K_2(1770)$ Particle Listings.

[ll] See the "Note on $K_2(1770)$ and the $K_2(1820)$ " in the $K_2(1770)$ Particle Listings.

[mm] This result applies to $Z^0 \rightarrow c\bar{c}$ decays only. Here ℓ^+ is an average (not a sum) of e^+ and μ^+ decays.

[nn] This is a weighted average of D^\pm (44%) and D^0 (56%) branching fractions. See " D^+ and $D^0 \rightarrow (\eta \text{ anything}) / (\text{total } D^+ \text{ and } D^0)$ " under " D^+ Branching Ratios" in the Particle Listings.

[oo] This value averages the e^+ and μ^+ branching fractions, after making a small phase-space adjustment to the μ^+ fraction to be able to use it as an e^+ fraction; hence our ℓ^+ here is really an e^+ .

[pp] An ℓ indicates an e or a μ mode, not a sum over these modes.

[qq] The branching fraction for this mode may differ from the sum of the submodes that contribute to it, due to interference effects. See the relevant papers in the Particle Listings.

[rr] The two experiments measuring this fraction are in serious disagreement. See the Particle Listings.

[ss] This mode is not a useful test for a $\Delta C=1$ weak neutral current because both quarks must change flavor in this decay.

[tt] This $D_1^0\text{-}D_2^0$ limit is inferred from the $D^0\text{-}\bar{D}^0$ mixing ratio $\Gamma(K^+\pi^-)$ (via \bar{D}^0) / $\Gamma(K^-\pi^+)$ near the end of the D^0 Listings.

[uu] The experiments on the division of this charge mode amongst its submodes disagree, and the submode branching fractions here add up to considerably more than the charged-mode fraction.

[vv] However, these upper limits are in serious disagreement with values obtained in another experiment.

[ww] For now, we average together measurements of the $X e^+ \nu_e$ and $X \mu^+ \nu_\mu$ branching fractions. This is the *average*, not the *sum*.

[xx] This branching fraction includes all the decay modes of the final-state resonance.

[yy] This value includes only K^+K^- decays of the $f_0(1710)$, because branching fractions of this resonance are not known.

[zz] This value includes only $\pi^+\pi^-$ decays of the $f_0(1500)$, because branching fractions of this resonance are not known.

[aaa] B^0 and B_S^0 contributions not separated. Limit is on weighted average of the two decay rates.

[bbb] These values are model dependent. See "Note on Semileptonic Decays" in the B^+ Particle Listings.

[ccc] D^{**} stands for the sum of the $D(1^1P_1)$, $D(1^3P_0)$, $D(1^3P_1)$, $D(1^3P_2)$, $D(2^1S_0)$, and $D(2^1S_1)$ resonances.

[ddd] $D^{(*)}\bar{D}^{(*)}$ stands for the sum of $D^*\bar{D}^*$, $D^*\bar{D}$, $D\bar{D}^*$, and $D\bar{D}$.

[eee] Inclusive branching fractions have a multiplicity definition and can be greater than 100%.

[fff] D_j represents an unresolved mixture of pseudoscalar and tensor D^{**} (P -wave) states.

[ggg] Not a pure measurement. See note at head of B_S^0 Decay Modes.

[hhh] Not a pure branching ratio, it is the fraction $(\Gamma_i/\Gamma) \times B(\bar{B} \rightarrow B_c)$.

[iii] Includes $\rho\bar{\rho}\pi^+\pi^-\gamma$ and excludes $\rho\bar{\rho}\eta$, $\rho\bar{\rho}\omega$, $\rho\bar{\rho}\eta'$.

[jjj] J^{PC} known by production in e^+e^- via single photon annihilation. J^G is not known; interpretation of this state as a single resonance is unclear because of the expectation of substantial threshold effects in this energy region.

[kkk] Spectroscopic labeling for these states is theoretical, pending experimental information.

Meson Summary Table

See also the table of suggested $q\bar{q}$ quark-model assignments in the Quark Model section.

• Indicates particles that appear in the preceding Meson Summary Table. We do not regard the other entries as being established.

† Indicates that the value of J given is preferred, but needs confirmation.

LIGHT UNFLAVORED ($S = C = B = 0$)		STRANGE ($S = \pm 1, C = B = 0$)		BOTTOM ($B = \pm 1$)			
$I^G(J^{PC})$	$I^G(J^{PC})$	$I(J^P)$	$I(J^P)$	$I^G(J^{PC})$	$I^G(J^{PC})$		
• π^\pm	$1^-(0^-)$	• $\pi_2(1670)$	$1^-(2^-+)$	• K^\pm	$1/2(0^-)$	• B^\pm	$1/2(0^-)$
• π^0	$1^-(0^-+)$	• $\phi(1680)$	$0^-(1^-)$	• K^0	$1/2(0^-)$	• B^0	$1/2(0^-)$
• η	$0^+(0^-+)$	• $\rho_3(1690)$	$1^+(3^-)$	• K_S^0	$1/2(0^-)$	• B^\pm/B^0 ADMIXTURE	
• $f_0(400-1200)$	$0^+(0^+)$	• $\rho(1700)$	$1^+(1^-)$	• K_L^0	$1/2(0^-)$	• $B^\pm/B^0/B_S^0/b$ -baryon ADMIXTURE	
• $\rho(770)$	$1^+(1^-)$	• $f_0(1710)$	$0^+(0^+)$	• $K^*(892)$	$1/2(1^-)$	• B^*	$1/2(1^-)$
• $\omega(782)$	$0^-(1^-)$	• $a_2(1750)$	$1^-(2^+)$	• $K_1(1270)$	$1/2(1^+)$	• $B_J^*(5732)$	$?(??)$
• $\eta'(958)$	$0^+(0^-+)$	• $\eta(1760)$	$0^+(0^-+)$	• $K_2(1400)$	$1/2(1^+)$		
• $f_0(980)$	$0^+(0^+)$	• $X(1775)$	$1^-(?^-+)$	• $K^*(1410)$	$1/2(1^-)$		
• $a_0(980)$	$1^-(0^+)$	• $\pi(1800)$	$1^-(0^-+)$	• $K_0^*(1430)$	$1/2(0^+)$		
• $\phi(1020)$	$0^-(1^-)$	• $f_2(1810)$	$0^+(2^+)$	• $K_2^*(1430)$	$1/2(2^+)$		
• $h_1(1170)$	$0^-(1^+)$	• $\phi_3(1850)$	$0^-(3^-)$	• $K(1460)$	$1/2(0^-)$		
• $b_1(1235)$	$1^+(1^+)$	• $\eta_2(1870)$	$0^+(2^-+)$	• $K_2(1580)$	$1/2(2^-)$		
• $a_1(1260)$	$1^-(1^+)$	• $X(1910)$	$0^+(?^+)$	• $K(1630)$	$1/2(??)$		
• $f_2(1270)$	$0^+(2^+)$	• $f_2(1950)$	$0^+(2^+)$	• $K_1(1650)$	$1/2(1^+)$		
• $f_1(1285)$	$0^+(1^+)$	• $X(2000)$	$1^-(?^+)$	• $K^*(1680)$	$1/2(1^-)$		
• $\eta(1295)$	$0^+(0^-+)$	• $f_2(2010)$	$0^+(2^+)$	• $K_2(1770)$	$1/2(2^-)$		
• $\pi(1300)$	$1^-(0^-+)$	• $f_0(2020)$	$0^+(0^+)$	• $K_3^*(1780)$	$1/2(3^-)$		
• $a_2(1320)$	$1^-(2^+)$	• $a_4(2040)$	$1^-(4^+)$	• $K_2(1820)$	$1/2(2^-)$		
• $f_0(1370)$	$0^+(0^+)$	• $f_4(2050)$	$0^+(4^+)$	• $K(1830)$	$1/2(0^-)$		
• $h_1(1380)$	$?^-(1^+)$	• $f_0(2060)$	$0^+(0^+)$	• $K_0^*(1950)$	$1/2(0^+)$		
• $\pi_1(1400)$	$1^-(1^-+)$	• $\pi_2(2100)$	$1^-(2^-+)$	• $K_2^*(1980)$	$1/2(2^+)$		
• $f_1(1420)$	$0^+(1^+)$	• $f_2(2150)$	$0^+(2^+)$	• $K_4^*(2045)$	$1/2(4^+)$		
• $\omega(1420)$	$0^-(1^-)$	• $\rho(2150)$	$1^+(1^-)$	• $K_2(2250)$	$1/2(2^-)$		
• $f_2(1430)$	$0^+(2^+)$	• $f_0(2200)$	$0^+(0^+)$	• $K_3(2320)$	$1/2(3^+)$		
• $\eta(1440)$	$0^+(0^-+)$	• $f_J(2220)$	$0^+(2^+)$ or 4^+	• $K_5^*(2380)$	$1/2(5^-)$		
• $a_0(1450)$	$1^-(0^+)$	• $\eta(2225)$	$0^+(0^-+)$	• $K_4(2500)$	$1/2(4^-)$		
• $\rho(1450)$	$1^+(1^-)$	• $\rho_3(2250)$	$1^+(3^-)$	• $K(3100)$	$?(???)$		
• $f_0(1500)$	$0^+(0^+)$	• $f_2(2300)$	$0^+(2^+)$	CHARMED ($C = \pm 1$)			
• $f_1(1510)$	$0^+(1^+)$	• $f_4(2300)$	$0^+(4^+)$	• D^\pm	$1/2(0^-)$		
• $f_2'(1525)$	$0^+(2^+)$	• $f_2(2340)$	$0^+(2^+)$	• D^0	$1/2(0^-)$		
• $f_2(1565)$	$0^+(2^+)$	• $\rho_5(2350)$	$1^+(5^-)$	• $D^*(2007)^0$	$1/2(1^-)$		
• $\pi_1(1600)$	$1^-(1^-+)$	• $a_6(2450)$	$1^-(6^+)$	• $D^*(2010)^\pm$	$1/2(1^-)$		
• $X(1600)$	$2^+(2^+)$	• $f_6(2510)$	$0^+(6^+)$	• $D_1(2420)^0$	$1/2(1^+)$		
• $a_1(1640)$	$1^+(1^+)$	• $X(3250)$	$?(???)$	• $D_1(2420)^\pm$	$1/2(??)$		
• $f_2(1640)$	$0^+(2^+)$	OTHER LIGHT UNFLAVORED ($S = C = B = 0$)		• $D_2^*(2460)^0$	$1/2(2^+)$		
• $\eta_2(1645)$	$0^+(2^-)$	• $e^+e^-(1100-2200) ?^?(1^-)$		• $D_2^*(2460)^+$	$1/2(2^+)$		
• $\omega(1650)$	$0^-(1^-)$	• $\bar{N}N(1100-3600)$		• $D^*(2640)^\pm$	$1/2(??)$		
• $X(1650)$	$0^-(?^-)$	• $X(1900-3600)$		CHARMED, STRANGE ($C = S = \pm 1$)			
• $a_2(1660)$	$1^-(2^+)$			• D_s^\pm	$0(0^-)$		
• $\omega_3(1670)$	$0^-(3^-)$			• $D_s^{*\pm}$	$0(??)$		
				• $D_{s1}(2536)^\pm$	$0(1^+)$		
				• $D_{sJ}(2573)^\pm$	$0(??)$		
				BOTTOM, STRANGE ($B = \pm 1, S = \mp 1$)			
				• B_s^0	$0(0^-)$		
				• B_s^*	$0(1^-)$		
				• $B_{sJ}^*(5850)$	$?(??)$		
				BOTTOM, CHARMED ($B = C = \pm 1$)			
				• B_c^\pm	$0(0^-)$		
				$c\bar{c}$			
				• $\eta_c(1S)$	$0^+(0^-+)$		
				• $J/\psi(1S)$	$0^-(1^-)$		
				• $\chi_{c0}(1P)$	$0^+(0^+)$		
				• $\chi_{c1}(1P)$	$0^+(1^+)$		
				• $h_c(1P)$	$?(???)$		
				• $\chi_{c2}(1P)$	$0^+(2^+)$		
				• $\eta_c(2S)$	$?(??+)$		
				• $\psi(2S)$	$0^-(1^-)$		
				• $\psi(3770)$	$0^-(1^-)$		
				• $\psi(3836)$	$0^-(2^-)$		
				• $\psi(4040)$	$0^-(1^-)$		
				• $\psi(4160)$	$0^-(1^-)$		
				• $\psi(4415)$	$0^-(1^-)$		
				$b\bar{b}$			
				• $T(1S)$	$0^-(1^-)$		
				• $\chi_{b0}(1P)$	$0^+(0^+)$		
				• $\chi_{b1}(1P)$	$0^+(1^+)$		
				• $\chi_{b2}(1P)$	$0^+(2^+)$		
				• $T(2S)$	$0^-(1^-)$		
				• $\chi_{b0}(2P)$	$0^+(0^+)$		
				• $\chi_{b1}(2P)$	$0^+(1^+)$		
				• $\chi_{b2}(2P)$	$0^+(2^+)$		
				• $T(3S)$	$0^-(1^-)$		
				• $T(4S)$	$0^-(1^-)$		
				• $T(10860)$	$0^-(1^-)$		
				• $T(11020)$	$0^-(1^-)$		
				NON- $q\bar{q}$ CANDIDATES			
				NON- $q\bar{q}$ CANDIDATES			

Baryon Summary Table

This short table gives the name, the quantum numbers (where known), and the status of baryons in the Review. Only the baryons with 3- or 4-star status are included in the main Baryon Summary Table. Due to insufficient data or uncertain interpretation, the other entries in the short table are not established as baryons. The names with masses are of baryons that decay strongly. See our 1986 edition (Physics Letters 170B) for listings of evidence for Z baryons (KN resonances).

p, n	P_{11}	****	$\Delta(1232)$	P_{33}	****	Λ	P_{01}	****	$\Sigma^+, \Sigma^0, \Sigma^-$	P_{11}	****	Ξ^0, Ξ^-	P_{11}	****
$N(1440)$	P_{11}	****	$\Delta(1600)$	P_{33}	***	$\Lambda(1405)$	S_{01}	****	$\Sigma(1385)$	P_{13}	****	$\Xi(1530)$	P_{13}	****
$N(1520)$	D_{13}	****	$\Delta(1620)$	S_{31}	****	$\Lambda(1520)$	D_{03}	****	$\Sigma(1480)$		*	$\Xi(1620)$		*
$N(1535)$	S_{11}	****	$\Delta(1700)$	D_{33}	****	$\Lambda(1600)$	P_{01}	***	$\Sigma(1560)$		**	$\Xi(1690)$		***
$N(1650)$	S_{11}	****	$\Delta(1750)$	P_{31}	*	$\Lambda(1670)$	S_{01}	****	$\Sigma(1580)$	D_{13}	**	$\Xi(1820)$	D_{13}	***
$N(1675)$	D_{15}	****	$\Delta(1900)$	S_{31}	**	$\Lambda(1690)$	D_{03}	****	$\Sigma(1620)$	S_{11}	**	$\Xi(1950)$		***
$N(1680)$	F_{15}	****	$\Delta(1905)$	F_{35}	****	$\Lambda(1800)$	S_{01}	***	$\Sigma(1660)$	P_{11}	***	$\Xi(2030)$		***
$N(1700)$	D_{13}	***	$\Delta(1910)$	P_{31}	****	$\Lambda(1810)$	P_{01}	***	$\Sigma(1670)$	D_{13}	****	$\Xi(2120)$		*
$N(1710)$	P_{11}	***	$\Delta(1920)$	P_{33}	***	$\Lambda(1820)$	F_{05}	****	$\Sigma(1690)$		**	$\Xi(2250)$		**
$N(1720)$	P_{13}	****	$\Delta(1930)$	D_{35}	***	$\Lambda(1830)$	D_{05}	****	$\Sigma(1750)$	S_{11}	***	$\Xi(2370)$		**
$N(1900)$	P_{13}	**	$\Delta(1940)$	D_{33}	*	$\Lambda(1890)$	P_{03}	****	$\Sigma(1770)$	P_{11}	*	$\Xi(2500)$		*
$N(1990)$	F_{17}	**	$\Delta(1950)$	F_{37}	****	$\Lambda(2000)$		*	$\Sigma(1775)$	D_{15}	****			
$N(2000)$	F_{15}	**	$\Delta(2000)$	F_{35}	**	$\Lambda(2020)$	F_{07}	*	$\Sigma(1840)$	P_{13}	*	Ω^-		****
$N(2080)$	D_{13}	**	$\Delta(2150)$	S_{31}	*	$\Lambda(2100)$	G_{07}	****	$\Sigma(1880)$	P_{11}	**	$\Omega(2250)^-$		***
$N(2090)$	S_{11}	*	$\Delta(2200)$	G_{37}	*	$\Lambda(2110)$	F_{05}	***	$\Sigma(1915)$	F_{15}	****	$\Omega(2380)^-$		**
$N(2100)$	P_{11}	*	$\Delta(2300)$	H_{39}	**	$\Lambda(2325)$	D_{03}	*	$\Sigma(1940)$	D_{13}	***	$\Omega(2470)^-$		**
$N(2190)$	G_{17}	****	$\Delta(2350)$	D_{35}	*	$\Lambda(2350)$	H_{09}	***	$\Sigma(2000)$	S_{11}	*			
$N(2200)$	D_{15}	**	$\Delta(2390)$	F_{37}	*	$\Lambda(2585)$		**	$\Sigma(2030)$	F_{17}	****	Λ_c^+		****
$N(2220)$	H_{19}	****	$\Delta(2400)$	G_{39}	**				$\Sigma(2070)$	F_{15}	*	$\Lambda_c(2593)^+$		***
$N(2250)$	G_{19}	****	$\Delta(2420)$	$H_{3,11}$	****				$\Sigma(2080)$	P_{13}	**	$\Lambda_c(2625)^+$		**
$N(2600)$	$h_{1,11}$	***	$\Delta(2750)$	$l_{3,13}$	**				$\Sigma(2100)$	G_{17}	*	$\Sigma_c(2455)$		****
$N(2700)$	$K_{1,13}$	**	$\Delta(2950)$	$K_{3,15}$	**				$\Sigma(2250)$		***	$\Sigma_c(2520)$		***
									$\Sigma(2455)$		**	Ξ_c^+, Ξ_c^0		***
									$\Sigma(2620)$		**	$\Xi_c^{'+}, \Xi_c^0$		***
									$\Sigma(3000)$		*	$\Xi_c(2645)$		***
									$\Sigma(3170)$		*	$\Xi_c(2815)$		***
												Ω_c^0		***
												Λ_b^0		***
												Ξ_b^0, Ξ_b^-		*
												b -baryon ADMIXTURE		

**** Existence is certain, and properties are at least fairly well explored.

*** Existence ranges from very likely to certain, but further confirmation is desirable and/or quantum numbers, branching fractions, etc. are not well determined.

** Evidence of existence is only fair.

* Evidence of existence is poor.

Baryon Summary Table

N BARYONS
(S = 0, I = 1/2)
p, N⁺ = uud; n, N⁰ = udd

p

$$I(J^P) = \frac{1}{2}(\frac{1}{2}^+)$$

Mass $m = 938.27200 \pm 0.00004$ MeV [a]
 $= 1.00727646688 \pm 0.00000000013$ u
 $|m_p - m_{\bar{p}}|/m_p < 5 \times 10^{-7}$ [b]
 $|g_p^2|/(g_p^2) = 0.99999999991 \pm 0.00000000009$
 $|q_p + q_{\bar{p}}|/e < 5 \times 10^{-7}$ [b]
 $|q_p + q_e|/e < 1.0 \times 10^{-21}$ [c]
 Magnetic moment $\mu = 2.792847337 \pm 0.000000029 \mu_N$
 $(\mu_p + \mu_{\bar{p}}) / \mu_p = (-2.6 \pm 2.9) \times 10^{-3}$
 Electric dipole moment $d = (-4 \pm 6) \times 10^{-23}$ e cm
 Electric polarizability $\bar{\alpha} = (12.1 \pm 0.9) \times 10^{-4}$ fm³
 Magnetic polarizability $\bar{\beta} = (2.1 \pm 0.9) \times 10^{-4}$ fm³
 Mean life $\tau > 1.6 \times 10^{25}$ years (independent of mode)
 $> 10^{31}$ to 10^{33} years [d] (mode dependent)

Below, for *N* decays, *p* and *n* distinguish proton and neutron partial lifetimes. See also the "Note on Nucleon Decay" in our 1994 edition (Phys. Rev. D50, 1673) for a short review.

The "partial mean life" limits tabulated here are the limits on τ/B_i , where τ is the total mean life and B_i is the branching fraction for the mode in question.

p DECAY MODES	Partial mean life (10 ³⁰ years)	Confidence level	<i>p</i> (MeV/c)
Antilepton + meson			
<i>N</i> → <i>e</i> ⁺ π	> 158 (<i>n</i>), > 1600 (<i>p</i>)	90%	459
<i>N</i> → <i>μ</i> ⁺ π	> 100 (<i>n</i>), > 473 (<i>p</i>)	90%	453
<i>N</i> → <i>ν</i> π	> 112 (<i>n</i>), > 25 (<i>p</i>)	90%	459
<i>p</i> → <i>e</i> ⁺ η	> 313	90%	309
<i>p</i> → <i>μ</i> ⁺ η	> 126	90%	296
<i>n</i> → <i>ν</i> η	> 158	90%	310
<i>N</i> → <i>e</i> ⁺ ρ	> 217 (<i>n</i>), > 75 (<i>p</i>)	90%	153
<i>N</i> → <i>μ</i> ⁺ ρ	> 228 (<i>n</i>), > 110 (<i>p</i>)	90%	119
<i>N</i> → <i>ν</i> ρ	> 19 (<i>n</i>), > 162 (<i>p</i>)	90%	153
<i>p</i> → <i>e</i> ⁺ ω	> 107	90%	142
<i>p</i> → <i>μ</i> ⁺ ω	> 117	90%	104
<i>n</i> → <i>ν</i> ω	> 108	90%	144
<i>N</i> → <i>e</i> ⁺ <i>K</i>	> 17 (<i>n</i>), > 150 (<i>p</i>)	90%	337
<i>p</i> → <i>e</i> ⁺ <i>K</i> _S ⁰	> 76	90%	337
<i>p</i> → <i>e</i> ⁺ <i>K</i> _L ⁰	> 44	90%	337
<i>N</i> → <i>μ</i> ⁺ <i>K</i>	> 26 (<i>n</i>), > 120 (<i>p</i>)	90%	326
<i>p</i> → <i>μ</i> ⁺ <i>K</i> _S ⁰	> 64	90%	326
<i>p</i> → <i>μ</i> ⁺ <i>K</i> _L ⁰	> 44	90%	326
<i>N</i> → <i>νK</i>	> 86 (<i>n</i>), > 670 (<i>p</i>)	90%	339
<i>p</i> → <i>e</i> ⁺ <i>K</i> [*] (892) ⁰	> 84	90%	45
<i>N</i> → <i>νK</i> [*] (892)	> 78 (<i>n</i>), > 51 (<i>p</i>)	90%	45
Antilepton + mesons			
<i>p</i> → <i>e</i> ⁺ π ⁺ π ⁻	> 82	90%	448
<i>p</i> → <i>e</i> ⁺ π ⁰ π ⁰	> 147	90%	449
<i>n</i> → <i>e</i> ⁺ π ⁻ π ⁰	> 52	90%	449
<i>p</i> → <i>μ</i> ⁺ π ⁺ π ⁻	> 133	90%	425
<i>p</i> → <i>μ</i> ⁺ π ⁰ π ⁰	> 101	90%	427
<i>n</i> → <i>μ</i> ⁺ π ⁻ π ⁰	> 74	90%	427
<i>n</i> → <i>e</i> ⁺ <i>K</i> ⁰ π ⁻	> 18	90%	319
Lepton + meson			
<i>n</i> → <i>e</i> ⁻ π ⁺	> 65	90%	459
<i>n</i> → <i>μ</i> ⁻ π ⁺	> 49	90%	453
<i>n</i> → <i>e</i> ⁻ ρ ⁺	> 62	90%	154
<i>n</i> → <i>μ</i> ⁻ ρ ⁺	> 7	90%	120
<i>n</i> → <i>e</i> ⁻ <i>K</i> ⁺	> 32	90%	340
<i>n</i> → <i>μ</i> ⁻ <i>K</i> ⁺	> 57	90%	330

Lepton + mesons			
<i>p</i> → <i>e</i> ⁻ π ⁺ π ⁺	> 30	90%	448
<i>n</i> → <i>e</i> ⁻ π ⁺ π ⁰	> 29	90%	449
<i>p</i> → <i>μ</i> ⁻ π ⁺ π ⁺	> 17	90%	425
<i>n</i> → <i>μ</i> ⁻ π ⁺ π ⁰	> 34	90%	427
<i>p</i> → <i>e</i> ⁻ π ⁺ <i>K</i> ⁺	> 75	90%	320
<i>p</i> → <i>μ</i> ⁻ π ⁺ <i>K</i> ⁺	> 245	90%	279
Antilepton + photon(s)			
<i>p</i> → <i>e</i> ⁺ γ	> 670	90%	469
<i>p</i> → <i>μ</i> ⁺ γ	> 478	90%	463
<i>n</i> → <i>ν</i> γ	> 28	90%	470
<i>p</i> → <i>e</i> ⁺ γγ	> 100	90%	469
<i>n</i> → <i>ν</i> γγ	> 219	90%	470
Three (or more) leptons			
<i>p</i> → <i>e</i> ⁺ <i>e</i> ⁺ <i>e</i> ⁻	> 793	90%	469
<i>p</i> → <i>e</i> ⁺ <i>μ</i> ⁺ <i>μ</i> ⁻	> 359	90%	457
<i>p</i> → <i>e</i> ⁺ <i>νν</i>	> 17	90%	469
<i>n</i> → <i>e</i> ⁺ <i>e</i> ⁻ <i>ν</i>	> 257	90%	470
<i>n</i> → <i>μ</i> ⁺ <i>e</i> ⁻ <i>ν</i>	> 83	90%	464
<i>n</i> → <i>μ</i> ⁺ <i>μ</i> ⁻ <i>ν</i>	> 79	90%	458
<i>p</i> → <i>μ</i> ⁺ <i>e</i> ⁺ <i>e</i> ⁻	> 529	90%	464
<i>p</i> → <i>μ</i> ⁺ <i>μ</i> ⁺ <i>μ</i> ⁻	> 675	90%	439
<i>p</i> → <i>μ</i> ⁺ <i>νν</i>	> 21	90%	463
<i>p</i> → <i>e</i> ⁻ <i>μ</i> ⁺ <i>μ</i> ⁺	> 6	90%	457
<i>n</i> → <i>3ν</i>	> 0.0005	90%	470
Inclusive modes			
<i>N</i> → <i>e</i> ⁺ anything	> 0.6 (<i>n, p</i>)	90%	-
<i>N</i> → <i>μ</i> ⁺ anything	> 12 (<i>n, p</i>)	90%	-
<i>N</i> → <i>e</i> ⁺ π ⁰ anything	> 0.6 (<i>n, p</i>)	90%	-

ΔB = 2 dinucleon modes			
The following are lifetime limits per iron nucleus.			
<i>pp</i> → π ⁺ π ⁺	> 0.7	90%	-
<i>pn</i> → π ⁺ π ⁰	> 2	90%	-
<i>nn</i> → π ⁺ π ⁻	> 0.7	90%	-
<i>nn</i> → π ⁰ π ⁰	> 3.4	90%	-
<i>pp</i> → <i>e</i> ⁺ <i>e</i> ⁺	> 5.8	90%	-
<i>pp</i> → <i>e</i> ⁺ <i>μ</i> ⁺	> 3.6	90%	-
<i>pp</i> → <i>μ</i> ⁺ <i>μ</i> ⁺	> 1.7	90%	-
<i>pn</i> → <i>e</i> ⁺ <i>ν</i>	> 2.8	90%	-
<i>pn</i> → <i>μ</i> ⁺ <i>ν</i>	> 1.6	90%	-
<i>nn</i> → <i>νeνe</i>	> 0.000012	90%	-
<i>nn</i> → <i>νμνμ</i>	> 0.000006	90%	-
p̄ DECAY MODES			
p̄ DECAY MODES	Partial mean life (years)	Confidence level	<i>p</i> (MeV/c)
<i>p̄</i> → <i>e</i> ⁻ γ	> 7 × 10 ⁵	90%	469
<i>p̄</i> → <i>μ</i> ⁻ γ	> 5 × 10 ⁴	90%	463
<i>p̄</i> → <i>e</i> ⁻ π ⁰	> 4 × 10 ⁵	90%	459
<i>p̄</i> → <i>μ</i> ⁻ π ⁰	> 5 × 10 ⁴	90%	453
<i>p̄</i> → <i>e</i> ⁻ η	> 2 × 10 ⁴	90%	309
<i>p̄</i> → <i>μ</i> ⁻ η	> 8 × 10 ³	90%	296
<i>p̄</i> → <i>e</i> ⁻ <i>K</i> _S ⁰	> 900	90%	337
<i>p̄</i> → <i>μ</i> ⁻ <i>K</i> _S ⁰	> 4 × 10 ³	90%	326
<i>p̄</i> → <i>e</i> ⁻ <i>K</i> _L ⁰	> 9 × 10 ³	90%	337
<i>p̄</i> → <i>μ</i> ⁻ <i>K</i> _L ⁰	> 7 × 10 ³	90%	326
<i>p̄</i> → <i>e</i> ⁻ γγ	> 2 × 10 ⁴	90%	469
<i>p̄</i> → <i>μ</i> ⁻ γγ	> 2 × 10 ⁴	90%	463
<i>p̄</i> → <i>e</i> ⁻ ρ	> 200	90%	153
<i>p̄</i> → <i>e</i> ⁻ ω	> 200	90%	142
<i>p̄</i> → <i>e</i> ⁻ <i>K</i> [*] (892) ⁰	> 1 × 10 ³	90%	141

Baryon Summary Table

n	$I(J^P) = \frac{1}{2}(\frac{1}{2}^+)$
Mass $m = 939.56533 \pm 0.00004$ MeV [a] = $1.00866491578 \pm 0.00000000055$ u	
$m_n - m_p = 1.2933318 \pm 0.0000005$ MeV = $0.0013884489 \pm 0.0000000006$ u	
Mean life $\tau = 886.7 \pm 1.9$ s (S = 1.2) $c\tau = 2.658 \times 10^8$ km	
Magnetic moment $\mu = -1.9130427 \pm 0.0000005 \mu_N$	
Electric dipole moment $d < 0.63 \times 10^{-25}$ e cm, CL = 90%	
Electric polarizability $\alpha = (0.98^{+0.19}_{-0.23}) \times 10^{-3}$ fm ³ (S = 1.1)	
Charge $q = (-0.4 \pm 1.1) \times 10^{-21}$ e	
Mean $n\bar{n}$ -oscillation time $> 8.6 \times 10^7$ s, CL = 90% (free n) $> 1.2 \times 10^8$ s, CL = 90% [e] (bound n)	

Decay parameters [f]

$\rho e^- \bar{\nu}_e$	$g_A/g_V = -1.2670 \pm 0.0035$ (S = 1.9)
"	$A = -0.1162 \pm 0.0013$ (S = 1.8)
"	$B = 0.983 \pm 0.004$
"	$a = -0.102 \pm 0.005$
"	$\phi_{AV} = (180.07 \pm 0.18)^\circ$ [g]
"	$D = (-0.5 \pm 1.4) \times 10^{-3}$

n DECAY MODES	Fraction (Γ_i/Γ)	Confidence level	ρ (MeV/c)
$\rho e^- \bar{\nu}_e$	100 %		1.19
Charge conservation (Q) violating mode			
$\rho \nu_e \bar{\nu}_e$	$Q < 8 \times 10^{-27}$	68%	1.29

$N(1440) P_{11}$	$I(J^P) = \frac{1}{2}(\frac{1}{2}^+)$
Breit-Wigner mass = 1430 to 1470 (≈ 1440) MeV	
Breit-Wigner full width = 250 to 450 (≈ 350) MeV	
$p_{\text{beam}} = 0.61$ GeV/c $4\pi\chi^2 = 31.0$ mb	
Re(pole position) = 1345 to 1385 (≈ 1365) MeV	
-2Im(pole position) = 160 to 260 (≈ 210) MeV	

$N(1440)$ DECAY MODES	Fraction (Γ_i/Γ)	ρ (MeV/c)
$N\pi$	60-70 %	397
$N\pi\pi$	30-40 %	342
$\Delta\pi$	20-30 %	143
$N\rho$	< 8 %	†
$N(\pi\pi)_{S\text{-wave}}^{I=0}$	5-10 %	-
$\rho\gamma$	0.035-0.048 %	414
$\rho\gamma$, helicity=1/2	0.035-0.048 %	414
$n\gamma$	0.009-0.032 %	413
$n\gamma$, helicity=1/2	0.009-0.032 %	413

$N(1520) D_{13}$	$I(J^P) = \frac{1}{2}(\frac{3}{2}^-)$
Breit-Wigner mass = 1515 to 1530 (≈ 1520) MeV	
Breit-Wigner full width = 110 to 135 (≈ 120) MeV	
$p_{\text{beam}} = 0.74$ GeV/c $4\pi\chi^2 = 23.5$ mb	
Re(pole position) = 1505 to 1515 (≈ 1510) MeV	
-2Im(pole position) = 110 to 120 (≈ 115) MeV	

$N(1520)$ DECAY MODES	Fraction (Γ_i/Γ)	ρ (MeV/c)
$N\pi$	50-60 %	456
$N\pi\pi$	40-50 %	410
$\Delta\pi$	15-25 %	228
$N\rho$	15-25 %	†
$N(\pi\pi)_{S\text{-wave}}^{I=0}$	< 8 %	-
$\rho\gamma$	0.46-0.56 %	470
$\rho\gamma$, helicity=1/2	0.001-0.034 %	470
$\rho\gamma$, helicity=3/2	0.44-0.53 %	470
$n\gamma$	0.30-0.53 %	470
$n\gamma$, helicity=1/2	0.04-0.10 %	470
$n\gamma$, helicity=3/2	0.25-0.45 %	470

$N(1535) S_{11}$	$I(J^P) = \frac{1}{2}(\frac{1}{2}^-)$
Breit-Wigner mass = 1520 to 1555 (≈ 1535) MeV	
Breit-Wigner full width = 100 to 250 (≈ 150) MeV	
$p_{\text{beam}} = 0.76$ GeV/c $4\pi\chi^2 = 22.5$ mb	
Re(pole position) = 1495 to 1515 (≈ 1505) MeV	
-2Im(pole position) = 90 to 250 (≈ 170) MeV	

$N(1535)$ DECAY MODES	Fraction (Γ_i/Γ)	ρ (MeV/c)
$N\pi$	35-55 %	467
$N\eta$	30-55 %	182
$N\pi\pi$	1-10 %	422
$\Delta\pi$	< 1 %	242
$N\rho$	< 4 %	†
$N(\pi\pi)_{S\text{-wave}}^{I=0}$	< 3 %	-
$N(1440)\pi$	< 7 %	†
$\rho\gamma$	0.15-0.35 %	481
$\rho\gamma$, helicity=1/2	0.15-0.35 %	481
$n\gamma$	0.004-0.29 %	480
$n\gamma$, helicity=1/2	0.004-0.29 %	480

$N(1650) S_{11}$	$I(J^P) = \frac{1}{2}(\frac{1}{2}^-)$
Breit-Wigner mass = 1640 to 1680 (≈ 1650) MeV	
Breit-Wigner full width = 145 to 190 (≈ 150) MeV	
$p_{\text{beam}} = 0.96$ GeV/c $4\pi\chi^2 = 16.4$ mb	
Re(pole position) = 1640 to 1680 (≈ 1660) MeV	
-2Im(pole position) = 150 to 170 (≈ 160) MeV	

$N(1650)$ DECAY MODES	Fraction (Γ_i/Γ)	ρ (MeV/c)
$N\pi$	55-90 %	547
$N\eta$	3-10 %	346
ΛK	3-11 %	161
$N\pi\pi$	10-20 %	511
$\Delta\pi$	1-7 %	344
$N\rho$	4-12 %	†
$N(\pi\pi)_{S\text{-wave}}^{I=0}$	< 4 %	-
$N(1440)\pi$	< 5 %	147
$\rho\gamma$	0.04-0.18 %	558
$\rho\gamma$, helicity=1/2	0.04-0.18 %	558
$n\gamma$	0.003-0.17 %	557
$n\gamma$, helicity=1/2	0.003-0.17 %	557

$N(1675) D_{15}$	$I(J^P) = \frac{1}{2}(\frac{5}{2}^-)$
Breit-Wigner mass = 1670 to 1685 (≈ 1675) MeV	
Breit-Wigner full width = 140 to 180 (≈ 150) MeV	
$p_{\text{beam}} = 1.01$ GeV/c $4\pi\chi^2 = 15.4$ mb	
Re(pole position) = 1655 to 1665 (≈ 1660) MeV	
-2Im(pole position) = 125 to 155 (≈ 140) MeV	

$N(1675)$ DECAY MODES	Fraction (Γ_i/Γ)	ρ (MeV/c)
$N\pi$	40-50 %	563
ΛK	< 1 %	209
$N\pi\pi$	50-60 %	529
$\Delta\pi$	50-60 %	364
$N\rho$	< 1-3 %	†
$\rho\gamma$	0.004-0.023 %	575
$\rho\gamma$, helicity=1/2	0.0-0.015 %	575
$\rho\gamma$, helicity=3/2	0.0-0.011 %	575
$n\gamma$	0.02-0.12 %	574
$n\gamma$, helicity=1/2	0.006-0.046 %	574
$n\gamma$, helicity=3/2	0.01-0.08 %	574

Baryon Summary Table

 $N(1680) F_{15}$

$$I(J^P) = \frac{1}{2}(\frac{5}{2}^+)$$

Breit-Wigner mass = 1675 to 1690 (\approx 1680) MeV
 Breit-Wigner full width = 120 to 140 (\approx 130) MeV
 $p_{\text{beam}} = 1.01 \text{ GeV}/c$ $4\pi\chi^2 = 15.2 \text{ mb}$
 Re(pole position) = 1665 to 1675 (\approx 1670) MeV
 $-2\text{Im}(\text{pole position}) = 105 \text{ to } 135$ (\approx 120) MeV

$N(1680)$ DECAY MODES	Fraction (Γ_i/Γ)	ρ (MeV/c)
$N\pi$	60–70 %	567
$N\pi\pi$	30–40 %	532
$\Delta\pi$	5–15 %	369
$N\rho$	3–15 %	†
$N(\pi\pi)_{S\text{-wave}}^{I=0}$	5–20 %	–
$\rho\gamma$	0.21–0.32 %	578
$\rho\gamma$, helicity=1/2	0.001–0.011 %	578
$\rho\gamma$, helicity=3/2	0.20–0.32 %	578
$n\gamma$	0.021–0.046 %	577
$n\gamma$, helicity=1/2	0.004–0.029 %	577
$n\gamma$, helicity=3/2	0.01–0.024 %	577

 $N(1700) D_{13}$

$$I(J^P) = \frac{1}{2}(\frac{3}{2}^-)$$

Breit-Wigner mass = 1650 to 1750 (\approx 1700) MeV
 Breit-Wigner full width = 50 to 150 (\approx 100) MeV
 $p_{\text{beam}} = 1.05 \text{ GeV}/c$ $4\pi\chi^2 = 14.5 \text{ mb}$
 Re(pole position) = 1630 to 1730 (\approx 1680) MeV
 $-2\text{Im}(\text{pole position}) = 50 \text{ to } 150$ (\approx 100) MeV

$N(1700)$ DECAY MODES	Fraction (Γ_i/Γ)	ρ (MeV/c)
$N\pi$	5–15 %	580
ΛK	<3 %	250
$N\pi\pi$	85–95 %	547
$N\rho$	<35 %	†
$\rho\gamma$	0.01–0.05 %	591
$\rho\gamma$, helicity=1/2	0.0–0.024 %	591
$\rho\gamma$, helicity=3/2	0.002–0.026 %	591
$n\gamma$	0.01–0.13 %	590
$n\gamma$, helicity=1/2	0.0–0.09 %	590
$n\gamma$, helicity=3/2	0.01–0.05 %	590

 $N(1710) P_{11}$

$$I(J^P) = \frac{1}{2}(\frac{1}{2}^+)$$

Breit-Wigner mass = 1680 to 1740 (\approx 1710) MeV
 Breit-Wigner full width = 50 to 250 (\approx 100) MeV
 $p_{\text{beam}} = 1.07 \text{ GeV}/c$ $4\pi\chi^2 = 14.2 \text{ mb}$
 Re(pole position) = 1670 to 1770 (\approx 1720) MeV
 $-2\text{Im}(\text{pole position}) = 80 \text{ to } 380$ (\approx 230) MeV

$N(1710)$ DECAY MODES	Fraction (Γ_i/Γ)	ρ (MeV/c)
$N\pi$	10–20 %	587
ΛK	5–25 %	264
$N\pi\pi$	40–90 %	554
$\Delta\pi$	15–40 %	393
$N\rho$	5–25 %	48
$N(\pi\pi)_{S\text{-wave}}^{I=0}$	10–40 %	–
$\rho\gamma$	0.002–0.05 %	598
$\rho\gamma$, helicity=1/2	0.002–0.05 %	598
$n\gamma$	0.0–0.02 %	597
$n\gamma$, helicity=1/2	0.0–0.02 %	597

 $N(1720) P_{13}$

$$I(J^P) = \frac{1}{2}(\frac{3}{2}^+)$$

Breit-Wigner mass = 1650 to 1750 (\approx 1720) MeV
 Breit-Wigner full width = 100 to 200 (\approx 150) MeV
 $p_{\text{beam}} = 1.09 \text{ GeV}/c$ $4\pi\chi^2 = 13.9 \text{ mb}$
 Re(pole position) = 1650 to 1750 (\approx 1700) MeV
 $-2\text{Im}(\text{pole position}) = 110 \text{ to } 390$ (\approx 250) MeV

$N(1720)$ DECAY MODES	Fraction (Γ_i/Γ)	ρ (MeV/c)
$N\pi$	10–20 %	594
ΛK	1–15 %	278
$N\pi\pi$	>70 %	561
$N\rho$	70–85 %	104
$\rho\gamma$	0.003–0.10 %	604
$\rho\gamma$, helicity=1/2	0.003–0.08 %	604
$\rho\gamma$, helicity=3/2	0.001–0.03 %	604
$n\gamma$	0.002–0.39 %	603
$n\gamma$, helicity=1/2	0.0–0.002 %	603
$n\gamma$, helicity=3/2	0.001–0.39 %	603

 $N(2190) G_{17}$

$$I(J^P) = \frac{1}{2}(\frac{7}{2}^-)$$

Breit-Wigner mass = 2100 to 2200 (\approx 2190) MeV
 Breit-Wigner full width = 350 to 550 (\approx 450) MeV
 $p_{\text{beam}} = 2.07 \text{ GeV}/c$ $4\pi\chi^2 = 6.21 \text{ mb}$
 Re(pole position) = 1950 to 2150 (\approx 2050) MeV
 $-2\text{Im}(\text{pole position}) = 350 \text{ to } 550$ (\approx 450) MeV

$N(2190)$ DECAY MODES	Fraction (Γ_i/Γ)	ρ (MeV/c)
$N\pi$	10–20 %	888

 $N(2220) H_{19}$

$$I(J^P) = \frac{1}{2}(\frac{9}{2}^+)$$

Breit-Wigner mass = 2180 to 2310 (\approx 2220) MeV
 Breit-Wigner full width = 320 to 550 (\approx 400) MeV
 $p_{\text{beam}} = 2.14 \text{ GeV}/c$ $4\pi\chi^2 = 5.97 \text{ mb}$
 Re(pole position) = 2100 to 2240 (\approx 2170) MeV
 $-2\text{Im}(\text{pole position}) = 370 \text{ to } 570$ (\approx 470) MeV

$N(2220)$ DECAY MODES	Fraction (Γ_i/Γ)	ρ (MeV/c)
$N\pi$	10–20 %	905

 $N(2250) G_{19}$

$$I(J^P) = \frac{1}{2}(\frac{9}{2}^-)$$

Breit-Wigner mass = 2170 to 2310 (\approx 2250) MeV
 Breit-Wigner full width = 290 to 470 (\approx 400) MeV
 $p_{\text{beam}} = 2.21 \text{ GeV}/c$ $4\pi\chi^2 = 5.74 \text{ mb}$
 Re(pole position) = 2080 to 2200 (\approx 2140) MeV
 $-2\text{Im}(\text{pole position}) = 280 \text{ to } 680$ (\approx 480) MeV

$N(2250)$ DECAY MODES	Fraction (Γ_i/Γ)	ρ (MeV/c)
$N\pi$	5–15 %	923

 $N(2600) h_{11}$

$$I(J^P) = \frac{1}{2}(\frac{11}{2}^-)$$

Breit-Wigner mass = 2550 to 2750 (\approx 2600) MeV
 Breit-Wigner full width = 500 to 800 (\approx 650) MeV
 $p_{\text{beam}} = 3.12 \text{ GeV}/c$ $4\pi\chi^2 = 3.86 \text{ mb}$

$N(2600)$ DECAY MODES	Fraction (Γ_i/Γ)	ρ (MeV/c)
$N\pi$	5–10 %	1126

Baryon Summary Table

Δ BARYONS (S = 0, I = 3/2)

$$\Delta^{++} = uuu, \quad \Delta^+ = uud, \quad \Delta^0 = udd, \quad \Delta^- = ddd$$

Δ(1232) P₃₃

$$I(J^P) = \frac{3}{2}(\frac{3}{2}^+)$$

Breit-Wigner mass (mixed charges) = 1230 to 1234 (≈ 1232) MeV
 Breit-Wigner full width (mixed charges) = 115 to 125 (≈ 120) MeV
 $p_{\text{beam}} = 0.30 \text{ GeV}/c$ $4\pi\chi^2 = 94.8 \text{ mb}$
 Re(pole position) = 1209 to 1211 (≈ 1210) MeV
 $-2\text{Im}(\text{pole position}) = 98 \text{ to } 102 (\approx 100) \text{ MeV}$

Δ(1232) DECAY MODES	Fraction (Γ _i /Γ)	ρ (MeV/c)
Nπ	>99 %	227
Nγ	0.52-0.60 %	259
Nγ, helicity=1/2	0.11-0.13 %	259
Nγ, helicity=3/2	0.41-0.47 %	259

Δ(1600) P₃₃

$$I(J^P) = \frac{3}{2}(\frac{3}{2}^+)$$

Breit-Wigner mass = 1550 to 1700 (≈ 1600) MeV
 Breit-Wigner full width = 250 to 450 (≈ 350) MeV
 $p_{\text{beam}} = 0.87 \text{ GeV}/c$ $4\pi\chi^2 = 18.6 \text{ mb}$
 Re(pole position) = 1500 to 1700 (≈ 1600) MeV
 $-2\text{Im}(\text{pole position}) = 200 \text{ to } 400 (\approx 300) \text{ MeV}$

Δ(1600) DECAY MODES	Fraction (Γ _i /Γ)	ρ (MeV/c)
Nπ	10-25 %	512
Nππ	75-90 %	473
Δπ	40-70 %	301
Nρ	<25 %	†
N(1440)π	10-35 %	74
Nγ	0.001-0.02 %	525
Nγ, helicity=1/2	0.0-0.02 %	525
Nγ, helicity=3/2	0.001-0.005 %	525

Δ(1620) S₃₁

$$I(J^P) = \frac{3}{2}(\frac{1}{2}^-)$$

Breit-Wigner mass = 1615 to 1675 (≈ 1620) MeV
 Breit-Wigner full width = 120 to 180 (≈ 150) MeV
 $p_{\text{beam}} = 0.91 \text{ GeV}/c$ $4\pi\chi^2 = 17.7 \text{ mb}$
 Re(pole position) = 1580 to 1620 (≈ 1600) MeV
 $-2\text{Im}(\text{pole position}) = 100 \text{ to } 130 (\approx 115) \text{ MeV}$

Δ(1620) DECAY MODES	Fraction (Γ _i /Γ)	ρ (MeV/c)
Nπ	20-30 %	526
Nππ	70-80 %	488
Δπ	30-60 %	318
Nρ	7-25 %	†
Nγ	0.004-0.044 %	538
Nγ, helicity=1/2	0.004-0.044 %	538

Δ(1700) D₃₃

$$I(J^P) = \frac{3}{2}(\frac{3}{2}^-)$$

Breit-Wigner mass = 1670 to 1770 (≈ 1700) MeV
 Breit-Wigner full width = 200 to 400 (≈ 300) MeV
 $p_{\text{beam}} = 1.05 \text{ GeV}/c$ $4\pi\chi^2 = 14.5 \text{ mb}$
 Re(pole position) = 1620 to 1700 (≈ 1660) MeV
 $-2\text{Im}(\text{pole position}) = 150 \text{ to } 250 (\approx 200) \text{ MeV}$

Δ(1700) DECAY MODES	Fraction (Γ _i /Γ)	ρ (MeV/c)
Nπ	10-20 %	580
Nππ	80-90 %	547
Δπ	30-60 %	385
Nρ	30-55 %	†
Nγ	0.12-0.26 %	591
Nγ, helicity=1/2	0.08-0.16 %	591
Nγ, helicity=3/2	0.025-0.12 %	591

Δ(1905) F₃₅

$$I(J^P) = \frac{3}{2}(\frac{5}{2}^+)$$

Breit-Wigner mass = 1870 to 1920 (≈ 1905) MeV
 Breit-Wigner full width = 280 to 440 (≈ 350) MeV
 $p_{\text{beam}} = 1.45 \text{ GeV}/c$ $4\pi\chi^2 = 9.62 \text{ mb}$
 Re(pole position) = 1800 to 1860 (≈ 1830) MeV
 $-2\text{Im}(\text{pole position}) = 230 \text{ to } 330 (\approx 280) \text{ MeV}$

Δ(1905) DECAY MODES	Fraction (Γ _i /Γ)	ρ (MeV/c)
Nπ	5-15 %	713
Nππ	85-95 %	687
Δπ	<25 %	542
Nρ	>60 %	421
Nγ	0.01-0.03 %	721
Nγ, helicity=1/2	0.0-0.1 %	721
Nγ, helicity=3/2	0.004-0.03 %	721

Δ(1910) P₃₁

$$I(J^P) = \frac{3}{2}(\frac{1}{2}^+)$$

Breit-Wigner mass = 1870 to 1920 (≈ 1910) MeV
 Breit-Wigner full width = 190 to 270 (≈ 250) MeV
 $p_{\text{beam}} = 1.46 \text{ GeV}/c$ $4\pi\chi^2 = 9.54 \text{ mb}$
 Re(pole position) = 1830 to 1880 (≈ 1855) MeV
 $-2\text{Im}(\text{pole position}) = 200 \text{ to } 500 (\approx 350) \text{ MeV}$

Δ(1910) DECAY MODES	Fraction (Γ _i /Γ)	ρ (MeV/c)
Nπ	15-30 %	716
Nγ	0.0-0.2 %	725
Nγ, helicity=1/2	0.0-0.2 %	725

Δ(1920) P₃₃

$$I(J^P) = \frac{3}{2}(\frac{3}{2}^+)$$

Breit-Wigner mass = 1900 to 1970 (≈ 1920) MeV
 Breit-Wigner full width = 150 to 300 (≈ 200) MeV
 $p_{\text{beam}} = 1.48 \text{ GeV}/c$ $4\pi\chi^2 = 9.37 \text{ mb}$
 Re(pole position) = 1850 to 1950 (≈ 1900) MeV
 $-2\text{Im}(\text{pole position}) = 200 \text{ to } 400 (\approx 300) \text{ MeV}$

Δ(1920) DECAY MODES	Fraction (Γ _i /Γ)	ρ (MeV/c)
Nπ	5-20 %	722

Δ(1930) D₃₅

$$I(J^P) = \frac{3}{2}(\frac{5}{2}^-)$$

Breit-Wigner mass = 1920 to 1970 (≈ 1930) MeV
 Breit-Wigner full width = 250 to 450 (≈ 350) MeV
 $p_{\text{beam}} = 1.50 \text{ GeV}/c$ $4\pi\chi^2 = 9.21 \text{ mb}$
 Re(pole position) = 1840 to 1940 (≈ 1890) MeV
 $-2\text{Im}(\text{pole position}) = 200 \text{ to } 300 (\approx 250) \text{ MeV}$

Δ(1930) DECAY MODES	Fraction (Γ _i /Γ)	ρ (MeV/c)
Nπ	10-20 %	729
Nγ	0.0-0.02 %	737
Nγ, helicity=1/2	0.0-0.01 %	737
Nγ, helicity=3/2	0.0-0.01 %	737

Δ(1950) F₃₇

$$I(J^P) = \frac{3}{2}(\frac{7}{2}^+)$$

Breit-Wigner mass = 1940 to 1960 (≈ 1950) MeV
 Breit-Wigner full width = 290 to 350 (≈ 300) MeV
 $p_{\text{beam}} = 1.54 \text{ GeV}/c$ $4\pi\chi^2 = 8.91 \text{ mb}$
 Re(pole position) = 1880 to 1890 (≈ 1885) MeV
 $-2\text{Im}(\text{pole position}) = 210 \text{ to } 270 (\approx 240) \text{ MeV}$

Δ(1950) DECAY MODES	Fraction (Γ _i /Γ)	ρ (MeV/c)
Nπ	35-40 %	741
Nππ		716
Δπ	20-30 %	574
Nρ	<10 %	469
Nγ	0.08-0.13 %	749
Nγ, helicity=1/2	0.03-0.055 %	749
Nγ, helicity=3/2	0.05-0.075 %	749

Baryon Summary Table

 $\Delta(2420) H_{3,11}$

$$I(J^P) = \frac{3}{2}(\frac{1}{2}^+)$$

Breit-Wigner mass = 2300 to 2500 (≈ 2420) MeV
 Breit-Wigner full width = 300 to 500 (≈ 400) MeV
 $p_{\text{beam}} = 2.64 \text{ GeV}/c$ $4\pi\chi^2 = 4.68 \text{ mb}$
 Re(pole position) = 2260 to 2400 (≈ 2330) MeV
 $-2\text{Im}(\text{pole position}) = 350 \text{ to } 750$ (≈ 550) MeV

$\Delta(2420)$ DECAY MODES	Fraction (Γ_i/Γ)	ρ (MeV/c)
$N\pi$	5–15 %	1023

Λ BARYONS

$(S = -1, I = 0)$

$$\Lambda^0 = uds$$

 Λ

$$I(J^P) = 0(\frac{1}{2}^+)$$

Mass $m = 1115.683 \pm 0.006 \text{ MeV}$
 $(m_\Lambda - m_{\bar{\Lambda}}) / m_\Lambda = (-0.1 \pm 1.1) \times 10^{-5}$ ($S = 1.6$)
 Mean life $\tau = (2.632 \pm 0.020) \times 10^{-10} \text{ s}$ ($S = 1.6$)
 $c\tau = 7.89 \text{ cm}$

Magnetic moment $\mu = -0.613 \pm 0.004 \mu_N$
 Electric dipole moment $d < 1.5 \times 10^{-16} \text{ ecm}$, CL = 95%

Decay parameters

$p\pi^-$	$\alpha_- = 0.642 \pm 0.013$
"	$\phi_- = (-6.5 \pm 3.5)^\circ$
"	$\gamma_- = 0.76$ [h]
"	$\Delta_- = (8 \pm 4)^\circ$ [h]
$n\pi^0$	$\alpha_0 = +0.65 \pm 0.05$
$p e^- \bar{\nu}_e$	$g_A/g_V = -0.718 \pm 0.015$ [f]

Λ DECAY MODES	Fraction (Γ_i/Γ)	ρ (MeV/c)
$p\pi^-$	$(63.9 \pm 0.5) \%$	101
$n\pi^0$	$(35.8 \pm 0.5) \%$	104
$n\gamma$	$(1.75 \pm 0.15) \times 10^{-3}$	162
$p\pi^- \gamma$	$[f] (8.4 \pm 1.4) \times 10^{-4}$	101
$p e^- \bar{\nu}_e$	$(8.32 \pm 0.14) \times 10^{-4}$	163
$p\mu^- \bar{\nu}_\mu$	$(1.57 \pm 0.35) \times 10^{-4}$	131

 $\Lambda(1405) S_{01}$

$$I(J^P) = 0(\frac{1}{2}^-)$$

Mass $m = 1406 \pm 4 \text{ MeV}$
 Full width $\Gamma = 50.0 \pm 2.0 \text{ MeV}$
 Below $\bar{K}N$ threshold

$\Lambda(1405)$ DECAY MODES	Fraction (Γ_i/Γ)	ρ (MeV/c)
$\Sigma\pi$	100 %	152

 $\Lambda(1520) D_{03}$

$$I(J^P) = 0(\frac{3}{2}^-)$$

Mass $m = 1519.5 \pm 1.0 \text{ MeV}$ [l]
 Full width $\Gamma = 15.6 \pm 1.0 \text{ MeV}$ [l]
 $p_{\text{beam}} = 0.39 \text{ GeV}/c$ $4\pi\chi^2 = 82.8 \text{ mb}$

$\Lambda(1520)$ DECAY MODES	Fraction (Γ_i/Γ)	ρ (MeV/c)
$N\bar{K}$	45 \pm 1%	244
$\Sigma\pi$	42 \pm 1%	267
$\Lambda\pi\pi$	10 \pm 1%	252
$\Sigma\pi\pi$	0.9 \pm 0.1%	152
$\Lambda\gamma$	0.8 \pm 0.2%	351

 $\Lambda(1600) P_{01}$

$$I(J^P) = 0(\frac{1}{2}^+)$$

Mass $m = 1560 \text{ to } 1700$ (≈ 1600) MeV
 Full width $\Gamma = 50 \text{ to } 250$ (≈ 150) MeV
 $p_{\text{beam}} = 0.58 \text{ GeV}/c$ $4\pi\chi^2 = 41.6 \text{ mb}$

$\Lambda(1600)$ DECAY MODES	Fraction (Γ_i/Γ)	ρ (MeV/c)
$N\bar{K}$	15–30 %	343
$\Sigma\pi$	10–60 %	336

 $\Lambda(1670) S_{01}$

$$I(J^P) = 0(\frac{1}{2}^-)$$

Mass $m = 1660 \text{ to } 1680$ (≈ 1670) MeV
 Full width $\Gamma = 25 \text{ to } 50$ (≈ 35) MeV
 $p_{\text{beam}} = 0.74 \text{ GeV}/c$ $4\pi\chi^2 = 28.5 \text{ mb}$

$\Lambda(1670)$ DECAY MODES	Fraction (Γ_i/Γ)	ρ (MeV/c)
$N\bar{K}$	15–25 %	414
$\Sigma\pi$	20–60 %	393
$\Lambda\eta$	15–35 %	64

 $\Lambda(1690) D_{03}$

$$I(J^P) = 0(\frac{3}{2}^-)$$

Mass $m = 1685 \text{ to } 1695$ (≈ 1690) MeV
 Full width $\Gamma = 50 \text{ to } 70$ (≈ 60) MeV
 $p_{\text{beam}} = 0.78 \text{ GeV}/c$ $4\pi\chi^2 = 26.1 \text{ mb}$

$\Lambda(1690)$ DECAY MODES	Fraction (Γ_i/Γ)	ρ (MeV/c)
$N\bar{K}$	20–30 %	433
$\Sigma\pi$	20–40 %	409
$\Lambda\pi\pi$	$\sim 25 \%$	415
$\Sigma\pi\pi$	$\sim 20 \%$	350

 $\Lambda(1800) S_{01}$

$$I(J^P) = 0(\frac{1}{2}^-)$$

Mass $m = 1720 \text{ to } 1850$ (≈ 1800) MeV
 Full width $\Gamma = 200 \text{ to } 400$ (≈ 300) MeV
 $p_{\text{beam}} = 1.01 \text{ GeV}/c$ $4\pi\chi^2 = 17.5 \text{ mb}$

$\Lambda(1800)$ DECAY MODES	Fraction (Γ_i/Γ)	ρ (MeV/c)
$N\bar{K}$	25–40 %	528
$\Sigma\pi$	seen	493
$\Sigma(1385)\pi$	seen	345
$N\bar{K}^*(892)$	seen	†

 $\Lambda(1810) P_{01}$

$$I(J^P) = 0(\frac{1}{2}^+)$$

Mass $m = 1750 \text{ to } 1850$ (≈ 1810) MeV
 Full width $\Gamma = 50 \text{ to } 250$ (≈ 150) MeV
 $p_{\text{beam}} = 1.04 \text{ GeV}/c$ $4\pi\chi^2 = 17.0 \text{ mb}$

$\Lambda(1810)$ DECAY MODES	Fraction (Γ_i/Γ)	ρ (MeV/c)
$N\bar{K}$	20–50 %	537
$\Sigma\pi$	10–40 %	501
$\Sigma(1385)\pi$	seen	356
$N\bar{K}^*(892)$	30–60 %	†

 $\Lambda(1820) F_{05}$

$$I(J^P) = 0(\frac{5}{2}^+)$$

Mass $m = 1815 \text{ to } 1825$ (≈ 1820) MeV
 Full width $\Gamma = 70 \text{ to } 90$ (≈ 80) MeV
 $p_{\text{beam}} = 1.06 \text{ GeV}/c$ $4\pi\chi^2 = 16.5 \text{ mb}$

$\Lambda(1820)$ DECAY MODES	Fraction (Γ_i/Γ)	ρ (MeV/c)
$N\bar{K}$	55–65 %	545
$\Sigma\pi$	8–14 %	508
$\Sigma(1385)\pi$	5–10 %	362

Baryon Summary Table

$\Lambda(1830) D_{05}$ $I(J^P) = 0(\frac{5}{2}^-)$
 Mass $m = 1810$ to 1830 (≈ 1830) MeV
 Full width $\Gamma = 60$ to 110 (≈ 95) MeV
 $p_{\text{beam}} = 1.08$ GeV/c $4\pi\chi^2 = 16.0$ mb

$\Lambda(1830)$ DECAY MODES	Fraction (Γ_i/Γ)	p (MeV/c)
$N\bar{K}$	3–10 %	553
$\Sigma\pi$	35–75 %	515
$\Sigma(1385)\pi$	>15 %	371

$\Lambda(1890) P_{03}$ $I(J^P) = 0(\frac{3}{2}^+)$
 Mass $m = 1850$ to 1910 (≈ 1890) MeV
 Full width $\Gamma = 60$ to 200 (≈ 100) MeV
 $p_{\text{beam}} = 1.21$ GeV/c $4\pi\chi^2 = 13.6$ mb

$\Lambda(1890)$ DECAY MODES	Fraction (Γ_i/Γ)	p (MeV/c)
$N\bar{K}$	20–35 %	599
$\Sigma\pi$	3–10 %	559
$\Sigma(1385)\pi$	seen	420
$N\bar{K}^*(892)$	seen	233

$\Lambda(2100) G_{07}$ $I(J^P) = 0(\frac{7}{2}^-)$
 Mass $m = 2090$ to 2110 (≈ 2100) MeV
 Full width $\Gamma = 100$ to 250 (≈ 200) MeV
 $p_{\text{beam}} = 1.68$ GeV/c $4\pi\chi^2 = 8.68$ mb

$\Lambda(2100)$ DECAY MODES	Fraction (Γ_i/Γ)	p (MeV/c)
$N\bar{K}$	25–35 %	751
$\Sigma\pi$	~ 5 %	704
$\Lambda\eta$	<3 %	617
ΞK	<3 %	483
$\Lambda\omega$	<8 %	443
$N\bar{K}^*(892)$	10–20 %	514

$\Lambda(2110) F_{05}$ $I(J^P) = 0(\frac{5}{2}^+)$
 Mass $m = 2090$ to 2140 (≈ 2110) MeV
 Full width $\Gamma = 150$ to 250 (≈ 200) MeV
 $p_{\text{beam}} = 1.70$ GeV/c $4\pi\chi^2 = 8.53$ mb

$\Lambda(2110)$ DECAY MODES	Fraction (Γ_i/Γ)	p (MeV/c)
$N\bar{K}$	5–25 %	757
$\Sigma\pi$	10–40 %	711
$\Lambda\omega$	seen	455
$\Sigma(1385)\pi$	seen	589
$N\bar{K}^*(892)$	10–60 %	524

$\Lambda(2350) H_{09}$ $I(J^P) = 0(\frac{9}{2}^+)$
 Mass $m = 2340$ to 2370 (≈ 2350) MeV
 Full width $\Gamma = 100$ to 250 (≈ 150) MeV
 $p_{\text{beam}} = 2.29$ GeV/c $4\pi\chi^2 = 5.85$ mb

$\Lambda(2350)$ DECAY MODES	Fraction (Γ_i/Γ)	p (MeV/c)
$N\bar{K}$	~ 12 %	915
$\Sigma\pi$	~ 10 %	867

Σ BARYONS ($S = -1, I = 1$)

$$\Sigma^+ = uus, \quad \Sigma^0 = uds, \quad \Sigma^- = dds$$

Σ^+ $I(J^P) = 1(\frac{1}{2}^+)$

Mass $m = 1189.37 \pm 0.07$ MeV ($S = 2.2$)
 Mean life $\tau = (0.8018 \pm 0.0026) \times 10^{-10}$ s
 $c\tau = 2.404$ cm
 $(\tau_{\Sigma^+} - \tau_{\Sigma^-}) / \tau_{\Sigma^+} = (-0.6 \pm 1.2) \times 10^{-3}$
 Magnetic moment $\mu = 2.458 \pm 0.010 \mu_N$ ($S = 2.1$)
 $\Gamma(\Sigma^+ \rightarrow n\ell^+\nu) / \Gamma(\Sigma^- \rightarrow n\ell^-\bar{\nu}) < 0.043$

Decay parameters

$p\pi^0$	$\alpha_0 = -0.980^{+0.017}_{-0.015}$
"	$\phi_0 = (36 \pm 34)^\circ$
"	$\gamma_0 = 0.16$ [h]
"	$\Delta_0 = (187 \pm 6)^\circ$ [h]
$n\pi^+$	$\alpha_+ = 0.068 \pm 0.013$
"	$\phi_+ = (167 \pm 20)^\circ$ ($S = 1.1$)
"	$\gamma_+ = -0.97$ [h]
"	$\Delta_+ = (-73^{+133}_{-10})^\circ$ [h]
$p\gamma$	$\alpha_\gamma = -0.76 \pm 0.08$

Σ^+ DECAY MODES	Fraction (Γ_i/Γ)	Confidence level	p (MeV/c)
$p\pi^0$	(51.57 ± 0.30) %		189
$n\pi^+$	(48.31 ± 0.30) %		185
$p\gamma$	$(1.23 \pm 0.05) \times 10^{-3}$		225
$n\pi^+\gamma$	[i] $(4.5 \pm 0.5) \times 10^{-4}$		185
$\Lambda e^+\nu_e$	$(2.0 \pm 0.5) \times 10^{-5}$		71

$\Delta S = \Delta Q$ (SQ) violating modes or $\Delta S = 1$ weak neutral current (SI) modes

$n e^+ \nu_e$	SQ	< 5	$\times 10^{-6}$	90%	224
$n \mu^+ \nu_\mu$	SQ	< 3.0	$\times 10^{-5}$	90%	202
$p e^+ e^-$	SI	< 7	$\times 10^{-6}$		225

Σ^0 $I(J^P) = 1(\frac{1}{2}^+)$

Mass $m = 1192.642 \pm 0.024$ MeV
 $m_{\Sigma^-} - m_{\Sigma^0} = 4.807 \pm 0.035$ MeV ($S = 1.1$)
 $m_{\Sigma^0} - m_\Lambda = 76.959 \pm 0.023$ MeV
 Mean life $\tau = (7.4 \pm 0.7) \times 10^{-20}$ s
 $c\tau = 2.22 \times 10^{-11}$ m
 Transition magnetic moment $|\mu_{\Sigma\Lambda}| = 1.61 \pm 0.08 \mu_N$

Σ^0 DECAY MODES	Fraction (Γ_i/Γ)	Confidence level	p (MeV/c)
$\Lambda\gamma$	100 %		74
$\Lambda\gamma\gamma$	< 3 %	90%	74
$\Lambda e^+ e^-$	[k] 5×10^{-3}		74

Baryon Summary Table

Σ^-	$I(J^P) = 1(\frac{1}{2}^+)$
Mass $m = 1197.449 \pm 0.030$ MeV (S = 1.2)	
$m_{\Sigma^-} - m_{\Sigma^+} = 8.08 \pm 0.08$ MeV (S = 1.9)	
$m_{\Sigma^-} - m_{\Lambda} = 81.766 \pm 0.030$ MeV (S = 1.2)	
Mean life $\tau = (1.479 \pm 0.011) \times 10^{-10}$ s (S = 1.3)	
$c\tau = 4.434$ cm	
Magnetic moment $\mu = -1.160 \pm 0.025 \mu_N$ (S = 1.7)	

Decay parameters

$n\pi^-$	$\alpha_- = -0.068 \pm 0.008$
"	$\phi_- = (10 \pm 15)^\circ$
"	$\gamma_- = 0.98$ [h]
"	$\Delta_- = (249^{+12}_{-120})^\circ$ [h]
$ne^- \bar{\nu}_e$	$g_A/g_V = 0.340 \pm 0.017$ [f]
"	$f_2(0)/f_1(0) = 0.97 \pm 0.14$
"	$D = 0.11 \pm 0.10$
$\Lambda e^- \bar{\nu}_e$	$g_V/g_A = 0.01 \pm 0.10$ [f] (S = 1.5)
"	$g_{WM}/g_A = 2.4 \pm 1.7$ [f]

Σ^- DECAY MODES	Fraction (Γ_i/Γ)	ρ (MeV/c)
$n\pi^-$	(99.848 ± 0.005) %	193
$n\pi^- \gamma$	[f] (4.6 ± 0.6) × 10 ⁻⁴	193
$ne^- \bar{\nu}_e$	(1.017 ± 0.034) × 10 ⁻³	230
$n\mu^- \bar{\nu}_\mu$	(4.5 ± 0.4) × 10 ⁻⁴	210
$\Lambda e^- \bar{\nu}_e$	(5.73 ± 0.27) × 10 ⁻⁵	79

$\Sigma(1385) P_{13}$	$I(J^P) = 1(\frac{3}{2}^+)$
$\Sigma(1385)^+$ mass $m = 1382.8 \pm 0.4$ MeV (S = 2.0)	
$\Sigma(1385)^0$ mass $m = 1383.7 \pm 1.0$ MeV (S = 1.4)	
$\Sigma(1385)^-$ mass $m = 1387.2 \pm 0.5$ MeV (S = 2.2)	
$\Sigma(1385)^+$ full width $\Gamma = 35.8 \pm 0.8$ MeV	
$\Sigma(1385)^0$ full width $\Gamma = 36 \pm 5$ MeV	
$\Sigma(1385)^-$ full width $\Gamma = 39.4 \pm 2.1$ MeV (S = 1.7)	
Below $\bar{K}N$ threshold	

$\Sigma(1385)$ DECAY MODES	Fraction (Γ_i/Γ)	ρ (MeV/c)
$\Lambda\pi$	88 ± 2 %	208
$\Sigma\pi$	12 ± 2 %	127

$\Sigma(1660) P_{11}$	$I(J^P) = 1(\frac{1}{2}^+)$
Mass $m = 1630$ to 1690 (≈ 1660) MeV	
Full width $\Gamma = 40$ to 200 (≈ 100) MeV	
$p_{\text{beam}} = 0.72$ GeV/c $4\pi\lambda^2 = 29.9$ mb	

$\Sigma(1660)$ DECAY MODES	Fraction (Γ_i/Γ)	ρ (MeV/c)
$N\bar{K}$	10–30 %	405
$\Lambda\pi$	seen	439
$\Sigma\pi$	seen	385

$\Sigma(1670) D_{13}$	$I(J^P) = 1(\frac{3}{2}^-)$
Mass $m = 1665$ to 1685 (≈ 1670) MeV	
Full width $\Gamma = 40$ to 80 (≈ 60) MeV	
$p_{\text{beam}} = 0.74$ GeV/c $4\pi\lambda^2 = 28.5$ mb	

$\Sigma(1670)$ DECAY MODES	Fraction (Γ_i/Γ)	ρ (MeV/c)
$N\bar{K}$	7–13 %	414
$\Lambda\pi$	5–15 %	447
$\Sigma\pi$	30–60 %	393

$\Sigma(1750) S_{11}$	$I(J^P) = 1(\frac{1}{2}^-)$
Mass $m = 1730$ to 1800 (≈ 1750) MeV	
Full width $\Gamma = 60$ to 160 (≈ 90) MeV	
$p_{\text{beam}} = 0.91$ GeV/c $4\pi\lambda^2 = 20.7$ mb	

$\Sigma(1750)$ DECAY MODES	Fraction (Γ_i/Γ)	ρ (MeV/c)
$N\bar{K}$	10–40 %	486
$\Lambda\pi$	seen	507
$\Sigma\pi$	< 8 %	455
$\Sigma\eta$	15–55 %	81

$\Sigma(1775) D_{15}$	$I(J^P) = 1(\frac{5}{2}^-)$
Mass $m = 1770$ to 1780 (≈ 1775) MeV	
Full width $\Gamma = 105$ to 135 (≈ 120) MeV	
$p_{\text{beam}} = 0.96$ GeV/c $4\pi\lambda^2 = 19.0$ mb	

$\Sigma(1775)$ DECAY MODES	Fraction (Γ_i/Γ)	ρ (MeV/c)
$N\bar{K}$	37–43%	508
$\Lambda\pi$	14–20%	525
$\Sigma\pi$	2–5%	474
$\Sigma(1385)\pi$	8–12%	324
$\Lambda(1520)\pi$	17–23%	198

$\Sigma(1915) F_{15}$	$I(J^P) = 1(\frac{5}{2}^+)$
Mass $m = 1900$ to 1935 (≈ 1915) MeV	
Full width $\Gamma = 80$ to 160 (≈ 120) MeV	
$p_{\text{beam}} = 1.26$ GeV/c $4\pi\lambda^2 = 12.8$ mb	

$\Sigma(1915)$ DECAY MODES	Fraction (Γ_i/Γ)	ρ (MeV/c)
$N\bar{K}$	5–15 %	618
$\Lambda\pi$	seen	622
$\Sigma\pi$	seen	577
$\Sigma(1385)\pi$	< 5 %	440

$\Sigma(1940) D_{13}$	$I(J^P) = 1(\frac{3}{2}^-)$
Mass $m = 1900$ to 1950 (≈ 1940) MeV	
Full width $\Gamma = 150$ to 300 (≈ 220) MeV	
$p_{\text{beam}} = 1.32$ GeV/c $4\pi\lambda^2 = 12.1$ mb	

$\Sigma(1940)$ DECAY MODES	Fraction (Γ_i/Γ)	ρ (MeV/c)
$N\bar{K}$	< 20 %	637
$\Lambda\pi$	seen	639
$\Sigma\pi$	seen	594
$\Sigma(1385)\pi$	seen	460
$\Lambda(1520)\pi$	seen	354
$\Delta(1232)\bar{K}$	seen	410
$N\bar{K}^*(892)$	seen	320

$\Sigma(2030) F_{17}$	$I(J^P) = 1(\frac{7}{2}^+)$
Mass $m = 2025$ to 2040 (≈ 2030) MeV	
Full width $\Gamma = 150$ to 200 (≈ 180) MeV	
$p_{\text{beam}} = 1.52$ GeV/c $4\pi\lambda^2 = 9.93$ mb	

$\Sigma(2030)$ DECAY MODES	Fraction (Γ_i/Γ)	ρ (MeV/c)
$N\bar{K}$	17–23 %	702
$\Lambda\pi$	17–23 %	700
$\Sigma\pi$	5–10 %	657
ΞK	< 2 %	412
$\Sigma(1385)\pi$	5–15 %	529
$\Lambda(1520)\pi$	10–20 %	430
$\Delta(1232)\bar{K}$	10–20 %	498
$N\bar{K}^*(892)$	< 5 %	438

Baryon Summary Table

$\Sigma(2250)$		$I(J^P) = 1(?^?)$
Mass $m = 2210$ to 2280 (≈ 2250) MeV		
Full width $\Gamma = 60$ to 150 (≈ 100) MeV		
$p_{\text{beam}} = 2.04$ GeV/c $4\pi\lambda^2 = 6.76$ mb		
$\Sigma(2250)$ DECAY MODES	Fraction (Γ_i/Γ)	p (MeV/c)
$N\bar{K}$	<10 %	851
$\Lambda\pi$	seen	842
$\Sigma\pi$	seen	803

Ξ BARYONS ($S = -2, I = 1/2$)

$$\Xi^0 = uss, \quad \Xi^- = dss$$

Ξ^0		$I(J^P) = \frac{1}{2}(\frac{1}{2}^+)$	
P is not yet measured; + is the quark model prediction.			
Mass $m = 1314.83 \pm 0.20$ MeV			
$m_{\Xi^-} - m_{\Xi^0} = 6.48 \pm 0.24$ MeV			
Mean life $\tau = (2.90 \pm 0.09) \times 10^{-10}$ s			
$c\tau = 8.71$ cm			
Magnetic moment $\mu = -1.250 \pm 0.014 \mu_N$			
Decay parameters			
$\Lambda\pi^0$	$\alpha = -0.411 \pm 0.022$ ($S = 2.1$)		
"	$\phi = (21 \pm 12)^\circ$		
"	$\gamma = 0.85$ [h]		
"	$\Delta = (218_{-19}^{+12})^\circ$ [h]		
$\Lambda\gamma$	$\alpha = 0.4 \pm 0.4$		
$\Sigma^0\gamma$	$\alpha = 0.20 \pm 0.32$		
Ξ^0 DECAY MODES	Fraction (Γ_i/Γ)	Scale factor/ Confidence level	p (MeV/c)
$\Lambda\pi^0$	$(99.51 \pm 0.05)\%$	$S=1.2$	135
$\Lambda\gamma$	$(1.18 \pm 0.30) \times 10^{-3}$	$S=2.0$	184
$\Sigma^0\gamma$	$(3.5 \pm 0.4) \times 10^{-3}$		117
$\Sigma^+ e^- \bar{\nu}_e$	$(2.7 \pm 0.4) \times 10^{-4}$		120
$\Sigma^+ \mu^- \bar{\nu}_\mu$	$< 1.1 \times 10^{-3}$	CL=90%	64
$\Delta S = \Delta Q$ (SQ) violating modes or $\Delta S = 2$ forbidden (S_2) modes			
$\Sigma^- e^+ \nu_e$	$SQ < 9 \times 10^{-4}$	CL=90%	112
$\Sigma^- \mu^+ \nu_\mu$	$SQ < 9 \times 10^{-4}$	CL=90%	49
$p\pi^-$	$S_2 < 4 \times 10^{-5}$	CL=90%	299
$p e^- \bar{\nu}_e$	$S_2 < 1.3 \times 10^{-3}$		323
$p \mu^- \bar{\nu}_\mu$	$S_2 < 1.3 \times 10^{-3}$		309

Ξ^-		$I(J^P) = \frac{1}{2}(\frac{1}{2}^+)$	
P is not yet measured; + is the quark model prediction.			
Mass $m = 1321.31 \pm 0.13$ MeV			
Mean life $\tau = (1.639 \pm 0.015) \times 10^{-10}$ s			
$c\tau = 4.91$ cm			
Magnetic moment $\mu = -0.6507 \pm 0.0025 \mu_N$			
Decay parameters			
$\Lambda\pi^-$	$\alpha = -0.456 \pm 0.014$ ($S = 1.8$)		
"	$\phi = (4 \pm 4)^\circ$		
"	$\gamma = 0.89$ [h]		
"	$\Delta = (188 \pm 8)^\circ$ [h]		
$\Lambda e^- \bar{\nu}_e$	$\mathcal{E}A/\mathcal{E}V = -0.25 \pm 0.05$ [f]		
Ξ^- DECAY MODES	Fraction (Γ_i/Γ)	Confidence level	p (MeV/c)
$\Lambda\pi^-$	$(99.887 \pm 0.035)\%$		139
$\Sigma^- \gamma$	$(1.27 \pm 0.23) \times 10^{-4}$		118
$\Lambda e^- \bar{\nu}_e$	$(5.63 \pm 0.31) \times 10^{-4}$		190
$\Lambda \mu^- \bar{\nu}_\mu$	$(3.5_{-2.2}^{+3.5}) \times 10^{-4}$		163
$\Sigma^0 e^- \bar{\nu}_e$	$(8.7 \pm 1.7) \times 10^{-5}$		122
$\Sigma^0 \mu^- \bar{\nu}_\mu$	$< 8 \times 10^{-4}$	90%	70
$\Xi^0 e^- \bar{\nu}_e$	$< 2.3 \times 10^{-3}$	90%	6

$\Delta S = 2$ forbidden (S_2) modes				
$n\pi^-$	$S_2 < 1.9$	$\times 10^{-5}$	90%	303
$ne^- \bar{\nu}_e$	$S_2 < 3.2$	$\times 10^{-3}$	90%	327
$n\mu^- \bar{\nu}_\mu$	$S_2 < 1.5$	%	90%	314
$p\pi^- \pi^-$	$S_2 < 4$	$\times 10^{-4}$	90%	223
$p\pi^- e^- \bar{\nu}_e$	$S_2 < 4$	$\times 10^{-4}$	90%	304
$p\pi^- \mu^- \bar{\nu}_\mu$	$S_2 < 4$	$\times 10^{-4}$	90%	250
$p\mu^- \mu^-$	$L < 4$	$\times 10^{-4}$	90%	272

$\Xi(1530) P_{13}$		$I(J^P) = \frac{1}{2}(\frac{3}{2}^+)$	
$\Xi(1530)^0$ mass $m = 1531.80 \pm 0.32$ MeV ($S = 1.3$)			
$\Xi(1530)^-$ mass $m = 1535.0 \pm 0.6$ MeV			
$\Xi(1530)^0$ full width $\Gamma = 9.1 \pm 0.5$ MeV			
$\Xi(1530)^-$ full width $\Gamma = 9.9_{-1.9}^{+1.7}$ MeV			
$\Xi(1530)$ DECAY MODES	Fraction (Γ_i/Γ)	Confidence level	p (MeV/c)
$\Xi\pi$	100 %		152
$\Xi\gamma$	<4 %	90%	200

$\Xi(1690)$		$I(J^P) = \frac{1}{2}(\frac{1}{2}^?)$
Mass $m = 1690 \pm 10$ MeV [J]		
Full width $\Gamma < 30$ MeV		
$\Xi(1690)$ DECAY MODES	Fraction (Γ_i/Γ)	p (MeV/c)
$\Lambda\bar{K}$	seen	240
$\Sigma\bar{K}$	seen	51
$\Xi\pi$	seen	-
$\Xi^- \pi^+ \pi^-$	possibly seen	214

$\Xi(1820) D_{13}$		$I(J^P) = \frac{1}{2}(\frac{3}{2}^-)$
Mass $m = 1823 \pm 5$ MeV [J]		
Full width $\Gamma = 24_{-10}^{+15}$ MeV [J]		
$\Xi(1820)$ DECAY MODES	Fraction (Γ_i/Γ)	p (MeV/c)
$\Lambda\bar{K}$	large	400
$\Sigma\bar{K}$	small	320
$\Xi\pi$	small	413
$\Xi(1530)\pi$	small	234

$\Xi(1950)$		$I(J^P) = \frac{1}{2}(\frac{1}{2}^?)$
Mass $m = 1950 \pm 15$ MeV [J]		
Full width $\Gamma = 60 \pm 20$ MeV [J]		
$\Xi(1950)$ DECAY MODES	Fraction (Γ_i/Γ)	p (MeV/c)
$\Lambda\bar{K}$	seen	522
$\Sigma\bar{K}$	possibly seen	460
$\Xi\pi$	seen	518

$\Xi(2030)$		$I(J^P) = \frac{1}{2}(\geq \frac{5}{2}^?)$
Mass $m = 2025 \pm 5$ MeV [J]		
Full width $\Gamma = 20_{-5}^{+15}$ MeV [J]		
$\Xi(2030)$ DECAY MODES	Fraction (Γ_i/Γ)	p (MeV/c)
$\Lambda\bar{K}$	$\sim 20\%$	589
$\Sigma\bar{K}$	$\sim 80\%$	533
$\Xi\pi$	small	573
$\Xi(1530)\pi$	small	421
$\Lambda\bar{K}\pi$	small	501
$\Sigma\bar{K}\pi$	small	430

Baryon Summary Table

 Ω BARYONS
($S = -3, I = 0$)

$$\Omega^- = sss$$

 Ω^-

$$I(J^P) = 0(\frac{3}{2}^+)$$

 J^P is not yet measured; $\frac{3}{2}^+$ is the quark model prediction.

Mass $m = 1672.45 \pm 0.29$ MeV

$(m_{\Omega^-} - m_{\Xi^-}) / m_{\Omega^-} = (-1 \pm 8) \times 10^{-5}$

Mean life $\tau = (0.821 \pm 0.011) \times 10^{-10}$ s

$c\tau = 2.461$ cm

$(\tau_{\Omega^-} - \tau_{\Xi^-}) / \tau_{\Omega^-} = -0.002 \pm 0.040$

Magnetic moment $\mu = -2.02 \pm 0.05 \mu_N$

Decay parameters

$\Lambda K^- \quad \alpha = -0.026 \pm 0.023$

$\frac{1}{2}[\alpha(\Lambda K^-) + \alpha(\bar{\Lambda} K^+)] = -0.004 \pm 0.040$

$\Xi^0 \pi^- \quad \alpha = 0.09 \pm 0.14$

$\Xi^- \pi^0 \quad \alpha = 0.05 \pm 0.21$

Ω^- DECAY MODES	Fraction (Γ_i/Γ)	Confidence level	p (MeV/c)
ΛK^-	(67.8 ± 0.7) %		211
$\Xi^0 \pi^-$	(23.6 ± 0.7) %		294
$\Xi^- \pi^0$	(8.6 ± 0.4) %		290
$\Xi^- \pi^+ \pi^-$	(4.3 ^{+3.4} _{-1.3}) × 10 ⁻⁴		190
$\Xi(1530)^0 \pi^-$	(6.4 ^{+5.1} _{-2.0}) × 10 ⁻⁴		17
$\Xi^0 e^- \bar{\nu}_e$	(5.6 ± 2.8) × 10 ⁻³		319
$\Xi^- \gamma$	< 4.6 × 10 ⁻⁴	90%	314
$\Delta S = 2$ forbidden (S_2) modes			
$\Lambda \pi^-$	S_2 < 1.9 × 10 ⁻⁴	90%	449

 $\Omega(2250)^-$

$$I(J^P) = 0(?^?)$$

Mass $m = 2252 \pm 9$ MeV

Full width $\Gamma = 55 \pm 18$ MeV

$\Omega(2250)^-$ DECAY MODES	Fraction (Γ_i/Γ)	p (MeV/c)
$\Xi^- \pi^+ K^-$	seen	531
$\Xi(1530)^0 K^-$	seen	437

CHARMED BARYONS
($C = +1$)

$$\Lambda_c^+ = udc, \quad \Sigma_c^{++} = uuc, \quad \Sigma_c^+ = udc, \quad \Sigma_c^0 = ddc,$$

$$\Xi_c^+ = usc, \quad \Xi_c^0 = dsc, \quad \Omega_c^0 = ssc$$

 Λ_c^+

$$I(J^P) = 0(\frac{1}{2}^+)$$

 J is not well measured; $\frac{1}{2}$ is the quark-model prediction.

Mass $m = 2284.9 \pm 0.6$ MeV

Mean life $\tau = (0.206 \pm 0.012) \times 10^{-12}$ s

$c\tau = 61.8 \mu\text{m}$

Decay asymmetry parameters

$\Lambda \pi^+ \quad \alpha = -0.98 \pm 0.19$

$\Sigma^+ \pi^0 \quad \alpha = -0.45 \pm 0.32$

$\Lambda \ell^+ \nu_\ell \quad \alpha = -0.82^{+0.11}_{-0.07}$

Nearly all branching fractions of the Λ_c^+ are measured relative to the $pK^- \pi^+$ mode, but there are no model-independent measurements of this branching fraction. We explain how we arrive at our value of $B(\Lambda_c^+ \rightarrow pK^- \pi^+)$ in a Note at the beginning of the branching-ratio measurements in the Listings. When this branching fraction is eventually well determined, all the other branching fractions will slide up or down proportionally as the true value differs from the value we use here.

 Λ_c^+ DECAY MODES

DECAY MODES	Fraction (Γ_i/Γ)	Scale factor/ Confidence level	p (MeV/c)
Hadronic modes with a p and one \bar{K}			
$p \bar{K}^0$	(2.3 ± 0.6) %		872
$p \bar{K}^- \pi^+$	[η] (5.0 ± 1.3) %		822
$p \bar{K}^*(892)^0$	[m] (1.6 ± 0.5) %		681
$\Delta(1232)^{++} K^-$	(8.6 ± 3.0) × 10 ⁻³		709
$\Lambda(1520) \pi^+$	[m] (5.9 ± 2.1) × 10 ⁻³		626
$p K^- \pi^+$ nonresonant	(2.8 ± 0.8) %		822
$p \bar{K}^0 \pi^0$	(3.3 ± 1.0) %		822
$p \bar{K}^0 \eta$	(1.2 ± 0.4) %		567
$p \bar{K}^0 \pi^+ \pi^-$	(2.6 ± 0.7) %		753
$p K^- \pi^+ \pi^0$	(3.4 ± 1.0) %		758
$p K^*(892)^- \pi^+$	[m] (1.1 ± 0.5) %		579
$p (K^- \pi^+)$ nonresonant π^0	(3.6 ± 1.2) %		758
$\Delta(1232) \bar{K}^*(892)$	seen		416
$p K^- \pi^+ \pi^+ \pi^-$	(1.1 ± 0.8) × 10 ⁻³		670
$p K^- \pi^+ \pi^0 \pi^0$	(8 ± 4) × 10 ⁻³		676
$p K^- \pi^+ \pi^0 \pi^0 \pi^0$	(5.0 ± 3.4) × 10 ⁻³		573
Hadronic modes with a p and zero or two K's			
$p \pi^+ \pi^-$	(3.5 ± 2.0) × 10 ⁻³		926
$p f_0(980)$	[m] (2.8 ± 1.9) × 10 ⁻³		621
$p \pi^+ \pi^+ \pi^- \pi^-$	(1.8 ± 1.2) × 10 ⁻³		851
$p K^+ K^-$	(2.3 ± 0.9) × 10 ⁻³		615
$p \phi$	[m] (1.2 ± 0.5) × 10 ⁻³		589

Baryon Summary Table

Hadronic modes with a hyperon			
$\Lambda\pi^+$		$(9.0 \pm 2.8) \times 10^{-3}$	863
$\Lambda\pi^+\pi^0$		$(3.6 \pm 1.3) \%$	843
$\Lambda\rho^+$		$< 5 \%$	638
		CL=95%	
$\Lambda\pi^+\pi^+\pi^-$		$(3.3 \pm 1.0) \%$	806
$\Lambda\pi^+\eta$		$(1.8 \pm 0.6) \%$	690
$\Sigma(1385)^+\eta$	[m]	$(8.5 \pm 3.3) \times 10^{-3}$	569
$\Lambda K^+\bar{K}^0$		$(6.0 \pm 2.1) \times 10^{-3}$	441
$\Sigma^0\pi^+$		$(9.9 \pm 3.2) \times 10^{-3}$	824
$\Sigma^+\pi^0$		$(1.00 \pm 0.34) \%$	826
$\Sigma^+\eta$		$(5.5 \pm 2.3) \times 10^{-3}$	712
$\Sigma^+\pi^+\pi^-$		$(3.4 \pm 1.0) \%$	803
$\Sigma^+\rho^0$		$< 1.4 \%$	578
		CL=95%	
$\Sigma^-\pi^+\pi^+$		$(1.8 \pm 0.8) \%$	798
$\Sigma^0\pi^+\pi^0$		$(1.8 \pm 0.8) \%$	802
$\Sigma^0\pi^+\pi^+\pi^-$		$(1.1 \pm 0.4) \%$	762
$\Sigma^+\pi^+\pi^-\pi^0$		—	766
$\Sigma^+\omega$	[m]	$(2.7 \pm 1.0) \%$	568
$\Sigma^+\pi^+\pi^+\pi^-\pi^-$		$(3.0 \pm 4.1) \times 10^{-3}$	707
$\Sigma^+K^+K^-$		$(3.5 \pm 1.2) \times 10^{-3}$	346
$\Sigma^+\phi$	[m]	$(3.5 \pm 1.7) \times 10^{-3}$	292
$\Sigma^+K^+\pi^-$		$(7 \pm 6) \times 10^{-3}$	668
$\Xi^0 K^+$		$(3.9 \pm 1.4) \times 10^{-3}$	652
$\Xi^- K^+\pi^+$		$(4.9 \pm 1.7) \times 10^{-3}$	564
$\Xi(1530)^0 K^+$	[m]	$(2.6 \pm 1.0) \times 10^{-3}$	471
Semileptonic modes			
$\Lambda\ell^+\nu_\ell$	[n]	$(2.0 \pm 0.6) \%$	—
$\Lambda e^+\nu_e$		$(2.1 \pm 0.6) \%$	870
$\Lambda\mu^+\nu_\mu$		$(2.0 \pm 0.7) \%$	866
Inclusive modes			
e^+ anything		$(4.5 \pm 1.7) \%$	—
ρe^+ anything		$(1.8 \pm 0.9) \%$	—
p anything		$(50 \pm 16) \%$	—
p anything (no Λ)		$(12 \pm 19) \%$	—
n anything		$(50 \pm 16) \%$	—
n anything (no Λ)		$(29 \pm 17) \%$	—
Λ anything		$(35 \pm 11) \%$	S=1.4
Σ^\pm anything	[o]	$(10 \pm 5) \%$	—

$\Delta C = 1$ weak neutral current (C1) modes, or
Lepton number (L) violating modes

$\rho\mu^+\mu^-$	C1	$< 3.4 \times 10^{-4}$	CL=90%	936
$\Sigma^-\mu^+\mu^+$	L	$< 7.0 \times 10^{-4}$	CL=90%	811

 $\Lambda_c(2593)^+$

$$I(J^P) = 0(\frac{1}{2}^-)$$

The spin-parity follows from the fact that $\Sigma_c(2455)\pi$ decays, with little available phase space, are dominant.

$$\text{Mass } m = 2593.9 \pm 0.8 \text{ MeV}$$

$$m - m_{\Lambda_c^+} = 308.9 \pm 0.6 \text{ MeV} \quad (S = 1.1)$$

$$\text{Full width } \Gamma = 3.6^{+2.0}_{-1.3} \text{ MeV}$$

$\Lambda_c^+\pi\pi$ and its submode $\Sigma_c(2455)\pi$ — the latter just barely — are the only strong decays allowed to an excited Λ_c^+ having this mass; and the submode seems to dominate.

$\Lambda_c(2593)^+$ DECAY MODES	Fraction (Γ_i/Γ)	ρ (MeV/c)
$\Lambda_c^+\pi^+\pi^-$	[ρ] $\approx 67 \%$	124
$\Sigma_c(2455)^+\pi^-$	$24 \pm 7 \%$	17
$\Sigma_c(2455)^0\pi^+$	$24 \pm 7 \%$	23
$\Lambda_c^+\pi^+\pi^-$ 3-body	$18 \pm 10 \%$	124
$\Lambda_c^+\pi^0$	not seen	261
$\Lambda_c^+\gamma$	not seen	290

 $\Lambda_c(2625)^+$

$$I(J^P) = 0(\frac{3}{2}^-)$$

J^P has not been measured; $\frac{3}{2}^-$ is the quark-model prediction.

$$\text{Mass } m = 2626.6 \pm 0.8 \text{ MeV} \quad (S = 1.2)$$

$$m - m_{\Lambda_c^+} = 341.7 \pm 0.6 \text{ MeV} \quad (S = 1.6)$$

$$\text{Full width } \Gamma < 1.9 \text{ MeV, CL} = 90\%$$

$\Lambda_c^+\pi\pi$ and its submode $\Sigma(2455)\pi$ are the only strong decays allowed to an excited Λ_c^+ having this mass.

$\Lambda_c(2625)^+$ DECAY MODES	Fraction (Γ_i/Γ)	Confidence level	ρ (MeV/c)
$\Lambda_c^+\pi^+\pi^-$	[ρ] $\approx 67 \%$		184
$\Sigma_c(2455)^+\pi^-$	< 5	90%	100
$\Sigma_c(2455)^0\pi^+$	< 5	90%	101
$\Lambda_c^+\pi^+\pi^-$ 3-body	large		184
$\Lambda_c^+\pi^0$	not seen		293
$\Lambda_c^+\gamma$	not seen		319

 $\Sigma_c(2455)$

$$I(J^P) = 1(\frac{1}{2}^+)$$

J^P has not been measured; $\frac{1}{2}^+$ is the quark-model prediction.

$$\Sigma_c(2455)^{++}\text{mass } m = 2452.8 \pm 0.6 \text{ MeV}$$

$$\Sigma_c(2455)^+\text{ mass } m = 2453.6 \pm 0.9 \text{ MeV}$$

$$\Sigma_c(2455)^0\text{ mass } m = 2452.2 \pm 0.6 \text{ MeV}$$

$$m_{\Sigma_c^{++}} - m_{\Lambda_c^+} = 167.87 \pm 0.19 \text{ MeV}$$

$$m_{\Sigma_c^+} - m_{\Lambda_c^+} = 168.7 \pm 0.6 \text{ MeV}$$

$$m_{\Sigma_c^0} - m_{\Lambda_c^+} = 167.30 \pm 0.20 \text{ MeV}$$

$$m_{\Sigma_c^{++}} - m_{\Sigma_c^0} = 0.57 \pm 0.23 \text{ MeV}$$

$$m_{\Sigma_c^+} - m_{\Sigma_c^0} = 1.4 \pm 0.6 \text{ MeV}$$

$\Lambda_c^+\pi$ is the only strong decay allowed to a Σ_c having this mass.

$\Sigma_c(2455)$ DECAY MODES	Fraction (Γ_i/Γ)	ρ (MeV/c)
$\Lambda_c^+\pi$	$\approx 100 \%$	90

 $\Sigma_c(2520)$

$$I(J^P) = 1(\frac{3}{2}^+)$$

J^P has not been measured; $\frac{3}{2}^+$ is the quark-model prediction.

$$\Sigma_c(2520)^{++}\text{mass } m = 2519.4 \pm 1.5 \text{ MeV}$$

$$\Sigma_c(2520)^0\text{ mass } m = 2517.5 \pm 1.4 \text{ MeV}$$

$$m_{\Sigma_c(2520)^{++}} - m_{\Lambda_c^+} = 234.5 \pm 1.4 \text{ MeV}$$

$$m_{\Sigma_c(2520)^0} - m_{\Lambda_c^+} = 232.6 \pm 1.3 \text{ MeV}$$

$$m_{\Sigma_c(2520)^{++}} - m_{\Sigma_c(2520)^0} = 1.9 \pm 1.7 \text{ MeV}$$

$$\Sigma_c(2520)^{++}\text{full width } \Gamma = 18 \pm 5 \text{ MeV}$$

$$\Sigma_c(2520)^0\text{ full width } \Gamma = 13 \pm 5 \text{ MeV}$$

$\Lambda_c^+\pi$ is the only strong decay allowed to a Σ_c having this mass.

$\Sigma_c(2520)$ DECAY MODES	Fraction (Γ_i/Γ)	ρ (MeV/c)
$\Lambda_c^+\pi$	$\approx 100 \%$	180

Baryon Summary Table

 Ξ_c^+

$I(J^P) = \frac{1}{2}(\frac{1}{2}^+)$

 J^P has not been measured; $\frac{1}{2}^+$ is the quark-model prediction.Mass $m = 2466.3 \pm 1.4$ MeVMean life $\tau = (0.33_{-0.04}^{+0.06}) \times 10^{-12}$ s $c\tau = 98$ μm No absolute branching fractions have been measured. The following are branching ratios relative to $\Xi^- \pi^+ \pi^+$.

Ξ_c^+ DECAY MODES	Fraction (Γ_i/Γ)	Confidence level	p (MeV/c)
$\Lambda K^- \pi^+ \pi^+$	[q] 0.58 \pm 0.18		785
$\Lambda \bar{K}^*(892)^0 \pi^+$	[m,q] <0.29	90%	603
$\Sigma(1385)^+ K^- \pi^+$	[m,q] <0.41	90%	677
$\Sigma^+ K^- \pi^+$	[q] 1.18 \pm 0.31		809
$\Sigma^+ \bar{K}^*(892)^0$	[m,q] 0.92 \pm 0.30		654
$\Sigma^0 K^- \pi^+ \pi^+$	[q] 0.49 \pm 0.26		734
$\Xi^0 \pi^+$	[q] 0.55 \pm 0.16		876
$\Xi^- \pi^+ \pi^+$	[q] \equiv 1.0		850
$\Xi(1530)^0 \pi^+$	[m,q] <0.2	90%	749
$\Xi^0 \pi^+ \pi^0$	[q] 2.34 \pm 0.68		855
$\Xi^0 \pi^+ \pi^+ \pi^-$	[q] 1.74 \pm 0.50		817
$\Xi^0 e^+ \nu_e$	[q] 2.3 $_{-0.9}^{+0.7}$		883
$p K^- \pi^+$	[q] 0.20 \pm 0.05		-

 Ξ_c^0

$I(J^P) = \frac{1}{2}(\frac{1}{2}^+)$

 J^P has not been measured; $\frac{1}{2}^+$ is the quark-model prediction.Mass $m = 2471.8 \pm 1.4$ MeV $m_{\Xi_c^0} - m_{\Xi_c^+} = 5.5 \pm 1.8$ MeVMean life $\tau = (0.098_{-0.015}^{+0.023}) \times 10^{-12}$ s $c\tau = 29$ μm

Ξ_c^0 DECAY MODES	Fraction (Γ_i/Γ)	p (MeV/c)
$\Lambda \bar{K}^0$	seen	907
$\Lambda \bar{K}^0 \pi^+ \pi^-$	seen	788
$\Lambda K^- \pi^+ \pi^+ \pi^-$	seen	704
$\Xi^- \pi^+$	seen	876
$\Xi^- \pi^+ \pi^+ \pi^-$	seen	817
$p K^- \bar{K}^*(892)^0$	seen	408
$\Omega^- K^+$	seen	523
$\Xi^- e^+ \nu_e$	seen	883
$\Xi^- \ell^+$ anything	seen	-

 $\Xi_c^{'+}$

$I(J^P) = \frac{1}{2}(\frac{1}{2}^+)$

 J^P has not been measured; $\frac{1}{2}^+$ is the quark-model prediction.Mass $m = 2574.1 \pm 3.3$ MeV $m_{\Xi_c^{'+}} - m_{\Xi_c^+} = 107.8 \pm 3.0$ MeVThe $\Xi_c^{'+} - \Xi_c^+$ mass difference is too small for any strong decay to occur.

$\Xi_c^{'+}$ DECAY MODES	Fraction (Γ_i/Γ)	p (MeV/c)
$\Xi_c^{'+} \gamma$	seen	106

 Ξ_c^0

$I(J^P) = \frac{1}{2}(\frac{1}{2}^+)$

 J^P has not been measured; $\frac{1}{2}^+$ is the quark-model prediction.Mass $m = 2578.8 \pm 3.2$ MeV $m_{\Xi_c^0} - m_{\Xi_c^+} = 107.0 \pm 2.9$ MeVThe $\Xi_c^0 - \Xi_c^+$ mass difference is too small for any strong decay to occur.

Ξ_c^0 DECAY MODES	Fraction (Γ_i/Γ)	p (MeV/c)
$\Xi_c^0 \gamma$	seen	105

 $\Xi_c(2645)$

$I(J^P) = \frac{1}{2}(\frac{3}{2}^+)$

 J^P has not been measured; $\frac{3}{2}^+$ is the quark-model prediction. $\Xi_c(2645)^+$ mass $m = 2647.4 \pm 2.0$ MeV ($S = 1.2$) $\Xi_c(2645)^0$ mass $m = 2644.5 \pm 1.8$ MeV $m_{\Xi_c(2645)^+} - m_{\Xi_c^0} = 175.6 \pm 1.4$ MeV ($S = 1.7$) $m_{\Xi_c(2645)^0} - m_{\Xi_c^+} = 178.2 \pm 1.1$ MeV $\Xi_c(2645)^+$ full width $\Gamma < 3.1$ MeV, CL = 90% $\Xi_c(2645)^0$ full width $\Gamma < 5.5$ MeV, CL = 90% $\Xi_c \pi$ is the only strong decay allowed to a Ξ_c resonance having this mass.

$\Xi_c(2645)$ DECAY MODES	Fraction (Γ_i/Γ)	p (MeV/c)
$\Xi_c^0 \pi^+$	seen	103
$\Xi_c^+ \pi^-$	seen	107

 $\Xi_c(2815)$

$I(J^P) = \frac{1}{2}(\frac{3}{2}^-)$

 J^P has not been measured; $\frac{3}{2}^-$ is the quark-model prediction. $\Xi_c(2815)^+$ mass $m = 2814.9 \pm 1.8$ MeV $\Xi_c(2815)^0$ mass $m = 2819.0 \pm 2.5$ MeV $m_{\Xi_c(2815)^+} - m_{\Xi_c^+} = 348.6 \pm 1.2$ MeV $m_{\Xi_c(2815)^0} - m_{\Xi_c^0} = 347.2 \pm 2.1$ MeV $\Xi_c(2815)^+$ full width $\Gamma < 3.5$ MeV, CL = 90% $\Xi_c(2815)^0$ full width $\Gamma < 6.5$ MeV, CL = 90%The $\Xi_c \pi \pi$ modes are consistent with being entirely via $\Xi_c(2645)\pi$.

$\Xi_c(2815)$ DECAY MODES	Fraction (Γ_i/Γ)	p (MeV/c)
$\Xi_c^+ \pi^+ \pi^-$	seen	196
$\Xi_c^0 \pi^+ \pi^-$	seen	193

 Ω_c^0

$I(J^P) = 0(\frac{1}{2}^+)$

 J^P has not been measured; $\frac{1}{2}^+$ is the quark-model prediction.Mass $m = 2704 \pm 4$ MeV ($S = 1.8$)Mean life $\tau = (0.064 \pm 0.020) \times 10^{-12}$ s $c\tau = 19$ μm

Ω_c^0 DECAY MODES	Fraction (Γ_i/Γ)	p (MeV/c)
$\Sigma^+ K^- K^- \pi^+$	seen	697
$\Xi^- K^- \pi^+ \pi^+$	seen	838
$\Omega^- \pi^+$	seen	827
$\Omega^- \pi^- \pi^+ \pi^+$	seen	759

Baryon Summary Table

BOTTOM BARYONS

($B = -1$)

$$\Lambda_b^0 = udb, \Xi_b^0 = usb, \Xi_b^- = dsb$$

Λ_b^0

$$I(J^P) = 0(\frac{1}{2}^+)$$

$I(J^P)$ not yet measured; $0(\frac{1}{2}^+)$ is the quark model prediction.

$$\text{Mass } m = 5624 \pm 9 \text{ MeV} \quad (S = 1.8)$$

$$\text{Mean life } \tau = (1.229 \pm 0.080) \times 10^{-12} \text{ s}$$

$$c\tau = 368 \text{ } \mu\text{m}$$

These branching fractions are actually an average over weakly decaying b -baryons weighted by their production rates in Z decay (or high-energy $p\bar{p}$), branching ratios, and detection efficiencies. They scale with the LEP b -baryon production fraction $B(b \rightarrow b\text{-baryon})$ and are evaluated for our value $B(b \rightarrow b\text{-baryon}) = (11.6 \pm 2.0)\%$.

The branching fractions $B(b\text{-baryon} \rightarrow \Lambda\ell^- \bar{\nu}_\ell \text{ anything})$ and $B(\Lambda_b^0 \rightarrow \Lambda_c^+ \ell^- \bar{\nu}_\ell \text{ anything})$ are not pure measurements because the underlying measured products of these with $B(b \rightarrow b\text{-baryon})$ were used to determine $B(b \rightarrow b\text{-baryon})$, as described in the note "Production and Decay of b -Flavored Hadrons."

Λ_b^0 DECAY MODES	Fraction (Γ_i/Γ)	Confidence level	p (MeV/c)
$J/\psi(1S)\Lambda$	$(4.7 \pm 2.8) \times 10^{-4}$		1744
$\Lambda_c^+ \pi^-$	seen		2345
$\Lambda_c^+ \pi_1(1260)^-$	seen		2156
$\Lambda_c^+ \ell^- \bar{\nu}_\ell \text{ anything}$	[r] $(7.9 \pm 1.9)\%$		—
$p\pi^-$	$< 5.0 \times 10^{-5}$	90%	2732
pK^-	$< 5.0 \times 10^{-5}$	90%	2711

b -baryon ADMIXTURE ($\Lambda_b, \Xi_b, \Sigma_b, \Omega_b$)

$$\text{Mean life } \tau = (1.208 \pm 0.051) \times 10^{-12} \text{ s}$$

These branching fractions are actually an average over weakly decaying b -baryons weighted by their production rates in Z decay (or high-energy $p\bar{p}$), branching ratios, and detection efficiencies. They scale with the LEP b -baryon production fraction $B(b \rightarrow b\text{-baryon})$ and are evaluated for our value $B(b \rightarrow b\text{-baryon}) = (11.6 \pm 2.0)\%$.

The branching fractions $B(b\text{-baryon} \rightarrow \Lambda\ell^- \bar{\nu}_\ell \text{ anything})$ and $B(\Lambda_b^0 \rightarrow \Lambda_c^+ \ell^- \bar{\nu}_\ell \text{ anything})$ are not pure measurements because the underlying measured products of these with $B(b \rightarrow b\text{-baryon})$ were used to determine $B(b \rightarrow b\text{-baryon})$, as described in the note "Production and Decay of b -Flavored Hadrons."

b -baryon ADMIXTURE ($\Lambda_b, \Xi_b, \Sigma_b, \Omega_b$)	Fraction (Γ_i/Γ)	p (MeV/c)
$p\mu^- \bar{\nu}$ anything	$(4.2 \pm 1.8)\%$	—
$p\ell \bar{\nu}_\ell$ anything	$(4.1 \pm 1.0)\%$	—
p anything	$(51 \pm 17)\%$	—
$\Lambda\ell^- \bar{\nu}_\ell$ anything	$(2.7 \pm 0.8)\%$	—
$\Lambda/\bar{\Lambda}$ anything	$(28 \pm 7)\%$	—
$\Xi^- \ell^- \bar{\nu}_\ell$ anything	$(4.8 \pm 1.3) \times 10^{-3}$	—

NOTES

This Summary Table only includes established baryons. The Particle Listings include evidence for other baryons. The masses, widths, and branching fractions for the resonances in this Table are Breit-Wigner parameters, but pole positions are also given for most of the N and Δ resonances.

For most of the resonances, the parameters come from various partial-wave analyses of more or less the same sets of data, and it is not appropriate to treat the results of the analyses as independent or to average them together. Furthermore, the systematic errors on the results are not well understood. Thus, we usually only give ranges for the parameters. We then also give a best guess for the mass (as part of the name of the resonance) and for the width. The *Note on N and Δ Resonances* and the *Note on Λ and Σ Resonances* in the Particle Listings review the partial-wave analyses.

When a quantity has "($S = \dots$)" to its right, the error on the quantity has been enlarged by the "scale factor" S , defined as $S = \sqrt{\chi^2/(N-1)}$, where N is the number of measurements used in calculating the quantity. We do this when $S > 1$, which often indicates that the measurements are inconsistent. When $S > 1.25$, we also show in the Particle Listings an ideogram of the measurements. For more about S , see the Introduction.

A decay momentum p is given for each decay mode. For a 2-body decay, p is the momentum of each decay product in the rest frame of the decaying particle. For a 3-or-more-body decay, p is the largest momentum any of the products can have in this frame. For any resonance, the *nominal* mass is used in calculating p . A dagger (" \dagger ") in this column indicates that the mode is forbidden when the nominal masses of resonances are used, but is in fact allowed due to the nonzero widths of the resonances.

[a] The masses of the p and n are most precisely known in u (unified atomic mass units). The conversion factor to MeV, $1 u = 931.494013 \pm 0.000037$ MeV, is less well known than are the masses in u .

[b] These two results are not independent, and both use the more precise measurement of $|q_p/m_p|/(q_p/m_p)$.

[c] The limit is from neutrality-of-matter experiments; it assumes $q_n = q_p + q_e$. See also the charge of the neutron.

[d] The first limit is geochemical and independent of decay mode. The second entry, a rough range of limits, assumes the dominant decay modes are among those investigated. For antiprotons the best limit, inferred from the observation of cosmic ray \bar{p} 's is $\tau_{\bar{p}} > 10^7$ yr, the cosmic-ray storage time, but this limit depends on a number of assumptions. The best direct observation of stored antiprotons gives $\tau_{\bar{p}}/B(\bar{p} \rightarrow e^- \gamma) > 7 \times 10^5$ yr.

[e] There is some controversy about whether nuclear physics and model dependence complicate the analysis for bound neutrons (from which the best limit comes). The first limit here is from reactor experiments with free neutrons.

[f] The parameters g_A, g_V , and g_{WM} for semileptonic modes are defined by $\bar{B}_f[\gamma_\lambda(g_V + g_A\gamma_5) + i(g_{WM}/m_{B_i})\sigma_{\lambda\nu}q^\nu]B_i$, and ϕ_{AV} is defined by $g_A/g_V = |g_A/g_V|e^{i\phi_{AV}}$. See the "Note on Baryon Decay Parameters" in the neutron Particle Listings.

[g] Time-reversal invariance requires this to be 0° or 180° .

[h] The decay parameters γ and Δ are calculated from α and ϕ using

$$\gamma = \sqrt{1-\alpha^2} \cos\phi, \quad \tan\Delta = -\frac{1}{\alpha} \sqrt{1-\alpha^2} \sin\phi.$$

See the "Note on Baryon Decay Parameters" in the neutron Particle Listings.

[i] See the Listings for the pion momentum range used in this measurement.

[j] The error given here is only an educated guess. It is larger than the error on the weighted average of the published values.

[k] A theoretical value using QED.

[l] See the "Note on Λ_c^+ Branching Fractions" in the Branching Fractions of the Λ_c^+ Particle Listings.

[m] This branching fraction includes all the decay modes of the final-state resonance.

[n] An ℓ indicates an e or a μ mode, not a sum over these modes.

[o] The value is for the sum of the charge states or particle/antiparticle states indicated.

[p] Assuming isospin conservation, so that the other third is $\Lambda_c^+ \pi^0 \pi^0$.

[q] No absolute branching fractions have been measured. The following are branching *ratios* relative to $\Xi^- \pi^+ \pi^+$.

[r] Not a pure measurement. See note at head of Λ_b^0 Decay Modes.

SEARCHES FOR MONOPOLES, SUPERSYMMETRY, TECHNICOLOR, COMPOSITENESS, etc.

Magnetic Monopole Searches

Isolated supermassive monopole candidate events have not been confirmed. The most sensitive experiments obtain negative results.

Best cosmic-ray supermassive monopole flux limit:
 $< 1.0 \times 10^{-15} \text{ cm}^{-2} \text{sr}^{-1} \text{s}^{-1}$ for $1.1 \times 10^{-4} < \beta < 0.1$

Supersymmetric Particle Searches

Limits are based on the Minimal Supersymmetric Standard Model.

Assumptions include: 1) $\tilde{\chi}_1^0$ (or $\tilde{\gamma}$) is lightest supersymmetric particle; 2) R -parity is conserved; 3) With the exception of \tilde{t} and \tilde{b} , all scalar quarks are assumed to be degenerate in mass and $m_{\tilde{q}_R} = m_{\tilde{q}_L}$. 4) Limits for sleptons refer to the \tilde{L}_R states.

See the Particle Listings for a Note giving details of supersymmetry.

$\tilde{\chi}_i^0$ — neutralinos (mixtures of $\tilde{\gamma}$, \tilde{Z}^0 , and \tilde{H}_i^0)

Mass $m_{\tilde{\chi}_1^0} > 32.5 \text{ GeV}$, CL = 95%

$[\tan\beta > 0.7, m_{\tilde{\chi}_2^0} - m_{\tilde{\chi}_1^0} > 5 \text{ GeV}]$

Mass $m_{\tilde{\chi}_2^0} > 55.9 \text{ GeV}$, CL = 95%

$[\tan\beta > 1.5, m_{\tilde{\chi}_2^0} - m_{\tilde{\chi}_1^0} > 10 \text{ GeV}]$

Mass $m_{\tilde{\chi}_3^0} > 106.6 \text{ GeV}$, CL = 95%

$[\tan\beta > 1.5, m_{\tilde{\chi}_2^0} - m_{\tilde{\chi}_1^0} > 10 \text{ GeV}]$

$\tilde{\chi}_i^\pm$ — charginos (mixtures of \tilde{W}^\pm and \tilde{H}_i^\pm)

Mass $m_{\tilde{\chi}_1^\pm} > 67.7 \text{ GeV}$, CL = 95%

$[\tan\beta > 0.7, m_{\tilde{\chi}_1^\pm} - m_{\tilde{\chi}_1^0} > 3 \text{ GeV}]$

\tilde{e} — scalar electron (selectron)

Mass $m > 87.1 \text{ GeV}$, CL = 95% $[m_{\tilde{e}_R} - m_{\tilde{\chi}_1^0} > 5 \text{ GeV}]$

$\tilde{\mu}$ — scalar muon (smuon)

Mass $m > 82.3 \text{ GeV}$, CL = 95% $[m_{\tilde{\mu}_R} - m_{\tilde{\chi}_1^0} > 3 \text{ GeV}]$

$\tilde{\tau}$ — scalar tau (stau)

Mass $m > 81.0 \text{ GeV}$, CL = 95% $[m_{\tilde{\tau}_R} - m_{\tilde{\chi}_1^0} > 8 \text{ GeV}]$

\tilde{q} — scalar quark (squark)

These limits include the effects of cascade decays, evaluated assuming a fixed value of the parameters μ and $\tan\beta$. The limits are weakly sensitive to these parameters over much of parameter space. Limits assume GUT relations between gaugino masses and the gauge coupling.

Mass $m > 250 \text{ GeV}$, CL = 95% $[\tan\beta = 2, \mu < 0, A = 0]$

\tilde{b} — scalar bottom (sbottom)

Mass m none 40–75 GeV, CL = 95%

$[\tilde{b} \rightarrow b\tilde{\chi}_1^0, \text{ all } \theta_b, m_{\tilde{b}} - m_{\tilde{\chi}_1^0} > 10 \text{ GeV}]$

\tilde{t} — scalar top (stop)

Mass $m > 86.4 \text{ GeV}$, CL = 95%

$[\tilde{t} \rightarrow t\tilde{\chi}_1^0, \text{ all } \theta_t, m_{\tilde{t}} - m_{\tilde{\chi}_1^0} > 5 \text{ GeV}]$

\tilde{g} — gluino

There is some controversy on whether gluinos in a low-mass window ($1 \lesssim m_{\tilde{g}} \lesssim 5 \text{ GeV}$) are excluded or not. See the Supersymmetry Listings for details.

The limits summarised here refer to the high-mass region ($m_{\tilde{g}} \gtrsim 5 \text{ GeV}$), and include the effects of cascade decays, evaluated assuming a fixed value of the parameters μ and $\tan\beta$.

The limits are weakly sensitive to these parameters over much of parameter space. Limits assume GUT relations between gaugino masses and the gauge coupling.

Mass $m > 190 \text{ GeV}$, CL = 95% $[\tan\beta = 2, \mu < 0, A = 0]$

Mass $m > 260 \text{ GeV}$, CL = 95% $[m_{\tilde{g}} = m_{\tilde{g}}, \tan\beta = 2, \mu < 0, A = 0]$

Technicolor

Searches for a color-octet techni- ρ constrain its mass to be greater than 260 to 480 GeV, depending on allowed decay channels. Similar bounds exist on the color-octet techni- ω .

Quark and Lepton Compositeness, Searches for

Scale Limits Λ for Contact Interactions (the lowest dimensional interactions with four fermions)

If the Lagrangian has the form

$$\pm \frac{g^2}{2\Lambda^2} \bar{\psi}_L \gamma_\mu \psi_L \bar{\psi}_L \gamma^\mu \psi_L$$

(with $g^2/4\pi$ set equal to 1), then we define $\Lambda \equiv \Lambda_{LL}^\pm$. For the full definitions and for other forms, see the Note in the Listings on Searches for Quark and Lepton Compositeness in the full Review and the original literature.

$\Lambda_{LL}^+(e e e e) > 3.5 \text{ TeV}$, CL = 95%

$\Lambda_{LL}^-(e e e e) > 3.8 \text{ TeV}$, CL = 95%

$\Lambda_{LL}^+(e e \mu \mu) > 4.5 \text{ TeV}$, CL = 95%

$\Lambda_{LL}^-(e e \mu \mu) > 4.7 \text{ TeV}$, CL = 95%

$\Lambda_{LL}^+(e e \tau \tau) > 3.9 \text{ TeV}$, CL = 95%

$\Lambda_{LL}^-(e e \tau \tau) > 4.0 \text{ TeV}$, CL = 95%

$\Lambda_{LL}^+(l l l l) > 5.3 \text{ TeV}$, CL = 95%

$\Lambda_{LL}^-(l l l l) > 5.5 \text{ TeV}$, CL = 95%

$\Lambda_{LL}^+(e e q q) > 5.4 \text{ TeV}$, CL = 95%

$\Lambda_{LL}^-(e e q q) > 6.2 \text{ TeV}$, CL = 95%

$\Lambda_{LL}^+(e e b b) > 5.6 \text{ TeV}$, CL = 95%

$\Lambda_{LL}^-(e e b b) > 4.9 \text{ TeV}$, CL = 95%

$\Lambda_{LL}^+(\mu \mu q q) > 2.9 \text{ TeV}$, CL = 95%

$\Lambda_{LL}^-(\mu \mu q q) > 4.2 \text{ TeV}$, CL = 95%

$\Lambda_{LR}^\pm(\nu_\mu \nu_e e e) > 3.1 \text{ TeV}$, CL = 90%

$\Lambda_{LL}^+(q q q q) > 2.7 \text{ TeV}$, CL = 95%

$\Lambda_{LL}^-(q q q q) > 2.4 \text{ TeV}$, CL = 95%

$\Lambda_{LL}^+(\nu \nu q q) > 5.0 \text{ TeV}$, CL = 95%

$\Lambda_{LL}^-(\nu \nu q q) > 5.4 \text{ TeV}$, CL = 95%

Searches Summary Table

Excited Leptons

The limits from $\ell^{*+}\ell^{*-}$ do not depend on λ (where λ is the $\ell\ell^*$ transition coupling). The λ -dependent limits assume chiral coupling, except for the third limit for e^* which is for nonchiral coupling. For chiral coupling, this limit corresponds to $\lambda_\gamma = \sqrt{2}$.

$e^{*\pm}$ — excited electron

Mass $m > 90.7$ GeV, CL = 95% (from $e^{*+}e^{*-}$)
 Mass $m =$ none 30–200 GeV, CL = 95% (from $e p \rightarrow e^* X$)
 Mass $m > 91$ GeV, CL = 95% (if $\lambda_Z > 1$)
 Mass $m > 306$ GeV, CL = 95% (if $\lambda_\gamma = 1$)

$\mu^{*\pm}$ — excited muon

Mass $m > 90.7$ GeV, CL = 95% (from $\mu^{*+}\mu^{*-}$)
 Mass $m > 91$ GeV, CL = 95% (if $\lambda_Z > 1$)

$\tau^{*\pm}$ — excited tau

Mass $m > 89.7$ GeV, CL = 95% (from $\tau^{*+}\tau^{*-}$)
 Mass $m > 90$ GeV, CL = 95% (if $\lambda_Z > 0.18$)

ν^* — excited neutrino

Mass $m > 90.0$ GeV, CL = 95% (from $\nu^*\bar{\nu}^*$)
 Mass $m > 91$ GeV, CL = 95% (if $\lambda_Z > 1$)
 Mass $m =$ none 40–96 GeV, CL = 95% (from $e p \rightarrow \nu^* X$)

q^* — excited quark

Mass $m > 45.6$ GeV, CL = 95% (from $q^*\bar{q}^*$)
 Mass $m > 88$ GeV, CL = 95% (if $\lambda_Z > 1$)
 Mass $m > 570$ GeV, CL = 95% ($p\bar{p} \rightarrow q^* X$)

Color Sextet and Octet Particles

Color Sextet Quarks (q_6)

Mass $m > 84$ GeV, CL = 95% (Stable q_6)

Color Octet Charged Leptons (ℓ_8)

Mass $m > 86$ GeV, CL = 95% (Stable ℓ_8)

Color Octet Neutrinos (ν_8)

Mass $m > 110$ GeV, CL = 90% ($\nu_8 \rightarrow \nu g$)

TESTS OF CONSERVATION LAWS

Revised by L. Wolfenstein and T.G. Trippe, May 2000.

In keeping with the current interest in tests of conservation laws, we collect together a Table of experimental limits on all weak and electromagnetic decays, mass differences, and moments, and on a few reactions, whose observation would violate conservation laws. The Table is given only in the full *Review of Particle Physics*, not in the Particle Physics Booklet. For the benefit of Booklet readers, we include the best limits from the Table in the following text. Limits in this text are for CL=90% unless otherwise specified. The Table is in two parts: "Discrete Space-Time Symmetries," *i.e.*, C , P , T , CP , and CPT ; and "Number Conservation Laws," *i.e.*, lepton, baryon, hadronic flavor, and charge conservation. The references for these data can be found in the the Particle Listings in the *Review*. A discussion of these tests follows.

CPT INVARIANCE

General principles of relativistic field theory require invariance under the combined transformation CPT . The simplest tests of CPT invariance are the equality of the masses and lifetimes of a particle and its antiparticle. The best test comes from the limit on the mass difference between K^0 and \bar{K}^0 . Any such difference contributes to the CP -violating parameter ϵ . Assuming CPT invariance, ϕ_ϵ , the phase of ϵ should be very close to 44° . (See the review " CP Violation" in this edition.) In contrast, if the entire source of CP violation in K^0 decays were a $K^0 - \bar{K}^0$ mass difference, ϕ_ϵ would be $44^\circ + 90^\circ$.

Assuming that there is no other source of CPT violation than this mass difference, it is possible to deduce that [1]

$$m_{\bar{K}^0} - m_{K^0} \approx \frac{2(m_{K_L^0} - m_{K_S^0})|\eta|(\frac{2}{3}\phi_{+-} + \frac{1}{3}\phi_{00} - \phi_0)}{\sin\phi_0},$$

where $\phi_0 = 43.5^\circ$ with an uncertainty of less than 0.1° . Using our best values of the CP -violation parameters, we get $|(m_{\bar{K}^0} - m_{K^0})/m_{K^0}| \leq 10^{-18}$ at CL=95%. Limits can also be placed on specific CPT -violating decay amplitudes. Given the small value of $(1 - |\eta_{00}/\eta_{+-}|)$, the value of $\phi_{00} - \phi_{+-}$ provides a measure of CPT violation in $K_L^0 \rightarrow 2\pi$ decay. Results from CERN [1] and Fermilab [2] indicate no CPT -violating effect.

CP AND T INVARIANCE

Given CPT invariance, CP violation and T violation are equivalent. So far most of the evidence for CP or T violation comes from the measurements of η_{+-} , η_{00} , $\eta_{+-\gamma}$, the semileptonic decay charge asymmetry for K_L , and the decay plane asymmetry in $K_L \rightarrow \pi^+\pi^-e^+e^-$, *e.g.*, $|\eta_{+-}| = |A(K_L^0 \rightarrow \pi^+\pi^-)/A(K_S^0 \rightarrow \pi^+\pi^-)| = (2.285 \pm 0.019) \times 10^{-3}$ and $[\Gamma(K_L^0 \rightarrow \pi^-e^+\nu) - \Gamma(K_L^0 \rightarrow \pi^+e^-\bar{\nu})]/[\text{sum}] = (0.333 \pm 0.014)\%$. There is also a measurement from CPLEAR of the difference between the oscillation probabilities of $K^0 \rightarrow \bar{K}^0$ and $\bar{K}^0 \rightarrow K^0$ [3]. In the Standard Model, much larger effects are expected in B decays and the first measurement of the CP -violating parameter $\sin 2\beta$ at Fermilab gives a value of 0.9 ± 0.4 . Other searches for CP or T violation involve effects that are expected to be unobservable in the Standard Model. The most sensitive are probably the searches for an electric dipole moment of the neutron, measured to be $< 6 \times 10^{-26}$ e cm, and the electron $(0.18 \pm 0.16) \times 10^{-26}$ e cm. A nonzero value requires both P and T violation.

CONSERVATION OF LEPTON NUMBERS

Present experimental evidence and the standard electroweak theory are consistent with the absolute conservation of three separate lepton numbers: electron number L_e , muon number L_μ , and tau number L_τ . Searches for violations are of the following types:

a) $\Delta L = 2$ for one type of charged lepton. The best limit comes from the search for neutrinoless double beta decay ($Z, A \rightarrow (Z+2, A) + e^- + e^-$). The best laboratory limit is $t_{1/2} > 1.6 \times 10^{25}$ yr (CL=90%) for ^{76}Ge .

b) Conversion of one charged-lepton type to another. For purely leptonic processes, the best limits are on $\mu \rightarrow e\gamma$ and $\mu \rightarrow 3e$, measured as $\Gamma(\mu \rightarrow e\gamma)/\Gamma(\mu \rightarrow \text{all}) < 1.2 \times 10^{-11}$ and $\Gamma(\mu \rightarrow 3e)/\Gamma(\mu \rightarrow \text{all}) < 1.0 \times 10^{-12}$. For semileptonic processes, the best limit comes from the coherent conversion process in a muonic atom, $\mu^-(Z, A) \rightarrow e^-(Z, A)$, measured as $\Gamma(\mu^- \text{Ti} \rightarrow e^- \text{Ti})/\Gamma(\mu^- \text{Ti} \rightarrow \text{all}) < 4 \times 10^{-12}$. Of special interest is the case in which the hadronic flavor also changes, as in $K_L \rightarrow e\mu$ and $K^+ \rightarrow \pi^+e^-\mu^+$, measured as $\Gamma(K_L \rightarrow e\mu)/\Gamma(K_L \rightarrow \text{all}) < 4.7 \times 10^{-12}$ and $\Gamma(K^+ \rightarrow \pi^+e^-\mu^+)/\Gamma(K^+ \rightarrow \text{all}) < 2.1 \times 10^{-10}$. Limits on the conversion of τ into e or μ are found in τ decay and are much less stringent than those for $\mu \rightarrow e$ conversion, *e.g.*, $\Gamma(\tau \rightarrow \mu\gamma)/\Gamma(\tau \rightarrow \text{all}) < 1.1 \times 10^{-6}$ and $\Gamma(\tau \rightarrow e\gamma)/\Gamma(\tau \rightarrow \text{all}) < 2.7 \times 10^{-6}$.

c) Conversion of one type of charged lepton into another type of charged antilepton. The case most studied is $\mu^- + (Z, A) \rightarrow e^+ + (Z-2, A)$, the strongest limit being $\Gamma(\mu^- \text{Ti} \rightarrow e^+ \text{Ca})/\Gamma(\mu^- \text{Ti} \rightarrow \text{all}) < 3.6 \times 10^{-11}$.

d) Neutrino oscillations. If neutrinos have mass, then it is expected even in the standard electroweak theory that the lepton numbers are not separately conserved, as a consequence of lepton mixing analogous to Cabibbo quark mixing. However, in this case lepton-number-violating processes such as $\mu \rightarrow e\gamma$ are expected to have extremely small probability. For small neutrino masses, the lepton-number violation would be observed first in neutrino oscillations, which have been the subject of extensive experimental searches. For example, searches for $\bar{\nu}_e$ disappearance, which we label as $\bar{\nu}_e \not\rightarrow \bar{\nu}_e$, give measured limits $\Delta(m^2) < 7 \times 10^{-4}$ eV² for $\sin^2(2\theta) = 1$, and $\sin^2(2\theta) < 0.02$ for large $\Delta(m^2)$, where θ is the neutrino mixing angle. Possible evidence for mixing has come from two sources. The deficit in the solar neutrino flux compared with solar model calculations could be explained by oscillations with $\Delta(m^2) \leq 10^{-4}$ eV² causing the disappearance of ν_e . In addition, underground detectors observing neutrinos produced by cosmic rays in the atmosphere have measured a ν_μ/ν_e ratio much less than expected and have also found a factor of 2 deficiency of upward going ν_μ compared to downward. This provides compelling evidence for ν_μ disappearance, for which the most probable explanation is $\nu_\mu \rightarrow \nu_\tau$ oscillations with nearly maximal mixing and $\Delta(m^2)$ of the order 0.001–0.01 eV².

CONSERVATION OF HADRONIC FLAVORS

In strong and electromagnetic interactions, hadronic flavor is conserved, *i.e.* the conversion of a quark of one flavor (d, u, s, c, b, t) into a quark of another flavor is forbidden. In the Standard Model, the weak interactions violate these conservation laws in a manner described by the Cabibbo-Kobayashi-Maskawa mixing (see the section "Cabibbo-Kobayashi-Maskawa Mixing Matrix"). The way in which these conservation laws are violated is tested as follows:

Tests of Conservation Laws

a) $\Delta S = \Delta Q$ rule. In the strangeness-changing semileptonic decay of strange particles, the strangeness change equals the change in charge of the hadrons. Tests come from limits on decay rates such as $\Gamma(\Sigma^+ \rightarrow ne^+\nu)/\Gamma(\Sigma^+ \rightarrow \text{all}) < 5 \times 10^{-6}$, and from a detailed analysis of $K_L \rightarrow \pi e \nu$, which yields the parameter x , measured to be $(\text{Re } x, \text{Im } x) = (-0.002 \pm 0.006, -0.0012 \pm 0.0019)$. Corresponding rules are $\Delta C = \Delta Q$ and $\Delta B = \Delta Q$.

b) **Change of flavor by two units.** In the Standard Model this occurs only in second-order weak interactions. The classic example is $\Delta S = 2$ via $K^0 - \bar{K}^0$ mixing, which is directly measured by $m(K_S) - m(K_L) = (3.489 \pm 0.008) \times 10^{-12}$ MeV. There is now evidence for $B^0 - \bar{B}^0$ mixing ($\Delta B = 2$), with the corresponding mass difference between the eigenstates ($m_{B_H^0} - m_{B_L^0}$) $= (0.730 \pm 0.029)\Gamma_{B^0} = (3.11 \pm 0.11) \times 10^{-10}$ MeV, and for $B_s^0 - \bar{B}_s^0$ mixing, with $(m_{B_H^0} - m_{B_L^0}) > 16\Gamma_{B_s^0}$ or $> 7 \times 10^{-9}$ MeV (CL=95%). For $D^0 - \bar{D}^0$ mixing $m_{D_H^0} - m_{D_L^0} < 5 \times 10^{-11}$ MeV; the value in the Standard Model is expected to be much smaller than this.

c) **Flavor-changing neutral currents.** In the Standard Model the neutral-current interactions do not change flavor. The low rate $\Gamma(K_L \rightarrow \mu^+\mu^-)/\Gamma(K_L \rightarrow \text{all}) = (7.2 \pm 0.5) \times 10^{-9}$ puts limits on such interactions; the nonzero value for this rate is attributed to a combination of the weak and electromagnetic interactions. The best test should come from $K^+ \rightarrow \pi^+\nu\bar{\nu}$, which occurs in the Standard Model only as a second-order weak process with a branching fraction of $(0.4 \text{ to } 1.2) \times 10^{-10}$. Recent results, including observation of one event, yields $\Gamma(K^+ \rightarrow \pi^+\nu\bar{\nu})/\Gamma(K^+ \rightarrow \text{all}) = (1.5^{+3.4}_{-1.2}) \times 10^{-10}$ [5]. Limits for charm-changing or bottom-changing neutral currents are much less stringent: $\Gamma(D^0 \rightarrow \mu^+\mu^-)/\Gamma(D^0 \rightarrow \text{all}) < 4 \times 10^{-6}$ and $\Gamma(B^0 \rightarrow \mu^+\mu^-)/\Gamma(B^0 \rightarrow \text{all}) < 7 \times 10^{-7}$. One cannot isolate flavor-changing neutral current (FCNC) effects in non leptonic decays. For example, the FCNC transition $s \rightarrow d + (\bar{u} + u)$ is equivalent to the charged-current transition $s \rightarrow u + (\bar{u} + d)$. Tests for FCNC are therefore limited to hadron decays into lepton pairs. Such decays are expected only in second-order in the electroweak coupling in the Standard Model.

References

1. R. Carosi *et al.*, Phys. Lett. **B237**, 303 (1990).
2. M. Karlsson *et al.*, Phys. Rev. Lett. **64**, 2976 (1990); L.K. Gibbons *et al.*, Phys. Rev. Lett. **70**, 1199 (1993).
3. A. Angelopoulos *et al.*, Phys. Lett. **B444**, 43 (1998).
4. B. Schwingerheuer *et al.*, Phys. Rev. Lett. **74**, 4376 (1995).
5. S. Adler *et al.*, Phys. Rev. Lett. **84**, 3768 (2000).

TESTS OF DISCRETE SPACE-TIME SYMMETRIES

CHARGE CONJUGATION (C) INVARIANCE

$\Gamma(\pi^0 \rightarrow 3\gamma)/\Gamma_{\text{total}}$	$< 3.1 \times 10^{-8}$, CL = 90%
η C-nonconserving decay parameters	
$\pi^+\pi^-\pi^0$ left-right asymmetry parameter	$(0.09 \pm 0.17) \times 10^{-2}$
$\pi^+\pi^-\pi^0$ sextant asymmetry parameter	$(0.18 \pm 0.16) \times 10^{-2}$
$\pi^+\pi^-\pi^0$ quadrant asymmetry parameter	$(-0.17 \pm 0.17) \times 10^{-2}$
$\pi^+\pi^-\gamma$ left-right asymmetry parameter	$(0.9 \pm 0.4) \times 10^{-2}$
$\pi^+\pi^-\gamma$ parameter β (D-wave)	0.05 ± 0.06 ($S = 1.5$)
$\Gamma(\eta \rightarrow 3\gamma)/\Gamma_{\text{total}}$	$< 5 \times 10^{-4}$, CL = 95%
$\Gamma(\eta \rightarrow \pi^0 e^+ e^-)/\Gamma_{\text{total}}$	[a] $< 4 \times 10^{-5}$, CL = 90%
$\Gamma(\eta \rightarrow \pi^0 \mu^+ \mu^-)/\Gamma_{\text{total}}$	[a] $< 5 \times 10^{-6}$, CL = 90%
$\Gamma(\omega(782) \rightarrow \eta \pi^0)/\Gamma_{\text{total}}$	$< 1 \times 10^{-3}$, CL = 90%
$\Gamma(\omega(782) \rightarrow 3\pi^0)/\Gamma_{\text{total}}$	$< 3 \times 10^{-4}$, CL = 90%
$\Gamma(\eta'(958) \rightarrow \gamma e^+ e^-)/\Gamma_{\text{total}}$	$< 9 \times 10^{-4}$, CL = 90%
$\Gamma(\eta'(958) \rightarrow \pi^0 e^+ e^-)/\Gamma_{\text{total}}$	[a] $< 1.4 \times 10^{-3}$, CL = 90%
$\Gamma(\eta'(958) \rightarrow \eta e^+ e^-)/\Gamma_{\text{total}}$	[a] $< 2.4 \times 10^{-3}$, CL = 90%
$\Gamma(\eta'(958) \rightarrow 3\gamma)/\Gamma_{\text{total}}$	$< 1.0 \times 10^{-4}$, CL = 90%
$\Gamma(\eta'(958) \rightarrow \mu^+ \mu^- \pi^0)/\Gamma_{\text{total}}$	[a] $< 6.0 \times 10^{-5}$, CL = 90%
$\Gamma(\eta'(958) \rightarrow \mu^+ \mu^- \eta)/\Gamma_{\text{total}}$	[a] $< 1.5 \times 10^{-5}$, CL = 90%

PARITY (P) INVARIANCE

e electric dipole moment	$(0.18 \pm 0.16) \times 10^{-26}$ ecm
μ electric dipole moment	$(3.7 \pm 3.4) \times 10^{-19}$ ecm
τ electric dipole moment (d_τ)	> -3.1 and $< 3.1 \times 10^{-16}$ ecm, CL = 95%
$\Gamma(\eta \rightarrow \pi^+\pi^-)/\Gamma_{\text{total}}$	$< 3.3 \times 10^{-4}$, CL = 90%
$\Gamma(\eta \rightarrow \pi^0\pi^0)/\Gamma_{\text{total}}$	$< 4.3 \times 10^{-4}$, CL = 90%
$\Gamma(\eta'(958) \rightarrow \pi^+\pi^-)/\Gamma_{\text{total}}$	$< 2 \times 10^{-2}$, CL = 90%
$\Gamma(\eta'(958) \rightarrow \pi^0\pi^0)/\Gamma_{\text{total}}$	$< 9 \times 10^{-4}$, CL = 90%
p electric dipole moment	$(-4 \pm 6) \times 10^{-23}$ ecm
n electric dipole moment d_n	$< 0.63 \times 10^{-25}$ ecm, CL = 90%
Λ electric dipole moment	$< 1.5 \times 10^{-16}$ ecm, CL = 95%

TIME REVERSAL (T) INVARIANCE

Limits on $e, \mu, \tau, p, n,$ and Λ electric dipole moments under Parity Invariance above are also tests of Time Reversal Invariance.

μ decay parameters	
transverse e^+ polarization normal to plane of μ spin, e^+ momentum	0.007 ± 0.023
α'/A	$(0 \pm 4) \times 10^{-3}$
β'/A	$(2 \pm 6) \times 10^{-3}$
$\text{Im}(\xi)$ in $K_{\mu 3}^\pm$ decay (from transverse μ pol.)	-0.014 ± 0.014
asymmetry A_T in $K^0 - \bar{K}^0$ mixing	$(6.6 \pm 1.6) \times 10^{-3}$
$\text{Im}(\xi)$ in $K_{\mu 3}^0$ decay (from transverse μ pol.)	-0.007 ± 0.026
$n \rightarrow p e^- \nu$ decay parameters	
ϕ_{AV} , phase of g_A relative to g_V	[b] $(180.07 \pm 0.18)^\circ$
triple correlation coefficient D	$(-0.5 \pm 1.4) \times 10^{-3}$
triple correlation coefficient D for $\Sigma^- \rightarrow n e^- \bar{\nu}_e$	0.11 ± 0.10

CP INVARIANCE

$\text{Re}(d_W^{\mu})$	$<0.56 \times 10^{-17}$ ecm, CL = 95%
$\text{Im}(d_W^{\mu})$	$<1.5 \times 10^{-17}$ ecm, CL = 95%
$\Gamma(\eta \rightarrow \pi^+ \pi^-) / \Gamma_{\text{total}}$	$<3.3 \times 10^{-4}$, CL = 90%
$\Gamma(\eta \rightarrow \pi^0 \pi^0) / \Gamma_{\text{total}}$	$<4.3 \times 10^{-4}$, CL = 90%
$\Gamma(\eta'(958) \rightarrow \pi^+ \pi^-) / \Gamma_{\text{total}}$	$<2 \times 10^{-2}$, CL = 90%
$\Gamma(\eta'(958) \rightarrow \pi^0 \pi^0) / \Gamma_{\text{total}}$	$<9 \times 10^{-4}$, CL = 90%
$K^{\pm} \rightarrow \pi^{\pm} \pi^+ \pi^-$ rate difference/average	(0.07 ± 0.12)%
$K^{\pm} \rightarrow \pi^{\pm} \pi^0 \pi^0$ rate difference/average	(0.0 ± 0.6)%
$K^{\pm} \rightarrow \pi^{\pm} \pi^0 \gamma$ rate difference/average	(0.9 ± 3.3)%
$(g_{\pi^+} - g_{\pi^-}) / (g_{\pi^+} + g_{\pi^-})$ for $K^{\pm} \rightarrow \pi^{\pm} \pi^+ \pi^-$	(-0.7 ± 0.5)%
$\text{Im}(\eta_{+-0}) = \text{Im}(A(K_S^0 \rightarrow \pi^+ \pi^- \pi^0, \text{CP-violating}) / A(K_L^0 \rightarrow \pi^+ \pi^- \pi^0))$	-0.002 ± 0.009
$\text{Im}(\eta_{000}) = \text{Im}(A(K_S^0 \rightarrow \pi^0 \pi^0 \pi^0) / A(K_L^0 \rightarrow \pi^0 \pi^0 \pi^0))$	-0.05 ± 0.13
linear coefficient f for $K_L^0 \rightarrow \pi^+ \pi^- \pi^0$	0.0011 ± 0.0008
$ e'_{+-\gamma} / \epsilon$ for $K_L^0 \rightarrow \pi^+ \pi^- \gamma$	<0.3 , CL = 90%
$\Gamma(K_L^0 \rightarrow \pi^0 \mu^+ \mu^-) / \Gamma_{\text{total}}$	[c] $<5.1 \times 10^{-9}$, CL = 90%
$\Gamma(K_L^0 \rightarrow \pi^0 e^+ e^-) / \Gamma_{\text{total}}$	[c] $<4.3 \times 10^{-9}$, CL = 90%
$\Gamma(K_L^0 \rightarrow \pi^0 \nu \bar{\nu}) / \Gamma_{\text{total}}$	[d] $<5.9 \times 10^{-7}$, CL = 90%
$A_{CP}(K^+ K^- \pi^{\pm})$ in $D^{\pm} \rightarrow K^+ K^- \pi^{\pm}$	-0.017 ± 0.027
$A_{CP}(K^{\pm} K^* 0)$ in $D^+ \rightarrow K^+ \bar{K}^* 0, D^- \rightarrow K^- K^* 0$	-0.02 ± 0.05
$A_{CP}(\phi \pi^{\pm})$ in $D^{\pm} \rightarrow \phi \pi^{\pm}$	-0.014 ± 0.033
$A_{CP}(\pi^+ \pi^- \pi^{\pm})$ in $D^{\pm} \rightarrow \pi^+ \pi^- \pi^{\pm}$	-0.02 ± 0.04
$A_{CP}(K^+ K^-)$ in $D^0, \bar{D}^0 \rightarrow K^+ K^-$	0.026 ± 0.035
$A_{CP}(\pi^+ \pi^-)$ in $D^0, \bar{D}^0 \rightarrow \pi^+ \pi^-$	-0.05 ± 0.08
$A_{CP}(K_S^0 \phi)$ in $D^0, \bar{D}^0 \rightarrow K_S^0 \phi$	-0.03 ± 0.09
$A_{CP}(K_S^0 \pi^0)$ in $D^0, \bar{D}^0 \rightarrow K_S^0 \pi^0$	-0.018 ± 0.030
$A_{CP}(K^{\pm} \pi^{\mp})$ in $D^0 \rightarrow K^+ \pi^-, \bar{D}^0 \rightarrow K^- \pi^+$	0.02 ± 0.20
$\text{Re}(\epsilon_{B^0}) / (1 + \epsilon_{B^0} ^2)$	0.002 ± 0.007
Parameters for $B^0 \rightarrow J/\psi K_S^0$	
$\sin(2\beta)$	0.9 ± 0.4
$[\alpha_-(A) + \alpha_+(\bar{A})] / [\alpha_-(A) - \alpha_+(\bar{A})]$	-0.03 ± 0.06
$[\alpha(\Omega^- \rightarrow \Lambda K^-) + \alpha(\bar{\Omega}^+ \rightarrow \bar{\Lambda} K^+)] / 2$	-0.004 ± 0.040

CP VIOLATION OBSERVED

charge asymmetry in K_{L3}^0 decays	
$\delta(\mu) = [\Gamma(\pi^- \mu^+ \nu_{\mu}) - \Gamma(\pi^+ \mu^- \bar{\nu}_{\mu})] / \text{sum}$	(0.304 ± 0.025)%
$\delta(e) = [\Gamma(\pi^- e^+ \nu_e) - \Gamma(\pi^+ e^- \bar{\nu}_e)] / \text{sum}$	(0.333 ± 0.014)%
parameters for $K_L^0 \rightarrow 2\pi$ decay	
$ \eta_{00} = A(K_L^0 \rightarrow 2\pi^0) / A(K_S^0 \rightarrow 2\pi^0) $	(2.262 ± 0.017) × 10 ⁻³
$ \eta_{+-} = A(K_L^0 \rightarrow \pi^+ \pi^-) / A(K_S^0 \rightarrow \pi^+ \pi^-) $	(2.276 ± 0.017) × 10 ⁻³
$\epsilon' / \epsilon \approx \text{Re}(\epsilon' / \epsilon) = (1 - \eta_{00} / \eta_{+-}) / 3$	[e] (2.1 ± 0.5) × 10 ⁻³ (S = 1.6)
ϕ_{+-} , phase of η_{+-}	(43.3 ± 0.5)°
ϕ_{00} , phase of η_{00}	(43.2 ± 1.0)°
CP asymmetry A in $K_L^0 \rightarrow \pi^+ \pi^- e^+ e^-$	(13.6 ± 2.8)%
parameters for $K_L^0 \rightarrow \pi^+ \pi^- \gamma$ decay	
$ \eta_{+-\gamma} = A(K_L^0 \rightarrow \pi^+ \pi^- \gamma, \text{CP violating}) / A(K_S^0 \rightarrow \pi^+ \pi^- \gamma) $	(2.35 ± 0.07) × 10 ⁻³
$\phi_{+-\gamma}$ = phase of $\eta_{+-\gamma}$	(44 ± 4)°
$\Gamma(K_L^0 \rightarrow \pi^+ \pi^-) / \Gamma_{\text{total}}$	(2.056 ± 0.033) × 10 ⁻³
$\Gamma(K_L^0 \rightarrow \pi^0 \pi^0) / \Gamma_{\text{total}}$	(9.27 ± 0.19) × 10 ⁻⁴

CPT INVARIANCE

$(m_{W^+} - m_{W^-}) / m_{\text{average}}$	-0.002 ± 0.007
$(m_{e^+} - m_{e^-}) / m_{\text{average}}$	$<8 \times 10^{-9}$, CL = 90%
$ q_{e^+} + q_{e^-} / e$	$<4 \times 10^{-8}$
$(g_{e^+} - g_{e^-}) / g_{\text{average}}$	(-0.5 ± 2.1) × 10 ⁻¹²
$(\tau_{\mu^+} - \tau_{\mu^-}) / \tau_{\text{average}}$	(2 ± 8) × 10 ⁻⁵
$(g_{\mu^+} - g_{\mu^-}) / g_{\text{average}}$	(-2.6 ± 1.6) × 10 ⁻⁸
$(m_{\pi^+} - m_{\pi^-}) / m_{\text{average}}$	(2 ± 5) × 10 ⁻⁴
$(\tau_{\pi^+} - \tau_{\pi^-}) / \tau_{\text{average}}$	(6 ± 7) × 10 ⁻⁴
$(m_{K^+} - m_{K^-}) / m_{\text{average}}$	(-0.6 ± 1.8) × 10 ⁻⁴
$(\tau_{K^+} - \tau_{K^-}) / \tau_{\text{average}}$	(0.11 ± 0.09)% (S = 1.2)
$K^{\pm} \rightarrow \mu^{\pm} \nu_{\mu}$ rate difference/average	(-0.5 ± 0.4)%
$K^{\pm} \rightarrow \pi^{\pm} \pi^0$ rate difference/average	[f] (0.8 ± 1.2)%
$ m_{K^0} - m_{\bar{K}^0} / m_{\text{average}}$	[g] $<10^{-18}$
CPT-violation parameters in K^0 - \bar{K}^0 mixing	
real part of Δ	(2.9 ± 2.7) × 10 ⁻⁴
imaginary part of Δ	(-0.8 ± 3.1) × 10 ⁻³
phase difference $\phi_{00} - \phi_{+-}$	(-0.1 ± 0.8)°
$ m_{\rho^+} - m_{\rho^0} / m_{\rho}$	[h] $<5 \times 10^{-7}$
$(\frac{q_{\rho^+}}{m_{\rho^+}} - \frac{q_{\rho^0}}{m_{\rho^0}}) / \frac{q_{\rho^0}}{m_{\rho}}$	(-9 ± 9) × 10 ⁻¹¹
$ q_{\rho^+} + q_{\rho^0} / e$	[h] $<5 \times 10^{-7}$
$(\mu_{\rho^+} + \mu_{\rho^0}) / \mu_{\rho}$	(-2.6 ± 2.9) × 10 ⁻³
$(m_{\eta} - m_{\bar{\eta}}) / m_{\eta}$	(9 ± 5) × 10 ⁻⁵
$(m_{\Lambda} - m_{\bar{\Lambda}}) / m_{\Lambda}$	(-0.1 ± 1.1) × 10 ⁻⁵ (S = 1.6)
$(\tau_{\Lambda} - \tau_{\bar{\Lambda}}) / \tau_{\Lambda}$	0.04 ± 0.09
$(\tau_{\Sigma^+} - \tau_{\Sigma^-}) / \tau_{\Sigma^+}$	(-0.6 ± 1.2) × 10 ⁻³
$(\mu_{\Sigma^+} + \mu_{\Sigma^-}) / \mu_{\Sigma^+}$	0.014 ± 0.015
$(m_{\Xi^-} - m_{\Xi^+}) / m_{\Xi^-}$	(1.1 ± 2.7) × 10 ⁻⁴
$(\tau_{\Xi^-} - \tau_{\Xi^+}) / \tau_{\Xi^-}$	0.02 ± 0.18
$(\mu_{\Xi^-} + \mu_{\Xi^+}) / \mu_{\Xi^-}$	+0.01 ± 0.05
$(m_{\Omega^-} - m_{\bar{\Omega}^+}) / m_{\Omega^-}$	(-1 ± 8) × 10 ⁻⁵
$(\tau_{\Omega^-} - \tau_{\bar{\Omega}^+}) / \tau_{\Omega^-}$	-0.002 ± 0.040

TESTS OF NUMBER CONSERVATION LAWS

LEPTON FAMILY NUMBER

Lepton family number conservation means separate conservation of each of L_e, L_{μ}, L_{τ} .

$\Gamma(Z \rightarrow e^{\pm} \mu^{\mp}) / \Gamma_{\text{total}}$	[j] $<1.7 \times 10^{-6}$, CL = 95%
$\Gamma(Z \rightarrow e^{\pm} \tau^{\mp}) / \Gamma_{\text{total}}$	[j] $<9.8 \times 10^{-6}$, CL = 95%
$\Gamma(Z \rightarrow \mu^{\pm} \tau^{\mp}) / \Gamma_{\text{total}}$	[j] $<1.2 \times 10^{-5}$, CL = 95%
limit on $\mu^- \rightarrow e^-$ conversion	
$\sigma(\mu^- 32S \rightarrow e^- 32S) / \sigma(\mu^- 32S \rightarrow \nu_{\mu} 32P^*)$	$<7 \times 10^{-11}$, CL = 90%
$\sigma(\mu^- \text{Ti} \rightarrow e^- \text{Ti}) / \sigma(\mu^- \text{Ti} \rightarrow \text{capture})$	$<4.3 \times 10^{-12}$, CL = 90%
$\sigma(\mu^- \text{Pb} \rightarrow e^- \text{Pb}) / \sigma(\mu^- \text{Pb} \rightarrow \text{capture})$	$<4.6 \times 10^{-11}$, CL = 90%
limit on muonium \rightarrow antimuonium conversion $R_g = G_C / G_F$	<0.0030 , CL = 90%
$\Gamma(\mu^- \rightarrow e^- \nu_e \bar{\nu}_{\mu}) / \Gamma_{\text{total}}$	[j] $<1.2 \times 10^{-2}$, CL = 90%
$\Gamma(\mu^- \rightarrow e^- \gamma) / \Gamma_{\text{total}}$	$<1.2 \times 10^{-11}$, CL = 90%
$\Gamma(\mu^- \rightarrow e^- e^+ e^-) / \Gamma_{\text{total}}$	$<1.0 \times 10^{-12}$, CL = 90%
$\Gamma(\mu^- \rightarrow e^- 2\gamma) / \Gamma_{\text{total}}$	$<7.2 \times 10^{-11}$, CL = 90%
$\Gamma(\tau^- \rightarrow e^- \gamma) / \Gamma_{\text{total}}$	$<2.7 \times 10^{-6}$, CL = 90%
$\Gamma(\tau^- \rightarrow \mu^- \gamma) / \Gamma_{\text{total}}$	$<1.1 \times 10^{-6}$, CL = 90%
$\Gamma(\tau^- \rightarrow e^- \pi^0) / \Gamma_{\text{total}}$	$<3.7 \times 10^{-6}$, CL = 90%
$\Gamma(\tau^- \rightarrow \mu^- \pi^0) / \Gamma_{\text{total}}$	$<4.0 \times 10^{-6}$, CL = 90%
$\Gamma(\tau^- \rightarrow e^- K^0) / \Gamma_{\text{total}}$	$<1.3 \times 10^{-3}$, CL = 90%
$\Gamma(\tau^- \rightarrow \mu^- K^0) / \Gamma_{\text{total}}$	$<1.0 \times 10^{-3}$, CL = 90%
$\Gamma(\tau^- \rightarrow e^- \eta) / \Gamma_{\text{total}}$	$<8.2 \times 10^{-6}$, CL = 90%
$\Gamma(\tau^- \rightarrow \mu^- \eta) / \Gamma_{\text{total}}$	$<9.6 \times 10^{-6}$, CL = 90%
$\Gamma(\tau^- \rightarrow e^- \rho^0) / \Gamma_{\text{total}}$	$<2.0 \times 10^{-6}$, CL = 90%

Tests of Conservation Laws

$\Gamma(\tau^- \rightarrow \mu^- \rho^0)/\Gamma_{\text{total}}$	$<6.3 \times 10^{-6}$, CL = 90%
$\Gamma(\tau^- \rightarrow e^- K^*(892)^0)/\Gamma_{\text{total}}$	$<5.1 \times 10^{-6}$, CL = 90%
$\Gamma(\tau^- \rightarrow \mu^- K^*(892)^0)/\Gamma_{\text{total}}$	$<7.5 \times 10^{-6}$, CL = 90%
$\Gamma(\tau^- \rightarrow e^- \bar{K}^*(892)^0)/\Gamma_{\text{total}}$	$<7.4 \times 10^{-6}$, CL = 90%
$\Gamma(\tau^- \rightarrow \mu^- \bar{K}^*(892)^0)/\Gamma_{\text{total}}$	$<7.5 \times 10^{-6}$, CL = 90%
$\Gamma(\tau^- \rightarrow e^- \phi)/\Gamma_{\text{total}}$	$<6.9 \times 10^{-6}$, CL = 90%
$\Gamma(\tau^- \rightarrow \mu^- \phi)/\Gamma_{\text{total}}$	$<7.0 \times 10^{-6}$, CL = 90%
$\Gamma(\tau^- \rightarrow e^- e^+ e^-)/\Gamma_{\text{total}}$	$<2.9 \times 10^{-6}$, CL = 90%
$\Gamma(\tau^- \rightarrow e^- \mu^+ \mu^-)/\Gamma_{\text{total}}$	$<1.8 \times 10^{-6}$, CL = 90%
$\Gamma(\tau^- \rightarrow e^+ \mu^- \mu^-)/\Gamma_{\text{total}}$	$<1.5 \times 10^{-6}$, CL = 90%
$\Gamma(\tau^- \rightarrow \mu^- e^+ e^-)/\Gamma_{\text{total}}$	$<1.7 \times 10^{-6}$, CL = 90%
$\Gamma(\tau^- \rightarrow \mu^+ e^- e^-)/\Gamma_{\text{total}}$	$<1.5 \times 10^{-6}$, CL = 90%
$\Gamma(\tau^- \rightarrow \mu^- \mu^+ \mu^-)/\Gamma_{\text{total}}$	$<1.9 \times 10^{-6}$, CL = 90%
$\Gamma(\tau^- \rightarrow e^- \pi^+ \pi^-)/\Gamma_{\text{total}}$	$<2.2 \times 10^{-6}$, CL = 90%
$\Gamma(\tau^- \rightarrow \mu^- \pi^+ \pi^-)/\Gamma_{\text{total}}$	$<8.2 \times 10^{-6}$, CL = 90%
$\Gamma(\tau^- \rightarrow e^- \pi^+ K^-)/\Gamma_{\text{total}}$	$<6.4 \times 10^{-6}$, CL = 90%
$\Gamma(\tau^- \rightarrow e^- \pi^- K^+)/\Gamma_{\text{total}}$	$<3.8 \times 10^{-6}$, CL = 90%
$\Gamma(\tau^- \rightarrow e^- K^+ K^-)/\Gamma_{\text{total}}$	$<6.0 \times 10^{-6}$, CL = 90%
$\Gamma(\tau^- \rightarrow \mu^- \pi^- K^+)/\Gamma_{\text{total}}$	$<7.4 \times 10^{-6}$, CL = 90%
$\Gamma(\tau^- \rightarrow \mu^- K^+ K^-)/\Gamma_{\text{total}}$	$<1.5 \times 10^{-5}$, CL = 90%
$\Gamma(\tau^- \rightarrow e^- \pi^0 \pi^0)/\Gamma_{\text{total}}$	$<6.5 \times 10^{-6}$, CL = 90%
$\Gamma(\tau^- \rightarrow \mu^- \pi^0 \pi^0)/\Gamma_{\text{total}}$	$<1.4 \times 10^{-5}$, CL = 90%
$\Gamma(\tau^- \rightarrow e^- \eta)/\Gamma_{\text{total}}$	$<3.5 \times 10^{-5}$, CL = 90%
$\Gamma(\tau^- \rightarrow \mu^- \eta)/\Gamma_{\text{total}}$	$<6.0 \times 10^{-5}$, CL = 90%
$\Gamma(\tau^- \rightarrow e^- \pi^0 \eta)/\Gamma_{\text{total}}$	$<2.4 \times 10^{-5}$, CL = 90%
$\Gamma(\tau^- \rightarrow \mu^- \pi^0 \eta)/\Gamma_{\text{total}}$	$<2.2 \times 10^{-5}$, CL = 90%
$\Gamma(\tau^- \rightarrow e^- \text{light boson})/\Gamma_{\text{total}}$	$<2.7 \times 10^{-3}$, CL = 95%
$\Gamma(\tau^- \rightarrow \mu^- \text{light boson})/\Gamma_{\text{total}}$	$<5 \times 10^{-3}$, CL = 95%
ν -flavor nonconservation via mixing from reactor and accelerator experiments . (For other lepton mixing, see the Particle Listings. In particular, there is now compelling evidence from SuperKamioyande for the disappearance of ν_μ , for which the most probable interpretation is ν_μ - ν_τ mixing with $\Delta m^2 = 0.001$ - 0.01 eV ² and $\sin^2 2\theta \approx 1$.)	
$\bar{\nu}_e \not\leftrightarrow \bar{\nu}_e$	
$\Delta(m^2)$ for $\sin^2(2\theta) = 1$	$<7 \times 10^{-4}$ eV ² , CL = 90%
$\sin^2(2\theta)$ for "Large" $\Delta(m^2)$	<0.02 , CL = 90%
$\nu_e \rightarrow \nu_\tau$	
$\Delta(m^2)$ for $\sin^2(2\theta) = 1$	<0.77 eV ² , CL = 90%
$\sin^2(2\theta)$ for "Large" $\Delta(m^2)$	<0.21 , CL = 90%
$\bar{\nu}_e \rightarrow \bar{\nu}_\tau$	
$\sin^2(2\theta)$ for "Large" $\Delta(m^2)$	<0.7 , CL = 90%
$\nu_\mu \rightarrow \nu_e$	
$\Delta(m^2)$ for $\sin^2(2\theta) = 1$	<0.09 eV ² , CL = 90%
$\sin^2(2\theta)$ for "Large" $\Delta(m^2)$	$<3.0 \times 10^{-3}$, CL = 90%
$\bar{\nu}_\mu \rightarrow \bar{\nu}_e$	
$\Delta(m^2)$ for $\sin^2(2\theta) = 1$	<0.14 eV ² , CL = 90%
$\sin^2(2\theta)$ for "Large" $\Delta(m^2)$	<0.004 , CL = 95%
$\nu_\mu(\bar{\nu}_\mu) \rightarrow \nu_e(\bar{\nu}_e)$	
$\Delta(m^2)$ for $\sin^2(2\theta) = 1$	<0.075 eV ² , CL = 90%
$\sin^2(2\theta)$ for "Large" $\Delta(m^2)$	$<1.8 \times 10^{-3}$, CL = 90%
$\nu_\mu \rightarrow \nu_\tau$	
$\Delta(m^2)$ for $\sin^2(2\theta) = 1$	<1.1 eV ² , CL = 90%
$\sin^2(2\theta)$ for "Large" $\Delta(m^2)$	<0.0012 , CL = 90%
$\bar{\nu}_\mu \rightarrow \bar{\nu}_\tau$	
$\Delta(m^2)$ for $\sin^2(2\theta) = 1$	<2.2 eV ² , CL = 90%
$\sin^2(2\theta)$ for "Large" $\Delta(m^2)$	$<4.4 \times 10^{-2}$, CL = 90%
$\nu_\mu(\bar{\nu}_\mu) \rightarrow \nu_\tau(\bar{\nu}_\tau)$	
$\Delta(m^2)$ for $\sin^2(2\theta) = 1$	<1.5 eV ² , CL = 90%
$\sin^2(2\theta)$ for "Large" $\Delta(m^2)$	$<8 \times 10^{-3}$, CL = 90%
$\nu_e \not\leftrightarrow \nu_e$	
$\Delta(m^2)$ for $\sin^2(2\theta) = 1$	<0.18 eV ² , CL = 90%
$\sin^2(2\theta)$ for "Large" $\Delta(m^2)$	$<7 \times 10^{-2}$, CL = 90%
$\nu_\mu \not\leftrightarrow \nu_\mu$	
$\Delta(m^2)$ for $\sin^2(2\theta) = 1$	<0.23 or >1500 eV ²
$\sin^2(2\theta)$ for $\Delta(m^2) = 100$ eV ²	[k] <0.02 , CL = 90%
$\bar{\nu}_\mu \not\leftrightarrow \bar{\nu}_\mu$	
$\Delta(m^2)$ for $\sin^2(2\theta) = 1$	<7 or >1200 eV ²
$\sin^2(2\theta)$ for 190 eV ² $< \Delta(m^2) < 320$ eV ²	[l] <0.02 , CL = 90%
$\Gamma(\pi^+ \rightarrow \mu^+ \nu_e)/\Gamma_{\text{total}}$	[m] $<8.0 \times 10^{-3}$, CL = 90%
$\Gamma(\pi^+ \rightarrow \mu^- e^+ e^+)/\Gamma_{\text{total}}$	$<1.6 \times 10^{-6}$, CL = 90%
$\Gamma(\pi^0 \rightarrow \mu^+ e^- + e^- \mu^+)/\Gamma_{\text{total}}$	$<1.72 \times 10^{-8}$, CL = 90%
$\Gamma(\eta \rightarrow \mu^+ e^- + \mu^- e^+)/\Gamma_{\text{total}}$	$<6 \times 10^{-6}$, CL = 90%

$\Gamma(\eta(958) \rightarrow e\mu)/\Gamma_{\text{total}}$	$<4.7 \times 10^{-4}$, CL = 90%
$\Gamma(K^+ \rightarrow \mu^- \nu e^+)/\Gamma_{\text{total}}$	$<2.0 \times 10^{-8}$, CL = 90%
$\Gamma(K^+ \rightarrow \mu^+ \nu_e)/\Gamma_{\text{total}}$	[m] $<4 \times 10^{-3}$, CL = 90%
$\Gamma(K^+ \rightarrow \pi^+ \mu^+ e^-)/\Gamma_{\text{total}}$	$<2.1 \times 10^{-10}$, CL = 90%
$\Gamma(K^+ \rightarrow \pi^+ \mu^- e^+)/\Gamma_{\text{total}}$	$<7 \times 10^{-9}$, CL = 90%
$\Gamma(K_L^0 \rightarrow e^\pm \mu^\mp)/\Gamma_{\text{total}}$	[l] $<4.7 \times 10^{-12}$, CL = 90%
$\Gamma(K_L^0 \rightarrow e^\pm e^\pm \mu^\mp \mu^\mp)/\Gamma_{\text{total}}$	[l] $<6.1 \times 10^{-9}$, CL = 90%
$\Gamma(K_L^0 \rightarrow \pi^0 \mu^\pm e^\mp)/\Gamma_{\text{total}}$	[l] $<6.2 \times 10^{-9}$, CL = 90%
$\Gamma(D^+ \rightarrow \pi^+ e^\pm \mu^\mp)/\Gamma_{\text{total}}$	[l] $<3.4 \times 10^{-5}$, CL = 90%
$\Gamma(D^+ \rightarrow K^+ e^\pm \mu^\mp)/\Gamma_{\text{total}}$	[l] $<6.8 \times 10^{-5}$, CL = 90%
$\Gamma(D^0 \rightarrow \mu^\pm e^\mp)/\Gamma_{\text{total}}$	[l] $<8.1 \times 10^{-6}$, CL = 90%
$\Gamma(D^0 \rightarrow \pi^0 e^\pm \mu^\mp)/\Gamma_{\text{total}}$	[l] $<8.6 \times 10^{-5}$, CL = 90%
$\Gamma(D^0 \rightarrow \eta e^\pm \mu^\mp)/\Gamma_{\text{total}}$	[l] $<1.0 \times 10^{-4}$, CL = 90%
$\Gamma(D^0 \rightarrow \rho^0 e^\pm \mu^\mp)/\Gamma_{\text{total}}$	[l] $<4.9 \times 10^{-5}$, CL = 90%
$\Gamma(D^0 \rightarrow \omega e^\pm \mu^\mp)/\Gamma_{\text{total}}$	[l] $<1.2 \times 10^{-4}$, CL = 90%
$\Gamma(D^0 \rightarrow \phi e^\pm \mu^\mp)/\Gamma_{\text{total}}$	[l] $<3.4 \times 10^{-5}$, CL = 90%
$\Gamma(D^0 \rightarrow \bar{K}^0 e^\pm \mu^\mp)/\Gamma_{\text{total}}$	[l] $<1.0 \times 10^{-4}$, CL = 90%
$\Gamma(D^0 \rightarrow \bar{K}^*(892)^0 e^\pm \mu^\mp)/\Gamma_{\text{total}}$	[l] $<1.0 \times 10^{-4}$, CL = 90%
$\Gamma(D_S^+ \rightarrow \pi^+ e^\pm \mu^\mp)/\Gamma_{\text{total}}$	[l] $<6.1 \times 10^{-4}$, CL = 90%
$\Gamma(D_S^+ \rightarrow K^+ e^\pm \mu^\mp)/\Gamma_{\text{total}}$	[l] $<6.3 \times 10^{-4}$, CL = 90%
$\Gamma(B^+ \rightarrow \pi^+ e^+ \mu^-)/\Gamma_{\text{total}}$	$<6.4 \times 10^{-3}$, CL = 90%
$\Gamma(B^+ \rightarrow \pi^+ e^- \mu^+)/\Gamma_{\text{total}}$	$<6.4 \times 10^{-3}$, CL = 90%
$\Gamma(B^+ \rightarrow K^+ e^+ \mu^-)/\Gamma_{\text{total}}$	$<6.4 \times 10^{-3}$, CL = 90%
$\Gamma(B^+ \rightarrow K^+ e^- \mu^+)/\Gamma_{\text{total}}$	$<6.4 \times 10^{-3}$, CL = 90%
$\Gamma(B^+ \rightarrow \pi^- e^+ \mu^+)/\Gamma_{\text{total}}$	$<6.4 \times 10^{-3}$, CL = 90%
$\Gamma(B^+ \rightarrow K^- e^+ \mu^+)/\Gamma_{\text{total}}$	$<6.4 \times 10^{-3}$, CL = 90%
$\Gamma(B^0 \rightarrow e^\pm \mu^\mp)/\Gamma_{\text{total}}$	[l] $<3.5 \times 10^{-6}$, CL = 90%
$\Gamma(B^0 \rightarrow e^\pm \tau^\mp)/\Gamma_{\text{total}}$	[l] $<5.3 \times 10^{-4}$, CL = 90%
$\Gamma(B^0 \rightarrow \mu^\pm \tau^\mp)/\Gamma_{\text{total}}$	[l] $<8.3 \times 10^{-4}$, CL = 90%
$\Gamma(B \rightarrow e^\pm \mu^\mp s)/\Gamma_{\text{total}}$	$<2.2 \times 10^{-5}$, CL = 90%
$\Gamma(B_S^0 \rightarrow e^\pm \mu^\mp)/\Gamma_{\text{total}}$	[l] $<6.1 \times 10^{-6}$, CL = 90%

TOTAL LEPTON NUMBER

Violation of total lepton number conservation also implies violation of lepton family number conservation.

$\Gamma(Z \rightarrow \nu e)/\Gamma_{\text{total}}$	$<1.8 \times 10^{-6}$, CL = 95%
$\Gamma(Z \rightarrow \nu \mu)/\Gamma_{\text{total}}$	$<1.8 \times 10^{-6}$, CL = 95%
limit on $\mu^- \rightarrow e^+$ conversion	
$\sigma(\mu^- 32S \rightarrow e^+ 32Si^*) / \sigma(\mu^- 32S \rightarrow \nu_\mu 32P^*)$	$<9 \times 10^{-10}$, CL = 90%
$\sigma(\mu^- 127I \rightarrow e^+ 127Sb^*) / \sigma(\mu^- 127I \rightarrow \text{anything})$	$<3 \times 10^{-10}$, CL = 90%
$\sigma(\mu^- \text{Ti} \rightarrow e^+ \text{Ca}) / \sigma(\mu^- \text{Ti} \rightarrow \text{capture})$	$<3.6 \times 10^{-11}$, CL = 90%
$\Gamma(\tau^- \rightarrow \pi^- \eta)/\Gamma_{\text{total}}$	$<2.8 \times 10^{-4}$, CL = 90%
$\Gamma(\tau^- \rightarrow \pi^- \pi^0)/\Gamma_{\text{total}}$	$<3.7 \times 10^{-4}$, CL = 90%
$\Gamma(\tau^- \rightarrow e^+ \pi^- \pi^-)/\Gamma_{\text{total}}$	$<1.9 \times 10^{-6}$, CL = 90%
$\Gamma(\tau^- \rightarrow \mu^+ \pi^- \pi^-)/\Gamma_{\text{total}}$	$<3.4 \times 10^{-6}$, CL = 90%
$\Gamma(\tau^- \rightarrow e^+ \pi^- K^-)/\Gamma_{\text{total}}$	$<2.1 \times 10^{-6}$, CL = 90%
$\Gamma(\tau^- \rightarrow e^+ K^- K^-)/\Gamma_{\text{total}}$	$<3.8 \times 10^{-6}$, CL = 90%
$\Gamma(\tau^- \rightarrow \mu^+ \pi^- K^-)/\Gamma_{\text{total}}$	$<7.0 \times 10^{-6}$, CL = 90%
$\Gamma(\tau^- \rightarrow \mu^+ K^- K^-)/\Gamma_{\text{total}}$	$<6.0 \times 10^{-6}$, CL = 90%
$\Gamma(\tau^- \rightarrow \bar{p} \gamma)/\Gamma_{\text{total}}$	$<3.5 \times 10^{-6}$, CL = 90%
$\Gamma(\tau^- \rightarrow \bar{p} \pi^0)/\Gamma_{\text{total}}$	$<1.5 \times 10^{-5}$, CL = 90%
$\Gamma(\tau^- \rightarrow \bar{p} 2\pi^0)/\Gamma_{\text{total}}$	$<3.3 \times 10^{-5}$, CL = 90%
$\Gamma(\tau^- \rightarrow \bar{p} \eta)/\Gamma_{\text{total}}$	$<8.9 \times 10^{-6}$, CL = 90%
$\Gamma(\tau^- \rightarrow \bar{p} \pi^0 \eta)/\Gamma_{\text{total}}$	$<2.7 \times 10^{-5}$, CL = 90%
$\nu_e \rightarrow (\bar{\nu}_e)_L$	
$\alpha \Delta(m^2)$ for $\sin^2(2\theta) = 1$	<0.14 eV ² , CL = 90%
$\alpha^2 \sin^2(2\theta)$ for "Large" $\Delta(m^2)$	<0.032 , CL = 90%
$\nu_\mu \rightarrow (\bar{\nu}_\mu)_L$	
$\alpha \Delta(m^2)$ for $\sin^2(2\theta) = 1$	<0.16 eV ² , CL = 90%
$\alpha^2 \sin^2(2\theta)$ for "Large" $\Delta(m^2)$	<0.001 , CL = 90%
$\Gamma(\pi^+ \rightarrow \mu^+ \bar{\nu}_e)/\Gamma_{\text{total}}$	[m] $<1.5 \times 10^{-3}$, CL = 90%
$\Gamma(K^+ \rightarrow \pi^- \mu^+ e^+)/\Gamma_{\text{total}}$	$<7 \times 10^{-9}$, CL = 90%
$\Gamma(K^+ \rightarrow \pi^- e^+ e^+)/\Gamma_{\text{total}}$	$<1.0 \times 10^{-8}$, CL = 90%
$\Gamma(K^+ \rightarrow \pi^- \mu^+ \mu^+)/\Gamma_{\text{total}}$	[m] $<1.5 \times 10^{-4}$, CL = 90%
$\Gamma(K^+ \rightarrow \mu^+ \bar{\nu}_e)/\Gamma_{\text{total}}$	[m] $<3.3 \times 10^{-3}$, CL = 90%
$\Gamma(K^+ \rightarrow \pi^0 e^+ \bar{\nu}_e)/\Gamma_{\text{total}}$	$<3 \times 10^{-3}$, CL = 90%

Unless otherwise stated, limits are given at the 90% confidence level, while errors are given as ± 1 standard deviation.

Tests of Conservation Laws

$\Gamma(D^+ \rightarrow \pi^- e^+ e^+)/\Gamma_{\text{total}}$	$<9.6 \times 10^{-5}$, CL = 90%
$\Gamma(D^+ \rightarrow \pi^- \mu^+ \mu^+)/\Gamma_{\text{total}}$	$<1.7 \times 10^{-5}$, CL = 90%
$\Gamma(D^+ \rightarrow \pi^- e^+ \mu^+)/\Gamma_{\text{total}}$	$<5.0 \times 10^{-5}$, CL = 90%
$\Gamma(D^+ \rightarrow \rho^- \mu^+ \mu^+)/\Gamma_{\text{total}}$	$<5.6 \times 10^{-4}$, CL = 90%
$\Gamma(D^+ \rightarrow K^- e^+ e^+)/\Gamma_{\text{total}}$	$<1.2 \times 10^{-4}$, CL = 90%
$\Gamma(D^+ \rightarrow K^- \mu^+ \mu^+)/\Gamma_{\text{total}}$	$<1.2 \times 10^{-4}$, CL = 90%
$\Gamma(D^+ \rightarrow K^- e^+ \mu^+)/\Gamma_{\text{total}}$	$<1.3 \times 10^{-4}$, CL = 90%
$\Gamma(D^+ \rightarrow K^*(892)^- \mu^+ \mu^+)/\Gamma_{\text{total}}$	$<8.5 \times 10^{-4}$, CL = 90%
$\Gamma(D_S^+ \rightarrow \pi^- e^+ e^+)/\Gamma_{\text{total}}$	$<6.9 \times 10^{-4}$, CL = 90%
$\Gamma(D_S^+ \rightarrow \pi^- \mu^+ \mu^+)/\Gamma_{\text{total}}$	$<8.2 \times 10^{-5}$, CL = 90%
$\Gamma(D_S^+ \rightarrow \pi^- e^+ \mu^+)/\Gamma_{\text{total}}$	$<7.3 \times 10^{-4}$, CL = 90%
$\Gamma(D_S^+ \rightarrow K^- e^+ e^+)/\Gamma_{\text{total}}$	$<6.3 \times 10^{-4}$, CL = 90%
$\Gamma(D_S^+ \rightarrow K^- \mu^+ \mu^+)/\Gamma_{\text{total}}$	$<1.8 \times 10^{-4}$, CL = 90%
$\Gamma(D_S^+ \rightarrow K^- e^+ \mu^+)/\Gamma_{\text{total}}$	$<6.8 \times 10^{-4}$, CL = 90%
$\Gamma(D_S^+ \rightarrow K^*(892)^- \mu^+ \mu^+)/\Gamma_{\text{total}}$	$<1.4 \times 10^{-3}$, CL = 90%
$\Gamma(B^+ \rightarrow \pi^- e^+ e^+)/\Gamma_{\text{total}}$	$<3.9 \times 10^{-3}$, CL = 90%
$\Gamma(B^+ \rightarrow \pi^- \mu^+ \mu^+)/\Gamma_{\text{total}}$	$<9.1 \times 10^{-3}$, CL = 90%
$\Gamma(B^+ \rightarrow K^- e^+ e^+)/\Gamma_{\text{total}}$	$<3.9 \times 10^{-3}$, CL = 90%
$\Gamma(B^+ \rightarrow K^- \mu^+ \mu^+)/\Gamma_{\text{total}}$	$<9.1 \times 10^{-3}$, CL = 90%
$\Gamma(\Xi^- \rightarrow \rho \mu^- \mu^-)/\Gamma_{\text{total}}$	$<4 \times 10^{-4}$, CL = 90%
$\Gamma(\Lambda_C^+ \rightarrow \Sigma^- \mu^+ \mu^+)/\Gamma_{\text{total}}$	$<7.0 \times 10^{-4}$, CL = 90%

BARYON NUMBER

$\Gamma(Z \rightarrow \rho e)/\Gamma_{\text{total}}$	$<1.8 \times 10^{-6}$, CL = 95%
$\Gamma(Z \rightarrow \rho \mu)/\Gamma_{\text{total}}$	$<1.8 \times 10^{-6}$, CL = 95%
$\Gamma(\tau^- \rightarrow \bar{p} \gamma)/\Gamma_{\text{total}}$	$<3.5 \times 10^{-6}$, CL = 90%
$\Gamma(\tau^- \rightarrow \bar{p} \pi^0)/\Gamma_{\text{total}}$	$<1.5 \times 10^{-5}$, CL = 90%
$\Gamma(\tau^- \rightarrow \bar{p} 2\pi^0)/\Gamma_{\text{total}}$	$<3.3 \times 10^{-5}$, CL = 90%
$\Gamma(\tau^- \rightarrow \bar{p} \eta)/\Gamma_{\text{total}}$	$<8.9 \times 10^{-6}$, CL = 90%
$\Gamma(\tau^- \rightarrow \bar{p} \pi^0 \eta)/\Gamma_{\text{total}}$	$<2.7 \times 10^{-5}$, CL = 90%
ρ mean life	$>1.6 \times 10^{25}$ years
A few examples of proton or bound neutron decay follow. For limits on many other nucleon decay channels, see the Baryon Summary Table.	
$\tau(N \rightarrow e^+ \pi)$	$> 158 (n), > 1600 (p) \times 10^{30}$ years, CL = 90%
$\tau(N \rightarrow \mu^+ \pi)$	$> 100 (n), > 473 (p) \times 10^{30}$ years, CL = 90%
$\tau(N \rightarrow e^+ K)$	$> 17 (n), > 150 (p) \times 10^{30}$ years, CL = 90%
$\tau(N \rightarrow \mu^+ K)$	$> 26 (n), > 120 (p) \times 10^{30}$ years, CL = 90%
limit on $n\bar{n}$ oscillations (free n)	$>0.86 \times 10^8$ s, CL = 90%
limit on $n\bar{n}$ oscillations (bound n)	$[n] >1.2 \times 10^8$ s, CL = 90%

ELECTRIC CHARGE (Q)

e^- mean life / branching fraction	$[p] >4.2 \times 10^{24}$ yr, CL = 68%
$\Gamma(n \rightarrow p \nu_e \bar{\nu}_e)/\Gamma_{\text{total}}$	$<8 \times 10^{-27}$, CL = 68%

 $\Delta S = \Delta Q$ RULE

Violations allowed in second-order weak interactions.

$\Gamma(K^+ \rightarrow \pi^+ \pi^+ e^- \bar{\nu}_e)/\Gamma_{\text{total}}$	$<1.2 \times 10^{-8}$, CL = 90%
$\Gamma(K^+ \rightarrow \pi^+ \pi^+ \mu^- \bar{\nu}_\mu)/\Gamma_{\text{total}}$	$<3.0 \times 10^{-6}$, CL = 95%
$x = A(K^0 \rightarrow \pi^- \ell^+ \nu)/A(K^0 \rightarrow \pi^- \ell^+ \nu) = A(\Delta S = -\Delta Q)/A(\Delta S = \Delta Q)$	
real part of x	-0.002 ± 0.006
imaginary part of x	0.0012 ± 0.0019
$\Gamma(\Sigma^+ \rightarrow n \ell^+ \nu)/\Gamma(\Sigma^- \rightarrow n \ell^- \bar{\nu})$	<0.043
$\Gamma(\Sigma^+ \rightarrow n e^+ \nu_e)/\Gamma_{\text{total}}$	$<5 \times 10^{-6}$, CL = 90%
$\Gamma(\Sigma^+ \rightarrow n \mu^+ \nu_\mu)/\Gamma_{\text{total}}$	$<3.0 \times 10^{-5}$, CL = 90%
$\Gamma(\Xi^0 \rightarrow \Sigma^- e^+ \nu_e)/\Gamma_{\text{total}}$	$<9 \times 10^{-4}$, CL = 90%
$\Gamma(\Xi^0 \rightarrow \Sigma^- \mu^+ \nu_\mu)/\Gamma_{\text{total}}$	$<9 \times 10^{-4}$, CL = 90%

 $\Delta S = 2$ FORBIDDEN

Allowed in second-order weak interactions.

$\Gamma(\Xi^0 \rightarrow p \pi^-)/\Gamma_{\text{total}}$	$<4 \times 10^{-5}$, CL = 90%
$\Gamma(\Xi^0 \rightarrow p e^- \bar{\nu}_e)/\Gamma_{\text{total}}$	$<1.3 \times 10^{-3}$
$\Gamma(\Xi^0 \rightarrow p \mu^- \bar{\nu}_\mu)/\Gamma_{\text{total}}$	$<1.3 \times 10^{-3}$
$\Gamma(\Xi^- \rightarrow n \pi^-)/\Gamma_{\text{total}}$	$<1.9 \times 10^{-5}$, CL = 90%
$\Gamma(\Xi^- \rightarrow n e^- \bar{\nu}_e)/\Gamma_{\text{total}}$	$<3.2 \times 10^{-3}$, CL = 90%
$\Gamma(\Xi^- \rightarrow n \mu^- \bar{\nu}_\mu)/\Gamma_{\text{total}}$	$<1.5 \times 10^{-2}$, CL = 90%
$\Gamma(\Xi^- \rightarrow p \pi^- \pi^-)/\Gamma_{\text{total}}$	$<4 \times 10^{-4}$, CL = 90%
$\Gamma(\Xi^- \rightarrow p \pi^- e^- \bar{\nu}_e)/\Gamma_{\text{total}}$	$<4 \times 10^{-4}$, CL = 90%
$\Gamma(\Xi^- \rightarrow p \pi^- \mu^- \bar{\nu}_\mu)/\Gamma_{\text{total}}$	$<4 \times 10^{-4}$, CL = 90%
$\Gamma(\Omega^- \rightarrow \Lambda \pi^-)/\Gamma_{\text{total}}$	$<1.9 \times 10^{-4}$, CL = 90%

 $\Delta S = 2$ VIA MIXING

Allowed in second-order weak interactions, e.g. mixing.

$m_{K_L^0} - m_{K_S^0}$	$(0.5300 \pm 0.0012) \times 10^{10} \hbar s^{-1}$
$m_{K_L^0} - m_{K_S^0}$	$(3.489 \pm 0.008) \times 10^{-12} \text{ MeV}$

 $\Delta C = 2$ VIA MIXING

Allowed in second-order weak interactions, e.g. mixing.

$ m_{D_1^0} - m_{D_2^0} $	$[p] <7 \times 10^{10} \hbar s^{-1}$, CL = 95%
$\Gamma(K^+ \ell^- \bar{\nu}_\ell \text{ (via } \bar{D}^0))/\Gamma(K^- \ell^+ \nu_\ell)$	<0.005 , CL = 90%
$\Gamma(K^+ \pi^- \text{ (via } \bar{D}^0))/\Gamma(K^- \pi^+)$	$<4.1 \times 10^{-4}$, CL = 95%
$\Gamma(D^0 \rightarrow K^+ \ell^- \bar{\nu}_\ell \text{ (via } \bar{D}^0))/\Gamma_{\text{total}}$	$<1.7 \times 10^{-4}$, CL = 90%
$\Gamma(D^0 \rightarrow K^+ \pi^- \text{ (via } \bar{D}^0))/\Gamma_{\text{total}}$	$<1.6 \times 10^{-5}$, CL = 95%
$\Gamma(D^0 \rightarrow K^+ \pi^- \pi^+ \pi^- \text{ (via } \bar{D}^0))/\Gamma_{\text{total}}$	$<4 \times 10^{-4}$, CL = 90%
$\Gamma(D^0 \rightarrow \mu^- \text{ anything (via } \bar{D}^0))/\Gamma_{\text{total}}$	$<4 \times 10^{-4}$, CL = 90%

 $\Delta B = 2$ VIA MIXING

Allowed in second-order weak interactions, e.g. mixing.

x_d	0.174 ± 0.009
$\Delta m_{B^0} = m_{B_H^0} - m_{B_L^0}$	$(0.472 \pm 0.017) \times 10^{12} \hbar s^{-1}$
$x_d = \Delta m_{B^0}/\Gamma_{B^0}$	0.730 ± 0.029
x_B at high energy	0.118 ± 0.005
$\Delta m_{B_s^0} = m_{B_{sH}^0} - m_{B_{sL}^0}$	$>10.6 \times 10^{12} \hbar s^{-1}$, CL = 95%
$x_s = \Delta m_{B_s^0}/\Gamma_{B_s^0}$	>15.7 , CL = 95%
x_s	>0.4980 , CL = 95%

 $\Delta S = 1$ WEAK NEUTRAL CURRENT FORBIDDEN

Allowed by higher-order electroweak interactions.

$\Gamma(K^+ \rightarrow \pi^+ e^+ e^-)/\Gamma_{\text{total}}$	$(2.88 \pm 0.13) \times 10^{-7}$
$\Gamma(K^+ \rightarrow \pi^+ \mu^+ \mu^-)/\Gamma_{\text{total}}$	$(7.6 \pm 2.1) \times 10^{-8}$ ($S = 3.4$)
$\Gamma(K^+ \rightarrow \pi^+ \nu \bar{\nu})/\Gamma_{\text{total}}$	$(1.5^{+3.4}_{-1.2}) \times 10^{-10}$
$\Gamma(K_S^0 \rightarrow \mu^+ \mu^-)/\Gamma_{\text{total}}$	$<3.2 \times 10^{-7}$, CL = 90%
$\Gamma(K_S^0 \rightarrow e^+ e^-)/\Gamma_{\text{total}}$	$<1.4 \times 10^{-7}$, CL = 90%
$\Gamma(K_S^0 \rightarrow \pi^0 e^+ e^-)/\Gamma_{\text{total}}$	$<1.1 \times 10^{-6}$, CL = 90%
$\Gamma(K_L^0 \rightarrow \mu^+ \mu^-)/\Gamma_{\text{total}}$	$(7.15 \pm 0.16) \times 10^{-9}$
$\Gamma(K_L^0 \rightarrow e^+ e^-)/\Gamma_{\text{total}}$	$(9^{+6}_{-4}) \times 10^{-12}$
$\Gamma(K_L^0 \rightarrow \pi^+ \pi^- e^+ e^-)/\Gamma_{\text{total}}$	$[q] (3.5 \pm 0.6) \times 10^{-7}$
$\Gamma(K_L^0 \rightarrow \mu^+ \mu^- e^+ e^-)/\Gamma_{\text{total}}$	$(2.9^{+6.7}_{-2.4}) \times 10^{-9}$
$\Gamma(K_L^0 \rightarrow e^+ e^- e^+ e^-)/\Gamma_{\text{total}}$	$(4.1 \pm 0.8) \times 10^{-8}$ ($S = 1.2$)
$\Gamma(K_L^0 \rightarrow \pi^0 \mu^+ \mu^-)/\Gamma_{\text{total}}$	$<5.1 \times 10^{-9}$, CL = 90%
$\Gamma(K_L^0 \rightarrow \pi^0 e^+ e^-)/\Gamma_{\text{total}}$	$<4.3 \times 10^{-9}$, CL = 90%
$\Gamma(K_L^0 \rightarrow \pi^0 \nu \bar{\nu})/\Gamma_{\text{total}}$	$<5.9 \times 10^{-7}$, CL = 90%
$\Gamma(\Sigma^+ \rightarrow p e^+ e^-)/\Gamma_{\text{total}}$	$<7 \times 10^{-6}$

$\Delta C = 1$ WEAK NEUTRAL CURRENT FORBIDDEN

NOTES

Allowed by higher-order electroweak interactions.

$\Gamma(D^+ \rightarrow \pi^+ e^+ e^-)/\Gamma_{\text{total}}$	$< 5.2 \times 10^{-5}$, CL = 90%
$\Gamma(D^+ \rightarrow \pi^+ \mu^+ \mu^-)/\Gamma_{\text{total}}$	$< 1.5 \times 10^{-5}$, CL = 90%
$\Gamma(D^+ \rightarrow \rho^+ \mu^+ \mu^-)/\Gamma_{\text{total}}$	$< 5.6 \times 10^{-4}$, CL = 90%
$\Gamma(D^0 \rightarrow e^+ e^-)/\Gamma_{\text{total}}$	$< 6.2 \times 10^{-6}$, CL = 90%
$\Gamma(D^0 \rightarrow \mu^+ \mu^-)/\Gamma_{\text{total}}$	$< 4.1 \times 10^{-6}$, CL = 90%
$\Gamma(D^0 \rightarrow \pi^0 e^+ e^-)/\Gamma_{\text{total}}$	$< 4.5 \times 10^{-5}$, CL = 90%
$\Gamma(D^0 \rightarrow \pi^0 \mu^+ \mu^-)/\Gamma_{\text{total}}$	$< 1.8 \times 10^{-4}$, CL = 90%
$\Gamma(D^0 \rightarrow \eta e^+ e^-)/\Gamma_{\text{total}}$	$< 1.1 \times 10^{-4}$, CL = 90%
$\Gamma(D^0 \rightarrow \eta \mu^+ \mu^-)/\Gamma_{\text{total}}$	$< 5.3 \times 10^{-4}$, CL = 90%
$\Gamma(D^0 \rightarrow \rho^0 e^+ e^-)/\Gamma_{\text{total}}$	$< 1.0 \times 10^{-4}$, CL = 90%
$\Gamma(D^0 \rightarrow \rho^0 \mu^+ \mu^-)/\Gamma_{\text{total}}$	$< 2.3 \times 10^{-4}$, CL = 90%
$\Gamma(D^0 \rightarrow \omega e^+ e^-)/\Gamma_{\text{total}}$	$< 1.8 \times 10^{-4}$, CL = 90%
$\Gamma(D^0 \rightarrow \omega \mu^+ \mu^-)/\Gamma_{\text{total}}$	$< 8.3 \times 10^{-4}$, CL = 90%
$\Gamma(D^0 \rightarrow \phi e^+ e^-)/\Gamma_{\text{total}}$	$< 5.2 \times 10^{-5}$, CL = 90%
$\Gamma(D^0 \rightarrow \phi \mu^+ \mu^-)/\Gamma_{\text{total}}$	$< 4.1 \times 10^{-4}$, CL = 90%
$\Gamma(D^0 \rightarrow \pi^+ \pi^- \pi^0 \mu^+ \mu^-)/\Gamma_{\text{total}}$	$< 8.1 \times 10^{-4}$, CL = 90%
$\Gamma(D_s^+ \rightarrow K^+ e^+ e^-)/\Gamma_{\text{total}}$	$< 1.6 \times 10^{-3}$, CL = 90%
$\Gamma(D_s^+ \rightarrow K^+ \mu^+ \mu^-)/\Gamma_{\text{total}}$	$< 1.4 \times 10^{-4}$, CL = 90%
$\Gamma(D_s^+ \rightarrow K^*(892)^+ \mu^+ \mu^-)/\Gamma_{\text{total}}$	$< 1.4 \times 10^{-3}$, CL = 90%
$\Gamma(\Lambda_c^+ \rightarrow p \mu^+ \mu^-)/\Gamma_{\text{total}}$	$< 3.4 \times 10^{-4}$, CL = 90%

 $\Delta B = 1$ WEAK NEUTRAL CURRENT FORBIDDEN

Allowed by higher-order electroweak interactions.

$\Gamma(B^+ \rightarrow \pi^+ e^+ e^-)/\Gamma_{\text{total}}$	$< 3.9 \times 10^{-3}$, CL = 90%
$\Gamma(B^+ \rightarrow \pi^+ \mu^+ \mu^-)/\Gamma_{\text{total}}$	$< 9.1 \times 10^{-3}$, CL = 90%
$\Gamma(B^+ \rightarrow K^+ e^+ e^-)/\Gamma_{\text{total}}$	$< 6 \times 10^{-5}$, CL = 90%
$\Gamma(B^+ \rightarrow K^+ \mu^+ \mu^-)/\Gamma_{\text{total}}$	$< 5.2 \times 10^{-6}$, CL = 90%
$\Gamma(B^+ \rightarrow K^*(892)^+ e^+ e^-)/\Gamma_{\text{total}}$	$< 6.9 \times 10^{-4}$, CL = 90%
$\Gamma(B^+ \rightarrow K^*(892)^+ \mu^+ \mu^-)/\Gamma_{\text{total}}$	$< 1.2 \times 10^{-3}$, CL = 90%
$\Gamma(B^0 \rightarrow e^+ e^-)/\Gamma_{\text{total}}$	$< 5.9 \times 10^{-6}$, CL = 90%
$\Gamma(B^0 \rightarrow \mu^+ \mu^-)/\Gamma_{\text{total}}$	$< 6.8 \times 10^{-7}$, CL = 90%
$\Gamma(B^0 \rightarrow K^0 e^+ e^-)/\Gamma_{\text{total}}$	$< 3.0 \times 10^{-4}$, CL = 90%
$\Gamma(B^0 \rightarrow K^0 \mu^+ \mu^-)/\Gamma_{\text{total}}$	$< 3.6 \times 10^{-4}$, CL = 90%
$\Gamma(B^0 \rightarrow K^*(892)^0 e^+ e^-)/\Gamma_{\text{total}}$	$< 2.9 \times 10^{-4}$, CL = 90%
$\Gamma(B^0 \rightarrow K^*(892)^0 \mu^+ \mu^-)/\Gamma_{\text{total}}$	$< 4.0 \times 10^{-6}$, CL = 90%
$\Gamma(B^0 \rightarrow K^*(892)^0 \nu \bar{\nu})/\Gamma_{\text{total}}$	$< 1.0 \times 10^{-3}$, CL = 90%
$\Gamma(B \rightarrow e^+ e^- s)/\Gamma_{\text{total}}$	$< 5.7 \times 10^{-5}$, CL = 90%
$\Gamma(B \rightarrow \mu^+ \mu^- s)/\Gamma_{\text{total}}$	$< 5.8 \times 10^{-5}$, CL = 90%
$\Gamma(\bar{b} \rightarrow \mu^+ \mu^- \text{anything})/\Gamma_{\text{total}}$	$< 3.2 \times 10^{-4}$, CL = 90%
$\Gamma(B_s^0 \rightarrow \mu^+ \mu^-)/\Gamma_{\text{total}}$	$< 2.0 \times 10^{-6}$, CL = 90%
$\Gamma(B_s^0 \rightarrow e^+ e^-)/\Gamma_{\text{total}}$	$< 5.4 \times 10^{-5}$, CL = 90%
$\Gamma(B_s^0 \rightarrow \phi \nu \bar{\nu})/\Gamma_{\text{total}}$	$< 5.4 \times 10^{-3}$, CL = 90%

 $\Delta T = 1$ WEAK NEUTRAL CURRENT FORBIDDEN

Allowed by higher-order electroweak interactions.

$\Gamma(t \rightarrow Z q(q=u,c))/\Gamma_{\text{total}}$	[r] $< 33 \times 10^{-2}$, CL = 95%
--	--------------------------------------

In this Summary Table:

When a quantity has "(S = ...)" to its right, the error on the quantity has been enlarged by the "scale factor" S, defined as $S = \sqrt{\chi^2/(N-1)}$, where N is the number of measurements used in calculating the quantity. We do this when $S > 1$, which often indicates that the measurements are inconsistent. When $S > 1.25$, we also show in the Particle Listings an ideogram of the measurements. For more about S, see the Introduction.

- [a] C parity forbids this to occur as a single-photon process.
- [b] Time-reversal invariance requires this to be 0° or 180° .
- [c] Allowed by higher-order electroweak interactions.
- [d] Violates CP in leading order. Test of direct CP violation since the indirect CP-violating and CP-conserving contributions are expected to be suppressed.
- [e] ϵ'/ϵ is derived from $|\eta_{00}/\eta_{+-}|$ measurements using theoretical input on phases.
- [f] Neglecting photon channels. See, e.g., A. Pais and S.B. Treiman, Phys. Rev. **D12**, 2744 (1975).
- [g] Derived from measured values of ϕ_{+-} , ϕ_{00} , $|\eta|$, $|m_{K_L^0} - m_{K_S^0}|$, and $\tau_{K_S^0}$, as described in the introduction to "Tests of Conservation Laws."
- [h] These two results are not independent, and both use the more precise measurement of $|q_{\bar{p}}/m_{\bar{p}}|/(q_p/m_p)$.
- [i] The value is for the sum of the charge states or particle/antiparticle states indicated.
- [j] A test of additive vs. multiplicative lepton family number conservation.
- [k] $\Delta(m^2) = 100 \text{ eV}^2$.
- [l] $190 \text{ eV}^2 < \Delta(m^2) < 320 \text{ eV}^2$.
- [m] Derived from an analysis of neutrino-oscillation experiments.
- [n] There is some controversy about whether nuclear physics and model dependence complicate the analysis for bound neutrons (from which the best limit comes). The first limit here is from reactor experiments with free neutrons.
- [o] This is the best "electron disappearance" limit. The best limit for the mode $e^- \rightarrow \nu \gamma$ is $> 2.35 \times 10^{25} \text{ yr}$ (CL=68%).
- [p] This D_1^0 - D_2^0 limit is inferred from the D^0 - \bar{D}^0 mixing ratio $\Gamma(K^+ \pi^- \text{ (via } \bar{D}^0)) / \Gamma(K^- \pi^+)$ near the end of the D^0 Listings.
- [q] See the K_L^0 Particle Listings for the energy limits used in this measurement.
- [r] This limit is for $\Gamma(t \rightarrow Z q)/\Gamma(t \rightarrow W b)$.

1. PHYSICAL CONSTANTS

Table 1.1. Reviewed 2000 by P.J. Mohr and B.N. Taylor (NIST). Based mainly on the “CODATA Recommended Values of the Fundamental Physical Constants: 1998” by P.J. Mohr and B.N. Taylor, *J. Phys. Chem. Ref. Data* **28**, 1713 (1999) and *Rev. Mod. Phys.* **72**, 351 (2000). The last group of constants (beginning with the Fermi coupling constant) comes from the Particle Data Group. The figures in parentheses after the values give the 1-standard-deviation uncertainties in the last digits; the corresponding uncertainties in parts per billion (ppb) are given in the last column. This set of constants (aside from the last group) is recommended for international use by CODATA (the Committee on Data for Science and Technology). The full 1998 CODATA set of constants may be found at <http://physics.nist.gov/constants>

Quantity	Symbol, equation	Value	Uncertainty (ppb)
speed of light in vacuum	c	299 792 458 m s ⁻¹	exact*
Planck constant	h	6.626 068 76(52) × 10 ⁻³⁴ J s	78
Planck constant, reduced	$\hbar \equiv h/2\pi$	1.054 571 596(82) × 10 ⁻³⁴ J s = 6.582 118 89(26) × 10 ⁻²² MeV s	78 39
electron charge magnitude	e	1.602 176 462(63) × 10 ⁻¹⁹ C = 4.803 204 20(19) × 10 ⁻¹⁰ esu	39, 39
conversion constant	$\hbar c$	197.326 960 2(77) MeV fm	39
conversion constant	$(\hbar c)^2$	0.389 379 292(30) GeV ² mbarn	78
electron mass	m_e	0.510 998 902(21) MeV/c ² = 9.109 381 88(72) × 10 ⁻³¹ kg	40, 79
proton mass	m_p	938.271 998(38) MeV/c ² = 1.672 621 58(13) × 10 ⁻²⁷ kg = 1.007 276 466 88(13) u = 1836.152 667 5(39) m_e	40, 79 0.13, 2.1
deuteron mass	m_d	1875.612 762(75) MeV/c ²	40
unified atomic mass unit (u)	(mass ¹² C atom)/12 = (1 g)/(N _A mol)	931.494 013(37) MeV/c ² = 1.660 538 73(13) × 10 ⁻²⁷ kg	40, 79
permittivity of free space	$\epsilon_0 = 1/\mu_0 c^2$	8.854 187 817 ... × 10 ⁻¹² F m ⁻¹	exact
permeability of free space	μ_0	4π × 10 ⁻⁷ N A ⁻² = 12.566 370 614 ... × 10 ⁻⁷ N A ⁻²	exact
fine-structure constant	$\alpha = e^2/4\pi\epsilon_0\hbar c$	7.297 352 533(27) × 10 ⁻³ = 1/137.035 999 76(50) [†]	3.7, 3.7
classical electron radius	$r_e = e^2/4\pi\epsilon_0 m_e c^2$	2.817 940 285(31) × 10 ⁻¹⁵ m	11
(e ⁻ Compton wavelength)/2π	$\lambda_e = \hbar/m_e c = r_e \alpha^{-1}$	3.861 592 642(28) × 10 ⁻¹³ m	7.3
Bohr radius ($m_{\text{nucleus}} = \infty$)	$a_\infty = 4\pi\epsilon_0 \hbar^2/m_e e^2 = r_e \alpha^{-2}$	0.529 177 208 3(19) × 10 ⁻¹⁰ m	3.7
wavelength of 1 eV/c particle	$\hbar c/e$	1.239 841 857(49) × 10 ⁻⁶ m	39
Rydberg energy	$\hbar c R_\infty = m_e e^4/2(4\pi\epsilon_0)^2 \hbar^2 = m_e c^2 \alpha^2/2$	13.605 691 72(53) eV	39
Thomson cross section	$\sigma_T = 8\pi r_e^2/3$	0.665 245 854(15) barn	22
Bohr magneton	$\mu_B = e\hbar/2m_e$	5.788 381 749(43) × 10 ⁻¹¹ MeV T ⁻¹	7.3
nuclear magneton	$\mu_N = e\hbar/2m_p$	3.152 451 238(24) × 10 ⁻¹⁴ MeV T ⁻¹	7.6
electron cyclotron freq./field	$\omega_{\text{cycl}}^e/B = e/m_e$	1.758 820 174(71) × 10 ¹¹ rad s ⁻¹ T ⁻¹	40
proton cyclotron freq./field	$\omega_{\text{cycl}}^p/B = e/m_p$	9.578 834 08(38) × 10 ⁷ rad s ⁻¹ T ⁻¹	40
gravitational constant [‡]	G_N	6.673(10) × 10 ⁻¹¹ m ³ kg ⁻¹ s ⁻² = 6.707(10) × 10 ⁻³⁹ $\hbar c$ (GeV/c ²) ⁻²	1.5 × 10 ⁶ 1.5 × 10 ⁶
standard grav. accel., sea level	g_n	9.806 65 m s ⁻²	exact
Avogadro constant	N_A	6.022 141 99(47) × 10 ²³ mol ⁻¹	79
Boltzmann constant	k	1.380 650 3(24) × 10 ⁻²³ J K ⁻¹ = 8.617 342(15) × 10 ⁻⁵ eV K ⁻¹	1700 1700
molar volume, ideal gas at STP	$N_A k(273.15 \text{ K})/(101 325 \text{ Pa})$	22.413 996(39) × 10 ⁻³ m ³ mol ⁻¹	1700
Wien displacement law constant	$b = \lambda_{\text{max}} T$	2.897 768 6(51) × 10 ⁻³ m K	1700
Stefan-Boltzmann constant	$\sigma = \pi^2 k^4/60\hbar^3 c^2$	5.670 400(40) × 10 ⁻⁸ W m ⁻² K ⁻⁴	7000
Fermi coupling constant**	$G_F/(\hbar c)^3$	1.166 39(1) × 10 ⁻⁵ GeV ⁻²	9000
weak-mixing angle	$\sin^2 \hat{\theta}(M_Z) (\overline{\text{MS}})$	0.23117(16) ^{††}	7 × 10 ⁵
W [±] boson mass	m_W	80.419(56) GeV/c ²	7 × 10 ⁵
Z ⁰ boson mass	m_Z	91.1882(22) GeV/c ²	2.4 × 10 ⁴
strong coupling constant	$\alpha_s(m_Z)$	0.1185(20)	1.7 × 10 ⁷
$\pi = 3.141 592 653 589 793 238$		$e = 2.718 281 828 459 045 235$	$\gamma = 0.577 215 664 901 532 861$
1 in ≡ 0.0254 m	1 G ≡ 10 ⁻⁴ T	1 eV = 1.602 176 462(63) × 10 ⁻¹⁹ J	kT at 300 K = [38.681 686(67)] ⁻¹ eV
1 Å ≡ 0.1 nm	1 dyne ≡ 10 ⁻⁵ N	1 eV/c ² = 1.782 661 731(70) × 10 ⁻³⁶ kg	0 °C ≡ 273.15 K
1 barn ≡ 10 ⁻²⁸ m ²	1 erg ≡ 10 ⁻⁷ J	2.997 924 58 × 10 ⁹ esu = 1 C	1 atmosphere ≡ 760 Torr ≡ 101 325 Pa

* The meter is the length of the path traveled by light in vacuum during a time interval of 1/299 792 458 of a second.

† At $Q^2 = 0$. At $Q^2 \approx m_W^2$ the value is approximately 1/128.

‡ Absolute lab measurements of G_N have been made only on scales of 1 mm to 1 m.

** See the discussion in Sec. 10, “Electroweak model and constraints on new physics.”

†† The corresponding $\sin^2 \theta$ for the effective angle is 0.23147(16).

2. ASTROPHYSICAL CONSTANTS

Table 2.1. Revised 2000 by D.E. Groom (LBNL). The figures in parentheses after some values give the one-standard deviation uncertainties in the last digit(s). Physical constants are from Ref. 1. While every effort has been made to obtain the most accurate current values of the listed quantities, the table does not represent a critical review or adjustment of the constants, and is not intended as a primary reference.

Quantity	Symbol, equation	Value	Reference, footnote
speed of light	c	$299\,792\,458\text{ m s}^{-1}$	defined2
Newtonian gravitational constant	G_N	$6.673(10) \times 10^{-11}\text{ m}^3\text{ kg}^{-1}\text{ s}^{-2}$	3
astronomical unit (mean \oplus - \odot distance)	au	$149\,597\,870\,660(20)\text{ m}$	4, 5
tropical year (equinox to equinox) (2001.0)	yr	$31\,556\,925.2\text{ s}$	4
sidereal year (fixed star to fixed star) (2001.0)		$31\,558\,149.8\text{ s}$	4
mean sidereal day (2001.0)		$23^{\text{h}}\,56^{\text{m}}\,04^{\text{s}}.090\,53$	4
Jansky	Jy	$10^{-26}\text{ W m}^{-2}\text{ Hz}^{-1}$	
Planck mass	$\sqrt{\hbar c/G_N}$	$1.2210(9) \times 10^{19}\text{ GeV}/c^2$ $= 2.176\,7(16) \times 10^{-8}\text{ kg}$	1
parsec (1 AU/1 arc sec)	pc	$3.085\,677\,580\,7(4) \times 10^{16}\text{ m} = 3.262\dots\text{ly}$	6
light year (deprecated unit)	ly	$0.306\,6\dots\text{ pc} = 0.946\,1\dots \times 10^{16}\text{ m}$	
Schwarzschild radius of the Sun	$2G_N M_{\odot}/c^2$	$2.953\,250\,08\text{ km}$	7
solar mass	M_{\odot}	$1.988\,9(30) \times 10^{30}\text{ kg}$	8
solar equatorial radius	R_{\odot}	$6.961 \times 10^8\text{ m}$	4
solar luminosity	L_{\odot}	$(3.846 \pm 0.008) \times 10^{26}\text{ W}$	9
Schwarzschild radius of the Earth	$2G_N M_{\oplus}/c^2$	$4.435\,028\,11\text{ mm}$	10
Earth mass	M_{\oplus}	$5.974(9) \times 10^{24}\text{ kg}$	11
Earth mean equatorial radius	R_{\oplus}	$6.378\,140 \times 10^6\text{ m}$	4
luminosity conversion	L	$3.02 \times 10^{28} \times 10^{-0.4 M_{\text{bol}}}\text{ W}$ (M_{bol} = absolute bolometric magnitude = bolometric magnitude at 10 pc)	12
flux conversion	\mathcal{F}	$2.52 \times 10^{-8} \times 10^{-0.4 m_{\text{bol}}}\text{ W m}^{-2}$ (m_{bol} = apparent bolometric magnitude)	from above
v_{\odot} around center of Galaxy	Θ_{\odot}	$220(20)\text{ km s}^{-1}$	13
solar distance from galactic center	R_{\odot}	$8.0(5)\text{ kpc}$	14
Hubble expansion rate [†]	H_0	$100\ h_0\text{ km s}^{-1}\text{ Mpc}^{-1}$ $= h_0 \times (9.778\,13\text{ Gyr})^{-1}$	15
normalized Hubble expansion rate [†]	h_0	$(0.71 \pm 0.07) \times 0.95^{1.15}$	16, 17
critical density of the universe [†]	$\rho_c = 3H_0^2/8\pi G_N$	$2.775\,366\,27 \times 10^{11}\ h_0^2\ M_{\odot}\text{Mpc}^{-3}$ $= 1.879(3) \times 10^{-29}\ h_0^2\ \text{g cm}^{-3}$ $= 1.053\,9(16) \times 10^{-5}\ h_0^2\ \text{GeV cm}^{-3}$	
local disk density	ρ_{disk}	$3\text{--}12 \times 10^{-24}\ \text{g cm}^{-3} \approx 2\text{--}7\ \text{GeV}/c^2\ \text{cm}^{-3}$	18
local halo density	ρ_{halo}	$2\text{--}13 \times 10^{-25}\ \text{g cm}^{-3} \approx 0.1\text{--}0.7\ \text{GeV}/c^2\ \text{cm}^{-3}$	19
pressureless matter density of the universe [†]	$\Omega_M \equiv \rho_M/\rho_c$	$0.15 \lesssim \Omega_M \lesssim 0.45$	16, 20
scaled cosmological constant [†]	$\Omega_{\Lambda} \equiv \Lambda c^2/3H_0^2$	$0.6 \lesssim \Omega_{\Lambda} \lesssim 0.8$	16
scale factor for cosmological constant [†]	$c^2/3H_0^2$	$2.853 \times 10^{51}\ h_0^{-2}\ \text{m}^2$	
$\Omega_M + \Omega_{\Lambda} + \dots$ [21]	Ω_{tot} [21]	see footnote 22	
age of the universe [†]	t_0	$12\text{--}18\ \text{Gyr}$	16
cosmic background radiation (CBR) temperature [†]	T_0	$2.725 \pm 0.001\ \text{K}$	23, 24
solar velocity with respect to CBR		$369.3 \pm 2.5\ \text{km s}^{-1}$	24, 25
energy density of CBR	ρ_{γ}	$4.641\,7 \times 10^{-34}\ (T/2.725)^4\ \text{g cm}^{-3}$ $= 0.260\,38\ (T/2.725)^4\ \text{eV cm}^{-3}$	12, 24
energy density of relativistic particles (CBR + ν)	ρ_R	$7.804\,2 \times 10^{-34}\ (T/2.725)^4\ \text{g cm}^{-3}$ $= 0.437\,78\ (T/2.725)^4\ \text{eV cm}^{-3}$	12, 24
number density of CBR photons	n_{γ}	$410.50\ (T/2.725)^3\ \text{cm}^{-3}$	12, 24
entropy density/Boltzmann constant	s/k	$2\,889.2\ (T/2.725)^3\ \text{cm}^{-3}$	12

[†] Subscript 0 indicates present-day values.

References:

1. P.J. Mohr and B.N. Taylor, "CODATA Recommended Values of the Fundamental Physical Constants: 1998," *J. Phys. Chem. Ref. Data* **28**, 1713–1852 (1999).
2. B.W. Petley, *Nature* **303**, 373 (1983).
3. The value of G_N [1] is the same as in Ref. 26, but the quoted error is 12 times larger. See *Measurement, Science, and Technology* **10**, No. 6 (June 1999), special section: "The gravitational constant: Theory and experiment 200 years after Cavendish."

In the context of the scale dependence of field theoretic quantities, it should be remarked that absolute lab measurements of G_N have been performed on scales of 0.01–1.0 m.
4. *The Astronomical Almanac for the year 2001*, U.S. Government Printing Office, Washington, and Her Majesty's Stationary Office, London (1999).
5. JPL Planetary Ephemerides, E. Myles Standish, Jr., private communication (1989).
6. 1 AU divided by $\pi/648000$; quoted error is from the JPL Planetary Ephemerides value of the AU [5].
7. Product of $2/c^2$ and the heliocentric gravitational constant [4]. The given 9-place accuracy seems consistent with uncertainties in defining the earth's orbital parameters.
8. Obtained from the heliocentric gravitational constant [4] and G_N [3]. The error is the 1500 ppm standard deviation of G_N .
9. 1996 mean total solar irradiance (TSI) = 1367.5 ± 2.7 [27]; the solar luminosity is $4\pi \times (1 \text{ AU})^2$ times this quantity. This value increased by 0.036% between the minima of solar cycles 21 and 22. It was modulated with an amplitude of 0.039% during solar cycle 21 [28].

Sackmann *et al.* [29] use TSI = $1370 \pm 2 \text{ W m}^{-2}$, but conclude that the solar luminosity ($L_\odot = 3.853 \times 10^{26} \text{ J s}^{-1}$) has an uncertainty of 1.5%. Their value comes from three 1977–83 papers, and they comment that the error is based on scatter among the reported values, which is substantially in excess of that expected from the individual quoted errors.

The conclusion of the 1971 review by Thekaekara and Drummond [30] ($1353 \pm 1\% \text{ W m}^{-2}$) is often quoted [31]. The conversion to luminosity is not given in the Thekaekara and Drummond paper, and we cannot exactly reproduce the solar luminosity given in Ref. 31.

Finally, a value based on the 1954 spectral curve due to Johnson [32] ($1395 \pm 1\% \text{ W m}^{-2}$, or $L_\odot = 3.92 \times 10^{26} \text{ J s}^{-1}$) has been used widely, and may be the basis for the higher value of the solar luminosity and the corresponding lower value of the solar absolute bolometric magnitude (4.72) still common in the literature [12].
10. Product of $2/c^2$, the heliocentric gravitational constant from Ref. 4, and the earth/sun mass ratio, also from Ref. 4. The given 9-place accuracy appears to be consistent with uncertainties in actually defining the earth's orbital parameters.
11. Obtained from the geocentric gravitational constant [4] and G_N [3]. The error is the 1500 ppm standard deviation of G_N .
12. E.W. Kolb and M.S. Turner, *The Early Universe*, Addison-Wesley (1990).
13. F.J. Kerr and D. Lynden-Bell, *Mon. Not. R. Astr. Soc.* **221**, 1023–1038 (1985). "On the basis of this review these [$R_\odot = 8.5 \pm 1.1 \text{ kpc}$ and $\Theta_\odot = 220 \pm 20 \text{ km s}^{-1}$] were adopted by resolution of IAU Commission 33 on 1985 November 21 at Delhi".
14. M.J. Reid, *Annu. Rev. Astron. Astrophys.* **31**, 345–372 (1993). Note that Θ_\odot from the 1985 IAU Commission 33 recommendations is adopted in this review, although the new value for R_\odot is smaller.
15. Conversion using length of tropical year.
16. M. Fukugita & C.J. Hogan, "Global Cosmological Parameters: H_0 , Ω_M , and Λ ," Sec. 17 of this *Review*.
17. The final uncertainty arises from dichotomous estimates of the distance to the Large Magellanic Cloud.
18. G. Gilmore, R.F.G. Wyse, and K. Kuijken, *Annu. Rev. Astron. Astrophys.* **27**, 555 (1989).
19. E.I. Gates, G. Gyuk, and M.S. Turner (*Astrophys. J.* **449**, L133 (1995)) find the local halo density to be $9.2^{+3.8}_{-3.1} \times 10^{-25} \text{ g cm}^{-3}$, but also comment that previously published estimates are in the range $1\text{--}10 \times 10^{-25} \text{ g cm}^{-3}$. The value $0.3 \text{ GeV}/c^2$ has been taken as "standard" in several papers setting limits on WIMP mass limits, *e.g.* in M. Mori *et al.*, *Phys. Lett.* **B289**, 463 (1992).
20. Fukugita & Hogan find a more restrictive limit, $0.2 \lesssim \Omega_M \lesssim 0.4$, if the Universe is flat.
21. In addition to the pressureless mass density Ω_M and the scaled cosmological constant Ω_Λ , Ω_{tot} contains very small contributions from the cosmic background radiation, the primordial neutrino energy density, and perhaps other sources. $1 - \Omega_{\text{tot}}$ is the three-dimensional scalar curvature scaled by the squared inverse Hubble length, variously written as $kc^2/(H_0 R(t_0))^2$ [12], Kc^2/H_0^2 [36], and Ω_k [37]. Thus $\Omega_{\text{tot}} = 1$ indicates a flat universe.
22. First results from both BOOMERANG [33] and MAXIMA-1 [34] indicate $\Omega_M + \Omega_\Lambda \approx 1$ with $\approx 10\%$ uncertainties, providing the strongest evidence to date for a flat universe. See discussions elsewhere in this *Review* concerning the remarkable consistency of Ω_M and Ω_Λ measurements by different methods [16,24,35].
23. J. Mather *et al.*, *Astrophys. J.* **512**, 511 (1999). We quote a one standard deviation uncertainty.
24. G.F. Smoot & D. Scott, "Cosmic Background Radiation," Sec. 19 of this *Review*.
25. C.H. Lineweaver *et al.*, *Astrophys. J.* **470**, 28 (1996). Dipole velocity is in the direction $(\ell, b) = (264^\circ.31 \pm 0^\circ.04 \pm 0^\circ.16, +48^\circ.05 \pm 0^\circ.02 \pm 0^\circ.09)$, or $(\alpha, \delta) = (11^{\text{h}}11^{\text{m}}57^{\text{s}} \pm -7^\circ.22 \pm 0^\circ.08)$ (JD2000).
26. E.R. Cohen and B.N. Taylor, *Rev. Mod. Phys.* **59**, 1121 (1987).
27. R.C. Willson, *Science* **277**, 1963 (1997); the 0.2% error estimate is from R.C. Willson, private correspondence (1998).
28. R.C. Willson and H.S. Hudson, *Nature* **332**, 810 (1988).
29. I.-J. Sackmann, A.I. Boothroyd, and K.E. Kraemer, *Astrophys. J.* **418**, 457 (1993).
30. M.P. Thekaekara and A.J. Drummond, *Nature Phys. Sci.* **229**, 6 (1971).
31. K.R. Lang, *Astrophysical Formulae*, Springer-Verlag (1974); K.R. Lang, *Astrophysical Data: Planets and Stars*, Springer-Verlag (1992).
32. F.S. Johnson, *J. Meteorol.* **11**, 431 (1954).
33. P. de Bernardis *et al.*, *Nature* **404**, 955 (2000).
34. A. Balbi *et al.*, astro-ph/0005124, submitted to *Astrophys. J. Lett.*
35. E.W. Kolb and M.S. Turner, "Pocket Cosmology," Sec. 15 of this *Review*.
36. S. Weinberg, *Gravitation and Cosmology*, John Wiley & Sons (1972).
37. P.J.E. Peebles, *Principles of Physical Cosmology*, Princeton (1993).

3. INTERNATIONAL SYSTEM OF UNITS (SI)

See "The International System of Units (SI)," NIST Special Publication 330, B.N. Taylor, ed. (USGPO, Washington, DC, 1991); and "Guide for the Use of the International System of Units (SI)," NIST Special Publication 811, 1995 edition, B.N. Taylor (USGPO, Washington, DC, 1995).

Physical quantity	Name of unit	Symbol
<i>Base units</i>		
length	meter	m
mass	kilogram	kg
time	second	s
electric current	ampere	A
thermodynamic temperature	kelvin	K
amount of substance	mole	mol
luminous intensity	candela	cd
<i>Derived units with special names</i>		
plane angle	radian	rad
solid angle	steradian	sr
frequency	hertz	Hz
energy	joule	J
force	newton	N
pressure	pascal	Pa
power	watt	W
electric charge	coulomb	C
electric potential	volt	V
electric resistance	ohm	Ω
electric conductance	siemens	S
electric capacitance	farad	F
magnetic flux	weber	Wb
inductance	henry	H
magnetic flux density	tesla	T
luminous flux	lumen	lm
illuminance	lux	lx
celsius temperature	degree celsius	$^{\circ}\text{C}$
activity (of a radioactive source)*	becquerel	Bq
absorbed dose (of ionizing radiation)*	gray	Gy
dose equivalent*	sievert	Sv

SI prefixes

10^{24}	yotta (Y)
10^{21}	zetta (Z)
10^{18}	exa (E)
10^{15}	peta (P)
10^{12}	tera (T)
10^9	giga (G)
10^6	mega (M)
10^3	kilo (k)
10^2	hecto (h)
10	deca (da)
10^{-1}	deci (d)
10^{-2}	centi (c)
10^{-3}	milli (m)
10^{-6}	micro (μ)
10^{-9}	nano (n)
10^{-12}	pico (p)
10^{-15}	femto (f)
10^{-18}	atto (a)
10^{-21}	zepto (z)
10^{-24}	yocto (y)

*See our section 25, on "Radioactivity and radiation protection," p. 186.

4. PERIODIC TABLE OF THE ELEMENTS

Table 4.1. Revised 1997 by C.G. Wohl (LBNL). Heavy element updates in May 2000 by D.E. Groom. The atomic number (top left) is the number of protons in the nucleus. The atomic mass (bottom) is weighted by isotopic abundances in the Earth's surface. Atomic masses are relative to the mass of the carbon-12 isotope, defined to be exactly 12 unified atomic mass units (u). Errors range from 1 to 9 in the last digit quoted. Relative isotopic abundances often vary considerably, both in natural and commercial samples. A number in parentheses is the mass of the longest-lived isotope of that element—no stable isotope exists. However, although Th, Pa, and U have no stable isotopes, they do have characteristic terrestrial compositions, and meaningful weighted masses can be given. For elements 110–112, the atomic numbers of known isotopes are given. Adapted from the Commission of Atomic Weights and Isotopic Abundances, "Atomic Weights of the Elements 1995," Pure and Applied Chemistry 68, 2339 (1996), and G. Audi and A.H. Wapstra, "The 1993 Mass Evaluation," Nucl. Phys. A565, 1 (1993).

1 IA		18 VIIIA									
2 He 4.002602		13 IIIA		14 IVA		15 VA		16 VIA		17 VIIA	
3 Li 6.941		4 Be 9.012182		5 B 10.811		6 C 12.0107		7 N 14.00674		8 O 15.9994	
9 F 18.9984032		10 Ne 20.1797		11 Na 22.989770		12 Mg 24.3050		13 Al 26.981538		14 Si 28.0855	
15 P 30.973761		16 S 32.066		17 Cl 35.4527		18 Ar 39.948		19 K 39.0983		20 Ca 40.078	
21 Sc 44.955910		22 Ti 47.867		23 V 50.9415		24 Cr 51.9961		25 Mn 54.938049		26 Fe 55.845	
27 Co 58.933200		28 Ni 58.6934		29 Cu 63.546		30 Zn 65.39		31 Ga 69.723		32 Ge 72.61	
33 As 74.92160		34 Se 78.96		35 Br 79.904		36 Kr 83.80		37 Rb 85.4678		38 Sr 87.62	
39 Y 88.90585		40 Zr 91.224		41 Nb 92.90638		42 Mo 95.94		43 Tc 97.907215		44 Ru 101.07	
45 Rh 102.90550		46 Pd 106.42		47 Ag 107.8682		48 Cd 112.411		49 In 114.818		50 Sn 118.710	
51 Sb 121.760		52 Te 127.60		53 I 126.90447		54 Xe 131.29		55 Cs 132.90545		56 Ba 137.327	
57 La 138.9055		58 Ce 140.116		59 Pr 140.90765		60 Nd 144.24		61 Pm (144.912745)		62 Sm 150.36	
63 Eu 151.964		64 Gd 157.25		65 Tb 158.92534		66 Dy 162.50		67 Ho 164.93032		68 Er 167.26	
69 Tm 168.93421		70 Yb 173.04		71 Lu 174.967		72 Hf 178.49		73 Ta 180.9479		74 W 183.84	
75 Re 186.207		76 Os 190.23		77 Ir 192.217		78 Pt 195.078		79 Au 196.96655		80 Hg 200.59	
81 Tl 204.3833		82 Pb 207.2		83 Bi 208.98038		84 Po (209)		85 At (209)		86 Rn (222)	
87 Fr (223.019731)		88 Ra (226.025402)		89 Ac (227)		90 Th (232)		91 Pa (231)		92 U (238)	
93 Np (237)		94 Pu (244)		95 Am (243)		96 Cm (247)		97 Bk (247)		98 Cf (251)	
99 Es (252)		100 Fm (257)		101 Md (258)		102 No (259)		103 Lr (262)		104 Lu (175)	
105 La 138.9055		106 Ce 140.116		107 Pr 140.90765		108 Nd 144.24		109 Pm (144.912745)		110 Sm 150.36	
111 Eu 151.964		112 Gd 157.25		113 Tb 158.92534		114 Dy 162.50		115 Ho 164.93032		116 Er 167.26	
117 Tm 168.93421		118 Yb 173.04		119 Lu 174.967		120 Hf 178.49		121 Ta 180.9479		122 W 183.84	
123 Re 186.207		124 Os 190.23		125 Ir 192.217		126 Pt 195.078		127 Au 196.96655		128 Hg 200.59	
129 Tl 204.3833		130 Pb 207.2		131 Bi 208.98038		132 Po (209)		133 At (209)		134 Rn (222)	
135 Fr (223)		136 Ra (226)		137 Ac (227)		138 Th (232)		139 Pa (231)		140 U (238)	
141 Np (237)		142 Pu (244)		143 Am (243)		144 Cm (247)		145 Bk (247)		146 Cf (251)	
147 Es (252)		148 Fm (257)		149 Md (258)		150 No (259)		151 Lr (262)		152 Lu (175)	

Lanthanide series

Actinide series

5. ELECTRONIC STRUCTURE OF THE ELEMENTS

Table 5.1. Reviewed 1999 by W.C. Martin (NIST). The electronic configurations and the ionization energies (except for a few newer values, marked with an *) are taken from "Atomic Spectroscopy," W.C. Martin and W.L. Wiese, in *Atomic, Molecular, and Optical Physics Reference Book*, G.W.F. Drake, ed., Amer. Inst. Phys., 1995. The electron configuration for, say, iron indicates an argon electronic core (see argon) plus six 3d electrons and two 4s electrons. The ionization energy is the least energy necessary to remove to infinity one electron from an atom of the element.

Element	Electron configuration (3d ⁵ = five 3d electrons, etc.)	Ground state $2S+1L_J$	Ionization energy (eV)
1 H Hydrogen	1s	$^2S_{1/2}$	13.5984
2 He Helium	1s ²	1S_0	24.5874
3 Li Lithium	(He) 2s	$^2S_{1/2}$	5.3917
4 Be Beryllium	(He) 2s ²	1S_0	9.3227
5 B Boron	(He) 2s ² 2p	$^2P_{1/2}$	8.2980
6 C Carbon	(He) 2s ² 2p ²	3P_0	11.2603
7 N Nitrogen	(He) 2s ² 2p ³	$^4S_{3/2}$	14.5341
8 O Oxygen	(He) 2s ² 2p ⁴	3P_2	13.6181
9 F Fluorine	(He) 2s ² 2p ⁵	$^2P_{3/2}$	17.4228
10 Ne Neon	(He) 2s ² 2p ⁶	1S_0	21.5646
11 Na Sodium	(Ne) 3s	$^2S_{1/2}$	5.1391
12 Mg Magnesium	(Ne) 3s ²	1S_0	7.6462
13 Al Aluminium	(Ne) 3s ² 3p	$^2P_{1/2}$	5.9858
14 Si Silicon	(Ne) 3s ² 3p ²	3P_0	8.1517
15 P Phosphorus	(Ne) 3s ² 3p ³	$^4S_{3/2}$	10.4867
16 S Sulfur	(Ne) 3s ² 3p ⁴	3P_2	10.3600
17 Cl Chlorine	(Ne) 3s ² 3p ⁵	$^2P_{3/2}$	12.9676
18 Ar Argon	(Ne) 3s ² 3p ⁶	1S_0	15.7596
19 K Potassium	(Ar) 4s	$^2S_{1/2}$	4.3407
20 Ca Calcium	(Ar) 4s ²	1S_0	6.1132
21 Sc Scandium	(Ar) 3d 4s ²	$^2D_{3/2}$	6.5615
22 Ti Titanium	(Ar) 3d ² 4s ²	3F_2	6.8281
23 V Vanadium	(Ar) 3d ³ 4s ²	$^4F_{3/2}$	6.7463
24 Cr Chromium	(Ar) 3d ⁵ 4s	7S_3	6.7665
25 Mn Manganese	(Ar) 3d ⁵ 4s ²	$^6S_{5/2}$	7.4340
26 Fe Iron	(Ar) 3d ⁶ 4s ²	5D_4	7.9024
27 Co Cobalt	(Ar) 3d ⁷ 4s ²	$^4F_{9/2}$	7.8810
28 Ni Nickel	(Ar) 3d ⁸ 4s ²	3F_4	7.6398
29 Cu Copper	(Ar) 3d ¹⁰ 4s	$^2S_{1/2}$	7.7264
30 Zn Zinc	(Ar) 3d ¹⁰ 4s ²	1S_0	9.3942
31 Ga Gallium	(Ar) 3d ¹⁰ 4s ² 4p	$^2P_{1/2}$	5.9993
32 Ge Germanium	(Ar) 3d ¹⁰ 4s ² 4p ²	3P_0	7.8994
33 As Arsenic	(Ar) 3d ¹⁰ 4s ² 4p ³	$^4S_{3/2}$	9.7886
34 Se Selenium	(Ar) 3d ¹⁰ 4s ² 4p ⁴	3P_2	9.7524
35 Br Bromine	(Ar) 3d ¹⁰ 4s ² 4p ⁵	$^2P_{3/2}$	11.8138
36 Kr Krypton	(Ar) 3d ¹⁰ 4s ² 4p ⁶	1S_0	13.9996
37 Rb Rubidium	(Kr) 5s	$^2S_{1/2}$	4.1771
38 Sr Strontium	(Kr) 5s ²	1S_0	5.6949
39 Y Yttrium	(Kr) 4d 5s ²	$^2D_{3/2}$	6.2171
40 Zr Zirconium	(Kr) 4d ² 5s ²	3F_2	6.6339
41 Nb Niobium	(Kr) 4d ⁴ 5s	$^6D_{1/2}$	6.7589
42 Mo Molybdenum	(Kr) 4d ⁵ 5s	7S_3	7.0924
43 Tc Technetium	(Kr) 4d ⁵ 5s ²	$^6S_{5/2}$	7.28
44 Ru Ruthenium	(Kr) 4d ⁷ 5s	5F_5	7.3605
45 Rh Rhodium	(Kr) 4d ⁸ 5s	$^4F_{9/2}$	7.4589
46 Pd Palladium	(Kr) 4d ¹⁰	1S_0	8.3369
47 Ag Silver	(Kr) 4d ¹⁰ 5s	$^2S_{1/2}$	7.5762*
48 Cd Cadmium	(Kr) 4d ¹⁰ 5s ²	1S_0	8.9938

49	In	Indium	(Kr)4d ¹⁰ 5s ² 5p			² P _{1/2}	5.7864
50	Sn	Tin	(Kr)4d ¹⁰ 5s ² 5p ²			³ P ₀	7.3439
51	Sb	Antimony	(Kr)4d ¹⁰ 5s ² 5p ³			⁴ S _{3/2}	8.6084
52	Te	Tellurium	(Kr)4d ¹⁰ 5s ² 5p ⁴			³ P ₂	9.0096
53	I	Iodine	(Kr)4d ¹⁰ 5s ² 5p ⁵			² P _{3/2}	10.4513
54	Xe	Xenon	(Kr)4d ¹⁰ 5s ² 5p ⁶			¹ S ₀	12.1298
55	Cs	Cesium	(Xe) 6s			² S _{1/2}	3.8939
56	Ba	Barium	(Xe) 6s ²			¹ S ₀	5.2117
57	La	Lanthanum	(Xe) 5d 6s ²			² D _{3/2}	5.5770
58	Ce	Cerium	(Xe)4f 5d 6s ²			¹ G ₄	5.5387
59	Pr	Praseodymium	(Xe)4f ³ 6s ²	L		⁴ I _{9/2}	5.464
60	Nd	Neodymium	(Xe)4f ⁴ 6s ²	a		⁵ I ₄	5.5250
61	Pm	Promethium	(Xe)4f ⁵ 6s ²	n		⁶ H _{5/2}	5.58
62	Sm	Samarium	(Xe)4f ⁶ 6s ²	t		⁷ F ₀	5.6436
63	Eu	Europium	(Xe)4f ⁷ 6s ²	h		⁸ S _{7/2}	5.6704
64	Gd	Gadolinium	(Xe)4f ⁷ 5d 6s ²	a		⁹ D ₂	6.1498*
65	Tb	Terbium	(Xe)4f ⁹ 6s ²	n		⁶ H _{15/2}	5.8638
66	Dy	Dysprosium	(Xe)4f ¹⁰ 6s ²	i		⁵ I ₈	5.9389
67	Ho	Holmium	(Xe)4f ¹¹ 6s ²	d		⁴ I _{15/2}	6.0215
68	Er	Erbium	(Xe)4f ¹² 6s ²	e		³ H ₆	6.1077
69	Tm	Thulium	(Xe)4f ¹³ 6s ²	s		² F _{7/2}	6.1843
70	Yb	Ytterbium	(Xe)4f ¹⁴ 6s ²			¹ S ₀	6.2542
71	Lu	Lutetium	(Xe)4f ¹⁴ 5d 6s ²			² D _{3/2}	5.4259
72	Hf	Hafnium	(Xe)4f ¹⁴ 5d ² 6s ²	T		³ F ₂	6.8251
73	Ta	Tantalum	(Xe)4f ¹⁴ 5d ³ 6s ²	r		⁴ F _{3/2}	7.5496
74	W	Tungsten	(Xe)4f ¹⁴ 5d ⁴ 6s ²	a		⁵ D ₀	7.8640
75	Re	Rhenium	(Xe)4f ¹⁴ 5d ⁵ 6s ²	n		⁶ S _{5/2}	7.8335
76	Os	Osmium	(Xe)4f ¹⁴ 5d ⁶ 6s ²	s		⁵ D ₄	8.4382*
77	Ir	Iridium	(Xe)4f ¹⁴ 5d ⁷ 6s ²	i		⁴ F _{9/2}	8.9670*
78	Pt	Platinum	(Xe)4f ¹⁴ 5d ⁹ 6s	t		³ D ₃	8.9587
79	Au	Gold	(Xe)4f ¹⁴ 5d ¹⁰ 6s	i		² S _{1/2}	9.2255
80	Hg	Mercury	(Xe)4f ¹⁴ 5d ¹⁰ 6s ²	o		¹ S ₀	10.4375
81	Tl	Thallium	(Xe)4f ¹⁴ 5d ¹⁰ 6s ² 6p	n		² P _{1/2}	6.1082
82	Pb	Lead	(Xe)4f ¹⁴ 5d ¹⁰ 6s ² 6p ²			³ P ₀	7.4167
83	Bi	Bismuth	(Xe)4f ¹⁴ 5d ¹⁰ 6s ² 6p ³			⁴ S _{3/2}	7.2855*
84	Po	Polonium	(Xe)4f ¹⁴ 5d ¹⁰ 6s ² 6p ⁴			³ P ₂	8.4167
85	At	Astatine	(Xe)4f ¹⁴ 5d ¹⁰ 6s ² 6p ⁵			² P _{3/2}	
86	Rn	Radon	(Xe)4f ¹⁴ 5d ¹⁰ 6s ² 6p ⁶			¹ S ₀	10.7485
87	Fr	Francium	(Rn) 7s			² S _{1/2}	4.0727
88	Ra	Radium	(Rn) 7s ²			¹ S ₀	5.2784
89	Ac	Actinium	(Rn) 6d 7s ²			² D _{3/2}	5.17
90	Th	Thorium	(Rn) 6d ² 7s ²			³ F ₂	6.3067
91	Pa	Protactinium	(Rn)5f ² 6d 7s ²	A		⁴ K _{11/2}	5.89
92	U	Uranium	(Rn)5f ³ 6d 7s ²	c		⁵ L ₆	6.1941
93	Np	Neptunium	(Rn)5f ⁴ 6d 7s ²	t		⁶ L _{11/2}	6.2657
94	Pu	Plutonium	(Rn)5f ⁶ 7s ²	i		⁷ F ₀	6.0262
95	Am	Americium	(Rn)5f ⁷ 7s ²	n		⁸ S _{7/2}	5.9738
96	Cm	Curium	(Rn)5f ⁷ 6d 7s ²	i		⁹ D ₂	5.9915*
97	Bk	Berkelium	(Rn)5f ⁹ 7s ²	d		⁶ H _{15/2}	6.1979*
98	Cf	Californium	(Rn)5f ¹⁰ 7s ²	e		⁵ I ₈	6.2817*
99	Es	Einsteinium	(Rn)5f ¹¹ 7s ²	s		⁴ I _{15/2}	6.42
100	Fm	Fermium	(Rn)5f ¹² 7s ²			³ H ₆	6.50
101	Md	Mendelevium	(Rn)5f ¹³ 7s ²			² F _{7/2}	6.58
102	No	Nobelium	(Rn)5f ¹⁴ 7s ²			¹ S ₀	6.65
103	Lr	Lawrencium	(Rn)5f ¹⁴ 7s ² 7p?			² P _{1/2} ?	
104	Rf	Rutherfordium	(Rn)5f ¹⁴ 6d ² 7s ² ?			³ F ₂ ?	6.0?

6. ATOMIC AND NUCLEAR PROPERTIES OF MATERIALS

Table 6.1. Revised May 2000 by D.E. Groom (LBNL). Gases are evaluated at 20°C and 1 atm (in parentheses) or at STP [square brackets]. Densities and refractive indices without parentheses or brackets are for solids or liquids, or are for cryogenic liquids at the indicated boiling point (BP) at 1 atm. Refractive indices are evaluated at the sodium D line. Data for compounds and mixtures are from Refs. 1 and 2. Further materials and properties are given in Ref. 3.

Material	Z	A	(Z/A)	Nuclear collision length λ_T {g/cm ² }	Nuclear α interaction length λ_I {g/cm ² }	Nuclear α $dE/dx _{\min}$ ^b $\left\{ \frac{\text{MeV}}{\text{g/cm}^2} \right\}$	Radiation length ^c X_0 {g/cm ² } {cm}	Density {g/cm ³ } {g/ℓ} for gas	Liquid boiling point at 1 atm(K)	Refractive index n (($n-1$) $\times 10^6$) for gas
H ₂ gas	1	1.00794	0.99212	43.3	50.8	(4.103)	61.28 ^d (731000)	(0.0838)[0.0899]		[139.2]
H ₂ liquid	1	1.00794	0.99212	43.3	50.8	4.034	61.28 ^d 866	0.0708	20.39	1.112
D ₂	1	2.0140	0.49652	45.7	54.7	(2.052)	122.4 724	0.169[0.179]	23.65	1.128 [138]
He	2	4.002602	0.49968	49.9	65.1	(1.937)	94.32 756	0.1249[0.1786]	4.224	1.024 [34.9]
Li	3	6.941	0.43221	54.6	73.4	1.639	82.76 155	0.534		—
Be	4	9.012182	0.44384	55.8	75.2	1.594	65.19 35.28	1.848		—
C	6	12.011	0.49954	60.2	86.3	1.745	42.70 18.8	2.265 ^e		—
N ₂	7	14.00674	0.49976	61.4	87.8	(1.825)	37.99 47.1	0.8073[1.250]	77.36	1.205 [298]
O ₂	8	15.9994	0.50002	63.2	91.0	(1.801)	34.24 30.0	1.141[1.428]	90.18	1.22 [296]
F ₂	9	18.9984032	0.47372	65.5	95.3	(1.675)	32.93 21.85	1.507[1.696]	85.24	[195]
Ne	10	20.1797	0.49555	66.1	96.6	(1.724)	28.94 24.0	1.204[0.9005]	27.09	1.092 [67.1]
Al	13	26.981539	0.48181	70.6	106.4	1.615	24.01 8.9	2.70		—
Si	14	28.0855	0.49848	70.6	106.0	1.664	21.82 9.36	2.33		3.95
Ar	18	39.948	0.45059	76.4	117.2	(1.519)	19.55 14.0	1.396[1.782]	87.28	1.233 [283]
Ti	22	47.867	0.45948	79.9	124.9	1.476	16.17 3.56	4.54		—
Fe	26	55.845	0.46556	82.8	131.9	1.451	13.84 1.76	7.87		—
Cu	29	63.546	0.45636	85.6	134.9	1.403	12.86 1.43	8.96		—
Ge	32	72.61	0.44071	88.3	140.5	1.371	12.25 2.30	5.323		—
Sn	50	118.710	0.42120	100.2	163	1.264	8.82 1.21	7.31		—
Xe	54	131.29	0.41130	102.8	169	(1.255)	8.48 2.87	2.953[5.858]	165.1	[701]
W	74	183.84	0.40250	110.3	185	1.145	6.76 0.35	19.3		—
Pt	78	195.08	0.39984	113.3	189.7	1.129	6.54 0.305	21.45		—
Pb	82	207.2	0.39575	116.2	194	1.123	6.37 0.56	11.35		—
U	92	238.0289	0.38651	117.0	199	1.082	6.00 ≈ 0.32	≈ 18.95		—
Air, (20°C, 1 atm.), [STP]			0.49919	62.0	90.0	(1.815)	36.66 [30420]	(1.205)[1.2931]	78.8	(273) [293]
H ₂ O			0.55509	60.1	83.6	1.991	36.08 36.1	1.00	373.15	1.33
CO ₂ gas			0.49989	62.4	89.7	(1.819)	36.2 [18310]	[1.977]		[410]
CO ₂ solid (dry ice)			0.49989	62.4	89.7	1.787	36.2 23.2	1.563	sublimes	—
Shielding concrete ^f			0.50274	67.4	99.9	1.711	26.7 10.7	2.5		—
SiO ₂ (fused quartz)			0.49926	66.5	97.4	1.699	27.05 12.3	2.20 ^g		1.458
Dimethyl ether, (CH ₃) ₂ O			0.54778	59.4	82.9	—	38.89	—	248.7	—
Methane, CH ₄			0.62333	54.8	73.4	(2.417)	46.22 [64850]	0.4224[0.717]	111.7	[444]
Ethane, C ₂ H ₆			0.59861	55.8	75.7	(2.304)	45.47 [34035]	0.509[1.356] ^h	184.5	(1.038) ^h
Propane, C ₃ H ₈			0.58962	56.2	76.5	(2.262)	45.20	(1.879)	231.1	—
Isobutane, (CH ₃) ₂ CHCH ₃			0.58496	56.4	77.0	(2.239)	45.07 [16930]	[2.67]	261.42	[1900]
Octane, liquid, CH ₃ (CH ₂) ₆ CH ₃			0.57778	56.7	77.7	2.123	44.86 63.8	0.703	398.8	1.397
Paraffin wax, CH ₃ (CH ₂) _{n\approx23} CH ₃			0.57275	56.9	78.2	2.087	44.71 48.1	0.93		—
Nylon, type 6 ⁱ			0.54790	58.5	81.5	1.974	41.84 36.7	1.14		—
Polycarbonate (Lexan) ^j			0.52697	59.5	83.9	1.886	41.46 34.6	1.20		—
Polyethylene terephthalate (Mylar) ^k			0.52037	60.2	85.7	1.848	39.95 28.7	1.39		—
Polyethylene ^l			0.57034	57.0	78.4	2.076	44.64 ≈ 47.9	0.92–0.95		—
Polyimide film (Kapton) ^m			0.51264	60.3	85.8	1.820	40.56 28.6	1.42		—
Lucite, Plexiglas ⁿ			0.53937	59.3	83.0	1.929	40.49 ≈ 34.4	1.16–1.20		≈ 1.49
Polystyrene, scintillator ^o			0.53768	58.5	81.9	1.936	43.72 42.4	1.032		1.581
Polytetrafluoroethylene (Teflon) ^p			0.47992	64.2	93.0	1.671	34.84 15.8	2.20		—
Polyvinyltoluene, scintillator ^q			0.54155	58.3	81.5	1.956	43.83 42.5	1.032		—
Aluminum oxide (Al ₂ O ₃)			0.49038	67.0	98.9	1.647	19.27 4.85	3.97		1.761
Barium fluoride (BaF ₂)			0.42207	92.0	145	1.303	9.91 2.05	4.89		1.56
Bismuth germanate (BGO) ^r			0.42065	98.2	157	1.251	7.97 1.12	7.1		2.15
Cesium iodide (CsI)			0.41569	102	167	1.243	8.39 1.85	4.53		1.80
Lithium fluoride (LiF)			0.46262	62.2	88.2	1.614	39.25 14.91	2.632		1.392
Sodium fluoride (NaF)			0.47632	66.9	98.3	1.69	29.87 11.68	2.558		1.336
Sodium iodide (NaI)			0.42697	94.6	151	1.305	9.49 2.59	3.67		1.775
Silica Aerogel ^s			0.52019	64	92	1.83	29.83 ≈ 150	0.1–0.3		1.0+0.25 ρ
NEMA G10 plate ^t				62.6	90.2	1.87	33.0 19.4	1.7		—

Material	Dielectric constant ($\kappa = \epsilon/\epsilon_0$) () is $(\kappa-1)\times 10^6$ for gas	Young's modulus [10^6 psi]	Coeff. of thermal expansion [10^{-6} cm/cm- $^{\circ}$ C]	Specific heat [cal/g- $^{\circ}$ C]	Electrical resistivity [$\mu\Omega$ cm(@ $^{\circ}$ C)]	Thermal conductivity [cal/cm- $^{\circ}$ C-sec]
H ₂	(253.9)	—	—	—	—	—
He	(64)	—	—	—	—	—
Li	—	—	56	0.86	8.55(0 $^{\circ}$)	0.17
Be	—	37	12.4	0.436	5.885(0 $^{\circ}$)	0.38
C	—	0.7	0.6-4.3	0.165	1375(0 $^{\circ}$)	0.057
N ₂	(548.5)	—	—	—	—	—
O ₂	(495)	—	—	—	—	—
Ne	(127)	—	—	—	—	—
Al	—	10	23.9	0.215	2.65(20 $^{\circ}$)	0.53
Si	11.9	16	2.8-7.3	0.162	—	0.20
Ar	(517)	—	—	—	—	—
Ti	—	16.8	8.5	0.126	50(0 $^{\circ}$)	—
Fe	—	28.5	11.7	0.11	9.71(20 $^{\circ}$)	0.18
Cu	—	16	16.5	0.092	1.67(20 $^{\circ}$)	0.94
Ge	16.0	—	5.75	0.073	—	0.14
Sn	—	6	20	0.052	11.5(20 $^{\circ}$)	0.16
Xe	—	—	—	—	—	—
W	—	50	4.4	0.032	5.5(20 $^{\circ}$)	0.48
Pt	—	21	8.9	0.032	9.83(0 $^{\circ}$)	0.17
Pb	—	2.6	29.3	0.038	20.65(20 $^{\circ}$)	0.083
U	—	—	36.1	0.028	29(20 $^{\circ}$)	0.064

1. R.M. Sternheimer, M.J. Berger, and S.M. Seltzer, Atomic Data and Nuclear Data Tables **30**, 261-271 (1984).
2. S.M. Seltzer and M.J. Berger, Int. J. Appl. Radiat. **33**, 1189-1218 (1982).
3. D.E. Groom, N.V. Mokhov, and S.I. Striganov, "Muon stopping-power and range tables," Atomic Data and Nuclear Data Tables, to be published (2000).
4. S.M. Seltzer and M.J. Berger, Int. J. Appl. Radiat. **35**, 665 (1984) and <http://physics.nist.gov/PhysRefData/Star/Text/contents.html>.
 - a. σ_T , λ_T and λ_I are energy dependent. Values quoted apply to high energy range, where energy dependence is weak. Mean free path between collisions (λ_T) or inelastic interactions (λ_I), calculated from $\lambda^{-1} = N_A \sum w_j \sigma_j / A_j$, where N is Avogadro's number and w_j is the weight fraction of the j th element in the element, compound, or mixture. σ_{total} at 80-240 GeV for neutrons ($\approx \sigma$ for protons) from Murthy *et al.*, Nucl. Phys. **B92**, 269 (1975). This scales approximately as $A^{0.77}$. $\sigma_{\text{inelastic}} = \sigma_{\text{total}} - \sigma_{\text{elastic}} - \sigma_{\text{quasielastic}}$; for neutrons at 60-375 GeV from Roberts *et al.*, Nucl. Phys. **B159**, 56 (1979). For protons and other particles, see Carroll *et al.*, Phys. Lett. **80B**, 319 (1979); note that $\sigma_I(p) \approx \sigma_I(n)$. σ_I scales approximately as $A^{0.71}$.
 - b. For minimum-ionizing muons (results are very slightly different for other particles). Minimum dE/dx from Ref. 3, using density effect correction coefficients from Ref. 1. For electrons and positrons see Ref. 4. Ionization energy loss is discussed in Sec. 23.
 - c. From Y.S. Tsai, Rev. Mod. Phys. **46**, 815 (1974); X_0 data for all elements up to uranium are given. Corrections for molecular binding applied for H₂ and D₂. For atomic H, $X_0 = 63.05$ g/cm².
 - d. For molecular hydrogen (deuterium). For atomic H, $X_0 = 63.047$ g cm⁻².
 - e. For pure graphite; industrial graphite density may vary 2.1-2.3 g/cm³.
 - f. Standard shielding blocks, typical composition O₂ 52%, Si 32.5%, Ca 6%, Na 1.5%, Fe 2%, Al 4%, plus reinforcing iron bars. The attenuation length, $\ell = 115 \pm 5$ g/cm², is also valid for earth (typical $\rho = 2.15$), from CERN-LRL-RHEL Shielding exp., UCRL-17841 (1968).
 - g. For typical fused quartz. The specific gravity of crystalline quartz is 2.64.
 - h. Solid ethane density at -60 $^{\circ}$ C; gaseous refractive index at 0 $^{\circ}$ C, 546 mm pressure.
 - i. Nylon, Type 6, (NH(CH₂)₅CO)_n
 - j. Polycarbonate (Lexan), (C₁₆H₁₄O₃)_n
 - k. Polyethylene terephthalate, monomer, C₅H₄O₂
 - l. Polyethylene, monomer CH₂=CH₂
 - m. Polyimide film (Kapton), (C₂₂H₁₀N₂O₅)_n
 - n. Polymethylmethacrylate, monomer CH₂=C(CH₃)CO₂CH₃
 - o. Polystyrene, monomer C₆H₅CH=CH₂
 - p. Teflon, monomer CF₂=CF₂
 - q. Polyvinyltolulene, monomer 2-CH₃C₆H₄CH=CH₂
 - r. Bismuth germanate (BGO), (Bi₂O₃)₂(GeO₂)₃
 - s. $n(\text{SiO}_2) + 2n(\text{H}_2\text{O})$ used in Čerenkov counters, ρ = density in g/cm³. From M. Cantin *et al.*, Nucl. Instrum. Methods **118**, 177 (1974).
 - t. G10-plate, typically 60% SiO₂ and 40% epoxy.

7. ELECTROMAGNETIC RELATIONS

Quantity	Gaussian CGS	SI
Conversion factors: Charge: Potential: Magnetic field:	$2.997\,924\,58 \times 10^9$ esu $(1/299.792\,458)$ statvolt (ergs/esu) 10^4 gauss = 10^4 dyne/esu	$= 1\text{ C} = 1\text{ A s}$ $= 1\text{ V} = 1\text{ J C}^{-1}$ $= 1\text{ T} = 1\text{ N A}^{-1}\text{m}^{-1}$
Lorentz force:	$\mathbf{F} = q(\mathbf{E} + \frac{\mathbf{v}}{c} \times \mathbf{B})$	$\mathbf{F} = q(\mathbf{E} + \mathbf{v} \times \mathbf{B})$
Maxwell equations:	$\nabla \cdot \mathbf{D} = 4\pi\rho$ $\nabla \times \mathbf{H} - \frac{1}{c} \frac{\partial \mathbf{D}}{\partial t} = \frac{4\pi}{c} \mathbf{J}$ $\nabla \cdot \mathbf{B} = 0$ $\nabla \times \mathbf{E} + \frac{1}{c} \frac{\partial \mathbf{B}}{\partial t} = 0$	$\nabla \cdot \mathbf{D} = \rho$ $\nabla \times \mathbf{H} - \frac{\partial \mathbf{D}}{\partial t} = \mathbf{J}$ $\nabla \cdot \mathbf{B} = 0$ $\nabla \times \mathbf{E} + \frac{\partial \mathbf{B}}{\partial t} = 0$
Constitutive relations:	$\mathbf{D} = \mathbf{E} + 4\pi\mathbf{P}$, $\mathbf{H} = \mathbf{B} - 4\pi\mathbf{M}$	$\mathbf{D} = \epsilon_0\mathbf{E} + \mathbf{P}$, $\mathbf{H} = \mathbf{B}/\mu_0 - \mathbf{M}$
Linear media: Permittivity of free space: Permeability of free space:	$\mathbf{D} = \epsilon\mathbf{E}$, $\mathbf{H} = \mathbf{B}/\mu$ 1 1	$\mathbf{D} = \epsilon\mathbf{E}$, $\mathbf{H} = \mathbf{B}/\mu$ $\epsilon_0 = 8.854\,187 \dots \times 10^{-12}$ F m ⁻¹ $\mu_0 = 4\pi \times 10^{-7}$ N A ⁻²
Fields from potentials:	$\mathbf{E} = -\nabla V - \frac{1}{c} \frac{\partial \mathbf{A}}{\partial t}$ $\mathbf{B} = \nabla \times \mathbf{A}$	$\mathbf{E} = -\nabla V - \frac{\partial \mathbf{A}}{\partial t}$ $\mathbf{B} = \nabla \times \mathbf{A}$
Static potentials: (coulomb gauge)	$V = \sum_{\text{charges}} \frac{q_i}{r_i} = \int \frac{\rho(\mathbf{r}')}{ \mathbf{r} - \mathbf{r}' } d^3x'$ $\mathbf{A} = \frac{1}{c} \oint \frac{I d\boldsymbol{\ell}}{ \mathbf{r} - \mathbf{r}' } = \frac{1}{c} \int \frac{\mathbf{J}(\mathbf{r}')}{ \mathbf{r} - \mathbf{r}' } d^3x'$	$V = \frac{1}{4\pi\epsilon_0} \sum_{\text{charges}} \frac{q_i}{r_i} = \frac{1}{4\pi\epsilon_0} \int \frac{\rho(\mathbf{r}')}{ \mathbf{r} - \mathbf{r}' } d^3x'$ $\mathbf{A} = \frac{\mu_0}{4\pi} \oint \frac{I d\boldsymbol{\ell}}{ \mathbf{r} - \mathbf{r}' } = \frac{\mu_0}{4\pi} \int \frac{\mathbf{J}(\mathbf{r}')}{ \mathbf{r} - \mathbf{r}' } d^3x'$
Relativistic transformations: (\mathbf{v} is the velocity of the primed frame as seen in the unprimed frame)	$\mathbf{E}'_{\parallel} = \mathbf{E}_{\parallel}$ $\mathbf{E}'_{\perp} = \gamma(\mathbf{E}_{\perp} + \frac{1}{c} \mathbf{v} \times \mathbf{B})$ $\mathbf{B}'_{\parallel} = \mathbf{B}_{\parallel}$ $\mathbf{B}'_{\perp} = \gamma(\mathbf{B}_{\perp} - \frac{1}{c} \mathbf{v} \times \mathbf{E})$	$\mathbf{E}'_{\parallel} = \mathbf{E}_{\parallel}$ $\mathbf{E}'_{\perp} = \gamma(\mathbf{E}_{\perp} + \mathbf{v} \times \mathbf{B})$ $\mathbf{B}'_{\parallel} = \mathbf{B}_{\parallel}$ $\mathbf{B}'_{\perp} = \gamma(\mathbf{B}_{\perp} - \frac{1}{c^2} \mathbf{v} \times \mathbf{E})$
	$\frac{1}{4\pi\epsilon_0} = c^2 \times 10^{-7} \text{ N A}^{-2} = 8.987\,55 \dots \times 10^9 \text{ m F}^{-1}$; $\frac{\mu_0}{4\pi} = 10^{-7} \text{ N A}^{-2}$; $c = \frac{1}{\sqrt{\mu_0\epsilon_0}} = 2.997\,924\,58 \times 10^8 \text{ m s}^{-1}$	

7.1. Impedances (SI units)

ρ = resistivity at room temperature in $10^{-8} \Omega \text{ m}$:
 ~ 1.7 for Cu ~ 5.5 for W
 ~ 2.4 for Au ~ 73 for SS 304
 ~ 2.8 for Al ~ 100 for Nichrome
 (Al alloys may have double the Al value.)

For alternating currents, instantaneous current I , voltage V , angular frequency ω :

$$V = V_0 e^{j\omega t} = ZI. \quad (7.1)$$

Impedance of self-inductance L : $Z = j\omega L$.

Impedance of capacitance C : $Z = 1/j\omega C$.

Impedance of free space: $Z = \sqrt{\mu_0/\epsilon_0} = 376.7 \Omega$.

High-frequency surface impedance of a good conductor:

$$Z = \frac{(1+j)\rho}{\delta}, \quad \text{where } \delta = \text{skin depth}; \quad (7.2)$$

$$\delta = \sqrt{\frac{\rho}{\pi\nu\mu}} \approx \frac{6.6 \text{ cm}}{\sqrt{\nu(\text{Hz})}} \quad \text{for Cu}. \quad (7.3)$$

7.2. Capacitance \hat{C} and inductance \hat{L} per unit length (SI units) [negligible skin depth]

Flat rectangular plates of width w , separated by $d \ll w$ with linear medium (ϵ, μ) between:

$$\hat{C} = \epsilon \frac{w}{d}; \quad \hat{L} = \mu \frac{d}{w}; \quad (7.4)$$

$$\epsilon/\epsilon_0 = 2 \text{ to } 6 \text{ for plastics; } 4 \text{ to } 8 \text{ for porcelain, glasses;} \quad (7.5)$$

$$\mu/\mu_0 \approx 1. \quad (7.6)$$

Coaxial cable of inner radius r_1 , outer radius r_2 :

$$\hat{C} = \frac{2\pi\epsilon}{\ln(r_2/r_1)}; \quad \hat{L} = \frac{\mu}{2\pi} \ln(r_2/r_1). \quad (7.7)$$

Transmission lines (no loss):

$$\text{Impedance: } Z = \sqrt{\hat{L}/\hat{C}}. \quad (7.8)$$

$$\text{Velocity: } v = 1/\sqrt{\hat{L}\hat{C}} = 1/\sqrt{\mu\epsilon}. \quad (7.9)$$

7.3. Synchrotron radiation (CGS units)

For a particle of charge e , velocity $v = \beta c$, and energy $E = \gamma mc^2$, traveling in a circular orbit of radius R , the classical energy loss per revolution δE is

$$\delta E = \frac{4\pi}{3} \frac{e^2}{R} \beta^3 \gamma^4. \quad (7.10)$$

For high-energy electrons or positrons ($\beta \approx 1$), this becomes

$$\delta E \text{ (in MeV)} \approx 0.0885 [E(\text{in GeV})]^4/R(\text{in m}). \quad (7.11)$$

For $\gamma \gg 1$, the energy radiated per revolution into the photon energy interval $d(\hbar\omega)$ is

$$dI = \frac{8\pi}{9} \alpha \gamma F(\omega/\omega_c) d(\hbar\omega), \quad (7.12)$$

where $\alpha = e^2/\hbar c$ is the fine-structure constant and

$$\omega_c = \frac{3\gamma^3 c}{2R} \quad (7.13)$$

is the critical frequency. The normalized function $F(y)$ is

$$F(y) = \frac{9}{8\pi} \sqrt{3} y \int_y^\infty K_{5/3}(x) dx, \quad (7.14)$$

where $K_{5/3}(x)$ is a modified Bessel function of the third kind. For electrons or positrons,

$$\hbar\omega_c \text{ (in keV)} \approx 2.22 [E(\text{in GeV})]^3/R(\text{in m}). \quad (7.15)$$

Fig. 7.1 shows $F(y)$ over the important range of y .

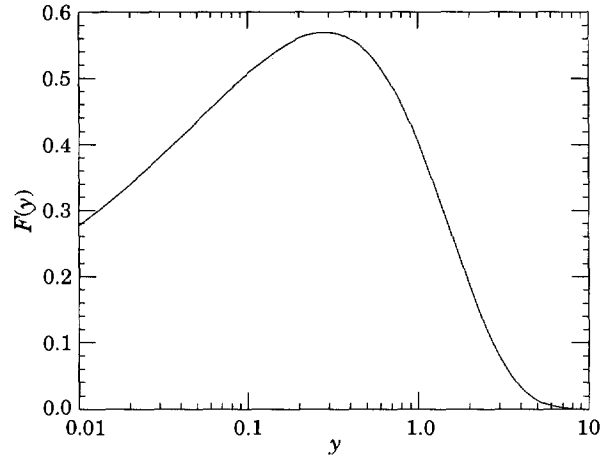


Figure 7.1: The normalized synchrotron radiation spectrum $F(y)$.

For $\gamma \gg 1$ and $\omega \ll \omega_c$,

$$\frac{dI}{d(\hbar\omega)} \approx 3.3\alpha (\omega R/c)^{1/3}, \quad (7.16)$$

whereas for

$$\gamma \gg 1 \text{ and } \omega \gtrsim 3\omega_c,$$

$$\frac{dI}{d(\hbar\omega)} \approx \sqrt{\frac{3\pi}{2}} \alpha \gamma \left(\frac{\omega}{\omega_c}\right)^{1/2} e^{-\omega/\omega_c} \left[1 + \frac{55}{72} \frac{\omega_c}{\omega} + \dots\right]. \quad (7.17)$$

The radiation is confined to angles $\lesssim 1/\gamma$ relative to the instantaneous direction of motion. The mean number of photons emitted per revolution is

$$N_\gamma = \frac{5\pi}{\sqrt{3}} \alpha \gamma, \quad (7.18)$$

and the mean energy per photon is

$$\langle \hbar\omega \rangle = \frac{8}{15\sqrt{3}} \hbar\omega_c. \quad (7.19)$$

When $\langle \hbar\omega \rangle \gtrsim O(E)$, quantum corrections are important.

See J.D. Jackson, *Classical Electrodynamics*, 2nd edition (John Wiley & Sons, New York, 1975) for more formulae and details. In his book, Jackson uses a definition of ω_c that is twice as large as the customary one given above.

8. NAMING SCHEME FOR HADRONS

Maintained 2000 by M. Roos (University of Finland) and C.G. Wohl (LBNL).

8.1. Introduction

We introduced in the 1986 edition [1] a new naming scheme for the hadrons. Changes from older terminology affected mainly the heavier mesons made of the light (u , d , and s) quarks. Old and new names were listed alongside until 1994. Names also change from edition to edition because some characteristic like mass or spin changes. The Summary Tables give both the new and old names whenever a change occurred.

8.2. “Neutral-flavor” mesons ($S=C=B=T=0$)

Table 8.1 shows the names for mesons having the strangeness and all heavy-flavor quantum numbers equal to zero. The scheme is designed for all ordinary non-exotic mesons, but it will work for many exotic types too, if needed.

Table 8.1: Symbols for mesons with the strangeness and all heavy-flavor quantum numbers equal to zero.

J^{PC}	$\begin{cases} 0^{-+} \\ 2^{-+} \\ \vdots \end{cases}$	$\begin{cases} 1^{+-} \\ 3^{+-} \\ \vdots \end{cases}$	$\begin{cases} 1^{--} \\ 2^{--} \\ \vdots \end{cases}$	$\begin{cases} 0^{++} \\ 1^{++} \\ \vdots \end{cases}$
$q\bar{q}$ content	${}^{2S+1}L_J = {}^1(L\text{ even})_J$	${}^1(L\text{ odd})_J$	${}^3(L\text{ even})_J$	${}^3(L\text{ odd})_J$
$u\bar{d}, u\bar{u} - d\bar{d}, d\bar{u}$ ($I=1$)	π	b	ρ	a
$d\bar{d} + u\bar{u}$ and/or $s\bar{s}$ } ($I=0$)	η, η'	h, h'	ω, ϕ	f, f'
$c\bar{c}$	η_c	h_c	ψ^1	χ_c
$b\bar{b}$	η_b	h_b	Υ	χ_b
$t\bar{t}$	η_t	h_t	θ	χ_t

[†]The J/ψ remains the J/ψ .

First, we assign names to those states with quantum numbers compatible with being $q\bar{q}$ states. The rows of the Table give the possible $q\bar{q}$ content. The columns give the possible parity/charge-conjugation states,

$$PC = --, +-, --, \text{ and } ++;$$

these combinations correspond one-to-one with the angular-momentum state ${}^{2S+1}L_J$ of the $q\bar{q}$ system being

$${}^1(L\text{ even})_J, {}^1(L\text{ odd})_J, {}^3(L\text{ even})_J, \text{ or } {}^3(L\text{ odd})_J.$$

Here S , L , and J are the spin, orbital, and total angular momenta of the $q\bar{q}$ system. The quantum numbers are related by

$$P = (-1)^{L+1}, C = (-1)^{L+S}, \text{ and } G \text{ parity} = (-1)^{L+S+I},$$

where of course the C quantum number is only relevant to neutral mesons.

The entries in the Table give the meson names. The spin J is added as a subscript except for pseudoscalar and vector mesons, and the mass is added in parentheses for mesons that decay strongly. However, for the lightest meson resonances, we omit the mass.

Measurements of the mass, quark content (where relevant), and quantum numbers I , J , P , and C (or G) of a meson thus fix its symbol. Conversely, these properties may be inferred unambiguously from the symbol.

If the main symbol cannot be assigned because the quantum numbers are unknown, X is used. Sometimes it is not known whether a meson is mainly the isospin-0 mix of $u\bar{u}$ and $d\bar{d}$ or is mainly $s\bar{s}$. A prime (or pair ω , ϕ) may be used to distinguish two such mixing states.

We follow custom and use spectroscopic names such as $T(1S)$ as the primary name for most of those ψ , T , and χ states whose spectroscopic identity is known. We use the form $T(9460)$ as an alternative, and as the primary name when the spectroscopic identity is not known.

Names are assigned for $t\bar{t}$ mesons, although the top quark is evidently so heavy that it is expected to decay too rapidly for bound states to form.

Gluonium states or other mesons that are not $q\bar{q}$ states are, if the quantum numbers are *not* exotic, to be named just as are the $q\bar{q}$ mesons. Such states will probably be difficult to distinguish from $q\bar{q}$ states and will likely mix with them, and we make no attempt to distinguish those “mostly gluonium” from those “mostly $q\bar{q}$.”

An “exotic” meson with J^{PC} quantum numbers that a $q\bar{q}$ system cannot have, namely $J^{PC} = 0^{-+}, 0^{+-}, 1^{-+}, 2^{+-}, 3^{-+}, \dots$, would use the same symbol as does an ordinary meson with all the same quantum numbers as the exotic meson except for the C parity. But then the J subscript may still distinguish it; for example, an isospin-0 1^{-+} meson could be denoted ω_1 .

8.3. Mesons with nonzero S , C , B , and/or T

Since the strangeness or a heavy flavor of these mesons is nonzero, none of them are eigenstates of charge conjugation, and in each of them one of the quarks is heavier than the other. The rules are:

1. The main symbol is an upper-case italic letter indicating the heavier quark as follows:

$$s \rightarrow \bar{K} \quad c \rightarrow D \quad b \rightarrow \bar{B} \quad t \rightarrow T.$$

We use the convention that *the flavor and the charge of a quark have the same sign*. Thus the strangeness of the s quark is negative, the charm of the c quark is positive, and the bottom of the b quark is negative. In addition, I_3 of the u and d quarks are positive and negative, respectively. The effect of this convention is as follows: *Any flavor carried by a charged meson has the same sign as its charge*. Thus the K^+ , D^+ , and B^+ have positive strangeness, charm, and bottom, respectively, and all have positive I_3 . The D_s^+ has positive charm *and* strangeness. Furthermore, the $\Delta(\text{flavor}) = \Delta Q$ rule, best known for the kaons, applies to every flavor.

2. If the lighter quark is not a u or a d quark, its identity is given by a subscript. The D_s^+ is an example.
3. If the spin-parity is in the “normal” series, $J^P = 0^+, 1^-, 2^+, \dots$, a superscript “*” is added.
4. The spin is added as a subscript except for pseudoscalar or vector mesons.

8.4. Baryons

The symbols N , Δ , Λ , Σ , Ξ , and Ω used for more than 30 years for the baryons made of light quarks (u , d , and s quarks) tell the isospin and quark content, and the same information is conveyed by the symbols used for the baryons containing one or more heavy quarks (c and b quarks). The rules are:

1. Baryons with *three* u and/or d quarks are N 's (isospin 1/2) or Δ 's (isospin 3/2).
2. Baryons with *two* u and/or d quarks are Λ 's (isospin 0) or Σ 's (isospin 1). If the third quark is a c , b , or t quark, its identity is given by a subscript.
3. Baryons with *one* u or d quark are Ξ 's (isospin 1/2). One or two subscripts are used if one or both of the remaining quarks are heavy: thus Ξ_c , Ξ_{cc} , Ξ_b , *etc.**
4. Baryons with *no* u or d quarks are Ω 's (isospin 0), and subscripts indicate any heavy-quark content.
5. A baryon that decays strongly has its mass as part of its name. Thus p , Σ^- , Ω^- , Λ_c^+ , *etc.*, but $\Delta(1232)^0$, $\Sigma(1385)^-$, $\Xi_c(2645)^+$, *etc.*

In short, the number of u plus d quarks together with the isospin determine the main symbol, and subscripts indicate any content of heavy quarks. A Σ always has isospin 1, an Ω always has isospin 0, *etc.*

Footnote and Reference:

- * Sometimes a prime is necessary to distinguish two Ξ_c 's in the same $SU(n)$ multiplet. See the “Note on Charmed Baryons” in the Charmed Baryon Listings.
1. Particle Data Group: M. Aguilar-Benitez *et al.*, Phys. Lett. **170B** (1986).

9. QUANTUM CHROMODYNAMICS

9.1. The QCD Lagrangian

Revised September 1999 by I. Hinchliffe (LBNL).

Quantum Chromodynamics (QCD), the gauge field theory which describes the strong interactions of colored quarks and gluons, is one of the components of the $SU(3) \times SU(2) \times U(1)$ Standard Model. A quark of specific flavor (such as a charm quark) comes in 3 colors; gluons come in eight colors; hadrons are color-singlet combinations of quarks, anti-quarks, and gluons. The Lagrangian describing the interactions of quarks and gluons is (up to gauge-fixing terms)

$$L_{\text{QCD}} = -\frac{1}{4} F_{\mu\nu}^{(a)} F^{(a)\mu\nu} + i \sum_q \bar{\psi}_q^i \gamma^\mu (D_\mu)_{ij} \psi_q^j - \sum_q m_q \bar{\psi}_q^i \psi_{qi}, \quad (9.1)$$

$$F_{\mu\nu}^{(a)} = \partial_\mu A_\nu^a - \partial_\nu A_\mu^a + g_s f_{abc} A_\mu^b A_\nu^c, \quad (9.2)$$

$$(D_\mu)_{ij} = \delta_{ij} \partial_\mu - i g_s \sum_a \frac{\lambda_{ij}^a}{2} A_\mu^a, \quad (9.3)$$

where g_s is the QCD coupling constant, and the f_{abc} are the structure constants of the $SU(3)$ algebra (the λ matrices and values for f_{abc} can be found in ‘‘SU(3) Isoscalar Factors and Representation Matrices,’’ Sec. 32 of this *Review*). The $\psi_q^i(x)$ are the 4-component Dirac spinors associated with each quark field of (3) color i and flavor q , and the $A_\mu^a(x)$ are the (8) Yang-Mills (gluon) fields. A complete list of the Feynman rules which derive from this Lagrangian, together with some useful color-algebra identities, can be found in Ref. 1.

The principle of ‘‘asymptotic freedom’’ (see below) determines that the renormalized QCD coupling is small only at high energies, and it is only in this domain that high-precision tests—similar to those in QED—can be performed using perturbation theory. Nonetheless, there has been in recent years much progress in understanding and quantifying the predictions of QCD in the nonperturbative domain, for example, in soft hadronic processes and on the lattice [2]. This short review will concentrate on QCD at short distances (large momentum transfers), where perturbation theory is the standard tool. It will discuss the processes that are used to determine the coupling constant of QCD. Other recent reviews of the coupling constant measurements may be consulted for a different perspective [3,4].

9.2. The QCD coupling and renormalization scheme

The renormalization scale dependence of the effective QCD coupling $\alpha_s = g_s^2/4\pi$ is controlled by the β -function:

$$\mu \frac{\partial \alpha_s}{\partial \mu} = -\frac{\beta_0}{2\pi} \alpha_s^2 - \frac{\beta_1}{4\pi^2} \alpha_s^3 - \frac{\beta_2}{64\pi^3} \alpha_s^4 - \dots, \quad (9.4a)$$

$$\beta_0 = 11 - \frac{2}{3} n_f, \quad (9.4b)$$

$$\beta_1 = 51 - \frac{19}{3} n_f, \quad (9.4c)$$

$$\beta_2 = 2857 - \frac{5033}{9} n_f + \frac{325}{27} n_f^2; \quad (9.4d)$$

where n_f is the number of quarks with mass less than the energy scale μ . The expression for the next term in this series (β_3) can be found in Ref. 5. In solving this differential equation for α_s , a constant of integration is introduced. This constant is the one fundamental constant of QCD that must be determined from experiment. The most sensible choice for this constant is the value of α_s at a fixed-reference scale μ_0 . It has become standard to choose $\mu_0 = M_Z$. It is also convenient to introduce the dimensional parameter Λ , since this provides a parameterization of the μ dependence of α_s . The definition of Λ is arbitrary. One way to define it (adopted here) is to write a solution of Eq. (9.4) as an expansion in inverse powers of $\ln(\mu^2)$:

$$\alpha_s(\mu) = \frac{4\pi}{\beta_0 \ln(\mu^2/\Lambda^2)} \left[1 - \frac{2\beta_1}{\beta_0^2} \frac{\ln[\ln(\mu^2/\Lambda^2)]}{\ln(\mu^2/\Lambda^2)} + \frac{4\beta_1^2}{\beta_0^3 \ln^2(\mu^2/\Lambda^2)} \right. \\ \left. \times \left(\left(\ln[\ln(\mu^2/\Lambda^2)] - \frac{1}{2} \right)^2 + \frac{\beta_2 \beta_0}{8\beta_1^2} - \frac{5}{4} \right) \right]. \quad (9.5a)$$

The last term in this expansion is

$$\mathcal{O} \left(\frac{\ln^2[\ln(\mu^2/\Lambda^2)]}{\ln^3(\mu^2/\Lambda^2)} \right), \quad (9.5b)$$

and is usually neglected in the definition of Λ . We choose to include it. For a fixed value of $\alpha_s(M_Z)$, the inclusion of this term shifts the value of Λ by ~ 15 MeV. This solution illustrates the *asymptotic freedom* property: $\alpha_s \rightarrow 0$ as $\mu \rightarrow \infty$.

Consider a ‘‘typical’’ QCD cross section which, when calculated perturbatively, starts at $\mathcal{O}(\alpha_s)$:

$$\sigma = A_1 \alpha_s + A_2 \alpha_s^2 + \dots \quad (9.6)$$

The coefficients A_1, A_2 come from calculating the appropriate Feynman diagrams. In performing such calculations, various divergences arise, and these must be regulated in a consistent way. This requires a particular renormalization scheme (RS). The most commonly used one is the modified minimal subtraction ($\overline{\text{MS}}$) scheme [6]. This involves continuing momentum integrals from 4 to $4-2\epsilon$ dimensions, and then subtracting off the resulting $1/\epsilon$ poles and also $(\ln 4\pi - \gamma_E)$, which is another artifact of continuing the dimension. (Here γ_E is the Euler-Mascheroni constant.) To preserve the dimensionless nature of the coupling, a mass scale μ must also be introduced: $g \rightarrow \mu^\epsilon g$. The finite coefficients A_i ($i \geq 2$) thus obtained depend implicitly on the renormalization convention used and explicitly on the scale μ .

The first two coefficients (β_0, β_1) in Eq. (9.4) are independent of the choice of RS's. In contrast, the coefficients of terms proportional to α_s^n for $n > 3$ are RS-dependent. The form given above for β_2 is in the $\overline{\text{MS}}$ scheme.

The fundamental theorem of RS dependence is straightforward. Physical quantities, in particular the cross section, calculated to all orders in perturbation theory, do not depend on the RS. It follows that a truncated series *does* exhibit RS dependence. In practice, QCD cross sections are known to leading order (LO), or to next-to-leading order (NLO), or in a few cases, to next-to-next-to-leading order (NNLO); and it is only the latter two cases, which have reduced RS dependence, that are useful for precision tests. At NLO the RS dependence is completely given by one condition which can be taken to be the value of the renormalization scale μ . At NNLO this is not sufficient, and μ is no longer equivalent to a choice of scheme; both must now be specified. One, therefore, has to address the question of what is the ‘‘best’’ choice for μ within a given scheme, usually $\overline{\text{MS}}$. There is no definite answer to this question—higher-order corrections do not ‘‘fix’’ the scale, rather they render the theoretical predictions less sensitive to its variation.

One should expect that choosing a scale μ characteristic of the typical energy scale (E) in the process would be most appropriate. In general, a poor choice of scale generates terms of order $\ln(E/\mu)$ in the A_i 's. Various methods have been proposed including choosing the scale for which the next-to-leading-order correction vanishes (‘‘Fastest Apparent Convergence [7]’’); the scale for which the next-to-leading-order prediction is stationary [8], (i.e., the value of μ where $d\sigma/d\mu = 0$); or the scale dictated by the effective charge scheme [9] or by the BLM scheme [10]. By comparing the values of α_s that different reasonable schemes give, an estimate of theoretical errors can be obtained. It has also been suggested to replace the perturbation series by its Padé approximant [11]. Results obtained using this method have, in certain cases, a reduced scale dependence [12,13]. One can also attempt to determine the scale from data by allowing it to vary and using a fit to determine it. This method can allow a determination of the error due to the scale choice and can give more confidence in the end result [14]. In many of the cases discussed below this scale uncertainty is the dominant error.

An important corollary is that if the higher-order corrections are naturally small, then the additional uncertainties introduced by the μ dependence are likely to be small. There are some processes, however, for which the choice of scheme *can* influence the extracted value of $\alpha_s(M_Z)$. There is no resolution to this problem other than to try to

calculate even more terms in the perturbation series. It is important to note that, since the perturbation series is an asymptotic expansion, there is a limit to the precision with which any theoretical quantity can be calculated. In some processes, the highest-order perturbative terms may be comparable in size to nonperturbative corrections (sometimes called higher-twist or renormalon effects, for a discussion see [15]); an estimate of these terms and their uncertainties is required if a value of α_s is to be extracted.

Cases occur where there is more than one large scale, say μ_1 and μ_2 . In these cases, terms appear of the form $\log(\mu_1/\mu_2)$. If the ratio μ_1/μ_2 is large, these logarithms can render naive perturbation theory unreliable and a modified perturbation expansion that takes these terms into account must be used. A few examples are discussed below.

In the cases where the higher-order corrections to a process are known and are large, some caution should be exercised when quoting the value of α_s . In what follows, we will attempt to indicate the size of the theoretical uncertainties on the extracted value of α_s . There are two simple ways to determine this error. First, we can estimate it by comparing the value of $\alpha_s(\mu)$ obtained by fitting data using the QCD formula to highest known order in α_s , and then comparing it with the value obtained using the next-to-highest-order formula (μ is chosen as the typical energy scale in the process). The corresponding Λ 's are then obtained by evolving $\alpha_s(\mu)$ to $\mu = M_Z$ using Eq. (9.4) to the same order in α_s as the fit. Alternatively, we can vary the value of μ over a reasonable range, extracting a value of Λ for each choice of μ . This method is by its nature imprecise, since "reasonable" involves a subjective judgment. In either case, if the perturbation series is well behaved, the resulting error on $\alpha_s(M_Z)$ will be small.

In the above discussion we have ignored quark-mass effects, *i.e.*, we have assumed an idealized situation where quarks of mass greater than μ are neglected completely. In this picture, the β -function coefficients change by discrete amounts as flavor thresholds (a quark of mass M) are crossed when integrating the differential equation for α_s . Now imagine an experiment at energy scale μ ; for example, this could be $e^+e^- \rightarrow$ hadrons at center-of-mass energy μ . If $\mu \gg M$, the mass M is negligible and the process is well described by QCD with n_f massless flavors and its parameter $\alpha_{(n_f)}$ up to terms of order M^2/μ^2 . Conversely if $\mu \ll M$, the heavy quark plays no role and the process is well described by QCD with $n_f - 1$ massless flavors and its parameter $\alpha_{(n_f-1)}$ up to terms of order μ^2/M^2 . If $\mu \sim M$, the effects of the quark mass are process-dependent and cannot be absorbed into the running coupling. The values of $\alpha_{(n_f)}$ and $\alpha_{(n_f-1)}$ are related so that a physical quantity calculated in both "theories" gives the same result [16]. This implies

$$\alpha_{(n_f)}(M) = \alpha_{(n_f-1)}(M) - \frac{7}{72\pi^2} \alpha_{(n_f-1)}^2(M) \quad (9.7)$$

which is almost identical to the naive result $\alpha_{(n_f)}(M) = \alpha_{(n_f-1)}(M)$. Here M is the mass of the value of the running quark mass defined in the $\overline{\text{MS}}$ scheme (see the note on "Quark Masses" in the Particle Listings for more details), *i.e.*, where $M_{\overline{\text{MS}}}(M) = M$.

It also follows that, for a relationship such as Eq. (9.5) to remain valid for all values of μ , Λ must also change as flavor thresholds are crossed, the value corresponds to an effective number of massless quarks: $\Lambda \rightarrow \Lambda^{(n_f)}$ [16,17]. The formulae are given in the previous edition of this review.

An alternative matching procedure can be used [18]. This procedure requires the equality $\alpha_s(\mu)^{(n_f)} = \alpha_s(\mu)^{(n_f-1)}$ for $\mu = M$. This matching is somewhat arbitrary; a different relation between $\Lambda^{(n_f)}$ and $\Lambda^{(n_f-1)}$ would result if $\mu = M/2$ were used. In practice, the differences between these procedures are very small. $\Lambda^{(5)} = 200$ MeV corresponds to $\Lambda^{(4)} = 289$ MeV in the scheme of Ref. 18 and $\Lambda^{(4)} = 280$ MeV in the scheme we adopt. Note that the differences between $\Lambda^{(5)}$ and $\Lambda^{(4)}$ are numerically very significant.

Data from deep-inelastic scattering are in a range of energy where the bottom quark is not readily excited, and hence, these experiments quote $\Lambda_{\overline{\text{MS}}}^{(4)}$. Most data from PEP, PETRA, TRISTAN, LEP, and SLC quote a value of $\Lambda_{\overline{\text{MS}}}^{(5)}$ since these data are in an energy range

where the bottom quark is light compared to the available energy. We have converted it to $\Lambda_{\overline{\text{MS}}}^{(4)}$ as required. A few measurements, including the lattice gauge theory values from the $J\psi$ system, and from τ decay are at sufficiently low energy that $\Lambda_{\overline{\text{MS}}}^{(3)}$ is appropriate.

In order to compare the values of α_s from various experiments, they must be evolved using the renormalization group to a common scale. For convenience, this is taken to be the mass of the Z boson. This evolution uses third-order perturbation theory and can introduce additional errors particularly if extrapolation from very small scales is used. The variation in the charm and bottom quark masses ($m_b = 4.3 \pm 0.2$ GeV and $m_c = 1.3 \pm 0.3$ GeV are used) can also introduce errors. These result in a fixed value of $\alpha_s(2 \text{ GeV})$ giving an uncertainty in $\alpha_s(M_Z) = \pm 0.001$ if only perturbative evolution is used. There could be additional errors from nonperturbative effects that enter at low energy.

9.3. QCD in deep-inelastic scattering

The original and still one of the most powerful quantitative tests of perturbative QCD is the breaking of Bjorken scaling in deep-inelastic lepton-hadron scattering. In the leading-logarithm approximation, the measured structure functions $F_i(x, Q^2)$ are related to the quark distribution functions $q_i(x, Q^2)$ according to the naive parton model, by the formulae in "Cross-section Formulae for Specific Processes," Sec. 35 of this Review. (In that section, q_i is denoted by the notation f_q .) In describing the way in which scaling is broken in QCD, it is convenient to define nonsinglet and singlet quark distributions:

$$F^{NS} = q_i - q_j \quad F^S = \sum_i (q_i + \bar{q}_i) \quad (9.8)$$

The nonsinglet structure functions have nonzero values of flavor quantum numbers such as isospin or baryon number. The variation with Q^2 of these is described by the so-called DGLAP equations [19,20]:

$$Q^2 \frac{\partial F^{NS}}{\partial Q^2} = \frac{\alpha_s(|Q|)}{2\pi} P^{qq} * F^{NS} \quad (9.9a)$$

$$Q^2 \frac{\partial}{\partial Q^2} \begin{pmatrix} F^S \\ G \end{pmatrix} = \frac{\alpha_s(|Q|)}{2\pi} \begin{pmatrix} P^{qq} & 2n_f P^{qg} \\ P^{gq} & P^{gg} \end{pmatrix} * \begin{pmatrix} F^S \\ G \end{pmatrix} \quad (9.9b)$$

where $*$ denotes a convolution integral:

$$f * g = \int_x^1 \frac{dy}{y} f(y) g\left(\frac{x}{y}\right) \quad (9.10)$$

The leading-order Altarelli-Parisi [20] splitting functions are

$$P^{qq} = \frac{4}{3} \left[\frac{1+x^2}{(1-x)_+} \right] + 2\delta(1-x), \quad (9.11a)$$

$$P^{qg} = \frac{1}{2} \left[x^2 + (1-x)^2 \right], \quad (9.11b)$$

$$P^{gq} = \frac{4}{3} \left[\frac{1+(1-x)^2}{x} \right], \quad (9.11c)$$

$$P^{gg} = 6 \left[\frac{1-x}{x} + x(1-x) + \frac{x}{(1-x)_+} + \frac{11}{12} \delta(1-x) \right] - \frac{n_f}{3} \delta(1-x). \quad (9.11d)$$

Here the gluon distribution $G(x, Q^2)$ has been introduced and $1/(1-x)_+$ means

$$\int_0^1 dx \frac{f(x)}{(1-x)_+} = \int_0^1 dx \frac{f(x) - f(1)}{(1-x)}. \quad (9.12)$$

The precision of contemporary experimental data demands that higher-order corrections also be included [21]. The above results are for massless quarks. At low Q^2 values, there are also important "higher-twist" (HT) contributions of the form:

$$F_i(x, Q^2) = F_i^{(LT)}(x, Q^2) + \frac{F_i^{(HT)}(x, Q^2)}{Q^2} + \dots \quad (9.13)$$

Leading twist (LT) indicates a term whose behavior is predicted by perturbative QCD. These corrections are numerically important only for $Q^2 < \mathcal{O}(\text{few GeV}^2)$ except for x very close to 1. At very large values of x perturbative corrections proportional to $\log(1-x)$ can become important [22].

A detailed review of the current status of the experimental data can be found, for example, in Refs. [23–26], and only a brief summary will be presented here. We shall only include determinations of Λ from the recently published results; the earlier editions of this *Review* should be consulted for the earlier data. Data now exist from HERA at much smaller values of x than the fixed-target data. They provide valuable information about the shape of the antiquark and gluon distribution functions at $x \sim 10^{-4}$ [27].

From Eq. (9.9), it is clear that a nonsinglet structure function offers in principle the most precise test of the theory, since the Q^2 evolution is independent of the unmeasured gluon distribution. The CCFR collaboration fit to the Gross-Llewellyn Smith sum rule [28] which is known to order α_s^3 [29,30] (Estimates of the order α_s^4 term are available [31])

$$\int_0^1 dx \left(F_3^{\bar{\nu}p}(x, Q^2) + F_3^{\nu p}(x, Q^2) \right) = 3 \left[1 - \frac{\alpha_s}{\pi} (1 + 3.58 \frac{\alpha_s}{\pi} + 19.0 \left(\frac{\alpha_s}{\pi} \right)^2) - \Delta HT \right], \quad (9.14)$$

where the higher-twist contribution ΔHT is estimated to be $(0.09 \pm 0.045)/Q^2$ in Refs. [29,32] and to be somewhat smaller by Ref. 33. The CCFR collaboration [35], combines their data with that from other experiments [36] and gives $\alpha_s(\sqrt{3} \text{ GeV}) = 0.28 \pm 0.035$ (expt.) ± 0.05 (sys) $_{-0.03}^{+0.035}$ (theory). The error from higher-twist terms (assumed to be $\Delta HT = 0.05 \pm 0.05$) dominates the theoretical error. If the higher twist result of Ref. 33 is used, the central value increases to 0.31 in agreement with the fit of [37]. This value corresponds to $\alpha_s(M_Z) = 0.118 \pm 0.011$.

Measurements involving singlet-dominated structure functions, such as F_2 , result in measurements of α_s and the gluon structure function. A full next-to-leading-order fit combining data from SLAC [38], BCDMS [39], E665 [40] and HERA [27] has been performed by Ref. 41. These authors extend the analysis to next-to-next-to-leading order (NNLO). In this case the full theoretical calculation is not available as not all the three loop anomalous dimensions are known; their analysis uses moments of structure functions and is restricted to those moments where the full calculation is available [21,42,37]. The NNLO result is $\alpha_s(M_Z) = 0.1172 \pm 0.0017$ (expt.) ± 0.0017 (sys). Here the first error is a combination of statistical and systematic experimental errors, and the second error is due to the uncertainties in the quark masses, higher twist and target mass corrections, and errors from the gluon distribution. If only a next-to-leading-order fit is performed then the value decreases to $\alpha_s(M_Z) = 0.116$ indicating that the theoretical results are stable. Scale uncertainties are not included. This result is consistent with earlier determinations [43,44,45]. The second of these authors estimated the scale uncertainty at ± 0.004 when a NLO fit was used. The error of Ref. 41 should be increased to take account of the possible scale error. We will therefore use $\alpha_s(M_Z) = 0.1172 \pm 0.0045$ in the final average.

The spin-dependent structure functions, measured in polarized lepton-nucleon scattering, can also be used to test QCD and to determine α_s . Here the values of $Q^2 \sim 2.5 \text{ GeV}^2$ are small, particularly for the E143 data [49], and higher-twist corrections are important. A fit [46] using the measured spin dependent structure functions for several experiments themselves from Refs. [48,49] gives $\alpha_s(M_Z) = 0.121 \pm 0.002$ (expt.) ± 0.006 (theory and syst.). Data from HERMES [50] are not included in this fit; they are consistent with the older data. α_s can also be determined from the Bjorken sum rule [51]; a fit gives [47] $\alpha_s(M_Z) = 0.118_{-0.024}^{+0.010}$; consistent with an earlier determination [52], the larger error being due to the extrapolation into the (unmeasured) small x region. Theoretically, the sum rule is preferable as the perturbative QCD result is known to higher order and these terms are important at the low Q^2 involved. It has been shown that the theoretical errors associated with the choice of scale are considerably reduced by the use of Padé approximants [12]

which results in $\alpha_s(1.7 \text{ GeV}) = 0.328 \pm 0.03$ (expt.) ± 0.025 (theory) corresponding to $\alpha_s(M_Z) = 0.116_{-0.003}^{+0.003}$ (expt.) ± 0.003 (theory). No error is included from the extrapolation into the region of x that is unmeasured. Should data become available at smaller values of x so that this extrapolation could be more tightly constrained, the sum rule method could provide the best determination of α_s ; the result from the structure functions themselves is used in the average.

At very small values of x and Q^2 , the x and Q^2 dependence of the structure functions is predicted by perturbative QCD [53]. Here terms to all orders in $\alpha_s \ln(1/x)$ are summed. The data from HERA [27] on $F_2^{\nu p}(x, Q^2)$ can be fitted to this form [54], including the NLO terms which are required to fix the Q^2 scale. The data are dominated by $4 \text{ GeV}^2 < Q^2 < 100 \text{ GeV}^2$. The fit [55] using H1 data [56] gives $\alpha_s(M_Z) = 0.122 \pm 0.004$ (expt.) ± 0.009 (theory). (The theoretical error is taken from Ref. 54.) The dominant part of the theoretical error is from the scale dependence; errors from terms that are suppressed by $1/\log(1/x)$ in the quark sector are included [57] while those from the gluon sector are not.

Typically, Λ is extracted from the deep inelastic scattering data by parameterizing the parton densities in a simple analytic way at some Q_0^2 , evolving to higher Q^2 using the next-to-leading-order evolution equations, and fitting globally to the measured structure functions to obtain $\Lambda_{\overline{\text{MS}}}^{(4)}$. Thus, an important by-product of such studies is the extraction of parton densities at a fixed-reference value of Q_0^2 . These can then be evolved in Q^2 and used as input for phenomenological studies in hadron-hadron collisions (see below). To avoid having to evolve from the starting Q_0^2 value each time, a parton density is required; it is useful to have available a simple analytic approximation to the densities valid over a range of x and Q^2 values. A package is available from the CERN computer library that includes an exhaustive set of fits [58]. Most of these fits are obsolete. In using a parameterization to predict event rates, a next-to-leading order fit must be used if the process being calculated is known to next-to-leading order in QCD perturbation theory. In such a case, there is an additional scheme dependence; this scheme dependence is reflected in the $\mathcal{O}(\alpha_s)$ corrections that appear in the relations between the structure functions and the quark distribution functions. There are two common schemes: a deep-inelastic scheme where there are no order α_s corrections in the formula for $F_2(x, Q^2)$ and the minimal subtraction scheme. It is important when these next-to-leading order fits are used in other processes (see below), that the same scheme is used in the calculation of the partonic rates. Most current sets of parton distributions are obtained using fits to all relevant event data [59]. In particular, data from purely hadronic initial states are used as they can provide important constraints on the gluon distributions.

9.4. QCD in decays of the τ lepton

The semi-leptonic branching ratio of the tau ($\tau \rightarrow \nu_\tau + \text{hadrons}$, R_τ) is an inclusive quantity. It is related to the contribution of hadrons to the imaginary part of the W self energy ($\text{Im}(\Pi(s))$). It is sensitive to a range of energies since it involves an integral

$$R_\tau \sim \int_0^{m_\tau^2} \frac{ds}{m_\tau^2} \left(1 - \frac{s}{m_\tau^2}\right)^2 \text{Im}(\Pi(s)) .$$

Since the scale involved is low, one must take into account nonperturbative (higher-twist) contributions which are suppressed by powers of the τ mass.

$$R_\tau = 3.058 \left[1 + \frac{\alpha_s(m_\tau)}{\pi} + 5.2 \left(\frac{\alpha_s(m_\tau)}{\pi} \right)^2 + 26.4 \left(\frac{\alpha_s(m_\tau)}{\pi} \right)^3 + a \frac{m^2}{m_\tau^2} + b \frac{m\psi\bar{\psi}}{m_\tau^4} + c \frac{\psi\bar{\psi}\psi\bar{\psi}}{m_\tau^6} + \dots \right]. \quad (9.15)$$

Here a , b , and c are dimensionless constants and m is a light quark mass. The term of order $1/m_\tau^2$ is a kinematical effect due to the light quark masses and is consequently very small. The nonperturbative terms are estimated using sum rules [60]. In total, they are estimated to be -0.014 ± 0.005 [61,62]. This estimate relies on there being no

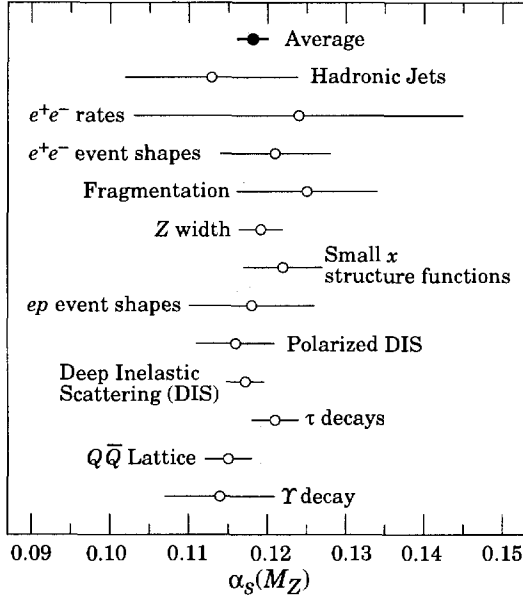


Figure 9.1: Summary of the values of $\alpha_s(M_Z)$ and $\Lambda^{(5)}$ from various processes. The values shown indicate the process and the measured value of α_s extrapolated up to $\mu = M_Z$. The error shown is the *total* error including theoretical uncertainties.

term of order Λ^2/m_τ^2 (note that $\frac{\alpha_s(m_\tau)}{\pi} \sim (\frac{0.5 \text{ GeV}}{m_\tau})^2$). The a , b , and c can be determined from the data [63] by fitting to moments of the $\Pi(s)$ and separately to the final states accessed by the vector and axial parts of the W coupling. The values so extracted [64,65] are consistent with the theoretical estimates. If the nonperturbative terms are omitted from the fit, the extracted value of $\alpha_s(m_\tau)$ decreases by ~ 0.02 .

For $\alpha_s(m_\tau) = 0.35$ the perturbative series for R_τ is $R_\tau \sim 3.058(1 + 0.112 + 0.064 + 0.036)$. The size (estimated error) of the nonperturbative term is 20% (7%) of the size of the order α_s^3 term. The perturbation series is not very well convergent; if the order α_s^3 term is omitted, the extracted value of $\alpha_s(m_\tau)$ increases by 0.05. The order α_s^4 term has been estimated [111] and attempts made to resum the entire series [67,68]. These estimates can be used to obtain an estimate of the errors due to these unknown terms [69,70]. We assign an uncertainty of ± 0.02 to $\alpha_s(m_\tau)$ from these sources.

R_τ can be extracted from the semi-leptonic branching ratio from the relation $R_\tau = 1/(B(\tau \rightarrow e\nu\bar{\nu}) - 1.97256)$; where $B(\tau \rightarrow e\nu\bar{\nu})$ is measured directly or extracted from the lifetime, the muon mass, and the muon lifetime assuming universality of lepton couplings. Using the average lifetime of 290.0 ± 1.2 fs and a τ mass of 1777.05 ± 0.29 MeV from the PDG fit gives $R_\tau = 3.655 \pm 0.023$. The direct measurement of $B(\tau \rightarrow e\nu\bar{\nu})$ can be combined with $B(\tau \rightarrow \mu\nu\bar{\nu})$ to give $B(\tau \rightarrow e\nu\bar{\nu}) = 0.1783 \pm 0.0007$ which gives $R_\tau = 3.636 \pm 0.021$. Averaging these yields $\alpha_s(m_\tau) = 0.351 \pm 0.008$ using the experimental error alone. We assign a theoretical error equal to 40% of the contribution from the order α_s^3 term and all of the nonperturbative contributions. This then gives $\alpha_s(m_\tau) = 0.35 \pm 0.03$ for the final result. This corresponds to $\alpha_s(M_Z) = 0.121 \pm 0.003$.

9.5. QCD in high-energy hadron collisions

There are many ways in which perturbative QCD can be tested in high-energy hadron colliders. The quantitative tests are only useful if the process in question has been calculated beyond leading order in QCD perturbation theory. The production of hadrons with large transverse momentum in hadron-hadron collisions provides a direct probe of the scattering of quarks and gluons: $qq \rightarrow qq$, $qg \rightarrow qg$, $gg \rightarrow gg$, etc. Higher-order QCD calculations of the jet rates [71] and shapes are in impressive agreement with data [72]. This agreement has led to the proposal that these data could be used to provide a determination of α_s [73]. A set of structure functions is assumed and

Tevatron collider data are fitted over a very large range of transverse momenta, to the QCD prediction for the underlying scattering process that depends on α_s . The evolution of the coupling over this energy range (40 to 250 GeV) is therefore tested in the analysis. CDF obtains $\alpha_s(M_Z) = 0.1129 \pm 0.0001$ (stat.) ± 0.0085 (syst.) [74]. Estimation of the theoretical errors is not straightforward. The structure functions used depend implicitly on α_s and an iteration procedure must be used to obtain a consistent result; different sets of structure functions yield different correlations between the two values of α_s . I estimate an uncertainty of ± 0.005 from examining the fits. Ref. 73 estimates the error from unknown higher order QCD corrections to be ± 0.005 . Combining these then gives $\alpha_s(M_Z) = 0.113 \pm 0.011$. Data are also available on the angular distribution of jets; these are also in agreement with QCD expectations [75,76].

QCD corrections to Drell-Yan type cross sections (*i.e.*, the production in hadron collisions by quark-antiquark annihilation of lepton pairs of invariant mass Q from virtual photons, or of real W or Z bosons), are known [77]. These $\mathcal{O}(\alpha_s)$ QCD corrections are sizable at small values of Q . The correction to W and Z production, as measured in $p\bar{p}$ collisions at $\sqrt{s} = 0.63$ TeV and $\sqrt{s} = 1.8$ TeV, is of order 30%. The NNLO corrections to this process are known [78].

The production of W and Z bosons and photons at large transverse momentum can also be used to test QCD. The leading-order QCD subprocesses are $q\bar{q} \rightarrow \gamma g$ and $qg \rightarrow \gamma q$. If the parton distributions are taken from other processes and a value of α_s assumed, then an absolute prediction is obtained. Conversely, the data can be used to extract information on quark and gluon distributions and on the value of α_s . The next-to-leading-order QCD corrections are known [79,80] (for photons), and for W/Z production [81], and so a precision test is possible. Data exist on photon production from the CDF and DØ collaborations [82,83] and from fixed target experiments [84]. Detailed comparisons with QCD predictions [85] may indicate an excess of the data over the theoretical prediction at low value of transverse momenta, although other authors [86] find smaller excesses.

The UA2 collaboration [87] extracted a value of $\alpha_s(M_W) = 0.123 \pm 0.018$ (stat.) ± 0.017 (syst.) from the measured ratio $R_W = \frac{\sigma(W + 1\text{jet})}{\sigma(W + 0\text{jet})}$. The result depends on the algorithm used to define a jet, and the dominant systematic errors due to fragmentation and corrections for underlying events (the former causes jet energy to be lost, the latter causes it to be increased) are connected to the algorithm. There is also dependence on the parton distribution functions, and hence, α_s appears explicitly in the formula for R_W , and implicitly in the distribution functions. This result is not used in the final average. Data from CDF and DØ on the $W p_t$ distribution [89] are in agreement with QCD but are not able to determine α_s with sufficient precision to have any weight in a global average.

In the region of low p_t , fixed order perturbation theory is not applicable; one must sum terms of order $\alpha_s^n \ln^n(p_t/M_W)$ [88]. Data from DØ [90] on the p_t distribution of Z bosons agree well with these predictions.

The production rates of b quarks in $p\bar{p}$ have been used to determine α_s [91]. The next-to-leading-order QCD production processes [92] have been used. By selecting events where the b quarks are back-to-back in azimuth, the next-to-leading-order calculation can be used to compare rates to the measured value and a value of α_s extracted. The errors are dominated by the measurement errors, the choice of μ and M , and uncertainties in the choice of structure functions. The last were estimated by varying the structure functions used. The result is $\alpha_s(M_Z) = 0.113^{+0.009}_{-0.013}$.

9.6. QCD in heavy-quarkonium decay

Under the assumption that the hadronic and leptonic decay widths of heavy $Q\bar{Q}$ resonances can be factorized into a nonperturbative part—dependent on the confining potential—and a calculable perturbative part, the ratios of partial decay widths allow measurements of α_s at the heavy-quark mass scale. The most precise data come from the decay widths of the $1^{--} J/\psi(1S)$ and Υ resonances. The total decay width of the Υ is predicted by perturbative QCD [93]

$$R_\mu(\Upsilon) = \frac{\Gamma(\Upsilon \rightarrow \text{hadrons})}{\Gamma(\Upsilon \rightarrow \mu^+\mu^-)} = \frac{10(\pi^2 - 9)\alpha_s^3(M)}{9\pi\alpha_{\text{em}}^2} \times \left[1 + \frac{\alpha_s}{\pi} \left(-19.4 + \frac{3\beta_0}{2} \left(1.162 + \ln\left(\frac{2M}{M_\Upsilon}\right) \right) \right) \right] \quad (9.16)$$

Data are available for the Υ , Υ' , Υ'' , and J/ψ . The result is very sensitive to α_s and the data are sufficiently precise ($R_\mu(\Upsilon) = 32.5 \pm 0.9$) [94] that the theoretical errors will dominate. There are theoretical corrections to this simple formula due to the relativistic nature of the $Q\bar{Q}$ system; $v^2/c^2 \sim 0.1$ for the Υ . They are more severe for the J/ψ . There are also nonperturbative corrections of the form Λ^2/M_Υ^2 ; again these are more severe for the J/ψ . A fit to Υ , Υ' , and Υ'' [95] gives $\alpha_s(M_Z) = 0.113 \pm 0.001$ (expt.). The results from each state separately and also from the J/ψ are consistent with each other. There is an uncertainty of order ± 0.005 from the choice of scale; the error from v^2/c^2 corrections is a little larger. The ratio of widths $\frac{\Upsilon \rightarrow \gamma\gamma\gamma}{\Upsilon \rightarrow ggg}$ has been measured by the CLEO collaboration who use it to determine $\alpha_s(9.45 \text{ GeV}) = 0.163 \pm 0.002 \pm 0.014$ [97] which corresponds to $\alpha_s(M_Z) = 0.110 \pm 0.001 \pm 0.007$. The error is dominated by theoretical uncertainties associated with the scale choice. The theoretical uncertainties due to the production of photons in fragmentation [96] are small [97]. Higher order QCD calculations of the photon energy distribution are available [98]; this distribution could now be used to further test the theory. The width $\Gamma(\Upsilon \rightarrow e^+e^-)$ can also be used to determine α_s by using moments of the quantity $R_b(s) = \frac{\sigma(e^+e^- \rightarrow b\bar{b})}{\sigma(e^+e^- \rightarrow \mu^+\mu^-)}$ defined by

$M_n = \int_0^\infty \frac{R_b(s)}{s^{n+1}} [99]$. At large values of n , M_n is dominated by $\Gamma(\Upsilon \rightarrow e^+e^-)$. Higher order corrections are available and the method gives [100] $\alpha_s(m_b) = 0.220 \pm 0.027$. The dominant error is theoretical and is dominated by the choice of scale and by uncertainties in Coulomb corrections. It corresponds to $\alpha_s(M_Z) = 0.119 \pm 0.008$. These various Υ measurements can be combined and give $\alpha_s(M_Z) = 0.114 \pm 0.008$.

9.7. Perturbative QCD in e^+e^- collisions

The total cross section for $e^+e^- \rightarrow \text{hadrons}$ is obtained (at low values of \sqrt{s}) by multiplying the muon-pair cross section by the factor $R = 3\Sigma_q e_q^2$. The higher-order QCD corrections to this quantity have been calculated, and the results can be expressed in terms of the factor:

$$R = R^{(0)} \left[1 + \frac{\alpha_s}{\pi} + C_2 \left(\frac{\alpha_s}{\pi} \right)^2 + C_3 \left(\frac{\alpha_s}{\pi} \right)^3 + \dots \right], \quad (9.17)$$

where $C_2 = 1.411$ and $C_3 = -12.8$ [101].

$R^{(0)}$ can be obtained from the formula for $d\sigma/d\Omega$ for $e^+e^- \rightarrow f\bar{f}$ by integrating over Ω . The formula is given in Sec. 35.2 of this *Review*. This result is only correct in the zero-quark-mass limit. The $\mathcal{O}(\alpha_s)$ corrections are also known for massive quarks [102]. The principal advantage of determining α_s from R in e^+e^- annihilation is that there is no dependence on fragmentation models, jet algorithms, etc.

A measurement by CLEO [103] at $\sqrt{s} = 10.52 \text{ GeV}$ yields $\alpha_s(10.52 \text{ GeV}) = 0.20 \pm 0.01 \pm 0.06$, which corresponds to $\alpha_s(M_Z) = 0.13 \pm 0.005 \pm 0.03$. A comparison of the theoretical prediction of Eq. (9.17) (corrected for the b -quark mass), with all the available data at values of \sqrt{s} between 20 and 65 GeV, gives [104]

$\alpha_s(35 \text{ GeV}) = 0.146 \pm 0.030$. The size of the order α_s^3 term is of order 40% of that of the order α_s^2 and 3% of the order α_s . If the order α_s^3 term is not included, a fit to the data yields $\alpha_s(34 \text{ GeV}) = 0.142 \pm 0.03$, indicating that the theoretical uncertainty is smaller than the experimental error.

Measurements of the ratio of hadronic to leptonic width of the Z at LEP and SLC, Γ_h/Γ_μ probe, the same quantity as R . Using the average of $\Gamma_h/\Gamma_\mu = 20.783 \pm 0.029$ gives $\alpha_s(M_Z) = 0.123 \pm 0.004$ [105]. There are theoretical errors arising from the values of top-quark and Higgs masses which enter due to electroweak corrections to the Z width and from the choice of scale.

While this method has small theoretical uncertainties from QCD itself, it relies sensitively on the electroweak couplings of the Z to quarks [106]. The presence of new physics which changes these couplings via electroweak radiative corrections would invalidate the value of $\alpha_s(M_Z)$. However, given the excellent agreement [107] of the many measurements at the Z , there is no reason not to use the value of $\alpha_s(M_Z) = 0.1192 \pm 0.0028 \pm 0.002$ (scale) from the global fits of the various precision measurements at LEP/SLC and the W and top masses in the world average (see the section on “Electroweak model and constraints on new physics,” Sec. 10 of this *Review*).

An alternative method of determining α_s in e^+e^- annihilation is from measuring quantities that are sensitive to the relative rates of two-, three-, and four-jet events. A review should be consulted for more details [108] of the issues mentioned briefly here. In addition to simply counting jets, there are many possible choices of such “shape variables”: thrust [109], energy-energy correlations [110], average jet mass, etc. All of these are infrared safe, which means they can be reliably calculated in perturbation theory. The starting point for all these quantities is the multijet cross section. For example, at order α_s , for the process $e^+e^- \rightarrow q\bar{q}g$: [111]

$$\frac{1}{\sigma} \frac{d^2\sigma}{dx_1 dx_2} = \frac{2\alpha_s}{3\pi} \frac{x_1^2 + x_2^2}{(1-x_1)(1-x_2)}, \quad (9.18)$$

$$x_i = \frac{2E_i}{\sqrt{s}} \quad (9.19)$$

where x_i are the center-of-mass energy fractions of the final-state (massless) quarks. A distribution in a “three-jet” variable, such as those listed above, is obtained by integrating this differential cross section over an appropriate phase space region for a fixed value of the variable. The order α_s^2 corrections to this process have been computed, as well as the 4-jet final states such as $e^+e^- \rightarrow q\bar{q}gg$ [112].

There are many methods used by the e^+e^- experimental groups to determine α_s from the event topology. The jet-counting algorithm, originally introduced by the JADE collaboration [113], has been used by many other groups. Here, particles of momenta p_i and p_j are combined into a pseudo-particle of momentum $p_i + p_j$ if the invariant mass of the pair is less than $y_0\sqrt{s}$. The process is then iterated until no more pairs of particles or pseudo-particles remain. The remaining number is then defined to be the number of jets in the event, and can be compared to the QCD prediction. The Durham algorithm is slightly different: in computing the mass of a pair of partons, it uses $M^2 = 2\min(E_i^2, E_j^2)(1 - \cos\theta_{ij})$ for partons of energies E_i and E_j separated by angle θ_{ij} [114].

There are theoretical ambiguities in the way this process is carried out. Quarks and gluons are massless, whereas the observed hadrons are not, so that the massive jets that result from this scheme cannot be compared directly to the massless jets of perturbative QCD. Different recombination schemes have been tried, for example combining 3-momenta and then rescaling the energy of the cluster so that it remains massless. These schemes result in the same data giving a slightly different values [115,116] of α_s . These differences can be used to determine a systematic error. In addition, since what is observed are hadrons rather than quarks and gluons, a model is needed to describe the evolution of a partonic final state into one involving hadrons, so that detector corrections can be applied. The QCD matrix elements are combined with a parton-fragmentation

model. This model can then be used to correct the data for a direct comparison with the parton calculation. The different hadronization models that are used [117–120] model the dynamics that are controlled by nonperturbative QCD effects which we cannot yet calculate. The fragmentation parameters of these Monte Carlos are tuned to get agreement with the observed data. The differences between these models contribute to the systematic errors. The systematic errors from recombination schemes and fragmentation effects dominate over the statistical and other errors of the LEP/SLD experiments.

The scale M at which $\alpha_s(M)$ is to be evaluated is not clear. The invariant mass of a typical jet (or $\sqrt{sy_0}$) is probably a more appropriate choice than the e^+e^- center-of-mass energy. While there is no justification for doing so, if the value is allowed to float in the fit to the data, the fit improves and the data tend to prefer values of order $\sqrt{s}/10$ GeV for some variables [116,121]; the exact value depends on the variable that is fitted.

The perturbative QCD formulae can break down in special kinematical configurations. For example, the thrust (T) distribution contains terms of the type $\alpha_s \ln^2(1-T)$. The higher orders in the perturbation expansion contain terms of order $\alpha_s^n \ln^m(1-T)$. For $T \sim 1$ (the region populated by 2-jet events), the perturbation expansion is unreliable. The terms with $n \leq m$ can be summed to all orders in α_s [122]. If the jet recombination methods are used higher-order terms involve $\alpha_s^n \ln^m(y_0)$, these too can be resummed [123]. The resummed results give better agreement with the data at large values of T . Some caution should be exercised in using these resummed results because of the possibility of overcounting; the showering Monte Carlos that are used for the fragmentation corrections also generate some of these leading-log corrections. Different schemes for combining the order α_s^2 and the resummations are available [124]. These different schemes result in shifts in α_s of order ± 0.002 . The use of the resummed results improves the agreement between the data and the theory. An average of the recent results at the Z resonance from SLD [116], OPAL [125], L3 [126], ALEPH [127], and DELPHI [128], using the combined α_s^2 and resummation fitting to a large set of shape variables, gives $\alpha_s(M_Z) = 0.122 \pm 0.007$. The errors in the values of $\alpha_s(M_Z)$ from these shape variables are totally dominated by the theoretical uncertainties associated with the choice of scale, and the effects of hadronization Monte Carlos on the different quantities fitted.

Similar studies on event shapes have been undertaken at lower energies at TRISTAN, PEP/PETRA, and CLEO. A combined result from various shape parameters by the TOPAZ collaboration gives $\alpha_s(58 \text{ GeV}) = 0.125 \pm 0.009$, using the fixed order QCD result, and $\alpha_s(58 \text{ GeV}) = 0.132 \pm 0.008$ (corresponding to $\alpha_s(M_Z) = 0.123 \pm 0.007$), using the same method as in the SLD and LEP average [129]. The measurements of event shapes at PEP/PETRA are summarized in earlier editions of this note. A recent reevaluation of the JADE data [130] obtained using resummed QCD results and by averaging over several shape variables gives $\alpha_s(35 \text{ GeV}) = 0.145^{+0.012}_{-0.007}$. An analysis by the TPC group [131] gives $\alpha_s(29 \text{ GeV}) = 0.160 \pm 0.012$, using the same method as TOPAZ. This value corresponds to $\alpha_s(M_Z) = 0.131 \pm 0.010$.

The CLEO collaboration fits to the order α_s^2 results for the two jet fraction at $\sqrt{s} = 10.53 \text{ GeV}$, and obtains $\alpha_s(10.93 \text{ GeV}) = 0.164 \pm 0.004$ (expt.) ± 0.014 (theory) [132]. The dominant systematic error arises from the choice of scale (μ), and is determined from the range of α_s that results from fit with $\mu = 10.53 \text{ GeV}$, and a fit where μ is allowed to vary to get the lowest χ^2 . The latter results in $\mu = 1.2 \text{ GeV}$. Since the quoted result corresponds to $\alpha_s(1.2 \text{ GeV}) = 0.35$, it is by no means clear that the perturbative QCD expression is reliable and the resulting error should, therefore, be treated with caution. A fit to many different variables as is done in the LEP/SLC analyses would give added confidence to the quoted error.

Recently studies have been carried out at energies between $\sim 130 \text{ GeV}$ [133] and $\sim 189 \text{ GeV}$ [134]. These can be combined to give $\alpha_s(130 \text{ GeV}) = 0.114 \pm 0.008$ and $\alpha_s(189 \text{ GeV}) = 0.1104 \pm 0.005$. The dominant errors are theoretical and systematic and, as most of these are in common at the two energies. These data and those at the

Z resonance provide clear confirmation of the expected decrease in α_s as the energy is increased.

Since the errors in the event shape measurements are dominantly systematic, and are common to the experiments, the results from PEP/PETRA, TRISTAN, LEP, SLC, and CLEO are combined to give $\alpha_s(M_Z) = 0.121 \pm 0.007$. All of the experiments are consistent with this average and, taken together, provide verification of the running of the coupling constant with energy.

Estimates are available for the nonperturbative corrections to the mean value of $1-T$ [136]. These are of order $1/E$ and involve a single parameter to be determined from experiment. These corrections can then be used as an alternative to those modeled by the fragmentation Monte-Carlos. The DELPHI collaboration [135] uses data up to the Z mass from many experiments and determines $\alpha_s(M_Z) = 0.119 \pm 0.006$, the error being dominated by the choice of scale. The value is also determined by a fit to a second variable (the mean jet mass); while the extracted values of $\alpha_s(M_Z)$ are consistent with each other, the values of the non perturbative parameter are not. The analysis is useful as one can directly determine the size of the $1/E$ corrections; they are approximately 20% (50%) of the perturbative result at $\sqrt{s} = 91(11) \text{ GeV}$.

9.8. Scaling violations in fragmentation functions

Measurements of the fragmentation function $d_i(z, E)$, (the probability that a hadron of type i be produced with energy zE in e^+e^- collisions at $\sqrt{s} = 2E$) can be used to determine α_s . As in the case of scaling violations in structure functions, QCD predicts only the E dependence. Hence, measurements at different energies are needed to extract a value of α_s . Because the QCD evolution mixes the fragmentation functions for each quark flavor with the gluon fragmentation function, it is necessary to determine each of these before α_s can be extracted. The ALEPH collaboration has used data from energies ranging from $\sqrt{s} = 22 \text{ GeV}$ to $\sqrt{s} = 91 \text{ GeV}$. A flavor tag is used to discriminate between different quark species, and the longitudinal and transverse cross sections are used to extract the gluon fragmentation function [137]. The result obtained is $\alpha_s(M_Z) = 0.126 \pm 0.007$ (expt.) ± 0.006 (theory) [138]. The theory error is due mainly to the choice of scale. The OPAL collaboration [139] has also extracted the separate fragmentation functions. DELPHI [140] has also performed a similar analysis using data from other experiments at lower energy with the result $\alpha_s(M_Z) = 0.124 \pm 0.007 \pm 0.009$ (theory). The larger theoretical error is due to the larger range of scales that were used in the fit. These results can be combined to give $\alpha_s(M_Z) = 0.125 \pm 0.005 \pm 0.008$ (theory).

9.9. Photon structure functions

e^+e^- can also be used to study photon-photon interactions, which can be used to measure the structure function of a photon [141], by selecting events of the type $e^+e^- \rightarrow e^+e^- + \text{hadrons}$ which proceeds via two photon scattering. If events are selected where one of the photons is almost on mass shell and the other has a large invariant mass Q , then the latter probes the photon structure function at scale Q ; the process is analogous to deep inelastic scattering where a highly virtual photon is used to probe the proton structure. This process was included in earlier versions of this *Review* which can be consulted for details on older measurements [142–145]. A recent review of the data can be found in Ref. 146. Data have become available from LEP [147–150] and from TRISTAN [151,152] which extend the range of Q^2 to of order 300 GeV^2 and x as low as 2×10^{-3} and show Q^2 dependence of the structure function that is consistent with QCD expectations. Experiments at HERA can also probe the photon structure function by looking at jet production in γp collisions; this is analogous to the jet production in hadron-hadron collisions which is sensitive to hadron structure functions. The data [153] are consistent with theoretical models [154].

9.10. Jet rates in ep collisions

At lowest order in α_s , the ep scattering process produces a final state of (1+1) jets, one from the proton fragment and the other from the quark knocked out by the process $e + quark \rightarrow e + quark$. At next order in α_s , a gluon can be radiated, and hence a (2+1) jet final state produced. By comparing the rates for these (1+1) and (2+1) jet processes, a value of α_s can be obtained. A NLO QCD calculation is available [155]. The basic methodology is similar to that used in the jet counting experiments in e^+e^- annihilation discussed above. Unlike those measurements, the ones in ep scattering are not at a fixed value of Q^2 . In addition to the systematic errors associated with the jet definitions, there are additional ones since the structure functions enter into the rate calculations. Results from H1 [156] and ZEUS [157] can be combined to give $\alpha_s(M_Z) = 0.118 \pm 0.0015$ (stat.) ± 0.009 (syst.). The contributions to the systematic errors from experimental effects (mainly the hadronic energy scale) are comparable to the theoretical ones arising from scale choice, structure functions, and jet definitions. The theoretical errors are common to the two measurements; therefore, we have not reduced the systematic error after forming the average.

9.11. QCD in diffractive events

In approximately 10% of the deep-inelastic scattering events at HERA a rapidity gap is observed [158]; that is events are seen where there are almost no hadrons produced in the direction of the incident proton. This was unexpected; QCD based models of the final state predicted that the rapidity interval between the quark that is hit by the electron and the proton remnant should be populated approximately evenly by the hadrons. Similar phenomena have been observed at the Tevatron in W and jet production. For a review see Ref. 159.

9.12. Lattice QCD

Lattice gauge theory calculations can be used to calculate, using non-perturbative methods, a physical quantity that can be measured experimentally. The value of this quantity can then be used to determine the QCD coupling that enters in the calculation. For a review of the methodology see Ref. 160. For example, the energy levels of a $Q\bar{Q}$ system can be determined and then used to extract α_s . The masses of the $Q\bar{Q}$ states depend only on the quark mass and on α_s . A limitation is that calculations cannot be performed for three light quark flavors. Results are available for zero ($n_f = 0$, quenched approximation) and two light flavors, which allow extrapolation to three. The coupling constant so extracted is in a lattice renormalization scheme, and must be converted to the \overline{MS} scheme for comparison with other results. Using the mass differences of Υ and Υ' and Υ'' and χ_b , Davies *et al.* [161] extract a value of $\alpha_s(M_Z) = 0.1174 \pm 0.0024$. A similar result with larger errors is reported by [162], where results are consistent with $\alpha_s(M_Z) = 0.111 \pm 0.006$. The SESAM collaboration [163] uses the Υ and Υ' and χ_b masses to obtain $\alpha_s(M_Z) = 0.1118 \pm 0.0017$ using Wilson fermions. These authors point out that their result is more than 3σ from that of Davies *et al.* which uses Kogut-Susskind fermions. A combination of the results from quenched [164] and ($n_f = 2$) [165] gives $\alpha_s(M_Z) = 0.116 \pm 0.003$ [166]. Calculations [167] using the strength of the force between two heavy quarks computed in the quenched approximation obtains a value of $\alpha_s(5 \text{ GeV})$ that is consistent with these results. There have also been investigations of the running of α_s [168]. These show remarkable agreement with the two loop perturbative result of Eq. (9.5).

There are several sources of error in these estimates of $\alpha_s(M_Z)$. The experimental error associated with the measurements of the particle masses is negligible. The conversion from the lattice coupling constant to the \overline{MS} constant is obtained using a perturbative expansion where one coupling expanded as a power series in the other. This series is only known to second order. A third order calculation exists only from the $n_f = 0$ case [169]. Its inclusion leads to a shift in the extracted value of $\alpha_s(M_Z)$ of $+0.002$. Other theoretical errors arising from the limited statistics of the Monte-Carlo calculation, extrapolation in n_f , and corrections for light quark masses are smaller than this.

The result of averaging [163,161,164] gives with a more conservative error $\alpha_s(M_Z) = 0.115 \pm 0.003$. This will be used in the average.

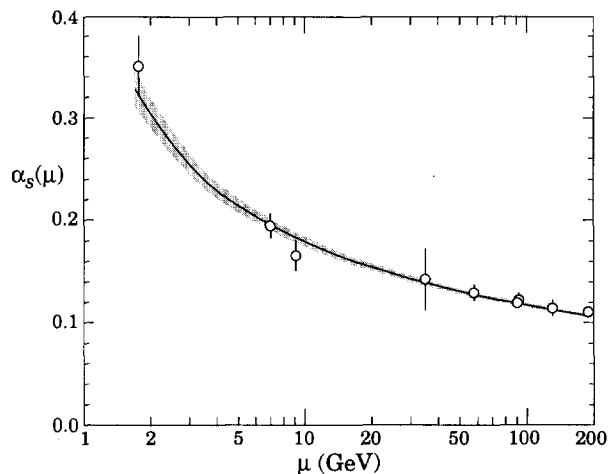


Figure 9.2: Summary of the values of $\alpha_s(\mu)$ at the values of μ where they are measured. The lines show the central values and the $\pm 1\sigma$ limits of our average. The figure clearly shows the decrease in $\alpha_s(\mu)$ with increasing μ . The data are, in increasing order of μ , τ width, deep inelastic scattering, T decays, e^+e^- event rate at 25 GeV, event shapes at TRISTAN, Z width, e^+e^- event shapes of M_Z , 135, and 189 GeV.

9.13. Conclusions

The need for brevity has meant that many other important topics in QCD phenomenology have had to be omitted from this review. One should mention in particular the study of exclusive processes (form factors, elastic scattering, ...), the behavior of quarks and gluons in nuclei, the spin properties of the theory, and QCD effects in hadron spectroscopy.

We have focused on those high-energy processes which currently offer the most quantitative tests of perturbative QCD. Figure 9.1 shows the values of $\alpha_s(M_Z)$ deduced from the various experiments. Figure 9.2 shows the values and the values of Q where they are measured. This figure clearly shows the experimental evidence for the variation of $\alpha_s(Q)$ with Q .

An average of the values in Fig. 9.1 gives $\alpha_s(M_Z) = 0.1181$, with a total χ^2 of 3.8 for twelve fitted points, showing good consistency among the data. The error on the average, assuming that all of the errors in the contributing results are uncorrelated, is ± 0.0014 , and may be an underestimate. Almost all of the values used in the average are dominated by systematic, usually theoretical, errors. Only some of these, notably from the choice of scale, are correlated. The average is not dominated by a single measurement; there are several results with comparable small errors: these are the ones from τ decay, lattice gauge theory, deep inelastic scattering, and the Z^0 width. We quote our average value as $\alpha_s(M_Z) = 0.1181 \pm 0.002$, which corresponds to $\Lambda^{(5)} = 208_{-23}^{+25}$ MeV using Eq. (9.5a). Future experiments can be expected to improve the measurements of α_s somewhat. Precision at the 1% level may be achievable if the systematic and theoretical errors can be reduced [170].

The value of α_s at any scale corresponding to our average can be obtained from <http://www-theory.lbl.gov/~ianh/alpha/alpha.html>

References:

1. R.K. Ellis, W.J. Stirling, and B.R. Webber, "QCD and Collider Physics" (Cambridge 1996).
2. For reviews see, for example, A.S. Kronfeld and P.B. Mackenzie, *Ann. Rev. Nucl. and Part. Sci.* **43**, 793 (1993); H. Wittig, *Int. J. Mod. Phys.* **A12**, 4477 (1997).
3. For example see, S. Bethke, in *Proceedings of the IVth Int. Symposium on Radiative Corrections*, Barcelona, Spain (Sept. 1998), [hep-ex/9812026](#);
M Davier, *33rd Rencontres de Moriond: Electroweak Interactions and Unified Theories*, Les Arcs, France (14–21 Mar. 1998);
P.N. Burrows, *Acta. Phys. Pol.* **28**, 701 (1997).
4. J. Womersley, *International Conference on Lepton Photon Interactions*, Stanford, USA (Aug. 1999).
5. S.A. Larin, T. van Ritbergen, and J.A.M. Vermaseren, *Phys. Lett.* **B400**, 379 (1997).
6. W.A. Bardeen *et al.*, *Phys. Rev.* **D18**, 3998 (1978).
7. G. Grunberg, *Phys. Lett.* **95B**, 70 (1980); *Phys. Rev.* **D29**, 2315 (1984).
8. P.M. Stevenson, *Phys. Rev.* **D23**, 2916 (1981); and *Nucl. Phys.* **B203**, 472 (1982).
9. S. Brodsky and H.J. Lu, SLAC-PUB-6389 (Nov. 1993).
10. S. Brodsky, G.P. Lepage, and P.B. Mackenzie, *Phys. Rev.* **D28**, 228 (1983).
11. M.A. Samuel, G. Li, and E. Steinfelds, *Phys. Lett.* **B323**, 188 (1994);
M.A. Samuel, J. Ellis, and M. Karliner, *Phys. Rev. Lett.* **74**, 4380 (1995).
12. J. Ellis *et al.*, *Phys. Rev.* **D54**, 6986 (1996).
13. P.N. Burrows *et al.*, *Phys. Lett.* **B382**, 157 (1996).
14. P. Abreu *et al.*, *Z. Phys.* **C54**, 55 (1992).
15. A.H. Mueller, *Phys. Lett.* **B308**, 355, (1993).
16. W. Bernreuther, *Annals of Physics* **151**, 127 (1983); Erratum *Nucl. Phys.* **B513**, 758 (1998);
S.A. Larin, T. van Ritbergen, and J.A.M. Vermaseren, *Nucl. Phys.* **B438**, 278 (1995).
17. K.G. Chetyrkin, B.A. Kniehl, and M. Steinhauser, *Phys. Rev. Lett.* **79**, 2184 (1977).
18. W. Marciano, *Phys. Rev.* **D29**, 580 (1984).
19. V.N. Gribov and L.N. Lipatov, *Sov. J. Nucl. Phys.* **15**, 438 (1972);
Yu.L. Dokshitzer, *Sov. Phys. JETP* **46**, 641 (1977).
20. G. Altarelli and G. Parisi, *Nucl. Phys.* **B126**, 298 (1977).
21. G. Curci, W. Furmanski, and R. Petronzio, *Nucl. Phys.* **B175**, 27 (1980);
W. Furmanski and R. Petronzio, *Phys. Lett.* **97B**, 437 (1980);
and *Z. Phys.* **C11**, 293 (1982);
E.G. Floratos, C. Kounnas, and R. Lacaze, *Phys. Lett.* **98B**, 89 (1981); *Phys. Lett.* **98B**, 285 (1981); and *Nucl. Phys.* **B192**, 417 (1981);
R.T. Herrod and S. Wada, *Phys. Lett.* **96B**, 195 (1981); and
Z. Phys. **C9**, 351 (1981).
22. G. Sterman, *Nucl. Phys.* **B281**, 310 (1987);
S. Catani and L. Trentadue, *Nucl. Phys.* **B327**, 323 (1989); *Nucl. Phys.* **B353**, 183 (1991).
23. R.D. Ball and A. DeRoeck, [hep-ph/9609309](#).
24. J. Feltesse, in *Proceedings of the XXVII International Conference on High Energy Physics*, Glasgow, Scotland, (July 1994).
25. M Klein at *International Conference on Lepton Photon Interactions*, Stanford, USA (August 1999).
26. F. Eisele, at the European Physical Society meeting, Brussels, (July 1995).
27. M. Derrick *et al.*, *Phys. Lett.* **B345**, 576 (1995); *Z. Phys.* **C62**, 399 (1999);
S. Aid *et al.*, *Phys. Lett.* **B354**, 494 (1995); *Nucl. Phys.* **B470**, 3 (1996).
28. D. Gross and C.H. Llewellyn Smith, *Nucl. Phys.* **B14**, 337 (1969).
29. J. Chyla and A.L. Kataev, *Phys. Lett.* **B297**, 385 (1992).
30. S.A. Larin and J.A.M. Vermaseren, *Phys. Lett.* **B259**, 345 (1991).
31. A.L. Kataev and V.V. Starchenko, *Mod. Phys. Lett.* **A10**, 235 (1995).
32. V.M. Braun and A.V. Kolesnichenko, *Nucl. Phys.* **B283**, 723 (1987).
33. M. Dasgupta and B. Webber, *Phys. Lett.* **B382**, 273 (1993).
34. M. Maul *et al.*, *Phys. Lett.* **401**, 100 (1997).
35. J. Kim *et al.*, *Phys. Rev. Lett.* **81**, 3595 (1998).
36. D. Allasia *et al.*, *Z. Phys.* **C28**, 321 (1985);
K. Varvell *et al.*, *Z. Phys.* **C36**, 1 (1997);
V.V. Ammosov *et al.*, *Z. Phys.* **C30**, 175 (1986);
P.C. Bosetti *et al.*, *Nucl. Phys.* **B142**, 1 (1978).
37. A.L. Kataev *et al.*, *Nucl. Phys.* **A666 & 667**, 184 (2000) [hep-ph/9907310](#).
38. L.W. Whitlow *et al.*, *Phys. Lett.* **B282**, 475 (1992).
39. A.C. Benvenuti *et al.*, *Phys. Lett.* **B223**, 490 (1989); *Phys. Lett.* **B223**, 485, (1989); *Phys. Lett.* **B237**, 592 (1990); and *Phys. Lett.* **B237**, 599 (1990).
40. M.R. Adams *et al.*, *Phys. Rev.* **D54**, 3006 (1996).
41. J. Santiago and F.J. Yndurain, *Nucl. Phys.* **B563**, 45 (1999) [hep-ph/9904344](#).
42. K. Adel, F. Barriero, and F.J. Yndurain, *Nucl. Phys.* **B495**, 221 (1997);
W.L. Van Neerven, and E.B. Zijlstra, *Phys. Lett.* **B272**, 127 (1991); *Nucl. Phys.* **B383**, 525 (1992);
S. A. Larin *et al.*, *Nucl. Phys.* **B427**, 41 (1994); *Nucl. Phys.* **B492**, 338 (1997).
43. M. Arneodo *et al.*, *Phys. Lett.* **B309**, 222 (1993).
44. M. Virchaux and A. Milsztajn, *Phys. Lett.* **B274**, 221 (1992).
45. P.Z. Quintas, *Phys. Rev. Lett.* **71**, 1307 (1993).
46. B. Adeva *et al.*, *Phys. Rev.* **D58**, 112002 (1998).
47. G. Altarelli *et al.*, *Nucl. Phys.* **B496**, 337 (1997), [hep-ph/9803237](#).
48. D. Adams *et al.*, *Phys. Lett.* **B329**, 399 (1995); *Phys. Rev.* **D56**, 5330 (1998); *Phys. Rev.* **D58**, 1112001 (1998).
49. K. Abe *et al.*, *Phys. Rev. Lett.* **74**, 346 (1995); *Phys. Lett.* **B364**, 61 (1995); *Phys. Rev. Lett.* **75**, 25 (1995);
P.L. Anthony *et al.*, *Phys. Rev.* **D54**, 6620 (1996).
50. A. Airapetian *et al.*, *Phys. Lett.* **B442**, 484 (1998), [hep-ex/99-06035](#).
51. J.D. Bjorken, *Phys. Rev.* **148**, 1467 (1966).
52. J. Ellis and M. Karliner, *Phys. Lett.* **B341**, 397 (1995).
53. A. DeRujula *et al.*, *Phys. Rev.* **D10**, 1669 (1974);
E.A. Kurayev, L.N. Lipatov, and V.S. Fadin, *Sov. Phys. JETP* **45**, 119 (1977);
Ya.Ya. Balitsky and L.N. Lipatov, *Sov. J. Nucl. Phys.* **28**, 882 (1978).
54. R.D. Ball and S. Forte, *Phys. Lett.* **B335**, 77 (1994); *Phys. Lett.* **B336**, 77 (1994);
H1Collaboration: S. Aid *et al.*, *Nucl. Phys.* **B470**, 3 (1996).
55. R.D. Ball and S. Forte, [hep-ph/9607289](#).
56. H1 Collaboration: T. Ahmed *et al.*, *Nucl. Phys.* **B439**, 471 (1995).
57. S. Catani and F. Hautmann, *Nucl. Phys.* **B427**, 475 (1994).
58. H. Plochow-Besch, *Comp. Phys. Comm.* **75**, 396 (1993).

59. H.L. Lai *et al.*, Eur. Phys. J. **C12**, 375 (2000) hep-ph/9903282; A.D. Martin *et al.*, Nucl. Phys. B Proc. Suppl. **79**, 105 (1999) hep-ph/9906231.
60. M.A. Shifman, A.I. Vainshtein, and V.I. Zakharov, Nucl. Phys. **B147**, 385 (1979).
61. S. Narison and A. Pich, Phys. Lett. **B211**, 183 (1988); E. Braaten, S. Narison, and A. Pich, Nucl. Phys. **B373**, 581 (1992).
62. M. Neubert, Nucl. Phys. **B463**, 511 (1996).
63. F. Le Diberder and A. Pich, Phys. Lett. **B289**, 165 (1992).
64. R. Barate *et al.*, Z. Phys. **C76**, 1 (1997); Z. Phys. **C76**, 15 (1997); K. Ackerstaff *et al.*, Eur. Phys. J. **C7**, 571 (1999).
65. T. Coan *et al.*, Phys. Lett. **B356**, 580 (1995).
66. A.L. Kataev and V.V. Starshenko, Mod. Phys. Lett. **A10**, 235 (1995).
67. F. Le Diberder and A. Pich, Phys. Lett. **B286**, 147 (1992).
68. C.J. Maxwell and D.J. Tong, Nucl. Phys. **B481**, 681 (1996).
69. G. Altarelli, Nucl. Phys. **B40**, 59 (1995); G. Altarelli, P. Nason, and G. Ridolfi, Z. Phys. **C68**, 257 (1995).
70. S. Narison, Nucl. Phys. **B40**, 47 (1995).
71. S.D. Ellis, Z. Kunszt, and D.E. Soper, Phys. Rev. Lett. **64**, 2121 (1990); F. Aversa *et al.*, Phys. Rev. Lett. **65**, 401 (1990); W.T. Giele, E.W.N. Glover, and D. Kosower, Phys. Rev. Lett. **73**, 2019 (1994); S. Frixione, Z. Kunszt, and A. Signer, Nucl. Phys. **B467**, 399 (1996).
72. F. Abe *et al.*, Phys. Rev. Lett. **77**, 438 (1996); B. Abbott *et al.*, Phys. Rev. Lett. **82**, 2451 (1999).
73. W.T. Giele, E.W.N. Glover, and J. Yu, Phys. Rev. **D53**, 120 (1996).
74. CDF Collaboration reported in [4].
75. UA1 Collaboration: G. Arnison *et al.*, Phys. Lett. **B177**, 244 (1986).
76. F. Abe *et al.*, Phys. Rev. Lett. **77**, 533 (1996); *ibid.*, erratum Phys. Rev. Lett. **78**, 4307 (1997); B. Abbott, Phys. Rev. Lett. **80**, 666 (1998); S. Abache *et al.*, Phys. Rev. **D53**, 6000 (1996).
77. G. Altarelli, R.K. Ellis, and G. Martinelli, Nucl. Phys. **B143**, 521 (1978).
78. R. Hamberg, W.L. Van Neerven, and T. Matsuura, Nucl. Phys. **B359**, 343 (1991).
79. P. Aurenche, R. Baier, and M. Fontannaz, Phys. Rev. **D42**, 1440 (1990); P. Aurenche *et al.*, Phys. Lett. **140B**, 87 (1984); P. Aurenche *et al.*, Nucl. Phys. **B297**, 661 (1988).
80. H. Baer, J. Ohnemus, and J.F. Owens, Phys. Lett. **B234**, 127 (1990).
81. H. Baer and M.H. Reno, Phys. Rev. **D43**, 2892 (1991); P.B. Arnold and M.H. Reno, Nucl. Phys. **B319**, 37 (1989).
82. F. Abe *et al.*, Phys. Rev. Lett. **73**, 2662 (1994).
83. S. Abachi *et al.*, Phys. Rev. Lett. **77**, 5011 (1996).
84. G. Alverson *et al.*, Phys. Rev. **D48**, 5 (1993).
85. L. Apanasevich *et al.*, Phys. Rev. **D59**, 074007 (1999); Phys. Rev. Lett. **81**, 2642 (1998).
86. W. Vogelsang and A. Vogt, Nucl. Phys. **B453**, 334 (1995); P. Aurenche *et al.*, Eur. Phys. J. **C9**, 107 (1999).
87. J. Alitti *et al.*, Phys. Lett. **B263**, 563 (1991).
88. R. K. Ellis and S. Veseli, Nucl. Phys. **B511**, 649 (1998); C.T. Davies, B.R. Webber, and W.J. Stirling, Nucl. Phys. **B256**, 413 (1985).
89. S. Abache *et al.*, Phys. Rev. Lett. **75**, 3226 (1995); J. Womersley, private communication; J. Huston, in the *Proceedings to the 29th International Conference on High-Energy Physics (ICHEP98)*, Vancouver, Canada (23–29 Jul 1998) hep-ph/9901352.
90. DØ Collaboration: B. Abbott *et al.*, Phys. Rev. **D61**, 032004 (2000) hep-ex/9907009; T. Affolder *et al.*, FERMILAB-PUB-99/220.
91. C. Albajar *et al.*, Phys. Lett. **B369**, 46 (1996).
92. M.L. Mangano, P. Nason, and G. Ridolfi, Nucl. Phys. **B373**, 295 (1992).
93. R. Barbieri *et al.*, Phys. Lett. **95B**, 93 (1980); B.P. Mackenzie and G.P. Lepage, Phys. Rev. Lett. **47**, 1244 (1981).
94. M. Kobel *et al.*, Z. Phys. **C53**, 193 (1992).
95. M. Kobel, DESY-F31-91-03 (thesis).
96. S. Catani and F. Hautmann, Nucl. Phys. **B** (Proc. Supp.), vol. **39BC**, 359 (1995).
97. B. Nemati *et al.*, Phys. Rev. **D55**, 5273 (1997).
98. M. Kramer, Phys. Rev. **D60**, 111503 (1999) hep-ph/9904416.
99. M. Voloshin, Int. J. Mod. Phys. **A10**, 2865 (1999).
100. M. Jamin and A. Pich, Nucl. Phys. **B507**, 334 (1997).
101. S.G. Gorishny, A. Kataev, and S.A. Larin, Phys. Lett. **B259**, 114 (1991); L.R. Surguladze and M.A. Samuel, Phys. Rev. Lett. **66**, 560 (1991).
102. K.G. Chetyrkin and J.H. Kuhn, Phys. Lett. **B308**, 127 (1993).
103. R. Ammar *et al.*, Phys. Rev. **D57**, 1350 (1998).
104. D. Haidt, in *Directions in High Energy Physics*, vol. 14, p. 201, ed. P. Langacker (World Scientific, 1995).
105. G. Quast, presented at the *International Europhysics Conference on High Energy Physics, EPS-HEP99*, Tampere, Finland (July 1999).
106. A. Blondel and C. Verzegrassi, Phys. Lett. **B311**, 346 (1993); G. Altarelli *et al.*, Nucl. Phys. **B405**, 3 (1993).
107. See the section on “Standard Model of Electroweak Interactions” (Sec. 10) in this *Review*.
108. S. Bethke and J. Pilcher, Ann. Rev. Nucl. and Part. Sci. **42**, 251 (1992).
109. E. Farhi, Phys. Rev. Lett. **39**, 1587 (1977).
110. C.L. Basham *et al.*, Phys. Rev. **D17**, 2298 (1978).
111. J. Ellis, M.K. Gaillard, and G. Ross, Nucl. Phys. **B111**, 253 (1976); *ibid.*, erratum Nucl. Phys. **B130**, 516 (1977); P. Hoyer *et al.*, Nucl. Phys. **B161**, 349 (1979).
112. R.K. Ellis, D.A. Ross, T. Terrano, Phys. Rev. Lett. **45**, 1226 (1980); Z. Kunszt and P. Nason, ETH-89-0836 (1989).
113. S. Bethke *et al.*, Phys. Lett. **B213**, 235 (1988).
114. S. Bethke *et al.*, Nucl. Phys. **B370**, 310 (1992).
115. M.Z. Akrawy *et al.*, Z. Phys. **C49**, 375 (1991).
116. K. Abe *et al.*, Phys. Rev. Lett. **71**, 2578 (1993); Phys. Rev. **D51**, 962 (1995).
117. B. Andersson *et al.*, Phys. Reports **97**, 33 (1983).
118. A. Ali *et al.*, Nucl. Phys. **B168**, 409 (1980); A. Ali and R. Barreiro, Phys. Lett. **118B**, 155 (1982).
119. B.R. Webber, Nucl. Phys. **B238**, 492 (1984); G. Marchesini *et al.*, Phys. Comm. **67**, 465 (1992).
120. T. Sjostrand and M. Bengtsson, Comp. Phys. Comm. **43**, 367 (1987); T. Sjostrand, CERN-TH-7112/93 (1993).

121. O. Adriani *et al.*, Phys. Lett. **B284**, 471 (1992);
M. Akrawy *et al.*, Z. Phys. **C47**, 505 (1990);
B. Adeva *et al.*, Phys. Lett. **B248**, 473 (1990);
D. Decamp *et al.*, Phys. Lett. **B255**, 623 (1991).
122. S. Catani *et al.*, Phys. Lett. **B263**, 491 (1991).
123. S. Catani *et al.*, Phys. Lett. **B269**, 432 (1991);
S. Catani, B.R. Webber, and G. Turnock, Phys. Lett. **B272**, 368 (1991);
N. Brown and J. Stirling, Z. Phys. **C53**, 629 (1992).
124. G. Catani *et al.*, Phys. Lett. **B269**, 632 (1991); Phys. Lett. **B295**, 269 (1992); Nucl. Phys. **B607**, 3 (1993); Phys. Lett. **B269**, 432 (1991).
125. P.D. Acton *et al.*, Z. Phys. **C55**, 1 (1992); Z. Phys. **C58**, 386 (1993).
126. O. Adriani *et al.*, Phys. Lett. **B284**, 471 (1992).
127. D. Decamp *et al.*, Phys. Lett. **B255**, 623 (1992); Phys. Lett. **B257**, 479 (1992).
128. P. Abreu *et al.*, Z. Phys. **C59**, 21 (1993);
M. Acciarri *et al.*, Phys. Lett. **B404**, 390 (1997).
129. Y. Ohnishi *et al.*, Phys. Lett. **B313**, 475 (1993).
130. P.A. Movilla Fernandez *et al.*, Eur. Phys. J. **C1**, 461 (1998);
O. Biebel *et al.*, Phys. Lett. **B459**, 326 (1999).
131. D.A. Bauer *et al.*, SLAC-PUB-6518.
132. L. Gibbons *et al.*, CLNS 95-1323 (1995).
133. DELPHI Collaboration: D. Buskulic *et al.*, Z. Phys. **C73**, 409 (1997); Z. Phys. **C73**, 229 (1997).
134. ALEPH Collaboration: 99-023 (1999); DELPHI Collaboration: 99-114 (1999); L3 Collaboration: L3-2414 (1999); OPAL Collaboration, PN-403 (1999); all submitted to *International Conference on Lepton Photon Interactions*, Stanford, USA (Aug. 1999);
OPAL Collaboration: M. Acciarri *et al.*, Phys. Lett. **B371**, 137 (1996); Z. Phys. **C72**, 191 (1996);
K. Ackerstaff *et al.*, Z. Phys. **C75**, 193 (1997);
ALEPH Collaboration: ALEPH 98-025 (1998).
135. DELPHI Collaboration: Phys. Lett. **B456**, 322 (1999).
136. Y.L. Dokshitzer and B.R. Webber Phys. Lett. **B352**, 451 (1995);
Y.L. Dokshitzer *et al.* Nucl. Phys. **B511**, 396 (1997);
Y.L. Dokshitzer *et al.* JHEP 9801,011 (1998).
137. P. Nason and B.R. Webber, Nucl. Phys. **B421**, 473 (1994).
138. D. Buskulic *et al.*, Phys. Lett. **B357**, 487 (1995);
ibid., erratum Phys. Lett. **B364**, 247 (1995).
139. OPAL Collaboration: R. Akers *et al.*, Z. Phys. **C68**, 203 (1995).
140. DELPHI Collaboration: P. Abreu *et al.*, Phys. Lett. **B398**, 194 (1997).
141. E. Witten, Nucl. Phys. **B120**, 189 (1977).
142. C. Berger *et al.*, Nucl. Phys. **B281**, 365 (1987).
143. H. Aihara *et al.*, Z. Phys. **C34**, 1 (1987).
144. M. Althoff *et al.*, Z. Phys. **C31**, 527 (1986).
145. W. Bartel *et al.*, Z. Phys. **C24**, 231 (1984).
146. J. Butterworth, *International Conference on Lepton Photon Interactions*, Stanford, USA (Aug. 1999).
147. K. Ackerstaff *et al.*, Phys. Lett. **B412**, 225 (1997); Phys. Lett. **B411**, 387 (1997).
148. R. Barate *et al.*, Phys. Lett. **B458**, 152 (1999).
149. M. Acciarri *et al.*, Phys. Lett. **B436**, 403 (1998).
150. P. Abreu *et al.*, Z. Phys. **C69**, 223 (1996).
151. K. Muramatsu *et al.*, Phys. Lett. **B332**, 477 (1994).
152. S.K. Sahu *et al.*, Phys. Lett. **B346**, 208 (1995).
153. H1 Collaboration: C. Adloff *et al.*, Eur. Phys. J. **C13**, 397 (2000) DESY-98-205;
J. Breitweg *et al.*, Eur. Phys. J. **C11**, 35 (1999) DESY 99-057.
154. S. Frixione, Nucl. Phys. **B507**, 295 (1997);
B.W. Harris and J.F. Owens, Phys. Rev. **D56**, 4007 (1997);
M. Klasen and G. Kramr, Z. Phys. **C72**, 107 (1996).
155. D. Graudenz, Phys. Rev. **D49**, 3921 (1994) hep-ph/9708362;
J.G. Korner, E. Mirkes, and G.A. Schuler, Int. J. Mod. Phys. **A4**, 1781, (1989);
S. Catani and M. Seymour, Nucl. Phys. **B485**, 291 (1997);
M. Dasgupta and B.R. Webber, Eur. Phys. J. **C1**, 539 (1998) hep-ph/9704297;
E. Mirkes and D. Zeppenfeld, Phys. Lett. **B380**, 205 (1996).
156. H1 Collaboration: T. Ahmed *et al.*, Phys. Lett. **B346**, 415 (1995); Eur. Phys. J. **C5**, 575 (1998).
157. ZEUS Collaboration: M. Derrick *et al.*, Phys. Lett. **B363**, 201 (1995).
158. M. Derrick *et al.*, Phys. Lett. **B**, 369 (1996);
H1 Collaboration: T. Ahmed *et al.*, Nucl. Phys. **B435**, 3 (1995).
159. D.M. Janson, M. Albrow, and R. Brugnera hep-ex/9905537.
160. P. Weisz, Nucl. Phys. **B** (Proc. Supp.) **47**, 71 (1996).
161. C.T.H. Davies *et al.*, Phys. Rev. **D56**, 2755 (1997).
162. S. Aoki *et al.*, Phys. Rev. Lett. **74**, 222 (1995).
163. A. Spitz *et al.*, Phys. Rev. **D60**, 074502 (1999) hep-lat/9906009.
164. A.X. El-Khadra *et al.*, Phys. Rev. Lett. **69**, 729 (1992);
A.X. El-Khadra *et al.*, FNAL 94-091/T (1994);
A.X. El-Khadra *et al.*, hep-ph/9608220.
165. S. Collins *et al.*, cited by [166].
166. J. Shigemitsu, Nucl. Phys. **B** (Proc. Supp.) **53**, 16 (1997).
167. G.S. Bali and K. Schilling, Phys. Rev. **D47**, 661 (1973);
S.P. Booth *et al.*, Phys. Lett. **B294**, 38 (1992).
168. G. de Divitiis *et al.*, Nucl. Phys. **B437**, 447 (1995);
M. Luscher *et al.*, Nucl. Phys. **B413**, 481 (1994).
169. M. Luscher and P. Weisz, Nucl. Phys. **B452**, 234 (1995).
170. P.N. Burrows *et al.*, in *Proceedings of 1996 DPF/DPB Snowmass Summer Study*, ed. D. Cassel *et al.*, (1997).

10. ELECTROWEAK MODEL AND CONSTRAINTS ON NEW PHYSICS

Revised August 1999 by J. Erler and P. Langacker (Univ. of Pennsylvania).

- 10.1 Introduction
- 10.2 Renormalization and radiative corrections
- 10.3 Cross-section and asymmetry formulas
- 10.4 W and Z decays
- 10.5 Experimental results
- 10.6 Constraints on new physics

10.1. Introduction

The standard electroweak model is based on the gauge group [1] $SU(2) \times U(1)$, with gauge bosons W_μ^i , $i = 1, 2, 3$, and B_μ for the $SU(2)$ and $U(1)$ factors, respectively, and the corresponding gauge coupling constants g and g' . The left-handed fermion fields $\psi_i = \begin{pmatrix} \nu_i \\ \ell_i^- \end{pmatrix}$ and $\begin{pmatrix} u_i \\ d_i^- \end{pmatrix}$ of the i^{th} fermion family transform as doublets under $SU(2)$, where $d_i^- \equiv \sum_j V_{ij} d_j$, and V is the Cabibbo-Kobayashi-Maskawa mixing matrix. (Constraints on V are discussed in the section on the Cabibbo-Kobayashi-Maskawa mixing matrix.) The right-handed fields are $SU(2)$ singlets. In the minimal model there are three fermion families and a single complex Higgs doublet $\phi \equiv \begin{pmatrix} \phi^+ \\ \phi^0 \end{pmatrix}$.

After spontaneous symmetry breaking the Lagrangian for the fermion fields is

$$\begin{aligned} \mathcal{L}_F = & \sum_i \bar{\psi}_i \left(i \not{\partial} - m_i - \frac{gm_i H}{2M_W} \right) \psi_i \\ & - \frac{g}{2\sqrt{2}} \sum_i \bar{\psi}_i \gamma^\mu (1 - \gamma^5) (T^+ W_\mu^+ + T^- W_\mu^-) \psi_i \\ & - e \sum_i q_i \bar{\psi}_i \gamma^\mu \psi_i A_\mu \\ & - \frac{g}{2 \cos \theta_W} \sum_i \bar{\psi}_i \gamma^\mu (g_V^i - g_A^i \gamma^5) \psi_i Z_\mu . \end{aligned} \quad (10.1)$$

$\theta_W \equiv \tan^{-1}(g'/g)$ is the weak angle; $e = g \sin \theta_W$ is the positron electric charge; and $A \equiv B \cos \theta_W + W^3 \sin \theta_W$ is the (massless) photon field. $W^\pm \equiv (W^1 \mp iW^2)/\sqrt{2}$ and $Z \equiv -B \sin \theta_W + W^3 \cos \theta_W$ are the massive charged and neutral weak boson fields, respectively. T^+ and T^- are the weak isospin raising and lowering operators. The vector and axial vector couplings are

$$g_V^i \equiv t_{3L}(i) - 2q_i \sin^2 \theta_W , \quad (10.2a)$$

$$g_A^i \equiv t_{3L}(i) , \quad (10.2b)$$

where $t_{3L}(i)$ is the weak isospin of fermion i ($+1/2$ for u_i and ν_i ; $-1/2$ for d_i and e_i) and q_i is the charge of ψ_i in units of e .

The second term in \mathcal{L}_F represents the charged-current weak interaction [2]. For example, the coupling of a W to an electron and a neutrino is

$$-\frac{e}{2\sqrt{2} \sin \theta_W} \left[W_\mu^- \bar{\nu} \gamma^\mu (1 - \gamma^5) \nu + W_\mu^+ \bar{\nu} \gamma^\mu (1 - \gamma^5) e \right] . \quad (10.3)$$

For momenta small compared to M_W , this term gives rise to the effective four-fermion interaction with the Fermi constant given (at tree level, *i.e.*, lowest order in perturbation theory) by $G_F/\sqrt{2} = g^2/8M_W^2$. CP violation is incorporated in the Standard Model by a single observable phase in V_{ij} . The third term in \mathcal{L}_F describes electromagnetic interactions (QED), and the last is the weak neutral-current interaction.

In Eq. (10.1), m_i is the mass of the i^{th} fermion ψ_i . For the quarks these are the current masses. For the light quarks, as described in the Particle Listings, $\hat{m}_u \approx 1\text{--}5$ MeV, $\hat{m}_d \approx 3\text{--}9$ MeV, and $\hat{m}_s \approx 75\text{--}170$ MeV. These are running $\overline{\text{MS}}$ masses evaluated at the scale $\mu = 2$ GeV. (In this section we denote quantities defined in the $\overline{\text{MS}}$ scheme by a caret; the exception is the strong coupling constant, α_s , which will always correspond to the $\overline{\text{MS}}$ definition and where the caret will be dropped.) For the heavier quarks,

$\hat{m}_c(\mu = \hat{m}_c) \approx 1.15\text{--}1.35$ GeV and $\hat{m}_b(\mu = \hat{m}_b) \approx 4.0\text{--}4.4$ GeV. The average of the recent CDF [4] and DØ [5] values for the top quark ‘‘pole’’ mass is $m_t = 174.3 \pm 5.1$ GeV. We will use this value for m_t (together with $M_H = 100$ GeV) for the numerical values quoted in Sec. 10.2–Sec. 10.4. See ‘‘The Note on Quark Masses’’ in the Particle Listings for more information.

H is the physical neutral Higgs scalar which is the only remaining part of ϕ after spontaneous symmetry breaking. The Yukawa coupling of H to ψ_i , which is flavor diagonal in the minimal model is $gm_i/2M_W$. In nonminimal models there are additional charged and neutral scalar Higgs particles [6].

10.2. Renormalization and radiative corrections

The Standard Model has three parameters (not counting the Higgs boson mass, M_H , and the fermion masses and mixings). A particularly useful set is:

- (a) The fine structure constant $\alpha = 1/137.0359895(61)$, determined from the quantum Hall effect. In most electroweak-renormalization schemes, it is convenient to define a running α dependent on the energy scale of the process, with $\alpha^{-1} \sim 137$ appropriate at very low energy. (The running has also been observed directly. [7]) For scales above a few hundred MeV this introduces an uncertainty due to the low-energy hadronic contribution to vacuum polarization. In the modified minimal subtraction ($\overline{\text{MS}}$) scheme [8] (used for this *Review*), and with $\alpha_s(M_Z) = 0.120$ for the QCD coupling at M_Z , one has $\hat{\alpha}(m_\tau)^{-1} = 133.513 \pm 0.026$ and $\hat{\alpha}(M_Z)^{-1} = 127.934 \pm 0.027$ [9]. The non-linear α_s dependence of $\hat{\alpha}(M_Z)$ and the resulting correlation with the input variable α_s , is fully taken into account in the fits. The uncertainty is from e^+e^- annihilation data below 1.8 GeV [10], from uncalculated higher order perturbative and non-perturbative QCD corrections, and from the $\overline{\text{MS}}$ quark masses, $\hat{m}_c(\hat{m}_c) = 1.31 \pm 0.07$ and $\hat{m}_b(\hat{m}_b) = 4.24 \pm 0.11$ [9]. Such a short distance mass definition (unlike the pole mass) is free from non-perturbative and renormalon uncertainties. Various recent evaluations of the contributions of the five light quark flavors, $\Delta\alpha_{\text{had}}^{(5)}$, to the conventional (on-shell) QED coupling, $\alpha(M_Z) = \frac{\alpha}{1 - \Delta\alpha}$, are summarized in Table 10.1. Most of the older results relied on $e^+e^- \rightarrow$ hadrons cross-section measurements up to energies of 40 GeV which were somewhat higher than the QCD prediction, suggested stronger running, and were less precise. The most recent results assume the validity of perturbative QCD (PQCD) at scales of 1.8 GeV and above (outside of resonance regions), and are in very good agreement with each other. They imply higher central values for the extracted M_H by $\mathcal{O}(20)$ GeV. On the other hand, the upper limits for M_H are all similar due to a compensation of the latter effect and the higher precision. Further improvement of this dominant theoretical uncertainty in the interpretation of precision data will require better measurements of the cross-section for $e^+e^- \rightarrow$ hadrons at low energy.
- (b) The Fermi constant, $G_F = 1.16637(1) \times 10^{-5}$ GeV $^{-2}$, determined from the muon lifetime formula [22,23],

$$\begin{aligned} \tau_\mu^{-1} = & \frac{G_F^2 m_\mu^5}{192\pi^3} F\left(\frac{m_e^2}{m_\mu^2}\right) \left(1 + \frac{3}{5} \frac{m_\mu^2}{M_W^2}\right) \\ & \times \left[1 + \left(\frac{25}{8} - \frac{\pi^2}{2}\right) \frac{\alpha(m_\mu)}{\pi} + C_2 \frac{\alpha^2(m_\mu)}{\pi^2}\right] , \end{aligned} \quad (10.4a)$$

where

$$F(x) = 1 - 8x + 8x^3 - x^4 - 12x^2 \ln x , \quad (10.4b)$$

$$C_2 = \frac{156815}{5184} - \frac{518}{81} \pi^2 - \frac{895}{36} \zeta(3) + \frac{67}{720} \pi^4 + \frac{53}{6} \pi^2 \ln(2) , \quad (10.4c)$$

and

$$\alpha(m_\mu)^{-1} = \alpha^{-1} - \frac{2}{3\pi} \ln\left(\frac{m_\mu}{m_e}\right) + \frac{1}{6\pi} \approx 136 . \quad (10.4d)$$

Table 10.1: Recent evaluations of the on-shell $\Delta\alpha_{\text{had}}^{(5)}(M_Z)$. For better comparison we adjusted central values and errors to correspond to a common and fixed value of $\alpha_s(M_Z) = 0.120$. References quoting results without the top quark decoupled are converted to the five flavor definition. Ref. [20] uses $\Lambda_{\text{QCD}} = 380 \pm 60$ MeV; for the conversion we assumed $\alpha_s(M_Z) = 0.118 \pm 0.003$.

Reference	Result	Comment
Martin&Zeppenfeld [11]	0.02744 ± 0.00036	PQCD for $\sqrt{s} > 3$ GeV
Eidelman&Jegerlehner [12]	0.02803 ± 0.00065	PQCD for $\sqrt{s} > 40$ GeV
Geshkenbein&Morgunov [13]	0.02780 ± 0.00006	$\mathcal{O}(\alpha_s)$ resonance model
Burkhardt&Pietrzyk [14]	0.0280 ± 0.0007	PQCD for $\sqrt{s} > 40$ GeV
Swartz [15]	0.02754 ± 0.00046	use of fitting function
Aleman, Davier, Höcker [16]	0.02816 ± 0.00062	includes τ decay data
Krasnikov&Rodenberg [17]	0.02737 ± 0.00039	PQCD for $\sqrt{s} > 2.3$ GeV
Davier&Höcker [10]	0.02784 ± 0.00022	PQCD for $\sqrt{s} > 1.8$ GeV
Kühn&Steinhauser [18]	0.02778 ± 0.00016	complete $\mathcal{O}(\alpha_s^2)$
Erlar [9]	0.02779 ± 0.00020	converted from $\overline{\text{MS}}$ scheme
Davier&Höcker [19]	0.02770 ± 0.00015	use of QCD sum rules
Groote <i>et al.</i> [20]	0.02787 ± 0.00032	use of QCD sum rules
Jegerlehner [21]	0.02778 ± 0.00024	converted from MOM scheme

The $\mathcal{O}(\alpha^2)$ corrections to μ decay have been completed recently [23]. The remaining uncertainty in G_F is from the experimental input.

- (c) The Z boson mass, $M_Z = 91.1872 \pm 0.0021$ GeV, determined from the Z lineshape scan at LEP 1 [24].

With these inputs, $\sin^2 \theta_W$ can be calculated when values for m_t and M_H are given; conversely (as is done at present), M_H can be constrained by $\sin^2 \theta_W$. The value of $\sin^2 \theta_W$ is extracted from Z pole observables, the W mass, and neutral-current processes [25], and depends on the renormalization prescription. There are a number of popular schemes [27–32] leading to values which differ by small factors depending on m_t and M_H . The notation for these schemes is shown in Table 10.2. Discussion of the schemes follows the table.

Table 10.2: Notations used to indicate the various schemes discussed in the text. Each definition of $\sin \theta_W$ leads to values that differ by small factors depending on m_t and M_H .

Scheme	Notation
On-shell	$s_W = \sin \theta_W$
NOV	$s_{M_Z} = \sin \theta_W$
$\overline{\text{MS}}$	$\hat{s}_Z = \sin \theta_W$
$\overline{\text{MS}} ND$	$\hat{s}_{ND} = \sin \theta_W$
Effective angle	$\bar{s}_f = \sin \theta_W$

- (i) The on-shell scheme [27] promotes the tree-level formula $\sin^2 \theta_W = 1 - M_W^2/M_Z^2$ to a definition of the renormalized $\sin^2 \theta_W$ to all orders in perturbation theory, *i.e.*, $\sin^2 \theta_W \rightarrow s_W^2 \equiv 1 - M_W^2/M_Z^2$. This scheme is simple conceptually. However, M_W is known much less precisely than M_Z and in practice one extracts s_W^2 from M_Z alone using

$$M_W = \frac{A_0}{s_W(1 - \Delta r)^{1/2}}, \quad (10.5a)$$

$$M_Z = \frac{M_W}{c_W}, \quad (10.5b)$$

where $c_W \equiv \cos \theta_W$, $A_0 = (\pi\alpha/\sqrt{2}G_F)^{1/2} = 37.2805(2)$ GeV, and Δr includes the radiative corrections relating α , $\alpha(M_Z)$, G_F , M_W , and M_Z . One finds $\Delta r \sim \Delta r_0 - \rho_t/\tan^2 \theta_W$, where $\Delta r_0 = 1 - \alpha/\hat{\alpha}(M_Z) = 0.0664(2)$ is due to the running of α and $\rho_t = 3G_F m_t^2/8\sqrt{2}\pi^2 = 0.00952(m_t/174.3 \text{ GeV})^2$ represents the dominant (quadratic) m_t dependence. There are additional contributions to Δr from bosonic loops, including those which depend logarithmically on M_H . One has $\Delta r = 0.0350 \mp 0.0019 \pm 0.0002$, where the second uncertainty is from $\alpha(M_Z)$. Thus the value of s_W^2 extracted from M_Z includes an uncertainty (∓ 0.0006) from the currently allowed range of m_t .

- (ii) A more precisely determined quantity $s_{M_Z}^2$ can be obtained from M_Z by removing the (m_t, M_H) dependent term from Δr [28], *i.e.*,

$$s_{M_Z}^2 c_{M_Z}^2 \equiv \frac{\pi\alpha(M_Z)}{\sqrt{2}G_F M_Z^2}. \quad (10.6)$$

Using $\alpha(M_Z)^{-1} = 128.92 \pm 0.03$ yields $s_{M_Z}^2 = 0.23105 \mp 0.00008$. The small uncertainty in $s_{M_Z}^2$ compared to other schemes is because most of the m_t dependence has been removed by definition. However, the m_t uncertainty reemerges when other quantities (*e.g.*, M_W or other Z pole observables) are predicted in terms of M_Z .

Both s_W^2 and $s_{M_Z}^2$ depend not only on the gauge couplings but also on the spontaneous-symmetry breaking, and both definitions are awkward in the presence of any extension of the Standard Model which perturbs the value of M_Z (or M_W). Other definitions are motivated by the tree-level coupling constant definition $\theta_W = \tan^{-1}(g'/g)$.

- (iii) In particular, the modified minimal subtraction ($\overline{\text{MS}}$) scheme introduces the quantity $\sin^2 \hat{\theta}_W(\mu) \equiv \hat{g}'^2(\mu)/[\hat{g}^2(\mu) + \hat{g}'^2(\mu)]$, where the couplings \hat{g} and \hat{g}' are defined by modified minimal subtraction and the scale μ is conveniently chosen to be M_Z for electroweak processes. The value of $\hat{s}_Z^2 = \sin^2 \hat{\theta}_W(M_Z)$ extracted from M_Z is less sensitive than s_W^2 to m_t (by a factor of $\tan^2 \theta_W$), and is less sensitive to most types of new physics than s_W^2 or $s_{M_Z}^2$. It is also very useful for comparing with the predictions of grand unification. There are actually several variant definitions of $\sin^2 \hat{\theta}_W(M_Z)$, differing according to whether or how finite $\alpha \ln(m_t/M_Z)$ terms are decoupled (subtracted from the couplings). One cannot entirely decouple the $\alpha \ln(m_t/M_Z)$ terms from all electroweak quantities because $m_t \gg m_b$ breaks SU(2) symmetry. The scheme that will be adopted here decouples the $\alpha \ln(m_t/M_Z)$ terms from the $\gamma - Z$ mixing [8,29], essentially eliminating any $\ln(m_t/M_Z)$ dependence in the formulae for asymmetries at the Z pole when written in terms of \hat{s}_Z^2 . (A similar definition is used for $\hat{\alpha}$.) The various definitions are related by

$$\hat{s}_Z^2 = c(m_t, M_H) s_W^2 = \bar{c}(m_t, M_H) s_{M_Z}^2, \quad (10.7)$$

where $c = 1.0371 \pm 0.0021$ and $\bar{c} = 1.0004 \mp 0.0007$. The quadratic m_t dependence is given by $c \sim 1 + \rho_t/\tan^2 \theta_W$ and $\bar{c} \sim 1 - \rho_t/(1 - \tan^2 \theta_W)$, respectively. The expressions for M_W and M_Z in the $\overline{\text{MS}}$ scheme are

$$M_W = \frac{A_0}{\hat{s}_Z(1 - \Delta \hat{r}_W)^{1/2}}, \quad (10.8a)$$

$$M_Z = \frac{M_W}{\hat{\rho}^{1/2} \hat{c}_Z}, \quad (10.8b)$$

and one predicts $\Delta \hat{r}_W = 0.0695 \pm 0.0001 \pm 0.0002$. $\Delta \hat{r}_W$ has no quadratic m_t dependence, because shifts in M_W are absorbed into the observed G_F , so that the error in $\Delta \hat{r}_W$ is dominated by $\Delta r_0 = 1 - \alpha/\hat{\alpha}(M_Z)$, which induces the second quoted uncertainty. The quadratic m_t dependence has been shifted into $\hat{\rho} \sim 1 + \rho_t$, where including bosonic loops, $\hat{\rho} = 1.0107 \pm 0.0006$.

- (iv) A variant $\overline{\text{MS}}$ quantity \hat{s}_{ND}^2 (used in the 1992 edition of this *Review*) does not decouple the $\alpha \ln(m_t/M_Z)$ terms [30]. It is

related to \hat{s}_Z^2 by

$$\hat{s}_Z^2 = \hat{s}_{\text{ND}}^2 / \left(1 + \frac{\hat{\alpha}}{\pi} d\right), \quad (10.9a)$$

$$d = \frac{1}{3} \left(\frac{1}{\hat{s}^2} - \frac{8}{3} \right) \left[\left(1 + \frac{\alpha_s}{\pi}\right) \ln \frac{m_t}{M_Z} - \frac{15\alpha_s}{8\pi} \right], \quad (10.9b)$$

Thus, $\hat{s}_Z^2 - \hat{s}_{\text{ND}}^2 \sim -0.0002$ for $m_t = 174.3$ GeV.

(v) Yet another definition, the effective angle [31,32] \hat{s}_f^2 for Z coupling to fermion f , is described in Sec. 10.3.

Experiments are now at such a level of precision that complete $\mathcal{O}(\alpha)$ radiative corrections must be applied. For neutral-current and Z pole processes, these corrections are conveniently divided into two classes:

1. QED diagrams involving the emission of real photons or the exchange of virtual photons in loops, but not including vacuum polarization diagrams. These graphs often yield finite and gauge-invariant contributions to observable processes. However, they are dependent on energies, experimental cuts, *etc.*, and must be calculated individually for each experiment.
2. Electroweak corrections, including $\gamma\gamma$, γZ , ZZ , and WW vacuum polarization diagrams, as well as vertex corrections, box graphs, *etc.*, involving virtual W 's and Z 's. Many of these corrections are absorbed into the renormalized Fermi constant defined in Eq. (10.4). Others modify the tree-level expressions for Z pole observables and neutral-current amplitudes in several ways [25]. One-loop corrections are included for all processes. In addition, certain two-loop corrections are also important. In particular, two-loop corrections involving the top-quark modify ρ_t in \bar{p} , Δr , and elsewhere by

$$\rho_t \rightarrow \rho_t [1 + R(M_H, m_t) \rho_t / 3]. \quad (10.10)$$

$R(M_H, m_t)$ is best described as an expansion in M_Z^2/m_t^2 . The unsuppressed terms were first obtained in Ref. 33, and are known analytically [34]. Contributions suppressed by M_Z^2/m_t^2 were studied in Ref. 35 with the help of small and large Higgs mass expansions, which can be interpolated. These contributions are about as large as the leading ones in Refs. 33 and 34. A subset of the relevant two-loop diagrams has also been calculated numerically without any heavy mass expansion [36]. This serves as a valuable check on the M_H dependence of the leading terms obtained in Refs. 33–35. The difference turned out to be small. For M_H above its lower direct limit, $-17 < R < -12$. Mixed QCD-electroweak loops of order $\alpha_s m_t^2$ [37] and $\alpha_s^2 m_t^2$ [38] increase the predicted value of m_t by 6%. This is, however, almost entirely an artifact of using the pole mass definition for m_t . The equivalent corrections when using the $\overline{\text{MS}}$ definition $\hat{m}_t(\hat{m}_t)$ increase m_t by less than 0.5%. The leading electroweak [33,34] and mixed [39] two-loop terms are also known for the $Z \rightarrow b\bar{b}$ vertex, but not the respective subleading ones. $\mathcal{O}(\alpha\alpha_s)$ -vertex corrections involving massless quarks have been obtained in Ref. [40]. Since they add coherently, the resulting effect is sizable, and shifts the extracted $\alpha_s(M_Z)$ by $\approx +0.0007$. Corrections of the same order to $Z \rightarrow b\bar{b}$ decays have also been completed [41].

Throughout this Review we utilize electroweak radiative corrections from the program GAPP, which works entirely in the $\overline{\text{MS}}$ scheme, and which is independent of the package ZFITTER.

10.3. Cross-section and asymmetry formulas

It is convenient to write the four-fermion interactions relevant to ν -hadron, ν - e , and parity violating e -hadron neutral-current processes in a form that is valid in an arbitrary gauge theory (assuming massless left-handed neutrinos). One has

$$-\mathcal{L}^{\nu\text{Hadron}} = \frac{G_F}{\sqrt{2}} \bar{\nu} \gamma^\mu (1 - \gamma^5) \nu \times \sum_i \left[\epsilon_L(i) \bar{q}_i \gamma_\mu (1 - \gamma^5) q_i + \epsilon_R(i) \bar{q}_i \gamma_\mu (1 + \gamma^5) q_i \right], \quad (10.11)$$

$$-\mathcal{L}^{\nu e} = \frac{G_F}{\sqrt{2}} \bar{\nu}_\mu \gamma^\mu (1 - \gamma^5) \nu_\mu \bar{e} \gamma_\mu (g_{V_e}^{\nu e} - g_{A_e}^{\nu e} \gamma^5) e \quad (10.12)$$

(for ν_e - e or $\bar{\nu}_e$ - e , the charged-current contribution must be included), and

$$-\mathcal{L}^{e\text{Hadron}} = -\frac{G_F}{\sqrt{2}} \times \sum_i \left[C_{1i} \bar{e} \gamma_\mu \gamma^5 e \bar{q}_i \gamma^\mu q_i + C_{2i} \bar{e} \gamma_\mu e \bar{q}_i \gamma^\mu \gamma^5 q_i \right]. \quad (10.13)$$

(One must add the parity-conserving QED contribution.)

The Standard Model expressions for $\epsilon_{L,R}(i)$, $g_{V,A}^{\nu e}$, and C_{ij} are given in Table 10.3. Note, that $g_{V,A}^{\nu e}$ and the other quantities are coefficients of effective four-fermi operators, which differ from the quantities defined in Eq. (10.2) in the radiative corrections and in the presence of possible physics beyond the Standard Model.

A precise determination of the on-shell s_W^2 , which depends only very weakly on m_t and M_H , is obtained from deep inelastic neutrino scattering from (approximately) isoscalar targets [42]. The ratio $R_\nu \equiv \sigma_{\nu N}^{NC} / \sigma_{\nu N}^{CC}$ of neutral- to charged-current cross-sections has been measured to 1% accuracy by the CDHS [43] and CHARM [44] collaborations at CERN, and the CCFR [45] collaboration at Fermilab has obtained an even more precise result, so it is important to obtain theoretical expressions for R_ν and $R_{\bar{\nu}} \equiv \sigma_{\bar{\nu} N}^{NC} / \sigma_{\bar{\nu} N}^{CC}$ to comparable accuracy. Fortunately, most of the uncertainties from the strong interactions and neutrino spectra cancel in the ratio. The largest theoretical uncertainty is associated with the c -threshold, which mainly affects σ^{CC} . Using the slow rescaling prescription [46] the central value of $\sin^2 \theta_W$ from CCFR varies as $0.0111(m_c [\text{GeV}] - 1.31)$, where m_c is the effective mass which is numerically close to the $\overline{\text{MS}}$ mass $\hat{m}_c(\hat{m}_c)$, but their exact relation is unknown at higher orders. For $m_c = 1.31 \pm 0.24$ GeV (determined from ν -induced dimuon production [47]) this contributes ± 0.003 to the total uncertainty $\Delta \sin^2 \theta_W \sim \pm 0.004$. (The experimental uncertainty is also ± 0.003 .) This uncertainty largely cancels, however, in the Paschos-Wolfenstein ratio [48],

$$R^- = \frac{\sigma_{\nu N}^{NC} - \sigma_{\bar{\nu} N}^{NC}}{\sigma_{\nu N}^{CC} - \sigma_{\bar{\nu} N}^{CC}}. \quad (10.14)$$

It was measured recently by the NuTeV collaboration [49] for the first time, and required a high-intensity and high-energy anti-neutrino beam.

A simple zeroth-order approximation is

$$R_\nu = g_L^2 + g_R^2, \quad (10.15a)$$

$$R_{\bar{\nu}} = g_L^2 + \frac{g_R^2}{r}, \quad (10.15b)$$

$$R^- = g_L^2 - g_R^2, \quad (10.15c)$$

where

$$g_L^2 \equiv \epsilon_L(u)^2 + \epsilon_L(d)^2 \approx \frac{1}{2} - \sin^2 \theta_W + \frac{5}{9} \sin^4 \theta_W, \quad (10.16a)$$

$$g_R^2 \equiv \epsilon_R(u)^2 + \epsilon_R(d)^2 \approx \frac{5}{9} \sin^4 \theta_W, \quad (10.16b)$$

and $r \equiv \sigma_{\bar{\nu} N}^{CC} / \sigma_{\nu N}^{CC}$ is the ratio of $\bar{\nu}$ and ν charged-current cross-sections, which can be measured directly. (In the simple parton model, ignoring hadron energy cuts, $r \approx (\frac{1}{3} + \epsilon) / (1 + \frac{1}{3}\epsilon)$, where $\epsilon \sim 0.125$ is the ratio of the fraction of the nucleon's momentum carried by antiquarks to that carried by quarks.) In practice, Eq. (10.15) must be corrected for quark mixing, quark sea effects, c -quark threshold effects, nonisoscality, $W - Z$ propagator differences, the finite muon mass, QED and electroweak radiative corrections. Details of the neutrino spectra, experimental cuts, x and Q^2 dependence of structure functions, and longitudinal structure functions enter only at the level of these corrections and therefore lead to very small uncertainties. The CCFR group quotes $s_W^2 = 0.2236 \pm 0.0041$ for $(m_t, M_H) = (175, 150)$ GeV with very little sensitivity to (m_t, M_H) . The NuTeV collaboration finds $s_W^2 = 0.2253 \pm 0.0022$ using the

Table 10.3: Standard Model expressions for the neutral-current parameters for ν -hadron, ν - e , and e -hadron processes. At tree level, $\rho = \kappa = 1$, $\lambda = 0$. If radiative corrections are included, $\rho_{\nu N}^{NC} = 1.0083$, $\widehat{\kappa}_{\nu N}(\langle Q^2 \rangle = -10 \text{ GeV}^2) = 0.9980$, $\widehat{\kappa}_{\nu N}(\langle Q^2 \rangle = -35 \text{ GeV}^2) = 0.9965$, $\lambda_{uL} = -0.0031$, $\lambda_{dL} = -0.0025$, and $\lambda_{dR} = 2\lambda_{uR} = 7.5 \times 10^{-5}$. For ν - e scattering, $\rho_{\nu e} = 1.0129$ and $\widehat{\kappa}_{\nu e} = 0.9967$ (at $\langle Q^2 \rangle = 0$). For atomic parity violation and the SLAC polarized electron experiment, $\rho'_{eq} = 0.9878$, $\rho_{eq} = 1.0008$, $\widehat{\kappa}'_{eq} = 1.0026$, $\widehat{\kappa}_{eq} = 1.0300$, $\lambda_{1d} = -2\lambda_{1u} = 3.7 \times 10^{-5}$, $\lambda_{2u} = -0.0121$ and $\lambda_{2d} = 0.0026$. The dominant m_t dependence is given by $\rho \sim 1 + \rho_t$, while $\widehat{\kappa} \sim 1$ ($\overline{\text{MS}}$) or $\kappa \sim 1 + \rho_t / \tan^2 \theta_W$ (on-shell).

Quantity	Standard Model Expression
$\epsilon_L(u)$	$\rho_{\nu N}^{NC} \left(\frac{1}{2} - \frac{2}{3} \widehat{\kappa}_{\nu N} \widehat{s}_Z^2 \right) + \lambda_{uL}$
$\epsilon_L(d)$	$\rho_{\nu N}^{NC} \left(-\frac{1}{2} + \frac{1}{3} \widehat{\kappa}_{\nu N} \widehat{s}_Z^2 \right) + \lambda_{dL}$
$\epsilon_R(u)$	$\rho_{\nu N}^{NC} \left(-\frac{2}{3} \widehat{\kappa}_{\nu N} \widehat{s}_Z^2 \right) + \lambda_{uR}$
$\epsilon_R(d)$	$\rho_{\nu N}^{NC} \left(\frac{1}{3} \widehat{\kappa}_{\nu N} \widehat{s}_Z^2 \right) + \lambda_{dR}$
$g_V^{\nu e}$	$\rho_{\nu e} \left(-\frac{1}{2} + 2\widehat{\kappa}_{\nu e} \widehat{s}_Z^2 \right)$
$g_A^{\nu e}$	$\rho_{\nu e} \left(-\frac{1}{2} \right)$
C_{1u}	$\rho'_{eq} \left(-\frac{1}{2} + \frac{4}{3} \widehat{\kappa}'_{eq} \widehat{s}_Z^2 \right) + \lambda_{1u}$
C_{1d}	$\rho'_{eq} \left(\frac{1}{2} - \frac{2}{3} \widehat{\kappa}'_{eq} \widehat{s}_Z^2 \right) + \lambda_{1d}$
C_{2u}	$\rho_{eq} \left(-\frac{1}{2} + 2\widehat{\kappa}_{eq} \widehat{s}_Z^2 \right) + \lambda_{2u}$
C_{2d}	$\rho_{eq} \left(\frac{1}{2} - 2\widehat{\kappa}_{eq} \widehat{s}_Z^2 \right) + \lambda_{2d}$

same reference values. Combining all of the precise deep-inelastic measurements, one obtains $s_W^2 = 0.2253 \pm 0.0021$.

The laboratory cross-section for $\nu_\mu e \rightarrow \nu_\mu e$ or $\bar{\nu}_\mu e \rightarrow \bar{\nu}_\mu e$ elastic scattering is

$$\frac{d\sigma_{\nu_\mu, \bar{\nu}_\mu}}{dy} = \frac{G_F^2 m_e E_\nu}{2\pi} \times \left[(g_V^{\nu e} \pm g_A^{\nu e})^2 + (g_V^{\nu e} \mp g_A^{\nu e})^2 (1-y)^2 - (g_V^{\nu e 2} - g_A^{\nu e 2}) \frac{y m_e}{E_\nu} \right], \quad (10.17)$$

where the upper (lower) sign refers to $\nu_\mu(\bar{\nu}_\mu)$, and $y \equiv E_e/E_\nu$ (which runs from 0 to $(1 + m_e/2E_\nu)^{-1}$) is the ratio of the kinetic energy of the recoil electron to the incident ν or $\bar{\nu}$ energy. For $E_\nu \gg m_e$ this yields a total cross-section

$$\sigma = \frac{G_F^2 m_e E_\nu}{2\pi} \left[(g_V^{\nu e} \pm g_A^{\nu e})^2 + \frac{1}{3} (g_V^{\nu e} \mp g_A^{\nu e})^2 \right]. \quad (10.18)$$

The most accurate leptonic measurements [50–52] of $\sin^2 \theta_W$ are from the ratio $R \equiv \sigma_{\nu_\mu e} / \sigma_{\bar{\nu}_\mu e}$ in which many of the systematic uncertainties cancel. Radiative corrections (other than m_t effects) are small compared to the precision of present experiments and have negligible effect on the extracted $\sin^2 \theta_W$. The most precise experiment (CHARM II) [52] determined not only $\sin^2 \theta_W$ but $g_V^{\nu e}$ as well. The cross-sections for $\nu_e e$ and $\bar{\nu}_e e$ may be obtained from Eq. (10.17) by replacing $g_V^{\nu e}$ by $g_V^{\nu e} + 1$, where the 1 is due to the charged-current contribution.

The SLAC polarized-electron experiment [53] measured the parity-violating asymmetry

$$A = \frac{\sigma_R - \sigma_L}{\sigma_R + \sigma_L}, \quad (10.19)$$

where $\sigma_{R,L}$ is the cross-section for the deep-inelastic scattering of a right- or left-handed electron: $e_{R,L} N \rightarrow eX$. In the quark parton model

$$\frac{A}{Q^2} = a_1 + a_2 \frac{1 - (1-y)^2}{1 + (1-y)^2}, \quad (10.20)$$

where $Q^2 > 0$ is the momentum transfer and y is the fractional energy transfer from the electron to the hadrons. For the deuteron or other isoscalar targets, one has, neglecting the s -quark and antiquarks,

$$a_1 = \frac{3G_F}{5\sqrt{2}\pi\alpha} \left(C_{1u} - \frac{1}{2} C_{1d} \right) \approx \frac{3G_F}{5\sqrt{2}\pi\alpha} \left(-\frac{3}{4} + \frac{5}{3} \sin^2 \theta_W \right), \quad (10.21a)$$

$$a_2 = \frac{3G_F}{5\sqrt{2}\pi\alpha} \left(C_{2u} - \frac{1}{2} C_{2d} \right) \approx \frac{9G_F}{5\sqrt{2}\pi\alpha} \left(\sin^2 \theta_W - \frac{1}{4} \right). \quad (10.21b)$$

There are now precise experiments measuring atomic parity violation [54] in cesium (at the 0.4% level) [55], thallium [56], lead [57], and bismuth [58]. The uncertainties associated with atomic wave functions are quite small for cesium [59], and have been reduced recently to about 0.4% [60]. In the past, the semi-empirical value of the tensor polarizability added another source of theoretical uncertainty [61]. The ratio of the off-diagonal hyperfine amplitude to the polarizability has now been measured directly by the Boulder group [60]. Combined with the precisely known hyperfine amplitude [62] one finds excellent agreement with the earlier results, reducing the overall theory uncertainty to only 0.5% (while slightly increasing the experimental error). The theoretical uncertainties are 3% for thallium [63] but larger for the other atoms. For heavy atoms one determines the “weak charge”

$$Q_W = -2[C_{1u}(2Z + N) + C_{1d}(Z + 2N)] \approx Z(1 - 4\sin^2 \theta_W) - N. \quad (10.22)$$

The recent Boulder experiment in cesium also observed the parity-violating weak corrections to the nuclear electromagnetic vertex (the anapole moment [64]).

In the future it should be possible to reduce the theoretical wave function uncertainties by taking the ratios of parity violation in different isotopes [54,65]. There would still be some residual uncertainties from differences in the neutron charge radii, however [66].

The forward-backward asymmetry for $e^+e^- \rightarrow \ell^+\ell^-$, $\ell = \mu$ or τ , is defined as

$$A_{FB} \equiv \frac{\sigma_F - \sigma_B}{\sigma_F + \sigma_B}, \quad (10.23)$$

where $\sigma_F(\sigma_B)$ is the cross-section for ℓ^- to travel forward (backward) with respect to the e^- direction. A_{FB} and R , the total cross-section relative to pure QED, are given by

$$R = F_1, \quad (10.24)$$

$$A_{FB} = 3F_2/4F_1, \quad (10.25)$$

where

$$F_1 = 1 - 2\chi_0 g_V^e g_V^\ell \cos \delta_R + \chi_0^2 (g_V^{e2} + g_A^{e2}) (g_V^{\ell 2} + g_A^{\ell 2}), \quad (10.26a)$$

$$F_2 = -2\chi_0 g_A^e g_A^\ell \cos \delta_R + 4\chi_0^2 g_A^e g_A^\ell g_V^e g_V^\ell, \quad (10.26b)$$

$$\tan \delta_R = \frac{M_Z \Gamma_Z}{M_Z^2 - s}, \quad (10.27)$$

$$\chi_0 = \frac{G_F}{2\sqrt{2}\pi\alpha} \frac{sM_Z^2}{[(M_Z^2 - s)^2 + M_Z^2 \Gamma_Z^2]^{1/2}}, \quad (10.28)$$

and \sqrt{s} is the CM energy. Eq. (10.26) is valid at tree level. If the data is radiatively corrected for QED effects (as described above), then the remaining electroweak corrections can be incorporated [67,68] (in an approximation adequate for existing PEP, PETRA, and TRISTAN data, which are well below the Z pole) by replacing χ_0 by $\chi(s) \equiv (1 + \rho_t)\chi_0(s)\alpha/\alpha(s)$, where $\alpha(s)$ is the running QED coupling, and evaluating g_V in the $\overline{\text{MS}}$ scheme. Formulas for $e^+e^- \rightarrow$ hadrons may be found in Ref. 69.

At LEP and SLC, there are high-precision measurements of various Z pole observables [70–78]. These include the Z mass and total width, Γ_Z , and partial widths $\Gamma(f\bar{f})$ for $Z \rightarrow f\bar{f}$ where fermion $f = e, \mu, \tau$, hadrons, b , or c . It is convenient to use the variables $M_Z, \Gamma_Z, R_\ell \equiv \Gamma(\text{had})/\Gamma(\ell^+\ell^-), \sigma_{\text{had}} \equiv 12\pi\Gamma(e^+e^-)\Gamma(\text{had})/M_Z^2\Gamma_Z^2, R_b \equiv \Gamma(b\bar{b})/\Gamma(\text{had}),$ and $R_c \equiv \Gamma(c\bar{c})/\Gamma(\text{had}),$ most of which are weakly correlated experimentally. ($\Gamma(\text{had})$ is the partial width into hadrons.) $\mathcal{O}(\alpha^3)$ QED corrections introduce a large anticorrelation (-28%) between Γ_Z and σ_{had} , while the anticorrelation between R_b and R_c (-14%) is smaller than previously. R_ℓ is insensitive to m_t except for the $Z \rightarrow b\bar{b}$ vertex and final state corrections and the implicit dependence through $\sin^2\theta_W$. Thus it is especially useful for constraining α_s . The width for invisible decays [24], $\Gamma(\text{inv}) = \Gamma_Z - 3\Gamma(\ell^+\ell^-) - \Gamma(\text{had}) = 498.8 \pm 1.5$ MeV, can be used to determine the number of neutrino flavors much lighter than $M_Z/2, N_\nu = \Gamma(\text{inv})/\Gamma^{\text{theory}}(\nu\bar{\nu}) = 2.983 \pm 0.009$ for $(m_t, M_H) = (174.3, 100)$ GeV.

There are also measurements of various Z pole asymmetries. These include the polarization or left-right asymmetry

$$A_{LR} \equiv \frac{\sigma_L - \sigma_R}{\sigma_L + \sigma_R}, \quad (10.29)$$

where $\sigma_L(\sigma_R)$ is the cross-section for a left-(right)-handed incident electron. A_{LR} has been measured precisely by the SLD collaboration at the SLC [71,72], and has the advantages of being extremely sensitive to $\sin^2\theta_W$ and that systematic uncertainties largely cancel. In addition, the SLD collaboration has extracted the final-state couplings A_b, A_c [24,73], A_s [74], A_τ , and A_μ [72,75] from left-right forward-backward asymmetries, using

$$A_{LR}^f(f) = \frac{\sigma_{LF}^f - \sigma_{LB}^f - \sigma_{RF}^f + \sigma_{RB}^f}{\sigma_{LF}^f + \sigma_{LB}^f + \sigma_{RF}^f + \sigma_{RB}^f} = \frac{3}{4}A_f, \quad (10.30)$$

where, for example, σ_{LF} is the cross-section for a left-handed incident electron to produce a fermion f traveling in the forward hemisphere. Similarly, A_τ is measured at LEP [24,76] through the negative total τ polarization, \mathcal{P}_τ , and A_e is extracted from the angular distribution of \mathcal{P}_τ . An equation such as (10.30) assumes that initial state QED corrections, photon exchange, $\gamma - Z$ interference, the tiny electroweak boxes, and corrections for $\sqrt{s} \neq M_Z$ are removed from the data, leaving the pure electroweak asymmetries. This allows the use of effective tree-level expressions,

$$A_{LR} = A_e P_e, \quad (10.31)$$

$$A_{FB} = \frac{3}{4}A_f \frac{A_e + P_e}{1 + P_e A_e}, \quad (10.32)$$

where

$$A_f \equiv \frac{2\bar{g}_V^f \bar{g}_A^f}{f_V^2 + \bar{g}_A^2}, \quad (10.33)$$

and

$$\bar{g}_V^f = \sqrt{\rho_f} (t_{3L}^{(f)} - 2q_f \kappa_f \sin^2\theta_W), \quad (10.33b)$$

$$\bar{g}_A^f = \sqrt{\rho_f} t_{3L}^{(f)}. \quad (10.33c)$$

P_e is the initial e^- polarization, so that the second equality in Eq. (10.30) is reproduced for $P_e = 1$, and the Z pole forward-backward asymmetries at LEP ($P_e = 0$) are given by $A_{FB}^{(0,f)} = \frac{3}{4}A_e A_f$ where $f = e, \mu, \tau, b, c, s$ [77], and q , and where $A_{FB}^{(0,g)}$ refers to the hadronic charge asymmetry. Corrections for t -channel exchange and s/t -channel interference cause $A_{FB}^{(0,e)}$ to be strongly anticorrelated with R_e (-36%). The initial state coupling, A_e , is also determined through the left-right charge asymmetry [78] and in polarized Bhabha scattering at the SLC [72,75].

The electroweak-radiative corrections have been absorbed into corrections $\rho_f - 1$ and $\kappa_f - 1$, which depend on the fermion f and on the renormalization scheme. In the on-shell scheme, the quadratic m_t dependence is given by $\rho_f \sim 1 + \rho_t, \kappa_f \sim 1 + \rho_t/\tan^2\theta_W$, while in $\overline{\text{MS}}$,

$\hat{\rho}_f \sim \hat{\kappa}_f \sim 1$, for $f \neq b$ ($\hat{\rho}_b \sim 1 - \frac{4}{3}\rho_t, \hat{\kappa}_b \sim 1 + \frac{2}{3}\rho_t$). In the $\overline{\text{MS}}$ scheme the normalization is changed according to $G_F M_Z^2/2\sqrt{2}\pi \rightarrow \hat{\alpha}/4\hat{s}_Z^2\hat{c}_Z^2$. (If one continues to normalize amplitudes by $G_F M_Z^2/2\sqrt{2}\pi$, as in the 1996 edition of this *Review*, then $\hat{\rho}_f$ contains an additional factor of $\hat{\rho}$.) In practice, additional bosonic and fermionic loops, vertex corrections, leading higher order contributions, etc., must be included. For example, in the $\overline{\text{MS}}$ scheme one has $\hat{\rho}_\ell = 0.9979, \hat{\kappa}_\ell = 1.0013, \hat{\rho}_b = 0.9866$ and $\hat{\kappa}_b = 1.0068$. It is convenient to define an effective angle $\bar{s}_f^2 \equiv \sin^2\bar{\theta}_{Wf} \equiv \hat{\kappa}_f \hat{s}_Z^2 = \kappa_f s_W^2$, in terms of which \bar{g}_V^f and \bar{g}_A^f are given by $\sqrt{\bar{\rho}_f}$ times their tree-level formulae. Because \bar{g}_V^f is very small, not only $A_{LR}^0 = A_e, A_{FB}^{(0,\ell)}$, and \mathcal{P}_τ , but also $A_{FB}^{(0,b)}, A_{FB}^{(0,c)}, A_{FB}^{(0,s)}$, and the hadronic asymmetries are mainly sensitive to \bar{s}_ℓ^2 . One finds that $\hat{\kappa}_f$ ($f \neq b$) is almost independent of (m_t, M_H) , so that one can write

$$\bar{s}_\ell^2 \sim \hat{s}_Z^2 + 0.00029. \quad (10.34)$$

Thus, the asymmetries determine values of \bar{s}_ℓ^2 and \hat{s}_Z^2 almost independent of m_t , while the κ 's for the other schemes are m_t dependent.

The Z boson properties are extracted assuming the Standard Model expressions for the $\gamma - Z$ interference terms. These have also been tested experimentally by performing more general fits [79] to the LEP data obtained at CM energies of about 91, 130, and 172 GeV. Assuming family universality this approach introduces three additional parameters relative to the standard fit [76],

$$j_{\text{had}}^{\text{tot}} \sim g_V^\ell g_V^{\text{had}} = 0.14 \pm 0.14, \quad (10.35a)$$

$$j_\ell^{\text{tot}} \sim g_V^\ell g_V^\ell = 0.004 \pm 0.012, \quad (10.35b)$$

$$j_\ell^{\text{fb}} \sim g_A^\ell g_A^\ell = 0.780 \pm 0.013, \quad (10.35c)$$

where the first two parameters describe the $\gamma - Z$ interference contribution to the total hadronic and leptonic cross-sections, and the third to the leptonic forward-backward asymmetries. The results in Eq. (10.35) are in good agreement with the Standard Model expectations [76], 0.22, 0.004, and 0.799, respectively. This is a valuable test of the Standard Model; but it should be cautioned that new physics is not expected to be described by this set of parameters, since (i) they do not account for extra interactions beyond the standard weak neutral current, and (ii) the photonic amplitude remains fixed to its Standard Model value.

As another test, strong constraints on anomalous triple gauge couplings were obtained at LEP 2 above the W^+W^- threshold and by $D\bar{O}$ at the Tevatron. While there are a total of 14 independent couplings, one can use $SU(2) \times U(1)$ gauge invariance, discrete symmetries, and LEP 1 constraints to reduce the number of triple gauge couplings to three. Each coupling is extracted from the data by setting the other two to zero (the SM value). Including the run at CM energy of 189 GeV, LEP 2 quotes the results [24],

$$\Delta\kappa_\gamma = 0.038_{-0.075}^{+0.079}, \quad (10.36a)$$

$$\Delta g_1^Z = -0.010 \pm 0.033, \quad (10.36b)$$

$$\lambda_\gamma = -0.037_{-0.036}^{+0.035}, \quad (10.36c)$$

in excellent agreement with Standard Model expectations. Eq. (10.36a) can be used to rule out Kaluza-Klein theories which predict $\Delta\kappa_\gamma = -3$ [80]. In addition, the first direct limits on anomalous quartic gauge couplings were obtained by OPAL [81] through measurements of the $W^+W^- \gamma$ cross-section and of acoplanar photon pair events.

The CLEO collaboration [82] reported a precise measurement of the flavor changing transition $b \rightarrow s\gamma$. The result for the branching fraction is

$$\mathcal{B}(b \rightarrow s\gamma) = (3.37 \pm 0.37 \pm 0.34 \pm 0.24_{-0.16}^{+0.35} \pm 0.38) \times 10^{-4}, \quad (10.37)$$

where the first three errors are the quoted statistical, systematical, and model uncertainties, respectively. The fourth uncertainty accounts for the extrapolation from the finite photon energy cutoff (2.1 GeV) to the

full theoretical branching ratio [83], and the last one is our estimate of the theory uncertainty (excluding parametric errors such as from α_s). It is advantageous to normalize the result with respect to the semi-leptonic branching fraction [84,85], $\mathcal{B}(b \rightarrow c\nu) = 0.1034 \pm 0.0046$, yielding

$$R = \frac{\mathcal{B}(b \rightarrow s\gamma)}{\mathcal{B}(b \rightarrow c\nu)} = (3.26_{-0.68}^{+0.75}) \times 10^{-3}, \quad (10.38)$$

and to use the variable $\ln R = -5.73 \pm 0.22$ in electroweak fits to assure an approximately Gaussian error [86]. This measurement is to be compared to the next-to-leading order calculations of Refs. 85,87.

The present world average of the muon anomalous magnetic moment is

$$a_\mu^{\text{exp}} = \frac{g_\mu - 2}{2} = (116592300 \pm 840) \times 10^{-11}, \quad (10.39)$$

while the estimated SM electroweak contribution [88], $a_\mu^{\text{EW}} = (151 \pm 4) \times 10^{-11}$, is much smaller than the uncertainty. However, a new experiment at BNL is expected to reduce the experimental error to $\pm 40 \times 10^{-11}$ or better. The limiting factor will then be the uncertainty from the hadronic contribution [19], $a_\mu^{\text{had}} = (6924 \pm 62) \times 10^{-11}$, which has recently been estimated with the help of τ decay data and finite-energy QCD sum rule techniques. This result constitutes a major improvement over previous ones which had more than twice the uncertainty [12]. It would be important to verify it, and reduce the error even further to meet the experimental precision. Additional hadronic uncertainties are induced by the light-by-light scattering contribution [89], $a_\mu^{\text{LBS}} = (-92 \pm 32) \times 10^{-11}$, and other subleading hadronic contributions [90], $a_\mu^{\text{had}} \left[\left(\frac{\alpha}{\pi} \right)^3 \right] = (-100 \pm 6) \times 10^{-11}$. The SM prediction is

$$a_\mu^{\text{theory}} = (116591596 \pm 67) \times 10^{-11}. \quad (10.40)$$

With the anticipated accuracy at BNL it will be possible to explore new physics (specifically supersymmetry in the large $\tan\beta$ region [91]) up to energies of 5 TeV and more. If greater precision is achieved, it will be important to properly correlate the theoretical error on a_μ^{had} with the one in $\Delta\alpha_{\text{had}}^{(5)}$.

10.4. W and Z decays

The partial decay width for gauge bosons to decay into massless fermions $f_1\bar{f}_2$ is

$$\Gamma(W^+ \rightarrow e^+\nu_e) = \frac{G_F M_W^3}{6\sqrt{2}\pi} \approx 226.5 \pm 0.3 \text{ MeV}, \quad (10.41a)$$

$$\Gamma(W^+ \rightarrow u_i\bar{d}_j) = \frac{CG_F M_W^3}{6\sqrt{2}\pi} |V_{ij}|^2 \approx (707 \pm 1) |V_{ij}|^2 \text{ MeV}, \quad (10.41b)$$

$$\Gamma(Z \rightarrow \psi_i\bar{\psi}_i) = \frac{CG_F M_Z^3}{6\sqrt{2}\pi} [g_V^i + g_A^i] \quad (10.41c)$$

$$\approx \begin{cases} 300.3 \pm 0.2 \text{ MeV} (u\bar{u}), & 167.24 \pm 0.08 \text{ MeV} (\nu\bar{\nu}), \\ 383.1 \pm 0.2 \text{ MeV} (d\bar{d}), & 84.01 \pm 0.05 \text{ MeV} (e^+e^-), \\ 375.9 \mp 0.1 \text{ MeV} (b\bar{b}). \end{cases}$$

For leptons $C = 1$, while for quarks $C = 3(1 + \alpha_s(M_V)/\pi + 1.409\alpha_s^2/\pi^2 - 12.77\alpha_s^3/\pi^3)$, where the 3 is due to color and the factor in parentheses represents the universal part of the QCD corrections [92] for massless quarks [93]. The $Z \rightarrow f\bar{f}$ widths contain a number of additional corrections: universal (non-singlet) top-mass contributions [94]; fermion mass effects and further QCD corrections proportional to $\hat{m}_q^2(M_Z^2)$ [95] which are different for vector and axial-vector partial widths; and singlet contributions starting from two-loop order which are large, strongly top-mass dependent, family universal, and flavor non-universal [96]. All QCD effects are known and included up to three loop order. The QED factor $1 + 3\alpha q_f^2/4\pi$, as well as two-loop α_s and α^2 self-energy corrections [97] are also included. Working in the on-shell scheme, *i.e.*, expressing the widths

in terms of $G_F M_{W,Z}^3$, incorporates the largest radiative corrections from the running QED coupling [27,98]. Electroweak corrections to the Z widths are then incorporated by replacing $g_{V,A}^i$ by $\bar{g}_{V,A}^i$. Hence, in the on-shell scheme the Z widths are proportional to $\rho_i \sim 1 + \rho_t$. The \bar{M}_5 normalization accounts also for the leading electroweak corrections [31]. There is additional (negative) quadratic m_t dependence in the $Z \rightarrow b\bar{b}$ vertex corrections [99] which causes $\Gamma(b\bar{b})$ to decrease with m_t . The dominant effect is to multiply $\Gamma(b\bar{b})$ by the vertex correction $1 + \delta\rho_{b\bar{b}}$, where $\delta\rho_{b\bar{b}} \sim 10^{-2}(-\frac{1}{2}\frac{m_t^2}{M_Z^2} + \frac{1}{5})$. In practice, the corrections are included in ρ_b and κ_b , as discussed before.

For 3 fermion families the total widths are predicted to be

$$\Gamma_Z \approx 2.4963 \pm 0.0012 \text{ GeV}, \quad (10.42)$$

$$\Gamma_W \approx 2.0927 \pm 0.0025 \text{ GeV}. \quad (10.43)$$

We have assumed $\alpha_s(M_Z) = 0.1200$. An uncertainty in α_s of ± 0.0028 introduces an additional uncertainty of 0.1% in the hadronic widths, corresponding to ± 1.4 MeV in Γ_Z . These predictions are to be compared with the experimental results $\Gamma_Z = 2.4944 \pm 0.0024$ GeV [24] and $\Gamma_W = 2.06 \pm 0.05$ GeV [100].

10.5. Experimental results

The values of the principal Z pole observables are listed in Table 10.4, along with the Standard Model predictions for $M_Z = 91.1870 \pm 0.0021$ GeV, $M_H = 98_{-38}^{+57}$ GeV, $m_t = 172.9 \pm 4.6$ GeV, $\alpha_s(M_Z) = 0.1192 \pm 0.0028$, and $\hat{\alpha}(M_Z)^{-1} = 127.938 \pm 0.027$ ($\Delta\alpha_{\text{had}}^{(5)} \approx 0.02776 \pm 0.00020$). Note, that the values of the Z pole observables (as well as M_W) differ from those in the Particle Listings because they include recent preliminary results [24,72]. The values and predictions of M_W [24,101]; the Q_W for cesium [55,60] and thallium [56]; deep inelastic [43–45,49] and ν_μ - e scattering [50–52]; and the $b \rightarrow s\gamma$ observable [82] are also listed. The agreement is very good. Even the largest discrepancies, $A_{FB}^{(0,b)}$ and $Q_W(\text{Cs})$, deviate by only 2.3 σ . The hadronic peak cross-section, σ_{had} , the A_{LR}^0 from hadronic final states, and the R^ν result by the CHARM collaboration deviate by 1.7 σ ; all the other observables agree with the Standard Model prediction at the 1.5 σ level or better. Other observables like $R_b = \Gamma(b\bar{b})/\Gamma(\text{had})$ and $R_c = \Gamma(c\bar{c})/\Gamma(\text{had})$ which showed significant deviations in the past, are now in reasonable agreement. In particular, R_b whose measured value deviated as much as 3.7 σ from the Standard Model prediction is now only 0.9 σ (0.3%) high.

A_b can be extracted from $A_{FB}^{(0,b)}$ when $A_e = 0.1497 \pm 0.0016$ is taken from a fit to leptonic asymmetries (using lepton universality), and combined with the measurement at the SLC. The result, $A_b = 0.892 \pm 0.016$, is 2.7 σ below the Standard Model prediction.† However, it would be extremely difficult to account for this nearly 5% deviation by new physics radiative corrections since a 25% correction to $\hat{\kappa}_b$ would be necessary to account for the central value of A_b . If this deviation is due to new physics, it is most likely of tree-level type affecting preferentially the third generation. It seems difficult, however, to simultaneously account for R_b , which has been measured on the Z peak, off-peak [103], and recently at LEP 2 [24]. $A_{FB}^{(b)} = 0.44 \pm 0.12$ has also been measured at LEP 2 [24], and found to be 1.2 σ below the Standard Model prediction (0.58).

The left-right asymmetry, $A_{LR}^0 = 0.15108 \pm 0.00218$ [72], based on all hadronic data from 1992–1998 has moved closer to the Standard Model expectation of 0.1475 ± 0.0013 than previous values. The combined value of $A_\ell = 0.1512 \pm 0.0020$ from SLD (using lepton-family universality) is still 1.8 σ above the Standard Model prediction; but there is now only a minor experimental difference of ~ 1.2 σ between this SLD value and the LEP value, $A_\ell = 0.1471 \pm 0.0026$, obtained from a fit to $A_{FB}^{(0,\ell)}$, $A_e(\mathcal{P}_\tau)$, and $A_\tau(\mathcal{P}_\tau)$, again assuming universality.

† Alternatively, one can use $A_\ell = 0.1471 \pm 0.0026$, which is from LEP alone and in excellent agreement with the Standard Model, and obtain $A_b = 0.904 \pm 0.018$ which is 1.7 σ low. This illustrates that some of the discrepancy is related to the one in A_{LR} .

Table 10.4: Principal Z -pole and other recent observables, compared with the Standard Model predictions for the global best fit values $M_Z = 91.1870 \pm 0.0021$ GeV, $M_H = 98_{-38}^{+57}$ GeV, $m_t = 172.9 \pm 4.6$ GeV, $\alpha_s(M_Z) = 0.1192 \pm 0.0028$, and $\hat{\alpha}(M_Z)^{-1} = 127.938 \pm 0.027$. The LEP averages of the ALEPH, DELPHI, L3, and OPAL results include common systematic errors and correlations [24,76]. The heavy flavour results of LEP and SLD are based on common inputs and correlated, as well [73]. $\hat{s}_Z^2(A_{FB}^{(0,q)})$ is the effective angle extracted from the hadronic charge asymmetry. The values of $\Gamma(\ell^+\ell^-)$, $\Gamma(\text{had})$, and $\Gamma(\text{inv})$ are not independent of Γ_Z , the R_ℓ , and σ_{had} . The first M_W value is from CDF, UA2, and DØ [101] while the second one is from LEP 2 [24]. The first M_W and M_Z are correlated, but the effect is negligible due to the tiny M_Z error. The three values of A_e are (i) from A_{LR} for hadronic final states [71]; (ii) from A_{LR} for leptonic final states and from polarized Bhabba scattering [75]; and (iii) from the angular distribution of the τ polarization. The two A_τ values are from SLD and the total τ polarization, respectively. The two values of R^ν from deep-inelastic scattering (DIS) are from CDHS [43] and CHARM [44], respectively; similarly, κ^ν (proportional to R^ν) is from CCFR [45]. The two values for $g_{V,A}^{\nu e}$ are from CHARM II [52] and the world average. The second errors in Q_W and DIS are theoretical. In the Standard Model predictions, the uncertainty is from M_Z , M_H , m_t , $\hat{\alpha}(M_Z)^{-1}$, and α_s , and their correlations have been accounted for. The errors in Γ_Z , $\Gamma(\text{had})$, R_ℓ , and σ_{had} are largely dominated by the uncertainty in α_s .

Quantity	Value	Standard Model	Pull
m_t [GeV]	174.3 ± 5.1	172.9 ± 4.6	0.3
M_W [GeV]	80.448 ± 0.062	80.378 ± 0.020	1.1
	80.350 ± 0.056		-0.5
M_Z [GeV]	91.1872 ± 0.0021	91.1870 ± 0.0021	0.1
Γ_Z [GeV]	2.4944 ± 0.0024	2.4956 ± 0.0016	-0.5
$\Gamma(\text{had})$ [GeV]	1.7439 ± 0.0020	1.7422 ± 0.0015	—
$\Gamma(\text{inv})$ [MeV]	498.8 ± 1.5	501.65 ± 0.15	—
$\Gamma(\ell^+\ell^-)$ [MeV]	83.96 ± 0.09	84.00 ± 0.03	—
σ_{had} [nb]	41.544 ± 0.037	41.480 ± 0.014	1.7
R_e	20.803 ± 0.049	20.740 ± 0.018	1.3
R_μ	20.786 ± 0.033	20.741 ± 0.018	1.4
R_τ	20.764 ± 0.045	20.786 ± 0.018	-0.5
R_b	0.21642 ± 0.00073	0.2158 ± 0.0002	0.9
R_c	0.1674 ± 0.0038	0.1723 ± 0.0001	-1.3
$A_{FB}^{(0,e)}$	0.0145 ± 0.0024	0.0163 ± 0.0003	-0.8
$A_{FB}^{(0,\mu)}$	0.0167 ± 0.0013		0.3
$A_{FB}^{(0,\tau)}$	0.0188 ± 0.0017		1.5
$A_{FB}^{(0,b)}$	0.0988 ± 0.0020	0.1034 ± 0.0009	-2.3
$A_{FB}^{(0,c)}$	0.0692 ± 0.0037	0.0739 ± 0.0007	-1.3
$A_{FB}^{(0,s)}$	0.0976 ± 0.0114	0.1035 ± 0.0009	-0.5
$\hat{s}_Z^2(A_{FB}^{(0,q)})$	0.2321 ± 0.0010	0.2315 ± 0.0002	0.6

Despite these discrepancies the goodness of the fit to all data is reasonable with a $\chi^2/\text{d.o.f.} = 42/37$. The probability of a larger χ^2 is 27%. The observables in Table 10.4, as well as some other less precise observables, are used in the global fits described below. The correlations on the LEP lineshape, the LEP/SLD heavy flavor, and the deep inelastic scattering observables, are included. There are also small correlations between some of the SLD measurements, and between the two observables from the τ polarization at LEP, which have not been fully investigated, yet.

The data allow a simultaneous determination of M_H , m_t , $\sin^2\theta_W$, and the strong coupling $\alpha_s(M_Z)$. ($\Delta\alpha_{\text{had}}^{(5)}$ is also allowed to float in the fits, subject to the theoretical constraints [9] described in

Table 10.4: (continued)

Quantity	Value	Standard Model	Pull
A_e	0.15108 ± 0.00218	0.1475 ± 0.0013	1.7
	0.1558 ± 0.0064		1.3
	0.1483 ± 0.0051		0.2
A_μ	0.137 ± 0.016		-0.7
A_τ	0.142 ± 0.016		-0.3
	0.1425 ± 0.0044		-1.1
A_b	0.911 ± 0.025	0.9348 ± 0.0001	-1.0
A_c	0.630 ± 0.026	0.6679 ± 0.0006	-1.5
A_s	0.85 ± 0.09	0.9357 ± 0.0001	-1.0
R^-	$0.2277 \pm 0.0021 \pm 0.0007$	0.2299 ± 0.0002	-1.0
κ^ν	$0.5820 \pm 0.0027 \pm 0.0031$	0.5831 ± 0.0004	-0.3
R^ν	$0.3096 \pm 0.0033 \pm 0.0028$	0.3091 ± 0.0002	0.1
	$0.3021 \pm 0.0031 \pm 0.0026$		-1.7
$g_V^{\nu e}$	-0.035 ± 0.017	-0.0397 ± 0.0003	—
	-0.041 ± 0.015		-0.1
$g_A^{\nu e}$	-0.503 ± 0.017	-0.5064 ± 0.0001	—
	-0.507 ± 0.014		0.0
$Q_W(\text{Cs})$	$-72.06 \pm 0.28 \pm 0.34$	-73.09 ± 0.03	2.3
$Q_W(\text{Tl})$	$-114.8 \pm 1.2 \pm 3.4$	-116.7 ± 0.1	0.5
$\frac{\Gamma(b \rightarrow s\gamma)}{\Gamma(b \rightarrow c\bar{c}\nu)}$	$3.26_{-0.68}^{+0.75} \times 10^{-3}$	$3.15_{-0.20}^{+0.21} \times 10^{-3}$	0.1

Table 10.5: Values of \hat{s}_Z^2 , s_W^2 , α_s , and M_H [in GeV] for various (combinations of) observables. Unless indicated otherwise, the top quark mass, $m_t = 174.3 \pm 5.1$ GeV, is used as an additional constraint in the fits. The (†) symbol indicates a fixed parameter.

Data	\hat{s}_Z^2	s_W^2	$\alpha_s(M_Z)$	M_H
All data	0.23117(16)	0.2230(4)	0.1192(28)	98_{-38}^{+57}
All data (incl. α_s)	0.23116(16)	0.2230(4)	0.1184(12)	97_{-37}^{+56}
All indirect (no m_t)	0.23114(17)	0.2232(5)	0.1190(28)	69_{-33}^{+80}
Z pole (no m_t)	0.23120(18)	0.2233(6)	0.1191(28)	77_{-38}^{+102}
LEP 1 (no m_t)	0.23156(23)	0.2240(7)	0.1208(30)	166_{-95}^{+270}
SLD + M_Z	0.23070(28)	0.2220(6)	0.1200 (†)	40_{-22}^{+38}
$A_{FB}^{(b,c)} + M_Z$	0.23204(34)	0.2251(9)	0.1200 (†)	516_{-258}^{+521}
$M_W + M_Z$	0.23107(42)	0.2227(9)	0.1200 (†)	85_{-60}^{+112}
M_Z	0.23115(18)	0.2229(6)	0.1200 (†)	100 (†)
Q_W	0.2269(18)	0.2186(19)	0.1200 (†)	100 (†)
DIS (isoscalar)	0.2335(22)	0.2252(21)	0.1200 (†)	100 (†)
SLAC eD	0.222(18)	0.213(19)	0.1200 (†)	100 (†)
elastic $\nu_\mu(\bar{\nu}_\mu)e$	0.229(8)	0.221(8)	0.1200 (†)	100 (†)
elastic $\nu_\mu(\bar{\nu}_\mu)p$	0.211(32)	0.203(32)	0.1200 (†)	100 (†)

Sec. 10.2.) α_s is determined mainly from R_ℓ , Γ_Z , and σ_{had} , and is only weakly correlated with the other variables. The global fit to all data, including the CDF/DØ value, $m_t = 174.3 \pm 5.1$ GeV, yields

$$\begin{aligned}
 M_H &= 98_{-38}^{+57} \text{ GeV} , \\
 m_t &= 172.9 \pm 4.6 \text{ GeV} , \\
 \hat{s}_Z^2 &= 0.23117 \pm 0.00016 , \\
 \alpha_s(M_Z) &= 0.1192 \pm 0.0028 .
 \end{aligned} \tag{10.44}$$

In the on-shell scheme one has $s_W^2 = 0.22302 \pm 0.00040$, the larger error due to the stronger sensitivity to m_t , while the corresponding

effective angle is related by Eq. (10.34), *i.e.*, $\hat{s}_f^2 = 0.23147 \pm 0.00016$. In all fits, the errors include full statistical, systematic, and theoretical uncertainties. The \hat{s}_f^2 (\hat{s}_f^2) error reflects the error on $\hat{s}_f^2 = 0.23151 \pm 0.00017$ from a fit to the Z pole asymmetries.

The weak mixing angle can be determined from Z pole observables, M_W , and from a variety of neutral-current processes spanning a very wide Q^2 range. The results (for the older low-energy neutral-current data see [25,26]) shown in Table 10.5, are in reasonable agreement with each other, indicating the quantitative success of the Standard Model. The largest discrepancy is the value $\hat{s}_Z^2 = 0.23204 \pm 0.00034$ from the forward-backward asymmetries into bottom and charm quarks combined with M_Z , which is 2.6 σ above the value 0.23117 ± 0.00016 from the global fit to all data. Similarly, the SLD asymmetries, when combined with M_Z , yield $\hat{s}_Z^2 = 0.23070 \pm 0.00028$, which is 1.7 σ low. The new value of Q_W from atomic parity violation corresponds (for $M_H = 100$ GeV) to $\hat{s}_Z^2 = 0.2269 \pm 0.0018$, which is 2.4 σ low.

The extracted value of $\alpha_s(M_Z)$ is based on a formula with negligible theoretical uncertainty (± 0.0005 in $\alpha_s(M_Z)$) if one assumes the exact validity of the Standard Model. It is in excellent agreement with other precise values, such as 0.1202 ± 0.0027 (ALEPH) and 0.1219 ± 0.0020 (OPAL) from τ decays [104], 0.120 ± 0.005 from jet-event shapes in e^+e^- annihilation, 0.119 ± 0.002 (exp) ± 0.004 (scale) from deep-inelastic scattering [105], and 0.1174 ± 0.0024 ($b\bar{b}$) [106] and 0.116 ± 0.003 ($c\bar{c}$) [107] from lattice calculations of quarkonium spectra. The results from the τ lifetime have been converted from the 3-flavor definition, $\alpha_s^{(3)}(m_\tau) = 0.334 \pm 0.022$ (ALEPH) and $\alpha_s^{(3)}(m_\tau) = 0.348 \pm 0.021$ (OPAL), to the 5-flavor definition at the Z scale using the four-loop QCD β -function [108] with three-loop matching [109]. We note, that this introduces an asymmetric error (the lower error bar being larger), and that the quoted OPAL error for $\alpha_s^{(5)}(M_Z)$ is slightly underestimated given their result for $\alpha_s^{(3)}(m_\tau)$. For more details, see our Section 9 on ‘‘Quantum Chromodynamics’’ in this *Review*. The average $\alpha_s(M_Z)$ obtained from Section 9 when ignoring the precision measurements discussed in this Section is 0.1182 ± 0.0013 . We use this value as an external constraint for the second fit in Table 10.5. The resulting value, $\alpha_s(M_Z) = 0.1184 \pm 0.0012$, can be regarded as the present world average. One should keep in mind, however, that the Z lineshape value of α_s is very sensitive to many types of new physics.

The data indicate a preference for a small Higgs mass. There is a strong correlation between the quadratic m_t and logarithmic M_H terms in $\hat{\rho}$ in all of the indirect data except for the $Z \rightarrow b\bar{b}$ vertex. Therefore, observables (other than R_b) which favor m_t values higher than the Tevatron range favor lower values of M_H . This effect is enhanced by R_b , which has little direct M_H dependence but favors the lower end of the Tevatron m_t range. M_W has additional M_H dependence through $\Delta\hat{\tau}_W$ which is not coupled to m_t^2 effects. The strongest individual pulls towards smaller M_H are from M_W and A_{LR}^0 . The difference in χ^2 for the global fit is $\Delta\chi^2 = \chi^2(M_H = 1000 \text{ GeV}) - \chi_{\min}^2 = 30.4$. Hence, the data favor a small value of M_H , as in supersymmetric extensions of the Standard Model, and m_t on the lower side of the Tevatron range. The central value of the global fit result, $M_H = 98^{+37}_{-38}$ GeV, is close to the present kinematic reach at LEP 2, and slightly above the direct lower bound, $M_H \geq 95.2$ GeV (95% CL) [110].

The 90% central confidence range from all precision data is

$$42 \text{ GeV} \leq M_H \leq 201 \text{ GeV} .$$

Including the results of the direct searches as an extra contribution to the likelihood function drives the 95% upper limit to $M_H \leq 231$ GeV. As two further refinements, we account for (i) theoretical uncertainties from uncalculated higher order contributions by allowing the T parameter (see next subsection) subject to the constraint $T = 0 \pm 0.02$, (ii) the M_H dependence of the correlation matrix which gives slightly more weight to lower Higgs masses [112]. The resulting limits at 95 (90, 99)% CL are

$$M_H \leq 235 \text{ (205, 306) GeV} ,$$

respectively. The extraction of M_H from the precision data depends strongly on the value used for $\alpha(M_Z)$. Upper limits, however, are more robust due to two compensating effects: the older results indicated more QED running and were less precise, yielding M_H distributions which were broader with centers shifted to smaller values.

One can also carry out a fit to the indirect data alone, *i.e.*, without including the value, $m_t = 174.3 \pm 5.1$ GeV, observed directly by CDF and DØ. (The indirect prediction is for the \overline{MS} mass, $\hat{m}_t(\hat{m}_t) = 158.7^{+9.1}_{-7.0}$ GeV, which is in the end converted to the pole mass using a BLM optimized [113] version of the two-loop perturbative QCD formula [114]; this should correspond approximately to the kinematic mass extracted from the collider events.) One obtains $m_t = 168.2^{+9.6}_{-7.4}$ GeV, with little change in the $\sin^2\theta_W$ and α_s values, in remarkable agreement with the direct CDF/DØ value. The central M_H value of this fit (see the third line of Table 10.5) is below the direct lower bound; keeping $M_H = 100$ GeV fixed results in $m_t = 172.2 \pm 4.0$ GeV in even better agreement. The relations between M_H and m_t for various observables are shown in Fig. 10.1.

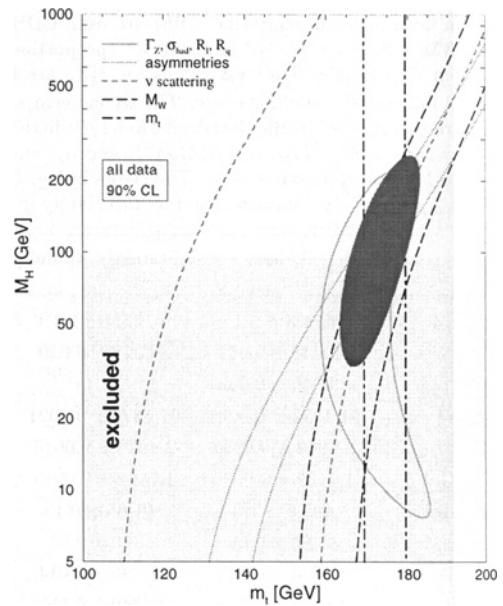


Figure 10.1: One-standard-deviation (39.35%) uncertainties in M_H as a function of m_t for various inputs, and the 90% CL region ($\Delta\chi^2 = 4.605$) allowed by all data. $\alpha_s(M_Z) = 0.120$ is assumed except for the fit to all data. The 95% direct lower limit from LEP 2 is also shown.

Using $\alpha(M_Z)$ and \hat{s}_Z^2 as inputs, one can predict $\alpha_s(M_Z)$ assuming grand unification. One predicts [115] $\alpha_s(M_Z) = 0.130 \pm 0.001 \pm 0.01$ for the simplest theories based on the minimal supersymmetric extension of the Standard Model, where the first (second) uncertainty is from the inputs (thresholds). This is slightly larger, but consistent with the experimental $\alpha_s(M_Z) = 0.1192 \pm 0.0028$ from the Z lineshape, and with the world average 0.1184 ± 0.0012 . Nonsupersymmetric unified theories predict the low value $\alpha_s(M_Z) = 0.073 \pm 0.001 \pm 0.001$. See also the note on ‘‘Low-Energy Supersymmetry’’ in the Particle Listings.

One can also determine the radiative correction parameters Δr : from the global fit one obtains $\Delta r = 0.0354 \pm 0.0012$ and $\Delta\hat{\tau}_W = 0.0694 \pm 0.0004$. M_W measurements [24,101] (when combined with M_Z) are equivalent to measurements of $\Delta r = 0.0345 \pm 0.0025$, in excellent agreement with the result from all indirect data, $\Delta r = 0.0357 \pm 0.0014$. Fig. 10.2 shows the 1σ contours in the $M_W - m_t$ plane from the direct and indirect determinations, as well as the combined 90% CL region. The indirect determination uses M_Z from LEP 1 as input, which is defined assuming an s -dependent decay width. M_W then corresponds to the s -dependent width definition, as well, and can be directly compared with the results from the Tevatron and LEP 2 which have been obtained using the same definition. The difference to a constant width definition is formally only of $\mathcal{O}(\alpha^2)$, but

is strongly enhanced since the decay channels add up coherently. It is about 34 MeV for M_Z and 27 MeV for M_W . The residual difference between working consistently with one or the other definition is about 3 MeV, *i.e.*, of typical size for non-enhanced (and generally uncalculated) $\mathcal{O}(\alpha^2)$ corrections.

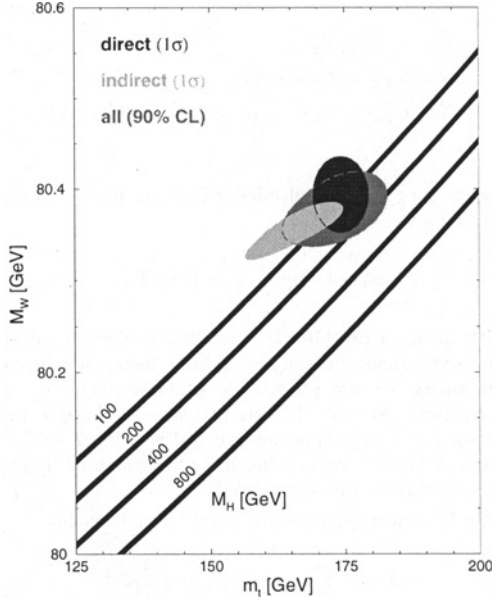


Figure 10.2: One-standard-deviation (39.35%) region in M_W as a function of m_t for the direct and indirect data, and the 90% CL region ($\Delta\chi^2 = 4.605$) allowed by all data. The Standard Model prediction as a function of M_H is also indicated. The widths of the M_H bands reflect the theoretical uncertainty from $\alpha(M_Z)$ for $\alpha_s(M_Z) = 0.120$.

Most of the parameters relevant to ν -hadron, ν - e , e -hadron, and e^+e^- processes are determined uniquely and precisely from the data in “model independent” fits (*i.e.*, fits which allow for an arbitrary electroweak gauge theory). The values for the parameters defined in Eqs. (10.11)–(10.13) are given in Table 10.6 along with the predictions of the Standard Model. The agreement is reasonable. The low-energy e^+e^- results are difficult to present in a model-independent way because Z propagator effects are non-negligible at TRISTAN, PETRA, and PEP energies. However, assuming e - μ - τ universality, the lepton asymmetries imply [69] $4(g_A^e)^2 = 0.99 \pm 0.05$, in good agreement with the Standard Model prediction $\simeq 1$.

The results presented here are generally in reasonable agreement with the ones obtained by the LEP Electroweak Working Group [24,76]. We obtain slightly higher best fit values for α_s and M_H . We could trace most of the differences to be due to (i) the inclusion of recent higher order radiative corrections, in particular, the leading $\mathcal{O}(\alpha_s^4)$ contribution to hadronic Z decays [111]; (ii) a different evaluation of $\alpha(M_Z)$ [9]; (iii) slightly different data sets; and (iv) scheme dependences. Taking into account these differences, the agreement is excellent.

10.6. Constraints on new physics

The Z pole, W mass, and neutral-current data can be used to search for and set limits on deviations from the Standard Model. In particular, the combination of these indirect data with the direct CDF and $D\bar{D}$ value for m_t allows to set stringent limits on new physics. We will mainly discuss the effects of exotic particles (with heavy masses $M_{\text{new}} \gg M_Z$ in an expansion in M_Z/M_{new}) on the gauge boson self-energies. (Brief remarks are made on new physics which is not of this type.) Most of the effects on precision measurements can be described by three gauge self-energy parameters S , T , and U . We will define these, as well as related parameters, such as ρ_0 , ϵ_i , and $\hat{\epsilon}_i$, to arise from new physics only. *I.e.*, they are equal to zero ($\rho_0 = 1$) exactly in the Standard Model, and do not include any contributions

Table 10.6: Values of the model-independent neutral-current parameters, compared with the Standard Model predictions for the global best fit values $M_Z = 91.1870 \pm 0.0021$ GeV, $M_H = 98_{-38}^{+57}$ GeV, $m_t = 172.9 \pm 4.6$ GeV, $\alpha_s(M_Z) = 0.1192 \pm 0.0028$, and $\hat{\alpha}(M_Z)^{-1} = 127.938 \pm 0.027$. There is a second $g_{V,A}^{\nu e}$ solution, given approximately by $g_{V,A}^{\nu e} \leftrightarrow g_{A,V}^{\nu e}$, which is eliminated by e^+e^- data under the assumption that the neutral current is dominated by the exchange of a single Z . The ϵ_L , as well as the ϵ_R , are strongly correlated and non-Gaussian, so that for implementations we recommend the parametrization using g_i and $\theta_i = \tan^{-1}[\epsilon_i(u)/\epsilon_i(d)]$, $i = L$ or R . θ_R is only weakly correlated with the g_i , while the correlation coefficient between θ_R and θ_L is 0.27.

Quantity	Experimental Value	Standard Model Prediction	Correlation	
$\epsilon_L(u)$	0.330 ± 0.016	0.3459 ± 0.0002		
$\epsilon_L(d)$	-0.439 ± 0.011	-0.4291 ± 0.0002	non-	
$\epsilon_R(u)$	$-0.176_{-0.006}^{+0.014}$	-0.1550 ± 0.0001	Gaussian	
$\epsilon_R(d)$	$-0.023_{-0.047}^{+0.070}$	0.0776		
g_L^2	0.3020 ± 0.0019	0.3038 ± 0.0003	0.32	-0.39
g_R^2	0.0315 ± 0.0016	0.0301		-0.10
θ_L	2.50 ± 0.034	2.4631 ± 0.0001		
θ_R	$4.58_{-0.27}^{+0.40}$	5.1765		
$g_{V,A}^{\nu e}$	-0.041 ± 0.015	-0.0397 ± 0.0003		-0.04
$g_{V,A}^e$	-0.507 ± 0.014	-0.5064 ± 0.0001		
C_{1u}	-0.211 ± 0.041	-0.1886 ± 0.0002	-0.9996	-0.78
C_{1d}	0.359 ± 0.037	0.3413 ± 0.0002		0.78
$C_{2u} - \frac{1}{2}C_{2d}$	-0.04 ± 0.12	-0.0491 ± 0.0005		

from m_t or M_H , which are treated separately. Our treatment differs from most of the original papers.

Many extensions of the Standard Model are described by the ρ_0 parameter,

$$\rho_0 \equiv M_W^2 / (M_Z^2 \hat{c}_Z^2 \hat{\rho}), \quad (10.45)$$

which describes new sources of SU(2) breaking that cannot be accounted for by the Standard Model Higgs doublet or m_t effects. In the presence of $\rho_0 \neq 1$, Eq. (10.45) generalizes Eq. (10.8b), while Eq. (10.8a) remains unchanged. Provided that the new physics which yields $\rho_0 \neq 1$ is a small perturbation which does not significantly affect the radiative corrections, ρ_0 can be regarded as a phenomenological parameter which multiplies G_F in Eqs. (10.11)–(10.13), (10.28), and Γ_Z in Eq. (10.41). There is enough data to determine ρ_0 , M_H , m_t , and α_s , simultaneously. From the global fit,

$$\rho_0 = 0.9998_{-0.0006}^{+0.0011}, \quad (10.46)$$

$$95 \text{ GeV} < M_H < 211 \text{ GeV}, \quad (10.47)$$

$$m_t = 173.6 \pm 4.9 \text{ GeV}, \quad (10.48)$$

$$\alpha_s(M_Z) = 0.1194 \pm 0.0028, \quad (10.49)$$

where the lower limit on M_H is the direct search bound. (If the direct limit is ignored one obtains $M_H = 72_{-36}^{+125}$ and $\rho_0 = 0.9995_{-0.0009}^{+0.0013}$). The error bar in Eq. (10.46) is highly asymmetric: at the 2σ level one has $\rho_0 = 0.9998_{-0.0012}^{+0.0034}$ and $M_H < 1002$ GeV. Clearly, in the presence of ρ_0 upper limits on M_H become very weak.

The result in Eq. (10.46) is in remarkable agreement with the Standard Model expectation, $\rho_0 = 1$. It can be used to constrain higher-dimensional Higgs representations to have vacuum expectation values of less than a few percent of those of the doublets. Indeed, the relation between M_W and M_Z is modified if there are Higgs multiplets with weak isospin $> 1/2$ with significant vacuum expectation values. In order to calculate to higher orders in such theories one must define a set of four fundamental renormalized parameters which one may

conveniently choose to be α , G_F , M_Z , and M_W , since M_W and M_Z are directly measurable. Then \hat{s}_Z^2 and ρ_0 can be considered dependent parameters.

Eq. (10.46) can also be used to constrain other types of new physics. For example, nondegenerate multiplets of heavy fermions or scalars break the vector part of weak SU(2) and lead to a decrease in the value of M_Z/M_W . A nondegenerate SU(2) doublet (f_2^1) yields a positive contribution to ρ_0 [116] of

$$\frac{C_{GF}}{8\sqrt{2}\pi^2} \Delta m^2, \quad (10.50)$$

where

$$\Delta m^2 \equiv m_1^2 + m_2^2 - \frac{4m_1^2 m_2^2}{m_1^2 - m_2^2} \ln \frac{m_1}{m_2} \geq (m_1 - m_2)^2, \quad (10.51)$$

and $C = 1$ (3) for color singlets (triplets). Thus, in the presence of such multiplets, one has

$$\frac{3G_F}{8\sqrt{2}\pi^2} \sum_i \frac{C_i}{3} \Delta m_i^2 = \rho_0 - 1, \quad (10.52)$$

where the sum includes fourth-family quark or lepton doublets, (ν') or (E^-), and scalar doublets such as (\hat{b}) in supersymmetry (in the absence of $L - R$ mixing). This implies

$$\sum_i \frac{C_i}{3} \Delta m_i^2 \leq (100 \text{ GeV})^2 \quad (10.53)$$

at 95% CL. The corresponding constraints on nondegenerate squark and slepton doublets are even stronger, $\Delta m_i^2 \leq (69 \text{ GeV})^2$. This is due to the MSSM Higgs mass bound, $m_{h_0} < 150 \text{ GeV}$, and the strong correlation between m_{h_0} and ρ_0 (81%).

Nondegenerate multiplets usually imply $\rho_0 > 1$. Similarly, heavy Z' bosons decrease the prediction for M_Z due to mixing and generally lead to $\rho_0 > 1$ [117]. On the other hand, additional Higgs doublets which participate in spontaneous symmetry breaking [118], heavy lepton doublets involving Majorana neutrinos [119], and the vacuum expectation values of Higgs triplets or higher-dimensional representations can contribute to ρ_0 with either sign. Allowing for the presence of heavy degenerate chiral multiplets (the S parameter, to be discussed below) affects the determination of ρ_0 from the data, at present leading to a smaller value (for fixed M_H).

A number of authors [120–125] have considered the general effects on neutral current and Z and W boson observables of various types of heavy (*i.e.*, $M_{\text{new}} \gg M_Z$) physics which contribute to the W and Z self-energies but which do not have any direct coupling to the ordinary fermions. In addition to nondegenerate multiplets, which break the vector part of weak SU(2), these include heavy degenerate multiplets of chiral fermions which break the axial generators. The effects of one degenerate chiral doublet are small, but in technicolor theories there may be many chiral doublets and therefore significant effects [120].

Such effects can be described by just three parameters, S , T , and U at the (electroweak) one loop level. (Three additional parameters are needed if the new physics scale is comparable to M_Z [126].) T is proportional to the difference between the W and Z self-energies at $Q^2 = 0$ (*i.e.*, vector SU(2)-breaking), while S ($S + U$) is associated with the difference between the Z (W) self-energy at $Q^2 = M_{Z,W}^2$ and $Q^2 = 0$ (axial SU(2)-breaking). Denoting the contributions of new physics to the various self-energies by Π_{ij}^{new} , we have

$$\hat{\alpha}(M_Z)T \equiv \frac{\Pi_{WW}^{\text{new}}(0)}{M_W^2} - \frac{\Pi_{ZZ}^{\text{new}}(0)}{M_Z^2}, \quad (10.54a)$$

$$\begin{aligned} \frac{\hat{\alpha}(M_Z)}{4\hat{s}_Z^2 \hat{c}_Z^2} S \equiv & \frac{\Pi_{ZZ}^{\text{new}}(M_Z^2) - \Pi_{ZZ}^{\text{new}}(0)}{M_Z^2} \\ & - \frac{\hat{c}_Z^2 - \hat{s}_Z^2}{\hat{c}_Z \hat{s}_Z} \frac{\Pi_{Z\gamma}^{\text{new}}(M_Z^2)}{M_Z^2} - \frac{\Pi_{\gamma\gamma}^{\text{new}}(M_Z^2)}{M_Z^2}, \end{aligned} \quad (10.54b)$$

$$\begin{aligned} \frac{\hat{\alpha}(M_Z)}{4\hat{s}_Z^2} (S + U) \equiv & \frac{\Pi_{WW}^{\text{new}}(M_W^2) - \Pi_{WW}^{\text{new}}(0)}{M_W^2} \\ & - \frac{\hat{c}_Z}{\hat{s}_Z} \frac{\Pi_{Z\gamma}^{\text{new}}(M_Z^2)}{M_Z^2} - \frac{\Pi_{\gamma\gamma}^{\text{new}}(M_Z^2)}{M_Z^2}. \end{aligned} \quad (10.54c)$$

S , T , and U are defined with a factor proportional to $\hat{\alpha}$ removed, so that they are expected to be of order unity in the presence of new physics. In the $\overline{\text{MS}}$ scheme as defined in Ref. [29], the last two terms in Eq. (10.54b) and Eq. (10.54c) can be omitted (as was done in earlier editions of this *Review*). They are related to other parameters (S_i , h_i , $\hat{\epsilon}_i$) defined in [29,121,122] by

$$\begin{aligned} T &= h_V = \hat{\epsilon}_1/\alpha, \\ S &= h_{AZ} = S_Z = 4\hat{s}_Z^2 \hat{\epsilon}_3/\alpha, \\ U &= h_{AW} - h_{AZ} = S_W - S_Z = -4\hat{s}_Z^2 \hat{\epsilon}_2/\alpha. \end{aligned} \quad (10.55)$$

A heavy nondegenerate multiplet of fermions or scalars contributes positively to T as

$$\rho_0 - 1 = \frac{1}{1 - \alpha T} - 1 \simeq \alpha T, \quad (10.56)$$

where ρ_0 is given in Eq. (10.52). The effects of nonstandard Higgs representations cannot be separated from heavy nondegenerate multiplets unless the new physics has other consequences, such as vertex corrections. Most of the original papers defined T to include the effects of loops only. However, we will redefine T to include all new sources of SU(2) breaking, including nonstandard Higgs, so that T and ρ_0 are equivalent by Eq. (10.56).

A multiplet of heavy degenerate chiral fermions yields

$$S = C \sum_i (t_{3L}(i) - t_{3R}(i))^2 / 3\pi, \quad (10.57)$$

where $t_{3L,R}(i)$ is the third component of weak isospin of the left-(right-) handed component of fermion i and C is the number of colors. For example, a heavy degenerate ordinary or mirror family would contribute $2/3\pi$ to S . In technicolor models with QCD-like dynamics, one expects [120] $S \sim 0.45$ for an isodoublet of technifermions, assuming $N_{TC} = 4$ technicolors, while $S \sim 1.62$ for a full technigeneration with $N_{TC} = 4$; T is harder to estimate because it is model dependent. In these examples one has $S \geq 0$. However, the QCD-like models are excluded on other grounds (flavor-changing neutral currents, and too-light quarks and pseudo-Goldstone bosons [127]). In particular, these estimates do not apply to models of walking technicolor [127], for which S can be smaller or even negative [128]. Other situations in which $S < 0$, such as loops involving scalars or Majorana particles, are also possible [129]. Supersymmetric extensions of the Standard Model generally give very small effects [130]. Most simple types of new physics yield $U = 0$, although there are counter-examples, such as the effects of anomalous triple-gauge vertices [122].

The Standard Model expressions for observables are replaced by

$$\begin{aligned} M_Z^2 &= M_{Z0}^2 \frac{1 - \alpha T}{1 - G_F M_{Z0}^2 S / 2\sqrt{2}\pi}, \\ M_W^2 &= M_{W0}^2 \frac{1}{1 - G_F M_{W0}^2 (S + U) / 2\sqrt{2}\pi}, \end{aligned} \quad (10.58)$$

where M_{Z0} and M_{W0} are the Standard Model expressions (as functions of m_t and M_H) in the $\overline{\text{MS}}$ scheme. Furthermore,

$$\begin{aligned} \Gamma_Z &= \frac{1}{1 - \alpha T} M_Z^3 \beta_Z, \\ \Gamma_W &= M_W^3 \beta_W, \\ A_i &= \frac{1}{1 - \alpha T} A_{i0}, \end{aligned} \quad (10.59)$$

where β_Z and β_W are the Standard Model expressions for the reduced widths Γ_{Z0}/M_{Z0}^3 and Γ_{W0}/M_{W0}^3 , M_Z and M_W are the physical masses, and A_i (A_{i0}) is a neutral current amplitude (in the Standard Model).

The data allow a simultaneous determination of \hat{s}_Z^2 (from the Z pole asymmetries), S (from M_Z), U (from M_W), T (mainly from

Γ_Z), α_s (from R_ℓ and σ_{had}), and m_t (from CDF and DØ), with little correlation among the Standard Model parameters:

$$\begin{aligned} S &= -0.07 \pm 0.11 (-0.09), \\ T &= -0.10 \pm 0.14 (+0.09), \\ U &= 0.11 \pm 0.15 (+0.01), \end{aligned} \quad (10.60)$$

and $\hat{s}_Z^2 = 0.23117 \pm 0.00017$, $\alpha_s(M_Z) = 0.1203 \pm 0.0031$, $m_t = 173.4 \pm 4.9$ GeV, where the uncertainties are from the inputs. The central values assume $M_H = 100$ GeV, and in parentheses we show the change for $M_H = 300$ GeV. As can be seen, the Standard Model parameters (U) can be determined with no (little) M_H dependence. On the other hand, S , T , and M_H cannot be obtained simultaneously, because the Higgs boson loops themselves are resembled approximately by oblique effects. The first Eq. (10.60) shows that negative contributions to the S parameter can weaken or entirely remove the strong constraints on M_H from the Standard Model fits. The parameters in Eqs. (10.60) which by definition are due to new physics only, are all consistent with the Standard Model values of zero. Using Eq. (10.56) the value of ρ_0 corresponding to T is $0.9992 \pm 0.0011 (+0.0007)$. The values of the $\hat{\epsilon}$ parameters defined in Eq. (10.55) are

$$\begin{aligned} \hat{\epsilon}_3 &= -0.0006 \pm 0.0009 (-0.0008), \\ \hat{\epsilon}_1 &= -0.0008 \pm 0.0011 (+0.0007), \\ \hat{\epsilon}_2 &= -0.0009 \pm 0.0013 (-0.0001). \end{aligned} \quad (10.61)$$

Unlike the original definition, we defined the quantities in Eqs. (10.61) to vanish identically in the absence of new physics and to correspond directly to the parameters S , T , and U in Eqs. (10.60). There is a strong correlation (81%) between the S and T parameters. The allowed region in $S - T$ is shown in Fig. 10.3. From Eqs. (10.60) one obtains $S \leq 0.11(0.01)$ and $T \leq 0.13(0.22)$ at 95% CL for $M_H = 100$ GeV (300 GeV). If one fixes $M_H = 600$ GeV and requires the constraint $S \geq 0$ (as is appropriate in QCD-like technicolor models) then $S \leq 0.09$. This rules out simple technicolor models with many techni-doublets and QCD-like dynamics.

An extra generation of ordinary fermions is excluded at the 99.6% CL on the basis of the S parameter alone. This result assumes that there are no new contributions to T or U . Allowing a contribution of 0.18 ± 0.08 to T reduces the CL to 97%. This is in agreement with a fit to the number of light neutrinos, $N_\nu = 2.985 \pm 0.008$ (which favors a larger value for $\alpha_s(M_Z) = 0.1229 \pm 0.0034$ mainly from R_ℓ). However, the S parameter fit is valid even for a very heavy fourth family neutrino.

Although S is consistent with zero, the electroweak asymmetries, especially the SLD left-right asymmetry and Q_W , favor $S < 0$. The simplest origin of $S < 0$ would probably be an additional heavy Z' boson [117], which could mimic $S < 0$. Similarly, there is a slight indication of negative T , while, as discussed above, nondegenerate scalar or fermion multiplets generally predict $T > 0$.

There is no simple parametrization that is powerful enough to describe the effects of every type of new physics on every possible observable. The S , T , and U formalism describes many types of heavy physics which affect only the gauge self-energies, and it can be applied to all precision observables. However, new physics which couples directly to ordinary fermions, such as heavy Z' bosons [117] or mixing with exotic fermions [131] cannot be fully parametrized in the S , T , and U framework. It is convenient to treat these types of new physics by parametrizations that are specialized to that particular class of theories (*e.g.*, extra Z' bosons), or to consider specific models (which might contain, *e.g.*, Z' bosons and exotic fermions with correlated parameters). Constraints on various types of new physics are reviewed in [26,132,133]. Fits to models with technicolor, extended technicolor, and supersymmetry are described, respectively, in [134], [135], and [86,136]. In a new development, the effects of compactified extra spatial dimensions at the TeV scale have been considered in Ref. 137.

An alternate formalism [138] defines parameters, ϵ_1 , ϵ_2 , ϵ_3 , ϵ_b in terms of the specific observables M_W/M_Z , $\Gamma_{\ell\ell}$, $A_{FB}^{(0,\ell)}$, and R_b .

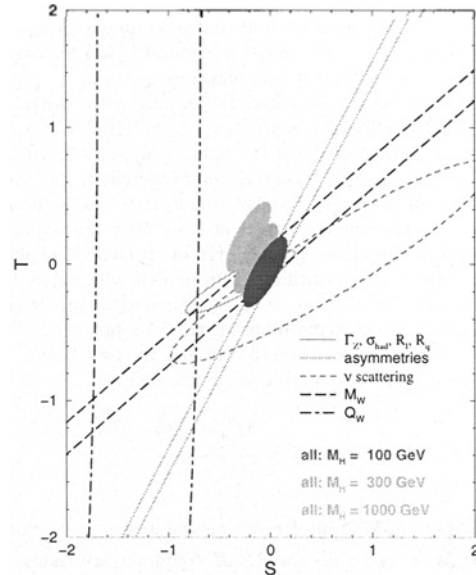


Figure 10.3: 1σ constraints (39.35%) on S and T from various inputs. S and T represent the contributions of new physics only. (Uncertainties from m_t are included in the errors.) The contours assume $M_H = 100$ GeV except for the central and upper 90% CL contours allowed by all data, which are for $M_H = 300$ GeV and 1000 GeV, respectively. Data sets not involving M_W are insensitive to U . Due to higher order effects, however, $U = 0$ has to be assumed in all fits. $\alpha_s(M_Z) = 0.120$ is assumed for the 1σ constraints, while in the fits to all data α_s is allowed to float.

The definitions coincide with those for $\hat{\epsilon}_i$ in Eqs. (10.54) and (10.55) for physics which affects gauge self-energies only, but the ϵ 's now parametrize arbitrary types of new physics. However, the ϵ 's are not related to other observables unless additional model-dependent assumptions are made. Another approach [139–141] parametrizes new physics in terms of gauge-invariant sets of operators. It is especially powerful in studying the effects of new physics on non-Abelian gauge vertices. The most general approach introduces deviation vectors [132]. Each type of new physics defines a deviation vector, the components of which are the deviations of each observable from its Standard Model prediction, normalized to the experimental uncertainty. The length (direction) of the vector represents the strength (type) of new physics.

Table 10.7: 95% CL lower mass limits (in GeV) on various extra Z' bosons, appearing in models of unification and string theory. ρ_0 free indicates a completely arbitrary Higgs sector, while $\rho_0 = 1$ restricts to Higgs doublets and singlets with still unspecified charges.

Z'	ρ_0 free	$\rho_0 = 1$
Z_χ	551	545
Z_ψ	151	146
Z_η	379	365
Z_{LR}	570	564
Z_{SM}	822	809
Z_{string}	582	578

One of the best motivated kinds of physics beyond the Standard Model besides supersymmetry are extra Z' bosons. They do not spoil the observed approximate gauge coupling unification, and appear copiously in many Grand Unified Theories (GUTs) and most superstring models. For example, the $SO(10)$ GUT contains an extra $U(1)$ as can be seen from its maximal subgroup,

$SU(5) \times U(1)_\chi$. Similarly, the E_6 GUT contains the subgroup $SO(10) \times U(1)_\psi$. It possesses only axial-vector couplings to the ordinary fermions, and its mass is generally less constrained. The Z_η boson is the linear combination $\sqrt{3/8}Z_\chi - \sqrt{5/8}Z_\psi$. The Z_{LR} boson occurs in left-right models with gauge group $SU(3)_C \times SU(2)_L \times SU(2)_R \times U(1)_{B-L} \subset SO(10)$. The sequential Z_{SM} boson is defined to have the same couplings to fermions as the SM Z boson. Such a boson is not expected in the context of gauge theories unless it has different couplings to exotic fermions than the ordinary Z . However, it serves as a useful reference case when comparing constraints from various sources. It could also play the role of an excited state of the ordinary Z in models with extra dimensions at the weak scale. Finally, we consider a superstring motivated Z_{string} boson appearing in a specific model [142]. The potential Z' boson is in general a superposition of the SM Z and the new boson associated with the extra $U(1)$. The mixing angle θ satisfies,

$$\tan^2 \theta = \frac{M_{Z_1^0}^2 - M_Z^2}{M_{Z'}^2 - M_{Z_1^0}^2},$$

where $M_{Z_1^0}$ is the SM value for M_Z in the absence of mixing. Note, that $M_Z < M_{Z_1^0}$, and that the SM Z couplings are changed by the mixing. If the Higgs $U(1)'$ quantum numbers are known, there will be an extra constraint,

$$\theta = C \frac{g_2}{g_1} \frac{M_Z^2}{M_{Z'}^2}, \quad (10.62)$$

where $g_{1,2}$ are the $U(1)$ and $U(1)'$ gauge couplings with $g_2 = \sqrt{\frac{3}{5}} \sin \theta_W \sqrt{\lambda} g_1$. $\lambda = 1$ (which we assume) if the GUT group breaks directly to $SU(3) \times SU(2) \times U(1) \times U(1)'$. C is a function of vacuum expectation values. For minimal Higgs sectors it can be found in reference [117]. Table 10.7 shows the 95% CL lower mass limits obtained from a somewhat earlier data set [143] for ρ_0 free and $\rho_0 = 1$, respectively. In cases of specific minimal Higgs sectors where C is known, the Z' mass limits are generally pushed into the TeV region. For more details see Ref. 143 and the Section on "The Z' Searches" in this Review. The more recent values for $Q_W(Cs)$ and σ_{had} used in this Review modify the results and even suggest the possible existence of Z' [144].

References:

1. S. Weinberg, Phys. Rev. Lett. **19**, 1264 (1967);
A. Salam, p. 367 of *Elementary Particle Theory*, ed. N. Svartholm (Almqvist and Wiksells, Stockholm, 1969);
S.L. Glashow, J. Iliopoulos, and L. Maiani, Phys. Rev. **D2**, 1285 (1970).
2. For reviews, see G. Barbiellini and C. Santoni, Riv. Nuovo Cimento **9(2)**, 1 (1986);
E.D. Commins and P.H. Bucksbaum, *Weak Interactions of Leptons and Quarks*, (Cambridge Univ. Press, Cambridge, 1983);
W. Fetscher and H.J. Gerber, p. 657 of Ref. 3;
J. Deutsch and P. Quin, p. 706 of Ref. 3.
3. *Precision Tests of the Standard Electroweak Model*, ed. P. Langacker (World Scientific, Singapore, 1995).
4. CDF: F. Abe *et al.*, Phys. Rev. Lett. **82**, 271 (1999).
5. DØ: B. Abbott *et al.*, Phys. Rev. **D58**, 052001 (1998).
6. For reviews, see the article on "The Higgs boson" in this Review;
J. Gunion, H.E. Haber, G.L. Kane, and S. Dawson, *The Higgs Hunter's Guide*, (Addison-Wesley, Redwood City, 1990);
M. Sher, Phys. Reports **179**, 273 (1989).
7. TOPAZ: I. Levine *et al.*, Phys. Rev. Lett. **78**, 424 (1997);
OPAL: hep-ex/9908008.
8. S. Fanchiotti, B. Kniehl, and A. Sirlin, Phys. Rev. **D48**, 307 (1993) and references therein.
9. J. Erler, Phys. Rev. **D59**, 054008 (1999).
10. M. Davier and A. Höcker, Phys. Lett. **B419**, 419 (1998).
11. A.D. Martin and D. Zeppenfeld, Phys. Lett. **B345**, 558 (1995).
12. S. Eidelman and F. Jegerlehner, Z. Phys. **C67**, 585 (1995).
13. B.V. Geshkenbein and V.L. Morgunov, Phys. Lett. **B340**, 185 (1995) and Phys. Lett. **B352**, 456 (1995).
14. H. Burkhardt and B. Pietrzyk, Phys. Lett. **B356**, 398 (1995).
15. M.L. Swartz, Phys. Rev. **D53**, 5268 (1996).
16. R. Alemany, M. Davier, and A. Höcker, Eur. Phys. J. **C2**, 123 (1998).
17. N.V. Krasnikov and R. Rodenberg, Nuovo Cimento **111A**, 217 (1998).
18. J.H. Kühn and M. Steinhauser, Phys. Lett. **B437**, 425 (1998).
19. M. Davier and A. Höcker, Phys. Lett. **B435**, 427 (1998).
20. S. Groote, J.G. Körner, K. Schilcher, N.F. Nasrallah, Phys. Lett. **B440**, 375 (1998).
21. F. Jegerlehner, hep-ph/9901386.
22. W.J. Marciano and A. Sirlin, Phys. Rev. Lett. **61**, 1815 (1988).
23. T. van Ritbergen and R.G. Stuart, Phys. Rev. Lett. **82**, 488 (1999).
24. J. Mnich and G. Quast for the LEP collaborations, presented at the *International Europhysics Conference on High Energy Physics* (Tampere, 1999).
25. Earlier analyses include U. Amaldi *et al.*, Phys. Rev. **D36**, 1385 (1987);
P. Langacker and M. Luo, Phys. Rev. **D44**, 817 (1991);
Very similar conclusions are reached in an analysis by G. Costa *et al.*, Nucl. Phys. **B297**, 244 (1988);
Deep inelastic scattering is considered by G.L. Fogli and D. Haidt, Z. Phys. **C40**, 379 (1988);
For recent analyses, see Ref. 26.
26. P. Langacker, p. 883 of Ref. 3;
J. Erler and P. Langacker, Phys. Rev. **D52**, 441 (1995).
27. A. Sirlin, Phys. Rev. **D22**, 971 (1980);
A. Sirlin, Phys. Rev. **D29**, 89 (1984);
W. Hollik, Fortsch. Phys. **38**, 165 (1990);
D.C. Kennedy *et al.*, Nucl. Phys. **B321**, 83 (1989);
D.C. Kennedy and B.W. Lynn, Nucl. Phys. **B322**, 1 (1989);
D.Yu. Bardin *et al.*, Z. Phys. **C44**, 493 (1989);
For recent reviews, see the articles by W. Hollik, pp. 37 and 117, and W. Marciano, p. 170 in Ref. 3. Extensive references to other papers are given in Ref. 25.
28. W. Hollik in Ref. 27 and references therein;
V.A. Novikov, L.B. Okun, and M.I. Vysotsky, Nucl. Phys. **B397**, 35 (1993).
29. W.J. Marciano and J.L. Rosner, Phys. Rev. Lett. **65**, 2963 (1990).
30. G. Degrassi, S. Fanchiotti, and A. Sirlin, Nucl. Phys. **B351**, 49 (1991).
31. G. Degrassi and A. Sirlin, Nucl. Phys. **B352**, 342 (1991).
32. P. Gambino and A. Sirlin, Phys. Rev. **D49**, 1160 (1994);
ZFITTER: D. Bardin *et al.*, CERN-TH.6443/92 and references therein.
33. R. Barbieri *et al.*, Phys. Lett. **B288**, 95 (1992);
R. Barbieri *et al.*, Nucl. Phys. **B409**, 105 (1993).
34. J. Fleischer, O.V. Tarasov, and F. Jegerlehner, Phys. Lett. **B319**, 249 (1993).
35. G. Degrassi, P. Gambino, and A. Vicini, Phys. Lett. **B383**, 219 (1996);
G. Degrassi, P. Gambino, and A. Sirlin, Phys. Lett. **B394**, 188 (1997).
36. S. Bauberger and G. Weiglein, Phys. Lett. **B419**, 333 (1998).

37. A. Djouadi and C. Verzegnassi, *Phys. Lett.* **B195**, 265 (1987);
A. Djouadi, *Nuovo Cimento* **100A**, 357 (1988);
B.A. Kniehl, *Nucl. Phys.* **B347**, 86 (1990);
A. Djouadi and P. Gambino, *Phys. Rev.* **D49**, 3499 (1994), **D49**, 4705 (1994), and **D53**, 4111(E) (1996).
38. K.G. Chetyrkin, J.H. Kühn, and M. Steinhauser, *Phys. Lett.* **B351**, 331 (1995);
L. Avdeev *et al.*, *Phys. Lett.* **B336**, 560 (1994) and **B349**, 597(E) (1995).
39. J. Fleischer *et al.*, *Phys. Lett.* **B293**, 437 (1992);
K.G. Chetyrkin, A. Kwiatkowski, and M. Steinhauser, *Mod. Phys. Lett.* **A8**, 2785 (1993).
40. A. Czarnecki and J.H. Kühn, *Phys. Rev. Lett.* **77**, 3955 (1996).
41. R. Harlander, T. Seidensticker, and M. Steinhauser, *Phys. Lett.* **B426**, 125 (1998);
J. Fleischer *et al.*, *hep-ph/9904256*.
42. For a review, see F. Perrier, p. 385 of Ref. 3.
43. CDHS: H. Abramowicz *et al.*, *Phys. Rev. Lett.* **57**, 298 (1986);
CDHS: A. Blondel *et al.*, *Z. Phys.* **C45**, 361 (1990).
44. CHARM: J.V. Allaby *et al.*, *Phys. Lett.* **B117**, 446 (1986);
CHARM: J.V. Allaby *et al.*, *Z. Phys.* **C36**, 611 (1987).
45. CCFR: C.G. Arroyo *et al.*, *Phys. Rev. Lett.* **72**, 3452 (1994);
CCFR: K.S. McFarland *et al.*, *Eur. Phys. J.* **C1**, 509 (1998).
46. H. Georgi and H.D. Politzer, *Phys. Rev.* **D14**, 1829 (1976);
R.M. Barnett, *Phys. Rev.* **D14**, 70 (1976).
47. LAB-E: S.A. Rabinowitz *et al.*, *Phys. Rev. Lett.* **70**, 134 (1993).
48. E.A. Paschos and L. Wolfenstein, *Phys. Rev.* **D7**, 91 (1973).
49. NuTeV: K.S. McFarland *et al.*, presented at the *International Europhysics Conference on High Energy Physics* (Tampere, 1999).
50. CHARM: J. Dorenbosch *et al.*, *Z. Phys.* **C41**, 567 (1989).
51. CALO: L.A. Ahrens *et al.*, *Phys. Rev.* **D41**, 3297 (1990).
52. CHARM II: P. Vilain *et al.*, *Phys. Lett.* **B335**, 246 (1994);
See also J. Panman, p. 504 of Ref. 3.
53. SSF: C.Y. Prescott *et al.*, *Phys. Lett.* **B84**, 524 (1979);
For a review, see P. Souder, p. 599 of Ref. 3.
54. For reviews and references to earlier work, see B.P. Masterson and C.E. Wieman, p. 545 of Ref. 3;
M.A. Bouchiat and L. Pottier, *Science* **234**, 1203 (1986).
55. Cesium (Boulder): C.S. Wood *et al.*, *Science* **275**, 1759 (1997).
56. Thallium (Oxford): N.H. Edwards *et al.*, *Phys. Rev. Lett.* **74**, 2654 (1995);
Thallium (Seattle): P.A. Vetter *et al.*, *Phys. Rev. Lett.* **74**, 2658 (1995).
57. Lead (Seattle): D.M. Meekhof *et al.*, *Phys. Rev. Lett.* **71**, 3442 (1993).
58. Bismuth (Oxford): M.J.D. MacPherson *et al.*, *Phys. Rev. Lett.* **67**, 2784 (1991).
59. V.A. Dzuba, V.V. Flambaum, and O.P. Sushkov, *Phys. Lett.* **141A**, 147 (1989);
S.A. Blundell, J. Sapirstein, and W.R. Johnson, *Phys. Rev. Lett.* **65**, 1411 (1990) and *Phys. Rev.* **D45**, 1602 (1992);
For a review, see S.A. Blundell, W.R. Johnson, and J. Sapirstein, p. 577 of Ref. 3.
60. S.C. Bennett and C.E. Wieman, *Phys. Rev. Lett.* **82**, 2484 (1999).
61. V.A. Dzuba, V.V. Flambaum, and O.P. Sushkov, *Phys. Rev.* **A56**, R4357 (1997).
62. M.A. Bouchiat and J. Guéna, *J. Phys. (France)* **49**, 2037 (1988).
63. V.A. Dzuba *et al.*, *J. Phys.* **B20**, 3297 (1987).
64. Ya.B. Zel'dovich, *Sov. Phys. JETP* **6**, 1184 (1958);
For a recent discussion, see V.V. Flambaum and D.W. Murray, *Phys. Rev.* **C56**, 1641 (1997) and references therein.
65. J.L. Rosner, *Phys. Rev.* **D53**, 2724 (1996).
66. S.J. Pollock, E.N. Fortson, and L. Willets, *Phys. Rev.* **C46**, 2587 (1992);
B.Q. Chen and P. Vogel, *Phys. Rev.* **C48**, 1392 (1993).
67. B.W. Lynn and R.G. Stuart, *Nucl. Phys.* **B253**, 216 (1985).
68. *Physics at LEP*, ed. J. Ellis and R. Peccei, CERN 86-02, Vol. 1.
69. C. Kiesling, *Tests of the Standard Theory of Electroweak Interactions*, (Springer-Verlag, New York, 1988);
R. Marshall, *Z. Phys.* **C43**, 607 (1989);
Y. Mori *et al.*, *Phys. Lett.* **B218**, 499 (1989);
D. Haidt, p. 203 of Ref. 3.
70. For reviews, see D. Schaile, p. 215, and A. Blondel, p. 277 of Ref. 3;
R. Clare, private communication.
71. SLD: K. Abe *et al.*, *Phys. Rev. Lett.* **78**, 2075 (1997).
72. SLD: J.E. Brau *et al.*, presented at the *International Europhysics Conference on High Energy Physics* (Tampere, 1999).
73. The LEP/SLD Heavy Flavour Working Group: D. Abbaneo *et al.*, LEPHF/99-01.
74. SLD: K. Abe *et al.*, submitted to the *International Europhysics Conference on High Energy Physics* (Tampere, 1999).
75. SLD: K. Abe *et al.*, *Phys. Rev. Lett.* **79**, 804 (1997).
76. The LEP Collaborations ALEPH, DELPHI, L3, OPAL, the LEP Electroweak Working Group and the SLD Heavy Flavour and Electroweak Groups: D. Abbaneo *et al.*, CERN-EP/99-15.
77. DELPHI: P. Abreu *et al.*, *Z. Phys.* **C67**, 1 (1995);
OPAL: K. Ackerstaff *et al.*, submitted to the *XXIXth Conference on High Energy Physics* (Vancouver, 1998).
78. SLD: K. Abe *et al.*, *Phys. Rev. Lett.* **78**, 17 (1997).
79. A. Leike, T. Riemann, and J. Rose, *Phys. Lett.* **B273**, 513 (1991);
T. Riemann, *Phys. Lett.* **B293**, 451 (1992).
80. L. Maiani and P. Zerwas, as quoted in Ref. 76.
81. OPAL: K. Ackerstaff *et al.*, submitted to the *International Europhysics Conference on High Energy Physics* (Tampere, 1999).
82. CLEO: M.S. Alam *et al.*, *Phys. Rev. Lett.* **74**, 2885 (1995);
CLEO: T. Skwarnicki *et al.*, presented at the *29th International Conference on High Energy Physics* (Vancouver, 1998).
83. A. Ali and C. Greub, *Phys. Lett.* **B259**, 182 (1991);
A.L. Kagan and M. Neubert, *Eur. Phys. J.* **C7**, 5 (1999).
84. B. Barish *et al.*, *Phys. Rev. Lett.* **76**, 1570 (1996).
85. A. Czarnecki and W.J. Marciano, *Phys. Rev. Lett.* **81**, 277 (1998).
86. J. Erler and D.M. Pierce, *Nucl. Phys.* **B526**, 53 (1998).
87. Y. Nir, *Phys. Lett.* **B221**, 184 (1989);
K. Adel and Y.P. Yao, *Phys. Rev.* **D49**, 4945 (1994);
C. Greub, T. Hurth, and D. Wyler, *Phys. Rev.* **D54**, 3350 (1996);
K.G. Chetyrkin, M. Misiak, and M. Münz, *Phys. Lett.* **B400**, 206 (1997);
C. Greub and T. Hurth, *Phys. Rev.* **D56**, 2934 (1997);
M. Ciuchini *et al.*, *Nucl. Phys.* **B527**, 21 (1998) and **B534**, 3 (1998);
F.M. Borzumati and C. Greub, *Phys. Rev.* **D58**, 074004 (1998) and **D59**, 057501 (1999);
A. Strumia, *Nucl. Phys.* **B532**, 28 (1998).
88. A. Czarnecki, B. Krause, and W.J. Marciano, *Phys. Rev. Lett.* **76**, 3267 (1996).
89. J. Bijnens, E. Pallante, and J. Prades, *Nucl. Phys.* **B474**, 379 (1996).
90. B. Krause, *Phys. Lett.* **B390**, 392 (1997).
91. M. Carena, G.F. Giudice, and C.E.M. Wagner, *Phys. Lett.* **B390**, 234 (1997).

92. A comprehensive report and further references can be found in K.G. Chetyrkin, J.H. Kühn, and A. Kwiatkowski, Phys. Reports **277**, 189 (1996).
93. J. Schwinger, *Particles, Sources and Fields*, Vol. II, (Addison-Wesley, New York, 1973);
K.G. Chetyrkin, A.L. Kataev, and F.V. Tkachev, Phys. Lett. **B85**, 277 (1979);
M. Dine and J. Sapiirstein, Phys. Rev. Lett. **43**, 668 (1979);
W. Celmater, R.J. Gonsalves, Phys. Rev. Lett. **44**, 560 (1980);
S.G. Gorishnii, A.L. Kataev, and S.A. Larin, Phys. Lett. **B212**, 238 (1988) and **B259**, 144 (1991);
L.R. Surguladze and M.A. Samuel, Phys. Rev. Lett. **66**, 560 (1991) and 2416(E);
For a discussion of higher order estimates, see A.L. Kataev and V.V. Starshenko, Mod. Phys. Lett. **A10**, 235 (1995).
94. W. Bernreuther and W. Wetzel, Z. Phys. **11**, 113 (1981);
W. Wetzel and W. Bernreuther, Phys. Rev. **D24**, 2724 (1982);
B.A. Kniehl, Phys. Lett. **B237**, 127 (1990);
K.G. Chetyrkin, Phys. Lett. **B307**, 169 (1993);
A.H. Hoang *et al.*, Phys. Lett. **B338**, 330 (1994);
S.A. Larin, T. van Ritbergen, and J.A.M. Vermaseren, Nucl. Phys. **B438**, 278 (1995).
95. T.H. Chang, K.J.F. Gaemers, and W.L. van Neerven, Nucl. Phys. **B202**, 407 (1980);
J. Jersak, E. Laermann, and P.M. Zerwas, Phys. Lett. **B98**, 363 (1981) and Phys. Rev. **D25**, 1218 (1982);
S.G. Gorishnii, A.L. Kataev, and S.A. Larin, Nuovo Cimento **92**, 117 (1986);
K.G. Chetyrkin and J.H. Kühn, Phys. Lett. **B248**, 359 (1990);
K.G. Chetyrkin, J.H. Kühn, and A. Kwiatkowski, Phys. Lett. **B282**, 221 (1992);
K.G. Chetyrkin and J.H. Kühn, Phys. Lett. **B406**, 102 (1997).
96. B.A. Kniehl and J.H. Kühn, Phys. Lett. **B224**, 229 (1990) and Nucl. Phys. **B329**, 547 (1990);
K.G. Chetyrkin and A. Kwiatkowski, Phys. Lett. **B305**, 285 (1993) and **B319**, 307 (1993);
S.A. Larin, T. van Ritbergen, and J.A.M. Vermaseren, Phys. Lett. **B320**, 159 (1994);
K.G. Chetyrkin and O.V. Tarasov, Phys. Lett. **B327**, 114 (1994).
97. A.L. Kataev, Phys. Lett. **B287**, 209 (1992).
98. D. Albert *et al.*, Nucl. Phys. **B166**, 460 (1980);
F. Jegerlehner, Z. Phys. **C32**, 425 (1986);
A. Djouadi, J.H. Kühn, and P.M. Zerwas, Z. Phys. **C46**, 411 (1990);
A. Borrelli *et al.*, Nucl. Phys. **B333**, 357 (1990).
99. A.A. Akhundov, D.Yu. Bardin, and T. Riemann, Nucl. Phys. **B276**, 1 (1986);
W. Beenakker and W. Hollik, Z. Phys. **C40**, 141 (1988);
B.W. Lynn and R.G. Stuart, Phys. Lett. **B352**, 676 (1990);
J. Bernabeu, A. Pich, and A. Santamaria, Nucl. Phys. **B363**, 326 (1991).
100. C. Caso *et al.*, from the *W* Particle Listings in the 1999 WWW edition of the "Review of Particle Physics", <http://pdg.lbl.gov>.
101. CDF: F. Abe *et al.*, Phys. Rev. Lett. **75**, 11 (1995);
CDF: F. Abe *et al.*, Phys. Rev. **D52**, 4784 (1995);
CDF: W. Carithers *et al.*, presented at the *International Europhysics Conference on High Energy Physics* (Tampere, 1999);
DØ: B. Abbott *et al.*, Phys. Rev. **D58**, 092003 (1998);
DØ: B. Abbott *et al.*, Phys. Rev. Lett. **80**, 3008 (1998);
DØ: B. Abbott *et al.*, submitted to the *International Europhysics Conference on High Energy Physics* (Tampere, 1999);
UA2: S. Alitti *et al.*, Phys. Lett. **B276**, 354 (1992).
102. J. Erler, Phys. Rev. **D52**, 28 (1995);
J. Erler, J.L. Feng, and N. Polonsky, Phys. Rev. Lett. **78**, 3063 (1997).
103. DELPHI: P. Abreu *et al.*, Z. Phys. **C**, 70 (1996);
DELPHI: P. Abreu *et al.*, submitted to the *International Europhysics Conference on High Energy Physics* (Jerusalem, 1997).
104. ALEPH: R. Barate *et al.*, Eur. Phys. J. **C4**, 409 (1998);
OPAL: K. Ackerstaff *et al.*, Eur. Phys. J. **C7**, 571 (1999).
105. CCFR: W.G. Seligman *et al.*, Phys. Rev. Lett. **79**, 1213 (1997).
106. NRQCD: C.T.H. Davies *et al.*, Phys. Rev. **D56**, 2755 (1997).
107. SCRI: A.X. El-Khadra *et al.*, presented at the 31st Rencontres de Moriond: Electroweak Interactions and Unified Theories, Les Arcs (1996).
108. T. van Ritbergen, J.A.M. Vermaseren, and S.A. Larin, Phys. Lett. **B400**, 379 (1997).
109. K.G. Chetyrkin, B.A. Kniehl, and M. Steinhauser, Phys. Rev. Lett. **79**, 2184 (1997).
110. ALEPH, DELPHI, L3, OPAL, and the LEP working group for Higgs boson searches, P. Bock *et al.*, submitted to the *International Europhysics Conference on High Energy Physics* (Tampere, 1999).
111. A.L. Kataev and V.V. Starshenko, Mod. Phys. Lett. **A10**, 235 (1995);
J. Erler, to be published.
112. J. Erler, presented at the *17th International Workshop on Weak Interactions and Neutrinos* (Cape Town, 1999).
113. S.J. Brodsky, G.P. Lepage, and P.B. Mackenzie, Phys. Rev. **D28**, 228 (1983).
114. N. Gray *et al.*, Z. Phys. **C48**, 673 (1990).
115. P. Langacker and N. Polonsky, Phys. Rev. **D52**, 3081 (1995) and references therein.
116. M. Veltman, Nucl. Phys. **B123**, 89 (1977);
M. Chanowitz, M.A. Furman, and I. Hinchliffe, Phys. Lett. **B78**, 285 (1978).
117. P. Langacker and M. Luo, Phys. Rev. **D45**, 278 (1992) and references therein.
118. A. Denner, R.J. Guth, and J.H. Kühn, Phys. Lett. **B240**, 438 (1990).
119. S. Bertolini and A. Sirlin, Phys. Lett. **B257**, 179 (1991).
120. M. Peskin and T. Takeuchi, Phys. Rev. Lett. **65**, 964 (1990);
M. Peskin and T. Takeuchi, Phys. Rev. **D46**, 381 (1992);
M. Golden and L. Randall, Nucl. Phys. **B361**, 3 (1991).
121. D. Kennedy and P. Langacker, Phys. Rev. Lett. **65**, 2967 (1990);
D. Kennedy and P. Langacker, Phys. Rev. **D44**, 1591 (1991).
122. G. Altarelli and R. Barbieri, Phys. Lett. **B253**, 161 (1990).
123. B. Holdom and J. Terning, Phys. Lett. **B247**, 88 (1990).
124. B.W. Lynn, M.E. Peskin, and R.G. Stuart, p. 90 of Ref. 68.
125. An alternative formulation is given by K. Hagiwara *et al.*, Z. Phys. **C64**, 559 (1994) and **C68**, 352(E) (1995);
K. Hagiwara, D. Haidt, and S. Matsumoto, Eur. Phys. J. **C2**, 95 (1998).
126. I. Maksymyk, C.P. Burgess, and D. London, Phys. Rev. **D50**, 529 (1994);
C.P. Burgess *et al.*, Phys. Lett. **B326**, 276 (1994).
127. K. Lane, presented at the *27th International Conference on High Energy Physics* (ICHEP 94) (Glasgow, 1994).
128. R. Sundrum and S.D.H. Hsu, Nucl. Phys. **B391**, 127 (1993);
R. Sundrum, Nucl. Phys. **B395**, 60 (1993);
M. Luty and R. Sundrum, Phys. Rev. Lett. **70**, 529 (1993);
T. Appelquist and J. Terning, Phys. Lett. **B315**, 139 (1993);
E. Gates and J. Terning, Phys. Rev. Lett. **67**, 1840 (1991).

129. H. Georgi, Nucl. Phys. **B363**, 301 (1991);
M.J. Dugan and L. Randall, Phys. Lett. **B264**, 154 (1991).
130. R. Barbieri *et al.*, Nucl. Phys. **B341**, 309 (1990).
131. For a review, see D. London, p. 951 of Ref. 3.
132. P. Langacker, M. Luo, and A.K. Mann, Rev. Mod. Phys. **64**, 87 (1992);
M. Luo, p. 977 of Ref. 3.
133. F.S. Merritt *et al.*, p. 19 of *Particle Physics: Perspectives and Opportunities: Report of the DPF Committee on Long Term Planning*, ed. R. Peccei *et al.* (World Scientific, Singapore, 1995).
134. R.S. Chivukula, E.H. Simmons, and J. Terning, Phys. Lett. **B331**, 383 (1994).
135. J. Ellis, G.L. Fogli, and E. Lisi, Phys. Lett. **B343**, 282 (1995).
136. G.L. Kane, R.G. Stuart, and J.D. Wells, Phys. Lett. **B354**, 350 (1995);
X. Wang, J.L. Lopez, and D.V. Nanopoulos, Phys. Rev. **D52**, 4116 (1995);
P.H. Chankowski and S. Pokorski, Phys. Lett. **B366**, 188 (1996).
137. M. Masip and A. Pomarol, Phys. Rev. **D60**, 096005 (1999) hep-ph/9902467;
K. Cheung, Phys. Lett. **B460**, 383 (1999);
T.G. Rizzo and J.D. Wells, Phys. Rev. **D61**, 016007 (2000) hep-ph/9906234;
A. Strumia, Phys. Lett. **B466**, 107 (1999) hep-ph/9906266;
R. Casalbuoni *et al.*, Phys. Lett. **B462**, 48 (1999) hep-ph/9907355;
C.D. Carone, Phys. Rev. **D61**, 015008 (2000) hep-ph/9907362;
A. Ioannisisian and A. Pilaftsis, hep-ph/9907522.
138. G. Altarelli, R. Barbieri, and S. Jadach, Nucl. Phys. **B369**, 3 (1992) and **B376**, 444(E) (1992).
139. A. De Rújula *et al.*, Nucl. Phys. **B384**, 3 (1992).
140. K. Hagiwara *et al.*, Phys. Rev. **D48**, 2182 (1993).
141. C.P. Burgess and D. London, Phys. Rev. **D48**, 4337 (1993).
142. S. Chaudhuri *et al.*, Nucl. Phys. **B456**, 89 (1995);
G. Cleaver *et al.*, Phys. Rev. **D59**, 055005 (1999).
143. J. Erler and P. Langacker, Phys. Lett. **B456**, 68 (1999).
144. R. Casalbuoni, S. De Curtis, D. Dominici, and R. Gatto, Phys. Lett. **B460**, 135 (1999);
J.L. Rosner, Phys. Rev. **D61**, 016006 (2000);
J. Erler and P. Langacker, Phys. Rev. Lett. **84**, 212 (2000).

11. THE CABIBBO-KOBAYASHI-MASKAWA QUARK-MIXING MATRIX

Revised 2000 by F.J. Gilman (Carnegie-Mellon University), K. Kleinknecht and B. Renk (Johannes-Gutenberg Universität Mainz).

In the Standard Model with $SU(2) \times U(1)$ as the gauge group of electroweak interactions, both the quarks and leptons are assigned to be left-handed doublets and right-handed singlets. The quark mass eigenstates are not the same as the weak eigenstates, and the matrix relating these bases was defined for six quarks and given an explicit parametrization by Kobayashi and Maskawa [1] in 1973. It generalizes the four-quark case, where the matrix is parametrized by a single angle, the Cabibbo angle [2].

By convention, the mixing is often expressed in terms of a 3×3 unitary matrix V operating on the charge $-\epsilon/3$ quark mass eigenstates (d , s , and b):

$$\begin{pmatrix} d' \\ s' \\ b' \end{pmatrix} = \begin{pmatrix} V_{ud} & V_{us} & V_{ub} \\ V_{cd} & V_{cs} & V_{cb} \\ V_{td} & V_{ts} & V_{tb} \end{pmatrix} \begin{pmatrix} d \\ s \\ b \end{pmatrix}. \quad (11.1)$$

The values of individual matrix elements can in principle all be determined from weak decays of the relevant quarks, or, in some cases, from deep inelastic neutrino scattering. Using the constraints discussed below together with unitarity, and assuming only three generations, the 90% confidence limits on the magnitude of the elements of the complete matrix are

$$\begin{pmatrix} 0.9742 \text{ to } 0.9757 & 0.219 \text{ to } 0.226 & 0.002 \text{ to } 0.005 \\ 0.219 \text{ to } 0.225 & 0.9734 \text{ to } 0.9749 & 0.037 \text{ to } 0.043 \\ 0.004 \text{ to } 0.014 & 0.035 \text{ to } 0.043 & 0.9990 \text{ to } 0.9993 \end{pmatrix}. \quad (11.2)$$

The ranges shown are for the individual matrix elements. The constraints of unitarity connect different elements, so choosing a specific value for one element restricts the range of others.

There are several parametrizations of the Cabibbo-Kobayashi-Maskawa (CKM) matrix. We advocate a "standard" parametrization [3] of V that utilizes angles θ_{12} , θ_{23} , θ_{13} , and a phase, δ_{13}

$$V = \begin{pmatrix} c_{12}c_{13} & s_{12}c_{13} & s_{13}e^{-i\delta_{13}} \\ -s_{12}c_{23} - c_{12}s_{23}s_{13}e^{i\delta_{13}} & c_{12}c_{23} - s_{12}s_{23}s_{13}e^{i\delta_{13}} & s_{23}c_{13} \\ s_{12}s_{23} - c_{12}c_{23}s_{13}e^{i\delta_{13}} & -c_{12}s_{23} - s_{12}c_{23}s_{13}e^{i\delta_{13}} & c_{23}c_{13} \end{pmatrix}, \quad (11.3)$$

with $c_{ij} = \cos\theta_{ij}$ and $s_{ij} = \sin\theta_{ij}$ for the "generation" labels $i, j = 1, 2, 3$. This has distinct advantages of interpretation, for the rotation angles are defined and labelled in a way that relates to the mixing of two specific generations and if one of these angles vanishes, so does the mixing between those two generations; in the limit $\theta_{23} = \theta_{13} = 0$ the third generation decouples, and the situation reduces to the usual Cabibbo mixing of the first two generations with θ_{12} identified with the Cabibbo angle [2]. The real angles θ_{12} , θ_{23} , θ_{13} can all be made to lie in the first quadrant by an appropriate redefinition of quark field phases.

The matrix elements in the first row and third column, which can be directly measured in decay processes, are all of a simple form, and, as c_{13} is known to deviate from unity only in the sixth decimal place, $V_{ud} = c_{12}$, $V_{us} = s_{12}$, $V_{ub} = s_{13}e^{-i\delta_{13}}$, $V_{cb} = s_{23}$, and $V_{tb} = c_{23}$ to an excellent approximation. The phase δ_{13} lies in the range $0 \leq \delta_{13} < 2\pi$, with nonzero values generally breaking CP invariance for the weak interactions. The generalization to the n generation case contains $n(n-1)/2$ angles and $(n-1)(n-2)/2$ phases. The range of matrix elements in Eq. (11.2) corresponds to 90% CL limits on the sines of the angles of $s_{12} = 0.219$ to 0.226 , $s_{23} = 0.037$ to 0.043 , and $s_{13} = 0.002$ to 0.005 .

Kobayashi and Maskawa [1] originally chose a parametrization involving the four angles θ_1 , θ_2 , θ_3 , and δ :

$$\begin{pmatrix} d' \\ s' \\ b' \end{pmatrix} = \begin{pmatrix} c_1 & -s_1c_3 & -s_1s_3 \\ s_1c_2 & c_1c_2c_3 - s_2s_3e^{i\delta} & c_1c_2s_3 + s_2c_3e^{i\delta} \\ s_1s_2 & c_1s_2c_3 + c_2s_3e^{i\delta} & c_1s_2s_3 - c_2c_3e^{i\delta} \end{pmatrix} \begin{pmatrix} d \\ s \\ b \end{pmatrix}, \quad (11.4)$$

where $c_i = \cos\theta_i$ and $s_i = \sin\theta_i$ for $i = 1, 2, 3$. In the limit $\theta_2 = \theta_3 = 0$, this reduces to the usual Cabibbo mixing with θ_1 identified (up to a sign) with the Cabibbo angle [2]. Several different forms of the Kobayashi-Maskawa parametrization are found in the literature. Since all these parametrizations are referred to as "the" Kobayashi-Maskawa form, some care about which one is being used is needed when the quadrant in which δ lies is under discussion.

A popular approximation that emphasizes the hierarchy in the size of the angles, $s_{12} \gg s_{23} \gg s_{13}$, is due to Wolfenstein [4], where one sets $\lambda \equiv s_{12}$, the sine of the Cabibbo angle, and then writes the other elements in terms of powers of λ :

$$V \approx \begin{pmatrix} 1 - \lambda^2/2 & \lambda & A\lambda^3(\rho - i\eta) \\ -\lambda & 1 - \lambda^2/2 & A\lambda^2 \\ A\lambda^3(1 - \rho - i\eta) & -A\lambda^2 & 1 \end{pmatrix}. \quad (11.5)$$

with A , ρ , and η real numbers that were intended to be of order unity.

More recently, another parametrization has been advocated [5]. It arises in many theories of quark masses and is particularly useful where one builds models in which initially $m_u = m_d = 0$ and there is no nontrivial phase in the CKM matrix. In this parametrization [5] no phases occur in the third row or third column of the CKM matrix, so that the CP -violating phase only occurs in the CKM matrix elements connecting first and second generation quarks. Consequently, the connection between measurements of CP -violating effects for B mesons and single CKM parameters is less obvious than in the standard parametrization.

No physics can depend on which of the above parametrizations (or any other) is used, as long as a single one is used consistently and care is taken to be sure that no other choice of phases is in conflict.

Our present knowledge of the matrix elements comes from the following sources:

(1)| V_{ud} |: Analyses have been performed comparing nuclear beta decays that proceed through a vector current to muon decay. Radiative corrections are essential to extracting the value of the matrix element. They already include [6] effects of order $Z\alpha^2$, and most of the theoretical argument centers on the nuclear mismatch and structure-dependent radiative corrections [7,8]. New data have been obtained on superallowed $0^+ \rightarrow 0^+$ beta decays [9].

Taking the complete data set, a value of $|V_{ud}| = 0.9740 \pm 0.0005$ has been obtained [10]. It has been argued [11] that the change in charge-symmetry-violation for quarks inside nucleons that are in nuclear matter results in an additional change in the predicted decay rate by 0.075 to 0.2%, leading to a systematic underestimate of $|V_{ud}|$. This reasoning has been used [12] to explain quantitatively the binding energy differences of the valence protons and neutrons of mirror nuclei. While it can be argued [10] that there may be double-counting of corrections, until this is settled, we take this correction as an additional uncertainty to obtain a value of $|V_{ud}| = 0.9740 \pm 0.0010$.

The theoretical uncertainties in extracting a value of $|V_{ud}|$ from neutron decays are significantly smaller than for decays of mirror nuclei, but the value depends on both the value of g_A/g_V and the neutron lifetime. Experimental progress has been made on the former quantity using very highly polarized cold neutrons together with improved detectors. Averaging over recent experiments [13] gives $g_A/g_V = -1.2715 \pm 0.0021$ and results in $|V_{ud}| = 0.9728 \pm 0.0012$ from neutron decay. Since most of the contributions to the errors in these two determinations of $|V_{ud}|$ are independent, we average them to obtain

$$|V_{ud}| = 0.9735 \pm 0.0008. \quad (11.6)$$

(2)| V_{us} |: Analysis of K_{e3} decays yields [14]

$$|V_{us}| = 0.2196 \pm 0.0023. \quad (11.7)$$

With isospin violation taken into account in K^+ and K^0 decays, the extracted values of $|V_{us}|$ are in agreement at the 1% level.

A reanalysis [8] obtains essentially the same value, but quotes a somewhat smaller error, which is only statistical. The analysis [15] of hyperon decay data has larger theoretical uncertainties because of first order SU(3) symmetry breaking effects in the axial-vector couplings. This has been redone incorporating second order SU(3) symmetry breaking corrections in models [16] applied to the WA2 data [17] to give a value of $|V_{us}| = 0.2176 \pm 0.0026$, which is consistent with Eq. (11.7) using the “best-fit” model. Since the values obtained in the models differ outside the errors and generally do not give good fits, we retain the value in Eq. (11.7) for $|V_{us}|$.

(3) $|V_{cd}|$: The magnitude of $|V_{cd}|$ may be deduced from neutrino and antineutrino production of charm off valence d quarks. The dimuon production cross sections of the CDHS group [18] yield $\overline{B}_c |V_{cd}|^2 = 0.41 \pm 0.07 \times 10^{-2}$, where \overline{B}_c is the semileptonic branching fraction of the charmed hadrons produced. The corresponding value from the more recent CCFR Tevatron experiment [19], where a next-to-leading-order QCD analysis has been carried out, is $0.534 \pm 0.021_{-0.051}^{+0.025} \times 10^{-2}$, where the last error is from the scale uncertainty. Assuming a similar scale error for the CDHS result and averaging these two results gives $0.49 \pm 0.05 \times 10^{-2}$. Supplementing this with data [20] on the mix of charmed particle species produced by neutrinos and PDG values for their semileptonic branching fractions (to give [19] $\overline{B}_c = 0.099 \pm 0.012$) then yields

$$|V_{cd}| = 0.224 \pm 0.016 . \quad (11.8)$$

(4) $|V_{cs}|$: Values of $|V_{cs}|$ from neutrino production of charm are dependent on assumptions about the strange-quark density in the parton sea. The most conservative assumption, that the strange-quark sea does not exceed the value corresponding to an SU(3)-symmetric sea, leads to a lower bound [18], $|V_{cs}| > 0.59$. It is more advantageous to proceed analogously to the method used for extracting $|V_{us}|$ from K_{e3} decay; namely, we compare the experimental value for the width of D_{e3} decay with the expression [21] that follows from the standard weak interaction amplitude:

$$\Gamma(D \rightarrow \overline{K} e^+ \nu_e) = |f_+^D(0)|^2 |V_{cs}|^2 (1.54 \times 10^{11} \text{ s}^{-1}) . \quad (11.9)$$

Here $f_+^D(q^2)$, with $q = p_D - p_K$, is the form factor relevant to D_{e3} decay; its variation has been taken into account with the parametrization $f_+^D(t)/f_+^D(0) = M^2/(M^2 - t)$ and $M = 2.1 \text{ GeV}/c^2$, a form and mass consistent with direct measurements [22]. Combining data on branching fractions for D_{e3} decays with accurate values for the D lifetimes [22] yields a value of $(0.818 \pm 0.041) \times 10^{11} \text{ s}^{-1}$ for $\Gamma(D \rightarrow \overline{K} e^+ \nu_e)$. Therefore

$$|f_+^D(0)|^2 |V_{cs}|^2 = 0.531 \pm 0.027 . \quad (11.10)$$

A very conservative assumption is that $|f_+^D(0)| < 1$, from which it follows that $|V_{cs}| > 0.62$. Calculations of the form factor either performed [23,24] directly at $q^2 = 0$, or done [25] at the maximum value of $q^2 = (m_D - m_K)^2$ and interpreted at $q^2 = 0$ using the measured q^2 dependence, give the value $f_+^D(0) = 0.7 \pm 0.1$. It follows that

$$|V_{cs}| = 1.04 \pm 0.16 . \quad (11.11)$$

Recent measurements [26] of $|V_{cs}|$ in charmed-tagged W decays give a consistent result of $|V_{cs}| = 0.97 \pm 0.09$ (stat.) ± 0.07 (syst.). The constraint of unitarity when there are only three generations gives a much tighter bound (see below).

(5) $|V_{cb}|$: The heavy quark effective theory [27] (HQET) provides a nearly model-independent treatment of B semileptonic decays to charmed mesons, assuming that both the b and c quarks are heavy enough for the theory to apply. Measurements of the exclusive decay $B \rightarrow \overline{D}^* \ell^+ \nu_\ell$ have been used primarily to extract a value of $|V_{cb}|$ using corrections based on the HQET. Exclusive $B \rightarrow \overline{D} \ell^+ \nu_\ell$ decays give a consistent but less precise result. Analysis of inclusive decays, where the measured semileptonic bottom hadron partial width is assumed to be that of a b quark decaying through the usual $V-A$ interaction, depends on going from the quark to the hadron level. This is also understood within the context of the HQET [28], and the results for $|V_{cb}|$ are again consistent with those from exclusive decays. Combining all the LEP data on both exclusive and inclusive decays gives [29]

$$|V_{cb}| = 0.0402 \pm 0.0019 , \quad (11.12)$$

which is consistent with the latest CLEO result [29] from exclusive and inclusive decays, $|V_{cb}| = 0.0404 \pm 0.0034$. The combination of large data samples and the HQET make this the third most accurately measured CKM matrix element, after $|V_{ud}|$ and $|V_{us}|$.

(6) $|V_{ub}|$: The decay $b \rightarrow u \ell \overline{\nu}$ and its charge conjugate can be observed from the semileptonic decay of B mesons produced on the $\Upsilon(4S)$ ($b\overline{b}$) resonance by measuring the lepton energy spectrum above the endpoint of the $b \rightarrow c \ell \overline{\nu}_\ell$ spectrum. There the $b \rightarrow u \ell \overline{\nu}_\ell$ decay rate can be obtained by subtracting the background from nonresonant e^+e^- reactions. This continuum background is determined from auxiliary measurements off the $\Upsilon(4S)$. The interpretation of the result in terms of $|V_{ub}|/|V_{cb}|$ depends fairly strongly on the theoretical model used to generate the lepton energy spectrum, especially for $b \rightarrow u$ transitions [24,25,30].

The LEP experiments ALEPH [31], L3 [32], and DELPHI [33] have presented new analyses that measure the $b \rightarrow u \ell \nu_\ell$ component in b decays at the Z^0 . Discrimination between u -like and c -like decays is based on up to 20 different event parameters which are sensitive to the mass of the quark of the final state. Using an extended range of the spectrum compared to the end-point analysis, this extraction of $|V_{ub}|$ is less sensitive to theoretical assumptions, but requires a detailed understanding of the decay $b \rightarrow c \ell \nu_\ell$.

The value of $|V_{ub}|$ can also be extracted from exclusive decays, such as $B \rightarrow \pi \ell \nu_\ell$ and $B \rightarrow \rho \ell \nu_\ell$, but there is an associated theoretical model dependence in the values of the matrix elements of the weak current between exclusive states. There has been a substantial increase in the data from CLEO for these exclusive decays [29], and the error on $|V_{ub}|$, arising primarily from the theoretical model dependence, is comparable to that obtained from inclusive decays. Enhanced awareness of the theoretical uncertainties and the difference between the results obtained from inclusive and exclusive analyses leads us to be even more conservative in setting the error bar than in previous reviews and we quote [34]

$$|V_{ub}|/|V_{cb}| = 0.090 \pm 0.025 . \quad (11.13)$$

(7) V_{tb} : The discovery of the top quark by the CDF and DØ collaborations utilized in part the semileptonic decays of t to b . One can set a (still rather crude) limit on the fraction of decays of the form $t \rightarrow b \ell^+ \nu_\ell$, as opposed to semileptonic t decays that involve s or d quarks, of [35]

$$\frac{|V_{tb}|^2}{|V_{td}|^2 + |V_{ts}|^2 + |V_{tb}|^2} = 0.99 \pm 0.29 . \quad (11.14)$$

(8)**Hadronic W decays**: The ratio of hadronic W decays to leptonic decays has been measured at LEP, with the result [36] that $\sum_{i,j} |V_{ij}|^2 = 2.032 \pm 0.032$, where the sum extends over $i = u, c$ and $j = d, s, b$. With a three-generation CKM matrix, from unitarity this sum would be expected to have the value 2. Since five of the CKM matrix elements are well measured or contribute negligibly to the sum of the squares, this measurement can also be used as a precision measurement of $|V_{cs}| = 0.9891 \pm 0.016$.

For most of these CKM matrix elements the principal error is no longer experimental, but rather theoretical. This arises from explicit model dependence in interpreting data or in the use of specific hadronic matrix elements to relate experimental measurements to weak transitions of quarks. This type of uncertainty arises even more strongly in extracting CKM matrix elements from loop diagrams, as discussed below. Such errors are not distributed in a Gaussian manner. We have taken the interpretation that a “ 1σ ” range in a theoretical error corresponds to a 68% likelihood that the true value lies within “ $\pm 1 \sigma$ ” of the central value. While we do use the central values with the quoted errors to make a best overall fit to the CKM matrix, the result should be taken with appropriate care, and we regard extending this to multi-standard-deviation determinations of allowed regions for CKM matrix elements as unfounded.

The results for three generations of quarks, from Eqs. (11.6)–(11.8) and Eqs. (11.11)–(11.14), plus unitarity, are summarized in the matrix in Eq. (11.2). The ranges given there are different from those given

in Eqs. (11.6)–(11.14) because of the inclusion of unitarity, but are consistent with the one-standard-deviation errors on the input matrix elements. Note in particular that the unitarity constraint has pushed $|V_{ud}|$ about one standard deviation higher than given in Eq. (11.6). If we had kept the error on $|V_{ud}|$ quoted by Hardy and Towner [10], we would have a violation of unitarity in the first row of the CKM matrix by about two standard deviations. While this bears watching and encourages another more accurate measurement of $|V_{us}|$, we do not see this presently as a major challenge to the validity of the three-generation Standard Model.

The data do not preclude there being more than three generations. Moreover, the entries deduced from unitarity might be altered when the CKM matrix is expanded to accommodate more generations. Conversely, the known entries restrict the possible values of additional elements if the matrix is expanded to account for additional generations. For example, unitarity and the known elements of the first row require that any additional element in the first row have a magnitude $|V_{ub'}| < 0.10$. When there are more than three generations, the allowed ranges (at 90% CL) of the matrix elements connecting the first three generations are

$$\begin{pmatrix} 0.9722 \text{ to } 0.9748 & 0.216 \text{ to } 0.223 & 0.002 & \text{to } 0.005 & \dots \\ 0.209 & \text{to } 0.228 & 0.959 \text{ to } 0.976 & 0.037 & \text{to } 0.043 & \dots \\ 0 & \text{to } 0.09 & 0 & \text{to } 0.16 & 0.07 & \text{to } 0.993 & \dots \\ \vdots & & \vdots & & \vdots & & \vdots \end{pmatrix}, \quad (11.15)$$

where we have used unitarity (or the expanded matrix) and the measurements of the magnitudes of the CKM matrix elements (including the constraint from hadronic W decays), resulting in the weak bound $|V_{tb}| > 0.07$.

Further information, particularly on CKM matrix elements involving the top quark, can be obtained from flavor-changing processes that occur at the one-loop level. We have not used this information in the discussion above since the derivation of values for V_{td} and V_{ts} in this manner from, for example, B mixing or $b \rightarrow s\gamma$, require an additional assumption that the top-quark loop, rather than new physics, gives the dominant contribution to the process in question. Conversely, the agreement of CKM matrix elements extracted from loop diagrams with the values based on direct measurements and three generations can be used to place restrictions on new physics.

The measured value [37] of $\Delta M_{B_d} = 0.473 \pm 0.016 \text{ ps}^{-1}$ from $B_d^0 - \bar{B}_d^0$ mixing can be turned in this way into information on $|V_{tb}^* V_{td}|$, assuming that the dominant contribution to the mass difference arises from the matrix element between a B_d and a \bar{B}_d of an operator that corresponds to a box diagram with W bosons and top quarks as sides. Using the characteristic hadronic matrix element that then occurs, $\widehat{B}_{B_d} f_{B_d}^2 = (210 \pm 40 \text{ MeV})^2$ from lattice QCD calculations [38], which we regard as having become the most reliable source of such matrix elements, next-to-leading-order QCD corrections ($\eta_{\text{QCD}} = 0.55$) [39], and the running top-quark mass, $\overline{m}_t(m_t) = 166 \pm 5 \text{ GeV}$, as input,

$$|V_{tb}^* \cdot V_{td}| = 0.0083 \pm 0.0016, \quad (11.16)$$

where the uncertainty comes primarily from that in the hadronic matrix elements, whose estimated errors are combined linearly.

In the ratio of B_s to B_d mass differences, many common factors (such as the QCD correction and dependence on the top-quark mass) cancel, and we have

$$\frac{\Delta M_{B_s}}{\Delta M_{B_d}} = \frac{M_{B_s}}{M_{B_d}} \frac{\widehat{B}_{B_s} f_{B_s}^2}{\widehat{B}_{B_d} f_{B_d}^2} \frac{|V_{tb}^* \cdot V_{ts}|^2}{|V_{tb}^* \cdot V_{td}|^2}. \quad (11.17)$$

With the experimentally measured masses [22], $\widehat{B}_{B_s}/\widehat{B}_{B_d} = (1.14 \pm 0.13)^2$ with quite conservative error bars from lattice QCD [38], and the improved experimental lower limit [37] at 95% CL of $\Delta M_{B_s} > 14.3 \text{ ps}^{-1}$,

$$|V_{td}|/|V_{ts}| < 0.24 \quad (11.18)$$

Since with three generations, $|V_{ts}| \approx |V_{cb}|$, this result converts to $|V_{td}| < 0.010$, which is a significant constraint by itself (see Fig. 11.2).

The CLEO observation [40] of $b \rightarrow s\gamma$ can be translated [41] similarly into $|V_{ts}|/|V_{cb}| = 1.1 \pm 0.43$, where the large uncertainty is again dominantly theoretical. In $K^+ \rightarrow \pi^+ \nu \bar{\nu}$ there are significant contributions from loop diagrams involving both charm and top quarks. Experiment is just beginning to probe the level predicted in the Standard Model [42].

All these additional indirect constraints are consistent with the matrix elements obtained from the direct measurements plus unitarity, assuming three generations; with the recent results on B mixing and theoretical improvements in lattice calculations, adding the indirect constraints to the fit reduces the range allowed for $|V_{td}|$.

Direct and indirect information on the CKM matrix is neatly summarized in terms of “the unitarity triangle,” one of six such triangles that correspond to the unitarity condition applied to two different rows or columns of the CKM matrix. Unitarity of the 3×3 CKM matrix applied to the first and third columns yields

$$V_{ud} V_{ub}^* + V_{cd} V_{cb}^* + V_{td} V_{tb}^* = 0. \quad (11.19)$$

The unitarity triangle is just a geometrical presentation of this equation in the complex plane [43]. We can always choose to orient the triangle so that $V_{cd} V_{cb}^*$ lies along the horizontal; in the parametrization we have chosen, V_{cb} is real, and V_{cd} is real to a very good approximation in any case. Setting cosines of small angles to unity, Eq. (11.19) becomes

$$V_{ub}^* + V_{td} = s_{12} V_{cb}^*, \quad (11.20)$$

which is shown as the unitarity triangle in Fig. 11.1(a). Rescaling the triangle by a factor $[1/s_{12} |V_{cb}|]$ so that the base is of unit length, the coordinates of the vertices become

$$A(\text{Re}(V_{ub})/|s_{12} V_{cb}|, -\text{Im}(V_{ub})/|s_{12} V_{cb}|), B(1,0), C(0,0). \quad (11.21)$$

In the Wolfenstein parametrization [4], the coordinates of the vertex A of the unitarity triangle are simply (ρ, η) , as shown in Fig. 11.1(b). The angle $\gamma = \delta_{13}$.

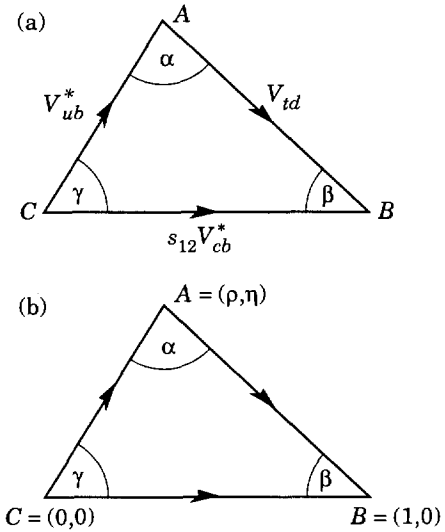


Figure 11.1: (a) Representation in the complex plane of the triangle formed by the CKM matrix elements V_{ub}^* , V_{td} , and $s_{12} V_{cb}^*$. (b) Rescaled triangle with vertices $A(\rho, \eta)$, $B(1,0)$, and $C(0,0)$.

CP -violating processes will involve the phase in the CKM matrix, assuming that the observed CP violation is solely related to a nonzero value of this phase. This allows additional constraints to be

brought to bear. More specifically, a necessary and sufficient condition for CP violation with three generations can be formulated in a parametrization-independent manner in terms of the nonvanishing of the determinant of the commutator of the mass matrices for the charge $2e/3$ and charge $-e/3$ quarks [44]. CP -violating amplitudes or differences of rates are all proportional to the CKM factor in this quantity. This is the product of factors $s_{12}s_{13}s_{23}c_{12}c_{13}^2c_{23}s_{\delta_{13}}$ in the parametrization adopted above, and is $s_1^2s_2s_3c_1c_2c_3s_\delta$ in that of Ref. 1. With the approximation of setting cosines to unity, this is just twice the area of the unitarity triangle.

While hadronic matrix elements whose values are imprecisely known generally enter the calculations, the constraints from CP violation in the neutral kaon system, taken together with the restrictions on the magnitudes of the CKM matrix elements shown above, are tight enough to restrict considerably the range of angles and the phase of the CKM matrix. For example, the constraint obtained from the CP -violating parameter ϵ in the neutral K system corresponds to the vertex A of the unitarity triangle lying on a hyperbola for fixed values of the hadronic matrix elements [45,46]. In addition, following the initial evidence [47], it is now established that direct CP violation in the weak transition from a neutral K to two pions exists, *i.e.*, that the parameter ϵ' is nonzero [48]. However, theoretical uncertainties in hadronic matrix elements of cancelling amplitudes presently preclude this measurement from giving a significant constraint on the unitarity triangle.

The constraints on the vertex of the unitarity triangle that follow from $|V_{ub}|$, B mixing, and ϵ are shown in Fig. 11.2. The improved limit in Eq. (11.18) that arises from the ratio of B_s to B_d mixing eliminates a significant region for the vertex A of the unitarity triangle, a region otherwise allowed by direct measurements of the CKM matrix elements, essentially limiting the vertex A to be in the first quadrant (ρ positive). The limit is not far from the value we would expect from the other information on the unitarity triangle. Thus a significant increase in experimental sensitivity to B_s mixing will lead either to an observation of mixing or an indication of physics beyond the Standard Model. This limit is more robust theoretically since it depends on ratios (rather than absolute values) of hadronic matrix elements and is independent of the top mass or QCD corrections (which cancel in the ratio).

Ultimately in the Standard Model, the CP -violating process $K_L \rightarrow \pi^0\nu\bar{\nu}$ offers high precision in measuring the imaginary part of $V_{td} \cdot V_{ts}^*$, which, given V_{ts} , will yield the altitude of the unitarity triangle. However, the experimental upper limit is presently many orders of magnitude away from the requisite sensitivity.

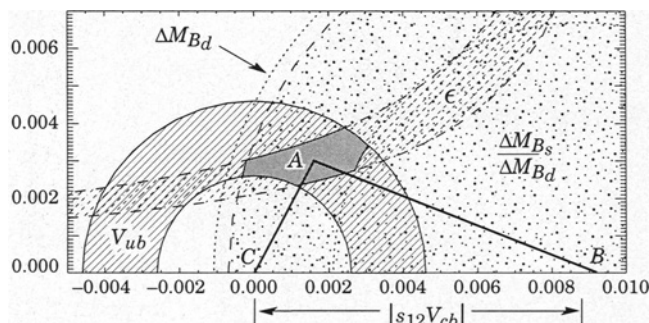


Figure 11.2: Constraints on the position of the vertex, A , of the unitarity triangle following from $|V_{ub}|$, B mixing, and ϵ . A possible unitarity triangle is shown with A in the preferred region.

For CP -violating asymmetries of neutral B mesons decaying to CP eigenstates, for certain final states arising from a single weak decay amplitude there is a direct relationship between the magnitude of the asymmetry in a given decay and $\sin 2\phi$, where $\phi = \alpha, \beta, \gamma$ is an appropriate angle of the unitarity triangle [43]. The CDF

Collaboration has used the decay $B_d(\bar{B}_d) \rightarrow \psi K_S$ to obtain a first indication [49] of a nonvanishing asymmetry, corresponding to a value of $\sin 2\beta$:

$$\sin 2\beta = 0.79_{-0.44}^{+0.41}. \quad (11.22)$$

This is consistent with the other information in Fig. 11.2 including having the correct sign, which is positive at the 93% CL. It presages the data that will be obtained in the next several years on both the magnitudes and relative phases of the CKM matrix elements, permitting incisive tests of this part of the Standard Model. (See Sec. 12 on CP Violation and the review on “ CP Violation in B decay—Standard Model Predictions” in the B Listings.)

References:

1. M. Kobayashi and T. Maskawa, Prog. Theor. Phys. **49**, 652 (1973).
2. N. Cabibbo, Phys. Rev. Lett. **10**, 531 (1963).
3. L.-L. Chau and W.-Y. Keung, Phys. Rev. Lett. **53**, 1802 (1984); H. Harari and M. Leurer, Phys. Lett. **B181**, 123 (1986); H. Fritzsch and J. Plankl, Phys. Rev. **D35**, 1732 (1987); F.J. Botella and L.-L. Chao, Phys. Lett. **B168**, 97 (1986).
4. L. Wolfenstein, Phys. Rev. Lett. **51**, 1945 (1983).
5. C.D. Froggatt and H.B. Nielsen, Nucl. Phys. **B147**, 277 (1979); H. Fritzsch, Nucl. Phys. **B155**, 189 (1979); S. Dimopoulos, L.J. Hall, and S. Rabi, Phys. Rev. Lett. **68**, 1984 (1992); H. Fritzsch and Z.-Z. Xing, Phys. Lett. **B413**, 396 (1997).
6. W.J. Marciano and A. Sirlin, Phys. Rev. Lett. **56**, 22 (1986); A. Sirlin and R. Zucchini, Phys. Rev. Lett. **57**, 1994 (1986); W. Jaus and G. Rasche, Phys. Rev. **D35**, 3420 (1987); A. Sirlin, Phys. Rev. **D35**, 3423 (1987).
7. B.A. Brown and W.E. Ormand, Phys. Rev. Lett. **62**, 866 (1989).
8. F.C. Barker *et al.*, Nucl. Phys. **A540**, 501 (1992); F.C. Barker *et al.*, Nucl. Phys. **A579**, 62 (1994).
9. G. Savard *et al.*, Phys. Rev. Lett. **74**, 1521 (1995).
10. J.C. Hardy and I.S. Towner, talk at WEIN98 (Santa Fe, June 14–21, 1998) and nucl-th/9809087.
11. K.P. Saito and A.W. Thomas, Phys. Lett. **B363**, 157 (1995).
12. K. Tsushima, K. Saito, and A.W. Thomas, nucl-th/9907101.
13. H. Abele *et al.*, Phys. Lett. **B407**, 212 (1997); J. Reich *et al.*, ILL Workshop, October 1998; E. Bopp *et al.*, Phys. Rev. Lett. **56**, 919 (1986); P. Liaud, Nucl. Phys. **A612**, 53 (1997).
14. H. Leutwyler and M. Roos, Z. Phys. **C25**, 91 (1984). See also the work of R.E. Shrock and L.-L. Wang, Phys. Rev. Lett. **41**, 1692 (1978).
15. J.F. Donoghue, B.R. Holstein, and S.W. Klimt, Phys. Rev. **D35**, 934 (1987).
16. R. Flores-Mendieta, A. García, and G. Sánchez-Colón, Phys. Rev. **D54**, 6855 (1996).
17. M. Bourquin *et al.*, Z. Phys. **C21**, 27 (1983).
18. H. Abramowicz *et al.*, Z. Phys. **C15**, 19 (1982).
19. S.A. Rabinowitz *et al.*, Phys. Rev. Lett. **70**, 134 (1993); A.O. Bazarko *et al.*, Z. Phys. **C65**, 189 (1995).
20. N. Ushida *et al.*, Phys. Lett. **B206**, 375 (1988).
21. F. Bletzacker, H.T. Nieh, and A. Soni, Phys. Rev. **D16**, 731 (1977).
22. C. Caso *et al.*, Review of Particle Physics, Eur. Phys. J. **C3**, 1 (1998).
23. T.M. Aliev *et al.*, Yad. Fiz. **40**, 823 (1984) [Sov. J. Nucl. Phys. **40**, 527 (1984)].
24. M. Bauer, B. Stech, and M. Wirbel, Z. Phys. **C29**, 637 (1985).

25. B. Grinstein, N. Isgur, and M.B. Wise, Phys. Rev. Lett. **56**, 298 (1986);
B. Grinstein *et al.*, Phys. Rev. **D39**, 799 (1989).
26. P. Abreu *et al.*, Phys. Lett. **B439**, 209 (1998);
R. Barate *et al.*, Phys. Lett. **B465**, 349 (1999).
27. N. Isgur and M.B. Wise, Phys. Lett. **B232**, 113 (1989) and Phys. Lett. **B237**, 527 (1990);
E.E. Eichten and B. Hill, Phys. Lett. **B234**, 511 (1990);
M.E. Luke, Phys. Lett. **B252**, 447 (1990).
28. M. Neubert, to appear in *Heavy Flavors*, Second Edition, edited by A.J. Buras and M. Lindner (World Scientific, Singapore, 1997), p. 239.
29. R. Poling, plenary talk at the *XIX International Symposium on Lepton and Photon Interactions at High Energies* (Stanford, August 9–14, 1999).
30. G. Altarelli *et al.*, Nucl. Phys. **B208**, 365 (1982).
31. R. Barate *et al.*, Eur. Phys. J. **C6**, 555 (1999).
32. M. Acciarri *et al.*, Phys. Lett. **B436**, 174 (1998).
33. P. Abreu *et al.*, Phys. Lett. **B478**, 14 (2000).
34. A. Falk, plenary talk at the *XIX International Symposium on Lepton and Photon Interactions at High Energies* (Stanford, August 9–14, 1999);
Z. Ligeti, invited talk at KAON'99 (Chicago, June 21–26, 1999), Fermilab preprint FERMILAB-Conf-99/213-T, and hep-ph/9908432.
35. A.P. Heinson, invited talk at the *Second International Conference on B Physics and CP Violation* (Honolulu, March 24–27, 1997) and hep-ex/9707026.
36. C. Sbarra, talk at the *Rencontres de Moriond*, Les Arcs, Savoie, France (March 11–18, 2000).
37. G. Blaylock, plenary talk at the *XIX International Conference on Lepton and Photon Interactions at High Energies* (Stanford, August 9–14, 1999).
38. S. Sharpe, plenary talk at the *International Conference on High Energy Physics* (Vancouver, July 23–29, 1998) and hep-lat/9811006.
39. A.J. Buras *et al.*, Nucl. Phys. **B347**, 491 (1990).
40. M.S. Alam *et al.*, Phys. Rev. Lett. **74**, 2885 (1995).
41. P.A. Griffin, M. Maslip, and M. McGuigan, Phys. Rev. **D50**, 5751 (1994).
42. S. Adler *et al.*, Phys. Rev. Lett. **79**, 2204 (1997);
G. Redlinger, talk at KAON99 (Chicago, June 21–26, 1999).
43. L.-L. Chau and W.Y. Keung, Ref. 3;
J.D. Bjorken, private communication and Phys. Rev. **D39**, 1396 (1989);
C. Jarlskog and R. Stora, Phys. Lett. **B208**, 268 (1988);
J.L. Rosner, A.I. Sanda, and M.P. Schmidt, in *Proceedings of the Workshop on High Sensitivity Beauty Physics at Fermilab*, Fermilab, November 11–14, 1987, edited by A.J. Slaughter, N. Lockyer, and M. Schmidt (Fermilab, Batavia, 1988), p. 165;
C. Hamzaoui, J.L. Rosner, and A.I. Sanda, *ibid.*, p. 215.
44. C. Jarlskog, Phys. Rev. Lett. **55**, 1039 (1985) and Z. Phys. **C29**, 491 (1985).
45. The relevant QCD corrections in leading order in F.J. Gilman and M.B. Wise, Phys. Lett. **B93**, 129 (1980) and Phys. Rev. **D27**, 1128 (1983), have been extended to next-to-leading-order by A. Buras, M. Jamin, and P.H. Weisz, Nucl. Phys. **B347**, 491 (1990);
S. Herrlich and H. Nierste, Nucl. Phys. **B419**, 292 (1992) and Nucl. Phys. **B476**, 27 (1996).
46. The limiting curves in Fig. 11.2 arising from the value of $|\epsilon|$ correspond to values of the hadronic matrix element, expressed in terms of the renormalization group invariant parameter \widehat{B}_K , from 0.75 to 1.10, following the lattice QCD calculations reported in Sharpe, Ref. 38.
47. H. Burkhardt *et al.*, Phys. Lett. **B206**, 169 (1988).
48. G.D. Barr *et al.*, Phys. Lett. **B317**, 233 (1993);
L.K. Gibbons *et al.*, Phys. Rev. Lett. **70**, 1203 (1993);
A. Alavi-Harati *et al.*, Phys. Rev. Lett. **83**, 22 (1999);
M. Sozzi, talk at KAON99 (Chicago, June 23–26, 1999);
G. Barr, plenary talk at the *XIX International Symposium on Lepton and Photon Interactions at High Energies* (Stanford, August 9–14, 1999).
49. M. Paulini, plenary talk at the *XIX International Conference on Lepton and Photon Interactions at High Energies* (Stanford, August 9–14, 1999);
CDF Collab: T. Affolder *et al.*, hep-ex/9909003.

12. CP VIOLATION

Revised April 2000 by L. Wolfenstein (Carnegie-Mellon Univ.).

The symmetries C (particle-antiparticle interchange) and P (space inversion) hold for strong and electromagnetic interactions. After the discovery of large C and P violation in the weak interactions, it appeared that the product CP was a good symmetry. In 1964 CP violation was observed in K^0 decays at a level given by the parameter $\epsilon \approx 2.3 \times 10^{-3}$. Larger CP -violation effects are anticipated in B^0 decays.

12.1. CP violation in Kaon decay

CP violation has been observed in the semi-leptonic decays $K_L^0 \rightarrow \pi^\mp \ell^\pm \nu$ and in the nonleptonic decay $K_L^0 \rightarrow 2\pi$. The experimental numbers that have been measured are

$$\delta = \frac{\Gamma(K_L^0 \rightarrow \pi^- \ell^+ \nu) - \Gamma(K_L^0 \rightarrow \pi^+ \ell^- \nu)}{\Gamma(K_L^0 \rightarrow \pi^- \ell^+ \nu) + \Gamma(K_L^0 \rightarrow \pi^+ \ell^- \nu)} \quad (12.1a)$$

$$\begin{aligned} \eta_{+-} &= A(K_L^0 \rightarrow \pi^+ \pi^-) / A(K_S^0 \rightarrow \pi^+ \pi^-) \\ &= |\eta_{+-}| e^{i\phi_{+-}} \end{aligned} \quad (12.1b)$$

$$\begin{aligned} \eta_{00} &= A(K_L^0 \rightarrow \pi^0 \pi^0) / A(K_S^0 \rightarrow \pi^0 \pi^0) \\ &= |\eta_{00}| e^{i\phi_{00}} \end{aligned} \quad (12.1c)$$

CP violation can occur either in the $K^0 - \bar{K}^0$ mixing or in the decay amplitudes. Assuming CPT invariance, the mass eigenstates of the $K^0 - \bar{K}^0$ system can be written

$$|K_S\rangle = p|K^0\rangle + q|\bar{K}^0\rangle, \quad |K_L\rangle = p|K^0\rangle - q|\bar{K}^0\rangle. \quad (12.2)$$

If CP invariance held, we would have $q = p$ so that K_S would be CP even and K_L CP odd. (We define $|\bar{K}^0\rangle$ as CP $|K^0\rangle$). CP violation in $K^0 - \bar{K}^0$ mixing is then given by the parameter $\bar{\epsilon}$ where

$$\frac{p}{q} = \frac{(1 + \bar{\epsilon})}{(1 - \bar{\epsilon})}. \quad (12.3)$$

CP violation can also occur in the decay amplitudes

$$A(K^0 \rightarrow \pi\pi(I)) = A_I e^{i\delta_I}, \quad A(\bar{K}^0 \rightarrow \pi\pi(I)) = A_I^* e^{i\delta_I}, \quad (12.4)$$

where I is the isospin of $\pi\pi$, δ_I is the final-state phase shift, and A_I would be real if CP invariance held. The CP -violating observables are usually expressed in terms of ϵ and ϵ' defined by

$$\eta_{+-} = \epsilon + \epsilon', \quad \eta_{00} = \epsilon - 2\epsilon', \quad (12.5a)$$

One can then show [1]

$$\epsilon = \bar{\epsilon} + i (\text{Im } A_0 / \text{Re } A_0), \quad (12.5b)$$

$$\sqrt{2}\epsilon' = i\bar{\epsilon} e^{i(\delta_2 - \delta_0)} (\text{Re } A_2 / \text{Re } A_0) (\text{Im } A_2 / \text{Re } A_2 - \text{Im } A_0 / \text{Re } A_0), \quad (12.5c)$$

$$\delta = 2\text{Re } \epsilon / (1 + |\epsilon|^2) \approx 2\text{Re } \epsilon. \quad (12.5d)$$

In Eq. (12.5c) small corrections of order $\epsilon' \times \text{Re } (A_2/A_0)$ are neglected and Eq. (12.5d) assumes the $\Delta S = \Delta Q$ rule.

The quantities $\text{Im } A_0$, $\text{Im } A_2$, and $\text{Im } \epsilon$ depend on the choice of phase convention since one can change the phases of K^0 and \bar{K}^0 by a transformation of the strange quark state $|s\rangle \rightarrow |s\rangle e^{i\alpha}$; of course, observables are unchanged. It is possible by a choice of phase convention to set $\text{Im } A_0$ or $\text{Im } A_2$ or $\text{Im } \bar{\epsilon}$ to zero, but none of these is zero with the usual phase conventions in the Standard Model. The choice $\text{Im } A_0 = 0$ is called the Wu-Yang phase convention [2] in which case $\epsilon = \bar{\epsilon}$. The value of ϵ' is independent of phase convention and a nonzero value demonstrates CP violation in the decay amplitudes, referred to as direct CP violation. The possibility that direct CP violation is essentially zero and that CP violation occurs only in the mixing matrix was referred to as the superweak theory [3].

By applying CPT invariance and unitarity the phase of ϵ is given approximately by

$$\phi(\epsilon) \approx \tan^{-1} \frac{2(m_{K_L} - m_{K_S})}{\Gamma_{K_S} - \Gamma_{K_L}} = 43.49 \pm 0.08^\circ \quad (12.6a)$$

while Eq. (12.5c) gives

$$\phi(\epsilon') = \delta_2 - \delta_0 + \frac{\pi}{2} \approx 48 \pm 4^\circ, \quad (12.6b)$$

where the numerical value is based on an analysis of $\pi\pi$ scattering [4]. The approximation in Eq. (12.6a) depends on the assumption that direct CP violation is very small in all K^0 decays. This is expected to be good to a few tenths of a degree as indicated by the small value of ϵ' and of η_{+-} , the CP violation parameter in the decay $K_S \rightarrow \pi^+ \pi^- \pi^0$ [5], although limits on η_{00} are still poor. The relation in Eq. (12.6a) is exact in the superweak theory so this is sometimes called the superweak phase. An important point for the analysis is that $\cos[\phi(\epsilon') - \phi(\epsilon)] \simeq 1$. The consequence is that only two real quantities need be measured, the magnitude of ϵ and the value of (ϵ'/ϵ) including its sign. The measured quantity $|\eta_{00}/\eta_{+-}|^2$, which is very close to unity, is given to a good approximation by

$$|\eta_{00}/\eta_{+-}|^2 \approx 1 - 6\text{Re } (\epsilon'/\epsilon) \approx 1 - 6\epsilon'/\epsilon. \quad (12.7)$$

From the experimental measurements, one finds

$$\epsilon = (2.271 \pm 0.017) \times 10^{-3}, \quad (12.8a)$$

$$\text{Re}(\epsilon'/\epsilon) \approx \epsilon'/\epsilon = (2.1 \pm 0.5) \times 10^{-3}, \quad (12.8b)$$

$$\phi_{+-} = 43.5 \pm 0.5^\circ, \quad (12.8c)$$

$$\phi_{00} - \phi_{+-} = -0.1 \pm 0.8, \quad (12.8d)$$

$$\delta = (3.33 \pm 0.14) \times 10^{-3}. \quad (12.8e)$$

Direct CP violation, as indicated by ϵ'/ϵ , is expected in the Standard Model; most calculations [6] give a somewhat smaller value, but they have a large uncertainty. The value of δ agrees with Eq. (12.5d). The values of ϕ_{+-} and $\phi_{00} - \phi_{+-}$ are used to set limits on CPT violation. [See Tests of Conservation Laws.]

In the Standard Model, CP violation arises as a result of a single phase entering the CKM matrix (Sec. 11). As a result in what is now the standard phase convention, two elements have large phases, $V_{ub} \sim e^{-i\gamma}$, $V_{td} \sim e^{-i\beta}$. Because these elements have small magnitudes and involve the third generation, CP violation in the K^0 system is small. On the other hand, large effects are expected in the B^0 system, which is a major motivation for B factories.

12.2. CP violation in B decay

CP violation in the B^0 system can be observed by comparing B^0 and \bar{B}^0 decays [7]. For a final CP eigenstate a , the decay rate has a time dependence given by

$$\begin{aligned} \Gamma_a \sim e^{-\Gamma t} & \left([1 + |\lambda_a|^2] \pm [1 - |\lambda_a|^2] \cos(\Delta M t) \right. \\ & \left. \mp \text{Im } \lambda_a \sin(\Delta M t) \right) \end{aligned} \quad (12.9)$$

where the top sign is for B^0 and the bottom for \bar{B}^0 and

$$\lambda_a = (q_B/p_B) \bar{A}_a/A_a. \quad (12.10)$$

The quantities p_B and q_B come from the analogue for B^0 of Eq. (12.2), and $A_a(\bar{A}_a)$ is the decay amplitude to state a for $B^0(\bar{B}^0)$. However, for B^0 the eigenstates are expected to have a negligible lifetime difference and are only distinguished by the mass difference ΔM ; also as a consequence $|q_B/p_B| \approx 1$ so that $\bar{\epsilon}_B$ is purely imaginary.

If only one quark weak transition contributes to the decay, $|\bar{A}_a/A_a| = 1$ so that $|\lambda_a| = 1$ and the $\cos(\Delta Mt)$ term vanishes. In this case, the difference between B^0 and \bar{B}^0 decays is given by the $\sin(\Delta Mt)$ term with the asymmetry coefficient

$$a_a = \frac{\Gamma_a(t) - \bar{\Gamma}_a(t)}{(\Gamma_a(t) + \bar{\Gamma}_a(t)) \sin(\Delta Mt)} = \eta_a \sin\left(2(\phi_M + \phi_D)\right), \quad (12.11)$$

where $2\phi_M$ is the phase of the B^0 - \bar{B}^0 mixing, ϕ_D is the weak phase of the decay transition, and η_a is the CP eigenvalue of a .

For $B^0(\bar{B}^0) \rightarrow \psi K_S$ from the transition $b \rightarrow c\bar{c}s$, one finds in the Standard Model that the asymmetry is given directly in terms of a CKM phase with no hadronic uncertainty:

$$a_{\psi K_S} = -\sin 2\beta. \quad (12.12)$$

From the constraints on the CKM matrix (Sec. 11) $\sin 2\beta$ is predicted to be between 0.3 and 0.9. A significantly different value could be a sign of new physics.

A second decay of interest is $B^0(\bar{B}^0) \rightarrow \pi^+\pi^-$ from the transition $b \rightarrow u\bar{u}d$ with

$$a_{\pi\pi} = \sin 2(\beta + \gamma). \quad (12.13)$$

While either of these asymmetries could be ascribed to B^0 - \bar{B}^0 mixing (q_B/p_B or $\bar{\epsilon}_B$), the difference between the two asymmetries is evidence for direct CP violation. From Eq. (12.10) it is seen that this corresponds to a phase difference between $A_{\psi K_S}$ and $A_{\pi^+\pi^-}$. Thus this is analogous to ϵ' . In the standard phase convention, 2β in Eqs. (12.12) and (12.13) arises from B^0 - \bar{B}^0 mixing whereas the γ in Eq. (12.13) comes from V_{ub} in the transition $b \rightarrow u\bar{u}d$. The result in Eq. (12.13) may have a sizeable correction due to what is called a penguin diagram. This is a one-loop graph producing $b \rightarrow d + \text{gluon}$ with a W and a quark, predominantly the t quark, in the loop. This leads to an amplitude proportional to $V_{tb}^* V_{td}$, which has a weak phase different from that of the original tree amplitude proportional to $V_{ub} V_{ud}^*$. There are several methods to approximately determine this correction using additional measurements [8].

CP violation in the decay amplitude is also revealed by the $\cos(\Delta Mt)$ term in Eq. (12.9) or by a difference in rates of B^+ and B^- to charge-conjugate states. These effects, however, require two contributing amplitudes to the decay (such as a tree amplitude plus a penguin) and also require final-state interaction phases. Predicted effects are very uncertain and are generally small [9].

In the case of the B_s system, the mass difference ΔM is much larger than for B^0 and has not yet been measured. As a result, it will be difficult to isolate the $\sin(\Delta Mt)$ term to measure asymmetries. Furthermore, in the Standard Model with the standard phase convention, ϕ_M is very small so that decays due to $b \rightarrow c\bar{c}s$, yielding $B_s \rightarrow \psi\eta'$, would have zero asymmetry. Decays due to $b \rightarrow u\bar{u}d$, yielding $B_s \rightarrow \rho^0 K_S$, would have an asymmetry $\sin 2\gamma$ in the tree approximation. The width difference $\Delta\Gamma$ is also expected to be much larger for B_s so that $\Delta\Gamma/\Gamma$ might be as large as 0.15. In this case, there might be a possibility of detecting CP violation as in the case of K^0 by observing the B_s states with different lifetimes decaying into the same CP eigenstate [10].

For further details, see the notes on CP violation in the K_L^0 , K_S^0 , and B^0 Particle Listings of this Review.

References:

1. B. Winstein and L. Wolfenstein, Rev. Mod. Phys. **65**, 1113 (1993).
2. T.T. Wu and C.N. Yang, Phys. Rev. Lett. **13**, 380 (1964).
3. L. Wolfenstein, Phys. Rev. Lett. **13**, 562 (1964);
L. Wolfenstein, Comm. Nucl. Part. Phys. **21**, 275 (1994).
4. E. Chell and M.G. Olsson, Phys. Rev. **D48**, 4076 (1993).
5. R. Adler *et al.*, (CLEAR Collaboration), Phys. Lett. **B407**, 193 (1997);
P. Bloch, to be published in *Proceedings of Workshop on K Physics* (Orsay 1996), ed. L. Iconomidou-Fayard, Edition Frontieres, Gif-sur-Yvette, France (1997) p. 307.
6. G. Buchalla, A.J. Buras, and M.E. Lautenbacher, Rev. Mod. Phys. **68**, 1125 (1996);
S. Bosch *et al.*, Nucl. Phys. **B565**, 3 (2000);
S. Bertolini, M. Fabrichesi, and J.O. Egg, Rev. Mod. Phys. **72**, 65 (2000).
7. For a review, see Y. Nir and H. Quinn in *B Decays* (ed. S. Stone) World Scientific 1994, p. 362 or Ann. Rev. Nucl. and Part. Sci. **42**, 211 (1992).
8. M. Gronau and D. London, Phys. Rev. Lett. **65**, 3361 (1990);
J.P. Silva and L. Wolfenstein, Phys. Rev. **D49**, R1151 (1994);
A.S. Dighe, M. Gronau, and J.L. Rosner, Phys. Rev. **D54**, 3309 (1996).
9. J.M. Gerard and W.S. Hou, Phys. Rev. **D43**, 2999 (1991).
10. I. Dunietz Phys. Rev. **D52**, 3048 (1995);
R. Fleischer and I. Dunietz, Phys. Rev. **D55**, 279 (1997).

13. QUARK MODEL

Revised April 2000 by C. Amsler (Univ. of Zürich) and C.G. Wohl (LBNL).

13.1. Quantum numbers of the quarks

Each quark has spin 1/2 and baryon number 1/3. Table 13.1 gives the additive quantum numbers (other than baryon number) of the three generations of quarks. Our convention is that the *flavor* of a quark (l_z , S, C, B, or T) has the same sign as its *charge*. With this convention, any flavor carried by a *charged* meson has the same sign as its charge; e.g., the strangeness of the K^+ is +1, the bottomness of the B^+ is +1, and the charm and strangeness of the D_s^- are each -1.

By convention, each quark is assigned positive parity. Then each antiquark has negative parity.

Table 13.1: Additive quantum numbers of the quarks.

Property	Quark	d	u	s	c	b	t
Q - electric charge		$-\frac{1}{3}$	$+\frac{2}{3}$	$-\frac{1}{3}$	$+\frac{2}{3}$	$-\frac{1}{3}$	$+\frac{2}{3}$
l_z - isospin z -component		$-\frac{1}{2}$	$+\frac{1}{2}$	0	0	0	0
S - strangeness		0	0	-1	0	0	0
C - charm		0	0	0	+1	0	0
B - bottomness		0	0	0	0	-1	0
T - topness		0	0	0	0	0	+1

13.2. Mesons: $q\bar{q}$ states

Nearly all known mesons are bound states of a quark q and an antiquark \bar{q}' (the flavors of q and q' may be different). If the orbital angular momentum of the $q\bar{q}'$ state is L , then the parity P is $(-1)^{L+1}$. A state $q\bar{q}$ of a quark and its own antiquark is also an eigenstate of charge conjugation, with $C = (-1)^{L+S}$, where the spin S is 0 or 1. The $L = 0$ states are the pseudoscalars, $J^P = 0^-$, and the vectors, $J^P = 1^-$. Assignments for many of the known mesons are given in Table 13.2. States in the "normal" spin-parity series, $P = (-1)^J$, must, according to the above, have $S = 1$ and hence $CP = +1$. Thus mesons with normal spin-parity and $CP = -1$ are forbidden in the $q\bar{q}'$ model. The $J^{PC} = 0^{- -}$ state is forbidden as well. Mesons with such J^{PC} may exist, but would lie outside the $q\bar{q}'$ model.

The nine possible $q\bar{q}'$ combinations containing u , d , and s quarks group themselves into an octet and a singlet:

$$3 \otimes \bar{3} = 8 \oplus 1 \quad (13.1)$$

States with the same IJ^P and additive quantum numbers can mix. (If they are eigenstates of charge conjugation, they must also have the same value of C .) Thus the $I = 0$ member of the ground-state pseudoscalar octet mixes with the corresponding pseudoscalar singlet to produce the η and η' . These appear as members of a nonet, which is shown as the middle plane in Fig. 13.1(a). Similarly, the ground-state vector nonet appears as the middle plane in Fig. 13.1(b).

A fourth quark such as charm can be included in this scheme by extending the symmetry to SU(4), as shown in Fig. 13.1. Bottom extends the symmetry to SU(5); to draw the multiplets would require four dimensions.

For the pseudoscalar mesons, the Gell-Mann-Okubo formula is

$$m_\eta^2 = \frac{1}{3}(4m_K^2 - m_\pi^2), \quad (13.2)$$

assuming no octet-singlet mixing. However, the octet η_8 and singlet η_1 mix because of SU(3) breaking. In general, the mixing angle is

mass dependent and becomes complex for resonances of finite width. Neglecting this, the physical states η and η' are given in terms of a mixing angle θ_P by

$$\eta = \eta_8 \cos \theta_P - \eta_1 \sin \theta_P \quad (13.3a)$$

$$\eta' = \eta_8 \sin \theta_P + \eta_1 \cos \theta_P. \quad (13.3b)$$

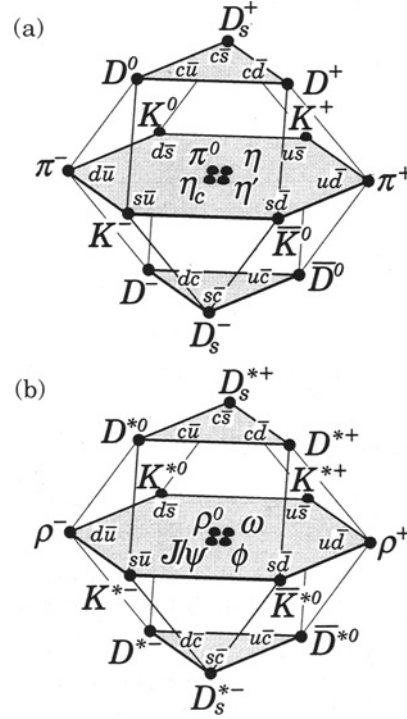


Figure 13.1: SU(4) 16-plets for the (a) pseudoscalar and (b) vector mesons made of u , d , s , and c quarks. The nonets of light mesons occupy the central planes, to which the $c\bar{c}$ states have been added. The neutral mesons at the centers of these planes are mixtures of $u\bar{u}$, $d\bar{d}$, $s\bar{s}$, and $c\bar{c}$ states.

These combinations diagonalize the mass-squared matrix

$$M^2 = \begin{pmatrix} M_{11}^2 & M_{18}^2 \\ M_{18}^2 & M_{88}^2 \end{pmatrix}, \quad (13.4)$$

where $M_{88}^2 = \frac{1}{3}(4m_K^2 - m_\pi^2)$. It follows that

$$\tan^2 \theta_P = \frac{M_{88}^2 - m_\eta^2}{m_\eta^2 - M_{88}^2}. \quad (13.5)$$

The sign of θ_P is meaningful in the quark model. If

$$\eta_1 = (u\bar{u} + d\bar{d} + s\bar{s})/\sqrt{3} \quad (13.6a)$$

$$\eta_8 = (u\bar{u} + d\bar{d} - 2s\bar{s})/\sqrt{6}, \quad (13.6b)$$

then the matrix element M_{18}^2 , which is due mostly to the strange quark mass, is negative. From the relation

$$\tan \theta_P = \frac{M_{88}^2 - m_\eta^2}{M_{18}^2}, \quad (13.7)$$

we find that $\theta_P < 0$. However, caution is suggested in the use of the η - η' mixing-angle formulas, as they are extremely sensitive to SU(3)

Table 13.2: Suggested $q\bar{q}$ quark-model assignments for most of the known mesons. Some assignments, especially for the 0^{++} multiplet and for some of the higher multiplets, are controversial. Mesons in bold face are included in the Meson Summary Table. Of the light mesons in the Summary Table, the $f_0(1500)$, $f_1(1510)$, $f_2(1950)$, $f_2(2300)$, $f_2(2340)$, and one of the two peaks in the $\eta(1440)$ entry are not in this table. Within the $q\bar{q}$ model, it is especially hard to find a place for the first two of these f mesons and for one of the $\eta(1440)$ peaks. See the "Note on Non- $q\bar{q}$ Mesons" at the end of the Meson Listings.

$N 2S+1L_J$	J^{PC}	$u\bar{d}, u\bar{u}, d\bar{d}$ $I = 1$	$u\bar{u}, d\bar{d}, s\bar{s}$ $I = 0$	$c\bar{c}$ $I = 0$	$b\bar{b}$ $I = 0$	$\bar{s}u, \bar{s}d$ $I = 1/2$	$c\bar{u}, c\bar{d}$ $I = 1/2$	$c\bar{s}$ $I = 0$	$\bar{b}u, \bar{b}d$ $I = 1/2$	$\bar{b}s$ $I = 0$	$\bar{b}c$ $I = 0$
1^1S_0	0^{-+}	π	η, η'	η_c		K	D	D_s	B	B_s	B_c
1^3S_1	1^{--}	ρ	ω, ϕ	$J/\psi(1S)$	$\Upsilon(1S)$	$K^*(892)$	$D^*(2010)$	D_s^*	B^*	B_s^*	
1^1P_1	1^{+-}	$b_1(1235)$	$h_1(1170), h_1(1380)$	$h_c(1P)$		K_{1B}^\dagger	$D_1(2420)$	$D_{s1}(2536)$			
1^3P_0	0^{++}	$a_0(1450)^*$	$f_0(1370)^*, f_0(1710)^*$	$\chi_{c0}(1P)$	$\chi_{b0}(1P)$	$K_0^*(1430)$					
1^3P_1	1^{++}	$a_1(1260)$	$f_1(1285), f_1(1420)$	$\chi_{c1}(1P)$	$\chi_{b1}(1P)$	K_{1A}^\dagger					
1^3P_2	2^{++}	$a_2(1320)$	$f_2(1270), f_2'(1525)$	$\chi_{c2}(1P)$	$\chi_{b2}(1P)$	$K_2^*(1430)$	$D_2^*(2460)$				
1^1D_2	2^{-+}	$\pi_2(1670)$	$\eta_2(1645), \eta_2(1870)$			$K_2(1770)$					
1^3D_1	1^{--}	$\rho(1700)$	$\omega(1650)$	$\psi(3770)$		$K^*(1680)^\ddagger$					
1^3D_2	2^{--}					$K_2(1820)$					
1^3D_3	3^{--}	$\rho_3(1690)$	$\omega_3(1670), \phi_3(1850)$			$K_3^*(1780)$					
1^3F_4	4^{++}	$a_4(2040)$	$f_4(2050), f_4(2220)$			$K_4^*(2045)$					
2^1S_0	0^{-+}	$\pi(1300)$	$\eta(1295), \eta(1440)$	$\eta_c(2S)$		$K(1460)$					
2^3S_1	1^{--}	$\rho(1450)$	$\omega(1420), \phi(1680)$	$\psi(2S)$	$\Upsilon(2S)$	$K^*(1410)^\ddagger$					
2^3P_2	2^{++}		$f_2(1810), f_2(2010)$		$\chi_{b2}(2P)$	$K_2^*(1980)$					
3^1S_0	0^{-+}	$\pi(1800)$	$\eta(1760)$			$K(1830)$					

* See our scalar minireview in the Particle Listings. The candidates for the $I = 1$ states are $a_0(980)$ and $a_0(1450)$, while for $I = 0$ they are: $f_0(400-1200)$, $f_0(980)$, $f_0(1370)$, and $f_0(1710)$. The light scalars are problematic, since there may be two poles for one $q\bar{q}$ state and $a_0(980)$, $f_0(980)$ may be $K\bar{K}$ bound states.

† The K_{1A} and K_{1B} are nearly equal (45°) mixes of the $K_1(1270)$ and $K_1(1400)$.

‡ The $K^*(1410)$ could be replaced by the $K^*(1680)$ as the 2^3S_1 state.

If we allow $M_{88}^2 = \frac{1}{3}(4m_K^2 - m_\pi^2)(1 + \Delta)$, the mixing angle is determined by

$$\tan^2 \theta_P = 0.0319(1 + 17\Delta) \quad (13.8)$$

$$\theta_P = -10.1^\circ(1 + 8.5\Delta) \quad (13.9)$$

to first order in Δ . A small breaking of the Gell-Mann-Okubo relation can produce a major modification of θ_P .

For the vector mesons, $\pi \rightarrow \rho$, $K \rightarrow K^*$, $\eta \rightarrow \phi$, and $\eta' \rightarrow \omega$, so that

$$\phi = \omega_8 \cos \theta_V - \omega_1 \sin \theta_V \quad (13.10)$$

$$\omega = \omega_8 \sin \theta_V + \omega_1 \cos \theta_V. \quad (13.11)$$

For "ideal" mixing, $\phi = s\bar{s}$, so $\tan \theta_V = 1/\sqrt{2}$ and $\theta_V = 35.3^\circ$. Experimentally, θ_V is near 35° , the sign being determined by a formula like that for $\tan \theta_P$. Following this procedure we find the mixing angles given in Table 13.3.

Table 13.3: Singlet-octet mixing angles for several nonets, neglecting possible mass dependence and imaginary parts. The sign conventions are given in the text. The values of θ_{quad} are obtained from the equations in the text, while those for θ_{lin} are obtained by replacing m^2 by m throughout. Of the two isosinglets in a nonet, the mostly octet one is listed first.

J^{PC}	Nonet members	θ_{quad}	θ_{lin}
0^{-+}	π, K, η, η'	-10°	-23°
1^{--}	$\rho, K^*(892), \phi, \omega$	39°	36°
2^{++}	$a_2(1320), K_2^*(1430), f_2'(1525), f_2(1270)$	28°	26°
3^{--}	$\rho_3(1690), K_3^*(1780), \phi_3(1850), \omega_3(1670)$	29°	28°

In the quark model, the coupling of neutral mesons to two photons is proportional to $\sum_i Q_i^2$, where Q_i is the charge of the i -th quark. This provides an alternative characterization of mixing. For example, defining

$$\text{Amp}[P \rightarrow \gamma(k_1) \gamma(k_2)] = M \epsilon^{\mu\nu\alpha\beta} \epsilon_{1\mu}^* k_{1\nu} \epsilon_{2\alpha}^* k_{2\beta}, \quad (13.12)$$

where $\epsilon_{i\lambda}$ is the λ component of the polarization vector of the i -th photon, one finds

$$\begin{aligned} \frac{M(\eta \rightarrow \gamma\gamma)}{M(\pi^0 \rightarrow \gamma\gamma)} &= \frac{1}{\sqrt{3}}(\cos\theta_P - 2\sqrt{2}\sin\theta_P) \\ &= \frac{1.73 \pm 0.18}{\sqrt{3}} \end{aligned} \quad (13.13a)$$

$$\begin{aligned} \frac{M(\eta' \rightarrow \gamma\gamma)}{M(\pi^0 \rightarrow \gamma\gamma)} &= 2\sqrt{2/3} \left(\cos\theta_P + \frac{\sin\theta_P}{2\sqrt{2}} \right) \\ &= 2\sqrt{2/3}(0.78 \pm 0.04), \end{aligned} \quad (13.13b)$$

where the numbers with errors are experimental. These data favor $\theta_P \approx -20^\circ$, which is compatible with the quadratic mass mixing formula with about 12% SU(3) breaking in M_{88}^2 .

13.3. Baryons: qqq states

All the established baryons are apparently 3-quark (qqq) states, and each such state is an SU(3) color singlet, a completely antisymmetric state of the three possible colors. Since the quarks are fermions, the state function for any baryon must be antisymmetric under interchange of any two equal-mass quarks (up and down quarks in the limit of isospin symmetry). Thus the state function may be written as

$$|qqq\rangle_A = |\text{color}\rangle_A \times |\text{space, spin, flavor}\rangle_S, \quad (13.14)$$

where the subscripts S and A indicate symmetry or antisymmetry under interchange of any two of the equal-mass quarks. Note the contrast with the state function for the three nucleons in ${}^3\text{H}$ or ${}^3\text{He}$:

$$|NNN\rangle_A = |\text{space, spin, isospin}\rangle_A. \quad (13.15)$$

This difference has major implications for internal structure, magnetic moments, *etc.* (For a nice discussion, see Ref. 1.)

The "ordinary" baryons are made up of u , d , and s quarks. The three flavors imply an approximate flavor SU(3), which requires that baryons made of these quarks belong to the multiplets on the right side of

$$\mathbf{3} \otimes \mathbf{3} \otimes \mathbf{3} = \mathbf{10}_S \oplus \mathbf{8}_M \oplus \mathbf{8}_M \oplus \mathbf{1}_A \quad (13.16)$$

(see Sec. 33, on "SU(n) Multiplets and Young Diagrams"). Here the subscripts indicate symmetric, mixed-symmetry, or antisymmetric states under interchange of any two quarks. The $\mathbf{1}$ is a uds state (Λ_1) and the octet contains a similar state (Λ_8). If these have the same spin and parity they can mix. An example is the mainly octet D_{03} $\Lambda(1690)$ and mainly singlet D_{03} $\Lambda(1520)$. In the ground state multiplet, the SU(3) flavor singlet Λ is forbidden by Fermi statistics. The mixing formalism is the same as for η - η' or ϕ - ω (see above), except that for baryons the mass M instead of M^2 is used. Section 32, on "SU(3) Isoscalar Factors and Representation Matrices", shows how relative decay rates in, say, $\mathbf{10} \rightarrow \mathbf{8} \otimes \mathbf{8}$ decays may be calculated. A summary of results of fits to the observed baryon masses and decay rates for the best-known SU(3) multiplets is given in Appendix II of our 1982 edition [2].

The addition of the c quark to the light quarks extends the flavor symmetry to SU(4). Figures 13.2(a) and 13.2(b) show the (badly broken) SU(4) baryon multiplets that have as their bottom levels an SU(3) octet, such as the octet that includes the nucleon, or an SU(3) decuplet, such as the decuplet that includes the $\Delta(1232)$. All the particles in a given SU(4) multiplet have the same spin and parity. The charmed baryons are discussed in more detail in the "Note on Charmed Baryons" in the Particle Listings. The addition of a b quark extends the flavor symmetry to SU(5); it would require four dimensions to draw the multiplets.

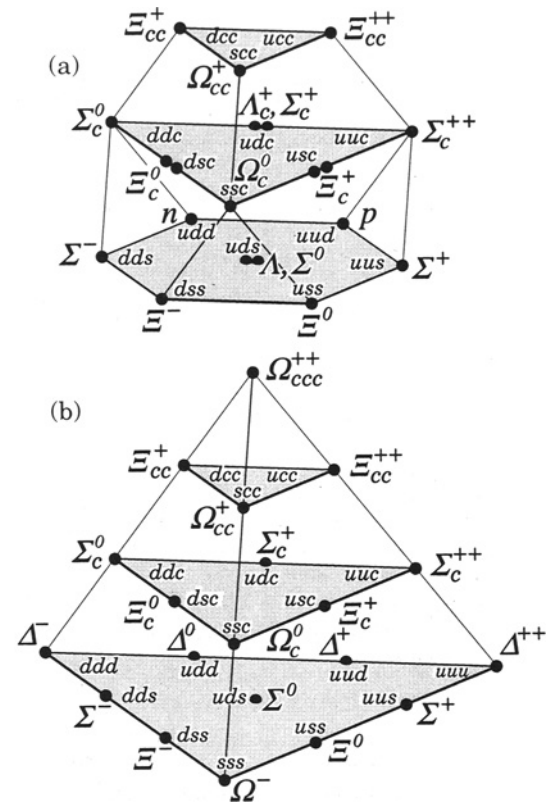


Figure 13.2: SU(4) multiplets of baryons made of u , d , s , and c quarks. (a) The 20-plet with an SU(3) octet. (b) The 20-plet with an SU(3) decuplet.

For the "ordinary" baryons (no c or b quark), flavor and spin may be combined in an approximate flavor-spin SU(6) in which the six basic states are $d \uparrow, d \downarrow, \dots, s \downarrow$ (\uparrow, \downarrow = spin up, down). Then the baryons belong to the multiplets on the right side of

$$\mathbf{6} \otimes \mathbf{6} \otimes \mathbf{6} = \mathbf{56}_S \oplus \mathbf{70}_M \oplus \mathbf{70}_M \oplus \mathbf{20}_A. \quad (13.17)$$

These SU(6) multiplets decompose into flavor SU(3) multiplets as follows:

$$\mathbf{56} = {}^4\mathbf{10} \oplus {}^2\mathbf{8} \quad (13.18a)$$

$$\mathbf{70} = {}^2\mathbf{10} \oplus {}^4\mathbf{8} \oplus {}^2\mathbf{8} \oplus {}^2\mathbf{1} \quad (13.18b)$$

$$\mathbf{20} = {}^2\mathbf{8} \oplus {}^4\mathbf{1}, \quad (13.18c)$$

where the superscript $(2S+1)$ gives the net spin S of the quarks for each particle in the SU(3) multiplet. The $J^P = 1/2^+$ octet containing the nucleon and the $J^P = 3/2^+$ decuplet containing the $\Delta(1232)$ together make up the "ground-state" 56-plet in which the orbital angular momenta between the quark pairs are zero (so that the spatial part of the state function is trivially symmetric). The $\mathbf{70}$ and $\mathbf{20}$ require some excitation of the spatial part of the state function in order to make the overall state function symmetric. States with nonzero orbital angular momenta are classified in SU(6) \otimes O(3) supermultiplets. Physical baryons with the same quantum numbers do not belong to a single supermultiplet, since SU(6) is broken by spin-dependent interactions, differences in quark masses, *etc.* Nevertheless, the SU(6) \otimes O(3) basis provides a suitable framework for describing baryon state functions.

It is useful to classify the baryons into bands that have the same number N of quanta of excitation. Each band consists of a number of supermultiplets, specified by (D, L_N^P) , where D is the dimensionality of the SU(6) representation, L is the total quark orbital angular momentum, and P is the total parity. Supermultiplets contained in bands up to $N = 12$ are given in Ref. 3. The $N = 0$ band,

which contains the nucleon and $\Delta(1232)$, consists only of the $(56, 0_0^+)$ supermultiplet. The $N = 1$ band consists only of the $(70, 1_1^-)$ multiplet and contains the negative-parity baryons with masses below about 1.9 GeV. The $N = 2$ band contains five supermultiplets: $(56, 0_2^+)$, $(70, 0_2^+)$, $(56, 2_2^+)$, $(70, 2_2^+)$, and $(20, 1_2^+)$. Baryons belonging to the $(20, 1_2^+)$ supermultiplet are not ever likely to be observed, since a coupling from the ground-state baryons requires a two-quark excitation. Selection rules are similarly responsible for the fact that many other baryon resonances have not been observed [4].

In Table 13.4, quark-model assignments are given for many of the established baryons whose $SU(6) \otimes O(3)$ compositions are relatively unmixed. We note that the unestablished resonances $\Sigma(1480)$, $\Sigma(1560)$, $\Sigma(1580)$, $\Sigma(1770)$, and $\Xi(1620)$ in our Baryon Particle Listings are too low in mass to be accommodated in most quark models [4,5].

Table 13.4: Quark-model assignments for many of the known baryons in terms of a flavor-spin $SU(6)$ basis. Only the dominant representation is listed. Assignments for some states, especially for the $\Lambda(1810)$, $\Lambda(2350)$, $\Xi(1820)$, and $\Xi(2030)$, are merely educated guesses. For assignments of the charmed baryons, see the “Note on Charmed Baryons” in the Particle Listings.

J^P	(D, L_N^P)	S	Octet members			Singlets
$1/2^+$	$(56, 0_0^+)$	$1/2$	$N(939)$	$\Lambda(1116)$	$\Sigma(1193)$	$\Xi(1318)$
$1/2^+$	$(56, 0_2^+)$	$1/2$	$N(1440)$	$\Lambda(1600)$	$\Sigma(1660)$	$\Xi(?)$
$1/2^-$	$(70, 1_1^-)$	$1/2$	$N(1535)$	$\Lambda(1670)$	$\Sigma(1620)$	$\Xi(?)$ $\Lambda(1405)$
$3/2^-$	$(70, 1_1^-)$	$1/2$	$N(1520)$	$\Lambda(1690)$	$\Sigma(1670)$	$\Xi(1820)$ $\Lambda(1520)$
$1/2^-$	$(70, 1_1^-)$	$3/2$	$N(1650)$	$\Lambda(1800)$	$\Sigma(1750)$	$\Xi(?)$
$3/2^-$	$(70, 1_1^-)$	$3/2$	$N(1700)$	$\Lambda(?)$	$\Sigma(?)$	$\Xi(?)$
$5/2^-$	$(70, 1_1^-)$	$3/2$	$N(1675)$	$\Lambda(1830)$	$\Sigma(1775)$	$\Xi(?)$
$1/2^+$	$(70, 0_2^+)$	$1/2$	$N(1710)$	$\Lambda(1810)$	$\Sigma(1880)$	$\Xi(?)$ $\Lambda(?)$
$3/2^+$	$(56, 2_2^+)$	$1/2$	$N(1720)$	$\Lambda(1890)$	$\Sigma(?)$	$\Xi(?)$
$5/2^+$	$(56, 2_2^+)$	$1/2$	$N(1680)$	$\Lambda(1820)$	$\Sigma(1915)$	$\Xi(2030)$
$7/2^-$	$(70, 3_3^-)$	$1/2$	$N(2190)$	$\Lambda(?)$	$\Sigma(?)$	$\Xi(?)$ $\Lambda(2100)$
$9/2^-$	$(70, 3_3^-)$	$3/2$	$N(2250)$	$\Lambda(?)$	$\Sigma(?)$	$\Xi(?)$
$9/2^+$	$(56, 4_4^+)$	$1/2$	$N(2220)$	$\Lambda(2350)$	$\Sigma(?)$	$\Xi(?)$
Decuplet members						
$3/2^+$	$(56, 0_0^+)$	$3/2$	$\Delta(1232)$	$\Sigma(1385)$	$\Xi(1530)$	$\Omega(1672)$
$1/2^-$	$(70, 1_1^-)$	$1/2$	$\Delta(1620)$	$\Sigma(?)$	$\Xi(?)$	$\Omega(?)$
$3/2^-$	$(70, 1_1^-)$	$1/2$	$\Delta(1700)$	$\Sigma(?)$	$\Xi(?)$	$\Omega(?)$
$5/2^+$	$(56, 2_2^+)$	$3/2$	$\Delta(1905)$	$\Sigma(?)$	$\Xi(?)$	$\Omega(?)$
$7/2^+$	$(56, 2_2^+)$	$3/2$	$\Delta(1950)$	$\Sigma(2030)$	$\Xi(?)$	$\Omega(?)$
$11/2^+$	$(56, 4_4^+)$	$3/2$	$\Delta(2420)$	$\Sigma(?)$	$\Xi(?)$	$\Omega(?)$

The quark model for baryons is extensively reviewed in Ref. 6 and 7.

13.4. Dynamics

Many specific quark models exist, but most contain the same basic set of dynamical ingredients. These include:

- i) A confining interaction, which is generally spin-independent.
- ii) A spin-dependent interaction, modeled after the effects of gluon exchange in QCD. For example, in the S -wave states, there is a spin-spin hyperfine interaction of the form

$$H_{HF} = -\alpha_S M \sum_{i>j} (\vec{\sigma}^i \lambda_a)_i (\vec{\sigma}^j \lambda_a)_j, \tag{13.19}$$

where M is a constant with units of energy, λ_a ($a = 1, \dots, 8$) is the set of $SU(3)$ unitary spin matrices, defined in Sec. 32, on “ $SU(3)$ Isoscalar Factors and Representation Matrices,” and the sum runs over constituent quarks or antiquarks. Spin-orbit interactions, although allowed, seem to be small.

- iii) A strange quark mass somewhat larger than the up and down quark masses, in order to split the $SU(3)$ multiplets.
- iv) In the case of isoscalar mesons, an interaction for mixing $q\bar{q}$ configurations of different flavors (e.g., $u\bar{u} \leftrightarrow d\bar{d} \leftrightarrow s\bar{s}$), in a manner which is generally chosen to be flavor independent.

These four ingredients provide the basic mechanisms that determine the hadron spectrum.

References:

1. F.E. Close, in *Quarks and Nuclear Forces* (Springer-Verlag, 1982), p. 56.
2. Particle Data Group, *Phys. Lett.* **111B** (1982).
3. R.H. Dalitz and L.J. Reinders, in *Hadron Structure as Known from Electromagnetic and Strong Interactions, Proceedings of the Hadron '77 Conference* (Veda, 1979), p. 11.
4. N. Isgur and G. Karl, *Phys. Rev.* **D18**, 4187 (1978); *ibid.* **D19**, 2653 (1979); *ibid.* **D20**, 1191 (1979); K.-T. Chao, N. Isgur, and G. Karl, *Phys. Rev.* **D23**, 155 (1981).
5. C.P. Forsyth and R.E. Cutkosky, *Z. Phys.* **C18**, 219 (1983).
6. A.J.G. Hey and R.L. Kelly, *Phys. Reports* **96**, 71 (1983). Also see S. Gasiorowicz and J.L. Rosner, *Am. J. Phys.* **49**, 954 (1981).
7. N. Isgur, *Int. J. Mod. Phys.* **E1**, 465 (1992); G. Karl, *Int. J. Mod. Phys.* **E1**, 491 (1992).

14. EXPERIMENTAL TESTS OF GRAVITATIONAL THEORY

Revised October 1999 by T. Damour (IHES, Bures-sur-Yvette, France).

Einstein's General Relativity, the current "standard" theory of gravitation, describes gravity as a universal deformation of the Minkowski metric:

$$g_{\mu\nu}(x^\lambda) = \eta_{\mu\nu} + h_{\mu\nu}(x^\lambda), \text{ where } \eta_{\mu\nu} = \text{diag}(-1, +1, +1, +1). \quad (14.1)$$

Alternatively, it can be defined as the unique, consistent, local theory of a massless spin-2 field $h_{\mu\nu}$, whose source must then be the total, conserved energy-momentum tensor [1]. General Relativity is classically defined by two postulates. One postulate states that the Lagrangian density describing the propagation and self-interaction of the gravitational field is

$$\mathcal{L}_{\text{Ein}}[g_{\mu\nu}] = \frac{c^4}{16\pi G_N} \sqrt{g} g^{\mu\nu} R_{\mu\nu}(g), \quad (14.2)$$

$$R_{\mu\nu}(g) = \partial_\alpha \Gamma_{\mu\nu}^\alpha - \partial_\nu \Gamma_{\mu\alpha}^\alpha + \Gamma_{\alpha\beta}^\beta \Gamma_{\mu\nu}^\alpha - \Gamma_{\nu\alpha}^\beta \Gamma_{\mu\beta}^\alpha, \quad (14.3)$$

$$\Gamma_{\mu\nu}^\lambda = \frac{1}{2} g^{\lambda\sigma} (\partial_\mu g_{\nu\sigma} + \partial_\nu g_{\mu\sigma} - \partial_\sigma g_{\mu\nu}), \quad (14.4)$$

where G_N is Newton's constant, $g = -\det(g_{\mu\nu})$, and $g^{\mu\nu}$ is the matrix inverse of $g_{\mu\nu}$. A second postulate states that $g_{\mu\nu}$ couples universally, and minimally, to all the fields of the Standard Model by replacing everywhere the Minkowski metric $\eta_{\mu\nu}$. Schematically (suppressing matrix indices and labels for the various gauge fields and fermions and for the Higgs doublet),

$$\begin{aligned} \mathcal{L}_{\text{SM}}[\psi, A_\mu, H, g_{\mu\nu}] = & -\frac{1}{4} \sum \sqrt{g} g^{\mu\alpha} g^{\nu\beta} F_{\mu\nu}^a F_{\alpha\beta}^a \\ & - \sum \sqrt{g} \bar{\psi} \gamma^\mu D_\mu \psi \\ & - \frac{1}{2} \sqrt{g} g^{\mu\nu} D_\mu H D_\nu H - \sqrt{g} V(H) \\ & - \sum \lambda \sqrt{g} \bar{\psi} H \psi, \end{aligned} \quad (14.5)$$

where $\gamma^\mu \gamma^\nu + \gamma^\nu \gamma^\mu = 2g^{\mu\nu}$, and where the covariant derivative D_μ contains, besides the usual gauge field terms, a (spin dependent) gravitational contribution $\Gamma_\mu(x)$ [2]. From the total action $S_{\text{tot}}[g_{\mu\nu}, \psi, A_\mu, H] = c^{-1} \int d^4x (\mathcal{L}_{\text{Ein}} + \mathcal{L}_{\text{SM}})$ follow Einstein's field equations,

$$R_{\mu\nu} - \frac{1}{2} R g_{\mu\nu} = \frac{8\pi G_N}{c^4} T_{\mu\nu}. \quad (14.6)$$

Here $R = g^{\mu\nu} R_{\mu\nu}$, $T_{\mu\nu} = g_{\mu\alpha} g_{\nu\beta} T^{\alpha\beta}$, and $T^{\mu\nu} = (2/\sqrt{g}) \delta \mathcal{L}_{\text{SM}} / \delta g_{\mu\nu}$ is the (symmetric) energy-momentum tensor of the Standard Model matter. The theory is invariant under arbitrary coordinate transformations: $x'^\mu = f^\mu(x^\nu)$. To solve the field equations Eq. (14.6) one needs to fix this coordinate gauge freedom. E.g. the "harmonic gauge" (which is the analogue of the Lorentz gauge, $\partial_\mu A^\mu = 0$, in electromagnetism) corresponds to imposing the condition $\partial_\nu (\sqrt{g} g^{\mu\nu}) = 0$.

In this *Review*, we only consider the classical limit of gravitation (*i.e.* classical matter and classical gravity). Considering quantum matter in a classical gravitational background already poses interesting challenges, notably the possibility that the zero-point fluctuations of the matter fields generate a nonvanishing vacuum energy density ρ_{vac} , corresponding to a term $-\sqrt{g} \rho_{\text{vac}}$ in \mathcal{L}_{SM} [3]. This is equivalent to adding a "cosmological constant" term $+\Lambda g_{\mu\nu}$ on the left-hand side of Einstein's equations Eq. (14.6), with $\Lambda = 8\pi G_N \rho_{\text{vac}}/c^4$. Cosmological observations set upper bounds (as well as, possibly, lower bounds) on Λ (see "Astrophysical Constants," Sec. 2 of this *Review*) which, when translated in particle physics units, appear suspiciously small: $\rho_{\text{vac}} \lesssim 10^{-46} \text{ GeV}^4$. This bound shows that ρ_{vac} , even if it is not strictly zero, has a negligible effect on the tests discussed below. Quantizing the gravitational field itself poses a very difficult challenge because of the perturbative non-renormalizability of Einstein's Lagrangian. Supergravity and superstring theory offer promising avenues toward solving this challenge.

14.1. Experimental tests of the coupling between matter and gravity

The universality of the coupling between $g_{\mu\nu}$ and the Standard Model matter postulated in Eq. (14.5) ("Equivalence Principle") has many observable consequences. First, it predicts that the outcome of a local non-gravitational experiment, referred to local standards, does not depend on where, when, and in which locally inertial frame, the experiment is performed. This means, for instance, that local experiments should neither feel the cosmological evolution of the universe (constancy of the "constants"), nor exhibit preferred directions in spacetime (isotropy of space, local Lorentz invariance). These predictions are consistent with many experiments and observations. The best limit on a possible time variation of the basic coupling constants concerns the fine-structure constant α_{em} and has been obtained by analyzing a natural fission reactor phenomenon which took place at Oklo, Gabon, two billion years ago [4]

$$-6.7 \times 10^{-17} \text{ yr}^{-1} < \frac{\dot{\alpha}_{\text{em}}}{\alpha_{\text{em}}} < 5.0 \times 10^{-17} \text{ yr}^{-1}. \quad (14.7)$$

The highest precision tests of the isotropy of space have been performed by looking to possible quadrupolar shifts of nuclear energy levels [5]. The (null) results can be interpreted as testing the fact that the various pieces in the matter Lagrangian Eq. (14.5) are indeed coupled to one and the same external metric $g_{\mu\nu}$ to the 10^{-27} level.

The universal coupling to $g_{\mu\nu}$ postulated in Eq. (14.5) implies that two (electrically neutral) test bodies dropped at the same location and with the same velocity in an external gravitational field fall in the same way, independently of their masses and compositions. The universality of the acceleration of free fall has been verified at the 10^{-12} level both for laboratory bodies [6],

$$\left(\frac{\Delta a}{a} \right)_{\text{BeCu}} = (-1.9 \pm 2.5) \times 10^{-12}, \quad (14.8)$$

and for the gravitational accelerations of the Moon and the Earth toward the Sun [7],

$$\left(\frac{\Delta a}{a} \right)_{\text{MoonEarth}} = (-3.2 \pm 4.6) \times 10^{-13}. \quad (14.9)$$

Finally, Eq. (14.5) also implies that two identically constructed clocks located at two different positions in a static external Newtonian potential $U(\mathbf{x}) = \sum G_N m/r$ exhibit, when intercompared by means of electromagnetic signals, the (apparent) difference in clock rate,

$$\frac{\tau_1}{\tau_2} = \frac{\nu_2}{\nu_1} = 1 + \frac{1}{c^2} [U(\mathbf{x}_1) - U(\mathbf{x}_2)] + O\left(\frac{1}{c^4}\right), \quad (14.10)$$

independently of their nature and constitution. This universal gravitational redshift of clock rates has been verified at the 10^{-4} level by comparing a hydrogen-maser clock flying on a rocket up to an altitude $\sim 10,000$ km to a similar clock on the ground [8]. For more details and references on experimental gravity see, *e.g.*, Refs. 9 and 10.

14.2. Tests of the dynamics of the gravitational field in the weak field regime

The effect on matter of one-graviton exchange, *i.e.* the interaction Lagrangian obtained when solving Einstein's field equations Eq. (14.6) written in, say, the harmonic gauge at first order in $h_{\mu\nu}$,

$$\square h_{\mu\nu} = -\frac{16\pi G_N}{c^4}(T_{\mu\nu} - \frac{1}{2}T\eta_{\mu\nu}) + O(h^2) + O(hT), \quad (14.11)$$

reads $-(8\pi G_N/c^4)T^{\mu\nu}\square^{-1}(T_{\mu\nu} - \frac{1}{2}T\eta_{\mu\nu})$. For a system of N moving point masses, with free Lagrangian $L^{(1)} = \sum_{A=1}^N -m_A c^2 \sqrt{1 - \mathbf{v}_A^2/c^2}$, this interaction, expanded to order v^2/c^2 , reads (with $r_{AB} \equiv |\mathbf{x}_A - \mathbf{x}_B|$, $\mathbf{n}_{AB} \equiv (\mathbf{x}_A - \mathbf{x}_B)/r_{AB}$)

$$L^{(2)} = \frac{1}{2} \sum_{A \neq B} \frac{G_N m_A m_B}{r_{AB}} \left[1 + \frac{3}{2c^2}(\mathbf{v}_A^2 + \mathbf{v}_B^2) - \frac{7}{2c^2}(\mathbf{v}_A \cdot \mathbf{v}_B) - \frac{1}{2c^2}(\mathbf{n}_{AB} \cdot \mathbf{v}_A)(\mathbf{n}_{AB} \cdot \mathbf{v}_B) + O\left(\frac{1}{c^4}\right) \right]. \quad (14.12)$$

The two-body interactions Eq. (14.12) exhibit v^2/c^2 corrections to Newton's $1/r$ potential induced by spin-2 exchange. Consistency at the “post-Newtonian” level $v^2/c^2 \sim G_N m/r c^2$ requires that one also considers the three-body interactions induced by some of the three-graviton vertices and other nonlinearities (terms $O(h^2)$ and $O(hT)$ in Eq. (14.11)),

$$L^{(3)} = -\frac{1}{2} \sum_{B \neq A \neq C} \frac{G_N^2 m_A m_B m_C}{r_{AB} r_{AC} c^2} + O\left(\frac{1}{c^4}\right). \quad (14.13)$$

All currently performed gravitational experiments in the solar system, including perihelion advances of planetary orbits, the bending and delay of electromagnetic signals passing near the Sun, and very accurate ranging data to the Moon obtained by laser echoes, are compatible with the post-Newtonian results Eqs. (14.11)–(14.13).

Similarly to what is done in discussions of precision electroweak experiments (see Section 10 in this *Review*), it is useful to quantify the significance of precision gravitational experiments by parameterizing plausible deviations from General Relativity. Endowing the spin-2 excitations with a (Pauli-Fierz) mass term is excluded both for phenomenological (discontinuities in observable predictions [11]) and theoretical (no energy lower bound [12]) reasons. Therefore, deviations from Einstein's pure spin-2 theory are defined by adding new, bosonic, ultra light or massless, macroscopically coupled fields. The addition of a vector (spin 1) field necessarily leads to violations of the universality of free fall and is constrained by “fifth force” experiments. See Refs. [6,13] for compilations of constraints. The addition of a scalar (spin 0) field is the most studied type of deviation from General Relativity, being motivated by many attempts to unify gravity with the Standard Model (Kaluza-Klein program, supergravity, string theory). The technically simplest class of tensor-scalar (spin $2 \oplus$ spin 0) theories consists in adding a massless scalar field φ coupled to the trace of the energy-momentum tensor $T = g_{\mu\nu} T^{\mu\nu}$ [14]. The most general such theory contains an arbitrary function $a(\varphi)$ of the scalar field, and can be defined by the Lagrangian

$$\mathcal{L}_{\text{tot}}[g_{\mu\nu}, \varphi, \psi, A_\mu, H] = \frac{c^4}{16\pi G} \sqrt{g}(R(g) - 2g^{\mu\nu} \partial_\mu \varphi \partial_\nu \varphi) + \mathcal{L}_{\text{SM}}[\psi, A_\mu, H, \tilde{g}_{\mu\nu}], \quad (14.14)$$

where G is a “bare” Newton constant, and where the Standard Model matter is coupled not to the “Einstein” (pure spin-2) metric $g_{\mu\nu}$, but to the conformally related (“Jordan-Fierz”) metric $\tilde{g}_{\mu\nu} = \exp(2a(\varphi))g_{\mu\nu}$. The scalar field equation $\square_g \varphi = -(4\pi G/c^4)\alpha(\varphi)T$ displays $\alpha(\varphi) \equiv \partial a(\varphi)/\partial \varphi$ as the basic (field-dependent) coupling between φ and matter [15]. The one-parameter Jordan-Fierz-Brans-Dicke theory [14] is the special case $a(\varphi) = \alpha_0 \varphi$ leading to a field-independent coupling $\alpha(\varphi) = \alpha_0$.

In the weak field, slow motion, limit appropriate to describing gravitational experiments in the solar system, the addition of φ modifies Einstein's predictions only through the appearance of two “post-Einstein” dimensionless parameters: $\bar{\gamma} = -2\alpha_0^2/(1 + \alpha_0^2)$ and $\bar{\beta} = +\frac{1}{2}\beta_0\alpha_0^2/(1 + \alpha_0^2)^2$, where $\alpha_0 \equiv \alpha(\varphi_0)$, $\beta_0 \equiv \partial\alpha(\varphi_0)/\partial\varphi_0$, φ_0 denoting the vacuum expectation value of φ . These parameters show up also naturally (in the form $\gamma_{\text{PPN}} = 1 + \bar{\gamma}$, $\beta_{\text{PPN}} = 1 + \bar{\beta}$) in phenomenological discussions of possible deviations from General Relativity [16,9]. The parameter $\bar{\gamma}$ measures the admixture of spin 0 to Einstein's graviton, and contributes an extra term $+\bar{\gamma}(\mathbf{v}_A - \mathbf{v}_B)^2/c^2$ in the square brackets of the two-body Lagrangian Eq. (14.12). The parameter $\bar{\beta}$ modifies the three-body interaction Eq. (14.13) by a factor $1 + 2\bar{\beta}$. Moreover, the combination $\eta \equiv 4\bar{\beta} - \bar{\gamma}$ parameterizes the lowest order effect of the self-gravity of orbiting masses by modifying the Newtonian interaction energy terms in Eq. (14.12) into $G_{AB} m_A m_B / r_{AB}$, with a body-dependent gravitational “constant” $G_{AB} = G_N [1 + \eta(E_A^{\text{grav}}/m_A c^2 + E_B^{\text{grav}}/m_B c^2) + O(1/c^4)]$, where $G_N = G \exp[2a(\varphi_0)](1 + \alpha_0^2)$ and where E_A^{grav} denotes the gravitational binding energy of body A .

The best current limits on the post-Einstein parameters $\bar{\gamma}$ and $\bar{\beta}$ are (at the 68% confidence level): (i) $-3.8 \times 10^{-4} < \bar{\gamma} < 2.6 \times 10^{-4}$ deduced from Very Long Baseline Interferometry (VLBI) measurements of the deflection of radio waves by the Sun [17], and (ii) $4\bar{\beta} - \bar{\gamma} = -0.0007 \pm 0.0010$ [7] from Lunar Laser Ranging measurements of a possible polarization of the Moon toward the Sun [18]. More stringent limits on $\bar{\gamma}$ are obtained in models (*e.g.*, string-inspired ones [19]) where scalar couplings violate the Equivalence Principle.

14.3. Tests of the dynamics of the gravitational field in the radiative and/or strong field regimes

The discovery of pulsars (*i.e.* rotating neutron stars emitting a beam of radio noise) in gravitationally bound orbits [20,21] has opened up an entirely new testing ground for relativistic gravity, giving us an experimental handle on the regime of radiative and/or strong gravitational fields. In these systems, the finite velocity of propagation of the gravitational interaction between the pulsar and its companion generates damping-like terms at order $(v/c)^5$ in the equations of motion [22]. These damping forces are the local counterparts of the gravitational radiation emitted at infinity by the system (“gravitational radiation reaction”). They cause the binary orbit to shrink and its orbital period P_b to decrease. The remarkable stability of the pulsar clock has allowed Taylor and collaborators to measure the corresponding very small orbital period decay $\dot{P}_b \equiv dP_b/dt \sim (v/c)^5 \sim 10^{-12}$ [21,23], thereby giving us a direct experimental confirmation of the propagation properties of the gravitational field. In addition, the surface gravitational potential of a neutron star $h_{00}(R) \simeq 2Gm/c^2 R \simeq 0.4$ being a factor $\sim 10^8$ higher than the surface potential of the Earth, and a mere factor 2.5 below the black hole limit ($h_{00} = 1$), pulsar data are sensitive probes of the strong-gravitational-field regime.

Binary pulsar timing data record the times of arrival of successive electromagnetic pulses emitted by a pulsar orbiting around the center of mass of a binary system. After correcting for the Earth motion around the Sun and for the dispersion due to propagation in the interstellar plasma, the time of arrival of the N th pulse t_N can be described by a generic, parameterized “timing formula [24]” whose functional form is common to the whole class of tensor-scalar gravitation theories:

$$t_N - t_0 = F[T_N(\nu_p, \dot{\nu}_p, \ddot{\nu}_p); \{p^K\}; \{p^{PK}\}]. \quad (14.15)$$

Here, T_N is the pulsar proper time corresponding to the N th turn given by $N/2\pi = \nu_p T_N + \frac{1}{2}\dot{\nu}_p T_N^2 + \frac{1}{6}\ddot{\nu}_p T_N^3$ (with $\nu_p \equiv 1/P_p$ the spin frequency of the pulsar, etc.), $\{p^K\} = \{P_b, T_0, e, \omega_0, x\}$ is the set of “Keplerian” parameters (notably, orbital period P_b , eccentricity e and projected semi-major axis $x = a \sin i/c$), and $\{p^{PK}\} = \{k, \gamma_{\text{timing}}, \dot{P}_b, r, s, \delta_\theta, \dot{e}, \dot{x}\}$ denotes the set of (separately measurable) “post-Keplerian” parameters. Most important among these are: the fractional periastron advance per orbit $k \equiv \dot{\omega} P_b / 2\pi$, a dimensionful time-dilation parameter γ_{timing} , the orbital period

derivative \dot{P}_b , and the “range” and “shape” parameters of the gravitational time delay caused by the companion, r and s .

Without assuming any specific theory of gravity, one can phenomenologically analyze the data from any binary pulsar by least-squares fitting the observed sequence of pulse arrival times to the timing formula Eq. (14.15). This fit yields the “measured” values of the parameters $\{\nu_p, \dot{\nu}_p, \ddot{\nu}_p\}$, $\{p^K\}$, $\{p^{PK}\}$. Now, each specific relativistic theory of gravity predicts that, for instance, k , γ_{timing} , \dot{P}_b , r and s (to quote parameters that have been successfully measured from some binary pulsar data) are some theory-dependent functions of the Keplerian parameters and of the (unknown) masses m_1 , m_2 of the pulsar and its companion. For instance, in General Relativity, one finds (with $M \equiv m_1 + m_2$, $n \equiv 2\pi/P_b$)

$$\begin{aligned} k^{\text{GR}}(m_1, m_2) &= 3(1 - e^2)^{-1} (G_N M n / c^3)^{2/3}, \\ \gamma_{\text{timing}}^{\text{GR}}(m_1, m_2) &= e n^{-1} (G_N M n / c^3)^{2/3} m_2 (m_1 + 2m_2) / M^2, \\ \dot{P}_b^{\text{GR}}(m_1, m_2) &= - (192\pi/5) (1 - e^2)^{-7/2} \left(1 + \frac{73}{24} e^2 + \frac{37}{96} e^4 \right) \\ &\quad \times (G_N M n / c^3)^{5/3} m_1 m_2 / M^2, \\ r(m_1, m_2) &= G_N m_2 / c^3, \\ s(m_1, m_2) &= n x (G_N M n / c^3)^{-1/3} M / m_2. \end{aligned} \quad (14.16)$$

In tensor-scalar theories, each of the functions $k^{\text{theory}}(m_1, m_2)$, $\gamma_{\text{timing}}^{\text{theory}}(m_1, m_2)$, $\dot{P}_b^{\text{theory}}(m_1, m_2)$, etc is modified by quasi-static strong field effects (associated with the self-gravities of the pulsar and its companion), while the particular function $\dot{P}_b^{\text{theory}}(m_1, m_2)$ is further modified by radiative effects (associated with the spin 0 propagator) [15,25].

Let us summarize the current experimental situation. In the first discovered binary pulsar PSR1913 + 16 [20,21], it has been possible to measure with accuracy the three post-Keplerian parameters k , γ_{timing} and \dot{P}_b . The three equations $k^{\text{measured}} = k^{\text{theory}}(m_1, m_2)$, $\gamma_{\text{timing}}^{\text{measured}} = \gamma_{\text{timing}}^{\text{theory}}(m_1, m_2)$, $\dot{P}_b^{\text{measured}} = \dot{P}_b^{\text{theory}}(m_1, m_2)$ determine, for each given theory, three curves in the two-dimensional mass plane. This yields one (combined radiative/strong-field) test of the specified theory, according to whether the three curves meet at one point, as they should. After subtracting a small ($\sim 10^{-14}$ level in $\dot{P}_b^{\text{obs}} = (-2.422 \pm 0.006) \times 10^{-12}$), but significant, Newtonian perturbing effect caused by the Galaxy [26], one finds that General Relativity passes this $(k - \gamma_{\text{timing}} - \dot{P}_b)_{1913+16}$ test with complete success at the 10^{-3} level [21,23]

$$\left[\frac{\dot{P}_b^{\text{obs}} - \dot{P}_b^{\text{galactic}}}{\dot{P}_b^{\text{GR}}[k^{\text{obs}}, \gamma_{\text{timing}}^{\text{obs}}]} \right]_{1913+16} = 1.0032 \pm 0.0023(\text{obs}) \pm 0.0026(\text{galactic}) = 1.0032 \pm 0.0035. \quad (14.17)$$

Here $\dot{P}_b^{\text{GR}}[k^{\text{obs}}, \gamma_{\text{timing}}^{\text{obs}}]$ is the result of inserting in $\dot{P}_b^{\text{GR}}(m_1, m_2)$ the values of the masses predicted by the two equations $k^{\text{obs}} = k^{\text{GR}}(m_1, m_2)$, $\gamma_{\text{timing}}^{\text{obs}} = \gamma_{\text{timing}}^{\text{GR}}(m_1, m_2)$. This experimental evidence for the reality of gravitational radiation damping forces at the 0.3% level is illustrated in Fig. 14.1, which shows actual orbital phase data (after subtraction of a linear drift).

The discovery of the binary pulsar PSR1534 + 12 [27] has allowed one to measure the four post-Keplerian parameters k , γ_{timing} , r and s , and thereby to obtain two (four observables minus two masses) tests of strong field gravity, without mixing of radiative effects [28]. General Relativity passes these tests within the measurement accuracy [28,21]. The most precise of these new, pure, strong-field tests is the one obtained by combining the measurements of k , γ , and s . Using the most recent data [29], one finds agreement at the 1% level:

$$\left[\frac{s^{\text{obs}}}{s^{\text{GR}}[k^{\text{obs}}, \gamma_{\text{timing}}^{\text{obs}}]} \right]_{1534+12} = 1.007 \pm 0.008. \quad (14.18)$$

It has also been possible to measure the orbital period change of PSR1534 + 12. General Relativity passes the corresponding $(k - \gamma_{\text{timing}} - \dot{P}_b)_{1534+12}$ test with success at the 15% level [29].

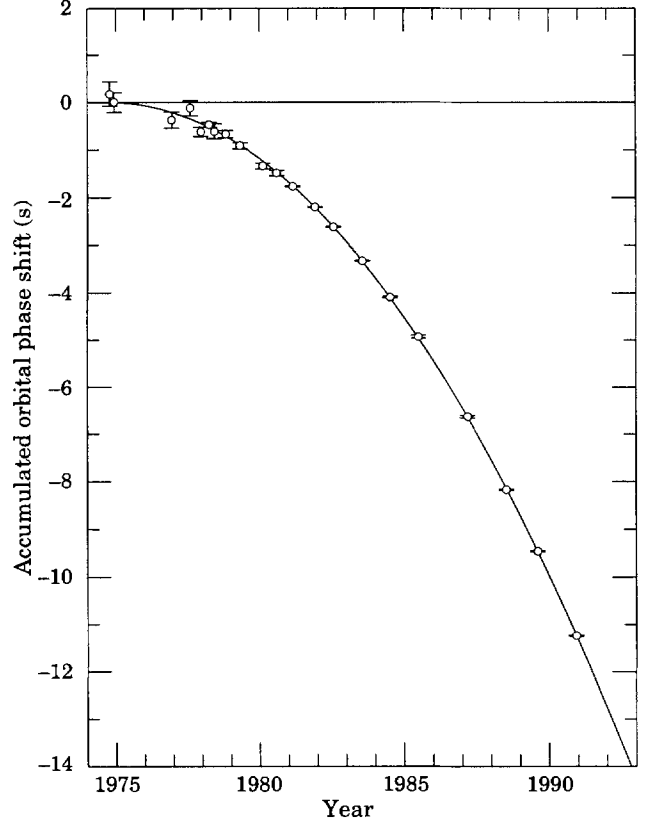


Figure 14.1: Accumulated shift of the times of periastron passage in the PSR 1913+16 system, relative to an assumed orbit with a constant period. The parabolic curve represents the general relativistic prediction, modified by Galactic effects, for orbital period decay from gravitational radiation damping forces. (Figure obtained with permission from Ref. 21.)

Several other binary pulsar systems, of a nonsymmetric type (nearly circular systems made of a neutron star and a white dwarf), can also be used to test relativistic gravity [30,31]. The constraints on tensor-scalar theories provided by three binary-pulsar “experiments” have been analyzed in [25] and shown to exclude a large portion of the parameter space allowed by solar-system tests. Recently, measurements of the pulse shape of PSR1913 + 16 [32] have detected a time variation of the pulse shape compatible with the prediction [33] that the general relativistic spin-orbit coupling should cause a secular change in the orientation of the pulsar beam with respect to the line of sight (“geodetic precession”).

The tests considered above have examined the gravitational interaction on scales between a few centimeters and a few astronomical units. Millimeter scale tests of Newtonian gravity have been reported in Ref. 34. On the other hand, the general relativistic action on light and matter of an external gravitational field on a length scale ~ 100 kpc has been verified to $\sim 30\%$ in some gravitational lensing systems (see, e.g., Ref. 35). Some tests on cosmological scales are also available. In particular, Big Bang Nucleosynthesis (see Section 15 of this Review) has been used to set significant constraints on the variability of the gravitational “constant” [36].

14.4. Conclusions

All present experimental tests are compatible with the predictions of the current “standard” theory of gravitation: Einstein’s General Relativity. The universality of the coupling between matter and gravity (Equivalence Principle) has been verified at the 10^{-12} level. Solar system experiments have tested the weak-field predictions of Einstein’s theory at the 10^{-3} level. The propagation properties of relativistic gravity, as well as several of its strong-field aspects, have been verified at the 10^{-3} level in binary pulsar experiments. Several

important new developments in experimental gravitation are expected in the near future. The approved NASA Gravity Probe B mission (a space gyroscope experiment; due for launch within the next two years) will directly measure the gravitational spin-orbit and spin-spin couplings, thereby measuring the weak-field post-Einstein parameter $\bar{\gamma}$ to the 10^{-5} level. The planned NASA-ESA MiniSTEP mission (a satellite test of the Equivalence Principle) should test the universality of acceleration of free fall down to the 10^{-18} level (an improvement by six orders of magnitude). Laboratory experiments (motivated by recent theoretical ideas [37]) plan to test possible deviations from standard Newtonian gravity on sub-millimeter distance scales. Finally, the various kilometer-size laser interferometers under construction (notably LIGO in the USA and VIRGO in Europe) should, soon after 2002, directly detect gravitational waves arriving on Earth. As the sources of these waves are expected to be extremely relativistic objects with strong internal gravitational fields (e.g., coalescing binary black holes), their detection will allow one to experimentally probe gravity in highly dynamical circumstances.

References:

1. S.N. Gupta, *Phys. Rev.* **96**, 1683 (1954);
R.H. Kraichnan, *Phys. Rev.* **98**, 1118 (1955);
R.P. Feynman, F.B. Morinigo, and W.G. Wagner, *Feynman Lectures on Gravitation*, edited by Brian Hatfield (Addison-Wesley, Reading, 1995);
S. Weinberg, *Phys. Rev.* **138**, B988 (1965);
V.I. Ogievetsky and I.V. Polubarinov, *Ann. Phys. (NY)* **35**, 167 (1965);
W. Wyss, *Helv. Phys. Acta* **38**, 469 (1965);
S. Deser, *Gen. Rel. Grav.* **1**, 9 (1970);
D.G. Boulware and S. Deser, *Ann. Phys. (NY)* **89**, 193 (1975);
J. Fang and C. Fronsdal, *J. Math. Phys.* **20**, 2264 (1979);
R.M. Wald, *Phys. Rev.* **D33**, 3613 (1986);
C. Cutler and R.M. Wald, *Class. Quantum Grav.* **4**, 1267 (1987);
R.M. Wald, *Class. Quantum Grav.* **4**, 1279 (1987).
2. S. Weinberg, *Gravitation and Cosmology* (John Wiley, New York, 1972).
3. S. Weinberg, *Rev. Mod. Phys.* **61**, 1 (1989).
4. A.I. Shlyakhter, *Nature* **264**, 340 (1976);
T. Damour and F. Dyson, *Nucl. Phys.* **B480**, 37 (1996).
5. J.D. Prestage *et al.*, *Phys. Rev. Lett.* **54**, 2387 (1985);
S.K. Lamoreaux *et al.*, *Phys. Rev. Lett.* **57**, 3125 (1986);
T.E. Chupp *et al.*, *Phys. Rev. Lett.* **63**, 1541 (1989).
6. Y. Su *et al.*, *Phys. Rev.* **D50**, 3614 (1994).
7. J.O. Dickey *et al.*, *Science* **265**, 482 (1994);
J.G. Williams, X.X. Newhall, and J.O. Dickey, *Phys. Rev.* **D53**, 6730 (1996).
8. R.F.C. Vessot and M.W. Levine, *Gen. Rel. Grav.* **10**, 181 (1978);
R.F.C. Vessot *et al.*, *Phys. Rev. Lett.* **45**, 2081 (1980).
9. C.M. Will, *Theory and Experiment in Gravitational Physics* (Cambridge University Press, Cambridge, 1993).
10. T. Damour, in *Gravitation and Quantizations*, ed. B. Julia and J. Zinn-Justin, Les Houches, Session LVII (Elsevier, Amsterdam, 1995), pp. 1-61.
11. H. van Dam and M. Veltman, *Nucl. Phys.* **B22**, 397 (1970).
12. D.G. Boulware and S. Deser, *Phys. Rev.* **D6**, 3368 (1972).
13. E. Fischbach and C. Talmadge, *Nature* **356**, 207 (1992).
14. P. Jordan, *Schwerkraft und Weltall* (Vieweg, Braunschweig, 1955);
M. Fierz, *Helv. Phys. Acta* **29**, 128 (1956);
C. Brans and R.H. Dicke, *Phys. Rev.* **124**, 925 (1961).
15. T. Damour and G. Esposito-Farèse, *Class. Quantum Grav.* **9**, 2093 (1992).
16. A.S. Eddington, *The Mathematical Theory of Relativity* (Cambridge University Press, Cambridge, 1923);
K. Nordtvedt, *Phys. Rev.* **169**, 1017 (1968);
C.M. Will, *Astrophys. J.* **163**, 611 (1971).
17. T.M. Eubanks *et al.*, *Bull. Am. Phys. Soc.*, Abstract # K 11.05 (1997).
18. K. Nordtvedt, *Phys. Rev.* **170**, 1186 (1968).
19. T.R. Taylor and G. Veneziano, *Phys. Lett.* **B213**, 450 (1988);
T. Damour and A.M. Polyakov, *Nucl. Phys.* **B423**, 532 (1994).
20. R.A. Hulse, *Rev. Mod. Phys.* **66**, 699 (1994).
21. J.H. Taylor, *Rev. Mod. Phys.* **66**, 711 (1994).
22. T. Damour and N. Deruelle, *Phys. Lett.* **A87**, 81 (1981);
T. Damour, *C.R. Acad. Sci. Paris* **294**, 1335 (1982).
23. J.H. Taylor, *Class. Quantum Grav.* **10**, S167 (Supplement 1993).
24. T. Damour and J.H. Taylor, *Phys. Rev.* **D45**, 1840 (1992).
25. T. Damour and G. Esposito-Farèse, *Phys. Rev.* **D54**, 1474 (1996).
26. T. Damour and J.H. Taylor, *Astrophys. J.* **366**, 501 (1991).
27. A. Wolszczan, *Nature* **350**, 688 (1991).
28. J.H. Taylor *et al.*, *Nature* **355**, 132 (1992).
29. I.H. Stairs *et al.*, *Astrophys. J.* **505**, 352 (1998);
I.H. Stairs *et al.*, *astro-ph/9903289*, to appear in the proceedings of "Gravitational Waves and Experimental Gravity," XXXIVth Rencontres de Moriond (January 23-30, 1999).
30. C.M. Will and H.W. Zaglauer, *Astrophys. J.* **346**, 366 (1989).
31. T. Damour and G. Schäfer, *Phys. Rev. Lett.* **66**, 2549 (1991).
32. M. Kramer, *Astrophys. J.* **509**, 856 (1998);
J.H. Taylor, talk given at the XXXIVth Rencontres de Moriond (January 23-30, 1999).
33. T. Damour and R. Ruffini, *C. R. Acad. Sc. Paris* **279**, série A, 971 (1974);
B.M. Barker and R.F. O'Connell, *Phys. Rev. D* **12**, 329 (1975).
34. V.P. Mitrofanov and O.I. Ponomareva, *Sov. Phys. JETP* **67**, 1963 (1988).
35. A. Dar, *Nucl. Phys. (Proc. Supp.)* **B28**, 321 (1992).
36. J. Yang *et al.*, *Astrophys. J.* **227**, 697 (1979);
T. Rothman and R. Matzner, *Astrophys. J.* **257**, 450 (1982);
F.S. Accetta, L.M. Krauss, and P. Romanelli, *Phys. Lett.* **B248**, 146 (1990).
37. I. Antoniadis, S. Dimopoulos, and G. Dvali, *Nucl. Phys.* **B516**, 70 (1998);
N. Arkani-Hamed, S. Dimopoulos, and G. Dvali, *Phys. Lett.* **B429**, 263 (1998).

15. THE POCKET COSMOLOGY

Written April 2000 by E.W. Kolb and M.S. Turner (The University of Chicago and Fermilab).

15.1. The Universe Observed

15.1.1. The Hubble expansion:

The most fundamental discovery of modern observational cosmology is the expansion of the Universe. The expansion is just a rescaling of the Universe: the proper distance between points at rest in the cosmic rest frame scales as the cosmic scale factor $R(t)$ [sometimes denoted as $a(t)$]. The expansion rate is given by

$$H(t) \equiv \dot{R}(t)/R(t). \quad (15.1)$$

In general, H is a function of time. The present value of the expansion rate, the Hubble constant H_0 , can be measured in a number of ways, all of which fundamentally involve dividing the recessional velocity of a distant galaxy by its distance. It is conventional to express H_0 in terms of a dimensionless constant h : $H_0 = 100 h \text{ km s}^{-1} \text{ Mpc}^{-1}$. While the linear nature of the distance-redshift relation for nearby objects (Hubble's Law) is clear (see Fig. 15.1), until recently there was a systematic uncertainty of almost a factor of two in the value of h . Today, virtually all methods are now consistent with $h = 0.65 \pm 0.05$ ($H_0 = 65 \pm 5 \text{ km s}^{-1} \text{ Mpc}^{-1}$), with a possible systematic error of about 10% [1].

The Hubble constant sets the scale of the Universe in both time and space: the time since the scale factor $R(t)$ was zero is measured in units of the Hubble time $H_0^{-1} = 9.778 h^{-1} \text{ Gyr}$, and the size of the observable Universe is set by the Hubble distance $cH_0^{-1} = 2998 h^{-1} \text{ Mpc} = 9.251 h^{-1} \times 10^{27} \text{ cm}$. The precise relationships between H_0 and the size and age depend upon the expansion history of the Universe and are discussed in Sec. 15.2.

Another fundamental parameter is the deceleration parameter, q_0 , which measures the rate of change of the expansion:

$$H_0^2 q_0 \equiv -\ddot{R}(t_0)/R(t_0). \quad (15.2)$$

In a universe comprised only of matter, q_0 equals $\Omega_M/2$, where Ω_M is the fraction of critical density contributed by matter. The critical density is determined by H_0 and the gravitational constant G :

$$\begin{aligned} \rho_{\text{crit}} &\equiv \frac{3H_0^2}{8\pi G} = 1.879 h^2 \times 10^{-29} \text{ g cm}^{-3} \\ &= 1.054 h^2 \times 10^4 \text{ eV cm}^{-3}. \end{aligned} \quad (15.3)$$

For a matter-dominated or radiation-dominated universe the density determines the fate of the universe: a sub-critical-density universe expands forever and a super-critical-density universe recollapses. A cosmological constant (or similar form of energy density) complicates the connection between destiny and energy density.

Measurements of the distances to very distant supernovae indicate that q_0 is actually negative, *i.e.*, the Universe is accelerating (see below). If correct, this illustrates dramatically that the energy density of the Universe is dominated by something other than matter or relativistic particles, since their gravity would slow (decelerate) the expansion.

15.1.2. The redshift:

As the Universe expands, all distances are stretched with the cosmic scale factor, including the wavelengths of photons. (The exception to this universal stretching is the size of a bound system, *e.g.*, a galaxy, a Hydrogen atom, or a proton.) Because the Universe is expanding, photons emitted long ago are redshifted:

$$1 + z \equiv \frac{\lambda_{\text{today}}}{\lambda_{\text{emission}}} = \frac{R(t_0)}{R(t_{\text{emission}})}. \quad (15.4)$$

Redshift (z) directly indicates the relative linear size of the Universe when that photon was emitted. For example, the most distant quasar has $z = 5.82$; when the light from that quasar was emitted, the Universe was a factor of $1 + z \approx 6.82$ times smaller. The relative size of the Universe is simply $(1 + z)^{-1}$, while its age at a given redshift depends upon the expansion history.

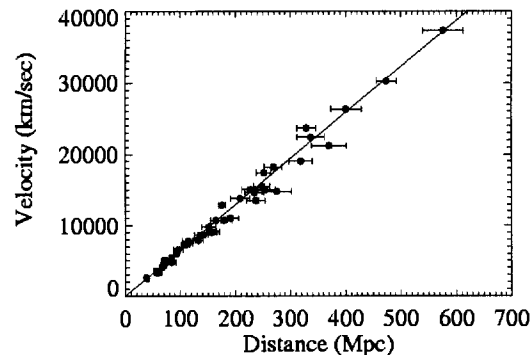


Figure 15.1: The distance-redshift diagram illustrates the expansion of the Universe. This “Hubble diagram” with linear axes is derived from a sample of type Ia supernovae and $H_0 = 65 \pm 2 \text{ km s}^{-1} \text{ Mpc}^{-1}$ (error purely statistical; figure courtesy of Adam Riess).

15.1.3. The age of the Universe:

The relationship between the expansion age (time since zero scale factor) and the Hubble age H_0^{-1} depends upon the slowing or speeding of the expansion rate. For plausible values of the Hubble constant and expansion histories, the expansion age is between 10 and 17 Gyr. The supernova measurements that indicate the Universe is accelerating also constrain the expansion history, and imply an expansion age of $15_{-1.1}^{+1.4} \text{ Gyr}$ [2].

An important cosmological consistency test is the comparison of the expansion age with independent age measurements of objects within the Universe: consistency requires the Universe to be older than any object within it. Independent age measurements include the ages of the oldest globular clusters dated by their stars, of the heavy elements as dated by radioactive decays, and of the oldest white-dwarf stars in the disk of our galaxy as measured by their cooling. The last two clocks are less easily compared to the expansion age because of the uncertainty of when the disk formed relative to the galaxy and the time history of heavy-element formation.

The reliability of the globular-cluster technique has improved in the last five years due to better stellar models, better atomic-physics data, and more accurate globular-cluster distance measurements. Current estimates for the age of the Universe based upon globular clusters are $t_0 = 14 \pm 2 \text{ Gyr}$, with a possible systematic error of similar size [3]. Ages for the Universe based upon white-dwarf cooling and nucleocosmochronology are consistent with this number. While the error bars are still significant, the expansion age is comfortably consistent with the independent estimates of the age of the Universe.

15.1.4. The composition of the Universe:

We have taken the first steps toward a full accounting of the composition of the Universe. In units of the critical density, our assessment is

$$\begin{aligned} \text{total: } \Omega_0 &= 1 \pm 0.1, \\ \text{matter: } \Omega_M &= 0.35 \pm 0.1, \\ \text{energy: } \Omega_E &= 0.8 \pm 0.2, \end{aligned} \quad (15.5)$$

where the errors quoted are meant to be 1σ . By matter we mean material that is nonrelativistic (*i.e.*, pressure p much smaller than its energy density). As discussed below, energy refers to components that are intrinsically relativistic; *e.g.*, photons (γ), massless neutrinos (ν), and vacuum energy (Λ).

The total of matter plus energy density has been determined by measurements of the dependence of the anisotropy of the cosmic

microwave background (CMB) upon angular scale (see the review on “Cosmic background radiation” (Sec. 19) in the full *Review* and Figure 15.2).

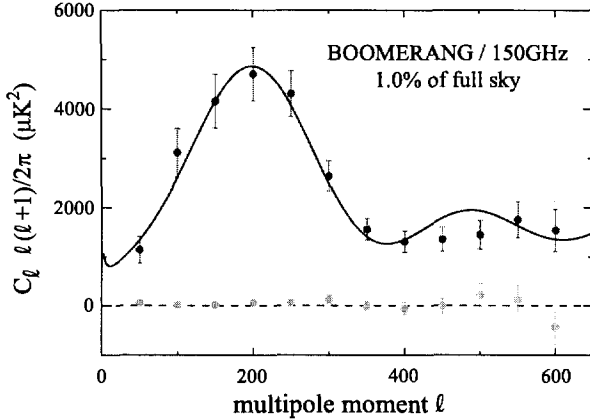


Figure 15.2: CMB angular power spectrum as determined by the Long Duration Balloon Flight of Boomerang, based on one frequency channel and 1% of the sky [4]. The curve is a flat CDM model with $\Omega_\Lambda = 0.65$. The Boomerang data by themselves imply $\Omega_0 = 1 \pm 0.06$. (The broken line and associated points show the difference of the two halves of the time stream of data; the absence of a difference indicates internal consistency.)

The matter density consists of several components: optically bright baryons in stars, optically dark baryons (in hot, cold, and warm gas, neutral atomic gas, molecular clouds, and stellar remnants), neutrinos, and nonbaryonic dark matter of an unknown form, here referred to as cold dark matter (CDM). The matter density breaks down as follows

$$\begin{aligned} \text{CDM} : \Omega_{\text{CDM}} &= 0.30 \pm 0.1 \\ \text{Baryons} : \Omega_B &= (0.019 \pm 0.001)h^{-2} \simeq 0.045 \pm 0.01 \\ &\quad \text{optically bright baryons } \Omega_* \sim 0.005 \\ &\quad \text{dark baryons } \Omega_B \sim 0.04 \\ \text{Neutrinos} : 0.10 &\gtrsim \Omega_\nu \gtrsim 0.003 . \end{aligned} \quad (15.6)$$

The baryon density is most precisely probed by comparing the big-bang production of deuterium and the measurements of the primeval deuterium abundances in high-redshift clouds of hydrogen (see the review on “Big-bang nucleosynthesis (BBN)” (Sec. 16) in the full *Review* and Ref. 5). The total matter density is determined many ways, all of which are consistent with $\Omega_M = 0.35 \pm 0.07$. We believe that it is most cleanly determined from the baryon density and the ratio of baryonic mass to total mass in clusters of galaxies ($\equiv f_B$): $\Omega_M = \Omega_B / f_B$ [6].

The lower bound to the contribution of light neutrinos is from the SuperKamionkande evidence for neutrino oscillations involving muon neutrinos and a mass difference squared of $\mathcal{O}(10^{-2} \text{ eV}^2)$ [7]. The upper bound to Ω_ν is from the requirement that neutrinos not interfere with the formation of structure in the Universe [8]. While the neutrino contribution is small, it is comparable to that of bright stars. Finally, the CDM mass density is derived from the difference of Ω_M and Ω_B , assuming that neutrinos do not contribute significantly and that the nonbaryonic dark matter is slowly moving cold particles (the “C” in CDM).

Almost seventy years ago Zwicky pointed out that the gravity of stars in clusters of galaxies is not great enough to hold together clusters. More precise measurements today show that the total matter density is almost 100 times that of stars and that the dark matter problem is manifold. The factor of seven discrepancy between Ω_M and Ω_B is strong evidence that most of the matter is nonbaryonic. Further, the study of the formation of structure in the Universe indicates

that the nonbaryonic dark matter must be slowly moving particles (cold dark matter), with the leading candidates being elementary particles left over from the earliest moments (see the review on “Dark matter” (Sec. 18) in the full *Review*). Finally, (optically) dark baryons outweigh those in stars by about a factor of ten.

Relativistic energy denoted by Ω_E appears in several forms today:

$$\begin{aligned} \text{photons} : \Omega_\gamma h^2 &= 2.471 \times 10^{-5} \\ \text{massless neutrinos} : \Omega_\nu h^2 &= 1.122 \times 10^{-5} \\ \text{dark energy} : \Omega_X &= 0.8 \pm 0.2 . \end{aligned} \quad (15.7)$$

The contribution of the photons in the cosmic microwave background and the (undetected) relativistic neutrino seas (two relativistic species assumed) are simple to calculate. Today, this relativistic contribution is negligible, but during the earliest moments it was the dominant component.

The mysterious entry, dark energy, is suggested by the type Ia supernovae measurements (SNeIa) that indicate the Universe is accelerating [2,9]. The supernovae data were analyzed assuming that the dark energy is a cosmological constant, and the results can be summarized by

$$\Omega_\Lambda = \frac{4}{3}\Omega_M + \frac{1}{3} \pm \frac{1}{6} . \quad (15.8)$$

All data are consistent with a cosmological constant of this size; however, theoretical estimates for the contribution to the cosmological constant coming from vacuum energy (zero-point energies) are at least 55 orders of magnitude larger than the critical density. This is the long-standing cosmological-constant problem.

It might well be that the resolution of the cosmological-constant puzzle is that vacuum energy does not contribute anything to the energy budget of the Universe today. If this is so, any acceleration of the expansion must be due to something else! The requirement for acceleration is an inequality involving the energy density and the pressure: $\rho + 3p < 0$. Since this component is clearly dark and relativistic ($|p| \sim \rho$ if $\rho > 0$), we have called it dark energy. Theorists have been busy, and there are already a number of interesting suggestions for the dark energy; they include a very light, slowly evolving scalar field (sometimes referred to as quintessence), vacuum energy, and a network of light, tangled topological defects. The supernova measurements, combined with other data, indicate that $-1 \leq p/\rho \leq -\frac{1}{2}$ [10].

As shown in Fig. 15.3 there is consistency between the independent determinations of the matter/energy content of the Universe. The emerging picture for the matter-energy of the Universe challenges the Standard Model of particle physics since nonbaryonic dark matter, massive neutrinos, and dark energy are not part of the Standard Model.

15.1.5. The cosmic microwave background:

The cosmic microwave background contributes only a tiny fraction of critical density today; however, its presence means that during early history ($t < 40,000$ yrs) radiation dominated the energy density of the Universe. See the review on “Cosmic background radiation” (Sec. 19) in the full *Review* for a summary of the CMB with references; here we touch upon the most salient features.

The CMB is to an extraordinary precision black-body radiation (any deviation from the Planck spectrum is less than 50 parts per million and statistically insignificant). The temperature has been measured to four significant figures: $T_0 = 2.725 \pm 0.001 \text{ K}$. This corresponds to a photon number density of $n_\gamma = 410.5 \text{ cm}^{-3}$ and fraction of critical density $\Omega_\gamma = 2.471 h^{-2} \times 10^{-5}$.

The CMB has a dipole anisotropy on the sky of amplitude $3.372 \pm 0.004 \text{ mK}$, which arises from the velocity of the solar system with respect to the cosmic rest frame (defined as the CMB rest frame). This implies a solar-system velocity of $371 \pm 0.5 \text{ km s}^{-1}$, and a velocity of the local group of $622 \pm 22 \text{ km s}^{-1}$.

CMB anisotropy has now been detected on angular scales from 90° (multipole $l = 2$) to a fraction of a degree ($l \sim 500$), with amplitudes of tens of μK (see Figure 15.2). This anisotropy is due to

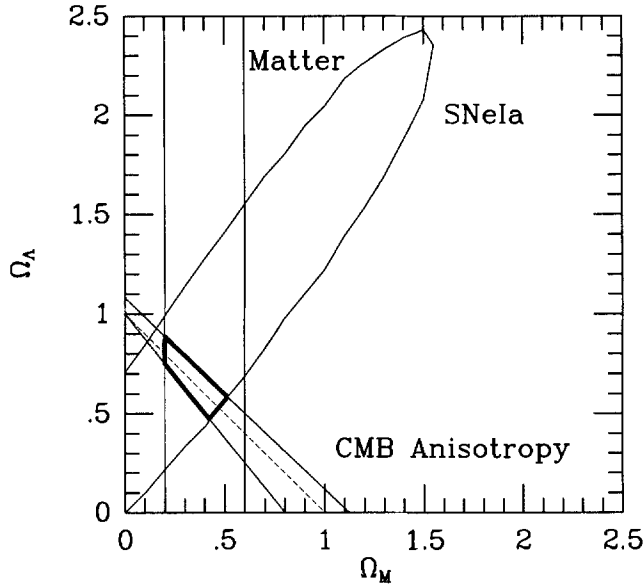


Figure 15.3: Summary of independent determinations of Ω_0 , Ω_X and Ω_M , assuming the dark energy is vacuum energy (cosmological constant). Note the consistency of the three 95% confidence contours. Data are consistent with $\Omega_o = \Omega_\Lambda + \Omega_M = 1$ (dashed line).

inhomogeneity in the distribution of matter of the same amplitude, $\delta\rho/\rho \sim \delta T/T \sim 10^{-5}$. Since the surface of last scattering for the CMB is the Universe at about 500,000 years after the bang, this CMB anisotropy implies that the Universe at that time was very smooth, but not perfectly smooth. The level of matter inhomogeneity indicated is what is needed to explain the structure that exists today, after taking into account the growth of inhomogeneity due to the attractive force of gravity over the past 14 Gyr.

15.1.6. Large-scale structure of the Universe:

Einstein and others assumed isotropy and homogeneity to simplify the field equations of general relativity. While the Universe on small scales (much less than 100 Mpc) is neither isotropic or homogeneous, at early times, and on large scales today, there is ample evidence for isotropy and homogeneity. The evidence at early times is provided by the uniformity of the CMB ($\delta T/T \sim \delta\rho/\rho \sim 10^{-5}$). Redshift surveys, three-dimensional maps of the distribution of galaxies, now probe the Universe on scales as large as $300 h^{-1}$ Mpc. They indicate that the distribution of galaxies becomes homogeneous and isotropic on scales much greater than 100 Mpc (see Fig. 15.4). Even larger surveys to be completed over the next five years [e.g., the Sloan Digital Sky Survey (SDSS) and the 2^o Field project (2dF)] will probe the distribution of matter on even larger scales.

On smaller scales the Universe is highly structured: there are galaxies, small groups of galaxies, great clusters containing thousands of galaxies, superclusters, and giant sheet-like structures extending across $100 h^{-1}$ Mpc. This structure can be explained by the level of inhomogeneity revealed by the CMB anisotropy and the subsequent growth due to gravitational amplification, provided there is nonbaryonic dark matter.

Redshift surveys reveal the distribution of light, rather than matter itself. In principle, the two could be very different. After all, the bulk of the matter is not even baryons. This problem is called biasing: light is likely to be a biased tracer of mass. The ratio of the inhomogeneity in the distribution of galaxies to that of matter is called the bias factor b . (The bias is likely to depend on scale and the type of galaxy.) A variety of studies show that biasing is important, but not overwhelming: b differs from unity by of order 50% or less. For example, the *rms* fluctuation in the number of galaxies within a sphere of radius $8 h^{-1}$ Mpc is unity; on the same scale the *rms* mass fluctuation has been inferred to be about 0.8, from the abundance of rich clusters and numerical simulations of structure formation.

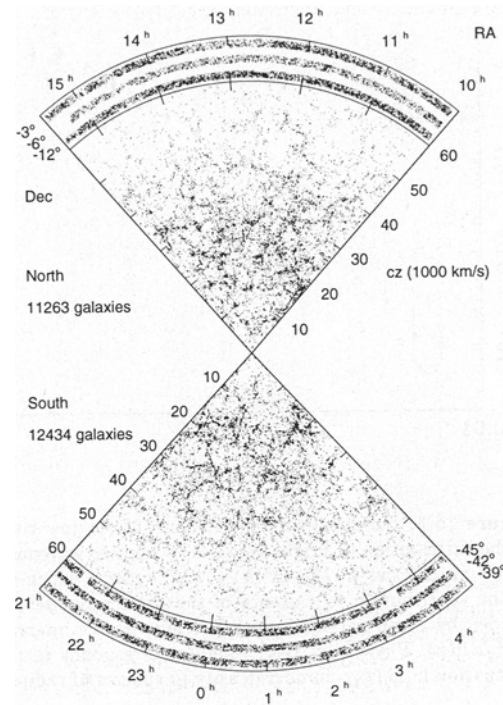


Figure 15.4: A slice from the Las Campanas Redshift Survey [11]. Each point represents a galaxy in the survey. Recessional velocity cz may be translated into distance d from us by Hubble's Law, $d = 10 h^{-1}$ Mpc ($cz/1000$ km/s).

Figure 15.5 summarizes the power spectrum $P(k) \equiv |\delta_k|^2$ of the distribution of galaxies today, where δ_k is the Fourier transform of the galaxy number density. On the very largest scales, $\lambda \gtrsim 10 h^{-1}$ Mpc, the inhomogeneity of matter is probed by the CMB anisotropy; on small scales it is probed by the present distribution of galaxies. When the MAP and Planck CMB anisotropy maps and the 2dF and SDSS redshift surveys are complete, there will be a range of scales, from about $10 h^{-1}$ Mpc up to about $500 h^{-1}$ Mpc, where both the matter and galaxy inhomogeneity will be probed. On these scales biasing will be directly examined.

15.2. The Standard Cosmology

15.2.1. Robertson-Walker line element:

The distribution of matter in the observable Universe today is isotropic and homogeneous on the largest scales ($\gg 10 h^{-1}$ Mpc). The smoothness of the CMB, $\delta T/T < 10^{-4}$ on all angular scales measured, indicates that at early times the distribution of matter and radiation were isotropic and homogeneous. Thus, for purposes of describing the present observable Universe on sufficiently large scales, as well as the Universe at early times, we may assume that the Universe is isotropic and homogeneous.

The metric for a space with homogeneous and isotropic spatial sections is the maximally symmetric Robertson-Walker (RW) metric, which can be written in the form

$$ds^2 = dt^2 - R^2(t) \left\{ \frac{dr^2}{1 - kr^2} + r^2 d\theta^2 + r^2 \sin^2 \theta d\phi^2 \right\}, \quad (15.9)$$

where (t, r, θ, ϕ) are coordinates (referred to as comoving coordinates), and $R(t)$ is the cosmic scale factor. With an appropriate rescaling of the coordinates, k can be chosen to be +1, -1, or 0 for spaces of constant positive, negative, or zero spatial curvature, respectively. Nonetheless, there are an infinity of RW models, distinguished

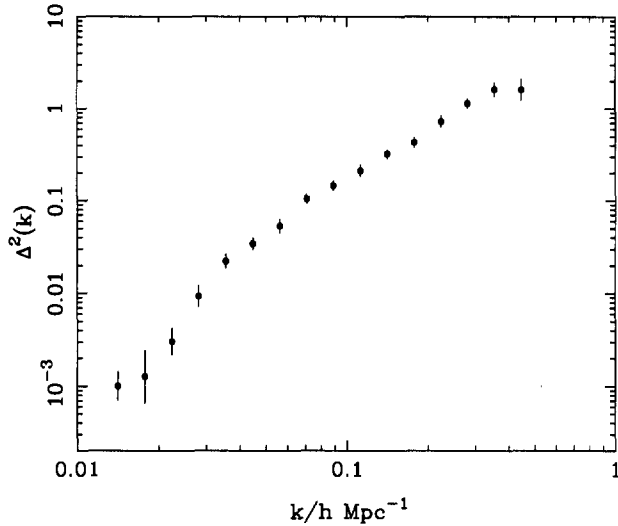


Figure 15.5: Summary of measurements of the power spectrum of the distribution of bright galaxies vs Fourier wavenumber k , shown as $\Delta^2(k)$ vs k [12]. $\Delta^2(k) = k^3 P(k)/2\pi^2$, which is equal to the contribution to variance of the galaxy number density divided by mean galaxy density per logarithmic interval in k ($d\sigma^2/d\ln k$). Physically, $\Delta(k)$ roughly corresponds to the rms fluctuation in galaxy-number density in spheres of radius $\approx \pi/k$.

by their radii of spatial curvature, $R_{\text{curv}} = R(t)/\sqrt{|k|}$. A convenient and widely used convention is to set the cosmic scale factor to unity today; then, the coordinate r and $1/\sqrt{|k|}$ have dimensions of length. We shall usually use this convention.

The time coordinate is just the proper (or clock) time measured by an observer at rest in the comoving frame, *i.e.*, $(r, \theta, \phi) = \text{const}$. The term *comoving* is well chosen: Observers at rest in the comoving frame remain at rest, *i.e.*, (r, θ, ϕ) remain unchanged, and observers initially moving with respect to this frame will eventually come to rest in it.

15.2.2. Particle kinematics and conservation of energy

If the stress-energy tensor has the form of a perfect fluid, the conservation of stress energy ($T^{\mu\nu}_{;\nu} = 0$) gives the first law of thermodynamics in the form

$$d(\rho R^3) = -pd(R^3), \quad (15.10)$$

or equivalently,

$$\begin{aligned} d \ln \rho &= -3(1+w)d \ln R \\ \Rightarrow \rho &\propto \exp \left[-3 \int (1+w) d \ln R \right], \end{aligned} \quad (15.11)$$

where $w \equiv p/\rho$ characterizes the equation of state of the fluid. The physical significance of the above equation is clear: The change in energy in a comoving volume element, $d(\rho R^3)$, is equal to minus the pressure times the change in volume, $-pd(R^3)$. If w is independent of time, the energy density evolves as $\rho \propto R^{-3(1+w)}$. Examples of interest include

$$\begin{aligned} \text{radiation:} \quad & p = \frac{1}{3}\rho \Rightarrow \rho \propto R^{-4} \\ \text{matter:} \quad & p = 0 \Rightarrow \rho \propto R^{-3} \\ \text{vacuum energy:} \quad & p = -\rho \Rightarrow \rho \propto \text{const}. \end{aligned} \quad (15.12)$$

The “early” Universe was radiation dominated, and the “adolescent” Universe was matter dominated. The Universe today appears to be dominated by a form of energy similar to vacuum energy ($w \approx -1$). If the Universe underwent inflation, there was a “very early” period when the stress-energy was dominated by vacuum energy.

The equation of motion for a freely falling particle in RW space-time is very simple: the three-momentum decreases as the inverse of the cosmic scale factor:

$$|p| \propto 1/R \quad (15.13)$$

For a massless particle, this is the cosmological redshift of wavelength. For a massive, nonrelativistic particle, this implies that any velocity with respect to the cosmic rest frame decreases as the inverse of the scale factor, with the particle eventually coming to rest in comoving RW coordinates.

15.2.3. Friedmann equations:

The dynamics of the expansion are determined from the Einstein equations. For the Robertson–Walker metric they are known as the Friedmann equations:

$$\begin{aligned} H^2 &= \frac{\dot{R}^2}{R^2} = \frac{8\pi G}{3}\rho - \frac{k}{R^2} \\ \frac{\ddot{R}}{R} &= -\frac{4\pi G}{3}(\rho + 3p). \end{aligned} \quad (15.14)$$

Note that the equation for the expansion rate is the first integral of the second Friedmann equation.

These equations can be used to write the deceleration parameter as

$$q_0 = \frac{1}{2}\Omega_0 + \frac{3}{2} \sum_i w_i \Omega_i. \quad (15.15)$$

This formula applies to any epoch, provided the values of Ω_i corresponding to that epoch are used. For example, assuming a flat Universe and matter and cosmological-constant components,

$$q_z = \frac{1}{2} - \frac{3}{2} \left[\frac{\Omega_\Lambda}{\Omega_\Lambda + (1+z)^3(1-\Omega_\Lambda)} \right] \quad (15.16)$$

where the factor following $3/2$ is $\Omega_\Lambda(z)$. It follows that the epoch of accelerated expansion ($q_z < 0$) began at redshift $z = (2\Omega_\Lambda/\Omega_M)^{1/3} - 1 \approx 0.6$ (taking $\Omega_M = 0.35$ and $\Omega_\Lambda = 0.65$).

In the simple case in which the right side of the Friedmann equation is dominated by a fluid whose pressure is given by $p = w\rho$, it follows that

$$\rho \propto R^{-3(1+w)} \quad R \propto t^{2/3(1+w)}, \quad (15.17)$$

This leads to the results: $R \propto t^{1/2}$ for $w = 1/3$ (radiation-dominated universe); $R \propto t^{2/3}$ for $w = 0$ (matter dominated); $R \propto \exp(H_0 t)$ for $w = -1$ (vacuum dominated); and $R \propto t$ for a curvature-dominated universe (*i.e.*, $H^2 = |k|/R^2$). Dark energy with $-1/3 > w \geq -1$ leads to the scale factor growing more rapidly than t and perhaps as rapidly as $\exp(H_0 t)$. Note that in terms of the dynamics of the expansion, curvature-domination and dark energy with $w = -1/3$ both lead to $R \propto t$.

15.2.4. The three ages of the Universe:

Because the energy density in relativistic particles (photons and neutrinos) evolves as R^{-4} , while that in matter evolves as R^{-3} , when $R(t) \leq R_{EQ} = 2.663 \times 10^{-4}/(\Omega_M h^2/0.156)$ the Universe was “radiation dominated.” This corresponds to temperatures $T \geq T_{EQ} = 0.8819 \text{ eV}/(\Omega_M h^2/0.156)$. (In computing R_{EQ} we have assumed that all three neutrino species were relativistic at early times.) During the radiation era, the scale factor $R(t) \propto t^{1/2}$. Note that the 1σ uncertainty in $\Omega_M h^2$ is nearly 30%; the fiducial value $\Omega_M h^2 = 0.156$ derives from the somewhat arbitrarily selected central values, $\Omega_M = 0.35$ and $h = 2/3$;

After matter-radiation equality, the Universe begins a matter-dominated phase with scale factor $R(t) \propto t^{2/3}$. During the matter-dominated era,

$$t(z) = 16.5 \text{ Gyr}/(1+z)^{3/2}(\Omega_M h^2/0.156)^{1/2}. \quad (15.18)$$

When the contributions to the energy density from both matter and radiation are comparable, the scale factor and age are related by

$$\frac{t}{t_{EQ}} = \frac{(R/R_{EQ} - 2)(R/R_{EQ} + 1)^{1/2} + 2}{2 - \sqrt{2}}, \quad (15.19)$$

This exact expression reduces to $R \propto t^{1/2}$ for $t \ll t_{EQ}$ and $R \propto t^{2/3}$ for $t \gg t_{EQ}$. The age of the Universe at matter-radiation equality is

$$t_{EQ} = 4(\sqrt{2} - 1)H_{EQ}^{-1}/3 \\ = 4.25 \times 10^4 \text{ yrs}/(\Omega_M h^2/0.156)^2. \quad (15.20)$$

Last scattering of the CMB photons occurs shortly after matter-radiation equality, at a redshift $z_{LS} \simeq 1100$, when the age of the Universe was

$$t_{LS} \simeq 4.5 \times 10^5 \text{ yrs}/(\Omega_M h^2/0.156)^{1/2}. \quad (15.21)$$

Acceleration implies that dark energy has recently begun to control the behavior of the expansion. Assuming that the dark energy exists in the form of a cosmological constant, the transition to a vacuum-energy dominated age occurred at

$$R_\Lambda = (\Omega_M/\Omega_\Lambda)^{1/3} = 0.814 \quad (15.22)$$

for $\Omega_M = 0.35$ and $\Omega_\Lambda = 0.65$, which corresponds to a redshift $z_\Lambda = 0.23$. Well into the Λ -dominated era, the scale factor evolves as

$$R(t) \propto \exp[\sqrt{\Omega_\Lambda} H_0 t]. \quad (15.23)$$

15.2.5. Destiny:

In a universe where all forms of energy density decrease more rapidly than R^{-2} ($w_i > -1/3$ for all i), there is a connection between geometry and destiny: open universes ($k \leq 0$) expand forever and closed universes ($k > 0$) recollapse. We thought until recently that we lived in this kind of universe *i.e.*, matter plus radiation. With the advent of a sizable dark energy component, all that goes out the window! For example, a closed universe with a positive cosmological constant ($w = -1$) can expand forever and an open universe with a negative cosmological constant must recollapse.

15.2.6. Age and deceleration parameter:

The equality $dt = RdR/H$ can be integrated to give the age of the Universe as a function of redshift:

$$t(z) = \int_z^\infty \frac{dz}{(1+z)H(z)}. \quad (15.24)$$

where the present age $t_0 = t(z=0)$ (see Fig. 15.6). An interesting example is a flat vacuum energy + matter universe:

$$t(z) = \frac{2}{3} H(z)^{-1} \Omega_\Lambda(z)^{-1/2} \ln \left[\frac{1 + \Omega_\Lambda(z)^{1/2}}{\sqrt{\Omega_M(z)}} \right]. \quad (15.25)$$

where

$$\Omega_M(z) = \frac{\Omega_M}{\Omega_M + \Omega_\Lambda(1+z)^3} \\ \Omega_\Lambda(z) = 1 - \Omega_M(z) \\ H^2(z) = H_0^2 [\Omega_M(1+z)^3 + \Omega_\Lambda]. \quad (15.26)$$

15.2.7. The classic tests:

The behavior of the expansion, and thereby the underlying mean properties of the mass and energy in the Universe, as well as the curvature of the Universe are probed by the classical kinematic cosmological tests: the magnitude vs redshift (Hubble) diagram, the angular diameter vs redshift diagram, and the number count vs redshift test. At the heart of all three tests is the comoving distance to an object with redshift z :

$$r(z) = \kappa^{-1/2} \sinh \left[\kappa^{-1/2} \int_0^z \frac{dx}{H(x)} \right] \\ \kappa = (1 - \Omega_0) H_0^2 \\ H^2(z) = H_0^2 \left[\Omega_M(1+z)^3 + \Omega_X \exp \left(3 \int (1+w) d \ln z \right) \right. \\ \left. + (1 - \Omega_0)(1+z)^2 \right]. \quad (15.27)$$

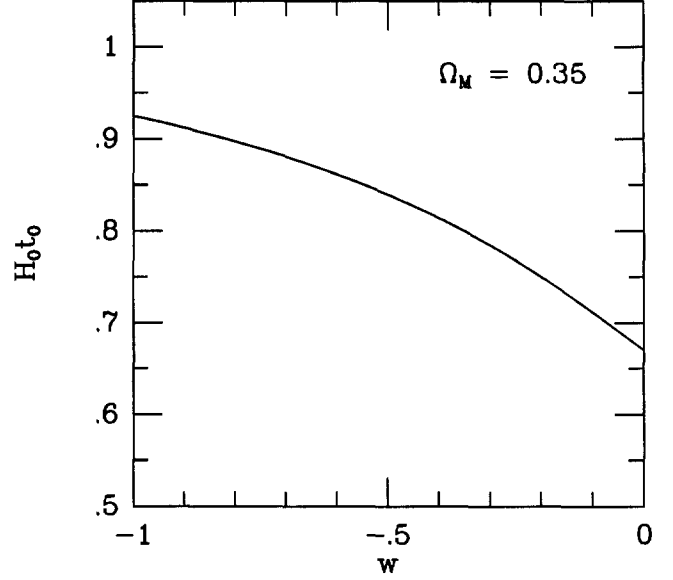


Figure 15.6: $H_0 t_0$ as a function of w , assuming a two-component universe with $\Omega_M = 0.35$ and $\Omega_X = 0.65$. $w = -1$ corresponds to a cosmological constant and $w = -1/3$ corresponds to an open universe with $\Omega_0 = \Omega_M = 0.35$. Accelerated expansion (or less decelerated expansion) leads to an older universe for a given present expansion rate; thus, $H_0 t_0$ increases with decreasing w .

For definiteness, $k < 0$ was assumed. For $k > 0$, $\sinh \rightarrow \sin$ and $\kappa \rightarrow k$.

Luminosity distance as a function of redshift

$$d_L(z) = (1+z)r(z) \quad (15.28)$$

can be inferred from flux measurements of standard (or standardizable) candles such as supernovae of type Ia:

$$d_L = \sqrt{\mathcal{L}/4\pi\mathcal{F}} \quad (15.29)$$

where \mathcal{L} is the luminosity of the standard candle and \mathcal{F} is the measured flux. It is this technique, used with type Ia supernovae, that has revealed the acceleration of the expansion.

The angular-diameter distance

$$d_A(z) = r(z)/(1+z) \quad (15.30)$$

can be inferred through measurements of the angular size of standard rules,

$$d_A = D/\theta \quad (15.31)$$

where D is the size of the standard ruler and θ is the subtended angle. This method is central to the determination of Ω_0 from CMB anisotropy. The standard ruler is the sound horizon distance at last scattering, $D \propto v_s t_{LS}$.

The comoving volume element is given by

$$\frac{dV}{d\Omega dr} = \frac{r^2}{\sqrt{1+\kappa r^2}} \Rightarrow \frac{dV}{d\Omega dz} = \frac{r^2(z)}{H(z)}. \quad (15.32)$$

It can be related to counts of objects of a constant (or known) comoving number density (*e.g.*, clusters or galaxies of a certain mass) vs a function of redshift,

$$\frac{dN}{dz d\Omega} = \frac{n(z)r^2(z)}{H(z)}. \quad (15.33)$$

Using this technique and theoretical expectations for the comoving number density of clusters in the CDM scenario, a matter density of about 0.3 has been inferred.

15.2.8. Thermal history.

During much of the history of the Universe, particularly the earliest history, conditions of thermal equilibrium existed. The total energy density and pressure of all species in equilibrium can be expressed in terms of the photon temperature T

$$\begin{aligned} \rho_R &= T^4 \sum_{i=\text{species}} \left(\frac{T_i}{T}\right)^4 \frac{g_i}{2\pi^2} \int_{x_i}^{\infty} \frac{(u^2 - x_i^2)^{1/2} u^2 du}{\exp(u - y_i) \pm 1} \\ p_R &= T^4 \sum_{i=\text{species}} \left(\frac{T_i}{T}\right)^4 \frac{g_i}{6\pi^2} \int_{x_i}^{\infty} \frac{(u^2 - x_i^2)^{3/2} du}{\exp(u - y_i) \pm 1}, \end{aligned} \quad (15.34)$$

where $x_i \equiv m_i/T$, $y_i \equiv \mu_i/T$, the + sign applies to fermions, the - sign to bosons, and we have taken into account the possibility that the species i may have a thermal distribution, but with a different temperature than that of the photons. We have used natural units, where $\hbar = c = k_B = 1$.

Since the energy density and pressure of a nonrelativistic species (*i.e.*, one with mass $m \gg T$) is exponentially smaller than that of a relativistic species (*i.e.*, one with mass $m \ll T$), it is a very convenient and a good approximation to include only the relativistic species in the sums for ρ_R and p_R , in which case the above expressions greatly simplify:

$$\begin{aligned} \rho_R &= \frac{\pi^2}{30} g_* T^4, \\ p_R &= \frac{\rho_R}{3} = \frac{\pi^2}{90} g_* T^4, \end{aligned} \quad (15.35)$$

where g_* counts the total number of effectively massless degrees of freedom (those species with mass $m_i \ll T$),

$$g_* = \sum_{i=\text{bosons}} g_i \left(\frac{T_i}{T}\right)^4 + \frac{7}{8} \sum_{i=\text{fermions}} g_i \left(\frac{T_i}{T}\right)^4. \quad (15.36)$$

Fig. 15.7 shows $g_*(T)$ for the degrees of freedom in the Standard Model of particle physics.

During the early radiation-dominated epoch ($t \lesssim 40,000$ yrs) $\rho \simeq \rho_R$; and further, when $g_* \simeq \text{const}$, $p_R = \rho_R/3$ (*i.e.*, $w = 1/3$) and $R(t) \propto t^{1/2}$. From this it follows

$$\begin{aligned} H &= 1.660 g_*^{1/2} \frac{T^2}{m_{\text{Pl}}} \\ t &= 0.3012 g_*^{-1/2} \frac{m_{\text{Pl}}}{T^2} \sim \frac{\text{MeV}}{T^2} \text{ s}, \end{aligned} \quad (15.37)$$

where m_{Pl} is the Planck mass 1.221×10^{19} GeV.

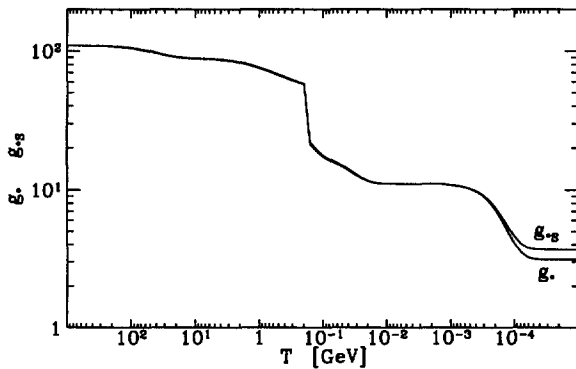


Figure 15.7: Number of relativistic degrees of freedom g_* and g_{*S} vs temperature according to the Standard Model of particle physics.

In the expanding Universe the entropy density s is given by

$$s \equiv \frac{\rho + p}{T}. \quad (15.38)$$

It is dominated by the contribution of relativistic particles, so that to a good approximation,

$$s = \frac{2\pi^2}{45} g_{*S} T^3, \quad (15.39)$$

where

$$g_{*S} = \sum_{i=\text{bosons}} g_i \left(\frac{T_i}{T}\right)^3 + \frac{7}{8} \sum_{i=\text{fermions}} g_i \left(\frac{T_i}{T}\right)^3. \quad (15.40)$$

For most of the history of the Universe all particle species had a common temperature, and g_{*S} can be replaced by g_* . The annihilation of electron-positron pairs after neutrinos ceased interacting with the electromagnetic plasma (“decoupled”) about 1 s after the bang leads to the slight heating of photons and $T_\gamma = (11/4)^{1/3} T_\nu$. Since then

$$\begin{aligned} g_* &= 2.0 + N_\nu \frac{7}{8} (4/11)^{4/3} = 3.363 \\ g_{*S} &= 2.0 + N_\nu \frac{7}{8} \frac{4}{11} = 43/11 = 3.91 \end{aligned} \quad (15.41)$$

where $N_\nu = 3$ has been used to obtain numerical values since much of the time since BBN all three neutrino species have been relativistic.

In the absence of an entropy producing event (*e.g.*, phase transition or particle decay), the entropy per comoving volume $S \propto R^3 s$ is conserved. The constancy of S implies that the temperature of the Universe evolves as

$$\begin{aligned} T &\propto g_{*S}^{-1/3} R^{-1} \\ \Rightarrow R &= 3.699 \times 10^{-10} g_{*S}(T)^{-1/3} \frac{\text{MeV}}{T}. \end{aligned} \quad (15.42)$$

Whenever g_{*S} is constant, the familiar result, $T \propto R^{-1}$, obtains. The factor of $g_{*S}^{-1/3}$ enters because whenever a particle species becomes nonrelativistic and disappears, its entropy is transferred to the other relativistic particle species still present in the thermal plasma, causing T to decrease *slightly less slowly*.

Constancy of S also implies that $s \propto R^{-3}$. This means the physical size of a comoving volume element is proportional to $R^3 \propto s^{-1}$. Thus the number of some species per unit comoving volume, $N \equiv R^3 n$, is equal to the number density of that species divided by s : $N \equiv n/s$. Particle-number conservation in the expanding Universe is thus simply expressed as the constancy of n/s .

The entropy density s is proportional to the number density of relativistic particles, and therefore, to the photon number density, $s = 1.80 g_{*S} n_\gamma$. Today $s = 7.04 n_\gamma$; g_{*S} is a function of temperature, and the factor relating s and n_γ has decreased with time. However, since about 1 s that factor has been constant.

As an example of the utility of the ratio n/s , consider the baryon number. The baryon number in a comoving volume is

$$\frac{n_B}{s} \equiv \frac{n_b - n_{\bar{b}}}{s}. \quad (15.43)$$

So long as baryon number nonconserving interactions are occurring very slowly, the baryon number in a comoving volume, n_B/s , is conserved. Today, there are only baryons and $s = 7.04 n_\gamma$; thus, the baryon number of the Universe $n_B/s \simeq \eta/7$, where η is the present baryon-to-photon ratio. From BBN we know $\eta = (5.1 \pm 0.3) \times 10^{-10}$, and so we can infer that the baryon number of the Universe $n_B/s = (7.2 \pm 0.4) \times 10^{-11}$. It is believed that this tiny asymmetry between matter and antimatter arises due to B , C , and CP violating interactions that occurred out of equilibrium in the early Universe (baryogenesis).

Finally, thermal equilibrium in the expanding Universe corresponds to the limit of particle interactions occurring much more rapidly than

the rate at which the temperature is dropping (set by expansion rate H). The opposite limit, a particle species that interacts slowly compared to the expansion rate (said to be decoupled), can be easily discussed. This limit applies to CMB photons after last scattering (redshift $z_{LS} \simeq 1100$) and neutrinos when the temperature of the Universe falls below about 1 MeV. The evolution of the phase-space distribution of a decoupled species is simple: particle momenta decrease as $1/R(t)$ and particle number density decrease as $1/R^3$. For a relativistic particle species that was in thermal equilibrium at decoupling (neutrinos and CMB photons), the phase-space distributions remain of the Fermi-Dirac or Bose-Einstein form, with a temperature that decreases precisely as $1/R(t)$. (Should the species eventually become nonrelativistic—for example a light neutrino species—the momentum phase-space distribution retains the FD or BE form, with $T \propto 1/R$.)

This fact explains why the CMB remains a perfect black body, and with some simple algebra and the constancy of S , how the factor of $(4/11)^{1/3}$ relating the neutrino and photon temperatures arises.

15.3. Beyond the Standard Cosmology: Inflation

Inflation is the most predictive and best developed idea about the earliest moments of the Universe. Further, its basic predictions—a flat Universe, a nearly scale-invariant spectrum of Gaussian, adiabatic density perturbations, and a nearly scale invariant spectrum of gravitational waves—are now being tested. The early results are consistent with the first two of these predictions; the third prediction will be much harder to test.

Inflation can provide insight about very fundamental issues not addressed by the standard cosmology: the origin of the large-scale isotropy and homogeneity; the origin of the small-scale inhomogeneity; the explanation for the oldness/flatness of the Universe; and in the context of simple grand unified theories, the monopole problem.

The key features of inflation are a period of accelerated expansion (typically exponential expansion), followed by an enormous release of entropy. During the period of exponential expansion a small, sub-horizon sized portion of the Universe is blown up to enormous size and made spatially flat. Quantum fluctuations in the field responsible for inflation, and in the metric of space time itself, are likewise stretched in size and eventually become density perturbations and gravitational waves. The entropy release that follows provides the heat that becomes the bath of radiation and other particles, thereby smoothly handing over the Universe to the standard hot big-bang phase. Provided that all of this occurs well before the epoch of big bang nucleosynthesis (*i.e.*, $T \gtrsim 1$ MeV and $t \lesssim 1$ s), inflation can successfully address the fundamental questions without upsetting the success of the standard hot big-bang cosmology.

15.3.1. Scalar-field dynamics:

While there is no standard model of inflation, essentially all models can be described by the evolution of a scalar field ϕ initially displaced from the minimum of its potential energy curve $V(\phi)$. The evolution of the field can be described by two phases: (1) the slow roll during which nearly exponential expansion is driven by the nearly constant potential energy; (2) the coherent oscillation/reheat phase, during which the field oscillates rapidly about the minimum of its potential and eventually decays into lighter fields reheating the Universe and producing the heat of the big bang.

During the first phase, the equation of motion for the homogeneous mode scalar field in the expanding Universe is

$$\ddot{\phi} + 3H\dot{\phi} + V'(\phi) = 0, \quad (15.44)$$

which is supplemented by the Friedmann equation

$$H^2 = \frac{8\pi}{3m_{\text{Pl}}^2} \left[\frac{1}{2}\dot{\phi}^2 + V(\phi) \right]. \quad (15.45)$$

Over a small patch of the Universe, the scalar field should be smooth enough to justify the homogeneity assumption, and as inflation proceeds, the inhomogeneities in the scalar field decay away rapidly. Likewise, the energy density associated with the scalar field quickly

come to dominate all other forms of energy in the Universe (*e.g.*, matter and radiation).

During the slow-roll phase the equations can be further simplified, as the $\ddot{\phi}$ term in the equation of motion and the $\dot{\phi}^2$ term in the expression for H^2 can be neglected:

$$\begin{aligned} \dot{\phi} &\simeq -\frac{V'}{3H} \\ dN \equiv d \ln R &= H dt = -\frac{8\pi}{m_{\text{Pl}}^2} \frac{d\phi}{V'/V}, \end{aligned} \quad (15.46)$$

where prime denotes $d/d\phi$. These equations hold until the potential steepens and the slow-roll conditions, $m_{\text{Pl}} V'/V \lesssim \sqrt{48\pi}$ and $m_{\text{Pl}}^2 V''/V \lesssim 24\pi$, are no longer valid.

During the slow-roll phase the Universe grows in size by a factor $\exp(N)$, where N is given by the integral of dN . To solve the flatness and horizon problems, N must be greater than about 60 (the precise number depends upon when inflation takes place and the temperature to which the Universe reheats after inflation). Quantum fluctuations in ϕ , which correspond to energy density fluctuations, $\Delta\rho \sim \Delta\phi V'$, are stretched exponentially from microscopic size to astrophysical size. Likewise, quantum fluctuations in the metric undergo similar exponential stretching.

When the slow-roll phase ends, accelerated expansion ends and the scale factor grows as a power law that depends upon the shape of the potential. Ultimately, the energy in the ϕ field is transferred to other, lighter fields. These fields interact and create the thermal bath of particles that we are confident existed during the earliest moments of the Universe.

Though there are many interesting intermediate details, the reheating of the Universe involves the transition from a cold Universe dominated by the zero-momentum mode of the scalar field to a hot Universe dominated by many degrees of freedom.

While there is no standard model for inflation, typically the energy scale of inflation is $V^{1/4} \sim 10^{14}$ GeV, though models exist with energy scales as small as 1 TeV. The potential V must be very flat, typically with a dimensionless coupling of the order of 10^{-14} (which is driven to be this small by the requirement of the density perturbation amplitude of 10^{-5}). The simplest model of inflation is a potential of the form $V(\phi) = \lambda\phi^4$, in this case, $\lambda \simeq 10^{-14}$ and the 60 or so e -folds of inflation needed to produce a large enough patch to contain our present Hubble volume occurs as ϕ rolls from $4.5m_{\text{Pl}}$ to $m_{\text{Pl}}/\sqrt{2\pi}$.

15.3.2. Predictions for observables:

The spectrum of gravity waves (tensor perturbations) and density (or scalar) perturbations are the basis of the observables associated with inflation. They can be directly calculated from the properties of the scalar-field potential. This fact is the basis for the belief that observations may someday pin down the underlying model of inflation.

In most models both scalar and tensor perturbations have an approximately scale-invariant spectrum. In physical terms, that means that the dimensionless strain amplitude of gravity waves when they re-enter the horizon after inflation is independent of scale; in terms of the inflationary potential, that amplitude is $h_{\text{HOR}} \sim H/m_{\text{Pl}} \sim V^{1/2}/m_{\text{Pl}}^2$. For density perturbations, it is the amplitude of the density perturbation at horizon crossing that is independent of scale: $(\delta\rho/\rho)_{\text{HOR}} \sim H^2/\dot{\phi} \sim V^{3/2}/m_{\text{Pl}}^3 V'$. Further, both spectra are expected to deviate from exact scale invariance by a small amount that depends upon the potential. Finally, the Fourier components of both scalar and tensor perturbations are approximately power-law in wavenumber k .

Primordial perturbations and gravity waves lead to CMB fluctuations, so measurable quantities may be expressed in terms of the inflationary potential. For instance, the scalar contribution (S) and the tensor contribution (T) to the CMB quadrupole anisotropy are

$$\begin{aligned} S &\equiv \frac{5C_2^S}{4\pi} \simeq 2.9 \frac{V/m_{\text{Pl}}^4}{(m_{\text{Pl}} V'/V)^2} \\ T &\equiv \frac{5C_2^T}{4\pi} \simeq 0.56 (V/m_{\text{Pl}}^4), \end{aligned} \quad (15.47)$$

where C_2^S and C_2^T are the contribution of scalar and tensor perturbations to the variance of the $l = 2$ multipole amplitude ($\langle |a_{2m}|^2 \rangle = C_2^S + C_2^T$) and V is the value of the inflationary potential when the scale $k = H_0$ (present horizon scale) crossed the Hubble radius during inflation. Note, that the numerical coefficients in these expressions depend upon the composition of the Universe; the numbers shown are for $\Omega_M = 0.35$ and $\Omega_\Lambda = 0.65$.

The power-law indices that characterize the scalar and gravity-wave spectra may also be expressed in terms of the inflationary potential and its derivatives:

$$\begin{aligned} n - 1 &= -\frac{1}{8\pi} \left(\frac{m_{\text{Pl}} V'}{V} \right)^2 + \frac{m_{\text{Pl}}}{4\pi} \left(\frac{m_{\text{Pl}} V'}{V} \right)' \\ n_T &= -\frac{1}{8\pi} \left(\frac{m_{\text{Pl}} V'}{V} \right)^2. \end{aligned} \quad (15.48)$$

Variations in the power-law indices with k may be expressed in terms of higher derivatives of V . For example,

$$\frac{dn}{d \ln k} = -\frac{m_{\text{Pl}}}{8\pi} \left(\frac{m_{\text{Pl}} V'}{V} \right) \frac{dn}{d\phi}. \quad (15.49)$$

Finally, one can in principle use these observables to solve for the inflationary potential and its first two derivatives at the value of ϕ when the scale that fixes the CMB quadrupole crossed the Hubble radius during inflation:

$$\begin{aligned} V &= 1.8T m_{\text{Pl}}^4, \\ V' &= \pm \sqrt{\frac{8\pi T}{7S}} V/m_{\text{Pl}}, \\ V'' &= 4\pi \left[(n-1) + \frac{3T}{7S} \right] V/m_{\text{Pl}}^2, \end{aligned} \quad (15.50)$$

where the factor 1.8 depends upon the composition of the Universe and is given for $\Omega_M = 0.35$ and $\Omega_\Lambda = 0.65$. The key to learning about the inflationary potential is measuring the ratio of the gravity-wave to density-perturbation contributions to the CMB quadrupole anisotropy. From that ratio, T/S , and the quadrupole anisotropy ($= T + S$), which has been measured by COBE, one can infer T . Further, if the spectrum of the inflation-produced gravity waves (n_T) can be measured, there is an important consistency test: inflation predicts $T/S = -4.9 n_T$ (for $\Omega_M = 0.35$ and $\Omega_\Lambda = 0.65$).

15.3.3. The new standard model:

Motivated by the predictions of inflation and the best fit for the matter/energy content of the Universe, a standard model is emerging: Λ CDM. The model is characterized by its energy/matter content; in terms of the critical density, 65% vacuum energy, 30% cold dark matter particles, and 5% baryons with a tiny bit of hot dark matter. It is a flat ($k = 0$) model with a Hubble constant of about $65 \text{ km s}^{-1} \text{ Mpc}^{-1}$ and inflation-produced density perturbations that are close to being scale invariant. This model embodies all the successes of the hot big-bang cosmology, as well as the aspirations of inner space/outer space connection. Just as importantly, it is consistent with a very large (and rapidly growing) body of cosmological observations, including, the age of the Universe, the power spectrum of inhomogeneity, the CMB anisotropy measurements from 0.1° to 100° , the studies of the abundance and evolution of galaxies and clusters, the mapping of dark matter in clusters and galaxies, further supernovae observations, and more.

But important questions remain: If there is dark energy, is it just a cosmological constant, and if so why is it so small? What is the nonbaryonic dark matter? What is the primeval spectrum of inhomogeneity and is it consistent with the simplest models of inflation? What are the underlying model parameters of inflation? How does baryogenesis work and can the baryon asymmetry be related to laboratory measurements of CP violation, neutrino masses or proton decay? Is there a fundamental explanation for the odd matter/energy recipe for our Universe? Will one of the seemingly minor puzzles that exist today (the sheet like structures separated by $125 h^{-1} \text{ Mpc}$ or the disagreement between theory and observation about the structure of CDM halos) unravel the whole picture? With the flood of observations and data that are coming, we can hope to answer these questions and more in the next decade or so.

References:

1. J.R. Mould *et al.*, *Astrophys. J.* **529**, 786 (2000).
2. S. Perlmutter *et al.*, *Astrophys. J.* **517**, 565 (1999).
3. B. Chaboyer *et al.*, *Astrophys. J.* **494**, 96 (1998).
4. P. de Bernardis *et al.*, *Nature* **404**, 955 (2000).
5. S. Burles *et al.*, *Phys. Rev. Lett.* **82**, 4176 (1999).
6. J. Mohr *et al.*, *Astrophys. J.* **517**, 627 (1999).
7. Y. Fukuda *et al.*, *Phys. Rev. Lett.* **81**, 1562 (1998).
8. S. Dodelson *et al.*, *Science* **274**, 69 (1996);
R.A.C. Croft, W. Hu, and R. Dave, *Phys. Rev. Lett.* **83**, 1092 (1999).
9. A.G. Riess, *et al.*, *Astron. J.* **116**, 1009 (1998).
10. P.M. Garnavich *et al.*, *Astrophys. J.* **507**, 74 (1998);
S. Perlmutter *et al.*, *Phys. Rev. Lett.* **83**, 670 (1999).
11. S.A. Shectman *et al.*, *Astrophys. J.* **470**, 172 (1996).
12. J. Peacock and S. Dodds, *Mon. Not. Roy. Astron. Soc.* **267**, 1020 (1994).

16. BIG-BANG NUCLEOSYNTHESIS

Revised September 1999 by K.A. Olive (Univ. of Minnesota).

Among the successes of the standard big-bang model is the agreement between the predictions of big-bang nucleosynthesis (BBN) for the abundances of the light elements, D, ^3He , ^4He , and ^7Li , and the primordial abundances inferred from observational data (see [1–4] for a more complete discussion). These abundances span some nine orders of magnitude: ^4He has an abundance by number relative to hydrogen of about 0.08 (accounting for about 25% of the baryonic mass), while ^7Li , the least abundant of the elements with a big-bang origin, has an abundance by number relative to hydrogen of about $\sim 10^{-10}$.

16.1. Big-bang nucleosynthesis theory

The BBN theory matches the observationally determined abundances with a single well-defined parameter, the baryon-to-photon ratio, η . All the light-element abundances can be explained with η in the range $(1.2\text{--}5.7) \times 10^{-10}$, or $\eta_{10} \equiv \eta \times 10^{10} = 1.2\text{--}5.7$. Equivalently, this range can be expressed as the allowed range for the baryon mass density, $\rho_B = 0.8\text{--}3.9 \times 10^{-31} \text{ g cm}^{-3}$, and can be converted to the fraction, Ω , of the critical density, ρ_c .

The synthesis of the light elements was affected by conditions in the early Universe at temperatures $T \lesssim 1 \text{ MeV}$, corresponding to an age as early as 1 s. At somewhat higher temperatures, weak-interaction rates were in equilibrium, thus fixing the ratio of the neutron and proton number densities. At $T \gg 1 \text{ MeV}$, $n/p \approx 1$, since the ratio was given approximately by the Saha relation, $n/p \approx e^{-Q/T}$, where Q is the neutron-proton mass difference. As the temperature fell, the Universe approached the point (“freeze-out”) where the weak-interaction rates were no longer fast enough to maintain equilibrium. The final abundance of ^4He is very sensitive to the n/p ratio at freeze-out.

The nucleosynthesis chain begins with the formation of deuterium in the process $pn \rightarrow D\gamma$. However, photo-dissociation by the high number density of photons ($n_\gamma/n_B = \eta^{-1} \sim 10^{10}$) delays production of deuterium (and other complex nuclei) well past the point where T reaches the binding energy of deuterium, $E_B = 2.2 \text{ MeV}$. (The average photon energy in a blackbody is $\bar{E}_\gamma \approx 2.7 T$.) When the quantity $\eta^{-1} \exp(-E_B/T)$ reaches about 1 (at $T \approx 0.1 \text{ MeV}$), the photo-dissociation rate finally falls below the nuclear production rate.

The 25% fraction of mass in ^4He due to BBN is easily estimated by counting the number of neutrons present when nucleosynthesis begins. When the weak-interaction rates freeze-out at about $T \approx 0.8 \text{ MeV}$, the n -to- p ratio is about 1/6. When free-neutron decays prior to deuterium formation are taken into account, the ratio drops to $n/p \lesssim 1/7$. Then simple counting yields a primordial ^4He mass fraction

$$Y_p = \frac{2(n/p)}{1 + n/p} \lesssim 0.25. \quad (16.1)$$

In the Standard Model, the ^4He mass fraction depends primarily on the baryon-to-photon ratio η , as it is this quantity that determines when nucleosynthesis via deuterium production may begin. But because the n/p ratio depends only weakly on η , the ^4He mass fraction is relatively flat as a function of η . The effect of the uncertainty in the neutron half-life, $\tau_n = 886.7 \pm 1.9 \text{ s}$, is now small. Lesser amounts of the other light elements are produced: D and ^3He at the level of a few times 10^{-5} by number relative to H, and $^7\text{Li}/\text{H}$ at the level of about 10^{-10} , when η is in the range $1 - 10 \times 10^{-10}$.

When we go beyond the Standard Model, the ^4He abundance is very sensitive to changes in the expansion rate, which can be related to the effective number of neutrino flavors. This will be discussed below.

The calculated abundances of the light elements are shown in Fig. 16.1 as a function of η_{10} . The curves for the ^4He mass fraction, Y_p , bracket the range based primarily on the uncertainty of the neutron mean-life. The spread in the ^7Li curves is due to the 1σ uncertainties in nuclear cross sections leading to ^7Li and ^7Be which subsequently decays to ^7Li [5–7]. Similarly, the spread in the curves for D and ^3He are 1σ uncertainties in the D and ^3He predictions. The

boxes show the observed abundances with their range of uncertainty, discussed below. Since the observational boxes line up on top of each other, there is an overall agreement between theory and observations for η_{10} in the range 1.2–5.7.

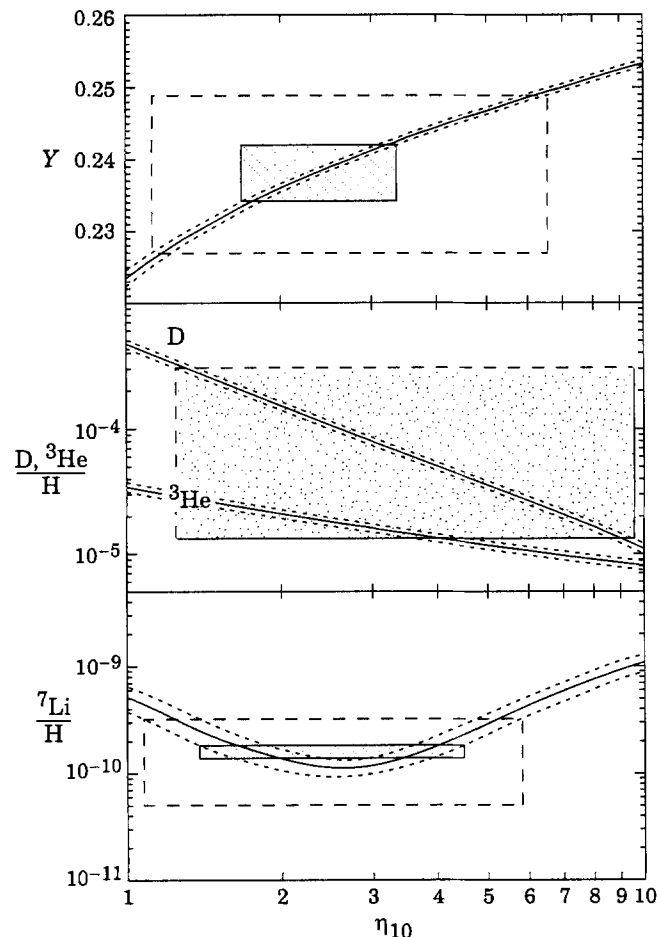


Figure 16.1: The abundances of D, ^3He , ^4He and ^7Li as predicted by the standard model of big-bang nucleosynthesis. Also shown by a series of boxes is the comparison between these predictions and the observational determination of the light element abundances. See text for details.

16.2. Observations

Because stars produce helium as well as heavier elements, one must search for primordial helium in regions where stellar processing has been minimal, *i.e.*, in regions where abundances of elements such as carbon, nitrogen and oxygen are very low. There are extensive compilations of observed abundances of ^4He , N, and O in many different extra-galactic regions of ionized H [8,9]. Extrapolating the ^4He abundances from the data leads to an observational estimate for Y_p of [10–13]

$$Y_p = 0.238 \pm 0.002 \pm 0.005. \quad (16.2)$$

(Here and elsewhere, the first error is the statistical standard deviation, and the second systematic.) The box in Fig. 16.1 bracketing the ^4He curves covers the range 0.234–0.242, where the half height is given as twice the statistical error. Of course the real uncertainty is dominated by systematic effects and the dashed box is obtained using a larger error (twice the statistical and systematic error when added in quadrature) allowing Y_p to take values in an extended range 0.227–0.249.

Observations for deuterium and ^3He abundances currently present certain difficulties. All deuterium is primordial [14], but some of the primordial deuterium has been destroyed. Thus, as can be seen in the figure, the present deuterium abundance gives us an absolute upper limit to η . However, to get more information requires either an understanding of galactic chemical evolution of deuterium or a direct measurement of primordial deuterium. Even more problematical is ^3He : Not only is primordial ^3He destroyed in stars but it is very likely that at least some low-mass stars are net producers of ^3He . Neither the galactic chemical evolution of ^3He nor the production of ^3He in stars is well understood with standard models and observations presenting an inconsistent picture.

It appears that D/H has decreased over the age of the galaxy. Samples obtained deep inside meteorites provide measurements of the true (pre)-solar system abundance of ^3He , while measurements on meteoritic near-surface samples, the solar wind, and lunar soil samples also contain ^3He converted from deuterium in the early pre-main-sequence stage of the sun. The best current values are [15]

$$\begin{aligned} \left(\frac{\text{D} + ^3\text{He}}{\text{H}}\right)_{\odot} &= (4.1 \pm 1.0) \times 10^{-5}, \\ \left(\frac{^3\text{He}}{\text{H}}\right)_{\odot} &= (1.5 \pm 0.3) \times 10^{-5}. \end{aligned} \quad (16.3)$$

The difference between these, is the pre-solar D abundance. There has also been a recent measurement of HD in the atmosphere of Jupiter [16] yielding a value $\text{D}/\text{H} = (2.7 \pm 0.7) \times 10^{-5}$ which is consistent with the above presolar value of D/H.

The present interstellar-medium abundance of D/H is [17]

$$\text{D}/\text{H} = 1.60 \pm 0.09_{-0.10}^{+0.05} \times 10^{-5}. \quad (16.4)$$

It is this lowest value of D/H that provides the most robust upper bound on η , since D is only destroyed. It is shown (decreased by twice the errors added in quadrature) as the lower right corner of the D and ^3He box in Fig. 16.1. Thus, with confidence we can be sure that $\eta_{10} < 9.5$ And correspondingly $\Omega_B h^2 < 0.035$.

Deuterium has also been detected in high-redshift, low-metallicity quasar absorption systems [18–20]. These measured abundances should represent the primordial value, but, they are at present not consistent: Two [18,19] give a relatively high value for $\text{D}/\text{H} \approx 2 \times 10^{-4}$ while another two [20] give $\text{D}/\text{H} \approx 3.4 \pm 0.3 \times 10^{-5}$. Although it appears that the quality of the low D/H data is better than those showing high D/H, the latter can be used at the very least as an upper limit to primordial D/H and this is shown by the dashed box in Fig. 16.1, taking a 2σ upper limit of $\text{D}/\text{H} < 3 \times 10^{-4}$. As one can see, the corresponding value of Y_p (at the same value of η as inferred by the observation of a high D/H) is in good agreement with the data. ^7Li is also in agreement at this value as well. However, due to the still somewhat preliminary status of this observation, it is premature to use it to fix the primordial abundance. A high value for the D abundance would require an even greater degree of D destruction over the age of the galaxy. The lower measurement for D/H requires that systematics work coherently for both ^4He and ^7Li to give an overlap with this data. Systematic effects [21] may, however, imply a higher D/H abundance (in the low D/H objects) which is in the range $3.5\text{--}5 \times 10^{-5}$. At the upper end of this range, all of the light element abundances are also in concordance. Eventually, the primordial D/H issue will hopefully be resolved and give a correspondingly narrow allowed range in η and perhaps change the nature of the ^3He and ^7Li (see below) arguments which are currently dominated by galactic and/or stellar evolution issues.

Finally, we turn to ^7Li . In old, hot, population-II stars, ^7Li is found to have a very nearly uniform abundance. For stars with a surface temperature $T > 5500$ K and a metallicity less than about 1/20th solar (so that effects such as stellar convection may not be important), the abundances show little or no dispersion beyond that consistent with the errors of individual measurements. Much data has been obtained recently from a variety of sources, and the best estimate for the mean ^7Li abundance and its statistical uncertainty in halo stars

is [22] (the estimate of the systematic uncertainty discussed below is our own)

$$\text{Li}/\text{H} = (1.6 \pm 0.1_{-0.3-0.6}^{+0.4+0.9}) \times 10^{-10}. \quad (16.5)$$

The first error is statistical. The box in Fig. 16.1 corresponds to a $2\sigma_{\text{stat}}$ spread. The second set of errors is a systematic uncertainty that covers the range of abundances derived by various methods. The third set of errors in Eq. (16.5) accounts for the possibility that some of the primordial ^7Li has been destroyed in stars, and that as much as 40% of the observed ^7Li was produced in cosmic ray collisions rather than in the Big Bang. This uncertainty has been constrained by recent observations showing some evidence for evolution in ^7Li [23]. These uncertainties (depicted with a half height of $2\sigma_{\text{stat}} + \sigma_{\text{syst}}$) are shown by the dashed box in Fig. 16.1. Observations of ^6Li , Be, and B help constrain the degree to which these effects play a role [24–26].

16.3. A consistent value for η

For the Standard Model of BBN to be deemed successful, theory and observation of the light element abundances must agree using a single value of η . We summarize the constraints on η from each of the light elements. From the ^4He mass fraction, $Y_p < (0.242\text{--}0.249)$, we have $\eta_{10} < (3.4\text{--}6.6)$ as a 2σ upper limit (the highest values use possible systematic errors as shown by the shaded box in the figure). Because of the sensitivity to the assumed upper limit on Y_p and Li/H, the upper limit on η from D/H, is still of value. From $\text{D}/\text{H} > 1.3 \times 10^{-5}$, we have $\eta_{10} \lesssim 9.5$.

The lower limit on η_{10} can be obtained from either D/H or ^7Li . From the high D/H measurement in quasar absorption systems, we obtain $\eta_{10} > 1.2$. ^7Li allows a broad range for η_{10} consistent with the other elements. When uncertainties in the reaction rates and systematic uncertainties in the observed abundances are both taken into account, ^7Li allows values of η_{10} between (1.1–5.7).

The determination of η depends on our certainty that the observations of the light elements abundances can be translated into primordial abundances. This is perhaps more straightforward for ^4He and ^7Li , where the element abundances are determined in primitive low metallicity environments. If it turns out that a consistent value for D/H can be obtained from quasar absorption systems, then because of the slope of D/H with respect to η , D/H will be the best isotope for the determination of η . Until then, the use of the D and ^3He abundance determinations is necessarily complicated by the evolution of the abundances of these elements over the star forming history of the galaxy. Uncertainties in the ^3He evolution are compounded by uncertainties of stellar production/destruction mechanisms. The resulting overall consistent range for η_{10} is extended to (1.2–5.7) when systematic errors are pushed to their limits. These bounds on η_{10} constrain the fraction of critical density in baryons, Ω_B , to be

$$0.004 < \Omega_B h_0^2 < 0.021. \quad (16.6)$$

For a Hubble parameter, h_0 , between 0.4 and 1.0, the corresponding range for Ω_B is 0.004–0.13.

Perhaps the best test of BBN will come when anisotropies in the microwave background check the determination of Ω_B . At present, other measurements (such as of hot X-ray gas in clusters of galaxies, Lyman- α clouds, or microwave anisotropies) of Ω_B give considerably larger uncertainties than those from BBN, but they are consistent with the BBN range.

16.4. Beyond the Standard Model

Limits on particle physics beyond the Standard Model come mainly from the observational bounds on the ^4He abundance. As discussed earlier, the neutron-to-proton ratio is fixed by its equilibrium value at the freeze-out of the weak-interaction rates at a temperature $T_f \sim 1$ MeV, with corrections for free neutron decay. Furthermore, freeze-out is determined by the competition between the weak-interaction rates and the expansion rate of the Universe,

$$G_F^2 T_f^5 \sim \Gamma_{\text{wk}}(T_f) = H(T_f) \sim \sqrt{G_{NN}} T_f^2, \quad (16.7)$$

where N counts the total (equivalent) number of relativistic particle species. The presence of additional neutrino flavors (or of any other relativistic species) at the time of nucleosynthesis increases the energy density of the Universe and hence the expansion rate, leading to a larger value of T_f , n/p , and ultimately Y_p . It is clear that just as one can place limits [27] on N , any changes in the weak or gravitational coupling constants can be similarly constrained.

In the Standard Model, the number of particle species can be written as $N = 5.5 + \frac{7}{4}N_\nu$; 5.5 accounts for photons and e^\pm , and N_ν is the number of (massless) neutrino flavors. The helium curves in Fig. 16.1 were computed assuming $N_\nu = 3$, and the computed ^4He abundance scales roughly as $\Delta Y_{\text{BBN}} \approx 0.012 - 0.014 \Delta N_\nu$. Clearly the central value for N_ν from BBN will depend on η . If the best value for the observed primordial ^4He abundance is 0.238, then, for $\eta_{10} \sim 1.8$, the central value for N_ν is very close to 3. By means of a likelihood analysis on η and N_ν based on ^4He and ^7Li [28,29](see also [30]) it was found that the 95% CL ranges are $1.7 \leq N_\nu \leq 4.3$, and $1.4 \leq \eta \leq 4.9$.

The limits on N_ν can be translated into limits on other types of particles or particle masses that would affect the expansion rate of the Universe just prior to nucleosynthesis. In some cases, it is the interaction strengths of new particles which are constrained. Particles with less than full weak strength interactions contribute less to the energy density than particles that remain in equilibrium up to the time of nucleosynthesis [31].

We close with a simple example. Suppose there exist three right-handed neutrinos with only right-handed interactions of strength $G_R < G_F$. The standard left-handed neutrinos are no longer in equilibrium at temperatures below ~ 1 MeV. Particles with weaker interactions decouple at higher temperatures, and their number density ($\propto T^3$) relative to neutrinos is reduced by the annihilations of particles more massive than 1 MeV. If we use the upper bound $N_\nu < 4.0$, then the three right-handed neutrinos must have a temperature $3(T_{\nu_R}/T_{\nu_L})^4 < 1$. Since the temperature of the decoupled ν_R 's is determined by entropy conservation, $T_{\nu_R}/T_{\nu_L} = [(43/4)/N(T_f)]^{1/3} < 0.76$, where T_f is the freeze-out temperature of the ν_R 's. Thus $N(T_f) > 24$ and decoupling must have occurred at $T_f > 140$ MeV. Finally, the decoupling temperature is related to G_R by $(G_R/G_F)^2 \sim (T_f/3 \text{ MeV})^{-3}$, where 3 MeV corresponds to the decoupling temperature for ν_L . This yields a limit $G_R \lesssim 10^{-2} G_F$. These limits are strongly dependent on the assumed upper limit to N_ν ; for $N_\nu < 3.5$, the limit on G_R strengthened to $G_R < 0.002 G_F$, since T_f is constrained to be larger than the temperature corresponding to the QCD transition in the early Universe.

References:

1. D.N. Schramm and R.V. Wagoner, *Ann. Rev. Nucl. and Part. Sci.* **27**, 37 (1977).
2. A. Boesgard and G. Steigman, *Ann. Rev. Astron. Astrophys.* **23**, 319 (1985).
3. T.P. Walker, G. Steigman, D.N. Schramm, K.A. Olive, and H.-S. Kang, *Astrophys. J.* **376**, 51 (1991).
4. K.A. Olive, G. Steigman, and T.P. Walker, *Phys. Rep.* (in press) astro-ph/9905320.
5. C.J. Copi, D.N. Schramm, and M.S. Turner, *Science* **267**, 192 (1995).
6. L.M. Krauss and P. Romanelli, *Astrophys. J.* **358**, 47 (1990).
7. N. Hata, R.J. Scherrer, G. Steigman, D. Thomas, and T.P. Walker, *Astrophys. J.* **458**, 637 (1996).
8. B.E.J. Pagel, E.A. Simonson, R.J. Terlevich, and M. Edmunds, *MNRAS* **255**, 325 (1992).
9. Y.I. Izotov, T.X. Thuan, and V.A. Lipovetsky, *Astrophys. J.* **435**, 647 (1994);
Y.I. Izotov and T.X. Thuan, *Astrophys. J. Supp.* **108**, 1 (1997);
Astrophys. J. **500**, 188 (1998).
10. K.A. Olive and G. Steigman, *Astrophys. J. Supp.* **97**, 49 (1995).
11. K.A. Olive and S.T. Scully, *Int. J. Mod. Phys. A* **11**, 409 (1996).
12. K.A. Olive, E. Skillman, and G. Steigman, *Astrophys. J.* **493**, 788 (1997).
13. B.D. Fields and K.A. Olive, *Astrophys. J.* **506**, 177 (1998).
14. H. Reeves, J. Audouze, W. Fowler, and D.N. Schramm, *Astrophys. J.* **179**, 909 (1973).
15. J. Geiss, in *Origin and Evolution of the Elements*, eds. N. Prantzos, E. Vangioni-Flam, and M. Cassé (Cambridge: Cambridge University Press, 1993), p. 89.
16. H.B. Niemann *et al.*, *Science*, **272**, 846 (1996);
P.R. Mahaffy *et al.*, *Sp. Sci. Rev.* **84**, 251 (1998).
17. J.L. Linsky, *et al.*, *Astrophys. J.* **402**, 695 (1993);
J.L. Linsky, *et al.*, *Astrophys. J.* **451**, 335 (1995).
18. R.F. Carswell, M. Rauch, R.J. Weymann, A.J. Cooke, J.K. Webb, *MNRAS* **268**, L1 (1994);
A. Songaila, L.L. Cowie, C. Hogan, M. Rugers, *Nature* **368**, 599 (1994).
19. J.K. Webb *et al.*, *Nature* **388**, 250 (1997);
D. Tytler *et al.*, *Astron. J.* **117**, 63 (1999).
20. D. Tytler, X.-M. Fan, and S. Burles, *Nature* **381**, 207 (1996);
D. Tytler, and S. Burles, *Astrophys. J.* **460**, 584 (1996);
D. Tytler, and S. Burles, *Astrophys. J.* **499**, 699 (1998);
D. Tytler, and S. Burles, *Astrophys. J.* **507**, 732 (1998).
21. S. Levshakov, D. Tytler, and S. Burles, astro-ph/9812114.
22. P. Molaro, F. Primas, and P. Bonifacio, *Astron. & Astrophys.* **295**, L47 (1995);
P. Bonifacio and P. Molaro, *MNRAS*, 285,847(1997).
23. S.G. Ryan, J.E. Norris, and T.C. Beers, *Astrophys. J.* (in press) astro-ph/9903059 (1999).
24. T.P. Walker, G. Steigman, D.N. Schramm, K.A. Olive, and B. Fields, *Astrophys. J.* **413**, 562 (1993).
25. K.A. Olive, and D.N. Schramm, *Nature* **360**, 439 (1993).
26. G. Steigman, B. Fields, K.A. Olive, D.N. Schramm, and T.P. Walker, *Astrophys. J.* **415**, L35 (1993);
E. Vangioni-Flam *et al.*, *New Astronomy* **4**, 245 (1999);
B.D. Fields and K.A. Olive, *New Astronomy* **4**, 255 (1999).
27. G. Steigman, D.N. Schramm, and J. Gunn, *Phys. Lett.* **B66**, 202 (1977).
28. B.D. Fields and K.A. Olive, *Phys. Lett.* **B368**, 103 (1996);
B.D. Fields, K. Kainulainen, D. Thomas, and K.A. Olive, *New Astronomy* **1**, 77 (1996).
29. K.A. Olive and D. Thomas, *Astro. Part. Phys.* **7**, 27 (1997);
K.A. Olive and D. Thomas, *Astro. Part. Phys.* **11**, 403 (1999).
30. C.J. Copi, D.N. Schramm, and M.S. Turner, *Phys. Rev.* **D55**, 3389 (1997).
31. G. Steigman, K.A. Olive, and D.N. Schramm, *Phys. Rev. Lett.* **43**, 239 (1979);
K.A. Olive, D.N. Schramm, and G. Steigman, *Nucl. Phys.* **B180**, 497 (1981).

17. GLOBAL COSMOLOGICAL PARAMETERS: H_0 , Ω_M , and Λ

Written April 2000 by M. Fukugita (University of Tokyo, Institute for Cosmic Ray Research) and C.J. Hogan (University of Washington).

This review surveys the current status of the determination of the three cosmological parameters, the Hubble constant H_0 , the mass density parameter Ω_M and the cosmological constant Λ . These quantities set the scale and characterize the mean mass-energy content and curvature in cosmological solutions of Einstein's equations which describe the geometry and evolution of the universe as a whole. For technical details, see Ref. 1.

We adopt the normalization $\Omega_M + \Omega_\Lambda = 1$ for zero curvature (flat universe), where $\Omega_\Lambda = \Lambda/3H_0^2$ with Λ being the cosmological constant entering in the Einstein equation. The case with $\Omega_M = 1$ and $\Omega_\Lambda = 0$ is referred to as the Einstein-de Sitter (EdS) universe. We often use distance modulus $m - M = 5 \log(d_L/10 \text{ pc})$ instead of the luminosity distance d_L , where m is the apparent magnitude of an object whose magnitude at 10 pc would be M . We omit the unit $\text{km s}^{-1}\text{Mpc}^{-1}$ for the Hubble constant and adopt the abbreviation $h = H_0/100$.

17.1. The Hubble Constant

17.1.1. Overview: The Hubble constant, which has dimension of inverse time, sets the scale of the size and age of the Universe. Recent efforts to measure it have almost solved the long-standing discrepancy concerning the extragalactic distance scale; at the same time, new uncertainties have been revealed in the Milky Way distance scale.

The global value of H_0 was uncertain by a factor of two for several decades. Before 1980 the dispute was between two schools: Sandage and collaborators insisted on $H_0 = 50$; de Vaucouleurs and collaborators preferred a high value, $H_0 = 90\text{--}100$. The dichotomy persisted even after the discovery of an empirical but tight relationship between a galaxy's luminosity and rotation velocity, known as the Tully-Fisher relation, which allowed relative distances between whole galaxies to be estimated far out into the smooth Hubble flow. A straightforward reading of the Tully-Fisher relation gave values $H_0 = 80\text{--}90$, but this result was challenged over the issue of the Malmquist bias—whether the sample selects preferentially bright galaxies, biasing towards a shorter distance. A related dispute concerned the distance to the Virgo cluster, 16 Mpc or 22 Mpc, depending on the sample used.

The next major advance came in 1989–1990 when new, more precise relative distance indicators were discovered: the apparently universal shape of the planetary nebula luminosity function (PNLF), and the surface brightness fluctuations (SBF) in galaxy images, utilizing the fact that a more distant galaxy shows a smoother light distribution. The two completely independent methods predicted relative distances to individual galaxies in excellent agreement with each other, and also with the Tully-Fisher relation (albeit with a somewhat larger scatter) [2]. These new techniques, when calibrated with the distance to M31, yielded a value around $H_0 = 80$ and a Virgo distance of 15 Mpc.

Around the same time Type Ia supernovae (SNeIa) were widely adopted as standard candles. This led to $H_0 = 50\text{--}55$, when calibrated with a Cepheid distance to the nearest SNIa host galaxy using the pre-refurbished *Hubble Space Telescope* (HST). Thus in the early nineties estimates were still dichotomous between $H_0 = 50$ and 80.

The refurbishment of HST allowed accurate measurements of Cepheids in galaxies as distant as 20 Mpc. This secured the distance to the Virgo cluster and tightened the calibrations of the extragalactic distance indicators, and resulted in $H_0 = (70\text{--}75) \pm 10$, 10% lower than the 'high value'. Another important contribution was the discovery that the maximum brightness of SNeIa varies from supernova to supernova, and that it correlates tightly with the decline rate of brightness. Direct calibration of the maximum brightness of several SNeIa with HST Cepheid observations yielded $H_0 = 65^{+5}_{-10}$, and nearly resolved the long-standing controversy.

All the methods mentioned above use distance ladders and take the distance to the Large Magellanic Cloud (LMC) to be 50 kpc ($m - M = 18.5$) as the zero point. Before 1997 few doubts were cast on the distance to LMC. With the exception of determinations using RR Lyr stars, the distance modulus converged to $m - M = 18.5 \pm 0.1$, i.e., with a 5% error, and the RR Lyr discrepancy was blamed on its larger calibration error. It had been believed that the Hipparcos astrometric satellite would secure the distance within the Milky Way and tighten the distance to LMC. To everyone's surprise, Hipparcos instead revealed the contrary: the distance to LMC was more uncertain than we had thought, introducing new uncertainties into the determination of H_0 . Connected to this, the age of the Universe turned out to be more uncertain than had been believed.

17.1.2. Extragalactic distance scale: The measurement of cosmological distances traditionally employs distance ladders, as shown in Table 17.1. The listings written in italics indicate new methods which circumvent intermediate rungs. The most important milestone of the ladder is the LMC distance, 50 kpc ($m - M = 18.5$). The century-old Cepheid period-luminosity (PL) relation is still given great weight, but requires a few lower rungs to calibrate its zero point.

The refurbishment of HST achieved sufficient resolution to resolve Cepheids in the Virgo cluster [3]. Now 23 nearby spiral galaxies within 25 Mpc are given distances measured using the Cepheid PL relation [4]. A typical random error is 4–5% (0.08–0.10 mag), and the systematic error (from photometry) is 5% (0.1 mag) excluding the uncertainty of the LMC distance, to which the HST-KP ("Key Project") group assigns 6.5% error (0.13 mag). The prime use of these galaxies is to calibrate secondary distance indicators, which penetrate to sufficient depth that perturbations in the Hubble flow are a minor component of the error budget. The results are summarized in Table 17.2. We include a few earlier SNIa results which employed a partial list of Cepheid calibrators.

Table 17.1: Traditional distance ladders.

Method	Distance range	typical targets
Population I stars		
trigonometric or kinematic methods (ground)	< 50 pc	Hyades, nearby dwarfs
main sequence fitting (FG stars) Pop. I	< 200 pc	Pleiades
<i>trigonometric method (Hipparcos)</i>	< 500 pc	nearby open clusters
main sequence fitting (B stars)	40 pc–10 kpc	open clusters
Cepheids [Population I] (ground)	1 kpc–3 Mpc	LMC, M31, M81
<i>Cepheids [Population I] (HST)</i>	< 30 Mpc	Virgo included
secondary (extragalactic) indicators	700 kpc–100 Mpc	
Population II stars		
<i>trigonometric method (Hipparcos)</i>	< 500 pc	nearby subdwarfs
subdwarf main sequence fitting	100 pc–10 kpc	global clusters
cluster RR Lyr	5 kpc–100 kpc	LMC, age determinations

Table 17.2: Hubble constant (uncertainties in the LMC distance are not included).

Secondary indicators	References	Hubble constant
Tully-Fisher	HST-KP (Sakai <i>et al.</i> , [8])	$71 \pm 4 \pm 7$
Fundamental plane	HST-KP (Kelson <i>et al.</i> , [9])	$78 \pm 8 \pm 10$
SBF	HST-KP (Ferrarese <i>et al.</i> , [10])	$69 \pm 4 \pm 6$
SBF	Tonry <i>et al.</i> , [7]	<u>$77 \pm 4 \pm 7$</u>
SBF (galaxy z survey)	Blakeslee <i>et al.</i> , [11]	$74 \pm 4 \pm 7$
SNeIa	Riess <i>et al.</i> , [12]	67 ± 7
SNeIa	Hamuy <i>et al.</i> , [13]	$63 \pm 3 \pm 3$
SNeIa	Jha <i>et al.</i> , [14]	$64.4^{+5.6}_{-5.1}$
SNeIa	Suntzeff <i>et al.</i> , [15]	65.6 ± 1.8
SNeIa	HST-KP (Gibson <i>et al.</i> , [16])	<u>$68 \pm 2 \pm 5$</u>
SNeIa	Saha <i>et al.</i> , ([17])	60 ± 2

We emphasize H_0 determinations by two methods, SBF and SNeIa, in particular those underlined in the table. A cross correlation analysis showed that the relative distances agree well between SBF and others, including the Cepheids [5,6], and that it is probably the best secondary indicator presently available together with SNeIa. It is also important that there are now 300 galaxies measured with SBF, which are essential to make corrections for peculiar velocity flows for the ≤ 4000 km s $^{-1}$ sample. The final value of Tonry *et al.* [7] is $H_0 = 77 \pm 8$, in which ± 4 is allotted to uncertainties in the flow model and another ± 4 to SBF calibration procedure in addition to the error of the Cepheid distance ± 6 (a quadrature sum is taken). When supplemented with peculiar velocity information from redshift surveys of galaxies, the value is further constrained to be 74 ± 4 up to the Cepheid distance error [11].

It is impressive that analyses of SNeIa Hubble diagram give virtually the same answer despite differences and corrections. The smaller H_0 of Saha *et al.* [17] arises from omission of the luminosity-decline rate correction; including this would push H_0 up by 10%. The other notable difference is a slightly higher value of HST-KP. Gibson *et al.* [16] made a reanalysis for all Cepheid observations performed by other groups and showed that the distances are all farther than would be derived from the HST-KP procedure. Taking the luminosity-decline rate correlation to be real and adopting Cepheid distances from the HST-KP data reduction, we adopt $H_0 = 68$ from SNeIa.

Leaving out the uncertainty of the Cepheid distance, H_0 from Tonry *et al.*'s [7] SBF determination is 77 ± 6 , and that from SNeIa (HST-KP) is 68 ± 4 . The difference is 13%, and the two values overlap at $H_0 = 71$. Allowing for individual 2σ errors, the overlap is in a range of $H_0 = 65$ –76. An additional uncertainty is the 6% error ($\delta H_0 = \pm 4.5$) from the Cepheid distance which is common to both, still excluding the uncertainty of the LMC distance. We may summarize $H_0 = 71 \pm 7$ or 64–78 as our current standard, provided that the LMC distance is 50 kpc.

The convergence is a great achievement, in spite of the fact that the SNeIa results are still lower than those from other secondary indicators by 10%. All analyses are based on the LMC distance modulus $m - M = 18.50$ [18,19]. Doubts about this distance are discussed next.

17.1.3. The Local Distance Scale: Distance to LMC: Most traditional paths to the LMC distance follow the ladder shown in the upper half of Table 17.1. The Hipparcos satellite can measure a parallax as small as 2 milliarcsec (mas), corresponding to a distance of 500 pc. It was a reasonable expectation that the geometric distance to the Pleiades cluster could be determined, circumventing the main sequence fitting from nearby parallax stars to the Pleiades and thus securing the Galactic distance scale. Hipparcos results have also opened new methods to estimate the distance to the LMC. However, the new detailed information has actually brought confusion.

The “Pleiades problem”: The Pleiades cluster at 130 pc has long been taken to be the first milestone of the distance work, since it has nearly solar abundance of heavy elements. Hipparcos results have led to a revision of the previous distance modulus, based on main sequence fitting of FGK dwarfs, shorter by 0.25 mag (12%) [20,21]. This is a serious problem, since the disagreement means that either our understanding of FGK dwarfs, for which we have the best knowledge about stellar evolution, is incomplete, or that the Hipparcos parallax measurements contain systematic errors [22,23].

Metallicity effects in the LMC Cepheid calibration: The Cepheid distance to LMC is based on calibration using open cluster Cepheids, the distances to which are estimated by B star main sequence fitting that ties to the Pleiades (see Ref. 18 and references therein). It is shown that the residual of the PL fit shows a strong metallicity (Z) dependence. This means *either* the Cepheid PL relation suffers from a large Z effect, or the distances to open clusters contain significant Z -dependent errors [24]. A correction for this effect changes the distance to LMC either way, depending upon which interpretation is correct. So far direct Hipparcos Cepheid distances are too noisy to resolve this issue directly [25–27].

Red clump: Hipparcos has recalibrated the “red clump,” the He burning stage of Population I stars, giving the distance modulus to LMC as 18.1 ± 0.1 . Although much shorter than distances from other methods, this value is substantially in agreement with earlier red clump results [28,29].

Eclipsing binaries: Double-spectroscopic eclipsing binaries in principle yield the distance in a semi-geometric way out to LMC or even farther. The LMC distance modulus is estimated to be $m - M = 18.30 \pm 0.07$ [30]. There is a claim that the extinction used is too small by an amount of $\Delta E(B - V) = 0.037$ mag, leading to $m - M = 18.19$ [31].

RR Lyr calibration: The absolute luminosity of RR Lyr depends on metallicity, usually expressed as

$$(M_V(\text{RR Lyr})) = a[\text{Fe}/\text{H}] + b. \quad (17.1)$$

(V means values obtained using a “visual” wideband filter.) Considerable effort has been invested in determining the coefficients (a, b). The problem is again how to estimate the distance to RR Lyr stars. The calibration from the ground, (a, b) = (0.2, 1.04), leads to an LMC distance of $m - M \approx 18.3$. Using Hipparcos field subdwarfs with parallax to calibrate RR Lyr in globular clusters gives (a, b) = (0.22 \pm 0.09, 0.76), which brings the LMC distance to $m - M = 18.5$ –18.6 [32]; see also Ref. 33. Statistical parallax for field RR Lyr in the Hipparcos catalogue [34,35], however, agrees better with the ground-based estimate. The uncertainties of 0.3 mag in the RR Lyr calibration translate to the LMC distance modulus 18.25–18.55.

Summary of the LMC distance problem: The distance modulus of the LMC is now uncertain by as much as 0.4 mag (20% in distance), ranging from 18.20 to 18.60. Recent observations with new techniques argue for the lower value. There is clearly a systematic effect, so that we cannot simply take an ‘average of all observations’. Rather, we should leave both possibilities open.

17.1.4. Direct and Physical Methods: Techniques called ‘physical methods,’ allow distance estimates without resorting to astronomical ladders. The advantage of the ladder is that the error of each ladder can be well documented, while the disadvantage is accumulation of errors. Physical methods are free from ‘accumulation of errors,’ but in this case the central problem is to minimize the model dependence and document realistic systematic errors. (The use of SNeIa maximum brightness was once taken to be a physical method; when it was ‘downgraded’ to an empirically-calibrated ladder, the accuracy and reliability were significantly enhanced.) A few direct results are reliable enough to be compared with the distances from ladders.

Geometrical calibration of the Cepheids: NGC4258 (M106) shows H $_2$ O maser emission from clouds orbiting around a black hole of

mass $4 \times 10^7 M_\odot$ located at the center. Precise VLBA measurements of Doppler velocities show that the motion of the clouds is very close to Keplerian and is perturbed very little. A complete determination is made for the orbital parameters, including centripetal acceleration and a bulk proper motion of the emission system. This yields a geometric distance to NGC4258 to be 7.2 ± 0.3 Mpc [36]. The distance is also measured using the conventional Cepheid PL relation to give 8.1 ± 0.4 Mpc with $(m - M)_{\text{LMC}} = 18.5$, 13% longer than that from the maser measurement [37]. The short LMC distance would bring the Cepheid distance in a perfect agreement with the geometric distance. However, this is only one example, and the difference could be merely a statistical effect: the deviation is only twice the error.

Expansion photosphere model (EPM) for Type II supernovae (SNeII): If a supernova is a black body emitter one can calculate source brightness from temperature. The distance can then be estimated by comparing source brightness with the observed flux. In SNeII atmospheres the flux is diluted due to electron scattering opacity, requiring more sophisticated model atmospheres. Schmidt *et al.* [38,39] developed this approach and obtained absolute distances of SNeII in agreement with those from the ladder. The Hubble constant they obtained is 73 ± 9 .

Gravitational lensing time delay: When a quasar image is split into two or more by gravitational lensing, a time delay arises among images from different path lengths and potentials at the image position of the galaxy. The time delay is written as a product of a cosmological factor and a deflector model. It is observable if the source is variable, and can be used to infer H_0 [40]. The cosmological factor depends on Ω_M only weakly; its Ω_Λ dependence is even weaker. However, a crucial ingredient in this argument is a well-constrained model of the mass distribution of the deflector.

The first estimates of H_0 used the 0957+561 lens system. The deflector is not simple but includes a giant elliptical galaxy embedded in a cluster. There is an ambiguity associated with a galaxy mass/cluster mass separation, which does not change any observed lens properties but affects the derived Hubble constant. One way to resolve this degeneracy is to use the velocity dispersion of the central galaxy [41]. While the long-standing issue as to the value of the time delay was settled and $H_0 = 64 \pm 13$ was reported [42], the inclusion of a wider class of models [43] produces a significantly wider range, $H_0 = 77^{+29}_{-24}$, representing uncertainties associated with the choice of models. The second example, PG1115+080, is again not a simple deflector but includes an elliptical galaxy embedded in a compact group of galaxies. Various models for this system yield $H_0 = 36\text{--}70$ [44–47], but, as is discussed in the papers, the derived H_0 depends on the assumption for the dark matter distribution, with H_0 varying from 44 ± 4 to 65 ± 5 .

Recently time delays have been measured for three simpler lenses, B0218+357, B1608+656 and PKS1830-211. Among them B0218+357 is a rather clean, isolated spiral galaxy lens, giving $H_0 = 69^{+13}_{-19}$ (the central value will be 74 if $\Omega_M = 0.3$) with a simple galaxy model of a singular isothermal ellipsoid [48]. For B1608+656 one obtained 64 ± 7 for $\Omega_M = 0.3$ (59 ± 7 for an EdS universe) and for PKS1830-211 75^{+18}_{-10} for EdS and 85^{+20}_{-11} for $\Omega_M = 0.3$ from the time delay measured by Koopmans and Fassnacht [49]. These authors concluded 74 ± 8 for low density cosmologies (69 ± 7 for EdS) from four (excluding the second) lensing systems with the simplest model of deflectors. It is encouraging to find such good agreement with the values from ladders from completely independent arguments.

Zeldovich-Sunyaev effect: The observation of the Zeldovich-Sunyaev (ZS) effect (the statistical heating of background photons by Compton scattering off hot electrons) for clusters tells us about the cluster depth (times electron density), which, when combined with angular diameter (times electron density squared) from x-ray observations, gives us the distance to the cluster provided that the cluster is spherical [50–52]. Although new and promising samples of ZS data are being assembled [52], we give little weight to this method for the time being since it is still subject to large systematic errors ($\pm 30\%$). Even with a large sample, selection effects would bias

towards clusters elongated along the line of sight because of higher surface brightness.

17.1.5. Age of globular clusters: The most restrictive estimate for cosmic age is obtained from the evolution of globular clusters. Here, the RR Lyr calibration is also crucial, since the stellar age is proportional to the inverse of luminosity, *i.e.*, inverse square of the distance. Modern calculated evolutionary tracks of the main sequence by different authors agree reasonably well. There are occasional disagreements of colors at around the turn-off point, largely depending on the treatment of convection, but the turnoff luminosity is little affected (see *e.g.*, Renzini [53] and Vandenberg *et al.* [54]). The absolute magnitude at the turn-off point M_V^{TO} of the main sequence is hence a good indicator of the age [53]:

$$\log t_9 = -0.41 + 0.37M_V^{TO} - 0.43Y - 0.13[\text{Fe}/\text{H}], \quad (17.2)$$

in units of Gyr, or

$$\log t_9 = -0.41 + (0.37a - 0.13)[\text{Fe}/\text{H}] + 0.37[(M_V^{TO} - M_V^{\text{RR}}) + b] - 0.43Y \quad (17.3)$$

if Eq. (17.1) is inserted. (Y is the helium mass fraction.) The difference of the magnitudes between the turn-off point and RR Lyr ($M_V^{TO} - M_V^{\text{RR}}$) depends little on clusters and is measured to be 3.5 ± 0.1 mag [55]. The a dependence appears in such a way that the metallicity dependence of the cluster age disappears if $a = 0.35$, *i.e.*, globular cluster formation appears coeval [56]. Current estimates (see above) give $a \approx 0.2$, which indicates that metal-poor clusters appear older.

The dichotomous calibrations of RR Lyr stars obviously affect the age of globular clusters. The result also depends on whether one takes the age-metallicity correlation to be real, as indicating metal-poor clusters being formed earlier, or merely due to a systematic error, the formation of globular clusters being coeval. The possibilities are four-fold:

b	$(m - M)_{\text{LMC}}$	t_0 (noncoeval)	t_0 (coeval)
1.05	18.25	18 Gyr	15 Gyr
0.75	18.55	14 Gyr	12 Gyr

In addition there are $\pm 10\%$ errors of various origin. The recent claims of Gratton *et al.* [32], Reid [33], and Chaboyer *et al.* [57] for young universe (11–12 Gyr) assume a coeval-formation interpretation together with the long RR Lyr calibration and the mean of globular cluster ages. The three other possibilities, however, are not excluded.

17.1.6. Conclusions on H_0 : Progress in the extragalactic distance scale has been substantial. The ladders yield values convergent within 10%, compared to a factor of 1.6 disagreement in early nineties. A new uncertainty, however, becomes manifest in the Galactic distance scale: there is a 15–20% uncertainty in the distance to LMC. Therefore, we may summarize

$$H_0 = (71 \pm 7) \times_{0.95}^{1.15} \quad (17.4)$$

as a currently acceptable value of the Hubble constant. This agrees with a HST-KP summary of Mould *et al.* [58] up to the uncertainty from the LMC distance, though we followed a different argument. This still allows $H_0 = 90$ at the high end (if Tonry *et al.*'s SBF [7,11] is given a higher weight) and 60 at the low end (if the SNeIa results are weighted). Note that H_0 from both EPM and gravitational lensing are consistent with the ladder value for $(m - M)_{\text{LMC}} = 18.5$. With the shorter LMC distance the overlap is marginal.

The short LMC distance also causes trouble for H_0 -age consistency. The LMC distance modulus of $m - M = 18.25$ would raise the lower limit of H_0 to 72, and increase the lower limit of age from ≈ 11.5 Gyr to ≈ 14.5 Gyr at the same time. There is then no solution for a $\Lambda = 0$ universe. Even with a non-zero Ω_Λ the solution is marginal (see Fig. 17.1 below).

17.2. The Density Parameter

The dimensionless cosmological density parameter directly controls the gravitational formation of cosmic structure. As our understanding of the cosmic structure formation is tightened, we should have a convergence of the Ω_M parameter. An important test is to examine whether estimates of Ω_M parameter extracted from cosmic structure formation agree with each other and with the values estimated in more direct ways.

17.2.1. Model-independent determinations:

Luminosity density $\times \langle M/L \rangle$: The mass density can be obtained by multiplying the luminosity density ($\mathcal{L}_B = (2.0 \pm 0.4) \times 10^8 h L_\odot \text{ Mpc}^{-3}$) with the average mass-to-light ratio (M/L). The M/L_B of galaxies is about 1–2 in galaxy disks and generally increases with the scale due to the increasing dominance of dark matter. If the dark matter distribution is isothermal within the virial radius ($r = 0.13 \text{ Mpc } \Omega_M^{-0.15} [M/10^{12} M_\odot]^{1/2} < 100 \text{ kpc}$ in a spherical collapse model), the value of M/L_B inside the virial radius is (150–400) h for L^* galaxies. This is about the value of M/L_B estimated for groups and clusters, (150–500) h , both from dynamics [59] and from lensing, (see e.g., Kaiser *et al.* [60]). Multiplying the two values we get [61] $\Omega_M = 0.20 \times 2^{\pm 1}$. The CNOC group [62] made a self-contained estimate using their cluster sample and built-in field galaxy sample. They estimated $M/L_r \approx (210 \pm 60) h$ (n.b.: $M/L_B \approx 1.4 \times M/L_r$) for field galaxies from the cluster value $(289 \pm 50) h$. Their luminosity density of field galaxies is $\mathcal{L}_r = (1.7 \pm 0.2) \times 10^8 h L_\odot \text{ Mpc}^{-3}$, and therefore $\Omega_M = 0.19 \pm 0.06$.

H_0 versus cosmic age: For $H_0 \geq 60$, the age is 10.9 Gyr for the EdS universe. Since this is too short, Ω_M must be smaller than unity. The limits on H_0 and Ω_M are best compared graphically (see Fig. 17.1 below).

Type Ia supernova Hubble diagram: The type Ia supernova Hubble diagram now reaches $z \approx 0.4$ –0.8. It can be used to infer the mass density parameter and the cosmological constant. As we discuss later, the observations favor a low Ω_M and a positive Λ . If we accept the published formal errors, $\Omega_M > 0.1$ is allowed only at three sigma for a zero Λ universe [63,64]. With some allowance for systematic effects, a zero Λ open universe may not be excluded yet, but an EdS geometry is far away from the observations. The favored value for Ω_M is approximately $0.8 \Omega_\Lambda - 0.4$.

Baryon fractions in Galaxy Clusters: If the gas in a galaxy cluster is in approximate hydrostatic equilibrium (at the virial temperature $T \approx 7 \times 10^7 (\sigma/1000 \text{ km s}^{-1})^2 \text{ K}$), its mass can be estimated by the luminosity and temperature of x-ray emission. In typical clusters baryon mass in the gas exceeds that in stars by an order of magnitude, so the gas gives the total baryon mass [65,66]. From 19 clusters White and Fabian [67] obtained $M_{\text{gas}}/M_{\text{grav}} = 0.056 h^{-2/3}$, where M_{grav} is the dynamical mass. By requiring that the cluster baryon fraction agrees with Ω_B/Ω_M in the field, we have $\Omega_M = 0.066 h^{-1/2} \eta_{10} = 0.39 (\eta_{10}/5)$, where η_{10} is the global baryon to photon ratio in units of 10^{-10} and the last number assumes $h = 0.7$. An independent estimate from the Zeldovich-Sunyaev effect observed in clusters [51,68] yields $M_{\text{gas}}/M_{\text{grav}} = 0.082 h^{-1}$, or $\Omega_M = 0.044 h^{-1} \eta_{10} = 0.31 (\eta_{10}/5)$. With $\eta_{10} = 3$ –5 from primordial nucleosynthesis (see Sec. 16 on “Big-bang nucleosynthesis” in this *Review*) we have $\Omega_M = 0.2$ –0.4.

Nonlinear Statistical Dynamics on Small Scales: For small scales ($r < 1 \text{ Mpc}$) perturbations are non-linear, and a statistical equilibrium argument is invoked for ensemble averages: the peculiar acceleration induced by a pair of galaxies is balanced by relative motions (the cosmic virial theorem). Current estimates [69] give $\Omega_M(10 \text{ kpc} \lesssim r \lesssim 1 \text{ Mpc}) = 0.15 \pm 0.10$ from the pairwise velocity dispersion (with samples excluding clusters) and the three point correlation function of galaxies via a statistical stability argument. Least action principle reconstruction of galaxy orbits in the Local Group gives $\Omega_M = 0.15 \pm 0.15$. All arguments involving velocity are uncertain regarding the extent to which galaxies trace the mass

distribution (biasing), or how much mass is present far away from galaxies.

Simple quasi-linear infall models: For larger scales ($r > 10 \text{ Mpc}$), where perturbations are still in a linear regime, the velocity field is described by

$$\nabla \cdot \vec{v} + H_0 \Omega_M^{0.6} \delta = 0, \quad (17.5)$$

where δ is the enclosed mass overdensity. An integral form of Eq. (17.5) for a spherically symmetric case, $v/H_0 r = \Omega_M^{0.6} \langle \delta \rangle / 3$, when applied to the Virgo-centric flow, gives $\Omega_M \approx 0.2$ for $v \approx 200$ –400 km s^{-1} and $\langle \delta \rangle \sim 2$, assuming no biasing, i.e., galaxies mass [70]. Recently, Tonry *et al.* [7] argued that the peculiar velocity ascribed to the Virgo cluster is only $\lesssim 140 \text{ km s}^{-1}$, while the rest of the peculiar velocity flow is attributed to the Hydra-Centarus supercluster and the quadrupole field.

Large-scale velocity flows: There are several methods to statistically compare large-scale velocity flows and density perturbations [71,72]. If δ is measured from galaxy clustering, Ω_M always appears in the measured combination $\beta = \Omega_M^{0.6} / b$ where b is a linear biasing factor of galaxies against the mass distribution. The value of $\Omega_M^{0.6} / b$ varies from 0.3 to 1.1, and tends to favor a high value. The most recent POTENT analysis using the Mark III compilation of velocities indicates a high-density universe, $\Omega_M = 0.5$ –0.7 with $\Omega_M < 0.3$ excluded at a 99% CL [73]. Blakeslee *et al.* [11] derived $\Omega_M \approx 0.25 \pm 0.05$, if b is close to unity, using better-determined distances from SBF. In spite of substantial effort the results are controversial. The difficulty is that one needs accurate information for velocity fields, for which an accurate estimate of distances and their errors is crucial. Random errors of the distance indicators introduce large noise in the velocity field. This seems particularly serious in the POTENT algorithm, in which the derivative $\nabla \cdot \vec{v} / \Omega_M^{0.6}$ and its square are numerically computed. This procedure enhances noise, especially for a small Ω_M .

17.2.2. Model-dependent determinations: The following derivations of the mass density parameter are based on the hierarchical clustering model of cosmic structure formation assuming the cold dark matter (CDM) model. The extraction of Ω_M is therefore indirect. On the other hand it is reasonable to appeal to such models, since Ω_M is the parameter that predominantly controls gravitational structure formation.

Shape parameter of the transfer function: Perturbations of density are described by the Fourier power spectrum $P(k)$, where k is the spatial wavenumber. CDM models predict a shape for the linear power spectrum $P(k) \propto k^{n-4}$ on small scales and $P(k) \propto k^n$ on large scales, where $n \approx 1$ is the primordial power law index. The transition scale is determined by $k_{\text{eq}} \approx 2\pi / c t_{\text{eq}}$, where the characteristic length $c t_{\text{eq}} = 6.5 (\Omega_M h)^{-1} h^{-1} \text{ Mpc}$ is the horizon size at the time of matter-radiation equality (in comoving units, appropriately stretched to the present epoch). The “shape parameter” $\Gamma \equiv \Omega_M h$ can be estimated from galaxy clustering, and to yield sufficient clustering power on scales of tens of Mpc must be small, about 0.2 [74–76].

Power spectrum in nonlinear galaxy clustering: It is argued that the power spectrum in a small scale region ($k^{-1} < 3h^{-1} \text{ Mpc}$), where nonlinear effects are dominant, shows more power than is expected in $\Omega_M = 1$ cosmological models. The excess power is understood if $\Omega_M \approx 0.3$ [77].

Evolution of the rich cluster abundance: The cluster abundance at $z \approx 0$ requires the rms mass fluctuation $\sigma_8 = ((\delta M/M)^{1/2})_{r=8h^{-1} \text{ Mpc}}$ to satisfy $\sigma_8 \approx 0.6 \Omega_M^{-0.5}$ [78, 79]. The evolution of the cluster abundance is sensitive to σ_8 in early epochs of growth, corresponding to $z \gtrsim 0.3$ for rich clusters. The rich cluster abundance at $z \sim 0.3$ –1, when compared with that at a low z , thus determines both σ_8 and Ω_M [80]. Carlberg [81] derived $\Omega_M = 0.4 \pm 0.2$, and Bahcall and Fan [82] obtained $\Omega_M = 0.2^{+0.3}_{-0.1}$, while Eke *et al.* [76] reported $\Omega_M = 0.43 \pm 0.25$ for an open universe, and $\Omega_M = 0.36 \pm 0.25$ for a flat universe, corresponding to a slow growth of the abundance. On the other hand, Blanchard and Bartlett [83] and Reichart *et al.* [84]

obtained $\Omega_M \approx 1$ from a more rapid growth. The controversy among authors arises from different estimates of the cluster mass at high z .

Cluster abundance versus the COBE normalization: The cluster abundance gives an accurate estimate of σ_8 for a low- z universe. Another place we can extract an accurate σ_8 is from the fluctuation power imprinted on cosmic microwave background radiation (CBR) anisotropies. Assuming the model CDM transfer function $\sigma_8 = \sigma_8(H_0, \Omega_M, \Omega_\Lambda, \Omega_B, n, \dots)$, matching of the COBE [85] with the cluster abundance gives a significant constraint on cosmological parameters $\Omega_M = \Omega_M(H_0, \Omega_\Lambda)$ [79,86], which improves by adding small-angle CBR data [87–90]. The presence of the tensor mode makes the range of n more uncertain, but notwithstanding these uncertainties, $\Omega_M > 0.5$ is difficult to reconcile with the matching condition whereas too-small $\Omega_M (\lesssim 0.15)$ is not consistent with the cluster abundance. These constraints will rapidly improve with new CBR data.

17.3. The Cosmological Constant

17.3.1. Type Ia supernova Hubble diagram: The luminosity distance receives a cosmology-dependent correction as z increases: Ω_M pulls down d_L and Ω_Λ pushes it up. In first order of z the correction enters in the combination of $q_0 = \Omega_M/2 - \Omega_\Lambda$, so this is historically referred to as a q_0 test, a measure of cosmic deceleration, although this single-parameter description is not adequate at the redshifts of the current samples. The discovery by two groups that distant supernovae are fainter than expected from the local sample, even fainter than expected for $q_0 = 0$, points to the reality of $\Lambda > 0$ [63,64]. The best fits are currently for $\Omega_\Lambda \approx 0.7$, $\Omega_M \approx 0.3$ —a flat, Λ -dominated universe.

The challenge of this analysis is to differentiate among interesting cosmologies with small differences of brightness. The samples are on average about 0.25 mag fainter than in the $\Omega_M = 0.2$, $\Omega_\Lambda = 0$ model, a difference most economically explained by adopting a cosmology with $\Lambda > 0$. On the other hand, at $z = 0.4$ where many supernovae are observed, the difference is $\Delta m = 0.12$ mag between $(\Omega_M, \Omega_\Lambda) = (0.3, 0.7)$ and $(0, 0)$, and $\Delta m = 0.22$ from $(0, 0)$ to $(1.0, 0)$. Therefore, an accuracy of $\lesssim 0.05$ mag ($\lesssim 5\%$) must be attained including systematics to prove the presence of Λ without appeal to other constraints (on Ω_M , $\Omega_M + \Omega_\Lambda$, etc.). Each SN data point contains at best ± 0.2 mag (20%) statistical error; the question is whether the total error is mostly random and systematics are controlled to a level of $\lesssim 0.05$ mag. A particular difficulty arises from a procedure to match high z SNe with the template at $z \approx 0$, which involves an integration over SN spectra dominated by strong features as well as a careful calibration of the flux zero points at different color bands. Even for spectrophotometric standard stars, the synthetic magnitude usually contains errors of 0.02–0.05 mag, especially when the color band involves the Balmer or Paschen regions. Dust obscuration may also be amplified into an important potential source of error, since, for example, a 0.02 mag error in color results in a 0.06 mag error in A_V . Perlmutter *et al.* [64] estimate 0.02 mag and Riess *et al.* [63] (see also Ref. 91) estimate 0.03 mag for K correction plus zero point errors, and 0.025 and 0.06 for dust extinction errors, respectively.

17.3.2. Gravitational lensing frequencies for quasars: The cosmological factor in the gravitational lensing optical depth is very sensitive to the cosmological constant, if $\Omega_\Lambda \gg \Omega_M$ [92,93]. On the other hand, it is nearly insensitive to the change of Λ when it is small ($\Omega_\Lambda \lesssim 0.6$, say); in that case the uncertainties in the normalization factor (galaxy number density and the mass distribution of galaxies) dominate. It is likely that $\Omega_\Lambda > 0.8$ is excluded. On the other hand, a more stringent limit or solid detection is liable to be elusive for a smaller Ω_Λ . Nearly a decade of continuous efforts have brought substantial improvement in reducing uncertainties in the normalization factor [94–96]. Nevertheless, the luminosity density of early type galaxies which dominate lensing is uncertain by about a factor of two. We should adopt a conservative limit at present $\Omega_\Lambda < 0.8$ which is insensitive to this concern.

17.3.3. Harmonics of CBR anisotropies: The angular scale of the first acoustic peak is particularly sensitive to a combination of Ω_M and Ω_Λ . The position of the first acoustic peak as estimated numerically using CMBFAST [97] is

$$\ell_1 \approx 220 \left(\frac{1 - \Omega_\Lambda}{\Omega_M} \right)^{1/2}, \quad (17.6)$$

valid to about 10% accuracy for the parameter range that concerns us. This means that the position of the acoustic peak is about $\ell \approx 220$ if $\Omega_M + \Omega_\Lambda = 1$, but it shifts to a high ℓ as $\Omega_M^{-1/2}$ if $\Omega_\Lambda = 0$. On the other hand, there is little power to determine Ω_M separately from Ω_Λ . The harmonics C_ℓ measured at small angles now reveal the acoustic peak [98], and its position favors a universe close to flat [87–89]. The most recent result [99] indicates $0.88 \leq \Omega_M + \Omega_\Lambda \leq 1.12$, which means that a zero Λ universe is not tenable when combined with Ω_M from other arguments.

Table 17.3: Summary of Ω and Ω_Λ .

Method	Ω_M	Ω_Λ
H_0 vs t_0	< 0.7	
luminosity density +M/L	0.1–0.4	
cluster baryon fraction	0.15–0.35	
SNeIa Hubble diagram	≤ 0.3	≈ 0.7
small-scale velocity field		
(summary)	0.2 ± 0.15	
(pairwise velocity)	0.15 ± 0.1	
(Local Group kinematics)	0.15 ± 0.15	
(Virgo-centric flow)	0.2 ± 0.2	
large-scale velocity field	0.2–1	
cluster evolution		
(low Ω_M sol'n)	$0.2^{+0.3*}_{-0.1}$	
(high Ω_M sol'n)	$\sim 1^*$	
COBE-cluster matching	0.35–0.45 (if $\Omega_\Lambda = 0$)*	
	0.20–0.40 (if $\Omega_\Lambda \neq 0$)*	
shape parameter Γ	0.2–0.4*	
CBR acoustic peak	$\approx (1 \pm 0.12) - \Omega_\Lambda^*$	$\approx (1 \pm 0.12) - \Omega_M$
gravitational lensing		< 0.8
Summary	0.15–0.45 (if open)	
	0.2–0.4 (if flat)	
		0.6–0.8

*CDM model used.

17.4. Conclusions

The status of Ω_M and Ω_Λ is summarized in Table 17.3. We have a reasonable convergence of the Ω_M parameter towards a low value $\Omega_M = 0.15$ –0.4. The convergence of Ω_M is significantly better with the presence of a cosmological constant that makes the universe flat. Particularly encouraging is the agreement of Ω_M derived with the most reliable arguments. Even so, the current ‘low Ω_M concordance’ means values that still vary by more than a factor of two. The indication of $\Omega_\Lambda \neq 0$ from the SNeIa Hubble diagram is very interesting and important, but on its own the conclusion is susceptible to small systematic effects. On the other hand small-scale CBR anisotropy observations confirming a nearly flat universe, in combination with the sum of the other evidence considered here, strongly suggest the presence of Λ or other exotic (highly negative pressure) form of dark mass-energy.

In conclusion we present in Fig. 17.1 allowed ranges of H_0 and Ω_M (and Ω_Λ) for the case of (a) flat and (b) open universes. With the flat case we cut the lower limit of Ω_M at 0.2 due to a strong constraint from lensing. An ample amount of parameter space is allowed for a

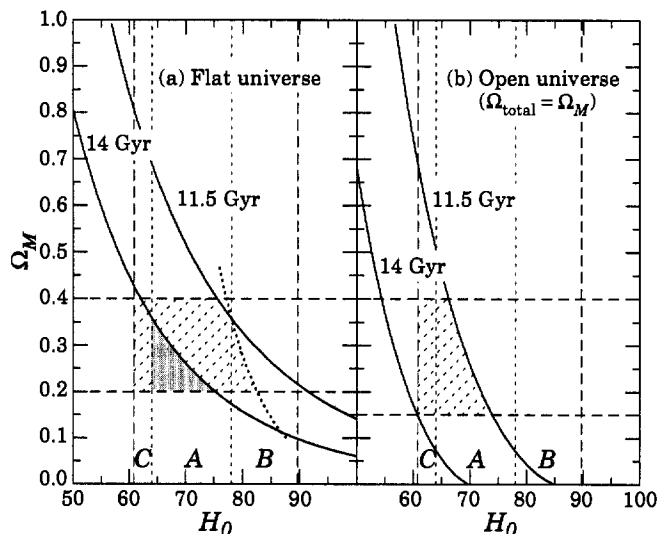


Figure 17.1: Consistent parameter ranges in the H_0 - Ω_M plane for (a) a flat universe and (b) an open universe. A is the range of the Hubble constant when $(m - M)_{\text{LMC}} = 18.5$. B is also allowed when the LMC distance is shorter by 0.3 mag, and C when longer by 0.1 mag. Note in panel (a) that most of the range of B is forbidden by the compatibility of age and H_0 that are simultaneously driven by the RR Lyr calibration (short dotted curve, see Sec. 17.1.6). Also note that the age range between ≈ 11.5 Gyr and ≈ 14 Gyr (light cross-hatched) is possible only with the interpretation that globular cluster formation is coeval (Sec. 17.1.5). The 'most natural' parameter region is dark gray.

flat universe. A high value of $H_0 > 82$, which would be driven only by a short LMC distance, is excluded by self-consistency with the age of globular clusters, as noted earlier. Therefore, we are led to the range $H_0 \approx 60$ -82 from consistency. For an open universe the coeval-formation interpretation is compelling for globular clusters, or else no region is allowed; the allowed H_0 is limited to 60-70. No solution is available if LMC is at the shorter distance.

References:

- M. Fukugita, in *Structure Formation in the Universe*, Proc. of the NATO ASI, Cambridge, 1999 (to be published, 2000); astro-ph/0005069.
- J.H. Jacoby *et al.*, Publ. Astron. Soc. Pac. **104**, 599 (1992).
- W.L. Freedman *et al.*, Nature **371**, 757 (1994).
- L. Ferrarese *et al.*, astro-ph/9910501 (1999).
- J.L. Tonry *et al.*, Astrophys. J. **475**, 399 (1997).
- W.L. Freedman, B.F. Madore, and R.C. Kennicutt, in *The Extragalactic distance scale*, eds. M. Livio, M. Donahue, and N. Panagia (Cambridge University Press, Cambridge), p. 171 (1997).
- J.L. Tonry *et al.*, Astrophys. J. **530**, 625 (2000).
- S. Sakai *et al.*, Astrophys. J. **529**, 698 (2000).
- D.D. Kelson *et al.*, Astrophys. J. **529**, 768 (2000).
- L. Ferrarese *et al.*, Astrophys. J. **529**, 745 (2000).
- J.P. Blakeslee *et al.*, Astron. J. **527**, L73 (1999).
- A.G. Riess, W.H. Press, and R.P. Kirshner, Astrophys. J. **438**, L17 (1995).
- M. Hamuy *et al.*, Astrophys. J. **112**, 2398 (1996).
- S. Jha *et al.*, Astrophys. J. Suppl. Ser. **125**, 73 (1999).
- N.B. Suntzeff *et al.*, Astrophys. J. **117**, 1175 (1999).
- B.K. Gibson *et al.*, Astrophys. J. **529**, 723 (2000).
- A. Saha *et al.*, Astrophys. J. **522**, 802 (1999).
- M.W. Feast and A.R. Walker, Ann. Rev. Astr. Astrophys. **25**, 345 (1987).
- B.F. Madore and W.L. Freedman, Publ. Astron. Soc. Pac. **103**, 933 (1991).
- F. van Leeuwen and C.S. Hansen-Ruiz, Mon. Not. of the R. Astron. Soc. **287**, 955 (1997).
- J.-C. Mermilliod *et al.*, in *Hipparcos Venice '97*, ed. B. Battarick (ESA, Noordwijk, 1997), p. 643.
- M.H. Pinsonneault *et al.*, Astrophys. J. **504**, 170 (1998).
- V.K. Narayanan and A. Gould, Astrophys. J. **523**, 328 (1999).
- M. Sekiguchi and M. Fukugita, Observatory **118**, 73 (1998).
- M.W. Feast and R.M. Catchpole, Mon. Not. of the R. Astron. Soc. **286**, L1 (1997).
- X. Luri, *et al.*, Astr. and Astrophys. **335**, L81 (1998).
- B.F. Madore and W.L. Freedman, Astrophys. J. **492**, 110 (1998).
- A. Udalski *et al.*, Acta Astron. **48**, 1 (1998).
- K.Z. Stanek and P.M. Garnavich, Astrophys. J. **503**, L131 (1998).
- E.F. Guinan *et al.*, Astrophys. J. **509**, L21 (1998).
- A. Udalski *et al.*, Astrophys. J. **509**, L25 (1998).
- R.G. Gratton *et al.*, Astrophys. J. **491**, 749 (1997).
- I.N. Reid, Astron. J. **114**, 161 (1997).
- J. Fernley *et al.*, Astr. and Astrophys. **330**, 515 (1998).
- A. Gould and P. Popowski, Astrophys. J. **508**, 844 (1998).
- J.R. Herrnstein *et al.*, Nature **400**, 539 (1999).
- E. Maoz *et al.*, Nature **401**, 351 (1999).
- B.P. Schmidt, R.P. Kirshner, and R.G. Eastman, Astrophys. J. **395**, 366 (1992).
- B.P. Schmidt *et al.*, Astrophys. J. **432**, 42 (1994).
- S. Refsdal, Mon. Not. of the R. Astron. Soc. **128**, 307 (1964).
- E.E. Falco, M.V. Gorenstein, and I.I. Shapiro, Astrophys. J. **372**, 364 (1991).
- T. Kundić *et al.*, Astrophys. J. **482**, 75 (1997).
- G. Bernstein and P. Fischer, Astron. J. **118**, 14 (1999).
- P.L. Schechter *et al.*, Astrophys. J. **475**, L85 (1997).
- C.R. Keeton and C.S. Kochanek, Astrophys. J. **487**, 42 (1997).
- F. Courbin *et al.*, Astr. and Astrophys. **324**, L1 (1997).
- C.D. Impey *et al.*, Astrophys. J. **509**, 551 (1998).
- A.D. Biggs *et al.*, Mon. Not. of the R. Astron. Soc. **304**, 349 (1999).
- L.V.E. Koopmans and C.D. Fassnacht, Astrophys. J. **527**, 513 (1999).
- M. Birkinshaw, J.P. Hughes, and K.A. Arnaud, Astrophys. J. **379**, 466 (1991).
- S.T. Myers *et al.*, Astrophys. J. **485**, 1 (1997).
- E.D. Reese *et al.*, Astrophys. J. **533**, 38 (2000).
- A. Renzini, in *Observational Tests of Cosmological Inflation*, ed. T. Shanks *et al.*, (Kluwer, Dordrecht), p. 131 (1991).
- D.A. Vandenberg, M. Bolte, and P.B. Stetson, Ann. Rev. Astr. Astrophys. **34**, 461 (1996).
- B. Chaboyer, P. Demarque, and A. Sarajedini, Astrophys. J. **459**, 558 (1996).
- A. Sandage, Astron. J. **106**, 703 (1993).
- B. Chaboyer *et al.*, Astrophys. J. **494**, 96 (1998).
- J.R. Mould *et al.*, Astrophys. J. **529**, 786 (2000).
- N.A. Bahcall, L.M. Lubin, and V. Dorman, Astrophys. J. **447**, L81 (1995).
- N. Kaiser *et al.*, astro-ph/9809268 (1998).
- M. Fukugita, C.J. Hogan, and P.J.E. Peebles, Astrophys. J. **503**, 518 (1998).
- R.G. Carlberg, H.K.C. Yee, and E. Ellingson, Astrophys. J. **478**, 462 (1997).
- A.G. Riess *et al.*, Astron. J. **116**, 1009 (1998).
- S. Perlmutter *et al.*, Astrophys. J. **517**, 565 (1999).

65. W. Forman, and C. Jones, *Ann. Rev. Astr. Astrophys.* **20**, 547 (1982).
66. S.D.M. White *et al.*, *Nature* **366**, 429 (1993).
67. D.A. White and A.C. Fabian, *Mon. Not. of the R. Astron. Soc.* **273**, 72 (1995).
68. L. Grego *et al.*, presented at the AAS meeting (194.5807G) (1999).
69. P.J.E. Peebles, in *Formation of Structure in the Universe*, eds Dekel, A. and Ostriker, J. P. (Cambridge University Press, Cambridge), p. 435 (1999).
70. M. Davis and P.J.E. Peebles, *Ann. Rev. Astr. Astrophys.* **21**, 109 (1983).
71. M.A. Strauss and J.A. Willick, *Phys. Reports* **261**, 271 (1995).
72. A.J.S Hamilton, in *The Evolving Universe*, ed. D. Hamilton, (Kluwer, Dordrecht, 1998), p. 185.
73. A. Dekel *et al.*, *Astrophys. J.* **522**, 1 (1999).
74. G. Efstathiou, W.J. Sutherland, and S.J. Maddox, *Nature* **348**, 705 (1990).
75. J.A. Peacock and S.J. Dodds, *Mon. Not. of the R. Astron. Soc.* **267**, 1020 (1994).
76. V.R. Eke *et al.*, *Mon. Not. of the R. Astron. Soc.* **298**, 1145 (1998).
77. J.A. Peacock, *Mon. Not. of the R. Astron. Soc.* **284**, 885 (1997).
78. S.D.M. White, G. Efstathiou, and C.S. Frenk, *Mon. Not. of the R. Astron. Soc.* **262**, 1023 (1993).
79. V.R. Eke, S. Cole, and C.S. Frenk, *Mon. Not. of the R. Astron. Soc.* **282**, 263 (1996).
80. J. Oukbir and A. Blanchard, *Astr. and Astrophys.* **262**, L21 (1992).
81. R.G. Carlberg *et al.*, *Astrophys. J.* **479**, L19 (1997).
82. N.A. Bahcall and X. Fan, *Astrophys. J.* **504**, 1 (1998).
83. A. Blanchard and J.G. Bartlett, *Astr. and Astrophys.* **332**, L49 (1998).
84. D.E. Reichart, *et al.*, *Astrophys. J.* **518**, 521 (1999).
85. C.L. Bennett *et al.*, *Astrophys. J.* **464**, L1 (1996).
86. G. Efstathiou, J.R. Bond, and S.D.M White, *Mon. Not. of the R. Astron. Soc.* **258**, 1 (1992).
87. S. Hancock *et al.*, *Mon. Not. of the R. Astron. Soc.* **294**, L1 (1998).
88. C.H. Lineweaver, *Astrophys. J.* **505**, L69 (1998).
89. G. Efstathiou *et al.*, *Mon. Not. of the R. Astron. Soc.* **303**, 47 (1999).
90. M. Tegmark, *Astrophys. J.* **514**, L69 (1999).
91. B.P. Schmidt *et al.*, *Astrophys. J.* **507**, 46 (1998).
92. M. Fukugita, T. Futamase, and M. Kasai, *Mon. Not. of the R. Astron. Soc.* **256**, 25 (1990).
93. E.L. Turner, *Astrophys. J.* **365**, L43 (1990).
94. D. Maoz and H.-W. Rix, *Astrophys. J.* **416**, 425 (1993).
95. C.S. Kochanek, *Astrophys. J.* **466**, 638 (1996).
96. E.E. Falco, C.S. Kochanek, and J.A. Muñoz, *Astrophys. J.* **494**, 47 (1998).
97. U. Seljak and M. Zaldarriaga, *Astrophys. J.* **469**, 437 (1996).
98. P.F. Scott *et al.*, *Astrophys. J.* **461**, L1 (1996).
99. P. deBernardis *et al.*, *Nature* **404**, 955 (2000).

18. DARK MATTER

Revised Sep. 1999 by M. Srednicki (University of California, Santa Barbara).

The total mass-energy of the Universe is composed of several constituents, each of which may be characterized by its energy density $\rho_i \equiv \Omega_i \rho_c$ and its pressure $p_i \equiv w_i \rho_i$. Here $\rho_c \equiv 3H_0^2/8\pi G_N$ is the critical density, and H_0 is the present value of the Hubble parameter. We will take $H_0 = 70 \text{ km s}^{-1} \text{ Mpc}^{-1}$ when a numerical value is needed; then $\rho_c = 5.2 \times 10^{-6} \text{ GeV/cm}^3$. We can express the total density as $\rho_0 = \Omega_0 \rho_c$, where $\Omega_0 = \sum_i \Omega_i$. The deceleration parameter $q_0 \equiv (\ddot{R}/R)_0/H_0^2$, where $R(t)$ is the scale factor and the subscript 0 denotes the present value, is then given by $q_0 = \frac{1}{2}\Omega_0 + \frac{3}{2}\sum_i \Omega_i w_i$.

In general, relativistic particles have an equation of state specified by $w = +\frac{1}{3}$, nonrelativistic particles have $w = 0$, and the cosmological constant (here treated as another form of matter) has $w = -1$. Spatially uniform scalar fields which are oscillating rapidly in time (that is, with a frequency much greater than the Hubble parameter H_0) also have $w = 0$. Spatially uniform scalar fields which are changing slowly in time have $-1 < w < 0$.

Certain contributions to the mass density are well determined. The photons of the cosmic microwave background radiation (CMB) have $\rho_\gamma = \pi^2 T_0^4/15$, where $T_0 = 2.73 \text{ K} = 2.35 \times 10^{-4} \text{ eV}$ is the present temperature of the CMB; this yields $\Omega_\gamma = 5.1 \times 10^{-5}$. Results from Big-Bang nucleosynthesis indicate that the total baryon density is in the range $0.008 < \Omega_b < 0.043$; of this, roughly 0.004 is accounted for by stars. A single species of neutrino with a Majorana mass m_ν would have $\Omega_\nu = 0.56 G_N T_0^3 H_0^{-2} m_\nu = m_\nu/(45 \text{ eV})$ and $w_\nu = 0$ if $m_\nu \gg T_0$, and $\Omega_\nu = 0.23 \Omega_\gamma$ and $w_\nu = \frac{1}{3}$ if $m_\nu \ll T_0$.

There is strong evidence from a variety of different observations for a large amount of dark matter in the Universe [1,2,3,4]. The phrase “dark matter” signifies matter whose existence has been inferred only through its gravitational effects. Two categories should be distinguished: baryonic dark matter, composed of baryons which are not seen (including black holes formed by stellar collapse), and nonbaryonic dark matter, composed either of massive neutrinos, or of elementary particles or fields which are as yet undiscovered (including primordial black holes). The particles or fields which comprise nonbaryonic dark matter must have survived from the Big Bang, and therefore must either be stable or have lifetimes in excess of the current age of the Universe.

There are a number of different observations which indicate the presence of dark matter (baryonic or nonbaryonic). These observations include rotation curves of spiral galaxies [5], which indicate that individual galaxies have halos of dark matter whose density falls off as $1/r^2$ at large distances r from the galaxy’s center. In our own Galaxy, estimates of the local density of dark matter typically give $\rho_{\text{dm}} \simeq 0.3 \text{ GeV/cm}^3$, but this result depends sensitively on how the dark-matter halo is modeled.

An estimate of the total pressureless matter density Ω_m (that is, of all components, baryonic and nonbaryonic, with $w_i = 0$) can be made from studies of rich clusters of galaxies. The baryonic mass of a cluster can be inferred from X-ray emissions, and the total mass from galactic velocities (via the virial theorem) or gas dynamics [6]. Assuming that the ratio of these masses is typical of the Universe as a whole, we obtain the value of Ω_m/Ω_b . Using the nucleosynthesis value of Ω_b then yields $\Omega_m = 0.4 \pm 0.1$. This is at least roughly consistent with a number of other estimates of Ω_m , such as from mass-to-light ratios for clusters [7] and from large-scale velocity fields [8]. This value of Ω_m would imply that 90% of the pressureless matter in the Universe is nonbaryonic.

An estimate of the total density Ω_0 can be made from fluctuations in the CMB (see Section 15 on “Big-Bang Cosmology” in this *Review*). The first acoustic peak in the power spectrum of these fluctuations is predicted to occur at a multipole $\ell \sim 220 \Omega_0^{-1/2}$; current data yields $\Omega_0 \sim 0.8 \pm 0.2$ [9]. This is consistent with the generic prediction $\Omega_0 = 1$ of inflationary models.

Type Ia supernovae can be used as standard candles to get information on the relationship between redshift and distance [10].

If we assume that the dominant contributions to Ω_0 are from pressureless matter and an unknown component X , then the results require $w_X < -0.6$ (at the 95% CL, ignoring any systematic errors). Assuming $w_X = -1$ (a cosmological constant), the results constrain the combination $0.8 \Omega_m - 0.6 \Omega_X$ to be -0.2 ± 0.1 .

None of these observations give us any direct indication of the nature of the dark matter. The halos of galaxies could have significant fractions of baryonic dark matter in the form of remnants (white dwarfs, neutron stars, black holes) of an early generation of massive stars, or smaller objects which never initiated nuclear burning (and would therefore have masses less than about $0.1 M_\odot$). These massive compact halo objects are collectively called MACHOs. Results from searches via gravitational lensing effects [11] show that MACHOs with masses from $10^{-6} M_\odot$ to $0.1 M_\odot$ each are not a significant component of our Galaxy’s halo. However, the results also indicate that MACHOs with masses of approximately $0.5 M_\odot$ each comprise roughly half the total mass of the halo. This situation is difficult to reconcile with models of star formation.

For purposes of galaxy formation models [12], nonbaryonic dark matter is classified as “hot” or “cold,” depending on whether the dark matter particles were relativistic or nonrelativistic at the time when the horizon of the Universe enclosed enough matter to form a galaxy. If the dark matter particles are in thermal equilibrium with the baryons and radiation, then only the mass of a dark matter particle is relevant to knowing whether the dark matter is hot or cold, with the dividing line being $m_{\text{dm}} \sim 1 \text{ keV}$. In addition, specifying a model requires giving the power spectrum of initial density fluctuations. Inflationary models generically predict a power spectrum which is nearly scale invariant. With these inputs, galaxy formation models require primarily cold dark matter, with significantly less hot dark matter. However, either a negative-pressure component or some hot dark matter is needed in addition to cold dark matter. For example, a model with $\Omega_{\text{cdm}} = 0.3$, $\Omega_{\text{hdm}} = 0$, $\Omega_X = 0.7$ and $w_X = -0.6$ gives a good fit to all current data [13].

There is a constraint on neutrinos (or any light fermions) if they are to comprise the halos of dwarf galaxies: the Fermi-Dirac distribution in phase space restricts the number of neutrinos that can be put into a halo [14], and this implies a lower limit on the neutrino mass of roughly $m_\nu > 80 \text{ eV}$.

There are no presently known particles which could be cold dark matter. However, many proposed extensions of the Standard Model predict a stable (or sufficiently long lived) particle. The key question then becomes the predicted value of Ω_{cdm} .

If the particle is its own antiparticle (or there are particles and antiparticles present in equal numbers), and these particles were in thermal equilibrium with radiation at least until they became nonrelativistic, then their relic abundance is determined by their annihilation cross section $\sigma_{\text{ann}}: \Omega_{\text{cdm}} \sim G_N^{3/2} T_0^3 H_0^{-2} \langle \sigma_{\text{ann}} v_{\text{rel}} \rangle^{-1}$. Here v_{rel} is the relative velocity of the two incoming dark matter particles, and the angle brackets denote an averaging over a thermal distribution of velocities for each at the freeze-out temperature T_{fr} when the dark matter particles go out of thermal equilibrium with radiation; typically $T_{\text{fr}} \simeq \frac{1}{20} m_{\text{dm}}$. One then finds (putting in appropriate numerical factors) that $\Omega_{\text{cdm}} \simeq 7 \times 10^{-27} \text{ cm}^3 \text{ s}^{-1} / \langle \sigma_{\text{ann}} v_{\text{rel}} \rangle$. The value of $\langle \sigma_{\text{ann}} v_{\text{rel}} \rangle$ needed for $\Omega_{\text{cdm}} \simeq 1$ is remarkably close to what one would expect for a weakly interacting massive particle (WIMP) with a mass of $m_{\text{dm}} = 100 \text{ GeV}$: $\langle \sigma_{\text{ann}} v_{\text{rel}} \rangle \sim \alpha^2/8\pi m_{\text{dm}}^2 \sim 3 \times 10^{-27} \text{ cm}^3 \text{ s}^{-1}$.

If the dark matter particle is not its own antiparticle, and the number of particles minus antiparticles is conserved, then an initial asymmetry in the abundances of particles and antiparticles will be preserved, and can give relic abundances much larger than those predicted above.

If the dark matter particles were never in thermal equilibrium with radiation, then their abundance today must be calculated in some other way, and will in general depend on the precise initial conditions which are assumed.

The two best known and most studied cold dark matter candidates are the neutralino and the axion. The neutralino is predicted by

the Minimal Supersymmetric extension of the Standard Model (MSSM) [15,16]. It qualifies as a WIMP, with a theoretically expected mass in the range of tens to hundreds of GeV. The axion is predicted by extensions of the Standard Model which resolve the strong CP problem [17]. Axions can occur in the early universe in the form of a Bose condensate which never comes into thermal equilibrium. The axions in this condensate are always nonrelativistic, and can be a significant component of the dark matter if the axion mass is approximately 10^{-5} eV. Axions can also arise from the decay of a network of axion strings and domain walls.

There are prospects for direct experimental detection of both these candidates (and other WIMP candidates as well). WIMPs will scatter off nuclei at a calculable rate, and produce observable nuclear recoils [2,16,19]; current data excludes certain regions of parameter space of the MSSM. Axions can be detected by axion to photon conversion in a microwave cavity in a strong magnetic field, and limits on the allowed axion-photon coupling have been set [18].

WIMP candidates can have indirect signatures as well, via present day annihilations into particles which can be detected as cosmic rays. The most promising possibility arises from the fact that WIMPs collect at the centers of the sun and the earth, thus greatly increasing their annihilation rate, and producing high energy neutrinos which can escape and arrive at the earth's surface in potentially observable numbers [16,20].

References:

1. V. Trimble, *Ann. Rev. Astron. Astrophys.* **25**, 425 (1987).
2. B. Sadoulet, *Rev. Mod. Phys.* **71**, S197 (1999).
3. M.S. Turner and J.A. Tyson, *Rev. Mod. Phys.* **71**, S145 (1999).
4. N.A. Bahcall *et al.*, *Science* **284**, 1481 (1999).
5. M. Persic, P. Salucci and F. Stel, *Mon. Not. Roy. Astron. Soc.* **281**, 27 (1996).
6. A.E. Evrard, *Mon. Not. Roy. Astron. Soc.* **292**, 289 (1997).
7. R.G. Carlberg *et al.*, *Astrophys. J.* **516**, 552 (1999).
8. A. Dekel, *Ann. Rev. Astron. Astrophys.* **32**, 371 (1994);
M.A. Strauss and J.A. Willick, *Phys. Reports* **261**, 271 (1995);
A. Dekel, in *Formation of Structure in the Universe*, ed. A. Dekel and J.P. Ostriker (Cambridge, New York, 1999).
9. C.H. Lineweaver, *Astrophys. J.* **505**, L69 (1998).
10. S. Perlmutter *et al.*, *Astrophys. J.* **483**, 565 (1997);
B.P. Schmidt *et al.*, *Astrophys. J.* **507**, 46 (1998);
A.G. Riess *et al.*, *Astron. J.* **116**, 1009 (1998);
P.M. Garnavich *et al.*, *Astrophys. J.* **509**, 74 (1998);
S. Perlmutter *et al.*, *Astrophys. J.* **517**, 565 (1999).
11. W. Sutherland, *Rev. Mod. Phys.* **71**, S421 (1999).
12. S. Dodelson, E.I. Gates, and M.S. Turner, *Science* **274**, 69 (1996);
J.R. Primack, in *Formation of Structure in the Universe*, ed. A. Dekel and J.P. Ostriker (Cambridge, New York, 1999).
13. M.S. Turner and M. White, *Phys. Rev.* **D56**, R4439 (1997);
S. Perlmutter, M.S. Turner, and M. White, *Phys. Rev. Lett.* **83**, 670 (1999).
14. S. Tremaine and J. E. Gunn, *Phys. Rev. Lett.* **42**, 407 (1979);
O. E. Gerhard and D. N. Spergel, *Astrophys. J.* **389**, L1 (1992).
15. H.E. Haber and G.L. Kane, *Phys. Reports* **117**, 75 (1985).
16. G. Jungman, M. Kamionkowski, and K. Griest, *Phys. Reports* **267**, 195 (1996).
17. M.S. Turner, *Phys. Reports* **197**, 67 (1990);
Azions '98, ed. P. Sikivie, *Nucl. Phys. B (Proc. Supp.)* **72** (1999).
18. C. Hagmann *et al.*, *Phys. Rev. Lett.* **80**, 2043 (1998).
19. J.R. Primack, B. Sadoulet, and D. Seckel, *Ann. Rev. Nucl. and Part. Sci.* **38**, 751 (1988);
P.F. Smith and J.D. Lewin, *Phys. Reports* **187**, 203 (1990);
TAUP 97, ed. A. Bottino *et al.*, *Nucl. Phys. B (Proc. Supp.)* **70** (1999).
20. F. Halzen, *Nucl. Phys. B (Proc. Supp.)* **77**, 474 (1999).

19. COSMIC BACKGROUND RADIATION

Revised February 2000 by G.F. Smoot (LBNL) and D. Scott (University of British Columbia).

19.1. Introduction

The observed cosmic microwave background (CMB) radiation provides strong evidence for the hot big bang. The success of primordial nucleosynthesis calculations (see Sec. 16, "Big-bang nucleosynthesis") requires a cosmic background radiation (CBR) characterized by a temperature $kT \sim 1$ MeV at a redshift of $z \simeq 10^9$. In their pioneering work, Gamow, Alpher, and Herman [1] realized this and predicted the existence of a faint residual relic, primordial radiation, with a present temperature of a few degrees. The observed CMB is interpreted as the current manifestation of the required CBR.

The CMB was serendipitously discovered by Penzias and Wilson [2] in 1965. Its spectrum is well characterized by a 2.73 K black-body (Planckian) spectrum over more than three decades in frequency (see Fig. 19.1). A non-interacting Planckian distribution of temperature T_i at redshift z_i transforms with the universal expansion to another Planckian distribution at redshift z_f with temperature $T_f/(1+z_f) = T_i/(1+z_i)$. Hence thermal equilibrium, once established (e.g. at the nucleosynthesis epoch), is preserved by the expansion, in spite of the fact that photons decoupled from matter at early times. Because there are about 10^9 photons per nucleon, the transition from the ionized primordial plasma to neutral atoms at $z \sim 1000$ does not significantly alter the CBR spectrum [3].

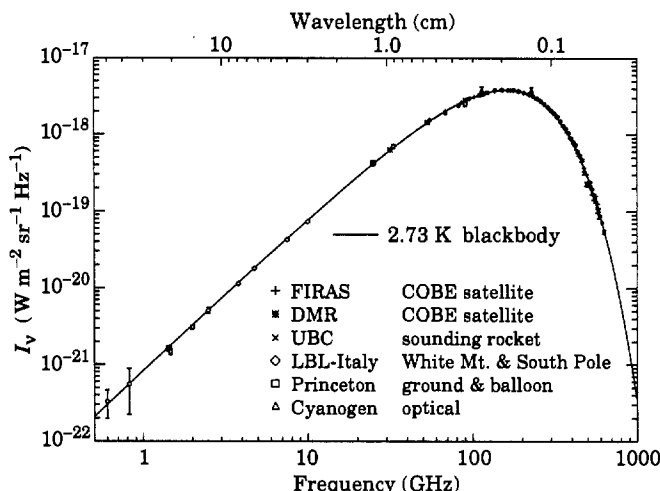


Figure 19.1: Precise measurements of the CMB spectrum. The line represents a 2.73 K blackbody, which describes the spectrum very well, especially around the peak of intensity. The spectrum is less well constrained at 10 cm and longer wavelengths. (References for this figure are at the end of this section under "CMB Spectrum References.")

19.2. The CMB frequency spectrum

The remarkable precision with which the CMB spectrum is fitted by a Planckian distribution provides limits on possible energy releases in the early Universe, at roughly the fractional level of 10^{-4} of the CBR energy, for redshifts $\lesssim 10^4$ (corresponding to epochs $\gtrsim 1$ year). The following three important classes of theoretical spectral distortions (see Fig. 19.2) generally correspond to energy releases at different epochs. The distortion results from the CBR photon interactions with a hot electron gas at temperature T_e .

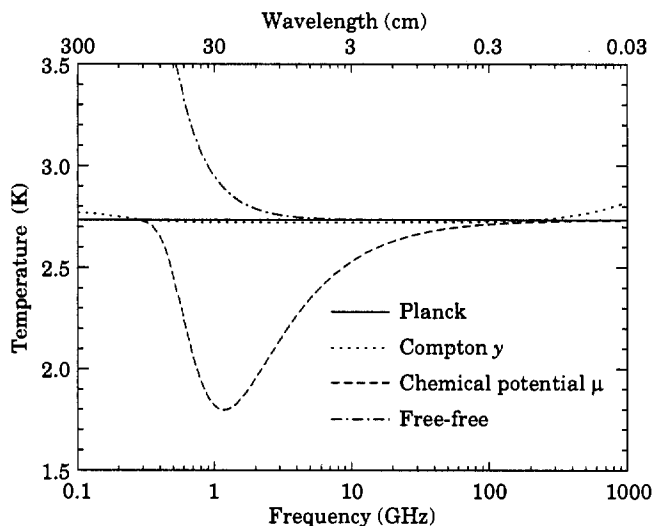


Figure 19.2: The shapes of expected, but so far unobserved, CMB distortions, resulting from energy-releasing processes at different epochs.

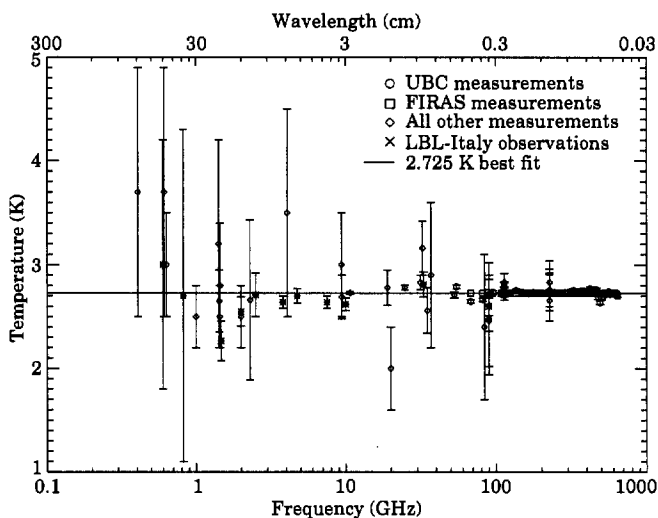


Figure 19.3: Observed thermodynamic temperature as a function frequency.

19.2.1. Compton distortion: Late energy release ($z \lesssim 10^5$). Compton scattering ($\gamma e \rightarrow \gamma' e'$) of the CBR photons by a hot electron gas creates spectral distortions by transferring energy from the electrons to the photons. Compton scattering cannot achieve thermal equilibrium for $y \lesssim 1$, where

$$y = \int_0^z \frac{kT_e(z') - kT_\gamma(z')}{m_e c^2} \sigma_T n_e(z') c \frac{dt}{dz'} dz', \quad (19.1)$$

is the integral of the number of interactions, $\sigma_T n_e(z) c dt$, times the mean-fractional photon-energy change per collision [4]. For $T_e \gg T_\gamma$ y is also proportional to the integral of the electron pressure $n_e k T_e$ along the line of sight. For standard thermal histories $y < 1$ for epochs later than $z \simeq 10^5$.

The resulting CMB distortion is a temperature decrement

$$\Delta T_{RJ} = -2y T_\gamma \quad (19.2)$$

in the Rayleigh-Jeans ($h\nu/kT \ll 1$) portion of the spectrum, and a rise in temperature in the Wien ($h\nu/kT \gg 1$) region, i.e. photons are

shifted from low to high frequencies. The magnitude of the distortion is related to the total energy transfer [4] ΔE by

$$\Delta E/E_{\text{CMB}} = e^{4y} - 1 \simeq 4y. \quad (19.3)$$

A prime candidate for producing a Comptonized spectrum is a hot intergalactic medium. A hot ($T_e > 10^5$ K) medium in clusters of galaxies can and does produce a partially Comptonized spectrum as seen through the cluster, known as the Sunyaev-Zel'dovich effect [5]. Based upon X-ray data, the predicted large angular scale total combined effect of the hot intracluster medium should produce $y \sim 10^{-6}$ [6].

19.2.2. Bose-Einstein or chemical potential distortion: Early energy release ($z \sim 10^5$ – 10^7). After many Compton scatterings ($y \gg 1$), the photons and electrons will reach statistical (not thermodynamic) equilibrium, because Compton scattering conserves photon number. This equilibrium is described by the Bose-Einstein distribution with non-zero chemical potential:

$$n = \frac{1}{e^{x+\mu_0} - 1}, \quad (19.4)$$

where $x \equiv h\nu/kT$ and $\mu_0 \simeq 1.4 \Delta E/E_{\text{CMB}}$, with μ_0 being the dimensionless chemical potential that is required to conserve photon number.

The collisions of electrons with nuclei in the plasma produce free-free (thermal bremsstrahlung) radiation: $eZ \rightarrow e'Z'\gamma$. Free-free emission thermalizes the spectrum to the plasma temperature at long wavelengths and Compton scattering begins to shift these photons upward. Including this effect, the chemical potential becomes frequency-dependent,

$$\mu(x) = \mu_0 e^{-2x_b/x}, \quad (19.5)$$

where x_b is the transition frequency at which Compton scattering of photons to higher frequencies is balanced by free-free creation of new photons. The resulting spectrum has a sharp drop in brightness temperature at centimeter wavelengths [7]. The minimum wavelength is determined by Ω_B .

The equilibrium Bose-Einstein distribution results from the oldest non-equilibrium processes ($10^5 < z < 10^7$), such as the decay of relic particles or primordial inhomogeneities. Note that free-free emission (thermal bremsstrahlung) and radiative-Compton scattering effectively erase any distortions [8] to a Planckian spectrum for epochs earlier than $z \sim 10^7$.

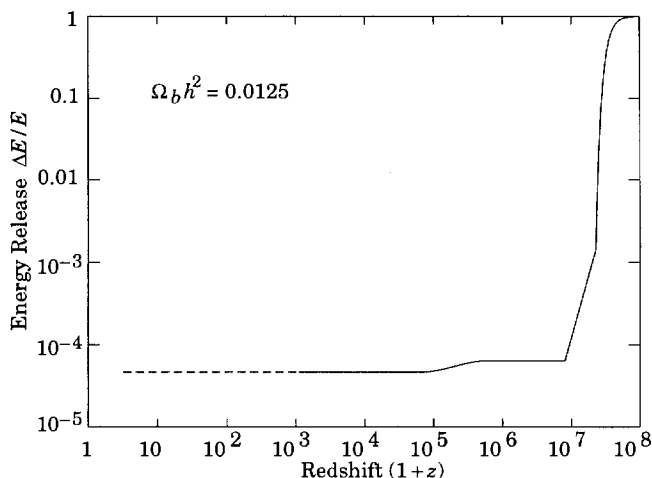


Figure 19.4: Upper Limits (95% CL) on fractional energy ($\Delta E/E_{\text{CMB}}$) releases from processes at different epochs as set by resulting lack of CMB spectral distortions. These can be translated into constraints on the mass, lifetime and photon branching ratio of unstable relic particles, with some additional dependence on cosmological parameters such as Ω_B [11,12].

19.2.3. Free-free distortion: Very late energy release ($z \ll 10^3$). Free-free emission can create rather than erase spectral distortion in the late Universe, for recent reionization ($z < 10^3$) and from a warm intergalactic medium. The distortion arises because of the lack of Comptonization at recent epochs. The effect on the present-day CMB spectrum is described by

$$\Delta T_{\text{ff}} = T_{\gamma} Y_{\text{ff}}/x^2, \quad (19.6)$$

where T_{γ} is the undistorted photon temperature, x is the dimensionless frequency, and Y_{ff}/x^2 is the optical depth to free-free emission:

$$Y_{\text{ff}} = \int_0^z \frac{T_e(z') - T_{\gamma}(z')}{T_e(z')} \frac{8\pi e^6 h^2 n_e^2 g}{3m_e (kT_{\gamma})^3 \sqrt{6\pi m_e kT_e}} dt dz'. \quad (19.7)$$

Here h is Planck's constant, n_e is the electron density and g is the Gaunt factor [9].

19.2.4. Spectrum summary: The CMB spectrum is consistent with a blackbody distribution over more than three decades of frequency around the peak. The best-fit to the COBE FIRAS data yields $T_{\gamma} = 2.725 \pm 0.002$ K (95% CL) [10]. The following table is a summary of all CMB spectrum measurements:

$$\begin{aligned} T_{\gamma} &= 2.725 \pm 0.002 \text{ K (95\% CL)}; \\ n_{\gamma} &= (2\zeta(3)/\pi^2) T_{\gamma}^3 \simeq 411 \text{ cm}^{-3}; \\ \rho_{\gamma} &= (\pi^2/15) T_{\gamma}^4 \simeq 4.64 \times 10^{-34} \text{ g cm}^{-3} \simeq 0.260 \text{ eV cm}^{-3}; \\ |y| &< 1.2 \times 10^{-5} \quad (95\% \text{ CL}); \\ |\mu_0| &< 9 \times 10^{-5} \quad (95\% \text{ CL}); \\ |Y_{\text{ff}}| &< 1.9 \times 10^{-5} \quad (95\% \text{ CL}). \end{aligned}$$

These limits [13] correspond to constraints [13–15] on energetic processes $\Delta E/E_{\text{CMB}} < 2 \times 10^{-4}$ occurring between redshifts 10^3 and 5×10^6 (see Fig. 19.4).

19.3. Deviations from isotropy

Penzias and Wilson reported that the CMB was isotropic and unpolarized at the 10% level. Current observations show that the CMB is unpolarized at the 10^{-5} level but has a dipole anisotropy at the 10^{-3} level, with smaller-scale anisotropies at the 10^{-5} level. Standard theories predict temperature anisotropies of roughly the amplitude now being detected, and anisotropies in linear polarization at a level which should soon be reached.

It is customary to express the CMB temperature anisotropies on the sky in a spherical harmonic expansion,

$$\frac{\Delta T}{T}(\theta, \phi) = \sum_{\ell m} a_{\ell m} Y_{\ell m}(\theta, \phi), \quad (19.8)$$

and to discuss the various multipole amplitudes. The power at a given angular scale is roughly $\ell \sum_m |a_{\ell m}|^2 / 4\pi$, with $\ell \sim 1/\theta$.

19.3.1. The dipole: The largest anisotropy is in the $\ell = 1$ (dipole) first spherical harmonic, with amplitude at the level of $\Delta T/T = 1.23 \times 10^{-3}$. The dipole is interpreted as the result of the Doppler shift caused by the solar system motion relative to the nearly isotropic blackbody field, as confirmed by measurements of the velocity field of local galaxies [16]. The motion of the observer (receiver) with velocity $\beta = v/c$ relative to an isotropic Planckian radiation field of temperature T_0 produces a Doppler-shifted temperature

$$\begin{aligned} T(\theta) &= T_0(1 - \beta^2)^{1/2} / (1 - \beta \cos \theta) \\ &= T_0 \left(1 + \beta \cos \theta + (\beta^2/2) \cos 2\theta + O(\beta^3) \right). \end{aligned} \quad (19.9)$$

The implied velocity [13,17] for the solar-system barycenter is $\beta = 0.01237 \pm 0.000002$ (68% CL) or $v = 371 \pm 0.5 \text{ km s}^{-1}$, assuming a value $T_0 = T_{\gamma}$, towards $(\alpha, \delta) = (11.20^{\text{h}} \pm 0.01^{\text{h}}, -7.22^{\circ} \pm 0.08^{\circ})$, or $(\ell, b) = (264.31^{\circ} \pm 0.17^{\circ}, 48.05^{\circ} \pm 0.10^{\circ})$. Such a solar-system velocity implies a velocity for the Galaxy and the Local Group of galaxies

relative to the CMB. The derived velocity is $v_{LG} = 627 \pm 22 \text{ km s}^{-1}$ toward $(\ell, b) = (276^\circ \pm 3^\circ, 30^\circ \pm 3^\circ)$, where most of the error comes from uncertainty in the velocity of the solar system relative to the Local Group.

The Doppler effect of this velocity and of the velocity of the Earth around the Sun, as well as any velocity of the receiver relative to the Earth, is normally removed for the purposes of CMB anisotropy study. The resulting high degree of CMB isotropy is the strongest evidence for the validity of the Robertson-Walker metric.

19.3.2. The quadrupole: The rms quadrupole anisotropy amplitude is defined through $Q_{\text{rms}}^2/T_\gamma^2 = \sum_m |a_{2m}|^2/4\pi$. The current estimate of its value is $4 \mu\text{K} \leq Q_{\text{rms}} \leq 28 \mu\text{K}$ for a 95% confidence interval [18]. The uncertainty here includes both statistical errors and systematic errors, which are dominated by the effects of galactic emission modelling. This level of quadrupole anisotropy allows one to set general limits on anisotropic expansion, shear, and vorticity; all such dimensionless quantities are constrained to be less than about 10^{-5} .

For specific homogeneous cosmologies, fits to the whole anisotropy pattern allow stringent limits to be placed on, for example, the global rotation at the level of about 10^{-7} of the expansion rate [19].

19.3.3. Smaller angular scales: The COBE-discovered [20] higher-order ($\ell > 2$) anisotropy is interpreted as being the result of perturbations in the energy density of the early Universe, manifesting themselves at the epoch of the CMB's last scattering. The detection of these anisotropies at just the right level for gravity to have grown all of the structure observed in today's Universe demonstrates that gravitational instability acting on primordial density perturbations was the main mechanism for structure formation.

Theoretical models generally predict a power spectrum in spherical harmonic amplitudes, since the models lead to primordial fluctuations and thus $a_{\ell m}$ that are Gaussian random fields, and hence the power spectrum in ℓ is sufficient to characterize the results. The power at each ℓ is $(2\ell + 1)C_\ell/(4\pi)$, where $C_\ell \equiv \langle |a_{\ell m}|^2 \rangle$ and a statistically isotropic sky means that all m 's are equivalent. For an idealized full-sky observation, the variance of each measured C_ℓ is $[2/(2\ell + 1)]C_\ell^2$. This sampling variance (known as cosmic variance) comes about because each C_ℓ is chi-squared distributed with $(2\ell + 1)$ degrees of freedom for our observable volume of the Universe [21].

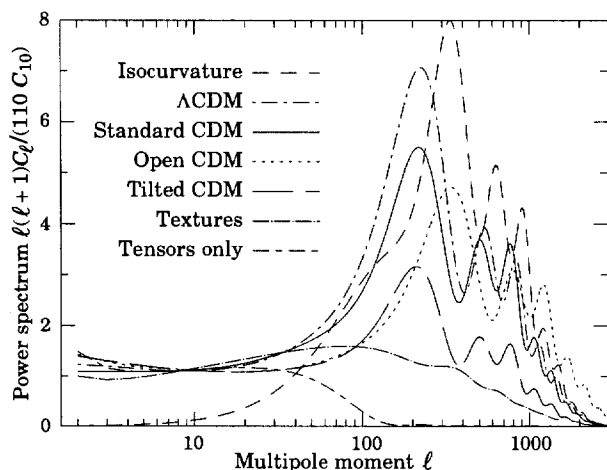


Figure 19.5: Theoretically predicted $\ell(\ell + 1)C_\ell$ or CMB anisotropy power spectra [24] for a range of models. The top curve is an isocurvature CDM model which has a characteristically different shape than the adiabatic models. The next four are variants of adiabatic Cold Dark Matter models. The textures model [25] is an example with perturbations seeded by topological defects. We also show the power spectrum from gravity waves (tensors), which could contribute at large angles. All the models have been normalized at $\ell = 10$ except for the isocurvature case, which was arbitrarily normalized to the height of the box. Such curves depend in detail on the precise values of the cosmological parameters, and those shown here are examples only.

Figure 19.5 shows the theoretically predicted anisotropy power spectrum for a sample of models, plotted as $\ell(\ell + 1)C_\ell$ versus ℓ which is the power per logarithmic interval in ℓ or, equivalently, the two-dimensional power spectrum. If the initial power spectrum of perturbations is the result of quantum mechanical fluctuations produced and amplified during inflation, then for simple models the shape of the anisotropy spectrum is coupled to the ratio of contributions from density (scalar) and gravitational wave (tensor) perturbations [22]. In such models the large angle contribution from tensors is constrained to be $\lesssim 0.5$ [23]. However, there are other inflationary models which allow higher tensor contribution. In particular if the energy scale of inflation at the appropriate epoch is $\approx 10^{16} \text{ GeV}$, then detection of the effect of gravitons is more likely and partial reconstruction of the inflaton potential may be feasible. However, if the energy scale is $\lesssim 10^{14} \text{ GeV}$, then typically density fluctuations dominate and less constraint is possible.

On angular scales corresponding to $\ell \gtrsim 50$ scalar modes certainly dominate. In the standard scenario the last scattering epoch happens at a redshift of approximately 1100, by which time the large number of photons was no longer able to keep the hydrogen ionized. The optical thickness of the cosmic photosphere is roughly $\Delta z \sim 100$ corresponding to about 5 arcminutes on the sky, so that features smaller than this size are damped.

Anisotropies have now been observed on angular scales above this damping scale by a large number of experiments (see Fig. 19.6), and are consistent with those expected from an initially scale-invariant (also referred to as 'flat') power spectrum of potential and thus metric fluctuations. The initial spectrum of density perturbations is reflected in the large angle (small ℓ) power spectrum, but perturbations can evolve significantly in the epoch $z \gtrsim 1100$ for causally connected regions (angles $\lesssim 1^\circ \Omega_{\text{tot}}^{1/2}$). The primary mode of evolution is through acoustic oscillations, leading to a series of peaks at small angular scales, which encode information about the primordial perturbations, geometry, matter and radiation content, and ionization history of the Universe [26]. Thus, precise measurement of the shape of the anisotropy power spectrum will provide information on the amplitude and slope of the initial conditions, as well as Ω_0 , Ω_B , Ω_Λ (cosmological constant), H_0 and other cosmological parameters.

Fits to experimental data are often quoted as the expected value of the quadrupole $\langle Q \rangle$ for some specific theory over some range of ℓ (e.g. a model with power-law initial conditions, having primordial density perturbation power spectrum $|\delta_k|^2 \propto k^n$). The full 4-year COBE DMR data give $\langle Q \rangle = 15.3_{-2.8}^{+3.7} \mu\text{K}$, after projecting out the slope dependence, while the best-fit slope is $n = 1.2 \pm 0.3$, and for a pure $n = 1$ (scale-invariant potential perturbation) spectrum $\langle Q \rangle (n = 1) = 18 \pm 1.6 \mu\text{K}$ [18,27]. The conventional notation is such that $\langle Q \rangle^2/T_\gamma^2 = 5C_2/4\pi$. An alternative convention is to quote the 'band-power' $\sqrt{\ell(2\ell + 1)C_\ell/4\pi}$. Many recent experiments give results for a number of band-powers covering different ranges of ℓ . $\langle Q \rangle^2/T_\gamma^2 = 5C_2/4\pi$ fluctuations measured by other experiments can be quoted in terms ($n = 1$)

The initial density perturbations can either be 'adiabatic' (meaning that there is no change to the entropy per particle for each species) or 'isocurvature' (meaning that, for example, matter perturbations compensate radiation perturbations so that the total energy density remains unchanged). Within the family of adiabatic models, the location of the first acoustic peak is predicted to be at $\ell \sim 220 \Omega_{\text{tot}}^{-1/2}$ or $\theta \sim 0.3^\circ \Omega_{\text{tot}}^{1/2}$ and its amplitude is a calculable function of the parameters (see Fig. 19.5).

It has been clear for several years that there is more power at sub-degree scales than at COBE scales [26]. More recently results have indicated that there is a localized peak, and the general shape of the power spectrum favors adiabatic-type perturbations (compare Fig. 19.5 and Fig. 19.6). Within the adiabatic scenario, the currently available data imply that the Universe is close to flat [28], with $0.62 < \Omega_{\text{tot}} < 1.24$ (95% CL) [29]. Together with a number of observations indicating that the matter density $\Omega_M \approx 0.3$ (e.g. see Ref. 37), this implies that there is some unknown contribution to the energy, 'dark energy,' which is independently indicated through distant supernova studies [30]. The height of the peak can also be used to constrain models, but currently the results depend sensitively on what range of models are considered and what other cosmological

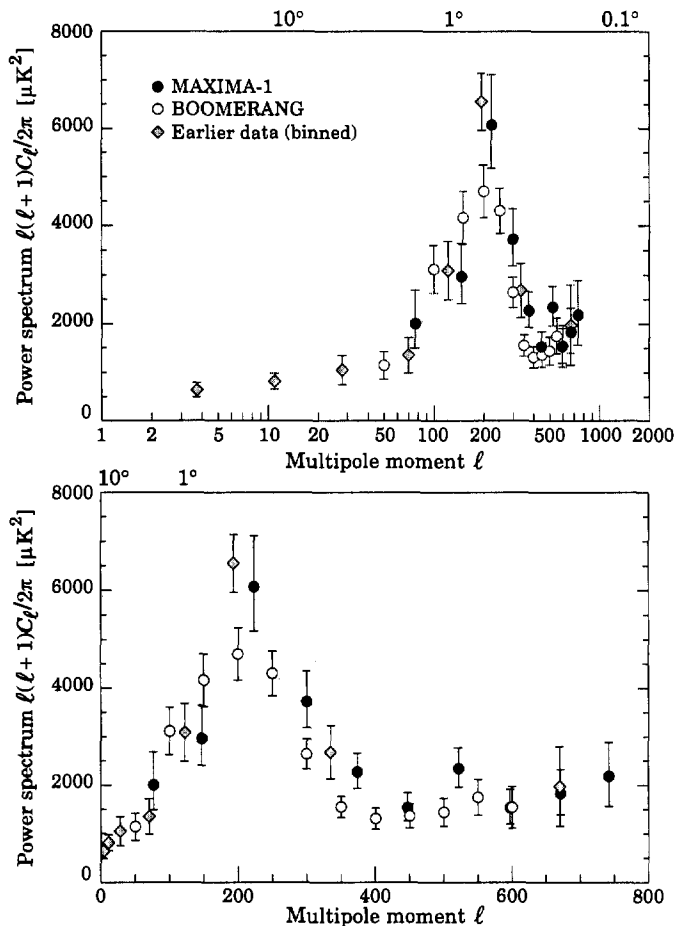


Figure 19.6: There is now so much CMB data that it is difficult and confusing to show all the individual results. Instead the figure shows the new BOOMERANG [32] (open circles) and MAXIMA-1 [33] data (filled circles), together with binned results of all previous experiments, based on data with references given at the end of this section under “CMB Anisotropy References.” The previous data are shown as grey diamonds, which were obtained [38] by maximizing the likelihood for a power spectrum assumed to be piece-wise constant between $\ell = 2$ and 1000, permitting experimental errors to be asymmetric, and allowing for correlated calibration uncertainties for each experiment [39]. These binned values are somewhat correlated, partly explaining the apparent discrepancy, which is consistent with calibration uncertainties between experiments. The sub-set of data from the first Antarctic flight of BOOMERANG and the data from the MAXIMA-1 flight are independent, with essentially no correlations between bins. The figure clearly shows a localized peak at $\ell \approx 200$ and some structure at higher ℓ . Upper limits at smaller angular scales, indicating further evidence for a falloff at high ℓ , have not been shown.

constraints are used [28,29,31]. Detailed measurements of parameters are expected to follow soon, but certainly some more general questions are already being answered.

Recent experimental results from the Boomerang 98 [32] and MAXIMA-1 [33] balloon flights have dramatically improved the power spectrum measurements. These new data indicate a very well-defined first acoustic peak, at close to the position expected in flat models with adiabatic fluctuations. It is difficult to generate this feature by an incoherent causal mechanism, such as with topological defects. The position of the first peak constrains the total density parameter to be $\Omega_{\text{tot}} \approx 1.0 \pm 0.1$ [34,35]. Intriguingly, the second peak does not appear as pronounced as had been expected in the previously favored models. There are several ways to explain this [36], including a combination of tilt, higher baryon density and some other mild

parameter variations, as well as more exotic explanations such as delayed recombination, partial loss of coherence of the oscillations, or features in the underlying power spectrum. Detailed measurement of the second and third peaks ought to distinguish among these possibilities.

Causal mechanisms, such as arise in topological defect models, cannot naturally account for the observed power spectrum (see Fig. 19.5), and isocurvature models also generically give the wrong shape. Thus the present data appear to point to models with adiabatic and apparently acausal fluctuations. Since inflation is the only mechanism we have to provide the large-scale homogeneity and anisotropy observed in the universe and to produce these apparently acausal fluctuations, one might consider the current CMB data as supporting the inflationary paradigm. A more stringent test of inflation will be provided with the arrival of data that have the fidelity to resolve the sub-degree region into the oscillating peaks and troughs which must be present in inflationary models.

New data are being acquired at an increasing rate, with a large number of improved ground- and balloon-based experiments being developed. The current suite of experiments promises to map out the CMB anisotropy power spectrum to about 10% accuracy, and determine several parameters at the 10 to 20% level in the very near future. A vigorous sub-orbital and interferometric program should push those numbers further in the next few years.

There are also now two approved satellite experiments: the NASA Microwave Anisotropy Probe (MAP), scheduled for launch in late 2000; and the ESA Planck mission, expected to launch in 2007. The improved sensitivity, freedom from earth-based systematics, and all-sky coverage allow a simultaneous determination of many of the cosmological parameters to unprecedented precision: for example, Ω_0 and n to about 1%, Ω_B and H_0 at the level of a few percent [40]. Just as with the frequency spectrum, precise measurement of the anisotropies should also lead to constraints on a particle physics effects at $z \sim 1000$ [41].

Since Thomson scattering of the anisotropic radiation field also generates linear polarization at the roughly 5% level [42], there is additional cosmological information to be gleaned from polarization measurements. Although difficult to detect, the polarization signal should act as a strong confirmation of the general paradigm. Furthermore, detailed measurement of the polarization signal provides more precise information on the physical parameters. In particular it allows a clear distinction of any gravity wave contribution, which is crucial to probing the $\sim 10^{16}$ GeV energy range. The fulfillment of this promise may await an even more sensitive generation of satellites.

References:

1. R.A. Alpher and R.C. Herman, *Physics Today* **41**, No. 8, p. 24 (1988).
2. A.A. Penzias and R. Wilson, *Astrophys. J.* **142**, 419 (1965); R.H. Dicke, P.J.E. Peebles, P.G. Roll, and D.T. Wilkinson, *Astrophys. J.* **142**, 414 (1965).
3. P.J.E. Peebles, “Principles of Physical Cosmology,” Princeton U. Press, p. 168 (1993).
4. R.A. Sunyaev and Ya.B. Zel’dovich, *Ann. Rev. Astron. Astrophys.* **18**, 537 (1980).
5. M. Birkinshaw, *Phys. Rep.* **310**, 98 (1999).
6. A.C. da Silva, D. Barbosa, A.R. Liddle, and P.A. Thomas, *MNRAS*, in press, astro-ph/9907224.
7. C. Burigana, L. Danese, and G.F. De Zotti, *Astron. & Astrophys.* **246**, 49 (1991).
8. L. Danese and G.F. De Zotti, *Astron. & Astrophys.* **107**, 39 (1982); G. De Zotti, *Prog. in Part. Nucl. Phys.* **17**, 117 (1987).
9. J.G. Bartlett and A. Stebbins, *Astrophys. J.* **371**, 8 (1991).
10. J.C. Mather *et al.*, *Astrophys. J.* **512**, 511 (1999).
11. E.L. Wright *et al.*, *Astrophys. J.* **420**, 450 (1994).
12. W. Hu and J. Silk, *Phys. Rev. Lett.* **70**, 2661 (1993).
13. D.J. Fixsen *et al.*, *Astrophys. J.* **473**, 576 (1996).
14. J.C. Mather *et al.*, *Astrophys. J.* **420**, 439 (1994).

15. M. Bersanelli *et al.*, *Astrophys. J.* **424**, 517 (1994).
 16. A. Dekel, in "Cosmic Flows: Towards an Understanding of Large-Scale Structure", ed. S. Courteau, M.A. Strauss, and J.A. Willick (ASP Conf. Ser.), in press, astro-ph/9911501.
 17. A. Kogut *et al.*, *Astrophys. J.* **419**, 1 (1993);
C. Lineweaver *et al.*, *Astrophys. J.* **470**, L28 (1996).
 18. C.L. Bennett *et al.*, *Astrophys. J.* **464**, L1 (1996).
 19. A. Kogut, G. Hinshaw, and A.J. Banday, *Phys. Rev.* **D55**, 1901 (1997);
E.F. Bunn, P. Ferreira, and J. Silk, *Phys. Rev. Lett.* **77**, 2883 (1996).
 20. G.F. Smoot *et al.*, *Astrophys. J.* **396**, L1 (1992).
 21. M. White, D. Scott, and J. Silk, *Ann. Rev. Astron. & Astrophys.* **32**, 329 (1994).
 22. D.H. Lyth and A. Riotto, *Phys. Rep.* **314**, 1 (1999).
 23. J.P. Zibin, D. Scott, and M. White, *Phys. Rev. D* **60**, 123513 (1999).
 24. U. Seljak and M. Zaldarriaga, *Astrophys. J.* **469**, 437 (1996).
 25. U.-L. Pen, U. Seljak, and N. Turok, *Phys. Rev. Lett.* **79**, 1611 (1997).
 26. D. Scott, J. Silk, and M. White, *Science* **268**, 829 (1995);
W. Hu, J. Silk, and N. Sugiyama, *Nature* **386**, 37 (1996).
 27. K.M. Górski *et al.*, *Astrophys. J.* **464**, L11 (1996).
 28. S. Dodelson and L. Knox, *Phys. Rev. Lett.*, in press, astro-ph/9909454;
A. Melchiorri *et al.*, *Astrophys. J.*, in press, astro-ph/9911445.
 29. M. Tegmark and M. Zaldarriaga, *Astrophys. J.*, in press, astro-ph/0002091.
 30. S. Perlmutter *et al.*, *Astrophys. J.* **517**, 565 (1999);
A.G. Riess *et al.*, *Astron. J.* **116**, 1009 (1998).
 31. C.H. Lineweaver, *Astrophys. J.* **505**, L69 (1998);
J.R. Bond and A.H. Jaffe, *Phil. Trans. Roy. Soc. A*, in press, astro-ph/98089043;
G. Efstathiou, *MNRAS* **310**, 842 (1999).
 32. P. de Bernardis *et al.*, *Nature* **404**, 955 (2000).
 33. S. Hanany *et al.*, astro-ph/0005123.
 34. A. Lange *et al.*, astro-ph/0005004.
 35. A. Balbi *et al.*, astro-ph/0005124.
 36. M. White, D. Scott, E. Pierpaoli, astro-ph/0004385.
 37. R.G. Carlberg *et al.*, *Astrophys. J.* **462**, 32 (1996);
P. Coles and G.F.R. Ellis, "Is the Universe Open or Closed?", Cambridge University Press, Cambridge (1997).
 38. E. Pierpaoli, D. Scott and M. White, *Science*, in press (2000).
 39. J. R. Bond, A.H. Jaffe, and L.E. Knox, *Astrophys. J.*, in press, astro-ph/9808264.
 40. G. Jungman, M. Kamionkowski, A. Kosowsky, and D.N. Spergel, *Phys. Rev.* **D54**, 1332 (1996);
W. Hu and M. White, *Phys. Rev. Lett.* **77**, 1687 (1996);
J.R. Bond, G. Efstathiou, and M. Tegmark, *MNRAS* **291**, L33 (1997);
M. Zaldarriaga, D. Spergel, and U. Seljak, *Astrophys. J.* **488**, 1 (1997).
 41. M. Kamionkowski, A. Kosowsky, *Ann. Rev. Nucl. Part. Sci.* **49**, 77 (1999).
 42. W. Hu, M. White, *New Astron.* **2**, 323 (1997).
- CMB Spectrum References:**
1. **FIRAS**: J.C. Mather *et al.*, *Astrophys. J.* **420**, 439 (1994);
D. Fixsen *et al.*, *Astrophys. J.* **420**, 445 (1994);
D. Fixsen *et al.*, *Astrophys. J.* **473**, 576 (1996);
J.C. Mather *et al.*, *Astrophys. J.* **512**, 511 (1999).
 2. **DMR**: A. Kogut *et al.*, *Astrophys. J.* **419**, 1 (1993);
A. Kogut *et al.*, *Astrophys. J.* **460**, 1 (1996).
 3. **UBC**: H.P. Gush, M. Halpern, and E.H. Wishnow, *Phys. Rev. Lett.* **65**, 537 (1990).
 4. **LBL-Italy**: G.F. Smoot *et al.*, *Phys. Rev. Lett.* **51**, 1099 (1983);
M. Bensadoun *et al.*, *Astrophys. J.* **409**, 1 (1993);
M. Bersanelli *et al.*, *Astrophys. J.* **424**, 517 (1994);
M. Bersanelli *et al.*, *Astrophys. Lett. and Comm.* **32**, 7 (1995);
G. De Amici *et al.*, *Astrophys. J.* **381**, 341 (1991);
A. Kogut *et al.*, *Astrophys. J.* **335**, 102 (1990);
N. Mandolesi *et al.*, *Astrophys. J.* **310**, 561 (1986);
G. Sironi, G. Bonelli, & M. Limon, *Astrophys. J.* **378**, 550 (1991).
 5. **Princeton**: S. Staggs *et al.*, *Astrophys. J.* **458**, 407 (1995);
S. Staggs *et al.*, *Astrophys. J.* **473**, L1 (1996);
D.G. Johnson and D.T. Wilkinson, *Astrophys. J.* **313**, L1 (1987).
 6. **Cyanogen**: K.C. Roth, D.M. Meyer, and I. Hawkins, *Astrophys. J.* **413**, L67 (1993);
K.C. Roth and D.M. Meyer, *Astrophys. J.* **441**, 129 (1995);
E. Palazzi *et al.*, *Astrophys. J.* **357**, 14 (1990).
- CMB Anisotropy References:**
1. **ARGO**: P. de Bernardis *et al.*, *Astrophys. J.* **422**, L33 (1994);
S. Masi *et al.*, *Astrophys. J.* **463**, L47 (1996).
 2. **ATCA**: R. Subrahmayan, M.J. Kesteven, R.D. Ekers, M. Sinclair, and J. Silk, *Monthly Not. Royal Astron. Soc.* **298**, 1189 (1993).
 3. **BAM**: G.S. Tucker *et al.*, *Astrophys. J.* **475**, L73 (1997).
 4. **BOOM97**: P.D. Mauskopf *et al.*, *Astrophys. J.*, in press, astro-ph/9911444.
 5. **CAT**: P.F.S. Scott *et al.*, *Astrophys. J.* **461**, L1 (1996);
J.C. Baker *et al.*, *Monthly Not. Royal Astron. Soc.* **308**, 1173 (1999).
 6. **COBE**: G. Hinshaw *et al.*, *Astrophys. J.* **464**, L17 (1996).
 7. **FIRS**: K. Ganga, L. Page, E. Cheng, and S. Meyers, *Astrophys. J.* **432**, L15 (1993).
 8. **IAB**: L. Piccirillo and P. Calisse, *Astrophys. J.* **413**, 529 (1993).
 9. **IAC**: S.R. Dicker *et al.*, *Monthly Not. Royal Astron. Soc.*, in press, astro-ph/9907118.
 10. **MAT**: E. Torbet *et al.*, *Astrophys. J.* **521**, L79 (1999);
A.D. Miller *et al.*, *Astrophys. J.* **524**, L1 (1999).
 11. **MAX**: S.T. Tanaka *et al.*, *Astrophys. J.* **468**, L81 (1996);
M. Lim *et al.*, *Astrophys. J.* **469**, L69 (1996).
 12. **MSAM**: G.W. Wilson *et al.*, *Astrophys. J.*, in press, astro-ph/9902047.
 13. **OVRO**: A.C.S. Readhead *et al.*, *Astrophys. J.* **346**, 566 (1989);
E. Leitch, A.C.S. Readhead, T.J. Pearson, S.T. Myers, and S. Gulkis, *Astrophys. J.*, in press, astro-ph/9807312.
 14. **Python**: S.R. Platt *et al.*, *Astrophys. J.* **475**, L1 (1997);
K. Coble *et al.*, *Astrophys. J.* **519**, L5 (1999).
 15. **QMAP**: A. de Oliveira-Costa *et al.*, *Astrophys. J.* **509**, L77 (1998).
 16. **Saskatoon**: C.B. Netterfield *et al.*, *Astrophys. J.* **474**, 47 (1997).
 17. **SP91**: J. Schuster *et al.*, *Astrophys. J.* **412**, L47 (1993).
 18. **SP94**: J.O. Gundersen *et al.*, *Astrophys. J.* **443**, L57 (1994).
 19. **SuZIE**: S. E. Church *et al.*, *Astrophys. J.* **484**, 523 (1997).
 20. **Tenerife**: C.M. Gutiérrez *et al.*, *Astrophys. J.* **529**, 47 (2000).
 21. **Viper**: J.B. Peterson *et al.*, *Astrophys. J.*, in press, astro-ph/9910503.
 22. **VLA**: B. Partridge *et al.*, *Astrophys. J.* **483**, 38 (1997).
 23. **WD**: G.S. Tucker, G.S. Griffin, H.T. Nguyen, and J.B. Peterson, *Astrophys. J.* **419**, L45 (1993).

20. COSMIC RAYS

Revised February 2000 by T.K. Gaisser and T. Stanev (Bartol Research Inst., Univ. of Delaware).

20.1. Primary spectra

The cosmic radiation incident at the top of the terrestrial atmosphere includes all stable charged particles and nuclei with lifetimes of order 10^6 years or longer. Technically, "primary" cosmic rays are those particles accelerated at astrophysical sources and "secondaries" are those particles produced in interaction of the primaries with interstellar gas. Thus electrons, protons and helium, as well as carbon, oxygen, iron, and other nuclei synthesized in stars, are primaries. Nuclei such as lithium, beryllium, and boron (which are not abundant end-products of stellar nucleosynthesis) are secondaries. Antiprotons and positrons are partly, if not entirely, secondaries, but the fraction of these particles that may be primary is a question of current interest.

Apart from particles associated with solar flares, the cosmic radiation comes from outside the solar system. The incoming charged particles are "modulated" by the solar wind, the expanding magnetized plasma generated by the Sun, which decelerates and partially excludes the lower energy galactic cosmic rays from the inner solar system. There is a significant anticorrelation between solar activity (which has an eleven-year cycle) and the intensity of the cosmic rays with energies below about 10 GeV. In addition, the lower-energy cosmic rays are affected by the geomagnetic field, which they must penetrate to reach the top of the atmosphere. Thus the intensity of any component of the cosmic radiation in the GeV range depends both on the location and time.

There are four different ways to describe the spectra of the components of the cosmic radiation: (1) By particles per unit rigidity. Propagation (and probably also acceleration) through cosmic magnetic fields depends on gyroradius or *magnetic rigidity*, R , which is gyroradius multiplied by the magnetic field strength:

$$R = \frac{pc}{Ze} = r_L B. \quad (20.1)$$

(2) By particles per energy-per-nucleon. Fragmentation of nuclei propagating through the interstellar gas depends on energy per nucleon, since that quantity is approximately conserved when a nucleus breaks up on interaction with the gas. (3) By nucleons per energy-per-nucleon. Production of secondary cosmic rays in the atmosphere depends on the intensity of nucleons per energy-per-nucleon, approximately independently of whether the incident nucleons are free protons or bound in nuclei. (4) By particles per energy-per-nucleus. Air shower experiments that use the atmosphere as a calorimeter generally measure a quantity that is related to total energy per particle.

The units of differential intensity I are $[\text{cm}^{-2}\text{s}^{-1}\text{sr}^{-1}\mathcal{E}^{-1}]$, where \mathcal{E} represents the units of one of the four variables listed above.

The intensity of primary nucleons in the energy range from several GeV to somewhat beyond 100 TeV is given approximately by

$$I_N(E) \approx 1.8 E^{-\alpha} \frac{\text{nucleons}}{\text{cm}^2 \text{ s sr GeV}}, \quad (20.2)$$

where E is the energy-per-nucleon (including rest mass energy) and α ($\equiv \gamma + 1$) = 2.7 is the differential spectral index of the cosmic ray flux and γ is the integral spectral index. About 79% of the primary nucleons are free protons and about 70% of the rest are nucleons bound in helium nuclei. The fractions of the primary nuclei are nearly constant over this energy range (possibly with small but interesting variations). Fractions of both primary and secondary incident nuclei are listed in Table 20.1. Figure 20.1 [1] shows the major components as a function of energy at a particular epoch of the solar cycle. There has been a series of more precise measurements of the primary spectrum of protons and helium in the past decade [2,3,4,5].

The spectrum of electrons and positrons incident at the top of the atmosphere is steeper than the spectra of protons and nuclei, as shown

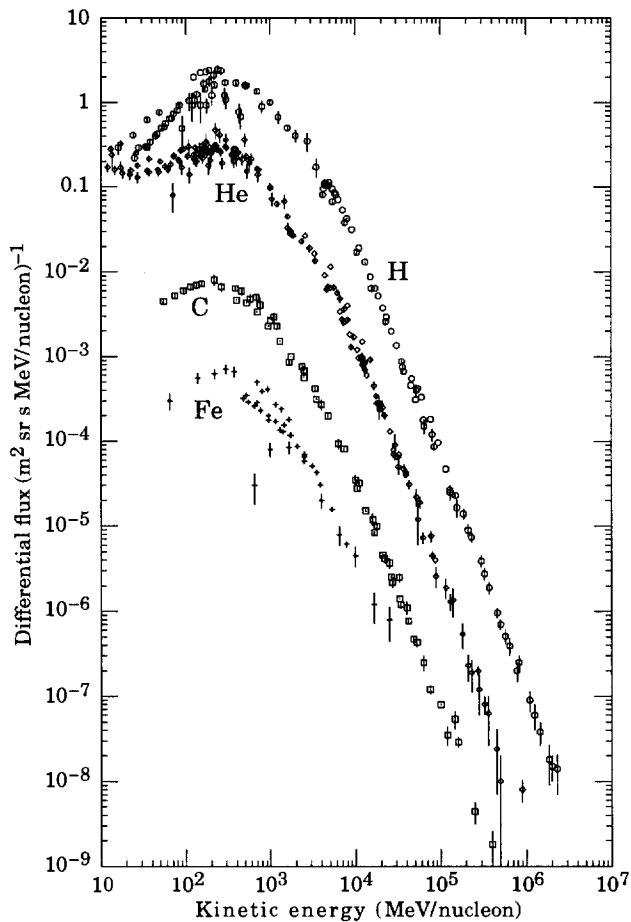


Figure 20.1: Major components of the primary cosmic radiation (from Ref. 1).

Table 20.1: Relative abundances F of cosmic-ray nuclei at 10.6 GeV/nucleon normalized to oxygen ($\equiv 1$) [6]. The oxygen flux at kinetic energy of 10.6 GeV/nucleon is $3.26 \times 10^{-6} \text{ cm}^{-2} \text{ s}^{-1} \text{ sr}^{-1} (\text{GeV/nucleon})^{-1}$. Abundances of hydrogen and helium are from Ref. 2.

Z	Element	F	Z	Element	F
1	H	485	13-14	Al-Si	0.19
2	He	26	15-16	P-S	0.03
3-5	Li-B	0.40	17-18	Cl-Ar	0.01
6-8	C-O	2.20	19-20	K-Ca	0.02
9-10	F-Ne	0.30	21-25	Sc-Mn	0.05
11-12	Na-Mg	0.22	26-28	Fe-Ni	0.12

in Fig. 20.2. The positron fraction is about 10% in the region in which it is measured (< 20 GeV), but it is not yet fully understood [8].

Above 10 GeV the fraction of antiprotons to protons is about 10^{-4} , and there is evidence for the kinematic suppression at lower energy expected for secondary antiprotons [9,10,11,12]. There is at this time no evidence for a significant primary component of antiprotons.

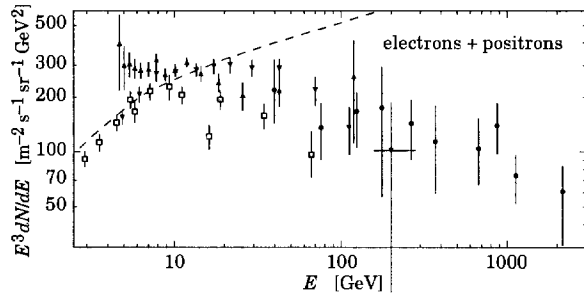


Figure 20.2: Differential spectrum of electrons plus positrons multiplied by E^3 (data summary from Ref. 7). The dashed line shows the proton spectrum multiplied by 0.01.

20.2. Cosmic rays in the atmosphere

Figure 20.3 shows the vertical fluxes of the major cosmic ray components in the atmosphere in the energy region where the particles are most numerous (except for electrons, which are most numerous near their critical energy, which is about 81 MeV in air). Except for protons and electrons near the top of the atmosphere, all particles are produced in interactions of the primary cosmic rays in the air. Muons and neutrinos are products of the decay of charged mesons, while electrons and photons originate in decays of neutral mesons.

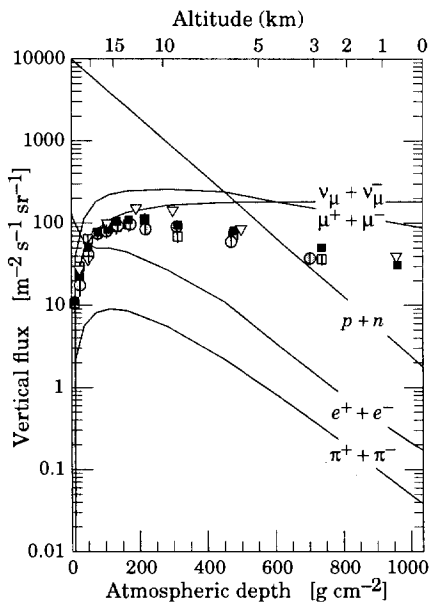


Figure 20.3: Vertical fluxes of cosmic rays in the atmosphere with $E > 1$ GeV estimated from the nucleon flux of Eq. (20.2). The points show measurements of negative muons with $E_\mu > 1$ GeV [3,13,14,15].

Most measurements are made at ground level or near the top of the atmosphere, but there are also measurements of muons and electrons from airplanes and balloons. Fig. 20.3 includes recent measurements of negative muons [3,13,14,15]. Since $\mu^+(\mu^-)$ are produced in association with $\nu_\mu(\bar{\nu}_\mu)$, the measurement of muons near the maximum of the intensity curve for the parent pions serves to calibrate the atmospheric ν_μ beam [16]. Because muons typically lose almost two GeV in passing through the atmosphere, the comparison near the production altitude is important for the sub-GeV range of $\nu_\mu(\bar{\nu}_\mu)$ energies.

The flux of cosmic rays through the atmosphere is described by a set of coupled cascade equations with boundary conditions at the top of the atmosphere to match the primary spectrum. Numerical or Monte Carlo calculations are needed to account accurately for decay and energy-loss processes, and for the energy-dependences of the cross sections and of the primary spectral index γ . Approximate analytic solutions are, however, useful in limited regions of energy [17]. For

example, the vertical intensity of nucleons at depth X (g cm^{-2}) in the atmosphere is given by

$$I_N(E, X) \approx I_N(E, 0) e^{-X/\Lambda}, \quad (20.3)$$

where Λ is the attenuation length of nucleons in air.

The corresponding expression for the vertical intensity of charged pions with energy $E_\pi \ll \epsilon_\pi = 115$ GeV is

$$I_\pi(E_\pi, X) \approx \frac{Z_{N\pi}}{\lambda_N} I_N(E_\pi, 0) e^{-X/\Lambda} \frac{X E_\pi}{\epsilon_\pi}. \quad (20.4)$$

This expression has a maximum at $t = \Lambda \approx 120$ g cm^{-2} , which corresponds to an altitude of 15 kilometers. The quantity $Z_{N\pi}$ is the spectrum-weighted moment of the inclusive distribution of charged pions in interactions of nucleons with nuclei of the atmosphere. The intensity of low-energy pions is much less than that of nucleons because $Z_{N\pi} \approx 0.079$ is small and because most pions with energy much less than the critical energy ϵ_π decay rather than interact.

20.3. Cosmic rays at the surface

20.3.1. Muons: Muons are the most numerous charged particles at sea level (see Fig. 20.3). Most muons are produced high in the atmosphere (typically 15 km) and lose about 2 GeV to ionization before reaching the ground. Their energy and angular distribution reflect a convolution of production spectrum, energy loss in the atmosphere, and decay. For example, 2.4 GeV muons have a decay length of 15 km, which is reduced to 8.7 km by energy loss. The mean energy of muons at the ground is ≈ 4 GeV. The energy spectrum is almost flat below 1 GeV, steepens gradually to reflect the primary spectrum in the 10–100 GeV range, and steepens further at higher energies because pions with $E_\pi > \epsilon_\pi \approx 115$ GeV tend to interact in the atmosphere before they decay. Asymptotically ($E_\mu \gg 1$ TeV), the energy spectrum of atmospheric muons is one power steeper than the primary spectrum. The integral intensity of vertical muons above 1 GeV/c at sea level is ≈ 70 $\text{m}^{-2}\text{s}^{-1}\text{sr}^{-1}$ [18,19]. Experimentalists are familiar with this number in the form $I \approx 1$ $\text{cm}^{-2}\text{min}^{-1}$ for horizontal detectors.

The overall angular distribution of muons at the ground is $\propto \cos^2 \theta$, which is characteristic of muons with $E_\mu \sim 3$ GeV. At lower energy the angular distribution becomes increasingly steeper, while at higher energy it flattens and approaches a $\sec \theta$ distribution for $E_\mu \gg \epsilon_\pi$ and $\theta < 70^\circ$.

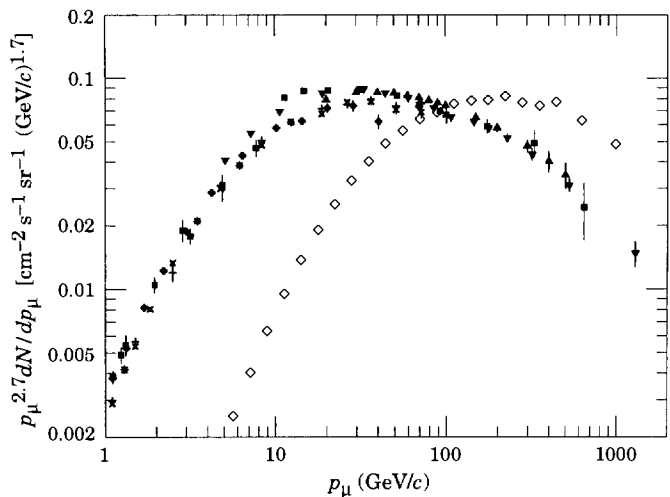


Figure 20.4: Spectrum of muons at $\theta = 0^\circ$ (\diamond [18], \blacksquare [20], \blacktriangledown [21], \blacktriangle [22], \times , $+$ [23]), and $\theta = 75^\circ$ (\diamond [24]).

Figure 20.4 shows the muon energy spectrum at sea level for two angles. At large angles low energy muons decay before reaching the surface and high energy pions decay before they interact, thus the average muon energy increases. An approximate extrapolation

formula valid when muon decay is negligible ($E_\mu > 100/\cos\theta$ GeV) and the curvature of the Earth can be neglected ($\theta < 70^\circ$) is

$$\frac{dN_\mu}{dE_\mu} \approx \frac{0.14 E_\mu^{-2.7}}{\text{cm}^2 \text{ s sr GeV}} \times \left\{ \frac{1}{1 + \frac{1.1 E_\mu \cos\theta}{115 \text{ GeV}}} + \frac{0.054}{1 + \frac{1.1 E_\mu \cos\theta}{850 \text{ GeV}}} \right\}, \quad (20.5)$$

where the two terms give the contribution of pions and charged kaons. Eq. (20.5) neglects a small contribution from charm and heavier flavors which is negligible except at very high energy [27].

The muon charge ratio reflects the excess of π^+ over π^- in the forward fragmentation region of proton initiated interactions together with the fact that there are more protons than neutrons in the primary spectrum. The charge ratio is between 1.1 and 1.4 from 1 GeV to 100 GeV [18,23]. Below 1 GeV there is a systematic dependence on location due to geomagnetic effects. [23]

20.3.2. Electromagnetic component: At the ground, this component consists of electrons, positrons, and photons primarily from electromagnetic cascades initiated by decay of neutral and charged mesons. Muon decay is the dominant source of low-energy electrons at sea level. Decay of neutral pions is more important at high altitude or when the energy threshold is high. Knock-on electrons also make a small contribution at low energy [25]. The integral vertical intensity of electrons plus positrons is very approximately 30, 6, and $0.2 \text{ m}^{-2}\text{s}^{-1}\text{sr}^{-1}$ above 10, 100, and 1000 MeV respectively [19,26], but the exact numbers depend sensitively on altitude, and the angular dependence is complex because of the different altitude dependence of the different sources of electrons [25,26,28]. The ratio of photons to electrons plus positrons is approximately 1.3 above a GeV and 1.7 below the critical energy [28].

20.3.3. Protons: Nucleons above 1 GeV/c at ground level are degraded remnants of the primary cosmic radiation. The intensity is approximately represented by Eq. (20.3) with the replacement $t \rightarrow t/\cos\theta$ for $\theta < 70^\circ$ and an attenuation length $\Lambda = 123 \text{ g cm}^{-2}$. At sea level, about 1/3 of the nucleons in the vertical direction are neutrons (up from $\approx 10\%$ at the top of the atmosphere as the n/p ratio approaches equilibrium). The integral intensity of vertical protons above 1 GeV/c at sea level is $\approx 0.9 \text{ m}^{-2}\text{s}^{-1}\text{sr}^{-1}$ [19,29].

20.4. Cosmic rays underground

Only muons and neutrinos penetrate to significant depths underground. The muons produce tertiary fluxes of photons, electrons, and hadrons.

20.4.1. Muons: As discussed in Section 23.6 of this *Review*, muons lose energy by ionization and by radiative processes: bremsstrahlung, direct production of e^+e^- pairs, and photonuclear interactions. The total muon energy loss may be expressed as a function of the amount of matter traversed as

$$-\frac{dE_\mu}{dX} = a + b E_\mu, \quad (20.6)$$

where a is the ionization loss and b is the fractional energy loss by the three radiation processes. Both are slowly varying functions of energy. The quantity $\epsilon \equiv a/b$ (≈ 500 GeV in standard rock) defines a critical energy below which continuous ionization loss is more important than radiative losses. Table 20.2 shows a and b values for standard rock as a function of muon energy. The second column of Table 20.2 shows the muon range in standard rock ($A = 22$, $Z = 11$, $\rho = 2.65 \text{ g cm}^{-3}$). These parameters are quite sensitive to the chemical composition of the rock, which must be evaluated for each experimental location.

The intensity of muons underground can be estimated from the muon intensity in the atmosphere and their rate of energy loss. To the extent that the mild energy dependence of a and b can be neglected, Eq. (20.6) can be integrated to provide the following relation between

Table 20.2: Average muon range R and energy loss parameters calculated for standard rock[30]. Range is given in km-water-equivalent, or 10^5 g cm^{-2} .

E_μ GeV	R km.w.e.	a MeV $\text{g}^{-1} \text{cm}^2$	b_{brems} —	b_{pair} $10^{-6} \text{ g}^{-1} \text{cm}^2$	b_{nucl} $\text{g}^{-1} \text{cm}^2$	$\sum b_i$ —
10	0.05	2.17	0.70	0.70	0.50	1.90
100	0.41	2.44	1.10	1.53	0.41	3.04
1000	2.45	2.68	1.44	2.07	0.41	3.92
10000	6.09	2.93	1.62	2.27	0.46	4.35

the energy $E_{\mu,0}$ of a muon at production in the atmosphere and its average energy E_μ after traversing a thickness X of rock (or ice or water):

$$E_\mu = (E_{\mu,0} + \epsilon) e^{-bX} - \epsilon. \quad (20.7)$$

Especially at high energy, however, fluctuations are important and an accurate calculation requires a simulation that accounts for stochastic energy-loss processes [31].

There are two depth regimes for Eq. (20.7). For $X \ll b^{-1} \approx 2.5$ km water equivalent, $E_{\mu,0} \approx E_\mu(X) + aX$, while for $X \gg b^{-1}$ $E_{\mu,0} \approx (\epsilon + E_\mu(X)) \exp(bX)$. Thus at shallow depths the differential muon energy spectrum is approximately constant for $E_\mu < aX$ and steepens to reflect the surface muon spectrum for $E_\mu > aX$, whereas for $X > 2.5$ km.w.e. the differential spectrum underground is again constant for small muon energies but steepens to reflect the surface muon spectrum for $E_\mu > \epsilon \approx 0.5$ TeV. In the deep regime the shape is independent of depth although the intensity decreases exponentially with depth. In general the muon spectrum at slant depth X is

$$\frac{dN_\mu(X)}{dE_\mu} = \frac{dN_\mu}{dE_{\mu,0}} \frac{dE_{\mu,0}}{dE_\mu} = \frac{dN_\mu}{dE_{\mu,0}} e^{bX}, \quad (20.8)$$

where $E_{\mu,0}$ is the solution of Eq. (20.7) in the approximation neglecting fluctuations.

Fig. 20.5 shows the vertical muon intensity versus depth. In constructing this “depth-intensity curve,” each group has taken account of the angular distribution of the muons in the atmosphere, the map of the overburden at each detector, and the properties of the local medium in connecting measurements at various slant depths and zenith angles to the vertical intensity. Use of data from a range of angles allows a fixed detector to cover a wide range of depths. The flat portion of the curve is due to muons produced locally by charged-current interactions of ν_μ .

20.4.2. Neutrinos: Because neutrinos have small interaction cross sections, measurements of atmospheric neutrinos require a deep detector to avoid backgrounds. There are two types of measurements: contained (or semi-contained) events, in which the vertex is determined to originate inside the detector, and neutrino-induced muons. The latter are muons that enter the detector from zenith angles so large (e.g., nearly horizontal or upward) that they cannot be muons produced in the atmosphere. In neither case is the neutrino flux measured directly. What is measured is a convolution of the neutrino flux and cross section with the properties of the detector (which includes the surrounding medium in the case of entering muons).

Contained and semi-contained events reflect neutrinos in the sub-GeV to multi-GeV region where the product of increasing cross section and decreasing flux is maximum. In the GeV region the neutrino flux and its angular distribution depend on the geomagnetic location of the detector and, to a lesser extent, on the phase of the solar cycle. Naively, we expect $\nu_\mu/\nu_e = 2$ from counting neutrinos of the two flavors coming from the chain of pion and muon decay. This ratio is only slightly modified by the details of the decay kinematics, but the fraction of electron neutrinos gradually decreases above a GeV as parent muons begin to reach the ground before decaying. Experimental measurements have to account for the ratio of $\bar{\nu}/\nu$, which have cross sections different by a factor of 3 in this energy range. In addition, detectors generally have different efficiencies for

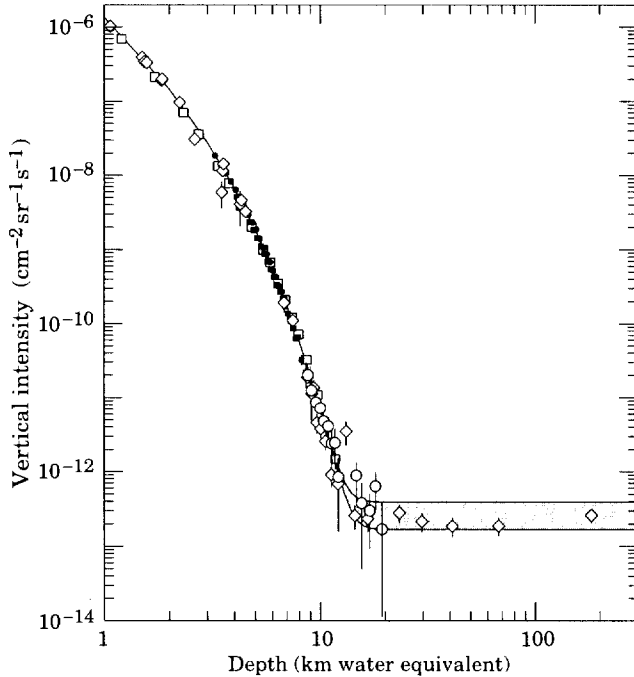


Figure 20.5: Vertical muon intensity vs depth (1 km.w.e. = 10^5 g cm^{-2} of standard rock). The experimental data are from: \diamond : the compilations of Crouch [32], \square : Baksan [33], \circ : LVD [34], \bullet : MACRO [35], \blacksquare : Frejus [36]. The shaded area at large depths represents neutrino induced muons of energy above 2 GeV. The upper line is for horizontal neutrino-induced muons, the lower one for vertically upward muons.

detecting muon neutrinos and electron neutrinos which need to be accounted for in comparing measurements with expectation. Fig. 20.6 shows the distributions of the visible energy in the Super-Kamiokande detector [39] for electron-like and muon-like charged current neutrino interactions. Contrary to expectation, the numbers of the two classes of events are similar rather than different by a factor of two. The exposure for the data sample shown here is 50 kiloton-years. The falloff of the muon-like events at high energy is a consequence of the poor containment for high energy muons. Corrections for detection efficiencies and backgrounds are, however, insufficient to account for the large difference from the expectation.

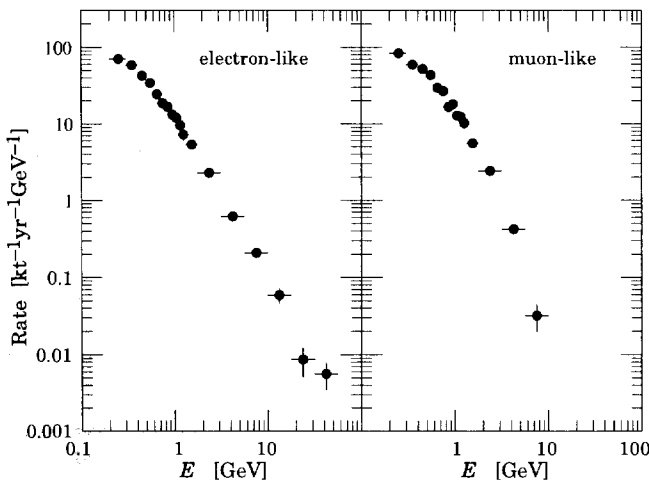


Figure 20.6: Sub-GeV and multi-GeV neutrino interactions from SuperKamiokande [39]. The plot shows the spectra of visible energy in the detector.

Two well-understood properties of atmospheric cosmic rays provide a standard for comparison of the measurements of atmospheric

neutrinos. These are the “ $\sec\theta$ effect” and the “east-west effect”. The former refers originally to the enhancement of the flux of $> 10 \text{ GeV}$ muons (and neutrinos) at large zenith angles because the parent pions propagate more in the low density upper atmosphere where decay is enhanced relative to interaction. For neutrinos from muon decay, the enhancement near the horizontal becomes important for $E_\nu > 1 \text{ GeV}$ and arises mainly from the increased pathlength through the atmosphere for muon decay in flight. Fig. 20.7 from Ref. 40 shows a comparison between measurement and expectation for the zenith angle dependence of multi-GeV electron-like (mostly ν_e) and muon-like (mostly ν_μ) events separately. The ν_e show an enhancement near the horizontal and approximate equality for nearly upward ($\cos\theta \approx -1$) and nearly downward ($\cos\theta \approx 1$) events. There is, however, a very significant deficit of upward ($\cos\theta < 0$) ν_μ events, which have long pathlengths comparable to the radius of the Earth. This pattern has been interpreted as evidence for oscillations involving muon neutrinos [39]. (See the article on neutrino properties in this Review.) Including three dimensional effects in the calculation of atmospheric neutrinos may change somewhat the expected angular distributions of neutrinos at low energy [41], but it does not change the fundamental expectation of up-down symmetry, which is the basis of the evidence for oscillations.

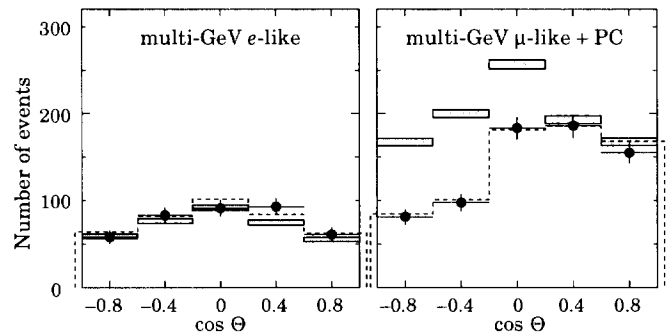


Figure 20.7: Zenith-angle dependence of multi-GeV neutrino interactions from SuperKamiokande [40]. The shaded boxes show the expectation in the absence of any oscillations. The lines show fits with some assumed oscillation parameters, as described in Ref. 40.

The east-west effect [42,43] is the enhancement, especially at low geomagnetic latitudes, of cosmic rays incident on the atmosphere from the west as compared to those from the east. This is a consequence of the fact that the cosmic rays are positively charged nuclei which are bent systematically in one sense in the geomagnetic field. Not all trajectories can reach the atmosphere from outside the geomagnetic field. The standard procedure to see which trajectories are allowed is to inject antiprotons outward from near the top of the atmosphere in various directions and see if they escape from the geomagnetic field without becoming trapped indefinitely or intersecting the surface of the Earth. Any direction in which an antiproton of a given momentum can escape is an allowed direction from which a proton of the opposite momentum can arrive. Since the geomagnetic field is oriented from south to north in the equatorial region, antiprotons injected toward the east are bent back towards the Earth. Thus there is a range of momenta and zenith angles for which positive particles cannot arrive from the east but can arrive from the west. This east-west asymmetry of the incident cosmic rays induces a similar asymmetry on the secondaries, including neutrinos. Since this is an azimuthal effect, the resulting asymmetry is independent of possible oscillations, which depend on pathlength (equivalently zenith angle), but not on azimuth. Fig. 20.8 (from Ref. 44) is a comparison of data and expectation for this effect, which serves as a consistency check of the measurement and analysis.

Muons that enter the detector from outside after production in charged-current interactions of neutrinos naturally reflect a higher energy portion of the neutrino spectrum than contained events because the muon range increases with energy as well as the cross section. The relevant energy range is $\sim 10 < E_\nu < 1000 \text{ GeV}$, depending somewhat on angle. Neutrinos in this energy range show a $\sec\theta$ effect similar

Table 20.3: Measured fluxes ($10^{-13} \text{ cm}^{-2} \text{ s}^{-1} \text{ sr}^{-1}$) of neutrino-induced muons as a function of the effective minimum muon energy E_μ .

$E_\mu >$	1 GeV	1 GeV	1 GeV	2 GeV	3 GeV	3 GeV
Ref.	CWI [45]	Baksan [46]	MACRO [47]	IMB [48]	Kam [49]	SuperK [50]
F_μ	2.17 ± 0.21	2.77 ± 0.17	2.29 ± 0.15	2.26 ± 0.11	1.94 ± 0.12	1.74 ± 0.07

to muons (see Eq. (20.5)). This causes the flux of horizontal neutrino induced muons to be approximately a factor two higher than the vertically upward flux. The upper and lower edges of the horizontal shaded region in Fig. 20.5 correspond to horizontal and vertical intensities of neutrino-induced muons. Table 20.3 gives the measured fluxes of upward-moving neutrino-induced muons averaged over the lower hemisphere. Generally the definition of minimum muon energy depends on where it passes through the detector. The tabulated effective minimum energy estimates the average over various accepted trajectories.

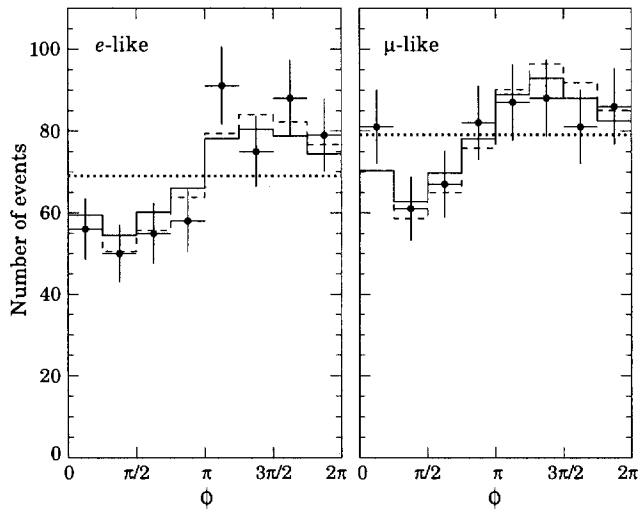


Figure 20.8: Azimuthal dependence of \sim GeV neutrino interactions from SuperKamiokande [44]. The cardinal points of the compass are S, E, N, W starting at 0. These are the direction from which the particles arrive. The lines show the expectation based on two different calculations, as described in Ref. 44.

20.5. Air showers

So far we have discussed inclusive or uncorrelated fluxes of various components of the cosmic radiation. An air shower is caused by a single cosmic ray with energy high enough for its cascade to be detectable at the ground. The shower has a hadronic core, which acts as a collimated source of electromagnetic subshowers, generated mostly from $\pi^0 \rightarrow \gamma\gamma$. The resulting electrons and positrons are the most numerous particles in the shower. The number of muons, produced by decays of charged mesons, is an order of magnitude lower.

Air showers spread over a large area on the ground, and arrays of detectors operated for long times are useful for studying cosmic rays with primary energy $E_0 > 100 \text{ TeV}$, where the low flux makes measurements with small detectors in balloons and satellites difficult.

Greisen [51] gives the following approximate expressions for the numbers and lateral distributions of particles in showers at ground level. The total number of muons N_μ with energies above 1 GeV is

$$N_\mu(> 1 \text{ GeV}) \approx 0.95 \times 10^5 \left(N_e / 10^6 \right)^{3/4}, \quad (20.9)$$

where N_e is the total number of charged particles in the shower (not just e^\pm). The number of muons per square meter, ρ_μ , as a function of the lateral distance r (in meters) from the center of the shower is

$$\rho_\mu = \frac{1.25 N_\mu}{2\pi \Gamma(1.25)} \left(\frac{1}{320} \right)^{1.25} r^{-0.75} \left(1 + \frac{r}{320} \right)^{-2.5}, \quad (20.10)$$

where Γ is the gamma function. The number density of charged particles is

$$\rho_e = C_1(s, d, C_2) x^{(s-2)} (1+x)^{(s-4.5)} (1+C_2 x^d). \quad (20.11)$$

Here s , d , and C_2 are parameters in terms of which the overall normalization constant $C_1(s, d, C_2)$ is given by

$$C_1(s, d, C_2) = \frac{N_e}{2\pi r_1^2} [B(s, 4.5 - 2s) + C_2 B(s + d, 4.5 - d - 2s)]^{-1}, \quad (20.12)$$

where $B(m, n)$ is the beta function. The values of the parameters depend on shower size (N_e), depth in the atmosphere, identity of the primary nucleus, etc. For showers with $N_e \approx 10^6$ at sea level, Greisen uses $s = 1.25$, $d = 1$, and $C_2 = 0.088$. Finally, x is r/r_1 , where r_1 is the Molière radius, which depends on the density of the atmosphere and hence on the altitude at which showers are detected. At sea level $r_1 \approx 78 \text{ m}$. It increases with altitude.

The lateral spread of a shower is determined largely by Coulomb scattering of the many low-energy electrons and is characterized by the Molière radius. The lateral spread of the muons (ρ_μ) is larger and depends on the transverse momenta of the muons at production as well as multiple scattering.

There are large fluctuations in development from shower to shower, even for showers of the same energy and primary mass—especially for small showers, which are usually well past maximum development when observed at the ground. Thus the shower size N_e and primary energy E_0 are only related in an average sense, and even this relation depends on depth in the atmosphere. One estimate of the relation is [52]

$$E_0 \sim 3.9 \times 10^6 \text{ GeV} (N_e / 10^6)^{0.9} \quad (20.13)$$

for vertical showers with $10^{14} < E < 10^{17} \text{ eV}$ at 920 g cm^{-2} (965 m above sea level). Because of fluctuations, N_e as a function of E_0 is not the inverse of Eq. (20.13). As E_0 increases the shower maximum (on average) moves down into the atmosphere and the relation between N_e and E_0 changes. At the maximum of shower development, there are approximately 2/3 particles per GeV of primary energy.

Detailed simulations and cross-calibrations between different types of detectors are necessary to establish the primary energy spectrum from air-shower experiments [52,53]. Figure 20.9 shows the “all-particle” spectrum. In establishing this spectrum, efforts have been made to minimize the dependence of the analysis on the primary composition. In the energy range above 10^{17} eV , the Fly’s Eye technique [71] is particularly useful because it can establish the primary energy in a model-independent way by observing most of the longitudinal development of each shower, from which E_0 is obtained by integrating the energy deposition in the atmosphere.

In Fig. 20.9 the differential energy spectrum has been multiplied by $E^{2.7}$ in order to display the features of the steep spectrum that are otherwise difficult to discern. The steepening that occurs between 10^{15} and 10^{16} eV is known as the *knee* of the spectrum. The feature between 10^{18} and 10^{19} eV is called the *ankle* of the spectrum.

If the cosmic ray spectrum below 10^{18} eV is of galactic origin, the *knee* could reflect the fact that some (but not all) cosmic accelerators have reached their maximum energy. Some types of expanding supernova remnants, for example, are estimated not to be able to accelerate particles above energies in the range of 10^{15} eV total energy per particle. Effects of propagation and confinement in the galaxy [61] also need to be considered.

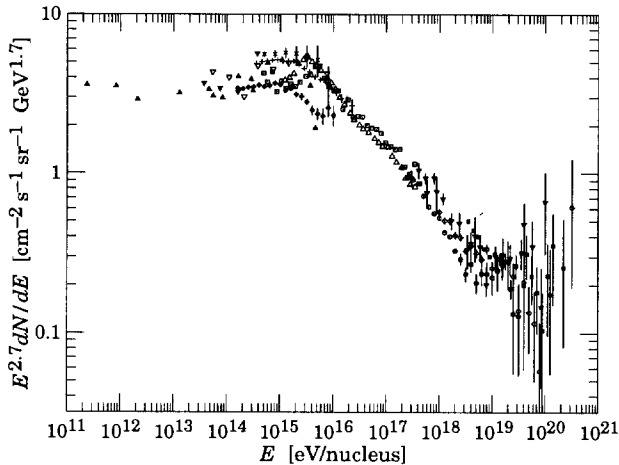


Figure 20.9: The all-particle spectrum: \square [52], \blacktriangle [54], \blacktriangledown [55], ∇ [56], \triangle [57], $+$ [58], \times [59], \blacklozenge [60]. References for the high energy portion of the spectrum are given in Fig. 20.10.

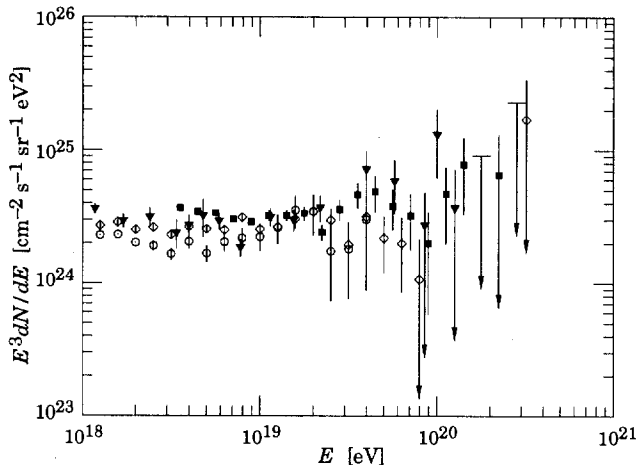


Figure 20.10: Expanded view of the highest energy portion of the cosmic-ray spectrum: \circ [71] (stereo), \diamond [71] (monocular) \blacksquare [72], \blacktriangledown [73].

The *ankle* has the classical characteristic shape [62] of a higher energy population of particles overtaking a lower energy population. A possible interpretation is that the higher energy population represents cosmic rays of extragalactic origin. If this is the case and if the cosmic rays are cosmological in origin, then there should be a cutoff around 5×10^{19} eV, resulting from interactions with the microwave background [63,64]. It is therefore of special interest that several events have been assigned energies above 10^{20} eV [65,66,67,68].

Figure 20.10 gives an expanded view of the high energy end of the spectrum. Not included in the figure are the preliminary results of the Hi-Res Fly's Eye group [69]. Their spectrum is consistent with the others and includes several events above 10^{20} eV. To expand the scale in Fig. 20.10, the differential flux is multiplied by E^3 , a process which amplifies small systematic differences in energy assignments into sizeable differences in rate. The different measurements agree with each other within 20% systematic shifts in energy scale and consistently show that the spectrum continues well past the expected cutoff for a cosmological distribution of sources. The implication is that some sources of the highest energy particles must be relatively nearby. For example, the attenuation length for protons at 2×10^{20} eV is 30 Mpc [70].

References:

1. J.A. Simpson, *Ann. Rev. Nucl. and Part. Sci.* **33**, 323 (1983).
2. M. Boezio *et al.*, *Astrophys. J.* **518**, 457 (1999).
3. R. Bellotti *et al.*, *Phys. Rev.* **D60**, 052002 (1999).

4. AMS Collaboration, *Phys. Lett.* **B** (to be published, 1999).
5. T. Sanuki *et al.*, in *Proc. 26th Int. Cosmic Ray Conf.*, Salt Lake City, **3**, 93 (1999).
6. J.J. Engemann *et al.*, *Astron. & Astrophys.* **233**, 96 (1990); See also *Cosmic Abundances of Matter* (ed. C. Jake Waddington) A.I.P. Conf. Proceedings No. 183 (1988) p. 111.
7. S.W. Barwick *et al.*, *Astrophys. J.* **498**, 779 (1998).
8. Stephane Coutu *et al.*, *Astropart. Phys.* **11**, 429 (1999).
9. J.W. Mitchell *et al.*, *Phys. Rev. Lett.* **76**, 3057 (1996).
10. M. Boezio *et al.*, *Astrophys. J.* **487**, 415 (1997).
11. M. Hof *et al.*, *Astrophys. J.* **467**, L33 (1996) See also G. Basini *et al.*, *Proc. 26th Int. Cosmic Ray Conf.*, Salt Lake City, **3**, 101 (1999).
12. H. Matsunaga *et al.*, *Phys. Rev. Lett.* **81**, 4052 (1998). See also S. Orito *et al.*, *astro-ph/9906426*.
13. R. Bellotti *et al.*, *Phys. Rev.* **D53**, 35 (1996).
14. M. Boezio *et al.*, *Phys. Rev. Lett.* **82**, 4757 (1999).
15. S. Coutu *et al.*, *Proc. 26th Int. Cosmic Ray Conf.*, Salt Lake City, **2**, 68 (1999).
16. D.H. Perkins, *Astropart. Phys.* **2**, 249 (1994).
17. T.K. Gaisser, *Cosmic Rays and Particle Physics*, Cambridge University Press (1990).
18. M.P. De Pascale *et al.*, *J. Geophys. Res.* **98**, 3501 (1993).
19. K. Allkofer and P.K.F. Grieder, *Cosmic Rays on Earth*, Fachinformationszentrum, Karlsruhe (1984).
20. O.C. Allkofer, K. Carstensen, and W.D. Dau, *Phys. Lett.* **B36**, 425 (1971).
21. B.C. Rastin, *J. Phys.* **G10**, 1609 (1984).
22. C.A. Ayre *et al.*, *J. Phys.* **G1**, 584 (1975).
23. J. Kremer *et al.*, *Phys. Rev. Lett.* **83**, 4241 (1999).
24. H. Jokisch *et al.*, *Phys. Rev.* **D19**, 1368 (1979).
25. S. Hayakawa, *Cosmic Ray Physics*, Wiley, Interscience, New York (1969).
26. R.R. Daniel and S.A. Stephens, *Revs. Geophysics & Space Sci.* **12**, 233 (1974).
27. F. Halzen, R. Vázquez, and E. Zas, *Astropart. Phys.* **1**, 297 (1993).
28. K.P. Beuermann and G. Wibberenz, *Can. J. Phys.* **46**, S1034 (1968).
29. I.S. Diggory *et al.*, *J. Phys.* **A7**, 741 (1974).
30. D.E. Groom, N.V. Mokhov, and S.I. Striganov, "Muon stopping-power and range tables," *Atomic Data and Nuclear Data Tables*, to be published (2000).
31. P. Lipari and T. Stanev, *Phys. Rev.* **D44**, 3543 (1991).
32. M. Crouch, in *Proc. 20th Int. Cosmic Ray Conf.*, Moscow, **6**, 165 (1987).
33. Yu.M. Andreev, V.I. Gurentsov, and I.M. Kogai, in *Proc. 20th Int. Cosmic Ray Conf.*, Moscow, **6**, 200 (1987).
34. M. Aglietta *et al.*, (LVD Collaboration), *Astropart. Phys.* **3**, 311 (1995).
35. M. Ambrosio *et al.*, (MACRO Collaboration), *Phys. Rev.* **D52**, 3793 (1995).
36. Ch. Berger *et al.*, (Frejus Collaboration), *Phys. Rev.* **D40**, 2163 (1989).
37. K.S. Hirata *et al.*, (Kam-II Collaboration), *Phys. Lett.* **B280**, 146 (1992); Y. Fukuda *et al.*, *Phys. Lett.* **B335**, 237 (1994).
38. R. Becker-Szendy *et al.*, (IMB Collaboration), *Phys. Rev.* **D46**, 3720 (1992); See also D. Casper *et al.*, *Phys. Rev. Lett.* **66**, 2561 (1991).
39. Y. Fukuda *et al.*, *Phys. Rev. Lett.* **81**, 1562 (1998).

40. K. Scholberg *et al.*, in *Proc. Eighth Int. Workshop on Neutrino Telescopes* (ed. Milla Baldo Ceolin, edizioni papergraf, Venezia, 1999) p. 183.
41. G. Battistoni *et al.*, *Astropart. Phys.* **12**, 315 (2000).
42. T.H. Johnson, *Phys. Rev.* **43**, 834 (1933). See also T.H. Johnson & E.C. Street, *Phys. Rev.* **44**, 125 (1933).
43. L.W. Alvarez and A.H. Compton, *Phys. Rev.* **43**, 835 (1933).
44. T. Futagami *et al.*, *Phys. Rev. Lett.* **82**, 5194 (1999).
45. F. Reines *et al.*, *Phys. Rev. Lett.* **15**, 429 (1965).
46. M.M. Boliev *et al.*, in *Proceedings 3rd Int. Workshop on Neutrino Telescopes* (ed. Milla Baldo Ceolin), 235 (1991).
47. M. Ambrosio *et al.*, (MACRO) *Phys. Lett.* **B434**, 451 (1998). The number quoted for MACRO is the average over 90% of the lower hemisphere, $\cos\theta < -0.1$; see F. Ronga *et al.*, [hep-ex/9905025](#).
48. R. Becker-Szendy *et al.*, *Phys. Rev. Lett.* **69**, 1010 (1992); *Proc. 25th Int. Conf. High-Energy Physics*, Singapore (ed. K.K. Phua and Y. Yamaguchi, World Scientific, 1991) p. 662.
49. S. Hatakeyama *et al.*, *Phys. Rev. Lett.* **81**, 2016 (1998).
50. Y. Fukuda *et al.*, *Phys. Rev. Lett.* **82**, 2644 (1999).
51. K. Greisen, *Ann. Rev. Nucl. Sci.* **10**, 63 (1960).
52. M. Nagano *et al.*, *J. Phys.* **G10**, 1295 (1984).
53. M. Teshima *et al.*, *J. Phys.* **G12**, 1097 (1986).
54. N.L. Grigorov *et al.*, *Yad. Fiz.* **11**, 1058 (1970) and *Proc. 12th Int. Cosmic Ray Conf.*, Hobart, **2**, 206 (1971).
55. K. Asakimori *et al.*, *Proc. 23rd Int. Cosmic Ray Conf.*, Calgary, **2**, 25 (1993); *Proc. 22nd Int. Cosmic Ray Conf.*, Dublin, **2**, 57 and 97 (1991).
56. T.V. Danilova *et al.*, *Proc. 15th Int. Cosmic Ray Conf.*, Plovdiv, **8**, 129 (1977).
57. Yu. A. Fomin *et al.*, *Proc. 22nd Int. Cosmic Ray Conf.*, Dublin, **2**, 85 (1991).
58. M. Amenomori *et al.*, *Astrophys. J.* **461**, 408 (1996).
59. A. Roehring *et al.*, *Proc. 26th Int. Cosmic Ray Conf.*, Salt Lake City, **1**, 214 (1999).
60. M.A.K. Glasmacher *et al.*, *Astropart. Phys.* **10**, 291 (1999).
61. V.S. Ptuskin *et al.*, *Astron. & Astrophys.* **268**, 726 (1993).
62. B. Peters, *Nuovo Cimento* **22**, 800 (1961).
63. K. Greisen, *Phys. Rev. Lett.* **16**, 748 (1966).
64. G.T. Zatsepin and V.A. Kuz'min, *Sov. Phys. JETP Lett.* **4**, 78 (1966).
65. J. Linsley, *Phys. Rev. Lett.* **10**, 146 (1963).
66. D.J. Bird *et al.*, *Astrophys. J.* **441**, 144 (1995).
67. N. Hayashima *et al.*, *Phys. Rev. Lett.* **73**, 3941 (1994).
68. A.A. Watson, *Proc. of the 1994 Summer Study on Nuclear and Particle Astrophysics and Cosmology for the Next Millennium*, Snowmass CO, 1994, ed. by E.W. Kolb *et al.* (World Scientific, Singapore, to be published, 1996).
69. C. Jui *et al.*, highlight talk, *26th International Cosmic Ray Conf.*, Salt Lake City, 1999, to be published in A.I.P. Conference Proceedings.
70. V.S. Berezinskii *et al.*, *Astrophysics of Cosmic Rays*, North-Holland (1990).
71. D.J. Bird *et al.*, *Astrophys. J.* **424**, 491 (1994).
72. M. Takeda *et al.*, *Phys. Rev. Lett.* **81**, 1163 (1998).
73. M.A. Lawrence, R.J.O. Reid, and A.A. Watson, *J. Phys.* **G17**, 733 (1991).

21. ACCELERATOR PHYSICS OF COLLIDERS

Revised October 1999 by K. Desler and D.A. Edwards (DESY).

21.1. Introduction

This article is intended to be a mini-introduction to accelerator physics, with emphasis on colliders. Essential data are summarized in the “Tables of Collider Parameters” (Sec. 22). Luminosity is the quantity of most immediate interest for HEP, and so we begin with its definition and a discussion of the various factors involved. Then we talk about some of the underlying beam dynamics. Finally, we comment on present limitations and possible future directions.

The focus is on colliders because they provide the highest c.m. energy, and so the longest potential discovery reach. All present-day colliders are synchrotrons with the exception of the SLAC Linear Collider. In the pursuit of higher c.m. energy with electrons, synchrotron radiation presents a formidable barrier to energy beyond LEP. The LHC will be the first proton collider in which synchrotron radiation has significant design impact.

21.2. Luminosity

The event rate R in a collider is proportional to the interaction cross section σ_{int} and the factor of proportionality is called the *luminosity*:

$$R = \mathcal{L} \sigma_{\text{int}} . \quad (21.1)$$

If two bunches containing n_1 and n_2 particles collide with frequency f , then the luminosity is

$$\mathcal{L} = f \frac{n_1 n_2}{4\pi\sigma_x\sigma_y} \quad (21.2)$$

where σ_x and σ_y characterize the Gaussian transverse beam profiles in the horizontal (bend) and vertical directions. Though the initial distribution at the source may be far from Gaussian, by the time the beam reaches high energy the normal form is a very good approximation thanks to the central limit theorem of probability and diminished importance of space charge effects.

Luminosity is normally expressed in units of $\text{cm}^{-2}\text{s}^{-1}$, and tends to be a large number. For example, as we write this update in late 1999, PEP II has just reached $1.3 \times 10^{33} \text{ cm}^{-2}\text{s}^{-1}$. The highest luminosity for protons so far is $2.3 \times 10^{32} \text{ cm}^{-2}\text{s}^{-1}$ at the now decommissioned ISR. The critical quantity for HEP is the integrated luminosity, often stated in pb^{-1} ; the two-year Tevatron run that concluded in February 1996 yielded 148 pb^{-1} , for instance.

The beam size can be expressed in terms of two quantities, one termed the *transverse emittance*, ϵ and the other, the *amplitude function*, β . The transverse emittance is a beam quality concept reflecting the process of bunch preparation, extending all the way back to the source for hadrons and, in the case of electrons, mostly dependent on synchrotron radiation. The amplitude function is a beam optics quantity and is determined by the accelerator magnet configuration.

The transverse emittance is a measure of the phase space area associated with either of the two transverse degrees of freedom, x and y . These coordinates represent the position of a particle with reference to some ideal design trajectory. Think of x as the “horizontal” displacement (in the bend plane for the case of a synchrotron), and y as the “vertical” displacement. The conjugate coordinates are the transverse momenta, which at constant energy are proportional to the angles of particle motion with respect to the design trajectory, x' and y' . Various conventions are in use to characterize the boundary of phase space. Beam sizes are usually given as the standard deviations characterizing Gaussian beam profiles in the two transverse degrees of freedom. In each degree of freedom, the one- σ contour in displacement and angle is frequently used and we will follow this choice.

Suppose that at some location in the collider, the phase space boundary appears as an upright ellipse where the coordinates are the displacement x (using the horizontal plane for instance) and the angle x' with respect to the beam axis. The choice of an elliptical

contour will be justified under Beam Dynamics below. If σ and σ' are the ellipse semi-axes in the x and x' directions respectively, then the emittance may be defined by $\epsilon \equiv \pi\sigma\sigma'$. Transverse emittance is often stated in units of mm-mrad.

The aspect ratio, σ/σ' , is the so-called *amplitude function*, β , and its value depends on position within the focussing structure. When expressed in terms of σ and β the transverse emittance becomes

$$\epsilon = \pi\sigma^2/\beta . \quad (21.3)$$

Of particular significance is the value of the amplitude function at the interaction point, β^* . To achieve high luminosity, one wants β^* to be as small as possible; how small depends on the capability of the hardware to make a near-focus at the interaction point. For example, in the HERA proton ring, β^* at one of the major detectors is 1 m while elsewhere in the synchrotron typical values of the amplitude function lie in the range 30–100 m.

Eq. (21.2) can now be recast in terms of emittances and amplitude functions as

$$\mathcal{L} = f \frac{n_1 n_2}{4\sqrt{\epsilon_x \beta_x^* \epsilon_y \beta_y^*}} . \quad (21.4)$$

Thus, to achieve high luminosity, all one has to do is make high population bunches of low emittance to collide at high frequency at locations where the beam optics provides as low values of the amplitude functions as possible.

Depending on the particular facility, there are other ways of stating the expression for the luminosity. In a multibunch collider, the various bunch populations will differ, in a facility such as HERA, the electron and proton bunches may differ in emittance, the variation of the beam size in the neighborhood of the interaction point may be significant, and so on.

21.3. Beam dynamics

A major concern of beam dynamics is stability: conservation of adequate beam properties over a sufficiently long time scale. Several time scales are involved, and the approximations used in writing the equations of motion reflect the time scale under consideration. For example, when, in Sec. 21.3.1 below, we write the equations for transverse stability no terms associated with phase stability or synchrotron radiation appear; the time scale associated with the last two processes is much longer than that demanded by the need for transverse stability.

21.3.1. *Betatron oscillations:*

Present-day high-energy accelerators employ alternating gradient focussing provided by quadrupole magnetic fields [1]. The equations of motion of a particle undergoing oscillations with respect to the design trajectory are

$$x'' + K_x(s)x = 0 , \quad y'' + K_y(s)y = 0 , \quad (21.5)$$

with

$$x' \equiv dx/ds , \quad y' \equiv dy/ds \quad (21.6)$$

$$K_x \equiv B'/(B\rho) + \rho^{-2} , \quad K_y \equiv -B'/(B\rho) \quad (21.7)$$

$$B' \equiv \partial B_y / \partial x . \quad (21.8)$$

The independent variable s is path length along the design trajectory. This motion is called a *betatron* oscillation because it was initially studied in the context of that type of accelerator. The functions K_x and K_y reflect the transverse focussing—primarily due to quadrupole fields except for the radius of curvature, ρ , term in K_x for a synchrotron—so each equation of motion resembles that for a harmonic oscillator but with spring constants that are a function of position. No terms relating to synchrotron oscillations appear, because their time scale is much longer and in this approximation play no role.

These equations have the form of Hill’s equation and so the solution in one plane may be written as

$$x(s) = A\sqrt{\beta(s)} \cos(\psi(s) + \delta) , \quad (21.9)$$

where A and δ are constants of integration and the phase advances according to $d\psi/ds = 1/\beta$. The dimension of A is the square root of length, reflecting the fact that the oscillation amplitude is modulated by the square root of the amplitude function. In addition to describing the envelope of the oscillation, β also plays the role of an 'instantaneous' λ . The wavelength of a betatron oscillation may be some tens of meters, and so typically values of the amplitude function are of the order of meters rather than on the order of the beam size. The beam optics arrangement generally has some periodicity and the amplitude function is chosen to reflect that periodicity. As noted above, at the interaction point a small value of the amplitude function is desired, and so the focussing optics is tailored in the neighborhood to provide a suitable β^* .

The number of betatron oscillations per turn in a synchrotron is called the *tune* and is given by

$$\nu = \frac{1}{2\pi} \oint \frac{ds}{\beta} . \quad (21.10)$$

Expressing the integration constant A in the solution above in terms of x , x' yields the *Courant-Snyder invariant*

$$A^2 = \gamma(s) x(s)^2 + 2\alpha(s) x(s) x'(s) + \beta(s) x'(s)^2$$

where

$$\alpha \equiv -\beta'/2, \quad \gamma \equiv \frac{1 + \alpha^2}{\beta} . \quad (21.11)$$

(The Courant-Snyder parameters α , β and γ employ three Greek letters which have other meanings and the significance at hand must often be recognized from context.) Because β is a function of position in the focussing structure, this ellipse changes orientation and aspect ratio from location to location but the area πA^2 remains the same.

As noted above the transverse emittance is a measure of the area in x , x' (or y , y') phase space occupied by an ensemble of particles. The definition used in Eq. (21.3) is the area that encloses 39% of a Gaussian beam.

For electron synchrotrons the equilibrium emittance results from the balance between synchrotron radiation damping and excitation from quantum fluctuations in the radiation rate. The equilibrium is reached in a time small compared with the storage time.

For present-day hadron synchrotrons, synchrotron radiation does not play a similar role in determining the transverse emittance. Rather the emittance during storage reflects the source properties and the abuse suffered by the particles throughout acceleration and storage. Nevertheless it is useful to argue as follows: Though x' and x can serve as canonically conjugate variables at constant energy this definition of the emittance would not be an adiabatic invariant when the energy changes during the acceleration cycle. However, $\gamma(v/c)x'$, where here γ is the Lorentz factor, is proportional to the transverse momentum and so qualifies as a variable conjugate to x . So often one sees a normalized emittance defined according to

$$\epsilon_N = \gamma \frac{v}{c} \epsilon . \quad (21.12)$$

21.3.2. Phase stability. The particles in a circular collider also undergo synchrotron oscillations. This is usually referred to as motion in the *longitudinal* degree-of-freedom because particles arrive at a particular position along the accelerator earlier or later than an ideal reference particle. This circumstance results in a finite bunch length, which is related to an energy spread.

For dynamical variables in longitudinal phase space, let us take ΔE and Δt , where these are the energy and time differences from that of the ideal particle. A positive Δt means a particle is behind the ideal particle. The equation of motion is the same as that for a physical pendulum and therefore is nonlinear. But for small oscillations, it reduces to a simple harmonic oscillator:

$$\frac{d^2 \Delta t}{dn^2} = -(2\pi\nu_s)^2 \Delta t \quad (21.13)$$

where the independent variable n is the turn number and ν_s is the number of synchrotron oscillations per turn, analogous to the betatron oscillation tune defined earlier.

In the high-energy limit, where $v/c \approx 1$,

$$\nu_s = \left[\frac{h\eta eV \cos \phi_s}{2\pi E} \right]^{1/2} . \quad (21.14)$$

There are four as yet undefined quantities in this expression: the harmonic number h , the slip factor η , the maximum energy eV gain per turn from the acceleration system, and the synchronous phase ϕ_s . The frequency of the RF system is normally a relatively high multiple, h , of the orbit frequency. The slip factor relates the fractional change in the orbit period τ to changes in energy according to

$$\frac{\Delta \tau}{\tau} = \eta \frac{\Delta E}{E} . \quad (21.15)$$

At sufficiently high energy, the slip factor just reflects the relationship between path length and energy, since the speed is a constant; η is positive for all the synchrotrons in the tables.

The synchronous phase is a measure of how far up on the RF wave the average particle must ride in order to maintain constant energy in the face of synchrotron radiation. That is, $\sin \phi_s$ is the ratio of the energy loss per turn to the maximum energy per turn that can be provided by the acceleration system. For hadron colliders built to date, $\sin \phi_s$ is effectively zero. This is not the case for electron storage rings; for example, the electron ring of HERA runs at a synchronous phase of 45° .

Now if one has a synchrotron oscillation with amplitudes $\widehat{\Delta t}$ and $\widehat{\Delta E}$,

$$\Delta t = \widehat{\Delta t} \sin(2\pi\nu_s n) , \quad \Delta E = \widehat{\Delta E} \cos(2\pi\nu_s n) \quad (21.16)$$

then the amplitudes are related according to

$$\widehat{\Delta E} = \frac{2\pi\nu_s E}{\eta\tau} \widehat{\Delta t} . \quad (21.17)$$

The longitudinal emittance ϵ_ℓ may be defined as the phase space area bounded by particles with amplitudes $\widehat{\Delta t}$ and $\widehat{\Delta E}$. In general, the longitudinal emittance for a given amplitude is found by numerical integrations. For $\sin \phi_s = 0$, an analytical expression is as follows:

$$\epsilon_\ell = \left[\frac{2\pi^3 E e V h}{\tau^2 \eta} \right]^{1/2} (\widehat{\Delta t})^2 \quad (21.18)$$

Again, a Gaussian is a reasonable representation of the longitudinal profile of a well-behaved beam bunch; if $\sigma_{\Delta t}$ is the standard deviation of the time distribution, then the bunch length can be characterized by

$$\ell = c \sigma_{\Delta t} . \quad (21.19)$$

In the electron case the longitudinal emittance is determined by the synchrotron radiation process just as in the transverse degrees of freedom. For the hadron case the history of acceleration plays a role and because energy and time are conjugate coordinates, the longitudinal emittance is a quasi-invariant.

For HEP bunch length is a significant quantity because if the bunch length becomes larger than β^* the luminosity is adversely affected. This is because β grows parabolically as one proceeds from the IP and so the beam size increases thus lowering the contribution to the luminosity from such locations.

21.3.3. Synchrotron radiation [2]: A relativistic particle undergoing centripetal acceleration radiates at a rate given by the Larmor formula multiplied by the 4th power of the Lorentz factor:

$$P = \frac{1}{6\pi\epsilon_0} \frac{e^2 a^2}{c^3} \gamma^4 . \quad (21.20)$$

Here, $a = v^2/\rho$ is the centripetal acceleration of a particle with speed v undergoing deflection with radius of curvature ρ . In a synchrotron

that has a constant radius of curvature within bending magnets, the energy lost due to synchrotron radiation per turn is the above multiplied by the time spent in bending magnets, $2\pi\rho/v$. Expressed in familiar units, this result may be written

$$W = 8.85 \times 10^{-5} E^4 / \rho \text{ MeV per turn} \quad (21.21)$$

for electrons at sufficiently high energy that $v \approx c$. The energy E is in GeV and ρ is in kilometers. The radiation has a broad energy spectrum which falls off rapidly above the *critical energy*, $E_c = (3c/2\rho)\hbar\gamma^3$. Typically, E_c is in the hard x-ray region.

The characteristic time for synchrotron radiation processes is the time during which the energy must be replenished by the acceleration system. If f_0 is the orbit frequency, then the characteristic time is given by

$$\tau_0 = \frac{E}{f_0 W} \quad (21.22)$$

Oscillations in each of the three degrees of freedom either damp or antidamp depending on the design of the accelerator. For a simple separated function alternating gradient synchrotron, all three modes damp. The damping time constants are related by Robinson's Theorem [3], which, expressed in terms of τ_0 , is

$$\frac{1}{\tau_x} + \frac{1}{\tau_y} + \frac{1}{\tau_s} = 2 \frac{1}{\tau_0} \quad (21.23)$$

Even though all three modes may damp, the emittances do not tend toward zero. Statistical fluctuations in the radiation rate excite synchrotron oscillations and radial betatron oscillations. Thus there is an equilibrium emittance at which the damping and excitation are in balance. The vertical emittance is non-zero due to horizontal-vertical coupling.

Polarization can develop from an initially unpolarized beam as a result of synchrotron radiation. A small fraction $\approx E_c/E$ of the radiated power flips the electron spin. Because the lower energy state is that in which the particle magnetic moment points in the same direction as the magnetic bend field, the transition rate toward this alignment is larger than the rate toward the reverse orientation. An equilibrium polarization of 92% is predicted, and despite a variety of depolarizing processes, polarization above 80% has been observed at a number of facilities.

The radiation rate for protons is of course down by a factor of the fourth power of the mass ratio, and is given by

$$W = 7.8 \times 10^{-3} E^4 / \rho \text{ keV per turn} \quad (21.24)$$

where E is now in TeV and ρ in km. For the LHC, synchrotron radiation presents a significant load to the cryogenic system, and impacts magnet design due to gas desorption and secondary electron emission from the wall of the cold beam tube.

21.3.4. Beam-beam tune shift: In a bunch-bunch collision the particles of one bunch see the other bunch as a nonlinear lens. Therefore the focussing properties of the ring are changed in a way that depends on the transverse oscillation amplitude. And so there is a spread in the frequency of betatron oscillations.

There is an extensive literature on the subject of how large this tune spread can be. In practice, the limiting value is hard to predict. It is consistently larger for electrons because of the beneficial effects of damping from synchrotron radiation.

In order that contributions to the total tune spread arise only at the detector locations, the beams in a multibunch collider are kept apart elsewhere by a variety of techniques. For equal energy particles of opposite charge circulating in the same vacuum chamber, electrostatic separators may be used assisted by a crossing angle if appropriate. For particles of equal energy and of the same charge, a crossing angle is needed not only for tune spread reasons but to steer the particles into two separate beam pipes. In HERA, because of the large ratio of proton to electron energy, separation can be achieved by bending magnets.

21.3.5. Luminosity lifetime: In electron synchrotrons the luminosity degrades during the store primarily due to particles leaving the phase stable region in longitudinal phase space as a result of quantum fluctuations in the radiation rate and bremsstrahlung. For hadron colliders the luminosity deteriorates due to emittance dilution resulting from a variety of processes. In practice, stores are intentionally terminated when the luminosity drops to the point where a refill will improve the integrated luminosity.

21.4. Status and prospects

Present facilities represent a balance among current technology, the desires of High Energy Physics, and public support. For forty-five years, beam optics has exploited the invention of alternating gradient focussing. This principle is employed in all colliders both linear and circular. Superconducting technology has grown dramatically in importance during the last two decades. Superconducting magnets are vital to the Tevatron, HERA, and to the future LHC. Superconducting accelerating structures are necessary to CESR, LEP, HERA, Jefferson Laboratory and other facilities requiring high-gradient long pulse length RF systems. Present room temperature accelerating structures produce very short pulses, but with gradients well in excess of the superconducting variety [7].

At present, the next potential facilities are perceived to include the LHC and an electron linear collider. The LHC is an approved project that will represent a major step forward in superconducting magnet technology. No linear collider project has been approved as yet, and the conventional and superconducting approaches compete for prominence. Of perhaps more immediate impact are the B and τ "factories" that are designed to go beyond the $10^{33} \text{ cm}^{-2}\text{s}^{-1}$ level in luminosity.

In addition to the possibilities of the preceding paragraph, there are other synchrotron-based collider studies underway. Despite formidable R&D challenges a muon-muon collider may become feasible. Proponents of a very large hadron collider at higher energy than the cancelled SSC project are exploring low-cost magnets and tunnels for a facility on the 100 TeV c.m. energy scale.

Ideas abound in accelerator R&D for the long term. Approaches such as wakefield accelerators, plasma-laser combinations, and related investigations may if successful deliver gradients far higher than anything realized today. These studies could potentially lead to a new vision for HEP facilities.

References:

1. E.D. Courant and H.S. Snyder, *Ann. Phys.* **3**, 1 (1958). This is the classic article on the alternating gradient synchrotron.
2. M. Sands, *The Physics of Electron Storage Rings—An Introduction*, SLAC Publication SLAC 121, UC-28 (ACC), 1970.
3. K. Robinson, *Phys. Rev.* **111**, 373 (1958).
4. D.A. Edwards and M.J. Syphers, *An Introduction to the Physics of High Energy Accelerators*, John Wiley & Sons, 1993. This is an elementary textbook on accelerator physics. The next two references are more advanced, and are cited here for readers who may wish to pursue beam physics in greater depth.
5. A. Wu Chao, *Physics of Collective Beam Instabilities in High Energy Accelerators*, John Wiley & Sons, 1993.
6. M. Reiser, *Theory and Design of Charged Particle Beams*, John Wiley & Sons, 1994.
7. *Handbook of Accelerator Physics and Engineering*, ed. A.W. Chao and M. Tigner, World Scientific Publishing Co. (Singapore, 1999).

HIGH-ENERGY COLLIDER PARAMETERS: e^+e^- Colliders (I)

The numbers here were received from representatives of the colliders in late 1999 (contact C.G. Wohl, LBNL). Many of the numbers of course change with time, and only the latest values (or estimates) are given here; those in brackets are for coming upgrades. Quantities are, where appropriate, r.m.s. H and V indicate horizontal and vertical directions. Parameters for the defunct SPEAR, DORIS, PETRA, PEP, and TRISTAN colliders may be found in our 1996 edition (Phys. Rev. **D54**, 1 July 1996, Part I).

	VEPP-2M (Novosibirsk)	VEPP-2000* (Novosibirsk)	VEPP-4M (Novosibirsk)	BEPC (China)	DAΦNE (Frascati)
Physics start date	1974	2001	1994	1989	1999
Maximum beam energy (GeV)	0.7	1.0	6	2.2	0.510 (0.75 max.)
Luminosity ($10^{30} \text{ cm}^{-2}\text{s}^{-1}$)	5	100	50	10 at 2 GeV 5 at 1.55 GeV	5(→50)
Time between collisions (μs)	0.03	0.04	0.6	0.8	0.0027–0.0108
Crossing angle ($\mu \text{ rad}$)	0	0	0	0	$\pm(1.0 \text{ to } 1.5) \times 10^4$
Energy spread (units 10^{-3})	0.36	0.64	1	0.58 at 2.2 GeV	0.40
Bunch length (cm)	3	4	5	≈ 5	2(→3)
Beam radius (10^{-6} m)	H : 300 V : 10	125 (round)	H : 1000 V : 30	H : 890 V : 37	H : 2100 V : 21
Free space at interaction point (m)	± 1	± 1	± 2	± 2.15	± 0.46 ($\pm 157 \text{ mrad cone}$)
Luminosity lifetime (hr)	continuous	continuous	2	7–12	1(→2)
Filling time (min)	continuous	continuous	15	30	2 (per beam)
Acceleration period (s)	—	—	150	120	—
Injection energy (GeV)	0.2–0.6	0.2–1.0	1.8	1.55	0.510
Transverse emittance ($10^{-9} \pi \text{ rad-m}$)	H : 110 V : 1.3	H : 250 V : 250	H : 400 V : 20	H : 660 V : 28	H : 1000 V : 10
β^* , amplitude function at interaction point (m)	H : 0.45 V : 0.045	H : 0.06 V : 0.06	H : 0.75 V : 0.05	H : 1.2 V : 0.05	H : 4.5 V : 0.045
Beam-beam tune shift per crossing (units 10^{-4})	H : 200 V : 500	H : 750 V : 750	500	350	400
RF frequency (MHz)	200	172	180	199.53	368.25
Particles per bunch (units 10^{10})	2	16	15	20 at 2 GeV 11 at 1.55 GeV	3(→ 9)
Bunches per ring per species	1	1	2	1	30–120
Average beam current per species (mA)	50	300	80	40 at 2 GeV 22 at 1.55 GeV	800(→1500)
Circumference or length (km)	0.018	0.024	0.366	0.2404	0.0977
Interaction regions	2	2	1	2	1(→2)
Utility insertions	1	2	1	4	2×2
Magnetic length of dipole (m)	1	1.2	2	1.6	e^+ : 1.21/0.99 e^- : 1.21/0.99
Length of standard cell (m)	4.5	12	7.2	6.6	—
Phase advance per cell (deg)	280	H : 738 V : 378	65	≈ 60	—
Dipoles in ring	8	8	78	40 + 4 weak	e^+ : 8(+4 wigglers) e^- : 8(+4 wigglers)
Quadrupoles in ring	20	20	150	68	e^+/e^- : 53/53
Peak magnetic field (T)	1.8	2.4	0.6	0.9028 at 2.8 GeV	1.2(→1.76) dipoles 1.8 wigglers

*VEPP-2000 is a major upgrade of VEPP-2M.

HIGH-ENERGY COLLIDER PARAMETERS: e^+e^- Colliders (II)

The numbers here were received from representatives of the colliders in late 1999. Many of the numbers of course change with time, and only the latest values (or estimates) are given here. Quantities are, where appropriate, r.m.s. H and V indicate horizontal and vertical directions; s.c. indicates superconducting.

	CESR (Cornell)	KEKB (KEK)	PEP-II (SLAC)	SLC (SLAC)	LEP (CERN)
Physics start date	1979	1999	1999	1989	1989
Maximum beam energy (GeV)	6	$e^- \times e^+$: 8×3.5	e^- : 7-12 (9.0 nominal) e^+ : 2.5-4 (3.1 ") (nominal $E_{cm} = 10.5$ GeV)	50	101 in 1999 (105=max. foreseen)
Luminosity (10^{30} $\text{cm}^{-2}\text{s}^{-1}$)	830 at 5.3 GeV	10000	3000	2.5	24 at Z^0 100 at > 90 GeV
Time between collisions (μs)	0.014 to 0.22	0.002	0.0042	8300	22
Crossing angle (μ rad)	± 2000	$\pm 11,000$	0	0	0
Energy spread (units 10^{-3})	0.6 at 5.3 GeV	0.7	e^-/e^+ : 0.61/0.77	1.2	0.7 \rightarrow 1.5
Bunch length (cm)	1.8	0.4	e^-/e^+ : 1.1/1.0	0.1	1.0
Beam radius (μm)	H : 500 V : 10	H : 77 V : 1.9	H : 157 V : 4.7	H : 1.5 V : 0.5	H : 200 \rightarrow 300 V : 2.5 \rightarrow 8
Free space at interaction point (m)	± 2.2 (± 0.6 to REC quads)	+0.75/-0.58 (+300/-500) mrad cone	± 0.2 , ± 300 mrad cone	± 2.8	± 3.5
Luminosity lifetime (hr)	2-3	2	2.5	—	20 at Z^0 10 at > 90 GeV
Filling time (min)	10 (topping up)	8 (topping up)	3 (topping up)	—	20 to setup 20 to accumulate
Acceleration period (s)	—	—	—	—	600
Injection energy (GeV)	6	e^-/e^+ : 8/3.5	2.5-12	45.64	22
Transverse emittance (π rad-nm)	H : 240 V : 6	H : 18 V : 0.36	e^- : 48 (H), 1.5 (V) e^+ : 48 (H), 1.5 (V)	H : 0.5 V : 0.05	H : 20-45 V : 0.25 \rightarrow 1
β^* , amplitude function at interaction point (m)	H : 1.0 V : 0.018	H : 0.33 V : 0.01	e^- : 0.50 (H), 0.015 (V) e^+ : 0.50 (H), 0.015 (V)	H : 0.0025 V : 0.0015	H : 1.5 V : 0.05
Beam-beam tune shift per crossing (units 10^{-4})	480	H : 390 V : 520	300	—	830
RF frequency (MHz)	500	508.887	476	—	352.2
Particles per bunch (units 10^{10})	1.15	e^-/e^+ : 1.3/3.2	e^-/e^+ : 2.1/5.9	4.0	45 in collision 60 in single beam
Bunches per ring per species	9 trains of 4 bunches	5120 (5-10% gap is necessary)	1658	1	4 trains of 1 or 2
Average beam current per species (mA)	260	e^-/e^+ : 1100/2600	e^-/e^+ : 750/2161	0.0008	4 at Z^0 4-6 at > 90 GeV
Beam polarization (%)	—	—	—	e^- : 80	55 at 45 GeV 5 at 61 GeV
Circumference or length (km)	0.768	3.016	2.2	1.45 +1.47	26.66
Interaction regions	1	1	1 (2 possible)	1	4
Utility insertions	3	3 per ring	5	—	4
Magnetic length of dipole (m)	1.6-6.6	e^-/e^+ : 5.86/0.915	e^-/e^+ : 5.4/0.45	2.5	11.66/pair
Length of standard cell (m)	16	e^-/e^+ : 75.7/76.1	15.2	5.2	79
Phase advance per cell (deg)	45-90 (no standard cell)	450	e^-/e^+ : 60/90	108	102/90
Dipoles in ring	86	e^-/e^+ : 116/112	e^-/e^+ : 192/192	460+440	3280+24 inj. + 64 weak
Quadrupoles in ring	104	e^-/e^+ : 452/452	e^-/e^+ : 290/326	—	520+288 + 8 s.c.
Peak magnetic field (T)	0.3 normal } at 8 0.8 high field } GeV	e^-/e^+ : 0.25/0.72	e^-/e^+ : 0.18/0.75	0.597	0.135

HIGH-ENERGY COLLIDER PARAMETERS: ep , $p\bar{p}$, and pp Colliders

The numbers here were received from representatives of the colliders in late 1999. Many of the numbers of course change with time, and only the latest values (or estimates) are given here. Quantities are, where appropriate, r.m.s. H , V , and, s.c. indicate horizontal and vertical directions, and superconducting. The SSC is kept for purposes of comparison.

	HERA (DESY)	SppS (CERN)	TEVATRON (Fermilab)	LHC (CERN)		SSC (USA)
Physics start date	1992	1981	1987	2005		Terminated
Physics end date	—	1990	—	—		—
Particles collided	ep	$p\bar{p}$	$p\bar{p}$	pp	Pb Pb	pp
Maximum beam energy (TeV)	e : 0.030 p : 0.92	0.315 (0.45 in pulsed mode)	1.0	7.0	2.76 TeV/u	20
Luminosity ($10^{30} \text{ cm}^{-2} \text{ s}^{-1}$)	14	6	210	1.0×10^4	0.002	1000
Time between collisions (μs)	0.096	3.8	0.396	0.025	0.125	0.016678
Crossing angle ($\mu \text{ rad}$)	0	0	0	≥ 200	≤ 200	100 to 200 (135 nominal)
Energy spread (units 10^{-3})	e : 0.91 p : 0.2	0.35	0.09	0.1	0.1	0.055
Bunch length (cm)	e : 0.83 p : 8.5	20	38	7.5	7.5	6.0
Beam radius (10^{-6} m)	e : 280(H), 50(V) p : 265(H), 50(V)	p : 73(H), 36(V) \bar{p} : 55(H), 27(V)	p : 34 \bar{p} : 29	16	15	4.8
Free space at interaction point (m)	± 5.8	16	± 6.5	38	38	± 20
Luminosity lifetime (hr)	10	15	7–30	10	6.7	~ 24
Filling time (min)	e : 60 p : 120	0.5	30	6	20	72
Acceleration period (s)	e : 200 p : 1500	10	86	1200		1500
Injection energy (TeV)	e : 0.012 p : 0.040	0.026	0.15	0.450	177.4 GeV/u	2
Transverse emittance ($10^{-9} \pi \text{ rad-m}$)	e : 42(H), 6(V) p : 5(H), 5(V)	p : 9 \bar{p} : 5	p : 3.5 \bar{p} : 2.5	0.5	0.5	0.047
β^* , amplitude function at interaction point (m)	e : 1(H), 0.7(V) p : 7(H), 0.5(V)	0.6 (H) 0.15 (V)	0.35	0.5	0.5	0.5
Beam-beam tune shift per crossing (units 10^{-4})	e : 190(H), 360(V) p : 12(H), 9(V)	50	p : 38 \bar{p} : 97	34	—	8 head on 13 long range
RF frequency (MHz)	e : 499.7 p : 208.2/52.05	100+200	53	400.8	400.8	359.75
Particles per bunch (units 10^{10})	e : 3 p : 7	p : 15 \bar{p} : 8	p : 27 \bar{p} : 7.5	10.5	0.0094	0.8
Bunches per ring per species	e : 189 p : 180	6	36	2835	608	17,424
Average beam current per species (mA)	e : 40 p : 90	p : 6 \bar{p} : 3	p : 81 \bar{p} : 22	536	7.8	71
Circumference (km)	6.336	6.911	6.28	26.659		87.12
Interaction regions	ep : 2; e , p : 1 each, internal fixed target	2	2 high \mathcal{L}	2 high \mathcal{L} +1	1	4
Utility insertions	4	—	4	4		2
Magnetic length of dipole (m)	e : 9.185 p : 8.82	6.26	6.12	14.3		Mostly 14.928
Length of standard cell (m)	e : 23.5 p : 47	64	59.5	106.90		180
Phase advance per cell (deg)	e : 60 p : 90	90	67.8	90		90
Dipoles in ring	e : 396 p : 416	744	774	1232 main dipoles		H : 8336 V : 88 } in 2 rings
Quadrupoles in ring	e : 580 p : 280	232	216	692 focussing +96 skew		2084 } 2 rings
Magnet type	e : C-shaped p : s.c., collared, cold iron	H type with bent-up coil ends	s.c. $\cos \theta$ warm iron	s.c. 2 in 1 cold iron		s.c. $\cos \theta$ cold iron
Peak magnetic field (T)	e : 0.274 p : 4.65	1.4 (2 in pulsed mode)	4.4	8.3		6.790
\bar{p} source accum. rate (hr^{-1})	—	6×10^{10}	20×10^{10}	—		—
Max. no. \bar{p} in accum. ring	—	1.2×10^{12}	2.6×10^{12}	—		—

23. PASSAGE OF PARTICLES THROUGH MATTER

Revised October 1999 by D.E. Groom and S.R. Klein (LBNL).

23.1. Notation

Table 23.1: Summary of variables used in this section. The kinematic variables β and γ have their usual meanings.

Symbol	Definition	Units or Value
α	Fine structure constant ($e^2/4\pi\epsilon_0\hbar c$)	1/137.035 999 76(50)
M	Incident particle mass	MeV/ c^2
E	Incident particle energy $\gamma M c^2$	MeV
T	Kinetic energy	MeV
$m_e c^2$	Electron mass $\times c^2$	0.510 998 902(21) MeV
r_e	Classical electron radius $e^2/4\pi\epsilon_0 m_e c^2$	2.817 940 285(31) fm
N_A	Avogadro's number	$6.022 141 99(47) \times 10^{23}$ mol $^{-1}$
ze	Charge of incident particle	
Z	Atomic number of medium	
A	Atomic mass of medium	g mol $^{-1}$
K/A	$4\pi N_A r_e^2 m_e c^2 / A$	0.307 075 MeV g $^{-1}$ cm 2 for $A = 1$ g mol $^{-1}$
I	Mean excitation energy	eV (<i>Note bene!</i>)
δ	Density effect correction to ionization energy loss	
$\hbar\omega_p$	Plasma energy ($\sqrt{4\pi N_e r_e^3} m_e c^2 / \alpha$)	28.816 $\sqrt{\rho(Z/A)}$ eV $^{(a)}$
N_c	Electron density	(units of r_e) $^{-3}$
w_j	Weight fraction of the j th element in a compound or mixture	
n_j	α number of j th kind of atoms in a compound or mixture	
X_0	Radiation length	g cm $^{-2}$
—	$4\alpha r_e^2 N_A / A$	(716.408 g cm $^{-2}$) $^{-1}$ for $A = 1$ g mol $^{-1}$
E_c	Critical energy	MeV
E_s	Scale energy $\sqrt{4\pi/\alpha} m_e c^2$	21.2052 MeV
R_M	Molière radius	g cm $^{-2}$

 (a) For ρ in g cm $^{-3}$.

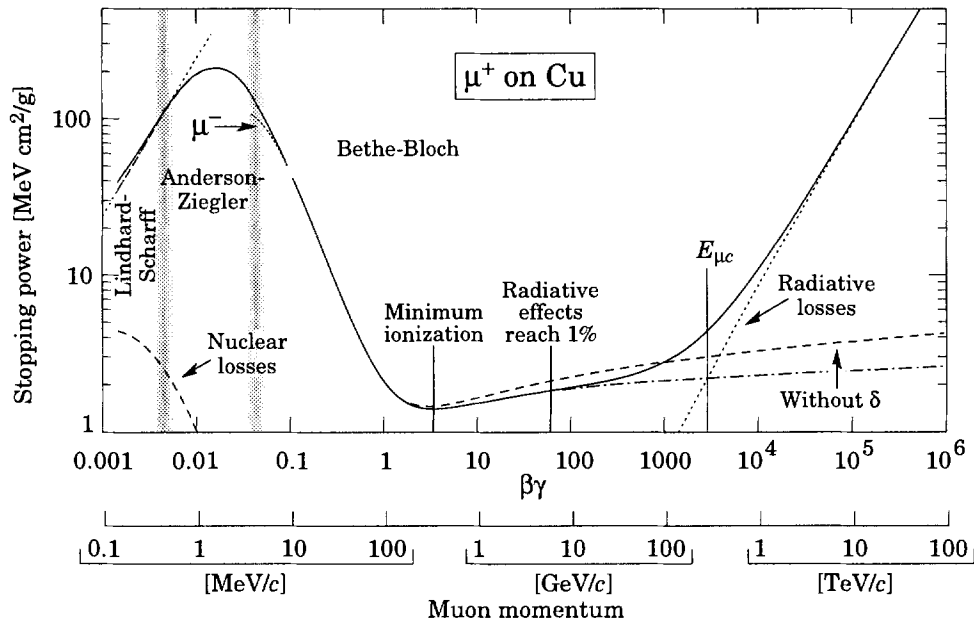
23.2. Ionization energy loss by heavy particles [4–1]

Moderately relativistic charged particles other than electrons lose energy in matter primarily by ionization. The mean rate of energy loss (or stopping power) is given by the Bethe-Bloch equation,

$$-\frac{dE}{dx} = K z^2 \frac{Z}{A} \frac{1}{\beta^2} \left[\frac{1}{2} \ln \frac{2m_e c^2 \beta^2 \gamma^2 T_{\max}}{I^2} - \beta^2 - \frac{\delta}{2} \right]. \quad (23.1)$$

 Here T_{\max} is the maximum kinetic energy which can be imparted to a free electron in a single collision, and the other variables are defined in Table 23.1. The units are chosen so that dx is measured in mass per unit area, e.g., in g cm $^{-2}$.

 In this form, the Bethe-Bloch equation describes the energy loss of pions in a material such as copper to about 1% accuracy for energies between about 6 MeV and 6 GeV (momenta between about 40 MeV/ c and 6 GeV/ c). At lower energies “ C/Z ” corrections for tightly-bound atomic electrons and other effects must be made, and at higher energies radiative effects begin to be important. These limits of validity depend on both the effective atomic number of the absorber and the mass of the slowing particle. Low-energy effects will be discussed in Sec. 23.2.2.

 The function as computed for muons on copper is shown by the solid curve in Fig. 23.1, and for pions on other materials in Fig. 23.3. A minor dependence on M at the highest energies is introduced through T_{\max} , but for all practical purposes in high-energy physics dE/dx in a given material is a function only of β . Except in hydrogen, particles of the same velocity have very similar rates of energy loss in different materials; there is a slow decrease in the rate of energy loss with increasing Z . The qualitative difference in stopping power behavior at high energies between a gas (He) and the other materials shown in Fig. 23.3 is due to the density-effect correction, δ , discussed below. The stopping power functions are characterized by broad minima whose position drops from $\beta\gamma = 3.5$ to 3.0 as Z goes from 7 to 100. The values of minimum ionization as a function of atomic number are shown in Fig. 23.2.

Fig. 23.1: Stopping power ($= \langle -dE/dx \rangle$) for positive muons in copper as a function of $\beta\gamma = p/Mc$ over nine orders of magnitude in momentum (12 orders of magnitude in kinetic energy) [1]. Solid curves indicate the total stopping power. Data below the break at $\beta\gamma \approx 0.1$ are taken from ICRU 49 [2], and data at higher energies are from Ref. 1. Vertical bands indicate boundaries between different approximations discussed in the text. The short dotted lines labeled “ μ^- ” illustrate the “Barkas effect,” the dependence of stopping power on projectile charge at very low energies [3].

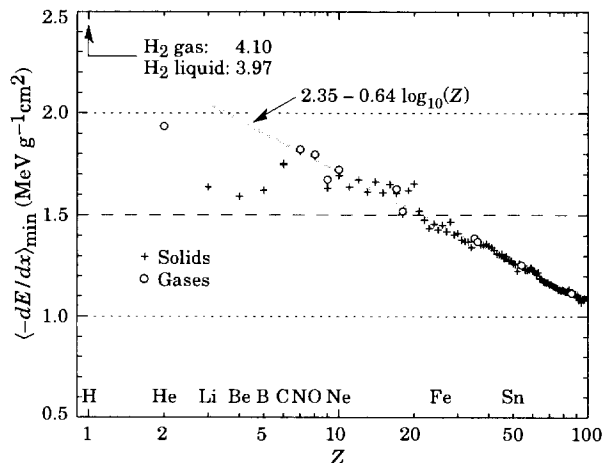


Figure 23.2: Stopping power at minimum ionization for the chemical elements. The straight line is fitted for $Z > 6$. A simple functional dependence is not to be expected, since $\langle -dE/dx \rangle$ depends on other properties than atomic number.

In practical cases, most relativistic particles (e.g., cosmic-ray muons) have energy loss rates close to the minimum, and are said to be minimum ionizing particles, or mip's.

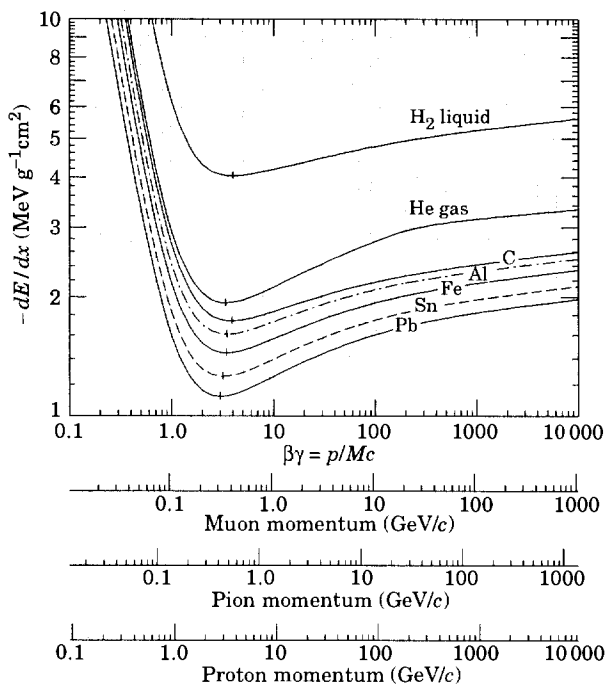


Figure 23.3: Energy loss rate in liquid (bubble chamber) hydrogen, gaseous helium, carbon, aluminum, tin, and lead.

Eq. (23.1) may be integrated to find the total range R for a particle which loses energy only through ionization. Since dE/dx depends only on β , R/M is a function of E/M or pc/M . In practice, range is a useful concept only for low-energy hadrons ($R \lesssim \lambda_I$, where λ_I is the nuclear interaction length), and for muons below a few hundred GeV (above which radiative effects dominate). R/M as a function of $\beta\gamma = p/Mc$ is shown for a variety of materials in Fig. 23.4.

For a particle with mass M and momentum $M\beta\gamma c$, T_{\max} is given by

$$T_{\max} = \frac{2m_e c^2 \beta^2 \gamma^2}{1 + 2\gamma m_e/M + (m_e/M)^2}. \quad (23.2)$$

It is usual [4,5] to make the "low-energy" approximation $T_{\max} = 2m_e c^2 \beta^2 \gamma^2$, valid for $2\gamma m_e/M \ll 1$; this, in fact, is done

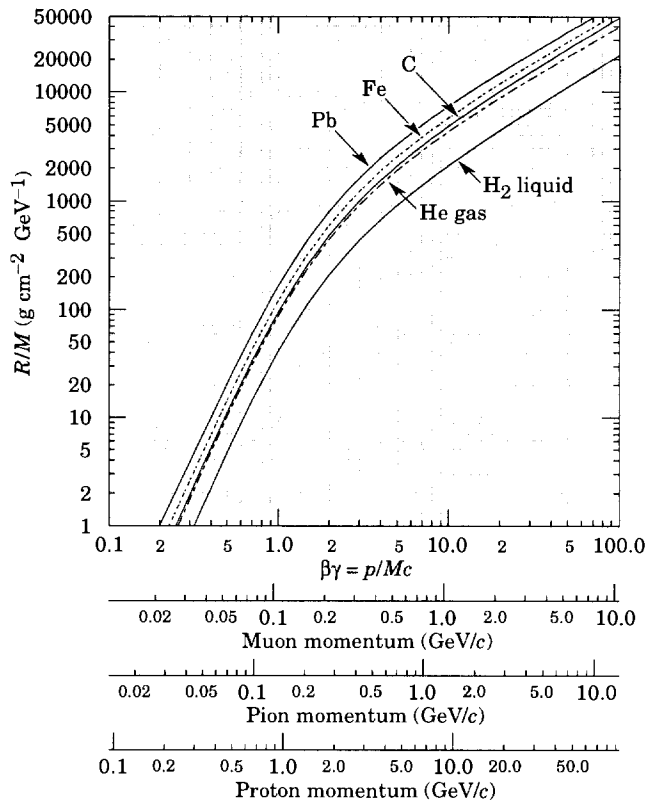


Figure 23.4: Range of heavy charged particles in liquid (bubble chamber) hydrogen, helium gas, carbon, iron, and lead. For example: For a K^+ whose momentum is 700 MeV/c, $\beta\gamma = 1.42$. For lead we read $R/M \approx 396$, and so the range is 195 g cm $^{-2}$.

implicitly in many standard references. For a pion in copper, the error thus introduced into dE/dx is greater than 6% at 100 GeV. The correct expression should be used.

At energies of order 100 GeV, the maximum 4-momentum transfer to the electron can exceed 1 GeV/c, where structure effects significantly modify the cross sections. This problem has been investigated by J.D. Jackson [6], who concluded that for hadrons (but not for large nuclei) corrections to dE/dx are negligible below energies where radiative effects dominate. While the cross section for rare hard collisions is modified, the average stopping power, dominated by many softer collisions, is almost unchanged.

"The determination of the mean excitation energy is the principal non-trivial task in the evaluation of the Bethe stopping-power formula" [7]. Recommended values have varied substantially with time. Estimates based on experimental stopping-power measurements for protons, deuterons, and alpha particles and on oscillator-strength distributions and dielectric-response functions were given in ICRU 37 [8]. These values, shown in Fig. 23.5, have since been widely used. Machine-readable versions can also be found [9].

23.2.1. The density effect: As the particle energy increases, its electric field flattens and extends, so that the distant-collision contribution to Eq. (23.1) increases as $\ln \beta\gamma$. However, real media become polarized, limiting the field extension and effectively truncating this part of the logarithmic rise [10,11–14]. At very high energies,

$$\delta/2 \rightarrow \ln(\hbar\omega_p/I) + \ln \beta\gamma - 1/2, \quad (23.3)$$

where $\delta/2$ is the density effect correction introduced in Eq. (23.1) and $\hbar\omega_p$ is the plasma energy defined in Table 23.1. A comparison with Eq. (23.1) shows that $|dE/dx|$ then grows as $\ln \beta\gamma$ rather than $\ln \beta^2 \gamma^2$, and that the mean excitation energy I is replaced by the plasma energy $\hbar\omega_p$. The ionization stopping power as calculated with and without the density effect correction is shown in Fig. 23.1. Since the plasma frequency scales as the square root of the electron density, the correction is much larger for a liquid or solid than for a gas, as is illustrated by the examples in Fig. 23.3.

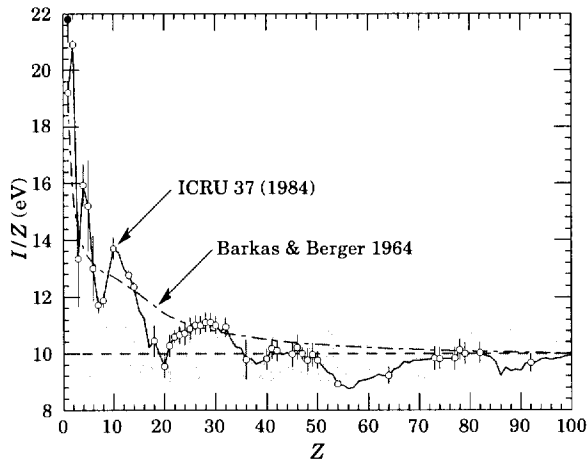


Figure 23.5: Excitation energies (divided by Z) as adopted by the ICRU [8]. Those based on measurement are shown by points with error flags; the interpolated values are simply joined. The solid point is for liquid H_2 ; the open point at 19.2 is for H_2 gas. Also shown are the $I/Z = 10 \pm 1$ eV band and an early approximation.

The density effect correction is usually computed using Sternheimer's parameterization [11]:

$$\delta = \begin{cases} 2(\ln 10)x - \bar{C} & \text{if } x \geq x_1; \\ 2(\ln 10)x - \bar{C} + a(x_1 - x)^k & \text{if } x_0 \leq x < x_1; \\ 0 & \text{if } x < x_0 \text{ (nonconductors);} \\ \delta_0 10^{2(x-x_0)} & \text{if } x < x_0 \text{ (conductors)} \end{cases} \quad (23.4)$$

Here $x = \log_{10} \eta = \log_{10}(p/Mc)$. \bar{C} (the negative of the C used in Ref. 11) is obtained by equating the high-energy case of Eq. (23.4) with the limit given in Eq. (23.3). The other parameters are adjusted to give a best fit to the results of detailed calculations for momenta below $Mc \exp(x_1)$. Parameters for elements and nearly 200 compounds and mixtures of interest are published in a variety of places, notably in Ref. 14. A recipe for finding the coefficients for nontabulated materials is given by Sternheimer and Peierls [13], and is summarized in Ref. 1.

The remaining relativistic rise can be attributed to large energy transfers to a few electrons. If these escape or are otherwise accounted for separately, the energy deposited in an absorbing layer (in contrast to the energy lost by the particle) approaches a constant value, the Fermi plateau (see Sec. 23.2.5 below). At extreme energies (e.g., > 332 GeV for muons in iron), radiative effects are more important than ionization losses. These are especially relevant for high-energy muons, as discussed in Sec. 23.6.

23.2.2. Energy loss at low energies: A shell correction C/Z is often included in the square brackets of Eq. (23.1) [2,8,15] to correct for atomic binding having been neglected in calculating some of the contributions to Eq. (23.1). We show the Barkas form [15] in Fig. 23.1. For copper it contributes about 1% at $\beta\gamma = 0.3$ (kinetic energy 6 MeV for a pion), and the correction decreases very rapidly with energy.

Eq. (23.1) is based on a first-order Born approximation. Higher-order corrections, again important only at lower energy, are normally included by adding a term $z^2 L_2(\beta)$ inside the square brackets.

An additional "Barkas correction" $zL_1(\beta)$ makes the stopping power for a negative particle somewhat larger than for a positive particle with the same mass and velocity. In a 1956 paper, Barkas *et al.* noted that negative pions had a longer range than positive pions [3]. The effect has been measured for a number of negative/positive particle pairs, most recently for antiprotons at the CERN LEAR facility [16].

A detailed discussion of low-energy corrections to the Bethe formula is given in ICRU Report 49 [2]. When the corrections are properly included, the accuracy of the Bethe-Bloch treatment is accurate to about 1% down to $\beta \approx 0.05$, or about 1 MeV for protons.

For $0.01 < \beta < 0.05$, there is no satisfactory theory. For protons, one usually relies on the empirical fitting formulae developed by

Andersen and Ziegler [2,17]. For particles moving more slowly than $\approx 0.01c$ (more or less the velocity of the outer atomic electrons), Lindhard has been quite successful in describing electronic stopping power, which is proportional to β [18,19]. Finally, we note that at low energies, e.g., for protons of less than several hundred eV, non-ionizing nuclear recoil energy loss dominates the total energy loss [2,19,20].

As shown in ICRU 49 [2] (using data taken from Ref. 17), the nuclear plus electronic proton stopping power in copper is $113 \text{ MeV cm}^2 \text{ g}^{-1}$ at $T = 10 \text{ keV}$, rises to a maximum of $210 \text{ MeV cm}^2 \text{ g}^{-1}$ at 100–150 keV, then falls to $120 \text{ MeV cm}^2 \text{ g}^{-1}$ at 1 MeV. Above 0.5–1.0 MeV the corrected Bethe-Bloch theory is adequate.

23.2.3. Fluctuations in energy loss: The quantity $(dE/dx)\delta x$ is the mean energy loss via interaction with electrons in a layer of the medium with thickness δx . For finite δx , there are fluctuations in the actual energy loss. The distribution is skewed toward high values (the Landau tail) [4,21]. Only for a thick layer [$(dE/dx)\delta x \gg T_{\text{max}}$] is the distribution nearly Gaussian. The large fluctuations in the energy loss are due to the small number of collisions involving large energy transfers. The fluctuations are smaller for the so-called restricted energy loss rate, as discussed in Sec. 23.2.5 below.

23.2.4. Energy loss in mixtures and compounds: A mixture or compound can be thought of as made up of thin layers of pure elements in the right proportion (Bragg additivity). In this case,

$$\frac{dE}{dx} = \sum w_j \left. \frac{dE}{dx} \right|_j, \quad (23.5)$$

where $dE/dx|_j$ is the mean rate of energy loss (in MeV g cm^{-2}) in the j th element. Eq. (23.1) can be inserted into Eq. (23.5) to find expressions for $\langle Z/A \rangle$, $\langle I \rangle$, and $\langle \delta \rangle$; for example, $\langle Z/A \rangle = \sum w_j Z_j / A_j = \sum n_j Z_j / \sum n_j A_j$. However, $\langle I \rangle$ as defined this way is an underestimate, because in a compound electrons are more tightly bound than in the free elements, and $\langle \delta \rangle$ as calculated this way has little relevance, because it is the electron density which matters. If possible, one uses the tables given in Refs. 14 and 22, which include effective excitation energies and interpolation coefficients for calculating the density effect correction for the chemical elements and nearly 200 mixtures and compounds. If a compound or mixture is not found, then one uses the recipe for δ given in Ref. 13 (or Ref. 23), and calculates $\langle I \rangle$ according to the discussion in Ref. 7. (Note the "13%" rule!)

23.2.5. Restricted energy loss rates for relativistic ionizing particles: Fluctuations in energy loss are due mainly to the production of a few high-energy knock-on electrons. Practical detectors often measure the energy deposited, not the energy lost. When energy is carried off by energetic knock-on electrons, it is more appropriate to consider the mean energy loss excluding energy transfers greater than some cutoff T_{cut} . The restricted energy loss rate is

$$-\left. \frac{dE}{dx} \right|_{T < T_{\text{cut}}} = K z^2 \frac{Z}{A} \frac{1}{\beta^2} \left[\frac{1}{2} \ln \frac{2m_e c^2 \beta^2 \gamma^2 T_{\text{upper}}}{T^2} - \frac{\beta^2}{2} \left(1 + \frac{T_{\text{upper}}}{T_{\text{max}}} \right) - \frac{\delta}{2} \right] \quad (23.6)$$

where $T_{\text{upper}} = \text{MIN}(T_{\text{cut}}, T_{\text{max}})$. This form agrees with the equation given in previous editions of this Review [24] for $T_{\text{cut}} \ll T_{\text{max}}$ but smoothly joins the normal Bethe-Bloch function (Eq. (23.1)) for $T_{\text{cut}} > T_{\text{max}}$.

23.2.6. Energetic knock-on electrons (δ rays): The distribution of secondary electrons with kinetic energies $T \gg I$ is given by [4]

$$\frac{d^2 N}{dT dx} = \frac{1}{2} K z^2 \frac{Z}{A} \frac{1}{\beta^2} \frac{F(T)}{T^2} \quad (23.7)$$

for $I < T \leq T_{\text{max}}$, where T_{max} is given by Eq. (23.2). The factor F is spin-dependent, but is about unity for $T \ll T_{\text{max}}$. For spin-0 particles $F(T) = (1 - \beta^2 T/T_{\text{max}})$; forms for spins 1/2 and 1 are also given by Rossi [4]. When Eq. (23.7) is integrated from T_{cut} to T_{max} , one obtains the difference between Eq. (23.1) and Eq. (23.6). For incident electrons, the indistinguishability of projectile and target means that the range of T extends only to half the kinetic energy of the incident

particle. Additional formulae are given in Ref. 25. Equation (23.7) is inaccurate for T close to I : for $2I \lesssim T \lesssim 10I$, the $1/T^2$ dependence above becomes approximately $T^{-\eta}$, with $3 \lesssim \eta \lesssim 5$ [26].

23.2.7. Ionization yields: Physicists frequently relate total energy loss to the number of ion pairs produced near the particle's track. This relation becomes complicated for relativistic particles due to the wandering of energetic knock-on electrons whose ranges exceed the dimensions of the fiducial volume. For a qualitative appraisal of the nonlocality of energy deposition in various media by such modestly energetic knock-on electrons, see Ref. 27. The mean local energy dissipation per local ion pair produced, W , while essentially constant for relativistic particles, increases at slow particle speeds [28]. For gases, W can be surprisingly sensitive to trace amounts of various contaminants [28]. Furthermore, ionization yields in practical cases may be greatly influenced by such factors as subsequent recombination [29].

23.3. Multiple scattering through small angles

A charged particle traversing a medium is deflected by many small-angle scatters. Most of this deflection is due to Coulomb scattering from nuclei, and hence the effect is called multiple Coulomb scattering. (However, for hadronic projectiles, the strong interactions also contribute to multiple scattering.) The Coulomb scattering distribution is well represented by the theory of Molière [30]. It is roughly Gaussian for small deflection angles, but at larger angles (greater than a few θ_0 , defined below) it behaves like Rutherford scattering, having larger tails than does a Gaussian distribution.

If we define

$$\theta_0 = \theta_{\text{plane}}^{\text{rms}} = \frac{1}{\sqrt{2}} \theta_{\text{space}}^{\text{rms}}. \quad (23.8)$$

then it is sufficient for many applications to use a Gaussian approximation for the central 98% of the projected angular distribution, with a width given by [31,32]

$$\theta_0 = \frac{13.6 \text{ MeV}}{\beta c p} z \sqrt{x/X_0} \left[1 + 0.038 \ln(x/X_0) \right]. \quad (23.9)$$

Here p , βc , and z are the momentum, velocity, and charge number of the incident particle, and x/X_0 is the thickness of the scattering medium in radiation lengths (defined below). This value of θ_0 is from a fit to Molière distribution [30] for singly charged particles with $\beta = 1$ for all Z , and is accurate to 11% or better for $10^{-3} < x/X_0 < 100$.

Eq. (23.9) describes scattering from a single material, while the usual problem involves the multiple scattering of a particle traversing many different layers and mixtures. Since it is from a fit to a Molière distribution, it is incorrect to add the individual θ_0 contributions in quadrature; the result is systematically too small. It is much more accurate to apply Eq. (23.9) once, after finding x and X_0 for the combined scatterer.

Lynch and Dahl have extended this phenomenological approach, fitting Gaussian distributions to a variable fraction of the Molière distribution for arbitrary scatterers [32], and achieve accuracies of 2% or better.

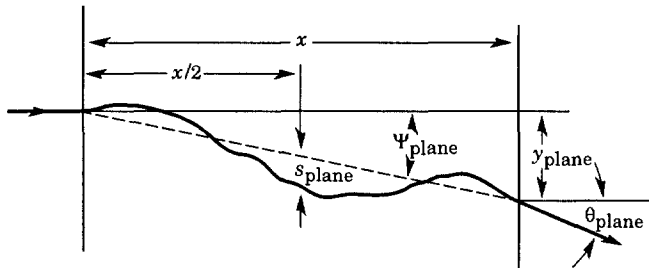


Figure 23.6: Quantities used to describe multiple Coulomb scattering. The particle is incident in the plane of the figure.

The nonprojected (space) and projected (plane) angular distributions are given approximately by [30]

$$\frac{1}{2\pi\theta_0^2} \exp\left(-\frac{\theta_{\text{space}}^2}{2\theta_0^2}\right) d\Omega, \quad (23.10)$$

$$\frac{1}{\sqrt{2\pi}\theta_0} \exp\left(-\frac{\theta_{\text{plane}}^2}{2\theta_0^2}\right) d\theta_{\text{plane}}, \quad (23.11)$$

where θ is the deflection angle. In this approximation, $\theta_{\text{space}}^2 \approx (\theta_{\text{plane},x}^2 + \theta_{\text{plane},y}^2)$, where the x and y axes are orthogonal to the direction of motion, and $d\Omega \approx d\theta_{\text{plane},x} d\theta_{\text{plane},y}$. Deflections into $\theta_{\text{plane},x}$ and $\theta_{\text{plane},y}$ are independent and identically distributed.

Figure 23.6 shows these and other quantities sometimes used to describe multiple Coulomb scattering. They are

$$\psi_{\text{plane}}^{\text{rms}} = \frac{1}{\sqrt{3}} \theta_{\text{plane}}^{\text{rms}} = \frac{1}{\sqrt{3}} \theta_0, \quad (23.12)$$

$$y_{\text{plane}}^{\text{rms}} = \frac{1}{\sqrt{3}} x \theta_{\text{plane}}^{\text{rms}} = \frac{1}{\sqrt{3}} x \theta_0, \quad (23.13)$$

$$s_{\text{plane}}^{\text{rms}} = \frac{1}{4\sqrt{3}} x \theta_{\text{plane}}^{\text{rms}} = \frac{1}{4\sqrt{3}} x \theta_0. \quad (23.14)$$

All the quantitative estimates in this section apply only in the limit of small $\theta_{\text{plane}}^{\text{rms}}$ and in the absence of large-angle scatters. The random variables s , ψ , y , and θ in a given plane are distributed in a correlated fashion (see Sec. 27.1 of this Review for the definition of the correlation coefficient). Obviously, $y \approx x\psi$. In addition, y and θ have the correlation coefficient $\rho_{y\theta} = \sqrt{3}/2 \approx 0.87$. For Monte Carlo generation of a joint $(y_{\text{plane}}, \theta_{\text{plane}})$ distribution, or for other calculations, it may be most convenient to work with independent Gaussian random variables (z_1, z_2) with mean zero and variance one, and then set

$$y_{\text{plane}} = z_1 x \theta_0 (1 - \rho_{y\theta}^2)^{1/2} / \sqrt{3} + z_2 \rho_{y\theta} x \theta_0 / \sqrt{3} \\ = z_1 x \theta_0 / \sqrt{12} + z_2 x \theta_0 / 2; \quad (23.15)$$

$$\theta_{\text{plane}} = z_2 \theta_0. \quad (23.16)$$

Note that the second term for y_{plane} equals $x\theta_{\text{plane}}/2$ and represents the displacement that would have occurred had the deflection θ_{plane} all occurred at the single point $x/2$.

For heavy ions the multiple Coulomb scattering has been measured and compared with various theoretical distributions [33].

23.4. Photon and electron interactions in matter

23.4.1. Radiation length: High-energy electrons predominantly lose energy in matter by bremsstrahlung, and high-energy photons by e^+e^- pair production. The characteristic amount of matter traversed for these related interactions is called the radiation length X_0 , usually measured in g cm^{-2} . It is the mean distance over which a high-energy electron loses all but $1/e$ of its energy by bremsstrahlung, and the e -folding distance for pair production by a high-energy photon is $\frac{7}{9}X_0$. It is also the appropriate scale length for describing high-energy electromagnetic cascades. X_0 has been calculated and tabulated by Y.S. Tsai [34]:

$$\frac{1}{X_0} = 4\alpha r_e^2 \frac{N_A}{A} \left\{ Z^2 [L_{\text{rad}} - f(Z)] + Z L'_{\text{rad}} \right\}. \quad (23.17)$$

For $A = 1 \text{ g mol}^{-1}$, $4\alpha r_e^2 N_A/A = (716.408 \text{ g cm}^{-2})^{-1}$. L_{rad} and L'_{rad} are given in Table 23.2. The function $f(Z)$ is an infinite sum, but for elements up to uranium can be represented to 4-place accuracy by

$$f(Z) = a^2 [(1 + a^2)^{-1} + 0.20206 \\ - 0.0369 a^2 + 0.0083 a^4 - 0.002 a^6], \quad (23.18)$$

where $a = \alpha Z$ [35].

Table 23.2: Tsai's L_{rad} and L'_{rad} , for use in calculating the radiation length in an element using Eq. (23.17).

Element	Z	L_{rad}	L'_{rad}
H	1	5.31	6.144
He	2	4.79	5.621
Li	3	4.74	5.805
Be	4	4.71	5.924
Others	> 4	$\ln(184.15 Z^{-1/3})$	$\ln(1194 Z^{-2/3})$

Although it is easy to use Eq. (23.17) to calculate X_0 , the functional dependence on Z is somewhat hidden. Dahl provides a compact fit to the data [36]:

$$X_0 = \frac{716.4 \text{ g cm}^{-2} A}{Z(Z+1) \ln(287/\sqrt{Z})} \quad (23.19)$$

Results obtained with this formula agree with Tsai's values to better than 2.5% for all elements except helium, where the result is about 5% low.

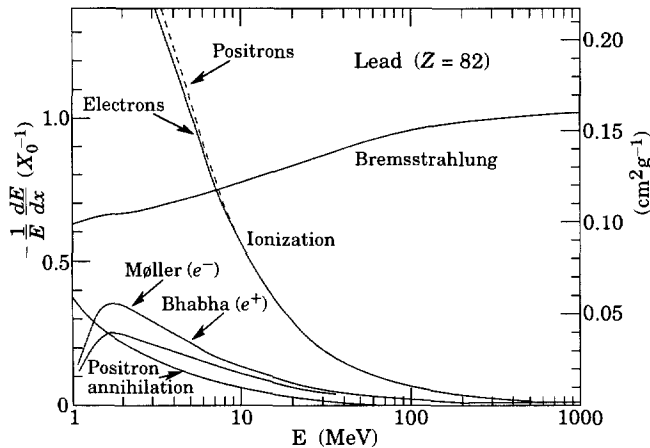


Figure 23.7: Fractional energy loss per radiation length in lead as a function of electron or positron energy. Electron (positron) scattering is considered as ionization when the energy loss per collision is below 0.255 MeV, and as Møller (Bhabha) scattering when it is above. Adapted from Fig. 3.2 from Messel and Crawford, *Electron-Photon Shower Distribution Function Tables for Lead, Copper, and Air Absorbers*, Pergamon Press, 1970. Messel and Crawford use $X_0(\text{Pb}) = 5.82 \text{ g/cm}^2$, but we have modified the figures to reflect the value given in the Table of Atomic and Nuclear Properties of Materials ($X_0(\text{Pb}) = 6.37 \text{ g/cm}^2$).

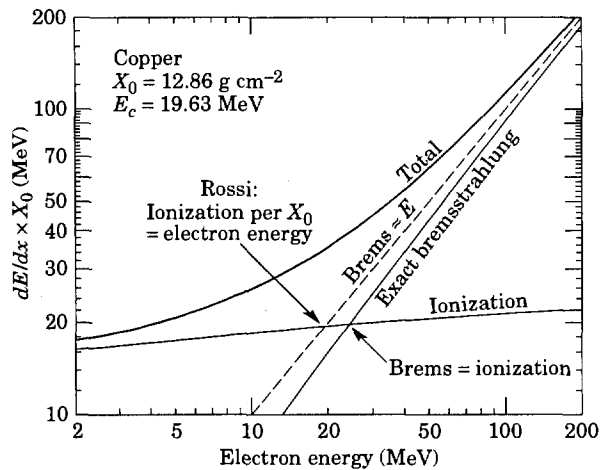


Figure 23.8: Two definitions of the critical energy E_c .

The radiation length in a mixture or compound may be approximated by

$$1/X_0 = \sum w_j/X_j, \quad (23.20)$$

where w_j and X_j are the fraction by weight and the radiation length for the j th element.

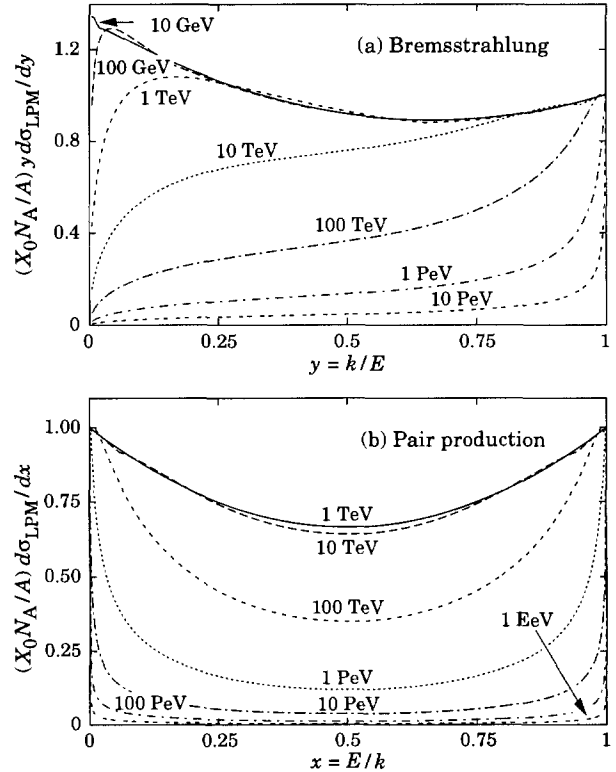


Figure 23.9: (a) The normalized bremsstrahlung cross section $k d\sigma_{LPM}/dk$ in lead versus the fractional photon energy $y = k/E$. The vertical axis has units of photons per radiation length. (b) The normalized pair production cross section $d\sigma_{LPM}/dy$, versus fractional electron energy $x = E/k$.

23.4.2. Energy loss by electrons: At low energies electrons and positrons primarily lose energy by ionization, although other processes (Møller scattering, Bhabha scattering, e^+ annihilation) contribute, as shown in Fig. 23.7. While ionization loss rates rise logarithmically with energy, bremsstrahlung losses rise nearly linearly (fractional loss is nearly independent of energy), and dominates above a few tens of MeV in most materials (see Fig. 23.8).

Ionization loss by electrons and positrons differs from loss by heavy particles because of the kinematics, spin, and the identity of the incident electron with the electrons which it ionizes. Complete discussions and tables can be found in Refs. 7, 8, and 22.

At very high energies and except at the high-energy tip of the bremsstrahlung spectrum, the cross section can be approximated in the "complete screening case" as [34]

$$\frac{d\sigma}{dk} = (1/k) 4\alpha r_e^2 \left\{ \left(\frac{4}{3} - \frac{4}{3}y + y^2 \right) [Z^2(L_{\text{rad}} - f(Z)) + Z L'_{\text{rad}}] + \frac{1}{3}(1-y)(Z^2 + Z) \right\}, \quad (23.21)$$

where $y = k/E$ is the fraction of the electron's energy transferred to the radiated photon. At small y (the "infrared limit") the term on the second line can reach 2.5%. If it is ignored and the first line simplified with the definition of X_0 given in Eq. (23.17), we have

$$\frac{d\sigma}{dk} = \frac{A}{X_0 N_A k} \left(\frac{4}{3} - \frac{4}{3}y + y^2 \right). \quad (23.22)$$

This cross section (times k) is shown by the top curve in Fig. 23.9(a).

This formula is accurate except in near $y = 1$, where screening may become incomplete, and near $y = 0$, where the infrared divergence is removed by the interference of bremsstrahlung amplitudes from nearby scattering centers (the LPM effect) [37,38] and dielectric suppression [39,40]. These and other suppression effects in bulk media are discussed in Sec. 23.4.5.

With decreasing energy ($E \lesssim 10 \text{ GeV}$) the high- y cross section drops and the curves become rounded as $y \rightarrow 1$. Curves of this familiar

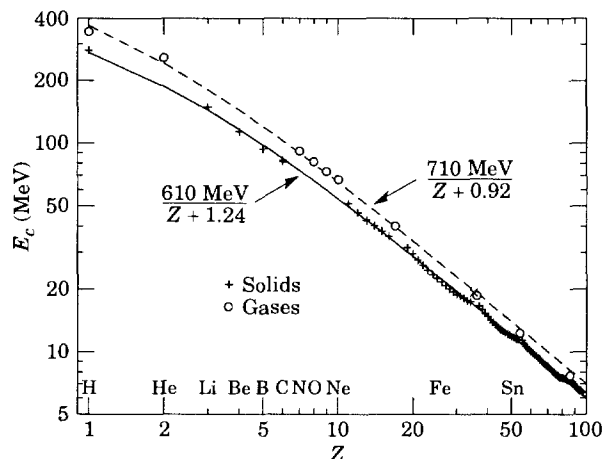


Figure 23.10: Electron critical energy for the chemical elements, using Rossi's definition [4]. The fits shown are for solids and liquids (solid line) and gases (dashed line). The rms deviation is 2.2% for the solids and 4.0% for the gases. (Computed with code supplied by A. Fassó.)

shape can be seen in Rossi [4] (Figs. 2.11,2,3); see also the review by Koch & Motz [41].

Except at these extremes, and still in the complete-screening approximation, the number of photons with energies between k_{\min} and k_{\max} emitted by an electron travelling a distance $d \ll X_0$ is

$$N_\gamma = \frac{d}{X_0} \left[\frac{4}{3} \ln \left(\frac{k_{\max}}{k_{\min}} \right) - \frac{4(k_{\max} - k_{\min})}{3E} + \frac{(k_{\max} - k_{\min})^2}{2E^2} \right] \quad (23.23)$$

23.4.3. Critical energy: An electron loses energy by bremsstrahlung at a rate nearly proportional to its energy, while the ionization loss rate varies only logarithmically with the electron energy. The *critical energy* E_c is sometimes defined as the energy at which the two loss rates are equal [42]. Berger and Seltzer [42] also give the approximation $E_c = (800 \text{ MeV})/(Z + 1.2)$. This formula has been widely quoted, and has been given in previous editions of this *Review* [24]. Among alternate definitions is that of Rossi [4], who defines the critical energy as the energy at which the ionization loss per radiation length is equal to the electron energy. Equivalently, it is the same as the first definition with the approximation $|dE/dx|_{\text{brems}} \approx E/X_0$. This form has been found to describe more accurately transverse electromagnetic shower development (see below). These definitions are illustrated in the case of copper in Fig. 23.8.

The accuracy of approximate forms for E_c has been limited by the failure to distinguish between gases and solid or liquids, where there is a substantial difference in ionization at the relevant energy because of the density effect. We distinguish these two cases in Fig. 23.10. Fits were also made with functions of the form $a/(Z + b)^\alpha$, but α was essentially unity. Since E_c also depends on A , I , and other factors, such forms are at best approximate.

23.4.4. Energy loss by photons: Contributions to the photon cross section in a light element (carbon) and a heavy element (lead) are shown in Fig. 23.11. At low energies it is seen that the photoelectric effect dominates, although Compton scattering, Rayleigh scattering, and photonuclear absorption also contribute. The photoelectric cross section is characterized by discontinuities (absorption edges) as thresholds for photoionization of various atomic levels are reached. Photon attenuation lengths for a variety of elements are shown in Fig. 23.12, and data for $30 \text{ eV} < k < 100 \text{ GeV}$ for all elements is available from the web pages given in the caption. Here k is the photon energy.

The increasing domination of pair production as the energy increases is shown in Fig. 23.13. Using approximations similar to those used to obtain Eq. (23.22), Tsai's formula for the differential cross section [34] reduces to

$$\frac{d\sigma}{dE} = \frac{A}{X_0 N_A} \left[1 - \frac{4}{3}x(1-x) \right] \quad (23.24)$$

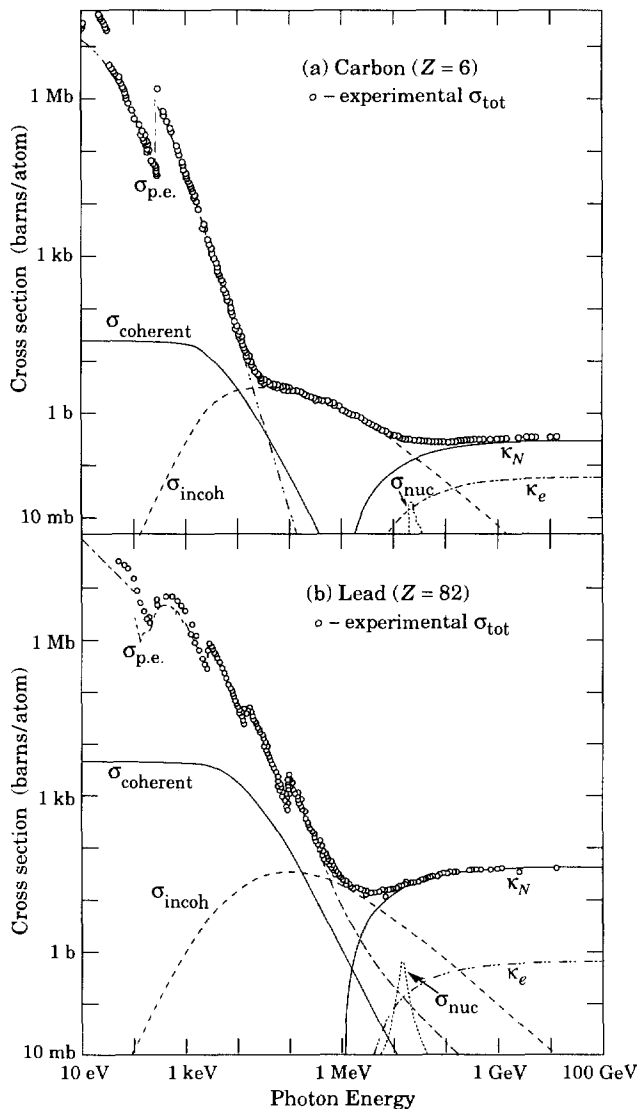


Figure 23.11: Photon total cross sections as a function of energy in carbon and lead, showing the contributions of different processes:

- $\sigma_{\text{p.e.}}$ = Atomic photoeffect (electron ejection, photon absorption)
- σ_{coherent} = Coherent scattering (Rayleigh scattering—atom neither ionized nor excited)
- $\sigma_{\text{incoherent}}$ = Incoherent scattering (Compton scattering off an electron)
- κ_n = Pair production, nuclear field
- κ_e = Pair production, electron field
- σ_{nuc} = Photonuclear absorption (nuclear absorption, usually followed by emission of a neutron or other particle)

From Hubbell, Gimm, and Øverbø, *J. Phys. Chem. Ref. Data* **9**, 1023 (1980). Data for these and other elements, compounds, and mixtures may be obtained from <http://physics.nist.gov/PhysRefData>. The photon total cross section is assumed approximately flat for at least two decades beyond the energy range shown. Figures courtesy J.H. Hubbell (NIST).

in the complete-screening limit valid at high energies. Here $x = E/k$ is the fractional energy transfer to the pair-produced electron (or positron), and k is the incident photon energy. The cross section is very closely related to that for bremsstrahlung, since the Feynman

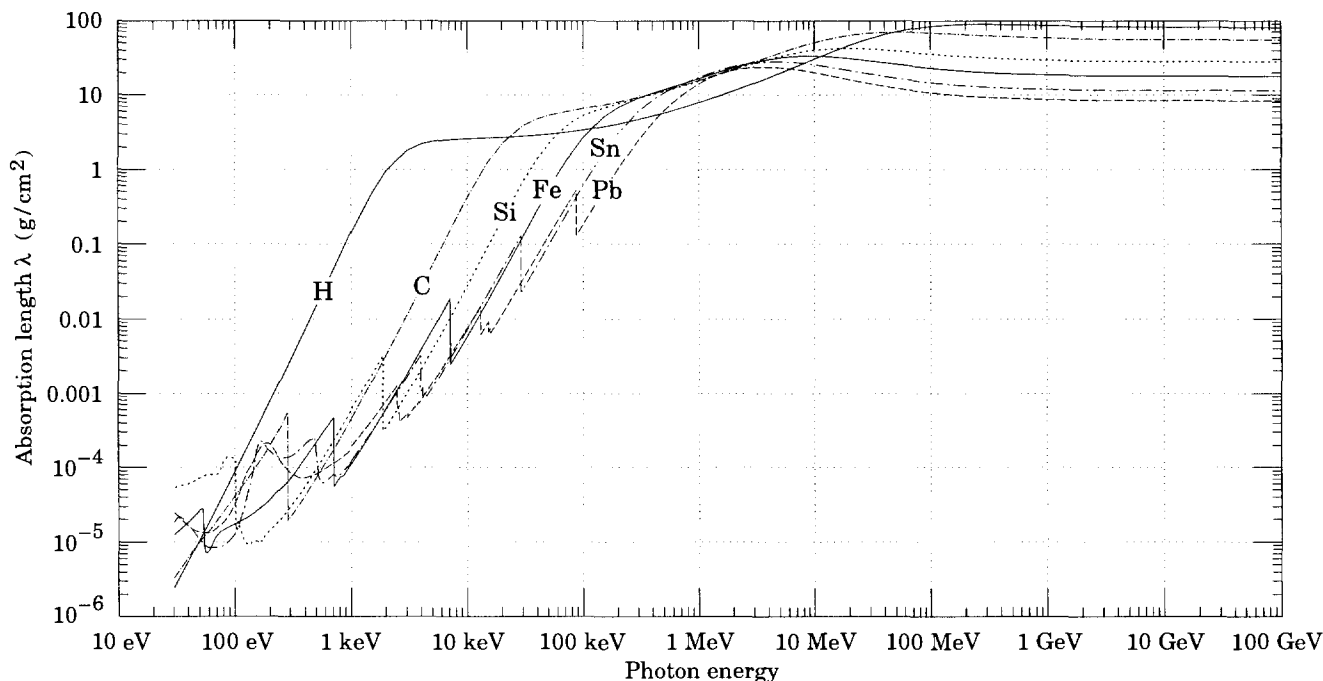


Fig. 23.12: The photon mass attenuation length (or mean free path) $\lambda = 1/(\mu/\rho)$ for various elemental absorbers as a function of photon energy. The mass attenuation coefficient is μ/ρ , where ρ is the density. The intensity I remaining after traversal of thickness t (in mass/unit area) is given by $I = I_0 \exp(-t/\lambda)$. The accuracy is a few percent. For a chemical compound or mixture, $1/\lambda_{\text{eff}} \approx \sum_{\text{elements}} w_Z/\lambda_Z$, where w_Z is the proportion by weight of the element with atomic number Z . The processes responsible for attenuation are given in not Fig. 23.7. Since coherent processes are included, not all these processes result in energy deposition. The data for $30 \text{ eV} < E < 1 \text{ keV}$ are obtained from http://www-cxro.lbl.gov/optical_constants (courtesy of Eric M. Gullikson, LBNL). The data for $1 \text{ keV} < E < 100 \text{ GeV}$ are from <http://physics.nist.gov/PhysRefData>, through the courtesy of John H. Hubbell (NIST).

diagrams are variants of one another. The cross section is of necessity symmetric between x and $1-x$, as can be seen by the solid curve in Fig. 23.9(b). See the review by Motz, Olsen, & Koch for a more detailed treatment [43].

Eq. (23.24) may be integrated to find the high-energy limit for the total e^+e^- pair-production cross section:

$$\sigma = \frac{7}{9}(A/X_0 N_A). \quad (23.25)$$

Equation Eq. (23.25) is accurate to within a few percent down to energies as low as 1 GeV, particularly for high- Z materials.

23.4.5. Bremsstrahlung and pair production at very high energies: At ultrahigh energies, Eqns. 23.21–23.25 will fail because of quantum mechanical interference between amplitudes from different scattering centers. Since the longitudinal momentum transfer to a given center is small ($\propto k/E^2$, in the case of bremsstrahlung), the interaction is spread over a comparatively long distance called the formation length ($\propto E^2/k$) via the uncertainty principle. In alternate language, the formation length is the distance over which the highly relativistic electron and the photon “split apart.” The interference is usually destructive. Calculations of the “Landau-Pomeranchuk-Migdal” effect may be made semi-classically based on the average multiple scattering, or more rigorously using a quantum transport approach [37,38].

In amorphous media, bremsstrahlung is suppressed if the photon energy is above $k > E^2/E_{LPM}$ [38], where*

$$E_{LPM} = \frac{(m_e c^2)^2 \alpha \rho X_0}{4\pi \hbar c} = (7.7 \text{ TeV/cm}) \times \rho X_0. \quad (23.26)$$

* This definition differs from that of Ref. 44 by a factor of two. It is also pointed out that E_{LPM} scales as the 4th power of the mass of the incident particle, so that $E_{LPM} = (1.4 \times 10^{10} \text{ TeV/cm}) \times \rho X_0$ for a muon.

Since physical distances are involved, ρX_0 , in cm, appears. The energy-weighted bremsstrahlung spectrum for lead, $k d\sigma_{LPM}/dk$, is shown in Fig. 23.9(a). With appropriate scaling by ρX_0 , other materials behave similarly.

For photons, pair production is reduced for $E(k-E) > k E_{LPM}$. The pair-production cross sections for different photon energies are shown in Fig. 23.9(b).

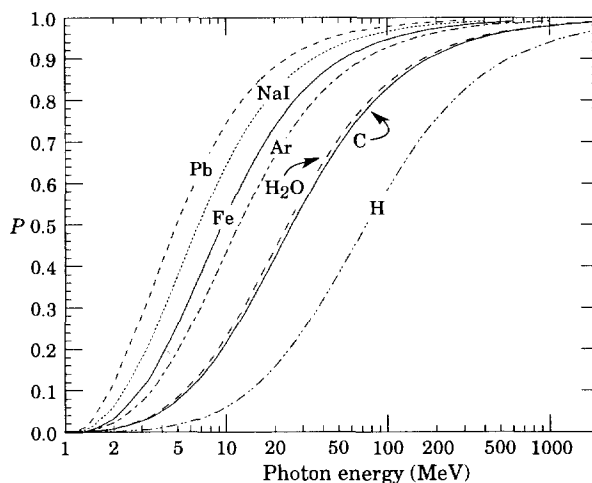


Figure 23.13: Probability P that a photon interaction will result in conversion to an e^+e^- pair. Except for a few-percent contribution from photonuclear absorption around 10 or 20 MeV, essentially all other interactions in this energy range result in Compton scattering off an atomic electron. For a photon attenuation length λ (Fig. 23.12), the probability that a given photon will produce an electron pair (without first Compton scattering) in thickness t of absorber is $P[1 - \exp(-t/\lambda)]$.

If $k \ll E$, several additional mechanisms can also produce suppression. When the formation length is long, even weak factors can perturb the interaction. For example, the emitted photon can coherently forward scatter off of the electrons in the media. Because of this, for $k < \omega_p E/m_e \sim 10^{-4}$, bremsstrahlung is suppressed by a factor $(km_e/\omega_p E)^2$ [40]. Magnetic fields can also suppress bremsstrahlung.

In crystalline media, the situation is more complicated, with coherent enhancement or suppression possible. The cross section depends on the electron and photon energies and the angles between the particle direction and the crystalline axes [38].

23.5. Electromagnetic cascades

When a high-energy electron or photon is incident on a thick absorber, it initiates an electromagnetic cascade as pair production and bremsstrahlung generate more electrons and photons with lower energy. The longitudinal development is governed by the high-energy part of the cascade, and therefore scales as the radiation length in the material. Electron energies eventually fall below the critical energy, and then dissipate their energy by ionization and excitation rather than by the generation of more shower particles. In describing shower behavior, it is therefore convenient to introduce the scale variables

$$\begin{aligned} t &= x/X_0 \\ y &= E/E_c, \end{aligned} \quad (23.27)$$

so that distance is measured in units of radiation length and energy in units of critical energy.

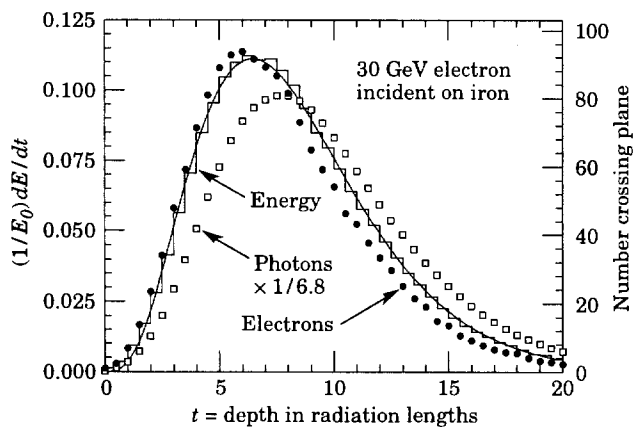


Figure 23.14: An EGS4 simulation of a 30 GeV electron-induced cascade in iron. The histogram shows fractional energy deposition per radiation length, and the curve is a gamma-function fit to the distribution. Circles indicate the number of electrons with total energy greater than 1.5 MeV crossing planes at $X_0/2$ intervals (scale on right) and the squares the number of photons with $E \geq 1.5$ MeV crossing the planes (scaled down to have same area as the electron distribution).

Longitudinal profiles for an EGS4 [23] simulation of a 30 GeV electron-induced cascade in iron are shown in Fig. 23.14. The number of particles crossing a plane (very close to Rossi's Π function [4]) is sensitive to the cutoff energy, here chosen as a total energy of 1.5 MeV for both electrons and photons. The electron number falls off more quickly than energy deposition. This is because, with increasing depth, a larger fraction of the cascade energy is carried by photons. Exactly what a calorimeter measures depends on the device, but it is not likely to be exactly any of the profiles shown. In gas counters it may be very close to the electron number, but in glass Čerenkov detectors and other devices with "thick" sensitive regions it is closer to the energy deposition (total track length). In such detectors the signal is proportional to the "detectable" track length T_d , which is in general less than the total track length T . Practical devices are sensitive to electrons with energy above some detection threshold E_d , and $T_d = T F(E_d/E_c)$. An analytic form for $F(E_d/E_c)$ obtained by Rossi [4] is given by Fabjan [45]; see also Amaldi [46].

The mean longitudinal profile of the energy deposition in an electromagnetic cascade is reasonably well described by a gamma distribution [47]:

$$\frac{dE}{dt} = E_0 b \frac{(bt)^{a-1} e^{-bt}}{\Gamma(a)} \quad (23.28)$$

The maximum t_{\max} occurs at $(a-1)/b$. We have made fits to shower profiles in elements ranging from carbon to uranium, at energies from 1 GeV to 100 GeV. The energy deposition profiles are well described by Eq. (23.28) with

$$t_{\max} = (a-1)/b = 1.0 \times (\ln y + C_j), \quad j = e, \gamma, \quad (23.29)$$

where $C_e = -0.5$ for electron-induced cascades and $C_\gamma = +0.5$ for photon-induced cascades. To use Eq. (23.28), one finds $(a-1)/b$ from Eq. (23.29) and Eq. (23.27), then finds a either by assuming $b \approx 0.5$ or by finding a more accurate value from Fig. 23.15. The results are very similar for the electron number profiles, but there is some dependence on the atomic number of the medium. A similar form for the electron number maximum was obtained by Rossi in the context of his "Approximation B," [4] (see Fabjan's review in Ref. 45), but with $C_e = -1.0$ and $C_\gamma = -0.5$; we regard this as superseded by the EGS4 result.

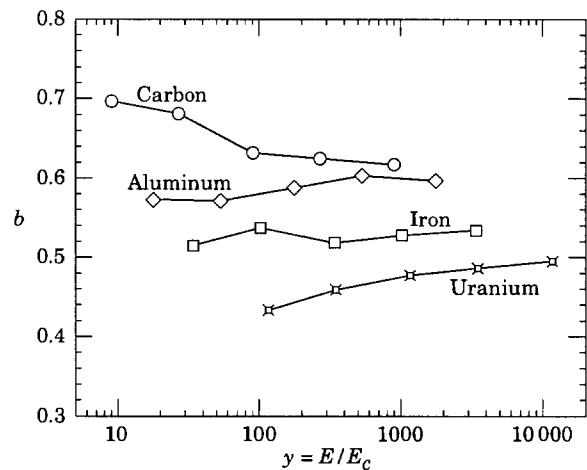


Figure 23.15: Fitted values of the scale factor b for energy deposition profiles obtained with EGS4 for a variety of elements for incident electrons with $1 \leq E_0 \leq 100$ GeV. Values obtained for incident photons are essentially the same.

The "shower length" $X_s = X_0/b$ is less conveniently parameterized, since b depends upon both Z and incident energy, as shown in Fig. 23.15. As a corollary of this Z dependence, the number of electrons crossing a plane near shower maximum is underestimated using Rossi's approximation for carbon and seriously overestimated for uranium. Essentially the same b values are obtained for incident electrons and photons. For many purposes it is sufficient to take $b \approx 0.5$.

The gamma distribution is very flat near the origin, while the EGS4 cascade (or a real cascade) increases more rapidly. As a result Eq. (23.28) fails badly for about the first two radiation lengths; it was necessary to exclude this region in making fits.

Because fluctuations are important, Eq. (23.28) should be used only in applications where average behavior is adequate. Grindhammer *et al.* have developed fast simulation algorithms in which the variance and correlation of a and b are obtained by fitting Eq. (23.28) to individually simulated cascades, then generating profiles for cascades using a and b chosen from the correlated distributions [48].

The transverse development of electromagnetic showers in different materials scales fairly accurately with the *Molière radius* R_M , given by [49,50]

$$R_M = X_0 E_s/E_c, \quad (23.30)$$

where $E_s \approx 21$ MeV (see Table 23.1), and the Rossi definition of E_c is used.

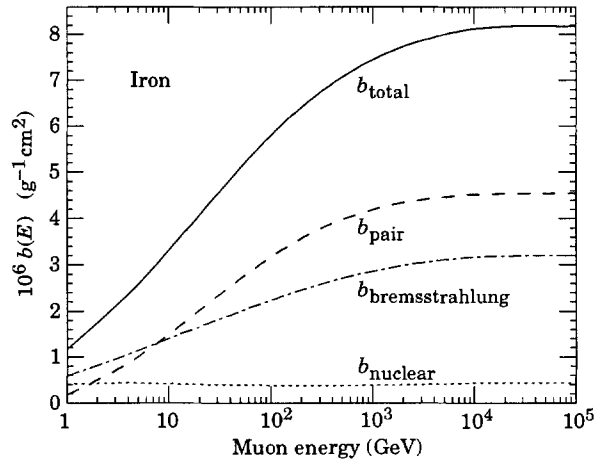


Figure 23.16: Contributions to the fractional energy loss by muons in iron due to e^+e^- pair production, bremsstrahlung, and photonuclear interactions, as obtained from Lohmann *et al.* [61].

In a material containing a weight fraction w_j of the element with critical energy E_{cj} and radiation length X_j , the Molière radius is given by

$$\frac{1}{R_M} = \frac{1}{E_s} \sum \frac{w_j E_{cj}}{X_j}. \quad (23.31)$$

Measurements of the lateral distribution in electromagnetic cascades are shown in Refs. 49 and 50. On the average, only 10% of the energy lies outside the cylinder with radius R_M . About 99% is contained inside of $3.5R_M$, but at this radius and beyond composition effects become important and the scaling with R_M fails. The distributions are characterized by a narrow core, and broaden as the shower develops. They are often represented as the sum of two Gaussians, and Grindhammer [48] describes them with the function

$$f(r) = \frac{2r R^2}{(r^2 + R^2)^2}, \quad (23.32)$$

where R is a phenomenological function of x/X_0 and $\ln E$.

At high enough energies, the LPM effect (Sec. 23.4.5) reduces the cross sections for bremsstrahlung and pair production, and hence can cause significant elongation of electromagnetic cascades [38].

23.6. Muon energy loss at high energy

At sufficiently high energies, radiative processes become more important than ionization for all charged particles. For muons and pions in materials such as iron, this “critical energy” occurs at several hundred GeV. Radiative effects dominate the energy loss of energetic muons found in cosmic rays or produced at the newest accelerators. These processes are characterized by small cross sections, hard spectra, large energy fluctuations, and the associated generation of electromagnetic and (in the case of photonuclear interactions) hadronic showers [51–59]. As a consequence, at these energies the treatment of energy loss as a uniform and continuous process is for many purposes inadequate.

It is convenient to write the average rate of muon energy loss as [60]

$$-dE/dx = a(E) + b(E)E. \quad (23.33)$$

Here $a(E)$ is the ionization energy loss given by Eq. (23.1), and $b(E)$ is the sum of e^+e^- pair production, bremsstrahlung, and photonuclear contributions. To the approximation that these slowly-varying functions are constant, the mean range x_0 of a muon with initial energy E_0 is given by

$$x_0 \approx (1/b) \ln(1 + E_0/E_{\mu c}), \quad (23.34)$$

where $E_{\mu c} = a/b$. Figure 23.16 shows contributions to $b(E)$ for iron. Since $a(E) \approx 0.002 \text{ GeV g}^{-1} \text{ cm}^2$, $b(E)E$ dominates the energy loss above several hundred GeV, where $b(E)$ is nearly constant. The rate of energy loss for muons in hydrogen, uranium, and iron is shown in Fig. 23.17 [61].

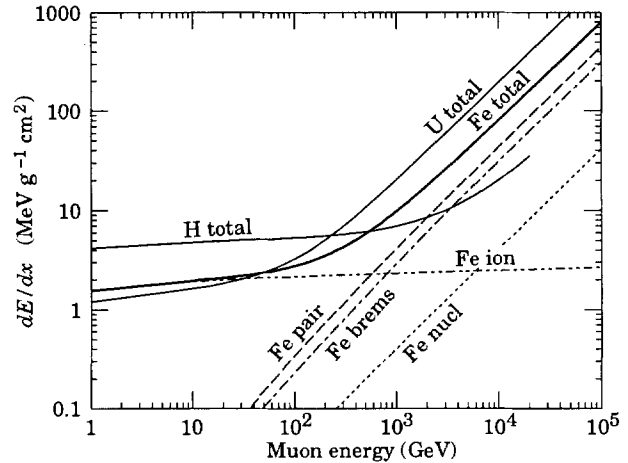


Figure 23.17: The average energy loss of a muon in hydrogen, iron, and uranium as a function of muon energy. Contributions to dE/dx in iron from ionization and the processes shown in Fig. 23.16 are also shown.

The “muon critical energy” $E_{\mu c}$ can be defined more exactly as the energy at which radiative and ionization losses are equal, and can be found by solving $E_{\mu c} = a(E_{\mu c})/b(E_{\mu c})$. This definition corresponds to the solid-line intersection in Fig. 23.8, and is different from the Rossi definition we used for electrons. It serves the same function: below $E_{\mu c}$ ionization losses dominate, and above $E_{\mu c}$ radiative losses dominate. The dependence of $E_{\mu c}$ on atomic number Z is shown in Fig. 23.18.

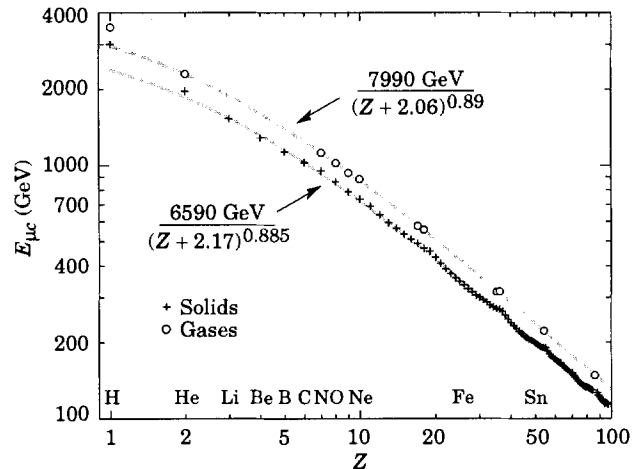


Figure 23.18: Muon critical energy for the chemical elements, defined as the energy at which radiative and ionization energy loss rates are equal. The equality comes at a higher energy for gases than for solids or liquids with the same atomic number because of a smaller density effect reduction of the ionization losses. The fits shown in the figure exclude hydrogen. Alkali metals fall 3–4% above the fitted function, while most other solids are within 2% of the function. Among the gases the worst fit is for neon (1.4% high). (Courtesy of N.V. Mokhov and S.I. Striganov.)

The radiative cross sections are expressed as functions of the fractional energy loss ν . The bremsstrahlung cross section goes roughly as $1/\nu$ over most of the range, while for the pair production case the distribution goes as ν^{-3} to ν^{-2} (see Ref. 62). “Hard” losses are therefore more probable in bremsstrahlung, and in fact energy losses due to pair production may very nearly be treated as continuous. The calculated momentum distribution of an incident 1 TeV/c muon beam after it crosses 3 m of iron is shown in Fig. 23.19. The most probable loss is 9 GeV, or $3.8 \text{ MeV g}^{-1} \text{ cm}^2$. The full width at half maximum is 7 GeV/c, or 0.7%. The radiative tail is almost entirely

due to bremsstrahlung; this includes most of the 10% that lost more than 2.8% of their energy. Most of the 3.3% that lost more than 10% of their incident energy experienced photonuclear interactions, which are concentrated in rare, relatively hard collisions. The latter can exceed nominal detector resolution [63], necessitating the reconstruction of lost energy. Electromagnetic and hadronic cascades in detector materials can obscure muon tracks in detector planes and reduce tracking efficiency [64].

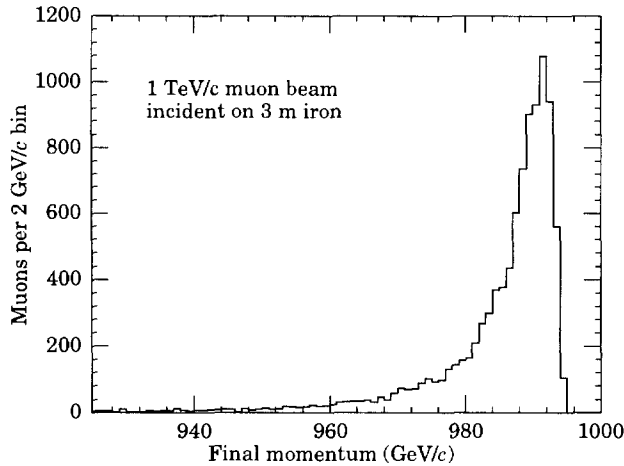


Figure 23.19: The momentum distribution of 1 TeV/c muons after traversing 3 m of iron, as obtained with Van Ginniken's TRAMU muon transport code [62].

23.7. Čerenkov and transition radiation [10,65,66]

A charged particle radiates if its velocity is greater than the local phase velocity of light (Čerenkov radiation) or if it crosses suddenly from one medium to another with different optical properties (transition radiation). Neither process is important for energy loss, but both are used in high-energy physics detectors.

Čerenkov Radiation. The half-angle θ_c of the Čerenkov cone for a particle with velocity βc in a medium with index of refraction n is

$$\theta_c = \arccos(1/n\beta) \approx \sqrt{2(1-1/n\beta)} \quad \text{for small } \theta_c, \text{ e.g. in gases.} \quad (23.35)$$

The threshold velocity β_t is $1/n$, and $\gamma_t = 1/(1-\beta_t^2)^{1/2}$. Therefore, $\beta_t \gamma_t = 1/(2\delta + \delta^2)^{1/2}$, where $\delta = n - 1$. Values of δ for various commonly used gases are given as a function of pressure and wavelength in Ref. 67. For values at atmospheric pressure, see Table 6.1. Data for other commonly used materials are given in Ref. 68.

The number of photons produced per unit path length of a particle with charge ze and per unit energy interval of the photons is

$$\frac{d^2 N}{dE dx} = \frac{\alpha z^2}{hc} \sin^2 \theta_c = \frac{\alpha^2 z^2}{r_e m_e c^2} \left(1 - \frac{1}{\beta^2 n^2(E)}\right) \approx 370 \sin^2 \theta_c(E) \text{ eV}^{-1} \text{ cm}^{-1} \quad (z=1), \quad (23.36)$$

or, equivalently,

$$\frac{d^2 N}{dx d\lambda} = \frac{2\pi \alpha z^2}{\lambda^2} \left(1 - \frac{1}{\beta^2 n^2(\lambda)}\right). \quad (23.37)$$

The index of refraction is a function of photon energy E , as is the sensitivity of the transducer used to detect the light. For practical use, Eq. (23.36) must be multiplied by the the transducer response function and integrated over the region for which $\beta n(E) > 1$. Further details are given in the discussion of Čerenkov detectors in the Detectors section (Sec. 24 of this Review).

Transition radiation. The energy radiated when a particle with charge ze crosses the boundary between vacuum and a medium with plasma frequency ω_p is

$$I = \alpha z^2 \gamma \hbar \omega_p / 3, \quad (23.38)$$

where

$$\begin{aligned} \hbar \omega_p &= \sqrt{4\pi N_e r_e^3} m_e c^2 / \alpha \\ &= \sqrt{4\pi N_e a_\infty^3} 2 \times 13.6 \text{ eV}. \end{aligned} \quad (23.39)$$

Here N_e is the electron density in the medium, r_e is the classical electron radius, and a_∞ is the Bohr radius. For styrene and similar materials, $\sqrt{4\pi N_e a_\infty^3} \approx 0.8$, so that $\hbar \omega_p \approx 20$ eV. The typical emission angle is $1/\gamma$.

The radiation spectrum is logarithmically divergent at low energies and decreases rapidly for $\hbar \omega / \gamma \hbar \omega_p > 1$. About half the energy is emitted in the range $0.1 \leq \hbar \omega / \gamma \hbar \omega_p \leq 1$. For a particle with $\gamma = 10^3$, the radiated photons are in the soft x-ray range 2 to 20 keV. The γ dependence of the emitted energy thus comes from the hardening of the spectrum rather than from an increased quantum yield. For a typical radiated photon energy of $\gamma \hbar \omega_p / 4$, the quantum yield is

$$\begin{aligned} N_\gamma &\approx \frac{1}{2} \frac{\alpha z^2 \gamma \hbar \omega_p}{3} \frac{\gamma \hbar \omega_p}{4} \\ &\approx \frac{2}{3} \alpha z^2 \approx 0.5\% \times z^2. \end{aligned} \quad (23.40)$$

More precisely, the number of photons with energy $\hbar \omega > \hbar \omega_0$ is given by [10]

$$N_\gamma(\hbar \omega > \hbar \omega_0) = \frac{\alpha z^2}{\pi} \left[\left(\ln \frac{\gamma \hbar \omega_p}{\hbar \omega_0} - 1 \right)^2 + \frac{\pi^2}{12} \right], \quad (23.41)$$

within corrections of order $(\hbar \omega_0 / \gamma \hbar \omega_p)^2$. The number of photons above a fixed energy $\hbar \omega_0 \ll \gamma \hbar \omega_p$ thus grows as $(\ln \gamma)^2$, but the number above a fixed fraction of $\gamma \hbar \omega_p$ (as in the example above) is constant. For example, for $\hbar \omega > \gamma \hbar \omega_p / 10$, $N_\gamma = 2.519 \alpha z^2 / \pi = 0.59\% \times z^2$.

The yield can be increased by using a stack of plastic foils with gaps between. However, interference can be important, and the soft x rays are readily absorbed in the foils. The first problem can be overcome by choosing thicknesses and spacings large compared to the "formation length" $D = \gamma c / \omega_p$, which in practical situations is tens of μm . Other practical problems are discussed in Sec. 24.

References:

1. D.E. Groom, N.V. Mokhov, and S.I. Striganov, "Muon stopping-power and range tables," Atomic Data and Nuclear Data Tables, to be published (2000).
2. "Stopping Powers and Ranges for Protons and Alpha Particles," ICRU Report No. 49 (1993); Tables and graphs of these data are available at <http://physics.nist.gov/PhysRefData/>.
3. W.H. Barkas, W. Birnbaum, and F.M. Smith, Phys. Rev. **101**, 778 (1956).
4. B. Rossi, *High Energy Particles*, Prentice-Hall, Inc., Englewood Cliffs, NJ, 1952.
5. U. Fano, Ann. Rev. Nucl. Sci. **13**, 1 (1963).
6. J. D. Jackson, Phys. Rev. **D59**, 017301 (1999).
7. S.M. Seltzer and M.J. Berger, Int. J. of Applied Rad. **33**, 1189 (1982).
8. "Stopping Powers for Electrons and Positrons," ICRU Report No. 37 (1984).
9. <http://physics.nist.gov/PhysRefData/XrayMassCoef/tab1.html>.
10. J.D. Jackson, *Classical Electrodynamics*, 3rd edition, (John Wiley & Sons, New York, 1998).
11. R.M. Sternheimer, Phys. Rev. **88**, 851 (1952).
12. A. Crispin and G.N. Fowler, Rev. Mod. Phys. **42**, 290 (1970).
13. R.M. Sternheimer and R.F. Peierls, Phys. Rev. **B3**, 3681 (1971).
14. R.M. Sternheimer, S.M. Seltzer, and M.J. Berger, "The Density Effect for the Ionization Loss of Charged Particles in Various Substances," Atomic Data & Nucl. Data Tables **30**, 261 (1984). An error resulting from an incorrect chemical formula for lanthanum oxysulfide is corrected in a footnote in Ref. 22. Chemical composition for the tabulated materials is given in Ref. 7.

15. W.H. Barkas and M.J. Berger, *Tables of Energy Losses and Ranges of Heavy Charged Particles*, NASA-SP-3013 (1964).
16. M. Agnello *et al.*, Phys. Rev. Lett. **74**, 371 (1995).
17. H.H. Andersen and J.F. Ziegler, *Hydrogen: Stopping Powers and Ranges in All Elements*. Vol. 3 of *The Stopping and Ranges of Ions in Matter* (Pergamon Press 1977).
18. J. Lindhard, Kgl. Danske Videnskab. Selskab, Mat.-Fys. Medd. **28**, No. 8 (1954).
19. J. Lindhard, M. Scharff, and H.E. Schiøtt, Kgl. Danske Videnskab. Selskab, Mat.-Fys. Medd. **33**, No. 14 (1963).
20. J.F. Ziegler, J.F. Biersac, and U. Littmark, *The Stopping and Range of Ions in Solids*, Pergamon Press 1985.
21. L.D. Landau, J. Exp. Phys. (USSR) **8**, 201 (1944); See, for instance, K.A. Ispirian, A.T. Margarian, and A.M. Zverev, Nucl. Instrum. Methods **117**, 125 (1974).
22. S.M. Seltzer and M.J. Berger, Int. J. of Applied Rad. **35**, 665 (1984). This paper corrects and extends the results of Ref. 7.
23. W.R. Nelson, H. Hirayama, and D.W.O. Rogers, "The EGS4 Code System," SLAC-265, Stanford Linear Accelerator Center (Dec. 1985).
24. K. Hikasa *et al.*, *Review of Particle Properties*, Phys. Rev. **D46** (1992) S1.
25. For unit-charge projectiles, see E.A. Uehling, Ann. Rev. Nucl. Sci. **4**, 315 (1954). For highly charged projectiles, see J.A. Doggett and L.V. Spencer, Phys. Rev. **103**, 1597 (1956). A Lorentz transformation is needed to convert these center-of-mass data to knock-on energy spectra.
26. N.F. Mott and H.S.W. Massey, *The Theory of Atomic Collisions*, Oxford Press, London, 1965.
27. L.V. Spencer "Energy Dissipation by Fast Electrons," Nat'l Bureau of Standards Monograph No. 1 (1959).
28. "Average Energy Required to Produce an Ion Pair," ICRU Report No. 31 (1979).
29. N. Hadley *et al.*, "List of Poisoning Times for Materials," Lawrence Berkeley Lab Report TPC-LBL-79-8 (1981).
30. H.A. Bethe, Phys. Rev. **89**, 1256 (1953). A thorough review of multiple scattering is given by W.T. Scott, Rev. Mod. Phys. **35**, 231 (1963). However, the data of Shen *et al.*, (Phys. Rev. **D20**, 1584 (1979)) show that Bethe's simpler method of including atomic electron effects agrees better with experiment than does Scott's treatment. For a thorough discussion of simple formulae for single scatters and methods of compounding these into multiple-scattering formulae, see W.T. Scott, Rev. Mod. Phys. **35**, 231 (1963). For detailed summaries of formulae for computing single scatters, see J.W. Motz, H. Olsen, and H.W. Koch, Rev. Mod. Phys. **36**, 881 (1964).
31. V.L. Highland, Nucl. Instrum. Methods **129**, 497 (1975), and Nucl. Instrum. Methods **161**, 171 (1979).
32. G.R. Lynch and O.I. Dahl, Nucl. Instrum. Methods **B58**, 6 (1991).
33. M. Wong *et al.*, Med. Phys. **17**, 163 (1990).
34. Y.S. Tsai, Rev. Mod. Phys. **46**, 815 (1974).
35. H. Davies, H.A. Bethe, and L.C. Maximon, Phys. Rev. **93**, 788 (1954).
36. O.I. Dahl, private communication.
37. L.D. Landau and I.J. Pomeranchuk, Dokl. Akad. Nauk. SSSR **92**, 535 (1953); **92**, 735 (1953). These papers are available in English in L. Landau, *The Collected Papers of L.D. Landau*, Pergamon Press, 1965; A.B. Migdal, Phys. Rev. **103**, 1811 (1956).
38. S. Klein, Rev. Mod. Phys. **71**, 1501 (1999).
39. M. L. Ter-Mikaelian, SSSR **94**, 1033 (1954);
M. L. Ter-Mikaelian, *High Energy Electromagnetic Processes in Condensed Media* (John Wiley & Sons, New York, 1972).
40. P. Anthony *et al.*, Phys. Rev. Lett. **76**, 3550 (1996).
41. H. W. Koch and J. W. Motz, Rev. Mod. Phys. **31**, 920 (1959).
42. M.J. Berger and S.M. Seltzer, "Tables of Energy Losses and Ranges of Electrons and Positrons," National Aeronautics and Space Administration Report NASA-SP-3012 (Washington DC 1964).
43. J. W. Motz, H. A. Olsen, and H. W. Koch, Rev. Mod. Phys. **41**, 581 (1969).
44. P. Anthony *et al.*, Phys. Rev. Lett. **75**, 1949 (1995).
45. *Experimental Techniques in High Energy Physics*, ed. by T. Ferbel (Addison-Wesley, Menlo Park CA 1987).
46. U. Amaldi, Phys. Scripta **23**, 409 (1981).
47. E. Longo and I. Sestili, Nucl. Instrum. Methods **128**, 283 (1975).
48. G. Grindhammer *et al.*, in *Proceedings of the Workshop on Calorimetry for the Supercollider*, Tuscaloosa, AL, March 13-17, 1989, edited by R. Donaldson and M.G.D. Gilchriese (World Scientific, Teaneck, NJ, 1989), p. 151.
49. W.R. Nelson, T.M. Jenkins, R.C. McCall, and J.K. Cobb, Phys. Rev. **149**, 201 (1966).
50. G. Bathow *et al.*, Nucl. Phys. **B20**, 592 (1970).
51. H.A. Bethe and W. Heitler, Proc. Roy. Soc. **A146**, 83 (1934);
H.A. Bethe, Proc. Cambridge Phil. Soc. **30**, 542 (1934).
52. A.A. Petrukhin and V.V. Shestakov, Can. J. Phys. **46**, S377 (1968).
53. V.M. Galitskii and S.R. Kel'ner, Sov. Phys. JETP **25**, 948 (1967).
54. S.R. Kel'ner and Yu.D. Kotov, Sov. J. Nucl. Phys. **7**, 237 (1968).
55. R.P. Kokoulin and A.A. Petrukhin, in *Proceedings of the International Conference on Cosmic Rays*, Hobart, Australia, August 16-25, 1971, Vol. 4, p. 2436.
56. A.I. Nikishov, Sov. J. Nucl. Phys. **27**, 677 (1978).
57. Y.M. Andreev *et al.*, Phys. Atom. Nucl. **57**, 2066 (1994).
58. L.B. Bezrukov and E.V. Bugaev, Sov. J. Nucl. Phys. **33**, 635 (1981).
59. N.V. Mokhov and J.D. Cossairt, Nucl. Instrum. Methods **A244**, 349 (1986);
N.V. Mokhov, Soviet J. Particles and Nuclei **18**(5), 408-426 (1987);
N.V. Mokhov, "The MARS Code System User's Guide, Version 13(95)," Fermilab-FN-628, (April 1995).
60. P.H. Barrett, L.M. Bollinger, G. Cocconi, Y. Eisenberg, and K. Greisen, Rev. Mod. Phys. **24**, 133 (1952).
61. W. Lohmann, R. Kopp, and R. Voss, "Energy Loss of Muons in the Energy Range 1-10000 GeV," CERN Report 85-03 (1985).
62. A. Van Ginneken, Nucl. Instrum. Methods **A251**, 21 (1986).
63. U. Becker *et al.*, Nucl. Instrum. Methods **A253**, 15 (1986).
64. J.J. Eastman and S.C. Loken, in *Proceedings of the Workshop on Experiments, Detectors, and Experimental Areas for the Supercollider*, Berkeley, CA, July 7-17, 1987, edited by R. Donaldson and M.G.D. Gilchriese (World Scientific, Singapore, 1988), p. 542.
65. *Methods of Experimental Physics*, L.C.L. Yuan and C.-S. Wu, editors, Academic Press, 1961, Vol. 5A, p. 163.
66. W.W.M. Allison and P.R.S. Wright, "The Physics of Charged Particle Identification: dE/dx , Čerenkov Radiation, and Transition Radiation," p. 371 in *Experimental Techniques in High Energy Physics*, T. Ferbel, editor, (Addison-Wesley 1987).
67. E.R. Hayes, R.A. Schluter, and A. Tamosaitis, "Index and Dispersion of Some Čerenkov Counter Gases," ANL-6916 (1964).
68. T. Ypsilantis, "Particle Identification at Hadron Colliders", CERN-EP/89-150 (1989), or ECFA 89-124, **2** 661 (1989).

24. PARTICLE DETECTORS

Revised 1999 (see the various sections for authors).

In this section we give various parameters for common detector components. The quoted numbers are usually based on typical devices, and should be regarded only as rough approximations for new designs. A more detailed discussion of detectors can be found in Ref. 1. In Table 24.1 are given typical spatial and temporal resolutions of common detectors.

Table 24.1: Typical detector characteristics.

Detector Type	Accuracy (rms)	Resolution Time	Dead Time
Bubble chamber	10 to 150 μm	1 ms	50 ms ^a
Streamer chamber	300 μm	2 μs	100 ns
Proportional chamber	$\geq 300 \mu\text{m}^{b,c}$	50 ns	200 ns
Drift chamber	50 to 300 μm	2 ns ^d	100 ns
Scintillator	—	150 ps	10 ns
Emulsion	1 μm	—	—
Silicon strip	pitch ^e	<i>f</i>	<i>f</i>
	3 to 7		
Silicon pixel	2 μm^g	<i>f</i>	<i>f</i>

^a Multiple pulsing time.

^b 300 μm is for 1 mm pitch.

^c Delay line cathode readout can give $\pm 150 \mu\text{m}$ parallel to anode wire.

^d For two chambers.

^e The highest resolution (“7”) is obtained for small-pitch detectors ($\lesssim 25 \mu\text{m}$) with pulse-height-weighted center finding.

^f Limited at present by properties of the readout electronics. (Time resolution of $\leq 25 \text{ ns}$ is planned for the ATLAS SCT.)

^g Analog readout of 34 μm pitch, monolithic pixel detectors.

24.1. Organic scintillators

Written October 1995 by K.F. Johnson (FSU).

Organic scintillators are broadly classed into three types, crystalline, liquid, and plastic, all of which utilize the ionization produced by charged particles (see the section on “Passage of particles through matter” (Sec. 23.2) of this *Review*) to generate optical photons, usually in the blue to green wavelength regions [2]. Plastic scintillators are by far the most widely used and we address them primarily; however, most of the discussion will also have validity for liquid scintillators with obvious caveats. Crystal organic scintillators are practically unused in high-energy physics.

Densities range from 1.03 to 1.20 g cm^{-3} . Typical photon yields are about 1 photon per 100 eV of energy deposit [3]. A one-cm-thick scintillator traversed by a minimum-ionizing particle will therefore yield $\approx 2 \times 10^4$ photons. The resulting photoelectron signal will depend on the collection and transport efficiency of the optical package and the quantum efficiency of the photodetector.

Plastic scintillators do not respond linearly to the ionization density. Very dense ionization columns emit less light than expected on the basis of dE/dx for minimum-ionizing particles. A widely used semi-empirical model by Birks’ posits that recombination and quenching effects between the excited molecules reduce the light yield [4]. These effects are more pronounced the greater the density of the excited molecules. Birks’ formula is

$$\frac{d\mathcal{L}}{dx} = \mathcal{L}_0 \frac{dE/dx}{1 + k_B dE/dx}, \quad (24.1)$$

where \mathcal{L} is the luminescence, \mathcal{L}_0 is the luminescence at low specific ionization density, and k_B is Birks’ constant, which must be determined for each scintillator by measurement.

Decay times are in the ns range; rise times are much faster. The combination of high light yield and fast response time allows the possibility of sub-ns timing resolution [5]. The fraction of light emitted during the decay “tail” can depend on the exciting particle. This allows pulse shape discrimination as a technique to carry out particle identification. Because of the hydrogen content (carbon to hydrogen ratio ≈ 1) plastic scintillator is sensitive to proton recoils from neutrons. Ease of fabrication into desired shapes and low cost has made plastic scintillators a common detector component. Recently, plastic scintillators in the form of scintillating fibers have found widespread use in tracking and calorimetry [6].

24.1.1. Scintillation mechanism :

Scintillation: A charged particle traversing matter leaves behind it a wake of excited molecules. Certain types of molecules, however, will release a small fraction ($\approx 3\%$) of this energy as optical photons. This process, scintillation, is especially marked in those organic substances which contain aromatic rings, such as polystyrene, polyvinyltoluene, and naphthalene. Liquids which scintillate include toluene and xylene.

Fluorescence: In fluorescence, the initial excitation takes place via the absorption of a photon, and de-excitation by emission of a longer wavelength photon. Fluors are used as “wavelength shifters” to shift scintillation light to a more convenient wavelength. Occurring in complex molecules, the absorption and emission are spread out over a wide band of photon energies, and have some overlap, that is, there is some fraction of the emitted light which can be re-absorbed [7]. This “self-absorption” is undesirable for detector applications because it causes a shortened attenuation length. The wavelength difference between the major absorption and emission peaks is called the Stokes’ shift. It is usually the case that the greater the Stokes’ shift, the smaller the self absorption—thus, a large Stokes’ shift is a desirable property for a fluor.

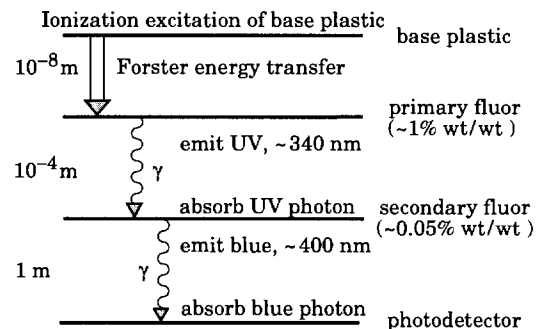


Figure 24.1: Cartoon of scintillation “ladder” depicting the operating mechanism of plastic scintillator. Approximate fluor concentrations and energy transfer distances for the separate sub-processes are shown.

Scintillators: The plastic scintillators used in high-energy physics are binary or ternary solutions of selected fluors in a plastic base containing aromatic rings. (See the appendix in Ref. 8 for a comprehensive list of plastic scintillator components.) Virtually all plastic scintillators contain as a base either polyvinyltoluene, polystyrene, or acrylic, whereby polyvinyltoluene-based scintillator can be up to 50% brighter than the others. Acrylic is non-aromatic and has therefore a very low scintillation efficiency. It becomes an acceptable scintillator when naphthalene, a highly aromatic compound, is dissolved into the acrylic at 5% to 20% weight fraction. Thus, in “acrylic” scintillator the active component is naphthalene. The fluors must satisfy additional conditions besides being fluorescent. They must be sufficiently stable, soluble, chemically inert, fast, radiation tolerant, and efficient.

The plastic base is the ionization-sensitive (*i.e.*, the scintillator) portion of the plastic scintillator (see Fig. 24.1). In the absence of fluors the base would emit UV photons with short attenuation length (several mm). Longer attenuation lengths are obtained by dissolving a “primary” fluor in high concentration (1% by weight) into the

25. RADIOACTIVITY AND RADIATION PROTECTION

Revised March 1998 by R.J. Donahue (LBNL) and A. Fassò (SLAC).

25.1. Definitions

The International Commission on Radiation Units and Measurements (ICRU) recommends the use of SI units. Therefore we list SI units first, followed by cgs (or other common) units in parentheses, where they differ.

- **Unit of activity** = becquerel (curie):
1 Bq = 1 disintegration s^{-1} [= 1/(3.7 × 10¹⁰) Ci]
 - **Unit of absorbed dose** = gray (rad):
1 Gy = 1 joule kg^{-1} (= 10⁴ erg g^{-1} = 100 rad)
= 6.24 × 10¹² MeV kg^{-1} deposited energy
 - **Unit of exposure**, the quantity of x - or γ - radiation at a point in space integrated over time, in terms of charge of either sign produced by showering electrons in a small volume of air about the point:
= 1 coul kg^{-1} of air (roentgen; 1 R = 2.58 × 10⁻⁴ coul kg^{-1})
= 1 esu cm^{-3} (= 87.8 erg released energy per g of air)
- Implicit in the definition is the assumption that the small test volume is embedded in a sufficiently large uniformly irradiated volume that the number of secondary electrons entering the volume equals the number leaving. This unit is somewhat historical, but appears on many measuring instruments.
- **Unit of equivalent dose** (for biological damage) = sievert [= 100 rem (roentgen equivalent for man)]: Equivalent dose in Sv = absorbed dose in grays × w_R , where w_R (radiation weighting factor, formerly the quality factor Q) expresses long-term risk (primarily cancer and leukemia) from low-level chronic exposure. It depends upon the type of radiation and other factors, as follows [2]:

Table 25.1: Radiation weighting factors.

Radiation	w_R
X- and γ -rays, all energies	1
Electrons and muons, all energies	1
Neutrons < 10 keV	5
10–100 keV	10
> 100 keV to 2 MeV	20
2–20 MeV	10
> 20 MeV	5
Protons (other than recoils) > 2 MeV	5
Alphas, fission fragments, & heavy nuclei	20

25.2. Radiation levels [3]

- **Natural annual background**, all sources: Most world areas, whole-body equivalent dose rate \approx (0.4–4) mSv (40–400 millirems). Can range up to 50 mSv (5 rems) in certain areas. U.S. average \approx 3.6 mSv, including \approx 2 mSv (\approx 200 mrem) from inhaled natural radioactivity, mostly radon and radon daughters (0.1–0.2 mSv in open areas. Average is for a typical house and varies by more than an order of magnitude. It can be more than two orders of magnitude higher in poorly ventilated mines).
- **Cosmic ray background** in counters (Earth's surface): \sim 1 $min^{-1} cm^{-2} sr^{-1}$. For more accurate estimates and details, see the Cosmic Rays section (Sec. 20 of this Review).
- **Fluxes** (per cm^2) to deposit one Gy, assuming uniform irradiation:
 \approx (charged particles) $6.24 \times 10^9 / (dE/dx)$, where dE/dx (MeV $g^{-1} cm^2$), the energy loss per unit length, may be obtained from the Mean Range and Energy Loss figures.
 $\approx 3.5 \times 10^9 cm^{-2}$ minimum-ionizing singly-charged particles in carbon.

\approx (photons) $6.24 \times 10^9 / [Ef/\lambda]$, for photons of energy E (MeV), attenuation length λ ($g cm^{-2}$) (see Photon Attenuation Length figure), and fraction $f \lesssim 1$ expressing the fraction of the photon's energy deposited in a small volume of thickness $\ll \lambda$ but large enough to contain the secondary electrons.

$\approx 2 \times 10^{11}$ photons cm^{-2} for 1 MeV photons on carbon ($f \approx 1/2$).

(Quoted fluxes are good to about a factor of 2 for all materials.)

- **Recommended limits to exposure of radiation workers (whole-body dose):***

CERN: 15 mSv yr^{-1}

U.K.: 15 mSv yr^{-1}

U.S.: 50 mSv yr^{-1} (5 rem yr^{-1})†

- **Lethal dose:** Whole-body dose from penetrating ionizing radiation resulting in 50% mortality in 30 days (assuming no medical treatment) 2.5–3.0 Gy (250–300 rads), as measured internally on body longitudinal center line. Surface dose varies due to variable body attenuation and may be a strong function of energy.

25.3. Prompt neutrons at accelerators

25.3.1. Electron beams: At electron accelerators neutrons are generated via photonuclear reactions from bremsstrahlung photons. Neutron yields from semi-infinite targets per unit electron beam power are plotted in Fig. 25.1 as a function of electron beam energy [4]. In the photon energy range 10–30 MeV neutron production results from the giant photonuclear resonance mechanism. Neutrons are produced roughly isotropically (within a factor of 2) and with a Maxwellian energy distribution described as:

$$\frac{dN}{dE_n} = \frac{E_n}{T^2} e^{-E_n/T}, \quad (25.1)$$

where T is the nuclear temperature characteristic of the target nucleus, generally in the range of $T = 0.5$ – 1.0 MeV. For higher energy photons the quasi-deuteron and photopion production mechanisms become important.

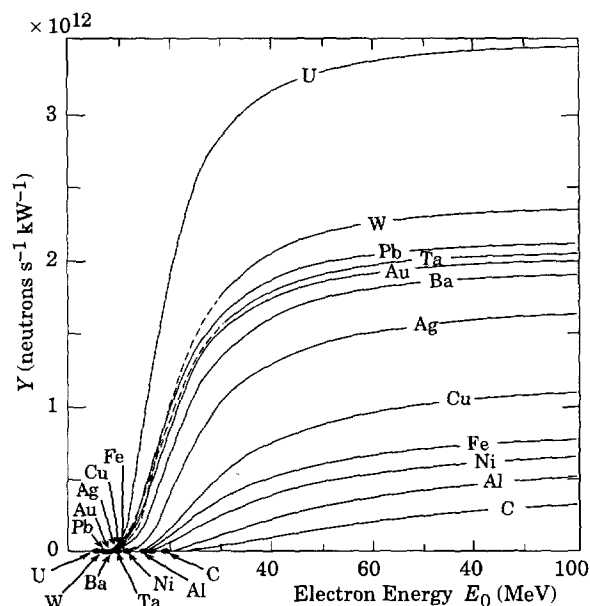


Figure 25.1: Neutron yields from semi-infinite targets, per kW of electron beam power, as a function of electron beam energy, disregarding target self-shielding.

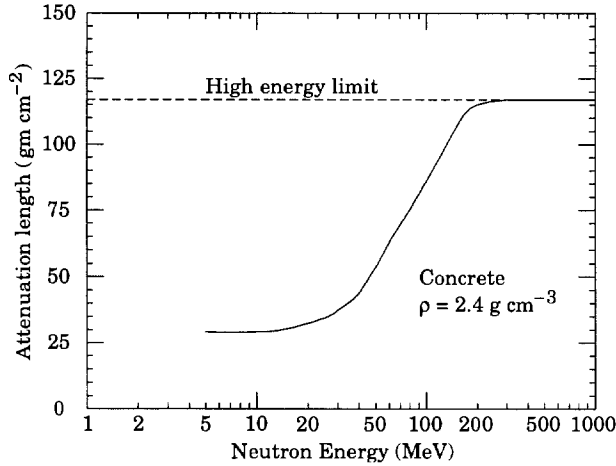


Figure 25.3: The variation of the attenuation length for monoenergetic neutrons in concrete as a function of neutron energy [5].

25.3.2. Proton beams: At proton accelerators neutron yields emitted per incident proton by different target materials are roughly independent [5] of proton energy between 20 MeV and 1 GeV and are given by the ratio C:Al:Cu:Fe:Sn:Ta:Pb = 0.3 : 0.6 : 1.0 : 1.5 : 1.7. Above 1 GeV neutron yield [6] is proportional to E^m , where $0.80 \leq m \leq 0.85$.

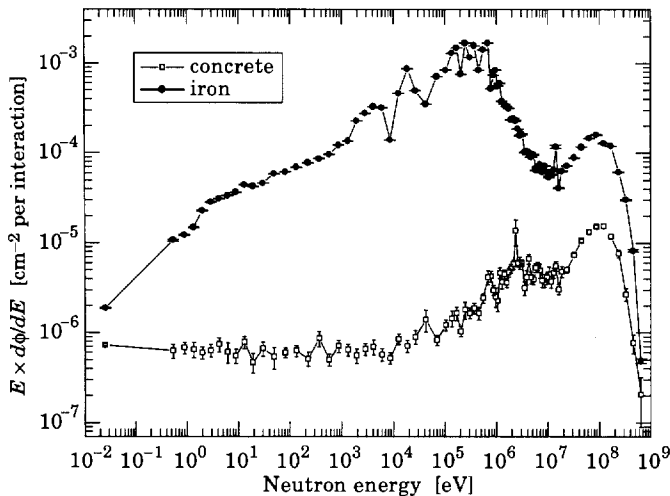


Figure 25.2: Calculated neutron spectrum from 205 GeV/c hadrons (2/3 protons and 1/3 π^+) on a thick copper target. Spectra are evaluated at 90° to beam and through 80 cm of normal density concrete or 40 cm of iron.

A typical neutron spectrum [7] outside a proton accelerator concrete shield is shown in Fig. 25.2. The shape of these spectra are generally characterized as having a thermal-energy peak which is very dependent on geometry and the presence of hydrogenic material, a low-energy evaporation peak around 2 MeV, and a high-energy spallation shoulder.

Letaw's [8] formula for the energy dependence of the inelastic proton cross-section (asymptotic values given in Table 6.1) for $E < 2$ GeV is:

$$\sigma(E) = \sigma_{\text{asympt}} \left[1 - 0.62e^{-E/200} \sin(10.9E^{-0.28}) \right], \quad (25.2)$$

and for $E > 2$ GeV:

$$\sigma_{\text{asympt}} = 45A^{0.7} [1 + 0.016 \sin(5.3 - 2.63 \ln A)], \quad (25.3)$$

where σ is in mb, E is the proton energy in MeV and A is the mass number.

The neutron-attenuation length, λ , is shown in Fig. 25.3 for monoenergetic broad-beam conditions. These values give a satisfactory representation at depths greater than 1 m in concrete.

25.4. Dose conversion factors

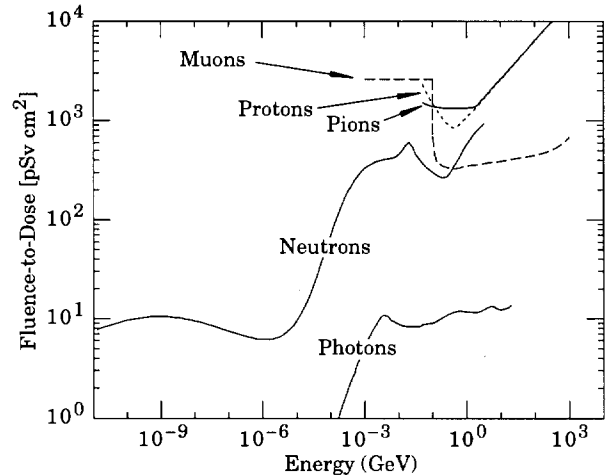


Figure 25.4: Fluence to dose equivalent conversion factors for various particles.

Fluence to dose equivalent factors are given in Fig. 25.4 for photons [9], neutrons [10], muons [11], protons and pions [12]. These factors can be used for converting particle fluence to dose for personnel protection purposes.

25.5. Accelerator-induced activity

The dose rate at 1 m due to spallation-induced activity by high energy hadrons in a 1 g medium atomic weight target can be estimated [13] from the following expression:

$$D = D_0 \Phi \ln[(T + t)/t], \quad (25.4)$$

where T is the irradiation time, t is the decay time since irradiation, Φ is the flux of irradiating hadrons ($\text{hadrons cm}^{-2} \text{ s}^{-1}$) and D_0 has a value of 5.2×10^{-17} [(Sv hr $^{-1}$)/(hadron $\text{cm}^{-2} \text{ s}^{-1}$)]. This relation is essentially independent of hadron energy above 200 MeV.

Dose due to accelerator-produced induced activity can also be estimated with the use of " ω factors" [5]. These factors give the dose rate per unit star density (inelastic reaction for $E > 50$ MeV) after a 30-day irradiation and 1-day decay. The ω factor for steel or iron is $\approx 3 \times 10^{-12}$ (Sv cm^3/star). This does not include possible contributions from thermal-neutron activation. Induced activity in concrete can vary widely depending on concrete composition, particularly with the concentration of trace quantities such as sodium. Additional information can be found in Barbier [14].

25.6. Photon sources

The dose rate from a gamma point source of C Curies emitting one photon of energy $0.07 < E < 4$ MeV per disintegration at a distance of 30 cm is $6CE$ (rem/hr), or $60CE$ (mSv/hr), $\pm 20\%$.

The dose rate from a semi-infinite uniform photon source of specific activity C ($\mu\text{Ci/g}$) and gamma energy E (MeV) is $1.07CE$ (rem/hr), or $10.7CE$ (mSv/hr).

25.7. Radiation levels in detectors at hadron colliders

An SSC Central Design Group task force studied the radiation levels to be expected in SSC detectors [15]. The study focused on scaling with energy, distance, and angle. As such, it is applicable to future detectors such as those at the LHC. Although superior detector-specific calculations have since been made, the scaling is in most cases not evident, and so the SSC results have some relevance. The SSC/CDG model assumed

- The machine luminosity at $\sqrt{s} = 40$ TeV is $\mathcal{L} = 10^{33} \text{ cm}^{-2}\text{s}^{-1}$, and the pp inelastic cross section is $\sigma_{\text{inel}} = 100$ mb. This luminosity is effectively achieved for 10^7 s yr^{-1} . The interaction rate is thus 10^8 s^{-1} , or 10^{15} yr^{-1} ;
- All radiation comes from pp collisions at the interaction point;
- The charged particle distribution is (a) flat in pseudorapidity for $|\eta| < 6$ and (b) has a momentum distribution whose perpendicular component is independent of rapidity, which is taken as independent of pseudorapidity:

$$\frac{d^2 N_{\text{ch}}}{d\eta dp_{\perp}} = H f(p_{\perp}) \quad (25.5)$$

(where $p_{\perp} = p \sin \theta$). Integrals involving $f(p_{\perp})$ are simplified by replacing $f(p_{\perp})$ by $\delta(p_{\perp} - \langle p_{\perp} \rangle)$; in the worst case this approximation introduces an error of less than 10%;

- Gamma rays from π^0 decay are as abundant as charged particles. They have approximately the same η distribution, but half the mean momentum;
- At the SSC ($\sqrt{s} = 40$ TeV), $H \approx 7.5$ and $\langle p_{\perp} \rangle \approx 0.6$ GeV/c; assumed values at other energies are given in Table 25.3. Together with the model discussed above, these values are thought to describe particle production to within a factor of two or better.

It then follows that the flux of charged particles from the interaction point passing through a normal area da located a distance r_{\perp} from the beam line is given by

$$\frac{dN_{\text{ch}}}{da} = \frac{1.2 \times 10^8 \text{ s}^{-1}}{r_{\perp}^2} \quad (25.6)$$

In a typical organic material, a relativistic charged particle flux of $3 \times 10^9 \text{ cm}^{-2}$ produces an ionizing radiation dose of 1 Gy, where $1 \text{ Gy} \equiv 1 \text{ joule kg}^{-1}$ ($= 100$ rads). The above result may thus be rewritten as dose rate,

$$\dot{D} = \frac{0.4 \text{ MGy yr}^{-1}}{(\tau_{\perp}/1 \text{ cm})^2} \quad (25.7)$$

If a magnetic field is present, “loopers” may increase this dose rate by a factor of two or more.

In a medium in which cascades can develop, the ionizing dose or neutron fluence is proportional to dN_{ch}/da multiplied by $\langle E \rangle^{\alpha}$, where $\langle E \rangle$ is the mean energy of the particles going through da and the power α is slightly less than unity. Since $E \approx p = p_{\perp}/\sin \theta$ and $r_{\perp} = r \sin \theta$, the above expression for dN_{ch}/da becomes

$$\text{Dose or fluence}^{\dagger} = \frac{A}{r^2} \cosh^{2+\alpha} \eta = \frac{A}{r^2 \sin^{2+\alpha} \theta} \quad (25.8)$$

The constant A contains the total number of interactions $\sigma_{\text{inel}} \int \mathcal{L} dt$, so the ionizing dose or neutron fluence at another accelerator scales as $\sigma_{\text{inel}} \int \mathcal{L} dt H \langle p_{\perp} \rangle^{\alpha}$.

The dose or fluence in a calorimeter scales as $1/r^2$, as does the neutron fluence inside a central cavity with characteristic dimension r .

Under all conditions so far studied, the neutron spectrum shows a broad log-normal distribution peaking at just under 1 MeV. In a 2 m radius central cavity of a detector with coverage down to $|\eta| = 3$, the average neutron flux is $2 \times 10^{12} \text{ cm}^{-2}\text{yr}^{-1}$, including secondary scattering contributions.

Values of A and α are given in Table 25.2 for several relevant situations. Examples of scaling to other accelerators are given in Table 25.3. It should be noted that the assumption that all radiation comes from the interaction point does not apply to the present generation of accelerators.

The constant A includes factors evaluated with cascade simulation programs as well as constants describing particle production at the interaction point. It is felt that each could introduce an error as large as a factor of two in the results.

Table 25.2: Coefficients $A/(100 \text{ cm})^2$ and α for the evaluation of calorimeter radiation levels at cascade maxima under SSC nominal operating conditions. At a distance r and angle θ from the interaction point the annual fluence or dose is $A/(r^2 \sin^{2+\alpha} \theta)$.

Quantity	$A/(100 \text{ cm})^2$	Units	$\langle p_{\perp} \rangle$	α
Neutron flux	1.5×10^{12}	$\text{cm}^{-2}\text{yr}^{-1}$	0.6 GeV/c	0.67
Dose rate from photons	124	Gy yr^{-1}	0.3 GeV/c	0.93
Dose rate from hadrons	29	Gy yr^{-1}	0.6 GeV/c	0.89

Table 25.3: A rough comparison of beam-collision induced radiation levels at the Tevatron, high-luminosity LHC, SSC, and a possible 100 TeV machine [16].

	Tevatron	LHC	SSC	100 TeV
\sqrt{s} (TeV)	1.8	15.4	40	100
\mathcal{L}_{nom} ($\text{cm}^{-2}\text{s}^{-1}$)	2×10^{30}	1.7×10^{34} ^a	1×10^{33}	1×10^{34}
σ_{inel}	56 mb	84 mb	100 mb	134 mb
H	3.9	6.2	7.5	10.6
$\langle p_{\perp} \rangle$ (GeV/c)	0.46	0.55	0.60	0.70
Relative dose rate ^b	5×10^{-4}	11	1	20

^a High-luminosity option.

^b Proportional to $\mathcal{L}_{\text{nom}} \sigma_{\text{inel}} H \langle p_{\perp} \rangle^{0.7}$

Footnotes:

- The ICRP recommendation [2] is 20 mSv yr^{-1} averaged over 5 years, with the dose in any one year ≤ 50 mSv.

[†] Many laboratories in the U.S. and elsewhere set lower limits.

[‡] Dose is the time integral of dose rate, and fluence is the time integral of flux.

References:

1. C. Birattari *et al.*, “Measurements and simulations in high energy neutron fields” Proceedings of the Second Shielding Aspects of Accelerators, Targets and Irradiation Facilities, in press (1995).
2. ICRP Publication 60, *1990 Recommendation of the International Commission on Radiological Protection* Pergamon Press (1991).
3. See E. Pochin, *Nuclear Radiation: Risks and Benefits* (Clarendon Press, Oxford, 1983).
4. W.P. Swanson, *Radiological Safety Aspects of the operation of Electron Linear Accelerators*, IAEA Technical Reports Series No. 188 (1979).
5. R.H. Thomas and G.R. Stevenson, *Radiological Safety Aspects of the Operation of Proton Accelerators*, IAEA Technical Report Series No. 283 (1988).
6. T.A. Gabriel *et al.*, “Energy Dependence of Hadronic Activity,” Nucl. Instrum. Methods **A338**, 336 (1994).
7. A.V. Sannikov, “BON94 Code for Neutron Spectra Unfolding from Bonner Spectrometer Data,” CERN/TIS-RP/IR/94-16 (1994).

8. Letaw, Silberberg, and Tsao, "Proton-nucleus Total Inelastic Cross Sections: An Empirical Formula for $E > 10$ MeV," *Astrophysical Journal Supplement Series*, **51**, 271 (1983);
For improvements to this formula see Shen Qing-bang, "Systematics of intermediate energy proton nonelastic and neutron total cross section," International Nuclear Data Committee INDC(CPR)-020 (July 1991).
9. A. Ferrari and M. Pelliccioni, "On the Conversion Coefficients from Fluence to Ambient Dose Equivalent," *Rad. Pro. Dosimetry* **51**, 251 (1994).
10. A.V. Sannikov and E.N. Savitskaya, "Ambient Dose and Ambient Dose Equivalent Conversion Factors for High-Energy neutrons," CERN/TIS-RP/93-14 (1993).
11. "Data for Use in Protection Against External Radiation," ICRP Publication 51 (1987).
12. G.R. Stevenson, "Dose Equivalent Per Star in Hadron Cascade Calculations," CERN TIS-RP/173 (1986).
13. A.H. Sullivan *A Guide To Radiation and Radioactivity Levels Near High Energy Particle Accelerators*, Nuclear Technology Publishing, Ashford, Kent, England (1992).
14. M. Barbier, *Induced Activity*, North-Holland, Amsterdam (1969).
15. Report of the Task Force on Radiation Levels in the SSC Interaction Regions, SSC Central Design Group Report SSC-SR-1033 (June 1988). An abridged version is D.E. Groom, *Nucl. Instrum. Methods* **A279**, 1 (1989).
16. D.E. Groom, pp. 311-326 in *Supercolliders and Superdetectors: Proc. 19th and 25th Workshops of the INFN Eloisatron Project*, Erice, Sicily, Italy, 17-22 Nov. 1992, ed. W.A. Barletta and H. Leutz (World Scientific, 1992); also appeared as CERN/LAA/SF/93-11.

26. COMMONLY USED RADIOACTIVE SOURCES

Table 26.1. Revised November 1993 by E. Browne (LBNL).

Nuclide	Half-life	Type of decay	Particle		Photon	
			Energy Emission (MeV)	prob.	Energy Emission (MeV)	prob.
$^{22}_{11}\text{Na}$	2.603 y	β^+ , EC	0.545	90%	0.511 Annih. 1.275 100%	
$^{54}_{25}\text{Mn}$	0.855 y	EC			0.835 100% Cr K x rays 26%	
$^{55}_{26}\text{Fe}$	2.73 y	EC			Mn K x rays: 0.00590 24.4% 0.00649 2.86%	
$^{57}_{27}\text{Co}$	0.744 y	EC			0.014 9% 0.122 86% 0.136 11% Fe K x rays 58%	
$^{60}_{27}\text{Co}$	5.271 y	β^-	0.316	100%	1.173 100% 1.333 100%	
$^{68}_{32}\text{Ge}$	0.742 y	EC			Ga K x rays 44%	
$\rightarrow ^{68}_{31}\text{Ga}$		β^+ , EC	1.899	90%	0.511 Annih. 1.077 3%	
$^{90}_{38}\text{Sr}$	28.5 y	β^-	0.546	100%		
$\rightarrow ^{90}_{39}\text{Y}$		β^-	2.283	100%		
$^{106}_{44}\text{Ru}$	1.020 y	β^-	0.039	100%		
$\rightarrow ^{106}_{45}\text{Rh}$		β^-	3.541	79%	0.512 21% 0.622 10%	
$^{109}_{48}\text{Cd}$	1.267 y	EC	0.063 e^- 0.084 e^- 0.087 e^-	41% 45% 9%	0.088 3.6% Ag K x rays 100%	
$^{113}_{50}\text{Sn}$	0.315 y	EC	0.364 e^- 0.388 e^-	29% 6%	0.392 65% In K x rays 97%	
$^{137}_{55}\text{Cs}$	30.2 y	β^-	0.514 e^- 1.176 e^-	94% 6%	0.662 85%	
$^{133}_{56}\text{Ba}$	10.54 y	EC	0.045 e^- 0.075 e^-	50% 6%	0.081 34% 0.356 62% Cs K x rays 121%	
$^{207}_{83}\text{Bi}$	31.8 y	EC	0.481 e^- 0.975 e^- 1.047 e^-	2% 7% 2%	0.569 98% 1.063 75% 1.770 7% Pb K x rays 78%	
$^{228}_{90}\text{Th}$	1.912 y	6α : $3\beta^-$:	5.341 to 8.785 0.334 to 2.246		0.239 44% 0.583 31% 2.614 36%	
$(\rightarrow ^{224}_{88}\text{Ra} \rightarrow ^{220}_{86}\text{Rn} \rightarrow ^{216}_{84}\text{Po} \rightarrow ^{212}_{82}\text{Pb} \rightarrow ^{212}_{83}\text{Bi} \rightarrow ^{212}_{84}\text{Po})$						
$^{241}_{95}\text{Am}$	432.7 y	α	5.443 5.486	13% 85%	0.060 36% Np L x rays 38%	
$^{241}_{95}\text{Am/Be}$	432.2 y	6×10^{-5} neutrons (4–8 MeV) and 4×10^{-5} γ 's (4.43 MeV) per Am decay				
$^{244}_{96}\text{Cm}$	18.11 y	α	5.763 5.805	24% 76%	Pu L x rays \sim 9%	
$^{252}_{98}\text{Cf}$	2.645 y (α 97%)	α	6.076 6.118	15% 82%		
		Fission (3.1%)				
		≈ 20 γ 's/fission; 80% < 1 MeV				
		≈ 4 neutrons/fission; $\langle E_n \rangle = 2.14$ MeV				

"Emission probability" is the probability per decay of a given emission; because of cascades these may total more than 100%. Only principal emissions are listed. EC means electron capture, and e^- means monoenergetic internal conversion (Auger) electron. The intensity of 0.511 MeV e^+e^- annihilation photons depends upon the number of stopped positrons. Endpoint β^\pm energies are listed. In some cases when energies are closely spaced, the γ -ray values are approximate weighted averages. Radiation from short-lived daughter isotopes is included where relevant.

Half-lives, energies, and intensities are from E. Browne and R.B. Firestone, *Table of Radioactive Isotopes* (John Wiley & Sons, New York, 1986), recent *Nuclear Data Sheets*, and *X-ray and Gamma-ray Standards for Detector Calibration*, IAEA-TECDOC-619 (1991).

Neutron data are from *Neutron Sources for Basic Physics and Applications* (Pergamon Press, 1983).

27. PROBABILITY

Revised May 1996 by D.E. Groom (LBNL) and F. James (CERN).
 Updated September 1999 by R. Cousins (UCLA).

27.1. General [1-6]

Let x be a possible outcome of an observation. The probability of x is the relative frequency with which that outcome occurs out of a (possibly hypothetical) large set of similar observations. If x can take any value from a *continuous* range, we write $f(x; \theta) dx$ as the probability of observing x between x and $x + dx$. The function $f(x; \theta)$ is the *probability density function* (p.d.f.) for the *random variable* x , which may depend upon one or more parameters θ . If x can take on only *discrete* values (e.g., the non-negative integers), then $f(x; \theta)$ is itself a probability, but we shall still call it a p.d.f. The p.d.f. is always normalized to unit area (unit sum, if discrete). Both x and θ may have multiple components and are then often written as column vectors. If θ is unknown and we wish to estimate its value from a given set of data measuring x , we may use statistics (see Sec. 28).

The *cumulative distribution function* $F(a)$ is the probability that $x \leq a$:

$$F(a) = \int_{-\infty}^a f(x) dx . \tag{27.1}$$

Here and below, if x is discrete-valued, the integral is replaced by a sum. The endpoint a is expressly included in the integral or sum. Then $0 \leq F(x) \leq 1$, $F(x)$ is nondecreasing, and $\text{Prob}(a < x \leq b) = F(b) - F(a)$. If x is discrete, $F(x)$ is flat except at allowed values of x , where it has discontinuous jumps equal to $f(x)$.

Any function of random variables is itself a random variable, with (in general) a different p.d.f. The *expectation value* of any function $u(x)$ is

$$E[u(x)] = \int_{-\infty}^{\infty} u(x) f(x) dx , \tag{27.2}$$

assuming the integral is finite. For $u(x)$ and $v(x)$ any two functions of x , $E(u + v) = E(u) + E(v)$. For c and k constants, $E(cu + k) = cE(u) + k$.

The n th moment of a distribution is

$$\alpha_n \equiv E(x^n) = \int_{-\infty}^{\infty} x^n f(x) dx , \tag{27.3a}$$

and the n th moment about the mean of x , α_1 , is

$$m_n \equiv E[(x - \alpha_1)^n] = \int_{-\infty}^{\infty} (x - \alpha_1)^n f(x) dx . \tag{27.3b}$$

The most commonly used moments are the mean μ and variance σ^2 :

$$\mu \equiv \alpha_1 \tag{27.4a}$$

$$\sigma^2 \equiv \text{Var}(x) \equiv m_2 = \alpha_2 - \mu^2 . \tag{27.4b}$$

The mean is the location of the “center of mass” of the probability density function, and the variance is a measure of the square of its width. Note that $\text{Var}(cx + k) = c^2 \text{Var}(x)$.

Any odd moment about the mean is a measure of the skewness of the p.d.f. The simplest of these is the dimensionless coefficient of skewness $\gamma_1 \equiv m_3/\sigma^3$.

Besides the mean, another useful indicator of the “middle” of the probability distribution is the *median* x_{med} , defined by $F(x_{\text{med}}) = 1/2$; i.e., half the probability lies above and half lies below x_{med} . For a given *sample* of events, x_{med} is the value such that half the events have larger x and half have smaller x (not counting any that have the same x as the median). If the sample median lies between two observed x values, it is set by convention halfway between them. If the p.d.f. for x has the form $f(x - \mu)$ and μ is both mean and median, then for a large number of events N , the variance of the median approaches $1/[4Nf^2(0)]$, provided $f(0) > 0$.

Let x and y be two random variables with a joint p.d.f. $f(x, y)$. The *marginal* p.d.f. of x (the distribution of x with y unobserved) is

$$f_1(x) = \int_{-\infty}^{\infty} f(x, y) dy , \tag{27.5}$$

and similarly for the marginal p.d.f. $f_2(y)$. We define $f_3(y|x)$, the *conditional* p.d.f. of y given fixed x , by

$$f_3(y|x) f_1(x) = f(x, y) . \tag{27.6a}$$

Similarly, $f_4(x|y)$, the conditional p.d.f. of x given fixed y , is

$$f_4(x|y) f_2(y) = f(x, y) . \tag{27.6b}$$

From these definitions we immediately obtain Bayes' theorem [2]:

$$f_4(x|y) = \frac{f_3(y|x) f_1(x)}{f_2(y)} = \frac{f_3(y|x) f_1(x)}{\int f_3(y|x) f_1(x) dx} . \tag{27.7}$$

The mean of x is

$$\mu_x = \int_{-\infty}^{\infty} \int_{-\infty}^{\infty} x f(x, y) dx dy = \int_{-\infty}^{\infty} x f_1(x) dx , \tag{27.8}$$

and similarly for y . The *correlation* between x and y is

$$\rho_{xy} = E[(x - \mu_x)(y - \mu_y)] / \sigma_x \sigma_y = \text{Cov}(x, y) / \sigma_x \sigma_y , \tag{27.9}$$

where σ_x and σ_y are defined in analogy with Eq. (27.4b). It can be shown that $-1 \leq \rho_{xy} \leq 1$. Here “Cov” is the covariance of x and y , a 2-dimensional generalization of the variance.

Two random variables are *independent* if and only if

$$f(x, y) = f_1(x) f_2(y) . \tag{27.10}$$

If x and y are independent then $\rho_{xy} = 0$; the converse is not necessarily true except for Gaussian-distributed x and y . If x and y are independent, $E[u(x) v(y)] = E[u(x)] E[v(y)]$, and $\text{Var}(x + y) = \text{Var}(x) + \text{Var}(y)$; otherwise, $\text{Var}(x + y) = \text{Var}(x) + \text{Var}(y) + 2\text{Cov}(x, y)$, and $E(u v)$ does not factor.

In a *change of continuous random variables* from $\mathbf{x} \equiv (x_1, \dots, x_n)$, with p.d.f. $f(\mathbf{x}) = f(x_1, \dots, x_n)$, to $\mathbf{y} \equiv (y_1, \dots, y_n)$, a one-to-one function of the x_i 's, the p.d.f. $g(\mathbf{y}) = g(y_1, \dots, y_n)$ is found by substitution for (x_1, \dots, x_n) in f followed by multiplication by the absolute value of the Jacobian of the transformation; that is,

$$g(\mathbf{y}) = f[w_1(\mathbf{y}), \dots, w_n(\mathbf{y})] |J| . \tag{27.11}$$

The functions w_i express the *inverse* transformation, $x_i = w_i(\mathbf{y})$ for $i = 1, \dots, n$, and $|J|$ is the absolute value of the determinant of the square matrix $J_{ij} = \partial x_i / \partial y_j$. If the transformation from \mathbf{x} to \mathbf{y} is not one-to-one, the situation is more complex and a unique solution may not exist. For example, if the change is to $m < n$ variables, then a given \mathbf{y} may correspond to more than one \mathbf{x} , leading to multiple integrals over the contributions [1].

To change variables for discrete random variables simply substitute; no Jacobian is necessary because now f is a probability rather than a probability density.

If f depends upon a parameter set α , a change to a different parameter set $\phi_i = \phi_i(\alpha)$ is made by simple substitution; no Jacobian is used.

27.2. Characteristic functions

The characteristic function $\phi(u)$ associated with the p.d.f. $f(x)$ is essentially its (inverse) Fourier transform, or the expectation value of $\exp(iux)$:

$$\phi(u) = E(e^{iux}) = \int_{-\infty}^{\infty} e^{iux} f(x) dx . \tag{27.12}$$

It is often useful, and several of its properties follow [1].

It follows from Eqs. (27.3a) and (27.12) that the n th moment of the distribution $f(x)$ is given by

$$i^{-n} \frac{d^n \phi}{du^n} \Big|_{u=0} = \int_{-\infty}^{\infty} x^n f(x) dx = \alpha_n . \tag{27.13}$$

Thus it is often easy to calculate all the moments of a distribution defined by $\phi(u)$, even when $f(x)$ is difficult to obtain.

If $f_1(x)$ and $f_2(y)$ have characteristic functions $\phi_1(u)$ and $\phi_2(u)$, then the characteristic function of the weighted sum $ax + by$ is $\phi_1(au)\phi_2(bu)$. The addition rules for common distributions (e.g., that the sum of two numbers from Gaussian distributions also has a Gaussian distribution) easily follow from this observation.

Let the (partial) characteristic function corresponding to the conditional p.d.f. $f_2(x|z)$ be $\phi_2(u|z)$, and the p.d.f. of z be $f_1(z)$. The characteristic function after integration over the conditional value is

$$\phi(u) = \int \phi_2(u|z) f_1(z) dz . \tag{27.14}$$

Suppose we can write ϕ_2 in the form

$$\phi_2(u|z) = A(u)e^{ig(u)z} . \tag{27.15}$$

Then

$$\phi(u) = A(u)\phi_1(g(u)) . \tag{27.16}$$

The semi-invariants κ_n are defined by

$$\phi(u) = \exp \left(\sum_1^{\infty} \frac{\kappa_n}{n!} (iu)^n \right) = \exp \left(i\kappa_1 u - \frac{1}{2} \kappa_2 u^2 + \dots \right) . \tag{27.17}$$

The κ_n 's are related to the moments α_n and m_n . The first few relations are

$$\begin{aligned} \kappa_1 &= \alpha_1 (= \mu, \text{ the mean}) \\ \kappa_2 &= m_2 = \alpha_2 - \alpha_1^2 (= \sigma^2, \text{ the variance}) \\ \kappa_3 &= m_3 = \alpha_3 - 3\alpha_1\alpha_2 + 2\alpha_1^3 . \end{aligned} \tag{27.18}$$

27.3. Some probability distributions

Table 27.1 gives a number of common probability density functions and corresponding characteristic functions, means, and variances. Further information may be found in Refs. 1-7; Ref. 7 has particularly detailed tables. Monte Carlo techniques for generating each of them may be found in our Sec. 29.4. We comment below on all except the trivial uniform distribution.

27.3.1. Binomial distribution: A random process with exactly two possible outcomes is called a *Bernoulli* process. If the probability of obtaining a certain outcome (a "success") in each trial is p , then the probability of obtaining exactly r successes ($r = 0, 1, 2, \dots, n$) in n trials, without regard to the order of the successes and failures, is given by the binomial distribution $f(r; n, p)$ in Table 27.1. If r successes are observed in n_r trials with probability p of a success, and if s successes are observed in n_s similar trials, then $t = r + s$ is also binomial with $n_t = n_r + n_s$.

27.3.2. Poisson distribution: The Poisson distribution $f(r; \mu)$ gives the probability of finding exactly r events in a given interval of x (e.g., space and time) when the events occur independently of one another and of x at an average rate of μ per the given interval. The variance σ^2 equals μ . It is the limiting case $p \rightarrow 0, n \rightarrow \infty, np = \mu$ of the binomial distribution. The Poisson distribution approaches the Gaussian distribution for large μ .

Two or more Poisson processes (e.g., *signal + background*, with parameters μ_s and μ_b) that independently contribute amounts n_s and n_b to a given measurement will produce an observed number $n = n_s + n_b$, which is distributed according to a new Poisson distribution with parameter $\mu = \mu_s + \mu_b$.

27.3.3. Normal or Gaussian distribution: The normal (or Gaussian) probability density function $f(x; \mu, \sigma^2)$ given in Table 27.1 has mean $\bar{x} = \mu$ and variance σ^2 . Comparison of the characteristic function $\phi(u)$ given in Table 27.1 with Eq. (27.17) shows that all semi-invariants κ_n beyond κ_2 vanish; this is a unique property of the Gaussian distribution. Some properties of the distribution are:

- rms deviation = σ
- probability x in the range $\mu \pm \sigma = 0.6827$
- probability x in the range $\mu \pm 0.6745\sigma = 0.5$
- expectation value of $|x - \mu|, E(|x - \mu|) = (2/\pi)^{1/2}\sigma = 0.7979\sigma$
- half-width at half maximum = $(2 \ln 2)^{1/2}\sigma = 1.177\sigma$

The cumulative distribution, Eq. (27.1), for a Gaussian with $\mu = 0$ and $\sigma^2 = 1$ is related to the error function $\text{erf}(y)$ by

$$F(x; 0, 1) = \frac{1}{2} \left[1 + \text{erf}(x/\sqrt{2}) \right] . \tag{27.19}$$

The error function is tabulated in Ref. 7 and is available in computer math libraries and personal computer spreadsheets. For a mean μ and variance σ^2 , replace x by $(x - \mu)/\sigma$. The probability of x in a given range can be calculated with Eq. (28.36).

For x and y independent and normally distributed, $z = ax + by$ obeys $f(z; a\mu_x + b\mu_y, a^2\sigma_x^2 + b^2\sigma_y^2)$; that is, the weighted means and variances add.

The Gaussian gets its importance in large part from the *central limit theorem*: If a continuous random variable x is distributed according to any p.d.f. with finite mean and variance, then the sample mean, \bar{x}_n , of n observations of x will have a p.d.f. that approaches a Gaussian as n increases. Therefore the end result $\sum^n x_i \equiv n\bar{x}_n$ of a large number of small fluctuations x_i will be distributed as a Gaussian, even if the x_i themselves are not.

(Note that the *product* of a large number of random variables is not Gaussian, but its logarithm is. The p.d.f. of the product is *lognormal*. See Ref. 6 for details.)

For a set of n Gaussian random variables \mathbf{x} with means $\boldsymbol{\mu}$ and corresponding Fourier variables \mathbf{u} , the characteristic function for a one-dimensional Gaussian is generalized to

$$\phi(\mathbf{x}; \boldsymbol{\mu}, S) = \exp \left[i\boldsymbol{\mu} \cdot \mathbf{u} - \frac{1}{2} \mathbf{u}^T S \mathbf{u} \right] . \tag{27.20}$$

From Eq. (27.13), the covariance about the mean is

$$E[(x_j - \mu_j)(x_k - \mu_k)] = S_{jk} . \tag{27.21}$$

If the \mathbf{x} are independent, then $S_{jk} = \delta_{jk}\sigma_j^2$, and Eq. (27.20) is the product of the c.f.'s of n Gaussians.

The covariance matrix S can be related to the correlation matrix defined by Eq. (27.9) (a sort of normalized covariance matrix). With the definition $\sigma_k^2 \equiv S_{kk}$, we have $\rho_{jk} = S_{jk}/\sigma_j\sigma_k$.

The characteristic function may be inverted to find the corresponding p.d.f.

$$f(\mathbf{x}; \boldsymbol{\mu}, S) = \frac{1}{(2\pi)^{n/2} \sqrt{|S|}} \exp \left[-\frac{1}{2} (\mathbf{x} - \boldsymbol{\mu})^T S^{-1} (\mathbf{x} - \boldsymbol{\mu}) \right] \tag{27.22}$$

where the determinant $|S|$ must be greater than 0. For diagonal S (independent variables), $f(\mathbf{x}; \boldsymbol{\mu}, S)$ is the product of the p.d.f.'s of n Gaussian distributions.

Table 27.1. Some common probability density functions, with corresponding characteristic functions and means and variances. In the Table, $\Gamma(k)$ is the gamma function, equal to $(k - 1)!$ when k is an integer.

Distribution	Probability density function f (variable; parameters)	Characteristic function $\phi(u)$	Mean	Variance σ^2
Uniform	$f(x; a, b) = \begin{cases} 1/(b-a) & a \leq x \leq b \\ 0 & \text{otherwise} \end{cases}$	$\frac{e^{ibu} - e^{iau}}{(b-a)iu}$	$\bar{x} = \frac{a+b}{2}$	$\frac{(b-a)^2}{12}$
Binomial	$f(r; n, p) = \frac{n!}{r!(n-r)!} p^r q^{n-r}$ $r = 0, 1, 2, \dots, n; \quad 0 \leq p \leq 1; \quad q = 1 - p$	$(q + pe^{iu})^n$	$\bar{r} = np$	npq
Poisson	$f(r; \mu) = \frac{\mu^r e^{-\mu}}{r!}; \quad r = 0, 1, 2, \dots; \quad \mu > 0$	$\exp[\mu(e^{iu} - 1)]$	$\bar{r} = \mu$	μ
Normal (Gaussian)	$f(x; \mu, \sigma^2) = \frac{1}{\sigma\sqrt{2\pi}} \exp(-(x-\mu)^2/2\sigma^2)$ $-\infty < x < \infty; \quad -\infty < \mu < \infty; \quad \sigma > 0$	$\exp(i\mu u - \frac{1}{2}\sigma^2 u^2)$	$\bar{x} = \mu$	σ^2
Multivariate Gaussian	$f(\mathbf{x}; \boldsymbol{\mu}, S) = \frac{1}{(2\pi)^{n/2} \sqrt{ S }}$ $\times \exp[-\frac{1}{2}(\mathbf{x} - \boldsymbol{\mu})^T S^{-1}(\mathbf{x} - \boldsymbol{\mu})]$ $-\infty < x_j < \infty; \quad -\infty < \mu_j < \infty; \quad \det S > 0$	$\exp[i\boldsymbol{\mu} \cdot \mathbf{u} - \frac{1}{2}\mathbf{u}^T S \mathbf{u}]$	$\boldsymbol{\mu}$	S_{jk}
χ^2	$f(z; n) = \frac{z^{n/2-1} e^{-z/2}}{2^{n/2} \Gamma(n/2)}; \quad z \geq 0$	$(1 - 2iu)^{-n/2}$	$\bar{z} = n$	$2n$
Student's t	$f(t; n) = \frac{1}{\sqrt{n\pi}} \frac{\Gamma[(n+1)/2]}{\Gamma(n/2)} \left(1 + \frac{t^2}{n}\right)^{-(n+1)/2}$ $-\infty < t < \infty; \quad n \text{ not required to be integer}$	—	$\bar{t} = 0$ for $n \geq 2$	$n/(n-2)$ for $n \geq 3$
Gamma	$f(x; \lambda, k) = \frac{x^{k-1} \lambda^k e^{-\lambda x}}{\Gamma(k)}; \quad 0 < x < \infty;$ $k \text{ not required to be integer}$	$(1 - iu/\lambda)^{-k}$	$\bar{x} = k/\lambda$	k/λ^2

For $n = 2$, $f(\mathbf{x}; \boldsymbol{\mu}, S)$ is

$$f(x_1, x_2; \mu_1, \mu_2, \sigma_1, \sigma_2, \rho) = \frac{1}{2\pi\sigma_1\sigma_2\sqrt{1-\rho^2}} \times \exp\left\{\frac{-1}{2(1-\rho^2)} \left[\frac{(x_1 - \mu_1)^2}{\sigma_1^2} - \frac{2\rho(x_1 - \mu_1)(x_2 - \mu_2)}{\sigma_1\sigma_2} + \frac{(x_2 - \mu_2)^2}{\sigma_2^2}\right]\right\}. \quad (27.23)$$

The marginal distribution of any x_i is a Gaussian with mean μ_i and variance S_{ii} . S is $n \times n$, symmetric, and positive definite. Therefore for any vector \mathbf{X} , the quadratic form $\mathbf{X}^T S^{-1} \mathbf{X} = C$, where C is any positive number, traces an n -dimensional ellipsoid as \mathbf{X} varies. If $\mathbf{X}_i = (x_i - \mu_i)/\sigma_i$, then C is a random variable obeying the $\chi^2(n)$ distribution, discussed in the following section. The probability that \mathbf{X} corresponding to a set of Gaussian random variables x_i lies outside the ellipsoid characterized by a given value of $C (= \chi^2)$ is given by Eq. (27.24) and may be read from Fig. 27.1. For example, the “ s -standard-deviation ellipsoid” occurs at $C = s^2$. For the two-variable case ($n = 2$), the point \mathbf{X} lies outside the one-standard-deviation ellipsoid with 61% probability. (This assumes that μ_i and σ_i are correct.) For $\mathbf{X}_i = x_i/\sigma_i$, the ellipsoids of constant χ^2 have the same size and orientation but are centered at $\boldsymbol{\mu}$. The use of these ellipsoids as indicators of probable error is described in Sec. 28.6.2.

27.3.4. χ^2 distribution: If x_1, \dots, x_n are independent Gaussian distributed random variables, the sum $z = \sum^n (x_i - \mu_i)^2/\sigma_i^2$ is distributed as a χ^2 with n degrees of freedom, $\chi^2(n)$. Under a linear transformation to n dependent Gaussian variables x'_i , the χ^2 at each transformed point retains its value; then $z = \mathbf{X}'^T V^{-1} \mathbf{X}'$ as in the previous section. For a set of z_i , each of which is $\chi^2(n_i)$, $\sum z_i$ is a new random variable which is $\chi^2(\sum n_i)$.

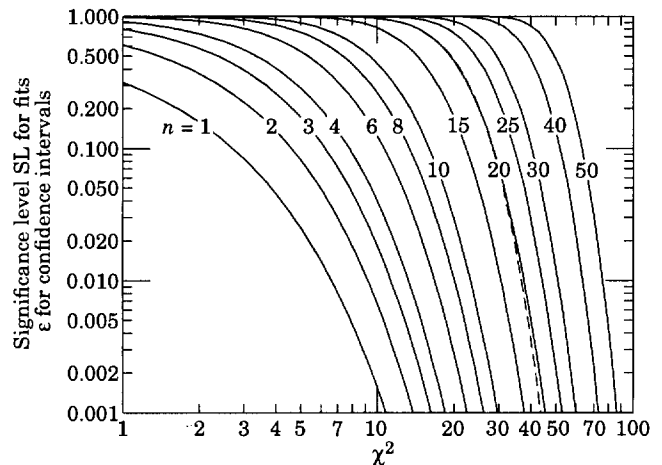


Figure 27.1: The significance level versus χ^2 for n degrees of freedom, as defined in Eq. (27.24). The curve for a given n gives the probability that a value at least as large as χ^2 will be obtained in an experiment; e.g., for $n = 10$, a value $\chi^2 \geq 18$ will occur in 5% of a large number of experiments. For a fit, the SL is a measure of goodness-of-fit, in that a good fit to a correct model is expected to yield a low χ^2 (see Sec. 28.5.0). For a confidence interval, ϵ measures the probability that the interval does not cover the true value of the quantity being estimated (see Sec. 28.6). The dashed curve for $n = 20$ is calculated using the approximation of Eq. (27.25).

Fig. 27.1 shows the significance level (SL) obtained by integrating the tail of $f(z; n)$:

$$SL(\chi^2) = \int_{\chi^2}^{\infty} f(z; n) dz . \quad (27.24)$$

This is shown for a special case in Fig. 27.2, and is equal to 1.0 minus the cumulative distribution function $F(z = \chi^2; n)$. It is useful in evaluating the consistency of data with a model (see Sec. 28): The SL is the probability that a random repeat of the given experiment would observe a greater χ^2 , assuming the model is correct. It is also useful for confidence intervals for statistical estimators (see Sec. 28.6), in which case one is interested in the unshaded area of Fig. 27.2.

Since the mean of the χ^2 distribution is equal to n , one expects in a "reasonable" experiment to obtain $\chi^2 \approx n$. Hence the "reduced χ^2 " $\equiv \chi^2/n$ is sometimes reported. Since the p.d.f. of χ^2/n depends on n , one must report n as well in order to make a meaningful statement. Figure 27.3 shows χ^2/n for useful SL's as a function of n .

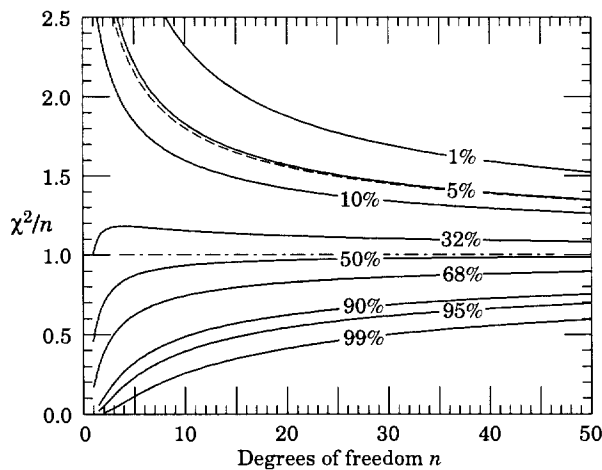


Figure 27.3: Significance levels as a function of the "reduced χ^2 " $\equiv \chi^2/n$ and the number of degrees of freedom n . Curves are labeled by the probability that a measurement will give a value of χ^2/n greater than that given on the y axis; e.g., for $n = 10$, a value $\chi^2/n \gtrsim 1.8$ can be expected 5% of the time.

For large n , the SL is approximately given by [1,8]

$$SL(\chi^2) \approx \frac{1}{\sqrt{2\pi}} \int_y^{\infty} e^{-x^2/2} dx , \quad (27.25)$$

where $y = \sqrt{2\chi^2} - \sqrt{2n-1}$. This approximation was used to draw the dashed curves in Fig. 27.1 (for $n = 20$) and Fig. 27.3 (for SL = 5%). Since all the functions and their inverses are now readily

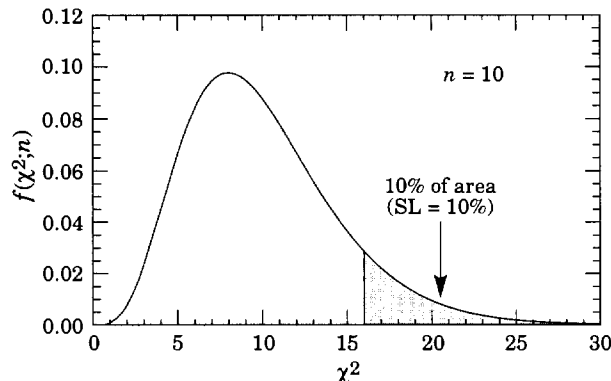


Figure 27.2: Illustration of the significance level integral given in Eq. (27.24). This particular example is for $n = 10$, where the area above 15.99 is 0.1.

available in standard mathematical libraries (such as IMSL, used to generate these figures, and personal computer spreadsheets, such as Microsoft® Excel [9]), the approximation (and even figures and tables) are seldom needed.

27.3.5. Student's t distribution: Suppose that x and x_1, \dots, x_n are independent and Gaussian distributed with mean 0 and variance 1. We then define

$$z = \sum_1^n x_i^2 , \quad \text{and} \quad t = \frac{x}{\sqrt{z/n}} . \quad (27.26)$$

The variable z thus belongs to a $\chi^2(n)$ distribution. Then t is distributed according to a Student's t distribution with n degrees of freedom, $f(t; n)$, given in Table 27.1.

The Student's t distribution resembles a Gaussian distribution with wide tails. As $n \rightarrow \infty$, the distribution approaches a Gaussian. If $n = 1$, the distribution is a *Cauchy* or *Breit-Wigner* distribution. The mean is finite only for $n > 1$ and the variance is finite only for $n > 2$, so for $n = 1$ or $n = 2$, the central limit theorem is not applicable to t .

As an example, consider the *sample mean* $\bar{x} = \sum x_i/n$ and the *sample variance* $s^2 = \sum (x_i - \bar{x})^2/(n-1)$ for normally distributed random variables x_i with unknown mean μ and variance σ^2 . The sample mean has a Gaussian distribution with a variance σ^2/n , so the variable $(\bar{x} - \mu)/\sqrt{\sigma^2/n}$ is normal with mean 0 and variance 1. Similarly, $(n-1)s^2/\sigma^2$ is independent of this and is χ^2 distributed with $n-1$ degrees of freedom. The ratio

$$t = \frac{(\bar{x} - \mu)/\sqrt{\sigma^2/n}}{\sqrt{(n-1)s^2/\sigma^2}/\sqrt{n-1}} = \frac{\bar{x} - \mu}{\sqrt{s^2/n}} \quad (27.27)$$

is distributed as $f(t; n-1)$. The unknown true variance σ^2 cancels, and t can be used to test the probability that the true mean is some particular value μ .

In Table 27.1, n in $f(t; n)$ is not required to be an integer. A Student's t distribution with nonintegral $n > 0$ is useful in certain applications.

27.3.6. Gamma distribution: For a process that generates events as a function of x (e.g., space or time) according to a Poisson distribution, the distance in x from an arbitrary starting point (which may be some particular event) to the k^{th} event belongs to a *gamma* distribution, $f(x; \lambda, k)$. The Poisson parameter μ is λ per unit x . The special case $k = 1$ (i.e., $f(x; \lambda, 1) = \lambda e^{-\lambda x}$) is called the *exponential* distribution. A sum of k' exponential random variables x_i is distributed as $f(\sum x_i; \lambda, k')$.

The parameter k is not required to be an integer. For $\lambda = 1/2$ and $k = n/2$, the gamma distribution reduces to the $\chi^2(n)$ distribution.

References:

1. H. Cramér, *Mathematical Methods of Statistics*, Princeton Univ. Press, New Jersey (1958).
2. A. Stuart and A.K. Ord, *Kendall's Advanced Theory of Statistics, Vol. 1 Distribution Theory* 5th Ed., (Oxford Univ. Press, New York, 1987), and earlier editions by Kendall and Stuart.
3. W.T. Eadie, D. Drijard, F.E. James, M. Roos, and B. Sadoulet, *Statistical Methods in Experimental Physics* (North Holland, Amsterdam and London, 1971).
4. L. Lyons, *Statistics for Nuclear and Particle Physicists* (Cambridge University Press, New York, 1986).
5. B.R. Roe, *Probability and Statistics in Experimental Physics*, (Springer-Verlag, New York, 1992).
6. G. Cowan, *Statistical Data Analysis* (Oxford University Press, Oxford, 1998).
7. M. Abramowitz and I. Stegun, eds., *Handbook of Mathematical Functions* (Dover, New York, 1972).
8. R.A. Fisher, *Statistical Methods for Research Workers*, 8th edition, Edinburgh and London (1941).
9. Microsoft® is a registered trademark of Microsoft corporation.

27. PROBABILITY

Revised May 1996 by D.E. Groom (LBNL) and F. James (CERN).
 Updated September 1999 by R. Cousins (UCLA).

27.1. General [1-6]

Let x be a possible outcome of an observation. The probability of x is the relative frequency with which that outcome occurs out of a (possibly hypothetical) large set of similar observations. If x can take any value from a *continuous* range, we write $f(x; \theta) dx$ as the probability of observing x between x and $x + dx$. The function $f(x; \theta)$ is the *probability density function* (p.d.f.) for the *random variable* x , which may depend upon one or more parameters θ . If x can take on only *discrete* values (e.g., the non-negative integers), then $f(x; \theta)$ is itself a probability, but we shall still call it a p.d.f. The p.d.f. is always normalized to unit area (unit sum, if discrete). Both x and θ may have multiple components and are then often written as column vectors. If θ is unknown and we wish to estimate its value from a given set of data measuring x , we may use statistics (see Sec. 28).

The *cumulative distribution function* $F(a)$ is the probability that $x \leq a$:

$$F(a) = \int_{-\infty}^a f(x) dx . \tag{27.1}$$

Here and below, if x is discrete-valued, the integral is replaced by a sum. The endpoint a is expressly included in the integral or sum. Then $0 \leq F(x) \leq 1$, $F(x)$ is nondecreasing, and $\text{Prob}(a < x \leq b) = F(b) - F(a)$. If x is discrete, $F(x)$ is flat except at allowed values of x , where it has discontinuous jumps equal to $f(x)$.

Any function of random variables is itself a random variable, with (in general) a different p.d.f. The *expectation value* of any function $u(x)$ is

$$E[u(x)] = \int_{-\infty}^{\infty} u(x) f(x) dx , \tag{27.2}$$

assuming the integral is finite. For $u(x)$ and $v(x)$ any two functions of x , $E(u + v) = E(u) + E(v)$. For c and k constants, $E(cu + k) = cE(u) + k$.

The n th moment of a distribution is

$$\alpha_n \equiv E(x^n) = \int_{-\infty}^{\infty} x^n f(x) dx , \tag{27.3a}$$

and the n th moment about the mean of x , α_1 , is

$$m_n \equiv E[(x - \alpha_1)^n] = \int_{-\infty}^{\infty} (x - \alpha_1)^n f(x) dx . \tag{27.3b}$$

The most commonly used moments are the mean μ and variance σ^2 :

$$\mu \equiv \alpha_1 \tag{27.4a}$$

$$\sigma^2 \equiv \text{Var}(x) \equiv m_2 = \alpha_2 - \mu^2 . \tag{27.4b}$$

The mean is the location of the “center of mass” of the probability density function, and the variance is a measure of the square of its width. Note that $\text{Var}(cx + k) = c^2 \text{Var}(x)$.

Any odd moment about the mean is a measure of the skewness of the p.d.f. The simplest of these is the dimensionless coefficient of skewness $\gamma_1 \equiv m_3/\sigma^3$.

Besides the mean, another useful indicator of the “middle” of the probability distribution is the *median* x_{med} , defined by $F(x_{\text{med}}) = 1/2$; i.e., half the probability lies above and half lies below x_{med} . For a given *sample* of events, x_{med} is the value such that half the events have larger x and half have smaller x (not counting any that have the same x as the median). If the sample median lies between two observed x values, it is set by convention halfway between them. If the p.d.f. for x has the form $f(x - \mu)$ and μ is both mean and median, then for a large number of events N , the variance of the median approaches $1/[4Nf^2(0)]$, provided $f(0) > 0$.

Let x and y be two random variables with a joint p.d.f. $f(x, y)$. The *marginal* p.d.f. of x (the distribution of x with y unobserved) is

$$f_1(x) = \int_{-\infty}^{\infty} f(x, y) dy , \tag{27.5}$$

and similarly for the marginal p.d.f. $f_2(y)$. We define $f_3(y|x)$, the *conditional* p.d.f. of y given fixed x , by

$$f_3(y|x) f_1(x) = f(x, y) . \tag{27.6a}$$

Similarly, $f_4(x|y)$, the conditional p.d.f. of x given fixed y , is

$$f_4(x|y) f_2(y) = f(x, y) . \tag{27.6b}$$

From these definitions we immediately obtain Bayes' theorem [2]:

$$f_4(x|y) = \frac{f_3(y|x) f_1(x)}{f_2(y)} = \frac{f_3(y|x) f_1(x)}{\int f_3(y|x) f_1(x) dx} . \tag{27.7}$$

The mean of x is

$$\mu_x = \int_{-\infty}^{\infty} \int_{-\infty}^{\infty} x f(x, y) dx dy = \int_{-\infty}^{\infty} x f_1(x) dx , \tag{27.8}$$

and similarly for y . The *correlation* between x and y is

$$\rho_{xy} = E[(x - \mu_x)(y - \mu_y)] / \sigma_x \sigma_y = \text{Cov}(x, y) / \sigma_x \sigma_y , \tag{27.9}$$

where σ_x and σ_y are defined in analogy with Eq. (27.4b). It can be shown that $-1 \leq \rho_{xy} \leq 1$. Here “Cov” is the covariance of x and y , a 2-dimensional generalization of the variance.

Two random variables are *independent* if and only if

$$f(x, y) = f_1(x) f_2(y) . \tag{27.10}$$

If x and y are independent then $\rho_{xy} = 0$; the converse is not necessarily true except for Gaussian-distributed x and y . If x and y are independent, $E[u(x) v(y)] = E[u(x)] E[v(y)]$, and $\text{Var}(x + y) = \text{Var}(x) + \text{Var}(y)$; otherwise, $\text{Var}(x + y) = \text{Var}(x) + \text{Var}(y) + 2\text{Cov}(x, y)$, and $E(u v)$ does not factor.

In a *change of continuous random variables* from $\mathbf{x} \equiv (x_1, \dots, x_n)$, with p.d.f. $f(\mathbf{x}) = f(x_1, \dots, x_n)$, to $\mathbf{y} \equiv (y_1, \dots, y_n)$, a one-to-one function of the x_i 's, the p.d.f. $g(\mathbf{y}) = g(y_1, \dots, y_n)$ is found by substitution for (x_1, \dots, x_n) in f followed by multiplication by the absolute value of the Jacobian of the transformation; that is,

$$g(\mathbf{y}) = f[w_1(\mathbf{y}), \dots, w_n(\mathbf{y})] |J| . \tag{27.11}$$

The functions w_i express the *inverse* transformation, $x_i = w_i(\mathbf{y})$ for $i = 1, \dots, n$, and $|J|$ is the absolute value of the determinant of the square matrix $J_{ij} = \partial x_i / \partial y_j$. If the transformation from \mathbf{x} to \mathbf{y} is not one-to-one, the situation is more complex and a unique solution may not exist. For example, if the change is to $m < n$ variables, then a given \mathbf{y} may correspond to more than one \mathbf{x} , leading to multiple integrals over the contributions [1].

To change variables for discrete random variables simply substitute; no Jacobian is necessary because now f is a probability rather than a probability density.

If f depends upon a parameter set α , a change to a different parameter set $\phi_i = \phi_i(\alpha)$ is made by simple substitution; no Jacobian is used.

27.2. Characteristic functions

The characteristic function $\phi(u)$ associated with the p.d.f. $f(x)$ is essentially its (inverse) Fourier transform, or the expectation value of $\exp(iux)$:

$$\phi(u) = E(e^{iux}) = \int_{-\infty}^{\infty} e^{iux} f(x) dx . \tag{27.12}$$

It is often useful, and several of its properties follow [1].

It follows from Eqs. (27.3a) and (27.12) that the n th moment of the distribution $f(x)$ is given by

$$i^{-n} \left. \frac{d^n \phi}{du^n} \right|_{u=0} = \int_{-\infty}^{\infty} x^n f(x) dx = \alpha_n . \tag{27.13}$$

28. STATISTICS

Revised April 1998 by F. James (CERN). Updated February 2000 by R. Cousins (UCLA).

A probability density function $f(x; \alpha)$ (p.d.f.) with known parameters α enables us to predict the frequency with which random data x will take on a particular value (if discrete) or lie in a given range (if continuous). Here we are concerned with the inverse problem, that of making inferences about α from a set of actual observations. Such inferences are part of a larger subject variously known as statistics, statistical inference, or inverse probability.

There are two different approaches to statistical inference, which we may call Frequentist and Bayesian. In the former, the frequency definition of probability (Sec. 27.1) is used, and it is usually meaningless to define a p.d.f. in α (for example, a parameter which is a constant of nature has a value which is fixed). In Frequentist statistics, one can compute confidence intervals as a function of the observed data, and they will contain ("cover") the unknown true value of α a specified fraction of the time in the long run, as defined in Sec. 28.6.

In Bayesian statistics, the concept of probability is not based on limiting frequencies, but is more general and includes *degree of belief*. With this definition, one may define p.d.f.'s in α , and then inverse probability simply obeys the general rules of probability. Bayesian methods allow for a natural way to input additional information such as physical boundaries and subjective information; in fact they *require* as input the *prior* p.d.f. for any parameter to be estimated. Using Bayes' Theorem (Eq. (27.7)), the prior degree of belief is updated by incoming data.

For many inference problems, the Frequentist and Bayesian approaches give the same numerical answers, even though they are based on fundamentally different assumptions. However, for exact results for small samples and for measurements near a physical boundary, the different approaches may yield very different confidence limits, so we are forced to make a choice. There is an enormous amount of literature devoted to the question of Bayesian vs non-Bayesian methods, much of it written by people who are fervent advocates of one or the other methodology, which often leads to exaggerated conclusions. For a reasonably balanced discussion, we recommend the following articles: by a statistician [1], and by a physicist [2]. A more advanced comparison is offered in Ref. 3.

In high energy physics, where experiments are repeatable (at least in principle) the frequentist definition of probability is normally used. However, Bayesian equations are often used to treat uncertainties on luminosity, background, etc. If the result has poor properties from a Frequentist point of view, one should note that the result is not a classical confidence interval.

Frequentist methods cannot provide the probability that a theory is true, or that a parameter has a particular value. (Such probabilities require input of prior belief.) Rather, Frequentist methods calculate probabilities that various data sets are obtained given specified theories or parameters; these frequencies are often calculated by Monte Carlo methods. As described below, confidence intervals are constructed from such frequencies, and therefore do not represent degree of belief.

The Bayesian methodology is particularly well-adapted to *decision-making*, which requires subjective input not only for prior belief, but also for risk tolerance, etc. Even primarily Frequentist texts such as Ref. 4 outline Bayesian decision theory. However, the usefulness of Bayesian methods as a means for the communication of experimental measurements is controversial.

Recently, the first Workshop on Confidence Limits [5] was held at CERN, where proponents of various statistical methods presented and discussed the issues. One sees that there was not a consensus on the best way to report confidence limits. We recommend the web site and eventual proceedings as a starting point for discussion of these issues. The methods described below use the Frequentist definition of probability, except where noted.

28.1. Parameter estimation [3, 4, 6–9]

Here we review *parametric* statistics in which one desires estimates of the parameters α from a set of actual observations.

A *statistic* is any function of the data, plus known constants, which does not depend upon any of the unknown parameters. A *statistic* is a random variable if the data have random errors. An *estimator* is any statistic whose value (the *estimate* $\hat{\alpha}$) is intended as a meaningful guess for the value of the parameter α , or the vector α if there is more than one parameter.

Since we are free to choose any function of the data as an estimator of the parameter α , we will try to choose that estimator which has the best properties. The most important properties are (a) *consistency*, (b) *bias*, (c) *efficiency*, and (d) *robustness*.

(a) An estimator is said to be *consistent* if the estimate $\hat{\alpha}$ converges to the true value α as the amount of data increases. This property is so important that it is possessed by all commonly used estimators.

(b) The *bias*, $b = E(\hat{\alpha}) - \alpha$, is the difference between the true value and the expectation of the estimates, where the expectation value is taken over a hypothetical set of similar experiments in which $\hat{\alpha}$ is constructed the same way. When $b = 0$ the estimator is said to be unbiased. The bias depends on the chosen metric, i.e., if $\hat{\alpha}$ is an unbiased estimator of α , then $(\hat{\alpha})^2$ is generally not an unbiased estimator of α^2 . The bias may be due to statistical properties of the estimator or to *systematic* errors in the experiment. If we can estimate the b we can subtract it from $\hat{\alpha}$ to obtain a new $\hat{\alpha}' \equiv \hat{\alpha} - b$. However, b may depend upon α or other unknowns, in which case we usually try to choose an estimator which minimizes its average size.

(c) *Efficiency* is the inverse of the ratio between the *variance of the estimates* $\text{Var}(\hat{\alpha})$ and the minimum possible value of the variance. Under rather general conditions, the minimum variance is given by the Rao-Cramér-Frechet bound:

$$\text{Var}_{\min} = [1 + \partial b / \partial \alpha]^2 / I(\alpha); \quad (28.1)$$

$$I(\alpha) = E \left\{ \left[\frac{\partial}{\partial \alpha} \sum_i \ln f(x_i; \alpha) \right]^2 \right\}.$$

(Compare with Eq. (28.6) below.) The sum is over all data and b is the bias, if any; the x_i are assumed independent and distributed as $f(x_i; \alpha)$, and the allowed range of x must not depend upon α . *Mean-squared error*, $\text{mse} = E[(\hat{\alpha} - \alpha)^2] = V(\hat{\alpha}) + b^2$ is a convenient quantity which combines in the appropriate way the errors due to bias and efficiency.

(d) *Robustness*; is the property of being insensitive to departures from assumptions in the p.d.f. due to such factors as noise.

For some common estimators the above properties are known exactly. More generally, it is always possible to evaluate them by Monte Carlo simulation. Note that they will often depend on the unknown α .

28.2. Data with a common mean

Suppose we have a set of N independent measurements y_i assumed to be unbiased measurements of the same unknown quantity μ with a common, but unknown, variance σ^2 resulting from measurement error. Then

$$\hat{\mu} = \frac{1}{N} \sum_{i=1}^N y_i \quad (28.2)$$

$$\hat{\sigma}^2 = \frac{1}{N-1} \sum_{i=1}^N (y_i - \hat{\mu})^2 \quad (28.3)$$

are unbiased estimators of μ and σ^2 . The variance of $\hat{\mu}$ is σ^2/N . If the common p.d.f. of the y_i is Gaussian, these estimates are uncorrelated. Then, for large N , the standard deviation of $\hat{\sigma}$ (the "error of the error") is $\sigma/\sqrt{2N}$. Again if the y_i are Gaussian, $\hat{\mu}$ is an efficient estimator for μ . Otherwise the mean is in general not the most

efficient estimator. For example, if the y follow a double-exponential distribution [$\sim \exp(-\sqrt{2}|y - \mu|/\sigma)$], the most efficient estimator of the mean is the sample median (the value for which half the y_i lie above and half below). This is discussed in more detail in Ref. 4, Sec. 8.7.

If σ^2 is known, it does not improve the estimate $\hat{\mu}$, as can be seen from Eq. (28.2); however, if μ is known, substitute it for $\hat{\mu}$ in Eq. (28.3) and replace $N - 1$ by N , to obtain a somewhat better estimator of σ^2 .

If the y_i have different, known, variances σ_i^2 , then the weighted average

$$\hat{\mu} = \frac{1}{w} \sum_{i=1}^N w_i y_i, \tag{28.4}$$

is an unbiased estimator for μ with smaller variance than an unweighted average; here $w_i = 1/\sigma_i^2$ and $w = \sum w_i$. The standard deviation of $\hat{\mu}$ is $1/\sqrt{w}$.

28.3. The method of maximum likelihood

28.3.1. Parameter estimation by maximum likelihood:

"From a theoretical point of view, the most important general method of estimation so far known is the *method of maximum likelihood*" [6]. We suppose that a set of independently measured quantities x_i came from a p.d.f. $f(x_i; \alpha)$, where α is an unknown set of parameters. The method of maximum likelihood consists of finding the set of values, $\hat{\alpha}$, which maximizes the joint probability density for all the data, given by

$$\mathcal{L}(\alpha) = \prod_i f(x_i; \alpha), \tag{28.5}$$

where \mathcal{L} is called the likelihood. It is usually easier to work with $\ln \mathcal{L}$, and since both are maximized for the same set of α , it is sufficient to solve the *likelihood equation*

$$\frac{\partial \ln \mathcal{L}}{\partial \alpha_n} = 0. \tag{28.6}$$

When the solution to Eq. (28.6) is a maximum, it is called the *maximum likelihood estimate* of α . The importance of the approach is shown by the following proposition, proved in Ref. 3:

If an efficient estimate $\hat{\alpha}$ of α exists, the likelihood equation will have a unique solution equal to $\hat{\alpha}$.

In evaluating \mathcal{L} , it is important that any normalization factors in the f 's which involve α be included. However, we will only be interested in the maximum of \mathcal{L} and in ratios of \mathcal{L} at different α 's; hence any multiplicative factors which do not involve the parameters we want to estimate may be dropped; this includes factors which depend on the data but not on α . The results of two or more independent experiments may be combined by forming the product of the \mathcal{L} 's, or the sum of the $\ln \mathcal{L}$'s.

Most commonly the solution to Eq. (28.6) will be found using a general numerical minimization program such as the CERN program MINUIT [10], which contains considerable code to take account of the many special cases and problems which can arise.

Under a one-to-one change of parameters from α to $\beta = \beta(\alpha)$, the maximum likelihood estimate $\hat{\alpha}$ transforms to $\beta(\hat{\alpha})$. That is, the maximum likelihood solution is invariant under change of parameter. However, many properties of $\hat{\alpha}$, in particular the bias, are not invariant under change of parameter.

28.3.2. Uses of \mathcal{L} : $\mathcal{L}(\alpha)$ is not a p.d.f. for α :

Recall the definition of a probability *density* function: a function $p(\alpha)$ is a p.d.f. for α if $p(\alpha)d\alpha$ is the *probability* for α to be within α and $\alpha + d\alpha$. The likelihood function $\mathcal{L}(\alpha)$ is *not* a p.d.f. for α , so in general it is nonsensical to integrate the likelihood function with respect to its parameter(s).

Consider, for example, the Poisson probability for obtaining n when sampling from a distribution with mean α : $f(n; \alpha) = \alpha^n \exp(-\alpha)/n!$. If one obtains $n = 3$ in a particular experiment, then

$\mathcal{L}(\alpha) = \alpha^3 \exp(-\alpha)/6$. Nothing in the construction of \mathcal{L} makes it a probability *density*, i.e., a function which one can multiply by $d\alpha$ in order to obtain a probability.

In Bayesian theory, one applies Bayes' Theorem to construct the posterior p.d.f. for α by multiplying the prior p.d.f. for α by \mathcal{L} :

$$p_{\text{posterior}}(\alpha) \propto \mathcal{L}(\alpha) \times p_{\text{prior}}(\alpha).$$

If the prior p.d.f. is uniform, integrating the posterior p.d.f. may give the appearance of integrating \mathcal{L} . But note that the prior p.d.f. crucially provides the *density* which makes it sensible to multiply by $d\alpha$ to obtain a probability. In non-Bayesian applications, such as those considered in the following subsections, only likelihood *ratios* are used (or equivalently, differences in $\ln \mathcal{L}$).

Because \mathcal{L} is so useful, we strongly encourage publishing it (or enough information to allow the reader to reconstruct it), when practical.

28.3.3. Confidence intervals from the likelihood function:

The covariance matrix V may be estimated from

$$V_{nm} = \left(E \left[- \frac{\partial^2 \ln \mathcal{L}}{\partial \alpha_n \partial \alpha_m} \Big|_{\hat{\alpha}} \right] \right)^{-1}. \tag{28.7}$$

(Here and below, the superscript -1 indicates matrix inversion, followed by application of the subscripts.)

In the large sample case (or a linear model with Gaussian errors), \mathcal{L} is Gaussian, $\ln \mathcal{L}$ is a (multidimensional) parabola, and the second derivative in Eq. (28.7) is constant, so the "expectation" operation has no effect. This leads to the usual approximation of calculating the error matrix of the parameters by inverting the second derivative matrix of $\ln \mathcal{L}$. In this asymptotic case, it can be seen that a numerically equivalent way of determining s -standard-deviation errors is from the contour given by the α' such that

$$\ln \mathcal{L}(\alpha') = \ln \mathcal{L}_{\text{max}} - s^2/2, \tag{28.8}$$

where $\ln \mathcal{L}_{\text{max}}$ is the value of $\ln \mathcal{L}$ at the solution point (compare with Eq. (28.32), below). The extreme limits of this contour parallel to the α_n axis give an approximate s -standard-deviation confidence interval in α_n . These intervals may not be symmetric and in pathological cases they may even consist of two or more disjoint intervals.

Although asymptotically Eq. (28.7) is equivalent to Eq. (28.8) with $s = 1$, the latter is a better approximation when the model deviates from linearity. This is because Eq. (28.8) is invariant with respect to even a non-linear transformation of parameters α , whereas Eq. (28.7) is not. Still, when the model is non-linear or errors are not Gaussian, confidence intervals obtained with both these formulas are only approximate. The true coverage of these confidence intervals can always be determined by a Monte Carlo simulation, or exact confidence intervals can be determined as in Sec. 28.6.1.

28.3.4. Application to Poisson-distributed data:

In the case of Poisson-distributed data in a counting experiment, the unbinned maximum likelihood method (where the index i in Eq. (28.5) labels events) is preferred if the total number of events is very small. (Sometimes it is "extended" to include the total number of events as a Poisson-distributed observable.) If there are enough events to justify binning them in a histogram, then one may alternatively maximize the likelihood function for the contents of the bins (so i labels bins). This is equivalent to minimizing [11]

$$\chi^2 = \sum_i \left[2(N_i^{\text{th}} - N_i^{\text{obs}}) + 2N_i^{\text{obs}} \ln(N_i^{\text{obs}}/N_i^{\text{th}}) \right]. \tag{28.9}$$

where N_i^{obs} and N_i^{th} are the observed and theoretical (from f) contents of the i th bin. In bins where $N_i^{\text{obs}} = 0$, the second term is zero. This function asymptotically behaves like a classical χ^2 for purposes of point estimation, interval estimation, and *goodness-of-fit*. It also guarantees that the area under the fitted function f is equal to the sum of the histogram contents (as long as the overall normalization of f is effectively left unconstrained during the fit), which is not the case for χ^2 statistics based on a least-squares procedure with traditional weights.

28.4. Propagation of errors

Suppose that $F(x; \alpha)$ is some function of variable(s) x and the fitted parameters α , with a value \hat{F} at $\hat{\alpha}$. The variance matrix of the parameters is V_{mn} . To first order in $\alpha_m - \hat{\alpha}_m$, F is given by

$$F = \hat{F} + \sum_m \frac{\partial F}{\partial \alpha_m} (\alpha_m - \hat{\alpha}_m), \tag{28.10}$$

and the variance of F about its estimator is given by

$$(\Delta F)^2 = E[(F - \hat{F})^2] = \sum_{mn} \frac{\partial F}{\partial \alpha_m} \frac{\partial F}{\partial \alpha_n} V_{mn}, \tag{28.11}$$

evaluated at the x of interest. For different functions F_j and F_k , the covariance is

$$E[(F_j - \hat{F}_j)(F_k - \hat{F}_k)] = \sum_{mn} \frac{\partial F_j}{\partial \alpha_m} \frac{\partial F_k}{\partial \alpha_n} V_{mn}. \tag{28.12}$$

If the first-order approximation is in serious error, the above results may be very approximate. \hat{F} may be a biased estimator of F even if the $\hat{\alpha}$ are unbiased estimators of α . Inclusion of higher-order terms or direct evaluation of F in the vicinity of $\hat{\alpha}$ will help to reduce the bias.

28.5. Method of least squares

The *method of least squares* can be derived from the maximum likelihood theorem. We suppose a set of N measurements at points x_i . The i th measurement y_i is assumed to be chosen from a Gaussian distribution with mean $F(x_i; \alpha)$ and variance σ_i^2 . Then

$$\chi^2 = -2 \ln \mathcal{L} + \text{constant} = \sum_i \frac{[y_i - F(x_i; \alpha)]^2}{\sigma_i^2}. \tag{28.13}$$

Finding the set of parameters α which maximizes \mathcal{L} is the same as finding the set which minimizes χ^2 .

In many practical cases one further restricts the problem to the situation in which $F(x_i; \alpha)$ is a linear function of the α_m 's,

$$F(x_i; \alpha) = \sum_n \alpha_n f_n(x_i), \tag{28.14}$$

where the f_n are k linearly independent functions (e.g., 1, x , x^2 , ..., or Legendre polynomials) which are single-valued over the allowed range of x . We require $k \leq N$, and at least k of the x_i must be distinct. We wish to estimate the linear coefficients α_n . Later we will discuss the nonlinear case.

If the point errors $\epsilon_i = y_i - F(x_i; \alpha)$ are Gaussian, then the minimum χ^2 will be distributed as a χ^2 random variable with $n = N - k$ degrees of freedom. We can then evaluate the goodness-of-fit (significance level) from Figs. 27.1 or 27.3, as per the earlier discussion. The significance level expresses the probability that a *worse* fit would be obtained in a large number of similar experiments under the assumptions that: (a) the model $y = \sum \alpha_n f_n$ is correct and (b) the errors ϵ_i are Gaussian and unbiased with variance σ_i^2 . If this probability is larger than an agreed-upon value (0.001, 0.01, or 0.05 are common choices), the data are *consistent* with the assumptions; otherwise we may want to find improved assumptions. As for the converse, most people do not regard a model as being truly *inconsistent* unless the probability is as low as that corresponding to four or five standard deviations for a Gaussian (6×10^{-3} or 6×10^{-5} ; see Sec. 28.6.2). If the ϵ_i are not Gaussian, the method of least squares still gives an answer, but the goodness-of-fit test would have to be done using the correct distribution of the random variable which is still called " χ^2 ."

Minimizing χ^2 in the linear case is straightforward:

$$-\frac{1}{2} \frac{\partial \chi^2}{\partial \alpha_m} = \sum_i f_m(x_i) \left(\frac{y_i - \sum_n \alpha_n f_n(x_i)}{\sigma_i^2} \right)$$

$$= \sum_i \frac{y_i f_m(x_i)}{\sigma_i^2} - \sum_n \alpha_n \sum_i \frac{f_n(x_i) f_m(x_i)}{\sigma_i^2}. \tag{28.15}$$

With the definitions

$$g_m = \sum_i y_i f_m(x_i) / \sigma_i^2 \tag{28.16}$$

and

$$V_{mn}^{-1} = \sum_i f_n(x_i) f_m(x_i) / \sigma_i^2, \tag{28.17}$$

the k -element column vector of solutions $\hat{\alpha}$, for which $\partial \chi^2 / \partial \alpha_m = 0$ for all m , is given by

$$\hat{\alpha} = V g. \tag{28.18}$$

With this notation, χ^2 for the special case of a linear fitting function (Eq. (28.14)) can be rewritten in the compact form

$$\chi^2 = \chi_{\min}^2 + (\alpha - \hat{\alpha})^T V^{-1} (\alpha - \hat{\alpha}). \tag{28.19}$$

Nonindependent y_i 's

Eq. (28.13) is based on the assumption that the likelihood function is the product of independent Gaussian distributions. More generally, the measured y_i 's are not independent, and we must consider them as coming from a multivariate distribution with nondiagonal covariance matrix S , as described in Sec. 27.3.3. The generalization of Eq. (28.13) is

$$\chi^2 = \sum_{jk} [y_j - F(x_j; \alpha)] S_{jk}^{-1} [y_k - F(x_k; \alpha)]. \tag{28.20}$$

In the case of a fitting function that is linear in the parameters, one may differentiate χ^2 to find the generalization of Eq. (28.15), and with the extended definitions

$$g_m = \sum_{jk} y_j f_m(x_k) S_{jk}^{-1} \\ V_{mn}^{-1} = \sum_{jk} f_n(x_j) f_m(x_k) S_{jk}^{-1} \tag{28.21}$$

solve Eq. (28.18) for the estimators $\hat{\alpha}$.

The problem of constructing the covariance matrix S is simplified by the fact that contributions to S (not to its inverse) are additive. For example, suppose that we have three variables, all of which have independent statistical errors. The first two also have a common error resulting in a positive correlation, perhaps because a common baseline with its own statistical error (variance s^2) was subtracted from each. In addition, the second two have a common error (variance a^2), but this time the values are anticorrelated. This might happen, for example, if the sum of the two variables is a constant. Then

$$S = \begin{pmatrix} \sigma_1^2 & 0 & 0 \\ 0 & \sigma_2^2 & 0 \\ 0 & 0 & \sigma_3^2 \end{pmatrix} + \begin{pmatrix} s^2 & s^2 & 0 \\ s^2 & s^2 & 0 \\ 0 & 0 & 0 \end{pmatrix} + \begin{pmatrix} 0 & 0 & 0 \\ 0 & a^2 & -a^2 \\ 0 & -a^2 & a^2 \end{pmatrix}. \tag{28.22}$$

If unequal amounts of the common baseline were subtracted from variables 1, 2, and 3—e.g., fractions f_1 , f_2 , and f_3 , then we would have

$$S = \begin{pmatrix} \sigma_1^2 & 0 & 0 \\ 0 & \sigma_2^2 & 0 \\ 0 & 0 & \sigma_3^2 \end{pmatrix} + \begin{pmatrix} f_1^2 s^2 & f_1 f_2 s^2 & f_1 f_3 s^2 \\ f_1 f_2 s^2 & f_2^2 s^2 & f_2 f_3 s^2 \\ f_1 f_3 s^2 & f_2 f_3 s^2 & f_3^2 s^2 \end{pmatrix}. \tag{28.23}$$

While in general this "two-vector" representation is not possible, it underscores the procedure: Add zero-determinant correlation matrices to the matrix expressing the independent variation.

Care must be taken when fitting to correlated data, since off-diagonal contributions to χ^2 are not necessarily positive. It is even possible for all of the residuals to have the same sign.

Example: straight-line fit

For the case of a straight-line fit, $y(x) = \alpha_1 + \alpha_2 x$, one obtains, for independent measurements y_i , the following estimates of α_1 and α_2 ,

$$\hat{\alpha}_1 = (g_1 \Lambda_{22} - g_2 \Lambda_{12})/D, \tag{28.24}$$

$$\hat{\alpha}_2 = (g_2 \Lambda_{11} - g_1 \Lambda_{12})/D, \tag{28.25}$$

where

$$(\Lambda_{11}, \Lambda_{12}, \Lambda_{22}) = \sum (1, x_i, x_i^2)/\sigma_i^2, \tag{28.26a}$$

$$(g_1, g_2) = \sum (1, x_i)y_i/\sigma_i^2. \tag{28.26b}$$

respectively, and

$$D = \Lambda_{11} \Lambda_{22} - (\Lambda_{12})^2. \tag{28.27}$$

The covariance matrix of the fitted parameters is:

$$\begin{pmatrix} V_{11} & V_{12} \\ V_{12} & V_{22} \end{pmatrix} = \frac{1}{D} \begin{pmatrix} \Lambda_{22} & -\Lambda_{12} \\ -\Lambda_{12} & \Lambda_{11} \end{pmatrix}. \tag{28.28}$$

The estimated variance of an interpolated or extrapolated value of y at point x is:

$$(\hat{y} - y_{\text{true}})^2 \Big|_{\text{est}} = \frac{1}{\Lambda_{11}} + \frac{\Lambda_{11}}{D} \left(x - \frac{\Lambda_{12}}{\Lambda_{11}} \right)^2. \tag{28.29}$$

28.5.1. Confidence intervals from the chisquare function:

If y is not linear in the fitting parameters α , the solution vector may have to be found by iteration. If we have a first guess α_0 , then we may expand to obtain

$$\frac{\partial \chi^2}{\partial \alpha} \Big|_{\alpha} = \frac{\partial \chi^2}{\partial \alpha} \Big|_{\alpha_0} + V_{\alpha_0}^{-1} \cdot (\alpha - \alpha_0) + \dots, \tag{28.30}$$

where $\partial \chi^2 / \partial \alpha$ is a vector whose m th component is $\partial \chi^2 / \partial \alpha_m$, and $(V_{\alpha_0}^{-1}) = \frac{1}{2} \partial^2 \chi^2 / \partial \alpha_m \partial \alpha_n$. (See Eqns. 28.7 and 28.17. When evaluated at $\hat{\alpha}$, V^{-1} is the inverse of the covariance matrix.) The next iteration toward $\hat{\alpha}$ can be obtained by setting $\partial \chi^2 / \partial \alpha_m |_{\alpha} = 0$ and neglecting higher-order terms:

$$\alpha = \alpha_0 - V_{\alpha_0} \cdot \partial \chi^2 / \partial \alpha |_{\alpha_0}. \tag{28.31}$$

If V is constant in the vicinity of the minimum, as it is when the model function is linear in the parameters, then χ^2 is parabolic as a function of α and Eq. (28.31) gives the solution immediately. Otherwise, further iteration is necessary. If the problem is highly nonlinear, considerable difficulty may be encountered. There may be secondary minima, and χ^2 may be decreasing at physical boundaries. Numerical methods have been devised to find such solutions without divergence [9,10]. In particular, the CERN program MINUIT [10] offers several iteration schemes for solving such problems.

Note that minimizing any function proportional to χ^2 (or maximizing any function proportional to $\ln \mathcal{L}$) will result in the same parameter set $\hat{\alpha}$. Hence, for example, if the variances σ_j^2 are known only up to a common constant, one can still solve for $\hat{\alpha}$. One cannot, however, evaluate goodness-of-fit, and the covariance matrix is known only to within the constant multiplier. The scale can be estimated at least roughly from the value of χ^2 compared to its expected value.

Additional information can be extracted from the behavior of the normalized residuals (known as "pulls"), $r_j = (y_j - F(x_j; \alpha))/\sigma_j$, which should themselves distribute normally with mean 0 and rms deviation 1.

If the data covariance matrix S has been correctly evaluated (or, equivalently, the σ_j 's, if the data are independent), then the s -standard deviation limits on each of the parameters are given by a set α' such that

$$\chi^2(\alpha') = \chi_{\text{min}}^2 + s^2. \tag{28.32}$$

This equation gives confidence intervals in the same sense as 28.8, and all the discussion of Sec. 28.3.3 applies as well here, substituting $-\chi^2/2$ for $\ln \mathcal{L}$.

28.6. Exact confidence intervals

The unqualified phrase "confidence intervals" refers to frequentist (also called classical) intervals obtained with a construction due to Neyman [12], described below. Approximate confidence intervals are obtained in classical statistics from likelihood ratios as described in the preceding subsections. The validity of the approximation (in terms of coverage; see below) should be checked (typically by the Monte Carlo method) when in doubt, as is usually the case with small numbers of events.

Intervals in Bayesian statistics, usually called credible intervals or Bayesian confidence intervals, are obtained by integrating the posterior p.d.f. (based on a non-frequency definition of probability), and in many cases do not obey the defining properties of confidence intervals. Correspondingly, confidence intervals do not in general behave like credible intervals.

In the Bayesian framework, all uncertainty including systematic and theoretical uncertainties can be treated in a straightforward manner: one includes in the p.d.f. one's degree of belief about background estimates, luminosity, etc. Then one integrates out such "nuisance parameters." In the Frequentist approach, one should have exact coverage no matter what the value of the nuisance parameters, and this is not in general possible. If one performs a Bayesian-style integration over nuisance parameters while constructing nominally Frequentist intervals, then coverage must be checked.

28.6.1. Neyman's Construction of Confidence intervals:

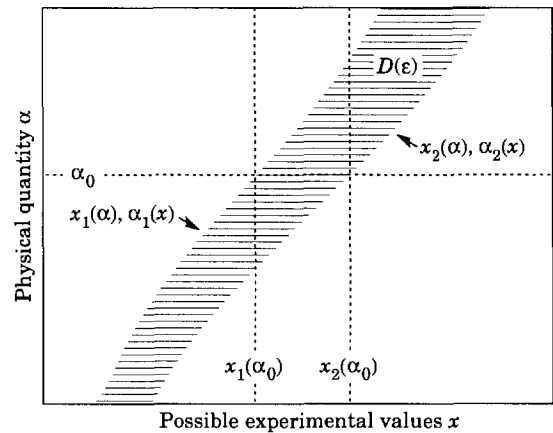


Figure 28.1: Confidence intervals for a single unknown parameter α . One might think of the p.d.f. $f(x; \alpha)$ as being plotted out of the paper as a function of x along each horizontal line of constant α . The domain $D(\epsilon)$ contains a fraction $1 - \epsilon$ of the area under each of these functions.

We consider the parameter α whose true value is fixed but unknown. The properties of our experimental apparatus are expressed in the function $f(x; \alpha)$ which gives the probability of observing data x if the true value of the parameter is α . This function must be known in order to interpret the results of an experiment. For a large complex experiment, f is usually determined numerically using Monte Carlo simulation.

Given $f(x; \alpha)$, we can find for every value of α , two values $x_1(\alpha, \epsilon)$ and $x_2(\alpha, \epsilon)$ such that

$$P(x_1 < x < x_2; \alpha) = 1 - \epsilon = \int_{x_1}^{x_2} f(x; \alpha) dx. \tag{28.33}$$

This is shown graphically in Fig. 28.1: a horizontal line segment $[x_1(\alpha, \epsilon), x_2(\alpha, \epsilon)]$ is drawn for representative values of α . The union of all intervals $[x_1(\alpha, \epsilon), x_2(\alpha, \epsilon)]$, designated in the figure as the domain $D(\epsilon)$, is known as the *confidence belt*. Typically the curves $x_1(\alpha, \epsilon)$ and $x_2(\alpha, \epsilon)$ are monotonic functions of α , which we assume for this discussion.

Upon performing an experiment to measure x and obtaining the value x_0 , one draws a vertical line through x_0 on the horizontal axis.

The confidence interval for α is the union of all values of α for which the corresponding line segment $[x_1(\alpha, \epsilon), x_2(\alpha, \epsilon)]$ is intercepted by this vertical line. The confidence interval is an interval $[\alpha_1(x_0), \alpha_2(x_0)]$, where $\alpha_1(x_0)$ and $\alpha_2(x_0)$ are on the boundary of $D(\epsilon)$. Thus, the boundaries of $D(\epsilon)$ can be considered to be functions $x(\alpha)$ when constructing D , and then to be functions $\alpha(x)$ when reading off confidence intervals.

Such confidence intervals are said to have Confidence Level (CL) equal to $1 - \epsilon$.

Now suppose that some unknown particular value of α , say α_0 (indicated in the figure), is the true value of α . We see from the figure that α_0 lies between $\alpha_1(x)$ and $\alpha_2(x)$ if and only if x lies between $x_1(\alpha_0)$ and $x_2(\alpha_0)$. Thus we can write:

$$P[x_1(\alpha_0) < x < x_2(\alpha_0)] = 1 - \epsilon = P[\alpha_2(x) < \alpha_0 < \alpha_1(x)] \tag{28.34}$$

And since, by construction, this is true for any value α_0 , we can drop the subscript 0 and obtain the relationship we wanted to establish for the probability that the confidence limits will contain the true value of α :

$$P[\alpha_2(x) < \alpha < \alpha_1(x)] = 1 - \epsilon \tag{28.35}$$

In this probability statement, α_1 and α_2 are the random variables (not α), and we can verify that the statement is true, as a limiting ratio of frequencies in random experiments, for any assumed value of α . In a particular real experiment, the numerical values α_1 and α_2 are determined by applying the algorithm to the real data, and the probability statement is (all too frequently) misinterpreted to be a statement about the true value α since this is the only unknown remaining in the equation. It should however be interpreted as the probability of obtaining values α_1 and α_2 which include the true value of α , in an ensemble of identical experiments. Any method which gives confidence intervals that contain the true value with probability $1 - \epsilon$ (no matter what the true value of α is) is said to have the correct *coverage*. The frequentist intervals as constructed above have the correct *coverage* by construction. Coverage is a critical property of confidence intervals [2]. (Power to exclude false values of α , related to the length of the intervals in a relevant measure, is also important.)

The condition of coverage Eq. (28.33) does not determine x_1 and x_2 uniquely, since any range which gives the desired value of the integral would give the same coverage. Additional criteria are thus needed. The most common criterion is to choose *central intervals* such that the area of the excluded tail on either side is $\epsilon/2$. This criterion is sufficient in most cases, but there is a more general *ordering principle* which reduces to centrality in the usual cases and produces confidence intervals with better properties when in the neighborhood of a physical limit. This ordering, which consists of taking the interval which includes the largest values of a likelihood ratio, is briefly outlined in Ref. 3 and has been applied to prototypical problems by Feldman and Cousins [13].

For the problem of a counting rate experiment in the presence of background, Roe and Woodroffe [14] have proposed a modification to Ref. 13 incorporating *conditioning*, i.e., conditional probabilities computed using constraints on the number of background events actually observed. This and other prescriptions giving frequentist intervals have not yet been fully explored [5].

28.6.2. Gaussian errors:

If the data are such that the distribution of the estimator(s) satisfies the central limit theorem discussed in Sec. 27.3.3, the function $f(x; \alpha)$ is the Gaussian distribution. If there is more than one parameter being estimated, the multivariate Gaussian is used. For the univariate case with known σ ,

$$1 - \epsilon = \int_{\mu - \delta}^{\mu + \delta} e^{-\frac{(x - \mu)^2}{2\sigma^2}} dx = \text{erf}\left(\frac{\delta}{\sqrt{2}\sigma}\right) \tag{28.36}$$

is the probability that the measured value x will fall within $\pm\delta$ of the true value μ . From the symmetry of the Gaussian with respect to x and μ , this is also the probability that the true value will be within

Table 28.1: Area of the tails ϵ outside $\pm\delta$ from the mean of a Gaussian distribution.

ϵ (%)	δ	ϵ (%)	δ
31.73	1σ	20	1.28σ
4.55	2σ	10	1.64σ
0.27	3σ	5	1.96σ
6.3×10^{-3}	4σ	1	2.58σ
5.7×10^{-5}	5σ	0.1	3.29σ
2.0×10^{-7}	6σ	0.01	3.89σ

$\pm\delta$ of the measured value. Fig. 28.2 shows a $\delta = 1.64\sigma$ confidence interval unshaded. The choice $\delta = \sqrt{\text{Var}(\mu)} \equiv \sigma$ gives an interval called the *standard error* which has $1 - \epsilon = 68.27\%$ if σ is known. Confidence coefficients ϵ for other frequently used choices of δ are given in Table 28.1.

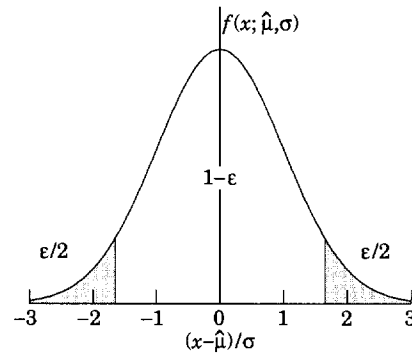


Figure 28.2: Illustration of a symmetric 90% confidence interval (unshaded) for a measurement of a single quantity with Gaussian errors. Integrated probabilities, defined by ϵ , are as shown.

For other δ , find ϵ as the ordinate of Fig. 27.1 on the $n = 1$ curve at $\chi^2 = (\delta/\sigma)^2$. We can set a one-sided (upper or lower) limit by excluding above $\mu + \delta$ (or below $\mu - \delta$); ϵ 's for such limits are 1/2 the values in Table 28.1.

For multivariate α the scalar $\text{Var}(\mu)$ becomes a full variance-covariance matrix. Assuming a multivariate Gaussian, Eq. (27.22), and subsequent discussion the standard error ellipse for the pair $(\hat{\alpha}_m, \hat{\alpha}_n)$ may be drawn as in Fig. 28.3.

The minimum χ^2 or maximum likelihood solution is at $(\hat{\alpha}_m, \hat{\alpha}_n)$. The standard errors σ_m and σ_n are defined as shown, where the ellipse is at a constant value of $\chi^2 = \chi_{\min}^2 + 1$ or $\ln \mathcal{L} = \ln \mathcal{L}_{\max} - 1/2$. The angle of the major axis of the ellipse is given by

$$\tan 2\phi = \frac{2\rho_{mn} \sigma_m \sigma_n}{\sigma_m^2 - \sigma_n^2} \tag{28.37}$$

For non-Gaussian or nonlinear cases, one may construct an analogous contour from the same χ^2 or $\ln \mathcal{L}$ relations. Any other parameters $\hat{\alpha}_\ell, \ell \neq m, n$ must be allowed freely to find their optimum values for every trial point.

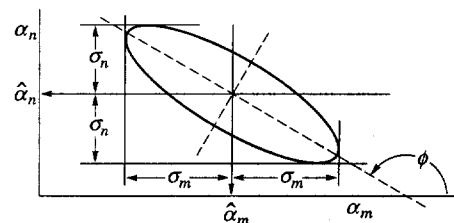


Figure 28.3: Standard error ellipse for the estimators $\hat{\alpha}_m$ and $\hat{\alpha}_n$. In this case the correlation is negative.

Table 28.2: $\Delta\chi^2$ corresponding to $(1 - \epsilon)$, for joint estimation of k parameters.

$(1 - \epsilon)$ (%)	$k = 1$	$k = 2$	$k = 3$
68.27	1.00	2.30	3.53
90.	2.71	4.61	6.25
95.45	4.00	6.18	8.03
99.	6.63	9.21	11.34
99.73	9.00	11.83	14.16

For any unbiased procedure (e.g., least squares or maximum likelihood) used to estimate k parameters α_i , $i = 1, \dots, k$, the probability $1 - \epsilon$ that the true values of all k parameters lie within an ellipsoid bounded by a fixed value of $\Delta\chi^2 = \chi^2 - \chi_{\min}^2$ may be found from Fig. 27.1. This is because the difference, $\Delta\chi^2 = \chi^2 - \chi_{\min}^2$, obeys the “ χ^2 ” p.d.f. given in Table 27.1, if the parameter n in the formula is taken to be k (rather than degrees-of-freedom in the fit). In Fig. 27.1, read the ordinate as ϵ and the abscissa as $\Delta\chi^2$. The correct values of ϵ are on the $n = k$ curve. For $k > 1$, the values of ϵ for given $\Delta\chi^2$ are much greater than for $k = 1$. Hence, using $\Delta\chi^2 = s^2$, which gives s -standard-deviation errors on a single parameter (irrespective of the other parameters), is not appropriate for a multi-dimensional ellipsoid. For example, for $k = 2$, the probability $(1 - \epsilon)$ that the true values of α_1 and α_2 simultaneously lie within the one-standard-deviation error ellipse ($s = 1$), centered on $\hat{\alpha}_1$ and $\hat{\alpha}_2$, is only 39%.

Values of $\Delta\chi^2$ corresponding to commonly used values of ϵ and k are given in Table 28.2. These probabilities assume Gaussian errors, unbiased estimators, and that the model describing the data in terms of the α_i is correct. When these assumptions are not satisfied, a Monte Carlo simulation is typically performed to determine the relation between $\Delta\chi^2$ and ϵ .

28.6.3. Upper limits and two-sided intervals:

When a measured value is close to a physical boundary, it is natural to report a one-sided confidence interval (often an upper limit). It is straightforward to force the procedure of Sec. 28.6.1 to produce only an upper limit, by setting $x_2 = \infty$ in Eq. (28.33). Then x_1 is uniquely determined. Clearly this procedure will have the desired coverage, but *only if we always choose to set an upper limit*. In practice one might decide after seeing the data whether to set an upper limit or a two-sided limit. In this case the upper limits calculated by Eq. (28.33) will not give exact coverage, as has been noted in Ref. 13.

In order to correct this problem and assure coverage in all circumstances, it is necessary to adopt a *unified procedure*, that is, a single ordering principle which will provide coverage globally. Then it is the *ordering principle* which decides whether a one-sided or two-sided interval will be reported for any given set of data. The unified procedure and ordering principle which follows from the theory of likelihood-ratio tests [3] is described in Ref. 13. We reproduce below the main results.

28.6.4. Gaussian data close to a boundary:

One of the most controversial statistical questions in physics is how to report a measurement which is close to the edge or even outside of the allowed physical region. This is because there are several admissible possibilities depending on how the result is to be used or interpreted. Normally one or more of the following should be reported:

(a) The actual measurement should be reported, even if it is outside the physical region. As with any other measurement, it is best to report the value of a quantity which is nearly Gaussian distributed if possible. Thus one may choose to report mass squared rather than mass, or $\cos\theta$ rather than θ . For a complex quantity z close to zero, report $\text{Re}(z)$ and $\text{Im}(z)$ rather than amplitude and phase of z . Data carefully reported in this way can be unbiased, objective, easily interpreted and combined (averaged) with other data in a straightforward way, even if they lie partly or wholly outside the physical region. The reported error is a direct measure of the intrinsic accuracy of the result, which cannot always be inferred from the upper limits proposed below.

(b) If the data are to be used to make a decision, for example to determine the dimensions of a new experimental apparatus for an improved measurement, it may be appropriate to report a Bayesian upper limit, which must necessarily contain subjective belief about the possible values of the parameter, as well as containing information about the physical boundary. Its interpretation requires knowledge of the prior distribution which was necessarily used to obtain it.

(c) If it is desired to report an upper limit that has a well-defined meaning in terms of a limiting frequency, then report the Frequentist confidence bound(s) as given by the unified approach [3], [13]. This algorithm always gives a non-null interval (that is, the confidence limits are always inside the physical region, even for a measurement well outside the physical region), and still has correct global coverage. These confidence limits for a Gaussian measurement close to a non-physical boundary are summarized in Fig. 28.4. Additional tables are given in Ref. 13.

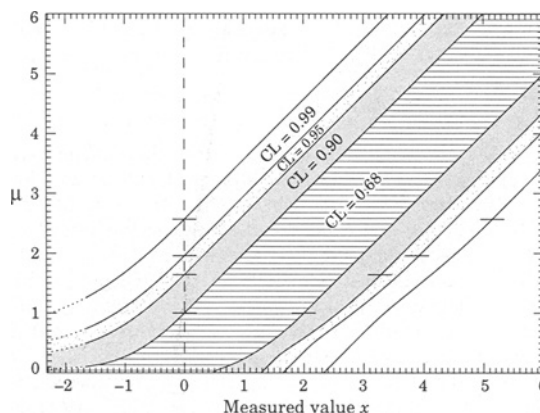


Figure 28.4: Plot of 99%, 95%, 90%, and 68.27% (“one σ ”) confidence intervals (using the unified approach as in Ref. 13) for a physical quantity μ based on a Gaussian measurement x (in units of standard deviations), for the case where the true value of μ cannot be negative. The curves become straight lines above the horizontal tick marks. The probability of obtaining an experimental value at least as negative as the left edge of the graph ($x = -2.33$) is less than 1%. Values of x more negative than -1.64 (dotted segments) are less than 5% probable, no matter what the true value of μ .

28.6.5. Poisson data for small samples:

When the observable is restricted to integer values (as in the case of Poisson and binomial distributions), it is not generally possible to construct confidence intervals with exact coverage for all values of α . In these cases the integral in Eq. (28.33) becomes a sum of finite contributions and it is no longer possible (in general) to find consecutive terms which add up exactly to the required confidence level $1 - \epsilon$ for all values of α . Thus one constructs intervals which happen to have exact coverage for a few values of α , and unavoidable over-coverage for all other values.

In addition to the problem posed by the discreteness of the data, we usually have to contend with possible background whose expectation must be evaluated separately and may not be known precisely. For these reasons, the reporting of this kind of data is even more controversial than the Gaussian data near a boundary as discussed above. This is especially true when the number of observed counts is greater than the expected background. As for the Gaussian case, there are at least three possibilities for reporting such results depending on how the result is to be used:

(a) The actual measurements should be reported, which means (1) the number of recorded counts, (2) the expected background, possibly with its error, and (3) normalization factor which turns the number of counts into a cross section, decay rate, etc. As with Gaussian data, these data can be combined with that of other experiments, to make improved upper limits for example.

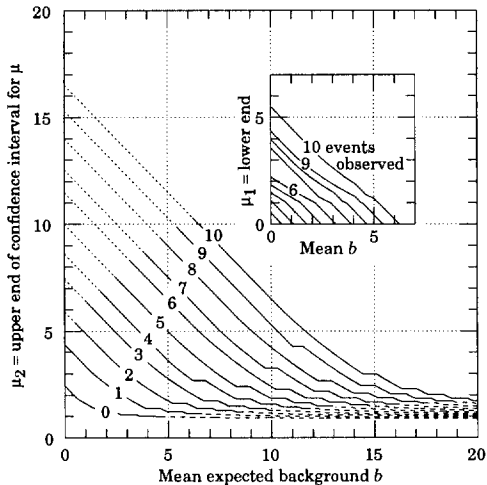


Figure 28.5: 90% confidence intervals $[\mu_1, \mu_2]$ on the number of signal events μ as a function of the expected number of background events b . For example, if the expected background is 8 events and 5 events are observed, then the signal is 2.60 or less with 90% confidence. Dotted portions of the μ_2 curves on the upper left indicate regions where μ_1 is non-zero (as shown by the inset). Dashed portions in the lower right indicate regions where the probability of obtaining the number of events observed or fewer is less than 1%, even if $\mu = 0$. Horizontal curve sections occur because of discrete number statistics. Tables showing these data as well as the CL = 68.27%, 95%, and 99% results are given in Ref. 13. There is considerable discussion about the behavior of the intervals when the number of observed events is less than the expected background; see Ref. 5

(b) A Bayesian upper limit may be reported. This has the advantages and disadvantages of any Bayesian result as discussed above. The noninformative priors (based on invariance principles rather than subjective degree of belief) recommended in the statistics literature for Poisson mean are rarely, if at all, used in high energy physics; they diverge for the case of zero events observed, and they give upper limits which undercover when evaluated by the Frequentist criterion of coverage. Rather, priors uniform in the counting rate have been used by convention; care must be used in interpreting such results either as “degree of belief” or as a limiting frequency.

(c) An upper limit (or confidence region) with optimal coverage can be reported using the unified approach of Ref. 13. At the moment these confidence limits have been calculated only for the case of exactly known background expectation. The main results can be read from Fig. 28.5 or from Table 28.3; more extensive tables can be found in Ref. 13.

Table 28.3: Poisson limits $[\mu_1, \mu_2]$ for n_0 observed events in the absence of background.

n_0	CI = 90%		CI = 95%	
	μ_1	μ_2	μ_1	μ_2
0	0.00	2.44	0.00	3.09
1	0.11	4.36	0.05	5.14
2	0.53	5.91	0.36	6.72
3	1.10	7.42	0.82	8.25
4	1.47	8.60	1.37	9.76
5	1.84	9.99	1.84	11.26
6	2.21	11.47	2.21	12.75
7	3.56	12.53	2.58	13.81
8	3.96	13.99	2.94	15.29
9	4.36	15.30	4.36	16.77
10	5.50	16.50	4.75	17.82

None of the above gives a single number which quantifies the quality or sensitivity of the experiment. This is a serious shortcoming of most upper limits including those of method (c), since it is impossible to distinguish, from the upper limit alone, between a clean experiment with no background and a lucky experiment with fewer observed counts than expected background. For this reason, we suggest that in addition to (a) and (c) above, a measure of the sensitivity should be reported whenever expected background is larger or comparable to the number of observed counts. The best such measure we know of is that proposed and tabulated in Ref. 13, defined as the average upper limit that would be attained by an ensemble of experiments with the expected background and no true signal.

References:

1. B. Efron, *Am. Stat.* **40**, 11 (1986).
2. R.D. Cousins, *Am. J. Phys.* **63**, 398 (1995).
3. A. Stuart and A. K. Ord, *Kendall's Advanced Theory of Statistics*, Vol. 2 *Classical Inference and Relationship* 5th Ed., (Oxford Univ. Press, 1991), and earlier editions by Kendall and Stuart. The likelihood-ratio ordering principle is described at the beginning of Ch. 23. Chapter 31 compares different schools of statistical inference.
4. W.T. Eadie, D. Drijard, F.E. James, M. Roos, and B. Sadoulet, *Statistical Methods in Experimental Physics* (North Holland, Amsterdam and London, 1971).
5. Workshop on Confidence Limits, CERN, 17-18 Jan. 2000, www.cern.ch/CERN/Divisions/EP/Events/CLW/. See also the later Fermilab workshop linked to the CERN web page.
6. H. Cramér, *Mathematical Methods of Statistics*, Princeton Univ. Press, New Jersey (1958).
7. B.P. Roe, *Probability and Statistics in Experimental Physics*, (Springer-Verlag, New York, 208 pp., 1992).
8. G. Cowan, *Statistical Data Analysis* (Oxford University Press, Oxford, 1998).
9. W.H. Press *et al.*, *Numerical Recipes* (Cambridge University Press, New York, 1986).
10. F. James and M. Roos, “MINUIT, Function Minimization and Error Analysis,” CERN D506 (Long Writeup). Available from the CERN Program Library Office, CERN-IT Division, CERN, CH-1211, Geneva 21, Switzerland.
11. For a review, see S. Baker and R. Cousins, *Nucl. Instrum. Methods* **221**, 437 (1984).
12. J. Neyman, *Phil. Trans. Royal Soc. London, Series A*, **236**, 333 (1937), reprinted in *A Selection of Early Statistical Papers on J. Neyman* (University of California Press, Berkeley, 1967).
13. G.J. Feldman and R.D. Cousins, *Phys. Rev.* **D57**, 3873 (1998). This paper does not specify what to do if the ordering principle gives equal rank to some values of x . Eq. 23.6 of Ref. 3 gives the rule: all such points are included in the acceptance region (the domain $D(\epsilon)$). Some authors have assumed the contrary, and shown that one can then obtain null intervals..
14. B.P. Roe and M.B. Woodrooffe, *Phys. Rev.* **D60**, 053009 (1999).

29. MONTE CARLO TECHNIQUES

Revised July 1995 by S. Youssef (SCRI, Florida State University). Updated February 2000 by R. Cousins (UCLA) in consultation with F. James (CERN).

Monte Carlo techniques are often the only practical way to evaluate difficult integrals or to sample random variables governed by complicated probability density functions. Here we describe an assortment of methods for sampling some commonly occurring probability density functions.

29.1. Sampling the uniform distribution

Most Monte Carlo sampling or integration techniques assume a "random number generator" which generates uniform statistically independent values on the half open interval $[0,1)$. There is a long history of problems with various generators on a finite digital computer, but recently, the RANLUX generator [1] has emerged with a solid theoretical basis in chaos theory. Based on the method of Lüscher, it allows the user to select different quality levels, trading off quality with speed.

Other generators are also available which pass extensive batteries of tests for statistical independence and which have periods which are so long that, for practical purposes, values from these generators can be considered to be uniform and statistically independent. In particular, the lagged-Fibonacci based generator introduced by Marsaglia, Zaman, and Tsang [2] is efficient, has a period of approximately 10^{43} , produces identical sequences on a wide variety of computers and, passes the extensive "DIEHARD" battery of tests [3]. Many commonly available congruential generators fail these tests and often have sequences (typically with periods less than 2^{32}) which can be easily exhausted on modern computers and should therefore be avoided [4].

29.2. Inverse transform method

If the desired probability density function is $f(x)$ on the range $-\infty < x < \infty$, its cumulative distribution function (expressing the probability that $x \leq a$) is given by Eq. (27.1). If a is chosen with probability density $f(a)$, then the integrated probability up to point a , $F(a)$, is itself a random variable which will occur with uniform probability density on $[0,1]$. If x can take on any value, and ignoring the endpoints, we can then find a unique x chosen from the p.d.f. $f(x)$ for a given u if we set

$$u = F(x), \tag{29.1}$$

provided we can find an inverse of F , defined by

$$x = F^{-1}(u). \tag{29.2}$$

This method is shown in Fig. 29.1a. It is most convenient when one can calculate by hand the inverse function of the indefinite integral of f . This is the case for some common functions $f(x)$ such as $\exp(x)$, $(1-x)^n$, and $1/(1+x^2)$ (Cauchy or Breit-Wigner), although it does not necessarily produce the fastest generator. CERNLIB contains routines to implement this method numerically, working from functions or histograms.

For a discrete distribution, $F(x)$ will have a discontinuous jump of size $f(x_k)$ at each allowed $x_k, k = 1, 2, \dots$. Choose u from a uniform distribution on $(0,1)$ as before. Find x_k such that

$$F(x_{k-1}) < u \leq F(x_k) \equiv \text{Prob}(x \leq x_k) = \sum_{i=1}^k f(x_i); \tag{29.3}$$

then x_k is the value we seek (note: $F(x_0) \equiv 0$). This algorithm is illustrated in Fig. 29.1b.

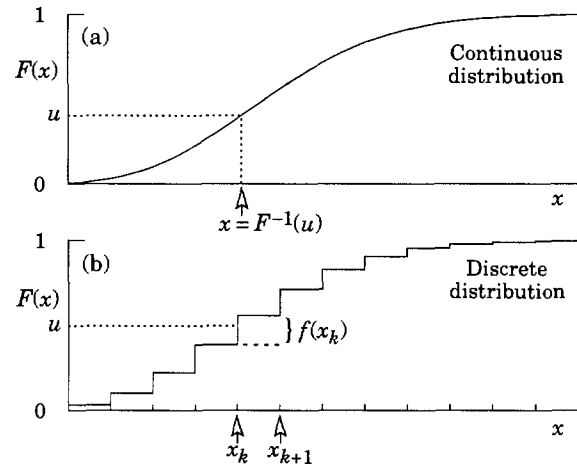


Figure 29.1: Use of a random number u chosen from a uniform distribution $(0,1)$ to find a random number x from a distribution with cumulative distribution function $F(x)$.

29.3. Acceptance-rejection method (Von Neumann)

Very commonly an analytic form for $F(x)$ is unknown or too complex to work with, so that obtaining an inverse as in Eq. (29.2) is impractical. We suppose that for any given value of x the probability density function $f(x)$ can be computed and further that enough is known about $f(x)$ that we can enclose it entirely inside a shape which is C times an easily generated distribution $h(x)$ as illustrated in Fig. 29.2.

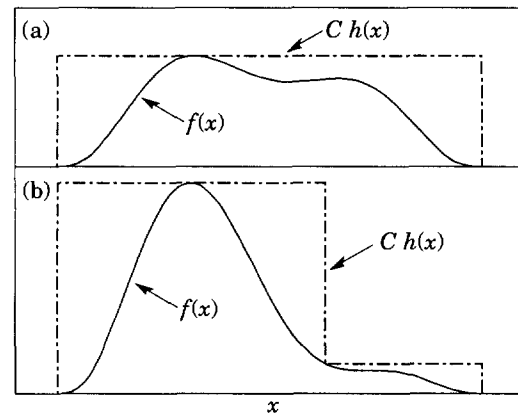


Figure 29.2: Illustration of the acceptance-rejection method. Random points are chosen inside the upper bounding figure, and rejected if the ordinate exceeds $f(x)$. Lower figure illustrates importance sampling.

Frequently $h(x)$ is uniform or is a normalized sum of uniform distributions. Note that both $f(x)$ and $h(x)$ must be normalized to unit area and therefore the proportionality constant $C > 1$. To generate $f(x)$, first generate a candidate x according to $h(x)$. Calculate $f(x)$ and the height of the envelope $C h(x)$; generate u and test if $u C h(x) \leq f(x)$. If so, accept x ; if not reject x and try again. If we regard x and $u C h(x)$ as the abscissa and ordinate of a point in a two-dimensional plot, these points will populate the entire area $C h(x)$ in a smooth manner; then we accept those which fall under $f(x)$. The efficiency is the ratio of areas, which must equal $1/C$; therefore we must keep C as close as possible to 1.0. Therefore we try to choose $C h(x)$ to be as close to $f(x)$ as convenience dictates, as in the lower part of Fig. 29.2. This practice is called importance sampling, because we generate more trial values of x in the region where $f(x)$ is most important.

29.4. Algorithms

Algorithms for generating random numbers belonging to many different distributions are given by Press [5], Ahrens and Dieter [6], Rubinstein [7], Everett and Cashwell [8], Devroye [9], and Walck [10]. For many distributions alternative algorithms exist, varying in complexity, speed, and accuracy. For time-critical applications, these algorithms may be coded in-line to remove the significant overhead often encountered in making function calls. Variables named "u" are assumed to be independent and uniform on (0,1). (Hence, u must be verified to be non-zero where relevant.)

In the examples given below, we use the notation for the variables and parameters given in Table 27.1.

29.4.1. Exponential decay:

This is a common application of the inverse transform method, also using the fact that (1 - u) is uniform if u is uniform. To generate decays between times t1 and t2 according to f(t) = exp(-t/τ): let r2 = exp(-t2/τ) and r1 = exp(-t1/τ); generate u and let

$$t = -\tau \ln(r_2 + u(r_1 - r_2)). \tag{29.4}$$

For (t1, t2) = (0, ∞), we have simply t = -τ ln u. (See also Sec. 29.4.6.)

29.4.2. Isotropic direction in 3D:

Isotropy means the density is proportional to solid angle, the differential element of which is dΩ = d(cos θ)dφ. Hence cos θ is uniform (2u1 - 1) and φ is uniform (2πu2). For alternative generation of sin φ and cos φ, see the next subsection.

29.4.3. Sine and cosine of random angle in 2D:

Generate u1 and u2. Then v1 = 2u1 - 1 is uniform on (-1,1), and v2 = u2 is uniform on (0,1). Calculate r2 = v1^2 + v2^2. If r2 > 1, start over. Otherwise, the sine (S) and cosine (C) of a random angle are given by

$$S = 2v_1v_2/r^2 \quad \text{and} \quad C = (v_1^2 - v_2^2)/r^2. \tag{29.5}$$

29.4.4. Gaussian distribution:

If u1 and u2 are uniform on (0,1), then

$$z_1 = \sin 2\pi u_1 \sqrt{-2 \ln u_2} \quad \text{and} \quad z_2 = \cos 2\pi u_1 \sqrt{-2 \ln u_2} \tag{29.6}$$

are independent and Gaussian distributed with mean 0 and σ = 1.

There are many faster variants of this basic algorithm. For example, construct v1 = 2u1 - 1 and v2 = 2u2 - 1, which are uniform on (-1,1). Calculate r2 = v1^2 + v2^2, and if r2 > 1 start over. If r2 < 1, it is uniform on (0,1). Then

$$z_1 = v_1 \sqrt{\frac{-2 \ln r^2}{r^2}} \quad \text{and} \quad z_2 = v_2 \sqrt{\frac{-2 \ln r^2}{r^2}} \tag{29.7}$$

are independent numbers chosen from a normal distribution with mean 0 and variance 1. zi = μ + σzi distributes with mean μ and variance σ2.

A recent implementation of the fast algorithm of Leva Ref. 11 is in CERNLIB.

For a multivariate Gaussian, see the algorithm in Ref. 12.

29.4.5. χ2(n) distribution:

For n even, generate n/2 uniform numbers ui; then

$$y = -2 \ln \left(\prod_{i=1}^{n/2} u_i \right) \quad \text{is} \quad \chi^2(n). \tag{29.8}$$

For n odd, generate (n - 1)/2 uniform numbers ui and one Gaussian z as in Sec. 29.4.4; then

$$y = -2 \ln \left(\prod_{i=1}^{(n-1)/2} u_i \right) + z^2 \quad \text{is} \quad \chi^2(n). \tag{29.9}$$

For n ≳ 30 the much faster Gaussian approximation for the χ2 may be preferable: generate z as in Sec. 29.4.4 and use

y = [z + √(2n - 1)]2 / 2; if z < -√(2n - 1) reject and start over.

29.4.6. Gamma distribution:

All of the following algorithms are given for λ = 1. For λ ≠ 1, divide the resulting random number x by λ.

- If k = 1 (the exponential distribution), accept x = -(ln u). (See also Sec. 29.4.1.)
- If 0 < k < 1, initialize with v1 = (e + k)/e (with e = 2.71828... being the natural log base). Generate u1, u2. Define v2 = v1u1.

Case 1: v2 ≤ 1. Define x = v2^{1/k}. If u2 ≤ e^{-x}, accept x and stop, else restart by generating new u1, u2.

Case 2: v2 > 1. Define x = -ln([v1 - v2]/k). If u2 ≤ x^{k-1}, accept x and stop, else restart by generating new u1, u2. Note that, for k < 1, the probability density has a pole at x = 0, so that return values of zero due to underflow must be accepted or otherwise dealt with.

- Otherwise, if k > 1, initialize with c = 3k - 0.75. Generate u1 and compute v1 = u1(1 - u1) and v2 = (u1 - 0.5)√c/v1. If x = k + v2 - 1 ≤ 0, go back and generate new u1; otherwise generate u2 and compute v3 = 64v1³u2². If v3 ≤ 1 - 2v2²/x or if ln v3 ≤ 2{[k - 1] ln[x/(k - 1)] - v2}, accept x and stop; otherwise go back and generate new u1.

29.4.7. Binomial distribution:

If p ≤ 1/2, iterate until a successful choice is made: begin with k = 1; compute Pk = qⁿ [for k ≠ 1 use Pk ≡ f(rk; n, p), and store Pk into B; generate u. If u ≤ B accept rk = k - 1 and stop; otherwise increment k by 1 and compute next Pk and add to B; generate a new u and repeat. If we arrive at k = n + 1, stop and accept rn+1 = n. If p > 1/2 it will be more efficient to generate r from f(r; n, q), i.e., with p and q interchanged, and then set rk = n - r.

29.4.8. Poisson distribution:

Iterate until a successful choice is made: Begin with k = 1 and set A = 1 to start. Generate u. Replace A with uA; if now A < exp(-μ), where μ is the Poisson parameter, accept nk = k - 1 and stop. Otherwise increment k by 1, generate a new u and repeat, always starting with the value of A left from the previous try. For large μ (≳ 10) it may be satisfactory (and much faster) to approximate the Poisson distribution by a Gaussian distribution (see our Probability chapter, Sec. 27.3.3) and generate z from f(z; 0, 1); then accept x = max(0, [μ + z√μ + 0.5]) where [] signifies the greatest integer ≤ the expression. [13]

29.4.9. Student's t distribution:

For n > 0 degrees of freedom (n not necessarily integer), generate x from a Gaussian with mean 0 and σ2 = 1 according to the method of 29.4.4. Next generate y, an independent gamma random variate with k = n/2 degrees of freedom. Then z = x√(2n)/√y is distributed as a t with n degrees of freedom.

For the special case n = 1, the Breit-Wigner distribution, generate u1 and u2; set v1 = 2u1 - 1 and v2 = 2u2 - 1. If v1² + v2² ≤ 1 accept z = v1/v2 as a Breit-Wigner distribution with unit area, center at 0.0, and FWHM 2.0. Otherwise start over. For center M0 and FWHM Γ, use W = zΓ/2 + M0.

References:

1. F. James, Comp. Phys. Comm. **79** 111 (1994), based on M. Lüscher, Comp. Phys. Comm. **79** 100 (1994). This generator is available as the CERNLIB routine V115, RANLUX.
2. G. Marsaglia, A. Zaman, and W.W. Tsang, *Towards a Universal Random Number Generator*, Supercomputer Computations Research Institute, Florida State University technical report FSU-SCRI-87-50 (1987). This generator is available as the CERNLIB routine V113, RANMAR, by F. Carminati and F. James.
3. Much of DIEHARD is described in: G. Marsaglia, *A Current View of Random Number Generators*, keynote address, *Computer Science and Statistics: 16th Symposium on the Interface*, Elsevier (1985).

4. Newer generators with periods even longer than the lagged-Fibonacci based generator are described in G. Marsaglia and A. Zaman, *Some Portable Very-Long-Period Random Number Generators*, *Compt. Phys.* **8**, 117 (1994). The Numerical Recipes generator **ran2** [W.H. Press and S.A. Teukolsky, *Portable Random Number Generators*, *Compt. Phys.* **6**, 521 (1992)] is also known to pass the DIEHARD tests.
5. W.H. Press *et al.*, *Numerical Recipes* (Cambridge University Press, New York, 1986).
6. J.H. Ahrens and U. Dieter, *Computing* **12**, 223 (1974).
7. R.Y. Rubinstein, *Simulation and the Monte Carlo Method* (John Wiley and Sons, Inc., New York, 1981).
8. C.J. Everett and E.D. Cashwell, *A Third Monte Carlo Sampler*, Los Alamos report LA-9721-MS (1983).
9. L. Devroye, *Non-Uniform Random Variate Generation* (Springer-Verlag, New York, 1986).
10. Ch. Walck, *Random Number Generation*, University of Stockholm Physics Department Report 1987-10-20 (Vers. 3.0).
11. J.L. Leva, *ACM Trans. Math. Softw.* **18** 449 (1992). This generator has been implemented by F. James in the CERNLIB routine V120, RNORML.
12. F. James, *Rept. on Prog. in Phys.* **43**, 1145 (1980).
13. This generator has been implemented by D. Drijard and K. Kölblig in the CERNLIB routine V136, RNPSSN.

30. MONTE CARLO PARTICLE NUMBERING SCHEME

Revised April 2000 by L. Garren (Fermilab), I.G. Knowles (Edinburgh U.), T. Sjöstrand (Lund U.), and T. Trippe (LBNL).

The Monte Carlo particle numbering scheme presented here is intended to facilitate interfacing between event generators, detector simulators, and analysis packages used in particle physics. The numbering scheme was introduced in 1988 [1] and a revised version [2,3] was adopted in 1998 in order to allow systematic inclusion of quark model states which are as yet undiscovered and hypothetical particles such as SUSY particles. The numbering scheme is used in several event generators, *e.g.* HERWIG and PYTHIA/JETSET, and in the /HEPEVT/ [4] standard interface.

The general form is a 7-digit number:

$$\pm n n_r n_L n_{q_1} n_{q_2} n_{q_3} n_J .$$

This encodes information about the particle's spin, flavor content, and internal quantum numbers. The details are as follows:

1. Particles are given positive numbers, antiparticles negative numbers. The PDG convention for mesons is used, so that K^+ and B^+ are particles.
2. Quarks and leptons are numbered consecutively starting from 1 and 11 respectively; to do this they are first ordered by family and within families by weak isospin.
3. In composite quark systems (diquarks, mesons, and baryons) $n_{q_{1-3}}$ are quark numbers used to specify the quark content, while the rightmost digit $n_J = 2J + 1$ gives the system's spin (except for the K_S^0 and K_L^0). The scheme does not cover particles of spin $J > 4$.
4. Diquarks have 4-digit numbers with $n_{q_1} \geq n_{q_2}$ and $n_{q_3} = 0$.
5. The numbering of mesons is guided by the nonrelativistic (L - S decoupled) quark model, as listed in Table 13.2.
 - a. The numbers specifying the meson's quark content conform to the convention $n_{q_1} = 0$ and $n_{q_2} \geq n_{q_3}$. The special case K_L^0 is the sole exception to this rule.
 - b. The quark numbers of flavorless, light (u, d, s) mesons are: 11 for the member of the isotriplet (π^0, ρ^0, \dots), 22 for the lighter isosinglet (η, ω, \dots), and 33 for the heavier isosinglet (η', ϕ, \dots). Since isosinglet mesons are often large mixtures of $u\bar{u} + d\bar{d}$ and $s\bar{s}$ states, 22 and 33 are assigned by mass and do not necessarily specify the dominant quark composition.
 - c. The special numbers 310 and 130 are given to the K_S^0 and K_L^0 respectively.
 - d. The fifth digit n_L is reserved to distinguish mesons of the same total (J) but different spin (S) and orbital (L) angular momentum quantum numbers. For $J > 0$ the numbers are: (L, S) = ($J - 1, 1$) $n_L = 0$, ($J, 0$) $n_L = 1$, ($J, 1$) $n_L = 2$ and ($J + 1, 1$) $n_L = 3$. For the exceptional case $J = 0$ the numbers are ($0, 0$) $n_L = 0$ and ($1, 1$) $n_L = 1$ (*i.e.* $n_L = L$). See Table 30.1.

Table 30.1: Meson numbering logic. Here qq stands for $n_{q_2} n_{q_3}$.

	$L = J - 1, S = 1$	$L = J, S = 0$	$L = J, S = 1$	$L = J + 1, S = 1$
J	code $J^{PC} L$	code $J^{PC} L$	code $J^{PC} L$	code $J^{PC} L$
0	— — —	00qq1 0 ⁺⁺ 0	— — —	10qq1 0 ⁺⁺ 1
1	00qq3 1 ⁻⁻ 0	10qq3 1 ⁺⁻ 1	20qq3 1 ⁺⁺ 1	30qq3 1 ⁻⁻ 2
2	00qq5 2 ⁺⁺ 1	10qq5 2 ⁻⁺ 2	20qq5 2 ⁻⁻ 2	30qq5 2 ⁺⁺ 3
3	00qq7 3 ⁻⁻ 2	10qq7 3 ⁺⁻ 3	20qq7 3 ⁺⁺ 3	30qq7 3 ⁻⁻ 4
4	00qq9 4 ⁺⁺ 3	10qq9 4 ⁺⁻ 4	20qq9 4 ⁻⁻ 4	30qq9 4 ⁺⁺ 5

- e. If a set of physical mesons correspond to a (non-negligible) mixture of basis states, differing in their internal quantum numbers, then the lightest physical state gets the smallest basis state number. For example the $K_1(1270)$ is numbered 10313 ($1^1 P_1 K_{1B}$) and the $K_1(1400)$ is numbered 20313 ($1^3 P_1 K_{1A}$).

- f. The sixth digit n_r is used to label mesons radially excited above the ground state.
 - g. Numbers have been assigned for complete $n_r = 0$ S - and P -wave multiplets, even where states remain to be identified.
 - h. In some instances assignments within the $q\bar{q}$ meson model are only tentative; here best guess assignments are made.
 - i. Many states appearing in the Meson Listings are not yet assigned within the $q\bar{q}$ model. Here $n_{q_{2-3}}$ and n_J are assigned according to the state's likely flavors and spin; all such unassigned light isoscalar states are given the flavor code 22. Within these groups $n_L = 0, 1, 2, \dots$ is used to distinguish states of increasing mass. These states are flagged using $n = 9$. It is to be expected that these numbers will evolve as the nature of the states are elucidated.
6. The numbering of baryons is again guided by the nonrelativistic quark model, see Table 13.4.
 - a. The numbers specifying a baryon's quark content are such that in general $n_{q_1} \geq n_{q_2} \geq n_{q_3}$.
 - b. Two states exist for $J = 1/2$ baryons containing 3 different types of quarks. In the lighter baryon ($\Lambda, \Xi, \Omega, \dots$) the light quarks are in an antisymmetric ($J = 0$) state while for the heavier baryon ($\Sigma^0, \Xi', \Omega', \dots$) they are in a symmetric ($J = 1$) state. In this situation n_{q_2} and n_{q_3} are reversed for the lighter state, so that the smaller number corresponds to the lighter baryon.
 - c. At present most Monte Carlos do not include excited baryons and no systematic scheme has been developed to denote them, though one is foreseen. In the meantime, use of the PDG 96 [5] numbers for excited baryons is recommended.
 7. The gluon, when considered as a gauge boson, has official number 21. In codes for glueballs, however, 9 is used to allow a notation in close analogy with that of hadrons.
 8. The pomeron and odderon trajectories and a generic reggeon trajectory of states in QCD are assigned codes 990, 9990, and 110 respectively, where the final 0 indicates the indeterminate nature of the spin, and the other digits reflect the expected "valence" flavor content. We do not attempt a complete classification of all reggeon trajectories, since there is currently no need to distinguish a specific such trajectory from its lowest-lying member.
 9. Two-digit numbers in the range 21–30 are provided for the Standard Model gauge bosons and Higgs.
 10. Codes 81–100 are reserved for generator-specific pseudoparticles and concepts.
 11. The search for physics beyond the Standard Model is an active area, so these codes are also standardized as far as possible.
 - a. A standard fourth generation of fermions is included by analogy with the first three.
 - b. The graviton and the boson content of a two-Higgs-doublet scenario and of additional $SU(2) \times U(1)$ groups are found in the range 31–40.
 - c. "One-of-a-kind" exotic particles are assigned numbers in the range 41–80.
 - d. Fundamental supersymmetric particles are identified by adding a nonzero n to the particle number. The superpartner of a boson or a left-handed fermion has $n = 1$ while the superpartner of a right-handed fermion has $n = 2$. When mixing occurs, such as between the winos and charged Higgsinos to give charginos, or between left and right sfermions, the lighter physical state is given the smaller basis state number.
 - e. Technicolor states have $n = 3$. In the absence of a unique theory we only number generic states whose digits reflect the techniquark content.
 - f. Excited (composite) quarks and leptons are identified by setting $n = 4$.
 12. Occasionally program authors add their own states. To avoid confusion, these should be flagged by setting $nn_r = 99$.
 13. Concerning the non-99 numbers, it may be noted that only quarks, excited quarks, squarks, and diquarks have $n_{q_3} = 0$;

only diquarks, baryons, and the odderon have $n_{q_1} \neq 0$; and only mesons, the reggeon, and the pomeron have $n_{q_1} = 0$ and $n_{q_2} \neq 0$. Concerning mesons (not antimesons), if n_{q_1} is odd then it labels a quark and an antiquark if even.

This text and lists of particle numbers can be found on the WWW [6]. The StdHep Monte Carlo standardization project [7] maintains the list of PDG particle numbers, as well as numbering schemes from most event generators and software to convert between the different schemes.

References:

1. G.P. Yost *et al.*, Particle Data Group, Phys. Lett. **B204**, 1 (1988).
2. I. G. Knowles *et al.*, in "Physics at LEP2", CERN 96-01, vol. 2, p. 103.
3. C. Caso *et al.*, Particle Data Group, Eur. Phys. J. **C3**, 1 (1998).
4. T. Sjöstrand *et al.*, in "Z physics at LEP1", CERN 89-08, vol. 3, p. 327.
5. R.M. Barnett *et al.*, Particle Data Group, Phys. Rev. **D54**, 1 (1996).
6. http://pdg.lbl.gov/mc_particle_id_contents.html.
7. L. Garren, StdHep, Monte Carlo Standardization at FNAL, Fermilab PM0091 and StdHep WWW site: <http://www-pat.fnal.gov/stdhep.html>.

QUARKS		DIQUARKS		SUSY PARTICLES		LIGHT $I = 1$ MESONS		LIGHT $I = 0$ MESONS ($u\bar{u}$, $d\bar{d}$, and $s\bar{s}$ Admixtures)	
d	1	$(dd)_1$	1103	\tilde{d}_L	1000001	π^0	111	π^+	211
u	2	$(ud)_0$	2101	\tilde{u}_L	1000002	$a_0(980)^0$	9000111	η	221
s	3	$(ud)_1$	2103	\tilde{s}_L	1000003	$a_0(980)^+$	9000211	$\eta'(958)$	331
c	4	$(uu)_1$	2203	\tilde{c}_L	1000004	$\pi(1300)^0$	100111	$f_0(400-1200)$	9000221
b	5	$(sd)_0$	3101	\tilde{b}_1	1000005 ^a	$\pi(1300)^+$	100211	$f_0(980)$	9010221
t	6	$(sd)_1$	3103	\tilde{t}_1	1000006 ^a	$a_0(1450)^0$	10111	$\eta(1295)$	100221
b'	7	$(su)_0$	3201	\tilde{e}_L	1000011	$a_0(1450)^+$	10211	$f_0(1370)$	10221
t'	8	$(su)_1$	3203	$\tilde{\nu}_{eL}$	1000012	$\pi(1800)^0$	200111	$\eta(1440)$	100331
LEPTONS		$(ss)_1$	3303	$\tilde{\mu}_L$	1000013	$\pi(1800)^+$	200211	$f_0(1500)$	9020221
e^-	11	$(cd)_0$	4101	$\tilde{\nu}_{\mu L}$	1000014	$\rho(770)^0$	113	$f_0(1710)$	10331*
ν_e	12	$(cd)_1$	4103	$\tilde{\tau}_1$	1000015 ^a	$\rho(770)^+$	213	$\eta(1760)$	200221
μ^-	13	$(cu)_0$	4201	$\tilde{\nu}_{\tau L}$	1000016	$b_1(1235)^0$	10113	$f_0(2020)$	9030221*
ν_μ	14	$(cu)_1$	4203	\tilde{d}_R	2000001	$b_1(1235)^+$	10213	$f_0(2060)$	9040221*
τ^-	15	$(cs)_0$	4301	\tilde{u}_R	2000002	$a_1(1260)^0$	20113	$f_0(2200)$	9050221*
ν_τ	16	$(cs)_1$	4303	\tilde{s}_R	2000003	$a_1(1260)^+$	20213	$\eta(2225)$	9060221*
τ'^-	17	$(cc)_1$	4403	\tilde{c}_R	2000004	$\pi_1(1400)^0$	9000113*	$\omega(782)$	223
$\nu_{\tau'}$	18	$(bd)_0$	5101	\tilde{b}_2	2000005 ^a	$\pi_1(1400)^+$	9000213*	$\phi(1020)$	333
EXCITED PARTICLES		$(bd)_1$	5103	\tilde{t}_2	2000006 ^a	$\rho(1450)^0$	100113	$h_1(1170)$	10223
d^*	4000001	$(bu)_0$	5201	\tilde{e}_R	2000011	$\rho(1450)^+$	100213	$f_1(1285)$	20223
u^*	4000002	$(bu)_1$	5203	$\tilde{\mu}_R$	2000013	$\pi_1(1600)^0$	9010113*	$h_1(1380)$	10333
e^*	4000011	$(bs)_0$	5301	$\tilde{\tau}_2$	2000015 ^a	$\pi_1(1600)^+$	9010213*	$f_1(1420)$	20333
ν_e^*	4000012	$(bs)_1$	5303	\tilde{g}	1000021	$\alpha_1(1640)^0$	9020113*	$\omega(1420)$	100223
GAUGE AND HIGGS BOSONS		$(bc)_0$	5401	$\tilde{\chi}_1^0$	1000022 ^b	$\alpha_1(1640)^+$	9020213*	$f_1(1510)$	9000223
g	(9) 21	$(bc)_1$	5403	$\tilde{\chi}_2^0$	1000023 ^b	$\rho(1700)^0$	30113	$\omega(1650)$	30223*
γ	22	TECHNICOLOR PARTICLES		$\tilde{\chi}_1^+$	1000024 ^b	$\rho(1700)^+$	30213	$\phi(1680)$	100333
Z^0	23	π_{tech}^0	3000111	$\tilde{\chi}_3^0$	1000025 ^b	$\rho(2150)^0$	9030113*	$f_2(1270)$	225
W^+	24	π_{tech}^+	3000211	$\tilde{\chi}_4^0$	1000035 ^b	$\rho(2150)^+$	9030213*	$f_2(1430)$	9000225
h^0/H_1^0	25	η_{tech}^0	3000221	$\tilde{\chi}_2^+$	1000037 ^b	$a_2(1320)^0$	115	$f_2'(1525)$	335
Z'/Z_2^0	32	ρ_{tech}^0	3000113	\tilde{G}	1000039	$a_2(1320)^+$	215	$f_2(1565)$	9010225
Z''/Z_3^0	33	ρ_{tech}^+	3000213	SPECIAL PARTICLES		$\alpha_2(1660)^0$	9000115*	$f_2(1640)$	9020225
W'/W_2^+	34	ω_{tech}^0	3000223	G (graviton)	39	$\alpha_2(1660)^+$	9000215*	$\eta_2(1645)$	10225
H^0/H_2^0	35			R^0	41	$\pi_2(1670)^0$	10115	$f_2(1810)$	100225
A^0/H_3^0	36			LQ^c	42	$\pi_2(1670)^+$	10215	$\eta_2(1870)$	10335
H^+	37			<i>reggeon</i>	110	$\alpha_2(1750)^0$	9010115*	$f_2(1950)$	9030225
				<i>pomeron</i>	990	$\alpha_2(1750)^+$	9010215*	$f_2(2010)$	100335
				<i>odderon</i>	9990	$\pi_2(2100)^0$	9020115*	$f_2(2150)$	9040225
						$\pi_2(2100)^+$	9020215*	$f_2(2300)$	9050225
						$\rho_3(1690)^0$	117	$f_2(2340)$	9060225
						$\rho_3(1690)^+$	217	$\omega_3(1670)$	227
						$\rho_3(2250)^0$	9000117	$\phi_3(1850)$	337
						$\rho_3(2250)^+$	9000217	$f_4(2050)$	229
						$a_4(2040)^0$	119	$f_J(2220)$	9000339
						$a_4(2040)^+$	219	$f_4(2300)$	9000229

31. CLEBSCH-GORDAN COEFFICIENTS, SPHERICAL HARMONICS, AND d FUNCTIONS

Note: A square-root sign is to be understood over every coefficient, e.g., for $-8/15$ read $-\sqrt{8/15}$.

Notation:

J	J	\dots
M	M	\dots
m_1	m_2	\dots
\vdots	\vdots	\vdots
\vdots	\vdots	\vdots
\vdots	\vdots	\vdots

Coefficients

$Y_1^0 = \sqrt{\frac{3}{4\pi}} \cos \theta$

$Y_1^1 = -\sqrt{\frac{3}{8\pi}} \sin \theta e^{i\phi}$

$Y_2^0 = \sqrt{\frac{5}{4\pi}} \left(\frac{3}{2} \cos^2 \theta - \frac{1}{2}\right)$

$Y_2^1 = -\sqrt{\frac{15}{8\pi}} \sin \theta \cos \theta e^{i\phi}$

$Y_2^2 = \frac{1}{4} \sqrt{\frac{15}{2\pi}} \sin^2 \theta e^{2i\phi}$

$Y_\ell^{-m} = (-1)^m Y_\ell^{m*}$

$d_{m,0}^\ell = \sqrt{\frac{4\pi}{2\ell+1}} Y_\ell^m e^{-im\phi}$

$(j_1 j_2 m_1 m_2 | j_1 j_2 JM)$

$= (-1)^{J-j_1-j_2} (j_2 j_1 m_2 m_1 | j_2 j_1 JM)$

$d_{m',m}^j = (-1)^{m-m'} d_{m,m'}^j = d_{-m,-m'}^j$

$d_{1,0}^1 = \cos \theta$

$d_{1/2,1/2}^{1/2} = \cos \frac{\theta}{2}$

$d_{1/2,-1/2}^{1/2} = -\sin \frac{\theta}{2}$

$d_{1,1}^1 = \frac{1 + \cos \theta}{2}$

$d_{1,0}^1 = -\frac{\sin \theta}{\sqrt{2}}$

$d_{1,-1}^1 = \frac{1 - \cos \theta}{2}$

$d_{3/2,3/2}^{3/2} = \frac{1 + \cos \theta}{2} \cos \frac{\theta}{2}$

$d_{3/2,1/2}^{3/2} = -\sqrt{3} \frac{1 + \cos \theta}{2} \sin \frac{\theta}{2}$

$d_{3/2,-1/2}^{3/2} = \sqrt{3} \frac{1 - \cos \theta}{2} \cos \frac{\theta}{2}$

$d_{3/2,-3/2}^{3/2} = -\frac{1 - \cos \theta}{2} \sin \frac{\theta}{2}$

$d_{1/2,1/2}^{3/2} = \frac{3 \cos \theta - 1}{2} \cos \frac{\theta}{2}$

$d_{1/2,-1/2}^{3/2} = -\frac{3 \cos \theta + 1}{2} \sin \frac{\theta}{2}$

$d_{2,2}^2 = \left(\frac{1 + \cos \theta}{2}\right)^2$

$d_{2,1}^2 = -\frac{1 + \cos \theta}{2} \sin \theta$

$d_{2,0}^2 = \frac{\sqrt{6}}{4} \sin^2 \theta$

$d_{2,-1}^2 = -\frac{1 - \cos \theta}{2} \sin \theta$

$d_{2,-2}^2 = \left(\frac{1 - \cos \theta}{2}\right)^2$

$d_{1,1}^2 = \frac{1 + \cos \theta}{2} (2 \cos \theta - 1)$

$d_{1,0}^2 = -\sqrt{\frac{3}{2}} \sin \theta \cos \theta$

$d_{1,-1}^2 = \frac{1 - \cos \theta}{2} (2 \cos \theta + 1)$

$d_{0,0}^2 = \left(\frac{3}{2} \cos^2 \theta - \frac{1}{2}\right)$

Figure 31.1: The sign convention is that of Wigner (*Group Theory*, Academic Press, New York, 1959), also used by Condon and Shortley (*The Theory of Atomic Spectra*, Cambridge Univ. Press, New York, 1953), Rose (*Elementary Theory of Angular Momentum*, Wiley, New York, 1957), and Cohen (*Tables of the Clebsch-Gordan Coefficients*, North American Rockwell Science Center, Thousand Oaks, Calif., 1974). The coefficients here have been calculated using computer programs written independently by Cohen and at LBNL.

32. SU(3) ISOSCALAR FACTORS AND REPRESENTATION MATRICES

Written by R.L. Kelly (LBNL).

The most commonly used SU(3) isoscalar factors, corresponding to the singlet, octet, and decuplet content of $8 \otimes 8$ and $10 \otimes 8$, are shown at the right. The notation uses particle names to identify the coefficients, so that the pattern of relative couplings may be seen at a glance. We illustrate the use of the coefficients below. See J.J. de Swart, Rev. Mod. Phys. **35**, 916 (1963) for detailed explanations and phase conventions.

A $\sqrt{\quad}$ is to be understood over every integer in the matrices; the exponent 1/2 on each matrix is a reminder of this. For example, the $\Xi \rightarrow \Omega K$ element of the $10 \rightarrow 10 \otimes 8$ matrix is $-\sqrt{6}/\sqrt{24} = -1/2$.

Intramultiplet relative decay strengths may be read directly from the matrices. For example, in decuplet \rightarrow octet + octet decays, the ratio of $\Omega^* \rightarrow \Xi \bar{K}$ and $\Delta \rightarrow N \pi$ partial widths is, from the $10 \rightarrow 8 \times 8$ matrix,

$$\frac{\Gamma(\Omega^* \rightarrow \Xi \bar{K})}{\Gamma(\Delta \rightarrow N \pi)} = \frac{12}{6} \times (\text{phase space factors}). \quad (32.1)$$

Including isospin Clebsch-Gordan coefficients, we obtain, e.g.,

$$\frac{\Gamma(\Omega^{*-} \rightarrow \Xi^0 K^-)}{\Gamma(\Delta^+ \rightarrow p \pi^0)} = \frac{1/2}{2/3} \times \frac{12}{6} \times p.s.f. = \frac{3}{2} \times p.s.f. \quad (32.2)$$

Partial widths for $8 \rightarrow 8 \otimes 8$ involve a linear superposition of 8_1 (symmetric) and 8_2 (antisymmetric) couplings. For example,

$$\Gamma(\Xi^* \rightarrow \Xi \pi) \sim \left(-\sqrt{\frac{9}{20}} g_1 + \sqrt{\frac{3}{12}} g_2 \right)^2. \quad (32.3)$$

The relations between g_1 and g_2 (with de Swart's normalization) and the standard D and F couplings that appear in the interaction Lagrangian,

$$\mathcal{L} = -\sqrt{2} D \text{Tr}(\{\bar{B}, B\}M) + \sqrt{2} F \text{Tr}([\bar{B}, B]M), \quad (32.4)$$

where $[\bar{B}, B] \equiv \bar{B}B - B\bar{B}$ and $\{\bar{B}, B\} \equiv \bar{B}B + B\bar{B}$, are

$$D = \frac{\sqrt{30}}{40} g_1, \quad F = \frac{\sqrt{6}}{24} g_2. \quad (32.5)$$

Thus, for example,

$$\Gamma(\Xi^* \rightarrow \Xi \pi) \sim (F - D)^2 \sim (1 - 2\alpha)^2, \quad (32.6)$$

where $\alpha \equiv F/(D + F)$. (This definition of α is de Swart's. The alternative $D/(D + F)$, due to Gell-Mann, is also used.)

The generators of SU(3) transformations, λ_a ($a = 1, 8$), are 3×3 matrices that obey the following commutation and anticommutation relationships:

$$[\lambda_a, \lambda_b] \equiv \lambda_a \lambda_b - \lambda_b \lambda_a = 2i f_{abc} \lambda_c \quad (32.7)$$

$$\{\lambda_a, \lambda_b\} \equiv \lambda_a \lambda_b + \lambda_b \lambda_a = \frac{4}{3} \delta_{ab} I + 2d_{abc} \lambda_c, \quad (32.8)$$

where I is the 3×3 identity matrix, and δ_{ab} is the Kronecker delta symbol. The f_{abc} are odd under the permutation of any pair of indices, while the d_{abc} are even. The nonzero values are

$1 \rightarrow 8 \otimes 8$

$$(A) \rightarrow (N \bar{K} \Sigma \pi \Lambda \eta \Xi K) = \frac{1}{\sqrt{8}} (2 \ 3 \ -1 \ -2)^{1/2}$$

$8_1 \rightarrow 8 \otimes 8$

$$\begin{pmatrix} N \\ \Sigma \\ \Lambda \\ \Xi \end{pmatrix} \rightarrow \begin{pmatrix} N\pi & N\eta & \Sigma K & \Lambda K \\ N\bar{K} & \Sigma\pi & \Lambda\pi & \Sigma\eta \Xi K \\ N\bar{K} & \Sigma\pi & \Lambda\eta & \Xi K \\ \Sigma\bar{K} & \Lambda\bar{K} & \Xi\pi & \Xi\eta \end{pmatrix} = \frac{1}{\sqrt{20}} \begin{pmatrix} 9 & -1 & -9 & -1 \\ -6 & 0 & 4 & 4 \\ 2 & -12 & -4 & -2 \\ 9 & -1 & -9 & -1 \end{pmatrix}^{1/2}$$

$8_2 \rightarrow 8 \otimes 8$

$$\begin{pmatrix} N \\ \Sigma \\ \Lambda \\ \Xi \end{pmatrix} \rightarrow \begin{pmatrix} N\pi & N\eta & \Sigma K & \Lambda K \\ N\bar{K} & \Sigma\pi & \Lambda\pi & \Sigma\eta \Xi K \\ N\bar{K} & \Sigma\pi & \Lambda\eta & \Xi K \\ \Sigma\bar{K} & \Lambda\bar{K} & \Xi\pi & \Xi\eta \end{pmatrix} = \frac{1}{\sqrt{12}} \begin{pmatrix} 3 & 3 & 3 & -3 \\ 2 & 8 & 0 & 0 \\ 6 & 0 & 0 & 6 \\ 3 & 3 & 3 & -3 \end{pmatrix}^{1/2}$$

$10 \rightarrow 8 \otimes 8$

$$\begin{pmatrix} \Delta \\ \Sigma \\ \Xi \\ \Omega \end{pmatrix} \rightarrow \begin{pmatrix} N\pi & \Sigma K \\ N\bar{K} & \Sigma\pi & \Lambda\pi & \Sigma\eta \Xi K \\ \Sigma\bar{K} & \Lambda\bar{K} & \Xi\pi & \Xi\eta \\ \Xi\bar{K} \end{pmatrix} = \frac{1}{\sqrt{12}} \begin{pmatrix} -6 & 6 \\ -2 & 2 & -3 & 3 & 2 \\ 3 & -3 & 3 & 3 \\ 12 \end{pmatrix}^{1/2}$$

$8 \rightarrow 10 \otimes 8$

$$\begin{pmatrix} N \\ \Sigma \\ \Lambda \\ \Xi \end{pmatrix} \rightarrow \begin{pmatrix} \Delta\pi & \Sigma K \\ \Delta\bar{K} & \Sigma\pi & \Sigma\eta \Xi K \\ \Sigma\pi & \Xi K \\ \Sigma\bar{K} & \Xi\pi & \Xi\eta \Omega K \end{pmatrix} = \frac{1}{\sqrt{15}} \begin{pmatrix} -12 & 3 \\ 8 & -2 & -3 & 2 \\ -9 & 6 \\ 3 & -3 & -3 & 6 \end{pmatrix}^{1/2}$$

$10 \rightarrow 10 \otimes 8$

$$\begin{pmatrix} \Delta \\ \Sigma \\ \Xi \\ \Omega \end{pmatrix} \rightarrow \begin{pmatrix} \Delta\pi & \Delta\eta & \Sigma K \\ \Delta\bar{K} & \Sigma\pi & \Sigma\eta \Xi K \\ \Sigma\bar{K} & \Xi\pi & \Xi\eta \Omega K \\ \Xi\bar{K} & \Omega\eta \end{pmatrix} = \frac{1}{\sqrt{24}} \begin{pmatrix} 15 & 3 & -6 \\ 8 & 8 & 0 & -8 \\ 12 & 3 & -3 & -6 \\ 12 & -12 \end{pmatrix}^{1/2}$$

abc	f_{abc}	abc	d_{abc}	abc	d_{abc}
123	1	118	$1/\sqrt{3}$	355	$1/2$
147	$1/2$	146	$1/2$	366	$-1/2$
156	$-1/2$	157	$1/2$	377	$-1/2$
246	$1/2$	228	$1/\sqrt{3}$	448	$-1/(2\sqrt{3})$
257	$1/2$	247	$-1/2$	558	$-1/(2\sqrt{3})$
345	$1/2$	256	$1/2$	668	$-1/(2\sqrt{3})$
367	$-1/2$	338	$1/\sqrt{3}$	778	$-1/(2\sqrt{3})$
458	$\sqrt{3}/2$	344	$1/2$	888	$-1/\sqrt{3}$
678	$\sqrt{3}/2$				

The λ_a 's are

$$\lambda_1 = \begin{pmatrix} 0 & 1 & 0 \\ 1 & 0 & 0 \\ 0 & 0 & 0 \end{pmatrix}, \quad \lambda_2 = \begin{pmatrix} 0 & -i & 0 \\ i & 0 & 0 \\ 0 & 0 & 0 \end{pmatrix}, \quad \lambda_3 = \begin{pmatrix} 1 & 0 & 0 \\ 0 & -1 & 0 \\ 0 & 0 & 0 \end{pmatrix}$$

$$\lambda_4 = \begin{pmatrix} 0 & 0 & 1 \\ 0 & 0 & 0 \\ 1 & 0 & 0 \end{pmatrix}, \quad \lambda_5 = \begin{pmatrix} 0 & 0 & -i \\ 0 & 0 & 0 \\ i & 0 & 0 \end{pmatrix}, \quad \lambda_6 = \begin{pmatrix} 0 & 0 & 0 \\ 0 & 0 & 1 \\ 0 & 1 & 0 \end{pmatrix}$$

$$\lambda_7 = \begin{pmatrix} 0 & 0 & 0 \\ 0 & 0 & -i \\ 0 & i & 0 \end{pmatrix}, \quad \lambda_8 = \frac{1}{\sqrt{3}} \begin{pmatrix} 1 & 0 & 0 \\ 0 & 1 & 0 \\ 0 & 0 & -2 \end{pmatrix}$$

Equation (32.7) defines the Lie algebra of SU(3). A general d -dimensional representation is given by a set of $d \times d$ matrices satisfying Eq. (32.7) with the f_{abc} given above. Equation (32.8) is specific to the defining 3-dimensional representation.

33. SU(n) MULTIPLETS AND YOUNG DIAGRAMMS

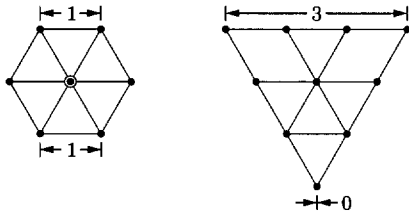
Written by C.G. Wohl (LBNL).

This note tells (1) how SU(n) particle multiplets are identified or labeled, (2) how to find the number of particles in a multiplet from its label, (3) how to draw the Young diagram for a multiplet, and (4) how to use Young diagrams to determine the overall multiplet structure of a composite system, such as a 3-quark or a meson-baryon system.

In much of the literature, the word "representation" is used where we use "multiplet," and "tableau" is used where we use "diagram."

33.1. Multiplet labels

An SU(n) multiplet is uniquely identified by a string of (n-1) nonnegative integers: (α, β, γ, ...). Any such set of integers specifies a multiplet. For an SU(2) multiplet such as an isospin multiplet, the single integer α is the number of steps from one end of the multiplet to the other (i.e., it is one fewer than the number of particles in the multiplet). In SU(3), the two integers α and β are the numbers of steps across the top and bottom levels of the multiplet diagram. Thus the labels for the SU(3) octet and decuplet



are (1,1) and (3,0). For larger n, the interpretation of the integers in terms of the geometry of the multiplets, which exist in an (n-1)-dimensional space, is not so readily apparent.

The label for the SU(n) singlet is (0, 0, ..., 0). In a flavor SU(n), the n quarks together form a (1, 0, ..., 0) multiplet, and the n antiquarks belong to a (0, ..., 0, 1) multiplet. These two multiplets are conjugate to one another, which means their labels are related by (α, β, ...) ↔ (... , β, α).

33.2. Number of particles

The number of particles in a multiplet, N = N(α, β, ...), is given as follows (note the pattern of the equations).

In SU(2), N = N(α) is

$$N = \frac{(\alpha + 1)}{1} \tag{33.1}$$

In SU(3), N = N(α, β) is

$$N = \frac{(\alpha + 1)}{1} \cdot \frac{(\beta + 1)}{1} \cdot \frac{(\alpha + \beta + 2)}{2} \tag{33.2}$$

In SU(4), N = N(α, β, γ) is

$$N = \frac{(\alpha + 1)}{1} \cdot \frac{(\beta + 1)}{1} \cdot \frac{(\gamma + 1)}{1} \cdot \frac{(\alpha + \beta + 2)}{2} \cdot \frac{(\beta + \gamma + 2)}{2} \cdot \frac{(\alpha + \beta + \gamma + 3)}{3} \tag{33.3}$$

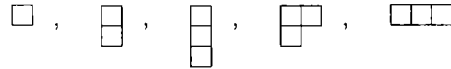
Note that in Eq. (33.3) there is no factor with (α + γ + 2): only a consecutive sequence of the label integers appears in any factor. One more example should make the pattern clear for any SU(n). In SU(5), N = N(α, β, γ, δ) is

$$N = \frac{(\alpha + 1)}{1} \cdot \frac{(\beta + 1)}{1} \cdot \frac{(\gamma + 1)}{1} \cdot \frac{(\delta + 1)}{1} \cdot \frac{(\alpha + \beta + 2)}{2} \cdot \frac{(\beta + \gamma + 2)}{2} \times \frac{(\gamma + \delta + 2)}{2} \cdot \frac{(\alpha + \beta + \gamma + 3)}{3} \cdot \frac{(\beta + \gamma + \delta + 3)}{3} \cdot \frac{(\alpha + \beta + \gamma + \delta + 4)}{4} \tag{33.4}$$

From the symmetry of these equations, it is clear that multiplets that are conjugate to one another have the same number of particles, but so can other multiplets. For example, the SU(4) multiplets (3,0,0) and (1,1,0) each have 20 particles. Try the equations and see.

33.3. Young diagrams

A Young diagram consists of an array of boxes (or some other symbol) arranged in one or more left-justified rows, with each row being at least as long as the row beneath. The correspondence between a diagram and a multiplet label is: The top row juts out α boxes to the right past the end of the second row, the second row juts out β boxes to the right past the end of the third row, etc. A diagram in SU(n) has at most n rows. There can be any number of "completed" columns of n boxes buttressing the left of a diagram; these don't affect the label. Thus in SU(3) the diagrams



represent the multiplets (1,0), (0,1), (0,0), (1,1), and (3,0). In any SU(n), the quark multiplet is represented by a single box, the antiquark multiplet by a column of (n-1) boxes, and a singlet by a completed column of n boxes.

33.4. Coupling multiplets together

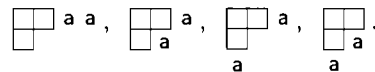
The following recipe tells how to find the multiplets that occur in coupling two multiplets together. To couple together more than two multiplets, first couple two, then couple a third with each of the multiplets obtained from the first two, etc.

First a definition: A sequence of the letters a, b, c, ... is admissible if at any point in the sequence at least as many a's have occurred as b's, at least as many b's have occurred as c's, etc. Thus abcd and aabcb are admissible sequences and abb and acb are not. Now the recipe:

(a) Draw the Young diagrams for the two multiplets, but in one of the diagrams replace the boxes in the first row with a's, the boxes in the second row with b's, etc. Thus, to couple two SU(3) octets (such as the π-meson octet and the baryon octet), we start with

and a. The unlettered diagram forms the upper left-hand corner of all the enlarged diagrams constructed below.

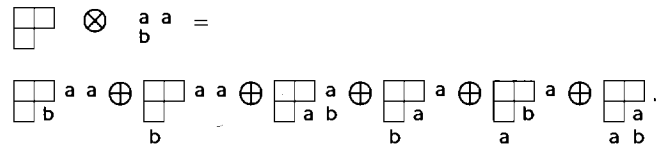
(b) Add the a's from the lettered diagram to the right-hand ends of the rows of the unlettered diagram to form all possible legitimate Young diagrams that have no more than one a per column. In general, there will be several distinct diagrams, and all the a's appear in each diagram. At this stage, for the coupling of the two SU(3) octets, we have:



(c) Use the b's to further enlarge the diagrams already obtained, subject to the same rules. Then throw away any diagram in which the full sequence of letters formed by reading right to left in the first row, then the second row, etc., is not admissible.

(d) Proceed as in (c) with the c's (if any), etc.

The final result of the coupling of the two SU(3) octets is:



Here only the diagrams with admissible sequences of a's and b's and with fewer than four rows (since n = 3) have been kept. In terms of multiplet labels, the above may be written

$$(1, 1) \otimes (1, 1) = (2, 2) \oplus (3, 0) \oplus (0, 3) \oplus (1, 1) \oplus (1, 1) \oplus (0, 0) .$$

In terms of numbers of particles, it may be written

$$8 \otimes 8 = 27 \oplus 10 \oplus \overline{10} \oplus 8 \oplus 8 \oplus 1 .$$

The product of the numbers on the left here is equal to the sum on the right, a useful check. (See also Sec. 13 on the Quark Model.)

34. KINEMATICS

Revised January 2000 by J.D. Jackson (LBNL).

Throughout this section units are used in which $\hbar = c = 1$. The following conversions are useful: $\hbar c = 197.3$ MeV fm, $(\hbar c)^2 = 0.3894$ (GeV)² mb.

34.1. Lorentz transformations

The energy E and 3-momentum \mathbf{p} of a particle of mass m form a 4-vector $p = (E, \mathbf{p})$ whose square $p^2 \equiv E^2 - |\mathbf{p}|^2 = m^2$. The velocity of the particle is $\boldsymbol{\beta} = \mathbf{p}/E$. The energy and momentum (E^*, \mathbf{p}^*) viewed from a frame moving with velocity $\boldsymbol{\beta}_f$ are given by

$$\begin{pmatrix} E^* \\ \mathbf{p}_{\parallel}^* \end{pmatrix} = \begin{pmatrix} \gamma_f & -\gamma_f \boldsymbol{\beta}_f \\ -\gamma_f \boldsymbol{\beta}_f & \gamma_f \end{pmatrix} \begin{pmatrix} E \\ \mathbf{p}_{\parallel} \end{pmatrix}, \quad \mathbf{p}_{\perp}^* = \mathbf{p}_{\perp}, \quad (34.1)$$

where $\gamma_f = (1 - \beta_f^2)^{-1/2}$ and p_{\perp} (p_{\parallel}) are the components of \mathbf{p} perpendicular (parallel) to $\boldsymbol{\beta}_f$. Other 4-vectors, such as the space-time coordinates of events, of course transform in the same way. The scalar product of two 4-momenta $\mathbf{p}_1 \cdot \mathbf{p}_2 = E_1 E_2 - \mathbf{p}_1 \cdot \mathbf{p}_2$ is invariant (frame independent).

34.2. Center-of-mass energy and momentum

In the collision of two particles of masses m_1 and m_2 the total center-of-mass energy can be expressed in the Lorentz-invariant form

$$\begin{aligned} E_{\text{cm}} &= \left[(E_1 + E_2)^2 - (\mathbf{p}_1 + \mathbf{p}_2)^2 \right]^{1/2}, \\ &= \left[m_1^2 + m_2^2 + 2E_1 E_2 (1 - \beta_1 \beta_2 \cos \theta) \right]^{1/2}, \end{aligned} \quad (34.2)$$

where θ is the angle between the particles. In the frame where one particle (of mass m_2) is at rest (lab frame),

$$E_{\text{cm}} = (m_1^2 + m_2^2 + 2E_{1\text{lab}} m_2)^{1/2}. \quad (34.3)$$

The velocity of the center-of-mass in the lab frame is

$$\boldsymbol{\beta}_{\text{cm}} = \mathbf{p}_{\text{lab}} / (E_{1\text{lab}} + m_2), \quad (34.4)$$

where $\mathbf{p}_{\text{lab}} \equiv \mathbf{p}_{1\text{lab}}$ and

$$\gamma_{\text{cm}} = (E_{1\text{lab}} + m_2) / E_{\text{cm}}. \quad (34.5)$$

The c.m. momenta of particles 1 and 2 are of magnitude

$$p_{\text{cm}} = p_{\text{lab}} \frac{m_2}{E_{\text{cm}}}. \quad (34.6)$$

For example, if a 0.80 GeV/c kaon beam is incident on a proton target, the center of mass energy is 1.699 GeV and the center of mass momentum of either particle is 0.442 GeV/c. It is also useful to note that

$$E_{\text{cm}} dE_{\text{cm}} = m_2 dE_{1\text{lab}} = m_2 \beta_{1\text{lab}} dp_{1\text{lab}}. \quad (34.7)$$

34.3. Lorentz-invariant amplitudes

The matrix elements for a scattering or decay process are written in terms of an invariant amplitude $-i\mathcal{M}$. As an example, the S -matrix for $2 \rightarrow 2$ scattering is related to \mathcal{M} by

$$\begin{aligned} \langle p'_1 p'_2 | S | p_1 p_2 \rangle &= I - i(2\pi)^4 \delta^4(p_1 + p_2 - p'_1 - p'_2) \\ &\times \frac{\mathcal{M}(p_1, p_2; p'_1, p'_2)}{(2E_1)^{1/2} (2E_2)^{1/2} (2E'_1)^{1/2} (2E'_2)^{1/2}}. \end{aligned} \quad (34.8)$$

The state normalization is such that

$$\langle p' | p \rangle = (2\pi)^3 \delta^3(\mathbf{p} - \mathbf{p}'). \quad (34.9)$$

34.4. Particle decays

The partial decay rate of a particle of mass M into n bodies in its rest frame is given in terms of the Lorentz-invariant matrix element \mathcal{M} by

$$d\Gamma = \frac{(2\pi)^4}{2M} |\mathcal{M}|^2 d\Phi_n(P; p_1, \dots, p_n), \quad (34.10)$$

where $d\Phi_n$ is an element of n -body phase space given by

$$d\Phi_n(P; p_1, \dots, p_n) = \delta^4(P - \sum_{i=1}^n p_i) \prod_{i=1}^n \frac{d^3 p_i}{(2\pi)^3 2E_i}. \quad (34.11)$$

This phase space can be generated recursively, viz.

$$\begin{aligned} d\Phi_n(P; p_1, \dots, p_n) &= d\Phi_j(q; p_1, \dots, p_j) \\ &\times d\Phi_{n-j+1}(P; q, p_{j+1}, \dots, p_n) (2\pi)^3 dq^2, \end{aligned} \quad (34.12)$$

where $q^2 = (\sum_{i=1}^j E_i)^2 - |\sum_{i=1}^j \mathbf{p}_i|^2$. This form is particularly useful in the case where a particle decays into another particle that subsequently decays.

34.4.1. Survival probability: If a particle of mass M has mean proper lifetime τ ($= 1/\Gamma$) and has momentum (E, \mathbf{p}) , then the probability that it lives for a time t_0 or greater before decaying is given by

$$P(t_0) = e^{-t_0 \Gamma / \gamma} = e^{-M t_0 \Gamma / E}, \quad (34.13)$$

and the probability that it travels a distance x_0 or greater is

$$P(x_0) = e^{-M x_0 \Gamma / |\mathbf{p}|}. \quad (34.14)$$

34.4.2. Two-body decays:

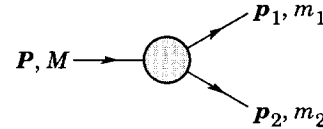


Figure 34.1: Definitions of variables for two-body decays.

In the rest frame of a particle of mass M , decaying into 2 particles labeled 1 and 2,

$$E_1 = \frac{M^2 - m_2^2 + m_1^2}{2M}, \quad (34.15)$$

$$|\mathbf{p}_1| = |\mathbf{p}_2|$$

$$= \frac{[(M^2 - (m_1 + m_2)^2)(M^2 - (m_1 - m_2)^2)]^{1/2}}{2M}, \quad (34.16)$$

and

$$d\Gamma = \frac{1}{32\pi^2} |\mathcal{M}|^2 \frac{|\mathbf{p}_1|}{M^2} d\Omega, \quad (34.17)$$

where $d\Omega = d\phi_1 d(\cos \theta_1)$ is the solid angle of particle 1.

34.4.3. Three-body decays:

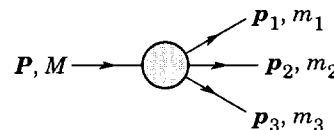


Figure 34.2: Definitions of variables for three-body decays.

Defining $p_{ij} = p_i + p_j$ and $m_{ij}^2 = p_{ij}^2$, then $m_{12}^2 + m_{23}^2 + m_{13}^2 = M^2 + m_1^2 + m_2^2 + m_3^2$ and $m_{12}^2 = (P - p_3)^2 = M^2 + m_3^2 - 2ME_3$, where E_3 is the energy of particle 3 in the rest frame of M . In that frame, the momenta of the three decay particles lie in a plane. The relative orientation of these three momenta is fixed if their energies are known. The momenta can therefore be specified in space by giving three Euler angles (α, β, γ) that specify the orientation of the final system relative to the initial particle [1]. Then

$$d\Gamma = \frac{1}{(2\pi)^5} \frac{1}{16M} |\mathcal{M}|^2 dE_1 dE_2 d\alpha d(\cos\beta) d\gamma. \quad (34.18)$$

Alternatively

$$d\Gamma = \frac{1}{(2\pi)^5} \frac{1}{16M^2} |\mathcal{M}|^2 |\mathbf{p}_1^*| |\mathbf{p}_3| dm_{12} d\Omega_1^* d\Omega_3, \quad (34.19)$$

where $(|\mathbf{p}_1^*|, \Omega_1^*)$ is the momentum of particle 1 in the rest frame of 1 and 2, and Ω_3 is the angle of particle 3 in the rest frame of the decaying particle. $|\mathbf{p}_1^*|$ and $|\mathbf{p}_3|$ are given by

$$|\mathbf{p}_1^*| = \frac{[(m_{12}^2 - (m_1 + m_2)^2)(m_{12}^2 - (m_1 - m_2)^2)]^{1/2}}{2m_{12}}, \quad (34.20a)$$

and

$$|\mathbf{p}_3| = \frac{[(M^2 - (m_{12} + m_3)^2)(M^2 - (m_{12} - m_3)^2)]^{1/2}}{2M}. \quad (34.20b)$$

[Compare with Eq. (34.16).]

If the decaying particle is a scalar or we average over its spin states, then integration over the angles in Eq. (34.18) gives

$$\begin{aligned} d\Gamma &= \frac{1}{(2\pi)^3} \frac{1}{8M} |\overline{\mathcal{M}}|^2 dE_1 dE_2 \\ &= \frac{1}{(2\pi)^3} \frac{1}{32M^3} |\overline{\mathcal{M}}|^2 dm_{12}^2 dm_{23}^2. \end{aligned} \quad (34.21)$$

This is the standard form for the Dalitz plot.

34.4.3.1. Dalitz plot: For a given value of m_{12}^2 , the range of m_{23}^2 is determined by its values when \mathbf{p}_2 is parallel or antiparallel to \mathbf{p}_3 :

$$(m_{23}^2)_{\max} = (E_2^* + E_3^*)^2 - \left(\sqrt{E_2^{*2} - m_2^2} - \sqrt{E_3^{*2} - m_3^2} \right)^2, \quad (34.22a)$$

$$(m_{23}^2)_{\min} = (E_2^* + E_3^*)^2 - \left(\sqrt{E_2^{*2} - m_2^2} + \sqrt{E_3^{*2} - m_3^2} \right)^2. \quad (34.22b)$$

Here $E_2^* = (m_{12}^2 - m_1^2 + m_2^2)/2m_{12}$ and $E_3^* = (M^2 - m_{12}^2 - m_3^2)/2m_{12}$ are the energies of particles 2 and 3 in the m_{12} rest frame. The scatter plot in m_{12}^2 and m_{23}^2 is called a Dalitz plot. If $|\overline{\mathcal{M}}|^2$ is constant, the allowed region of the plot will be uniformly populated with events [see Eq. (34.21)]. A nonuniformity in the plot gives immediate information on $|\overline{\mathcal{M}}|^2$. For example, in the case of $D \rightarrow K\pi\pi$, bands appear when $m_{(K\pi)} = m_{K^*(892)}$, reflecting the appearance of the decay chain $D \rightarrow K^*(892)\pi \rightarrow K\pi\pi$.

34.4.4. Kinematic limits: In a three-body decay the maximum of $|\mathbf{p}_3|$, [given by Eq. (34.20)], is achieved when $m_{12} = m_1 + m_2$, i.e., particles 1 and 2 have the same vector velocity in the rest frame of the decaying particle. If, in addition, $m_3 > m_1, m_2$, then $|\mathbf{p}_3|_{\max} > |\mathbf{p}_1|_{\max}, |\mathbf{p}_2|_{\max}$.

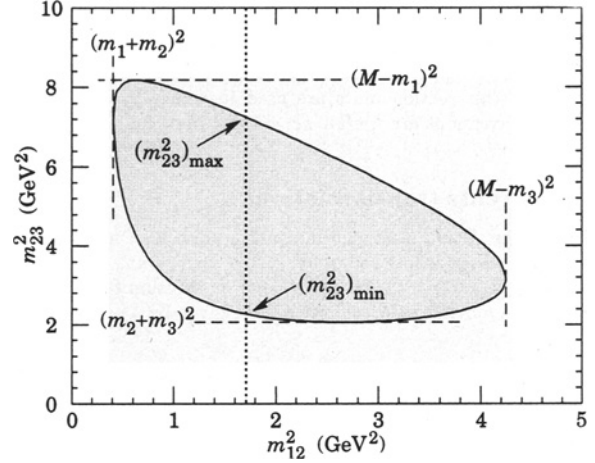


Figure 34.3: Dalitz plot for a three-body final state. In this example, the state is $\pi^+\bar{K}^0 p$ at 3 GeV. Four-momentum conservation restricts events to the shaded region.

34.4.5. Multibody decays: The above results may be generalized to final states containing any number of particles by combining some of the particles into “effective particles” and treating the final states as 2 or 3 “effective particle” states. Thus, if $p_{ijk\dots} = p_i + p_j + p_k + \dots$, then

$$m_{ijk\dots} = \sqrt{p_{ijk\dots}^2}, \quad (34.23)$$

and $m_{ijk\dots}$ may be used in place of e.g., m_{12} in the relations in Sec. 34.4.3 or 34.4.3.1 above.

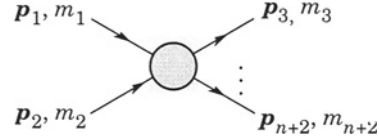


Figure 34.4: Definitions of variables for production of an n -body final state.

34.5. Cross sections

The differential cross section is given by

$$\begin{aligned} d\sigma &= \frac{(2\pi)^4 |\overline{\mathcal{M}}|^2}{4\sqrt{(p_1 \cdot p_2)^2 - m_1^2 m_2^2}} \\ &\times d\Phi_n(p_1 + p_2; p_3, \dots, p_{n+2}). \end{aligned} \quad (34.24)$$

[See Eq. (34.11).] In the rest frame of m_2 (lab),

$$\sqrt{(p_1 \cdot p_2)^2 - m_1^2 m_2^2} = m_2 p_{1\text{lab}}; \quad (34.25a)$$

while in the center-of-mass frame

$$\sqrt{(p_1 \cdot p_2)^2 - m_1^2 m_2^2} = p_{\text{cm}} \sqrt{s}. \quad (34.25b)$$

34.5.1. Two-body reactions:

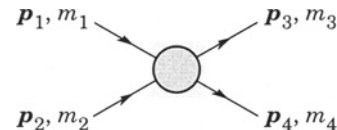


Figure 34.5: Definitions of variables for a two-body final state.

Two particles of momenta p_1 and p_2 and masses m_1 and m_2 scatter to particles of momenta p_3 and p_4 and masses m_3 and m_4 ; the Lorentz-invariant Mandelstam variables are defined by

$$s = (p_1 + p_2)^2 = (p_3 + p_4)^2 = m_1^2 + 2E_1E_2 - 2\mathbf{p}_1 \cdot \mathbf{p}_2 + m_2^2, \quad (34.26)$$

$$t = (p_1 - p_3)^2 = (p_2 - p_4)^2 = m_1^2 - 2E_1E_3 + 2\mathbf{p}_1 \cdot \mathbf{p}_3 + m_3^2, \quad (34.27)$$

$$u = (p_1 - p_4)^2 = (p_2 - p_3)^2 = m_1^2 - 2E_1E_4 + 2\mathbf{p}_1 \cdot \mathbf{p}_4 + m_4^2, \quad (34.28)$$

and they satisfy

$$s + t + u = m_1^2 + m_2^2 + m_3^2 + m_4^2. \quad (34.29)$$

The two-body cross section may be written as

$$\frac{d\sigma}{dt} = \frac{1}{64\pi s} \frac{1}{|\mathbf{p}_{1\text{cm}}|^2} |\mathcal{M}|^2. \quad (34.30)$$

In the center-of-mass frame

$$t = (E_{1\text{cm}} - E_{3\text{cm}})^2 - (\mathbf{p}_{1\text{cm}} - \mathbf{p}_{3\text{cm}})^2 - 4p_{1\text{cm}}p_{3\text{cm}}\sin^2(\theta_{\text{cm}}/2) = t_0 - 4p_{1\text{cm}}p_{3\text{cm}}\sin^2(\theta_{\text{cm}}/2), \quad (34.31)$$

where θ_{cm} is the angle between particle 1 and 3. The limiting values t_0 ($\theta_{\text{cm}} = 0$) and t_1 ($\theta_{\text{cm}} = \pi$) for $2 \rightarrow 2$ scattering are

$$t_0(t_1) = \left[\frac{m_1^2 - m_3^2 - m_2^2 + m_4^2}{2\sqrt{s}} \right]^2 - (\mathbf{p}_{1\text{cm}} \mp \mathbf{p}_{3\text{cm}})^2. \quad (34.32)$$

In the literature the notation t_{\min} (t_{\max}) for t_0 (t_1) is sometimes used, which should be discouraged since $t_0 > t_1$. The center-of-mass energies and momenta of the incoming particles are

$$E_{1\text{cm}} = \frac{s + m_1^2 - m_2^2}{2\sqrt{s}}, \quad E_{2\text{cm}} = \frac{s + m_2^2 - m_1^2}{2\sqrt{s}}, \quad (34.33)$$

For $E_{3\text{cm}}$ and $E_{4\text{cm}}$, change m_1 to m_3 and m_2 to m_4 . Then

$$p_{i\text{cm}} = \sqrt{E_{i\text{cm}}^2 - m_i^2} \quad \text{and} \quad p_{1\text{cm}} = \frac{p_{1\text{lab}} m_2}{\sqrt{s}}. \quad (34.34)$$

Here the subscript lab refers to the frame where particle 2 is at rest. [For other relations see Eqs. (34.2)–(34.4).]

34.5.2. Inclusive reactions: Choose some direction (usually the beam direction) for the z -axis; then the energy and momentum of a particle can be written as

$$E = m_T \cosh y, \quad p_x, p_y, p_z = m_T \sinh y, \quad (34.35)$$

where m_T is the transverse mass

$$m_T^2 = m^2 + p_x^2 + p_y^2, \quad (34.36)$$

and the rapidity y is defined by

$$y = \frac{1}{2} \ln \left(\frac{E + p_z}{E - p_z} \right) = \ln \left(\frac{E + p_z}{m_T} \right) = \tanh^{-1} \left(\frac{p_z}{E} \right). \quad (34.37)$$

Under a boost in the z -direction to a frame with velocity β , $y \rightarrow y - \tanh^{-1} \beta$. Hence the shape of the rapidity distribution dN/dy is invariant. The invariant cross section may also be rewritten

$$E \frac{d^3\sigma}{d^3p} = \frac{d^3\sigma}{d\phi dy p_T dp_T} \Rightarrow \frac{d^2\sigma}{\pi dy d(p_T^2)}. \quad (34.38)$$

The second form is obtained using the identity $dy/dp_z = 1/E$, and the third form represents the average over ϕ .

Feynman's x variable is given by

$$x = \frac{p_z}{p_{z\text{max}}} \approx \frac{E + p_z}{(E + p_z)_{\text{max}}} \quad (p_T \ll |p_z|). \quad (34.39)$$

In the c.m. frame,

$$x \approx \frac{2p_{z\text{cm}}}{\sqrt{s}} = \frac{2m_T \sinh y_{\text{cm}}}{\sqrt{s}} \quad (34.40)$$

and

$$= (y_{\text{cm}})_{\text{max}} = \ln(\sqrt{s}/m). \quad (34.41)$$

For $p \gg m$, the rapidity [Eq. (34.37)] may be expanded to obtain

$$y = \frac{1}{2} \ln \frac{\cos^2(\theta/2) + m^2/4p^2 + \dots}{\sin^2(\theta/2) + m^2/4p^2 + \dots} \approx -\ln \tan(\theta/2) \equiv \eta \quad (34.42)$$

where $\cos \theta = p_z/p$. The pseudorapidity η defined by the second line is approximately equal to the rapidity y for $p \gg m$ and $\theta \gg 1/\gamma$, and in any case can be measured when the mass and momentum of the particle is unknown. From the definition one can obtain the identities

$$\sinh \eta = \cot \theta, \quad \cosh \eta = 1/\sin \theta, \quad \tanh \eta = \cos \theta. \quad (34.43)$$

34.5.3. Partial waves: The amplitude in the center of mass for elastic scattering of spinless particles may be expanded in Legendre polynomials

$$f(k, \theta) = \frac{1}{k} \sum_{\ell} (2\ell + 1) a_{\ell} P_{\ell}(\cos \theta), \quad (34.44)$$

where k is the c.m. momentum, θ is the c.m. scattering angle, $a_{\ell} = (\eta_{\ell} e^{2i\delta_{\ell}} - 1)/2i$, $0 \leq \eta_{\ell} \leq 1$, and δ_{ℓ} is the phase shift of the ℓ^{th} partial wave. For purely elastic scattering, $\eta_{\ell} = 1$. The differential cross section is

$$\frac{d\sigma}{d\Omega} = |f(k, \theta)|^2. \quad (34.45)$$

The optical theorem states that

$$\sigma_{\text{tot}} = \frac{4\pi}{k} \text{Im} f(k, 0), \quad (34.46)$$

and the cross section in the ℓ^{th} partial wave is therefore bounded:

$$\sigma_{\ell} = \frac{4\pi}{k^2} (2\ell + 1) |a_{\ell}|^2 \leq \frac{4\pi(2\ell + 1)}{k^2}. \quad (34.47)$$

The evolution with energy of a partial-wave amplitude a_{ℓ} can be displayed as a trajectory in an Argand plot, as shown in Fig. 34.6.

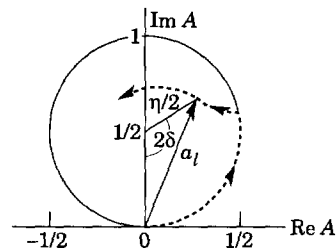


Figure 34.6: Argand plot showing a partial-wave amplitude a_{ℓ} as a function of energy. The amplitude leaves the unitary circle where inelasticity sets in ($\eta_{\ell} < 1$).

The usual Lorentz-invariant matrix element \mathcal{M} (see Sec. 34.3 above) for the elastic process is related to $f(k, \theta)$ by

$$\mathcal{M} = -8\pi\sqrt{s} f(k, \theta), \quad (34.48)$$

so

$$\sigma_{\text{tot}} = -\frac{1}{2p_{\text{lab}} m_2} \text{Im} \mathcal{M}(t=0), \quad (34.49)$$

where s and t are the center-of-mass energy squared and momentum transfer squared, respectively (see Sec. 34.4.1).

34.5.3.1. Resonances: The Breit-Wigner (nonrelativistic) form for an elastic amplitude a_ℓ with a resonance at c.m. energy E_R , elastic width Γ_{el} , and total width Γ_{tot} is

$$a_\ell = \frac{\Gamma_{\text{el}}/2}{E_R - E - i\Gamma_{\text{tot}}/2}, \quad (34.50)$$

where E is the c.m. energy. As shown in Fig. 34.7, in the absence of background the elastic amplitude traces a counterclockwise circle with center $ix_{\text{el}}/2$ and radius $x_{\text{el}}/2$, where the elasticity $x_{\text{el}} = \Gamma_{\text{el}}/\Gamma_{\text{tot}}$. The amplitude has a pole at $E = E_R - i\Gamma_{\text{tot}}/2$.

The spin-averaged Breit-Wigner cross section for a spin- J resonance produced in the collision of particles of spin S_1 and S_2 is

$$\sigma_{BW}(E) = \frac{(2J+1)}{(2S_1+1)(2S_2+1)} \frac{\pi}{k^2} \frac{B_{\text{in}}B_{\text{out}}\Gamma_{\text{tot}}^2}{(E - E_R)^2 + \Gamma_{\text{tot}}^2/4}, \quad (34.51)$$

where k is the c.m. momentum, E is the c.m. energy, and B_{in} and B_{out} are the branching fractions of the resonance into the entrance and exit channels. The $2S+1$ factors are the multiplicities of the incident spin states, and are replaced by 2 for photons. This expression is valid only for an isolated state. If the width is not small, Γ_{tot} cannot be treated as a constant independent of E . There are many other forms for σ_{BW} , all of which are equivalent to the one given here in the narrow-width case. Some of these forms may be more appropriate if the resonance is broad.

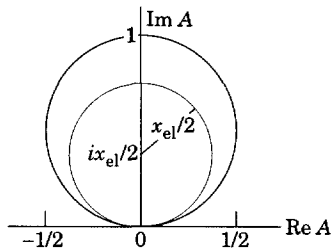


Figure 34.7: Argand plot for a resonance.

The relativistic Breit-Wigner form corresponding to Eq. (34.50) is:

$$a_\ell = \frac{-m\Gamma_{\text{el}}}{s - m^2 + im\Gamma_{\text{tot}}}. \quad (34.52)$$

A better form incorporates the known kinematic dependences, replacing $m\Gamma_{\text{tot}}$ by $\sqrt{s}\Gamma_{\text{tot}}(s)$, where $\Gamma_{\text{tot}}(s)$ is the width the resonance particle would have if its mass were \sqrt{s} , and correspondingly $m\Gamma_{\text{el}}$ by $\sqrt{s}\Gamma_{\text{el}}(s)$ where $\Gamma_{\text{el}}(s)$ is the partial width in the incident channel for a mass \sqrt{s} :

$$a_\ell = \frac{-\sqrt{s}\Gamma_{\text{el}}(s)}{s - m^2 + i\sqrt{s}\Gamma_{\text{tot}}(s)}. \quad (34.53)$$

For the Z boson, all the decays are to particles whose masses are small enough to be ignored, so on dimensional grounds $\Gamma_{\text{tot}}(s) = \sqrt{s}\Gamma_0/m_Z$, where Γ_0 defines the width of the Z , and $\Gamma_{\text{el}}(s)/\Gamma_{\text{tot}}(s)$ is constant. A full treatment of the line shape requires consideration of dynamics, not just kinematics. For the Z this is done by calculating the radiative corrections in the Standard Model.

References:

1. See, for example, J.J. Sakurai, *Modern Quantum Mechanics*, Addison-Wesley (1985), p. 172, or D.M. Brink and G.R. Satchler, *Angular Momentum*, 2nd ed., Oxford University Press (1968), p. 20.

35. CROSS-SECTION FORMULAE FOR SPECIFIC PROCESSES

Revised April 1998 by R.N. Cahn (LBNL).

35.1. Leptonproduction

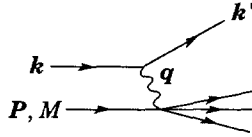


Figure 35.1: Kinematic quantities for description of lepton-nucleon scattering. k and k' are the four-momenta of incoming and outgoing leptons, P is the four-momentum of a nucleon with mass M . The exchanged particle is a γ , W^\pm , or Z^0 ; it transfers four-momentum $q = k - k'$ to the target.

Invariant quantities:

$\nu = \frac{q \cdot P}{M} = E - E'$ is the lepton's energy loss in the lab (in earlier literature sometimes $\nu = q \cdot P$). Here, E and E' are the initial and final lepton energies in the lab.

$Q^2 = -q^2 = 2(E E' - \vec{k} \cdot \vec{k}') - m_\ell^2 - m_{\ell'}^2$ where m_ℓ ($m_{\ell'}$) is the initial (final) lepton mass. If $E E' \sin^2(\theta/2) \gg m_\ell^2, m_{\ell'}^2$, then $\approx 4E E' \sin^2(\theta/2)$, where θ is the lepton's scattering angle in the lab.

$x = \frac{Q^2}{2M\nu}$ In the parton model, x is the fraction of the target nucleon's momentum carried by the struck quark. [See section on Quantum Chromodynamics (Sec. 9 of this Review.)]

$y = \frac{q \cdot P}{k \cdot P} = \frac{\nu}{E}$ is the fraction of the lepton's energy lost in the lab.

$W^2 = (P + q)^2 = M^2 + 2M\nu - Q^2$ is the mass squared of the system recoiling against the lepton.

$s = (k + P)^2 = \frac{Q^2}{xy} + M^2$

35.1.1. Leptonproduction cross sections:

$$\begin{aligned} \frac{d^2\sigma}{dx dy} &= \nu (s - M^2) \frac{d^2\sigma}{d\nu dQ^2} = \frac{2\pi M\nu}{E'} \frac{d^2\sigma}{d\Omega_{\text{lab}} dE'} \\ &= x(s - M^2) \frac{d^2\sigma}{dx dQ^2}. \end{aligned} \quad (35.1)$$

35.1.2. Leptonproduction structure functions: The neutral-current process, $eN \rightarrow eX$, at low Q^2 is just electromagnetic and parity conserving. It can be written in terms of two structure functions $F_1^{\text{em}}(x, Q^2)$ and $F_2^{\text{em}}(x, Q^2)$:

$$\begin{aligned} \frac{d^2\sigma}{dx dy} &= \frac{4\pi\alpha^2(s - M^2)}{Q^4} \\ &\times \left[(1 - y) F_2^{\text{em}} + y^2 x F_1^{\text{em}} - \frac{M^2}{(s - M^2)} xy F_2^{\text{em}} \right]. \end{aligned} \quad (35.2)$$

The charged-current processes, $e^-N \rightarrow \nu X$, $\nu N \rightarrow e^-X$, and $\bar{\nu}N \rightarrow e^+X$, are parity violating and can be written in terms of three structure functions $F_1^{\text{CC}}(x, Q^2)$, $F_2^{\text{CC}}(x, Q^2)$, and $F_3^{\text{CC}}(x, Q^2)$:

$$\begin{aligned} \frac{d^2\sigma}{dx dy} &= \frac{G_F^2 (s - M^2)}{2\pi} \frac{M_W^4}{(Q^2 + M_W^2)^2} \\ &\times \left\{ \left[1 - y - \frac{M^2 xy}{(s - M^2)} \right] F_2^{\text{CC}} + \frac{y^2}{2} 2x F_1^{\text{CC}} \pm (y - \frac{y^2}{2}) x F_3^{\text{CC}} \right\}, \end{aligned} \quad (35.3)$$

where the last term is positive for the e^- and ν reactions and negative for $\bar{\nu}N \rightarrow e^+X$. As explained below there are different structure functions for charge-raising and charge-lowering currents.

35.1.3. Structure functions in the QCD parton model: In the QCD parton model, the structure functions defined above can be expressed in terms of parton distribution functions. The quantity $f_i(x, Q^2)dx$ is the probability that a parton of type i (quark, antiquark, or gluon), carries a momentum fraction between x and $x + dx$ of the nucleon's momentum in a frame where the nucleon's momentum is large. For the cross section corresponding to the *neutral-current process* $ep \rightarrow eX$, we have for $s \gg M^2$ (in the case where the incoming electron is either left- (L) or right- (R) handed):

$$\begin{aligned} \frac{d^2\sigma}{dx dy} &= \frac{\pi\alpha^2}{sx^2 y^2} \left[\sum_q \left(x f_q(x, Q^2) + x f_{\bar{q}}(x, Q^2) \right) \right] \\ &\times \left[A_q + (1 - y)^2 B_q \right]. \end{aligned} \quad (35.4)$$

Here the index q refers to a quark flavor (i.e., u, d, s, c, b , or t), and

$$A_q = \left(-q_q + g_{Lq} g_{Le} \frac{Q^2}{Q^2 + M_Z^2} \right)^2 + \left(-q_q + g_{Rq} g_{Re} \frac{Q^2}{Q^2 + M_Z^2} \right)^2, \quad (35.5)$$

$$B_q = \left(-q_q + g_{Rq} g_{Le} \frac{Q^2}{Q^2 + M_Z^2} \right)^2 + \left(-q_q + g_{Lq} g_{Re} \frac{Q^2}{Q^2 + M_Z^2} \right)^2. \quad (35.6)$$

Here q_q is the charge of flavor q . For a left-handed electron, $g_{Re} = 0$ and $g_{Le} = (-1/2 + \sin^2 \theta_W)/(\sin \theta_W \cos \theta_W)$, while for a right-handed electron, $g_{Le} = 0$ and $g_{Re} = (\sin^2 \theta_W)/(\sin \theta_W \cos \theta_W)$. For the quarks, $g_{Lq} = (T_3 - q_q \sin^2 \theta_W)/(\sin \theta_W \cos \theta_W)$, and $g_{Rq} = (-q_q \sin^2 \theta_W)/(\sin \theta_W \cos \theta_W)$.

For neutral-current *neutrino (antineutrino) scattering*, the same formula applies with g_{Le} replaced by $g_{L\nu} = 1/(2 \sin \theta_W \cos \theta_W)$ ($g_{L\bar{\nu}} = 0$) and g_{Re} replaced by $g_{R\nu} = 0$ [$g_{R\bar{\nu}} = -1/(2 \sin \theta_W \cos \theta_W)$].

In the case of the *charged-current processes* $e^-_L p \rightarrow \nu X$ and $\bar{\nu} p \rightarrow e^+ X$, Eq. (35.3) applies with

$$\begin{aligned} F_2 &= 2xF_1 = 2x \left[f_u(x, Q^2) + f_c(x, Q^2) + f_t(x, Q^2) \right. \\ &\quad \left. + f_{\bar{d}}(x, Q^2) + f_{\bar{s}}(x, Q^2) + f_{\bar{b}}(x, Q^2) \right], \end{aligned} \quad (35.7)$$

$$\begin{aligned} F_3 &= 2 \left[f_u(x, Q^2) + f_c(x, Q^2) + f_t(x, Q^2) \right. \\ &\quad \left. - f_{\bar{d}}(x, Q^2) - f_{\bar{s}}(x, Q^2) - f_{\bar{b}}(x, Q^2) \right]. \end{aligned} \quad (35.8)$$

For the process $\nu p \rightarrow e^- X$:

$$\begin{aligned} F_2 &= 2xF_1 = 2x \left[f_d(x, Q^2) + f_s(x, Q^2) + f_b(x, Q^2) \right. \\ &\quad \left. + f_{\bar{u}}(x, Q^2) + f_{\bar{c}}(x, Q^2) + f_{\bar{t}}(x, Q^2) \right], \end{aligned} \quad (35.9)$$

$$\begin{aligned} F_3 &= 2 \left[f_d(x, Q^2) + f_s(x, Q^2) + f_b(x, Q^2) \right. \\ &\quad \left. - f_{\bar{u}}(x, Q^2) - f_{\bar{c}}(x, Q^2) - f_{\bar{t}}(x, Q^2) \right]. \end{aligned} \quad (35.10)$$

 35.2. e^+e^- annihilation

For pointlike, spin-1/2 fermions, the differential cross section in the c.m. for $e^+e^- \rightarrow f\bar{f}$ via single photon annihilation is (θ is the angle between the incident electron and the produced fermion; $N_c = 1$ if f is a lepton and $N_c = 3$ if f is a quark).

$$\frac{d\sigma}{d\Omega} = N_c \frac{\alpha^2}{4s} \beta [1 + \cos^2 \theta + (1 - \beta^2) \sin^2 \theta] Q_f^2, \quad (35.11)$$

where β is the velocity of the final state fermion in the c.m. and Q_f is the charge of the fermion in units of the proton charge. For $\beta \rightarrow 1$,

$$\sigma = N_c \frac{4\pi\alpha^2}{3s} Q_f^2 = N_c \frac{86.8 Q_f^2 \text{ nb}}{s (\text{GeV}/c^2)^2}. \quad (35.12)$$

At higher energies, the Z^0 (mass M_Z and width Γ_Z) must be included. If the mass of a fermion f is much less than the mass of the Z^0 , then the differential cross section for $e^+e^- \rightarrow f\bar{f}$ is

$$\frac{d\sigma}{d\Omega} = N_c \frac{\alpha^2}{4s} \left\{ (1 + \cos^2 \theta) \left[Q_f^2 - 2\chi_1 v_e v_f Q_f + \chi_2 (a_e^2 + v_e^2) (a_f^2 + v_f^2) \right] + 2 \cos \theta \left[-2\chi_1 a_e a_f Q_f + 4\chi_2 a_e a_f v_e v_f \right] \right\} \quad (35.13)$$

where

$$\begin{aligned} \chi_1 &= \frac{1}{16 \sin^2 \theta_W \cos^2 \theta_W} \frac{s(s - M_Z^2)}{(s - M_Z^2)^2 + M_Z^2 \Gamma_Z^2}, \\ \chi_2 &= \frac{1}{256 \sin^4 \theta_W \cos^4 \theta_W} \frac{s^2}{(s - M_Z^2)^2 + M_Z^2 \Gamma_Z^2}, \\ a_e &= -1, \\ v_e &= -1 + 4 \sin^2 \theta_W, \\ a_f &= 2T_{3f}, \\ v_f &= 2T_{3f} - 4Q_f \sin^2 \theta_W, \end{aligned} \quad (35.14)$$

where $T_{3f} = 1/2$ for u, c and neutrinos, while $T_{3f} = -1/2$ for d, s, b , and negatively charged leptons.

At LEP II it may be possible to produce the orthodox Higgs boson, H , (see the mini-review on Higgs bosons) in the reaction $e^+e^- \rightarrow HZ^0$, which proceeds dominantly through a virtual Z^0 . The Standard Model prediction for the cross section [3] is

$$\sigma(e^+e^- \rightarrow HZ^0) = \frac{\pi\alpha^2}{24} \cdot \frac{2K}{\sqrt{s}} \cdot \frac{K^2 + 3M_Z^2}{(s - M_Z^2)^2} \cdot \frac{1 - 4 \sin^2 \theta_W + 8 \sin^4 \theta_W}{\sin^4 \theta_W \cos^4 \theta_W}. \quad (35.15)$$

where K is the c.m. momentum of the produced H or Z^0 . Near the production threshold, this formula needs to be corrected for the finite width of the Z^0 .

35.3. Two-photon process at e^+e^- colliders

When an e^+ and an e^- collide with energies E_1 and E_2 , they emit dn_1 and dn_2 virtual photons with energies ω_1 and ω_2 and 4-momenta q_1 and q_2 . In the equivalent photon approximation, the cross section for $e^+e^- \rightarrow e^+e^-X$ is related to the cross section for $\gamma\gamma \rightarrow X$ by (Ref. 1)

$$d\sigma_{e^+e^- \rightarrow e^+e^-X}(s) = dn_1 dn_2 d\sigma_{\gamma\gamma \rightarrow X}(W^2) \quad (35.16)$$

where $s = 4E_1E_2$, $W^2 = 4\omega_1\omega_2$ and

$$dn_i = \frac{\alpha}{\pi} \left[1 - \frac{\omega_i}{E_i} + \frac{\omega_i^2}{2E_i^2} - \frac{m_e^2 \omega_i^2}{(-q_i^2)E_i^2} \right] \frac{d\omega_i}{\omega_i} \frac{d(-q_i^2)}{(-q_i^2)}. \quad (35.17)$$

After integration (including that over q_i^2 in the region $m_e^2 \omega_i^2 / E_i(E_i - \omega_i) \leq -q_i^2 \leq (-q_i^2)_{\max}$), the cross section is

$$\begin{aligned} \sigma_{e^+e^- \rightarrow e^+e^-X}(s) &= \frac{\alpha^2}{\pi^2} \int_{z_{\min}}^1 \frac{dz}{z} \left[f(z) \left(\ln \frac{(-q^2)_{\max}}{m_e^2 z} - 1 \right)^2 - \frac{1}{3} \left(\ln \frac{1}{z} \right)^3 \right] \sigma_{\gamma\gamma \rightarrow X}(zs); \\ f(z) &= \left(1 + \frac{1}{2}z \right)^2 \ln \frac{1}{z} - \frac{1}{2}(1-z)(3+z); \\ z &= \frac{W^2}{s}. \end{aligned} \quad (35.18)$$

The quantity $(-q^2)_{\max}$ depends on properties of the produced system X , in particular, $(-q^2)_{\max} \sim m_p^2$ for hadron production ($X = h$) and $(-q^2)_{\max} \sim W^2$ for lepton pair production ($X = \ell^+\ell^-$, $\ell = e, \mu, \tau$).

For production of a resonance of mass m_R and spin $J \neq 1$

$$\begin{aligned} \sigma_{e^+e^- \rightarrow e^+e^-R}(s) &= (2J+1) \frac{8\alpha^2 \Gamma_{R \rightarrow \gamma\gamma}}{m_R^3} \\ &\times \left[f(m_R^2/s) \left(\ln \frac{sm_V^2}{m^2 m_R^2} - 1 \right)^2 - \frac{1}{3} \left(\ln \frac{s}{m_R^2} \right)^3 \right] \end{aligned} \quad (35.19)$$

where m_V is the mass that enters into the form factor of the $\gamma\gamma \rightarrow R$ transition: $m_V \sim m_\rho$ for $R = \pi^0, \eta, f_2(1270), \dots$, $m_V \sim m_R$ for $R = c\bar{c}$ or $b\bar{b}$ resonances.

35.4. Inclusive hadronic reactions

One-particle inclusive cross sections $E d^3\sigma/d^3p$ for the production of a particle of momentum p are conveniently expressed in terms of rapidity (see above) and the momentum p_T transverse to the beam direction (defined in the center-of-mass frame)

$$E \frac{d^3\sigma}{d^3p} = \frac{d^3\sigma}{d\phi dy p_T dp_T}. \quad (35.20)$$

In the case of processes where p_T is large or the mass of the produced particle is large (here large means greater than 10 GeV), the parton model can be used to calculate the rate. Symbolically

$$\sigma_{\text{hadronic}} = \sum_{ij} \int f_i(x_1, Q^2) f_j(x_2, Q^2) dx_1 dx_2 \hat{\sigma}_{\text{partonic}}, \quad (35.21)$$

where $f_i(x, Q^2)$ is the parton distribution introduced above and Q is a typical momentum transfer in the partonic process and $\hat{\sigma}$ is the partonic cross section. Some examples will help to clarify. The production of a W^+ in pp reactions at rapidity y in the center-of-mass frame is given by

$$\begin{aligned} \frac{d\sigma}{dy} &= \frac{G_F \pi \sqrt{2}}{3} \\ &\times \tau \left[\cos^2 \theta_c \left(u(x_1, M_W^2) \bar{d}(x_2, M_W^2) + u(x_2, M_W^2) \bar{d}(x_1, M_W^2) \right) + \sin^2 \theta_c \left(u(x_1, M_W^2) \bar{s}(x_2, M_W^2) + s(x_2, M_W^2) \bar{u}(x_1, M_W^2) \right) \right], \end{aligned} \quad (35.22)$$

where $x_1 = \sqrt{\tau} e^y$, $x_2 = \sqrt{\tau} e^{-y}$, and $\tau = M_W^2/s$. Similarly the production of a jet in pp (or $p\bar{p}$) collisions is given by

$$\begin{aligned} \frac{d^3\sigma}{d^2p_T dy} &= \sum_{ij} \int f_i(x_1, p_T^2) f_j(x_2, p_T^2) \\ &\times \left[\hat{s} \frac{d\hat{\sigma}}{d\hat{t}} \right]_{ij} dx_1 dx_2 \delta(\hat{s} + \hat{t} + \hat{u}), \end{aligned} \quad (35.23)$$

where the summation is over quarks, gluons, and antiquarks. Here

$$s = (p_1 + p_2)^2, \quad (35.24)$$

$$t = (p_1 - p_{\text{jet}})^2, \quad (35.25)$$

$$u = (p_2 - p_{\text{jet}})^2, \quad (35.26)$$

p_1 and p_2 are the momenta of the incoming p and p (or \bar{p}) and \hat{s} , \hat{t} , and \hat{u} are s , t , and u with $p_1 \rightarrow x_1 p_1$ and $p_2 \rightarrow x_2 p_2$. The partonic cross section $\hat{\sigma}[(d\hat{\sigma})/(d\hat{t})]$ can be found in Ref. 2. Example: for the process $gg \rightarrow q\bar{q}$,

$$\hat{s} \frac{d\sigma}{d\hat{t}} = 3\alpha_s^2 \frac{(\hat{t}^2 + \hat{u}^2)}{8\hat{s}} \left[\frac{4}{9\hat{t}\hat{u}} - \frac{1}{\hat{s}^2} \right]. \quad (35.27)$$

The prediction of Eq. (35.23) is compared to data from the UA1 and UA2 collaborations in Fig. 37.8 in the Plots of Cross Sections and Related Quantities section of this Review.

The associated production of a Higgs boson and a gauge boson is analogous to the process $e^+e^- \rightarrow HZ^0$ in Sec. 35.2. The required parton-level cross sections [4], averaged over initial quark colors, are

$$\begin{aligned} \sigma(q_i \bar{q}_j \rightarrow W^\pm H) &= \frac{\pi\alpha^2 |V_{ij}|^2}{36 \sin^4 \theta_W} \cdot \frac{2K}{\sqrt{s}} \cdot \frac{K^2 + 3M_W^2}{(s - M_W^2)^2} \\ \sigma(q\bar{q} \rightarrow Z^0 H) &= \frac{\pi\alpha^2 (a_q^2 + v_q^2)}{144 \sin^4 \theta_W \cos^4 \theta_W} \cdot \frac{2K}{\sqrt{s}} \cdot \frac{K^2 + 3M_Z^2}{(s - M_Z^2)^2}. \end{aligned}$$

Here V_{ij} is the appropriate element of the Kobayashi-Maskawa matrix and K is the c.m. momentum of the produced H . The axial and vector couplings are defined as in Sec. 35.2.

35.5. One-particle inclusive distributions

In order to describe one-particle inclusive production in e^+e^- annihilation or deep inelastic scattering, it is convenient to introduce a fragmentation function $D_i^h(z, Q^2)$ where $D_i^h(z, Q^2)$ is the number of hadrons of type h and momentum between zp and $(z + dz)p$ produced in the fragmentation of a parton of type i . The Q^2 evolution is predicted by QCD and is similar to that of the parton distribution functions [see section on Quantum Chromodynamics (Sec. 9 of this *Review*)]. The $D_i^h(z, Q^2)$ are normalized so that

$$\sum_h \int z D_i^h(z, Q^2) dz = 1. \quad (35.28)$$

If the contributions of the Z boson and three-jet events are neglected, the cross section for producing a hadron h in e^+e^- annihilation is given by

$$\frac{1}{\sigma_{\text{had}}} \frac{d\sigma}{dz} = \frac{\sum_i e_i^2 D_i^h(z, Q^2)}{\sum_i e_i^2}, \quad (35.29)$$

where e_i is the charge of quark-type i , σ_{had} is the total hadronic cross section, and the momentum of the hadron is $zE_{\text{cm}}/2$.

In the case of deep inelastic muon scattering, the cross section for producing a hadron of energy E_h is given by

$$\frac{1}{\sigma_{\text{tot}}} \frac{d\sigma}{dz} = \frac{\sum_i e_i^2 q_i(x, Q^2) D_i^h(z, Q^2)}{\sum_i e_i^2 q_i(x, Q^2)}, \quad (35.30)$$

where $E_h = \nu z$. (For the kinematics of deep inelastic scattering, see Sec. 34.4.2 of the Kinematics section of this *Review*.) The fragmentation functions for light and heavy quarks have a different z dependence; the former peak near $z = 0$. They are illustrated in Figs. 36.1 and 36.2 in the section on "Heavy Quark Fragmentation in e^+e^- Annihilation" (Sec. 36 of this *Review*).

References:

1. V.M. Budnev, I.F. Ginzburg, G.V. Meledin, and V.G. Serbo, Phys. Reports **15C**, 181 (1975);
See also S. Brodsky, T. Kinoshita, and H. Terazawa, Phys. Rev. **D4**, 1532 (1971).
2. G.F. Owens, F. Reya, and M. Glück, Phys. Rev. **D18**, 1501 (1978).
3. B.W. Lee, C. Quigg, and B. Thacker, Phys. Rev. **D16**, 1519 (1977).
4. E. Eichten, I. Hinchliffe, K. Lane, and C. Quigg, Rev. Mod. Phys. **56**, 579 (1984).

36. HEAVY-QUARK FRAGMENTATION IN e^+e^- ANNIHILATION

Written January 1998 by D. Besson (University of Kansas).

Measurement of the fragmentation functions of heavy quarks provides information about non-perturbative particle production in a variety of experimental environments. The CDF observation of high p_T $J/\psi(1S)$ production rates far in excess of the extant theoretical predictions prompted the development of the color octet model (e.g., $p\bar{p} \rightarrow gg \rightarrow \chi_c \rightarrow \psi + X$) and highlighted the role of gluon fragmentation in charmonium production. Recent results from both LEP and HERA have also helped elucidate the gluonic contribution to charmed meson production. Current estimates from LEP are that gluon fragmentation accounts for approximately half of the D^* production in the lowest momentum region (the lowest quarter of the allowed kinematic region).

Many functional forms have been suggested to describe these momentum spectra for heavy quarks produced in e^+e^- annihilations. The functional form given by Peterson *et al.* [1] in terms of just one free parameter ϵ_P has found widespread use; other parameterizations are also given in the literature [2]. The earliest Peterson form was a function of one variable z , defined for a heavy-quark Q , light-quark \bar{q} system as the ratio of the energy plus the longitudinal momentum of the hadron $Q\bar{q}$ to the sum of the energy and momentum of the heavy quark after accounting for initial state radiation, gluon bremsstrahlung, and final state radiation: $z = (E + p_{\parallel})_{Q\bar{q}} / (E + p_Q)$. The main advantage of this variable is that it is relativistically invariant with respect to boosts in the direction of the primary quark. Unfortunately, as this quantity is not directly accessible, experiments typically use other scaling variables which are close approximations to z —either $x^+ = (p_{\parallel} + E)_{\text{hadron}} / (p_{\parallel} + E)_{\text{max}}$, $x_p = p/p_{\text{max}}$, or $x_E = E_{\text{hadron}}/E_{\text{beam}}$.

The Peterson functional form is:

$$\frac{dN}{dz} = \frac{1}{z[1 - (1/z) - \epsilon_P/(1-z)]^2} \quad (36.1)$$

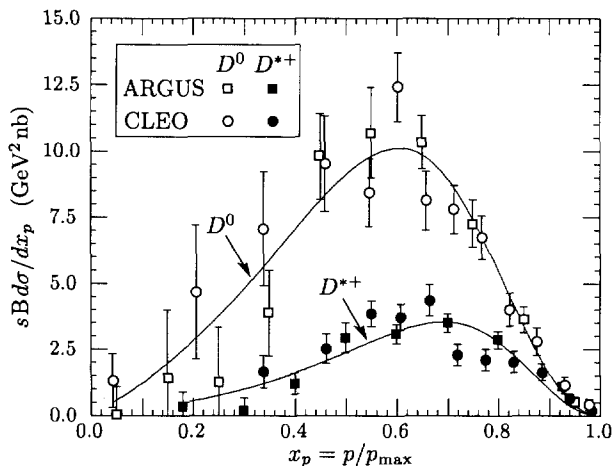


Figure 36.1: Efficiency-corrected inclusive cross section measurements for the production of D^0 and D^{*+} in e^+e^- annihilations at $\sqrt{s} \approx 10$ GeV. The variable x_p is related to the Peterson variable z , but is not identical to it.

The bulk of the available fragmentation function data on charmed mesons (excluding $J/\psi(1S)$) is from measurements at $\sqrt{s} = 10$ GeV. Shown in Fig. 36.1 are the efficiency-corrected (but not branching ratio corrected) CLEO [3] and ARGUS [4] inclusive cross sections ($s \cdot B d\sigma/dx_p$ in units of $\text{GeV}^2\text{-nb}$, with $x_p = p/p_{\text{max}}$) for the production of pseudoscalar D^0 and vector D^{*+} in e^+e^- annihilations at $\sqrt{s} \approx 10$ GeV. For the D^0 , B represents the branching fraction for $D^0 \rightarrow K^-\pi^+$; for the D^{*+} , B represents the product branching fraction: $D^{*+} \rightarrow D^0\pi^+$; $D^0 \rightarrow K^-\pi^+$. These inclusive spectra have not been corrected for cascades from higher states, nor for radiative effects. Note that since the momentum spectra are sensitive to

radiative corrections, comparison of charm spectra at $\sqrt{s} = 10$ GeV cannot be compared directly with spectra at higher center-of-mass energies, and must be appropriately evolved.

Fits to the combined CLEO and ARGUS D^0 and D^{*+} data give $\epsilon_P(D^0) = 0.135 \pm 0.01$ and $\epsilon_P(D^{*+}) = 0.078 \pm 0.008$; these are indicated in the solid curves. Measurement of the fragmentation functions for a variety of particles has allowed comparisons between mesons and baryons, and particles of different spin structure, as shown in Table 36.1

Table 36.1: The Peterson momentum hardness parameter ϵ_P as obtained from $e^+e^- \rightarrow (\text{particle}) + X$ measurements.

Particle	L	\sqrt{s}	ϵ_P	Reference
D^0	0	10 GeV	0.135 ± 0.01	[3]
D^{*+}	0	10 GeV	0.078 ± 0.008	[3]
D_s^*	0	10 GeV	$0.04^{+0.03}_{-0.01}$	[5]
$D_1^0(2420)$	1	10 GeV	$0.034^{+0.018}_{-0.012}$	[6]
$D_2^0(2460)$	1	10 GeV	0.015 ± 0.004	[6]
$D_1^+(2420)$	1	10 GeV	$0.020^{+0.011}_{-0.006}$	[7]
$D_2^+(2460)$	1	10 GeV	0.013 ± 0.007	[7]
$D_{s1}(2536)$	1	10 GeV	$0.06^{+0.035}_{-0.03}$	[8]
$D_{s2}(2573)$	1	10 GeV	$0.027^{+0.043}_{-0.016}$	[9]
Λ_c	0	10 GeV	0.25 ± 0.03	[10,11]
Ξ_c	0	10 GeV	0.23 ± 0.05	[12,13]
Σ_c	0	10 GeV	0.29 ± 0.06	[14,15]
Σ_c^*	0	10 GeV	$0.30^{+0.10}_{-0.07}$	[16]
Ξ_c^{*+}	0	10 GeV	$0.24^{+0.22}_{-0.10}$	[17]
Ξ_c^{*0}	0	10 GeV	$0.22^{+0.15}_{-0.08}$	[18]
$\Lambda_{c,1}$	1	10 GeV	0.059 ± 0.028	[19,20]
$\Lambda_{c,2}$	1	10 GeV	0.053 ± 0.012	[19,21]
$\Xi_{c,2}$	1	10 GeV	$0.058^{+0.037}_{-0.021}$	[22]
b hadrons	—	90 GeV	$0.0047^{+0.0010}_{-0.0008}$	[23]

We note from Table 36.1 that the mass dependence of ϵ_P is less marked than the dependence on the orbital angular momentum structure of the charmed hadron being measured. Orbitally excited $L = 1$ charmed hadrons (D_J , $D_{s,J}$, and $\Lambda_{c,J}$) show consistently harder spectra (i.e., smaller values of ϵ_P) than the $L = 0$ ground states, whereas the data for the ground state charmed baryons Λ_c and Ξ_c show agreement with the lighter (by ≈ 400 – 600 MeV) ground-state D and D_s charmed mesons. To some extent, the harder spectra of $L = 1$ hadrons can be attributed to the fact that all the $L = 1$ charmed hadrons will eventually decay into $L = 0$ hadrons.

Bottom-flavored hadrons at LEP have been measured to have an even harder momentum spectrum than charmed hadrons at lower energies [23–25]. Qualitatively, whereas charm spectra peak at $x_p \approx 0.6$, the spectra of bottom hadrons peak at $x_p \approx 0.8$. This is as expected in the Peterson model, where the value ϵ_P is expected to vary as the ratio of the effective light quark mass to the heavy quark mass in a heavy quark + light (di)quark hadron. In the case of charm, the Peterson functional form provides an acceptable description of the shape of the x_p distribution, provided the appropriate ϵ_P value is independently determined for each separate species of charmed particle. However, unlike charm, the numbers of fully reconstructed b -flavored hadrons is too small to allow a statistically compelling measure of ϵ_P for each separate bottom hadron. Consequently, a b -enriched sample is isolated kinematically, using, e.g., a high p_T lepton and/or a displaced vertex to tag a primary b quark. The x_p distribution therefore includes all b -flavored hadrons in the sample, and

does not yet allow a straightforward species-by-species ϵ_P extraction. Additional uncertainties in the case of bottom arise from the sensitivity of ϵ_P to the fragmentation model used to non-perturbatively evolve the initial $q\bar{q}$ system into final state hadrons.

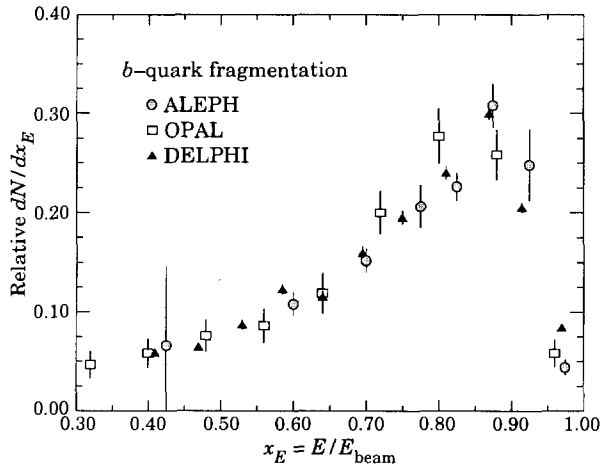


Figure 36.2: Fractional energy distribution for b -quark fragmentation for inclusive b production at LEP.

In general, the b -quark fragmentation function distribution is found to be somewhat narrower than the shape of the Peterson function; this may be due to a systematic underestimate of soft gluon emission in event generators, and/or uncertainties in the appropriate mix of b -flavored hadrons. The match of a single Peterson function to data is therefore much more difficult for bottom than charm at this time, although there is relatively good agreement from experiment to experiment, as seen in Fig. 36.2, which displays the fragmentation function data from OPAL [23], ALEPH [24], and DELPHI [25].

References:

1. C. Peterson, D. Schlatter, I. Schmitt, and P. M. Zerwas, Phys. Rev. **D27**, 105 (1983).
2. M.G. Bowler, Z. Phys. **C11**, 169 (1981); V.G. Kartvelishvili *et al.*, Phys. Lett. **B78**, 615 (1978); B. Andersson *et al.*, Z. Phys. **C20**, 317 (1983).
3. D. Bortoletto *et al.*, Phys. Rev. **D37**, 1719 (1988).
4. H. Albrecht *et al.*, Z. Phys. **C52**, 353 (1991).
5. J. A. McKenna, Ph.D. thesis, U. of Toronto, Toronto, Canada (1987), unpublished.
6. P. Avery *et al.*, Phys. Lett. **B331**, 236 (1994).
7. T. Bergfeld *et al.*, Phys. Lett. **B341**, 435 (1995).
8. R. Kutschke, presented at Intl. Conf. on Heavy Quark Physics, Ithaca, NY, 1989.
9. H. Albrecht *et al.*, Z. Phys. **C69**, 405 (1996).
10. G. Crawford *et al.*, Phys. Rev. **D45**, 752 (1992).
11. C. E. K. Charlesworth, A Study of the Decay Properties of the Charmed Baryon Λ_c^+ , Ph. D. Thesis, University of Toronto (1992).
12. H. Albrecht *et al.*, Phys. Lett. **B247**, 121 (1990).
13. K. W. Edwards *et al.*, Phys. Lett. **B373**, 261 (1996).
14. H. Albrecht *et al.*, Phys. Lett. **B207**, 489 (1988).
15. T. Bowcock *et al.*, Phys. Rev. Lett. **62**, 2233 (1989).
16. G. Brandenburg *et al.*, Phys. Rev. Lett. **78**, 2304 (1997).
17. L. Gibbons *et al.*, Phys. Rev. Lett. **77**, 810 (1996).
18. P. Avery *et al.*, Phys. Rev. Lett. **75**, 4364 (1995).
19. K. W. Edwards *et al.*, Phys. Rev. Lett. **74**, 3331 (1995).
20. H. Albrecht *et al.*, Phys. Lett. **B402**, 207 (1997).
21. H. Albrecht *et al.*, Phys. Lett. **B317**, 227 (1993).
22. G. Brandenburg *et al.*, CLEO-CONF 97-17, EPS97-398, submitted to the 1997 European Physical Society Conf. on High Energy Physics, Jerusalem, Israel, Aug. 18-25, 1997.
23. G. Alexander *et al.*, The OPAL Collaboration, Phys. Lett. **B364**, 93 (1995).
24. D. Buskulic *et al.*, The ALEPH Collaboration, Phys. Lett. **B357**, 699 (1995).
25. O. Podobrin, M. Feindt, *et al.*, The DELPHI Collaboration, DELPHI 95-103 PHYS 538.

37. PLOTS OF CROSS SECTIONS AND RELATED QUANTITIES

NOTE: THE FIGURES IN THIS SECTION ARE INTENDED TO SHOW THE REPRESENTATIVE DATA.
THEY ARE NOT MEANT TO BE COMPLETE COMPILATIONS OF ALL THE WORLD'S RELIABLE DATA.

Structure Functions

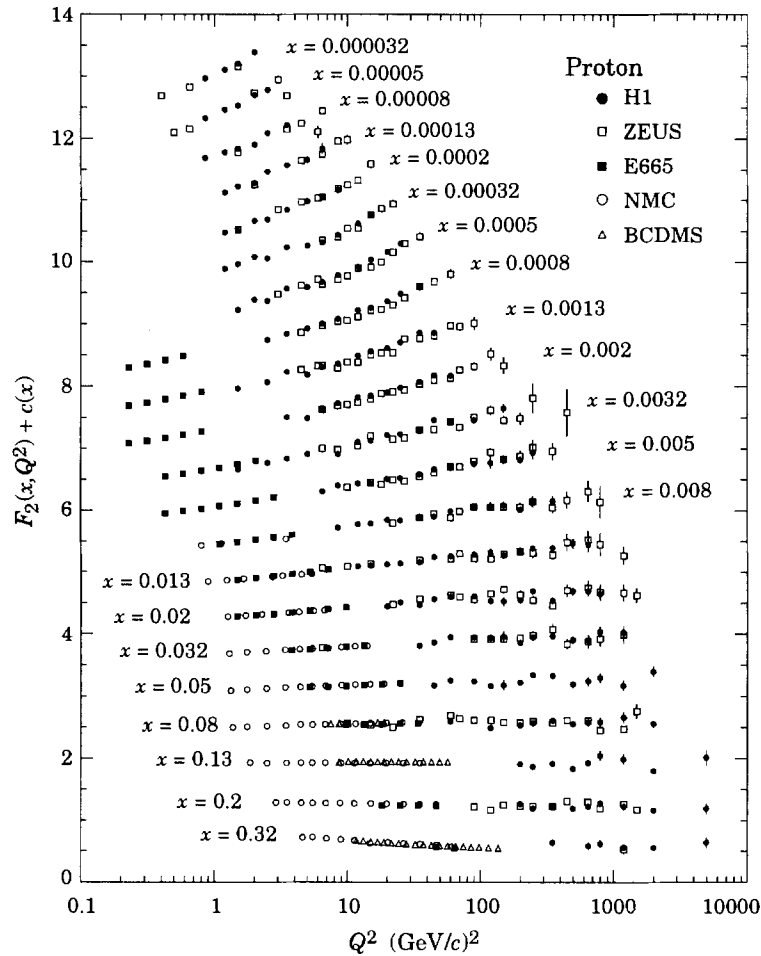


Figure 37.1: The proton structure function F_2^p measured in electromagnetic scattering of electrons (H1, ZEUS) and muons (BCDMS, E665, NMC), in the kinematic domain of the HERA data, for $x > 0.00003$; cf. Fig. 37.2 for data at smaller x . Only statistical errors are shown. The data are plotted as a function of Q^2 in bins of fixed x . The H1 binning in x is used in this plot; the ZEUS, BCDMS, E665 and NMC data are rebinned to the x values of the H1 data using a phenomenological parametrization. For the purpose of plotting, a constant $c(x) = 0.6(i_x - 0.4)$ is added to F_2^p , where i_x is the number of the x bin ranging from $i_x = 1$ ($x = 0.32$) to $i_x = 21$ ($x = 0.000032$). References: **H1**—S. Aid *et al.*, Nucl. Phys. **B470**, 3 (1996); C. Adloff *et al.*, Nucl. Phys. **B497**, 3 (1997); **ZEUS**—M. Derrick *et al.*, Z. Phys. **C72**, 399 (1996); J. Breitweg *et al.*, Phys. Lett. **B407**, 432 (1997); **BCDMS**—A.C. Benvenuti *et al.*, Phys. Lett. **B223**, 485 (1989); **E665**—M.R. Adams *et al.*, Phys. Rev. **D54**, 3006 (1996); **NMC**—M. Arneodo *et al.*, Phys. Lett. **B364**, 107 (1995). (Courtesy of R. Voss, 1997.)

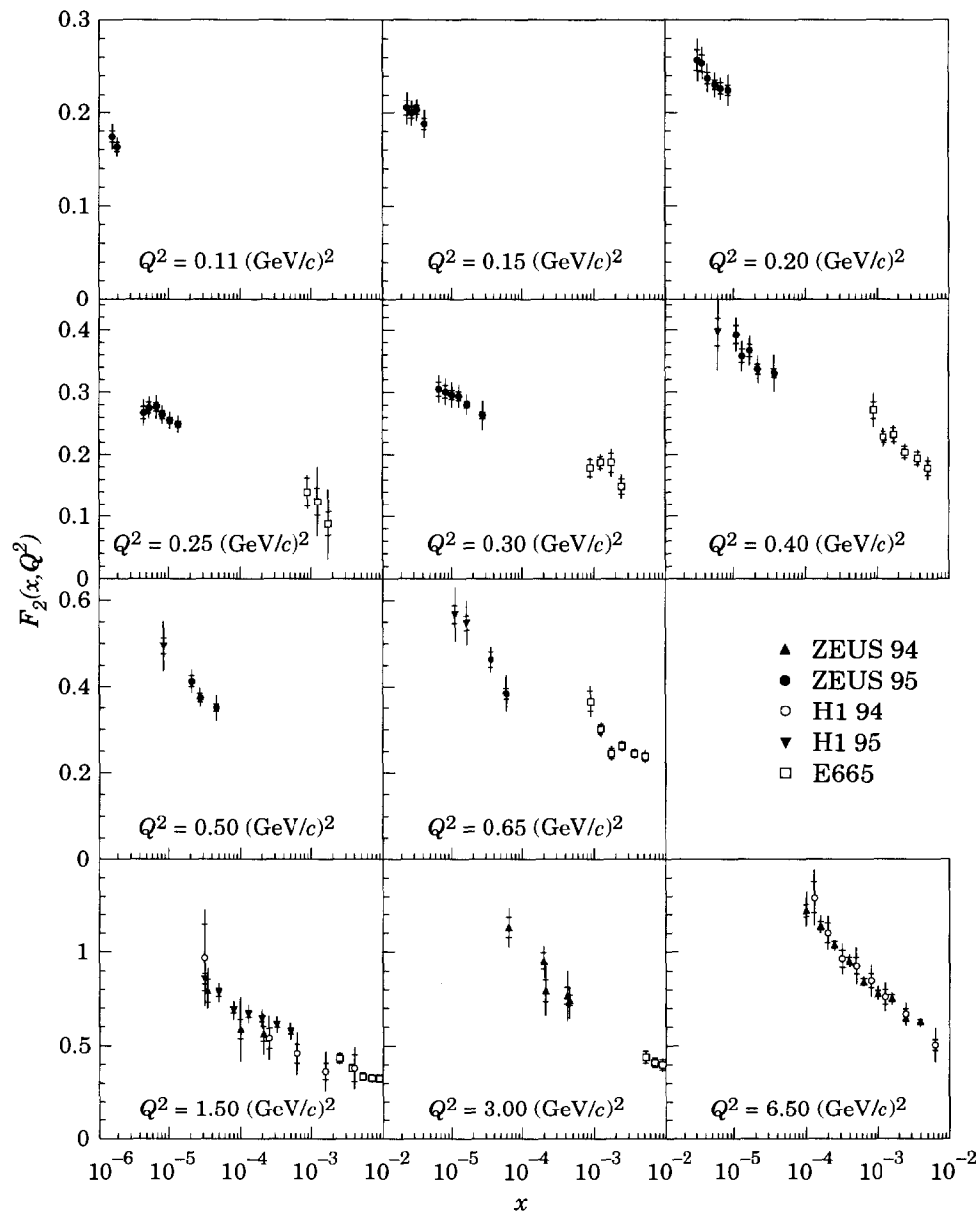


Figure 37.2: The proton structure function F_2^p at small x and Q^2 , measured in electromagnetic scattering of electrons (H1, ZEUS) and muons (E665). The data are plotted as a function of x in bins of fixed Q^2 . References: **ZEUS 94**—M. Derrick *et al.*, *Z. Phys.* **C72**, 399 (1996); **ZEUS 95**—J. Breitweg *et al.*, *Phys. Lett.* **B407**, 432 (1997); **H1 94**—S. Aid *et al.*, *Nucl. Phys.* **B470**, 3 (1996); **H1 95**—C. Adloff *et al.*, *Nucl. Phys.* **B497**, 3 (1997); **E665**—M.R. Adams *et al.*, *Phys. Rev.* **D54**, 3006 (1996). (Courtesy of R. Voss, 1997.)

Structure Functions

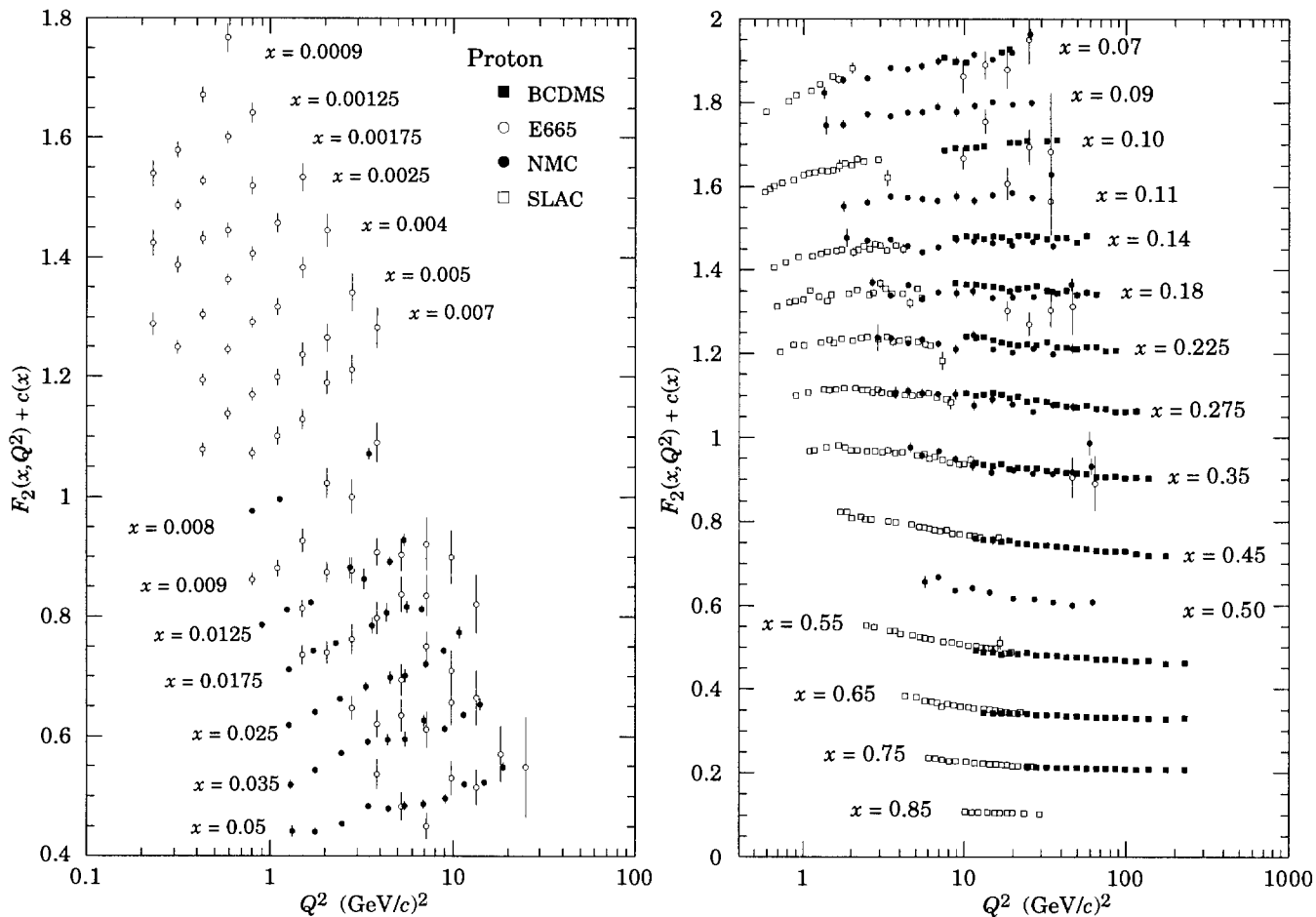


Figure 37.3: The proton structure function F_2^p measured in electromagnetic scattering of electrons (SLAC) and muons (BCDMS, E665, NMC), shown as a function of Q^2 for bins of fixed x . Only statistical errors are shown. For the purpose of plotting, a constant $c(x) = 0.1i_x$ is added to F_2^p where i_x is the number of the x bin, ranging from 1 ($x = 0.05$) to 14 ($x = 0.0009$) on the left-hand figure, and from 1 ($x = 0.07$) to 15 ($x = 0.85$) on the right-hand figure. For HERA data in the kinematic range of this figure, see Fig. 37.1. References: **BCDMS**—A.C. Benvenuti *et al.*, Phys. Lett. **B223**, 485 (1989); **E665**—M.R. Adams *et al.*, Phys. Rev. **D54**, 3006 (1996); **NMC**—M. Arneodo *et al.*, Phys. Lett. **B364**, 107 (1995). **SLAC**—L.W. Whitlow *et al.*, Phys. Lett. **B282**, 475 (1992). (Courtesy of R. Voss, 1996.)

Structure Functions

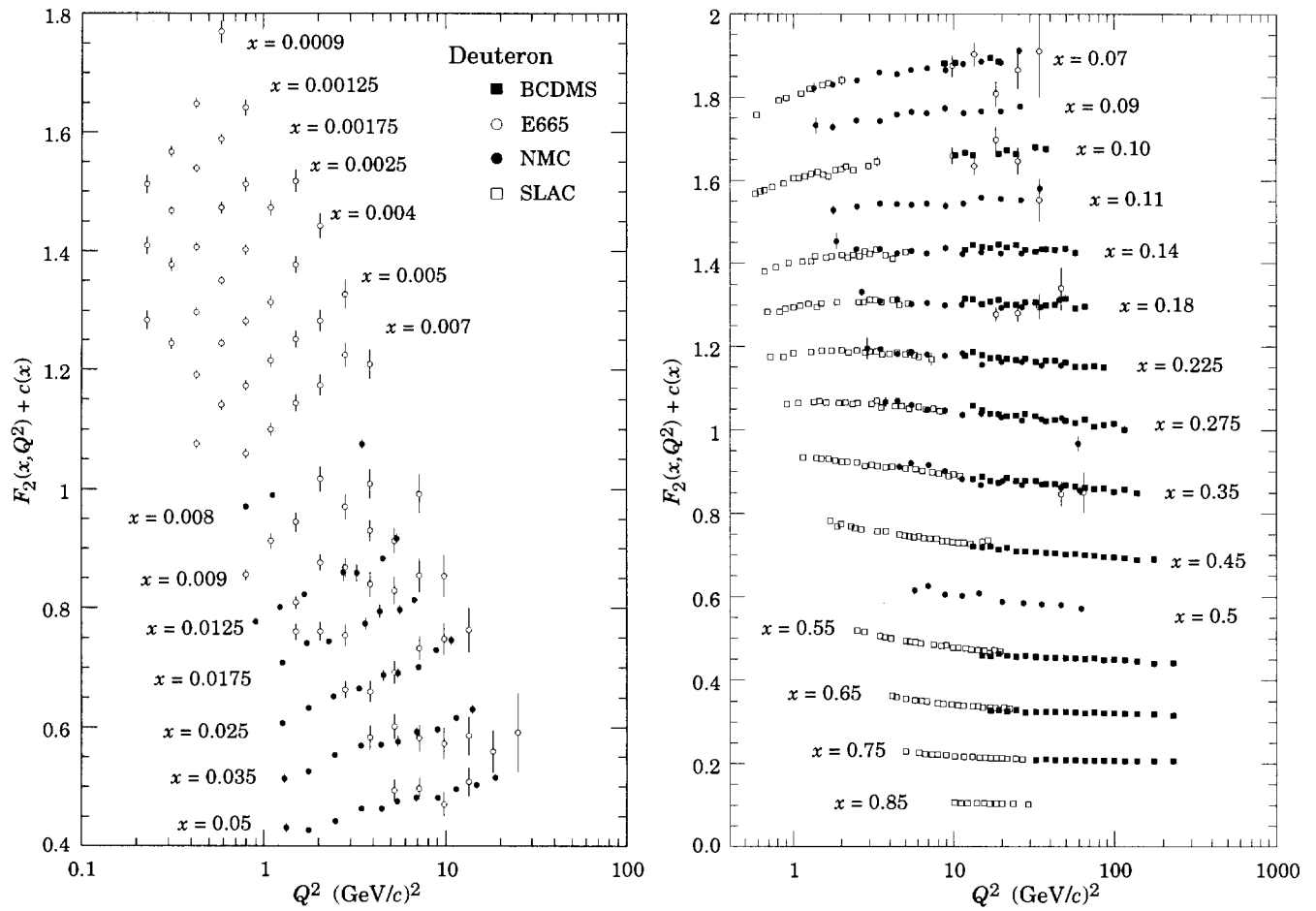


Figure 37.4: As Fig. 37.3, for the deuteron structure function F_2^d . References: **BCDMS**—A.C. Benvenuti *et al.*, Phys. Lett. **B237**, 592 (1990). **E665**, **NMC**, **SLAC**—same references as Fig. 37.3. (Courtesy of R. Voss, 1996.)

Structure Functions

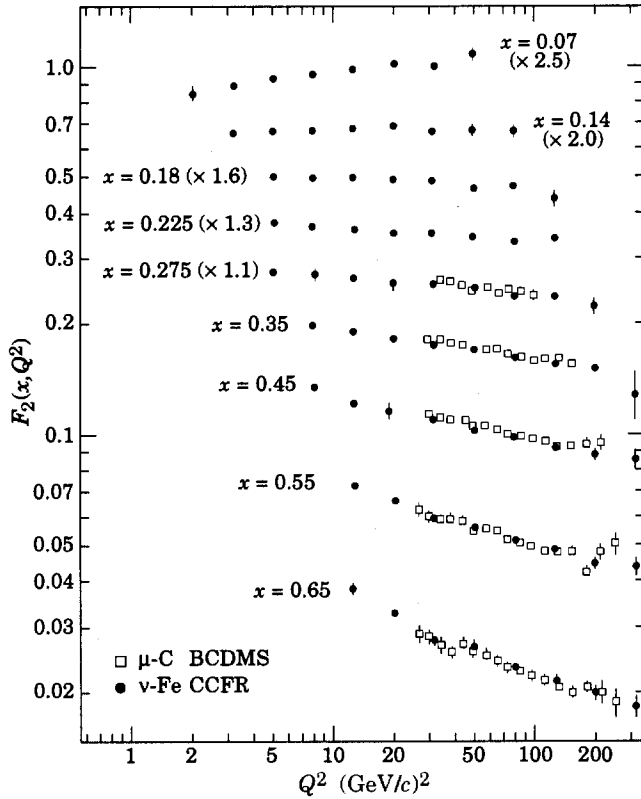


Figure 37.5: The nucleon structure function F_2 measured in deep inelastic scattering of muons on carbon (BCDMS) and neutrinos on iron (CCFR). The data are shown versus Q^2 , for bins of fixed x , and have been scaled by the factors shown in parentheses. References: BCDMS—A.C. Benvenuti *et al.*, Phys. Lett. **B195**, 91 (1987); CCFR—S.R. Mishra *et al.*, NEVIS-1465 (1992). (Courtesy of R. Voss, 1996.)

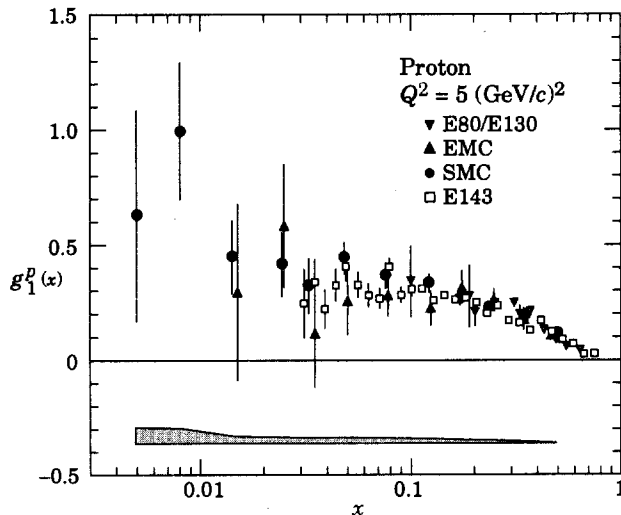


Figure 37.6: The spin-dependent structure function $g_1(x)$ of the proton measured in deep inelastic scattering of polarized electrons (E80, E130, E143) and muons (EMC, SMC), shown at $Q^2 = 5 \text{ GeV}^2$. Only statistical errors are shown with the data points. As an example, the SMC systematic error is indicated by the shaded

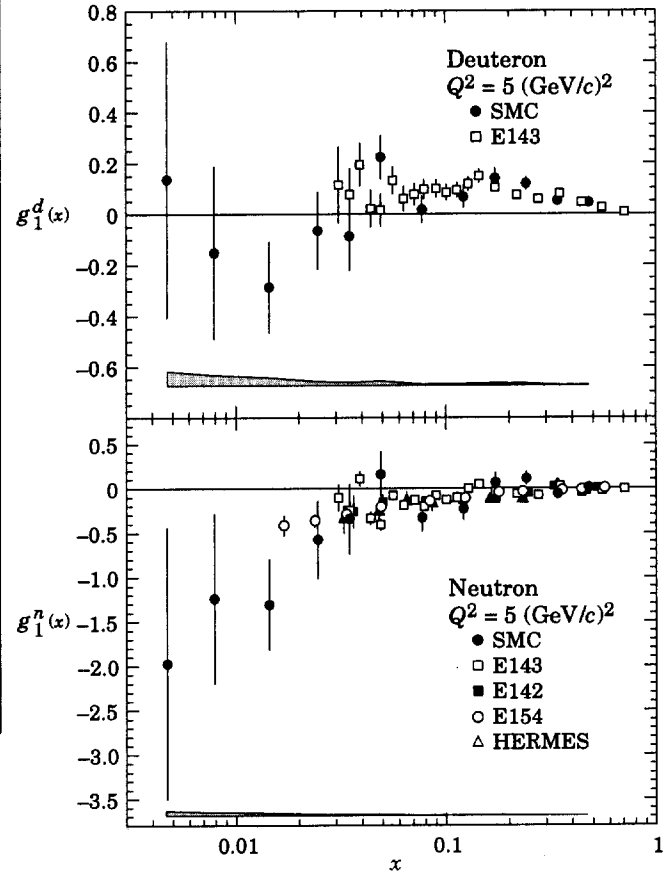


Figure 37.7: The spin-dependent structure function $g_1(x)$ of the deuteron (top) and the neutron (bottom) measured in deep inelastic scattering of polarized electrons (E142, E143, E154, HERMES) and muons (SMC). The SMC and E143 results for the neutron are evaluated from the difference of deuteron and proton data; the E142, E154, and HERMES results were obtained with polarized ^3He targets. Only statistical errors are shown with the data points. As an example, the SMC systematic error is indicated by the shaded area. All results except the HERMES data are shown at $Q^2 = 5 \text{ GeV}^2$; the HERMES results are shown at the average Q^2 of the respective data point which varies from $Q^2 = 1.22 \text{ GeV}^2$ at $x = 0.033$ to $Q^2 = 5.25 \text{ GeV}^2$ at $x = 0.464$. References: E142—P.L. Anthony *et al.*, Phys. Rev. Lett. **71**, 959 (1993); E143—K. Abe *et al.*, Phys. Rev. Lett. **75**, 25 (1995); E154—K. Abe *et al.*, Phys. Lett. **B405**, 180 (1997) and hep-ph/9705344 v2 (1997); HERMES—K. Ackerstaff *et al.*, Phys. Lett. **B404**, 383 (1997); SMC—D. Adams *et al.*, Phys. Lett. **B396**, 338 (1997). (Courtesy of R. Voss, 1997.)

area. References: E80—M.J. Alguard *et al.*, Phys. Rev. Lett. **37**, 1261 (1976); *ibid.* **41**, 70 (1978); E130—G. Baum *et al.*, Phys. Rev. Lett. **51**, 1135 (1983); E143—K. Abe *et al.*, Phys. Rev. Lett. **74**, 346 (1995); EMC—J. Ashman *et al.*, Nucl. Phys. **B328**, 1 (1989); SMC—B. Adeva *et al.*, Phys. Lett. **B412**, 414 (1997). In this plot, the E80, E130 and EMC data have been reevaluated using up-to-date parametrizations of F_2^p and $R = \sigma_L/\sigma_T$. (Courtesy of R. Voss, 1997.)

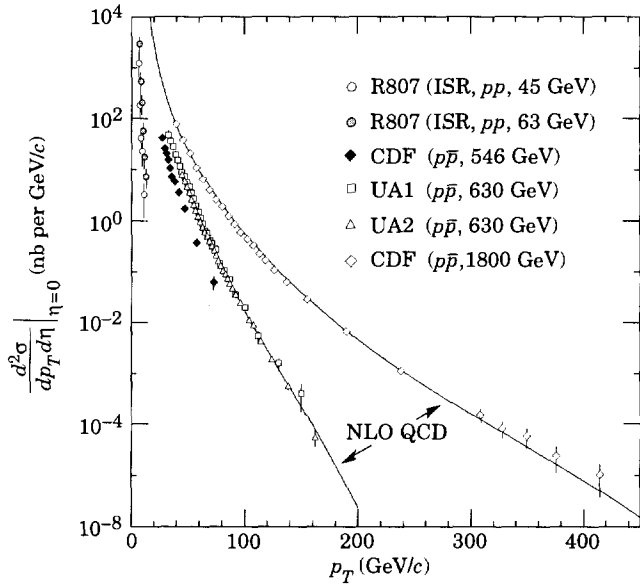
Jet Production in pp and $p\bar{p}$ Interactions


Figure 37.8: Differential cross sections for observation of a single jet of pseudorapidity $\eta = 0$ as a function of the jet transverse momentum. CDF—F. Abe *et al.*, Phys. Rev. Lett. **70**, 1376 (1993); UA1—G. Arnison *et al.*, Phys. Lett. **B172**, 461 (1986); UA2—J. Alitti *et al.*, Phys. Lett. **B257**, 232 (1991); R807—T. Akesson *et al.*, Phys. Lett. **B123**, 133 (1983). Next-to-leading order QCD curves are shown for 630 GeV and 1800 GeV. (Courtesy of S. Geer, FNAL, 1995.)

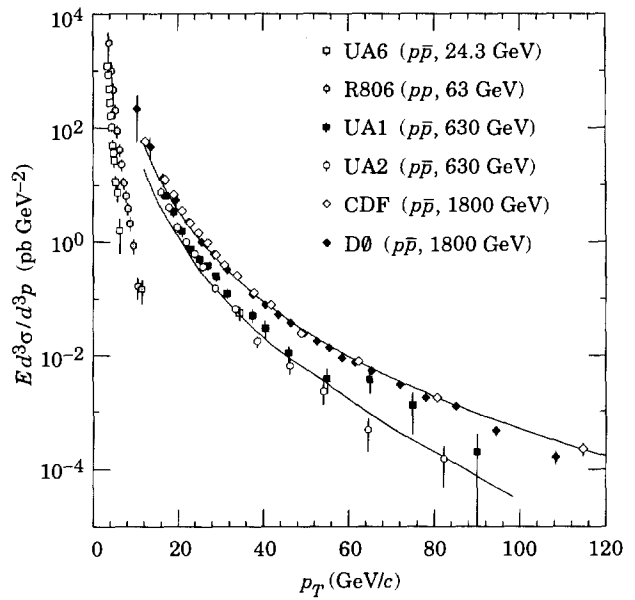
 Direct γ Production in $p\bar{p}$ Interactions


Figure 37.9: Differential cross sections for observation of a single photon of pseudorapidity $\eta = 0$ as a function of the photon transverse momentum R806—E. Anassontzis *et al.*, Z. Phys. **C13**, 277 (1982); UA6—A. Bernasconi *et al.*, Phys. Lett. **B206**, 163 (1988); UA1—C. Albajar *et al.*, Phys. Lett. **B209**, 385 (1988); UA2—J. Alitti *et al.*, Phys. Lett. **B288**, 386 (1992); CDF—F. Abe *et al.*, Phys. Rev. Lett. **73**, 2662 (1994); D0—S. Abachi *et al.*, Phys. Rev. Lett. **77**, 5011 (1996). Next-to-leading order QCD curves are shown for 630 GeV and 1800 GeV. (Courtesy of S. Geer, FNAL, 1995.)

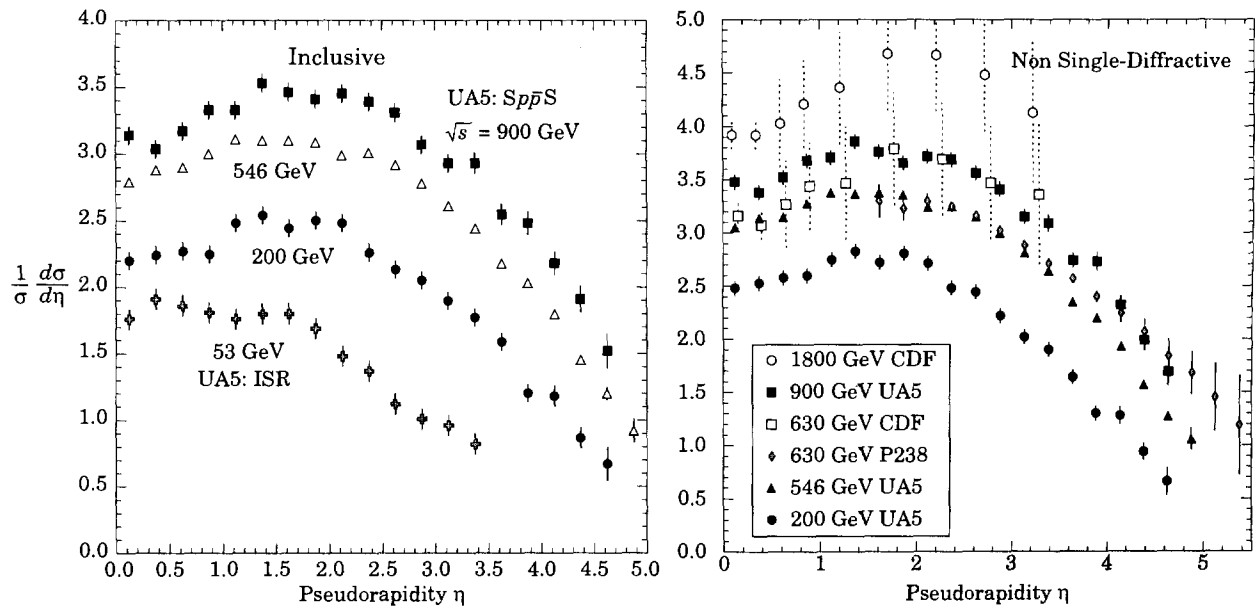
 Pseudorapidity Distributions in $p\bar{p}$ Interactions


Figure 37.10: Charged particle pseudorapidity distributions in $p\bar{p}$ collisions for $53 \text{ GeV} \leq \sqrt{s} \leq 1800 \text{ GeV}$. UA5 data from the $Spp\bar{S}$ are taken from G.J. Alner *et al.*, Z. Phys. **C33**, 1 (1986), and from the ISR from K. Alpgård *et al.*, Phys. Lett. **112B**, 193 (1982). The UA5 data are shown for both the full inelastic cross-section and with singly diffractive events excluded. Additional non single-diffractive measurements are available from CDF at the Tevatron, F. Abe *et al.*, Phys. Rev. **D41**, 2330 (1990) and Experiment P238 at the $Spp\bar{S}$, R. Harr *et al.*, Phys. Lett. **B401**, 176 (1997). (Courtesy of D.R. Ward, Cambridge Univ., 1999.)

Average Hadron Multiplicities in Hadronic e^+e^- Annihilation Events

Table 37.1: Average hadronic multiplicities per hadronic e^+e^- annihilation event at $\sqrt{s} \approx 10, 29\text{--}35,$ and 91 GeV. The rates given include decay products from resonances with $c\tau < 10$ cm, and include charge conjugated states. Correlations of the systematic uncertainties were considered for the calculation of the averages. (Updated July 1999 by O. Biebel.)

Particle	$\sqrt{s} \approx 10$ GeV	$\sqrt{s} = 29\text{--}35$ GeV	$\sqrt{s} = 91$ GeV
Pseudoscalar mesons:			
π^+	6.6 ± 0.2	10.3 ± 0.4	16.99 ± 0.27
π^0	3.2 ± 0.3	5.83 ± 0.28	9.47 ± 0.54
K^+	0.90 ± 0.04	1.48 ± 0.09	2.242 ± 0.063
K^0	0.91 ± 0.05	1.48 ± 0.07	2.013 ± 0.033
η	0.20 ± 0.04	0.61 ± 0.07	0.971 ± 0.030
$\eta'(958)$	0.03 ± 0.01	0.26 ± 0.10	0.156 ± 0.021
D^+	0.16 ± 0.03	0.17 ± 0.03	0.175 ± 0.016
D^0	0.37 ± 0.06	0.45 ± 0.07	0.454 ± 0.030
D_s^+	0.13 ± 0.02	0.45 ± 0.20 ^(a)	0.131 ± 0.021
B^+, B_d^0	—	—	0.165 ± 0.026 ^(b)
B_s^0	—	—	0.057 ± 0.013 ^(b)
Scalar mesons:			
$f_0(980)$	0.024 ± 0.006	0.05 ± 0.02 ^(c)	0.146 ± 0.012
$a_0(980)^\pm$	—	—	0.27 ± 0.11 ^(d)
Vector mesons:			
$\rho(770)^0$	0.35 ± 0.04	0.81 ± 0.08	1.231 ± 0.098
$\rho(770)^\pm$	—	—	2.40 ± 0.43 ^(d)
$\omega(782)$	0.30 ± 0.08	—	1.08 ± 0.12
$K^*(892)^+$	0.27 ± 0.03	0.64 ± 0.05	0.715 ± 0.059
$K^*(892)^0$	0.29 ± 0.03	0.56 ± 0.06	0.738 ± 0.024
$\phi(1020)$	0.044 ± 0.003	0.085 ± 0.011	0.0963 ± 0.0032
$D^*(2010)^+$	0.22 ± 0.04	0.43 ± 0.07	0.183 ± 0.010
$D^*(2007)^0$	0.23 ± 0.06	0.27 ± 0.11	—
$D_s^*(2112)^+$	—	—	0.101 ± 0.048 ^(f)
B^* ^(e)	—	—	0.288 ± 0.026
$J/\psi(1S)$	—	—	0.0052 ± 0.0004 ^(g)
$\psi(2S)$	—	—	0.0023 ± 0.0004 ^(g)
$\Upsilon(1S)$	—	—	0.00014 ± 0.00007 ^(g)
Pseudovector mesons:			
$\chi_{c1}(3510)$	—	—	0.0041 ± 0.0011 ^(g)
Tensor mesons:			
$f_2(1270)$	0.09 ± 0.02	0.14 ± 0.04	0.166 ± 0.020
$f_2'(1525)$	—	—	0.012 ± 0.006
$K_2^*(1430)^+$	—	0.09 ± 0.03	—
$K_2^*(1430)^0$	—	0.12 ± 0.06	0.084 ± 0.022 ^(g)
B^{**} ^(h)	—	—	0.118 ± 0.024
Baryons:			
p	0.253 ± 0.016	0.640 ± 0.050	1.048 ± 0.045
Λ	0.080 ± 0.007	0.205 ± 0.010	0.374 ± 0.009
Σ^0	0.023 ± 0.008	—	0.070 ± 0.012
Σ^-	—	—	0.081 ± 0.010
Σ^+	—	—	0.099 ± 0.015
Σ^\pm	—	—	0.174 ± 0.009
Ξ^-	0.0059 ± 0.0007	0.0176 ± 0.0027	0.0258 ± 0.0010
$\Delta(1232)^{++}$	0.040 ± 0.010	—	0.085 ± 0.014
$\Sigma(1385)^-$	0.006 ± 0.002	0.017 ± 0.004	0.0240 ± 0.0017
$\Sigma(1385)^+$	0.005 ± 0.001	0.017 ± 0.004	0.0239 ± 0.0015
$\Sigma(1385)^\pm$	0.0106 ± 0.0020	0.033 ± 0.008	0.0462 ± 0.0028
$\Xi(1530)^0$	0.0015 ± 0.0006	—	0.0055 ± 0.0005
Ω^-	0.0007 ± 0.0004	0.014 ± 0.007	0.0016 ± 0.0003
Λ_c^+	0.100 ± 0.030 ⁽ⁱ⁾	0.110 ± 0.050	0.078 ± 0.017
Λ_b^0	—	—	0.031 ± 0.016
$\Sigma_c^{++}, \Sigma_c^0$	0.014 ± 0.007	—	—
$\Lambda(1520)$	0.008 ± 0.002	—	0.0222 ± 0.0027

All average multiplicities are per hadronic e^+e^- annihilation event.

- (a) $B(D_s \rightarrow \eta\pi, \eta'\pi)$ was used (RPP94).
- (b) The Standard Model $B(Z \rightarrow b\bar{b}) = 0.217$ was used.
- (c) $x_p = p/p_{\text{beam}} > 0.1$ only.
- (d) Both charge states.
- (e) Any charge state (i.e., B_d^* , B_u^* , or B_s^*).
- (f) $B(D_s^* \rightarrow D_s^+\gamma), B(D_s^+ \rightarrow \phi\pi^+), B(\phi \rightarrow K^+K^-)$ have been used (RPP98).
- (g) $B(Z \rightarrow \text{hadrons}) = 0.699$ was used (RPP94).
- (h) Any charge state (i.e., $B_d^{**}, B_u^{**},$ or B_s^{**}).
- (i) The value was derived from the cross section of $A_c^+ \rightarrow p\pi K$, assuming the branching fraction to be $(3.2 \pm 0.7)\%$ (RPP92).

References:

- RPP92:** Phys. Rev. **D45** (1992) and references therein
RPP94: Phys. Rev. **D50**, 1173 (1994) and references therein
RPP96: Phys. Rev. **D54**, 1 (1996) and references therein
RPP98: Eur. Phys. J. **C3**, 1 (1998) and references therein
R. Marshall, Rep. Prog. Phys. **52**, 1329 (1989)
A. De Angelis, J. Phys. **G19**, 1233 (1993) and references therein
ALEPH: D. Buskulic *et al.*: Phys. Lett. **B295**, 396 (1992);
Z. Phys. **C64**, 361 (1994); **C69**, 15 (1996); **C69**, 379 (1996);
C73, 409 (1997); and R. Barate *et al.*: Z. Phys. **C74**, 451
(1997); Phys. Reports **294**, 1 (1998); Eur. Phys. J. **C5**, 205
(1998)
ARGUS: H. Albrecht *et al.*: Phys. Lett. **230B**, 169 (1989);
Z. Phys. **C44**, 547 (1989); **C46**, 15 (1990); **C54**, 1 (1992);
C58, 199 (1993); **C61**, 1 (1994); Phys. Rep. **276**, 223 (1996)
CELLO: H.J. Behrend *et al.*: Z. Phys. **C46**, 397 (1990); **C47**,
1 (1990)
CLEO: D. Bortoletto *et al.*, Phys. Rev. **D37**, 1719 (1988)
Crystal Ball: Ch. Bieler *et al.*, Z. Phys. **C49**, 225 (1991)
DELPHI: P. Abreu *et al.*: Z. Phys. **C57**, 181 (1993); **C59**, 533
(1993); **C61**, 40 7(1994); **C65**, 587 (1995); **C67**, 543 (1995);
C68, 353 (1995); **C73**, 61 (1996); Nucl. Phys. **B444**, 3 (1995);
Phys. Lett. **B341**, 109 (1994); **B345**, 598 (1995); **B361**,
207 (1995); **B372**, 172 (1996); **B379**, 309 (1996); **B416**, 233
(1998); **B449**, 364 (1999); Eur. Phys. J. **C6**, 19 (1999); **C5**,
585 (1998); CERN-EP/2000-009 (accepted by Phys. Lett.);
W. Adam *et al.*: Z. Phys. **C69**, 561 (1996); **C70**, 371 (1996)
HRS: S. Abachi *et al.*, Phys. Rev. Lett. **57**, 1990 (1986); and
M. Derrick *et al.*, Phys. Rev. **D35**, 2639 (1987)
L3: M. Acciarri *et al.*: Phys. Lett. **B328**, 223 (1994); **B345**,
589 (1995); **B371**, 126 (1996); **B371**, 137 (1996); **B393**, 465
(1997); **B404**, 390 (1997); **B407**, 351 (1997); **B407**, 389 (1997),
erratum ibid. **B427**, 409 (1998); **B453**, 94 (1999);
MARK II: H. Schellman *et al.*, Phys. Rev. **D31**, 3013 (1985);
and G. Wormser *et al.*, Phys. Rev. Lett. **61**, 1057 (1988)
JADE: W. Bartel *et al.*, Z. Phys. **C20**, 187 (1983); and D.D.
Pietzl *et al.*, Z. Phys. **C46**, 1 (1990)
OPAL: R. Akers *et al.*: Z. Phys. **C63**, 181 (1994); **C66**, 555
(1995); **C67**, 389 (1995); **C68**, 1 (1995); and G. Alexander
et al.: Phys. Lett. **B358**, 162 (1995); Z. Phys. **C70**, 197
(1996); **C72**, 1 (1996); **C72**, 191 (1996); **C73**, 569 (1997);
C73, 587 (1997); Phys. Lett. **B370**, 185 (1996); and K.
Ackerstaff *et al.*: Z. Phys. **C75**, 192 (1997); Phys. Lett. **B412**,
210 (1997); Eur. Phys. J. **C1**, 439 (1998); **C4**, 19 (1998); **C5**,
1 (1998); **C5**, 411 (1998);
PLUTO: Ch. Berger *et al.*, Phys. Lett. **104B**, 79 (1981)
SLD: K. Abe, Phys. Rev. **D59**, 052001 (1999)
TASSO: H. Aihara *et al.*, Z. Phys. **C27**, 27 (1985)
TPC: H. Aihara *et al.*, Phys. Rev. Lett. **53**, 2378 (1984)

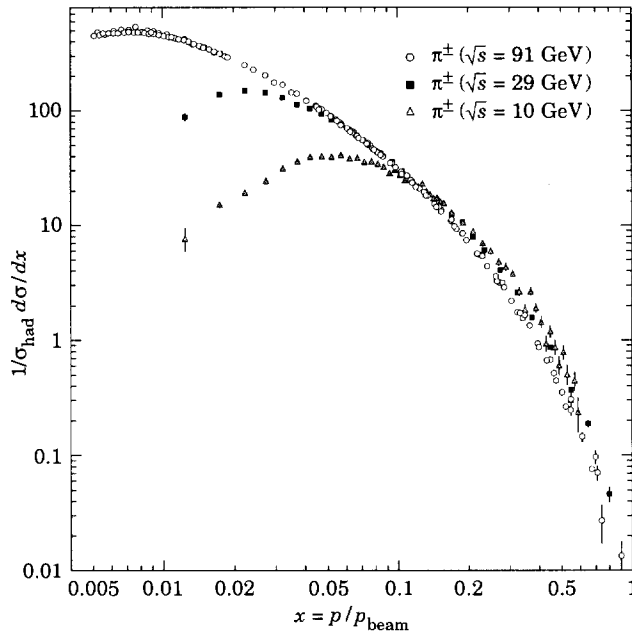
Fragmentation in e^+e^- Annihilation

Figure 37.11: Fragmentation into π^\pm in e^+e^- annihilations: Inclusive cross sections $(1/\sigma_{\text{had}})(d\sigma/dx)$, with $x = p/p_{\text{beam}}$. The indicated errors are statistical and systematic errors added in quadrature. Files of the data shown in this figure are given in <http://home.cern.ch/b/biebel/www/RPP00>

Δ : rate at $\sqrt{s} = 9.98$ GeV; an overall uncertainty of 1.8%:

ARGUS—H. Albrecht *et al.*, *Z. Phys.* **C44**, 547 (1989).

\blacksquare : rate at $\sqrt{s} = 29$ GeV

TPC—H. Aihara *et al.*, *Phys. Rev. Lett.* **61**, 1263 (1988).

\circ : rate for hadronic decays of the Z at $\sqrt{s} = 91.2$ GeV

ALEPH—D. Buskulic *et al.*, *Z. Phys.* **C66**, 355 (1995);

DELPHI—P. Abreu *et al.*, *Eur. Phys. J.* **C5**, 585 (1998);

OPAL—R. Akers *et al.*, *Z. Phys.* **C63**, 181 (1994);

SLD—K. Abe *et al.*, *Phys. Rev.* **D59**, 052001 (1999).

(Courtesy of O. Biebel, Max-Planck-Institut für Physik, München, 1999.)

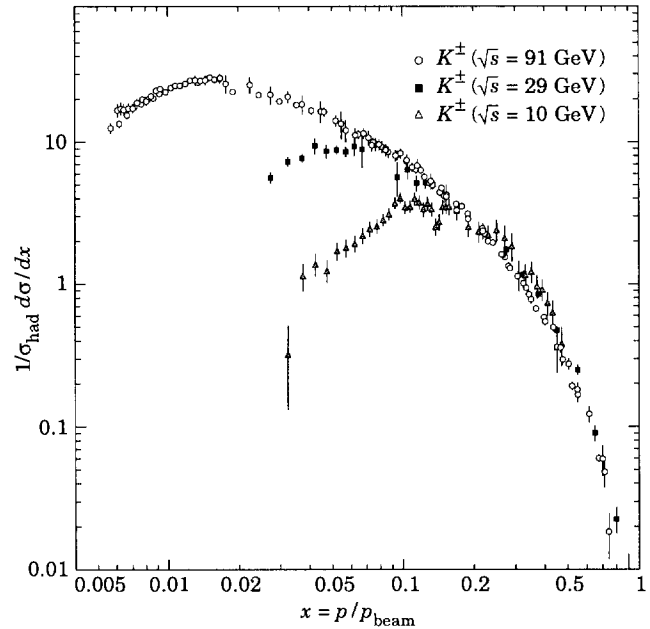


Figure 37.12: Fragmentation into K^\pm in e^+e^- annihilations: Inclusive cross sections $(1/\sigma_{\text{had}})(d\sigma/dx)$, with $x = p/p_{\text{beam}}$. The indicated errors are statistical and systematic errors added in quadrature. Files of the data shown in this figure are given in <http://home.cern.ch/b/biebel/www/RPP00>

Δ : rate at $\sqrt{s} = 9.98$ GeV; an overall uncertainty of 1.8%:

ARGUS—H. Albrecht *et al.*, *Z. Phys.* **C44**, 547 (1989).

\blacksquare : rate at $\sqrt{s} = 29$ GeV **TPC**—H. Aihara *et al.*, *Phys. Rev. Lett.* **61**, 1263 (1988).

\circ : rate for hadronic decays of the Z at $\sqrt{s} = 91.2$ GeV

ALEPH—D. Buskulic *et al.*, *Z. Phys.* **C66**, 355 (1995);

DELPHI—P. Abreu *et al.*, *Eur. Phys. J.* **C5**, 585 (1998);

OPAL—R. Akers *et al.*, *Z. Phys.* **C63**, 181 (1994).

SLD—K. Abe *et al.*, *Phys. Rev.* **D59**, 052001 (1999).

(Courtesy of O. Biebel, Max-Planck-Institut für Physik, München, 1999.)

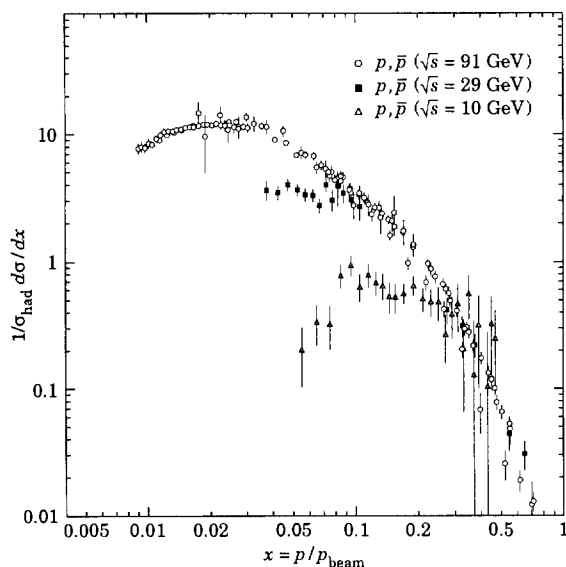


Figure 37.13: Fragmentation into $p\bar{p}$ in e^+e^- annihilations: Inclusive cross sections $(1/\sigma_{\text{had}})(d\sigma/dx)$, with $x = p/p_{\text{beam}}$. The indicated errors are statistical and systematic errors added in quadrature. Files of the data shown in this figure are given in <http://home.cern.ch/b/biebel/www/RPP00>

Δ : rate at $\sqrt{s} = 9.98$ GeV; an overall uncertainty of 1.8%. This rate is obtained from the measured \bar{p} rate by scaling with a factor of two: **ARGUS**—H. Albrecht *et al.*, *Z. Phys.* **C44**, 547 (1989).

\blacksquare : rate at $\sqrt{s} = 29$ GeV: **TPC**—H. Aihara *et al.*, *Phys. Rev. Lett.* **61**, 1263 (1988).

\circ : rate for hadronic decays of the Z at $\sqrt{s} = 91.2$ GeV:

ALEPH—D. Buskulic *et al.*, *Z. Phys.* **C66**, 355 (1995);

DELPHI—P. Abreu *et al.*, *Eur. Phys. J.* **C5**, 585 (1998);

OPAL—R. Akers *et al.*, *Z. Phys.* **C63**, 181 (1994);

SLD—K. Abe *et al.*, *Phys. Rev.* **D59**, 052001 (1999).

(Courtesy of O. Biebel, Max-Planck-Institut für Physik, München, 1999.)

Annihilation Cross Section Near M_Z

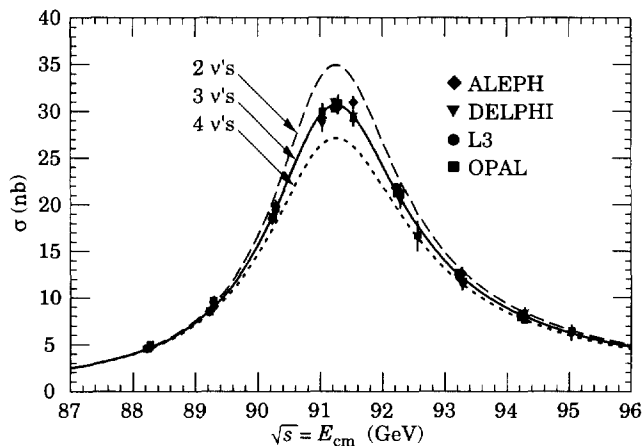


Figure 37.14: Data from the ALEPH, DELPHI, L3, and OPAL Collaborations for the cross section in e^+e^- annihilation into hadronic final states as a function of c.m. energy near the Z . LEP detectors obtained data at the same energies; some of the points are obscured by overlap. The curves show the predictions of the Standard Model with three species (solid curve) and four species (dashed curve) of light neutrinos. The asymmetry of the curves is produced by initial-state radiation. References:

- ALEPH:** D. Decamp *et al.*, *Z. Phys.* **C53**, 1 (1992).
- DELPHI:** P. Abreu *et al.*, *Nucl. Phys.* **B367**, 511 (1992).
- L3:** B. Adeva *et al.*, *Z. Phys.* **C51**, 179 (1991).
- OPAL:** G. Alexander *et al.*, *Z. Phys.* **C52**, 175 (1991).

Average e^+e^- , pp , and $p\bar{p}$ Multiplicity

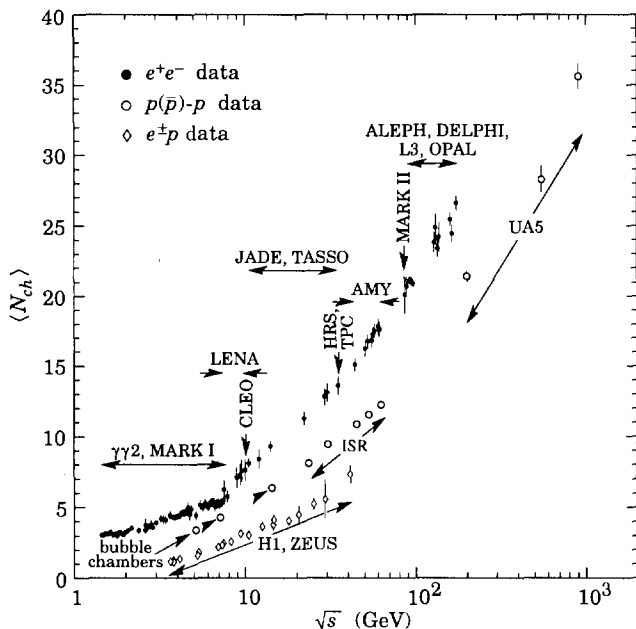


Figure 37.15: Average multiplicity as a function of \sqrt{s} for e^+e^- and $p\bar{p}$ annihilations, and pp and ep collisions. The indicated errors are statistical and systematic errors added in quadrature, except when no systematic errors are given. Files of the data shown in this figure are given in <http://home.cern.ch/b/biebel/www/RPP00>

e^+e^- : All e^+e^- measurements include contributions from K_S^0 and Λ decays with the exception of the L3 measurements. The $\gamma\gamma 2$ and MARK I measurements contain a systematic 5% error. Points at identical energies have been spread horizontally for clarity:

- ALEPH:** D. Buskulic *et al.*, *Z. Phys.* **C69**, 15 (1995) and *Z. Phys.* **C73**, 409 (1997)
- DELPHI:** P. Abreu *et al.*, *Eur. Phys. J.* **C6**, 19 (1999); *et al.*, *Phys. Lett.* **B372**, 172 (1996); and *et al.*, *Phys. Lett.* **B416**, 233 (1998)
- L3:** M. Acciarri *et al.*, *Phys. Lett.* **B371**, 137 (1996); *Phys. Lett.* **B404**, 390 (1997); and *Phys. Lett.* **B444**, 569 (1998)
- OPAL:** K. Ackerstaff *et al.*, *Z. Phys.* **C75**, 193 (1997); P.D. Acton *et al.*, *Z. Phys.* **C53**, 539 (1992) and references therein; R. Akers *et al.*, *Z. Phys.* **C68**, 203 (1995)
- TOPAZ:** K. Nakabayashi *et al.*, *Phys. Lett.* **B413**, 447 (1997),
- VENUS:** K. Okabe *et al.*, *Phys. Lett.* **B423**, 407 (1998).

$e^\pm p$: Multiplicities have been measured in the current fragmentation region of the Breit frame:

- H1:** C. Adloff *et al.*, *Nucl. Phys.* **B504**, 3 (1997)
- ZEUS:** M. Derrick *et al.*, *Z. Phys.* **C67**, 93 (1995).

$p(\bar{p})$: The errors of the $p(\bar{p})$ measurements are the quadratically added statistical and systematic errors, except for the bubble chamber measurements for which only statistical errors are given in the references. The values measured by UA5 exclude single diffractive dissociation:

- bubble chamber:** J. Benecke *et al.*, *Nucl. Phys.* **B76**, 29 (1976), W.M. Morse *et al.*, *Phys. Rev.* **D15**, 66 (1977),
- ISR:** A. Breakstone *et al.*, *Phys. Rev.* **D30**, 528 (1984),
- UA5:** G.J. Alner *et al.*, *Phys. Lett.* **167B**, 476 (1986), R.E. Ansgore *et al.*, *Z. Phys.* **C43**, 357 (1989).

(Courtesy of O. Biebel, Max-Planck-Institut für Physik, München, 1999.)

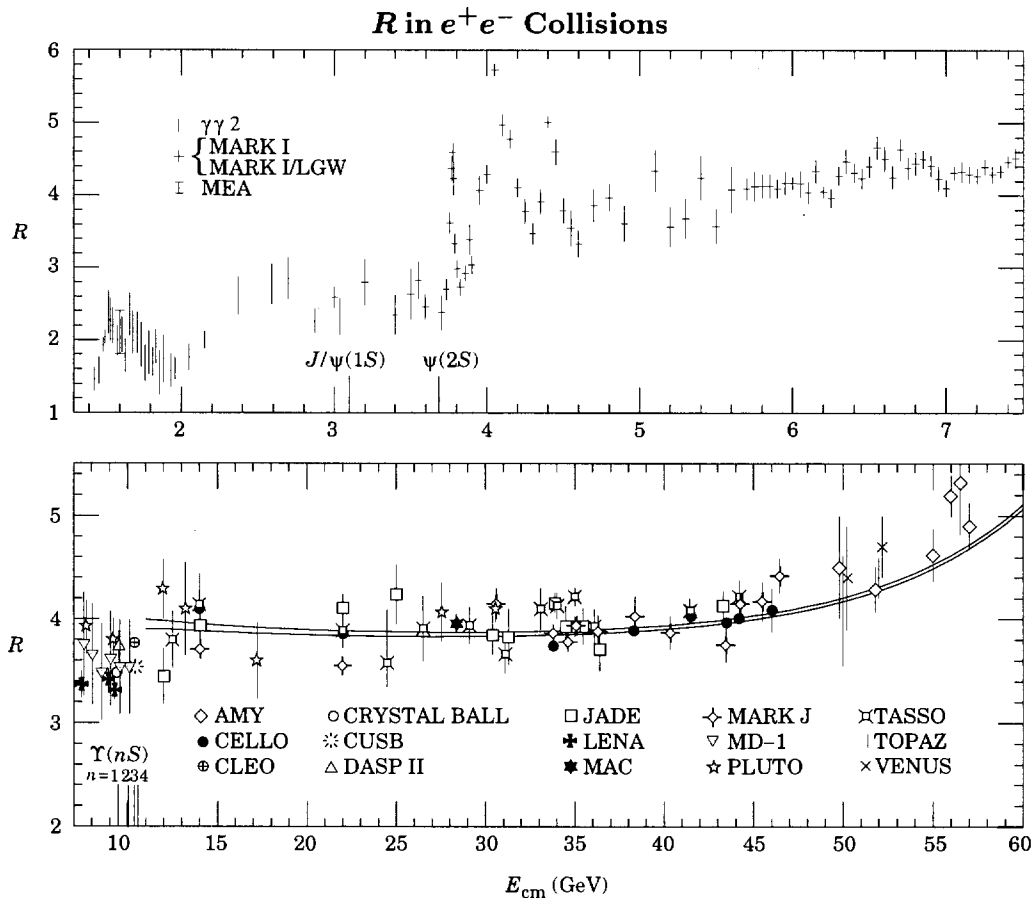


Figure 37.16: Selected measurements of $R \equiv \sigma(e^+e^- \rightarrow \text{hadrons})/\sigma(e^+e^- \rightarrow \mu^+\mu^-)$, where the annihilation in the numerator proceeds via one photon or via the Z . Measurements in the vicinity of the Z mass are shown in the following figure. The denominator is the calculated QED single-photon process; see the section on Cross-Section Formulae for Specific Processes. Radiative corrections and, where important, corrections for two-photon processes and τ production have been made. Note that the ADONE data ($\gamma\gamma 2$ and MEA) is for ≥ 3 hadrons. The points in the $\psi(3770)$ region are from the MARK I—Lead Glass Wall experiment. To preserve clarity only a representative subset of the available measurements is shown—references to additional data are included below. Also for clarity, some points have been combined or shifted slightly ($< 4\%$) in E_{cm} , and some points with low statistical significance have been omitted. Systematic normalization errors are not included; they range from ~ 5 – 20% , depending on experiment. We caution that especially the older experiments tend to have large normalization uncertainties. Note the suppressed zero. The horizontal extent of the plot symbols has no significance. The positions of the $J/\psi(1S)$, $\psi(2S)$, and the four lowest Υ vector-meson resonances are indicated. Two curves are overlaid for $E_{\text{cm}} > 11$ GeV, showing the theoretical prediction for R , including higher order QCD [M. Dine and J. Sapirstein, Phys. Rev. Lett. **43**, 668 (1979)] and electroweak corrections. The Λ values are for 5 flavors in the $\overline{\text{MS}}$ scheme and are $\Lambda_{\overline{\text{MS}}}^{(5)} = 60$ MeV (lower curve) and $\Lambda_{\overline{\text{MS}}}^{(5)} = 250$ MeV (upper curve). (Courtesy of F. Porter, 1992.) References (including several references to data not appearing in the figure and some references to preliminary data):

- AMY:** T. Mori *et al.*, Phys. Lett. **B218**, 499 (1989);
CELLO: H.-J. Behrend *et al.*, Phys. Lett. **144B**, 297 (1984);
 and H.-J. Behrend *et al.*, Phys. Lett. **183B**, 400 (1987);
CLEO: R. Giles *et al.*, Phys. Rev. **D29**, 1285 (1984);
 and D. Besson *et al.*, Phys. Rev. Lett. **54**, 381 (1985);
CUSB: E. Rice *et al.*, Phys. Rev. Lett. **48**, 906 (1982);
CRYSTAL BALL: A. Osterheld *et al.*, SLAC-PUB-4160;
 and Z. Jakubowski *et al.*, Z. Phys. **C40**, 49 (1988);
DASP: R. Brandelik *et al.*, Phys. Lett. **76B**, 361 (1978);
DASP II: Phys. Lett. **116B**, 383 (1982);
DCI: G. Cosme *et al.*, Nucl. Phys. **B152**, 215 (1979);
DHHM: P. Bock *et al.* (DESY-Hamburg-Heidelberg-
 MPI München Collab.), Z. Phys. **C6**, 125 (1980);
 $\gamma\gamma 2$: C. Bacci *et al.*, Phys. Lett. **86B**, 234 (1979);
HRS: D. Bender *et al.*, Phys. Rev. **D31**, 1 (1985);
JADE: W. Bartel *et al.*, Phys. Lett. **129B**, 145 (1983);
 and W. Bartel *et al.*, Phys. Lett. **160B**, 337 (1985);
LENA: B. Niczyporuk *et al.*, Z. Phys. **C15**, 299 (1982);
MAC: E. Fernandez *et al.*, Phys. Rev. **D31**, 1537 (1985);
MARK J: B. Adeva *et al.*, Phys. Rev. Lett. **50**, 799 (1983);
 and B. Adeva *et al.*, Phys. Rev. **D34**, 681 (1986);
MARK I: J.L. Siegrist *et al.*, Phys. Rev. **D26**, 969 (1982);
MARK I + Lead Glass Wall: P.A. Rapidis *et al.*,
 Phys. Rev. Lett. **39**, 526 (1977); and P.A. Rapidis, thesis,
 SLAC-Report-220 (1979);
MARK II: J. Patrick, Ph.D. thesis, LBL-14585 (1982);
MD-1: A.E. Blinov *et al.*, Z. Phys. **C70**, 31 (1996);
MEA: B. Esposito *et al.*, Lett. Nuovo Cimento **19**, 21 (1977);
PLUTO: A. Bäcker, thesis Gesamthochschule Siegen,
 DESY F33-77/03 (1977); C. Gerke, thesis, Hamburg Univ. (1979);
 Ch. Berger *et al.*, Phys. Lett. **81B**, 410 (1979);
 and W. Lackas, thesis, RWTH Aachen, DESY Pluto-81/11 (1981);
TASSO: R. Brandelik *et al.*, Phys. Lett. **113B**, 499 (1982);
 and M. Althoff *et al.*, Phys. Lett. **138B**, 441 (1984);
TOPAZ: I. Adachi *et al.*, Phys. Rev. Lett. **60**, 97 (1988); and
VENUS: H. Yoshida *et al.*, Phys. Lett. **198B**, 570 (1987).

Muon Neutrino and Anti-Neutrino Charged-Current Total Cross Section

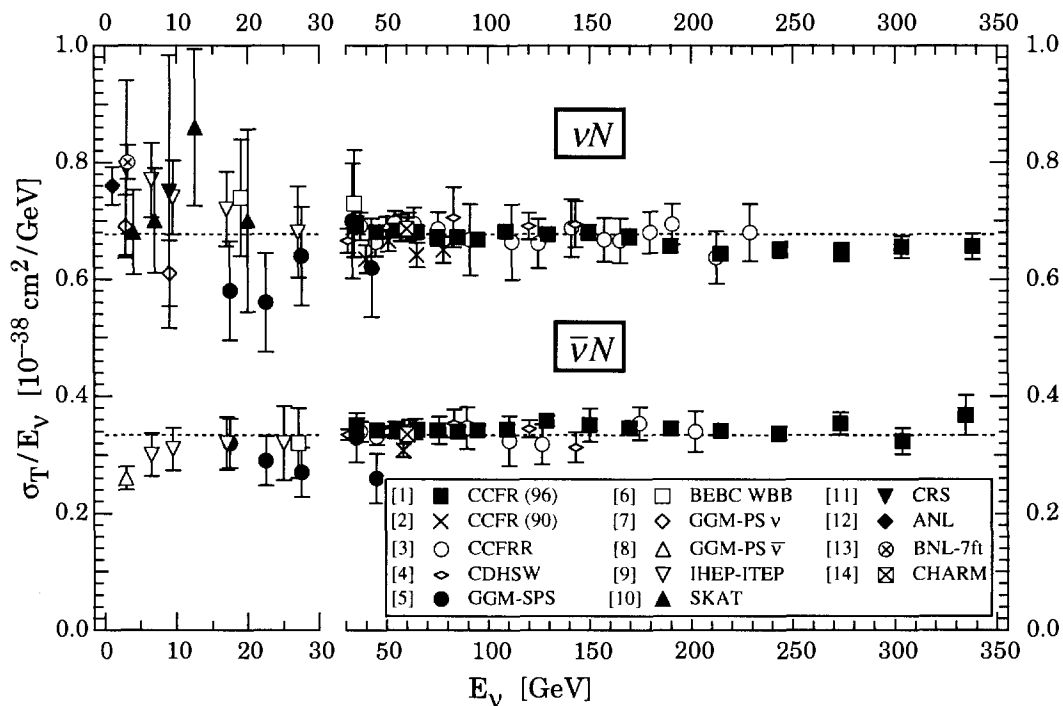


Figure 37.17: σ_T/E_ν , for the muon neutrino and anti-neutrino charged-current total cross section as a function of neutrino energy. The error bars include both statistical and systematic errors. The straight lines are the averaged values over all energies as measured by the experiments in Refs. [1–4]: $= 0.677 \pm 0.014$ (0.334 ± 0.008) $\times 10^{-38}$ cm²/GeV. Note the change in the energy scale at 30 GeV. (Courtesy W. Seligman and M.H. Shaevitz, Columbia University, 2000.)

- [1] W. Seligman, Ph.D. Thesis, Nevis Report 292 (1996);
- [2] P.S. Auchincloss *et al.*, *Z. Phys.* **C48**, 411 (1990);
- [3] D.B. MacFarlane *et al.*, *Z. Phys.* **C26**, 1 (1984);
- [4] P. Berge *et al.*, *Z. Phys.* **C35**, 443 (1987);
- [5] J. Morfin *et al.*, *Phys. Lett.* **104B**, 235 (1981);
- [6] D.C. Colley *et al.*, *Z. Phys.* **C2**, 187 (1979);
- [7] S. Campolillo *et al.*, *Phys. Lett.* **84B**, 281 (1979);

- [8] O. Erriquez *et al.*, *Phys. Lett.* **80B**, 309 (1979);
- [9] A.S. Vovenko *et al.*, *Sov. J. Nucl. Phys.* **30**, 527 (1979);
- [10] D.S. Baranov *et al.*, *Phys. Lett.* **81B**, 255 (1979);
- [11] C. Baltay *et al.*, *Phys. Rev. Lett.* **44**, 916 (1980);
- [12] S.J. Barish *et al.*, *Phys. Rev.* **D19**, 2521 (1979);
- [13] N.J. Baker *et al.*, *Phys. Rev.* **D25**, 617 (1982);
- [14] J.V. Allaby *et al.*, *Z. Phys.* **C38**, 403 (1988).

Table 37.2: Total hadronic cross section. Regge theory suggests a parameterization of total cross sections as

$$\sigma_{AB} = X_{AB}s^\epsilon + Y_{1AB}s^{-\eta_1} - Y_{2AB}s^{-\eta_2}, \quad \sigma_{\bar{A}B} = X_{AB}s^\epsilon + Y_{1AB}s^{-\eta_1} + Y_{2AB}s^{-\eta_2}$$

where X_{AB}, Y_{iAB} are in mb and s is in GeV^2 . The exponents ϵ, η_1 , and η_2 are independent of the particles A, \bar{A} , and B and represent the pomeron, and lower-lying C -even and C -odd exchanges, respectively. Requiring $\eta_1 = \eta_2$ results in much poorer fits. In addition to total cross section, the measured ratio of the real to the imaginary part of the forward scattering amplitudes were included in the fits by assuming that the C -even and C -odd amplitudes have the simple behavior $(-s)^\alpha \pm s^\alpha$, where $\alpha = 1 + \epsilon, 1 - \eta_1, 1 - \eta_2$. Fits were made to the 1999-updated data for $p^\pm p, \pi^\pm p, K^\pm p, \gamma p$, and $\gamma\gamma$. The exponents $\epsilon = 0.093(2), \eta_1 = 0.358(15)$, and $\eta_2 = 0.560(17)$ thus obtained were then fixed and used as inputs to a fit to a larger data sample that included cross sections on deuterons and neutrons. In the initial fit only data above $\sqrt{s_{\min}} = 9$ GeV were used. In the subsequent fit, data above $p_{\text{lab}} = 10$ GeV (hadronic collisions) and $\sqrt{s_{\min}} = 4$ GeV (γp and $\gamma\gamma$) collisions were used.

Fits to $\bar{p}(p)p, \pi^\pm p, K^\pm p, \gamma p, \gamma\gamma$			Colliding particles	Fits to groups			χ^2/dof by groups
X	Y_1	Y_2		X	Y_1	Y_2	
18.751(27)	63.58(26)	35.46(34)	$\bar{p}(p)p$	18.760(22)	63.52(23)	35.43(34)	1.23
			$\bar{p}(p)n$	18.760(22)	64.74(33)	31.42(63)	
11.883(21)	28.59(14)	5.90(12)	$\pi^\pm p$	11.883(23)	28.59(15)	5.90(13)	1.50
10.546(27)	16.42(20)	13.84(18)	$K^\pm p$	10.587(22)	16.13(17)	13.82(18)	1.21
			$K^\pm n$	10.587(22)	14.68(38)	7.78(38)	
0.0593(4)	0.1202(26)		γp	0.0593(2)	0.1202(17)		0.7
1.56(11)E-4	0.37(10)E-3		$\gamma\gamma$	1.56(7)E-4	0.37(7)E-3		
$\chi^2/dof = 1.23$ with fixed $\epsilon = 0.093(2)$, $\eta_1 = 0.358(15), \eta_2 = 0.560(17)$ at their central values			$\bar{p}(p)d$	33.290(47)	154.3(8)	91.6(1.1)	1.69
			$\pi^\pm d$	21.550(36)	68.87(53)	1.42(63)	1.74
			$K^\pm d$	19.327(38)	37.53(50)	30.49(61)	1.46

The fitted functions are shown in the following figures, along with one-standard-deviation error bands. When the reduced χ^2 is greater than one, a scale factor has been included. Where appropriate, statistical and systematic errors were combined quadratically in constructing weights for all fits. On the plots only statistical error bars are shown. Vertical arrows indicate lower limits on the p_{lab} or E_{cm} range used in the fits. The user may decide on the range of applicability of the extrapolated curves.

One can find the details of the fits and exact parameterizations of the ratio of the real to imaginary part of the forward scattering amplitude in J.R. Cudell *et al.*, Phys. Rev. **D61**, 034019 (2000), as well as comparisons of the simple pole pomeron parameterization with the “unitarized” pomeron parameterizations. It should be noted that parameterization with linear logarithmic pomeron

$$\sigma_{AB} = X_{AB} \ln\left(\frac{s}{s_0}\right) + Y_{1AB} \left(\frac{s}{s_0}\right)^{-\eta_1} - Y_{2AB} \left(\frac{s}{s_0}\right)^{-\eta_2}, \quad \sigma_{\bar{A}B} = X_{AB} \ln\left(\frac{s}{s_0}\right) + Y_{1AB} \left(\frac{s}{s_0}\right)^{-\eta_1} + Y_{2AB} \left(\frac{s}{s_0}\right)^{-\eta_2}$$

gives much better data description picture under the same fits strategy. The data were extracted from the PPDS accessible at

<http://wwwppds.ihep.su:8001/ppds.html>

or

<http://pdg.lbl.gov>

Computer-readable data files are also available at <http://pdg.lbl.gov>. (Courtesy of V.V. Ezhela, S.B. Lugovsky, and N.P. Tkachenko, COMPAS group, IHEP, Protvino, Russia, August 1999.)

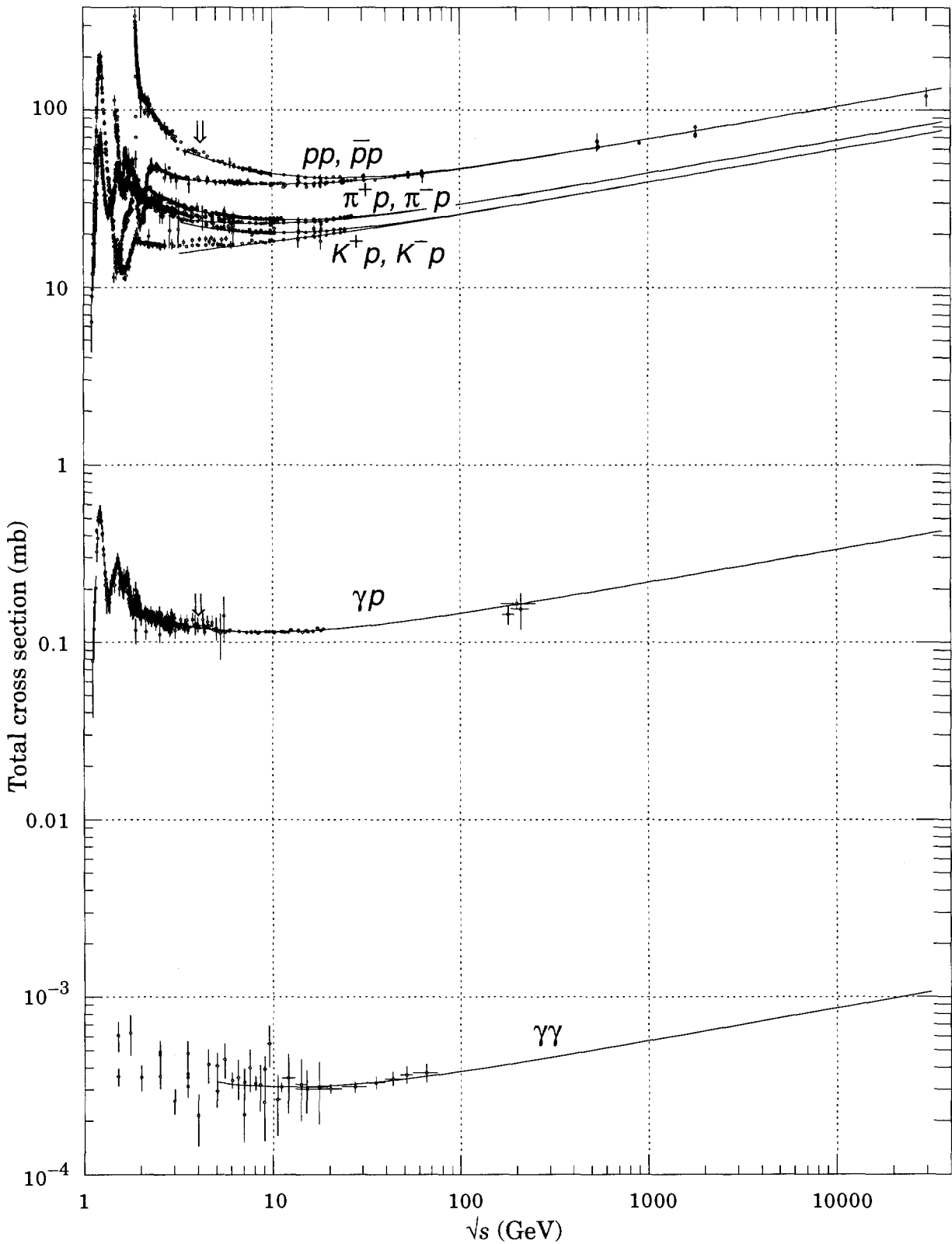


Figure 37.18: Summary of hadronic, γp , and $\gamma\gamma$ total cross sections. Corresponding computer-readable data files may be found at <http://pdg.lbl.gov/xsect/contents.html> (Courtesy of the COMPAS group, IHEP, Protvino, Russia, August 1999.)

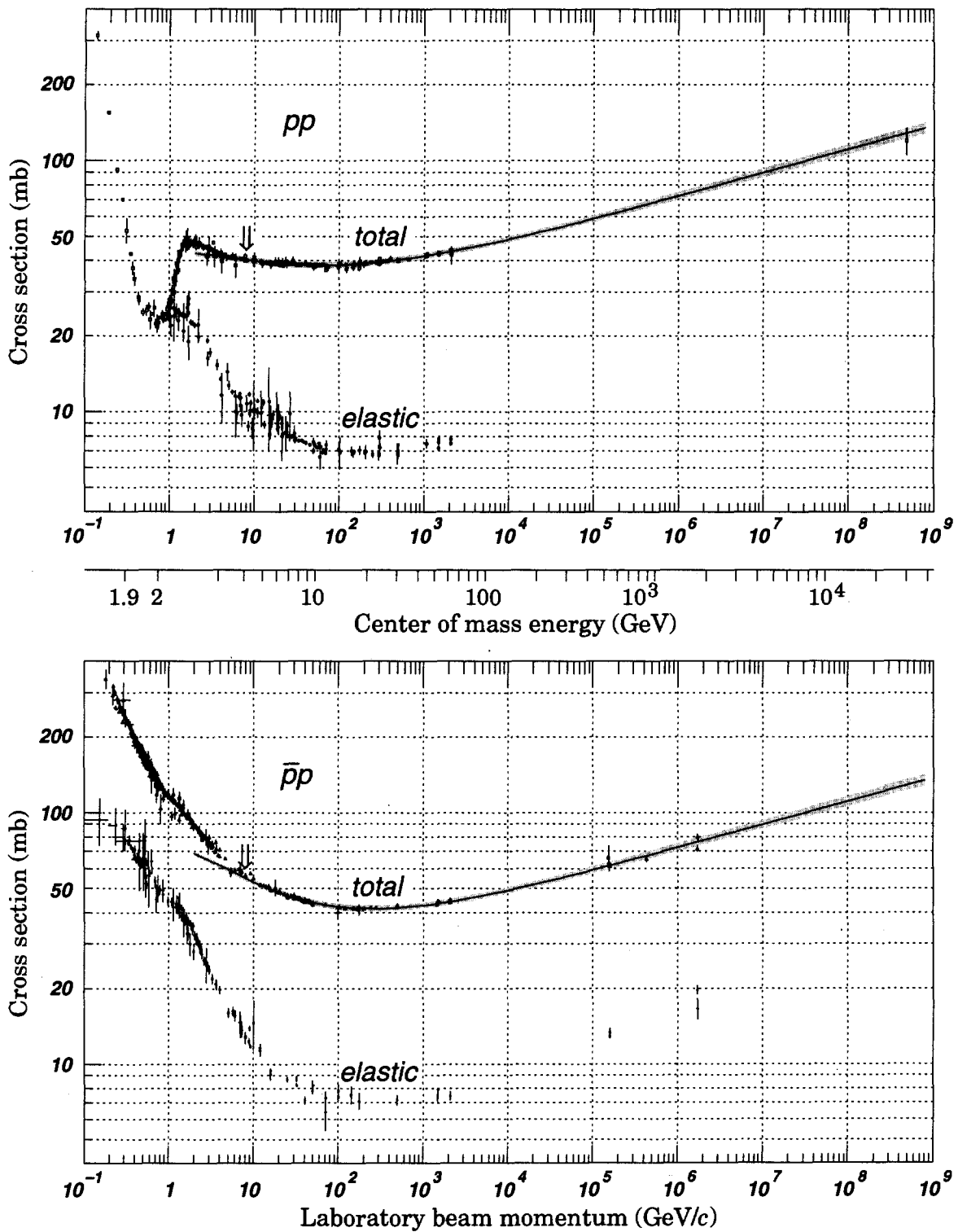


Figure 37.19: Total and elastic cross sections for pp and $\bar{p}p$ collisions as a function of laboratory beam momentum and total center-of-mass energy. Corresponding computer-readable data files may be found at <http://pdg.lbl.gov/xsect/contents.html> (Courtesy of the COMPAS Group, IHEP, Protvino, Russia, August 1999.)

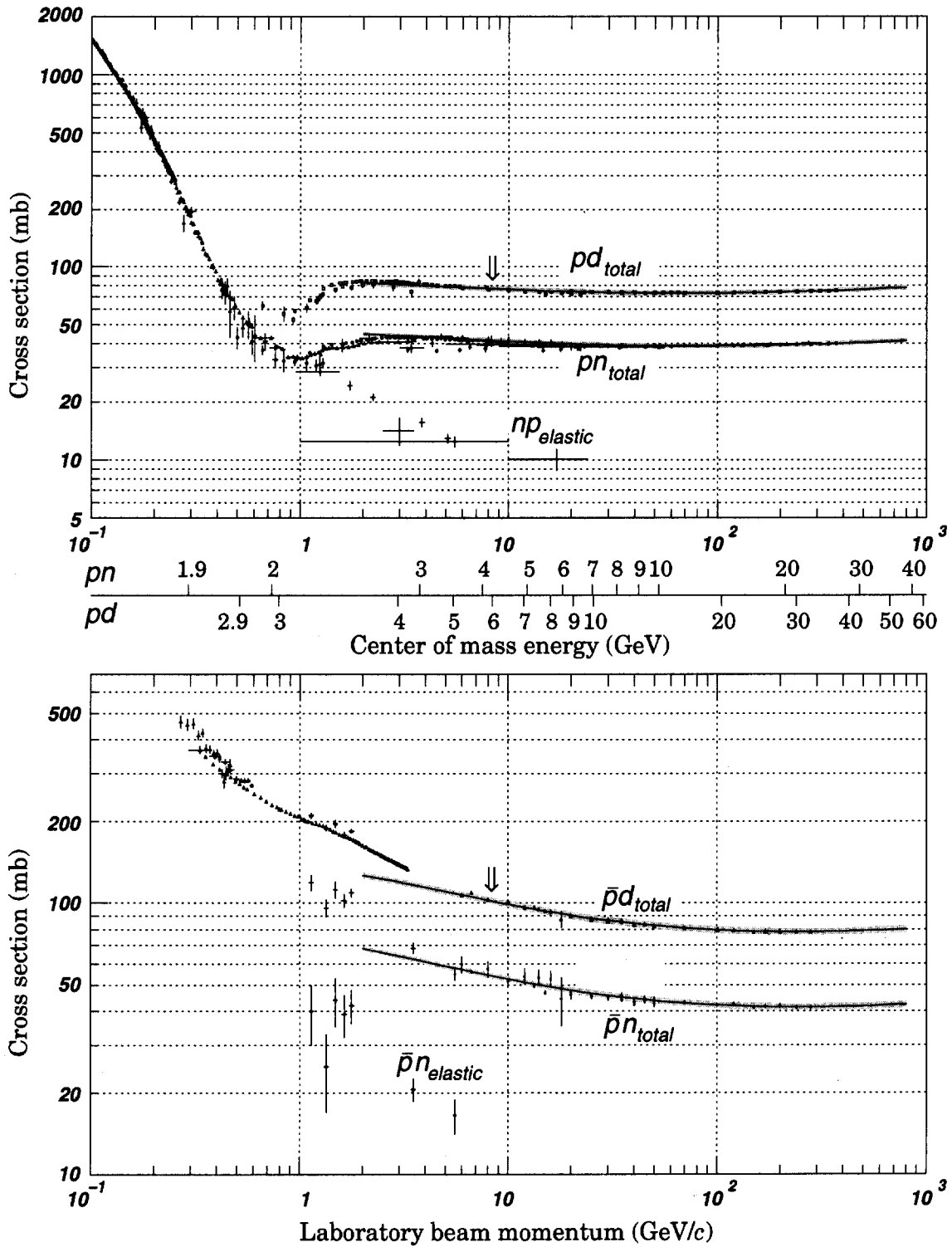


Figure 37.20: Total and elastic cross sections for pd (total only), np , $\bar{p}d$ (total only), and $\bar{p}n$ collisions as a function of laboratory beam momentum and total center-of-mass energy. Corresponding computer-readable data files may be found at <http://pdg.lbl.gov/xsect/contents.html> (Courtesy of the COMPAS Group, IHEP, Protvino, Russia, August 1999.)

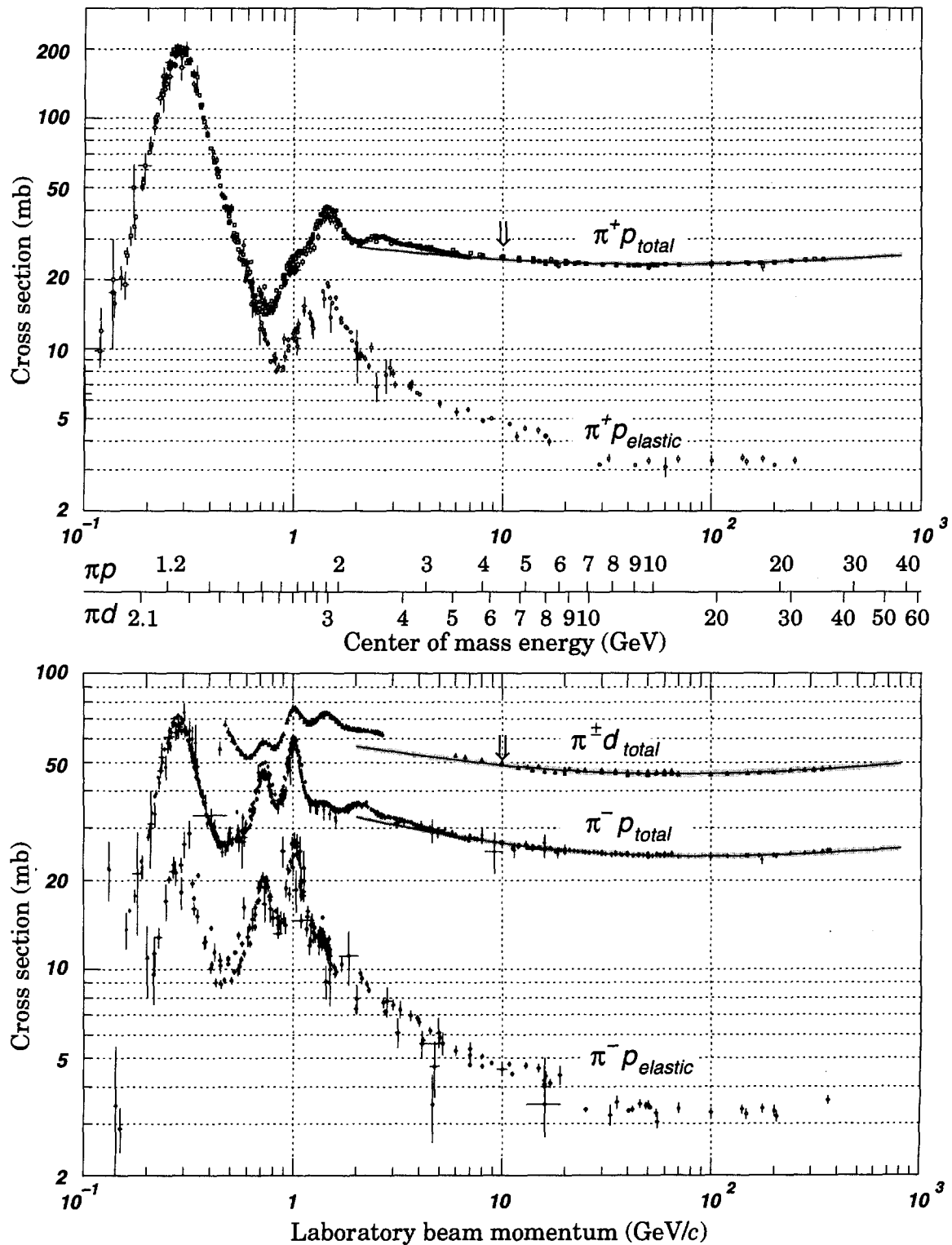


Figure 37.21: Total and elastic cross sections for $\pi^\pm p$ and $\pi^\pm d$ (total only) collisions as a function of laboratory beam momentum and total center-of-mass energy. Corresponding computer-readable data files may be found at <http://pdg.lbl.gov/xsect/contents.html> (Courtesy of the COMPAS Group, IHEP, Protvino, Russia, August 1999.)

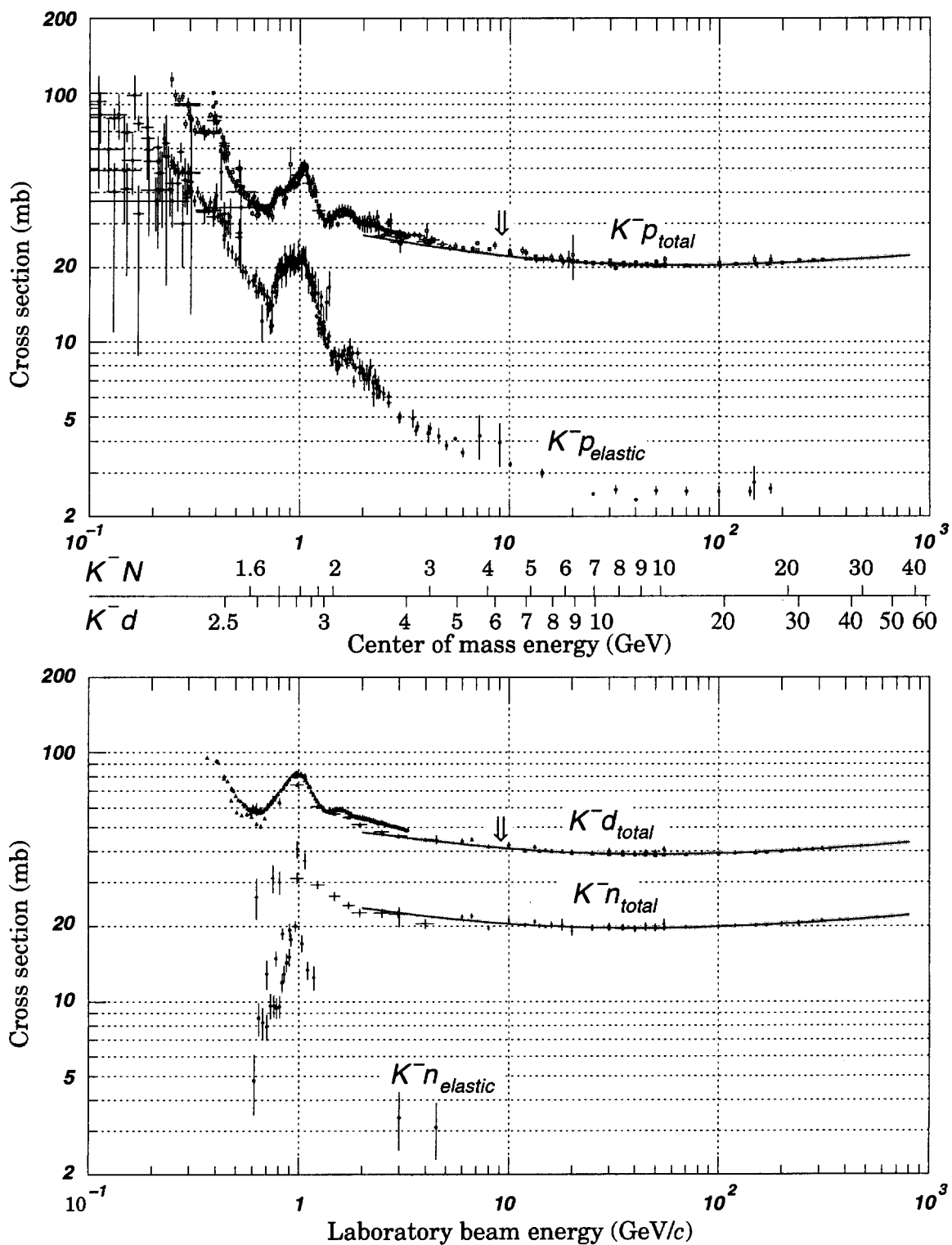


Figure 37.22: Total and elastic cross sections for $K^- p$ and $K^- d$ (total only), and $K^- n$ collisions as a function of laboratory beam momentum and total center-of-mass energy. Corresponding computer-readable data files may be found at <http://pdg.lbl.gov/xsect/contents.html> (Courtesy of the COMPAS Group, IHEP, Protvino, Russia, August 1999.)

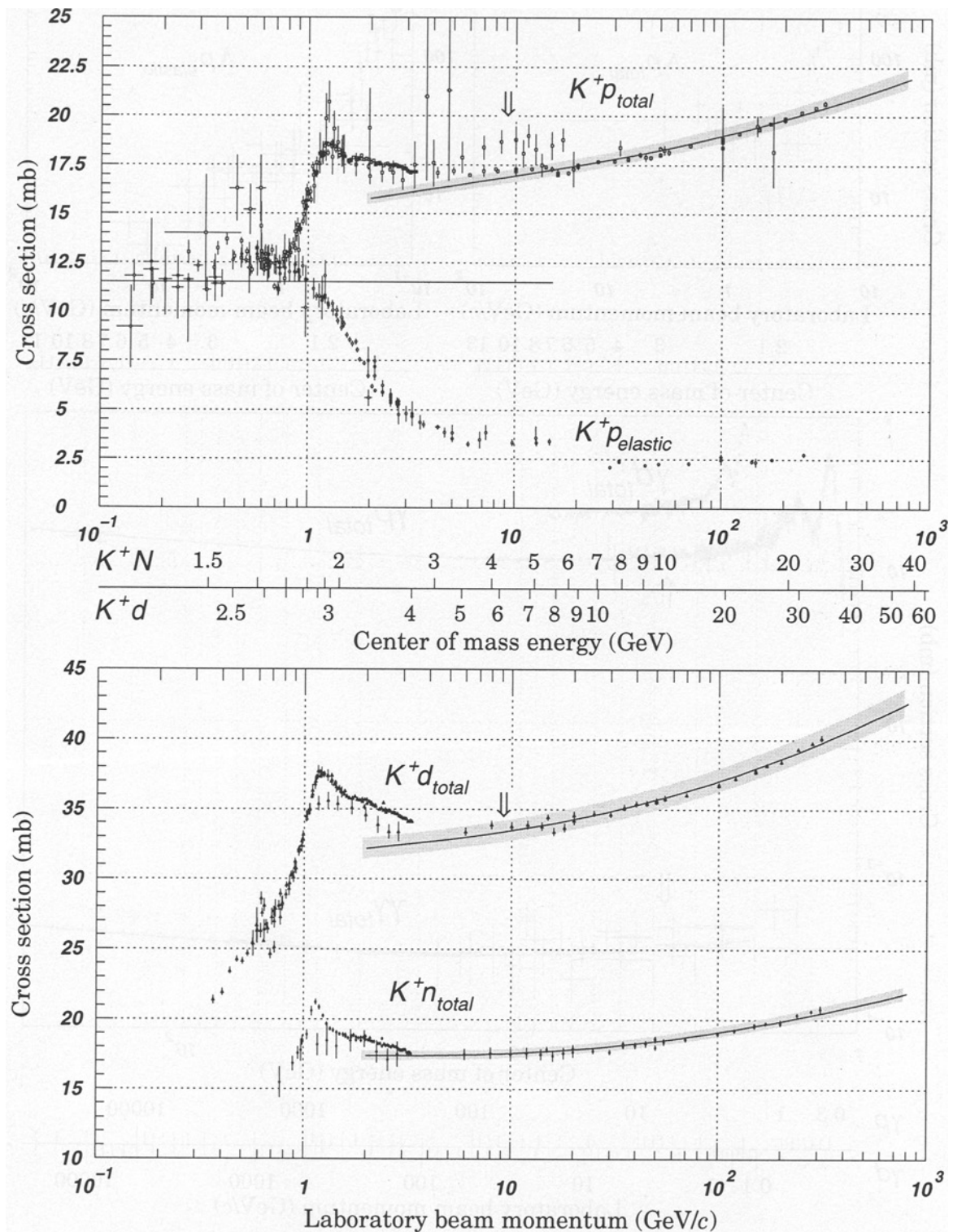


Figure 37.23: Total and elastic cross sections for K^+p and total cross sections for K^+d and K^+n collisions as a function of laboratory beam momentum and total center-of-mass energy. Corresponding computer-readable data files may be found at <http://pdg.lbl.gov/xsect/contents.html> (Courtesy of the COMPAS Group, IHEP, Protvino, Russia, August 1999.)

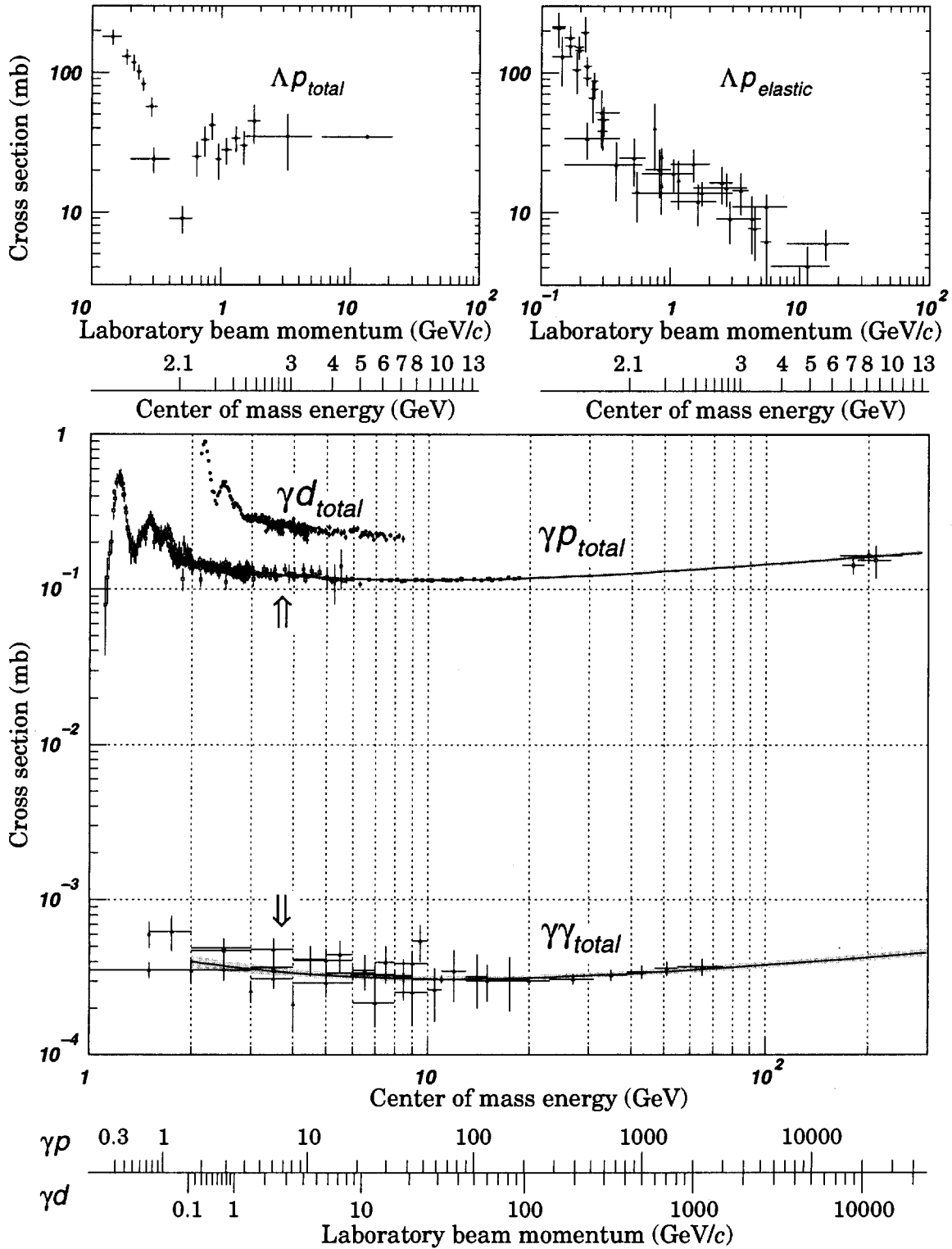


Figure 37.24: Total and elastic cross sections for Λp and total hadronic cross sections for γd , γp , and $\gamma\gamma$ collisions as a function of laboratory beam momentum and the total center-of-mass energy. Corresponding computer-readable data files may be found at <http://pdg.lbl.gov/xsect/contents.html> (Courtesy of the COMPAS group, IHEP, Protvino, Russia, August 1999.)

See key on page 239

Gauge & Higgs Boson Particle Listings

$\gamma, g, \text{graviton}, W$

GAUGE AND HIGGS BOSONS

γ

$$I(J^{PC}) = 0,1(1^{--})$$

γ MASS

For a review of the photon mass, see BYRNE 77.

VALUE (eV)	CL%	DOCUMENT ID	TECN	COMMENT
< 2	$\times 10^{-16}$	¹ LAKES	98	Torque on toroid balance
••• We do not use the following data for averages, fits, limits, etc. •••				
< 9	$\times 10^{-16}$	² FISCHBACH	94	Earth magnetic field
< (4.73 ± 0.45) × 10 ⁻¹²		³ CHERNIKOV	92	SQID Ampere-law null test
< (9.0 ± 8.1) × 10 ⁻¹⁰		⁴ RYAN	85	Coulomb-law null test
< 3	$\times 10^{-27}$	⁵ CHIBISOV	76	Galactic magnetic field
< 6	$\times 10^{-16}$	DAVIS	75	Jupiter magnetic field
< 7.3	$\times 10^{-16}$	HOLLWEG	74	Alfven waves
< 6	$\times 10^{-17}$	FRANKEN	71	Low freq. res. cir.
< 1	$\times 10^{-14}$	WILLIAMS	71	CNTR Tests Gauss law
< 2.3	$\times 10^{-15}$	GOLDHABER	68	Satellite data
< 6	$\times 10^{-15}$	⁶ PATEL	65	Satellite data
< 6	$\times 10^{-15}$	GINTSBURG	64	Satellite data

- ¹ LAKES 98 report limits on torque on a toroid Cavendish balance, obtaining a limit on $\mu^2 A$ via the Maxwell-Proca equations, where μ is the photon mass and A is the ambient vector potential in the Lorentz gauge. This is the most conservative limit reported, in which $A \approx (1 \mu G) \times (600 \text{ pc})$ is based on the Galactic field.
- ² FISCHBACH 94 report $< 8 \times 10^{-16}$ with unknown CL. We report Bayesian CL used elsewhere in these Listings and described in the Statistics section.
- ³ CHERNIKOV 92 measures the photon mass at 1.24 K, following a theoretical suggestion that electromagnetic gauge invariance might break down at some low critical temperature. See the erratum for a correction, included here, to the published result.
- ⁴ RYAN 85 measures the photon mass at 1.36 K (see the footnote to CHERNIKOV 92).
- ⁵ CHIBISOV 76 depends in critical way on assumptions such as applicability of virial theorem. Some of the arguments given only in unpublished references.
- ⁶ See criticism questioning the validity of these results in KROLL 71 and GOLDHABER 71.

γ CHARGE

VALUE (e)	DOCUMENT ID	TECN	COMMENT
< 5 × 10 ⁻³⁰	⁷ RAFFELT	94	TOF Pulsar $f_1 - f_2$
••• We do not use the following data for averages, fits, limits, etc. •••			
< 2 × 10 ⁻²⁸	⁸ COCCONI	92	VLBA radio telescope resolution
< 2 × 10 ⁻³²	COCCONI	88	TOF Pulsar $f_1 - f_2$ TOF

- ⁷ RAFFELT 94 notes that COCCONI 88 neglects the fact that the time delay due to dispersion by free electrons in the interstellar medium has the same photon energy dependence as that due to bending of a charged photon in the magnetic field. His limit is based on the assumption that the entire observed dispersion is due to photon charge. It is a factor of 200 less stringent than the COCCONI 88 limit.
- ⁸ See COCCONI 92 for less stringent limits in other frequency ranges. Also see RAFFELT 94 note.

γ REFERENCES

LAKES	98	PRL 80 1826	R. Lakes	(WISC)
FISCHBACH	94	PRL 73 514	E. Fischbach et al.	(PURD, JHU+)
RAFFELT	94	PR D50 7729	G. Raffelt	(MPIM)
CHERNIKOV	92	PRL 68 3383	M.A. Chernikov et al.	(ETH)
Also	92B	PRL 69 2999 (erratum)	M.A. Chernikov et al.	(ETH)
COCCONI	92	AJP 60 750	G. Cocconi	(CERN)
COCCONI	88	PL B206 705	G. Cocconi	(CERN)
RYAN	85	PR D32 802	J.J. Ryan, F. Accetta, R.H. Austin	(PRIN)
BYRNE	77	Adv. Sp. Sci. 46 115	J. Byrne	(LOFC)
CHIBISOV	76	SFU 19 624	G.V. Chibisov	(LEBD)
DAVIS	75	PRL 35 1402	L. Davis, A.S. Goldhaber, M.M. Nieto	(CIT, STON+)
HOLLWEG	74	PRL 32 961	J.V. Hollweg	(NCAR)
FRANKEN	71	PRL 26 115	P.A. Franken, G.W. Ampulski	(MICH)
GOLDHABER	71	RMP 43 277	A.S. Goldhaber, M.M. Nieto	(STON, BOHR, UCSB)
KROLL	71	PRL 26 1395	N.M. Kroll	(SLAC)
WILLIAMS	71	PRL 26 721	E.R. Williams, J.E. Faller, H.A. Hill	(WESL)
GOLDHABER	68	PRL 21 567	A.S. Goldhaber, M.M. Nieto	(STON)
PATEL	65	PL 14 105	V.L. Patel	(DUKE)
GINTSBURG	64	Sov. Astr. AJ7 536	Gintsburg	(ASCI)

g
or gluon

$$I(J^P) = 0(1^-)$$

SU(3) color octet

Mass $m = 0$. Theoretical value. A mass as large as a few MeV may not be precluded, see YNDURAIN 95.

VALUE	DOCUMENT ID	TECN	COMMENT
••• We do not use the following data for averages, fits, limits, etc. •••			
	ABREU	92E DLPH	Spin 1, not 0
	ALEXANDER	91H OPAL	Spin 1, not 0
	BEHREND	82D CELL	Spin 1, not 0
	BERGER	80D PLUT	Spin 1, not 0
	BRANDELIK	80C TASS	Spin 1, not 0

gluon REFERENCES

YNDURAIN	95	PL B345 524	F.J. Yndurain	(MADU)
ABREU	92E	PL B274 498	F. Abreu et al.	(DELPHI Collab.)
ALEXANDER	91H	ZPHY C52 543	G. Alexander et al.	(OPAL Collab.)
BEHREND	82D	PL B110 329	H.J. Behrend et al.	(CELLO Collab.)
BERGER	80D	PL B97 459	C. Berger et al.	(PLUTO Collab.)
BRANDELIK	80C	PL B97 453	R. Brandelik et al.	(TASSO Collab.)

graviton

$$J = 2$$

OMITTED FROM SUMMARY TABLE

graviton MASS

All of the following limits are obtained assuming Yukawa potential in weak field limit. VANDAM 70 argue that a massive field cannot approach general relativity in the zero-mass limit; however, see GOLDHABER 74 and references therein. h_0 is the Hubble constant in units of $100 \text{ km s}^{-1} \text{ Mpc}^{-1}$.

VALUE (eV)	DOCUMENT ID	COMMENT
••• We do not use the following data for averages, fits, limits, etc. •••		
< 2 × 10 ⁻²⁹ h_0^{-1}	¹ DAMOUR	91 Binary pulsar PSR 1913+16
< 7 × 10 ⁻²⁸	GOLDHABER	74 Rich clusters
< 8 × 10 ⁴	HARE	73 Galaxy
	HARE	73 2 γ decay

- ¹ DAMOUR 91 is an analysis of the orbital period change in binary pulsar PSR 1913+16, and confirms the general relativity prediction to 0.8%. "The theoretical importance of the [rate of orbital period decay] measurement has long been recognized as a direct confirmation that the gravitational interaction propagates with velocity c (which is the immediate cause of the appearance of a damping force in the binary pulsar system) and thereby as a test of the existence of gravitational radiation and of its quadrupolar nature." TAYLOR 93 adds that orbital parameter studies now agree with general relativity to 0.5%, and set limits on the level of scalar contribution in the context of a family of tensor [spin 2]-biscalar theories.

graviton REFERENCES

TAYLOR	93	Nature 355 132	J.N. Taylor et al.	(PRIN, ARCOB, BURE+)
DAMOUR	91	APJ 366 501	T. Damour, J.H. Taylor	(BURE, MEUD, PRIN)
GOLDHABER	74	PR D9 1119	A.S. Goldhaber, M.M. Nieto	(LANL, STON)
HARE	73	CJP 51 431	Hare	(SASK)
VANDAM	70	NP B22 397	H. van Dam, M. Veltman	(UTRE)

W

$$J = 1$$

THE MASS OF THE W BOSON

Revised March 2000 by C. Caso (Univ. of Genova) and A. Gurtu (Tata Inst.)

Till 1995 the production and study of the W boson was the exclusive domain of the $\bar{p}p$ colliders at CERN and FNAL. W production in these hadron colliders is tagged by a high p_T lepton from W decay. Owing to unknown parton-parton effective energy and missing energy in the longitudinal direction, the experiments reconstruct only the transverse mass of the W and derive the W mass from comparing the transverse mass distribution with Monte Carlo predictions as a function of M_{TW} .

Beginning 1996 the energy of LEP increased to above 161 GeV, the threshold for W -pair production. A precise knowledge of the e^+e^- centre of mass energy enables one to reconstruct the W mass even if one of them decays leptonically. At LEP two methods have been used to obtain the W mass. In the first method the measured W -pair production cross sections, $\sigma(e^+e^- \rightarrow W^+W^-)$, have been used to determine the W mass using the predicted dependence of this cross section on M_W (see Fig. 1). At 161 GeV, which is just above the W -pair production threshold, this dependence is a much more sensitive function of the W mass than at the higher energies (172 to 202 GeV) at which LEP has run during 1996-99. In the second method, which is used at the higher energies, the

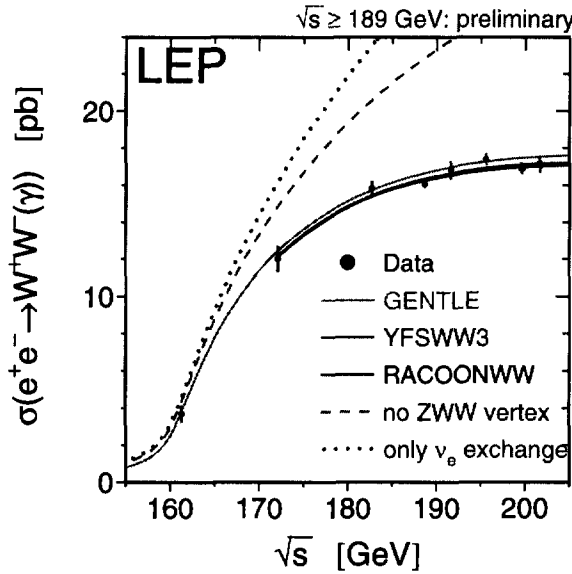


Figure 1: The W -pair cross section as a function of the center-of-mass energy. The data points are the LEP averages. The solid lines are predictions from different models of WW production. For comparison the figure contains also the cross section if the ZWW coupling did not exist (dashed line), or if only the t -channel ν_e exchange diagram existed (dotted line).

W mass has been determined by directly reconstructing the W from its decay products.

Each LEP experiment has combined their own mass values properly taking into account the common systematic errors. In order to compute the LEP average W mass each experiment has provided its measured W mass for the $qqqq$ and $qql\nu$ channels at each center-of-mass energy along with a detailed break-up of errors (statistical and uncorrelated, partially correlated and fully correlated systematics [1]). These have been properly combined to obtain a preliminary [2] LEP W mass = 80.401 ± 0.048 GeV. Errors due to uncertainties in LEP energy (17 MeV) and possible effect of color reconnection (CR) and Bose-Einstein (BE) correlations between quarks from different W 's (18 MeV) are included. The mass difference between $qqqq$ and $qql\nu$ final states (due to possible CR and BE effects) is 35 ± 55 MeV.

The two Tevatron experiments have also carried out the exercise of identifying common systematic errors and averaging with CERN UA2 data obtain an average W mass = 80.448 ± 0.062 GeV.

Combining all the published and unpublished $p\bar{p}$ Collider and LEP results (as of mid-March 2000) yields an average W -boson mass of 80.419 ± 0.038 GeV assuming no common systematics between LEP and hadron collider measurements.

The Standard Model prediction from the electroweak fit, excluding the direct W mass measurements from LEP and Tevatron, gives a W -boson mass of 80.382 ± 0.026 GeV.

OUR EVALUATION in the listing below is obtained by combining only published LEP and $p\bar{p}$ Collider results using the same procedure as above.

References

1. The LEP Collaborations: ALEPH, DELPHI, L3, OPAL, the LEP Electroweak Working Group, and the SLD Heavy Flavour and Electroweak Groups, CERN-EP-2000-016 (January 21, 2000).
2. A. Straessner and C. Sbarra, talks presented at the XXXV Rencontres de Moriond, "Electroweak Interactions and Unified Theories," (Les Arcs, France, 11-18 March 2000).

W MASS

OUR FIT uses the W and Z mass, mass difference, and mass ratio measurements.

To obtain OUR EVALUATION the correlation between systematics is properly taken into account.

VALUE (GeV)	EVTS	DOCUMENT ID	TECN	COMMENT
80.419 ± 0.056 OUR EVALUATION				
80.43 ± 0.05 OUR FIT				
80.482 ± 0.091	45394	1 ABBOTT	00 D0	$E_{cm}^{p\bar{p}} = 1.8$ TeV
80.38 ± 0.12 ± 0.05	701	2 ABBIENDI	99C OPAL	$E_{cm}^{e^+e^-} = 161+172+183$ GeV
80.270 ± 0.137 ± 0.048	809	3 ABREU	99T DLPH	$E_{cm}^{e^+e^-} = 161+172+183$ GeV
80.61 ± 0.15	801	4 ACCIARRI	99 L3	$E_{cm}^{e^+e^-} = 161+172+183$ GeV
80.423 ± 0.112 ± 0.054	812	5 BARATE	99 ALEP	$E_{cm}^{e^+e^-} = 161+172+183$ GeV
80.41 ± 0.18	8986	6 ABE	95P CDF	$E_{cm}^{p\bar{p}} = 1.8$ TeV
79.91 ± 0.39	1722	7 ABE	90G CDF	$E_{cm}^{p\bar{p}} = 1.8$ TeV
• • • We do not use the following data for averages, fits, limits, etc. • • •				
80.49 ± 0.43 ± 0.095	871	8 ABREU	99K DLPH	Repl. by ABREU 99T
80.44 ± 0.10 ± 0.07	28323	9 ABBOTT	98O D0	Repl. by ABBOTT 00
80.22 ± 0.41 ± 0.07	72	10 ABREU	98B DLPH	Repl. by ABREU 99T
80.32 ± 0.30 ± 0.094	96	11 ACKERSTAFF	98D OPAL	Repl. by ABBIENDI 99C
80.5 +1.4 +0.5 -2.2 -0.6	104	12 ACKERSTAFF	98D OPAL	Repl. by ABBIENDI 99C
80.80 ± 0.32 ± 0.114	95	13 BARATE	98B ALEP	Repl. by BARATE 99
80.80 +0.48 +0.03 -0.42	20	14 ACCIARRI	97 L3	Repl. by ACCIARRI 99
80.5 +1.4 +0.3 -2.4	94	15 ACCIARRI	97M L3	Repl. by ACCIARRI 99
80.71 +0.34 +0.09 -0.35	101	16 ACCIARRI	97S L3	Repl. by ACCIARRI 99
80.14 ± 0.34 ± 0.095	32	17 BARATE	97 ALEP	Repl. by BARATE 99
81.17 +1.15 +1.62	106	18 BARATE	97S ALEP	Repl. by BARATE 99
80.35 ± 0.14 ± 0.23	5982	19 ABACHI	96E D0	Repl. by ABBOTT 00
80.40 +0.44 +0.09 -0.41 -0.10	23	20 ACKERSTAFF	96B OPAL	Repl. by ABBIENDI 99C
84 +10 -7	13	21 AID	96D H1	$e^\pm p \rightarrow \nu_e(\bar{\nu}_e) + X$ $\sqrt{s} \approx 300$ GeV
80.84 ± 0.22 ± 0.83	2065	22 ALITTI	92B UA2	See W/Z ratio below
80.79 ± 0.31 ± 0.84		23 ALITTI	90B UA2	$E_{cm}^{p\bar{p}} = 546,630$ GeV
80.0 ± 3.3 ± 2.4	22	24 ABE	89I CDF	$E_{cm}^{p\bar{p}} = 1.8$ TeV
82.7 ± 1.0 ± 2.7	149	25 ALBAJAR	89 UA1	$E_{cm}^{p\bar{p}} = 546,630$ GeV
81.8 +6.0 +2.6 -5.3	46	26 ALBAJAR	89 UA1	$E_{cm}^{p\bar{p}} = 546,630$ GeV
89 ± 3 ± 6	32	27 ALBAJAR	89 UA1	$E_{cm}^{p\bar{p}} = 546,630$ GeV
81. ± 5.	6	ARNISON	83 UA1	$E_{cm}^{e^+e^-} = 546$ GeV
80. +10. -6.	4	BANNER	83B UA2	Repl. by ALITTI 90B

¹ ABBOTT 00 use $W \rightarrow e\nu_e$ events to measure the W mass with a fit to the transverse mass distribution. The result quoted here corresponds to electrons detected both in the forward and in the central calorimeters for the data recorded in 1992-1995. For the large rapidity electrons recorded in 1994-1995, the analysis combines results obtained from $m_T, p_T(e)$, and $p_T(\nu)$.

² ABBIENDI 99C obtain this value properly combining results from a direct W mass reconstruction at 172 and 183 GeV with that from the measurement of the total W -pair production cross section at 161 GeV. The systematic error includes an uncertainty of ± 0.02 GeV due to the possible color-reconnection and Bose-Einstein effects in the purely hadronic final states and an uncertainty of ± 0.02 GeV due to the beam energy.

³ ABREU 99T obtain this value properly combining results obtained from a direct W mass reconstruction at 172 and 183 GeV with those from measurement of W -pair production cross sections at 161, 172, and 183 GeV. The systematic error includes ± 0.021 GeV due to the beam energy uncertainty and ± 0.030 GeV due to possible color reconnection and Bose-Einstein effects in the purely hadronic final state.

- ⁴ ACCIARRI 99 obtain this value properly combining results obtained from a direct W mass reconstruction at 172 and 183 GeV with those from the measurements of the total W -pair production cross sections at 161 and 172 GeV. The value of the mass obtained from the direct reconstruction at 172 and 183 GeV is $M(W) = 80.58 \pm 0.14 \pm 0.08$ GeV.
- ⁵ BARATE 99 obtain this value properly combining results from a direct W mass reconstruction at 172 and 183 GeV with those from the measurements of the total W -pair production cross sections at 161 and 172 GeV. The systematic error includes ± 0.023 GeV due to LEP energy uncertainty and ± 0.021 GeV due to theory uncertainty on account of possible color reconnection and Bose-Einstein correlations.
- ⁶ ABE 95P use 3268 $W \rightarrow \mu\nu_\mu$ events to find $M = 80.310 \pm 0.205 \pm 0.130$ GeV and 5718 $W \rightarrow e\nu_e$ events to find $M = 80.490 \pm 0.145 \pm 0.175$ GeV. The result given here combines these while accounting for correlated uncertainties.
- ⁷ ABE 90C result from $W \rightarrow e\nu$ is $79.91 \pm 0.35 \pm 0.24 \pm 0.19$ (scale) GeV and from $W \rightarrow \mu\nu$ is $79.90 \pm 0.53 \pm 0.32 \pm 0.08$ (scale) GeV.
- ⁸ ABREU 99k derive this value using the Standard Model dependence on M_W of the W - W production cross sections measured at 161, 172, and 183 GeV. The systematics include an error of ± 0.03 GeV arising from the beam energy uncertainty.
- ⁹ ABBOTT 980 fit the transverse mass distribution of 28323 $W \rightarrow e\nu_e$ events. The systematic error includes a detector related uncertainty of ± 60 MeV and a model uncertainty of ± 30 MeV. Combining with ABACHI 96E DØ obtain a W mass value of 80.43 ± 0.11 GeV.
- ¹⁰ ABREU 98b obtain this value from a fit to the reconstructed W mass distribution. The W width was taken as its Standard Model value at the fitted W mass. The systematic error includes ± 0.03 GeV due to the beam energy uncertainty and ± 0.05 GeV due to the possible color reconnection and Bose-Einstein effects in the purely hadronic final state.
- ¹¹ ACKERSTAFF 98b obtain this value from a fit to the reconstructed W mass distribution. The W width was taken as its Standard Model value at the fitted W mass. When both W mass and width are varied they obtain $M(W) = 80.30 \pm 0.27 \pm 0.095$ GeV. The systematic error includes ± 0.03 GeV due to the beam energy uncertainty and ± 0.05 GeV due to the possible color reconnection and Bose-Einstein effects in the purely hadronic final state. Combining both values of ACKERSTAFF 98b with ACKERSTAFF 96b authors find: $M(W) = 80.35 \pm 0.24 \pm 0.07 \pm 0.03$ (LEP) GeV.
- ¹² ACKERSTAFF 98d derive this value from their measured W - W production cross section $\sigma_{WW} = 12.3 \pm 1.3 \pm 0.4$ pb using the Standard Model dependence of σ_{WW} on M_W at the given c.m. energy.
- ¹³ BARATE 98b obtain this value from a fit to the reconstructed W mass distribution. The W width was taken as its Standard Model value at the fitted W mass. The systematic error includes ± 0.03 GeV due to the beam energy uncertainty and ± 0.032 GeV due to the possible color reconnection and Bose-Einstein effects in the purely hadronic final state. Combining with the M_W values from cross section measurements at 161 and 172 GeV (BARATE 97 and BARATE 97s) authors find: $M(W) = 80.51 \pm 0.23 \pm 0.08$ GeV.
- ¹⁴ ACCIARRI 97 derive this value from their measured W - W production cross section $\sigma_{WW} = 2.89^{+0.81}_{-0.70} \pm 0.14$ pb using the Standard Model dependence of σ_{WW} on M_W at the given c.m. energy. Statistical and systematic errors are added in quadrature and the last error of ± 0.03 GeV arises from the beam energy uncertainty. The same result is given by a fit of the production cross sections to the data.
- ¹⁵ ACCIARRI 97m derive this value from their measured W - W production cross section $\sigma_{WW} = 12.27^{+1.41}_{-1.32} \pm 0.23$ pb using the Standard Model dependence of σ_{WW} on M_W at the given c.m. energy. Combining with ACCIARRI 97 authors find $M(W) = 80.78^{+0.45}_{-0.41} \pm 0.03$ GeV where the last error is due to beam energy uncertainty.
- ¹⁶ ACCIARRI 97s obtain this value from a fit to the reconstructed W mass distribution. The W width was taken as its Standard Model value at the fitted W mass. When both W mass and width are varied they obtain $M(W) = 80.72^{+0.31}_{-0.33} \pm 0.09$ GeV. The systematic error includes ± 0.03 GeV due to the beam energy uncertainty and ± 0.05 GeV due to the possible color reconnection and Bose-Einstein effects in the purely hadronic final state. Combining with ACCIARRI 97 and ACCIARRI 97m authors find: $M(W) = 80.75^{+0.26}_{-0.27} \pm 0.03$ (LEP) GeV.
- ¹⁷ BARATE 97 derive this value from their measured W - W production cross section $\sigma_{WW} = 4.23 \pm 0.73 \pm 0.19$ pb using the Standard Model dependence of σ_{WW} on M_W at the given c.m. energy. The systematics include an error of ± 0.03 GeV arising from the beam energy uncertainty.
- ¹⁸ BARATE 97s derive this value from their measured W - W production cross section $\sigma_{WW} = 11.71 \pm 1.23 \pm 0.28$ pb using the Standard Model dependence of σ_{WW} on M_W at the given c.m. energy. The errors quoted on the mass are statistical only. Combining with BARATE 97 authors find: $M(W) = 80.20 \pm 0.33 \pm 0.09 \pm 0.03$ (LEP) GeV.
- ¹⁹ ABACHI 96E fit the transverse mass distribution of 5982 $W \rightarrow e\nu_e$ decays. An error of ± 160 MeV due to the uncertainty in the absolute energy scale of the EM calorimeter is included in the total systematics.
- ²⁰ ACKERSTAFF 96b derive this value from an analysis of the predicted M_W dependence of their accepted four-fermion cross section, explicitly taking into account interference effects. The systematics include an error of ± 0.03 GeV arising from the beam energy uncertainty.
- ²¹ AID 96d derive this value as a propagator mass using the Q^2 shape and magnitude of the e^\pm charged-current cross sections. $Q^2 > 5000$ GeV² events with p_T of the outgoing lepton > 25 GeV/ c are used.
- ²² ALITTI 92b result has two contributions to the systematic error (± 0.83); one (± 0.81) cancels in m_W/m_Z and one (± 0.17) is noncancelling. These were added in quadrature. We choose the ALITTI 92b value without using the LEP m_Z value, because we perform our own combined fit.
- ²³ There are two contributions to the systematic error (± 0.84): one (± 0.81) which cancels in m_W/m_Z and one (± 0.21) which is non-cancelling. These were added in quadrature.
- ²⁴ ABE 89j systematic error dominated by the uncertainty in the absolute energy scale.
- ²⁵ ALBAJAR 89 result is from a total sample of 299 $W \rightarrow e\nu$ events.
- ²⁶ ALBAJAR 89 result is from a total sample of 67 $W \rightarrow \mu\nu$ events.
- ²⁷ ALBAJAR 89 result is from $W \rightarrow \tau\nu$ events.

W/Z MASS RATIO

The fit uses the W and Z mass, mass difference, and mass ratio measurements.

VALUE	EVTs	DOCUMENT ID	TECN	COMMENT
0.8820 ± 0.0005 OUR FIT				
0.8821 ± 0.0011 ± 0.0008	28323	28 ABBOTT	98N D0	$E_{cm}^{PD} = 1.8$ TeV
0.88114 ± 0.00154 ± 0.00252	5982	29 ABBOTT	98P D0	$E_{cm}^{PD} = 1.8$ TeV
0.8813 ± 0.0036 ± 0.0019	156	30 ALITTI	92B UA2	$E_{cm}^{PD} = 630$ GeV

- ²⁸ ABBOTT 98n obtain this from a study of 28323 $W \rightarrow e\nu_e$ and 3294 $Z \rightarrow e^+e^-$ decays. Of this latter sample, 2179 events are used to calibrate the electron energy scale.
- ²⁹ ABBOTT 98p obtain this from a study of 5982 $W \rightarrow e\nu_e$ events. The systematic error includes an uncertainty of ± 0.00175 due to the electron energy scale.
- ³⁰ Scale error cancels in this ratio.

 $m_Z - m_W$

The fit uses the W and Z mass, mass difference, and mass ratio measurements.

VALUE (GeV)	DOCUMENT ID	TECN	COMMENT
10.76 ± 0.05 OUR FIT			
10.4 ± 1.4 ± 0.8	ALBAJAR 89 UA1	UA1	$E_{cm}^{PD} = 546,630$ GeV
• • • We do not use the following data for averages, fits, limits, etc. • • •			
11.3 ± 1.3 ± 0.9	ANSARI 87 UA2	UA2	$E_{cm}^{PD} = 546,630$ GeV

 $m_{W^+} - m_{W^-}$

Test of CPT invariance.

VALUE (GeV)	EVTs	DOCUMENT ID	TECN	COMMENT
-0.19 ± 0.58	1722	ABE	90G CDF	$E_{cm}^{PD} = 1.8$ TeV

W WIDTH

The CDF and DØ widths labelled "extracted value" are obtained by measuring $R = [\sigma(W)/\sigma(Z)] [\Gamma(W \rightarrow \ell\nu_\ell)]/[\Gamma(B \rightarrow \ell\ell)\Gamma(W)]$ where the bracketed quantities can be calculated with plausible reliability. $\Gamma(W)$ is then extracted by using a value of $B(Z \rightarrow \ell\ell)$ measured at LEP. The UA1 and UA2 widths used $R = [\sigma(W)/\sigma(Z)] [\Gamma(W \rightarrow \ell\nu_\ell)/\Gamma(Z \rightarrow \ell\ell)] \Gamma(Z)/\Gamma(W)$ and the measured value of $\Gamma(Z)$. The Standard Model prediction is 2.067 ± 0.021 (ROSNER 94).

VALUE (GeV)	CL%	EVTs	DOCUMENT ID	TECN	COMMENT
2.12 ± 0.05 OUR AVERAGE					
2.152 ± 0.066		79176	31 ABBOTT	00B D0	Extracted value
1.84 ± 0.32 ± 0.20		674	32 ABBIENDI	99C OPAL	$E_{cm}^{PD} = 172+183$ GeV
2.48 ± 0.40 ± 0.10		737	33 ABREU	99T DLPH	$E_{cm}^{PD} = 183$ GeV
1.97 ± 0.34 ± 0.17		687	34 ACCIARRI	99 L3	$E_{cm}^{PD} = 172+183$ GeV
2.11 ± 0.28 ± 0.16		58	35 ABE	95C CDF	Direct meas.
2.064 ± 0.060 ± 0.059			36 ABE	95W CDF	Extracted value
2.10 $^{+0.14}_{-0.13}$ ± 0.09		3559	37 ALITTI	92 UA2	Extracted value
2.18 $^{+0.26}_{-0.24}$ ± 0.04			38 ALBAJAR	91 UA1	Extracted value
• • • We do not use the following data for averages, fits, limits, etc. • • •					
2.044 ± 0.097		11858	39 ABBOTT	99H D0	Repl. by ABBOTT 00B
2.126 $^{+0.052}_{-0.048}$ ± 0.035			40 BARATE	99I ALEP	$E_{cm}^{PD} = 161+172+183$ GeV
1.30 $^{+0.70}_{-0.55}$ ± 0.18		92	41 ACKERSTAFF	98D OPAL	Repl. by ABBIENDI 99c
1.74 $^{+0.88}_{-0.78}$ ± 0.25		101	42 ACCIARRI	97s L3	Repl. by ACCIARRI 99
2.30 ± 0.19 ± 0.06			43 ALITTI	90C UA2	Extracted value
2.8 $^{+1.4}_{-1.5}$ ± 1.3		149	44 ALBAJAR	89 UA1	$E_{cm}^{PD} = 546,630$ GeV
<7		90 119	APPEL	86 UA2	$E_{cm}^{PD} = 546,630$ GeV
<6.5		90 86	45 ARNISON	86 UA1	$E_{cm}^{PD} = 546,630$ GeV

- ³¹ ABBOTT 00b measure $R = 10.43 \pm 0.27$ for the $W \rightarrow e\nu_e$ decay channel. They use the SM theoretical predictions for $\sigma(W)/\sigma(Z)$ and $\Gamma(W \rightarrow e\nu_e)$ and the world average for $B(Z \rightarrow e\bar{e})$. The value quoted here is obtained combining this result (2.169 ± 0.070 GeV) with that of ABBOTT 99h.
- ³² ABBIENDI 99c obtain this value from a fit to the reconstructed W mass distribution using data at 172 and 183 GeV. The systematic error includes an uncertainty of ± 0.12 GeV due to the possible color-reconnection and Bose-Einstein effects in the purely hadronic final states and an uncertainty of ± 0.01 GeV due to the beam energy.
- ³³ ABREU 99t obtain this value using W - $W \rightarrow \ell\nu_\ell q\bar{q}$ and W - $W \rightarrow q\bar{q} q\bar{q}$ events. The systematic error includes an uncertainty of ± 0.080 GeV due to possible color reconnection and Bose-Einstein effects in the purely hadronic final state.
- ³⁴ ACCIARRI 99 obtain this value from a fit to the reconstructed W mass distribution using data at 172 and 183 GeV.
- ³⁵ ABE 95c use the tail of the transverse mass distribution of $W \rightarrow e\nu_e$ decays.

Gauge & Higgs Boson Particle Listings

W

- ³⁶ ABE 95w measured $R = 10.90 \pm 0.32 \pm 0.29$. They use $m_W = 80.23 \pm 0.18$ GeV, $\sigma(W)/\sigma(Z) = 3.35 \pm 0.03$, $\Gamma(W \rightarrow e\nu) = 225.9 \pm 0.9$ MeV, $\Gamma(Z \rightarrow e^+e^-) = 83.98 \pm 0.18$ MeV, and $\Gamma(Z) = 2.4969 \pm 0.0038$ GeV.
- ³⁷ ALITTI 92 measured $R = 10.4^{+0.7}_{-0.6} \pm 0.3$. The values of $\sigma(Z)$ and $\sigma(W)$ come from $O(\alpha_s^2)$ calculations using $m_W = 80.14 \pm 0.27$ GeV, and $m_Z = 91.175 \pm 0.021$ GeV along with the corresponding value of $\sin^2\theta_W = 0.2274$. They use $\sigma(W)/\sigma(Z) = 3.26 \pm 0.07 \pm 0.05$ and $\Gamma(Z) = 2.467 \pm 0.010$ GeV.
- ³⁸ ALBAJAR 91 measured $R = 9.5^{+1.1}_{-1.0}$ (stat. + syst.). $\sigma(W)/\sigma(Z)$ is calculated in QCD at the parton level using $m_W = 80.18 \pm 0.28$ GeV and $m_Z = 91.172 \pm 0.031$ GeV along with $\sin^2\theta_W = 0.2322 \pm 0.0014$. They use $\sigma(W)/\sigma(Z) = 3.23 \pm 0.05$ and $\Gamma(Z) = 2.498 \pm 0.020$ GeV. This measurement is obtained combining both the electron and muon channels.
- ³⁹ ABBOTT 99H measure $R = 10.90 \pm 0.52$ combining electron and muon channels. They use $M_W = 80.39 \pm 0.06$ GeV and the SM theoretical predictions for $\sigma(W)/\sigma(Z)$, $B(Z \rightarrow \ell\ell)$, and $\Gamma(W \rightarrow \ell\nu_\ell)$.
- ⁴⁰ BARATE 99I obtain this result with a fit to the WW measured cross sections at 161, 172, and 183 GeV. The theoretical prediction takes into account the sensitivity to the W total width.
- ⁴¹ ACKERSTAFF 98D obtain this value from a fit to the reconstructed W mass distribution.
- ⁴² ACCIARRI 97S obtain this value from a fit to the reconstructed W mass distribution.
- ⁴³ ALITTI 90C used the same technique as described for ABE 90. They measured $R = 9.38^{+0.82}_{-0.72} \pm 0.25$, obtained $\Gamma(W)/\Gamma(Z) = 0.902 \pm 0.074 \pm 0.024$. Using $\Gamma(Z) = 2.546 \pm 0.032$ GeV, they obtained the $\Gamma(W)$ value quoted above and the limits $\Gamma(W) < 2.56$ (2.64) GeV at the 90% (95%) CL. $E_{cm}^{pp} = 546,630$ GeV.
- ⁴⁴ ALBAJAR 89 result is from a total sample of 299 $W \rightarrow e\nu$ events.
- ⁴⁵ If systematic error is neglected, result is $2.7^{+1.4}_{-1.5}$ GeV. This is enhanced subsample of 172 total events.

W⁺ DECAY MODES

W^- modes are charge conjugates of the modes below.

Mode	Fraction (Γ_i/Γ)	Confidence level
Γ_1 $\ell^+\nu$	[a] (10.56 ± 0.14) %	
Γ_2 $e^+\nu$	(10.66 ± 0.20) %	
Γ_3 $\mu^+\nu$	(10.49 ± 0.29) %	
Γ_4 $\tau^+\nu$	(10.4 ± 0.4) %	
Γ_5 hadrons	(68.5 ± 0.6) %	
Γ_6 $\pi^+\gamma$	< 7 × 10 ⁻⁵	95%
Γ_7 $D_s^+\gamma$	< 1.3 × 10 ⁻³	95%
Γ_8 $c\bar{X}$	(35 ± 4) %	
Γ_9 $c\bar{s}$	(32 $^{+13}_{-11}$) %	
Γ_{10} invisible	[b] (1.4 ± 2.8) %	

[a] ℓ indicates each type of lepton (e , μ , and τ), not sum over them.

[b] This represents the width for the decay of the W boson into a charged particle with momentum below detectability, $p < 200$ MeV.

W PARTIAL WIDTHS

$\Gamma(\text{invisible})$	Γ_{10}		
This represents the width for the decay of the W boson into a charged particle with momentum below detectability, $p < 200$ MeV.			
VALUE (MeV)	DOCUMENT ID	TECN	COMMENT
$30^{+52}_{-48} \pm 33$	46 BARATE	99I ALEP	$E_{cm}^{ee} = 161+172+183$ GeV
• • • We do not use the following data for averages, fits, limits, etc. • • •			
	47 BARATE	99L ALEP	$E_{cm}^{ee} = 161+172+183$ GeV
⁴⁶ BARATE 99I measure this quantity using the dependence of the total cross section σ_{WW} upon a change in the total width. The fit is performed to the WW measured cross sections at 161, 172, and 183 GeV. This partial width is < 139 MeV at 95%CL.			
⁴⁷ BARATE 99L use W -pair production to search for effectively invisible W decays, tagging with the decay of the other W boson to Standard Model particles. The partial width for effectively invisible decay is < 27 MeV at 95%CL.			

W BRANCHING RATIOS

Overall fits are performed to determine the branching ratios of the W . For each LEP experiment the correlation matrix of the leptonic branching ratios is used and the common systematic errors among LEP experiments are properly taken into account. A first fit determines three individual leptonic branching ratios, $B(W \rightarrow e\nu_e)$, $B(W \rightarrow \mu\nu_\mu)$, and $B(W \rightarrow \tau\nu_\tau)$. This fit has a $\chi^2 = 10.5$ for 20 degrees of freedom. A second fit assumes lepton universality and determines the leptonic branching ratio $B(W \rightarrow \ell\nu_\ell)$. This fit has a $\chi^2 = 11.0$ for 22 degrees of freedom. A separate fit is performed only to hadronic branching ratio data taking into account the common systematic errors. This fit has a $\chi^2 = 2.3$ for 3 degrees of freedom.

$$\Gamma(\ell^+\nu)/\Gamma_{\text{total}} \quad \Gamma_1/\Gamma$$

ℓ indicates average over e , μ , and τ modes, not sum over modes.

Data marked "fit" are used for the fit. The other data is highly correlated with data appearing elsewhere in the Listings and are therefore not used in the fit.

VALUE	EVTS	DOCUMENT ID	TECN	COMMENT
0.1056 ± 0.0014 OUR FIT				
0.1071 ± 0.0024 ± 0.0014	1237	ABREU	00K DLPH	$E_{cm}^{ee} = 161+172+183+189$ GeV
0.107 ± 0.004 ± 0.002	461	ABBIENDI	99D OPAL	$E_{cm}^{ee} = 161+172+183$ GeV
0.1102 ± 0.0052	fit 11858	48 ABBOTT	99H D0	$E_{cm}^{pp} = 1.8$ TeV
0.1036 ± 0.0040 ± 0.0017	532	BARATE	99I ALEP	$E_{cm}^{ee} = 161+172+183$ GeV
0.100 ± 0.004 ± 0.001	324	ACCIARRI	98P L3	$E_{cm}^{ee} = 161+172+183$ GeV
0.104 ± 0.008	fit 3642	49 ABE	92I CDF	$E_{cm}^{pp} = 1.8$ TeV
• • • We do not use the following data for averages, fits, limits, etc. • • •				
0.1085 ± 0.0048 ± 0.0017	170	ABREU	99K DLPH	Repl. by ABREU 00K
0.101 $^{+0.011}_{-0.010} \pm 0.002$	61	ACKERSTAFF	98D OPAL	Repl. by ABBIENDI 99D
0.119 $^{+0.013}_{-0.012} \pm 0.002$	51	ACCIARRI	97M L3	Repl. by ACCIARRI 98P

⁴⁸ ABBOTT 99H measure $R \equiv [\sigma_{WW} B(W \rightarrow \ell\nu_\ell)]/[\sigma_Z B(Z \rightarrow \ell\ell)] = 10.90 \pm 0.52$ combining electron and muon channels. They use $M_W = 80.39 \pm 0.06$ GeV and the SM theoretical predictions for $\sigma(W)/\sigma(Z)$ and $B(Z \rightarrow \ell\ell)$.

⁴⁹ 1216 ± 38 $^{+27}_{-31}$ $W \rightarrow \mu\nu$ events from ABE 92I and 2426 $W \rightarrow e\nu$ events of ABE 91C. ABE 92I give the inverse quantity as 9.6 ± 0.7 and we have inverted.

$$\Gamma(e^+\nu)/\Gamma_{\text{total}} \quad \Gamma_2/\Gamma$$

VALUE	EVTS	DOCUMENT ID	TECN	COMMENT
0.1066 ± 0.0020 OUR FIT				
0.1044 ± 0.0015 ± 0.0028	67318	50 ABBOTT	00B D0	$E_{cm}^{pp} = 1.8$ TeV
0.1018 ± 0.0054 ± 0.0026	352	ABREU	00K DLPH	$E_{cm}^{ee} = 161+172+183+189$ GeV
0.117 ± 0.009 ± 0.002	191	ABBIENDI	99D OPAL	$E_{cm}^{ee} = 161+172+183$ GeV
0.1115 ± 0.0085 ± 0.0024	193	BARATE	99I ALEP	$E_{cm}^{ee} = 161+172+183$ GeV
0.105 ± 0.009 ± 0.002	128	ACCIARRI	98P L3	$E_{cm}^{ee} = 161+172+183$ GeV
0.1094 ± 0.0033 ± 0.0031		51 ABE	95W CDF	$E_{cm}^{pp} = 1.8$ TeV
0.10 ± 0.014 $^{+0.02}_{-0.03}$	248	52 ANSARI	87C UA2	$E_{cm}^{pp} = 546,630$ GeV
• • • We do not use the following data for averages, fits, limits, etc. • • •				
0.1012 ± 0.0107 ± 0.0028	56	ABREU	99K DLPH	Repl. by ABREU 00K
0.098 $^{+0.022}_{-0.020} \pm 0.003$	21	ACKERSTAFF	98D OPAL	Repl. by ABBIENDI 99D
0.165 $^{+0.037}_{-0.033} \pm 0.005$	23	ACCIARRI	97M L3	Repl. by ACCIARRI 98P
0.097 ± 0.02 ± 0.005	21	BARATE	97S ALEP	Repl. by BARATE 99I
seen	119	APPEL	86 UA2	$E_{cm}^{pp} = 546,630$ GeV
seen	172	ARNISON	86 UA1	$E_{cm}^{pp} = 546,630$ GeV

⁵⁰ ABBOTT 00B measure $R \equiv [\sigma_{WW} B(W \rightarrow e\nu_e)]/[\sigma_Z B(Z \rightarrow ee)] = 10.43 \pm 0.27$ for the $W \rightarrow e\nu_e$ decay channel. They use the SM theoretical prediction for $\sigma(W)/\sigma(Z)$ and the world average for $B(Z \rightarrow ee)$.

⁵¹ ABE 95w result is from a measurement of $\sigma B(W \rightarrow e\nu)/\sigma B(Z \rightarrow e^+e^-) = 10.90 \pm 0.32 \pm 0.29$, the theoretical prediction for the cross section ratio, the experimental knowledge of $\Gamma(Z \rightarrow e^+e^-) = 83.98 \pm 0.18$ MeV, and $\Gamma(Z) = 2.4969 \pm 0.0038$ GeV.

⁵² The first error was obtained by adding the statistical and systematic experimental uncertainties in quadrature. The second error reflects the dependence on theoretical prediction of total W cross section: $\sigma(546 \text{ GeV}) = 4.7^{+1.4}_{-0.7}$ nb and $\sigma(630 \text{ GeV}) = 5.8^{+1.8}_{-1.0}$ nb. See ALTARELLI 85B.

See key on page 239

Gauge & Higgs Boson Particle Listings

W

$\Gamma(\mu^+\nu)/\Gamma_{total}$					Γ_3/Γ
VALUE	EVTs	DOCUMENT ID	TECN	COMMENT	
0.1049 ± 0.0029 OUR FIT					
0.1092 ± 0.0048 ± 0.0012	461	ABREU	00K DLPH	$E_{cm}^{ee} = 161+172+183+189$ GeV	
0.102 ± 0.008 ± 0.002	169	ABBIENDI	99D OPAL	$E_{cm}^{ee} = 161+172+183$ GeV	
0.1006 ± 0.0078 ± 0.0021	179	BARATE	99I ALEP	$E_{cm}^{ee} = 161+172+183$ GeV	
0.102 ± 0.009 ± 0.002	115	ACCIARRI	98P L3	$E_{cm}^{ee} = 161+172+183$ GeV	
0.10 ± 0.01	1216	53 ABE	92I CDF	$E_{cm}^{pp} = 1.8$ TeV	
• • • We do not use the following data for averages, fits, limits, etc. • • •					
0.1139 ± 0.0096 ± 0.0023	67	ABREU	99K DLPH	Repl. by ABREU 00k	
0.073 ± 0.017 ± 0.002	16	ACKERSTAFF	98D OPAL	Repl. by ABBIENDI 99D	
0.084 ± 0.028 ± 0.003	13	ACCIARRI	97M L3	Repl. by ACCIARRI 98P	
0.112 ± 0.02 ± 0.006	25	BARATE	97S ALEP	Repl. by BARATE 99I	

53 ABE 92I quote the inverse quantity as 9.9 ± 1.2 which we have inverted.

$\Gamma(\tau^+\nu)/\Gamma_{total}$					Γ_4/Γ
VALUE	EVTs	DOCUMENT ID	TECN	COMMENT	
0.1043 ± 0.0041 OUR FIT					
0.1105 ± 0.0075 ± 0.0032	424	ABREU	00K DLPH	$E_{cm}^{ee} = 161+172+183+189$ GeV	
0.101 ± 0.010 ± 0.003	144	ABBIENDI	99D OPAL	$E_{cm}^{ee} = 161+172+183$ GeV	
0.0976 ± 0.0101 ± 0.0033	160	BARATE	99I ALEP	$E_{cm}^{ee} = 161+172+183$ GeV	
0.090 ± 0.012 ± 0.003	81	ACCIARRI	98P L3	$E_{cm}^{ee} = 161+172+183$ GeV	
• • • We do not use the following data for averages, fits, limits, etc. • • •					
0.1095 ± 0.0149 ± 0.0041	47	ABREU	99K DLPH	Repl. by ABREU 00k	
0.140 ± 0.030 ± 0.005	23	ACKERSTAFF	98D OPAL	Repl. by ABBIENDI 99D	
0.109 ± 0.042 ± 0.005	15	ACCIARRI	97M L3	Repl. by ACCIARRI 98P	
0.113 ± 0.027 ± 0.006	37	BARATE	97S ALEP	Repl. by BARATE 99I	

$\Gamma(\text{hadrons})/\Gamma_{total}$					Γ_5/Γ
VALUE	EVTs	DOCUMENT ID	TECN	COMMENT	
0.6848 ± 0.0059 OUR FIT					
0.6789 ± 0.0073 ± 0.0043	1773	ABREU	00K DLPH	$E_{cm}^{ee} = 161+172+183+189$ GeV	
0.679 ± 0.012 ± 0.005	395	ABBIENDI	99D OPAL	$E_{cm}^{ee} = 161+172+183$ GeV	
0.6893 ± 0.0121 ± 0.0051	1255	BARATE	99I ALEP	$E_{cm}^{ee} = 161+172+183$ GeV	
0.701 ± 0.013 ± 0.004	462	ACCIARRI	98P L3	$E_{cm}^{ee} = 161+172+183$ GeV	
• • • We do not use the following data for averages, fits, limits, etc. • • •					
0.6746 ± 0.0143 ± 0.0052	465	ABREU	99K DLPH	Repl. by ABREU 00k	
0.698 ± 0.032 ± 0.007	52	ACKERSTAFF	98D OPAL	Repl. by ABBIENDI 99D	
0.642 ± 0.037 ± 0.005	70	ACCIARRI	97M L3	Repl. by ACCIARRI 98P	
0.677 ± 0.031 ± 0.007	65	BARATE	97S ALEP	Repl. by BARATE 99I	

$\Gamma(\mu^+\nu)/\Gamma(e^+\nu)$					Γ_3/Γ_2
VALUE	EVTs	DOCUMENT ID	TECN	COMMENT	
0.984 ± 0.032 OUR FIT					
0.89 ± 0.10	13k	54 ABACHI	95D D0	$E_{cm}^{pp} = 1.8$ TeV	
1.02 ± 0.08	1216	55 ABE	92I CDF	$E_{cm}^{pp} = 1.8$ TeV	
• • • We do not use the following data for averages, fits, limits, etc. • • •					
1.00 ± 0.14 ± 0.08	67	ALBAJAR	89 UA1	$E_{cm}^{pp} = 546,630$ GeV	
1.24 ± 0.6 ± 0.4	14	ARNISON	84D UA1	Repl. by ALBAJAR 89	

54 ABACHI 95D obtain this result from the measured $\sigma_{WB}(W \rightarrow \mu\nu) = 2.09 \pm 0.23 \pm 0.11$ nb and $\sigma_{WB}(W \rightarrow e\nu) = 2.36 \pm 0.07 \pm 0.13$ nb in which the first error is the combined statistical and systematic uncertainty, the second reflects the uncertainty in the luminosity.

55 ABE 92I obtain $\sigma_{WB}(W \rightarrow \mu\nu) = 2.21 \pm 0.07 \pm 0.21$ and combine with ABE 91C $\sigma_{WB}(W \rightarrow e\nu)$ to give a ratio of the couplings from which we derive this measurement.

$\Gamma(\tau^+\nu)/\Gamma(e^+\nu)$					Γ_4/Γ_2
VALUE	EVTs	DOCUMENT ID	TECN	COMMENT	
0.979 ± 0.044 OUR FIT					
0.94 ± 0.14	179	56 ABE	92E CDF	$E_{cm}^{pp} = 1.8$ TeV	
1.04 ± 0.08 ± 0.08	754	57 ALITTI	92F UA2	$E_{cm}^{pp} = 630$ GeV	
1.02 ± 0.20 ± 0.12	32	ALBAJAR	89 UA1	$E_{cm}^{pp} = 546,630$ GeV	
• • • We do not use the following data for averages, fits, limits, etc. • • •					
0.995 ± 0.112 ± 0.083	198	ALITTI	91C UA2	Repl. by ALITTI 92F	
1.02 ± 0.20 ± 0.10	32	ALBAJAR	87 UA1	Repl. by ALBAJAR 89	
56 ABE 92E use two procedures for selecting $W \rightarrow \tau\nu$ events. The missing E_T trigger leads to $132 \pm 14 \pm 8$ events and the τ trigger to $47 \pm 9 \pm 4$ events. Proper statistical and systematic correlations are taken into account to arrive at $\sigma_B(W \rightarrow \tau\nu) = 2.05 \pm 0.27$ nb. Combined with ABE 91C result on $\sigma_B(W \rightarrow e\nu)$, ABE 92E quote a ratio of the couplings from which we derive this measurement.					
57 This measurement is derived by us from the ratio of the couplings of ALITTI 92F.					

$\Gamma(\pi^+\gamma)/\Gamma(e^+\nu)$					Γ_6/Γ_2
VALUE	CL%	DOCUMENT ID	TECN	COMMENT	
$< 7 \times 10^{-4}$	95	ABE	98H CDF	$E_{cm}^{pp} = 1.8$ TeV	
$< 4.9 \times 10^{-3}$	95	58 ALITTI	92D UA2	$E_{cm}^{pp} = 630$ GeV	
$< 58 \times 10^{-3}$	95	59 ALBAJAR	90 UA1	$E_{cm}^{pp} = 546, 630$ GeV	
58 ALITTI 92D limit is 3.8×10^{-3} at 90%CL.					
59 ALBAJAR 90 obtain < 0.048 at 90%CL.					

$\Gamma(D_s^+\gamma)/\Gamma(e^+\nu)$					Γ_7/Γ_2
VALUE	CL%	DOCUMENT ID	TECN	COMMENT	
$< 1.2 \times 10^{-2}$	95	ABE	98P CDF	$E_{cm}^{pp} = 1.8$ TeV	

$\Gamma(cX)/\Gamma(\text{hadrons})$					Γ_8/Γ_5
VALUE	EVTs	DOCUMENT ID	TECN	COMMENT	
0.51 ± 0.05 ± 0.03	746	60 BARATE	99M ALEP	$E_{cm}^{ee} = 172 + 183$ GeV	
60 BARATE 99M tag c jets using a neural network algorithm. From this measurement $ V_{cs} $ is determined to be $1.00 \pm 0.11 \pm 0.07$.					

$R_{cS} = \Gamma(c\bar{s})/\Gamma(\text{hadrons})$					Γ_9/Γ_5
VALUE		DOCUMENT ID	TECN	COMMENT	
0.46 ± 0.18 ± 0.07		61 ABREU	98N DLPH	$E_{cm}^{ee} = 161+172$ GeV	
61 ABREU 98N tag c and s jets by identifying a charged kaon as the highest momentum particle in a hadronic jet. They also use a lifetime tag to independently identify a c jet, based on the impact parameter distribution of charged particles in a jet. From this measurement $ V_{cs} $ is determined to be $0.94^{+0.32}_{-0.26} \pm 0.13$.					

AVERAGE PARTICLE MULTIPLICITIES IN HADRONIC W DECAY

Summed over particle and antiparticle, when appropriate.

$\langle N_{charged} \rangle$				
VALUE		DOCUMENT ID	TECN	COMMENT
19.3 ± 0.4 OUR AVERAGE				
19.3 ± 0.3 ± 0.3		62 ABBIENDI	99N OPAL	$E_{cm}^{ee} = 183$ GeV
19.23 ± 0.74		63 ABREU	98C DLPH	$E_{cm}^{ee} = 172$ GeV
62 ABBIENDI 99N use the final states $W^+W^- \rightarrow q\bar{q}l\bar{l}$ to derive this value.				
63 ABREU 98C combine results from both the fully hadronic as well semileptonic WW final states after demonstrating that the W decay charged multiplicity is independent of the topology within errors.				

TRIPLE GAUGE COUPLINGS (TGC'S)

Revised March 2000 by C. Caso (Univ. of Genova) and A. Gurtu (Tata Inst.)

Fourteen independent couplings, 7 each for ZWW and γWW , completely describe the VWW vertices within the most general framework of the electroweak Standard Model (SM) consistent with Lorentz invariance and $U(1)$ gauge invariance. Of each of the 7 TGC's, 3 conserve C and P individually, 3 violate CP , and one TGC violates C and P individually while conserving CP . Assumption of C and P conservation and electromagnetic gauge invariance reduces the independent VWW couplings to five: one common set is $(\kappa_\gamma, \kappa_Z, \lambda_\gamma, \lambda_Z, g_1^Z)$, where $\kappa_\gamma = \kappa_Z = g_1^Z = 1$ and $\lambda_\gamma = \lambda_Z = 0$ in the Standard Model at the tree level. The W magnetic dipole moment, μ_W , and the W electric quadrupole moment, q_W , are expressed as $\mu_W = e(1 + \kappa_\gamma + \lambda_\gamma)/2M_W$ and $q_W = -e(\kappa_\gamma - \lambda_\gamma)/M_W^2$.

Gauge & Higgs Boson Particle Listings

W

Precision measurements of suitable observables at LEP1 has already led to an exploration of much of the TGC parameter space. Three linear combinations of the TGC's, $\alpha_{W\phi}$, $\alpha_{B\phi}$ and α_W , have been proposed to investigate the leftover "blind" directions in the CP -conserving TGC parameter space, and two linear couplings, $\tilde{\alpha}_{BW}$ and $\tilde{\alpha}_W$ in the CP -violating TGC parameter space (see *e.g.*, papers by Hagiwara [1], Bilenky [2], and Gounaris [3,4]). The relations between these parameters and those contained in the above set, expressed as *deviations* from the SM, are $\Delta g_1^Z = \alpha_{W\phi}/c_w^2$, $\Delta\kappa_\gamma = \alpha_{W\phi} + \alpha_{B\phi}$, $\Delta\kappa_Z = \alpha_{W\phi} - t_w^2\alpha_{B\phi}$ and $\lambda_\gamma = \lambda_Z = \alpha_W$, where c_w and t_w are the cosine and tangent of the electroweak mixing angle. Similarly, $\tilde{\kappa}_\gamma = \tilde{\alpha}_{BW}$, $\tilde{\kappa}_Z = t_w^2\tilde{\alpha}_{BW}$ and $\tilde{\lambda}_\gamma = \tilde{\lambda}_Z = \tilde{\alpha}_W$ within the CP -violating sector. The LEP Collaborations have recently agreed to express their results directly in terms of the parameters Δg_1^Z , $\Delta\kappa_\gamma$ and λ_γ .

At LEP2 the VWW coupling arises in W -pair production via s -channel exchange or in single W production via the radiation of a virtual photon off the incident e^+ or e^- . At the TEVATRON hard photon bremsstrahlung off a produced W or Z signals the presence of a triple gauge vertex. In order to extract the value of one TGC the others are generally kept fixed to their SM values.

References

1. K. Hagiwara *et al.*, Nucl. Phys. **B282**, 253 (1987).
2. M. Bilenky *et al.*, Nucl. Phys. **B409**, 22 (1993).
3. G. Gounaris *et al.*, CERN 96-01 525.
4. G. Gounaris *et al.*, Eur. Phys. J. **C2**, 365 (1998).

Δg_1^Z

VALUE	EVTS	DOCUMENT ID	TECN	COMMENT
0.01	+0.09			OUR AVERAGE
	-0.08			
0.01	+0.13 -0.12	853 64	ABBIENDI 99D	OPAL $E_{cm}^{ee} = 161+172+183$ GeV
-0.04	+0.14 -0.12	566 65	ABREU 99L	DLPH $E_{cm}^{ee} = 183$ GeV
0.11	+0.19 -0.18	±0.10 1154 66	ACCIARRI 99Q	L3 $E_{cm}^{ee} = 161+172+183$ GeV

• • • We do not use the following data for averages, fits, limits, etc. • • •

		331 67	ABBOTT 99I	D0 $E_{cm}^{pp} = 1.8$ TeV
-0.017	+0.018 -0.003	±0.018	68	MOLNAR 99 THEO LEP1, SLAC+Tevatron

64 ABBIENDI 99D combine results from W^+W^- production at different energies. The 95% confidence interval is $-0.23 < \Delta g_1^Z < 0.26$.

65 ABREU 99L use W^+W^- , $W\nu_e$, and $\nu\bar{\nu}\gamma$ final states. The 95% confidence interval is $-0.28 < \Delta g_1^Z < 0.24$.

66 ACCIARRI 99Q study W -pair, single- W , and single photon events.

67 ABBOTT 99I perform a simultaneous fit to the $W\gamma$, $WW \rightarrow$ dilepton, $WW/WZ \rightarrow e\nu jj$, $WW/WZ \rightarrow \mu\nu jj$, and $WZ \rightarrow$ trilepton data samples. For $\Lambda = 2.0$ TeV, the 95%CL limits are $-0.37 < \Delta g_1^Z < 0.57$, fixing $\lambda_Z = \Delta\kappa_Z = 0$ and assuming Standard Model values for the $WV\gamma$ couplings.

68 MOLNAR 99 extract this value indirectly by fitting high energy electroweak data within the framework of the Standard Model. The central value of the Higgs mass used is 300 GeV and the quoted systematic error is due to its variation between 90 to 1000 GeV.

$\Delta\kappa_\gamma$

VALUE	EVTS	DOCUMENT ID	TECN	COMMENT
0.08	+0.17			OUR AVERAGE
	-0.37			
0.11	+0.52 -0.37	853 69	ABBIENDI 99D	OPAL $E_{cm}^{ee} = 161+172+183$ GeV
-0.08	±0.34	331 70	ABBOTT 99I	D0 $E_{cm}^{pp} = 1.8$ TeV
0.19	+0.32 -0.34	566 71	ABREU 99L	DLPH $E_{cm}^{ee} = 183$ GeV
0.11	±0.25	±0.17 1154 72	ACCIARRI 99Q	L3 $E_{cm}^{ee} = 161+172+183$ GeV
0.05	+1.15 -1.10	±0.25 207 73	BARATE,R 98	ALEP $E_{cm}^{ee} = 161+172+183$ GeV

• • • We do not use the following data for averages, fits, limits, etc. • • •

		15 74	BARATE 99L	ALEP $E_{cm}^{ee} = 161+172+183$ GeV
0.016	+0.019 -0.013	75	MOLNAR 99	THEO LEP1, SLAC+Tevatron
0.06	+0.27 -0.26	86 76	ACCIARRI 98N	L3 Repl. by ACCIARRI 99Q

69 ABBIENDI 99D combine results from W^+W^- production at different energies. The 95% confidence interval is $-0.55 < \Delta\kappa_\gamma < 1.28$.

70 ABBOTT 99I perform a simultaneous fit to the $W\gamma$, $WW \rightarrow$ dilepton, $WW/WZ \rightarrow e\nu jj$, $WW/WZ \rightarrow \mu\nu jj$, and $WZ \rightarrow$ trilepton data samples. For $\Lambda = 2.0$ TeV, the 95%CL limits are $-0.25 < \Delta\kappa_\gamma < 0.39$.

71 ABREU 99L use W^+W^- , $W\nu_e$, and $\nu\bar{\nu}\gamma$ final states. The 95% confidence interval is $-0.46 < \Delta\kappa_\gamma < 0.84$.

72 ACCIARRI 99Q study W -pair, single- W , and single photon events.

73 BARATE,R 98 study single photon production in e^+e^- interactions from 161 to 183 GeV. A likelihood fit is performed to the cross section and to the photon energy and angular distributions, taking into account systematic uncertainties. The 95%CL limits are $-2.2 < \Delta\kappa_\gamma < 2.3$.

74 BARATE 99I study single W production in e^+e^- interactions from 161 to 183 GeV. They obtain 95%CL limits of $-1.6 < \kappa_\gamma < 1.5$, which we convert to $-2.6 < \Delta\kappa_\gamma < 0.5$ for $\lambda_\gamma = 0$.

75 MOLNAR 99 extract this value indirectly by fitting high energy electroweak data within the framework of the Standard Model. The central value of the Higgs mass used is 300 GeV and the quoted systematic error is due to its variation between 90 to 1000 GeV.

76 ACCIARRI 98N study single W production in e^+e^- interactions from 130 to 183 GeV. The 95%CL limits are $-0.46 < \Delta\kappa_\gamma < 0.57$.

λ_γ

VALUE	EVTS	DOCUMENT ID	TECN	COMMENT
-0.04	+0.07			OUR AVERAGE
	-0.06			
-0.10	+0.13 -0.12	853 77	ABBIENDI 99D	OPAL $E_{cm}^{ee} = 161+172+183$ GeV
0.00	+0.10 -0.09	331 78	ABBOTT 99I	D0 $E_{cm}^{pp} = 1.8$ TeV
-0.15	+0.19 -0.15	566 79	ABREU 99L	DLPH $E_{cm}^{ee} = 183$ GeV
0.10	+0.22 -0.20	±0.10 1154 80	ACCIARRI 99Q	L3 $E_{cm}^{ee} = 161+172+183$ GeV
-0.05	+1.55 -1.45	±0.30 207 81	BARATE,R 98	ALEP $E_{cm}^{ee} = 161+172+183$ GeV

• • • We do not use the following data for averages, fits, limits, etc. • • •

		15 82	BARATE 99L	ALEP $E_{cm}^{ee} = 161+172+183$ GeV
-0.48	+0.44 -0.21	86 83	ACCIARRI 98N	L3 Repl. by ACCIARRI 99Q

77 ABBIENDI 99D combine results from W^+W^- production at different energies. The 95% confidence interval is $-0.33 < \lambda_\gamma < 0.16$.

78 ABBOTT 99I perform a simultaneous fit to the $W\gamma$, $WW \rightarrow$ dilepton, $WW/WZ \rightarrow e\nu jj$, $WW/WZ \rightarrow \mu\nu jj$, and $WZ \rightarrow$ trilepton data samples. For $\Lambda = 2.0$ TeV, the 95%CL limits are $-0.18 < \lambda_\gamma < 0.19$.

79 ABREU 99L use W^+W^- , $W\nu_e$, and $\nu\bar{\nu}\gamma$ final states. The 95% confidence interval is $-0.44 < \lambda_\gamma < 0.24$.

80 ACCIARRI 99Q study W -pair, single- W , and single photon events.

81 BARATE,R 98 study single photon production in e^+e^- interactions from 161 to 183 GeV. A likelihood fit is performed to the cross section and to the photon energy and angular distributions, taking into account systematic uncertainties. The 95%CL limits are $-3.1 < \lambda_\gamma < 3.2$.

82 BARATE 99I study single W production in e^+e^- interactions from 161 to 183 GeV. The 95%CL limits are $-1.6 < \lambda_\gamma < 1.6$ for $\Delta\kappa_\gamma = 0$.

83 ACCIARRI 98N study single W production in e^+e^- interactions from 130 to 183 GeV. The 95%CL limits are $-0.86 < \lambda_\gamma < 0.75$.

Δg_5^Z

VALUE	EVTS	DOCUMENT ID	TECN	COMMENT
-0.44	+0.23			OUR AVERAGE
	-0.22			
-0.44	+0.23 -0.22	±0.12 1154 84	ACCIARRI 99Q	L3 $E_{cm}^{ee} = 161+172+183$ GeV

84 ACCIARRI 99Q study W -pair, single- W , and single photon events.

$\alpha_W\phi$

VALUE	EVTS	DOCUMENT ID	TECN	COMMENT
0.05	±0.20			OUR AVERAGE
0.22	+0.25 -0.28	±0.06 89 85	ABREU 98K	DLPH $E_{cm}^{ee} = 161+172$ GeV
-0.14	+0.27 -0.25	+0.14 -0.12 78 86	BARATE 98V	ALEP $E_{cm}^{ee} = 172$ GeV
		331 87	ABBOTT 99I	D0 $E_{cm}^{pp} = 1.8$ TeV

• • • We do not use the following data for averages, fits, limits, etc. • • •

85 ABREU 98K obtain this result using both W pair production and single W ($W\nu_e$) production.

86 BARATE 98V obtain this value using semileptonic and hadronic decay modes in W pair production.

87 ABBOTT 99I perform a simultaneous fit to the $W\gamma$, $WW \rightarrow$ dilepton, $WW/WZ \rightarrow e\nu jj$, $WW/WZ \rightarrow \mu\nu jj$, and $WZ \rightarrow$ trilepton data samples. For $\Lambda = 2.0$ TeV, the 95%CL limits are $-0.18 < \alpha_W\phi < 0.36$, fixing $\alpha_{B\phi} = \alpha_W = 0$.

See key on page 239

Gauge & Higgs Boson Particle Listings

W

α_W

VALUE	EVTs	DOCUMENT ID	TECN	COMMENT
0.1 ± 0.4 OUR AVERAGE				
0.11 ^{+0.48} _{-0.49} ± 0.09	89	88 ABREU	98k DLPH	$E_{cm}^{ee} = 161+172$ GeV
0.06 ^{+0.56} _{-0.50} ± 0.12	78	89 BARATE	98Y ALEP	$E_{cm}^{ee} = 172$ GeV
• • • We do not use the following data for averages, fits, limits, etc. • • •				
	331	90 ABBOTT	99i D0	$E_{cm}^{pp} = 1.8$ TeV

88 ABREU 98k obtain this result using both W pair production and single $W(W\ell\nu_e)$ production.
 89 BARATE 98Y obtain this value using semileptonic and hadronic decay modes in W pair production.
 90 ABBOTT 99i perform a simultaneous fit to the $W\gamma$, $WW \rightarrow$ dilepton, $WW/WZ \rightarrow e\nu jj$, $WW/WZ \rightarrow \mu\nu jj$, and $WZ \rightarrow$ trilepton data samples. For $\Lambda = 2.0$ TeV, the 95%CL limits are $-0.18 < \alpha_W < 0.19$, fixing $\alpha_B\phi = \alpha_W\phi = 0$.

$\alpha_B\phi$

VALUE	EVTs	DOCUMENT ID	TECN	COMMENT
0.4 ± 0.5 OUR AVERAGE				
0.22 ^{+0.66} _{-0.83} ± 0.24	89	91 ABREU	98k DLPH	$E_{cm}^{ee} = 161+172$ GeV
1.01 ^{+0.71} _{-1.75} ± 0.33	78	92 BARATE	98Y ALEP	$E_{cm}^{ee} = 172$ GeV
• • • We do not use the following data for averages, fits, limits, etc. • • •				
	331	93 ABBOTT	99i D0	$E_{cm}^{pp} = 1.8$ TeV

91 ABREU 98k obtain this result using both W pair production and single $W(W\ell\nu_e)$ production.
 92 BARATE 98Y obtain this value using semileptonic and hadronic decay modes in W pair production.
 93 ABBOTT 99i perform a simultaneous fit to the $W\gamma$, $WW \rightarrow$ dilepton, $WW/WZ \rightarrow e\nu jj$, $WW/WZ \rightarrow \mu\nu jj$, and $WZ \rightarrow$ trilepton data samples. For $\Lambda = 2.0$ TeV, the 95%CL limits are $-0.67 < \alpha_B\phi < 0.56$, fixing $\alpha_W\phi = \alpha_W = 0$.

$\tilde{\alpha}_{BW}$

VALUE	EVTs	DOCUMENT ID	TECN	COMMENT
0.11 ± 0.71 OUR AVERAGE				
0.11 ^{+0.71} _{-0.88} ± 0.09	89	94 ABREU	98k DLPH	$E_{cm}^{ee} = 161+172$ GeV
94 ABREU 98k obtain this result using both W pair production and single $W(W\ell\nu_e)$ production.				

$\tilde{\alpha}_W$

VALUE	EVTs	DOCUMENT ID	TECN	COMMENT
0.19 ± 0.28 OUR AVERAGE				
0.19 ^{+0.28} _{-0.41} ± 0.11	89	95 ABREU	98k DLPH	$E_{cm}^{ee} = 161+172$ GeV
95 ABREU 98k obtain this result using both W pair production and single $W(W\ell\nu_e)$ production.				

W ANOMALOUS MAGNETIC MOMENT ($\Delta\kappa$)

The full magnetic moment is given by $\mu_W = e(1+\kappa+\lambda)/2m_W$. In the Standard Model, at tree level, $\kappa = 1$ and $\lambda = 0$. Some papers have defined $\Delta\kappa = 1-\kappa$ and assume that $\lambda = 0$. Note that the electric quadrupole moment is given by $-e(\kappa-\lambda)/m_W^2$. A description of the parameterization of these moments and additional references can be found in HAGIWARA 87 and BAUR 88. The parameter Λ appearing in the theoretical limits below is a regularization cutoff which roughly corresponds to the energy scale where the structure of the W boson becomes manifest.

VALUE ($e/2m_W$)	DOCUMENT ID	TECN
• • • We do not use the following data for averages, fits, limits, etc. • • •		
	96 ABE	95G CDF
	97 ALITTI	92C UA2
	98 SAMUEL	92 THEO
	99 SAMUEL	91 THEO
	100 GRIFOLS	88 THEO
	101 GROTCHE	87 THEO
	102 VANDERBIJ	87 THEO
	103 GRAU	85 THEO
	104 SUZUKI	85 THEO
	105 HERZOG	84 THEO

- 96 ABE 95G report $-1.3 < \kappa < 3.2$ for $\lambda=0$ and $-0.7 < \lambda < 0.7$ for $\kappa=1$ in $p\bar{p} \rightarrow e\nu_e\gamma X$ and $\mu\nu_\mu\gamma X$ at $\sqrt{s} = 1.8$ TeV.
 97 ALITTI 92C measure $\kappa = 1 \pm 2.6$ and $\lambda = 0 \pm 1.7$ in $p\bar{p} \rightarrow e\nu\gamma + X$ at $\sqrt{s} = 630$ GeV. At 95%CL they report $-3.5 < \kappa < 5.9$ and $-3.6 < \lambda < 3.5$.
 98 SAMUEL 92 use preliminary CDF and UA2 data and find $-2.4 < \kappa < 3.7$ at 96%CL and $-3.1 < \kappa < 4.2$ at 95%CL respectively. They use data for $W\gamma$ production and radiative W decay.
 99 SAMUEL 91 use preliminary CDF data for $p\bar{p} \rightarrow W\gamma X$ to obtain $-11.3 \leq \Delta\kappa \leq 10.9$. Note that their $\kappa = 1 - \Delta\kappa$.
 100 GRIFOLS 88 uses deviation from ρ parameter to set limit $\Delta\kappa \lesssim 65 (M_W^2/\Lambda^2)$.
 101 GROTCHE 87 finds the limit $-37 < \Delta\kappa < 73.5$ (90% CL) from the experimental limits on $e^+e^- \rightarrow \nu\bar{\nu}\gamma$ assuming three neutrino generations and $-19.5 < \Delta\kappa < 56$ for four generations. Note their $\Delta\kappa$ has the opposite sign as our definition.
 102 VANDERBIJ 87 uses existing limits to the photon structure to obtain $|\Delta\kappa| < 33 (m_W/\Lambda)$. In addition VANDERBIJ 87 discusses problems with using the ρ parameter of the Standard Model to determine $\Delta\kappa$.

- 103 GRAU 85 uses the muon anomaly to derive a coupled limit on the anomalous magnetic dipole and electric quadrupole (λ) moments $1.05 > \Delta\kappa \ln(\Lambda/m_W) + \lambda/2 > -2.77$. In the Standard Model $\lambda = 0$.
 104 SUZUKI 85 uses partial-wave unitarity at high energies to obtain $|\Delta\kappa| \lesssim 190 (m_W/\Lambda)^2$. From the anomalous magnetic moment of the muon, SUZUKI 85 obtains $|\Delta\kappa| \lesssim 2.2 \ln(\Lambda/m_W)$. Finally SUZUKI 85 uses deviations from the ρ parameter and obtains a very qualitative, order-of-magnitude limit $|\Delta\kappa| \lesssim 150 (m_W/\Lambda)^4$ if $|\Delta\kappa| \ll 1$.
 105 HERZOG 84 consider the contribution of W -boson to muon magnetic moment including anomalous coupling of $WW\gamma$. Obtain a limit $-1 < \Delta\kappa < 3$ for $\Lambda \gtrsim 1$ TeV.

W REFERENCES

ABBOTT 00	PRL 84 222	B. Abbott et al.	(D0 Collab.)
ABBOTT 00B	PR D61 072001	B. Abbott et al.	(D0 Collab.)
ABREU 00K	PL B479 89	P. Abreu et al.	(DELPHI Collab.)
ABBIENDI 95C	PL B453 138	G. Abbiendi et al.	(OPAL Collab.)
ABBIENDI 99D	EPJ C8 191	G. Abbiendi et al.	(OPAL Collab.)
ABBIENDI 99N	PL B453 153	G. Abbiendi et al.	(OPAL Collab.)
ABBOTT 99H	PR D60 052003	B. Abbott et al.	(D0 Collab.)
ABBOTT 99I	PR D60 072002	B. Abbott et al.	(D0 Collab.)
ABREU 99K	PL B456 310	P. Abreu et al.	(DELPHI Collab.)
ABREU 99L	PL B459 382	P. Abreu et al.	(DELPHI Collab.)
ABREU 99T	PL B462 410	P. Abreu et al.	(DELPHI Collab.)
ACCIARRI 99	PL B454 386	M. Acciari et al.	(L3 Collab.)
ACCIARRI 99Q	PL B467 171	M. Acciari et al.	(L3 Collab.)
BARATE 99	PL B453 121	R. Barate et al.	(ALEPH Collab.)
BARATE 99I	PL B453 107	R. Barate et al.	(ALEPH Collab.)
BARATE 99L	PL B462 389	R. Barate et al.	(ALEPH Collab.)
BARATE 99M	PL B465 349	R. Barate et al.	(ALEPH Collab.)
MOLNAR 99	PL B461 149	F. Molnar, M. Grunewald	(ALEPH Collab.)
ABBOTT 98N	PR D58 092003	B. Abbott et al.	(D0 Collab.)
ABBOTT 98O	PRL 80 3008	B. Abbott et al.	(D0 Collab.)
ABBOTT 98P	PR D58 012002	B. Abbott et al.	(D0 Collab.)
ABE 98H	PR C58 031101	F. Abe et al.	(CDF Collab.)
ABE 98R	PR D58 091101	F. Abe et al.	(CDF Collab.)
ABREU 98B	EPJ C2 581	P. Abreu et al.	(DELPHI Collab.)
ABREU 98C	PL B416 233	P. Abreu et al.	(DELPHI Collab.)
ABREU 98K	PL B423 194	P. Abreu et al.	(DELPHI Collab.)
ABREU 98N	PL B439 209	P. Abreu et al.	(DELPHI Collab.)
ACCIARRI 98N	PL B436 417	M. Acciari et al.	(L3 Collab.)
ACCIARRI 98P	PL B436 437	M. Acciari et al.	(L3 Collab.)
ACKERSTAFF 98D	EPJ C1 395	K. Ackerstaff et al.	(OPAL Collab.)
BARATE 98B	PL B422 384	R. Barate et al.	(ALEPH Collab.)
BARATE 98Y	PL B422 369	R. Barate et al.	(ALEPH Collab.)
BARATE,R 98	PL B445 239	R. Barate et al.	(ALEPH Collab.)
ACCIARRI 97	PL B398 223	M. Acciari et al.	(L3 Collab.)
ACCIARRI 97M	PL B407 419	M. Acciari et al.	(L3 Collab.)
ACCIARRI 97S	PL B413 176	M. Acciari et al.	(L3 Collab.)
BARATE 97	PL B401 347	R. Barate et al.	(ALEPH Collab.)
BARATE 97S	PL B415 435	R. Barate et al.	(ALEPH Collab.)
ABACHI 96E	PRL 77 3309	S. Abachi et al.	(D0 Collab.)
ACKERSTAFF 96B	PL B389 416	K. Ackerstaff et al.	(OPAL Collab.)
AID 96D	PL B379 319	S. Aid et al.	(H1 Collab.)
ABACHI 95D	PRL 75 1456	S. Abachi et al.	(D0 Collab.)
ABE 95C	PRL 74 341	F. Abe et al.	(CDF Collab.)
ABE 95G	PRL 74 1936	F. Abe et al.	(CDF Collab.)
ABE 95P	PRL 75 11	F. Abe et al.	(CDF Collab.)
ABE Also 95Q	PR D52 4784	F. Abe et al.	(CDF Collab.)
ABE 95W	PR D52 2624	F. Abe et al.	(CDF Collab.)
ABE Also 94B	PRL 73 220	F. Abe et al.	(CDF Collab.)
ROSNER 94	PR D49 1363	J.L. Rosner, M.P. Worah, T. Takeuchi	(EFI, FNAL)
ABE 92E	PRL 68 3398	F. Abe et al.	(CDF Collab.)
ABE 92I	PRL 69 28	F. Abe et al.	(CDF Collab.)
ALITTI 92	PL B276 365	J. Alitti et al.	(UA2 Collab.)
ALITTI 92B	PL B276 354	J. Alitti et al.	(UA2 Collab.)
ALITTI 92C	PL B277 194	J. Alitti et al.	(UA2 Collab.)
ALITTI 92D	PL B277 203	J. Alitti et al.	(UA2 Collab.)
ALITTI 92F	PL B280 137	J. Alitti et al.	(UA2 Collab.)
SAMUEL 92	PL B280 124	M.A. Samuel et al.	(OKSU, CARL)
ABE 91C	PR D44 29	F. Abe et al.	(CDF Collab.)
ALBAJAR 91	PL B253 503	C. Albajar et al.	(UA1 Collab.)
ALITTI 91C	ZPHY C52 209	J. Alitti et al.	(UA2 Collab.)
SAMUEL 91I	PRL 67 9	M.A. Samuel et al.	(OKSU, CARL)
Also 91C	PRL 67 2920 erratum		
ABE 90	PRL 64 152	F. Abe et al.	(CDF Collab.)
Also 91C	PR D44 29	F. Abe et al.	(CDF Collab.)
ABE 90G	PRL 65 2243	F. Abe et al.	(CDF Collab.)
Also 91B	PR D43 2070	F. Abe et al.	(CDF Collab.)
ALBAJAR 90	PL B241 283	C. Albajar et al.	(UA1 Collab.)
ALITTI 90B	PL B241 150	J. Alitti et al.	(UA2 Collab.)
ALITTI 90C	ZPHY C47 11	J. Alitti et al.	(UA2 Collab.)
ABE 89I	PRL 62 1005	F. Abe et al.	(CDF Collab.)
ALBAJAR 89I	ZPHY C44 15	C. Albajar et al.	(UA1 Collab.)
BAUR 88	NP B308 127	U. Baur, D. Zeppenfeld	(FSU, WISC)
GRIFOLS 88	JMP A3 225	J.A. Grifols, S. Peris, J. Sola	(BARC, DESY)
Also 87	PL B197 437	J.A. Grifols, S. Peris, J. Sola	(BARC, DESY)
ALBAJAR 87	PL B185 233	C. Albajar et al.	(UA1 Collab.)
ANSARI 87	PL B186 440	R. Ansari et al.	(UA2 Collab.)
ANSARI 87C	PL B194 158	R. Ansari et al.	(UA2 Collab.)
GROTCHE 87	PR D36 2153	H. Grötsch, R.W. Robinett	(PSU)
HAGIWARA 87	NP B282 253	K. Hagiwara et al.	(KEK, UCLA, FSU)
VANDERBIJ 87	PR D35 1088	J.J. van der Bij	(FNAL)
APPEL 86	ZPHY C30 1	J.A. Appel et al.	(UA2 Collab.)
ARNISON 86	PL 166B 484	G.T.J. Aronson et al.	(UA1 Collab.)
ALTARELLI 85B	ZPHY C27 617	G. Altarelli, R.K. Ellis, G. Martinelli	(CERN+)
GRAU 85	PL 154B 283	A. Grau, J.A. Grifols	(BARC)
SUZUKI 85	PL 153B 289	M. Suzuki	(LBL)
ARNISON 84D	PL 134B 469	G.T.J. Aronson et al.	(UA1 Collab.)
HERZOG 84	PL 148B 355	F. Herzog	(WISC)
Also 84B	PL 155B 468 erratum	F. Herzog	(WISC)
ARNISON 84	PL 122B 103	G.T.J. Aronson et al.	(UA1 Collab.)
BANNER 83B	PL 122B 476	M. Banner et al.	(UA1 Collab.)



J = 1

THE Z BOSON

Revised March 2000 by C. Caso (Univ. of Genova) and A. Gurtu (Tata Inst.)

Precision measurements at the Z -boson resonance using electron-positron colliding beams began in 1989 at the SLC and at LEP. During 1989–95, the four CERN experiments have made high-statistics studies of the Z . The availability of longitudinally polarized electron beams at the SLC since 1993 has enabled a precision determination of the effective electroweak mixing angle $\sin^2\bar{\theta}_W$ that is competitive with the CERN results on this parameter.

The Z -boson properties reported in this section may broadly be categorized as:

- The standard ‘lineshape’ parameters of the Z consisting of its mass, M_Z , its total width, Γ_Z , and its partial decay widths, $\Gamma(\text{hadrons})$, and $\Gamma(\ell\bar{\ell})$ where $\ell = e, \mu, \tau, \nu$;
- Z asymmetries in leptonic decays and extraction of Z couplings to charged and neutral leptons;
- The b - and c -quark-related partial widths and charge asymmetries which require special techniques;
- Determination of Z decay modes and the search for modes that violate known conservation laws;
- Average particle multiplicities in hadronic Z decay;
- Z anomalous couplings.

Details on Z -parameter determination and the study of $Z \rightarrow b\bar{b}, c\bar{c}$ at LEP and SLC are given in this note.

The standard ‘lineshape’ parameters of the Z are determined from an analysis of the production cross sections of these final states in e^+e^- collisions. The $Z \rightarrow \nu\bar{\nu}(\gamma)$ state is identified directly by detecting single photon production and indirectly by subtracting the visible partial widths from the total width. Inclusion in this analysis of the forward-backward asymmetry of charged leptons, $A_{FB}^{(0,\ell)}$, of the τ polarization, $P(\tau)$, and its forward-backward asymmetry, $P(\tau)^{fb}$, enables the separate determination of the effective vector (\bar{g}_V) and axial vector (\bar{g}_A) couplings of the Z to these leptons and the ratio (\bar{g}_V/\bar{g}_A) which is related to the effective electroweak mixing angle $\sin^2\bar{\theta}_W$ (see the ‘‘Electroweak Model and Constraints on New Physics’’ Review).

Determination of the b - and c -quark-related partial widths and charge asymmetries involves tagging the b and c quarks. Traditionally this was done by requiring the presence of a prompt lepton in the event with high momentum and high transverse momentum (with respect to the accompanying jet). Precision vertex measurement with high-resolution detectors enabled one to do impact parameter and lifetime tagging. Neural-network techniques have also been used to classify events as b or non- b on a statistical basis using event-shape variables. Finally, the presence of a charmed meson (D/D^*) has been used to tag heavy quarks.

Z -parameter determination

LEP was run at energy points on and around the Z mass (88–94 GeV) constituting an energy ‘scan.’ The shape of the cross-section variation around the Z peak can be described by a Breit-Wigner ansatz with an energy-dependent total width [1–3]. The **three** main properties of this distribution, viz., the **position** of the peak, the **width** of the distribution, and the **height** of the peak, determine respectively the values of M_Z , Γ_Z , and $\Gamma(e^+e^-) \times \Gamma(f\bar{f})$, where $\Gamma(e^+e^-)$ and $\Gamma(f\bar{f})$ are the electron and fermion partial widths of the Z . The quantitative determination of these parameters is done by writing analytic expressions for these cross sections in terms of the parameters and fitting the calculated cross sections to the measured ones by varying these parameters, taking properly into account all the errors. Single-photon exchange (σ_γ^0) and γ - Z interference ($\sigma_{\gamma Z}^0$) are included, and the large ($\sim 25\%$) initial-state radiation (ISR) effects are taken into account by convoluting the analytic expressions over a ‘Radiator Function’ [1–6] $H(s, s')$. Thus for the process $e^+e^- \rightarrow f\bar{f}$:

$$\sigma_f(s) = \int H(s, s') \sigma_f^0(s') ds' \quad (1)$$

$$\sigma_f^0(s) = \sigma_Z^0 + \sigma_\gamma^0 + \sigma_{\gamma Z}^0 \quad (2)$$

$$\sigma_Z^0 = \frac{12\pi}{M_Z^2} \frac{\Gamma(e^+e^-)\Gamma(f\bar{f})}{\Gamma_Z^2} \frac{s \Gamma_Z^2}{(s - M_Z^2)^2 + s^2\Gamma_Z^2/M_Z^2} \quad (3)$$

$$\sigma_\gamma^0 = \frac{4\pi\alpha^2(s)}{3s} Q_f^2 N_c^f \quad (4)$$

$$\sigma_{\gamma Z}^0 = -\frac{2\sqrt{2}\alpha(s)}{3} (Q_f G_F N_c^f G_{V_e} G_{V_f}) \times \frac{(s - M_Z^2)M_Z^2}{(s - M_Z^2)^2 + s^2\Gamma_Z^2/M_Z^2} \quad (5)$$

where Q_f is the charge of the fermion, $N_c^f = 3(1)$ for quark (lepton) and G_{V_f} is the neutral vector coupling of the Z to the fermion-antifermion pair $f\bar{f}$.

Since $\sigma_{\gamma Z}^0$ is expected to be much less than σ_Z^0 , the LEP Collaborations have generally calculated the interference term in the framework of the Standard Model. This fixing of $\sigma_{\gamma Z}^0$ leads to a tighter constraint on M_Z and consequently a smaller error on its fitted value.

In the above framework, the QED radiative corrections have been explicitly taken into account by convoluting over the ISR and allowing the electromagnetic coupling constant to run [10]: $\alpha(s) = \alpha/(1 - \Delta\alpha)$. On the other hand, weak radiative corrections that depend upon the assumptions of the electroweak theory and on the values of the unknown M_{top} and M_{Higgs} are accounted for by **absorbing them into the couplings**, which are then called the *effective* couplings \mathcal{G}_V and \mathcal{G}_A (or alternatively the effective parameters of the \star scheme of Kennedy and Lynn [11]).

\mathcal{G}_{Vf} and \mathcal{G}_{Af} are complex numbers with a small imaginary part. As experimental data does not allow simultaneous extraction of both real and imaginary parts of the effective couplings,

the convention $g_{Af} = \text{Re}(\mathcal{G}_{Af})$ and $g_{Vf} = \text{Re}(\mathcal{G}_{Vf})$ is used and the imaginary parts are added in the fitting code [4].

Defining

$$A_f = 2 \frac{g_{Vf} \cdot g_{Af}}{(g_{Vf}^2 + g_{Af}^2)} \quad (6)$$

the lowest-order expressions for the various lepton-related asymmetries on the Z pole are [7–9] $A_{FB}^{(0,\ell)} = (3/4)A_e A_f$, $P(\tau) = -A_\tau$, $P(\tau)^{fb} = -(3/4)A_e$, $A_{LR} = A_e$. The full analysis takes into account the energy dependence of the asymmetries. Experimentally A_{LR} is defined as $(\sigma_L - \sigma_R)/(\sigma_L + \sigma_R)$ where $\sigma_{L(R)}$ are the $e^+e^- \rightarrow Z$ production cross sections with left-(right)-handed electrons.

The definition of the partial decay width of the Z to $f\bar{f}$ includes the effects of QED and QCD final state corrections as well as the contribution due to the imaginary parts of the couplings:

$$\Gamma(f\bar{f}) = \frac{G_F M_Z^3}{6\sqrt{2}\pi} N_c^f (|\mathcal{G}_{Vf}|^2 R_A^f + |\mathcal{G}_{VA}|^2 R_V^f) + \Delta_{ew/QCD} \quad (7)$$

where R_V^f and R_A^f are radiator factors to account for final state QED and QCD corrections as well as effects due to nonzero fermion masses, and $\Delta_{ew/QCD}$ represents the non-factorizable electroweak/QCD corrections.

S-matrix approach to the Z

While practically all experimental analyses of LEP/SLC data have followed the ‘Breit-Wigner’ approach described above, an alternative S-matrix-based analysis is also possible. The Z , like all unstable particles, is associated with a complex pole in the S matrix. The pole position is process independent and gauge invariant. The mass, \bar{M}_Z , and width, $\bar{\Gamma}_Z$, can be defined in terms of the pole in the energy plane via [12–15]

$$\bar{s} = \bar{M}_Z^2 - i\bar{M}_Z\bar{\Gamma}_Z \quad (8)$$

leading to the relations

$$\begin{aligned} \bar{M}_Z &= M_Z / \sqrt{1 + \Gamma_Z^2/M_Z^2} \\ &\approx M_Z - 34.1 \text{ MeV} \end{aligned} \quad (9)$$

$$\begin{aligned} \bar{\Gamma}_Z &= \Gamma_Z / \sqrt{1 + \Gamma_Z^2/M_Z^2} \\ &\approx \Gamma_Z - 0.9 \text{ MeV} . \end{aligned} \quad (10)$$

Some authors [16] choose to define the Z mass and width via

$$\bar{s} = (\bar{M}_Z - \frac{i}{2}\bar{\Gamma}_Z)^2 \quad (11)$$

which yields $\bar{M}_Z \approx M_Z - 26 \text{ MeV}$, $\bar{\Gamma}_Z \approx \Gamma_Z - 1.2 \text{ MeV}$.

The L3 and OPAL Collaborations at LEP (ACCIARRI 97K and ACKERSTAFF 97C) have analyzed their data using the S-matrix approach as defined in Eq. (8), in addition to the conventional one. They observe a downward shift in the Z mass as expected.

Handling the large-angle e^+e^- final state

Unlike other $f\bar{f}$ decay final states of the Z , the e^+e^- final state has a contribution not only from the s -channel but also from the t -channel and s - t interference. The full amplitude is not amenable to fast calculation, which is essential if one has to carry out minimization fits within reasonable computer time. The usual procedure is to calculate the non- s channel part of the cross section separately using the Standard Model programs ALIBABA [17] or TOPAZO [18] with the measured value of M_{top} , and $M_{\text{Higgs}} = 150 \text{ GeV}$ and add it to the s -channel cross section calculated as for other channels. This leads to two additional sources of error in the analysis: firstly, the theoretical calculation in ALIBABA itself is known to be accurate to $\sim 0.5\%$, and secondly, there is uncertainty due to the error on M_{top} and the unknown value of M_{Higgs} (100–1000 GeV). These additional errors are propagated into the analysis by including them in the systematic error on the e^+e^- final state. As these errors are common to the four LEP experiments, this is taken into account when performing the LEP average.

Errors due to uncertainty in LEP energy determination [19–23]

The systematic errors related to the LEP energy measurement can be classified as:

- The absolute energy scale error;
- Energy-point-to-energy-point errors due to the non-linear response of the magnets to the exciting currents;
- Energy-point-to-energy-point errors due to possible higher-order effects in the relationship between the dipole field and beam energy;
- Energy reproducibility errors due to various unknown uncertainties in temperatures, tidal effects, corrector settings, RF status, *etc.*

Precise energy calibration was done outside normal data taking using the resonant depolarization technique. Run-time energies were determined every 10 minutes by measuring the relevant machine parameters and using a model which takes into account all the known effects, including leakage currents produced by trains in the Geneva area and the tidal effects due to gravitational forces of the Sun and the Moon. The LEP Energy Working Group has provided a covariance matrix from the determination of LEP energies for the different running periods during 1993–1995 [5].

Choice of fit parameters

The LEP Collaborations have chosen the following primary set of parameters for fitting: M_Z , Γ_Z , σ_{hadron}^0 , $R(\text{lepton})$, $A_{FB}^{(0,\ell)}$, where $R(\text{lepton}) = \Gamma(\text{hadrons})/\Gamma(\text{lepton})$, $\sigma_{\text{hadron}}^0 = 12\pi\Gamma(e^+e^-)\Gamma(\text{hadrons})/M_Z^2\Gamma_Z^2$. With a knowledge of these fitted parameters and their covariance matrix, any other parameter can be derived. The main advantage of these parameters is that they form the **least correlated** set of parameters, so that it becomes easy to combine results from the different LEP experiments.

Thus, the most general fit carried out to cross section and asymmetry data determines the **nine parameters**: M_Z , Γ_Z , σ_{hadron}^0 , $R(e)$, $R(\mu)$, $R(\tau)$, $A_{FB}^{(0,e)}$, $A_{FB}^{(0,\mu)}$, $A_{FB}^{(0,\tau)}$. Assumption of lepton universality leads to a **five-parameter fit** determining M_Z , Γ_Z , σ_{hadron}^0 , $R(\text{lepton})$, $A_{FB}^{(0,\ell)}$. The use of **only** cross-section data leads to six- or four-parameter fits if lepton universality is or is not assumed, *i.e.*, $A_{FB}^{(0,\ell)}$ values are not determined.

In order to determine the best values of the effective vector and axial vector couplings of the charged leptons to the Z , the above mentioned nine- and five-parameter fits are carried out with added constraints from the measured values of A_τ and A_e obtained from τ polarization studies at LEP and the determination of A_{LR} at SLC.

Combining results from the LEP and SLC experiments [24]

Each LEP experiment provides the values of the parameters mentioned above together with the full covariance matrix. The statistical and experimental systematic errors are assumed to be uncorrelated among the four experiments. The sources of **common** systematic errors are i) the LEP energy uncertainties, ii) the effect of theoretical uncertainty in calculating the small-angle Bhabha cross section for luminosity determination and in estimating the non- s channel contribution to the large-angle Bhabha cross section, and iii) common theory errors. Using this information, a full covariance matrix, V , of all the input parameters is constructed and a combined parameter set is obtained by minimizing $\chi^2 = \Delta^T V^{-1} \Delta$, where Δ is the vector of residuals of the combined parameter set to the results of individual experiments.

Non-LEP measurement of a Z parameter, (*e.g.*, $\Gamma(e^+e^-)$ from SLD) is included in the overall fit by calculating its value using the fit parameters and constraining it to the measurement.

Study of $Z \rightarrow b\bar{b}$ and $Z \rightarrow c\bar{c}$

In the sector of c - and b -physics the LEP experiments have measured the ratios of partial widths $R_b = \Gamma(Z \rightarrow b\bar{b})/\Gamma(Z \rightarrow \text{hadrons})$ and $R_c = \Gamma(Z \rightarrow c\bar{c})/\Gamma(Z \rightarrow \text{hadrons})$ and the forward-backward (charge) asymmetries $A_{FB}^{b\bar{b}}$ and $A_{FB}^{c\bar{c}}$. Several of the analyses have also determined other quantities, in particular the semileptonic branching ratios, $B(b \rightarrow \ell)$, $B(b \rightarrow c \rightarrow \ell^+)$, and $B(c \rightarrow \ell)$, the average $B^0\bar{B}^0$ mixing parameter $\bar{\chi}$ and the probabilities for a c -quark to fragment into a D^+ , a D_s , a D^{*+} , or a charmed baryon. The latter measurements do not concern properties of the Z boson and hence they do not appear in the listing below. However, for completeness, we will report at the end of this minireview their values as obtained fitting the data contained in the Z section. All these quantities are correlated with the electroweak parameters, and since the mixture of b hadrons is different from the one at the $\Upsilon(4S)$, their values might differ from those measured at the $\Upsilon(4S)$.

All the above quantities are correlated to each other since:

- Several analyses (for example the lepton fits) determine more than one parameter simultaneously;
- Some of the electroweak parameters depend explicitly on the values of other parameters (for example R_b depends on R_c);
- Common tagging and analysis techniques produce common systematic uncertainties.

The LEP Electroweak Heavy Flavour Working Group has developed [25] a procedure for combining the measurements taking into account known sources of correlation. The combining procedure determines twelve parameters: the four parameters of interest in the electroweak sector, R_b , R_c , $A_{FB}^{b\bar{b}}$, and $A_{FB}^{c\bar{c}}$ and, in addition, $B(b \rightarrow \ell)$, $B(b \rightarrow c \rightarrow \ell^+)$, $B(c \rightarrow \ell)$, $\bar{\chi}$, $f(D^+)$, $f(D_s)$, $f(c_{\text{baryon}})$ and $P(c \rightarrow D^{*+}) \times B(D^{*+} \rightarrow \pi^+ D^0)$, to take into account their correlations with the electroweak parameters. Before the fit both the peak and off-peak asymmetries are translated to the common energy $\sqrt{s} = 91.26$ GeV using the predicted dependence from ZFITTER [6].

Summary of the measurements and of the various kinds of analysis

The measurements of R_b and R_c fall into two classes. In the first, named single-tag measurement, a method for selecting b and c events is applied and the number of tagged events is counted. The second technique, named double-tag measurement, is based on the following principle: if the number of events with a single hemisphere tagged is N_t and with both hemispheres tagged is N_{tt} , then given a total number of N_{had} hadronic Z decays one has:

$$\frac{N_t}{2N_{\text{had}}} = \varepsilon_b R_b + \varepsilon_c R_c + \varepsilon_{uds}(1 - R_b - R_c) \quad (12)$$

$$\frac{N_{tt}}{N_{\text{had}}} = C_b \varepsilon_b^2 R_b + C_c \varepsilon_c^2 R_c + C_{uds} \varepsilon_{uds}^2 (1 - R_b - R_c) \quad (13)$$

where ε_b , ε_c , and ε_{uds} are the tagging efficiencies per hemisphere for b , c , and light quark events, and $C_q \neq 1$ accounts for the fact that the tagging efficiencies between the hemispheres may be correlated. In tagging the b one has $\varepsilon_b \gg \varepsilon_c \gg \varepsilon_{uds}$, $C_b \approx 1$. Neglecting the c and uds background and the hemisphere correlations, these equations give:

$$\varepsilon_b = 2N_{tt}/N_t \quad (14)$$

$$R_b = N_t^2 / (4N_{tt}N_{\text{had}}) . \quad (15)$$

The double-tagging method has thus the great advantage that the tagging efficiency is directly derived from the data, reducing the systematic error of the measurement. The backgrounds, dominated by $c\bar{c}$ events, obviously complicate this simple picture, and their level must still be inferred by other means. The rate of charm background in these analyses depends explicitly on the value of R_c . The correlations in the tagging efficiencies between the hemispheres (due for instance to correlations in momentum between the b hadrons in the two hemispheres) are small but nevertheless lead to further systematic uncertainties.

The measurements in the b - and c -sector can be essentially grouped in the following categories:

- Lifetime (and lepton) double-tagging measurements of R_b . These are the most precise measurements of R_b and obviously dominate the combined result. The main sources of systematics come from the charm contamination and from estimating the hemisphere b -tagging efficiency correlation. The charm rejection has been improved (and hence the systematic errors reduced) by using either the information of the secondary vertex invariant mass or the information from the energy of all particles at the secondary vertex and their rapidity;
- Analyses with $D/D^{*\pm}$ to measure R_c . These measurements make use of several different tagging techniques (inclusive/exclusive double tag, exclusive double tag, reconstruction of all weakly decaying charmed states) and no assumptions are made on the energy dependence of charm fragmentation;
- Lepton fits which use hadronic events with one or more leptons in the final state to measure $A_{FB}^{b\bar{b}}$ and $A_{FB}^{c\bar{c}}$. Each analysis usually gives several other electroweak parameters. The dominant sources of systematics are due to lepton identification, to other semileptonic branching ratios and to the modeling of the semileptonic decay;
- Measurements of $A_{FB}^{b\bar{b}}$ using lifetime tagged events with a hemisphere charge measurement. Their contribution to the combined result has roughly the same weight as the lepton fits;
- Analyses with $D/D^{*\pm}$ to measure $A_{FB}^{c\bar{c}}$ or simultaneously $A_{FB}^{b\bar{b}}$ and $A_{FB}^{c\bar{c}}$;
- Measurements of A_b and A_c from SLD, using several tagging methods (lepton, kaon, D/D^* , and vertex mass). These quantities are directly extracted from a measurement of the left–right forward–backward asymmetry in $c\bar{c}$ and $b\bar{b}$ production using a polarized electron beam.

Averaging procedure

All the measurements are provided by the LEP Collaborations in the form of tables with a detailed breakdown of the systematic errors of each measurement and its dependence on other electroweak parameters.

The averaging proceeds via the following steps:

- Define and propagate a consistent set of external inputs such as branching ratios, hadron lifetimes, fragmentation models *etc.* All the measurements are also consistently checked to ensure that all use a common set of assumptions (for instance since the QCD corrections for the forward–backward asymmetries are strongly dependent on the experimental conditions, the data are corrected before combining);

- Form the full (statistical and systematic) covariance matrix of the measurements. The systematic correlations between different analyses are calculated from the detailed error breakdown in the measurement tables. The correlations relating several measurements made by the same analysis are also used;
- Take into account any explicit dependence of a measurement on the other electroweak parameters. As an example of this dependence we illustrate the case of the double-tag measurement of R_b , where c -quarks constitute the main background. The normalization of the charm contribution is not usually fixed by the data and the measurement of R_b depends on the assumed value of R_c , which can be written as:

$$R_b = R_b^{\text{meas}} + a(R_c) \frac{(R_c - R_c^{\text{used}})}{R_c}, \quad (16)$$

where R_b^{meas} is the result of the analysis which assumed a value of $R_c = R_c^{\text{used}}$ and $a(R_c)$ is the constant which gives the dependence on R_c ;

- Perform a χ^2 minimization with respect to the combined electroweak parameters.

After the fit the average peak asymmetries $A_{FB}^{c\bar{c}}$ and $A_{FB}^{b\bar{b}}$ are corrected for the energy shift from 91.26 GeV to M_Z and for QED (initial state radiation), γ exchange, and γZ interference effects to obtain the corresponding pole asymmetries $A_{FB}^{0,c}$ and $A_{FB}^{0,b}$.

This averaging procedure, using the twelve parameters described above and applied to the data contained in the Z particle listing below, gives the following results:

$$R_b^0 = 0.21644 \pm 0.00075$$

$$R_c^0 = 0.1671 \pm 0.0048$$

$$A_{FB}^{0,b} = 0.1003 \pm 0.0022$$

$$A_{FB}^{0,c} = 0.0701 \pm 0.0045$$

$$B(b \rightarrow \ell) = 0.1056 \pm 0.0026$$

$$B(b \rightarrow c \rightarrow \ell^+) = 0.0807 \pm 0.0034$$

$$B(c \rightarrow \ell) = 0.0990 \pm 0.0037$$

$$\bar{\chi} = 0.1177 \pm 0.0055$$

$$f(D^+) = 0.239 \pm 0.016$$

$$f(D_s) = 0.116 \pm 0.025$$

$$f(c_{\text{baryon}}) = 0.084 \pm 0.023$$

$$P(c \rightarrow D^{*+}) \times B(D^{*+} \rightarrow \pi^+ D^0) = 0.1657 \pm 0.0057$$

Gauge & Higgs Boson Particle Listings

Z

References

1. R.N. Cahn, Phys. Rev. **D36**, 2666 (1987).
2. F.A. Berends *et al.*, "Z Physics at LEP 1", CERN Report 89-08 (1989), Vol. 1, eds. G. Altarelli, R. Kleiss, and C. Verzegnassi, p. 89.
3. A. Borrelli *et al.*, Nucl. Phys. **B333**, 357 (1990).
4. D. Bardin and G. Passarino, "Upgrading of Precision Calculations for Electroweak Observables," hep-ph/9803425; D. Bardin, G. Passarino, and M. Grunewald, "Precision Calculation Project Report," hep-ph/9902452.
5. R. Billen *et al.* (Working Group on LEP Energy), Eur. Phys. J. **C6**, 187 (1999).
6. D. Bardin *et al.*, Nucl. Phys. **B351**, 1 (1991).
7. M. Consoli *et al.*, "Z Physics at LEP 1", CERN Report 89-08 (1989), Vol. 1, eds. G. Altarelli, R. Kleiss, and C. Verzegnassi, p. 7.
8. M. Bohm *et al.*, *ibid.*, p. 203.
9. S. Jadach *et al.*, *ibid.*, p. 235.
10. G. Burgers *et al.*, *ibid.*, p. 55.
11. D.C. Kennedy and B.W. Lynn, SLAC-PUB 4039 (1986, revised 1988).
12. R. Stuart, Phys. Lett. **B262**, 113 (1991).
13. A. Sirlin, Phys. Rev. Lett. **67**, 2127 (1991).
14. A. Leike, T. Riemann, and J. Rose, Phys. Lett. **B273**, 513 (1991).
15. See also D. Bardin *et al.*, Phys. Lett. **B206**, 539 (1988).
16. S. Willenbrock and G. Valencia, Phys. Lett. **B259**, 373 (1991).
17. W. Beenakker, F.A. Berends, and S.C. van der Marck, Nucl. Phys. **B349**, 323 (1991).
18. K. Miyabayashi *et al.* (TOPAZ Collaboration) Phys. Lett. **B347**, 171 (1995).
19. R. Assmann *et al.* (Working Group on LEP Energy), Z. Phys. **C66**, 567 (1995).
20. L. Arnaudon *et al.* (Working Group on LEP Energy and LEP Collaborations), Phys. Lett. **B307**, 187 (1993).
21. L. Arnaudon *et al.* (Working Group on LEP Energy), CERN-PPE/92-125 (1992).
22. L. Arnaudon *et al.*, Phys. Lett. **B284**, 431 (1992).
23. R. Bailey *et al.*, 'LEP Energy Calibration' CERN-SL 90-95.
24. The LEP Collaborations: ALEPH, DELPHI, L3, OPAL, the LEP Electroweak Working Group, and the SLD Heavy Flavour Group: CERN-EP/2000-016 (1999); CERN-EP/99-15 (1998); CERN-PPE/97-154 (1997); CERN-PPE/96-183 (1996); CERN-PPE/95-172 (1995); CERN-PPE/94-187 (1994); CERN-PPE/93-157 (1993).
25. The LEP Experiments: ALEPH, DELPHI, L3, and OPAL Nucl. Instrum. Methods **A378**, 101 (1996).

Z MASS

OUR FIT is obtained using the fit procedure and correlations as determined by the LEP Electroweak Working Group (see the "Note on the Z boson"). The fit is performed using the Z mass and width, the Z hadronic pole cross section, the ratios of hadronic to leptonic partial widths, and the Z pole forward-backward lepton asymmetries. This set is believed to be most free of correlations.

The Z-boson mass listed here corresponds to a Breit-Wigner resonance parameter. The value is 34 MeV greater than the real part of the position of the pole (in the energy-squared plane) in the Z-boson propagator. Also the LEP experiments have generally assumed a fixed value of the $\gamma - Z$ interferences term based on the standard model. Keeping this term as free parameter leads to a somewhat larger error on the fitted Z mass. See ACCIARRI 97k and ACKERSTAFF 97c for a detailed investigation of both these issues.

VALUE (GeV)	EVTS	DOCUMENT ID	TECN	COMMENT
91.1882 ± 0.0022 OUR FIT				
91.1863 ± 0.0028	4.08M	¹ ABREU	00F DLPH	$E_{cm}^{ee} = 88-94$ GeV
91.1898 ± 0.0031	3.96M	² ACCIARRI	00C L3	$E_{cm}^{ee} = 88-94$ GeV
91.1885 ± 0.0031	4.57M	³ BARATE	00C ALEP	$E_{cm}^{ee} = 88-94$ GeV
• • • We do not use the following data for averages, fits, limits, etc. • • •				
91.193 ± 0.010	1.2M	⁴ ACCIARRI	97k L3	$E_{cm}^{ee} = \text{LEP1} + 130-136 \text{ GeV} + 161-172 \text{ GeV}$
91.185 ± 0.010		⁵ ACKERSTAFF	97c OPAL	$E_{cm}^{ee} = \text{LEP1} + 130-136 \text{ GeV} + 161 \text{ GeV}$
91.162 ± 0.011	1.2M	⁶ ACCIARRI	96B L3	Repl. by ACCIARRI 97k
91.192 ± 0.011	1.33M	⁷ ALEXANDER	96x OPAL	Repl. by ACKERSTAFF 97c
91.151 ± 0.008		⁸ MIYABAYASHI	95 TOPZ	$E_{cm}^{ee} = 57.8$ GeV
91.187 ± 0.007 ± 0.006	1.16M	⁹ ABREU	94 DLPH	Repl. by ABREU 00f
91.195 ± 0.006 ± 0.007	1.19M	⁹ ACCIARRI	94 L3	Repl. by ACCIARRI 00c
91.182 ± 0.007 ± 0.006	1.33M	⁹ AKERS	94 OPAL	$E_{cm}^{ee} = 88-94$ GeV
91.187 ± 0.007 ± 0.006	1.27M	⁹ BUSKULIC	94 ALEP	Repl. by BARATE 00c
91.74 ± 0.28 ± 0.93	156	¹⁰ ALITTI	92b UA2	$E_{cm}^{pp} = 630$ GeV
89.2 ^{+2.1} _{-1.8}		¹¹ ADACHI	90f RVUE	
90.9 ± 0.3 ± 0.2	188	¹² ABE	89c CDF	$E_{cm}^{pp} = 1.8$ TeV
91.14 ± 0.12	480	¹³ ABRAMS	89b MRK2	$E_{cm}^{ee} = 89-93$ GeV
93.1 ± 1.0 ± 3.0	24	¹⁴ ALBAJAR	89 UA1	$E_{cm}^{pp} = 546,630$ GeV

¹ The error includes 1.6 MeV due to LEP energy uncertainty.

² The error includes 1.8 MeV due to LEP energy uncertainty.

³ BARATE 00c error includes approximately 2.4 MeV due to statistics, 0.2 MeV due to experimental systematics, and 1.7 MeV due to LEP energy uncertainty.

⁴ ACCIARRI 97k interpret the s-dependence of the cross sections and lepton forward-backward asymmetries in the framework of the S-matrix formalism with a combined fit to their cross section and asymmetry data at the Z peak (ACCIARRI 94) and their data at 130, 136, 161, and 172 GeV. The authors have corrected the measurement for the 34.1 MeV shift with respect to the Breit-Wigner fits. The error contains a contribution of ±3 MeV due to the uncertainty on the γZ interference.

⁵ ACKERSTAFF 97c obtain this using the S-matrix formalism for a combined fit to their cross-section and asymmetry data at the Z peak (AKERS 94) and their data at 130, 136, and 161 GeV. The authors have corrected the measurement for the 34 MeV shift with respect to the Breit-Wigner fits.

⁶ ACCIARRI 96B interpret the s-dependence of the cross sections and lepton forward-backward asymmetries in the framework of the S-matrix ansatz. The 130-136 GeV data constrains the γZ interference terms. As expected, this result is below the mass values obtained with a standard Breit-Wigner parametrization.

⁷ ALEXANDER 96x obtain this using the S-matrix formalism for a combined fit to their cross-section and asymmetry data at the Z peak (AKERS 94) and their data at 130 and 136 GeV. The authors have corrected the measurement for the 34 MeV shift with respect to the Breit-Wigner fits.

⁸ MIYABAYASHI 95 combine their low energy total hadronic cross-section measurement with the ACTON 930 data and perform a fit using an S-matrix formalism. As expected, this result is below the mass values obtained with the standard Breit-Wigner parametrization.

⁹ The second error of 6.3 MeV is due to a common LEP energy uncertainty.

¹⁰ Enters fit through W/Z mass ratio given in the W Particle Listings. The ALITTI 92b systematic error (±0.93) has two contributions: one (±0.92) cancels in m_W/m_Z and one (±0.12) is noncancelling. These were added in quadrature.

¹¹ ADACHI 90f use a Breit-Wigner resonance shape fit and combine their results with published data of PEP and PETRA.

¹² First error of ABE 89 is combination of statistical and systematic contributions; second is mass scale uncertainty.

¹³ ABRAMS 89b uncertainty includes 35 MeV due to the absolute energy measurement.

¹⁴ ALBAJAR 89 result is from a total sample of 33 Z → e⁺e⁻ events.

Z WIDTH

OUR FIT is obtained using the fit procedure and correlations as determined by the LEP Electroweak Working Group (see the "Note on the Z boson").

VALUE (GeV)	EVTS	DOCUMENT ID	TECN	COMMENT
2.4952 ± 0.0026 OUR FIT				
2.4876 ± 0.0041	4.08M	15 ABREU	00f DLPH	$E_{cm}^{ee} = 88-94$ GeV
2.5024 ± 0.0042	3.96M	16 ACCIARRI	00c L3	$E_{cm}^{ee} = 88-94$ GeV
2.4951 ± 0.0043	4.57M	17 BARATE	00c ALEP	$E_{cm}^{ee} = 88-94$ GeV
• • • We do not use the following data for averages, fits, limits, etc. • • •				
2.494 ± 0.010	1.2M	18 ACCIARRI	97k L3	$E_{cm}^{ee} = \text{LEP1} + 130-136$ GeV + 161-172 GeV
2.50 ± 0.21 ± 0.06		19 ABREU	96R DLPH	$E_{cm}^{ee} = 91.2$ GeV
2.492 ± 0.010	1.2M	20 ACCIARRI	96B L3	Repl. by ACCIARRI 97k
2.483 ± 0.011 ± 0.0045	1.16M	21 ABREU	94 DLPH	Repl. by ABREU 00f
2.494 ± 0.009 ± 0.0045	1.19M	21 ACCIARRI	94 L3	Repl. by ACCIARRI 00c
2.483 ± 0.011 ± 0.0045	1.33M	21 AKERS	94 OPAL	$E_{cm}^{ee} = 88-94$ GeV
2.501 ± 0.011 ± 0.0045	1.27M	21 BUSKULIC	94 ALEP	Repl. by BARATE 00c
3.8 ± 0.8 ± 1.0	188	ABE	89c CDF	$E_{cm}^{pp} = 1.8$ TeV
2.42 ± 0.45 ± 0.35	480	22 ABRAMS	89B MRK2	$E_{cm}^{ee} = 89-93$ GeV
2.7 ± 1.2 ± 1.0	24	23 ALBAJAR	89 UA1	$E_{cm}^{pp} = 546,630$ GeV
2.7 ± 2.0 ± 1.0	25	24 ANSARI	87 UA2	$E_{cm}^{pp} = 546,630$ GeV

- 15 The error includes 1.2 MeV due to LEP energy uncertainty.
- 16 The error includes 1.3 MeV due to LEP energy uncertainty.
- 17 BARATE 00c error includes approximately 3.8 MeV due to statistics, 0.9 MeV due to experimental systematics, and 1.3 MeV due to LEP energy uncertainty.
- 18 ACCIARRI 97k interpret the s-dependence of the cross sections and lepton forward-backward asymmetries in the framework of the S-matrix formalism with a combined fit to their cross section and asymmetry data at the Z peak (ACCIARRI 94) and their data at 130, 136, 161, and 172 GeV. The authors have corrected the measurement for the 0.9 MeV shift with respect to the Breit-Wigner fits.
- 19 ABREU 96R obtain this value from a study of the interference between initial and final state radiation in the process $e^+e^- \rightarrow Z \rightarrow \mu^+\mu^-$.
- 20 ACCIARRI 96B interpret the s-dependence of the cross sections and lepton forward-backward asymmetries in the framework of the S-matrix ansatz. The 130-136 GeV data constrains the γ Z interference terms. The fitted width is expected to be 0.9 MeV less than that obtained using the standard Breit-Wigner parametrization (see "Note on the Z Boson").
- 21 The second error of 4.5 MeV is due to a common LEP energy uncertainty.
- 22 ABRAMS 89B uncertainty includes 50 MeV due to the miniSAM background subtraction error.
- 23 ALBAJAR 89 result is from a total sample of 33 Z $\rightarrow e^+e^-$ events.
- 24 Quoted values of ANSARI 87 are from direct fit. Ratio of Z and W production gives either $\Gamma(Z) < (1.09 \pm 0.07) \times \Gamma(W)$, CL = 90% or $\Gamma(Z) = (0.82^{+0.19}_{-0.14} \pm 0.06) \times \Gamma(W)$. Assuming Standard-Model value $\Gamma(W) = 2.65$ GeV then gives $\Gamma(Z) < 2.89 \pm 0.19$ or $= 2.17^{+0.50}_{-0.37} \pm 0.16$.

Z DECAY MODES

Mode	Fraction (Γ_i/Γ)	Scale factor/ Confidence level
$\Gamma_1 e^+e^-$	(3.367 ± 0.005) %	
$\Gamma_2 \mu^+\mu^-$	(3.367 ± 0.008) %	
$\Gamma_3 \tau^+\tau^-$	(3.371 ± 0.009) %	
$\Gamma_4 \ell^+\ell^-$	[a] (3.3688 ± 0.0026) %	
Γ_5 invisible	(20.02 ± 0.06) %	
Γ_6 hadrons	(69.89 ± 0.07) %	
$\Gamma_7 (u\bar{u} + c\bar{c})/2$	(10.1 ± 1.1) %	
$\Gamma_8 (d\bar{d} + s\bar{s} + b\bar{b})/3$	(16.6 ± 0.6) %	
$\Gamma_9 c\bar{c}$	(11.68 ± 0.34) %	
$\Gamma_{10} b\bar{b}$	(15.13 ± 0.05) %	
$\Gamma_{11} b\bar{b}b\bar{b}$	(4.2 ± 1.6) × 10 ⁻⁴	
$\Gamma_{12} gg$	< 1.1 %	CL=95%
$\Gamma_{13} \pi^0\gamma$	< 5.2 × 10 ⁻⁵	CL=95%
$\Gamma_{14} \eta\gamma$	< 5.1 × 10 ⁻⁵	CL=95%
$\Gamma_{15} \omega\gamma$	< 6.5 × 10 ⁻⁴	CL=95%
$\Gamma_{16} \eta'(958)\gamma$	< 4.2 × 10 ⁻⁵	CL=95%
$\Gamma_{17} \gamma\gamma$	< 5.2 × 10 ⁻⁵	CL=95%
$\Gamma_{18} \gamma\gamma\gamma$	< 1.0 × 10 ⁻⁵	CL=95%
$\Gamma_{19} \pi^\pm W^\mp$	[b] < 7 × 10 ⁻⁵	CL=95%
$\Gamma_{20} \rho^\pm W^\mp$	[b] < 8.3 × 10 ⁻⁵	CL=95%
$\Gamma_{21} J/\psi(1S)X$	(3.51 ± 0.23 ± 0.25) × 10 ⁻³	S=1.1
$\Gamma_{22} \psi(2S)X$	(1.60 ± 0.29) × 10 ⁻³	
$\Gamma_{23} \chi_{c1}(1P)X$	(2.9 ± 0.7) × 10 ⁻³	

$\Gamma_{24} \chi_{c2}(1P)X$	< 3.2 × 10 ⁻³	CL=90%
$\Gamma_{25} \Upsilon(1S)X + \Upsilon(2S)X + \Upsilon(3S)X$	(1.0 ± 0.5) × 10 ⁻⁴	
$\Gamma_{26} \Upsilon(1S)X$	< 4.4 × 10 ⁻⁵	CL=95%
$\Gamma_{27} \Upsilon(2S)X$	< 1.39 × 10 ⁻⁴	CL=95%
$\Gamma_{28} \Upsilon(3S)X$	< 9.4 × 10 ⁻⁵	CL=95%
$\Gamma_{29} (D^0/\bar{D}^0)X$	(20.7 ± 2.0) %	
$\Gamma_{30} D^\pm X$	(12.2 ± 1.7) %	
$\Gamma_{31} D^*(2010)^\pm X$	[b] (11.4 ± 1.3) %	
$\Gamma_{32} B^+X$		
$\Gamma_{33} B^0X$		
$\Gamma_{34} B_s^0X$	seen	
$\Gamma_{35} B_c^+X$	searched for	
Γ_{36} anomalous γ + hadrons	[c] < 3.2 × 10 ⁻³	CL=95%
$\Gamma_{37} e^+e^-\gamma$	[c] < 5.2 × 10 ⁻⁴	CL=95%
$\Gamma_{38} \mu^+\mu^-\gamma$	[c] < 5.6 × 10 ⁻⁴	CL=95%
$\Gamma_{39} \tau^+\tau^-\gamma$	[c] < 7.3 × 10 ⁻⁴	CL=95%
$\Gamma_{40} \ell^+\ell^-\gamma\gamma$	[d] < 6.8 × 10 ⁻⁶	CL=95%
$\Gamma_{41} q\bar{q}\gamma\gamma$	[d] < 5.5 × 10 ⁻⁶	CL=95%
$\Gamma_{42} \nu\bar{\nu}\gamma\gamma$	[d] < 3.1 × 10 ⁻⁶	CL=95%
$\Gamma_{43} e^\pm\mu^\mp$	LF [b] < 1.7 × 10 ⁻⁶	CL=95%
$\Gamma_{44} e^\pm\tau^\mp$	LF [b] < 9.8 × 10 ⁻⁶	CL=95%
$\Gamma_{45} \mu^\pm\tau^\mp$	LF [b] < 1.2 × 10 ⁻⁵	CL=95%
$\Gamma_{46} p e$	L,B < 1.8 × 10 ⁻⁶	CL=95%
$\Gamma_{47} p \mu$	L,B < 1.8 × 10 ⁻⁶	CL=95%

- [a] ℓ indicates each type of lepton ($e, \mu,$ and τ), not sum over them.
- [b] The value is for the sum of the charge states or particle/antiparticle states indicated.
- [c] See the Particle Listings below for the γ energy range used in this measurement.
- [d] For $m_{\gamma\gamma} = (60 \pm 5)$ GeV.

Z PARTIAL WIDTHS

$\Gamma(e^+e^-)$ Γ_1
For the LEP experiments, this parameter is not directly used in the overall fit but is derived using the fit results; see the "Note on the Z Boson."

VALUE (MeV)	EVTS	DOCUMENT ID	TECN	COMMENT
84.015 ± 0.139 OUR FIT				
83.54 ± 0.27	117.8k	ABREU	00f DLPH	$E_{cm}^{ee} = 88-94$ GeV
84.16 ± 0.22	124.4k	ACCIARRI	00c L3	$E_{cm}^{ee} = 88-94$ GeV
83.88 ± 0.19		BARATE	00c ALEP	$E_{cm}^{ee} = 88-94$ GeV
82.89 ± 1.20 ± 0.89		25 ABE	95J SLD	$E_{cm}^{ee} = 91.31$ GeV
• • • We do not use the following data for averages, fits, limits, etc. • • •				
83.63 ± 0.53	42k	AKERS	94 OPAL	$E_{cm}^{ee} = 88-94$ GeV

25 ABE 95J obtain this measurement from Bhabha events in a restricted fiducial region to improve systematics. They use the values 91.187 and 2.489 GeV for the Z mass and total decay width to extract this partial width.

$\Gamma(\mu^+\mu^-)$ Γ_2
This parameter is not directly used in the overall fit but is derived using the fit results; see the "Note on the Z Boson."

VALUE (MeV)	EVTS	DOCUMENT ID	TECN	COMMENT
84.003 ± 0.210 OUR FIT				
84.48 ± 0.40	157.6k	ABREU	00f DLPH	$E_{cm}^{ee} = 88-94$ GeV
83.95 ± 0.44	113.4k	ACCIARRI	00c L3	$E_{cm}^{ee} = 88-94$ GeV
84.02 ± 0.28		BARATE	00c ALEP	$E_{cm}^{ee} = 88-94$ GeV
• • • We do not use the following data for averages, fits, limits, etc. • • •				
83.83 ± 0.65	57k	AKERS	94 OPAL	$E_{cm}^{ee} = 88-94$ GeV

$\Gamma(\tau^+\tau^-)$ Γ_3
This parameter is not directly used in the overall fit but is derived using the fit results; see the "Note on the Z Boson."

VALUE (MeV)	EVTS	DOCUMENT ID	TECN	COMMENT
84.113 ± 0.245 OUR FIT				
83.71 ± 0.58	104.0k	ABREU	00f DLPH	$E_{cm}^{ee} = 88-94$ GeV
84.23 ± 0.58	103.0k	ACCIARRI	00c L3	$E_{cm}^{ee} = 88-94$ GeV
84.38 ± 0.31		BARATE	00c ALEP	$E_{cm}^{ee} = 88-94$ GeV
• • • We do not use the following data for averages, fits, limits, etc. • • •				
82.90 ± 0.77	47k	AKERS	94 OPAL	$E_{cm}^{ee} = 88-94$ GeV

Gauge & Higgs Boson Particle Listings

Z

$\Gamma(\ell^+\ell^-)$ Γ_4

In our fit $\Gamma(\ell^+\ell^-)$ is defined as the partial Z width for the decay into a pair of massless charged leptons. This parameter is not directly used in the 5-parameter fit assuming lepton universality but is derived using the fit results. See the 'Note on the Z Boson.'

VALUE (MeV)	EVTS	DOCUMENT ID	TECN	COMMENT
84.057 ± 0.099 OUR FIT				
83.85 ± 0.17	379.4k	ABREU	00F DLPH	$E_{cm}^{ee} = 88-94$ GeV
84.14 ± 0.17	340.8k	ACCIARRI	00C L3	$E_{cm}^{ee} = 88-94$ GeV
84.02 ± 0.15	500k	BARATE	00C ALEP	$E_{cm}^{ee} = 88-94$ GeV
• • • We do not use the following data for averages, fits, limits, etc. • • •				
83.55 ± 0.44	146k	AKERS	94 OPAL	$E_{cm}^{ee} = 88-94$ GeV

• • • We do not use the following data for averages, fits, limits, etc. • • •

20.54 ± 0.14	45.6k	ABREU	94 DLPH	Repl. by ABREU 00F
21.02 ± 0.16	34k	ACCIARRI	94 L3	Repl. by ACCIARRI 00C
20.78 ± 0.11	57k	AKERS	94 OPAL	$E_{cm}^{ee} = 88-94$ GeV
20.83 ± 0.15	46.4k	BUSKULIC	94 ALEP	Repl. by BARATE 00C
18.9 +7.1 -5.3	13	32 ABRAMS	89D MRK2	$E_{cm}^{ee} = 89-93$ GeV

³¹BARATE 00C error includes approximately 0.053 due to statistics and 0.021 due to experimental systematics.

³²ABRAMS 89D have included both statistical and systematic uncertainties in their quoted errors.

$\Gamma(\text{invisible})$ Γ_5

We use only direct measurements of the invisible partial width using the single photon channel to obtain the average value quoted below. OUR FIT value is obtained as a difference between the total and the observed partial widths assuming lepton universality.

VALUE (MeV)	EVTS	DOCUMENT ID	TECN	COMMENT
499.4 ± 1.7 OUR FIT				
503 ± 16 OUR AVERAGE	Error includes scale factor of 1.2.			
498 ± 12 ± 12	1791	ACCIARRI	98G L3	$E_{cm}^{ee} = 88-94$ GeV
539 ± 26 ± 17	410	AKERS	95C OPAL	$E_{cm}^{ee} = 88-94$ GeV
450 ± 34 ± 34	258	BUSKULIC	93L ALEP	$E_{cm}^{ee} = 88-94$ GeV
540 ± 80 ± 40	52	ADEVA	92 L3	$E_{cm}^{ee} = 88-94$ GeV
• • • We do not use the following data for averages, fits, limits, etc. • • •				
498.1 ± 3.2	26	ABREU	00F DLPH	$E_{cm}^{ee} = 88-94$ GeV
499.1 ± 2.9	26	ACCIARRI	00C L3	$E_{cm}^{ee} = 88-94$ GeV
499.1 ± 2.5	26	BARATE	00C ALEP	$E_{cm}^{ee} = 88-94$ GeV
490.3 ± 7.3	26	AKERS	94 OPAL	$E_{cm}^{ee} = 88-94$ GeV
524 ± 40 ± 20	172	27 ADRIANI	92E L3	Repl. by ACCIARRI 98G

²⁶This is an indirect determination of $\Gamma(\text{invisible})$ from a fit to the visible Z decay modes.
²⁷ADRIANI 92E improves but does not supersede ADEVA 92, obtained with 1990 data only.

$\Gamma(\text{hadrons})$ Γ_6

This parameter is not directly used in the 5-parameter fit assuming lepton universality, but is derived using the fit results. See the 'Note on the Z Boson.'

VALUE (MeV)	EVTS	DOCUMENT ID	TECN	COMMENT
1743.8 ± 2.2 OUR FIT				
1738.1 ± 4.0	3.70M	ABREU	00F DLPH	$E_{cm}^{ee} = 88-94$ GeV
1751.1 ± 3.8	3.54M	ACCIARRI	00C L3	$E_{cm}^{ee} = 88-94$ GeV
1744.0 ± 3.4	4.07M	BARATE	00C ALEP	$E_{cm}^{ee} = 88-94$ GeV
• • • We do not use the following data for averages, fits, limits, etc. • • •				
1741 ± 10	1.19M	28 AKERS	94 OPAL	$E_{cm}^{ee} = 88-94$ GeV

²⁸AKERS 94 assumes lepton universality. Without this assumption, it becomes 1742 ± 11 MeV.

Z BRANCHING RATIOS

OUR FIT is obtained using the fit procedure and correlations as determined by the LEP Electroweak Working Group (see the "Note on the Z boson").

$\Gamma(\text{hadrons})/\Gamma(e^+e^-)$ Γ_6/Γ_1

VALUE	EVTS	DOCUMENT ID	TECN	COMMENT
20.766 ± 0.056 OUR FIT				
20.88 ± 0.12	117.8k	ABREU	00F DLPH	$E_{cm}^{ee} = 88-94$ GeV
20.816 ± 0.089	124.4k	ACCIARRI	00C L3	$E_{cm}^{ee} = 88-94$ GeV
20.677 ± 0.075		29 BARATE	00C ALEP	$E_{cm}^{ee} = 88-94$ GeV
• • • We do not use the following data for averages, fits, limits, etc. • • •				
20.74 ± 0.18	31.4k	ABREU	94 DLPH	Repl. by ABREU 00F
20.96 ± 0.15	38k	ACCIARRI	94 L3	Repl. by ACCIARRI 00C
20.83 ± 0.16	42k	AKERS	94 OPAL	$E_{cm}^{ee} = 88-94$ GeV
20.59 ± 0.15	45.8k	BUSKULIC	94 ALEP	Repl. by BARATE 00C
27.0 +11.7 -8.8	12	30 ABRAMS	89D MRK2	$E_{cm}^{ee} = 89-93$ GeV

²⁹BARATE 00C error includes approximately 0.062 due to statistics, 0.033 due to experimental systematics, and 0.026 due to the theoretical uncertainty in t-channel prediction.

³⁰ABRAMS 89D have included both statistical and systematic uncertainties in their quoted errors.

$\Gamma(\text{hadrons})/\Gamma(\mu^+\mu^-)$ Γ_6/Γ_2

OUR FIT is obtained using the fit procedure and correlations as determined by the LEP Electroweak Working Group (see the "Note on the Z boson").

VALUE	EVTS	DOCUMENT ID	TECN	COMMENT
20.769 ± 0.041 OUR FIT				
20.65 ± 0.08	157.6k	ABREU	00F DLPH	$E_{cm}^{ee} = 88-94$ GeV
20.861 ± 0.097	113.4k	ACCIARRI	00C L3	$E_{cm}^{ee} = 88-94$ GeV
20.799 ± 0.056		31 BARATE	00C ALEP	$E_{cm}^{ee} = 88-94$ GeV

$\Gamma(\text{hadrons})/\Gamma(\tau^+\tau^-)$ Γ_6/Γ_3

OUR FIT is obtained using the fit procedure and correlations as determined by the LEP Electroweak Working Group (see the "Note on the Z boson").

VALUE	EVTS	DOCUMENT ID	TECN	COMMENT
20.742 ± 0.051 OUR FIT				
20.84 ± 0.13	104.0k	ABREU	00F DLPH	$E_{cm}^{ee} = 88-94$ GeV
20.792 ± 0.133	103.0k	ACCIARRI	00C L3	$E_{cm}^{ee} = 88-94$ GeV
20.707 ± 0.062		33 BARATE	00C ALEP	$E_{cm}^{ee} = 88-94$ GeV
• • • We do not use the following data for averages, fits, limits, etc. • • •				
20.68 ± 0.18	25k	ABREU	94 DLPH	Repl. by ABREU 00F
20.80 ± 0.20	25k	ACCIARRI	94 L3	Repl. by ACCIARRI 00C
21.01 ± 0.15	47k	AKERS	94 OPAL	$E_{cm}^{ee} = 88-94$ GeV
20.70 ± 0.16	45.1k	BUSKULIC	94 ALEP	Repl. by BARATE 00C
15.2 +4.8 -3.9	21	34 ABRAMS	89D MRK2	$E_{cm}^{ee} = 89-93$ GeV

³³BARATE 00C error includes approximately 0.054 due to statistics and 0.033 due to experimental systematics.

³⁴ABRAMS 89D have included both statistical and systematic uncertainties in their quoted errors.

$\Gamma(\text{hadrons})/\Gamma(\ell^+\ell^-)$ Γ_6/Γ_4

ℓ indicates each type of lepton (e, μ , and τ), not sum over them.

Our fit result is obtained requiring lepton universality.

VALUE	EVTS	DOCUMENT ID	TECN	COMMENT
20.744 ± 0.029 OUR FIT				
20.730 ± 0.060	379.4k	ABREU	00F DLPH	$E_{cm}^{ee} = 88-94$ GeV
20.810 ± 0.060	340.8k	ACCIARRI	00C L3	$E_{cm}^{ee} = 88-94$ GeV
20.725 ± 0.039	500k	35 BARATE	00C ALEP	$E_{cm}^{ee} = 88-94$ GeV
• • • We do not use the following data for averages, fits, limits, etc. • • •				
20.62 ± 0.10	102k	ABREU	94 DLPH	Repl. by ABREU 00F
20.93 ± 0.10	97k	ACCIARRI	94 L3	Repl. by ACCIARRI 00C
20.835 ± 0.086	146k	AKERS	94 OPAL	$E_{cm}^{ee} = 88-94$ GeV
20.69 ± 0.09	137.3k	BUSKULIC	94 ALEP	Repl. by BARATE 00C
18.9 +3.6 -3.2	46	ABRAMS	89B MRK2	$E_{cm}^{ee} = 89-93$ GeV

³⁵BARATE 00C error includes approximately 0.033 due to statistics, 0.020 due to experimental systematics, and 0.005 due to the theoretical uncertainty in t-channel prediction.

$\Gamma(\text{hadrons})/\Gamma_{\text{total}}$ Γ_6/Γ

This parameter is not directly used in the overall fit but is derived using the fit results; see the 'Note on the Z Boson.'

VALUE (%)	EVTS	DOCUMENT ID	TECN	COMMENT
69.886 ± 0.065 OUR FIT				
69.83 ± 0.23	1.14M	BUSKULIC	94 ALEP	$E_{cm}^{ee} = 88-94$ GeV

$\Gamma(e^+e^-)/\Gamma_{\text{total}}$ Γ_1/Γ

This parameter is not directly used in the overall fit but is derived using the fit results; see the 'Note on the Z Boson.'

VALUE (%)	EVTS	DOCUMENT ID	TECN	COMMENT
3.3671 ± 0.0047 OUR FIT				
3.383 ± 0.013	45.8k	BUSKULIC	94 ALEP	$E_{cm}^{ee} = 88-94$ GeV

$\Gamma(\mu^+\mu^-)/\Gamma_{\text{total}}$ Γ_2/Γ

This parameter is not directly used in the overall fit but is derived using the fit results; see the 'Note on the Z Boson.'

VALUE (%)	EVTS	DOCUMENT ID	TECN	COMMENT
3.3666 ± 0.0079 OUR FIT				
3.344 ± 0.026	46.4k	BUSKULIC	94 ALEP	$E_{cm}^{ee} = 88-94$ GeV

$\Gamma(\tau^+\tau^-)/\Gamma_{\text{total}}$ Γ_3/Γ

This parameter is not directly used in the overall fit but is derived using the fit results; see the 'Note on the Z Boson.'

VALUE (%)	EVTS	DOCUMENT ID	TECN	COMMENT
3.3710 ± 0.0094 OUR FIT				
3.366 ± 0.028	45.1k	BUSKULIC	94 ALEP	$E_{cm}^{ee} = 88-94$ GeV

$\Gamma(\ell^+ \ell^-)/\Gamma_{total}$ Γ_4/Γ
 ℓ indicates each type of lepton ($e, \mu,$ and τ), not sum over them.
 Our fit result assumes lepton universality.

This parameter is not directly used in the overall fit but is derived using the fit results; see the 'Note on the Z Boson.'

VALUE (%)	EVTS	DOCUMENT ID	TECN	COMMENT
3.3688 ± 0.0026 OUR FIT				
• • •	• • •	• • •	• • •	• • •
3.375 ± 0.009	137.3k	BUSKULIC	94 ALEP	$E_{cm}^{ee} = 88-94$ GeV

$\Gamma(invisible)/\Gamma_{total}$ Γ_5/Γ
 See the data, the note, and the fit result for the partial width, Γ_5 , above.

VALUE (%)	DOCUMENT ID
20.016 ± 0.063 OUR FIT	

$\Gamma(\mu^+ \mu^-)/\Gamma(\ell^+ \ell^-)$ Γ_2/Γ_1
 This parameter is not directly used in the overall fit but is derived using the fit results; see the 'Note on the Z Boson.'

$\Gamma(\tau^+ \tau^-)/\Gamma(\ell^+ \ell^-)$ Γ_3/Γ_1
 This parameter is not directly used in the overall fit but is derived using the fit results; see the 'Note on the Z Boson.'

$\Gamma((u\bar{u} + c\bar{c})/2)/\Gamma(hadrons)$ Γ_7/Γ_6
 This quantity is the branching ratio of $Z \rightarrow$ "up-type" quarks to $Z \rightarrow$ hadrons. Except ACKERSTAFF 97T the values of $Z \rightarrow$ "up-type" and $Z \rightarrow$ "down-type" branchings are extracted from measurements of $\Gamma(hadrons)$, and $\Gamma(Z \rightarrow \gamma + jets)$ where γ is a high-energy (>5 GeV) isolated photon. As the experiments use different procedures and slightly different values of M_Z , $\Gamma(hadrons)$ and α_s in their extraction procedures, our average has to be taken with caution.

VALUE	DOCUMENT ID	TECN	COMMENT
0.145 ± 0.015 OUR AVERAGE			
0.160 ± 0.019 ± 0.019	36	ACKERSTAFF 97T OPAL	$E_{cm}^{ee} = 88-94$ GeV
0.137 ^{+0.038} _{-0.054}	37	ABREU 95x DLPH	$E_{cm}^{ee} = 88-94$ GeV
0.139 ± 0.026	38	ACTON 93f OPAL	$E_{cm}^{ee} = 88-94$ GeV
0.137 ± 0.033	39	ADRIANI 93 L3	$E_{cm}^{ee} = 91.2$ GeV
<p>36 ACKERSTAFF 97T measure $\Gamma_{u\bar{u}}/(\Gamma_{d\bar{d}} + \Gamma_{u\bar{u}} + \Gamma_{s\bar{s}}) = 0.258 \pm 0.031 \pm 0.032$. To obtain this branching ratio authors use $R_c + R_b = 0.380 \pm 0.010$. This measurement is fully negatively correlated with the measurement of $\Gamma_{d\bar{d}, s\bar{s}}/(\Gamma_{d\bar{d}} + \Gamma_{u\bar{u}} + \Gamma_{s\bar{s}})$ given in the next data block.</p> <p>37 ABREU 95x use $M_Z = 91.187 \pm 0.009$ GeV, $\Gamma(hadrons) = 1725 \pm 12$ MeV and $\alpha_s = 0.123 \pm 0.005$. To obtain this branching ratio we divide their value of $C_{2/3} = 0.91 \pm^{+0.25}_{-0.36}$ by their value of $(3C_{1/3} + 2C_{2/3}) = 6.66 \pm 0.05$.</p> <p>38 ACTON 93f use the LEP 92 value of $\Gamma(hadrons) = 1740 \pm 12$ MeV and $\alpha_s = 0.122 \pm^{+0.006}_{-0.005}$.</p> <p>39 ADRIANI 93 use $M_Z = 91.181 \pm 0.022$ GeV, $\Gamma(hadrons) = 1742 \pm 19$ MeV and $\alpha_s = 0.125 \pm 0.009$. To obtain this branching ratio we divide their value of $C_{2/3} = 0.92 \pm^{+0.22}_{-0.22}$ by their value of $(3C_{1/3} + 2C_{2/3}) = 6.720 \pm 0.076$.</p>			

$\Gamma((d\bar{d} + s\bar{s} + b\bar{b})/3)/\Gamma(hadrons)$ Γ_8/Γ_6
 This quantity is the branching ratio of $Z \rightarrow$ "down-type" quarks to $Z \rightarrow$ hadrons. Except ACKERSTAFF 97T the values of $Z \rightarrow$ "up-type" and $Z \rightarrow$ "down-type" branchings are extracted from measurements of $\Gamma(hadrons)$, and $\Gamma(Z \rightarrow \gamma + jets)$ where γ is a high-energy (>5 GeV) isolated photon. As the experiments use different procedures and slightly different values of M_Z , $\Gamma(hadrons)$ and α_s in their extraction procedures, our average has to be taken with caution.

VALUE	DOCUMENT ID	TECN	COMMENT
0.237 ± 0.009 OUR AVERAGE			
0.230 ± 0.010 ± 0.010	40	ACKERSTAFF 97T OPAL	$E_{cm}^{ee} = 88-94$ GeV
0.243 ^{+0.036} _{-0.026}	41	ABREU 95x DLPH	$E_{cm}^{ee} = 88-94$ GeV
0.241 ± 0.017	42	ACTON 93f OPAL	$E_{cm}^{ee} = 88-94$ GeV
0.243 ± 0.022	43	ADRIANI 93 L3	$E_{cm}^{ee} = 91.2$ GeV
<p>40 ACKERSTAFF 97T measure $\Gamma_{d\bar{d}, s\bar{s}}/(\Gamma_{d\bar{d}} + \Gamma_{u\bar{u}} + \Gamma_{s\bar{s}}) = 0.371 \pm 0.016 \pm 0.016$. To obtain this branching ratio authors use $R_c + R_b = 0.380 \pm 0.010$. This measurement is fully negatively correlated with the measurement of $\Gamma_{u\bar{u}}/(\Gamma_{d\bar{d}} + \Gamma_{u\bar{u}} + \Gamma_{s\bar{s}})$ presented in the previous data block.</p> <p>41 ABREU 95x use $M_Z = 91.187 \pm 0.009$ GeV, $\Gamma(hadrons) = 1725 \pm 12$ MeV and $\alpha_s = 0.123 \pm 0.005$. To obtain this branching ratio we divide their value of $C_{1/3} = 1.62 \pm^{+0.24}_{-0.17}$ by their value of $(3C_{1/3} + 2C_{2/3}) = 6.66 \pm 0.05$.</p> <p>42 ACTON 93f use the LEP 92 value of $\Gamma(hadrons) = 1740 \pm 12$ MeV and $\alpha_s = 0.122 \pm^{+0.006}_{-0.005}$.</p> <p>43 ADRIANI 93 use $M_Z = 91.181 \pm 0.022$ GeV, $\Gamma(hadrons) = 1742 \pm 19$ MeV and $\alpha_s = 0.125 \pm 0.009$. To obtain this branching ratio we divide their value of $C_{1/3} = 1.63 \pm 0.15$ by their value of $(3C_{1/3} + 2C_{2/3}) = 6.720 \pm 0.076$.</p>			

$R_c = \Gamma(c\bar{c})/\Gamma(hadrons)$ Γ_9/Γ_6
 OUR FIT is obtained by a simultaneous fit to several c - and b -quark measurements as explained in the "Note on the Z boson." As a cross check we have also performed a weighted average of the R_c measurements taking into account the various common systematic errors. Assuming that the smallest common systematic error is fully correlated, we obtain $R_c = 0.1683 \pm 0.0049$.

Because of the high current interest, we mention the following preliminary results here, but do not average them or include them in the Listings or Tables. Combining published and unpublished preliminary LEP and SLD electroweak results (as of March 2000) yields $R_c = 0.1674 \pm 0.0038$. The Standard Model predicts $R_c = 0.1723$ for $m_t = 174.3$ GeV and $M_H = 150$ GeV.

VALUE	DOCUMENT ID	TECN	COMMENT
0.1671 ± 0.0048 OUR FIT			
0.1665 ± 0.0051 ± 0.0081	44	ABREU 00 DLPH	$E_{cm}^{ee} = 88-94$ GeV
0.1698 ± 0.0069	45	BARATE 00b ALEP	$E_{cm}^{ee} = 88-94$ GeV
0.180 ± 0.011 ± 0.013	46	ACKERSTAFF 98E OPAL	$E_{cm}^{ee} = 88-94$ GeV
0.167 ± 0.011 ± 0.012	47	ALEXANDER 96R OPAL	$E_{cm}^{ee} = 88-94$ GeV
• • •	• • •	• • •	• • •
0.1675 ± 0.0062 ± 0.0103	48	BARATE 98T ALEP	Repl. by BARATE 00b
0.1689 ± 0.0095 ± 0.0068	49	BARATE 98T ALEP	Repl. by BARATE 00b
0.1623 ± 0.0085 ± 0.0209	50	ABREU 95D DLPH	$E_{cm}^{ee} = 88-94$ GeV
0.142 ± 0.008 ± 0.014	51	AKERS 95O OPAL	Repl. by ACKERSTAFF 98E
0.165 ± 0.005 ± 0.020	52	BUSKULIC 94G ALEP	Repl. by BARATE 00b

44 ABREU 00 obtain this result properly combining the measurement from the D^{*+} production rate ($R_c = 0.1610 \pm 0.0104 \pm 0.0077 \pm 0.0043$ (BR)) with that from the overall charm counting ($R_c = 0.1692 \pm 0.0047 \pm 0.0063 \pm 0.0074$ (BR)) in $c\bar{c}$ events. The systematic error includes an uncertainty of ± 0.0054 due to the uncertainty on the charmed hadron branching fractions.

45 BARATE 00b use exclusive decay modes to independently determine the quantities $R_c \times f(c \rightarrow X)$, $X = D^0, D^+, D_s^+$, and A_c . Estimating $R_c \times f(c \rightarrow \Xi_c / \Omega_c) = 0.0034$, they simply sum over all the charm decays to obtain $R_c = 0.1738 \pm 0.0047 \pm 0.0088 \pm 0.0075$ (BR). This is combined with all previous ALEPH measurements (BARATE 98T and BUSKULIC 94G, $R_c = 0.1681 \pm 0.0054 \pm 0.0062$) to obtain the quoted value.

46 ACKERSTAFF 98E use an inclusive/exclusive double tag. In one jet D^{*+} mesons are exclusively reconstructed in several decay channels and in the opposite jet a slow pion (opposite charge inclusive D^{*+}) tag is used. The b content of this sample is measured by the simultaneous detection of a lepton in one jet and an inclusively reconstructed D^{*+} meson in the opposite jet. The systematic error includes an uncertainty of ± 0.006 due to the external branching ratios.

47 ALEXANDER 96R obtain this value via direct charm counting, summing the partial contributions from D^0, D^+, D_s^+ , and A_c^+ , and assuming that strange-charmed baryons account for the 15% of the A_c^+ production. An uncertainty of ± 0.005 due to the uncertainties in the charm hadron branching ratios is included in the overall systematics.

48 BARATE 98T perform a simultaneous fit to the p and p_T spectra of electrons from hadronic Z decays. The semileptonic branching ratio $B(c \rightarrow e)$ is taken as 0.098 ± 0.005 and the systematic error includes an uncertainty of ± 0.0084 due to this.

49 BARATE 98T obtain this result combining two double-tagging techniques. Searching for a D meson in each hemisphere by full reconstruction in an exclusive decay mode gives $R_c = 0.173 \pm 0.014 \pm 0.0009$. The same tag in combination with inclusive identification using the slow pion from the $D^{*+} \rightarrow D^0 \pi^+$ decay in the opposite hemisphere yields $R_c = 0.166 \pm 0.012 \pm 0.009$. The R_D dependence is given by $R_c = 0.1689 - 0.023 \times (R_D - 0.2159)$. The three measurements of BARATE 98T are combined with BUSKULIC 94G to give the average $R_c = 0.1681 \pm 0.0054 \pm 0.0062$.

50 ABREU 95D perform a maximum likelihood fit to the combined p and p_T distributions of single and dilepton samples. The second error includes an uncertainty of ± 0.0124 due to models and branching ratios.

51 AKERS 95O use the presence of a D^{*+} to tag $Z \rightarrow c\bar{c}$ with $D^{*+} \rightarrow D^0 \pi^+$ and $D^0 \rightarrow K \pi$. They measure $P_c \times f(c\bar{c})/\Gamma(hadrons)$ to be $(1.006 \pm 0.055 \pm 0.061) \times 10^{-3}$, where P_c is the product branching ratio $B(c \rightarrow D^*)B(D^* \rightarrow D^0 \pi)B(D^0 \rightarrow K \pi)$. Assuming that P_c remains unchanged with energy, they use its value $(7.1 \pm 0.5) \times 10^{-3}$ determined at CESR/PETRA to obtain $\Gamma(c\bar{c})/\Gamma(hadrons)$. The second error of AKERS 95O includes an uncertainty of ± 0.011 from the uncertainty on P_c .

52 BUSKULIC 94G perform a simultaneous fit to the p and p_T spectra of both single and dilepton events.

$R_b = \Gamma(b\bar{b})/\Gamma(hadrons)$ Γ_{10}/Γ_6
 OUR FIT is obtained by a simultaneous fit to several c - and b -quark measurements as explained in the "Note on the Z boson." As a cross check we have also performed a weighted average of the R_b measurements taking into account the various common systematic errors. We have assumed that the smallest common systematic error is fully correlated. For $R_c = 0.1671$ (as given by OUR FIT above), we obtain $R_b = 0.21653 \pm 0.00070$. For an expected Standard Model value of $R_c = 0.1723$, our weighted average gives $R_b = 0.21631 \pm 0.00070$.

Because of the high current interest, we mention the following preliminary results here, but do not average them or include them in the Listings or Tables. Combining published and unpublished preliminary LEP and SLD electroweak results (as of March 2000) yields $R_b = 0.21642 \pm 0.00073$. The Standard Model predicts $R_b = 0.21581$ for $m_t = 174.3$ GeV and $M_H = 150$ GeV.

VALUE	EVTS	DOCUMENT ID	TECN	COMMENT
0.21644 ± 0.00075 OUR FIT				
0.2174 ± 0.0015 ± 0.0028	53	ACCIARRI 00 L3	$E_{cm}^{ee} = 89-93$ GeV	
0.2178 ± 0.0011 ± 0.0013	54	ABBIENDI 99b OPAL	$E_{cm}^{ee} = 88-94$ GeV	
0.21634 ± 0.00067 ± 0.00060	55	ABREU 99b DLPH	$E_{cm}^{ee} = 88-94$ GeV	
0.2142 ± 0.0034 ± 0.0015	56	ABE 98D SLD	$E_{cm}^{ee} = 91.2$ GeV	
0.2159 ± 0.0009 ± 0.0011	57	BARATE 97F ALEP	$E_{cm}^{ee} = 88-94$ GeV	

Gauge & Higgs Boson Particle Listings

Z

$\Gamma(e^\pm\tau^\mp)/\Gamma_{total}$ Γ_{44}/Γ
 Test of lepton family number conservation. The value is for the sum of the charge states indicated.

VALUE	CL%	DOCUMENT ID	TECN	COMMENT
$<2.2 \times 10^{-5}$	95	ABREU	97c DLPH	$E_{cm}^{95} = 88-94$ GeV
$<9.8 \times 10^{-6}$	95	AKERS	95w OPAL	$E_{cm}^{95} = 88-94$ GeV
$<1.3 \times 10^{-5}$	95	ADRIANI	93i L3	$E_{cm}^{95} = 88-94$ GeV
$<1.2 \times 10^{-4}$	95	DECAMP	92 ALEP	$E_{cm}^{95} = 88-94$ GeV

$\Gamma(\mu^\pm\tau^\mp)/\Gamma_{total}$ Γ_{45}/Γ
 Test of lepton family number conservation. The value is for the sum of the charge states indicated.

VALUE	CL%	DOCUMENT ID	TECN	COMMENT
$<1.2 \times 10^{-5}$	95	ABREU	97c DLPH	$E_{cm}^{95} = 88-94$ GeV
$<1.7 \times 10^{-5}$	95	AKERS	95w OPAL	$E_{cm}^{95} = 88-94$ GeV
$<1.9 \times 10^{-5}$	95	ADRIANI	93i L3	$E_{cm}^{95} = 88-94$ GeV
$<1.0 \times 10^{-4}$	95	DECAMP	92 ALEP	$E_{cm}^{95} = 88-94$ GeV

$\Gamma(pe)/\Gamma_{total}$ Γ_{46}/Γ
 Test of baryon number and lepton number conservations. Charge conjugate states are implied.

VALUE	CL%	DOCUMENT ID	TECN	COMMENT
$<1.8 \times 10^{-6}$	95	105 ABBIENDI	99i OPAL	$E_{cm}^{99} = 88-94$ GeV

105 ABBIENDI 99i give the 95%CL limit on the partial width $\Gamma(Z^0 \rightarrow pe) < 4.6$ KeV and we have transformed it into a branching ratio.

$\Gamma(p\mu)/\Gamma_{total}$ Γ_{47}/Γ
 Test of baryon number and lepton number conservations. Charge conjugate states are implied.

VALUE	CL%	DOCUMENT ID	TECN	COMMENT
$<1.8 \times 10^{-6}$	95	106 ABBIENDI	99i OPAL	$E_{cm}^{99} = 88-94$ GeV

106 ABBIENDI 99i give the 95%CL limit on the partial width $\Gamma(Z^0 \rightarrow p\mu) < 4.4$ KeV and we have transformed it into a branching ratio.

AVERAGE PARTICLE MULTIPLICITIES IN HADRONIC Z DECAY

Summed over particle and antiparticle, when appropriate.

$\langle N_\gamma \rangle$

VALUE	DOCUMENT ID	TECN	COMMENT
$20.97 \pm 0.02 \pm 1.15$	ACKERSTAFF	98A OPAL	$E_{cm}^{98} = 91.2$ GeV

$\langle N_{\pi^\pm} \rangle$

VALUE	DOCUMENT ID	TECN	COMMENT
16.99 ± 0.20 OUR AVERAGE			
16.84 ± 0.37	ABE	99E SLD	$E_{cm}^{99} = 91.2$ GeV
$17.26 \pm 0.10 \pm 0.88$	ABREU	98L DLPH	$E_{cm}^{98} = 91.2$ GeV
17.04 ± 0.31	BARATE	98v ALEP	$E_{cm}^{98} = 91.2$ GeV
17.05 ± 0.43	AKERS	94P OPAL	$E_{cm}^{94} = 91.2$ GeV

$\langle N_{\pi^0} \rangle$

VALUE	DOCUMENT ID	TECN	COMMENT
9.76 ± 0.26 OUR AVERAGE			
$9.55 \pm 0.06 \pm 0.75$	ACKERSTAFF	98A OPAL	$E_{cm}^{98} = 91.2$ GeV
$9.63 \pm 0.13 \pm 0.63$	BARATE	97J ALEP	$E_{cm}^{97} = 91.2$ GeV
$9.90 \pm 0.02 \pm 0.33$	ACCIARRI	96 L3	$E_{cm}^{96} = 91.2$ GeV
$9.2 \pm 0.2 \pm 1.0$	ADAM	96 DLPH	$E_{cm}^{96} = 91.2$ GeV
• • • We do not use the following data for averages, fits, limits, etc. • • •			
$9.18 \pm 0.03 \pm 0.73$	ACCIARRI	94B L3	Repl. by ACCIARRI 96

$\langle N_\eta \rangle$

VALUE	DOCUMENT ID	TECN	COMMENT
0.95 ± 0.07 OUR AVERAGE			
$0.97 \pm 0.03 \pm 0.11$	ACKERSTAFF	98A OPAL	$E_{cm}^{98} = 91.2$ GeV
$0.93 \pm 0.01 \pm 0.09$	ACCIARRI	96 L3	$E_{cm}^{96} = 91.2$ GeV
• • • We do not use the following data for averages, fits, limits, etc. • • •			
$0.91 \pm 0.02 \pm 0.11$	ACCIARRI	94B L3	Repl. by ACCIARRI 96

$\langle N_{\rho^\pm} \rangle$

VALUE	DOCUMENT ID	TECN	COMMENT
$2.40 \pm 0.06 \pm 0.43$	ACKERSTAFF	98A OPAL	$E_{cm}^{98} = 91.2$ GeV

$\langle N_{\rho^0} \rangle$

VALUE	DOCUMENT ID	TECN	COMMENT
1.24 ± 0.10 OUR AVERAGE			Error includes scale factor of 1.1.
1.19 ± 0.10	ABREU	99J DLPH	$E_{cm}^{99} = 91.2$ GeV
$1.45 \pm 0.06 \pm 0.20$	BUSKULIC	96H ALEP	$E_{cm}^{96} = 91.2$ GeV
• • • We do not use the following data for averages, fits, limits, etc. • • •			
$1.21 \pm 0.04 \pm 0.15$	ABREU	95L DLPH	Repl. by ABREU 99J

$\langle N_w \rangle$

VALUE	DOCUMENT ID	TECN	COMMENT
1.08 ± 0.09 OUR AVERAGE			
$1.04 \pm 0.04 \pm 0.14$	ACKERSTAFF	98A OPAL	$E_{cm}^{98} = 91.2$ GeV
$1.17 \pm 0.09 \pm 0.15$	ACCIARRI	97D L3	$E_{cm}^{97} = 91.2$ GeV
$1.07 \pm 0.06 \pm 0.13$	BUSKULIC	96H ALEP	$E_{cm}^{96} = 91.2$ GeV

$\langle N_\eta' \rangle$

VALUE	DOCUMENT ID	TECN	COMMENT
0.17 ± 0.05 OUR AVERAGE			Error includes scale factor of 2.4.
$0.14 \pm 0.01 \pm 0.02$	ACKERSTAFF	98A OPAL	$E_{cm}^{98} = 91.2$ GeV
0.25 ± 0.04	107 ACCIARRI	97D L3	$E_{cm}^{97} = 91.2$ GeV
• • • We do not use the following data for averages, fits, limits, etc. • • •			
$0.068 \pm 0.018 \pm 0.016$	108 BUSKULIC	92D ALEP	$E_{cm}^{92} = 91.2$ GeV
107 ACCIARRI 97D obtain this value averaging over the two decay channels $\eta' \rightarrow \pi^+\pi^-\eta$ and $\eta' \rightarrow \rho^0\gamma$.			
108 BUSKULIC 92D obtain this value for $x > 0.1$.			

$\langle N_{\eta(980)} \rangle$

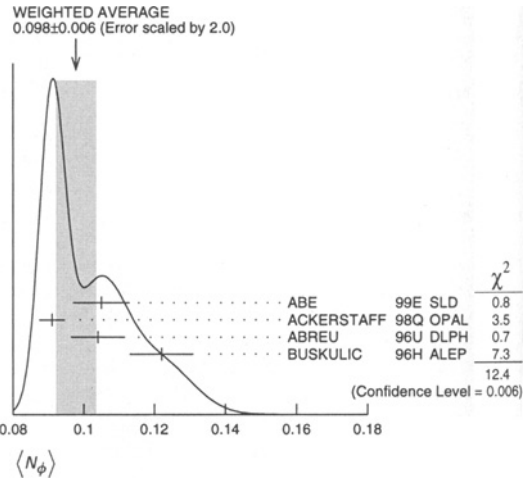
VALUE	DOCUMENT ID	TECN	COMMENT
0.147 ± 0.011 OUR AVERAGE			
0.164 ± 0.021	ABREU	99J DLPH	$E_{cm}^{99} = 91.2$ GeV
$0.141 \pm 0.007 \pm 0.011$	ACKERSTAFF	98Q OPAL	$E_{cm}^{98} = 91.2$ GeV

$\langle N_{\eta(980)^\pm} \rangle$

VALUE	DOCUMENT ID	TECN	COMMENT
$0.27 \pm 0.04 \pm 0.10$	ACKERSTAFF	98A OPAL	$E_{cm}^{98} = 91.2$ GeV

$\langle N_\phi \rangle$

VALUE	DOCUMENT ID	TECN	COMMENT
0.098 ± 0.006 OUR AVERAGE			Error includes scale factor of 2.0. See the ideogram below.
0.105 ± 0.008	ABE	99E SLD	$E_{cm}^{99} = 91.2$ GeV
$0.091 \pm 0.002 \pm 0.003$	ACKERSTAFF	98Q OPAL	$E_{cm}^{98} = 91.2$ GeV
$0.104 \pm 0.003 \pm 0.007$	ABREU	96U DLPH	$E_{cm}^{96} = 91.2$ GeV
$0.122 \pm 0.004 \pm 0.008$	BUSKULIC	96H ALEP	$E_{cm}^{96} = 91.2$ GeV
• • • We do not use the following data for averages, fits, limits, etc. • • •			
$0.100 \pm 0.004 \pm 0.007$	AKERS	95x OPAL	Repl. by ACKERSTAFF 98q



$\langle N_{K(1270)} \rangle$

VALUE	DOCUMENT ID	TECN	COMMENT
0.169 ± 0.025 OUR AVERAGE			Error includes scale factor of 1.4.
0.214 ± 0.038	ABREU	99J DLPH	$E_{cm}^{99} = 91.2$ GeV
$0.155 \pm 0.011 \pm 0.018$	ACKERSTAFF	98Q OPAL	$E_{cm}^{98} = 91.2$ GeV

$\langle N_{K^*(1525)} \rangle$

VALUE	DOCUMENT ID	TECN	COMMENT
0.012 ± 0.006	ABREU	99J DLPH	$E_{cm}^{99} = 91.2$ GeV
• • • We do not use the following data for averages, fits, limits, etc. • • •			
$0.020 \pm 0.005 \pm 0.006$	ABREU	96C DLPH	Repl. by ABREU 99J

$\langle N_{K^\pm} \rangle$

VALUE	DOCUMENT ID	TECN	COMMENT
2.25 ± 0.05 OUR AVERAGE			
2.22 ± 0.16	ABE	99E SLD	$E_{cm}^{99} = 91.2$ GeV
$2.21 \pm 0.05 \pm 0.05$	ABREU	98L DLPH	$E_{cm}^{98} = 91.2$ GeV
2.26 ± 0.12	BARATE	98v ALEP	$E_{cm}^{98} = 91.2$ GeV
2.42 ± 0.13	AKERS	94P OPAL	$E_{cm}^{94} = 91.2$ GeV
• • • We do not use the following data for averages, fits, limits, etc. • • •			
$2.26 \pm 0.01 \pm 0.18$	ABREU	95F DLPH	Repl. by ABREU 98L

See key on page 239

Gauge & Higgs Boson Particle Listings

Z

$\langle N_{K^0} \rangle$

VALUE	DOCUMENT ID	TECN	COMMENT
2.013 ± 0.022 OUR AVERAGE			
2.01 ± 0.08	ABE	99E SLD	$E_{cm}^{ee} = 91.2$ GeV
2.024 ± 0.006 ± 0.042	ACCIARRI	97L L3	$E_{cm}^{ee} = 91.2$ GeV
1.962 ± 0.022 ± 0.056	ABREU	95L DLPH	$E_{cm}^{ee} = 91.2$ GeV
1.99 ± 0.01 ± 0.04	AKERS	95U OPAL	$E_{cm}^{ee} = 91.2$ GeV
2.061 ± 0.047	BUSKULIC	94K ALEP	$E_{cm}^{ee} = 91.2$ GeV
• • • We do not use the following data for averages, fits, limits, etc. • • •			
2.04 ± 0.02 ± 0.14	ACCIARRI	94B L3	Repl. by ACCIARRI 97L

$\langle N_{K^*(892)^+} \rangle$

VALUE	DOCUMENT ID	TECN	COMMENT
0.72 ± 0.05 OUR AVERAGE			
0.712 ± 0.031 ± 0.059	ABREU	95L DLPH	$E_{cm}^{ee} = 91.2$ GeV
0.72 ± 0.02 ± 0.08	ACTON	93 OPAL	$E_{cm}^{ee} = 91.2$ GeV

$\langle N_{K^*(892)^0} \rangle$

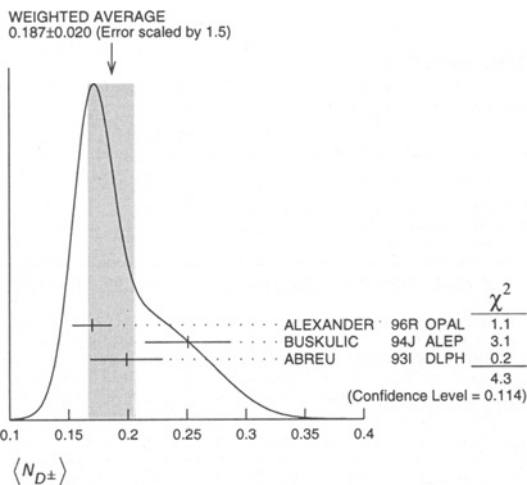
VALUE	DOCUMENT ID	TECN	COMMENT
0.739 ± 0.022 OUR AVERAGE			
0.707 ± 0.041	ABE	99E SLD	$E_{cm}^{ee} = 91.2$ GeV
0.74 ± 0.02 ± 0.02	ACKERSTAFF	97S OPAL	$E_{cm}^{ee} = 91.2$ GeV
0.77 ± 0.02 ± 0.07	ABREU	96U DLPH	$E_{cm}^{ee} = 91.2$ GeV
0.83 ± 0.01 ± 0.09	BUSKULIC	96H ALEP	$E_{cm}^{ee} = 91.2$ GeV
0.97 ± 0.18 ± 0.31	ABREU	93 DLPH	$E_{cm}^{ee} = 91.2$ GeV
• • • We do not use the following data for averages, fits, limits, etc. • • •			
0.74 ± 0.03 ± 0.03	AKERS	95X OPAL	Repl. by ACKERSTAFF 97S

$\langle N_{K_2^*(1430)} \rangle$

VALUE	DOCUMENT ID	TECN	COMMENT
0.073 ± 0.023	ABREU	99J DLPH	$E_{cm}^{ee} = 91.2$ GeV
• • • We do not use the following data for averages, fits, limits, etc. • • •			
0.079 ± 0.026 ± 0.031	ABREU	96U DLPH	Repl. by ABREU 99J
0.19 ± 0.04 ± 0.06	109 AKERS	95X OPAL	$E_{cm}^{ee} = 91.2$ GeV
109 AKERS 95X obtain this value for $x < 0.3$.			

$\langle N_{D^\pm} \rangle$

VALUE	DOCUMENT ID	TECN	COMMENT
0.187 ± 0.020 OUR AVERAGE	Error includes scale factor of 1.5. See the ideogram below.		
0.170 ± 0.009 ± 0.014	ALEXANDER	96R OPAL	$E_{cm}^{ee} = 91.2$ GeV
0.251 ± 0.026 ± 0.025	BUSKULIC	94J ALEP	$E_{cm}^{ee} = 91.2$ GeV
0.199 ± 0.019 ± 0.024	110 ABREU	93I DLPH	$E_{cm}^{ee} = 91.2$ GeV
110 See ABREU 95 (erratum).			



$\langle N_{D^0} \rangle$

VALUE	DOCUMENT ID	TECN	COMMENT
0.462 ± 0.026 OUR AVERAGE			
0.465 ± 0.017 ± 0.027	ALEXANDER	96R OPAL	$E_{cm}^{ee} = 91.2$ GeV
0.518 ± 0.052 ± 0.035	BUSKULIC	94J ALEP	$E_{cm}^{ee} = 91.2$ GeV
0.403 ± 0.038 ± 0.044	111 ABREU	93I DLPH	$E_{cm}^{ee} = 91.2$ GeV
111 See ABREU 95 (erratum).			

$\langle N_{D_s^\pm} \rangle$

VALUE	DOCUMENT ID	TECN	COMMENT
0.131 ± 0.010 ± 0.018	ALEXANDER	96R OPAL	$E_{cm}^{ee} = 91.2$ GeV

$\langle N_{D^*(2010)^\pm} \rangle$

VALUE	DOCUMENT ID	TECN	COMMENT
0.183 ± 0.008 OUR AVERAGE			
0.1854 ± 0.0041 ± 0.0091	112 ACKERSTAFF	98E OPAL	$E_{cm}^{ee} = 91.2$ GeV
0.187 ± 0.015 ± 0.013	BUSKULIC	94J ALEP	$E_{cm}^{ee} = 91.2$ GeV
0.171 ± 0.012 ± 0.016	113 ABREU	93I DLPH	$E_{cm}^{ee} = 91.2$ GeV
• • • We do not use the following data for averages, fits, limits, etc. • • •			
0.183 ± 0.009 ± 0.011	114 AKERS	95O OPAL	Repl. by ACKERSTAFF 98E
112 ACKERSTAFF 98E systematic error includes an uncertainty of ± 0.0069 due to the branching ratios $B(D^{*+} \rightarrow D^0 \pi^+) = 0.683 \pm 0.014$ and $B(D^0 \rightarrow K^- \pi^+) = 0.0383 \pm 0.0012$.			
113 See ABREU 95 (erratum).			
114 AKERS 95O systematic error includes an uncertainty of ± 0.008 due to the $D^{*\pm}$ and D^0 branching ratios [they use $B(D^{*+} \rightarrow D^0 \pi) = 0.681 \pm 0.016$ and $B(D^0 \rightarrow K \pi) = 0.0401 \pm 0.0014$ to obtain this measurement].			

$\langle N_{D_{s1}(2536)^+} \rangle$

VALUE (units 10^{-3})	DOCUMENT ID	TECN	COMMENT
2.9^{+0.7}_{-0.6} ± 0.2	115 ACKERSTAFF	97W OPAL	$E_{cm}^{ee} = 91.2$ GeV
115 ACKERSTAFF 97W obtain this value for $x > 0.6$ and with the assumption that its decay width is saturated by the $D^* K$ final states.			

$\langle N_{B^*} \rangle$

VALUE	DOCUMENT ID	TECN	COMMENT
0.28 ± 0.01 ± 0.03	116 ABREU	95R DLPH	$E_{cm}^{ee} = 91.2$ GeV
116 ABREU 95R quote this value for a flavor-averaged excited state.			

$\langle N_{J/\psi(1S)} \rangle$

VALUE	DOCUMENT ID	TECN	COMMENT
0.0056 ± 0.0003 ± 0.0004	117 ALEXANDER	96B OPAL	$E_{cm}^{ee} = 91.2$ GeV
117 ALEXANDER 96B identify $J/\psi(1S)$ from the decays into lepton pairs.			

$\langle N_{\psi(2S)} \rangle$

VALUE	DOCUMENT ID	TECN	COMMENT
0.0023 ± 0.0004 ± 0.0003	ALEXANDER	96B OPAL	$E_{cm}^{ee} = 91.2$ GeV

$\langle N_p \rangle$

VALUE	DOCUMENT ID	TECN	COMMENT
1.04 ± 0.04 OUR AVERAGE			
1.03 ± 0.13	ABE	99E SLD	$E_{cm}^{ee} = 91.2$ GeV
1.08 ± 0.04 ± 0.03	ABREU	98L DLPH	$E_{cm}^{ee} = 91.2$ GeV
1.00 ± 0.07	BARATE	98V ALEP	$E_{cm}^{ee} = 91.2$ GeV
0.92 ± 0.11	AKERS	94P OPAL	$E_{cm}^{ee} = 91.2$ GeV
1.07 ± 0.01 ± 0.14	ABREU	95F DLPH	Repl. by ABREU 98L
• • • We do not use the following data for averages, fits, limits, etc. • • •			

$\langle N_{\Delta(1232)^{++}} \rangle$

VALUE	DOCUMENT ID	TECN	COMMENT
0.087 ± 0.033 OUR AVERAGE	Error includes scale factor of 2.4.		
0.079 ± 0.009 ± 0.011	ABREU	95W DLPH	$E_{cm}^{ee} = 91.2$ GeV
0.22 ± 0.04 ± 0.04	ALEXANDER	95D OPAL	$E_{cm}^{ee} = 91.2$ GeV

$\langle N_\Lambda \rangle$

VALUE	DOCUMENT ID	TECN	COMMENT
0.374 ± 0.007 OUR AVERAGE			
0.395 ± 0.022	ABE	99E SLD	$E_{cm}^{ee} = 91.2$ GeV
0.364 ± 0.004 ± 0.017	ACCIARRI	97L L3	$E_{cm}^{ee} = 91.2$ GeV
0.374 ± 0.002 ± 0.010	ALEXANDER	97D OPAL	$E_{cm}^{ee} = 91.2$ GeV
0.386 ± 0.016	BUSKULIC	94K ALEP	$E_{cm}^{ee} = 91.2$ GeV
0.357 ± 0.003 ± 0.017	ABREU	93L DLPH	$E_{cm}^{ee} = 91.2$ GeV
• • • We do not use the following data for averages, fits, limits, etc. • • •			
0.37 ± 0.01 ± 0.04	ACCIARRI	94B L3	Repl. by ACCIARRI 97L

$\langle N_{\Lambda(1520)} \rangle$

VALUE	DOCUMENT ID	TECN	COMMENT
0.0213 ± 0.0021 ± 0.0019	ALEXANDER	97D OPAL	$E_{cm}^{ee} = 91.2$ GeV

$\langle N_{\Sigma^+} \rangle$

VALUE	DOCUMENT ID	TECN	COMMENT
0.099 ± 0.008 ± 0.013	ALEXANDER	97E OPAL	$E_{cm}^{ee} = 91.2$ GeV

$\langle N_{\Sigma^-} \rangle$

VALUE	DOCUMENT ID	TECN	COMMENT
0.083 ± 0.006 ± 0.009	ALEXANDER	97E OPAL	$E_{cm}^{ee} = 91.2$ GeV

Gauge & Higgs Boson Particle Listings

Z

$\langle N_{\Sigma^{++}\Sigma^-} \rangle$

VALUE	DOCUMENT ID	TECN	COMMENT
0.181 ± 0.018 OUR AVERAGE			
0.182 ± 0.010 ± 0.016	118 ALEXANDER	97E OPAL	$E_{cm}^{ee} = 91.2$ GeV
0.170 ± 0.014 ± 0.061	ABREU	95O DLPH	$E_{cm}^{ee} = 91.2$ GeV

118 We have combined the values of $\langle N_{\Sigma^+} \rangle$ and $\langle N_{\Sigma^-} \rangle$ from ALEXANDER 97E adding the statistical and systematic errors of the two final states separately in quadrature. If isospin symmetry is assumed this value becomes $0.174 \pm 0.010 \pm 0.015$.

$\langle N_{\Sigma^0} \rangle$

VALUE	DOCUMENT ID	TECN	COMMENT
0.070 ± 0.011 OUR AVERAGE			
0.071 ± 0.012 ± 0.013	ALEXANDER	97E OPAL	$E_{cm}^{ee} = 91.2$ GeV
0.070 ± 0.010 ± 0.010	ADAM	96B DLPH	$E_{cm}^{ee} = 91.2$ GeV

$\langle N_{(\Sigma^+ + \Sigma^- + \Sigma^0)/3} \rangle$

VALUE	DOCUMENT ID	TECN	COMMENT
0.084 ± 0.005 ± 0.008	ALEXANDER	97E OPAL	$E_{cm}^{ee} = 91.2$ GeV

$\langle N_{\Sigma(1385)^+} \rangle$

VALUE	DOCUMENT ID	TECN	COMMENT
0.0239 ± 0.0009 ± 0.0012	ALEXANDER	97D OPAL	$E_{cm}^{ee} = 91.2$ GeV

$\langle N_{\Sigma(1385)^-} \rangle$

VALUE	DOCUMENT ID	TECN	COMMENT
0.0240 ± 0.0010 ± 0.0014	ALEXANDER	97D OPAL	$E_{cm}^{ee} = 91.2$ GeV

$\langle N_{\Sigma(1385)^+ + \Sigma(1385)^-} \rangle$

VALUE	DOCUMENT ID	TECN	COMMENT
0.046 ± 0.004 OUR AVERAGE			Error includes scale factor of 1.6.
0.0479 ± 0.0013 ± 0.0026	ALEXANDER	97D OPAL	$E_{cm}^{ee} = 91.2$ GeV
0.0382 ± 0.0028 ± 0.0045	ABREU	95O DLPH	$E_{cm}^{ee} = 91.2$ GeV

$\langle N_{\Xi^-} \rangle$

VALUE	DOCUMENT ID	TECN	COMMENT
0.0258 ± 0.0009 OUR AVERAGE			
0.0259 ± 0.0004 ± 0.0009	ALEXANDER	97D OPAL	$E_{cm}^{ee} = 91.2$ GeV
0.0250 ± 0.0009 ± 0.0021	ABREU	95O DLPH	$E_{cm}^{ee} = 91.2$ GeV

$\langle N_{\Xi(1530)^0} \rangle$

VALUE	DOCUMENT ID	TECN	COMMENT
0.0053 ± 0.0013 OUR AVERAGE			Error includes scale factor of 3.2.
0.0068 ± 0.0005 ± 0.0004	ALEXANDER	97D OPAL	$E_{cm}^{ee} = 91.2$ GeV
0.0041 ± 0.0004 ± 0.0004	ABREU	95O DLPH	$E_{cm}^{ee} = 91.2$ GeV

$\langle N_{\Omega^-} \rangle$

VALUE	DOCUMENT ID	TECN	COMMENT
0.00164 ± 0.00028 OUR AVERAGE			
0.0018 ± 0.0003 ± 0.0002	ALEXANDER	97D OPAL	$E_{cm}^{ee} = 91.2$ GeV
0.0014 ± 0.0002 ± 0.0004	ADAM	96B DLPH	$E_{cm}^{ee} = 91.2$ GeV

$\langle N_{\Lambda_c^+} \rangle$

VALUE	DOCUMENT ID	TECN	COMMENT
0.078 ± 0.012 ± 0.012	ALEXANDER	96R OPAL	$E_{cm}^{ee} = 91.2$ GeV

$\langle N_{charged} \rangle$

VALUE	DOCUMENT ID	TECN	COMMENT
21.07 ± 0.11 OUR AVERAGE			
21.21 ± 0.01 ± 0.20	ABREU	99 DLPH	$E_{cm}^{ee} = 91.2$ GeV
21.05 ± 0.20	AKERS	95Z OPAL	$E_{cm}^{ee} = 91.2$ GeV
20.91 ± 0.03 ± 0.22	BUSKULIC	95R ALEP	$E_{cm}^{ee} = 91.2$ GeV
21.40 ± 0.43	ACTON	92B OPAL	$E_{cm}^{ee} = 91.2$ GeV
20.71 ± 0.04 ± 0.77	ABREU	91H DLPH	$E_{cm}^{ee} = 91.2$ GeV
20.7 ± 0.7	ADEVA	91I L3	$E_{cm}^{ee} = 91.2$ GeV
20.1 ± 1.0 ± 0.9	ABRAMS	90 MRK2	$E_{cm}^{ee} = 91.1$ GeV

Z HADRONIC POLE CROSS SECTION

OUR FIT is obtained using the fit procedure and correlations as determined by the LEP Electroweak Working Group (see the "Note on the Z boson"). This quantity is defined as

$$\sigma_h^0 = \frac{12\pi}{M_Z^2} \frac{\Gamma(e^+e^-)\Gamma(\text{hadrons})}{\Gamma_Z^2}$$

It is one of the parameters used in the Z lineshape fit.

VALUE (nb)	EVTS	DOCUMENT ID	TECN	COMMENT
41.561 ± 0.042 OUR FIT				
41.578 ± 0.069	3.70M	ABREU	00F DLPH	$E_{cm}^{ee} = 88-94$ GeV
41.535 ± 0.055	3.54M	ACCIARRI	00C L3	$E_{cm}^{ee} = 88-94$ GeV
41.559 ± 0.058	4.07M	119 BARATE	00C ALEP	$E_{cm}^{ee} = 88-94$ GeV

• • • We do not use the following data for averages, fits, limits, etc. • • •

41.23 ± 0.20	1.05M	ABREU	94 DLPH	Repl. by ABREU 00F
41.39 ± 0.26	1.09M	ACCIARRI	94 L3	Repl. by ACCIARRI 00C
41.70 ± 0.23	1.19M	AKERS	94 OPAL	$E_{cm}^{ee} = 88-94$ GeV
41.60 ± 0.16	1.27M	BUSKULIC	94 ALEP	Repl. by BARATE 00C
42 ± 4	450	ABRAMS	89B MRK2	$E_{cm}^{ee} = 89.2-93.0$ GeV

119 BARATE 00C error includes approximately 0.030 due to statistics, 0.026 due to experimental systematics, and 0.025 due to uncertainty in luminosity measurement.

Z VECTOR COUPLINGS TO CHARGED LEPTONS

These quantities are the effective vector couplings of the Z to charged leptons. Their magnitude is derived from a measurement of the Z lineshape and the forward-backward lepton asymmetries as a function of energy around the Z mass. The relative sign among the vector to axial-vector couplings is obtained from a measurement of the Z asymmetry parameters, A_e , A_μ , and A_τ . By convention the sign of g_A^e is fixed to be negative (and opposite to that of g_V^e obtained using ν_e scattering measurements). The fit values quoted below correspond to global nine- or five-parameter fits to lineshape, lepton forward-backward asymmetry, and A_e , A_μ , and A_τ measurements. See "Note on the Z boson" for details.

g_V^e

VALUE	EVTS	DOCUMENT ID	TECN	COMMENT
-0.03874 ± 0.00094 OUR FIT				
-0.0412 ± 0.0027	124.4k	120 ACCIARRI	00C L3	$E_{cm}^{ee} = 88-94$ GeV
-0.0400 ± 0.0037		BARATE	00C ALEP	$E_{cm}^{ee} = 88-94$ GeV
-0.0414 ± 0.0020		121 ABE	95J SLD	$E_{cm}^{ee} = 91.31$ GeV

120 ACCIARRI 00C use their measurement of the τ polarization in addition to forward-backward lepton asymmetries.

121 ABE 95J obtain this result combining polarized Bhabha results with the A_{FB} measurement of ABE 94c. The Bhabha results alone give $-0.0507 \pm 0.0096 \pm 0.0020$.

g_V^μ

VALUE	EVTS	DOCUMENT ID	TECN	COMMENT
-0.0359 ± 0.0033 OUR FIT				
-0.0386 ± 0.0073	113.4k	122 ACCIARRI	00C L3	$E_{cm}^{ee} = 88-94$ GeV
-0.0362 ± 0.0061		BARATE	00C ALEP	$E_{cm}^{ee} = 88-94$ GeV

122 ACCIARRI 00C use their measurement of the τ polarization in addition to forward-backward lepton asymmetries.

g_V^τ

VALUE	EVTS	DOCUMENT ID	TECN	COMMENT
-0.0366 ± 0.0014 OUR FIT				
-0.0384 ± 0.0026	103.0k	123 ACCIARRI	00C L3	$E_{cm}^{ee} = 88-94$ GeV
-0.0361 ± 0.0068		BARATE	00C ALEP	$E_{cm}^{ee} = 88-94$ GeV

123 ACCIARRI 00C use their measurement of the τ polarization in addition to forward-backward lepton asymmetries.

g_V^e

VALUE	EVTS	DOCUMENT ID	TECN	COMMENT
-0.03795 ± 0.00071 OUR FIT				
-0.0397 ± 0.0020	379.4k	124 ABREU	00F DLPH	$E_{cm}^{ee} = 88-94$ GeV
-0.0397 ± 0.0017	340.8k	125 ACCIARRI	00C L3	$E_{cm}^{ee} = 88-94$ GeV
-0.0383 ± 0.0018	500k	BARATE	00C ALEP	$E_{cm}^{ee} = 88-94$ GeV

• • • We do not use the following data for averages, fits, limits, etc. • • •

-0.034 ± 0.004	146k	124 AKERS	94 OPAL	$E_{cm}^{ee} = 88-94$ GeV
----------------	------	-----------	---------	---------------------------

124 Using forward-backward lepton asymmetries.

125 ACCIARRI 00C use their measurement of the τ polarization in addition to forward-backward lepton asymmetries.

Z AXIAL-VECTOR COUPLINGS TO CHARGED LEPTONS

These quantities are the effective axial-vector couplings of the Z to charged leptons. Their magnitude is derived from a measurement of the Z lineshape and the forward-backward lepton asymmetries as a function of energy around the Z mass. The relative sign among the vector to axial-vector couplings is obtained from a measurement of the Z asymmetry parameters, A_e , A_μ , and A_τ . By convention the sign of g_A^e is fixed to be negative (and opposite to that of g_V^e obtained using ν_e scattering measurements). The fit values quoted below correspond to global nine- or five-parameter fits to lineshape, lepton forward-backward asymmetry, and A_e , A_μ , and A_τ measurements. See "Note on the Z boson" for details.

g_A^e

VALUE	EVTS	DOCUMENT ID	TECN	COMMENT
-0.50133 ± 0.00040 OUR FIT				
-0.5015 ± 0.0007	124.4k	126 ACCIARRI	00C L3	$E_{cm}^{ee} = 88-94$ GeV
-0.50166 ± 0.00057		BARATE	00C ALEP	$E_{cm}^{ee} = 88-94$ GeV
-0.4977 ± 0.0045		127 ABE	95J SLD	$E_{cm}^{ee} = 91.31$ GeV

126 ACCIARRI 00C use their measurement of the τ polarization in addition to forward-backward lepton asymmetries.

127 ABE 95J obtain this result combining polarized Bhabha results with the A_{FB} measurement of ABE 94c. The Bhabha results alone give $-0.4968 \pm 0.0039 \pm 0.0027$.

g_A^μ

VALUE	EVTS	DOCUMENT ID	TECN	COMMENT
-0.50139 ± 0.00066 OUR FIT				
-0.5009 ± 0.0014	113.4k	128 ACCIARRI	00C L3	$E_{cm}^{ee} = 88-94$ GeV
-0.50046 ± 0.00093		BARATE	00C ALEP	$E_{cm}^{ee} = 88-94$ GeV

128 ACCIARRI 00C use their measurement of the τ polarization in addition to forward-backward lepton asymmetries.

g_A^τ

VALUE	EVTS	DOCUMENT ID	TECN	COMMENT
-0.50223 ± 0.00073 OUR FIT				
-0.5023 ± 0.0017	103.0k	129 ACCIARRI	00C L3	$E_{cm}^{ee} = 88-94$ GeV
-0.50150 ± 0.00100		BARATE	00C ALEP	$E_{cm}^{ee} = 88-94$ GeV

129 ACCIARRI 00C use their measurement of the τ polarization in addition to forward-backward lepton asymmetries.

g_A^e

VALUE	EVTS	DOCUMENT ID	TECN	COMMENT
-0.50145 ± 0.00030 OUR FIT				
-0.5007 ± 0.0005	379.4k	ABREU	00F DLPH	$E_{cm}^{ee} = 88-94$ GeV
-0.50153 ± 0.00053	340.8k	130 ACCIARRI	00C L3	$E_{cm}^{ee} = 88-94$ GeV
-0.50150 ± 0.00046	500k	BARATE	00C ALEP	$E_{cm}^{ee} = 88-94$ GeV

• • • We do not use the following data for averages, fits, limits, etc. • • •

-0.500 ± 0.001	146k	AKERS	94 OPAL	$E_{cm}^{ee} = 88-94$ GeV
----------------	------	-------	---------	---------------------------

130 ACCIARRI 00C use their measurement of the τ polarization in addition to forward-backward lepton asymmetries.

Z COUPLINGS TO NEUTRAL LEPTONS

These quantities are the effective couplings of the Z to neutral leptons. $\nu_e e$ and $\nu_\mu e$ scattering results are combined with g_A^e and g_V^e measurements at the Z mass to obtain $g^{\nu e}$ and $g^{\nu\mu}$ following NOVIKOV 93c.

$g^{\nu e}$

VALUE	DOCUMENT ID	TECN	COMMENT
0.528 ± 0.085	131 VILAIN	94 CHM2	From $\nu_\mu e$ and $\nu_e e$ scattering

131 VILAIN 94 derive this value from their value of $g^{\nu\mu}$ and their ratio $g^{\nu e}/g^{\nu\mu} = 1.05^{+0.15}_{-0.18}$.

$g^{\nu\mu}$

VALUE	DOCUMENT ID	TECN	COMMENT
0.502 ± 0.017	132 VILAIN	94 CHM2	From $\nu_\mu e$ scattering

132 VILAIN 94 derive this value from their measurement of the couplings $g_A^{\nu\mu} = -0.503 \pm 0.017$ and $g_V^{\nu\mu} = -0.035 \pm 0.017$ obtained from $\nu_\mu e$ scattering. We have re-evaluated this value using the current PDG values for g_A^e and g_V^e .

Z ASYMMETRY PARAMETERS

For each fermion-antifermion pair coupling to the Z these quantities are defined as

$$A_f = \frac{2g_V^f g_A^f}{(g_V^f)^2 + (g_A^f)^2}$$

where g_V^f and g_A^f are the effective vector and axial-vector couplings. For their relation to the various lepton asymmetries see the 'Note on the Z Boson.'

A_e Using polarized beams, this quantity can also be measured as $(\sigma_L - \sigma_R)/(\sigma_L + \sigma_R)$, where σ_L and σ_R are the e^+e^- production cross sections for Z bosons produced with left-handed and right-handed electrons respectively.

VALUE	EVTS	DOCUMENT ID	TECN	COMMENT
0.152 ± 0.004 OUR AVERAGE				Error includes scale factor of 1.2.
0.1382 ± 0.0116 ± 0.0005	105000	133 ABREU	00E DLPH	$E_{cm}^{ee} = 88-94$ GeV
0.1678 ± 0.0127 ± 0.0030	137092	134 ACCIARRI	98H L3	$E_{cm}^{ee} = 88-94$ GeV
0.162 ± 0.041 ± 0.014	89838	135 ABE	97 SLD	$E_{cm}^{ee} = 91.27$ GeV
0.1543 ± 0.0039	93644	136 ABE	97E SLD	$E_{cm}^{ee} = 91.27$ GeV
0.152 ± 0.012		137 ABE	97N SLD	$E_{cm}^{ee} = 91.27$ GeV
0.129 ± 0.014 ± 0.005	89075	138 ALEXANDER	96U OPAL	$E_{cm}^{ee} = 88-94$ GeV
0.202 ± 0.038 ± 0.008		139 ABE	95J SLD	$E_{cm}^{ee} = 91.31$ GeV
0.129 ± 0.016 ± 0.005	33000	140 BUSKULIC	95Q ALEP	$E_{cm}^{ee} = 88-94$ GeV
• • • We do not use the following data for averages, fits, limits, etc. • • •				
0.136 ± 0.027 ± 0.003		134 ABREU	95I DLPH	Repl. by ABREU 00E
0.122 ± 0.030 ± 0.012	30663	134 AKERS	95 OPAL	Repl. by ALEXANDER 96U
0.1656 ± 0.0071 ± 0.0028	49392	141 ABE	94C SLD	Repl. by ABE 97E
0.157 ± 0.020 ± 0.005	86000	134 ACCIARRI	94E L3	Repl. by ACCIARRI 98H

133 ABREU 00E obtain this result fitting the τ polarization as a function of the polar τ production angle. This measurement is a combination of different analyses (exclusive τ decay modes, inclusive hadronic 1-prong reconstruction, and a neural network analysis).

134 Derived from the measurement of forward-backward τ polarization asymmetry.

135 ABE 97 obtain this result from a measurement of the observed left-right charge asymmetry, $A_{LR}^{Obs} = 0.225 \pm 0.056 \pm 0.019$, in hadronic Z decays. If they combine this value of A_{LR}^{Obs} with their earlier measurement of A_{LR}^{Obs} they determine A_e to be $0.1574 \pm 0.0197 \pm 0.0067$ independent of the beam polarization.

136 ABE 97E measure the left-right asymmetry in hadronic Z production. This value (statistical and systematic errors added in quadrature) leads to $\sin^2\theta_{eff}^{\nu} = 0.23060 \pm 0.00050$.

137 ABE 97N obtain this direct measurement using the left-right cross section asymmetry and the left-right forward-backward asymmetry in leptonic decays of the Z boson obtained with a polarized electron beam.

138 ALEXANDER 96U measure the τ -lepton polarization and the forward-backward polarization asymmetry.

139 ABE 95J obtain this result from polarized Bhabha scattering.

140 BUSKULIC 95Q obtain this result fitting the τ polarization as a function of the polar τ production angle.

141 ABE 94C measured the left-right asymmetry in Z production. This value leads to $\sin^2\theta_{\nu\nu} = 0.2292 \pm 0.0009 \pm 0.0004$.

A_μ This quantity is directly extracted from a measurement of the left-right forward-backward asymmetry in $\mu^+\mu^-$ production at SLC using a polarized electron beam. This double asymmetry eliminates the dependence on the Z-e-e coupling parameter A_e .

VALUE	EVTS	DOCUMENT ID	TECN	COMMENT
0.102 ± 0.034	3788	142 ABE	97N SLD	$E_{cm}^{ee} = 91.27$ GeV

142 ABE 97N obtain this direct measurement using the left-right cross section asymmetry and the left-right forward-backward asymmetry in $\mu^+\mu^-$ decays of the Z boson obtained with a polarized electron beam.

A_τ The LEP Collaborations derive this quantity from the measurement of the τ polarization in $Z \rightarrow \tau^+\tau^-$. The SLD Collaboration directly extracts this quantity from its measured left-right forward-backward asymmetry in $Z \rightarrow \tau^+\tau^-$ produced using a polarized e^- beam. This double asymmetry eliminates the dependence on the Z-e-e coupling parameter A_e .

VALUE	EVTS	DOCUMENT ID	TECN	COMMENT
0.141 ± 0.006 OUR AVERAGE				
0.1359 ± 0.0079 ± 0.0055	105000	143 ABREU	00E DLPH	$E_{cm}^{ee} = 88-94$ GeV
0.1476 ± 0.0088 ± 0.0062	137092	ACC IARRI	98H L3	$E_{cm}^{ee} = 88-94$ GeV
0.195 ± 0.034		144 ABE	97N SLD	$E_{cm}^{ee} = 91.27$ GeV
0.134 ± 0.009 ± 0.010	89075	145 ALEXANDER	96U OPAL	$E_{cm}^{ee} = 88-94$ GeV
0.136 ± 0.012 ± 0.009	33000	146 BUSKULIC	95Q ALEP	$E_{cm}^{ee} = 88-94$ GeV
• • • We do not use the following data for averages, fits, limits, etc. • • •				
0.148 ± 0.017 ± 0.014		ABREU	95I DLPH	Repl. by ABREU 00E
0.153 ± 0.019 ± 0.013	30663	AKERS	95 OPAL	Repl. by ALEXANDER 96U
0.150 ± 0.013 ± 0.009	86000	ACCIARRI	94E L3	Repl. by ACCIARRI 98H

143 ABREU 00E obtain this result fitting the τ polarization as a function of the polar τ production angle. This measurement is a combination of different analyses (exclusive τ decay modes, inclusive hadronic 1-prong reconstruction, and a neural network analysis).

144 ABE 97N obtain this direct measurement using the left-right cross section asymmetry and the left-right forward-backward asymmetry in $\tau^+\tau^-$ decays of the Z boson obtained with a polarized electron beam.

145 ALEXANDER 96U measure the τ -lepton polarization and the forward-backward polarization asymmetry.

146 BUSKULIC 95Q obtain this result fitting the τ polarization as a function of the polar τ production angle.

A_c This quantity is directly extracted from a measurement of the left-right forward-backward asymmetry in $c\bar{c}$ production at SLC using polarized electron beam. This double asymmetry eliminates the dependence on the Z-e-e coupling parameter A_e .

VALUE	DOCUMENT ID	TECN	COMMENT
0.66 ± 0.11 OUR AVERAGE			
0.642 ± 0.110 ± 0.063	147 ABE	990 SLD	$E_{cm}^{ee} = 91.27$ GeV
0.73 ± 0.22 ± 0.10	148 ABE,K	95 SLD	$E_{cm}^{ee} = 91.26$ GeV
• • • We do not use the following data for averages, fits, limits, etc. • • •			
0.37 ± 0.23 ± 0.21	149 ABE	95L SLD	Repl. by ABE 990

147 ABE 990 tag b and c quarks through their semileptonic decays into electrons and muons. A maximum likelihood fit is performed to extract simultaneously A_b and A_c .

148 ABE,K 95 tag Z $\rightarrow c\bar{c}$ events using D^{*+} and D^+ meson production. To take care of the $b\bar{b}$ contamination in their analysis they use $A_b^D = 0.64 \pm 0.11$ (which is A_b from D^*/D tagging). This is obtained by starting with a Standard Model value of 0.935, assigning it an estimated error of ± 0.105 to cover LEP and SLD measurements, and finally taking into account $B-\bar{B}$ mixing ($1-2\chi_{mix} = 0.72 \pm 0.09$).

149 ABE 95I tag b and c quarks through their semileptonic decays into electrons and muons. A maximum likelihood fit is performed to extract A_b and A_c .

Gauge & Higgs Boson Particle Listings

Z

 A_b

This quantity is directly extracted from a measurement of the left-right forward-backward asymmetry in $b\bar{b}$ production at SLC using polarized electron beam. This double asymmetry eliminates the dependence on the Z - e - e coupling parameter A_e .

VALUE	EVTs	DOCUMENT ID	TECN	COMMENT
0.905 ± 0.051	150	ABE	990 SLD	$E_{cm}^{ee} = 91.27$ GeV
• • • We do not use the following data for averages, fits, limits, etc. • • •				
0.855 ± 0.088 ± 0.102	7473	151 ABE	99L SLD	Repl. by ABE 990
0.911 ± 0.045 ± 0.045	11092	152 ABE	98I SLD	Repl. by ABE 990
0.91 ± 0.14 ± 0.07	153	ABE	95L SLD	Repl. by ABE 990
150 ABE 990 tag b and c quarks through their semileptonic decays into electrons and muons. A maximum likelihood fit is performed to extract simultaneously A_b and A_c . The value of A_b so extracted, $0.910 \pm 0.068 \pm 0.037$, is then combined with A_b from ABE 99L and ABE 99I to obtain the resulting SLD average value quoted here.				
151 ABE 99L obtain an enriched sample of $b\bar{b}$ events tagging with an inclusive vertex mass cut. For distinguishing b and \bar{b} quarks they use the charge of identified K^\pm .				
152 ABE 98I obtain an enriched sample of $b\bar{b}$ events tagging with an inclusive vertex mass cut. A momentum-weighted track charge is used to identify the sign of the charge of the underlying b quark.				
153 ABE 95L tag b and c quarks through their semileptonic decays into electrons and muons. A maximum likelihood fit is performed to extract A_b and A_c .				

TRANSVERSE SPIN CORRELATIONS IN $Z \rightarrow \tau^+ \tau^-$

The correlations between the transverse spin components of $\tau^+ \tau^-$ produced in Z decays may be expressed in terms of the vector and axial-vector couplings:

$$C_{TT} = \frac{|g_A^\tau|^2 - |g_V^\tau|^2}{|g_A^\tau|^2 + |g_V^\tau|^2}$$

$$C_{TN} = -2 \frac{|g_A^\tau| |g_V^\tau|}{|g_A^\tau|^2 + |g_V^\tau|^2} \sin(\Phi_{g_V^\tau} - \Phi_{g_A^\tau})$$

C_{TT} refers to the transverse-transverse (within the collision plane) spin correlation and C_{TN} refers to the transverse-normal (to the collision plane) spin correlation.

The longitudinal τ polarization P_τ ($= -A_\tau$) is given by:

$$P_\tau = -2 \frac{|g_A^\tau| |g_V^\tau|}{|g_A^\tau|^2 + |g_V^\tau|^2} \cos(\Phi_{g_V^\tau} - \Phi_{g_A^\tau})$$

Here Φ is the phase and the phase difference $\Phi_{g_V^\tau} - \Phi_{g_A^\tau}$ can be obtained using both the measurements of C_{TN} and P_τ .

 C_{TT}

VALUE	EVTs	DOCUMENT ID	TECN	COMMENT
1.01 ± 0.12 OUR AVERAGE				
0.87 ± 0.20 ^{+0.10} _{-0.12}	9.1k	ABREU	97G DLPH	$E_{cm}^{ee} = 91.2$ GeV
1.06 ± 0.13 ± 0.05	120k	BARATE	97D ALEP	$E_{cm}^{ee} = 91.2$ GeV

 C_{TN}

VALUE	EVTs	DOCUMENT ID	TECN	COMMENT
0.08 ± 0.13 ± 0.04	120k	154 BARATE	97D ALEP	$E_{cm}^{ee} = 91.2$ GeV
154 BARATE 97D combine their value of C_{TN} with the world average $P_\tau = -0.140 \pm 0.007$ to obtain $\tan(\Phi_{g_V^\tau} - \Phi_{g_A^\tau}) = -0.57 \pm 0.97$.				

 $A_{FB}^{(0,e)}$ CHARGE ASYMMETRY IN $e^+ e^- \rightarrow e^+ e^-$

OUR FIT is obtained using the fit procedure and correlations as determined by the LEP Electroweak Working Group (see the "Note on the Z boson"). For the Z peak, we report the pole asymmetry defined by $(3/4)A_e^2$ as determined by the nine-parameter fit to cross-section and lepton forward-backward asymmetry data.

ASYMMETRY (%)	STD. MODEL	\sqrt{s} (GeV)	DOCUMENT ID	TECN
1.64 ± 0.27 OUR FIT				
1.71 ± 0.49		91.2	ABREU	00F DLPH
1.06 ± 0.58		91.2	ACCIARRI	00C L3
1.88 ± 0.34		91.2	155 BARATE	00C ALEP
• • • We do not use the following data for averages, fits, limits, etc. • • •				
2.5 ± 0.9		91.2	ABREU	94 DLPH
1.04 ± 0.92		91.2	ACCIARRI	94 L3
0.62 ± 0.80		91.2	AKERS	94 OPAL
1.85 ± 0.66		91.2	BUSKULIC	94 ALEP
155 BARATE 00C error includes approximately 0.31 due to statistics, 0.06 due to experimental systematics, and 0.13 due to the theoretical uncertainty in t -channel prediction.				

 $A_{FB}^{(0,\mu)}$ CHARGE ASYMMETRY IN $e^+ e^- \rightarrow \mu^+ \mu^-$

OUR FIT is obtained using the fit procedure and correlations as determined by the LEP Electroweak Working Group (see the "Note on the Z boson"). For the Z peak, we report the pole asymmetry defined by $(3/4)A_e A_\mu$ as determined by the nine-parameter fit to cross-section and lepton forward-backward asymmetry data.

ASYMMETRY (%)	STD. MODEL	\sqrt{s} (GeV)	DOCUMENT ID	TECN
1.73 ± 0.16 OUR FIT				
1.65 ± 0.25		91.2	ABREU	00F DLPH
1.88 ± 0.33		91.2	ACCIARRI	00C L3
1.71 ± 0.24		91.2	156 BARATE	00C ALEP
• • • We do not use the following data for averages, fits, limits, etc. • • •				
9 ± 30	-2	20	157 ABREU	95M DLPH
7 ± 26	-10	40	157 ABREU	95M DLPH
-11 ± 33	-25	57	157 ABREU	95M DLPH
-62 ± 17	-45	69	157 ABREU	95M DLPH
-56 ± 10	-58	79	157 ABREU	95M DLPH
-13 ± 5	-23	87.5	157 ABREU	95M DLPH
1.4 ± 0.5		91.2	ABREU	94 DLPH
1.79 ± 0.61		91.2	ACCIARRI	94 L3
0.99 ± 0.42		91.2	AKERS	94 OPAL
1.46 ± 0.48		91.2	BUSKULIC	94 ALEP
-29.0 ± 5.0 ± 0.5	-32.1	56.9	158 ABE	90I VNS
-9.9 ± 1.5 ± 0.5	-9.2	35	HEGNER	90 JADE
0.05 ± 0.22	0.026	91.14	159 ABRAMS	89D MRK2
-43.4 ± 17.0	-24.9	52.0	160 BACALA	89 AMY
-11.0 ± 16.5	-29.4	55.0	160 BACALA	89 AMY
-30.0 ± 12.4	-31.2	56.0	160 BACALA	89 AMY
-46.2 ± 14.9	-33.0	57.0	160 BACALA	89 AMY
-29 ± 13	-25.9	53.3	ADACHI	88C TOPZ
+5.3 ± 5.0 ± 0.5	-1.2	14.0	ADEVA	88 MRKJ
-10.4 ± 1.3 ± 0.5	-8.6	34.8	ADEVA	88 MRKJ
-12.3 ± 5.3 ± 0.5	-10.7	38.3	ADEVA	88 MRKJ
-15.6 ± 3.0 ± 0.5	-14.9	43.8	ADEVA	88 MRKJ
-1.0 ± 6.0	-1.2	13.9	BRAUNSCH...	88D TASS
-9.1 ± 2.3 ± 0.5	-8.6	34.5	BRAUNSCH...	88D TASS
-10.6 ± 2.2 ± 0.5	-8.9	35.0	BRAUNSCH...	88D TASS
-17.6 ± 4.4 ± 0.5	-15.2	43.6	BRAUNSCH...	88D TASS
-4.8 ± 6.5 ± 1.0	-11.5	39	BEHREND	87C CELL
-18.8 ± 4.5 ± 1.0	-15.5	44	BEHREND	87C CELL
+2.7 ± 4.9	-1.2	13.9	BARTEL	86C JADE
-11.1 ± 1.8 ± 1.0	-8.6	34.4	BARTEL	86C JADE
-17.3 ± 4.8 ± 1.0	-13.7	41.5	BARTEL	86C JADE
-22.8 ± 5.1 ± 1.0	-16.6	44.8	BARTEL	86C JADE
-6.3 ± 0.8 ± 0.2	-6.3	29	ASH	85 MAC
-4.9 ± 1.5 ± 0.5	-5.9	29	DERRICK	85 HRS
-7.1 ± 1.7	-5.7	29	LEVI	83 MRK2
-16.1 ± 3.2	-9.2	34.2	BRANDELIK	82C TASS

156 BARATE 00C error is almost entirely on account of statistics.

157 ABREU 95M perform this measurement using radiative muon-pair events associated with high-energy isolated photons.

158 ABE 90I measurements in the range $50 \leq \sqrt{s} \leq 60.8$ GeV.

159 ABRAMS 89D asymmetry includes both $9 \mu^+ \mu^-$ and $15 \tau^+ \tau^-$ events.

160 BACALA 89 systematic error is about 5%.

 $A_{FB}^{(0,\tau)}$ CHARGE ASYMMETRY IN $e^+ e^- \rightarrow \tau^+ \tau^-$

OUR FIT is obtained using the fit procedure and correlations as determined by the LEP Electroweak Working Group (see the "Note on the Z boson"). For the Z peak, we report the pole asymmetry defined by $(3/4)A_e A_\tau$ as determined by the nine-parameter fit to cross-section and lepton forward-backward asymmetry data.

ASYMMETRY (%)	STD. MODEL	\sqrt{s} (GeV)	DOCUMENT ID	TECN
2.07 ± 0.20 OUR FIT				
2.41 ± 0.37		91.2	ABREU	00F DLPH
2.60 ± 0.47		91.2	ACCIARRI	00C L3
1.70 ± 0.28		91.2	161 BARATE	00C ALEP
• • • We do not use the following data for averages, fits, limits, etc. • • •				
2.2 ± 0.7		91.2	ABREU	94 DLPH
2.65 ± 0.88		91.2	ACCIARRI	94 L3
2.05 ± 0.52		91.2	AKERS	94 OPAL
1.97 ± 0.56		91.2	BUSKULIC	94 ALEP
-32.8 ± 6.4 ± 1.5	-32.1	56.9	162 ABE	90I VNS
-8.1 ± 2.0 ± 0.6	-9.2	35	HEGNER	90 JADE
-18.4 ± 19.2	-24.9	52.0	163 BACALA	89 AMY
-17.7 ± 26.1	-29.4	55.0	163 BACALA	89 AMY
-45.9 ± 16.6	-31.2	56.0	163 BACALA	89 AMY
-49.5 ± 18.0	-33.0	57.0	163 BACALA	89 AMY

-20 ± 14	-25.9	53.3	ADACHI	88c	TOPZ
-10.6 ± 3.1 ± 1.5	-8.5	34.7	ADEVA	88	MRKJ
- 8.5 ± 6.6 ± 1.5	-15.4	43.8	ADEVA	88	MRKJ
- 6.0 ± 2.5 ± 1.0	8.8	34.6	BARTEL	85F	JADE
-11.8 ± 4.6 ± 1.0	14.8	43.0	BARTEL	85F	JADE
- 5.5 ± 1.2 ± 0.5	-0.063	29.0	FERNANDEZ	85	MAC
- 4.2 ± 2.0	0.057	29	LEVI	83	MRK2
-10.3 ± 5.2	-9.2	34.2	BEHREND	82	CELL
- 0.4 ± 6.6	-9.1	34.2	BRANDELIK	82c	TASS

161 BARATE 00c error includes approximately 0.26 due to statistics and 0.11 due to experimental systematics.

162 ABE 90f measurements in the range $50 \leq \sqrt{s} \leq 60.8$ GeV.

163 BACALA 89 systematic error is about 5%.

$A_{FB}^{(0,d)}$ CHARGE ASYMMETRY IN $e^+e^- \rightarrow \ell^+\ell^-$

For the Z peak, we report the pole asymmetry defined by $(3/4)A_2^2$ as determined by the five-parameter fit to cross-section and lepton forward-backward asymmetry data assuming lepton universality. For details see the "Note on the Z boson."

ASYMMETRY (%)	STD. MODEL	\sqrt{s} (GeV)	DOCUMENT ID	TECN
1.82 ± 0.11 OUR FIT				
1.87 ± 0.19		91.2	ABREU	00F DLPH
1.92 ± 0.24		91.2	ACCIARRI	00C L3
1.73 ± 0.16		91.2	164 BARATE	00C ALEP
• • • We do not use the following data for averages, fits, limits, etc. • • •				
1.77 ± 0.37		91.2	ABREU	94 DLPH
1.84 ± 0.45		91.2	ACCIARRI	94 L3
1.28 ± 0.30		91.2	AKERS	94 OPAL
1.71 ± 0.33		91.2	BUSKULIC	94 ALEP

164 BARATE 00c error includes approximately 0.15 due to statistics, 0.04 due to experimental systematics, and 0.02 due to the theoretical uncertainty in t -channel prediction.

$A_{FB}^{(0,u)}$ CHARGE ASYMMETRY IN $e^+e^- \rightarrow u\bar{u}$

ASYMMETRY (%)	STD. MODEL	\sqrt{s} (GeV)	DOCUMENT ID	TECN
4.0 ± 6.7 ± 2.8	6	91.2	165 ACKERSTAFF	97T OPAL

165 ACKERSTAFF 97T measure the forward-backward asymmetry of various fast hadrons made of light quarks. Then using SU(2) isospin symmetry and flavor independence for down and strange quarks authors solve for the different quark types.

$A_{FB}^{(0,s)}$ CHARGE ASYMMETRY IN $e^+e^- \rightarrow s\bar{s}$

The s -quark asymmetry is derived from measurements of the forward-backward asymmetry of fast hadrons containing an s quark.

ASYMMETRY (%)	STD. MODEL	\sqrt{s} (GeV)	DOCUMENT ID	TECN
9.8 ± 1.1 OUR AVERAGE				
10.08 ± 1.13 ± 0.40		91.2	166 ABREU	00b DLPH
6.8 ± 3.5 ± 1.1	10	91.2	167 ACKERSTAFF	97T OPAL
• • • We do not use the following data for averages, fits, limits, etc. • • •				
13.1 ± 3.5 ± 1.3		91.2	168 ABREU	95G DLPH

166 ABREU 00b tag the presence of an s quark requiring a high-momentum-identified charged kaon. The s -quark pole asymmetry is extracted from the charged-kaon asymmetry taking the expected d - and u -quark asymmetries from the Standard Model and using the measured values for the c - and b -quark asymmetries.

167 ACKERSTAFF 97T measure the forward-backward asymmetry of various fast hadrons made of light quarks. Then using SU(2) isospin symmetry and flavor independence for down and strange quarks authors solve for the different quark types. The value reported here corresponds then to the forward-backward asymmetry for "down-type" quarks.

168 ABREU 95G require the presence of a high-momentum charged kaon or A^0 to tag the s quark. An unresolved s - and d -quark asymmetry of $(11.2 \pm 3.1 \pm 5.4)\%$ is obtained by tagging the presence of a high-energy neutron or neutral kaon in the hadron calorimeter. Superseded by ABREU 00b.

$A_{FB}^{(0,c)}$ CHARGE ASYMMETRY IN $e^+e^- \rightarrow c\bar{c}$

OUR FIT, which is obtained by a simultaneous fit to several c - and b -quark measurements as explained in the "Note on the Z boson," refers to the Z pole asymmetry. As a cross check we have also performed a weighted average of the "near peak" measurements taking into account the various common systematic errors. We have assumed that the smallest common systematic error is fully correlated. Applying to this combined "peak" measurement QED and energy-dependence corrections, our weighted average gives a pole asymmetry of $(7.18 \pm 0.49)\%$.

ASYMMETRY (%)	STD. MODEL	\sqrt{s} (GeV)	DOCUMENT ID	TECN
7.01 ± 0.45 OUR FIT				
6.59 ± 0.94 ± 0.35		91.235	169 ABREU	99Y DLPH
6.3 ± 0.9 ± 0.3		91.22	170 BARATE	98O ALEP
6.3 ± 1.2 ± 0.6		91.22	171 ALEXANDER	97C OPAL
6.00 ± 0.67 ± 0.52		91.24	172 ALEXANDER	96 OPAL
8.3 ± 2.2 ± 1.6		91.27	173 ABREU	95K DLPH
9.9 ± 2.0 ± 1.7		91.24	174 BUSKULIC	94G ALEP
8.3 ± 3.8 ± 2.7	5.6	91.24	175 ADRIANI	92D L3

• • • We do not use the following data for averages, fits, limits, etc. • • •

- 4.96 ± 3.68 ± 0.53	89.434	169 ABREU	99Y DLPH	
- 11.80 ± 3.18 ± 0.62	92.990	169 ABREU	99Y DLPH	
- 1.0 ± 4.3 ± 1.0	89.37	170 BARATE	98O ALEP	
11.0 ± 3.3 ± 0.8	92.96	170 BARATE	98O ALEP	
3.9 ± 5.1 ± 0.9	89.45	171 ALEXANDER	97C OPAL	
15.8 ± 4.1 ± 1.1	93.00	171 ALEXANDER	97C OPAL	
- 7.5 ± 3.4 ± 0.6	-3.5	89.52	172 ALEXANDER	96 OPAL
14.1 ± 2.8 ± 0.9	12.0	92.94	172 ALEXANDER	96 OPAL
7.7 ± 2.9 ± 1.2	91.27	176 ABREU	95E DLPH	
6.99 ± 2.05 ± 1.02	91.24	177 BUSKULIC	95I ALEP	
- 12.9 ± 7.8 ± 5.5	-13.6	35	BEHREND	90D CELL
7.7 ± 13.4 ± 5.0	-22.1	43	BEHREND	90D CELL
- 12.8 ± 4.4 ± 4.1	-13.6	35	ELSEN	90 JADE
- 10.9 ± 12.9 ± 4.6	-23.2	44	ELSEN	90 JADE
- 14.9 ± 6.7	-13.3	35	OULD-SAADA	89 JADE

169 ABREU 99Y tag $Z \rightarrow b\bar{b}$ and $Z \rightarrow c\bar{c}$ events by an exclusive reconstruction of several D meson decay modes (D^{*+} , D^0 , and D^+ with their charge-conjugate states).

170 BARATE 98o tag $Z \rightarrow c\bar{c}$ events requiring the presence of high-momentum reconstructed D^{*+} , D^+ , or D^0 mesons.

171 ALEXANDER 97c identify the b and c events using a D/D^* tag.

172 ALEXANDER 96 tag heavy flavors using one or two identified leptons. This allows the simultaneous fitting of the b and c quark forward-backward asymmetries as well as the average B^0 - \bar{B}^0 mixing.

173 ABREU 95k identify c and b quarks using both electron and muon semileptonic decays.

174 BUSKULIC 94G perform a simultaneous fit to the p and p_T spectra of both single and dilepton events.

175 ADRIANI 92D use both electron and muon semileptonic decays.

176 ABREU 95E require the presence of a $D^{*\pm}$ to identify c and b quarks. Replaced by ABREU 99Y.

177 BUSKULIC 95i require the presence of a high momentum $D^{*\pm}$ to have an enriched sample of $Z \rightarrow c\bar{c}$ events. Replaced by BARATE 98o.

$A_{FB}^{(0,b)}$ CHARGE ASYMMETRY IN $e^+e^- \rightarrow b\bar{b}$

OUR FIT, which is obtained by a simultaneous fit to several c - and b -quark measurements as explained in the "Note on the Z boson," refers to the Z pole asymmetry. As a cross check we have also performed a weighted average of the "near peak" measurements taking into account the various common systematic errors. We have assumed that the smallest common systematic error is fully correlated. Applying to this combined "peak" measurement QED and energy-dependence corrections, our weighted average gives a pole asymmetry of $(10.09 \pm 0.22)\%$. For the jet-charge measurements (where the QCD effects are included since they represent an inherent part of the analysis), we use the corrections given by the authors.

ASYMMETRY (%)	STD. MODEL	\sqrt{s} (GeV)	DOCUMENT ID	TECN
10.03 ± 0.22 OUR FIT				
9.82 ± 0.47 ± 0.16		91.26	178 ABREU	99M DLPH
7.62 ± 1.94 ± 0.85		91.235	179 ABREU	99Y DLPH
9.60 ± 0.66 ± 0.33		91.26	180 ACCIARRI	99D L3
9.31 ± 1.01 ± 0.55		91.24	181 ACCIARRI	98U L3
10.40 ± 0.40 ± 0.32		91.25	182 BARATE	98M ALEP
9.94 ± 0.52 ± 0.44		91.21	183 ACKERSTAFF	97P OPAL
9.4 ± 2.7 ± 2.2		91.22	184 ALEXANDER	97C OPAL
9.06 ± 0.51 ± 0.23		91.24	185 ALEXANDER	96 OPAL
9.65 ± 0.44 ± 0.26		91.21	186 BUSKULIC	96Q ALEP
10.4 ± 1.3 ± 0.5		91.27	187 ABREU	95K DLPH

• • • We do not use the following data for averages, fits, limits, etc. • • •

6.8 ± 1.8 ± 0.13	89.55	178 ABREU	99M DLPH
12.3 ± 1.6 ± 0.27	92.94	178 ABREU	99M DLPH
5.67 ± 7.56 ± 1.17	89.434	179 ABREU	99Y DLPH
8.82 ± 6.33 ± 1.22	92.990	179 ABREU	99Y DLPH
6.11 ± 2.93 ± 0.43	89.50	180 ACCIARRI	99D L3
13.71 ± 2.40 ± 0.44	93.10	180 ACCIARRI	99D L3
4.95 ± 5.23 ± 0.40	89.45	181 ACCIARRI	98U L3
11.37 ± 3.99 ± 0.65	92.99	181 ACCIARRI	98U L3
7.46 ± 1.78 ± 0.24	89.43	182 BARATE	98M ALEP
9.24 ± 1.79 ± 0.52	92.97	182 BARATE	98M ALEP
4.1 ± 2.1 ± 0.2	89.44	183 ACKERSTAFF	97P OPAL
14.5 ± 1.7 ± 0.7	92.91	183 ACKERSTAFF	97P OPAL
- 8.6 ± 10.8 ± 2.9	89.45	184 ALEXANDER	97C OPAL
- 2.1 ± 9.0 ± 2.6	93.00	184 ALEXANDER	97C OPAL
5.5 ± 2.4 ± 0.3	89.52	185 ALEXANDER	96 OPAL
11.7 ± 2.0 ± 0.3	92.94	185 ALEXANDER	96 OPAL
- 3.4 ± 11.2 ± 0.7	88.38	186 BUSKULIC	96Q ALEP
5.3 ± 2.0 ± 0.2	89.38	186 BUSKULIC	96Q ALEP
8.9 ± 5.9 ± 0.4	90.21	186 BUSKULIC	96Q ALEP
3.8 ± 5.1 ± 0.2	92.05	186 BUSKULIC	96Q ALEP
10.3 ± 1.6 ± 0.4	92.94	186 BUSKULIC	96Q ALEP
8.8 ± 7.5 ± 0.5	93.90	186 BUSKULIC	96Q ALEP
5.9 ± 6.2 ± 2.4	91.27	188 ABREU	95E DLPH
11.5 ± 1.7 ± 1.0	91.27	189 ABREU	95K DLPH
6.2 ± 3.4 ± 0.2	89.52	190 AKERS	95S OPAL
9.63 ± 0.67 ± 0.38	91.25	190 AKERS	95S OPAL
17.2 ± 2.8 ± 0.7	92.94	190 AKERS	95S OPAL

Gauge & Higgs Boson Particle Listings

Z

8.7 ± 1.1 ± 0.4	91.3	191 ACCIARRI	94D L3
8.7 ± 1.4 ± 0.2	91.24	192 BUSKULIC	94G ALEP
9.92 ± 0.84 ± 0.46	91.19	193 BUSKULIC	94I ALEP
-71 ± 34 ± 7/8	-58	58.3 SHIMONAKA	91 TOPZ
-22.2 ± 7.7 ± 3.5	-26.0	35 BEHREND	90D CELL
-49.1 ± 16.0 ± 5.0	-39.7	43 BEHREND	90D CELL
-28 ± 11	-23	35 BRAUNSCH...	90 TASS
-16.6 ± 7.7 ± 4.8	-24.3	35 ELSÉN	90 JADE
-33.6 ± 22.2 ± 5.2	-39.9	44 ELSÉN	90 JADE
3.4 ± 7.0 ± 3.5	-16.0	29.0 BAND	89 MAC
-72 ± 28 ± 13	-56	55.2 SAGAWA	89 AMY

178 ABREU 99M tag $Z \rightarrow b\bar{b}$ events using lifetime and vertex charge. The original quark charge is obtained from the charge flow, the difference between the forward and backward hemisphere charges.

179 ABREU 99Y tag $Z \rightarrow b\bar{b}$ and $Z \rightarrow c\bar{c}$ events by an exclusive reconstruction of several D meson decay modes (D^{*+} , D^0 , and D^+ with their charge-conjugate states).

180 ACCIARRI 99D tag $Z \rightarrow b\bar{b}$ events using high p and p_T leptons. The analysis determines simultaneously a mixing parameter $\chi_b = 0.1192 \pm 0.0068 \pm 0.0051$ which is used to correct the observed asymmetry.

181 ACCIARRI 98U tag $Z \rightarrow b\bar{b}$ events using lifetime and measure the jet charge using the hemisphere charge.

182 BARATE 98M tag $Z \rightarrow b\bar{b}$ events using lifetime and measure the jet charge using the hemisphere charge. The analysis is performed as a function of the b quark purity and b polar angle.

183 ACKERSTAFF 97P tag b quarks using lifetime. The quark charge is measured using both jet charge and vertex charge, a weighted sum of the charges of tracks in a jet which contains a tagged secondary vertex.

184 ALEXANDER 97C identify the b and c events using a D/D^* tag.

185 ALEXANDER 96 tag heavy flavors using one or two identified leptons. This allows the simultaneous fitting of the b and c quark forward-backward asymmetries as well as the average B^0 - \bar{B}^0 mixing.

186 BUSKULIC 96Q tag b -quark flavor and charge using high transverse momentum leptons. The asymmetry value at the Z peak is obtained using a charm charge asymmetry of 6.17%.

187 ABREU 95K identify c and b quarks using both electron and muon semileptonic decays. The systematic error includes an uncertainty of ± 0.3 due to the mixing correction ($\chi = 0.115 \pm 0.011$).

188 ABREU 95E require the presence of a D^{*+} to identify c and b quarks. Replaced by ABREU 99Y.

189 ABREU 95K tag b quarks using lifetime; the quark charge is identified using jet charge. The systematic error includes an uncertainty of ± 0.3 due to the mixing correction ($\chi = 0.115 \pm 0.011$). Replaced by ABREU 99M.

190 AKERS 95S tag b quarks using lifetime; the quark charge is measured using jet charge. These asymmetry values are obtained using $R_b = \Gamma(bb)/\Gamma(\text{hadrons}) = 0.216$. For a value of R_b different from this by an amount ΔR_b , the change in the asymmetry values is given by $-K\Delta R_b$, where $K = 0.082, 0.471$, and 0.855 for \sqrt{s} values of 89.52, 91.25, and 92.94 GeV respectively. Replaced by ACKERSTAFF 97P.

191 ACCIARRI 94D use both electron and muon semileptonic decays. Replaced by ACCIARRI 99D.

192 BUSKULIC 94G perform a simultaneous fit to the p and p_T spectra of both single and dilepton events. Replaced by BUSKULIC 96Q.

193 BUSKULIC 94I use the lifetime tag method to obtain a high purity sample of $Z \rightarrow b\bar{b}$ events and the hemisphere charge technique to obtain the jet charge. Replaced by BARATE 98M.

CHARGE ASYMMETRY IN $e^+e^- \rightarrow q\bar{q}$

Summed over five lighter flavors.

Experimental and Standard Model values are somewhat event-selection dependent. Standard Model expectations contain some assumptions on B^0 - \bar{B}^0 mixing and on other electroweak parameters.

ASYMMETRY (%)	STD. MODEL	\sqrt{s} (GeV)	DOCUMENT ID	TECN
• • • We do not use the following data for averages, fits, limits, etc. • • •				
-0.76 ± 0.12 ± 0.15		91.2	194 ABREU	92I DLPH
4.0 ± 0.4 ± 0.63	4.0	91.3	195 ACTON	92L OPAL
9.1 ± 1.4 ± 1.6	9.0	57.9	ADACHI	91 TOPZ
-0.84 ± 0.15 ± 0.04		91	DECAMP	91B ALEP
8.3 ± 2.9 ± 1.9	8.7	56.6	STUART	90 AMY
11.4 ± 2.2 ± 2.1	8.7	57.6	ABE	89L VNS
6.0 ± 1.3	5.0	34.8	GREENSHAW	89 JADE
8.2 ± 2.9	8.5	43.6	GREENSHAW	89 JADE

- 194 ABREU 92I has 0.14 systematic error due to uncertainty of quark fragmentation.
- 195 ACTON 92L use the weight function method on 259k selected $Z \rightarrow$ hadrons events. The systematic error includes a contribution of 0.2 due to B^0 - \bar{B}^0 mixing effect, 0.4 due to Monte Carlo (MC) fragmentation uncertainties and 0.3 due to MC statistics. ACTON 92L derive a value of $\sin^2\theta_W^{\text{eff}}$ to be $0.2321 \pm 0.0017 \pm 0.0028$.

CHARGE ASYMMETRY IN $p\bar{p} \rightarrow Z \rightarrow e^+e^-$

ASYMMETRY (%)	STD. MODEL	\sqrt{s} (GeV)	DOCUMENT ID	TECN
• • • We do not use the following data for averages, fits, limits, etc. • • •				
5.2 ± 5.9 ± 0.4		91	ABE	91E CDF

ANOMALOUS $ZZ\gamma$, $Z\gamma\gamma$, AND ZZV COUPLINGS

Revised March 2000 by C. Caso (Univ. of Genova) and A. Gurtu (Tata Inst.)

In the reaction $e^+e^- \rightarrow Z\gamma$, deviations from the Standard Model for the $ZV\gamma$ couplings may be described in terms of 8 parameters, h_i^V ($i = 1, 4; V = \gamma, Z$) [1]. In this formalism h_1^V and h_2^V lead to CP -violating and h_3^V and h_4^V to CP -conserving effects. All these anomalous contributions to the cross section increase rapidly with center-of-mass energy. In order to ensure unitarity, these parameters are usually described by a form-factor representation, $h_i^V(s) = h_{i0}^V/(1 + s/\Lambda^2)^n$, where Λ is the energy scale for the manifestation of a new phenomenon and n is a sufficiently large power. By convention one uses $n = 3$ for $h_{1,3}^V$ and $n = 4$ for $h_{2,4}^V$. Usually limits on h_i^V 's are put assuming some value of Λ (sometimes ∞).

Above the $e^+e^- \rightarrow ZZ$ threshold, deviations from the Standard Model may be described by means of four anomalous couplings f_i^V ($i = 4, 5; V = \gamma, Z$) [2]. The anomalous couplings f_3^V lead to violation of C and P symmetries while f_4^V introduces CP violation. These couplings are zero at tree level in the Standard Model.

Reference

- U. Baur and E.L. Berger Phys. Rev. **D47**, 4889 (1993).
- K. Hagiwara *et al.*, Nucl. Phys. **B282**, 253 (1987).

 h_i^V

• • • We do not use the following data for averages, fits, limits, etc. • • •

VALUE	DOCUMENT ID	TECN
196 ABBOTT	98M D0	
197 ABREU	98K DLPH	
198 ACCIARRI	98L L3	

- 196 ABBOTT 98M study $p\bar{p} \rightarrow Z\gamma + X$, with $Z \rightarrow e^+e^-, \mu^+\mu^-, \nu\nu$ at 1.8 TeV, to obtain 95% CL limits at $\Lambda = 750$ GeV: $|h_{30}^Z| < 0.36$, $|h_{40}^Z| < 0.05$ (keeping $h_1^Z = 0$) and $|h_{30}^Z| < 0.37$, $|h_{40}^Z| < 0.05$ (keeping $h_1^Z = 0$). Limits on the CP -violating couplings are $|h_{10}^Z| < 0.36$, $|h_{20}^Z| < 0.05$ (keeping $h_1^Z = 0$), and $|h_{10}^Z| < 0.37$, $|h_{20}^Z| < 0.05$ (keeping $h_1^Z = 0$).

- 197 ABREU 98K determine a 95% CL upper limit on $\sigma(e^+e^- \rightarrow \gamma + \text{invisible particles}) < 2.5$ pb using 161 and 172 GeV data. This is used to set 95% CL limits on $|h_{30}^Z| < 0.8$ and $|h_{30}^Z| < 1.3$, derived at a scale $\Lambda = 1$ TeV and with $n = 3$ in the form factor representation.

- 198 ACCIARRI 98L study 161, 172, and 183 GeV $e^+e^- \rightarrow q\bar{q}\gamma$ and $e^+e^- \rightarrow \nu\bar{\nu}\gamma$ events to derive 95% CL limits on h_i^V . For deriving each limit the others are fixed at zero. For $\Lambda = \infty$ they report: $-0.54 < h_1^Z < 0.17$, $-0.11 < h_2^Z < 0.37$, $-0.50 < h_3^Z < 0.36$, $-0.12 < h_4^Z < 0.39$, $-0.25 < h_1^T < 0.23$, $-0.18 < h_2^T < 0.18$, $-0.33 < h_3^T < 0.01$, $-0.02 < h_4^T < 0.24$.

 f_i^V

• • • We do not use the following data for averages, fits, limits, etc. • • •

VALUE	DOCUMENT ID	TECN
199 ACCIARRI	99O L3	

- 199 ACCIARRI 99O study ZZ production in e^+e^- collisions at 183 and 189 GeV to derive 95%CL limits on f_i^V . For deriving each limit the others are fixed at zero. They report: $-1.9 < f_4^Z < 1.9$, $-5.0 < f_5^Z < 4.5$, $-1.1 < f_4^T < 1.2$, $-3.0 < f_5^T < 2.9$.

Gauge & Higgs Boson Particle Listings

Higgs Bosons — H^0 and H^\pm

Higgs Bosons — H^0 and H^\pm , Searches for

SEARCHES FOR HIGGS BOSONS

Written February 2000 by P. Igo-Kemenes (Physikalisches Institut, Heidelberg, Germany)

I. Introduction

One of the main challenges in high energy physics is the discovery of Higgs bosons. Their existence is related to the generation of elementary particle masses. In the Standard Model (SM) [1], the electroweak interaction is described by a gauge field theory based on the $SU(2)_L \times U(1)_Y$ symmetry group. Masses can be introduced by the Higgs mechanism [2], where fundamental scalar “Higgs” fields interact with each other such that they acquire a nonzero vacuum expectation value and the $SU(2)_L \times U(1)_Y$ symmetry is spontaneously broken down to the electromagnetic $U(1)_{EM}$ symmetry. Gauge bosons and fermions obtain their masses by interacting with the vacuum Higgs field. Associated with this mechanism is the existence of massive scalar particles called Higgs bosons, and the proof for the above mechanism would come from the direct observation of this novel particle species.

In its minimal version, the SM requires one Higgs field doublet and predicts a single neutral Higgs boson. Beyond the SM, supersymmetric (SUSY) models [3] are considered. They provide a consistent framework for the unification of the gauge interactions at a high energy scale $\Lambda_{GUT} \approx 10^{16}$ GeV and an explanation for the stability of the electroweak energy scale in the presence of quantum corrections (the “scale hierarchy problem”). Moreover, their predictions are compatible with existing high-precision data. The Minimal Supersymmetric Standard Model (MSSM) [4] is the SUSY extension of the SM with minimal new particle content. It needs two Higgs field doublets and predicts the existence of three neutral and a pair of charged Higgs bosons. While in the SM the mass of the Higgs boson is not predicted, in SUSY models the Higgs masses are related to the gauge couplings. As a consequence, one of the neutral Higgs bosons must have its mass close to the electroweak energy scale. In the MSSM this mass is predicted to be less than about 135 GeV [5].

Prior to 1989, when the e^+e^- collider LEP at CERN came into operation, Higgs boson searches were sensitive to masses below a few GeV only (see Ref. 6 for a review). The LEP collider, operating for five years at a center-of-mass energy $\sqrt{s} \approx M_{Z^0}$ (the LEP1 phase), definitively excluded a SM Higgs boson with a mass between zero and about 65 GeV [7]. Since 1995, the center-of-mass energy has increased each year (the LEP2 phase) and has reached $\sqrt{s} = 204$ GeV in 1999, within a few GeV of the highest energy expected. When the full data of the four LEP experiments are combined, the sensitivity for discovery will extend to SM Higgs boson masses of approximately 110 GeV. After the LEP experiments finish taking data, searches for Higgs bosons will be pursued primarily

at the Tevatron $p\bar{p}$ collider. The sensitivity to Higgs bosons in the Run I data is rather limited, though the planned energy and luminosity upgrades (Run II [8]) would extend the sensitivity well beyond the LEP range. The searches will continue later at the LHC pp collider [9] covering the canonical mass range up to about 1 TeV. If Higgs bosons are discovered, the Higgs mechanism can be studied in great detail at future e^+e^- [10] and $\mu^+\mu^-$ colliders [11].

The sensitivity of current searches is continuously improving with increasing collider energies and sample sizes. There is also ongoing activity in refining the phenomenology relevant to Higgs boson searches. In order to provide an up to date description, recent documents are quoted even though in some cases they are not published. Such documents (indicated by **name** in the Reference list) can be accessed conveniently from the web page <http://home.cern.ch/p/pik/www/pdg2000/index.html>.

II. Higgs boson masses

In the Standard Model, the Higgs mass $m_{H^0} = \sqrt{2\lambda}v$ is proportional to the vacuum expectation value v of the Higgs field, which is fixed by the Fermi coupling. The quartic Higgs coupling λ , and thus m_{H^0} , is not determined, but arguments of self-consistency of the theory can be used to place upper and lower bounds on m_{H^0} .

Since the running coupling λ rises indefinitely with energy, the theory would eventually become non-perturbative. The requirement that in the SM this does not occur at a scale lower than Λ defines an upper bound for the Higgs mass [12]. On the other hand, a lower bound for m_{H^0} is obtained from top-loop induced quantum corrections to the Higgs interaction potential [13]. The requirement that the electroweak minimum is an absolute minimum up to the scale Λ yields a “vacuum stability” condition which limits m_{H^0} from below. These theoretical bounds are summarized in Fig. 1 [14] as a function of Λ . Self-consistency of the SM up to $\Lambda = \Lambda_{GUT}$ allows only the narrow band from about 130 to 190 GeV for the mass. This range is beyond the reach of LEP2, which implies that the discovery of a Higgs boson at LEP would indicate new physics beyond the SM at energies lower than Λ_{GUT} .

Indirect experimental bounds for the Higgs mass are obtained from fits to precision measurements of electroweak observables, primarily from Z^0 decay data, and to the measured top and W^\pm masses [15]. These measurements are sensitive to $\log(m_{H^0})$ through radiative corrections. Currently the best fit value is $m_{H^0} = 77_{-39}^{+69}$ GeV, and $m_{H^0} < 215$ GeV is obtained at the 95% confidence level (CL) [16], still consistent with the SM being valid up to the GUT scale.

In the MSSM, one of the two Higgs field doublets, with vacuum expectation value v_1 , couples to “down” quarks and charged leptons while the second, with v_2 , couples to “up” quarks only. Assuming CP invariance, the spectrum of physical Higgs bosons [4] consists of two CP -even neutral scalars h^0 and H^0 (h^0 is the one with the smaller mass), one CP -odd neutral scalar A^0 , and one pair of charged Higgs bosons H^\pm .

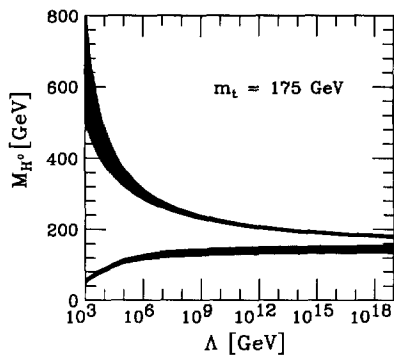


Figure 1: Bounds on the Higgs mass based on arguments of self-consistency of the SM [14]. Λ denotes the energy scale at which the SM would become non-perturbative or the electroweak potential unstable. The dark bands represent the theoretical uncertainties.

At the tree level, only two parameters are required (beyond the Z^0 mass) to fix all Higgs masses and couplings. A convenient choice is the ratio $\tan\beta = v_2/v_1$ and the mass (m_{A^0}) of the CP -odd scalar A^0 . The mixing angle α which diagonalizes the CP -even Higgs mass matrix can also be expressed in terms of $\tan\beta$ and m_{A^0} . The following ordering of masses is valid at the tree level: $m_{h^0} < M_Z$, $m_{A^0} < m_{H^0}$, and $m_{A^0}, M_W < m_{H^\pm}$. These relations are modified by radiative corrections; the largest contribution is a consequence of the incomplete cancellation between virtual-top and scalar-top (stop) loops. The corrections affect mainly the masses and decay branching ratios in the neutral Higgs sector. They depend strongly on the top quark mass ($\sim m_t^4$) and logarithmically on the stop masses, and involve a detailed parameterization of SUSY breaking and of the mixing between the SUSY partners of the left- and right-handed top quarks [17].

The Higgs masses, after radiative corrections, are displayed in Fig. 2 as a function of m_{A^0} for two representative values of $\tan\beta$ within the range from 1 to $\approx m_t/m_b$ which is preferred in grand unification schemes [18]. One observes that m_{h^0} may exceed M_Z .

III. Higgs boson production and decay

A comprehensive discussion of the Higgs boson phenomenology is given in Ref. 19. In this section the focus is on Higgs production in e^+e^- collisions at energies below 210 GeV (LEP2) [20] by which most of the recent search results have been obtained. Extensions to higher e^+e^- energies [10] and to production in hadron collisions [8,9] are discussed briefly in Sections V and VI.

Higgs boson production in e^+e^- collisions:

The principal mechanism for producing the *SM Higgs particle* in e^+e^- collisions at current energies is Higgs-strahlung in the s -channel [21], $e^+e^- \rightarrow H^0 Z^0$, where a Higgs boson is radiated off an intermediate Z^0 boson. The Z^0 boson in the final state is either virtual (LEP1) or on the mass shell (LEP2).

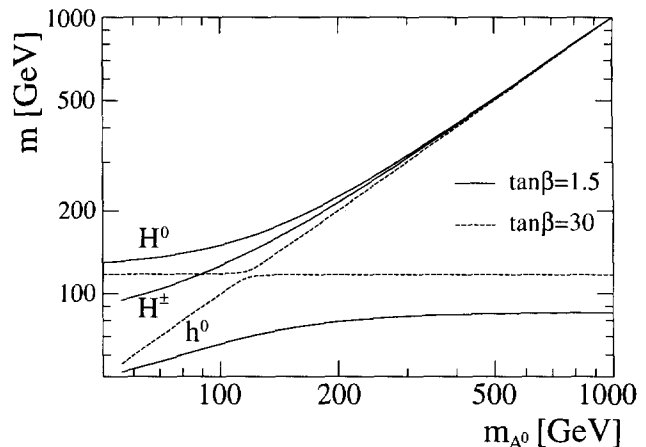


Figure 2: Higgs masses in the MSSM after radiative corrections, as a function of m_{A^0} for two representative values of $\tan\beta$; 1.5 and 30 (in the case of H^\pm the variation with $\tan\beta$ is invisible on the scale of the figure).

In the latter case (at energies far from the Z^0 resonance) the cross section is given by

$$\sigma(e^+e^- \rightarrow Z^0 H^0) = \frac{G_F^2 M_Z^4}{96\pi s} (v_e^2 + a_e^2) \lambda^{1/2} \frac{\lambda + 12M_Z^2/s}{(1 - M_Z^2/s)^2} \equiv \sigma_{\text{SM}} \quad (1)$$

where s denotes the center-of-mass energy squared, $a_e = -1$, $v_e = -1 + 4s_W^2$ ($s_W = \sin\theta_W$ is the *sine* of the weak-mixing angle), and $\lambda = [1 - (m_{H^0} + M_Z)^2/s][1 - (m_{H^0} - M_Z)^2/s]$ is the two-particle phase-space function. The cross section [21,22] is shown in Fig. 3 as a function of \sqrt{s} , together with that of other SM processes.

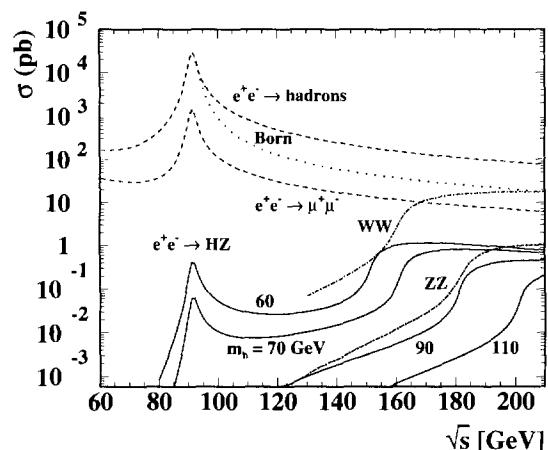


Figure 3: Cross sections for the Higgs-strahlung process in the SM for fixed values of m_{H^0} (full lines) and for other SM processes which contribute to the background, as a function of \sqrt{s} .

Gauge & Higgs Boson Particle Listings

Higgs Bosons — H^0 and H^\pm

The SM Higgs boson can also be produced by W^+W^- fusion in the t -channel [23], $e^+e^- \rightarrow \bar{\nu}_e\nu_e H^0$, but at current energies this process has a small contribution to the cross section, except for Higgs masses which cannot be reached by the Higgs-strahlung process. The W^+W^- fusion process may extend slightly the ultimate range of sensitivity at LEP2 [20].

In the *MSSM*, the main production mechanisms of the neutral Higgs bosons h^0 and A^0 are [24] the Higgs-strahlung process $e^+e^- \rightarrow h^0 Z^0$ and the pair-production process $e^+e^- \rightarrow h^0 A^0$. As in the SM case, the fusion process plays a marginal role at current energies. Furthermore, the production of the heavy neutral CP -even Higgs boson H^0 is suppressed over most of the parameter space currently accessible. The cross sections for the Higgs-strahlung and pair-production processes may be expressed in terms of σ_{SM} given in Eq. (1) and the angles α and β introduced before:

$$\sigma(e^+e^- \rightarrow Z^0 h^0) = \sin^2(\beta - \alpha) \sigma_{\text{SM}} \quad (2)$$

$$\sigma(e^+e^- \rightarrow A^0 h^0) = \cos^2(\beta - \alpha) \bar{\lambda} \sigma_{\text{SM}}, \quad (3)$$

with the kinematic factor $\bar{\lambda} = \lambda_{A^0 h^0}^{3/2} / [\lambda_{Z^0 h^0}^{1/2} (12M_Z^2/s + \lambda_{Z^0 h^0})]$ and $\lambda_{ij} = [1 - (m_i + m_j)^2/s][1 - (m_i - m_j)^2/s]$. The cross sections are complementary due to the *MSSM* suppression factors $\sin^2(\beta - \alpha)$ and $\cos^2(\beta - \alpha)$. At small $\tan\beta$ the process $e^+e^- \rightarrow Z^0 h^0$ has the larger cross section while at large $\tan\beta$ it is $e^+e^- \rightarrow h^0 A^0$, unless the latter is suppressed kinematically.

In models with *two Higgs field doublets* (2HD models), including the *MSSM*, charged Higgs bosons are expected to be produced in pairs [19,25], $e^+e^- \rightarrow H^+H^-$, and the cross section is fixed at the tree level by the mass m_{H^\pm} :

$$\sigma(e^+e^- \rightarrow H^+H^-) = \frac{2G_F^2 M_W^4 s_W^4}{3\pi s} \times \left[1 + \frac{v_e v_H}{4s_W^2 c_W^2 (1 - M_Z^2/s)} + \frac{(a_e^2 + v_e^2) v_H^2}{64s_W^4 c_W^4 (1 - M_Z^2/s)^2} \right] \beta_H^3 \quad (4)$$

with $c_W = \cos\theta_W$, $v_H = -1 + 2s_W^2$, and $\beta_H = (1 - 4m_{H^\pm}^2/s)^{1/2}$.

Higgs boson decay:

In the case of the *SM Higgs boson*, the most relevant decay branching ratios [22,26] are summarized in Fig. 4. For masses below about 135 GeV, decays to fermion anti-fermion pairs dominate, and $H^0 \rightarrow b\bar{b}$ has the largest branching ratio. Decays to $\tau^+\tau^-$, $c\bar{c}$, and gluon pairs (*via* loops) are below 10%. The decay width is less than 10 MeV. For larger masses, the W^+W^- , $Z^0 Z^0$ final states dominate [10] and the decay width rises rapidly with mass, reaching about 1 GeV for $m_{H^0} = 200$ GeV and 100 GeV for $m_{H^0} = 500$ GeV.

In the *MSSM*, the couplings of the neutral Higgs bosons to quarks, leptons, and gauge bosons are modified with respect to those of the SM Higgs boson by factors which depend upon the mixing angles α and β . These factors, valid at leading order, are summarized in Table 1. The decays are discussed in [19,24]. Some features relevant to current searches are discussed below.

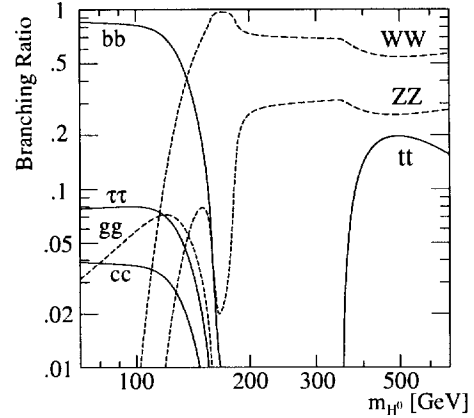


Figure 4: Branching ratios for the main decay modes of the SM Higgs boson [10].

Table 1: Factors relating the SM Higgs couplings to the corresponding couplings in the *MSSM*.

	“Up” fermions	“Down” fermions	Vector bosons
SM-Higgs:	1	1	1
<i>MSSM</i> h^0 :	$\cos\alpha/\sin\beta$	$-\sin\alpha/\cos\beta$	$\sin(\beta - \alpha)$
H^0 :	$\sin\alpha/\sin\beta$	$\cos\alpha/\cos\beta$	$\cos(\beta - \alpha)$
A^0 :	$1/\tan\beta$	$\tan\beta$	0

- The h^0 boson will decay mainly to fermion pairs since the mass is smaller than about 135 GeV. The A^0 boson also decays predominantly to fermion pairs, independently of its mass, since its coupling to vector bosons is zero at leading order (see Table 1). For $\tan\beta > 1$, decays to $b\bar{b}$ and $\tau^+\tau^-$ pairs are preferred, with branching ratios of about 90% and 8%, respectively, while the decays to $c\bar{c}$ and gluon pairs are suppressed. Decays to $c\bar{c}$ may become important for $\tan\beta < 1$.
- The decay $h^0 \rightarrow A^0 A^0$ may become dominant if it is kinematically allowed [25].
- Other possible decays are into SUSY particles such as sfermions, charginos or neutralinos, which may lead to invisible or barely visible final states. The branching fractions can be large, even dominant in parts of the *MSSM* parameter space, thus requiring a different search strategy.

Charged Higgs bosons in 2HD models decay mainly *via* $H^\pm \rightarrow \tau^+\nu_\tau$ if $\tan\beta$ is large. For small $\tan\beta$, the decay to $c\bar{c}$ is dominant at low mass, and the decay to $H^\pm \rightarrow t^*\bar{b} \rightarrow W^+\bar{b}\bar{b}$ is dominant for H^\pm masses larger than about 130 GeV [27].

IV. The search environment at LEP

During the first phase of LEP, the experiments ALEPH, DELPHI, L3, and OPAL analysed over four million Z^0 decays each. They have set lower bounds of approximately 65 GeV

on the mass of the SM Higgs boson, and of about 45 GeV on the masses of the h^0 , A^0 (valid for $\tan\beta > 1$) and also for H^\pm bosons. At energies above the Z^0 resonance (the LEP2 phase) the experimental environment is different in many respects. The signal-to-background ratio at LEP2 is more favorable (see Fig. 3), despite the additional backgrounds from the processes $e^+e^- \rightarrow W^+W^-$ and Z^0Z^0 . The latter have kinematic properties similar to the signal process $e^+e^- \rightarrow H^0Z^0$, but since at LEP2 the Z^0 boson is on the mass shell, constrained kinematic fits allow a good overall signal-to-background ratio to be achieved. Furthermore, since neutral Higgs bosons decay preferentially to $b\bar{b}$, the LEP Collaborations have considerably upgraded their b -tagging capabilities for the LEP2 phase. Jets with B hadrons are recognized by the presence of secondary decay vertices or tracks with large impact parameters, identified by means of high-precision silicon microvertex detectors. Other indicators for B hadron decays are high- p_T leptons ($\ell = e, \mu$) from $b \rightarrow c\ell^-\bar{\nu}_\ell$ decays and several jet properties.

The following final states provide good sensitivity for neutral Higgs bosons (here h^0 may designate either the SM Higgs boson or the light CP -even neutral scalar in the MSSM).

(a) The **four-jet final state** is produced by the processes ($h^0 \rightarrow b\bar{b}$)($Z^0 \rightarrow q\bar{q}$) and ($h^0 \rightarrow b\bar{b}$)($A^0 \rightarrow b\bar{b}$). In the SM it occurs with a branching ratio of 58%. In the first process, the invariant mass of two of the jets is close to M_Z , while the other two jets contain B hadrons. In the second process, the Z^0 mass constraint cannot be used, but B hadrons are expected in all four jets. The Higgs mass can be reconstructed with a typical resolution of 2.5 GeV.

(b) The **missing-energy final state** is produced mainly by the process ($h^0 \rightarrow b\bar{b}$)($Z^0 \rightarrow \nu\bar{\nu}$). In the SM it occurs with a branching ratio of 17%. The signal has two jets with B hadrons, substantial missing transverse momentum and missing mass compatible with M_Z . A similar event topology would also occur in h^0Z^0 and h^0A^0 if the h^0 or the A^0 boson decayed into “invisible” SUSY particles (*e.g.*, neutralinos), or in the W^+W^- fusion process leading to $b\bar{b}\nu_e\bar{\nu}_e$ events. The reconstruction of the Higgs boson requires good knowledge of the detector acceptance and energy resolution; it is achieved with a typical resolution of 3 GeV, but the distribution usually has a pronounced non-Gaussian tail.

(c) The **leptonic final states** are produced in the processes ($h^0 \rightarrow b\bar{b}$)($Z^0 \rightarrow e^+e^-, \mu^+\mu^-$). In the SM the branching ratios add up to 6%. The two leptons reconstruct to M_Z and the two jets contain B hadrons. Although the branching ratio is small, this channel adds considerably to the overall search sensitivity since it has low background and good mass resolution, typically 1.5 GeV, if m_{h^0} is taken to be the mass recoiling against the reconstructed Z^0 boson.

(d) The **tau final states** are produced in the SM and MSSM processes ($h^0 \rightarrow \tau^+\tau^-$)($Z^0 \rightarrow q\bar{q}$), ($h^0 \rightarrow q\bar{q}$)($Z^0 \rightarrow \tau^+\tau^-$), ($h^0 \rightarrow \tau^+\tau^-$)($A^0 \rightarrow q\bar{q}$), and ($h^0 \rightarrow q\bar{q}$)($A^0 \rightarrow \tau^+\tau^-$). In the SM they occur with a branching ratio of about 10% in total. These channels play an important role in some subsets

of the MSSM parameter space where the decays to $b\bar{b}$ are suppressed.

To summarize, the conjunction of constrained kinematic fits and sophisticated b tagging allows the searches at LEP2 to be conducted with increased sensitivity. With the inclusion of the abundant four-jet final states, which had to be discarded at LEP1 from searches for the SM Higgs boson, about 95% of the signal cross section is utilized.

Searches for the charged Higgs process $e^+e^- \rightarrow H^+H^-$ make use of the decays $H^+ \rightarrow c\bar{s}$ and $\tau^+\nu_\tau$. The process $e^+e^- \rightarrow W^+W^-$ constitutes a high background at $m_{H^\pm} \approx M_W$.

In the SM and the MSSM, the signal and background rates are predicted channel by channel. The corresponding search results can thus be combined for a better overall sensitivity. Furthermore, datasets from different LEP energies and experiments can also be added. The combined LEP data are used to test two hypotheses: the *background-only* (“ b ”) hypothesis, which assumes no Higgs boson to be present in the mass range investigated, and the *signal + background* (“ $s + b$ ”) hypothesis, where Higgs bosons are assumed to be produced according to the model under consideration. A global *test-statistic* X is constructed [28] which allows the experimental result X_{observed} to be classified between the b -like and $s + b$ -like situations. It utilizes the number of selected events and various distributions which provide discrimination between signal and background (*e.g.*, the reconstructed mass or b -tag variables). The test-statistic takes into account experimental details such as detection efficiencies, signal-to-background ratios, resolution functions, and provides a single value for a given model hypothesis (*e.g.*, the test-mass m_{H^0} in the SM).

To set the scale for X , a large number of Monte Carlo experiments are generated, separately for the b and the $s + b$ hypotheses, and separately for each model hypothesis (*e.g.*, m_{H^0}). The resulting distributions of $X(m_{H^0})$ are normalized to become probability density functions, and integrated to form the confidence levels $\text{CL}_b(m_{H^0})$ and $\text{CL}_{s+b}(m_{H^0})$. The integration starts in both cases from the b -like end and runs up to X_{observed} ; thus $\text{CL}_b(m_{H^0})$ and $\text{CL}_{s+b}(m_{H^0})$ express the probabilities that the outcome of an experiment is more b -like or less $s + b$ -like, respectively, than the outcome represented by the set of selected events.

The 95% CL lower limit for the SM Higgs mass is defined as the lowest value of the test mass m_{H^0} which yields* $\text{CL}_s(m_{H^0}) = \text{CL}_{s+b}(m_{H^0}) / \text{CL}_b(m_{H^0}) = 0.05$. The quantity $1 - \text{CL}_b(m_{H^0})$ is an indicator for a possible signal: a SM Higgs boson with true mass m_0 would produce a pronounced drop in this quantity for $m_{H^0} \approx m_0$. Values of $1 - \text{CL}_b < 5.7 \times 10^{-7}$ would indicate a five-standard deviation (5σ) discovery.

If values of X_{observed} (and thus the integration bounds) are obtained from Monte Carlo simulations of the real experiment, the average expected confidence levels $\langle 1 - \text{CL}_b(m_{H^0}) \rangle$ and $\langle \text{CL}_s(m_{H^0}) \rangle$ are obtained. Of particular interest are $\langle 1 - \text{CL}_b(m_{H^0}) \rangle$ from simulated $s + b$ experiments and

Gauge & Higgs Boson Particle Listings

Higgs Bosons — H^0 and H^\pm

$\langle CL_s(m_{H^0}) \rangle$ from simulated b experiments, since these indicate the expected ranges of sensitivity of the available data set for discovery and exclusion, respectively.

V. Latest results

We summarize below the search results obtained recently by the LEP Collaborations, the CDF, DØ, and other experiments. Some of the LEP results presented are obtained by combining [29] preliminary data from the four experimental groups [30] according to the procedure outlined above.

Results relevant to the SM and the MSSM:

(a) For the **SM Higgs boson**, the confidence levels $1 - CL_b$ and CL_s obtained from combining the data of the four LEP experiments are shown in Fig. 5 [29]. One can see in the upper part that the observed behavior of $1 - CL_b$ (full line) is compatible with the expected behaviors for background within 2σ (light-shaded band). The expected behavior in the presence of a signal (dashed line) indicates that the data have sensitivity for a 5σ discovery ($1 - CL_b < 5.7 \times 10^{-7}$) up to $m_{H^0} \approx 98$ GeV. In the lower part of the figure, the curves of CL_s observed (full line) and expected from background (dashed line) follow each other closely, as anticipated in the absence of a signal. The curves cross the value $CL_s = 0.05$ in the vicinity of $m_{H^0} = 103$ GeV. After cross checking with several test-statistics, the value 102.6 GeV is quoted in Ref. 29 as the 95% CL lower bound for the SM Higgs mass.

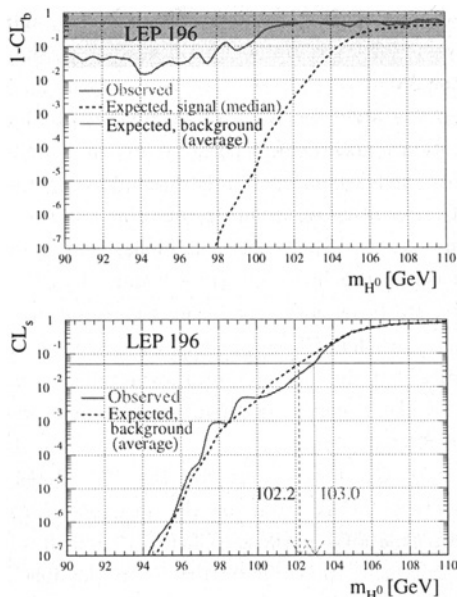


Figure 5: The confidence levels $1 - CL_b$ (upper) and CL_s (lower part), observed and expected, as a function of the test mass m_{H^0} , obtained from combining [29] preliminary data of the four LEP experiments. The dark (light) shaded areas represent the \pm one- (two-) standard deviation bands around the expected average (0.5) from simulated *background only* experiments.

At the Tevatron, the SM Higgs boson would be produced primarily by gluon fusion, $gg \rightarrow H^0$ [31]. However, the signal processes providing best sensitivity to masses below 140 GeV are those where a Higgs boson is produced in association with a W^\pm or Z^0 boson, or in association with heavy quarks, $p\bar{p} \rightarrow W^\pm H^0 X$, $Z^0 H^0 X$, $Q\bar{Q}H^0 X$ [32]. The Run I data samples, of about 110 pb^{-1} from both CDF and DØ, are far too small for a discovery of the SM Higgs boson but allow upper bounds to be set on the cross section. For $m_{H^0} > 70$ GeV, these bounds are higher by an order of magnitude at least than the SM prediction [33,34].

(b) For the **MSSM Higgs bosons h^0 and A^0** , the search results are used to test a ‘constrained’ MSSM where universal SUSY-breaking masses m_{SUSY} and M_2 are assumed for sfermions and gauginos, respectively, at the electroweak scale. With these assumptions, the number of MSSM parameters is reduced to only six [4,19]. All masses, cross sections, and decay branching ratios can be calculated by fixing m_{SUSY} , M_2 , $\tan \beta$, m_{A^0} , the Higgs mixing parameter μ , and the trilinear coupling A_t which controls stop mixing. The top mass has also an impact on the predictions through loop corrections.

Although more general parameter scans have been reported [35,36], most interpretations of the results are limited to less general scenarios (*e.g.*, those proposed in Ref. 20), where some of the parameters are fixed: $m_{\text{SUSY}} = 1 \text{ TeV}/c^2$, $M_2 = 1.6 \text{ TeV}/c^2$, $\mu = -100 \text{ GeV}$, and $m_t = 175 \text{ GeV}$. Two separate cases are considered, with $A_t = 0$ and $\sqrt{6} \text{ TeV}$, which correspond to *no mixing* and *large stop-mixing*. The remaining parameters, m_{A^0} and $\tan \beta$, are scanned independently.

The current LEP limits in the MSSM parameter space [29], valid for *large mixing*, are shown in Fig. 6 in the $(m_{h^0}, \tan \beta)$ and $(m_{A^0}, \tan \beta)$ projections (for *no mixing* the available parameter space is more restricted). The current 95% CL bounds are: $m_{h^0} > 84.3 \text{ GeV}$, $m_{A^0} > 84.5 \text{ GeV}$. Furthermore, values of $\tan \beta$ from 0.8 to 1.9 are excluded for the parameter sets considered; however, that exclusion can be reduced considerably in other scenarios [37].

The CDF experiment has searched for the process $p\bar{p} \rightarrow b\bar{b}X \rightarrow b\bar{b}b\bar{b}$ [33] where a particle $X (\equiv h^0, H^0, A^0)$ is radiated from a b quark and decays subsequently to $b\bar{b}$. This process is enhanced in the MSSM at large $\tan \beta$ where the Yukawa coupling to the b quark is large. The domains excluded by CDF are indicated in Fig. 6 together with the limits from LEP.

Interpretations in models beyond the SM and the MSSM:

Any model, to be acceptable, has to reproduce the available precision electroweak data. 2HD models with any number of additional singlet or doublet fields satisfy this criterion. This has been demonstrated [38] for 2HD models of class II where the ‘up’ and ‘down’ fermions couple to separate Higgs doublets. In the case of higher representations (*e.g.*, triplet fields) the parameters can also be tuned to obtain agreement, in particular to preserve the value of $\rho = M_W^2/M_Z^2 \cos^2 \theta_W$

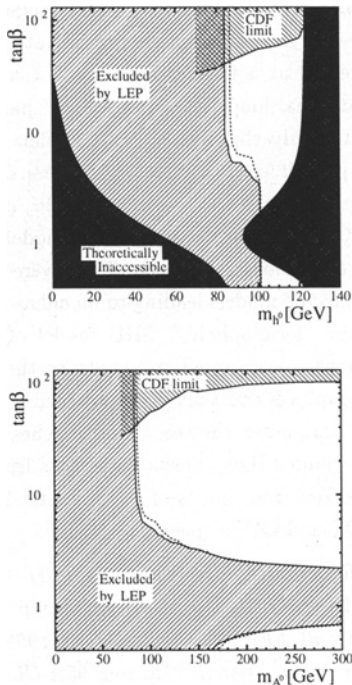


Figure 6: The 95% CL bounds on m_{h^0} , m_{A^0} , and $\tan\beta$, for the case of large mixing, from combining the data of the four LEP experiments up to $\sqrt{s} = 196$ GeV [29]. The dashed lines indicate the expected limits. The exclusions at large $\tan\beta$ from the CDF experiment [33] are also indicated.

and to avoid excessive rates of flavor-changing neutral currents. Search results are discussed below in theoretical contexts which are more general than the SM and the MSSM.

(a) The searches for $e^+e^- \rightarrow h^0 Z^0$ and $h^0 A^0$ have been used to derive *model-independent bounds* for the rates of *generic processes* where h^0 and A^0 can be any CP -even and CP -odd scalar particles [36,40]. In deriving these limits it is generally assumed that the decay properties of the generic particles are identical to those of the SM Higgs boson. Models with CP violation [39] and non-SM decay properties have also been addressed [40].

(b) The searches for *charged Higgs bosons* are guided by predictions of 2HD models. The mass m_{H^\pm} is not constrained. In the LEP searches [41] it is assumed that the decay modes $H^+ \rightarrow c\bar{s}$ and $\tau^+\nu_\tau$ fully exhaust the decay width, but the relative branching ratio is unknown. They therefore include the $e^+e^- \rightarrow H^+H^-$ final states $(c\bar{s})(\bar{c}s)$, $(\tau^+\nu_\tau)(\tau^-\bar{\nu}_\tau)$ and $(c\bar{s})(\tau^-\bar{\nu}_\tau) + (\bar{c}s)(\tau^+\nu_\tau)$. The current combined limits from LEP [29] are reproduced in Fig. 7 as a function of the branching ratio $B(H^+ \rightarrow \tau^+\nu_\tau)$. The lowest value, independent of the branching ratio, is currently 77 GeV.

At the Tevatron, charged Higgs bosons may be produced in the decay of the top quark, $t \rightarrow bH^+$. While the SM requires the top quark to decay almost exclusively via $t \rightarrow bW^+$, in 2HD models the process $t \rightarrow bH^+$ may compete with the SM process if $m_{H^+} < m_t - m_b$ and if $\tan\beta$ is either large (> 30)

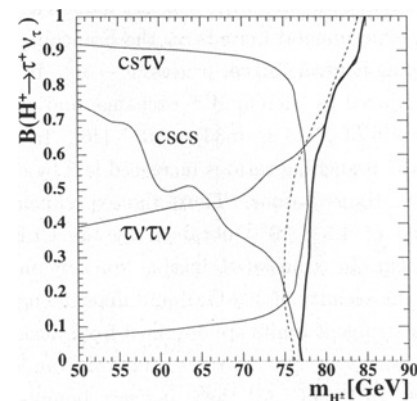


Figure 7: The 95% CL bounds on m_{H^\pm} as a function of the branching ratio $B(H^+ \rightarrow \tau^+\nu_\tau)$, from combining the data collected by the LEP experiments at energies up to 196 GeV [29]. The expected exclusion limit is indicated by the dashed line and the observed limits, channel-by-channel (light) and total (heavy), by the full lines.

or less than one. To search for H^\pm , the $D\bar{O}$ experiment has adopted an indirect “disappearance technique [42],” optimized for the detection of the SM background process $t \rightarrow bW^+$. The CDF Collaboration reported on a direct search for the process $t \rightarrow H^+b \rightarrow \tau^+\nu_\tau b$ [43] and on an indirect approach [44] in which the rate of di-leptons and lepton+jets in $t\bar{t}$ decay is compared to the SM prediction. The 2HD model of class II is assumed by both collaborations, and that the H^+ decays into three channels: (i) $c\bar{s}$, which is dominant at low $\tan\beta$ and small m_{H^\pm} , (ii) $t^*b \rightarrow W^+b\bar{b}$, dominant at low $\tan\beta$ and for $m_{H^\pm} \approx m_t + m_b$ [27], and (iii) $\tau^+\nu_\tau$, dominant at high $\tan\beta$. The results are summarized in Fig. 8, where the LEP limits of Fig. 7 are also reproduced. All these limits are subject to potentially large theoretical uncertainties [45].

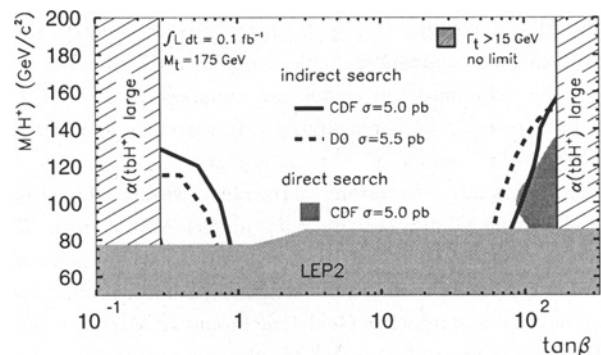


Figure 8: Summary of the 95% CL exclusions in the $(m_{H^+}, \tan\beta)$ plane obtained by the $D\bar{O}$ [42] and CDF [43] collaborations, using various indirect and direct observation techniques. The limits quoted by the two collaborations were obtained assuming slightly different $t\bar{t}$ cross sections and using different statistical procedures. The LEP limits from Fig. 7 are also reproduced.

Gauge & Higgs Boson Particle Listings

Higgs Bosons — H^0 and H^\pm

Indirect limits in the $(m_{H^\pm}, \tan\beta)$ plane can also be derived using experimental bounds on the branching ratio of the flavor-changing neutral current process $b \rightarrow s\gamma$. In the SM, this process is induced by virtual W^\pm exchange and gives rise to a branching ratio of $(3.28 \pm 0.33) \times 10^{-4}$ [46]. In 2HD models of class II, the branching ratio is increased [47] by contributions from charged Higgs bosons. Thus, the experimental 95% CL upper bound of 4.5×10^{-4} obtained by the CLEO Collaboration [48] can be translated into a lower bound on m_{H^\pm} , which is in the vicinity of 300 GeV and depends moderately on $\tan\beta$. Less stringent limits are obtained from measurements of the $b \rightarrow s\gamma$ and $b \rightarrow \tau^-\bar{\nu}_\tau X$ rates and from tau-lepton decay properties at LEP [49]. All these indirect bounds are model-dependent and may be invalidated, *e.g.*, by sparticle loops or anomalous couplings.

(c) Higgs bosons with **double-electric charge**, $H^{\pm\pm}$, are predicted by several models [50,19] *e.g.*, with triplet scalar fields. The OPAL Collaboration has searched for the process $Z^0 \rightarrow H^{++}H^{--}$ in final states with four prompt electrons or muons. An alternative selection, sensitive to long-lived $H^{\pm\pm}$ and giving rise to isolated tracks with ionization energy loss typical for two electron charges, was also used. By combining the two searches, $H^{\pm\pm}$ bosons with mass less than $M_Z/2$ could almost completely be excluded [51].

(d) The addition of a **singlet scalar field** to the MSSM [52], gives rise to two additional neutral scalars, one CP -even and one CP -odd. The radiative corrections to the masses are similar to those in the MSSM and arguments of perturbative continuation to the GUT scale lead again to an upper bound of about 135-140 GeV for the mass of the lightest neutral CP -even scalar. The DELPHI Collaboration has used the searches for neutral Higgs bosons to constrain such models [53].

(e) Higgs bosons can be produced by **Yukawa processes** in which they are radiated from a massive fermion, *e.g.*, b or τ^\pm . The CDF search for this process [33] has already been discussed in the MSSM context of Fig. 6. In a broader context, this process can be dominant in regions of the 2HD model space where the “standard” processes are suppressed. The LEP1 data have recently been reanalyzed [54], searching specifically for $b\bar{b}b\bar{b}$, $b\bar{b}\tau^+\tau^-$, and $\tau^+\tau^-\tau^+\tau^-$ final states.

(f) Decays into **“invisible” particles** (weakly interacting neutral particles) may occur, *e.g.*, in the MSSM with R -parity conservation, if the Higgs bosons decay to pairs of neutralinos [55]. In a different context, Higgs bosons could also decay into pairs of massless Goldstone bosons or Majorons [56]. In Higgs-strahlung, $e^+e^- \rightarrow h^0 Z^0$, the mass of the invisible Higgs boson can be inferred from the Z^0 boson which is reconstructed in the $Z^0 \rightarrow e^+e^-$, $\mu^+\mu^-$, and $q\bar{q}$ final states, and using the beam energy constraint. Assuming the SM production rate, the LEP experiments exclude the existence a Higgs boson of mass less than about 95 GeV decaying exclusively to invisible final states [57].

(g) **Photonic final states** from the processes $Z^0/\gamma^* \rightarrow H^0\gamma$ and $H^0 \rightarrow \gamma\gamma$ do not occur in the SM at the tree level, but may be present at a low rate due to W^\pm and top-quark loops [58]. Additional loops, *e.g.*, from SUSY particles, would increase the rates only slightly [59], but models with anomalous couplings predict enhancements by orders of magnitude. Searches for the processes $e^+e^- \rightarrow (H^0 \rightarrow b\bar{b})\gamma$, $(H^0 \rightarrow \gamma\gamma)q\bar{q}$, and $(H^0 \rightarrow \gamma\gamma)\gamma$ have been used to set model-independent limits on such anomalous couplings. They were also used to constrain very specific models leading to an enhanced $H^0 \rightarrow \gamma\gamma$ rate, such as the “fermiophobic” 2HD model of class I [60], where all fermions are assumed to couple to the same scalar field, and the couplings can thus be suppressed simultaneously by appropriate parameter choices. The searches at LEP [61] exclude a fermiophobic Higgs boson with mass less than about 95 GeV. At the Tevatron, limits of 82 GeV and 78.5 GeV are obtained by CDF and DØ, respectively [33,62].

Note: Very Recent Results (March 2000)

Very recently, the LEP Higgs working group updated their results including all LEP data collected in 1999 [63]. They report no indication for a signal. The new 95% CL mass bounds, replacing the ones quoted in this section, are the following. For the SM Higgs boson, $m_{H^0} > 107.7$ GeV; for the h^0 and A^0 bosons of MSSM, $m_{h^0} > 88.9$ GeV and $m_{A^0} > 88.4$ GeV; finally, for charged Higgs bosons in 2HD models, $m_{H^\pm} > 78.6$ GeV.

VI. Outlook

The LEP collider is scheduled to stop producing data in the year 2000. At the Tevatron, the Run I sensitivity is rather limited for Higgs boson searches, but a powerful luminosity upgrade is in preparation. Performance studies [8] provide a high motivation for collecting large data samples in excess of 10 fb^{-1} per experiment. Such samples will extend the combined sensitivity of CDF and DØ well beyond the LEP reach and allow large domains in the MSSM parameter space to be investigated.

The Large Hadron Collider (LHC) will deliver proton-proton collisions at 14 TeV energy in the year 2005. The ATLAS and CMS detectors have been optimized for Higgs boson searches [9]. The discovery of the SM Higgs boson will be possible over the full canonical mass range between 100 GeV and 1 TeV. This broad range is covered by a variety of production and decay processes. The LHC experiments will provide full coverage of the MSSM parameter space *via* their searches for the h^0 , H^0 , A^0 , and H^\pm bosons and by detecting the h^0 boson in cascade decays of SUSY particles. The discovery of several Higgs bosons is possible over extended domains of the parameter space. Decay branching fractions can be determined, and masses measured with accuracies between 10^{-3} (at 400 GeV mass) and 10^{-2} (at 700 GeV).

It is conceivable that a high-energy e^+e^- linear collider will be realized after the year 2010. Initially it could run at energies up to 500 GeV, with 1 TeV and more in perspective [10]. One of the prime goals of such a collider is to extend the

precision measurements, typical of e^+e^- colliders, to the Higgs sector. The Higgs couplings to fermions and vector bosons can be measured through production cross sections and decay branching ratios, with precisions of a few percent. The MSSM parameters can be studied in great detail. At the highest collider energies and luminosities, the self-coupling of the Higgs fields can be studied directly through final states with two Higgs bosons [64].

At a future $\mu^+\mu^-$ collider [11], the Higgs bosons can be generated as s -channel resonances. Mass measurements with precisions of a few MeV would be possible and the widths could be obtained directly from Breit-Wigner scans. The heavy CP -even and CP -odd Higgs bosons H^0 and A^0 , degenerate over most of the MSSM parameter space, could be disentangled experimentally.

Finally, if Higgs bosons are not discovered at the TeV scale, both the LHC and the future lepton colliders will be in a position to test alternative theories of electroweak symmetry breaking such as those with strongly interacting vector bosons [65], expected in theories with dynamical symmetry breaking [66].

Notes and References

- * The ratio CL_s replaces CL_{s+b} in order to avoid situations where a downward fluctuation of the event count would exclude even the b -like hypothesis. In such situations, the exclusion of the $s + b$ hypothesis would incorrectly appear as an exclusion of a signal for which there is insufficient experimental sensitivity.
- S.L. Glashow, Nucl. Phys. **20**, 579 (1961); S. Weinberg, Phys. Rev. Lett. **19**, 1264 (1967); A. Salam, *Elementary Particle Theory*, ed.: N. Svartholm, Almquist, and Wiksells, Stockholm, 1968; S. Glashow, J. Iliopoulos, and L. Maiani, Phys. Rev. **D2**, 1285 (1970).
 - P.W. Higgs, Phys. Rev. Lett. **12**, 132 (1964); Phys. Rev. **145**, 1156 (1966); F. Englert and R. Brout, Phys. Rev. Lett. **13**, 321 (1964); G.S. Guralnik, C.R. Hagen, and T.W. Kibble, Phys. Rev. Lett. **13**, 585 (1964).
 - J. Wess, B. Zumino, Nucl. Phys. **B70**, 39 (1974); *idem*, Phys. Lett. **49B**, 52 (1974); P. Fayet, Phys. Lett. **69B**, 489 (1977); *ibid.* **84B** 421, (1979); **86B**, 272 (1979); H.E. Haber, *Supersymmetry*, elsewhere in this Review.
 - K. Inoue, A. Kakuto, H. Komatsu, and S. Takeshita, Prog. Theor. Phys. **68**, 927 (1982); *ibid.* **70**, 330 (1983); *ibid.* **71**, 413 (1984); H.E. Haber and G.L. Kane, Phys. Rep. **C117**, 75 (1985).
 - Y. Okada, M. Yamaguchi, and T. Yanagida, Theor. Phys. **85**, 1 (1991); H. Haber and R. Hempfling, Phys. Lett. **66**, 1815 (1991); J. Ellis, G. Ridolfi, and F. Zwirner, Phys. Lett. **B257**, 83 (1991); R. Barbieri and M. Frigeni, Phys. Lett. **B258**, 395 (1991).
 - P.J. Franzini and P. Taxil, in *Z physics at LEP 1*, CERN 89-08 (1989).
 - For complete documentation of published results, the reader should consult the Particle Listings in this Review and in the 1998 Edition (Eur. Phys. J. **C3**, 1 (1998)).
 - Tevatron Run II workshop, <http://fnth37.fnal.gov/higgs.html>; M. Spira, hep-ph/9810289; J.S. Conway, FERMILAB-CONF-99/156-E.
 - ATLAS TDR on Physics performance, Vol. II, Chap. 19, *Higgs Bosons* (1999); CMS TP, CERN/LHC 94-38 (1994)..
 - E. Accomando *et al.*, Physics Reports **299**, 1 (1998); H. Murayama and M.E. Peskin, Ann. Rev. Nucl. and Part. Sci. **46**, 583 (1996); ACFA Workshop, KEK Report 99-12, 1999; K. Hübner, *Future Accelerators*, Proceedings of ICHEP'98, Vancouver, Canada, July 1998; G. Borisov and F. Richard, hep-ph/9905413; M. Battaglia, hep-ph/9910271.
 - B. Autin, A. Blondel, and J. Ellis (eds.), CERN 99-02; C.M. Ankenbrandt *et al.*, Phys. Rev. ST Acc. Beams **2**, 081001 (1999).
 - N. Cabibbo, L. Maiani, G. Parisi, and R. Petronzio, Nucl. Phys. **B158**, 295 (1979); R. Dashen and H. Neuberger, Phys. Rev. Lett. **50**, 1897 (1983).
 - M. Lindner, M. Sher, and H.W. Zaglauer, Phys. Lett. **B228**, 139 (1989); M. Sher, Phys. Lett. **B317**, 159 (1993); *ibid.* **331B**, 448 (1994); G. Altarelli and I. Isidori, Phys. Lett. **B337**, 141 (1994); J.A. Casas, J.R. Espinosa, and M. Quirós, Phys. Lett. **B342**, 89 (1995).
 - T. Hambye and K. Riesselmann, Phys. Rev. **D55**, 7255 (1997).
 - J. Erler and P. Langacker, *Electroweak Model and Constraints on New Physics*, elsewhere in this Review.
 - G. Quast, *ew-fits*.
 - M. Carena, M. Quiros, and C.E.M. Wagner, Nucl. Phys. **B461**, 407 (1996); H. Haber, R. Hempfling, and A. Hoang, Z. Phys. **C75**, 539 (1997); S. Heinemeyer, W. Hollik, and G. Weiglein, Phys. Lett. **B455**, 179 (1999); *idem*, Eur. Phys. J. **C9**, 343 (1999).
 - M. Carena, S. Pokorski, and C. Wagner, Nucl. Phys. **B406**, 45 (1993); V. Barger, M.S. Berger, and P. Ohmann, Phys. Rev. **D47**, 1093 (1993); M. Carena and C. Wagner, Nucl. Phys. **B452**, 45 (1995).
 - J.F. Gunion, H.E. Haber, G.L. Kane, and S. Dawson, *The Higgs Hunter's Guide* (Addison-Wesley) 1990.
 - M. Carena *et al.*, LEP2 Workshop, CERN 96-01, (1996) Vol. 1, p. 351.
 - J. Ellis, M.K. Gaillard, and D.V. Nanopoulos, Nucl. Phys. **B106**, 292 (1976); B.L. Ioffe and V.A. Khoze, Sov. J. Nucl. Phys. **9**, 50 (1978).
 - E. Gross, B.A. Kniehl, and G. Wolf, Z. Phys. **C63**, 417 (1994); erratum *ibid.* **C66**, 32 (1995).
 - D.R.T. Jones and S.T. Petcov, Phys. Lett. **84B**, 440 (1979); G. Altarelli, B. Mele, and F. Pitolli, Nucl. Phys. **B287**, 205 (1987); W. Kilian, M. Krämer, and P.M. Zerwas, Phys. Lett. **B373**, 135 (1996).
 - J.F. Gunion and H.E. Haber, Nucl. Phys. **B272**, 1 (1986); *ibid.* **B278**, 449 (1986); *ibid.* **B307**, 445 (1988); erratum: *ibid.* **B402**, 567 (1993).

Gauge & Higgs Boson Particle Listings

Higgs Bosons — H^0 and H^\pm

-
25. A. Brignole, J. Ellis, G. Ridolfi, and F. Zwirner, Phys. Lett. **B271**, 123 (1991).
26. A. Djouadi, M. Spira, P.M. Zerwas, Z. Phys. **C70**, 675 (1996).
27. A. Djouadi *et al.*, Z. Phys. **C70**, 435 (1996); E. Ma, D.P. Roy, and J. Wudka, Phys. Rev. Lett. **80**, 1162 (1998).
28. LEP Higgs working group: CERN-EP/98-046, CERN-EP/99-060; *lephiggs-1*.
29. LEP Higgs working group: *lephiggs-2*.
30. *ALEPH 99-084*, *ALEPH 99-070*, *DELPHI 99-86*, *DELPHI 99-95*, *DELPHI 99-92*, M. Acciarri *et al.*, Phys. Lett. **B461**, 376 (1999); *idem* **B466**, 71 (1999); CERN-EP/99-145; *OPAL-PN/99-373*, *OPAL-PN/99-414*, CERN-EP/99-096.
31. H. Georgi, S. Glashow, M. Machacek, and D.V. Nanopoulos, Phys. Rev. Lett. **40**, 692 (1978); M. Spira, A. Djouadi, D. Graudenz and P.M. Zerwas, Nucl. Phys. **B453**, 17 (1995).
32. S.L. Glashow, D.V. Nanopoulos, and A. Yildiz, Phys. Rev. **D18**, 1724 (1978); Z. Kunszt, Nucl. Phys. **B247**, 339 (1984); D. Dicus and S. Willenbrock, Phys. Rev. **D39**, 751 (1989).
33. Xin Wu, FERMILAB-CONF-99/053-E; J.A. Walls, FERMILAB-CONF-99/263-E.
34. F. Abe *et al.*, Phys. Rev. Lett. **79**, 3819 (1997); *ibid.*, **81**, 5748 (1998); W.-M. Yao, FERMILAB-CONF-99/100.
35. R. Barate *et al.*, Phys. Lett. **B440**, 419 (1998); *DELPHI 98-124*.
36. G. Abbiendi *et al.*, Eur. Phys. J. **C7**, 407 (1999).
37. G. Weiglein, S. Heinemeyer, W. Hollik, hep-ph/9909540; M. Carena *et al.*, hep-ph/9912223.
38. P. Chankowski, M. Krawczyk, J. Zochowski, hep-ph/9905436.
39. J.F. Gunion, B. Grzadkowski, H.E. Haber, J. Kalinowski, Phys. Rev. Lett. **79**, 982 (1997).
40. *ALEPH 99-053*, *DELPHI 99-86*, *OPAL-PN/99-416*.
41. *ALEPH 99-070*, CERN-EP/99-011, CERN-EP/98-149, *DEPHI 99-92*, M. Acciarri *et al.*, Phys. Lett. **B466**, 71 (1999); *OPAL-PN/99-373*, *OPAL-PN/99-414*.
42. B. Abbott *et al.*, Phys. Rev. Lett. **82**, 4975 (1999).
43. F. Abe *et al.*, Phys. Rev. Lett. **79**, 357 (1997); T. Affolder *et al.*, hep-ex/9912013.
44. B. Bevensee, FERMILAB-CONF-98/155-E.
45. J.A. Coarasa, J. Guach, and J. Solá, hep-ph/9903212; J.A. Coarasa, J. Guach, J. Solá, and W. Hollik, hep-ph/9808278; F.M. Borzumati and A. Djouadi, hep-ph/9806301.
46. K. Chetyrkin *et al.*, Phys. Lett. **B400**, 206 (1997); *idem* Phys. Lett. **B425**, 414 (1998); A. Kagan and M. Neubert, Eur. Phys. J. **C7**, 5 (1999).
47. R. Ellis *et al.*, Phys. Lett. **B179**, 119 (1986); V. Barger, J. Hewett, and R. Phillips, Phys. Rev. **D41**, 3421 (1990).
48. M.S. Alam *et al.*, Phys. Rev. Lett. **74**, 2885 (1995); S. Ahmed *et al.*, hep-ex/9908022.
49. O. Adriani *et al.*, Phys. Lett. **B317**, 637 (1993); D. Buskulic *et al.*, Phys. Lett. **B343**, 444 (1995); W. Adam *et al.*, Z. Phys. **C72**, 207 (1996); R. Barate *et al.*, Phys. Lett. **B429**, 169 (1998); K. Ackerstaff *et al.*, Eur. Phys. J. **C8**, 3 (1999).
50. G.B. Gelmini and M. Roncadelli, Phys. Lett. **99B**, 411 (1981); R.N. Mohapatra and J.D. Vergados, Phys. Rev. Lett. **47**, 1713 (1981); V. Barger, H. Baer, W.Y. Keung, and R.J.N. Phillips, Phys. Rev. **D26**, 218 (1982).
51. P.D. Acton *et al.*, Phys. Lett. **B295**, 347 (1992).
52. P. Fayet, Nucl. Phys. **B90**, 104 (1975); S.A. Abel, S. Sarkar, P.L. White, Nucl. Phys. **B454**, 663 (1995); S.F. King, P.L. White, Phys. Rev. **D53**, 4049 (1996).
53. *DELPHI 99-97*.
54. *ALEPH PA13-027*, *DELPHI 99-76*.
55. A. Djouadi, P. Janot, J. Kalinowski, and P.M. Zerwas, Phys. Lett. **B376**, 220 (1996).
56. Y. Chikashige, R.N. Mohapatra, and P.D. Peccei, Phys. Lett. **98B**, 265 (1981); F. de Campos, O.J.Éboli, J. Rosiek, and J.W.F. Valle, Phys. Rev. **D55**, 1316 (1997).
57. *ALEPH 99-069*, *DELPHI 99-83*, *L3 Note 2435*, *OPAL-PN/99-399*.
58. J. Ellis, M.K. Gaillard, and D.V. Nanopoulos, Nucl. Phys. **B106**, 292 (1976); R.N. Cahn, M.S. Chanowitz, and N. Fleishon, Phys. Lett. **B82**, 113 (1997); J. Leveille, Phys. Lett. **B83**, 123 (1997); A.I. Vainshtein *et al.*, Sov. J. Nucl. Phys. **30**, 711 (1979); A. Barroso, J. Pulido, J.C. Romão, Nucl. Phys. **B267**, 509 (1986); A. Abbasabadi *et al.*, Phys. Rev. **D52**, 3919 (1995).
59. G. Gamberini, G.F. Giudice, and G. Ridolfi, Nucl. Phys. **B292**, 237 (1987); R. Bates, J.N. Ng, and P. Kalyniak, Phys. Rev. **D34**, 172 (1986); K. Hagiwara, R. Szalapski, and D. Zeppenfeld, Phys. Lett. **B318**, 155 (1993); O.J.P. Éboli, M.C. Gonzalez-Garcia, S.M. Lietti, and S.F. Novaes, Phys. Lett. **B434**, 340 (1998).
60. A.G. Akeroyd, Phys. Lett. **B368**, 89 (1996); H. Haber, G. Kane, and T. Stirling, Nucl. Phys. **B161**, 493 (1979) 493.
61. *ALEPH 99-054*, *DELPHI 99-72*, CERN-EP/99-058, *L3 Note 2429*, G. Abbiendi *et al.*, Phys. Lett. **B464**, 311 (1999).
62. B. Abbott *et al.*, hep-ex/9902028.
63. *lephiggs-3*.
64. G.J. Gounaris, F. Renard, D. Schildknecht, Phys. Lett. **83B**, 191 (1979); V. Barger, T. Han, R.J.N. Phillips, Phys. Rev. **D38**, 2766 (1988); F. Boudjema and E. Chopin, Z. Phys. **C37**, 85 (1996); A. Djouadi, W. Kilian, M. Mühlleitner, and P.M. Zerwas, Eur. Phys. J. **C10**, 27 (1999).
65. B.W. Lee, C. Quigg, and H.B. Thacker, Phys. Rev. **D16**, 1519 (1977); R.S. Chivukula *et al.*, hep-ph/9503202,; C. Yuan, hep-ph/9712513; M. Chanowitz, hep-ph/9812215.
66. S. Weinberg, Phys. Rev. **D13**, 974 (1976); *ibid.* **D19**, 1277 (1979); L. Susskind, Phys. Rev. **D20**, 2619 (1979).
-

STANDARD MODEL H^0 (Higgs Boson) MASS LIMITS

These limits apply to the Higgs boson of the three-generation Standard Model with the minimal Higgs sector. For a review and a bibliography, see the above Note on 'Searches for Higgs Bosons' by P. Igo-Kemenes.

Limits from Coupling to Z/W^\pm

Limits on the Standard Model Higgs obtained from the study of Z^0 decays rule out conclusively its existence in the whole mass region $m_{H^0} \lesssim 60$ GeV. These limits, as well as stronger limits obtained from e^+e^- collisions at LEP at energies up to 172 GeV, and weaker limits obtained from other sources, have been superseded by the most recent data of LEP. They have been removed from this compilation, and are documented in the 1998 Edition (The European Physical Journal **C3** 1 (1998)) of this Review of Particle Physics.

In this Section, unless otherwise stated, limits from the four LEP experiments (ALEPH, DELPHI, L3, and OPAL) are obtained from the study of the $e^+e^- \rightarrow H^0 Z$ process, at center-of-mass energies reported in the comment lines.

A recent combination (LEP 00B) of preliminary, unpublished results relative to data taken at LEP in the Summer of 1999 at energies up to 202 GeV gives the limit $m_{H^0} > 107.7$ GeV.

VALUE (GeV)	CL%	DOCUMENT ID	TECN	COMMENT
>91.0	95	¹ ABBIENDI	00F OPAL	$E_{cm} \leq 189$ GeV
>94.6	95	¹ ABREU	00G DLPH	$E_{cm} \leq 189$ GeV
>95.3	95	¹ ACCIARRI	99I L3	$E_{cm} = 189$ GeV
>87.9	95	² BARATE	99B ALEP	$E_{cm} \leq 183$ GeV
• • • We do not use the following data for averages, fits, limits, etc. • • •				
>88.3	95	¹ ABBIENDI	99E OPAL	$E_{cm} = 183$ GeV
>85.7	95	¹ ABREU	99I DLPH	$E_{cm} \leq 183$ GeV
		³ ABE	98T CDF	$p\bar{p} \rightarrow H^0 WX, H^0 ZX$
>87.6	95	¹ ACCIARRI	98I L3	$E_{cm} \leq 183$ GeV

¹ Search for $e^+e^- \rightarrow H^0 Z$ in the final states $H^0 \rightarrow q\bar{q}$ with $Z \rightarrow \ell^+\ell^-, \nu\bar{\nu}, q\bar{q}$, and $\tau^+\tau^-$, and $H^0 \rightarrow \tau^+\tau^-$ with $Z \rightarrow q\bar{q}$.

² Search for $e^+e^- \rightarrow H^0 Z$ in the final states $H^0 \rightarrow q\bar{q}$ with $Z \rightarrow \ell^+\ell^-, \nu\bar{\nu}, q\bar{q}$, and $\tau^+\tau^-$, and $H^0 \rightarrow \tau^+\tau^-$ with $Z \rightarrow \ell^+\ell^-, \nu\bar{\nu}$, and $q\bar{q}$.

³ ABE 98T search for associated $H^0 W$ and $H^0 Z$ production in $p\bar{p}$ collisions at $\sqrt{s} = 1.8$ TeV with $W(Z) \rightarrow q\bar{q}(\ell)$, $H^0 \rightarrow b\bar{b}$. The results are combined with the search in ABE 97W, resulting in the cross-section limit $\sigma(H^0 + W/Z) \cdot B(H^0 \rightarrow b\bar{b}) < (23-17)$ pb (95%CL) for $m_H = 70-140$ GeV. This limit is one to two orders of magnitude larger than the expected cross section in the Standard Model.

 H^0 Indirect Mass Limits from Electroweak Analysis

For limits obtained before the direct measurement of the top quark mass, see the 1996 (Physical Review **D54** 1 (1996)) Edition of this Review. Other studies based on data available prior to 1996 can be found in the 1998 Edition (The European Physical Journal **C3** 1 (1998)) of this Review. For indirect limits obtained from other considerations of theoretical nature, see the Note on "Searches for Higgs Bosons."

Because of the high current interest, we mention here the following unpublished result (LEP 00, and update, presented by A. Straessner at the 2000 Electroweak Rencontres de Moriond) although we do not include it in the Listings or Tables: $m_H = 66.5^{+60}_{-33}$ GeV. This is obtained from a fit to LEP, SLD, W mass, top mass, and neutrino scattering data available in the Spring of 2000, with $1/\alpha(m_Z) = 128.878 \pm 0.090$. The 95%CL upper limit is 188 GeV.

VALUE (GeV)	CL%	DOCUMENT ID	TECN	COMMENT
• • • We do not use the following data for averages, fits, limits, etc. • • •				
<290	95	⁴ CHANOWITZ	99 RVUE	
<211	95	⁵ D'AGOSTINI	99 RVUE	
		⁶ FIELD	99 RVUE	
		⁷ CHANOWITZ	98 RVUE	
170^{+150}_{-90}		⁸ HAGIWARA	98B RVUE	
141^{+140}_{-77}		⁹ DEBOER	97B RVUE	
127^{+143}_{-71}		¹⁰ DEGRASSI	97 RVUE	$\sin^2\theta_{W}(\text{eff, lept})$
158^{+148}_{-84}		¹¹ DITTMAYER	97 RVUE	
149^{+148}_{-82}		¹² RENTON	97 RVUE	
145^{+164}_{-77}		¹³ ELLIS	96C RVUE	
185^{+251}_{-134}		¹⁴ GURTU	96 RVUE	

⁴ CHANOWITZ 99 studies LEP/SLD data on 9 observables related $\sin^2\theta_{eff}^{\text{lep}}$, available in the Spring of 1998. A scale factor method is introduced to perform a global fit, in view of the conflicting data. m_H as large as 750 GeV is allowed at 95% CL.

⁵ D'AGOSTINI 99 use m_t, m_W , and effective $\sin^2\theta_{W}$ from LEP/SLD available in the Fall 1998 and combine with direct Higgs search constraints from LEP2 at $E_{cm} = 183$ GeV. $\alpha(m_Z)$ given by DAVIER 98.

⁶ FIELD 99 studies the data on b asymmetries from $Z^0 \rightarrow b\bar{b}$ decays at LEP and SLD (from LEP 99). The limit uses $1/\alpha(m_Z) = 128.90 \pm 0.09$, the variation in the fitted top quark mass, $m_t = 171.2^{+3.7}_{-3.8}$ GeV, and excludes b -asymmetry data. It is argued that exclusion of these data, which deviate from the Standard Model expectation, from the electroweak fits reduces significantly the upper limit on m_H . Including the b -asymmetry data gives instead the 95%CL limit $m_H < 284$ GeV. See also FIELD 00.

⁷ CHANOWITZ 98 fits LEP and SLD Z -decay-asymmetry data (as reported in ABBA-NEO 97), and explores the sensitivity of the fit to the weight ascribed to measurements that are individually in significant contradiction with the direct-search limits. Various prescriptions are discussed, and significant variations of the 95%CL Higgs-mass upper limits are found. The Higgs-mass central value varies from 100 to 250 GeV and the 95%CL upper limit from 340 GeV to the TeV scale.

⁸ HAGIWARA 98B fit to LEP, SLD, W mass, and neutrino scattering data as reported in ALCARAZ 96, with $m_t = 175 \pm 6$ GeV, $1/\alpha(m_Z) = 128.90 \pm 0.09$ and $\alpha_s(m_Z) = 0.118 \pm 0.003$. Strong dependence on m_t is found.

⁹ DEBOER 97B fit to LEP and SLD data (as reported in ALCARAZ 96), as well as m_W and m_t from CDF/DØ and CLEO $b \rightarrow s\gamma$ data (ALAM 95). $1/\alpha(m_Z) = 128.90 \pm 0.09$ and $\alpha_s(m_Z) = 0.120 \pm 0.003$ are used. Exclusion of SLD data yields $m_H = 241^{+218}_{-123}$ GeV. $\sin^2\theta_{eff}$ from SLD (0.23061 \pm 0.00047) would give $m_H = 16^{+16}_{-9}$ GeV.

¹⁰ DEGRASSI 97 is a two-loop calculation of M_W and $\sin^2\theta_{eff}^{\text{lep}}$ as a function of m_H , using $\sin^2\theta_{eff}^{\text{lep}} = 0.23165(24)$ as reported in ALCARAZ 96, $m_t = 175 \pm 6$ GeV, and $1/\alpha(m_Z) = 128.90 \pm 0.09$.

¹¹ DITTMAYER 97 fit to m_W and LEP/SLC data as reported in ALCARAZ 96, with $m_t = 175 \pm 6$ GeV, $1/\alpha(m_Z) = 128.89 \pm 0.09$. Exclusion of the SLD data gives $m_H = 261^{+224}_{-128}$ GeV. Taking only the data on $m_t, m_W, \sin^2\theta_{eff}^{\text{lep}}$, and I_Z^{lep} , the authors get $m_H = 190^{+174}_{-102}$ GeV and $m_H = 296^{+243}_{-143}$ GeV, with and without SLD data, respectively. The 95% CL upper limit is given by 550 GeV (800 GeV removing the SLD data).

¹² RENTON 97 fit to LEP and SLD data (as reported in ALCARAZ 96), as well as m_W and m_t from $p\bar{p}$, and low-energy νN data available in early 1997. $1/\alpha(m_Z) = 128.90 \pm 0.09$ is used.

¹³ ELLIS 96C fit to LEP, SLD, m_W , neutral-current data available in the summer of 1996, plus $m_t = 175 \pm 6$ GeV from CDF/DØ. The fit yields $m_t = 172 \pm 6$ GeV.

¹⁴ GURTU 96 studies the effect of the mutually incompatible SLD and LEP asymmetry data on the determination of m_H . Use is made of data available in the Summer of 1996. The quoted value is obtained by increasing the errors *à la* PDG. A fit ignoring the SLD data yields 267^{+242}_{-135} GeV.

MASS LIMITS FOR NON-STANDARD MODEL HIGGS BOSONS

This section covers the following cases:

- Neutral scalar and pseudoscalar Higgs bosons in the MSSM,
- Neutral Higgs bosons in extended Higgs models,
- Charged Higgs bosons, and
- Doubly-charged Higgs bosons

 H_1^0 (Higgs Boson) MASS LIMITS in Supersymmetric Models

The minimal supersymmetric model has two complex doublets of Higgs bosons. The resulting physical states are two scalars [H_1^0 and H_2^0], where we define $m_{H_1^0} < m_{H_2^0}$,

a pseudoscalar (A^0), and a charged Higgs pair (H^\pm). H_1^0 and H_2^0 are also called h and H in the literature. There are two free parameters in the theory which can be chosen to be m_{A^0} and $\tan\beta = v_2/v_1$, the ratio of vacuum expectation values of the two Higgs doublets. Tree-level Higgs masses are constrained by the model to be $m_{H_1^0} \leq m_Z, m_{H_2^0} \geq m_Z, m_{A^0} \geq m_{H_1^0}$, and $m_{H^\pm} \geq m_W$. However, as described in the Review on Supersymmetry in this Volume these relations are violated by radiative corrections.

The mass region $m_{H_1^0} \lesssim 45$ GeV has been by now entirely ruled out by measurements at the Z pole. The relative limits, as well as other by now obsolete limits from different techniques, have been removed from this compilation, and can be found in the 1998 Edition (The European Physical Journal **C3** 1 (1998)) of this Review. Unless otherwise stated, the following results assume no invisible H_1^0 or A^0 decays.

A recent combination (LEP 00B) of preliminary, unpublished results relative to data taken at LEP in the Summer of 1999 at energies up to 202 GeV gives the limit $m_{H_1^0} > 88.3$ GeV.

VALUE (GeV)	CL%	DOCUMENT ID	TECN	COMMENT
>74.8	95	¹⁵ ABBIENDI	00F OPAL	$E_{cm} \leq 189$ GeV, $\tan\beta > 1$
>82.6	95	¹⁶ ABREU	00G DLPH	$E_{cm} \leq 189$ GeV, $\tan\beta > 0.6$
>77.1		¹⁷ ACCIARRI	99U L3	$E_{cm} \leq 189$ GeV, $\tan\beta > 1$
>72.2	95	¹⁸ BARATE	98A ALEP	$E_{cm} \leq 183$ GeV
• • • We do not use the following data for averages, fits, limits, etc. • • •				
>70.5	95	¹⁹ ABBIENDI	99E OPAL	$E_{cm} \leq 183$ GeV, $\tan\beta > 1$
>74.4	95	²⁰ ABREU	99I DLPH	$E_{cm} \leq 183$ GeV, $\tan\beta > 0.6$
>59.5	95	²¹ ABREU	98E DLPH	$E_{cm} \leq 172$ GeV, $\tan\beta > 1$
>70.7	95	²² ACCIARRI	98M L3	$E_{cm} \leq 183$ GeV, $\tan\beta > 1$
>59.0	95	²³ ACKERSTAFF	98S OPAL	
		²⁴ ACCIARRI	97N L3	$E_{cm} \leq 172$ GeV
		²⁵ BARATE	97P ALEP	

¹⁵ ABBIENDI 00F search for $e^+e^- \rightarrow H_1^0 A^0$ in the final states $b\bar{b}b\bar{b}, b\bar{b}\tau^+\tau^-$, and $A^0 A^0 \rightarrow b\bar{b}b\bar{b}b\bar{b}$, and $e^+e^- \rightarrow H_1^0 Z$. Universal scalar mass of 1 TeV, SU(2) gaugino mass of 1.63 TeV and Higgsino mass parameter $\mu = -0.1$ TeV are assumed. $m_t = 175$ GeV is used. The cases of maximal and no-stop mixing are examined. Limits obtained from scans of the Supersymmetric parameter space can be found in the paper.

¹⁶ ABREU 00G search for $e^+e^- \rightarrow H_1^0 A^0$ in the final states $b\bar{b}b\bar{b}$ and $b\bar{b}\tau^+\tau^-$, and $e^+e^- \rightarrow H_1^0 Z$. $m_{A^0} > 20$ GeV is assumed. Universal scalar mass of 1 TeV, SU(2) gaugino mass of 0.2 TeV, and Higgsino mass parameter $\mu = -0.2$ TeV are assumed. $m_t = 175$ GeV is used. The scenarios of no-stop mixing, and of mixing with the maximal impact on the Higgs mass limit, are examined.

Gauge & Higgs Boson Particle Listings

Higgs Bosons — H^0 and H^\pm

- ¹⁷ ACCIARRI 99u searched for $e^+e^- \rightarrow H_1^0 A^0$ in the final state $b\bar{b}b\bar{b}$ and $b\bar{b}\tau^+\tau^-$, and $e^+e^- \rightarrow H_1^0 Z$. Universal scalar mass and SU(2) gaugino mass of 1 TeV and Higgsino mass parameter $\mu = -0.1$ TeV are assumed. The cases of minimal and maximal stop mixing are examined.
- ¹⁸ BARATE 98A search for $e^+e^- \rightarrow H_1^0 A^0$ in the final states $b\bar{b}b\bar{b}$ and $b\bar{b}\tau^+\tau^-$ and combine with BARATE 99b limit on $e^+e^- \rightarrow H_1^0 Z$. The limit is for $M_{\text{SUSY}} = 1$ TeV with minimal/maximal stop mixing. See paper for the result from a scan in more general MSSM parameters.
- ¹⁹ ABBIENDI 99E search for $e^+e^- \rightarrow H_1^0 A^0$ in the final states $b\bar{b}b\bar{b}$, $q\bar{q}\tau^+\tau^-$, and $6b$ and $e^+e^- \rightarrow H_1^0 Z$ for various final states. $M_{\text{top}}=175$ GeV, $M_{\text{SUSY}}=1$ TeV, and minimal/maximal scalar top mixing. See paper for results of more general scans.
- ²⁰ ABREU 99i search for $e^+e^- \rightarrow H_1^0 A^0$ in the final state $b\bar{b}b\bar{b}$, and $b\bar{b}\tau^+\tau^-$ and $e^+e^- \rightarrow H_1^0 Z$ for various final states. The limit is for the universal scalar mass of 1 TeV, SU(2) gaugino mass of 1.6 TeV, and Higgsino mass parameter $\mu = -100$ GeV, with typical/maximal/no-stop mixing. $m_t = 173.9$ GeV.
- ²¹ ABREU 98E search for $e^+e^- \rightarrow H_1^0 A^0$ in the final state $b\bar{b}b\bar{b}$ and $q\bar{q}\tau^+\tau^-$. The results from the SM Higgs search described in the same paper are also used to set these limits. $m_{\text{top}} = 175$ GeV, $M_{\text{SUSY}} = 1$ TeV, and maximal scalar top mixings.
- ²² ACCIARRI 98M search for $e^+e^- \rightarrow H_1^0 A^0$ in the final state $b\bar{b}b\bar{b}$ and $b\bar{b}\tau^+\tau^-$, and $e^+e^- \rightarrow H_1^0 Z$. $m_{\text{top}} = 175$ GeV, $M_{\text{SUSY}} = 1$ TeV, SU(2) gaugino mass of 1 TeV and various scalar top mixing scenarios.
- ²³ ACKERSTAFF 98S search for $e^+e^- \rightarrow H_1^0 A^0$ in the final state $b\bar{b}b\bar{b}$, $q\bar{q}\tau^+\tau^-$, and $6b$ and combine with ACKERSTAFF 98H limit on $e^+e^- \rightarrow H_1^0 Z$. $m_{\text{top}} = 175$ GeV, $M_{\text{SUSY}} = 1$ TeV, SU(2) gaugino mass of 1 TeV and maximal scalar stop mixing. The more general scan of the MSSM parameter space does not reduce the limit significantly.
- ²⁴ ACCIARRI 97N search for $e^+e^- \rightarrow H_1^0 A^0$ in four-jet final states. Cross-section limits are obtained for $|m_{H_1^0} - m_{A^0}| = 0, 10, \text{ and } 20$ GeV.
- ²⁵ BARATE 97P search for $e^+e^- \rightarrow H_1^0 A^0$ in the final state $b\bar{b}b\bar{b}$ and $b\bar{b}\tau^+\tau^-$ and combine with BARATE 97O limit on $e^+e^- \rightarrow H_1^0 Z$. $m_{\text{top}} = 175$ GeV and $M_{\text{SUSY}} = 1$ TeV, and maximal scalar top mixings. The invisible decays $H_1^0 \rightarrow \tilde{\chi}^0 \tilde{\chi}^0$ are not allowed in the analysis, as ruled out in the relevant kinematic region by BUSKULIC 96K.

 A^0 (Pseudoscalar Higgs Boson) MASS LIMITS in Supersymmetric Models

Limits on the A^0 mass from e^+e^- collisions arise from direct searches in the $e^+e^- \rightarrow A^0 H_1^0$ channel and indirectly from the relations valid in the minimal supersymmetric model between m_{A^0} and $m_{H_1^0}$. As discussed in the "Note on Supersymmetry," these relations depend on the masses of the t quark and \tilde{t} squarks. The limits are weaker for larger t and \tilde{t} masses, while they increase with the inclusion of two-loop radiative corrections. Some specific examples of these dependences are provided in the footnotes to the listed papers. Unless otherwise stated, two-loop radiative corrections have been included, where relevant, in the limits presented here.

Limits obtained at the Z pole have been made obsolete by more recent results from higher energy e^+e^- collision data at LEP. Together with other by now obsolete results, they have been omitted from this compilation, and can be found in the 1998 Edition (The European Physical Journal **C3** (1998)) of this Review. Unless otherwise stated, the following results assume no invisible H_1^0 or A^0 decays. Limits quoted for a given value of E_{cm} may include data from lower energies.

A recent combination (LEP 00b) of preliminary, unpublished results relative to data taken at LEP in the Summer of 1999 at energies up to 202 GeV gives the limit $m_{A^0} > 88.4$ GeV.

VALUE (GeV)	CL%	DOCUMENT ID	TECN	COMMENT
>76.5	95	26 ABBIENDI	00F OPAL	$E_{\text{cm}} \leq 189$ GeV, $\tan\beta > 1$
>84.1	95	27 ABREU	00G DLPH	$E_{\text{cm}} \leq 189$ GeV, $\tan\beta > 0.6$
>77.1	95	28 ACCIARRI	99U L3	$E_{\text{cm}} \leq 189$ GeV, $\tan\beta > 1$
>76.1	95	29 BARATE	98A ALEP	$E_{\text{cm}} \leq 183$ GeV
• • • We do not use the following data for averages, fits, limits, etc. • • •				
>72.0	95	30 ABBIENDI	99E OPAL	$E_{\text{cm}} \leq 183$ GeV, $\tan\beta > 1$
>75.3	95	31 ABREU	99I DLPH	$E_{\text{cm}} \leq 183$ GeV, $\tan\beta > 0.6$
>51.0	95	32 ABREU	98C DLPH	$E_{\text{cm}} \leq 172$ GeV, $\tan\beta > 1$
>71.0	95	33 ACCIARRI	98M L3	$E_{\text{cm}} \leq 183$ GeV, $\tan\beta > 1$
>59.5	95	34 ACKERSTAFF	98S OPAL	$E_{\text{cm}} \leq 172$ GeV, $\tan\beta > 1$
		35 DREES	98 RVUE	$\rho\bar{\rho} \rightarrow b\bar{b}H^0/A^0 + \text{any}$
		36 ACCIARRI	97N L3	$E_{\text{cm}} \leq 172$ GeV
>62.5	95	37 BARATE	97P ALEP	$E_{\text{cm}} \leq 172$ GeV, $\tan\beta > 1$
²⁶ ABBIENDI 00F search for $e^+e^- \rightarrow H_1^0 A^0$ in the final states $b\bar{b}b\bar{b}$, $b\bar{b}\tau^+\tau^-$, and $A^0 A^0 \rightarrow b\bar{b}b\bar{b}b\bar{b}$, and $e^+e^- \rightarrow H_1^0 Z$. Universal scalar mass of 1 TeV, SU(2) gaugino mass of 1.63 TeV and Higgsino mass parameter $\mu = -0.1$ TeV are assumed. $m_t = 175$ GeV is used. The cases of maximal and no-stop mixing are examined. Limits obtained from scans of the Supersymmetric parameter space can be found in the paper.				
²⁷ ABREU 00G search for $e^+e^- \rightarrow H_1^0 A^0$ in the final states $b\bar{b}b\bar{b}$ and $b\bar{b}\tau^+\tau^-$, and $e^+e^- \rightarrow H_1^0 Z$. $m_{A^0} > 20$ GeV is assumed. Universal scalar mass of 1 TeV, SU(2) gaugino mass of 0.2 TeV, and Higgsino mass parameter $\mu = -0.2$ TeV are assumed. $m_t = 175$ GeV is used. The scenarios of no-stop mixing, and of mixing with the maximal impact on the Higgs mass limit, are examined.				
²⁸ ACCIARRI 99u searched for $e^+e^- \rightarrow H_1^0 A^0$ in the final state $b\bar{b}b\bar{b}$ and $b\bar{b}\tau^+\tau^-$, and $e^+e^- \rightarrow H_1^0 Z$. Universal scalar mass and SU(2) gaugino mass of 1 TeV and Higgsino mass parameter $\mu = -0.1$ TeV are assumed. The cases of minimal and maximal stop mixing are examined.				
²⁹ BARATE 98A search for $e^+e^- \rightarrow H_1^0 A^0$ in the final states $b\bar{b}b\bar{b}$ and $b\bar{b}\tau^+\tau^-$ and combine with BARATE 99b limit on $e^+e^- \rightarrow H_1^0 Z$. The limit is for $M_{\text{SUSY}} = 1$ TeV				

- with minimal/maximal stop mixing. See paper for the result from a scan in more general MSSM parameters.
- ³⁰ ABBIENDI 99E search for $e^+e^- \rightarrow H_1^0 A^0$ in the final states $b\bar{b}b\bar{b}$, $q\bar{q}\tau^+\tau^-$, and $6b$ and $e^+e^- \rightarrow H_1^0 Z$ for various final states. $M_{\text{top}}=175$ GeV, $M_{\text{SUSY}}=1$ TeV, and minimal/maximal scalar top mixing. See paper for results of more general scans.
- ³¹ ABREU 99i search for $e^+e^- \rightarrow H_1^0 A^0$ in the final state $b\bar{b}b\bar{b}$, and $b\bar{b}\tau^+\tau^-$ and $e^+e^- \rightarrow H_1^0 Z$ for various final states. The limit is for the universal scalar mass of 1 TeV, SU(2) gaugino mass of 1.6 TeV, and Higgsino mass parameter $\mu = -100$ GeV, with typical/maximal/no-stop mixing. $m_t = 173.9$ GeV.
- ³² ABREU 98E search for $e^+e^- \rightarrow H_1^0 A^0$ in the final state $b\bar{b}b\bar{b}$ and $q\bar{q}\tau^+\tau^-$. The results from the SM Higgs search described in the same paper are also used to set these limits. $m_{\text{top}} = 175$ GeV, $M_{\text{SUSY}} = 1$ TeV, and maximal scalar top mixings.
- ³³ ACCIARRI 98M search for $e^+e^- \rightarrow H_1^0 A^0$ in the final state $b\bar{b}b\bar{b}$ and $b\bar{b}\tau^+\tau^-$, and $e^+e^- \rightarrow H_1^0 Z$. $m_{\text{top}} = 175$ GeV, $M_{\text{SUSY}} = 1$ TeV, SU(2) gaugino mass of 1 TeV and various scalar top mixing scenarios.
- ³⁴ ACKERSTAFF 98S search for $e^+e^- \rightarrow H_1^0 A^0$ in the final state $b\bar{b}b\bar{b}$, $q\bar{q}\tau^+\tau^-$, and $6b$ and combine with ACKERSTAFF 98H limit on $e^+e^- \rightarrow H_1^0 Z$. $m_{\text{top}} = 175$ GeV, $M_{\text{SUSY}} = 1$ TeV, SU(2) gaugino mass of 1 TeV and maximal scalar stop mixing. The more general scan of the MSSM parameter space does not reduce the limit significantly.
- ³⁵ DREES 98 (and Erratum in DREES 98b) use the CDF third-generation leptoquark search results (ABE 97f) to constrain possible Higgs production in association with $b\bar{b}$ in $\rho\bar{\rho}$ collision. In the framework of MSSM, m_A less than 130 GeV is excluded for $\tan\beta=100$. No significant limit is obtained for $\tan\beta < 80$.
- ³⁶ ACCIARRI 97N search for $e^+e^- \rightarrow H_1^0 A^0$ in four-jet final states. Cross-section limits are obtained for $|m_{H_1^0} - m_{A^0}| = 0, 10, \text{ and } 20$ GeV.
- ³⁷ BARATE 97P search for $e^+e^- \rightarrow H_1^0 A^0$ in the final state $b\bar{b}b\bar{b}$ and $b\bar{b}\tau^+\tau^-$ and combine with BARATE 97O limit on $e^+e^- \rightarrow H_1^0 Z$. $m_{\text{top}} = 175$ GeV and $M_{\text{SUSY}} = 1$ TeV, and maximal scalar top mixings. The invisible decays $H_1^0 \rightarrow \tilde{\chi}^0 \tilde{\chi}^0$ are not allowed in the analysis, as ruled out in the relevant kinematic region by BUSKULIC 96K.

 H^0 (Higgs Boson) MASS LIMITS in Extended Higgs Models

This Section covers models which do not fit into either the Standard Model or its simplest minimal Supersymmetric extension (MSSM), leading to anomalous production rates, or nonstandard final states and branching ratios. In particular, this Section covers limits which may apply to generic two-Higgs-doublet models (2HDM), or to special regions of the MSSM parameter space where decays to invisible particles or to photon pairs are dominant (see the Note on "Searches for Higgs Bosons" at the beginning of this Chapter). See the footnotes or the comment lines for details on the nature of the models to which the limits apply.

VALUE (GeV)	CL%	DOCUMENT ID	TECN	COMMENT
• • • We do not use the following data for averages, fits, limits, etc. • • •				
>68.0	95	38 ABBIENDI	99E OPAL	$\tan\beta > 1$
>96.2	95	39 ABBIENDI	99O OPAL	$e^+e^- \rightarrow H^0 Z, H^0 \rightarrow \gamma\gamma$
>78.5	95	40 ABBOTT	99B D0	$\rho\bar{\rho} \rightarrow H^0 W/Z, H^0 \rightarrow \gamma\gamma$
		41 ABREU	99P DLPH	$e^+e^- \rightarrow H^0 \gamma$ and/or $H^0 \rightarrow \gamma\gamma$
>76.1	95	42 ABREU	99Q DLPH	Invisible H^0
>80	95	43 BARATE	99C ALEP	Invisible H^0
>95.4	95	44 BARATE	99O ALEP	Invisible H^0
>69.6	95	45 ACCIARRI	98B L3	Invisible H^0
>56.0	95	46 ACKERSTAFF	98S OPAL	$\tan\beta > 1$
>90	95	47 ACKERSTAFF	98Y OPAL	$e^+e^- \rightarrow H^0 Z, H^0 \rightarrow \gamma\gamma$
		48 GONZALEZ-G.	98B RVUE	Anomalous coupling
		49 KRAWCZYK	97 RVUE	$(g-2)_\mu$
		50 ACCIARRI	96J L3	$Z \rightarrow H^0 Z^*, H^0 \rightarrow \gamma\gamma$
		51 ACCIARRI	96J L3	$Z \rightarrow H^0 \gamma$
		52 ALEXANDER	96H OPAL	$Z \rightarrow H^0 \gamma$
		53 ABREU	95H DLPH	$Z \rightarrow H^0 Z^*, H^0 A^0$
		54 PICH	92 RVUE	Very light Higgs
³⁸ ABBIENDI 99E search for $e^+e^- \rightarrow H^0 A^0$ and $H^0 Z$ at $E_{\text{cm}} = 183$ GeV. The limit is with $m_H = m_A$ in general two Higgs-doublet models. See their Fig. 18 for the exclusion limit in the $m_H - m_A$ plane. The limit includes searches at lower energy between m_Z and 172 GeV.				
³⁹ ABBIENDI 99o search for associated production of a $\gamma\gamma$ resonance with a $q\bar{q}, \nu\bar{\nu}$, or t^+t^- pair in e^+e^- collisions at 189 GeV. The limit is for a H^0 with SM production cross section and $B(H^0 \rightarrow f\bar{f})=0$, for all fermions f . See their Fig. 4 for limits on $\sigma(e^+e^- \rightarrow H^0 Z^0) \times B(H^0 \rightarrow \gamma\gamma) \times B(X^0 \rightarrow f\bar{f})$ for various masses.				
⁴⁰ ABBOTT 99B search for associated production of a $\gamma\gamma$ resonance and a dijet pair. The limit assumes Standard Model values for the production cross section and for the couplings of the H^0 to W and Z bosons. Limits in the range of $\sigma(H^0 + Z/W) \cdot B(H^0 \rightarrow \gamma\gamma) = 0.80-0.34$ pb are obtained in the mass range $m_{H^0} = 65-150$ GeV.				
⁴¹ ABREU 99P search for $e^+e^- \rightarrow H^0 \gamma$ with $H^0 \rightarrow b\bar{b}$ or $\gamma\gamma$, and $e^+e^- \rightarrow H^0 q\bar{q}$ with $H^0 \rightarrow \gamma\gamma$. See their Fig. 4 for limits on $\sigma \times B$. Explicit limits within an effective interaction framework are also given.				
⁴² ABREU 99Q search for $e^+e^- \rightarrow H^0 Z$ with H^0 decaying invisibly at E_{cm} between 161 and 183 GeV. The limit assumes SM production cross section, and holds for any $B(H^0 \rightarrow \text{invisible})$. In the case of invisible decays in the MSSM, the excluded region of the $(M_2, \tan\beta)$ plane overlaps the exclusion region from direct searches for charginos and neutralinos (ABREU 99E in the Supersymmetry Listings). See their Fig. 6(d) for limits on a Majoron model.				
⁴³ BARATE 99C search for $e^+e^- \rightarrow H^0 Z$ with H^0 decaying invisibly at \sqrt{s} between 161 and 184 GeV, and update the search for $Z^0 \rightarrow H^0 Z^*$ at m_Z . The limit assumes SM				

- production cross section, and $B(H^0 \rightarrow \text{invisible}) = 100\%$. See their Fig. 6 for limit on the ZZH^0 coupling vs. m_{H^0} .
- 44 BARATE 99o search for $e^+e^- \rightarrow H^0 Z$ with H^0 decaying invisibly at $E_{\text{cm}} = 189$ GeV. The limit assumes SM production cross section and $B(H^0 \rightarrow \text{invisible}) = 100\%$. See their Fig. 7 for limits on the ZZH^0 coupling vs. m_{H^0} .
- 45 ACCIARRI 98b searches for $e^+e^- \rightarrow ZH^0$ events, with $Z \rightarrow$ hadrons and H^0 decaying invisibly. The limit assumes SM production cross section, and $B(H^0 \rightarrow \text{invisible}) = 1$. For limits under other assumptions, see their Fig. 5b.
- 46 ACKERSTAFF 98s search for $e^+e^- \rightarrow H^0 A^0$ and $H^0 Z$ at E_{cm} between 130 and 172 GeV. The limit is for $m_H = m_A$. The limit is 41 GeV for all values of $\tan\beta$. See also their Fig. 10 for the exclusion limit in the $m_H - m_A$ plane.
- 47 ACKERSTAFF 98y search for associate production of a $\gamma\gamma$ resonance and a $q\bar{q}, \nu\bar{\nu}$, or $\ell^+\ell^-$ pair in e^+e^- annihilation at $E_{\text{cm}} = 183$ GeV. The limit assumes SM production cross section and $B(H^0 \rightarrow \gamma\gamma) = 1$. See their Fig. 3 for limit on $\sigma(H^0) \cdot B(H^0 \rightarrow \gamma\gamma) / \sigma(H^0_{\text{SM}})$. Supersedes ACKERSTAFF 98b.
- 48 GONZALEZ-GARCIA 98b use $D\bar{D}$ limit for $\gamma\gamma$ events with missing E_T in $p\bar{p}$ collisions (ABBOTT 98) to constrain possible ZH or WH production followed by unconventional $H \rightarrow \gamma\gamma$ decay which is induced by higher-dimensional operators. See their Figs. 1 and 2 for limits on the anomalous couplings.
- 49 KRAWCZYK 97 analyse the muon anomalous magnetic moment in a two-doublet Higgs model (with type II Yukawa couplings) assuming no $H^0_Z Z$ coupling and obtain $m_{H^\pm} \gtrsim 5$ GeV or $m_{A^0} \gtrsim 5$ GeV for $\tan\beta > 50$. Other Higgs bosons are assumed to be much heavier.
- 50 ACCIARRI 96j give $B(Z \rightarrow H^0 + \text{hadrons}) \times B(H^0 \rightarrow \gamma\gamma) < 2.3 - 6.9 \times 10^{-6}$ for $20 < m_{H^0} < 70$ GeV.
- 51 ACCIARRI 96j give $B(Z \rightarrow H^0 \gamma) \times B(H^0 \rightarrow q\bar{q}) < 6.9 - 22.9 \times 10^{-6}$ (95%CL) for $20 < m_{H^0} < 80$ GeV.
- 52 ALEXANDER 96h give $B(Z \rightarrow H^0 \gamma) \times B(H^0 \rightarrow q\bar{q}) < 1 - 4 \times 10^{-5}$ (95%CL) and $B(Z \rightarrow H^0 \gamma) \times B(H^0 \rightarrow b\bar{b}) < 0.7 - 2 \times 10^{-5}$ (95%CL) in the range $20 < m_{H^0} < 80$ GeV.
- 53 See Fig. 4 of ABREU 95h for the excluded region in the $m_{H^0} - m_{A^0}$ plane for general two-doublet models. For $\tan\beta > 1$, the region $m_{H^0} + m_{A^0} \lesssim 87$ GeV, $m_{H^0} < 47$ GeV is excluded at 95% CL.
- 54 PICH 92 analyse H^0 with $m_{H^0} < 2m_\mu$ in general two-doublet models. Excluded regions in the space of mass-mixing angles from LEP, beam dump, and π^\pm, η rare decays are shown in Figs. 3, 4. The considered mass region is not totally excluded.

H^\pm (Charged Higgs) MASS LIMITS

Unless otherwise stated, the limits below assume $B(H^+ \rightarrow \tau^+\nu) + B(H^+ \rightarrow c\bar{s}) = 1$, and hold for all values of $B(H^+ \rightarrow \tau^+\nu)$, and assume H^\pm weak isospin of $T_3 = +1/2$. In the following, $\tan\beta$ is the ratio of the two vacuum expectation values in two-doublet models (2HDM).

The limits are also applicable to point-like technipions. For a discussion of techniparticles, see the Review of Dynamical Electroweak Symmetry Breaking in this Review.

For limits obtained in hadronic collisions before the observation of the top quark, and based on the top mass values inconsistent with the current measurements, see the 1996 (Physical Review D54 1 (1996)) Edition of this Review.

Searches in e^+e^- collisions at and above the Z pole have conclusively ruled out the existence of a charged Higgs in the region $m_{H^\pm} \lesssim 45$ GeV, and are now superseded by the most recent searches in higher energy e^+e^- collisions at LEP. Results by now obsolete are therefore not included in this compilation, and can be found in the 1998 Edition (The European Physical Journal C3 1 (1998)) of this Review.

In the following, and unless otherwise stated, results from the LEP experiments (ALEPH, DELPHI, L3, and OPAL) are assumed to derive from the study of the $e^+e^- \rightarrow H^+H^-$ process. Limits from $b \rightarrow s\gamma$ decays are usually stronger in generic 2HDM models than in Supersymmetric models.

'OUR LIMIT' is taken from the LEP Higgs Boson Searches Working Group (LEP 99b), where the combination of the results of ABBIENDI 99e, ABREU 99r, ACCIARRI 99b, BARATE 99d was performed.

A recent combination (LEP 00b) of preliminary, unpublished results relative to data taken at LEP in the Summer of 1999 at energies up to 202 GeV gives the limit $m_{H^\pm} > 78.6$ GeV.

VALUE (GeV)	CL%	DOCUMENT ID	TECN	COMMENT
> 69.0 (CL = 95%) OUR LIMIT				
> 59.5	95	ABBIENDI 99e OPAL		$E_{\text{cm}} \leq 183$ GeV
> 56.3	95	ABREU 99r DLPH		$E_{\text{cm}} \leq 183$ GeV
> 65.5	95	55 ACCIARRI 99p L3		$E_{\text{cm}} = 189$ GeV
> 59	95	BARATE 99d ALEP		$E_{\text{cm}} \leq 183$ GeV
• • • We do not use the following data for averages, fits, limits, etc. • • •				
> 82.8	95	ABBIENDI 00g OPAL		$E_{\text{cm}} \leq 189$ GeV, $B(\tau\nu) = 1$
		56 ABBOTT 99e D0		$t \rightarrow bH^+$
> 57.5	95	ACCIARRI 99b L3		$E_{\text{cm}} \leq 183$ GeV
		57 ACKERSTAFF 99d OPAL		$\tau \rightarrow e\nu\nu, \mu\nu\nu$
> 54.5	95	ABREU 98f DLPH		$E_{\text{cm}} \leq 172$ GeV
> 52.0	95	ACKERSTAFF 98i RVUE		$E_{\text{cm}} \leq 172$ GeV

> 52	95	BARATE 98g ALEP		$E_{\text{cm}} \leq 172$ GeV
		58 ABE 97L CDF		$t \rightarrow bH^+, H \rightarrow \tau\nu$
		59 ACCIARRI 97F L3		$B \rightarrow \tau\nu_\tau$
		60 AMMAR 97b CLEO		$\tau \rightarrow \mu\nu\nu$
		61 COARASA 97 RVUE		$B \rightarrow \tau\nu_\tau X$
		62 GUCHAIT 97 RVUE		$t \rightarrow bH^+, H \rightarrow \tau\nu$
		63 MANGANO 97 RVUE		$B_u(c) \rightarrow \tau\nu_\tau$
		64 STAHL 97 RVUE		$\tau \rightarrow \mu\nu\nu$
> 244	95	65 ALAM 97 CLE2		$b \rightarrow s\gamma$
		66 BUSKULIC 95 ALEP		$b \rightarrow \tau\nu_\tau X$

- 55 The limit improves to 71.6 GeV for $B(\tau\nu) > 0.2$ (see Fig. 4).
- 56 ABBOTT 99e search for a charged Higgs boson in top decays in $p\bar{p}$ collisions at $E_{\text{cm}} = 1.8$ TeV, by comparing the observed $t\bar{t}$ cross section (extracted from the data assuming the dominant decay $t \rightarrow bW^+$) with theoretical expectation. The search is sensitive to regions of the domains $\tan\beta \lesssim 1, 50 < m_{H^\pm} (\text{GeV}) \lesssim 120$ and $\tan\beta \gtrsim 40, 50 < m_{H^\pm} (\text{GeV}) \lesssim 160$. See Fig. 3 for the details of the excluded region.
- 57 ACKERSTAFF 99d measure the Michel parameters ρ, ξ, η , and δ in leptonic τ decays from $Z \rightarrow \tau\tau$. Assuming $e-\mu$ universality, the limit $m_{H^\pm} > 0.97 \tan\beta$ GeV (95%CL) is obtained for two-doublet models in which only one doublet couples to leptons.
- 58 ABE 97L search for a charged Higgs boson in top decays in $p\bar{p}$ collisions at $E_{\text{cm}} = 1.8$ TeV, with $H^\pm \rightarrow \tau^+\nu_\tau, \tau$ decaying hadronically. The limits depend on the choice of the $t\bar{t}$ cross section. See Fig. 3 for the excluded region. The excluded mass region extends to over 140 GeV for $\tan\beta$ values above 100.
- 59 ACCIARRI 97F give a limit $m_{H^\pm} > 2.6 \tan\beta$ GeV (90%CL) from their limit on the exclusive $B \rightarrow \tau\nu_\tau$ branching ratio.
- 60 AMMAR 97b measure the Michel parameter ρ from $\tau \rightarrow e\nu\nu$ decays and assume e/μ universality to extract the Michel η parameter from $\tau \rightarrow \mu\nu\nu$ decays. The measurement is translated to a lower limit on m_{H^\pm} in a two-doublet model $m_{H^\pm} > 0.97 \tan\beta$ GeV (90%CL).
- 61 COARASA 97 reanalyzed the constraint on the $(m_{H^\pm}, \tan\beta)$ plane derived from the inclusive $B \rightarrow \tau\nu_\tau X$ branching ratio in GROSSMAN 95b and BUSKULIC 95. They show that the constraint is quite sensitive to supersymmetric one-loop effects.
- 62 GUCHAIT 97 studies the constraints on m_{H^\pm} set by Tevatron data on $\ell\tau$ final states in $t\bar{t} \rightarrow (Wb)(Hb), W \rightarrow \ell\nu, H \rightarrow \tau\nu_\tau$. See Fig. 2 for the excluded region.
- 63 MANGANO 97 reconsiders the limit in ACCIARRI 97F including the effect of the potentially large $B_c \rightarrow \tau\nu_\tau$ background to $B_u \rightarrow \tau\nu_\tau$ decays. Stronger limits are obtained.
- 64 STAHL 97 fit τ lifetime, leptonic branching ratios, and the Michel parameters and derive limit $m_{H^\pm} > 1.5 \tan\beta$ GeV (90%CL) for a two-doublet model. See also STAHL 94.
- 65 ALAM 95 measure the inclusive $b \rightarrow s\gamma$ branching ratio at $\Upsilon(4S)$ and give $B(b \rightarrow s\gamma) < 4.2 \times 10^{-4}$ (95%CL), which translates to the limit $m_{H^\pm} > [244 + 63/(\tan\beta)]^{1.3}$ GeV in the Type II two-doublet model. Light supersymmetric particles can invalidate this bound.
- 66 BUSKULIC 95 give a limit $m_{H^\pm} > 1.9 \tan\beta$ GeV (90%CL) for Type-II models from $b \rightarrow \tau\nu_\tau X$ branching ratio, as proposed in GROSSMAN 94.

MASS LIMITS for $H^{\pm\pm}$ (doubly-charged Higgs boson)

VALUE (GeV)	CL%	DOCUMENT ID	TECN	COMMENT
> 45.6	95	67 ACTON 92M OPAL		
• • • We do not use the following data for averages, fits, limits, etc. • • •				
		68 GORDEEV 97 SPEC		muonium conversion
		69 ASAKA 95 THEO		
> 30.4	95	70 ACTON 92M OPAL		$T_3(H^{++}) = +1$
> 25.5	95	70 ACTON 92M OPAL		$T_3(H^{++}) = 0$
none 6.5-36.6	95	71 SWARTZ 90 MRK2		$T_3(H^{++}) = +1$
none 7.3-34.3	95	71 SWARTZ 90 MRK2		$T_3(H^{++}) = 0$
67 ACTON 92M limit assumes $H^{\pm\pm} \rightarrow \ell^\pm\ell^\pm$ or $H^{\pm\pm}$ does not decay in the detector. Thus the region $g_{\ell\ell} \approx 10^{-7}$ is not excluded.				
68 GORDEEV 97 search for muonium-antimuonium conversion and find $G_{M\bar{M}}/G_F < 0.14$ (90%CL), where $G_{M\bar{M}}$ is the lepton-flavor violating effective four-fermion coupling. This limit may be converted to $m_{H^{++}} > 210$ GeV if the Yukawa couplings of H^{++} to ee and $\mu\mu$ are as large as the weak gauge coupling. For similar limits on muonium-antimuonium conversion, see the muon Particle Listings.				
69 ASAKA 95 point out that H^{++} decays dominantly to four fermions in a large region of parameter space where the limit of ACTON 92M from the search of dilepton modes does not apply.				
70 ACTON 92M from $\Delta F_Z < 40$ MeV.				
71 SWARTZ 90 assume $H^{\pm\pm} \rightarrow \ell^\pm\ell^\pm$ (any flavor). The limits are valid for the Higgs-lepton coupling $g(H\ell\ell) \gtrsim 7.4 \times 10^{-7} / [m_H/\text{GeV}]^{1/2}$. The limits improve somewhat for ee and $\mu\mu$ decay modes.				

Gauge & Higgs Boson Particle Listings

Higgs Bosons — H^0 and H^\pm , Heavy Bosons Other than Higgs Bosons H^0 and H^\pm REFERENCES

ABBIENDI	00F	EPJ C12 567	G. Abbiendi et al.	(OPAL Collab.)
ABBIENDI	00G	EPJ C14 91	G. Abbiendi et al.	(OPAL Collab.)
ABREU	00G	CERN-EP-2000-038	P. Abreu et al.	(DELPHI Collab.)
FIELD	00	PR D61 013010	J.H. Field	
LEP	00	CERN-EP-2000-016		(ALEPH, DELPHI, L3, OPAL, SLD+)
LEP	00B	CERN-EP-2000-055		(ALEPH, DELPHI, L3, OPAL, LEP Higgs Working Group)
ABBIENDI	99E	EPJ C7 407	G. Abbiendi et al.	(OPAL Collab.)
ABBIENDI	99O	PL B464 311	G. Abbiendi et al.	(OPAL Collab.)
ABBOTT	99B	PRL 82 2244	B. Abbott et al.	(DO Collab.)
ABBOTT	99E	PRL 82 4975	B. Abbott et al.	(DO Collab.)
ABREU	99E	PL B446 75	P. Abreu et al.	(DELPHI Collab.)
Also	99N	PL B451 447 (erratum)		
ABREU	99I	EPJ C10 563	P. Abreu et al.	(DELPHI Collab.)
ABREU	99P	PL B458 431	P. Abreu et al.	(DELPHI Collab.)
ABREU	99Q	PL B459 367	P. Abreu et al.	(DELPHI Collab.)
ABREU	99R	PL B460 484	P. Abreu et al.	(DELPHI Collab.)
ACCIARRI	99B	PL B446 368	M. Acciari et al.	(L3 Collab.)
ACCIARRI	99J	PL B461 376	M. Acciari et al.	(L3 Collab.)
ACCIARRI	99P	PL B466 71	M. Acciari et al.	(L3 Collab.)
ACCIARRI	99U	PL B471 321	M. Acciari et al.	(L3 Collab.)
ACKERSTAFF	99D	EPJ C8 3	K. Ackerstaff et al.	(OPAL Collab.)
BARATE	99B	PL B447 336	R. Barate et al.	(ALEPH Collab.)
BARATE	99B	replaces the misprinted version in BARATE 98Z.		
BARATE	99C	PL B450 301	R. Barate et al.	(ALEPH Collab.)
BARATE	99D	PL B450 467	R. Barate et al.	(ALEPH Collab.)
BARATE	99O	PL B466 50	R. Barate et al.	(ALEPH Collab.)
CHANOWITZ	99	PR D59 073005	M.S. Chanowitz	
D'AGOSTINI	99	EPJ C10 663	G. D'Agostini, G. Degrassi	
FIELD	99	MPL A14 1815	J.H. Field	
LEP	99	CERN-EP/99-15		(ALEPH, DELPHI, L3, OPAL, LEP EWG+)
LEP	99B	CERN-EP/99-060		(ALEPH, DELPHI, L3, OPAL, LEP Higgs Working Group)
ABBOTT	98	PRL 80 442	B. Abbott et al.	(DO Collab.)
ABE	98T	PRL 81 5748	F. Abe et al.	(CDF Collab.)
ABREU	98E	EPJ C2 1	P. Abreu et al.	(DELPHI Collab.)
ABREU	98F	PL B420 140	P. Abreu et al.	(DELPHI Collab.)
ACCIARRI	98B	PL B418 389	M. Acciari et al.	(L3 Collab.)
ACCIARRI	98I	PL B431 437	M. Acciari et al.	(L3 Collab.)
ACCIARRI	98M	PL B436 389	M. Acciari et al.	(L3 Collab.)
ACKERSTAFF	98B	EPJ C1 31	K. Ackerstaff et al.	(OPAL Collab.)
ACKERSTAFF	98H	EPJ C1 425	K. Ackerstaff et al.	(OPAL Collab.)
ACKERSTAFF	98I	PL B426 180	K. Ackerstaff et al.	(OPAL Collab.)
ACKERSTAFF	98S	EPJ C5 19	K. Ackerstaff et al.	(OPAL Collab.)
ACKERSTAFF	98Y	PL B437 218	K. Ackerstaff et al.	(OPAL Collab.)
BARATE	98A	PL B440 419	R. Barate et al.	(ALEPH Collab.)
Also	99H	PL B447 355 (erratum)		
BARATE	98G	PL B418 419	R. Barate et al.	(ALEPH Collab.)
CHANOWITZ	98	PRL 80 2521	M. Chanowitz	
DAVIER	98	PL B435 427	M. Davier, A. Hoecker	
DREES	98	PRL 80 2047	M. Drees, M. Guchait, P. Roy	
Also	98B	PRL 81 2394 (erratum)		
DREES	98B	PRL 81 2394 (erratum)	M. Drees, M. Guchait, P. Roy	
GONZALEZ-G.	98B	PR D57 7045	M.C. Gonzalez-Garcia, S.M. Lietti, S.F. Novaez	
HAGIWARA	98B	EPJ C2 95	K. Hagiwara, D. Haidt, S. Matsumoto	
PDC	98	EPJ C3 1	C. Caso et al.	
ABBANEONE	97	CERN-PPE/97-154	D. Abbaneone et al.	
ALEPH, DELPHI, L3, OPAL, and SLD Collaborations, and the LEP Electroweak Working Group.				
ABE	97F	PRL 78 2906	F. Abe et al.	(CDF Collab.)
ABE	97L	PRL 79 357	F. Abe et al.	(CDF Collab.)
ABE	97W	PRL 79 3819	F. Abe et al.	(CDF Collab.)
ACCIARRI	97F	PL B396 327	M. Acciari et al.	(L3 Collab.)
ACCIARRI	97N	PL B411 330	M. Acciari et al.	(L3 Collab.)
AMMAR	97B	PRL 78 4856	R. Ammar et al.	(CLEO Collab.)
BARATE	97O	PL B412 155	R. Barate et al.	(ALEPH Collab.)
BARATE	97P	PL B412 173	R. Barate et al.	(ALEPH Collab.)
COARASA	97	PL B406 337	J.A. Coarasa, R.A. Jimenez, J. Sola	
DEBOER	97B	ZPHY C75 627	W. de Boer et al.	
DEGRASSI	97	PL B394 188	G. Degrassi, P. Gambino, A. Sirin	(MPIM, NYU)
DITTMAYER	97	PL B391 420	S. Dittmaier, D. Schildknecht	(BIEL)
GORDEEV	97	PAN 60 1164	V.A. Gordeev et al.	(PNPI)
GUCHAIT	97	Translated from YAF 60 1291.	M. Guchait, D.P. Roy	(TATA)
KRAWCZYK	97	PR D55 6968	M. Krawczyk, J. Zochowski	(WARSA)
MANGANO	97	PL B410 299	M. Mangano, S. Slabospitsky	
RENTON	97	IJMP A12 4109	P.B. Renton	
STAHL	97	ZPHY C74 73	A. Stahl, H. Voss	(BONN)
ACCIARRI	96J	PL B388 409	M. Acciari et al.	(L3 Collab.)
ALCARAZ	96	CERN-PPE/96-183	J. Alcaraz et al.	
The ALEPH, DELPHI, L3, OPAL, and SLD Collaborations and the LEP Electroweak Working Group.				
ALEXANDER	96H	ZPHY C71 1	G. Alexander et al.	(OPAL Collab.)
BUSKULIC	96K	PL B373 245	D. Buskalic et al.	(ALEPH Collab.)
ELLIS	96C	PL B389 321	J. Ellis, G.L. Fogli, E. Lisi	(CERN, BARI)
GURTU	96	PL B385 415	A. Gurtu	(TATA)
PDG	96	PR D54 1		
ABREU	95H	ZPHY C67 69	P. Abreu et al.	(DELPHI Collab.)
ALAM	95	PRL 74 2885	M.S. Alam et al.	(CLEO Collab.)
ASAKA	95	PL B345 36	T. Asaka, K.I. Hikasa	(TOHOK)
BUSKULIC	95	PL B343 444	D. Buskalic et al.	(ALEPH Collab.)
GROSSMAN	95B	PL B357 630	Y. Grossman, H. Haber, Y. Nir	
GROSSMAN	94	PL B332 373	Y. Grossman, Z. Ligeti	
STAHL	94	PL B324 121	A. Stahl	(BONN)
ACTON	92M	PL B295 347	P.D. Acton et al.	(OPAL Collab.)
PICH	92	NP B388 31	A. Pich, J. Prades, P. Yepes	(CERN, CPPM)
SWARTZ	90	PL B4 2877	M.L. Swartz et al.	(Mark II Collab.)

Heavy Bosons Other Than Higgs Bosons, Searches for

We list here various limits on charged and neutral heavy vector bosons (other than W 's and Z 's), heavy scalar bosons (other than Higgs bosons), vector or scalar leptoquarks, and axiglons.

 W_R (Right-Handed W Boson) MASS LIMITS

Assuming a light right-handed neutrino, except for BEALL 82, LANGACKER 89b, and COLANGELO 91. $g_R = g_L$ assumed. [Limits in the section MASS LIMITS for W' below are also valid for W_R if $m_{\nu_R} \ll m_{W_R}$.] Some limits assume manifest left-right symmetry, i.e., the equality of left- and right Cabibbo-Kobayashi-Maskawa matrices. For a comprehensive review, see LANGACKER 89b. Limits on the W_L - W_R mixing angle ζ are found in the next section. Values in brackets are from cosmological and astrophysical considerations and assume a light right-handed neutrino.

VALUE (GeV)	CL%	DOCUMENT ID	TECN	COMMENT
> 715	90	¹ CZAKON	99	RVUE Electroweak
> 137	95	² ACKERSTAFF	99D	OPAL τ decay
> 1400	68	³ BARENBOIM	98	RVUE Electroweak, Z - Z' mixing
> 549	68	⁴ BARENBOIM	97	RVUE μ decay
> 220	95	⁵ STAHL	97	RVUE τ decay
> 220	90	⁶ ALLET	96	CNTR β^+ decay
> 281	90	⁷ KUZNETSOV	95	CNTR Polarized neutron decay
> 282	90	⁸ KUZNETSOV	94B	CNTR Polarized neutron decay
> 439	90	⁹ BHATTACH...	93	RVUE Z - Z' mixing
> 250	90	¹⁰ SEVERIJNS	93	CNTR β^+ decay
> 475	90	¹¹ IMAZATO	92	CNTR K^+ decay
> 240	90	¹² POLAK	92B	RVUE μ decay
> 496	90	¹³ AQUINO	91	RVUE Neutron decay
> 700	90	¹³ AQUINO	91	RVUE Neutron and muon decay
> 477	90	¹⁴ COLANGELO	91	THEO $m_{K_0^+} - m_{K_0^0}$
[none 540-23000]		¹⁵ POLAK	91	RVUE μ decay
> 300	90	¹⁶ BARBIERI	89B	ASTR SN 1987A; light ν_R
> 160	90	¹⁷ LANGACKER	89B	RVUE General
> 406	90	¹⁸ BALKE	88	CNTR $\mu \rightarrow e\nu\bar{\nu}$
> 482	90	¹⁹ JODIDIO	86	ELEC Any ζ
> 800	90	¹⁹ JODIDIO	86	ELEC $\zeta = 0$
> 400	95	²⁰ MOHAPATRA	86	RVUE $SU(2)_L \times SU(2)_R \times U(1)$
> 475	95	²⁰ STOKER	85	ELEC Any ζ
> 380	90	²¹ STOKER	85	ELEC $\zeta < 0.041$
> 1600	90	²² BERGSMA	83	CHRM $\nu_\mu e \rightarrow \mu\nu_e$
> 4000		²³ CARR	83	ELEC μ^+ decay
> 4000		²³ BEALL	82	THEO $m_{K_0^+} - m_{K_0^0}$
> 4000		STEIGMAN	79	COSM Nucleosynthesis; light ν_R

- ¹ CZAKON 99 perform a simultaneous fit to charged and neutral sectors.
- ² ACKERSTAFF 99D limit is from τ decay parameters. Limit increase to 145 GeV for zero mixing.
- ³ BARENBOIM 98 assumes minimal left-right model with Higgs of $SU(2)_R$ in $SU(2)_L$ doublet. For Higgs in $SU(2)_L$ triplet, $m_{W_R} > 1100$ GeV. Bound calculated from effect of corresponding Z_{LR} on electroweak data through Z - Z_{LR} mixing.
- ⁴ The quoted limit is from μ decay parameters. BARENBOIM 97 also evaluate limit from K_L - K_S mass difference.
- ⁵ STAHL 97 limit is from fit to τ -decay parameters.
- ⁶ ALLET 96 measured polarization-asymmetry correlation in $^{12}N\beta^+$ decay. The listed limit assumes zero L - R mixing.
- ⁷ KUZNETSOV 95 limit is from measurements of the asymmetry $\langle \bar{\nu}_\nu \sigma_n \rangle$ in the β decay of polarized neutrons. Zero mixing assumed. See also KUZNETSOV 94B.
- ⁸ KUZNETSOV 94B limit is from measurements of the asymmetry $\langle \bar{\nu}_\nu \sigma_n \rangle$ in the β decay of polarized neutrons. Zero mixing assumed.
- ⁹ BHATTACHARYYA 93 uses Z - Z' mixing limit from LEP '90 data, assuming a specific Higgs sector of $SU(2)_L \times SU(2)_R \times U(1)$ gauge model. The limit is for $m_t = 200$ GeV and slightly improves for smaller m_t .
- ¹⁰ SEVERIJNS 93 measured polarization-asymmetry correlation in $^{107}In\beta^+$ decay. The listed limit assumes zero L - R mixing. Value quoted here is from SEVERIJNS 94 erratum.
- ¹¹ IMAZATO 92 measure positron asymmetry in $K^+ \rightarrow \mu^+ \nu_\mu$ decay and obtain $\langle \bar{\nu}_\mu \rangle = 0.990$ (90%CL). If W_R couples to $u\bar{s}$ with full weak strength ($V_{us}^R = 1$), the result corresponds to $m_{W_R} > 653$ GeV. See their Fig. 4 for m_{W_R} limits for general $|V_{us}^R|^2 = 1 - |V_{ud}^R|^2$.
- ¹² POLAK 92B limit is from fit to muon decay parameters and is essentially determined by JODIDIO 86 data assuming $\zeta = 0$. Supersedes POLAK 91.
- ¹³ AQUINO 91 limits obtained from neutron lifetime and asymmetries together with unitarity of the CKM matrix. Manifest left-right symmetry assumed. Stronger of the two limits also includes muon decay results.
- ¹⁴ COLANGELO 91 limit uses hadronic matrix elements evaluated by QCD sum rule and is less restrictive than BEALL 82 limit which uses vacuum saturation approximation. Manifest left-right symmetry assumed.
- ¹⁵ POLAK 91 limit is from fit to muon decay parameters and is essentially determined by JODIDIO 86 data assuming $\zeta = 0$. Superseded by POLAK 92B.
- ¹⁶ BARBIERI 89B limit holds for $m_{\nu_R} \leq 10$ MeV.
- ¹⁷ LANGACKER 89B limit is for any ν_R mass (either Dirac or Majorana) and for a general class of right-handed quark mixing matrices.

See key on page 239

Gauge & Higgs Boson Particle Listings

Heavy Bosons Other than Higgs Bosons

- ¹⁸BALKE 88 limit is for $m_{\nu_{eR}} = 0$ and $m_{\nu_{\mu R}} \leq 50$ MeV. Limits come from precise measurements of the muon decay asymmetry as a function of the positron energy.
- ¹⁹JODIDIO 86 is the same TRIUMF experiment as STOKER 85 (and CARR 83); however, it uses a different technique. The results given here are combined results of the two techniques. The technique here involves precise measurement of the end-point e^+ spectrum in the decay of the highly polarized μ^+ .
- ²⁰STOKER 85 is same TRIUMF experiment as CARR 83. Here they measure the decay e^+ spectrum asymmetry above 46 MeV/c using a muon-spin-rotation technique. Assumed a light right-handed neutrino. Quoted limits are from combining with CARR 83.
- ²¹BERGSMA 83 set limit $m_{W_2}/m_{W_1} > 1.9$ at CL = 90%.
- ²²CARR 83 is TRIUMF experiment with a highly polarized μ^+ beam. Looked for deviation from $V-A$ at the high momentum end of the decay e^+ energy spectrum. Limit from previous world-average muon polarization parameter is $m_{W_R} > 240$ GeV. Assumes a light right-handed neutrino.
- ²³BEALL 82 limit is obtained assuming that W_R contribution to $K_L^0-K_S^0$ mass difference is smaller than the standard one, neglecting the top quark contributions. Manifest left-right symmetry assumed.

Limit on W_L - W_R Mixing Angle ζ

Lighter mass eigenstate $W_1 = W_L \cos \zeta - W_R \sin \zeta$. Light ν_R assumed unless noted. Values in brackets are from cosmological and astrophysical considerations.

VALUE	CL%	DOCUMENT ID	TECN	COMMENT
• • • We do not use the following data for averages, fits, limits, etc. • • •				
< 0.12	95	24 ACKERSTAFF	99D OPAL	τ decay
< 0.013	90	25 CZAKON	99 RVUE	Electroweak
< 0.0333		26 BARENBOIM	97 RVUE	μ decay
< 0.04	90	27 MISHRA	92 CCFR	νN scattering
-0.0006 to 0.0028	90	28 AQUINO	91 RVUE	
[none 0.00001-0.02]		29 BARBIERI	89B ASTR	SN 1987A
< 0.040	90	30 JODIDIO	86 ELEC	μ decay
-0.056 to 0.040	90	30 JODIDIO	86 ELEC	μ decay

- ²⁴ACKERSTAFF 99D limit is from τ decay parameters.
- ²⁵CZAKON 99 perform a simultaneous fit to charged and neutral sectors.
- ²⁶The quoted limit is from μ decay parameters. BARENBOIM 97 also evaluate limit from K_L-K_S mass difference.
- ²⁷MISHRA 92 limit is from the absence of extra large- x , large- y $\bar{\nu}_\mu N \rightarrow \bar{\nu}_\mu X$ events at Tevatron, assuming left-handed ν and right-handed $\bar{\nu}$ in the neutrino beam. The result gives $\zeta^2(1-2m_{W_1}^2/m_{W_2}^2) < 0.0015$. The limit is independent of ν_R mass.
- ²⁸AQUINO 91 limits obtained from neutron lifetime and asymmetries together with unitarity of the CKM matrix. Manifest left-right asymmetry is assumed.
- ²⁹BARBIERI 89B limit holds for $m_{\nu_R} \leq 10$ MeV.
- ³⁰First JODIDIO 86 result assumes $m_{W_R} = \infty$, second is for unconstrained m_{W_R} .

THE W' SEARCHES

Written October 1997 by K.S. Babu, C. Kolda, and J. March-Russell (IAS/Princeton).

Any electrically charged gauge boson outside of the Standard Model is generically denoted W' . A W' always couples to two different flavors of fermions, similar to the W boson. In particular, if a W' couples quarks to leptons it is a leptoquark gauge boson.

The most attractive candidate for W' is the W_R gauge boson associated with the left-right symmetric models [1]. These models seek to provide a spontaneous origin for parity violation in weak interactions. Here the gauge group is extended to $SU(3)_C \times SU(2)_L \times SU(2)_R \times U(1)_{B-L}$ with the Standard Model hypercharge identified as $Y = T_{3R} + (B-L)/2$, T_{3R} being the third component of $SU(2)_R$. The fermions transform under the gauge group in a left-right symmetric fashion: $q_L(3, 2, 1, 1/3) + q_R(3, 1, 2, 1/3)$ for quarks and $\ell_L(1, 2, 1, -1) + \ell_R(1, 1, 2, -1)$ for leptons. Note that the model requires the introduction of right-handed neutrinos, which can facilitate the see-saw mechanism for explaining the smallness of the ordinary neutrino masses. A Higgs bidoublet $\Phi(1, 2, 2, 0)$ is usually employed to generate quark and lepton masses and to participate in the electroweak symmetry breaking. Under left-right (or parity) symmetry, $q_L \leftrightarrow q_R$, $\ell_L \leftrightarrow \ell_R$, $W_L \leftrightarrow W_R$ and $\Phi \leftrightarrow \Phi^\dagger$.

After spontaneous symmetry breaking, the two W bosons of the model, W_L and W_R , will mix. The physical mass eigenstates are denoted as

$$W_1 = \cos \zeta W_L + \sin \zeta W_R, \quad W_2 = -\sin \zeta W_L + \cos \zeta W_R \quad (1)$$

with W_1 identified as the observed W boson. The most general Lagrangian that describes the interactions of the $W_{1,2}$ with the quarks can be written as [2]

$$\mathcal{L} = -\frac{1}{\sqrt{2}} \bar{u} \gamma_\mu \left[(g_L \cos \zeta V^L P_L - g_R e^{i\omega} \sin \zeta V^R P_R) W_1^\mu + (g_L \sin \zeta V^L P_L + g_R e^{i\omega} \cos \zeta V^R P_R) W_2^\mu \right] d + h.c. \quad (2)$$

where $g_{L,R}$ are the $SU(2)_{L,R}$ gauge couplings, $P_{L,R} = (1 \mp \gamma_5)/2$ and $V^{L,R}$ are the left- and right-handed CKM matrices in the quark sector. The phase ω reflects a possible complex mixing parameter in the W_L - W_R mass-squared matrix. Note that there is CP violation in the model arising from the right-handed currents even with only two generations. The Lagrangian for leptons is identical to that for quarks, with the replacements $u \rightarrow \nu$, $d \rightarrow e$ and the identification of $V^{L,R}$ with the CKM matrices in the leptonic sector.

If parity invariance is imposed on the Lagrangian, then $g_L = g_R$. Furthermore, the Yukawa coupling matrices that arise from coupling to the Higgs bidoublet Φ will be Hermitian. If in addition the vacuum expectation values of Φ are assumed to be real, the quark and lepton mass matrices will also be Hermitian, leading to the relation $V^L = V^R$. Such models are called *manifest* left-right symmetric models and are approximately realized with a minimal Higgs sector [3]. If instead parity and CP are both imposed on the Lagrangian, then the Yukawa coupling matrices will be real symmetric and, after spontaneous CP violation, the mass matrices will be complex symmetric. In this case, which is known in the literature as *pseudo-manifest* left-right symmetry, $V^L = (V^R)^*$.

Indirect constraints: In minimal version of manifest or pseudo-manifest left-right symmetric models with $\omega = 0$ or π , there are only two free parameters, ζ and M_{W_2} , and they can be constrained from low energy processes. In the large M_{W_2} limit, stringent bounds on the angle ζ arise from three processes. (i) Nonleptonic K decays: The decays $K \rightarrow 3\pi$ and $K \rightarrow 2\pi$ are sensitive to small admixtures of right-handed currents. Assuming the validity of PCAC relations in the Standard Model it has been argued in Ref. 4 that the success in the $K \rightarrow 3\pi$ prediction will be spoiled unless $|\zeta| \leq 4 \times 10^{-3}$. (ii) $b \rightarrow s\gamma$: The amplitude for this process has an enhancement factor m_t/m_b relative to the Standard Model and thus can be used to constrain ζ yielding the limit $-0.01 \leq \zeta \leq 0.003$ [5]. (iii) Universality in weak decays: If the right-handed neutrinos are heavy, the right-handed admixture in the charged current will contribute to β decay and K decay, but not to the μ decay. This will modify the extracted values of V_{ud}^L and V_{us}^L . Demanding that the difference not upset the three generation

Gauge & Higgs Boson Particle Listings

Heavy Bosons Other than Higgs Bosons

unitarity of the CKM matrix, a bound $|\zeta| \leq 10^{-3}$ has been derived [6].

If the ν_R are heavy, leptonic and semileptonic processes do not constrain ζ since the emission of ν_R will not be kinematically allowed. However, if the ν_R is light enough to be emitted in μ decay and β decay, stringent limits on ζ do arise. For example, $|\zeta| \leq 0.039$ can be obtained from polarized μ decay [7] in the large M_{W_2} limit of the manifest left-right model. Alternatively, in the $\zeta = 0$ limit, there is a constraint $M_{W_2} \geq 484$ GeV from direct W_2 exchange. For the constraint on the case in which M_{W_2} is not taken to be heavy, see Ref. 2. There are also cosmological and astrophysical constraints on M_{W_2} and ζ in scenarios with a light ν_R . During nucleosynthesis the process $e^+e^- \rightarrow \nu_R\bar{\nu}_R$, proceeding via W_2 exchange, will keep the ν_R in equilibrium leading to an overproduction of ${}^4\text{He}$ unless M_{W_2} is greater than about 1 TeV [8]. Likewise the ν_{eR} produced via $e_R^-p \rightarrow n\nu_R$ inside a supernova must not drain too much of its energy, leading to limits $M_{W_2} > 16$ TeV and $|\zeta| \leq 3 \times 10^{-5}$ [9]. Note that models with light ν_R do not have a see-saw mechanism for explaining the smallness of the neutrino masses, though other mechanisms may arise in variant models [10].

The mass of W_2 is severely constrained (independent of the value of ζ) from K_L - K_S mass-splitting. The box diagram with exchange of one W_L and one W_R has an anomalous enhancement and yields the bound $M_{W_2} \geq 1.6$ TeV [11] for the case of manifest or pseudo-manifest left-right symmetry. If the ν_R have Majorana masses, another constraint arises from neutrinoless double β decay. Combining the experimental limit from ${}^{76}\text{Ge}$ decay with arguments of vacuum stability, a limit of $M_{W_2} \geq 1.1$ TeV has been obtained [12].

Direct search limits: Limits on M_{W_2} from direct searches depend on the available decay channels of W_2 . If ν_R is heavier than W_2 , the decay $W_2^+ \rightarrow \ell_R^+\nu_R$ will be forbidden kinematically. Assuming that ζ is small, the dominant decay of W_2 will be into dijets. UA2 [13] has excluded a W_2 in the mass range of 100 to 251 GeV in this channel. DØ excludes the mass range of 340 to 680 GeV [14], while CDF excludes the mass range of 300 to 420 GeV for such a W_2 [15]. If ν_R is lighter than W_2 , the decay $W_2^+ \rightarrow e_R^+\nu_R$ is allowed. The ν_R can then decay into $e_R W_R^*$, leading to an $eejj$ signature. DØ has a limit of $M_{W_2} > 720$ GeV if $m_{\nu_R} \ll M_{W_2}$; the bound weakens, for example, to 650 GeV for $m_{\nu_R} = M_{W_2}/2$ [16]. CDF finds $M_{W_2} > 652$ GeV if ν_R is stable and much lighter than W_2 [17]. All of these limits assume manifest or pseudo-manifest left-right symmetry. See [16] for some variations in the limits if the assumption of left-right symmetry is relaxed.

Alternative models: W' gauge bosons can also arise in other models. We shall briefly mention some such popular models, but for details we refer the reader to the original literature. The *alternate* left-right model [18] is based on the same gauge group as the left-right model, but arises in the following way:

In E_6 unification, there is an option to identify the right-handed down quarks as $SU(2)_R$ singlets or doublets. If they are $SU(2)_R$ doublets, one recovers the conventional left-right model; if they are singlets it leads to the alternate left-right model. A similar ambiguity exists in the assignment of left-handed leptons; the alternate left-right model assigns them to a $(1, 2, 2, 0)$ multiplet. As a consequence, the ordinary neutrino remains exactly massless in the model. One important difference from the usual left-right model is that the limit from the K_L - K_S mass difference is no longer applicable, since the d_R do not couple to the W_R . There is also no limit from polarized μ decay, since the $SU(2)_R$ partner of e_R can receive a large Majorana mass. Other W' models include the un-unified Standard Model of Ref. 19 where there are two different $SU(2)$ gauge groups, one each for the quarks and leptons; models with separate $SU(2)$ gauge factors for each generation [20]; and the $SU(3)_C \times SU(3)_L \times U(1)$ model of Ref. 21.

Leptoquark gauge bosons: The $SU(3)_C \times U(1)_{B-L}$ part of the gauge symmetry discussed above can be embedded into a simple $SU(4)_C$ gauge group [22]. The model then will contain leptoquark gauge boson as well, with couplings of the type $\{(\bar{e}_L\gamma_\mu d_L + \bar{\nu}_L\gamma_\mu u_L)W'^\mu + (L \rightarrow R)\}$. The best limit on such leptoquark W' comes from nonobservation of $K_L \rightarrow \mu e$, which requires $M_{W'} \geq 1400$ TeV; for the corresponding limits on less conventional leptoquark flavor structures, see Ref. 23. Thus such a W' is inaccessible to direct searches with present machines which are sensitive to vector leptoquark masses of order 300 GeV only.

References

- J.C. Pati and A. Salam, Phys. Rev. **D10**, 275 (1974); R.N. Mohapatra and J.C. Pati, Phys. Rev. **D11**, 566 (1975); *ibid.* Phys. Rev. **D11**, 2558 (1975); G. Senjanovic and R.N. Mohapatra, Phys. Rev. **D12**, 1502 (1975).
- P. Langacker and S. Uma Sankar, Phys. Rev. **D40**, 1569 (1989).
- A. Masiero, R.N. Mohapatra, and R. Peccei, Nucl. Phys. **B192**, 66 (1981); J. Basecq, *et al.*, Nucl. Phys. **B272**, 145 (1986).
- J. Donoghue and B. Holstein, Phys. Lett. **113B**, 383 (1982).
- K.S. Babu, K. Fujikawa, and A. Yamada, Phys. Lett. **B333**, 196 (1994); P. Cho and M. Misiak, Phys. Rev. **D49**, 5894 (1994); T.G. Rizzo, Phys. Rev. **D50**, 3303 (1994).
- L. Wolfenstein, Phys. Rev. **D29**, 2130 (1984).
- P. Herczeg, Phys. Rev. **D34**, 3449 (1986).
- G. Steigman, K.A. Olive, and D. Schramm, Nucl. Phys. **B180**, 497 (1981).
- R. Barbieri and R.N. Mohapatra, Phys. Rev. **D39**, 1229 (1989); G. Raffelt and D. Seckel, Phys. Rev. Lett. **60**, 1793 (1988).
- D. Chang and R.N. Mohapatra, Phys. Rev. Lett. **58**, 1600 (1987); K.S. Babu and X.G. He, Mod. Phys. Lett. **A4**, 61 (1989).

See key on page 239

Gauge & Higgs Boson Particle Listings Heavy Bosons Other than Higgs Bosons

11. G. Beall, M. Bender, and A. Soni, Phys. Rev. Lett. **48**, 848 (1982).
12. R.N. Mohapatra, Phys. Rev. **D34**, 909 (1986).
13. J. Alitti, *et al.* (UA2 Collaboration), Nucl. Phys. **B400**, 3 (1993).
14. B. Abbott, *et al.* (DØ Collaboration), International Europhysics Conference on High Energy Physics, August 19-26, 1997, Jerusalem, Israel.
15. F. Abe, *et al.* (CDF Collaboration), Phys. Rev. **D55**, R5263 (1997).
16. S. Abachi, *et al.* (DØ Collaboration), Phys. Rev. Lett. **76**, 3271 (1996).
17. F. Abe, *et al.* (CDF Collaboration), Phys. Rev. Lett. **74**, 2900 (1995).
18. E. Ma, Phys. Rev. **D36**, 274 (1987);
K.S. Babu, X-G. He and E. Ma, Phys. Rev. **D36**, 878 (1987).
19. H. Georgi and E. Jenkins, Phys. Rev. Lett. **62**, 2789 (1989);
Nucl. Phys. **B331**, 541 (1990).
20. X. Li and E. Ma, Phys. Rev. Lett. **47**, 1788 (1981);
R.S. Chivukula, E.H. Simmons, and J. Terning, Phys. Lett. **B331**, 383 (1994);
D.J. Muller and S. Nandi, Phys. Lett. **B383**, 345 (1996).
21. F. Pisano, V. Pleitez, Phys. Rev. **D46**, 410 (1992);
P. Frampton, Phys. Rev. Lett. **69**, 2889 (1992).
22. J.C. Pati and A. Salam, Phys. Rev. **D10**, 275 (1974).
23. A. Kuznetsov and N. Mikheev, Phys. Lett. **B329**, 295 (1994);
G. Valencia and S. Willenbrock, Phys. Rev. **D50**, 6843 (1994).

MASS LIMITS for W' (A Heavy-Charged Vector Boson Other Than W) in Hadron Collider Experiments

Couplings of W' to quarks and leptons are taken to be identical with those of W . The following limits are obtained from $p\bar{p} \rightarrow W'X$ with W' decaying to the mode indicated in the comments. New decay channels (e.g., $W' \rightarrow WZ$) are assumed to be suppressed. UA1 and UA2 experiments assume that the $t\bar{b}$ channel is not open.

VALUE (GeV)	CL%	DOCUMENT ID	TECN	COMMENT
>720	95	31 ABACHI	96C D0	$W' \rightarrow e\nu_e$
••• We do not use the following data for averages, fits, limits, etc. •••				
none 300-420	95	32 ABE	97G CDF	$W' \rightarrow q\bar{q}$
>610	95	33 ABACHI	95E D0	$W' \rightarrow e\nu_e$ and $W' \rightarrow \tau\nu_\tau \rightarrow e\nu\nu$
>652	95	34 ABE	95M CDF	$W' \rightarrow e\nu_e$
>251	90	35 ALITTI	93 UA2	$W' \rightarrow q\bar{q}$
none 260-600	95	36 RIZZO	93 RVUE	$W' \rightarrow q\bar{q}$
>520	95	37 ABE	91F CDF	$W' \rightarrow e\nu, \mu\nu$
none 101-158	90	38 ALITTI	91 UA2	$W' \rightarrow q\bar{q}$
>220	90	39 ALBAJAR	89 UA1	$W' \rightarrow e\nu$
>209	90	40 ANSARI	87D UA2	$W' \rightarrow e\nu$
>210	90	41 ARNISON	86B UA1	$W' \rightarrow e\nu$
>170	90	42 ARNISON	83D UA1	$W' \rightarrow e\nu$

³¹ For bounds on W_R with nonzero right-handed mass, see Fig. 5 from ABACHI 96c.

³² ABE 97G search for new particle decaying to dijets.

³³ ABACHI 95E assume that the decay $W' \rightarrow WZ$ is suppressed and that the neutrino from W' decay is stable and has a mass significantly less than $m_{W'}$.

³⁴ ABE 95M assume that the decay $W' \rightarrow WZ$ is suppressed and the (right-handed) neutrino is light, noninteracting, and stable. If $m_\nu = 60$ GeV, for example, the effect on the mass limit is negligible.

³⁵ ALITTI 93 search for resonances in the two-jet invariant mass. The limit assumes $\Gamma(W')/m_{W'} = \Gamma(W)/m_W$ and $B(W' \rightarrow jj) = 2/3$. This corresponds to W_R with $m_{\nu_R} > m_{W_R}$ (no leptonic decay) and $W_R \rightarrow t\bar{b}$ allowed. See their Fig. 4 for limits in the $m_{W'} - B(q\bar{q})$ plane.

³⁶ RIZZO 93 analyses CDF limit on possible two-jet resonances. The limit is sensitive to the inclusion of the assumed K factor.

³⁷ ABE 91F assume leptonic branching ratio of 1/12 for each lepton flavor. The limit from the $e\nu$ ($\mu\nu$) mode alone is 490 (435) GeV. These limits apply to W_R if $m_{\nu_R} \lesssim 15$ GeV and ν_R does not decay in the detector. Cross section limit $\sigma \cdot B < (1-10)$ pb is given for $m_{W'} = 100-550$ GeV; see Fig. 2.

³⁸ ALITTI 91 search is based on two-jet invariant mass spectrum, assuming $B(W' \rightarrow q\bar{q}) = 67.6\%$. Limit on $\sigma \cdot B$ as a function of two-jet mass is given in Fig. 7.

³⁹ ALBAJAR 89 cross section limit at 630 GeV is $\sigma(W') B(e\nu) < 4.1$ pb (90% CL).

⁴⁰ See Fig. 5 of ANSARI 87D for the excluded region in the $m_{W'} - [(\hat{g}_{W'q})^2 B(W' \rightarrow e\bar{\nu})]$ plane. Note that the quantity $(\hat{g}_{W'q})^2 B(W' \rightarrow e\bar{\nu})$ is normalized to unity for the standard W couplings.

⁴¹ ARNISON 86B find no excess at large p_T in 148 $W \rightarrow e\nu$ events. Set limit $\sigma \times B(e\nu) < 10$ pb at CL = 90% at $E_{cm} = 546$ and 630 GeV.

⁴² ARNISON 83D find among 47 $W \rightarrow e\nu$ candidates no event with excess p_T . Also set $\sigma \times B(e\nu) < 30$ pb with CL = 90% at $E_{cm} = 540$ GeV.

THE Z' SEARCHES

Written October 1997 by K.S. Babu, C. Kolda, and J. March-Russell (IAS/Princeton).

If the Standard Model is enhanced by additional gauge symmetries or embedded into a larger gauge group, there will arise new heavy gauge bosons, some of which generically are electrically neutral. Such a gauge boson is called a Z' . Consider the most general renormalizable Lagrangian describing the complete set of interactions of the neutral gauge bosons among themselves and with fermions, which is that of the Standard Model plus the following new pieces [1,2,3]:

$$\mathcal{L}_{Z'} = -\frac{1}{4}\hat{F}'_{\mu\nu}\hat{F}'^{\mu\nu} - \frac{\sin\chi}{2}\hat{F}'_{\mu\nu}\hat{F}^{\mu\nu} + \frac{1}{2}\hat{M}_Z^2\hat{Z}'_\mu\hat{Z}'^\mu + \delta\hat{M}^2\hat{Z}'_\mu\hat{Z}'^\mu - \frac{\hat{g}'}{2}\sum_i\bar{\psi}_i\gamma^\mu(f_V^i - f_A^i\gamma^5)\psi_i\hat{Z}'_\mu \quad (1)$$

where $\hat{F}'_{\mu\nu}, \hat{F}_{\mu\nu}$ are the field strength tensors for the hypercharge \hat{B}_μ gauge boson and the Z' respectively before any diagonalizations are performed, ψ_i are the matter fields with Z' vector and axial charges f_V^i and f_A^i , and \hat{Z}'_μ is the electroweak Z boson in this basis. (See the Review on "Electroweak Model and Constraints on New Physics" for the Standard Model pieces of the Lagrangian.) The mass terms are assumed to come from spontaneous symmetry breaking via scalar expectation values. The above Lagrangian is general to all abelian and non-abelian extensions, except that $\chi = 0$ for the non-abelian case since then $\hat{F}'_{\mu\nu}$ is not gauge invariant. Most analyses take $\chi = 0$ even for the abelian case.

Going to the physical eigenbasis requires diagonalizing both the gauge kinetic and mass terms, with mass eigenstates denoted Z_1 and Z_2 , where we choose Z_1 to be the observed Z boson. The interaction Lagrangian for Z_1 has the form, to leading order in the mixing angle ξ ($s_W \equiv \sin\theta_W$, etc.):

$$\mathcal{L}_{Z_1} = -\frac{e}{2s_W c_W} \left(1 + \frac{\alpha T}{2}\right) \bar{\psi}_i \gamma^\mu \left\{ \left(g_V^i + \xi \tilde{f}_V^i\right) - \left(g_A^i + \xi \tilde{f}_A^i\right) \gamma^5 \right\} \psi_i Z_{1\mu} \quad (2)$$

where

$$\xi \simeq \frac{-\cos\chi(\delta\hat{M}^2 + \hat{M}_Z^2 s_W \sin\chi)}{\hat{M}_Z^2 - \hat{M}_Z^2 \cos^2\chi + \hat{M}_Z^2 s_W^2 \sin^2\chi + 2\delta\hat{M}^2 s_W \sin\chi} \quad (3)$$

We have made the identifications $g_A^i = T_3^i$, $g_V^i = T_3^i - 2Q^i s_W^2$, $\tilde{f}_{V,A}^i = (\hat{g}' s_W c_W / e \cos\chi) f_{V,A}^i$, and s_W^2 is identified to be the $s_{M_Z}^2$ defined in the "Electroweak Model and Constraints on New Physics" review. Note that the value of the weak angle

See key on page 239

Gauge & Higgs Boson Particle Listings Heavy Bosons Other than Higgs Bosons

11. G. Beall, M. Bender, and A. Soni, Phys. Rev. Lett. **48**, 848 (1982).
12. R.N. Mohapatra, Phys. Rev. **D34**, 909 (1986).
13. J. Alitti, *et al.* (UA2 Collaboration), Nucl. Phys. **B400**, 3 (1993).
14. B. Abbott, *et al.* (DØ Collaboration), International Europhysics Conference on High Energy Physics, August 19-26, 1997, Jerusalem, Israel.
15. F. Abe, *et al.* (CDF Collaboration), Phys. Rev. **D55**, R5263 (1997).
16. S. Abachi, *et al.* (DØ Collaboration), Phys. Rev. Lett. **76**, 3271 (1996).
17. F. Abe, *et al.* (CDF Collaboration), Phys. Rev. Lett. **74**, 2900 (1995).
18. E. Ma, Phys. Rev. **D36**, 274 (1987);
K.S. Babu, X-G. He and E. Ma, Phys. Rev. **D36**, 878 (1987).
19. H. Georgi and E. Jenkins, Phys. Rev. Lett. **62**, 2789 (1989);
Nucl. Phys. **B331**, 541 (1990).
20. X. Li and E. Ma, Phys. Rev. Lett. **47**, 1788 (1981);
R.S. Chivukula, E.H. Simmons, and J. Terning, Phys. Lett. **B331**, 383 (1994);
D.J. Muller and S. Nandi, Phys. Lett. **B383**, 345 (1996).
21. F. Pisano, V. Pleitez, Phys. Rev. **D46**, 410 (1992);
P. Frampton, Phys. Rev. Lett. **69**, 2889 (1992).
22. J.C. Pati and A. Salam, Phys. Rev. **D10**, 275 (1974).
23. A. Kuznetsov and N. Mikheev, Phys. Lett. **B329**, 295 (1994);
G. Valencia and S. Willenbrock, Phys. Rev. **D50**, 6843 (1994).

MASS LIMITS for W' (A Heavy-Charged Vector Boson Other Than W) in Hadron Collider Experiments

Couplings of W' to quarks and leptons are taken to be identical with those of W . The following limits are obtained from $p\bar{p} \rightarrow W'X$ with W' decaying to the mode indicated in the comments. New decay channels (e.g., $W' \rightarrow WZ$) are assumed to be suppressed. UA1 and UA2 experiments assume that the $t\bar{b}$ channel is not open.

VALUE (GeV)	CL%	DOCUMENT ID	TECN	COMMENT
>720	95	31 ABACHI	96C D0	$W' \rightarrow e\nu_e$
••• We do not use the following data for averages, fits, limits, etc. •••				
none 300-420	95	32 ABE	97G CDF	$W' \rightarrow q\bar{q}$
>610	95	33 ABACHI	95E D0	$W' \rightarrow e\nu_e$ and $W' \rightarrow \tau\nu_\tau \rightarrow e\nu\nu$
>652	95	34 ABE	95M CDF	$W' \rightarrow e\nu_e$
>251	90	35 ALITTI	93 UA2	$W' \rightarrow q\bar{q}$
none 260-600	95	36 RIZZO	93 RVUE	$W' \rightarrow q\bar{q}$
>520	95	37 ABE	91F CDF	$W' \rightarrow e\nu, \mu\nu$
none 101-158	90	38 ALITTI	91 UA2	$W' \rightarrow q\bar{q}$
>220	90	39 ALBAJAR	89 UA1	$W' \rightarrow e\nu$
>209	90	40 ANSARI	87D UA2	$W' \rightarrow e\nu$
>210	90	41 ARNISON	86B UA1	$W' \rightarrow e\nu$
>170	90	42 ARNISON	83D UA1	$W' \rightarrow e\nu$

³¹ For bounds on W_R with nonzero right-handed mass, see Fig. 5 from ABACHI 96c.

³² ABE 97G search for new particle decaying to dijets.

³³ ABACHI 95E assume that the decay $W' \rightarrow WZ$ is suppressed and that the neutrino from W' decay is stable and has a mass significantly less than $m_{W'}$.

³⁴ ABE 95M assume that the decay $W' \rightarrow WZ$ is suppressed and the (right-handed) neutrino is light, noninteracting, and stable. If $m_\nu = 60$ GeV, for example, the effect on the mass limit is negligible.

³⁵ ALITTI 93 search for resonances in the two-jet invariant mass. The limit assumes $\Gamma(W')/m_{W'} = \Gamma(W)/m_W$ and $B(W' \rightarrow jj) = 2/3$. This corresponds to W_R with $m_{\nu_R} > m_{W_R}$ (no leptonic decay) and $W_R \rightarrow t\bar{b}$ allowed. See their Fig. 4 for limits in the $m_{W'}-B(q\bar{q})$ plane.

³⁶ RIZZO 93 analyses CDF limit on possible two-jet resonances. The limit is sensitive to the inclusion of the assumed K factor.

³⁷ ABE 91F assume leptonic branching ratio of 1/12 for each lepton flavor. The limit from the $e\nu$ ($\mu\nu$) mode alone is 490 (435) GeV. These limits apply to W_R if $m_{\nu_R} \lesssim 15$ GeV and ν_R does not decay in the detector. Cross section limit $\sigma \cdot B < (1-10)$ pb is given for $m_{W'} = 100-550$ GeV; see Fig. 2.

³⁸ ALITTI 91 search is based on two-jet invariant mass spectrum, assuming $B(W' \rightarrow q\bar{q}) = 67.6\%$. Limit on $\sigma \cdot B$ as a function of two-jet mass is given in Fig. 7.

³⁹ ALBAJAR 89 cross section limit at 630 GeV is $\sigma(W') B(e\nu) < 4.1$ pb (90% CL).

⁴⁰ See Fig. 5 of ANSARI 87D for the excluded region in the $m_{W'}-[(g_{W'q})^2 B(W' \rightarrow e\bar{\nu})]$ plane. Note that the quantity $(g_{W'q})^2 B(W' \rightarrow e\bar{\nu})$ is normalized to unity for the standard W couplings.

⁴¹ ARNISON 86B find no excess at large p_T in 148 $W \rightarrow e\nu$ events. Set limit $\sigma \times B(e\nu) < 10$ pb at CL = 90% at $E_{cm} = 546$ and 630 GeV.

⁴² ARNISON 83D find among 47 $W \rightarrow e\nu$ candidates no event with excess p_T . Also set $\sigma \times B(e\nu) < 30$ pb with CL = 90% at $E_{cm} = 540$ GeV.

THE Z' SEARCHES

Written October 1997 by K.S. Babu, C. Kolda, and J. March-Russell (IAS/Princeton).

If the Standard Model is enhanced by additional gauge symmetries or embedded into a larger gauge group, there will arise new heavy gauge bosons, some of which generically are electrically neutral. Such a gauge boson is called a Z' . Consider the most general renormalizable Lagrangian describing the complete set of interactions of the neutral gauge bosons among themselves and with fermions, which is that of the Standard Model plus the following new pieces [1,2,3]:

$$\mathcal{L}_{Z'} = -\frac{1}{4}\hat{F}'_{\mu\nu}\hat{F}'^{\mu\nu} - \frac{\sin\chi}{2}\hat{F}'_{\mu\nu}\hat{F}^{\mu\nu} + \frac{1}{2}\hat{M}_Z^2\hat{Z}'_\mu\hat{Z}'^\mu + \delta\hat{M}^2\hat{Z}'_\mu\hat{Z}'^\mu - \frac{\hat{g}'}{2}\sum_i\bar{\psi}_i\gamma^\mu(f_V^i - f_A^i\gamma^5)\psi_i\hat{Z}'_\mu \quad (1)$$

where $\hat{F}'_{\mu\nu}, \hat{F}_{\mu\nu}$ are the field strength tensors for the hypercharge \hat{B}_μ gauge boson and the Z' respectively before any diagonalizations are performed, ψ_i are the matter fields with Z' vector and axial charges f_V^i and f_A^i , and \hat{Z}'_μ is the electroweak Z boson in this basis. (See the Review on "Electroweak Model and Constraints on New Physics" for the Standard Model pieces of the Lagrangian.) The mass terms are assumed to come from spontaneous symmetry breaking via scalar expectation values. The above Lagrangian is general to all abelian and non-abelian extensions, except that $\chi = 0$ for the non-abelian case since then $\hat{F}'_{\mu\nu}$ is not gauge invariant. Most analyses take $\chi = 0$ even for the abelian case.

Going to the physical eigenbasis requires diagonalizing both the gauge kinetic and mass terms, with mass eigenstates denoted Z_1 and Z_2 , where we choose Z_1 to be the observed Z boson. The interaction Lagrangian for Z_1 has the form, to leading order in the mixing angle ξ ($s_W \equiv \sin\theta_W$, etc.):

$$\mathcal{L}_{Z_1} = -\frac{e}{2s_W c_W} \left(1 + \frac{\alpha T}{2}\right) \bar{\psi}_i \gamma^\mu \left\{ \left(g_V^i + \xi \tilde{f}_V^i\right) - \left(g_A^i + \xi \tilde{f}_A^i\right) \gamma^5 \right\} \psi_i Z_{1\mu} \quad (2)$$

where

$$\xi \simeq \frac{-\cos\chi(\delta\hat{M}^2 + \hat{M}_Z^2 s_W \sin\chi)}{\hat{M}_Z^2 - \hat{M}_Z^2 \cos^2\chi + \hat{M}_Z^2 s_W^2 \sin^2\chi + 2\delta\hat{M}^2 s_W \sin\chi} \quad (3)$$

We have made the identifications $g_A^i = T_3^i$, $g_V^i = T_3^i - 2Q^i s_W^2$, $\tilde{f}_{V,A}^i = (\hat{g}' s_W c_W / e \cos\chi) f_{V,A}^i$, and s_W^2 is identified to be the $s_{M_Z}^2$ defined in the "Electroweak Model and Constraints on New Physics" review. Note that the value of the weak angle

Gauge & Higgs Boson Particle Listings

Heavy Bosons Other than Higgs Bosons

that appears in the vector coupling is shifted by the S and T oblique parameters:

$$s_*^2 = s_W^2 + \frac{1}{s_W^2 - c_W^2} \left(\frac{1}{4} \alpha S - c_W^2 s_W^2 \alpha T \right) . \quad (4)$$

Recall that $\rho = 1 + \alpha T$ defines the usual ρ parameter. In the presence of Z - Z' mixing, the oblique parameters receive contributions [4]:

$$\begin{aligned} \alpha S &= 4\xi c_W^2 s_W \tan \chi \\ \alpha T &= \xi^2 \left(\frac{M_{Z_2}^2}{M_{Z_1}^2} - 1 \right) + 2\xi s_W \tan \chi \\ \alpha U &= 0 \end{aligned} \quad (5)$$

to leading order in small ξ . These contributions are in addition to those coming from top quark and Higgs boson loops in the Standard Model. (This is in contrast to the ‘‘Electroweak Model and Constraints on New Physics’’ Review in which oblique parameters are defined to be zero for reference values of m_t and M_H .) Note that nonzero Z - Z' contributions to S arise only in the presence of kinetic mixing.

The corresponding $Z_2 \bar{\psi}\psi$ interaction Lagrangian is:

$$\mathcal{L}_{Z_2} = -\frac{e}{2s_W c_W} \bar{\psi}_i \gamma^\mu \{ (h_V^i - g_V^i \xi) - (h_A^i - g_A^i \xi) \gamma^5 \} \psi_i Z_{2\mu} \quad (6)$$

with the following definitions:

$$\begin{aligned} h_V^i &= \tilde{f}_V^i + \tilde{s}(T_3^i - 2Q^i) \tan \chi \\ h_A^i &= \tilde{f}_A^i + \tilde{s}T_3^i \tan \chi \\ \tilde{s} &= s_W + \frac{s_W^3}{c_W^2 - s_W^2} \left(\frac{1}{4c_W^2} \alpha S - \frac{1}{2} \alpha T \right) \end{aligned} \quad (7)$$

where the last equation defines a weak angle appropriate for the Z_2 interactions.

If the Z' charges are generation-dependent, there exist severe constraints in the first two generations coming from precision measurements such as the K_L - K_S mass splitting and $B(\mu \rightarrow 3e)$ owing to the lack of GIM suppression in the Z' interactions; however, constraints on a Z' which couples differently only to the third generation are somewhat weaker. (It will be assumed in the Z -pole constraint section that the Z' couples identically to all three generations of matter; all other results are general.) If the new Z' interactions commute with the Standard Model gauge group, then per generation, there are only five independent $Z' \bar{\psi}\psi$ couplings; we can choose them to be $\tilde{f}_V^u, \tilde{f}_A^u, \tilde{f}_V^d, \tilde{f}_A^d$, and \tilde{f}_A^e . All other couplings can be determined in terms of these, e.g., $\tilde{f}_V^e = (\tilde{f}_V^e + \tilde{f}_A^e)/2$.

Canonical models: One of the prime motivations for an additional Z' has come from string theory in which certain compactifications lead naturally to an E_6 gauge group, or one of its subgroups. E_6 contains two $U(1)$ factors beyond the Standard Model, a basis for which is formed by the two groups $U(1)_\chi$ and $U(1)_\psi$, defined via the decompositions $E_6 \rightarrow SO(10) \times U(1)_\psi$ and $SO(10) \rightarrow SU(5) \times U(1)_\chi$; one special case

often encountered is $U(1)_\eta$ where $Z_\eta = \sqrt{\frac{3}{8}} Z_\chi + \sqrt{\frac{5}{8}} Z_\psi$. The charges of the SM fermions under these $U(1)$'s, and a discussion of their experimental signals, can be found in Ref. 5.

It is also common to express experimental bounds in terms of a toy Z' usually denoted Z_{SM} . This Z_{SM} , of arbitrary mass, couples to the SM fermions identically to the usual Z .

Almost all analyses of Z' physics have worked with one of these canonical models and have assumed zero kinetic mixing at the weak scale.

Experimental constraints: There are three primary sets of constraints on the existence of a Z' which will be considered here: precision measurements of neutral-current processes at low energies, Z -pole constraints on Z - Z' mixing, and direct search constraints from production at very high energies. In principle, one usually expects other new states to appear at the same scale as the Z' , including its symmetry-breaking sector and any additional fermions necessary for anomaly cancellation. However, because these states are highly model-dependent, we will not include searches for them, or Z' decays to them, in the bounds that follow.

Low-energy constraints: After the breaking of the new gauge group and the usual electroweak breaking, the Z of the Standard Model can mix with the Z' , with mixing angle ξ defined above. As already discussed, this Z - Z' mixing implies a shift in the usual oblique parameters [S, T, U defined in Eq. (5)]. Current bounds on S and T translate into stringent constraints on the mixing angle, ξ , requiring $\xi \ll 1$; similar constraints on ξ arise from the LEP Z -pole data. Thus we will only consider the small- ξ limit henceforth.

Whether or not the new gauge interactions are parity violating, stringent constraints can arise from atomic parity violation (APV) and polarized electron-nucleon scattering experiments [6]. At low energies, the effective neutral-current Lagrangian is conventionally written:

$$\mathcal{L}_{NC} = \frac{G_F}{\sqrt{2}} \sum_{q=u,d} \{ C_{1q} (\bar{e} \gamma_\mu \gamma^5 e) (\bar{q} \gamma^\mu q) + C_{2q} (\bar{e} \gamma_\mu e) (\bar{q} \gamma^\mu \gamma^5 q) \} \quad (8)$$

APV experiments are sensitive only to C_{1u} and C_{1d} (see the ‘‘Electroweak Model and Constraints on New Physics’’ Review for the nuclear weak charge, Q_W , in terms of the C_{1q}) where in the presence of the Z and Z' :

$$C_{1q} = 2(1 + \alpha T) (g_A^e + \xi \tilde{f}_A^e) (g_V^q + \xi \tilde{f}_V^q) + 2r (h_A^e - \xi g_A^e) (h_V^q - \xi g_V^q) \quad (9)$$

where $r = (M_{Z_1}/M_{Z_2})^2$. The r -dependent terms arise from Z_2 exchange and can interfere constructively or destructively with the Z_1 contribution. In the limit $\xi = r = 0$, this reduces to the Standard Model expression. Polarized electron scattering is sensitive to both the C_{1q} and C_{2q} couplings, again as discussed in the ‘‘Electroweak Model and Constraints on New Physics’’ Review. The C_{2q} can be derived from the expression for C_{1q} with the complete interchange $V \leftrightarrow A$.

Table 1: Expansion coefficients for shifts in Z -pole observables normalized to the Standard Model value of the observable [7,3].

\mathcal{O}	$\mathcal{A}_\mathcal{O}^S$	$\mathcal{A}_\mathcal{O}^T$	$\mathcal{B}_\mathcal{O}^{V^u}$	$\mathcal{B}_\mathcal{O}^{A^u}$	$\mathcal{B}_\mathcal{O}^{V^d}$	$\mathcal{B}_\mathcal{O}^{V^e}$	$\mathcal{B}_\mathcal{O}^{A^e}$
Γ_Z	-0.49	1.35	-0.89	-0.40	0.37	0.37	0
R_ℓ	-0.39	0.28	-1.3	-0.56	0.52	0.30	4.0
σ_h	0.046	-0.033	0.50	0.22	-0.21	-1.0	-4.0
R_b	0.085	-0.061	-1.4	-2.1	0.29	0	0
R_c	-0.16	0.12	2.7	4.1	-0.59	0	0
\bar{A}_e	-24.9	17.7	0	0	0	-26.7	2.0
\bar{A}_b	-0.32	0.23	0.71	0.71	-1.73	0	0
\bar{A}_c	-2.42	1.72	3.89	-1.49	0	0	0
M_W^2	-0.93	1.43	0	0	0	0	0

Stringent limits also arise from neutrino-hadron scattering. One usually expresses experimental results in terms of the effective 4-fermion operators $(\bar{\nu}\gamma_\mu\nu)(\bar{q}_{L,R}\gamma^\mu q_{L,R})$ with coefficients $(2\sqrt{2}G_F)\epsilon_{L,R}(q)$. (Again, see the ‘‘Electroweak Model and Constraints on New Physics’’ Review.) In the presence of the Z and Z' , the $\epsilon_{L,R}(q)$ are given by:

$$\begin{aligned} \epsilon_{L,R}(q) = & \frac{1 + \alpha T}{2} \left\{ (g_V^q \pm g_A^q)[1 + \xi(\tilde{f}_V \pm \tilde{f}_A)] + \xi(\tilde{f}_V \pm \tilde{f}_A) \right\} \\ & + \frac{\tau}{2} \left\{ (h_V^q \pm h_A^q)(h_V^\nu \pm h_A^\nu) - \xi(g_V^q \pm g_A^q)(h_V^\nu \pm h_A^\nu) \right. \\ & \left. - \xi(h_V^q \pm h_A^q) \right\}. \end{aligned} \quad (10)$$

Again, the τ -dependent terms arise from Z_2 -exchange.

Z -pole constraints: Electroweak measurements made at LEP and SLC while sitting on the Z resonance are generally sensitive to Z' physics only through the mixing with the Z unless the Z and Z' are very nearly degenerate, a possibility we ignore. Constraints on the allowed mixing angle and Z couplings arise by fitting all data simultaneously to the *ansatz* of Z - Z' mixing. For any observable, \mathcal{O} , the shift in that observable, $\Delta\mathcal{O}$, can be expressed (following the procedure of Ref. 7) as:

$$\frac{\Delta\mathcal{O}}{\mathcal{O}} = \mathcal{A}_\mathcal{O}^S \alpha S + \mathcal{A}_\mathcal{O}^T \alpha T + \xi \sum_i \mathcal{B}_\mathcal{O}^{(i)} \tilde{f}^i \quad (11)$$

where i runs over the 5 independent $Z'\bar{\psi}\psi$ couplings listed earlier (assuming a Z' couplings commute with the generation and gauge symmetries of the Standard Model; this is the only place where we enforce such a restriction). The coefficients $\mathcal{A}_\mathcal{O}^{S,T}$ and $\mathcal{B}_\mathcal{O}^{(i)}$, which are functions only of the Standard Model parameters, are given in Table 1. The first 5 observables are directly measured at LEP and SLC, while \bar{A}_e , \bar{A}_b and \bar{A}_c are measured via the asymmetries $\bar{A}_{FB}^{(0,f)} = \frac{3}{4}\bar{A}_e\bar{A}_f$ and $A_{LR}^0 = \bar{A}_e$ as defined in the ‘‘Electroweak Model and Constraints on New Physics’’ Review. As an example, the shift in \bar{A}_e due to Z' physics is given by

$$\frac{\Delta\bar{A}_e}{\bar{A}_e} = -24.9 \alpha S + 17.7 \alpha T - 26.7 \xi \tilde{f}_V^e + 2.0 \xi \tilde{f}_A^e. \quad (12)$$

High-energy indirect constraints: At $\sqrt{s} < M_{Z_2}$, but off the Z_1 pole, strong constraints on new Z' physics arise from measurements of deviations of asymmetries and leptonic and hadronic cross sections from their Standard Model predictions. These processes are sensitive not only to Z - Z' mixing but also to direct Z_2 exchange primarily through γ - Z_2 and Z_1 - Z_2 interference; therefore information on the Z_2 couplings and mass can be extracted that is not accessible via Z - Z' mixing alone.

Far below the Z_2 mass scale, experiment is only sensitive to the scaled Z_2 couplings $(\sqrt{s}/M_{Z_2}) \cdot h_{V,A}^i$ so the Z_2 mass and overall magnitude of the couplings cannot both be extracted. However as \sqrt{s} approaches M_{Z_2} the Z_2 exchange can no longer be approximated by a contact interaction and the mass and couplings can be simultaneously extracted.

Z' studies done before LEP relied heavily on this approach; see, *e.g.*, Ref. 8. LEP has also done similar work using data collected above the Z peak; see, *e.g.*, Ref. 9. For indirect Z' searches at future facilities, see, *e.g.* Refs. 10 and 11.

Direct-search constraints: Finally, high-energy experiments have searched for on-shell Z' (here Z_2) production and decay. Searches can be classified by the initial state off of which the Z' is produced, and the final state into which the Z' decays; we will not include here exotic decays of a Z' . Experiments to date have been sensitive to Z' production via their coupling to quarks ($p\bar{p}$ colliders), to electrons (e^+e^-) or to both (ep).

For a heavy Z' ($M_{Z_2} \gg M_{Z_1}$), the best limits come from $p\bar{p}$ machines via Drell-Yan production and subsequent decay to charged leptons. For $M_{Z_2} > 600$ GeV, CDF [12] quotes limits on $\sigma(p\bar{p} \rightarrow Z_2 X) \cdot B(Z_2 \rightarrow \ell^+\ell^-) < 0.04$ pb at 95% C.L. for $\ell = e + \mu$ combined; DØ [13] quotes $\sigma \cdot B < 0.025$ pb for $\ell = e$. For $M_{Z_2} < 600$ GeV, the mass dependence is complicated and one should refer to the original literature. For studies of the search capabilities of future facilities, see *e.g.* Ref. 10.

If the Z' has suppressed, or no, couplings to leptons (*i.e.*, it is leptophobic) then experimental sensitivities are much weaker. In particular, searches for a Z' via hadronic decays at DØ [14] are able to rule out a Z' with quark couplings identical to those of the Z only in the mass range $365 \text{ GeV} < M_{Z_2} < 615 \text{ GeV}$; CDF [15] cannot exclude even this range. Additionally, UA2 [16] finds $\sigma \cdot B(Z' \rightarrow jj) < 11.7$ pb at 90% C.L. for $M_{Z'} > 200$ GeV and more complicated bounds in the range $130 \text{ GeV} < M_{Z'} < 200 \text{ GeV}$.

For a light Z' ($M_{Z'} < M_Z$) direct searches in e^+e^- colliders have ruled out any Z' unless it has extremely weak couplings to leptons. For a combined analysis of the various pre-LEP experiments see Ref. 8.

References

1. B. Holdom, Phys. Lett. **166B**, 196 (1986).
2. F. del Aguila, Acta Phys. Polon. **B25**, 1317 (1994);
F. del Aguila, M. Cvetič and P. Langacker, Phys. Rev. **D52**, 37 (1995).

Gauge & Higgs Boson Particle Listings

Heavy Bosons Other than Higgs Bosons

3. K.S. Babu, C. Kolda and J. March-Russell, Phys. Rev. D**54**, 4635 (1996);
K.S. Babu, C. Kolda, and J. March-Russell, Phys. Rev. D**57**, 6788 (1998).
4. B. Holdom, Phys. Lett. B**259**, 329 (1991).
5. J. Hewett and T. Rizzo, Phys. Rept. **183**, 193 (1989).
6. J. Kim, *et al.*, Rev. Mod. Phys. **53**, 211 (1981);
U. Amaldi, *et al.*, Phys. Rev. D**36**, 1385 (1987);
W. Marciano and J. Rosner, Phys. Rev. Lett. **65**, 2963 (1990) (*Erratum: 68* 898 (1992));
K. Mahanthappa and P. Mohapatra, Phys. Rev. D**43**, 3093 (1991) (*Erratum: D44* 1616 (1991));
P. Langacker and M. Luo, Phys. Rev. D**45**, 278 (1992);
P. Langacker, M. Luo and A. Mann, Rev. Mod. Phys. **64**, 87 (1992).
7. G. Altarelli, *et al.*, Mod. Phys. Lett. A**5**, 495 (1990);
ibid., Phys. Lett. B**263**, 459 (1991).
8. L. Durkin and P. Langacker, Phys. Lett. **166B**, 436 (1986).
9. P. Abreu *et al.*, (DELPHI Collaboration), Eur. Phys. J. C**11**, 383 (1999);
R. Barate *et al.*, (ALEPH Collaboration), Eur. Phys. J. C**12**, 183 (1999).
10. M. Cvetič and S. Godfrey, hep-ph/9504216, in *Electroweak Symmetry Breaking and Beyond the Standard Model*, Eds. T. Barklow, *et al.* (World Scientific 1995).
11. T. Rizzo, Phys. Rev. D**55**, 5483 (1997).
12. F. Abe *et al.*, (CDF Collaboration), Phys. Rev. Lett. **79**, 2191 (1997).
13. DØ Collab., *XVIII International Conf. on Lepton Photon Interactions* (June 1997), <http://www-d0.fnal.gov/public/new/conferences/lp97.html>.
14. DØ Collaboration, *XVIII International Conference on Lepton Photon Interactions* (June 1997), see URL above.
15. F. Abe *et al.*, (CDF Collaboration), Phys. Rev. D**55**, 5263R (1997).
16. J. Alitti, *et al.*, (UA2 Collaboration), Nucl. Phys. B**400**, 3 (1993).

MASS LIMITS for Z' (Heavy Neutral Vector Boson Other Than Z)

Limits for Z'_{SM}

Z'_{SM} is assumed to have couplings with quarks and leptons which are identical to those of Z, and decays only to known fermions.

VALUE (GeV)	CL%	DOCUMENT ID	TECN	COMMENT
>898	95	43 BARATE	00i ALEP	e ⁺ e ⁻
>690	95	44 ABE	97s CDF	p \bar{p} ; Z' _{SM} → e ⁺ e ⁻ , μ ⁺ μ ⁻
>809	95	45 ERLER	99 RVUE	Electroweak
>490	95	ABACHI	96D D0	p \bar{p} ; Z' _{SM} → e ⁺ e ⁻
>505	95	46 ABE	95 CDF	p \bar{p} ; Z' _{SM} → e ⁺ e ⁻
>398	95	47 VILAIN	94B CHM2	ν _μ e → ν _μ e and ν̄ _μ e → ν̄ _μ e
>237	90	48 ALITTI	93 UA2	p \bar{p} ; Z' _{SM} → q \bar{q}
none 260-600	95	49 RIZZO	93 RVUE	p \bar{p} ; Z' _{SM} → q \bar{q}
>426	90	50 ABE	90F VNS	e ⁺ e ⁻

⁴³BARATE 00i search for deviations in cross section and asymmetries in e⁺e⁻ → fermions at √s=90 to 183 GeV. Assume θ=0. Bounds in the mass-mixing plane are shown in their Figure 18.

⁴⁴ABE 97s find σ(Z')×B(e⁺e⁻, μ⁺μ⁻) < 40 fb for m_{Z'} > 600 GeV at √s=1.8 TeV.

⁴⁵ERLER 99 give 90%CL limit on the Z-Z' mixing -0.0041 < θ < 0.0003. ρ₀=1 is assumed.

⁴⁶ABE 97s find σ(Z')×B(e⁺e⁻) < 350 fb for m_{Z'} > 350 GeV at √s=1.8 TeV.

⁴⁷VILAIN 94B assume m_t = 150 GeV.

⁴⁸ALITTI 93 search for resonances in the two-jet invariant mass. The limit assumes B(Z' → q \bar{q})=0.7. See their Fig. 5 for limits in the m_{Z'}-B(q \bar{q}) plane.

⁴⁹RIZZO 93 analyses CDF limit on possible two-jet resonances.

⁵⁰ABE 90F use data for R, R_{ℓℓ}, and A_{ℓℓ}. They fix m_W = 80.49 ± 0.43 ± 0.24 GeV and m_Z = 91.13 ± 0.03 GeV.

Limits for Z_LR

Z_LR is the extra neutral boson in left-right symmetric models. g_L = g_R is assumed unless noted. Values in parentheses assume stronger constraint on the Higgs sector, usually motivated by specific left-right symmetric models (see the Note on the W'). Values in brackets are from cosmological and astrophysical considerations and assume a light right-handed neutrino. Direct search bounds assume decays to Standard Model fermions only, unless noted.

VALUE (GeV)	CL%	DOCUMENT ID	TECN	COMMENT
>564	95	51 ERLER	99 RVUE	Electroweak
>630	95	52 ABE	97s CDF	p \bar{p} ; Z' _{LR} → e ⁺ e ⁻ , μ ⁺ μ ⁻
>436	95	53 BARATE	00i ALEP	e ⁺ e ⁻
>550	95	54 CHAY	00 RVUE	Electroweak
>230	95	55 ERLER	00 RVUE	Cs
>230	95	56 ABREU	99A DLPH	e ⁺ e ⁻
>230	95	57 CASALBUONI	99 RVUE	Cs
>230	95	58 CZAKON	99 RVUE	Electroweak
>230	95	59 ERLER	99 RVUE	Electroweak
>230	95	60 BARENBOIM	98 RVUE	Electroweak
>244	95	61 CONRAD	98 RVUE	ν _μ N scattering
>190	95	62 BARATE	97B ALEP	e ⁺ e ⁻ → μ ⁺ μ ⁻ and hadronic cross section
>445	95	63 ABE	95 CDF	p \bar{p} ; Z' _{LR} → e ⁺ e ⁻
>253	95	64 VILAIN	94B CHM2	ν _μ e → ν _μ e and ν̄ _μ e → ν̄ _μ e
>130	95	65 ADRIANI	93D L3	Z parameters
>1500	90	66 ALTARELLI	93B RVUE	Z parameters
none 200-600	95	67 RIZZO	93 RVUE	p \bar{p} ; Z' _{LR} → q \bar{q}
>2000	95	WALKER	91 COSM	Nucleosynthesis; light ν _R
none 200-500	95	68 GRIFOLS	90 ASTR	SN 1987A; light ν _R
none 350-2400	95	69 BARBIERI	89B ASTR	SN 1987A; light ν _R

• • • We do not use the following data for averages, fits, limits, etc. • • •

⁵¹ERLER 99 give 90%CL limit on the Z-Z' mixing -0.0009 < θ < 0.0017.

⁵²ABE 97s find σ(Z')×B(e⁺e⁻, μ⁺μ⁻) < 40 fb for m_{Z'} > 600 GeV at √s=1.8 TeV.

⁵³BARATE 00i search for deviations in cross section and asymmetries in e⁺e⁻ → fermions at √s=90 to 183 GeV. Assume θ=0. Bounds in the mass-mixing plane are shown in their Figure 18.

⁵⁴CHAY 00 also find -0.0003 < θ < 0.0019. For g_R free, m_{Z'} > 430 GeV.

⁵⁵ERLER 00 discuss the possibility that a discrepancy between the observed and predicted values of Q_W(Cs) is due to the exchange of Z'. The data are better described in a certain class of the Z' models including Z_{LR} and Z_χ.

⁵⁶ABREU 99A give 95%CL limit on the Z-Z' mixing |θ| < 0.0031. For the limit contour in the mass-mixing plane, see their Fig. 16. Data taken at √s=130-172 GeV.

⁵⁷CASALBUONI 99 discuss the discrepancy between the observed and predicted values of Q_W(Cs). It is shown that the data are better described in a class of models including the Z_{LR} model.

⁵⁸CZAKON 99 perform a simultaneous fit to charged and neutral sectors. Assumes manifest left-right symmetric model. Finds |θ| < 0.0042.

⁵⁹ERLER 99 assumes 2 Higgs doublets, transforming as 10 of SO(10), embedded in E₆. Assumes Higgs sector of minimal left-right model.

⁶⁰BARENBOIM 98 also gives 68% CL limits on the Z-Z' mixing -0.0005 < θ < 0.0033.

⁶¹CONRAD 98 limit is from measurements at CCFR, assuming no Z-Z' mixing.

⁶²BARATE 97B gives 95% CL limits on Z-Z' mixing -0.0017 < θ < 0.0035. The bounds are computed with α_s = 0.120 ± 0.003, m_t = 175 ± 6 GeV, and M_H = 150⁺¹⁵⁰₋₉₀ GeV.

⁶³ABE 97s find σ(Z')×B(e⁺e⁻) < 350 fb for m_{Z'} > 350 GeV at √s=1.8 TeV. See their Fig. 3 for the mass bound of Z' decaying to all allowed fermions and supersymmetric fermions.

⁶⁴VILAIN 94B assume m_t = 150 GeV and θ=0. See Fig. 2 for limit contours in the mass-mixing plane.

⁶⁵ADRIANI 93D give limits on the Z-Z' mixing -0.002 < θ < 0.015 assuming m_{Z'} > 310 GeV.

⁶⁶ALTARELLI 93B limit is from LEP data available in summer '93 and is for m_t = 110 GeV, m_H = 100 GeV and α_s = 0.118 assumed. The limit improves for larger m_t (see their Fig. 5). The 90%CL limit on the Z-Z' mixing angle is in Table 4.

⁶⁷RIZZO 93 analyses CDF limit on possible two-jet resonances.

⁶⁸GRIFOLS 90 limit holds for m_{ν_R} ≲ 1 MeV. A specific Higgs sector is assumed. See also GRIFOLS 90D, RIZZO 91.

⁶⁹BARBIERI 89B limit holds for m_{ν_R} ≤ 10 MeV. Bounds depend on assumed supernova core temperature.

Limits for Z_χ

Z_χ is the extra neutral boson in SO(10) → SU(5) × U(1)_χ. g_χ = e/cosθ_W is assumed unless otherwise stated. We list limits with the assumption ρ = 1 but with no further constraints on the Higgs sector. Values in parentheses assume stronger constraint on the Higgs sector motivated by superstring models. Values in brackets are from cosmological and astrophysical considerations and assume a light right-handed neutrino.

VALUE (GeV)	CL%	DOCUMENT ID	TECN	COMMENT
>545	95	70 ERLER	99 RVUE	Electroweak
>595	95	71 ABE	97s CDF	p \bar{p} ; Z' _χ → e ⁺ e ⁻ , μ ⁺ μ ⁻

Gauge & Higgs Boson Particle Listings
Heavy Bosons Other than Higgs Bosons

• • • We do not use the following data for averages, fits, limits, etc. • • •

Table listing particle data for Z bosons, including columns for value, document ID, and comment. Includes entries like BARATE 001 ALEP e+e- and ERLER 00 RVUE Cs.

70 ERLER 99 give 90%CL limit on the Z-Z' mixing -0.0020 < theta < 0.0015.
71 ABE 97s find sigma(Z') x B(e+e- -> mu+mu-) < 40 fb for mZ' > 600 GeV at sqrt(s) = 1.8 TeV.
72 BARATE 00i search for deviations in cross section and asymmetries in e+e- -> fermions at sqrt(s)=90 to 183 GeV.
73 ERLER 00 discuss the possibility that a discrepancy between the observed and predicted values of QW(Cs) is due to the exchange of Z'.
74 ROSNER 00 discusses the possibility that a discrepancy between the observed and predicted values of QW(Cs) is due to the exchange of Z'.
75 ABREU 99A give 95%CL limit on the Z-Z' mixing |theta| < 0.0033.
76 ERLER 99 assumes 2 Higgs doublets, transforming as 10 of SO(10), embedded in E6.
77 CHO 98 limit is from constraints on four-Fermi contact interactions obtained from low-energy electroweak experiments, and assumes no Z-Z' mixing.
78 CHO 98b use various electroweak data to constrain Z' models assuming mH=100 GeV. rho=1 is not assumed.
79 CONRAD 98 limit is from measurements at CCFR, assuming no Z-Z' mixing.
80 Z-Z' mixing is assumed to be zero. sqrt(s)=57.77 GeV.
81 BARATE 97b gives 95% CL limits on Z-Z' mixing -0.0016 < theta < 0.0036.
82 ABE 95 limit is obtained assuming that Z' decays to known fermions only.
83 ABREU 95M limit is for alpha_s=0.123, m_t=150 GeV, and mH=300 GeV.
84 VILAIN 94b assume m_t = 150 GeV and theta=0.
85 ADRIANI 93d give limits on the Z-Z' mixing -0.004 < theta < 0.015.
86 ALTARELLI 93b limit is from LEP data available in summer '93.
87 FARAGGI 91 limit assumes the nucleosynthesis bound on the effective number of neutrinos delta N_nu < 0.5.
88 ABE 90f use data for R, Rf, and Afl.
89 Assumes the nucleosynthesis bound on the effective number of light neutrinos (delta N_nu < 1) and that nu_R is light (< 1 MeV).
90 GRIFOLS 90 limit holds for m_nu_R < 1 MeV.

Limits for Zeta

Zeta is the extra neutral boson in E6 -> SO(10) x U(1)_psi. g_psi = e/cos theta_W is assumed unless otherwise stated. We list limits with the assumption rho=1 but with no further constraints on the Higgs sector.

Table listing particle data for Zeta bosons, including columns for value, document ID, and comment. Includes entries like BARATE 001 ALEP e+e- and ABE 92 CDF p anti-p; Zeta prime -> e+e-, mu+mu-.

• • • We do not use the following data for averages, fits, limits, etc. • • •

Table listing particle data for Zeta bosons, including columns for value, document ID, and comment. Includes entries like ABREU 99A DLPH e+e- and ERLER 99 RVUE Electroweak.

Table listing particle data for Zeta bosons, including columns for value, document ID, and comment. Includes entries like CONRAD 97 RVUE nu_mu N scattering and BARATE 98 ALEP e+e- -> mu+mu- and hadronic cross section.

91 BARATE 00i search for deviations in cross section and asymmetries in e+e- -> fermions at sqrt(s)=90 to 183 GeV. Assume theta=0.
92 ABE 97s find sigma(Z') x B(e+e- -> mu+mu-) < 40 fb for mZ' > 600 GeV at sqrt(s) = 1.8 TeV.
93 ABREU 99A give 95%CL limit on the Z-Z' mixing |theta| < 0.0021.
94 ERLER 99 give 90%CL limit on the Z-Z' mixing -0.0013 < theta < 0.0024.
95 CHO 98 limit is from constraints on four-Fermi contact interactions obtained from low-energy electroweak experiments and assumes no Z-Z' mixing.
96 CHO 98b use various electroweak data to constrain Z' models.
97 CONRAD 98 limit is from measurements at CCFR, assuming no Z-Z' mixing.
98 BARATE 97b gives 95% CL limits on Z-Z' mixing -0.0020 < theta < 0.0038.
99 See ABE 95 Fig. 3 for the mass bound of Z' decaying to all allowed fermions and supersymmetric fermions.

100 ABREU 95M limit is for alpha_s=0.123, m_t=150 GeV, and mH=300 GeV.
101 VILAIN 94b assume m_t = 150 GeV and theta=0.
102 ADRIANI 93d give limits on the Z-Z' mixing -0.003 < theta < 0.020.
103 ABE 90f use data for R, Rf, and Afl.
104 Assumes the nucleosynthesis bound on the effective number of light neutrinos (delta N_nu < 1) and that nu_R is light (< 1 MeV).
105 GRIFOLS 90d limit holds for m_nu_R < 1 MeV.

Limits for Zeta

Zeta is the extra neutral boson in E6 models, corresponding to Qeta = sqrt(3/8) QX - sqrt(5/8) Qpsi. g_eta = e/cos theta_W is assumed unless otherwise stated.

Table listing particle data for Zeta bosons, including columns for value, document ID, and comment. Includes entries like ERLER 99 RVUE Electroweak and ABE 97s CDF p anti-p; Zeta prime -> e+e-, mu+mu-.

• • • We do not use the following data for averages, fits, limits, etc. • • •

Table listing particle data for Zeta bosons, including columns for value, document ID, and comment. Includes entries like BARATE 001 ALEP e+e- and ABREU 99A DLPH e+e-.

106 ERLER 99 give 90%CL limit on the Z-Z' mixing -0.0062 < theta < 0.0011.

107 ABE 97s find sigma(Z') x B(e+e- -> mu+mu-) < 40 fb for mZ' > 600 GeV at sqrt(s) = 1.8 TeV.
108 BARATE 00i search for deviations in cross section and asymmetries in e+e- -> fermions at sqrt(s)=90 to 183 GeV.
109 ABREU 99A give 95%CL limit on the Z-Z' mixing |theta| < 0.0046.
110 CHO 98 limit is from constraints on four-Fermi contact interactions obtained from low-energy electroweak experiments, and assumes no Z-Z' mixing.
111 CHO 98b use various electroweak data to constrain Z' models assuming mH=100 GeV. rho=1 is not assumed.
112 CONRAD 98 limit is from measurements at CCFR, assuming no Z-Z' mixing.

Gauge & Higgs Boson Particle Listings

Heavy Bosons Other than Higgs Bosons

- ¹¹³ BARATE 97B gives 95% CL limits on Z - Z' mixing $-0.021 < \theta < 0.012$. The bounds are computed with $\alpha_s = 0.120 \pm 0.003$, $m_t = 175 \pm 6$ GeV, and $M_H = 150_{-90}^{+150}$ GeV. Data was taken at $\sqrt{s} = 20$ -136 GeV.
- ¹¹⁴ See ABE 95 Fig. 3 for the mass bound of Z' decaying to all allowed fermions and supersymmetric fermions.
- ¹¹⁵ ABREU 95M limit is for $\alpha_s = 0.123$, $m_t = 150$ GeV, and $m_H = 300$ GeV. For the limit contour in the mass-mixing plane, see their Fig. 13.
- ¹¹⁶ VILAIN 94B assume $m_t = 150$ GeV and $\theta = 0$. See Fig. 2 for limit contours in the mass-mixing plane.
- ¹¹⁷ ADRIANI 93D give limits on the Z - Z' mixing $-0.029 < \theta < 0.010$ assuming the ABE 92B mass limit.
- ¹¹⁸ ALTARELLI 93B limit is from LEP data available in summer '93 and is for $m_t = 110$ GeV, $m_H = 100$ GeV and $\alpha_s = 0.118$ assumed. The 90%CL limit on the Z - Z' mixing angle is in Fig. 2.
- ¹¹⁹ ABE 90F use data for R , $R_{\ell\ell}$, and $A_{\ell\ell}$. ABE 90F fix $m_W = 80.49 \pm 0.43 \pm 0.24$ GeV and $m_Z = 91.13 \pm 0.03$ GeV.
- ¹²⁰ These authors claim that the nucleosynthesis bound on the effective number of light neutrinos ($\delta N_\nu < 1$) constrains Z' masses if ν_R is light ($\lesssim 1$ MeV).
- ¹²¹ GRIFOLS 90 limit holds for $m_{\nu_R} \lesssim 1$ MeV. See also GRIFOLS 90D, RIZZO 91.

Limits for other Z'

$$Z_\beta = Z_X \cos\beta + Z_\psi \sin\beta$$

VALUE (GeV)	DOCUMENT ID	TECN	COMMENT
• • • We do not use the following data for averages, fits, limits, etc. • • •			
	122 CHO	98 RVUE	E_6 -motivated
	123 CHO	98B RVUE	E_6 -motivated

¹²² CHO 98 study constraints on four-Fermi contact interactions obtained from low-energy electroweak experiments, assuming no Z - Z' mixing.

¹²³ CHO 98B use various electroweak data to constrain Z' models.

LEPTOQUARK QUANTUM NUMBERS

Written December 1997 by M. Tanabashi (Tohoku U.).

Leptoquarks are particles carrying both baryon number (B) and lepton number (L). They are expected to exist in various extensions of the Standard Model (SM). The possible quantum numbers of leptoquark states can be restricted by assuming that their direct interactions with the ordinary SM fermions are dimensionless and invariant under the SM gauge group. Table 1 shows the list of all possible quantum numbers with this assumption [1]. The columns of $SU(3)_C$, $SU(2)_W$, and $U(1)_Y$ in Table 1 indicate the QCD representation, the weak isospin representation, and the weak hypercharge, respectively. Naming conventions of leptoquark states are taken from Ref. 1. The spin of a leptoquark state is taken to be 1 (vector leptoquark) or 0 (scalar leptoquark).

Table 1: Possible leptoquarks and their quantum numbers.

Leptoquarks	Spin	$3B + L$	$SU(3)_c$	$SU(2)_W$	$U(1)_Y$
S_1	0	-2	$\bar{3}$	1	1/3
\tilde{S}_1	0	-2	$\bar{3}$	1	4/3
S_3	0	-2	$\bar{3}$	3	1/3
V_2	1	-2	$\bar{3}$	2	5/6
\tilde{V}_2	1	-2	$\bar{3}$	2	-1/6
R_2	0	0	3	2	7/6
\tilde{R}_2	0	0	3	2	1/6
U_1	1	0	3	1	2/3
\tilde{U}_1	1	0	3	1	5/3
U_3	1	0	3	3	2/3

If we do not require leptoquark states to couple directly with SM fermions, different assignments of quantum numbers become possible.

The Pati-Salam model [2] is an example predicting the existence of a leptoquark state. In this model a vector leptoquark appears at the scale where the Pati-Salam $SU(4)$ "color" gauge group breaks into the familiar QCD $SU(3)_C$ group (or $SU(3)_C \times U(1)_{B-L}$). The Pati-Salam leptoquark is a weak isosinglet and its hypercharge is 2/3 (U_1 leptoquark in Table 1). The coupling strength of the Pati-Salam leptoquark is given by the QCD coupling at the Pati-Salam symmetry breaking scale.

Bounds on leptoquark states are obtained both directly and indirectly. Direct limits are from their production cross sections at colliders, while indirect limits are calculated from the bounds on the leptoquark induced four-fermion interactions which are obtained from low energy experiments.

The pair production cross sections of leptoquarks are evaluated from their interactions with gauge bosons. The gauge couplings of a scalar leptoquark are determined uniquely according to its quantum numbers in Table 1. The magnetic-dipole-type and the electric-quadrupole-type interactions of a vector leptoquark are, however, not determined even if we fix its gauge quantum numbers as listed in the table [3]. We need extra assumptions about these interactions to evaluate the pair production cross section for a vector leptoquark.

If a leptoquark couples to fermions of more than a single generation in the mass eigenbasis of the SM fermions, it can induce four-fermion interactions causing flavor-changing-neutral-currents and lepton-family-number violations. Non-chiral leptoquarks, which couple simultaneously to both left- and right-handed quarks, cause four-fermion interactions affecting the $(\pi \rightarrow e\nu)/(\pi \rightarrow \mu\nu)$ ratio [4]. Indirect limits provide stringent constraints on these leptoquarks. Since the Pati-Salam leptoquark has non-chiral coupling with both e and μ , indirect limits from the bounds on $K_L \rightarrow \mu e$ lead to severe bounds on the Pati-Salam leptoquark mass. For detailed bounds obtained in this way, see the Boson Particle Listings for "Indirect Limits for Leptoquarks" and its references.

It is therefore often assumed that a leptoquark state couples only to a single generation in a chiral interaction, where indirect limits become much weaker. This assumption gives strong constraints on concrete models of leptoquarks, however. Leptoquark states which couple only to left- or right-handed quarks are called chiral leptoquarks. Leptoquark states which couple only to the first (second, third) generation are referred as the first (second, third) generation leptoquarks in this section.

Reference

1. W. Buchmüller, R. Rückl, and D. Wyler, Phys. Lett. **B191**, 442 (1987).
2. J.C. Pati and A. Salam, Phys. Rev. **D10**, 275 (1974).
3. J. Blümlein, E. Boos, and A. Kryukov, Z. Phys. **C76**, 137 (1997).
4. O. Shanker, Nucl. Phys. **B204**, 375 (1982).

See key on page 239

Gauge & Higgs Boson Particle Listings
Heavy Bosons Other than Higgs Bosons

MASS LIMITS for Leptoquarks from Pair Production

Table with columns: VALUE (GeV), CL%, EVTS, DOCUMENT ID, TECN, COMMENT. Contains entries for various leptoquark searches and limits, including references to ABBOTT, ABE, ADRIANI, etc.

MASS LIMITS for Leptoquarks from Single Production

Table with columns: VALUE (GeV), CL%, DOCUMENT ID, TECN, COMMENT. Contains entries for single production limits for leptoquarks, including references to ADLOFF, ABREU, DERRICK, etc.

Indirect Limits for Leptoquarks

Table with columns: VALUE (TeV), CL%, DOCUMENT ID, TECN, COMMENT. Contains indirect limits for leptoquarks, including references to BARATE, ABBIENDI, ABE, ACCIARRI, etc.

Gauge & Higgs Boson Particle Listings

Heavy Bosons Other than Higgs Bosons

MASS LIMITS for Diquarks

VALUE (GeV)	CL%	DOCUMENT ID	TECN	COMMENT
• • • We do not use the following data for averages, fits, limits, etc. • • •				
none 290-420	95	162 ABE	97G CDF	E_6 diquark
none 15-31.7	95	163 ABREU	940 DLPH	SUSY E_6 diquark
162 ABE 97G search for new particle decaying to dijets.				
163 ABREU 940 limit is from $e^+ e^- \rightarrow \tau 3cs$. Range extends up to 43 GeV if diquarks are degenerate in mass.				

MASS LIMITS for g_A (axigluon)

Axigluons are massive color-octet gauge bosons in chiral color models and have axial-vector coupling to quarks with the same coupling strength as gluons.

VALUE (GeV)	CL%	DOCUMENT ID	TECN	COMMENT
• • • We do not use the following data for averages, fits, limits, etc. • • •				
>365	95	164 DONCHESKI	98 RVUE	$\Gamma(Z \rightarrow \text{hadron})$
none 200-980	95	165 ABE	97G CDF	$p\bar{p} \rightarrow g_A X, X \rightarrow 2 \text{ jets}$
none 200-870	95	166 ABE	95N CDF	$p\bar{p} \rightarrow g_A X, g_A \rightarrow q\bar{q}$
none 240-640	95	167 ABE	93G CDF	$p\bar{p} \rightarrow g_A X, g_A \rightarrow 2\text{jets}$
> 50	95	168 CUYPERS	91 RVUE	$\sigma(e^+ e^- \rightarrow \text{hadrons})$
none 120-210	95	169 ABE	90H CDF	$p\bar{p} \rightarrow g_A X, g_A \rightarrow 2\text{jets}$
> 29		170 ROBINETT	89 THEO	Partial-wave unitarity
none 150-310	95	171 ALBAJAR	88b UA1	$p\bar{p} \rightarrow g_A X, g_A \rightarrow 2\text{jets}$
> 20		BERGSTROM	88 RVUE	$p\bar{p} \rightarrow \gamma X$ via $g_A g$
> 9		172 CUYPERS	88 RVUE	γ decay
> 25		173 DONCHESKI	88b RVUE	γ decay
164 DONCHESKI 98 compare α_S derived from low-energy data and that from $\Gamma(Z \rightarrow \text{hadrons})/\Gamma(Z \rightarrow \text{leptons})$.				
165 ABE 97G search for new particle decaying to dijets.				
166 ABE 95N assume axigluons decaying to quarks in the Standard Model only.				
167 ABE 93G assume $\Gamma(g_A) = N\alpha_S m_{g_A}/6$ with $N = 10$.				
168 CUYPERS 91 compare α_S measured in γ decay and that from R at PEP/PETRA energies.				
169 ABE 90H assumes $\Gamma(g_A) = N\alpha_S m_{g_A}/6$ with $N = 5$ ($\Gamma(g_A) = 0.09m_{g_A}$). For $N = 10$, the excluded region is reduced to 120-150 GeV.				
170 ROBINETT 89 result demands partial-wave unitarity of $J = 0$ $t\bar{t} \rightarrow t\bar{t}$ scattering amplitude and derives a limit $m_{g_A} > 0.5 m_t$. Assumes $m_t > 56$ GeV.				
171 ALBAJAR 88b result is from the nonobservation of a peak in two-jet invariant mass distribution. $\Gamma(g_A) < 0.4 m_{g_A}$ assumed. See also BAGGER 88.				
172 CUYPERS 88 requires $\Gamma(T \rightarrow g g_A) < \Gamma(T \rightarrow g g g)$. A similar result is obtained by DONCHESKI 88.				
173 DONCHESKI 88b requires $\Gamma(T \rightarrow g q q)/\Gamma(T \rightarrow g g g) < 0.25$, where the former decay proceeds via axigluon exchange. A more conservative estimate of < 0.5 leads to $m_{g_A} > 21$ GeV.				

X^0 (Heavy Boson) Searches in Z Decays

Searches for radiative transition of Z to a lighter spin-0 state X^0 decaying to hadrons, a lepton pair, a photon pair, or invisible particles as shown in the comments. The limits are for the product of branching ratios.

VALUE	CL%	DOCUMENT ID	TECN	COMMENT
• • • We do not use the following data for averages, fits, limits, etc. • • •				
		174 BARATE	98U ALEP	$X^0 \rightarrow \ell\ell, q\bar{q}, g\bar{g}, \gamma\gamma, \nu\bar{\nu}$
		175 ACCIARRI	97Q L3	$X^0 \rightarrow$ invisible particle(s)
		176 ACTON	93E OPAL	$X^0 \rightarrow \gamma\gamma$
		177 ABREU	92b DLPH	$X^0 \rightarrow$ hadrons
		178 ADRIANI	92F L3	$X^0 \rightarrow$ hadrons
		179 ACTON	91 OPAL	$X^0 \rightarrow$ anything
<1.1 x 10 ⁻⁴	95	180 ACTON	91b OPAL	$X^0 \rightarrow e^+ e^-$
<9 x 10 ⁻⁵	95	180 ACTON	91b OPAL	$X^0 \rightarrow \mu^+ \mu^-$
<1.1 x 10 ⁻⁴	95	180 ACTON	91b OPAL	$X^0 \rightarrow \tau^+ \tau^-$
<2.8 x 10 ⁻⁴	95	181 ADEVA	91D L3	$X^0 \rightarrow e^+ e^-$
<2.3 x 10 ⁻⁴	95	181 ADEVA	91D L3	$X^0 \rightarrow \mu^+ \mu^-$
<4.7 x 10 ⁻⁴	95	182 ADEVA	91D L3	$X^0 \rightarrow$ hadrons
<8 x 10 ⁻⁴	95	183 AKRAWY	90J OPAL	$X^0 \rightarrow$ hadrons
174 BARATE 98U obtain limits on $B(Z \rightarrow \gamma X^0)B(X^0 \rightarrow \ell\ell, q\bar{q}, g\bar{g}, \gamma\gamma, \nu\bar{\nu})$. See their Fig. 17.				
175 See Fig. 4 of ACCIARRI 97Q for the upper limit on $B(Z \rightarrow \gamma X^0; E_\gamma > E_{\text{min}})$ as a function of E_{min} .				
176 ACTON 93E give $\sigma(e^+ e^- \rightarrow X^0 \gamma) \cdot B(X^0 \rightarrow \gamma\gamma) < 0.4$ pb (95%CL) for $m_{X^0} = 60 \pm 2.5$ GeV. If the process occurs via s-channel γ exchange, the limit translates to $\Gamma(X^0) \cdot B(X^0 \rightarrow \gamma\gamma)^2 < 20$ MeV for $m_{X^0} = 60 \pm 1$ GeV.				
177 ABREU 92D give $\sigma_Z \cdot B(Z \rightarrow \gamma X^0) \cdot B(X^0 \rightarrow \text{hadrons}) < (3-10)$ pb for $m_{X^0} = 10-78$ GeV. A very similar limit is obtained for spin-1 X^0 .				
178 ADRIANI 92f search for isolated γ in hadronic Z decays. The limit $\sigma_Z \cdot B(Z \rightarrow \gamma X^0) \cdot B(X^0 \rightarrow \text{hadrons}) < (2-10)$ pb (95%CL) is given for $m_{X^0} = 25-85$ GeV.				
179 ACTON 91 searches for $Z \rightarrow Z^* X^0, Z^* \rightarrow e^+ e^-, \mu^+ \mu^-, \text{ or } \nu\bar{\nu}$. Excludes any new scalar X^0 with $m_{X^0} < 9.5$ GeV/c if it has the same coupling to $Z Z^*$ as the MSM Higgs boson.				
180 ACTON 91B limits are for $m_{X^0} = 60-85$ GeV.				

- 181 ADEVA 91D limits are for $m_{X^0} = 30-89$ GeV.
- 182 ADEVA 91D limits are for $m_{X^0} = 30-86$ GeV.
- 183 AKRAWY 90J give $\Gamma(Z \rightarrow \gamma X^0) \cdot B(X^0 \rightarrow \text{hadrons}) < 1.9$ MeV (95%CL) for $m_{X^0} = 32-80$ GeV. We divide by $\Gamma(Z) = 2.5$ GeV to get product of branching ratios. For nonresonant transitions, the limit is $B(Z \rightarrow \gamma q\bar{q}) < 8.2$ MeV assuming three-body phase space distribution.

MASS LIMITS for a Heavy Neutral Boson Coupling to $e^+ e^-$

VALUE (GeV)	CL%	DOCUMENT ID	TECN	COMMENT
• • • We do not use the following data for averages, fits, limits, etc. • • •				
none 55-61		184 ODAKA	89 VNS	$\Gamma(X^0 \rightarrow e^+ e^-) \cdot B(X^0 \rightarrow \text{hadrons}) > 0.2$ MeV
>45	95	185 DERRICK	86 HRS	$\Gamma(X^0 \rightarrow e^+ e^-) = 6$ MeV
>46.6	95	186 ADEVA	85 MRKJ	$\Gamma(X^0 \rightarrow e^+ e^-) = 10$ keV
>48	95	186 ADEVA	85 MRKJ	$\Gamma(X^0 \rightarrow e^+ e^-) = 4$ MeV
		187 BERGER	85B PLUT	
none 39.8-45.5		188 ADEVA	84 MRKJ	$\Gamma(X^0 \rightarrow e^+ e^-) = 10$ keV
>47.8	95	188 ADEVA	84 MRKJ	$\Gamma(X^0 \rightarrow e^+ e^-) = 4$ MeV
none 39.8-45.2		188 BEHREND	84C CELL	
>47	95	188 BEHREND	84C CELL	$\Gamma(X^0 \rightarrow e^+ e^-) = 4$ MeV
184 ODAKA 89 looked for a narrow or wide scalar resonance in $e^+ e^- \rightarrow \text{hadrons}$ at $E_{\text{cm}} = 55.0-60.8$ GeV.				
185 DERRICK 86 found no deviation from the Standard Model Bhabha scattering at $E_{\text{cm}} = 29$ GeV and set limits on the possible scalar boson $e^+ e^-$ coupling. See their figure 4 for excluded region in the $\Gamma(X^0 \rightarrow e^+ e^-) - m_{X^0}$ plane. Electronic chiral invariance requires a parity doublet of X^0 , in which case the limit applies for $\Gamma(X^0 \rightarrow e^+ e^-) = 3$ MeV.				
186 ADEVA 85 first limit is from $2\gamma, \mu^+ \mu^-$, hadrons assuming X^0 is a scalar. Second limit is from $e^+ e^-$ channel. $E_{\text{cm}} = 40-47$ GeV. Supersedes ADEVA 84.				
187 BERGER 85b looked for effect of spin-0 boson exchange in $e^+ e^- \rightarrow e^+ e^-$ and $\mu^+ \mu^-$ at $E_{\text{cm}} = 34.7$ GeV. See Fig. 5 for excluded region in the $m_{X^0} - \Gamma(X^0)$ plane.				
188 ADEVA 84 and BEHREND 84c have $E_{\text{cm}} = 39.8-45.5$ GeV. MARK-J searched X^0 in $e^+ e^- \rightarrow \text{hadrons}, 2\gamma, \mu^+ \mu^-, e^+ e^-$ and CELLO in the same channels plus τ pair. No narrow or broad X^0 is found in the energy range. They also searched for the effect of X^0 with $m_X > E_{\text{cm}}$. The second limits are from Bhabha data and for spin-0 singlet. The same limits apply for $\Gamma(X^0 \rightarrow e^+ e^-) = 2$ MeV if X^0 is a spin-0 doublet. The second limit of BEHREND 84c was read off from their figure 2. The original papers also list limits in other channels.				

Search for X^0 Resonance in $e^+ e^-$ Collisions

The limit is for $\Gamma(X^0 \rightarrow e^+ e^-) \cdot B(X^0 \rightarrow f)$, where f is the specified final state. Spin 0 is assumed for X^0 .

VALUE (keV)	CL%	DOCUMENT ID	TECN	COMMENT
• • • We do not use the following data for averages, fits, limits, etc. • • •				
<10 ³	95	189 ABE	93C VNS	$\Gamma(ee)$
<(0.4-10)	95	190 ABE	93C VNS	$f = \gamma\gamma$
<(0.3-5)	95	191,192 ABE	93D TOPZ	$f = \gamma\gamma$
<(2-12)	95	191,192 ABE	93D TOPZ	$f = \text{hadrons}$
<(4-200)	95	192,193 ABE	93D TOPZ	$f = ee$
<(0.1-6)	95	192,193 ABE	93D TOPZ	$f = \mu\mu$
<(0.5-8)	90	194 STERNER	93 AMY	$f = \gamma\gamma$
189 Limit is for $\Gamma(X^0 \rightarrow e^+ e^-) m_{X^0} = 56-63.5$ GeV for $\Gamma(X^0) = 0.5$ GeV.				
190 Limit is for $m_{X^0} = 56-61.5$ GeV and is valid for $\Gamma(X^0) \ll 100$ MeV. See their Fig. 5 for limits for $\Gamma = 1, 2$ GeV.				
191 Limit is for $m_{X^0} = 57.2-60$ GeV.				
192 Limit is valid for $\Gamma(X^0) \ll 100$ MeV. See paper for limits for $\Gamma = 1$ GeV and those for $J = 2$ resonances.				
193 Limit is for $m_{X^0} = 56.6-60$ GeV.				
194 STERNER 93 limit is for $m_{X^0} = 57-59.6$ GeV and is valid for $\Gamma(X^0) < 100$ MeV. See their Fig. 2 for limits for $\Gamma = 1, 3$ GeV.				

Search for X^0 Resonance in Two-Photon Process

The limit is for $\Gamma(X^0) \cdot B(X^0 \rightarrow \gamma\gamma)^2$. Spin 0 is assumed for X^0 .

VALUE (MeV)	CL%	DOCUMENT ID	TECN	COMMENT
• • • We do not use the following data for averages, fits, limits, etc. • • •				
<2.6	95	195 ACTON	93E OPAL	$m_{X^0} = 60 \pm 1$ GeV
<2.9	95	BUSKULIC	93F ALEP	$m_{X^0} \sim 60$ GeV
195 ACTON 93E limit for a $J = 2$ resonance is 0.8 MeV.				

Search for X^0 Resonance in $e^+ e^- \rightarrow X^0 \gamma$

VALUE (GeV)	DOCUMENT ID	TECN	COMMENT
• • • We do not use the following data for averages, fits, limits, etc. • • •			
	196 ADAM	96C DLPH	X^0 decaying invisibly
196 ADAM 96c is from the single photon production cross at $\sqrt{s} = 130, 136$ GeV. The upper bound is less than 3 pb for X^0 masses between 60 and 130 GeV. See their Fig. 5 for the exact bound on the cross section $\sigma(e^+ e^- \rightarrow \gamma X^0)$.			

Gauge & Higgs Boson Particle Listings

Heavy Bosons Other than Higgs Bosons, Axions (A^0) and Other Very Light Bosons

GRIFOLS	90	NP B331 244	J.A. Grifols, E. Masso	(BARC)
GRIFOLS	90D	PR D42 3293	J.A. Grifols, E. Masso, T.G. Rizzo	(BARC, CERN+)
KIM	90	PL B240 243	G.N. Kim <i>et al.</i>	(AMY Collab.)
LOPEZ	90	PL B241 392	J.L. Lopez, D.V. Nanopoulos	(TAMU)
ALBAJAR	89	ZPHY C44 15	C. Albajar <i>et al.</i>	(UA1 Collab.)
ALBRECHT	89	ZPHY C42 349	H. Albrecht <i>et al.</i>	(ARGUS Collab.)
BARBIERI	89B	PR D39 1229	R. Barbieri, R.N. Mohapatra	(PISA, UMD)
LANGACKER	89B	PR D40 1569	P. Langacker, S. Uma Sankar	(PENNY)
ODAKA	89	JPSJ 58 3037	S. Odaoka <i>et al.</i>	(VENUS Collab.)
ROBINETT	89	PR D39 834	R.W. Robinett	(PSU)
ALBAJAR	88B	PL B209 127	C. Albajar <i>et al.</i>	(UA1 Collab.)
BAGGER	88	PR D37 1188	J. Bagger, C. Schmidt, S. King	(HARV, BOST)
BALKE	88	PR D37 587	B. Balke <i>et al.</i>	(LBL, UCB, COLO, NWES+)
BERGSTROM	88	PL B212 386	L. Bergstrom	(STOH)
CUYPERS	88	PRL 60 1237	F. Cuypers, P.H. Frampton	(UNCCH)
DONCHESKI	88	PL B206 137	M.A. Doncheski, H. Grotch, R. Robinett	(PSU)
DONCHESKI	88B	PR D38 412	M.A. Doncheski, H. Grotch, R.W. Robinett	(PSU)
ANSARI	87D	PL B195 613	R. Ansari <i>et al.</i>	(UA2 Collab.)
BARTEL	87B	ZPHY C36 15	W. Bartel <i>et al.</i>	(JADE Collab.)
ARNISON	86B	EPL 1 327	G.T.J. Arnison <i>et al.</i>	(UA1 Collab.)
BEHREND	86B	PL B178 452	H.J. Behrend <i>et al.</i>	(CELLO Collab.)
DERRICK	86	PL 166B 463	M. Derrick <i>et al.</i>	(HRS Collab.)
Also	86B	PR D34 3286	M. Derrick <i>et al.</i>	(HRS Collab.)
JODIDIO	86	PR D34 1967	A. Jodidio <i>et al.</i>	(LBL, NWES, TRIU)
Also	88	PR D37 237 erratum	A. Jodidio <i>et al.</i>	(LBL, NWES, TRIU)
MOHAPATRA	86	PR D34 909	R.N. Mohapatra	(UMD)
ADEVA	85	PL 152B 439	B. Adeva <i>et al.</i>	(Mark-J Collab.)
BERGER	85B	ZPHY C27 341	C. Berger <i>et al.</i>	(PLUTO Collab.)
STOKER	85	PRL 54 1887	D.P. Stoker <i>et al.</i>	(LBL, NWES, TRIU)
ADEVA	84	PRL 53 134	B. Adeva <i>et al.</i>	(Mark-J Collab.)
BEHREND	84C	PL 140B 130	H.J. Behrend <i>et al.</i>	(CELLO Collab.)
ARNISON	83D	PL 129B 273	G.T.J. Arnison <i>et al.</i>	(UA1 Collab.)
BERGSMA	83	PL 122B 465	F. Bergsma <i>et al.</i>	(CHARM Collab.)
CARR	83	PRL 51 627	J. Carr <i>et al.</i>	(LBL, NWES, TRIU)
DESHPANDE	83	PR D27 1193	N.G. Deshpande, R.J. Johnson	(OREG)
BEALL	82	PRL 48 848	G. Beall, M. Bander, A. Soni	(UCI, UCLA)
SHANKER	82	NP B204 375	O. Shanker	(TRIUM)
DIMOPOULOS	81	NP B182 77	S. Dimopoulos, S. Raby, G.L. Kane	(STAN, MICH)
STEIGMAN	79	PRL 43 239	G. Steigman, K.A. Olive, D.N. Schramm	(BART+)

where J^μ is the Noether current of the spontaneously broken global symmetry.

An axion gives a natural solution to the strong CP problem: why the effective θ -parameter in the QCD Lagrangian $\mathcal{L}_\theta = \theta_{\text{eff}} \frac{\alpha_s}{8\pi} F^{\mu\nu a} \tilde{F}_{\mu\nu}^a$ is so small ($\theta_{\text{eff}} \lesssim 10^{-9}$) as required by the current limits on the neutron electric dipole moment, even though $\theta_{\text{eff}} \sim O(1)$ is perfectly allowed by the QCD gauge invariance. Here, θ_{eff} is the effective θ parameter after the diagonalization of the quark masses, and $F^{\mu\nu a}$ is the gluon field strength and $\tilde{F}_{\mu\nu}^a = \frac{1}{2} \epsilon_{\mu\nu\rho\sigma} F^{\rho\sigma a}$. An axion is a pseudo-NG boson of a spontaneously broken Peccei–Quinn symmetry, which is an exact symmetry at the classical level, but is broken quantum mechanically due to the triangle anomaly with the gluons. The definition of the Peccei–Quinn symmetry is model dependent. As a result of the triangle anomaly, the axion acquires an effective coupling to gluons

$$\mathcal{L} = \left(\theta_{\text{eff}} - \frac{\phi_A}{f_A} \right) \frac{\alpha_s}{8\pi} F^{\mu\nu a} \tilde{F}_{\mu\nu}^a, \quad (2)$$

where ϕ_A is the axion field. It is often convenient to *define* the axion decay constant f_A with this Lagrangian [6]. The QCD nonperturbative effect induces a potential for ϕ_A whose minimum is at $\phi_A = \theta_{\text{eff}} f_A$ cancelling θ_{eff} and solving the strong CP problem. The mass of the axion is inversely proportional to f_A as

$$m_A = 0.62 \times 10^{-3} \text{eV} \times (10^{10} \text{GeV}/f_A). \quad (3)$$

The original axion model [1,5] assumes $f_A \sim v$, where $v = (\sqrt{2}G_F)^{-1/2} = 247 \text{ GeV}$ is the scale of the electroweak symmetry breaking, and has two Higgs doublets as minimal ingredients. By requiring tree-level flavor conservation, the axion mass and its couplings are completely fixed in terms of one parameter ($\tan\beta$): the ratio of the vacuum expectation values of two Higgs fields. This model is excluded after extensive experimental searches for such an axion [7]. Observation of a narrow-peak structure in positron spectra from heavy ion collisions [8] suggested a particle of mass 1.8 MeV that decays into e^+e^- . Variants of the original axion model, which keep $f_A \sim v$, but drop the constraints of tree-level flavor conservation, were proposed [9]. Extensive searches for this particle, $A^0(1.8 \text{ MeV})$, ended up with another negative result [10].

The popular way to save the Peccei–Quinn idea is to introduce a new scale $f_A \gg v$. Then the A^0 coupling becomes weaker, thus one can easily avoid all the existing experimental limits; such models are called invisible axion models [11,12]. Two classes of models are discussed commonly in the literature. One introduces new heavy quarks which carry Peccei–Quinn charge while the usual quarks and leptons do not (KSVZ axion or “hadronic axion”) [11]. The other does not need additional quarks but requires two Higgs doublets, and all quarks and leptons carry Peccei–Quinn charges (DFSZ axion or “GUT-axion”) [12]. All models contain at least one electroweak singlet scalar boson which acquires an expectation value and breaks Peccei–Quinn symmetry. The invisible axion with a large decay

Axions (A^0) and Other Very Light Bosons, Searches for

AXIONS AND OTHER VERY LIGHT BOSONS

Written October 1997 by H. Murayama (University of California, Berkeley) Part I; April 1998 by G. Raffelt (Max-Planck Institute, München) Part II; and April 1998 by C. Haggmann, K. van Bibber (Lawrence Livermore National Laboratory), and L.J. Rosenberg (Massachusetts Institute of Technology) Part III.

This review is divided into three parts:

Part I (Theory)

Part II (Astrophysical Constraints)

Part III (Experimental Limits)

AXIONS AND OTHER VERY LIGHT BOSONS, PART I (THEORY)

(by H. Murayama)

In this section we list limits for very light neutral (pseudo) scalar bosons that couple weakly to stable matter. They arise if there is a global continuous symmetry in the theory that is spontaneously broken in the vacuum. If the symmetry is exact, it results in a massless Nambu–Goldstone (NG) boson. If there is a small explicit breaking of the symmetry, either already in the Lagrangian or due to quantum mechanical effects such as anomalies, the would-be NG boson acquires a finite mass; then it is called a pseudo-NG boson. Typical examples are axions (A^0) [1], familons [2], and Majorons [3,4], associated, respectively, with spontaneously broken Peccei–Quinn [5], family, and lepton-number symmetries. This Review provides brief descriptions of each of them and their motivations.

One common characteristic for all these particles is that their coupling to the Standard Model particles are suppressed by the energy scale of symmetry breaking, *i.e.* the decay constant f , where the interaction is described by the Lagrangian

$$\mathcal{L} = \frac{1}{f} (\partial_\mu \phi) J^\mu, \quad (1)$$

constant $f_A \sim 10^{12}$ GeV was found to be a good candidate of the cold dark matter component of the Universe [13](see Dark Matter review). The energy density is stored in the low-momentum modes of the axion field which are highly occupied and thus represent essentially classical field oscillations.

The constraints on the invisible axion from astrophysics are derived from interactions of the axion with either photons, electrons or nucleons. The strengths of the interactions are model dependent (*i.e.*, not a function of f_A only), and hence one needs to specify a model in order to place lower bounds on f_A . Such constraints will be discussed in Part II. Serious experimental searches for an invisible axion are underway; they typically rely on axion-photon coupling, and some of them assume that the axion is the dominant component of our galactic halo density. Part III will discuss experimental techniques and limits.

Familons arise when there is a global family symmetry broken spontaneously. A family symmetry interchanges generations or acts on different generations differently. Such a symmetry may explain the structure of quark and lepton masses and their mixings. A familon could be either a scalar or a pseudoscalar. For instance, an SU(3) family symmetry among three generations is non-anomalous and hence the familons are exactly massless. In this case, familons are scalars. If one has larger family symmetries with separate groups of left-handed and right-handed fields, one also has pseudoscalar familons. Some of them have flavor-off-diagonal couplings such as $\partial_\mu \phi_F \bar{d} \gamma^\mu s / F_{ds}$ or $\partial_\mu \phi_F \bar{e} \gamma^\mu \mu / F_{\mu e}$, and the decay constant F can be different for individual operators. The decay constants have lower bounds constrained by flavor-changing processes. For instance, $B(K^+ \rightarrow \pi^+ \phi_F) < 3 \times 10^{-10}$ [14] gives $F_{ds} > 3.4 \times 10^{11}$ GeV [15]. The constraints on familons primarily coupled to third generation are quite weak [15].

If there is a global lepton-number symmetry and if it breaks spontaneously, there is a Majoron. The triplet Majoron model [4] has a weak-triplet Higgs boson, and Majoron couples to Z . It is now excluded by the Z invisible-decay width. The model is viable if there is an additional singlet Higgs boson and if the Majoron is mainly a singlet [16]. In the singlet Majoron model [3], lepton-number symmetry is broken by a weak-singlet scalar field, and there are right-handed neutrinos which acquire Majorana masses. The left-handed neutrino masses are generated by a “seesaw” mechanism [17]. The scale of lepton number breaking can be much higher than the electroweak scale in this case. Astrophysical constraints require the decay constant to be $\gtrsim 10^9$ GeV [18].

There is revived interest in a long-lived neutrino, to improve Big-Bang Nucleosynthesis [19] or large scale structure formation theories [20]. Since a decay of neutrinos into electrons or photons is severely constrained, these scenarios require a familon (Majoron) mode $\nu_1 \rightarrow \nu_2 \phi_F$ (see, *e.g.*, Ref. 15 and references therein).

Other light bosons (scalar, pseudoscalar, or vector) are constrained by “fifth force” experiments. For a compilation of constraints, see Ref. 21.

It has been widely argued that a fundamental theory will not possess global symmetries; gravity, for example, is expected to violate them. Global symmetries such as baryon number arise by accident, typically as a consequence of gauge symmetries. It has been noted [22] that the Peccei-Quinn symmetry, from this perspective, must also arise by accident and must hold to an extraordinary degree of accuracy in order to solve the strong CP problem. Possible resolutions to this problem, however, have been discussed [22,23]. String theory also provides sufficiently good symmetries, especially using a large compactification radius motivated by recent developments in M-theory [24].

References

1. S. Weinberg, Phys. Rev. Lett. **40**, 223 (1978); F. Wilczek, Phys. Rev. Lett. **40**, 279 (1978).
2. F. Wilczek, Phys. Rev. Lett. **49**, 1549 (1982).
3. Y. Chikashige, R.N. Mohapatra, and R.D. Peccei, Phys. Lett. **98B**, 265 (1981).
4. G.B. Gelmini and M. Roncadelli, Phys. Lett. **99B**, 411 (1981).
5. R.D. Peccei and H. Quinn, Phys. Rev. Lett. **38**, 1440 (1977); also Phys. Rev. **D16**, 1791 (1977).
6. Our normalization here is the same as f_a used in G.G. Raffelt, Phys. Reports **198**, 1 (1990). See this *Review* for the relation to other conventions in the literature.
7. T.W. Donnelly *et al.*, Phys. Rev. **D18**, 1607 (1978); S. Barshay *et al.*, Phys. Rev. Lett. **46**, 1361 (1981); A. Barroso and N.C. Mukhopadhyay, Phys. Lett. **106B**, 91 (1981); R.D. Peccei, in *Proceedings of Neutrino '81*, Honolulu, Hawaii, Vol. 1, p. 149 (1981); L.M. Krauss and F. Wilczek, Phys. Lett. **B173**, 189 (1986).
8. J. Schweppe *et al.*, Phys. Rev. Lett. **51**, 2261 (1983); T. Cowan *et al.*, Phys. Rev. Lett. **54**, 1761 (1985).
9. R.D. Peccei, T.T. Wu, and T. Yanagida, Phys. Lett. **B172**, 435 (1986).
10. W.A. Bardeen, R.D. Peccei, and T. Yanagida, Nucl. Phys. **B279**, 401 (1987).
11. J.E. Kim, Phys. Rev. Lett. **43**, 103 (1979); M.A. Shifman, A.I. Vainstein, and V.I. Zakharov, Nucl. Phys. **B166**, 493 (1980).
12. A.R. Zhitnitsky, Sov. J. Nucl. Phys. **31**, 260 (1980); M. Dine and W. Fischler, Phys. Lett. **120B**, 137 (1983).
13. J. Preskill, M. Wise, F. Wilczek, Phys. Lett. **120B**, 127 (1983); L. Abbott and P. Sikivie, Phys. Lett. **120B**, 133 (1983); M. Dine and W. Fischler, Phys. Lett. **120B**, 137 (1983); M.S. Turner, Phys. Rev. **D33**, 889 (1986).
14. S. Adler *et al.*, hep-ex/9708031.
15. J. Feng, T. Moroi, H. Murayama, and E. Schnapka, UCB-PTH-97/47.
16. K. Choi and A. Santamaria, Phys. Lett. **B267**, 504 (1991).
17. T. Yanagida, in *Proceedings of Workshop on the Unified Theory and the Baryon Number in the Universe*, Tsukuba,

Gauge & Higgs Boson Particle Listings

Axions (A^0) and Other Very Light Bosons

- Japan, 1979, edited by A. Sawada and A. Sugamoto (KEK, Tsukuba, 1979), p. 95;
M. Gell-Mann, P. Ramond, and R. Slansky, in *Supergravity*, Proceedings of the Workshop, Stony Brook, New York, 1979, edited by P. Van Nieuwenhuizen and D.Z. Freedman (North-Holland, Amsterdam, 1979), p. 315.
18. For a recent analysis of the astrophysical bound on axion-electron coupling, see G. Raffelt and A. Weiss, *Phys. Rev. D* **51**, 1495 (1995). A bound on Majoron decay constant can be inferred from the same analysis..
 19. M. Kawasaki, P. Kernan, H.-S. Kang, R.J. Scherrer, G. Steigman, and T.P. Walker, *Nucl. Phys. B* **419**, 105 (1994);
S. Dodelson, G. Gyuk, and M.S. Turner, *Phys. Rev. D* **49**, 5068 (1994);
J.R. Rehm, G. Raffelt, and A. Weiss, *astro-ph/9612085*;
M. Kawasaki, K. Kohri, and K. Sato, *astro-ph/9705148*.
 20. M. White, G. Gelmini, and J. Silk, *Phys. Rev. D* **51**, 2669 (1995);
S. Bharadwaj and S.K. Kethi, *astro-ph/9707143*.
 21. E.G. Adelberger, B.R. Heckel, C.W. Stubbs, and W.F. Rogers, *Ann. Rev. Nucl. and Part. Sci.* **41**, 269 (1991).
 22. M. Kamionkowski and J. March-Russell, *Phys. Lett. B* **282**, 137 (1992);
R. Holman *et al.*, *Phys. Lett. B* **282**, 132 (1992).
 23. R. Kallosh, A. Linde, D. Linde, and L. Susskind, *Phys. Rev. D* **52**, 912 (1995).
 24. See, for instance, T. Banks and M. Dine, *Nucl. Phys. B* **479**, 173 (1996); *Nucl. Phys. B* **505**, 445 (1997).

AXIONS AND OTHER VERY LIGHT BOSONS: PART II (ASTROPHYSICAL CONSTRAINTS)

(by G.G. Raffelt)

Low-mass weakly-interacting particles (neutrinos, gravitons, axions, baryonic or leptonic gauge bosons, *etc.*) are produced in hot plasmas and thus represent an energy-loss channel for stars. The strength of the interaction with photons, electrons, and nucleons can be constrained from the requirement that stellar-evolution time scales are not modified beyond observational limits. For detailed reviews see Refs. [1,2].

The energy-loss rates are steeply increasing functions of temperature T and density ρ . Because the new channel has to compete with the standard neutrino losses which tend to increase even faster, the best limits arise from low-mass stars, notably from horizontal-branch (HB) stars which have a helium-burning core of about 0.5 solar masses at $(\rho) \approx 0.6 \times 10^4 \text{ g cm}^{-3}$ and $\langle T \rangle \approx 0.7 \times 10^8 \text{ K}$. The new energy-loss rate must not exceed about $10 \text{ ergs g}^{-1} \text{ s}^{-1}$ to avoid a conflict with the observed number ratio of HB stars in globular clusters. Likewise the ignition of helium in the degenerate cores of the preceding red-giant phase is delayed too much unless the same constraint holds at $\langle \rho \rangle \approx 2 \times 10^5 \text{ g cm}^{-3}$ and $\langle T \rangle \approx 1 \times 10^8 \text{ K}$. The white-dwarf luminosity function also yields useful bounds.

The new bosons X^0 interact with electrons and nucleons with a dimensionless strength g . For scalars it is a Yukawa coupling, for new gauge bosons (*e.g.*, from a baryonic or leptonic gauge symmetry) a gauge coupling. Axion-like pseudoscalars couple derivatively as $f^{-1} \bar{\psi} \gamma_\mu \gamma_5 \psi \partial^\mu \phi_X$ with f an energy scale.

Usually this is equivalent to $(2m/f) \bar{\psi} \gamma_5 \psi \phi_X$ with m the mass of the fermion ψ so that $g = 2m/f$. For the coupling to electrons, globular-cluster stars yield the constraint

$$g_{Xe} \lesssim \begin{cases} 0.5 \times 10^{-12} & \text{for pseudoscalars [3] ,} \\ 1.3 \times 10^{-14} & \text{for scalars [4] ,} \end{cases} \quad (1)$$

if $m_X \lesssim 10 \text{ keV}$. The Compton process $\gamma + {}^4\text{He} \rightarrow {}^4\text{He} + X^0$ limits the coupling to nucleons to $g_{XN} \lesssim 0.4 \times 10^{-10}$ [4].

Scalar and vector bosons mediate long-range forces which are severely constrained by "fifth-force" experiments [5]. In the massless case the best limits come from tests of the equivalence principle in the solar system, leading to

$$g_{B,L} \lesssim 10^{-23} \quad (2)$$

for a baryonic or leptonic gauge coupling [6].

In analogy to neutral pions, axions A^0 couple to photons as $g_{A\gamma} \mathbf{E} \cdot \mathbf{B} \phi_A$ which allows for the Primakoff conversion $\gamma \leftrightarrow A^0$ in external electromagnetic fields. The most restrictive limit arises from globular-cluster stars [2]

$$g_{A\gamma} \lesssim 0.6 \times 10^{-10} \text{ GeV}^{-1} . \quad (3)$$

The often-quoted "red-giant limit" [7] is slightly weaker.

The duration of the SN 1987A neutrino signal of a few seconds proves that the newborn neutron star cooled mostly by neutrinos rather than through an "invisible channel" such as right-handed (sterile) neutrinos or axions [8]. Therefore,

$$3 \times 10^{-10} \lesssim g_{AN} \lesssim 3 \times 10^{-7} \quad (4)$$

is excluded for the pseudoscalar Yukawa coupling to nucleons [2]. The "strong" coupling side is allowed because axions then escape only by diffusion, quenching their efficiency as an energy-loss channel [9]. Even then the range

$$10^{-6} \lesssim g_{AN} \lesssim 10^{-3} \quad (5)$$

is excluded to avoid excess counts in the water Cherenkov detectors which registered the SN 1987A neutrino signal [11].

In terms of the Peccei-Quinn scale f_A , the axion couplings to nucleons and photons are $g_{AN} = C_N m_N / f_A$ ($N = n$ or p) and $g_{A\gamma} = (\alpha / 2\pi f_A) (E/N - 1.92)$ where C_N and E/N are model-dependent numerical parameters of order unity. With $m_A = 0.62 \text{ eV} (10^7 \text{ GeV} / f_A)$, Eq. (3) yields $m_A \lesssim 0.4 \text{ eV}$ for $E/N = 8/3$ as in GUT models or the DFSZ model. The SN 1987A limit is $m_A \lesssim 0.008 \text{ eV}$ for KSVZ axions while it varies between about 0.004 and 0.012 eV for DFSZ axions, depending on the angle β which measures the ratio of two Higgs vacuum expectation values [10]. In view of the large uncertainties it is good enough to remember $m_A \lesssim 0.01 \text{ eV}$ as a generic limit (Fig. 1).

In the early universe, axions come into thermal equilibrium only if $f_A \lesssim 10^8 \text{ GeV}$ [12]. Some fraction of the relic axions end up in galaxies and galaxy clusters. Their decay $a \rightarrow 2\gamma$ contributes to the cosmic extragalactic background light and to line emissions from galactic dark-matter haloes and galaxy

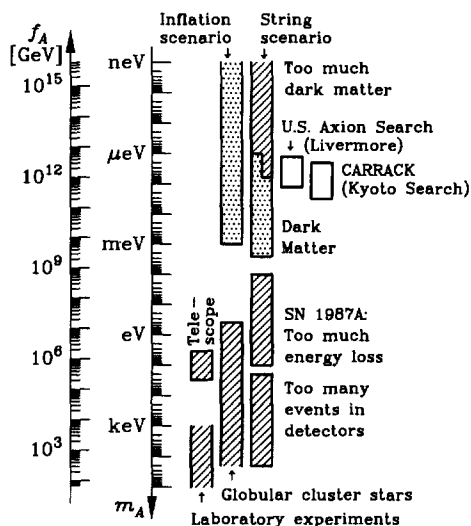


Figure 1: Astrophysical and cosmological exclusion regions (hatched) for the axion mass m_A or equivalently, the Peccei-Quinn scale f_A . An “open end” of an exclusion bar means that it represents a rough estimate; its exact location has not been established or it depends on detailed model assumptions. The globular cluster limit depends on the axion-photon coupling; it was assumed that $E/N = 8/3$ as in GUT models or the DFSZ model. The SN 1987A limits depend on the axion-nucleon couplings; the shown case corresponds to the KSVZ model and approximately to the DFSZ model. The dotted “inclusion regions” indicate where axions could plausibly be the cosmic dark matter. Most of the allowed range in the inflation scenario requires fine-tuned initial conditions. In the string scenario the plausible dark-matter range is controversial as indicated by the step in the low-mass end of the “inclusion bar” (see main text for a discussion). Also shown is the projected sensitivity range of the search experiments for galactic dark-matter axions.

clusters. An unsuccessful “telescope search” for such features yields $m_a < 3.5$ eV [13]. For $m_a \gtrsim 30$ eV, the axion lifetime is shorter than the age of the universe.

For $f_A \gtrsim 10^8$ GeV cosmic axions are produced nonthermally. If inflation occurred after the Peccei-Quinn symmetry breaking or if $T_{\text{reheat}} < f_A$, the “misalignment mechanism” [14] leads to a contribution to the cosmic critical density of

$$\Omega_A h^2 \approx 1.9 \times 3^{\pm 1} (1 \mu\text{eV}/m_A)^{1.175} \Theta_i^2 F(\Theta_i) \quad (6)$$

where h is the Hubble constant in units of $100 \text{ km s}^{-1} \text{ Mpc}^{-1}$. The stated range reflects recognized uncertainties of the cosmic conditions at the QCD phase transition and of the temperature-dependent axion mass. The function $F(\Theta)$ with $F(0) = 1$ and $F(\pi) = \infty$ accounts for anharmonic corrections to the axion potential. Because the initial misalignment angle Θ_i can be very small or very close to π , there is no real prediction for

the mass of dark-matter axions even though one would expect $\Theta_i^2 F(\Theta_i) \sim 1$ to avoid fine-tuning the initial conditions.

A possible fine-tuning of Θ_i is limited by inflation-induced quantum fluctuations which in turn lead to temperature fluctuations of the cosmic microwave background [15,16]. In a broad class of inflationary models one thus finds an upper limit to m_A where axions could be the dark matter. According to the most recent discussion [16] it is about 10^{-3} eV (Fig. 1).

If inflation did not occur at all or if it occurred before the Peccei-Quinn symmetry breaking with $T_{\text{reheat}} > f_A$, cosmic axion strings form by the Kibble mechanism [17]. Their motion is damped primarily by axion emission rather than gravitational waves. After axions acquire a mass at the QCD phase transition they quickly become nonrelativistic and thus form a cold dark matter component. Battye and Shellard [18] found that the dominant source of axion radiation are string loops rather than long strings. At a cosmic time t the average loop creation size is parametrized as $\langle \ell \rangle = \alpha t$ while the radiation power is $P = \kappa \mu$ with μ the renormalized string tension. The loop contribution to the cosmic axion density is [18]

$$\Omega_A h^2 \approx 88 \times 3^{\pm 1} \left[(1 + \alpha/\kappa)^{3/2} - 1 \right] (1 \mu\text{eV}/m_A)^{1.175}, \quad (7)$$

where the stated nominal uncertainty has the same source as in Eq. (6). The values of α and κ are not known, but probably $0.1 < \alpha/\kappa < 1.0$ [18], taking the expression in square brackets to 0.15–1.83. If axions are the dark matter, we have

$$0.05 \lesssim \Omega_A h^2 \lesssim 0.50, \quad (8)$$

where it was assumed that the universe is older than 10 Gyr, that the dark-matter density is dominated by axions with $\Omega_A \gtrsim 0.2$, and that $h \gtrsim 0.5$. This implies $m_A = 6\text{--}2500 \mu\text{eV}$ for the plausible mass range of dark-matter axions (Fig. 1).

Contrary to Ref. 18, Sikivie *et al.* [19] find that the motion of global strings is strongly damped, leading to a flat axion spectrum. In Battye and Shellard’s treatment the axion radiation is strongly peaked at wavelengths of order the loop size. In Sikivie *et al.*’s picture more of the string radiation goes into kinetic axion energy which is redshifted so that ultimately there are fewer axions. In this scenario the contributions from string decay and vacuum realignment are of the same order of magnitude; they are both given by Eq. (6) with Θ_i of order one. As a consequence, Sikivie *et al.* allow for a plausible range of dark-matter axions which reaches to smaller masses as indicated in Fig. 1.

The work of both groups implies that the low-mass end of the plausible mass interval in the string scenario overlaps with the projected sensitivity range of the U.S. search experiment for galactic dark-matter axions (Livermore) [20] and of the Kyoto search experiment CARRACK [21] as indicated in Fig. 1. (See also Part III of this Review by Hagmann, van Bibber, and Rosenberg.)

In summary, a variety of robust astrophysical arguments and laboratory experiments (Fig. 1) indicate that $m_A \lesssim 10^{-2}$ eV.

Gauge & Higgs Boson Particle Listings

Axions (A^0) and Other Very Light Bosons

The exact value of this limit may change with a more sophisticated treatment of supernova physics and/or the observation of the neutrino signal from a future galactic supernova, but a dramatic modification is not expected unless someone puts forth a completely new argument. The stellar-evolution limits shown in Fig. 1 depend on the axion couplings to various particles and thus can be irrelevant in fine-tuned models where, for example, the axion-photon coupling strictly vanishes. For nearly any m_A in the range generically allowed by stellar evolution, axions could be the cosmic dark matter, depending on the cosmological scenario realized in nature. It appears that our only practical chance to discover these “invisible” particles rests with the ongoing or future search experiments for galactic dark-matter.

References

1. M.S. Turner, Phys. Reports **197**, 67 (1990);
G.G. Raffelt, Phys. Reports **198**, 1 (1990).
2. G.G. Raffelt, Stars as Laboratories for Fundamental Physics (Univ. of Chicago Press, Chicago, 1996).
3. D.A. Dicus, E.W. Kolb, V.L. Teplitz, and R.V. Wagoner, Phys. Rev. **D18**, 1829 (1978);
G.G. Raffelt and A. Weiss, Phys. Rev. **D51**, 1495 (1995).
4. J.A. Grifols and E. Massó, Phys. Lett. **B173**, 237 (1986);
J.A. Grifols, E. Massó, and S. Peris, Mod. Phys. Lett. **A4**, 311 (1989).
5. E. Fischbach and C. Talmadge, Nature **356**, 207 (1992).
6. L.B. Okun, Yad. Fiz. **10**, 358 (1969) [Sov. J. Nucl. Phys. **10**, 206 (1969)];
S.I. Blinnikov *et al.*, Nucl. Phys. **B458**, 52 (1996).
7. G.G. Raffelt, Phys. Rev. **D33**, 897 (1986);
G.G. Raffelt and D. Dearborn, *ibid.* **36**, 2211 (1987).
8. J. Ellis and K.A. Olive, Phys. Lett. **B193**, 525 (1987);
G.G. Raffelt and D. Seckel, Phys. Rev. Lett. **60**, 1793 (1988).
9. M.S. Turner, Phys. Rev. Lett. **60**, 1797 (1988);
A. Burrows, T. Ressel, and M. Turner, Phys. Rev. **D42**, 3297 (1990).
10. H.-T. Janka, W. Keil, G. Raffelt, and D. Seckel, Phys. Rev. Lett. **76**, 2621 (1996);
W. Keil *et al.*, Phys. Rev. **D56**, 2419 (1997).
11. J. Engel, D. Seckel, and A.C. Hayes, Phys. Rev. Lett. **65**, 960 (1990).
12. M.S. Turner, Phys. Rev. Lett. **59**, 2489 (1987).
13. M.A. Bershad, M.T. Ressell, and M.S. Turner, Phys. Rev. Lett. **66**, 1398 (1991);
M.T. Ressell, Phys. Rev. **D44**, 3001 (1991);
J.M. Overduin and P.S. Wesson, Astrophys. J. **414**, 449 (1993).
14. J. Preskill, M. Wise, and F. Wilczek, Phys. Lett. **B120**, 127 (1983);
L. Abbott and P. Sikivie, *ibid.* 133;
M. Dine and W. Fischler, *ibid.* 137;
M.S. Turner, Phys. Rev. **D33**, 889 (1986).
15. D.H. Lyth, Phys. Lett. **B236**, 408 (1990);
M.S. Turner and F. Wilczek, Phys. Rev. Lett. **66**, 5 (1991);
A. Linde, Phys. Lett. **B259**, 38 (1991).
16. E.P.S. Shellard and R.A. Battye, “Inflationary axion cosmology revisited”, in preparation (1998);
The main results can be found in: E.P.S. Shellard and R.A. Battye, astro-ph/9802216.
17. R.L. Davis, Phys. Lett. **B180**, 225 (1986);
R.L. Davis and E.P.S. Shellard, Nucl. Phys. **B324**, 167 (1989).
18. R.A. Battye and E.P.S. Shellard, Nucl. Phys. **B423**, 260 (1994);
Phys. Rev. Lett. **73**, 2954 (1994) (E) *ibid.* **76**, 2203 (1996);
astro-ph/9706014, to be published in: Proceedings Dark Matter 96, Heidelberg, ed. by H.V. Klapdor-Kleingrothaus and Y. Ramacher.
19. D. Harari and P. Sikivie, Phys. Lett. **B195**, 361 (1987);
C. Hagmann and P. Sikivie, Nucl. Phys. **B363**, 247 (1991).
20. C. Hagmann *et al.*, Phys. Rev. Lett. **80**, 2043 (1998).
21. I. Ogawa, S. Matsuki, and K. Yamamoto, Phys. Rev. **D53**, R1740 (1996).

AXIONS AND OTHER VERY LIGHT BOSONS, PART III (EXPERIMENTAL LIMITS)

(by C. Hagmann, K. van Bibber, and L.J. Rosenberg)

In this section we review the experimental methodology and limits on light axions and light pseudoscalars in general. (A comprehensive overview of axion theory is given by H. Murayama in the Part I of this Review, whose notation we follow [1].) Within its scope are searches where the axion is assumed to be dark matter, searches where the Sun is presumed to be a source of axions, and purely laboratory experiments. We restrict the discussion to axions of mass $m_A < O(\text{eV})$, as the allowed range for the axion mass is nominally $10^{-6} < m_A < 10^{-2}$ eV. Experimental work in this range predominantly has been through the axion-photon coupling $g_{A\gamma}$, to which the present review is confined. As discussed in Part II of this Review by G. Raffelt, the lower bound derives from a cosmological overclosure argument, and the upper bound from SN1987A [2]. Limits from stellar evolution overlap seamlessly above that, connecting with accelerator-based limits which ruled out the original axion. There it was assumed that the Peccei-Quinn symmetry-breaking scale was the electroweak scale, *i.e.*, $f_A \sim 250$ GeV, implying axions of mass $m_A \sim O(100 \text{ keV})$. These earlier limits from nuclear transitions, particle decays, *etc.*, while not discussed here, are included in the Listings.

While the axion mass is well determined by the Peccei-Quinn scale, *i.e.*, $m_A = 0.62 \text{ eV} (10^7 \text{ GeV}/f_A)$, the axion-photon coupling $g_{A\gamma}$ is not: $g_{A\gamma} = (\alpha/\pi f_A) g_\gamma$, with $g_\gamma = (E/N - 1.92)/2$, where E/N is a model-dependent number. It is noteworthy however, that two quite distinct models lead to axion-photon couplings which are not very different. For the case of axions imbedded in Grand Unified Theories, the DFSZ axion [3], $g_\gamma = 0.37$, whereas in one popular implementation of the “hadronic” class of axions, the KSVZ axion [4], $g_\gamma = -0.96$. The Lagrangian $L = g_{A\gamma} \mathbf{E} \cdot \mathbf{B} \phi_A$, with ϕ_A the axion field, permits the conversion of an axion into a single real photon in an external electromagnetic field, *i.e.*, a Primakoff interaction. In the case of relativistic axions, $k_\gamma - k_A \sim m_A^2/2\omega \ll \omega$, pertinent to several experiments below, coherent axion-photon

See key on page 239

Gauge & Higgs Boson Particle Listings Axions (A^0) and Other Very Light Bosons

mixing in long magnetic fields results in significant conversion probability even for very weakly coupled axions [5].

Below are discussed several experimental techniques constraining $g_{A\gamma}$, and their results. Also included are recent but yet-unpublished results, and projected sensitivities for experiments soon to be upgraded.

III.1. Microwave cavity experiments: Possibly the most promising avenue to the discovery of the axion presumes that axions constitute a significant fraction of the dark matter halo of our galaxy. The maximum likelihood density for the Cold Dark Matter (CDM) component of our galactic halo is $\rho_{\text{CDM}} = 7.5 \times 10^{-25} \text{g/cm}^3 (450 \text{MeV/cm}^3)$ [6]. That the CDM halo is in fact made of axions (rather than *e.g.* WIMPs) is in principle an independent assumption, however should very light axions exist they would almost necessarily be cosmologically abundant [2]. As shown by Sikivie [7], halo axions may be detected by their resonant conversion into a quasi-monochromatic microwave signal in a high- Q cavity permeated by a strong magnetic field. The cavity is tunable and the signal is maximum when the frequency $\nu = m_A(1 + O(10^{-6}))$, the width of the peak representing the virial distribution of thermalized axions in the galactic gravitational potential. The signal may possess ultra-fine structure due to axions recently fallen into the galaxy and not yet thermalized [8]. The feasibility of the technique was established in early experiments of small sensitive volume, $V = O(1 \text{ liter})$ [9,10] with High Electron Mobility Transistor (HEMT) amplifiers, which set limits on axions in the mass range $4.5 < m_A < 16.3 \mu\text{eV}$, but at power sensitivity levels 2–3 orders of magnitude too high to see KSVZ and DFSZ axions (the conversion power $P_{A \rightarrow \gamma} \propto g_{A\gamma}^2$). A recent large-scale experiment ($B \sim 7.5 \text{ T}, V \sim 200 \text{ liter}$) has achieved sensitivity to KSVZ axions over a narrow mass range $2.77 < m_A < 3.3 \mu\text{eV}$, and continues to take data [11]. The exclusion regions shown in Fig. 1 for Refs. [9–12] are all normalized to the best-fit Cold Dark Matter density $\rho_{\text{CDM}} = 7.5 \times 10^{-25} \text{g/cm}^3 (450 \text{MeV/cm}^3)$, and 90% CL. Recent developments in DC SQUID amplifiers [12] and Rydberg atom single-quantum detectors [13] promise dramatic improvements in noise temperature, which will enable rapid scanning of the axion mass range at or below the DFSZ limit. The region of the microwave cavity experiments is shown in detail in Fig. 2.

III.2. Telescope search for eV axions: For axions of mass greater than about 10^{-1} eV , their cosmological abundance is no longer dominated by vacuum misalignment or string radiation mechanisms, but rather by thermal production. Their contribution to the critical density is small, $\Omega \sim 0.01 (m_A/\text{eV})$. However, the spontaneous-decay lifetime of axions, $\tau(A \rightarrow 2\gamma) \sim 10^{25} \text{sec} (m_A/\text{eV})^{-5}$ while irrelevant for μeV axions, is short enough to afford a powerful constraint on such thermally produced axions in the eV range, by looking for a quasi-monochromatic photon line from galactic clusters. This line, corrected for Doppler shift, would be at half the axion mass and its width would be consistent with the observed virial motion,

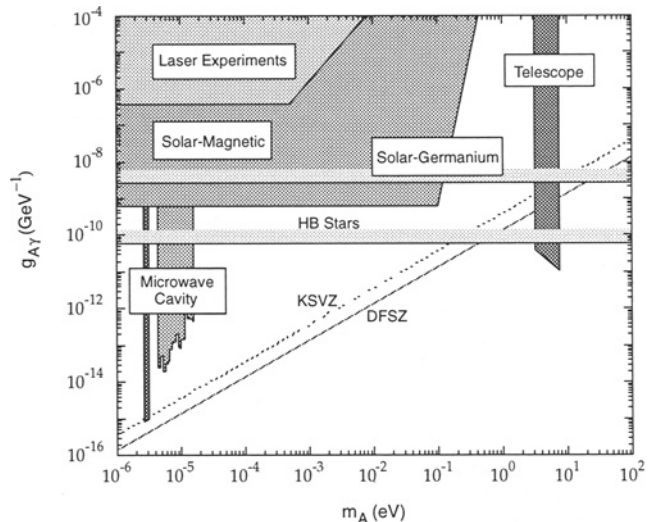


Figure 1: Exclusion region in mass vs. axion-photon coupling ($m_A, g_{A\gamma}$) for various experiments. The limit set by globular cluster Horizontal Branch Stars (“HB Stars”) is shown for Ref. 2.

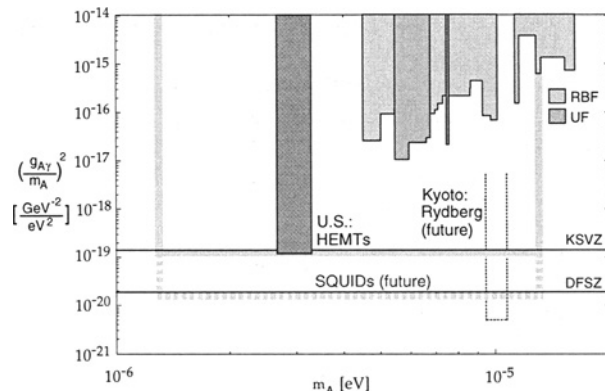


Figure 2: Exclusion region from the microwave cavity experiments, where the plot is flattened by presenting $(g_{A\gamma}/m_A)^2$ vs. m_A . The first-generation experiments (Rochester-BNL-FNAL, “RBF” [9]; University of Florida, “UF” [10]) and the US large-scale experiment in progress (“US” [11]) are all HEMT-based. Shown also is the full mass range to be covered by the latter experiment (shaded line), and the improved sensitivity when upgraded with DC SQUID amplifiers [12] (shaded dashed line). The expected performance of the Kyoto experiment based on a Rydberg atom single-quantum receiver (dotted line) is also shown [13].

typically $\Delta\lambda/\lambda \sim 10^{-2}$. The expected line intensity would be of the order $I_A \sim 10^{-17} (m_A/3 \text{ eV})^7 \text{ erg cm}^{-2} \text{ arcsec}^{-2} \text{ \AA}^{-1} \text{ sec}^{-1}$ for DFSZ axions, comparable to the continuum night emission.

Gauge & Higgs Boson Particle Listings Axions (A^0) and Other Very Light Bosons

The conservative assumption is made that the relative density of thermal axions fallen into the cluster gravitational potential reflects their overall cosmological abundance. A search for thermal axions in three rich Abell clusters was carried out at Kitt Peak National Laboratory [14]; no such line was observed between 3100–8300 Å ($m_A = 3\text{--}8$ eV) after “on-off field” subtraction of the atmospheric molecular background spectra. A limit everywhere stronger than $g_{A\gamma} < 10^{-10}\text{GeV}^{-1}$ is set, which is seen from Fig. 1 to easily exclude DFSZ axions throughout the mass range.

III.3. A search for solar axions: As with the telescope search for thermally produced axions above, the search for solar axions was stimulated by the possibility of there being a “1 eV window” for hadronic axions (*i.e.*, axions with no tree-level coupling to leptons), a “window” subsequently closed by an improved understanding of the evolution of globular cluster stars and SN1987A [2]. Hadronic axions would be copiously produced within our Sun’s interior by a Primakoff process. Their flux at the Earth of $\sim 10^{12}\text{cm}^{-2}\text{sec}^{-1}(m_A/\text{eV})^2$, which is independent of the details of the solar model, is sufficient for a definitive test via the axion reconversion to photons in a large magnetic field. However, their average energy is ~ 4 keV, implying an oscillation length in the vacuum of $2\pi(m_A^2/2\omega)^{-1} \sim O(\text{mm})$, precluding the mixing from achieving its theoretically maximum value in any practical magnet. It was recognized that one could endow the photon with an effective mass in a gas, $m_\gamma = \omega_{\text{pl}}$, thus permitting the axion and photon dispersion relationships to be matched [15]. A first simple implementation of this proposal was carried out using a conventional dipole magnet with a conversion volume of variable-pressure helium gas and a xenon proportional chamber as the x-ray detector [16]. The magnet was fixed in orientation to take data for ~ 1000 sec/day. Axions were excluded for $g_{A\gamma} < 3.6 \times 10^{-9}\text{GeV}^{-1}$ for $m_A < 0.03$ eV, and $g_{A\gamma} < 7.7 \times 10^{-9}\text{GeV}^{-1}$ for $0.03\text{ eV} < m_A < 0.11$ eV (95% CL). A more ambitious experiment has recently been commissioned, using a superconducting magnet on a telescope mount to track the Sun continuously. A preliminary exclusion limit of $g_{A\gamma} < 6 \times 10^{-10}\text{GeV}^{-1}$ (95% CL) has been set for $m_A < 0.03$ eV [17].

Another search for solar axions has been carried out, using a single crystal germanium detector. It exploits the coherent conversion of axions into photons when their angle of incidence satisfies a Bragg condition with a crystalline plane. Analysis of 1.94 kg-yr of data from a 1 kg germanium detector yields a bound of $g_{A\gamma} < 2.7 \times 10^{-9}\text{GeV}^{-1}$ (95% CL), independent of mass up to $m_A \sim 1$ keV [18].

III.4. Photon regeneration (“invisible light shining through walls”): Photons propagating through a transverse field (with $\mathbf{E} \parallel \mathbf{B}$) may convert into axions. For light axions with $m_A^2 l / 2\omega \ll 2\pi$, where l is the length of the magnetic field, the axion beam produced is colinear and coherent with the photon beam, and the conversion probability Π is given by $\Pi \sim (1/4)(g_{A\gamma} B l)^2$. An ideal implementation for this limit

is a laser beam propagating down a long, superconducting dipole magnet like those for high-energy physics accelerators. If another such dipole magnet is set up in line with the first, with an optical barrier interposed between them, then photons may be regenerated from the pure axion beam in the second magnet and detected [19]. The overall probability $P(\gamma \rightarrow A \rightarrow \gamma) = \Pi^2$. Such an experiment has been carried out, utilizing two magnets of length $l = 4.4$ m and $B = 3.7$ T. Axions with mass $m_A < 10^{-3}$ eV, and $g_{A\gamma} > 6.7 \times 10^{-7}\text{GeV}^{-1}$ were excluded at 95% CL [20,21]. With sufficient effort, limits comparable to those from stellar evolution would be achievable. Due to the $g_{A\gamma}^4$ rate suppression however, it does not seem feasible to reach standard axion couplings.

III.5. Polarization experiments: The existence of axions can affect the polarization of light propagating through a transverse magnetic field in two ways [22]. First, as the E_{\parallel} component, but not the E_{\perp} component will be depleted by the production of real axions, there will be in general a small rotation of the polarization vector of linearly polarized light. This effect will be a constant for all sufficiently light m_A such that the oscillation length is much longer than the magnet ($m_A^2 l / 2\omega \ll 2\pi$). For heavier axions, the effect oscillates and diminishes with increasing m_A , and vanishes for $m_A > \omega$. The second effect is birefringence of the vacuum, again because there can be a mixing of virtual axions in the E_{\parallel} state, but not for the E_{\perp} state. This will lead to light which is initially linearly polarized becoming elliptically polarized. Higher-order QED also induces vacuum birefringence, and is much stronger than the contribution due to axions. A search for both polarization-rotation and induced ellipticity has been carried out with the same magnets described in Sec. (III.4) above [21,23]. As in the case of photon regeneration, the observables are boosted linearly by the number of passes the laser beam makes in an optical cavity within the magnet. The polarization-rotation resulted in a stronger limit than that from ellipticity, $g_{A\gamma} < 3.6 \times 10^{-7}\text{GeV}^{-1}$ (95% CL) for $m_A < 5 \times 10^{-4}$ eV. The limits from ellipticity are better at higher masses, as they fall off smoothly and do not terminate at m_A . There are two experiments in construction with greatly improved sensitivity which while still far from being able to detect standard axions, should measure the QED “light-by-light” contribution for the first time [24,25]. The overall envelope for limits from the laser-based experiments in Sec. (III.4) and Sec. (III.5) is shown schematically in Fig. 1.

References

1. H. Murayama, Part I (Theory) of this Review.
2. G. Raffelt, Part II (Astrophysical Constraints) of this Review.
3. M. Dine *et al.*, Phys. Lett. **B104**, 199 (1981);
A. Zhitnitsky, Sov. J. Nucl. Phys. **31**, 260 (1980).
4. J. Kim, Phys. Rev. Lett. **43**, 103 (1979);
M. Shifman *et al.*, Nucl. Phys. **B166**, 493 (1980).
5. G. Raffelt and L. Stodolsky, Phys. Rev. **D37**, 1237 (1988).

See key on page 239

Gauge & Higgs Boson Particle Listings

Axions (A^0) and Other Very Light Bosons

6. E. Gates *et al.*, Ap. J. **449**, 123 (1995).
7. P. Sikivie, Phys. Rev. Lett. **51**, 1415 (1983); **52(E)**, 695 (1984); Phys. Rev. **D32**, 2988 (1985).
8. P. Sikivie and J. Ipser, Phys. Lett. **B291**, 288 (1992); P. Sikivie *et al.*, Phys. Rev. Lett. **75**, 2911 (1995).
9. S. DePanfilis *et al.*, Phys. Rev. Lett. **59**, 839 (1987); W. Wuensch *et al.*, Phys. Rev. **D40**, 3153 (1989).
10. C. Hagmann *et al.*, Phys. Rev. **D42**, 1297 (1990).
11. C. Hagmann *et al.*, Phys. Rev. Lett. **80**, 2043 (1998).
12. M. Mück *et al.*, to be published in Appl. Phys. Lett.
13. I. Ogawa *et al.*, Proceedings II. RESCEU Conference on "Dark Matter in the Universe and its Direct Detection," p. 175, Universal Academy Press, ed. M. Minowa (1997).
14. M. Bershadsky *et al.*, Phys. Rev. Lett. **66**, 1398 (1991); M. Ressel, Phys. Rev. **D44**, 3001 (1991).
15. K. van Bibber *et al.*, Phys. Rev. **D39**, 2089 (1989).
16. D. Lazarus *et al.*, Phys. Rev. Lett. **69**, 2333 (1992).
17. M. Minowa, Proceedings International Workshop Non-Accelerator New Physics, Dubna (1997), and private communication (1998).
18. F. Avignone III *et al.*, *ibid.*
19. K. van Bibber *et al.*, Phys. Rev. Lett. **59**, 759 (1987). A similar proposal has been made for exactly massless pseudoscalars: A. Ansel'm, Sov. J. Nucl. Phys. **42**, 936 (1985).
20. G. Ruoso *et al.*, Z. Phys. **C56**, 505 (1992).
21. R. Cameron *et al.*, Phys. Rev. **D47**, 3707 (1993).
22. L. Maiani *et al.*, Phys. Lett. **B175**, 359 (1986).
23. Y. Semertzidis *et al.*, Phys. Rev. Lett. **64**, 2988 (1990).
24. S. Lee *et al.*, Fermilab proposal E-877 (1995).
25. D. Bakalov *et al.*, Quantum Semiclass. Opt. **10**, 239 (1998).

$<6 \times 10^{-5}$	90	7 AMSLER	94B CBAR	$\eta \rightarrow \gamma X^0$, $m_{X^0}=200-525$ MeV
<0.007	90	8 MEIJERDREES94	CNTR	$\pi^0 \rightarrow \gamma X^0$, $m_{X^0}=25$ MeV
<0.002	90	8 MEIJERDREES94	CNTR	$\pi^0 \rightarrow \gamma X^0$, $m_{X^0}=100$ MeV
$<2 \times 10^{-7}$	90	9 ATIYA	93B B787	$K^+ \rightarrow \pi^+ A^0$
$<3 \times 10^{-13}$	90	10 NG	93 COSM	$\pi^0 \rightarrow \gamma X^0$
$<1.1 \times 10^{-8}$	90	11 ALLIEGRO	92 SPEC	$K^+ \rightarrow \pi^+ A^0$ ($A^0 \rightarrow e^+ e^-$)
$<5 \times 10^{-4}$	90	12 ATIYA	92 B787	$\pi^0 \rightarrow \gamma X^0$
$<4 \times 10^{-6}$	90	13 MEIJERDREES92	SPEC	$\pi^0 \rightarrow \gamma X^0$, $X^0 \rightarrow e^+ e^-$, $m_{X^0}=100$ MeV
$<1 \times 10^{-7}$	90	14 ATIYA	90B B787	Sup. by KITCH- ING 97
$<1.3 \times 10^{-8}$	90	15 KORENCHEN...	87 SPEC	$\pi^+ \rightarrow e^+ \nu A^0$ ($A^0 \rightarrow e^+ e^-$)
$<1 \times 10^{-9}$	90	0	16 EICHLER	86 SPEC Stopped $\pi^+ \rightarrow$ $e^+ \nu A^0$
$<2 \times 10^{-5}$	90	17 YAMAZAKI	84 SPEC	For $160 < m < 260$ MeV
$<(1.5-4) \times 10^{-6}$	90	17 YAMAZAKI	84 SPEC	K decay, $m_{A^0} \ll$ 100 MeV
	0	18 ASANO	82 CNTR	Stopped $K^+ \rightarrow$ $\pi^+ A^0$
	0	19 ASANO	81B CNTR	Stopped $K^+ \rightarrow$ $\pi^+ A^0$
		20 ZHITNITSKII	79	Heavy axion

³ ALTEGOER 98 looked for X^0 from π^0 decay which penetrate the shielding and convert to π^0 in the external Coulomb field of a nucleus.
⁴ ADLER 97 bound is for massless A^0 .
⁵ KITCHING 97 limit is for $B(K^+ \rightarrow \pi^+ A^0) \cdot B(A^0 \rightarrow \gamma\gamma)$ and applies for $m_{A^0} \approx 50$ MeV, $\tau_{A^0} < 10^{-10}$ s. Limits are provided for $0 < m_{A^0} < 100$ MeV, $\tau_{A^0} < 10^{-8}$ s.
⁶ ADLER 96 looked for a peak in missing-mass distribution. This work is an update of ATIYA 93. The limit is for massless stable A^0 particles and extends to $m_{A^0}=80$ MeV at the same level. See paper for dependence on finite lifetime.
⁷ AMSLER 94B and AMSLER 96B looked for a peak in missing-mass distribution.
⁸ The MEIJERDREES 94 limit is based on inclusive photon spectrum and is independent of X^0 decay modes. It applies to $\tau(X^0) > 10^{-23}$ sec.
⁹ ATIYA 93B looked for a peak in missing mass distribution. The bound applies for stable A^0 of $m_{A^0}=150-250$ MeV, and the limit becomes stronger (10^{-8}) for $m_{A^0}=180-240$ MeV.
¹⁰ NG 93 studied the production of X^0 via $\gamma\gamma \rightarrow \pi^0 \rightarrow \gamma X^0$ in the early universe at $T \approx 1$ MeV. The bound on extra neutrinos from nucleosynthesis $\Delta N_\nu < 0.3$ (WALKER 91) is employed. It applies to $m_{X^0} \ll 1$ MeV in order to be relativistic down to nucleosynthesis temperature. See paper for heavier X^0 .
¹¹ ALLIEGRO 92 limit applies for $m_{A^0}=150-340$ MeV and is the branching ratio times the decay probability. Limit is $< 1.5 \times 10^{-8}$ at 99%CL.
¹² ATIYA 92 looked for a peak in missing mass distribution. The limit applies to $m_{X^0}=0-130$ MeV in the narrow resonance limit. See paper for the dependence on lifetime. Covariance requires X^0 to be a vector particle.
¹³ MEIJERDREES 92 limit applies for $\tau_{X^0} = 10^{-23}-10^{-11}$ sec. Limits between 2×10^{-4} and 4×10^{-6} are obtained for $m_{X^0} = 25-120$ MeV. Angular momentum conservation requires that X^0 has spin ≥ 1 .
¹⁴ ATIYA 90B limit is for $B(K^+ \rightarrow \pi^+ A^0) \cdot B(A^0 \rightarrow \gamma\gamma)$ and applies for $m_{A^0} = 50$ MeV, $\tau_{A^0} < 10^{-10}$ s. Limits are also provided for $0 < m_{A^0} < 100$ MeV, $\tau_{A^0} < 10^{-8}$ s.
¹⁵ KORENCHENKO 87 limit assumes $m_{A^0} = 1.7$ MeV, $\tau_{A^0} \lesssim 10^{-12}$ s, and $B(A^0 \rightarrow e^+ e^-) = 1$.
¹⁶ EICHLER 86 looked for $\pi^+ \rightarrow e^+ \nu A^0$ followed by $A^0 \rightarrow e^+ e^-$. Limits on the branching fraction depend on the mass and lifetime of A^0 . The quoted limits are valid when $\tau(A^0) \gtrsim 3 \times 10^{-10}$ s if the decays are kinematically allowed.
¹⁷ YAMAZAKI 84 looked for a discrete line in $K^+ \rightarrow \pi^+ X$. Sensitive to wide mass range (5-300 MeV), independent of whether X decays promptly or not.
¹⁸ ASANO 82 at KEK set limits for $B(K^+ \rightarrow \pi^+ A^0)$ for $m_{A^0} < 100$ MeV as BR $< 4 \times 10^{-8}$ for $\tau(A^0 \rightarrow n\gamma's) > 1 \times 10^{-9}$ s, BR $< 1.4 \times 10^{-6}$ for $\tau < 1 \times 10^{-9}$ s.
¹⁹ ASANO 81B is KEK experiment. Set $B(K^+ \rightarrow \pi^+ A^0) < 3.8 \times 10^{-8}$ at CL = 90%.
²⁰ ZHITNITSKII 79 argue that a heavy axion predicted by YANG 78 ($3 < m < 40$ MeV) contradicts experimental muon anomalous magnetic moments.

A^0 (Axion) MASS LIMITS from Astrophysics and Cosmology

These bounds depend on model-dependent assumptions (i.e. — on a combination of axion parameters).

VALUE (MeV)	DOCUMENT ID	TECN	COMMENT
>0.2	BARROSO 82	ASTR	Standard Axion
>0.25	1 RAFFELT 82	ASTR	Standard Axion
>0.2	2 DICUS 78c	ASTR	Standard Axion
	MIKAELIAN 78	ASTR	Stellar emission
>0.3	2 SATO 78	ASTR	Standard Axion
>0.2	VYSOTSKII 78	ASTR	Standard Axion

¹ Lower bound from 5.5 MeV γ -ray line from the sun.
² Lower bound from requiring the red giants' stellar evolution not be disrupted by axion emission.

A^0 (Axion) and Other Light Boson (X^0) Searches in Stable Particle Decays

Limits are for branching ratios.

VALUE	CL%	EVTS	DOCUMENT ID	TECN	COMMENT
$<3.3 \times 10^{-5}$	90		3 ALTEGOER 98	NOMD	$\pi^0 \rightarrow \gamma X^0$, $m_{X^0} < 120$ MeV
$<3.0 \times 10^{-10}$	90		4 ADLER 97	B787	$K^+ \rightarrow \pi^+ A^0$
$<5.0 \times 10^{-8}$	90		5 KITCHING 97	B787	$K^+ \rightarrow \pi^+ A^0$ ($A^0 \rightarrow \gamma\gamma$)
$<5.2 \times 10^{-10}$	90		6 ADLER 96	B787	$K^+ \rightarrow \pi^+ A^0$
$<2.8 \times 10^{-4}$	90		7 AMSLER 96B	CBAR	$\pi^0 \rightarrow \gamma X^0$, $m_{X^0} < 65$ MeV
$<3 \times 10^{-4}$	90		7 AMSLER 96B	CBAR	$\eta \rightarrow \gamma X^0$, $m_{X^0}=50-200$ MeV
$<4 \times 10^{-5}$	90		7 AMSLER 96B	CBAR	$\eta' \rightarrow \gamma X^0$, $m_{X^0}=50-925$ MeV
$<6 \times 10^{-5}$	90		7 AMSLER 94B	CBAR	$\pi^0 \rightarrow \gamma X^0$, $m_{X^0}=65-125$ MeV

A^0 (Axion) Searches in Quarkonium Decays

Decay or transition of quarkonium. Limits are for branching ratio.

VALUE	CL%	EVTS	DOCUMENT ID	TECN	COMMENT
$<1.3 \times 10^{-5}$	90		21 BALEST 95	CLEO	$\Upsilon(1S) \rightarrow A^0 \gamma$
$<4.0 \times 10^{-5}$	90		ANTREASYAN 90C	CBAL	$\Upsilon(1S) \rightarrow A^0 \gamma$
			22 ANTREASYAN 90C	RVUE	
$<5 \times 10^{-5}$	90		23 DRUZHININ 87	ND	$\phi \rightarrow A^0 \gamma$ ($A^0 \rightarrow e^+ e^-$)
$<2 \times 10^{-3}$	90		24 DRUZHININ 87	ND	$\phi \rightarrow A^0 \gamma$ ($A^0 \rightarrow \gamma\gamma$)
$<7 \times 10^{-6}$	90		25 DRUZHININ 87	ND	$\phi \rightarrow A^0 \gamma$ ($A^0 \rightarrow$ missing)
$<3.1 \times 10^{-4}$	90	0	26 ALBRECHT 86D	ARG	$\Upsilon(1S) \rightarrow A^0 \gamma$ ($A^0 \rightarrow e^+ e^-$)

$\bullet \bullet \bullet$ We do not use the following data for averages, fits, limits, etc. $\bullet \bullet \bullet$

Gauge & Higgs Boson Particle Listings

Axions (A^0) and Other Very Light Bosons

$<4 \times 10^{-4}$	90	0	26 ALBRECHT	86D ARG	$T(1S) \rightarrow A^0 \gamma$ ($A^0 \rightarrow \mu^+ \mu^-$, $\pi^+ \pi^-, K^+ K^-$)
$<8 \times 10^{-4}$	90	1	27 ALBRECHT	86D ARG	$T(1S) \rightarrow A^0 \gamma$
$<1.3 \times 10^{-3}$	90	0	28 ALBRECHT	86D ARG	$T(1S) \rightarrow A^0 \gamma$ ($A^0 \rightarrow e^+ e^-, \gamma \gamma$)
$<2. \times 10^{-3}$	90		29 BOWCOCK	86 CLEO	$T(2S) \rightarrow T(1S) \rightarrow A^0$
$<5. \times 10^{-3}$	90		30 MAGERAS	86 CUSB	$T(1S) \rightarrow A^0 \gamma$
$<3. \times 10^{-4}$	90		31 ALAM	83 CLEO	$T(1S) \rightarrow A^0 \gamma$
$<9.1 \times 10^{-4}$	90		32 NICZYPORUK	83 LENA	$T(1S) \rightarrow A^0 \gamma$
$<1.4 \times 10^{-5}$	90		33 EDWARDS	82 CBAL	$J/\psi \rightarrow A^0 \gamma$
$<3.5 \times 10^{-4}$	90		34 SIVERTZ	82 CUSB	$T(1S) \rightarrow A^0 \gamma$
$<1.2 \times 10^{-4}$	90		34 SIVERTZ	82 CUSB	$T(3S) \rightarrow A^0 \gamma$

- ²¹BALEST 95 looked for a monochromatic γ from $T(1S)$ decay. The bound is for $m_{A^0} < 5.0$ GeV. See Fig. 7 in the paper for bounds for heavier m_{A^0} . They also quote a bound on branching ratios 10^{-3} – 10^{-5} of three-body decay $\gamma X \bar{X}$ for $0 < m_X < 3.1$ GeV.
- ²²The combined limit of ANTREASIAN 90C and EDWARDS 82 excludes standard axion with $m_{A^0} < 2m_e$ at 90% CL as long as $C_{\gamma} C_{J/\psi} > 0.09$, where $C_V (V = T, J/\psi)$ is the reduction factor for $\Gamma(V \rightarrow A^0 \gamma)$ due to QCD and/or relativistic corrections. The same data excludes $0.02 < x < 260$ (90% CL) if $C_{\gamma} = C_{J/\psi} = 0.5$, and further combining with ALBRECHT 86D result excludes $5 \times 10^{-5} < x < 260$. x is the ratio of the vacuum expectation values of the two Higgs fields. These limits use conventional assumption $\Gamma(A^0 \rightarrow ee) \propto x^{-2}$. The alternative assumption $\Gamma(A^0 \rightarrow ee) \propto x^2$ gives a somewhat different excluded region 0.00075 $< x < 44$.
- ²³The first DRUZHININ 87 limit is valid when $\tau_{A^0}/m_{A^0} < 3 \times 10^{-13}$ s/MeV and $m_{A^0} < 20$ MeV.
- ²⁴The second DRUZHININ 87 limit is valid when $\tau_{A^0}/m_{A^0} < 5 \times 10^{-13}$ s/MeV and $m_{A^0} < 20$ MeV.
- ²⁵The third DRUZHININ 87 limit is valid when $\tau_{A^0}/m_{A^0} > 7 \times 10^{-12}$ s/MeV and $m_{A^0} < 200$ MeV.
- ²⁶ $\tau_{A^0} < 1 \times 10^{-13}$ s and $m_{A^0} < 1.5$ GeV. Applies for $A^0 \rightarrow \gamma \gamma$ when $m_{A^0} < 100$ MeV.
- ²⁷ $\tau_{A^0} > 1 \times 10^{-7}$ s.
- ²⁸Independent of τ_{A^0} .
- ²⁹BOWCOCK 86 looked for A^0 that decays into $e^+ e^-$ in the cascade decay $T(2S) \rightarrow T(1S) \pi^+ \pi^-$ followed by $T(1S) \rightarrow A^0 \gamma$. The limit for $B(T(1S) \rightarrow A^0 \gamma) B(A^0 \rightarrow e^+ e^-)$ depends on m_{A^0} and τ_{A^0} . The quoted limit for $m_{A^0} = 1.8$ MeV is at $\tau_{A^0} \sim 2. \times 10^{-12}$ s, where the limit is the worst. The same limit $2. \times 10^{-3}$ applies for all lifetimes for masses $2m_e < m_{A^0} < 2m_\mu$ when the results of this experiment are combined with the results of ALAM 83.
- ³⁰MAGERAS 86 looked for $T(1S) \rightarrow \gamma A^0$ ($A^0 \rightarrow e^+ e^-$). The quoted branching fraction limit is for $m_{A^0} = 1.7$ MeV, at $\tau(A^0) \sim 4. \times 10^{-13}$ s where the limit is the worst.
- ³¹ALAM 83 is at CESR. This limit combined with limit for $B(J/\psi \rightarrow A^0 \gamma)$ (EDWARDS 82) excludes standard axion.
- ³²NICZYPORUK 83 is DESY-DORIS experiment. This limit together with lower limit 9.2×10^{-4} of $B(T \rightarrow A^0 \gamma)$ derived from $B(J/\psi(1S) \rightarrow A^0 \gamma)$ limit (EDWARDS 82) excludes standard axion.
- ³³EDWARDS 82 looked for $J/\psi \rightarrow \gamma A^0$ decays by looking for events with a single γ [of energy $\sim 1/2$ the $J/\psi(1S)$ mass], plus nothing else in the detector. The limit is inconsistent with the axion interpretation of the FAISSNER 81B result.
- ³⁴SIVERTZ 82 is CESR experiment. Looked for $T \rightarrow \gamma A^0, A^0$ undetected. Limit for 1S (3S) is valid for $m_{A^0} < 7$ GeV (4 GeV).

A^0 (Axion) Searches in Positronium Decays

Decay or transition of positronium. Limits are for branching ratio.

VALUE	CL%	DOCUMENT ID	TECN	COMMENT
$<2 \times 10^{-4}$	90	MAENO	95 CNTR	α -Ps $\rightarrow A^0 \gamma$ $m_{A^0} = 850$ – 1013 keV
$<3.0 \times 10^{-3}$	90	35 ASAI	94 CNTR	α -Ps $\rightarrow A^0 \gamma$ $m_{A^0} = 30$ – 500 keV
$<2.8 \times 10^{-5}$	90	36 AKOPYAN	91 CNTR	α -Ps $\rightarrow A^0 \gamma$ ($A^0 \rightarrow \gamma \gamma$), $m_{A^0} < 30$ keV
$<1.1 \times 10^{-6}$	90	37 ASAI	91 CNTR	α -Ps $\rightarrow A^0 \gamma$, $m_{A^0} < 800$ keV
$<3.8 \times 10^{-4}$	90	GNINENKO	90 CNTR	α -Ps $\rightarrow A^0 \gamma, m_{A^0} < 30$ keV
$<(1-5) \times 10^{-4}$	95	38 TSUCHIAKI	90 CNTR	α -Ps $\rightarrow A^0 \gamma, m_{A^0} = 300$ – 900 keV
$<6.4 \times 10^{-5}$	90	39 ORITO	89 CNTR	α -Ps $\rightarrow A^0 \gamma$, $m_{A^0} < 30$ keV
		40 AMALDI	85 CNTR	Ortho-positronium
		41 CARBONI	83 CNTR	Ortho-positronium

- ³⁵The ASAI 94 limit is based on inclusive photon spectrum and is independent of A^0 decay modes.
- ³⁶The AKOPYAN 91 limit applies for a short-lived A^0 with $\tau_{A^0} < 10^{-13}$ m_{A^0} [keV] s.
- ³⁷ASAI 91 limit translates to $g_{A^0 e^+ e^-}^2 / 4\pi < 1.1 \times 10^{-11}$ (90%CL) for $m_{A^0} < 800$ keV.
- ³⁸The TSUCHIAKI 90 limit is based on inclusive photon spectrum and is independent of A^0 decay modes.

³⁹ORITO 89 limit translates to $g_{A^0 e^+ e^-}^2 / 4\pi < 6.2 \times 10^{-10}$. Somewhat more sensitive limits are obtained for larger m_{A^0} : $B < 7.6 \times 10^{-6}$ at 100 keV.

⁴⁰AMALDI 85 set limits $B(A^0 \gamma) / B(\gamma \gamma \gamma) < (1-5) \times 10^{-6}$ for $m_{A^0} = 900$ – 100 keV which are about 1/10 of the CARBONI 83 limits.

⁴¹CARBONI 83 looked for orthopositronium $\rightarrow A^0 \gamma$. Set limit for A^0 electron coupling squared, $g(e e A^0)^2 / (4\pi) < 6. \times 10^{-10}$ – $7. \times 10^{-9}$ for m_{A^0} from 150–900 keV (CL = 99.7%). This is about 1/10 of the bound from $g=2$ experiments.

A^0 (Axion) Search in Photoproduction

VALUE	DOCUMENT ID	COMMENT
• • • We do not use the following data for averages, fits, limits, etc. • • •		
	42 BASSOMPIERRE... 95	$m_{A^0} = 1.8 \pm 0.2$ MeV

⁴²BASSOMPIERRE 95 is an extension of BASSOMPIERRE 93. They looked for a peak in the invariant mass of $e^+ e^-$ pairs in the region $m_{e^+ e^-} = 1.8 \pm 0.2$ MeV. They obtained bounds on the production rate A^0 for $\tau(A^0) = 10^{-18}$ – 10^{-9} sec. They also found an excess of events in the range $m_{e^+ e^-} = 2.1$ – 3.5 MeV.

A^0 (Axion) Production in Hadron Collisions

Limits are for $\sigma(A^0) / \sigma(\pi^0)$.

VALUE	CL%	EVTS	DOCUMENT ID	TECN	COMMENT
• • • We do not use the following data for averages, fits, limits, etc. • • •					
			43 AHMAD	97 SPEC	e^+ production
			44 LEINBERGER	97 SPEC	$A^0 \rightarrow e^+ e^-$
			45 GANZ	96 SPEC	$A^0 \rightarrow e^+ e^-$
			46 KAMEL	96 EMUL	^{32}S emulsion, $A^0 \rightarrow$
			47 BLUEMLEIN	92 BDMP	$A^0 N_Z \rightarrow \ell^+ \ell^- N_Z$
			48 MEIJERDREES	92 SPEC	$\pi^- p \rightarrow n A^0, A^0 \rightarrow$
			49 BLUEMLEIN	91 BDMP	$A^0 \rightarrow e^+ e^-, 2\gamma$
			50 FAISSNER	89 OSPK	Beam dump, $A^0 \rightarrow e^+ e^-$
			51 DEBOER	88 RVUE	$A^0 \rightarrow e^+ e^-$
			52 EL-NADI	88 EMUL	$A^0 \rightarrow e^+ e^-$
			53 FAISSNER	88 OSPK	Beam dump, $A^0 \rightarrow 2\gamma$
			54 BADIER	86 BDMP	$A^0 \rightarrow e^+ e^-$
$<2. \times 10^{-11}$	90	0	55 BERGSMA	85 CHRM	CERN beam dump
$<1. \times 10^{-13}$	90	0	55 BERGSMA	85 CHRM	CERN beam dump
		24	56 FAISSNER	83 OSPK	Beam dump, $A^0 \rightarrow 2\gamma$
			57 FAISSNER	83B RVUE	LAMPF beam dump
			58 FRANK	83B RVUE	LAMPF beam dump
			59 HOFFMAN	83 CNTR	$\pi p \rightarrow n A^0$ ($A^0 \rightarrow e^+ e^-$)
			60 FETSCHER	82 RVUE	See FAISSNER 81B
		12	61 FAISSNER	81 OSPK	CERN PS ν widband
		15	62 FAISSNER	81B OSPK	Beam dump, $A^0 \rightarrow 2\gamma$
		8	63 KIM	81 OSPK	26 GeV $pN \rightarrow A^0 X$
		0	64 FAISSNER	80 OSPK	Beam dump, $A^0 \rightarrow e^+ e^-$
$<1. \times 10^{-8}$	90		65 JACQUES	80 HLBC	28 GeV protons
$<1. \times 10^{-14}$	90		65 JACQUES	80 HLBC	Beam dump
			66 SOUKAS	80 CALO	28 GeV p beam dump
			67 BECHIS	79 CNTR	
$<1. \times 10^{-8}$	90		68 COTEUS	79 OSPK	Beam dump
$<1. \times 10^{-3}$	95		69 DISHAW	79 CALO	400 GeV pp
$<1. \times 10^{-8}$	90		ALIBRAN	78 HYBR	Beam dump
$<6. \times 10^{-9}$	95		ASRATYAN	78B CALO	Beam dump
$<1.5 \times 10^{-8}$	90		70 BELLOTTI	78 HLBC	Beam dump
$<5.4 \times 10^{-14}$	90		70 BELLOTTI	78 HLBC	$m_{A^0} = 1.5$ MeV
$<4.1 \times 10^{-9}$	90		70 BELLOTTI	78 HLBC	$m_{A^0} = 1$ MeV
$<1. \times 10^{-8}$	90		71 BOSETTI	78B HYBR	Beam dump
			72 DONNELLY	78	
$<0.5 \times 10^{-8}$	90		HANSL	78D WIRE	Beam dump
			73 MICELMAC...	78	
			74 VYSOTSKII	78	

⁴³AHMAD 97 reports a result of APEX Collaboration which studied positron production in $^{238}\text{U} + ^{232}\text{Th}$ and $^{238}\text{U} + ^{181}\text{Ta}$ collisions, without requiring a coincident electron. No narrow lines were found for $250 < E_{e^+} < 750$ keV.

⁴⁴LEINBERGER 97 (ORANGE Collaboration) at GSI looked for a narrow sum-energy $e^+ e^-$ line at ~ 635 keV in $^{238}\text{U} + ^{181}\text{Ta}$ collision. Limits on the production probability for a narrow sum-energy $e^+ e^-$ line are set. See their Table 2.

⁴⁵GANZ 96 (EPOS II Collaboration) has placed upper bounds on the production cross section of $e^+ e^-$ pairs from $^{238}\text{U} + ^{181}\text{Ta}$ and $^{238}\text{U} + ^{232}\text{Th}$ collisions at GSI. See Table 2 for limits both for back-to-back and isotropic configurations of $e^+ e^-$ pairs. These limits rule out the existence of peaks in the $e^+ e^-$ sum-energy distribution, reported by an earlier version of this experiment.

⁴⁶KAMEL 96 looked for $e^+ e^-$ pairs from the collision of ^{32}S (200 GeV/nucleon) and emulsion. No evidence of mass peaks is found in the region of sensitivity $m_{ee} > 2$ MeV.

⁴⁷BLUEMLEIN 92 is a proton beam dump experiment at Serpukhov with a secondary target to induce Bethe-Heitler production of $e^+ e^-$ or $\mu^+ \mu^-$ from the produce A^0 . See Fig. 5 for the excluded region in m_{A^0} - x plane. For the standard axion, $0.3 < x < 25$ is excluded at 95% CL. If combined with BLUEMLEIN 91, $0.008 < x < 32$ is excluded.

See key on page 239

Gauge & Higgs Boson Particle Listings
Axions (A^0) and Other Very Light Bosons

- 48 MEIJERDREES 92 give $\Gamma(\pi^- p \rightarrow n A^0) \cdot B(A^0 \rightarrow e^+ e^-) / \Gamma(\pi^- p \rightarrow \text{all}) < 10^{-5}$ (90% CL) for $m_{A^0} = 100$ MeV, $\tau_{A^0} = 10^{-11} - 10^{-23}$ sec. Limits ranging from 2.5×10^{-3} to 10^{-7} are given for $m_{A^0} = 25 - 136$ MeV.
- 49 BLUEMLEIN 91 is a proton beam dump experiment at Serpukhov. No candidate event for $A^0 \rightarrow e^+ e^-$, 2γ are found. Fig. 6 gives the excluded region in m_{A^0} - x plane ($x = \tan\beta = v_2/v_1$). Standard axion is excluded for $0.2 < m_{A^0} < 3.2$ MeV for most $x > 1$, 0.2-11 MeV for most $x < 1$.
- 50 FAISSNER 89 searched for $A^0 \rightarrow e^+ e^-$ in a proton beam dump experiment at SIN. No excess of events was observed over the background. A standard axion with mass $2m_e - 20$ MeV is excluded. Lower limit on f_{A^0} of $\approx 10^4$ GeV is given for $m_{A^0} = 2m_e - 20$ MeV.
- 51 DEBOER 88 reanalyze EL-NADI 88 data and claim evidence for three distinct states with mass $\sim 1.1, \sim 2.1$, and ~ 9 MeV, lifetimes $10^{-16} - 10^{-15}$ s decaying to $e^+ e^-$ and note the similarity of the data with those of a cosmic-ray experiment by Bristol Group (B.M. Anand, Proc. of the Royal Society of London, Section A **A22** 183 (1953)). For a criticism see PERKINS 89, who suggests that the events are compatible with π^0 Dalitz decay. DEBOER 89b is a reply which contests the criticism.
- 52 EL-NADI 88 claim the existence of a neutral particle decaying into $e^+ e^-$ with mass 1.60 ± 0.59 MeV, lifetime $(0.15 \pm 0.01) \times 10^{-14}$ s, which is produced in heavy ion interactions with emulsion nuclei at ~ 4 GeV/c/nucleon.
- 53 FAISSNER 88 is a proton beam dump experiment at SIN. They found no candidate event for $A^0 \rightarrow \gamma\gamma$. A standard axion decaying to 2γ is excluded except for a region $x \geq 1$. Lower limit on f_{A^0} of $10^2 - 10^3$ GeV is given for $m_{A^0} = 0.1 - 1$ MeV.
- 54 BADIER 86 did not find long-lived A^0 in 300 GeV π^- Beam Dump Experiment that decays into $e^+ e^-$ in the mass range $m_{A^0} = (20 - 200)$ MeV, which excludes the A^0 decay constant $f(A^0)$ in the interval (60-600) GeV. See their figure 6 for excluded region on $f(A^0)$ - m_{A^0} plane.
- 55 BERGSMAN 85 look for $A^0 \rightarrow 2\gamma, e^+ e^-, \mu^+ \mu^-$. First limit above is for $m_{A^0} = 1$ MeV; second is for 200 MeV. See their figure 4 for excluded region on f_{A^0} - m_{A^0} plane, where f_{A^0} is A^0 decay constant. For Peccel-Quinn PECCEL 77 $A^0, m_{A^0} < 180$ keV and $\tau > 0.037$ s. (CL = 90%). For the axion of FAISSNER 81b at 250 keV, BERGSMAN 85 expect 15 events but observe zero.
- 56 FAISSNER 83 observed 19 $1-\gamma$ and 12 $2-\gamma$ events where a background of 4.8 and 2.3 respectively is expected. A small-angle peak is observed even if iron wall is set in front of the decay region.
- 57 FAISSNER 83b extrapolate SIN γ signal to LAMPF ν experimental condition. Resulting 370 γ 's are not at variance with LAMPF upper limit of 450 γ 's. Derived from LAMPF limit that $[d\sigma(A^0)/d\omega \text{ at } 90^\circ] m_{A^0}/\tau_{A^0} < 14 \times 10^{-35} \text{ cm}^2 \text{ sr}^{-1} \text{ MeV ms}^{-1}$. See comment on FRANK 83b.
- 58 FRANK 83b stress the importance of LAMPF data bins with negative net signal. By statistical analysis say that LAMPF and SIN-A0 are at variance when extrapolation by phase-space model is done. They find LAMPF upper limit is 248 not 450 γ 's. See comment on FAISSNER 83b.
- 59 HOFFMAN 83 set CL = 90% limit $d\sigma/dt B(e^+ e^-) < 3.5 \times 10^{-32} \text{ cm}^2/\text{GeV}^2$ for 140 $< m_{A^0} < 160$ MeV. Limit assumes $\tau(A^0) < 10^{-9}$ s.
- 60 FETSCHER 82 reanalyzes SIN beam-dump data of FAISSNER 81. Claims no evidence for axion since $2-\gamma$ peak rate remarkably decreases if iron wall is set in front of the decay region.
- 61 FAISSNER 81 see excess μe events. Suggest axion interactions.
- 62 FAISSNER 81b is SIN 590 MeV proton beam dump. Observed 14.5 ± 5.0 events of 2γ decay of long-lived neutral penetrating particle with $m_{2\gamma} \lesssim 1$ MeV. Axion interpretation with η - A^0 mixing gives $m_{A^0} = 250 \pm 25$ keV, $\tau(2\gamma) = (7.3 \pm 3.7) \times 10^{-3}$ s from above rate. See critical remarks below in comments of FETSCHER 82, FAISSNER 83, FAISSNER 83b, FRANK 83b, and BERGSMAN 85. Also see in the next subsection ALEKSEEV 82, CAVIGNAC 83, and ANANEV 85.
- 63 KIM 81 analyzed 8 candidates for $A^0 \rightarrow 2\gamma$ obtained by Aachen-Padova experiment at CERN with 26 GeV protons on Be. Estimated axion mass is about 300 keV and lifetime is $(0.86 \sim 5.6) \times 10^{-3}$ s depending on models. Faissner (private communication), says axion production underestimated and mass overestimated. Correct value around 200 keV.
- 64 FAISSNER 80 is SIN beam dump experiment with 590 MeV protons looking for $A^0 \rightarrow e^+ e^-$ decay. Assuming $A^0/\pi^0 = 5.5 \times 10^{-7}$, obtained decay rate limit $20/(A^0 \text{ mass}) \text{ MeV/s}$ (CL = 90%), which is about 10^{-7} below theory and interpreted as upper limit to $m_{A^0} < 2m_e$.
- 65 JACQUES 80 is a BNL beam dump experiment. First limit above comes from nonobservation of excess neutral-current-type events $[\sigma(\text{production})\sigma(\text{interaction}) < 7. \times 10^{-68} \text{ cm}^4, \text{ CL} = 90\%]$. Second limit is from nonobservation of axion decays into 2γ 's or $e^+ e^-$, and for axion mass a few MeV.
- 66 SOUKAS 80 at BNL observed no excess of neutral-current-type events in beam dump.
- 67 BECHIS 79 looked for the axion production in low energy electron Bremsstrahlung and the subsequent decay into either 2γ or $e^+ e^-$. No signal found. CL = 90% limits for model parameter(s) are given.
- 68 COTEUS 79 is a beam dump experiment at BNL.
- 69 DISHAW 79 is a calorimetric experiment and looks for low energy tail of energy distributions due to energy lost to weakly interacting particles.
- 70 BELLOTTI 78 first value comes from search for $A^0 \rightarrow e^+ e^-$. Second value comes from search for $A^0 \rightarrow 2\gamma$, assuming mass $< 2m_e$. For any mass satisfying this, limit is above value $\times (\text{mass}^{-4})$. Third value uses data of PL 60B 401 and quotes $\sigma(\text{production})\sigma(\text{interaction}) < 10^{-67} \text{ cm}^4$.
- 71 BOSETTI 78b quotes $\sigma(\text{production})\sigma(\text{interaction}) < 2. \times 10^{-67} \text{ cm}^4$.
- 72 DONNELLY 78 examines data from reactor neutrino experiments of REINES 76 and GURR 74 as well as SLAC beam dump experiment. Evidence is negative.
- 73 MICELMACHER 78 finds no evidence of axion existence in reactor experiments of REINES 76 and GURR 74. (See reference under DONNELLY 78 below).
- 74 VYSOTSKI 78 derived lower limit for the axion mass 25 keV from luminosity of the sun and 200 keV from red supergiants.

 A^0 (Axion) Searches in Reactor Experiments

VALUE	DOCUMENT ID	TECN	COMMENT
• • • We do not use the following data for averages, fits, limits, etc. • • •			
	75 ALTMANN	95 CNTR	Reactor; $A^0 \rightarrow e^+ e^-$
	76 KETOV	86 SPEC	Reactor; $A^0 \rightarrow \gamma\gamma$
	77 KOCH	86 SPEC	Reactor; $A^0 \rightarrow \gamma\gamma$
	78 DATAR	82 CNTR	Light water reactor
	79 VUILLEUMIER	81 CNTR	Reactor; $A^0 \rightarrow 2\gamma$
75 ALTMANN 95 looked for A^0 decaying into $e^+ e^-$ from the Bugey 5 nuclear reactor. They obtain an upper limit on the A^0 production rate of $\omega(A^0)/\omega(\gamma) \times B(A^0 \rightarrow e^+ e^-) < 10^{-16}$ for $m_{A^0} = 1.5$ MeV at 90% CL. The limit is weaker for heavier A^0 . In the case of a standard axion, this limit excludes a mass in the range $2m_e < m_{A^0} < 4.8$ MeV at 90% CL. See Fig. 5 of their paper for exclusion limits of axion-like resonances Z^0 in the (m_{X^0}, f_{X^0}) plane.			
76 KETOV 86 searched for A^0 at the Rovno nuclear power plant. They found an upper limit on the A^0 production probability of $0.8 [100 \text{ keV}/m_{A^0}]^6 \times 10^{-6}$ per fission. In the standard axion model, this corresponds to $m_{A^0} > 150$ keV. Not valid for $m_{A^0} \gtrsim 1$ MeV.			
77 KOCH 86 searched for $A^0 \rightarrow \gamma\gamma$ at nuclear power reactor Biblis A. They found an upper limit on the A^0 production rate of $\omega(A^0)/\omega(\gamma(M1)) < 1.5 \times 10^{-10}$ (CL=95%). Standard axion with $m_{A^0} = 250$ keV gives 10^{-5} for the ratio. Not valid for $m_{A^0} > 1022$ keV.			
78 DATAR 82 looked for $A^0 \rightarrow 2\gamma$ in neutron capture ($n p \rightarrow d A^0$) at Tarapur 500 MW reactor. Sensitive to sum of $l = 0$ and $l = 1$ amplitudes. With ZEHNDER 81 ($l = 0$) - ($l = 1$) result, assert nonexistence of standard A^0 .			
79 VUILLEUMIER 81 is at Grenoble reactor. Set limit $m_{A^0} < 280$ keV.			

 A^0 (Axion) and Other Light Boson (X^0) Searches in Nuclear Transitions

Limits are for branching ratio.					
VALUE	CL%	EVTS	DOCUMENT ID	TECN	COMMENT
• • • We do not use the following data for averages, fits, limits, etc. • • •					
			80 DEBOER	97c RVUE	M1 transitions
			81 TSUNODA	95 CNTR	^{252}Cf fission, $A^0 \rightarrow e e$
			82 MINOWA	93 CNTR	$^{139}\text{La}^* \rightarrow ^{139}\text{La} A^0$
			83 HICKS	92 CNTR	^{35}S decay, $A^0 \rightarrow \gamma\gamma$
			84 ASANUMA	90 CNTR	^{241}Am decay
			85 DEBOER	90 CNTR	$^8\text{Be}^* \rightarrow ^8\text{Be} A^0$, $A^0 \rightarrow e^+ e^-$, $^{16}\text{O}^* \rightarrow ^{16}\text{O} X^0$, $X^0 \rightarrow e^+ e^-$
			86 BINI	89 CNTR	$^{16}\text{O}^* \rightarrow ^{16}\text{O} X^0$, $X^0 \rightarrow e^+ e^-$
			87 AVIGNONE	88 CNTR	$\text{Cu}^* \rightarrow \text{Cu} A^0$ ($A^0 \rightarrow 2\gamma, A^0 e \rightarrow \gamma e$, $A^0 Z \rightarrow \gamma Z$)
			88 DATAR	88 CNTR	$^{12}\text{C}^* \rightarrow ^{12}\text{C} A^0$, $A^0 \rightarrow e^+ e^-$
			89 DEBOER	88c CNTR	$^{16}\text{O}^* \rightarrow ^{16}\text{O} X^0$, $X^0 \rightarrow e^+ e^-$
			90 DOEHNER	88 SPEC	$^2\text{H}^*, A^0 \rightarrow e^+ e^-$
			91 SAVAGE	88 CNTR	Nuclear decay (isovector)
			91 SAVAGE	88 CNTR	Nuclear decay (isoscalar)
			92 HALLIN	86 SPEC	^6Li isovector decay
			92 HALLIN	86 SPEC	^{10}B isoscalar decays
			92 HALLIN	86 SPEC	^{14}N isoscalar decays
			93 SAVAGE	86b CNTR	$^{14}\text{N}^*$
			94 ANANEV	85 CNTR	$\text{Li}^*, \text{deut}^* A^0 \rightarrow 2\gamma$
			95 CAVIGNAC	83 CNTR	$^{97}\text{Nb}^*, \text{deut}^* \text{ transition } A^0 \rightarrow 2\gamma$
			96 ALEKSEEV	82b CNTR	$\text{Li}^*, \text{deut}^* \text{ transition } A^0 \rightarrow 2\gamma$
			97 LEHMANN	82 CNTR	$\text{Cu}^* \rightarrow \text{Cu} A^0$ ($A^0 \rightarrow 2\gamma$)
			98 ZEHNDER	82 CNTR	$\text{Li}^*, \text{Nb}^* \text{ decay, } n\text{-capt.}$
			99 ZEHNDER	81 CNTR	$\text{Ba}^* \rightarrow \text{Ba} A^0$ ($A^0 \rightarrow 2\gamma$)
			100 CALAPRICE	79	Carbon
80 DEBOER 97c reanalyzed the existent data on Nuclear M1 transitions and find that a 9 MeV boson decaying into $e^+ e^-$ would explain the excess of events with large opening angles.					
81 TSUNODA 95 looked for axion emission when ^{252}Cf undergoes a spontaneous fission, with the axion decaying into $e^+ e^-$. The bound is for $m_{A^0} = 40$ MeV. It improves to 2.5×10^{-5} for $m_{A^0} = 200$ MeV.					
82 MINOWA 93 studied chain process, $^{139}\text{Ce} \rightarrow ^{139}\text{La}^*$ by electron capture and M1 transition of $^{139}\text{La}^*$ to the ground state. It does not assume decay modes of A^0 . The bound applies for $m_{A^0} < 166$ keV.					
83 HICKS 92 bound is applicable for $\tau_{X^0} < 4 \times 10^{-11}$ sec.					
84 THE ASANUMA 90 limit is for the branching fraction of X^0 emission per ^{241}Am decay and valid for $\tau_{X^0} < 3 \times 10^{-11}$ s.					
85 THE DEBOER 90 limit is for the branching ratio $^8\text{Be}^* (18.15 \text{ MeV}, 1^+) \rightarrow ^8\text{Be} A^0, A^0 \rightarrow e^+ e^-$ for the mass range $m_{A^0} = 4 - 15$ MeV.					
86 THE BINI 89 limit is for the branching fraction of $^{16}\text{O}^* (6.05 \text{ MeV}, 0^+) \rightarrow ^{16}\text{O} X^0, X^0 \rightarrow e^+ e^-$ for $m_X = 1.5 - 3.1$ MeV. $\tau_{X^0} \lesssim 10^{-11}$ s is assumed. The spin-parity of X is restricted to 0^+ or 1^- .					

Gauge & Higgs Boson Particle Listings

Axions (A^0) and Other Very Light Bosons

- 87 AVIGNONE 88 looked for the 1115 keV transition $C^* \rightarrow Cu A^0$, either from $A^0 \rightarrow 2\gamma$ in-flight decay or from the secondary A^0 interactions by Compton and by Primakoff processes. Limits for axion parameters are obtained for $m_{A^0} < 1.1$ MeV.
- 88 DATAR 88 rule out light pseudoscalar particle emission through its decay $A^0 \rightarrow e^+e^-$ in the mass range 1.02–2.5 MeV and lifetime range 10^{-13} – 10^{-8} s. The above limit is for $\tau = 5 \times 10^{-13}$ s and $m = 1.7$ MeV; see the paper for the τ - m dependence of the limit.
- 89 The limit is for the branching fraction of $^{16}O^*(6.05 \text{ MeV}, 0^+) \rightarrow ^{16}O X^0, X^0 \rightarrow e^+e^-$ against internal pair conversion for $m_{X^0} = 1.7$ MeV and $\tau_{X^0} < 10^{-11}$ s. Similar limits are obtained for $m_{X^0} = 1.3$ – 3.2 MeV. The spin parity of X^0 must be either 0^+ or 1^- . The limit at 1.7 MeV is translated into a limit for the X^0 -nucleon coupling constant: $g_{X^0 NN}^2/4\pi < 2.3 \times 10^{-9}$.
- 90 The DOEHNER 88 limit is for $m_{A^0} = 1.7$ MeV, $\tau(A^0) < 10^{-10}$ s. Limits less than 10^{-4} are obtained for $m_{A^0} = 1.2$ – 2.2 MeV.
- 91 SAVAGE 88 looked for A^0 that decays into e^+e^- in the decay of the 9.17 MeV $J^P = 2^+$ state in ^{14}N , 17.64 MeV state $J^P = 1^+$ in 8Be , and the 18.15 MeV state $J^P = 1^+$ in 9Be . This experiment constrains the isovector coupling of A^0 to hadrons, if $m_{A^0} = (1.1 \rightarrow 2.2)$ MeV and the isoscalar coupling of A^0 to hadrons, if $m_{A^0} = (1.1 \rightarrow 2.6)$ MeV. Both limits are valid only if $\tau(A^0) \lesssim 1 \times 10^{-11}$ s.
- 92 Limits are for $\Gamma(A^0(1.8 \text{ MeV})/\Gamma(\pi^0 M1))$; i.e., for 1.8 MeV axion emission normalized to the rate for internal emission of e^+e^- pairs. Valid for $\tau_{A^0} < 2 \times 10^{-11}$ s. 6Li isovector decay data strongly disfavor PECCEI 86 model I, whereas the ^{10}B and ^{14}N isoscalar decay data strongly reject PECCEI 86 model II and III.
- 93 SAVAGE 86B looked for A^0 that decays into e^+e^- in the decay of the 9.17 MeV $J^P = 2^+$ state in ^{14}N . Limit on the branching fraction is valid if $\tau_{A^0} \lesssim 1 \times 10^{-11}$ s for $m_{A^0} = (1.1$ – $1.7)$ MeV. This experiment constrains the iso-vector coupling of A^0 to hadrons.
- 94 ANANEV 85 with IBR-2 pulsed reactor exclude standard A^0 at CL = 95% masses below 470 keV (Li^* decay) and below $2m_e$ for deuteron* decay.
- 95 CAVAIGNAC 83 at Bugey reactor exclude axion at any $m_{97}Nb^*$ decay and axion with m_{A^0} between 275 and 288 keV (deuteron* decay).
- 96 ALEKSEEV 82 with IBR-2 pulsed reactor exclude standard A^0 at CL = 95% mass-ranges $m_{A^0} < 400$ keV (Li^* decay) and 330 keV $< m_{A^0} < 2.2$ MeV. (deuteron* decay).
- 97 LEHMANN 82 obtained $A^0 \rightarrow 2\gamma$ rate $< 6.2 \times 10^{-5}/s$ (CL = 95%) excluding m_{A^0} between 100 and 1000 keV.
- 98 ZEHNDER 82 used Goesgen 2.8GW light-water reactor to check A^0 production. No 2γ peak in Li^* , Nb^* decay (both single p transition) nor in n capture (combined with previous Ba^* negative result) rules out standard A^0 . Set limit $m_{A^0} < 60$ keV for any A^0 .
- 99 ZEHNDER 81 looked for $Ba^* \rightarrow A^0 Ba$ transition with $A^0 \rightarrow 2\gamma$. Obtained 2γ coincidence rate $< 2.2 \times 10^{-5}/s$ (CL = 95%) excluding $m_{A^0} > 160$ keV (or 200 keV depending on Higgs mixing). However, see BARROSO 81.
- 100 CALAPRICE 79 saw no axion emission from excited states of carbon. Sensitive to axion mass between 1 and 15 MeV.

A^0 (Axion) Limits from Its Electron Coupling

Limits are for $\tau(A^0 \rightarrow e^+e^-)$.

VALUE (s)	CL%	DOCUMENT ID	TECN	COMMENT
none 4×10^{-16} – 4.5×10^{-12}	90	101 BROSS	91 BDMP	$eN \rightarrow eA^0 N$ ($A^0 \rightarrow ee$)
		102 GUO	90 BDMP	$eN \rightarrow eA^0 N$ ($A^0 \rightarrow ee$)
		103 BJORKEN	88 CALO	$A \rightarrow e^+e^-$ or 2γ
		104 BLINOV	88 MDI	$ee \rightarrow eeA^0$ ($A^0 \rightarrow ee$)
none 1×10^{-14} – 1×10^{-10}	90	105 RIORDAN	87 BDMP	$eN \rightarrow eA^0 N$ ($A^0 \rightarrow ee$)
none 1×10^{-14} – 1×10^{-11}	90	106 BROWN	86 BDMP	$eN \rightarrow eA^0 N$ ($A^0 \rightarrow ee$)
none 6×10^{-14} – 9×10^{-11}	95	107 DAVIER	86 BDMP	$eN \rightarrow eA^0 N$ ($A^0 \rightarrow ee$)
none 3×10^{-13} – 1×10^{-7}	90	108 KONAKA	86 BDMP	$eN \rightarrow eA^0 N$ ($A^0 \rightarrow ee$)

- 101 The listed BROSS 91 limit is for $m_{A^0} = 1.14$ MeV. $B(A^0 \rightarrow e^+e^-) = 1$ assumed. Excluded domain in the τ_{A^0} - m_{A^0} plane extends up to $m_{A^0} \approx 7$ MeV (see Fig. 5). Combining with electron $g-2$ constraint, axions coupling only to e^+e^- ruled out for $m_{A^0} < 4.8$ MeV (90%CL).
- 102 GUO 90 use the same apparatus as BROWN 86 and improve the previous limit in the shorter lifetime region. Combined with $g-2$ constraint, axions coupling only to e^+e^- are ruled out for $m_{A^0} < 2.7$ MeV (90% CL).
- 103 BJORKEN 88 reports limits on axion parameters (f_A, m_A, τ_A) for $m_{A^0} < 200$ MeV from electron beam-dump experiment with production via Primakoff photoproduction, bremsstrahlung from electrons, and resonant annihilation of positrons on atomic electrons.
- 104 BLINOV 88 assume zero spin, $m = 1.8$ MeV and lifetime $< 5 \times 10^{-12}$ s and find $\Gamma(A^0 \rightarrow \gamma\gamma)B(A^0 \rightarrow e^+e^-) < 2$ eV (CL=90%).
- 105 Assumes $A^0\gamma\gamma$ coupling is small and hence Primakoff production is small. Their figure 2 shows limits on axions for $m_{A^0} < 15$ MeV.
- 106 Uses electrons in hadronic showers from an incident 800 GeV proton beam. Limits for $m_{A^0} < 15$ MeV are shown in their figure 3.

107 $m_{A^0} = 1.8$ MeV assumed. The excluded domain in the τ_{A^0} - m_{A^0} plane extends up to $m_{A^0} \approx 14$ MeV, see their figure 4.

108 The limits are obtained from their figure 3. Also given is the limit on the $A^0\gamma\gamma \rightarrow A^0 e^+e^-$ coupling plane by assuming Primakoff production.

Search for A^0 (Axion) Resonance in Bhabha Scattering

The limit is for $\Gamma(A^0)[B(A^0 \rightarrow e^+e^-)]^2$.

VALUE (10^{-3} eV)	CL%	DOCUMENT ID	TECN	COMMENT
• • • We do not use the following data for averages, fits, limits, etc. • • •				
< 1.3	97	109 HALLIN	92 CNTR	$m_{A^0} = 1.75$ – 1.88 MeV
none 0.0016–0.47	90	110 HENDERSON	92c CNTR	$m_{A^0} = 1.5$ – 1.86 MeV
< 2.0	90	111 WU	92 CNTR	$m_{A^0} = 1.56$ – 1.86 MeV
< 0.013	95	TSERTOS	91 CNTR	$m_{A^0} = 1.832$ MeV
none 0.19–3.3	95	112 WIDMANN	91 CNTR	$m_{A^0} = 1.78$ – 1.92 MeV
< 5	97	BAUER	90 CNTR	$m_{A^0} = 1.832$ MeV
none 0.09–1.5	95	113 JUDGE	90 CNTR	$m_{A^0} = 1.832$ MeV, elastic
< 1.9	97	114 TSERTOS	89 CNTR	$m_{A^0} = 1.82$ MeV
$< (10$ – $40)$	97	114 TSERTOS	89 CNTR	$m_{A^0} = 1.51$ – 1.65 MeV
$< (1$ – $2.5)$	97	114 TSERTOS	89 CNTR	$m_{A^0} = 1.80$ – 1.86 MeV
< 31	95	LORENZ	88 CNTR	$m_{A^0} = 1.646$ MeV
< 94	95	LORENZ	88 CNTR	$m_{A^0} = 1.726$ MeV
< 23	95	LORENZ	88 CNTR	$m_{A^0} = 1.782$ MeV
< 19	95	LORENZ	88 CNTR	$m_{A^0} = 1.837$ MeV
< 3.8	97	115 TSERTOS	88 CNTR	$m_{A^0} = 1.832$ MeV
		116 VANKLINKEN	88 CNTR	
		117 MAIER	87 CNTR	
< 2500	90	MILLS	87 CNTR	$m_{A^0} = 1.8$ MeV
		118 VONWIMMER	87 CNTR	

109 HALLIN 92 quote limits on lifetime, 8×10^{-14} – 5×10^{-13} sec depending on mass, assuming $B(A^0 \rightarrow e^+e^-) = 100\%$. They say that TSERTOS 91 overstated their sensitivity by a factor of 3.

110 HENDERSON 92c exclude axion with lifetime $\tau_{A^0} = 1.4 \times 10^{-12}$ – 4.0×10^{-10} s, assuming $B(A^0 \rightarrow e^+e^-) = 100\%$. HENDERSON 92c also exclude a vector boson with $\tau = 1.4 \times 10^{-12}$ – 6.0×10^{-10} s.

111 WU 92 quote limits on lifetime $> 3.3 \times 10^{-13}$ s assuming $B(A^0 \rightarrow e^+e^-) = 100\%$. They say that TSERTOS 89 overestimate the limit by a factor of $\pi/2$. WU 92 also quote a bound for vector boson, $\tau > 8.2 \times 10^{-13}$ s.

112 WIDMANN 91 bound applies exclusively to the case $B(A^0 \rightarrow e^+e^-) = 1$, since the detection efficiency varies substantially as $\Gamma(A^0)_{\text{total}}$ changes. See their Fig. 6.

113 JUDGE 90 excludes an elastic pseudoscalar e^+e^- resonance for 4.5×10^{-13} s $< \tau(A^0) < 7.5 \times 10^{-12}$ s (95% CL) at $m_{A^0} = 1.832$ MeV. Comparable limits can be set for $m_{A^0} = 1.776$ – 1.856 MeV.

114 See also TSERTOS 88b in references.

115 The upper limit listed in TSERTOS 88 is too large by a factor of 4. See TSERTOS 88b, footnote 3.

116 VANKLINKEN 88 looked for relatively long-lived resonance ($\tau = 10^{-10}$ – 10^{-12} s). The sensitivity is not sufficient to exclude such a narrow resonance.

117 MAIER 87 obtained limits $R\Gamma \lesssim 60$ eV (100 eV) at $m_{A^0} \approx 1.64$ MeV (1.83 MeV) for energy resolution $\Delta E_{cm} \approx 3$ keV, where R is the resonance cross section normalized to that of Bhabha scattering, and $\Gamma = \Gamma_{e^+e^-}^2/\Gamma_{\text{total}}$. For a discussion implying that $\Delta E_{cm} \approx 10$ keV, see TSERTOS 89.

118 VONWIMMERSPERG 87 measured Bhabha scattering for $E_{cm} = 1.37$ – 1.86 MeV and found a possible peak at 1.73 with $f\sigma_{e^+e^-} = 14.5 \pm 6.8$ keV-b. For a comment and a reply, see VANKLINKEN 88b and VONWIMMERSPERG 88. Also see CONNELL 88.

Search for A^0 (Axion) Resonance in $e^+e^- \rightarrow \gamma\gamma$

The limit is for $\Gamma(A^0 \rightarrow e^+e^-)\Gamma(A^0 \rightarrow \gamma\gamma)/\Gamma_{\text{total}}$

VALUE (10^{-3} eV)	CL%	DOCUMENT ID	TECN	COMMENT
• • • We do not use the following data for averages, fits, limits, etc. • • •				
< 0.18	95	VO	94 CNTR	$m_{A^0} = 1.1$ MeV
< 1.5	95	VO	94 CNTR	$m_{A^0} = 1.4$ MeV
< 12	95	VO	94 CNTR	$m_{A^0} = 1.7$ MeV
< 6.6	95	119 TRZASKA	91 CNTR	$m_{A^0} = 1.8$ MeV
< 4.4	95	WIDMANN	91 CNTR	$m_{A^0} = 1.78$ – 1.92 MeV
		120 FOX	89 CNTR	
< 0.11	95	121 MINOWA	89 CNTR	$m_{A^0} = 1.062$ MeV
< 33	97	CONNELL	88 CNTR	$m_{A^0} = 1.580$ MeV
< 42	97	CONNELL	88 CNTR	$m_{A^0} = 1.642$ MeV
< 73	97	CONNELL	88 CNTR	$m_{A^0} = 1.782$ MeV
< 79	97	CONNELL	88 CNTR	$m_{A^0} = 1.832$ MeV

119 TRZASKA 91 also give limits in the range $(6.6$ – $30) \times 10^{-3}$ eV (95%CL) for $m_{A^0} = 1.6$ – 2.0 MeV.

120 FOX 89 measured positron annihilation with an electron in the source material into two photons and found no signal at 1.062 MeV ($< 9 \times 10^{-5}$ of two-photon annihilation at rest).

121 Similar limits are obtained for $m_{A^0} = 1.045$ – 1.085 MeV.

See key on page 239

Gauge & Higgs Boson Particle Listings

Axions (A^0) and Other Very Light Bosons

Search for X^0 (Light Boson) Resonance in $e^+e^- \rightarrow \gamma\gamma\gamma$

The limit is for $\Gamma(X^0 \rightarrow e^+e^-) \cdot \Gamma(X^0 \rightarrow \gamma\gamma\gamma) / \Gamma_{\text{total}}$. C invariance forbids spin-0 X^0 coupling to both e^+e^- and $\gamma\gamma\gamma$.

VALUE (10^{-3} eV)	CL%	DOCUMENT ID	TECN	COMMENT
• • • We do not use the following data for averages, fits, limits, etc. • • •				
< 0.2	95	122 VO	94 CNTR	$m_{X^0} = 1.1-1.9$ MeV
< 1.0	95	123 VO	94 CNTR	$m_{X^0} = 1.1$ MeV
< 2.5	95	123 VO	94 CNTR	$m_{X^0} = 1.4$ MeV
< 120	95	123 VO	94 CNTR	$m_{X^0} = 1.7$ MeV
< 3.8	95	124 SKALSEY	92 CNTR	$m_{X^0} = 1.5$ MeV
122 VO 94 looked for $X^0 \rightarrow \gamma\gamma\gamma$ decaying at rest. The precise limits depend on m_{X^0} . See Fig. 2(b) in paper.				
123 VO 94 looked for $X^0 \rightarrow \gamma\gamma\gamma$ decaying in flight.				
124 SKALSEY 92 also give limits 4.3 for $m_{X^0} = 1.54$ and 7.5 for 1.64 MeV. The spin of X^0 is assumed to be one.				

Light Boson (X^0) Search in Nonresonant e^+e^- Annihilation at Rest

Limits are for the ratio of $n\gamma + X^0$ production relative to $\gamma\gamma$.

VALUE (units 10^{-6})	CL%	DOCUMENT ID	TECN	COMMENT
• • • We do not use the following data for averages, fits, limits, etc. • • •				
< 4.2	90	125 MITSUI	96 CNTR	γX^0
< 4	68	126 SKALSEY	95 CNTR	γX^0
< 40	68	127 SKALSEY	95 RVUE	γX^0
< 0.18	90	128 ADACHI	94 CNTR	$\gamma\gamma X^0, X^0 \rightarrow \gamma\gamma$
< 0.26	90	129 ADACHI	94 CNTR	$\gamma\gamma X^0, X^0 \rightarrow \gamma\gamma$
< 0.33	90	130 ADACHI	94 CNTR	$\gamma X^0, X^0 \rightarrow \gamma\gamma\gamma$
125 MITSUI 96 looked for a monochromatic γ . The bound applies for a vector X^0 with $C = -1$ and $m_{X^0} < 200$ keV. They derive an upper bound on eX^0 coupling and hence on the branching ratio $B(\sigma\text{-Ps} \rightarrow \gamma\gamma X^0) < 6.2 \times 10^{-6}$. The bounds weaken for heavier X^0 .				
126 SKALSEY 95 looked for a monochromatic γ without an accompanying γ in e^+e^- annihilation. The bound applies for scalar and vector X^0 with $C = -1$ and $m_{X^0} = 100-1000$ keV.				
127 SKALSEY 95 reinterpreted the bound on γA^0 decay of $\sigma\text{-Ps}$ by ASAI 91 where 3% of delayed annihilations are not from 3S_1 states. The bound applies for scalar and vector X^0 with $C = -1$ and $m_{X^0} = 0-800$ keV.				
128 ADACHI 94 looked for a peak in the $\gamma\gamma$ invariant mass distribution in $\gamma\gamma\gamma\gamma$ production from e^+e^- annihilation. The bound applies for $m_{X^0} = 70-800$ keV.				
129 ADACHI 94 looked for a peak in the missing-mass mass distribution in $\gamma\gamma$ channel, using $\gamma\gamma\gamma\gamma$ production from e^+e^- annihilation. The bound applies for $m_{X^0} < 800$ keV.				
130 ADACHI 94 looked for a peak in the missing mass distribution in $\gamma\gamma\gamma$ channel, using $\gamma\gamma\gamma\gamma$ production from e^+e^- annihilation. The bound applies for $m_{X^0} = 200-900$ keV.				

Searches for Goldstone Bosons (X^0)

(Including Horizontal Bosons and Majorons.) Limits are for branching ratios.

VALUE	CL%	EVTs	DOCUMENT ID	TECN	COMMENT
• • • We do not use the following data for averages, fits, limits, etc. • • •					
			131 DIAZ	98 THEO	$H^0 \rightarrow X^0 X^0, A^0 \rightarrow X^0 X^0 X^0$, Majoron interaction
			132 BOBRAKOV	91	Electron quasi-magnetic interaction
$< 3.3 \times 10^{-2}$	95		133 ALBRECHT	90E ARG	$\tau \rightarrow \mu X^0$, Familon
$< 1.8 \times 10^{-2}$	95		133 ALBRECHT	90E ARG	$\tau \rightarrow e X^0$, Familon
$< 6.4 \times 10^{-9}$	90		134 ATIYA	90 B787	$K^+ \rightarrow \pi^+ X^0$, Familon
$< 1.1 \times 10^{-9}$	90		135 BOLTON	88 CBOX	$\mu^+ \rightarrow e^+ \gamma X^0$, Familon
			136 CHANDA	88 ASTR	Sun, Majoron
			137 CHOI	88 ASTR	Majoron, SN 1987A
$< 5 \times 10^{-6}$	90		138 PICCIOTTO	88 CNTR	$\pi \rightarrow e\nu X^0$, Majoron
$< 1.3 \times 10^{-9}$	90		139 GOLDMAN	87 CNTR	$\mu \rightarrow e\gamma X^0$, Familon
$< 3 \times 10^{-4}$	90		140 BRYMAN	86B RVUE	$\mu \rightarrow e X^0$, Familon
$< 1 \times 10^{-10}$	90	0	141 EICHLER	86 SPEC	$\mu^+ \rightarrow e^+ X^0$, Familon
$< 2.6 \times 10^{-6}$	90		142 JODIDIO	86 SPEC	$\mu^+ \rightarrow e^+ X^0$, Familon
			143 BALTRUSAITIS	85 MRK3	$\tau \rightarrow \ell X^0$, Familon
			144 DICUS	83 COSM	$\nu(\text{hvy}) \rightarrow \nu(\text{light}) X^0$

131 DIAZ 98 studied models of spontaneously broken lepton number with both singlet and triplet Higgses. They obtain limits on the parameter space from invisible decay $Z \rightarrow H^0 A^0 \rightarrow X^0 X^0 X^0 X^0$ and $e^+e^- \rightarrow Z H^0$ with $H^0 \rightarrow X^0 X^0$.

132 BOBRAKOV 91 searched for anomalous magnetic interactions between polarized electrons expected from the exchange of a massless pseudoscalar boson (arion). A limit $\chi_e^2 < 2 \times 10^{-4}$ (95%CL) is found for the effective anomalous magneton parametrized as $\chi_e(G_F/8\pi\sqrt{2})^{1/2}$.

133 ALBRECHT 90E limits are for $B(\tau \rightarrow \ell X^0)/B(\tau \rightarrow \ell\nu\bar{\nu})$. Valid for $m_{X^0} < 100$ MeV. The limits rise to 7.1% (for μ), 5.0% (for e) for $m_{X^0} = 500$ MeV.

134 ATIYA 90 limit is for $m_{X^0} = 0$. The limit $B < 1 \times 10^{-8}$ holds for $m_{X^0} < 95$ MeV. For the reduction of the limit due to finite lifetime of X^0 , see their Fig. 3.

135 BOLTON 88 limit corresponds to $F > 3.1 \times 10^9$ GeV, which does not depend on the chirality property of the coupling.

136 CHANDA 88 find $v_T < 10$ MeV for the weak-triplet Higgs vev. in Gelmini-Roncadelli model, and $v_S > 5.8 \times 10^6$ GeV in the singlet Majoron model.

137 CHOI 88 used the observed neutrino flux from the supernova SN 1987A to exclude the neutrino Majoron Yukawa coupling h in the range $2 \times 10^{-5} < h < 3 \times 10^{-4}$ for the interaction $L_{\text{int}} = \frac{1}{2} h \bar{\psi}_\nu^c \gamma_5 \psi_\nu \phi_X$. For several families of neutrinos, the limit applies for $(\Sigma h_i^2)^{1/4}$.

138 PICCIOTTO 88 limit applies when $m_{X^0} < 55$ MeV and $\tau_{X^0} > 2$ ns, and it decreases to 4×10^{-7} at $m_{X^0} = 125$ MeV, beyond which no limit is obtained.

139 GOLDMAN 87 limit corresponds to $F > 2.9 \times 10^9$ GeV for the family symmetry breaking scale from the Lagrangian $L_{\text{int}} = (1/F) \bar{\psi}_\mu \gamma^\mu (a + b\gamma_5) \psi_e \theta_\mu \phi_{X^0}$ with $a^2 + b^2 = 1$. This is not as sensitive as the limit $F > 9.9 \times 10^9$ GeV derived from the search for $\mu^+ \rightarrow e^+ X^0$ by JODIDIO 86, but does not depend on the chirality property of the coupling.

140 Limits are for $\Gamma(\mu \rightarrow e X^0) / \Gamma(\mu \rightarrow e\nu\bar{\nu})$. Valid when $m_{X^0} = 0-93.4, 98.1-103.5$ MeV.

141 EICHLER 86 looked for $\mu^+ \rightarrow e^+ X^0$ followed by $X^0 \rightarrow e^+e^-$. Limits on the branching fraction depend on the mass and lifetime of X^0 . The quoted limits are valid when $\tau_{X^0} \lesssim 3 \times 10^{-10}$ s if the decays are kinematically allowed.

142 JODIDIO 86 corresponds to $F > 9.9 \times 10^9$ GeV for the family symmetry breaking scale with the parity-conserving effective Lagrangian $L_{\text{int}} = (1/F) \bar{\psi}_\mu \gamma^\mu \psi_e \theta_\mu \phi_{X^0}$.

143 BALTRUSAITIS 85 search for light Goldstone boson (X^0) of broken $U(1)$. CL = 95% limits are $B(\tau \rightarrow \mu^+ X^0) / B(\tau \rightarrow \mu^+ \nu\bar{\nu}) < 0.125$ and $B(\tau \rightarrow e^+ X^0) / B(\tau \rightarrow e^+ \nu\bar{\nu}) < 0.04$. Inferred limit for the symmetry breaking scale is $m > 3000$ TeV.

144 The primordial heavy neutrino must decay into ν and familon, f_A , early so that the red-shifted decay products are below critical density, see their table. In addition, $K \rightarrow \pi f_A$ and $\mu \rightarrow e f_A$ are unseen. Combining these excludes $m_{\text{heavy}\nu}$ between 5×10^{-5} and 5×10^{-4} MeV (μ decay) and $m_{\text{heavy}\nu}$ between 5×10^{-5} and 0.1 MeV (K -decay).

Majoron Searches in Neutrinoless Double β Decay

Limits are for the half-life of neutrinoless $\beta\beta$ decay with a Majoron emission.

Previous indications for neutrinoless double beta decay with majoron emission have been superseded. No experiment currently claims any such evidence. Also see the recent reviews ZUBER 98 and FAESSLER 98B.

$t_{1/2}(10^{21}$ yr)	CL%	ISOTOPE	TRANSITION	METHOD	DOCUMENT ID
>7200		90 ¹²⁸Te		CNTR	145 BERNATOW... 92
• • • We do not use the following data for averages, fits, limits, etc. • • •					
> 0.35	90	⁹⁶ Zr	$0\nu\chi$	NEMO-2	146 ARNOLD 99
> 1.2	90	¹¹⁶ Cd	$0\nu\chi$	SCIN	147 DANEVICH 98
> 0.26	90	¹¹⁶ Cd	$0\nu 2\chi$	SCIN	148 DANEVICH 98
> 7.2	90	¹³⁶ Xe	$0\nu 2\chi$	TPC	149 LUESCHER 98
> 7.91	90	⁷⁶ Ge		SPEC	150 GUENTHER 96
> 17	90	⁷⁶ Ge		CNTR	BECK 93
> 0.79	68	¹⁰⁰ Mo		SPEC	151 TANAKA 93
> 0.19	68	¹³⁶ Xe		CNTR	BARABASH 89
> 1.0	90	⁷⁶ Ge		CNTR	FISHER 89
> 0.33	90	¹⁰⁰ Mo		CNTR	ALSTON... 88
> 0.6 \pm 0.1	90	⁷⁶ Ge		CNTR	AVIGNONE 87
> 1.4	90	⁷⁶ Ge		CNTR	CALDWELL 87
> 0.44	90	⁸² Se		SPEC	ELLIOTT 87
> 1.2	90	⁷⁶ Ge		CNTR	FISHER 87
				CNTR	152 VERGADOS 82

145 BERNATOWICZ 92 studied double- β decays of ¹²⁸Te and ¹³⁰Te, and found the ratio $\tau(^{130}\text{Te})/\tau(^{128}\text{Te}) = (3.52 \pm 0.11) \times 10^{-4}$ in agreement with relatively stable theoretical predictions. The bound is based on the requirement that Majoron-emitting decay cannot be larger than the observed double-beta rate of ¹²⁸Te of $(7.7 \pm 0.4) \times 10^{24}$ year. We calculated 90% CL limit as $(7.7-1.28 \times 0.4=7.2) \times 10^{24}$.

146 ARNOLD 99 use enriched ⁹⁶Zr and give a limit based on the matrix elements of STAUDT 90.

147 DANEVICH 98 use cadmium tungstate crystals, enriched to 83% in ¹¹⁶Cd. The spectrum was analysed in the region of expected majoron emission. Using a variety of nuclear matrix elements, they obtain a limit $\langle g_{\nu\chi} \rangle < (1-3) \times 10^{-4}$.

148 DANEVICH 98 obtain a limit on the 0ν decay with emission of 2 majorons.

149 LUESCHER 98 report a limit for the 0ν decay with Majoron emission of ¹³⁶Xe using Xe TPC. This result is more stringent than BARABASH 89. Using the matrix elements of ENGEL 88, they obtain a limit on $\langle g_{\nu\chi} \rangle$ of 2.0×10^{-4} .

150 See Table 1 in GUENTHER 96 for limits on the Majoron coupling in different models.

151 TANAKA 93 also quote limit 5.3×10^{19} years on two Majoron emission.

152 VERGADOS 82 sets limit $g_H < 4 \times 10^{-3}$ for (dimensionless) lepton-number violating coupling, g_H of scalar boson (Majoron) to neutrinos, from analysis of data on double β decay of ⁴⁸Ca.

Invisible A^0 (Axion) MASS LIMITS from Astrophysics and Cosmology

$\nu_1 = \nu_2$ is usually assumed (ν_i = vacuum expectation values). For a review of these limits, see RAFFELT 90C and TURNER 90. In the comment lines below, D and K refer to DFSZ and KSVZ axion types, discussed in the above minireview.

VALUE (eV)	DOCUMENT ID	TECN	COMMENT
• • • We do not use the following data for averages, fits, limits, etc. • • •			
3 to 20	153 MOROI	98 COSM	K, hot dark matter
< 0.007	154 BORISOV	97 ASTR	D, neutron star
< 4	155 KACHELRIESS	97 ASTR	D, neutron star cooling
$< (0.5-6) \times 10^{-3}$	156 KEIL	97 ASTR	SN 1987A

Gauge & Higgs Boson Particle Listings

Axions (A^0) and Other Very Light Bosons

< 0.018	157 RAFFELT	95 ASTR	D, red giant
< 0.010	158 ALTHERR	94 ASTR	D, red giants, white dwarfs
< 0.01	159 CHANG	93 ASTR	K, SN 1987A
< 0.03	WANG	92 ASTR	D, white dwarf
none 3-8	WANG	92C ASTR	D, C-O burning
< 10	160 BERSHADY	91 ASTR	D, K, intergalactic light
< 1	161 KIM	91C COSM	D, K, mass density of the universe, super-symmetry
< 1	162 RAFFELT	91B ASTR	D, K, SN 1987A
none 10^{-3-3}	163 RESSELL	91 ASTR	K, intergalactic light
< 0.02	BURROWS	90 ASTR	D, K, SN 1987A
< 1	164 ENGEL	90 ASTR	D, K, SN 1987A
< $(1.4-10) \times 10^{-3}$	165 RAFFELT	90D ASTR	D, red giant
< 3.6×10^{-4}	166 BURROWS	89 ASTR	D, K, SN 1987A
< 12	167 ERICSON	89 ASTR	D, K, SN 1987A
< 1	168 MAYLE	89 ASTR	D, K, SN 1987A
< 1×10^{-3}	CHANDA	88 ASTR	D, Sun
< 0.07	RAFFELT	88 ASTR	D, K, SN 1987A
< 0.7	169 RAFFELT	88B ASTR	red giant
< 2-5	FRIEMAN	87 ASTR	D, red giant
< 0.01	170 RAFFELT	87 ASTR	K, red giant
< 0.06	TURNER	87 COSM	K, thermal production
< 0.7	171 DEARBORN	86 ASTR	D, red giant
< 0.03	RAFFELT	86 ASTR	D, red giant
< 1	172 RAFFELT	86 ASTR	K, red giant
< 0.003-0.02	RAFFELT	86B ASTR	D, white dwarf
> 1	173 KAPLAN	85 ASTR	K, red giant
> 1×10^{-5}	IWAMOTO	84 ASTR	D, K, neutron star
> 1	ABBOTT	83 COSM	D, K, mass density of the universe
> 1×10^{-5}	DINE	83 COSM	D, K, mass density of the universe
< 0.04	ELLIS	83B ASTR	D, red giant
> 1	PRESKILL	83 COSM	D, K, mass density of the universe
< 0.1	BARROSO	82 ASTR	D, red giant
< 1	174 FUKUGITA	82 ASTR	D, stellar cooling
< 0.07	FUKUGITA	82B ASTR	D, red giant

153 MOROI 98 points out that a KSVZ axion of this mass range (see CHANG 93) can be a viable hot dark matter of Universe, as long as the model-dependent $g_{A\gamma}$ is accidentally small enough as originally emphasized by KAPLAN 85; see Fig. 1.

154 BORISOV 97 bound is on the axion-electron coupling $g_{ae} < 1 \times 10^{-13}$ from the photo-production of axions off of electric fields in the outer layers of neutron stars.

155 KACHELRIESS 97 bound is on the axion-electron coupling $g_{ae} < 1 \times 10^{-10}$ from the production of axions in strongly magnetized neutron stars. The authors also quote a stronger limit, $g_{ae} < 9 \times 10^{-13}$ which is strongly dependent on the strength of the magnetic field in white dwarfs.

156 KEIL 97 uses new measurements of the axial-vector coupling strength of nucleons, as well as a reanalysis of many-body effects and pion-emission processes in the core of the neutron star, to update limits on the invisible-axion mass.

157 RAFFELT 95 reexamined the constraints on axion emission from red giants due to the axion-electron coupling. They improve on DEARBORN 86 by taking into proper account degeneracy effects in the bremsstrahlung rate. The limit comes from requiring the red giant core mass at helium ignition not to exceed its standard value by more than 5% (0.025 solar masses).

158 ALTHERR 94 bound is on the axion-electron coupling $g_{ae} < 1.5 \times 10^{-13}$, from energy loss via axion emission.

159 CHANG 93 updates ENGEL 90 bound with the Kaplan-Mahohar ambiguity in $z = m_{\mu}/m_d$ (see the Note on the Quark Masses in the Quark Particle Listings). It leaves the window $f_A = 3 \times 10^5 - 3 \times 10^6$ GeV open. The constraint from Big-Bang Nucleosynthesis is satisfied in this window as well.

160 BERSHADY 91 searched for a line at wave length from 3100-8300 Å expected from 2γ decays of relic thermal axions in intergalactic light of three rich clusters of galaxies.

161 KIM 91C argues that the bound from the mass density of the universe will change drastically for the supersymmetric models due to the entropy production of saxion (scalar component in the axionic chiral multiplet) decay. Note that it is an upperbound rather than a lowerbound.

162 RAFFELT 91B argue that previous SN 1987A bounds must be relaxed due to corrections to nucleon bremsstrahlung processes.

163 RESSELL 91 uses absence of any intracuster line emission to set limit.

164 ENGEL 90 rule out $10^{-10} \lesssim g_{AN} \lesssim 10^{-3}$, which for a hadronic axion with EMC motivated axion-nucleon couplings corresponds to $2.5 \times 10^{-3} \text{ eV} \lesssim m_{A^0} \lesssim 2.5 \times 10^4 \text{ eV}$. The constraint is loose in the middle of the range, i.e. for $g_{AN} \sim 10^{-6}$.

165 RAFFELT 90D is a re-analysis of DEARBORN 86.

166 The region $m_{A^0} \gtrsim 2 \text{ eV}$ is also allowed.

167 ERICSON 89 considered various nuclear corrections to axion emission in a supernova core, and found a reduction of the previous limit (MAYLE 88) by a large factor.

168 MAYLE 89 limit based on naive quark model couplings of axion to nucleons. Limit based on couplings motivated by EMC measurements is 2-4 times weaker. The limit from axion-electron coupling is weak: see HATSUDA 88B.

169 RAFFELT 88B derives a limit for the energy generation rate by exotic processes in helium-burning stars $\epsilon < 100 \text{ erg g}^{-1} \text{ s}^{-1}$, which gives a firmer basis for the axion limits based on red giant cooling.

170 RAFFELT 87 also gives a limit $g_{A\gamma} < 1 \times 10^{-10} \text{ GeV}^{-1}$.

171 DEARBORN 86 also gives a limit $g_{A\gamma} < 1.4 \times 10^{-11} \text{ GeV}^{-1}$.

172 RAFFELT 86 gives a limit $g_{A\gamma} < 1.1 \times 10^{-10} \text{ GeV}^{-1}$ from red giants and $< 2.4 \times 10^{-9} \text{ GeV}^{-1}$ from the sun.

173 KAPLAN 85 says $m_{A^0} < 23 \text{ eV}$ is allowed for a special choice of model parameters.

174 FUKUGITA 82 gives a limit $g_{A\gamma} < 2.3 \times 10^{-10} \text{ GeV}^{-1}$.

Search for Relic Invisible Axions

Limits are for $[G_{A\gamma\gamma}/m_{A^0}]^2 \rho_A$ where $G_{A\gamma\gamma}$ denotes the axion two-photon coupling, $L_{\text{int}} = \frac{G_{A\gamma\gamma}}{4} \phi_A F_{\mu\nu} \tilde{F}^{\mu\nu} = G_{A\gamma\gamma} \phi_A \mathbf{E} \cdot \mathbf{B}$, and ρ_A is the axion energy density near the earth.

VALUE	CL%	DOCUMENT ID	TECN	COMMENT
$< 5.5 \times 10^{-43}$	95	175 HAGMANN	98 CNTR	$m_{A^0} = 2.9-3.3 \times 10^{-6} \text{ eV}$
		176 KIM	98 THEO	
$< 2 \times 10^{-41}$		177 HAGMANN	90 CNTR	$m_{A^0} = (5.4-5.9)10^{-6} \text{ eV}$
$< 1.3 \times 10^{-42}$	95	178 WUENSCH	89 CNTR	$m_{A^0} = (4.5-10.2)10^{-6} \text{ eV}$
$< 2 \times 10^{-41}$	95	178 WUENSCH	89 CNTR	$m_{A^0} = (11.3-16.3)10^{-6} \text{ eV}$

175 Based on the conversion of halo axions to microwave photons. Limit assumes $\rho_A = 0.45 \text{ GeV cm}^{-3}$. At 90%CL this result excludes a version of KSVZ axions as dark matter in the halo of our Galaxy, for the quoted axion mass range.

176 KIM 98 calculated the axion-to-photon couplings for various axion models and compared them to the HAGMANN 90 bounds. This analysis demonstrates a strong model dependence of $G_{A\gamma\gamma}$ and hence the bound from relic axion search.

177 HAGMANN 90 experiment is based on the proposal of SIKIVIE 83.

178 WUENSCH 89 looks for condensed axions near the earth that could be converted to photons in the presence of an intense electromagnetic field via the Primakoff effect, following the proposal of SIKIVIE 83. The theoretical prediction with $[G_{A\gamma\gamma}/m_{A^0}]^2 = 2 \times 10^{-14} \text{ MeV}^{-4}$ (the three generation DFSZ model) and $\rho_A = 300 \text{ MeV/cm}^3$ that makes up galactic halos gives $(G_{A\gamma\gamma}/m_{A^0})^2 \rho_A = 4 \times 10^{-44}$. Note that our definition of $G_{A\gamma\gamma}$ is $(1/4\pi)$ smaller than that of WUENSCH 89.

Invisible A^0 (Axion) Limits from Photon Coupling

Limits are for the axion-two-photon coupling $G_{A\gamma\gamma}$ defined by $L = G_{A\gamma\gamma} \phi_A \mathbf{E} \cdot \mathbf{B}$. Related limits from astrophysics can be found in the "Invisible A^0 (Axion) Mass Limits from Astrophysics and Cosmology" section.

VALUE (GeV^{-1})	CL%	DOCUMENT ID	TECN	COMMENT
$< 2.7 \times 10^{-9}$		179 MASSO	00 THEO	induced photon coupling
$< 6.0 \times 10^{-10}$	95	180 AVIGNONE	98	$m_{A^0} < 1 \text{ keV}$
$< 3.6 \times 10^{-7}$	95	181 MORIYAMA	98	$m_{A^0} < 0.03 \text{ eV}$
	95	182 CAMERON	93	$m_{A^0} < 10^{-3} \text{ eV}$, optical rotation
$< 6.7 \times 10^{-7}$	95	183 CAMERON	93	$m_{A^0} < 10^{-3} \text{ eV}$, photon regeneration
$< 3.6 \times 10^{-9}$	99.7	184 LAZARUS	92	$m_{A^0} < 0.03 \text{ eV}$
$< 7.7 \times 10^{-9}$	99.7	184 LAZARUS	92	$m_{A^0} = 0.03-0.11 \text{ eV}$
$< 7.7 \times 10^{-7}$	99	185 RUOSO	92	$m_{A^0} < 10^{-3} \text{ eV}$
$< 2.5 \times 10^{-6}$		186 SEMERTZIDIS	90	$m_{A^0} < 7 \times 10^{-4} \text{ eV}$

179 MASSO 00 studied limits on axion-proton coupling using the induced axion-photon coupling through the proton loop and CAMERON 93 bound on the axion-photon coupling using optical rotation. They obtained the bound $g_D^2/4\pi < 1.7 \times 10^{-9}$ for the coupling $g_D \bar{\psi} \gamma_5 \rho \psi$.

180 AVIGNONE 98 result is based on the coherent conversion of solar axions to photons via the Primakoff effect in a single crystal germanium detector.

181 Based on the conversion of solar axions to X-rays in a strong laboratory magnetic field.

182 Experiment based on proposal by MAIANI 86.

183 Experiment based on proposal by VANBIBBER 87.

184 LAZARUS 92 experiment is based on proposal found in VANBIBBER 89.

185 RUOSO 92 experiment is based on the proposal by VANBIBBER 87.

186 SEMERTZIDIS 90 experiment is based on the proposal of MAIANI 86. The limit is obtained by taking the noise amplitude as the upper limit. Limits extend to $m_{A^0} = 4 \times 10^{-3} \text{ eV}$ where $G_{A\gamma\gamma} < 1 \times 10^{-4} \text{ GeV}^{-1}$.

Limit on Invisible A^0 (Axion) Electron Coupling

The limit is for $G_{Aee} \delta_{\mu\nu} \phi_A \tilde{e} \gamma^{\mu} \gamma_5 e$ in GeV^{-1} , or equivalently, the dipole-dipole potential $\frac{G_{Aee}^2}{4\pi} ((\sigma_1 \cdot \sigma_2) - 3(\sigma_1 \cdot \mathbf{n})(\sigma_2 \cdot \mathbf{n}))/r^3$ where $\mathbf{n} = \mathbf{r}/r$.

The limits below apply to invisible axion of $m_A \leq 10^{-6} \text{ eV}$.

VALUE (GeV^{-1})	CL%	DOCUMENT ID	TECN	COMMENT
$< 5.3 \times 10^{-5}$	66	187 NI	94	Induced magnetism
$< 6.7 \times 10^{-5}$	66	187 CHUI	93	Induced magnetism
$< 3.6 \times 10^{-4}$	66	188 PAN	92	Torsion pendulum
$< 2.7 \times 10^{-5}$	95	187 BOBRAKOV	91	Induced magnetism
$< 1.9 \times 10^{-3}$	66	189 WINELAND	91	NMR
$< 8.9 \times 10^{-4}$	66	188 RITTER	90	Torsion pendulum
$< 6.6 \times 10^{-5}$	95	187 VOROBYOV	88	Induced magnetism

See key on page 239

Gauge & Higgs Boson Particle Listings
Axions (A⁰) and Other Very Light Bosons

- 187 These experiments measured induced magnetization of a bulk material by the spin-dependent potential generated from other bulk material with aligned electron spins, where the magnetic field is shielded with superconductor.
188 These experiments used a torsion pendulum to measure the potential between two bulk matter objects where the spins are polarized but without a net magnetic field in either of them.
189 WINELAND 91 looked for an effect of bulk matter with aligned electron spins on atomic hyperfine splitting using nuclear magnetic resonance.

Invisible A⁰ (Axion) Limits from Nucleon Coupling

Limits are for the axion mass in eV.

Table with columns: VALUE (eV), CL%, DOCUMENT ID, TECN, COMMENT. Includes entries for <745, 190 KRCMAR 98 CNTR Solar axion, 190 KRCMAR 98 looked for solar axions emitted by the M1 transition of thermally excited 57Fe nuclei in the Sun, following MORIYAMA 95b.

Axion Limits from T-violating Medium-Range Forces

The limit is for the coupling g in a T-violating potential between nucleons or nucleon and electron of the form V = (g hbar^2 / 8 pi m_p (sigma . sigma)) (1/r^2 + m_A c / h r) e^-m_A c r / h

Table with columns: VALUE, DOCUMENT ID, TECN, COMMENT. Includes entries for 191 NI 99 paramagnetic Tb F3, 192 POSPELOV 98 THEO neutron EDM, 193 YODIN 96 torsion pendulum, 194 RITTER 93 nuclear spin-precession frequencies, 195 VENEMA 92 NMR.

- 191 NI 99 searched for a T-violating medium-range force acting on paramagnetic Tb F3 salt. See their Fig. 1 for the result.
192 POSPELOV 98 studied the possible contribution of T-violating Medium-Range Force to the neutron electric dipole moment, which is possible when axion interactions violate CP. The size of the force among nucleons must be smaller than gravity by a factor of 2 x 10^-10 (1 cm/lambda_A), where lambda_A = hbar/m_A c.
193 YODIN 96 compared the precession frequencies of atomic 199Hg and Cs when a large mass is positioned near the cells, relative to an applied magnetic field. See Fig. 3 for their limits.
194 RITTER 93 used a torsion pendulum to study the influence of bulk mass with polarized electrons on the pendulum.
195 VENEMA 92 looked for an effect of Earth's gravity on nuclear spin-precession frequencies of 199Hg and 201Hg atoms.
196 WINELAND 91 looked for an effect of bulk matter with aligned electron spins on atomic hyperfine resonances in stored 9Be+ ions using nuclear magnetic resonance.

REFERENCES FOR Searches for Axions (A⁰) and Other Very Light Bosons

MASSO 00 PR D61 011701R E. Masso (NEMO Collab.)
ARNOLD 99 NP A658 298 R. Arnold et al.
NI 99 PRL 82 2439 W.-T. Ni et al.
ALTEGOER 98 PL B428 197 J. Altegoer et al.
AVIGNONE 98 PRL 81 5068 F.T. Avignone et al.
DANEVICH 98 NP A643 317 F.A. Danevich et al.
DIAZ 98 NP B527 44 M.A. Diaz et al.
FAESSLER 98B JP G24 2139 C. Hagmann et al.
HAGMANN 98 PRL 80 2043 J.E. Kim
KIM 98 PR D56 055006 M. Kim et al.
KRCMAR 98 PL B442 38 M. Krcmar et al.
LUESCHER 98 PL B434 407 R. Luescher et al.
MORIYAMA 98 PL B434 147 S. Moriyama et al.
MOROI 98 PL B440 69 T. Moroi, H. Murayama
POSPELOV 98 PR D58 097703 M. Pospelov
ZUBER 98 PRPL 305 295 S. Adler et al.
ADLER 97 PRL 79 2204 (BNL 787 Collab.)
AHMAD 97 PRL 78 618 I. Ahmad et al. (APEX Collab.)
BORISOV 97 JETP 93 868 A.V. Borisov, V.Y. Grishina (MOSU)
DEBOER 97C JP G23 185 F.W.N. de Boer et al.
KACHELRIESS 97 PR D56 1313 M. Kachelriess, C. Wilke, G. Wunner (BOCH)
KEIL 97 PR D56 2419 W. Keil et al.
KITCHING 97 PRL 79 4079 P. Kitching et al. (BNL 787 Collab.)
LEINBERGER 97 PL B394 16 U. Leinberger et al. (ORANGE Collab.)
ADLER 96 PRL 76 1421 S. Adler et al. (BNL 787 Collab.)
AMSLER 96B ZPHY C70 219 C. AMSler et al. (Crystal Barrel Collab.)
GANZ 96 PL B389 4 R. Ganz et al. (GSI, HEID, FRAN, JAGL+)
GUENTHER 96 PR D54 3641 M. Gunther et al. (MPIH, SASSO)
KAMEI 96 PL B368 291 S. Kamei (SHAMS)
MITSUI 96 EPL 33 111 T. Mitsui et al. (TOKY)
YODIN 96 PRL 77 2170 A.N. Yodin et al. (AMHT, WASH)
ALTMANN 95 ZPHY C68 221 M. Altmann et al. (MUNT, LAPP, CPPM)
BALEST 95 PR D51 2053 R. Balest et al. (CLEO Collab.)
BASSOMPIERRE... 95 PL B355 584 G. Bassompierre et al. (LAPP, LCGT, LYON)
MAENO 95 PL B351 574 T. Maeno et al. (TOKY)
MORIYAMA 95B PRL 75 3222 S. Moriyama
RAFFELT 95 PR D51 1495 G. Raffelt, A. Weiss (MPIM, MPIA)
SKALSEY 95 PR D51 6292 M. Skalsey, R.S. Conti (MICH)
TSUNODA 95 EPL 30 273 T. Tsunoda et al. (TOKY)
ADACHI 94 PR A49 3201 S. Adachi et al. (TMU)
ALTHERR 94 ASP 2 175 T. Altherr, E. Pettigirard, del Rio Gaztelurrutia (Crystal Barrel Collab.)
AMSLER 94B PL B333 271 C. AMSler et al. (TOKY)
ASAI 94 PL B323 90 S. Asai et al. (TOKY)
MEIJERDREES 94 PR D49 4937 M.R. Drees et al. (BRCO, OREG, TRIU)
NI 94 Physica B194 153 W.T. Ni et al. (NTHU)
YO 94 PR C49 1351 D.T. Yo et al. (ISU, LBL, LLNL, UCSD)
ATIYA 93 PRL 70 2521 M.S. Atiya et al. (BNL 787 Collab.)
Also 93C PRL 71 305 (erratum) M.S. Atiya et al. (BNL 787 Collab.)

ATIYA 93B PR D48 R1 M.S. Atiya et al. (BNL 787 Collab.)
BASSOMPIERRE... 93 EPL 22 239 G. Bassompierre et al. (LAPP, TORI, LYON)
BECK 93 PRL 70 2853 M. Beck et al. (MPIH, KIAE, SASSO)
CAMERON 93 PR D47 3707 R.E. Cameron et al. (ROCH, BNL, FNAL+)
CHANG 93 PL B316 51 S. Chang, K. Choi
CHUI 93 PRL 71 3247 T.C.P. Chui, W.T. Ni (NTHU)
MINOWA 93 PRL 71 4120 M. Minowa et al. (TOKY)
NG 93 PR D48 2941 K.W. Ng (AST)
RITTER 93 PRL 70 701 R.C. Ritter et al.
TANAKA 93 PR D48 5412 J. Tanaka, H. Ejiri (OSAK)
ALLIEGRO 92 PRL 68 278 C. Alliegro et al. (BNL, FNAL, PSI+)
ATIYA 92 PRL 69 733 M.S. Atiya et al. (BNL, LANL, PRIN+)
BERNATOW... 92 PRL 69 2341 T. Bernatowicz et al. (WUSL, TATA)
BLUMLLEIN 92 IJMP A7 3835 J. Blumlein et al. (BERL, BUDA, JINR+)
HALLIN 92 PR D45 3955 A.L. Hallin et al. (PRIN)
HENDERSON 92C PRL 69 1733 S.D. Henderson et al. (YALE, BNL)
HICKS 92 PL B276 423 K.H. Hicks, D.E. Alburger (OHIO, BNL)
LAZARUS 92 PRL 69 2333 D.M. Lazarus et al. (BNL, RDCH, FNAL)
MEIJERDREES 92 PRL 68 2845 R. Meijer Drees et al. (SINDRUM 1 Collab.)
PAN 92 MPL 7 1287 S.S. Pan, W.T. Ni, S.C. Chen (NTHU)
RUOSO 92 ZPHY C56 505 G. Ruoso et al. (ROCH, BNL, FNAL, TRST)
SKALSEY 92 PRL 68 456 M. Skalsey, J.J. Kolata (MICH, NDAM)
VENEMA 92 PRL 68 135 B.J. Venema et al.
WANG 92 MPL A7 1497 J. Wang (ILL)
WANG 92C PL B291 97 J. Wang (ILL)
WU 92 PRL 69 1729 X.Y. Wu et al. (BNL, YALE, CUNY)
AKOPYAN 91 PL B272 445 M.V. Akopyan et al. (INRM)
ASAI 91 PRL 66 2449 S. Asai et al. (ICEPP)
BERSHADY 91 PRL 66 1398 M.A. Bershad, M.T. Ressell, M.S. Turner (CHIC+)
BLUMLLEIN 91 ZPHY C51 341 J. Blumlein et al. (BERL, BUDA, JINR+)
BOBRAKOV 91 JETPL 53 294 V.F. Bobrov et al. (PNPI)
Translated from ZETFP 53 283
BROSS 91 PRL 67 2942 A.D. Bross et al. (FNAL, ILL)
KIM 91C PRL 67 3465 J.E. Kim (SEOUL)
RAFFELT 91B PRL 67 2605 G. Raffelt, D. Seckel (MPIM, BART)
RESSELL 91 PR D44 3001 M.T. Ressell (CHIC, FNAL)
TRZASKA 91 PL B269 54 W.H. Trzaska et al. (TAMU)
TSERTOS 91 PL B266 259 H. Tsertos et al. (ILL, GSI)
WALKER 91 APJ 376 51 T.P. Walker et al. (HSCA, OSU, CHIC+)
WIDMANN 91 ZPHY A340 209 E. Widmann et al. (STUT, GSI, STUBM)
WINELAND 91 PRL 67 1735 D.J. Wineland et al. (NBSB)
ALBRECHT 90E PL B246 278 H. Albrecht et al. (ARGUS Collab.)
ANTREASYAN 90C PL B251 204 D. Antreasyan et al. (Crystal Ball Collab.)
ASANUMA 90 PL B237 588 T. Asanuma et al. (TOKY)
ATIYA 90 PRL 64 21 M.S. Atiya et al. (BNL 787 Collab.)
ATIYA 90B PRL 65 1188 M.S. Atiya et al. (BNL 787 Collab.)
BAUER 90 NIM B50 300 W. Bauer et al. (STUT, VILL, GSI)
BURROWS 90 PR D42 3297 A. Burrows, M.T. Ressell, M.S. Turner (ARIZ+)
DEBBER 90 JGP 16 L1 F.W.N. de Boer, J. Lehmann, J. Steyaert (LOUV)
ENGEL 90 PRL 65 960 J. Engel, D. Seckel, A.C. Hayes (BART, LANL)
GINNENKO 90 PL B237 287 S.N. Ginenko et al. (INRM)
GUO 90 PR D41 2924 R. Guo et al. (FNAL)
HAGMANN 90 PR D42 1297 C. Hagmann et al. (NIU, LANL, FNAL, CASE+)
JUDGE 90 PRL 65 972 C. Judge et al. (FLOR)
RAFFELT 90C PRPL 198 1 G.G. Raffelt et al. (ILL, GSI)
RAFFELT 90D PR D41 1324 G.G. Raffelt (MPIM)
RITTER 90 PR D42 977 R.C. Ritter et al. (VIRG)
SEMERTZIDIS 90 PRL 64 2988 Y.K. Semertzidis et al. (ROCH, BNL, FNAL+)
STAUDT 90 EPL 13 31 A. Staudt, K. Muto, H.V. Klapdor-Kleingrothaus (ICEPP)
TSUCHIYAKI 90 PL B236 81 M. Tsuchiyaki et al. (FNAL)
TURNER 90 PRL 65 677 M.S. Turner (ITER, INRM)
BARABASH 89 PL B223 275 A.S. Barabash et al. (ITER, INRM)
BINI 89 PL B221 99 M. Bini et al. (FIRZ, CERN, AARH)
BURROWS 89 PR D39 1020 A. Burrows, M.S. Turner, R.P. Brinkmann (ARIZ+)
Also 89B PRL 60 1797 M.S. Turner (FNAL, EFI)
DEBOER 89B PRL 62 2639 F.W.N. de Boer, R. van Dantzig (ANIK)
ERICSON 89 PL B219 507 T.E.O. Ericson, J.F. Mathiot (CERN, IPN)
FAISSNER 89 ZPHY C44 557 H. Faissner et al. (AACH3, BERL, PSI)
FISHER 89 PL B218 257 P.H. Fisher et al. (CIT, NEUC, PSI)
FOX 89 PR 65 288 J.D. Fox et al.
MAYLE 89 PL B219 515 R. Mayle et al. (LLL, CERN, MINN, FNAL+)
Also 89B PL B203 188 R. Mayle et al. (LLL, CERN, MINN, FNAL+)
MINOWA 89 PRL 62 1091 M. Minowa et al. (ICEPP)
ORITO 89 PRL 63 597 S. Orito et al. (ICEPP)
PERKINS 89 PRL 62 2638 D.H. Perkins (OXF)
TSERTOS 89 PR D40 1397 H. Tsertos et al. (GSI, ILLG)
VANBIBBER 89 PR D39 2089 K. van Bibber et al. (LLL, TAMU, LBL)
WUENSCH 89 PR D40 3153 W.U. Wuensch et al. (ROCH, BNL, FNAL)
Also 89B PRL 62 2639 S. de Panfilis et al. (ROCH, BNL, FNAL)
ALSTON... 88 PRL 60 1928 M. Alston-Garnjost et al. (LBL, MTHO+)
AVIGNONE 88 PR D37 618 F.T. Avignone et al. (PRIN, SCUC, ORNL+)
BJORKEN 88 PR D38 3375 J.D. Bjorken et al. (FNAL, SLAC, VPI)
BLINOV 88 SJNP 47 563 A.E. Blinov et al. (NOVO)
Translated from YAF 47 889
BOLTON 88 PR D38 2077 R.D. Bolton et al. (LANL, STAN, CHIC+)
Also 88 PRL 60 2461 R.D. Bolton et al. (LANL, STAN, CHIC+)
Also 86 PRL 57 3241 D. Grosnick et al. (CHIC, LANL, STAN+)
CHANDA 88 PR D37 2714 R. Chanda, J.F. Nieves, P.B. Pal (UMD, UPR+)
CHOI 88 PR D37 3225 K. Choi et al. (JHU)
CONNELL 88 PRL 60 2242 S.H. Connell et al. (WITW)
DATAR 88 PR C37 250 V.M. Datar et al. (IPN)
DEBOER 88 PRL 61 1274 F.W.N. de Boer, R. van Dantzig (ANIK)
Also 89 PRL 62 2644 erratum F.W.N. de Boer, R. van Dantzig (ANIK)
Also 89B PRL 62 2638 D.H. Perkins (OXF)
DEBOER 88C JGP 14 L131 F.W.N. de Boer et al. (LOUV)
DOEHNER 88 PR D38 2722 J. Doehner et al. (HEIDP, ANL, ILLG)
EL-NADI 88 PRL 61 1271 M. el Nadi, O.E. Badawy (CAIR)
ENGEL 88 PR C37 731 J. Engel, P. Vogel, M.R. Zirnbauer (AACH3, BERL, SIN)
FAISSNER 88 ZPHY C37 231 H. Faissner et al. (KEK)
HATSUDA 88B PL B203 469 T. Hatsuda, M. Yoshimura (KEK)
LORENZ 88 PL B214 10 E. Lorenz et al. (MPIM, PSI)
MAYLE 88 PL B203 188 R. Mayle et al. (LLL, CERN, MINN, FNAL+)
PICCIOTTO 88 PR D37 1131 C.E. Picciotto et al. (TRIU, CNRC)
RAFFELT 88 PRL 60 1793 G. Raffelt, D. Seckel (UCB, LLL, UCSC)
RAFFELT 88B PR D37 349 G.G. Raffelt, D.S.P. Dearborn (UCB, LLL)
SAVAGE 88 PR D37 1134 M.J. Savage, B.W. Filippone, L.W. Mitchell (CIT)
TSERTOS 88 PL B207 273 A. Tsertos et al. (GSI, ILLG)
TSERTOS 88B ZPHY A331 103 A. Tsertos et al. (GSI, ILLG)
VANKLINKEN 88 PL B205 223 J. van Kiinen et al. (GRON, GSI)
VANKLINKEN 88B PRL 60 2442 J. van Kiinen (GRON)
VONWIMMERSBERG 88 PRL 60 2443 U. von Wimmersberg (BNL)
VOROBOV 88 PL B208 146 P.V. Vorobiev, A.I. Gitars (NOVO)
AVIGNONE 87 AIP Conf. 1987 F.T. Avignone et al. (SCUC, PNLO)
AIP Conf. Proc. Salt Lake City, UT
CALDWELL 87 PRL 59 419 D.O. Caldwell et al. (UCSB, LBL)
DRUZHININ 87 ZPHY C37 1 V.P. Druzhinin et al. (NOVO)
ELLIOTT 87 PRL 59 1649 S.R. Elliott, A.A. Hahn, M.K. Moe (UCI)
FISHER 87 PL B192 460 P.H. Fisher et al. (CIT, NEUC, SIN)
FRIEMAN 87 PR D36 2203 I.A. Frieman, S. Dimopoulos, M.S. Turner (SLAC+)
GOLDMAN 87 PR D36 543 T. Goldman et al. (LANL, CHIC, STAN)
KORENCHENKO... 87 SJNP 46 192 S.M. Korenchenko et al. (JINR)
Translated from YAF 46 313

Gauge & Higgs Boson Particle Listings

Axions (A^0) and Other Very Light Bosons

MAIER	87	ZPHY A326 527	K. Maier <i>et al.</i>	(STUT, GSI)	ASANO	82	PL 113B 195	Y. Asano <i>et al.</i>	(KEK, TOKY, INUS, OSAK)
MILLS	87	PR D36 707	A.P. Mills, J. Levy	(BELL)	BARROSO	82	PL 116B 247	A. Barrosa, G.C. Branco	(LISB)
RAFFELT	87	PR D36 2211	G.G. Raffelt, D.S.P. Dearborn	(LLL, UCIB)	DATAR	82	PL 114B 63	V.M. Datar <i>et al.</i>	(BHAB)
RIORDAN	87	PRL 59 755	E.M. Riordan <i>et al.</i>	(ROCH, CIT+)	EDWARDS	82	PRL 48 903	C. Edwards <i>et al.</i>	(Crystal Ball Collab.)
TURNER	87	PRL 59 2489	M.S. Turner	(FNAL, EFI)	FETSCHER	82	JPG 8 L147	W. Fetscher	(ETH)
VANBIBBER	87	PRL 59 759	K. van Bibber <i>et al.</i>	(LLL, CIT, MIT+)	FUKUGITA	82	PRL 48 1522	M. Fukugita, S. Watamura, M. Yoshimura	(KEK)
VONWIMMER	87	PRL 59 266	U. von Wimmersperg <i>et al.</i>	(WITW)	FUKUGITA	82B	PR D26 1840	M. Fukugita, S. Watamura, M. Yoshimura	(KEK)
ALBRECHT	86D	PL B179 403	H. Albrecht <i>et al.</i>	(ARGUS Collab.)	LEHMANN	82	PL 115B 270	P. Lehmann <i>et al.</i>	(SACL)
BADIER	86	ZPHY C31 21	J. Badier <i>et al.</i>	(NA3 Collab.)	RAFFELT	82	PL 119B 323	G. Raffelt, L. Stodolsky	(MPIM)
BOWCOCK	86	PRL 56 2676	T.J.V. Bowcock <i>et al.</i>	(CLEO Collab.)	SIVERTZ	82	PR D26 717	J.M. Sivertz <i>et al.</i>	(CUSB Collab.)
BROWN	86	PRL 57 2101	C.N. Brown <i>et al.</i>	(FNAL, WASH, KYOT+)	VERGADOS	82	PL 109B 96	J.D. Vergados	(CERN)
BRYMAN	86B	PRL 57 2787	D.A. Bryman, E.T.H. Clifford	(TRIU)	ZEHNDER	82	PL 110B 419	A. Zehnder, K. Gabathuler, J.L. Vuilleumier	(ETH+)
DAVIER	86	PL B180 295	M. Davier, J. Jeanjean, H. Nguyen Ngoc	(LALO)	ASANO	81B	PL 107B 159	Y. Asano <i>et al.</i>	(KEK, TOKY, INUS, OSAK)
DEARBORN	86	PRL 56 26	D.S.P. Dearborn, D.N. Schramm, G. Steigman	(LL+)	BARROSO	81	PL 106B 91	A. Barrosa, N.C. Mukhopadhyay	(SIN)
EICHLER	86	PL B175 101	R.A. Eichler <i>et al.</i>	(SINDRUM Collab.)	FAISSNER	81	ZPHY C10 95	H. Faissner <i>et al.</i>	(AACH3)
HALLIN	86	PRL 57 2105	A.L. Hallin <i>et al.</i>	(PRIN)	FAISSNER	81B	PL 103B 234	H. Faissner <i>et al.</i>	(AACH3)
JODIDIO	86	PR D34 1967	A. Jodidio <i>et al.</i>	(LBL, NWES, TRIU)	KIM	81	PL 105B 55	B.R. Kim, C. Stamm	(AACH3)
Also		PR D37 237 erratum	A. Jodidio <i>et al.</i>	(LBL, NWES, TRIU)	VUILLEUMIER	81	PL 101B 341	J.L. Vuilleumier <i>et al.</i>	(CIT, MUNI)
KETOV	86	JETPL 44 146	S.N. Ketov <i>et al.</i>	(KIAE)	ZEHNDER	81	PL 104B 494	A. Zehnder	(ETH)
Also		Translated from ZETFP			FAISSNER	80	PL 96B 201	H. Faissner <i>et al.</i>	(AACH3)
KOCH	86	NC 96A 182	H.R. Koch, O.W.B. Schult	(JULI)	JACQUES	80	PR D21 1206	P.F. Jacques <i>et al.</i>	(RUTG, STEV, COLU)
KONAKA	86	PRL 57 659	A. Konaka <i>et al.</i>	(KYOT, KEK)	SOUKAS	80	PRL 44 564	A. Soukas <i>et al.</i>	(BNL, HARV, ORNL, PENN)
MAGERAS	86	PRL 56 2672	G. Mageras <i>et al.</i>	(MPIM, COLU, STON)	BECHIS	79	PRL 42 1511	D.J. Bechis <i>et al.</i>	(UMD, COLL, AFRR)
MAIANI	86	PL B175 359	L. Maiani, R. Petronzio, E. Zavattini	(CERN)	CALAPRICE	79	PR D20 2708	F.P. Calaprice <i>et al.</i>	(PRIN)
PECCCI	86	PL B172 435	R.D. Peccei, T.T. Wu, T. Yanagida	(DESY)	COTEUS	79	PRL 42 1438	P. Coteus <i>et al.</i>	(COLU, ILL, BNL)
RAFFELT	86	PR D33 897	G.G. Raffelt	(MPIM)	DISHAW	79	PL 85B 142	J.P. Dishaw <i>et al.</i>	(SLAC, CIT)
RAFFELT	86B	PL 166B 402	G.G. Raffelt	(MPIM)	ZHITNITSKII	79	SJNP 29 517	A.R. Zhitnitsky, Y.I. Skovpen	(NOVO)
SAVAGE	86B	PRL 57 178	M.J. Savage <i>et al.</i>	(CIT)	ALIBRAN	78	PL 74B 134	P. Alibran <i>et al.</i>	(Gargamelle Collab.)
AMALDI	85	PL 153B 444	U. Amaldi <i>et al.</i>	(CERN)	ASRATYAN	78B	PL 79B 497	A.E. Asratyan <i>et al.</i>	(ITEP, SERP)
ANANEV	85	SJNP 41 585	V.D. Ananev <i>et al.</i>	(JINR)	RELOTTI	78	PL 76B 223	E. Bellotti, E. Fiorini, L. Zanotti	(MILA)
Also		Translated from YAF 41 912			BOSETTI	78B	PL 74B 143	P.C. Bosetti <i>et al.</i>	(BEBE Collab.)
BALTRUSAITIS...	85	PRL 55 1842	R.M. Baltrusaitis <i>et al.</i>	(Mark III Collab.)	DICUS	78C	PR D18 1829	D.A. Dicus <i>et al.</i>	(TEXA, VPI, STAN)
BERGSMÄ	85	PL 157B 458	F. Bergsmä <i>et al.</i>	(CHARM Collab.)	DONNELLY	78	PR D18 1607	T.W. Donnelly <i>et al.</i>	(STAN)
KAPLAN	85	NP B260 215	D.B. Kaplan	(HARV)	Also	76	PRL 37 315	F. Reines, H.S. Gurr, H.W. Sobel	(UCI)
IWAMOTO	84	PRL 53 1198	N. Iwamoto	(UCSB, WUSL)	HANSI	78D	PL 74B 139	T. Hansi <i>et al.</i>	(UCI)
YAMAZAKI	84	PRL 52 1089	T. Yamazaki <i>et al.</i>	(INUS, KEK)	MICELMAC...	78	LNIC 21 441	G.V. Mitselmakher, B. Pontecorvo	(CDHS Collab.)
ABBOTT	83	PL 120B 133	L.F. Abbott, P. Sikivie	(BRAN, FLOR)	MIKAEILIAN	78	PR D18 3605	K.O. Mikaelian	(JINR)
ALAM	83	PR D27 1665	M.S. Alam <i>et al.</i>	(VAND, CORN, ITHA, HARV+)	SATO	78	PTP 60 1942	K. Sato	(FNAL, NWES)
CARBONI	83	PL 123B 349	G. Carboni, W. Dahme	(CERN, MUNI)	VYSOTSKII	78	JETPL 27 502	M.I. Vysotsky <i>et al.</i>	(KYOT)
CAVAIGNAC	83	PL 121B 193	J.F. Cavaignac <i>et al.</i>	(ISNG, LAPP)	Also	78	Translated from ZETFP		(ASCI)
DICUS	83	PR D28 1778	D.A. Dicus, V.L. Tepilitz	(TEXA, UMD)	YANG	78	PRL 41 523	T.C. Yang	(MASA)
DINE	83	PL 120B 137	M. Dine, W. Fischer	(IAS, PENN)	PECCCI	77	PR D16 1791	R.D. Peccei, H.R. Quinn	(STAN, SLAC)
ELLIS	83B	NP B223 252	J. Ellis, K.A. Olive	(CERN)	Also	77B	PR 38 1440	R.D. Peccei, H.R. Quinn	(STAN, SLAC)
FAISSNER	83	PR D28 1190	H. Faissner <i>et al.</i>	(AACH)	REINES	76	PRL 37 315	F. Reines, H.S. Gurr, H.W. Sobel	(UCI)
FAISSNER	83B	PR D28 1787	H. Faissner <i>et al.</i>	(AACH3)	GURR	74	PR 33 179	H.S. Gurr, F. Reines, H.W. Sobel	(UCI)
FRANK	83B	PR D28 1790	J.S. Frank <i>et al.</i>	(LANL, YALE, LBL+)	ANAND	53	PRSL A22 183	Anand	(UCI)
HOFFMAN	83	PR D28 660	C.M. Hoffman <i>et al.</i>	(LANL, AR25)					
NICZYPORUK	83	ZPHY C17 197	B. Niczyporuk <i>et al.</i>	(LENA Collab.)					
PRESKILL	83	PL 120B 127	J. Preskill, M.B. Wise, F. Wilczek	(HARV, UCSBT)					
SIKIVIE	83	PRL 51 1415	P. Sikivie	(FLOR)					
Also		PRL 52 695 erratum	P. Sikivie	(FLOR)					
ALEKSEEV	82	JETP 55 591	E.A. Alekseeva <i>et al.</i>	(KIAE)					
Also		Translated from ZETF 82 1007							
ALEKSEEV	82B	JETPL 36 116	G.D. Alekseev <i>et al.</i>	(MOSU, JINR)					
Also		Translated from ZETFP 36 94							

OTHER RELATED PAPERS

SREDNICKI	85	NP B260 689	M. Srednicki	(UCSB)
BARDEEN	78	PL 74B 229	W.A. Bardeen, S.-H.H. Tye	(FNAL)

LEPTONS

e

$$J = \frac{1}{2}$$

e MASS

The mass is known much more precisely in u (atomic mass units) than in MeV; see the footnote. The conversion from u to MeV, $1 u = 931.494013 \pm 0.000037 \text{ MeV}/c^2$ (MOHR 99, the 1998 CODATA value), involves the relatively poorly known electronic charge.

VALUE (MeV)	DOCUMENT ID	TECN	COMMENT
0.510998902 ± 0.000000021	¹ MOHR	99 RVUE	1998 CODATA value
• • • We do not use the following data for averages, fits, limits, etc. • • •			
0.51099907 ± 0.00000015	² FARNHAM	95 CNTR	Penning
0.51099906 ± 0.00000015	³ COHEN	87 RVUE	1986 CODATA value
0.5110034 ± 0.0000014	COHEN	73 RVUE	1973 CODATA value

- ¹ MOHR 99 (1998 CODATA) value in atomic mass units is 0.0005485799110(12).
- ² FARNHAM 95 compares cyclotron frequency of trapped electrons with that of a single trapped $^{12}\text{C}^{+6}$ ion. The result is $m_e = 0.000548579911(12) u$, where the figure in parenthesis is the 1σ uncertainty in the last digit. The uncertainty after conversion to MeV is dominated by the uncertainty in the electron charge.
- ³ COHEN 87 (1986 CODATA) value in atomic mass units is 0.000548579903(13). See footnote on FARNHAM 95.

$$(m_{e^+} - m_{e^-}) / m_{\text{average}}$$

A test of CPT invariance.

VALUE	CL%	DOCUMENT ID	TECN	COMMENT
< 8 × 10⁻⁹	90	⁴ FEE	93 CNTR	Positronium spectroscopy
• • • We do not use the following data for averages, fits, limits, etc. • • •				
< 4 × 10 ⁻⁸	90	CHU	84 CNTR	Positronium spectroscopy

- ⁴ FEE 93 value is obtained under the assumption that the positronium Rydberg constant is exactly half the hydrogen one.

$$|q_{e^+} + q_{e^-}|/e$$

A test of CPT invariance. See also similar tests involving the proton.

VALUE	DOCUMENT ID	TECN	COMMENT
< 4 × 10⁻⁸	⁵ HUGHES	92 RVUE	
• • • We do not use the following data for averages, fits, limits, etc. • • •			
< 2 × 10 ⁻¹⁸	⁶ SCHAEFER	95 THEO	Vacuum polarization
< 1 × 10 ⁻¹⁸	⁷ MUELLER	92 THEO	Vacuum polarization

- ⁵ HUGHES 92 uses recent measurements of Rydberg-energy and cyclotron-frequency ratios.
- ⁶ SCHAEFER 95 removes model dependency of MUELLER 92.
- ⁷ MUELLER 92 argues that an inequality of the charge magnitudes would, through higher-order vacuum polarization, contribute to the net charge of atoms.

e MAGNETIC MOMENT ANOMALY

$$\mu_e/\mu_B - 1 = (g-2)/2$$

For the most accurate theoretical calculation, see KINOSHITA 81.

VALUE (units 10 ⁻⁶)	DOCUMENT ID	TECN	CHG	COMMENT
1159.6521869 ± 0.0000041	⁸ MOHR	99 RVUE		1998 CODATA value
• • • We do not use the following data for averages, fits, limits, etc. • • •				
1159.652193 ± 0.000010	⁸ COHEN	87 RVUE		1986 CODATA value
1159.6521884 ± 0.0000043	VANDYCK	87 MRS	-	Single electron
1159.6521879 ± 0.0000043	VANDYCK	87 MRS	+	Single positron

- ⁸ The CODATA value assumes the $g/2$ values for e^+ and e^- are equal, as required by CPT.

$$(g_{e^+} - g_{e^-}) / g_{\text{average}}$$

A test of CPT invariance.

VALUE (units 10 ⁻¹²)	CL%	DOCUMENT ID	TECN	COMMENT
- 0.5 ± 2.1		⁹ VANDYCK	87 MRS	Penning trap
• • • We do not use the following data for averages, fits, limits, etc. • • •				
< 12	95	¹⁰ VASSERMAN	87 CNTR	Assumes $m_{e^+} = m_{e^-}$
22 ± 64		SCHWINBERG	81 MRS	Penning trap

- ⁹ VANDYCK 87 measured $(g_-/g_+) - 1$ and we converted it.
- ¹⁰ VASSERMAN 87 measured $(g_+ - g_-)/(g-2)$. We multiplied by $(g-2)/g = 1.2 \times 10^{-3}$.

e ELECTRIC DIPOLE MOMENT

A nonzero value is forbidden by both T invariance and P invariance.

VALUE (10 ⁻²⁶ ecm)	CL%	DOCUMENT ID	TECN	COMMENT
0.18 ± 0.12 ± 0.10		¹¹ COMMINS	94 MRS	205 Tl beams
• • • We do not use the following data for averages, fits, limits, etc. • • •				
- 0.27 ± 0.83		¹¹ ABDULLAH	90 MRS	205 Tl beams
- 14 ± 24		CHO	89 NMR	Tl F molecules
- 1.5 ± 5.5 ± 1.5		MURTHY	89	Cesium, no B field
- 50 ± 110		LAMOREAUX	87 NMR	199 Hg
190 ± 340	90	SANDARS	75 MRS	Thallium
70 ± 220	90	PLAYER	70 MRS	Xenon
< 300	90	WEISSKOPF	68 MRS	Cesium

- ¹¹ ABDULLAH 90 and COMMINS 94 use the relativistic enhancement of a valence electron's electric dipole moment in a high-Z atom.

e- MEAN LIFE / BRANCHING FRACTION

A test of charge conservation. See the "Note on Testing Charge Conservation and the Pauli Exclusion Principle" following this section in our 1992 edition (Physical Review D45, 1 June, Part II (1992), p.VI.10).

Most of these experiments are one of three kinds: Attempts to observe (a) the (K) shell x-ray produced when an electron decays without additional energy deposit, e.g., $e^- \rightarrow \nu_e \bar{\nu}_e \nu_e$ ("disappearance" experiments), (b) the 255.5 keV gamma ray produced in $e^- \rightarrow \nu_e \gamma$, and (c) nuclear de-excitation gamma rays after the electron disappears from an atomic shell and the nucleus is left in an excited state. The last can include both weak boson and photon mediating processes. We use the best "disappearance" limit for the Summary Tables. The best limit for the specific channel $e^- \rightarrow \nu \gamma$ is much better.

Note that we use the mean life rather than the half life, which is often reported.

VALUE (yr)	CL%	DOCUMENT ID	TECN	COMMENT
> 4.2 × 10²⁴	68	BELLI	99 DAMA	1 L-shell disappearance
• • • We do not use the following data for averages, fits, limits, etc. • • •				
> 6.4 × 10 ²⁴	68	¹² BELLI	99B DAMA	Disappearance in ¹²⁹ Xe
> 2.4 × 10 ²³	90	¹³ BELLI	99D DAMA	Disappear in ¹²⁷ I (in NaI)
> 4.3 × 10 ²³	68	AHARONOV	95B CNTR	Ge K-shell disappearance
> 3.7 × 10 ²⁵	68	AHARONOV	95B CNTR	$e^- \rightarrow \nu \gamma$
> 2.35 × 10 ²⁵	68	BALYSH	93 CNTR	$e^- \rightarrow \nu \gamma$, ⁷⁶ Ge detector
> 2.7 × 10 ²³	68	REUSSER	91 CNTR	Ge K-shell disappearance
> 1.5 × 10 ²⁵	68	AVIGNONE	86 CNTR	$e^- \rightarrow \nu \gamma$
> 1 × 10 ³⁹		¹⁴ ORITO	85 ASTR	Astrophysical argument
> 3 × 10 ²³	68	BELLOTTI	83B CNTR	$e^- \rightarrow \nu \gamma$
> 2 × 10 ²²	68	BELLOTTI	83B CNTR	Ge K-shell disappearance

- ¹² BELLI 99B limit on charge nonconserving e^- capture involving excitation of the 236.1 keV nuclear state of ¹²⁹Xe. Less stringent limits for other states are also given.
- ¹³ BELLI 99D limit on charge nonconserving e^- capture involving excitation of the 57.6 keV nuclear state of ¹²⁷I. Less stringent limits for the other states and for the state of ²³Na are also given.
- ¹⁴ ORITO 85 assumes that electromagnetic forces extend out to large enough distances and that the age of our galaxy is 10¹⁰ years.

e REFERENCES

BELLI 99	PL B460 236	P. Belli et al.	(DAMA Collab.)
BELLI 99B	PL B465 315	P. Belli et al.	(DAMA Collab.)
BELLI 99D	PR C60 065501	P. Belli et al.	(DAMA Collab.)
MOHR 99	JPCRD 28 1713	P.J. Mohr, B.N. Taylor	(NIST)
Also	00 RMP 72 351	F.J. Mohr, B.N. Taylor	(NIST)
AHARONOV 95B	PR D52 3785	Y. Aharonov et al.	(SCUC, PNL, ZAGR+)
Also	95 PL B353 168	Y. Aharonov et al.	(SCUC, PNL, ZAGR+)
FARNHAM 95	PRL 75 3598	D.L. Farnham, R.S. van Dyck, P.B. Schwinberg	(WASH)
SCHAEFER 95	PR A51 838	A. Schaefer, J. Reinhardt	(FRAN)
COMMINS 94	PR A50 2960	E.D. Commins et al.	
BALYSH 93	PL B298 278	A. Balysh et al.	(KIAE, MPH, SASSO)
FEE 93	PR A48 192	M.S. Fee et al.	
HUGHES 92	PRL 69 578	R.J. Hughes, B.I. Deutch	(LANL, AARR)
MUELLER 92	PRL 69 3432	B. Muller, M.H. Thoma	(DUKE)
PDG 92	PR D45, 1 June, Part II	K. Hikasa et al.	(KEK, LBL, BOST+)
REUSSER 91	PL B255 143	D. Reusser et al.	(NEUC, CIT, PSI)
ABDULLAH 90	PRL 65 2347	K. Abdullah et al.	(LBL, UCB)
CHO 89	PRL 63 2559	D. Cho, K. Sangster, E.A. Hinds	(YALE)
MURTHY 89	PRL 63 965	S.A. Murthy et al.	(AMHT)
COHEN 87	RMP 59 1121	E.R. Cohen, B.N. Taylor	(RISC, NBS)
LAMOREAUX 87	PRL 59 2275	S.K. Lamoreaux et al.	(WASH)
VANDYCK 87	PRL 59 26	R.S. van Dyck, P.B. Schwinberg, H.G. Dehmelt	(WASH)
VASSERMAN 87	PL B198 302	I.B. Vasserma et al.	(NOVO)
Also	87B PL B187 172	I.B. Vasserma et al.	(NOVO)
AVIGNONE 86	PR D34 97	F.T. Avignone et al.	(PNL, SCUC)
ORITO 85	PRL 54 2457	S. Orito, M. Yoshimura	(TOKY, KEK)
CHU 84	PRL 52 1689	S. Chu, A.P. Mills, J.L. Hall	(BELL, NBS, COLO)
BELLOTTI 83B	PL 124B 435	E. Bellotti et al.	(MILA)
KINOSHITA 81	PRL 47 1573	T. Kinoshita, W.B. Lindquist	(CORN)
SCHWINBERG 81	PRL 47 1679	P.B. Schwinberg, R.S. van Dyck, H.G. Dehmelt	(WASH)
SANDARS 75	PR A11 473	P.G.H. Sandars, D.M. Sternheimer	(OXF, BNL)
COHEN 73	JPCRD 2 663	E.R. Cohen, B.N. Taylor	(RISC, NBS)
PLAYER 70	JPB 3 1620	M.A. Player, P.G.H. Sandars	(OXF)
WEISSKOPF 68	PRL 21 1645	M.C. Weisskopf et al.	(BRAN)

Lepton Particle Listings

μ



$$J = \frac{1}{2}$$

μ MASS

The mass is known much more precisely in u (atomic mass units) than in MeV. The conversion from u to MeV, $1 u = 931.494013 \pm 0.000037$ MeV/ c^2 (MOHR 99, the 1998 CODATA value), involves the relatively poorly known electronic charge.

Where m_μ/m_e was measured, we have used the 1986 CODATA value for $m_e = 0.51099906 \pm 0.00000015$ MeV.

VALUE (MeV)	DOCUMENT ID	TECN	CHG	COMMENT
105.6583568 ± 0.0000052	¹ MOHR	99	RVUE	1998 CODATA value
• • • We do not use the following data for averages, fits, limits, etc. • • •				
105.658389 ± 0.000034	² COHEN	87	RVUE	1986 CODATA value
105.658386 ± 0.000044	³ MARIAM	82	CNTR +	
105.65836 ± 0.00026	⁴ CROWE	72	CNTR	
105.65865 ± 0.00044	⁵ CRANE	71	CNTR	

- ¹ The mass is known much more precisely in u : $0.1134289168(34) u$.
- ² The mass is known more precisely in u : $m = 0.113428913 \pm 0.000000017 u$. COHEN 87 makes use of the other entries below.
- ³ MARIAM 82 gives $m_\mu/m_e = 206.768259(62)$.
- ⁴ CROWE 72 gives $m_\mu/m_e = 206.7682(5)$.
- ⁵ CRANE 71 gives $m_\mu/m_e = 206.76878(85)$.

μ MEAN LIFE τ

Measurements with an error $> 0.001 \times 10^{-6}$ s have been omitted.

VALUE (10^{-6} s)	DOCUMENT ID	TECN	CHG	COMMENT
2.19703 ± 0.00004 OUR AVERAGE				
2.197078 ± 0.000073	BARDIN	84	CNTR +	
2.197025 ± 0.000155	BARDIN	84	CNTR -	
2.19695 ± 0.00006	GIOVANETTI	84	CNTR +	
2.19711 ± 0.00008	BALANDIN	74	CNTR +	
2.1973 ± 0.0003	DUCCLOS	73	CNTR +	

$\tau_{\mu^+}/\tau_{\mu^-}$ MEAN LIFE RATIO

A test of CPT invariance.

VALUE	DOCUMENT ID	TECN	CHG	COMMENT
1.000024 ± 0.000078	BARDIN	84	CNTR	
• • • We do not use the following data for averages, fits, limits, etc. • • •				
1.0008 ± 0.0010	BAILEY	79	CNTR	Storage ring
1.000 ± 0.001	MEYER	63	CNTR	Mean life μ^+/μ^-

$$(\tau_{\mu^+} - \tau_{\mu^-}) / \tau_{\text{average}}$$

A test of CPT invariance. Calculated from the mean-life ratio, above.

VALUE	DOCUMENT ID
(2 ± 8) × 10⁻⁵ OUR EVALUATION	

μ MAGNETIC MOMENT ANOMALY

The CODATA value (MOHR 99) comes from the current theoretical expression, based on the Standard Model and implicitly assuming that corrections beyond the Standard Model are negligible at the level of the quoted uncertainty. See reviews HUGHES 99 and FARLEY 90.

$$\mu_\mu / (e\hbar/2m_\mu) - 1 = (g_\mu - 2)/2$$

VALUE (units 10^{-6})	DOCUMENT ID	TECN	CHG	COMMENT
1165.9160 ± 0.0006 OUR EVALUATION	From MOHR 99			(theoretical)
1165.923 ± 0.008 OUR AVERAGE	Error includes scale factor of 1.1.			
1165.925 ± 0.015	⁶ CAREY	99	CNTR +	Storage ring
1165.910 ± 0.011	⁷ BAILEY	79	CNTR +	Storage ring
1165.936 ± 0.012	⁷ BAILEY	79	CNTR -	Storage ring
• • • We do not use the following data for averages, fits, limits, etc. • • •				
1165.91602 ± 0.00064	MOHR	99	RVUE	1998 CODATA value
1165.9230 ± 0.0084	COHEN	87	RVUE	1986 CODATA value
1162.0 ± 5.0	CHARPAK	62	CNTR +	

- ⁶ CAREY 99 measure ratio R to the free proton Larmor precession frequency, and then convert this to the magnetic moment anomaly using $\mu_\mu/\mu_p = 3.18334547(47)$ (COHEN 87).
- ⁷ BAILEY 79 values recalculated by HUGHES 99 using the COHEN 87 μ/p magnetic moment. The improved MOHR 99 value does not change the result.

$$(g_{\mu^+} - g_{\mu^-}) / g_{\text{average}}$$

A test of CPT invariance.

VALUE (units 10^{-8})	DOCUMENT ID
-2.6 ± 1.6	BAILEY 79

μ/p MAGNETIC MOMENT RATIO

This ratio is used to obtain a precise value of the muon mass and to reduce experimental muon Larmor frequency measurements to the muon magnetic moment anomaly. Measurements with an error > 0.00001 have been omitted.

VALUE	DOCUMENT ID	TECN	CHG	COMMENT
3.18334539 ± 0.00000010	⁸ MOHR	99	RVUE	1998 CODATA value
• • • We do not use the following data for averages, fits, limits, etc. • • •				
3.18334513 ± 0.00000039	LIU	99	CNTR +	HFS in muonium
3.18334547 ± 0.00000047	⁸ COHEN	87	RVUE	1986 CODATA value
3.1833441 ± 0.0000017	KLEMPPT	82	CNTR +	Precession strob
3.1833461 ± 0.0000011	MARIAM	82	CNTR +	HFS splitting
3.1833448 ± 0.0000029	CAMANI	78	CNTR +	See KLEMPPT 82
3.1833403 ± 0.0000044	CASPERSON	77	CNTR +	HFS splitting
3.1833402 ± 0.0000072	COHEN	73	RVUE	1973 CODATA value
3.1833467 ± 0.0000082	CROWE	72	CNTR +	Precession phase

⁸ CODATA values fitted using their selection of data, plus other data from multiparameter fits.

μ ELECTRIC DIPOLE MOMENT

A nonzero value is forbidden by both T invariance and P invariance.

VALUE (10^{-19} ecm)	DOCUMENT ID	TECN	CHG	COMMENT
3.7 ± 3.4	⁹ BAILEY	78	CNTR ±	Storage ring
• • • We do not use the following data for averages, fits, limits, etc. • • •				
8.6 ± 4.5	BAILEY	78	CNTR +	Storage rings
0.8 ± 4.3	BAILEY	78	CNTR -	Storage rings

⁹ This is the combination of the two BAILEY 78 results given below.

μ^- DECAY MODES

μ^+ modes are charge conjugates of the modes below.

Mode	Fraction (Γ_i/Γ)	Confidence level
Γ_1 $e^- \bar{\nu}_e \nu_\mu$	$\approx 100\%$	
Γ_2 $e^- \bar{\nu}_e \nu_\mu \gamma$	[a] $(1.4 \pm 0.4)\%$	
Γ_3 $e^- \bar{\nu}_e \nu_\mu e^+ e^-$	[b] $(3.4 \pm 0.4) \times 10^{-5}$	
Lepton Family number (LF) violating modes		
Γ_4 $e^- \nu_e \bar{\nu}_\mu$	LF [c] < 1.2	% 90%
Γ_5 $e^- \gamma$	LF < 1.2	$\times 10^{-11}$ 90%
Γ_6 $e^- e^+ e^-$	LF < 1.0	$\times 10^{-12}$ 90%
Γ_7 $e^- 2\gamma$	LF < 7.2	$\times 10^{-11}$ 90%

[a] This only includes events with the γ energy > 10 MeV. Since the $e^- \bar{\nu}_e \nu_\mu$ and $e^- \bar{\nu}_e \nu_\mu \gamma$ modes cannot be clearly separated, we regard the latter mode as a subset of the former.

[b] See the Particle Listings below for the energy limits used in this measurement.

[c] A test of additive vs. multiplicative lepton family number conservation.

μ^- BRANCHING RATIOS

$\Gamma(e^- \bar{\nu}_e \nu_\mu \gamma) / \Gamma_{\text{total}}$	Γ_2 / Γ				
VALUE	EVTS	DOCUMENT ID	TECN	CHG	COMMENT
0.014 ± 0.004		CRITTENDEN	61	CNTR	γ KE > 10 MeV
• • • We do not use the following data for averages, fits, limits, etc. • • •					
	862	BOGART	67	CNTR	γ KE > 14.5 MeV
0.0033 ± 0.0013		CRITTENDEN	61	CNTR	γ KE > 20 MeV
	27	ASHKIN	59	CNTR	
$\Gamma(e^- \bar{\nu}_e \nu_\mu e^+) / \Gamma_{\text{total}}$	Γ_3 / Γ				
VALUE (units 10^{-5})	EVTS	DOCUMENT ID	TECN	CHG	COMMENT
3.4 ± 0.2 ± 0.3	7443	¹⁰ BERTL	85	SPEC +	SINDRUM
• • • We do not use the following data for averages, fits, limits, etc. • • •					
2.2 ± 1.5	7	¹¹ CRITTENDEN	61	HLBC +	$E(e^+ e^-) > 10$ MeV
2	1	¹² GUREVICH	60	EMUL +	
1.5 ± 1.0	3	¹³ LEE	59	HBC +	

- ¹⁰ BERTL 85 has transverse momentum cut $p_T > 17$ MeV/ c . Systematic error was increased by us.
- ¹¹ CRITTENDEN 61 count only those decays where total energy of either (e^+ , e^-) combination is > 10 MeV.
- ¹² GUREVICH 60 interpret their event as either virtual or real photon conversion. e^+ and e^- energies not measured.
- ¹³ In the three LEE 59 events, the sum of energies $E(e^+) + E(e^-) + E(\gamma)$ was 51 MeV, 55 MeV, and 33 MeV.

Lepton Particle Listings

Neutrinos

NEUTRINO MASS

Written February 1998 and updated October 1999 by B. Kayser (NSF).

There is now rather convincing evidence that neutrinos have nonzero masses. This evidence comes from the apparent observation of neutrino oscillation. Let us recall the physics of this phenomenon, and its relation to neutrino mass.

In the decay

$$W^+ \rightarrow \ell^+ \nu_\ell \quad (1)$$

of a W boson into a charged lepton of “flavor” ℓ (e, μ , or τ), the accompanying neutrino is referred to as ν_ℓ , the neutrino of flavor ℓ . Neutrinos of different flavor are different objects. When an energetic ν_ℓ undergoes a charged-current weak interaction, it produces a charged lepton ℓ of the same flavor as the neutrino [1].

If neutrinos have masses, then a neutrino of definite flavor, ν_ℓ , need not be a mass eigenstate. Indeed, if leptons behave like quarks, the ν_ℓ is a coherent linear superposition of mass eigenstates, given by

$$|\nu_\ell\rangle = \sum_m U_{\ell m} |\nu_m\rangle. \quad (2)$$

Here, the ν_m are the mass eigenstates, and the coefficients $U_{\ell m}$ form a matrix U known as the leptonic mixing matrix. There are at least three ν_m , and perhaps more. However, it is most often assumed that no more than three ν_m make significant contributions to Eq. (2). Then U is a 3×3 matrix, and according to the electroweak Standard Model (SM), extended to include neutrino masses, it is unitary.

The relation Eq. (2) means that when, for example, a W^+ decays to an e^+ and a neutrino, the neutrino with probability $|U_{e1}|^2$ is a ν_1 , with probability $|U_{e2}|^2$ is a ν_2 , and so on. This behavior is an exact leptonic analogue of what is known to occur when a W^+ decays to quarks.

If each neutrino of definite flavor is a coherent superposition of mass eigenstates, then a neutrino of one flavor can spontaneously change into one of another flavor as it propagates [2]. This is the phenomenon referred to as neutrino oscillation.

To understand neutrino oscillation, let us consider how a neutrino born as the ν_ℓ of Eq. (2) evolves in time. First, we apply Schrödinger’s equation to the ν_m component of ν_ℓ in the rest frame of that component. This tells us that [3]

$$|\nu_m(\tau_m)\rangle = e^{-iM_m\tau_m} |\nu_m(0)\rangle, \quad (3)$$

where M_m is the mass of ν_m , and τ_m is time in the ν_m frame. In terms of the time t and position L in the laboratory frame, the Lorentz-invariant phase factor in Eq. (3) may be written

$$e^{-iM_m\tau_m} = e^{-i(E_m t - p_m L)}. \quad (4)$$

Here, E_m and p_m are respectively the energy and momentum of ν_m in the laboratory frame. In practice, our neutrino will be extremely relativistic, so we will be interested in evaluating

the phase factor of Eq. (4) where $t \approx L$, where it becomes $\exp[-i(E_m - p_m)L]$.

Imagine now that our ν_ℓ has been produced with a definite momentum p , so that all of its mass-eigenstate components have this common momentum. Then the ν_m component has $E_m = \sqrt{p^2 + M_m^2} \approx p + M_m^2/2p$, assuming that all neutrino masses M_m are small compared to the neutrino momentum. The phase factor of Eq. (4) is then approximately

$$e^{-i(M_m^2/2p)L}. \quad (5)$$

Alternatively, suppose that our ν_ℓ has been produced with a definite energy E , so that all of its mass-eigenstate components have this common energy [4]. Then the ν_m component has $p_m = \sqrt{E^2 - M_m^2} \approx E - M_m^2/2E$. The phase factor of Eq. (4) is then approximately

$$e^{-i(M_m^2/2E)L}. \quad (6)$$

Since highly relativistic neutrinos have $E \approx p$, the phase factors (5) and (6) are approximately equal. Thus, it doesn’t matter whether our ν_ℓ is created with definite momentum or definite energy.

From Eq. (2) and either Eq. (5) or Eq. (6), it follows that after a neutrino born as a ν_ℓ has propagated a distance L , its state vector has become

$$|\nu_\ell(L)\rangle \approx \sum_m U_{\ell m} e^{-i(M_m^2/2E)L} |\nu_m\rangle. \quad (7)$$

Using the unitarity of U to invert Eq. (2), and inserting the result in Eq. (7), we find that

$$|\nu_\ell(L)\rangle \approx \sum_{\ell'} \left[\sum_m U_{\ell m} e^{-i(M_m^2/2E)L} U_{\ell' m}^* \right] |\nu_{\ell'}\rangle. \quad (8)$$

We see that our ν_ℓ , in traveling the distance L , has turned into a superposition of all the flavors. The probability that it has flavor ℓ' , $P(\nu_\ell \rightarrow \nu_{\ell'}; L)$, is obviously given by

$$P(\nu_\ell \rightarrow \nu_{\ell'}; L) = |\langle \nu_{\ell'} | \nu_\ell(L) \rangle|^2 = \left| \sum_m U_{\ell m} e^{-i(M_m^2/2E)L} U_{\ell' m}^* \right|^2. \quad (9)$$

If it should turn out that the number of neutrino flavors, N , is greater than three, and that the N neutrinos of definite flavor are made up out of N light neutrino mass eigenstates, then the neutrino oscillation probability will still be given by this equation, but with U an $N \times N$, rather than 3×3 , unitary matrix.

The mixing matrix U is often called the “Maki-Nakagawa-Sakata matrix” in recognition of the very insightful early work of these three authors on neutrino mixing and oscillation [2].

The quantum mechanics of neutrino oscillation leading to the result Eq. (9) is somewhat subtle. It has been analyzed using wave packets [5], treating a propagating neutrino as a virtual particle [6], evaluating the phase acquired by a propagating mass eigenstate in terms of the proper time of propagation [3], requiring that a neutrino’s flavor cannot change

See key on page 239

unless the neutrino travels [4], and taking different neutrino mass eigenstates to have both different momenta and different energies [7]. The subtleties of oscillation are still being explored.

Frequently, a neutrino oscillation experiment is analyzed assuming that only two neutrino flavors, ν_e and ν_μ for example, mix appreciably. Then the mixing matrix U takes the form

$$U = \begin{pmatrix} \cos \theta_{e\mu} & \sin \theta_{e\mu} \\ -\sin \theta_{e\mu} & \cos \theta_{e\mu} \end{pmatrix}, \quad (10)$$

where $\theta_{e\mu}$ is the ν_e - ν_μ mixing angle. Inserting this matrix into Eq. (9), we find that

$$P(\nu_e \rightarrow \nu_\mu; L) = \sin^2 2\theta_{e\mu} \sin^2 (\Delta M_{21}^2 L/4E). \quad (11)$$

Here, $\Delta M_{21}^2 \equiv M_2^2 - M_1^2$, where ν_1 and ν_2 are the mass eigenstates which make up ν_e and ν_μ . If the omitted factors of \hbar and c are inserted into the argument $\Delta M_{21}^2 L/4E$ of the oscillatory sine function, it becomes $1.27 \Delta M_{21}^2 (\text{eV}^2)L (\text{km})/E (\text{GeV})$. The probability that a ν_e will retain its original flavor during propagation over a distance L is simply

$$P(\nu_e \rightarrow \nu_e; L) = 1 - P(\nu_e \rightarrow \nu_\mu; L). \quad (12)$$

When ν_e , ν_μ , and ν_τ all mix, but two of the three corresponding mass eigenstate neutrinos ν_m are nearly degenerate, neutrino oscillation is described by an expression nearly identical to the “two-neutrino formula” of Eq. (11). To be more precise, suppose that $|\Delta M_{21}^2| \ll |\Delta M_{31}^2| \cong |\Delta M_{32}^2|$, where $\Delta M_{mm'}^2 \equiv M_m^2 - M_{m'}^2$ is the splitting between the squared masses of mass eigenstates ν_m and $\nu_{m'}$. That is, ν_2 and ν_1 form a pair with a much smaller splitting than that between ν_3 and this pair. Now, suppose an oscillation experiment has L/E such that $|\Delta M_{31}^2|L/E$ is of order unity, so that $|\Delta M_{21}^2|L/E \ll 1$. For this experiment, it follows from Eq. (9) and the unitarity of U that [8]

$$P(\nu_\ell \rightarrow \nu_{\ell' \neq \ell}; L) \cong |2U_{\ell 3}U_{\ell' 3}|^2 \sin^2 (\Delta M_{31}^2 L/4E). \quad (13)$$

Because $|\Delta M_{21}^2|L/E \ll 1$, this experiment cannot “see” the splitting between ν_2 and ν_1 , so these two mass eigenstates behave as if they were a single one. Thus, in this experiment there appear to be only two mass eigenstates altogether, so it is no surprise that the expression for neutrino oscillation, Eq. (13), is very similar to the “two-neutrino” result of Eq. (11).

In a beam of neutrinos born with flavor ℓ_a , neutrino oscillation can be sought in two ways: First, one may seek the *appearance* in the beam of neutrinos of a different flavor, ℓ_b . Secondly, one may seek a *disappearance* of some of the original ν_{ℓ_a} flux, or an L - or E -dependence of this flux.

Clearly, no oscillation is expected unless L/E of the experiment is sufficiently large that the phase factors $\exp(-iM_m^2 L/2E)$ in Eq. (9) differ appreciably from one another. Otherwise, $P(\nu_\ell \rightarrow \nu_{\ell'}; L) = |\sum_m U_{\ell m}U_{\ell' m}^*|^2 = \delta_{\ell\ell'}$. Now, with omitted factors of \hbar and c inserted, the relative phase of $\exp(-iM_m^2 L/2E)$ and $\exp(-iM_{m'}^2 L/2E)$ is $2.54 \Delta M_{mm'}^2 (\text{eV}^2) L(\text{km})/E(\text{GeV})$. Thus, for example, an

experiment in which neutrinos with $E \approx 1$ GeV travel 1 km between production and detection will be sensitive to $\Delta M^2 \gtrsim 1 \text{ eV}^2$.

A more direct way than neutrino oscillation experiments to search for neutrino mass is to look for its kinematical effects in decays which produce a neutrino. In the decay $X \rightarrow Y\ell^+\nu_\ell$, where X is a hadron and Y is zero or more hadrons, the momenta of ℓ^+ and the particles in Y will obviously be modified if ν_ℓ has a mass. If ν_ℓ is a superposition of mass eigenstates ν_m , then $X \rightarrow Y\ell^+\nu_\ell$ is actually the sum of the decays $X \rightarrow Y\ell^+\nu_m$ yielding every ν_m light enough to be emitted. Thus, if, for example, one ν_m is much heavier than the others, the energy spectrum of ℓ^+ may show a threshold rise where the ℓ^+ energy becomes low enough for the heavy ν_m to be emitted [9]. However, if neutrino mixing is small, then the decays $X \rightarrow Y\ell^+\nu_m$ yield almost always the neutrino mass eigenstate which is the dominant component of ν_ℓ . The kinematics of ℓ^+ and Y then reflect the mass of this mass eigenstate.

From kinematical studies of the particles produced in ${}^3\text{H} \rightarrow {}^3\text{He} e^- \bar{\nu}_e$, $\pi \rightarrow \mu\nu_\mu$, and $\tau \rightarrow n\pi\nu_\tau$, various upper bounds on neutrino mass have been obtained. In the case of the decay ${}^3\text{H} \rightarrow {}^3\text{He} e^- \bar{\nu}_e$, the upper bound on the neutrino mass is derived from study of the e^- energy spectrum. It should be noted that in several experiments, the observed spectrum is not well fit by the standard theoretical expression, either with vanishing or nonvanishing neutrino mass. However, progress is being made in understanding the spectral anomalies [10].

Neutrinos carry neither electric charge nor, as far as we know, any other charge-like quantum numbers. To be sure, it may be that the reason an interacting “neutrino” creates an ℓ^- , while an “antineutrino” creates an ℓ^+ , is that neutrinos and antineutrinos carry opposite values of a conserved “lepton number.” However, there may be no lepton number. Even then, the fact that “neutrinos” and “antineutrinos” interact differently can be easily understood. One need only note that, in practice, the particles we call “neutrinos” are always left-handed, while the ones we call “antineutrinos” are right-handed. Since the weak interactions are not invariant under parity, it is then possible to attribute the difference between the interactions of “neutrinos” and “antineutrinos” to the fact that these particles are oppositely polarized.

If the neutrino mass eigenstates do not carry any charge-like attributes, they may be their own antiparticles. A neutrino which is its own antiparticle is called a Majorana neutrino, while one which is not is called a Dirac neutrino.

If neutrinos are of Majorana character, we can have neutrinoless double beta-decay ($\beta\beta_{0\nu}$), in which one nucleus decays to another by emitting two electrons and nothing else. This process can be initiated through the emission of two virtual W bosons by the parent nucleus. One of these W bosons then emits an electron and an accompanying virtual “antineutrino.” In the Majorana case, this “antineutrino” is no different from a “neutrino,” except for its right-handed helicity. If the virtual

Lepton Particle Listings

Neutrinos

neutrino has a mass, then (like the e^+ in nuclear β -decay), it is not fully right-handed, but has a small amplitude, proportional to its mass, for being left-handed. Its left-handed component is precisely what we call a “neutrino,” and can be absorbed by the second virtual W boson to create the second outgoing electron. This mechanism yields for $\beta\beta_{0\nu}$ an amplitude proportional to an effective neutrino mass $\langle M \rangle$, given in a common phase convention by [11]

$$\langle M \rangle = \sum_m U_{em}^2 M_m . \quad (14)$$

Experimental upper bounds on the $\beta\beta_{0\nu}$ rate are used to derive upper bounds on $\langle M \rangle$. Note that, owing to possible phases in the mixing matrix elements U_{em} , the relation between $\langle M \rangle$ and the actual masses M_m of the neutrino mass eigenstates can be somewhat complicated. The process $\beta\beta_{0\nu}$ is discussed further by P. Vogel in this *Review*.

If neutrinos are their own antiparticles, then their magnetic and electric dipole moments must vanish. To see why, recall that CPT invariance requires that the dipole moments of the electron and its antiparticle be equal and opposite. Similarly, CPT invariance would require that the dipole moments of a neutrino and its antiparticle be equal and opposite. But, if the antiparticle of the neutrino is the neutrino itself, this means that the dipole moments must vanish [12].

If neutrinos are not their own antiparticles, then they can have dipole moments. However, for a Dirac neutrino mass eigenstate ν_m , the magnetic dipole moment μ_m predicted by the Standard Model (extended to include neutrino masses) is only [13]

$$\mu_m = 3.2 \times 10^{-19} M_m (\text{eV}) \mu_B , \quad (15)$$

where μ_B is the Bohr magneton.

Whether neutrinos are their own antiparticles or not, there may be *transition* magnetic and electric dipole moments. These induce the transitions $\nu_m \rightarrow \nu_{m' \neq m} \gamma$.

A Majorana neutrino, being its own antiparticle, obviously consists of just two states: spin up and spin down. In contrast, a Dirac neutrino, together with its antiparticle, consists of four states: the spin-up and spin-down neutrino states, plus the spin-up and spin-down antineutrino states. A four-state Dirac neutrino may be pictured as comprised of two degenerate two-state Majorana neutrinos. Conversely, in the field-theory description of neutrinos, by introducing so-called Majorana mass terms, one can split a Dirac neutrino, D , into two nondegenerate Majorana neutrinos, ν and N . In some extensions of the SM, it is natural for the D , ν , and N masses, M_D , M_ν , and M_N , to be related by

$$M_\nu M_N \approx M_D^2 . \quad (16)$$

In these extensions, it is also natural for M_D to be of the order of $M_{\ell \text{ or } q}$, the mass of a typical charged lepton or quark. Then we have [14]

$$M_\nu M_N \sim M_{\ell \text{ or } q}^2 . \quad (17)$$

Suppose now that $M_N \gg M_{\ell \text{ or } q}$, so that N is a very heavy neutrino which has not yet been observed. Then relation Eq. (17), known as the seesaw relation, implies that $M_\nu \ll M_{\ell \text{ or } q}$. Thus, ν is a candidate for one of the light neutrino mass eigenstates which make up ν_e , ν_μ , and ν_τ . So long as N is heavy, the seesaw relation explains, without fine tuning, why a mass eigenstate component of ν_e , ν_μ , or ν_τ will be light. Interestingly, the picture from which the seesaw relation arises predicts that the mass eigenstate components of ν_e , ν_μ , and ν_τ are Majorana neutrinos.

There are three reported indications that neutrinos actually oscillate in nature, and thus have mass. There is rather convincing evidence that the atmospheric neutrinos oscillate, fairly strong evidence that the solar neutrinos do, and so-far unconfirmed evidence that the neutrinos studied by the LSND experiment do as well.

The atmospheric neutrinos are produced in the earth's atmosphere by cosmic rays, and then detected in an underground detector. Incident on this detector are neutrinos coming from all directions, created in the atmosphere all around the earth. The most compelling evidence that something very interesting happens to these atmospheric neutrinos en route to the detector is the fact that the detected upward-going atmospheric ν_μ flux U (coming from all directions below the horizontal at the detector) differs from the corresponding downward-going flux D . Suppose that neither neutrino oscillation nor any other mechanism decreases or increases the ν_μ flux as the neutrinos travel from their points of origin to the detector. Then, as illustrated in Fig. 1, any ν_μ that enters the sphere S defined in the figure caption will later exit this sphere. Thus, since we are dealing with a steady-state situation, the total ν_μ fluxes entering and exiting S per unit time must be equal. Now, for neutrino energies above a few GeV, the flux of cosmic rays which produce the atmospheric neutrinos is isotropic. Consequently, these neutrinos are being created at the same rate all around the earth. Owing to this spherical symmetry, the equality between the ν_μ fluxes entering and exiting S must hold at any point of S , such as the location of the detector. Now, as shown in Fig. 1, a ν_μ entering S through the detector must be part of the downward-going flux D . One exiting S through the detector must be part of the upward-going flux U . Thus, the equality of the ν_μ fluxes entering and exiting S at the detector implies that $D = U$. (It is easily shown that this equality must hold not only for the integrated downward and upward fluxes, but angle by angle. That is, the flux coming down from zenith angle θ_Z must equal that coming up from angle $\pi - \theta_Z$.)

The underground Super-Kamiokande detector (Super-K) finds that for multi-GeV atmospheric muon neutrinos [15],

$$\frac{\text{Flux Up}(-1.0 < \cos \theta_Z < -0.2)}{\text{Flux Down}(+0.2 < \cos \theta_Z < +1.0)} = 0.52 \pm 0.05 , \quad (18)$$

in strong disagreement with the requirement that the upward and downward fluxes be equal. Thus, some mechanism must be changing the ν_μ flux as the neutrinos travel to the detector.

See key on page 239

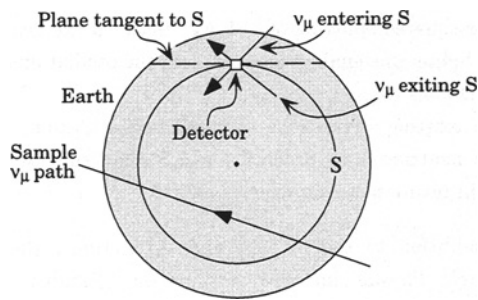


Figure 1: Atmospheric muon neutrino fluxes at an underground detector. S is a sphere centered at the center of the earth and passing through the detector.

The most attractive candidate for this mechanism is neutrino oscillation. Since the atmospheric ν_e flux is compatible with up-down symmetry, the electron neutrinos do not seem to be involved significantly in this oscillation. All of the detailed Super-K atmospheric neutrino data are well described by the hypothesis that $\nu_\mu \rightarrow \nu_\tau$ oscillation is occurring, with [16]

$$2 \times 10^{-3} \text{eV}^2 \lesssim \Delta M^2 \lesssim 6 \times 10^{-3} \text{eV}^2 \quad (19)$$

and

$$\sin^2 2\theta \approx 1. \quad (20)$$

Other experiments favor roughly similar regions of parameter space [17].

The order of magnitude of the splitting ΔM^2 in Eq. (19) may be understood by noting that for $E \sim 1$ GeV, upward-going neutrinos have $L/E \sim 10^4 \text{km}/1 \text{GeV}$, while downward-going ones have $L/E \sim 10 \text{km}/1 \text{GeV}$. Thus, if $\Delta M^2 \sim 10^{-3} \text{eV}^2$, the argument $[1.27\Delta M^2(\text{eV}^2)L(\text{km})/E(\text{GeV})]$ of the oscillatory factor in Eq. (11) (applied to the relevant observation channel) exceeds unity for the upward-going neutrinos, but is quite small for the downward-going ones. As a result, the upward-going muon neutrinos oscillate away into neutrinos of another flavor, but the downward-going ones do not. This explains why the flux ratio of Eq. (18) is less than unity.

Conceivably, upward-going muon neutrinos are disappearing, not as a result of neutrino oscillation, but through neutrino decay. This possibility is theoretically less likely than oscillation. However, it is interesting to note that it is not at all excluded by the present data [18]. Of course, neutrino decay, like neutrino oscillation, implies neutrino mass.

The flux of solar neutrinos has been detected on earth by several experiments [19] with different neutrino energy thresholds. In every experiment, the flux is found to be below the corresponding prediction of the Standard Solar Model (SSM) [20]. The discrepancies between the observed fluxes and the SSM predictions have proven very difficult to explain by simply modifying the SSM, without invoking neutrino mass [21]. Indeed, we know of no attempt which has succeeded despite very serious

and clever attempts [22–24]. By contrast, all the existing observations can successfully and elegantly be explained if one does invoke neutrino mass. The most popular explanation of this type is based on the Mikheyev-Smirnov-Wolfenstein (MSW) effect—a matter-enhanced neutrino oscillation [25].

The neutrinos produced by the nuclear processes that power the sun are electron neutrinos ν_e . With some probability, the MSW effect converts a ν_e into a neutrino ν_x of another flavor. Depending on the specific version of the effect, ν_x is a ν_μ , a ν_τ , a ν_μ - ν_τ mixture, or perhaps a sterile neutrino ν_s . Since present solar neutrino detectors are sensitive to a ν_e , but wholly, or at least largely, insensitive to a ν_μ , ν_τ , or ν_s , the flavor conversion accounts for the low observed fluxes.

The MSW $\nu_e \rightarrow \nu_x$ conversion results from interaction between neutrinos and solar electrons as the neutrinos travel outward from the solar core, where they were produced. When, for example, the neutrino mixing is small, the conversion requires that, somewhere in the sun, the total energy of a ν_e of given momentum, including the energy of its interaction with the solar electrons, equal the total energy of the ν_x of the same momentum, so that we have an energy level crossing. Given the typical density of solar electrons, and the typical momenta of solar neutrinos, the condition that there be a level crossing requires that

$$M_{\nu_x}^2 - M_{\nu_e}^2 \equiv \Delta M_{\nu_x \nu_e}^2 \sim 10^{-5} \text{eV}^2, \quad (21)$$

where M_{ν_e} , continuing to assume small mixing, is the mass of the dominant mass eigenstate component of ν_e , and similarly for M_{ν_x} .

The observed solar neutrino fluxes can also be explained by supposing that on their way from the sun to the earth, the electron neutrinos produced in the solar core undergo vacuum oscillation into neutrinos of another flavor [26]. Assuming that only two neutrino flavors are important to this oscillation, the oscillation probability is described by an expression of the form given by Eq. (11). To explain the observed suppression of the solar ν_e flux to less than half the predicted value at some energies, and to accommodate the observation that the suppression is energy-dependent, the argument $[1.27\Delta M^2(\text{eV}^2)L(\text{km})/E(\text{GeV})]$ of the oscillatory factor in Eq. (11) must be of order unity when L is the distance from the sun to the earth, and $E \simeq 1$ MeV is the typical energy of a solar neutrino. Perhaps this apparent coincidence makes the vacuum oscillation explanation of the solar neutrino observations less likely than the MSW explanation. To have $[1.27\Delta M^2(\text{eV}^2)L(\text{km})/E(\text{GeV})] \sim 1$, we require that $\Delta M^2 \sim 10^{-10} \text{eV}^2$.

In addition to measuring the solar neutrino fluxes, one can explore the physics of the solar neutrinos by studying the solar ν_e energy spectrum [27], by probing the dependence of the solar ν_e flux on whether it is day or night, and on the time of night [28], and by measuring the solar ν_e flux as a function of the season of the year. The Super-K experiment is doing all of these things [29].

Lepton Particle Listings

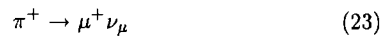
Neutrinos

The solar neutrino experiments, and the comparison between their results and theoretical predictions, are discussed in some detail by K. Nakamura in this *Review*.

The LSND experiment [30] has studied neutrinos from stopped positively-charged pions, which decay via the chain



We note that this chain does not produce $\bar{\nu}_e$, but an excess of $\bar{\nu}_e$ over expected background is reported by the experiment. This excess is interpreted as arising from oscillation of the $\bar{\nu}_\mu$ which the chain does produce into $\bar{\nu}_e$. Since the experiment has $L(\text{km})/E(\text{GeV}) \sim 1$, the implied mass splitting is $\Delta M^2 \gtrsim 1 \text{ eV}^2$. LSND finds supporting evidence for its reported oscillation in a study of the neutrinos from the decay



of positively-charged pions in flight [31].

Other experiments do not observe the oscillation seen by LSND, and allow only some of the $(\Delta M^2, \sin^2 2\theta)$ region favored by LSND. However, these other experiments do not exclude the oscillation interpretation of the LSND data [32,33].

Suppose we assume that the behavior of the atmospheric, solar, and LSND neutrinos are all to be understood in terms of neutrino oscillation. What neutrino masses are then suggested?

If there are only three neutrinos of definite flavor, ν_e , ν_μ , and ν_τ , made up out of just three neutrinos of definite mass, ν_1 , ν_2 , and ν_3 , then there are only three mass splittings $\Delta M_{mm'}^2$, and they obviously satisfy

$$\begin{aligned} \Delta M_{32}^2 + \Delta M_{21}^2 + \Delta M_{13}^2 = \\ (M_3^2 - M_2^2) + (M_2^2 - M_1^2) + (M_1^2 - M_3^2) = 0. \end{aligned} \quad (24)$$

Now, as we have seen, the ΔM^2 values required to explain the atmospheric, solar, and LSND oscillations are of three different orders of magnitude. Thus, they cannot possibly obey the constraint of Eq. (24). Hence, to explain all three of the reported neutrino oscillations, one must introduce a fourth neutrino. Since this neutrino is known to make no contribution to the width of the Z^0 [34], it must be a neutrino which does not participate in the normal weak interactions—a “sterile” neutrino.

One four-neutrino scheme which accounts for all three reported oscillations contains the following neutrino mass eigenstates: A nearly degenerate pair, ν_3 , ν_2 , with $M_3 \approx M_2 \sim 1 \text{ eV}$, and a much lighter pair, ν_1 , ν_0 , with the mass of ν_0 , M_0 , roughly $3 \times 10^{-3} \text{ eV}$, and $M_1 \ll M_0$. The mass splitting $M_3^2 - M_2^2$ is chosen to be $\sim 4 \times 10^{-3} \text{ eV}^2$ to explain the oscillation of the atmospheric neutrinos. Interpreting that oscillation as $\nu_\mu \rightarrow \nu_\tau$ with near maximal mixing, we take ν_2 and ν_3 to be approximately 50-50 mixtures of ν_μ and ν_τ . The splitting $M_0^2 - M_1^2 \approx M_0^2 \sim 10^{-5} \text{ eV}^2$ allows us to interpret the solar neutrino observations in terms of the MSW effect. We take ν_1

to be largely ν_e , and ν_0 to be largely a sterile neutrino ν_s , so that the MSW effect converts ν_e to a sterile neutrino. Finally, the mass-squared splitting of $\sim 1 \text{ eV}^2$ between the heavier pair and the lighter one enables us to explain the oscillation reported by LSND [35].

The existing indications of neutrino oscillation, and the possible neutrino-mass scenarios which they suggest, will be probed in future neutrino experiments.

In addition to the ν_e , ν_μ , and ν_τ sections, the *Review of Particle Physics* includes sections on “Number of Light Neutrino Types,” “Heavy Lepton Searches,” and “Searches for Massive Neutrinos and Lepton Mixing.” Also see other recent reviews [36].

References

1. G. Danby *et al.*, Phys. Rev. Lett. **9**, 36 (1962).
2. Z. Maki, M. Nakagawa, and S. Sakata, Prog. Theor. Phys. **28**, 870 (1962); B. Pontecorvo, Zh. Eksp. Teor. Fiz. **53**, 1717 (1967) [Sov. Phys. JETP **26**, 984 (1968)]; V. Gribov and B. Pontecorvo, Phys. Lett. **B28**, 493 (1969); S. Bilenky and B. Pontecorvo, Phys. Reports **C41**, 225 (1978); A. Mann and H. Primakoff, Phys. Rev. **D15**, 655 (1977).
3. B. Kayser and L. Stodolsky, Phys. Lett. **B359**, 343 (1995). See also Y. Srivastava, A. Widom, and E. Sassaroli, Z. Phys. **C66**, 601 (1995).
4. Y. Grossman and H. Lipkin, Phys. Rev. **D55**, 2760 (1997); H. Lipkin, Phys. Lett. **B348**, 604 (1995).
5. B. Kayser, Phys. Rev. **D24**, 110 (1981); C. Giunti, C. Kim, and U. Lee, Phys. Rev. **D44**, 3635 (1991).
6. J. Rich, Phys. Rev. **D48**, 4318 (1993); W. Grimus and P. Stockinger, Phys. Rev. **D54**, 3414 (1996); W. Grimus, S. Mohanty, and P. Stockinger, eprint hep-ph/9904340.
7. T. Goldman, eprint hep-ph/9604357; F. Boehm and P. Vogel, *Physics of Massive Neutrinos* (Cambridge University Press, Cambridge, 1987) p. 87.
8. S. Bilenky, *Proceedings of the XV Workshop on Weak Interactions and Neutrinos*, eds. G. Bonneaud, V. Brisson, T. Kafka, and J. Schneps (Tufts University, Medford, 1995) p. 1122.
9. R. Shrock, Phys. Lett. **B96**, 159 (1980); Phys. Rev. **D24**, 1232 (1981); Phys. Rev. **D24**, 1275 (1981).
10. E. Otten, talk presented at the Workshop on Low-Energy Neutrino Physics, Institute for Nuclear Theory, Univ. of Washington, July 1999; V. Lobashev, *ibid.*; R.G.H. Robertson *et al.*, Phys. Rev. Lett. **67**, 957 (1991); H. Kawakami *et al.*, Phys. Lett. **B256**, 105 (1991); E. Holzschuh *et al.*, Phys. Lett. **B287**, 381 (1992); W. Stoeffl and D. Decman, Phys. Rev. Lett. **75**, 3237 (1995); H. Backe *et al.*, *Proceedings of the 17th Int. Conf. on Neutrino Physics and Astrophysics*, eds. K. Engvist, K. Huitu, and J. Maalampi (World Scientific, Singapore, 1997) p. 259; V. Lobashev *et al.*, *ibid.*, p. 264.

-
11. M. Doi *et al.*, Phys. Lett. **B102**, 323 (1981);
L. Wolfenstein, Phys. Lett. **B107**, 77 (1981);
B. Kayser and A. Goldhaber, Phys. Rev. **D28**, 2341 (1983);
B. Kayser, Phys. Rev. **D30**, 1023 (1984);
S. Bilenky, N. Nedelcheva, and S. Petcov, Nucl. Phys. **B247**, 61 (1984).
 12. For further discussion of the physics of Majorana neutrinos, see, for example, B. Kayser, F. Gibrat-Debu, and F. Perrier, *The Physics of Massive Neutrinos* (World Scientific, Singapore, 1989).
 13. B.W. Lee and R. Shrock, Phys. Rev. **D16**, 1444 (1977);
K. Fujikawa and R. Shrock, Phys. Rev. Lett. **45**, 963 (1980).
 14. M. Gell-Mann, P. Ramond, and R. Slansky, in *Supergravity*, eds. D. Freedman and P. van Nieuwenhuizen (North Holland, Amsterdam, 1979) p. 315;
T. Yanagida, in *Proceedings of the Workshop on Unified Theory and Baryon Number in the Universe*, eds. O. Sawada and A. Sugamoto (KEK, Tsukuba, Japan, 1979);
R. Mohapatra and G. Senjanovic, Phys. Rev. Lett. **44**, 912 (1980) and Phys. Rev. **D23**, 165 (1981).
 15. A. Mann, talk presented at the XIX Int. Symposium on Lepton-Photon Interactions, Stanford University, August, 1999, eprint hep-ex/9912007.
 16. R. Wilkes, talk presented on behalf of the Super-K Collaboration on 27 July 1999, at the Workshop on Low-Energy Neutrino Physics at the Inst. for Nucl. Theory, Univ. of Washington, Seattle.
 17. D. Michael, for the MACRO Collaboration, in *Proc. 29th Int. Conf. High Energy Phys.*, edited by A. Astbury, D. Axen, and J. Robinson (World Scientific, Singapore, 1999) p. 584;
H. Gallagher, for the Soudan 2 Collaboration, *ibid.* p. 579;
Y. Fukuda *et al.*, Phys. Lett. **B335**, 237 (1994).
 18. V. Barger *et al.*, Phys. Lett. **B462**, 109 (1999).
 19. Y. Fukuda *et al.*, Phys. Rev. Lett. **81**, 1158 (1998);
B. Cleveland *et al.*, Ap. J. **496**, 505 (1998);
T. Kirsten for the GALLEX and GNO Collaborations, Nucl. Phys. Proc. Suppl. **77**, 26 (1999);
Dzh. Abdurashitov for the SAGE Collaboration, *ibid.*, p. 20.
 20. J. Bahcall, S. Basu, and M. Pinsonneault, Phys. Lett. **B433**, 1 (1998).
 21. J. Bahcall and H. Bethe, Phys. Rev. Lett. **65**, 2233 (1990) and Phys. Rev. **D44**, 2962 (1991);
N. Hata and P. Langacker, Phys. Rev. **D56**, 6107 (1997).
 22. N. Hata, S. Bludman, and P. Langacker, Phys. Rev. **D49**, 3622 (1994).
 23. K.M. Heeger and R.G.H. Robertson, Phys. Rev. Lett. **77**, 3720 (1996).
 24. J.N. Bahcall, P.I. Krastev, and A.Yu. Smirnov, Phys. Rev. **D58**, 096016 (1998).
 25. L. Wolfenstein, Phys. Rev. **D17**, 2369 (1978) and Phys. Rev. **D20**, 2634 (1979);
S. Mikheyev and A. Smirnov, Yad. Fiz. **42**, 1441 (1985) [Sov. J. Nucl. Phys. **42**, 913 (1985)]; Nuovo Cimento **9C**, 17 (1986).
 26. P. Krastev and S. Petcov, Phys. Rev. **D53**, 1665 (1996).
 27. However, this spectrum may be modified by unexpectedly large contributions from sources other than ^8B decay, as emphasized in R. Escrivano, J.-M. Frere, A. Gevaert, and D. Monderen, Phys. Lett. **B444**, 397 (1998).
 28. M. Maris and S. Petcov, Phys. Rev. **D56**, 7444 (1997);
S. Petcov, Phys. Lett. **B434**, 321 (1998).
 29. Y. Fukuda *et al.*, (the Super-Kamiokande Collaboration), Phys. Rev. Lett. **82**, 2430 (1999); *ibid.* p. 1810.
 30. C. Athanassopoulos *et al.*, (LSND Collaboration), Phys. Rev. **C54**, 2685 (1996) and Phys. Rev. Lett. **77**, 3082 (1996).
 31. C. Athanassopoulos *et al.*, (LSND Collaboration), Phys. Rev. Lett. **81**, 1774 (1998) and Phys. Rev. **C58**, 2511 (1998).
 32. R. Maschuw, talk presented at the 17th Int. Workshop on Weak Interactions and Neutrinos, Cape Town, South Africa, January 1999;
K. Eitel, eprint hep-ex/9909036.
 33. There is an interesting argument that the r process in supernovae may be an additional hint of neutrino oscillation. See Y.-Z. Qian and G. Fuller, Phys. Rev. **D52**, 656 (1995), and references therein.
 34. D. Karlen, in this *Review*.
 35. This is a somewhat modified version of a neutrino-mass scenario proposed in D. Caldwell and R. Mohapatra, Phys. Rev. **D48**, 3259 (1993). In constructing this scenario, we have not assumed that neutrinos are a component of the dark matter in the universe. See also J. Peltoniemi, D. Tommasini, and J. Valle, Phys. Lett. **B298**, 383 (1993);
V. Barger, S. Pakvasa, T. Weiler, and K. Whisnant, Phys. Rev. **D58**, 093016 (1998).
 36. Recent detailed reviews of neutrino mass and oscillation include K. Zuber, Phys. Rept. **305**, 295 (1998);
S. Bilenky, C. Giunti, and W. Grimus, Prog. Part. Nucl. Phys. **43**, 1 (1999);
G. Altarelli and F. Feruglio, in *Venice 1999, Neutrino Telescopes*, **2**, 353;
P. Fisher, B. Kayser, and K. McFarland, *Ann. Rev. Nucl. Part. Sci.*, **49**, eds. C. Quigg, V. Luth, and P. Paul (Annual Reviews, Palo Alto, California, 1999) p. 481.
-

Number of Light Neutrino Types

The neutrinos referred to in this section are those of the Standard $SU(2) \times U(1)$ Electroweak Model possibly extended to allow nonzero neutrino masses. Light neutrinos are those with $m_\nu < m_Z/2$. The limits are on the number of neutrino families or species, including ν_e, ν_μ, ν_τ .

THE NUMBER OF LIGHT NEUTRINO TYPES FROM COLLIDER EXPERIMENTS

Revised August 1999 by D. Karlen (Carleton University).

The most precise measurements of the number of light neutrino types, N_ν , come from studies of Z production in e^+e^- collisions. The invisible partial width, Γ_{inv} , is determined by subtracting the measured visible partial widths, corresponding to Z decays into quarks and charged leptons, from the total Z width. The invisible width is assumed to be due to N_ν light neutrino species each contributing the neutrino partial width Γ_ν as given by the Standard Model. In order to reduce the model dependence, the Standard Model value for the ratio of the neutrino to charged leptonic partial widths, $(\Gamma_\nu/\Gamma_\ell)_{\text{SM}} = 1.991 \pm 0.001$, is used instead of $(\Gamma_\nu)_{\text{SM}}$ to determine the number of light neutrino types:

$$N_\nu = \frac{\Gamma_{\text{inv}}}{\Gamma_\ell} \left(\frac{\Gamma_\ell}{\Gamma_\nu} \right)_{\text{SM}} \quad (1)$$

The combined result from the four LEP experiments is $N_\nu = 2.984 \pm 0.008$ [1].

In the past, when only small samples of Z decays had been recorded by the LEP experiments and by the Mark II at SLC, the uncertainty in N_ν was reduced by using Standard Model fits to the measured hadronic cross sections at several center-of-mass energies near the Z resonance. Since this method is much more dependent on the Standard Model, the approach described above is favored.

Before the advent of the SLC and LEP, limits on the number of neutrino generations were placed by experiments at lower-energy e^+e^- colliders by measuring the cross section of the process $e^+e^- \rightarrow \nu\bar{\nu}\gamma$. The ASP, CELLO, MAC, MARK J, and VENUS experiments observed a total of 3.9 events above background [2], leading to a 95% CL limit of $N_\nu < 4.8$. This process has a much larger cross section at center-of-mass energies near the Z mass and has been measured at LEP by the ALEPH, DELPHI, L3, and OPAL experiments [3]. These experiments have observed several thousand such events, and the combined result is $N_\nu = 3.00 \pm 0.08$. The same process has been measured by the LEP experiments at center-of-mass energies approaching 100 GeV above the Z mass, in searches for new physics. Combined, the measured cross section is 0.965 \pm 0.028 of that expected for 3 light neutrino generations [1].

Experiments at $p\bar{p}$ colliders also placed limits on N_ν by determining the total Z width from the observed ratio of $W^\pm \rightarrow \ell^\pm\nu$ to $Z \rightarrow \ell^+\ell^-$ events [4]. This involved a calculation that assumed Standard Model values for the total W width and the ratio of W and Z leptonic partial widths, and used an estimate of the ratio of Z to W production cross sections.

Now that the Z width is very precisely known from the LEP experiments, the approach is now one of those used to determine the W width.

References

1. The LEP Collaborations and the LEP Electroweak Working Group, as reported by J. Mnich at the International Europhysics Conference, Tampere, Finland (July 1999).
2. VENUS: K. Abe *et al.*, Phys. Lett. **B232**, 431 (1989); ASP: C. Hearty *et al.*, Phys. Rev. **D39**, 3207 (1989); CELLO: H.J. Behrend *et al.*, Phys. Lett. **B215**, 186 (1988); MAC: W.T. Ford *et al.*, Phys. Rev. **D33**, 3472 (1986); MARK J: H. Wu, Ph.D. Thesis, Univ. Hamburg (1986).
3. L3: M. Acciarri *et al.*, Phys. Lett. **B431**, 199 (1998); DELPHI: P. Abreu *et al.*, Z. Phys. **C74**, 577 (1997); OPAL: R. Akers *et al.*, Z. Phys. **C65**, 47 (1995); ALEPH: D. Buskulic *et al.*, Phys. Lett. **B313**, 520 (1993).
4. UA1: C. Albajar *et al.*, Phys. Lett. **B198**, 271 (1987); UA2: R. Ansari *et al.*, Phys. Lett. **B186**, 440 (1987).

Number from e^+e^- Colliders**Number of Light ν Types**

Our evaluation uses the invisible and leptonic widths of the Z boson from our combined fit shown in the Particle Listings for the Z Boson, and the Standard Model value $\Gamma_\nu/\Gamma_\ell = 1.9908 \pm 0.0015$.

VALUE	DOCUMENT ID	TECN
2.994 \pm 0.012 OUR EVALUATION	Combined fit to all LEP data.	
• • • We do not use the following data for averages, fits, limits, etc. • • •		
3.00 \pm 0.05	¹ LEP	92 RVUE

¹ Simultaneous fits to all measured cross section data from all four LEP experiments.

Number of Light ν Types from Direct Measurement of Invisible Z Width

In the following, the invisible Z width is obtained from studies of single-photon events from the reaction $e^+e^- \rightarrow \nu\bar{\nu}\gamma$. All are obtained from LEP runs in the $E_{\text{cm}}^{\text{eff}}$ range 88–94 GeV.

VALUE	DOCUMENT ID	TECN	COMMENT
3.00 \pm 0.06 OUR AVERAGE			
3.01 \pm 0.08	ACCIARRI	99R L3	1998 LEP run
2.98 \pm 0.07 \pm 0.07	ACCIARRI	98G L3	LEP 1991–1994
2.89 \pm 0.32 \pm 0.19	ABREU	97J DLPH	1993–1994 LEP runs
3.23 \pm 0.16 \pm 0.10	AKERS	95C OPAL	1990–1992 LEP runs
2.68 \pm 0.20 \pm 0.20	BUSKULIC	93L ALEP	1990–1991 LEP runs
• • • We do not use the following data for averages, fits, limits, etc. • • •			
3.1 \pm 0.6 \pm 0.1	ADAM	96C DLPH	$\sqrt{s} = 130, 136$ GeV

Limits from Astrophysics and Cosmology**Number of Light ν Types**

("light" means $<$ about 1 MeV). See also OLIVE 81. For a review of limits based on Nucleosynthesis, Supernovae, and also on terrestrial experiments, see DENEGR1 90. Also see "Big-Bang Nucleosynthesis" in this Review.

VALUE	DOCUMENT ID	COMMENT
• • • We do not use the following data for averages, fits, limits, etc. • • •		
2 < N_ν < 4	LISI	99 BBN
< 4.3	OLIVE	99 BBN
< 4.9	COPI	97 Cosmology
< 3.6	HATA	97B High D/H quasar abs.
< 4.0	OLIVE	97 BBN; high ⁴ He and ⁷ Li
< 4.7	CARDALL	96B Cosmology, High D/H quasar abs.
< 3.9	FIELDS	96 Cosmology, BBN; high ⁴ He and ⁷ Li
< 4.5	KERNAN	96 Cosmology, High D/H quasar abs.
< 3.6	OLIVE	95 BBN; ≥ 3 massless ν
< 3.3	WALKER	91 Cosmology
< 3.4	OLIVE	90 Cosmology
< 4	YANG	84 Cosmology
< 4	YANG	79 Cosmology
< 7	STEIGMAN	77 Cosmology
	PEEBLES	71 Cosmology
< 16	² SHVARTSMAN	69 Cosmology
	HOYLE	64 Cosmology

² SHVARTSMAN 69 limit inferred from his equations.

Number Coupling with Less Than Full Weak Strength

VALUE	DOCUMENT ID	TECN
• • • We do not use the following data for averages, fits, limits, etc. • • •		
< 20	³ OLIVE	81C COSM
< 20	³ STEIGMAN	79 COSM

³ Limit varies with strength of coupling. See also WALKER 91.

Lepton Particle Listings

Number of Light Neutrino Types, Massive Neutrinos and Lepton Mixing

REFERENCES FOR Limits on Number of Light Neutrino Types

ACCIARRI	99R	PL B470 268	M. Acciari et al.	(L3 Collab.)
LISI	99	PR D59 123520	E. Lisi, S. Sarkar, F.L. Villante	
OLIVE	99	ASP 11 403	K.A. Olive, D. Thomas	
ACCIARRI	98G	PL B431 199	M. Acciari et al.	(L3 Collab.)
ABREU	97J	ZPHY C74 577	P. Abreu et al.	(DELPHI Collab.)
COPI	97	PR D55 3389	C.J. Copi, D.N. Schramm, M.S. Turner	(CHIC)
HATA	97B	PR D55 540	N. Hata et al.	(OSU, PENN)
OLIVE	97	ASP 7 27	K.A. Olive, D. Thomas	(MINN, FLOR)
AOAM	96C	PL B380 471	W. Adam et al.	(DELPHI Collab.)
CARDALL	96B	APJ 472 435	C.Y. Cardall, G.M. Fuller	(UCSD)
FIELDS	96	New Ast 1 77	B.D. Fields et al.	(NDAM, CERN, MINN+)
KERNAN	96	PR D54 3681	P.S. Kernan, S. Sarkar	(CASE, OXFTRP)
AKERS	95C	ZPHY C65 47	R. Akers et al.	(OPAL Collab.)
OLIVE	95	PL B354 357	K.A. Olive, G. Steigman	(MINN, OSU)
BUSKULIC	93L	PL B313 520	D. Buskulic et al.	(ALEPH Collab.)
LEP	92	PL B276 247	LEP et al.	(LEP Collab.)
WALKER	91	APJ 376 51	T.P. Walker et al.	(HSCA, OSU, CHIC+)
DENEGRİ	90	RMP 62 1	D. Deneğri, B. Sadoulet, M. Spiro	(CERN, UCB+)
OLIVE	90	PL B236 454	K.A. Olive et al.	(MINN, CHIC, OSU+)
YANG	84	APJ 281 493	J. Yang et al.	(CHIC, BART)
OLIVE	81	APJ 246 557	K.A. Olive et al.	(CHIC, BART)
OLIVE	81C	NP B189 497	K.A. Olive, D.N. Schramm, G. Steigman	(EFI+)
STEIGMAN	79	PRL 43 239	G. Steigman, K.A. Olive, D.N. Schramm	(BART+)
YANG	79	APJ 227 697	J. Yang et al.	(CHIC, YALE, VIRG)
STEIGMAN	77	PL 66B 202	G. Steigman, D.N. Schramm, J.R. Gunn	(YALE, CHIC+)
PEEBLES	71	Physical Cosmology	P.Z. Peebles	(PRIN)
		Princeton Univ. Press (1971)		
SHVARTSMAN	69	JETPL 9 184	Shvartsman	(MOSU)
		Translated from ZETFP 9 315.		
HOYLE	64	Nature 203 1106	Hoyle, Tayler	(CAMB)

Massive Neutrinos and Lepton Mixing, Searches for

SEARCHES FOR MASSIVE NEUTRINOS

Revised April 2000 by D.E. Groom (LBNL).

Searches for massive neutral leptons and the effects of nonzero neutrino masses are listed here. These results are divided into the following main sections:

- A. Heavy neutral lepton mass limits;
- B. Sum of neutrino masses;
- C. Searches for neutrinoless double- β decay (see the note by P. Vogel on "Searches for neutrinoless double- β decay" preceding this section);
- D. Other bounds from nuclear and particle decays;
- E. Solar ν experiments (see the note on "Solar Neutrinos" by K. Nakamura preceding this section);
- F. Astrophysical neutrino observations;
- G. Reactor $\bar{\nu}_e$ disappearance experiments;
- H. Accelerator neutrino appearance experiments;
- I. Disappearance experiments with accelerator and radioactive source neutrinos.

Direct searches for masses of dominantly coupled neutrinos are listed in the appropriate sections on ν_e , ν_μ , or ν_τ , where it is assumed that the mass eigenstates ν_1 , ν_2 , and ν_3 predominately couple to ν_e , ν_μ , and ν_τ , respectively. Note that the assumptions made in these Listings, that ν_2 predominately couples to ν_μ and ν_3 to ν_τ , may not be true. Searches for massive charged leptons are listed elsewhere, and searches for the mixing of $(\mu^- e^+)$ and $(\mu^+ e^-)$ are given in the muon Listings.

Discussion of the current neutrino mass limits and the theory of mixing are given in the note on "Neutrino Mass" by Boris Kayser just before the ν_e Listings.

In many of the following Listings (e.g. neutrino disappearance and appearance experiments), results are presented assuming that mixing occurs only between two neutrino species, such as $\nu_\tau \leftrightarrow \nu_e$. This assumption is also made for lepton-number violating mixing between two states, such as $\nu_e \leftrightarrow \bar{\nu}_\mu$

or $\nu_\mu \leftrightarrow \bar{\nu}_\mu$. As discussed in Kayser's review, the assumption of mixing between only two states is valid if (a) all mixing angles are small or (b) there is a mass hierarchy such that one ΔM_{ij}^2 , e.g. $\Delta M_{21}^2 = M_{\nu_2}^2 - M_{\nu_1}^2$, is small compared with the others, so that there is a region in L/E (the ratio of the distance L that the neutrino travels to its energy E) where $\Delta M_{21}^2 L/E$ is negligible, but $\Delta M_{32}^2 L/E$ is not.

In this case limits or results can be shown as allowed regions on a plot of $|\Delta M^2|$ as a function of $\sin^2 2\theta$. The simplest situation occurs in an "appearance" experiment, where one searches for interactions by neutrinos of a variety not expected in the beam. An example is the search for ν_e interactions in a detector in a ν_μ beam. For oscillation between two states, the probability that the "wrong" state will appear is given by Eq. 11 in Kayser's review, which may be written as

$$P = \sin^2 2\theta \sin^2(1.27\Delta M^2 L/E), \quad (1)$$

where $|\Delta M^2|$ is in eV^2 and L/E is in km/GeV or m/MeV . In a real experiment L and E have some spread, so that one must average P over the distribution of L/E . As an example, let us make the somewhat unrealistic assumption that $b \equiv 1.27L/E$ has a Gaussian distribution with standard deviation σ_b about a central value b_0 . Then:

$$\langle P \rangle = \frac{1}{2} \sin^2 2\theta [1 - \cos(2b_0\Delta M^2) \exp(-2\sigma_b^2(\Delta M^2)^2)] \quad (2)$$

The value of $\langle P \rangle$ is set by the experiment. For example, if 230 interactions of the expected flavor are detected and none of the wrong flavor are seen, then $P = 0.010$ at the 90% CL.* We can then solve the above expression for $\sin^2 2\theta$ as a function of $|\Delta M^2|$. This function is shown in Fig. 1.[†] Note that:

- (a) since the fast oscillations are completely washed out by the resolution for large $|\Delta M^2|$, $\sin^2 2\theta = 2\langle P \rangle$ in this region (If b is taken as much smaller than experimental resolution, Eq. (2) can be used in Monte Carlo calculations to avoid the pathology if Eq. (1) at large Δm^2);
- (b) the maximum excursion of the curve to the left is to $\sin^2 2\theta = \langle P \rangle$ with good resolution, with smaller excursion for worse resolution. This "bump" occurs at $|\Delta M^2| = \pi/2b_0 \text{ eV}^2$;
- (c) for large $\sin^2 2\theta$, $\Delta M^2 \approx (\langle P \rangle / \sin^2 2\theta)^{1/2} / b_0$; and, consequently,
- (d) the intercept at $\sin^2 2\theta = 1$ is at $\Delta M^2 = \sqrt{\langle P \rangle} / b_0$.

The intercept for large $|\Delta M^2|$ is a measure of running time and backgrounds, while the intercept at $\sin^2 2\theta = 1$ depends also on the mean value of L/E . The wiggles depend on experimental features such as the size of the source, the neutrino energy distribution, and detector and analysis features. Aside from such details, the two intercepts completely describe the exclusion region: For large $|\Delta M^2|$, $\sin^2 2\theta$ is constant and equal to $2\langle P \rangle$, and for large $\sin^2 2\theta$ the slope is known from the intercept. For these reasons, it is (nearly) sufficient to summarize the results of an experiment by stating the two intercepts, as is done in the

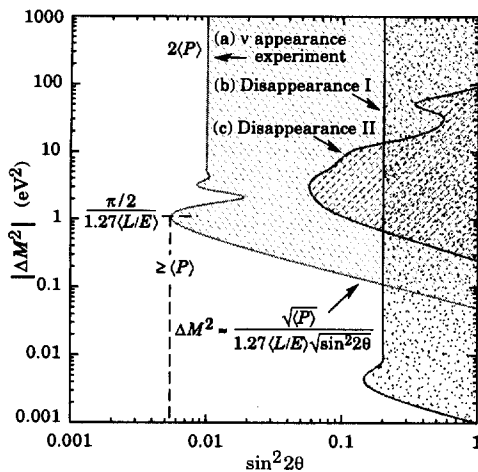


Figure 1: Neutrino oscillation parameter ranges excluded by two hypothetical experiments

(a and b) described by Eq. (2) and one real one (c). Parameters for the first two cases are given in the footnotes. In case (a) one searches for the appearance of neutrinos not expected in the beam. The probability of appearance, in this case 0.5% at some specified CL, is set by the number of right-flavor events observed and/or information about the flux and cross sections. Case (b) represents a disappearance experiment in which the flux is known in the absence of mixing. In case (c), the information comes from measured fluxes at two distances from the target [4].

following tables. The reader is referred to the original papers for the two-dimensional plots expressing the actual limits.

If a positive effect is claimed, then the excluded region is replaced by an allowed band or allowed regions. This is the case for the LSND experiment [2] and the SuperKamiokande analysis of $R(\mu/e)$ for atmospheric neutrinos [3].

In a “disappearance” experiment, one looks for the attenuation of the beam neutrinos (for example, ν_k) by mixing with at least one other neutrino eigenstate. (We label such experiments as $\nu_k \nrightarrow \nu_k$.) The probability that a neutrino remains the same neutrino from the production point to detector is given by

$$P(\nu_k \rightarrow \nu_k) = 1 - P(\nu_k \rightarrow \nu_j), \quad (3)$$

where mixing occurs between the k th and j th species with $P(\nu_k \rightarrow \nu_j)$ given by Eq. (1) or Eq. (2).

In contrast to the detection of even a few “wrong-flavor” neutrinos establishing mixing in an appearance experiment, the disappearance of a few “right-flavor” neutrinos in a disappearance experiment goes unobserved because of statistical fluctuations. For this reason, disappearance experiments usually cannot establish small-probability (small $\sin^2 2\theta$) mixing.

Disappearance experiments fall into two general classes:

- I. Those in which the beam neutrino flux is known, from theory or from other measurements. Examples are reactor $\bar{\nu}_e$ experiments and certain accelerator experiments. Although such experiments cannot establish very small- $\sin^2 2\theta$ mixing, they can establish small limits on ΔM^2 for large $\sin^2 2\theta$ because L/E can be very large. An example, based on the Chooz reactor measurements [5], is labeled “Disappearance I” in Fig. 1.[†]
- II. Those in which attenuation or oscillation of the beam neutrino flux is measured in the apparatus itself (two detectors, or a “long” detector). Above some minimum $|\Delta M^2|$ the equilibrium is established upstream, and there is no change in intensity over the length of the apparatus. As a result, sensitivity is lost at high $|\Delta M^2|$, as can be seen by the curve labeled “Disappearance II” in Fig. 1 [4]. Such experiments have not been competitive for a long time. However, a new generation of long-baseline experiments with a “near” detector and a “far” detector with very large L , *e.g.*, MINOS, will be able to use this strategy to advantage.

Finally, there are more complicated cases, such as analyses of solar neutrino data in terms of the MSW parameters [6]. For a variety of physical reasons, an irregular region in the $|\Delta M^2|$ vs $\sin^2 2\theta$ plane is allowed. It is difficult to represent these graphical data adequately within the strictures of our tables.

Experimental two-neutrino mixing limits and positive signals are shown on the following page.

Footnotes and References

* A superior statistical analysis of confidence limits in the $\sin^2 2\theta - |\Delta M^2|$ plane is given in Ref. 1.

[†] Curve generated with $\langle P \rangle = 0.005$, $\langle L/E \rangle = 1.11$, and $\sigma_b/b_0 = 0.08$.

[‡] Curve parameters $\langle P \rangle = 0.1$, $\langle L/E \rangle = 237$, and $\sigma_b/b_0 = 0.5$. For the actual Chooz experiment [5], $\langle L/E \rangle \approx 300$ and the limit on $\langle P \rangle$ is 0.09.

1. G.J. Feldman and R.D. Cousins, Phys. Rev. **D3873** (1998).
2. C. Athanassopoulos *et al.*, Phys. Rev. **C54** (1996).
3. Y. Fukuda *et al.*, eprint hep-ex/9803005.
4. F. Dydak *et al.*, Phys. Lett. **134B** (1984).
5. M. Apollonio *et al.*, Phys. Lett. **B420**, 397 (1998).
6. N. Hata and P. Langacker, Phys. Rev. **D56**, 6107 (1997).

TWO-FLAVOR OSCILLATION PARAMETERS AND LIMITS

Written April 2000 by H. Murayama (LBNL).

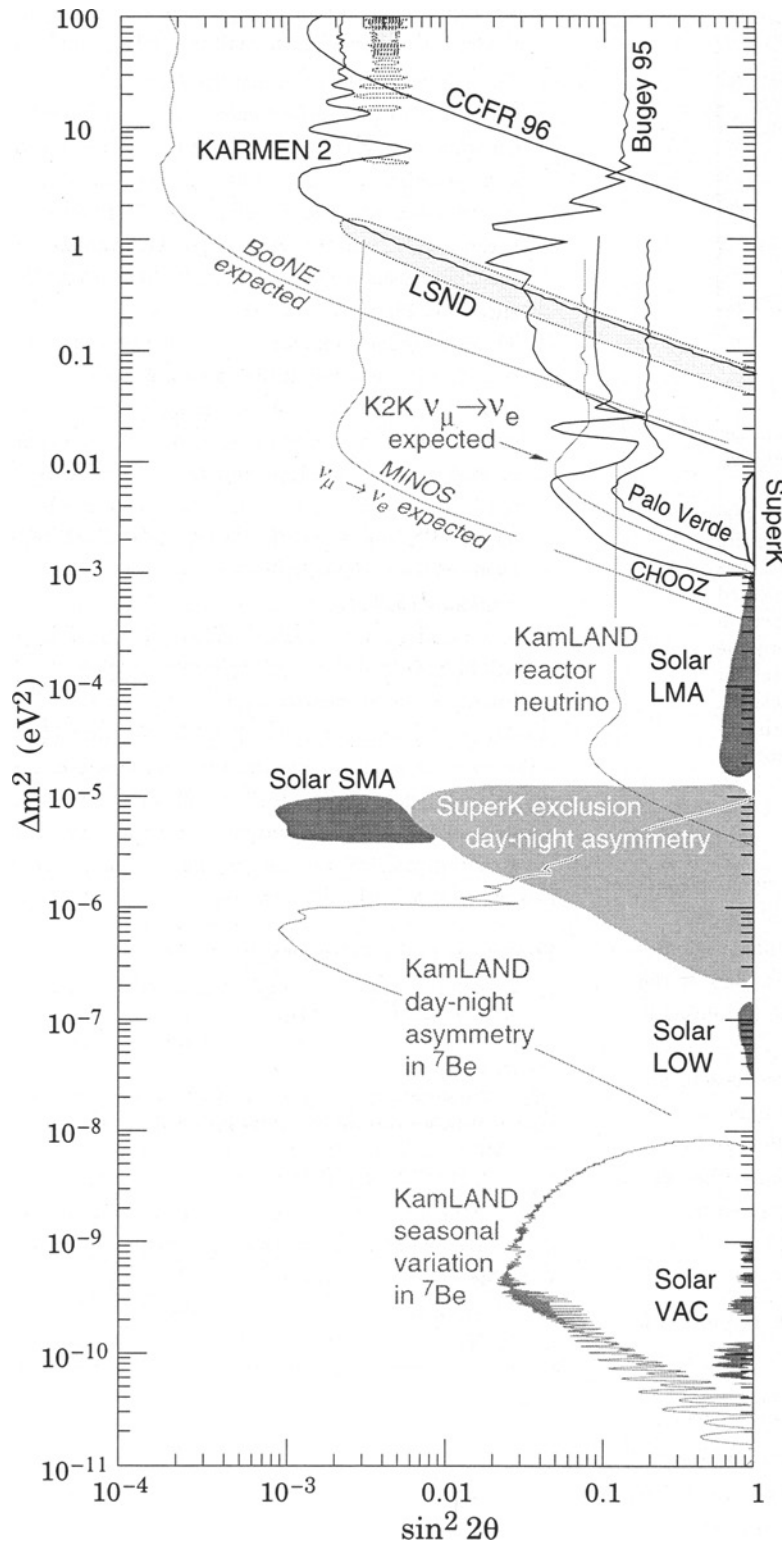


Figure 1: The most important exclusion limits as well as preferred parameter regions from neutrino oscillation experiments in the context of two-flavor oscillations. Beware that the plot shows oscillation modes on different pairs of neutrinos at the same time. All of them are 90% confidence limits unless otherwise noted. From the top,

- CCFR 96 limit is on ν_μ to ν_e oscillation from ROMOSAN 97
- KARMEN 2 excluded region and LSND preferred region are for $\bar{\nu}_e$ appearance from $\bar{\nu}_\mu$ taken from Klaus Eitel, *New J. Phys.* **2**, 1 (2000), Fig. 12
- Bugey 95 limit is on $\bar{\nu}_e$ disappearance from ACHKAR 95
- CHOOZ limit is on $\bar{\nu}_e$ disappearance from APOLLONIO 99, Fig. 9
- Palo Verde limit is on $\bar{\nu}_e$ disappearance from BOEHM 00, Fig. 3, curve (b)
- SuperKamiokande preferred region is on $\bar{\nu}_\mu$ disappearance from FUKUDA 98C
- Solar neutrino preferred regions (solar LMA, solar SMA, solar LOW, and solar VAC) are on ν_e disappearance from J.N. Bahcall, P.I. Krastev, and A.Yu. Smirnov, *Phys. Rev. D* **58**, 096016 (1998) based on solar neutrino rates only at 99% CL
- SuperKamiokande exclusion is based on the absence of day-night asymmetry in the neutrino rate from FUKUDA 99, Fig. 2, at 99% CL
- Some projected improvements by near-future experiments on ν_e oscillations are shown in grey

Note that the plot shows only half of the parameter space $\Delta m^2 \cos 2\theta > 0$, while the other half $\Delta m^2 \cos 2\theta < 0$ should show different regions excluded/preferred, especially for solar neutrino oscillations (de Gouvêa *et al.*, [hep-ph/0002064](#)) once experiments report their data. References in upper-case letters are given at the end of the Listings for "Massive Neutrinos and Lepton Mixing."

See key on page 239

Lepton Particle Listings

Massive Neutrinos and Lepton Mixing

(A) Heavy neutral leptons**Stable Neutral Heavy Lepton MASS LIMITS**

Note that LEP results in combination with REUSSER 91 exclude a fourth stable neutrino with $m < 2400$ GeV.

VALUE (GeV)	CL%	DOCUMENT ID	TECN	COMMENT
>45.0	95	ABREU	92B DLPH	Dirac
>39.5	95	ABREU	92B DLPH	Majorana
>44.1	95	ALEXANDER	91F OPAL	Dirac
>37.2	95	ALEXANDER	91F OPAL	Majorana
none 3-100	90	SATO	91 KAM2	Kamiokande II
>42.8	95	¹ ADEVA	90S L3	Dirac
>34.8	95	¹ ADEVA	90S L3	Majorana
>42.7	95	DECAMP	90F ALEP	Dirac

¹ADEVA 90s limits for the heavy neutrino apply if the mixing with the charged leptons satisfies $|U_{1j}|^2 + |U_{2j}|^2 + |U_{3j}|^2 > 6.2 \times 10^{-8}$ at $m_{L0} = 20$ GeV and $> 5.1 \times 10^{-10}$ for $m_{L0} = 40$ GeV.

Neutral Heavy Lepton MASS LIMITS

Limits apply only to heavy lepton type given in comment at right of data Listings. See review above for description of types.

See the "Quark and Lepton Compositeness, Searches for" Listings for limits on radiatively decaying excited neutral leptons, i.e. $\nu^* \rightarrow \nu\gamma$.

VALUE (GeV)	CL%	DOCUMENT ID	TECN	COMMENT
>76.5	95	ABREU	99O DLPH	Dirac coupling to e
>79.5	95	ABREU	99O DLPH	Dirac coupling to μ
>60.5	95	ABREU	99O DLPH	Dirac coupling to τ
>92.4	95	ACCIARRI	99L L3	Dirac coupling to e
>81.8	95	ACCIARRI	99L L3	Majorana coupling to e
>93.3	95	ACCIARRI	99L L3	Dirac coupling to μ
>84.1	95	ACCIARRI	99L L3	Majorana coupling to μ
>83.3	95	ACCIARRI	99L L3	Dirac coupling to τ
>73.5	95	ACCIARRI	99L L3	Majorana coupling to τ
>69.8	95	² ACKERSTAFF	98C OPAL	Majorana, coupling to e
>79.1	95	² ACKERSTAFF	98C OPAL	Dirac, coupling to e
>68.7	95	² ACKERSTAFF	98C OPAL	Majorana, coupling to μ
>78.5	95	² ACKERSTAFF	98C OPAL	Dirac, coupling to μ
>54.4	95	² ACKERSTAFF	98C OPAL	Majorana, coupling to τ
>69.0	95	² ACKERSTAFF	98C OPAL	Dirac, coupling to τ
>63	95	^{3,4} BUSKULIC	96S ALEP	Dirac
>54.3	95	^{3,5} BUSKULIC	96S ALEP	Majorana

²The decay length of the heavy lepton is assumed to be < 1 cm, limiting the square of the mixing angle $|U_{ej}|^2$ to 10^{-12} .

³BUSKULIC 96s requires the decay length of the heavy lepton to be < 1 cm, limiting the square of the mixing angle $|U_{ej}|^2$ to 10^{-10} .

⁴BUSKULIC 96s limit for mixing with τ . Mass is > 63.6 GeV for mixing with e or μ .

⁵BUSKULIC 96s limit for mixing with τ . Mass is > 55.2 GeV for mixing with e or μ .

Astrophysical Limits on Neutrino MASS for $m_\nu > 1$ GeV

VALUE (GeV)	CL%	DOCUMENT ID	TECN	COMMENT
none 60-115		⁶ FARGION	95 ASTR	Dirac
none 9.2-2000		⁷ GARCIA	95 COSM	Nucleosynthesis
none 26-4700		⁷ BECK	94 COSM	Dirac
none 6 - hundreds		^{8,9} MORI	92B KAM2	Dirac neutrino
none 24 - hundreds		^{8,9} MORI	92B KAM2	Majorana neutrino
none 10-2400	90	¹⁰ REUSSER	91 CNTR	HPGe search
none 3-100	90	SATO	91 KAM2	Kamiokande II
none 12-1400		¹¹ ENQVIST	89 COSM	
none 4-16	90	^{7,8} OLIVE	88 COSM	Dirac ν
none 4-35	90	^{7,8} OLIVE	88 COSM	Dirac ν
>4.2 to 4.7		SREDNICKI	88 COSM	Majorana ν
>5.3 to 7.4		SREDNICKI	88 COSM	Dirac ν
none 20-1000	95	⁷ AHLEN	87 COSM	Majorana ν
>4.1		GRIEST	87 COSM	Dirac ν

⁶FARGION 95 bound is sensitive to assumed ν concentration in the Galaxy. See also KONOPLICH 94.

⁷These results assume that neutrinos make up dark matter in the galactic halo.

⁸Limits based on annihilations in the sun and are due to an absence of high energy neutrinos detected in underground experiments.

⁹MORI 92B results assume that neutrinos make up dark matter in the galactic halo. Limits based on annihilations in earth are also given.

¹⁰REUSSER 91 uses existing $\beta\beta$ detector (see FISHER 89) to search for CDM Dirac neutrinos.

¹¹ENQVIST 89 argue that there is no cosmological upper bound on heavy neutrinos.

(B) Sum of neutrino masses

Revised April 1998 by K.A. Olive (University of Minnesota).

The limits on low mass ($m_\nu \lesssim 1$ MeV) neutrinos apply to m_{tot} given by

$$m_{\text{tot}} = \sum_{\nu} (g_\nu/2)m_\nu,$$

where g_ν is the number of spin degrees of freedom for ν plus $\bar{\nu}$: $g_\nu = 4$ for neutrinos with Dirac masses; $g_\nu = 2$ for Majorana neutrinos. Stable neutrinos in this mass range make a contribution to the total energy density of the Universe which is given by

$$\rho_\nu = m_{\text{tot}} n_\nu = m_{\text{tot}} (3/11) n_\gamma,$$

where the factor 3/11 is the ratio of (light) neutrinos to photons. Writing $\Omega_\nu = \rho_\nu/\rho_c$, where ρ_c is the critical energy density of the Universe, and using $n_\gamma = 412 \text{ cm}^{-3}$, we have

$$\Omega_\nu h^2 = m_{\text{tot}} / (94 \text{ eV}).$$

Therefore, a limit on $\Omega_\nu h^2$ such as $\Omega_\nu h^2 < 0.25$ gives the limit

$$m_{\text{tot}} < 24 \text{ eV}.$$

The limits on high mass ($m_\nu > 1$ MeV) neutrinos apply separately to each neutrino type.

Limit on Total ν MASS, m_{tot}

(Defined in the above note), of effectively stable neutrinos (i.e., those with mean lives greater than or equal to the age of the universe). These papers assumed Dirac neutrinos. When necessary, we have generalized the results reported so they apply to m_{tot} . For other limits, see SZALAY 76, VYSOTSKY 77, BERNSTEIN 81, FREESE 84, SCHRAMM 84, and COWSIK 85.

VALUE (eV)	DOCUMENT ID	TECN	COMMENT
< 5.5	¹² CROFT	99 ASTR	Ly α power spec
<180	SZALAY	74 COSM	
<132	COWSIK	72 COSM	
<280	MARX	72 COSM	
<400	GRSHEIN	66 COSM	

¹²CROFT 99 result based on the power spectrum of the Ly α forest. If $\Omega_{\text{matter}} < 0.5$, the limit is improved to $m_\nu < 2.4 (\Omega_{\text{matter}}/0.17-1)$ eV.

Limits on MASSES of Light Stable Right-Handed ν (with necessarily suppressed interaction strengths)

VALUE (eV)	DOCUMENT ID	TECN	COMMENT
<100-200	¹³ OLIVE	82 COSM	Dirac ν
<200-2000	¹³ OLIVE	82 COSM	Majorana ν

¹³Depending on interaction strength G_R where $G_R < G_F$.

Limits on MASSES of Heavy Stable Right-Handed ν (with necessarily suppressed interaction strengths)

VALUE (GeV)	DOCUMENT ID	TECN	COMMENT
> 10	¹⁴ OLIVE	82 COSM	$G_R/G_F < 0.1$
>100	¹⁴ OLIVE	82 COSM	$G_R/G_F < 0.01$

¹⁴These results apply to heavy Majorana neutrinos and are summarized by the equation: $m_\nu > 1.2 \text{ GeV} (G_F/G_R)$. The bound saturates, and if G_R is too small no mass range is allowed.

Lepton Particle Listings

Massive Neutrinos and Lepton Mixing

(C) Searches for neutrinoless double- β decayLIMITS FROM NEUTRINOLESS $\beta\beta$ DECAY

Revised September 1999 by P. Vogel (Caltech).

Neutrinoless double beta decay, if observed, would signal violation of the total lepton number conservation. The process can be mediated by an exchange of light Majorana neutrino, or by an exchange of other particles. As long as only a limit on its lifetime is available, limits on the effective Majorana neutrino mass, and on the lepton-number violating right-handed current admixture can be obtained, independently on the actual mechanism. These are considered in the following three tables.

The derived quantities are nuclear model-dependent, so the half-life measurements are given first. Where possible, we list the references for the nuclear matrix elements used in the subsequent analysis. Since rates for the more conventional $2\nu\beta\beta$ decay serve to calibrate the theory, results for this process are also given. As an indication of the spread among different ways of evaluating the matrix elements, we show in Fig. 1 some representative examples for the most popular nuclei.

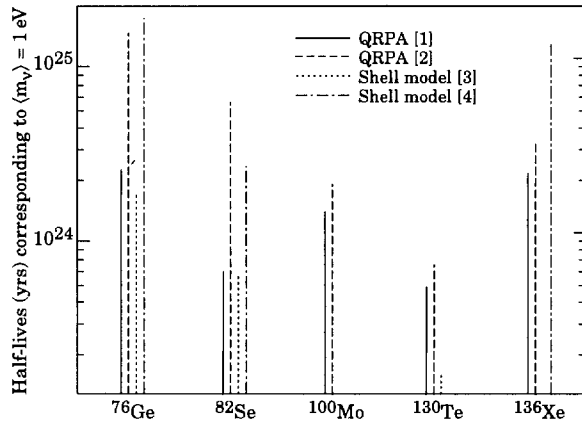


Figure 1: Half-lives (in years) calculated for $\langle m_\nu \rangle = 1 \text{ eV}$ by various representative methods and different authors for the most popular double-beta decay candidate nuclei. Solid lines are QRPA from [1], dashed lines are QRPA from [2] (recalculated for $g_A = 1.25$ and $\alpha' = -390 \text{ MeV fm}^3$, dotted lines are shell model [3], and dot-and-dashed lines are shell model [4].

To define the limits on lepton-number violating right-handed current admixtures, we display the relevant part of a phenomenological current-current weak interaction Hamiltonian:

$$H_W = (G_F/\sqrt{2}) \times (J_L \cdot j_L^\dagger + \kappa J_R \cdot j_R^\dagger + \eta J_L \cdot j_R^\dagger + \lambda J_R \cdot j_L^\dagger) + \text{h.c.} \quad (1)$$

where $j_L^\mu = \bar{e}_L \gamma^\mu \nu_{eL}$, $j_R^\mu = \bar{e}_R \gamma^\mu \nu_{eR}$, and J_L^μ and J_R^μ are left-handed and right-handed hadronic weak currents. Experiments are not sensitive to κ , but quote limits on quantities

proportional to η and λ .^{*} In analogy to $\langle m_\nu \rangle$ (see Eq. 17 in the “Neutrino mass” at the beginning of the Neutrino Particle Listings), the quantities extracted from experiments are $\langle \eta \rangle = \eta \sum U_{1j} V_{1j}$ and $\langle \lambda \rangle = \lambda \sum U_{1j} V_{1j}$, where V_{ij} is a matrix analogous to U_{ij} (see Eq. 2 in the “Neutrino mass”), but describing the mixing among right-handed neutrinos. The quantities $\langle \eta \rangle$ and $\langle \lambda \rangle$ therefore vanish for massless or unmixed neutrinos. Also, as in the case of $\langle m_\nu \rangle$, cancellations are possible in $\langle \eta \rangle$ and $\langle \lambda \rangle$. The limits on $\langle \eta \rangle$ are of order 10^{-8} while the limits on $\langle \lambda \rangle$ are of order 10^{-6} . The reader is warned that a number of earlier experiments did not distinguish between η and λ . Because of evolving reporting conventions and matrix element calculations, we have not tabulated the admixture parameters for experiments published earlier than 1989.

See the section on Majoron searches for additional limits set by these experiments.

Footnotes and References

^{*} We have previously used a less accepted but more explicit notation in which $\eta_{RL} \equiv \kappa$, $\eta_{LR} \equiv \eta$, and $\eta_{RR} \equiv \lambda$.

1. A. Staudt, K. Muto, and H.V. Klapdor-Kleingrothaus, *Europhys. Lett.* **13**, 31 (1990).
2. J. Engel, P. Vogel, and M.R. Zirnbauer, *Phys. Rev.* **C37**, 731 (1988).
3. W.C. Haxton and G.J. Stephenson Jr., *Prog. in Part. Nucl. Phys.* **12**, 409 (1984).
4. E. Caurier, F. Nowacki, A. Poves, and J. Retamosa *Phys. Rev. Lett.* **77**, 1954 (1996).

Half-life Measurements and Limits for Double β Decay

In all cases of double beta decay, $(Z,A) \rightarrow (Z+2,A) + 2e^- + (0 \text{ or } 2)\nu_e$. In the following Listings, only best or comparable limits or lifetimes for each isotope are reported.

$t_{1/2}(10^{21} \text{ yr})$	CL% ISOTOPE	TRANSITION	METHOD	DOCUMENT ID
> 8000	90 ^{76}Ge 0ν		Enriched HPGe	15 AALSETH 99
$0.021^{+0.008}_{-0.004} \pm 0.002$	96Zr 2ν		NEMO-2	16 ARNOLD 99
> 1.0	90 ^{96}Zr 0ν		NEMO-2	16 ARNOLD 99
> 0.39	90 ^{96}Zr 0ν	$0^0 \rightarrow 2^+$	NEMO-2	16 ARNOLD 99
>16000(57000)	90 ^{76}Ge 0ν		Enriched HPGe	17 BAUDIS 99b
> 56	90 ^{130}Te 0ν		Cryog. det.	18 ALESSAND... 98
> 16	90 ^{130}Te 0ν	$0^+ \rightarrow 2^+$	Cryog. det.	18 ALESSAND... 98
> 17	90 ^{128}Te 0ν		Cryog. det.	18 ALESSAND... 98
> 440	90 ^{136}Xe 0ν		Xe TPC	19 LUESCHER 98
> 0.36	90 ^{136}Xe 2ν		Xe TPC	20 LUESCHER 98
$(7.6^{+2.2}_{-1.4})\text{E-3}$	100Mo 2ν		Si(Li)	21 ALSTON... 97
> 0.19	90 ^{92}Mo $0\nu+2\nu$	$0^+ \rightarrow 0^+$	γ in HPGe	22 BARABASH 97
> 0.81	90 ^{92}Mo $0\nu+2\nu$	$0^+ \rightarrow 0^+_1$	γ in HPGe	22 BARABASH 97
> 0.89	90 ^{92}Mo $0\nu+2\nu$	$0^+ \rightarrow 2^+_1$	γ in HPGe	22 BARABASH 97
>11000	90 ^{76}Ge 0ν	$0^+ \rightarrow 0^+$	Enriched HPGe	23 BAUDIS 97
$(6.82^{+0.38}_{-0.53} \pm 0.68)\text{E-3}$	100Mo 2ν		TPC	24 DESILVA 97
$(6.75^{+0.37}_{-0.42} \pm 0.68)\text{E-3}$	150Nd 2ν		TPC	25 DESILVA 97
> 1.2	90 ^{150}Nd 0ν		TPC	26 DESILVA 97
$1.77 \pm 0.01^{+0.13}_{-0.11}$	76Ge 2ν		Enriched HPGe	27 GUENTHER 97
$(3.75 \pm 0.35 \pm 0.21)\text{E-2}$	^{116}Cd 2ν	$0^+ \rightarrow 0^+$	NEMO 2	28 ARNOLD 96
$0.043^{+0.024}_{-0.011} \pm 0.014$	48Ca 2ν		TPC	29 BALYSH 96
> 52	68 ^{100}Mo $0\nu, \langle m_\nu \rangle^+$	$0^+ \rightarrow 0^+$	ELEGANT V	30 EJIRI 96
> 39	68 ^{100}Mo $0\nu, \langle \lambda \rangle$	$0^+ \rightarrow 0^+$	ELEGANT V	30 EJIRI 96
> 51	68 ^{100}Mo $0\nu, \langle \eta \rangle$	$0^+ \rightarrow 0^+$	ELEGANT V	30 EJIRI 96
0.79 ± 0.10	130Te $0\nu+2\nu$		Geochem	31 TAKAOKA 96
$0.61^{+0.18}_{-0.11}$	100Mo $0\nu+2\nu$	$0^+ \rightarrow 0^+_1$	γ in HPGe	32 BARABASH 95
> 0.00013	99 ^{160}Gd 2ν	$0^+ \rightarrow 0^+$	$\text{Gd}_2\text{SiO}_5:\text{Ce scint}^{33}$	BURACHAS 95
> 0.00012	99 ^{160}Gd 2ν	$0^+ \rightarrow 2^+$	$\text{Gd}_2\text{SiO}_5:\text{Ce scint}^{33}$	BURACHAS 95

See key on page 239

Lepton Particle Listings

Massive Neutrinos and Lepton Mixing

> 0.014	90	¹⁶⁰ Gd 0ν	0 ⁺ → 0 ⁺	Gd ₂ SiO ₅ :Ce scint ³³	BURACHAS	95
> 0.013	90	¹⁶⁰ Gd 0ν	0 ⁺ → 2 ⁺	Gd ₂ SiO ₅ :Ce scint ³³	BURACHAS	95
(9.5 ± 0.4 ± 0.9)E18	100	¹⁰⁰ Mo 2ν		NEMO 2	DASSIE	95
> 0.6	90	¹⁰⁰ Mo 0ν	0 ⁺ → 0 ⁺	NEMO 2	DASSIE	95
0.026 +0.009 −0.005	116	¹¹⁶ Cd 2ν	0 ⁺ → 0 ⁺	ELEGANT IV	EJIRI	95
> 29	90	¹¹⁶ Cd 0ν	0 ⁺ → 0 ⁺	¹¹⁶ CdWO ₄ scint ³⁴	GEORGADZE	95
> 0.3	68	¹⁶⁰ Gd 0ν		Gd ₂ SiO ₅ :Ce scint	KOBAYASHI	95
> 2.37	90	¹¹⁶ Cd 0ν+2ν	0 ⁺ → 2 ⁺	γ in HPGe	³⁵ PIEPKE	94
> 2.05	90	¹¹⁶ Cd 0ν+2ν	0 ⁺ → 0 ⁺	γ in HPGe	³⁵ PIEPKE	94
> 2.05	90	¹¹⁶ Cd 0ν+2ν	0 ⁺ → 0 ⁺	γ in HPGe	³⁵ PIEPKE	94
0.017 +0.010 −0.005 ± 0.0035	150	¹⁵⁰ Nd 2ν	0 ⁺ → 0 ⁺	TPC	ARTEMEV	93
0.039 ± 0.009	96	⁹⁶ Zr 0ν+2ν		Geochem	KAWASHIMA	93
> 430	90	⁷⁶ Ge 0ν	0 ⁺ → 2 ⁺	Enriched HPGe	BALYSH	92
2.7 ± 0.1	130	¹³⁰ Te		Geochem	BERNATOW...	92
7200 ± 400	128	¹²⁸ Te		Geochem	BERNATOW...	92
> 27	68	⁸² Se 0ν	0 ⁺ → 0 ⁺	TPC	ELLIOTT	92
0.108 +0.026 −0.006	82	⁸² Se 2ν	0 ⁺ → 0 ⁺	TPC	ELLIOTT	92
0.92 +0.07 −0.04	76	⁷⁶ Ge 2ν	0 ⁺ → 0 ⁺	Enriched HPGe	37 AVIGNONE	91
> 3.3	95	¹³⁶ Xe 0ν	0 ⁺ → 2 ⁺	Prop cntr	38 BELLOTTI	91
> 0.16	95	¹³⁶ Xe 2ν		Prop cntr	BELLOTTI	91
2.0 ± 0.6	238	²³⁸ U		Radiochem	39 TURKEVICH	91
> 9.5	76	⁴⁸ Ca 0ν		CaF ₂ scint.	YOU	91
1.12 +0.48 −0.26	76	⁷⁶ Ge 2ν	0 ⁺ → 0 ⁺	HPGe	40 MILEY	90
0.9 ± 0.1	76	⁷⁶ Ge 2ν		Enriched Ge(Li)	VASENKO	90
> 4.7	68	¹²⁸ Te	0 ⁺ → 2 ⁺	Ge(Li)	33 BELLOTTI	87
> 4.5	68	¹³⁰ Te	0 ⁺ → 2 ⁺	Ge(Li)	33 BELLOTTI	87
> 800	95	¹²⁸ Te		Geochem	41 KIRSTEN	83
2.60 ± 0.28	130	¹³⁰ Te		Geochem	41 KIRSTEN	83

predict a ratio of 2ν decay widths ... in fair agreement with observation." Further details of the experiment are given in BERNATOWICZ 93. Our listed half-life has been revised downward from the published value by the authors, on the basis of reevaluated cosmic-ray ¹²⁸Xe production corrections.

37 AVIGNONE 91 reports confirmation of the MILEY 90 and VASENKO 90 observations of 2νββ decay of ⁷⁶Ge. Error is 2σ.

38 BELLOTTI 91 uses difference between natural and enriched ¹³⁶Xe runs to obtain ββ0ν limits, leading to "less stringent, but safer limits."

39 TURKEVICH 91 observes activity in old U sample. The authors compare their results with theoretical calculations. They state "Using the phase-space factors of Boehm and Vogel (BOEHM 87) leads to matrix element values for the ²³⁸U transition in the same range as deduced for ¹³⁰Te and ⁷⁶Ge. On the other hand, the latest theoretical estimates (STAUDT 90) give an upper limit that is 10 times lower. This large discrepancy implies either a defect in the calculations or the presence of a faster path than the standard two-neutrino mode in this case." See BOEHM 87 and STAUDT 90.

40 MILEY 90 claims only "suggestive evidence" for the decay. Error is 2σ.

41 KIRSTEN 83 reports "2σ" error. References are given to earlier determinations of the ¹³⁰Te lifetime.

⟨m_ν⟩, The Effective Weighted Sum of Majorana Neutrino Masses Contributing to Neutrinoless Double β Decay

$\langle m_\nu \rangle = \left[\sum U_{ej}^2 m_{\nu_j} \right]$, where the sum goes from 1 to n and where $n =$ number of neutrino generations, and ν_j is a Majorana neutrino. Note that U_{ej}^2 , not $|U_{ej}|^2$, occurs in the sum. The possibility of cancellations has been stressed. In the following Listings, only best or comparable limits or lifetimes for each isotope are reported.

VALUE (eV)	CL% ISOTOPE	TRANSITION	METHOD	DOCUMENT ID
• • • We do not use the following data for averages, fits, limits, etc. • • •				
< 0.5–1.5	90 ⁷⁶ Ge		Enriched HPGe	42 AALSETH 99
< 23	90 ⁹⁶ Zr		NEMO-2	43 ARNOLD 99
< 0.4(0.2)–1.0(0.6)	90 ⁷⁶ Ge		Enriched HPGe	44 BAUDIS 99B
< 2.4–2.7	90 ¹³⁶ Xe 0ν		Xe TPC	45 LUESCHER 98
< 9.3	68 ¹⁰⁰ Mo 0ν		Si(Li)	46 ALSTON... 97
< 0.46	90 ⁷⁶ Ge 0ν	0 ⁺ → 0 ⁺	Enriched HPGe	47 BAUDIS 97
< 2.2	68 ¹⁰⁰ Mo 0ν	0 ⁺ → 0 ⁺	ELEGANT V	48 EJIRI 96
< 4.1	90 ¹¹⁶ Cd 0ν		¹¹⁶ CdWO ₄ scint	49 DANEVICH 95
< 2.8–4.3	90 ¹³⁶ Xe 0ν	0 ⁺ → 0 ⁺	TPC	50 VUILLEUMIER 93
< 1.1–1.5	128 ¹²⁸ Te		Geochem	51 BERNATOW... 92
< 5	68 ⁸² Se		TPC	52 ELLIOTT 92
< 8.3	76 ⁴⁸ Ca 0ν		CaF ₂ scint.	YOU 91
< 5.6	95 ¹²⁸ Te		Geochem	KIRSTEN 83

42 In AALSETH 99, the range given in the limit reflects the spread of the corresponding nuclear matrix elements. This limit is not competitive with BAUDIS 99B.

43 ARNOLD 99 limit based on the nuclear matrix elements of STAUDT 90.

44 BAUDIS 99B derive a limit for ⟨m_ν⟩ using the matrix elements of STAUDT 90. The uncertainty given for ⟨m_ν⟩ reflects theoretical uncertainty in the matrix element calculations. The less restrictive limit is based on the quoted experimental sensitivity while the lower value in parentheses makes use of measured rates significantly below background.

45 LUESCHER 98 limit for ⟨m_ν⟩ is based on the matrix elements of ENGEL 88.

46 ALSTON-GARNJOST 97 obtain the limit for ⟨m_ν⟩ using the matrix elements of ENGEL 88. The limit supersedes ALSTON-GARNJOST 93.

47 BAUDIS 97 limit for ⟨m_ν⟩ is based on the matrix elements of STAUDT 90. This is the most stringent bound on ⟨m_ν⟩. It supersedes the limit of GUENTHER 97.

48 EJIRI 96 obtain the limit for ⟨m_ν⟩ using the matrix elements of TOMODA 91.

49 DANEVICH 95 is identical to GEORGADZE 95.

50 VUILLEUMIER 93 mass range from parameter range in the Caltech calculations (ENGEL 88). On the basis of these calculations, the BALYSH 92 mass range would be < 2.2–4.4 eV.

51 BERNATOWICZ 92 finds these majoron mass limits assuming that the measured geochemical decay width is a limit on the 0ν decay width. The range is the range found using matrix elements from HAXTON 84, TOMODA 87, and SUHONEN 91. Further details of the experiment are given in BERNATOWICZ 93.

52 ELLIOTT 92 uses the matrix elements of HAXTON 84.

Limits on Lepton-Number Violating (V+A) Current Admixture

For reasons given in the discussion at the beginning of this section, we list only results from 1989 and later. $\langle \lambda \rangle = \lambda \sum U_{ej} V_{ej}$ and $\langle \eta \rangle = \eta \sum U_{ej} V_{ej}$, where the sum is over the number of neutrino generations. This sum vanishes for massless or unmixed neutrinos. In the following Listings, only best or comparable limits or lifetimes for each isotope are reported.

⟨λ⟩ (10 ⁻⁶)	CL%	⟨η⟩ (10 ⁻⁸)	CL%	ISOTOPE	METHOD	DOCUMENT ID
• • • We do not use the following data for averages, fits, limits, etc. • • •						
< 1.1	90	< 0.64	90	⁷⁶ Ge	Enriched HPGe	53 GUENTHER 97
< 3.7	68	< 2.5	68	¹⁰⁰ Mo	Elegant V	54 EJIRI 96
< 5.3	90	< 5.9	90	¹¹⁶ Cd	¹¹⁶ CdWO ₄ scint	55 DANEVICH 95
< 4.4	90	< 2.3	90	¹³⁶ Xe	TPC	56 VUILLEUMIER 93
		< 5.3		¹²⁸ Te	Geochem	57 BERNATOW... 92

53 GUENTHER 97 limits use the matrix elements of STAUDT 90. Supersedes BALYSH 95 and BALYSH 92.

54 EJIRI 96 obtain limits for ⟨λ⟩ and ⟨η⟩ using the matrix elements of TOMODA 91.

55 DANEVICH 95 is identical to GEORGADZE 95.

56 VUILLEUMIER 93 uses the matrix elements of MUTO 89.

57 BERNATOWICZ 92 takes the measured geochemical decay width as a limit on the 0ν width, and uses the SUHONEN 91 coefficients to obtain the least restrictive limit on η. Further details of the experiment are given in BERNATOWICZ 93.

Lepton Particle Listings

Massive Neutrinos and Lepton Mixing

Limits on $|U_{ax}|^2$ Where $a = e, \mu$ from ρ parameter in μ decay.

VALUE	CL%	DOCUMENT ID	TECN	COMMENT
••• We do not use the following data for averages, fits, limits, etc. •••				
$<1 \times 10^{-2}$	68	SHROCK	81B THEO	$m_{\nu_x} = 10$ GeV
$<2 \times 10^{-3}$	68	SHROCK	81B THEO	$m_{\nu_x} = 40$ MeV
$<4 \times 10^{-2}$	68	SHROCK	81B THEO	$m_{\nu_x} = 70$ MeV

Limits on $|U_{1j} \times U_{2j}|$ as Function of m_{ν_j}

VALUE	CL%	DOCUMENT ID	TECN	COMMENT
••• We do not use the following data for averages, fits, limits, etc. •••				
$<3 \times 10^{-5}$	90	⁹⁹ BARANOV 93		$m_{\nu_j} = 80$ MeV
$<3 \times 10^{-6}$	90	⁹⁹ BARANOV 93		$m_{\nu_j} = 160$ MeV
$<6 \times 10^{-7}$	90	⁹⁹ BARANOV 93		$m_{\nu_j} = 240$ MeV
$<2 \times 10^{-7}$	90	⁹⁹ BARANOV 93		$m_{\nu_j} = 320$ MeV
$<9 \times 10^{-5}$	90	BERNARDI 86	CNTR	$m_{\nu_j} = 25$ MeV
$<3.6 \times 10^{-7}$	90	BERNARDI 86	CNTR	$m_{\nu_j} = 100$ MeV
$<3 \times 10^{-8}$	90	BERNARDI 86	CNTR	$m_{\nu_j} = 200$ MeV
$<6 \times 10^{-9}$	90	BERNARDI 86	CNTR	$m_{\nu_j} = 350$ MeV
$<1 \times 10^{-2}$	90	BERGSMAN 83B	CNTR	$m_{\nu_j} = 10$ MeV
$<1 \times 10^{-5}$	90	BERGSMAN 83B	CNTR	$m_{\nu_j} = 140$ MeV
$<7 \times 10^{-7}$	90	BERGSMAN 83B	CNTR	$m_{\nu_j} = 370$ MeV

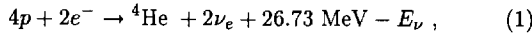
⁹⁹BARANOV 93 is a search for neutrino decays into $e^+ e^- \nu_e$ using a beam dump experiment at the 70 GeV Serpukhov proton synchrotron.

(E) Solar ν Experiments

SOLAR NEUTRINOS

Revised January 2000 by K. Nakamura (KEK, High Energy Accelerator Research Organization, Japan).

The Sun is a main-sequence star at a stage of stable hydrogen burning. It produces an intense flux of electron neutrinos as a consequence of nuclear fusion reactions which generate solar energy, and whose combined effect is



where E_ν represents the energy taken away by neutrinos, with an average value being $\langle E_\nu \rangle \sim 0.6$ MeV. Each neutrino-producing reaction, the resulting flux, and contributions to the event rates in chlorine and gallium solar-neutrino experiments predicted by the recent Bahcall, Basu, and Pinsonneault standard solar model (SSM) calculation [1] are listed in Table 1. This SSM is regarded as the best with helium and heavy-element diffusion. Figure 1 shows the energy spectra of solar neutrinos from these reactions quoted from Ref. 1. Recently, the SSM has been shown to predict accurately the helioseismological sound velocities with a precision of 0.1% rms throughout essentially the entire Sun, greatly strengthening confidence in the solar model [1,2].

Observation of solar neutrinos directly addresses the SSM and, more generally, the theory of stellar structure and evolution which is the basis of the SSM. The Sun as a well-defined neutrino source also provides extremely important opportunities to investigate nontrivial neutrino properties such as nonzero mass and mixing, because of the wide range of matter density and the very long distance from the Sun to the Earth. In fact, the currently available solar-neutrino data seem to require such neutrino properties, if one tries to understand them consistently.

So far, five solar-neutrino experiments have published results. Three of them are radiochemical experiments using ${}^{37}\text{Cl}$

Table 1: Neutrino-producing reactions in the Sun (the first column) and their abbreviations (second column). The neutrino fluxes and event rates in chlorine and gallium solar-neutrino experiments predicted by Bahcall, Basu, and Pinsonneault [1] are listed in the third, fourth, and fifth columns respectively.

Reaction	Abbr.	BAHCALL 98C [1]		
		Flux ($\text{cm}^{-2} \text{s}^{-1}$)	Cl (SNU*)	Ga (SNU*)
$pp \rightarrow de^+ \nu$	<i>pp</i>	$5.94(1.00^{+0.01}_{-0.01}) \times 10^{10}$	—	69.6
$pe^- p \rightarrow d \nu$	<i>pep</i>	$1.39(1.00^{+0.01}_{-0.01}) \times 10^8$	0.2	2.8
${}^3\text{He} p \rightarrow {}^4\text{He} e^+ \nu$	<i>hep</i>	2.10×10^3	0.0	0.0
${}^7\text{Be} e^- \rightarrow {}^7\text{Li} \nu + (\gamma)$	${}^7\text{Be}$	$4.80(1.00^{+0.09}_{-0.09}) \times 10^9$	1.15	34.4
${}^8\text{B} \rightarrow {}^8\text{Be}^* e^+ \nu$	${}^8\text{B}$	$5.15(1.00^{+0.19}_{-0.14}) \times 10^6$	5.9	12.4
${}^{13}\text{N} \rightarrow {}^{13}\text{C} e^+ \nu$	${}^{13}\text{N}$	$6.05(1.00^{+0.19}_{-0.13}) \times 10^8$	0.1	3.7
${}^{15}\text{O} \rightarrow {}^{15}\text{N} e^+ \nu$	${}^{15}\text{O}$	$5.32(1.00^{+0.23}_{-0.15}) \times 10^8$	0.4	6.0
${}^{17}\text{F} \rightarrow {}^{17}\text{O} e^+ \nu$	${}^{17}\text{F}$	$6.48(1.00^{+0.12}_{-0.11}) \times 10^6$	0.0	0.1
Total			$7.7^{+1.2}_{-1.0}$	129^{+8}_{-6}

* 1 SNU (Solar Neutrino Unit) = 10^{-36} captures per atom per second.

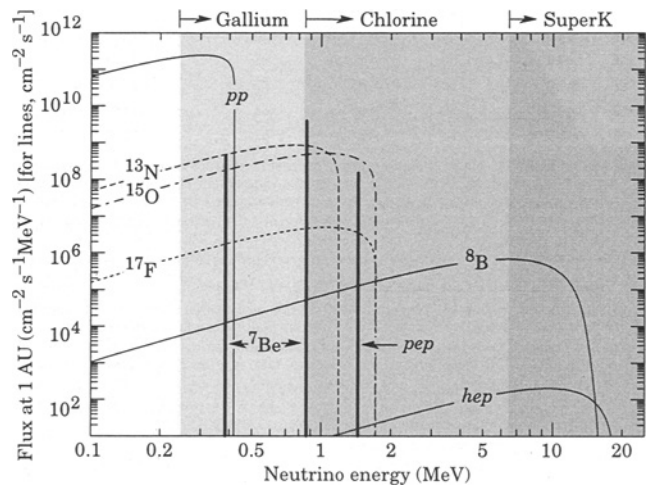


Figure 1: The solar neutrino spectrum predicted by the standard solar model. The neutrino fluxes from continuum sources are given in units of number $\text{cm}^{-2} \text{s}^{-1} \text{MeV}^{-1}$ at one astronomical unit, and the line fluxes are given in number $\text{cm}^{-2} \text{s}^{-1}$. Spectra for the *pp* chain, shown by the solid curves, are courtesy of J.N. Bahcall (1999), and reflect updates in BAHCALL 98C. Spectra for the CNO chain are shown by the dotted curves, and are courtesy of J.N. Bahcall (1995).

(Homestake in USA) or ${}^{71}\text{Ga}$ (GALLEX at Gran Sasso in Italy and SAGE at Baksan in Russia) to capture neutrinos: ${}^{37}\text{Cl} \nu_e \rightarrow {}^{37}\text{Ar} e^-$ (threshold 814 keV) or ${}^{71}\text{Ga} \nu_e \rightarrow {}^{71}\text{Ge} e^-$ (threshold 233 keV). The produced ${}^{37}\text{Ar}$ and ${}^{71}\text{Ge}$ are both radioactive nuclei, with half lives ($\tau_{1/2}$) of 34.8 days and 11.43 days, respectively. After an exposure of the detector for two to three times $\tau_{1/2}$, the reaction products are extracted and introduced into

a low-background proportional counter, and are counted for a sufficiently long period to determine the exponentially decaying signal and a constant background. In the chlorine experiment, the dominant contribution comes from ${}^8\text{B}$ neutrinos, but ${}^7\text{Be}$, pep , ${}^{13}\text{N}$, and ${}^{15}\text{O}$ neutrinos also contribute. At present, the most abundant pp neutrinos can be detected only in gallium experiments. Even so, almost half of the capture rate in the gallium experiments is due to other solar neutrinos.

The other experiments are real-time experiments utilizing νe scattering in a large water-Cherenkov detector (Kamiokande and Super-Kamiokande in Japan). These experiments take advantage of the directional correlation between the incoming neutrino and the recoil electron. This feature greatly helps the clear separation of the solar-neutrino signal from the background. Due to the high thresholds (7 MeV in Kamiokande and 5.5 MeV at present in Super-Kamiokande) the experiments observe pure ${}^8\text{B}$ solar neutrinos because hep neutrinos contribute negligibly according to the SSM. (However, the recent Super-Kamiokande results on the recoil-electron energy spectrum at > 13 MeV raised some discussion on the possibility of an enhanced hep neutrino contribution [3,4].)

In May, 1999, a new realtime solar-neutrino experiment, SNO (Sudbury Neutrino Observatory) started observation. This experiment uses 1000 tons of heavy water (D_2O) to measure solar neutrinos through both inverse β decay ($\nu_e d \rightarrow e^- pp$) and neutral-current interactions ($\nu_x d \rightarrow \nu_x pn$). In addition, νe scattering events will be measured.

Solar neutrinos were first observed in the Homestake chlorine experiment in the late 1960's. From the very beginning, it was recognized that the observed capture rate was significantly smaller than the SSM prediction provided nothing happens to the electron neutrinos after they are created in the solar interior. This deficit has been called "the solar-neutrino problem."

The Kamiokande-II Collaboration started observing the ${}^8\text{B}$ solar neutrinos at the beginning of 1987. Because of the strong directional correlation of νe scattering, this result gave the first direct evidence that the Sun emits neutrinos (no directional information is available in radiochemical solar-neutrino experiments.) The observed solar-neutrino flux was also significantly less than the SSM prediction. In addition, Kamiokande-II obtained the energy spectrum of recoil electrons and the fluxes separately measured in the daytime and nighttime. The Kamiokande-II experiment came to an end at the beginning of 1995.

GALLEX presented the first evidence of pp solar-neutrino observation in 1992. Here also, the observed capture rate is significantly less than the SSM prediction. SAGE, after the initial confusion which is ascribed to statistics by the group, observed a similar capture rate to that of GALLEX. Both GALLEX and SAGE groups tested the overall detector response with intense man-made ${}^{51}\text{Cr}$ neutrino sources, and observed good agreement between the measured ${}^{71}\text{Ge}$ production rate and that predicted from the source activity, demonstrating the reliability of these

experiments. The GALLEX Collaboration formally finished observations in early 1997. Since April, 1998, a newly defined collaboration, GNO (Gallium Neutrino Observatory) resumed the observations.

Super-Kamiokande is a 50-kton second-generation solar-neutrino detector, which is characterized by a significantly larger counting rate than the first-generation experiments. This experiment started observation in April 1996. The average solar-neutrino flux is smaller than, but consistent with, the Kamiokande-II result. However, the flux measured in the nighttime shows an excess over that measured in the daytime [5,6], though the significance is not yet high. Super-Kamiokande also observed the recoil-electron energy spectrum [7]. Its shape showed an excess at the high-energy end (> 13 MeV) compared to the SSM expectation, though its statistical significance is not very high. More recent results indicate that the high-energy excess is reduced with the accumulation of statistics.

The most recent published results on the average capture rates or flux from solar-neutrino experiments are listed in Table 2 and compared to the results from SSM calculations which are taken from "Lepton Particle Listings (E) Solar ν Experiments" in this edition of "Review of Particle Physics." In these calculations, BAHCALL 98C [1], BRUN 98 [12], BAHCALL 95B [14], and DAR 96 [13] take into account helium and heavy-element diffusion, but other calculations do not. SSM calculations give essentially the same results for the same input parameters and physics. This statement applies to the most recent BAHCALL 98C [1] and BRUN 98 [12] models. The BAHCALL 98C model [1] differs from the BAHCALL 95B model [14] in that BAHCALL 98C [1] uses the nuclear fusion rates systematically reevaluated and recommended by Adelberger *et al.* [24], and other best available input data. The ${}^7\text{Be}(p, \gamma){}^8\text{B}$ cross section adopted by Adelberger *et al.* [24] is 15% lower than the value used by BAHCALL 95B [14]. This is the principal reason why the ${}^8\text{B}$ neutrino flux and the ${}^{37}\text{Cl}$ and ${}^{71}\text{Ga}$ capture rates calculated by the BAHCALL 98C model [1] are lower than those calculated by the BAHCALL 95B model [14]. The BAHCALL 95B [14] model and the TURCK-CHIEZE 93B [15] model differ primarily in that BAHCALL 95B [14] includes element diffusion. The DAR 96 [13] model differs significantly from the BAHCALL 95B [14] model mostly due to the use of nonstandard reaction rates, different treatments of diffusion, and the equation of state.

All results from the present solar-neutrino experiments indicate significantly less flux than expected from SSM calculations except those of DAR 96 [13]. The DAR 96 [13] model predicts the ${}^8\text{B}$ solar-neutrino flux which is consistent with the Kamiokande-II and Super-Kamiokande results, but even this model predicts ${}^{37}\text{Cl}$ and ${}^{71}\text{Ga}$ capture rates significantly larger than the Homestake, GALLEX, and SAGE results.

Is there any possible consistent explanation of all the results of solar-neutrino observations in the framework of the standard solar model? This is difficult because the Homestake result and the Kamiokande result, taken at face value, are mutually

Lepton Particle Listings

Massive Neutrinos and Lepton Mixing

Table 2: Recent results from the five solar-neutrino experiments and a comparison with theoretical solar-model predictions. Solar model calculations are also presented. The evolution of these results over the years gives some feeling for their robustness as the models have become more sophisticated and complete.

	$^{37}\text{Cl} \rightarrow ^{37}\text{Ar}$ (SNU)	$^{71}\text{Ga} \rightarrow ^{71}\text{Ge}$ (SNU)	^8B ν flux ($10^6 \text{cm}^{-2} \text{s}^{-1}$)
Homestake			
(CLEVELAND 98)[8]	$2.56 \pm 0.16 \pm 0.16$	—	—
GALLEX			
(HAMPEL 99)[9]	—	$77.5 \pm 6.2^{+4.3}_{-4.7}$	—
SAGE			
(ABDURASHI...99B)[10]	—	$67.2^{+7.2+3.5}_{-7.0-3.0}$	—
Kamiokande			
(FUKUKDA 96)[11]	—	—	$2.80 \pm 0.19 \pm 0.33$
Super-Kamiokande			
(FUKUKDA 99)[5]	—	—	$2.436^{+0.053+0.085}_{-0.047-0.071}$
(BAHCALL 98C)[1]	$7.7^{+1.2}_{-1.0}$	129^{+8}_{-6}	$5.15(1.00^{+0.19}_{-0.14})$
(BRUN 98)[12]	7.18	127.2	4.82
(DAR 96)[13]	4.1 ± 1.2	115 ± 6	2.49
(BAHCALL 95B)[14]	$9.3^{+1.2}_{-1.4}$	137^{+8}_{-7}	$6.6(1.00^{+0.14}_{-0.17})$
(TURCK-CHIEZE 93B)[15]	6.4 ± 1.4	123 ± 7	4.4 ± 1.1
(BAHCALL 92)[16]	$8.0 \pm 3.0^\dagger$	$132^{+21\dagger}_{-17}$	$5.69(1.00 \pm 0.43)^\dagger$
(BAHCALL 88)[17]	$7.9 \pm 2.6^\dagger$	$132^{+20\dagger}_{-17}$	$5.8(1.00 \pm 0.37)^\dagger$
(TURCK-CHIEZE 88)[18]	5.8 ± 1.3	125 ± 5	$3.8(1.00 \pm 0.29)$
(FILIPPONE 83)[19]	5.6	—	—
(BAHCALL 82)[20]	$7.6 \pm 3.3^\dagger$	$106^{+13\dagger}_{-8}$	5.6
(FILIPPONE 82)[21]	7.0 ± 3.0	111 ± 13	4.8
(FOWLER 82)[22]	6.9 ± 1.0	—	—
(BAHCALL 80)[23]	7.3	—	—

* 1 SNU (Solar Neutrino Unit) = 10^{-36} captures per atom per second.

† “ 3σ ” errors.

inconsistent if one assumes standard neutrino spectra. That is, with the reduction factor of the ^8B solar-neutrino flux as determined from the Kamiokande result, the Homestake ^{37}Cl capture rate would be oversaturated, and there would be no room to accommodate the ^7Be solar neutrinos. This makes astrophysical solutions untenable because ^8B nuclei are produced from ^7Be nuclei in the Sun.

Several authors made more elaborate analyses using the constraint of observed solar luminosity, and found (see for example, Refs. 25–28)

- that both the comparison of the Kamiokande and gallium results and the comparison of the gallium and chlorine results also indicate strong suppression of the ^7Be solar-neutrino flux, and
- that not only the SSM but also nonstandard solar models are incompatible with the observed data.

In view of the above situation, it is attractive to invoke nontrivial neutrino properties. Neutrino oscillation in matter (MSW mechanism) is particularly attractive in explaining all

the experimental data on the average solar-neutrino flux consistently, without any *a priori* assumptions or fine tuning. Several authors made extensive MSW analyses using all the available data and ended up with similar results. For example, Bahcall, Krastev, and Smirnov [28] analyzed the solar-neutrino data as of 1998 in terms of two-flavor oscillations. In addition, they analyzed the case of vacuum oscillations. They obtained the following solutions for the BAHCALL 98C [1] SSM: Using only the total event rates in the five solar-neutrino experiments, there are three MSW solutions and one vacuum-oscillation solution at the 99% confidence level for oscillations into active neutrinos (ν_μ or ν_τ).

- Small mixing-angle (SMA) solution:
 $\Delta m^2 = 5.4 \times 10^{-6} \text{ eV}^2$, $\sin^2 2\theta = 6.0 \times 10^{-3}$
- Large mixing-angle (LMA) solution:
 $\Delta m^2 = 1.8 \times 10^{-5} \text{ eV}^2$, $\sin^2 2\theta = 0.76$
- LOW (low probability or low mass) solution:
 $\Delta m^2 = 7.9 \times 10^{-8} \text{ eV}^2$, $\sin^2 2\theta = 0.96$
- Vacuum (VAC) solution:
 $\Delta m^2 = 8.0 \times 10^{-11} \text{ eV}^2$, $\sin^2 2\theta = 0.75$.

In the case of oscillations into sterile neutrinos, only the SMA and VAC solutions are allowed at the 99% confidence level with the best-fit parameters similar to the ones given above.

Bahcall, Krastev, and Smirnov [28] also made global analyses using all of the available solar-neutrino data, *i.e.*, total event rates plus the Super-Kamiokande recoil-electron energy spectrum and day-night asymmetry. At the 99% confidence level, acceptable solutions are found to be SMA (oscillations into both active and sterile neutrinos) and VAC. The LMA and LOW solutions are marginally ruled out.

Assuming that the solution to the solar-neutrino problem will really be provided by neutrino oscillations, how can one discriminate various solutions? The MSW SMA solution causes an energy-spectrum distortion. In the Super-Kamiokande and SNO observations, the flux will be more suppressed at lower energies. The MSW LMA solution predicts the day-night flux difference, a hint of which is seen in the recent Super-Kamiokande results [6]. However, the LMA solution gives almost no spectrum distortion. Thus, should LMA be a correct solution, one needs to explain the high-energy excess in the recoil-electron spectrum observed by Super-Kamiokande [7], if it turns out to be a real effect, due to a very large contribution from *hep* neutrinos or from other possibilities [4]. The VAC solution is characterized by seasonal variation of the flux, which is different from the trivial variation due to the eccentricity of Earth's orbit [29,30]. Also, the VAC solution can explain the high-energy excess of the recoil-electron spectrum observed by Super-Kamiokande [30].

SNO's observations of solar-neutrino flux by neutral-current reactions will give decisive evidence for neutrino oscillations into active neutrinos, if that flux is consistent with the SSM prediction and larger than the flux measured by charged-current reactions. On the other hand, the signal for oscillations into sterile neutrinos will be the same amount of reduction of the fluxes measured by neutral- and charged-current reactions.

See key on page 239

Lepton Particle Listings

Massive Neutrinos and Lepton Mixing

An important task of the second-generation solar neutrino experiments is the measurement of monochromatic ${}^7\text{Be}$ solar neutrinos. If the VAC solution is correct, the flux of ${}^7\text{Be}$ neutrinos shows larger seasonal variations than the flux of ${}^8\text{B}$ neutrinos. The ${}^7\text{Be}$ neutrino flux will be measured by a new experiment, Borexino, at Gran Sasso *via* νe scattering in 300 tons of ultra-pure liquid scintillator with a detection threshold as low as 250 keV. The Borexino detector is expected to be completed in 2001.

KamLAND, which is under construction at Kamioka and will be completed in 2001, is a multi-purpose neutrino experiment with 1000 tons of ultra-pure liquid scintillator. This experiment will also observe ${}^7\text{Be}$ neutrinos if the detection threshold can be lowered to a level similar to that of Borexino. However, one of the primary purposes of this experiment is the observation of oscillations of neutrinos produced by power reactors. The sensitivity region of KamLAND includes the MSW LMA solution. Thus, the LMA solution may be proved or excluded by KamLAND.

The second-generation solar-neutrino experiments, Super-Kamiokande, SNO, and Borexino, as well as KamLAND, will provide a variety of data with high statistical accuracy. It is hoped that these experiments will solve the long-standing solar-neutrino problem in coming years.

References

1. J.N. Bahcall, S. Basu, and M.H. Pinsonneault, Phys. Lett. **B433**, 1 (1998).
2. J.N. Bahcall *et al.*, Phys. Rev. Lett. **78**, 171 (1997).
3. J.N. Bahcall and P.I. Kratsev, Phys. Lett. **B436**, 243 (1998).
4. J.N. Bahcall, P.I. Kratsev, and A.Yu. Smirnov, Phys. Rev. **D60**, 093001 (1999).
5. Y. Fukuda *et al.*, Phys. Rev. Lett. **82**, 1810 (1999).
6. Y. Suzuki, talk at the *XIX Int. Symposium on Lepton and Photon Interactions at High Energies*, Stanford (August 1999).
7. Y. Fukuda *et al.*, Phys. Rev. Lett. **82**, 2430 (1999).
8. B.T. Cleveland *et al.*, Ap. J. **496**, 505 (1998).
9. W. Hampel *et al.*, Phys. Lett. **B447**, 127 (1999);
W. Hampel *et al.*, Phys. Lett. **B388**, 384 (1996).
10. J.N. Abdurashitov *et al.*, Phys. Rev. **C60**, 0055801 (1999)
11. Y. Fukuda *et al.*, Phys. Rev. Lett. **77**, 1683 (1996).
12. A.S. Brun, S. Turck-Chieze, and P. Morel, Astrophys. J. **506**, 913 (1998).
13. A. Dar and G. Shaviv, Astrophys. J. **468**, 933 (1996).
14. J.N. Bahcall and M. H. Pinsonneault, Rev. Mod. Phys. **67**, 781 (1995).
15. S. Turck-Chieze and I. Lopez, Astrophys. J. **408**, 347 (1993).
16. J.N. Bahcall and M. H. Pinsonneault, Rev. Mod. Phys. **64**, 885 (1992).
17. J.N. Bahcall and R.K. Ulrich, Rev. Mod. Phys. **60**, 297 (1988).
18. S. Turck-Chieze *et al.*, Astrophys. J. **335**, 415 (1988).
19. B.W. Filippone *et al.*, Phys. Rev. Lett. **50**, 412 (1983).
20. J.N. Bahcall *et al.*, Rev. Mod. Phys. **54**, 767 (1982).
21. B.W. Filippone and D.N. Schramm, Astrophys. J. **253**, 393 (1982).
22. W.A. Fowler, AIP Conf. Proceedings 96 80 (1982).
23. J.N. Bahcall *et al.*, Phys. Rev. Lett. **45**, 945 (1980).
24. E.G. Adelberger *et al.*, Rev. Mod. Phys. **70**, 1265 (1998).
25. N. Hata and P. Langacker, Phys. Rev. **D52**, 420 (1995).
26. N. Hata and P. Langacker, Phys. Rev. **D56**, 6107 (1997).
27. K.M. Heeger and R.G.H. Robertson, Phys. Rev. Lett. **77**, 3720 (1996).
28. J.N. Bahcall, P.I. Kratsev, and A.Yu. Smirnov, Phys. Rev. **D58**, 096016 (1998).
29. S.L. Glashow, P.J. Kerman, and L.M. Krauss, Phys. Lett. **B445**, 412 (1999).
30. V. Barger and K. Whismant, Phys. Lett. **B456**, 54 (1999).

1 SNU (Solar Neutrino Unit) = 10^{-36} captures per atom per second.

VALUE	DOCUMENT ID	TECN	COMMENT
$67.2^{+7.2+3.5}_{-7.0-3.0}$ SNU	100 ABDURASHI...	99B SAGE	${}^{71}\text{Ge} \rightarrow {}^{71}\text{Ge}$
$(2.44 \pm 0.05^{+0.09}_{-0.07}) \times 10^6 \text{ cm}^{-2}\text{s}^{-1}$	101 FUKUDA	99 SKAM	${}^8\text{B} \nu$ flux (all)
$(2.37 \pm 0.07) \times 10^6 \text{ cm}^{-2}\text{s}^{-1}$	101 FUKUDA	99 SKAM	${}^8\text{B} \nu$ flux (day)
$(2.48^{+0.07}_{-0.06}) \times 10^6 \text{ cm}^{-2}\text{s}^{-1}$	101 FUKUDA	99 SKAM	${}^8\text{B} \nu$ flux (night)
	102 FUKUDA	99B SKAM	Recoil e spectrum
$77.5 \pm 6.2^{+4.3}_{-4.7}$ SNU	103 HAMPEL	99 GALX	${}^{71}\text{Ge} \rightarrow {}^{71}\text{Ge}$
$2.56 \pm 0.16 \pm 0.16$ SNU	104 CLEVELAND	98 HOME	${}^{37}\text{Cl}$ radiochem.
$(2.80 \pm 0.19 \pm 0.33) \times 10^6 \text{ cm}^{-2}\text{s}^{-1}$	105 FUKUDA	96 KAMI	${}^8\text{B} \nu$ flux
$(2.70 \pm 0.27) \times 10^6 \text{ cm}^{-2}\text{s}^{-1}$	105 FUKUDA	96 KAMI	${}^8\text{B} \nu$ flux (day)
$(2.87^{+0.27}_{-0.26}) \times 10^6 \text{ cm}^{-2}\text{s}^{-1}$	105 FUKUDA	96 KAMI	${}^8\text{B} \nu$ flux (night)

100 ABDURASHITOV 99B is a detailed report of the SAGE solar-neutrino experiment during the period January 1990 through December 1997, and updates the ABDURASHITOV 94 result. However the data in the period November 1993 through June 1994 were not used in determining the neutrino capture rate due to some uncertainty with respect to experimental control. A total of 211 ${}^{71}\text{Ge}$ events were observed.

101 FUKUDA 99 results are for a total of 503.8 live days with Super-Kamiokande between 31 May 1996 and 25 March 1998, with threshold $E_\nu > 6.5$ MeV, and replace FUKUDA 98B results. The day-night solar-neutrino flux asymmetry is given as $N/D - 1 = 0.047 \pm 0.042 \pm 0.008$. The results are also given for night fluxes subdivided into five data sets according to nadir of the Sun at the time of the neutrino event. FUKUDA 99 set an absolute flux-independent exclusion region in the two-neutrino oscillation parameter space from the absence of a significant day-night variation. Except for $+0.6\%/ -0.5\%$, the systematic errors are common to day and night fluxes.

102 FUKUDA 99B reports the energy spectrum of recoil electrons from elastic scattering of solar neutrinos for a total of 503.8 live days of Super-Kamiokande observation. A comparison of the observed spectrum with the expectation is in poor agreement at the 4.6% confidence level.

103 HAMPEL 99 report the combined result for GALLEX I+II+III+IV (65 runs in total), which update the HAMPEL 96 result. The GALLEX IV result (12 runs) is $118.4 \pm 17.8 \pm 6.6$ SNU. (HAMPEL 99 discuss the consistency of partial results with the mean.) The GALLEX experimental program has been completed with these runs. The total run data cover the period 14 May 1991 through 23 January 1997. A total of 300 ${}^{71}\text{Ge}$ events were observed.

104 CLEVELAND 98 is a detailed report of the ${}^{37}\text{Cl}$ experiment at the Homestake Mine. The average solar neutrino-induced ${}^{37}\text{Ar}$ production rate from 108 runs between 1970 and 1994 updates the DAVIS 89 result.

105 FUKUDA 96 results are for a total of 2079 live days with Kamiokande II and III from January 1987 through February 1995, covering the entire solar cycle 22, with threshold $E_\nu > 9.3$ MeV (first 449 days), > 7.5 MeV (middle 794 days), and > 7.0 MeV (last 836 days). These results update the HIRATA 90 result for the average ${}^8\text{B}$ solar-neutrino flux and HIRATA 91 result for the day-night variation in the ${}^8\text{B}$ solar-neutrino flux. The total data sample was also analyzed for short-term variations: within experimental errors, no strong correlation of the solar-neutrino flux with the sunspot numbers was found.

(F) Astrophysical neutrino observations

Neutrinos and antineutrinos produced in the atmosphere induce μ -like and e -like events in underground detectors. The ratio of the numbers of the two kinds of events is defined as μ/e . It has the advantage that systematic effects, such as flux uncertainty, tend to cancel, for both experimental and theoretical values of the ratio. The "ratio of the ratios" of experimental to theoretical μ/e , $R(\mu/e)$, or that of experimental to theoretical μ/total , $R(\mu/\text{total})$ with $\text{total} = \mu + e$, is reported below. If the actual value is not unity, the value obtained in a given experiment may depend on the experimental conditions.

$R(\mu/e) = (\text{Measured Ratio } \mu/e) / (\text{Expected Ratio } \mu/e)$

VALUE	DOCUMENT ID	TECN	COMMENT
$0.64 \pm 0.11 \pm 0.06$	106 ALLISON	99 SOU2	Calorimeter
$0.61 \pm 0.03 \pm 0.05$	107 FUKUDA	98 SKAM	sub-GeV

• • • We do not use the following data for averages, fits, limits, etc. • • •

Lepton Particle Listings

Massive Neutrinos and Lepton Mixing

$0.66 \pm 0.06 \pm 0.08$	108 FUKUDA	98E SKAM	multi-GeV
	109 FUKUDA	96B KAMI	Water Cerenkov
$1.00 \pm 0.15 \pm 0.08$	110 DAUM	95 FREJ	Calorimeter
$0.60^{+0.06}_{-0.05} \pm 0.05$	111 FUKUDA	94 KAMI	sub-GeV
$0.57^{+0.08}_{-0.07} \pm 0.07$	112 FUKUDA	94 KAMI	multi-GeV
	113 BECKER-SZ...	92B IMB	Water Cerenkov

106 ALLISON 99 result is based on an exposure of 3.9 kton yr, 2.6 times the exposure reported in ALLISON 97, and replaces that result.

107 FUKUDA 98 result is based on an exposure of 25.5 kton yr. The analyzed data sample consists of fully-contained e-like events with $0.1 \text{ GeV}/c < p_e$ and μ -like events with $0.2 \text{ GeV}/c < p_\mu$, both having a visible energy $< 1.33 \text{ GeV}$. These criteria match the definition used by FUKUDA 94.

108 FUKUDA 98 result is based on an exposure of 25.5 kton yr. The analyzed data sample consists of fully-contained single-ring events with visible energy $> 1.33 \text{ GeV}$ and partially contained events. All partially contained events are classified as μ -like.

109 FUKUDA 96B studied neutron background in the atmospheric neutrino sample observed in the Kamiokande detector. No evidence for the background contamination was found.

110 DAUM 95 results are based on an exposure of 2.0 kton yr which includes the data used by BERGER 90B. This ratio is for the contained and semicontained events. DAUM 95 also report $R(\mu/e) = 0.99 \pm 0.13 \pm 0.08$ for the total neutrino induced data sample which includes upward going stopping muons and horizontal muons in addition to the contained and semicontained events.

111 FUKUDA 94 result is based on an exposure of 7.7 kton yr and updates the HIRATA 92 result. The analyzed data sample consists of fully-contained e-like events with $0.1 < p_e < 1.33 \text{ GeV}/c$ and fully-contained μ -like events with $0.2 < p_\mu < 1.5 \text{ GeV}/c$.

112 FUKUDA 94 analyzed the data sample consisting of fully contained events with visible energy $> 1.33 \text{ GeV}$ and partially contained μ -like events.

113 BECKER-SZENDY 92B reports the fraction of nonshowering events (mostly muons from atmospheric neutrinos) as $0.36 \pm 0.02 \pm 0.02$, as compared with expected fraction $0.51 \pm 0.01 \pm 0.05$. After cutting the energy range to the Kamiokande limits, BEIER 92 finds $R(\mu/e)$ very close to the Kamiokande value.

$R(\nu_\mu) = (\text{Measured Flux of } \nu_\mu) / (\text{Expected Flux of } \nu_\mu)$

VALUE	DOCUMENT ID	TECN	COMMENT
• • • We do not use the following data for averages, fits, limits, etc. • • •			
$0.74 \pm 0.036 \pm 0.046$	114 AMBROSIO	98 MCRO	Streamer tubes
	115 CASPER	91 IMB	Water Cherenkov
	116 AGLIETTA	89 NUSX	
0.95 ± 0.22	117 BOLIEV	81	Baksan
0.62 ± 0.17	CROUCH	78	Case Western/UCI

114 AMBROSIO 98 result is for all nadir angles and updates AHLEN 95 result. The lower cutoff on the muon energy is 1 GeV. In addition to the statistical and systematic errors, there is a Monte Carlo flux error (theoretical error) of ± 0.13 . With a neutrino oscillation hypothesis, the fit either to the flux or zenith distribution independently yields $\sin^2 2\theta = 1.0$ and $\Delta(m^2) \sim$ a few times 10^{-3} eV^2 . However, the fit to the observed zenith distribution gives a maximum probability for χ^2 of only 5% for the best oscillation hypothesis.

115 CASPER 91 correlates showering/nonshowering signature of single-ring events with parent atmospheric-neutrino flavor. They find nonshowering ($\approx \nu_\mu$ induced) fraction is $0.41 \pm 0.03 \pm 0.02$, as compared with expected 0.51 ± 0.05 (syst).

116 AGLIETTA 89 finds no evidence for any anomaly in the neutrino flux. They define $\rho = (\text{measured number of } \nu_e) / (\text{measured number of } \nu_\mu)$. They report $\rho(\text{measured}) = \rho(\text{expected}) = 0.96^{+0.32}_{-0.28}$.

117 From this data BOLIEV 81 obtain the limit $\Delta(m^2) \leq 6 \times 10^{-3} \text{ eV}^2$ for maximal mixing, $\nu_\mu \leftrightarrow \nu_\mu$ type oscillation.

$R(\mu/\text{total}) = (\text{Measured Ratio } \mu/\text{total}) / (\text{Expected Ratio } \mu/\text{total})$

VALUE	DOCUMENT ID	TECN	COMMENT
• • • We do not use the following data for averages, fits, limits, etc. • • •			
$1.1^{+0.07}_{-0.12} \pm 0.11$	118 CLARK	97 IMB	multi-GeV

118 CLARK 97 obtained this result by an analysis of fully contained and partially contained events in the IMB water-Cerenkov detector with visible energy $> 0.95 \text{ GeV}$.

$N_{\text{up}}(\mu) / N_{\text{down}}(\mu)$

VALUE	DOCUMENT ID	TECN	COMMENT
• • • We do not use the following data for averages, fits, limits, etc. • • •			
$0.52^{+0.07}_{-0.06} \pm 0.01$	119 FUKUDA	98E SKAM	multi-GeV

119 FUKUDA 98E result is based on an exposure of 25.5 kton yr. The analyzed data sample consists of fully-contained single-ring μ -like events with visible energy $> 1.33 \text{ GeV}$ and partially contained events. All partially contained events are classified as μ -like. Upward-going events are those with $-1 < \cos(\text{zenith angle}) < -0.2$ and downward-going events with those with $0.2 < \cos(\text{zenith angle}) < 1$. FUKUDA 98E result strongly deviates from an expected value of $0.98 \pm 0.03 \pm 0.02$.

$N_{\text{up}}(e) / N_{\text{down}}(e)$

VALUE	DOCUMENT ID	TECN	COMMENT
• • • We do not use the following data for averages, fits, limits, etc. • • •			
$0.84^{+0.14}_{-0.12} \pm 0.02$	120 FUKUDA	98E SKAM	multi-GeV

120 FUKUDA 98E result is based on an exposure of 25.5 kton yr. The analyzed data sample consists of fully-contained single-ring e-like events with visible energy $> 1.33 \text{ GeV}$. Upward-going events are those with $-1 < \cos(\text{zenith angle}) < -0.2$ and downward-going events are those with $0.2 < \cos(\text{zenith angle}) < 1$. FUKUDA 98E result is compared to an expected value of $1.01 \pm 0.06 \pm 0.03$.

$\sin^2(2\theta)$ for given $\Delta(m^2) (\nu_e \leftrightarrow \nu_\mu)$

For a review see BAHCALL 89.

VALUE	CL%	DOCUMENT ID	TECN	COMMENT
• • • We do not use the following data for averages, fits, limits, etc. • • •				
< 0.6	90	121 OYAMA	98 KAMI	$\Delta(m^2) > 0.1 \text{ eV}^2$
< 0.5		122 CLARK	97 IMB	$\Delta(m^2) > 0.1 \text{ eV}^2$
> 0.55	90	123 FUKUDA	94 KAMI	$\Delta(m^2) = 0.007-0.08 \text{ eV}^2$
< 0.47	90	124 BERGER	90B FREJ	$\Delta(m^2) > 1 \text{ eV}^2$
< 0.14	90	LOSECCO	87 IMB	$\Delta(m^2) = 0.00011 \text{ eV}^2$

121 OYAMA 98 obtained this result by an analysis of upward-going muons in Kamiokande. The data sample used is essentially the same as that used by HATAKEYAMA 98.

122 CLARK 97 obtained this result by an analysis of fully contained and partially contained events in the IMB water-Cerenkov detector with visible energy $> 0.95 \text{ GeV}$.

123 FUKUDA 94 obtained this result by a combined analysis of sub- and multi-GeV atmospheric neutrino events in Kamiokande.

124 BERGER 90B uses the Frejus detector to search for oscillations of atmospheric neutrinos. Bounds are for both neutrino and antineutrino oscillations.

$\Delta(m^2)$ for $\sin^2(2\theta) = 1 (\nu_e \leftrightarrow \nu_\mu)$

VALUE (10^{-5} eV^2)	CL%	DOCUMENT ID	TECN	COMMENT
• • • We do not use the following data for averages, fits, limits, etc. • • •				
< 560	90	125 OYAMA	98 KAMI	
< 980		126 CLARK	97 IMB	
$700 < \Delta(m^2) < 7000$	90	127 FUKUDA	94 KAMI	
< 150	90	128 BERGER	90B FREJ	

125 OYAMA 98 obtained this result by an analysis of upward-going muons in Kamiokande. The data sample used is essentially the same as that used by HATAKEYAMA 98.

126 CLARK 97 obtained this result by an analysis of fully contained and partially contained events in the IMB water-Cerenkov detector with visible energy $> 0.95 \text{ GeV}$.

127 FUKUDA 94 obtained this result by a combined analysis of sub- and multi-GeV atmospheric neutrino events in Kamiokande.

128 BERGER 90B uses the Frejus detector to search for oscillations of atmospheric neutrinos. Bounds are for both neutrino and antineutrino oscillations.

$\sin^2(2\theta)$ for given $\Delta(m^2) (\bar{\nu}_e \leftrightarrow \bar{\nu}_\mu)$

VALUE (10^{-5} eV^2)	CL%	DOCUMENT ID	TECN	COMMENT
• • • We do not use the following data for averages, fits, limits, etc. • • •				
< 0.9	99	129 SMIRNOV	94 THEO	$\Delta(m^2) > 3 \times 10^{-4} \text{ eV}^2$
< 0.7	99	129 SMIRNOV	94 THEO	$\Delta(m^2) < 10^{-11} \text{ eV}^2$

129 SMIRNOV 94 analyzed the data from SN 1987A using stellar-collapse models. They also give less stringent upper limits on $\sin^2 2\theta$ for $10^{-11} < \Delta(m^2) < 3 \times 10^{-7} \text{ eV}^2$ and $10^{-5} < \Delta(m^2) < 3 \times 10^{-4} \text{ eV}^2$. The same results apply to $\bar{\nu}_e \leftrightarrow \bar{\nu}_\tau$, ν_μ , and ν_τ .

$\sin^2(2\theta)$ for given $\Delta(m^2) (\nu_\mu \leftrightarrow \nu_\tau)$

VALUE	CL%	DOCUMENT ID	TECN	COMMENT
• • • We do not use the following data for averages, fits, limits, etc. • • •				
> 0.4	90	130 FUKUDA	99C SKAM	$\Delta(m^2) = 0.001-0.1 \text{ eV}^2$
> 0.7	90	131 FUKUDA	99D SKAM	$\Delta(m^2) = 0.0015-0.015 \text{ eV}^2$
> 0.82	90	132 AMBROSIO	98 MCRO	$\Delta(m^2) \sim 0.0025 \text{ eV}^2$
> 0.82	90	133 FUKUDA	98C SKAM	$\Delta(m^2) = 0.0005-0.006 \text{ eV}^2$
> 0.3	90	134 HATAKEYAMA98	KAMI	$\Delta(m^2) = 0.00055-0.14 \text{ eV}^2$
> 0.73	90	135 HATAKEYAMA98	KAMI	$\Delta(m^2) = 0.004-0.025 \text{ eV}^2$
< 0.7		136 CLARK	97 IMB	$\Delta(m^2) > 0.1 \text{ eV}^2$
> 0.65	90	137 FUKUDA	94 KAMI	$\Delta(m^2) = 0.005-0.03 \text{ eV}^2$
< 0.5	90	138 BECKER-SZ...	92 IMB	$\Delta(m^2) = 1-2 \times 10^{-4} \text{ eV}^2$
< 0.6	90	139 BERGER	90B FREJ	$\Delta(m^2) > 1 \text{ eV}^2$

130 FUKUDA 99C obtained this result from a total of 537 live days of upward through-going muon data in Super-Kamiokande between April 1996 to January 1998. With a threshold of $E_\mu > 1.6 \text{ GeV}$, the observed flux of upward through-going muons is $(1.74 \pm 0.07 \pm 0.02) \times 10^{-13} \text{ cm}^{-2} \text{ s}^{-1} \text{ sr}^{-1}$. The zenith-angle dependence of the flux does not agree with no-oscillation predictions. For the $\nu_\mu \rightarrow \nu_\tau$ hypothesis, FUKUDA 99C obtained the best fit at $\sin^2 2\theta = 0.95$ and $\Delta(m^2) = 5.9 \times 10^{-3} \text{ eV}^2$. FUKUDA 99C also reports 68% and 99% confidence-level allowed regions for the same hypothesis.

131 FUKUDA 99D obtained this result from a simultaneous fitting to zenith angle distributions of upward-stopping and through-going muons. The flux of upward-stopping muons of minimum energy of 1.6 GeV measured between April 1996 and January 1998 is $(0.39 \pm 0.04 \pm 0.02) \times 10^{-13} \text{ cm}^{-2} \text{ s}^{-1} \text{ sr}^{-1}$. This is compared to the expected flux of $(0.73 \pm 0.16 \text{ (theoretical error)}) \times 10^{-13} \text{ cm}^{-2} \text{ s}^{-1} \text{ sr}^{-1}$. The flux of upward through-going muons is taken from FUKUDA 99C. For the $\nu_\mu \rightarrow \nu_\tau$ hypothesis, FUKUDA 99D obtained the best fit in the physical region at $\sin^2 2\theta = 1.0$ and $\Delta(m^2) = 3.9 \times 10^{-3} \text{ eV}^2$. FUKUDA 99D also reports 68% and 99% confidence-level allowed regions for the same hypothesis. FUKUDA 99D further reports the result of the oscillation analysis using the zenith-angle dependence of upward-stopping/through-going flux ratio. The best fit in the physical region is obtained at $\sin^2 2\theta = 1.0$ and $\Delta(m^2) = 3.1 \times 10^{-3} \text{ eV}^2$.

132 AMBROSIO 98 result is only 17% probable at maximum because of relatively low flux for $\cos\theta < -0.8$.

133 FUKUDA 98C obtained this result by an analysis of 33.0 kton yr atmospheric-neutrino data which include the 25.5 kton yr data used by FUKUDA 98 (sub-GeV) and FUKUDA 98E (multi-GeV). Inside the physical region, the best fit was obtained at $\sin^2 2\theta = 1.0$ and $\Delta(m^2) = 2.2 \times 10^{-3} \text{ eV}^2$. In addition, FUKUDA 98C gave the 99% confidence interval, $\sin^2 2\theta > 0.73$ and $3 \times 10^{-4} < \Delta(m^2) < 8.5 \times 10^{-3} \text{ eV}^2$. FUKUDA 98C also tested the $\nu_\mu \rightarrow \nu_e$ hypothesis, and concluded that it is not favored.

134 HATAKEYAMA 98 obtained this result from a total of 2456 live days of upward-going muon data in Kamiokande between December 1985 and May 1995. With a threshold of $E_\mu > 1.6 \text{ GeV}$, the observed flux of upward through-going muon is

See key on page 239

Lepton Particle Listings
Massive Neutrinos and Lepton Mixing

$(1.94 \pm 0.10^{+0.07}_{-0.06}) \times 10^{-13} \text{ cm}^{-2} \text{ s}^{-1} \text{ sr}^{-1}$. This is compared to the expected flux of $(2.46 \pm 0.54 \text{ (theoretical error)}) \times 10^{-13} \text{ cm}^{-2} \text{ s}^{-1} \text{ sr}^{-1}$. For the $\nu_\mu \rightarrow \nu_\tau$ hypothesis, the best fit inside the physical region was obtained at $\sin^2 2\theta=1.0$ and $\Delta(m^2)=3.2 \times 10^{-3} \text{ eV}^2$.

- 135 HATAKEYAMA 98 obtained this result from a combined analysis of Kamiokande's contained events (FUKUDA 94) and upward-going muon events. The best fit was obtained at $\sin^2 2\theta=0.95$ and $\Delta(m^2)=1.3 \times 10^{-2} \text{ eV}^2$.
- 136 CLARK 97 obtained this result by an analysis of fully contained and partially contained events in the IMB water-Cherenkov detector with visible energy $> 0.95 \text{ GeV}$.
- 137 FUKUDA 94 obtained this result by a combined analysis of sub-and multi-GeV atmospheric neutrino events in Kamiokande.
- 138 BECKER-SZENDY 92 uses upward-going muons to search for atmospheric ν_μ oscillations. The fraction of muons which stop in the detector is used to search for deviations in the expected spectrum. No evidence for oscillations is found.
- 139 BERGER 90B uses the Frejus detector to search for oscillations of atmospheric neutrinos. Bounds are for both neutrino and antineutrino oscillations.

 $\Delta(m^2)$ for $\sin^2(2\theta) = 1$ ($\nu_\mu \leftrightarrow \nu_\tau$)

VALUE (10^{-3} eV^2)	CL%	DOCUMENT ID	TECN
----------------------------------	-----	-------------	------

• • • We do not use the following data for averages, fits, limits, etc. • • •

$100 < \Delta(m^2) < 5000$	90	140 FUKUDA	99C SKAM
$150 < \Delta(m^2) < 1500$	90	141 FUKUDA	99D SKAM
$50 < \Delta(m^2) < 600$	90	142 AMBROSIO	98 MCRO
$50 < \Delta(m^2) < 600$	90	143 FUKUDA	98C SKAM
$55 < \Delta(m^2) < 5000$	90	144 HATAKEYAMA 98	KAMI
$400 < \Delta(m^2) < 2300$	90	145 HATAKEYAMA 98	KAMI
< 1500		146 CLARK	97 IMB
$500 < \Delta(m^2) < 2500$	90	147 FUKUDA	94 KAMI
< 350	90	148 BERGER	90B FREJ

- 140 FUKUDA 99C obtained this result from a total of 537 live days of upward through-going muon data in Super-Kamiokande between April 1996 to January 1998. With a threshold of $E_\mu > 1.6 \text{ GeV}$, the observed flux of upward through-going muon is $(1.74 \pm 0.07 \pm 0.02) \times 10^{-13} \text{ cm}^{-2} \text{ s}^{-1} \text{ sr}^{-1}$. The zenith-angle dependence of the flux does not agree with no-oscillation predictions. For the $\nu_\mu \rightarrow \nu_\tau$ hypothesis, FUKUDA 99C obtained the best fit at $\sin^2 2\theta=0.95$ and $\Delta(m^2)=5.9 \times 10^{-3} \text{ eV}^2$. FUKUDA 99C also reports 68% and 99% confidence-level allowed regions for the same hypothesis.
- 141 FUKUDA 99D obtained this result from a simultaneous fitting to zenith angle distributions of upward-stopping and through-going muons. The flux of upward-stopping muons of minimum energy of 1.6 GeV measured between April 1996 and January 1998 is $(0.39 \pm 0.04 \pm 0.02) \times 10^{-13} \text{ cm}^{-2} \text{ s}^{-1} \text{ sr}^{-1}$. This is compared to the expected flux of $(0.73 \pm 0.16 \text{ (theoretical error)}) \times 10^{-13} \text{ cm}^{-2} \text{ s}^{-1} \text{ sr}^{-1}$. The flux of upward through-going muons is taken from FUKUDA 99C. For the $\nu_\mu \rightarrow \nu_\tau$ hypothesis, FUKUDA 99D obtained the best fit in the physical region at $\sin^2 2\theta=1.0$ and $\Delta(m^2)=3.9 \times 10^{-3} \text{ eV}^2$. FUKUDA 99D also reports 68% and 99% confidence-level allowed regions for the same hypothesis. FUKUDA 99D further reports the result of the oscillation analysis using the zenith-angle dependence of upward-stopping/through-going flux ratio. The best fit in the physical region is obtained at $\sin^2 2\theta=1.0$ and $\Delta(m^2)=3.1 \times 10^{-3} \text{ eV}^2$.

- 142 AMBROSIO 98 result is only 17% probable at maximum because of relatively low flux for $\cos\theta < -0.8$.
- 143 FUKUDA 98C obtained this result by an analysis of 33.0 kton yr atmospheric-neutrino data which include the 25.5 kton yr data used by FUKUDA 98 (sub-GeV) and FUKUDA 98E (multi-GeV). Inside the physical region, the best fit was obtained at $\sin^2 2\theta=1.0$ and $\Delta(m^2)=2.2 \times 10^{-3} \text{ eV}^2$. In addition, FUKUDA 98C gave the 99% confidence interval, $\sin^2 2\theta > 0.73$ and $3 \times 10^{-4} < \Delta(m^2) < 8.5 \times 10^{-3} \text{ eV}^2$. FUKUDA 98C also tested the $\nu_\mu \rightarrow \nu_e$ hypothesis, and concluded that it is not favored.
- 144 HATAKEYAMA 98 obtained this result from a total of 2456 live days of upward-going muon data in Kamiokande between December 1985 and May 1995. With a threshold of $E_\mu > 1.6 \text{ GeV}$, the observed flux of upward through-going muon is $(1.94 \pm 0.10^{+0.07}_{-0.06}) \times 10^{-13} \text{ cm}^{-2} \text{ s}^{-1} \text{ sr}^{-1}$. This is compared to the expected flux of $(2.46 \pm 0.54 \text{ (theoretical error)}) \times 10^{-13} \text{ cm}^{-2} \text{ s}^{-1} \text{ sr}^{-1}$. For the $\nu_\mu \rightarrow \nu_\tau$ hypothesis, the best fit inside the physical region was obtained at $\sin^2 2\theta=1.0$ and $\Delta(m^2)=3.2 \times 10^{-3} \text{ eV}^2$.

- 145 HATAKEYAMA 98 obtained this result from a combined analysis of Kamiokande's contained events (FUKUDA 94) and upward-going muon events. The best fit was obtained at $\sin^2 2\theta=0.95$ and $\Delta(m^2)=1.3 \times 10^{-2} \text{ eV}^2$.
- 146 CLARK 97 obtained this result by an analysis of fully contained and partially contained events in the IMB water-Cherenkov detector with visible energy $> 0.95 \text{ GeV}$.
- 147 FUKUDA 94 obtained this result by a combined analysis of sub-and multi-GeV atmospheric neutrino events in Kamiokande.
- 148 BERGER 90B uses the Frejus detector to search for oscillations of atmospheric neutrinos. Bounds are for both neutrino and antineutrino oscillations.

 $\Delta(m^2)$ for $\sin^2(2\theta) = 1$ ($\nu_\mu \rightarrow \nu_s$)

ν_s means ν_τ or any sterile (noninteracting) ν .

VALUE (10^{-3} eV^2)	CL%	DOCUMENT ID	TECN	COMMENT
----------------------------------	-----	-------------	------	---------

• • • We do not use the following data for averages, fits, limits, etc. • • •

< 3000 (or < 550)	90	149 OYAMA	89 KAMI	Water Cherenkov
< 4.2 or > 54 .	90	BIONTA	88 IMB	Flux has $\nu_\mu, \bar{\nu}_\mu, \nu_e,$ and $\bar{\nu}_e$

- 149 OYAMA 89 gives a range of limits, depending on assumptions in their analysis. They argue that the region $\Delta(m^2) = (100-1000) \times 10^{-5} \text{ eV}^2$ is not ruled out by any data for large mixing.

(G) Reactor $\bar{\nu}_e$ disappearance experiments

In most cases, the reaction $\bar{\nu}_e p \rightarrow e^+ n$ is observed at different distances from one or more reactors in a complex.

Events (Observed/Expected) from Reactor $\bar{\nu}_e$ Experiments

VALUE	DOCUMENT ID	TECN	COMMENT
• • • We do not use the following data for averages, fits, limits, etc. • • •			
$1.01 \pm 0.028 \pm 0.027$	150 APOLLONIO	99 CHOZ	Chooz reactors 1 km
$0.987 \pm 0.006 \pm 0.037$	151 GREENWOOD	96	Savannah River, 18.2 m
$0.988 \pm 0.004 \pm 0.05$	ACHKAR	95 CNTR	Bugey reactor, 15 m
$0.994 \pm 0.010 \pm 0.05$	ACHKAR	95 CNTR	Bugey reactor, 40 m
$0.915 \pm 0.132 \pm 0.05$	ACHKAR	95 CNTR	Bugey reactor, 95 m
$0.987 \pm 0.014 \pm 0.027$	152 DECLAIS	94 CNTR	Bugey reactor, 15 m
$0.985 \pm 0.018 \pm 0.034$	KUVSHINN...	91 CNTR	Rovno reactor
$1.05 \pm 0.02 \pm 0.05$	VUILLEUMIER	82	Gösgen reactor
$0.955 \pm 0.035 \pm 0.110$	153 KWON	81	$\bar{\nu}_e p \rightarrow e^+ n$
0.89 ± 0.15	153 BOEHM	80	$\bar{\nu}_e p \rightarrow e^+ n$
0.38 ± 0.21	154,155 REINES	80	
0.40 ± 0.22	154,155 REINES	80	

- 150 APOLLONIO 99, APOLLONIO 98 search for neutrino oscillations at 1.1 km fixed distance from Chooz reactors. They use $\bar{\nu}_e p \rightarrow e^+ n$ in Gd-loaded scintillator target. APOLLONIO 99 supersedes APOLLONIO 98.
- 151 GREENWOOD 96 search for neutrino oscillations at 18 m and 24 m from the reactor at Savannah River.
- 152 DECLAIS 94 result based on integral measurement of neutrons only. Result is ratio of measured cross section to that expected in standard V-A theory. Replaced by ACHKAR 95.
- 153 KWON 81 represents an analysis of a larger set of data from the same experiment as BOEHM 80.
- 154 REINES 80 involves comparison of neutral- and charged-current reactions $\bar{\nu}_e d \rightarrow n p \bar{\nu}_e$ and $\bar{\nu}_e d \rightarrow n n e^+$ respectively. Combined analysis of reactor $\bar{\nu}_e$ experiments was performed by SILVERMAN 81.
- 155 The two REINES 80 values correspond to the calculated $\bar{\nu}_e$ fluxes of AVIGNONE 80 and DAVIS 79 respectively.

 $\bar{\nu}_e \neq \nu_e$ $\Delta(m^2)$ for $\sin^2(2\theta) = 1$

VALUE (eV^2)	CL%	DOCUMENT ID	TECN	COMMENT
-------------------------	-----	-------------	------	---------

- < 0.0007
- • • We do not use the following data for averages, fits, limits, etc. • • •
- < 0.0011 90 157 BOEHM 00 Palo Verde react. 0.8 km
- < 0.01 90 158 ACHKAR 95 CNTR Bugey reactor
- < 0.0075 90 159 VIDYAKIN 94 Krasnoyarsk reactors
- < 0.04 90 160 AFONIN 88 CNTR Rovno reactor
- < 0.014 68 161 VIDYAKIN 87 $\bar{\nu}_e p \rightarrow e^+ n$
- < 0.019 90 162 ZACEK 86 Gösgen reactor
- 156 APOLLONIO 99 search for neutrino oscillations at 1.1 km fixed distance from Chooz reactors. They use $\bar{\nu}_e p \rightarrow e^+ n$ in Gd-loaded scintillator target. APOLLONIO 99 supersedes APOLLONIO 98. This is the most sensitive search in terms of $\Delta(m^2)$ for $\bar{\nu}_e$ disappearance.
- 157 BOEHM 00 is a disappearance search for neutrino oscillations at 0.75 and 0.89 km distance from Palo Verde reactors. The detection reaction is $\bar{\nu}_e p \rightarrow e^+ n$ in a segmented Gd loaded scintillator target. Result is less restrictive than APOLLONIO 99.
- 158 ACHKAR 95 bound is for $L=15, 40, \text{ and } 95 \text{ m}$.
- 159 VIDYAKIN 94 bound is for $L=57.0 \text{ m}, 57.6 \text{ m}, \text{ and } 231.4 \text{ m}$. Supersedes VIDYAKIN 90.
- 160 AFONIN 86 and AFONIN 87 also give limits on $\sin^2(2\theta)$ for intermediate values of $\Delta(m^2)$. (See also KETOV 92). Supersedes AFONIN 87, AFONIN 86, AFONIN 85, AFONIN 83, and BELENKII 83.
- 161 VIDYAKIN 87 bound is for $L = 32.8 \text{ and } 92.3 \text{ m}$ distance from two reactors.
- 162 This bound is from data for $L=37.9 \text{ m}, 45.9 \text{ m}, \text{ and } 64.7 \text{ m}$.

- 157 BOEHM 00 is a disappearance search for neutrino oscillations at 0.75 and 0.89 km distance from Palo Verde reactors. The detection reaction is $\bar{\nu}_e p \rightarrow e^+ n$ in a segmented Gd loaded scintillator target. Result is less restrictive than APOLLONIO 99.

- 158 ACHKAR 95 bound is for $L=15, 40, \text{ and } 95 \text{ m}$.
- 159 VIDYAKIN 94 bound is for $L=57.0 \text{ m}, 57.6 \text{ m}, \text{ and } 231.4 \text{ m}$. Supersedes VIDYAKIN 90.
- 160 AFONIN 86 and AFONIN 87 also give limits on $\sin^2(2\theta)$ for intermediate values of $\Delta(m^2)$. (See also KETOV 92). Supersedes AFONIN 87, AFONIN 86, AFONIN 85, AFONIN 83, and BELENKII 83.

- 161 VIDYAKIN 87 bound is for $L = 32.8 \text{ and } 92.3 \text{ m}$ distance from two reactors.

- 162 This bound is from data for $L=37.9 \text{ m}, 45.9 \text{ m}, \text{ and } 64.7 \text{ m}$.

 $\sin^2(2\theta)$ for "Large" $\Delta(m^2)$

VALUE	CL%	DOCUMENT ID	TECN	COMMENT
-------	-----	-------------	------	---------

- < 0.02 90 163 ACHKAR 95 CNTR For $\Delta(m^2) = 0.6 \text{ eV}^2$
- • • We do not use the following data for averages, fits, limits, etc. • • •
- < 0.21 90 164 BOEHM 00 Palo Verde react. 0.8 km
- < 0.10 90 165 APOLLONIO 99 CHOZ Chooz reactors 1 km
- < 0.24 90 166 GREENWOOD 96
- < 0.04 90 166 GREENWOOD 96 For $\Delta(m^2) = 1.0 \text{ eV}^2$
- < 0.087 68 167 VYRODOV 95 CNTR For $\Delta(m^2) > 2 \text{ eV}^2$
- < 0.15 90 168 VIDYAKIN 94 For $\Delta(m^2) > 5.0 \times 10^{-2} \text{ eV}^2$
- < 0.2 90 169 AFONIN 88 CNTR $\bar{\nu}_e p \rightarrow e^+ n$
- < 0.14 68 170 VIDYAKIN 87 $\bar{\nu}_e p \rightarrow e^+ n$
- < 0.21 90 171 ZACEK 86 $\bar{\nu}_e p \rightarrow e^+ n$
- < 0.19 90 172 ZACEK 85 Gösgen reactor
- < 0.16 90 173 GABATHULER 84 $\bar{\nu}_e p \rightarrow e^+ n$

- 163 ACHKAR 95 bound is from data for $L=15, 40, \text{ and } 95 \text{ m}$ distance from the Bugey reactor.
- 164 BOEHM 00 search for neutrino oscillations at 0.75 and 0.89 km distance from Palo Verde reactors.
- 165 APOLLONIO 99 search for neutrino oscillations at 1.1 km fixed distance from Chooz reactors.
- 166 GREENWOOD 96 search for neutrino oscillations at 18 m and 24 m from the reactor at Savannah River by observing $\bar{\nu}_e p \rightarrow e^+ n$ in a Gd loaded scintillator target. Their region of sensitivity in $\Delta(m^2)$ and $\sin^2 2\theta$ is already excluded by ACHKAR 95.
- 167 The VYRODOV 95 bound is from data for $L=15 \text{ m}$ distance from the Bugey-5 reactor.

Lepton Particle Listings

Massive Neutrinos and Lepton Mixing

- ¹⁶⁸ The VIDYAKIN 94 bound is from data for $L=57.0$ m, 57.6 m, and 231.4 m from three reactors in the Krasnoyarsk Reactor complex.
- ¹⁶⁹ Several different methods of data analysis are used in AFONIN 88. We quote the most stringent limits. Different upper limits on $\sin^2 2\theta$ apply at intermediate values of $\Delta(m^2)$. Supersedes AFONIN 87, AFONIN 85, and BELENKII 83.
- ¹⁷⁰ VIDYAKIN 87 bound is for $L=32.8$ and 92.3 m distance from two reactors.
- ¹⁷¹ This bound is from data for $L=37.9$ m, 45.9 m, and 64.7 m distance from Gosgen reactor.
- ¹⁷² ZACEK 85 gives two sets of bounds depending on what assumptions are used in the data analysis. The bounds in figure 3(a) of ZACEK 85 are progressively poorer for large $\Delta(m^2)$ whereas those of figure 3(b) approach a constant. We list the latter. Both sets of bounds use combination of data from 37.9 , 45.9 , and 64.7 m distance from reactor. ZACEK 85 states "Our experiment excludes this area (the oscillation parameter region allowed by the Bugey data, CAVIGNAC 84) almost completely, thus disproving the indications of neutrino oscillations of CAVIGNAC 84 with a high degree of confidence."
- ¹⁷³ This bound comes from a combination of the VUILLEUMIER 82 data at distance 37.9 m from Gosgen reactor and new data at 45.9 m.

(H) Accelerator neutrino appearance experiments

$$\nu_e \rightarrow \nu_\tau$$

$\Delta(m^2)$ for $\sin^2(2\theta) = 1$

VALUE (eV ²)	CL%	DOCUMENT ID	TECN	COMMENT
< 0.77	90	¹⁷⁴ ARMBRUSTER98	KARM	
• • • We do not use the following data for averages, fits, limits, etc. • • •				
< 17	90	NAPLES	99 CCFR	FNAL
< 44	90	TALEBZADEH 87	HLBC	BEBC
< 9	90	USHIDA	86c EMUL	FNAL

- ¹⁷⁴ ARMBRUSTER 98 use KARMEN detector with ν_e from muon decay at rest and observe $^{12}\text{C}(\nu_e, e^-)^{12}\text{N}_{gs}$, essentially free from this background. The reported limits on the parameters of ν_e disappearance are not competitive. A three-flavor analysis is also presented.

$\sin^2(2\theta)$ for "Large" $\Delta(m^2)$

VALUE	CL%	DOCUMENT ID	TECN	COMMENT
< 0.21	90	NAPLES	99 CCFR	FNAL
• • • We do not use the following data for averages, fits, limits, etc. • • •				
< 0.338	90	¹⁷⁵ ARMBRUSTER98	KARM	
< 0.36	90	TALEBZADEH 87	HLBC	BEBC
< 0.25	90	¹⁷⁶ USHIDA	86c EMUL	FNAL

- ¹⁷⁵ See footnote in preceding table (ARMBRUSTER 98) for further details, and see the paper for a plot showing allowed regions. A three-flavor analysis is also presented here.
- ¹⁷⁶ USHIDA 86c published result is $\sin^2 2\theta < 0.12$. The quoted result is corrected for a numerical mistake incurred in calculating the expected number of ν_e CC events, normalized to the total number of neutrino interactions (3886) rather than to the total number of ν_μ CC events (1870).

$$\bar{\nu}_e \rightarrow \bar{\nu}_\tau$$

$\sin^2(2\theta)$ for "Large" $\Delta(m^2)$

VALUE	CL%	DOCUMENT ID	TECN	COMMENT
< 0.7	90	¹⁷⁷ FRITZE	80 HYBR	BEBC CERN SPS

- ¹⁷⁷ Authors give $P(\nu_e \rightarrow \nu_\tau) < 0.35$, equivalent to above limit.

$$\nu_\mu \rightarrow \nu_e$$

$\Delta(m^2)$ for $\sin^2(2\theta) = 1$

VALUE (eV ²)	CL%	DOCUMENT ID	TECN	COMMENT
< 0.09	90	ANGELINI	86 HLBC	BEBC CERN PS
• • • We do not use the following data for averages, fits, limits, etc. • • •				
0.03 to 0.3	95	¹⁷⁸ ATHANASSO...98	LSND	$\nu_\mu \rightarrow \nu_e$
< 2.3	90	¹⁷⁹ LOVERRE	96	CHARM/CDHS
< 0.9	90	VILAIN	94c CHM2	CERN SPS
< 0.1	90	BLUMENFELD	89 CNTR	
< 1.3	90	AMMOSOV	88 HLBC	SKAT at Serpukhov
< 0.19	90	BERGSMASMA	88 CHRM	
		¹⁸⁰ LOVERRE	88 RVUE	
< 2.4	90	AHRENS	87 CNTR	BNL AGS
< 1.8	90	BOFILL	87 CNTR	FNAL
< 2.2	90	¹⁸¹ BRUCKER	86 HLBC	15-ft FNAL
< 0.43	90	AHRENS	85 CNTR	BNL AGS E734
< 0.20	90	BERGSMASMA	84 CHRM	
< 1.7	90	ARMENISE	81 HLBC	GGM CERN PS
< 0.6	90	BAKER	81 HLBC	15-ft FNAL
< 1.7	90	ERRIQUEZ	81 HLBC	BEBC CERN PS
< 1.2	95	BLIETSCHAU	78 HLBC	GGM CERN PS
< 1.2	95	BELLOTTI	76 HLBC	GGM CERN PS

- ¹⁷⁸ ATHANASSOPOULOS 98 is a search for the $\nu_\mu \rightarrow \nu_e$ oscillations using ν_μ from π^+ decay in flight. The 40 observed beam-on electron events are consistent with $\nu_e C \rightarrow e^- X$; the expected background is 21.9 ± 2.1 . Authors interpret this excess as evidence for an oscillation signal corresponding to oscillations with probability $(0.26 \pm 0.10 \pm 0.05)\%$. Although the significance is only 2.3σ , this measurement is an important and consistent cross check of ATHANASSOPOULOS 96 who reported evidence for $\bar{\nu}_\mu \rightarrow \bar{\nu}_e$ oscillations from μ^+ decay at rest. See also ATHANASSOPOULOS 98b.
- ¹⁷⁹ LOVERRE 96 uses the charged-current to neutral-current ratio from the combined CHARM (ALLABY 86) and CDHS (ABRAMOWICZ 86) data from 1986.
- ¹⁸⁰ LOVERRE 88 reports a less stringent, indirect limit based on theoretical analysis of neutral to charged current ratios.
- ¹⁸¹ 15ft bubble chamber at FNAL.

$\sin^2(2\theta)$ for "Large" $\Delta(m^2)$

VALUE (units 10^{-3})	CL%	DOCUMENT ID	TECN	COMMENT
< 3.0	90	¹⁸² LOVERRE	96	CHARM/CDHS
< 2.5	90	AMMOSOV	88 HLBC	SKAT at Serpukhov
• • • We do not use the following data for averages, fits, limits, etc. • • •				
0.0005 to 0.03	95	¹⁸³ ATHANASSO...98	LSND	$\nu_\mu \rightarrow \nu_e$
< 9.4	90	VILAIN	94c CHM2	CERN SPS
< 5.6	90	¹⁸⁴ VILAIN	94c CHM2	CERN SPS
< 16	90	BLUMENFELD	89 CNTR	
< 8	90	BERGSMASMA	88 CHRM	$\Delta(m^2) \geq 30 \text{ eV}^2$
		¹⁸⁵ LOVERRE	88 RVUE	
< 10	90	AHRENS	87 CNTR	BNL AGS
< 15	90	BOFILL	87 CNTR	FNAL
< 20	90	¹⁸⁶ ANGELINI	86 HLBC	BEBC CERN PS
20	to 40	¹⁸⁷ BERNARDI	86b CNTR	$\Delta(m^2)=5-10$
< 11	90	¹⁸⁸ BRUCKER	86 HLBC	15-ft FNAL
< 3.4	90	AHRENS	85 CNTR	BNL AGS E734
< 240	90	BERGSMASMA	84 CHRM	
< 10	90	ARMENISE	81 HLBC	GGM CERN PS
< 6	90	BAKER	81 HLBC	15-ft FNAL
< 10	90	ERRIQUEZ	81 HLBC	BEBC CERN PS
< 4	95	BLIETSCHAU	78 HLBC	GGM CERN PS
< 10	95	BELLOTTI	76 HLBC	GGM CERN PS

- ¹⁸² LOVERRE 96 uses the charged-current to neutral-current ratio from the combined CHARM (ALLABY 86) and CDHS (ABRAMOWICZ 86) data from 1986.
- ¹⁸³ ATHANASSOPOULOS 98 report $(0.26 \pm 0.10 \pm 0.05)\%$ for the oscillation probability; the value of $\sin^2 2\theta$ for large Δm^2 is deduced from this probability. See footnote in preceding table for further details, and see the paper for a plot showing allowed regions. If effect is due to oscillation, it is most likely to be intermediate $\sin^2 2\theta$ and Δm^2 . See also ATHANASSOPOULOS 98b.
- ¹⁸⁴ VILAIN 94c limit derived by combining the ν_μ and $\bar{\nu}_\mu$ data assuming CP conservation.
- ¹⁸⁵ LOVERRE 88 reports a less stringent, indirect limit based on theoretical analysis of neutral to charged current ratios.
- ¹⁸⁶ ANGELINI 86 limit reaches 13×10^{-3} at $\Delta(m^2) \approx 2 \text{ eV}^2$.
- ¹⁸⁷ BERNARDI 86b is a typical fit to the data, assuming mixing between two species. As the authors state, this result is in conflict with earlier upper bounds on this type of neutrino oscillations.
- ¹⁸⁸ 15ft bubble chamber at FNAL.

$$\bar{\nu}_\mu \rightarrow \bar{\nu}_e$$

$\Delta(m^2)$ for $\sin^2(2\theta) = 1$

VALUE (eV ²)	CL%	DOCUMENT ID	TECN	COMMENT
< 0.14	90	¹⁸⁹ FREEDMAN	93 CNTR	LAMPF
• • • We do not use the following data for averages, fits, limits, etc. • • •				
0.05-0.08	90	¹⁹⁰ ATHANASSO...96	LSND	LAMPF
0.048-0.090	80	¹⁹¹ ATHANASSO...95		
< 0.07	90	¹⁹² HILL	95	
< 0.9	90	VILAIN	94c CHM2	CERN SPS
< 3.1	90	BOFILL	87 CNTR	FNAL
< 2.4	90	TAYLOR	83 HLBC	15-ft FNAL
< 0.91	90	¹⁹³ NEMETHY	81b CNTR	LAMPF
< 1	95	BLIETSCHAU	78 HLBC	GGM CERN PS

- ¹⁸⁹ FREEDMAN 93 is a search at LAMPF for $\bar{\nu}_e$ generated from any of the three neutrino types ν_μ , $\bar{\nu}_\mu$, and ν_e which come from the beam stop. The $\bar{\nu}_e$'s would be detected by the reaction $\bar{\nu}_e p \rightarrow e^+ n$. FREEDMAN 93 replaces DURKIN 88.
- ¹⁹⁰ ATHANASSOPOULOS 96 is a search for $\bar{\nu}_e$ 30 m from LAMPF beam stop. Neutrinos originate mainly from π^+ decay at rest. $\bar{\nu}_e$ could come from either $\bar{\nu}_\mu \rightarrow \bar{\nu}_e$ or $\nu_e \rightarrow \bar{\nu}_e$; our entry assumes the first interpretation. They are detected through $\bar{\nu}_e p \rightarrow e^+ n$ ($20 \text{ MeV} < E_{e^+} < 60 \text{ MeV}$) in delayed coincidence with $n p \rightarrow d \gamma$. Authors observe $51 \pm 20 \pm 8$ total excess events over an estimated background 12.5 ± 2.9 . ATHANASSOPOULOS 96b is a shorter version of this paper.
- ¹⁹¹ ATHANASSOPOULOS 95 error corresponds to the 1.6σ band in the plot. The expected background is 2.7 ± 0.4 events. Corresponds to an oscillation probability of $(0.34^{+0.20}_{-0.18} \pm 0.07)\%$. For a different interpretation, see HILL 95. Replaced by ATHANASSOPOULOS 96.
- ¹⁹² HILL 95 is a report by one member of the LSND Collaboration, reporting a different conclusion from the analysis of the data of this experiment (see ATHANASSOPOULOS 95). Contrary to the rest of the LSND Collaboration, Hill finds no evidence for the neutrino oscillation $\bar{\nu}_\mu \rightarrow \bar{\nu}_e$ and obtains only upper limits.
- ¹⁹³ In reaction $\bar{\nu}_e p \rightarrow e^+ n$.

$\sin^2(2\theta)$ for "Large" $\Delta(m^2)$

VALUE	CL%	DOCUMENT ID	TECN	COMMENT
< 0.004	95	BLIETSCHAU	78 HLBC	GGM CERN PS
• • • We do not use the following data for averages, fits, limits, etc. • • •				
0.0062 \pm 0.0024 \pm 0.0010		¹⁹⁴ ATHANASSO...96	LSND	LAMPF
0.003-0.012	80	¹⁹⁵ ATHANASSO...95		
< 0.006	90	¹⁹⁶ HILL	95	
< 4.8	90	VILAIN	94c CHM2	CERN SPS
< 5.6	90	¹⁹⁷ VILAIN	94c CHM2	CERN SPS
< 0.024	90	¹⁹⁸ FREEDMAN	93 CNTR	LAMPF
< 0.04	90	BOFILL	87 CNTR	FNAL
< 0.013	90	TAYLOR	83 HLBC	15-ft FNAL
< 0.2	90	¹⁹⁹ NEMETHY	81b CNTR	LAMPF

See key on page 239

Lepton Particle Listings

Massive Neutrinos and Lepton Mixing

- 194 ATHANASSOPOULOS 96 reports $(0.31 \pm 0.12 \pm 0.05)\%$ for the oscillation probability; the value of $\sin^2 2\theta$ for large $\Delta(m^2)$ should be twice this probability. See footnote in preceding table for further details, and see the paper for a plot showing allowed regions.
- 195 ATHANASSOPOULOS 95 error corresponds to the 1.6σ band in the plot. The expected background is 2.7 ± 0.4 events. Corresponds to an oscillation probability of $(0.34_{-0.20}^{+0.18} \pm 0.07)\%$. For a different interpretation, see HILL 95. Replaced by ATHANASSOPOULOS 96.
- 196 HILL 95 is a report by one member of the LSND Collaboration, reporting a different conclusion from the analysis of the data of this experiment (see ATHANASSOPOULOS 95). Contrary to the rest of the LSND Collaboration, Hill finds no evidence for the neutrino oscillation $\bar{\nu}_\mu \rightarrow \bar{\nu}_e$ and obtains only upper limits.
- 197 VILAIN 94C limit derived by combining the ν_μ and $\bar{\nu}_\mu$ data assuming CP conservation.
- 198 FREDMAN 93 is a search at LAMPF for $\bar{\nu}_e$ generated from any of the three neutrino types ν_μ , $\bar{\nu}_\mu$, and ν_e which come from the beam stop. The $\bar{\nu}_e$'s would be detected by the reaction $\bar{\nu}_e p \rightarrow e^+ n$. FREDMAN 93 replaces DURKIN 88.
- 199 In reaction $\bar{\nu}_e p \rightarrow e^+ n$.

$\nu_\mu(\bar{\nu}_\mu) \rightarrow \nu_e(\bar{\nu}_e)$

$\Delta(m^2)$ for $\sin^2(2\theta) = 1$

VALUE (eV ²)	CL%	DOCUMENT ID	TECN	COMMENT
<0.075	90	BORODOV... 92	CNTR	BNL E776
<1.6	90	200 ROMOSAN 97	CCFR	FNAL

• • • We do not use the following data for averages, fits, limits, etc. • • •

$\sin^2(2\theta)$ for "Large" $\Delta(m^2)$

VALUE (units 10 ⁻³)	CL%	DOCUMENT ID	TECN	COMMENT
<1.8	90	201 ROMOSAN 97	CCFR	FNAL
<3.8	90	202 MCFARLAND 95	CCFR	FNAL
<3	90	BORODOV... 92	CNTR	BNL E776

- 201 ROMOSAN 97 uses wideband beam with a 0.5 km decay region.
- 202 MCFARLAND 95 state that "This result is the most stringent to date for $250 < \Delta(m^2) < 450$ eV² and also excludes at 90%CL much of the high $\Delta(m^2)$ region favored by the recent LSND observation." See ATHANASSOPOULOS 95 and ATHANASSOPOULOS 96.

$\nu_\mu \rightarrow \nu_\tau$

$\Delta(m^2)$ for $\sin^2(2\theta) = 1$

VALUE (eV ²)	CL%	DOCUMENT ID	TECN	COMMENT
< 1.1	90	203 ESKUT 98B	CHRS	CERN SPS
< 1.2	90	204 ASTIER 99	NOMD	CERN SPS
< 1.4	90	205 ALTEGOER 98B	NOMD	CERN SPS
< 1.5	90	206 ESKUT 98	CHRS	CERN SPS
< 3.3	90	207 LOVERRE 96	CHARM/CDHS	
< 1.4	90	MCFARLAND 95	CCFR	FNAL
< 4.5	90	BATUSOV 90B	EMUL	FNAL
< 10.2	90	BOFILL 87	CNTR	FNAL
< 6.3	90	BRUCKER 86	HLBC	15-ft FNAL
< 0.9	90	USHIDA 86C	EMUL	FNAL
< 4.6	90	ARMENISE 81	HLBC	GGM CERN SPS
< 3	90	BAKER 81	HLBC	15-ft FNAL
< 6	90	ERRIQUEZ 81	HLBC	BECB CERN SPS
< 3	90	USHIDA 81	EMUL	FNAL

- 203 ESKUT 98B search for $\tau^- \rightarrow \mu^- \nu_\tau \bar{\nu}_\mu$ or $h^- \nu_\tau \bar{\nu}_\mu$, where h^- is a negatively charged hadron. The μ^- sample is somewhat larger than in ESKUT 98, which this result supercedes. Bayesian limit.
- 204 ASTIER 99 limits are based on data corresponding to ~ 950000 ν_μ CC interactions in the 1995, 1996, and (most) 1997 runs. This is a "blind" analysis using the FELDMAN 98 classical CL approach, and other algorithms have also been improved since ALTEGOER 98B.
- 205 ALTEGOER 98B is the NOMAD 1995 data sample result, searching for events with $\tau^- \rightarrow e^- \nu_e \bar{\nu}_e$, hadron $^- \nu_\tau$, or $\pi^- \pi^+ \pi^-$ decay modes using classical CL approach of FELDMAN 98.
- 206 ESKUT 98 search for events with one μ^- with indication of a kink from τ^- decay in the nuclear emulsion. No candidates were found in a 31,423 event subsample.
- 207 LOVERRE 96 uses the charged-current to neutral-current ratio from the combined CHARM (ALLABY 86) and CDHS (ABRAMOWICZ 86) data from 1986.

$\sin^2(2\theta)$ for "Large" $\Delta(m^2)$

VALUE	CL%	DOCUMENT ID	TECN	COMMENT
<0.0012	90	208 ASTIER 99	NOMD	CERN SPS
<0.0042	90	209 ALTEGOER 98B	NOMD	CERN SPS
<0.0035	90	210 ESKUT 98	CHRS	CERN SPS

• • • We do not use the following data for averages, fits, limits, etc. • • •

<0.0018	90	211 ESKUT 98B	CHRS	CERN SPS
<0.006	90	212 LOVERRE 96	CHARM/CDHS	
<0.0081	90	MCFARLAND 95	CCFR	FNAL
<0.06	90	BATUSOV 90B	EMUL	FNAL
<0.34	90	BOFILL 87	CNTR	FNAL
<0.088	90	BRUCKER 86	HLBC	15-ft FNAL
<0.004	90	USHIDA 86C	EMUL	FNAL
<0.11	90	BALLAGH 84	HLBC	15-ft FNAL
<0.017	90	ARMENISE 81	HLBC	GGM CERN SPS
<0.06	90	BAKER 81	HLBC	15-ft FNAL
<0.05	90	ERRIQUEZ 81	HLBC	BECB CERN SPS
<0.013	90	USHIDA 81	EMUL	FNAL

- 208 ASTIER 99 limits are based on data corresponding to ~ 950000 ν_μ CC interactions in the 1995, 1996, and (most) 1997 runs. This is a "blind" analysis using the FELDMAN 98 classical CL approach, and other algorithms have also been improved since ALTEGOER 98B.
- 209 ALTEGOER 98B is the NOMAD 1995 data sample result, searching for events with $\tau^- \rightarrow e^- \nu_e \bar{\nu}_e$, hadron $^- \nu_\tau$, or $\pi^- \pi^+ \pi^-$ decay modes using classical CL approach of FELDMAN 98.
- 210 ESKUT 98 search for events with one μ^- with indication of a kink from τ^- decay in the nuclear emulsion. No candidates were found in a 31,423 event subsample.
- 211 ESKUT 98B search for $\tau^- \rightarrow \mu^- \nu_\tau \bar{\nu}_\mu$ or $h^- \nu_\tau \bar{\nu}_\mu$, where h^- is a negatively charged hadron. The μ^- sample is somewhat larger than in ESKUT 98, which this result supercedes. Bayesian limit.
- 212 LOVERRE 96 uses the charged-current to neutral-current ratio from the combined CHARM (ALLABY 86) and CDHS (ABRAMOWICZ 86) data from 1986.

$\bar{\nu}_\mu \rightarrow \bar{\nu}_\tau$

$\Delta(m^2)$ for $\sin^2(2\theta) = 1$

VALUE (eV ²)	CL%	DOCUMENT ID	TECN	COMMENT
<2.2	90	ASRATYAN 81	HLBC	FNAL
<1.4	90	MCFARLAND 95	CCFR	FNAL
<6.5	90	BOFILL 87	CNTR	FNAL
<7.4	90	TAYLOR 83	HLBC	15-ft FNAL

• • • We do not use the following data for averages, fits, limits, etc. • • •

$\sin^2(2\theta)$ for "Large" $\Delta(m^2)$

VALUE	CL%	DOCUMENT ID	TECN	COMMENT
<4.4 x 10 ⁻²	90	ASRATYAN 81	HLBC	FNAL
<0.0081	90	MCFARLAND 95	CCFR	FNAL
<0.15	90	BOFILL 87	CNTR	FNAL
<8.8 x 10 ⁻²	90	TAYLOR 83	HLBC	15-ft FNAL

$\nu_\mu(\bar{\nu}_\mu) \rightarrow \nu_\tau(\bar{\nu}_\tau)$

$\Delta(m^2)$ for $\sin^2(2\theta) = 1$

VALUE (eV ²)	CL%	DOCUMENT ID	TECN	COMMENT
<1.5	90	213 GRUWE 93	CHM2	CERN SPS

213 GRUWE 93 is a search using the CHARM II detector in the CERN SPS wide-band neutrino beam for $\nu_\mu \rightarrow \nu_\tau$ and $\bar{\nu}_\mu \rightarrow \bar{\nu}_\tau$ oscillations signalled by quasi-elastic ν_τ and $\bar{\nu}_\tau$ interactions followed by the decay $\tau \rightarrow \nu_\tau \pi$. The maximum sensitivity in $\sin^2 2\theta$ ($< 6.4 \times 10^{-3}$ at the 90% CL) is reached for $\Delta(m^2) \simeq 50$ eV².

$\sin^2(2\theta)$ for "Large" $\Delta(m^2)$

VALUE (units 10 ⁻³)	CL%	DOCUMENT ID	TECN	COMMENT
<8	90	214 GRUWE 93	CHM2	CERN SPS

214 GRUWE 93 is a search using the CHARM II detector in the CERN SPS wide-band neutrino beam for $\nu_\mu \rightarrow \nu_\tau$ and $\bar{\nu}_\mu \rightarrow \bar{\nu}_\tau$ oscillations signalled by quasi-elastic ν_τ and $\bar{\nu}_\tau$ interactions followed by the decay $\tau \rightarrow \nu_\tau \pi$. The maximum sensitivity in $\sin^2 2\theta$ ($< 6.4 \times 10^{-3}$ at the 90% CL) is reached for $\Delta(m^2) \simeq 50$ eV².

$\nu_e \rightarrow (\bar{\nu}_e)_L$

This is a limit on lepton family-number violation and total lepton-number violation. $(\bar{\nu}_e)_L$ denotes a hypothetical left-handed $\bar{\nu}_e$. The bound is quoted in terms of $\Delta(m^2)$, $\sin(2\theta)$, and α , where α denotes the fractional admixture of $(V+A)$ charged current.

$\alpha \Delta(m^2)$ for $\sin^2(2\theta) = 1$

VALUE (eV ²)	CL%	DOCUMENT ID	TECN	COMMENT
<0.14	90	215 FREDMAN 93	CNTR	LAMPF
<7	90	216 COOPER 82	HLBC	BECB CERN SPS

• • • We do not use the following data for averages, fits, limits, etc. • • •

- 215 FREDMAN 93 is a search at LAMPF for $\bar{\nu}_e$ generated from any of the three neutrino types ν_μ , $\bar{\nu}_\mu$, and ν_e which come from the beam stop. The $\bar{\nu}_e$'s would be detected by the reaction $\bar{\nu}_e p \rightarrow e^+ n$.
- 216 COOPER 82 states that existing bounds on V+A currents require α to be small.

Lepton Particle Listings

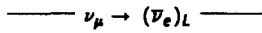
Massive Neutrinos and Lepton Mixing

$\alpha^2 \sin^2(2\theta)$ for "Large" $\Delta(m^2)$

VALUE	CL%	DOCUMENT ID	TECN	COMMENT
<0.032	90	217 FREEDMAN	93 CNTR	LAMPF
• • • We do not use the following data for averages, fits, limits, etc. • • •				
<0.05	90	218 COOPER	82 HLBC	BEBC CERN SPS

217 FREEDMAN 93 is a search at LAMPF for $\bar{\nu}_e$ generated from any of the three neutrino types $\nu_\mu, \bar{\nu}_\mu,$ and ν_e which come from the beam stop. The $\bar{\nu}_e$'s would be detected by the reaction $\bar{\nu}_e p \rightarrow e^+ n$.

218 COOPER 82 states that existing bounds on V+A currents require α to be small.



See note above for $\nu_e \rightarrow (\bar{\nu}_e)_L$ limit

$\alpha \Delta(m^2)$ for $\sin^2(2\theta) = 1$

VALUE (eV ²)	CL%	DOCUMENT ID	TECN	COMMENT
<0.16	90	219 FREEDMAN	93 CNTR	LAMPF
• • • We do not use the following data for averages, fits, limits, etc. • • •				
<0.7	90	220 COOPER	82 HLBC	BEBC CERN SPS

219 FREEDMAN 93 is a search at LAMPF for $\bar{\nu}_e$ generated from any of the three neutrino types $\nu_\mu, \bar{\nu}_\mu,$ and ν_e which come from the beam stop. The $\bar{\nu}_e$'s would be detected by the reaction $\bar{\nu}_e p \rightarrow e^+ n$. The limit on $\Delta(m^2)$ is better than the CERN BEBC experiment, but the limit on $\sin^2\theta$ is almost a factor of 100 less sensitive.

220 COOPER 82 states that existing bounds on V+A currents require α to be small.

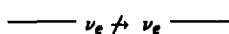
$\alpha^2 \sin^2(2\theta)$ for "Large" $\Delta(m^2)$

VALUE	CL%	DOCUMENT ID	TECN	COMMENT
<0.001	90	221 COOPER	82 HLBC	BEBC CERN SPS
• • • We do not use the following data for averages, fits, limits, etc. • • •				
<0.07	90	222 FREEDMAN	93 CNTR	LAMPF

221 COOPER 82 states that existing bounds on V+A currents require α to be small.

222 FREEDMAN 93 is a search at LAMPF for $\bar{\nu}_e$ generated from any of the three neutrino types $\nu_\mu, \bar{\nu}_\mu,$ and ν_e which come from the beam stop. The $\bar{\nu}_e$'s would be detected by the reaction $\bar{\nu}_e p \rightarrow e^+ n$. The limit on $\Delta(m^2)$ is better than the CERN BEBC experiment, but the limit on $\sin^2\theta$.

(I) Disappearance experiments with accelerator & radioactive source neutrinos



$\Delta(m^2)$ for $\sin^2(2\theta) = 1$

VALUE (eV ²)	CL%	DOCUMENT ID	TECN	COMMENT
< 0.18	90	223 HAMPEL	98 GALX	51Cr source
• • • We do not use the following data for averages, fits, limits, etc. • • •				
<40	90	224 BORISOV	96 CNTR	IHEP-JINR detector
<14.9	90	BRUCKER	86 HLBC	15-ft FNAL
< 8	90	BAKER	81 HLBC	15-ft FNAL
<56	90	DEDEN	81 HLBC	BEBC CERN SPS
<10	90	ERRIQUEZ	81 HLBC	BEBC CERN SPS
<2.3 OR >8	90	NEMETHY	81B CNTR	LAMPF

223 HAMPEL 98 analyzed the GALEX calibration results with ⁵¹Cr neutrino sources and updates the BAHCALL 95 analysis result. They also gave 95% and 99% CL limits of < 0.2 and < 0.22, respectively.

224 BORISOV 96 exclusion curve extrapolated to obtain this value; however, it does not have the right curvature in this region.

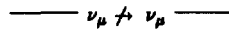
$\sin^2(2\theta)$ for "Large" $\Delta(m^2)$

VALUE	CL%	DOCUMENT ID	TECN	COMMENT
<7 × 10⁻²	90	225 ERRIQUEZ	81 HLBC	BEBC CERN SPS
• • • We do not use the following data for averages, fits, limits, etc. • • •				
<0.4	90	226 HAMPEL	98 GALX	51Cr source
<0.115	90	227 BORISOV	96 CNTR	$\Delta(m^2) = 175 \text{ eV}^2$
<0.54	90	BRUCKER	86 HLBC	15-ft FNAL
<0.6	90	BAKER	81 HLBC	15-ft FNAL
<0.3	90	225 DEDEN	81 HLBC	BEBC CERN SPS

225 Obtained from a Gaussian centered in the unphysical region.

226 HAMPEL 98 analyzed the GALEX calibration results with ⁵¹Cr neutrino sources and updates the BAHCALL 95 analysis result. They also gave 95% and 99% CL limits of < 0.45 and < 0.56, respectively.

227 BORISOV 96 sets less stringent limits at large $\Delta(m^2)$, but exclusion curve does not have clear asymptotic behavior.



$\Delta(m^2)$ for $\sin^2(2\theta) = 1$

VALUE (eV ²)	CL%	DOCUMENT ID	TECN	COMMENT
<0.23 OR >1500 OUR LIMIT				
<0.23 OR >100	90	DYDAK	84 CNTR	
<13 OR >1500	90	STOCKDALE	84 CNTR	
• • • We do not use the following data for averages, fits, limits, etc. • • •				
< 0.29 OR >22	90	BERGSMA	88 CHRM	
<7	90	BELIKOV	85 CNTR	Serpukhov
<8.0 OR >1250	90	STOCKDALE	85 CNTR	
<0.29 OR >22	90	BERGSMA	84 CHRM	
<8.0	90	BELIKOV	83 CNTR	

$\sin^2(2\theta)$ for $\Delta(m^2) = 100 \text{ eV}^2$

VALUE	CL%	DOCUMENT ID	TECN	COMMENT
<0.02	90	228 STOCKDALE	85 CNTR	FNAL
• • • We do not use the following data for averages, fits, limits, etc. • • •				
<0.17	90	229 BERGSMA	88 CHRM	
<0.07	90	230 BELIKOV	85 CNTR	Serpukhov
<0.27	90	229 BERGSMA	84 CHRM	CERN PS
<0.1	90	231 DYDAK	84 CNTR	CERN PS
<0.02	90	232 STOCKDALE	84 CNTR	FNAL
<0.1	90	233 BELIKOV	83 CNTR	Serpukhov

228 This bound applies for $\Delta(m^2) = 100 \text{ eV}^2$. Less stringent bounds apply for other $\Delta(m^2)$; these are nontrivial for $8 < \Delta(m^2) < 1250 \text{ eV}^2$.

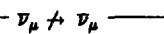
229 This bound applies for $\Delta(m^2) = 0.7-9 \text{ eV}^2$. Less stringent bounds apply for other $\Delta(m^2)$; these are nontrivial for $0.28 < \Delta(m^2) < 22 \text{ eV}^2$.

230 This bound applies for a wide range of $\Delta(m^2) > 7 \text{ eV}^2$. For some values of $\Delta(m^2)$, the value is less stringent; the least restrictive, nontrivial bound occurs approximately at $\Delta(m^2) = 300 \text{ eV}^2$ where $\sin^2(2\theta) < 0.13$ at CL = 90%.

231 This bound applies for $\Delta(m^2) = 1-10 \text{ eV}^2$. Less stringent bounds apply for other $\Delta(m^2)$; these are nontrivial for $0.23 < \Delta(m^2) < 90 \text{ eV}^2$.

232 This bound applies for $\Delta(m^2) = 110 \text{ eV}^2$. Less stringent bounds apply for other $\Delta(m^2)$; these are nontrivial for $13 < \Delta(m^2) < 1500 \text{ eV}^2$.

233 Bound holds for $\Delta(m^2) = 20-1000 \text{ eV}^2$.



$\Delta(m^2)$ for $\sin^2(2\theta) = 1$

VALUE (eV ²)	CL%	DOCUMENT ID	TECN
<7 OR >1200 OUR LIMIT			
<7 OR >1200	90	STOCKDALE	85 CNTR

$\sin^2(2\theta)$ for $190 \text{ eV}^2 < \Delta(m^2) < 320 \text{ eV}^2$

VALUE	CL%	DOCUMENT ID	TECN	COMMENT
<0.02	90	234 STOCKDALE	85 CNTR	FNAL

234 This bound applies for $\Delta(m^2)$ between 190 and 320 or = 530 eV². Less stringent bounds apply for other $\Delta(m^2)$; these are nontrivial for $7 < \Delta(m^2) < 1200 \text{ eV}^2$.

REFERENCES FOR Searches for Massive Neutrinos and Lepton Mixing

BOEHM 00 PRL 84 (to be publ.) F. Boehm et al.

AALSETH 99 PR C59 2108 C.E. Aalseth et al. (IGEX Collab.)

ABDURASH... 99B PR C60 058001 J.N. Abdurashitov et al. (SAGE Collab.)

ABREU 990 EPJ C8 41 P. Abreu et al. (DELPHI Collab.)

ACCIARRI 99K PL B461 397 M. Acciari et al. (L3 Collab.)

ACCIARRI 99L PL B462 354 M. Acciari et al. (L3 Collab.)

ALLISON 99 PL B449 137 W.W.M. Allison et al. (Soudan 2 Collab.)

APOLLONIO 99 PL B466 415 M. Apollonio et al. (CHOOZ Collab.)

ARNOLD 99 NP A658 299 R. Arnold et al. (MEMO Collab.)

ASTIER 99 PL B453 169 P. Astier et al. (NOMAD Collab.)

BAUDIS 99B PRL 83 41 L. Baudis et al.

CROFT 99 PRL 83 1092 R.A.C. Croft, W. Hu, R. Dave

DRAGOUN 99 JP G25 1839 O. Dragoun et al.

FUKUDA 99 PRL 82 1810 Y. Fukuda et al. (Super-Kamiokande Collab.)

FUKUDA 99B PRL 82 2430 Y. Fukuda et al. (Super-Kamiokande Collab.)

FUKUDA 99C PRL 82 2644 Y. Fukuda et al. (Super-Kamiokande Collab.)

FUKUDA 99D PL B467 185 Y. Fukuda et al. (Super-Kamiokande Collab.)

HAMPEL 99 PL B447 127 W. Hampel et al. (GALEX Collab.)

HOLESCHUH 99 PL B451 247 E. Holeschuh et al.

NAPLES 99 PR D59 031101 D. Naples et al. (CCFR Collab.)

VAITAITIS 99 PRL 83 4943 A. Vaitaitis et al. (CCFR Collab.)

ACKERSTAFF 98C EPJ C1 45 K. Ackerstaff et al. (OPAL Collab.)

ALESSAND... 98 PL B433 156 A. Alessandrello et al.

ALTEGOER 98B PRL 81 219 S. Altengo et al. (NOMAD Collab.)

AMBROSIO 98 PL B434 451 M. Ambrosio et al. (MACRO Collab.)

APOLLONIO 98 PL B420 397 M. Apollonio et al. (CHOOZ Collab.)

ARMBRUSTER 98 PR C57 3414 B. Armbruster et al. (KARMEN Collab.)

ASSMAGAN 98 PL B434 158 K. Assmagan et al.

ATHANASSO... 98 PRL 81 1774 C. Athanassopoulos et al. (LSND Collab.)

ATHANASSO... 98B PR C58 2489 C. Athanassopoulos et al. (LSND Collab.)

CLEVELAND 98 APJ 496 505 B.T. Cleveland et al. (Homestake Collab.)

ESKUT 98 PL B424 202 E. Eskut et al. (CHORUS Collab.)

ESKUT 98B PL B434 205 E. Eskut et al. (CHORUS Collab.)

FELDMAN 98 PR D57 3873 G.J. Feldman, R.D. Cousins

FUKUDA 98 PL B433 9 Y. Fukuda et al. (Super-Kamiokande Collab.)

FUKUDA 98B PRL 81 1158 Y. Fukuda et al. (Super-Kamiokande Collab.)

FUKUDA 98C PRL 81 1562 Y. Fukuda et al. (Super-Kamiokande Collab.)

FUKUDA 98E PL B436 33 Y. Fukuda et al. (Super-Kamiokande Collab.)

HAMPEL 98 PL B420 114 W. Hampel et al. (GALEX Collab.)

HATAKEYAMA 98 PRL 81 2016 S. Hatakeyama et al. (Kamiokande Collab.)

HINDI 98 PR C58 2512 M.M. Hindi et al.

LUESCHER 98 PL B434 407 R. Luescher et al.

OVAMA 98 PR D57 R6594 Y. Oyama

PR C53 1 C. Caso et al.

ABREU 97I ZPHY C74 57 P. Abreu et al. (DELPHI Collab.)

Also 97L ZPHY C75 580 erratum P. Abreu et al. (DELPHI Collab.)

ALLISON 97 PL B391 491 W.W.M. Allison et al. (Soudan 2 Collab.)

ALSTON... 97 PR C55 474 M. Alston-Garnjost et al. (LBL, MTHO+)

BARABASH 97 ZPHY A357 351 A.S. Barabash et al. (ITEP, BCEN)

BAUDIS 97 PL B407 219 L. Baudis et al. (MPIH, KIAE, SASSO)

CLARK 97 PRL 79 345 R. Clark et al. (IMB Collab.)

DESILVA 97 PR C56 2451 A. de Silva et al. (UCI)

GUENTHER 97 PR D55 54 M. Guenther et al. (MPH, KIAE, SASSO)

ROMOSAN 97 PRL 78 2912 A. Romosan et al. (CCFR Collab.)

ALESSAND... 96B NPBS 48 239 A. Alessandrello et al. (MILA, SASSO)

ARNOLD 96 ZPHY C72 293 R. Arnold et al. (BCEN, CAEN, JINR+)

ATHANASSO... 96 PR C54 2685 C. Athanassopoulos et al. (LSND Collab.)

ATHANASSO... 96B PRL 77 3082 C. Athanassopoulos et al. (LSND Collab.)

BALYSH 96 PRL 77 5186 A. Balysh et al.

BORISOV 96 PL B369 39 A.A. Borisov et al. (SERP, JINR)

BRYSMAN 96 PR D53 558 D.A. Brysman, T. Numao

BUSKULIC 95 PL B384 439 D. Buskulic et al. (TRU)

EJRI 96 NP A611 85 H. Ejri et al. (ALEPH Collab.)

Also 96 PL A611 85 H. Ejri et al. (OSAK)

FUKUDA 96 PRL 77 1683 Y. Fukuda et al. (Kamiokande Collab.)

FUKUDA 96B PL B388 397 Y. Fukuda et al. (Kamiokande Collab.)

GREENWOOD 96 PR D53 6054 Z.D. Greenwood et al. (UCI, SVR, SCUC)

HAMPEL 96 PL B388 384 W. Hampel et al. (GALEX Collab.)

QUARKS

QUARK MASSES

Written by A. Manohar (University of California, San Diego).

A. Introduction

This note discusses some of the theoretical issues involved in the determination of quark masses. Unlike the leptons, quarks are confined inside hadrons and are not observed as physical particles. Quark masses cannot be measured directly, but must be determined indirectly through their influence on hadron properties. As a result, the values of the quark masses depend on precisely how they are defined; there is no one definition that is the obvious choice. Though one often speaks loosely of quark masses as one would of the electron or muon mass, any careful statement of a quark mass value must make reference to a particular computational scheme that is used to extract the mass from observations. It is important to keep this scheme dependence in mind when using the quark mass values tabulated in the data listings.

The simplest way to define the mass of a quark is by making a fit of the hadron mass spectrum to a nonrelativistic quark model. The quark masses are defined as the values obtained from the fit. The resulting masses only make sense in the limited context of a particular quark model. They depend on the phenomenological potential used, and on how relativistic effects are modelled. The quark masses used in potential models also cannot be connected with the quark mass parameters in the QCD Lagrangian. Fortunately, there exist other definitions of the quark mass that have a more general significance, though they also depend on the method of calculation. The purpose of this review is to explain the most important such definitions and their interrelations.

B. Mass parameters and the QCD Lagrangian

The QCD Lagrangian for N_F quark flavors is

$$\mathcal{L} = \sum_{k=1}^{N_F} \bar{q}_k (i\mathcal{D} - m_k) q_k - \frac{1}{4} G_{\mu\nu} G^{\mu\nu}, \quad (1)$$

where $\mathcal{D} = (\partial_\mu - igA_\mu) \gamma^\mu$ is the gauge covariant derivative, A_μ is the gluon field, $G_{\mu\nu}$ is the gluon field strength, m_k is the mass parameter of the k^{th} quark, and q_k is the quark Dirac field. The QCD Lagrangian Eq. (1) gives finite scattering amplitudes after renormalization, a procedure that invokes a subtraction scheme to render the amplitudes finite, and requires the introduction of a dimensionful scale parameter μ . The mass parameters in the QCD Lagrangian Eq. (1) depend on the renormalization scheme used to define the theory, and also on the scale parameter μ . The most commonly used renormalization scheme for QCD perturbation theory is the $\overline{\text{MS}}$ scheme.

The QCD Lagrangian has a chiral symmetry in the limit that the quark masses vanish. This symmetry is spontaneously broken by dynamical chiral symmetry breaking, and explicitly

broken by the quark masses. The nonperturbative scale of dynamical chiral symmetry breaking, Λ_χ , is around 1 GeV. It is conventional to call quarks heavy if $m > \Lambda_\chi$, so that explicit chiral symmetry breaking dominates, and light if $m < \Lambda_\chi$, so that spontaneous chiral symmetry breaking dominates. The c , b , and t quarks are heavy, and the u , d and s quarks are light. The computations for light quarks involve an expansion in m_q/Λ_χ about the limit $m_q = 0$, whereas for heavy quarks, they involve an expansion in Λ_χ/m_q about $m_q = \infty$. The corrections are largest for the s and c quarks, which are the heaviest light quark and the lightest heavy quark, respectively.

At high energies or short distances, nonperturbative effects such as chiral symmetry breaking are unimportant, and one can in principle analyze mass-dependent effects using QCD perturbation theory to extract the quark mass values. The QCD computations are conventionally performed using the $\overline{\text{MS}}$ scheme at a scale $\mu \gg \Lambda_\chi$, and give the $\overline{\text{MS}}$ “running” mass $\bar{m}(\mu)$. The μ dependence of $\bar{m}(\mu)$ at short distances can be calculated using the renormalization group equations.

For heavy quarks, one can obtain useful information on the quark masses by studying the spectrum and decays of hadrons containing heavy quarks. One method of calculation uses the heavy quark effective theory (HQET), which defines a HQET quark mass m_Q . Other commonly used definitions of heavy quark masses such as the pole mass are discussed in Sec. C. QCD perturbation theory at the heavy quark scale $\mu = m_Q$ can be used to relate the various heavy quark masses to the $\overline{\text{MS}}$ mass $\bar{m}(\mu)$, and to each other.

For light quarks, one can obtain useful information on the quark mass ratios by studying the properties of the light pseudoscalar mesons using chiral perturbation theory, which utilizes the symmetries of the QCD Lagrangian Eq. (1). The quark mass ratios determined using chiral perturbation theory are those in a subtraction scheme that is independent of the quark masses themselves, such as the $\overline{\text{MS}}$ scheme.

A more detailed discussion of the masses for heavy and light quarks is given in the next two sections. The $\overline{\text{MS}}$ scheme applies to both heavy and light quarks. It is also commonly used for predictions of quark masses in unified theories, and for computing radiative corrections in the Standard Model. For this reason, we use the $\overline{\text{MS}}$ scheme as the standard scheme in reporting quark masses. One can easily convert the $\overline{\text{MS}}$ masses into other schemes using the formulæ given in this review.

C. Heavy quarks

The commonly used definitions of the quark mass for heavy quarks are the pole mass, the $\overline{\text{MS}}$ mass, the Georgi-Politzer mass, the potential model mass used in ψ and Υ spectroscopy, and the HQET mass.

The strong interaction coupling constant at the heavy quark scale is small, and one can compute the heavy quark propagator using QCD perturbation theory. For an observable particle such as the electron, the position of the pole in the propagator is the definition of the particle mass. In QCD this definition of the quark mass is known as the pole mass m_P , and is

Quark Particle Listings

Quarks

independent of the renormalization scheme used. It is known that the on-shell quark propagator has no infrared divergences in perturbation theory [1], so this provides a perturbative definition of the quark mass. The pole mass cannot be used to arbitrarily high accuracy because of nonperturbative infrared effects in QCD. The full quark propagator has no pole because the quarks are confined, so that the pole mass cannot be defined outside of perturbation theory.

The $\overline{\text{MS}}$ running mass $\overline{m}(\mu)$ is defined by regulating the QCD theory using dimensional regularization, and subtracting the divergences using the modified minimal subtraction scheme. The $\overline{\text{MS}}$ scheme is particularly convenient for Feynman diagram computations, and is the most commonly used subtraction scheme.

The Georgi-Politzer mass \widehat{m} is defined using the momentum space subtraction scheme at the spacelike point $-p^2 = \widehat{m}^2$ [2]. A generalization of the Georgi-Politzer mass that is often used in computations involving QCD sum rules [3] is $\widehat{m}(\xi)$, defined at the subtraction point $p^2 = -(\xi + 1)m_p^2$. QCD sum rules are discussed in more detail in the next section on light quark masses.

Lattice gauge theory calculations can be used to obtain heavy quark masses from ψ and Υ spectroscopy. The quark masses are obtained by comparing a nonperturbative computation of the meson spectrum with the experimental data. The lattice quark mass values can then be converted into quark mass values in the continuum QCD Lagrangian Eq. (1) using lattice perturbation theory at a scale given by the inverse lattice spacing. A recent computation determines the b -quark pole mass to be 5.0 ± 0.2 GeV, and the $\overline{\text{MS}}$ mass to be 4.0 ± 0.1 GeV [4].

Potential model calculations of the hadron spectrum also involve the heavy quark mass. There is no way to relate the quark mass as defined in a potential model to the quark mass parameter of the QCD Lagrangian, or to the pole mass. Even in the heavy quark limit, the two masses can differ by nonperturbative effects of order Λ_{QCD} . There is also no reason why the potential model quark mass should be independent of the particular form of the potential used.

Recent work on the heavy quark effective theory [5–9] has provided a definition of the quark mass for a heavy quark that is valid when one includes nonperturbative effects and will be called the HQET mass m_Q . The HQET mass is particularly useful in the analysis of the $1/m_Q$ corrections in HQET. The HQET mass agrees with the pole mass to all orders in perturbation theory when only one quark flavor is present, but differs from the pole mass at order α_s^2 when there are additional flavors [10]. Physical quantities such as hadron masses can in principle be computed in the heavy quark effective theory in terms of the HQET mass m_Q . The computations cannot be done analytically in practice because of nonperturbative effects in QCD, which also prevent a direct extraction of the quark masses from the original QCD Lagrangian, Eq. (1). Nevertheless, for heavy quarks, it is possible to parametrize the nonperturbative effects to a given order in the $1/m_Q$ expansion

in terms of a few unknown constants that can be obtained from experiment. For example, the B and D meson masses in the heavy quark effective theory are given in terms of a single nonperturbative parameter $\overline{\Lambda}$,

$$M(B) = m_b + \overline{\Lambda} + \mathcal{O}\left(\frac{\overline{\Lambda}^2}{m_b}\right),$$

$$M(D) = m_c + \overline{\Lambda} + \mathcal{O}\left(\frac{\overline{\Lambda}^2}{m_c}\right). \quad (2)$$

This allows one to determine the mass difference $m_b - m_c = M(B) - M(D) = 3.4$ GeV up to corrections of order $\overline{\Lambda}^2/m_b - \overline{\Lambda}^2/m_c$. The extraction of the individual quark masses m_b and m_c requires some knowledge of $\overline{\Lambda}$. An estimate of $\overline{\Lambda}$ using QCD sum rules gives $\overline{\Lambda} = 0.57 \pm 0.07$ GeV [11]. The HQET masses with this value of $\overline{\Lambda}$ are $m_b = 4.74 \pm 0.14$ GeV and $m_c = 1.4 \pm 0.2$ GeV, where the spin averaged meson masses $(3M(B^*) + M(B))/4$ and $(3M(D^*) + M(D))/4$ have been used to eliminate the spin-dependent $\mathcal{O}(\overline{\Lambda}^2/m_Q)$ correction terms. The errors reflect the uncertainty in $\overline{\Lambda}$ and the unknown spin-averaged $\mathcal{O}(\overline{\Lambda}^2/m_Q)$ correction. The errors do not include any theoretical uncertainty in the QCD sum rules, which could be large. A quark model estimate suggests that $\overline{\Lambda}$ is the constituent quark mass (≈ 350 MeV), which differs significantly from the sum rule estimate. In HQET, the $1/m_Q$ corrections to heavy meson decay form-factors are also given in terms of $\overline{\Lambda}$. Thus an accurate enough measurement of these form-factors could be used to extract $\overline{\Lambda}$ directly from experiment, which then determines the quark masses up to corrections of order $1/m_Q$.

The quark mass m_Q of HQET can be related to other quark mass parameters using QCD perturbation theory at the scale m_Q . The relation between m_Q and $\widehat{m}_Q(\xi)$ at one loop is [12]

$$m_Q = \widehat{m}_Q(\xi) \left[1 + \frac{\widehat{\alpha}_s(\xi)}{\pi} \frac{\xi + 2}{\xi + 1} \log(\xi + 2) \right], \quad (3)$$

where $\widehat{\alpha}_s(\xi)$ is the strong interaction coupling constant in the momentum space subtraction scheme. The relation between m_Q and the $\overline{\text{MS}}$ mass \overline{m}_Q is known to two loops [13],

$$m_Q = \overline{m}_Q(\overline{m}_Q) \left[1 + \frac{4\overline{\alpha}_s(\overline{m}_Q)}{3\pi} + \left(13.44 - 1.04 \sum_k \left(1 - \frac{4\overline{m}_{Q_k}}{3\overline{m}_Q} \right) \right) \left(\frac{\overline{\alpha}_s(\overline{m}_Q)}{\pi} \right)^2 \right], \quad (4)$$

where $\overline{\alpha}_s(\mu)$ is the strong interaction coupling constants in the $\overline{\text{MS}}$ scheme, and the sum on k extends over all flavors Q_k lighter than Q . For the b -quark, Eq. (4) reads

$$m_b = \overline{m}_b(\overline{m}_b) [1 + 0.09 + 0.05], \quad (5)$$

where the contributions from the different orders in α_s are shown explicitly. The two loop correction is comparable in size and has the same sign as the one loop term. There is

presumably an error of order 0.05 in the relation between m_b and $\bar{m}_b(\bar{m}_b)$ from the uncalculated higher order terms.

D. Light quarks

For light quarks, one can use the techniques of chiral perturbation theory to extract quark mass ratios. The light quark part of the QCD Lagrangian Eq. (1) has a chiral symmetry in the limit that the light quark masses are set to zero, under which left- and right-handed quarks transform independently. The mass term explicitly breaks the chiral symmetry, since it couples the left- and right-handed quarks to each other. A systematic analysis of this explicit chiral symmetry breaking provides some information on the light quark masses.

It is convenient to think of the three light quarks u , d and s as a three component column vector Ψ , and to write the mass term for the light quarks as

$$\bar{\Psi}M\Psi = \bar{\Psi}_L M \Psi_R + \bar{\Psi}_R M \Psi_L, \quad (6)$$

where M is the quark mass matrix M ,

$$M = \begin{pmatrix} m_u & 0 & 0 \\ 0 & m_d & 0 \\ 0 & 0 & m_s \end{pmatrix}. \quad (7)$$

The mass term $\bar{\Psi}M\Psi$ is the only term in the QCD Lagrangian that mixes left- and right-handed quarks. In the limit that $M \rightarrow 0$, there is an independent $SU(3)$ flavor symmetry for the left- and right-handed quarks. This $G_\chi = SU(3)_L \times SU(3)_R$ chiral symmetry of the QCD Lagrangian is spontaneously broken, which leads to eight massless Goldstone bosons, the π 's, K 's, and η , in the limit $M \rightarrow 0$. The symmetry G_χ is only an approximate symmetry, since it is explicitly broken by the quark mass matrix M . The Goldstone bosons acquire masses which can be computed in a systematic expansion in M in terms of certain unknown nonperturbative parameters of the theory. For example, to first order in M one finds that [14,15]

$$\begin{aligned} m_{\pi^0}^2 &= B(m_u + m_d), \\ m_{\pi^\pm}^2 &= B(m_u + m_d) + \Delta_{em}, \\ m_{K^0}^2 = m_{K^+}^2 &= B(m_d + m_s), \\ m_{K^\pm}^2 &= B(m_u + m_s) + \Delta_{em}, \\ m_\eta^2 &= \frac{1}{3}B(m_u + m_d + 4m_s), \end{aligned} \quad (8)$$

with two unknown parameters B and Δ_{em} , the electromagnetic mass difference. From Eq. (8), one can determine the quark mass ratios [14]

$$\begin{aligned} \frac{m_u}{m_d} &= \frac{2m_{\pi^0}^2 - m_{\pi^\pm}^2 + m_{K^+}^2 - m_{K^0}^2}{m_{K^0}^2 - m_{K^+}^2 + m_{\pi^\pm}^2} = 0.56, \\ \frac{m_s}{m_d} &= \frac{m_{K^0}^2 + m_{K^+}^2 - m_{\pi^\pm}^2}{m_{K^0}^2 + m_{\pi^\pm}^2 - m_{K^+}^2} = 20.1, \end{aligned} \quad (9)$$

to lowest order in chiral perturbation theory. The error on these numbers is the size of the second-order corrections, which

are discussed at the end of this section. Chiral perturbation theory cannot determine the overall scale of the quark masses, since it uses only the symmetry properties of M , and any multiple of M has the same G_χ transformation law as M . This can be seen from Eq. (8), where all quark masses occur only in the form Bm , so that B and m cannot be determined separately.

The mass parameters in the QCD Lagrangian have a scale dependence due to radiative corrections, and are renormalization scheme dependent. Since the mass ratios extracted using chiral perturbation theory use the symmetry transformation property of M under the chiral symmetry G_χ , it is important to use a renormalization scheme for QCD that does not change this transformation law. Any quark mass independent subtraction scheme such as \overline{MS} is suitable. The ratios of quark masses are scale independent in such a scheme.

The absolute normalization of the quark masses can be determined by using methods that go beyond chiral perturbation theory, such as QCD sum rules [3]. Typically, one writes a sum rule for a quantity such as B in terms of a spectral integral over all states with certain quantum numbers. This spectral integral is then evaluated by assuming it is dominated by one (or two) of the lowest resonances, and using the experimentally measured resonance parameters [16]. There are many subtleties involved, which cannot be discussed here [16].

Another method for determining the absolute normalization of the quark masses, is to assume that the strange quark mass is equal to the $SU(3)$ mass splitting in the baryon multiplets [14,16]. There is an uncertainty in this method since in the baryon octet one can use either the Σ - N or the Λ - N mass difference, which differ by about 75 MeV, to estimate the strange quark mass. But more importantly, there is no way to relate this normalization to any more fundamental definition of quark masses.

One can extend the chiral perturbation expansion Eq. (8) to second order in the quark masses M to get a more accurate determination of the quark mass ratios. There is a subtlety that arises at second order [17], because

$$M (M^\dagger M)^{-1} \det M^\dagger \quad (10)$$

transforms in the same way under G_χ as M . One can make the replacement $M \rightarrow M(\lambda) = M + \lambda M (M^\dagger M)^{-1} \det M^\dagger$ in all formulæ,

$$\begin{aligned} M(\lambda) &= \text{diag}(m_u(\lambda), m_d(\lambda), m_s(\lambda)) \\ &= \text{diag}(m_u + \lambda m_d m_s, m_d + \lambda m_u m_s, m_s + \lambda m_u m_d), \end{aligned} \quad (11)$$

so it is not possible to determine λ by fitting to data. One can only determine the ratios $m_i(\lambda)/m_j(\lambda)$ using second-order chiral perturbation theory, not the desired ratios $m_i/m_j = m_i(\lambda=0)/m_j(\lambda=0)$.

Dimensional analysis can be used to estimate [18] that second-order corrections in chiral perturbation theory due to the

Quark Particle Listings

Quarks

strange quark mass are of order $\lambda m_s \sim 0.25$. The ambiguity due to the redefinition Eq. (11) (which corresponds to a second-order correction) can produce a sizeable uncertainty in the ratio m_u/m_d . The lowest-order value $m_u/m_d = 0.56$ gets corrections of order $\lambda m_s(m_d/m_u - m_u/m_d) \sim 30\%$, whereas m_s/m_d gets a smaller correction of order $\lambda m_s(m_u/m_d - m_u m_d/m_s^2) \sim 15\%$. A more quantitative discussion of second-order effects can be found in Refs. 17,19,20. Since the second-order terms have a single parameter ambiguity, the value of m_u/m_d is related to the value of m_s/m_d .

The ratio m_u/m_d is of great interest since there is no strong CP problem if $m_u = 0$. To determine m_u/m_d requires fixing λ in the mass redefinition Eq. (11). There has been considerable effort to determine the chiral Lagrangian parameters accurately enough to determine m_u/m_d , for example from the analysis of the decays $\psi' \rightarrow \psi + \pi^0, \eta$, the decay $\eta \rightarrow 3\pi$, using sum rules, and from the heavy meson mass spectrum [16,21–24]. A recent paper giving a critique of these estimates is Ref. 25.

Eventually, lattice gauge theory methods will be accurate enough to be able to compute meson masses directly from the QCD Lagrangian Eq. (1), and thus determine the light quark masses. For a reliable determination of quark masses, these computations will have to be done with dynamical fermions, and with a small enough lattice spacing that one can accurately compute the relation between lattice and continuum Lagrangians.

The quark masses for light quarks discussed so far are often referred to as current quark masses. Nonrelativistic quark models use constituent quark masses, which are of order 350 MeV for the u and d quarks. Constituent quark masses model the effects of dynamical chiral symmetry breaking, and are not related to the quark mass parameters m_k of the QCD Lagrangian Eq. (1). Constituent masses are only defined in the context of a particular hadronic model.

E. Numerical values and caveats

The quark masses in the particle data listings have been obtained by using the wide variety of theoretical methods outlined above. Each method involves its own set of approximations and errors. In most cases, the errors are a best guess at the size of neglected higher-order corrections. The expansion parameter for the approximations is not much smaller than unity (for example it is $m_K^2/\Lambda_\chi^2 \approx 0.25$ for the chiral expansion), so an unexpectedly large coefficient in a neglected higher-order term could significantly alter the results. It is also important to note that the quark mass values can be significantly different in the different schemes. For example, assuming that the b -quark pole mass is 5.0 GeV, and $\bar{\alpha}_s(m_b) \approx 0.22$ gives the \overline{MS} b -quark mass $\bar{m}_b(\mu = m_b) = 4.6$ GeV using the one-loop term in Eq. (4), and $\bar{m}_b(\mu = m_b) = 4.3$ GeV including the one-loop and two-loop terms. The heavy quark masses obtained using HQET, QCD sum rules, or lattice gauge theory are consistent with each other if they are all converted into the same scheme. When using the data listings, it is important to remember that

the numerical value for a quark mass is meaningless without specifying the particular scheme in which it was obtained. All non- \overline{MS} quark masses have been converted to \overline{MS} values in the data listings using one-loop formulæ, unless an explicit two-loop conversion is given by the authors in the original article.

References

1. R. Tarrach, Nucl. Phys. **B183**, 384 (1981).
2. H. Georgi and H.D. Politzer, Phys. Rev. **D14**, 1829 (1976).
3. M.A. Shifman, A.I. Vainshtein, and V.I. Zakharov, Nucl. Phys. **B147**, 385 (1979).
4. C.T.H. Davies, *et al.*, Phys. Rev. Lett. **73**, 2654 (1994).
5. N. Isgur and M.B. Wise, Phys. Lett. **B232**, 113 (1989), *ibid* **B237**, 527 (1990); M.B. Voloshin and M. Shifman, Sov. J. Nucl. Phys. **45**, 292 (1987), *ibid* **47**, 511 (1988); S. Nussinov and W. Wetzel, Phys. Rev. **D36**, 130 (1987).
6. H. Georgi, Phys. Lett. **B240**, 447 (1990).
7. E. Eichten and B. Hill, Phys. Lett. **B234**, 511 (1990).
8. H. Georgi, in *Perspectives of the Standard Model*, ed. R.K. Ellis, C.T. Hill, and J.D. Lykken (World Scientific, Singapore, 1992); B. Grinstein, in *High Energy Phenomenology*, ed. R. Huerta and M.A. Pérez (World Scientific, Singapore, 1992).
9. A.F. Falk, M. Neubert, and M.E. Luke, Nucl. Phys. **B388**, 363 (1992).
10. A.V. Manohar and M.B. Wise, (unpublished).
11. M. Neubert, Phys. Reports **245**, 259 (1994).
12. S. Narison, Phys. Lett. **B197**, 405 (1987).
13. N. Gray, D.J. Broadhurst, W. Grafe, and K. Schilcher, Z. Phys. **C48**, 673 (1990); D.J. Broadhurst, N. Gray, and K. Schilcher, Z. Phys. **C52**, 111 (1991); K.G. Chetyrkin, J.H. Kuhn, and A. Kwiatkowski, Phys. Reports **277**, 189 (1996).
14. S. Weinberg, Trans. N.Y. Acad. Sci. **38**, 185 (1977).
15. See for example, H. Georgi, *Weak Interactions and Modern Particle Theory* (Benjamin/Cummings, Menlo Park, 1984).
16. J. Gasser and H. Leutwyler, Phys. Reports **87**, 77 (1982).
17. D.B. Kaplan and A.V. Manohar, Phys. Rev. Lett. **56**, 2004 (1986).
18. A.V. Manohar and H. Georgi, Nucl. Phys. **B234**, 189 (1984).
19. J. Gasser and H. Leutwyler, Nucl. Phys. **B250**, 465 (1985).
20. H. Leutwyler, Nucl. Phys. **B337**, 108 (1990).
21. P. Langacker and H. Pagels, Phys. Rev. **D19**, 2070 (1979); H. Pagels and S. Stokar, Phys. Rev. **D22**, 2876 (1980); H. Leutwyler, Nucl. Phys. **B337**, 108 (1990); J. Donoghue and D. Wyler, Phys. Rev. Lett. **69**, 3444 (1992); K. Maltman, T. Goldman and G.L. Stephenson Jr., Phys. Lett. **B234**, 158 (1990).
22. K. Choi, Nucl. Phys. **B383**, 58 (1992).
23. J. Donoghue and D. Wyler, Phys. Rev. **D45**, 892 (1992).
24. M.A. Luty and R. Sundrum, e-print hep-ph/9502398.
25. T. Banks, Y. Nir, and N. Seiberg, *Proceedings of the 2nd IFT Workshop on Yukawa Couplings and the Origins of Mass*, Gainesville, Florida (1994).

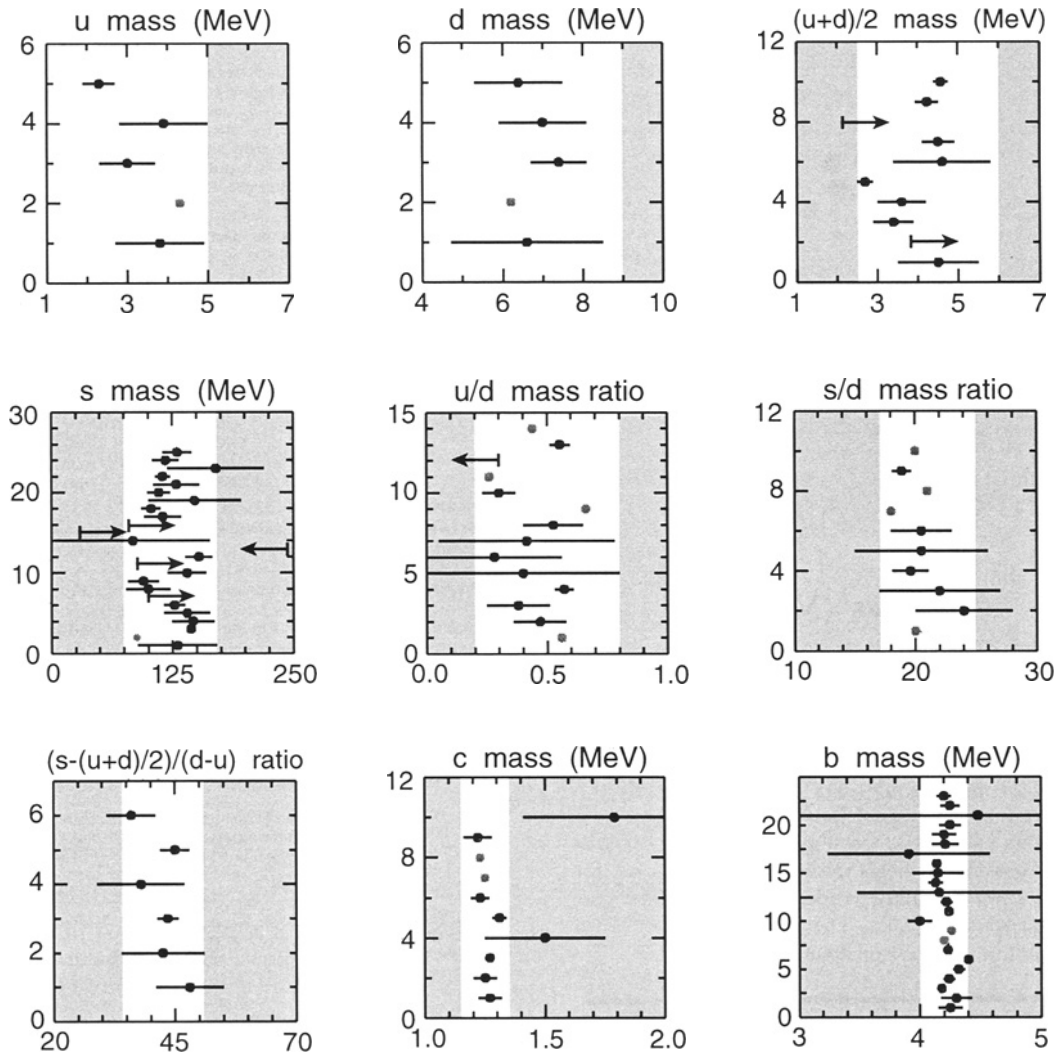


Figure 1: The values of each quark mass parameter taken from the Data Listings. Points from papers reporting no error bars are colored grey. Arrows indicate limits reported. The grey regions indicate values excluded by our evaluations; some regions were determined in part through examination of Fig. 2.

Quark Particle Listings

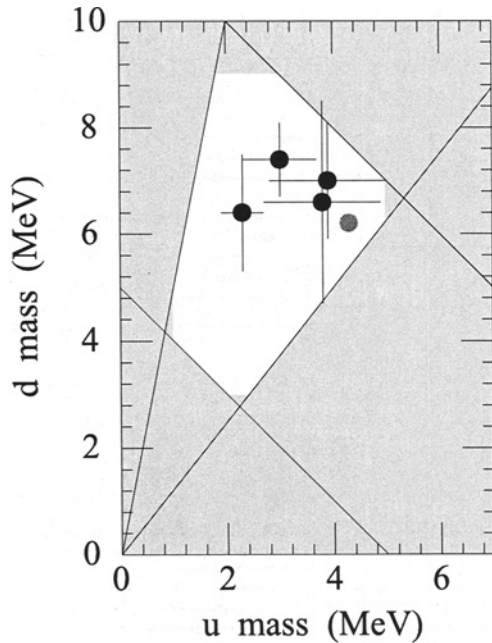
Quarks, u, d, s , Light Quarks (u, d, s)

Figure 2: The allowed region (shown in white) for up quark and down quark masses. This region was determined in part from papers reporting values for m_u and m_d (data points shown) and in part from analysis of the allowed ranges of other mass parameters (see Fig. 1). The parameter $(m_u + m_d)/2$ yields the two downward-sloping lines, while m_u/m_d yields the two rising lines originating at (0,0). The grey point is from a paper giving no error bars.

u	$I(J^P) = \frac{1}{2}(\frac{1}{2}^+)$
Mass $m = 1.5$ to 5 MeV $m_u/m_d = 0.20$ to 0.70	Charge = $\frac{2}{3} e$ $I_z = +\frac{1}{2}$
d	$I(J^P) = \frac{1}{2}(\frac{1}{2}^+)$
Mass $m = 3$ to 9 MeV $m_s/m_d = 17$ to 25 $\bar{m} = (m_u + m_d)/2 = 2$ to 6 MeV	Charge = $-\frac{1}{3} e$ $I_z = -\frac{1}{2}$
s	$I(J^P) = 0(\frac{1}{2}^+)$
Mass $m = 60$ to 170 MeV $(m_s - (m_u + m_d)/2)/(m_d - m_u) = 34$ to 51	Charge = $-\frac{1}{3} e$ Strangeness = -1

LIGHT QUARKS (u, d, s)

OMITTED FROM SUMMARY TABLE

u-QUARK MASS

The u -, d -, and s -quark masses are estimates of so-called "current-quark masses," in a mass-independent subtraction scheme such as \overline{MS} . The ratios m_u/m_d and m_s/m_d are extracted from pion and kaon masses using chiral symmetry. The estimates of d and u masses are not without controversy and remain under active investigation. Within the literature there are even suggestions that the u quark could be essentially massless. The s -quark mass is estimated from SU(3) splittings in hadron masses.

We have normalized the \overline{MS} masses at a renormalization scale of $\mu = 2$ GeV. Results quoted in the literature at $\mu = 1$ GeV have been rescaled by dividing by 1.35. The values of "Our Evaluation" were determined in part via Figures 1 and 2.

VALUE (MeV)	DOCUMENT ID	TECN	COMMENT
1 to 5 OUR EVALUATION			
• • • We do not use the following data for averages, fits, limits, etc. • • •			
2.3 ± 0.4	1 NARISON	99 THEO	\overline{MS} scheme
3.9 ± 1.1	2 JAMIN	95 THEO	\overline{MS} scheme
3.0 ± 0.7	3 NARISON	95c THEO	\overline{MS} scheme
4.3	4 CHOI	92b THEO	
3.8 ± 1.1	5 BARDUCCI	88 THEO	
	6 GASSER	82 THEO	
1 NARISON 99 uses sum rules to order α_s^3 for ϕ meson decays to get m_s , and finds m_u by combining with sum rule estimates of $m_u + m_d$ and Dashen's formula.			
2 JAMIN 95 uses QCD sum rules at next-to-leading order. We have rescaled $m_u(1 \text{ GeV}) = 5.3 \pm 1.5$ to $\mu = 2$ GeV.			
3 For NARISON 95c, we have rescaled $m_u(1 \text{ GeV}) = 4 \pm 1$ to $\mu = 2$ GeV.			
4 CHOI 92b argues that $m_u = 0$ is okay based on instanton contributions to the chiral coefficients. Disagrees with DONOGHUE 92 and DONOGHUE 92b.			
5 BARDUCCI 88 uses a calculation of the effective potential for $\bar{\psi}\psi$ in QCD, and estimates for $\Sigma(\rho^2)$. We have rescaled $m_u(1 \text{ GeV}) = 5.8$ to $\mu = 2$ GeV.			
6 GASSER 82 uses chiral perturbation theory for the mass ratios, and uses QCD sum rules to extract the absolute values. We have rescaled $m_u(1 \text{ GeV}) = 5.1 \pm 1.5$ to $\mu = 2$ GeV.			

d-QUARK MASSSee the comment for the u quark above.

We have normalized the \overline{MS} masses at a renormalization scale of $\mu = 2$ GeV. Results quoted in the literature at $\mu = 1$ GeV have been rescaled by dividing by 1.35. The values of "Our Evaluation" were determined in part via Figures 1 and 2.

VALUE (MeV)	DOCUMENT ID	TECN	COMMENT
3 to 9 OUR EVALUATION			
• • • We do not use the following data for averages, fits, limits, etc. • • •			
6.4 ± 1.1	7 NARISON	99 THEO	\overline{MS} scheme
7.0 ± 1.1	8 JAMIN	95 THEO	\overline{MS} scheme
7.4 ± 0.7	9 NARISON	95c THEO	\overline{MS} scheme
	10 ADAMI	93 THEO	
	11 NEFKENS	92 THEO	
6.2	12 BARDUCCI	88 THEO	
	13 DOMINGUEZ	87 THEO	
	14 KREMER	84 THEO	
6.6 ± 1.9	15 GASSER	82 THEO	
7 NARISON 99 uses sum rules to order α_s^3 for ϕ meson decays to get m_s , and finds m_d by combining with sum rule estimates of $m_u + m_d$ and Dashen's formula.			
8 JAMIN 95 uses QCD sum rules at next-to-leading order. We have rescaled $m_d(1 \text{ GeV}) = 9.4 \pm 1.5$ to $\mu = 2$ GeV.			
9 For NARISON 95c, we have rescaled $m_d(1 \text{ GeV}) = 10 \pm 1$ to $\mu = 2$ GeV.			
10 ADAMI 93 obtain $m_d - m_u = 3 \pm 1$ MeV at $\mu = 0.5$ GeV using isospin-violating effects in QCD sum rules.			
11 NEFKENS 92 results for $m_d - m_u$ are 3.1 ± 0.4 MeV from meson masses and 3.6 ± 0.4 MeV from baryon masses.			
12 BARDUCCI 88 uses a calculation of the effective potential for $\bar{\psi}\psi$ in QCD, and estimates for $\Sigma(\rho^2)$. We have rescaled $m_d(1 \text{ GeV}) = 8.4$ to $\mu = 2$ GeV.			
13 DOMINGUEZ 87 uses QCD sum rules to obtain $m_u + m_d = 15.5 \pm 2.0$ MeV and $m_d - m_u = 6 \pm 1.5$ MeV.			
14 KREMER 84 obtain $m_u + m_d = 21 \pm 2$ MeV at $Q^2 = 1 \text{ GeV}^2$ using SVZ values for quark condensates; they obtain $m_u + m_d = 35 \pm 3$ MeV at $Q^2 = 1 \text{ GeV}^2$ using factorization values for quark condensates.			
15 GASSER 82 uses chiral perturbation theory for the mass ratios, and uses QCD sum rules to extract the absolute values. We have rescaled $m_d(1 \text{ GeV}) = 8.9 \pm 2.6$ to $\mu = 2$ GeV.			

See key on page 239

Quark Particle Listings

Light Quarks (u, d, s)

$$\bar{m} = (m_u + m_d)/2$$

See the comments for the u quark above.

We have normalized the \overline{MS} masses at a renormalization scale of $\mu = 2$ GeV. Results quoted in the literature at $\mu = 1$ GeV have been rescaled by dividing by 1.35. The values of "Our Evaluation" were determined in part via Figures 1 and 2.

VALUE (MeV)	DOCUMENT ID	TECN	COMMENT
2.5 to 6 OUR EVALUATION			
• • • We do not use the following data for averages, fits, limits, etc. • • •			
4.57 ± 0.18	16 AOKI	00 LATT	
4.23 ± 0.29	17 AOKI	99 LATT	\overline{MS} scheme
> 2.1	18 STEELE	99 THEO	\overline{MS} scheme
4.5 ± 0.4	19 BECIREVIC	98 LATT	\overline{MS} scheme
4.6 ± 1.2	20 DOSCH	98 THEO	\overline{MS} scheme
2.7 ± 0.2	21 EICKER	97 LATT	\overline{MS} scheme
3.6 ± 0.6	22 GOUGH	97 LATT	\overline{MS} scheme
3.4 ± 0.4 ± 0.3	23 GUPTA	97 LATT	\overline{MS} scheme
> 3.8	24 LELLOUCH	97 THEO	\overline{MS} scheme
4.5 ± 1.0	25 BIJNENS	95	
16 AOKI 00	obtain the light quark masses from a quenched lattice simulation of the meson and baryon spectrum with the Wilson quark action.		
17 AOKI 99	obtain the light quark masses from a quenched lattice simulation of the meson spectrum with the Staggered quark action employing the regularization independent scheme.		
18 STEELE 99	obtain a bound on the light quark masses by applying the Holder inequality to a sum rule. We have converted their bound of $(m_u + m_d)/2 \geq 3$ GeV at $\mu=1$ GeV to $\mu=2$ GeV.		
19 BECIREVIC 98	compute the quark mass using the Alpha action in the quenched approximation. The conversion from the regularization independent scheme to the \overline{MS} scheme is at NNLO.		
20 DOSCH 98	use sum rule determinations of the quark condensate and chiral perturbation theory to obtain $9.4 \leq (m_u + m_d)(1 \text{ GeV}) \leq 15.7$ MeV. We have converted to result to $\mu=2$ GeV.		
21 EICKER 97	use lattice gauge computations with two dynamical light flavors.		
22 GOUGH 97	use lattice gauge computations in the quenched approximation. Correcting for quenching gives $2.1 < \bar{m} < 3.5$ MeV at $\mu=2$ GeV.		
23 GUPTA 97	use Lattice Monte Carlo computations in the quenched approximation. The value for two light dynamic flavors at $\mu = 2$ GeV is $2.7 \pm 0.3 \pm 0.3$ MeV.		
24 LELLOUCH 97	obtain lower bounds on quark masses using hadronic spectral functions.		
25 BIJNENS 95	determines $m_u + m_d(1 \text{ GeV}) = 12 \pm 2.5$ MeV using finite energy sum rules. We have rescaled this to 2 GeV.		

s-QUARK MASS

See the comment for the u quark above.

We have normalized the \overline{MS} masses at a renormalization scale of $\mu = 2$ GeV. Results quoted in the literature at $\mu = 1$ GeV have been rescaled by dividing by 1.35.

VALUE (MeV)	DOCUMENT ID	TECN	COMMENT
75 to 170 OUR EVALUATION			
• • • We do not use the following data for averages, fits, limits, etc. • • •			
130 ± 15	26 AOKI	00 LATT	
118 ± 14	27 AOKI	99 LATT	\overline{MS} scheme
170 +44 -55	28 BARATE	99R	\overline{MS} scheme
115 ± 8	29 MALTMAN	99 THEO	\overline{MS} scheme
129 ± 24	30 NARISON	99 THEO	\overline{MS} scheme
111 ± 12	31 BECIREVIC	98	\overline{MS} scheme
148 ± 48	32 CHETYRKIN	98 THEO	\overline{MS} scheme
103 ± 10	33 CUCCHIERI	98 LATT	\overline{MS} scheme
115 ± 19	34 DOMINGUEZ	98 THEO	\overline{MS} scheme
> 90 ± 9	35 DOSCH	98 THEO	\overline{MS} scheme
> 30	36 LEBED	98 THEO	\overline{MS} scheme
84 ± 80	37 MALTMAN	98 THEO	\overline{MS} scheme
< 163 ± 81	38 MALTMAN	98B THEO	\overline{MS} scheme
152.4 ± 14.1	39 CHETYRKIN	97 THEO	\overline{MS} scheme
≥ 89	40 COLANGELO	97 THEO	\overline{MS} scheme
140 ± 20	41 EICKER	97 LATT	\overline{MS} scheme
95 ± 16	42 GOUGH	97 LATT	\overline{MS} scheme
100 ± 21 ± 10	43 GUPTA	97 LATT	\overline{MS} scheme
> 100	44 LELLOUCH	97 THEO	\overline{MS} scheme
127 ± 11	45 CHETYRKIN	95 THEO	\overline{MS} scheme
140 ± 24	46 JAMIN	95 THEO	\overline{MS} scheme
146 ± 22	47 NARISON	95C THEO	\overline{MS} scheme
	48 NEFKENS	92 THEO	
144 ± 3	49 DOMINGUEZ	91 THEO	
88	50 BARDUCCI	88 THEO	
	51 KREMER	84 THEO	
130 ± 41	52 GASSER	82 THEO	
26 AOKI 00	obtain the light quark masses from a quenched lattice simulation of the meson and baryon spectrum with the Wilson quark action. We have averaged their results of $m_s = 115.6 \pm 2.3$ and $m_s = 143.7 \pm 5.8$ obtained using m_K and m_ϕ , respectively, to normalize the spectrum.		
27 AOKI 99	obtain the light quark masses from a quenched lattice simulation of the meson spectrum with the Staggered quark action employing the regularization independent		

scheme. We have averaged their results of $m_s = 106.0 \pm 7.1$ and $m_s = 129 \pm 12$ obtained using m_K and m_ϕ , respectively, to normalize the spectrum.

- 28 BARATE 99R obtain the strange quark mass from an analysis of the observed mass spectra in τ decay. We have converted their value of $m_s(m_\tau) = 176^{+46}_{-57}$ MeV to $\mu=2$ GeV.
- 29 MALTMAN 99 determines the strange quark mass using finite energy sum rules.
- 30 NARISON 99 uses sum rules to order α_s^3 for ϕ meson decays.
- 31 BECIREVIC 98 compute the quark mass using the Alpha action in the quenched approximation. The conversion from the regularization independent scheme to the \overline{MS} scheme is at NNLO.
- 32 CHETYRKIN 98 uses spectral moments of hadronic τ decays to determine $m_s(1 \text{ GeV}) = 200 \pm 70$ MeV. We have rescaled the result to $\mu=2$ GeV.
- 33 CUCCHIERI 98 obtains the quark mass using a quenched lattice computation of the hadronic spectrum.
- 34 DOMINGUEZ 98 uses hadronic spectral function sum rules (to four loops, and including dimension six operators) to determine $m_s(1 \text{ GeV}) < 155 \pm 25$ MeV. We have rescaled the result to $\mu=2$ GeV.
- 35 DOSCH 98 use sum rule determinations of the quark condensate and chiral perturbation theory to obtain $m_s(1 \text{ GeV}) > 121 \pm 12$ MeV. We have converted the result to $\mu=2$ GeV.
- 36 LEBED 98 obtain lower bounds of 41, 90, and 139 MeV for $m_s(1 \text{ GeV})$ using dispersion relations and chiral perturbation theory. The numbers assume the chiral perturbation theory form factor is accurate to 5%, 1%, and 0.05%, respectively. We have used the first number converted to $\mu=2$.
- 37 MALTMAN 98 uses τ -decay-like sum rules involving electromagnetic spectral data to determine $m_s(1 \text{ GeV}) = 113 \pm 107$ MeV. We have rescaled the result to $\mu=2$ GeV.
- 38 MALTMAN 98B uses spectral moments of hadronic τ decays to determine $m_s(1 \text{ GeV}) < 220 \pm 110$ MeV. We have rescaled the result to $\mu=2$ GeV.
- 39 CHETYRKIN 97 obtains 205.5 ± 19.1 MeV at $\mu=1$ GeV from QCD sum rules including fourth-order QCD corrections. We have rescaled the result to 2 GeV.
- 40 COLANGELO 97 is QCD sum rule computation. We have rescaled $m_s(1 \text{ GeV}) > 120$ to $\mu = 2$ GeV.
- 41 EICKER 97 use lattice gauge computations with two dynamical light flavors.
- 42 GOUGH 97 use lattice gauge computations in the quenched approximation. Correcting for quenching gives $54 < m_s < 92$ MeV at $\mu=2$ GeV.
- 43 GUPTA 97 use Lattice Monte Carlo computations in the quenched approximation. The value for two light dynamical flavors at $\mu = 2$ GeV is $68 \pm 12 \pm 7$ MeV.
- 44 LELLOUCH 97 obtain lower bounds on quark masses using hadronic spectral functions.
- 45 CHETYRKIN 95 uses QCD sum rules at next-to-leading order. We have rescaled $m_s(1 \text{ GeV}) = 171 \pm 15$ to $\mu = 2$ GeV.
- 46 JAMIN 95 uses QCD sum rules at next-to-leading order. We have rescaled $m_s(1 \text{ GeV}) = 189 \pm 32$ to $\mu = 2$ GeV.
- 47 For NARISON 95C, we have rescaled $m_s(1 \text{ GeV}) = 197 \pm 29$ to $\mu = 2$ GeV.
- 48 NEFKENS 92 results for $m_s - (m_u + m_d)/2$ are 111 ± 10 MeV from meson masses and 163 ± 15 MeV from baryon masses.
- 49 DOMINGUEZ 91 uses QCD sum rules with $\Lambda_{\text{QCD}} = 100\text{--}200$ MeV and the SVZ value for the gluon condensate. We have rescaled $m_s(1 \text{ GeV}) = 194 \pm 9$ to $\mu = 2$ GeV.
- 50 BARDUCCI 88 uses a calculation of the effective potential for $\bar{\psi}\psi$ in QCD, and estimates for $\Sigma(\rho^2)$. We have rescaled $m_s(1 \text{ GeV}) = 118$ to $\mu = 2$ GeV.
- 51 KREMER 84 obtain $m_u + m_s = 245 \pm 10$ MeV at $Q^2 = 1 \text{ GeV}^2$ using SVZ values for quark condensates; they obtain $m_u + m_s = 270 \pm 10$ MeV at $Q^2 = 1 \text{ GeV}^2$ using factorization values for quark condensates.
- 52 GASSER 82 uses chiral perturbation theory for the mass ratios, and uses QCD sum rules to extract the absolute values. We have rescaled $m_s(1 \text{ GeV}) = 175 \pm 55$ to $\mu = 2$ GeV.

LIGHT QUARK MASS RATIOS

u/d MASS RATIO

VALUE	DOCUMENT ID	TECN	COMMENT
0.2 to 0.8 OUR EVALUATION			
• • • We do not use the following data for averages, fits, limits, etc. • • •			
0.44	53 GAO	97 THEO	\overline{MS} scheme
0.553 ± 0.043	54 LEUTWYLER	96 THEO	Compilation
< 0.3	55 CHOI	92 THEO	
0.26	56 DONOGHUE	92 THEO	
0.30 ± 0.07	57 DONOGHUE	92B THEO	
0.66	58 GERARD	90 THEO	
0.4 to 0.65	59 LEUTWYLER	90B THEO	
0.05 to 0.78	60 MALTMAN	90 THEO	
0.0 to 0.56	61 CHOI	89B THEO	
0.0 to 0.8	62 KAPLAN	86 THEO	
0.57 ± 0.04	63 GASSER	82 THEO	
0.38 ± 0.13	64 LANGACKER	79 THEO	
0.47 ± 0.11	65 LANGACKER	79B THEO	
0.56	66 WEINBERG	77 THEO	
53 GAO 97	uses electromagnetic mass splittings of light mesons.		
54 LEUTWYLER 96	uses a combined fit to $\eta \rightarrow 3\pi$ and $\psi' \rightarrow J/\psi(\pi, \eta)$ decay rates, and the electromagnetic mass differences of the π and K .		
55 CHOI 92	result obtained from the decays $\psi(2S) \rightarrow J/\psi(1S)\pi$ and $\psi(2S) \rightarrow J/\psi(1S)\eta$, and a dilute instanton gas estimate of some unknown matrix elements.		
56 DONOGHUE 92	result is from a combined analysis of meson masses, $\eta \rightarrow 3\pi$ using second-order chiral perturbation theory including nonanalytic terms, and $\langle \psi(2S) \rightarrow J/\psi(1S)\pi \rangle / \langle \psi(2S) \rightarrow J/\psi(1S)\eta \rangle \rightarrow J/\psi(1S)\pi / J/\psi(1S)\eta$.		
57 DONOGHUE 92B	computes quark mass ratios using $\langle \psi(2S) \rightarrow J/\psi(1S)\pi \rangle / \langle \psi(2S) \rightarrow J/\psi(1S)\eta \rangle$, and an estimate of L_{14} using Weinberg sum rules.		
58 GERARD 90	uses large N and η - η' mixing.		
59 LEUTWYLER 90B	determines quark mass ratios using second-order chiral perturbation theory for the meson and baryon masses, including nonanalytic corrections. Also uses Weinberg sum rules to determine L_7 .		

Quark Particle Listings

Light Quarks (*u, d, s*), *c*

- ⁶⁰ MALTMAN 90 uses second-order chiral perturbation theory including nonanalytic terms for the meson masses. Uses a criterion of "maximum reasonableness" that certain coefficients which are expected to be of order one are ≤ 3 .
- ⁶¹ CHOI 89 uses second-order chiral perturbation theory and a dilute instanton gas estimate of second-order coefficients in the chiral lagrangian.
- ⁶² KAPLAN 86 uses second-order chiral perturbation theory including nonanalytic terms for the meson masses. Assumes that less than 30% of the mass squared of the pion is due to second-order corrections.
- ⁶³ GASSER 82 uses chiral perturbation theory for the meson and baryon masses.
- ⁶⁴ LANGACKER 79 result is from a fit to the meson and baryon mass spectrum, and the decay $\eta \rightarrow 3\pi$. The electromagnetic contribution is taken from Socolow rather than from Dashen's formula.
- ⁶⁵ LANGACKER 79b result uses LANGACKER 79 and also ρ - ω mixing.
- ⁶⁶ WEINBERG 77 uses lowest-order chiral perturbation theory for the meson and baryon masses and Dashen's formula for the electromagnetic mass differences.

s/d MASS RATIO

VALUE	DOCUMENT ID	TECN	COMMENT
17 to 25 OUR EVALUATION			
••• We do not use the following data for averages, fits, limits, etc. •••			
20.0	⁶⁷ GAO 97	THEO	\overline{MS} scheme
18.9 ± 0.8	⁶⁸ LEUTWYLER 96	THEO	Compilation
21	⁶⁹ DONOGHUE 92	THEO	
18	⁷⁰ GERARD 90	THEO	
18 to 23	⁷¹ LEUTWYLER 90b	THEO	
15 to 26	⁷² KAPLAN 86	THEO	
19.6 ± 1.5	⁷³ GASSER 82	THEO	
22 ± 5	⁷⁴ LANGACKER 79	THEO	
24 ± 4	⁷⁵ LANGACKER 79b	THEO	
20	⁷⁶ WEINBERG 77	THEO	

- ⁶⁷ GAO 97 uses electromagnetic mass splittings of light mesons.
- ⁶⁸ LEUTWYLER 96 uses a combined fit to $\eta \rightarrow 3\pi$ and $\psi' \rightarrow J/\psi(\pi,\eta)$ decay rates, and the electromagnetic mass differences of the π and K .
- ⁶⁹ DONOGHUE 92 result is from a combined analysis of meson masses, $\eta \rightarrow 3\pi$ using second-order chiral perturbation theory including nonanalytic terms, and $\langle\psi(2S) \rightarrow J/\psi(1S)\pi\rangle/\langle\psi(2S) \rightarrow J/\psi(1S)\eta\rangle$.
- ⁷⁰ GERARD 90 uses large N and η - η' mixing.
- ⁷¹ LEUTWYLER 90b determines quark mass ratios using second-order chiral perturbation theory for the meson and baryon masses, including nonanalytic corrections. Also uses Weinberg sum rules to determine L_7 .
- ⁷² KAPLAN 86 uses second-order chiral perturbation theory including nonanalytic terms for the meson masses. Assumes that less than 30% of the mass squared of the pion is due to second-order corrections.
- ⁷³ GASSER 82 uses chiral perturbation theory for the meson and baryon masses.
- ⁷⁴ LANGACKER 79 result is from a fit to the meson and baryon mass spectrum, and the decay $\eta \rightarrow 3\pi$. The electromagnetic contribution is taken from Socolow rather than from Dashen's formula.
- ⁷⁵ LANGACKER 79b result uses LANGACKER 79 and also ρ - ω mixing.
- ⁷⁶ WEINBERG 77 uses lowest-order chiral perturbation theory for the meson and baryon masses and Dashen's formula for the electromagnetic mass differences.

($m_s - m$)/($m_d - m_u$) MASS RATIO

VALUE	DOCUMENT ID	TECN	COMMENT
34 to 51 OUR EVALUATION			
••• We do not use the following data for averages, fits, limits, etc. •••			
36 ± 5	⁷⁷ ANISOVICH 96	THEO	
45 ± 3	⁷⁸ NEFKENS 92	THEO	
38 ± 9	⁷⁹ NEFKENS 92	THEO	
43.5 ± 2.2	⁸⁰ AMETTLER 84	THEO	
34 to 51	GASSER 82	THEO	
48 ± 7	GASSER 81	THEO	
	MINKOWSKI 80	THEO	

- ⁷⁷ ANISOVICH 96 find $Q=22.7 \pm 0.8$ with $Q^2 \equiv (m_s^2 - m^2)/(m_d^2 - m_u^2)$ from $\eta \rightarrow \pi^+\pi^-\pi^0$ decay using dispersion relations and chiral perturbation theory.
- ⁷⁸ NEFKENS 92 result is from an analysis of meson masses, mixing, and decay.
- ⁷⁹ NEFKENS 92 result is from an analysis of baryon masses.
- ⁸⁰ AMETTLER 84 uses $\eta \rightarrow \pi^+\pi^-\pi^0$ and ρ dominance.

LIGHT QUARKS (*u, d, s*) REFERENCES

AOKI 00	PRL 84 238	S. Aoki et al.	(CP-PACS Collab.)
AOKI 99	PRL 82 4392	S. Aoki et al.	(JLQCD Collab.)
BARATE 99b	EPJ C11 599	R. Barate et al.	(ALEPH Collab.)
MALTMAN	99	K. Maltman	
NARISON	99	S. Narison	
STEELE	99	T.G. Steele, K. Kostuik, J. Kwan	
BEĆIREVIC	98	D. Bećirevic et al.	
CHETYRKIN	98	K.G. Chetyrkin, J.H. Kuehn, A.A. Pivovarov	
CUCCHIERI	98	A. Chuchieri et al.	
DOMINGUEZ	98	C.A. Dominguez, L. Pirovano, K. Schilcher	
DOSCHI	98	H.G. Dosch, S. Narison	
LEBED	98	R.F. Lebed, K. Schilcher	
MALTMAN	98	K. Maltman	
MALTMAN	98b	K. Maltman	
CHETYRKIN	97	K.G. Chetyrkin, D. Pirjol, K. Schilcher	
COLANGELO	97	P. Colangelo et al.	
EICKER	97	N. Eicker et al.	(SESAM Collab.)

GAO 97	PR D56 4115	D.-N. Gao, B.A. Li, M.-L. Yan	
GOUGH 97	PRL 79 1622	B. Gough et al.	
GUPTA 97	PR D55 7203	R. Gupta, T. Bhattacharya	
LELLOUCH 97	PL B414 195	L. Lellouch, E. de Rafael, J. Taron	
ANISOVICH 96	PL B375 335	A.V. Anisovich, H. Leutwyler	
LEUTWYLER 96	PL B378 313	H. Leutwyler	
BIJNENS 95	PL B348 226	J. Bijnens, J. Prades, E. de Rafael	(NORO, BOHR+)
CHETYRKIN 95	PR D51 5090	K.G. Chetyrkin et al.	(INRM, CAPE, MANZ)
JAMIN 95	ZPHY C66 633	M. Jamin, M. Munz	(HEIDT, MUNT)
NARISON 95c	PL B358 113	S. Narison	(MONP)
ADAMI 93	PR D48 2304	C. Adami, E.G. Drukarev, B.I. Ioffe	(CIT, ITEP+)
CHOI 92	PL B292 159	K.W. Choi	(UCSD)
CHOI 92b	NP B383 58	K.W. Choi	(UCSD)
DONOGHUE 92	PRL 69 3444	J.F. Donoghue, B.R. Holstein, D. Wyler	(MASA+)
DONOGHUE 92b	PR D45 892	J.F. Donoghue, D. Wyler	(MASA, ZUR, UCSBT)
NEFKENS 92	CNPP 20 221	B.M.K. Nefkens, G.A. Miller, I. Slaus	(UCLA+)
DOMINGUEZ 91	PL B253 241	C.A. Dominguez, C. van Gend, N. Paver	(CAPE+)
GERARD 90	MPL A5 391	J.M. Gerard	(MPIM)
LEUTWYLER 90b	NP B337 108	H. Leutwyler	(BERN)
MALTMAN 90	PL B234 158	K. Maltman, T. Goldman, Stephenson Jr.	(YORKC+)
CHOI 89	PRL 62 849	K. Choi, C.W. Kim	(CMU, JHU)
CHOI 89b	PR D40 890	A. Barducci et al.	(FIRZ, INFN, LECE+)
BARDUCCI 88	PR D38 238	A. Barducci et al.	(FIRZ, INFN, LECE+)
Also	87	PL B193 305	
DOMINGUEZ 87	ANP 174 372	C.A. Dominguez, E. de Rafael	(ICTP, MARS, WIEN+)
KAPLAN 86	PR 56 2004	D.D. Kaplan, A.V. Manohar	(HARV)
AMETTLER 84	PL D30 674	L. Ametller, C. Ayala, A. Bramon	(BARC)
KREMER 84	PL 143B 476	M. Kremer, N.A. Papadopoulos, K. Schilcher	(MANZ)
GASSER 82	PRPL 87 77	J. Gasser, H. Leutwyler	(BERN)
GASSER 81	ANP 136 62	J. Gasser	(BERN)
MINKOWSKI 80	NP B164 25	P. Minkowski, A. Zepeda	(BERN)
LANGACKER 79	PR D19 2070	P. Langacker, H. Pagels	(DESY, PRIN)
LANGACKER 79b	PR D20 2983	P. Langacker	(PENN)
WEINBERG 77	ANYAS 38 185	S. Weinberg	(HARV)



$$I(J^P) = 0(\frac{1}{2}^+)$$

$$\text{Charge} = \frac{2}{3} e \quad \text{Charm} = +1$$

c-QUARK MASS

The *c*-quark mass is estimated from charmonium and *D* masses. It corresponds to the "running" mass $m_c(\mu = m_c)$ in the \overline{MS} scheme. We have converted masses in other schemes to the \overline{MS} scheme using one-loop QCD perturbation theory with $\alpha_s(\mu = m_c) = 0.39$. The range 1.0–1.6 GeV for the \overline{MS} mass corresponds to 1.2–1.9 GeV for the pole mass (see the "Note on Quark Masses").

VALUE (GeV)	DOCUMENT ID	TECN	COMMENT
1.15 to 1.35 OUR EVALUATION			
••• We do not use the following data for averages, fits, limits, etc. •••			
1.79 ± 0.38	¹ VILAIN 99	THEO	Assumes \overline{MS} scheme
1.22 ± 0.06	² DOMINGUEZ 94	THEO	\overline{MS} scheme
≥ 1.23	³ LIGETI 94	THEO	\overline{MS} scheme
≥ 1.25	⁴ LUKE 94	THEO	\overline{MS} scheme
1.23 ± 0.04	⁵ NARISON 94	THEO	\overline{MS} scheme
1.31 ± 0.03	⁶ TITARD 94	THEO	\overline{MS} scheme
1.5 +0.2 -0.1 ± 0.2	⁷ ALVAREZ 93	THEO	
1.27 ± 0.02	⁸ NARISON 89	THEO	
1.25 ± 0.05	⁹ NARISON 87	THEO	
1.27 ± 0.05	¹⁰ GASSER 82	THEO	

- ¹ VILAIN 99 obtain the charm quark mass from an analysis of charm production in neutrino scattering.
- ² DOMINGUEZ 94 uses QCD sum rules for $J/\psi(1S)$ system and finds a pole mass of 1.46 ± 0.07 GeV.
- ³ LIGETI 94 computes lower bound of 1.43 GeV on pole mass using HQET, and experimental data on inclusive *B* and *D* decays.
- ⁴ LUKE 94 computes lower bound of 1.46 GeV on pole mass using HQET, and experimental data on inclusive *B* and *D* decays.
- ⁵ NARISON 94 uses spectral sum rules to two loops, and $J/\psi(1S)$ and Υ systems.
- ⁶ TITARD 94 uses one-loop computation of the quark potential with nonperturbative gluon condensate effects to fit $J/\psi(1S)$ and Υ states.
- ⁷ ALVAREZ 93 method is to fit the measured x_F and p_T^2 charm photoproduction distributions to the theoretical predictions of ELLIS 89c.
- ⁸ NARISON 89 determines the Georgi-Politzer mass at $p^2 = -m^2$ to be 1.26 ± 0.02 GeV using QCD sum rules.
- ⁹ NARISON 87 computes pole mass of 1.46 ± 0.05 GeV using QCD sum rules, with $\Lambda(\overline{MS}) = 180 \pm 80$ MeV.
- ¹⁰ GASSER 82 uses SVZ sum rules. The renormalization point is $\mu =$ quark mass.

c-QUARK REFERENCES

VILAIN 99	EPJ C11 19	P. Vilain et al.	(CHARM II Collab.)
DOMINGUEZ 94	PL B333 184	C.A. Dominguez, G.R. Gluckman, N. Paver	(CAPE+)
LIGETI 94	PR D49 R4331	Z. Ligeti, Y. Nir	(REHO)
LUKE 94	PL B321 88	M. Luke, M.L. Savage	(TNTO, UCSD, CMU)
NARISON 94	PL B341 73	S. Narison	(CERN, MONP)
TITARD 94	PR D49 6007	S. Titard, F.J. Yndurain	(MICH, MADU)
ALVAREZ 93	ZPHY C60 53	M.P. Alvarez et al.	(CERN NA14/2 Collab.)
ELLIS 89c	NP B312 551	R.K. Ellis, P. Nason	(FNAL, ETH)
NARISON 89	PL B216 191	S. Narison	(ICTP)
NARISON 87	PL B197 405	S. Narison	(CERN)
GASSER 82	PRPL 87 77	J. Gasser, H. Leutwyler	(BERN)

b

$$I(J^P) = 0(\frac{1}{2}^+)$$

$$\text{Charge} = -\frac{1}{3} e \quad \text{Bottom} = -1$$

b-QUARK MASS

The *b*-quark mass is estimated from bottomonium and *B* masses. It corresponds to the "running" mass $m_b(\mu = m_b)$ in the $\overline{\text{MS}}$ scheme. We have converted masses in other schemes to the $\overline{\text{MS}}$ scheme using one-loop QCD perturbation theory with $\alpha_s(\mu=m_b) = 0.22$. The range 4.1–4.5 GeV for the $\overline{\text{MS}}$ mass corresponds to 4.5–4.9 GeV for the pole mass (see the "Note on Quark Masses").

VALUE (GeV)	DOCUMENT ID	TECN	COMMENT
4.0 to 4.4 OUR EVALUATION			
• • • We do not use the following data for averages, fits, limits, etc. • • •			
4.20 ± 0.06	¹ HOANG	00 THEO	Assumes $\overline{\text{MS}}$ scheme
4.25 ± 0.08	² BENEKE	99 THEO	Assumes $\overline{\text{MS}}$ scheme
4.48 $^{+1.1}_{-2.7}$	³ BRANDENB...	99	Assumes $\overline{\text{MS}}$ scheme
4.25 ± 0.09	⁴ HOANG	99 THEO	$\overline{\text{MS}}$ scheme
4.2 ± 0.1	⁵ MELNIKOV	99 THEO	Assumes $\overline{\text{MS}}$ scheme
4.21 ± 0.11	⁶ PENIN	99 THEO	Assumes $\overline{\text{MS}}$ scheme
3.91 ± 0.67	⁷ ABREU	98i DLPH	$\overline{\text{MS}}$ scheme
4.14 ± 0.04	⁸ KUEHN	98 THEO	$\overline{\text{MS}}$ scheme
4.15 ± 0.05 ± 0.20	⁹ GIMENEZ	97 LATT	$\overline{\text{MS}}$ scheme
4.13 ± 0.06	¹⁰ JAMIN	97 THEO	$\overline{\text{MS}}$ scheme
4.16 ± 0.32 ± 0.60	¹¹ RODRIGO	97 THEO	$\overline{\text{MS}}$ scheme
4.22 ± 0.05	¹² NARISON	95b THEO	$\overline{\text{MS}}$ scheme
4.238 ± 0.006	¹³ VOLOSHIN	95 THEO	$\overline{\text{MS}}$ scheme
4.0 ± 0.1	¹⁴ DAVIES	94 THEO	$\overline{\text{MS}}$ scheme
≥ 4.26	¹⁵ LIGETI	94 THEO	$\overline{\text{MS}}$ scheme
≥ 4.2	¹⁶ LUKE	94 THEO	$\overline{\text{MS}}$ scheme
4.23 ± 0.04	¹⁷ NARISON	94 THEO	$\overline{\text{MS}}$ scheme
4.397 ± 0.025	¹⁸ TITARD	94 THEO	$\overline{\text{MS}}$ scheme
4.32 ± 0.05	¹⁹ DOMINGUEZ	92 THEO	
4.24 ± 0.05	²⁰ NARISON	89 THEO	
4.18 ± 0.02	²¹ REINDERS	88 THEO	
4.30 ± 0.13	²² NARISON	87 THEO	
4.25 ± 0.1	²³ GASSER	82 THEO	

- ¹ HOANG 00 uses a NNLO calculation of the vacuum polarization function to determine spectral moments of the masses and electronic decay widths of the Υ mesons.
- ² BENEKE 99 uses a calculation of the $b\bar{b}$ production cross section and the mass of the Υ meson at NNLO.
- ³ BRANDENBURG 99 obtain a *b*-quark mass of $m_b(M_Z) = 2.56 \pm 0.27 + 0.28 - 0.49$ from a study of three-jet events at the Z . We have converted this to $\mu = m_b$.
- ⁴ HOANG 99 uses a NNLO calculation of the vacuum polarization function to determine spectral moments of the masses and electronic decay widths of the Υ mesons.
- ⁵ MELNIKOV 99 compute the quark mass using Υ sum rules at NNLO.
- ⁶ PENIN 99 compute the quark mass using Υ sum rules at NNLO.
- ⁷ ABREU 98i determines the $\overline{\text{MS}}$ mass $m_b = 2.67 \pm 0.25 \pm 0.34 \pm 0.27$ GeV at $\mu = M_Z$ from three jet heavy quark production at LEP. ABREU 98i have rescaled the result to $\mu = m_b$ using $\alpha_s = 0.118 \pm 0.003$.
- ⁸ KUEHN 98 uses a calculation of the vacuum polarization function, including resumming threshold effects, to determine spectral moments of the masses of the Υ mesons. We have converted their extracted value of 4.75 ± 0.04 for the pole mass to the $\overline{\text{MS}}$ scheme.
- ⁹ GIMENEZ 97 uses lattice computations of the *B*-meson propagator and the *B*-meson binding energy $\bar{\Lambda}$ in the HQET. Their systematic (second) error for the $\overline{\text{MS}}$ mass is an estimate of the effects of higher-order corrections in the matching of the HQET operators (renormalon effects).
- ¹⁰ JAMIN 97 apply the QCD moment method to the Υ system. They also find a pole mass of 4.60 ± 0.02 .
- ¹¹ RODRIGO 97 determines the $\overline{\text{MS}}$ mass $m_b = 2.85 \pm 0.22 \pm 0.20 \pm 0.36$ GeV at $\mu = M_Z$ from three jet heavy quark production at LEP. We have rescaled the result.
- ¹² NARISON 95b uses finite energy sum rules to two-loop accuracy to determine a *b*-quark pole mass of 4.61 ± 0.05 GeV.
- ¹³ VOLOSHIN 95 uses moments of the total cross section for $e^+e^- \rightarrow b$ hadrons. We have converted the value of 4.827 ± 0.007 MeV for the pole mass to the $\overline{\text{MS}}$ scheme using the two-loop formula.
- ¹⁴ DAVIES 94 uses lattice computation of Υ spectroscopy. They also quote a value of 5.0 ± 0.2 GeV for the *b*-quark pole mass. The numerical computation includes quark vacuum polarization (unquenched); they find that the masses are independent of n_f within their errors. Their error for the pole mass is larger than the error for the $\overline{\text{MS}}$ mass, because both are computed from the bare lattice quark mass, and the conversion for the pole mass is less accurate.
- ¹⁵ LIGETI 94 computes lower bound of 4.66 GeV on pole mass using HQET, and experimental data on inclusive *B* and *D* decays.
- ¹⁶ LUKE 94 computes lower bound of 4.60 GeV on pole mass using HQET, and experimental data on inclusive *B* and *D* decays.
- ¹⁷ NARISON 94 uses spectral sum rules to two loops, and $J/\psi(1S)$ and Υ systems.
- ¹⁸ TITARD 94 uses one-loop computation of the quark potential with nonperturbative gluon condensate effects to fit $J/\psi(1S)$ and Υ states.
- ¹⁹ DOMINGUEZ 92 determines pole mass to be 4.72 ± 0.05 using next-to-leading order in $1/m$ in moment sum rule.
- ²⁰ NARISON 89 determines the Georgi-Politzer mass at $p^2 = -m^2$ to be 4.23 ± 0.05 GeV using QCD sum rules.
- ²¹ REINDERS 88 determines the Georgi-Politzer mass at $p^2 = -m^2$ to be 4.17 ± 0.02 using moments of $\bar{b}\gamma^\mu b$. This technique leads to a value for the mass of the *B* meson of 5.25 ± 0.15 GeV.
- ²² NARISON 87 determines the pole mass to be 4.70 ± 0.14 using QCD sum rules, with $\Lambda(\overline{\text{MS}}) = 180 \pm 80$ MeV.
- ²³ GASSER 82 uses SVZ sum rules. The renormalization point is $\mu =$ quark mass.

 $m_b - m_c$ MASS DIFFERENCE

The mass difference $m_b - m_c$ in the HQET scheme is 3.4 ± 0.2 GeV (see the "Note on Quark Masses").

VALUE (GeV)	DOCUMENT ID
• • • We do not use the following data for averages, fits, limits, etc. • • •	
≥ 3.29	²⁴ GROSSE 78
²⁴ GROSSE 78 obtain $(m_b - m_c) \geq 3.29$ GeV based on eigenvalue inequalities in potential models.	

b-QUARK REFERENCES

HOANG	00	PR D61 034005	A.H. Hoang
BENEKE	99	PL B471 233	M. Beneke, A. Signer
BRANDENB...	99	PL B468 168	A. Brandenburg <i>et al.</i>
HOANG	99	PR D59 014039	A.H. Hoang
MELNIKOV	99	PR D59 114009	K. Melnikov, A. Yelkhovsky
PENIN	99	NP B549 217	A.A. Penin, A.A. Pivovarov
ABREU	98i	PL B418 430	P. Abreu <i>et al.</i> (DELPHI Collab.)
KUEHN	98	NP B534 356	J.H. Kuehn, A.A. Penin, A.A. Pivovarov
GIMENEZ	97	PL B393 124	V. Gimenez, G. Martinelli, C.T. Sachrajda
JAMIN	97	NP B507 334	M. Jamin, A. Pich
RODRIGO	97	PRL 79 193	G. Rodrigo, A. Santamaría, M.S. Bilenky
NARISON	95b	PL B352 122	S. Narison (MONP)
VOLOSHIN	95	IJMP A10 2865	M.B. Voloshin (MINN)
DAVIES	94	PRL 73 2654	C.T.H. Davies <i>et al.</i> (GLAS, SMU, CORN+)
LIGETI	94	PR D49 R4331	Z. Ligeti, Y. Nir (REHO)
LUKE	94	PL B321 88	M. Luke, M.L. Savage (TNTO, UCSD, CMU)
NARISON	94	PL B341 73	S. Narison (CERN, MONP)
TITARD	94	PR D49 6007	S. Titard, F.J. Yndurain (MICH, MADU)
DOMINGUEZ	92	PL B293 197	C.A. Dominguez, N. Paver (CAPE, TRST, INFN)
NARISON	89	PL B216 191	S. Narison (CTF)
REINDERS	88	PR D38 947	L.J. Reinders (BONN)
NARISON	87	PL B197 405	S. Narison (CERN)
GASSER	82	PRPL 87 77	J. Gasser, H. Leutwyler (BERN)
GROSSE	78	PL 79B 103	H. Grosse, A. Martin (CERN)

t

$$I(J^P) = 0(\frac{1}{2}^+)$$

$$\text{Charge} = \frac{2}{3} e \quad \text{Top} = +1$$

THE TOP QUARK

Revised April 2000 by M. Mangano (CERN) and T. Trippe (LBNL).

A. Introduction: The top quark is the $Q = 2/3$, $T_3 = +1/2$ member of the weak-isospin doublet containing the bottom quark (see our review on the "Standard Model of Electroweak Interactions" for more information). This note summarizes its currently measured properties, and provides a discussion of the experimental and theoretical issues involved in the determination of its parameters (mass, production cross section, decay branching ratios, *etc.*); it also comments on prospects for future improvements.

B. Top quark production at the Tevatron: All direct measurements of top quark production and decay have been made by the CDF and DØ experiments at the Fermilab Tevatron collider in $p\bar{p}$ collisions at $\sqrt{s} = 1.8$ TeV. Here top quarks are produced dominantly in pairs from the QCD processes $q\bar{q} \rightarrow t\bar{t}$ and $gg \rightarrow t\bar{t}$. At this energy, the production cross section in these channels is expected to be approximately 5 pb for $m_t = 175$ GeV/ c^2 , with a 90% contribution from $q\bar{q}$ annihilation. Smaller contributions are expected from electroweak single-top production mechanisms, namely $q\bar{q}' \rightarrow W^* \rightarrow t\bar{b}$ and $gg \rightarrow q't\bar{b}$, the latter mediated by virtual-*W* exchange ("*W*-gluon fusion"). The combined rate from these processes is approximately 2.5 pb at $m_t = 175$ GeV/ c^2 (see Ref. 1 and references therein). The expected contribution of these channels is further reduced relative to the dominant pair-production mechanisms because of larger backgrounds and poor detection efficiency.

With a mass above the *Wb* threshold, the decay width of the top quark is expected to be dominated by the two-body

Quark Particle Listings

t

channel $t \rightarrow Wb$. Neglecting terms of order m_b^2/m_t^2 , α_s^2 and those of order $(\alpha_s/\pi)m_W^2/m_t^2$, this is predicted in the Standard Model to be [2]:

$$\Gamma_t = \frac{G_F m_t^3}{8\pi\sqrt{2}} \left(1 - \frac{M_W^2}{m_t^2}\right)^2 \left(1 + 2\frac{M_W^2}{m_t^2}\right) \left[1 - \frac{2\alpha_s}{3\pi} \left(\frac{2\pi^2}{3} - \frac{5}{2}\right)\right]. \quad (1)$$

The use of G_F in this equation accounts for the largest part of the one-loop electroweak radiative corrections, providing an expression accurate to better than 2%. The width increases with mass, going for example from 1.02 GeV/c² at $m_t = 160$ GeV/c² to 1.56 GeV/c² at $m_t = 180$ GeV/c² (we used $\alpha_s(M_Z) = 0.118$). With such a correspondingly short lifetime, the top quark is expected to decay before top-flavored hadrons or $t\bar{t}$ -quarkonium bound states can form [3]. Recently, the order α_s^2 QCD corrections to Γ_t have also been calculated [4], thereby improving the overall theoretical accuracy to better than 1%.

In top decay, the Ws and Wd final states are expected to be suppressed relative to Wb by the square of the CKM matrix elements V_{ts} and V_{td} , whose values can be estimated under the assumption of unitarity of the three-generation CKM matrix to be less than 0.043 and 0.014, respectively (see our review “The Cabibbo-Kobayashi-Maskawa Mixing Matrix” in the current edition for more information). Typical final states for the leading pair-production process therefore belong to three classes:

- A. $t\bar{t} \rightarrow WbW\bar{b} \rightarrow q\bar{q}'bq''\bar{q}'''\bar{b}$,
- B. $t\bar{t} \rightarrow WbW\bar{b} \rightarrow q\bar{q}'b\ell\bar{\nu}_\ell\bar{b} + \bar{\ell}\nu_\ell b q\bar{q}'\bar{b}$,
- C. $t\bar{t} \rightarrow WbW\bar{b} \rightarrow \bar{\ell}\nu_\ell b\ell'\bar{\nu}_{\ell'}\bar{b}$,

where A, B, and C are referred to as the all-jets, lepton + jets, and dilepton channels, respectively.

The final state quarks can emit radiation and eventually evolve into jets of hadrons. The precise number of jets reconstructed by the detectors varies event by event, as it depends on the decay kinematics, as well as on the precise definition of jet used in the analysis. (Additional gluon radiation can also be emitted from the initial states.) The transverse momenta of the neutrinos are reconstructed via the large imbalance in detected transverse momentum of the event (missing E_T).

The observation of $t\bar{t}$ pairs has been reported in all of the above decay modes. As discussed below, the production and decay properties of the top quark extracted from the above three decay channels are all consistent with each other within experimental uncertainty. In particular, the $t \rightarrow Wb$ decay mode is supported through the reconstruction of the $W \rightarrow jj$ invariant mass in the $\ell\bar{\nu}_\ell b\bar{b}jj$ final state [5].

The extraction of top-quark properties from Tevatron data requires a good understanding of the production and decay mechanisms of the top, as well as of the large background processes. Because only leading order QCD calculations are available for most of the relevant processes ($W+3$ and 4 jets, or $WW+2$ jets), theoretical estimates of the backgrounds have large uncertainties. While this limitation affects estimates of the overall $t\bar{t}$ production rates, it is believed that the LO

determination of the event kinematics and of the fraction of W + multi-jet events containing b quarks is relatively accurate. In particular, for the background one expects the E_T spectrum of jets to fall rather steeply, the jet direction to peak at small angles to the beams, and the fraction of events with b quarks to be of the order of a few percent. On the contrary, for the top signal, the b fraction is $\sim 100\%$ and the jets are rather energetic, since they come from the decay of a massive object. It is therefore possible to improve the S/B ratio either by requiring the presence of a b quark, or by selecting very energetic and central kinematic configurations.

A detailed study of control samples with features similar to those of the relevant backgrounds, but free from possible top contamination, is required to provide a reliable check on background estimates.

C. Measured top properties: Current measurements of top properties are based on the full Run I integrated luminosity of 109 pb⁻¹ for CDF and 125 pb⁻¹ for DØ. DØ and CDF determine the $t\bar{t}$ cross section $\sigma_{t\bar{t}}$ from their number of observed top candidates, estimated background, $t\bar{t}$ acceptance, and integrated luminosity, assuming the Standard-Model decay $t \rightarrow Wb$ with unity branching ratio. Table 1 shows the measured cross sections from DØ and CDF along with the range of theoretical expectations, evaluated at the m_t values used by the experiments in calculating their acceptances. The DØ results have been updated in conference proceedings [7] to adjust to the current DØ value of the top mass. The CDF results have been updated in conference proceedings [16] to include improvements in their Monte Carlo determination of secondary-vertex tagging efficiency, calibration of the background estimate of the heavy-flavor fraction in inclusive W +jets events, and an updated total luminosity. This has brought the CDF cross section into better agreement with theoretical expectations. The agreement of both DØ and CDF $t\bar{t}$ cross sections with theory supports the hypothesis that the excess of events over background in all of these channels can be attributed to $t\bar{t}$ production.

More precise measurements of the top production cross section will test current understanding of the production mechanisms [9–12]. This is important for the extrapolation to higher energies of colliders such as the LHC, where the larger expected cross section will permit more extensive studies [17]. Discrepancies in rate between theory and data, even at the Tevatron, would be quite exciting, and might indicate the presence of exotic production or decay channels, as predicted in certain models. Such new sources of top would lead to a modification of kinematic distributions such as the invariant mass of the top pair or the transverse momentum of the top quark. Studies by CDF of the former [18] and of the latter [19] distributions, show no deviation from expected QCD behavior. DØ [20] also finds these kinematic distributions consistent with Standard Model expectations.

The top mass has been measured in the lepton + jets and dilepton channels by both DØ and CDF, and in the

Table 1: Cross section for $t\bar{t}$ production in $p\bar{p}$ collisions at $\sqrt{s} = 1.8$ TeV from DØ ($m_t = 172.1$ GeV/ c^2), CDF ($m_t = 175$ GeV/ c^2), and theory.

$\sigma_{t\bar{t}}(pb)$	Source	Ref.	Method
4.1 ± 2.1	DØ	[6,7]	ℓ + jets/topological
8.3 ± 3.5	DØ	[6,7]	ℓ + jets/soft μ b-tag
6.4 ± 3.3	DØ	[6,7]	$\ell\ell$ + $e\nu$
7.1 ± 3.2	DØ	[8]	all jets
5.9 ± 1.7	DØ	[8]	all combined
$5.2 - 6.0$	Theory	[9–12]	$m_t = 172.1$ GeV/ c^2
5.1 ± 1.5	CDF	[13,16]	ℓ + jets/vtx b-tag
9.2 ± 4.3	CDF	[13,16]	ℓ + jets/soft ℓ b-tag
$8.4^{+4.5}_{-3.5}$	CDF	[14,16]	$\ell\ell$
$7.6^{+3.5}_{-2.7}$	CDF	[15,16]	all jets
$6.5^{+1.7}_{-1.4}$	CDF	[16]	all combined
$4.75 - 5.5$	Theory	[9–12]	$m_t = 175$ GeV/ c^2

all-jets channel by CDF. At present, the most precise measurements come from the lepton + jets channel, with four or more jets and large missing E_T . In this channel, each event is subjected to a two-constraint kinematic fit to the hypothesis $t\bar{t} \rightarrow W^+ b W^- \bar{b} \rightarrow \ell \nu_\ell q \bar{q}' b \bar{b}$, assuming that the four highest E_T jets are the quarks from $t\bar{t}$ decay. The shape of the distribution of fitted top masses from these events is compared to templates expected from a mixture of background and signal distributions for a series of assumed top masses. This comparison yields values of the likelihood as a function of top mass, from which a best value of the top mass and its uncertainty can be obtained. The results are shown in Table 2. The systematic uncertainty (second uncertainty shown) is comparable to the statistical uncertainty, and is primarily due to uncertainties in the jet energy scale and in the Monte Carlo modeling.

Less precise determinations of the top mass come from the dilepton channel with two or more jets and large missing E_T , and from the all-jets channel. In the dilepton channel, a kinematically constrained fit is not possible because there are two missing neutrinos, so experiments must use other mass estimators than the reconstructed top mass. In principle, any quantity which is correlated with the top mass can be used as such an estimator. The DØ method uses the fact that if a value for m_t is assumed, the $t\bar{t}$ system can be reconstructed (up to a four-fold ambiguity). They compare the resulting kinematic configurations to expectations from $t\bar{t}$ production, and obtain an m_t -dependent weight curve for each event, which they histogram in five bins to obtain four shape-sensitive quantities as their multidimensional mass estimator. This method yields a significant increase in precision over one-dimensional estimators. CDF has employed a similar method, thereby reducing their previous systematic uncertainty in the $\ell\ell$ + jets channel by a factor of two. DØ and CDF obtain the top mass and uncertainty

from these mass estimators using the same type of template likelihood method as for the lepton + jets channel. CDF also measures the mass in the all-jets channel using events with six or more jets, at least one of which is tagged as a b jet through the detection of a secondary vertex.

Table 2: Top mass measurements from DØ and CDF.

m_t (GeV/ c^2)	Source	Ref.	Method
$173.3 \pm 5.6 \pm 5.5$	DØ	[20]	ℓ + jets
$168.4 \pm 12.3 \pm 3.6$	DØ	[21]	$\ell\ell$
$172.1 \pm 5.2 \pm 4.9$	DØ	[20]	DØ comb.
$175.9 \pm 4.8 \pm 5.3$	CDF	[22,23]	ℓ + jet
$167.4 \pm 10.3 \pm 4.8$	CDF	[22]	$\ell\ell$
$186.0 \pm 10.0 \pm 5.7$	CDF	[22,15]	all jets
$176.0 \pm 4.0 \pm 5.1$	CDF	[22]	CDF comb.
$174.3 \pm 3.2 \pm 4.0$ *	DØ & CDF	[24]	PDG best

* PDG uses this Top Averaging Group result as its best value

As seen in Table 2, all results are in good agreement with a unique mass for the top quark, giving further support to the hypothesis that these events are due to $t\bar{t}$ production. The Top Averaging Group, a joint CDF/DØ working group, produced the combined CDF/DØ average top mass in Table 2, taking into account correlations between systematic uncertainties in different measurements. They assume that the uncertainty in jet energy scale is completely correlated within CDF and within DØ but uncorrelated between the two experiments, and that the signal model and Monte Carlo generator uncertainties are completely correlated between all measurements. The uncertainties from uranium noise and multiple interactions relate only to DØ and are assumed completely correlated between their two measurements. The uncertainty on the background model is taken to be completely correlated between the CDF and the DØ ℓ +jets measurements, and similarly for the $\ell\ell$ measurements. The Particle Data Group uses this combined top mass, $m_t = 174.3 \pm 5.1$ GeV/ c^2 (statistical and systematic uncertainties combined in quadrature), as our PDG best value.

Given the experimental technique used to extract the top mass, these mass values should be taken as representing the top pole mass (see our review “Note on Quark Masses” in the current edition for more information).

With a smaller uncertainty on the top mass, and with improved measurements of other electroweak parameters, it will be possible to get important constraints on the value of the Higgs mass. Current global fits performed within the Standard Model and its minimal supersymmetric extension provide indications for a relatively light Higgs (see the review “ H^0 Indirect Mass Limits from Electroweak Analysis” in the Particle Listings of the current edition for more information).

Other properties of top decays are being studied. CDF reports a direct measurement of the $t \rightarrow Wb$ branching ratio [25]. Their preliminary result, obtained by comparing the number of events with 0, 1 and 2 tagged b jets and using the known b -tagging efficiency, is: $R = B(t \rightarrow Wb) / \sum_{q=d,s,b} B(t \rightarrow Wq) = 0.99 \pm 0.29$ where statistical and systematic uncertainties are included, or as a lower limit, $R > 0.58$ at 95% CL. Assuming that non- W decays of top can be neglected, that only three generations of fermions exist, and that the CKM matrix is unitary, they extract a CKM matrix-element $|V_{tb}| = 0.99 \pm 0.15$ or $|V_{tb}| > 0.76$ at 95% CL. A more direct measurement of the Wtb coupling constant will be possible when enough data are accumulated to detect the less frequent single-top production processes, such as $q\bar{q}' \rightarrow W^* \rightarrow t\bar{b}$ (a.k.a. s -channel W exchange) and $qb \rightarrow q't$ via W exchange (a.k.a. Wg fusion). The cross sections for these processes are proportional to $|V_{tb}|^2$, and there is no assumption needed on the number of families or the unitarity of the CKM matrix in the extraction of $|V_{tb}|$. Preliminary CDF results [19] give 95% CL limits of 15.8 and 15.4 pb for the single-top production rates in the s -channel and Wg -fusion channels, respectively. Comparison with the expected Standard Model rates of 0.73 ± 0.10 pb and 1.70 ± 0.30 pb, respectively, shows that far better statistics will be required before significant measurements can be achieved. For the prospects of these measurements at the LHC, see [17].

Both CDF and $D\bar{O}$ have searched for non-Standard Model top decays [26,27], particularly those expected in supersymmetric models. These studies search for $t \rightarrow H^+b$, followed by $H^+ \rightarrow \tau\nu$ or $c\bar{s}$. The $t \rightarrow H^+b$ branching ratio is a minimum at $\tan\beta = \sqrt{m_t/m_b} \simeq 6$ and is large in the region of either $\tan\beta \ll 6$ or $\tan\beta \gg 6$. In the former range $H^+ \rightarrow c\bar{s}$ is the dominant decay, while $H^+ \rightarrow \tau\nu$ dominates in the latter range. These studies are based either on direct searches for these final states, or on top disappearance. In the standard lepton + jets or dilepton cross section analyses, the charged Higgs decays are not detected as efficiently as $t \rightarrow W^\pm b$, primarily because the selection criteria are optimized for the standard decays, and because of the absence of energetic isolated leptons in the Higgs decays. With a significant $t \rightarrow H^+b$ contribution, this would give rise to measured cross sections lower than the prediction from the Standard Model (assuming that non-Standard contributions to $t\bar{t}$ production are negligible). More details, and the results of these studies, can be found in the review ‘‘Search for Higgs bosons’’ and in the ‘‘ H^+ Mass Limits’’ section of the Higgs Particle Listings of the current edition.

CDF reports a search for flavor changing neutral current (FCNC) decays of the top quark $t \rightarrow q\gamma$ and $t \rightarrow qZ$ [28], for which the Standard Model predicts such small rates that their observation here would indicate new physics. They assume that one top decays via FCNC while the other decays via Wb . For the $t \rightarrow q\gamma$ search, they examine two signatures, depending on whether the W decays leptonically or hadronically. For leptonic W decay, the signature is $\gamma\ell$ and missing E_T and two or more jets, while for hadronic W decay, it is γ plus four or more jets,

one with a secondary vertex b tag. They observe one event ($\mu\gamma$) with an expected background of less than half an event, giving an upper limit on the top branching ratio of $B(t \rightarrow q\gamma) < 3.2\%$ at 95% CL.

For the $t \rightarrow qZ$ FCNC search, they look for $Z \rightarrow \mu\mu$ or ee and $W \rightarrow$ hadrons, giving a $Z +$ four jets signature. They observe one $\mu\mu$ event with an expected background of 1.2 events, giving an upper limit on the top branching ratio of $B(t \rightarrow qZ) < 33\%$ at 95% CL. Both the γ and Z limits are non-background subtracted (i.e. conservative) estimates.

Indirect constraints on FCNC couplings of the top quark can be obtained from single-top production in e^+e^- collisions, via the process $e^+e^- \rightarrow \gamma, Z^* \rightarrow t\bar{q}$ and its charge-conjugate ($q = u, c$). Limits on the cross-section for this reaction have been obtained by DELPHI [29] using LEP2 data at energies between 183 and 189 GeV. When interpreted in terms of top decay branching ratios [30,17], these limits lead to a bound of $B(t \rightarrow qZ) < 22\%$ at 95% CL, which is stronger than the direct CDF limit.

Studies of the decay angular distributions allow a direct analysis of the $V-A$ nature of the Wtb coupling, and provide information on the relative coupling of longitudinal and transverse W bosons to the top quark. In the Standard Model, the fraction of decays to longitudinally polarized W bosons is expected to be $\mathcal{F}_0^{\text{SM}} = x/(1+x)$, $x = m_t^2/2M_W^2$ ($\mathcal{F}_0^{\text{SM}} \sim 70\%$ for $m_t = 175$ GeV/ c^2). Deviations from this value would bring into question the validity of the Higgs mechanism of spontaneous symmetry breaking. CDF has recently measured $\mathcal{F}_0^{\text{SM}} = 0.91 \pm 0.37_{\text{stat}} \pm 0.13_{\text{sys}}$ [31], in agreement with the expectations.

$D\bar{O}$ has studied $t\bar{t}$ spin correlation [32]. Top quark pairs produced at the Tevatron are expected to be unpolarized but to have correlated spins. Since top quarks decay before hadronizing, their spins are transmitted to their decay daughters. Spin correlation is studied by analyzing the joint decay angular distribution of one t daughter and one \bar{t} daughter. The sensitivity to top spin is greatest when the daughters are charged leptons or d -type quarks, in which case, the joint distribution is

$$\frac{1}{\sigma} \frac{d^2\sigma}{d(\cos\theta_+)d(\cos\theta_-)} = \frac{1 + \kappa \cos\theta_+ \cos\theta_-}{4}, \quad (2)$$

where θ_+ and θ_- are the angles of the daughters in the top rest frames with respect to a particular quantization axis, the optimal off-diagonal basis [33]. In this basis, the Standard Model predicts maximum correlation with $\kappa = 0.88$ at the Tevatron. $D\bar{O}$ analyzes their six dilepton events and obtains a likelihood as a function of κ which weakly favors the Standard Model ($\kappa = 0.88$) over no correlation ($\kappa = 0$) or anticorrelation ($\kappa = -1$, as would be expected for $t\bar{t}$ produced via an intermediate scalar). They quote a limit $\kappa > -0.25$ at 68% CL. With improved statistics, an observation of $t\bar{t}$ spin correlation could yield a lower limit on $|V_{tb}|$, independent of the assumption of three quark families [34].

References

1. T. Stelzer, Z. Sullivan, and S. Willenbrock, Phys. Rev. **D56**, 5919 (1997).
2. M. Jezabek and J.H. Kühn, Nucl. Phys. **B314**, 1 (1989).
3. I.I.Y. Bigi, Yu.L. Dokshitzer, V. Khoze, J.H. Kühn, P. Zerwas, Phys. Lett. **B181**, 157 (1986).
4. A. Czarnecki, K. Melnikov, Nucl. Phys. **B544**, 520 (1999); K.G. Chetyrkin, R. Harlander, T. Seidensticker, M. Steinhauser, Phys. Rev. **D60**, 114015 (1999).
5. F. Abe *et al.*, CDF Collab., Phys. Rev. Lett. **80**, 5720 (1998).
6. S. Abachi *et al.*, DØ Collab., Phys. Rev. Lett. **79**, 1203 (1997).
7. R. Partridge, 29th Intl. Conf. on High Energy Physics (ICHEP 98), Vancouver, Canada, 23-29 July, 1998, hep-ex/9811035.
8. B. Abbott *et al.*, DØ Collab., Phys. Rev. Lett. **83**, 1908 (1999); B. Abbott *et al.*, DØ Collab., Phys. Rev. **D60**, 012001 (1999).
9. P. Nason, S. Dawson, and R.K. Ellis, Nucl. Phys. **B303**, 607 (1988); W. Beenakker, H. Kuijf, W.L. van Neerven, and J. Smith, Phys. Rev. **D40**, 54 (1989).
10. E. Berger and H. Contopanagos, Phys. Lett. **B361**, 115 (1995).
11. E. Laenen, J. Smith, and W. van Neerven, Phys. Lett. **B321**, 254 (1994).
12. S. Catani, M. Mangano, P. Nason, and L. Trentadue, Phys. Lett. **B378**, 329 (1996); R. Bonciani, S. Catani, M.L. Mangano, P. Nason, Nucl. Phys. **B529**, 424 (1998); M.L. Mangano, hep-ph/9911256, to appear in Procs. of Intl. Europhysics Conf. on High Energy Physics (EPS-HEP 99), Tampere, Finland, 15-21 Jul 1999.
13. F. Abe *et al.*, CDF Collab., Phys. Rev. Lett. **80**, 2773 (1998).
14. F. Abe *et al.*, CDF Collab., Phys. Rev. Lett. **80**, 2779 (1998).
15. F. Abe *et al.*, CDF Collab., Phys. Rev. Lett. **79**, 1992 (1997).
16. F. Ptohos, Representing the CDF Collab., Procs. of Intl. Europhysics Conf. on High Energy Physics (EPS-HEP 99), Tampere, Finland, 15-21 July 1999, to be publ.
17. M. Beneke, I. Efthymiopoulos, M.L. Mangano, J. Womersley *et al.*, hep-ph/0003033, to appear in Proceedings of 1999 CERN Workshop on Standard Model Physics (and more) at the LHC, G. Altarelli and M.L. Mangano eds.
18. T. Affolder *et al.*, CDF Collab., FERMILAB-PUB-00-051, hep-ex/0003005.
19. P. Koehn, for the CDF Collab., FERMILAB-CONF-99-306-E, to be publ. in Procs. of Intl. Europhysics Conf. on High-Energy Physics (EPS-HEP 99), Tampere, Finland, 15-21 Jul 1999.
20. B. Abbott *et al.*, DØ Collab., Phys. Rev. **D58**, 052001 (1998); S. Abachi *et al.*, DØ Collab., Phys. Rev. Lett. **79**, 1197 (1997).
21. B. Abbott *et al.*, DØ Collab., Phys. Rev. **D60**, 052001 (1999); B. Abbott *et al.*, DØ Collab., Phys. Rev. Lett. **80**, 2063 (1998).
22. F. Abe *et al.*, CDF Collab., Phys. Rev. Lett. **82**, 271 (1999).
23. F. Abe *et al.*, CDF Collab., Phys. Rev. Lett. **80**, 2767 (1998).
24. L. Demortier *et al.*, The Top Averaging Group, For the CDF and DØ Collaborations, FERMILAB-TM-2084, September, 1999.
25. G. Chiarelli, Int. J. Mod. Phys. **A13**, 2883 (1998).
26. F. Abe *et al.*, CDF Collab., Phys. Rev. Lett. **79**, 357 (1997); B. Bevensee, for the CDF Collab., FERMILAB-CONF-98/155-E; T. Affolder *et al.*, CDF Collab., hep-ex/9912013.
27. B. Abbott *et al.*, Phys. Rev. Lett. **82**, 4975 (1999).
28. F. Abe *et al.*, CDF Collab., Phys. Rev. Lett. **80**, 2525 (1998).
29. P. Abreu *et al.*, DELPHI Collab., Phys. Lett. **B446**, 62 (1998); P. Abreu *et al.*, DELPHI Collab., DELPHI Note 99-85, submitted to the Intl. Europhysics Conference on High Energy Physics, Tampere, Finland, 15-21 July 1999.
30. V.F. Obraztsov, S.R. Slabospitsky, O.P. Yushchenko, Phys. Lett. **B426**, 393 (1998).
31. T. Affolder *et al.*, CDF Collab., Phys. Rev. Lett. **84**, 216 (2000).
32. B. Abbott *et al.*, DØ Collaboration, FERMILAB-PUB-00/046-E, submitted to Phys. Rev. Lett., hep-ex/0002058.
33. G. Mahlon and S. Parke, Phys. Rev. **D53**, 4886 (1996); G. Mahlon and S. Parke, Phys. Lett. **B411**, 173 (1997).
34. T. Stelzer and S. Willenbrock, Phys. Lett. **B374**, 169 (1996).

t-Quark Mass in $p\bar{p}$ Collisions

The t quark has been observed. Its mass is sufficiently high that decay is expected to occur before hadronization. OUR EVALUATION is an AVERAGE which incorporates correlations between systematic errors of the five different measurements. The average was done by a joint CDF/DØ working group and is reported in DEMORTIER 99, an FNAL Technical Memo. They report $174.3 \pm 3.2 \pm 4.0$ GeV, which yields "OUR EVALUATION" when statistical and systematic errors are combined.

For earlier search limits see the *Review of Particle Physics*, Phys. Rev. **D54**,1 (1996).

VALUE (GeV)	DOCUMENT ID	TECN	COMMENT
174.3 ± 5.1 OUR EVALUATION			
167.4 ± 10.3 ± 4.8	¹ ABE	99B CDF	dilepton
168.4 ± 12.3 ± 3.6	² ABBOTT	98D D0	dilepton
173.3 ± 5.6 ± 5.5	² ABBOTT	98F D0	lepton + jets
175.9 ± 4.8 ± 5.3	^{1,3} ABE	98E CDF	lepton + jets
186 ± 10 ± 5.7	^{1,4} ABE	97R CDF	6 or more jets
• • • We do not use the following data for averages, fits, limits, etc. • • •			
172.1 ± 5.2 ± 4.9	⁵ ABBOTT	99G D0	di-lepton, lepton+jets
176.0 ± 6.5	⁶ ABE	99B CDF	dilepton, lepton+jets, and all jets
161 ± 17 ± 10	¹ ABE	98F CDF	dilepton
172.1 ± 5.2 ± 4.9	⁷ BHAT	98b RVUE	dilepton and lepton+jets
173.8 ± 5.0	⁸ BHAT	98b RVUE	dilepton, lepton+jets, and all jets
173.3 ± 5.6 ± 6.2	² ABACHI	97E D0	lepton + jets
199 ⁺¹⁹ ₋₂₁ ± 22	ABACHI	95 D0	lepton + jets
176 ± 8 ± 10	ABE	95F CDF	lepton + b-jet
174 ± 10 ⁺¹³ ₋₁₂	ABE	94E CDF	lepton + b-jet

¹ Result is based on $109 \pm 7 \text{ pb}^{-1}$ of data at $\sqrt{s} = 1.8 \text{ TeV}$.

² Result is based on $125 \pm 7 \text{ pb}^{-1}$ of data at $\sqrt{s} = 1.8 \text{ TeV}$.

³ The updated systematic error is listed. See ABE 99b.

⁴ ABE 97R result is based on the first observation of all hadronic decays of $t\bar{t}$ pairs. Single b-quark tagging with jet-shape variable constraints was used to select signal enriched multi-jet events. The updated systematic error is listed. See ABE 99b.

⁵ ABBOTT 99G result is obtained by combining the D0 result m_t (GeV) = $168.4 \pm 12.3 \pm 3.6$ from 6 di-lepton events (see also ABBOTT 98D) and m_t (GeV) = $173.3 \pm 5.6 \pm 5.5$ from lepton+jet events (ABBOTT 98F).

Quark Particle Listings

t

⁶ ABE 99b result is obtained by combining the CDF results of m_t (GeV)=167.4 ± 10.3 ± 4.8 from 8 dilepton events, m_t (GeV)=175.9 ± 4.8 ± 5.3 from lepton+jet events (ABE 98e), and m_t (GeV)=186.0 ± 10.0 ± 5.7 from all-jet events (ABE 97R). The systematic errors in the latter two measurements are changed in this paper.
⁷ BHAT 98b result is obtained by combining the DØ results of m_t (GeV)=168.4 ± 12.3 ± 3.6 from 6 dilepton events and m_t (GeV)=173.3 ± 5.6 ± 5.5 from 77 lepton+jet events.
⁸ BHAT 98b result is obtained by combining the DØ results from dilepton and lepton+jet events, and the CDF results (ABE 99b) from dilepton, lepton+jet events, and all-jet events.

Indirect *t*-Quark Mass from Standard Model Electroweak Fit

"OUR EVALUATION" below is from the fit to electroweak data described in the "Electroweak Model and Constraints on New Physics" section of this Review. This fit result does not include direct measurements of m_t .

The RVUE values are based on the data described in the footnotes. RVUE's published before 1994 and superseded analyses are now omitted. For more complete listings of earlier results, see the 1994 edition (Physical Review D50 1173 (1994)).

VALUE (GeV)	DOCUMENT ID	TECN	COMMENT
168.2^{+9.6}_{-7.4}	OUR EVALUATION		
• • •	We do not use the following data for averages, fits, limits, etc. • • •		
171.2 ^{+3.7} _{-3.8}	⁹ FIELD	99 RVUE	Z parameters without <i>b</i> jet + Direct
172.0 ^{+5.8} _{-5.7}	¹⁰ DEBOER	97b RVUE	Electroweak + Direct
157 ⁺¹⁶ ₋₁₂	¹¹ ELLIS	96c RVUE	Z parameters, M_W , low energy
175 ± 11 ⁺¹⁷ ₋₁₉	¹² ERLER	95 RVUE	Z parameters, M_W , low energy
180 ± 9 ⁺¹⁹ ₋₂₁ ± 2.6 ± 4.8	¹³ MATSUMOTO	95 RVUE	
157 ⁺³⁶ ₋₄₈ ⁺¹⁹ ₋₂₀	¹⁴ ABREU	94 DLPH	Z parameters
158 ⁺³² ₋₄₀ ± 19	¹⁵ ACCIARRI	94 L3	Z parameters
132 ⁺⁴¹ ₋₄₈ ⁺²⁴ ₋₁₈	¹⁶ AKERS	94 OPAL	Z parameters
190 ⁺³⁹ ₋₄₈ ⁺¹² ₋₁₄	¹⁷ ARROYO	94 CCFR	ν_μ iron scattering
184 ⁺²⁵ ₋₂₉ ⁺¹⁷ ₋₁₈	¹⁸ BUSKULIC	94 ALEP	Z parameters
153 ± 15	¹⁹ ELLIS	94b RVUE	Electroweak
177 ± 9 ⁺¹⁶ ₋₂₀	²⁰ GURTU	94 RVUE	Electroweak
174 ⁺¹¹ ₋₁₃ ⁺¹⁷ ₋₁₈	²¹ MONTAGNA	94 RVUE	Electroweak
171 ± 12 ⁺¹⁵ ₋₂₁	²² NOVIKOV	94b RVUE	Electroweak
160 ⁺⁵⁰ ₋₆₀	²³ ALITTI	92b UA2	M_W , m_Z

⁹ FIELD 99 result is from the two-parameter fit with free m_t and m_H , yielding also $m_H = 47.2^{+29.8}_{-24.5}$ GeV. Only the lepton and charm-jet asymmetry data are used together with the direct measurement constraint $m_t = 173.8 \pm 5.0$ GeV, and $1/\alpha(m_Z) = 128.896$.
¹⁰ DEBOER 97b result is from the five-parameter fit which varies m_Z , m_t , m_H , α_s , and $\alpha(m_Z)$ under the constraints: $m_t = 175 \pm 6$ GeV, $1/\alpha(m_Z) = 128.896 \pm 0.09$. They found $m_H = 141^{+140}_{-77}$ GeV and $\alpha_s(m_Z) = 0.1197 \pm 0.0031$.
¹¹ ELLIS 96c result is a the two-parameter fit with free m_t and m_H , yielding also $m_H = 65^{+117}_{-37}$ GeV.
¹² ERLER 95 result is from fit with free m_t and $\alpha_s(m_Z)$, yielding $\alpha_s(m_Z) = 0.127(5)(2)$.
¹³ MATSUMOTO 95 result is from fit with free m_t to Z parameters, M_W , and low-energy neutral-current data. The second error is for $m_H = 300^{+700}_{-240}$ GeV, the third error is for $\alpha_s(m_Z) = 0.116 \pm 0.005$, the fourth error is for $\delta\alpha_{had} = 0.0283 \pm 0.0007$.
¹⁴ ABREU 94 value is for $\alpha_s(m_Z)$ constrained to 0.123 ± 0.005 . The second error corresponds to $m_H = 300^{+700}_{-240}$ GeV.
¹⁵ ACCIARRI 94 value is for $\alpha_s(m_Z)$ constrained to 0.124 ± 0.006 . The second error corresponds to $m_H = 300^{+700}_{-240}$ GeV.
¹⁶ AKERS 94 result is from fit with free α_s . The second error corresponds to $m_H = 300^{+700}_{-240}$ GeV. The 95%CL limit is $m_t < 210$ GeV.
¹⁷ ARROYO 94 measures the ratio of the neutral-current and charged-current deep inelastic scattering of ν_μ on an iron target. By assuming the SM electroweak correction, they obtain $1 - m_W^2/m_Z^2 = 0.2218 \pm 0.0059$, yielding the quoted m_t value. The second error corresponds to $m_H = 300^{+700}_{-240}$ GeV.
¹⁸ BUSKULIC 94 result is from fit with free α_s . The second error is from $m_H = 300^{+700}_{-240}$ GeV.
¹⁹ ELLIS 94b result is fit to electroweak data available in spring 1994, including the 1994 A_{LR} data from SLD. m_t and m_H are two free parameters of the fit for $\alpha_s(m_Z) = 0.118 \pm 0.007$ yielding m_t above, and $m_H = 35^{+70}_{-22}$ GeV. ELLIS 94b also give results for fits including constraints from CDF's direct measurement of m_t and CDF's and DØ 's production cross-section measurements. Fits excluding the A_{LR} data from SLD are also given.
²⁰ GURTU 94 result is from fit with free m_t and $\alpha_s(m_Z)$, yielding m_t above and $\alpha_s(m_Z) = 0.125 \pm 0.005^{+0.003}_{-0.001}$. The second errors correspond to $m_H = 300^{+700}_{-240}$ GeV. Uses LEP, M_W , νN , and SLD electroweak data available in spring 1994.
²¹ MONTAGNA 94 result is from fit with free m_t and $\alpha_s(m_Z)$, yielding m_t above and $\alpha_s(m_Z) = 0.124$. The second errors correspond to $m_H = 300^{+700}_{-240}$ GeV. Errors in

$\alpha(m_Z)$ and m_b are taken into account in the fit. Uses LEP, SLC, and M_W/M_Z data available in spring 1994.
²² NOVIKOV 94b result is from fit with free m_t and $\alpha_s(m_Z)$, yielding m_t above and $\alpha_s(m_Z) = 0.125 \pm 0.005 \pm 0.002$. The second errors correspond to $m_H = 300^{+700}_{-240}$ GeV. Uses LEP and CDF electroweak data available in spring 1994.
²³ ALITTI 92b assume $m_H = 100$ GeV. The 95%CL limit is $m_t < 250$ GeV for $m_H < 1$ TeV.

t DECAY MODES

Mode	Fraction (Γ_i/Γ)	Confidence level
Γ_1 <i>Wb</i>		
Γ_2 $\ell\nu_\ell$ anything	[a,b] (9.4 ± 2.4) %	
Γ_3 $\tau\nu_\tau b$		
Γ_4 γq ($q=u,c$)	[c] < 3.2 %	95%
$\Delta T = 1$ weak neutral current (<i>T1</i>) modes		
Γ_5 $Z q$ ($q=u,c$)	<i>T1</i> [d] < 33 %	95%

[a] ℓ means *e* or μ decay mode, not the sum over them.
 [b] Assumes lepton universality and *W*-decay acceptance.
 [c] This limit is for $\Gamma(t \rightarrow \gamma q)/\Gamma(t \rightarrow Wb)$.
 [d] This limit is for $\Gamma(t \rightarrow Z q)/\Gamma(t \rightarrow Wb)$.

t BRANCHING RATIOS

$\Gamma(\ell\nu_\ell \text{ anything})/\Gamma_{\text{total}}$				Γ_2/Γ
VALUE	DOCUMENT ID	TECN	COMMENT	
0.094 ± 0.024	²⁴ ABE	98x CDF		
²⁴ ℓ means <i>e</i> or μ decay mode, not the sum. Assumes lepton universality and <i>W</i> -decay acceptance.				
$\Gamma(\tau\nu_\tau b)/\Gamma_{\text{total}}$				Γ_3/Γ
VALUE	DOCUMENT ID	TECN	COMMENT	
• • •	We do not use the following data for averages, fits, limits, etc. • • •			
	²⁵ ABE	97v CDF	$\ell\tau + \text{jets}$	
²⁵ ABE 97v searched for $t\bar{t} \rightarrow (\ell\nu_\ell)(\tau\nu_\tau)b\bar{b}$ events in 109 pb ⁻¹ of $p\bar{p}$ collisions at $\sqrt{s} = 1.8$ TeV. They observed 4 candidate events where one expects ~ 1 signal and ~ 2 background events. Three of the four observed events have jets identified as <i>b</i> candidates.				
$\Gamma(\gamma q (q=u,c))/\Gamma_{\text{total}}$				Γ_4/Γ
VALUE	CL%	DOCUMENT ID	TECN	
< 0.032	95	²⁶ ABE	98G CDF	
²⁶ ABE 98G looked for $t\bar{t}$ events where one <i>t</i> decays into $q\gamma$ while the other decays into bW . The quoted bound is for $\Gamma(\gamma q)/\Gamma(Wb)$.				
$\Gamma(Z q (q=u,c))/\Gamma_{\text{total}}$				Γ_5/Γ
Test for $\Delta T = 1$ weak neutral current. Allowed by higher-order electroweak interaction.				
VALUE	CL%	DOCUMENT ID	TECN	
< 0.33	95	²⁷ ABE	98G CDF	
²⁷ ABE 98G looked for $t\bar{t}$ events where one <i>t</i> decays into three jets and the other decays into qZ with $Z \rightarrow \ell\ell$. The quoted bound is for $\Gamma(Z q)/\Gamma(Wb)$.				

t-Quark REFERENCES

ABBOTT 99G PR D60 052001	B. Abbott et al.	(DØ Collab.)
ABE 99B PRL 82 271	F. Abe et al.	(CDF Collab.)
Also 99G PRL 82 2808 (erratum)	F. Abe et al.	(CDF Collab.)
DEMORTIER 99 FNAL-TM-2084	L. Demortier et al.	(CDF/DØ Working Group)
FIELD 99 MPL A14 1815	J.H. Field	
ABBOTT 98D PRL 80 2063	B. Abbott et al.	(DØ Collab.)
ABBOTT 98F PR D58 052001	B. Abbott et al.	(DØ Collab.)
ABE 98E PRL 80 2767	F. Abe et al.	(CDF Collab.)
ABE 98F PRL 80 2779	F. Abe et al.	(CDF Collab.)
ABE 98G PRL 80 2525	F. Abe et al.	(CDF Collab.)
ABE 98X PRL 80 2773	F. Abe et al.	(CDF Collab.)
BHAT 98B JIMP A13 5113	P.C. Bhat, H.B. Prosper, S.S. Snyder	
ABACHI 97E PRL 79 1197	S. Abachi et al.	(DØ Collab.)
ABE 97R PRL 79 1992	F. Abe et al.	(CDF Collab.)
ABE 97V PRL 79 3585	F. Abe et al.	(CDF Collab.)
DEBOER 97B ZPHY C75 627	W. de Boer et al.	
ELLIS 96C PL B389 321	J. Ellis, G.L. Fogli, E. Lisi	(CERN, BARI)
ABACHI 95 PRL 74 2632	S. Abachi et al.	(DØ Collab.)
ABE 95F PRL 74 2626	F. Abe et al.	(CDF Collab.)
ERLER 95 PR D52 441	J. Erler, P. Langacker	(PENN)
MATSUMOTO 95 MPL A10 2553	S. Matsumoto	(KEK)
ABE 94E PR D50 2966	F. Abe et al.	(CDF Collab.)
Also 94F PRL 73 225	F. Abe et al.	(CDF Collab.)
ABREU 94 NP B418 403	P. Abreu et al.	(DELPHI Collab.)
ACCIARRI 94 ZPHY C62 551	M. Acciari et al.	(L3 Collab.)
AKERS 94 ZPHY C61 19	R. Akers et al.	(OPAL Collab.)
ARROYO 94 PRL 72 3452	C.G. Arroyo et al.	(COLU, CHIC, FNAL+)
BUSKULIC 94 ZPHY C62 539	D. Buskulic et al.	(ALEPH Collab.)
ELLIS 94B PL B333 118	J. Ellis, G.L. Fogli, E. Lisi	(CERN, BARI)
GURTU 94 MPL A9 3301	A. Gurttu	(TATA)
MONTAGNA 94 PL B335 484	G. Montagna et al.	(INFN, PAVI, CERN+)
NOVIKOV 94B MPL A9 2641	V.A. Novikov et al.	(GUEL, CERN, ITEP)
PDG 94 PR D50 1173	L. Montanet et al.	(CERN, LBL, BOST+)
ALITTI 92B PL B276 354	J. Alitti et al.	(UA2 Collab.)

See key on page 239

Quark Particle Listings

b' (Fourth Generation) Quark

b' (4th Generation) Quark, Searches for

MASS LIMITS for b' (4th Generation) Quark or Hadron in $p\bar{p}$ Collisions

VALUE (GeV)	CL%	DOCUMENT ID	TECN	COMMENT
>199	95	1 AFFOLDER	00 CDF	NC: $b' \rightarrow bZ$
>128	95	2 ABACHI	95F D0	$\ell\ell + \text{jets}, \ell + \text{jets}$
••• We do not use the following data for averages, fits, limits, etc. •••				
>148	95	3 ABE	98N CDF	NC: $b' \rightarrow bZ + \text{decay vertex}$
> 96	95	4 ABACHI	97D D0	NC: $b' \rightarrow b\gamma$
> 75	95	5 MUKHOPAD...	93 RVUE	NC: $b' \rightarrow b\ell\ell$
> 85	95	6 ABE	92 CDF	CC: $\ell\ell$
> 72	95	7 ABE	90B CDF	CC: $e + \mu$
> 54	95	8 AKESSON	90 UA2	CC: $e + \text{jets} + \text{missing } E_T$
> 43	95	9 ALBAJAR	90B UA1	CC: $\mu + \text{jets}$
> 34	95	10 ALBAJAR	88 UA1	CC: $e \text{ or } \mu + \text{jets}$

- AFFOLDER 00 looked for b' that decays in to $b+Z$. The signal searched for is $bbZZ$ events where one Z decays into e^+e^- or $\mu^+\mu^-$ and the other Z decays hadronically. The bound assumes $B(b' \rightarrow bZ) = 100\%$. Between 100 GeV and 199 GeV, the 95%CL upper bound on $\sigma(b' \rightarrow \bar{b}') \times B^2(b' \rightarrow bZ)$ is also given (see their Fig. 2).
- ABACHI 95F bound on the top-quark also applies to b' and t' quarks that decay predominantly into W . See FROGGATT 97.
- ABE 98N looked for $Z \rightarrow e^+e^-$ decays with displaced vertices. Quoted limit assumes $B(b' \rightarrow bZ)=1$ and $c\tau_{b'}=1$ cm. The limit is lower than 96 GeV ($m_Z+m_{b'}$) if $c\tau > 22$ cm or $c\tau < 0.009$ cm. See their Fig. 4.
- ABACHI 97D searched for b' that decays mainly via FCNC. They obtained 95%CL upper bounds on $B(b'\bar{b}' \rightarrow \gamma + 3 \text{ jets})$ and $B(b'\bar{b}' \rightarrow 2\gamma + 2 \text{ jets})$, which can be interpreted as the lower mass bound $m_{b'} > m_Z + m_b$.
- MUKHOPADHYAYA 93 analyze CDF dilepton data of ABE 92G in terms of a new quark decaying via flavor-changing neutral current. The above limit assumes $B(b' \rightarrow b\ell^+\ell^-)=1\%$. For an exotic quark decaying only via virtual Z [$B(b\ell^+\ell^-) = 3\%$], the limit is 85 GeV.
- ABE 92 dilepton analysis limit of >85 GeV at $CL=95\%$ also applies to b' quarks, as discussed in ABE 90B.
- ABE 90B exclude the region 28–72 GeV.
- AKESSON 90 searched for events having an electron with $p_T > 12$ GeV, missing momentum > 15 GeV, and a jet with $E_T > 10$ GeV, $|\eta| < 2.2$, and excluded $m_{b'}$ between 30 and 69 GeV.
- For the reduction of the limit due to non-charged-current decay modes, see Fig. 19 of ALBAJAR 90B.
- ALBAJAR 88 study events at $E_{cm} = 546$ and 630 GeV with a muon or isolated electron, accompanied by one or more jets and find agreement with Monte Carlo predictions for the production of charm and bottom, without the need for a new quark. The lower mass limit is obtained by using a conservative estimate for the $b'\bar{b}'$ production cross section and by assuming that it cannot be produced in W decays. The value quoted here is revised using the full $O(\alpha_s^3)$ cross section of ALTARELLI 88.

- | | | | | |
|-------|----|--------------|----------|--|
| >42.0 | 95 | 19 ABRAMS | 89C MRK2 | Any decay; event shape |
| >28.4 | 95 | 20,21 ADACHI | 89C TOPZ | $B(CC) = 1; \mu$ |
| >28.8 | 95 | 22 ENO | 89 AMY | $B(CC) \gtrsim 90\%; \mu, e$ |
| >27.2 | 95 | 22,23 ENO | 89 AMY | any decay; event shape |
| >29.0 | 95 | 22 ENO | 89 AMY | $B(b' \rightarrow b\gamma) \gtrsim 85\%;$
event shape |
| >24.4 | 95 | 24 IGARASHI | 88 AMY | μ, e |
| >23.8 | 95 | 25 SAGAWA | 88 AMY | event shape |
| >22.7 | 95 | 26 ADEVA | 86 MRKJ | μ |
| >21 | | 27 ALTHOFF | 84C TASS | R , event shape |
| >19 | | 28 ALTHOFF | 84I TASS | Aplanarity |
- DECAMP 90F looked for isolated charged particles, for isolated photons, and for four-jet final states. The modes $b' \rightarrow b\gamma$ for $B(b' \rightarrow b\gamma) > 65\%$ or $b' \rightarrow b\gamma$ for $B(b' \rightarrow b\gamma) > 5\%$ are excluded. Charged Higgs decay were not discussed.
 - ADRIANI 93G search for vector quarkonium states near Z and give limit on quarkonium- Z mixing parameter $\delta m^2 < (10-30)$ GeV² (95%CL) for the mass 88–94.5 GeV. Using Richardson potential, a 1S ($b'\bar{b}'$) state is excluded for the mass range 87.7–94.7 GeV. This range depends on the potential choice.
 - ABREU 90d assumed $m_{b'} < m_{b'} - 3$ GeV.
 - Superseded by ABREU 91F.
 - AKRAWY 90B search was restricted to data near the Z peak at $E_{cm} = 91.26$ GeV at LEP. The excluded region is between 23.6 and 41.4 GeV if no H^\pm decays exist. For charged Higgs decays the excluded regions are between $(m_{H^\pm} + 1.5 \text{ GeV})$ and 45.5 GeV.
 - AKRAWY 90J search for isolated photons in hadronic Z decay and derive $B(Z \rightarrow b'\bar{b}') \cdot B(b' \rightarrow \gamma X) / B(Z \rightarrow \text{hadrons}) < 2.2 \times 10^{-3}$. Mass limit assumes $B(b' \rightarrow \gamma X) > 10\%$.
 - ABE 89E search at $E_{cm} = 56-57$ GeV at TRISTAN for multihadron events with a spherical shape (using thrust and acoplanarity) or containing isolated leptons.
 - ABE 89G search was at $E_{cm} = 55-60.8$ GeV at TRISTAN.
 - If the photonic decay mode is large ($B(b' \rightarrow b\gamma) > 25\%$), the ABRAMS 89C limit is 45.4 GeV. The limit for for Higgs decay ($b' \rightarrow cH^\pm, H^\pm \rightarrow \bar{c}s$) is 45.2 GeV.
 - ADACHI 89C search was at $E_{cm} = 56.5-60.8$ GeV at TRISTAN using multi-hadron events accompanying muons.
 - ADACHI 89C also gives limits for any mixture of CC and $b\gamma$ decays.
 - ENO 89 search at $E_{cm} = 50-60.8$ at TRISTAN.
 - ENO 89 considers arbitrary mixture of the charged current, $b\gamma$, and $b\gamma$ decays.
 - IGARASHI 88 searches for leptons in low-thrust events and gives $\Delta R(b') < 0.26$ (95% CL) assuming charged current decay, which translates to $m_{b'} > 24.4$ GeV.
 - SAGAWA 88 set limit $\sigma(\text{top}) < 6.1$ pb at $CL=95\%$ for top-flavored hadron production from event shape analyses at $E_{cm} = 52$ GeV. By using the quark parton model cross-section formula near threshold, the above limit leads to lower mass bounds of 23.8 GeV for charge $-1/3$ quarks.
 - ADEVA 86 give 95%CL upper bound on an excess of the normalized cross section, ΔR , as a function of the minimum c.m. energy (see their figure 3). Production of a pair of $1/3$ charge quarks is excluded up to $E_{cm} = 45.4$ GeV.
 - ALTHOFF 84C narrow state search sets limit $\Gamma(e^+e^- \rightarrow b\text{hadrons}) < 2.4$ keV $CL = 95\%$ and heavy charge $1/3$ quark pair production $m > 21$ GeV, $CL = 95\%$.
 - ALTHOFF 84I exclude heavy quark pair production for $7 < m < 19$ GeV ($1/3$ charge) using aplanarity distributions ($CL = 95\%$).

MASS LIMITS for b' (4th Generation) Quark or Hadron in e^+e^- Collisions

Search for hadrons containing a fourth-generation $-1/3$ quark denoted b' .

The last column specifies the assumption for the decay mode (CC denotes the conventional charged-current decay) and the event signature which is looked for.

VALUE (GeV)	CL%	DOCUMENT ID	TECN	COMMENT
>46.0	95	11 DECAMP	90F ALEP	any decay
••• We do not use the following data for averages, fits, limits, etc. •••				
>44.7	95	12 ADRIANI	93G L3	Quarkonium
>45	95	ADRIANI	93M L3	$\Gamma(Z)$
none 19.4–28.2	95	ABREU	91F DLPH	$\Gamma(Z)$
>45.0	95	ABE	90D VNS	Any decay; event shape
	95	ABREU	90D DLPH	$B(CC) = 1$; event shape
>44.5	95	13 ABREU	90D DLPH	$b' \rightarrow cH^\pm, H^\pm \rightarrow \bar{c}s, \tau^- \nu$
>40.5	95	14 ABREU	90D DLPH	$\Gamma(Z \rightarrow \text{hadrons})$
>28.3	95	ADACHI	90 TOPZ	$B(\text{FCNC})=100\%$; isol. γ or 4 jets
>41.4	95	15 AKRAWY	90B OPAL	Any decay; acoplanarity
>45.2	95	15 AKRAWY	90B OPAL	$B(CC) = 1$; acoplanarity
>46	95	16 AKRAWY	90J OPAL	$b' \rightarrow \gamma + \text{any}$
>27.5	95	17 ABE	89E VNS	$B(CC) = 1; \mu, e$
none 11.4–27.3	95	18 ABE	89G VNS	$B(b' \rightarrow b\gamma) > 10\%$; isolated γ
>44.7	95	19 ABRAMS	89C MRK2	$B(CC) = 100\%$; isol. track
>42.7	95	19 ABRAMS	89C MRK2	$B(b\gamma) = 100\%$; event shape

REFERENCES FOR Searches for (Fourth Generation) b' Quark

AFFOLDER 00	PRL 84 835	A. Affolder et al.	(CDF Collab.)
ABE 98N	PR D58 051102	F. ABE et al.	(CDF Collab.)
ABACHI 97D	PRL 78 3818	S. Abachi et al.	(D0 Collab.)
FROGGATT 97	ZPHY C73 333	C.D. Froggatt, D.J. Smith, H.B. Nielsen	(GLAS+)
ABACHI 95F	PR D52 4877	S. Abachi et al.	(D0 Collab.)
ADRIANI 93G	PL B313 326	O. Adriani et al.	(L3 Collab.)
ADRIANI 93M	PRPL 236 1	O. Adriani et al.	(L3 Collab.)
MUKHOPAD... 93	PR D48 2105	B. Mukhopadhyaya, D.P. Roy	(TATA)
ABE 92	PRL 68 447	F. ABE et al.	(CDF Collab.)
Also 92G	PR D45 3921	F. ABE et al.	(CDF Collab.)
ABE 92G	PR D45 3921	F. ABE et al.	(CDF Collab.)
ABREU 91F	NP B367 511	P. Abreu et al.	(DELPHI Collab.)
ABE 90B	PRL 64 147	F. ABE et al.	(CDF Collab.)
ABE 90D	PL B234 382	K. ABE et al.	(VENUS Collab.)
ABREU 90D	PL B242 536	P. Abreu et al.	(DELPHI Collab.)
ADACHI 90	PL B234 197	I. Adachi et al.	(TOPAZ Collab.)
AKESSON 90	ZPHY C46 179	T. Akesson et al.	(UA2 Collab.)
AKRAWY 90B	PL B236 364	M.Z. Akrawy et al.	(OPAL Collab.)
AKRAWY 90J	PL B246 285	M.Z. Akrawy et al.	(OPAL Collab.)
ALBAJAR 90B	ZPHY C48 1	C. Albajar et al.	(UA1 Collab.)
DECAMP 90F	PL B236 511	D. Decamp et al.	(ALEPH Collab.)
ABE 89E	PR D39 3524	K. ABE et al.	(VENUS Collab.)
ABE 89G	PRL 63 1776	K. ABE et al.	(VENUS Collab.)
ABRAMS 89C	PRL 63 2447	G.S. Abrams et al.	(Mark II Collab.)
ADACHI 89C	PL B229 427	I. Adachi et al.	(TOPAZ Collab.)
ENO 89	PRL 63 1910	S. Eno et al.	(AMY Collab.)
ALBAJAR 88	ZPHY C37 505	C. Albajar et al.	(UA1 Collab.)
ALTARELLI 88	NP B308 724	G. Altarelli et al.	(CERN, ROMA, ETH)
IGARASHI 88	PRL 60 2359	S. Igarashi et al.	(AMY Collab.)
SAGAWA 88	PRL 60 93	H. Sagawa et al.	(AMY Collab.)
ADEVA 86	PR D34 681	B. Adeva et al.	(Mark-J Collab.)
ALTHOFF 84C	PL 138B 441	M. Althoff et al.	(TASSO Collab.)
ALTHOFF 84I	ZPHY C22 307	M. Althoff et al.	(TASSO Collab.)

Quark Particle Listings

Free Quark Searches

Free Quark Searches

FREE QUARK SEARCHES

The basis for much of the theory of particle scattering and hadron spectroscopy is the construction of the hadrons from a set of fractionally charged constituents (quarks). A central but unproven hypothesis of this theory, Quantum Chromodynamics, is that quarks cannot be observed as free particles but are confined to mesons and baryons.

Experiments show that it is at best difficult to "unglue" quarks. Accelerator searches at increasing energies have produced no evidence for free quarks, while only a few cosmic-ray and matter searches have produced uncorroborated events.

This compilation is only a guide to the literature, since the quoted experimental limits are often only indicative. Reviews can be found in Refs. 1-3.

References

1. P.F. Smith, Ann. Rev. Nucl. and Part. Sci. **39**, 73 (1989).
2. L. Lyons, Phys. Reports **129**, 225 (1985).
3. M. Marinelli and G. Morpurgo, Phys. Reports **85**, 161 (1982).

Quark Production Cross Section — Accelerator Searches

X-SECT (cm ²)	CHG (e/3)	MASS (GeV)	ENERGY (GeV)	BEAM	EVTS	DOCUMENT ID	TECN
<1.3E-36	±2	45-84	130-172	e ⁺ e ⁻	0	ABREU 97D DLPH	
<2.E-35	+2	250	1800	p \bar{p}	0	¹ ABE 92J CDF	
<1.E-35	+4	250	1800	p \bar{p}	0	¹ ABE 92J CDF	
<3.8E-28		14.5A	²⁸ Si-Pb		0	² HE 91 PLAS	
<3.2E-28		14.5A	²⁸ Si-Cu		0	² HE 91 PLAS	
<1.E-40	±1,2	<10		p, $\nu, \bar{\nu}$	0	BERGSMAN 84B CHRM	
<1.E-36	±1,2	<9	200	μ	0	AUBERT 83C SPEC	
<2.E-10	±2,4	1-3	200	p	0	³ BUSSIÈRE 80 CNTR	
<5.E-38	+1,2	>5	300	p	0	^{4,5} STEVENSON 79 CNTR	
<1.E-33	±1	<20	52	pp	0	BASILE 78 SPEC	
<9.E-39	±1,2	<6	400	p	0	⁴ ANTREASYAN 77 SPEC	
<8.E-35	+1,2	<20	52	pp	0	⁶ FABJAN 75 CNTR	
<5.E-38	-1,2	4-9	200	p	0	NASH 74 CNTR	
<1.E-32	+2,4	4-24	52	pp	0	ALPER 73 SPEC	
<5.E-31	+1,2,4	<12	300	p	0	LEIPUNER 73 CNTR	
<6.E-34	±1,2	<13	52	pp	0	BOTT 72 CNTR	
<1.E-36	-4	4	70	p	0	ANTIPOV 71 CNTR	
<1.E-35	±1,2	2	28	p	0	⁷ ALLABY 69B CNTR	
<4.E-37	-2	<5	70	p	0	³ ANTIPOV 69 CNTR	
<3.E-37	-1,2	2-5	70	p	0	⁷ ANTIPOV 69B CNTR	
<1.E-35	+1,2	<7	30	p	0	DORFAN 65 CNTR	
<2.E-35	-2	<2.5-5	30	p	0	⁸ FRANZINI 65B CNTR	
<5.E-35	+1,2	<2.2	21	p	0	BINGHAM 64 HLBC	
<1.E-32	+1,2	<4.0	28	p	0	BLUM 64 HBC	
<1.E-35	+1,2	<2.5	31	p	0	⁸ HAGOPIAN 64 HBC	
<1.E-34	+1	<2	28	p	0	LEIPUNER 64 CNTR	
<1.E-33	+1,2	<2.4	24	p	0	MORRISON 64 HBC	

¹ ABE 92J flux limits decrease as the mass increases from 50 to 500 GeV.

² HE 91 limits are for charges of the form $N \pm 1/3$ from 23/3 to 38/3.

³ Hadronic or leptonic quarks.

⁴ Cross section cm²/GeV².

⁵ 3×10^{-5} < lifetime < 1×10^{-3} s.

⁶ Includes BOTT 72 results.

⁷ Assumes isotropic cm production.

⁸ Cross section inferred from flux.

Quark Differential Production Cross Section — Accelerator Searches

X-SECT (cm ² sr ⁻¹ GeV ⁻¹)	CHG (e/3)	MASS (GeV)	ENERGY (GeV)	BEAM	EVTS	DOCUMENT ID	TECN
<4.E-36	-2,4	1.5-6	70	p	0	BALDIN 76 CNTR	
<2.E-33	±4	5-20	52	pp	0	ALBROW 75 SPEC	
<5.E-34	<7	7-15	44	pp	0	JOVANOV... 75 CNTR	
<5.E-35			20	γ	0	⁹ GALIK 74 CNTR	
<9.E-35	-1,2		200	p	0	NASH 74 CNTR	
<4.E-36	-4	2.3-2.7	70	p	0	ANTIPOV 71 CNTR	
<3.E-35	±1,2	<2.7	27	p	0	ALLABY 69B CNTR	
<7.E-38	-1,2	<2.5	70	p	0	ANTIPOV 69B CNTR	

⁹ Cross section in cm²/sr/equivalent quanta.

Quark Flux — Accelerator Searches

The definition of FLUX depends on the experiment

- (a) is the ratio of measured free quarks to predicted free quarks if there is no "confinement."
- (b) is the probability of fractional charge on nuclear fragments. Energy is in GeV/nucleon.
- (c) is the 90%CL upper limit on fractionally-charged particles produced per interaction.
- (d) is quarks per collision.
- (e) is inclusive quark-production cross-section ratio to $\sigma(e^+e^- \rightarrow \mu^+\mu^-)$.
- (f) is quark flux per charged particle.
- (g) is the flux per ν -event.
- (h) is quark yield per π^- yield.
- (i) is 2-body exclusive quark-production cross-section ratio to $\sigma(e^+e^- \rightarrow \mu^+\mu^-)$.

FLUX	CHG (e/3)	MASS (GeV)	ENERGY (GeV)	BEAM	EVTS	DOCUMENT ID	TECN
<1.6E-3	b	see note	200	³² S-Pb	0	¹⁰ HUENTRUP 96 PLAS	
<6.2E-4	b	see note	10.6	³² S-Pb	0	¹⁰ HUENTRUP 96 PLAS	
<0.94E-4	e	±2	2-30	88-94 e ⁺ e ⁻	0	AKERS 95R OPAL	
<1.7E-4	e	±2	30-40	88-94 e ⁺ e ⁻	0	AKERS 95R OPAL	
<3.6E-4	e	±4	5-30	88-94 e ⁺ e ⁻	0	AKERS 95R OPAL	
<1.9E-4	e	±4	30-45	88-94 e ⁺ e ⁻	0	AKERS 95R OPAL	
<2.E-3	e	+1	5-40	88-94 e ⁺ e ⁻	0	¹¹ BUSKULIC 93C ALEP	
<6.E-4	e	+2	5-30	88-94 e ⁺ e ⁻	0	¹¹ BUSKULIC 93C ALEP	
<1.2E-3	e	+4	15-40	88-94 e ⁺ e ⁻	0	¹¹ BUSKULIC 93C ALEP	
<3.6E-4	i	+4	5.0-10.2	88-94 e ⁺ e ⁻	0	BUSKULIC 93C ALEP	
<3.6E-4	i	+4	16.5-26.0	88-94 e ⁺ e ⁻	0	BUSKULIC 93C ALEP	
<6.9E-4	i	+4	26.0-33.3	88-94 e ⁺ e ⁻	0	BUSKULIC 93C ALEP	
<9.1E-4	i	+4	33.3-38.6	88-94 e ⁺ e ⁻	0	BUSKULIC 93C ALEP	
<1.1E-3	i	+4	38.6-44.9	88-94 e ⁺ e ⁻	0	BUSKULIC 93C ALEP	
<1.6E-4	b	see note	see note		0	¹² CECCHINI 93 PLAS	
	b	4,5,7,8	2.1A	¹⁶ O	0,2,0,6	¹³ GHOSH 92 EMUL	
<6.4E-5	g	1		$\nu, \bar{\nu}$	1	¹⁴ BASILE 91 CNTR	
<3.7E-5	g	2		$\nu, \bar{\nu}$	0	¹⁴ BASILE 91 CNTR	
<3.9E-5	g	1		$\nu, \bar{\nu}$	1	¹⁵ BASILE 91 CNTR	
<2.8E-5	g	2		$\nu, \bar{\nu}$	0	¹⁵ BASILE 91 CNTR	
<1.9E-4	c		14.5A	²⁸ Si-Pb	0	¹⁶ HE 91 PLAS	
<3.9E-4	c		14.5A	²⁸ Si-Cu	0	¹⁶ HE 91 PLAS	
<1.E-9	c	±1,2,4	14.5A	¹⁶ O-Ar	0	MATIS 91 MDRP	
<5.1E-10	c	±1,2,4	14.5A	¹⁶ O-Hg	0	MATIS 91 MDRP	
<8.1E-9	c	±1,2,4	14.5A	Si-Hg	0	MATIS 91 MDRP	
<1.7E-6	c	±1,2,4	60A	¹⁶ O-Hg	0	MATIS 91 MDRP	
<3.5E-7	c	±1,2,4	200A	¹⁶ O-Hg	0	MATIS 91 MDRP	
<1.3E-6	c	±1,2,4	200A	S-Hg	0	MATIS 91 MDRP	
<5E-2	e	2	19-27	52-60 e ⁺ e ⁻	0	ADACHI 90C TOPZ	
<5E-2	e	4	<24	52-60 e ⁺ e ⁻	0	ADACHI 90C TOPZ	
<1.E-4	e	+2	<3.5	10 e ⁺ e ⁻	0	BOWCOCK 89B CLEO	
<1.E-6	d	±1,2	60	¹⁶ O-Hg	0	CALLOWAY 89 MDRP	
<3.5E-7	d	±1,2	200	¹⁶ O-Hg	0	CALLOWAY 89 MDRP	
<1.3E-6	d	±1,2	200	S-Hg	0	CALLOWAY 89 MDRP	
<1.2E-10	d	±1	1	800 p-Hg	0	MATIS 89 MDRP	
<1.1E-10	d	±2	1	800 p-Hg	0	MATIS 89 MDRP	
<1.2E-10	d	±1	1	800 p-N ₂	0	MATIS 89 MDRP	
<7.7E-11	d	±2	1	800 p-N ₂	0	MATIS 89 MDRP	
<6.E-9	h	-5	0.9-2.3	12 p	0	NAKAMURA 89 SPEC	
<5.E-5	g	1,2	<0.5	$\nu, \bar{\nu}, d$	0	ALLASIA 88 BEBC	
<3.E-4	b	See note	14.5	¹⁶ O-Pb	0	¹⁷ HOFFMANN 88 PLAS	
<2.E-4	b	See note	200	¹⁶ O-Pb	0	¹⁸ HOFFMANN 88 PLAS	

Quark Particle Listings

Free Quark Searches

Table with 5 columns: Energy/Condition, Fractional Charge, Search Method, Author, and Reference Number. Rows include searches for water+/atom beam, levitated graphite, water+/uv spec, etc.

- 31 Also set limits for Q = +/- e/6.
32 Note that in PHILLIPS 88 these authors report a subtle magnetic effect which could account for the apparent fractional charges.
33 Limit inferred by JONES 77b.

REFERENCES FOR Free Quark Searches

Main reference table with 5 columns: Author, Reference Number, Search Method, Author, and Reference Number. Lists various experimental searches and collaborations.

Continuation of the reference table from the previous section, listing authors like Boyd, Lund, Puff, etc.

Continuation of the reference table, listing authors like Baldin, Briatore, Stevens, etc.

OTHER RELATED PAPERS

Table listing other related papers with 3 columns: Author, Reference Number, and Author.

LIGHT UNFLAVORED MESONS ($S = C = B = 0$)

For $l = 1$ (π, b, ρ, a): $u\bar{d}, (u\bar{u}-d\bar{d})/\sqrt{2}, d\bar{u}$;
for $l = 0$ ($\eta, \eta', h, h', \omega, \phi, f, f'$): $c_1(u\bar{u} + d\bar{d}) + c_2(s\bar{s})$

PSUEDOSCALAR-MESON DECAY CONSTANTS

Revised April 2000 by M. Suzuki (LBNL).

Charged mesons

The decay constant f_P for a charged pseudoscalar meson P is defined by

$$\langle 0 | A_\mu(0) | P(\mathbf{q}) \rangle = i f_P q_\mu, \quad (1)$$

where A_μ is the axial-vector part of the charged weak current after a Cabibbo-Kobayashi-Maskawa mixing-matrix element $V_{qq'}$ has been removed. The state vector is normalized by $\langle P(\mathbf{q}) | P(\mathbf{q}') \rangle = (2\pi)^3 2E_q \delta(\mathbf{q} - \mathbf{q}')$, and its phase is chosen to make f_P real and positive. Note, however, that in many theoretical papers our $f_P/\sqrt{2}$ is denoted by f_P .

In determining f_P experimentally, radiative corrections must be taken into account. Since the photon-loop correction introduces an infrared divergence that is canceled by soft-photon emission, we can determine f_P only from the combined rate for $P^\pm \rightarrow \ell^\pm \nu_\ell$ and $P^\pm \rightarrow \ell^\pm \nu_\ell \gamma$. This rate is given by

$$\Gamma(P \rightarrow \ell \nu_\ell + \ell \nu_\ell \gamma) = \frac{G_F^2 |V_{qq'}|^2}{8\pi} f_P^2 m_\ell^2 m_P \left(1 - \frac{m_\ell^2}{m_P^2} \right) [1 + \mathcal{O}(\alpha)]. \quad (2)$$

Here m_ℓ and m_P are the masses of the lepton and meson. Radiative corrections include inner bremsstrahlung, which is independent of the structure of the meson [1-3], and also a structure-dependent term [4,5]. After radiative corrections are made, there are ambiguities in extracting f_P from experimental measurements. In fact, the definition of f_P is no longer unique.

It is desirable to define f_P such that it depends only on the properties of the pseudoscalar meson, not on the final decay products. The short-distance corrections to the fundamental electroweak constants like $G_F |V_{qq'}|$ should be separated out. Following Marciano and Sirlin [6], we define f_P with the following form for the $\mathcal{O}(\alpha)$ corrections:

$$1 + \mathcal{O}(\alpha) = \left[1 + \frac{2\alpha}{\pi} \ln\left(\frac{m_Z}{m_\rho}\right) \right] \left[1 + \frac{\alpha}{\pi} F(x) \right] \times \left\{ 1 - \frac{\alpha}{\pi} \left[\frac{3}{2} \ln\left(\frac{m_\rho}{m_P}\right) + C_1 + C_2 \frac{m_\ell^2}{m_\rho^2} \ln\left(\frac{m_\rho}{m_\ell}\right) + C_3 \frac{m_\ell^2}{m_\rho^2} + \dots \right] \right\}, \quad (3)$$

where m_ρ and m_Z are the masses of the ρ meson and Z boson. Here

$$F(x) = 3 \ln x + \frac{13 - 19x^2}{8(1-x^2)} - \frac{8 - 5x^2}{2(1-x^2)^2} x^2 \ln x - 2 \left(\frac{1+x^2}{1-x^2} \ln x + 1 \right) \ln(1-x^2) + 2 \left(\frac{1+x^2}{1-x^2} \right) L(1-x^2),$$

with

$$x \equiv m_\ell/m_P, \quad L(z) \equiv \int_0^z \frac{\ln(1-t)}{t} dt. \quad (4)$$

The first bracket in the expression for $1 + \mathcal{O}(\alpha)$ is the short-distance electroweak correction. A quarter of $(2\alpha/\pi) \ln(m_Z/m_\rho)$ is subject to the QCD correction $(1 - \alpha_s/\pi)$, which leads to a reduction of the total short-distance correction of 0.00033 from the electroweak contribution alone [6]. The second bracket together with the term $-(3\alpha/2\pi) \ln(m_\rho/m_P)$ in the third bracket corresponds to the radiative corrections to the point-like pion decay ($\Lambda_{\text{cutoff}} \approx m_\rho$) [2]. The rest of the corrections in the third bracket are expanded in powers of m_ℓ/m_ρ . The expansion coefficients C_1, C_2 , and C_3 depend on the hadronic structure of the pseudoscalar meson and in most cases cannot be computed accurately. In particular, C_1 absorbs the uncertainty in the matching energy scale between short- and long-distance strong interactions and thus is the main source of uncertainty in determining f_{π^+} accurately.

With the experimental value for the decay $\pi^+ \rightarrow \mu^+ \nu_\mu + \mu^+ \nu_\mu \gamma$, one obtains

$$f_{\pi^+} = 130.7 \pm 0.1 \pm 0.36 \text{ MeV}, \quad (5)$$

where the first error comes from the experimental uncertainty on $|V_{ud}|$ and the second comes from the uncertainty on C_1 ($= 0 \pm 0.24$) [6]. Similarly, one obtains from the decay $K^+ \rightarrow \mu^+ \nu_\mu + \mu^+ \nu_\mu \gamma$ the decay constant

$$f_{K^+} = 159.8 \pm 1.4 \pm 0.44 \text{ MeV}, \quad (6)$$

where the first error is due to the uncertainty on $|V_{us}|$.

For the heavy pseudoscalar mesons, uncertainties in the experimental values for the decay rates are much larger than the radiative corrections. For the D^+ , a value (as opposed to an upper limit) has been obtained for the first time:

$$f_{D^+} = 300_{-150-40}^{+180+80} \text{ MeV}, \quad (7)$$

but it is based on only one $D^+ \rightarrow \mu^+ \nu_\mu$ event [7]. For the D_s^+ , the decay constant has been obtained from both the $D_s^+ \rightarrow \mu^+ \nu_\mu$ and the $D_s^+ \rightarrow \tau^+ \nu_\tau$ branching fractions. There are altogether six reported values ranging from about 200 to 450 MeV, but the errors are getting smaller; the best and most recent value, from 182 $D_s^+ \rightarrow \mu^+ \nu_\mu$ events, gives [8]

$$f_{D_s^+} = 280 \pm 19 \pm 28 \pm 34 \text{ MeV}. \quad (8)$$

(See the measurements of the $D_s^+ \rightarrow \ell^+ \nu_\ell$ modes in the Particle Listings for the numbers quoted by individual experiments.)

There have been many attempts to extract f_P from spectroscopy and nonleptonic decays using theoretical models. Since it is difficult to estimate uncertainties for them, we have listed here only values of decay constants that are obtained directly from the observation of $P^\pm \rightarrow \ell^\pm \nu_\ell$.

Meson Particle Listings

 π^\pm **Light neutral mesons**

The decay constants for the light neutral pseudoscalar mesons π^0 , η , and η' are defined by

$$\sqrt{2} \langle 0 | A_\mu^a(0) | P(q) \rangle = i f_P^a q_\mu \quad (9)$$

where A_μ^a is a neutral axial-vector current [9,10]. Restricting ourselves to the three light flavors, the index $a = 0, 3, 8$ refers to the usual set of Gell-Mann matrices, including the flavor singlet. In case of exact isospin symmetry (which is for most applications a very good approximation) we have only one decay constant for the π^0 meson ($f_{\pi^0}^3 \equiv f_{\pi^0}$) and two decay constants each for η and η' (f_η^8, f_η^0 , and $f_{\eta'}^8, f_{\eta'}^0$).

In the limit of $m_P \rightarrow 0$, the Adler-Bell-Jackiw anomaly [11,12] determines the matrix elements of the two-photon decay $P \rightarrow \gamma\gamma$ through the decay constants f_P^a . In the case of f_{π^0} , the extrapolation to $m_\pi \neq 0$ gives only a tiny effect, and the value of f_{π^0} can be extracted from the $\pi^0 \rightarrow \gamma\gamma$ decay width. The experimental uncertainty in the π^0 lifetime dominates in the uncertainty of f_{π^0} :

$$f_{\pi^0} = 130 \pm 5 \text{ MeV} . \quad (10)$$

This value is compatible with f_{π^\pm} , as it is expected from isospin symmetry.

The four decay constants of the η - η' system cannot be extracted from the two-photon decay widths alone. Also, the extrapolation to $m_{\eta(\eta')} \neq 0$ may give a larger effect here, and therefore the dominance of the Adler-Bell-Jackiw anomaly is perhaps questionable. Thus, an assessment of the values of the η and η' decay constants requires additional theoretical and phenomenological input about flavor symmetry breaking and η - η' mixing; see Ref. 13 for a review. Most analyses find similar values for the octet decay constants: $f_\eta^8 \simeq 1.2 f_\pi$ and $f_{\eta'}^8 \simeq -0.45 f_\pi$. The situation concerning the singlet decay constants, f_P^0 , is less clear.

References

1. S. Berman, Phys. Rev. Lett. **1**, 468 (1958).
2. T. Kinoshita, Phys. Rev. Lett. **2**, 477 (1959).
3. A. Sirlin, Phys. Rev. **D5**, 436 (1972).
4. M.V. Terent'ev, Yad. Fiz. **18**, 870 (1973) [Sov. J. Nucl. Phys. **18**, 449 (1974)].
5. T. Goldman and W.J. Wilson, Phys. Rev. **D15**, 709 (1977).
6. W.J. Marciano and A. Sirlin, Phys. Rev. Lett. **71**, 3629 (1993).
7. J.Z. Bai *et al.*, Phys. Lett. **B429**, 188 (1998).
8. M. Chada *et al.*, Phys. Rev. **D58**, 032002 (1998).
9. J. Gasser and H. Leutwyler, Nucl. Phys. **B250**, 465 (1985).
10. H. Leutwyler, Nucl. Phys. Proc. Suppl. **64**, 223 (1998).
11. S.L. Adler, Phys. Rev. **177**, 2426 (1969).
12. J.S. Bell and R. Jackiw, Nuovo Cimento **60A**, 46 (1969).
13. T. Feldmann, Int. J. Mod. Phys. **A15**, 159 (2000).

 π^\pm

$$J^G(J^P) = 1^-(0^-)$$

We have omitted some results that have been superseded by later experiments. The omitted results may be found in our 1988 edition Physics Letters **B204** (1988).

 π^\pm MASS

The most accurate charged pion mass measurements are based upon x-ray wavelength measurements for transitions in π^- -mesonic atoms. The observed line is the blend of three components, corresponding to different K-shell occupancies. JECKELMANN 94 revisits the occupancy question, with the conclusion that two sets of occupancy ratios, resulting in two different pion masses (Solutions A and B), are equally probable. We choose the higher Solution B since only this solution is consistent with a positive mass-squared for the muon neutrino, given the precise muon momentum measurements now available (DAUM 91, ASSAMAGAN 94, and ASSAMAGAN 96) for the decay of pions at rest. Earlier mass determinations with pi-mesonic atoms may have used incorrect K-shell screening corrections.

Measurements with an error of > 0.005 MeV have been omitted from this listing.

VALUE (MeV)	DOCUMENT ID	TECN	CHG	COMMENT
139.57018 ± 0.00035 OUR FIT				Error includes scale factor of 1.2.
139.57018 ± 0.00035 OUR AVERAGE				Error includes scale factor of 1.2.
139.57071 ± 0.00053	¹ LENZ	98	CNTR	- pionic N2-atoms gas target
139.56995 ± 0.00035	² JECKELMANN 94	CNTR	-	π^- atom, Soln. B
• • • We do not use the following data for averages, fits, limits, etc. • • •				
139.57022 ± 0.00014	³ ASSAMAGAN 96	SPEC	+	$\pi^+ \rightarrow \mu^+ \nu_\mu$
139.56782 ± 0.00037	⁴ JECKELMANN 94	CNTR	-	π^- atom, Soln. A
139.56996 ± 0.00067	⁵ DAUM 91	SPEC	+	$\pi^+ \rightarrow \mu^+ \nu$
139.56752 ± 0.00037	⁶ JECKELMANN 86B	CNTR	-	Mesonic atoms
139.5704 ± 0.0011	⁵ ABELA 84	SPEC	+	See DAUM 91
139.5664 ± 0.0009	⁷ LU 80	CNTR	-	Mesonic atoms
139.5686 ± 0.0020	⁸ CARTER 76	CNTR	-	Mesonic atoms
139.5660 ± 0.0024	^{7,8} MARUSHEN... 76	CNTR	-	Mesonic atoms

¹ LENZ 98 result does not suffer K-electron configuration uncertainties as does JECKELMANN 94.

² JECKELMANN 94 Solution B (dominant 2-electron K-shell occupancy), chosen for consistency with positive $m_{\nu_\mu}^2$.

³ ASSAMAGAN 96 measures the μ^+ momentum p_μ in $\pi^+ \rightarrow \mu^+ \nu_\mu$ decay at rest to be 29.79200 ± 0.00011 MeV/c. Combined with the μ^+ mass and the assumption $m_{\nu_\mu} = 0$, this gives the π^+ mass above; if $m_{\nu_\mu} > 0$, m_{π^+} given above is a lower limit. Combined instead with m_μ and (assuming *CPT*) the π^- mass of JECKELMANN 94, p_μ gives an upper limit on m_{ν_μ} (see the ν_μ).

⁴ JECKELMANN 94 Solution A (small 2-electron K-shell occupancy) in combination with either the DAUM 91 or ASSAMAGAN 94 pion decay muon momentum measurement yields a significantly negative $m_{\nu_\mu}^2$. It is accordingly not used in our fits.

⁵ The DAUM 91 value includes the ABELA 84 result. The value is based on a measurement of the μ^+ momentum for π^+ decay at rest, $p_\mu = 29.79179 \pm 0.00053$ MeV, uses $m_\mu = 105.658389 \pm 0.000034$ MeV, and assumes that $m_{\nu_\mu} = 0$. The last assumption means that in fact the value is a lower limit.

⁶ JECKELMANN 86B gives $m_\pi/m_e = 273.12677(71)$. We use $m_e = 0.51099906(15)$ MeV from COHEN 87. The authors note that two solutions for the probability distribution of K-shell occupancy fit equally well, and use other data to choose the lower of the two possible π^\pm masses.

⁷ These values are scaled with a new wavelength-energy conversion factor $\lambda A = 1.23984244(37) \times 10^{-6}$ eV m from COHEN 87. The LU 80 screening correction relies upon a theoretical calculation of inner-shell refilling rates.

⁸ This MARUSHENKO 76 value used at the authors' request to use the accepted set of calibration γ energies. Error increased from 0.0017 MeV to include QED calculation error of 0.0017 MeV (12 ppm).

 $m_{\pi^+} - m_{\mu^+}$

Measurements with an error > 0.05 MeV have been omitted from this listing.

VALUE (MeV)	EVTS	DOCUMENT ID	TECN	CHG	COMMENT
• • • We do not use the following data for averages, fits, limits, etc. • • •					
33.91157 ± 0.00067		⁹ DAUM 91	SPEC	+	$\pi^+ \rightarrow \mu^+ \nu$
33.9111 ± 0.0011		ABELA 84	SPEC	+	See DAUM 91
33.925 ± 0.025		BOOTH 70	CNTR	+	Magnetic spect.
33.881 ± 0.035	145	HYMAN 67	HEBC	+	K^- He

⁹ The DAUM 91 value assumes that $m_{\nu_\mu} = 0$ and uses our $m_\mu = 105.658389 \pm 0.000034$ MeV.

$$(m_{\pi^+} - m_{\pi^-}) / m_{\text{average}}$$

A test of CPT invariance.

VALUE (units 10^{-4})	DOCUMENT ID	TECN
2 ± 5	AYRES	71 CNTR

π^\pm MEAN LIFE

Measurements with an error > 0.02×10^{-8} s have been omitted.

VALUE (10^{-8} s)	DOCUMENT ID	TECN	CHG	COMMENT
2.6033 ± 0.0005 OUR AVERAGE	Error includes scale factor of 1.2.			
2.60361 ± 0.00052	¹⁰ KOPTEV	95	SPEC +	Surface μ^+ 's
2.60231 ± 0.00050 ± 0.00084	NUMAO	95	SPEC +	Surface μ^+ 's
2.609 ± 0.008	DUNAITSEV	73	CNTR +	
2.602 ± 0.004	AYRES	71	CNTR ±	
2.604 ± 0.005	NORDBERG	67	CNTR +	
2.602 ± 0.004	ECKHAUSE	65	CNTR +	
• • • We do not use the following data for averages, fits, limits, etc. • • •				
2.640 ± 0.008	¹¹ KINSEY	66	CNTR +	

¹⁰KOPTEV 95 combines the statistical and systematic errors; the statistical error dominates.

¹¹Systematic errors in the calibration of this experiment are discussed by NORDBERG 67.

$$(\tau_{\pi^+} - \tau_{\pi^-}) / \tau_{\text{average}}$$

A test of CPT invariance.

VALUE (units 10^{-4})	DOCUMENT ID	TECN
5.5 ± 7.1	AYRES	71 CNTR
• • • We do not use the following data for averages, fits, limits, etc. • • •		
-14 ± 29	PETRUKHIN	68 CNTR
40 ± 70	BARDON	66 CNTR
23 ± 40	¹² LOBKOWICZ	66 CNTR

¹²This is the most conservative value given by LOBKOWICZ 66.

π^+ DECAY MODES

π^- modes are charge conjugates of the modes below.

Mode	Fraction (Γ_i/Γ)	Confidence level
Γ_1 $\mu^+ \nu_\mu$	[a] (99.98770 ± 0.00004) %	
Γ_2 $\mu^+ \nu_\mu \gamma$	[b] (2.00 ± 0.25) × 10^{-4}	
Γ_3 $e^+ \nu_e$	[a] (1.230 ± 0.004) × 10^{-4}	
Γ_4 $e^+ \nu_e \gamma$	[b] (1.61 ± 0.23) × 10^{-7}	
Γ_5 $e^+ \nu_e \pi^0$	(1.025 ± 0.034) × 10^{-8}	
Γ_6 $e^+ \nu_e e^+ e^-$	(3.2 ± 0.5) × 10^{-9}	
Γ_7 $e^+ \nu_e \nu \bar{\nu}$	< 5 × 10^{-6}	90%
Lepton Family number (LF) or Lepton number (L) violating modes		
Γ_8 $\mu^+ \bar{\nu}_e$	L [c] < 1.5	× 10^{-3} 90%
Γ_9 $\mu^+ \nu_e$	LF [c] < 8.0	× 10^{-3} 90%
Γ_{10} $\mu^- e^+ e^+ \nu$	LF < 1.6	× 10^{-6} 90%

[a] Measurements of $\Gamma(e^+ \nu_e)/\Gamma(\mu^+ \nu_\mu)$ always include decays with γ 's, and measurements of $\Gamma(e^+ \nu_e \gamma)$ and $\Gamma(\mu^+ \nu_\mu \gamma)$ never include low-energy γ 's. Therefore, since no clean separation is possible, we consider the modes with γ 's to be subreactions of the modes without them, and let $[\Gamma(e^+ \nu_e) + \Gamma(\mu^+ \nu_\mu)]/\Gamma_{\text{total}} = 100\%$.

[b] See the Particle Listings below for the energy limits used in this measurement; low-energy γ 's are not included.

[c] Derived from an analysis of neutrino-oscillation experiments.

π^+ BRANCHING RATIOS

$\Gamma(e^+ \nu_e)/\Gamma_{\text{total}}$ Γ_3/Γ
See note [a] in the list of π^+ decay modes just above, and see also the next block of data.

VALUE (units 10^{-4})	DOCUMENT ID
1.230 ± 0.004 OUR EVALUATION	

$[\Gamma(e^+ \nu_e) + \Gamma(e^+ \nu_e \gamma)]/[\Gamma(\mu^+ \nu_\mu) + \Gamma(\mu^+ \nu_\mu \gamma)]$ $(\Gamma_3 + \Gamma_4)/(\Gamma_1 + \Gamma_2)$

See note [a] in the list of π^+ decay modes above. See NUMAO 92 for a discussion of $e-\mu$ universality.

VALUE (units 10^{-4})	EVTS	DOCUMENT ID	TECN	COMMENT
1.230 ± 0.004 OUR AVERAGE				
1.2346 ± 0.0035 ± 0.0036	120k	CZAPEK	93 CALO	Stopping π^+
1.2265 ± 0.0034 ± 0.0044	190k	BRITTON	92 CNTR	Stopping π^+
1.218 ± 0.014	32k	BRYMAN	86 CNTR	Stopping π^+
• • • We do not use the following data for averages, fits, limits, etc. • • •				
1.273 ± 0.028	11k	¹³ DICAPUA	64 CNTR	
1.21 ± 0.07		ANDERSON	60 SPEC	
¹³ DICAPUA 64 has been updated using the current mean life.				

$\Gamma(\mu^+ \nu_\mu \gamma)/\Gamma_{\text{total}}$ Γ_2/Γ
Note that measurements here do not cover the full kinematic range.

VALUE (units 10^{-4})	EVTS	DOCUMENT ID	TECN	CHG	COMMENT
2.0 ± 0.24 ± 0.08		¹⁴ BRESSI	98 CALO	+	Stopping π^+
• • • We do not use the following data for averages, fits, limits, etc. • • •					
1.24 ± 0.25	26	CASTAGNOLI	58 EMUL		$KE_\mu < 3.38$ MeV

¹⁴BRESSI 98 result is given for $E_\gamma > 1$ MeV only. Result agrees with QED expectation, 2.283×10^{-4} and does not confirm discrepancy of earlier experiment CASTAGNOLI 58.

$\Gamma(e^+ \nu_e \gamma)/\Gamma_{\text{total}}$ Γ_4/Γ
Note that measurements here do not cover the full kinematic range.

VALUE (units 10^{-8})	EVTS	DOCUMENT ID	TECN	COMMENT
16.1 ± 2.3		¹⁵ BOLOTOV	90B SPEC	17 GeV $\pi^- \rightarrow e^- \bar{\nu}_e \gamma$
• • • We do not use the following data for averages, fits, limits, etc. • • •				
5.6 ± 0.7	226	¹⁶ STETZ	78 SPEC	$P_e > 56$ MeV/c
3.0	143	DEPOMMIER	63B CNTR	(KE) $_{e^+ \gamma} > 48$ MeV

¹⁵BOLOTOV 90B is for $E_\gamma > 21$ MeV, $E_e > 70 - 0.8 E_\gamma$.

¹⁶STETZ 78 is for an $e^- \gamma$ opening angle > 132° . Obtains 3.7 when using same cutoffs as DEPOMMIER 63B.

$\Gamma(e^+ \nu_e \pi^0)/\Gamma_{\text{total}}$ Γ_5/Γ

VALUE (units 10^{-8})	EVTS	DOCUMENT ID	TECN	CHG	COMMENT
1.025 ± 0.034 OUR AVERAGE					
1.026 ± 0.039	1224	¹⁷ MCFARLANE	85 CNTR	+	Decay in flight
1.00 ^{+0.08} _{-0.10}	332	DEPOMMIER	68 CNTR	+	
1.07 ± 0.21	38	¹⁸ BACASTOW	65 OSPK	+	
1.10 ± 0.26		¹⁸ BERTRAM	65 OSPK	+	
1.1 ± 0.2	43	¹⁸ DUNAITSEV	65 CNTR	+	
0.97 ± 0.20	36	¹⁸ BARTLETT	64 OSPK	+	
• • • We do not use the following data for averages, fits, limits, etc. • • •					
1.15 ± 0.22	52	¹⁸ DEPOMMIER	63 CNTR	+	See DEPOMMIER 68

¹⁷MCFARLANE 85 combines a measured rate (0.394 ± 0.015)/s with 1982 PDG mean life.

¹⁸DEPOMMIER 68 says the result of DEPOMMIER 63 is at least 10% too large because of a systematic error in the π^0 detection efficiency, and that this may be true of all the previous measurements (also V. Soergel, private communication, 1972).

$\Gamma(e^+ \nu_e e^+ e^-)/\Gamma(\mu^+ \nu_\mu)$ Γ_6/Γ_1

VALUE (units 10^{-3})	CL%	EVTS	DOCUMENT ID	TECN	COMMENT
3.2 ± 0.5 ± 0.2		98	EGLI	89 SPEC	Uses $R_{P_{CAC}} = 0.068 \pm 0.004$
• • • We do not use the following data for averages, fits, limits, etc. • • •					
0.46 ± 0.16 ± 0.07		7	¹⁹ BARANOV	92 SPEC	Stopped π^+
< 4.8	90		KORENCHE...	76B SPEC	
< 34	90		KORENCHE...	71 OSPK	

¹⁹This measurement by BARANOV 92 is of the structure-dependent part of the decay. The value depends on values assumed for ratios of form factors.

$\Gamma(e^+ \nu_e \nu \bar{\nu})/\Gamma_{\text{total}}$ Γ_7/Γ

VALUE (units 10^{-6})	CL%	DOCUMENT ID	TECN
< 5	90	PICCIOTTO	88 SPEC

$\Gamma(\mu^+ \bar{\nu}_e)/\Gamma_{\text{total}}$ Γ_8/Γ
Forbidden by total lepton number conservation.

VALUE (units 10^{-3})	CL%	DOCUMENT ID	TECN	COMMENT
< 1.5	90	²⁰ COOPER	82 HLBC	Wideband ν beam

²⁰COOPER 82 limit on $\bar{\nu}_e$ observation is here interpreted as a limit on lepton number violation.

Meson Particle Listings

 π^\pm

$\Gamma(\mu^+\nu_e)/\Gamma_{\text{total}}$					Γ_9/Γ
Forbidden by lepton family number conservation.					
VALUE (units 10^{-3})	CL%	DOCUMENT ID	TECN	COMMENT	
<8.0	90	21 COOPER	82 HLBC	Wideband ν beam	
²¹ COOPER 82 limit on ν_e observation is here interpreted as a limit on lepton family number violation.					
$\Gamma(\mu^-e^+e^+\nu)/\Gamma_{\text{total}}$					Γ_{10}/Γ
Forbidden by lepton family number conservation.					
VALUE (units 10^{-6})	CL%	DOCUMENT ID	TECN	CHG	
<1.6	90	BARANOV	91B SPEC	+	
• • • We do not use the following data for averages, fits, limits, etc. • • •					
<7.7	90	KORENCHE...	87 SPEC	+	

 π^+ — POLARIZATION OF EMITTED μ^+

$\pi^+ \rightarrow \mu^+\nu$				
Tests the Lorentz structure of leptonic charged weak interactions.				
VALUE	CL%	DOCUMENT ID	TECN	COMMENT
<(-0.9959)	90	²² FETSCHER	84 RVUE	+
-0.99±0.16		²³ ABELA	83 SPEC	- μ X-rays
²² FETSCHER 84 uses only the measurement of CARR 83.				
²³ Sign of measurement reversed in ABELA 83 to compare with μ^+ measurements.				

 $\pi^\pm \rightarrow \ell^\pm\nu\gamma$ AND $K^\pm \rightarrow \ell^\pm\nu\gamma$ FORM FACTORS

Written by H.S. Pruis (Zürich University).

In the radiative decays $\pi^\pm \rightarrow \ell^\pm\nu\gamma$ and $K^\pm \rightarrow \ell^\pm\nu\gamma$, where ℓ is an e or a μ and γ is a real or virtual photon (e^+e^- pair), both the vector and the axial-vector weak hadronic currents contribute to the decay amplitude. Each current gives a structure-dependent term (SD_V and SD_A) from virtual hadronic states, and the axial-vector current also gives a contribution from inner bremsstrahlung (IB) from the lepton and meson. The IB amplitudes are determined by the meson decay constants f_π and f_K [1]. The SD_V and SD_A amplitudes are parameterized in terms of the vector form factor F_V and the axial-vector form factors F_A and R [1-4]:

$$M(SD_V) = \frac{-eG_F V_{qq'}}{\sqrt{2} m_P} \epsilon^\mu \ell^\nu F_V \epsilon_{\mu\nu\sigma\tau} k^\sigma q^\tau,$$

$$M(SD_A) = \frac{-ieG_F V_{qq'}}{\sqrt{2} m_P} \epsilon^\mu \ell^\nu \{F_A [(s-t)g_{\mu\nu} - q_\mu k_\nu] + R t g_{\mu\nu}\}. \quad (1)$$

Here $V_{qq'}$ is the Cabibbo-Kobayashi-Maskawa mixing-matrix element; ϵ^μ is the polarization vector of the photon (or the effective vertex, $\epsilon^\mu = (e/t)\bar{u}(p_-)\gamma^\mu v(p_+)$, of the e^+e^- pair); $\ell^\nu = \bar{u}(p_\nu)\gamma^\nu(1-\gamma_5)v(p_\ell)$ is the lepton-neutrino current; q and k are the meson and photon four-momenta, with $s = q \cdot k$ and $t = k^2 (= (p_+ + p_-)^2)$; and P stands for π or K . In the analysis of data, the s and t dependence of the form factors is neglected, which is a good approximation for pions [2] but not for kaons [4]. The pion vector form factor F_V^π is related via CVC to the π^0 lifetime, $|F_V^\pi| = (1/\alpha)\sqrt{2}\Gamma_{\pi^0}/\pi m_{\pi^0}$ [1]. PCAC relates R to the electromagnetic radius of the meson [2,4], $R^P = \frac{1}{3}m_P f_P \langle r_P^2 \rangle$. The calculation of the other form factors, F_A^π , F_V^K , and F_A^K , is model dependent [1,4].

When the photon is real, the partial decay rate can be given analytically [1,5]:

$$\frac{d^2\Gamma_{P\rightarrow\ell\nu\gamma}}{dx dy} = \frac{d^2(\Gamma_{\text{IB}} + \Gamma_{\text{SD}} + \Gamma_{\text{INT}})}{dx dy}, \quad (2)$$

where Γ_{IB} , Γ_{SD} , and Γ_{INT} are the contributions from inner bremsstrahlung, structure-dependent radiation, and their interference, and the Γ_{SD} term is given by

$$\frac{d^2\Gamma_{\text{SD}}}{dx dy} = \frac{\alpha}{8\pi} \Gamma_{P\rightarrow\ell\nu} \frac{1}{r(1-r)^2} \left(\frac{m_P}{f_P}\right)^2 \times [(F_V + F_A)^2 \text{SD}^+ + (F_V - F_A)^2 \text{SD}^-]. \quad (3)$$

Here

$$\text{SD}^+ = (x + y - 1 - r)[(x + y - 1)(1 - x) - r],$$

$$\text{SD}^- = (1 - y + r)[(1 - x)(1 - y) + r], \quad (4)$$

where $x = 2E_\gamma/m_P$, $y = 2E_\ell/m_P$, and $r = (m_\ell/m_P)^2$.

In $\pi^\pm \rightarrow e^\pm\nu\gamma$ and $K^\pm \rightarrow e^\pm\nu\gamma$ decays, the interference terms are small, and thus only the absolute values $|F_A + F_V|$ and $|F_A - F_V|$ can be obtained. In $K^\pm \rightarrow \mu^\pm\nu\gamma$ decay, the interference term is important, and thus the signs of F_V and F_A can be obtained. In $\pi^\pm \rightarrow \mu^\pm\nu\gamma$ decay, bremsstrahlung completely dominates. In $\pi^\pm \rightarrow e^\pm\nu e^+e^-$ and $K^\pm \rightarrow \ell^\pm\nu e^+e^-$ decays, all three form factors, F_V , F_A , and R , can be determined.

We give the π^\pm form factors F_V , F_A , and R in the Listings below. In the K^\pm Listings, we give the sum $F_A + F_V$ and difference $F_A - F_V$.

The electroweak decays of the pseudoscalar mesons are investigated to learn something about the unknown hadronic structure of these mesons, assuming a standard $V-A$ structure of the weak leptonic current. The experiments are quite difficult, and it is not meaningful to analyse the results using parameters for both the hadronic structure (decay constants, form factors) and the leptonic weak current (e.g., to add pseudoscalar or tensor couplings to the $V-A$ coupling). Deviations from the $V-A$ interactions are much better studied in purely leptonic systems such as muon decay.

References

1. D.A. Bryman *et al.*, Phys. Reports **88**, 151 (1982). See also our note on "Pseudoscalar-Meson Decay Constants," above.
2. A. Kersch and F. Scheck, Nucl. Phys. **B263**, 475 (1986).
3. W.T. Chu *et al.*, Phys. Rev. **166**, 1577 (1968).
4. D.Yu. Bardin and E.A. Ivanov, Sov. J. Part. Nucl. **7**, 286 (1976).
5. S.G. Brown and S.A. Bludman, Phys. Rev. **136**, B1160 (1964).

 π^\pm FORM FACTORS F_V , VECTOR FORM FACTOR

VALUE	EVTS	DOCUMENT ID	TECN	COMMENT
0.017±0.008 OUR AVERAGE				
0.014±0.009		²⁴ BOLOTOV	90B SPEC	17 GeV $\pi^- \rightarrow e^- \bar{\nu}_e \gamma$
0.023 ^{+0.015} _{-0.013}	98	EGLI	89 SPEC	$\pi^+ \rightarrow e^+ \nu_e e^+ e^-$

²⁴BOLOTOV 90B only determines the absolute value.

See key on page 239

Meson Particle Listings

π^\pm, π^0

F_A , AXIAL-VECTOR FORM FACTOR

VALUE	EVTS	DOCUMENT ID	TECN	COMMENT
0.0116 ± 0.0016 OUR AVERAGE		Error includes scale factor of 1.3. See the ideogram below.		
0.0106 ± 0.0060	25	BOLOTOV	90B SPEC	17 GeV $\pi^- \rightarrow e^- \bar{\nu}_e \gamma$
0.0135 ± 0.0016	25	BAY	86 SPEC	$\pi^+ \rightarrow e^+ \nu \gamma$
0.006 ± 0.003	25	PILONEN	86 SPEC	$\pi^+ \rightarrow e^+ \nu \gamma$
0.011 ± 0.003	25,26	STETZ	78 SPEC	$\pi^+ \rightarrow e^+ \nu \gamma$

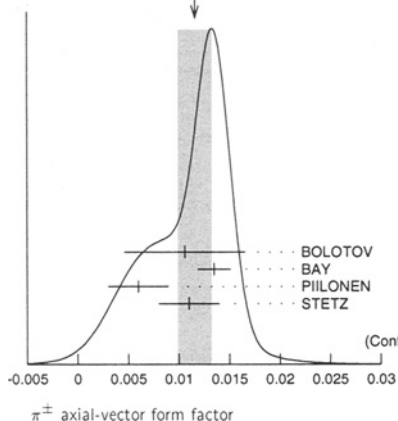
• • • We do not use the following data for averages, fits, limits, etc. • • •

0.021 ^{+0.011} _{-0.013} 98 EGLI 89 SPEC $\pi^+ \rightarrow e^+ \nu_e e^+ e^-$

²⁵ Using the vector form factor from CVC prediction $F_V = 0.0259 \pm 0.0005$. Only the absolute value of F_A is determined.

²⁶ The result of STETZ 78 has a two-fold ambiguity. We take the solution compatible with later determinations.

WEIGHTED AVERAGE
0.0116 ± 0.0016 (Error scaled by 1.3)



F_2 , SECOND AXIAL-VECTOR FORM FACTOR

VALUE	EVTS	DOCUMENT ID	TECN	COMMENT
0.059 ^{+0.009} _{-0.008} OUR AVERAGE	98	EGLI	89 SPEC	$\pi^+ \rightarrow e^+ \nu_e e^+ e^-$

π^\pm REFERENCES

We have omitted some papers that have been superseded by later experiments. The omitted papers may be found in our 1988 edition Physics Letters **B204** (1988).

BRESSI 98	NP B513 555	G. Bressi et al.		
LENZ 98	PL B416 50	S. Lenz et al.		
ASSAMAGAN 96	PR D53 6065	K.A. Assamagan et al.	(PSI, ZURI, VILL+)	
KOPEV 95	JETPL 61 877	V.P. Koptev et al.	(PNPI)	
	Translated from ZETFP 61 865.			
NUMAO 95	PR D52 4855	T. Numao et al.	(TRIUM, BRCCO)	
ASSAMAGAN 94	PL B335 231	K.A. Assamagan et al.	(PSI, ZURI, VILL+)	
JECKELMANN 94	PL B335 326	B. Jeckelmann, P.F.A. Goudsmit, H.J. Leisi	(WABRN+)	
CZAPEK 93	PRL 70 17	G. Czapek et al.	(BERN, VILL)	
BARANOV 92	SJNP 55 1644	V.A. Baranov et al.	(JINR)	
	Translated from YAF 55 2940.			
BRITTON 92	PRL 68 3000	D.J. Britton et al.	(TRIUM, CARL)	
Also	PR D49 28	D.J. Britton et al.	(TRIUM, CARL)	
NUMAO 92	MPL A7 3357	T. Numao	(TRIUM)	
BARANOV 91B	SJNP 54 790	V.A. Baranov et al.	(JINR)	
	Translated from YAF 54 1296.			
DAUM 91	PL B265 425	M. Daum et al.	(VILL)	
BOLOTOV 90B	PL B243 308	V.N. Bolotov et al.	(INRM)	
EGLI 89	PL B222 533	S. Egli et al.	(SINDRUM Collab.)	
Also	PL B175 97	S. Egli et al.	(AACH3, ETH, SIN, ZURI)	
PDG 88	PL B204	G.P. Yost et al.	(LBL+)	
PICCIOTTO 88	PR D37 1131	C.E. Picciotto et al.	(TRIUM, CNRC)	
COHEN 87	RMP 59 1121	E.R. Cohen, B.N. Taylor	(RISC, NBS)	
KORENCHENKO 87	SJNP 46 192	S.M. Korenchenko et al.	(JINR)	
	Translated from YAF 46 313.			
BAY 86	PL B174 445	A. Bay et al.	(LAUS, ZURI)	
BRYMAN 86	PR D33 1211	D.A. Bryman et al.	(TRIUM, CNRC)	
Also	PR 50 7	D.A. Bryman et al.	(TRIUM, CNRC)	
JECKELMANN 86B	NP A457 709	B. Jeckelmann et al.	(ETH, FRIB)	
Also	PRL 56 1444	B. Jeckelmann et al.	(ETH, FRIB)	
PILONEN 86	PRL 57 1402	L.E. Pilonen et al.	(LANL, TEMP, CHIC)	
MCFARLANE 85	PR D32 547	W.K. McFarlane et al.	(TEMP, LANL)	
ABELA 84	PL 146B 431	R. Abela et al.	(SIN)	
Also	PL 74B 126	M. Daum et al.	(SIN)	
Also	PR D20 2632	M. Daum et al.	(SIN)	
FETSCHER 84	PL 140B 117	W. Fetscher	(ETH)	
ABELA 83	NP A395 413	R. Abela et al.	(BASL, KARLK, KARLE)	
CARR 83	PRL 51 627	J. Carr et al.	(LBL, NWES, TRIUM)	
COOPER 82	PL 112B 97	A.M. Cooper et al.	(RL)	
LU 80	PRL 45 1066	D.C. Lu et al.	(YALE, COLU, JHU)	
STETZ 78	NP B138 285	A.W. Stetz et al.	(LBL, UCLA)	
CARTER 76	PRL 37 1380	A.L. Carter et al.	(CARL, CNRC, CHIC+)	
KORENCHENKO 76B	JETP 44 35	S.M. Korenchenko et al.	(JINR)	
	Translated from ZETFP 71 69.			
MARUSHENKO 76	JETPL 23 72	V.I. Marushenko et al.	(PNPI)	
	Translated from ZETFP 23 80.			
Also	Private Comm.	R.E. Shafer	(FNAL)	
Also	Private Comm.	Srinow	(PNPI)	
OUNAITSEV 73	SJNP 16 292	A.F. Dunaitsev et al.	(SERP)	
	Translated from YAF 16 524.			

AYRES 71	PR D3 1051	D.S. Ayres et al.	(LRL, UCSB)
Also	PR 157 1288	D.S. Ayres et al.	(LRL)
Also	PRL 21 261	D.S. Ayres et al.	(LRL, UCSB)
Also	Thesis UCRL 18369	D.S. Ayres	(LRL)
Also	PRL 23 1267	A.J. Greenberg et al.	(LRL, UCSB)
KORENCHENKO 71	SJNP 13 189	S.M. Korenchenko et al.	(JINR)
	Translated from YAF 13 339.		
BOOTH 70	PL 32B 723	P.S.L. Booth et al.	(LIVP)
DEPOMMIER 68	NP B4 189	P. Depommier et al.	(CERN)
PETRUKHIN 68	JINR P1 3862	V.I. Petrukhin et al.	(JINR)
HYMAN 67	PL 25B 376	L.G. Hyman et al.	(ANL, CMU, NWES)
NORDBERG 67	PL 24B 594	M.E. Nordberg, F. Lobkowicz, R.L. Burman	(ROCH)
BAROON 66	PRL 16 775	M. Baroon et al.	(COLU)
KINSEY 66	PRL 144 1132	K.F. Kinsey, F. Lobkowicz, M.E. Nordberg	(ROCH)
LOBKOWICZ 66	PRL 17 548	F. Lobkowicz et al.	(ROCH, BNL)
BACASTOW 65	PR 139B 407	R.B. Bacastow et al.	(LRL, SLAC)
BERTRAM 65	PR 139B 617	W.K. Bertram et al.	(MICH, CMU)
DUNAITSEV 65	JETP 20 58	A.F. Dunaitsev et al.	(JINR)
	Translated from ZETFP 47 64.		
ECKHAUSE 65	PL 19 348	M. Eckhause et al.	(WILL)
BARTLETT 64	PR 136B 1452	D. Bartlett et al.	(COLU)
DICAPUA 64	PR 133B 1333	M. di Capua et al.	(COLU)
Also	Private Comm.	L. Pondrom	(WISC)
DEPOMMIER 63	PL 5 61	P. Depommier et al.	(CERN)
DEPOMMIER 63B	PL 7 285	P. Depommier et al.	(CERN)
ANDERSON 60	PR 119 2050	H.L. Anderson et al.	(EFI)
CASTAGNOLI 58	PR 112 1779	C. Castagnoli, M. Muchnik	(ROMA)

π^0

$$JG(J^{PC}) = 1^-(0^-+)$$

We have omitted some results that have been superseded by later experiments. The omitted results may be found in our 1988 edition Physics Letters **B204** (1988).

π^0 MASS

The value is calculated from m_{π^\pm} and $(m_{\pi^\pm} - m_{\pi^0})$. See notes under the π^\pm Mass Listings concerning revision of the charged pion mass.

VALUE (MeV)	DOCUMENT ID	TECN	COMMENT
134.9766 ± 0.0006 OUR FIT		Error includes scale factor of 1.1.	

$m_{\pi^\pm} - m_{\pi^0}$

Measurements with an error > 0.01 MeV have been omitted.

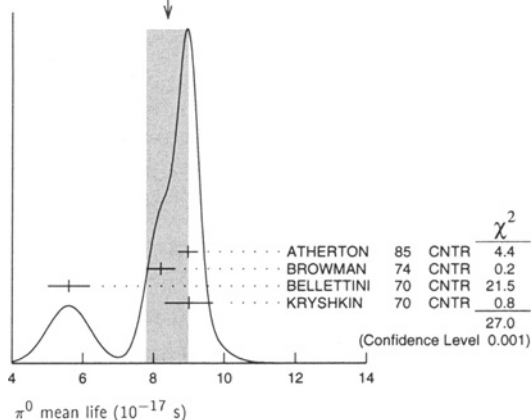
VALUE (MeV)	DOCUMENT ID	TECN	COMMENT
4.5936 ± 0.0005 OUR FIT			
4.5936 ± 0.0005 OUR AVERAGE			
4.59364 ± 0.00048	CRAWFORD 91	CNTR	$\pi^- p \rightarrow \pi^0 n, n$ TOF
4.5930 ± 0.0013	CRAWFORD 86	CNTR	$\pi^- p \rightarrow \pi^0 n, n$ TOF
• • • We do not use the following data for averages, fits, limits, etc. • • •			
4.59366 ± 0.00048	CRAWFORD 88B	CNTR	See CRAWFORD 91
4.6034 ± 0.0052	VASILEVSKY 66	CNTR	
4.6056 ± 0.0055	CZIRR 63	CNTR	

π^0 MEAN LIFE

Measurements with an error > 1×10^{-17} s have been omitted.

VALUE (10^{-17} s)	EVTS	DOCUMENT ID	TECN	COMMENT
8.4 ± 0.6 OUR AVERAGE		Error includes scale factor of 3.0. See the ideogram below.		
8.97 ± 0.22 ± 0.17		ATHERTON 85	CNTR	
8.2 ± 0.4		¹ BROWMAN 74	CNTR	Primakoff effect
5.6 ± 0.6		BELLETTINI 70	CNTR	Primakoff effect
9 ± 0.68		KRYSHKIN 70	CNTR	Primakoff effect
• • • We do not use the following data for averages, fits, limits, etc. • • •				
8.4 ± 0.5 ± 0.5	1182	² WILLIAMS 88	CBAL	$e^+ e^- \rightarrow e^+ e^- \pi^0$
		¹ BROWMAN 74		gives a π^0 width $\Gamma = 8.02 \pm 0.42$ eV. The mean life is \hbar/Γ .
		² WILLIAMS 88		gives $\Gamma(\gamma\gamma) = 7.7 \pm 0.5 \pm 0.5$ eV. We give here $\tau = \hbar/\Gamma$ (total).

WEIGHTED AVERAGE
8.4 ± 0.6 (Error scaled by 3.0)



Meson Particle Listings

π^0

π^0 DECAY MODES

Mode	Fraction (Γ_i/Γ)	Scale factor/ Confidence level
Γ_1 2γ	$(98.798 \pm 0.032) \%$	S=1.1
Γ_2 $e^+ e^- \gamma$	$(1.198 \pm 0.032) \%$	S=1.1
Γ_3 γ positronium	$(1.82 \pm 0.29) \times 10^{-9}$	
Γ_4 $e^+ e^+ e^- e^-$	$(3.14 \pm 0.30) \times 10^{-5}$	
Γ_5 $e^+ e^-$	$(6.2 \pm 0.5) \times 10^{-8}$	
Γ_6 4γ	< 2	CL=90%
Γ_7 $\nu\bar{\nu}$	$[a] < 8.3$	$\times 10^{-7}$ CL=90%
Γ_8 $\nu_e \bar{\nu}_e$	< 1.7	$\times 10^{-6}$ CL=90%
Γ_9 $\nu_\mu \bar{\nu}_\mu$	< 3.1	$\times 10^{-6}$ CL=90%
Γ_{10} $\nu_\tau \bar{\nu}_\tau$	< 2.1	$\times 10^{-6}$ CL=90%

Charge conjugation (C) or Lepton Family number (LF) violating modes

Γ_{11} 3γ	C	< 3.1	$\times 10^{-8}$ CL=90%
Γ_{12} $\mu^+ e^-$			
Γ_{13} $\mu^+ e^- + e^- \mu^+$	LF	< 1.72	$\times 10^{-8}$ CL=90%

[a] Astrophysical and cosmological arguments give limits of order 10^{-13} ; see the Particle Listings below.

CONSTRAINED FIT INFORMATION

An overall fit to 2 branching ratios uses 4 measurements and one constraint to determine 3 parameters. The overall fit has a $\chi^2 = 1.9$ for 2 degrees of freedom.

The following *off-diagonal* array elements are the correlation coefficients $\langle \delta x_i \delta x_j \rangle / (\delta x_i \delta x_j)$, in percent, from the fit to the branching fractions, $x_i \equiv \Gamma_i / \Gamma_{\text{total}}$. The fit constrains the x_i whose labels appear in this array to sum to one.

x_2	-100	
x_4	-1	0
	x_1	x_2

π^0 BRANCHING RATIOS

$\Gamma(e^+ e^- \gamma) / \Gamma(2\gamma)$	Γ_2 / Γ_1			
VALUE (%)	EVTS	DOCUMENT ID	TECN	COMMENT
1.213 ± 0.033 OUR FIT				Error includes scale factor of 1.1.
1.213 ± 0.030 OUR AVERAGE				
1.25 ± 0.04		SCHARDT	81	SPEC $\pi^- p \rightarrow n \pi^0$
1.166 ± 0.047	3071	³ SAMIOS	61	HBC $\pi^- p \rightarrow n \pi^0$
1.17 ± 0.15	27	BUDAGOV	60	HBC
• • • We do not use the following data for averages, fits, limits, etc. • • •				
1.196		JOSEPH	60	THEO QED calculation
³ SAMIOS 61 value uses a Panofsky ratio = 1.62.				

$\Gamma(\gamma \text{ positronium}) / \Gamma(2\gamma)$	Γ_3 / Γ_1			
VALUE (units 10^{-9})	EVTS	DOCUMENT ID	TECN	COMMENT
1.84 ± 0.29	277	AFANASYEV	90	CNTR pC 70 GeV

$\Gamma(e^+ e^+ e^- e^-) / \Gamma(2\gamma)$	Γ_4 / Γ_1			
VALUE (units 10^{-5})	EVTS	DOCUMENT ID	TECN	COMMENT
3.18 ± 0.30 OUR FIT				
3.18 ± 0.30	146	⁴ SAMIOS	62B	HBC
⁴ SAMIOS 62B value uses a Panofsky ratio = 1.62.				

$\Gamma(e^+ e^-) / \Gamma_{\text{total}}$	Γ_5 / Γ				
Experimental results are listed; branching ratios corrected for radiative effects are given in the footnotes. BERMAN 60 found $B(\pi^0 \rightarrow e^+ e^-) \geq 4.69 \times 10^{-8}$ via an exact QED calculation.					
VALUE (units 10^{-8})	EVTS	DOCUMENT ID	TECN	CHG	COMMENT
6.2 ± 0.5 OUR AVERAGE					
6.09 ± 0.40 ± 0.24	275	⁵ ALAVI-HARATI99c	SPEC	0	$K_L^0 \rightarrow 3\pi^0$ in flight
6.9 ± 2.3 ± 0.6	21	⁶ DESHPANDE	93	SPEC	$K^+ \rightarrow \pi^+ \pi^0$
7.6 $^{+2.9}_{-2.8}$ ± 0.5	8	⁷ MCFARLAND	93	SPEC	$K_L^0 \rightarrow 3\pi^0$ in flight

⁵ALAVI-HARATI 99c quote result for $B[\pi^0 \rightarrow e^+ e^-, (m_{e^+ e^-} / m_{\pi^0})^2 > 0.95]$ to minimize radiative contributions from $\pi^0 \rightarrow e^+ e^- \gamma$. After radiative corrections they obtain $(7.04 \pm 0.46 \pm 0.28) \times 10^{-8}$.

⁶The DESHPANDE 93 result with bremsstrahlung radiative corrections is $(8.0 \pm 2.6 \pm 0.6) \times 10^{-8}$.

⁷The MCFARLAND 93 result is for $B[\pi^0 \rightarrow e^+ e^-, (m_{e^+ e^-} / m_{\pi^0})^2 > 0.95]$. With radiative corrections it becomes $(8.8^{+4.5}_{-3.2} \pm 0.6) \times 10^{-8}$.

$\Gamma(e^+ e^-) / \Gamma(2\gamma)$	Γ_5 / Γ_1			
VALUE (units 10^{-7})	CL% EVTS	DOCUMENT ID	TECN	COMMENT
< 1.3	90	NIEBUHR	89	SPEC $\pi^- p \rightarrow \pi^0 n$ at rest
< 5.3	90	ZEPHAT	87	SPEC $\pi^- p \rightarrow \pi^0 n$ 0.3 GeV/c
1.7 ± 0.6 ± 0.3	59	FRANK	83	SPEC $\pi^- p \rightarrow n \pi^0$
1.8 ± 0.6	58	MISCHKE	82	SPEC See FRANK 83
2.23 $^{+2.40}_{-1.10}$	90	8	FISCHER	78B SPRK $K^+ \rightarrow \pi^+ \pi^0$

$\Gamma(4\gamma) / \Gamma_{\text{total}}$	Γ_6 / Γ			
VALUE (units 10^{-8})	CL% EVTS	DOCUMENT ID	TECN	COMMENT
< 2	90	MCDONOUGH	88	CBOX $\pi^- p$ at rest
• • • We do not use the following data for averages, fits, limits, etc. • • •				
< 160	90	BOLOTOV	86c	CALO
< 440	90	0	AUERBACH	80 CNTR

$\Gamma(\nu\bar{\nu}) / \Gamma_{\text{total}}$	Γ_7 / Γ			
The astrophysical and cosmological limits are many orders of magnitude lower, but we use the best laboratory limit for the Summary Tables.				
VALUE (units 10^{-8})	CL% EVTS	DOCUMENT ID	TECN	COMMENT
< 0.83	90	⁸ ATIYA	91	B787 $K^+ \rightarrow \pi^+ \nu\bar{\nu}$
• • • We do not use the following data for averages, fits, limits, etc. • • •				
$< 2.9 \times 10^{-7}$		⁹ LAM	91	Cosmological limit
$< 3.2 \times 10^{-7}$		¹⁰ NATALE	91	SN 1987A
< 6.5	90	DORENBOS...	88	CHRM Beam dump, prompt
< 24	90	0	⁸ HERCZEG	81 RVUE $K^+ \rightarrow \pi^+ \nu\bar{\nu}$

$\Gamma(\nu_e \bar{\nu}_e) / \Gamma_{\text{total}}$	Γ_8 / Γ			
VALUE (units 10^{-6})	CL%	DOCUMENT ID	TECN	COMMENT
< 1.7	90	DORENBOS...	88	CHRM Beam dump, prompt ν
• • • We do not use the following data for averages, fits, limits, etc. • • •				
< 3.1	90	¹¹ HOFFMAN	88	RVUE Beam dump, prompt ν
¹¹ HOFFMAN 88 analyzes data from a 400-GeV BEBC beam-dump experiment.				

$\Gamma(\nu_\mu \bar{\nu}_\mu) / \Gamma_{\text{total}}$	Γ_9 / Γ			
VALUE (units 10^{-6})	CL%	DOCUMENT ID	TECN	COMMENT
< 3.1	90	¹² HOFFMAN	88	RVUE Beam dump, prompt ν
• • • We do not use the following data for averages, fits, limits, etc. • • •				
< 7.8	90	DORENBOS...	88	CHRM Beam dump, prompt ν
¹² HOFFMAN 88 analyzes data from a 400-GeV BEBC beam-dump experiment.				

$\Gamma(\nu_\tau \bar{\nu}_\tau) / \Gamma_{\text{total}}$	Γ_{10} / Γ			
VALUE (units 10^{-6})	CL%	DOCUMENT ID	TECN	COMMENT
< 2.1	90	¹³ HOFFMAN	88	RVUE Beam dump, prompt ν
• • • We do not use the following data for averages, fits, limits, etc. • • •				
< 4.1	90	DORENBOS...	88	CHRM Beam dump, prompt ν
¹³ HOFFMAN 88 analyzes data from a 400-GeV BEBC beam-dump experiment.				

$\Gamma(3\gamma) / \Gamma_{\text{total}}$	Γ_{11} / Γ			
Forbidden by C invariance.				
VALUE (units 10^{-8})	CL% EVTS	DOCUMENT ID	TECN	COMMENT
< 3.1	90	MCDONOUGH	88	CBOX $\pi^- p$ at rest
• • • We do not use the following data for averages, fits, limits, etc. • • •				
< 38	90	0	HIGHLAND	80 CNTR
< 150	90	0	AUERBACH	78 CNTR
< 490	90	0	¹⁴ DUCLOS	65 CNTR
< 490	90	0	¹⁴ KUTIN	65 CNTR
¹⁴ These experiments give $B(3\gamma/2\gamma) < 5.0 \times 10^{-6}$.				

$\Gamma(\mu^+ e^-) / \Gamma_{\text{total}}$	Γ_{12} / Γ			
Forbidden by lepton family number conservation.				
VALUE (units 10^{-9})	CL%	DOCUMENT ID	TECN	COMMENT
• • • We do not use the following data for averages, fits, limits, etc. • • •				
< 16	90	LEE	90	SPEC $K^+ \rightarrow \pi^+ \mu^+ e^-$
< 78	90	CAMPAGNARI	88	SPEC See LEE 90

See key on page 239

Meson Particle Listings

 π^0, η

$[\Gamma(\mu^+e^-) + \Gamma(e^-\mu^+)]/\Gamma_{\text{total}}$
Forbidden by lepton family number conservation.

VALUE (units 10^{-9})	CL%	DOCUMENT ID	TECN	COMMENT
< 17.2	90	KROLAK 94 E799		$\ln K_L^0 \rightarrow 3\pi^0$
• • • We do not use the following data for averages, fits, limits, etc. • • •				
< 140		HERCZEG 84	RVUE	$K^+ \rightarrow \pi^+ \mu e$
< 2×10^{-6}		HERCZEG 84	THEO	$\mu^- \rightarrow e^-$ conversion
< 70	90	BRYMAN 82	RVUE	$K^+ \rightarrow \pi^+ \mu e$

 π^0 ELECTROMAGNETIC FORM FACTOR

The amplitude for the process $\pi^0 \rightarrow e^+e^-\gamma$ contains a form factor $F(x)$ at the $\pi^0\gamma\gamma$ vertex, where $x = [m_{e^+e^-}/m_{\pi^0}]^2$. The parameter a in the linear expansion $F(x) = 1 + ax$ is listed below.

All the measurements except that of BEHREND 91 are in the time-like region of momentum transfer.

LINEAR COEFFICIENT OF π^0 ELECTROMAGNETIC FORM FACTOR

VALUE	EVTS	DOCUMENT ID	TECN	COMMENT
0.032 ± 0.004	OUR AVERAGE			
+0.026 ± 0.024 ± 0.048	7548	FARZANPAY 92	SPEC	$\pi^-p \rightarrow \pi^0n$ at rest
+0.025 ± 0.014 ± 0.026	54k	MEIJERDREES 92b	SPEC	$\pi^-p \rightarrow \pi^0n$ at rest
+0.0326 ± 0.0026 ± 0.0026	127	15 BEHREND 91	CELL	$e^+e^- \rightarrow e^+e^-\pi^0$
-0.11 ± 0.03 ± 0.08	32k	FONVIEILLE 89	SPEC	Radiation corr.
• • • We do not use the following data for averages, fits, limits, etc. • • •				
0.12 +0.05 -0.04		16 TUPPER 83	THEO	FISCHER 78 data
+0.10 ± 0.03	31k	17 FISCHER 78	SPEC	Radiation corr.
+0.01 ± 0.11	2200	DEVONS 69	OSP	No radiation corr.
-0.15 ± 0.10	7676	KOBRAK 61	HBC	No radiation corr.
-0.24 ± 0.16	3071	SAMIOS 61	HBC	No radiation corr.

15 BEHREND 91 estimates that their systematic error is of the same order of magnitude as their statistical error, and so we have included a systematic error of this magnitude. The value of a is obtained by extrapolation from the region of large space-like momentum transfer assuming vector dominance.

16 TUPPER 83 is a theoretical analysis of FISCHER 78 including 2-photon exchange in the corrections.

17 The FISCHER 78 error is statistical only. The result without radiation corrections is $+0.05 \pm 0.03$.

 π^0 REFERENCES

We have omitted some papers that have been superseded by later experiments. The omitted papers may be found in our 1988 edition Physics Letters B204 (1988).

ALAVI-HARATI 99C	PRL 83 922	A. Alavi-Harati et al.	(KTeV Collab.)
KROLAK 94	PL B320 407	P. Krolik et al.	(EFI, UCLA, COLO, ELMT+)
DESHAPANDE 93	PRL 71 27	A. Deshpande et al.	(BNL E851 Collab.)
MC FARLAND 93	PRL 71 31	K.S. McFarland et al.	(EFI, UCLA, COLO+)
FARZANPAY 92	PL B278 413	F. Farzanpay et al.	(ORST, TRIU, BRCCO+)
MEIJERDREES 92B	PR D45 1439	R. Meijer Drees et al.	
ATYIA 91	PRL 66 2189	M.S. Atyia et al.	(BNL, LANL, PRIN+)
BEHREND 91	ZPHY C49 401	H.J. Behrend et al.	(CELLO Collab.)
CRAWFORD 91	PR D43 46	J.F. Crawford et al.	(VILL, VIRG)
LAM 91	PR D44 3345	W.P. Lam, K.W. Ng	(AST)
NATALE 91	PL B258 227	A.A. Natale	(SPIFT)
AFANASYEV 90B	PL B236 116	L.G. Afanasyev et al.	(JINR, MOSU, SERP)
Also	SJNP 51 664	L.G. Afanasyev et al.	(JINR)
	Translated from YAF 51 1040.		
LEE 90	PRL 64 165	A.M. Lee et al.	(BNL, FNAL, VILL, WASH+)
FONVIEILLE 89	PL B233 65	H. Fonvieille et al.	(CLER, LYON, SACL)
NIEBUHR 89	PR D40 2796	C. Niebuhr et al.	(SINDRUM Collab.)
CAMPAGNARI 88	PRL 61 2062	C. Campagnari et al.	(BNL, FNAL, PSI+)
CRAWFORD 88B	PL B213 391	J.F. Crawford et al.	(PSI, VIRG)
DORENBOS... 88	ZPHY C40 497	J. Dorenbosch et al.	(CHARM Collab.)
HOFFMAN 88	PL B208 149	C.M. Hoffman	(LANL)
MCDONOUGH 88	PR D38 2121	J.M. McDonough et al.	(TEMP, LANL, CHIC)
PDG 88	PL B204	G.P. Yost et al.	(LBL+)
WILLIAMS 88	PR D38 1365	D.A. Williams et al.	(Crystal Ball Collab.)
ZEPHAT 87	JPG 13 1375	A.G. Zephat et al.	(OMICRON Collab.)
BOLOTOV 86C	JETPL 43 520	V.N. Bolotov et al.	(INRM)
	Translated from ZETFP 43 405		
CRAWFORD 86	PRL 56 1043	J.F. Crawford et al.	(SIN, VIRG)
ATHERTON 85	PL 158B 81	H.W. Atherton et al.	(CERN, ISU, LUND+)
HERCZEG 84	PR D29 1954	P. Herczeg, C.M. Hoffman	(LANL)
FRANK 83	PR D28 423	J.S. Frank et al.	(LANL, ARZS)
TUPPER 83	PR D28 2905	G.B. Tupper, T.R. Grose, M.A. Samuel	(OKSU)
BRYMAN 82	PR D25 2538	D.A. Bryman	(TRIU)
MISCHKE 82	PRL 48 1153	R.E. Mischke et al.	(LANL, ARZS)
HERCZEG 81	PL 100B 347	P. Herczeg, C.M. Hoffman	(LANL)
SCHARDT 81	PR D23 639	M.A. Schardt et al.	(ARZS, LANL)
AUERBACH 80	PL 90B 317	L.B. Auerbach et al.	(TEMP, LASL)
HIGHLAND 80	PRL 44 628	V.L. Highland et al.	(TEMP, LASL)
AUERBACH 78	PRL 41 275	L.B. Auerbach et al.	(TEMP, LASL)
FISCHER 78B	PL 73B 359	J. Fischer et al.	(GEVA, SACL)
FISCHER 78B	PL 73B 364	J. Fischer et al.	(GEVA, SACL)
BROWMAN 74	PRL 33 1400	A. Browman et al.	(CORN, BING)
BELLETTINI 70	NC 66A 243	G. Bellettini et al.	(PISA, BONN)
KRYSHKIN 70	JETP 30 1037	V.I. Kryshkin, A.G. Sterligov, Y.P. Usov	(TMSK)
	Translated from ZETF 57 1917		
DEVONS 69	PR 184 1356	S. Devons et al.	(COLU, ROMA)
VASILEVSKY 66	PL 23 281	I.M. Vasilevsky et al.	(JINR)
DUCLOS 65	PL 19 253	J. Duclos et al.	(CERN, HEID)
KUTIN 65	JETPL 2 243	V.M. Kutin, V.I. Petrukhin, Y.D. Prokoshkin	(JINR)
	Translated from unknown journal.		
CZIRR 63	PR 130 341	J.B. Czirr	(LRL)
SAMIOS 62B	PR 126 1844	N.P. Samios et al.	(COLU, BNL)
KOBRAK 61	NC 20 1115	H. Kobrak	(EFI)
SAMIOS 61	PR 121 275	N.P. Samios	(COLU, BNL)
BERMAN 60	NC XVIII 1192	S. Berman, D. Geffen	
BUDAGOV 60	JETP 11 755	Y.A. Budagov et al.	(JINR)
	Translated from ZETF 38 1047		
JOSEPH 60	NC 16 997	D.W. Joseph	(EFI)

 η

$$I^G(J^{PC}) = 0^+(0^-+)$$

We have omitted some results that have been superseded by later experiments. The omitted results may be found in our 1988 edition Physics Letters B204 (1988).

 η MASS

We no longer use the bubble-chamber measurements from the 1960's, which seem to have been systematically high by about 1 MeV. Some early results have been omitted altogether.

VALUE (MeV)	EVTS	DOCUMENT ID	TECN	COMMENT
547.30 ± 0.12	OUR AVERAGE			
547.12 ± 0.06 ± 0.25		KRUSCHKE 95D	SPEC	$\gamma p \rightarrow \eta p$, threshold
547.30 ± 0.15		PLOUIN 92	SPEC	$d p \rightarrow \eta^3\text{He}$
547.45 ± 0.25		DUANE 74	SPEC	$\pi^- p \rightarrow n$ neutrals
• • • We do not use the following data for averages, fits, limits, etc. • • •				
548.2 ± 0.65		FOSTER 65c	HBC	
549.0 ± 0.7	148	FOELSCHE 64	HBC	
548.0 ± 1.0	91	ALFF... 62	HBC	
549.0 ± 1.2	53	BASTIEN 62	HBC	

 η WIDTH

This is the partial decay rate $\Gamma(\eta \rightarrow \gamma\gamma)$ divided by the fitted branching fraction for that mode. See the "Note on the Decay Width $\Gamma(\eta \rightarrow \gamma\gamma)$ " in our 1994 edition, Phys. Rev. D50, 1 August 1994, Part I, p. 1451.

VALUE (keV)	DOCUMENT ID
1.18 ± 0.11	OUR FIT

Error includes scale factor of 1.8.

 η DECAY MODES

Mode	Fraction (Γ_i/Γ)	Scale factor/ Confidence level
Neutral modes		
Γ_1 neutral modes	(71.6 ± 0.4) %	S=1.2
Γ_2 2γ	[a] (39.33 ± 0.25) %	S=1.1
Γ_3 $3\pi^0$	(32.24 ± 0.29) %	S=1.2
Γ_4 $\pi^0 2\gamma$	(7.1 ± 1.4) × 10 ⁻⁴	
Γ_5 other neutral modes	< 2.8 %	CL=90%
Charged modes		
Γ_6 charged modes	(28.3 ± 0.4) %	S=1.2
Γ_7 $\pi^+ \pi^- \pi^0$	(23.0 ± 0.4) %	S=1.2
Γ_8 $\pi^+ \pi^- \gamma$	(4.75 ± 0.11) %	S=1.1
Γ_9 $e^+ e^- \gamma$	(4.9 ± 1.1) × 10 ⁻³	
Γ_{10} $\mu^+ \mu^- \gamma$	(3.1 ± 0.4) × 10 ⁻⁴	
Γ_{11} $e^+ e^-$	< 7.7 × 10 ⁻⁵	CL=90%
Γ_{12} $\mu^+ \mu^-$	(5.8 ± 0.8) × 10 ⁻⁶	
Γ_{13} $\pi^+ \pi^- e^+ e^-$	(1.3 +1.2 -0.8) × 10 ⁻³	
Γ_{14} $\pi^+ \pi^- 2\gamma$	< 2.1 × 10 ⁻³	
Γ_{15} $\pi^+ \pi^- \pi^0 \gamma$	< 6 × 10 ⁻⁴	CL=90%
Γ_{16} $\pi^0 \mu^+ \mu^- \gamma$	< 3 × 10 ⁻⁶	CL=90%
Charge conjugation (C), Parity (P), Charge conjugation × Parity (CP), or Lepton Family number (LF) violating modes		
Γ_{17} $\pi^+ \pi^-$	P, CP < 3.3 × 10 ⁻⁴	CL=90%
Γ_{18} $\pi^0 \pi^0$	P, CP < 4.3 × 10 ⁻⁴	CL=90%
Γ_{19} 3γ	C < 5 × 10 ⁻⁴	CL=95%
Γ_{20} $\pi^0 e^+ e^-$	C [b] < 4 × 10 ⁻⁵	CL=90%
Γ_{21} $\pi^0 \mu^+ \mu^-$	C [b] < 5 × 10 ⁻⁶	CL=90%
Γ_{22} $\mu^+ e^- + \mu^- e^+$	LF < 6 × 10 ⁻⁶	CL=90%

[a] See the "Note on the Decay Width $\Gamma(\eta \rightarrow \gamma\gamma)$ " in our 1994 edition, Phys. Rev. D50, 1 August 1994, Part I, p. 1451.

[b] C parity forbids this to occur as a single-photon process.

Meson Particle Listings

η

CONSTRAINED FIT INFORMATION

An overall fit to a decay rate and 16 branching ratios uses 42 measurements and one constraint to determine 9 parameters. The overall fit has a $\chi^2 = 32.8$ for 34 degrees of freedom.

The following *off-diagonal* array elements are the correlation coefficients $\langle \delta x_i \delta x_j \rangle / (\delta x_i \delta x_j)$, in percent, from the fit to the branching fractions, $x_i \equiv \Gamma_i / \Gamma_{\text{total}}$. The fit constrains the x_i whose labels appear in this array to sum to one.

x_3	39												
x_4	1	1											
x_7	-74	-79	-4										
x_8	-58	-62	-3	64									
x_9	-12	-13	-1	-9	-8								
x_{10}	0	0	0	-1	0	0							
x_{13}	-9	-10	0	-16	-11	-2	0						
Γ	-7	-3	0	5	4	1	0	1					
		x_2	x_3	x_4	x_7	x_8	x_9	x_{10}	x_{13}				

Mode	Rate (keV)	Scale factor
Γ_2 2γ	[a] 0.46 ± 0.04	1.8
Γ_3 $3\pi^0$	0.381 ± 0.035	1.8
Γ_4 $\pi^0 2\gamma$	(8.4 ± 1.9) × 10 ⁻⁴	1.1
Γ_7 $\pi^+ \pi^- \pi^0$	0.271 ± 0.025	1.8
Γ_8 $\pi^+ \pi^- \gamma$	0.056 ± 0.005	1.7
Γ_9 $e^+ e^- \gamma$	0.0058 ± 0.0014	
Γ_{10} $\mu^+ \mu^- \gamma$	(3.7 ± 0.6) × 10 ⁻⁴	1.1
Γ_{13} $\pi^+ \pi^- e^+ e^-$	0.0016 ^{+0.0014} _{-0.0010}	

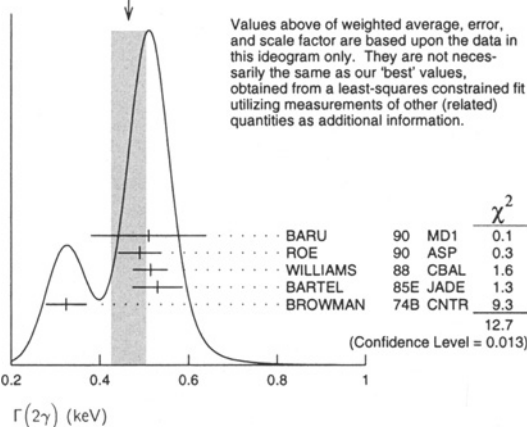
η DECAY RATES

$\Gamma(2\gamma)$ Γ_2
 See the table immediately above giving the fitted decay rates. See also the "Note on the Decay Width $\Gamma(\eta \rightarrow \gamma\gamma)$," in our 1994 edition, Phys. Rev. **D50**, 1 August 1994, Part I, p. 1451.

VALUE (keV)	EVTs	DOCUMENT ID	TECN	COMMENT
0.46 ± 0.04 OUR FIT				Error includes scale factor of 1.8.
0.46 ± 0.04 OUR AVERAGE				Error includes scale factor of 1.8. See the ideogram below.
0.51 ± 0.12 ± 0.05	36	BARU	90 MD1	$e^+ e^- \rightarrow e^+ e^- \eta$
0.490 ± 0.010 ± 0.048	2287	ROE	90 ASP	$e^+ e^- \rightarrow e^+ e^- \eta$
0.514 ± 0.017 ± 0.035	1295	WILLIAMS	88 CBAL	$e^+ e^- \rightarrow e^+ e^- \eta$
0.53 ± 0.04 ± 0.04		BARTEL	85E JADE	$e^+ e^- \rightarrow e^+ e^- \eta$
0.324 ± 0.046		BROWMAN	74B CNTR	Primakoff effect
• • • We do not use the following data for averages, fits, limits, etc. • • •				
0.64 ± 0.14 ± 0.13		AIHARA	86 TPC	$e^+ e^- \rightarrow e^+ e^- \eta$
0.56 ± 0.16	56	WEINSTEIN	83 CBAL	$e^+ e^- \rightarrow e^+ e^- \eta$
1.00 ± 0.22		BEMPORAD	67 CNTR	Primakoff effect

¹ BEMPORAD 67 gives $\Gamma(2\gamma) = 1.21 \pm 0.26$ keV assuming $\Gamma(2\gamma)/\Gamma(\text{total}) = 0.314$. Bemporad private communication gives $\Gamma(2\gamma)^2/\Gamma(\text{total}) = 0.380 \pm 0.083$. We evaluate this using $\Gamma(2\gamma)/\Gamma(\text{total}) = 0.38 \pm 0.01$. Not included in average because the uncertainty resulting from the separation of the coulomb and nuclear amplitudes has apparently been underestimated.

WEIGHTED AVERAGE
0.46 ± 0.04 (Error scaled by 1.8)



η BRANCHING RATIOS

Neutral modes

$\Gamma(\text{neutral modes})/\Gamma_{\text{total}}$	EVTs	DOCUMENT ID	TECN	COMMENT
0.716 ± 0.004 OUR FIT				Error includes scale factor of 1.2.
0.705 ± 0.008	16k	BASILE	71D CNTR	MM spectrometer
• • • We do not use the following data for averages, fits, limits, etc. • • •				
0.79 ± 0.08		BUNIATOV	67 OSPK	

$\Gamma(2\gamma)/\Gamma_{\text{total}}$	EVTs	DOCUMENT ID	TECN	COMMENT
0.3933 ± 0.0025 OUR FIT				Error includes scale factor of 1.1.
0.3949 ± 0.0017 ± 0.0030	65k	ABEGG	96 SPEC	$p d \rightarrow {}^3\text{He} \eta$

$\Gamma(2\gamma)/\Gamma(\text{neutral modes})$	EVTs	DOCUMENT ID	TECN	COMMENT
0.5490 ± 0.0021 OUR FIT				Error includes scale factor of 1.1.
0.549 ± 0.004 OUR AVERAGE				

VALUE	EVTs	DOCUMENT ID	TECN	COMMENT
0.549 ± 0.004		ALDE	84 GAM2	
0.535 ± 0.018		BUTTRAM	70 OSPK	
0.59 ± 0.033		BUNIATOV	67 OSPK	
• • • We do not use the following data for averages, fits, limits, etc. • • •				
0.52 ± 0.09	88	ABROSIMOV	80 HLBC	
0.60 ± 0.14	113	KENDALL	74 OSPK	
0.57 ± 0.09		STRUGALSKI	71 HLBC	
0.579 ± 0.052		FELDMAN	67 OSPK	
0.416 ± 0.044		DIGIUGNO	66 CNTR	Error doubled
0.44 ± 0.07		GRUNHAUS	66 OSPK	
0.39 ± 0.06		² JONES	66 CNTR	

² This result from combining cross sections from two different experiments.

$\Gamma(3\pi^0)/\Gamma(\text{neutral modes})$	EVTs	DOCUMENT ID	TECN	COMMENT
0.4500 ± 0.0021 OUR FIT				Error includes scale factor of 1.1.
0.450 ± 0.004 OUR AVERAGE				

VALUE	EVTs	DOCUMENT ID	TECN	COMMENT
0.450 ± 0.004		ALDE	84 GAM2	
0.439 ± 0.024		BUTTRAM	70 OSPK	
• • • We do not use the following data for averages, fits, limits, etc. • • •				
0.44 ± 0.08	75	ABROSIMOV	80 HLBC	
0.32 ± 0.09		STRUGALSKI	71 HLBC	
0.41 ± 0.033		BUNIATOV	67 OSPK	Not indep. of $\Gamma(2\gamma)/\Gamma(\text{neutral modes})$
0.177 ± 0.035		FELDMAN	67 OSPK	
0.209 ± 0.054		DIGIUGNO	66 CNTR	Error doubled
0.29 ± 0.10		GRUNHAUS	66 OSPK	

$\Gamma(3\pi^0)/\Gamma(2\gamma)$	EVTs	DOCUMENT ID	TECN	COMMENT
0.820 ± 0.007 OUR FIT				Error includes scale factor of 1.1.
0.825 ± 0.011 OUR AVERAGE				

VALUE	EVTs	DOCUMENT ID	TECN	COMMENT
0.796 ± 0.016 ± 0.016		ACHASOV	00 SND	$e^+ e^- \rightarrow \phi \rightarrow \eta\gamma$
0.832 ± 0.005 ± 0.012		KRUSCHE	95D SPEC	$\eta p \rightarrow \eta p$, threshold
0.841 ± 0.034		AMSLER	93 CBAR	$\bar{p} p \rightarrow \pi^+ \pi^- \eta$ at rest
• • • We do not use the following data for averages, fits, limits, etc. • • •				
0.822 ± 0.009		³ ALDE	84 GAM2	
0.91 ± 0.14		COX	70B HBC	
0.75 ± 0.09		DEVONS	70 OSPK	
0.88 ± 0.16		BALTAY	67D DBC	
1.1 ± 0.2		CENCE	67 OSPK	
1.25 ± 0.39		BACCI	63 CNTR	Inverse BR reported

³ This result is not independent of other ALDE 84 results in this Listing, and so is omitted from the fit and average.

$\Gamma(\pi^0 2\gamma)/\Gamma(\text{neutral modes})$	EVTs	DOCUMENT ID	TECN	COMMENT
(1.00 ± 0.20) × 10⁻³ OUR FIT				
0.0010 ± 0.0002		ALDE	84 GAM2	

$\Gamma(\pi^0 2\gamma)/\Gamma_{\text{total}}$	EVTs	DOCUMENT ID	TECN	COMMENT
7.1 ± 1.4 OUR FIT				
9.5 ± 2.3	70	BINON	82 GAM2	See ALDE 84
< 30	90	0	DAVYDOV	81 GAM2 $\pi^- p \rightarrow \eta n$

These results are summarized in the review by LANDSBERG 85.

• • • We do not use the following data for averages, fits, limits, etc. • • •

See key on page 239

Meson Particle Listings

 η

$$\Gamma(\text{neutral modes}) / [\Gamma(\pi^+\pi^-\pi^0) + \Gamma(\pi^+\pi^-\gamma) + \Gamma(e^+e^-\gamma)]$$

$$\Gamma_1 / (\Gamma_7 + \Gamma_8 + \Gamma_9) = (\Gamma_2 + \Gamma_3 + \Gamma_4) / (\Gamma_7 + \Gamma_8 + \Gamma_9)$$

VALUE	EVTs	DOCUMENT ID	TECN	COMMENT
2.54 ± 0.06 OUR FIT				Error includes scale factor of 1.3.
2.64 ± 0.23		BALTAY	67B	DBC
• • • We do not use the following data for averages, fits, limits, etc. • • •				
4.5 ± 1.0	280	⁴ JAMES	66	HBC
3.20 ± 1.26	53	⁴ BASTIEN	62	HBC
2.5 ± 1.0	10	⁴ PICKUP	62	HBC

⁴ These experiments are not used in the averages as they do not separate clearly $\eta \rightarrow \pi^+\pi^-\pi^0$ and $\eta \rightarrow \pi^+\pi^-\gamma$ from each other. The reported values thus probably contain some unknown fraction of $\eta \rightarrow \pi^+\pi^-\gamma$.

$$\Gamma(2\gamma) / [\Gamma(\pi^+\pi^-\pi^0) + \Gamma(\pi^+\pi^-\gamma) + \Gamma(e^+e^-\gamma)] \quad \Gamma_2 / (\Gamma_7 + \Gamma_8 + \Gamma_9)$$

VALUE	EVTs	DOCUMENT ID	TECN	COMMENT
1.395 ± 0.030 OUR FIT				Error includes scale factor of 1.2.
1.1 ± 0.4 OUR AVERAGE				
1.51 ± 0.93	75	KENDALL	74	OSPK
0.99 ± 0.48		CRAWFORD	63	HBC

$$\Gamma(\text{neutral modes}) / \Gamma(\pi^+\pi^-\pi^0) \quad \Gamma_1 / \Gamma_7 = (\Gamma_2 + \Gamma_3 + \Gamma_4) / \Gamma_7$$

VALUE	EVTs	DOCUMENT ID	TECN	COMMENT
3.12 ± 0.07 OUR FIT				Error includes scale factor of 1.3.
3.26 ± 0.30 OUR AVERAGE				
2.54 ± 1.89	74	KENDALL	74	OSPK
3.4 ± 1.1	29	AGUILAR...	72B	HBC
2.83 ± 0.80	70	⁵ BLOODWO...	72B	HBC
3.6 ± 0.6	244	FLATTE	67B	HBC
2.89 ± 0.56		ALFF...	66	HBC
3.6 ± 0.8	50	KRAEMER	64	DBC
3.8 ± 1.1		PAULI	64	DBC

⁵ Error increased from published value 0.5 by Bloodworth (private communication).

$$\Gamma(2\gamma) / \Gamma(\pi^+\pi^-\pi^0) \quad \Gamma_2 / \Gamma_7$$

VALUE	EVTs	DOCUMENT ID	TECN	COMMENT
1.71 ± 0.04 OUR FIT				Error includes scale factor of 1.2.
1.75 ± 0.13 OUR AVERAGE				
1.78 ± 0.10 ± 0.13	1077	AMSLER	95	CBAR $\bar{p}p \rightarrow \pi^+\pi^-\eta$ at rest
1.72 ± 0.25	401	BAGLIN	69	HLBC
1.61 ± 0.39		FOSTER	65	HBC

$$\Gamma(3\pi^0) / \Gamma(\pi^+\pi^-\pi^0) \quad \Gamma_3 / \Gamma_7$$

VALUE	EVTs	DOCUMENT ID	TECN	COMMENT
1.404 ± 0.034 OUR FIT				Error includes scale factor of 1.3.
1.34 ± 0.10 OUR AVERAGE				Error includes scale factor of 1.2.
1.44 ± 0.09 ± 0.10	1627	AMSLER	95	CBAR $\bar{p}p \rightarrow \pi^+\pi^-\eta$ at rest
1.50 ^{+0.15} / _{-0.29}	199	BAGLIN	69	HLBC
1.47 ^{+0.20} / _{-0.17}		BULLOCK	68	HLBC
1.3 ± 0.4		BAGLIN	67B	HLBC
0.90 ± 0.24		FOSTER	65	HBC
2.0 ± 1.0		FOELSCH	64	HBC
0.83 ± 0.32		CRAWFORD	63	HBC

$$\Gamma(\text{other neutral modes}) / \Gamma_{\text{total}} \quad \Gamma_5 / \Gamma$$

These are neutral modes other than $\gamma\gamma$, $3\pi^0$, and $\pi^0\gamma\gamma$; nearly any such mode one can think of would violate P, or C, or both.

VALUE	CL%	DOCUMENT ID	TECN	COMMENT
<0.028		ABEGG	96	SPEC $p\bar{d} \rightarrow {}^3\text{He}\eta$

Charged modes

$$\Gamma(\pi^+\pi^-\pi^0) / [\Gamma(2\gamma) + \Gamma(3\pi^0)] \quad \Gamma_7 / (\Gamma_2 + \Gamma_3)$$

VALUE	DOCUMENT ID	TECN	COMMENT
0.321 ± 0.007 OUR FIT			Error includes scale factor of 1.2.
0.3141 ± 0.0081 ± 0.0058	ACHASOV	00B	SND $e^+e^- \rightarrow \phi \rightarrow \eta\gamma$

$$\Gamma(\pi^+\pi^-\gamma) / \Gamma(\pi^+\pi^-\pi^0) \quad \Gamma_8 / \Gamma_7$$

VALUE	EVTs	DOCUMENT ID	TECN	COMMENT
0.207 ± 0.004 OUR FIT				Error includes scale factor of 1.1.
0.207 ± 0.004 OUR AVERAGE				Error includes scale factor of 1.1.
0.209 ± 0.004	18k	THALER	73	ASPK
0.201 ± 0.006	7250	GORMLEY	70	ASPK
• • • We do not use the following data for averages, fits, limits, etc. • • •				
0.28 ± 0.04		BALTAY	67B	DBC
0.25 ± 0.035		LITCHFIELD	67	DBC
0.30 ± 0.06		CRAWFORD	66	HBC
0.196 ± 0.041		FOSTER	65C	HBC

$$\Gamma(e^+e^-\gamma) / \Gamma(\pi^+\pi^-\pi^0) \quad \Gamma_9 / \Gamma_7$$

VALUE (units 10 ⁻²)	EVTs	DOCUMENT ID	TECN	COMMENT
2.1 ± 0.5 OUR FIT				
2.1 ± 0.5	80	JANE	75B	OSPK See the erratum

$$\Gamma(\mu^+\mu^-\gamma) / \Gamma_{\text{total}} \quad \Gamma_{10} / \Gamma$$

VALUE (units 10 ⁻⁴)	EVTs	DOCUMENT ID	TECN	COMMENT
3.1 ± 0.4 OUR FIT				
3.1 ± 0.4	600	DZHELADIN	80	SPEC $\pi^-p \rightarrow \eta n$
• • • We do not use the following data for averages, fits, limits, etc. • • •				
1.5 ± 0.75	100	BUSHNIN	78	SPEC See DZHELADIN 80

$$\Gamma(e^+e^-) / \Gamma_{\text{total}} \quad \Gamma_{11} / \Gamma$$

VALUE (units 10 ⁻⁴)	CL%	DOCUMENT ID	TECN	COMMENT
<0.77		BROWDER	97B	CLE2 $e^+e^- \simeq 10.5$ GeV
• • • We do not use the following data for averages, fits, limits, etc. • • •				
<2	90	WHITE	96	SPEC $p\bar{d} \rightarrow \eta {}^3\text{He}$
<3	90	DAVIES	74	RVUE Uses ESTEN 67

$$\Gamma(\mu^+\mu^-) / \Gamma_{\text{total}} \quad \Gamma_{12} / \Gamma$$

VALUE (units 10 ⁻⁶)	CL%	EVTs	DOCUMENT ID	TECN	COMMENT
5.8 ± 0.8 OUR AVERAGE					
5.7 ± 0.7 ± 0.5	114	ABEGG	94	SPEC $p\bar{d} \rightarrow \eta {}^3\text{He}$	
6.5 ± 2.1	27	DZHELADIN	80B	SPEC $\pi^-p \rightarrow \eta n$	
• • • We do not use the following data for averages, fits, limits, etc. • • •					
5.6 ^{+0.6} / _{-0.7} ± 0.5	100	KESSLER	93	SPEC See ABEGG 94	
<20	95	0	WEHMANN	68	OSPK

$$\Gamma(\mu^+\mu^-) / \Gamma(2\gamma) \quad \Gamma_{12} / \Gamma_2$$

VALUE (units 10 ⁻⁵)	DOCUMENT ID	TECN	COMMENT
5.9 ± 2.2	HYAMS	69	OSPK

$$\Gamma(\pi^+\pi^-e^+e^-) / \Gamma(\pi^+\pi^-\gamma) \quad \Gamma_{13} / \Gamma_8$$

VALUE	EVTs	DOCUMENT ID	TECN	COMMENT
0.026 ± 0.026				
0.026 ± 0.026	1	GROSSMAN	66	HBC

$$\Gamma(\pi^+\pi^-e^+e^-) / \Gamma_{\text{total}} \quad \Gamma_{13} / \Gamma$$

VALUE (units 10 ⁻²)	DOCUMENT ID	TECN	COMMENT
0.13 ^{+0.12}/_{-0.08} OUR FIT			

• • • We do not use the following data for averages, fits, limits, etc. • • •

$$\Gamma(\pi^+\pi^-2\gamma) / \Gamma(\pi^+\pi^-\pi^0) \quad \Gamma_{14} / \Gamma_7$$

VALUE	CL%	DOCUMENT ID	TECN	COMMENT
<0.009		PRICE	67	HBC
• • • We do not use the following data for averages, fits, limits, etc. • • •				
<0.016	95	BALTAY	67B	DBC

$$\Gamma(\pi^+\pi^-\pi^0\gamma) / \Gamma(\pi^+\pi^-\pi^0) \quad \Gamma_{15} / \Gamma_7$$

VALUE (units 10 ⁻²)	CL%	EVTs	DOCUMENT ID	TECN	COMMENT	
<0.24		90	0	THALER	73	ASPK
• • • We do not use the following data for averages, fits, limits, etc. • • •						
<1.7	90			ARNOLD	68	HLBC
<1.6	95			BALTAY	67B	DBC
<7.0				FLATTE	67	HBC
<0.9				PRICE	67	HBC

$$\Gamma(\pi^0\mu^+\mu^-) / \Gamma_{\text{total}} \quad \Gamma_{16} / \Gamma$$

VALUE (units 10 ⁻⁶)	CL%	DOCUMENT ID	TECN	COMMENT
<3		90		DZHELADIN 81 SPEC $\pi^-p \rightarrow \eta n$

Rare or forbidden modes

$$\Gamma(\pi^+\pi^-) / \Gamma_{\text{total}} \quad \Gamma_{17} / \Gamma$$

Forbidden by P and CP invariance.					
VALUE (units 10 ⁻⁴)	CL%	EVTs	DOCUMENT ID	TECN	COMMENT
< 3.3		90			AKHMETSHIN 99B CMD2 $e^+e^- \rightarrow \phi \rightarrow \eta\gamma$
• • • We do not use the following data for averages, fits, limits, etc. • • •					
< 9	90				AKHMETSHIN 97C CMD2 See AKHMETSHIN 99B
<15	0				THALER 73 ASPK

$$\Gamma(\pi^0\pi^0) / \Gamma_{\text{total}} \quad \Gamma_{18} / \Gamma$$

Forbidden by P and CP invariance.					
VALUE (units 10 ⁻⁴)	CL%	DOCUMENT ID	TECN	COMMENT	
<4.3		90			AKHMETSHIN 99C CMD2 $e^+e^- \rightarrow \phi \rightarrow \eta\gamma$
• • • We do not use the following data for averages, fits, limits, etc. • • •					
<6	90	⁶ ACHASOV	98	SND $e^+e^- \rightarrow \phi \rightarrow \eta\gamma$	

⁶ ACHASOV 98 observes one event in a $\pm 3\sigma$ region around the η mass, while a Monte Carlo calculation gives 10 ± 5 events. The limit here is the Poisson upper limit for one observed event and no background.

Meson Particle Listings

η

$\Gamma(3\gamma)/\Gamma(\text{neutral modes})$ Forbidden by C invariance. $\Gamma_{19}/\Gamma_1 = \Gamma_{19}/(\Gamma_2+\Gamma_3+\Gamma_4)$

VALUE (units 10^{-4})	CL%	DOCUMENT ID	TECN
<7	95	ALDE 84	GAM2

$\Gamma(\pi^0 e^+ e^-)/\Gamma(\pi^+ \pi^- \pi^0)$ C parity forbids this to occur as a single-photon process. Γ_{20}/Γ_7

VALUE (units 10^{-4})	CL%	EVTs	DOCUMENT ID	TECN
< 1.9	90		JANE 75	OSPK
< 42	90		BAGLIN 67	HLBC
< 16	90	0	BILLING 67	HLBC
< 77		0	FOSTER 65B	HBC
<110			PRICE 65	HBC

$\Gamma(\pi^0 e^+ e^-)/\Gamma_{\text{total}}$ C parity forbids this to occur as a single-photon process. Γ_{20}/Γ

VALUE (units 10^{-2})	CL%	EVTs	DOCUMENT ID	TECN
<0.016	90	0	MARTYNOV 76	HLBC
<0.084	90		BAZIN 68	DBC
<0.7			RITTENBERG 65	HBC

$\Gamma(\pi^0 \mu^+ \mu^-)/\Gamma_{\text{total}}$ C parity forbids this to occur as a single-photon process. Γ_{21}/Γ

VALUE (units 10^{-4})	CL%	DOCUMENT ID	TECN	COMMENT
<0.05	90	DZHELADIN 81	SPEC	$\pi^- p \rightarrow \eta n$
<5		WEHMANN 68	OSPK	

$[\Gamma(\mu^+ e^-) + \Gamma(\mu^- e^+)]/\Gamma_{\text{total}}$ Forbidden by lepton family number conservation. Γ_{22}/Γ

VALUE (units 10^{-6})	CL%	DOCUMENT ID	TECN	COMMENT
<6	90	WHITE 96	SPEC	$pd \rightarrow \eta^3 \text{He}$

η C-NONCONSERVING DECAY PARAMETERS

$\pi^+ \pi^- \pi^0$ LEFT-RIGHT ASYMMETRY PARAMETER

Measurements with an error $> 1.0 \times 10^{-2}$ have been omitted.

VALUE (units 10^{-2})	EVTs	DOCUMENT ID	TECN
0.09 ± 0.17 OUR AVERAGE			
0.28 ± 0.26	165k	JANE 74	OSPK
-0.05 ± 0.22	220k	LAYTER 72	ASPK
1.5 ± 0.5	37k	GORMLEY 68c	ASPK

⁷ The GORMLEY 68c asymmetry is probably due to unmeasured ($\mathbf{E} \times \mathbf{B}$) spark chamber effects. New experiments with ($\mathbf{E} \times \mathbf{B}$) controls don't observe an asymmetry.

$\pi^+ \pi^- \pi^0$ SEXTANT ASYMMETRY PARAMETER

Measurements with an error $> 2.0 \times 10^{-2}$ have been omitted.

VALUE (units 10^{-2})	EVTs	DOCUMENT ID	TECN
0.18 ± 0.16 OUR AVERAGE			
0.20 ± 0.25	165k	JANE 74	OSPK
0.10 ± 0.22	220k	LAYTER 72	ASPK
0.5 ± 0.5	37k	GORMLEY 68c	WIRE

$\pi^+ \pi^- \pi^0$ QUADRANT ASYMMETRY PARAMETER

VALUE (units 10^{-2})	EVTs	DOCUMENT ID	TECN
-0.17 ± 0.17 OUR AVERAGE			
-0.30 ± 0.25	165k	JANE 74	OSPK
-0.07 ± 0.22	220k	LAYTER 72	ASPK

$\pi^+ \pi^- \gamma$ LEFT-RIGHT ASYMMETRY PARAMETER

Measurements with an error $> 2.0 \times 10^{-2}$ have been omitted.

VALUE (units 10^{-2})	EVTs	DOCUMENT ID	TECN
0.9 ± 0.4 OUR AVERAGE			
1.2 ± 0.6	35k	JANE 74b	OSPK
0.5 ± 0.6	36k	THALER 72	ASPK
1.22 ± 1.56	7257	GORMLEY 70	ASPK

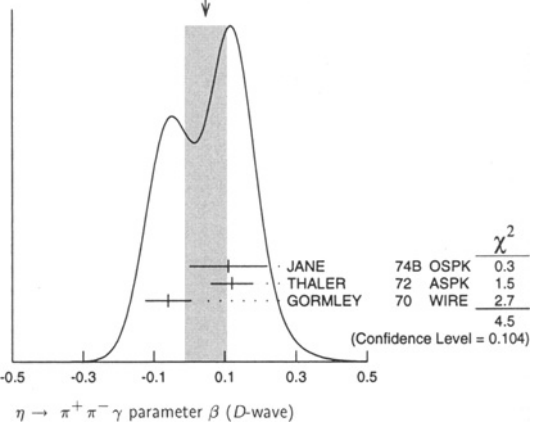
$\pi^+ \pi^- \gamma$ PARAMETER β (D-wave)

Sensitive to a D-wave contribution: $dN/d\cos\theta = \sin^2\theta (1 + \beta \cos^2\theta)$

VALUE	EVTs	DOCUMENT ID	TECN
0.05 ± 0.06 OUR AVERAGE			
0.11 ± 0.11	35k	JANE 74b	OSPK
0.12 ± 0.06		⁸ THALER 72	ASPK
-0.060 ± 0.065	7250	GORMLEY 70	WIRE

⁸ The authors don't believe this indicates D-wave because the dependence of β on the γ energy is inconsistent with theoretical prediction. A $\cos^2\theta$ dependence may also come from P- and F-wave interference.

WEIGHTED AVERAGE
0.05±0.06 (Error scaled by 1.5)



ENERGY DEPENDENCE OF $\eta \rightarrow 3\pi$ DALITZ PLOTS

PARAMETERS FOR $\eta \rightarrow \pi^+ \pi^- \pi^0$

See the "Note on η Decay Parameters" in our 1994 edition, Phys. Rev. **D50**, 1 August 1994, Part I, p. 1454. The following experiments fit to one or more of the coefficients a, b, c, d, e for $|\text{matrix element}|^2 = 1 + ay + by^2 + cx + dx^2 + exy$.

VALUE	EVTs	DOCUMENT ID	TECN	COMMENT
3230	⁹ ABELE	98D CBAR		$\bar{p}p \rightarrow \pi^0 \pi^0 \eta$ at rest
1077	¹⁰ AMSLER	95 CBAR		$\bar{p}p \rightarrow \pi^+ \pi^- \eta$ at rest
81k	LAYTER	73 ASPK		
220k	LAYTER	72 ASPK		
1138	CARPENTER	70 HBC		
349	DANBURG	70 DBC		
7250	GORMLEY	70 WIRE		
526	BAGLIN	69 HLBC		
7170	CNOPS	68 OSPK		
37k	GORMLEY	68c WIRE		
1300	CLPWY	66 HBC		
705	LARRIBE	66 HBC		

⁹ ABELE 98D obtain $a = -1.22 \pm 0.07$ and $b = 0.22 \pm 0.11$ when c (our d) is fixed at 0.06.
¹⁰ AMSLER 95 fits to $(1+ay+by^2)$ and obtains $a = -0.94 \pm 0.15$ and $b = 0.11 \pm 0.27$.

α PARAMETER FOR $\eta \rightarrow 3\pi^0$

See the "Note on η Decay Parameters" in our 1994 edition, Phys. Rev. **D50**, 1 August 1994, Part I, p. 1454. The value here is of α in $|\text{matrix element}|^2 = 1 + 2\alpha z$.

VALUE	EVTs	DOCUMENT ID	TECN	COMMENT
-0.039 ± 0.015 OUR AVERAGE				
-0.052 ± 0.017 ± 0.010	98k	ABELE 98C	CBAR	$\bar{p}p \rightarrow 5\pi^0$
-0.022 ± 0.023	50k	ALDE 84	GAM2	
-0.32 ± 0.37	192	BAGLIN 70	HLBC	

η REFERENCES

ACHASOV 00	EPJ C12 25	M.N. Achasov et al.	(Novosibirsk SND Collab.)
ACHASOV 00B	JETP 90 17	M.N. Achasov et al.	(Novosibirsk SND Collab.)
	Translated from ZHETF 117 22.		
AKHMETSHIN 99B	PL B462 371	R.R. Akhmetshin et al.	(CMD-2 Collab.)
AKHMETSHIN 99C	PL B462 380	R.R. Akhmetshin et al.	(CMD-2 Collab.)
ABELE 98C	PL B417 193	A. Abele et al.	(Crystal Barrel Collab.)
ABELE 98D	PL B417 197	A. Abele et al.	(Crystal Barrel Collab.)
ACHASOV 98	PL B425 388	M.M. Achasov et al.	(Novosibirsk SND Collab.)
AKHMETSHIN 97C	PL B415 452	R.R. Akhmetshin et al.	(CMD-2 Collab.)
BROWDER 97B	PR D56 5359	T.E. Browder et al.	(CLEO Collab.)
ABEGG 96	PR D53 11	R. Abegg et al.	(Saturne SPES2 Collab.)
WHITE 96	PR D53 6658	D.B. White et al.	(Saturne SPES2 Collab.)
AMSLER 95	PL B346 203	C. Amstler et al.	(Crystal Barrel Collab.)
KRUSCHE 95D	ZPHY A351 237	B. Krusche et al.	(TAPS + A2 Collab.)
ABEGG 94	PR D50 92	R. Abegg et al.	(Saturne SPES2 Collab.)
AMSLER 93	ZPHY C58 175	C. Amstler et al.	(Crystal Barrel Collab.)
KESSLER 93	PRL 70 892	R.S. Kessler et al.	(Saturne SPES2 Collab.)
PILOIN 92	PL B276 526	F. Piloïn et al.	(Saturne SPES4 Collab.)
BARU 90	ZPHY C48 581	S.E. Baru et al.	(MD-1 Collab.)
ROE 90	PR D41 17	N.A. Roe et al.	(ASP Collab.)
WILLIAMS 88	PR D38 1365	D.A. Williams et al.	(Crystal Ball Collab.)
AHARA 86	PR D33 844	H. Ahara et al.	(TPC-2 γ Collab.)
BARTEL 85E	PL 160B 421	W. Bartel et al.	(JADE Collab.)
LANDSBERG 85	PR D128 310	L.G. Landsberg et al.	(SERP)
ALDE 84	ZPHY C25 225	D.M. Alde et al.	(SERP, BELG, LAPP)
	Also 84B	SJNP 40 918	(SERP, BELG, LAPP)
		Translated from YAF 40 1447.	
WEINSTEIN 83	PR D28 2896	A.J. Weinstein et al.	(Crystal Ball Collab.)
BINON 82	SJNP 36 391	F.G. Binon et al.	(SERP, BELG, LAPP+)
		Translated from YAF 36 670.	
	Also 82B	NC 71A 497	(SERP, BELG, LAPP+)
DAVYDOV 81	LNJ 32 45	V.A. Davydov et al.	(SERP, BELG, LAPP+)
	Also 81B	SJNP 33 825	(SERP, BELG, LAPP+)
		Translated from YAF 33 1534.	
DZHELADIN 81	PL 105B 239	R.I. Dzhelezadin et al.	(SERP)
	Also 81C	SJNP 33 822	(SERP)
		Translated from YAF 33 1529.	

Meson Particle Listings

$f_0(400-1200), \rho(770)$

- 23 Breit-Wigner fit to S-wave intensity measured in $\pi^- N \rightarrow \pi^- \pi^+ N$ on polarized targets. The fit does not include $f_0(980)$.
- 24 Uses data from ASTON 88, OCHS 73, HYAMS 73, ARMSTRONG 91B, GRAYER 74, CASON 83, ROSSELET 77, and BEIER 72B. Coupled channel analysis with flavor symmetry and all light two-pseudoscalars systems.
- 25 Uses $\pi^0 \pi^0$ data from ANISOVICH 94, AMSLER 94D, and ALDE 95B, $\pi^+ \pi^-$ data from OCHS 73, GRAYER 74 and ROSSELET 77, and $\eta \eta$ data from ANISOVICH 94.
- 26 The pole is on Sheet III. Demonstrates explicitly that $f_0(400-1200)$ and $f_0(1370)$ are two different poles.
- 27 Analysis of data from OCHS 73, ESTABROOKS 75, ROSSELET 77, and MUKHIN 80.

$f_0(400-1200)$ DECAY MODES

Mode	Fraction (Γ_i/Γ)
$\Gamma_1 \quad \pi\pi$	dominant
$\Gamma_2 \quad \gamma\gamma$	seen

$f_0(400-1200)$ PARTIAL WIDTHS

$\Gamma(\gamma\gamma)$	DOCUMENT ID	TECN	COMMENT	Γ_2
VALUE (keV)				
seen	28 MORGAN	90 RVUE	$\gamma\gamma \rightarrow \pi^+ \pi^- \pi^0 \pi^0$	

• • • We do not use the following data for averages, fits, limits, etc. • • •

10 ± 6	COURAU	86 DMI	$e^+ e^- \rightarrow \pi^+ \pi^- e^+ e^-$
------------	--------	--------	---

28 Analysis of data from BOYER 90 and MARSISKE 90.

$f_0(400-1200)$ REFERENCES

ALEKSEEV 99 NP B541 3	I.G. Aleksev et al.
HANNAH 99 PR D50 017502	T. Hannah
KAMINSKI 99 EPJ C9 141	R. Kaminski, L. Lesniak, B. Loiseau
OLLER 99 PR D60 099906	J.A. Oller et al.
OLLER 99B NP A652 407	J.A. Oller, E. Oset
OLLER 99C PR D60 074023	J.A. Oller, E. Oset
ALEKSEEV 98 PAN 61 174	I.G. Aleksev et al.
ANISOVICH 98B UFN 41 419	V.V. Anisovich et al.
LOCHER 98 EPJ C4 317	M.P. Locher et al.
TROYAN 98 JINRRC 5 33	Yu. Troyan et al.
ALDE 97 PL B397 350	D.M. Alde et al.
ISHIDA 97 PTP 95 1005	S. Ishida et al.
KAMINSKI 97B PL B413 130	R. Kaminski et al.
Also 96 PTP 95 745	S. Ishida et al.
SVEC 96 PR D53 2343	M. Svec
TORNQVIST 96 PRL 76 1575	N.A. Tornqvist, M. Roos
ALDE 95B ZPHY C66 375	D.M. Alde et al.
AMSLER 95B PL B342 433	C. Amstler et al.
AMSLER 95D PL B355 425	C. Amstler et al.
ANISOVICH 95 PL B355 363	V.V. Anisovich et al.
JANSSEN 95 PR D52 2690	G. Janssen et al.
ACHASOV 94 PR D49 5779	N.N. Achasov, G.N. Shestakov
AMSLER 94D PL B333 277	C. Amstler et al.
ANISOVICH 94 PL B323 233	V.V. Anisovich et al.
KAMINSKI 94 PR D50 3145	R. Kaminski et al.
ZOU 94B PR D50 591	B.S. Zou, D.V. Bugg
ZOU 93 PR D48 R3948	B.S. Zou, D.V. Bugg
ARMSTRONG 91B ZPHY C52 359	T.A. Armstrong et al.
BOYER 90 PR D42 1350	J. Boyer et al.
MARSISKE 90 PR D41 3324	H. Marsiske et al.
MORGAN 90 ZPHY C48 623	D. Morgan, M.R. Pennington
AUGUSTIN 89 NP B320 1	J.E. Augustin, G. Cosme
ASTON 88 NP B296 493	D. Aston et al.
FALVARD 88 PR D38 2706	A. Falvard et al.
AU 87 PR D35 1633	K.L. Au, D. Morgan, M.R. Pennington
BEVEREN 86 ZPHY C30 615	E. van Beveren et al.
COURAU 86 NP B271 1	A. Courau et al.
CASON 83 PR D28 1586	N.M. Cason et al.
BISWAS 81 PRL 47 1378	N.N. Biswas et al.
MUKHIN 80 JETPL 32 601	K.N. Mukhin et al.
Translated from ZETFP 32 616.	
BECKER 79 NP B151 46	H. Becker et al.
CORDEN 79 NP B157 250	M.J. Corden et al.
ESTABROOKS 79 PR D19 2578	P. Estabrooks
FROGGATT 77 NP B129 89	C.D. Froggatt, J.L. Petersen
PAWLICKI 77 PR D15 3196	A.J. Pawlicki et al.
ROSSELET 77 PR D15 574	L. Rosselet et al.
CASON 76 PRL 36 1485	N.M. Cason et al.
ESTABROOKS 75 NP B95 322	P.G. Estabrooks, A.D. Martin
HYAMS 75 NP B100 205	B.D. Hyams et al.
SRINIVASAN 75 PR D12 661	V. Srinivasan et al.
ESTABROOKS 74 NP B79 301	P.G. Estabrooks, A.D. Martin
GRAYER 74 NP B75 189	G. Grayer et al.
APEL 73 PL 41B 542	W.D. Apel et al.
HYAMS 73 NP B64 134	B.D. Hyams et al.
OCHS 73 Thesis	W. Ochs
PROTOPOP... 73 PR D7 1279	S.D. Protopopescu et al.
BAILLON 72 PL 38B 555	P.H. Baillon et al.
BASDEVANT 72 PL 41B 178	J.L. Basdevant, C.D. Froggatt, J.L. Petersen
BEIER 72B PRL 29 511	E.W. Beier et al.
BENSINGER 71 PL 36B 134	J.R. Bensinger et al.
COLTON 71 PR D3 2028	E.P. Colton et al.
BATON 70 PL 33B 528	J.P. Baton, G. Laurens, J. Reigner
WALKER 67 RMP 39 695	W.D. Walker

OTHER RELATED PAPERS

BLACK 99 PR D59 074026	D. Black et al.
IGI 99 PR D59 034005	K. Igi, K. Hikasa
MINKOWSKI 99 EPJ C9 283	P. Minkowski, W. Ochs
SCADRON 99 EPJ C6 141	M. Scadron
TAKAMATSU 99 PAN 62 435	K. Takamatsu
ABELE 98 PR D57 3860	A. Abele et al.
ANISOVICH 98 PL B437 209	V.V. Anisovich et al.
DELBURGO 98 JUMP A13 657	R. Delbourgo et al.
OLLER 98 PRL 80 3452	J.A. Oller et al.
ANISOVICH 97 PL B395 125	V.V. Anisovich, A.V. Sarantsev
ANISOVICH 97B ZPHY A357 123	A.V. Anisovich et al.
ANISOVICH 97C PL B413 137	
ANISOVICH 97D ZPHY A359 173	
CLDSE 97B PR D55 5749	F. Close et al.
MALTMAN 97 PL B393 19	K. Maltman, C.E. Wolfe
OLLER 97 NP A620 438	J.A. Oller et al.
SVEC 97 PR D55 4355	M. Svec
SVEC 97B PR D55 5727	
ABELE 97 PL B380 453	A. Abele et al.
AMSLER 96 PR D53 295	C. Amstler, F.E. Close
BUNENS 96 PL B374 210	J. Bunens et al.
BONUTTI 96 PRL 77 603	F. Bonutti et al.
BUGG 96 NP B471 59	D.V. Bugg, A.V. Sarantsev, B.S. Zou
HARADA 96 PR D54 1991	M. Harasa et al.
ISHIDA 96 PTP 95 745	S. Ishida et al.
AMSLER 95C PL B353 571	C. Amstler et al.
AMSLER 95F PL B350 389	C. Amstler et al.
ANTINORI 95 PL B353 589	F. Antinori et al.
BUGG 95 PL B353 378	D.V. Bugg et al.
GASPERO 95 NP A588 861	M. Gaspero
TORNQVIST 95 ZPHY C68 647	N.A. Tornqvist
AMSLER 94 PL B322 431	C. Amstler et al.
BUGG 94 PR D50 4412	D.V. Bugg et al.
KAMINSKI 94 PR D50 3145	R. Kaminski et al.
ADAMO 93 NP A558 13C	A. Adamo et al.
GASPERO 93 NP A552 407	M. Gaspero
MORGAN 93 PR D48 1185	D. Morgan, M.R. Pennington
Also 93C NC A Conf. Suppl.	
BOLTON 92B PRL 69 1328	T. Bolton et al.
SVEC 92 PR D45 55	M. Svec, A. de Lesquen, L. van Rossum
SVEC 92B PR D45 1518	M. Svec, A. de Lesquen, L. van Rossum
SVEC 92C PR D46 949	M. Svec, A. de Lesquen, L. van Rossum
RIGGENBACH 91 PR D43 127	C. Riggenbach et al.
BAI 90C PRL 65 2507	Z. Bai et al.
WEINSTEIN 90 PR D41 2236	J. Weinstein, N. Isgur
WEINSTEIN 89 UTPT 89 03	J. Weinstein, N. Isgur
ASTON 88D NP B301 525	D. Aston et al.
LONGACRE 86 PL B177 223	R.S. Longacre et al.
ACHASOV 84 ZPHY C22 53	N.N. Achasov, S.A. Devyanin, G.N. Shestakov
GASSER 84 ANP 158 142	
BINON 83 NC 78A 313	F.G. Binon et al.
ETKIN 82B PR D25 1786	A. Etkin et al.
TORNQVIST 82 PR 49 629	N.A. Tornqvist
COHEN 80 PR D22 2955	D. Cohen et al.
COSTA 80 NP B175 402	G. Costa et al.
BECKER 79B NP B150 301	H. Becker et al.
NAGELS 79 PR D20 1633	M.M. Nagels, T.A. Rijken, J.J. de Swart
POLYCHRO... 79 PR D19 1317	V.A. Polychronakos et al.
CORDEN 78 NP B144 253	M.J. Corden et al.
JAFFE 77 PR D15 267,281	R. Jaffe
FLATTE 76 PL 63B 224	S.M. Flatte
WETZEL 76 NP B115 298	W. Wetzel et al.
DEFOIX 72 NP B44 125	C. Defoix et al.

$\rho(770)$

$$I_G(J^{PC}) = 1 + (1 - \dots)$$

THE $\rho(770)$

Updated March 2000 by S. Eidelman (Novosibirsk).

Determination of the parameters of the $\rho(770)$ is beset with many difficulties because of its large width. In physical region fits, the line shape does not correspond to a relativistic Breit-Wigner function with a P -wave width, but requires some additional shape parameter. This dependence on parameterization was demonstrated long ago by PISUT 68. Bose-Einstein correlations are another source of shifts in the $\rho(770)$ line shape, particularly in multiparticle final state systems (LAFPERTY 93).

The same model dependence afflicts any other source of resonance parameters, such as the energy dependence of the phase shift δ_1^1 , or the pole position. It is, therefore, not surprising that a study of $\rho(770)$ dominance in the decays of the η and η' reveals the need for specific dynamical effects, in addition to the $\rho(770)$ pole (BENAYOUN 93, ABELE 97B). Recently, BENAYOUN 98 compared the predictions of different Vector Meson Dominance (VMD)-based models with the data on the $e^+e^- \rightarrow \pi^+\pi^-$ cross section below 1 GeV, as well as with the phase and near-threshold behavior of the time-like

See key on page 239

Meson Particle Listings

$\rho(770)$

pion form factor. They showed that only the model based on hidden local symmetry (HLS) is able to account consistently for all low-energy information, if one also requires a point-like coupling $\gamma\pi^+\pi^-$, which is excluded by common VMD but predicted by HLS.

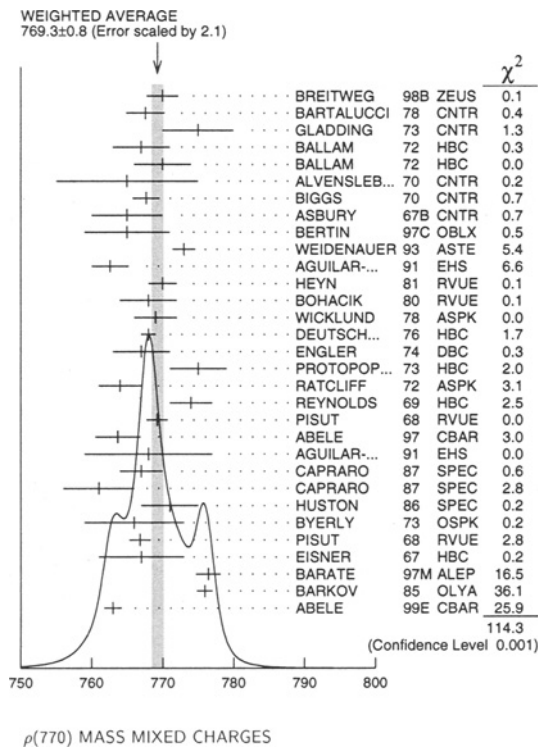
The cleanest determination of the $\rho(770)$ mass and width comes from the e^+e^- annihilation and τ -lepton decays. BARATE 97M showed that the charged $\rho(770)$ parameters measured from τ -lepton decays are consistent with those of the neutral one determined from e^+e^- data of BARKOV 85. This conclusion is qualitatively supported by the high statistics study of ANDERSON 00. However, model-independent comparison of the two-pion mass spectrum in τ decays and the $e^+e^- \rightarrow \pi^+\pi^-$ cross section gives indications of discrepancies between the overall normalization: τ data are about 3% higher than e^+e^- data (ANDERSON 99, EIDELMAN 99). This effect is too big to be explained by isospin violation (ALEMANY 98).

$\rho(770)$ MASS

We no longer list S-wave Breit-Wigner fits, or data with high combinatorial background.

MIXED CHARGES

VALUE (MeV) DOCUMENT ID
769.3±0.8 OUR AVERAGE Includes data from the 5 datablocks that follow this one. Error includes scale factor of 2.1. See the ideogram below.



MIXED CHARGES, τ DECAYS and e^+e^-

VALUE (MeV)	DOCUMENT ID	TECN	CHG	COMMENT
The data in this block is included in the average printed for a previous datablock.				
776.0±0.9 OUR AVERAGE				
776.4±0.9±1.5	¹ BARATE	97M ALEP		$\tau^- \rightarrow \pi^- \pi^0 \nu_\tau$
775.9±1.1	² BARKOV	85 OLYA	0	$e^+e^- \rightarrow \pi^+\pi^-$
• • • We do not use the following data for averages, fits, limits, etc. • • •				
775.1±0.7±5.3	³ BENAYOUN	98 RVUE		$e^+e^- \rightarrow \pi^+\pi^-, \mu^+\mu^-$
770.5±1.9±5.1	⁴ GARDNER	98 RVUE		$0.28-0.92 e^+e^- \rightarrow \pi^+\pi^-$
764.1±0.7	⁵ O'CONNELL	97 RVUE		$e^+e^- \rightarrow \pi^+\pi^-$
757.5±1.5	⁶ BERNICA	94 RVUE		$e^+e^- \rightarrow \pi^+\pi^-$
768 ± 1	⁷ GESHKEN...	89 RVUE		$e^+e^- \rightarrow \pi^+\pi^-$

MIXED CHARGES, OTHER REACTIONS

VALUE (MeV)	EVTS	DOCUMENT ID	TECN	CHG	COMMENT
The data in this block is included in the average printed for a previous datablock.					
763.0±0.3±1.2	600k	⁸ ABELE	99E CBAR	0±	$0.0 \bar{p}p \rightarrow \pi^+\pi^-\pi^0$

CHARGED ONLY, HADROPRODUCED

VALUE (MeV)	EVTS	DOCUMENT ID	TECN	CHG	COMMENT
The data in this block is included in the average printed for a previous datablock.					
766.5±1.1 OUR AVERAGE					
763.7±3.2		ABELE 97	CBAR		$\bar{p}n \rightarrow \pi^- \pi^0 \pi^0$
768 ± 9		AGUILAR...	91 EHS		400 pp
767 ± 3	2935	⁹ CAPRARO	87 SPEC	-	$200 \pi^- \text{Cu} \rightarrow \pi^- \pi^0 \text{Cu}$
761 ± 5	967	⁹ CAPRARO	87 SPEC	-	$200 \pi^- \text{Pb} \rightarrow \pi^- \pi^0 \text{Pb}$
771 ± 4		HUSTON 86	SPEC	+	$202 \pi^+ A \rightarrow \pi^+ \pi^0 A$
766 ± 7	6500	¹⁰ BYERLY	73 OSPK	-	5 π^-p
766.8±1.5	9650	¹¹ PISUT	68 RVUE	-	$1.7-3.2 \pi^-p, t < 10$
767 ± 6	900	⁹ EISNER	67 HBC	-	$4.2 \pi^-p, t < 10$

NEUTRAL ONLY, PHOTOPRODUCED

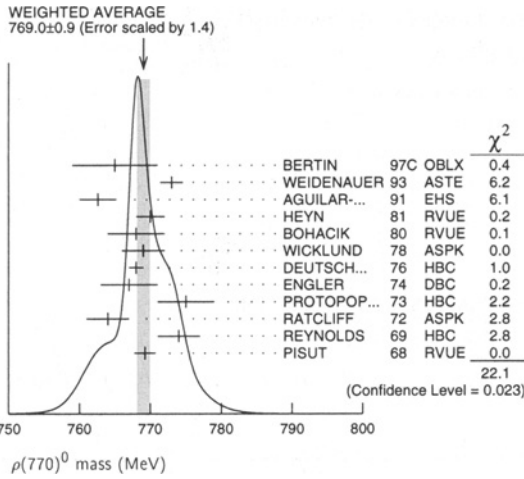
VALUE (MeV)	EVTS	DOCUMENT ID	TECN	CHG	COMMENT
The data in this block is included in the average printed for a previous datablock.					
776.5 ± 1.1 OUR AVERAGE					
770 ± 2 ± 1	79k	¹² BREITWEG	98B ZEUS	0	50-100 γp
767.6 ± 2.7		BARTALUCCI 78	CNTR	0	$\gamma p \rightarrow e^+e^-p$
775 ± 5		GLADDING 73	CNTR	0	2.9-4.7 γp
767 ± 4	1930	BALLAM 72	HBC	0	2.8 γp
770 ± 4	2430	BALLAM 72	HBC	0	4.7 γp
765 ± 10		ALVENSLEB... 70	CNTR	0	$\gamma A, t < 0.01$
767.7 ± 1.9	140k	BIGGS 70	CNTR	0	$< 4.1 \gamma C \rightarrow \pi^+\pi^-C$
765 ± 5	4000	ASBURY 67B	CNTR	0	$\gamma + Pb$
• • • We do not use the following data for averages, fits, limits, etc. • • •					
771 ± 2	79k	¹³ BREITWEG	98B ZEUS	0	50-100 γp

NEUTRAL ONLY, OTHER REACTIONS

VALUE (MeV)	EVTS	DOCUMENT ID	TECN	CHG	COMMENT
The data in this block is included in the average printed for a previous datablock.					
769.0±0.9 OUR AVERAGE Error includes scale factor of 1.4. See the ideogram below.					
765 ± 6		BERTIN 97C	OBLX		$0.0 \bar{p}p \rightarrow \pi^+\pi^-\pi^0$
773 ± 1.6		WEIDENAUER 93	ASTE		$\bar{p}p \rightarrow \pi^+\pi^-\omega$
762.6±2.6		AGUILAR... 91	EHS		400 pp
770 ± 2		¹⁴ HEYN 81	RVUE		Pion form factor
768 ± 4		^{15,16} BOHACIK 80	RVUE	0	$3,4,6 \pi^\pm N$
769 ± 3		¹⁰ WICKLUND 78	ASPK	0	$16 \pi^+p$
768 ± 1	76000	DEUTSCH... 76	HBC	0	$6 \pi^+n \rightarrow \pi^+\pi^-p$
767 ± 4	4100	ENGLER 74	DBC	0	$7.1 \pi^+p, t < 0.4$
775 ± 4	32000	¹⁵ PROTOPOP... 73	HBC	0	$15 \pi^-p, t < 0.3$
764 ± 3	6800	RATCLIFF 72	ASPK	0	$2.26 \pi^-p$
774 ± 3	1700	REYNOLDS 69	HBC	0	$1.7-3.2 \pi^-p, t < 10$
769.2±1.5	13300	¹⁷ PISUT 68	RVUE	0	$0.0 \bar{p}p \rightarrow \pi^+\pi^-\pi^0$
• • • We do not use the following data for averages, fits, limits, etc. • • •					
762.3±0.5±1.2	600k	¹⁸ ABELE 99E	CBAR	0	$0.0 \bar{p}p \rightarrow \pi^+\pi^-\pi^0$
777 ± 2	4943	¹⁹ ADAMS 97	E665		$470 \mu p \rightarrow \mu XB$
770 ± 2		²⁰ BOGOLYUB... 97	MIRA		$32 \bar{p}p \rightarrow \pi^+\pi^-X$
768 ± 8		²⁰ BOGOLYUB... 97	MIRA		$32 pp \rightarrow \pi^+\pi^-X$
761.1±2.9		DUBNICKA 89	RVUE		π form factor
777.4±2.0		²¹ CHABAUD 83	ASPK	0	$17 \pi^-p$ polarized
769.5±0.7		^{15,16} LANG 79	RVUE	0	$3,4,6 \pi^\pm N$
770 ± 9		¹⁶ ESTABROOKS 74	RVUE	0	$17 \pi^-p \rightarrow \pi^+\pi^-n$
773.5±1.7	11200	⁹ JACOBS 72	HBC	0	2.8 π^-p
775 ± 3	2250	HYAMS 68	OSPK	0	11.2 π^-p

Meson Particle Listings

$\rho(770)$



- From the Gounaris-Sakurai parametrization of the pion form factor. The second error is a model error taking into account different parametrizations of the pion form factor.
- From the Gounaris-Sakurai parametrization of the pion form factor.
- Using the data of BARKOV 85 in the hidden local symmetry model.
- From the fit to $e^+e^- \rightarrow \pi^+\pi^-$ data from the compilations of HEYN 81 and BARKOV 85, including the Gounaris-Sakurai parametrization of the pion form factor.
- A fit of BARKOV 85 data assuming the direct $\omega\pi\pi$ coupling.
- Applying the S-matrix formalism to the BARKOV 85 data.
- Includes BARKOV 85 data. Model-dependent width definition.
- Assuming the equality of ρ^+ and ρ^- masses and widths.
- Mass errors enlarged by us to Γ/\sqrt{N} ; see the note with the $K^*(892)$ mass.
- Phase shift analysis. Systematic errors added corresponding to spread of different fits.
- From fit of 3-parameter relativistic P-wave Breit-Wigner to total mass distribution. Includes BATON 68, MILLER 67b, ALFF-STEINBERGER 66, HAGOPIAN 66, HAGOPIAN 66b, JACOBS 66b, JAMES 66, WEST 66, BLIEDEN 65 and CARMONY 64.
- From the parametrization according to SOEDING 66.
- From the parametrization according to ROSS 66.
- HEYN 81 includes all spacelike and timelike F_π values until 1978.
- From pole extrapolation.
- From phase shift analysis of GRAYER 74 data.
- Includes MALAMUD 69, ARMENISE 68, BACON 67, HUWE 67, MILLER 67b, ALFF-STEINBERGER 66, HAGOPIAN 66, HAGOPIAN 66b, JACOBS 66b, JAMES 66, WEST 66, GOLDHABER 64, ABOLINS 63.
- Using relativistic Breit-Wigner and taking into account ρ - ω interference.
- Systematic errors not evaluated.
- Systematic effects not studied.
- From fit of 3-parameter relativistic Breit-Wigner to helicity-zero part of P-wave intensity. CHABAUD 83 includes data of GRAYER 74.

$m_{\rho(770)^0} - m_{\rho(770)^\pm}$

VALUE (MeV)	EVTs	DOCUMENT ID	TECN	CHG	COMMENT
0.4 ± 0.8 OUR AVERAGE					
1.6 ± 0.6 ± 1.7	600k	ABELE	99E	CBAR	0 ± 0.0 $\bar{p}p \rightarrow \pi^+\pi^-\pi^0\nu_\tau$
0.0 ± 1.0		22 BARATE	97M	ALEP	$\tau^- \rightarrow \pi^-\pi^0\nu_\tau$
-4 ± 4	3000	23 REYNOLDS	69	HBC	-0 2.26 π^-p
-5 ± 5	3600	23 FOSTER	68	HBC	± 0.0 $\bar{p}p$
2.4 ± 2.1	22950	24 PISUT	68	RVUE	$\pi N \rightarrow \rho N$

22 Using the compilation of e^+e^- data from BARKOV 85.
23 From quoted masses of charged and neutral modes.
24 Includes MALAMUD 69, ARMENISE 68, BATON 68, BACON 67, HUWE 67, MILLER 67b, ALFF-STEINBERGER 66, HAGOPIAN 66, HAGOPIAN 66b, JACOBS 66b, JAMES 66, WEST 66, BLIEDEN 65, CARMONY 64, GOLDHABER 64, ABOLINS 63.

$\rho(770)$ RANGE PARAMETER

The range parameter R enters an energy-dependent correction to the width, of the form $(1 + q^2 R^2) / (1 + q^2 R^2)$, where q is the momentum of one of the pions in the $\pi\pi$ rest system. At resonance, $q = q_r$.

VALUE (GeV ⁻¹)	DOCUMENT ID	TECN	CHG	COMMENT
5.3 ± 0.9 -0.7	CHABAUD	83	ASPK	0 17 π^-p polarized

$\rho(770)$ WIDTH

We no longer list S-wave Breit-Wigner fits, or data with high combinatorial background.

MIXED CHARGES

VALUE (MeV)	DOCUMENT ID
150.2 ± 0.8 OUR AVERAGE	Includes data from the 5 datablocks that follow this one.

MIXED CHARGES, τ DECAYS and e^+e^-

VALUE (MeV)	DOCUMENT ID	TECN	CHG	COMMENT
The data in this block is included in the average printed for a previous datablock.				
150.5 ± 2.7 OUR AVERAGE				
150.5 ± 1.6 ± 6.3	25 BARATE	97M	ALEP	$\tau^- \rightarrow \pi^-\pi^0\nu_\tau$
150.5 ± 3.0	26 BARKOV	85	OLYA	0 $e^+e^- \rightarrow \pi^+\pi^-$
• • • We do not use the following data for averages, fits, limits, etc. • • •				
147.9 ± 1.5 ± 7.5	27 BENAYOUN	98	RVUE	$e^+e^- \rightarrow \pi^+\pi^-, \mu^+\mu^-$
153.5 ± 1.3 ± 4.6	28 GARDNER	98	RVUE	0.28-0.92 $e^+e^- \rightarrow \pi^+\pi^-$
145.0 ± 1.7	29 O'CONNELL	97	RVUE	$e^+e^- \rightarrow \pi^+\pi^-$
142.5 ± 3.5	30 BERNICHA	94	RVUE	$e^+e^- \rightarrow \pi^+\pi^-$
138 ± 1	31 GESHKEN...	89	RVUE	$e^+e^- \rightarrow \pi^+\pi^-$

MIXED CHARGES, OTHER REACTIONS

VALUE (MeV)	EVTs	DOCUMENT ID	TECN	CHG	COMMENT
The data in this block is included in the average printed for a previous datablock.					
149.5 ± 1.3	600k	32 ABELE	99E	CBAR	0 ± 0.0 $\bar{p}p \rightarrow \pi^+\pi^-\pi^0$

CHARGED ONLY, HADROPRODUCED

VALUE (MeV)	EVTs	DOCUMENT ID	TECN	CHG	COMMENT
The data in this block is included in the average printed for a previous datablock.					
150.2 ± 2.4 OUR FIT					
150.2 ± 2.4 OUR AVERAGE					
152.8 ± 4.3		ABELE	97	CBAR	$\bar{p}n \rightarrow \pi^-\pi^0\pi^0$
155 ± 11	2935	33 CAPRARO	87	SPEC	- 200 $\pi^-Cu \rightarrow \pi^-\pi^0Cu$
154 ± 20	967	33 CAPRARO	87	SPEC	- 200 $\pi^-Pb \rightarrow \pi^-\pi^0Pb$
150 ± 5		HUSTON	86	SPEC	+ 202 $\pi^+A \rightarrow \pi^+\pi^0A$
146 ± 12	6500	34 BYERLY	73	OSPK	- 5 π^-p
148.2 ± 4.1	9650	35 PISUT	68	RVUE	- 1.7-3.2 $\pi^-p, t < 10$
146 ± 13	900	EISNER	67	HBC	- 4.2 $\pi^-p, t < 10$

NEUTRAL ONLY, PHOTOPRODUCED

VALUE (MeV)	EVTs	DOCUMENT ID	TECN	CHG	COMMENT
The data in this block is included in the average printed for a previous datablock.					
150.7 ± 2.9 OUR AVERAGE					
146 ± 3 ± 13	79k	36 BREITWEG	98B	ZEUS	0 50-100 γp
150.9 ± 3.0		BARTALUCCI	78	CNTR	0 $\gamma p \rightarrow e^+e^-p$
• • • We do not use the following data for averages, fits, limits, etc. • • •					
138 ± 3	79k	37 BREITWEG	98B	ZEUS	0 50-100 γp
147 ± 11		GLADDING	73	CNTR	0 2.9-4.7 γp
155 ± 12	2430	BALLAM	72	HBC	0 4.7 γp
145 ± 13	1930	BALLAM	72	HBC	0 2.8 γp
140 ± 5		ALVENSLEB...	70	CNTR	0 $\gamma A, t < 0.01$
146.1 ± 2.9	140k	BIGGS	70	CNTR	0 < 4.1 $\gamma C \rightarrow \pi^+\pi^-C$
160 ± 10		LANZEROTTI	68	CNTR	0 γp
130 ± 5	4000	ASBURY	67b	CNTR	0 $\gamma + Pb$

NEUTRAL ONLY, OTHER REACTIONS

VALUE (MeV)	EVTs	DOCUMENT ID	TECN	CHG	COMMENT
The data in this block is included in the average printed for a previous datablock.					
150.9 ± 2.0 OUR FIT					Error includes scale factor of 1.3.
150.9 ± 1.7 OUR AVERAGE					Error includes scale factor of 1.1.
122 ± 20		BERTIN	97C	OBLX	0.0 $\bar{p}p \rightarrow \pi^+\pi^-\pi^0$
145.7 ± 5.3		WEIDENAUER	93	ASTE	$\bar{p}p \rightarrow \pi^+\pi^-\omega$
144.9 ± 3.7		DUBNICKA	89	RVUE	π form factor
148 ± 6	38,39	BOHACIK	80	RVUE	0
152 ± 9	34	WICKLUND	78	ASPK	0 3,4,6 $\pi^\pm pN$
154 ± 2	76000	DEUTSCH...	76	HBC	0 16 π^+p
157 ± 8	6800	RATCLIFF	72	ASPK	0 15 $\pi^-p, t < 0.3$
143 ± 8	1700	REYNOLDS	69	HBC	0 2.26 π^-p
• • • We do not use the following data for averages, fits, limits, etc. • • •					
147.0 ± 2.5	600k	40 ABELE	99E	CBAR	0 0.0 $\bar{p}p \rightarrow \pi^+\pi^-\pi^0$
146 ± 3	4943	41 ADAMS	97	E665	470 $\mu p \rightarrow \mu XB$
160.0 ^{+4.1} -4.0		42 CHABAUD	83	ASPK	0 17 π^-p polarized
155 ± 1		43 HEYN	81	RVUE	0 π form factor
148.0 ± 1.3	38,39	LANG	79	RVUE	0
146 ± 14	4100	ENGLER	74	DBC	0 6 $\pi^+n \rightarrow \pi^+\pi^-p$
143 ± 13	39	ESTABROOKS	74	RVUE	0 17 $\pi^-p \rightarrow \pi^+\pi^-n$
160 ± 10	32000	38 PROTOPOP...	73	HBC	0 7.1 $\pi^+p, t < 0.4$
145 ± 12	2250	33 HYAMS	68	OSPK	0 11.2 π^-p
163 ± 15	13300	44 PISUT	68	RVUE	0 1.7-3.2 $\pi^-p, t < 10$

- From the Gounaris-Sakurai parametrization of the pion form factor. The second error is a model error taking into account different parametrizations of the pion form factor.
- From the Gounaris-Sakurai parametrization of the pion form factor.
- Using the data of BARKOV 85 in the hidden local symmetry model.
- From the fit to $e^+e^- \rightarrow \pi^+\pi^-$ data from the compilations of HEYN 81 and BARKOV 85, including the Gounaris-Sakurai parametrization of the pion form factor.
- A fit of BARKOV 85 data assuming the direct $\omega\pi\pi$ coupling.
- Applying the S-matrix formalism to the BARKOV 85 data.
- Includes BARKOV 85 data. Model-dependent width definition.

- 32 Assuming the equality of ρ^+ and ρ^- masses and widths.
- 33 Width errors enlarged by us to $4\Gamma/\sqrt{N}$; see the note with the $K^*(892)$ mass.
- 34 Phase shift analysis. Systematic errors added corresponding to spread of different fits.
- 35 From fit of 3-parameter relativistic P -wave Breit-Wigner to total mass distribution. Includes BATON 68, MILLER 67b, ALFF-STEINBERGER 66, HAGOPIAN 66, HAGOPIAN 66b, JACOBS 66b, JAMES 66, WEST 66, BLIEDEN 65 and CARMONY 64.
- 36 From the parametrization according to SOEDING 66.
- 37 From the parametrization according to ROSS 66.
- 38 From pole extrapolation.
- 39 From phase shift analysis of GRAYER 74 data.
- 40 Using relativistic Breit-Wigner and taking into account ρ - ω interference.
- 41 Systematic errors not evaluated.
- 42 From fit of 3-parameter relativistic Breit-Wigner to helicity-zero part of P -wave intensity. CHABAUD 83 includes data of GRAYER 74.
- 43 HEYN 81 includes all spacelike and timelike F_π values until 1978.
- 44 Includes MALAMUD 69, ARMENISE 68, BACON 67, HUWE 67, MILLER 67b, ALFF-STEINBERGER 66, HAGOPIAN 66, HAGOPIAN 66b, JACOBS 66b, JAMES 66, WEST 66, GOLDBERGER 64, ABOLINS 63.

$\Gamma_{\rho(770)^0} - \Gamma_{\rho(770)^\pm}$	DOCUMENT ID	TECN	COMMENT
VALUE -0.1 ± 1.9	45	BARATE	97M ALEP $\tau^- \rightarrow \pi^- \pi^0 \nu_\tau$

45 Using the compilation of e^+e^- data from BARKOV 85.

$\rho(770)$ DECAY MODES

Mode	Fraction (Γ_i/Γ)	Scale factor/ Confidence level
Γ_1 $\pi\pi$	~ 100	%
$\rho(770)^\pm$ decays		
Γ_2 $\pi^\pm \pi^0$	~ 100	%
Γ_3 $\pi^\pm \gamma$	(4.5 ± 0.5) × 10 ⁻⁴	S=2.2
Γ_4 $\pi^\pm \eta$	< 6	CL=84%
Γ_5 $\pi^\pm \pi^+ \pi^- \pi^0$	< 2.0	CL=84%
$\rho(770)^0$ decays		
Γ_6 $\pi^+ \pi^-$	~ 100	%
Γ_7 $\pi^+ \pi^- \gamma$	(9.9 ± 1.6) × 10 ⁻³	
Γ_8 $\pi^0 \gamma$	(6.8 ± 1.7) × 10 ⁻⁴	
Γ_9 $\eta \gamma$	(2.4 ^{+0.8} / _{-0.9}) × 10 ⁻⁴	S=1.6
Γ_{10} $\mu^+ \mu^-$	[a] (4.60 ± 0.28) × 10 ⁻⁵	
Γ_{11} $e^+ e^-$	[a] (4.49 ± 0.22) × 10 ⁻⁵	
Γ_{12} $\pi^+ \pi^- \pi^0$	< 1.2	CL=90%
Γ_{13} $\pi^+ \pi^- \pi^+ \pi^-$	(1.8 ± 0.9) × 10 ⁻⁵	
Γ_{14} $\pi^+ \pi^- \pi^0 \pi^0$	< 4	CL=90%

[a] The e^+e^- branching fraction is from $e^+e^- \rightarrow \pi^+\pi^-$ experiments only. The $\omega\rho$ interference is then due to $\omega\rho$ mixing only, and is expected to be small. If $e\mu$ universality holds, $\Gamma(\rho^0 \rightarrow \mu^+\mu^-) = \Gamma(\rho^0 \rightarrow e^+e^-) \times 0.99785$.

CONSTRAINED FIT INFORMATION

An overall fit to the total width and a partial width uses 10 measurements and one constraint to determine 3 parameters. The overall fit has a $\chi^2 = 10.7$ for 8 degrees of freedom.

The following *off-diagonal* array elements are the correlation coefficients $\langle \delta p_i \delta p_j \rangle / (\delta p_i \delta p_j)$, in percent, from the fit to parameters p_i , including the branching fractions, $x_i \equiv \Gamma_i / \Gamma_{\text{total}}$. The fit constrains the x_i whose labels appear in this array to sum to one.

x_3	-100	
Γ	15	-15
	x_2	x_3

Mode	Rate (MeV)	Scale factor
Γ_2 $\pi^\pm \pi^0$	150.2 ± 2.4	
Γ_3 $\pi^\pm \gamma$	0.068 ± 0.007	2.3

CONSTRAINED FIT INFORMATION

An overall fit to the total width, a partial width, and a branching ratio uses 10 measurements and one constraint to determine 4 parameters. The overall fit has a $\chi^2 = 9.9$ for 7 degrees of freedom.

The following *off-diagonal* array elements are the correlation coefficients $\langle \delta p_i \delta p_j \rangle / (\delta p_i \delta p_j)$, in percent, from the fit to parameters p_i , including the branching fractions, $x_i \equiv \Gamma_i / \Gamma_{\text{total}}$. The fit constrains the x_i whose labels appear in this array to sum to one.

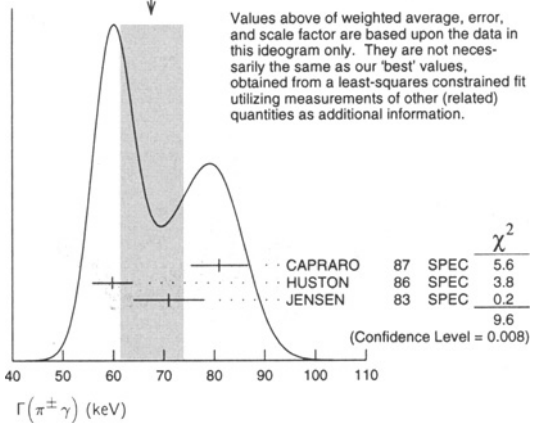
x_{10}	-79		
x_{11}	-61	0	
Γ	16	0	-27
	x_6	x_{10}	x_{11}

Mode	Rate (MeV)	Scale factor
Γ_6 $\pi^+ \pi^-$	150.8 ± 2.0	1.3
Γ_{10} $\mu^+ \mu^-$	[a] 0.0069 ± 0.0004	
Γ_{11} $e^+ e^-$	[a] 0.00677 ± 0.00032	

$\rho(770)$ PARTIAL WIDTHS

$\Gamma(\pi^\pm \gamma)$	DOCUMENT ID	TECN	CHG	COMMENT
68 ± 7	OUR FIT			Error includes scale factor of 2.3.
68 ± 7	OUR AVERAGE			Error includes scale factor of 2.2. See the ideogram below.
81 ± 4 ± 4	CAPRARO	87	SPEC	- 200 $\pi^- \pi^0 \pi^+ \rightarrow \pi^- \pi^0 \pi^+ \gamma$
59.8 ± 4.0	HUSTON	86	SPEC	+ 202 $\pi^+ \pi^0 \pi^+ \rightarrow \pi^+ \pi^0 \pi^+ \gamma$
71 ± 7	JENSEN	83	SPEC	- 156-260 $\pi^- \pi^0 \pi^+ \rightarrow \pi^- \pi^0 \pi^+ \gamma$

WEIGHTED AVERAGE
68 ± 7 (Error scaled by 2.2)



Values above of weighted average, error, and scale factor are based upon the data in this ideogram only. They are not necessarily the same as our 'best' values, obtained from a least-squares constrained fit utilizing measurements of other (related) quantities as additional information.

$\Gamma(e^+e^-)$	DOCUMENT ID	TECN	COMMENT
6.77 ± 0.32	OUR FIT		
6.77 ± 0.10 ± 0.30	BARKOV	85	OLYA $e^+e^- \rightarrow \pi^+\pi^-$

• • • We do not use the following data for averages, fits, limits, etc. • • •
6.3 ± 0.1 46 BENAYOUN 98 RVUE $e^+e^- \rightarrow \pi^+\pi^-, \mu^+\mu^-$

46 Using the data of BARKOV 85 in the hidden local symmetry model.

$\Gamma(\pi^0 \gamma)$	DOCUMENT ID	TECN	COMMENT
121 ± 31	DOLINSKY	89	ND $e^+e^- \rightarrow \pi^0 \gamma$

• • • We do not use the following data for averages, fits, limits, etc. • • •

$\Gamma(\eta \gamma)$	DOCUMENT ID	TECN	COMMENT
62 ± 17	47 DOLINSKY	89	ND $e^+e^- \rightarrow \eta \gamma$

• • • We do not use the following data for averages, fits, limits, etc. • • •

47 Solution corresponding to constructive ω - ρ interference.

$\Gamma(\pi^+ \pi^- \pi^+ \pi^-)$	DOCUMENT ID	TECN	COMMENT
2.8 ± 1.4 ± 0.5	153	AKHMETSHIN 00	CMD2 0.6-0.97 $e^+e^- \rightarrow \pi^+\pi^-\pi^+\pi^-$

• • • We do not use the following data for averages, fits, limits, etc. • • •

Meson Particle Listings

$\rho(770)$

$\rho(770)$ BRANCHING RATIOS

Table with 5 columns: VALUE, CL%, DOCUMENT ID, TECN, CHG, COMMENT. Row for $\Gamma(\pi^+\eta)/\Gamma(\pi\pi)$ with value <60 and CL% 84.

Table with 5 columns: VALUE, CL%, DOCUMENT ID, TECN, CHG, COMMENT. Row for $\Gamma(\pi^+\pi^+\pi^-\pi^0)/\Gamma(\pi\pi)$ with value <20 and CL% 84.

Table with 5 columns: VALUE, CL%, DOCUMENT ID, TECN, CHG, COMMENT. Rows for $\Gamma(\mu^+\mu^-)/\Gamma(\pi^+\pi^-)$ and $\Gamma(\pi^0\gamma)/\Gamma_{total}$.

48 Possibly large $\rho\omega$ interference leads us to increase the minus error.
49 Result contains $11 \pm 11\%$ correction using SU(3) for central value.
50 HYAMS 67's mass resolution is 20 MeV. The ω region was excluded.

Table with 5 columns: VALUE, CL%, DOCUMENT ID, TECN, COMMENT. Row for $\Gamma(e^+e^-)/\Gamma(\pi\pi)$ with value 0.41 ± 0.05 and DOCUMENT ID BENAKSAS 72.

Table with 5 columns: VALUE, CL%, DOCUMENT ID, TECN, CHG, COMMENT. Row for $\Gamma(\eta\gamma)/\Gamma_{total}$ with value $2.4^{+0.9}_{-0.8}$ and DOCUMENT ID DOLINSKY 89.

51 Reanalysis of DRUZHININ 84, DOLINSKY 89, and DOLINSKY 91 taking into account a triangle anomaly contribution.
52 Solution corresponding to constructive ω - ρ interference.

Table with 5 columns: VALUE, CL%, EVTS, DOCUMENT ID, TECN, COMMENT. Row for $\Gamma(\pi^+\pi^-\pi^+\pi^-)/\Gamma_{total}$ with value $1.8 \pm 0.9 \pm 0.3$ and DOCUMENT ID AKHMETSHIN 00.

Table with 5 columns: VALUE, CL%, DOCUMENT ID, TECN, CHG, COMMENT. Row for $\Gamma(\pi^+\pi^-\pi^+\pi^-)/\Gamma(\pi\pi)$ with value <20 and CL% 90.

Table with 5 columns: VALUE, CL%, DOCUMENT ID, TECN, COMMENT. Row for $\Gamma(\pi^+\pi^-\pi^0)/\Gamma_{total}$ with value <1.2 and CL% 90.

Table with 5 columns: VALUE, CL%, DOCUMENT ID, TECN, CHG, COMMENT. Row for $\Gamma(\pi^+\pi^-\pi^0)/\Gamma(\pi\pi)$ with value <0.01 and CL% 84.

Table with 5 columns: VALUE, CL%, DOCUMENT ID, TECN, CHG, COMMENT. Row for $\Gamma(\pi^+\pi^-\pi^0\pi^0)/\Gamma_{total}$ with value <0.4 and CL% 90.

Table with 5 columns: VALUE, CL%, DOCUMENT ID, TECN, CHG, COMMENT. Row for $\Gamma(\pi^+\pi^-\pi^0\pi^0)/\Gamma_{total}$ with value <2 and CL% 90.

Table with 5 columns: VALUE, CL%, DOCUMENT ID, TECN, COMMENT. Row for $\Gamma(\pi^+\pi^-\gamma)/\Gamma_{total}$ with value 0.0099 ± 0.0016 and DOCUMENT ID DOLINSKY 91.

54 Bremsstrahlung from a decay pion and for photon energy above 50 MeV.
55 Superseded by DOLINSKY 91.
56 Structure radiation due to quark rearrangement in the decay.

Table with 5 columns: VALUE, CL%, DOCUMENT ID, TECN, COMMENT. Row for $\Gamma(\pi^0\gamma)/\Gamma_{total}$ with value 6.8 ± 1.7 and DOCUMENT ID BENAYOUN 96.

57 Reanalysis of DRUZHININ 84, DOLINSKY 89, and DOLINSKY 91 taking into account a triangle anomaly contribution.

$\rho(770)$ REFERENCES

Akhmetshin 00, Abele 99E, Benayoun 98, Britweg 98B, Gardner 98, Abele 97, Adams 97, Barate 97M, Bertin -97C, Bogolyub... 97, O'Connell 97, Benayoun 96, Bernicha 94, Weidenauer 93, Aguilari... 91, Dolinsky 91, Antipov 89, Dolinsky 89, Dubnicka 89, Kurdadze 88, Vasserman 88B, Aulchenko 87C, Capraro 87, Bramon 86, Huston 86, Kurdadze 86, Barkov 85, Druzhinin 84, Chabaud 83, Jensen 83, Heyn 81, Bohacik 80, Lang 79, Bartalucci 78, Wicklund 78, Andrews 77, Deusch... 76, Engler 74, Estabrooks 74, Grayer 74, Byerly 73, Gladding 73, Protopop... 73, Ballam 72, Benaksas 72, Jacobs 72, Ratcliff 72, Abrams 71, Alvensleb... 70, Biggs 70, Erbe 69, Malamud 69, Reynolds 69, Rothwell 69, Wehm... 69, Armenise 68, Baton 68, Chung 68, Foster 68, Henson 68, Hyams 68, Lanzerotti 68, Pisut 68, Asbury 67B, Bacon 67, Eisner 67, Huwe 67, Hyams 67, Miller 67B, Alf... 66, Ferbel 66, Hagopian 66, Hagopian 66B, Jacobs 66B, James 66, Ross 66, Soeding 66, West 66, Bliden 65, Carmony 64, Goldhaber 64, Abolins 63, R.R. Akhmetshin et al. (CMD-2 Collab.), A. Abele et al. (Crystal Barrel Collab.), M. Benayoun et al. (IPNP, NOVO, ADL+), J. Britweg et al. (ZEUS Collab.), S. Gardner, H.B. O'Connell (Crystal Barrel Collab.), M.R. Adams et al. (E665 Collab.), R. Barate et al. (ALEPH Collab.), A. Bertin et al. (OBELIX Collab.), M.Y. Bogolyubskiy et al. (MOSU, SERP), H.B. O'Connell et al. (AOLD), M. Benayoun et al. (IPNP, NOVO), A. Bernicha, G. Lopez Castro, J. Pestieau (LOUV+), P. Weidenauer et al. (ASTERIX Collab.), M. Aguilar-Benitez et al. (LEBC-EHS Collab.), S.I. Dolinsky et al. (NOVO), Y.M. Antipov et al. (SERP, JINR, BGNA+), S.I. Dolinsky et al. (NOVO), S. Dubnicka et al. (JINR, SLOV), B.V. Geshkenbein (ITEP), L.M. Kurdadze et al. (NOVO), I.B. Vasserman et al. (NOVO), I.B. Vasserman et al. (NOVO), V.M. Aulchenko et al. (NOVO), L. Capraro et al. (CLER, FRAS, MILA+), A. Bramon, J. Casulleras (BARC), J. Huston et al. (ROCH, FNAL, MINN), L.M. Kurdadze et al. (NOVO), L.M. Barkov et al. (NOVO), V.P. Druzhinin et al. (NOVO), V. Chabaud et al. (CERN, CRAC, MPIM), T. Jensen et al. (ROCH, FNAL, MINN), M.F. Heyn, C.B. Lang (GRAZ), J. Bohacik, H. Kuhnelt (SLOV, WIEN), C.B. Lang, A. Mas-Parareda (GRAZ), S. Bartalucci et al. (DESY, FRAS), A.B. Wicklund et al. (ANL), D.E. Andrews et al. (ROCH), N. Deuschmann et al. (AACH3, BERL, BONN+), A. Engler et al. (CMU, CASE), P.G. Estabrooks, A.D. Martin (DURH), G. Grayer et al. (CERN, MPIM), W.L. Byerly et al. (MICH), S.E. Gladding et al. (HARV), G.D. Protopopescu et al. (LBL), J. Ballam et al. (SLAC, LBL, TUFTS), L. Benaksas et al. (ORSAV), D. Jacobs (SACL), B.N. Ratcliff et al. (SACL), G.S. Abrams et al. (LBL), H. Alvensleben et al. (DESY), P.J. Biggs et al. (DARE), R. Erbe et al. (UCLA), E.I. Malamud, P.E. Schlein (FSU), B.G. Reynolds et al. (NEAS), P.L. Rothwell et al. (HARV, CASE, SLAC+), N. Armenise et al. (BARI, BGNA, FIRZ+), J.P. Baton, G. Laurens (SACL), S.U. Chung et al. (LRL), M. Foster et al. (CERN, CDEF), R. Huseon et al. (ORSAV, MILA, UCLA), B.D. Hyams et al. (CERN, MPIM), L.J. Lanzerotti et al. (HARV), J. Pisut, M. Rous (CERN), J.G. Asbury et al. (DESY, COLU), T.C. Bacon et al. (BNL), R.L. Eisner et al. (PURD), D.O. Huwe et al. (COLU), B.D. Hyams et al. (CERN, MPIM), D.H. Miller et al. (PURD), C. Alf-Steinberger et al. (COLU, RUTG), T. Ferbel (ROCH), V. Hagopian et al. (PENN, SACL), V. Hagopian, Y.L. Pan (PENN, LRL), L.D. Jacobs (LRL), F.E. James, H.L. Kraybill (YALE, BNL), M. Ross, L. Stodolsky (WISC), P. Soeding (WISC), E. West et al. (WISC), H.R. Bliden et al. (UCB), D.D. Carmony et al. (UCB), G. Goldhaber et al. (LRL, UCB), M.A. Abolins et al. (UCSD).

OTHER RELATED PAPERS

ANDERSON	00	CLNS 99/1635	
BENAYOUN	99	PR D59 074020	M. Benayoun et al.
EIDELMAN	99	NPBPS 76 319	S. Eidelman, V. Ivanchenko
MARCO	99	PL B470 20	E. Marco et al.
ROOS	99	APS 49 N2 vii	M. Roos
ALEMANY	98	EPJ C2 123	R. Alemany et al.
ABELE	97B	PL B402 195	A. Abele et al. (Crystal Barrel Collab.)
ABELE	97F	PL B411 354	A. Abele et al. (Crystal Barrel Collab.)
BENAYOUN	93	ZPHY 58 31	M. Benayoun et al. (CDEF, CERN, BARI)
LAFFERTY	93	ZPHY C60 659	G.D. Lafferty (MCHS)
KAMAL	92	PL B284 421	A.N. Kamal, Q.P. Xu (ALBE)
KUHN	90	ZPHY C48 445	J.H. Kuhn et al. (MPIM)
ERKAL	85	ZPHY C29 485	C. Erkal, M.G. Olsson (WISC)
RYBICKI	85	ZPHY C28 65	K. Rybicki, I. Sakrejda (CRAC)
KURDADZE	83	JETPL 37 733	L.M. Kurdadze et al. (NOVO)
ALEKSEEV	82	JETP 55 591	E.A. Alekseeva et al. (KIAE)
KENNEY	62	PR 126 735	V.P. Kenney, W.D. Shephard, C.D. Gall (KNTY)
SAMIOS	62	PRL 9 139	N.P. Samios et al. (BNL, CUNY, COLU+)
XUONG	62	PR 128 1849	H. Nguyen Ngoc, G.R. Lynch (LRL)
ANDERSON	61	PRL 6 365	J.A. Anderson et al. (LRL)
ERWIN	61	PRL 6 628	A.R. Erwin et al. (WISC)

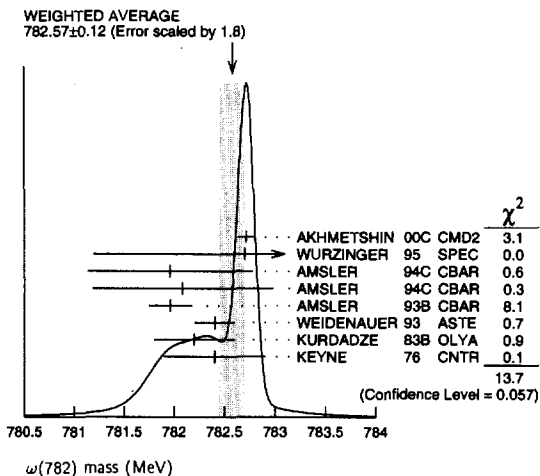
$\omega(782)$

$$J^{G(J^{PC})} = 0^{-}(1^{-}-)$$

$\omega(782)$ MASS

VALUE (MeV)	EVTS	DOCUMENT ID	TECN	COMMENT
782.57 ± 0.12 OUR AVERAGE				Error includes scale factor of 1.8. See the ideogram below.
782.71 ± 0.07 ± 0.04	11200	AKHMETSHIN 00C CMD2		$e^+e^- \rightarrow \pi^+\pi^-\pi^0$
782.7 ± 0.1 ± 1.5	19500	WURZINGER 95 SPEC		1.33 $\rho d \rightarrow {}^3\text{He}\omega$
781.96 ± 0.17 ± 0.80	11k	AMSLER 94C CBAR		$0.0 \bar{p}p \rightarrow \omega\pi^0\pi^0$
782.08 ± 0.36 ± 0.82	3463	AMSLER 94C CBAR		$0.0 \bar{p}p \rightarrow \omega\eta\pi^0$
781.96 ± 0.13 ± 0.17	15k	AMSLER 93B CBAR		$0.0 \bar{p}p \rightarrow \omega\pi^0\pi^0$
782.4 ± 0.2	270k	WEIDENAUER 93 ASTE		$\bar{p}p \rightarrow 2\pi^+2\pi^-\pi^0$
782.2 ± 0.4	1488	KURDADZE 83B OLYA		$e^+e^- \rightarrow \pi^+\pi^-\pi^0$
782.4 ± 0.5	7000	1 KEYNE 76 CNTR		$\pi^-\rho \rightarrow \omega n$
781.76 ± 0.10		2 BARKOV 87 CMD		$e^+e^- \rightarrow \pi^+\pi^-\pi^0$
783.3 ± 0.4		CORDIER 80 WIRE		$e^+e^- \rightarrow \pi^+\pi^-\pi^0$
782.5 ± 0.8	33260	ROOS 80 RVUE		0.0-3.6 $\bar{p}p$
782.6 ± 0.8	3000	BENKHEIRI 79 OMEG		9-12 $\pi^\pm p$
781.8 ± 0.6	1430	COOPER 78B HBC		0.7-0.8 $\bar{p}p \rightarrow 5\pi$
782.7 ± 0.9	535	VANAPEL... 78 HBC		7.2 $\bar{p}p \rightarrow \bar{p}\rho\omega$
783.5 ± 0.8	2100	GESSAROLI 77 HBC		11 $\pi^-\rho \rightarrow \omega n$
782.5 ± 0.8	418	AGUILAR... 72B HBC		3.9,4.6 $K^-\rho$
783.4 ± 1.0	248	BIZZARRI 71 HBC		0.0 $\rho\bar{p} \rightarrow K^+K^-\omega$
781.0 ± 0.6	510	BIZZARRI 71 HBC		0.0 $\rho\bar{p} \rightarrow K_1^+K_1^-\omega$
783.7 ± 1.0	3583	3 COYNE 71 HBC		3.7 $\pi^+\rho \rightarrow \rho\pi^+\pi^+\pi^-\pi^0$
784.1 ± 1.2	750	ABRAMOVI... 70 HBC		3.9 $\pi^-\rho$
783.2 ± 1.6		4 BIGGS 70B CNTR		<4.1 $\gamma C \rightarrow \pi^+\pi^-\pi^0$
782.4 ± 0.5	2400	BIZZARRI 69 HBC		0.0 $\bar{p}p$

1 Observed by threshold-crossing technique. Mass resolution = 4.8 MeV FWHM.
 2 Systematic uncertainties underestimated. Superseded by AKHMETSHIN 00C.
 3 From best-resolution sample of COYNE 71.
 4 From ω - ρ interference in the $\pi^+\pi^-\pi^0$ mass spectrum assuming ω width 12.6 MeV.



$\omega(782)$ WIDTH

VALUE (MeV)	EVTS	DOCUMENT ID	TECN	COMMENT
8.44 ± 0.09 OUR AVERAGE				
8.68 ± 0.23 ± 0.10	11200	AKHMETSHIN 00C CMD2		$e^+e^- \rightarrow \pi^+\pi^-\pi^0$
8.2 ± 0.3	19500	WURZINGER 95 SPEC		1.33 $\rho d \rightarrow {}^3\text{He}\omega$
8.4 ± 0.1		5 AULCHENKO 87 ND		$e^+e^- \rightarrow \pi^+\pi^-\pi^0$
8.30 ± 0.40		BARKOV 87 CMD		$e^+e^- \rightarrow \pi^+\pi^-\pi^0$
9.8 ± 0.9	1488	KURDADZE 83B OLYA		$e^+e^- \rightarrow \pi^+\pi^-\pi^0$
9.0 ± 0.8		CORDIER 80 WIRE		$e^+e^- \rightarrow \pi^+\pi^-\pi^0$
9.1 ± 0.8		BENAKSAS 72B OSPK		e^+e^-
• • • We do not use the following data for averages, fits, limits, etc. • • •				
12 ± 2	1430	COOPER 78B HBC		0.7-0.8 $\bar{p}p \rightarrow 5\pi$
9.4 ± 2.5	2100	GESSAROLI 77 HBC		11 $\pi^-\rho \rightarrow \omega n$
10.22 ± 0.43	20000	6 KEYNE 76 CNTR		$\pi^-\rho \rightarrow \omega n$
13.3 ± 2	418	AGUILAR... 72B HBC		3.9,4.6 $K^-\rho$
10.5 ± 1.5		BORENSTEIN 72 HBC		2.18 $K^-\rho$
7.70 ± 0.9 ± 1.15	940	BROWN 72 MMS		2.5 $\pi^-\rho \rightarrow nMM$
10.3 ± 1.4	510	BIZZARRI 71 HBC		0.0 $\rho\bar{p} \rightarrow K_1^+K_1^-\omega$
12.8 ± 3.0	248	BIZZARRI 71 HBC		0.0 $\rho\bar{p} \rightarrow K^+K^-\omega$
9.5 ± 1.0	3583	COYNE 71 HBC		3.7 $\pi^+\rho \rightarrow \rho\pi^+\pi^+\pi^-\pi^0$

5 Relativistic Breit-Wigner includes radiative corrections.
 6 Observed by threshold-crossing technique. Mass resolution = 4.8 MeV FWHM.

$\omega(782)$ DECAY MODES

Mode	Fraction (Γ_i/Γ)	Scale factor/ Confidence level
Γ_1 $\pi^+\pi^-\pi^0$	(88.8 ± 0.7) %	
Γ_2 $\pi^0\gamma$	(8.5 ± 0.5) %	
Γ_3 $\pi^+\pi^-$	(2.21 ± 0.30) %	
Γ_4 neutrals (excluding $\pi^0\gamma$)	(5.3 $^{+8.7}_{-3.5}$) × 10 ⁻³	
Γ_5 $\eta\gamma$	(6.5 ± 1.0) × 10 ⁻⁴	
Γ_6 $\pi^0e^+e^-$	(5.9 ± 1.9) × 10 ⁻⁴	
Γ_7 $\pi^0\mu^+\mu^-$	(9.6 ± 2.3) × 10 ⁻⁵	
Γ_8 e^+e^-	(7.07 ± 0.19) × 10 ⁻⁵	S=1.1
Γ_9 $\pi^+\pi^-\pi^0\pi^0$	< 2 %	CL=90%
Γ_{10} $\pi^+\pi^-\gamma$	< 3.6 × 10 ⁻³	CL=95%
Γ_{11} $\pi^+\pi^-\pi^+\pi^-$	< 1 × 10 ⁻³	CL=90%
Γ_{12} $\pi^0\pi^0\gamma$	(7.2 ± 2.5) × 10 ⁻⁵	
Γ_{13} $\mu^+\mu^-$	< 1.8 × 10 ⁻⁴	CL=90%
Γ_{14} 3γ	< 1.9 × 10 ⁻⁴	CL=95%
Charge conjugation (C) violating modes		
Γ_{15} $\eta\pi^0$	C < 1 × 10 ⁻³	CL=90%
Γ_{16} $3\pi^0$	C < 3 × 10 ⁻⁴	CL=90%

CONSTRAINED FIT INFORMATION

An overall fit to 6 branching ratios uses 20 measurements and one constraint to determine 4 parameters. The overall fit has a $\chi^2 = 10.3$ for 17 degrees of freedom.

The following off-diagonal array elements are the correlation coefficients $\langle \delta x_i \delta x_j \rangle / (\delta x_i \delta x_j)$, in percent, from the fit to the branching fractions, $x_i \equiv \Gamma_i/\Gamma_{\text{total}}$. The fit constrains the x_i whose labels appear in this array to sum to one.

x_2	13		
x_3	-39	-5	
x_4	-74	-68	-1
	x_1	x_2	x_3

$\omega(782)$ PARTIAL WIDTHS

VALUE (MeV)	EVTS	DOCUMENT ID	TECN	COMMENT
0.60 ± 0.02 OUR EVALUATION				
0.595 ± 0.014 ± 0.009	11200	7 AKHMETSHIN 00C CMD2		$e^+e^- \rightarrow \pi^+\pi^-\pi^0$
7 Using $B(\omega \rightarrow \pi^+\pi^-\pi^0) = 0.888 \pm 0.007$.				

$\omega(782)$ $\Gamma(i)\Gamma(e^+e^-)/\Gamma(\text{total})$

VALUE (MeV)	EVTS	DOCUMENT ID	TECN	COMMENT
0.528 ± 0.012 ± 0.007	11200	AKHMETSHIN 00C CMD2		$e^+e^- \rightarrow \pi^+\pi^-\pi^0$

Meson Particle Listings

 $\omega(782)$ $\omega(782)$ BRANCHING RATIOS

$\Gamma(\text{neutrals})/\Gamma(\pi^+\pi^-\pi^0)$ $(\Gamma_2+\Gamma_4)/\Gamma_1$

VALUE	EVTS	DOCUMENT ID	TECN	COMMENT
0.102 ± 0.008				OUR FIT
0.103^{+0.011}_{-0.010}				OUR AVERAGE
0.15 ± 0.04	46	AGUILAR...	72b HBC	3.9,4.6 K^-p
0.10 ± 0.03	19	BARASH	67b HBC	0.0 $\bar{p}p$
0.134 ± 0.026	850	DIGIUGNO	66b CNTR	1.4 π^-p
0.097 ± 0.016	348	FLATTE	66 HBC	1.4 - 1.7 $K^-p \rightarrow$ AMM
0.06 ^{+0.05} _{-0.02}		JAMES	66 HBC	2.1 π^+p
0.08 ± 0.03	35	KRAEMER	64 DBC	1.2 π^+d
• • • We do not use the following data for averages, fits, limits, etc. • • •				
0.11 ± 0.02	20	BUSCHBECK	63 HBC	1.5 K^-p

$\Gamma(\pi^+\pi^-)/\Gamma(\pi^+\pi^-\pi^0)$ Γ_3/Γ_1

See also $\Gamma(\pi^+\pi^-)/\Gamma_{\text{total}}$.

VALUE	DOCUMENT ID	TECN	COMMENT
0.0249 ± 0.0035			OUR FIT
0.026 ± 0.005			OUR AVERAGE
0.021 ^{+0.028} _{-0.009}	8 RATCLIFF	72 ASPK	15 $\pi^-p \rightarrow n2\pi$
0.028 ± 0.006	BEHREND	71 ASPK	Photoproduction
0.022 ^{+0.009} _{-0.01}	9 ROOS	70 RVUE	

⁸ Significant interference effect observed. NB of $\omega \rightarrow 3\pi$ comes from an extrapolation.
⁹ ROOS 70 combines ABRAMOVICH 70 and BIZZARRI 70.

$\Gamma(\pi^0\gamma)/\Gamma(\pi^+\pi^-\pi^0)$ Γ_2/Γ_1

VALUE	DOCUMENT ID	TECN	COMMENT
0.096 ± 0.006			OUR FIT
0.096 ± 0.006			OUR AVERAGE
0.099 ± 0.007	DOLINSKY	89 ND	$e^+e^- \rightarrow \pi^0\gamma$
0.084 ± 0.013	KEYNE	76 CNTR	$\pi^-p \rightarrow \omega n$
0.109 ± 0.025	BENAKSAS	72c OSPK	e^+e^-
0.081 ± 0.020	BALDIN	71 HLBC	2.9 π^+p
0.13 ± 0.04	JACQUET	69b HLBC	

$\Gamma(\pi^+\pi^-\gamma)/\Gamma(\pi^+\pi^-\pi^0)$ Γ_{10}/Γ_1

VALUE	CL%	DOCUMENT ID	TECN	COMMENT
• • • We do not use the following data for averages, fits, limits, etc. • • •				
<0.066		90	KALBFLEISCH 75 HBC	2.18 $K^-p \rightarrow$ $\Lambda\pi^+\pi^-\gamma$
<0.05		90	FLATTE 66 HBC	1.2 - 1.7 $K^-p \rightarrow$ $\Lambda\pi^+\pi^-\gamma$

$\Gamma(\pi^+\pi^-\gamma)/\Gamma_{\text{total}}$ Γ_{10}/Γ

VALUE	CL%	DOCUMENT ID	TECN	COMMENT
<0.0036		95	WEIDENAUER 90 ASTE	$\rho\bar{p} \rightarrow \pi^+\pi^-\pi^+\pi^-\gamma$
• • • We do not use the following data for averages, fits, limits, etc. • • •				
<0.004		95	BITYUKOV 88b SPEC	32 $\pi^-p \rightarrow \pi^+\pi^-\gamma X$

$\Gamma(\pi^+\pi^-\pi^+\pi^-)/\Gamma_{\text{total}}$ Γ_{11}/Γ

VALUE	CL%	DOCUMENT ID	TECN	COMMENT
<1 × 10⁻³		90	KURDADZE 88 OLYA	$e^+e^- \rightarrow$ $\pi^+\pi^-\pi^+\pi^-$

$\Gamma(\pi^+\pi^-\pi^0)/\Gamma_{\text{total}}$ Γ_9/Γ

VALUE (units 10 ⁻²)	CL%	DOCUMENT ID	TECN	COMMENT
<2		90	KURDADZE 86 OLYA	$e^+e^- \rightarrow \pi^+\pi^-\pi^0\pi^0$

$\Gamma(\mu^+\mu^-)/\Gamma(\pi^+\pi^-\pi^0)$ Γ_{13}/Γ_1

VALUE (units 10 ⁻³)	CL%	DOCUMENT ID	TECN	COMMENT
<0.2		90	WILSON 69 OSPK	12 $\pi^-C \rightarrow Fe$
• • • We do not use the following data for averages, fits, limits, etc. • • •				
<1.7		74	FLATTE 66 HBC	1.2 - 1.7 $K^-p \rightarrow$ $\Lambda\mu^+\mu^-$
<1.2			BARBARO... 65 HBC	2.7 K^-p

$\Gamma(\pi^0\pi^0\gamma)/\Gamma(\pi^0\gamma)$ Γ_{12}/Γ_2

VALUE	CL%	EVTS	DOCUMENT ID	TECN	COMMENT
0.00085 ± 0.00029		40 ± 14	ALDE	94b GAM2	38 $\pi^-p \rightarrow$ $\pi^0\pi^0\gamma n$
• • • We do not use the following data for averages, fits, limits, etc. • • •					
< 0.005		90	DOLINSKY	89 ND	$e^+e^- \rightarrow$ $\pi^0\pi^0\gamma$
< 0.18		95	KEYNE	76 CNTR	$\pi^-p \rightarrow \omega n$
< 0.15		90	BENAKSAS	72c OSPK	e^+e^-
< 0.14			BALDIN	71 HLBC	2.9 π^+p
< 0.1		90	BARMIN	64 HLBC	1.3-2.8 π^-p

$\Gamma(\eta\pi^0)/\Gamma_{\text{total}}$ Γ_{15}/Γ

Violates C conservation.

VALUE	CL%	DOCUMENT ID	TECN	COMMENT	
<0.001		90	ALDE	94b GAM2	38 $\pi^-p \rightarrow \eta\pi^0 n$

$[\Gamma(\eta\gamma) + \Gamma(\eta\pi^0)]/\Gamma(\pi^+\pi^-\pi^0)$ $(\Gamma_5+\Gamma_{15})/\Gamma_1$

VALUE	CL%	DOCUMENT ID	TECN	COMMENT	
<0.016		90	10 FLATTE	66 HBC	1.2 - 1.7 $K^-p \rightarrow$ $\Lambda\pi^+\pi^-MM$
• • • We do not use the following data for averages, fits, limits, etc. • • •					
<0.045		95	JACQUET	69b HLBC	
¹⁰ Restated by us using $B(\eta \rightarrow \text{charged modes}) = 29.2\%$.					

$\Gamma(\text{neutrals})/\Gamma(\text{charged particles})$ $(\Gamma_2+\Gamma_4)/(\Gamma_1+\Gamma_3)$

VALUE	DOCUMENT ID	TECN	COMMENT
0.099 ± 0.008			OUR FIT
0.124 ± 0.021			OUR AVERAGE
	FELDMAN	67c OSPK	1.2 π^-p

$\Gamma(\pi^0\pi^0\gamma)/\Gamma(\pi^+\pi^-\pi^0)$ Γ_{12}/Γ_1

VALUE	CL%	DOCUMENT ID	TECN	COMMENT	
<0.00045		90	DOLINSKY	89 ND	$e^+e^- \rightarrow \pi^0\pi^0\gamma$
• • • We do not use the following data for averages, fits, limits, etc. • • •					
<0.08		95	JACQUET	69b HLBC	

$\Gamma(\eta\gamma)/\Gamma(\pi^0\gamma)$ Γ_5/Γ_2

VALUE	DOCUMENT ID	TECN	COMMENT
• • • We do not use the following data for averages, fits, limits, etc. • • •			
0.0098 ± 0.0024	11 ALDE	93 GAM2	38 $\pi^-p \rightarrow \omega n$
0.0082 ± 0.0033	12 DOLINSKY	89 ND	$e^+e^- \rightarrow \eta\gamma$
0.010 ± 0.045	APEL	72b OSPK	4-8 $\pi^-p \rightarrow n3\gamma$
¹¹ Model independent determination.			
¹² Solution corresponding to constructive ω - ρ interference.			

$\Gamma(\pi^0\mu^+\mu^-)/\Gamma_{\text{total}}$ Γ_7/Γ

VALUE (units 10 ⁻⁴)	DOCUMENT ID	TECN	COMMENT
0.96 ± 0.23			OUR AVERAGE
	DZHELJADIN	81b CNTR	25-33 $\pi^-p \rightarrow \omega n$

$\Gamma(\pi^0e^+e^-)/\Gamma_{\text{total}}$ Γ_8/Γ

VALUE (units 10 ⁻⁴)	EVTS	DOCUMENT ID	TECN	COMMENT	
5.9 ± 1.9		43	DOLINSKY	88 ND	$e^+e^- \rightarrow \pi^0e^+e^-$

$\Gamma(e^+e^-)/\Gamma_{\text{total}}$ Γ_8/Γ

VALUE (units 10 ⁻⁴)	EVTS	DOCUMENT ID	TECN	COMMENT
0.707 ± 0.019				OUR AVERAGE
Error includes scale factor of 1.1.				
0.714 ± 0.036		DOLINSKY	89 ND	$e^+e^- \rightarrow \pi^+\pi^-\pi^0$
0.72 ± 0.03		BARKOV	87 CMD	$e^+e^- \rightarrow \pi^+\pi^-\pi^0$
0.64 ± 0.04	1488	KURDADZE	83b OLYA	$e^+e^- \rightarrow \pi^+\pi^-\pi^0$
0.675 ± 0.069		CORDIER	80 WIRE	$e^+e^- \rightarrow 3\pi$
0.83 ± 0.10		BENAKSAS	72b OSPK	$e^+e^- \rightarrow 3\pi$
0.77 ± 0.06		13 AUGUSTIN	69b OSPK	$e^+e^- \rightarrow 2\pi$

• • • We do not use the following data for averages, fits, limits, etc. • • •

0.685 ± 0.016 11200 14 AKHMETSHIN 00c CMD2 $e^+e^- \rightarrow \pi^+\pi^-\pi^0$

0.65 ± 0.13 33 15 ASTVACAT... 68 OSPK Assume SU(3)+mixing

$\Gamma(\text{neutrals})/\Gamma_{\text{total}}$ $(\Gamma_2+\Gamma_4)/\Gamma$

VALUE	EVTS	DOCUMENT ID	TECN	COMMENT
0.090 ± 0.006				OUR FIT
0.081 ± 0.011				OUR AVERAGE
0.075 ± 0.025		BIZZARRI	71 HBC	0.0 $\rho\bar{p}$
0.079 ± 0.019		DEINET	69b OSPK	1.5 π^-p
0.084 ± 0.015		BOLLINI	68c CNTR	2.1 π^-p
• • • We do not use the following data for averages, fits, limits, etc. • • •				
0.073 ± 0.018	42	BASILE	72b CNTR	1.67 π^-p

$\Gamma(\pi^+\pi^-)/\Gamma_{\text{total}}$ Γ_3/Γ

See also $\Gamma(\pi^+\pi^-)/\Gamma(\pi^+\pi^-\pi^0)$.

VALUE	DOCUMENT ID	TECN	COMMENT
0.0221 ± 0.0030			OUR FIT
0.021 ± 0.004			OUR AVERAGE
0.023 ± 0.005	BARKOV	85 OLYA	e^+e^-
0.016 ^{+0.009} _{-0.007}	QUENZER	78 CNTR	e^+e^-

Meson Particle Listings

 $\eta'(958)$

$$I^G(J^{PC}) = 0^+(0^{-+})$$

$\eta'(958)$ MASS		DOCUMENT ID	TECN	COMMENT
VALUE (MeV)	EVTS			
957.78 ± 0.14 OUR AVERAGE				
957.9 ± 0.2 ± 0.6	4800	WURZINGER 96	SPEC	1.68 $p d \rightarrow {}^3\text{He} \eta'$
959 ± 1	630	BELADIDZE 92c	VES	36 $\pi^- \text{Be} \rightarrow \pi^- \eta' \eta \text{Be}$
958 ± 1	340	ARMSTRONG 91b	OMEG	300 $p p \rightarrow p p \eta \pi^+ \pi^-$
958.2 ± 0.4	622	AUGUSTIN 90	DM2	$J/\psi \rightarrow \gamma \eta \pi^+ \pi^-$
957.8 ± 0.2	2420	AUGUSTIN 90	DM2	$J/\psi \rightarrow \gamma \gamma \pi^+ \pi^-$
956.3 ± 1.0	143	GIDAL 87	MRK2	$e^+ e^- \rightarrow \eta \pi^+ \pi^-$
957.46 ± 0.33		DUANE 74	MMS	$\pi^- p \rightarrow n \text{MM}$
958.2 ± 0.5	1414	DANBURG 73	HBC	2.2 $K^- p \rightarrow \Lambda \chi^0$
958 ± 1	400	JACOBS 73	HBC	2.9 $K^- p \rightarrow \Lambda \chi^0$
956.1 ± 1.1	3415	BASILE 71	CNTR	1.6 $\pi^- p \rightarrow n \chi^0$
957.4 ± 1.4	535	BASILE 71	CNTR	1.6 $\pi^- p \rightarrow n \chi^0$
957 ± 1		RITTENBERG 69	HBC	1.7-2.7 $K^- p$

$\eta'(958)$ WIDTH		DOCUMENT ID	TECN	CHG	COMMENT
VALUE (MeV)	EVTS				
0.202 ± 0.016 OUR FIT	Error includes scale factor of 1.3.				
0.30 ± 0.09 OUR AVERAGE					
0.40 ± 0.22	4800	WURZINGER 96	SPEC		1.68 $p d \rightarrow {}^3\text{He} \eta'$
0.28 ± 0.10	1000	BINNIE 79	MMS	0	$\pi^- p \rightarrow n \text{MM}$

$\eta'(958)$ DECAY MODES		Fraction (Γ_i/Γ)	Scale factor/ Confidence level
Γ_1	$\pi^+ \pi^- \eta$	(44.3 ± 1.5) %	S=1.2
Γ_2	$\rho^0 \gamma$ (including non-resonant $\pi^+ \pi^- \gamma$)	(29.5 ± 1.0) %	S=1.2
Γ_3	$\pi^0 \pi^0 \eta$	(20.9 ± 1.2) %	S=1.2
Γ_4	$\omega \gamma$	(3.03 ± 0.31) %	
Γ_5	$\gamma \gamma$	(2.12 ± 0.14) %	S=1.3
Γ_6	$3\pi^0$	(1.56 ± 0.26) × 10 ⁻³	
Γ_7	$\mu^+ \mu^- \gamma$	(1.04 ± 0.26) × 10 ⁻⁴	
Γ_8	$\pi^+ \pi^- \pi^0$	< 5 %	CL=90%
Γ_9	$\pi^0 \rho^0$	< 4 %	CL=90%
Γ_{10}	$\pi^+ \pi^+ \pi^- \pi^-$	< 1 %	CL=90%
Γ_{11}	$\pi^+ \pi^+ \pi^- \pi^-$ neutrals	< 1 %	CL=95%
Γ_{12}	$\pi^+ \pi^+ \pi^- \pi^- \pi^0$	< 1 %	CL=90%
Γ_{13}	6π	< 1 %	CL=90%
Γ_{14}	$\pi^+ \pi^- e^+ e^-$	< 6 × 10 ⁻³	CL=90%
Γ_{15}	$\pi^0 \gamma \gamma$	< 8 × 10 ⁻⁴	CL=90%
Γ_{16}	$4\pi^0$	< 5 × 10 ⁻⁴	CL=90%
Γ_{17}	$e^+ e^-$	< 2.1 × 10 ⁻⁷	CL=90%

Charge conjugation (C), Parity (P),
Lepton family number (LF) violating modes

Γ_{18}	$\pi^+ \pi^-$	P, CP	< 2 %	CL=90%
Γ_{19}	$\pi^0 \pi^0$	P, CP	< 9 × 10 ⁻⁴	CL=90%
Γ_{20}	$\gamma e^+ e^-$	C	< 9 × 10 ⁻⁴	CL=90%
Γ_{21}	$\pi^0 e^+ e^-$	C	[a] < 1.4 × 10 ⁻³	CL=90%
Γ_{22}	$\eta e^+ e^-$	C	[a] < 2.4 × 10 ⁻³	CL=90%
Γ_{23}	3γ	C	< 1.0 × 10 ⁻⁴	CL=90%
Γ_{24}	$\mu^+ \mu^- \pi^0$	C	[a] < 6.0 × 10 ⁻⁵	CL=90%
Γ_{25}	$\mu^+ \mu^- \eta$	C	[a] < 1.5 × 10 ⁻⁵	CL=90%
Γ_{26}	$e \mu$	LF	< 4.7 × 10 ⁻⁴	CL=90%

[a] C parity forbids this to occur as a single-photon process.

CONSTRAINED FIT INFORMATION

An overall fit to the total width, a partial width, 2 combinations of partial widths obtained from integrated cross section, and 16 branching ratios uses 48 measurements and one constraint to determine 7 parameters. The overall fit has a $\chi^2 = 35.6$ for 42 degrees of freedom.

The following off-diagonal array elements are the correlation coefficients $\langle \delta p_i \delta p_j \rangle / (\delta p_i \delta p_j)$, in percent, from the fit to parameters p_i , including the branching fractions, $x_i \equiv \Gamma_i / \Gamma_{\text{total}}$. The fit constrains the x_i whose labels appear in this array to sum to one.

x_2	-39					
x_3	-74	-29				
x_4	-33	-24	32			
x_5	-25	-12	26	8		
x_6	-27	-11	35	11	9	
Γ	32	-3	-24	-5	-88	-8
	x_1	x_2	x_3	x_4	x_5	x_6

Mode	Rate (MeV)	Scale factor	
Γ_1	$\pi^+ \pi^- \eta$	0.090 ± 0.008	1.2
Γ_2	$\rho^0 \gamma$ (including non-resonant $\pi^+ \pi^- \gamma$)	0.060 ± 0.005	1.3
Γ_3	$\pi^0 \pi^0 \eta$	0.042 ± 0.004	1.6
Γ_4	$\omega \gamma$	0.0061 ± 0.0008	1.2
Γ_5	$\gamma \gamma$	0.00429 ± 0.00015	1.1
Γ_6	$3\pi^0$	(3.1 ± 0.6) × 10 ⁻⁴	1.1

 $\eta'(958)$ PARTIAL WIDTHS

$\Gamma(\gamma\gamma)$		DOCUMENT ID	TECN	COMMENT
VALUE (keV)	EVTS			
4.29 ± 0.15 OUR FIT	Error includes scale factor of 1.1.			
4.28 ± 0.19 OUR AVERAGE				
4.17 ± 0.10 ± 0.27	2000	1 ACCIARRI 98B	L3	$e^+ e^- \rightarrow \pi^+ \pi^- \gamma$
4.53 ± 0.29 ± 0.51	266	KARCH 92	CBAL	$e^+ e^- \rightarrow \pi^+ \pi^0 \pi^0$
3.61 ± 0.13 ± 0.48		2 BEHREND 91	CELL	$e^+ e^- \rightarrow \eta' (958)$
4.6 ± 1.1 ± 0.6	23	BARU 90	MD1	$e^+ e^- \rightarrow \pi^+ \pi^- \gamma$
4.57 ± 0.25 ± 0.44		BUTLER 90	MRK2	$e^+ e^- \rightarrow \eta' (958)$
5.08 ± 0.24 ± 0.71	547	3 ROE 90	ASP	$e^+ e^- \rightarrow e^+ e^- 2\gamma$
3.8 ± 0.7 ± 0.6	34	AIHARA 88c	TPC	$e^+ e^- \rightarrow \pi^+ \pi^- \pi^0$
4.9 ± 0.5 ± 0.5	136	4 WILLIAMS 88	CBAL	$e^+ e^- \rightarrow e^+ e^- 2\gamma$
• • • We do not use the following data for averages, fits, limits, etc. • • •				
4.7 ± 0.6 ± 0.9	143	5 GIDAL 87	MRK2	$e^+ e^- \rightarrow \pi^+ \pi^- \pi^0$
4.0 ± 0.9		6 BARTEL 85E	JADE	$e^+ e^- \rightarrow e^+ e^- 2\gamma$

- 1 No non-resonant $\pi^+ \pi^-$ contribution found.
- 2 Revaluated by us using $B(\eta' \rightarrow \rho(770)\gamma) = (30.2 \pm 1.3)\%$.
- 3 Revaluated by us using $B(\eta' \rightarrow \gamma\gamma) = (2.11 \pm 0.13)\%$.
- 4 Revaluated by us using $B(\eta' \rightarrow \gamma\gamma) = (2.11 \pm 0.13)\%$.
- 5 Superseded by BUTLER 90.
- 6 Systematic error not evaluated.

 $\eta'(958) \Gamma(i)\Gamma(\gamma\gamma)/\Gamma(\text{total})$

This combination of a partial width with the partial width into $\gamma\gamma$ and with the total width is obtained from the integrated cross section into channel(i) in the $\gamma\gamma$ annihilation.

$\Gamma(\gamma\gamma) \times \Gamma(\rho^0 \gamma \text{ (including non-resonant } \pi^+ \pi^- \gamma)) / \Gamma_{\text{total}}$		DOCUMENT ID	TECN	COMMENT
VALUE (keV)	EVTS			
1.27 ± 0.05 OUR FIT	Error includes scale factor of 1.2.			
1.26 ± 0.07 OUR AVERAGE	Error includes scale factor of 1.2.			
1.09 ± 0.04 ± 0.13		BEHREND 91	CELL	$e^+ e^- \rightarrow \pi^+ \pi^- \rho(770)^0 \gamma$
1.35 ± 0.09 ± 0.21		AIHARA 87	TPC	$e^+ e^- \rightarrow e^+ e^- \rho\gamma$
1.13 ± 0.04 ± 0.13	867	ALBRECHT 87b	ARG	$e^+ e^- \rightarrow e^+ e^- \rho\gamma$
1.53 ± 0.09 ± 0.21		ALTHOFF 84E	TASS	$e^+ e^- \rightarrow e^+ e^- \rho\gamma$
1.14 ± 0.08 ± 0.11	243	BERGER 84B	PLUT	$e^+ e^- \rightarrow e^+ e^- \rho\gamma$
1.73 ± 0.34 ± 0.35	95	JENNI 83	MRK2	$e^+ e^- \rightarrow e^+ e^- \rho\gamma$
1.49 ± 0.13 ± 0.027	213	BARTEL 82B	JADE	$e^+ e^- \rightarrow e^+ e^- \rho\gamma$
• • • We do not use the following data for averages, fits, limits, etc. • • •				
1.85 ± 0.31 ± 0.24	43	BEHREND 83B	CELL	$e^+ e^- \rightarrow e^+ e^- \rho\gamma$

See key on page 239

Meson Particle Listings

 $\eta'(958)$

$\Gamma(\gamma\gamma) \times \Gamma(\pi^0\pi^0\eta)/\Gamma_{total}$				Γ_5/Γ
VALUE (keV)	DOCUMENT ID	TECN	COMMENT	
0.90 ± 0.06 OUR FIT			Error includes scale factor of 1.2.	
0.92 ± 0.06 ± 0.11	⁷ KARCH	92	CBAL $e^+e^- \rightarrow e^+e^-\eta\pi^0\pi^0$	
• • • We do not use the following data for averages, fits, limits, etc. • • •				
0.95 ± 0.05 ± 0.08	⁸ KARCH	90	CBAL $e^+e^- \rightarrow e^+e^-\eta\pi^0\pi^0$	
1.00 ± 0.08 ± 0.10	^{8,9} ANTREASYAN	87	CBAL $e^+e^- \rightarrow e^+e^-\eta\pi^0\pi^0$	
⁷ Revaluated by us using $B(\eta \rightarrow \gamma\gamma) = (39.21 \pm 0.34)\%$. Supersedes ANTREASYAN 87 and KARCH 90.				
⁸ Superseded by KARCH 92.				
⁹ Using $BR(\eta \rightarrow 2\gamma) = (38.9 \pm 0.5)\%$.				

 $\eta'(958)$ α PARAMETER

$ \text{MATRIX ELEMENT} ^2 = (1 + \alpha)^2 + \alpha^2$			
VALUE	DOCUMENT ID	TECN	COMMENT
-0.058 ± 0.013	¹⁰ ALDE	86	GAM2 $38\pi^-p \rightarrow n\eta 2\pi^0$
• • • We do not use the following data for averages, fits, limits, etc. • • •			
-0.08 ± 0.03	¹⁰ KALBFLEISCH	74	RVUE $\eta' \rightarrow \eta\pi^+\pi^-$
¹⁰ May not necessarily be the same for $\eta' \rightarrow \eta\pi^+\pi^-$ and $\eta' \rightarrow \eta\pi^0\pi^0$.			

 $\eta'(958)$ β PARAMETER

See the "Note on η Decay Parameters" in our 1994 edition Physical Review D50 1173 (1994), p. 1454.

$ \text{MATRIX ELEMENT} ^2 = (1 + 2\beta Z)$			
VALUE	DOCUMENT ID	TECN	COMMENT
-0.1 ± 0.3	ALDE	87B	GAM2 $38\pi^-p \rightarrow n3\pi^0$

 $\eta'(958)$ BRANCHING RATIOS

$\Gamma(\pi^+\pi^-\eta(\text{neutral decay}))/\Gamma_{total}$				$0.714\Gamma_1/\Gamma$
VALUE	EVTS	DOCUMENT ID	TECN	COMMENT
0.316 ± 0.010 OUR FIT				Error includes scale factor of 1.2.
0.314 ± 0.026	281	RITTENBERG	69	HBC 1.7-2.7 K^-p
$\Gamma(\pi^+\pi^-\text{neutrals})/\Gamma_{total}$				$(0.714\Gamma_1 + 0.286\Gamma_3 + 0.89\Gamma_4)/\Gamma$
VALUE	EVTS	DOCUMENT ID	TECN	COMMENT
0.403 ± 0.008 OUR FIT				Error includes scale factor of 1.2.
0.36 ± 0.05 OUR AVERAGE				
0.4 ± 0.1	39	LONDON	66	HBC 2.24 $K^-p \rightarrow \Lambda\pi^+\pi^-\text{neutrals}$
0.35 ± 0.06	33	BADIER	65B	HBC 3 K^-p
$\Gamma(\pi^+\pi^-\eta(\text{charged decay}))/\Gamma_{total}$				$0.286\Gamma_1/\Gamma$
VALUE	EVTS	DOCUMENT ID	TECN	COMMENT
0.127 ± 0.004 OUR FIT				Error includes scale factor of 1.2.
0.116 ± 0.013 OUR AVERAGE				
0.123 ± 0.014	107	RITTENBERG	69	HBC 1.7-2.7 K^-p
0.10 ± 0.04	10	LONDON	66	HBC 2.24 $K^-p \rightarrow \Lambda\pi^+\pi^-\pi^0$
0.07 ± 0.04	7	BADIER	65B	HBC 3 K^-p
$[\Gamma(\pi^0\pi^0\eta(\text{charged decay})) + \Gamma(\omega(\text{charged decay})\gamma)]/\Gamma_{total}$				$(0.286\Gamma_3 + 0.89\Gamma_4)/\Gamma$
VALUE	EVTS	DOCUMENT ID	TECN	COMMENT
0.087 ± 0.005 OUR FIT				Error includes scale factor of 1.2.
0.045 ± 0.029	42	RITTENBERG	69	HBC 1.7-2.7 K^-p
$\Gamma(\text{neutrals})/\Gamma_{total}$				$(0.714\Gamma_3 + 0.09\Gamma_4 + \Gamma_5)/\Gamma$
VALUE	EVTS	DOCUMENT ID	TECN	COMMENT
0.173 ± 0.009 OUR FIT				Error includes scale factor of 1.2.
0.187 ± 0.017 OUR AVERAGE				
0.185 ± 0.022	535	BASILE	71	CNTR 1.6 $\pi^-p \rightarrow nX^0$
0.189 ± 0.026	123	RITTENBERG	69	HBC 1.7-2.7 K^-p
$\Gamma(\rho^0\gamma(\text{including non-resonant}\pi^+\pi^-\gamma))/\Gamma_{total}$				Γ_2/Γ
VALUE	EVTS	DOCUMENT ID	TECN	COMMENT
0.295 ± 0.010 OUR FIT				Error includes scale factor of 1.2.
0.319 ± 0.030 OUR AVERAGE				
0.329 ± 0.033	298	RITTENBERG	69	HBC 1.7-2.7 K^-p
0.2 ± 0.1	20	LONDON	66	HBC 2.24 $K^-p \rightarrow \Lambda\pi^+\pi^-\gamma$
0.34 ± 0.09	35	BADIER	65B	HBC 3 K^-p
$\Gamma(\rho^0\gamma(\text{including non-resonant}\pi^+\pi^-\gamma))/\Gamma(\pi\pi\eta)$				$\Gamma_2/(\Gamma_1 + \Gamma_3)$
VALUE	DOCUMENT ID	TECN	COMMENT	
0.453 ± 0.022 OUR FIT			Error includes scale factor of 1.2.	
0.426 ± 0.028 OUR AVERAGE				
0.43 ± 0.02 ± 0.02	BARBERIS	98C	OMEG 450 $pp \rightarrow p\eta'\rho_3$	
0.31 ± 0.15	DAVIS	68	HBC 5.5 K^-p	

$\Gamma(\gamma e^+e^-)/\Gamma_{total}$				Γ_{20}/Γ
VALUE (units 10^{-3})	CL%	DOCUMENT ID	TECN	COMMENT
<0.9	90	BRIERE	00	CLEO 10.6 e^+e^-
$\Gamma(\pi^0 e^+e^-)/\Gamma_{total}$				Γ_{21}/Γ
VALUE (units 10^{-3})	CL%	DOCUMENT ID	TECN	COMMENT
<1.4	90	BRIERE	00	CLEO 10.6 e^+e^-
<13	90	RITTENBERG	65	HBC 2.7 K^-p
• • • We do not use the following data for averages, fits, limits, etc. • • •				
$\Gamma(\eta e^+e^-)/\Gamma_{total}$				Γ_{22}/Γ
VALUE (units 10^{-3})	CL%	DOCUMENT ID	TECN	COMMENT
<2.4	90	BRIERE	00	CLEO 10.6 e^+e^-
<11	90	RITTENBERG	65	HBC 2.7 K^-p
• • • We do not use the following data for averages, fits, limits, etc. • • •				
$\Gamma(\pi^0\rho^0)/\Gamma_{total}$				Γ_9/Γ
VALUE	CL%	DOCUMENT ID	TECN	COMMENT
<0.04	90	RITTENBERG	65	HBC 2.7 K^-p
$\Gamma(\pi^+\pi^-e^+e^-)/\Gamma_{total}$				Γ_{14}/Γ
VALUE	CL%	DOCUMENT ID	TECN	COMMENT
<0.006	90	RITTENBERG	65	HBC 2.7 K^-p
$\Gamma(6\pi)/\Gamma_{total}$				Γ_{13}/Γ
VALUE	CL%	DOCUMENT ID	TECN	COMMENT
<0.01	90	LONDON	66	HBC Compilation
$\Gamma(\omega\gamma)/\Gamma(\pi^+\pi^-\eta)$				Γ_4/Γ_1
VALUE	EVTS	DOCUMENT ID	TECN	COMMENT
0.069 ± 0.008 OUR FIT				Error includes scale factor of 1.1.
0.068 ± 0.013	68	ZANFINO	77	ASPK 8.4 π^-p
$\Gamma(\rho^0\gamma(\text{including non-resonant}\pi^+\pi^-\gamma))/[\Gamma(\pi^+\pi^-\eta) + \Gamma(\pi^0\pi^0\eta) + \Gamma(\omega\gamma)]$				$\Gamma_2/(\Gamma_1 + \Gamma_3 + \Gamma_4)$
VALUE	DOCUMENT ID	TECN	COMMENT	
0.433 ± 0.021 OUR FIT			Error includes scale factor of 1.2.	
0.25 ± 0.14	DAUBER	64	HBC 1.95 K^-p	
$\Gamma(\gamma\gamma)/\Gamma_{total}$				Γ_5/Γ
VALUE	EVTS	DOCUMENT ID	TECN	COMMENT
0.0212 ± 0.0014 OUR FIT				Error includes scale factor of 1.3.
0.0196 ± 0.0015 OUR AVERAGE				
0.0200 ± 0.0018		¹¹ STANTON	80	SPEC 8.45 $\pi^-p \rightarrow n\pi^+\pi^-2\gamma$
0.025 ± 0.007		DUANE	74	MMS $\pi^-p \rightarrow nMM$
0.0171 ± 0.0033	68	DALPIAZ	72	CNTR 1.6 $\pi^-p \rightarrow nX^0$
0.020 ± 0.008	31	HARVEY	71	OSPK 3.65 $\pi^-p \rightarrow nX^0$
-0.006				
• • • We do not use the following data for averages, fits, limits, etc. • • •				
0.018 ± 0.002	6000	¹² APEL	79	NICE 15-40 $\pi^-p \rightarrow n2\gamma$
¹¹ Includes APEL 79 result.				
¹² Data is included in STANTON 80 evaluation.				
$\Gamma(e^+e^-)/\Gamma_{total}$				Γ_{17}/Γ
VALUE (units 10^{-7})	CL%	DOCUMENT ID	TECN	COMMENT
<2.1	90	VOROBYEV	88	ND $e^+e^- \rightarrow \pi^+\pi^-\eta$
$\Gamma(\pi^+\pi^-)/\Gamma_{total}$				Γ_{18}/Γ
VALUE	CL%	DOCUMENT ID	TECN	COMMENT
<0.02	90	RITTENBERG	69	HBC 1.7-2.7 K^-p
• • • We do not use the following data for averages, fits, limits, etc. • • •				
<0.08	95	DANBURG	73	HBC 2.2 $K^-p \rightarrow \Lambda X^0$
$\Gamma(\pi^+\pi^-\pi^0)/\Gamma_{total}$				Γ_8/Γ
VALUE	CL%	DOCUMENT ID	TECN	COMMENT
<0.05	90	RITTENBERG	69	HBC 1.7-2.7 K^-p
• • • We do not use the following data for averages, fits, limits, etc. • • •				
<0.09	95	DANBURG	73	HBC 2.2 $K^-p \rightarrow \Lambda X^0$
$\Gamma(\pi^+\pi^+\pi^-\pi^-\text{neutrals})/\Gamma_{total}$				Γ_{11}/Γ
VALUE	CL%	DOCUMENT ID	TECN	COMMENT
<0.01	95	DANBURG	73	HBC 2.2 $K^-p \rightarrow \Lambda X^0$
• • • We do not use the following data for averages, fits, limits, etc. • • •				
<0.01	90	RITTENBERG	69	HBC 1.7-2.7 K^-p
$\Gamma(\pi^+\pi^+\pi^-\pi^0)/\Gamma_{total}$				Γ_{12}/Γ
VALUE	CL%	DOCUMENT ID	TECN	COMMENT
<0.01	90	RITTENBERG	69	HBC 1.7-2.7 K^-p

See key on page 239

Meson Particle Listings

$f_0(980)$

$f_0(980)$

$$I^G(J^{PC}) = 0^+(0^{++})$$

See also the minireview on scalar mesons under $f_0(1370)$. (See the index for the page number.)

$f_0(980)$ MASS

VALUE (MeV)	EVTs	DOCUMENT ID	TECN	COMMENT
980 ± 10 OUR ESTIMATE				
976 ± 5 ± 6		1 AKHMETSHIN 99B CMD2		$e^+e^- \rightarrow \pi^+\pi^-\gamma$
977 ± 3 ± 6	268	1 AKHMETSHIN 99C CMD2		$e^+e^- \rightarrow \pi^0\pi^0\gamma$
975 ± 4 ± 6		2 AKHMETSHIN 99C CMD2		$e^+e^- \rightarrow \pi^0\pi^0\gamma$
975 ± 4 ± 6		3 AKHMETSHIN 99C CMD2		$e^+e^- \rightarrow \pi^+\pi^-\gamma, \pi^0\pi^0\gamma$
985 ± 10		BARBERIS 99 OMEG	450	$pp \rightarrow \rho_S \rho_f K^+ K^-$
982 ± 3		BARBERIS 99B OMEG	450	$pp \rightarrow \rho_S \rho_f \pi^+ \pi^-$
982 ± 3		BARBERIS 99C OMEG	450	$pp \rightarrow \rho_S \rho_f \pi^0 \pi^0$
987 ± 6 ± 6		4 BARBERIS 99D OMEG	450	$pp \rightarrow K^+ K^-, \pi^+ \pi^-$
989 ± 15		BELLAZZINI 99 GAM4	450	$pp \rightarrow pp \pi^0 \pi^0$
991 ± 3		5 KAMINSKI 99 RVUE		$\pi\pi \rightarrow \pi\pi, K\bar{K}, \sigma\sigma$
~ 980		5 OLLER 99 RVUE		$\pi\pi \rightarrow \pi\pi, K\bar{K}$
~ 993.5		5 OLLER 99B RVUE		$\pi\pi \rightarrow \pi\pi, K\bar{K}$
~ 987		5 OLLER 99C RVUE		$\pi\pi \rightarrow \pi\pi, K\bar{K}, \eta\eta$
984 ± 12	164	6 ACHASOV 98I SND		$e^+e^- \rightarrow 5\gamma$
971 ± 6	164	7 ACHASOV 98I SND		$e^+e^- \rightarrow 5\gamma$
957 ± 6		8 ACKERSTAFF 98Q OPAL		$Z \rightarrow f_0 X$
960 ± 10		ALDE 98 GAM4		
1015 ± 15		5 ANISOVICH 98B RVUE		Compilation
1008		9 LOCHER 98 RVUE		$\pi\pi \rightarrow \pi\pi, K\bar{K}$
955 ± 10		8 ALDE 97 GAM2	450	$pp \rightarrow pp \pi^0 \pi^0$
994 ± 9		10 BERTIN 97C OBLX	0.0	$\bar{p}p \rightarrow \pi^+ \pi^- \pi^0$
993.2 ± 6.5 ± 6.9		11 ISHIDA 96 RVUE		$\pi\pi \rightarrow \pi\pi, K\bar{K}$
1006		TORNQVIST 96 RVUE		$\pi\pi \rightarrow \pi\pi, K\bar{K}, K\pi, \eta\pi$
997 ± 5	3k	12 ALDE 95B GAM2	38	$\pi^- p \rightarrow \pi^0 \pi^0 n$
960 ± 10	10k	13 ALDE 95B GAM2	38	$\pi^- p \rightarrow \pi^0 \pi^0 n$
994 ± 5		AMSLER 95B CBAR	0.0	$\bar{p}p \rightarrow 3\pi^0$
~ 996		14 AMSLER 95D CBAR	0.0	$\bar{p}p \rightarrow \pi^0 \pi^0 \pi^0, \pi^0 \eta, \pi^0 \pi^0 \eta$
987 ± 6		15 ANISOVICH 95 RVUE		
1015		JANSSEN 95 RVUE		$\pi\pi \rightarrow \pi\pi, K\bar{K}$
983		16 BUGG 94 RVUE		$\bar{p}p \rightarrow \eta 2\pi^0$
973 ± 2		17 KAMINSKI 94 RVUE		$\pi\pi \rightarrow \pi\pi, K\bar{K}$
988		18 ZOU 94B RVUE		
988 ± 10		19 MORGAN 93 RVUE		$\pi\pi(K\bar{K}) \rightarrow \pi\pi(K\bar{K}), J/\psi \rightarrow \phi\pi\pi(K\bar{K}), D_s \rightarrow \pi(\pi\pi)$
971.1 ± 4.0		8 AGUILAR... 91 EHS	400	pp
979 ± 4		20 ARMSTRONG 91 OMEG	300	$pp \rightarrow pp\pi\pi, ppK\bar{K}$
956 ± 12		BREAKSTONE 90 SFM		$pp \rightarrow pp\pi^+\pi^-$
959.4 ± 6.5		8 AUGUSTIN 89 DM2		$J/\psi \rightarrow \omega\pi^+\pi^-$
978 ± 9		8 ABACHI 86B HRS		$e^+e^- \rightarrow \pi^+\pi^-\chi$
985.0 ± 9.0 -39.0		ETKIN 82B MPS	23	$\pi^- p \rightarrow n 2K_S^0$
974 ± 4		20 GIDAL 81 MRK2		$J/\psi \rightarrow \pi^+\pi^-\chi$
975		21 ACHASOV 80 RVUE		
986 ± 10		20 AGUILAR... 78 HBC	0.7	$\bar{p}p \rightarrow K_S^0 K_S^0$
969 ± 5		20 LEEPER 77 ASPK	2-2.4	$\pi^- p \rightarrow \pi^+\pi^-n, K^+K^-n$
987 ± 7		20 BINNIE 73 CNTR		$\pi^- p \rightarrow nMM$
1012 ± 6		22 GRAYEY 73 ASPK	17	$\pi^- p \rightarrow \pi^+\pi^-n$
1007 ± 20		22 HYAMS 73 ASPK	17	$\pi^- p \rightarrow \pi^+\pi^-n$
997 ± 6		22 PROTOPOP... 73 HBC		$7\pi^+ p \rightarrow \pi^+ p\pi^+\pi^-$

1 Assuming $\Gamma(f_0) = 40$ MeV.
 2 From a narrow pole fit taking into account $f_0(980)$ and $f_0(1200)$ intermediate mechanisms.
 3 From the combined fit of the photon spectra in the reactions $e^+e^- \rightarrow \pi^+\pi^-\gamma, \pi^0\pi^0\gamma$.
 4 Supersedes BARBERIS 99 and BARBERIS 99B
 5 T-matrix pole.
 6 In the "narrow resonance" approximation.
 7 Using the "broad resonance" formulae of ACHASOV 97C.
 8 From invariant mass fit.
 9 On sheet II in a 2 pole solution. The other pole is found on sheet III at (1039-93i) MeV.
 10 On sheet II in a 2 pole solution. The other pole is found on sheet III at (963-29i) MeV.
 11 Reanalysis of data from HYAMS 73, GRAYEY 74, SRINIVASAN 75, and ROSSELET 77 using the interfering amplitude method.
 12 At high $|t|$.

13 At low $|t|$.
 14 On sheet II in a 4-pole solution, the other poles are found on sheet III at (953-55f) MeV and on sheet IV at (938-35f) MeV.
 15 Combined fit of ALDE 95B, ANISOVICH 94, AMSLER 94D.
 16 On sheet II in a 2 pole solution. The other pole is found on sheet III at (996-103j) MeV.
 17 From sheet II pole position.
 18 On sheet II in a 2 pole solution. The other pole is found on sheet III at (797-185f) MeV and can be interpreted as a shadow pole.
 19 On sheet II in a 2 pole solution. The other pole is found on sheet III at (978-28j) MeV.
 20 From coupled channel analysis.
 21 Coupled channel analysis with finite width corrections.
 22 Included in AGUILAR-BENITEZ 78 fit.

$f_0(980)$ WIDTH

Width determination very model dependent. Peak width in $\pi\pi$ is about 50 MeV, but decay width can be much larger.

VALUE (MeV)	EVTs	DOCUMENT ID	TECN	COMMENT
40 to 100 OUR ESTIMATE				
56 ± 20		23 AKHMETSHIN 99C CMD2		$e^+e^- \rightarrow \pi^0\pi^0\gamma$
65 ± 20		BARBERIS 99 OMEG	450	$pp \rightarrow \rho_S \rho_f K^+ K^-$
80 ± 10		BARBERIS 99B OMEG	450	$pp \rightarrow \rho_S \rho_f \pi^+ \pi^-$
80 ± 10		BARBERIS 99C OMEG	450	$pp \rightarrow \rho_S \rho_f \pi^0 \pi^0$
48 ± 12 ± 8		24 BARBERIS 99D OMEG	450	$pp \rightarrow K^+ K^-, \pi^+ \pi^-$
65 ± 25		BELLAZZINI 99 GAM4	450	$pp \rightarrow pp \pi^0 \pi^0$
71 ± 14		25 KAMINSKI 99 RVUE		$\pi\pi \rightarrow \pi\pi, K\bar{K}, \sigma\sigma$
~ 28		25 OLLER 99 RVUE		$\pi\pi \rightarrow \pi\pi, K\bar{K}$
~ 25		99B RVUE		$\pi\pi \rightarrow \pi\pi, K\bar{K}$
~ 14		25 OLLER 99C RVUE		$\pi\pi \rightarrow \pi\pi, K\bar{K}, \eta\eta$
74 ± 12	164	26 ACHASOV 98I SND		$e^+e^- \rightarrow 5\gamma$
188 + 48 - 33	164	27 ACHASOV 98I SND		$e^+e^- \rightarrow 5\gamma$
70 ± 20		ALDE 98 GAM4		
86 ± 16		25 ANISOVICH 98B RVUE		Compilation
54		28 LOCHER 98 RVUE		$\pi\pi \rightarrow \pi\pi, K\bar{K}$
69 ± 15		29 ALDE 97 GAM2	450	$pp \rightarrow pp \pi^0 \pi^0$
38 ± 20		30 BERTIN 97C OBLX	0.0	$\bar{p}p \rightarrow \pi^+ \pi^- \pi^0$
~ 100		31 ISHIDA 96 RVUE		$\pi\pi \rightarrow \pi\pi, K\bar{K}$
34		TORNQVIST 96 RVUE		$\pi\pi \rightarrow \pi\pi, K\bar{K}, K\pi, \eta\pi$
48 ± 10	3k	32 ALDE 95B GAM2	38	$\pi^- p \rightarrow \pi^0 \pi^0 n$
95 ± 20	10k	33 ALDE 95B GAM2	38	$\pi^- p \rightarrow \pi^0 \pi^0 n$
26 ± 10		AMSLER 95B CBAR	0.0	$\bar{p}p \rightarrow 3\pi^0$
~ 112		34 AMSLER 95D CBAR	0.0	$\bar{p}p \rightarrow \pi^0 \pi^0 \pi^0, \pi^0 \eta, \pi^0 \pi^0 \eta$
80 ± 12		35 ANISOVICH 95 RVUE		
30		JANSSEN 95 RVUE		$\pi\pi \rightarrow \pi\pi, K\bar{K}$
74		36 BUGG 94 RVUE		$\bar{p}p \rightarrow \eta 2\pi^0$
29 ± 2		37 KAMINSKI 94 RVUE		$\pi\pi \rightarrow \pi\pi, K\bar{K}$
46		38 ZOU 94B RVUE		
48 ± 12		39 MORGAN 93 RVUE		$\pi\pi(K\bar{K}) \rightarrow \pi\pi(K\bar{K}), J/\psi \rightarrow \phi\pi\pi(K\bar{K}), D_s \rightarrow \pi(\pi\pi)$
37.4 ± 10.6		29 AGUILAR... 91 EHS	400	pp
72 ± 8		40 ARMSTRONG 91 OMEG	300	$pp \rightarrow pp\pi\pi, ppK\bar{K}$
110 ± 30		BREAKSTONE 90 SFM		$pp \rightarrow pp\pi^+\pi^-$
29 ± 13		29 ABACHI 86B HRS		$e^+e^- \rightarrow \pi^+\pi^-\chi$
120 ± 281 ± 20		ETKIN 82B MPS	23	$\pi^- p \rightarrow n 2K_S^0$
28 ± 10		40 GIDAL 81 MRK2		$J/\psi \rightarrow \pi^+\pi^-\chi$
70 to 300		41 ACHASOV 80 RVUE		
100 ± 80		42 AGUILAR... 78 HBC	0.7	$\bar{p}p \rightarrow K_S^0 K_S^0$
30 ± 8		40 LEEPER 77 ASPK	2-2.4	$\pi^- p \rightarrow \pi^+\pi^-n, K^+K^-n$
48 ± 14		40 BINNIE 73 CNTR		$\pi^- p \rightarrow nMM$
32 ± 10		43 GRAYEY 73 ASPK	17	$\pi^- p \rightarrow \pi^+\pi^-n$
30 ± 10		43 HYAMS 73 ASPK	17	$\pi^- p \rightarrow \pi^+\pi^-n$
54 ± 16		43 PROTOPOP... 73 HBC		$7\pi^+ p \rightarrow \pi^+ p\pi^+\pi^-$

23 From the combined fit of the photon spectra in the reactions $e^+e^- \rightarrow \pi^+\pi^-\gamma, \pi^0\pi^0\gamma$.
 24 Supersedes BARBERIS 99 and BARBERIS 99B
 25 T-matrix pole.
 26 In the "narrow resonance" approximation.
 27 Using the "broad resonance" formulae of ACHASOV 97C.
 28 On sheet II in a 2 pole solution. The other pole is found on sheet III at (1039-93j) MeV.
 29 From invariant mass fit.
 30 On sheet II in a 2 pole solution. The other pole is found on sheet III at (963-29i) MeV.
 31 Reanalysis of data from HYAMS 73, GRAYEY 74, SRINIVASAN 75, and ROSSELET 77 using the interfering amplitude method.
 32 At high $|t|$.
 33 At low $|t|$.

Meson Particle Listings

$f_0(980)$

- ³⁴ On sheet II in a 4-pole solution, the other poles are found on sheet III at (953–557) MeV and on sheet IV at (938–357) MeV.
- ³⁵ Combined fit of ALDE 95B, ANISOVICH 94.
- ³⁶ On sheet II in a 2-pole solution. The other pole is found on sheet III at (996–1037) MeV.
- ³⁷ From sheet II pole position.
- ³⁸ On sheet II in a 2-pole solution. The other pole is found on sheet III at (797–1857) MeV and can be interpreted as a shadow pole.
- ³⁹ On sheet II in a 2-pole solution. The other pole is found on sheet III at (978–287) MeV.
- ⁴⁰ From coupled channel analysis.
- ⁴¹ Coupled channel analysis with finite width corrections.
- ⁴² From coupled channel fit to the HYAMS 73 and PROTOPOESCU 73 data. With a simultaneous fit to the $\pi\pi$ phase-shifts, inelasticity and to the $K_S^0 K_S^0$ invariant mass.
- ⁴³ Included in AGUILAR-BENITEZ 78 fit.

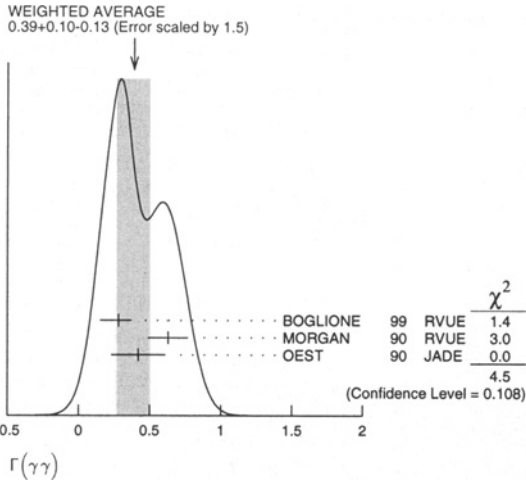
$f_0(980)$ DECAY MODES

Mode	Fraction (Γ_i/Γ)
Γ_1 $\pi\pi$	dominant
Γ_2 $K\bar{K}$	seen
Γ_3 $\gamma\gamma$	
Γ_4 e^+e^-	

$f_0(980)$ PARTIAL WIDTHS

$\Gamma(\gamma\gamma)$					Γ_3
VALUE (keV)	EVTS	DOCUMENT ID	TECN	COMMENT	
$0.39^{+0.10}_{-0.13}$	OUR AVERAGE	Error includes scale factor of 1.5. See the ideogram below.			
$0.28^{+0.09}_{-0.13}$		44 BOGLIONE 99 RVUE	$\gamma\gamma \rightarrow \pi^+\pi^-, \pi^0\pi^0$		
0.63 ± 0.14		45 MORGAN 90 RVUE	$\gamma\gamma \rightarrow \pi^+\pi^-, \pi^0\pi^0$		
$0.42 \pm 0.06 \pm 0.18$		60 46 OEST 90 JADE	$e^+e^- \rightarrow e^+e^-\pi^0\pi^0$		
••• We do not use the following data for averages, fits, limits, etc. •••					
$0.29 \pm 0.07 \pm 0.12$		47,48 BOYER 90 MRK2	$e^+e^- \rightarrow \pi^+\pi^-$		
$0.31 \pm 0.14 \pm 0.09$		47,48 MARSISKE 90 CBAL	$e^+e^- \rightarrow \pi^+\pi^-, \pi^0\pi^0$		

- ⁴⁴ Supersedes MORGAN 90.
- ⁴⁵ From amplitude analysis of BOYER 90 and MARSISKE 90, data corresponds to resonance parameters $m = 989$ MeV, $\Gamma = 61$ MeV.
- ⁴⁶ OEST 90 quote systematic errors ± 0.08 . We use ± 0.18 .
- ⁴⁷ From analysis allowing arbitrary background unconstrained by unitarity.
- ⁴⁸ Data included in MORGAN 90, BOGLIONE 99 analyses.



$\Gamma(e^+e^-)$					Γ_4
VALUE (eV)	CL%	DOCUMENT ID	TECN	COMMENT	
<8.4	90	VOROBYEV 88 ND		$e^+e^- \rightarrow \pi^0\pi^0$	

$f_0(980)$ BRANCHING RATIOS

$\Gamma(\pi\pi) / [\Gamma(\pi\pi) + \Gamma(K\bar{K})]$					$\Gamma_1/(\Gamma_1+\Gamma_2)$
VALUE	DOCUMENT ID	TECN	COMMENT		
••• We do not use the following data for averages, fits, limits, etc. •••					
~ 0.68	OLLER 99B	RVUE	$\pi\pi \rightarrow \pi\pi, K\bar{K}$		
0.67 ± 0.09	49 LOVERRE 80	HBC	$4\pi^-p \rightarrow n2K_S^0$		
$0.81^{+0.09}_{-0.04}$	49 CASON 78	STRC	$7\pi^-p \rightarrow n2K_S^0$		
0.78 ± 0.03	49 WETZEL 76	OSPK	$8.9\pi^-p \rightarrow n2K_S^0$		

- ⁴⁹ Measure $\pi\pi$ elasticity assuming two resonances coupled to the $\pi\pi$ and $K\bar{K}$ channels only.

$f_0(980)$ REFERENCES

AKHMETSHIN 99B	PL B462 371	R.R. Akhmetshin et al.	(CMD-2 Collab.)
AKHMETSHIN 99C	PL B462 380	R.R. Akhmetshin et al.	(CMD-2 Collab.)
BARBERIS 99	PL B453 305	D. Barberis et al.	(Omega expt.)
BARBERIS 99B	PL B453 316	D. Barberis et al.	(Omega expt.)
BARBERIS 99C	PL B453 325	D. Barberis et al.	(Omega expt.)
BARBERIS 99D	PL B462 462	D. Barberis et al.	(Omega expt.)
BELLAZZINI 99	PL B467 296	R. Bellazzini et al.	
BOGLIONE 99	EPJ C9 11	M. Boglione, M.R. Pennington	
KAMINSKI 99	EPJ C9 141	R. Kaminski, L. Lesniak, B. Loiseau	
OLLER 99	PR D60 099906	J.A. Oller et al.	
OLLER 99B	NP A652 407	J.A. Oller, E. Oset	
OLLER 99C	PR D60 074023	J.A. Oller, E. Oset	
ACHASOV 981	PL B440 442	M.N. Achasov et al.	
ACHERSTAFF 98Q	EPJ C4 19	K. Acherstaff et al.	(OPAL Collab.)
ALDE 98	EPJ A3 361	D. Alde et al.	(GAMA Collab.)
ALDE 99	PAN 62 405	D. Alde et al.	(GAMS Collab.)
ANISOVICH 98B	UFN 41 419	V.V. Anisovich et al.	
LOCHER 98	EPJ C4 317	M.P. Locher et al.	(PSI)
ACHASOV 97C	PR D56 4084	N.N. Achasov et al.	
ALDE 97	PL B397 350	D.M. Alde et al.	(GAMS Collab.)
BERTIN 97C	PL B408 476	A. Bertin et al.	(OBELIX Collab.)
ISHIDA 96	PTP 95 745	S. Ishida et al.	(TOKY, MIYA, KEK)
TORNQVIST 96	PR L76 1575	N.A. Tornqvist, M. Roos	(HEL5)
ALDE 95B	ZPHY C56 375	D.M. Alde et al.	(GAMS Collab.)
AMSLER 95B	PL B342 433	C. Amstler et al.	(Crystal Barrel Collab.)
AMSLER 95D	PL B355 425	C. Amstler et al.	(Crystal Barrel Collab.)
ANISOVICH 95	PL B355 363	V.V. Anisovich et al.	(PNPI, SERP)
JANSEN 95	PR D52 2690	G. Jansen et al.	(STON, ADL, JULI)
AMSLER 94D	PL B333 277	C. Amstler et al.	(Crystal Barrel Collab.)
ANISOVICH 94	PL B323 235	V.V. Anisovich et al.	
BUGG 94	PR D50 4412	D.V. Bugg et al.	(LOQM)
KAMINSKI 94	PR D50 3145	R. Kaminski et al.	(CRAC, IPN)
ZOU 94B	PR D50 591	B.S. Zou, D.V. Bugg	(LOQM)
MORGAN 93	PR D48 1185	D. Morgan, M.R. Pennington	(RAL, DURH)
AGUILAR... 91	ZPHY C50 405	M. Aguilar-Benitez et al.	(LEBC-EHS Collab.)
ARMSTRONG 91	ZPHY C51 351	T.A. Armstrong et al.	(ATHU, BARI, BIRM+)
BOYER 90	PR D42 1350	J. Boyer et al.	(Mark II Collab.)
BREAKSTONE 90	ZPHY C48 569	A.M. Breakstone et al.	(ISU, BGNA, CERN+)
MARSISKE 90	PR D41 3324	H. Marsiske et al.	(Crystal Ball Collab.)
MORGAN 90	ZPHY C48 623	D. Morgan, M.R. Pennington	(RAL, DURH)
OEST 90	ZPHY C47 343	T. Oest et al.	(JADE Collab.)
AUGUSTIN 89	NP B320 1	J.E. Augustin, G. Cosme	(DM2 Collab.)
VOROBYEV 88	SJNP 48 273	P.V. Vorobyev et al.	(NOVO)
Translated from YAF 48 436.			
ABACHI 86B	PRL 57 1990	S. Abachi et al.	(PURD, ANL, IND, MICH+)
ETKIN 82B	PR D25 1786	A. Etkin et al.	(BNL, CUNY, TUFTS, VAND)
GIDAL 81	PL 107B 153	G. Gidal et al.	(SLAC, LBL)
ACHASOV 80	SJNP 32 566	N.N. Achasov, S.A. Devyanin, G.N. Shestakov	(NOVM)
Translated from YAF 32 109B.			
LOVERRE 80	ZPHY C6 187	P.F. Loverre et al.	(CERN, CDEF, MADR+IJP)
AGUILAR... 78	NP B140 73	M. Aguilar-Benitez et al.	(MADR, BOMB+)
CASON 78	PRL 41 271	N.M. Cason et al.	(NDAM, ANL)
LEEPER 77	PR D16 2054	R.J. Leeper et al.	(ISU)
ROSSELET 77	PR D15 574	L. Rosselet et al.	(GEVA, SACL)
WETZEL 76	NP B115 208	W. Wetzel et al.	(ETH, CERN, LOIC)
SRINIVASAN 75	PR D12 1681	V. Srinivasan et al.	(NDAM, ANL)
GRAY 74	NP B75 189	G. Gray et al.	(CERN, MPIM)
BINNIE 73	PR L31 1534	D.M. Binnie et al.	(LOIC, SHMP)
GRAY 73	Tallahassee	G. Gray et al.	(CERN, MPIM)
HYAMS 73	NP B64 134	B.D. Hyams et al.	(CERN, MPIM)
PROTOPO... 73	PR D7 1279	S.D. Protopopescu et al.	(LBL)

OTHER RELATED PAPERS

ABREU 99J	PL B449 364	P. Abreu et al.	(DELPHI Collab.)
ANISOVICH 99D	PL B452 180	A.V. Anisovich et al.	
Also 99F	NP A651 253	A.V. Anisovich et al.	
ANISOVICH 99H	PL B467 289	A.V. Anisovich, V.V. Anisovich	
BLACK 99	PR D59 074026	D. Black et al.	
DELBOURGO 99	PL B445 332	R. Delbourgo, D. Liu, M. Scadron	
MARCO 99	PL B470 20	E. Marco et al.	
MINKOWSKI 99	EPJ C9 283	P. Minkowski, W. Ochs	
ACHASOV 98C	PR D57 1987	N.N. Achasov et al.	
ACHASOV 98G	JETP 67 464	N.N. Achasov et al.	
ACHASOV 98J	SPU 41 1149	N.N. Achasov et al.	
CHLIAPNIK... 98	PL B423 401	N.N. Achasov et al.	
ACHASOV 97C	PR D56 4084	N.N. Achasov et al.	
ACHASOV 97D	PR D56 203	N.N. Achasov et al.	
ACHASOV 97E	IAMP A32 5019	N.N. Achasov et al.	
PROKOSHNIK 97	SPD 42 117	Y.D. Prokoshkin et al.	(SERP)
Translated from DANS 353 323.			
AU 87	PR D35 1633	K.L. Au, D. Morgan, M.R. Pennington	(DURH, RAL)
AKESSON 86	NP B264 154	T. Akesson et al.	(Axial Field Spec. Collab.)
BEVEREN 86	ZPHY C30 615	E. van Beveren et al.	(NIJM, BIEL)
MENNESSIER 83	ZPHY C16 291	G. Mennessier	(MONP)
BARBER 82	ZPHY C12 1	D.P. Barber et al.	(DARE, LANC, SHEF)
ETKIN 82C	PR D25 2446	A. Etkin et al.	(BNL, CUNY, TUFTS, VAND)
SRINIVASAN 75	PR D12 681	V. Srinivasan et al.	(NDAM, ANL)
BIGI 62	CERN Conf. 247	A. Bigi et al.	(CERN)
BINGHAM 62	CERN Conf. 240	H.H. Bingham et al.	(EPOL, CERN)
ERWIN 62	PRL 9 34	A.R. Erwin et al.	(WISC, BERN)
WANG 61	JETP 13 323	Wang et al.	(JINR)
Translated from ZETF 40 464.			

See key on page 239

Meson Particle Listings

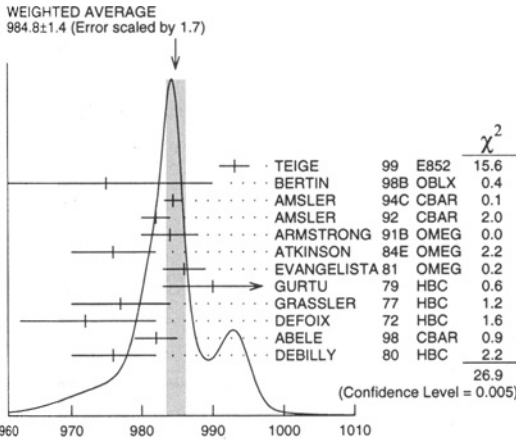
$a_0(980)$

$a_0(980)$ $I^G(J^{PC}) = 1^-(0^{++})$

See our minireview on scalar mesons under $f_0(1370)$. (See the index for the page number.)

$a_0(980)$ MASS

VALUE (MeV) DOCUMENT ID
984.8 ± 1.4 OUR AVERAGE Includes data from the 2 datablocks that follow this one. Error includes scale factor of 1.7. See the ideogram below.



$a_0(980)$ MASS

$\eta\pi$ FINAL STATE ONLY

VALUE (MeV) EVTS DOCUMENT ID TECN CHG COMMENT
 The data in this block is included in the average printed for a previous datablock.

985.2 ± 1.5 OUR AVERAGE Error includes scale factor of 1.7. See the ideogram below.

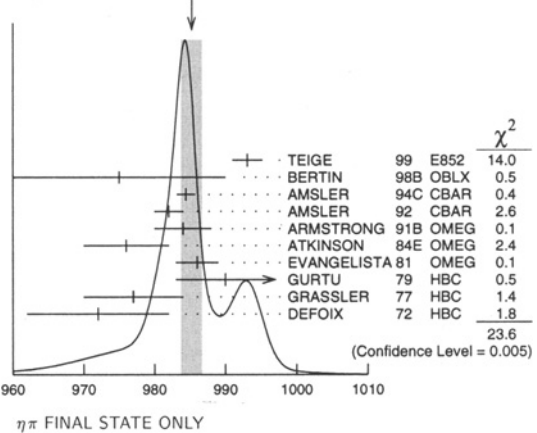
VALUE (MeV)	EVTS	DOCUMENT ID	TECN	CHG	COMMENT
993.1 ± 2.1	1	TEIGE	99 E852		18.3 $\pi^- p \rightarrow \eta\pi^+\pi^- n$
975 ± 15		BERTIN	98B OBLX		0.0 $\bar{p} p \rightarrow K^\pm K_S^0 \pi^\mp$
984.45 ± 1.23 ± 0.34		AMSLER	94C CBAR		0.0 $\bar{p} p \rightarrow \omega\eta\pi^0$
982 ± 2	2	AMSLER	92 CBAR		0.0 $\bar{p} p \rightarrow \eta\eta\pi^0$
984 ± 4	1040	2 ARMSTRONG	91B OMEG ±		300 $pp \rightarrow \rho\rho\eta\pi^+\pi^-$
976 ± 6		ATKINSON	84E OMEG ±		25-55 $\gamma p \rightarrow \eta\pi n$
986 ± 3	500	3 EVANGELISTA	81 OMEG ±		12 $\pi^- p \rightarrow \eta\pi^+\pi^-\pi^- p$
990 ± 7	145	3 GURTU	79 HBC ±		4.2 $K^- p \rightarrow \Lambda\eta 2\pi$
977 ± 7		GRASSLER	77 HBC		16 $\pi^+ p \rightarrow p\eta 3\pi$
972 ± 10	150	DEFOIX	72 HBC ±		0.7 $\bar{p} p \rightarrow 7\pi$

• • • We do not use the following data for averages, fits, limits, etc. • • •

~ 1055	4	OLLER	99 RVUE		$\eta\pi, K\bar{K}$
~ 1009.2	4	OLLER	99B RVUE		$\pi\pi \rightarrow \pi\pi, K\bar{K}$
986 $\begin{smallmatrix} +23 \\ -10 \end{smallmatrix}$	20	5 ACHASOV	98B SND		$e^+e^- \rightarrow 5\gamma$
988 ± 6	4	ANISOVICH	98B RVUE		Compilation
987		TORNQVIST	96 RVUE		$\pi\pi \rightarrow \pi\pi, K\bar{K}, K\pi, \eta\pi$
991		JANSSEN	95 RVUE		$\eta\pi \rightarrow \eta\pi, K\bar{K}, K\pi, \eta\pi$
980 ± 11	47	CONFORTO	78 OSPK		4.5 $\pi^- p \rightarrow \rho X^-$
978 ± 16	50	CORDEN	78 OMEG ±		12-15 $\pi^- p \rightarrow \eta\eta 2\pi$
989 ± 4	70	WELLS	75 HBC		3.1-6 $K^- p \rightarrow \Lambda\eta 2\pi$
970 ± 15	20	BARNES	69C HBC		4-5 $K^- p \rightarrow \Lambda\eta 2\pi$
980 ± 10		CAMPBELL	69 DBC		2.7 $\pi^+ d$
980 ± 10	15	MILLER	69B HBC		4.5 $K^- N \rightarrow \eta\pi\Lambda$
980 ± 10	30	AMMAR	68 HBC ±		5.5 $K^- p \rightarrow \Lambda\eta 2\pi$

1 Breit-Wigner fit, average between a_0^+ and a_0^0 . The fit favors a slightly heavier a_0^+ .
 2 From a single Breit-Wigner fit.
 3 From $f_1(1285)$ decay.
 4 T-matrix pole.
 5 Assuming $g_{a_0\eta\pi} = 0.85 g_{a_0 K^+ K^-}$. Systematic uncertainties not estimated.

WEIGHTED AVERAGE
 985.2 ± 1.5 (Error scaled by 1.7)



$\eta\pi$ FINAL STATE ONLY

$K\bar{K}$ ONLY

VALUE (MeV) EVTS DOCUMENT ID TECN CHG COMMENT
 The data in this block is included in the average printed for a previous datablock.

980.8 ± 2.7 OUR AVERAGE

982 ± 3	6	ABELE	98 CBAR		0.0 $\bar{p} p \rightarrow K_L^0 K^\pm \pi^\mp$
976 ± 6	316	DEBILLY	80 HBC ±		1.2-2 $\bar{p} p \rightarrow f_1(1285)\omega$

• • • We do not use the following data for averages, fits, limits, etc. • • •

~ 1053	7	OLLER	99C RVUE		$\pi\pi \rightarrow \pi\pi, K\bar{K}$
1016 ± 10	100	8 ASTIER	67 HBC ±		0.0 $\bar{p} p$
1003.3 ± 7.0	143	9 ROSENFELD	65 RVUE ±		

6 T-matrix pole on sheet II, the pole on sheet III is at 1006-i49 MeV.
 7 T-matrix pole.
 8 ASTIER 67 includes data of BARLOW 67, CONFORTO 67, ARMENTEROS 65.
 9 Plus systematic errors.

$a_0(980)$ WIDTH

VALUE (MeV) EVTS DOCUMENT ID TECN CHG COMMENT
50 to 100 OUR ESTIMATE Width determination very model dependent. Peak width in $\eta\pi$ is about 60 MeV, but decay width can be much larger.

• • • We do not use the following data for averages, fits, limits, etc. • • •

~ 42	10	OLLER	99 RVUE		$\eta\pi, K\bar{K}$
~ 112	10	OLLER	99B RVUE		$\pi\pi \rightarrow \eta\pi, K\bar{K}$
71 ± 7		TEIGE	99 E852		18.3 $\pi^- p \rightarrow \eta\pi^+\pi^- n$
92 ± 20		ANISOVICH	98B RVUE		Compilation
65 ± 10		BERTIN	98B OBLX		0.0 $\bar{p} p \rightarrow K^\pm K_S^0 \pi^\mp$
~ 100		TORNQVIST	96 RVUE		$\pi\pi \rightarrow \pi\pi, K\bar{K}, K\pi, \eta\pi$
202		JANSSEN	95 RVUE		$\eta\pi \rightarrow \eta\pi, K\bar{K}, K\pi, \eta\pi$
54.12 ± 0.34 ± 0.12		AMSLER	94C CBAR		0.0 $\bar{p} p \rightarrow \omega\eta\pi^0$
54 ± 10		11 AMSLER	92 CBAR		0.0 $\bar{p} p \rightarrow \eta\eta\pi^0$
95 ± 14	1040	11 ARMSTRONG	91B OMEG ±		300 $pp \rightarrow \rho\rho\eta\pi^+\pi^-$
62 ± 15	500	12 EVANGELISTA	81 OMEG ±		12 $\pi^- p \rightarrow \eta\pi^+\pi^-\pi^- p$
60 ± 20	145	12 GURTU	79 HBC ±		4.2 $K^- p \rightarrow \Lambda\eta 2\pi$
60 $\begin{smallmatrix} +50 \\ -30 \end{smallmatrix}$	47	CONFORTO	78 OSPK		4.5 $\pi^- p \rightarrow \rho X^-$
86.0 $\begin{smallmatrix} +60.0 \\ -50.0 \end{smallmatrix}$	50	CORDEN	78 OMEG ±		12-15 $\pi^- p \rightarrow \eta\eta 2\pi$
44 ± 22		GRASSLER	77 HBC		16 $\pi^+ p \rightarrow p\eta 3\pi$
80 to 300		13 FLATTE	76 RVUE		4.2 $K^- p \rightarrow \Lambda\eta 2\pi$
16.0 $\begin{smallmatrix} +25.0 \\ -16.0 \end{smallmatrix}$	70	WELLS	75 HBC		3.1-6 $K^- p \rightarrow \Lambda\eta 2\pi$
30 ± 5	150	DEFOIX	72 HBC ±		0.7 $\bar{p} p \rightarrow 7\pi$
40 ± 15		CAMPBELL	69 DBC		2.7 $\pi^+ d$
60 ± 30	15	MILLER	69B HBC		4.5 $K^- N \rightarrow \eta\pi\Lambda$
80 ± 30	30	AMMAR	68 HBC ±		5.5 $K^- p \rightarrow \Lambda\eta 2\pi$

10 T-matrix pole.
 11 From a single Breit-Wigner fit.
 12 From $f_1(1285)$ decay.
 13 Using a two-channel resonance parametrization of GAY 76B data.

$K\bar{K}$ ONLY

VALUE (MeV) EVTS DOCUMENT ID TECN CHG COMMENT

92 ± 8

14	ABELE	98 CBAR		0.0 $\bar{p} p \rightarrow K_L^0 K^\pm \pi^\mp$
----	-------	---------	--	---

• • • We do not use the following data for averages, fits, limits, etc. • • •

~ 24	15	OLLER	99C RVUE		$\pi\pi \rightarrow \pi\pi, K\bar{K}$
~ 25	100	16 ASTIER	67 HBC ±		
57 ± 13	143	17 ROSENFELD	65 RVUE ±		

14 T-matrix pole on sheet II, the pole on sheet III is at 1006-i49 MeV.
 15 T-matrix pole.
 16 ASTIER 67 includes data of BARLOW 67, CONFORTO 67, ARMENTEROS 65.
 17 Plus systematic errors.

Meson Particle Listings

$a_0(980), \phi(1020)$

$a_0(980)$ DECAY MODES

Mode	Fraction (Γ_i/Γ)
$\Gamma_1 \eta\pi$	dominant
$\Gamma_2 K\bar{K}$	seen
$\Gamma_3 \rho\pi$	
$\Gamma_4 \gamma\gamma$	seen
$\Gamma_5 e^+e^-$	

$a_0(980)$ PARTIAL WIDTHS

$\Gamma(\gamma\gamma)$	DOCUMENT ID	TECN	COMMENT
VALUE (keV)			
0.30 ± 0.10	18 AMSLER	98 RVUE	
¹⁸ Using $\Gamma_{\gamma\gamma}B(a_0(980) \rightarrow \eta\pi) = 0.24 \pm 0.08$ keV.			

$a_0(980)$ $\Gamma(\eta)\Gamma(\gamma\gamma)/\Gamma(\text{total})$

$\Gamma(\eta\pi) \times \Gamma(\gamma\gamma)/\Gamma(\text{total})$	EVTS	DOCUMENT ID	TECN	COMMENT
VALUE (keV)				
$0.24^{+0.08}_{-0.07}$ OUR AVERAGE				
$0.28 \pm 0.04 \pm 0.10$	44	OEST	90 JADE	$e^+e^- \rightarrow e^+e^-\pi^0\eta$
$0.19 \pm 0.07^{+0.10}_{-0.07}$		ANTREASYAN 86	CBAL	$e^+e^- \rightarrow e^+e^-\pi^0\eta$

$a_0(980)$ BRANCHING RATIOS

$\Gamma(K\bar{K})/\Gamma(\eta\pi)$	DOCUMENT ID	TECN	CHG	COMMENT
VALUE				
0.177 ± 0.024 OUR AVERAGE	Error includes scale factor of 1.2.			
0.23 ± 0.05	19 ABELE	98 CBAR		$0.0 \bar{p}p \rightarrow K_S^0 K^\pm \pi^\mp$
$0.166 \pm 0.01 \pm 0.02$	20 BARBERIS	98C OMEG		$450 \bar{p}p \rightarrow p \bar{p} f_1(1285) p_S$
• • • We do not use the following data for averages, fits, limits, etc. • • •				
~ 0.60	OLLER	99B RVUE		$\pi\pi \rightarrow \eta\pi, K\bar{K}$
1.16 ± 0.18	21 BUGG	94 RVUE		$\bar{p}p \rightarrow \eta\eta\pi^0$
0.7 ± 0.3	20 CORDEN	78 OMEG		$12-15 \pi^-\pi^0 \rightarrow n\eta 2\pi$
0.25 ± 0.08	20 DEFOIX	72 HBC	\pm	$0.7 \bar{p} \rightarrow 7\pi$
¹⁹ Using $\pi^0\pi^0\eta$ from AMSLER 94D.				
²⁰ From the decay of $f_1(1285)$.				
²¹ BUGG 94 uses AMSLER 94C data. This is a ratio of couplings.				

$a_0(980)$ REFERENCES

OLLER	99	PR D60 099906	J.A. Oller et al.
OLLER	99B	NP A652 407	J.A. Oller, E. Oset
OLLER	99C	PR D60 074023	J.A. Oller, E. Oset
TEIGE	99	PR D59 012001	S. Teige et al.
ABELE	98	PR D57 3860	A. Abele et al.
ACHASOV	98B	PL B438 441	M.N. Achasov et al.
AMSLER	98	RMP 70 1293	C. Amsler
ANISOVICH	98B	UFN 43 419	V.V. Anisovich et al.
BARBERIS	98C	PL B440 225	D. Barberis et al.
BERTIN	98B	PL B434 180	A. Bertin et al.
TORNQVIST	96	PRL 76 1575	N.A. Tornqvist, M. Roos
JANSEN	95	PR D52 2690	G. Janssen et al.
AMSLER	94C	PL B327 425	C. Amsler et al.
AMSLER	94D	PL B333 277	C. Amsler et al.
BUGG	94	PR D50 4412	D.V. Bugg et al.
AMSLER	92	PL B291 347	C. Amsler et al.
ARMSTRONG	91B	ZPHY C52 389	T.A. Armstrong et al.
OEST	90	ZPHY C47 343	T. Oest et al.
VOROBYEV	88	SJNP 48 273	P.V. Vorobiev et al.
Translated from YAF 48 436.			

ANTREASYAN	86	PR D33 1847	D. Antreasyan et al.	(Crystal Ball Collab.)
ATKINSON	84E	PL 1308 459	M. Atkinson et al.	(BONN, CERN, GLAS+)
EVANGELISTA	81	NP B378 197	C. Evangelista et al.	(BARI, BONN, CERN+)
DEBILLY	80	NP B176 1	L. de Billy et al.	(CURIN, LAUS, NEUC+)
GURTU	79	NP B151 181	A. Gurtu et al.	(CERN, ZEEB, NIJM, OXF)
CONFORTO	78	LNC 23 419	B. Conforto et al.	(RHEL, TINTO, CHIC+)
CORDEN	78	NP B144 253	M.J. Corden et al.	(BIRM, RHEL, TELA+)
GRASSLER	77	NP B121 189	H. Grassler et al.	(AACH3, BERL, BONN+)
FLATTE	76	PL 63B 224	S.M. Flatte	(CERN)
GAY	76B	PL 63B 220	J.B. Gay et al.	(CERN, AMST, NIJM) JP
WELLS	75	NP B101 333	J. Wells et al.	(OXF)
DEFOIX	72	NP B44 125	C. Defoix et al.	(CDEF, CERN)
AMMAR	70	PR D2 430	R. Ammar et al.	(KANS, NWES, ANL, WISC)
BARNES	69C	PRL 23 610	V.E. Barnes et al.	(BNL, SYRA)
CAMPBELL	69	PRL 22 1204	J.H. Campbell et al.	(PURD)
MILLER	69B	PL 29B 255	D.H. Miller et al.	(PURD)
Also	69	PR 108 2011	W.L. Yen et al.	(PURD)
AMMAR	68	PRL 21 1832	R. Ammar et al.	(NWES, ANL)
ASTIER	67	PL 25B 294	A. Astier et al.	(CDEF, CERN, IRAD)
Includes data of BARLOW 67, CONFORTO 67, and ARMENTEROS 65.				
BARLOW	67	NC 50A 701	J. Barlow et al.	(CERN, CDEF, IRAD, LVP)
CONFORTO	67	NP B3 469	G. Conforto et al.	(CERN, CDEF, IPNP+)
ARMENTEROS	65	PL 17 344	R. Armenteros et al.	(CERN, CDEF)
ROSENFELD	65	Oxford Conf. 58	A.H. Rosenfeld	(LRL)

OTHER RELATED PAPERS

ANISOVICH	99D	PL B452 180	A.V. Anisovich et al.	
Also	99F	NP A651 253	A.V. Anisovich et al.	
MARCO	99	PL B470 20	E. Marco et al.	
ACHASOV	98J	SFU 41 1149		
ACHASOV	97C	PR D56 4084	N.N. Achasov et al.	
ACHASOV	97D	PR D56 203	N.N. Achasov et al.	
ACHASOV	97E	LMP A12 5019	N.N. Achasov et al.	
AMSLER	94D	PL B333 277	C. Amsler et al.	(Crystal Barrel Collab.)
TORNQVIST	90	NPBPS 21 196	N.A. Tornqvist	(HEL5)
WEINSTEIN	89	UTPT 89 03	J. Weinstein, N. Isgur	(TINTO)
ACHASOV	88B	ZPHY C41 309	N.N. Achasov, G.N. Shestakov	(NOVM)
BEVEREN	86	ZPHY C30 615	E. van Beveren et al.	(NIJM, BIEL)
WEINSTEIN	83B	PR D27 588	J. Weinstein, N. Isgur	(TINTO)
TORNQVIST	82	PRL 49 624	N.A. Tornqvist	(HEL5)
BRAMON	80	PL 93B 65	A. Bramon, E. Masso	(BARC)
TURKOT	63	Siena Conf. 1 661	F. Turkot et al.	(BNL, PITT)

$\phi(1020)$

$$I^{G(J^{PC})} = 0^-(1^{--})$$

$\phi(1020)$ MASS

We average mass and width values only when the systematic errors have been evaluated.

VALUE (MeV)	EVTS	DOCUMENT ID	TECN	COMMENT
1019.417 ± 0.014 OUR AVERAGE		Error includes scale factor of 1.8. See the ideogram below.		
1019.36 ± 0.12		1 ACHASOV	00B SND	$e^+e^- \rightarrow \eta\gamma$
$1019.504 \pm 0.011 \pm 0.033$	314k	AKHMETSHIN 99D	CMD2	$e^+e^- \rightarrow K_L^0 K_S^0$
$1019.38 \pm 0.07 \pm 0.08$	2200	2 AKHMETSHIN 99F	CMD2	$e^+e^- \rightarrow \pi^+\pi^- \geq 2\gamma$
$1019.51 \pm 0.07 \pm 0.10$	11169	AKHMETSHIN 98	CMD2	$e^+e^- \rightarrow \pi^+\pi^-\pi^0$
1019.5 ± 0.4		BARBERIS	98 OMEG	$450 \bar{p}p \rightarrow pp2K^+2K^-$
1019.42 ± 0.06	55600	AKHMETSHIN 95	CMD2	$e^+e^- \rightarrow \text{hadrons}$
1019.7 ± 0.3	2012	DAVENPORT	86 MPFS	$400 \bar{p}p \rightarrow 4KK$
1019.411 ± 0.008	642k	3 DIJKSTRA	86 SPEC	$100-200 \pi^\pm, \bar{p}, p, K^\pm, \text{on Be}$
$1019.7 \pm 0.1 \pm 0.1$	5079	ALBRECHT	85D ARG	$10 e^+e^- \rightarrow K^+K^-X$
1019.3 ± 0.1	1500	ARENTON	82 AEMS	11.8 polar. $\bar{p}p \rightarrow KK$
1019.67 ± 0.17	25080	4 PELLINEN	82 RVUE	$e^+e^- \rightarrow \text{hadrons}$
1019.52 ± 0.13	3681	BUKIN	78C OLYA	$e^+e^- \rightarrow \text{hadrons}$
• • • We do not use the following data for averages, fits, limits, etc. • • •				
1019.8 ± 0.7		ARMSTRONG	86 OMEG	$85 \pi^+/\bar{p}p \rightarrow \pi^+/p4KK$
1020.1 ± 0.11	5526	5 ATKINSON	86 OMEG	$20-70 \gamma p$
1019.7 ± 1.0		BEBEK	86 CLEO	$e^+e^- \rightarrow T(4S)$
1020.9 ± 0.2		5 FRAME	86 OMEG	$13 K^+\pi^0 \rightarrow \phi K^+\pi$
1021.0 ± 0.2		5 ARMSTRONG	83B OMEG	$18.5 K^-\pi^0 \rightarrow K^-\pi^+\pi^0$
1020.0 ± 0.5		5 ARMSTRONG	83B OMEG	$18.5 K^-\pi^0 \rightarrow K^-\pi^+\pi^0$
1019.7 ± 0.3		5 BARATE	83 GOLI	$190 \pi^-\text{Be} \rightarrow 2\mu X$
$1019.8 \pm 0.2 \pm 0.5$	766	IVANOV	81 OLYA	$1-1.4 e^+e^- \rightarrow K^+K^-$
1019.4 ± 0.5	337	COOPER	78B HBC	$0.7-0.8 \bar{p}p \rightarrow K_S^0 K_L^0 \pi^+\pi^-$
1020 ± 1	383	5 BALDI	77 CNTR	$10 \pi^-\pi^0 \rightarrow \pi^-\phi p$

See key on page 239

Meson Particle Listings

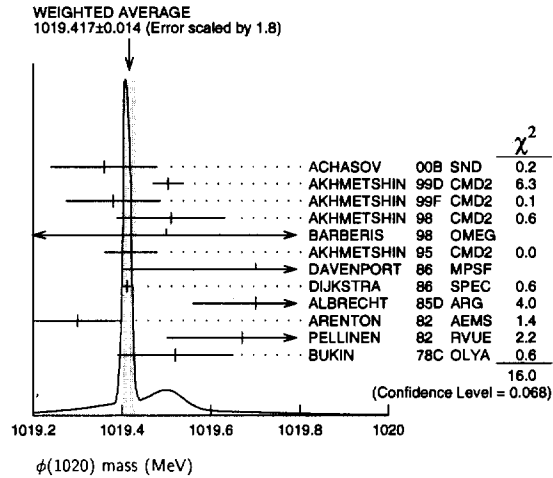
$\phi(1020)$

1018.9 ± 0.6	800	COHEN	77	ASPK	$6 \pi^\pm N \rightarrow K^+ K^- N$
1019.7 ± 0.5	454	KALBFLEISCH	76	HBC	$2.18 K^- p \rightarrow AK\bar{K}$
1019.4 ± 0.8	984	BESCH	74	CNTR	$2 \gamma p \rightarrow \rho K^+ K^-$
1020.3 ± 0.4	100	BALLAM	73	HBC	$2.8-9.3 \gamma p$
1019.4 ± 0.7		BINNIE	73B	CNTR	$\pi^- p \rightarrow \phi n$
1019.6 ± 0.5	120	⁶ AGUILAR...	72B	HBC	$3.9, 4.6 K^- p \rightarrow AK^+ K^-$
1019.9 ± 0.5	100	⁶ AGUILAR...	72B	HBC	$3.9, 4.6 K^- p \rightarrow K^- \rho K^+ K^-$
1020.4 ± 0.5	131	COLLEY	72	HBC	$10 K^+ p \rightarrow K^+ \rho \phi$
1019.9 ± 0.3	410	STOTTLE...	71	HBC	$2.9 K^- p \rightarrow \Sigma / AK\bar{K}$

$\phi(1020)$ DECAY MODES

Mode	Fraction (Γ_i/Γ)	Scale factor/ Confidence level
$\Gamma_1 K^+ K^-$	(49.2 ± 0.7) %	S=1.2
$\Gamma_2 K_L^0 K_S^0$	(33.8 ± 0.6) %	S=1.2
$\Gamma_3 \rho \pi^+ \pi^- \pi^0$	(15.5 ± 0.6) %	S=1.4
$\Gamma_4 \rho \pi$		
$\Gamma_5 \pi^+ \pi^- \pi^0$		
$\Gamma_6 \eta \gamma$	(1.297 ± 0.033) %	S=1.2
$\Gamma_7 \pi^0 \gamma$	(1.26 ± 0.10) × 10 ⁻³	
$\Gamma_8 e^+ e^-$	(2.91 ± 0.07) × 10 ⁻⁴	S=1.2
$\Gamma_9 \mu^+ \mu^-$	(3.7 ± 0.5) × 10 ⁻⁴	
$\Gamma_{10} \eta e^+ e^-$	(1.3 +0.8 -0.6) × 10 ⁻⁴	
$\Gamma_{11} \pi^+ \pi^-$	(7.5 ± 1.4) × 10 ⁻⁵	
$\Gamma_{12} \omega \pi^0$	(4.8 ± 2.0) × 10 ⁻⁵	
$\Gamma_{13} \omega \gamma$	< 5 %	CL=84%
$\Gamma_{14} \rho \gamma$	< 1.2 × 10 ⁻⁵	CL=90%
$\Gamma_{15} \pi^+ \pi^- \gamma$	(4.1 ± 1.3) × 10 ⁻⁵	
$\Gamma_{16} f_0(980) \gamma$	(3.4 ± 0.4) × 10 ⁻⁴	
$\Gamma_{17} \pi^0 \pi^0 \gamma$	(1.08 ± 0.19) × 10 ⁻⁴	
$\Gamma_{18} \pi^+ \pi^- \pi^+ \pi^-$	< 8.7 × 10 ⁻⁴	CL=90%
$\Gamma_{19} \pi^+ \pi^+ \pi^- \pi^- \pi^0$	< 1.5 × 10 ⁻⁴	CL=95%
$\Gamma_{20} \pi^0 e^+ e^-$	< 1.2 × 10 ⁻⁴	CL=90%
$\Gamma_{21} \pi^0 \eta \gamma$	(8.6 ± 1.8) × 10 ⁻⁵	
$\Gamma_{22} a_0(980) \gamma$	< 5 × 10 ⁻³	CL=90%
$\Gamma_{23} \eta'(958) \gamma$	(6.7 +3.5 -3.1) × 10 ⁻⁵	
$\Gamma_{24} \eta \pi^0 \pi^0 \gamma$	< 2 × 10 ⁻⁵	CL=90%
$\Gamma_{25} \mu^+ \mu^- \gamma$	(1.4 ± 0.5) × 10 ⁻⁵	
$\Gamma_{26} \rho \gamma \gamma$	< 5 × 10 ⁻⁴	CL=90%
$\Gamma_{27} \eta \pi^+ \pi^-$	< 3 × 10 ⁻⁴	CL=90%

- Using a total width of 4.43 ± 0.05 MeV. Systematic uncertainty included.
- Using a total width of 4.43 ± 0.05 MeV.
- Weighted and scaled average of 12 measurements of DIJKSTRA 86.
- PELLINEN 82 review includes AKERLOF 77, DAUM 81, BALDI 77, AYRES 74, DE-GROOT 74.
- Systematic errors not evaluated.
- Mass errors enlarged by us to Γ/\sqrt{N} ; see the note with the $K^*(892)$ mass.



CONSTRAINED FIT INFORMATION

An overall fit to 15 branching ratios uses 42 measurements and one constraint to determine 8 parameters. The overall fit has a $\chi^2 = 38.2$ for 35 degrees of freedom.

The following off-diagonal array elements are the correlation coefficients $\langle \delta x_i \delta x_j \rangle / (\delta x_i \delta x_j)$, in percent, from the fit to the branching fractions, $x_i \equiv \Gamma_i / \Gamma_{total}$. The fit constrains the x_i whose labels appear in this array to sum to one.

x_2	-66						
x_3	-58	-22					
x_6	-19	16	1				
x_7	-14	14	1	11			
x_8	44	-47	-4	-37	-30		
x_9	-8	8	1	6	5	-18	
x_{11}	-6	6	1	5	4	-13	2
	x_1	x_2	x_3	x_6	x_7	x_8	x_9

$\phi(1020)$ PARTIAL WIDTHS

$\Gamma(\eta\gamma)$	VALUE (keV)	DOCUMENT ID	TECN	COMMENT	Γ_6	
	••• We do not use the following data for averages, fits, limits, etc. •••					
	58.9 ± 0.5 ± 2.4	ACHASOV	00	SND	$e^+ e^- \rightarrow \eta \gamma$	
$\Gamma(\pi^0 \gamma)$	VALUE (keV)	DOCUMENT ID	TECN	COMMENT	Γ_7	
	••• We do not use the following data for averages, fits, limits, etc. •••					
	5.40 ± 0.16 ^{+0.43} _{-0.40}	ACHASOV	00	SND	$e^+ e^- \rightarrow \pi^0 \gamma$	
$\Gamma(e^+ e^-)$	VALUE (keV)	EVTS	DOCUMENT ID	TECN	COMMENT	Γ_8
	••• We do not use the following data for averages, fits, limits, etc. •••					
	1.32 ± 0.02 ± 0.04	314k	⁹ AKHMETSHIN	99D	CMD2	$e^+ e^- \rightarrow K_L^0 K_S^0$
	⁹ Using $B(\phi \rightarrow K_L^0 K_S^0) = 0.331 \pm 0.009$.					

$\phi(1020) \Gamma(l)\Gamma(e^+ e^-) / \Gamma^2(total)$

$\Gamma(e^+ e^-) \times \Gamma(K_L^0 K_S^0) / \Gamma_{total}^2$	VALUE (units 10 ⁻⁵)	EVTS	DOCUMENT ID	TECN	COMMENT	$\Gamma_8 \Gamma_2 / \Gamma^2$
	9.85 ± 0.22	OUR FIT	Error includes scale factor of 1.3.			
	9.756 ± 0.114 ± 0.146	314k	¹⁰ AKHMETSHIN	99D	CMD2	$e^+ e^- \rightarrow K_L^0 K_S^0$

$\phi(1020)$ WIDTH

We average mass and width values only when the systematic errors have been evaluated.

VALUE (MeV)	EVTS	DOCUMENT ID	TECN	COMMENT
4.458 ± 0.032	OUR AVERAGE			
4.477 ± 0.036 ± 0.022	314k	AKHMETSHIN 99D	CMD2	$e^+ e^- \rightarrow K_L^0 K_S^0$
4.44 ± 0.09	55600	AKHMETSHIN 95	CMD2	$e^+ e^- \rightarrow$ hadrons
4.45 ± 0.06	271k	DIJKSTRA 86	SPEC	100 $\pi^- Be$
4.5 ± 0.7	1500	ARENTON 82	AEMS	11.8 polar. $pp \rightarrow K K$
4.2 ± 0.6	766	⁷ IVANOV 81	OLYA	1-1.4 $e^+ e^- \rightarrow K^+ K^-$
4.3 ± 0.6		⁷ CORDIER 80	WIRE	$e^+ e^- \rightarrow \pi^+ \pi^- \pi^0$
4.36 ± 0.29	3681	⁷ BUKIN 78C	OLYA	$e^+ e^- \rightarrow$ hadrons
4.4 ± 0.6	984	⁷ BESCH 74	CNTR	$2 \gamma p \rightarrow \rho K^+ K^-$
4.67 ± 0.72	681	⁷ BALAKIN 71	OSPK	$e^+ e^- \rightarrow$ hadrons
4.09 ± 0.29		BIZOT 70	OSPK	$e^+ e^- \rightarrow$ hadrons
••• We do not use the following data for averages, fits, limits, etc. •••				
3.6 ± 0.8	337	⁷ COOPER 78B	HBC	0.7-0.8 $\bar{p} p \rightarrow K_S^0 K_L^0 \pi^+ \pi^-$
4.5 ± 0.50	1300	^{7,8} AKERLOF 77	SPEC	400 $pA \rightarrow K^+ K^- X$
4.5 ± 0.8	500	^{7,8} AYRES 74	ASPK	3-6 $\pi^- p \rightarrow K^+ K^- n, K^- p \rightarrow K^+ K^- \Lambda / \Sigma^0$
3.81 ± 0.37		COSME 74B	OSPK	$e^+ e^- \rightarrow K_L^0 K_S^0$
3.8 ± 0.7	454	⁷ BORENSTEIN 72	HBC	2.18 $K^- p \rightarrow K \bar{K} n$

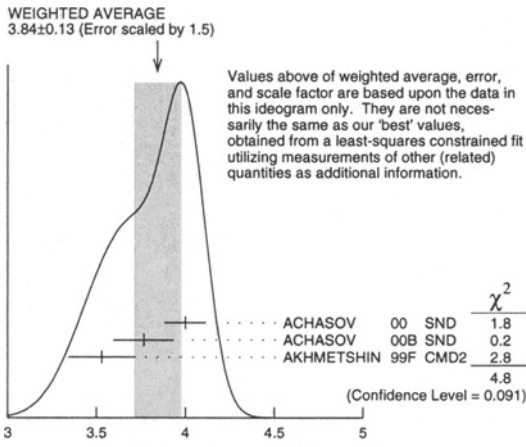
- Width errors enlarged by us to $4\Gamma/\sqrt{N}$; see the note with the $K^*(892)$ mass.
- Systematic errors not evaluated.

Meson Particle Listings

$\phi(1020)$

$\Gamma(e^+e^-) \times [\Gamma(\rho\pi) + \Gamma(\pi^+\pi^-\pi^0)]/\Gamma_{total}^2$			$\Gamma_8\Gamma_3/\Gamma^2$
VALUE (units 10^{-5})	EVTs	DOCUMENT ID	TECN COMMENT
4.50 ± 0.19 OUR FIT			Error includes scale factor of 1.3.
4.35 ± 0.27 ± 0.08	11169	10 AKHMETSHIN 98	CMD2 $e^+e^- \rightarrow \pi^+\pi^-\pi^0$

$\Gamma(e^+e^-) \times \Gamma(\eta\gamma)/\Gamma_{total}^2$			$\Gamma_8\Gamma_6/\Gamma^2$
VALUE (units 10^{-6})	EVTs	DOCUMENT ID	TECN COMMENT
3.77 ± 0.11 OUR FIT			Error includes scale factor of 1.4.
3.84 ± 0.13 OUR AVERAGE			Error includes scale factor of 1.5. See the ideogram below.
4.00 ± 0.04 ± 0.11		11 ACHASOV 00 SND	$e^+e^- \rightarrow \eta\gamma$
3.765 ± 0.092 ± 0.143		12 ACHASOV 00B SND	$e^+e^- \rightarrow \eta\gamma$
3.53 ± 0.08 ± 0.17	2200	12,13 AKHMETSHIN 99F CMD2	$e^+e^- \rightarrow \eta\gamma$
... We do not use the following data for averages, fits, limits, etc. ...			
3.848 ± 0.036 ± 0.070		14 ACHASOV 00B SND	$e^+e^- \rightarrow \eta\gamma$



$\Gamma(e^+e^-) \times \Gamma(\pi^0\gamma)/\Gamma_{total}^2$			$\Gamma_8\Gamma_7/\Gamma^2$
VALUE (units 10^{-7})	DOCUMENT ID	TECN COMMENT	
3.67 ± 0.28 OUR FIT			
3.67 ± 0.10 ± 0.27 -0.25	15 ACHASOV 00 SND	$e^+e^- \rightarrow \pi^0\gamma$	

$\Gamma(e^+e^-) \times \Gamma(\mu^+\mu^-)/\Gamma_{total}^2$			$\Gamma_8\Gamma_9/\Gamma^2$
VALUE (units 10^{-8})	DOCUMENT ID	TECN COMMENT	
10.8 ± 1.4 OUR FIT			
10.8 ± 1.4 OUR AVERAGE			
9.9 ± 1.4 ± 0.9	13 ACHASOV 99C SND	$e^+e^- \rightarrow \mu^+\mu^-$	
14.4 ± 3.0	10 VASSERMAN 81 OLYA	$e^+e^- \rightarrow \mu^+\mu^-$	
8.6 ± 5.9	10 AUGUSTIN 73 OSPK	$e^+e^- \rightarrow \mu^+\mu^-$	

$\Gamma(e^+e^-) \times \Gamma(\pi^+\pi^-)/\Gamma_{total}^2$			$\Gamma_8\Gamma_{11}/\Gamma^2$
VALUE (units 10^{-8})	DOCUMENT ID	TECN COMMENT	
2.2 ± 0.4 OUR FIT			
2.2 ± 0.4 OUR AVERAGE			
2.1 ± 0.3 ± 0.3	13 ACHASOV 00C SND	$e^+e^- \rightarrow \pi^+\pi^-$	
1.95 +1.15 -0.87	10 GOLUBEV 86 ND	$e^+e^- \rightarrow \pi^+\pi^-$	
6.01 +3.19 -2.51	10 VASSERMAN 81 OLYA	$e^+e^- \rightarrow \pi^+\pi^-$	

¹⁰ Recalculated by us from the cross section in the peak.
¹¹ From the $\eta \rightarrow 2\gamma$ decay and using $B(\eta \rightarrow 2\gamma) = (39.21 \pm 0.34) \times 10^{-2}$.
¹² From the $\eta \rightarrow \pi^+\pi^-\pi^0$ decay and using $B(\eta \rightarrow \pi^+\pi^-\pi^0) = (23.1 \pm 0.5) \times 10^{-2}$.
¹³ Recalculated by the authors from the cross section in the peak.
¹⁴ Using various decay modes of the η from ACHASOV 98F, ACHASOV 00, and ACHASOV 00B.
¹⁵ From the $\pi^0 \rightarrow 2\gamma$ decay and using $B(\pi^0 \rightarrow 2\gamma) = (98.798 \pm 0.032) \times 10^{-2}$.

$\phi(1020)$ BRANCHING RATIOS

$\Gamma(K^+K^-)/\Gamma_{total}$			Γ_1/Γ
VALUE	EVTs	DOCUMENT ID	TECN COMMENT
0.492 ± 0.007 OUR FIT			Error includes scale factor of 1.2.
0.493 ± 0.010 OUR AVERAGE			
0.492 ± 0.012	2913	AKHMETSHIN 95 CMD2	$e^+e^- \rightarrow K^+K^-$
0.44 ± 0.05	321	KALBFLEISCH 76 HBC	$2.18 K^-p \rightarrow \Lambda K^+K^-$
0.49 ± 0.06	270	DEGROOT 74 HBC	$4.2 K^-p \rightarrow \Lambda\phi$
0.540 ± 0.034	565	BALAKIN 71 OSPK	$e^+e^- \rightarrow K^+K^-$
0.48 ± 0.04	252	LINDSEY 66 HBC	$2.1-2.7 K^-p \rightarrow \Lambda K^+K^-$

$\Gamma(K_L^0K_S^0)/\Gamma_{total}$			Γ_2/Γ
VALUE	EVTs	DOCUMENT ID	TECN COMMENT
0.338 ± 0.006 OUR FIT			Error includes scale factor of 1.2.
0.331 ± 0.009 OUR AVERAGE			
0.335 ± 0.010	40644	AKHMETSHIN 95 CMD2	$e^+e^- \rightarrow K_L^0K_S^0$
0.326 ± 0.035		DOLINSKY 91 ND	$e^+e^- \rightarrow K_L^0K_S^0$
0.310 ± 0.024		DRUZHININ 84 ND	$e^+e^- \rightarrow K_L^0K_S^0$

0.329 ± 0.006 ± 0.010	314k	16 AKHMETSHIN 99D CMD2	$e^+e^- \rightarrow K_L^0K_S^0$
0.27 ± 0.03	133	KALBFLEISCH 76 HBC	$2.18 K^-p \rightarrow \Lambda K_L^0K_S^0$
0.257 ± 0.030	95	BALAKIN 71 OSPK	$e^+e^- \rightarrow K_L^0K_S^0$
0.40 ± 0.04	167	LINDSEY 66 HBC	$2.1-2.7 K^-p \rightarrow \Lambda K_L^0K_S^0$

$[\Gamma(\rho\pi) + \Gamma(\pi^+\pi^-\pi^0)]/\Gamma_{total}$			Γ_3/Γ
VALUE	EVTs	DOCUMENT ID	TECN COMMENT
0.155 ± 0.006 OUR FIT			Error includes scale factor of 1.4.
0.151 ± 0.009 OUR AVERAGE			Error includes scale factor of 1.7.
0.161 ± 0.008	11761	AKHMETSHIN 95 CMD2	$e^+e^- \rightarrow \pi^+\pi^-\pi^0$
0.143 ± 0.007		DOLINSKY 91 ND	$e^+e^- \rightarrow \pi^+\pi^-\pi^0$

0.145 ± 0.009 ± 0.003	11169	17 AKHMETSHIN 98 CMD2	$e^+e^- \rightarrow \pi^+\pi^-\pi^0$
0.139 ± 0.007	18	PARROUR 76B OSPK	e^+e^-

... We do not use the following data for averages, fits, limits, etc. ...

$\Gamma(K_L^0K_S^0)/\Gamma(K\bar{K})$			$\Gamma_2/(\Gamma_1+\Gamma_2)$
VALUE	EVTs	DOCUMENT ID	TECN COMMENT
0.407 +0.008 -0.007 OUR FIT			Error includes scale factor of 1.2.
0.45 ± 0.04 OUR AVERAGE			
0.44 ± 0.07		LONDON 66 HBC	$2.24 K^-p \rightarrow \Lambda K\bar{K}$
0.48 ± 0.07	52	BADIER 65B HBC	$3 K^-p$
0.40 ± 0.10	34	SCHLEIN 63 HBC	$1.95 K^-p \rightarrow \Lambda K\bar{K}$

$[\Gamma(\rho\pi) + \Gamma(\pi^+\pi^-\pi^0)]/\Gamma(K\bar{K})$			$\Gamma_3/(\Gamma_1+\Gamma_2)$
VALUE	DOCUMENT ID	TECN COMMENT	
0.186 ± 0.008 OUR FIT			Error includes scale factor of 1.4.
0.24 ± 0.04 OUR AVERAGE			
0.237 ± 0.039	CERRADA 77B HBC	$4.2 K^-p \rightarrow \Lambda 3\pi$	
0.30 ± 0.15	LONDON 66 HBC	$2.24 K^-p \rightarrow \Lambda\pi^+\pi^-\pi^0$	

$[\Gamma(\rho\pi) + \Gamma(\pi^+\pi^-\pi^0)]/\Gamma(K_L^0K_S^0)$			Γ_3/Γ_2
VALUE	EVTs	DOCUMENT ID	TECN COMMENT
0.457 ± 0.020 OUR FIT			Error includes scale factor of 1.3.
0.51 ± 0.05 OUR AVERAGE			
0.56 ± 0.07	3681	BUKIN 78C OLYA	$e^+e^- \rightarrow K_L^0K_S^0$

0.47 ± 0.06	516	COSME 74 OSPK	$e^+e^- \rightarrow \pi^+\pi^-\pi^0$
-------------	-----	---------------	--------------------------------------

$\Gamma(\eta\gamma)/\Gamma(\pi^0\gamma)$			Γ_6/Γ_7
VALUE	DOCUMENT ID	TECN COMMENT	
... We do not use the following data for averages, fits, limits, etc. ...			
10.9 ± 0.3 ± 0.7 -0.8		ACHASOV 00 SND	$e^+e^- \rightarrow \eta\gamma, \pi^0\gamma$

$\Gamma(\mu^+\mu^-)/\Gamma_{total}$			Γ_9/Γ
VALUE (units 10^{-4})	DOCUMENT ID	TECN COMMENT	
2.5 ± 0.4 OUR AVERAGE			
2.69 ± 0.46	19 HAYES 71 CNTR	$8.3, 9.8 \gamma C \rightarrow \mu^+\mu^-X$	
2.17 ± 0.60	19 EARLES 70 CNTR	$6.0 \gamma C \rightarrow \mu^+\mu^-X$	

3.30 ± 0.45 ± 0.32	17 ACHASOV 99C SND	$e^+e^- \rightarrow \mu^+\mu^-$
4.83 ± 1.02	20 VASSERMAN 81 OLYA	$e^+e^- \rightarrow \mu^+\mu^-$
2.87 ± 1.98	20 AUGUSTIN 73 OSPK	$e^+e^- \rightarrow \mu^+\mu^-$

$\Gamma(\eta\gamma)/\Gamma_{total}$			Γ_6/Γ
VALUE	EVTs	DOCUMENT ID	TECN COMMENT
0.01297 ± 0.00033 OUR FIT			Error includes scale factor of 1.2.
0.0125 ± 0.0004 OUR AVERAGE			
0.01246 ± 0.00025 ± 0.00057	10k	21 ACHASOV 98F SND	$e^+e^- \rightarrow 7\gamma$
0.0118 ± 0.0011	279	22 AKHMETSHIN 95 CMD2	$e^+e^- \rightarrow \pi^+\pi^-\pi^0\gamma$
0.0130 ± 0.0006		23 DRUZHININ 84 ND	$e^+e^- \rightarrow 3\gamma$
0.014 ± 0.002		24 DRUZHININ 84 ND	$e^+e^- \rightarrow 6\gamma$
0.0088 ± 0.0020	290	KURDADZE 83C OLYA	$e^+e^- \rightarrow 3\gamma$
0.0135 ± 0.0029		ANDREWS 77 CNTR	$6.7-10 \gamma Cu$
0.015 ± 0.004	54	23 COSME 76 OSPK	e^+e^-

... We do not use the following data for averages, fits, limits, etc. ...

0.01338 ± 0.00012 ± 0.00052	25 ACHASOV 00 SND	$e^+e^- \rightarrow \eta\gamma$	
0.01287 ± 0.00012 ± 0.00042	26 ACHASOV 00B SND	$e^+e^- \rightarrow \eta\gamma$	
0.01259 ± 0.00030 ± 0.00059	27 ACHASOV 00B SND	$e^+e^- \rightarrow \eta\gamma$	
0.0118 ± 0.0003 ± 0.0006	2200	28 AKHMETSHIN 99F CMD2	$e^+e^- \rightarrow \eta\gamma$
0.0121 ± 0.0007	29	BENAYOUN 96 RVUE	$0.54-1.04 e^+e^- \rightarrow \eta\gamma$

See key on page 239

Meson Particle Listings

$h_1(1170), b_1(1235)$

$h_1(1170)$ WIDTH

VALUE (MeV)	DOCUMENT ID	TECN	CHG	COMMENT
360 ± 40 OUR ESTIMATE				
• • • We do not use the following data for averages, fits, limits, etc. • • •				
345 ± 6	ANDO	92	SPEC	$8 \pi^- p \rightarrow \pi^+ \pi^- \pi^0 n$
375 ± 6 ± 34	³ ANDO	92	SPEC	$8 \pi^- p \rightarrow \pi^+ \pi^- \pi^0 n$
320 ± 50	⁴ DANKOWY...	81	SPEC	$8 \pi p \rightarrow 3 \pi n$

³Average and spread of values using 2 variants of the model of BOWLER 75.
⁴Uses the model of BOWLER 75.

$h_1(1170)$ DECAY MODES

Mode	Fraction (Γ_i/Γ)
Γ_1 $\rho\pi$	seen

$h_1(1170)$ BRANCHING RATIOS

$\Gamma(\rho\pi)/\Gamma_{total}$	DOCUMENT ID	TECN	COMMENT	Γ_1/Γ
• • • We do not use the following data for averages, fits, limits, etc. • • •				
seen	ANDO	92	SPEC $8 \pi^- p \rightarrow \pi^+ \pi^- \pi^0 n$	
seen	ATKINSON	84	OMEG $20-70 \gamma p \rightarrow \pi^+ \pi^- \pi^0 p$	
seen	DANKOWY...	81	SPEC $8 \pi p \rightarrow 3 \pi n$	

$h_1(1170)$ REFERENCES

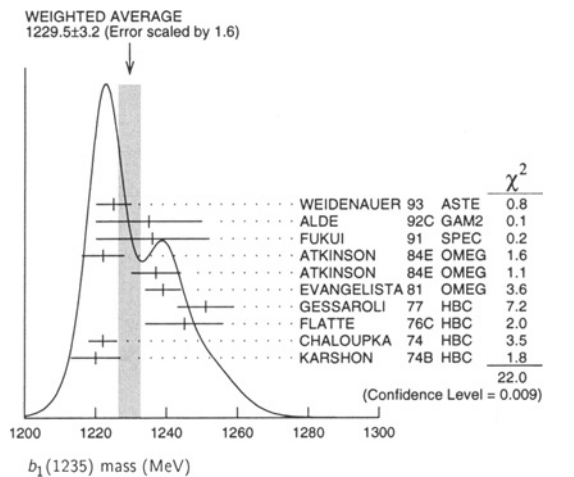
ANDO	92	PL B231 496	A. Ando et al.	(KEK, KYOT, NIRS, SAGA+)
ATKINSON	84	NP B231 15	M. Atkinson et al.	(BONN, CERN, GLAS+)
DANKOWY...	81	PRL 46 580	J.A. Dankowych et al.	(TNTO, BNL, CARL+)
BOWLER	75	NP B97 227	M.G. Bowler et al.	(OXFTP, DARE)

$b_1(1235)$

$$I^G(J^{PC}) = 1^+(1^-)$$

$b_1(1235)$ MASS

VALUE (MeV)	EVTS	DOCUMENT ID	TECN	CHG	COMMENT
1229.5 ± 3.2 OUR AVERAGE					Error includes scale factor of 1.6. See the ideogram below.
1225 ± 5		WEIDENAUER 93	ASTE		$\bar{p}p \rightarrow 2\pi^+ 2\pi^- \pi^0$
1235 ± 15		ALDE	92C GAM2		$38,100 \pi^- p \rightarrow \omega \pi^0 n$
1236 ± 16		FUKUI	91	SPEC	$8.95 \pi^- p \rightarrow \omega \pi^0 n$
1222 ± 6		ATKINSON	84E OMEG ±		$25-55 \gamma p \rightarrow \omega \pi X$
1237 ± 7		ATKINSON	84E OMEG 0		$25-55 \gamma p \rightarrow \omega \pi X$
1239 ± 5		EVANGELISTA 81	OMEG -		$12 \pi^- p \rightarrow \omega \pi p$
1251 ± 8	450	GESSAROLI 77	HBC -		$11 \pi^- p \rightarrow \pi^- \omega p$
1245 ± 11	890	FLATTE	76C HBC -		$4.2 K^- p \rightarrow \pi^- \omega \Sigma^+$
1222 ± 4	1400	CHALOUPKA 74	HBC -		$3.9 \pi^- p$
1220 ± 7	600	KARSHON	74B HBC +		$4.9 \pi^+ p$
• • • We do not use the following data for averages, fits, limits, etc. • • •					
1190 ± 10		AUGUSTIN	89 DM2 ±		$e^+ e^- \rightarrow 5\pi$
1213 ± 5		ATKINSON	84C OMEG 0		$20-70 \gamma p$
1271 ± 11		COLLICK	84	SPEC +	$200 \pi^+ Z \rightarrow Z \pi \omega$



$b_1(1235)$ WIDTH

VALUE (MeV)	EVTS	DOCUMENT ID	TECN	CHG	COMMENT
142 ± 9 OUR AVERAGE					Error includes scale factor of 1.2.
113 ± 12		WEIDENAUER 93	ASTE		$\bar{p}p \rightarrow 2\pi^+ 2\pi^- \pi^0$
160 ± 30		ALDE	92C GAM2		$38,100 \pi^- p \rightarrow \omega \pi^0 n$
151 ± 31		FUKUI	91	SPEC	$8.95 \pi^- p \rightarrow \omega \pi^0 n$
170 ± 15		EVANGELISTA 81	OMEG -		$12 \pi^- p \rightarrow \omega \pi p$
170 ± 50	225	BALTAY	78B HBC +		$15 \pi^+ p \rightarrow p 4\pi$
155 ± 32	450	GESSAROLI 77	HBC -		$11 \pi^- p \rightarrow \pi^- \omega p$
182 ± 45	890	FLATTE	76C HBC -		$4.2 K^- p \rightarrow \pi^- \omega \Sigma^+$
135 ± 20	1400	CHALOUPKA 74	HBC -		$3.9 \pi^- p$
156 ± 22	600	KARSHON	74B HBC +		$4.9 \pi^+ p$
• • • We do not use the following data for averages, fits, limits, etc. • • •					
210 ± 19		AUGUSTIN	89 DM2 ±		$e^+ e^- \rightarrow 5\pi$
231 ± 14		ATKINSON	84C OMEG 0		$20-70 \gamma p$
232 ± 29		COLLICK	84	SPEC +	$200 \pi^+ Z \rightarrow Z \pi \omega$

$b_1(1235)$ DECAY MODES

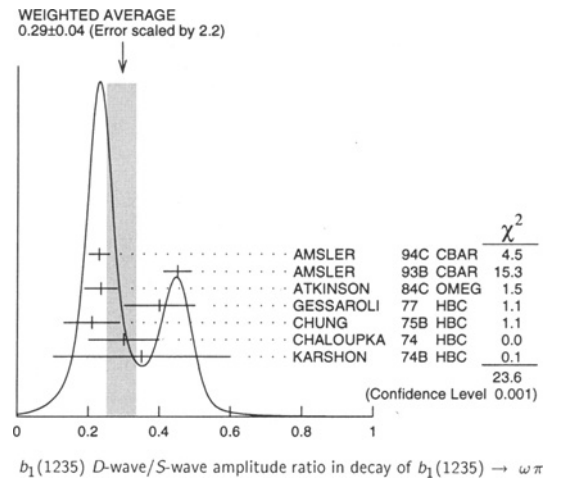
Mode	Fraction (Γ_i/Γ)	Confidence level
Γ_1 $\omega\pi$	dominant	
Γ_2 $\pi^\pm \gamma$	$[D/S \text{ amplitude ratio} = 0.29 \pm 0.04]$	
Γ_3 $\eta\rho$	$(1.6 \pm 0.4) \times 10^{-3}$	
Γ_4 $\pi^+ \pi^+ \pi^- \pi^0$	seen	
Γ_5 $(K\bar{K})^\pm \pi^0$	< 50 %	84%
Γ_6 $K_S^0 K_S^0 \pi^\pm$	< 8 %	90%
Γ_7 $K_S^0 K_S^0 \pi^\pm$	< 6 %	90%
Γ_8 $\phi\pi$	< 2 %	90%
	< 1.5 %	84%

$b_1(1235)$ PARTIAL WIDTHS

$\Gamma(\pi^\pm \gamma)$	DOCUMENT ID	TECN	CHG	COMMENT	Γ_2
230 ± 60	COLLICK	84	SPEC +	$200 \pi^+ Z \rightarrow Z \pi \omega$	

$b_1(1235)$ D-wave/S-wave AMPLITUDE RATIO IN DECAY OF $b_1(1235) \rightarrow \omega\pi$

VALUE	EVTS	DOCUMENT ID	TECN	CHG	COMMENT
0.29 ± 0.04 OUR AVERAGE					Error includes scale factor of 2.2. See the ideogram below.
0.23 ± 0.03		AMSLER	94C CBAR		$0.0 \bar{p}p \rightarrow \omega \eta \pi^0$
0.45 ± 0.04		AMSLER	93B CBAR		$0.0 \bar{p}p \rightarrow \omega \pi^0 \pi^0$
0.235 ± 0.047		ATKINSON	84C OMEG		$20-70 \gamma p$
0.4 + 0.1 - 0.1		GESSAROLI 77	HBC -		$11 \pi^- p \rightarrow \pi^- \omega p$
0.21 ± 0.08		CHUNG	75B HBC +		$7.1 \pi^+ p$
0.3 ± 0.1		CHALOUPKA 74	HBC -		$3.9-7.5 \pi^- p$
0.35 ± 0.25	600	KARSHON	74B HBC +		$4.9 \pi^+ p$



Meson Particle Listings

 $b_1(1235)$, $a_1(1260)$ $b_1(1235)$ BRANCHING RATIOS

$\Gamma(\eta\rho)/\Gamma(\omega\pi)$		Γ_3/Γ_1	
VALUE	DOCUMENT ID	TECN	COMMENT
<0.10	ATKINSON	84D OMEG	20-70 γ p
$\Gamma(\pi^+\pi^+\pi^-\pi^0)/\Gamma(\omega\pi)$		Γ_4/Γ_1	
VALUE	DOCUMENT ID	TECN	CHG
<0.5	ABOLINS	63 HBC	+ 3.5 $\pi^+\rho$
$\Gamma((K\bar{K})^\pm\pi^0)/\Gamma(\omega\pi)$		Γ_5/Γ_1	
VALUE	CL%	DOCUMENT ID	TECN
<0.08	90	BALTAY	67 HBC \pm 0.0 $\bar{p}p$
$\Gamma(K_S^0 K_L^0 \pi^\pm)/\Gamma(\omega\pi)$		Γ_6/Γ_1	
VALUE	CL%	DOCUMENT ID	TECN
<0.06	90	BALTAY	67 HBC \pm 0.0 $\bar{p}p$
$\Gamma(K_S^0 K_S^0 \pi^\pm)/\Gamma(\omega\pi)$		Γ_7/Γ_1	
VALUE	CL%	DOCUMENT ID	TECN
<0.02	90	BALTAY	67 HBC \pm 0.0 $\bar{p}p$
$\Gamma(\phi\pi)/\Gamma(\omega\pi)$		Γ_8/Γ_1	
VALUE	CL%	DOCUMENT ID	TECN
<0.004	95	VIKTOROV	96 SPEC 0 32.5 $\pi^-p \rightarrow K^+K^-\pi^0 n$

• • • We do not use the following data for averages, fits, limits, etc. • • •

<0.04	95	BIZZARRI	69 HBC \pm 0.0 $\bar{p}p$
<0.015		DAHL	67 HBC 1.6-4.2 π^-p

 $b_1(1235)$ REFERENCES

VIKTOROV	96	PAN 59 1184 Translated from YAF 59 1239.	V.A. Viktorov et al. (SERP)
AMSLER	94C	PL B327 425	C. Anisler et al. (Crystal Barrel Collab.)
AMSLER	93B	PL B311 362	C. Anisler et al. (Crystal Barrel Collab.)
WEIDENAUER	93	ZPHY C59 387	P. Weidenauer et al. (ASTERIX Collab.)
ALDE	92C	ZPHY C54 553	D.M. Alde et al. (BELG, SERP, KEK, LANL+)
FUKUI	91	PL B257 241	S. Fukui et al. (SUGI, NAGO, KEK, KYOT+)
AUGUSTIN	89	NP B320 1	J.E. Augustin, G. Cosme (DM2 Collab.)
ATKINSON	84C	NP B243 1	M. Atkinson et al. (BONN, CERN, GLAS+) ^{JP}
ATKINSON	84D	NP B242 269	M. Atkinson et al. (BONN, CERN, GLAS+)
ATKINSON	84E	PL 138B 459	M. Atkinson et al. (BONN, CERN, GLAS+)
COLLICK	84	PRL 53 2374	B. Collick et al. (MINN, ROCH, FNAL)
EVANGELISTA	81	NP B179 197	C. Evangelista et al. (BARI, BONN, CERN+)
BALTAY	78B	PR D17 62	C. Baltay et al. (COLU, BING)
GESSAROLI	77	NP B126 382	R. Gessaroli et al. (BGNA, FIRZ, GENO+) ^{JP}
FLATTE	76C	PL 64B 225	S.M. Flatte et al. (CERN, AMST, NIJ+) ^{JP}
CHUNG	75B	PR O11 2426	S.U. Chung et al. (BNL, LBL, UCSC) ^{JP}
CHALOUPOKA	74	PL 51B 407	V. Chaloupka et al. (CERN) ^{JP}
KARSHON	74B	PR D10 3608	U. Karshon et al. (REHO) ^{JP}
BIZZARRI	69	NP B14 169	R. Bizzarri et al. (CERN, CDEF)
BALTAY	67	PRL 18 93	C. Baltay et al. (COLU)
DAHL	67	PR 163 1377	O.I. Dahl et al. (LRL)
ABOLINS	63	PRL 11 381	M.A. Abolins et al. (UCSD)

OTHER RELATED PAPERS

GOLOVKIN	97	ZPHY A359 4335	S.V. Golovkin et al. (SERP, ITEP)
BRAU	88	PR D37 2379	J.E. Brau et al. ^{JP}
ATKINSON	84C	NP B243 1	M. Atkinson et al. (BONN, CERN, GLAS+) ^{JP}
GOLDBERGER	65	PRL 15 118	G. Goldhaber et al. (LRL)
CARMONY	64	PRL 12 254	D.D. Carmony et al. (UCB) ^{JP}
BONDAR	63B	PL 5 209	L. Bondar et al. (AACH, BIRM, HAMB, LOIC+)

 $a_1(1260)$

$$I^G(J^{PC}) = 1^-(1^+ +)$$

THE $a_1(1260)$

Updated March 2000 by S. Eidelman (Novosibirsk).

The main experimental data on the $a_1(1260)$ may be grouped into two classes:

(1) **Hadronic Production:** This comprises diffractive production with incident π^- (DAUM 80, 81B) and charge-exchange production with low-energy π^- (DANKOWYCH 81, ANDO 92). The 1980's experiments explain the $I^G L J^P = 1^+ S 0^+$ data using a phenomenological amplitude consisting of a rescattered Deck amplitude, plus a direct resonance-production term. They agree on a mass of about 1270 MeV and a width of 300-380 MeV. ANDO 92 finds rather lower values for the mass (1121 MeV) and width (239 MeV), in a partial-wave analysis based on the isobar model of the $\pi^+\pi^-\pi^0$ system. However, in this analysis, only Breit-Wigner terms were considered. Recently,

BARBERIS 98B studied central production of the $\pi^+\pi^-\pi^0$ system, and observed the $a_1(1260)$ meson with a mass of 1240 MeV and a width of about 400 MeV.

(2) **τ Decay:** Various experiments reported good data on $\tau \rightarrow a_1(1260)\nu_\tau \rightarrow \rho\pi\nu_\tau$ (RUCKSTUHL 86, SCHMIDKE 86, ALBRECHT 86B, BAND 87, ACKERSTAFF 97R, ABREU 98G, and ASNER 00). They are somewhat inconsistent concerning the $a_1(1260)$ mass, which can, however, be attributed to model-dependent systematic uncertainties (BOWLER 86, ALBRECHT 93C, ACKERSTAFF 97R). They all find a width greater than 400 MeV.

The discrepancies between the hadronic and τ decay results have stimulated several reanalyses. BASDEVANT 77, 78 used the early diffractive dissociation and τ -decay data, and showed that they could be well reproduced with an a_1 resonance mass of 1180 ± 50 MeV and width of 400 ± 50 MeV. Later, BOWLER 86, TORNQVIST 87, ISGUR 89, and IVANOV 91 have studied the process $\tau \rightarrow 3\pi\nu_\tau$. Despite quite different approaches, they all found a good overall description of the τ -decay data with an $a_1(1260)$ mass near 1230 MeV, consistent with the hadronic data. However, their widths remain significantly larger (400-600 MeV) than those extracted from diffractive-hadronic data. This is also the case with the later OPAL experiment (ACKERSTAFF 97R). In the high statistics analysis of ACKERSTAFF 97R, the models of ISGUR 89 and KUHN 90 are used to fit distributions of the 3π invariant mass, as well as the 2π invariant mass projections of the Dalitz plot. Neither model is found to provide a completely satisfactory description of the data. Another recent high statistics analysis of ABREU 98G obtains a good description of the $\tau \rightarrow 3\pi$ data using the model of FEINDT 90, which includes the a_1' meson, a radial excitation of the $a_1(1260)$ meson, with a mass of 1700 MeV and a width of 300 MeV. A similar signal has been observed by AMELIN 95B in the D and S waves of the $\rho\pi$ state, as well as by GOUZ 92 in the $f_1(1285)\pi$ state. The existence of such a resonance is also suggested by the very big data sample of ASNER 00, which shows an excess of events at high 3π mass. Their data are better described by the a_1' contribution, though at a level below that reported by ABREU 98G. Since the statistical significance of the a_1' contribution is $2-3\sigma$ only, they conclude that more data is needed to establish the existence of the a_1' .

ASNER 00 has also performed an analysis of the substructures in the Dalitz plot, and found significant contributions of the a_1 decay to $\sigma\pi$, $f_0(1370)\pi$, and $f_2(1270)\pi$. The contribution of the $a_1 \rightarrow \sigma\pi$ at a similar level has independently been observed in $e^+e^- \rightarrow 4\pi$ annihilation (AKHMETSCHIN 99E), where the $2\pi^+2\pi^-$ final state was shown to be dominated by the $a_1(1260)\pi$ mechanism. Note that the existence of isoscalar contributions to the two-pion state, in addition to the isovector one ($\rho\pi$), will influence the ratio $B(a_1^- \rightarrow \pi^-\pi^+\pi^-)/B(a_1^- \rightarrow \pi^-\pi^0\pi^0)$, which should be equal to 1 for the pure $\rho\pi$ state.

BOWLER 88 showed that good fits to both the hadronic and the τ -decay data could be obtained with a width of about

See key on page 239

Meson Particle Listings

$a_1(1260)$

400 MeV. However, applying the same type of analysis to the ANDO 92 data, the low mass and narrow width they obtained with the Breit-Wigner PWA do not change appreciably.

CONDO 93 found no evidence for charge-exchange photoproduction of the $a_1(1260)$ (but found a clear signal of $a_2(1320)$ photoproduction). They show that it is consistent with either an extremely large $a_1(1260)$ hadronic width, or with a small radiative width to $\pi\gamma$, which could be accommodated if the a_1 mass is somewhat below 1260 MeV.

$a_1(1260)$ MASS

VALUE (MeV) EVTS DOCUMENT ID TECN CHG COMMENT
1230 ± 40 OUR ESTIMATE

• • • We do not use the following data for averages, fits, limits, etc. • • •

VALUE (MeV)	EVTS	DOCUMENT ID	TECN	CHG	COMMENT
1331 ± 10 ± 3	37k	1 ASNER	00 CLE2		10.6 $e^+e^- \rightarrow \tau^+\tau^-\tau^-\tau^+ \rightarrow \pi^-\pi^0\pi^0\nu_\tau$
1255 ± 7 ± 6	5904	2 ABREU	98G DLPH		e^+e^-
1207 ± 5 ± 8	5904	3 ABREU	98G DLPH		e^+e^-
1196 ± 4 ± 5	5904	4,5 ABREU	98G DLPH		e^+e^-
1240 ± 10		BARBERIS	98B		450 $p\bar{p} \rightarrow \rho f \pi^+\pi^-\pi^0 p_S$
1262 ± 9 ± 7		2,6 ACKERSTAFF	97R OPAL		$E_{CM}^{ee} = 88-94, \tau \rightarrow 3\pi\nu$
1210 ± 7 ± 2		3,6 ACKERSTAFF	97R OPAL		$E_{CM}^{ee} = 88-94, \tau \rightarrow 3\pi\nu$
1211 ± 7 ± 50		3 ALBRECHT	93C ARG		$\tau^+ \rightarrow \pi^+\pi^+\pi^-\nu$
1121 ± 8		7 ANDO	92 SPEC		$8 \pi^-\rho \rightarrow \pi^+\pi^-\pi^0 n$
1242 ± 37		8 IVANOV	91 RVUE		$\tau \rightarrow \pi^+\pi^+\pi^-\nu$
1260 ± 14		9 IVANOV	91 RVUE		$\tau \rightarrow \pi^+\pi^+\pi^-\nu$
1250 ± 9		10 IVANOV	91 RVUE		$\tau \rightarrow \pi^+\pi^+\pi^-\nu$
1208 ± 15		ARMSTRONG	90 OMEG 0		300.0 $p\bar{p} \rightarrow p\bar{p}\pi^+\pi^-\pi^0$
1220 ± 15		11 ISGUR	89 RVUE		$\tau^+ \rightarrow \pi^+\pi^+\pi^-\nu$
1260 ± 25		12 BOWLER	88 RVUE		$\tau^+ \rightarrow \pi^+\pi^+\pi^-\nu$
1166 ± 18 ± 11		BAND	87 MAC		$\tau^+ \rightarrow \pi^+\pi^+\pi^-\nu$
1164 ± 41 ± 23		BAND	87 MAC		$\tau^+ \rightarrow \pi^+\pi^+\pi^-\nu$
1250 ± 40		11 TORNVIST	87 RVUE		$\tau^+ \rightarrow \pi^+\pi^+\pi^-\nu$
1046 ± 11		ALBRECHT	86B ARG		$\tau^+ \rightarrow \pi^+\pi^+\pi^-\nu$
1056 ± 20 ± 15		RUCKSTUHL	86 DLCO		$\tau^+ \rightarrow \pi^+\pi^+\pi^-\nu$
1194 ± 14 ± 10		SCHMIDKE	86 MRK2		$\tau^+ \rightarrow \pi^+\pi^+\pi^-\nu$
1255 ± 23		BELLINI	85 SPEC		40 $\pi^-A \rightarrow \pi^-\pi^+\pi^-A$
1240 ± 80		13 DANKOWY...	81 SPEC 0		8.45 $\pi^-\rho \rightarrow n3\pi$
1280 ± 30		13 DAUM	81B CNTR		63.94 $\pi^-\rho \rightarrow p3\pi$
1041 ± 13		14 GAVILLET	77 HBC +		4.2 $K^-\rho \rightarrow \Sigma 3\pi$

1 From a fit to the 3π mass spectrum including the $K\bar{K}^*(892)$ threshold.
 2 Uses the model of KUHN 90.
 3 Uses the model of ISGUR 89.
 4 Includes the effect of a possible a_1' state.
 5 Uses the model of FEINDT 90.
 6 Supersedes AKERS 95P.
 7 Average and spread of values using 2 variants of the model of BOWLER 75.
 8 Reanalysis of RUCKSTUHL 86.
 9 Reanalysis of SCHMIDKE 86.
 10 Reanalysis of ALBRECHT 86B.
 11 From a combined reanalysis of ALBRECHT 86B, SCHMIDKE 86, and RUCKSTUHL 86.
 12 From a combined reanalysis of ALBRECHT 86B and DAUM 81B.
 13 Uses the model of BOWLER 75.
 14 Produced in K^- backward scattering.

$a_1(1260)$ WIDTH

VALUE (MeV) EVTS DOCUMENT ID TECN CHG COMMENT
250 to 600 OUR ESTIMATE

• • • We do not use the following data for averages, fits, limits, etc. • • •

VALUE (MeV)	EVTS	DOCUMENT ID	TECN	CHG	COMMENT
814 ± 36 ± 13	37k	15 ASNER	00 CLE2		10.6 $e^+e^- \rightarrow \tau^+\tau^-\tau^-\tau^+ \rightarrow \pi^-\pi^0\pi^0\nu_\tau$
450 ± 50	22k	16 AKHMETSHIN	99E CMD2		1.05-1.38 $e^+e^- \rightarrow \pi^+\pi^-\pi^0\pi^0$
570 ± 10		17 BONDAR	99 RVUE		$e^+e^- \rightarrow 4\pi, \tau \rightarrow 3\pi\nu_\tau$
587 ± 27 ± 21	5904	18 ABREU	98G DLPH		e^+e^-

478 ± 3 ± 15	5904	19 ABREU	98G DLPH		e^+e^-
425 ± 14 ± 8	5904	20,21 ABREU	98G DLPH		e^+e^-
400 ± 35		BARBERIS	98B		450 $p\bar{p} \rightarrow \rho f \pi^+\pi^-\pi^0 p_S$
621 ± 32 ± 58		18,22 ACKERSTAFF	97R OPAL		$E_{CM}^{ee} = 88-94, \tau \rightarrow 3\pi\nu$
457 ± 15 ± 17		19,22 ACKERSTAFF	97R OPAL		$E_{CM}^{ee} = 88-94, \tau \rightarrow 3\pi\nu$
446 ± 21 ± 140		19 ALBRECHT	93C ARG		$\tau^+ \rightarrow \pi^+\pi^+\pi^-\nu$
239 ± 11		ANDO	92 SPEC		$8 \pi^-\rho \rightarrow \pi^+\pi^-\pi^0 n$
266 ± 13 ± 4		23 ANDO	92 SPEC		$8 \pi^-\rho \rightarrow \pi^+\pi^-\pi^0 n$
465 ± 228		24 IVANOV	91 RVUE		$\tau \rightarrow \pi^+\pi^+\pi^-\nu$
298 ± 40		25 IVANOV	91 RVUE		$\tau \rightarrow \pi^+\pi^+\pi^-\nu$
488 ± 32		26 IVANOV	91 RVUE		$\tau \rightarrow \pi^+\pi^+\pi^-\nu$
430 ± 50		ARMSTRONG	90 OMEG 0		300.0 $p\bar{p} \rightarrow p\bar{p}\pi^+\pi^-\pi^0$
420 ± 40		27 ISGUR	89 RVUE		$\tau^+ \rightarrow \pi^+\pi^+\pi^-\nu$
396 ± 43		28 BOWLER	88 RVUE		$\tau^+ \rightarrow \pi^+\pi^+\pi^-\nu$
405 ± 75 ± 25		BAND	87 MAC		$\tau^+ \rightarrow \pi^+\pi^+\pi^-\nu$
419 ± 108 ± 57		BAND	87 MAC		$\tau^+ \rightarrow \pi^+\pi^+\pi^-\nu$
521 ± 27		ALBRECHT	86B ARG		$\tau^+ \rightarrow \pi^+\pi^+\pi^-\nu$
476 ± 132		RUCKSTUHL	86 DLCO		$\tau^+ \rightarrow \pi^+\pi^+\pi^-\nu$
462 ± 56 ± 30		SCHMIDKE	86 MRK2		$\tau^+ \rightarrow \pi^+\pi^+\pi^-\nu$
292 ± 40		BELLINI	85 SPEC		40 $\pi^-A \rightarrow \pi^-\pi^+\pi^-A$
380 ± 100		29 DANKOWY...	81 SPEC 0		8.45 $\pi^-\rho \rightarrow n3\pi$
300 ± 50		29 DAUM	81B CNTR		63.94 $\pi^-\rho \rightarrow p3\pi$
230 ± 50		30 GAVILLET	77 HBC +		4.2 $K^-\rho \rightarrow \Sigma 3\pi$

15 From a fit to the 3π mass spectrum including the $K\bar{K}^*(892)$ threshold.
 16 Using the $a_1(1260)$ mass of 1230 MeV.
 17 From AKHMETSHIN 99E and ASNER 00 data using the $a_1(1260)$ mass of 1230 MeV.
 18 Uses the model of KUHN 90.
 19 Uses the model of ISGUR 89.
 20 Includes the effect of a possible a_1' state.
 21 Uses the model of FEINDT 90.
 22 Supersedes AKERS 95P.
 23 Average and spread of values using 2 variants of the model of BOWLER 75.
 24 Reanalysis of RUCKSTUHL 86.
 25 Reanalysis of SCHMIDKE 86.
 26 Reanalysis of ALBRECHT 86B.
 27 From a combined reanalysis of ALBRECHT 86B, SCHMIDKE 86, and RUCKSTUHL 86.
 28 From a combined reanalysis of ALBRECHT 86B and DAUM 81B.
 29 Uses the model of BOWLER 75.
 30 Produced in K^- backward scattering.

$a_1(1260)$ DECAY MODES

Mode	Fraction (Γ_i/Γ)
$\Gamma_1 (\rho\pi)_S$ -wave	seen
$\Gamma_2 (\rho\pi)_D$ -wave	seen
$\Gamma_3 (\rho(1450)\pi)_S$ -wave	seen
$\Gamma_4 (\rho(1450)\pi)_D$ -wave	seen
$\Gamma_5 \sigma\pi$	seen
$\Gamma_6 f_0(980)\pi$	not seen
$\Gamma_7 f_0(1370)\pi$	seen
$\Gamma_8 f_2(1270)\pi$	seen
$\Gamma_9 K\bar{K}^*(892)+c.c.$	seen
$\Gamma_{10} \pi(1300)\pi$	not seen
$\Gamma_{11} \pi\gamma$	seen

$a_1(1260)$ PARTIAL WIDTHS

$\Gamma(\pi\gamma)$	VALUE (keV)	DOCUMENT ID	TECN	COMMENT
	640 ± 246	ZIELINSKI	84C SPEC	200 $\pi^+Z \rightarrow Z3\pi$

D-wave/S-wave AMPLITUDE RATIO IN DECAY OF $a_1(1260) \rightarrow \rho\pi$

VALUE	DOCUMENT ID	TECN	COMMENT
-0.107 ± 0.016 OUR AVERAGE			
-0.10 ± 0.02 ± 0.02	31,32 ACKERSTAFF	97R OPAL	$E_{CM}^{ee} = 88-94, \tau \rightarrow 3\pi\nu$
-0.11 ± 0.02	31 ALBRECHT	93C ARG	$\tau^+ \rightarrow \pi^+\pi^+\pi^-\nu$

31 Uses the model of ISGUR 89.
 32 Supersedes AKERS 95P.

See key on page 239

Meson Particle Listings

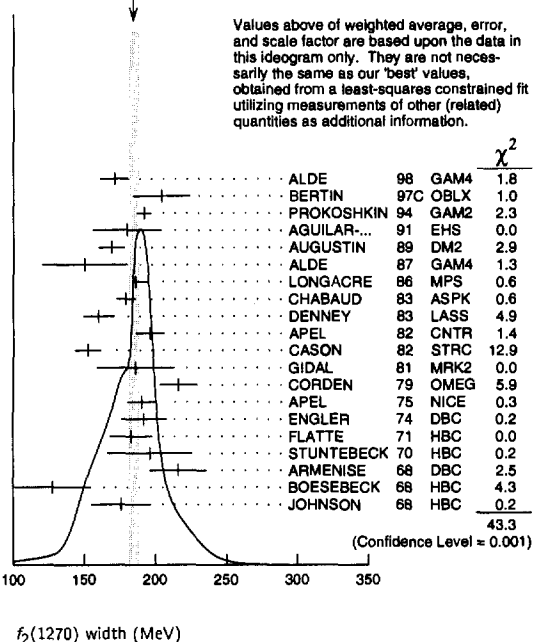
$f_2(1270)$

$f_2(1270)$ WIDTH

VALUE (MeV)	EVTS	DOCUMENT ID	TECN	COMMENT
$185.1^{+3.4}_{-2.6}$				OUR FIT Error includes scale factor of 1.5.
$184.3^{+4.0}_{-2.6}$				OUR AVERAGE Error includes scale factor of 1.6. See the ideogram below.
171 ± 10		ALDE 98	GAM4	100 $\pi^- \rho \rightarrow \pi^0 \pi^0 \pi^0$
204 ± 20		⁹ BERTIN 97c	OBLX	0.0 $\bar{p} p \rightarrow \pi^+ \pi^- \pi^0$
192 ± 5	200k	PROKOSHKIN 94	GAM2	38 $\pi^- \rho \rightarrow \pi^0 \pi^0 \pi^0$
180 ± 24		AGUILAR... 91	EHS	400 $p p$
169 ± 9	5730	¹⁰ AUGUSTIN 89	DM2	$e^+ e^- \rightarrow 5\pi$
150 ± 30	400	¹⁰ ALDE 87	GAM4	100 $\pi^- \rho \rightarrow 4\pi^0 \pi^0$
186^{+9}_{-2}		¹¹ LONGACRE 86	MPS	22 $\pi^- \rho \rightarrow n2K_S^0$
$179.2^{+6.9}_{-6.6}$		¹² CHABAUD 83	ASPK	17 $\pi^- \rho$ polarized
160 ± 11		DENNEY 83	LASS	10 $\pi^+ N$
196 ± 10	3k	APEL 82	CNTR	25 $\pi^- \rho \rightarrow n2\pi^0$
152 ± 9		¹³ CASON 82	STRC	8 $\pi^+ \rho \rightarrow \Delta^{++} \pi^0 \pi^0$
186 ± 27	11600	GIDAL 81	MRK2	J/ψ decay
216 ± 13		¹⁴ CORDEN 79	OMEG	12-15 $\pi^- \rho \rightarrow n2\pi$
190 ± 10	10k	APEL 75	NICE	40 $\pi^- \rho \rightarrow n2\pi^0$
192 ± 16	4600	ENGLER 74	DBC	6 $\pi^+ n \rightarrow \pi^+ \pi^- \rho$
183 ± 15	5300	FLATTE 71	HBC	7 $\pi^+ \rho \rightarrow \Delta^+ f_2$
196 ± 30		¹⁰ STUNTEBECK 70	HBC	8 $\pi^- \rho, 5.4 \pi^+ d$
216 ± 20	1960	¹⁰ ARMENISE 68	DBC	5.1 $\pi^+ n \rightarrow p\pi^+ MM^-$
128 ± 27		¹⁰ BOESEBECK 68	HBC	8 $\pi^+ \rho$
176 ± 21		^{10,15} JOHNSON 68	HBC	3.7-4.2 $\pi^- \rho$

- • • We do not use the following data for averages, fits, limits, etc. • • •
- 16 ALDE 97 GAM2 450 $p p \rightarrow p p \pi^0 \pi^0$
- 184 ± 10 ¹⁶GRYGOREV 96 SPEC 40 $\pi^- N \rightarrow K_S^0 K_S^0 X$
- 200 ± 10 AKER 91 CBAR 0.0 $\bar{p} p \rightarrow 3\pi^0$
- 240 ± 40 3k BINON 83 GAM2 38 $\pi^- \rho \rightarrow n2\eta$
- 187 ± 30 650 ¹⁰ANTIPOV 77 CIBS 25 $\pi^- \rho \rightarrow p3\pi$
- 225 ± 38 16000 DEUTSCH... 76 HBC 16 $\pi^+ \rho$
- 166 ± 28 600 ¹⁰TAKAHASHI 72 HBC 8 $\pi^- \rho \rightarrow n2\pi$
- 173 ± 53 ¹⁰ARMENISE 70 HBC 9 $\pi^+ n \rightarrow p\pi^+ \pi^-$

WEIGHTED AVERAGE
184.3±4.0-2.6 (Error scaled by 1.6)



Values above of weighted average, error, and scale factor are based upon the data in this ideogram only. They are not necessarily the same as our 'best' values, obtained from a least-squares constrained fit utilizing measurements of other (related) quantities as additional information.

DOCUMENT ID	TECN	COMMENT	χ^2
ALDE 98	GAM4	1.8	
BERTIN 97c	OBLX	1.0	
PROKOSHKIN 94	GAM2	2.3	
AGUILAR... 91	EHS	0.0	
AUGUSTIN 89	DM2	2.9	
ALDE 87	GAM4	1.3	
LONGACRE 86	MPS	0.6	
CHABAUD 83	ASPK	0.6	
DENNEY 83	LASS	4.9	
APEL 82	CNTR	1.4	
CASON 82	STRC	12.9	
GIDAL 81	MRK2	0.0	
CORDEN 79	OMEG	5.9	
APEL 75	NICE	0.3	
ENGLER 74	DBC	0.2	
FLATTE 71	HBC	0.0	
STUNTEBECK 70	HBC	0.2	
ARMENISE 68	DBC	2.5	
BOESEBECK 68	HBC	4.3	
JOHNSON 68	HBC	0.2	

(Confidence Level = 0.001)

$f_2(1270)$ DECAY MODES

Mode	Fraction (Γ_i/Γ)	Scale factor/Confidence level
Γ_1 $\pi\pi$	(84.7 $^{+2.4}_{-1.3}$) %	S=1.3
Γ_2 $\pi^+ \pi^- 2\pi^0$	(7.1 $^{+1.5}_{-2.6}$) %	S=1.3
Γ_3 $K\bar{K}$	(4.6 ± 0.5) %	S=2.8
Γ_4 $2\pi^+ 2\pi^-$	(2.8 ± 0.4) %	S=1.2
Γ_5 $\eta\eta$	(4.5 ± 1.0) × 10 ⁻³	S=2.4
Γ_6 $4\pi^0$	(3.0 ± 1.0) × 10 ⁻³	
Γ_7 $\gamma\gamma$	(1.41 ± 0.13) × 10 ⁻⁵	
Γ_8 $\eta\pi\pi$	< 8 × 10 ⁻³	CL=95%
Γ_9 $K^0 K^- \pi^+ + c.c.$	< 3.4 × 10 ⁻³	CL=95%
Γ_{10} $e^+ e^-$	< 9 × 10 ⁻⁹	CL=90%

CONSTRAINED FIT INFORMATION

An overall fit to the total width, 4 partial widths, a combination of partial widths obtained from integrated cross sections, and 6 branching ratios uses 41 measurements and one constraint to determine 8 parameters. The overall fit has a $\chi^2 = 73.5$ for 34 degrees of freedom.

The following off-diagonal array elements are the correlation coefficients $\langle \delta p_i \delta p_j \rangle / (\delta p_i \delta p_j)$, in percent, from the fit to parameters p_i , including the branching fractions, $x_i \equiv \Gamma_i/\Gamma_{total}$. The fit constrains the x_i whose labels appear in this array to sum to one.

x_2	-91						
x_3	11	-39					
x_4	11	-36	1				
x_5	2	-9	0	0			
x_6	0	-7	0	0	0		
x_7	11	-7	-9	1	0	0	
Γ	-79	73	-11	-8	-3	0	
	x_1	x_2	x_3	x_4	x_5	x_6	x_7

Mode	Rate (MeV)	Scale factor
Γ_1 $\pi\pi$	156.9 $^{+3.8}_{-1.3}$	
Γ_2 $\pi^+ \pi^- 2\pi^0$	13.1 $^{+3.0}_{-4.9}$	1.3
Γ_3 $K\bar{K}$	8.6 ± 0.8	2.9
Γ_4 $2\pi^+ 2\pi^-$	5.2 ± 0.7	1.2
Γ_5 $\eta\eta$	0.83 ± 0.18	2.4
Γ_6 $4\pi^0$	0.55 ± 0.19	
Γ_7 $\gamma\gamma$	0.00260 ± 0.00024	

$f_2(1270)$ PARTIAL WIDTHS

$\Gamma(\pi\pi)$	DOCUMENT ID	TECN	COMMENT	Γ_1
$156.9^{+3.8}_{-1.3}$			OUR FIT	
$157.0^{+6.0}_{-1.0}$	¹⁸ LONGACRE 86	MPS	22 $\pi^- \rho \rightarrow n2K_S^0$	
$\Gamma(K\bar{K})$	DOCUMENT ID	TECN	COMMENT	Γ_3
8.6 ± 0.8			Error includes scale factor of 2.9.	
$9.0^{+0.7}_{-0.3}$	¹⁸ LONGACRE 86	MPS	22 $\pi^- \rho \rightarrow n2K_S^0$	
$\Gamma(\eta\eta)$	DOCUMENT ID	TECN	COMMENT	Γ_5
0.83 ± 0.18			Error includes scale factor of 2.4.	
1.0 ± 0.1	¹⁸ LONGACRE 86	MPS	22 $\pi^- \rho \rightarrow n2K_S^0$	
$\Gamma(\gamma\gamma)$	DOCUMENT ID	TECN	COMMENT	Γ_7
2.60 ± 0.24			OUR FIT	
$2.71^{+0.25}_{-0.23}$			OUR AVERAGE	
2.84 ± 0.35	BOGLIONE 99	RVUE	$\gamma\gamma \rightarrow \pi^+ \pi^-, \pi^0 \pi^0$	
$2.58 \pm 0.13^{+0.36}_{-0.27}$	¹⁹ BEHREND 92	CELL	$e^+ e^- \rightarrow e^+ e^- \pi^+ \pi^-$	

Meson Particle Listings

f₂(1270)

• • • We do not use the following data for averages, fits, limits, etc. • • •

Table listing experimental data for various decays of f2(1270). Columns include experiment name (e.g., YABUKI, BLINOV), document ID, decay mode (e.g., e+e- -> pi+ pi-), and branching ratio values.

¹⁷With a narrow scalar state around 1220 MeV.

Table for Gamma(e+e-) with columns: VALUE (eV), CL%, DOCUMENT ID, TECN, COMMENT. Value is <1.7.

¹⁸From a partial-wave analysis of data using a K-matrix formalism with 5 poles.

¹⁹Using a unitarized model with a 300 - 500 keV wide scalar at 1100 MeV.

²⁰Using the unitarized model of LYTH 85.

²¹Error includes spread of different solutions. Data of MARK2 and CRYSTAL BALL used in the analysis. Authors report strong correlations with gamma-gamma width of f0(1370) : Gamma(f2) + 1/4 Gamma(f0) = 3.6 +/- 0.3 KeV.

²²Radiative corrections modify the partial widths; for instance the COURAU 84 value becomes 2.66 +/- 0.21 in the calculation of LANDRO 86.

²³Using the MENNESSIER 83 model.

²⁴Superseded by BOYER 90.

²⁵If helicity = 2 assumption is not made.

²⁶Using mass, width and B(f2(1270) -> 2pi) from PDG 78.

Table for Gamma(KK) x Gamma(gamma gamma) / Gamma(total). Columns include VALUE (keV), DOCUMENT ID, TECN, COMMENT. Value is 0.121 +/- 0.015.

• • • We do not use the following data for averages, fits, limits, etc. • • •

Table entry for ALBRECHT 90G ARG with value 0.104 +/- 0.007 +/- 0.072.

²⁷Using an incoherent background.

²⁸Using a coherent background.

f2(1270) BRANCHING RATIOS

Table for Gamma(pi pi) / Gamma(total) with columns: VALUE, EVTS, DOCUMENT ID, TECN, COMMENT. Value is 0.847 +/- 0.024.

0.837 +/- 0.020 OUR AVERAGE

Table entry for CHABAUD 83 ASPK with value 0.849 +/- 0.025.

Table entry for BEAUPRE 71 HBC with value 0.85 +/- 0.05.

Table entry for OH 70 HBC with value 0.8 +/- 0.04.

Table for Gamma(pi+ pi- 2pi0) / Gamma(pi pi) with columns: VALUE, EVTS, DOCUMENT ID, TECN, COMMENT.

0.083 +/- 0.019 OUR FIT Error includes scale factor of 1.3.

Table entry for EISENBERG 74 HBC with value 0.15 +/- 0.06.

• • • We do not use the following data for averages, fits, limits, etc. • • •

Table entry for EMMS 75D DBC with value 0.07.

Gamma(KK) / Gamma(pi pi) and Gamma3/Gamma1

We average only experiments which either take into account f2(1270)-a2(1320) interference explicitly or demonstrate that a2(1320) production is negligible.

Table for Gamma(KK) / Gamma(pi pi) with columns: VALUE, EVTS, DOCUMENT ID, TECN, COMMENT. Value is 0.055 +/- 0.005.

• • • We do not use the following data for averages, fits, limits, etc. • • •

Table for Gamma(2pi+ 2pi-) / Gamma(pi pi) with columns: VALUE, EVTS, DOCUMENT ID, TECN, COMMENT. Value is 0.033 +/- 0.005.

²⁹Re-evaluated by CHABAUD 83.

³⁰Includes PAWLICKI 77 data.

³¹Takes into account the f2(1270)-f2'(1525) interference.

Table for Gamma(Gamma pi pi) / Gamma(total) with columns: VALUE (units 10^-3), DOCUMENT ID, TECN, COMMENT. Value is 4.5 +/- 1.0.

• • • We do not use the following data for averages, fits, limits, etc. • • •

Table for Gamma(Gamma pi pi) / Gamma(pi pi) with columns: VALUE, CL%, DOCUMENT ID, TECN, COMMENT. Value is <0.05.

• • • We do not use the following data for averages, fits, limits, etc. • • •

Table for Gamma(4pi0) / Gamma(total) with columns: VALUE, EVTS, DOCUMENT ID, TECN, COMMENT. Value is 0.0030 +/- 0.0010.

• • • We do not use the following data for averages, fits, limits, etc. • • •

Table for Gamma(Gamma pi pi) / Gamma(pi pi) with columns: VALUE, CL%, DOCUMENT ID, TECN, COMMENT. Value is <0.010.

• • • We do not use the following data for averages, fits, limits, etc. • • •

Table for Gamma(K0 K- pi+ + c.c.) / Gamma(pi pi) with columns: VALUE, CL%, DOCUMENT ID, TECN, COMMENT. Value is <0.004.

Table for Gamma(K0 K- pi+ + c.c.) / Gamma(pi pi) with columns: VALUE, CL%, DOCUMENT ID, TECN, COMMENT. Value is <0.004.

f2(1270) REFERENCES

List of references for f2(1270) decays, including authors like BOGLIONE, ALDE, and institutions like GAMMA Collab., CELLO Collab., etc.

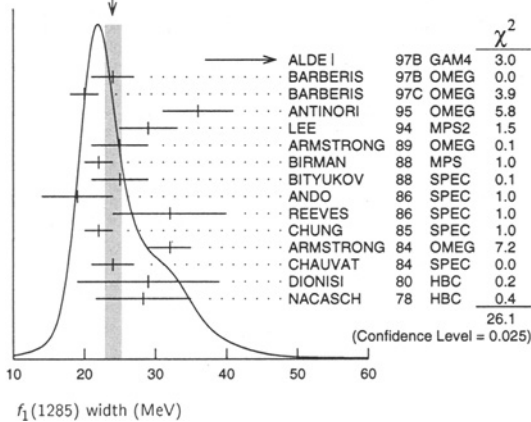
Meson Particle Listings

$f_1(1285)$

25 ± 4	504	BITYUKOV	88	SPEC	32.5 $\pi^- \rho^- \rightarrow K^+ K^- \pi^0 \eta$
19 ± 5		ANDO	86	SPEC	8 $\pi^- \rho^- \rightarrow \eta \pi^+ \pi^- \pi^-$
32 ± 8	420	REEVES	86	SPEC	6.6 $\rho \bar{\rho} \rightarrow K K \pi X$
22 ± 2		CHUNG	85	SPEC	8 $\pi^- \rho^- \rightarrow N K \bar{K} \pi$
32 ± 3	604	ARMSTRONG	84	OMEG	85 $\pi^+ \rho^- \rightarrow K \bar{K} \pi \pi \rho$, $\rho \rho \rightarrow K \bar{K} \pi \rho \rho$
24 ± 3		CHAUVAT	84	SPEC	ISR 31.5 $\rho \rho$
29 ± 10	103	DIONISI	80	HBC	4 $\pi^- \rho^- \rightarrow K \bar{K} \pi \eta$
28.3 ± 6.7	320	NACASCH	78	HBC	0.7, 0.76 $\bar{\rho} \rho \rightarrow K \bar{K} 3\pi$
18.2 ± 1.2		⁹ SOSA	99	SPEC	$\rho \rho \rightarrow \rho_{slow}^0 (K_S^0 K^+ \pi^-) P_{fast}$
19.4 ± 1.5		⁹ SOSA	99	SPEC	$\rho \rho \rightarrow \rho_{slow}^0 (K_S^0 K^- \pi^+) P_{fast}$
40 ± 5		ABATZIS	94	OMEG	450 $\rho \rho \rightarrow \rho \rho 2(\pi^+ \pi^-)$
44 ± 20		AUGUSTIN	90	DM2	$J/\psi \rightarrow \gamma \eta \pi^+ \pi^-$
31 ± 5		ARMSTRONG	89E	OMEG	300 $\rho \rho \rightarrow \rho \rho 2(\pi^+ \pi^-)$
41 ± 12		ARMSTRONG	89G	OMEG	85 $\pi^+ \rho^- \rightarrow 4\pi \pi \rho$, $\rho \rho \rightarrow 4\pi \rho \rho$
17.9 ± 10.9	60	RATH	89	MPS	21.4 $\pi^- \rho^- \rightarrow K_S^0 K_S^0 \pi^0 \eta$
14 ⁺²⁰ ₋₁₄ ± 10	16	BECKER	87	MRK3	$e^+ e^- \rightarrow \phi K \bar{K} \pi$
26 ± 12		EVANGELISTA	81	OMEG	12 $\pi^- \rho^- \rightarrow \eta \pi^+ \pi^- \pi^- \rho$
25 ± 15	200	GURTU	79	HBC	4.2 $K^- \rho^- \rightarrow \eta 2\pi$
~ 10		¹⁰ STANTON	79	CNTR	8.5 $\pi^- \rho^- \rightarrow \eta 2\gamma 2\pi$
24 ± 18	210	GRASSLER	77	HBC	16 $\pi^+ \rho^-$
28 ± 5	150	¹¹ DEFOIX	72	HBC	0.7 $\bar{\rho} \rho \rightarrow 7\pi$
46 ± 9	180	¹¹ DUBOC	72	HBC	1.2 $\bar{\rho} \rho \rightarrow 2K 4\pi$
37 ± 5	500	¹² THUN	72	MMS	13.4 $\pi^- \rho^-$
10 ± 10		BOESEBECK	71	HBC	16.0 $\pi \rho \rightarrow \rho 5\pi$
30 ± 15		CAMPBELL	69	DBC	2.7 $\pi^+ d$
60 ± 15		¹¹ LORSTAD	69	HBC	0.7 $\bar{\rho} \rho$, 4,5-body
35 ± 10		¹¹ DAHL	67	HBC	1.6-4.2 $\pi^- \rho^-$

⁷ Supersedes ABATZIS 94, ARMSTRONG 89E.
⁸ From partial wave analysis of $K^+ \bar{K}^0 \pi^-$ system.
⁹ No systematic error given.
¹⁰ From phase shift analysis of $\eta \pi^+ \pi^-$ system.
¹¹ Resolution is not unfolded.
¹² Seen in the missing mass spectrum.

WEIGHTED AVERAGE
24.0 ± 1.2 (Error scaled by 1.4)



$f_1(1285)$ DECAY MODES

Mode	Fraction (Γ_i/Γ)	Scale factor/Confidence level
Γ_1 4π	(33.1 ^{+2.1} _{-1.8}) %	S=1.3
Γ_2 $\pi^0 \pi^0 \pi^+ \pi^-$	(22.0 ^{+1.4} _{-1.2}) %	S=1.3
Γ_3 $2\pi^+ 2\pi^-$	(11.0 ^{+0.7} _{-0.6}) %	S=1.3
Γ_4 $\rho^0 \pi^+ \pi^-$	(11.0 ^{+0.7} _{-0.6}) %	S=1.3
Γ_5 $4\pi^0$	< 7 $\times 10^{-4}$	CL=90%

Γ_6 $\eta \pi \pi$	(52 ± 16) %
Γ_7 $a_0(980) \pi$ [ignoring $a_0(980) \rightarrow K \bar{K}$]	(36 ± 7) %
Γ_8 $\eta \pi \pi$ [excluding $a_0(980) \pi$]	(16 ± 7) %
Γ_9 $K \bar{K} \pi$	(9.0 ± 0.4) %
Γ_{10} $K \bar{K}^*(892)$	not seen
Γ_{11} $\gamma \rho^0$	(5.5 ± 1.3) %
Γ_{12} $\phi \gamma$	(7.4 ± 2.6) $\times 10^{-4}$
Γ_{13} $\gamma \gamma^*$	
Γ_{14} $\gamma \gamma$	

CONSTRAINED FIT INFORMATION

An overall fit to 7 branching ratios uses 16 measurements and one constraint to determine 5 parameters. The overall fit has a $\chi^2 = 24.7$ for 12 degrees of freedom.

The following off-diagonal array elements are the correlation coefficients $\langle \delta x_i \delta x_j \rangle / (\delta x_i \delta x_j)$, in percent, from the fit to the branching fractions, $x_i \equiv \Gamma_i/\Gamma_{total}$. The fit constrains the x_i whose labels appear in this array to sum to one.

x_7	-17				
x_8	-8	-95			
x_9	46	-9	-4		
x_{11}	-36	-4	-2	-34	
		x_1	x_7	x_8	x_9

$f_1(1285) \Gamma(1)(\gamma\gamma)/\Gamma_{total}$

VALUE (keV)	CL%	DOCUMENT ID	TECN	COMMENT
<0.62	95	GIDAL	87	MRK2 $e^+ e^- \rightarrow e^+ e^- \eta \pi^+ \pi^-$

$f_1(1285) \Gamma(\gamma\gamma^*)/\Gamma_{total}$

VALUE (keV)	EVTS	DOCUMENT ID	TECN	COMMENT
1.4 ± 0.4	OUR AVERAGE			Error includes scale factor of 1.4.
1.18 ± 0.25 ± 0.20	26	^{13,14} AIHARA	88B	TPC $e^+ e^- \rightarrow e^+ e^- \eta \pi^+ \pi^-$
2.30 ± 0.61 ± 0.42	13,15	GIDAL	87	MRK2 $e^+ e^- \rightarrow e^+ e^- \eta \pi^+ \pi^-$

¹³ Assuming a ρ -pole form factor.
¹⁴ Published value multiplied by $\eta \pi \pi$ branching ratio 0.49.
¹⁵ Published value divided by 2 and multiplied by the $\eta \pi \pi$ branching ratio 0.49.

$f_1(1285)$ BRANCHING RATIOS

$\Gamma(K \bar{K} \pi)/\Gamma(4\pi)$ Γ_9/Γ_1

VALUE	DOCUMENT ID	TECN	COMMENT
0.271 ± 0.016	OUR FIT		Error includes scale factor of 1.3.
0.271 ± 0.016	OUR AVERAGE		Error includes scale factor of 1.2.
0.265 ± 0.014	¹⁶ BARBERIS	97C OMEG 450 $\rho \rho \rightarrow \rho \rho K_S^0 K^\pm \pi^\mp$	
0.28 ± 0.05	¹⁷ ARMSTRONG	89E OMEG 300 $\rho \rho \rightarrow \rho \rho f_1(1285)$	
0.37 ± 0.03 ± 0.05	¹⁸ ARMSTRONG	89G OMEG 85 $\pi \rho \rightarrow 4\pi X$	

¹⁶ Using $2(\pi^+ \pi^-)$ data from BARBERIS 97B.
¹⁷ Assuming $\rho \pi \pi$ and $a_0(980) \pi$ intermediate states.
¹⁸ 4π consistent with being entirely $\rho \pi \pi$.

$\Gamma(\pi^0 \pi^0 \pi^+ \pi^-)/\Gamma_{total}$ $\Gamma_2/\Gamma = \frac{2}{3} \Gamma_1/\Gamma$

VALUE	DOCUMENT ID
0.220 ^{+0.014} _{-0.012}	OUR FIT
	Error includes scale factor of 1.3.

$\Gamma(2\pi^+ 2\pi^-)/\Gamma_{total}$ $\Gamma_3/\Gamma = \frac{1}{3} \Gamma_1/\Gamma$

VALUE	DOCUMENT ID
0.110 ^{+0.007} _{-0.006}	OUR FIT
	Error includes scale factor of 1.3.

$\Gamma(\rho^0 \pi^+ \pi^-)/\Gamma_{total}$ $\Gamma_4/\Gamma = \frac{1}{3} \Gamma_1/\Gamma$

VALUE	DOCUMENT ID
0.110 ^{+0.007} _{-0.006}	OUR FIT
	Error includes scale factor of 1.3.

$\Gamma(K \bar{K} \pi)/\Gamma(\eta \pi \pi)$ $\Gamma_9/\Gamma_6 = \Gamma_9/(\Gamma_7 + \Gamma_8)$

VALUE	DOCUMENT ID	TECN	COMMENT
0.171 ± 0.013	OUR FIT		Error includes scale factor of 1.1.
0.170 ± 0.012	OUR AVERAGE		
0.166 ± 0.01 ± 0.008	BARBERIS	98C OMEG 450 $\rho \rho \rightarrow \rho f_1(1285) \rho_S$	
0.42 ± 0.15	GURTU	79 HBC 4.2 $K^- \rho^-$	
0.5 ± 0.2	CORDEN	78 OMEG 12-15 $\pi^- \rho^-$	
0.20 ± 0.08	¹⁹ DEFOIX	72 HBC 0.7 $\bar{\rho} \rho \rightarrow 7\pi$	
0.16 ± 0.08	CAMPBELL	69 DBC 2.7 $\pi^+ d$	

¹⁹ $K \bar{K}$ system characterized by the $l = 1$ threshold enhancement. (See under $a_0(980)$).

See key on page 239

Meson Particle Listings
f1(1285), eta(1295)

Gamma(a0(980) pi [ignoring a0(980) -> K Kbar]) / Gamma(eta pi pi) Gamma7/Gamma6 = Gamma7/(Gamma7+Gamma6)

Table with columns: VALUE, EVTS, DOCUMENT ID, TECN, COMMENT. Contains data for Gamma(a0(980) pi) / Gamma(eta pi pi) and Gamma7/Gamma6.

Gamma(4 pi) / Gamma(eta pi pi) Gamma1/Gamma6 = Gamma1/(Gamma7+Gamma6)

Table with columns: VALUE, DOCUMENT ID, TECN, COMMENT. Contains data for Gamma(4 pi) / Gamma(eta pi pi) and Gamma1/Gamma6.

Gamma(K Kbar*(892)) / Gamma_total Gamma10/Gamma7

Table with columns: VALUE, DOCUMENT ID, TECN, COMMENT. Contains data for Gamma(K Kbar*(892)) / Gamma_total.

Gamma(rho0 pi+ pi-) / Gamma(2 pi+ 2 pi-) Gamma4/Gamma3

Table with columns: VALUE, DOCUMENT ID, TECN, COMMENT. Contains data for Gamma(rho0 pi+ pi-) / Gamma(2 pi+ 2 pi-).

Gamma(4 pi0) / Gamma_total Gamma5/Gamma7

Table with columns: VALUE (units 10^-4), CL%, DOCUMENT ID, TECN, COMMENT. Contains data for Gamma(4 pi0) / Gamma_total.

Gamma(phi gamma) / Gamma(K Kbar pi) Gamma12/Gamma9

Table with columns: VALUE (units 10^-2), CL%, EVTS, DOCUMENT ID, TECN, COMMENT. Contains data for Gamma(phi gamma) / Gamma(K Kbar pi).

Gamma(gamma rho0) / Gamma(K Kbar pi) Gamma11/Gamma9

Table with columns: VALUE, CL%, EVTS, DOCUMENT ID, TECN, COMMENT. Contains data for Gamma(gamma rho0) / Gamma(K Kbar pi).

Gamma(gamma rho0) / Gamma(2 pi+ 2 pi-) Gamma11/Gamma3 = Gamma11/Gamma3

Table with columns: VALUE, DOCUMENT ID, TECN, COMMENT. Contains data for Gamma(gamma rho0) / Gamma(2 pi+ 2 pi-).

Gamma(gamma rho0) / Gamma_total Gamma11/Gamma7

Table with columns: VALUE, CL%, DOCUMENT ID, TECN, COMMENT. Contains data for Gamma(gamma rho0) / Gamma_total.

Gamma(eta pi pi) / Gamma(rho0) Gamma6/Gamma11 = (Gamma7+Gamma8)/Gamma11

Table with columns: VALUE, DOCUMENT ID, TECN, COMMENT. Contains data for Gamma(eta pi pi) / Gamma(rho0).

²³Published value multiplied by 1.5.

f1(1285) REFERENCES

List of references for f1(1285) from various experiments and collaborations, including Sosa et al., Barberis et al., ALDE, etc.

OTHER RELATED PAPERS

List of other related papers for eta(1295) from various experiments and collaborations, including Aihara et al., Aston et al., etc.

eta(1295) $I^G(J^{PC}) = 0^+(0^{-+})$

See also the mini-review under non-q-qbar candidates. (See the index for the page number.)

eta(1295) MASS

Table with columns: VALUE (MeV), EVTS, DOCUMENT ID, TECN, COMMENT. Contains mass measurements for eta(1295).

eta(1295) WIDTH

Table with columns: VALUE (MeV), EVTS, DOCUMENT ID, TECN, COMMENT. Contains width measurements for eta(1295).

eta(1295) DECAY MODES

Table with columns: Mode, Fraction (Gamma_i/Gamma). Lists decay modes and their relative fractions for eta(1295).

Meson Particle Listings

$\eta(1295)$, $\pi(1300)$, $a_2(1320)$

$\eta(1295) \Gamma(I)\Gamma(\gamma\gamma)/\Gamma(\text{total})$

$\Gamma(\eta\pi^+\pi^-) \times \Gamma(\gamma\gamma)/\Gamma_{\text{total}}$	CL%	DOCUMENT ID	TECN	COMMENT	$\Gamma_1\Gamma_3/\Gamma$
VALUE (keV)					
<0.3		ANTREASIAN 87	CBAL	$e^+e^- \rightarrow e^+e^-\eta\pi\pi$	
• • • We do not use the following data for averages, fits, limits, etc. • • •					
<0.6	90	AIHARA	88c	TPC $e^+e^- \rightarrow e^+e^-\eta\pi^+\pi^-$	

$\eta(1295)$ BRANCHING RATIOS

$\Gamma(a_0(980)\pi)/\Gamma_{\text{total}}$	DOCUMENT ID	TECN	COMMENT	Γ_2/Γ
VALUE				
• • • We do not use the following data for averages, fits, limits, etc. • • •				
not seen	BERTIN	97	OBLX	$0.0 \bar{p}p \rightarrow \kappa^\pm(\kappa^0)\pi^\mp\pi^+\pi^-$
seen	BIRMAN	88	MPS	$8 \pi^-\rho \rightarrow \kappa^+\kappa^0\pi^-n$
large	ANDO	86	SPEC	$8 \pi^-\rho \rightarrow \eta\pi^+\pi^-n$
large	STANTON	79	CNTR	$8.4 \pi^-\rho \rightarrow n\eta 2\pi$

$\Gamma(a_0(980)\pi)/\Gamma(\eta\pi^0\pi^0)$	DOCUMENT ID	TECN	COMMENT	Γ_2/Γ_4
VALUE				
0.65 ± 0.10	1 ALDE	97b	GAM4	$100 \pi^-\rho \rightarrow \eta\pi^0\pi^0 n$
1 Assuming that $a_0(980)$ decays only to $\eta\pi$.				

$\Gamma(\eta(\pi\pi)_S\text{-wave})/\Gamma(\eta\pi^0\pi^0)$	DOCUMENT ID	TECN	COMMENT	Γ_5/Γ_4
VALUE				
0.35 ± 0.10	ALDE	97b	GAM4	$100 \pi^-\rho \rightarrow \eta\pi^0\pi^0 n$

$\eta(1295)$ REFERENCES

ALDE	97b	PAN 60 386	D. Alde et al.	(GAMS Collab.)
BERTIN	97	PL B400 226	A. Bertin et al.	(OBELIX Collab.)
FUKUI	91c	PL B267 293	S. Fukui et al.	(SUGI, NAGO, KEK, KYOT+)
AIHARA	88c	PR D38 1	H. Aihara et al.	(TPC-2\(\gamma\)) Collab.)
BIRMAN	88	PRL 61 1557	A. Birman et al.	(BNL, FSU, IND, MASD) JP
ANTREASIAN	87	PR D36 2633	D. Antreasian et al.	(Crystal Ball Collab.)
ANDO	86	PRL 57 1296	A. Ando et al.	(KEK, KYOT, NIRS, SAGA+) IJP
STANTON	79	PRL 42 346	N.R. Stanton et al.	(OSU, CARL, MCGI+) JP

$\pi(1300)$

$$I^{G(J^{PC})} = 1^-(0^-+)$$

$\pi(1300)$ MASS

VALUE (MeV)	DOCUMENT ID	TECN	COMMENT
1300 ± 100	OUR ESTIMATE		
• • • We do not use the following data for averages, fits, limits, etc. • • •			
1275 ± 15	BERTIN	97d	OBLX $0.05 \bar{p}p \rightarrow 2\pi^+2\pi^-$
~ 1114	ABELE	96	CBAR $0.0 \bar{p}p \rightarrow 5\pi^0$
1190 ± 30	ZIELINSKI	84	SPEC $200 \pi^+Z \rightarrow Z3\pi$
1240 ± 30	BELLINI	82	SPEC $40 \pi^-A \rightarrow A3\pi$
1273 ± 50	1 AARON	81	RVUE
1342 ± 20	BONESINI	81	OMEG $12 \pi^-\rho \rightarrow \rho 3\pi$
~ 1400	DAUM	81b	SPEC $63,94 \pi^-\rho$
1 Uses multichannel Aitchison-Bowler model (BOWLER 75). Uses data from DAUM 80 and DANKOWYCH 81.			

$\pi(1300)$ WIDTH

VALUE (MeV)	DOCUMENT ID	TECN	COMMENT
200 to 600	OUR ESTIMATE		
• • • We do not use the following data for averages, fits, limits, etc. • • •			
218 ± 100	BERTIN	97d	OBLX $0.05 \bar{p}p \rightarrow 2\pi^+2\pi^-$
~ 340	ABELE	96	CBAR $0.0 \bar{p}p \rightarrow 5\pi^0$
440 ± 80	ZIELINSKI	84	SPEC $200 \pi^+Z \rightarrow Z3\pi$
360 ± 120	BELLINI	82	SPEC $40 \pi^-A \rightarrow A3\pi$
580 ± 100	2 AARON	81	RVUE
220 ± 70	BONESINI	81	OMEG $12 \pi^-\rho \rightarrow \rho 3\pi$
~ 600	DAUM	81b	SPEC $63,94 \pi^-\rho$
2 Uses multichannel Aitchison-Bowler model (BOWLER 75). Uses data from DAUM 80 and DANKOWYCH 81.			

$\pi(1300)$ DECAY MODES

Mode	Fraction (Γ_i/Γ)
Γ_1 $\rho\pi$	seen
Γ_2 $\pi(\pi\pi)_S\text{-wave}$	seen
Γ_3 $\gamma\gamma$	

$\pi(1300) \Gamma(I)\Gamma(\gamma\gamma)/\Gamma(\text{total})$

$\Gamma(\rho\pi) \times \Gamma(\gamma\gamma)/\Gamma_{\text{total}}$	CL%	DOCUMENT ID	TECN	COMMENT	$\Gamma_1\Gamma_3/\Gamma$
VALUE (keV)					
<0.085	90	ACCIARRI	97T	L3 $e^+e^- \rightarrow e^+e^-\pi^+\pi^-0$	
<0.54	90	ALBRECHT	97b	ARG $e^+e^- \rightarrow e^+e^-\pi^+\pi^-0$	

$\Gamma(\pi(\pi\pi)_S\text{-wave})/\Gamma(\rho\pi)$

VALUE	DOCUMENT ID	TECN	COMMENT	Γ_2/Γ_1
• • • We do not use the following data for averages, fits, limits, etc. • • •				
2.12	3 AARON	81	RVUE	
3 Uses multichannel Aitchison-Bowler model (BOWLER 75). Uses data from DAUM 80 and DANKOWYCH 81.				

$\pi(1300)$ REFERENCES

ACCIARRI	97T	PL B413 147	M. Acciarri et al.	(L3 Collab.)
ALBRECHT	97b	ZPHY C74 469	H. Albrecht et al.	(ARGUS Collab.)
BERTIN	97d	PL B414 220	A. Bertin et al.	(OBELIX Collab.)
ABELE	96	PL B380 453	A. Abele et al.	(Crystal Barrel Collab.)
ZIELINSKI	84	PR D30 1855	M. Zielinski et al.	(ROCH, MINN, FNAL)
BELLINI	82	PRL 48 1697	G. Bellini et al.	(MILA, BGNA, JINR)
AARON	81	PR D24 1207	R.A. Aaron, R.S. Longacre	(NEAS, BNL)
BONESINI	81	PL 103B 75	M. Bonesini et al.	(MILA, LVP, DARE+)
DANKOWYCH...	81	PRL 46 580	J.A. Dankowych et al.	(TNTO, BNL, CARL+)
DAUM	81b	NP B182 269	C. Daum et al.	(AMST, CERN, CRAC, MPIM+)
DAUM	80	PL 99B 281	C. Daum et al.	(AMST, CERN, CRAC, MPIM+)
BOWLER	75	NP B97 227	M.G. Bowler et al.	(OXFTF, DARE)

OTHER RELATED PAPERS

ASNER	00	PR D61 012002	D.M. Asner et al.	(CLEO Collab.)
ZAIMIDOROGA	99	PAN 30 1	O.A. Zaimidzoga	
Translated from SJPN 30 5.				
ACKERSTAFF	97R	ZPHY C75 593	K. Ackerstaff et al.	(OPAL Collab.)
ALBRECHT	95c	PL B349 576	H. Albrecht et al.	(ARGUS Collab.)

$a_2(1320)$

$$I^{G(J^{PC})} = 1^-(2^{++})$$

$a_2(1320)$ MASS

VALUE (MeV)	DOCUMENT ID	COMMENT
1318.0 ± 0.6	OUR AVERAGE	Includes data from the 4 datablocks that follow this one. Error includes scale factor of 1.1.

3π MODE

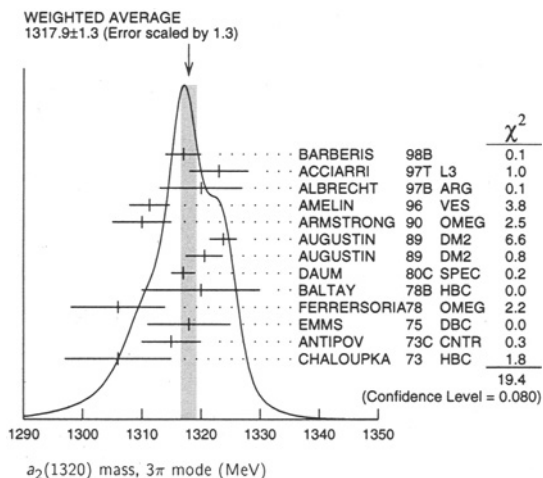
VALUE (MeV)	EVTs	DOCUMENT ID	TECN	CHG	COMMENT
The data in this block is included in the average printed for a previous datablock.					
1317.9 ± 1.3	OUR AVERAGE	Error includes scale factor of 1.3. See the ideogram below.			
1317 ± 3		BARBERIS	98b		$450 \rho\rho \rightarrow \rho_f\pi^+\pi^-\pi^0\rho_s$
$1323 \pm 4 \pm 3$		ACCIARRI	97T	L3	$e^+e^- \rightarrow e^+e^-\pi^+\pi^-\pi^0$
1320 ± 7		ALBRECHT	97b	ARG	$e^+e^- \rightarrow e^+e^-\pi^+\pi^-\pi^0$
$1311.3 \pm 1.6 \pm 3.0$	72400	AMELIN	96	VES	$36 \pi^-\rho \rightarrow e^+e^-\pi^+\pi^-\pi^0 n$
1310 ± 5		ARMSTRONG	90	OMEG 0	$300.0 \rho\rho \rightarrow \rho\rho\pi^+\pi^-\pi^0$
1323.8 ± 2.3	4022	AUGUSTIN	89	DM2 \pm	$J/\psi \rightarrow \rho^\pm a_2^\mp$
1320.6 ± 3.1	3562	AUGUSTIN	89	DM2 0	$J/\psi \rightarrow \rho^0 a_2^0$
1317 ± 2	25000	1 DAUM	80c	SPEC	$63,94 \pi^-\rho \rightarrow 3\pi\rho$
1320 ± 10	1097	1 BALTAY	78b	HBC $+0$	$15 \pi^+\rho \rightarrow \rho 4\pi$
1306 ± 8		FERRERSORIA	78	OMEG	$9 \pi^-\rho \rightarrow \rho 3\pi$
1318 ± 7	1600	1 EMMS	75	DBC 0	$4 \pi^+n \rightarrow \rho(3\pi)^0$
1315 ± 5		1 ANTIPOV	73c	CNTR	$25,40 \pi^-\rho \rightarrow \rho\eta\pi^-$
1306 ± 9	1580	CHALOUKKA	73	HBC	$3.9 \pi^-\rho$
• • • We do not use the following data for averages, fits, limits, etc. • • •					
1305 ± 14		CONDO	93	SHF	$\gamma\rho \rightarrow \eta\pi^+\pi^+\pi^-$
1310 ± 2		1 EVANGELISTA	81	OMEG	$12 \pi^-\rho \rightarrow 3\pi\rho$
1343 ± 11	490	BALTAY	78b	HBC 0	$15 \pi^+\rho \rightarrow \Delta 3\pi$
1309 ± 5	5000	BINNIE	71	MMS	$\pi^-\rho$ near a_2 thresh-old
1299 ± 6	28000	BOWEN	71	MMS	$5 \pi^-\rho$
1300 ± 6	24000	BOWEN	71	MMS	$5 \pi^+\rho$
1309 ± 4	17000	BOWEN	71	MMS	$7 \pi^-\rho$
1306 ± 4	941	ALSTON...	70	HBC	$7.0 \pi^+\rho \rightarrow 3\pi\rho$

1 From a fit to $J^P = 2^+ \rho\pi$ partial wave.

See key on page 239

Meson Particle Listings

$a_2(1320)$



$K^\pm K_S^0$ MODE

VALUE (MeV)	EVTS	DOCUMENT ID	TECN	CHG	COMMENT
The data in this block is included in the average printed for a previous datablock.					
1318.1 ± 0.7 OUR AVERAGE					
1319 ± 5	4700	2,3 CLELAND	82B SPEC	+	$50 \pi^+ p \rightarrow K_S^0 K^+ p$
1324 ± 6	5200	2,3 CLELAND	82B SPEC	-	$50 \pi^- p \rightarrow K_S^0 K^- p$
1320 ± 2	4000	CHABAUD	80 SPEC	-	$17 \pi^- A \rightarrow K_S^0 K^- A$
1312 ± 4	11000	CHABAUD	78 SPEC	-	$9.8 \pi^- p \rightarrow K^- K_S^0 p$
1316 ± 2	4730	CHABAUD	78 SPEC	-	$18.8 \pi^- p \rightarrow K^- K_S^0 p$
1318 ± 1		2,4 MARTIN	78D SPEC	-	$10 \pi^- p \rightarrow K_S^0 K^- p$
1320 ± 2	2724	MARGULIE	76 SPEC	-	$23 \pi^- p \rightarrow K^- K_S^0 p$
1313 ± 4	730	FOLEY	72 CNTR	-	$20.3 \pi^- p \rightarrow K^- K_S^0 p$
1319 ± 3	1500	4 GRAYER	71 ASPK	-	$17.2 \pi^- p \rightarrow K^- K_S^0 p$
• • • We do not use the following data for averages, fits, limits, etc. • • •					
1330 ± 11	1000	2,3 CLELAND	82B SPEC	+	$30 \pi^+ p \rightarrow K_S^0 K^+ p$
1324 ± 5	350	HYAMS	78 ASPK	+	$12.7 \pi^+ p \rightarrow K^+ K_S^0 p$

²From a fit to $J^P = 2^+$ partial wave.
³Number of events evaluated by us.
⁴Systematic error in mass scale subtracted.

$\eta\pi$ MODE

VALUE (MeV)	EVTS	DOCUMENT ID	TECN	CHG	COMMENT
The data in this block is included in the average printed for a previous datablock.					
1318.0 ± 1.5 OUR AVERAGE					
1317 ± 1 ± 2		THOMPSON	97 MPS		$18 \pi^- p \rightarrow \eta\pi^- p$
1315 ± 5 ± 2		5 AMSLER	94D CBAR		$0.0 \bar{p} p \rightarrow \pi^0 \pi^0 \eta$
1325.1 ± 5.1		AOYAGI	93 BKEI		$\pi^- p \rightarrow \eta\pi^- p$
1317.7 ± 1.4 ± 2.0		BELADIDZE	93 VES		$37 \pi^- N \rightarrow \eta\pi^- N$
1323 ± 8	1000	6 KEY	73 OSPK	-	$6 \pi^- p \rightarrow \rho\pi^- \eta$
• • • We do not use the following data for averages, fits, limits, etc. • • •					
1324 ± 5		ARMSTRONG	93C E760	0	$\bar{p} p \rightarrow \pi^0 \eta \eta \rightarrow 6\gamma$
1336.2 ± 1.7	2561	DELFOSSSE	81 SPEC	+	$\pi^\pm p \rightarrow \rho\pi^\pm \eta$
1330.7 ± 2.4	1653	DELFOSSSE	81 SPEC	-	$\pi^\pm p \rightarrow \rho\pi^\pm \eta$
1324 ± 8	6200	6,7 CONFORTO	73 OSPK	-	$6 \pi^- p \rightarrow \rho MM^-$
• • • We do not use the following data for averages, fits, limits, etc. • • •					
⁵ The systematic error of 2 MeV corresponds to the spread of solutions. ⁶ Error includes 5 MeV systematic mass-scale error. ⁷ Missing mass with enriched MMS = $\eta\pi^-$, $\eta = 2\gamma$.					

$\eta'\pi$ MODE

VALUE (MeV)	DOCUMENT ID	TECN	COMMENT
The data in this block is included in the average printed for a previous datablock.			
1327.0 ± 10.7			
	BELADIDZE	93 VES	$37 \pi^- N \rightarrow \eta'\pi^- N$

$a_2(1320)$ WIDTH

3π MODE

VALUE (MeV)	EVTS	DOCUMENT ID	TECN	CHG	COMMENT
104.7 ± 1.9 OUR AVERAGE					
120 ± 10		BARBERIS	98B		$450 \rho p \rightarrow \rho_f \pi^+ \pi^- \pi^0 \rho_S$
105 ± 10 ± 11		ACCIARRI	97T L3		$e^+ e^- \rightarrow \pi^+ \pi^- \pi^0$
120 ± 10		ALBRECHT	97B ARG		$e^+ e^- \rightarrow \pi^+ \pi^- \pi^0$
103.0 ± 6.0 ± 3.3	72400	AMELIN	96 VES		$36 \pi^- p \rightarrow \pi^+ \pi^- \pi^0 n$
120 ± 10		ARMSTRONG	90 OMEG	0	$300.0 \rho p \rightarrow \rho \rho \pi^+ \pi^- \pi^0$
107.0 ± 9.7	4022	AUGUSTIN	89 DM2	±	$J/\psi \rightarrow \rho^\pm a_2^\mp$
118.5 ± 12.5	3562	AUGUSTIN	89 DM2	0	$J/\psi \rightarrow \rho^0 a_2^0$
97 ± 5		8 EVANGELISTA	81 OMEG	-	$12 \pi^- p \rightarrow 3\pi\rho$
96 ± 9	25000	8 DAUM	80C SPEC	-	$63.94 \pi^- p \rightarrow 3\pi\rho$
110 ± 15	1097	8 BALTAY	78B HBC	+0	$15 \pi^+ p \rightarrow \rho 4\pi$
112 ± 18	1600	8 EMMS	75 DBC	0	$4 \pi^+ n \rightarrow \rho(3\pi)^0$
122 ± 14	1200	8,9 WAGNER	75 HBC	0	$7 \pi^+ p \rightarrow \Delta^+(3\pi)^0$
115 ± 15		8 ANTIPOV	73C CNTR	-	$25.40 \pi^- p \rightarrow \rho\eta\pi^-$
99 ± 15	1580	CHALOUKPA	73 HBC	-	$3.9 \pi^- p$
105 ± 5	28000	BOWEN	71 MMS	-	$5 \pi^- p$
99 ± 5	24000	BOWEN	71 MMS	+	$5 \pi^+ p$
103 ± 5	17000	BOWEN	71 MMS	-	$7 \pi^- p$
• • • We do not use the following data for averages, fits, limits, etc. • • •					
120 ± 40		CONDO	93 SHF		$\gamma p \rightarrow \eta\pi^+ \pi^+ \pi^-$
115 ± 14	490	BALTAY	78B HBC	0	$15 \pi^+ p \rightarrow \Delta 3\pi$
72 ± 16	5000	BINNIE	71 MMS	-	$\pi^- p$ near a_2 threshold
79 ± 12	941	ALSTON-...	70 HBC	+	$7.0 \pi^+ p \rightarrow 3\pi\rho$

⁸From a fit to $J^P = 2^+$ $\rho\pi$ partial wave.
⁹Width errors enlarged by us to $4\Gamma/\sqrt{N}$; see the note with the $K^*(892)$ mass.

$K^\pm K_S^0$ AND $\eta\pi$ MODES

VALUE (MeV)	DOCUMENT ID
107 ± 5 OUR ESTIMATE	
110.3 ± 1.7 OUR AVERAGE Includes data from the 2 datablocks that follow this one.	

$K^\pm K_S^0$ MODE

VALUE (MeV)	EVTS	DOCUMENT ID	TECN	CHG	COMMENT
The data in this block is included in the average printed for a previous datablock.					
109.8 ± 2.4 OUR AVERAGE					
112 ± 20	4700	10,11 CLELAND	82B SPEC	+	$50 \pi^+ p \rightarrow K_S^0 K^+ p$
120 ± 25	5200	10,11 CLELAND	82B SPEC	-	$50 \pi^- p \rightarrow K_S^0 K^- p$
106 ± 4	4000	CHABAUD	80 SPEC	-	$17 \pi^- A \rightarrow K_S^0 K^- A$
126 ± 11	11000	CHABAUD	78 SPEC	-	$9.8 \pi^- p \rightarrow K^- K_S^0 p$
101 ± 8	4730	CHABAUD	78 SPEC	-	$18.8 \pi^- p \rightarrow K^- K_S^0 p$
113 ± 4		10,12 MARTIN	78D SPEC	-	$10 \pi^- p \rightarrow K_S^0 K^- p$
105 ± 8	2724	12 MARGULIE	76 SPEC	-	$23 \pi^- p \rightarrow K^- K_S^0 p$
113 ± 19	730	FOLEY	72 CNTR	-	$20.3 \pi^- p \rightarrow K^- K_S^0 p$
123 ± 13	1500	12 GRAYER	71 ASPK	-	$17.2 \pi^- p \rightarrow K^- K_S^0 p$
• • • We do not use the following data for averages, fits, limits, etc. • • •					
121 ± 51	1000	10,11 CLELAND	82B SPEC	+	$30 \pi^+ p \rightarrow K_S^0 K^+ p$
110 ± 18	350	HYAMS	78 ASPK	+	$12.7 \pi^+ p \rightarrow K^+ K_S^0 p$

¹⁰From a fit to $J^P = 2^+$ partial wave.
¹¹Number of events evaluated by us.
¹²Width errors enlarged by us to $4\Gamma/\sqrt{N}$; see the note with the $K^*(892)$ mass.

$\eta\pi$ MODE

VALUE (MeV)	EVTS	DOCUMENT ID	TECN	CHG	COMMENT
The data in this block is included in the average printed for a previous datablock.					
111.0 ± 2.5 OUR AVERAGE					
112 ± 3 ± 2		13 AMSLER	94D CBAR		$0.0 \bar{p} p \rightarrow \pi^0 \pi^0 \eta$
103 ± 6 ± 3		BELADIDZE	93 VES		$37 \pi^- N \rightarrow \eta\pi^- N$
112.2 ± 5.7	2561	DELFOSSSE	81 SPEC	+	$\pi^\pm p \rightarrow \rho\pi^\pm \eta$
116.6 ± 7.7	1653	DELFOSSSE	81 SPEC	-	$\pi^\pm p \rightarrow \rho\pi^\pm \eta$
108 ± 9	1000	KEY	73 OSPK	-	$6 \pi^- p \rightarrow \rho\pi^- \eta$
• • • We do not use the following data for averages, fits, limits, etc. • • •					
127 ± 2 ± 2		14 THOMPSON	97 MPS		$18 \pi^- p \rightarrow \eta\pi^- p$
118 ± 10		ARMSTRONG	93C E760	0	$\bar{p} p \rightarrow \pi^0 \eta \eta \rightarrow 6\gamma$
104 ± 9	6200	15 CONFORTO	73 OSPK	-	$6 \pi^- p \rightarrow \rho MM^-$

¹³The systematic error of 2 MeV corresponds to the spread of solutions.
¹⁴Resolution is not unfolded.
¹⁵Missing mass with enriched MMS = $\eta\pi^-$, $\eta = 2\gamma$.

Meson Particle Listings

 $a_2(1320)$ η/π MODE

VALUE (MeV)	DOCUMENT ID	TECN	COMMENT
106±32	BELADIDZE 93	VES	$37\pi^- N \rightarrow \eta^+ \pi^- N$

 $a_2(1320)$ DECAY MODES

Mode	Fraction (Γ_i/Γ)	Scale factor/ Confidence level
Γ_1 $\rho\pi$	(70.1±2.7) %	S=1.2
Γ_2 $\eta\pi$	(14.5±1.2) %	
Γ_3 $\omega\pi\pi$	(10.6±3.2) %	S=1.3
Γ_4 $K\bar{K}$	(4.9±0.8) %	
Γ_5 $\eta'(958)\pi$	(5.3±0.9) × 10 ⁻³	
Γ_6 $\pi^\pm\gamma$	(2.8±0.6) × 10 ⁻³	
Γ_7 $\gamma\gamma$	(9.4±0.7) × 10 ⁻⁶	
Γ_8 $\pi^+\pi^-\pi^-$	< 8 %	CL=90%
Γ_9 e^+e^-	< 2.3 × 10 ⁻⁷	CL=90%

CONSTRAINED FIT INFORMATION

An overall fit to 5 branching ratios uses 18 measurements and one constraint to determine 4 parameters. The overall fit has a $\chi^2 = 9.3$ for 15 degrees of freedom.

The following *off-diagonal* array elements are the correlation coefficients $\langle \delta x_i \delta x_j \rangle / (\delta x_i \delta x_j)$, in percent, from the fit to the branching fractions, $x_i \equiv \Gamma_i/\Gamma_{\text{total}}$. The fit constrains the x_i whose labels appear in this array to sum to one.

x_2	10		
x_3	-89	-46	
x_4	-1	-2	-24
	x_1	x_2	x_3

 $a_2(1320)$ PARTIAL WIDTHS

$\Gamma(\pi^\pm\gamma)$	DOCUMENT ID	TECN	CHG	COMMENT	Γ_6
VALUE (keV)					
295±60	CIHANGIR 82	SPEC	+	200 $\pi^+ A$	
••• We do not use the following data for averages, fits, limits, etc. •••					
461±110	MAY 77	SPEC	±	9.7 γA	

$\Gamma(\gamma\gamma)$	DOCUMENT ID	TECN	CHG	COMMENT	Γ_7
VALUE (keV)					
1.00±0.06 OUR AVERAGE					
0.98±0.05±0.09	ACCIARRI 97T	L3		$e^+e^- \rightarrow e^+e^-\pi^+\pi^-\pi^0$	
0.96±0.03±0.13	ALBRECHT 97B	ARG		$e^+e^- \rightarrow e^+e^-\pi^+\pi^-\pi^0$	
1.26±0.26±0.18	36 BARU 90	MD1		$e^+e^- \rightarrow e^+e^-\pi^+\pi^-\pi^0$	
1.00±0.07±0.15	415 BEHREND 90C	CELL 0		$e^+e^- \rightarrow e^+e^-\pi^+\pi^-\pi^0$	
1.03±0.13±0.21	BUTLER 90	MRK2		$e^+e^- \rightarrow e^+e^-\pi^+\pi^-\pi^0$	
1.01±0.14±0.22	85 OEST 90	JADE		$e^+e^- \rightarrow e^+e^-\pi^0\eta$	
0.90±0.27±0.15	56 16 ALTHOFF 86	TASS 0		$e^+e^- \rightarrow e^+e^-\pi^0\eta$	
1.14±0.20±0.26	17 ANTREASIAN 86	CBAL 0		$e^+e^- \rightarrow e^+e^-\pi^0\eta$	
1.06±0.18±0.19	BERGER 84C	PLUT 0		$e^+e^- \rightarrow e^+e^-\pi^0\eta$	
••• We do not use the following data for averages, fits, limits, etc. •••					
0.81±0.19 ^{+0.42} _{-0.11}	35 16 BEHREND 83B	CELL 0		$e^+e^- \rightarrow e^+e^-\pi^0\eta$	
0.77±0.18±0.27	22 17 EDWARDS 82F	CBAL 0		$e^+e^- \rightarrow e^+e^-\pi^0\eta$	

¹⁶From $\rho\pi$ decay mode.
¹⁷From $\eta\pi^0$ decay mode.

$\Gamma(e^+e^-)$	DOCUMENT ID	TECN	COMMENT	Γ_9
VALUE (eV)				
<25	90 VOROBYEV 88	ND	$e^+e^- \rightarrow \pi^0\eta$	

 $a_2(1320)$ $\Gamma(\eta)\Gamma(\gamma\gamma)/\Gamma(\text{total})$

$\Gamma(K\bar{K}) \times \Gamma(\gamma\gamma)/\Gamma_{\text{total}}$	DOCUMENT ID	TECN	COMMENT	$\Gamma_4\Gamma_7/\Gamma$
VALUE (keV)				
0.126±0.007±0.028	18 ALBRECHT 90G	ARG	$e^+e^- \rightarrow e^+e^-K^+K^-$	
••• We do not use the following data for averages, fits, limits, etc. •••				
0.081±0.006±0.027	19 ALBRECHT 90G	ARG	$e^+e^- \rightarrow e^+e^-K^+K^-$	

¹⁸Using an incoherent background.
¹⁹Using a coherent background.

 $a_2(1320)$ BRANCHING RATIOS

$\Gamma(K\bar{K})/\Gamma(\rho\pi)$	DOCUMENT ID	TECN	CHG	COMMENT	Γ_4/Γ_1
VALUE					
0.070±0.012 OUR FIT					
0.078±0.017	CHABAUD 78	RVUE			
••• We do not use the following data for averages, fits, limits, etc. •••					
0.011±0.003	20 BERTIN 98B	OBLX		0.0 $\bar{p}p \rightarrow K^\pm K_S^0 \pi^\mp$	
0.056±0.014	50 21 CHALOUPKA 73	HBC	-	3.9 $\pi^- p$	
0.097±0.018	113 21 ALSTON-... 71	HBC	+	7.0 $\pi^+ p$	
0.06 ± 0.03	21 ABRAMOVI... 70B	HBC	-	3.93 $\pi^- p$	
0.054±0.022	21 CHUNG 68	HBC	-	3.2 $\pi^- p$	
20 Using 4 π data from BERTIN 97D. 21 Included in CHABAUD 78 review.					

$\Gamma(\eta\pi)/[\Gamma(\rho\pi) + \Gamma(\eta\pi) + \Gamma(K\bar{K})]$	DOCUMENT ID	TECN	CHG	COMMENT	$\Gamma_2/(\Gamma_1 + \Gamma_2 + \Gamma_4)$
VALUE					
0.162±0.012 OUR FIT					
0.140±0.028 OUR AVERAGE					
0.13 ± 0.04	ESPIGAT 72	HBC	±	0.0 $\bar{p}p$	
0.15 ± 0.04	34 BARNHAM 71	HBC	+	3.7 $\pi^+ p$	

$\Gamma(\eta\pi)/\Gamma(\rho\pi)$	DOCUMENT ID	TECN	CHG	COMMENT	Γ_2/Γ_1
VALUE					
0.207±0.018 OUR FIT					
0.213±0.020 OUR AVERAGE					
0.18 ± 0.05	FORINO 76	HBC		11 $\pi^- p$	
0.22 ± 0.05	52 ANTIPOV 73	CNTR	-	40 $\pi^- p$	
0.211±0.044	149 CHALOUPKA 73	HBC	-	3.9 $\pi^- p$	
0.246±0.042	167 ALSTON-... 71	HBC	+	7.0 $\pi^+ p$	
0.25 ± 0.09	15 BOECKMANN 70	HBC	+	5.0 $\pi^+ p$	
0.23 ± 0.08	22 ASCOLI 68	HBC	-	5 $\pi^- p$	
0.12 ± 0.08	CHUNG 68	HBC	-	3.2 $\pi^- p$	
0.22 ± 0.09	CONTE 67	HBC	-	11.0 $\pi^- p$	

$\Gamma(\eta'(958)\pi)/\Gamma_{\text{total}}$	DOCUMENT ID	TECN	CHG	COMMENT	Γ_5/Γ
VALUE					
CL%					
<0.006	95 ALDE 92B	GAM2		38,100 $\pi^- p \rightarrow \eta'^0 n$	
<0.02	97 BARNHAM 71	HBC	+	3.7 $\pi^+ p$	
0.004±0.004	BOESEBECK 68	HBC	+	8 $\pi^+ p$	

$\Gamma(\eta'(958)\pi)/\Gamma(\rho\pi)$	DOCUMENT ID	TECN	CHG	COMMENT	Γ_5/Γ_1
VALUE					
CL%					
<0.011	90 EISENSTEIN 73	HBC	-	5 $\pi^- p$	
<0.04	ALSTON-... 71	HBC	+	7.0 $\pi^+ p$	
0.04 ^{+0.03} _{-0.04}	BOECKMANN 70	HBC	0	5.0 $\pi^+ p$	

$\Gamma(K\bar{K})/[\Gamma(\rho\pi) + \Gamma(\eta\pi) + \Gamma(K\bar{K})]$	DOCUMENT ID	TECN	CHG	COMMENT	$\Gamma_4/(\Gamma_1 + \Gamma_2 + \Gamma_4)$
VALUE					
0.054±0.009 OUR FIT					
0.048±0.012 OUR AVERAGE					
0.05 ± 0.02	TOET 73	HBC	+	5 $\pi^+ p$	
0.09 ± 0.04	TOET 73	HBC	0	5 $\pi^+ p$	
0.03 ± 0.02	8 DAMERI 72	HBC	-	11 $\pi^- p$	
0.06 ± 0.03	17 BARNHAM 71	HBC	+	3.7 $\pi^+ p$	
••• We do not use the following data for averages, fits, limits, etc. •••					
0.020±0.004	22 ESPIGAT 72	HBC	±	0.0 $\bar{p}p$	
22 Not averaged because of discrepancy between masses from $K\bar{K}$ and $\rho\pi$ modes.					

$\Gamma(\pi^+\pi^-\pi^-)/\Gamma(\rho\pi)$	DOCUMENT ID	TECN	CHG	COMMENT	Γ_8/Γ_1
VALUE					
CL%					
<0.12	90 ABRAMOVI... 70B	HBC	-	3.93 $\pi^- p$	

$\Gamma(\pi^\pm\gamma)/\Gamma_{\text{total}}$	DOCUMENT ID	TECN	COMMENT	Γ_6/Γ
VALUE				
0.005±0.005	23 EISENBERG 72	HBC	4.3,5.25,7.5 γp	
-0.003				
23 Pion-exchange model used in this estimation.				

$\Gamma(\omega\pi\pi)/\Gamma(\rho\pi)$	DOCUMENT ID	TECN	CHG	COMMENT	Γ_3/Γ_1
VALUE					
0.15±0.05 OUR FIT					
0.15±0.05 OUR AVERAGE					
0.28 ± 0.09	60 DIAZ 74	DBC	0	6 $\pi^+ n$	
0.18 ± 0.08	24 KARSHON 74	HBC		Avg. of above two	
0.10 ± 0.05	279 CHALOUPKA 73	HBC	-	3.9 $\pi^- p$	

See key on page 239

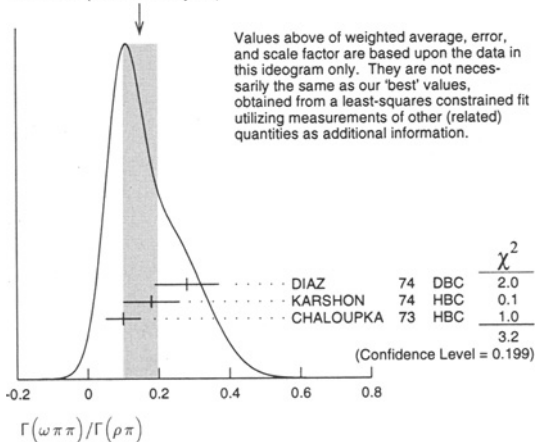
Meson Particle Listings

 $a_2(1320), f_0(1370)$

• • • We do not use the following data for averages, fits, limits, etc. • • •

0.29 ± 0.08	140	24 KARSHON	74	HBC	0	$4.9 \pi^+ p$
0.10 ± 0.04	60	24 KARSHON	74	HBC	+	$4.9 \pi^+ p$
0.19 ± 0.08		DEFOIX	73	HBC	0	$0.7 \bar{p} p$

24 KARSHON 74 suggest an additional $I = 0$ state strongly coupled to $\omega \pi \pi$ which could explain discrepancies in branching ratios and masses. We use a central value and a systematic spread.

WEIGHTED AVERAGE
0.15±0.05 (Error scaled by 1.3) $\Gamma(\eta(958)\pi)/\Gamma(\eta\pi)$

VALUE	DOCUMENT ID	TECN	COMMENT	Γ_5/Γ_2
-------	-------------	------	---------	---------------------

0.037±0.006 OUR AVERAGE

0.032±0.009

0.047±0.010±0.004

0.034±0.008±0.005

25 Using $B(\eta' \rightarrow \pi^+ \pi^- \eta) = 0.441$, $B(\eta \rightarrow \gamma\gamma) = 0.389$ and $B(\eta \rightarrow \pi^+ \pi^- \pi^0) = 0.236$.

 $\Gamma(K\bar{K})/\Gamma(\eta\pi)$

VALUE	DOCUMENT ID	TECN	COMMENT	Γ_4/Γ_2
-------	-------------	------	---------	---------------------

0.08±0.02

• • • We do not use the following data for averages, fits, limits, etc. • • •

0.08±0.02	26 BERTIN	98B	OBLX	$0.0 \bar{p} p \rightarrow K^\pm K_S \pi^\mp$
-----------	----------------	-----	------	---

26 Using $\eta\pi\pi$ data from AMSLER 94D.

 $a_2(1320)$ REFERENCES

BARBERIS	98B	PL B422 399	D. Barberis et al.	(WA102 Collab.)
BERTIN	98B	PL B434 180	A. Bertin et al.	(OBELIX Collab.)
ABELE	97C	PL B404 179	A. Abele et al.	(Crystal Barrel Collab.)
ACCIARRI	97T	PL B413 147	M. Acciari et al.	(L3 Collab.)
ALBRECHT	97B	ZPHY C74 469	H. Albrecht et al.	(ARGUS Collab.)
THOMPSON	97	PRL 79 1630	D.R. Thompson et al.	(E852 Collab.)
AMELIN	96	ZPHY C70 71	D.V. Amelin et al.	(SERP, TBIL.)
AMSLER	94D	PL B333 277	C. Amisler et al.	(Crystal Barrel Collab.)
AOYAGI	93	PL B314 246	H. Aoyagi et al.	(BKEI Collab.)
ARMSTRONG	93C	PL B307 394	T.A. Armstrong et al.	(FNAL, FERR, GENO+)
BELADIDZE	93	PL 313 276	G.M. Beladidze et al.	(VES Collab.)
CONDO	93	PR D48 3045	G.T. Condo et al.	(SLAC Hybrid Collab.)
ALDE	92B	ZPHY C54 549	D.M. Alde et al.	(SERP, BELG, LANL, LAPP+)
BELADIDZE	92	ZPHY C54 235	G.M. Beladidze et al.	(VES Collab.)
ALBRECHT	90G	ZPHY C48 183	H. Albrecht et al.	(ARGUS Collab.)
ARMSTRONG	90	ZPHY C48 213	T.A. Armstrong, M. Benayoun, W. Beusch	(MD-1 Collab.)
BARU	90	ZPHY C48 581	S.E. Baru et al.	(CELLO Collab.)
BEHREND	90C	ZPHY C46 583	H.J. Behrend et al.	(Mark II Collab.)
BUTLER	90	PR D42 1368	F. Butler et al.	(JADE Collab.)
OEST	90	ZPHY C47 343	T. Oest et al.	(DM2 Collab.)
AUGUSTIN	89	NP B320 1	J.E. Augustin, G. Cosme	(NOVO)
VOROBYEV	88	SJNP 48 273	P.V. Vorobiev et al.	(NOVO)
ALTHOFF	86	ZPHY C31 537	M. Althoff et al.	(TASSO Collab.)
ANTREASVAM	86	PR D33 1847	D. Antreasyan et al.	(Crystal Ball Collab.)
BERGER	84C	PL 149B 427	C. Berger et al.	(PLUTO Collab.)
BEHREND	83B	PL 125B 518	H.J. Behrend et al.	(CELLO Collab.)
CHANGIR	82	PL 117B 123	S. Cihangir et al.	(FNAL, MINN, ROCH)
CLELAND	82B	NP B208 228	W.E. Cleland et al.	(DURH, GEVA, LAUS+)
EDWARDS	82F	PL 110B 82	C. Edwards et al.	(CIT, HARV, PRIN+)
DELFOSE	81	NP B183 349	A. Delfosse et al.	(GEVA, LAUS)
EVANGELISTA	81	NP B178 197	C. Evangelista et al.	(BARI, BONN, CERN+)
CHABAUD	80	NP B175 189	V. Chabaud et al.	(CERN, MPIM, AMST)
DAUM	80C	PL 89B 276	C. Daum et al.	(AMST, CERN, CRAC, MPIM+)
BALTAY	78B	PR D17 62	C. Baltay et al.	(COLU, BING)
CHABAUD	78	NP B145 349	V. Chabaud et al.	(CERN, MPIM)
FERRERSORIA	78	PL 74B 287	A. Ferrer Soria et al.	(ORSAY, CERN, COEF+)
HYAMS	78	NP B146 303	B.D. Hyams et al.	(CERN, MPIM, ATEN)
MARTIN	78D	PL 74B 417	A.D. Martin et al.	(DURH, GEVA) JP
MAY	77	PR D16 1983	E.N. May et al.	(ROCH, CORN)
FORINO	76	NC 35A 465	A. Forino et al.	(BGNA, FIRZ, GENO, MILA+)
MARGULIE	75	PR D14 667	M. Margulies et al.	(BNL, CUNY)

EMMS	75	PL 98B 117	M.J. Emms et al.	(BIRM, DURH, RHEL) JP
WAGNER	75	PL 98B 201	F. Wagner, M. Tabak, D.M. Chew	(LBL) JP
DIAZ	74	PRL 32 260	F. Diaz et al.	(CASE, CMU)
KARSHON	74	PRL 32 852	U. Karshon et al.	(REHO)
ANTIPOV	73	NP B63 175	Y.M. Antipov et al.	(CERN, SERP) JP
ANTIPOV	73C	NP B63 153	Y.M. Antipov et al.	(CERN, SERP) JP
CHALOUKPA	73	PL 44B 211	V. Chaloupka et al.	(CERN)
CONFORTO	73	PL 45B 154	G. Conforto et al.	(EFI, FNAL, TATO+)
DEFOIX	73	PL 43B 141	C. Defoix et al.	(CDEF)
EISENSTEIN	73	PR D7 278	L. Eisenstein et al.	(ILL)
KEY	73	PRL 30 503	A.W. Key et al.	(TNTO, EFI, FNAL, WISC)
TOET	73	NP B63 298	D.Z. Toet et al.	(NIJM, BONN, DURH, TORI)
DAMERI	72	NC 9A 1	M. Dameri et al.	(GENO, MILA, SACL)
EISENBERG	72	PR D5 15	Y. Eisenberg et al.	(REHO, SLAC, TELA)
ESPIGAT	72	NP B36 93	P. Espigat et al.	(CERN, CDEF)
FOLEY	72	PR D6 747	K.J. Foley et al.	(BNL, CUNY)
ALSTON...	71	PL 34B 156	M. Alston-Garnjost et al.	(LRL)
BARNHAM	71	PRL 26 1494	K.W.J. Barnham et al.	(LRL)
BINNIE	71	PL 36B 257	D.M. Binnie et al.	(LOIC, SHMP)
BOWEN	71	PRL 26 1663	D.R. Bowen et al.	(NEAS, STON)
GRAVER	71	PL 34B 156	G. Graver et al.	(CERN, MPIM)
ABRAMOV...	70B	NP B23 466	M. Abramovich et al.	(CERN) JP
ALSTON...	70	PL 33B 607	M. Alston-Garnjost et al.	(LRL)
BOECKMANN	70	NP B16 221	K. Boeckmann et al.	(BONN, DURH, NIJM+)
ASCOLI	68	PRL 20 1321	G. Ascoli et al.	(ILL) JP
BOESEBECK	68	NP B4 501	K. Boesebeck et al.	(AACH, BERL, CERN)
CHUNG	68	PR 165 1491	S.U. Chung et al.	(LRL)
CONTE	67	NC 51A 175	F. Conte et al.	(GENO, HAMB, MILA, SACL)

OTHER RELATED PAPERS

ALDE	99B	PAN 62 421	D. Alde et al.	(GAMS Collab.)
JENNI	83	Translated from YAF 62 462	P. Jenni et al.	(SLAC, LBL)
BEHREND	82C	PL 114B 378	H.J. Behrend et al.	(CELLO Collab.)
ADERHOLZ	65	PR 138B 897	M. Aderholz (AACH3, BERL, BIRM, BONN, HAMB+)	(CELLO Collab.)
ALITTI	65	PL 15 69	J. Alitti et al.	(SACL, BGNA) JP
CHUNG	65	PRL 15 325	S.U. Chung et al.	(LRL)
FORINO	65B	PL 19 68	A. Forino et al.	(BGNA, BARI, FIRZ, ORSAY+)
LEFEBVRES	65	PL 19 434	F. Lefebvres et al.	(LRL)
SEIDLITZ	65	PRL 15 217	L. Seidlitz, O.J. Dahl, D.H. Miller	(LRL)
ADERHOLZ	64	PL 10 226	M. Aderholz et al.	(AACH3, BERL, BIRM+)
CHUNG	64	PRL 12 621	S.U. Chung et al.	(LRL)
GOLDBABER	64	PRL 12 336	G. Goldhaber et al.	(LRL, UCSD)
LANDER	64	PRL 13 346A	R.L. Lander et al.	(UCSD)

 $f_0(1370)$

$$I^G(J^{PC}) = 0^+(0^{++})$$

SCALAR MESONS

Written April 2000 by S. Spanier (SLAC) and N.A. Törnqvist (Helsinki).

Introduction: In contrast to the vector and tensor mesons, the identification of the scalar mesons is a long-standing puzzle. The number of publications since our last issue indicates great activity in that field. Scalar resonances are difficult to resolve because of their large decay widths causing a strong overlap between resonances and background, and at the same time, several decay channels open up within a short mass interval. In addition, especially the $\bar{K}K$ and $\eta\eta$ thresholds produce important sharp cusps in the energy dependence of the resonant amplitude. Furthermore, one expects non- $\bar{q}q$ scalar objects, like glueballs and multiquark states, in the mass range below 1800 MeV.

Scalars are produced, for example, in $\bar{p}p$ annihilation (high statistics), πN scattering on polarized/unpolarized targets, central production, J/ψ decays, D - and K -meson decays, $\gamma\gamma$ formation, and ϕ radiative decays. Experiments are accompanied by the development of theoretical models for the reaction amplitudes, which are based on common fundamental principles of two-body unitarity, analyticity, Lorentz invariance, and chiral- and flavor-symmetry using different techniques (K -matrix formalism, N/D -method, Dalitz Tuan ansatz, unitarized quark models with coupled channels, effective chiral field theories like the linear sigma model, etc.).

The mass and width of a resonance are found from the position of the nearest pole in the T matrix (or equivalently, in the S matrix) at an unphysical sheet of the complex energy plane: $(E - i\frac{\Gamma}{2})$. It is important to realize that only in the

Meson Particle Listings

 $f_0(1370)$

case of well-separated resonances, far away from the opening of decay channels, does the naive Breit-Wigner parameterization (or K -matrix pole parameterization) agree with the T -matrix pole position in the amplitude.

In this note, we discuss all light scalars organized in the listings under the entries ($I = 1/2$) $K^*(1430)$, ($I = 1$) $a_0(980)$, $a_0(1450)$, and ($I = 0$) σ or $f_0(400-1200)$, $f_0(980)$, $f_0(1370)$, and $f_0(1500)$. This list is minimal and does not necessarily exhaust the list of actual resonances. The ($I = 2$) $\pi\pi$ and ($I = 3/2$) $K\pi$ phase shifts do not exhibit any resonant behavior.

See also our notes in previous issues for further comments on *e.g.*, scattering lengths and older papers.

The $I = 1/2$ States: The $K^*(1430)$ (ASTON 88) is perhaps the least controversial of the light scalar mesons. The $K\pi$ phase shift rises smoothly from the threshold, passes 90° at 1350 MeV, and continues to rise to about 170° at 1600 MeV, the first important inelastic threshold $K\eta'(958)$. Thus, it behaves like a single broad, nearly elastic resonance. ABELE 98, analyzing the $\bar{K}K\pi$ channel of $\bar{p}p$ annihilation at rest, finds the T -matrix pole parameters, $m \approx 1430$ MeV and $\Gamma \approx 290$ MeV, while the K -matrix pole of the same data is about 1340 MeV. This agrees with the LASS (ASTON 88) determination.

It should, however, be noted that several authors (BLACK 98, 99, DELBOURGO 98, ISHIDA 99, OLLER 99,99C, BEVEREN 99) have introduced a light " $\kappa(900)$ " meson, which in the model interferes destructively with a large background. This makes the existence of a such light state very model dependent.

The $I = 1$ States: Two isovector states are known, the established $a_0(980)$ and the $a_0(1450)$ found by the Crystal Barrel experiment (AMSLER 94D). Independently of any model about the nature of the $a_0(980)$, the $\bar{K}K$ component in the wave function of this state must be large: the $a_0(980)$ lies close to the opening of the $\bar{K}K$ channel to which it couples strongly. This gives an important cusp-like behavior in the resonant amplitude. Hence, its mass and width parameters are strongly distorted. To reveal its true coupling constants, a coupled channel model with energy-dependent widths and mass shift contributions must be applied.

In our previous editions, the relative coupling $\bar{K}K/\pi\eta$ was only determined indirectly from $f_1(1285)$ (CORDEN 78, DEFOIX 72) or $\eta(1410)$ decays (BAI 90C, BOLTON 92B, AMSLER 95C), or from the line shape observed in the $\pi\eta$ decay mode (FLATTE 76, AMSLER 94D, BUGG 94, JANSSEN 95). From the analysis of $\pi\pi\eta$ and $\bar{K}K\pi$ final states of $\bar{p}p$ annihilation at rest, a relative production ratio $B(\bar{p}p \rightarrow \pi a_0; a_0 \rightarrow \bar{K}K)/B(\bar{p}p \rightarrow \pi a_0; a_0 \rightarrow \pi\eta) = 0.23 \pm 0.05$ is obtained by (ABELE 98). Tuning of the couplings in a coupled channel formula to reproduce the production ratio for the integrated mass distributions gives a relative branching ratio $\Gamma(\bar{K}K)/\Gamma(\pi\eta) = 1.03 \pm 0.14$. The analysis of the $\bar{p}p$ annihilation data also found that the width determined from the T -matrix pole is 92 ± 8 MeV, while the observed width of the peak in the $\pi\eta$ mass spectrum is about 45 MeV. In all

measurements listed in our table, the mass position agrees on a value near 980 MeV, but the width takes values between 50 and 300 MeV due to the different applied models.

The $a_0(1450)$ is seen by the Crystal Barrel experiment in its $\pi\eta$, $\bar{K}K$, and $\pi\eta'(958)$ decay modes. The relative couplings to the different final states are found to be close to SU(3)-flavor predictions for an ordinary $\bar{q}q$ meson. The OBELIX experiment (BERTIN 98B) finds two solutions in the $K_S K^\pm \pi^\mp$ final state of the $\bar{p}p$ annihilation, one at 1480 MeV and one with a mass value close to that of $a_2(1320)$, which is preferred by their fit, and by the low angular momentum in the production. The broad structure at about 1300 MeV observed in $\pi N \rightarrow \bar{K}KN$ reactions needs further confirmation in existence and isospin assignment.

The $I = 0$ States: The $I = 0 J^{PC} = 0^{++}$ sector is the most complex one, both experimentally and theoretically. The data have been obtained from $\pi\pi$, $\bar{K}K$, $\eta\eta$, 4π , and $\eta\eta'(958)$ systems produced in S wave. From the high-statistics data sets collected from $\bar{p}p$ annihilation at rest into $\pi^0 f_0$, where the f_0 decays into the channels mentioned above, one concludes that at least four poles are needed in the mass range from the $\pi\pi$ threshold to about 1600 MeV. The claimed isoscalar resonances are found under separate entries σ or $f_0(400-1200)$, $f_0(980)$, $f_0(1370)$, and $f_0(1500)$.

Below 1100 MeV, the important data come from the $\pi\pi$ and $\bar{K}K$ final states. Information on the $\pi\pi$ S -wave phase shift $\delta_0^I = \delta_0^0$ was already extracted 20 years ago from the πN scattering with unpolarized (GRAYER 74) and polarized targets (BECKER 79), and near threshold from the K_{e4} -decay (ROSSELET 77). The $\pi\pi$ S -wave inelasticity is not accurately known, and the reported $\pi\pi \rightarrow \bar{K}K$ cross sections (WETZEL 76, POLYCHRONAKOS 79, COHEN 80, and ETKIN 82B) may have large uncertainties. The πN data (GRAYER 74, BECKER 79) have been reanalyzed in combination with the $\bar{p}p$ annihilation data (KAMINSKI 97). Two out of four relevant solutions are found, with the S -wave phase shift rising slower than the P wave [$\rho(770)$], which is used as a reference. One of these corresponds to the well-known "down" solution of GRAYER 74. The other "up" solution shows a decrease of the modulus in the mass interval between 800–980 MeV. Both solutions exhibit a sudden drop in the modulus and inelasticity at 1 GeV, due to the appearance of $f_0(980)$, which is very close to the opening of the $\bar{K}K$ threshold. The phase shift δ_0^0 rises smoothly up to this point, where it jumps by 120° (in the "up") or 140° (in the "down") solution to reach 230° , and then both continue to rise slowly.

SVEC 97 suggests the existence of a narrow state at 750 MeV, with a small width of 100 to 200 MeV in his analysis of the πN (polarized) data, from 600 to 900 MeV. Such a solution is also found by (KAMINSKI 97) using the CERN-Munich (-Cracow) data considering both the π - and $a_1(1260)$ -exchange in the reaction amplitudes. However, they show that unitarity is violated for this solution. Therefore, a narrow, light f_0 state below 900 MeV is excluded (KAMINSKI 97, 00). Also, the

$2\pi^0$ invariant mass spectra of the $\bar{p}p$ annihilation at rest (AMSLER 95, ABELE 96), and the central collision (ALDE 97), do not show a narrow resonance below 900 MeV, and these data are consistently described with the standard “down” solution (GRAYNER 74, KAMINSKI 97), which allows for the existence of the broad ($\Gamma \approx 500$ MeV) σ listed under $f_0(400-1200)$. The σ is difficult to establish experimentally without models. It is expected to be very broad, and so can be easily distorted by large background from contact terms, crossed channel exchanges, the $f_0(1370)$, and other dynamical features. Further information on this object is expected from the analysis of three body decays of the D meson, *e.g.*, $D \rightarrow \sigma\pi \rightarrow 3\pi$ (E791 experiment).

The $f_0(980)$ interferes destructively with the background leading to a dip in the $\pi\pi$ spectrum at the $\bar{K}K$ threshold. It changes from a dip into a peak structure in the $\pi^0\pi^0$ invariant mass spectrum of the reaction $\pi^-p \rightarrow \pi^0\pi^0n$ (ACHASOV 98E), with increasing four-momentum transfer to the $\pi^0\pi^0$ system, which means increasing the a_1 -exchange contribution in the amplitude, while the π -exchange decreases.

A meson resonance very well studied experimentally, is the $f_0(1500)$, seen by the Crystal Barrel experiment in five decay modes: $\pi\pi$, $\bar{K}K$, $\eta\eta$, $\eta\eta'$ (958), and 4π (AMSLER 95D, ABELE 96, and ABELE 98). Due to its interference with the $f_0(1370)$, the peak attributed to $f_0(1500)$ can appear shifted in mass to 1590 MeV, where it was observed by the GAMS Collaboration (BINON 83) in the $\eta\eta$ mass spectrum. For the dynamics in the resonant amplitude, they applied a sum of Breit-Wigner functions. In the central production (ANTINORI 95), a peak at a mass of 1450 MeV, having a width of 60 MeV, can be interpreted as the coherent sum of $f_0(1370)$ and $f_0(1500)$. The $\bar{p}p$ and $\bar{n}p/\bar{p}n$ reactions show a single enhancement at 1400 MeV in the invariant 4π mass (GASPERO 93, ADAMO 93, AMSLER 94, and ABELE 96). In the $5\pi^0$ channel (ABELE 96), this structure was resolved into $f_0(1500)$ and $f_0(1370)$, where the latter was found at somewhat lower mass at around 1300 MeV. An additional scalar had to be introduced in the reanalysis of the reaction $J/\psi(1S) \rightarrow \gamma 4\pi$ with a mass above 1700 MeV (BUGG 95). According to these investigations, the $f_0(1500)$ decay proceeds dominantly via $\sigma\sigma \rightarrow 4\pi$, where σ denotes the $\pi\pi$ S wave below the $\bar{K}K$ threshold. The $\bar{K}K$ decay of $f_0(1500)$ is suppressed (ABELE 98).

The determination of the $\pi\pi$ coupling of $f_0(1370)$ is aggravated by the strong overlap with the broad background from the $f_0(400-1200)$. Since it does not show up prominently in the 2π spectra, its mass and width are difficult to determine. As mentioned under the $I = 1$ states section, data on $\pi\pi \rightarrow \bar{K}K$ show an enhancement in the scalar partial wave at around 1300 MeV (WETZEL 76, COHEN 80, POLYCHRONAKOS 79, COSTA 80, and LONGACRE 86). According to the phase shift, the resonance is found at about 1400 MeV (COHEN 80), while a reanalysis (BUGG 96) claims a trend towards lower mass. The recent three-channel approach (KAMINSKI 99) supports the Crystal Barrel findings, and yields a broad $f_0(1370)$

with a mass above 1400 MeV and a narrow $f_0(1500)$. Here, the $f_0(1370)$ couples more strongly to $\pi\pi$ than to $\bar{K}K$. The $f_0(1370)$ appears explicitly as $\eta\eta$ resonance in the $\pi^0\eta\eta$ final state of the $\bar{p}p$ annihilation at rest (AMSLER 95D). Further information about the $\bar{K}K$ decay of scalars are most welcome, in particular those that can clearly distinguish the $I = 0$ from the $I = 1$ system.

For numerical estimates of coupling constants of the lightest scalars to two pseudoscalars, see ACHASOV 89E,G,I, KAMINSKI 99, AKHMETSHIN 99C. For example, from these estimates, the $f_0(980)$ coupling to $K\bar{K}$ is much larger than its coupling to $\pi\pi$, which is an important constraint to model builders.

Interpretation: Almost every model on scalar states agrees that the $K^*(1430)$ is the quark model $s\bar{u}$ or $s\bar{d}$ state.

If one uses the naive quark model (which may be too naive because of lack of chiral symmetry constraints), it is natural to assume the $f_0(1370)$, $a_0(1450)$, and the $K^*(1430)$ are in the same SU(3) flavor nonet being the $(\bar{u}u + \bar{d}d)$, $u\bar{d}$ and $u\bar{s}$ state, respectively. In this picture, the choice of the ninth member of the nonet is ambiguous. The controversially discussed candidates are $f_0(1500)$ and $f_0(1710)$ (assuming $J = 0$). Compared to the above states, the $f_0(1500)$ is very narrow. Thus, it is unlikely to be their isoscalar partner. It is also too light to be the first radial excitation. Allowing for a gluonic admixture, one can come to an arrangement among these states. See our note on “Non- $\bar{q}q$ states.”

The $f_0(980)$ and $a_0(980)$ are often interpreted as being multi-quark states (JAFJE 77), $\bar{K}K$ bound states (WEINSTEIN 90), or vacuum scalars (CLOSE 93A). These pictures are supported by the two-photon widths of these states, which are smaller than expected for naive $\bar{q}q$ mesons neglecting the large $\bar{K}K$ components in the wave function (BARNES 85, LI 91). The results from SND (ACHASOV 98I) reveal a much higher branching ratio for radiative $\phi \rightarrow \gamma f_0$ decays than expected for naive $\bar{q}q$ mesons, but also for $\bar{K}K$ molecules (CLOSE 93B).

On the other hand, the states $f_0(980)$ and $a_0(980)$ may form a low-mass state nonet with the σ as a central ingredient, and the $K^*(1430)$ (or “ $\kappa(900)$ ”). Attempts have been made to start directly from chiral symmetry or chiral Lagrangians (SCADRON 99, OLLER 98, 99, HANNAH 99, IGI 99, ISHIDA 99, and TORNQVIST 99), which all predict the existence of the σ meson near 500 MeV. Hence, *e.g.*, in the chiral linear sigma model, the σ is the $(\bar{u}u + \bar{d}d)$ state, and at the same time, also the chiral partner of the π . Hence, an experimental proof of its existence has become very important.

In the unitarized quark model with coupled channels, six of the light scalars are understood as different manifestations of bare quark model $\bar{q}q$ states (TORNQVIST 82,95,96, BEVEREN 86). The σ , $f_0(980)$, $f_0(1370)$, $a_0(980)$, $a_0(1450)$, and $K^*(1430)$ are described as unitarized remnants of strongly shifted and mixed $\bar{q}q$ 1^3P_0 states using six parameters. The $f_0(980)$ and $f_0(1370)$, as well as $a_0(980)$ and $a_0(1450)$, are two manifestations of the same $\bar{q}q$ state.

Meson Particle Listings

$f_0(1370)$

QCD sum rule techniques (ELIAS 99) generally find that the lightest scalars are nearly decoupled from $q\bar{q}$, which would suggest a non- $q\bar{q}$ structure. But this is also consistent with them being unitarized remnants of $q\bar{q}$ surrounded by large "clouds" of light mesons (forming part of the $q\bar{q}$ sea).

Other detailed models exist, which arrive at different groupings of the observed resonances. Further publications discussing the light scalar resonances are (see also our previous issues): AU 87, MORGAN 93, ZOU 94B, JANSSEN 95, KLEMPPT 95, ANISOVICH 98, LOCHER 98, ACHASOV 98D, NARISON 98, and MINKOWSKI 99.

$f_0(1370)$ T-MATRIX POLE POSITION

Note that $\Gamma \approx 2 \text{Im}(\sqrt{s_{\text{pole}}})$.

VALUE (MeV)	DOCUMENT ID	TECN	COMMENT
(1200-1500)-i(150-250) OUR ESTIMATE			
• • • We do not use the following data for averages, fits, limits, etc. • • •			
$(1312 \pm 25 \pm 10) - i(109 \pm 22 \pm 15)$	BARBERIS	99D OMEG	$450 \rho\rho \rightarrow K^+ K^-$, $\pi^+ \pi^-$
$(1406 \pm 27) - i(80 \pm 6)$	¹ KAMINSKI	99 RVUE	$\pi\pi \rightarrow \pi\pi, K\bar{K}, \sigma\sigma$
$(1300 \pm 20) - i(120 \pm 20)$	ANISOVICH	98B RVUE	Compilation
$(1290 \pm 15) - i(145 \pm 15)$	BARBERIS	97B OMEG	$450 \rho\rho \rightarrow pp2(\pi^+ \pi^-)$
$(1548 \pm 40) - i(560 \pm 40)$	BERTIN	97C OBLX	$0.0 \bar{p}p \rightarrow \pi^+ \pi^- \pi^0$
$(1380 \pm 40) - i(180 \pm 25)$	ABELE	96B CBAR	$0.0 \bar{p}p \rightarrow \pi^0 K_L^0 K_L^0$
$(1300 \pm 15) - i(115 \pm 8)$	BUGG	96 RVUE	
$(1330 \pm 50) - i(150 \pm 40)$	² AMSLER	95B CBAR	$\bar{p}p \rightarrow 3\pi^0$
$(1360 \pm 35) - i(150-300)$	² AMSLER	95C CBAR	$\bar{p}p \rightarrow \pi^0 \eta\eta$
$(1390 \pm 30) - i(190 \pm 40)$	³ AMSLER	95D CBAR	$\bar{p}p \rightarrow 3\pi^0, \pi^0 \eta\eta, \pi^0 \pi^0 \eta$
$1346 - i249$	^{4,5} JANSSEN	95 RVUE	$\pi\pi \rightarrow \pi\pi, K\bar{K}$
$1214 - i168$	^{5,6} TORNVQVIST	95 RVUE	$\pi\pi \rightarrow \pi\pi, K\bar{K}, K\pi, \eta\pi$
$1364 - i139$	AMSLER	94D CBAR	$\bar{p}p \rightarrow \pi^0 \pi^0 \eta$
$(1365^{+20}_{-55}) - i(134 \pm 35)$	ANISOVICH	94 CBAR	$\bar{p}p \rightarrow 3\pi^0, \pi^0 \eta\eta$
$(1340 \pm 40) - i(127^{+30}_{-20})$	⁷ BUGG	94 RVUE	$\bar{p}p \rightarrow 3\pi^0, \eta\pi\pi^0, \eta\pi^0 \pi^0$
$(1430 \pm 5) - i(73 \pm 13)$	⁸ KAMINSKI	94 RVUE	$\pi\pi \rightarrow \pi\pi, K\bar{K}$
$1515 - i214$	^{5,9} ZOU	93 RVUE	$\pi\pi \rightarrow \pi\pi, K\bar{K}$
$1420 - i220$	¹⁰ AU	87 RVUE	$\pi\pi \rightarrow \pi\pi, K\bar{K}$

¹ T-matrix pole on sheet -+.
² Supersedes ANISOVICH 94.
³ Coupled-channel analysis of $\bar{p}p \rightarrow 3\pi^0, \pi^0 \eta\eta$, and $\pi^0 \pi^0 \eta$ on sheet IV. Demonstrates explicitly that $f_0(400-1200)$ and $f_0(1370)$ are two different poles.
⁴ Analysis of data from FALVARD 88.
⁵ The pole is on Sheet III. Demonstrates explicitly that $f_0(400-1200)$ and $f_0(1370)$ are two different poles.
⁶ Uses data from BEIER 72b, OCHS 73, HYAMS 73, GRAYER 74, ROSSELET 77, CASON 83, ASTON 88, and ARMSTRONG 91b. Coupled channel analysis with flavor symmetry and all light two-pseudoscalars systems.
⁷ Reanalysis of ANISOVICH 94 data.
⁸ T-matrix pole on sheet III.
⁹ Analysis of data from OCHS 73, GRAYER 74, and ROSSELET 77.
¹⁰ Analysis of data from OCHS 73, GRAYER 74, BECKER 79, and CASON 83.

$f_0(1370)$ BREIT-WIGNER MASS OR K-MATRIX POLE PARAMETER

VALUE (MeV)	DOCUMENT ID	TECN	COMMENT
1200 to 1500 OUR ESTIMATE			
• • • We do not use the following data for averages, fits, limits, etc. • • •			
1308 ± 10	BARBERIS	99B OMEG	$450 \rho\rho \rightarrow p_S p_f \pi^+ \pi^-$
1315 ± 50	BELLAZZINI	99 GAM4	$450 \rho\rho \rightarrow \rho\rho \pi^0 \pi^0$
1315 ± 30	ALDE	98 GAM4	$100 \pi^- p \rightarrow \pi^0 \pi^0 \eta$
1280 ± 55	BERTIN	98 OBLX	$0.05-0.405 \bar{p}p \rightarrow \pi^+ \pi^+ \pi^-$
1186	¹¹ TORNVQVIST	95 RVUE	$\pi\pi \rightarrow \pi\pi, K\bar{K}, K\pi, \eta\pi$
1472 ± 12	ARMSTRONG	91 OMEG	$300 \rho\rho \rightarrow \rho\rho \pi\pi, \rho\rho K\bar{K}$
1275 ± 20	BREAKSTONE	90 SFM	$62 \rho\rho \rightarrow \rho\rho \pi^+ \pi^-$
1420 ± 20	AKESSON	86 SPEC	$63 \rho\rho \rightarrow \rho\rho \pi^+ \pi^-$
1256	FROGGATT	77 RVUE	$\pi^+ \pi^-$ channel

¹¹ Uses data from BEIER 72b, OCHS 73, HYAMS 73, GRAYER 74, ROSSELET 77, CASON 83, ASTON 88, and ARMSTRONG 91b. Coupled channel analysis with flavor symmetry and all light two-pseudoscalars systems.

$K\bar{K}$ MODE

VALUE (MeV)	DOCUMENT ID	TECN	COMMENT
• • • We do not use the following data for averages, fits, limits, etc. • • •			
1440 ± 50	BOLONKIN	88 SPEC	$40 \pi^- p \rightarrow K_S^0 K_S^0 \eta$
1463 ± 9	ETKIN	82b MPS	$23 \pi^- p \rightarrow n 2K_S^0$
1425 ± 15	WICKLUND	80 SPEC	$6 \pi N \rightarrow K^+ K^- N$
~ 1300	POLYCHRO...	79 STRC	$7 \pi^- p \rightarrow n 2K_S^0$

4π MODE $2(\pi\pi)_S + \rho\rho$

VALUE (MeV)	DOCUMENT ID	TECN	COMMENT
• • • We do not use the following data for averages, fits, limits, etc. • • •			
1374 ± 38	AMSLER	94 CBAR	$0.0 \bar{p}p \rightarrow \pi^+ \pi^- 3\pi^0$
1345 ± 12	ADAMO	93 OBLX	$\bar{p}p \rightarrow 3\pi^+ 2\pi^-$
1386 ± 30	GASPERO	93 DBC	$0.0 \bar{p}p \rightarrow 2\pi^+ 3\pi^-$

$\eta\eta$ MODE

VALUE (MeV)	DOCUMENT ID	TECN	COMMENT
• • • We do not use the following data for averages, fits, limits, etc. • • •			
1430	AMSLER	92 CBAR	$0.0 \bar{p}p \rightarrow \pi^0 \eta\eta$
1220 ± 40	ALDE	86D GAM4	$100 \pi^- p \rightarrow n 2\eta$

$f_0(1370)$ BREIT-WIGNER WIDTH

VALUE (MeV)	DOCUMENT ID	TECN	COMMENT
200 to 500 OUR ESTIMATE			
• • • We do not use the following data for averages, fits, limits, etc. • • •			
222 ± 20	BARBERIS	99B OMEG	$450 \rho\rho \rightarrow p_S p_f \pi^+ \pi^-$
255 ± 60	BELLAZZINI	99 GAM4	$450 \rho\rho \rightarrow \rho\rho \pi^0 \pi^0$
190 ± 50	ALDE	98 GAM4	$100 \pi^- p \rightarrow \pi^0 \pi^0 \eta$
323 ± 13	BERTIN	98 OBLX	$0.05-0.405 \bar{p}p \rightarrow \pi^+ \pi^+ \pi^-$
350	¹² TORNVQVIST	95 RVUE	$\pi\pi \rightarrow \pi\pi, K\bar{K}, K\pi, \eta\pi$
195 ± 33	ARMSTRONG	91 OMEG	$300 \rho\rho \rightarrow \rho\rho \pi\pi, \rho\rho K\bar{K}$
285 ± 60	BREAKSTONE	90 SFM	$62 \rho\rho \rightarrow \rho\rho \pi^+ \pi^-$
460 ± 50	AKESSON	86 SPEC	$63 \rho\rho \rightarrow \rho\rho \pi^+ \pi^-$
~ 400	¹³ FROGGATT	77 RVUE	$\pi^+ \pi^-$ channel

¹² Uses data from BEIER 72b, OCHS 73, HYAMS 73, GRAYER 74, ROSSELET 77, CASON 83, ASTON 88, and ARMSTRONG 91b. Coupled channel analysis with flavor symmetry and all light two-pseudoscalars systems.
¹³ Width defined as distance between 45 and 135° phase shift.

$K\bar{K}$ MODE

VALUE (MeV)	DOCUMENT ID	TECN	COMMENT
• • • We do not use the following data for averages, fits, limits, etc. • • •			
250 ± 80	BOLONKIN	88 SPEC	$40 \pi^- p \rightarrow K_S^0 K_S^0 \eta$
118^{+138}_{-16}	ETKIN	82b MPS	$23 \pi^- p \rightarrow n 2K_S^0$
160 ± 30	WICKLUND	80 SPEC	$6 \pi N \rightarrow K^+ K^- N$
~ 150	POLYCHRO...	79 STRC	$7 \pi^- p \rightarrow n 2K_S^0$

4π MODE $2(\pi\pi)_S + \rho\rho$

VALUE (MeV)	DOCUMENT ID	TECN	COMMENT
• • • We do not use the following data for averages, fits, limits, etc. • • •			
375 ± 61	AMSLER	94 CBAR	$0.0 \bar{p}p \rightarrow \pi^+ \pi^- 3\pi^0$
398 ± 26	ADAMO	93 OBLX	$\bar{p}p \rightarrow 3\pi^+ 2\pi^-$
310 ± 50	GASPERO	93 DBC	$0.0 \bar{p}p \rightarrow 2\pi^+ 3\pi^-$

$\eta\eta$ MODE

VALUE (MeV)	DOCUMENT ID	TECN	COMMENT
• • • We do not use the following data for averages, fits, limits, etc. • • •			
250	AMSLER	92 CBAR	$0.0 \bar{p}p \rightarrow \pi^0 \eta\eta$
320 ± 40	ALDE	86D GAM4	$100 \pi^- p \rightarrow n 2\eta$

$f_0(1370)$ DECAY MODES

Mode	Fraction (Γ_i/Γ)
Γ_1 $\pi\pi$	seen
Γ_2 4π	seen
Γ_3 $4\pi^0$	seen
Γ_4 $2\pi^+ 2\pi^-$	seen
Γ_5 $\pi^+ \pi^- 2\pi^0$	seen
Γ_6 $\rho\rho$	
Γ_7 $2(\pi\pi)_S$ -wave	seen
Γ_8 $\eta\eta$	seen
Γ_9 $K\bar{K}$	seen
Γ_{10} $\gamma\gamma$	seen
Γ_{11} $e^+ e^-$	not seen

Meson Particle Listings

$\pi_1(1400)$, $f_1(1420)$

$\pi_1(1400)$
was $\hat{\rho}(1405)$

$$I^G(J^{PC}) = 1^-(1^-+)$$

OMITTED FROM SUMMARY TABLE

See also the mini-review under non- $q\bar{q}$ candidates. (See the index for the page number.)

$\pi_1(1400)$ MASS

VALUE (MeV)	DOCUMENT ID	TECN	CHG	COMMENT
1376 ± 17 OUR AVERAGE				
1360 ± 25	ABELE 99	CBAR		0.0 $\bar{p}p \rightarrow \pi^0 \pi^0 \eta$
1400 ± 20 ± 20	ABELE 98B	CBAR		0.0 $\bar{p}n \rightarrow \pi^- \pi^0 \eta$
1370 ± 16 ⁺⁵⁰ / ₋₃₀	¹ THOMPSON 97	MPS		18 $\pi^- p \rightarrow \eta \pi^- p$
• • • We do not use the following data for averages, fits, limits, etc. • • •				
1323.1 ± 4.6	² AOYAGI 93	BKEI		$\pi^- p \rightarrow \eta \pi^- p$
1406 ± 20	³ ALDE 88B	GAM4 0		100 $\pi^- p \rightarrow \eta \pi^0 n$

- ¹ Natural parity exchange.
- ² Unnatural parity exchange.
- ³ Seen in the P_0 -wave intensity of the $\eta \pi^0$ system, unnatural parity exchange.

$\pi_1(1400)$ WIDTH

VALUE (MeV)	DOCUMENT ID	TECN	CHG	COMMENT
300 ± 40 OUR AVERAGE				
220 ± 90	ABELE 99	CBAR		0.0 $\bar{p}p \rightarrow \pi^0 \pi^0 \eta$
310 ± 50 ⁺⁵⁰ / ₋₃₀	ABELE 98B	CBAR		0.0 $\bar{p}n \rightarrow \pi^- \pi^0 \eta$
385 ± 40 ⁺⁶⁵ / ₋₁₀₅	⁴ THOMPSON 97	MPS		18 $\pi^- p \rightarrow \eta \pi^- p$
• • • We do not use the following data for averages, fits, limits, etc. • • •				
143.2 ± 12.5	⁵ AOYAGI 93	BKEI		$\pi^- p \rightarrow \eta \pi^- p$
180 ± 20	⁶ ALDE 88B	GAM4 0		100 $\pi^- p \rightarrow \eta \pi^0 n$

- ⁴ Resolution is not unfolded, natural parity exchange.
- ⁵ Unnatural parity exchange.
- ⁶ Seen in the P_0 -wave intensity of the $\eta \pi^0$ system, unnatural parity exchange.

$\pi_1(1400)$ DECAY MODES

Mode	Fraction (Γ_i/Γ)
$\Gamma_1 \quad \eta \pi^0$	seen
$\Gamma_2 \quad \eta \pi^-$	seen
$\Gamma_3 \quad \eta' \pi$	possibly seen

$\pi_1(1400)$ BRANCHING RATIOS

$\Gamma(\eta \pi^0)/\Gamma_{total}$	DOCUMENT ID	TECN	CHG	COMMENT	Γ_1/Γ
VALUE					
• • • We do not use the following data for averages, fits, limits, etc. • • •					
not seen	PROKOSHKIN 95B	GAM4		100 $\pi^- p \rightarrow \eta \pi^0 n$	
not seen	⁷ BUGG 94	RVUE		$\bar{p}p \rightarrow \eta 2\pi^0$	
not seen	⁸ APEL 81	NICE 0		40 $\pi^- p \rightarrow \eta \pi^0 n$	

- ⁷ Using Crystal Barrel data.
- ⁸ A general fit allowing S, D, and P waves (including $m=0$) is not done because of limited statistics.

$\Gamma(\eta \pi^-)/\Gamma_{total}$	DOCUMENT ID	TECN	COMMENT	Γ_2/Γ
VALUE				
• • • We do not use the following data for averages, fits, limits, etc. • • •				
possibly seen	BELADIDZE 93	VES	$37\pi^- N \rightarrow \eta \pi^- N$	

$\Gamma(\eta' \pi)/\Gamma_{total}$	DOCUMENT ID	TECN	COMMENT	Γ_3/Γ
VALUE				
• • • We do not use the following data for averages, fits, limits, etc. • • •				
possibly seen	BELADIDZE 93	VES	$37\pi^- N \rightarrow \eta \pi^- N$	

$\Gamma(\eta' \pi)/\Gamma(\eta \pi^0)$	DOCUMENT ID	TECN	COMMENT	Γ_3/Γ_1
VALUE				
• • • We do not use the following data for averages, fits, limits, etc. • • •				
<0.80	95 BOUTEMEUR 90	GAM4	100 $\pi^- p \rightarrow 4\gamma n$	

$\pi_1(1400)$ REFERENCES

ABELE 99	PL B446 349	A. Abele et al.	(Crystal Barrel Collab.)
ABELE 98B	PL B423 175	A. Abele et al.	(Crystal Barrel Collab.)
THOMPSON 97	PRL 79 1630	D.R. Thompson et al.	(E852 Collab.)
PROKOSHKIN 95B	PAN 58 606	Y.D. Prokoshkin, S.A. Sadovsky	(SERP)
	Translated from YAF 58 662.		
BUGG 94	PR D50 4412	D.V. Bugg et al.	(LOQM)
AOYAGI 93	PL B314 246	H. Aoyagi et al.	(BKEI Collab.)
BELADIDZE 93	PL 313 276	G.M. Beladidze et al.	(VES Collab.)
BOUTEMEUR 90	Hadron 89 Conf. p 119	M. Boutemur, M. Poulet	(SERP, BELG, LANL+)
ALDE 88B	PL B205 397	D.M. Alde et al.	(SERP, BELG, LANL, LAPP) IGJPC
APEL 81	NP B193 269	W.D. Apel et al.	(SERP, CERN)

OTHER RELATED PAPERS

SADOVSKY 00	NP A655 131c	S.A. Sadovsky	(GAMS Collab.)
ALDE 99B	PAN 62 421	D. Alde et al.	
	Translated from YAF 62 462.		
CHUNG 99	PR D60 092001	S.U. Chung et al.	(BNL E852 Collab.)
GODFREY 99	RMP 71 1411	S. Godfrey, J. Napolitano	
DONNACHIE 98	PR D58 114012	A. Donnachie et al.	
LACOCK 97	PL B401 308	P. Lacock et al.	(EDIN, LIVP)
SVEC 97C	PR D56 4355	M. Svec	(MCGI)
PROKOSHKIN 95C	PAN 58 853	Y.D. Prokoshkin, S.A. Sadovsky	(SERP)
	Translated from YAF 58 921.		
KALASHNIK... 94	ZPHY C62 323	Y.S. Kalashnikova	(ITEP)
IDDIR 88	PL B205 564	F. Idir et al.	(ORSAY, TOKY)
TUAN 88	PL B213 537	S.F. Tuan, T. Ferbel, R.H. Dalitz	(HAWA, ROCH+)
ZIELINSKI 87	ZPHY C34 255	M. Zielinski	(ROCH)

$f_1(1420)$

$$I^G(J^{PC}) = 0^+(1^++)$$

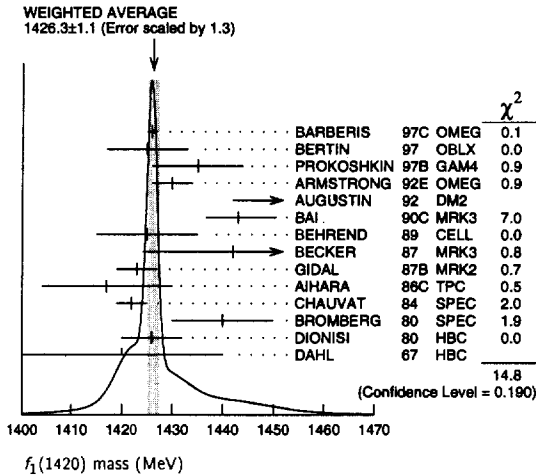
See the minireview under $\eta(1440)$.

$f_1(1420)$ MASS

VALUE (MeV)	EVTS	DOCUMENT ID	TECN	COMMENT
1426.3 ± 1.1 OUR AVERAGE				Error includes scale factor of 1.3. See the ideogram below.
1426 ± 1		BARBERIS 97C	OMEG	450 $pp \rightarrow \rho p K_S^0 K^\pm \pi^\mp$
1425 ± 8		BERTIN 97	OBLX	0.0 $\bar{p}p \rightarrow K^\pm(K^0) \pi^\mp \pi^+ \pi^-$
1435 ± 9		PROKOSHKIN 97B	GAM4	100 $\pi^- p \rightarrow \eta \pi^0 \pi^0 n$
1430 ± 4		¹ ARMSTRONG 92E	OMEG	85,300 $\pi^+ p, pp \rightarrow \pi^+ p, \rho p(K \bar{K} \pi)$
1462 ± 20		² AUGUSTIN 92	DM2	$J/\psi \rightarrow \gamma K \bar{K} \pi$
1443 ⁺⁷ / ₋₆ ⁺³ / ₋₂	1100	BAI 90C	MRK3	$J/\psi \rightarrow \gamma K_S^0 K^\pm \pi^\mp$
1425 ± 10	17	BEHREND 89	CELL	$\gamma \gamma \rightarrow K_S^0 K^\pm \pi^\mp$
1442 ± 5 ⁺¹⁰ / ₋₁₇	111	BECKER 87	MRK3	$e^+ e^- \rightarrow \omega K \bar{K} \pi$
1423 ± 4		GIDAL 87B	MRK2	$e^+ e^- \rightarrow e^+ e^- K \bar{K} \pi$
1417 ± 13	13	AIHARA 86C	TPC	$e^+ e^- \rightarrow e^+ e^- K \bar{K} \pi$
1422 ± 3		CHAUVAT 84	SPEC	ISR 31.5 pp
1440 ± 10		³ BROMBERG 80	SPEC	100 $\pi^- p \rightarrow K \bar{K} \pi X$
1426 ± 6	221	DIONISI 80	HBC	$4 \pi^- p \rightarrow K \bar{K} \pi n$
1420 ± 20		DAHL 67	HBC	1.6-4.2 $\pi^- p$
• • • We do not use the following data for averages, fits, limits, etc. • • •				
1430.8 ± 0.9		⁴ SOSA 99	SPEC	$pp \rightarrow P_{slow} (K_S^0 K^+ \pi^-) P_{fast}$
1433.4 ± 0.8		⁴ SOSA 99	SPEC	$pp \rightarrow P_{slow} (K_S^0 K^- \pi^+) P_{fast}$
1429 ± 3	389	ARMSTRONG 89	OMEG	300 $pp \rightarrow K \bar{K} \pi pp$
1425 ± 2	1520	ARMSTRONG 84	OMEG	85 $\pi^+ p, pp \rightarrow (\pi^+, \rho)(K \bar{K} \pi) p$
~ 1420		BITYUKOV 84	SPEC	32 $K^- p \rightarrow K^+ K^- \pi^0 \gamma$

- ¹ This result supersedes ARMSTRONG 84, ARMSTRONG 89.
- ² From fit to the $K^*(892) K 1^++$ partial wave.
- ³ Mass error increased to account for $a_0(980)$ mass cut uncertainties.
- ⁴ No systematic error given.

$f_1(1420)$



$f_1(1420)$ WIDTH

VALUE (MeV)	EVTS	DOCUMENT ID	TECN	COMMENT
55.5 ± 2.9 OUR AVERAGE				
58 ± 4		BARBERIS	97C OMEG	450 $pp \rightarrow p\bar{p}K_S^0 K^\pm \pi^\mp$
45 ± 10		BERTIN	97 OBLX	0.0 $\bar{p}p \rightarrow K^\pm(K^0)\pi^\mp\pi^\pm\pi^\mp$
90 ± 25		PROKOSHKIN	97B GAM4	100 $\pi^-p \rightarrow \eta\pi^0\pi^0n$
58 ± 10		⁵ ARMSTRONG	92E OMEG	85,300 $\pi^+p, pp \rightarrow \pi^+p, p\bar{p}(K\bar{K}\pi)$
129 ± 41		⁶ AUGUSTIN	92 DM2	$J/\psi \rightarrow \gamma K\bar{K}\pi$
68 ⁺²⁹ ₋₁₈ ⁺⁸ ₋₉	1100	BAI	90C MRK3	$J/\psi \rightarrow \gamma K_S^0 K^\pm \pi^\mp$
42 ± 22	17	BEHREND	89 CELL	$\gamma\gamma \rightarrow K_S^0 K^\pm \pi^\mp$
40 ⁺¹⁷ ₋₁₃ ± 5	111	BECKER	87 MRK3	$e^+e^- \rightarrow \omega K\bar{K}\pi$
35 ⁺⁴⁷ ₋₂₀	13	AIHARA	86C TPC	$e^+e^- \rightarrow e^+e^-K\bar{K}\pi$
47 ± 10		CHAUVAT	84 SPEC	ISR 31.5 pp
62 ± 14		BROMBERG	80 SPEC	100 $\pi^-p \rightarrow K\bar{K}\pi X$
40 ± 15	221	DIONISI	80 HBC	4 $\pi^-p \rightarrow K\bar{K}\pi n$
60 ± 20		DAHL	67 HBC	1.6-4.2 π^-p
^{•••} We do not use the following data for averages, fits, limits, etc. ^{•••}				
68.7 ± 2.9		⁷ SOSA	99 SPEC	$pp \rightarrow p_{slow}(K_S^0 K^+ \pi^-) p_{fast}$
58.8 ± 3.3		⁷ SOSA	99 SPEC	$pp \rightarrow p_{slow}(K_S^0 K^- \pi^+) p_{fast}$
58 ± 8	389	ARMSTRONG	89 OMEG	300 $pp \rightarrow K\bar{K}\pi pp$
62 ± 5	1520	ARMSTRONG	84 OMEG	85 $\pi^+p, pp \rightarrow (\pi^+, p)(K\bar{K}\pi)p$
~ 50		BITYUKOV	84 SPEC	32 $K^-p \rightarrow K^+K^- \pi^0 \gamma$

⁵ This result supersedes ARMSTRONG 84, ARMSTRONG 89.
⁶ From fit to the $K^*(892)K1^{++}$ partial wave.
⁷ No systematic error given.

$f_1(1420)$ DECAY MODES

Mode	Fraction (Γ_i/Γ)
Γ_1 $K\bar{K}\pi$	dominant
Γ_2 $K\bar{K}^*(892) + c.c.$	dominant
Γ_3 $\eta\pi\pi$	possibly seen
Γ_4 $a_0(980)\pi$	
Γ_5 $\pi\pi\rho$	
Γ_6 4π	
Γ_7 $\rho^0\gamma$	
Γ_8 $\phi\gamma$	seen

$f_1(1420)$ $\Gamma(i)\Gamma(\gamma\gamma)/\Gamma(\text{total})$

VALUE (keV)	CL%	DOCUMENT ID	TECN	COMMENT	$\Gamma_1\Gamma_0/\Gamma$
1.7 ± 0.4 OUR AVERAGE					
3.0 ± 0.9 ± 0.7		^{8,9} BEHREND	89 CELL	$e^+e^- \rightarrow e^+e^-K_S^0 K\pi$	
2.3 ^{+1.0} _{-0.9} ± 0.8		HILL	89 JADE	$e^+e^- \rightarrow e^+e^-K^\pm K_S^0 \pi^\mp$	
1.3 ± 0.5 ± 0.3		AIHARA	88B TPC	$e^+e^- \rightarrow e^+e^-K^\pm K_S^0 \pi^\mp$	
1.6 ± 0.7 ± 0.3		^{8,10} GIDAL	87B MRK2	$e^+e^- \rightarrow e^+e^-K\bar{K}\pi$	

^{•••} We do not use the following data for averages, fits, limits, etc. ^{•••}
 <8.0 95 JENNI 83 MRK2 $e^+e^- \rightarrow e^+e^-K\bar{K}\pi$
⁸ Assume a ρ -pole form factor.
⁹ A ϕ -pole form factor gives considerably smaller widths.
¹⁰ Published value divided by 2.

$f_1(1420)$ BRANCHING RATIOS

$\Gamma(K\bar{K}^*(892) + c.c.)/\Gamma(K\bar{K}\pi)$		Γ_2/Γ_1	
VALUE	DOCUMENT ID	TECN	COMMENT
^{•••} We do not use the following data for averages, fits, limits, etc. ^{•••}			
0.76 ± 0.06	BROMBERG	80 SPEC	100 $\pi^-p \rightarrow K\bar{K}\pi X$
0.86 ± 0.12	DIONISI	80 HBC	4 $\pi^-p \rightarrow K\bar{K}\pi n$

$\Gamma(\pi\pi\rho)/\Gamma(K\bar{K}\pi)$		Γ_5/Γ_1		
VALUE	CL%	DOCUMENT ID	TECN	COMMENT
^{•••} We do not use the following data for averages, fits, limits, etc. ^{•••}				
<0.3	95	CORDEN	78 OMEG	12-15 π^-p
<2.0		DAHL	67 HBC	1.6-4.2 π^-p

$\Gamma(\eta\pi\pi)/\Gamma(K\bar{K}\pi)$		Γ_3/Γ_1		
VALUE	CL%	DOCUMENT ID	TECN	COMMENT
<0.1	95	ARMSTRONG	91B OMEG	300 $pp \rightarrow p\bar{p}\eta\pi^+\pi^-$
^{•••} We do not use the following data for averages, fits, limits, etc. ^{•••}				
1.35 ± 0.75		KOPKE	89 MRK3	$J/\psi \rightarrow \omega\eta\pi\pi(K\bar{K}\pi)$
<0.6	90	GIDAL	87 MRK2	$e^+e^- \rightarrow e^+e^-\eta\pi^+\pi^-$
<0.5	95	CORDEN	78 OMEG	12-15 π^-p
1.5 ± 0.8		DEFOIX	72 HBC	0.7 $\bar{p}p$

$\Gamma(a_0(980)\pi)/\Gamma(\eta\pi\pi)$		Γ_4/Γ_3		
VALUE	CL%	DOCUMENT ID	TECN	COMMENT
>0.1	90	PROKOSHKIN	97B GAM4	100 $\pi^-p \rightarrow \eta\pi^0\pi^0n$
^{•••} We do not use the following data for averages, fits, limits, etc. ^{•••}				
not seen in either mode		ANDO	86 SPEC	8 π^-p
not seen in either mode		CORDEN	78 OMEG	12-15 π^-p
0.4 ± 0.2		DEFOIX	72 HBC	0.7 $\bar{p}p \rightarrow 7\pi$

$\Gamma(4\pi)/\Gamma(K\bar{K}^*(892) + c.c.)$		Γ_6/Γ_2		
VALUE	CL%	DOCUMENT ID	TECN	COMMENT
^{•••} We do not use the following data for averages, fits, limits, etc. ^{•••}				
<0.90	95	DIONISI	80 HBC	4 π^-p

$\Gamma(K\bar{K}\pi)/[\Gamma(K\bar{K}^*(892) + c.c.) + \Gamma(a_0(980)\pi)]$		$\Gamma_1/(\Gamma_2 + \Gamma_4)$		
VALUE	CL%	DOCUMENT ID	TECN	COMMENT
^{•••} We do not use the following data for averages, fits, limits, etc. ^{•••}				
0.65 ± 0.27		¹¹ DIONISI	80 HBC	4 π^-p
¹¹ Calculated using $\Gamma(K\bar{K})/\Gamma(\eta\pi) = 0.24 \pm 0.07$ for $a_0(980)$ fractions.				

$\Gamma(a_0(980)\pi)/\Gamma(K\bar{K}^*(892) + c.c.)$		Γ_4/Γ_2		
VALUE	CL%	DOCUMENT ID	TECN	COMMENT
0.04 ± 0.01 ± 0.01		BARBERIS	98C OMEG	450 $pp \rightarrow p_f f_1(1420) p_s$
^{•••} We do not use the following data for averages, fits, limits, etc. ^{•••}				
<0.04	68	ARMSTRONG	84 OMEG	85 π^+p

$\Gamma(4\pi)/\Gamma(K\bar{K}\pi)$		Γ_6/Γ_1		
VALUE	CL%	DOCUMENT ID	TECN	COMMENT
<0.62	95	ARMSTRONG	89G OMEG	85 $\pi p \rightarrow 4\pi X$

$\Gamma(\rho^0\gamma)/\Gamma_{\text{total}}$		Γ_7/Γ		
VALUE	CL%	DOCUMENT ID	TECN	COMMENT
<0.08	95	¹² ARMSTRONG	92C SPEC	300 $pp \rightarrow p\bar{p}\pi^+\pi^-\gamma$
¹² Using the data on the $\bar{K}K\pi$ mode from ARMSTRONG 89.				

$\Gamma(\rho^0\gamma)/\Gamma(K\bar{K}\pi)$		Γ_7/Γ_1		
VALUE	CL%	DOCUMENT ID	TECN	COMMENT
<0.02	95	BARBERIS	98C OMEG	450 $pp \rightarrow p_f f_1(1420) p_s$

$\Gamma(\phi\gamma)/\Gamma(K\bar{K}\pi)$		Γ_8/Γ_1		
VALUE	CL%	DOCUMENT ID	TECN	COMMENT
0.003 ± 0.001 ± 0.001		BARBERIS	98C OMEG	450 $pp \rightarrow p_f f_1(1420) p_s$

Meson Particle Listings

$f_1(1420), \omega(1420), f_2(1430)$

$f_1(1420)$ REFERENCES

SOSA	99	PRL 83 913	M. Sosa <i>et al.</i>	
BARBERIS	98C	PL B440 225	D. Barberis <i>et al.</i>	(WA102 Collab.)
BARBERIS	97C	PL B413 225	D. Barberis <i>et al.</i>	(WA102 Collab.)
BERTIN	97	PL B400 226	A. Bertin <i>et al.</i>	(OBELIX Collab.)
PROKOSHKIN	97B	SPD 42 298		
Translated from DANS 354 751.				
ARMSTRONG	92C	ZPHY C54 371	T.A. Armstrong <i>et al.</i>	(ATHU, BARI, BIRM+)
ARMSTRONG	92E	ZPHY 56 29	T.A. Armstrong <i>et al.</i>	(ATHU, BARI, BIRM+) JPC
AUGUSTIN	92	PR D46 1951	J.E. Augustin, G. Cosme	(DM2 Collab.)
ARMSTRONG	91B	ZPHY C52 389	T.A. Armstrong <i>et al.</i>	(ATHU, BARI, BIRM+)
BAI	90C	PRL 65 2507	Z. Bai <i>et al.</i>	(Mark III Collab.)
ARMSTRONG	89	PL B221 216	T.A. Armstrong <i>et al.</i>	(CERN, CDF, BIRM+) JPC
ARMSTRONG	89G	ZPHY C43 55	T.A. Armstrong <i>et al.</i>	(CERN, BIRM, BARI+)
BEHREND	89	ZPHY C42 357	H.J. Behrend <i>et al.</i>	(CELLIO Collab.)
HILL	89	ZPHY C42 355	P. Hill <i>et al.</i>	(JADE Collab.) JP
KOPKE	89	PRPL 174 67	L. Kopke <i>et al.</i>	(TPC-2 γ Collab.)
AIHARA	88B	PL B209 107	H. Aihsara <i>et al.</i>	(TPC-2 γ Collab.) JP
BECKER	87	PRL 59 186	J.J. Becker <i>et al.</i>	(Mark III Collab.) JP
GIDAL	87	PRL 59 2012	G. Gidal <i>et al.</i>	(LBL, SLAC, HARV)
GIDAL	87B	PRL 59 2013	G. Gidal <i>et al.</i>	(LBL, SLAC, HARV)
AIHARA	86C	PRL 57 2500	H. Aihsara <i>et al.</i>	(TPC-2 γ Collab.) JP
ANDO	86	PRL 57 1296	A. Ando <i>et al.</i>	(KEK, KYOT, NIRS, SAGA+)
ARMSTRONG	84	PL 146B 273	T.A. Armstrong <i>et al.</i>	(ATHU, BARI, BIRM+) JPC
BITYUKOV	84	SJNP 39 735	S. Bitiyukov <i>et al.</i>	(SERP)
Translated from YAF 39 1165.				
CHAUVAT	84	PL 148B 382	P. Chauvat <i>et al.</i>	(CERN, CLER, UCLA+)
JENNI	83	PR D27 1031	P. Jenni <i>et al.</i>	(SLAC, LBL)
BROMBERG	80	PR D22 1513	C.M. Bromberg <i>et al.</i>	(CIT, FNAL, ILLCL+)
DIONISI	80	NP B169 1	H. Dionisi <i>et al.</i>	(CERN, MADR, CDEF+) JPC
CORDEN	78	NP B144 253	M.J. Corden <i>et al.</i>	(BIRM, RHEL, TELA+)
DEFOIX	72	NP B44 125	C. Defoix <i>et al.</i>	(CDEF, CERN)
DAHL	67	PR 163 1377	O.I. Dahl <i>et al.</i>	(LRL) JPC
Also	65	PRL 14 1074	D.H. Miller <i>et al.</i>	(LRL, UCB)

OTHER RELATED PAPERS

GODFREY	99	RMP 71 1411	S. Godfrey, J. Napolitano	
PROKOSHKIN	99	PAN 62 356	Yu.D. Prokoshkin <i>et al.</i>	
Translated from YAF 62 396.				
IZUKA	91	PTP 86 885	J. Iizuka, H. Koibuchi	(NAGO)
ISHIDA	89	PR D32 119	S. Ishida <i>et al.</i>	(NIHO)
AIHARA	88C	PR D38 1	H. Aihsara <i>et al.</i>	(TPC-2 γ Collab.) JPC
BITYUKOV	88	PL B203 327	S.I. Bitiyukov <i>et al.</i>	(SERP)
PROTOPOPOV..	87B	Hadron 87 Conf.	S.D. Protopopescu, S.U. Chung	(BNL)

$\omega(1420)$

$I^G(J^{PC}) = 0^-(1^{--})$

$\omega(1420)$ MASS

VALUE (MeV)	EVTs	DOCUMENT ID	TECN	COMMENT
1419 ± 31	315	¹ ANTONELLI 92 DM2	DM2	1.34-2.4e ⁺ e ⁻ → $\rho\pi$
••• We do not use the following data for averages, fits, limits, etc. •••				
1170 ± 10		² ACHASOV 99E RVUE	99E RVUE	0.75-1.80 e ⁺ e ⁻ → $\pi^+\pi^-\pi^0$
1400 ⁺ ₋₂₀₀		³ ACHASOV 98H RVUE	98H RVUE	e ⁺ e ⁻ → $\pi^+\pi^-\pi^0$
~ 1400		⁴ ACHASOV 98H RVUE	98H RVUE	e ⁺ e ⁻ → $\omega\pi^+\pi^-$
~ 1460		⁵ ACHASOV 98H RVUE	98H RVUE	e ⁺ e ⁻ → K ⁺ K ⁻
1440 ± 70		⁶ CLEGG 94 RVUE	94 RVUE	

¹ From a fit to two Breit-Wigner functions interfering between them and with the ω, ϕ tails with fixed (+,-,+) phases.
² Using the data of DOLINSKY 91, ANTONELLI 92, AKHMETSHIN 98, and ACHASOV 99E. From a fit to two Breit-Wigner functions interfering between them and with the ω, ϕ tails with fixed (+,-,+) phases.
³ Using data from BARKOV 87, DOLINSKY 91, and ANTONELLI 92.
⁴ Using the data from ANTONELLI 92.
⁵ Using the data from IVANOV 81 and BISELLO 88b.
⁶ Using data published by ANTONELLI 92.

$\omega(1420)$ WIDTH

VALUE (MeV)	EVTs	DOCUMENT ID	TECN	COMMENT
174 ± 59	315	⁷ ANTONELLI 92 DM2	DM2	1.34-2.4e ⁺ e ⁻ → $\rho\pi$
••• We do not use the following data for averages, fits, limits, etc. •••				
187 ± 15		⁸ ACHASOV 99E RVUE	99E RVUE	0.75-1.80 e ⁺ e ⁻ → $\pi^+\pi^-\pi^0$
240 ± 70		⁹ CLEGG 94 RVUE	94 RVUE	

⁷ From a fit to two Breit-Wigner functions interfering between them and with the ω, ϕ tails with fixed (+,-,+) phases.
⁸ Using the data of DOLINSKY 91, ANTONELLI 92, AKHMETSHIN 98, and ACHASOV 99E. From a fit to two Breit-Wigner functions interfering between them and with the ω, ϕ tails with fixed (+,-,+) phases.
⁹ Using data published by ANTONELLI 92.

$\omega(1420)$ DECAY MODES

Mode	Fraction (Γ_i/Γ)
Γ_1 $\rho\pi$	dominant
Γ_2 e ⁺ e ⁻	

$\omega(1420)$ $\Gamma(\rho\pi)/\Gamma(\text{total})$

$\Gamma(\rho\pi) \times \Gamma(e^+e^-)/\Gamma_{\text{total}}$	VALUE (eV)	EVTs	DOCUMENT ID	TECN	COMMENT	$\Gamma_1\Gamma_2/\Gamma$
81 ± 31	315		¹⁰ ANTONELLI 92 DM2	DM2	1.34-2.4e ⁺ e ⁻ → $\rho\pi$	
••• We do not use the following data for averages, fits, limits, etc. •••						
137 ± 3 ± 15			¹¹ ACHASOV 99E RVUE	99E RVUE	0.75-1.80 e ⁺ e ⁻ → $\pi^+\pi^-\pi^0$	

¹⁰ From a fit to two Breit-Wigner functions interfering between them and with the ω, ϕ tails with fixed (+,-,+) phases.
¹¹ Using the data of DOLINSKY 91, ANTONELLI 92, AKHMETSHIN 98, and ACHASOV 99E. From a fit to two Breit-Wigner functions interfering between them and with the ω, ϕ tails with fixed (+,-,+) phases.

$\omega(1420)$ REFERENCES

ACHASOV	99E	PL B462 365	M.N. Achasov <i>et al.</i>	(Novosibirsk SND Collab.)
ACHASOV	98H	PR D57 4334	N.N. Achasov, A.A. Kozhevnikov	
AKHMETSHIN	98	PL B434 426	R.R. Akhmetshin <i>et al.</i>	
CLEGG	94	ZPHY C62 455	A.B. Clegg, A. Donnachie	(LANC, MCHS)
ANTONELLI	92	ZPHY C56 15	A. Antonelli <i>et al.</i>	(DM2 Collab.)
DOLINSKY	91	PRPL 202 99	S.I. Dolinsky <i>et al.</i>	(NOVO)
BISELLO	88B	ZPHY C39 13	D. Bisello <i>et al.</i>	(PADO, CLER, FRAS+)
BARKOV	87	JETPL 46 164	L.M. Barkov <i>et al.</i>	(NOVO)
IVANOV	81	PL 107B 297	P.M. Ivanov <i>et al.</i>	(NOVO)

OTHER RELATED PAPERS

ABELE	99D	PL B468 178	A. Abele <i>et al.</i>	(Crystal Barrel Collab.)
BELOZEROVA	98	PPN 29 63	T.S. Belozerovala, V.K. Hener	
Translated from FECAV 29 148.				
ACHASOV	97F	PAN 60 2029	N.N. Achasov, A.A. Kozhevnikov	(NOVM)
Translated from YAF 60 2212.				
ATKINSON	87	ZPHY C34 157	M. Atkinson <i>et al.</i>	(BONN, CERN, GLAS+)
ATKINSON	84	NP B231 15	M. Atkinson <i>et al.</i>	(BONN, CERN, GLAS+)
ATKINSON	83B	PL 127B 132	M. Atkinson <i>et al.</i>	(BONN, CERN, GLAS+)

$f_2(1430)$

$I^G(J^{PC}) = 0^+(2^{++})$

OMITTED FROM SUMMARY TABLE
 This entry lists nearby peaks observed in the D wave of the $K\bar{K}$ and $\pi^+\pi^-$ systems. Needs confirmation.

$f_2(1430)$ MASS

VALUE (MeV)	DOCUMENT ID	TECN	COMMENT
~ 1430 OUR ESTIMATE			
••• We do not use the following data for averages, fits, limits, etc. •••			
1421 ± 5	AUGUSTIN 87 DM2	DM2	$J/\psi \rightarrow \gamma\pi^+\pi^-$
1480 ± 50	AKESSON 86 SPEC	SPEC	$\rho\rho \rightarrow \rho\rho\pi^+\pi^-$
1436 ⁺ ₋₁₆	DAUM 84 CNTR	CNTR	17-18 $\pi^-p \rightarrow$
1412 ± 3	DAUM 84 CNTR	CNTR	$K^+K^-n \rightarrow K_S^0 K_S^0 n,$ K^+K^-n
1439 ⁺ ₋₆	¹ BEUSCH 67 OSPK	OSPK	5,7,12 $\pi^-p \rightarrow$ $K_S^0 K_S^0 n$

¹ Not seen by WETZEL 76.

$f_2(1430)$ WIDTH

VALUE (MeV)	DOCUMENT ID	TECN	COMMENT
••• We do not use the following data for averages, fits, limits, etc. •••			
30 ± 9	AUGUSTIN 87 DM2	DM2	$J/\psi \rightarrow \gamma\pi^+\pi^-$
150 ± 50	AKESSON 86 SPEC	SPEC	$\rho\rho \rightarrow \rho\rho\pi^+\pi^-$
81 ⁺ ₋₂₉	DAUM 84 CNTR	CNTR	17-18 $\pi^-p \rightarrow$ K^+K^-n
14 ± 6	DAUM 84 CNTR	CNTR	63 $\pi^-p \rightarrow K_S^0 K_S^0 n,$ K^+K^-n
43 ⁺ ₋₁₈	² BEUSCH 67 OSPK	OSPK	5,7,12 $\pi^-p \rightarrow$ $K_S^0 K_S^0 n$

² Not seen by WETZEL 76.

$f_2(1430)$ DECAY MODES

Mode
Γ_1 $K\bar{K}$
Γ_2 $\pi\pi$

$f_2(1430)$ REFERENCES

AUGUSTIN	87	ZPHY C36 369	J.E. Augustin <i>et al.</i>	(LALO, CLER, FRAS+)
AKESSON	86	NP B264 154	T. Akesson <i>et al.</i>	(Axial Field Spec. Collab.)
DAUM	84	ZPHY C23 339	C. Daum <i>et al.</i>	(AMST, CERN, CRAC, MPIM+) JPC
WETZEL	76	NP B115 208	W. Wetzel <i>et al.</i>	(ETH, CERN, LOIC)
BEUSCH	67	PL 25B 357	W. Beusch <i>et al.</i>	(ETH, CERN)

$\eta(1440)$

$$I^G(J^{PC}) = 0^+(0^{-+})$$

See also the mini-review under non- $q\bar{q}$ candidates. (See the index for the page number.)

THE $\eta(1440)$, $f_1(1420)$, AND $f_1(1510)$

Written April 2000 by M. Aguilar-Benitez (CIEMAT, Madrid), C. Amsler (Zürich), and A. Masoni (INFN Cagliari).

The first observation of $\eta(1440)$ was made in $p\bar{p}$ annihilation at rest into $\eta(1440)\pi^+\pi^-$, $\eta(1440) \rightarrow K\bar{K}\pi$ (BAILLON 67). This state was reported to decay through $a_0(980)\pi$ and $K^*(892)\bar{K}$ with roughly equal contributions. The $\eta(1440)$ has also been observed in radiative $J/\psi(1S)$ decay to $K\bar{K}\pi$ (SCHARRE 80, EDWARDS 82E, AUGUSTIN 90).

The $f_1(1420)$, decaying to $K^*\bar{K}$, was reported in π^-p reactions at 4 GeV/c (DIONISI 80). However, later analyses found that the 1400–1500 MeV region is far more complex. In π^-p experiments, (CHUNG 85, REEVES 86, BIRMAN 88) reported 0^{-+} with a dominant $a_0(980)\pi$ contribution to $K\bar{K}\pi$. The π^-p data of RATH 89 at 21 GeV/c suggest the presence of two pseudoscalars decaying to $K\bar{K}\pi$, one around 1410 MeV decaying through $a_0(980)\pi$, and the other around 1470 MeV, decaying to $K^*\bar{K}$. A reanalysis of the MARK III data in radiative $J/\psi(1S)$ decay to $K\bar{K}\pi$ (BAI 90C) also claims the existence of two pseudoscalars in the 1400–1500 MeV range, the lower mass state decaying through $a_0(980)\pi$, and the higher mass state decaying via $K^*\bar{K}$. In addition, $f_1(1420)$ is observed to decay into $K^*\bar{K}$.

In $\pi^-p \rightarrow \eta\pi\pi n$ charge-exchange reactions at 8–9 GeV/c, the $\eta\pi\pi$ mass spectrum is dominated by $\eta(1440)$ and $\eta(1295)$ (ANDO 86, FUKUI 91C), and at 100 GeV/c, ALDE 97B reports $\eta(1295)$ and $\eta(1440)$ decaying to $\eta\pi^0\pi^0$ with a weak $f_1(1285)$ signal, and no evidence for $f_1(1420)$.

An experiment in $p\bar{p}$ annihilation at rest into $K\bar{K}3\pi$ (BERTIN 95) reports two pseudoscalars with decay properties similar to BAI 90C, although the lower state shows, apart from $a_0(980)\pi$, a large contribution from the direct decay $\eta(1440) \rightarrow K\bar{K}\pi$.

The result of BERTIN 95 was supported by further $p\bar{p}$ data from the same experiment (BERTIN 97, CICALO 99). In particular, the data of CICALO 99 provided a decisive evidence for the presence of two pseudoscalar states.

We note that the data from AUGUSTIN 92 also suggest two states, but their intermediate states, $a_0(980)\pi$ and $K^*\bar{K}$, are reversed relative to BAI 90C.

Actually the interpretation of AUGUSTIN 92 is disfavored for several reasons: first, it disagrees with all the other $K\bar{K}3\pi$ results reporting two pseudoscalar states (they all agree in assigning the $K^*(892)\bar{K}$ decay mode to the higher mass pseudoscalar); second, it also disagrees with the $\eta\pi\pi$ results, because if the high mass pseudoscalar decays into $a_0(980)\pi$, then this state (and not the one at lower mass) should be seen in $\eta\pi\pi$ (see below).

In $J/\psi(1S)$ radiative decay, the $\eta(1440)$ decays to $K\bar{K}\pi$ through $a_0(980)\pi$, and hence a signal is also expected in the $\eta\pi\pi$

mass spectrum. This has indeed been observed by MARK III in $\eta\pi^+\pi^-$ (BOLTON 92B), which report a mass of 1400 MeV, in line with the existence of a low mass pseudoscalar, in the $\eta(1440)$ structure, decaying to $a_0(980)\pi$. This state is also observed in $p\bar{p}$ annihilation at rest into $\eta\pi^+\pi^-\pi^0\pi^0$, where it decays to $\eta\pi\pi$ (AMSLER 95F). The intermediate $a_0(980)\pi$ accounts for roughly half of the $\eta\pi\pi$ signal, in agreement with MARK III (BOLTON 92B) and DM2 (AUGUSTIN 90). However, ALDE 97B reports only a very small contribution due to $a_0(980)\pi$.

There is now a fairly consistent picture for the existence of two pseudoscalars. We call them η_L and η_H . The first one decays mainly through $a_0(980)\pi$ or direct $K\bar{K}\pi$. The second one decays mainly to $K^*(892)\bar{K}$. The η_L is seen both in $K\bar{K}\pi$ and $\eta\pi\pi$ experiments. The η_H is seen only in $K\bar{K}\pi$ experiments. The simultaneous observation of two pseudoscalars is reported in three production mechanisms by four different experiments: π^-p (RATH 89); radiative $J/\psi(1S)$ decay (BAI 90C, AUGUSTIN 92); and $p\bar{p}$ annihilation at rest (BERTIN 95, BERTIN 97, CICALO 99). All of them give values for the masses, widths and decay modes (with the exception of AUGUSTIN 92 quoted above) in reasonable agreement.

A recent paper reports only one pseudoscalar state seen in $J/\psi(1S)$ decay to $K\bar{K}\pi$ (BAI 98C), but its statistics are poorer, by a factor six, with respect to MARK III on the same final state (BAI 90C), and by more than an order of magnitude with respect to $p\bar{p}$ data (BERTIN 95, BERTIN 97, CICALO 99). It is, therefore, not surprising that their analysis is not capable to discriminate between the two states.

One of these two pseudoscalars could be the first radial excitation of the η' , with the $\eta(1295)$ being the first radial excitation of the η . Ideal mixing, suggested by the $\eta(1295)$ and $\pi(1300)$ mass degeneracy, would then imply that the second isoscalar in the nonet is mainly $s\bar{s}$, and hence, couples to $K^*\bar{K}$, in agreement with observations for the upper $\eta(1440)$ state.

Also its width matches the expected width for the radially excited $\eta^{s\bar{s}}$ (CLOSE 97, BARNES 97).

This scheme then favors an exotic interpretation of the lower state, perhaps gluonium mixed with $q\bar{q}$ (CLOSE 97B) or a bound state of gluinos (FARRAR 96). The gluonium interpretation is, however, not favored by lattice gauge theories, which predict the 0^{-+} state above 2 GeV (BALI 93).

Axial (1^{++}) mesons are not observed in $p\bar{p}$ annihilation at rest in liquid hydrogen, which proceeds dominantly through S -wave annihilation. However, in gaseous hydrogen, P -wave annihilation is enhanced and, indeed, BERTIN 97 reports $f_1(1420)$ decaying to $K^*\bar{K}$, while confirming their earlier evidence for two pseudoscalars (BERTIN 95).

In $\gamma\gamma$ fusion from e^+e^- annihilations, a signal around 1420 MeV is seen in single-tag events (GIDAL 87B, AIHARA 88B, BEHREND 89, HILL 89), where one of the two photons is off-shell. However, it is totally absent in the untagged events where both photons are real. This points to a spin 1 object, which is not produced by two real (massless) photons (Yang-Landau theorem). The 2γ decay also implies $C = +1$. For the

Meson Particle Listings

 $\eta(1440)$

parity, AIHARA 88C and BEHREND 89 both find angular distributions with positive parity preferred, but negative parity cannot be excluded.

The $f_1(1420)$, decaying in $K\bar{K}\pi$, is definitely seen in pp central production at 300 and 450 GeV/c, together with $f_1(1285)$. The latter decays via $a_0(980)\pi$, and the former only via $K^*\bar{K}$, while $\eta(1440)$ is absent (ARMSTRONG 89, BARBERIS 97C). The $K_S K_S \pi^0$ decay mode of $f_1(1420)$ establishes unambiguously $C=+1$. On the other hand, there is no evidence for any state decaying to $\eta\pi\pi$ around 1400 MeV, and hence, the $\eta\pi\pi$ mode of $f_1(1420)$ is suppressed (ARMSTRONG 91B).

We now turn to the experimental evidence for $f_1(1510)$. Two states, $f_1(1420)$ and $f_1(1510)$, decaying to $K^*\bar{K}$, compete for the $s\bar{s}$ assignment in the 1^{++} nonet. The $f_1(1510)$ was seen in $K^-p \rightarrow \Lambda K\bar{K}\pi$ at 4 GeV/c (GAVILLET 82), and at 11 GeV/c (ASTON 88C). Evidence is also reported in π^-p at 8 GeV/c, based on the phase motion of the $1^{++} K^*\bar{K}$ wave (BIRMAN 88).

The absence of $f_1(1420)$ in K^-p (ASTON 88C) argues against $f_1(1420)$ being the $s\bar{s}$ member of the 1^{++} nonet. However, $f_1(1420)$ has been reported in K^-p , but not in π^-p (BITYUKOV 84) while two experiments do not observe $f_1(1510)$ in K^-p (BITYUKOV 84, KING 91). It is also not seen in radiative $J/\psi(1S)$ decay (BAI 90C, AUGUSTIN 92), central collisions (BARBERIS 97C), or in $\gamma\gamma$ collisions (AIHARA 88C), although, surprisingly for an $s\bar{s}$ state, a signal is reported in 4π decays (BAUER 93B). These facts led to the conclusion that $f_1(1510)$ is not well established, and that its assignment as $s\bar{s}$ member of the 1^{++} nonet is premature (CLOSE 97D). The Particle Data Group has removed this state from the Summary Table. Assigning, instead, the $f_1(1420)$ to the 1^{++} nonet, one finds a nonet mixing angle of $\sim 50^\circ$ (CLOSE 97D). This is derived from the mass formula, and from $f_1(1285)$ radiative decays to $\phi\gamma$ (BITYUKOV 88) and $\rho\gamma$ (AMELIN 95).

Arguments favoring $f_1(1420)$ being a hybrid $q\bar{q}g$ meson or a four-quark state are put forward by ISHIDA 89 and CALDWELL 90, respectively, while LONGACRE 90 argues that this particle is a molecular state formed by the π orbiting in a P -wave around an S -wave $K\bar{K}$ state.

Summarizing, there is rather convincing evidence for $f_1(1420)$, mostly produced in central collisions and decaying to $K^*\bar{K}$, and for $\eta(1440)$, mostly produced in radiative $J/\psi(1S)$ decay and $\bar{p}p$ annihilation at rest, and decaying to $K^*\bar{K}$ and $a_0(980)\pi$. Confusion remains as to which states are observed in π^-p interactions. The $f_1(1510)$ is not well established.

Furthermore, there are fairly strong experimental indications for the presence of two pseudoscalars in the $\eta(1440)$ structure

The available information has led the Particle Data Group to split the $K\bar{K}\pi$ entry for $\eta(1440)$ into $a_0(980)\pi$ and $K^*\bar{K}$.

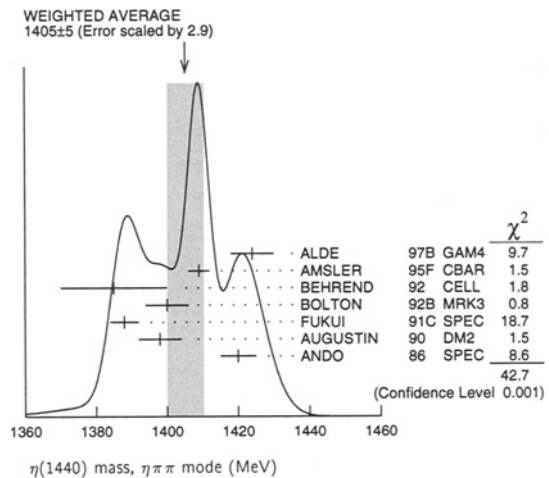
 $\eta(1440)$ MASS

VALUE (MeV) DOCUMENT ID
1400 - 1470 OUR ESTIMATE Contains possibly two overlapping pseudoscalars.

 $\eta\pi\pi$ MODE

VALUE (MeV)	EVTS	DOCUMENT ID	TECN	COMMENT
1405 ± 5 OUR AVERAGE	Error	includes scale factor of 2.9. See the ideogram below.		
1424 ± 6	2200	ALDE	97B GAM4	100 $\pi^-p \rightarrow \eta\pi^0\pi^0n$
1409 ± 3		AMSLER	95F CBAR	0 $\bar{p}p \rightarrow \pi^+\pi^-\pi^0\pi^0\eta$
1385 ± 15		1 BEHREND	92 CELL	$J/\psi \rightarrow \gamma\eta\pi^+\pi^-$
1400 ± 6		1 BOLTON	92B MRK3	$J/\psi \rightarrow \gamma\eta\pi^+\pi^-$
1388 ± 4		FUKUI	91C SPEC	8.95 $\pi^-p \rightarrow \eta\pi^+\pi^-n$
1398 ± 6	261	2 AUGUSTIN	90 DM2	$J/\psi \rightarrow \gamma\eta\pi^+\pi^-$
1420 ± 5		ANDO	86 SPEC	8 $\pi^-p \rightarrow \eta\pi^+\pi^-n$
1385 ± 7		BAI	99 BES	$J/\psi \rightarrow \gamma\pi^+\pi^-$

• • • We do not use the following data for averages, fits, limits, etc. • • •
1 From fit to the $a_0(980)\pi^0$ partial wave.
2 Best fit with a single Breit Wigner.

 $\pi\pi\gamma$ MODE

VALUE (MeV)	DOCUMENT ID	TECN	COMMENT
1401 ± 18	3,4 AUGUSTIN	90 DM2	$J/\psi \rightarrow \pi^+\pi^-\gamma\gamma$
1432 ± 8	4 COFFMAN	90 MRK3	$J/\psi \rightarrow \pi^+\pi^-\gamma$

• • • We do not use the following data for averages, fits, limits, etc. • • •
3 Best fit with a single Breit Wigner.
4 This peak in the $\gamma\rho$ channel may not be related to the $\eta(1440)$.

 4π MODE

VALUE (MeV)	EVTS	DOCUMENT ID	TECN	COMMENT
1420 ± 20		BUGG	95 MRK3	$J/\psi \rightarrow \gamma\pi^+\pi^-\pi^+\pi^-$
1489 ± 12	3270	5 BISELLO	89B DM2	$J/\psi \rightarrow 4\pi\gamma$

• • • We do not use the following data for averages, fits, limits, etc. • • •
5 Estimated by us from various fits.

 $K\bar{K}\pi$ MODE ($a_0(980)\pi$ dominant)

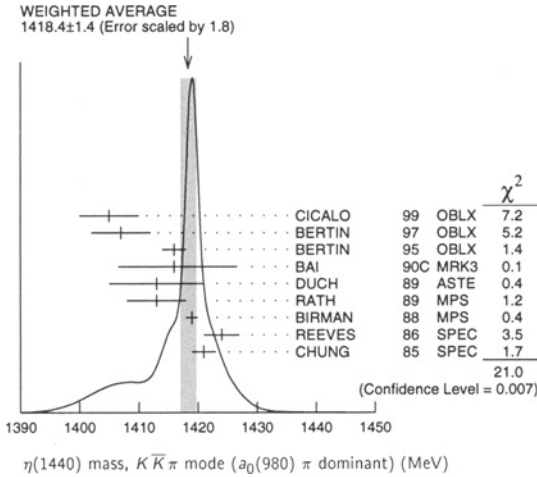
VALUE (MeV)	EVTS	DOCUMENT ID	TECN	COMMENT
1418.4 ± 1.4 OUR AVERAGE	Error	includes scale factor of 1.8. See the ideogram below.		
1405 ± 5		6 CICALO	99 OBLX	0 $\bar{p}p \rightarrow K^\pm K_S^0 \pi^\mp \pi^+$
1407 ± 5		6 BERTIN	97 OBLX	0 $\bar{p}p \rightarrow K^\pm (K^0) \pi^\mp \pi^+$
1416 ± 2		6 BERTIN	95 OBLX	0 $\bar{p}p \rightarrow K\bar{K}\pi\pi$
1416 ± 8 $^{+7}_{-5}$	700	7 BAI	90C MRK3	$J/\psi \rightarrow \gamma K_S^0 K^\pm \pi^\mp$
1413 ± 8	500	DUCH	89 ASTE	$\bar{p}p \rightarrow \pi^+\pi^- K^\pm \pi^\mp K^0$
1413 ± 5		7 RATH	89 MPS	21.4 $\pi^-p \rightarrow n K_S^0 K_S^0 \pi^0$
1419 ± 1	8800	BIRMAN	88 MPS	8 $\pi^-p \rightarrow K^+\bar{K}^0\pi^-n$
1424 ± 3	620	REEVES	86 SPEC	6.6 $\rho\bar{p} \rightarrow K\bar{K}\pi X$
1421 ± 2		CHUNG	85 SPEC	8 $\pi^-p \rightarrow K\bar{K}\pi n$
1459 ± 5		8 AUGUSTIN	92 DM2	$J/\psi \rightarrow \gamma K\bar{K}\pi$

• • • We do not use the following data for averages, fits, limits, etc. • • •
6 Decaying into $(K\bar{K})_S\pi$, $(K\pi)_S\bar{K}$, and $a_0(980)\pi$.
7 From fit to the $a_0(980)\pi^0$ partial wave. Cannot rule out a $a_0(980)\pi^+ \pi^+$ partial wave.
8 Excluded from averaging because averaging would be meaningless.

See key on page 239

Meson Particle Listings

$\eta(1440)$

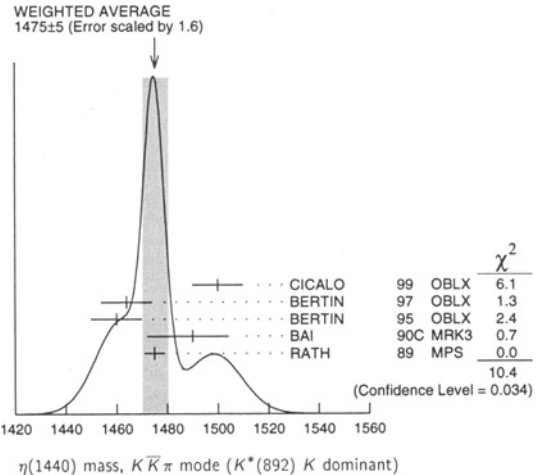


$K\bar{K}\pi$ MODE ($K^*(892)K$ dominant)

VALUE (MeV)	EVTS	DOCUMENT ID	TECN	COMMENT
1475 ± 5 OUR AVERAGE				Error includes scale factor of 1.6. See the ideogram below.
1500 ± 10		CICALO	99 OBLX	$0\bar{p}p \rightarrow K^\pm K_S^0 \pi^\mp \pi^+ \pi^-$
1464 ± 10		BERTIN	97 OBLX	$0\bar{p}p \rightarrow K^\pm (K^0) \pi^\mp \pi^+ \pi^-$
1460 ± 10		BERTIN	95 OBLX	$0\bar{p}p \rightarrow K\bar{K}\pi\pi\pi$
1490 ⁺¹⁴⁺³ ₋₈₋₁₆	1100	BAI	90C MRK3	$J/\psi \rightarrow \gamma K_S^0 K^\pm \pi^\mp$
1475 ± 4		RATH	89 MPS	$21.4 \pi^- p \rightarrow n K_S^0 K_S^0 \pi^0$
1442 ± 10	410	BAI	98c BES	$J/\psi \rightarrow \gamma K^+ K^- \pi^0$
1421 ± 14		⁹ AUGUSTIN	92 DM2	$J/\psi \rightarrow \gamma K\bar{K}\pi$

• • • We do not use the following data for averages, fits, limits, etc. • • •

⁹ Excluded from averaging because averaging would be meaningless.



$K\bar{K}\pi$ MODE (unresolved)

VALUE (MeV)	EVTS	DOCUMENT ID	TECN	COMMENT
1445 ± 8	693	AUGUSTIN	90 DM2	$J/\psi \rightarrow \gamma K_S^0 K^\pm \pi^\mp$
1433 ± 8	296	AUGUSTIN	90 DM2	$J/\psi \rightarrow \gamma K^+ K^- \pi^0$
1453 ± 7	170	RATH	89 MPS	$21.4 \pi^- p \rightarrow K_S^0 K_S^0 \pi^0 n$
1440 ⁺²⁰ ₋₁₅	174	EDWARDS	82E CBAL	$J/\psi \rightarrow \gamma K^+ K^- \pi^0$
1440 ⁺¹⁰ ₋₁₅		SCHARRE	80 MRK2	$J/\psi \rightarrow \gamma K_S^0 K^\pm \pi^\mp$
1425 ± 7	800	¹⁰ BAILLON	67 HBC	$0\bar{p}p \rightarrow K\bar{K}\pi\pi\pi$

• • • We do not use the following data for averages, fits, limits, etc. • • •

¹⁰ From best fit of 0^-+ partial wave, 50% $K^*(892)K$, 50% $a_0(980)\pi$.

$\eta(1440)$ WIDTH

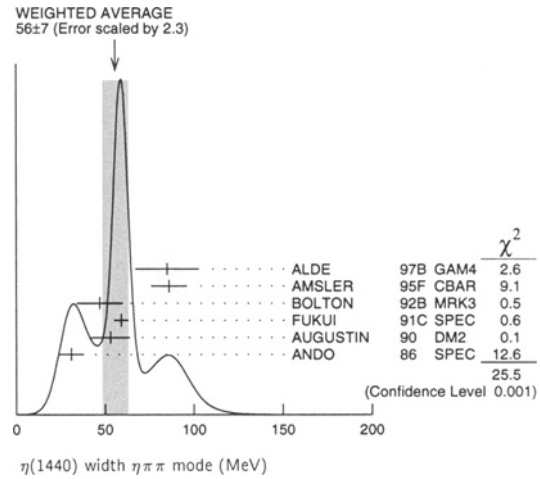
VALUE (MeV) DOCUMENT ID
50 - 80 OUR ESTIMATE Contains possibly two overlapping pseudoscalars.

$\eta\pi\pi$ MODE

VALUE (MeV)	EVTS	DOCUMENT ID	TECN	COMMENT
56 ± 7 OUR AVERAGE				Error includes scale factor of 2.3. See the ideogram below.
85 ± 18	2200	ALDE	97B GAM4	$100 \pi^- p \rightarrow \eta \pi^0 \pi^0 n$
86 ± 10		AMSLER	95F CBAR	$0\bar{p}p \rightarrow \pi^+ \pi^- \pi^0 \pi^0 \eta$
47 ± 13		¹¹ BOLTON	92B MRK3	$J/\psi \rightarrow \gamma \eta \pi^+ \pi^-$
59 ± 4		FUKUI	91C SPEC	$8.95 \pi^- p \rightarrow \eta \pi^+ \pi^- n$
53 ± 11		¹² AUGUSTIN	90 DM2	$J/\psi \rightarrow \gamma \eta \pi^+ \pi^-$
31 ± 7		ANDO	86 SPEC	$8 \pi^- p \rightarrow \eta \pi^+ \pi^- n$
~ 50		¹² BEHREND	92 CELL	$J/\psi \rightarrow \gamma \eta \pi^+ \pi^-$

• • • We do not use the following data for averages, fits, limits, etc. • • •

¹¹ From fit to the $a_0(980)\pi$ 0^-+ partial wave.
¹² From $\eta\pi^+\pi^-$ mass distribution - mainly $a_0(980)\pi$ - no spin-parity determination available.



$\pi\pi\gamma$ MODE

VALUE (MeV)	DOCUMENT ID	TECN	COMMENT
174 ± 44	AUGUSTIN	90 DM2	$J/\psi \rightarrow \pi^+ \pi^- \gamma \gamma$
90 ± 26	¹³ COFFMAN	90 MRK3	$J/\psi \rightarrow \pi^+ \pi^- 2\gamma$

¹³ This peak in the $\gamma\rho$ channel may not be related to the $\eta(1440)$.

4π MODE

VALUE (MeV)	EVTS	DOCUMENT ID	TECN	COMMENT
160 ± 30		BUGG	95 MRK3	$J/\psi \rightarrow \gamma \pi^+ \pi^- \pi^+ \pi^-$
144 ± 13	3270	¹⁴ BISELLO	89B DM2	$J/\psi \rightarrow 4\pi\gamma$

• • • We do not use the following data for averages, fits, limits, etc. • • •

¹⁴ Estimated by us from various fits.

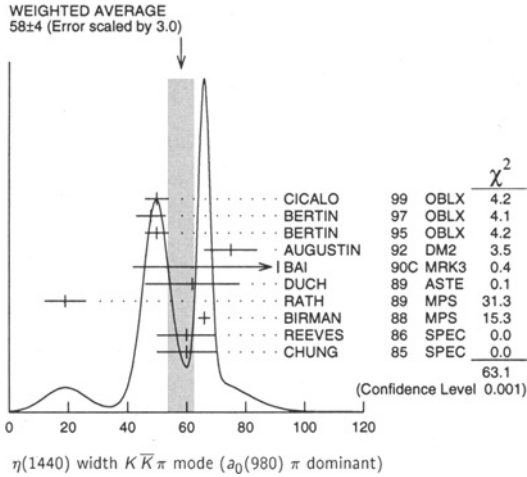
$K\bar{K}\pi$ MODE ($a_0(980)\pi$ dominant)

VALUE (MeV)	EVTS	DOCUMENT ID	TECN	COMMENT
50 ± 4 OUR AVERAGE				Error includes scale factor of 3.0. See the ideogram below.
50 ± 4		CICALO	99 OBLX	$0\bar{p}p \rightarrow K^\pm K_S^0 \pi^\mp \pi^+ \pi^-$
48 ± 5		¹⁵ BERTIN	97 OBLX	$0.0\bar{p}p \rightarrow K^\pm (K^0) \pi^\mp \pi^+ \pi^-$
50 ± 4		¹⁵ BERTIN	95 OBLX	$0\bar{p}p \rightarrow K\bar{K}\pi\pi\pi$
75 ± 9		AUGUSTIN	92 DM2	$J/\psi \rightarrow \gamma K\bar{K}\pi$
91 ⁺⁶⁷⁺¹⁵ ₋₃₁₋₃₈		¹⁶ BAI	90C MRK3	$J/\psi \rightarrow \gamma K_S^0 K^\pm \pi^\mp$
62 ± 16	500	DUCH	89 ASTE	$\bar{p}p \rightarrow K\bar{K}\pi\pi\pi$
19 ± 7		¹⁶ RATH	89 MPS	$21.4 \pi^- p \rightarrow n K_S^0 K_S^0 \pi^0$
66 ± 2	8800	BIRMAN	88 MPS	$8 \pi^- p \rightarrow K^+ \bar{K}^0 \pi^- n$
60 ± 10	620	REEVES	86 SPEC	$6.6 \bar{p}p \rightarrow K\bar{K}\pi\pi\pi$
60 ± 10		CHUNG	85 SPEC	$8 \pi^- p \rightarrow K\bar{K}\pi n$

¹⁵ Decaying into $(K\bar{K})_S \pi$, $(K\pi)_S \bar{K}$, and $a_0(980)\pi$.
¹⁶ From fit to the $a_0(980)\pi$ 0^-+ partial wave, but $a_0(980)\pi$ 1^++ cannot be excluded.

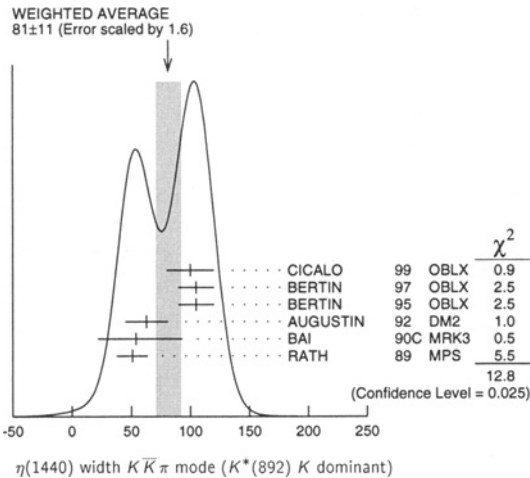
Meson Particle Listings

$\eta(1440)$



$K\bar{K}\pi$ MODE ($K^*(892)K$ dominant)

VALUE	DOCUMENT ID	TECN	COMMENT
81 ± 11 OUR AVERAGE	Error includes scale factor of 1.6. See the ideogram below.		
100 ± 20	CICALO 99	OBLX	$0 \bar{p}p \rightarrow K^\pm K_S^0 \pi^\mp \pi^+ \pi^-$
105 ± 15	BERTIN 97	OBLX	$0.0 \bar{p}p \rightarrow K^\pm (K^0) \pi^\mp \pi^+ \pi^-$
105 ± 15	BERTIN 95	OBLX	$0 \bar{p}p \rightarrow K\bar{K}\pi\pi\pi$
63 ± 18	AUGUSTIN 92	DM2	$J/\psi \rightarrow \gamma K\bar{K}\pi$
54^{+37+13}_{-21-24}	BAI 90C	MRK3	$J/\psi \rightarrow \gamma K_S^0 K^\pm \pi^\mp$
51 ± 13	RATH 89	MPS	$21.4 \pi^- p \rightarrow n K_S^0 K_S^0 \pi^0$



$K\bar{K}\pi$ MODE (unresolved)

VALUE	EVTs	DOCUMENT ID	TECN	COMMENT
93 ± 14	296	AUGUSTIN 90	DM2	$J/\psi \rightarrow \gamma K^+ K^- \pi^0$
105 ± 10	693	AUGUSTIN 90	DM2	$J/\psi \rightarrow \gamma K_S^0 K^\pm \pi^\mp$
100 ± 11	170	RATH 89	MPS	$21.4 \pi^- p \rightarrow K_S^0 K_S^0 \pi^0 n$
55^{+20}_{-30}	174	EDWARDS 82E	CBAL	$J/\psi \rightarrow \gamma K^+ K^- \pi^0$
50^{+30}_{-20}		SCHARRE 80	MRK2	$J/\psi \rightarrow \gamma K_S^0 K^\pm \pi^\mp$
80 ± 10	800	¹⁷ BAILLON 67	HBC	$0.0 \bar{p}p \rightarrow K\bar{K}\pi\pi\pi$

¹⁷ From best fit to 0^-+ partial wave, 50% $K^*(892)K$, 50% $a_0(980)\pi$.

$\eta(1440)$ DECAY MODES

Mode	Fraction (Γ_i/Γ)
Γ_1	$K\bar{K}\pi$ seen
Γ_2	$K\bar{K}^*(892) + c.c.$ seen
Γ_3	$\eta\pi\pi$ seen
Γ_4	$a_0(980)\pi$ seen
Γ_5	$\eta(\pi\pi)s$ -wave seen

Γ_6	$f_0(980)\eta$	seen
Γ_7	4π	seen
Γ_8	$\gamma\gamma$	
Γ_9	$\rho^0\gamma$	

$\eta(1440) \Gamma(i)/\Gamma(\gamma\gamma)/\Gamma(\text{total})$

VALUE (keV)	CL%	DOCUMENT ID	TECN	COMMENT	$\Gamma_1\Gamma_8/\Gamma$
<1.2	95	BEHREND 89	CELL	$\gamma\gamma \rightarrow K_S^0 K^\pm \pi^\mp$	
• • • We do not use the following data for averages, fits, limits, etc. • • •					
<1.6	95	AIHARA 86D	TPC	$e^+e^- \rightarrow e^+e^- K_S^0 K^\pm \pi^\mp$	
<2.2	95	ALTHOFF 85B	TASS	$e^+e^- \rightarrow e^+e^- K\bar{K}\pi$	
<8.0	95	JENNI 83	MRK2	$e^+e^- \rightarrow e^+e^- K\bar{K}\pi$	

$\Gamma(\eta\pi\pi) \times \Gamma(\gamma\gamma)/\Gamma(\text{total})$

VALUE (keV)	DOCUMENT ID	TECN	COMMENT	$\Gamma_3\Gamma_8/\Gamma$
• • • We do not use the following data for averages, fits, limits, etc. • • •				
<0.3	ANTREASYAN 87	CBAL	$e^+e^- \rightarrow e^+e^- \eta\pi\pi$	

$\Gamma(\rho^0\gamma) \times \Gamma(\gamma\gamma)/\Gamma(\text{total})$

VALUE (keV)	CL%	DOCUMENT ID	TECN	COMMENT	$\Gamma_9\Gamma_8/\Gamma$
• • • We do not use the following data for averages, fits, limits, etc. • • •					
<1.5	95	ALTHOFF 84E	TASS	$e^+e^- \rightarrow e^+e^- \pi^+ \pi^- \gamma$	

$\eta(1440)$ BRANCHING RATIOS

$\Gamma(\eta\pi\pi)/\Gamma(K\bar{K}\pi)$

VALUE	CL%	DOCUMENT ID	TECN	COMMENT	Γ_3/Γ_1
• • • We do not use the following data for averages, fits, limits, etc. • • •					
<0.5	90	EDWARDS 83B	CBAL	$J/\psi \rightarrow \eta\pi\pi\gamma$	
<1.1	90	SCHARRE 80	MRK2	$J/\psi \rightarrow \eta\pi\pi\gamma$	
<1.5	95	FOSTER 68B	HBC	$0.0 \bar{p}p$	

$\Gamma(a_0(980)\pi)/\Gamma(K\bar{K}\pi)$

VALUE	EVTs	DOCUMENT ID	TECN	COMMENT	Γ_4/Γ_1
• • • We do not use the following data for averages, fits, limits, etc. • • •					
~ 0.15	18	BERTIN 95	OBLX	$0 \bar{p}p \rightarrow K\bar{K}\pi\pi\pi$	
~ 0.8	500	¹⁸ DUCH 89	ASTE	$\bar{p}p \rightarrow \pi^+ \pi^- K^\pm \pi^\mp K^0$	
~ 0.75	18	REEVES 86	SPEC	$6.6 \rho\bar{p} \rightarrow K K \pi X$	

¹⁸ Assuming that the $a_0(980)$ decays only into $K\bar{K}$.

$\Gamma(a_0(980)\pi)/\Gamma(\eta\pi\pi)$

VALUE	EVTs	DOCUMENT ID	TECN	COMMENT	Γ_4/Γ_3
• • • We do not use the following data for averages, fits, limits, etc. • • •					
0.29 ± 0.10		ABELE 98E	CBAR	$0 \rho\bar{p} \rightarrow \eta\pi^0 \pi^0$	
0.19 ± 0.04	2200	¹⁹ ALDE 97B	GAM4	$100 \pi^- p \rightarrow \eta\pi^0 \pi^0 n$	
$0.56 \pm 0.04 \pm 0.03$		¹⁹ AMSLER 95F	CBAR	$0 \bar{p}p \rightarrow \pi^+ \pi^- \pi^0 \pi^0 \eta$	

¹⁹ Assuming that the $a_0(980)$ decays only into $\eta\pi$.

$\Gamma(a_0(980)\pi)/\Gamma(\eta\pi\pi)s$ -wave

VALUE	DOCUMENT ID	TECN	COMMENT	Γ_4/Γ_5
• • • We do not use the following data for averages, fits, limits, etc. • • •				
$0.70 \pm 0.12 \pm 0.20$	²⁰ BAI 99	BES	$J/\psi \rightarrow \gamma\eta\pi^+ \pi^-$	

²⁰ Assuming that the $a_0(980)$ decays only into $\eta\pi$.

$\Gamma(K\bar{K}^*(892) + c.c.)/\Gamma(K\bar{K}\pi)$

VALUE	DOCUMENT ID	TECN	COMMENT	Γ_2/Γ_1
0.50 ± 0.10	BAILLON 67	HBC	$0.0 \bar{p}p \rightarrow K\bar{K}\pi\pi\pi$	

$\Gamma(K\bar{K}^*(892) + c.c.) / [\Gamma(K\bar{K}^*(892) + c.c.) + \Gamma(a_0(980)\pi)]$

VALUE	CL%	DOCUMENT ID	TECN	COMMENT	$\Gamma_2/(\Gamma_2+\Gamma_4)$
• • • We do not use the following data for averages, fits, limits, etc. • • •					
<0.25	90	EDWARDS 82E	CBAL	$J/\psi \rightarrow K^+ K^- \pi^0 \gamma$	

$\Gamma(\rho^0\gamma)/\Gamma(K\bar{K}\pi)$

VALUE	DOCUMENT ID	TECN	COMMENT	Γ_9/Γ_1
0.0152 ± 0.0038	²¹ COFFMAN 90	MRK3	$J/\psi \rightarrow \gamma\eta\pi^+ \pi^-$	

²¹ Using $B(J/\psi \rightarrow \gamma\eta(1440) \rightarrow \gamma K\bar{K}\pi) = 4.2 \times 10^{-3}$ and $B(J/\psi \rightarrow \gamma\eta(1440) \rightarrow \gamma\rho^0) = 6.4 \times 10^{-5}$ and assuming that the $\gamma\rho^0$ signal does not come from the $f_1(1420)$.

$\Gamma(\eta(\pi\pi)s$ -wave)/ $\Gamma(\eta\pi\pi)$

VALUE	EVTs	DOCUMENT ID	TECN	COMMENT	Γ_5/Γ_3
• • • We do not use the following data for averages, fits, limits, etc. • • •					
0.81 ± 0.04	2200	ALDE 97B	GAM4	$100 \pi^- p \rightarrow \eta\pi^0 \pi^0 n$	

See key on page 239

Meson Particle Listings
 $\eta(1440), a_0(1450), \rho(1450)$

$\Gamma(a_0(980)\pi)/\Gamma(\eta(\pi\pi)\text{-s-wave})$		Γ_4/Γ_5	
VALUE	DOCUMENT ID	TECN	COMMENT
• • • We do not use the following data for averages, fits, limits, etc. • • •			
0.32 ± 0.07	22 ANISOVICH	99i SPEC	0.9–1.2 $\bar{p}p \rightarrow \eta 3\pi^0$
22 Using preliminary Crystal Barrel data.			

$\eta(1440)$ REFERENCES

ANISOVICH	99i PL B468 304	A.V. Anisovich et al.	
BAI	99 PL B446 356	J.Z. Bai et al.	(BES Collab.)
CICALO	99 PL B462 453	C. Cicalo et al.	(OBELIX Collab.)
ABELE	98E NP B514 45	A. Abele et al.	(Crystal Barrel Collab.)
BAI	98C PL B440 217	J.Z. Bai et al.	(BES Collab.)
ALDE	97B PAN 60 386	D. Alde et al.	(GAMS Collab.)
	Translated from YAF 60 456.		
BERTIN	97 PL B400 226	A. Bertin et al.	(OBELIX Collab.)
AMSLER	95F PL B358 389	C. Amisler et al.	(Crystal Barrel Collab.)
BERTIN	95 PL B361 187	A. Bertin et al.	(OBELIX Collab.)
BUGG	95 PL B353 378	D.V. Bugg et al.	(LOQM, PNPI, WASH)
AUGUSTIN	92 PR D46 1951	J.E. Augustin, G. Cosme	(DM2 Collab.)
BEHREND	92 ZPHY C56 381	H.J. Behrend	(CELLO Collab.)
BOLTON	92B PRL 69 1328	T. Bolton et al.	(Mark III Collab.)
FUKUI	91C PL B267 293	S. Fukui et al.	(SUGI, NAGO, KEK, KYOT+)
AUGUSTIN	90 PR D42 10	J.E. Augustin et al.	(DM2 Collab.)
BAI	90C PRL 65 2507	A. Ando et al.	(Mark III Collab.)
COFFMAN	90 PR D41 1410	D.M. Coffman et al.	(Mark III Collab.)
BEHREND	89 ZPHY C42 367	H.J. Behrend et al.	(CELLO Collab.)
BISELLO	89B PR D39 701	G. Busetto et al.	(DM2 Collab.)
DUCH	89 ZPHY 45 223	K.D. Duch et al.	(ASTERIX Collab.) JP
RATH	89 PR D40 693	M.G. Rath et al.	(NDAM, BRAN, BNLC, CUNY+)
BIRMAN	88 PRL 61 1557	A. Birman et al.	(BNL, FSU, IND, MASD) JP
ANTREASANYAN	87 PR D36 2633	D. Antreasanyan et al.	(Crystal Ball Collab.)
ALHARAZ	86D PRL 57 51	H. Alhara et al.	(TPC-2 γ Collab.)
ANDO	86 PRL 57 1296	G.S. Baif et al.	(BNL)
REEVES	86 PR 34 1960	D.F. Reeves et al.	(KEK, KYOT, NIRS, SAGA+) IJP
ALTHOFF	85B ZPHY C29 189	M. Althoff et al.	(FLOR, BNL, IND+) JP
CHUNG	85 PRL 55 779	S.U. Chung et al.	(TASSO Collab.)
ALTHOFF	84E PL 147B 487	M. Althoff et al.	(BNL, FLOR, IND+) JP
EDWARDS	83B PRL 51 859	C. Edwards et al.	(CIT, HARV, PRIN+)
JENNI	83 PR D27 1031	P. Jenni et al.	(SLAC, LBL)
EDWARDS	82E PRL 49 259	C. Edwards et al.	(CIT, HARV, PRIN+)
Also	83 PRL 50 219	C. Edwards et al.	(CIT, HARV, PRIN+)
SCHARRER	80C PL 97B 329	D.L. Scharrer et al.	(SLAC, LBL)
FOSTER	68B NP B8 174	M. Foster et al.	(CERN, CDF)
BAILLON	67 NC 50A 393	P.H. Bailion et al.	(CERN, CDF, IRAD)

OTHER RELATED PAPERS

CARVALHO	99 EPJ C7 95	W.S. Carvalho et al.	
GOOFREY	99 RMP 71 1411	S. Godfrey, J. Napolitano	
NEKRASOV	98 EPJ C5 507		
CLOSE	97B PR D55 5749	F. Close et al.	(RAL, RUTG, BEUT)
BERTIN	96 PL B385 493	A. Bertin et al.	(Obelix Collab.)
FARRAR	96 PRL 76 4111	G.R. Farrar	(RUTG)
AMELIN	95 ZPHY C66 71	D.V. Amelin et al.	(VES Collab.)
GENOVESE	94 ZPHY C61 425	M. Genovese, D.B. Lichtenberg, E. Predazzi	(TORI+)
BALI	93 PL B309 378	R.S. Ball et al.	(LIVP)
LONGACRE	90 PR D42 874	R.S. Longacre	(BNL)
AHMAD	89 NP B (PROC.) 8 50	S. Ahmad et al.	(ASTERIX Collab.)
ARMSTRONG	89 PL B221 216	T.A. Armstrong et al.	(CERN, CDF, BIRM+)
ARMSTRONG	87 ZPHY C34 23	T.A. Armstrong et al.	(CERN, BIRM, BARI+)
ASTON	87 NP B292 693	D. Aston et al.	(SLAC, NAGO, CINC, INUS)
ARMSTRONG	84 PL 146B 273	T.A. Armstrong et al.	(ATHU, BARI, BIRM+)
DIONISI	80 NP B169 1	C. Dionisi et al.	(CERN, MADR, CDEF+)
DEFOIX	72 NP B44 125	C. Defoix et al.	(CDEF, CERN)
OUBOC	72 NP B46 429	J. Duboc et al.	(PARIS, LIVP)
LORSTAD	69 NP B14 63	B. Lorstad et al.	(CDEF, CERN)

$a_0(1450)$ $I^G(J^{PC}) = 1^-(0^{++})$
 See minireview on scalar mesons under $f_0(1370)$.

$a_0(1450)$ MASS

VALUE (MeV)	DOCUMENT ID	TECN	COMMENT
1474 ± 19 OUR AVERAGE			
1480 ± 30			
1470 ± 25	1 AMSLER	95D CBAR	0.0 $\bar{p}p \rightarrow K^0 K^{\pm} \pi^{\mp}$ $\pi^0 \bar{p}p \rightarrow \pi^0 \pi^0 \pi^0$ $\pi^0 \eta \eta, \pi^0 \pi^0 \eta$
• • • We do not use the following data for averages, fits, limits, etc. • • •			
1565 ± 30	2 ANISOVICH	98b RVUE	Compilation
1290 ± 10	BERTIN	98b OBLX	0.0 $\bar{p}p \rightarrow K^{\pm} K_S^{\mp} \pi^{\mp}$
1450 ± 40	AMSLER	94D CBAR	0.0 $\bar{p}p \rightarrow \pi^0 \pi^0 \eta$
1435 ± 40	BUGG	94 RVUE	$\bar{p}p \rightarrow \eta 2\pi^0$
1410 ± 25	ETKIN	82c MPS	23 $\pi^- p \rightarrow n 2K_S^0$
~ 1300	MARTIN	78 SPEC	10 $K^{\pm} p \rightarrow K_S^0 \pi p$
1255 ± 5	3 CASON	76	
1 Coupled-channel analysis of AMSLER 95b, AMSLER 95c, and AMSLER 94d. 2 T-matrix pole. 3 Isospin 0 not excluded.			

$a_0(1450)$ WIDTH

VALUE (MeV)	DOCUMENT ID	TECN	COMMENT
265 ± 13 OUR AVERAGE			
265 ± 15			
265 ± 30	4 AMSLER	95D CBAR	0.0 $\bar{p}p \rightarrow K^0 K^{\pm} \pi^{\mp}$ $\pi^0 \bar{p}p \rightarrow \pi^0 \pi^0 \pi^0$ $\pi^0 \eta \eta, \pi^0 \pi^0 \eta$

• • • We do not use the following data for averages, fits, limits, etc. • • •

292 ± 40	5 ANISOVICH	98B RVUE	Compilation
80 ± 5	BERTIN	98B OBLX	0.0 $\bar{p}p \rightarrow K^{\pm} K_S^{\mp} \pi^{\mp}$
270 ± 40	AMSLER	94D CBAR	0.0 $\bar{p}p \rightarrow \pi^0 \pi^0 \eta$
270 ± 40	BUGG	94 RVUE	$\bar{p}p \rightarrow \eta 2\pi^0$
230 ± 30	ETKIN	82c MPS	23 $\pi^- p \rightarrow n 2K_S^0$
~ 250	MARTIN	78 SPEC	10 $K^{\pm} p \rightarrow K_S^0 \pi p$
79 ± 10	6 CASON	76	
4 Coupled-channel analysis of AMSLER 95b, AMSLER 95c, and AMSLER 94d. 5 T-matrix pole. 6 Isospin 0 not excluded.			

$a_0(1450)$ DECAY MODES

Mode	Fraction (Γ_i/Γ)
$\Gamma_1 \pi \eta$	seen
$\Gamma_2 \pi \eta'(958)$	seen
$\Gamma_3 K \bar{K}$	seen

$\Gamma(\pi \eta'(958))/\Gamma(\pi \eta)$ Γ_2/Γ_1

VALUE	DOCUMENT ID	TECN	COMMENT
0.35 ± 0.16	7 ABELE	98 CBAR	0.0 $\bar{p}p \rightarrow K_L^0 K^{\pm} \pi^{\mp}$
• • • We do not use the following data for averages, fits, limits, etc. • • •			
0.43 ± 0.19	ABELE	97C CBAR	0.0 $\bar{p}p \rightarrow \pi^0 \pi^0 \eta'$
0.7 Using $\pi^0 \eta$ from AMSLER 94d.			

$\Gamma(K \bar{K})/\Gamma(\pi \eta)$ Γ_3/Γ_1

VALUE	DOCUMENT ID	TECN	COMMENT
0.88 ± 0.23	7 ABELE	98 CBAR	0.0 $\bar{p}p \rightarrow K_L^0 K^{\pm} \pi^{\mp}$

$a_0(1450)$ REFERENCES

ABELE	98 PR D57 3860	A. Abele et al.	(Crystal Barrel Collab.)
ANISOVICH	98B UFN 41 419	V.V. Anisovich et al.	
BERTIN	98B PL B434 180	A. Bertin et al.	(OBELIX Collab.)
ABELE	97C PL B404 179	A. Abele et al.	(Crystal Barrel Collab.)
AMSLER	95B PL B342 433	C. Amisler et al.	(Crystal Barrel Collab.)
AMSLER	95C PL B353 571	C. Amisler et al.	(Crystal Barrel Collab.)
AMSLER	95D PL B355 425	C. Amisler et al.	(Crystal Barrel Collab.)
AMSLER	94D PL B333 277	C. Amisler et al.	(Crystal Barrel Collab.) IGJPC
BUGG	94 PR D50 4412	D.V. Bugg et al.	(LOQM)
ETKIN	82C PR D25 2446	A. Etkin et al.	(BNL, CUNY, TUFTS, VANO)
MARTIN	78 NP B134 392	A.D. Martin et al.	(DURH, GEVA)
CASON	76 PRL 36 1485	N.M. Cason et al.	(NDAM, ANL)

OTHER RELATED PAPERS

MASONI	99 EPJ C8 385	A. Masoni	
AMSLER	98 RMP 70 1293	C. Amisler	

$\rho(1450)$ $I^G(J^{PC}) = 1^+(1^{--})$
 See the mini-review under the $\rho(1700)$.

$\rho(1450)$ MASS

VALUE (MeV)	DOCUMENT ID	TECN	COMMENT
1465 ± 25 OUR ESTIMATE This is only an educated guess; the error given is larger than the error on the average of the published values.			
1452 ± 8 OUR AVERAGE Includes data from the 2 datablocks that follow this one.			

$\eta \rho^0$ MODE

VALUE (MeV)	DOCUMENT ID	TECN	COMMENT
The data in this block is included in the average printed for a previous datablock.			
1470 ± 20	ANTONELLI	88 DM2	$e^+ e^- \rightarrow \eta \pi^+ \pi^-$
1446 ± 10	FUKUI	88 SPEC	8.95 $\pi^- p \rightarrow \eta \pi^+ \pi^- n$

$\omega \pi$ MODE

VALUE (MeV)	DOCUMENT ID	TECN	COMMENT
The data in this block is included in the average printed for a previous datablock.			
1463 ± 25	1 CLEGG	94 RVUE	

• • • We do not use the following data for averages, fits, limits, etc. • • •

1250	2 ASTON	80c OMEG	20–70 $\gamma p \rightarrow \omega \pi^0 p$
1290 ± 40	2 BARBER	80c SPEC	3–5 $\gamma p \rightarrow \omega \pi^0 p$
1 Using data from BISELLO 91b, DOLINSKY 86 and ALBRECHT 87L. 2 Not separated from $b_1(1235)$, not pure $J^P = 1^-$ effect.			

Meson Particle Listings

$\rho(1450)$

$\pi\pi$ MODE

VALUE (MeV)	DOCUMENT ID	TECN	COMMENT
• • • We do not use the following data for averages, fits, limits, etc. • • •			
~ 1368	3 ABELE	99C CBAR	$0.0 \bar{p}d \rightarrow \pi^+ \pi^- \pi^- p$
1348 ± 33	BERTIN	98 OBLX	$0.05-0.405 \bar{n}p \rightarrow \pi^+ \pi^+ \pi^-$
1411 ± 14	4 ABELE	97 CBAR	$\bar{p}n \rightarrow \pi^- \pi^0 \pi^0$
1370 +90 -70	ACHASOV	97 RVUE	$e^+e^- \rightarrow \pi^+ \pi^-$
1380 ± 24	5 BARATE	97M ALEP	$\tau^- \rightarrow \pi^- \pi^0 \nu_\tau$
1359 ± 40	6 BERTIN	97C OBLX	$0.0 \bar{p}p \rightarrow \pi^+ \pi^- \pi^0$
1282 ± 37	BERTIN	97D OBLX	$0.05 \bar{p}p \rightarrow 2\pi^+ 2\pi^-$
1424 ± 25	BISELLO	89 DM2	$e^+e^- \rightarrow \pi^+ \pi^-$
1292 ± 17	7 KURDADZE	83 OLYA	$0.64-1.4 e^+e^- \rightarrow \pi^+ \pi^-$
3 $\rho(1700)$ mass and width fixed at 1780 MeV and 275 MeV respectively.			
4 T-matrix pole.			
5 Fixing $\rho(1450)$ width to 310 MeV and $\rho(1700)$ mass and width to 1700 MeV and 235 MeV respectively.			
6 $\rho(1700)$ mass and width fixed at 1700 MeV and 235 MeV, respectively.			
7 Using for $\rho(1700)$ mass and width 1600 ± 20 and 300 ± 10 MeV respectively.			

$\pi^+ \pi^- \pi^+ \pi^-$ MODE

VALUE (MeV)	DOCUMENT ID	TECN	COMMENT
• • • We do not use the following data for averages, fits, limits, etc. • • •			
1350 ± 50	ACHASOV	97 RVUE	$e^+e^- \rightarrow 2(\pi^+ \pi^-)$
1449 ± 4	8 ARMSTRONG	89E OMEG	$300 pp \rightarrow p\rho 2(\pi^+ \pi^-)$
8 Not clear whether this observation has $I=1$ or 0.			

$\phi\pi$ MODE

VALUE (MeV)	DOCUMENT ID	TECN	CHG	COMMENT
• • • We do not use the following data for averages, fits, limits, etc. • • •				
1480 ± 40	9,10 BITYUKOV	87 SPEC	0	$32.5 \pi^- p \rightarrow \phi \pi^0 n$
9 DONNACHIE 91 suggests this is a different particle.				
10 Not seen by ABELE 97H.				

$K\bar{K}$ MODE

VALUE (MeV)	EVTS	DOCUMENT ID	TECN	CHG	COMMENT
• • • We do not use the following data for averages, fits, limits, etc. • • •					
1422.8 ± 6.5	27k	11 ABELE	99D CBAR	±	$0.0 \bar{p}p \rightarrow K^+ K^- \pi^0$
11 K-matrix pole. Isospin not determined, could be $\omega(1420)$.					

MIXED MODES

VALUE (MeV)	DOCUMENT ID	TECN	COMMENT
• • • We do not use the following data for averages, fits, limits, etc. • • •			
1265.5 ± 75.3	DUBNICKA	89 RVUE	$e^+e^- \rightarrow \pi^+ \pi^-$

$\rho(1450)$ WIDTH

VALUE (MeV) DOCUMENT ID
310 ± 60 OUR ESTIMATE This is only an educated guess; the error given is larger than the error on the average of the published values.

$\eta\rho^0$ MODE

VALUE (MeV)	DOCUMENT ID	TECN	COMMENT
• • • We do not use the following data for averages, fits, limits, etc. • • •			
230 ± 30	ANTONELLI	88 DM2	$e^+e^- \rightarrow \eta \pi^+ \pi^-$
60 ± 15	FUKUI	88 SPEC	$8.95 \pi^- p \rightarrow \eta \pi^+ \pi^- n$

$\omega\pi$ MODE

VALUE (MeV)	DOCUMENT ID	TECN	COMMENT
The data in this block is included in the average printed for a previous datablock.			
311 ± 62	12 CLEGG	94 RVUE	
• • • We do not use the following data for averages, fits, limits, etc. • • •			
300	13 ASTON	80C OMEG	$20-70 \gamma p \rightarrow \omega \pi^0 p$
320 ± 100	13 BARBER	80C SPEC	$3-5 \gamma p \rightarrow \omega \pi^0 p$
12 Using data from BISELLO 91B, DOLINSKY 86 and ALBRECHT 87L.			
13 Not separated from $b_1(1235)$, not pure $J^P = 1^-$ effect.			

$\pi\pi$ MODE

VALUE (MeV)	DOCUMENT ID	TECN	COMMENT
• • • We do not use the following data for averages, fits, limits, etc. • • •			
~ 374	14 ABELE	99C CBAR	$0.0 \bar{p}d \rightarrow \pi^+ \pi^- \pi^- p$
275 ± 10	BERTIN	98 OBLX	$0.05-0.405 \bar{n}p \rightarrow \pi^+ \pi^+ \pi^-$
343 ± 20	15 ABELE	97 CBAR	$\bar{p}n \rightarrow \pi^- \pi^0 \pi^0$
310 ± 40	16 BERTIN	97C OBLX	$0.0 \bar{p}p \rightarrow \pi^+ \pi^- \pi^0$
236 ± 36	BERTIN	97D OBLX	$0.05 \bar{p}p \rightarrow 2\pi^+ 2\pi^-$
269 ± 31	BISELLO	89 DM2	$e^+e^- \rightarrow \pi^+ \pi^-$
218 ± 46	17 KURDADZE	83 OLYA	$0.64-1.4 e^+e^- \rightarrow \pi^+ \pi^-$
14 $\rho(1700)$ mass and width fixed at 1780 MeV and 275 MeV respectively.			
15 T-matrix pole.			
16 $\rho(1700)$ mass and width fixed at 1700 MeV and 235 MeV, respectively.			
17 Using for $\rho(1700)$ mass and width 1600 ± 20 and 300 ± 10 MeV respectively.			

$\phi\pi$ MODE

VALUE (MeV)	DOCUMENT ID	TECN	CHG	COMMENT
• • • We do not use the following data for averages, fits, limits, etc. • • •				
130 ± 60	18,19 BITYUKOV	87 SPEC	0	$32.5 \pi^- p \rightarrow \phi \pi^0 n$
18 DONNACHIE 91 suggests this is a different particle.				
19 Not seen by ABELE 97H.				

$K\bar{K}$ MODE

VALUE (MeV)	EVTS	DOCUMENT ID	TECN	CHG	COMMENT
• • • We do not use the following data for averages, fits, limits, etc. • • •					
146.5 ± 10.5	27k	20 ABELE	99D CBAR	±	$0.0 \bar{p}p \rightarrow K^+ K^- \pi^0$
20 K-matrix pole. Isospin not determined, could be $\omega(1420)$.					

MIXED MODES

VALUE (MeV)	DOCUMENT ID	TECN	COMMENT
• • • We do not use the following data for averages, fits, limits, etc. • • •			
391 ± 70	DUBNICKA	89 RVUE	$e^+e^- \rightarrow \pi^+ \pi^-$

$\rho(1450)$ DECAY MODES

Mode	Fraction (Γ_i/Γ)	Confidence level
$\Gamma_1 \pi\pi$	seen	
$\Gamma_2 4\pi$	seen	
$\Gamma_3 \omega\pi$	<2.0 %	95%
$\Gamma_4 e^+e^-$	seen	
$\Gamma_5 \eta\rho$	<4 %	
$\Gamma_6 \rho_2(1320)\pi$	not seen	
$\Gamma_7 \phi\pi$	<1 %	
$\Gamma_8 K\bar{K}$	<1.6 × 10 ⁻³	95%

$\rho(1450) \Gamma(I)\Gamma(e^+e^-)/\Gamma(\text{total})$

$\Gamma(\pi\pi) \times \Gamma(e^+e^-)/\Gamma_{\text{total}}$	VALUE (keV)	DOCUMENT ID	TECN	COMMENT	$\Gamma_1\Gamma_4/\Gamma$
• • • We do not use the following data for averages, fits, limits, etc. • • •					
0.12	21 DIEKMANN	88 RVUE		$e^+e^- \rightarrow \pi^+ \pi^-$	
0.027 + 0.015 - 0.010	22 KURDADZE	83 OLYA		$0.64-1.4 e^+e^- \rightarrow \pi^+ \pi^-$	
21 Using total width = 235 MeV.					
22 Using for $\rho(1700)$ mass and width 1600 ± 20 and 300 ± 10 MeV respectively.					

$\Gamma(\eta\rho) \times \Gamma(e^+e^-)/\Gamma_{\text{total}}$	VALUE (eV)	DOCUMENT ID	TECN	COMMENT	$\Gamma_5\Gamma_4/\Gamma$
91 ± 19	ANTONELLI	88 DM2		$e^+e^- \rightarrow \eta \pi^+ \pi^-$	

$\Gamma(\phi\pi) \times \Gamma(e^+e^-)/\Gamma_{\text{total}}$	VALUE (eV)	CL%	DOCUMENT ID	TECN	COMMENT	$\Gamma_7\Gamma_4/\Gamma$
<70	90	23	AULCHENKO	87B ND	$e^+e^- \rightarrow K_S^0 K_L^0 \pi^0$	
23 Using mass 1480 ± 40 MeV and total width 130 ± 60 MeV of BITYUKOV 87.						

$\rho(1450)$ BRANCHING RATIOS

$\Gamma(\eta\rho)/\Gamma_{\text{total}}$	VALUE	DOCUMENT ID	TECN	COMMENT	Γ_5/Γ
<0.04	DONNACHIE	87B RVUE			

$\Gamma(\rho_2(1320)\pi)/\Gamma_{\text{total}}$	VALUE	DOCUMENT ID	TECN	COMMENT	Γ_6/Γ
• • • We do not use the following data for averages, fits, limits, etc. • • •					
not seen	AMELIN	00 VES		$37 \pi^- p \rightarrow \eta \pi^+ \pi^- n$	

$\Gamma(\phi\pi)/\Gamma(\omega\pi)$	VALUE	CL%	DOCUMENT ID	TECN	CHG	COMMENT	Γ_7/Γ_3
>0.5	95		BITYUKOV	87 SPEC	0	$32.5 \pi^- p \rightarrow \phi \pi^0 n$	

$\Gamma(\omega\pi)/\Gamma(4\pi)$	VALUE	DOCUMENT ID	TECN	COMMENT	Γ_3/Γ_2
<0.14	CLEGG	88 RVUE			

$\Gamma(\eta\rho)/\Gamma(\omega\pi)$	VALUE	DOCUMENT ID	TECN	COMMENT	Γ_5/Γ_3
~ 0.24	24 DONNACHIE	91 RVUE			
• • • We do not use the following data for averages, fits, limits, etc. • • •					
>2	FUKUI	91 SPEC		$8.95 \pi^- p \rightarrow \omega \pi^0 n$	

$\Gamma(\omega\pi)/\Gamma_{\text{total}}$	VALUE	DOCUMENT ID	TECN	COMMENT	Γ_3/Γ
~ 0.21	CLEGG	94 RVUE			

See key on page 239

Meson Particle Listings

$\rho(1450), f_0(1500)$

$\Gamma(\pi\pi)/\Gamma(\omega\pi)$	DOCUMENT ID	TECN	Γ_1/Γ_3
VALUE			
~ 0.32	CLEGG	94 RVUE	
$\Gamma(\phi\pi)/\Gamma_{total}$	DOCUMENT ID	TECN	COMMENT
VALUE			
< 0.01	24 DONNACHIE	91 RVUE	
• • • We do not use the following data for averages, fits, limits, etc. • • •			
not seen	ABELE	97H CBAR	$\bar{p}p \rightarrow K_L^0 K_S^0 \pi^0 \pi^0$
$\Gamma(K\bar{K})/\Gamma(\omega\pi)$	DOCUMENT ID	TECN	Γ_8/Γ_3
VALUE			
< 0.08	24 DONNACHIE	91 RVUE	
24 Using data from BISELLO 91b, DOLINSKY 86 and ALBRECHT 87L.			

• • • We do not use the following data for averages, fits, limits, etc. • • •			
1497 ± 10	4 BARBERIS	99 OMEG	450 $pp \rightarrow \rho_S \rho_f K^+ K^-$
1502 ± 10	4 BARBERIS	99B OMEG	450 $pp \rightarrow \rho_S \rho_f \pi^+ \pi^-$
1502 ± 12 ± 10	5 BARBERIS	99D OMEG	450 $pp \rightarrow K^+ K^-, \pi^+ \pi^-$
1530 ± 45	4 BELLAZZINI	99 GAM4	450 $pp \rightarrow \rho \rho \pi^0 \pi^0$
1505 ± 18	4 FRENCH	99	300 $pp \rightarrow \rho_f(K^+ K^-) \rho_S \pi^0 n$
1580 ± 80	4 ALDE	98 GAM4	100 $\pi^- p \rightarrow \pi^0 \pi^0 n$
1499 ± 8	1 ANISOVICH	98B RVUE	Compilation
~ 1520	REYES	98 SPEC	800 $pp \rightarrow \rho_S \rho_f K_S^0 K_S^0$
~ 1475	FRABETTI	97D E687	$D_S^\pm \rightarrow \pi^\mp \pi^\pm \pi^\pm$
~ 1505	ABELE	96 CBAR	0.0 $\bar{p}p \rightarrow 5\pi^0$
1500 ± 8	1 ABELE	96C RVUE	Compilation
1460 ± 20	4 AMELIN	96B VES	37 $\pi^- A \rightarrow \eta \eta \pi^- A$
1500 ± 8	BUGG	96 RVUE	
1500 ± 10	6 AMSLER	95D CBAR	0.0 $\bar{p}p \rightarrow \pi^0 \pi^0 \pi^0, \pi^0 \eta, \pi^0 \pi^0 \eta$
1445 ± 5	7 ANTINORI	95 OMEG	300,450 $pp \rightarrow \rho \rho 2(\pi^+ \pi^-)$
1497 ± 30	4 ANTINORI	95 OMEG	300,450 $pp \rightarrow \rho \rho \pi^+ \pi^-$
~ 1505	BUGG	95 MRK3	J/ $\psi \rightarrow \gamma \pi^+ \pi^- \pi^+ \pi^-$
1446 ± 5	4 ABATZIS	94 OMEG	450 $pp \rightarrow \rho \rho 2(\pi^+ \pi^-)$
1545 ± 25	4 AMSLER	94E CBAR	0.0 $\bar{p}p \rightarrow \pi^0 \eta \eta'$
1520 ± 25	1,8 ANISOVICH	94 CBAR	0.0 $\bar{p}p \rightarrow 3\pi^0, \pi^0 \eta \eta$
1505 ± 20	1,9 BUGG	94 RVUE	$\bar{p}p \rightarrow 3\pi^0, \eta \eta \pi^0, \eta \pi^0 \pi^0$
1560 ± 25	4 AMSLER	92 CBAR	0.0 $\bar{p}p \rightarrow \pi^0 \eta \eta$
1550 ± 45 ± 30	4 BELADIDZE	92C VES	36 $\pi^- Be \rightarrow \pi^- \eta' \eta Be$
1449 ± 4	4 ARMSTRONG	89E OMEG	300 $pp \rightarrow \rho \rho 2(\pi^+ \pi^-)$
1610 ± 20	4 ALDE	88 GAM4	300 $\pi^- N \rightarrow \pi^- N 2\eta$
~ 1525	ASTON	88D LASS	11 $K^- p \rightarrow K_S^0 K_S^0 \Lambda$
1570 ± 20	4 ALDE	87 GAM4	100 $\pi^- p \rightarrow 4\pi^0 n$
1575 ± 45	10 ALDE	86D GAM4	100 $\pi^- p \rightarrow 2\eta n$
1568 ± 33	4 BINON	84C GAM2	38 $\pi^- p \rightarrow \eta \eta' n$
1592 ± 25	4 BINON	83 GAM2	38 $\pi^- p \rightarrow 2\eta n$
1525 ± 5	4 GRAY	83 DBC	0.0 $\bar{p}N \rightarrow 3\pi$

$\rho(1450)$ REFERENCES

AMELIN	00	NP B668 83	D. Amelin <i>et al.</i>	(VES Collab.)
ABELE	99C	PL B450 275	A. Abele <i>et al.</i>	(Crystal Barrel Collab.)
ABELE	99D	PL B468 178	A. Abele <i>et al.</i>	(Crystal Barrel Collab.)
BERTIN	98	PR D57 55	A. Bertin <i>et al.</i>	(OBELIX Collab.)
ABELE	97	PL B391 191	A. Abele <i>et al.</i>	(Crystal Barrel Collab.)
ABELE	97H	PL B415 280	A. Abele <i>et al.</i>	(Crystal Barrel Collab.)
ACHASOV	97	PR D55 2663	N.N. Achasov <i>et al.</i>	(NOVM)
BARATE	97M	ZPHY C76 15	R. Barate <i>et al.</i>	(ALEPH Collab.)
BERTIN	97C	PL B408 476	A. Bertin <i>et al.</i>	(OBELIX Collab.)
BERTIN	97D	PL B414 220	A. Bertin <i>et al.</i>	(OBELIX Collab.)
CLEGG	94	ZPHY C62 455	A.B. Clegg, A. Donnachie	(LANC, MCHS)
BISELLO	91B	NP B21 111 (suppl)	D. Bisello	(DM2 Collab.)
DONNACHIE	91	ZPHY C51 689	A. Donnachie, A.B. Clegg	(MCHS, LANC)
FUKUI	91	PL B257 241	S. Fukui <i>et al.</i>	(SUGI, NAGO, KEK, KYOT+)
ARMSTRONG	89E	PL B228 536	T.A. Armstrong, M. Benayoun	(ATHU, BARI, BIRM+)
BISELLO	89	PL B220 321	O. Bisello <i>et al.</i>	(DM2 Collab.)
DUBNICKA	89	JPG 15 1349	S. Dubnicka <i>et al.</i>	(JINR, SLOV)
ANTONELLI	88	PL B212 133	A. Antonelli <i>et al.</i>	(DM2 Collab.)
CLEGG	88	ZPHY C40 313	A.B. Clegg, A. Donnachie	(MCHS, LANC)
DIEMAN	88	PRPL 159 101	B. Diekmann	(BONN)
FUKUI	88	PL B202 441	S. Fukui <i>et al.</i>	(SUGI, NAGO, KEK, KYOT+)
ALBRECHT	87L	PL B185 223	H. Albrecht <i>et al.</i>	(ARGUS Collab.)
AULCHENKO	87B	JETPL 45 145	V.M. Aulcherko <i>et al.</i>	(NOVO)
Translated from ZETFP 45 118.				
BITUYKOV	87	PL B188 383	S.I. Bituykov <i>et al.</i>	(SERP)
DONNACHIE	87B	ZPHY C34 257	A. Donnachie, A.B. Clegg	(MCHS, LANC)
DOLINSKY	86	PL B174 453	S.I. Dolinsky <i>et al.</i>	(NOVO)
KURDADZE	83	JETPL 37 733	L.M. Kurdadze <i>et al.</i>	(NOVO)
Translated from ZETFP 37 613.				
ASTON	80C	PL 92B 211	D. Aston	(BONN, CERN, EPOL, GLAS, LANC+)
BARBER	80C	ZPHY C4 169	D.P. Barber <i>et al.</i>	(DARE, LANC, SHEF)

OTHER RELATED PAPERS

BELOZEROVA	98	PPN 29 63	T.S. Belozeroval, V.K. Henner	
Translated from FECAV 29 148.				
ABELE	97H	PL B415 280	A. Abele <i>et al.</i>	(Crystal Barrel Collab.)
BARNES	97	PR D55 4157	T. Barnes <i>et al.</i>	(ORNL, RAL, MCHS)
CLOSE	97C	PR D56 1584	F.E. Close <i>et al.</i>	(RAL, MCHS)
URHEIM	97	NPBPS 55C 359	J. Urheim	(CLEO Collab.)
ACHASOV	96B	PAN 59 1262	N.N. Achasov, G.N. Shestakov	(NOVM)
Translated from YAF 59 1319.				
MURADOV	94	PAN 57 864	R.K. Muradov	(BAKU)
LANDSBERG	92	SJNP 55 1051		(SERP)
Translated from YAF 55 1896.				
BRAU	88	PR D37 2379	J.E. Brau <i>et al.</i>	
ASTON	87	NP B292 693	D. Aston <i>et al.</i>	(SLAC, NAGO, CINC, INUS)
KURDADZE	86	JETPL 43 643	L.M. Kurdadze <i>et al.</i>	(NOVO)
Translated from ZETFP 43 497.				
BARKOV	85	NP B256 365	L.M. Barkov <i>et al.</i>	(NOVO)
BISELLO	85	LAL 85-15	D. Bisello <i>et al.</i>	(PADO, LALO, CLER+)
ABE	84B	PR 53 751	K. Abe <i>et al.</i>	
ATKINSON	84C	NP B243 1	M. Atkinson <i>et al.</i>	(BONN, CERN, GLAS+)
CORDIER	82	PL 109B 129	A. Cordier <i>et al.</i>	(LALO)
KILLIAN	80	PR D21 3005	T.J. Killian <i>et al.</i>	(CORN)
COSME	76	PL 63B 352	G. Cosme <i>et al.</i>	(ORSAY)
BINGHAM	72B	PL 41B 635	H.H. Bingham <i>et al.</i>	(LBL, UCB, SLAC)
FRENKIEL	72	NP B47 61	P. Frenkiel <i>et al.</i>	(CDEF, CERN)
LAYSAC	71	NC 6A 134	J. Laysac, F.M. Renard	(MONP)

$f_0(1500)$

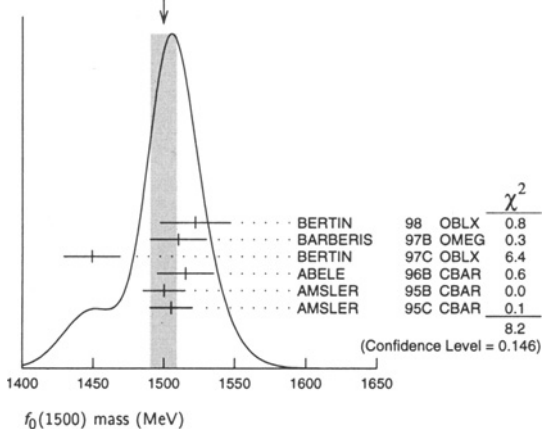
$$J^{PC} = 0^+(0^{++})$$

See also the mini-reviews on scalar mesons under $f_0(1370)$ and on non- $q\bar{q}$ candidates. (See the index for the page number.)

$f_0(1500)$ MASS

VALUE (MeV)	EVTS	DOCUMENT ID	TECN	COMMENT
1500 ± 10 OUR AVERAGE		Error includes scale factor of 1.3. See the ideogram below.		
1522 ± 25		BERTIN	98 OBLX	0.05–0.405 $\bar{n}p \rightarrow \pi^+ \pi^+ \pi^-$
1510 ± 20		1 BARBERIS	97B OMEG	450 $pp \rightarrow \rho \rho 2(\pi^+ \pi^-)$
1449 ± 20		1 BERTIN	97C OBLX	0.0 $\bar{p}p \rightarrow \pi^+ \pi^- \pi^0$
1515 ± 20		ABELE	96B CBAR	0.0 $\bar{p}p \rightarrow \pi^0 K_L^0 K_L^0$
1500 ± 15		2 AMSLER	95B CBAR	0.0 $\bar{p}p \rightarrow 3\pi^0$
1505 ± 15		3 AMSLER	95C CBAR	0.0 $\bar{p}p \rightarrow \eta \eta \pi^0$

WEIGHTED AVERAGE
1500 ± 10 (Error scaled by 1.3)



Meson Particle Listings

 $f_0(1500)$ $f_0(1500)$ WIDTH

VALUE (MeV)	EVTs	DOCUMENT ID	TECN	COMMENT
112 ± 10 OUR AVERAGE				
108 ± 33		BERTIN 98	OBLX	0.05–0.405 $\bar{p}p \rightarrow \pi^+ \pi^+ \pi^-$
120 ± 35		11 BARBERIS 97B	OMEG	450 $\rho\rho \rightarrow \rho\rho 2(\pi^+ \pi^-)$
114 ± 30		11 BERTIN 97C	OBLX	0.0 $\bar{p}p \rightarrow \pi^+ \pi^- \pi^0$
105 ± 15		ABELE 96B	CBAR	0.0 $\bar{p}p \rightarrow \pi^0 K_L^0 K_L^0$
120 ± 25		12 AMSLER 95B	CBAR	0.0 $\bar{p}p \rightarrow 3\pi^0$
120 ± 30		13 AMSLER 95C	CBAR	0.0 $\bar{p}p \rightarrow \eta\eta\pi^0$
• • • We do not use the following data for averages, fits, limits, etc. • • •				
104 ± 25		14 BARBERIS 99	OMEG	450 $\rho\rho \rightarrow \rho_S \rho_f K^+ K^-$
131 ± 15		14 BARBERIS 99B	OMEG	450 $\rho\rho \rightarrow \rho_S \rho_f \pi^+ \pi^-$
98 ± 18 ± 16		15 BARBERIS 99D	OMEG	450 $\rho\rho \rightarrow K^+ K^-$
160 ± 50		14 BELLAZZINI 99	GAM4	450 $\rho\rho \rightarrow \rho\rho\pi^0\pi^0$
100 ± 33		14 FRENCH 99		300 $\rho\rho \rightarrow \rho_f(K^+ K^-) \rho_S$
280 ± 100		16 ALDE 98	GAM4	100 $\pi^- p \rightarrow \pi^0 \pi^0 n$
130 ± 20		11 ANISOVICH 98B	RVUE	Compilation
~100		FRABETTI 97D	E687	$D_S^\pm \rightarrow \pi^\mp \pi^\pm \pi^\pm$
~169		ABELE 96	CBAR	0.0 $\bar{p}p \rightarrow 5\pi^0$
100 ± 30	120	14 AMELIN 96B	VES	37 $\pi^- A \rightarrow \eta\eta\pi^- A$
132 ± 15		96	RVUE	
154 ± 30		17 AMSLER 95D	CBAR	0.0 $\bar{p}p \rightarrow \pi^0 \pi^0 \pi^0, \pi^0 \eta\eta, \pi^0 \pi^0 \eta$
65 ± 10		18 ANTINORI 95	OMEG	300,450 $\rho\rho \rightarrow \rho\rho 2(\pi^+ \pi^-)$
199 ± 30		14 ANTINORI 95	OMEG	300,450 $\rho\rho \rightarrow \rho\rho \pi^+ \pi^-$
56 ± 12		14 ABATZIS 94	OMEG	450 $\rho\rho \rightarrow \rho\rho 2(\pi^+ \pi^-)$
100 ± 40		14 AMSLER 94E	CBAR	0.0 $\bar{p}p \rightarrow \pi^0 \eta\eta'$
148 ± 20		11,19 ANISOVICH 94	CBAR	0.0 $\bar{p}p \rightarrow 3\pi^0, \pi^0 \eta\eta$
150 ± 20		11,20 BUGG 94	RVUE	$\bar{p}p \rightarrow 3\pi^0, \eta\eta\pi^0, \eta\pi^0 \pi^0$
245 ± 50		14 AMSLER 92	CBAR	0.0 $\bar{p}p \rightarrow \pi^0 \eta\eta$
153 ± 67 ± 50		14 BELADIDZE 92C	VES	36 $\pi^- Be \rightarrow \pi^- \eta' \eta Be$
78 ± 18		14 ARMSTRONG 89E	OMEG	300 $\rho\rho \rightarrow \rho\rho 2(\pi^+ \pi^-)$
170 ± 40		14 ALDE 88	GAM4	300 $\pi^- N \rightarrow \pi^- N 2\eta$
150 ± 20	600	14 ALDE 87	GAM4	100 $\pi^- p \rightarrow 4\pi^0 n$
265 ± 65		21 ALDE 86D	GAM4	100 $\pi^- p \rightarrow 2\eta n$
260 ± 60		84C BINON 84C	GAM2	38 $\pi^- p \rightarrow \eta\eta' n$
210 ± 40		14 BINON 83	GAM2	38 $\pi^- p \rightarrow 2\eta n$
101 ± 13		14 GRAY 83	DBC	0.0 $\bar{p}N \rightarrow 3\pi$

11 T-matrix pole.

12 T-matrix pole, supersedes ANISOVICH 94.

13 T-matrix pole, supersedes ANISOVICH 94 and AMSLER 92.

14 Breit-Wigner mass.

15 Supersedes BARBERIS 99 and BARBERIS 99B.

16 Breit-Wigner width.

17 T-matrix pole. Coupled-channel analysis of AMSLER 95B, AMSLER 95C, and AMSLER 94D.

18 Supersedes ABATZIS 94, ARMSTRONG 89E. Breit-Wigner mass.

19 From a simultaneous analysis of the annihilations $\bar{p}p \rightarrow 3\pi^0, \pi^0 \eta\eta$.

20 Reanalysis of ANISOVICH 94 data.

21 From central value and spread of two solutions. Breit-Wigner mass.

 $f_0(1500)$ DECAY MODES

Mode	Fraction (Γ_i/Γ)
Γ_1 $\eta\eta'(958)$	seen
Γ_2 $\eta\eta$	seen
Γ_3 4π	seen
Γ_4 $4\pi^0$	seen
Γ_5 $2\pi^+ 2\pi^-$	seen
Γ_6 $\pi\pi$	seen
Γ_7 $\pi^+ \pi^-$	seen
Γ_8 $2\pi^0$	seen
Γ_9 $K\bar{K}$	seen
Γ_{10} $\gamma\gamma$	

 $f_0(1500)$ $\Gamma(i)\Gamma(\gamma\gamma)/\Gamma(\text{total})$

VALUE (keV)	CL%	DOCUMENT ID	TECN	COMMENT
<0.46	95	BARATE 95	00E ALEP	$\gamma\gamma \rightarrow \pi^+ \pi^-$

 $f_0(1500)$ BRANCHING RATIOS

$\Gamma(\eta\eta'(958))/\Gamma(\eta\eta)$	DOCUMENT ID	TECN	COMMENT	Γ_1/Γ_2
0.29 ± 0.10	22 AMSLER 95C	CBAR	0.0 $\bar{p}p \rightarrow \eta\eta\pi^0$	
• • • We do not use the following data for averages, fits, limits, etc. • • •				
0.84 ± 0.23	ABELE 96C	RVUE	Compilation	
2.7 ± 0.8	BINON 84C	GAM2	38 $\pi^- p \rightarrow \eta\eta' n$	
22 Using AMSLER 94E ($\eta\eta' \pi^0$).				

$\Gamma(\eta\eta)/\Gamma_{\text{total}}$	DOCUMENT ID	TECN	COMMENT	Γ_2/Γ
• • • We do not use the following data for averages, fits, limits, etc. • • •				
large	ALDE 88	GAM4	300 $\pi^- N \rightarrow \eta\eta\pi^- N$	
large	BINON 83	GAM2	38 $\pi^- p \rightarrow 2\eta n$	

$\Gamma(4\pi^0)/\Gamma(\eta\eta)$	DOCUMENT ID	TECN	COMMENT	Γ_4/Γ_2
• • • We do not use the following data for averages, fits, limits, etc. • • •				
0.8 ± 0.3	ALDE 87	GAM4	100 $\pi^- p \rightarrow 4\pi^0 n$	

$\Gamma(2\pi^0)/\Gamma(\eta\eta)$	DOCUMENT ID	TECN	COMMENT	Γ_8/Γ_2
1.45 ± 0.61	23 AMSLER 95C	CBAR	0.0 $\bar{p}p \rightarrow \eta\eta\pi^0$	
• • • We do not use the following data for averages, fits, limits, etc. • • •				
4.29 ± 0.72	24 ABELE 96C	RVUE	Compilation	
2.12 ± 0.81	25 AMSLER 95D	CBAR	0.0 $\bar{p}p \rightarrow \pi^0 \pi^0 \pi^0, \pi^0 \eta\eta, \pi^0 \pi^0 \eta$	
<0.3	BINON 83	GAM2	38 $\pi^- p \rightarrow 2\eta n$	
23 Using AMSLER 95B ($3\pi^0$).				
24 2π width determined to be 60 ± 12 MeV.				
25 Coupled-channel analysis of AMSLER 95B, AMSLER 95C, and AMSLER 94D.				

$\Gamma(K\bar{K})/\Gamma(\eta\eta)$	DOCUMENT ID	TECN	COMMENT	Γ_9/Γ_2
<0.6	26 BINON 83	GAM2	38 $\pi^- p \rightarrow 2\eta n$	
• • • We do not use the following data for averages, fits, limits, etc. • • •				
<0.4	90	27 PROKOSHKIN 91	GAM4 300 $\pi^- p \rightarrow \pi^- p \eta\eta$	
26 Using ETKIN 82B and COHEN 80.				
27 Combining results of GAM4 with those of WA76 on $K\bar{K}$ central production.				

$\Gamma(K\bar{K})/\Gamma_{\text{total}}$	DOCUMENT ID	TECN	COMMENT	Γ_9/Γ
<0.6	• • • We do not use the following data for averages, fits, limits, etc. • • •			
0.044 ± 0.021	BUGG 96	RVUE		

$\Gamma(K\bar{K})/\Gamma(\pi\pi)$	DOCUMENT ID	TECN	COMMENT	Γ_9/Γ_6
0.19 ± 0.07	28 ABELE 98	CBAR	0.0 $\bar{p}p \rightarrow K_L^0 K_S^\pm \pi^\mp$	
• • • We do not use the following data for averages, fits, limits, etc. • • •				
0.33 ± 0.03 ± 0.07	BARBERIS 99D	OMEG	450 $\rho\rho \rightarrow K^+ K^-$	
0.20 ± 0.08	29 ABELE 96B	CBAR	0.0 $\bar{p}p \rightarrow \pi^0 K_L^0 K_L^0$	
28 Using $\pi^0 \pi^0$ from AMSLER 95B.				
29 Using AMSLER 95B ($3\pi^0$), AMSLER 94C ($2\pi^0 \eta$) and SU(3).				

$\Gamma(\pi\pi)/\Gamma_{\text{total}}$	DOCUMENT ID	TECN	COMMENT	Γ_6/Γ
• • • We do not use the following data for averages, fits, limits, etc. • • •				
0.454 ± 0.104	BUGG 96	RVUE		

$\Gamma(4\pi)/\Gamma(\pi\pi)$	DOCUMENT ID	TECN	COMMENT	Γ_3/Γ_6
• • • We do not use the following data for averages, fits, limits, etc. • • •				
3.4 ± 0.8	30 ABELE 96	CBAR	0.0 $\bar{p}p \rightarrow 5\pi^0$	
30 Excluding $\rho\rho$ contribution to 4π .				

$\Gamma(\pi^+ \pi^-)/\Gamma_{\text{total}}$	DOCUMENT ID	TECN	COMMENT	Γ_7/Γ
• • • We do not use the following data for averages, fits, limits, etc. • • •				
seen	BERTIN 98	OBLX	0.05–0.405 $\bar{p}p \rightarrow \pi^+ \pi^+ \pi^-$	
possibly seen	FRABETTI 97D	E687	$D_S^\pm \rightarrow \pi^\mp \pi^\pm \pi^\pm$	

See key on page 239

Meson Particle Listings

$f_0(1500), f_1(1510)$

$f_0(1500)$ REFERENCES

BARATE 00E PL B472 189	R. Barate <i>et al.</i>	(ALEPH Collab.)
BARBERIS 99 PL B453 305	D. Barberis <i>et al.</i>	(Omega expt.)
BARBERIS 99B PL B453 316	D. Barberis <i>et al.</i>	(Omega expt.)
BARBERIS 99D PL B462 462	D. Barberis <i>et al.</i>	(Omega expt.)
BELLAZZINI 99 PL B467 296	R. Bellazzini <i>et al.</i>	
FRENCH 99 PL B214 213	B. French <i>et al.</i>	(WA76 Collab.)
ABELE 98 PR D57 3860	A. Abele <i>et al.</i>	(Crystal Barrel Collab.)
ALDE 98 EPJ A3 361	D. Alde <i>et al.</i>	(GAM4 Collab.)
Also 99 PAN 62 405	D. Alde <i>et al.</i>	(GAMS Collab.)
ANISOVICH 98B UFN 41 419	V.V. Anisovich <i>et al.</i>	
BERTIN 98 PR D57 55	A. Bertin <i>et al.</i>	(OBELIX Collab.)
REYES 98 PRL 81 4079	M.A. Reyes <i>et al.</i>	
BARBERIS 97B PL B413 217	D. Barberis <i>et al.</i>	(WA102 Collab.)
BERTIN 97C PL B408 476	A. Bertin <i>et al.</i>	(OBELIX Collab.)
FRABETTI 97D PL B407 79	P.L. Frabetti <i>et al.</i>	(FNAL E687 Collab.)
ABELE 96 PL B380 453	A. Abele <i>et al.</i>	(Crystal Barrel Collab.)
ABELE 96B PL B385 425	A. Abele <i>et al.</i>	(Crystal Barrel Collab.)
ABELE 96C NP A609 562	A. Abele <i>et al.</i>	(Crystal Barrel Collab.)
AMELIN 96B PAN 59 976	D.V. Amelin <i>et al.</i>	(SERP, TBIL)
BUGG 96 NP B471 59	D.V. Bugg, A.V. Sarantsev, B.S. Zou	(LOQM, PNPI)
AMSLER 95B PL B342 433	C. Amisler <i>et al.</i>	(Crystal Barrel Collab.)
AMSLER 95C PL B353 571	C. Amisler <i>et al.</i>	(Crystal Barrel Collab.)
AMSLER 95D PL B355 425	C. Amisler <i>et al.</i>	(Crystal Barrel Collab.)
ANTINORI 95 PL B353 589	F. Antinori <i>et al.</i>	(ATHU, BARI, BIRM+)
BUGG 95 PL B353 378	D.V. Bugg <i>et al.</i>	(LOQM, PNPI, WASH)
ABATZIS 94 PL B324 509	S. Abatzis <i>et al.</i>	(ATHU, BARI, BIRM+)
AMSLER 94C PL B327 425	C. Amisler <i>et al.</i>	(Crystal Barrel Collab.)
AMSLER 94D PL B333 277	C. Amisler <i>et al.</i>	(Crystal Barrel Collab.)
AMSLER 94E PL B340 259	C. Amisler <i>et al.</i>	(Crystal Barrel Collab.)
ANISOVICH 94 PL B323 233	V.V. Anisovich <i>et al.</i>	
BUGG 94 PR D50 4412	D.V. Bugg <i>et al.</i>	(LOQM)
AMSLER 92 PL B291 347	C. Amisler <i>et al.</i>	(Crystal Barrel Collab.)
BEHADIDZE 92C SJNP 55 1535	G.M. Beladidze, S.I. Bitiyukov, G.V. Borisov	(SERP+)
Translated from YAF 55 2748.		
PROKOSHKIN 91 SPD 36 155	Y.D. Prokoshkin	(GAM2, GAM4 Collab.)
Translated from DANS 316 900.		
ARMSTRONG 89E PL B228 536	T.A. Armstrong, M. Benayoun	(ATHU, BARI, BIRM+)
ALDE 88 PL B201 160	D.M. Alde <i>et al.</i>	(SERP, BELG, LANL, LAPP+)
ASTON 88D NP B301 525	D. Aston <i>et al.</i>	(SLAC, NAGO, CINC, INUS)
ALDE 87 PL B198 286	D.M. Alde <i>et al.</i>	(LANL, BRUX, SERP, LAPP)
ALDE 86D NP B269 485	D.M. Alde <i>et al.</i>	(BELG, LAPP, SERP, CERN+)
BINON 84C NC B0A 363	F.G. Binon <i>et al.</i>	(BELG, LAPP, SERP+)
BINON 83 NC 78A 313	F.G. Binon <i>et al.</i>	(BELG, LAPP, SERP+)
Also 83B SJNP 38 561	F.G. Binon <i>et al.</i>	(BELG, LAPP, SERP+)
Translated from YAF 38 934.		
GRAY 83 PR D27 307	L. Gray <i>et al.</i>	(SYRA)
ETKIN 82B PR D25 1786	A. Etkin <i>et al.</i>	(BNL, CUNY, TUFTS, VAND)
COHEN 80 PR D22 2595	D. Cohen <i>et al.</i>	(ANL)

OTHER RELATED PAPERS

ANISOVICH 99H PL B467 289	A.V. Anisovich, V.V. Anisovich	
AMSLER 98 RMP 70 1293	C. Amisler	
STROHMEIER 98 PL B438 21	M. Strohmeier <i>et al.</i>	
ANISOVICH 97 PL B395 123	A.V. Anisovich, A.V. Sarantsev	(PNPI)
ANISOVICH 97B ZPHY A357 123	A.V. Anisovich <i>et al.</i>	(PNPI)
ANISOVICH 97C PL B413 137		
ANISOVICH 97E PAN 60 1892	A.V. Anisovich <i>et al.</i>	(PNPI)
Translated from YAF 60 2065.		
PROKOSHKIN 97 SPD 42 117	Y.D. Prokoshkin <i>et al.</i>	(SERP)
Translated from DANS 353 323.		
AMSLER 96 PR D53 295	C. Amisler, F.E. Close	(ZURI, RAL)
AMSLER 95E PL B353 385	C. Amisler, F.E. Close	(ZURI, RAL)
GASPERO 95 NP A588 861	M. Gaspero	(ROMA)
SLAUGHTER 88 MPL A3 1361	M.D. Slaughter	(LANL)

$f_1(1510)$

$$J^{G(J^{PC})} = 0^+(1^{++})$$

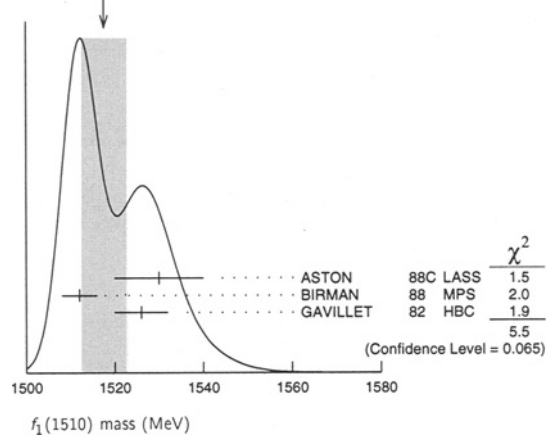
OMITTED FROM SUMMARY TABLE
See the minireview under $\eta(1440)$.

$f_1(1510)$ MASS

VALUE (MeV)	EVTS	DOCUMENT ID	TECN	COMMENT
1518 ± 5 OUR AVERAGE		Error includes scale factor of 1.7. See the ideogram below.		
1530 ± 10		ASTON	88C LASS	11 $K^- p \rightarrow K_S^0 K^\pm \pi^\mp \Lambda$
1512 ± 4	600	¹ BIRMAN	88 MPS	8 $\pi^- p \rightarrow K^+ \bar{K}^0 \pi^- n$
1526 ± 6	271	GAVILLET	82 HBC	4.2 $K^- p \rightarrow \Lambda K K \pi$
• • • We do not use the following data for averages, fits, limits, etc. • • •				
~ 1525		² BAUER	93B	$\gamma \gamma^* \rightarrow \pi^+ \pi^- \pi^0 \pi^0$

¹ From partial wave analysis of $K^+ \bar{K}^0 \pi^-$ state.
² Not seen by AIHARA 88C in the $K_S^0 K^\pm \pi^\mp$ final state.

WEIGHTED AVERAGE
1518 ± 5 (Error scaled by 1.7)

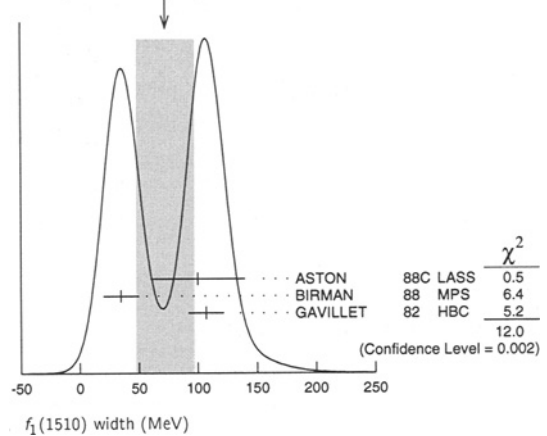


$f_1(1510)$ WIDTH

VALUE (MeV)	EVTS	DOCUMENT ID	TECN	COMMENT
73 ± 25 OUR AVERAGE		Error includes scale factor of 2.5. See the ideogram below.		
100 ± 40		ASTON	88C LASS	11 $K^- p \rightarrow K_S^0 K^\pm \pi^\mp \Lambda$
35 ± 15	600	³ BIRMAN	88 MPS	8 $\pi^- p \rightarrow K^+ \bar{K}^0 \pi^- n$
107 ± 15	271	GAVILLET	82 HBC	4.2 $K^- p \rightarrow \Lambda K K \pi$

³ From partial wave analysis of $K^+ \bar{K}^0 \pi^-$ state.

WEIGHTED AVERAGE
73 ± 25 (Error scaled by 2.5)



$f_1(1510)$ DECAY MODES

Mode	Fraction (Γ_i/Γ)
Γ_1 $K \bar{K}^*(892) + c.c.$	seen

$f_1(1510)$ REFERENCES

BAUER 93B PR D48 3976	D.A. Bauer <i>et al.</i>	(SLAC)
AIHARA 88C PR D38 1	H. Aihara <i>et al.</i>	(TPC-2 γ Collab.)
ASTON 88C PL B201 573	D. Aston <i>et al.</i>	(SLAC, NAGO, CINC, INUS) JP
BIRMAN 88 PRL 61 1557	A. Birman <i>et al.</i>	(BNL, FSU, IND, MASD) JP
GAVILLET 82 ZPHY C16 119	P. Gavillet <i>et al.</i>	(CERN, CDFE, PADO+)

OTHER RELATED PAPERS

ABELE 97G PL B415 289	A. Abele <i>et al.</i>	
BARBERIS 97C PL B413 225	D. Barberis <i>et al.</i>	(WA102 Collab.)
CLOSE 97D ZPHY C76 469	F.E. Close <i>et al.</i>	
KING 91 NP B21 11 (suppl)	E. King <i>et al.</i>	(FSU, BNL+)
AIHARA 88C PR D38 1	H. Aihara <i>et al.</i>	(TPC-2 γ Collab.)
BITYUKOV 84 SJNP 39 735	S. Bitiyukov <i>et al.</i>	(SERP)
Translated from YAF 39 1165.		

Meson Particle Listings

 $f_2'(1525)$ $f_2'(1525)$

$$I^G(J^{PC}) = 0^+(2^{++})$$

 $f_2'(1525)$ MASS

VALUE (MeV) DOCUMENT ID
1525 ± 5 OUR ESTIMATE This is only an educated guess; the error given is larger than the error on the average of the published values.

PRODUCED BY PION BEAM

VALUE (MeV)	EVTS	DOCUMENT ID	TECN	COMMENT
1547 ⁺¹⁰ ₋₂		1 LONGACRE	86 MPS	22 $\pi^- p \rightarrow K_S^0 K_S^0 n$
1496 ⁺⁹ ₋₈		2 CHABAUD	81 ASPK	6 $\pi^- p \rightarrow K^+ K^- n$
1497 ⁺⁸ ₋₉		CHABAUD	81 ASPK	18.4 $\pi^- p \rightarrow K^+ K^- n$
1492 ± 29		GORLICH	80 ASPK	17 $\pi^- p$ polarized → $K^+ K^- n$
1502 ± 25		3 CORDEN	79 OMEG	12-15 $\pi^- p \rightarrow$ $\pi^+ \pi^- n$
1480	14	CRENNELL	66 HBC	6.0 $\pi^- p \rightarrow K_S^0 K_S^0 n$

¹ From a partial-wave analysis of data using a K-matrix formalism with 5 poles.

² CHABAUD 81 is a reanalysis of PAWLICKI 77 data.

³ From an amplitude analysis where the $f_2'(1525)$ width and elasticity are in complete disagreement with the values obtained from $K\bar{K}$ channel, making the solution dubious.

PRODUCED BY K^\pm BEAM

VALUE (MeV)	EVTS	DOCUMENT ID	TECN	COMMENT
1524.6 ± 1.4 OUR AVERAGE	Includes data from the datablock that follows this one. Error includes scale factor of 1.1.			
1526.8 ± 4.3		ASTON	88b LASS	11 $K^- p \rightarrow K_S^0 K_S^0 \Lambda$
1504 ± 12		BOLONKIN	86 SPEC	40 $K^- p \rightarrow K_S^0 K_S^0 \gamma$
1529 ± 3		ARMSTRONG	83b OMEG	18.5 $K^- p \rightarrow K^- K^+ \Lambda$
1521 ± 6	650	AGUILAR...	81b HBC	4.2 $K^- p \rightarrow \Lambda K^+ K^-$
1521 ± 3	572	ALHARRAN	81 HBC	8.25 $K^- p \rightarrow \Lambda K\bar{K}$
1522 ± 6	123	BARREIRO	77 HBC	4.15 $K^- p \rightarrow \Lambda K_S^0 K_S^0$
1528 ± 7	166	EVANGELISTA	77 OMEG	10 $K^- p \rightarrow$ $K^+ K^- (\Lambda, \Sigma)$
1527 ± 3	120	BRANDENB...	76c ASPK	13 $K^- p \rightarrow$ $K^+ K^- (\Lambda, \Sigma)$
1519 ± 7	100	AGUILAR...	72b HBC	3.9, 4.6 $K^- p \rightarrow$ $K\bar{K} (\Lambda, \Sigma)$

• • • We do not use the following data for averages, fits, limits, etc. • • •

1513 ± 10 ⁴ BARKOV 99 SPEC 40 $K^- p \rightarrow K_S^0 K_S^0 \gamma$

⁴ Systematic errors not estimated.

PRODUCED IN e^+e^- ANNIHILATION

VALUE (MeV) DOCUMENT ID TECN COMMENT
 The data in this block is included in the average printed for a previous datablock.

VALUE (MeV)	EVTS	DOCUMENT ID	TECN	COMMENT
1524 ± 4 OUR AVERAGE	Error includes scale factor of 1.2.			
1535 ± 5 ± 4		ABREU	96c DLPH	$Z^0 \rightarrow K^+ K^-$
1516 ± 5 ⁺⁹ ₋₁₅		BAI	96c BES	$J/\psi \rightarrow \gamma K^+ K^-$
1529 ± 10		ACCIARRI	95j L3	$\gamma\gamma \rightarrow K_S^0 K_S^0 E_{cm}^{ee} =$ 88-94 GeV
1531.6 ± 10.0		AUGUSTIN	88 DM2	$J/\psi \rightarrow \gamma K^+ K^-$
1515 ± 5		⁵ FALVARD	88 DM2	$J/\psi \rightarrow \phi K^+ K^-$
1525 ± 10 ± 10		BALTRUSAIT..87	MRK3	$J/\psi \rightarrow \gamma K^+ K^-$
• • • We do not use the following data for averages, fits, limits, etc. • • •				
1496 ± 2		⁶ FALVARD	88 DM2	$J/\psi \rightarrow \phi K^+ K^-$

CENTRAL PRODUCTION

VALUE (MeV)	DOCUMENT ID	TECN	COMMENT
1515 ± 15	BARBERIS	99 OMEG	450 $pp \rightarrow$ $p_S p_f K^+ K^-$

⁵ From an analysis ignoring interference with $f_0(1710)$.

⁶ From an analysis including interference with $f_0(1710)$.

 $f_2'(1525)$ WIDTH

VALUE (MeV) DOCUMENT ID COMMENT
76 ± 10 OUR ESTIMATE This is only an educated guess; the error given is larger than the error on the average of the published values.

73⁺⁶₋₅ OUR FIT

76 ± 10 PDG 90 For fitting

PRODUCED BY PION BEAM

VALUE (MeV)	DOCUMENT ID	TECN	COMMENT
• • • We do not use the following data for averages, fits, limits, etc. • • •			
108 ⁺⁵ ₋₂	7 LONGACRE	86 MPS	22 $\pi^- p \rightarrow K_S^0 K_S^0 n$
69 ⁺²² ₋₁₆	8 CHABAUD	81 ASPK	6 $\pi^- p \rightarrow K^+ K^- n$
137 ⁺²³ ₋₂₁	CHABAUD	81 ASPK	18.4 $\pi^- p \rightarrow K^+ K^- n$
150 ⁺⁸³ ₋₅₀	GORLICH	80 ASPK	17 $\pi^- p$ polarized → $K^+ K^- n$
165 ± 42	⁹ CORDEN	79 OMEG	12-15 $\pi^- p \rightarrow$ $\pi^+ \pi^- n$
92 ⁺³⁹ ₋₂₂	¹⁰ POLYCHRO...	79 STRC	7 $\pi^- p \rightarrow n K_S^0 K_S^0$

⁷ From a partial-wave analysis of data using a K-matrix formalism with 5 poles.

⁸ CHABAUD 81 is a reanalysis of PAWLICKI 77 data.

⁹ From an amplitude analysis where the $f_2'(1525)$ width and elasticity are in complete disagreement with the values obtained from $K\bar{K}$ channel, making the solution dubious.

¹⁰ From a fit to the D with $f_2(1270)$ - $f_2'(1525)$ interference. Mass fixed at 1516 MeV.

PRODUCED BY K^\pm BEAM

VALUE (MeV)	EVTS	DOCUMENT ID	TECN	COMMENT
76 ± 5 OUR AVERAGE	Includes data from the datablock that follows this one.			
90 ± 12		ASTON	88b LASS	11 $K^- p \rightarrow K_S^0 K_S^0 \Lambda$
73 ± 18		BOLONKIN	86 SPEC	40 $K^- p \rightarrow K_S^0 K_S^0 \gamma$
83 ± 15		ARMSTRONG	83b OMEG	18.5 $K^- p \rightarrow K^- K^+ \Lambda$
85 ± 16	650	AGUILAR...	81b HBC	4.2 $K^- p \rightarrow \Lambda K^+ K^-$
80 ⁺¹⁴ ₋₁₁	572	ALHARRAN	81 HBC	8.25 $K^- p \rightarrow \Lambda K\bar{K}$
72 ± 25	166	EVANGELISTA	77 OMEG	10 $K^- p \rightarrow$ $K^+ K^- (\Lambda, \Sigma)$
69 ± 22	100	AGUILAR...	72b HBC	3.9, 4.6 $K^- p \rightarrow$ $K\bar{K} (\Lambda, \Sigma)$
• • • We do not use the following data for averages, fits, limits, etc. • • •				
75 ± 20		¹¹ BARKOV	99 SPEC	40 $K^- p \rightarrow K_S^0 K_S^0 \gamma$
62 ⁺¹⁹ ₋₁₄	123	BARREIRO	77 HBC	4.15 $K^- p \rightarrow \Lambda K_S^0 K_S^0$
61 ± 8	120	BRANDENB...	76c ASPK	13 $K^- p \rightarrow$ $K^+ K^- (\Lambda, \Sigma)$

¹¹ Systematic errors not estimated.

PRODUCED IN e^+e^- ANNIHILATION

VALUE (MeV) DOCUMENT ID TECN COMMENT
 The data in this block is included in the average printed for a previous datablock.

VALUE (MeV)	DOCUMENT ID	TECN	COMMENT
66 ± 8 OUR AVERAGE			
60 ± 20 ± 19	ABREU	96c DLPH	$Z^0 \rightarrow K^+ K^-$
60 ± 23 ⁺¹³ ₋₂₀	BAI	96c BES	$J/\psi \rightarrow \gamma K^+ K^-$
103 ± 30	AUGUSTIN	88 DM2	$J/\psi \rightarrow \gamma K^+ K^-$
62 ± 10	¹² FALVARD	88 DM2	$J/\psi \rightarrow \phi K^+ K^-$
85 ± 35	BALTRUSAIT..87	MRK3	$J/\psi \rightarrow \gamma K^+ K^-$
• • • We do not use the following data for averages, fits, limits, etc. • • •			
76 ± 40	ACCIARRI	95j L3	$\gamma\gamma \rightarrow K_S K_S E_{cm}^{ee} =$ 88-94 GeV
100 ± 3	¹³ FALVARD	88 DM2	$J/\psi \rightarrow \phi K^+ K^-$

CENTRAL PRODUCTION

VALUE (MeV)	DOCUMENT ID	TECN	COMMENT
70 ± 25	BARBERIS	99 OMEG	450 $pp \rightarrow$ $p_S p_f K^+ K^-$

¹² From an analysis ignoring interference with $f_0(1710)$.

¹³ From an analysis including interference with $f_0(1710)$.

 $f_2'(1525)$ DECAY MODES

Mode	Fraction (Γ_i/Γ)
Γ_1 $K\bar{K}$	(88.8 ± 3.1) %
Γ_2 $\eta\eta$	(10.3 ± 3.1) %
Γ_3 $\pi\pi$	(8.2 ± 1.5) × 10 ⁻³
Γ_4 $\gamma\gamma$	(1.32 ± 0.21) × 10 ⁻⁶
Γ_5 $K\bar{K}^*(892) + c.c.$	
Γ_6 $\pi\pi\eta$	
Γ_7 $\pi K\bar{K}$	
Γ_8 $\pi^+ \pi^+ \pi^- \pi^-$	

CONSTRAINED FIT INFORMATION

An overall fit to the total width, 2 partial widths, a combination of partial widths obtained from integrated cross sections, and 3 branching ratios uses 14 measurements and one constraint to determine 5 parameters. The overall fit has a $\chi^2 = 11.4$ for 10 degrees of freedom.

The following *off-diagonal* array elements are the correlation coefficients $\langle \delta p_i \delta p_j \rangle / (\delta p_i \delta p_j)$, in percent, from the fit to parameters p_i , including the branching fractions, $x_i \equiv \Gamma_i / \Gamma_{\text{total}}$. The fit constrains the x_i whose labels appear in this array to sum to one.

x_2	-100			
x_3	-3	-1		
x_4	-7	7	1	
Γ	-32	32	-1	-42
	x_1	x_2	x_3	x_4

Mode	Rate (MeV)
Γ_1 $K\bar{K}$	65 $^{+5}_{-4}$
Γ_2 $\eta\eta$	7.6 ± 2.6
Γ_3 $\pi\pi$	0.60 ± 0.12
Γ_4 $\gamma\gamma$	(9.7 ± 1.4) $\times 10^{-5}$

$f_2'(1525)$ PARTIAL WIDTHS

$\Gamma(K\bar{K})$	Γ_1
VALUE (MeV)	DOCUMENT ID

65 $^{+5}_{-4}$ OUR FIT	
63 $^{+6}_{-5}$	14 LONGACRE 86 MPS 22 $\pi^- p \rightarrow K_S^0 K_S^0 n$

$\Gamma(\pi\pi)$	Γ_3
VALUE (MeV)	DOCUMENT ID

0.60 ± 0.12 OUR FIT	
1.4 $^{+1.0}_{-0.5}$	14 LONGACRE 86 MPS 22 $\pi^- p \rightarrow K_S^0 K_S^0 n$

$\Gamma(\eta\eta)$	Γ_2
VALUE (MeV)	DOCUMENT ID

7.6 ± 2.5 OUR FIT	
24 $^{+3}_{-1}$	14 LONGACRE 86 MPS 22 $\pi^- p \rightarrow K_S^0 K_S^0 n$

¹⁴From a partial-wave analysis of data using a K-matrix formalism with 5 poles.

$f_2'(1525)$ $\Gamma(\eta)\Gamma(\gamma\gamma)/\Gamma(\text{total})$

$\Gamma(K\bar{K}) \times \Gamma(\gamma\gamma)/\Gamma_{\text{total}}$	$\Gamma_1\Gamma_4/\Gamma$
VALUE (MeV)	DOCUMENT ID

0.086 ± 0.012 OUR FIT	
0.086 ± 0.012 OUR AVERAGE	
0.093 ± 0.018 ± 0.022	15 ACCIARRI 95J L3 $E_{\text{cm}}^{\text{ee}} = 88-94$ GeV
0.067 ± 0.008 ± 0.015	15 ALBRECHT 90G ARG $e^+e^- \rightarrow K^+K^-$
0.11 $^{+0.03}_{-0.02}$ ± 0.02	BEHREND 89C CELL $e^+e^- \rightarrow K_S^0 K_S^0$
0.10 $^{+0.04}_{-0.03}$ $^{+0.03}_{-0.02}$	BERGER 88 PLUT $e^+e^- \rightarrow K_S^0 K_S^0$
0.12 ± 0.07 ± 0.04	15 AIHARA 86B TPC $e^+e^- \rightarrow K^+K^-$
0.11 ± 0.02 ± 0.04	15 ALTHOFF 83 TASS $e^+e^- \rightarrow e^+e^- K\bar{K}$
0.0314 ± 0.0050 ± 0.0077	16 ALBRECHT 90G ARG $e^+e^- \rightarrow K^+K^-$

¹⁵Using an incoherent background.
¹⁶Using a coherent background.

$f_2'(1525)$ BRANCHING RATIOS

$\Gamma(\eta\eta)/\Gamma(K\bar{K})$	Γ_2/Γ_1
VALUE	DOCUMENT ID

0.12 ± 0.04 OUR FIT	
0.11 ± 0.04	17 PROKOSHKIN 91 GAM4 300 $\pi^- p \rightarrow \pi^- \rho \eta \eta$
<0.50	BARNES 67 HBC 4.6, 5.0 $K^- p$

¹⁷Combining results of GAM4 with those of WA76 on $K\bar{K}$ central production and results of CBAL, MRK3 and DM2 on $J/\psi \rightarrow \gamma \eta \eta$.

$\Gamma(\pi\pi)/\Gamma_{\text{total}}$

VALUE	CL%	DOCUMENT ID	TECN	COMMENT
0.0082 ± 0.0016 OUR FIT				
0.0075 ± 0.0016 OUR AVERAGE				
0.007 ± 0.002		COSTA...	80 OMEG	10 $\pi^- p \rightarrow K^+ K^- n$
0.027 $^{+0.071}_{-0.013}$		18 GORLICH	80 ASPK	17, 18 $\pi^- p$
0.0075 ± 0.0025		18, 19 MARTIN	79 RVUE	
<0.06	95	AGUILAR-...	81b HBC	4.2 $K^- p \rightarrow \Lambda K^+ K^-$
0.19 ± 0.03		CORDEN	79 OMEG	12-15 $\pi^- p \rightarrow \pi^+ \pi^- n$
<0.045	95	BARREIRO	77 HBC	4.15 $K^- p \rightarrow \Lambda K_S^0 K_S^0$
0.012 ± 0.004		18 PAWLICKI	77 SPEC	6 $\pi N \rightarrow K^+ K^- N$
<0.063	90	BRANDENB...	76c ASPK	13 $K^- p \rightarrow K^+ K^- (\Lambda, \Sigma)$
<0.0086		18 BEUSCH	75b OSPK	8.9 $\pi^- p \rightarrow K^0 \bar{K}^0 n$

¹⁸ Assuming that the $f_2'(1525)$ is produced by a one-pion exchange production mechanism.

$\Gamma(\pi\pi)/\Gamma(K\bar{K})$	Γ_3/Γ_1
VALUE	DOCUMENT ID

0.0092 ± 0.0018 OUR FIT	
0.075 ± 0.035	AUGUSTIN 87 DM2 $J/\psi \rightarrow \gamma \pi^+ \pi^-$

$\Gamma(\pi\pi\eta)/\Gamma(K\bar{K})$	Γ_6/Γ_1
VALUE	DOCUMENT ID

<0.41	95 AGUILAR-...	81b HBC	3.9, 4.6 $K^- p$
<0.3	67 AMMAR	67 HBC	

$[\Gamma(K\bar{K}^*(892) + c.c.) + \Gamma(\pi K\bar{K})]/\Gamma(K\bar{K})$	$(\Gamma_5 + \Gamma_7)/\Gamma_1$
VALUE	DOCUMENT ID

<0.35	95 AGUILAR-...	72b HBC	3.9, 4.6 $K^- p$
<0.4	67 AMMAR	67 HBC	

$\Gamma(\pi^+ \pi^+ \pi^- \pi^-)/\Gamma(K\bar{K})$	Γ_8/Γ_1
VALUE	DOCUMENT ID

<0.32	95 AGUILAR-...	72b HBC	3.9, 4.6 $K^- p$
-------	----------------	---------	------------------

$\Gamma(\eta\eta)/\Gamma_{\text{total}}$	Γ_2/Γ
VALUE	DOCUMENT ID

0.10 ± 0.03	20 PROKOSHKIN 91 GAM4 300 $\pi^- p \rightarrow \pi^- \rho \eta \eta$
-----------------	--

²⁰ Combining results of GAM4 with those of WA76 on $K\bar{K}$ central production and results of CBAL, MRK3 and DM2 on $J/\psi \rightarrow \gamma \eta \eta$.

$f_2'(1525)$ REFERENCES

BARBERIS 99 PL B453 305	D. Barberis et al.	(Omega expt.)
BARKOV 99 JETPL 70 248	B.P. Barkov et al.	
ABREU 96C PL B379 309	P. Abreu et al.	(DELPHI Collab.)
BAI 96C PRL 77 3959	J.Z. Bai et al.	(BES Collab.)
ACCIARRI 95J PL B363 118	M. Acciari et al.	(L3 Collab.)
PROKOSHKIN 91 SPD 36 155	Y.D. Prokoshkin	(GAM2, GAM4 Collab.)
ALBRECHT 90G ZPHY C48 183	H. Albrecht et al.	(ARGUS Collab.)
PDG 90 PL B239	J.J. Hernandez et al.	(IFIC, BOST, CIT+)
BEHREND 89C ZPHY C43 91	H.J. Behrend et al.	(CELLO Collab.)
ASTON 88D NP B301 525	D. Aston et al.	(SLAC, NAGO, CINC, INUS)
AUGUSTIN 88 PRL 60 2238	J.E. Augustin et al.	(DM2 Collab.)
BERGER 88 ZPHY C37 329	C. Berger et al.	(PLUTO Collab.)
FALVARD 88 PR D38 2706	A. Falvard et al.	(CLER, FRAS, LALO+)
AUGUSTIN 87 ZPHY C36 369	J.E. Augustin et al.	(LALO, CLER, FRAS+)
BALTRUSAITIS 87 PR D35 2077	R.M. Baltrusaitis et al.	(Mark III Collab.)
AIHARA 86B PRL 57 404	H. Aihara et al.	(TPC-2\gamma Collab.)
BOLONKIN 86 SJP 43 976	B.V. Bolonkin et al.	(ITEP) JP
LONGACRE 86 PL B177 223	R.S. Longacre et al.	(BNL, BRAN, CUNY+)
ALTHOFF 83 PL 121B 216	M. Althoff et al.	(TASSO Collab.)
ARMSTRONG 83B NP B224 193	T.A. Armstrong et al.	(BARI, BIRM, CERN+)
AGUILAR-... 81B ZPHY C8 313	M. Aguilar-Benitez et al.	(CERN, CDEF+)
ALHARRAN 81 NP B191 26	S. Al-Harran et al.	(BIRM, CERN, GLAS+)
CHABAUD 81 APP B12 575	V. Chabaud et al.	(CERN, CRAC, MPIM)
COSTA... 80 NP B175 402	G. Costa de Beaugard et al.	(BARI, BONN+)
GORLICH 80 NP B174 16	L. Gorlich et al.	(CRAC, MPIM, CERN+)
CORDEN 79 NP B157 250	M.J. Corden et al.	(BIRM, RHEL, TELA+)-JP
MARTIN 79 NP B158 520	A.D. Martin, E.N. Ozmutlu	(DURH)
POLYCHRO... 79 PR D19 1317	V.A. Polychronakos et al.	(NDAM, ANL)
BARREIRO 77 NP B121 237	F. Barreiro et al.	(CERN, AMST, NIJM+)
EVANGELISTA 77 NP B127 384	C. Evangelista et al.	(BARI, BONN, CERN+)
PAWLICKI 77 PR D15 3196	A.J. Pawlicki et al.	(ANL) JIP
BRANDENB... 76C NP B104 413	G.W. Brandenburg et al.	(SLAC)
BEUSCH 75B PL 60B 101	W. Beusch et al.	(CERN, ETH)
AGUILAR-... 72B PR D6 29	M. Aguilar-Benitez et al.	(BNL)
AMMAR 67 PRL 19 1071	R. Ammar et al.	(NWES, ANL) JP
BARNES 67 PRL 19 964	V.E. Barnes et al.	(BNL, SYRA)
CRENNELL 66 PRL 16 1025	D.J. Crennell et al.	(BNL)!

Meson Particle Listings

$f_2'(1525), f_2(1565)$

OTHER RELATED PAPERS

ALBERICO 98	PL B438 430	A. Alberico <i>et al.</i>	(Obelix Collab.)
JENNI 83	PR D27 1031	P. Jenni <i>et al.</i>	(SLAC, LBL)
ARMSTRONG 82	PL 110B 77	T.A. Armstrong <i>et al.</i>	(BARI, BIRM, CERN+)
ETKIN 82B	PR D25 1786	A. Etkin <i>et al.</i>	(BNL, CUNY, TUFTS, VAND)
ABRAMS 67B	PRL 18 620	G.S. Abrams <i>et al.</i>	(UMD)
BARNES 65	PRL 15 322	V.E. Barnes <i>et al.</i>	(BNL, SYRA)

$f_2(1565)$

$$IG(J^{PC}) = 0^+(2^+ +)$$

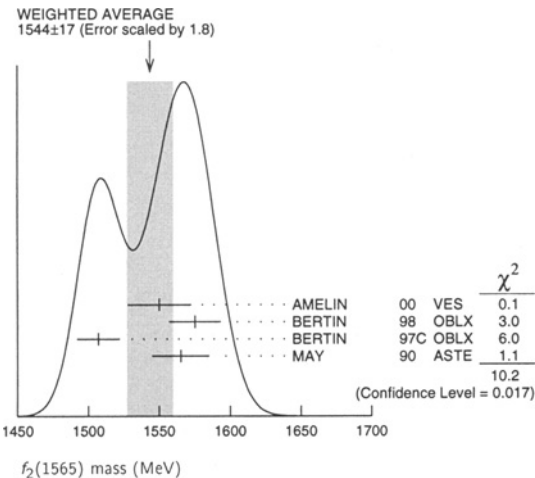
OMITTED FROM SUMMARY TABLE

Seen in antinucleon-nucleon annihilation at rest. See also minireview under non- $q\bar{q}$ candidates. (See the index for the page number.) Needs confirmation.

$f_2(1565)$ MASS

VALUE (MeV)	DOCUMENT ID	TECN	COMMENT
1544 ± 17 OUR AVERAGE	Error includes scale factor of 1.8. See the ideogram below.		
1550 ± 10 ± 20	AMELIN 00	VES	$37 \pi^- p \rightarrow \eta \pi^+ \pi^- n$
1575 ± 18	BERTIN 98	OBLX	$0.05-0.405 \bar{p} p \rightarrow \pi^+ \pi^+ \pi^-$
1507 ± 15	¹ BERTIN 97C	OBLX	$0.0 \bar{p} p \rightarrow \pi^+ \pi^- \pi^0$
1565 ± 20	MAY 90	ASTE	$0.0 \bar{p} p \rightarrow \pi^+ \pi^- \pi^0$
1598 ± 11 ± 9	BAKER 99B	SPEC	$0 \bar{p} p \rightarrow \omega \omega \pi^0$
1534 ± 20	² ABELE 96C	RVUE	Compilation
~ 1552	³ AMSLER 95D	CBAR	$0.0 \bar{p} p \rightarrow \pi^0 \pi^0 \pi^0, \pi^0 \eta \eta, \pi^0 \pi^0 \eta$
1598 ± 72	BALOSHIN 95	SPEC	$40 \pi^- C \rightarrow K_S^0 K_S^0 X$
1566 ⁺⁸⁰ ₋₅₀	⁴ ANISOVICH 94	CBAR	$0.0 \bar{p} p \rightarrow 3\pi^0, \eta \eta \pi^0$
1502 ± 9	ADAMO 93	OBLX	$\bar{p} p \rightarrow \pi^+ \pi^+ \pi^-$
1488 ± 10	⁵ ARMSTRONG 93C	E760	$\bar{p} p \rightarrow \pi^0 \eta \eta \rightarrow 6\gamma$
1508 ± 10	⁵ ARMSTRONG 93D	E760	$\bar{p} p \rightarrow 3\pi^0 \rightarrow 6\gamma$
1525 ± 10	⁵ ARMSTRONG 93D	E760	$\bar{p} p \rightarrow \eta \pi^0 \pi^0 \rightarrow 6\gamma$
~ 1504	⁶ WEIDENAUER 93	ASTE	$0.0 \bar{p} N \rightarrow 3\pi^- 2\pi^+$
1540 ± 15	⁵ ADAMO 92	OBLX	$\bar{p} p \rightarrow \pi^+ \pi^+ \pi^-$
1515 ± 10	⁷ AKER 91	CBAR	$0.0 \bar{p} p \rightarrow 3\pi^0$
1477 ± 5	BRIDGES 86C	DBC	$0.0 \bar{p} N \rightarrow 3\pi^- 2\pi^+$

- • • We do not use the following data for averages, fits, limits, etc. • • •
- ¹ T-matrix pole.
- ² T-matrix pole, large coupling to $\rho\rho$ and $\omega\omega$, could be $f_2(1640)$.
- ³ Coupled-channel analysis of AMSLER 95b, AMSLER 95c, and AMSLER 94d.
- ⁴ From a simultaneous analysis of the annihilations $\bar{p} p \rightarrow 3\pi^0, \pi^0 \eta \eta$ including AKER 91 data.
- ⁵ J^P not determined, could be partly $f_0(1500)$.
- ⁶ J^P not determined.
- ⁷ Superseded by AMSLER 95b.



$f_2(1565)$ WIDTH

VALUE (MeV)	DOCUMENT ID	TECN	COMMENT
131 ± 14 OUR AVERAGE			
130 ± 20 ± 40	AMELIN 00	VES	$37 \pi^- p \rightarrow \eta \pi^+ \pi^- n$
119 ± 24	BERTIN 98	OBLX	$0.05-0.405 \bar{p} p \rightarrow \pi^+ \pi^+ \pi^-$
130 ± 20	⁸ BERTIN 97C	OBLX	$0.0 \bar{p} p \rightarrow \pi^+ \pi^- \pi^0$
170 ± 40	MAY 90	ASTE	$0.0 \bar{p} p \rightarrow \pi^+ \pi^- \pi^0$

• • • We do not use the following data for averages, fits, limits, etc. • • •

180 ± 60	⁹ ABELE 96C	RVUE	Compilation
~ 142	¹⁰ AMSLER 95D	CBAR	$0.0 \bar{p} p \rightarrow \pi^0 \pi^0 \pi^0, \pi^0 \eta \eta, \pi^0 \pi^0 \eta$
263 ± 101	BALOSHIN 95	SPEC	$40 \pi^- C \rightarrow K_S^0 K_S^0 X$
166 ⁺⁸⁰ ₋₂₀	¹¹ ANISOVICH 94	CBAR	$0.0 \bar{p} p \rightarrow 3\pi^0, \eta \eta \pi^0$
130 ± 10	¹² ADAMO 93	OBLX	$\bar{p} p \rightarrow \pi^+ \pi^+ \pi^-$
148 ± 27	¹³ ARMSTRONG 93C	E760	$\bar{p} p \rightarrow \pi^0 \eta \eta \rightarrow 6\gamma$
103 ± 15	¹³ ARMSTRONG 93D	E760	$\bar{p} p \rightarrow 3\pi^0 \rightarrow 6\gamma$
111 ± 10	¹³ ARMSTRONG 93D	E760	$\bar{p} p \rightarrow \eta \pi^0 \pi^0 \rightarrow 6\gamma$
~ 206	¹⁴ WEIDENAUER 93	ASTE	$0.0 \bar{p} N \rightarrow 3\pi^- 2\pi^+$
132 ± 37	¹³ ADAMO 92	OBLX	$\bar{p} p \rightarrow \pi^+ \pi^+ \pi^-$
120 ± 10	¹⁵ AKER 91	CBAR	$0.0 \bar{p} p \rightarrow 3\pi^0$
116 ± 9	BRIDGES 86C	DBC	$0.0 \bar{p} N \rightarrow 3\pi^- 2\pi^+$

- ⁸ T-matrix pole.
- ⁹ T-matrix pole, large coupling to $\rho\rho$ and $\omega\omega$, could be $f_2(1640)$.
- ¹⁰ Coupled-channel analysis of AMSLER 95b, AMSLER 95c, and AMSLER 94d.
- ¹¹ From a simultaneous analysis of the annihilations $\bar{p} p \rightarrow 3\pi^0, \pi^0 \eta \eta$ including AKER 91 data.
- ¹² Supersedes ADAMO 92.
- ¹³ J^P not determined, could be partly $f_0(1500)$.
- ¹⁴ J^P not determined.
- ¹⁵ Superseded by AMSLER 95b.

$f_2(1565)$ DECAY MODES

Mode	Fraction (Γ_i/Γ)
$\Gamma_1 \pi \pi$	seen
$\Gamma_2 \pi^+ \pi^-$	seen
$\Gamma_3 \pi^0 \pi^0$	seen
$\Gamma_4 \rho^0 \rho^0$	seen
$\Gamma_5 2\pi^+ 2\pi^-$	seen
$\Gamma_6 \eta \eta$	seen
$\Gamma_7 a_2(1320) \pi$	not seen
$\Gamma_8 \omega \omega$	seen

$f_2(1565)$ BRANCHING RATIOS

VALUE	DOCUMENT ID	TECN	COMMENT	Γ_1/Γ
• • • We do not use the following data for averages, fits, limits, etc. • • •				
seen	BAKER 99B	SPEC	$0 \bar{p} p \rightarrow \omega \omega \pi^0$	

VALUE	DOCUMENT ID	TECN	COMMENT	Γ_2/Γ
• • • We do not use the following data for averages, fits, limits, etc. • • •				
seen	BERTIN 98	OBLX	$0.05-0.405 \bar{p} p \rightarrow \pi^+ \pi^+ \pi^-$	
not seen	¹⁶ ANISOVICH 94B	RVUE	$\bar{p} p \rightarrow \pi^+ \pi^- \pi^0$	
seen	MAY 89	ASTE	$\bar{p} p \rightarrow \pi^+ \pi^- \pi^0$	
¹⁶ ANISOVICH 94B is from a reanalysis of MAY 90.				

VALUE	DOCUMENT ID	TECN	COMMENT	Γ_2/Γ_4
• • • We do not use the following data for averages, fits, limits, etc. • • •				
0.042 ± 0.013	BRIDGES 86B	DBC	$\bar{p} N \rightarrow 3\pi^- 2\pi^+$	

VALUE	DOCUMENT ID	TECN	COMMENT	Γ_3/Γ
• • • We do not use the following data for averages, fits, limits, etc. • • •				
seen	AMSLER 95B	CBAR	$0.0 \bar{p} p \rightarrow 3\pi^0$	

VALUE	DOCUMENT ID	TECN	COMMENT	Γ_6/Γ_3
• • • We do not use the following data for averages, fits, limits, etc. • • •				
0.024 ± 0.005 ± 0.012	¹⁷ ARMSTRONG 93C	E760	$\bar{p} p \rightarrow \pi^0 \eta \eta \rightarrow 6\gamma$	
¹⁷ J^P not determined, could be partly $f_0(1500)$.				

VALUE	DOCUMENT ID	TECN	COMMENT	Γ_8/Γ
• • • We do not use the following data for averages, fits, limits, etc. • • •				
seen	BAKER 99B	SPEC	$0 \bar{p} p \rightarrow \omega \omega \pi^0$	

See key on page 239

Meson Particle Listings

$f_2(1565), \pi_1(1600), X(1600), a_1(1640), f_2(1640)$

$f_2(1565)$ REFERENCES

AMELIN 00 NP B668 83	D. Amelin <i>et al.</i>	(VES Collab.)
BAKER 99B PL B467 147	C.A. Baker <i>et al.</i>	(OBELIX Collab.)
BERTIN 98 PR D57 55	A. Bertin <i>et al.</i>	(OBELIX Collab.)
BERTIN 97C PL B408 476	A. Bertin <i>et al.</i>	(OBELIX Collab.)
ABELE 96C NP A609 562	A. Abele <i>et al.</i>	(Crystal Barrel Collab.)
AMSLER 95B PL B342 433	C. Amisler <i>et al.</i>	(Crystal Barrel Collab.)
AMSLER 95C PL B353 571	C. Amisler <i>et al.</i>	(Crystal Barrel Collab.)
AMSLER 95D PL B355 425	C. Amisler <i>et al.</i>	(Crystal Barrel Collab.)
BALOSHIN 95 PAN 58 46	O.N. Baloshin <i>et al.</i>	(ITEP)
Translated from YAF 58 50.		
AMSLER 94D PL B333 277	C. Amisler <i>et al.</i>	(Crystal Barrel Collab.)
ANISOVICH 94 PL B323 233	V.V. Anisovich <i>et al.</i>	
ANISOVICH 94B PR D50 1972	V.V. Anisovich <i>et al.</i>	(LOQM)
ADAMO 93 NP A558 13C	A. Adamo <i>et al.</i>	(OBELIX Collab.)
ARMSTRONG 93C PL B307 394	T.A. Armstrong <i>et al.</i>	(FNAL, FERR, GENO+)
ARMSTRONG 93D PL B307 399	T.A. Armstrong <i>et al.</i>	(FNAL, FERR, GENO+)
WEIDENAUER 93 ZPHY C59 387	P. Weidenaue <i>et al.</i>	(ASTERIX Collab.)
ADAMO 92 PL B287 368	A. Adamo <i>et al.</i>	(OBELIX Collab.)
AKER 91 PL B260 249	E. Aker <i>et al.</i>	(Crystal Barrel Collab.)
MAY 90 ZPHY C45 203	B. May <i>et al.</i>	(ASTERIX Collab.)
MAY 89 PL B225 450	B. May <i>et al.</i>	(ASTERIX Collab.)
BRIDGES 86B PRL 56 215	D.L. Bridges <i>et al.</i>	(SYRA, CASE)
BRIDGES 86C PRL 57 1534	D.L. Bridges <i>et al.</i>	(SYRA)

$\pi_1(1600)$ $I^G(J^{PC}) = 1^-(1^-+)$

OMITTED FROM SUMMARY TABLE

$\pi_1(1600)$ MASS

VALUE (MeV)	DOCUMENT ID	COMMENT
$1593 \pm 8^{+29}_{-47}$	¹ ADAMS 98B 18.3 $\pi^- p \rightarrow \pi^+ \pi^- \pi^- p$	

¹ Natural parity exchange.

$\pi_1(1600)$ WIDTH

VALUE (MeV)	DOCUMENT ID	COMMENT
$168 \pm 20^{+150}_{-12}$	² ADAMS 98B 18.3 $\pi^- p \rightarrow \pi^+ \pi^- \pi^- p$	

² Natural parity exchange.

$\pi_1(1600)$ REFERENCES

ADAMS 98B PRL 81 5760	G.S. Adams <i>et al.</i>	(MPS Collab.)
-----------------------	--------------------------	---------------

$X(1600)$ $I^G(J^{PC}) = 2^+(2^{++})$

OMITTED FROM SUMMARY TABLE

Observed in the reaction $\gamma\gamma \rightarrow \rho\rho$ near threshold. See also minireview under non- $q\bar{q}$ candidates. (See the index for the page number.)

$X(1600)$ MASS

VALUE (MeV)	DOCUMENT ID	TECN	CHG	COMMENT
1600 ± 100	¹ ALBRECHT 91F ARG 0			$10.2 e^+ e^- \rightarrow e^+ e^- 2(\pi^+ \pi^-)$

¹ Our estimate.

$X(1600)$ WIDTH

VALUE (MeV)	DOCUMENT ID	TECN	CHG	COMMENT
400 ± 200	² ALBRECHT 91F ARG 0			$10.2 e^+ e^- \rightarrow e^+ e^- 2(\pi^+ \pi^-)$

² Our estimate.

$X(1600)$ REFERENCES

ALBRECHT 91F ZPHY C50 1	H. Albrecht <i>et al.</i>	(ARGUS Collab.)
-------------------------	---------------------------	-----------------

OTHER RELATED PAPERS

BAJC 96 ZPHY A356 187	B. Bajc <i>et al.</i>	
ALBRECHT 89M PL B217 205	H. Albrecht <i>et al.</i>	(ARGUS Collab.)
BEHREND 89D PL B219 494	H.J. Behrend <i>et al.</i>	(CELLO Collab.)

$a_1(1640)$

$I^G(J^{PC}) = 1^+(1^{++})$

OMITTED FROM SUMMARY TABLE

Seen in the amplitude analysis of the $3\pi^0$ system produced in $\bar{p}p \rightarrow 4\pi^0$. Possibly seen in the study of the hadronic structure in decay $\tau \rightarrow 3\pi\nu_\tau$ (ABREU 98G). Needs confirmation.

$a_1(1640)$ MASS

VALUE (MeV)	DOCUMENT ID	TECN	COMMENT
$1640 \pm 12 \pm 30$	¹ BAKER 99 SPEC		$1.94 \bar{p}p \rightarrow 4\pi^0$
• • • We do not use the following data for averages, fits, limits, etc. • • •			
1670 ± 90	BELLINI 85 SPEC		$40 \pi^- A \rightarrow \pi^- \pi^+ \pi^- A$

¹ Using preliminary CBAR data.

$a_1(1640)$ WIDTH

VALUE (MeV)	DOCUMENT ID	TECN	COMMENT
$300 \pm 22 \pm 40$	² BAKER 99 SPEC		$1.94 \bar{p}p \rightarrow 4\pi^0$
• • • We do not use the following data for averages, fits, limits, etc. • • •			
300 ± 100	BELLINI 85 SPEC		$40 \pi^- A \rightarrow \pi^- \pi^+ \pi^- A$

² Using preliminary CBAR data.

$a_1(1640)$ DECAY MODES

Mode	Γ_1	Γ_2
$f_2(1270)\pi$		
$\sigma\pi$		

$a_1(1640)$ BRANCHING RATIOS

$\Gamma(f_2(1270)\pi)/\Gamma(\sigma\pi)$	DOCUMENT ID	TECN	COMMENT	Γ_1/Γ_2
0.24 ± 0.07	³ BAKER 99 SPEC		$1.94 \bar{p}p \rightarrow 4\pi^0$	

³ Using preliminary CBAR data.

$a_1(1640)$ REFERENCES

BAKER 99 PL B449 114	C.A. Baker <i>et al.</i>	
ABREU 98G PL B426 411	P. Abreu <i>et al.</i>	(DELPHI Collab.)
BELLINI 85	G. Bellini <i>et al.</i>	
Translated from YAF 41 1223.		

$f_2(1640)$

$I^G(J^{PC}) = 0^+(2^{++})$

OMITTED FROM SUMMARY TABLE

$f_2(1640)$ MASS

VALUE (MeV)	DOCUMENT ID	TECN	COMMENT
1638 ± 6 OUR AVERAGE	Error includes scale factor of 1.2.		
1620 ± 16	BUGG 95 MRK3		$J/\psi \rightarrow \gamma\pi^+\pi^-\pi^+\pi^-$
1647 ± 7	ADAMO 92 OBLX		$\bar{n}p \rightarrow 3\pi^+2\pi^-$
1590 ± 30	BELADIDZE 92B VES		$36 \pi^- p \rightarrow \omega\omega\eta$
1635 ± 7	ALDE 90 GAM2		$38 \pi^- p \rightarrow \omega\omega\eta$
• • • We do not use the following data for averages, fits, limits, etc. • • •			
1643 ± 7	¹ ALDE 89B GAM2		$38 \pi^- p \rightarrow \omega\omega\eta$

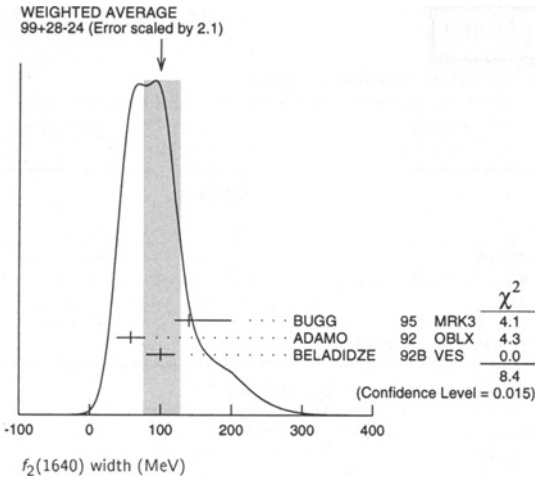
¹ Superseded by ALDE 90.

$f_2(1640)$ WIDTH

VALUE (MeV)	CL%	DOCUMENT ID	TECN	COMMENT
99^{+28}_{-24} OUR AVERAGE		Error includes scale factor of 2.1. See the ideogram below.		
140^{+60}_{-20}		BUGG 95 MRK3		$J/\psi \rightarrow \gamma\pi^+\pi^-\pi^+\pi^-$
58 ± 20		ADAMO 92 OBLX		$\bar{n}p \rightarrow 3\pi^+2\pi^-$
100 ± 20		BELADIDZE 92B VES		$36 \pi^- p \rightarrow \omega\omega\eta$
• • • We do not use the following data for averages, fits, limits, etc. • • •				
< 70		90 ALDE 90		$38 \pi^- p \rightarrow \omega\omega\eta$

Meson Particle Listings

$f_2(1640), \eta_2(1645), \omega(1650)$



$f_2(1640)$ DECAY MODES

Mode	Fraction (Γ_i/Γ)
Γ_1 $\omega\omega$	seen
Γ_2 4π	seen

$f_2(1640)$ REFERENCES

BUGG 95 PL B353 378	D.V. Bugg <i>et al.</i>	(LOQM, PNPI, WASH) JP
ADAMO 92 PL B287 368	A. Adamo <i>et al.</i>	(OBELIX Collab.)
BELADIDZE 92B ZPHY C54 367	G.M. Beladidze <i>et al.</i>	(VES Collab.)
ALDE 90 PL B241 600	D.M. Alde <i>et al.</i>	(SERP, BELG, LANL, LAPP+)
ALDE 89B PL B216 451	D.M. Alde <i>et al.</i>	(SERP, BELG, LANL, LAPP+)IGJPC

OTHER RELATED PAPERS

PROKOSHIN 99 PAN 62 356	Yu.D. Prokoshin <i>et al.</i>
Translated from YAF 62 396.	

$\eta_2(1645)$

$$I^G(J^{PC}) = 0^+(2^{-+})$$

OMITTED FROM SUMMARY TABLE

$\eta_2(1645)$ MASS

VALUE (MeV)	DOCUMENT ID	TECN	CHG	COMMENT
1632 ± 14 OUR AVERAGE				
1620 ± 20	BARBERIS 97B OMEG			450 $pp \rightarrow \rho\rho 2(\pi^+\pi^-)$
1645 ± 14 ± 15	ADOMEIT 96 CBAR 0			1.94 $\bar{p}p \rightarrow \eta 3\pi^0$

$\eta_2(1645)$ WIDTH

VALUE (MeV)	DOCUMENT ID	TECN	CHG	COMMENT
180⁺²²₋₂₀ OUR AVERAGE				
180 ± 25	BARBERIS 97B OMEG			450 $pp \rightarrow \rho\rho 2(\pi^+\pi^-)$
180 ⁺⁴⁰ ₋₂₁ ± 25	ADOMEIT 96 CBAR 0			1.94 $\bar{p}p \rightarrow \eta 3\pi^0$

$\eta_2(1645)$ DECAY MODES

Mode	Fraction (Γ_i/Γ)
Γ_1 $a_2(1320)\pi$	
Γ_2 $K\bar{K}\pi$	
Γ_3 $K^*\bar{K}$	
Γ_4 $\eta\pi^+\pi^-$	not seen

$\eta_2(1645)$ BRANCHING RATIOS

$\Gamma(K\bar{K}\pi)/\Gamma(a_2(1320)\pi)$	DOCUMENT ID	TECN	COMMENT	Γ_2/Γ_1
0.07 ± 0.03	¹ BARBERIS 97C OMEG		450 $pp \rightarrow \rho\rho K\bar{K}\pi$	

¹ Using $2(\pi^+\pi^-)$ data from BARBERIS 97B.

$\Gamma(\eta\pi^+\pi^-)/\Gamma_{total}$

VALUE	DOCUMENT ID	TECN	COMMENT
not seen	AMELIN 00 VES		$37 \pi^-\rho \rightarrow \eta\pi^+\pi^-\pi$

$\eta_2(1645)$ REFERENCES

AMELIN 00 NP B668 83	D. Amelin <i>et al.</i>	(VES Collab.)
BARBERIS 97B PL B413 217	D. Barberis <i>et al.</i>	(WA102 Collab.)
BARBERIS 97C PL B413 225	D. Barberis <i>et al.</i>	(WA102 Collab.)
ADOMEIT 96 ZPHY C71 227	J. Adomeit <i>et al.</i>	(Crystal Barrel Collab.)

$\omega(1650)$ was $\omega(1600)$

$$I^G(J^{PC}) = 0^-(1^{--})$$

$\omega(1650)$ MASS

VALUE (MeV)	EVTS	DOCUMENT ID	TECN	CHG	COMMENT
1649 ± 24 OUR AVERAGE					Error includes scale factor of 2.3.
1609 ± 20	315	¹ ANTONELLI 92 DM2			1.34-2.4e ⁺ e ⁻ → $\rho\pi$
1663 ± 12	435	² ANTONELLI 92 DM2			1.34-2.4e ⁺ e ⁻ → $\omega\pi\pi$
1643 ± 14		³ ACHASOV 99E RVUE			0.75-1.80 e ⁺ e ⁻ → $\pi^+\pi^-\pi^0$
1820 ⁺¹⁹⁰ ₋₁₅₀		⁴ ACHASOV 98H RVUE			e ⁺ e ⁻ → $\pi^+\pi^-\pi^0$
1840 ⁺¹⁰⁰ ₋₇₀		⁵ ACHASOV 98H RVUE			e ⁺ e ⁻ → $\omega\pi\pi$
1780 ⁺¹⁷⁰ ₋₃₀₀		⁶ ACHASOV 98H RVUE			e ⁺ e ⁻ → K^+K^-
~ 2100		⁷ ACHASOV 98H RVUE			e ⁺ e ⁻ → $K_S^0 K_{S,L}^\pm \pi^\mp$
1600 ± 30		¹ CLEGG 94 RVUE			e ⁺ e ⁻ → $\rho\pi$
1607 ± 10		² CLEGG 94 RVUE			e ⁺ e ⁻ → $\omega\pi\pi$
1635 ± 35		⁸ CLEGG 94 RVUE			e ⁺ e ⁻ → $\rho\pi$
1625 ± 21		⁸ CLEGG 94 RVUE			e ⁺ e ⁻ → $\omega\pi\pi$
1670 ± 20		ATKINSON 83B OMEG			20-70 $\gamma\rho \rightarrow 3\pi X$
1657 ± 13		CORDIER 81 DM1			e ⁺ e ⁻ → $\omega 2\pi$
1679 ± 34	21	ESPOSITO 80 FRAM			e ⁺ e ⁻ → 3π
1652 ± 17		COSME 79 OSPK 0			e ⁺ e ⁻ → 3π

¹ From a two Breit-Wigner fit.

² From a single Breit-Wigner plus background fit.

³ Using the data of DOLINSKY 91, ANTONELLI 92, AKHMETSHIN 98, and ACHASOV 99E. From a fit to two Breit-Wigner functions interfering between them and with the ω, ϕ tails with fixed (+, -, +) phases.

⁴ Using data from BARKOV 87, DOLINSKY 91, and ANTONELLI 92.

⁵ Using the data from ANTONELLI 92.

⁶ Using the data from IVANOV 81 and BISELLO 88b.

⁷ Using the data from BISELLO 91c.

⁸ From a single Breit-Wigner fit.

$\omega(1650)$ WIDTH

VALUE (MeV)	EVTS	DOCUMENT ID	TECN	CHG	COMMENT
220 ± 35 OUR AVERAGE					Error includes scale factor of 1.6.
159 ± 43	315	⁹ ANTONELLI 92 DM2			1.34-2.4e ⁺ e ⁻ → $\rho\pi$
240 ± 25	435	¹⁰ ANTONELLI 92 DM2			1.34-2.4e ⁺ e ⁻ → $\omega\pi\pi$
272 ± 29		¹¹ ACHASOV 99E RVUE			0.75-1.80 e ⁺ e ⁻ → $\pi^+\pi^-\pi^0$
140 ± 50		⁹ CLEGG 94 RVUE			e ⁺ e ⁻ → $\rho\pi$
86 ± 20		¹⁰ CLEGG 94 RVUE			e ⁺ e ⁻ → $\omega\pi\pi$
350 ± 80		¹² CLEGG 94 RVUE			e ⁺ e ⁻ → $\rho\pi$
401 ± 63		¹² CLEGG 94 RVUE			e ⁺ e ⁻ → $\omega\pi\pi$
160 ± 20		ATKINSON 83B OMEG			20-70 $\gamma\rho \rightarrow 3\pi X$
136 ± 46		CORDIER 81 DM1			e ⁺ e ⁻ → $\omega 2\pi$
99 ± 49	21	ESPOSITO 80 FRAM			e ⁺ e ⁻ → 3π
42 ± 17		COSME 79 OSPK 0			e ⁺ e ⁻ → 3π

⁹ From a two Breit-Wigner fit.

¹⁰ From a single Breit-Wigner plus background fit.

¹¹ Using the data of DOLINSKY 91, ANTONELLI 92, AKHMETSHIN 98, and ACHASOV 99E. From a fit to two Breit-Wigner functions interfering between them and with the ω, ϕ tails with fixed (+, -, +) phases.

¹² From a single Breit-Wigner fit.

See key on page 239

Meson Particle Listings

$\omega(1650)$, $X(1650)$, $a_2(1660)$

 $\omega(1650)$ DECAY MODES

Mode	Fraction (Γ_j/Γ)
Γ_1 $\rho\pi$	seen
Γ_2 $\omega\pi\pi$	seen
Γ_3 e^+e^-	seen

 $\omega(1650)$ $\Gamma(e^+e^-)/\Gamma(\text{total})$

$\Gamma(\rho\pi) \times \Gamma(e^+e^-)/\Gamma_{\text{total}}$	$\Gamma_1\Gamma_3/\Gamma$
---	---------------------------

VALUE (eV)	EVTs	DOCUMENT ID	TECN	COMMENT
134±14	435	¹³ ANTONELLI	92 DM2	1.34–2.4e ⁺ e ⁻ → hadrons
27±7		¹⁴ ACHASOV	99E RVUE	0.75–1.80 e ⁺ e ⁻ → $\pi^+\pi^-\pi^0$
93±27	315	ANTONELLI	92 DM2	1.34–2.4e ⁺ e ⁻ → $\rho\pi$
96±35		DONNACHIE	89 RVUE	e ⁺ e ⁻ → $\rho\pi$

• • • We do not use the following data for averages, fits, limits, etc. • • •
¹³From a coupled fit of $\rho\pi$ and $\omega\pi\pi$ channels.
¹⁴Using the data of DOLINSKY 91, ANTONELLI 92, AKHMETSHIN 98, and ACHASOV 99E. From a fit to two Breit-Wigner functions interfering between them and with the ω, ϕ tails with fixed (+, -, +) phases.

$\Gamma(\omega\pi\pi) \times \Gamma(e^+e^-)/\Gamma_{\text{total}}$	$\Gamma_2\Gamma_3/\Gamma$
--	---------------------------

VALUE (keV)	EVTs	DOCUMENT ID	TECN	COMMENT
170±17	435	¹⁵ ANTONELLI	92 DM2	1.34–2.4e ⁺ e ⁻ → hadrons
135±16	435	¹⁶ ANTONELLI	92 DM2	1.34–2.4e ⁺ e ⁻ → $\omega\pi\pi$
56±31		DONNACHIE	89 RVUE	e ⁺ e ⁻ → $\omega 2\pi$

• • • We do not use the following data for averages, fits, limits, etc. • • •
¹⁵From a coupled fit of $\rho\pi$ and $\omega\pi\pi$ channels.
¹⁶From a single Breit-Wigner fit.

 $\omega(1650)$ BRANCHING RATIOS

$\Gamma(\rho\pi)/\Gamma(\omega\pi\pi)$	Γ_1/Γ_2
--	---------------------

VALUE	DOCUMENT ID	TECN	COMMENT
0.17±0.05	¹⁷ ACHASOV	99E RVUE	0.75–1.80 e ⁺ e ⁻ → $\pi^+\pi^-\pi^0$

¹⁷Using the data of DOLINSKY 91, ANTONELLI 92, AKHMETSHIN 98, and ACHASOV 99E. From a fit to two Breit-Wigner functions interfering between them and with the ω, ϕ tails with fixed (+, -, +) phases.

 $\omega(1650)$ REFERENCES

ACHASOV	99E	PL B462 365	M.N. Achasov <i>et al.</i>	(Novosibirsk SND Collab.)
ACHASOV	98H	PR D57 4334	N.N. Achasov, A.A. Kozhevnikov	
AKHMETSHIN	98	PL B434 426	R.R. Akhmetshin <i>et al.</i>	
CLEGG	94	ZPHY C62 455	A.B. Clegg, A. Donnachie	(LANC, MCHS)
ANTONELLI	92	ZPHY C56 15	A. Antonelli <i>et al.</i>	(DM2 Collab.)
BISELLO	91C	ZPHY C52 227	D. Bisello <i>et al.</i>	(DM2 Collab.)
DOLINSKY	91	PRPL 202 99	S.I. Dolinsky <i>et al.</i>	(NOVO)
DONNACHIE	89	ZPHY C42 663	A. Donnachie, A.B. Clegg	(CERN, MCHS)
BISELLO	88B	ZPHY C39 13	D. Bisello <i>et al.</i>	(PADO, CLER, FRAS+)
BARKOV	87	JETPL 46 164	L.M. Barkov <i>et al.</i>	(NOVO)
ATKINSON	83B	PL 127B 132	M. Atkinson <i>et al.</i>	(BONN, CERN, GLAS+)
CORDIER	81	PL 106B 155	A. Cordier <i>et al.</i>	(ORSAY)
IVANOV	81	PL 107B 297	P.M. Ivanov <i>et al.</i>	(NOVO)
ESPOSITO	80	LCN 28 195	B. Esposito <i>et al.</i>	(FRAS, NAPL, PADO+)
COSME	79	NP B152 215	G. Cosme <i>et al.</i>	(IPN)

OTHER RELATED PAPERS

ABELE	99D	PL B468 178	A. Abele <i>et al.</i>	(Crystal Barrel Collab.)
BELOZEROVA	98	PPN 29 63	T.S. Belozerova, V.K. Henner	
		Translated from FECAJ 29 148.		
ACHASOV	97F	PAN 60 2029	N.N. Achasov, A.A. Kozhevnikov	(NOVM)
		Translated from YAF 60 2212.		
DOLINSKY	91	PRPL 202 99	S.I. Dolinsky <i>et al.</i>	(NOVO)
ATKINSON	87	ZPHY C34 157	M. Atkinson <i>et al.</i>	(BONN, CERN, GLAS+)
ATKINSON	84	NP B231 15	M. Atkinson <i>et al.</i>	(BONN, CERN, GLAS+)

 $X(1650)$

$$J^G(J^{PC}) = 0^-(?^{?}-)$$

J, P need confirmation.

OMITTED FROM SUMMARY TABLE

Observed in a study of the $\omega\eta$ effective mass distribution. Needs confirmation. **$X(1650)$ MASS**

VALUE (MeV)	EVTs	DOCUMENT ID	TECN	CHG	COMMENT
1652±7	100	¹ PROKOSHKIN	96 GAM2	0	32,38 $\pi\rho \rightarrow \omega\eta\pi$

¹Supersedes SAMOILENKO 91.

 $X(1650)$ WIDTH

VALUE (MeV)	CL%	DOCUMENT ID	TECN	CHG	COMMENT
<50	90	² PROKOSHKIN	96 GAM2	0	32,38 $\pi\rho \rightarrow \omega\eta\pi$

²Supersedes SAMOILENKO 91.

 $X(1650)$ DECAY MODES

Mode	Fraction (Γ_j/Γ)
Γ_1 $\omega\eta$	seen

 $X(1650)$ REFERENCES

PROKOSHKIN	96	SPD 41 247	Y.D. Prokoshkin, V.D. Samoilenko	(SERP)
		Translated from DANS 348 481.		
SAMOILENKO	91	SPD 36 473	V.D. Samoilenko	(SERP)
		Translated from DANS 318 1367.		

 $a_2(1660)$

$$J^G(J^{PC}) = 1^-(2^{++})$$

OMITTED FROM SUMMARY TABLE

 $a_2(1660)$ MASS

VALUE (MeV)	DOCUMENT ID	TECN	COMMENT
1660±40	ABELE	99B CBAR	1.94 $\bar{p}p \rightarrow \pi^0\eta\eta$

 $a_2(1660)$ WIDTH

VALUE (MeV)	DOCUMENT ID	TECN	COMMENT
280±70	ABELE	99B CBAR	1.94 $\bar{p}p \rightarrow \pi^0\eta\eta$

 $a_2(1660)$ DECAY MODES

Mode	Fraction (Γ_j/Γ)
Γ_1 $\eta\pi$	seen

 $a_2(1660)$ REFERENCES

ABELE	99B	EPJ C8 67	A. Abele <i>et al.</i>	(Crystal Barrel Collab.)
-------	-----	-----------	------------------------	--------------------------

Meson Particle Listings

$\omega_3(1670), \pi_2(1670)$

$\omega_3(1670)$ $I^G(J^{PC}) = 0^-(3^{--})$

$\omega_3(1670)$ MASS

VALUE (MeV)	EVTS	DOCUMENT ID	TECN	COMMENT
1667 ± 4 OUR AVERAGE				
1665.3 ± 5.2 ± 4.5	23400	AMELIN	96 VES	36 $\pi^- p \rightarrow \pi^+ \pi^- \pi^0 n$
1685 ± 20	60	BAUBILLIER	79 HBC	8.2 $K^- p$ backward
1673 ± 12	430	1,2 BALTAY	78E HBC	15 $\pi^+ p \rightarrow \Delta 3\pi$
1650 ± 12		CORDEN	78B OMEG	8-12 $\pi^- p \rightarrow N 3\pi$
1669 ± 11	600	2 WAGNER	75 HBC	7 $\pi^+ p \rightarrow \Delta^{++} 3\pi$
1678 ± 14	500	DIAZ	74 DBC	6 $\pi^+ n \rightarrow p 3\pi^0$
1660 ± 13	200	DIAZ	74 DBC	6 $\pi^+ n \rightarrow p \omega \pi^0 \pi^0$
1679 ± 17	200	MATTHEWS	71D DBC	7.0 $\pi^+ n \rightarrow p 3\pi^0$
1670 ± 20		KENYON	69 DBC	8 $\pi^+ n \rightarrow p 3\pi^0$
• • • We do not use the following data for averages, fits, limits, etc. • • •				
~ 1700	110	1 CERRADA	77B HBC	4.2 $K^- p \rightarrow \Lambda 3\pi$
1695 ± 20		BARNES	69B HBC	4.6 $K^- p \rightarrow \omega 2\pi X$
1636 ± 20		ARMENISE	68B DBC	5.1 $\pi^+ n \rightarrow p 3\pi^0$
1 Phase rotation seen for $J^P = 3^- \rho \pi$ wave. 2 From a fit to $I(J^P) = 0(3^-) \rho \pi$ partial wave.				

$\omega_3(1670)$ WIDTH

VALUE (MeV)	EVTS	DOCUMENT ID	TECN	COMMENT
168 ± 10 OUR AVERAGE				
149 ± 19 ± 7	23400	AMELIN	96 VES	36 $\pi^- p \rightarrow \pi^+ \pi^- \pi^0 n$
160 ± 80	60	3 BAUBILLIER	79 HBC	8.2 $K^- p$ backward
173 ± 16	430	4,5 BALTAY	78E HBC	15 $\pi^+ p \rightarrow \Delta 3\pi$
253 ± 39		CORDEN	78B OMEG	8-12 $\pi^- p \rightarrow N 3\pi$
173 ± 28	600	3,5 WAGNER	75 HBC	7 $\pi^+ p \rightarrow \Delta^{++} 3\pi$
167 ± 40	500	DIAZ	74 DBC	6 $\pi^+ n \rightarrow p 3\pi^0$
122 ± 39	200	DIAZ	74 DBC	6 $\pi^+ n \rightarrow p \omega \pi^0 \pi^0$
155 ± 40	200	3 MATTHEWS	71D DBC	7.0 $\pi^+ n \rightarrow p 3\pi^0$
• • • We do not use the following data for averages, fits, limits, etc. • • •				
90 ± 20		BARNES	69B HBC	4.6 $K^- p \rightarrow \omega 2\pi$
100 ± 40		KENYON	69 DBC	8 $\pi^+ n \rightarrow p 3\pi^0$
112 ± 60		ARMENISE	68B DBC	5.1 $\pi^+ n \rightarrow p 3\pi^0$
3 Width errors enlarged by us to $4\Gamma/\sqrt{N}$; see the note with the $K^*(892)$ mass. 4 Phase rotation seen for $J^P = 3^- \rho \pi$ wave. 5 From a fit to $I(J^P) = 0(3^-) \rho \pi$ partial wave.				

$\omega_3(1670)$ DECAY MODES

Mode	Fraction (Γ_i/Γ)
$\Gamma_1 \rho \pi$	seen
$\Gamma_2 \omega \pi \pi$	seen
$\Gamma_3 b_1(1235)\pi$	possibly seen

$\omega_3(1670)$ BRANCHING RATIOS

$\Gamma(\omega \pi \pi)/\Gamma(\rho \pi)$	Γ_2/Γ_1			
VALUE	EVTS	DOCUMENT ID	TECN	COMMENT
• • • We do not use the following data for averages, fits, limits, etc. • • •				
0.71 ± 0.27	100	DIAZ	74 DBC	6 $\pi^+ n \rightarrow p 5\pi^0$
$\Gamma(b_1(1235)\pi)/\Gamma(\rho \pi)$	Γ_3/Γ_1			
VALUE	DOCUMENT ID	TECN	COMMENT	
possibly seen	DIAZ	74 DBC	6 $\pi^+ n \rightarrow p 5\pi^0$	
$\Gamma(b_1(1235)\pi)/\Gamma(\omega \pi \pi)$	Γ_3/Γ_2			
VALUE	CL%	DOCUMENT ID	TECN	COMMENT
• • • We do not use the following data for averages, fits, limits, etc. • • •				
> 0.75	68	BAUBILLIER	79 HBC	8.2 $K^- p$ backward

$\omega_3(1670)$ REFERENCES

AMELIN	96	ZPHY C70 71	D.V. Amelin et al.	(SERP, TBIL)
BAUBILLIER	79	PL 89B 131	M. Baubillier et al.	(BIRM, CERN, GLAS+)
BALTAY	78E	PRL 40 87	C. Baltay, C.V. Cautis, M. Kalekar	(COLU) JP
CORDEN	78B	NP B138 235	M.J. Corden et al.	(BIRM, RHEL, TELA+)
CERRADA	77B	NP B126 241	M. Cerrada et al.	(AMST, CERN, NIJIM+) JP
WAGNER	75	PL 58B 201	F. Wagner, M. Tabak, D.M. Chew	(LBL) JP
DIAZ	74	PRL 32 260	J. Diaz et al.	(CASE, CMU)
MATTHEWS	71D	PR D3 2561	J.A.J. Matthews et al.	(TNTO, WISC)
BARNES	69B	PRL 23 142	V.E. Barnes et al.	(BNL)
KENYON	69	PRL 23 146	I.R. Kenyon et al.	(BNL, UCND, ORNL)
ARMENISE	68B	PL 26B 336	N. Armenise et al.	(BARI, BGNA, FIRZ+)

OTHER RELATED PAPERS

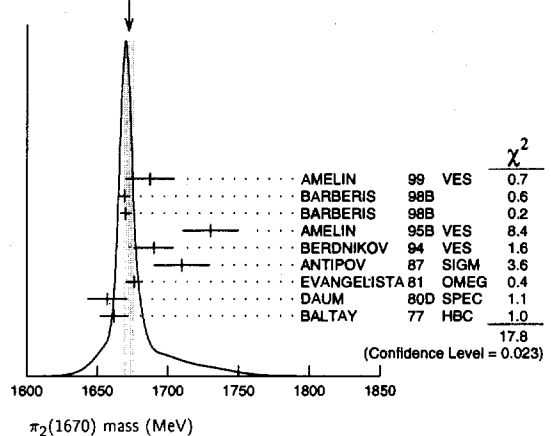
MATTHEWS	71	LCN 1 361	J.A.J. Matthews et al.	(TNTO, WISC)
ARMENISE	70	LCN 4 199	N. Armenise et al.	(BARI, BGNA, FIRZ)

$\pi_2(1670)$ $I^G(J^{PC}) = 1^-(2^{-+})$

$\pi_2(1670)$ MASS

VALUE (MeV)	EVTS	DOCUMENT ID	TECN	CHG	COMMENT
1670 ± 20 OUR ESTIMATE					This is only an educated guess; the error given is larger than the error on the average of the published values.
1672.0 ± 3.5 OUR AVERAGE					Error includes scale factor of 1.5. See the ideogram below.
1687 ± 9 ± 15		AMELIN	99 VES		37 $\pi^- A \rightarrow \omega \pi^- \pi^0 A^*$
1669 ± 4		BARBERIS	98B		450 $\rho \rho \rightarrow \rho f \rho \pi \rho_S$
1670 ± 4		BARBERIS	98B		450 $\rho \rho \rightarrow \rho f f_2(1270) \pi \rho_S$
1730 ± 20		1 AMELIN	95B VES		36 $\pi^- A \rightarrow \pi^+ \pi^- \pi^- A$
1690 ± 14		2 BERDNIKOV	94 VES		37 $\pi^- A \rightarrow K^+ K^- \pi^- A$
1710 ± 20	700	ANTIPOV	87 SIGM	-	50 $\pi^- Cu \rightarrow \mu^+ \mu^- \pi^- Cu$
1676 ± 6		2 EVANGELISTA	81 OMEG	-	12 $\pi^- p \rightarrow 3\pi \rho$
1657 ± 14		2,3 DAUM	80D SPEC	-	63-94 $\pi \rho \rightarrow 3\pi X$
1662 ± 10	2000	2 BALTAY	77 HBC	+	15 $\pi^+ p \rightarrow p 3\pi$
• • • We do not use the following data for averages, fits, limits, etc. • • •					
1742 ± 31 ± 49		ANTREASYAN	90 CBAL		$e^+ e^- \rightarrow e^+ e^- \pi^0 \pi^0 \pi^0$
1624 ± 21		4 BELLINI	85 SPEC		40 $\pi^- \pi^+ \pi^- A$
1622 ± 35		5 BELLINI	85 SPEC		40 $\pi^- \pi^+ \pi^- A$
1693 ± 28		6 BELLINI	85 SPEC		40 $\pi^- \pi^+ \pi^- A$
1710 ± 20		7 DAUM	81B SPEC	-	63,94 $\pi^- \rho$
1660 ± 10		2 ASCOLI	73 HBC	-	5-25 $\pi^- p \rightarrow p \pi_2$
1 From a fit to $J^{PC} = 2^-+ f_2(1270)\pi, f_0(1370)\pi$ waves. 2 From a fit to $J^P = 2^- S$ -wave $f_2(1270)\pi$ partial wave. 3 Clear phase rotation seen in $2^- S, 2^- P, 2^- D$ waves. We quote central value and spread of single-resonance fits to three channels. 4 From $f_2(1270)\pi$ decay. 5 From $\rho \pi$ decay. 6 From $\sigma \pi$ decay. 7 From a two-resonance fit to four $2^- 0^+$ waves. This should not be averaged with all the single resonance fits.					

WEIGHTED AVERAGE
1672.0 ± 3.5 (Error scaled by 1.5)



$\pi_2(1670)$ WIDTH

VALUE (MeV)	EVTS	DOCUMENT ID	TECN	CHG	COMMENT
259 ± 11 OUR AVERAGE					Error includes scale factor of 1.5. See the ideogram below.
168 ± 43 ± 53		AMELIN	99 VES		37 $\pi^- A \rightarrow \omega \pi^- \pi^0 A^*$
268 ± 15		BARBERIS	98B		450 $\rho \rho \rightarrow \rho f \rho \pi \rho_S$
256 ± 15		BARBERIS	98B		450 $\rho \rho \rightarrow \rho f f_2(1270) \pi \rho_S$
310 ± 20		8 AMELIN	95B VES		36 $\pi^- A \rightarrow \pi^+ \pi^- \pi^- A$
190 ± 50		9 BERDNIKOV	94 VES		37 $\pi^- A \rightarrow K^+ K^- \pi^- A$
170 ± 80	700	ANTIPOV	87 SIGM	-	50 $\pi^- Cu \rightarrow \mu^+ \mu^- \pi^- Cu$
260 ± 20		9 EVANGELISTA	81 OMEG	-	12 $\pi^- p \rightarrow 3\pi \rho$
219 ± 20		9,10 DAUM	80D SPEC	-	63-94 $\pi \rho \rightarrow 3\pi X$
285 ± 60	2000	9 BALTAY	77 HBC	+	15 $\pi^+ p \rightarrow p 3\pi$

See key on page 239

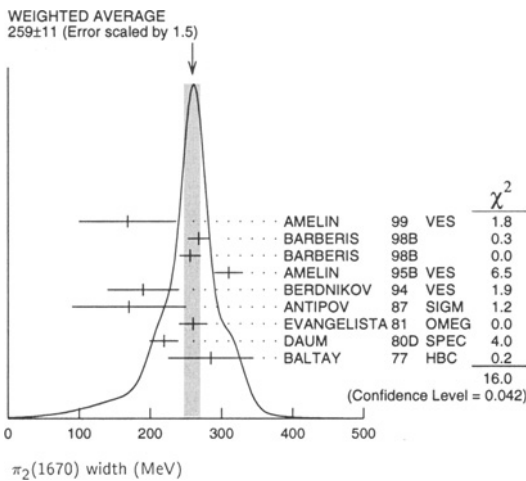
Meson Particle Listings

$\pi_2(1670)$

• • • We do not use the following data for averages, fits, limits, etc. • • •

236 ± 49 ± 36	ANTREASYAN 90	CBAL	$e^+e^- \rightarrow \pi^0\pi^0\pi^0$
304 ± 22	11 BELLINI	85 SPEC	$40 \pi^- A \rightarrow \pi^- \pi^+ \pi^- A$
404 ± 108	12 BELLINI	85 SPEC	$40 \pi^- A \rightarrow \pi^- \pi^+ \pi^- A$
330 ± 90	13 BELLINI	85 SPEC	$40 \pi^- A \rightarrow \pi^- \pi^+ \pi^- A$
312 ± 50	14 DAUM	81B SPEC	$63,94 \pi^- \rho$
270 ± 60	9 ASCOLI	73 HBC	$5-25 \pi^- \rho \rightarrow \rho \pi_2$

- ⁸ From a fit to $J^{PC} = 2^{-+} f_2(1270)\pi, f_0(1370)\pi$ waves.
- ⁹ From a fit to $J^P = 2^{-} f_2(1270)\pi$ partial wave.
- ¹⁰ Clear phase rotation seen in $2^{-}S, 2^{-}P, 2^{-}D$ waves. We quote central value and spread of single-resonance fits to three channels.
- ¹¹ From $f_2(1270)\pi$ decay.
- ¹² From $\rho\pi$ decay.
- ¹³ From $\sigma\pi$ decay.
- ¹⁴ From a two-resonance fit to four $2^{-}0^{+}$ waves. This should not be averaged with all the single resonance fits.



$\pi_2(1670)$ DECAY MODES

Mode	Fraction (Γ_i/Γ)	Confidence level
Γ_1 3π	(95.8 ± 1.4) %	
Γ_2 $f_2(1270)\pi$	(56.2 ± 3.2) %	
Γ_3 $\rho\pi$	(31 ± 4) %	
Γ_4 $\sigma\pi$	(13 ± 6) %	
Γ_5 $f_0(1370)\pi$	(8.7 ± 3.4) %	
Γ_6 $K\bar{K}^*(892) + c.c.$	(4.2 ± 1.4) %	
Γ_7 $\omega\rho$	(2.7 ± 1.1) %	
Γ_8 $\gamma\gamma$		
Γ_9 $\eta\pi$		
Γ_{10} $\pi^\pm 2\pi^+ 2\pi^-$		
Γ_{11} $\rho(1450)\pi$	< 3.6 × 10 ⁻³	97.7%
Γ_{12} $b_1(1235)\pi$	< 1.9 × 10 ⁻³	97.7%

CONSTRAINED FIT INFORMATION

An overall fit to 4 branching ratios uses 6 measurements and one constraint to determine 4 parameters. The overall fit has a $\chi^2 = 1.9$ for 3 degrees of freedom.

The following off-diagonal array elements are the correlation coefficients $\langle \delta x_i \delta x_j \rangle / (\delta x_i \delta x_j)$, in percent, from the fit to the branching fractions, $x_i \equiv \Gamma_i / \Gamma_{total}$. The fit constrains the x_i whose labels appear in this array to sum to one.

x_3	-53		
x_5	-29	-59	
x_6	-8	-21	-9
	x_2	x_3	x_5

$\pi_2(1670)$ PARTIAL WIDTHS

$\Gamma(\gamma\gamma)$	CL%	DOCUMENT ID	TECN	CHG	COMMENT	Γ_8
<0.072	90	15 ACCIARRI	97T	L3	$e^+e^- \rightarrow e^+e^- \pi^+ \pi^- \pi^0$	
<0.19	90	15 ALBRECHT	97B	ARG	$e^+e^- \rightarrow e^+e^- \pi^+ \pi^- \pi^0$	
1.41 ± 0.23 ± 0.28		ANTREASYAN 90	CBAL	0	$e^+e^- \rightarrow e^+e^- \pi^0 \pi^0 \pi^0$	
0.8 ± 0.3 ± 0.12		16 BEHREND	90C	CELL	$e^+e^- \rightarrow e^+e^- \pi^+ \pi^- \pi^0$	
1.3 ± 0.3 ± 0.2		17 BEHREND	90C	CELL	$e^+e^- \rightarrow e^+e^- \pi^+ \pi^- \pi^0$	

• • • We do not use the following data for averages, fits, limits, etc. • • •

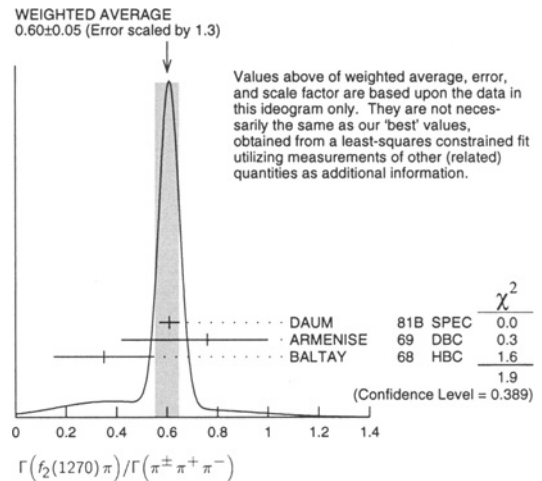
- ¹⁵ Decaying into $f_2(1270)\pi$ and $\rho\pi$.
- ¹⁶ Constructive interference between $f_2(1270)\pi, \rho\pi$ and background.
- ¹⁷ Incoherent Ansatz.

$\pi_2(1670)$ BRANCHING RATIOS

$\Gamma(3\pi)/\Gamma_{total}$	$\Gamma_1/\Gamma = (\Gamma_2 + \Gamma_3 + \Gamma_5)/\Gamma$
0.958 ± 0.014 OUR FIT	
$\Gamma(\rho\pi)/\Gamma(\pi^\pm \pi^+ \pi^-)$	$\frac{1}{2}\Gamma_3/(0.567\Gamma_2 + \frac{1}{2}\Gamma_3 + 0.624\Gamma_5)$
0.29 ± 0.05 OUR FIT	
0.61 ± 0.04	18 DAUM 81B SPEC 63,94 $\pi^- \rho$
<0.3	BARTSCH 68 HBC + $8\pi^+ \rho \rightarrow 3\pi\rho$
$\Gamma(f_2(1270)\pi)/\Gamma(\pi^\pm \pi^+ \pi^-)$	$0.567\Gamma_2/(0.567\Gamma_2 + \frac{1}{2}\Gamma_3 + 0.624\Gamma_5)$
0.604 ± 0.035 OUR FIT	
0.60 ± 0.05 OUR AVERAGE	Error includes scale factor of 1.3. See the ideogram below.
0.76 ± 0.24	19 DAUM 81B SPEC 63,94 $\pi^- \rho$
-0.34	ARMENISE 69 DBC + $5.1 \pi^+ d \rightarrow d3\pi$
0.35 ± 0.20	BALTAY 68 HBC + $7-8.5 \pi^+ \rho$
0.59	BARTSCH 68 HBC + $8\pi^+ \rho \rightarrow 3\pi\rho$

• • • We do not use the following data for averages, fits, limits, etc. • • •

- ¹⁸ From a two-resonance fit to four $2^{-}0^{+}$ waves.
- ¹⁹ From a two-resonance fit to four $2^{-}0^{+}$ waves.



$\Gamma(\rho\pi)/\Gamma(f_2(1270)\pi)$	$\Gamma_3/0.564\Gamma_2$
1.01 ± 0.05	
$\Gamma(\eta\pi)/\Gamma(\pi^\pm \pi^+ \pi^-)$	$\Gamma_9/(0.567\Gamma_2 + \frac{1}{2}\Gamma_3 + 0.624\Gamma_5)$
<0.09	
<0.10	CRENNELL 70 HBC - $6\pi^- \rho \rightarrow f_2 \pi^- N$

• • • We do not use the following data for averages, fits, limits, etc. • • •

Meson Particle Listings

$\pi_2(1670), \phi(1680)$

$\Gamma(\pi^\pm 2\pi^\pm 2\pi^-)/\Gamma(\pi^\pm \pi^\pm \pi^-)$		$\Gamma_{10}/(0.567\Gamma_2 + \frac{1}{2}\Gamma_3 + 0.624\Gamma_5)$			
VALUE		DOCUMENT ID	TECN	CHG	COMMENT
<0.10		CRENNELL	70	HBC	- $6\pi^- \rho \rightarrow f_2 \pi^- N$
<0.1		BALTAY	68	HBC	+ $7.8.5 \pi^+ \rho$

$\Gamma(\rho(1450)\pi)/\Gamma_{total}$		Γ_{11}/Γ			
VALUE	CL%	DOCUMENT ID	TECN	COMMENT	
<0.0036	97.7	AMELIN	99	VES	$37\pi^- A \rightarrow \omega\pi^- \pi^0 A^*$

$\Gamma(b_1(1235)\pi)/\Gamma_{total}$		Γ_{12}/Γ			
VALUE	CL%	DOCUMENT ID	TECN	COMMENT	
<0.0019	97.7	AMELIN	99	VES	$37\pi^- A \rightarrow \omega\pi^- \pi^0 A^*$

$\Gamma(f_0(1370)\pi)/\Gamma(\pi^\pm \pi^\pm \pi^-)$		$0.624\Gamma_5/(0.567\Gamma_2 + \frac{1}{2}\Gamma_3 + 0.624\Gamma_5)$			
VALUE		DOCUMENT ID	TECN	COMMENT	
0.10 ± 0.04 OUR FIT					
0.10 ± 0.05		20 DAUM	81B	SPEC	$63.94 \pi^- \rho$
20 From a two-resonance fit to four 2^-0^+ waves.					

$\Gamma(K\bar{K}^*(892) + c.c.)/\Gamma(f_2(1270)\pi)$		Γ_6/Γ_2			
VALUE		DOCUMENT ID	TECN	CHG	COMMENT
0.075 ± 0.025 OUR FIT					
0.075 ± 0.025		21 ARMSTRONG	82B	OMEG	- $16\pi^- \rho \rightarrow K^+ K^- \pi^- \rho$
21 From a partial-wave analysis of $K^+ K^- \pi^-$ system.					

$\Gamma(\omega\rho)/\Gamma_{total}$		Γ_7/Γ			
VALUE		DOCUMENT ID	TECN	COMMENT	
$0.027 \pm 0.004 \pm 0.010$		23 AMELIN	99	VES	$37\pi^- A \rightarrow \omega\pi^- \pi^0 A^*$

$\Gamma(\sigma\pi)/\Gamma(f_2(1270)\pi)$		Γ_4/Γ_2			
VALUE		DOCUMENT ID	TECN	COMMENT	
0.24 ± 0.10		24,25 BAKER	99	SPEC	$1.94 \bar{p} \rho \rightarrow 4\pi^0$

D-wave/S-wave RATIO FOR $\pi_2(1670) \rightarrow f_2(1270)\pi$					
VALUE		DOCUMENT ID	TECN	COMMENT	
-0.18 ± 0.06		24 BAKER	99	SPEC	$1.94 \bar{p} \rho \rightarrow 4\pi^0$
0.22 ± 0.10		22 DAUM	81B	SPEC	$63.94 \pi^- \rho$
22 From a two-resonance fit to four 2^-0^+ waves.					
23 Normalized to the $B(\pi_2(1670) \rightarrow f_2\pi)$.					
24 Using preliminary CBAR data.					
25 With the $\sigma\pi$ in $L=2$ and the $f_2(1270)\pi$ in $L=0$.					

$\pi_2(1670)$ REFERENCES

AMELIN	99	PAN 62 445	D.V. Amelin et al.	(VES Collab.)
BAKER	99	PL B449 114	C.A. Baker et al.	
BARBERIS	98B	PL B422 399	D. Barberis et al.	(WA102 Collab.)
ACCIARRI	97T	PL B413 147	M. Acciarri et al.	(L3 Collab.)
ALBRECHT	97B	ZPHY C74 469	H. Albrecht et al.	(ARGUS Collab.)
AMELIN	95B	PL B356 595	D.V. Amelin et al.	(SERP, TBIL)
BERDNIKOV	94	PL B337 219	E.B. Berdnikov et al.	(SERP, TBIL)
ANTREASANYAN	90	ZPHY C48 561	D. Antreasyan et al.	(Crystal Ball Collab.)
BEHREND	90C	ZPHY C46 583	H.J. Behrend et al.	(CELLO Collab.)
ANTIPOV	87	EPL 4 403	Y.M. Antipov et al.	(SERP, JINR, INRM+)
BELLINI	85	Translated from YAF 41 1223.	G. Bellini et al.	
ARMSTRONG	82B	NP B202 1	T.A. Armstrong, B. Bacchari	(AACH3, BARI, BONN+)
DAUM	81B	NP B182 269	C. Daum et al.	(AMST, CERN, CRAC, MPIM+)
EVANGELISTA	81	NP B178 197	C. Evangelista et al.	(BARI, BONN, CERN+)
Also	81B	NP B186 594	C. Evangelista	
DAUM	80D	PL 89B 285	C. Daum et al.	(AMST, CERN, CRAC, MPIM+)
BALTAY	77	PL 39 591	I.D. Baltay, C.V. Cautis, M. Kalekar	(COLU)JP
ASCOLI	73	PR D7 669	G. Ascoli et al.	(ILL, TNTO, GENO, HAMB, MILA+)
CRENNELL	70	PRL 24 781	D.J. Crennell et al.	(BNL)
ARMENISE	69	LCN 2 501	N. Armenise et al.	(BARI, BGNA, FIRZ)
BALTAY	68	PRL 20 887	C. Baltay et al.	(COLU, ROCH, RUTG, YALE)I
BARTSCH	68	NP B7 345	J. Bartsch et al.	(AACH, BERL, CERN)JP

OTHER RELATED PAPERS

ZAIMIDOROGA	99	PAN 30 1	O.A. Zaimidorga	
Also	99	Translated from SJPN 30 5.		
ABELE	96	PL B380 453	A. Abele et al.	(Crystal Barrel Collab.)
CHEN	83B	PR D28 2304	T.Y. Chen et al.	(ARIZ, FNAL, FLOR, NDAM+)
LEEDOM	83	PR D27 1426	I.D. Leedom et al.	(PURD, TINTO)
BELLINI	82B	NP B199 1	G. Bellini et al.	(CERN, MILA, JINR+)
DAUM	81B	NP B182 269	C. Daum et al.	(AMST, CERN, CRAC, MPIM+)
PERNEGR	78	NP B134 436	J. Pernegr et al.	(ETH, CERN, LOIC+)
FOCACCI	66	PRL 17 890	M.N. Focacci et al.	(CERN)
LEVRAT	66	PL 22 714	B. Levrat et al.	
VETLITSKY	66	PL 21 579	I.A. Vetlitsky et al.	(ITEP)
FORINO	65B	PL 19 68	A. Forino et al.	(BGNA, BARI, FIRZ, ORSAY+)

$\phi(1680)$

$$I^G(J^{PC}) = 0^-(1^{--})$$

$\phi(1680)$ MASS

e^+e^- PRODUCTION					
VALUE (MeV)	EVTS	DOCUMENT ID	TECN	COMMENT	
1680 ± 20 OUR ESTIMATE					
1681 ± 8 OUR AVERAGE					
1700 ± 20		1 CLEGG	94	RVUE	$e^+e^- \rightarrow K^+ K^-$, $K_S^0 K\pi$
1657 ± 27	367	BISELLO	91C	DM2	$e^+e^- \rightarrow K_S^0 K^\pm \pi^\mp$
1680 ± 10		2 BUON	82	DM1	$e^+e^- \rightarrow$ hadrons
~ 1500		3 ACHASOV	98H	RVUE	$e^+e^- \rightarrow \pi^+ \pi^- \pi^0$, $\omega \pi^+ \pi^-$, $K^+ K^-$
~ 1900		4 ACHASOV	98H	RVUE	$e^+e^- \rightarrow K_S^0 K^\pm \pi^\mp$
1655 ± 17		5 BISELLO	88B	DM2	$e^+e^- \rightarrow K^+ K^-$
1677 ± 12		6 MANE	82	DM1	$e^+e^- \rightarrow K_S^0 K\pi$

PHOTOPRODUCTION					
VALUE (MeV)		DOCUMENT ID	TECN	COMMENT	
1726 ± 22		BUSENITZ	89	TPS	$\gamma p \rightarrow K^+ K^- X$
1760 ± 20		ATKINSON	85C	OMEG	$20-70 \gamma p \rightarrow K\bar{K}X$
1690 ± 10		ASTON	81F	OMEG	$25-70 \gamma p \rightarrow K^+ K^- X$
1 Using BISELLO 88B and MANE 82 data.					
2 From global fit of ρ, ω, ϕ and their radial excitations to channels $\omega\pi^+\pi^-, K^+K^-, K_S^0 K_L^0, K_S^0 K^\pm \pi^\mp$. Assume mass 1570 MeV and width 510 MeV for ρ radial excitations, mass 1570 and width 500 MeV for ω radial excitation.					
3 Using data from IVANOV 81, BARKOV 87, BISELLO 88B, DOLINSKY 91, and AN-TONELLI 92.					
4 Using the data from BISELLO 91C.					
5 From global fit including ρ, ω, ϕ and $\rho(1700)$ assume mass 1570 MeV and width 510 MeV for ρ radial excitation.					
6 Fit to one channel only, neglecting interference with $\omega, \rho(1700)$.					

$\phi(1680)$ WIDTH

e^+e^- PRODUCTION					
VALUE (MeV)	EVTS	DOCUMENT ID	TECN	COMMENT	
150 ± 50 OUR ESTIMATE					This is only an educated guess; the error given is larger than the error on the average of the published values.
300 ± 60		7 CLEGG	94	RVUE	$e^+e^- \rightarrow K^+ K^-$, $K_S^0 K\pi$
146 ± 55	367	BISELLO	91C	DM2	$e^+e^- \rightarrow K_S^0 K^\pm \pi^\mp$
207 ± 45		8 BISELLO	88B	DM2	$e^+e^- \rightarrow K^+ K^-$
185 ± 22		9 BUON	82	DM1	$e^+e^- \rightarrow$ hadrons
102 ± 36		10 MANE	82	DM1	$e^+e^- \rightarrow K_S^0 K\pi$

PHOTOPRODUCTION					
VALUE (MeV)		DOCUMENT ID	TECN	COMMENT	
121 ± 47		BUSENITZ	89	TPS	$\gamma p \rightarrow K^+ K^- X$
80 ± 40		ATKINSON	85C	OMEG	$20-70 \gamma p \rightarrow K\bar{K}X$
100 ± 40		ASTON	81F	OMEG	$25-70 \gamma p \rightarrow K^+ K^- X$
7 Using BISELLO 88B and MANE 82 data.					
8 From global fit including ρ, ω, ϕ and $\rho(1700)$.					
9 From global fit of ρ, ω, ϕ and their radial excitations to channels $\omega\pi^+\pi^-, K^+K^-, K_S^0 K_L^0, K_S^0 K^\pm \pi^\mp$. Assume mass 1570 MeV and width 510 MeV for ρ radial excitations, mass 1570 and width 500 MeV for ω radial excitation.					
10 Fit to one channel only, neglecting interference with $\omega, \rho(1700)$.					

$\phi(1680)$ DECAY MODES

Mode	Fraction (Γ_i/Γ)
Γ_1 $K\bar{K}^*(892) + c.c.$	dominant
Γ_2 $K_S^0 K\pi$	seen
Γ_3 $K\bar{K}$	seen
Γ_4 e^+e^-	seen
Γ_5 $\omega\pi\pi$	not seen
Γ_6 $K^+K^-\pi^0$	

See key on page 239

Meson Particle Listings

 $\phi(1680), \rho_3(1690)$ $\phi(1680) \Gamma(I)\Gamma(e^+e^-)/\Gamma(\text{total})$

This combination of a partial width with the partial width into e^+e^- and with the total width is obtained from the integrated cross section into channel (I) in e^+e^- annihilation. We list only data that have not been used to determine the partial width $\Gamma(I)$ or the branching ratio $\Gamma(I)/\text{total}$.

VALUE (keV)	EVTs	DOCUMENT ID	TECN	COMMENT	$\Gamma_1/\Gamma_4/\Gamma$
0.48 ± 0.14	367	BISELLO	91c DM2	$e^+e^- \rightarrow K_S^0 K^\pm \pi^\mp$	

 $\phi(1680)$ BRANCHING RATIOS

VALUE	DOCUMENT ID	TECN	COMMENT	Γ_1/Γ_2
dominant	MANE	82 DM1	$e^+e^- \rightarrow K_S^0 K^\pm \pi^\mp$	

VALUE	DOCUMENT ID	TECN	COMMENT	Γ_3/Γ_1
0.07 ± 0.01	BUON	82 DM1	e^+e^-	

VALUE	DOCUMENT ID	TECN	COMMENT	Γ_5/Γ_1
< 0.10	BUON	82 DM1	e^+e^-	

 $\phi(1680)$ REFERENCES

ACHASOV	98H PR D57 4334	N.N. Achasov, A.A. Kozhevnikov
CLEGG	94 ZPHY C62 455	A.B. Clegg, A. Donnachie (LANC, MCHS)
ANTONELLI	92 ZPHY C56 15	A. Antonelli et al. (DM2 Collab.)
BISELLO	91C ZPHY C52 227	D. Bisello et al. (DM2 Collab.)
DOLINSKY	91 PRPL 202 99	S.I. Dolinsky et al. (NOVO)
BUSENITZ	89 PR D40 1	J.K. Busenitz et al. (ILL, FNAL)
BISELLO	88B ZPHY C39 13	D. Bisello et al. (PADO, CLER, FRAS+)
BARKOV	87 JETPL 46 164	I.M. Barkov et al. (NOVO)
	Translated from ZETFP 46 132.	
ATKINSON	85C ZPHY C27 233	M. Atkinson et al. (BONN, CERN, GLAS+)
BUON	82 PL 118B 221	J. Buon et al. (LALO, MONP)
MANE	82 PL 112B 178	F. Mane et al. (LALO)
ASTON	81F PL 104B 231	D. Aston (BONN, CERN, EPOL, GLAS, LANC+)
IVANOV	81 PL 107B 237	P.M. Ivanov et al. (NOVO)

OTHER RELATED PAPERS

ABELE	99D PL B468 178	A. Abele et al. (Crystal Barrel Collab.)
ACHASOV	97F PAN 60 2029	N.N. Achasov, A.A. Kozhevnikov (NOVM)
	Translated from YAF 60 2212.	
ATKINSON	86C ZPHY C30 541	M. Atkinson et al. (BONN, CERN, GLAS+)
ATKINSON	84 NP B231 15	M. Atkinson et al. (BONN, CERN, GLAS+)
ATKINSON	84B NP B231 1	M. Atkinson et al. (BONN, CERN, GLAS+)
ATKINSON	83C NP B229 269	M. Atkinson et al. (BONN, CERN, GLAS+)
CORDIER	81 PL 106B 155	A. Cordier et al. (ORSAY)
MANE	81 PL 99B 261	F. Mane et al. (ORSAY)
ASTON	80F NP B174 269	D. Aston (BONN, CERN, EPOL, GLAS, LANC+)

 $\rho_3(1690)$

$$I^G(J^{PC}) = 1^+(3^{--})$$

 $\rho_3(1690)$ MASS

VALUE (MeV)	DOCUMENT ID	COMMENT
1691 ± 5	OUR ESTIMATE	This is only an educated guess; the error given is larger than the error on the average of the published values.
1688.8 ± 2.1	OUR AVERAGE	Includes data from the 5 datablocks that follow this one.

 2π MODE

VALUE (MeV)	EVTs	DOCUMENT ID	TECN	CHG	COMMENT
-------------	------	-------------	------	-----	---------

The data in this block is included in the average printed for a previous datablock.

 1686 ± 4 OUR AVERAGE

1677 ± 14		EVANGELISTA 81	OMEG	-	$12 \pi^- p \rightarrow 2\pi p$
1679 ± 11	476	BALTAY	78b	HBC	0 $15 \pi^+ p \rightarrow \pi^+ \pi^- n$
					$\pi^+ \pi^- p \rightarrow p 3\pi$
1678 ± 12	175	¹ ANTIPOV	77	CIBS	0 $25 \pi^- p \rightarrow \pi^+ \pi^- p$
1690 ± 7	600	¹ ENGLER	74	DBC	0 $6 \pi^+ n \rightarrow \pi^+ \pi^- p$
1693 ± 8		² GRAYER	74	ASPK	0 $17 \pi^- p \rightarrow \pi^+ \pi^- n$
					$\pi^+ \pi^- n$
1678 ± 12		MATTHEWS	71c	DBC	0 $7 \pi^+ N$
• • • We do not use the following data for averages, fits, limits, etc. • • •					
1734 ± 10		³ CORDEN	79	OMEG	$12-15 \pi^- p \rightarrow n 2\pi$
1692 ± 12		^{2,4} ESTABROOKS	75	RVUE	$17 \pi^- p \rightarrow \pi^+ \pi^- n$
					$9 \pi^+ N$
1737 ± 23		ARMENISE	70	DBC	0 $8 \pi^+ p \rightarrow N 2\pi$
1650 ± 35	122	BARTSCH	70b	HBC	+ $8 \pi^+ p \rightarrow N 2\pi$
1687 ± 21		STUNTEBECK	70	HDBC	0 $8 \pi^- p, 5.4 \pi^+ d$
1683 ± 13		ARMENISE	68	DBC	0 $5.1 \pi^+ d$
1670 ± 30		GOLDBERG	65	HBC	0 $6 \pi^+ d, 8 \pi^- p$

¹ Mass errors enlarged by us to Γ/\sqrt{N} ; see the note with the $K^*(892)$ mass.² Uses same data as HYAMS 75.³ From a phase shift solution containing a $f_2'(1525)$ width two times larger than the $K\bar{K}$ result.⁴ From phase-shift analysis. Error takes account of spread of different phase-shift solutions. $K\bar{K}$ AND $K\bar{K}\pi$ MODES

VALUE (MeV)	EVTs	DOCUMENT ID	TECN	CHG	COMMENT
-------------	------	-------------	------	-----	---------

The data in this block is included in the average printed for a previous datablock.

 1696 ± 4 OUR AVERAGE

1699 ± 5		ALPER	80	CNTR	0 $62 \pi^- p \rightarrow K^+ K^- n$
1698 ± 12	6k	^{5,6} MARTIN	78d	SPEC	$10 \pi p \rightarrow K_S^0 K^- p$
1692 ± 6		BLUM	75	ASPK	0 $18.4 \pi^- p \rightarrow n K^+ K^-$
1690 ± 16		ADERHOLZ	69	HBC	+ $8 \pi^+ p \rightarrow K\bar{K}\pi$
• • • We do not use the following data for averages, fits, limits, etc. • • •					
1694 ± 8		⁷ COSTA...	80	OMEG	$10 \pi^- p \rightarrow K^+ K^- n$

⁵ From a fit to $J^P = 3^-$ partial wave.⁶ Systematic error on mass scale subtracted.⁷ They cannot distinguish between $\rho_3(1690)$ and $\omega_3(1670)$. $(4\pi)^\pm$ MODE

VALUE (MeV)	EVTs	DOCUMENT ID	TECN	CHG	COMMENT
-------------	------	-------------	------	-----	---------

The data in this block is included in the average printed for a previous datablock.

 1686 ± 5 OUR AVERAGE Error includes scale factor of 1.1.

1694 ± 6		⁸ EVANGELISTA 81	OMEG	-	$12 \pi^- p \rightarrow p 4\pi$
1665 ± 15	177	BALTAY	78b	HBC	+ $15 \pi^+ p \rightarrow p 4\pi$
1670 ± 10		THOMPSON	74	HBC	+ $13 \pi^+ p$
1687 ± 20		CASON	73	HBC	- $8.18.5 \pi^- p$
1685 ± 14		⁹ CASON	73	HBC	- $8.18.5 \pi^- p$
1680 ± 40	144	BARTSCH	70b	HBC	+ $8 \pi^+ p \rightarrow N 4\pi$
1689 ± 20	102	⁹ BARTSCH	70b	HBC	+ $8 \pi^+ p \rightarrow N 2p$
1705 ± 21		CASO	70	HBC	- $11.2 \pi^- p \rightarrow n p 2\pi$
• • • We do not use the following data for averages, fits, limits, etc. • • •					
1718 ± 10		¹⁰ EVANGELISTA 81	OMEG	-	$12 \pi^- p \rightarrow p 4\pi$
1673 ± 9		¹¹ EVANGELISTA 81	OMEG	-	$12 \pi^- p \rightarrow p 4\pi$
1733 ± 9	66	⁹ KLIGER	74	HBC	- $4.5 \pi^- p \rightarrow p 4\pi$
1630 ± 15		HOLMES	72	HBC	+ $10-12 K^+ p$
1720 ± 15		BALTAY	68	HBC	+ $7, 8.5 \pi^+ p$

⁸ From $p^- \rho^0$ mode, not independent of the other two EVANGELISTA 81 entries.⁹ From $p^\pm \rho^0$ mode.¹⁰ From $a_2(1320)^- \pi^0$ mode, not independent of the other two EVANGELISTA 81 entries.¹¹ From $a_2(1320)^0 \pi^-$ mode, not independent of the other two EVANGELISTA 81 entries. $\omega\pi$ MODE

VALUE (MeV)	DOCUMENT ID	TECN	CHG	COMMENT
-------------	-------------	------	-----	---------

The data in this block is included in the average printed for a previous datablock.

 1681 ± 7 OUR AVERAGE

1670 ± 25		¹² ALDE	95	GAM2	$38 \pi^- p \rightarrow \omega \pi^0 n$
1690 ± 15		EVANGELISTA 81	OMEG	-	$12 \pi^- p \rightarrow \omega \pi p$
1666 ± 14		GESSAROLI	77	HBC	$11 \pi^- p \rightarrow \omega \pi p$
1686 ± 9		THOMPSON	74	HBC	+ $13 \pi^+ p$
• • • We do not use the following data for averages, fits, limits, etc. • • •					
1654 ± 24		BARNHAM	70	HBC	+ $10 K^+ p \rightarrow \omega \pi X$

¹² Supersedes ALDE 92c. $\eta\pi^+\pi^-$ MODE(For difficulties with MMS experiments, see the $a_2(1320)$ mini-review in the 1973 edition.)

VALUE (MeV)	DOCUMENT ID	TECN	CHG	COMMENT
-------------	-------------	------	-----	---------

The data in this block is included in the average printed for a previous datablock.

 1682 ± 12 OUR AVERAGE

1685 ± 10 ± 20		AMELIN	00	VES	$37 \pi^- p \rightarrow \eta \pi^+ \pi^- n$
1680 ± 15		FUKUI	88	SPEC	0 $8.95 \pi^- p \rightarrow \eta \pi^+ \pi^- n$
• • • We do not use the following data for averages, fits, limits, etc. • • •					
1700 ± 47		¹³ ANDERSON	69	MMS	- $16 \pi^- p$ backward
1632 ± 15		^{13,14} FOCACCI	66	MMS	- $7-12 \pi^- p \rightarrow pMM$
1700 ± 15		^{13,14} FOCACCI	66	MMS	- $7-12 \pi^- p \rightarrow pMM$
1748 ± 15		^{13,14} FOCACCI	66	MMS	- $7-12 \pi^- p \rightarrow pMM$

¹³ Seen in 2.5-3 GeV/c $\bar{p}p$. $2\pi^+ 2\pi^-$, with 0, 1, 2 $\pi^+ \pi^-$ pairs in p band not seen by OREN 74 (2.3 GeV/c $\bar{p}p$) with more statistics. (Jan. 1976)¹⁴ Not seen by BOWEN 72.

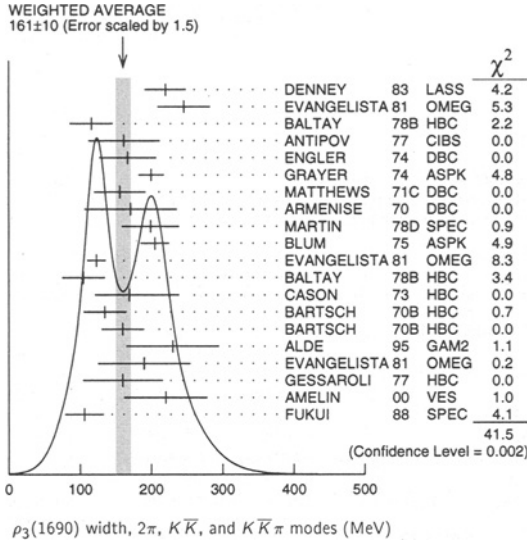
Meson Particle Listings

$\rho_3(1690)$

$\rho_3(1690)$ WIDTH

$2\pi, K\bar{K},$ AND $K\bar{K}\pi$ MODES

VALUE (MeV) DOCUMENT ID
161±10 OUR AVERAGE Includes data from the 5 datablocks that follow this one. Error includes scale factor of 1.5. See the ideogram below.



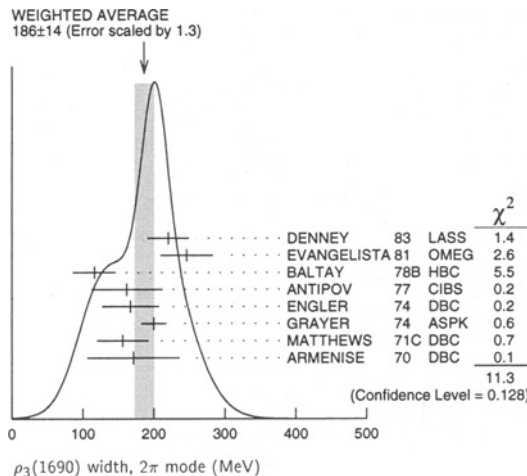
2π MODE

VALUE (MeV) EVTS DOCUMENT ID TECN CHG COMMENT
 The data in this block is included in the average printed for a previous datablock.

186±14 OUR AVERAGE Error includes scale factor of 1.3. See the ideogram below.

220±29		DENNEY 83 LASS			$10 \pi^+ N$
246±37		EVANGELISTA 81 OMEG	-		$12 \pi^- p \rightarrow 2\pi p$
116±30	476	BALTAY 78B HBC	0		$15 \pi^+ p \rightarrow \pi^+ \pi^- n$
162±50	175	15 ANTIPOV 77 CIBS	0		$25 \pi^- p \rightarrow p 3\pi$
167±40	600	ENGLER 74 DBC	0		$6 \pi^+ n \rightarrow \pi^+ \pi^- p$
200±18		16 GRAYER 74 ASPK	0		$17 \pi^- p \rightarrow \pi^+ \pi^- n$
156±36		MATTHEWS 71C DBC	0		$7 \pi^+ N$
171±65		ARMENISE 70 DBC	0		$9 \pi^+ d$
322±35		17 CORDEN 79 OMEG			$12-15 \pi^- p \rightarrow n 2\pi$
240±30		16,18 ESTABROOKS 75 RVUE			$17 \pi^- p \rightarrow \pi^+ \pi^- n$
180±30	122	BARTSCH 70B HBC	+		$8 \pi^+ p \rightarrow N 2\pi$
267±72		STUNTEBECK 70 HDBC	0		$8 \pi^- p, 5.4 \pi^+ d$
188±49		ARMENISE 68 DBC	0		$5.1 \pi^+ d$
180±40		GOLDBERG 65 HBC	0		$6 \pi^+ d, 8 \pi^- p$

¹⁵ Width errors enlarged by us to $4\Gamma/\sqrt{N}$; see the note with the $K^*(892)$ mass.
¹⁶ Uses same data as HYAMS 75 and BECKER 79.
¹⁷ From a phase shift solution containing a $f_2'(1525)$ width two times larger than the $K\bar{K}$ result.
¹⁸ From phase-shift analysis. Error takes account of spread of different phase-shift solutions.



$K\bar{K}$ AND $K\bar{K}\pi$ MODES

VALUE (MeV) EVTS DOCUMENT ID TECN CHG COMMENT
 The data in this block is included in the average printed for a previous datablock.

204±18 OUR AVERAGE

199±40	6000	19 MARTIN	78D SPEC		$10 \pi p \rightarrow K_S^0 K^- p$
205±20		BLUM 75 ASPK	0		$18.4 \pi^- p \rightarrow n K^+ K^-$
219±4		ALPER 80 CNTR	0		$62 \pi^- p \rightarrow K^+ K^- n$
186±11		20 COSTA...	80 OMEG		$10 \pi^- p \rightarrow K^+ K^- n$
112±60		ADERHOLZ 69 HBC	+		$8 \pi^+ p \rightarrow K\bar{K}\pi$

• • • We do not use the following data for averages, fits, limits, etc. • • •

¹⁹ From a fit to $J^P = 3^-$ partial wave.
²⁰ They cannot distinguish between $\rho_3(1690)$ and $\omega_3(1670)$.

$(4\pi)^\pm$ MODE

VALUE (MeV) EVTS DOCUMENT ID TECN CHG COMMENT
 The data in this block is included in the average printed for a previous datablock.

129±10 OUR AVERAGE

123±13		21 EVANGELISTA 81 OMEG	-		$12 \pi^- p \rightarrow p 4\pi$
105±30	177	BALTAY 78B HBC	+		$15 \pi^+ p \rightarrow p 4\pi$
169±70		CASON 73 HBC	-		$8, 18.5 \pi^- p$
135±30	144	BARTSCH 70B HBC	+		$8 \pi^+ p \rightarrow N 4\pi$
160±30	102	BARTSCH 70B HBC	+		$8 \pi^+ p \rightarrow N 2p$
230±28		22 EVANGELISTA 81 OMEG	-		$12 \pi^- p \rightarrow p 4\pi$
184±33		23 EVANGELISTA 81 OMEG	-		$12 \pi^- p \rightarrow p 4\pi$
150	66	24 KLIGER 74 HBC	-		$4.5 \pi^- p \rightarrow p 4\pi$
106±25		THOMPSON 74 HBC	+		$13 \pi^+ p$
125±83		24 CASON 73 HBC	-		$8, 18.5 \pi^- p$
130±30		HOLMES 72 HBC	+		$10-12 K^+ p$
180±30	90	24 BARTSCH 70B HBC	+		$8 \pi^+ p \rightarrow N a_2 \pi$
100±35		BALTAY 68 HBC	+		$7, 8.5 \pi^+ p$

²¹ From $\rho^- \rho^0$ mode, not independent of the other two EVANGELISTA 81 entries.
²² From $a_2(1320)^- \pi^0$ mode, not independent of the other two EVANGELISTA 81 entries.
²³ From $a_2(1320)^0 \pi^-$ mode, not independent of the other two EVANGELISTA 81 entries.
²⁴ From $\rho^\pm \rho^0$ mode.

$\omega\pi$ MODE

VALUE (MeV) DOCUMENT ID TECN CHG COMMENT
 The data in this block is included in the average printed for a previous datablock.

190±40 OUR AVERAGE

230±65		25 ALDE 95 GAM2			$38 \pi^- p \rightarrow \omega \pi^0 n$
190±65		EVANGELISTA 81 OMEG	-		$12 \pi^- p \rightarrow \omega \pi p$
160±56		GESSAROLI 77 HBC			$11 \pi^- p \rightarrow \omega \pi p$
89±25		THOMPSON 74 HBC	+		$13 \pi^+ p$
130±73		BARNHAM 70 HBC	+		$10 K^+ p \rightarrow \omega \pi X$

²⁵ Supersedes ALDE 92c.

$\eta\pi^+\pi^-$ MODE

(For difficulties with MMS experiments, see the $a_2(1320)$ mini-review in the 1973 edition.)

VALUE (MeV) DOCUMENT ID TECN CHG COMMENT
 The data in this block is included in the average printed for a previous datablock.

126±40 OUR AVERAGE Error includes scale factor of 1.8.

220±30±50		AMELIN 00 VES			$37 \pi^- p \rightarrow \eta \pi^+ \pi^- n$
106±27		FUKUI 88 SPEC	0		$8.95 \pi^- p \rightarrow \eta \pi^+ \pi^- n$

• • • We do not use the following data for averages, fits, limits, etc. • • •

195		26 ANDERSON 69 MMS	-		$16 \pi^- p$ backward
< 21		26,27 FOCACCI 66 MMS	-		$7-12 \pi^- p \rightarrow p MM$
< 30		26,27 FOCACCI 66 MMS	-		$7-12 \pi^- p \rightarrow p MM$
< 38		26,27 FOCACCI 66 MMS	-		$7-12 \pi^- p \rightarrow p MM$

²⁶ Seen in 2.5-3 GeV/c $\bar{p}p$. $2\pi^+ 2\pi^-$, with 0, 1, 2 $\pi^+ \pi^-$ pairs in ρ^0 band not seen by OREN 74 (2.3 GeV/c $\bar{p}p$) with more statistics. (Jan. 1979)
²⁷ Not seen by BOWEN 72.

See key on page 239

Meson Particle Listings

$\rho_3(1690)$

$\rho_3(1690)$ DECAY MODES

Mode	Fraction (Γ_i/Γ)	Scale factor
Γ_1 4π	(71.1 ± 1.9) %	
Γ_2 $\pi^\pm \pi^+ \pi^- \pi^0$	(67 ± 22) %	
Γ_3 $\omega \pi$	(16 ± 6) %	
Γ_4 $\pi \pi$	(23.6 ± 1.3) %	
Γ_5 $K \bar{K} \pi$	(3.8 ± 1.2) %	
Γ_6 $K \bar{K}$	(1.58 ± 0.26) %	1.2
Γ_7 $\eta \pi^+ \pi^-$	seen	
Γ_8 $\rho(770) \eta$	seen	
Γ_9 $\pi \pi \rho$		
Excluding 2ρ and $a_2(1320) \pi$.		
Γ_{10} $a_2(1320) \pi$		
Γ_{11} $\rho \rho$		
Γ_{12} $\phi \pi$		
Γ_{13} $\eta \pi$		
Γ_{14} $\pi^\pm 2\pi^+ 2\pi^- \pi^0$		

CONSTRAINED FIT INFORMATION

An overall fit to 5 branching ratios uses 10 measurements and one constraint to determine 4 parameters. The overall fit has a $\chi^2 = 14.7$ for 7 degrees of freedom.

The following off-diagonal array elements are the correlation coefficients $\langle \delta x_i \delta x_j \rangle / (\delta x_i \delta x_j)$, in percent, from the fit to the branching fractions, $x_i \equiv \Gamma_i / \Gamma_{\text{total}}$. The fit constrains the x_i whose labels appear in this array to sum to one.

x_4	-77		
x_5	-74	17	
x_6	-15	2	0
	x_1	x_4	x_5

$\rho_3(1690)$ BRANCHING RATIOS

$\Gamma(\pi\pi)/\Gamma_{\text{total}}$	DOCUMENT ID	TECN	CHG	COMMENT	Γ_4/Γ
0.236 ± 0.013 OUR FIT					
0.243 ± 0.013 OUR AVERAGE					
0.259 ^{+0.018} _{-0.019}	BECKER	79 ASPK	0	17 $\pi^- \rho$ polarized	
0.23 ± 0.02	CORDEN	79 OMEG		12-15 $\pi^- \rho \rightarrow n 2\pi$	
0.22 ± 0.04	²⁸ MATTHEWS	71c HDBC	0	7 $\pi^+ n \rightarrow \pi^- \rho$	
• • • We do not use the following data for averages, fits, limits, etc. • • •					
0.245 ± 0.006	²⁹ ESTABROOKS	75 RVUE		17 $\pi^- \rho \rightarrow \pi^+ \pi^- n$	

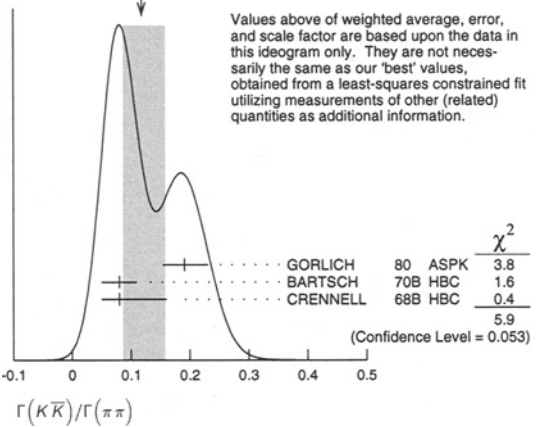
²⁸ One-pion-exchange model used in this estimation.
²⁹ From phase-shift analysis of HYAMS 75 data.

$\Gamma(a_2 \pi)/\Gamma(\pi^\pm \pi^+ \pi^- \pi^0)$	DOCUMENT ID	TECN	CHG	COMMENT	Γ_4/Γ_2
0.35 ± 0.11	CASON	73 HBC	-	8.18.5 $\pi^- \rho$	
• • • We do not use the following data for averages, fits, limits, etc. • • •					
<0.2	HOLMES	72 HBC	+	10-12 $K^+ \rho$	
<0.12	BALLAM	71b HBC	-	16 $\pi^- \rho$	

$\Gamma(\pi\pi)/\Gamma(4\pi)$	DOCUMENT ID	TECN	CHG	COMMENT	Γ_4/Γ_1
0.332 ± 0.026 OUR FIT				Error includes scale factor of 1.1.	
0.30 ± 0.10	BALTAY	78b HBC	0	15 $\pi^+ \rho \rightarrow \rho 4\pi$	

$\Gamma(K \bar{K})/\Gamma(\pi\pi)$	DOCUMENT ID	TECN	CHG	COMMENT	Γ_6/Γ_4
0.067 ± 0.011 OUR FIT				Error includes scale factor of 1.2.	
0.118^{+0.039}_{-0.032} OUR AVERAGE				Error includes scale factor of 1.7. See the ideogram below.	
0.191 ^{+0.040} _{-0.037}	GORLICH	80 ASPK	0	17.18 $\pi^- \rho$ polarized	
0.08 ± 0.03	BARTSCH	70b HBC	+	8 $\pi^+ \rho$	
0.08 ^{+0.08} _{-0.03}	CRENNELL	68b HBC		6.0 $\pi^- \rho$	

WEIGHTED AVERAGE
0.118 ± 0.039-0.032 (Error scaled by 1.7)



$\Gamma(K \bar{K} \pi)/\Gamma(\pi\pi)$	DOCUMENT ID	TECN	CHG	COMMENT	Γ_5/Γ_4
0.16 ± 0.05 OUR FIT					
0.16 ± 0.05	³⁰ BARTSCH	70b HBC	+	8 $\pi^+ \rho$	

³⁰ Increased by us to correspond to $B(\rho_3(1690) \rightarrow \pi\pi) = 0.24$.

$[\Gamma(\pi\pi\rho) + \Gamma(a_2(1320)\pi) + \Gamma(\rho\rho)]/\Gamma(\pi^\pm \pi^+ \pi^- \pi^0)$	DOCUMENT ID	TECN	CHG	COMMENT	$(\Gamma_9 + \Gamma_{10} + \Gamma_{11})/\Gamma_2$
0.94 ± 0.09 OUR AVERAGE					
0.96 ± 0.21	BALTAY	78b HBC	+	15 $\pi^+ \rho \rightarrow \rho 4\pi$	
0.88 ± 0.15	BALLAM	71b HBC	-	16 $\pi^- \rho$	
1 ± 0.15	BARTSCH	70b HBC	+	8 $\pi^+ \rho$	
consistent with 1	CASO	68 HBC	-	11 $\pi^- \rho$	

$\Gamma(\rho\rho)/\Gamma(\pi^\pm \pi^+ \pi^- \pi^0)$	DOCUMENT ID	TECN	CHG	COMMENT	Γ_{11}/Γ_2
• • • We do not use the following data for averages, fits, limits, etc. • • •					
0.12 ± 0.11	BALTAY	78b HBC	+	15 $\pi^+ \rho \rightarrow \rho 4\pi$	
0.56	KLIGER	74 HBC	-	4.5 $\pi^- \rho \rightarrow \rho 4\pi$	
0.13 ± 0.09	³¹ THOMPSON	74 HBC	+	13 $\pi^+ \rho$	
0.7 ± 0.15	BARTSCH	70b HBC	+	8 $\pi^+ \rho$	
³¹ $\rho\rho$ and $a_2(1320)\pi$ modes are indistinguishable.					

$\Gamma(\rho\rho)/[\Gamma(\pi\pi\rho) + \Gamma(a_2(1320)\pi) + \Gamma(\rho\rho)]$	DOCUMENT ID	TECN	CHG	COMMENT	$\Gamma_{11}/(\Gamma_9 + \Gamma_{10} + \Gamma_{11})$
• • • We do not use the following data for averages, fits, limits, etc. • • •					
0.48 ± 0.16	CASO	68 HBC	-	11 $\pi^- \rho$	

$\Gamma(a_2(1320)\pi)/\Gamma(\pi^\pm \pi^+ \pi^- \pi^0)$	DOCUMENT ID	TECN	CHG	COMMENT	Γ_{10}/Γ_2
• • • We do not use the following data for averages, fits, limits, etc. • • •					
0.66 ± 0.08	BALTAY	78b HBC	+	15 $\pi^+ \rho \rightarrow \rho 4\pi$	
0.36 ± 0.14	³² THOMPSON	74 HBC	+	13 $\pi^+ \rho$	
not seen	CASON	73 HBC	-	8.18.5 $\pi^- \rho$	
0.6 ± 0.15	BARTSCH	70b HBC	+	8 $\pi^+ \rho$	
0.6	BALTAY	68 HBC	+	7.8.5 $\pi^+ \rho$	
³² $\rho\rho$ and $a_2(1320)\pi$ modes are indistinguishable.					

$\Gamma(\omega\pi)/\Gamma(\pi^\pm \pi^+ \pi^- \pi^0)$	DOCUMENT ID	TECN	CHG	COMMENT	Γ_3/Γ_2
0.23 ± 0.05 OUR AVERAGE				Error includes scale factor of 1.2.	
0.33 ± 0.07	THOMPSON	74 HBC	+	13 $\pi^+ \rho$	
0.12 ± 0.07	BALLAM	71b HBC	-	16 $\pi^- \rho$	
0.25 ± 0.10	BALTAY	68 HBC	+	7.8.5 $\pi^+ \rho$	
0.25 ± 0.10	JOHNSTON	68 HBC	-	7.0 $\pi^- \rho$	
• • • We do not use the following data for averages, fits, limits, etc. • • •					
<0.11	95	BALTAY	78b HBC	+	15 $\pi^+ \rho \rightarrow \rho 4\pi$
<0.09		KLIGER	74 HBC	-	4.5 $\pi^- \rho \rightarrow \rho 4\pi$

$\Gamma(\phi\pi)/\Gamma(\pi^\pm \pi^+ \pi^- \pi^0)$	DOCUMENT ID	TECN	CHG	COMMENT	Γ_{12}/Γ_2
• • • We do not use the following data for averages, fits, limits, etc. • • •					
<0.11		BALTAY	68 HBC	+	7.8.5 $\pi^+ \rho$

$\Gamma(\pi^\pm 2\pi^+ 2\pi^- \pi^0)/\Gamma(\pi^\pm \pi^+ \pi^- \pi^0)$	DOCUMENT ID	TECN	CHG	COMMENT	Γ_{14}/Γ_2
• • • We do not use the following data for averages, fits, limits, etc. • • •					
<0.15		BALTAY	68 HBC	+	7.8.5 $\pi^+ \rho$

Meson Particle Listings

 $\rho_3(1690)$, $\rho(1700)$

$\Gamma(\eta\pi)/\Gamma(\pi^+\pi^-\pi^0)$						Γ_{13}/Γ_2
VALUE	DOCUMENT ID	TECN	CHG	COMMENT		
• • • We do not use the following data for averages, fits, limits, etc. • • •						
<0.02	THOMPSON	74	HBC	+	13	$\pi^+\rho$
$\Gamma(K\bar{K})/\Gamma_{total}$						Γ_6/Γ
VALUE	DOCUMENT ID	TECN	CHG	COMMENT		
• • • We do not use the following data for averages, fits, limits, etc. • • •						
0.0150 ± 0.0026 OUR FIT	Error includes scale factor of 1.2.					
0.0130 ± 0.0024 OUR AVERAGE						
0.013 \pm 0.003	COSTA...	80	OMEG	0	10	$\pi^-\rho \rightarrow K^+K^-\pi$
0.013 \pm 0.004	³³ MARTIN	78B	SPEC	-	10	$\pi\rho \rightarrow K_S^0K^-\pi$
³³ From $(\Gamma_4\Gamma_6)^{1/2} = 0.056 \pm 0.034$ assuming $B(\rho_3(1690) \rightarrow \pi\pi) = 0.24$.						
$\Gamma(\omega\pi)/[\Gamma(\omega\pi) + \Gamma(\rho\rho)]$						$\Gamma_3/(\Gamma_3 + \Gamma_{11})$
VALUE	DOCUMENT ID	TECN	CHG	COMMENT		
• • • We do not use the following data for averages, fits, limits, etc. • • •						
0.22 \pm 0.08	CASON	73	HBC	-	8,18,5	$\pi^-\rho$
$\Gamma(\eta\pi^+\pi^-)/\Gamma_{total}$						Γ_7/Γ
VALUE	DOCUMENT ID	TECN	COMMENT			
seen	FUKUI	88	SPEC	8.95	$\pi^-\rho \rightarrow \eta\pi^+\pi^-\pi$	
$\Gamma(\rho_2(1320)\pi)/\Gamma(\rho(770)\pi)$						Γ_{10}/Γ_8
VALUE	DOCUMENT ID	TECN	COMMENT			
5.5 ± 2.0	AMELIN	00	VES	37	$\pi^-\rho \rightarrow \eta\pi^+\pi^-\pi$	

 $\rho_3(1690)$ REFERENCES

AMELIN	00	NP B668 83	D. Amelin <i>et al.</i>	(VES Collab.)
ALDE	95	ZPHY C66 379	D.M. Alde <i>et al.</i>	(GAMS Collab.) JP
ALDE	92C	ZPHY C54 553	D.M. Alde <i>et al.</i>	(BELG, SERP, KEK, LANL+)
FUKUI	88	PL B202 441	S. Fukui <i>et al.</i>	(SUGI, NAGO, KEK, KYOT+)
DENNEY	83	PR D28 2726	D.L. Denney <i>et al.</i>	(IOWA, MICH)
EVANGELISTA	81	NP B178 197	C. Evangelista <i>et al.</i>	(BARI, BONN, CERN+)
ALPER	80	PL 94B 422	B. Alper <i>et al.</i>	(AMST, CERN, CRAC, MPIM+)
COSTA...	80	NP B175 402	G. Costa de Beauregard <i>et al.</i>	(BARI, BONN+)
GORLICH	80	NP B174 16	L. Gorlich <i>et al.</i>	(CRAC, MPIM, CERN+)
BECKER	79	NP B151 46	H. Becker <i>et al.</i>	(MPIM, CERN, ZEEM, CRAC)
CORDEN	79	NP B157 250	M.J. Corden <i>et al.</i>	(BIRM, RHEL, TELA+)
BALTAY	78B	PR D17 62	C. Baltay <i>et al.</i>	(COLL, BING)
MARTIN	78B	NP B140 158	A.D. Martin <i>et al.</i>	(DURH, GEVA)
MARTIN	78D	PL 74B 417	A.D. Martin <i>et al.</i>	(DURH, GEVA)
ANTIPOV	77	NP B119 45	Y.M. Antipov <i>et al.</i>	(SERP, GEVA)
GESSAROLI	77	NP B126 382	R. Gessaroli <i>et al.</i>	(BGNA, FIRZ, GENO+)
BLUM	75	PL 57B 403	W. Blum <i>et al.</i>	(CERN, MPIM) JP
ESTABROOKS	75	NP B95 322	P.G. Estabrooks, A.D. Martin	(DURH)
HYAMS	75	NP B100 205	B.D. Hyams <i>et al.</i>	(CERN, MPIM)
ENGLER	74	PR D10 2070	A. Engler <i>et al.</i>	(CMU, CASE)
GRAVER	74	NP B75 189	G. Grayer <i>et al.</i>	(CERN, MPIM)
KLIGER	74	SJNP 19 428	G.K. Kliger <i>et al.</i>	(ITEP)
Translated from YAF 19 839.				
OREN	74	NP B71 189	Y. Oren <i>et al.</i>	(ANL, OXF)
THOMPSON	74	NP B69 220	G. Thompson <i>et al.</i>	(PURD)
CASON	73	PR D7 1971	N.M. Cason <i>et al.</i>	(NOAM)
BOWEN	72	PRL 29 890	D.R. Bowen <i>et al.</i>	(NEAS, STON)
HOLMES	72	PR D6 3336	R. Holmes <i>et al.</i>	(ROCH)
BALLAM	71B	PR D3 2606	J. Ballam <i>et al.</i>	(SLAC)
MATTHEWS	71C	NP B33 1	J.A.J. Matthews <i>et al.</i>	(TNTO, WISC) JP
ARMENISE	70	LNK 4 199	N. Armenise <i>et al.</i>	(BARI, BGNA, FIRZ)
BARNHAM	70	PRL 24 1083	K.W.J. Barnham <i>et al.</i>	(BIRM)
BARTSCH	70B	NP B22 109	J. Bartsch <i>et al.</i>	(AACH, BERL, CERN)
CASO	70	LNK 3 707	C. Caso <i>et al.</i>	(GENO, HAMB, MILA, SACL)
STUNTEBECK	70	PL 32B 391	P.H. Stuntebeck <i>et al.</i>	(NDAM)
ADERHOLZ	69	NP B11 259	M. Aderholz <i>et al.</i>	(AACH3, BERL, CERN+)
ANDERSON	69	PRL 22 1390	E.W. Anderson <i>et al.</i>	(BNL, CMU)
ARMENISE	68	NC 54A 999	N. Armenise <i>et al.</i>	(BARI, BGNA, FIRZ+)
BALTAY	68	PRL 20 887	C. Baltay <i>et al.</i>	(COLL, ROCH, RUTG, YALE)†
CASO	68	NC 54A 983	C. Caso <i>et al.</i>	(GENO, HAMB, MILA, SACL)
CRENNELL	68B	PL 28B 136	D.J. Crennell <i>et al.</i>	(BNL)
JOHNSTON	68	PRL 20 1414	T.F. Johnston <i>et al.</i>	(TNTO, WISC) IJP
FOCACCI	66	PRL 17 890	M.N. Focacci <i>et al.</i>	(CERN)
GOLDBERG	65	PL 17 354	M. Goldberg <i>et al.</i>	(CERN, EPOL, ORSAY+)

OTHER RELATED PAPERS

BARNETT	83B	PL 120B 455	B. Barnett <i>et al.</i>	(JHU)
EHRICH	66	PR 152 1194	R. Ehrlich, W. Selove, H. Yuta	(PENN)
LEVRAT	66	PL 22 714	B. Levrat <i>et al.</i>	
SEGUNTO	66	PL 19 712	J. Segunto <i>et al.</i>	
BELLINI	65	NC 40A 948	G. Bellini <i>et al.</i>	(MILA)
DEUTSCH...	65	PL 18 351	M. Deutschnann <i>et al.</i>	(AACH3, BERL, CERN)
FORINO	65	PL 19 65	A. Forino <i>et al.</i>	(BGNA, ORSAY, SACL)

 $\rho(1700)$

$$I^G(J^{PC}) = 1^+(1^{--})$$

THE $\rho(1450)$ AND THE $\rho(1700)$

Updated March 2000 by S. Eidelman (Novosibirsk) and J. Hernandez (Valencia).

In our 1988 edition, we replaced the $\rho(1600)$ entry with two new ones, the $\rho(1450)$ and the $\rho(1700)$, because there was emerging evidence that the 1600-MeV region actually contains two ρ -like resonances. ERKAL 86 had pointed out this possibility with a theoretical analysis on the consistency of 2π and 4π electromagnetic form factors and the $\pi\pi$ scattering length. DONNACHIE 87, with a full analysis of data on the 2π and 4π final states in e^+e^- annihilation and photoproduction reactions, had also argued that in order to obtain a consistent picture, two resonances were necessary. The existence of $\rho(1450)$ was supported by the analysis of $\eta\rho^0$ mass spectra obtained in photoproduction and e^+e^- annihilation (DONNACHIE 87B), as well as that of $e^+e^- \rightarrow \omega\pi$ (DONNACHIE 91).

The analysis of DONNACHIE 87 was further extended by CLEGG 88, 94 to include new data on 4π systems produced in e^+e^- annihilation, and in τ decays (τ decays to 4π and e^+e^- annihilation to 4π can be related by the Conserved Vector Current assumption). These systems were successfully analyzed using interfering contributions from two ρ -like states, and from the tail of the $\rho(770)$ decaying into two-body states. While specific conclusions on $\rho(1450) \rightarrow 4\pi$ were obtained, little could be said about the $\rho(1700)$.

An analysis by CLEGG 90 of 6π mass spectra from e^+e^- annihilation and from diffractive photoproduction provides evidence for two ρ mesons at about 2.1 and 1.8 GeV that decay strongly into 6π states. While the former is a candidate for a new resonance ($\rho(2150)$), the latter could be a manifestation of the $\rho(1700)$ distorted by threshold effects.

Independent evidence for two 1^- states is provided by KILLIAN 80 in 4π electroproduction at $(Q^2) = 1$ (GeV/c)², and by FUKUI 88 in a high-statistics sample of the $\eta\pi\pi$ system in $\pi^-\rho$ charge exchange.

This scenario with two overlapping resonances is supported by other data. BISELLO 89 measured the pion form factor in the interval 1.35–2.4 GeV and observed a deep minimum around 1.6 GeV. The best fit was obtained with the hypothesis of ρ -like resonances at 1420 and 1770 MeV, with widths of about 250 MeV. ANTONELLI 88 found that the $e^+e^- \rightarrow \eta\pi^+\pi^-$ cross section is better fitted with two fully interfering Breit-Wigners, with parameters in fair agreement with those of DONNACHIE 87 and BISELLO 89. These results can be considered as a confirmation of the $\rho(1450)$.

Decisive evidence for the $\pi\pi$ decay mode of both $\rho(1450)$ and $\rho(1700)$ came from recent results in $\bar{p}p$ annihilation at rest (ABELE 97). It was shown that these resonances also possess a $K\bar{K}$ decay mode (ABELE 98, BERTIN 98B, ABELE 99D). High statistics studies of the decays $\tau \rightarrow \pi\pi\nu_\tau$ (BARATE 97M, URHEIM 97), and $\tau \rightarrow 4\pi\nu_\tau$ (EDWARDS 00), also require the

$\rho(1450)$, but are not sensitive to the $\rho(1700)$, because it is too close to the τ mass.

The structure of these ρ states is not yet completely clear. BARNES 97 and CLOSE 97C claim that $\rho(1450)$ has a mass consistent with radial $2S$, but its decays show characteristics of hybrids, and suggest that this state may be a $2S$ -hybrid mixture. DONNACHIE 99 argues that hybrid states could have a 4π decay mode dominated by the $a_1\pi$. Such behavior has recently been observed by AKHMETSHIN 99E in $e^+e^- \rightarrow 4\pi$ in the energy range 1.05–1.38 GeV, and by EDWARDS 00 in $\tau \rightarrow 4\pi$ decays. More data should be collected to clarify the nature of the ρ states, particularly in the energy range above 1.6 GeV.

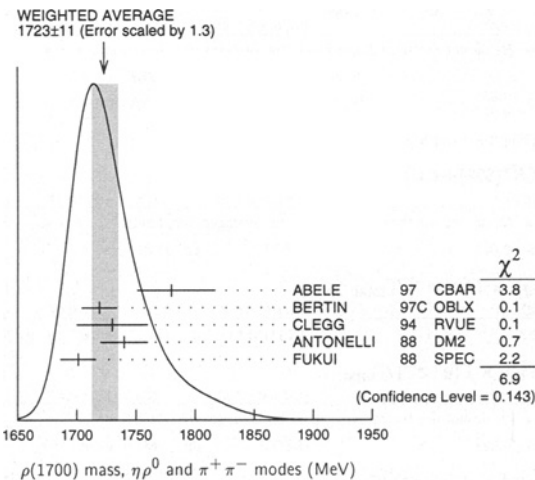
We also list under the $\rho(1450)$ the $\phi\pi$ state with $J^{PC} = 1^{--}$ or $C(1480)$ observed by BITYUKOV 87. While ACHASOV 96B shows that it may be a threshold effect, CLEGG 88 and LANDSBERG 92 suggest two independent vector states with this decay mode. Note, however, that $C(1480)$ in its $\phi\pi$ decay mode was not confirmed by e^+e^- (DOLINSKY 91, BISELLO 91C) and $\bar{p}p$ (ABELE 97H) experiments.

Several observations on the $\omega\pi$ system in the 1200-MeV region (FRENKIEL 72, COSME 76, BARBER 80C, ASTON 80C, ATKINSON 84C, BRAU 88, AMSLER 93B) may be interpreted in terms of either $J^P = 1^- \rho(770) \rightarrow \omega\pi$ production (LAYSSAC 71), or $J^P = 1^+ b_1(1235)$ production (BRAU 88, AMSLER 93B). We argue that no special entry for a $\rho(1250)$ is needed. The LASS amplitude analysis (ASTON 91B) showing evidence for $\rho(1270)$ is preliminary and needs confirmation. For completeness, the relevant observations are listed under the $\rho(1450)$.

$\rho(1700)$ MASS

$\eta\rho^0$ AND $\pi^+\pi^-$ MODES

VALUE (MeV)	DOCUMENT ID
1700 ± 20 OUR ESTIMATE	
1723 ± 11 OUR AVERAGE	Includes data from the 2 datablocks that follow this one. Error includes scale factor of 1.3. See the ideogram below.



$\eta\rho^0$ MODE

VALUE (MeV)	DOCUMENT ID	TECN	COMMENT
1740 ± 20	ANTONELLI	88 DM2	$e^+e^- \rightarrow \eta\pi^+\pi^-$
1701 ± 15	2 FUKUI	88 SPEC	$8.95 \pi^-\rho \rightarrow \eta\pi^+\pi^-n$

$\pi\pi$ MODE

VALUE (MeV)	DOCUMENT ID	TECN	COMMENT
The data in this block is included in the average printed for a previous datablock.			
1780 +37 -29	3 ABELE	97 CBAR	$\bar{p}n \rightarrow \pi^-\pi^0\pi^0$
1719 ± 15	3 BERTIN	97C OBLX	$0.0 \bar{p}p \rightarrow \pi^+\pi^-\pi^0$
1730 ± 30	CLEGG	94 RVUE	$e^+e^- \rightarrow \pi^+\pi^-$
• • • We do not use the following data for averages, fits, limits, etc. • • •			
1768 ± 21	BISELLO	89 DM2	$e^+e^- \rightarrow \pi^+\pi^-$
1745.7 ± 91.9	DUBNICKA	89 RVUE	$e^+e^- \rightarrow \pi^+\pi^-$
1546 ± 26	GESHKEN...	89 RVUE	
1650	4 ERKAL	85 RVUE	$20-70 \gamma\rho \rightarrow \gamma\pi$
1550 ± 70	ABE	84B HYBR	$20 \gamma\rho \rightarrow \pi^+\pi^-\rho$
1590 ± 20	5 ASTON	80 OMEG	$20-70 \gamma\rho \rightarrow p2\pi$
1600 ± 10	6 ATIYA	79B SPEC	$50 \gamma C \rightarrow C2\pi$
1598 +24 -22	BECKER	79 ASPK	$17 \pi^-\rho$ polarized
1659 ± 25	4 LANG	79 RVUE	
1575	4 MARTIN	78C RVUE	$17 \pi^-\rho \rightarrow \pi^+\pi^-n$
1610 ± 30	4 FROGGATT	77 RVUE	$17 \pi^-\rho \rightarrow \pi^+\pi^-n$
1590 ± 20	7 HYAMS	73 ASPK	$17 \pi^-\rho \rightarrow \pi^+\pi^-n$

$\pi\omega$ MODE

VALUE	DOCUMENT ID	TECN	COMMENT
• • • We do not use the following data for averages, fits, limits, etc. • • •			
1710 ± 90	ACHASOV	97 RVUE	$e^+e^- \rightarrow \omega\pi^0$

$K\bar{K}$ MODE

VALUE (MeV)	EVTS	DOCUMENT ID	TECN	CHG	COMMENT
• • • We do not use the following data for averages, fits, limits, etc. • • •					
1740.8 ± 22.2	27k	1 ABELE	99D CBAR	±	$0.0 \bar{p}p \rightarrow K^+K^-\pi^0$
1582 ± 36	1600	CLELAND	82B SPEC	±	$50 \pi\rho \rightarrow K_S^0 K^\pm\rho$

¹ K-matrix pole. Isospin not determined, could be $\omega(1650)$ or $\phi(1680)$.

$2(\pi^+\pi^-)$ MODE

VALUE (MeV)	EVTS	DOCUMENT ID	TECN	COMMENT
• • • We do not use the following data for averages, fits, limits, etc. • • •				
1851 +27 -24		ACHASOV	97 RVUE	$e^+e^- \rightarrow 2(\pi^+\pi^-)$
1570 ± 20		8 CORDIER	82 DM1	$e^+e^- \rightarrow 2(\pi^+\pi^-)$
1520 ± 30		5 ASTON	81E OMEG	$20-70 \gamma\rho \rightarrow p4\pi$
1654 ± 25		9 DIBIANCA	81 DBC	$\pi^+d \rightarrow pp2(\pi^+\pi^-)$
1666 ± 39		8 BACCI	80 FRAG	$e^+e^- \rightarrow 2(\pi^+\pi^-)$
1780	34	KILLIAN	80 SPEC	$11 e^-\rho \rightarrow 2(\pi^+\pi^-)$
1500	10	ATIYA	79B SPEC	$50 \gamma C \rightarrow C4\pi^\pm$
1570 ± 60	65	11 ALEXANDER	75 HBC	$7.5 \gamma\rho \rightarrow p4\pi$
1550 ± 60		5 CONVERSI	74 OSPK	$e^+e^- \rightarrow 2(\pi^+\pi^-)$
1550 ± 50	160	SCHACHT	74 STRC	$5.5-9 \gamma\rho \rightarrow p4\pi$
1450 ± 100	340	SCHACHT	74 STRC	$9-18 \gamma\rho \rightarrow p4\pi$
1430 ± 50	400	BINGHAM	72B HBC	$9.3 \gamma\rho \rightarrow p4\pi$

$\pi^+\pi^-\pi^0\pi^0$ MODE

VALUE (MeV)	DOCUMENT ID	TECN	COMMENT
• • • We do not use the following data for averages, fits, limits, etc. • • •			
1660 ± 30	ATKINSON	85B OMEG	$20-70 \gamma\rho$

$3(\pi^+\pi^-)$ AND $2(\pi^+\pi^-\pi^0)$ MODES

VALUE (MeV)	DOCUMENT ID	TECN	COMMENT
• • • We do not use the following data for averages, fits, limits, etc. • • •			
1783 ± 15	CLEGG	90 RVUE	$e^+e^- \rightarrow 3(\pi^+\pi^-)2(\pi^+\pi^-\pi^0)$

² Assuming $\rho^+\rho_0(1370)$ decay mode interferes with $a_1(1260)^+\pi$ background. From a two Breit-Wigner fit.

³ T-matrix pole.

⁴ From phase shift analysis of HYAMS 73 data.

⁵ Simple relativistic Breit-Wigner fit with constant width.

⁶ An additional 40 MeV uncertainty in both the mass and width is present due to the choice of the background shape.

⁷ Included in BECKER 79 analysis.

⁸ Simple relativistic Breit-Wigner fit with model dependent width.

⁹ One peak fit result.

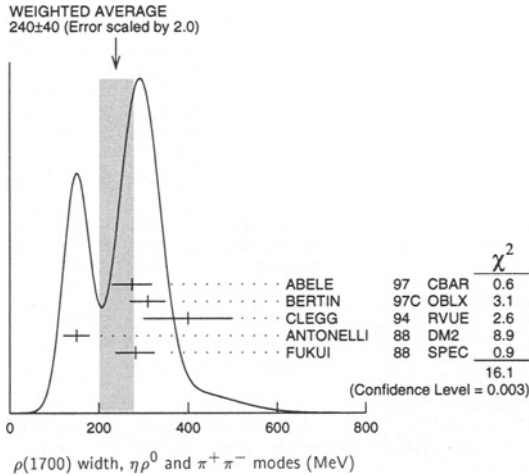
¹⁰ Parameters roughly estimated, not from a fit.

¹¹ Skew mass distribution compensated by Ross-Stodolsky factor.

Meson Particle Listings

 $\rho(1700)$ $\rho(1700)$ WIDTH $\eta\rho^0$ AND $\pi^+\pi^-$ MODES

VALUE (MeV) DOCUMENT ID
240±60 OUR ESTIMATE
240±40 OUR AVERAGE Includes data from the 2 datablocks that follow this one. Error includes scale factor of 2.0. See the ideogram below.

 $\eta\rho^0$ MODE

VALUE (MeV) DOCUMENT ID TECN COMMENT
 The data in this block is included in the average printed for a previous datablock.

150±30 ANTONELLI 88 DM2 $e^+e^- \rightarrow \eta\pi^+\pi^-$
 282±44 13 FUKUI 88 SPEC 8.95 $\pi^-p \rightarrow \eta\pi^+\pi^-n$

 $\pi\pi$ MODE

VALUE (MeV) DOCUMENT ID TECN COMMENT
 The data in this block is included in the average printed for a previous datablock.

275 ± 45 14 ABELE 97 CBAR $\bar{p}n \rightarrow \pi^-\pi^0\pi^0$
 310 ± 40 14 BERTIN 97C OBLX 0.0 $\bar{p}p \rightarrow \pi^+\pi^-\pi^0$
 400 ± 100 CLEGG 94 RVUE $e^+e^- \rightarrow \pi^+\pi^-$

• • • We do not use the following data for averages, fits, limits, etc. • • •

224 ± 22 BISELLO 89 DM2 $e^+e^- \rightarrow \pi^+\pi^-$
 242.5±163.0 DUBNICKA 89 RVUE $e^+e^- \rightarrow \pi^+\pi^-$
 620 ± 60 GESHKEN... 89 RVUE
 <315 15 ERKAL 85 RVUE 20-70 $\gamma p \rightarrow \gamma\pi$
 280 + 30 ABE 84B HYBR 20 $\gamma p \rightarrow \pi^+\pi^-p$
 - 80
 230 ± 80 16 ASTON 80 OMEG 20-70 $\gamma p \rightarrow \rho 2\pi$
 283 ± 14 17 ATIYA 79B SPEC 50 $\gamma C \rightarrow C 2\pi$
 175 + 98 BECKER 79 ASPK 17 π^-p polarized
 - 53
 232 ± 34 15 LANG 79 RVUE
 340 15 MARTIN 78C RVUE 17 $\pi^-p \rightarrow \pi^+\pi^-n$
 300 ± 100 15 FROGGATT 77 RVUE 17 $\pi^-p \rightarrow \pi^+\pi^-n$
 180 ± 50 18 HYAMS 73 ASPK 17 $\pi^-p \rightarrow \pi^+\pi^-n$

 $K\bar{K}$ MODE

VALUE (MeV) EVTS DOCUMENT ID TECN CHG COMMENT
 • • • We do not use the following data for averages, fits, limits, etc. • • •

187.2± 26.7 27k 12 ABELE 99D CBAR ± 0.0 $\bar{p}p \rightarrow K^+K^-\pi^0$
 265 ± 120 1600 CLELAND 82B SPEC ± 50 $\pi p \rightarrow K_S^0 K^\pm p$

¹²K-matrix pole. Isospin not determined, could be $\omega(1650)$ or $\phi(1680)$.

 $2(\pi^+\pi^-)$ MODE

VALUE (MeV) EVTS DOCUMENT ID TECN COMMENT
 • • • We do not use the following data for averages, fits, limits, etc. • • •

510± 40 19 CORDIER 82 DM1 $e^+e^- \rightarrow 2(\pi^+\pi^-)$
 400± 50 16 ASTON 81E OMEG 20-70 $\gamma p \rightarrow p 4\pi$
 400±146 20 DIBIANCA 81 DBC $\pi^+d \rightarrow pp 2(\pi^+\pi^-)$
 700±160 19 BACCI 80 FRAG $e^+e^- \rightarrow 2(\pi^+\pi^-)$
 100 34 KILLIAN 80 SPEC 11 $e^-p \rightarrow 2(\pi^+\pi^-)$
 600 21 ATIYA 79B SPEC 50 $\gamma C \rightarrow C 4\pi^\pm$
 340±160 65 22 ALEXANDER 75 HBC 7.5 $\gamma p \rightarrow p 4\pi$
 360±100 16 CONVERSI 74 OSPK $e^+e^- \rightarrow 2(\pi^+\pi^-)$
 400±120 160 23 SCHACHT 74 STRC 5.5-9 $\gamma p \rightarrow p 4\pi$
 850±200 340 23 SCHACHT 74 STRC 9-18 $\gamma p \rightarrow p 4\pi$
 650±100 400 BINGHAM 72B HBC 9.3 $\gamma p \rightarrow p 4\pi$

 $\pi^+\pi^-\pi^0\pi^0$ MODE

VALUE (MeV) DOCUMENT ID TECN COMMENT
 • • • We do not use the following data for averages, fits, limits, etc. • • •
 300±50 ATKINSON 85B OMEG 20-70 γp

 $3(\pi^+\pi^-)$ AND $2(\pi^+\pi^-\pi^0)$ MODES

VALUE (MeV) DOCUMENT ID TECN COMMENT
 • • • We do not use the following data for averages, fits, limits, etc. • • •
 285±20 CLEGG 90 RVUE $e^+e^- \rightarrow 3(\pi^+\pi^-)2(\pi^+\pi^-\pi^0)$

¹³ Assuming $\rho^+ f_0(1370)$ decay mode interferes with $a_1(1260)^+\pi$ background. From a two Breit-Wigner fit.
¹⁴ T-matrix pole.
¹⁵ From phase shift analysis of HYAMS 73 data.
¹⁶ Simple relativistic Breit-Wigner fit with constant width.
¹⁷ An additional 40 MeV uncertainty in both the mass and width is present due to the choice of the background shape.
¹⁸ Included in BECKER 79 analysis.
¹⁹ Simple relativistic Breit-Wigner fit with model-dependent width.
²⁰ One peak fit result.
²¹ Parameters roughly estimated, not from a fit.
²² Skew mass distribution compensated by Ross-Stodolsky factor.
²³ Width errors enlarged by us to $4\Gamma/\sqrt{N}$; see the note with the $K^*(892)$ mass.

 $\rho(1700)$ DECAY MODES

Mode	Fraction (Γ_i/Γ)
Γ_1 $\rho\pi\pi$	dominant
Γ_2 $\rho^0\pi^+\pi^-$	large
Γ_3 $\rho^0\pi^0\pi^0$	
Γ_4 $\rho^\pm\pi^\mp\pi^0$	large
Γ_5 $2(\pi^+\pi^-)$	large
Γ_6 $\pi^+\pi^-$	seen
Γ_7 $\pi^-\pi^0$	seen
Γ_8 $K\bar{K}^*(892) + c.c.$	seen
Γ_9 $\eta\rho$	seen
Γ_{10} $a_2(1320)\pi$	not seen
Γ_{11} $K\bar{K}$	seen
Γ_{12} e^+e^-	seen
Γ_{13} $\pi^0\omega$	seen

 $\rho(1700)$ $\Gamma(i)\Gamma(e^+e^-)/\Gamma(\text{total})$

This combination of a partial width with the partial width into e^+e^- and with the total width is obtained from the cross-section into channel i in e^+e^- annihilation.

 $\Gamma(2(\pi^+\pi^-)) \times \Gamma(e^+e^-)/\Gamma_{\text{total}}$

VALUE (keV) DOCUMENT ID TECN COMMENT $\Gamma_5\Gamma_{12}/\Gamma$
2.83±0.42 BACCI 80 FRAG $e^+e^- \rightarrow 2(\pi^+\pi^-)$
 • • • We do not use the following data for averages, fits, limits, etc. • • •
 2.6 ± 0.2 DELCOURT 81B DM1 $e^+e^- \rightarrow 2(\pi^+\pi^-)$

 $\Gamma(\pi^+\pi^-) \times \Gamma(e^+e^-)/\Gamma_{\text{total}}$

VALUE (keV) DOCUMENT ID TECN COMMENT $\Gamma_6\Gamma_{12}/\Gamma$
 • • • We do not use the following data for averages, fits, limits, etc. • • •
 0.13 24 DIEKMANN 88 RVUE $e^+e^- \rightarrow \pi^+\pi^-$
 0.029 +0.016 KURDADZE 83 OLYA 0.64-1.4 $e^+e^- \rightarrow \pi^+\pi^-$
 -0.012
²⁴ Using total width = 220 MeV.

 $\Gamma(K\bar{K}^*(892) + c.c.) \times \Gamma(e^+e^-)/\Gamma_{\text{total}}$

VALUE (keV) DOCUMENT ID TECN COMMENT $\Gamma_8\Gamma_{12}/\Gamma$
 • • • We do not use the following data for averages, fits, limits, etc. • • •
 0.305±0.071 25 BIZOT 80 DM1 e^+e^-

 $\Gamma(\eta\rho) \times \Gamma(e^+e^-)/\Gamma_{\text{total}}$

VALUE (eV) DOCUMENT ID TECN COMMENT $\Gamma_9\Gamma_{12}/\Gamma$
7 ± 3 ANTONELLI 88 DM2 $e^+e^- \rightarrow \eta\pi^+\pi^-$

 $\Gamma(K\bar{K}) \times \Gamma(e^+e^-)/\Gamma_{\text{total}}$

VALUE (keV) DOCUMENT ID TECN COMMENT $\Gamma_{11}\Gamma_{12}/\Gamma$
 • • • We do not use the following data for averages, fits, limits, etc. • • •
 0.035±0.029 25 BIZOT 80 DM1 e^+e^-

 $\Gamma(\rho\pi\pi) \times \Gamma(e^+e^-)/\Gamma_{\text{total}}$

VALUE (keV) DOCUMENT ID TECN COMMENT $\Gamma_1\Gamma_{12}/\Gamma$
 • • • We do not use the following data for averages, fits, limits, etc. • • •
 3.510±0.090 25 BIZOT 80 DM1 e^+e^-
²⁵ Model dependent.

See key on page 239

Meson Particle Listings
ρ(1700)

ρ(1700) BRANCHING RATIOS

Table with columns: Γ(π+π-)/Γtotal, VALUE, DOCUMENT ID, TECN, COMMENT, Γ6/Γ. Includes data for BECKER, MARTIN, COSTA, FROGGATT, EISENBERG, HYAMS.

Table with columns: Γ(π+π-)/Γ(2(π+π-)), VALUE, DOCUMENT ID, TECN, COMMENT, Γ6/Γ5. Includes data for ASTON, DAVIER, BINGHAM.

Table with columns: Γ(KK*(892)+c.c.)/Γ(2(π+π-)), VALUE, DOCUMENT ID, TECN, COMMENT, Γ8/Γ5. Includes data for DELCOURT.

Table with columns: Γ(ηρ)/Γtotal, VALUE, CL%, DOCUMENT ID, TECN, COMMENT, Γ9/Γ. Includes data for DONNACHIE, ATKINSON.

Table with columns: Γ(ρ2(1320)π)/Γtotal, VALUE, DOCUMENT ID, TECN, COMMENT, Γ10/Γ. Includes data for AMELIN.

Table with columns: Γ(ηρ)/Γ(2(π+π-)), VALUE, DOCUMENT ID, TECN, COMMENT, Γ9/Γ5. Includes data for DELCOURT, ASTON.

Table with columns: Γ(π+π-neutrals)/Γ(2(π+π-)), VALUE, DOCUMENT ID, TECN, COMMENT, (Γ3+Γ4+0.714Γ9)/Γ5. Includes data for BALLAM.

Table with columns: Γ(π0ω)/Γtotal, VALUE, DOCUMENT ID, TECN, COMMENT, Γ13/Γ. Includes data for ACHASOV.

Table with columns: Γ(KK)/Γ(2(π+π-)), VALUE, CL%, DOCUMENT ID, TECN, CHG, COMMENT, Γ11/Γ5. Includes data for DELCOURT, BINGHAM.

Table with columns: Γ(KK)/Γ(KK*(892)+c.c.), VALUE, DOCUMENT ID, TECN, COMMENT, Γ11/Γ8. Includes data for BUON.

Table with columns: Γ(ρ0π+π-)/Γ(2(π+π-)), VALUE, EVTS, DOCUMENT ID, TECN, COMMENT, Γ2/Γ5. Includes data for DELCOURT, SCHACHT, BINGHAM.

Table with columns: Γ(ρ0π0π0)/Γ(ρ±π±π0), VALUE, DOCUMENT ID, TECN, CHG, COMMENT, Γ3/Γ4. Includes data for ATKINSON.

ρ(1700) REFERENCES

Large table listing references for ρ(1700) with columns: AUTHOR, YEAR, DOCUMENT ID, TECN, COMMENT, COLLABORATION.

OTHER RELATED PAPERS

Table listing other related papers with columns: AUTHOR, YEAR, DOCUMENT ID, TECN, COMMENT, COLLABORATION.

Meson Particle Listings

$f_0(1710)$

$I^G(J^{PC}) = 0^+(0^{++})$

THE $f_0(1710)$

Updated April 2000 by M. Doser (CERN).

The $f_0(1710)$ is seen in the radiative decay $J/\psi(1S) \rightarrow \gamma f_0(1710)$; therefore $C = +1$. It decays into $\eta\eta$ and $K_S^0 K_S^0$, which implies $I^G J^{PC} = 0^+(even)^{++}$. The spin of the $f_0(1710)$ has been controversial, but evidence for spin 0 has accumulated recently in all production modes.

An analysis of radiative J/ψ decays at BES into $\pi^+\pi^-\pi^+\pi^-$ (BAI 00) clearly favors spin 0. Combined amplitude analyses of the K^+K^- , $K_S^0 K_S^0$ and $\pi^+\pi^-$ systems produced in $J/\psi(1S)$ radiative decay by MARK III (CHEN 91 and more recently DUNWOODIE 97) find a large spin-0 component, and at the same time reproduce known parameters of the $f_2(1270)$ and $f_2'(1525)$. In addition, a recent reanalysis (BUGG 95) of the 4π channel from MARK III, allowing both $\rho\rho$ and two $\pi\pi$ S-waves, also finds a 0^{++} assignment for the $f_0(1710)$. Earlier analyses of this final state (BISELLO 89B, BALTRUSAITIS 86B) found only pseudoscalar activity in the $f_0(1710)$ region, but considered only the process $J/\psi \rightarrow \gamma\rho\rho$. Similarly, earlier analyses of the K^+K^- system based on less statistics (BALTRUSAITIS 87, BAI 96) found a spin of 2 for the $f_0(1710)$.

A similar situation is present in central production, with earlier analyses favoring spin 2 over spin 0 (ARMSTRONG 89D). More recent analyses with greater statistics by BARBERIS 99 (K^+K^- , $K_S^0 K_S^0$), BARBERIS 99B ($\pi^+\pi^-$), and FRENCH 99 (K^+K^-) however clearly indicate spin 0, and exclude spin 2. Generally, analyses preferring spin 2 concentrate on angular distributions in the $f_0(1710)$ region, and do not include possible interferences or distortion due to the nearby $f_2'(1525)$.

The $f_0(1710)$ is also observed in $K\bar{K}$ (FALVARD 88) in $J/\psi(1S) \rightarrow \omega K\bar{K}$ and $J/\psi(1S) \rightarrow \phi K\bar{K}$, but with no spin-parity analysis, as well as in $\eta\eta$ in radiative J/ψ decays (EDWARDS 82). It is also clearly seen in 300-GeV/c pp central production in both K^+K^- and $K_S^0 K_S^0$ (ARMSTRONG 89D). Mass and width are determined via a fit to non-interfering Breit-Wigners over a polynomial background, which leads to large systematic errors for the width. ARMSTRONG 93C also sees a broad peak in $\eta\eta$ at 1747 MeV, which may be the $f_0(1710)$.

This resonance is not observed in the hypercharge-exchange reactions $K^-p \rightarrow K_S^0 K_S^0 \Lambda$ (ASTON 88D) and $K^-p \rightarrow K_S^0 K_S^0 Y^*$ (BOLONKIN 86); these non-observations are explained by a spin of 0 (LINDENBAUM 92). A possible observation in $\gamma\gamma$ collisions leading to $K_S^0 K_S^0$ (BRACCINI 99, but no spin determination), and a non-observation in $\gamma\gamma \rightarrow \pi^+\pi^-$ (BARATE 00E) is consistent with a large $\bar{s}s$ component.

$f_0(1710)$ MASS

VALUE (MeV)	CL%	EVTS	DOCUMENT ID	TECN	COMMENT
1715 ± 7		OUR AVERAGE			
1740 ⁺³⁰ ₋₂₅			1 BAI	00 BES	$J/\psi \rightarrow \gamma(\pi^+\pi^-\pi^+\pi^-)$
1710 ± 25			2 FRENCH	99	$300 \rho\rho \rightarrow \rho_f(K^+K^-)\rho_S$
1707 ± 10			3 AUGUSTIN	88 DM2	$J/\psi \rightarrow \gamma K^+K^-, K_S^0 K_S^0$
1698 ± 15			3 AUGUSTIN	87 DM2	$J/\psi \rightarrow \gamma\pi^+\pi^-$
1720 ± 10 ± 10			4 BALTRUSAITIS..87	MRK3	$J/\psi \rightarrow \gamma K^+K^-$
1742 ± 15			3 WILLIAMS	84 MPSF	$200 \pi^- N \rightarrow 2K_S^0 X$
1670 ± 50			BLOOM	83 CBAL	$J/\psi \rightarrow \gamma 2\eta$
1770 ± 12			5 ANISOVICH	99B SPEC	0.6-1.2 $\rho\bar{p} \rightarrow \eta\eta\pi^0$
1730 ± 15			1 BARBERIS	99 OMEG	$450 \rho\rho \rightarrow \rho_S \rho_f K^+K^-$
1750 ± 20			1 BARBERIS	99B OMEG	$450 \rho\rho \rightarrow \rho_S \rho_f \pi^+\pi^-$
1710 ± 12 ± 11			6 BARBERIS	99D OMEG	$450 \rho\rho \rightarrow K^+K^-, \pi^+\pi^-$
1750 ± 30			7 ANISOVICH	98B RVUE	Compilation
1720 ± 39			BAI	98H BES	$J/\psi \rightarrow \gamma\pi^0\pi^0$
1775 ± 1.5		57	8 BARKOV	98	$\pi^- p \rightarrow K_S^0 K_S^0 n$
1690 ± 11			9 ABREU	96C DLPH	$Z^0 \rightarrow K^+K^- X$
1696 ± 5 ⁺⁹ ₋₃₄			4 BAI	96C BES	$J/\psi \rightarrow \gamma K^+K^-$
1781 ± 8 ⁺¹⁰ ₋₃₁			1 BAI	96C BES	$J/\psi \rightarrow \gamma K^+K^-$
1768 ± 14			BALOSHIN	95 SPEC	$40 \pi^- C \rightarrow K_S^0 K_S^0 X$
1750 ± 15			10 BUGG	95 MRK3	$J/\psi \rightarrow \gamma\pi^+\pi^-\pi^+\pi^-$
1620 ± 16			4 BUGG	95 MRK3	$J/\psi \rightarrow \gamma\pi^+\pi^-\pi^+\pi^-$
1748 ± 10			3 ARMSTRONG	93C E760	$\bar{p}p \rightarrow \pi^0\eta\eta \rightarrow 6\gamma$
~ 1750			BREAKSTONE	93 SFM	$\rho\rho \rightarrow \rho\rho\pi^+\pi^-\pi^+\pi^-$
1744 ± 15			11 ALDE	92D GAM2	$38 \pi^- p \rightarrow \eta\eta n$
1713 ± 10			12 ARMSTRONG	89D OMEG	$300 \rho\rho \rightarrow \rho\rho K^+K^-$
1706 ± 10			12 ARMSTRONG	89D OMEG	$300 \rho\rho \rightarrow \rho\rho K_S^0 K_S^0$
1700 ± 15			4 BOLONKIN	88 SPEC	$40 \pi^- p \rightarrow K_S^0 K_S^0 n$
1720 ± 60			1 BOLONKIN	88 SPEC	$40 \pi^- p \rightarrow K_S^0 K_S^0 n$
1638 ± 10			13 FALVARD	88 DM2	$J/\psi \rightarrow \phi K^+K^-, K_S^0 K_S^0$
1690 ± 4			14 FALVARD	88 DM2	$J/\psi \rightarrow \phi K^+K^-, K_S^0 K_S^0$
1755 ± 8			15 ALDE	86C GAM2	$38 \pi^- p \rightarrow n 2\eta$
1730 ⁺² ₋₁₀			16 LONGACRE	86 RVUE	$22 \pi^- p \rightarrow n 2K_S^0$
1650 ± 50			BURKE	82 MRK2	$J/\psi \rightarrow \gamma 2\rho$
1640 ± 50			17,18 EDWARDS	82D CBAL	$J/\psi \rightarrow \gamma 2\eta$
1730 ± 10 ± 20			19 ETKIN	82C MPS	$23 \pi^- p \rightarrow n 2K_S^0$

• • • We do not use the following data for averages, fits, limits, etc. • • •
 1 $J^P = 0^+$.
 2 $J^P = 0^+$, superseded by ARMSTRONG 89D.
 3 No J^{PC} determination.
 4 $J^P = 2^+$.
 5 Preliminary data from CBAR, $J^P = 0^+$.
 6 Supersedes BARBERIS 99 and BARBERIS 99B.
 7 T-matrix pole, assuming $J^P = 0^+$.
 8 No J^{PC} determination.
 9 No J^{PC} determination, width not determined.
 10 From a fit to the 0^+ partial wave.
 11 ALDE 92D combines all the GAMS-2000 data.
 12 $J^P = 2^+$, superseded by FRENCH 99.
 13 From an analysis ignoring interference with $f_2'(1525)$.
 14 From an analysis including interference with $f_2'(1525)$.
 15 Superseded by ALDE 92D.
 16 Uses MRK3 data. From a partial-wave analysis of data using a K-matrix formalism with 5 poles, but assuming spin 2. Fit with constrained inelasticity.
 17 $J^P = 2^+$ preferred.
 18 From fit neglecting nearby $f_2'(1525)$. Replaced by BLOOM 83.
 19 Superseded by LONGACRE 86.

$f_0(1710)$ WIDTH

VALUE (MeV)	CL%	EVTS	DOCUMENT ID	TECN	COMMENT
125 ± 12		OUR AVERAGE			
120 ⁺⁵⁰ ₋₄₀			20 BAI	00 BES	$J/\psi \rightarrow \gamma(\pi^+\pi^-\pi^+\pi^-)$
105 ± 34			21 FRENCH	99	$300 \rho\rho \rightarrow \rho_f(K^+K^-)\rho_S$
166.4 ± 33.2			22 AUGUSTIN	88 DM2	$J/\psi \rightarrow \gamma K^+K^-, K_S^0 K_S^0$
136 ± 28			22 AUGUSTIN	87 DM2	$J/\psi \rightarrow \gamma\pi^+\pi^-$
130 ± 20			23 BALTRUSAITIS..87	MRK3	$J/\psi \rightarrow \gamma K^+K^-$
57 ± 38			3 WILLIAMS	84 MPSF	$200 \pi^- N \rightarrow 2K_S^0 X$
160 ± 80			BLOOM	83 CBAL	$J/\psi \rightarrow \gamma 2\eta$

••• We do not use the following data for averages, fits, limits, etc. •••

Table listing experimental data for f0(1710) decay modes, including columns for mode, value, document ID, and comment.

- 20 JP = 0+.
21 JP = 0+, supersedes by ARMSTRONG 89D.
22 No JPC determination.
23 JP = 2+.
24 Preliminary data from CBAR, JP = 0+.
25 Supersedes BARBERIS 99 and BARBERIS 99B.
26 T-matrix pole, assuming JP = 0+.
27 No JPC determination.
28 From a fit to the 0+ partial wave.
29 ALDE 92D combines all the GAMS-2000 data.
30 JP = 2+, (0+ excluded).
31 From an analysis ignoring interference with f'2(1525).
32 From an analysis including interference with f'2(1525).
33 Uses MRK3 data. From a partial-wave analysis of data using a K-matrix formalism with 5 poles, but assuming spin 2. Fit with constrained inelasticity.
34 JP = 2+ preferred.
35 From fit neglecting nearby f'2(1525). Replaced by BLOOM 83.
36 From an amplitude analysis of the K0S K0S system, superseded by LONGACRE 86.

f0(1710) DECAY MODES

Table showing decay modes (Gamma1, Gamma2, Gamma3, Gamma4) and their corresponding fractions (Gamma_i/Gamma).

f0(1710) Gamma(i)Gamma(gamma)/Gamma(total)

Table for Gamma(KKbar) x Gamma(gamma)/Gamma(total) with columns for value, CL%, document ID, and comment.

••• We do not use the following data for averages, fits, limits, etc. •••

Table listing data for Gamma(KKbar) x Gamma(gamma)/Gamma(total) with values and document IDs.

Table for Gamma(pi pi) x Gamma(gamma)/Gamma(total) with columns for value, CL%, document ID, and comment.

38 Assuming spin 0.

f0(1710) BRANCHING RATIOS

Table for Gamma(KKbar)/Gamma(total) with columns for value, document ID, and comment.

••• We do not use the following data for averages, fits, limits, etc. •••

Table listing data for Gamma(KKbar)/Gamma(total) with values and document IDs.

Table for Gamma(eta eta)/Gamma(total) with columns for value, document ID, and comment.

••• We do not use the following data for averages, fits, limits, etc. •••

Table listing data for Gamma(eta eta)/Gamma(total) with values and document IDs.

Table for Gamma(pi pi)/Gamma(total) with columns for value, document ID, and comment.

••• We do not use the following data for averages, fits, limits, etc. •••

Table listing data for Gamma(pi pi)/Gamma(total) with values and document IDs.

Table for Gamma(pi pi)/Gamma(KKbar) with columns for value, document ID, and comment.

••• We do not use the following data for averages, fits, limits, etc. •••

Table listing data for Gamma(pi pi)/Gamma(KKbar) with values and document IDs.

Table for Gamma(eta eta)/Gamma(KKbar) with columns for value, CL%, document ID, and comment.

••• We do not use the following data for averages, fits, limits, etc. •••

Table listing data for Gamma(eta eta)/Gamma(KKbar) with values and document IDs.

- 39 From a partial-wave analysis of data using a K-matrix formalism with 5 poles, but assuming spin 2.
40 Fit with constrained inelasticity.
41 Combining results of GAM4 with those of ARMSTRONG 89D.

f0(1710) REFERENCES

List of references for f0(1710) including authors, document IDs, and journal information.

OTHER RELATED PAPERS

List of other related papers including authors, document IDs, and journal information.

Meson Particle Listings

$a_2(1750)$, $\eta(1760)$, $X(1775)$, $\pi(1800)$

$a_2(1750)$ $I^G(J^{PC}) = 1^-(2^{++})$

OMITTED FROM SUMMARY TABLE

$a_2(1750)$ MASS

VALUE (MeV)	DOCUMENT ID	TECN	COMMENT
1752 ± 21 ± 4	ACCIARRI	97T L3	$\gamma\gamma \rightarrow \pi^+\pi^-\pi^0$
• • • We do not use the following data for averages, fits, limits, etc. • • •			
~1775	¹ GRYGOREV	99 SPEC	$40 \pi^-\rho \rightarrow K_S^0 K_S^0 \eta$
¹ Possibly two $J^P = 2^+$ resonances with isospins 0 and 1.			

$a_2(1750)$ WIDTH

VALUE (MeV)	DOCUMENT ID	TECN	COMMENT
150 ± 110 ± 34	ACCIARRI	97T L3	$\gamma\gamma \rightarrow \pi^+\pi^-\pi^0$

$a_2(1750)$ DECAY MODES

Mode
Γ_1 $\gamma\gamma$
Γ_2 $\rho\pi$
Γ_3 $f_2(1270)\pi$

$a_2(1750)$ $\Gamma(I)\Gamma(\gamma\gamma)/\Gamma(\text{total})$

VALUE (keV)	DOCUMENT ID	TECN	COMMENT
0.29 ± 0.04 ± 0.02	ACCIARRI	97T L3	$\gamma\gamma \rightarrow \pi^+\pi^-\pi^0$

$a_2(1750)$ REFERENCES

GRYGOREV	99	PAN 62 470	V.K. Grygorev et al.
		Translated from YAF 62 513.	
ACCIARRI	97T	PL B413 147	M. Acciari et al. (L3 Collab.)

$\eta(1760)$ $I^G(J^{PC}) = 0^+(0^{-+})$

OMITTED FROM SUMMARY TABLE

Seen by DM2 in the $\rho\rho$ system (BISELLO 89B). Structure in this region has been reported before in the same system (BALTRUSAITIS 86B) and in the $\omega\omega$ system (BALTRUSAITIS 85C, BISELLO 87). Needs confirmation.

$\eta(1760)$ MASS

VALUE (MeV)	EVTS	DOCUMENT ID	TECN	COMMENT
1760 ± 11	320	¹ BISELLO	89B DM2	$J/\psi \rightarrow 4\pi\gamma$
¹ Estimated by us from various fits.				

$\eta(1760)$ WIDTH

VALUE (MeV)	EVTS	DOCUMENT ID	TECN	COMMENT
60 ± 16	320	² BISELLO	89B DM2	$J/\psi \rightarrow 4\pi\gamma$
² Estimated by us from various fits.				

$\eta(1760)$ REFERENCES

BISELLO	89B	PR D39 701	G. Busetto et al. (DM2 Collab.)
BISELLO	87	PL B192 239	D. Bisello et al. (PADO, CLER, FRAS+)
BALTRUSAITIS...	86B	PR D33 1222	R.M. Baltrusaitis et al. (Mark III Collab.)
BALTRUSAITIS...	85C	PRL 55 1723	R.M. Baltrusaitis et al. (CIT, UCSC+)

OTHER RELATED PAPERS

BAI	99	PL B446 356	J.Z. Bai et al. (BES Collab.)
BUGG	99	PL B458 511	D.V. Bugg et al.

$X(1775)$ $I^G(J^{PC}) = 1^-(?^{-+})$

OMITTED FROM SUMMARY TABLE

Needs confirmation.

$X(1775)$ MASS

VALUE (MeV)	DOCUMENT ID	TECN	COMMENT
1776 ± 13 OUR AVERAGE			
1763 ± 20	CONDO	91 SHF	$\gamma\rho \rightarrow (\rho\pi^+)(\pi^+\pi^-\pi^-)$
1787 ± 18	CONDO	91 SHF	$\gamma\rho \rightarrow \eta\pi^+\pi^+\pi^-$

$X(1775)$ WIDTH

VALUE (MeV)	DOCUMENT ID	TECN	COMMENT
155 ± 40 OUR AVERAGE			
192 ± 60	CONDO	91 SHF	$\gamma\rho \rightarrow (\rho\pi^+)(\pi^+\pi^-\pi^-)$
118 ± 60	CONDO	91 SHF	$\gamma\rho \rightarrow \eta\pi^+\pi^+\pi^-$

$X(1775)$ DECAY MODES

Mode
Γ_1 $\rho\pi$
Γ_2 $f_2(1270)\pi$

$X(1775)$ BRANCHING RATIOS

$\Gamma(\rho\pi)/\Gamma(f_2(1270)\pi)$	DOCUMENT ID	TECN	COMMENT	Γ_1/Γ_2
1.43 ± 0.26 OUR AVERAGE				
1.3 ± 0.3	CONDO	91 SHF	$\gamma\rho \rightarrow (\rho\pi^+)(\pi^+\pi^-\pi^-)$	
1.8 ± 0.5	CONDO	91 SHF	$\gamma\rho \rightarrow \eta\pi^+\pi^+\pi^-$	

$X(1775)$ REFERENCES

CONDO	91	PR D43 2787	G.T. Condo et al. (SLAC Hybrid Collab.)
-------	----	-------------	---

$\pi(1800)$ $I^G(J^{PC}) = 1^-(0^{-+})$

See also minireview under non- $q\bar{q}$ candidates. (See the index for the page number.)

$\pi(1800)$ MASS

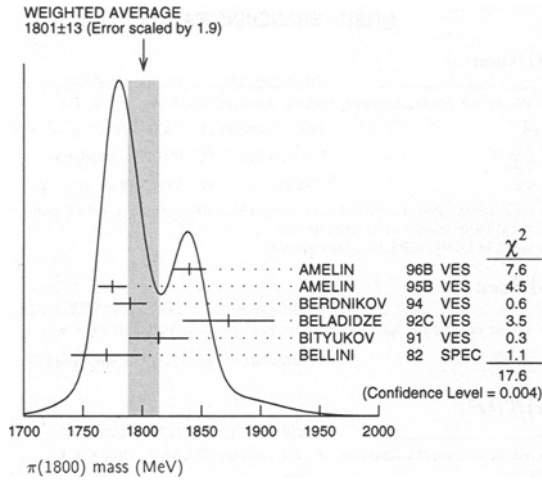
VALUE (MeV)	EVTS	DOCUMENT ID	TECN	CHG	COMMENT
1801 ± 13 OUR AVERAGE					Error includes scale factor of 1.9. See the ideogram below.
1840 ± 10 ± 10	1200	AMELIN	96B VES	-	$37 \pi^- A \rightarrow \eta\eta\pi^- A$
1775 ± 7 ± 10		¹ AMELIN	95B VES	-	$36 \pi^- A \rightarrow \pi^+\pi^-\pi^- A$
1790 ± 14		² BERDNIKOV	94 VES	-	$37 \pi^- A \rightarrow K^+K^-\pi^- A$
1873 ± 33 ± 20		BELADIDZE	92C VES	-	$36 \pi^- Be \rightarrow \pi^- \eta Be$
1814 ± 10 ± 23	426 ± 57	BITYUKOV	91 VES	-	$36 \pi^- C \rightarrow \pi^- \eta C$
1770 ± 30	1100	BELLINI	82 SPEC	-	$40 \pi^- A \rightarrow 3\pi A$
1737 ± 5 ± 15		AMELIN	99 VES	-	$37 \pi^- A \rightarrow \omega\pi^- \pi^0 A^*$

- • • We do not use the following data for averages, fits, limits, etc. • • •
- ¹ From a fit to $J^{PC} = 0^{-+}$ $f_0(980)\pi$, $f_0(1370)\pi$ waves.
- ² From a fit to $J^{PC} = 0^{-+}$ $K_0^*(1430)K^-$ and $f_0(980)\pi^-$ waves.

See key on page 239

Meson Particle Listings

$\pi(1800)$, $f_2(1810)$



$\Gamma(\eta\eta'(958)\pi^-)/\Gamma(\eta\eta\pi^-)$

VALUE	EVTs	DOCUMENT ID	TECN	CHG	COMMENT	Γ_8/Γ_5
0.29 ± 0.06	OUR AVERAGE					
0.29 ± 0.07		BELADIDZE	92c	VES	—	36 $\pi^- \text{Be} \rightarrow \pi^- \eta' \eta \text{Be}$
0.3 ± 0.1	426 ± 57	BITYUKOV	91	VES	—	36 $\pi^- \text{C} \rightarrow \pi^- \eta \eta \text{C}$

$\Gamma(K_0^*(1430)K^-)/\Gamma_{\text{total}}$

VALUE	DOCUMENT ID	TECN	CHG	COMMENT	Γ_9/Γ
seen	BERDNIKOV	94	VES	—	37 $\pi^- A \rightarrow K^+ K^- \pi^- A$

$\Gamma(K^*(892)K^-)/\Gamma_{\text{total}}$

VALUE	DOCUMENT ID	TECN	CHG	COMMENT	Γ_{10}/Γ
not seen	BERDNIKOV	94	VES	—	37 $\pi^- A \rightarrow K^+ K^- \pi^- A$

$\Gamma(\rho\pi^-)/\Gamma(f_0(980)\pi^-)$

VALUE	CL%	DOCUMENT ID	TECN	CHG	COMMENT	Γ_4/Γ_2
< 0.14	90	AMELIN	95b	VES	—	36 $\pi^- A \rightarrow \pi^+ \pi^- \pi^- A$

$\Gamma(\rho\pi^-)/\Gamma_{\text{total}}$

VALUE	DOCUMENT ID	TECN	CHG	COMMENT	Γ_4/Γ
not seen	BELLINI	82	SPEC	—	40 $\pi^- A \rightarrow 3\pi A$

$\pi(1800)$ WIDTH

VALUE (MeV)	EVTs	DOCUMENT ID	TECN	CHG	COMMENT
210 ± 15	OUR AVERAGE				
210 ± 30 ± 30	1200	AMELIN	96b	VES	—
190 ± 15 ± 15		3 AMELIN	95b	VES	—
210 ± 70		4 BERDNIKOV	94	VES	—
225 ± 35 ± 20		BELADIDZE	92c	VES	—
205 ± 18 ± 32	426 ± 57	BITYUKOV	91	VES	—
310 ± 50	1100	BELLINI	82	SPEC	—
259 ± 19 ± 6		AMELIN	99	VES	—

3 From a fit to $J^{PC} = 0^{-+} f_0(980)\pi, f_0(1370)\pi$ waves.
 4 From a fit to $J^{PC} = 0^{-+} K_0^*(1430)K^-$ and $f_0(980)\pi^-$ waves.

$\pi(1800)$ REFERENCES

AMELIN	99	PAN 62 445	D.V. Amelin et al.	(VES Collab.)
AMELIN	96B	PAN 59 976	D.V. Amelin et al.	(SERP, TBIL) IG/JPC
AMELIN	95B	PL B356 595	D.V. Amelin et al.	(SERP, TBIL)
BERDNIKOV	94	PL B337 219	E.B. Berdnikov et al.	(SERP, TBIL)
BELADIDZE	92C	SJNP 55 1535	G.M. Beladidze, S.I. Bityukov, G.V. Borisov	(SERP+)
BITYUKOV	91	PL B268 137	S.I. Bityukov et al.	(SERP, TBIL)
BELLINI	82	PRL 48 1697	G. Bellini et al.	(MILA, BGNA, JINR)

OTHER RELATED PAPERS

LANDSBERG	99	SPU 42 871	L.G. Landsberg	
ZAIMIDOROGA	99	PAN 30 1	O.A. Zaimidoroga	
BORISOV	92	SJNP 55 1441	G.V. Borisov, S.S. Gerstein, A.M. Zaitsev	(SERP)

$\pi(1800)$ DECAY MODES

Mode	Fraction (Γ_i/Γ)
Γ_1 $\pi^+ \pi^- \pi^-$	seen
Γ_2 $f_0(980)\pi^-$	seen
Γ_3 $f_0(1370)\pi^-$	seen
Γ_4 $\rho\pi^-$	not seen
Γ_5 $\eta\eta\pi^-$	seen
Γ_6 $a_0(980)\eta$	seen
Γ_7 $f_0(1500)\pi^-$	seen
Γ_8 $\eta\eta'(958)\pi^-$	seen
Γ_9 $K_0^*(1430)K^-$	seen
Γ_{10} $K^*(892)K^-$	not seen

$\pi(1800)$ BRANCHING RATIOS

$\Gamma(f_0(980)\pi^-)/\Gamma(f_0(1370)\pi^-)$	Γ_2/Γ_3				
VALUE	DOCUMENT ID	TECN	CHG	COMMENT	
1.7 ± 1.3	AMELIN	95b	VES	—	
$\Gamma(f_0(1370)\pi^-)/\Gamma_{\text{total}}$	Γ_3/Γ				
VALUE	DOCUMENT ID	TECN	CHG	COMMENT	
seen	BELLINI	82	SPEC	—	
$\Gamma(\eta\eta\pi^-)/\Gamma(\pi^+ \pi^- \pi^-)$	Γ_5/Γ_1				
VALUE	EVTs	DOCUMENT ID	TECN	CHG	COMMENT
0.5 ± 0.1	1200	AMELIN	96a	VES	—
$\Gamma(f_0(1500)\pi^-)/\Gamma(a_0(980)\eta)$	Γ_7/Γ_6				
VALUE	EVTs	DOCUMENT ID	TECN	CHG	COMMENT
0.08 ± 0.03	1200	5 AMELIN	96b	VES	—

5 Assuming that $f_0(1500)$ decays only to $\eta\eta$ and $a_0(980)$ decays only to $\eta\pi$.

$f_2(1810)$

$I^G(J^{PC}) = 0^+(2^{++})$

OMITTED FROM SUMMARY TABLE
Needs confirmation.

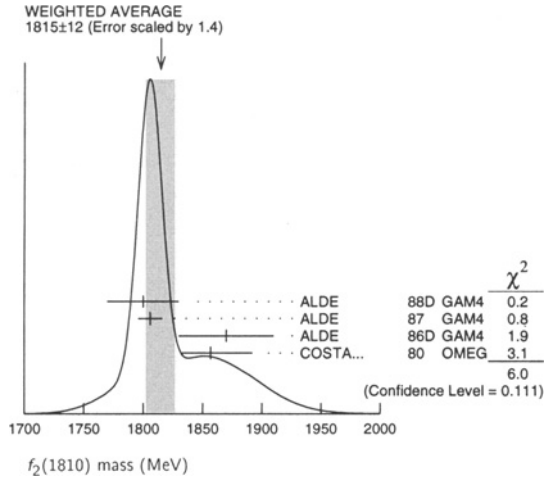
$f_2(1810)$ MASS

VALUE (MeV)	EVTs	DOCUMENT ID	TECN	COMMENT
1815 ± 12	OUR AVERAGE			Error includes scale factor of 1.4. See the ideogram below.
1800 ± 30	40	ALDE	88D	GAM4 300 $\pi^- \rho \rightarrow \pi^- \rho 4\pi^0$
1806 ± 10	1600	ALDE	87	GAM4 100 $\pi^- \rho \rightarrow 4\pi^0 n$
1870 ± 40		1 ALDE	86D	GAM4 100 $\pi^- \rho \rightarrow \eta\eta n$
1857 ⁺³⁵ ₋₂₄		2 COSTA...	80	OMEG 10 $\pi^- \rho \rightarrow K^+ K^- n$
1858 ⁺¹⁸ ₋₇₁		3 LONGACRE	86	RVUE Compilation
1799 ± 15		4 CASON	82	STRC 8 $\pi^+ \rho \rightarrow \Delta^{++} \pi^0 \pi^0$

1 Seen in only one solution.
 2 Error increased by spread of two solutions. Included in LONGACRE 86 global analysis.
 3 From a partial-wave analysis of data using a K-matrix formalism with 5 poles. Includes compilation of several other experiments.
 4 From an amplitude analysis of the reaction $\pi^+ \pi^- \rightarrow 2\pi^0$. The resonance in the $2\pi^0$ final state is not confirmed by PROKOSHKIN 97.

Meson Particle Listings

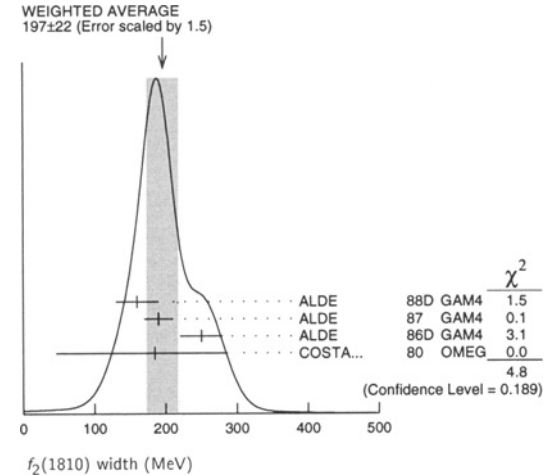
$f_2(1810), \phi_3(1850)$



$f_2(1810)$ WIDTH

VALUE (MeV)	EVTS	DOCUMENT ID	TECN	COMMENT
197 ± 22 OUR AVERAGE		Error includes scale factor of 1.5. See the ideogram below.		
160 ± 30	40	ALDE	88D GAM4	$300 \pi^- p \rightarrow \pi^- p 4\pi^0$
190 ± 20	1600	ALDE	87 GAM4	$100 \pi^- p \rightarrow 4\pi^0 n$
250 ± 30		⁵ ALDE	86D GAM4	$100 \pi^- p \rightarrow \eta\eta n$
185 ⁺¹⁰² ₋₁₃₉		⁶ COSTA...	80 OMEG	$10 \pi^- p \rightarrow K^+ K^- n$
388 ⁺¹⁵ ₋₂₁		⁷ LONGACRE	86 RVUE	Compilation
280 ⁺⁴² ₋₃₅		⁸ CASON	82 STRC	$8 \pi^+ p \rightarrow \Delta^{++} \pi^0 n$

⁵ Seen in only one solution.
⁶ Error increased by spread of two solutions. Included in LONGACRE 86 global analysis.
⁷ From a partial-wave analysis of data using a K-matrix formalism with 5 poles. Includes compilation of several other experiments.
⁸ From an amplitude analysis of the reaction $\pi^+ \pi^- \rightarrow 2\pi^0$. The resonance in the $2\pi^0$ final state is not confirmed by PROKOSHKIN 97.



$f_2(1810)$ DECAY MODES

Mode	Fraction (Γ_j/Γ)
$\Gamma_1 \pi\pi$	
$\Gamma_2 \eta\eta$	
$\Gamma_3 4\pi^0$	seen
$\Gamma_4 K^+ K^-$	

$f_2(1810)$ BRANCHING RATIOS

$\Gamma(\pi\pi)/\Gamma_{total}$	DOCUMENT ID	TECN	COMMENT	Γ_1/Γ
...	We do not use the following data for averages, fits, limits, etc. ...			
not seen	PROKOSHKIN 97	GAM2	$38 \pi^- p \rightarrow \pi^0 \pi^0 n$	
0.21 ^{+0.02} _{-0.03}	⁹ LONGACRE 86	RVUE	Compilation	
0.44 ± 0.03	¹⁰ CASON 82	STRC	$8 \pi^+ p \rightarrow \Delta^{++} \pi^0 n$	

⁹ From a partial-wave analysis of data using a K-matrix formalism with 5 poles. Includes compilation of several other experiments.
¹⁰ Included in LONGACRE 86 global analysis.

$\Gamma(\eta\eta)/\Gamma_{total}$	DOCUMENT ID	TECN	COMMENT	Γ_2/Γ
...	We do not use the following data for averages, fits, limits, etc. ...			
0.008 ^{+0.028} _{-0.003}	⁹ LONGACRE 86	RVUE	Compilation	

$\Gamma(\pi\pi)/\Gamma(4\pi^0)$	DOCUMENT ID	TECN	COMMENT	Γ_1/Γ_3
...	We do not use the following data for averages, fits, limits, etc. ...			
<0.75	ALDE 87	GAM4	$100 \pi^- p \rightarrow 4\pi^0 n$	

$\Gamma(4\pi^0)/\Gamma(\eta\eta)$	DOCUMENT ID	TECN	COMMENT	Γ_3/Γ_2
...	We do not use the following data for averages, fits, limits, etc. ...			
0.8 ± 0.3	ALDE 87	GAM4	$100 \pi^- p \rightarrow 4\pi^0 n$	

$\Gamma(K^+ K^-)/\Gamma_{total}$	DOCUMENT ID	TECN	COMMENT	Γ_4/Γ
...	We do not use the following data for averages, fits, limits, etc. ...			
0.003 ^{+0.019} _{-0.002}	⁹ LONGACRE 86	RVUE	Compilation	
seen	COSTA... 80	OMEG	$10 \pi^- p \rightarrow K^+ K^- n$	

$f_2(1810)$ REFERENCES

PROKOSHKIN 97	SPD 42 117	Y.D. Prokoshkin et al.	(SERP)
ALDE 88D	5JNP 47 810	D.M. Alde et al.	(SERP, BELG, LANL, LAPP+)
ALDE 87	PL B198 286	D.M. Alde et al.	(LANL, BRUX, SERP, LAPP)
ALDE 86D	NP B369 485	D.M. Alde et al.	(BELG, LAPP, SERP, CERN+)
LONGACRE 86	PL B177 223	R.S. Longacre et al.	(BNL, BRAN, CUNY+)
CASON 82	PRL 48 1316	N.M. Cason et al.	(NDAM, ANL)
COSTA... 80	NP B175 402	G. Costa de Beaugard et al.	(BARI, BONN+)

OTHER RELATED PAPERS

AKER 91	PL B260 249	E. Aker et al.	(Crystal Barrel Collab.)
CASON 83	PR D28 1586	N.M. Cason et al.	(NDAM, ANL)
ETKIN 82B	PR D25 1786	A. Etkin et al.	(BNL, CUNY, TUFTS, VAND)

$\phi_3(1850)$

$$I^G(J^{PC}) = 0^-(3^{--})$$

$\phi_3(1850)$ MASS

VALUE (MeV)	EVTS	DOCUMENT ID	TECN	COMMENT
1854 ± 7 OUR AVERAGE		Error includes scale factor of 1.2.		
1855 ± 10		ASTON 88E	LASS	$11 K^- p \rightarrow K^- K^+ \Lambda, K_S^0 K^\pm \pi^\mp \Lambda$
1870 ⁺³⁰ ₋₂₀	430	ARMSTRONG 82	OMEG	$18.5 K^- p \rightarrow K^- K^+ \Lambda$
1850 ± 10	123	ALHARRAN 81B	HBC	$8.25 K^- p \rightarrow K \bar{K} \Lambda$

$\phi_3(1850)$ WIDTH

VALUE (MeV)	EVTS	DOCUMENT ID	TECN	COMMENT
87⁺²⁸₋₂₃ OUR AVERAGE		Error includes scale factor of 1.2.		
64 ± 31		ASTON 88E	LASS	$11 K^- p \rightarrow K^- K^+ \Lambda, K_S^0 K^\pm \pi^\mp \Lambda$
160 ⁺⁹⁰ ₋₅₀	430	ARMSTRONG 82	OMEG	$18.5 K^- p \rightarrow K^- K^+ \Lambda$
80 ⁺⁴⁰ ₋₃₀	123	ALHARRAN 81B	HBC	$8.25 K^- p \rightarrow K \bar{K} \Lambda$

$\phi_3(1850)$ DECAY MODES

Mode	Fraction (Γ_j/Γ)
$\Gamma_1 K \bar{K}$	seen
$\Gamma_2 K \bar{K}^*(892) + c.c.$	seen

See key on page 239

Meson Particle Listings
 $\phi_3(1850)$, $\eta_2(1870)$, $X(1910)$

$\phi_3(1850)$ BRANCHING RATIOS

$\Gamma(K\bar{K}^*(892) + c.c.) / \Gamma(K\bar{K})$		Γ_2 / Γ_1	
VALUE	DOCUMENT ID	TECN	COMMENT
$0.55^{+0.05}_{-0.45}$	ASTON	88E LASS	$11 K^- p \rightarrow K^- K^+ \Lambda$, $K_S^0 K^\pm \pi^\mp \Lambda$
• • • We do not use the following data for averages, fits, limits, etc. • • •			
0.8 ± 0.4	ALHARRAN	81B HBC	$8.25 K^- p \rightarrow K\bar{K}\pi\Lambda$

$\phi_3(1850)$ REFERENCES

ASTON	88E	PL B208 324	D. Aston <i>et al.</i>	(SLAC, NAGO, CINC, INUS) IGJPC
ARMSTRONG	82	PL 110B 77	T.A. Armstrong <i>et al.</i>	(BARI, BIRM, CERN+) JP
ALHARRAN	81B	PL 101B 357	S. Al-Harran <i>et al.</i>	(BIRM, CERN, GLAS+)

OTHER RELATED PAPERS

CORDIER	82B	PL 110B 335	A. Cordier <i>et al.</i>	(LALO)
ASTON	80B	PL 92B 219	D. Aston	(BONN, CERN, EPOL, GLAS, LANC+)

$\eta_2(1870)$

$I^G(J^{PC}) = 0^+(2^{-+})$

OMITTED FROM SUMMARY TABLE
 Needs confirmation.

$\eta_2(1870)$ MASS

VALUE (MeV)	EVT5	DOCUMENT ID	TECN	CHG	COMMENT
1854 ± 20		OUR AVERAGE			
1840 ± 25		BARBERIS	97B OMEG		$450 pp \rightarrow pp2(\pi^+ \pi^-)$
$1875 \pm 20 \pm 35$		ADOMEIT	96 CBAR 0		$1.94 \bar{p}p \rightarrow \eta 3\pi^0$
$1881 \pm 32 \pm 40$	26	KARCH	92 CBAL		$e^+ e^- \rightarrow e^+ e^- \eta \pi^0 \pi^0$
• • • We do not use the following data for averages, fits, limits, etc. • • •					
1840 ± 15		BAI	99 BES		$J/\psi \rightarrow \gamma \eta \pi^+ \pi^-$

$\eta_2(1870)$ WIDTH

VALUE (MeV)	EVT5	DOCUMENT ID	TECN	CHG	COMMENT
202 ± 30		OUR AVERAGE			
200 ± 40		BARBERIS	97B OMEG		$450 pp \rightarrow pp2(\pi^+ \pi^-)$
$200 \pm 25 \pm 45$		ADOMEIT	96 CBAR 0		$1.94 \bar{p}p \rightarrow \eta 3\pi^0$
$221 \pm 92 \pm 44$	26	KARCH	92 CBAL		$e^+ e^- \rightarrow e^+ e^- \eta \pi^0 \pi^0$
• • • We do not use the following data for averages, fits, limits, etc. • • •					
170 ± 40		BAI	99 BES		$J/\psi \rightarrow \gamma \eta \pi^+ \pi^-$

$\eta_2(1870)$ DECAY MODES

Mode	Γ
$\eta \pi \pi$	Γ_1
$a_2(1320) \pi$	Γ_2
$f_2(1270) \eta$	Γ_3

$\eta_2(1870)$ BRANCHING RATIOS

$\Gamma(a_2(1320)\pi) / \Gamma(f_2(1270)\eta)$		Γ_2 / Γ_3	
VALUE	DOCUMENT ID	TECN	COMMENT
4.1 ± 2.3	ADOMEIT	96 CBAR 0	$1.94 \bar{p}p \rightarrow \eta 3\pi^0$
• • • We do not use the following data for averages, fits, limits, etc. • • •			
$\Gamma(\eta \pi \pi) / \Gamma_{total}$		Γ_1 / Γ	
VALUE	DOCUMENT ID	TECN	COMMENT
not seen	AMELIN	00 VES	$37 \pi^- p \rightarrow \eta \pi^+ \pi^- n$

$\eta_2(1870)$ REFERENCES

AMELIN	00	NP B668 83	D. Amelin <i>et al.</i>	(VES Collab.)
BAI	99	PL B446 356	J.Z. Bai <i>et al.</i>	(BES Collab.)
BARBERIS	97B	PL B413 217	D. Barberis <i>et al.</i>	(WA102 Collab.)
ADOMEIT	96	ZPHY C71 227	J. Adomeit <i>et al.</i>	(Crystal Barrel Collab.)
KARCH	92	ZPHY C54 33	K. Karch <i>et al.</i>	(Crystal Ball Collab.)

OTHER RELATED PAPERS

KARCH	90	PL B249 353	K. Karch <i>et al.</i>	(Crystal Ball Collab.)
-------	----	-------------	------------------------	------------------------

$X(1910)$

$I^G(J^{PC}) = 0^+(?^{?+})$

OMITTED FROM SUMMARY TABLE

We list here two different peaks with close masses and widths seen in the mass distributions of $\omega\omega$ and $\eta\eta'$ final states. ALDE 91B argues that they are of different nature.

$X(1910)$ MASS

VALUE (MeV)	DOCUMENT ID		
1810 to 1920	OUR ESTIMATE		
$X(1910) \omega\omega$ MODE			
VALUE (MeV)	DOCUMENT ID	TECN	COMMENT
1921 ± 8	OUR AVERAGE		
1920 ± 10	¹ BELADIDZE	92B VES	$36 \pi^- p \rightarrow \omega\omega n$
1924 ± 14	¹ ALDE	90 GAM2	$38 \pi^- p \rightarrow \omega\omega n$
$1 J^{PC} = 2^{++}$.			

$X(1910) \eta\eta'$ MODE

VALUE (MeV)	DOCUMENT ID	TECN	COMMENT
1911 ± 10	ALDE	91B GAM2	$38 \pi^- p \rightarrow \eta\eta' n$

$X(1910)$ WIDTH

VALUE (MeV)	DOCUMENT ID		
90 to 250	OUR ESTIMATE		
$X(1910) \omega\omega$ MODE			
VALUE (MeV)	DOCUMENT ID	TECN	COMMENT
90 ± 20	OUR AVERAGE		
90 ± 20	² BELADIDZE	92B VES	$36 \pi^- p \rightarrow \omega\omega n$
91 ± 50	² ALDE	90 GAM2	$38 \pi^- p \rightarrow \omega\omega n$
$2 J^{PC} = 2^{++}$.			

$X(1910) \eta\eta'$ MODE

VALUE (MeV)	DOCUMENT ID	TECN	COMMENT
90 ± 35	ALDE	91B GAM2	$38 \pi^- p \rightarrow \eta\eta' n$

$X(1910)$ DECAY MODES

Mode	Γ
$\pi^0 \pi^0$	Γ_1
$K_S^0 K_S^0$	Γ_2
$\eta\eta$	Γ_3
$\omega\omega$	Γ_4
$\eta\eta'$	Γ_5
$\eta'\eta'$	Γ_6

$X(1910)$ BRANCHING RATIOS

$\Gamma(\omega\omega) / \Gamma_{total}$		Γ_4 / Γ		
VALUE	DOCUMENT ID	TECN	COMMENT	
• • • We do not use the following data for averages, fits, limits, etc. • • •				
seen	ALDE	89B GAM2	$38 \pi^- p \rightarrow \omega\omega n$	
$\Gamma(\pi^0 \pi^0) / \Gamma(\eta\eta')$		Γ_1 / Γ_5		
VALUE	DOCUMENT ID	TECN	COMMENT	
• • • We do not use the following data for averages, fits, limits, etc. • • •				
< 0.1	ALDE	89	GAM2 $38 \pi^- p \rightarrow \eta\eta' n$	
$\Gamma(\eta\eta) / \Gamma(\eta\eta')$		Γ_3 / Γ_5		
VALUE	CL%	DOCUMENT ID	TECN	COMMENT
• • • We do not use the following data for averages, fits, limits, etc. • • •				
< 0.05		90	ALDE	91B GAM2 $38 \pi^- p \rightarrow \eta\eta' n$
$\Gamma(K_S^0 K_S^0) / \Gamma(\eta\eta')$		Γ_2 / Γ_5		
VALUE	CL%	DOCUMENT ID	TECN	COMMENT
• • • We do not use the following data for averages, fits, limits, etc. • • •				
< 0.066		90	BALOSHIN	86 SPEC $40 \pi^- p \rightarrow K_S^0 K_S^0 n$
$\Gamma(\eta'\eta') / \Gamma_{total}$		Γ_6 / Γ		
VALUE	DOCUMENT ID	TECN	COMMENT	
• • • We do not use the following data for averages, fits, limits, etc. • • •				
possibly seen	BELADIDZE	92D VES	$37 \pi^- p \rightarrow \eta'\eta' n$	

Meson Particle Listings

 $X(1910)$, $f_2(1950)$, $X(2000)$ $X(1910)$ REFERENCES

BELADIDZE	92B	ZPHY C54 357	G.M. Beladidze <i>et al.</i>	(VES Collab.)
BELADIDZE	92D	ZPHY C57 13	G.M. Beladidze <i>et al.</i>	(VES Collab.)
ALDE	91B	SJNP 54 455	D.M. Alde <i>et al.</i>	(SERP, BELG, LANL, LAPP+)
		Translated from YAF 54 751.		
Also	92	PL B276 375	D.M. Alde <i>et al.</i>	(BELG, SERP, KEK, LANL+)
ALDE	90	PL B241 600	D.M. Alde <i>et al.</i>	(SERP, BELG, LANL, LAPP+)
ALDE	89	PL B216 447	D.M. Alde <i>et al.</i>	(SERP, BELG, LANL, LAPP+)
Also	88E	SJNP 48 1035	D.M. Alde <i>et al.</i>	(BELG, SERP, LANL, LAPP)
ALDE	89B	Translated from YAF 48 1724.		
BALOSHIN	86	PL B216 451	D.M. Alde <i>et al.</i>	(SERP, BELG, LANL, LAPP+)
		SJNP 43 959	O.N. Baloshin <i>et al.</i>	(ITEP)
		Translated from YAF 43 1487.		

OTHER RELATED PAPERS

LEE	94	PL B323 227	J.H. Lee <i>et al.</i>	(BNL, IND, KYUN, MASD+)
-----	----	-------------	------------------------	-------------------------

 $f_2(1950)$

$$I^G(J^{PC}) = 0^+(2^{++})$$

OMITTED FROM SUMMARY TABLE

Needs confirmation.

 $f_2(1950)$ MASS

VALUE (MeV)	DOCUMENT ID	TECN	CHG	COMMENT
1960 ± 30	¹ BARBERIS	97B	OMEG	450 $pp \rightarrow \rho\rho 2(\pi^+\pi^-)$

• • • We do not use the following data for averages, fits, limits, etc. • • •

1940 ± 50	BAI	00	BES	$J/\psi \rightarrow \gamma(\pi^+\pi^-\pi^+\pi^-)$
1980 ± 50	² ANISOVICH	99B	SPEC	$1.35-1.94 \rho\bar{\rho} \rightarrow \eta\eta\pi^0$
1918 ± 12	ANTINORI	95	OMEG	$300,450 \rho\rho \rightarrow \rho\rho 2(\pi^+\pi^-)$
~ 1996	HASAN	94	RVUE	$\bar{p}p \rightarrow \pi\pi$
~ 1990	OAKDEN	94	RVUE	$0.36-1.55 \bar{p}p \rightarrow \pi\pi$
1950 ± 15	⁴ ASTON	91	LASS 0	$11 K^-p \rightarrow \Lambda K \bar{K} \pi\pi$

¹ Possibly two states.² Using preliminary CBAR data.³ From solution B of amplitude analysis of data on $\bar{p}p \rightarrow \pi\pi$. See however KLOET 96 who fit $\pi^+\pi^-$ only and find waves only up to $J=3$ to be important but not significantly resonant.⁴ Cannot determine spin to be 2. $f_2(1950)$ WIDTH

VALUE (MeV)	DOCUMENT ID	TECN	CHG	COMMENT
460 ± 40	⁵ BARBERIS	97B	OMEG	450 $pp \rightarrow \rho\rho 2(\pi^+\pi^-)$

• • • We do not use the following data for averages, fits, limits, etc. • • •

380^{+120}_{-90}	BAI	00	BES	$J/\psi \rightarrow \gamma(\pi^+\pi^-\pi^+\pi^-)$
500 ± 100	⁶ ANISOVICH	99B	SPEC	$1.35-1.94 \rho\bar{\rho} \rightarrow \eta\eta\pi^0$
390 ± 60	ANTINORI	95	OMEG	$300,450 \rho\rho \rightarrow \rho\rho 2(\pi^+\pi^-)$
~ 134	HASAN	94	RVUE	$\bar{p}p \rightarrow \pi\pi$
~ 100	⁷ OAKDEN	94	RVUE	$0.36-1.55 \bar{p}p \rightarrow \pi\pi$
250 ± 50	⁸ ASTON	91	LASS 0	$11 K^-p \rightarrow \Lambda K \bar{K} \pi\pi$

⁵ Possibly two states.⁶ Using preliminary CBAR data.⁷ From solution B of amplitude analysis of data on $\bar{p}p \rightarrow \pi\pi$. See however KLOET 96 who fit $\pi^+\pi^-$ only and find waves only up to $J=3$ to be important but not significantly resonant.⁸ Cannot determine spin to be 2. $f_2(1950)$ DECAY MODES

Mode	Fraction (Γ_i/Γ)
Γ_1 $K^*(892)\bar{K}^*(892)$	seen
Γ_2 $\pi^+\pi^-$	seen
Γ_3 $\pi^+\pi^-\pi^+\pi^-$	possibly seen
Γ_4 $a_2(1320)\pi$	
Γ_5 $f_2(1270)\pi\pi$	

 $f_2(1950)$ BRANCHING RATIOS

$\Gamma(K^*(892)\bar{K}^*(892))/\Gamma_{\text{total}}$	DOCUMENT ID	TECN	CHG	COMMENT
seen	ASTON	91	LASS 0	$11 K^-p \rightarrow \Lambda K \bar{K} \pi\pi$

 $\Gamma(a_2(1320)\pi)/\Gamma_{\text{total}}$

VALUE	DOCUMENT ID	TECN	COMMENT
• • • We do not use the following data for averages, fits, limits, etc. • • •			
possibly seen	BARBERIS	97B	OMEG 450 $pp \rightarrow \rho\rho 2(\pi^+\pi^-)$

 Γ_4/Γ $f_2(1950)$ REFERENCES

BAI	00	PL B472 207	J.Z. Bai <i>et al.</i>	(BES Collab.)
ANISOVICH	99B	PL B449 154	A.V. Anisovich <i>et al.</i>	
BARBERIS	97B	PL B413 217	D. Barberis <i>et al.</i>	(WA102 Collab.)
KLOET	96	PR D53 6120	W.M. Kloet, F. Myhrer	(RUTG, NORD)
ANTINORI	95	PL B353 589	F. Antinori <i>et al.</i>	(ATHU, BARI, BIRM+) ^{JP}
HASAN	94	PL B334 215	A. Hasan, D.V. Bugg	(LOQM)
OAKDEN	94	NPA 574 731	M.N. Oakden, M.R. Pennington	(DURH)
ASTON	91	NP B21 5 (suppl)	D. Aston <i>et al.</i>	(LASS Collab.)

OTHER RELATED PAPERS

ALBRECHT	88N	PL B212 528	H. Albrecht <i>et al.</i>	(ARGUS Collab.)
ALBRECHT	87Q	PL B198 255	H. Albrecht <i>et al.</i>	(ARGUS Collab.)
ARMSTRONG	87C	ZPHY C34 33	T.A. Armstrong <i>et al.</i>	(CERN, BIRM, BARI+)

 $X(2000)$

$$I^G(J^{PC}) = 1^-(?^{?+})$$

OMITTED FROM SUMMARY TABLE

BALTAY 77 favors $J^P = 3^+$. Needs confirmation. $X(2000)$ MASS

VALUE (MeV)	EVTS	DOCUMENT ID	TECN	CHG	COMMENT
1964 ± 35		¹ ARMSTRONG	93D	E760	$\bar{p}p \rightarrow 3\pi^0 \rightarrow 6\gamma$
~ 2100		¹ ANTIPOV	77	CIBS	$25 \pi^- p \rightarrow \rho\pi^- \rho_3$
2214 ± 15		BALTAY	77	HBC 0	$15 \pi^- p \rightarrow \Delta^{++} 3\pi$
2080 ± 40	208	KALELKAR	75	HBC +	$15 \pi^+ p \rightarrow \rho\pi^+ \rho_3$

¹ Cannot determine spin to be 3. $X(2000)$ WIDTH

VALUE (MeV)	EVTS	DOCUMENT ID	TECN	CHG	COMMENT
225 ± 50		² ARMSTRONG	93D	E760	$\bar{p}p \rightarrow 3\pi^0 \rightarrow 6\gamma$
~ 500		² ANTIPOV	77	CIBS	$25 \pi^- p \rightarrow \rho\pi^- \rho_3$
355 ± 21		BALTAY	77	HBC 0	$15 \pi^- p \rightarrow \Delta^{++} 3\pi$
340 ± 80	208	KALELKAR	75	HBC +	$15 \pi^+ p \rightarrow \rho\pi^+ \rho_3$

² Cannot determine spin to be 3. $X(2000)$ DECAY MODES

Mode	Fraction (Γ_i/Γ)
Γ_1 3π	
Γ_2 $\rho_3(1690)\pi$	dominant

 $X(2000)$ BRANCHING RATIOS

$\Gamma(\rho_3(1690)\pi)/\Gamma(3\pi)$	DOCUMENT ID	TECN	CHG	COMMENT
dominant	KALELKAR	75	HBC +	$15 \pi^+ p \rightarrow \rho_3\pi$

 $X(2000)$ REFERENCES

ARMSTRONG	93D	PL B307 399	T.A. Armstrong <i>et al.</i>	(FNAL, FERR, GENO+)
ANTIPOV	77	NP B119 45	Y.M. Antipov <i>et al.</i>	(SERP, GEVA)
BALTAY	77	PRL 39 591	C. Baltay, C.V. Cautis, M. Kalelkar	(COLU) ^{JP}
KALELKAR	75	Thesis Nevis 207	M.S. Kalelkar	(COLU)

OTHER RELATED PAPERS

HARRIS	81	ZPHY C9 275	R.M. Harris <i>et al.</i>	(SEAT, UCB)
HUSON	68	PL 28B 208	R. Huson <i>et al.</i>	(ORSAY, MILA, UCLA)
DANYSZ	67B	NC 51A 801	J.A. Danysz, B.R. French, V. Simak	(CERN)

See key on page 239

Meson Particle Listings
 $f_2(2010)$, $f_0(2020)$, $a_4(2040)$ $f_2(2010)$

$$I^G(J^{PC}) = 0^+(2^{++})$$

See also the mini-review under non- $q\bar{q}$ candidates. (See the index for the page number.) $f_2(2010)$ MASS

VALUE (MeV)	DOCUMENT ID	TECN	COMMENT
$2011 \pm \frac{62}{76}$	¹ ETKIN	88 MPS	$22 \pi^- \rho \rightarrow \phi \phi \pi$
• • • We do not use the following data for averages, fits, limits, etc. • • •			
2010 ± 60	ALDE	98 GAM4	$100 \pi^- \rho \rightarrow \pi^0 \pi^0 n$
1980 ± 20	² BOLONKIN	88 SPEC	$40 \pi^- \rho \rightarrow K_S^0 K_S^0 n$
$2050 \pm \frac{90}{50}$	ETKIN	85 MPS	$22 \pi^- \rho \rightarrow 2 \phi n$
$2120 \pm \frac{20}{120}$	LINDENBAUM	84 RVUE	
2160 ± 50	ETKIN	82 MPS	$22 \pi^- \rho \rightarrow 2 \phi n$

¹ Includes data of ETKIN 85. The percentage of the resonance going into $\phi \phi 2^{++} S_2$, D_2 , and D_0 is $98 \frac{+1}{-3}$, $0 \frac{+1}{-0}$, and $2 \frac{+2}{-1}$, respectively.² Statistically very weak, only 1.4 s.d. $f_2(2010)$ WIDTH

VALUE (MeV)	DOCUMENT ID	TECN	COMMENT
$202 \pm \frac{67}{62}$	³ ETKIN	88 MPS	$22 \pi^- \rho \rightarrow \phi \phi \pi$
• • • We do not use the following data for averages, fits, limits, etc. • • •			
240 ± 100	ALDE	98 GAM4	$100 \pi^- \rho \rightarrow \pi^0 \pi^0 n$
145 ± 50	⁴ BOLONKIN	88 SPEC	$40 \pi^- \rho \rightarrow K_S^0 K_S^0 n$
$200 \pm \frac{160}{50}$	ETKIN	85 MPS	$22 \pi^- \rho \rightarrow 2 \phi n$
$300 \pm \frac{150}{50}$	LINDENBAUM	84 RVUE	
310 ± 70	ETKIN	82 MPS	$22 \pi^- \rho \rightarrow 2 \phi n$

³ Includes data of ETKIN 85.⁴ Statistically very weak, only 1.4 s.d. $f_2(2010)$ DECAY MODES

Mode	Fraction (Γ_i/Γ)
$\Gamma_1 \phi \phi$	seen

 $f_2(2010)$ REFERENCES

ALDE	98 EPJ A3 361	D. Alde <i>et al.</i>	(GAM4 Collab.)
Also	99 PAN 62 405	D. Alde <i>et al.</i>	(GAMS Collab.)
BOLONKIN	88 NP B309 426	B.V. Bolonkin <i>et al.</i>	(ITEP, SERP)
ETKIN	88 PL B201 568	A. Etkin <i>et al.</i>	(BNL, CUNY)
ETKIN	85 PL 165B 217	A. Etkin <i>et al.</i>	(BNL, CUNY)
LINDENBAUM	84 CNPP 13 285	S.J. Lindenbaum	(CUNY)
ETKIN	82 PRL 49 1620	A. Etkin <i>et al.</i>	(BNL, CUNY)
Also	83 Brighton Conf. 351	S.J. Lindenbaum	(BNL, CUNY)

OTHER RELATED PAPERS

ANISOVICH	99D PL B452 180	A.V. Anisovich <i>et al.</i>	
Also	99F NP A651 253	A.V. Anisovich <i>et al.</i>	
ANISOVICH	99F NP A651 253	A.V. Anisovich <i>et al.</i>	
LANDBERG	96 PR D53 2839	C. Landberg <i>et al.</i>	(BNL, CUNY, RPI)
ARMSTRONG	89B PL B221 221	T.A. Armstrong <i>et al.</i>	(CERN, CDEF, BIRM+)
GREEN	86 PRL 56 1639	D.R. Green <i>et al.</i>	(FNAL, ARIZ, FSU+)
BOOTH	84 NP B242 51	P.S.L. Booth <i>et al.</i>	(LIVP, GLAS, CERN)
EISENHAND...	75 NP B95 109	E. Eisenhandler <i>et al.</i>	(LOQM, LIVP, DARE+)

 $f_0(2020)$

$$I^G(J^{PC}) = 0^+(0^{++})$$

OMITTED FROM SUMMARY TABLE
Needs confirmation. $f_0(2020)$ MASS

VALUE (MeV)	DOCUMENT ID	TECN	COMMENT
2020 ± 35	BARBERIS	97B OMEG	$450 \rho \rho \rightarrow \rho \rho 2(\pi^+ \pi^-)$
• • • We do not use the following data for averages, fits, limits, etc. • • •			
2010 ± 60	ALDE	98 GAM4	$100 \pi^- \rho \rightarrow \pi^0 \pi^0 n$

 $f_0(2020)$ WIDTH

VALUE (MeV)	DOCUMENT ID	TECN	COMMENT
410 ± 50	BARBERIS	97B OMEG	$450 \rho \rho \rightarrow \rho \rho 2(\pi^+ \pi^-)$
• • • We do not use the following data for averages, fits, limits, etc. • • •			
240 ± 100	ALDE	98 GAM4	$100 \pi^- \rho \rightarrow \pi^0 \pi^0 n$

 $f_0(2020)$ DECAY MODES

Mode	Fraction (Γ_i/Γ)
$\Gamma_1 \rho \pi \pi$	seen
$\Gamma_2 \pi^0 \pi^0$	seen

 $f_0(2020)$ REFERENCES

ALDE	98 EPJ A3 361	D. Alde <i>et al.</i>	(GAM4 Collab.)
Also	99 PAN 62 405	D. Alde <i>et al.</i>	(GAMS Collab.)
BARBERIS	97B PL B413 217	D. Barberis <i>et al.</i>	(WA102 Collab.)

 $a_4(2040)$

$$I^G(J^{PC}) = 1^-(4^{++})$$

 $a_4(2040)$ MASS

VALUE (MeV)	DOCUMENT ID	TECN	CHG	COMMENT
2014 ± 15 OUR AVERAGE				
$1944 \pm 8 \pm 50$	¹ AMELIN	99 VES		$37 \pi^- A \rightarrow \omega \pi^- \pi^0 A^*$
2010 ± 20	² DONSKOV	96 GAM2	0	$38 \pi^- \rho \rightarrow \eta \pi^0 n$
2040 ± 30	³ CLELAND	82B SPEC	\pm	$50 \pi \rho \rightarrow K_S^0 K^\pm \rho$
2030 ± 50	⁴ CORDEN	78C OMEG	0	$15 \pi^- \rho \rightarrow 3 \pi n$
• • • We do not use the following data for averages, fits, limits, etc. • • •				
1903 ± 10	⁵ BALDI	78 SPEC	-	$10 \pi^- \rho \rightarrow \rho K_S^0 K^-$

¹ May be a different state.² From a simultaneous fit to the G_+ and G_0 wave intensities.³ From an amplitude analysis.⁴ $J^P = 4^+$ is favored, though $J^P = 2^+$ cannot be excluded.⁵ From a fit to the γ_8^0 moment. Limited by phase space. $a_4(2040)$ WIDTH

VALUE (MeV)	DOCUMENT ID	TECN	CHG	COMMENT
361 ± 50 OUR AVERAGE				
$324 \pm 26 \pm 75$	⁶ AMELIN	99 VES		$37 \pi^- A \rightarrow \omega \pi^- \pi^0 A^*$
370 ± 80	⁷ DONSKOV	96 GAM2	0	$38 \pi^- \rho \rightarrow \eta \pi^0 n$
380 ± 150	⁸ CLELAND	82B SPEC	\pm	$50 \pi \rho \rightarrow K_S^0 K^\pm \rho$
510 ± 200	⁹ CORDEN	78C OMEG	0	$15 \pi^- \rho \rightarrow 3 \pi n$
• • • We do not use the following data for averages, fits, limits, etc. • • •				
166 ± 43	¹⁰ BALDI	78 SPEC	-	$10 \pi^- \rho \rightarrow \rho K_S^0 K^-$

⁶ May be a different state.⁷ From a simultaneous fit to the G_+ and G_0 wave intensities.⁸ From an amplitude analysis.⁹ $J^P = 4^+$ is favored, though $J^P = 2^+$ cannot be excluded.¹⁰ From a fit to the γ_8^0 moment. Limited by phase space.

Meson Particle Listings

$a_4(2040)$, $f_4(2050)$

$a_4(2040)$ DECAY MODES

Mode	Fraction (Γ_i/Γ)
Γ_1 $K\bar{K}$	seen
Γ_2 $\pi^+\pi^-\pi^0$	seen
Γ_3 $\eta\pi^0$	seen

$a_4(2040)$ BRANCHING RATIOS

$\Gamma(K\bar{K})/\Gamma_{total}$		Γ_1/Γ	
VALUE	DOCUMENT ID	TECN	CHG
seen	BALDI	78	SPEC \pm
COMMENT: $10 \pi^- p \rightarrow K_S^0 K^- p$			
$\Gamma(\pi^+\pi^-\pi^0)/\Gamma_{total}$		Γ_2/Γ	
VALUE	DOCUMENT ID	TECN	CHG
seen	CORDEN	78c	OMEG 0
COMMENT: $15 \pi^- p \rightarrow 3\pi n$			
$\Gamma(\eta\pi^0)/\Gamma_{total}$		Γ_3/Γ	
VALUE	DOCUMENT ID	TECN	CHG
seen	DONSKOV	96	GAM2 0
COMMENT: $38 \pi^- p \rightarrow \eta\pi^0 n$			

$a_4(2040)$ REFERENCES

NAME	YEAR	DOCUMENT ID	TECN	CHG	COMMENT
AMELIN	99	PAN 62 445	D.V. Amelin et al.		(VES Collab.)
		Translated from YAF 62 487.			
DONSKOV	96	PAN 59 382	S.V. Donskov et al.		(GAMS Collab.) IGJPC
		Translated from YAF 59 1027.			
CLELAND	82B	NP B208 228	W.E. Cleland et al.		(DURH, GEVA, LAUS+)
BALDI	78	PL 74B 413	R. Baldi et al.		(GEVA) JP
CORDEN	78C	NP B136 77	M.J. Corden et al.		(BIRM, RHEL, TELA+) JP

OTHER RELATED PAPERS

DELFOSSÉ	81	NP B183 349	A. Delfosse et al.		(GEVA, LAUS)
----------	----	-------------	--------------------	--	--------------

$f_4(2050)$

$$I^G(J^{PC}) = 0^+(4^{++})$$

$f_4(2050)$ MASS

VALUE (MeV)	EVTS	DOCUMENT ID	TECN	COMMENT
2034 ± 11	OUR AVERAGE	Error includes scale factor of 1.6. See the ideogram below.		
1998 ± 15		ALDE	98 GAM4	$100 \pi^- p \rightarrow \pi^0 \pi^0 n$
1970 ± 30		BELADIDZE	92B VES	$36 \pi^- p \rightarrow \omega \omega n$
2060 ± 20		ALDE	90 GAM2	$38 \pi^- p \rightarrow \omega \omega n$
2038 ± 30		AUGUSTIN	87 DM2	$J/\psi \rightarrow \gamma \pi^+ \pi^-$
2086 ± 15		BALTRUSAIT..	87 MRK3	$J/\psi \rightarrow \gamma \pi^+ \pi^-$
2000 ± 60		ALDE	86D GAM4	$100 \pi^- p \rightarrow n2\eta$
2020 ± 20	40k	¹ BINON	84B GAM2	$38 \pi^- p \rightarrow n2\pi^0$
2015 ± 28		² CASON	82 STRC	$8 \pi^+ p \rightarrow \Delta^{++} \pi^0 \pi^0$
2031 ⁺²⁵ ₋₃₆		ETKIN	82B MPS	$23 \pi^- p \rightarrow n2K_S^0$
2020 ± 30	700	APEL	75 NICE	$40 \pi^- p \rightarrow n2\pi^0$
2050 ± 25		BLUM	75 ASPK	$18.4 \pi^- p \rightarrow nK^+ K^-$

• • • We do not use the following data for averages, fits, limits, etc. • • •

~ 2000	³ MARTIN	98 RVUE	$N\bar{N} \rightarrow \pi\pi$	
~ 2010	⁴ MARTIN	97 RVUE	$\bar{N}N \rightarrow \pi\pi$	
~ 2040	⁵ OAKDEN	94 RVUE	$0.36-1.55 \bar{p}p \rightarrow \pi\pi$	
~ 1990	⁶ OAKDEN	94 RVUE	$0.36-1.55 \bar{p}p \rightarrow \pi\pi$	
1978 ± 5	⁷ ALPER	80 CNTR	$62 \pi^- p \rightarrow K^+ K^- n$	
2040 ± 10	⁷ ROZANSKA	80 SPRK	$18 \pi^- p \rightarrow p\bar{p}n$	
1935 ± 13	⁷ CORDEN	79 OMEG	$12-15 \pi^- p \rightarrow n2\pi$	
1988 ± 7		EVANGELISTA	79B OMEG	$10 \pi^- p \rightarrow K^+ K^- n$
1922 ± 14	⁸ ANTIPOV	77 CIB5	$25 \pi^- p \rightarrow p3\pi$	

¹ From a partial-wave analysis of the data.

² From an amplitude analysis of the reaction $\pi^+ \pi^- \rightarrow 2\pi^0$.

³ Energy-dependent analysis.

⁴ Single energy analysis.

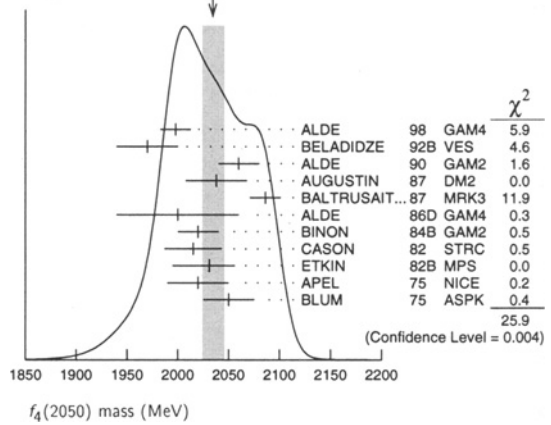
⁵ From solution A of amplitude analysis of data on $\bar{p}p \rightarrow \pi\pi$. See however KLOET 96 who fit $\pi^+ \pi^-$ only and find waves only up to $J = 3$ to be important but not significantly resonant.

⁶ From solution B of amplitude analysis of data on $\bar{p}p \rightarrow \pi\pi$. See however KLOET 96 who fit $\pi^+ \pi^-$ only and find waves only up to $J = 3$ to be important but not significantly resonant.

⁷ $I(J^{PC}) = 0(4^+)$ from amplitude analysis assuming one-pion exchange.

⁸ Width errors enlarged by us to $4\Gamma/\sqrt{N}$; see the note with the $K^*(892)$ mass.

WEIGHTED AVERAGE
2034 ± 11 (Error scaled by 1.6)



$f_4(2050)$ WIDTH

VALUE (MeV)	EVTS	DOCUMENT ID	TECN	COMMENT
222 ± 19	OUR AVERAGE	Error includes scale factor of 1.8. See the ideogram below.		
395 ± 40		ALDE	98 GAM4	$100 \pi^- p \rightarrow \pi^0 \pi^0 n$
300 ± 50		BELADIDZE	92B VES	$36 \pi^- p \rightarrow \omega \omega n$
170 ± 60		ALDE	90 GAM2	$38 \pi^- p \rightarrow \omega \omega n$
304 ± 60		AUGUSTIN	87 DM2	$J/\psi \rightarrow \gamma \pi^+ \pi^-$
210 ± 63		BALTRUSAIT..	87 MRK3	$J/\psi \rightarrow \gamma \pi^+ \pi^-$
400 ± 100		ALDE	86D GAM4	$100 \pi^- p \rightarrow n2\eta$
240 ± 40	40k	⁹ BINON	84B GAM2	$38 \pi^- p \rightarrow n2\pi^0$
190 ± 14		DENNEY	83 LASS	$10 \pi^+ n/\pi^+ p$
186 ⁺¹⁰³ ₋₅₈		¹⁰ CASON	82 STRC	$8 \pi^+ p \rightarrow \Delta^{++} \pi^0 \pi^0$
305 ⁺³⁶ ₋₁₁₉		ETKIN	82B MPS	$23 \pi^- p \rightarrow n2K_S^0$
180 ± 60	700	APEL	75 NICE	$40 \pi^- p \rightarrow n2\pi^0$
225 ± 120		BLUM	75 ASPK	$18.4 \pi^- p \rightarrow nK^+ K^-$

• • • We do not use the following data for averages, fits, limits, etc. • • •

~ 170	¹¹ MARTIN	98 RVUE	$N\bar{N} \rightarrow \pi\pi$	
~ 200	¹² MARTIN	97 RVUE	$\bar{N}N \rightarrow \pi\pi$	
~ 60	¹³ OAKDEN	94 RVUE	$0.36-1.55 \bar{p}p \rightarrow \pi\pi$	
~ 80	¹⁴ OAKDEN	94 RVUE	$0.36-1.55 \bar{p}p \rightarrow \pi\pi$	
243 ± 16	¹⁵ ALPER	80 CNTR	$62 \pi^- p \rightarrow K^+ K^- n$	
140 ± 15	¹⁵ ROZANSKA	80 SPRK	$18 \pi^- p \rightarrow p\bar{p}n$	
263 ± 57	¹⁵ CORDEN	79 OMEG	$12-15 \pi^- p \rightarrow n2\pi$	
100 ± 28		EVANGELISTA	79B OMEG	$10 \pi^- p \rightarrow K^+ K^- n$
107 ± 56	¹⁶ ANTIPOV	77 CIB5	$25 \pi^- p \rightarrow p3\pi$	

⁹ From a partial-wave analysis of the data.

¹⁰ From an amplitude analysis of the reaction $\pi^+ \pi^- \rightarrow 2\pi^0$.

¹¹ Energy-dependent analysis.

¹² Single energy analysis.

¹³ From solution A of amplitude analysis of data on $\bar{p}p \rightarrow \pi\pi$. See however KLOET 96 who fit $\pi^+ \pi^-$ only and find waves only up to $J = 3$ to be important but not significantly resonant.

¹⁴ From solution B of amplitude analysis of data on $\bar{p}p \rightarrow \pi\pi$. See however KLOET 96 who fit $\pi^+ \pi^-$ only and find waves only up to $J = 3$ to be important but not significantly resonant.

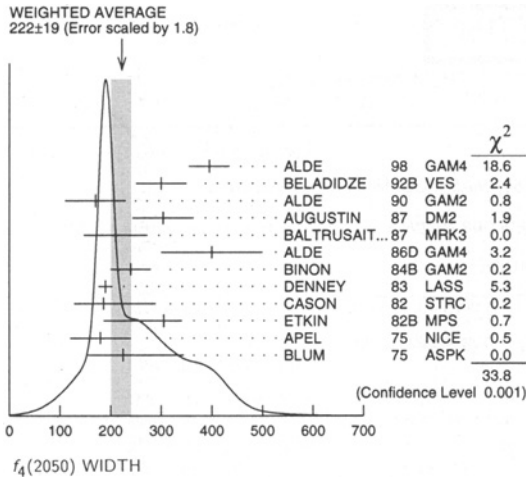
¹⁵ $I(J^{PC}) = 0(4^+)$ from amplitude analysis assuming one-pion exchange.

¹⁶ Width errors enlarged by us to $4\Gamma/\sqrt{N}$; see the note with the $K^*(892)$ mass.

See key on page 239

Meson Particle Listings

$f_4(2050)$, $f_0(2060)$



$f_4(2050)$ REFERENCES

AMELIN	00	NP B668 83	D. Amelin <i>et al.</i>	(VES Collab.)
ALDE	98	EPJ A3 361	D. Alde <i>et al.</i>	(GAM4 Collab.)
Also	99	PAN 62 405	D. Alde <i>et al.</i>	(GAMS Collab.)
MARTIN	98	PR C57 3492	B.R. Martin <i>et al.</i>	(LOUC, AARH)
MARTIN	97	PR C56 1114	B.R. Martin, G.C. Oades	(RUTG, NORD)
KLOET	96	PR D53 6120	W.M. Kloet, F. Myhrer	(DURH)
OAKDEN	94	NPA 574 731	M.N. Oakden, M.R. Pennington	(VES Collab.)
BELADIDZE	92B	ZPHY C54 367	G.M. Beladidze <i>et al.</i>	(SERP, BELG, LANL, LAPP+)
ALDE	90	PL B241 600	D.M. Alde <i>et al.</i>	(JADE Collab.)
OEST	90	ZPHY C47 343	T. Oest <i>et al.</i>	(LANL, BRUX, SERP, LAPP)
ALDE	87	PL B198 286	D.M. Alde <i>et al.</i>	(LALO, CLER, FRAS+)
AUGUSTIN	87	ZPHY C36 369	J.E. Augustin <i>et al.</i>	(Mark II Collab.)
BALTRUSAITIS...	87	PR D35 2077	R.M. Baltrusaitis <i>et al.</i>	(BELG, LAPP, SERP, CERN+)
ALDE	86D	NP B269 485	D.M. Alde <i>et al.</i>	(TASSO Collab.)
ALTHOFF	85B	ZPHY C29 189	M. Althoff <i>et al.</i>	(SERP, BELG, LAPP)
BINON	84B	LNC 39 41	F.G. Binon <i>et al.</i>	(SERP, BRUX+)
BINON	83C	SJNP 38 723	F.G. Binon <i>et al.</i>	(IOWA, MICH)
Translated from YAF 38 1199.				
DENNEY	83	PR D28 2726	D.L. Denney <i>et al.</i>	(NDAM, ANL)
CASON	82	PRL 48 1316	N.M. Cason <i>et al.</i>	(BNL, CUNY, TUFTS, VAND)
ETKIN	82B	PL D25 1756	A. Etkin <i>et al.</i>	(AMST, CERN, CRAC, MPIM+)
ALPER	80	PL 94B 422	B. Alper <i>et al.</i>	(MPIM, CERN)
ROZANSKA	80	NP B162 505	M. Rozanska <i>et al.</i>	(BIRM, RHEL, TELA+)
CORDEN	79	NP B157 250	M.J. Corden <i>et al.</i>	(BARI, BONN, CERN+)
EVANGELISTA	79B	NP B154 381	E. Evangelista <i>et al.</i>	(SERP, GEVA)
ANTIPOV	77	NP B119 45	Y.M. Antipov <i>et al.</i>	(KARLK, KARLE, PISA, SERP+)
APEL	75	PL 57B 398	W.D. Apel <i>et al.</i>	(CERN, MPIM)
BLUM	75	PL 57B 403	W. Blum <i>et al.</i>	

OTHER RELATED PAPERS

ANISOVICH	99D	PL B452 180	A.V. Anisovich <i>et al.</i>	(SERP)
Also	99F	NP A651 253	A.V. Anisovich <i>et al.</i>	
ANISOVICH	99F	NP A651 253	A.V. Anisovich <i>et al.</i>	
PROKOSHIN	97	SPD 42 117	Y.D. Prokoshin <i>et al.</i>	
Translated from DANS 353 323.				
CASON	83	PR D28 1586	N.M. Cason <i>et al.</i>	(NDAM, ANL)
GOTTESMAN	80	PR D22 1503	S.R. Gottesman <i>et al.</i>	(SYRA, BRAN, BNL+)
EISENHAND...	75	NP B96 109	E. Eisenhandler <i>et al.</i>	(LOQM, LIVP, DARE+)
WAGNER	74	London Conf. 2 27	F. Wagner	(MPIM)

$f_0(2060)$

$$I^{G(J^{PC})} = 0^{+}(0^{+}++)$$

OMITTED FROM SUMMARY TABLE
Needs confirmation.

$f_0(2060)$ MASS

VALUE	DOCUMENT ID	TECN	COMMENT
• • • We do not use the following data for averages, fits, limits, etc. • • •			
~ 2050	¹ OAKDEN	94 RVUE	0.36-1.55 $\bar{p}p \rightarrow \pi\pi$
~ 2060	² OAKDEN	94 RVUE	0.36-1.55 $\bar{p}p \rightarrow \pi\pi$
¹ From solution A of amplitude analysis of data on $\bar{p}p \rightarrow \pi\pi$ See however KLOET 96 who fit $\pi^+\pi^-$ only and find waves only up to $J = 3$ to be important but not significantly resonant.			
² From solution B of amplitude analysis of data on $\bar{p}p \rightarrow \pi\pi$ See however KLOET 96 who fit $\pi^+\pi^-$ only and find waves only up to $J = 3$ to be important but not significantly resonant.			

$f_0(2060)$ WIDTH

VALUE	DOCUMENT ID	TECN	COMMENT
• • • We do not use the following data for averages, fits, limits, etc. • • •			
~ 120	³ OAKDEN	94 RVUE	0.36-1.55 $\bar{p}p \rightarrow \pi\pi$
~ 50	⁴ OAKDEN	94 RVUE	0.36-1.55 $\bar{p}p \rightarrow \pi\pi$
³ From solution A of amplitude analysis of data on $\bar{p}p \rightarrow \pi\pi$ See however KLOET 96 who fit $\pi^+\pi^-$ only and find waves only up to $J = 3$ to be important but not significantly resonant.			
⁴ From solution B of amplitude analysis of data on $\bar{p}p \rightarrow \pi\pi$ See however KLOET 96 who fit $\pi^+\pi^-$ only and find waves only up to $J = 3$ to be important but not significantly resonant.			

$f_0(2060)$ DECAY MODES

Mode	Fraction (Γ_i/Γ)
$\Gamma_1 \pi^+\pi^-$	seen

$f_0(2060)$ REFERENCES

KLOET	96	PR D53 6120	W.M. Kloet, F. Myhrer	(RUTG, NORD)
OAKDEN	94	NPA 574 731	M.N. Oakden, M.R. Pennington	(DURH)

OTHER RELATED PAPERS

SEMENOV	99	SFU 42 847	S.V. Semenov	
Translated from UFN 42 937.				

$f_4(2050)$ DECAY MODES

Mode	Fraction (Γ_i/Γ)
$\Gamma_1 \omega\omega$	(26 ± 6) %
$\Gamma_2 \pi\pi$	(17.0 ± 1.5) %
$\Gamma_3 K\bar{K}$	(6.8 ^{+3.4} _{-1.8}) × 10 ⁻³
$\Gamma_4 \eta\eta$	(2.1 ± 0.8) × 10 ⁻³
$\Gamma_5 4\pi^0$	< 1.2 %
$\Gamma_6 \gamma\gamma$	seen
$\Gamma_7 a_2(1320)\pi$	seen

$f_4(2050)$ $\Gamma(i)\Gamma(\gamma\gamma)/\Gamma(\text{total})$

$\Gamma(K\bar{K}) \times \Gamma(\gamma\gamma)/\Gamma(\text{total})$	CL%	CL%	DOCUMENT ID	TECN	COMMENT	$\Gamma_3\Gamma_6/\Gamma$
• • • We do not use the following data for averages, fits, limits, etc. • • •						
<0.29	95		ALTHOFF	85B TASS	$\gamma\gamma \rightarrow K\bar{K}\pi$	
$\Gamma(\pi\pi) \times \Gamma(\gamma\gamma)/\Gamma(\text{total})$	CL%	EVTS	DOCUMENT ID	TECN	COMMENT	$\Gamma_2\Gamma_6/\Gamma$
<1.1	95	13 ± 4	OEST	90 JADE	$e^+e^- \rightarrow e^+e^-\pi^0\pi^0$	

$f_4(2050)$ BRANCHING RATIOS

$\Gamma(\omega\omega)/\Gamma(\pi\pi)$	DOCUMENT ID	TECN	COMMENT	Γ_1/Γ_2
1.5 ± 0.3	ALDE	90 GAM2	38 $\pi^-p \rightarrow \omega\omega n$	
$\Gamma(\pi\pi)/\Gamma(\text{total})$	DOCUMENT ID	TECN	COMMENT	Γ_2/Γ
0.170 ± 0.015 OUR AVERAGE				
0.18 ± 0.03	17 BINON	83C GAM2	38 $\pi^-p \rightarrow n4\gamma$	
0.16 ± 0.03	17 CASON	82 STRC	8 $\pi^+p \rightarrow \Delta^{++}\pi^0\pi^0$	
0.17 ± 0.02	17 CORDEN	79 OMEG	12-15 $\pi^-p \rightarrow n2\pi$	
¹⁷ Assuming one pion exchange.				
$\Gamma(K\bar{K})/\Gamma(\pi\pi)$	DOCUMENT ID	TECN	COMMENT	Γ_3/Γ_2
0.04 ^{+0.02} _{-0.01}	ETKIN	82B MPS	23 $\pi^-p \rightarrow n2K_S^0$	
$\Gamma(\eta\eta)/\Gamma(\text{total})$	DOCUMENT ID	TECN	COMMENT	Γ_4/Γ
2.1 ± 0.8	ALDE	86D GAM4	100 $\pi^-p \rightarrow n4\gamma$	
$\Gamma(4\pi^0)/\Gamma(\text{total})$	DOCUMENT ID	TECN	COMMENT	Γ_5/Γ
<0.012	ALDE	87 GAM4	100 $\pi^-p \rightarrow 4\pi^0 n$	
$\Gamma(a_2(1320)\pi)/\Gamma(\text{total})$	DOCUMENT ID	TECN	COMMENT	Γ_7/Γ
seen	AMELIN	00 VES	37 $\pi^-p \rightarrow \eta\pi^+\pi^- n$	

Meson Particle Listings

 $\pi_2(2100)$, $f_2(2150)$ $\pi_2(2100)$

$I^G(J^{PC}) = 1^-(2^-)$

OMITTED FROM SUMMARY TABLE
Needs confirmation. $\pi_2(2100)$ MASS

VALUE (MeV)	DOCUMENT ID	TECN	COMMENT
2090 ± 29 OUR AVERAGE			
2090 ± 30	¹ AMELIN	95B VES	36 $\pi^- A \rightarrow \pi^+ \pi^- \pi^- A$
2100 ± 150	² DAUM	81B CNTR	63,94 $\pi^- p \rightarrow 3\pi X$
¹ From a fit to $J^{PC} = 2^-+$ $f_2(1270)\pi$, $(\pi\pi)_S\pi$ waves.			
² From a two-resonance fit to four 2^-0^+ waves.			

 $\pi_2(2100)$ WIDTH

VALUE (MeV)	DOCUMENT ID	TECN	COMMENT
625 ± 50 OUR AVERAGE			Error includes scale factor of 1.2.
520 ± 100	³ AMELIN	95B VES	36 $\pi^- A \rightarrow \pi^+ \pi^- \pi^- A$
651 ± 50	⁴ DAUM	81B CNTR	63,94 $\pi^- p \rightarrow 3\pi X$
³ From a fit to $J^{PC} = 2^-+$ $f_2(1270)\pi$, $(\pi\pi)_S\pi$ waves.			
⁴ From a two-resonance fit to four 2^-0^+ waves.			

 $\pi_2(2100)$ DECAY MODES

Mode	Fraction (Γ_i/Γ)
Γ_1 3π	seen
Γ_2 $\rho\pi$	seen
Γ_3 $f_2(1270)\pi$	seen
Γ_4 $(\pi\pi)_S\pi$	seen

 $\pi_2(2100)$ BRANCHING RATIOS

$\Gamma(\rho\pi)/\Gamma(3\pi)$	Γ_2/Γ_1		
VALUE	DOCUMENT ID	TECN	COMMENT
0.19 ± 0.05	⁵ DAUM	81B CNTR	63,94 $\pi^- p$
$\Gamma(f_2(1270)\pi)/\Gamma(3\pi)$	Γ_3/Γ_1		
VALUE	DOCUMENT ID	TECN	COMMENT
0.36 ± 0.09	⁵ DAUM	81B CNTR	63,94 $\pi^- p$
$\Gamma((\pi\pi)_S\pi)/\Gamma(3\pi)$	Γ_4/Γ_1		
VALUE	DOCUMENT ID	TECN	COMMENT
0.45 ± 0.07	⁵ DAUM	81B CNTR	63,94 $\pi^- p$
D-wave/S-wave RATIO FOR $\pi_2(2100) \rightarrow f_2(1270)\pi$			
VALUE	DOCUMENT ID	TECN	COMMENT
0.39 ± 0.23	⁵ DAUM	81B CNTR	63,94 $\pi^- p$
⁵ From a two-resonance fit to four 2^-0^+ waves.			

 $\pi_2(2100)$ REFERENCES

AMELIN	95B PL B356 595	D.V. Amelin et al.	(SERP, TBIL)
DAUM	81B NP B182 269	C. Daum et al.	(AMST, CERN, CRAC, MPIM+)

 $f_2(2150)$

$I^G(J^{PC}) = 0^+(2^+)$

OMITTED FROM SUMMARY TABLE
This entry was previously called T_0 . $f_2(2150)$ MASS $f_2(2150)$ MASS, COMBINED MODES (MeV)

VALUE (MeV)	DOCUMENT ID
2161 ± 16 OUR AVERAGE	

Includes data from the 2 datablocks that follow this one.

 $\eta\eta$ MODE

VALUE (MeV)	DOCUMENT ID	TECN	COMMENT
The data in this block is included in the average printed for a previous datablock.			

2164 ± 19 OUR AVERAGE Error includes scale factor of 1.1.

2175 ± 20	PROKOSHKIN 95D GAM4	300 $\pi^- N \rightarrow \pi^- N 2\eta$, 450 $\rho\rho \rightarrow \rho\rho 2\eta$
2130 ± 35	SINGOVSKI 94 GAM4	450 $\rho\rho \rightarrow \rho\rho 2\eta$
• • • We do not use the following data for averages, fits, limits, etc. • • •		
2140 ± 30	¹ ABELE	99B CBAR
seen	² ANISOVICH	99B SPEC 1.35-1.94 $\bar{p}p \rightarrow \eta\eta\pi^0$
2105 ± 10	³ ANISOVICH	99K RVUE 0.6-1.94 $\bar{p}p \rightarrow \eta\eta, \eta\eta'$
2104 ± 20	⁴ ARMSTRONG	93C E760 $\bar{p}p \rightarrow \pi^0\eta\eta \rightarrow 6\gamma$

¹ Spin not determined.² $J^{PC} = 0^+ +$ ³ Using preliminary CBAR data. PWA gives $J^{PC} = 0^+ +$.⁴ No J^{PC} determination. $\eta\pi\pi$ MODE

VALUE (MeV)	DOCUMENT ID	TECN	CHG	COMMENT
The data in this block is included in the average printed for a previous datablock.				

2135 ± 20 ± 45ADOMEIT 96 CBAR 0 1.94 $\bar{p}p \rightarrow \eta\pi 3\pi^0$ $\bar{p}p \rightarrow \pi\pi$

VALUE (MeV)	DOCUMENT ID	TECN	COMMENT
• • • We do not use the following data for averages, fits, limits, etc. • • •			
~ 2226	HASAN 94 RVUE	$\bar{p}p \rightarrow \pi\pi$	
~ 2090	⁵ OAKDEN 94 RVUE	0.36-1.55 $\bar{p}p \rightarrow \pi\pi$	
~ 2120	⁶ OAKDEN 94 RVUE	0.36-1.55 $\bar{p}p \rightarrow \pi\pi$	
~ 2170	⁷ MARTIN 80B RVUE		
~ 2150	⁷ MARTIN 80C RVUE		
~ 2150	⁸ DULUDE 78B OSPK	1-2 $\bar{p}p \rightarrow \pi^0\pi^0$	
⁵ OAKDEN 94 makes an amplitude analysis of LEAR data on $\bar{p}p \rightarrow \pi\pi$ using a method based on Barrelet zeros. This is solution A. The amplitude analysis of HASAN 94 includes earlier data as well, and assume that the data can be parametrized in terms of towers of nearly degenerate resonances on the leading Regge trajectory. See also KLOET 96 and MARTIN 97 who make related analyses.			
⁶ From solution B of amplitude analysis of data on $\bar{p}p \rightarrow \pi\pi$.			
⁷ $I(J^P) = 0(2^+)$ from simultaneous analysis of $p\bar{p} \rightarrow \pi^- \pi^+ \pi^0$ and $\pi^0\pi^0$.			
⁸ $I^G(J^P) = 0^+(2^+)$ from partial-wave amplitude analysis.			

S-CHANNEL $\bar{p}p$, $\bar{N}N$ or $\bar{K}K$

VALUE (MeV)	DOCUMENT ID	TECN	CHG	COMMENT
• • • We do not use the following data for averages, fits, limits, etc. • • •				
2139 $^{+8}_{-9}$	⁹ EVANGELISTA 97 SPEC			0.6-2.4 $\bar{p}p \rightarrow K_S^0 K_S^0$
~ 2190	¹⁰ CUTTS 78B CNTR			0.97-3 $\bar{p}p \rightarrow \bar{N}N$
2155 ± 15	^{10,11} COUPLAND 77 CNTR	0		0.7-2.4 $\bar{p}p \rightarrow \bar{p}p$
2193 ± 2	^{10,12} ALSPECTOR 73 CNTR			$\bar{p}p$ S channel
⁹ Isospin 0 and 1 not separated.				
¹⁰ Isospins 0 and 1 not separated.				
¹¹ From a fit to the total elastic cross section.				
¹² Referred to as T or T' region by ALSPECTOR 73.				

 $K\bar{K}$ MODE

VALUE (MeV)	DOCUMENT ID	TECN	COMMENT
2130 ± 35	BARBERIS 99 OMEG	450 $\rho\rho \rightarrow \rho_S \rho_f K^+ K^-$	

 $f_2(2150)$ WIDTH $f_2(2150)$ WIDTH, COMBINED MODES (MeV)

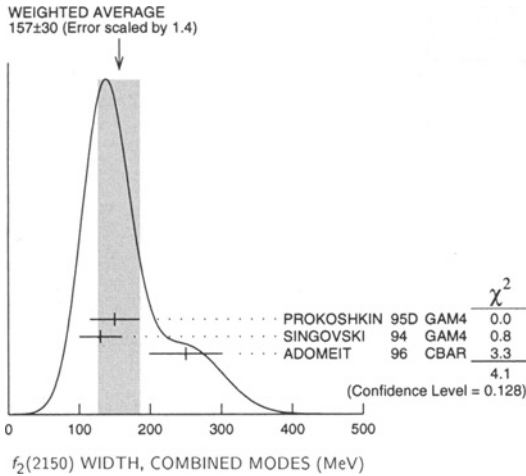
VALUE (MeV)	DOCUMENT ID
157 ± 30 OUR AVERAGE	

Includes data from the 2 datablocks that follow this one. Error includes scale factor of 1.4. See the ideogram below.

See key on page 239

Meson Particle Listings

$f_2(2150)$, $\rho(2150)$



$f_2(2150)$ BRANCHING RATIOS

$\Gamma(K\bar{K})/\Gamma(\eta\eta)$	CL%	DOCUMENT ID	TECN	COMMENT	Γ_3/Γ_2
<0.1	95	23 PROKOSHKIN 95D GAM4		$300 \pi^- N \rightarrow \pi^- N 2\eta$ $450 \rho\rho \rightarrow \rho\rho 2\eta$	
23 Using data from ARMSTRONG 89D.					
$\Gamma(\pi\pi)/\Gamma(\eta\eta)$	CL%	DOCUMENT ID	TECN	COMMENT	Γ_1/Γ_2
<0.33	95	24 PROKOSHKIN 95D GAM4		$300 \pi^- N \rightarrow \pi^- N 2\eta$ $450 \rho\rho \rightarrow \rho\rho 2\eta$	
24 Derived from a $\pi^0\pi^0/\eta\eta$ limit.					
$\Gamma(f_2(1270)\eta)/\Gamma(a_2(1320)\pi)$		DOCUMENT ID	TECN	COMMENT	Γ_4/Γ_5
0.79 ± 0.11		25 ADOMEIT 96 CBAR		$1.94 \bar{p}p \rightarrow \eta 3\pi^0$	
25 Using $B(a_2(1320) \rightarrow \eta\pi) = 0.145$					

$f_2(2150)$ REFERENCES

ABELE 99B EPJ C8 67	A. Abele et al.	(Crystal Barrel Collab.)
ANISOVICH 99B PL B449 154	A.V. Anisovich et al.	
ANISOVICH 99K PL B468 309	A.V. Anisovich et al.	
BARBERIS 99 PL B453 305	D. Barberis et al.	(Omega expt.)
EVANGELISTA 97 PR D56 3803	C. Evangelista et al.	(LEAR Collab.)
MARTIN 97 PR C56 1114	B.R. Martin, G.C. Oades	(LOU, AARH)
ADOMEIT 96 ZPHY C71 227	J. Adomeit et al.	(Crystal Barrel Collab.)
KLOET 96 PR D53 5129	W.M. Kloet, F. Myhrer	(RUTG, NORD)
PROKOSHKIN 95D SPD 40 495	Y.D. Prokoshkin	(SERP) IGJPC
Translated from DANS 344 469.		
HASAN 94 PL B334 215	A. Hasan, D.V. Bugg	(LOQM)
OAKDEN 94 NPA 574 731	M.N. Oakden, M.R. Pennington	(DURH)
SINGOVSKI 94 NC 107 1911	A.V. Singovsky	(SERP)
ARMSTRONG 93C PL B307 394	T.A. Armstrong et al.	(FNAL, FERR, GENO+)
ARMSTRONG 89D PL B227 136	T.A. Armstrong, M. Benayoun	(ATHU, BARI, BIRM+)
MARTIN 80B NP B176 355	B.R. Martin, D. Morgan	(LOU, RHEL) JP
MARTIN 80C NP B169 216	A.D. Martin, M.R. Pennington	(DURH) JP
CUTTS 78B PR D17 16	D. Cutts et al.	(STON, WISC)
DULUDE 78B PL 79B 335	R.S. Dulude et al.	(BROW, MIT, BARI) JP
COUPLAND 77 PL 71B 460	M. Coupland et al.	(LOQM, RHEL)
ALSPECTOR 73 PRL 30 511	J. Alspector et al.	(RUTG, UPNJ)

OTHER RELATED PAPERS

EISENHAND... 75 NP B96 109	E. Eisenhandler et al.	(LOQM, LVP, DARE+)
FIELDS 71 PRL 27 1749	T. Fields et al.	(ANL, OXF)
YOH 71 PRL 26 922	J.K. Yoh et al.	(CIT, BNL, ROCH)

$\rho(2150)$

$$I^G(J^{PC}) = 1^+(1^-)$$

OMITTED FROM SUMMARY TABLE
This entry was previously called $T_1(2190)$.

$\rho(2150)$ MASS

$e^+e^- \rightarrow \pi^+\pi^-, K^+K^-, 6\pi$	VALUE (MeV)	DOCUMENT ID	TECN	CHG	COMMENT
2149±17 OUR AVERAGE		Includes data from the datablock that follows this one.			
2153±37		BIAGINI 91 RVUE			$e^+e^- \rightarrow \pi^+\pi^-, K^+K^-$
2110±50		2 CLEGG 90 RVUE 0			$e^+e^- \rightarrow 3(\pi^+\pi^-), 2(\pi^+\pi^-\pi^0)$

$\bar{p}p \rightarrow \pi\pi$

VALUE (MeV)	DOCUMENT ID	TECN	COMMENT
<0.1	We do not use the following data for averages, fits, limits, etc.		
~2191	HASAN 94 RVUE		$\bar{p}p \rightarrow \pi\pi$
~1988	HASAN 94 RVUE		$\bar{p}p \rightarrow \pi\pi$
~2070	1 OAKDEN 94 RVUE		$0.36-1.55 \bar{p}p \rightarrow \pi\pi$
~2170	3 MARTIN 80B RVUE		
~2100	3 MARTIN 80C RVUE		

1 See however KLOET 96 who fit $\pi^+\pi^-$ only and find waves only up to $J = 3$ to be important but not significantly resonant.

S-CHANNEL $\bar{N}N$

VALUE (MeV)	DOCUMENT ID	TECN	CHG	COMMENT
<0.1	We do not use the following data for averages, fits, limits, etc.			
~2190	4 CUTTS 78B CNTR			$0.97-3 \bar{p}p \rightarrow \bar{N}N$
2155±15	4,5 COUPLAND 77 CNTR 0			$0.7-2.4 \bar{p}p \rightarrow \bar{p}p$
2193±2	4,6 ALSPECTOR 73 CNTR			$\bar{p}p$ S channel
2190±10	7 ABRAMS 70 CNTR			S channel $\bar{p}N$

$\eta\eta$ MODE

VALUE (MeV)	DOCUMENT ID	TECN	COMMENT
157 ± 30	The data in this block is included in the average printed for a previous datablock.		

138±23 OUR AVERAGE

130±30	PROKOSHKIN 95D GAM4		$300 \pi^- N \rightarrow \pi^- N 2\eta$ $450 \rho\rho \rightarrow \rho\rho 2\eta$
130±30	SINGOVSKI 94 GAM4		$450 \rho\rho \rightarrow \rho\rho 2\eta$

• • • We do not use the following data for averages, fits, limits, etc. • • •

310±50	13 ABELE 99B CBAR		
200±25	14 ANISOVICH 99B SPEC		$1.35-1.94 \bar{p}p \rightarrow \eta\eta\pi^0$
203±10	15 ANISOVICH 99K RVUE		$0.6-1.94 \bar{p}p \rightarrow \eta\eta, \eta\eta'$
203±10	16 ARMSTRONG 93C E760		$\bar{p}p \rightarrow \pi^0\eta\eta \rightarrow 6\gamma$

13 Spin not determined.

14 Using preliminary Crystal Barrel data, $J^{PC} = 0^{++}$

15 pWA gives $J^{PC} = 0^{++}$.

16 No J^{PC} determination.

$\eta\pi\pi$ MODE

VALUE (MeV)	DOCUMENT ID	TECN	CHG	COMMENT
$250 \pm 25 \pm 45$	ADOMEIT 96 CBAR 0			$1.94 \bar{p}p \rightarrow \eta 3\pi^0$

The data in this block is included in the average printed for a previous datablock.

$\bar{p}p \rightarrow \pi\pi$

VALUE (MeV)	DOCUMENT ID	TECN	COMMENT
250 OUR ESTIMATE	We do not use the following data for averages, fits, limits, etc.		
~226	HASAN 94 RVUE		$\bar{p}p \rightarrow \pi\pi$
~70	17 OAKDEN 94 RVUE		$0.36-1.55 \bar{p}p \rightarrow \pi\pi$
~250	18 MARTIN 80B RVUE		
~250	18 MARTIN 80C RVUE		
~250	19 DULUDE 78B OSPK		$1-2 \bar{p}p \rightarrow \pi^0\pi^0$

17 See however KLOET 96 who fit $\pi^+\pi^-$ only and find waves only up to $J = 3$ to be important but not significantly resonant.

18 $I(J^P) = 0(2^+)$ from simultaneous analysis of $\rho\bar{p} \rightarrow \pi^-\pi^+$ and $\pi^0\pi^0$.

19 $I^G(J^P) = 0^+(2^+)$ from partial-wave amplitude analysis.

S-CHANNEL $\bar{p}p, \bar{N}N$ or $\bar{K}K$

VALUE (MeV)	DOCUMENT ID	TECN	CHG	COMMENT
56^{+31}_{-16}	20 EVANGELISTA 97 SPEC			$0.6-2.4 \bar{p}p \rightarrow K_S^0 K_S^0$
135±75	21,22 COUPLAND 77 CNTR 0			$0.7-2.4 \bar{p}p \rightarrow \bar{p}p$
98±8	22 ALSPECTOR 73 CNTR			$\bar{p}p$ S channel

20 Isospin 0 and 2 not separated.

21 From a fit to the total elastic cross section.

22 Isospins 0 and 1 not separated.

$K\bar{K}$ MODE

VALUE (MeV)	DOCUMENT ID	TECN	COMMENT
270 ± 50	BARBERIS 99 OMEG		$450 \rho\rho \rightarrow P_S P_f K^+ K^-$

$f_2(2150)$ DECAY MODES

Mode	Branching Ratio
$\Gamma_1 \pi\pi$	
$\Gamma_2 \eta\eta$	
$\Gamma_3 K\bar{K}$	
$\Gamma_4 f_2(1270)\eta$	
$\Gamma_5 a_2(1320)\pi$	

Meson Particle Listings

 $\rho(2150)$, $f_0(2200)$, $f_J(2220)$ $\pi^- p \rightarrow \omega \pi^0 n$

VALUE (MeV)	DOCUMENT ID	TECN	COMMENT
The data in this block is included in the average printed for a previous datablock.			

2155 ± 21 OUR AVERAGE

2140 ± 30	ALDE	95	GAM2 38 $\pi^- p \rightarrow \omega \pi^0 n$
2170 ± 30	ALDE	92c	GAM4 100 $\pi^- p \rightarrow \omega \pi^0 n$

- ²Includes ATKINSON 85.
³ $I(J^P) = 1(1^-)$ from simultaneous analysis of $p\bar{p} \rightarrow \pi^- \pi^+$ and $\pi^0 \pi^0$.
⁴Isospins 0 and 1 not separated.
⁵From a fit to the total elastic cross section.
⁶Referred to as T or T region by ALSPECTOR 73.
⁷Seen as bump in $I = 1$ state. See also COOPER 68. PEASLEE 75 confirm $\bar{p}p$ results of ABRAMS 70, no narrow structure.

 $\rho(2150)$ WIDTH $e^+ e^- \rightarrow \pi^+ \pi^-, K^+ K^-, 6\pi$

VALUE (MeV)	DOCUMENT ID	TECN	CHG	COMMENT
363 ± 50 OUR AVERAGE Includes data from the datablock that follows this one.				

389 ± 79	BIAGINI	91	RVUE	$e^+ e^- \rightarrow \pi^+ \pi^-, K^+ K^-, 6\pi$
410 ± 100	⁹ CLEGG	90	RVUE 0	$e^+ e^- \rightarrow 3(\pi^+ \pi^-), 2(\pi^+ \pi^- \pi^0)$

 $\bar{p}p \rightarrow \pi\pi$

VALUE (MeV)	DOCUMENT ID	TECN	COMMENT
• • • We do not use the following data for averages, fits, limits, etc. • • •			

~ 296	HASAN	94	RVUE	$\bar{p}p \rightarrow \pi\pi$
~ 244	HASAN	94	RVUE	$\bar{p}p \rightarrow \pi\pi$
~ 40	⁸ OAKDEN	94	RVUE	0.36-1.55 $\bar{p}p \rightarrow \pi\pi$
~ 250	¹⁰ MARTIN	80b	RVUE	
~ 200	¹⁰ MARTIN	80c	RVUE	

- ⁸See however KLOET 96 who fit $\pi^+ \pi^-$ only and find waves only up to $J = 3$ to be important but not significantly resonant.

S-CHANNEL $\bar{N}N$

VALUE (MeV)	DOCUMENT ID	TECN	CHG	COMMENT
• • • We do not use the following data for averages, fits, limits, etc. • • •				

135 ± 75	^{11,12} COUPLAND	77	CNTR 0	0.7-2.4 $\bar{p}p \rightarrow \bar{p}p$
98 ± 8	¹² ALSPECTOR	73	CNTR	$\bar{p}p$ S channel
~ 85	¹³ ABRAMS	70	CNTR	S channel $\bar{p}N$

 $\pi^- p \rightarrow \omega \pi^0 n$

VALUE (MeV)	DOCUMENT ID	TECN	COMMENT
The data in this block is included in the average printed for a previous datablock.			

320 ± 70	ALDE	95	GAM2 38 $\pi^- p \rightarrow \omega \pi^0 n$
-----------------	------	----	--

- • • We do not use the following data for averages, fits, limits, etc. • • •
- ~ 300 ALDE 92c GAM4 100 $\pi^- p \rightarrow \omega \pi^0 n$
- ⁹Includes ATKINSON 85.
¹⁰ $I(J^P) = 1(1^-)$ from simultaneous analysis of $p\bar{p} \rightarrow \pi^- \pi^+$ and $\pi^0 \pi^0$.
¹¹From a fit to the total elastic cross section.
¹²Isospins 0 and 1 not separated.
¹³Seen as bump in $I = 1$ state. See also COOPER 68. PEASLEE 75 confirm $\bar{p}p$ results of ABRAMS 70, no narrow structure.

 $\rho(2150)$ REFERENCES

KLOET 96	PR D53 6120	W.M. Kloet, F. Myhrer	(RUTG, NORD)
ALDE 95	ZPHY C66 379	D.M. Alde et al.	(GAMS Collab.) JP
HASAN 94	PL B334 215	A. Hasan, D.V. Bugg	(LOQM)
OAKDEN 94	NPA 574 731	M.N. Oakden, M.R. Pennington	(DURH)
ALDE 92c	ZPHY C54 553	D.M. Alde et al.	(BELG, SERP, KEK, LANL+)
BIAGINI 91	NC 104A 363	M.E. Biagini et al.	(FRAS, PRAG)
CLEGG 90	ZPHY C45 677	A.B. Clegg, A. Donnachie	(LANC, MCHS)
ATKINSON 85	ZPHY C29 333	M. Atkinson et al.	(BONN, CERN, GLAS+)
MARTIN 80b	NP B176 355	B.R. Martin, D. Morgan	(LOUC, RHEL) JP
MARTIN 80c	NP B159 216	A.D. Martin, M.R. Pennington	(DURH) JP
CUTTS 78b	PR D17 15	D. Cutts et al.	(STON, WISC)
COUPLAND 77	PL 71B 460	M. Coupland et al.	(LOQM, RHEL)
PEASLEE 75	PL 57B 189	D.C. Peaslee et al.	(CANB, BARI, BROW+)
ALSPECTOR 73	PRL 30 511	J. Alspector et al.	(RUTG, UPNJ)
ABRAMS 70	PR D1 1917	R.J. Abrams et al.	(BNL)
COOPER 68	PRL 20 1059	W.A. Cooper et al.	(ANL)

OTHER RELATED PAPERS

AMELIN 00	NP B668 83	D. Amelin et al.	(VES Collab.)
EISENHAND... 75	NP B96 109	E. Eisenhandler et al.	(LOQM, LIVP, DARE+)
BRICMAN 69	PL 29B 451	C. Bricman et al.	(CERN, CAEN, SACL)
ABRAMS 67c	PRL 18 1209	R.J. Abrams et al.	(BNL)

 $f_0(2200)$

$$I^G(J^{PC}) = 0^+(0^{++})$$

OMITTED FROM SUMMARY TABLE

Seen at DCI in the $K_S^0 K_S^0$ system. Not seen in T radiative decays (BARU 89). Needs confirmation. **$f_0(2200)$ MASS**

VALUE (MeV)	DOCUMENT ID	TECN	CHG	COMMENT
2197 ± 17	¹ AUGUSTIN	88	DM2 0	$J/\psi \rightarrow \gamma K_S^0 K_S^0$

- • • We do not use the following data for averages, fits, limits, etc. • • •
- ~ 2122 HASAN 94 RVUE $\bar{p}p \rightarrow \pi\pi$
 ~ 2321 HASAN 94 RVUE $\bar{p}p \rightarrow \pi\pi$
- ¹Cannot determine spin to be 0.

 $f_0(2200)$ WIDTH

VALUE (MeV)	DOCUMENT ID	TECN	CHG	COMMENT
201 ± 51	² AUGUSTIN	88	DM2 0	$J/\psi \rightarrow \gamma K_S^0 K_S^0$

- • • We do not use the following data for averages, fits, limits, etc. • • •
- ~ 273 HASAN 94 RVUE $\bar{p}p \rightarrow \pi\pi$
 ~ 223 HASAN 94 RVUE $\bar{p}p \rightarrow \pi\pi$
- ²Cannot determine spin to be 0.

 $f_0(2200)$ REFERENCES

HASAN 94	PL B334 215	A. Hasan, D.V. Bugg	(LOQM)
BARU 89	ZPHY C42 505	S.E. Baru et al.	(NOVO)
AUGUSTIN 88	PRL 60 2238	J.E. Augustin et al.	(DM2 Collab.)

OTHER RELATED PAPERS

EISENHAND... 75	NP B96 109	E. Eisenhandler et al.	(LOQM, LIVP, DARE+)
-----------------	------------	------------------------	---------------------

 $f_J(2220)$

$$I^G(J^{PC}) = 0^+(2^{++} \text{ or } 4^{++})$$

OMITTED FROM SUMMARY TABLE

THE $f_J(2220)$

Updated April 2000 by M. Doser (CERN).

This state has been observed in $J/\psi(1S)$ radiative decay into $K\bar{K}$ (K^+K^- and $K_S^0 K_S^0$ modes seen (BALTRUSAITIS 86D, BAI 96B)). An upper limit from DM2 for these modes (AUGUSTIN 88) is at the level at which observation is claimed. There are also indications for further decay modes ($\pi^+ \pi^-$ and $\bar{p}p$ (BAI 96B) and $\pi^0 \pi^0$ (BAI 98H)) in the same production process, although again at the level at which previous upper limits had been obtained (BALTRUSAITIS 86D). This was also seen in $\eta\eta$ (ALDE 86B), $K_S^0 K_S^0$ (ASTON 88D), and $K^+ K^-$ (ALDE 88 F), albeit with very low statistics. Its J^{PC} is determined from the angular distributions of these observations.

It is not seen in T radiative decays (BARU 89), B inclusive decays (BEHRENDIS 84), nor in $\gamma\gamma$ (GODANG 97, ALAM 98C), which is not surprising, since if it were a glueball, its two-photon width would be expected to be small. It is also not seen in formation in $\bar{p}p \rightarrow K^+ K^-$ (BARDIN 87, SCULLI 87), in $\bar{p}p \rightarrow K_S K_S$ (BARNES 93, EVANGELISTA 97), $\bar{p}p \rightarrow \phi\phi$ (EVANGELISTA 98), nor in $\bar{p}p \rightarrow \pi^+ \pi^-$ (HASAN 96). The upper limit in $\bar{p}p$ formation can be related to the claimed decay into $\bar{p}p$ to give a lower limit for the process $J/\psi \rightarrow \gamma f_J(2220)$ of $\sim 2.3 \times 10^{-3}$ (GODFREY 99). Such a signal should be visible in the inclusive photon spectrum (BLOOM 85). The limit also leads to the surprising conclusion that the reported two-body final states constitute only a small fraction of all decay modes of the $f_J(2220)$. Observation of further decay modes and confirmation of the $\bar{p}p$ decay would be very desirable.

See key on page 239

Meson Particle Listings

$f_j(2220), \eta(2225)$

$f_j(2220)$ MASS

VALUE (MeV)	CL%	EVTS	DOCUMENT ID	TECN	COMMENT
2231.1 ± 3.5 OUR AVERAGE					
2235 ± 4 ± 6		74	BAI	96B BES	$e^+e^- \rightarrow J/\psi \rightarrow \gamma\pi^+\pi^-$
2230 + ⁶ / ₋₇ ± 16		46	BAI	96B BES	$e^+e^- \rightarrow J/\psi \rightarrow \gamma K^+K^-$
2232 + ⁸ / ₋₇ ± 15		23	BAI	96B BES	$e^+e^- \rightarrow J/\psi \rightarrow \gamma K_S^0 K_S^0$
2235 ± 4 ± 5		32	BAI	96B BES	$e^+e^- \rightarrow J/\psi \rightarrow \gamma\rho\bar{\rho}$
2209 + ¹⁷ / ₋₁₅ ± 10			ASTON	88F LASS	$11 K^-p \rightarrow K^+K^-A$
2230 ± 20			BOLONKIN	88 SPEC	$40 \pi^-p \rightarrow K_S^0 K_S^0 n$
2220 ± 10		41	¹ ALDE	86B GA24	$38-100 \pi\rho \rightarrow n\eta\eta'$
2230 ± 6 ± 14		93	BALTRUSAIT...86D	MRK3	$e^+e^- \rightarrow \gamma K^+K^-$
2232 ± 7 ± 7		23	BALTRUSAIT...86D	MRK3	$e^+e^- \rightarrow \gamma K_S^0 K_S^0$
• • • We do not use the following data for averages, fits, limits, etc. • • •					
2246 ± 36			BAI	98B BES	$J/\psi \rightarrow \gamma\pi^0\pi^0$

¹ALDE 86B uses data from both the GAMS-2000 and GAMS-4000 detectors.

$f_j(2220)$ WIDTH

VALUE (MeV)	CL%	EVTS	DOCUMENT ID	TECN	COMMENT
23 ±⁸/₇ OUR AVERAGE					
19 + ¹³ / ₋₁₁ ± 12		74	BAI	96B BES	$e^+e^- \rightarrow J/\psi \rightarrow \gamma\pi^+\pi^-$
20 + ²⁰ / ₋₁₅ ± 17		46	BAI	96B BES	$e^+e^- \rightarrow J/\psi \rightarrow \gamma K^+K^-$
20 + ²⁵ / ₋₁₆ ± 14		23	BAI	96B BES	$e^+e^- \rightarrow J/\psi \rightarrow \gamma K_S^0 K_S^0$
15 + ¹² / ₋₉ ± 9		32	BAI	96B BES	$e^+e^- \rightarrow J/\psi \rightarrow \gamma\rho\bar{\rho}$
60 + ¹⁰⁷ / ₋₅₇			ASTON	88F LASS	$11 K^-p \rightarrow K^+K^-A$
80 ± 30			BOLONKIN	88 SPEC	$40 \pi^-p \rightarrow K_S^0 K_S^0 n$
26 + ²⁰ / ₋₁₆ ± 17		93	BALTRUSAIT...86D	MRK3	$e^+e^- \rightarrow \gamma K^+K^-$
18 + ²³ / ₋₁₅ ± 10		23	BALTRUSAIT...86D	MRK3	$e^+e^- \rightarrow \gamma K_S^0 K_S^0$
• • • We do not use the following data for averages, fits, limits, etc. • • •					
<80	90		ALDE	87C GAM2	$38 \pi^-p \rightarrow \eta'\eta n$

$f_j(2220)$ DECAY MODES

Mode	Fraction (Γ_i/Γ)
$\Gamma_1 \pi\pi$	seen
$\Gamma_2 \pi^+\pi^-$	seen
$\Gamma_3 K\bar{K}$	seen
$\Gamma_4 \rho\bar{\rho}$	seen
$\Gamma_5 \gamma\gamma$	not seen
$\Gamma_6 \eta\eta'(958)$	seen
$\Gamma_7 \phi\phi$	not seen

$f_j(2220) \Gamma(1)\Gamma(\gamma\gamma)/\Gamma(\text{total})$

VALUE (eV)	CL%	DOCUMENT ID	TECN	COMMENT	$\Gamma_3\Gamma_5/\Gamma$
< 5.6	95	² GODANG 97	CLE2	$\gamma\gamma \rightarrow K_S^0 K_S^0$	

• • • We do not use the following data for averages, fits, limits, etc. • • •

< 86	95	² ALBRECHT 90G	ARG	$\gamma\gamma \rightarrow K^+K^-$
<1000	95	³ ALTHOFF 85B	TASS	$\gamma\gamma, K\bar{K}\pi$

² Assuming $J^P = 2^+$.
³ True for $J^P = 0^+$ and $J^P = 2^+$.

VALUE (eV)	CL%	DOCUMENT ID	TECN	COMMENT	$\Gamma_1\Gamma_5/\Gamma$
<3.8	95	ALAM 98C	CLE2	$\gamma\gamma \rightarrow \pi^+\pi^-$	

$f_j(2220) \Gamma(1)\Gamma(\rho\rho)/\Gamma(\text{total})$

VALUE (keV)	CL%	DOCUMENT ID	TECN	COMMENT	$\Gamma_4\Gamma_2/\Gamma$
<3.9	99	⁴ HASAN 96	SPEC	$\bar{p}p \rightarrow \pi^-\pi^+$	

⁴ Assuming $\Gamma = 15$ MeV and $J^P = 2^+$

VALUE (keV)	CL%	DOCUMENT ID	TECN	COMMENT	$\Gamma_4\Gamma_7/\Gamma$
<0.9	95	⁵ EVANGELISTA 98	SPEC	$1.1-2.0 \rho\bar{\rho} \rightarrow \phi\phi$	

⁵ Assuming $J^P = 2^+$, $M=2235$ MeV and $\Gamma_{\text{total}} = 15$ MeV.

$f_j(2220)$ BRANCHING RATIOS

VALUE (units 10^{-4})	CL%	DOCUMENT ID	TECN	COMMENT	Γ_4/Γ
<3.0	95	⁶ EVANGELISTA 97	SPEC	$1.96-2.40\bar{p}p \rightarrow K_S^0 K_S^0$	
<1.1	99.7	⁷ BARNES 93	SPEC	$1.3-1.57\bar{p}p \rightarrow K_S^0 K_S^0$	
<2.6	99.7	⁷ BARDIN 87	CNTR	$1.3-1.5\bar{p}p \rightarrow K^+K^-$	
<3.6	99.7	⁷ SCULLI 87	CNTR	$1.29-1.55\bar{p}p \rightarrow K^+K^-$	

⁶ Assuming $\Gamma \sim 20$ MeV, $J^P = 2^+$ and $B(f_j(2220) \rightarrow K\bar{K}) = 100\%$.
⁷ Assuming $\Gamma = 30-35$ MeV, $J^P = 2^+$ and $B(f_j(2220) \rightarrow K\bar{K}) = 100\%$.

VALUE	DOCUMENT ID	TECN	COMMENT	Γ_1/Γ_3
1.0 ± 0.5	BAI	96B BES	$e^+e^- \rightarrow J/\psi \rightarrow \gamma 2\pi, K\bar{K}$	

VALUE	DOCUMENT ID	TECN	COMMENT	Γ_4/Γ_3
0.17 ± 0.09	BAI	96B BES	$e^+e^- \rightarrow J/\psi \rightarrow \gamma\rho\bar{\rho}, K\bar{K}$	

$f_j(2220)$ REFERENCES

ALAM 98C	PRL 81 3328	M.S. Alam et al.	(CLEO Collab.)
BAI 98B	PRL 81 1179	J.Z. Bai et al.	(BES Collab.)
EVANGELISTA 98	PR D57 5370	C. Evangelista et al.	
EVANGELISTA 97	PR D56 3803	C. Evangelista et al.	(LEAR Collab.)
GODANG 97	PRL 79 3829	R. Godang et al.	(CLEO Collab.)
BAI 96B	PRL 76 3502	J.Z. Bai et al.	(BES Collab.)
HASAN 96	PL B388 376	A. Hasan, D.V. Bugg	(BRUN, LOQM)
BARNES 93	PL B309 469	P.D. Barnes, P. Birien, W.H. Breunlich	
ALBRECHT 90G	ZPHY C48 183	H. Albrecht et al.	(ARGUS Collab.)
ASTON 88F	PL B215 199	D. Aston et al.	(SLAC, NAGO, CINC, INUS) JP
BOLONKIN 88	NP B309 426	B.V. Bolonkin et al.	(ITER, SERP)
ALDE 87C	SJNP 45 255	D. Alde et al.	
BARDIN 87	PL B195 292	G. Bardin et al.	(SACL, FERR, CERN, PADO+)
SCULLI 87	PRL 58 1715	J. Sculli et al.	(NYU, BNL)
ALDE 86B	PL B177 120	D.M. Alde et al.	(SERP, BELG, LANL, LAPP)
BALTRUSAIT...86D	PRL 56 107	R.M. Baltrusaitis	(CIT, UCSC, ILL, SLAC+)
ALTHOFF 85B	ZPHY C29 189	M. Althoff et al.	(TASSO Collab.)

OTHER RELATED PAPERS

ANISOVICH 99D	PL B452 180	A.V. Anisovich et al.	
Also 99F	NP A651 253	A.V. Anisovich et al.	
ANISOVICH 99F	NP A651 253	A.V. Anisovich et al.	
GODFREY 99	RMP 71 1411	S. Godfrey, J. Napolitano	
PROKOSHNIK 99	PAN 62 356	Yu.D. Prokoshkin et al.	
Translated from YAF 62 395.			
HUANG 96	PL B380 189	T. Huang et al.	(BHEP, BEJ)
BARDIN 87	PL B195 292	G. Bardin et al.	(SACL, FERR, CERN, PADO+)
YAOUANC 85	ZPHY C28 309	A. Le Yaouanc et al.	(ORSAY, TOKY)
GODFREY 84	PL 141B 439	S. Godfrey, R. Kokoski, N. Isgur	(TNTO)
SHATZ 84	PL 138B 209	M.P. Shatz	(CIT)
WILLEY 84	PRL 52 585	R.S. Willey	(PITT)
EISENHAND... 75	NP B96 109	E. Eisenhandler et al.	(LOQM, LIVP, DARE+)

$\eta(2225)$

$I^G(J^{PC}) = 0^+(0^-+)$

OMITTED FROM SUMMARY TABLE
Seen in $J/\psi \rightarrow \gamma\phi\phi$. Needs confirmation.

$\eta(2225)$ MASS

VALUE (MeV)	DOCUMENT ID	TECN	COMMENT
2230 ± 25 ± 15	BAI	90B MRK3	$J/\psi \rightarrow \gamma K^+ K^- K^+ K^-$
2214 ± 20 ± 13	BAI	90B MRK3	$J/\psi \rightarrow \gamma K^+ K^- K_S^0 K_S^0$
~ 2220	BISELLO	86B DM2	$J/\psi \rightarrow \gamma K^+ K^- K^+ K^-$

• • • We do not use the following data for averages, fits, limits, etc. • • •

$\eta(2225)$ WIDTH

VALUE (MeV)	DOCUMENT ID	TECN	COMMENT
150+--300-60+60	BAI	90B MRK3	$J/\psi \rightarrow \gamma K^+ K^- K^+ K^-$

• • • We do not use the following data for averages, fits, limits, etc. • • •

~ 80	BISELLO	86B DM2	$J/\psi \rightarrow \gamma K^+ K^- K^+ K^-$
------	---------	---------	---

$\eta(2225)$ REFERENCES

BAI 90B	PRL 65 1309	Z. Bai et al.	(Mark III Collab.)
BISELLO 86B	PL B179 294	D. Bisello et al.	(DM2 Collab.)

Meson Particle Listings

 $\rho_3(2250), f_2(2300)$ $\rho_3(2250)$

$$1G(J^{PC}) = 1^+(3^-)$$

OMITTED FROM SUMMARY TABLE

Contains results mostly from formation experiments. For further production experiments see the $\bar{N}N(1100-3600)$ entry. See also $\rho(2150), f_2(2150), f_4(2300), \rho_5(2350)$.

 $\rho_3(2250)$ MASS $\bar{p}p \rightarrow \pi\pi \text{ or } K\bar{K}$

VALUE (MeV)	DOCUMENT ID	TECN	CHG	COMMENT
• • • We do not use the following data for averages, fits, limits, etc. • • •				
~ 2232	HASAN 94 RVUE			$\bar{p}p \rightarrow \pi\pi$
~ 2007	HASAN 94 RVUE			$\bar{p}p \rightarrow \pi\pi$
~ 2090	¹ OAKDEN 94 RVUE			$0.36-1.55 \bar{p}p \rightarrow \pi\pi$
~ 2250	² MARTIN 80B RVUE			
~ 2300	² MARTIN 80C RVUE			
~ 2140	³ CARTER 78B CNTR 0			$0.7-2.4 \bar{p}p \rightarrow \pi\pi$
~ 2150	⁴ CARTER 77 CNTR 0			$0.7-2.4 \bar{p}p \rightarrow \pi\pi$

¹ See however KLOET 96 who fit $\pi^+\pi^-$ only and find waves only up to $J = 3$ to be important but not significantly resonant.

² $J(J^P) = 1(3^-)$ from simultaneous analysis of $\bar{p}p \rightarrow \pi^-\pi^+$ and $\pi^0\pi^0$.

³ $l = 0, 1, J^P = 3^-$ from Barrelet-zero analysis.

⁴ $J(J^P) = 1(3^-)$ from amplitude analysis.

S-CHANNEL $\bar{N}N$

VALUE (MeV)	DOCUMENT ID	TECN	CHG	COMMENT
• • • We do not use the following data for averages, fits, limits, etc. • • •				
~ 2190	⁵ CUTTS 78B CNTR			$0.97-3 \bar{p}p \rightarrow \bar{N}N$
2155 ± 15	^{5,6} COUPLAND 77 CNTR 0			$0.7-2.4 \bar{p}p \rightarrow \bar{p}p$
2193 ± 2	^{5,7} ALSPECTOR 73 CNTR			$\bar{p}p$ S channel
2190 ± 10	⁸ ABRAMS 70 CNTR			S channel $\bar{p}N$

⁵ Isospins 0 and 1 not separated.

⁶ From a fit to the total elastic cross section.

⁷ Referred to as T or T region by ALSPECTOR 73.

⁸ Seen as bump in $l = 1$ state. See also COOPER 68. PEASLEE 75 confirm $\bar{p}p$ results of ABRAMS 70, no narrow structure.

 $\pi^-p \rightarrow \eta\pi\pi$

VALUE (MeV)	DOCUMENT ID	TECN	COMMENT
• • • We do not use the following data for averages, fits, limits, etc. • • •			
2290 ± 20 ± 30	AMELIN 00 VES		$37 \pi^-p \rightarrow \eta\pi^+\pi^-n$

 $\rho_3(2250)$ WIDTH $\bar{p}p \rightarrow \pi\pi \text{ or } K\bar{K}$

VALUE (MeV)	DOCUMENT ID	TECN	CHG	COMMENT
• • • We do not use the following data for averages, fits, limits, etc. • • •				
~ 220	HASAN 94 RVUE			$\bar{p}p \rightarrow \pi\pi$
~ 287	HASAN 94 RVUE			$\bar{p}p \rightarrow \pi\pi$
~ 60	⁹ OAKDEN 94 RVUE			$0.36-1.55 \bar{p}p \rightarrow \pi\pi$
~ 250	¹⁰ MARTIN 80B RVUE			
~ 200	¹⁰ MARTIN 80C RVUE			
~ 150	¹¹ CARTER 78B CNTR 0			$0.7-2.4 \bar{p}p \rightarrow K^-K^+$
~ 200	¹² CARTER 77 CNTR 0			$0.7-2.4 \bar{p}p \rightarrow \pi\pi$

⁹ See however KLOET 96 who fit $\pi^+\pi^-$ only and find waves only up to $J = 3$ to be important but not significantly resonant.

¹⁰ $J(J^P) = 1(3^-)$ from simultaneous analysis of $\bar{p}p \rightarrow \pi^-\pi^+$ and $\pi^0\pi^0$.

¹¹ $l = 0, 1, J^P = 3^-$ from Barrelet-zero analysis.

¹² $J(J^P) = 1(3^-)$ from amplitude analysis.

S-CHANNEL $\bar{N}N$

VALUE (MeV)	DOCUMENT ID	TECN	CHG	COMMENT
• • • We do not use the following data for averages, fits, limits, etc. • • •				
135 ± 75	^{13,14} COUPLAND 77 CNTR 0			$0.7-2.4 \bar{p}p \rightarrow \bar{p}p$
98 ± 8	¹⁴ ALSPECTOR 73 CNTR			$\bar{p}p$ S channel
~ 85	¹⁵ ABRAMS 70 CNTR			S channel $\bar{p}N$

¹³ From a fit to the total elastic cross section.

¹⁴ Isospins 0 and 1 not separated.

¹⁵ Seen as bump in $l = 1$ state. See also COOPER 68. PEASLEE 75 confirm $\bar{p}p$ results of ABRAMS 70, no narrow structure.

 $\pi^-p \rightarrow \eta\pi\pi$

VALUE (MeV)	DOCUMENT ID	TECN	COMMENT
• • • We do not use the following data for averages, fits, limits, etc. • • •			
230 ± 50 ± 80	AMELIN 00 VES		$37 \pi^-p \rightarrow \eta\pi^+\pi^-n$

 $\rho_3(2250)$ REFERENCES

AMELIN 00 NP B668 83	D. Amelin <i>et al.</i>	(VES Collab.)
KLOET 96 PR D53 6120	W.M. Kloet, F. Myhrer	(RUTG, NORD)
HASAN 94 PL B334 215	A. Hasan, D.V. Bugg	(LOQM)
OAKDEN 94 NPA 574 731	M.N. Oakden, M.R. Pennington	(DURH)
MARTIN 80B NP B376 355	B.R. Martin, D. Morgan	(LOUC, RHEL) JP
MARTIN 80C NP B169 216	A.D. Martin, M.R. Pennington	(DURH) JP
CARTER 78B NP B141 467	A.A. Carter	(LOQM)
CUTTS 78B PR D17 16	D. Cutts <i>et al.</i>	(STON, WISC)
CARTER 77 PL 67B 117	A.A. Carter <i>et al.</i>	(LOQM, RHEL) JP
COUPLAND 77 PL 71B 460	M. Coupland <i>et al.</i>	(LOQM, RHEL)
PEASLEE 75 PL 57B 189	D.C. Peaslee <i>et al.</i>	(CANB, BARI, BROW+)
ALSPECTOR 73 PRL 30 511	J. Alspector <i>et al.</i>	(RUTG, UPN)
ABRAMS 70 PR D1 1917	R.J. Abrams <i>et al.</i>	(BNL)
COOPER 68 PRL 20 1059	W.A. Cooper <i>et al.</i>	(ANL)

OTHER RELATED PAPERS

MARTIN 79B PL 86B 93	A.D. Martin, M.R. Pennington	(DURH)
CARTER 78 NP B132 176	A.A. Carter	(LOQM) JP
CARTER 77B PL 67B 122	A.A. Carter	(LOQM) JP
CARTER 77C NP B127 202	A.A. Carter <i>et al.</i>	(LOQM, DARE, RHEL)
ZEMANY 76 NP B103 537	P.D. Zemany <i>et al.</i>	(MSU)
EISENHAND... 75 NP B96 109	E. Eisenhandler <i>et al.</i>	(LOQM, LIVP, DARE+)
BERTANZA 74 NC 23A 209	L. Bertanza <i>et al.</i>	(PISA, PADO, TORI)
BETTINI 73 NC 15A 563	A. Bettini <i>et al.</i>	(PADO, LBL, PISA+)
DONNACHIE 73 LNC 7 285	A. Donnachie, P.R. Thomas	(MCHS)
NICHOLSON 73 PR D7 2572	H. Nicholson <i>et al.</i>	(CIT, ROCH, BNL)
FIELDS 71 PRL 27 1749	T. Fields <i>et al.</i>	(ANL, OXF)
YOH 71 PRL 26 922	J.K. Yoh <i>et al.</i>	(CIT, BNL, ROCH)
ABRAMS 67C PRL 18 1209	R.J. Abrams <i>et al.</i>	(BNL)

 $f_2(2300)$

$$1G(J^{PC}) = 0^+(2^{++})$$

See also the mini-review under non- $q\bar{q}$ candidates. (See the index for the page number.)

 $f_2(2300)$ MASS

VALUE (MeV)	DOCUMENT ID	TECN	COMMENT
• • • We do not use the following data for averages, fits, limits, etc. • • •			
2297 ± 28	¹ ETKIN 88 MPS		$22 \pi^-p \rightarrow \phi\phi n$
2231 ± 10	BOOTH 86 OMEG		$85 \pi^-Be \rightarrow 2\phi Be$
2220 ⁺⁹⁰ ₋₂₀	LINDENBAUM 84 RVUE		
2320 ± 40	ETKIN 82 MPS		$22 \pi^-p \rightarrow 2\phi n$

¹ Includes data of ETKIN 85. The percentage of the resonance going into $\phi\phi 2^{++} + S_2$, D_2 , and D_0 is 6^{+15}_-5 , 25^{+18}_-14 , and 69^{+16}_-27 , respectively.

 $f_2(2300)$ WIDTH

VALUE (MeV)	DOCUMENT ID	TECN	COMMENT
• • • We do not use the following data for averages, fits, limits, etc. • • •			
149 ± 41	² ETKIN 88 MPS		$22 \pi^-p \rightarrow \phi\phi n$
133 ± 50	BOOTH 86 OMEG		$85 \pi^-Be \rightarrow 2\phi Be$
200 ± 50	LINDENBAUM 84 RVUE		
220 ± 70	ETKIN 82 MPS		$22 \pi^-p \rightarrow 2\phi n$

² Includes data of ETKIN 85.

 $f_2(2300)$ DECAY MODES

Mode	Fraction (Γ_i/Γ)
$\Gamma_1 \phi\phi$	seen

 $f_2(2300)$ REFERENCES

ETKIN 88 PL B201 568	A. Etkin <i>et al.</i>	(BNL, CUNY)
BOOTH 86 NP B273 677	P.S.L. Booth <i>et al.</i>	(LIVP, GLAS, CERN)
ETKIN 85 PL 165B 217	A. Etkin <i>et al.</i>	(BNL, CUNY)
LINDENBAUM 84 CNPP 13 285	S.J. Lindenbaum	(CUNY)
ETKIN 82 PRL 49 1620	A. Etkin <i>et al.</i>	(BNL, CUNY)

OTHER RELATED PAPERS

AMELIN 00 NP B668 83	D. Amelin <i>et al.</i>	(VES Collab.)
BARBERIS 98 PL B432 436	D. Barberis <i>et al.</i>	(Omega exp.)
LANDBERG 96 PR D53 2839	C. Landberg <i>et al.</i>	(BNL, CUNY, RPI)
ARMSTRONG 89B PL B221 221	T.A. Armstrong <i>et al.</i>	(CERN, CDF, BIRM+)
GREEN 86 PRL 56 1639	D.R. Green <i>et al.</i>	(FNAL, ARIZ, FSU+)
BOOTH 84 NP B242 51	P.S.L. Booth <i>et al.</i>	(LIVP, GLAS, CERN)
EISENHAND... 75 NP B96 109	E. Eisenhandler <i>et al.</i>	(LOQM, LIVP, DARE+)

See key on page 239

Meson Particle Listings

$f_4(2300)$, $f_2(2340)$, $\rho_5(2350)$

$f_4(2300)$

$$I^G(J^{PC}) = 0^+(4^{++})$$

OMITTED FROM SUMMARY TABLE
 This entry was previously called $U_0(2350)$. Contains results mostly from formation experiments. For further production experiments see the $\bar{N}N(1100-3600)$ entry. See also $\rho(2150)$, $f_2(2150)$, $\rho_3(2250)$, $\rho_5(2350)$.

$f_4(2300)$ MASS

$\bar{p}p \rightarrow \pi\pi$ or $\bar{K}K$

VALUE (MeV)	DOCUMENT ID	TECN	COMMENT
• • • We do not use the following data for averages, fits, limits, etc. • • •			
~ 2314	HASAN	94 RVUE	$\bar{p}p \rightarrow \pi\pi$
~ 2300	¹ MARTIN	80B RVUE	
~ 2300	¹ MARTIN	80C RVUE	
~ 2340	² CARTER	78B CNTR	$0.7-2.4 \bar{p}p \rightarrow K^- K^+$
~ 2330	DULUDE	78B OSPK	$1-2 \bar{p}p \rightarrow \pi^0 \pi^0$
~ 2310	³ CARTER	77 CNTR	$0.7-2.4 \bar{p}p \rightarrow \pi\pi$
¹ $I(J^P) = 0(4^+)$ from simultaneous analysis of $p\bar{p} \rightarrow \pi^- \pi^+$ and $\pi^0 \pi^0$.			
² $I(J^P) = 0(4^+)$ from Barrelet-zero analysis.			
³ $I(J^P) = 0(4^+)$ from amplitude analysis.			

S-CHANNEL $\bar{p}p$ or $\bar{N}N$

VALUE (MeV)	DOCUMENT ID	TECN	COMMENT
• • • We do not use the following data for averages, fits, limits, etc. • • •			
~ 2380	⁴ CUTTS	78B CNTR	$0.97-3 \bar{p}p \rightarrow \bar{N}N$
2345 ± 15	^{4,5} COUPLAND	77 CNTR	$0.7-2.4 \bar{p}p \rightarrow \bar{p}p$
2359 ± 2	^{4,6} ALSPECTOR	73 CNTR	$\bar{p}p$ S channel
2375 ± 10	ABRAMS	70 CNTR	S channel $\bar{N}N$
⁴ Isospins 0 and 1 not separated.			
⁵ From a fit to the total elastic cross section.			
⁶ Referred to as U or U region by ALSPECTOR 73.			

$\pi^- p \rightarrow \eta\pi\pi$

VALUE (MeV)	DOCUMENT ID	TECN	COMMENT
• • • We do not use the following data for averages, fits, limits, etc. • • •			
2330 ± 20 ± 40	AMELIN	00 VES	$37 \pi^- p \rightarrow \eta\pi^+\pi^- n$

$f_4(2300)$ WIDTH

$\bar{p}p \rightarrow \pi\pi$ or $\bar{K}K$

VALUE (MeV)	DOCUMENT ID	TECN	COMMENT
• • • We do not use the following data for averages, fits, limits, etc. • • •			
~ 278	HASAN	94 RVUE	$\bar{p}p \rightarrow \pi\pi$
~ 200	⁷ MARTIN	80C RVUE	
~ 150	⁸ CARTER	78B CNTR	$0.7-2.4 \bar{p}p \rightarrow K^- K^+$
~ 210	⁹ CARTER	77 CNTR	$0.7-2.4 \bar{p}p \rightarrow \pi\pi$
⁷ $I(J^P) = 0(4^+)$ from simultaneous analysis of $p\bar{p} \rightarrow \pi^- \pi^+$ and $\pi^0 \pi^0$.			
⁸ $I(J^P) = 0(4^+)$ from Barrelet-zero analysis.			
⁹ $I(J^P) = 0(4^+)$ from amplitude analysis.			

S-CHANNEL $\bar{p}p$ or $\bar{N}N$

VALUE (MeV)	DOCUMENT ID	TECN	COMMENT
• • • We do not use the following data for averages, fits, limits, etc. • • •			
135^{+150}_{-65}	^{10,11} COUPLAND	77 CNTR	$0.7-2.4 \bar{p}p \rightarrow \bar{p}p$
165^{+18}_{-8}	¹¹ ALSPECTOR	73 CNTR	$\bar{p}p$ S channel
~ 190	ABRAMS	70 CNTR	S channel $\bar{N}N$
¹⁰ From a fit to the total elastic cross section.			
¹¹ Isospins 0 and 1 not separated.			

$\pi^- p \rightarrow \eta\pi\pi$

VALUE (MeV)	DOCUMENT ID	TECN	COMMENT
• • • We do not use the following data for averages, fits, limits, etc. • • •			
235 ± 50 ± 40	AMELIN	00 VES	$37 \pi^- p \rightarrow \eta\pi^+\pi^- n$

$f_4(2300)$ REFERENCES

AMELIN	00	NP B668 83	D. Amelin et al.	(VES Collab.)
HASAN	94	PL B334 215	A. Hasan, D.V. Bugg	(LOQM)
MARTIN	80B	NP B176 355	B.R. Martin, D. Morgan	(LOUC, RHEL) JP
MARTIN	80C	NP B169 216	A.D. Martin, M.R. Pennington	(DURH) JP
CARTER	78B	NP B141 467	A.A. Carter	(LOQM)
CUTTS	78B	PR D17 16	D. Cutts et al.	(STON, WISC)
DULUDE	78B	PL 79B 335	R.S. Dulude et al.	(BROW, MIT, BARI) JP
CARTER	77	PL 67B 117	A.A. Carter et al.	(LOQM, RHEL) JP
COUPLAND	77	PL 71B 450	M. Coupland et al.	(LOQM, RHEL)
ALSPECTOR	73	PRL 30 511	J. Alspector et al.	(RUTG, UPN)
ABRAMS	70	PR D1 1917	R.J. Abrams et al.	(BNL)

OTHER RELATED PAPERS

ANISOVICH	99D	PL B452 180	A.V. Anisovich et al.	
Also	99F	NP A651 253	A.V. Anisovich et al.	
ANISOVICH	99F	NP A651 253	A.V. Anisovich et al.	
EISENHAND...	75	NP B96 109	E. Eisenhandler et al.	(LOQM, LIVP, DARE+)
FIELDS	71	PRL 27 1749	T. Fields et al.	(ANL, OXF)
YOH	71	PRL 26 922	J.K. Yoh et al.	(CIT, BNL, ROCH)
BRICMAN	69	PL 29B 451	C. Bricman et al.	(CERN, CAEN, SACL)

$f_2(2340)$

$$I^G(J^{PC}) = 0^+(2^{++})$$

See also the mini-review under non- $q\bar{q}$ candidates. (See the index for the page number.)

$f_2(2340)$ MASS

VALUE (MeV)	DOCUMENT ID	TECN	COMMENT
• • • We do not use the following data for averages, fits, limits, etc. • • •			
2339 ± 55	¹ ETKIN	88 MPS	$22 \pi^- p \rightarrow \phi\phi n$
2392 ± 10	BOOTH	86 OMEG	$85 \pi^- Be \rightarrow 2\phi Be$
2360 ± 20	LINDENBAUM	84 RVUE	
¹ Includes data of ETKIN 85. The percentage of the resonance going into $\phi\phi 2^{++} + S_2$, D_2 , and D_0 is 37 ± 19 , 4^{+12}_{-4} , and 59^{+21}_{-19} , respectively.			

$f_2(2340)$ WIDTH

VALUE (MeV)	DOCUMENT ID	TECN	COMMENT
• • • We do not use the following data for averages, fits, limits, etc. • • •			
319^{+81}_{-69}	² ETKIN	88 MPS	$22 \pi^- p \rightarrow \phi\phi n$
198 ± 50	BOOTH	86 OMEG	$85 \pi^- Be \rightarrow 2\phi Be$
150^{+150}_{-50}	LINDENBAUM	84 RVUE	
² Includes data of ETKIN 85.			

$f_2(2340)$ DECAY MODES

Mode	Fraction (Γ_i/Γ)
$\Gamma_1 \phi\phi$	seen

$f_2(2340)$ REFERENCES

ETKIN	88	PL B201 568	A. Etkin et al.	(BNL, CUNY)
BOOTH	86	NP B273 677	P.S.L. Booth et al.	(LIVP, GLAS, CERN)
ETKIN	85	PL 165B 217	A. Etkin et al.	(BNL, CUNY)
LINDENBAUM	84	CNPP 13 285	S.J. Lindenbaum	(CUNY)

OTHER RELATED PAPERS

ANISOVICH	99D	PL B452 180	A.V. Anisovich et al.	
Also	99F	NP A651 253	A.V. Anisovich et al.	
ANISOVICH	99F	NP A651 253	A.V. Anisovich et al.	
LANDBERG	96	PR D53 2639	C. Landberg et al.	(BNL, CUNY, RPI)
ARMSTRONG	89B	PL B221 221	T.A. Armstrong et al.	(CERN, CDEF, BIRM+)
GREEN	86	PRL 56 1639	D.R. Green et al.	(FNAL, ARIZ, FSU+)
BOOTH	84	NP B242 51	P.S.L. Booth et al.	(LIVP, GLAS, CERN)
EISENHAND...	75	NP B96 109	E. Eisenhandler et al.	(LOQM, LIVP, DARE+)

$\rho_5(2350)$

$$I^G(J^{PC}) = 1^+(5^{--})$$

OMITTED FROM SUMMARY TABLE
 This entry was previously called $U_1(2400)$. See also the $\bar{N}N(1100-3600)$ and $X(1900-3600)$ entries. See also $\rho(2150)$, $f_2(2150)$, $\rho_3(2250)$, $f_4(2300)$.

$\rho_5(2350)$ MASS

VALUE (MeV)	DOCUMENT ID	TECN	COMMENT
• • • We do not use the following data for averages, fits, limits, etc. • • •			
2330 ± 35	ALDE	95 GAM2	$38 \pi^- p \rightarrow \omega\pi^0 n$

$\bar{p}p \rightarrow \pi\pi$ or $\bar{K}K$

VALUE (MeV)	DOCUMENT ID	TECN	CHG	COMMENT
• • • We do not use the following data for averages, fits, limits, etc. • • •				
~ 2303	HASAN	94 RVUE		$\bar{p}p \rightarrow \pi\pi$
~ 2300	¹ MARTIN	80B RVUE		
~ 2250	¹ MARTIN	80C RVUE		
~ 2500	² CARTER	78B CNTR	0	$0.7-2.4 \bar{p}p \rightarrow K^- K^+$
~ 2480	³ CARTER	77 CNTR	0	$0.7-2.4 \bar{p}p \rightarrow \pi\pi$

Meson Particle Listings

 $\rho_5(2350)$, $a_6(2450)$, $f_6(2510)$ S-CHANNEL $\bar{N}N$

VALUE (MeV)	DOCUMENT ID	TECN	CHG	COMMENT
~ 2380	4 CUTTS	78B CNTR		0.97-3 $\bar{p}p \rightarrow \bar{N}N$
2345 ± 15	4,5 COUPLAND	77 CNTR 0		0.7-2.4 $\bar{p}p \rightarrow \bar{p}p$
2359 ± 2	4,6 ALSPECTOR	73 CNTR		$\bar{p}p$ S channel
2350 ± 10	7 ABRAMS	70 CNTR		S channel $\bar{N}N$
2360 ± 25	8 OH	70B HDIBC -0		$\bar{p}(p\eta)$, $K^*K2\pi$

- 1 $I(J^P) = 1(5^-)$ from simultaneous analysis of $p\bar{p} \rightarrow \pi^- \pi^+$ and $\pi^0 \pi^0$.
 2 $I = 0(1)$; $J^P = 5^-$ from Barrelet-zero analysis.
 3 $I(J^P) = 1(5^-)$ from amplitude analysis.
 4 Isospins 0 and 1 not separated.
 5 From a fit to the total elastic cross section.
 6 Referred to as U or U region by ALSPECTOR 73.
 7 For $J = 1 \bar{N}N$.
 8 No evidence for this bump seen in the $\bar{p}p$ data of CHAPMAN 71B. Narrow state not confirmed by OH 73 with more data.

 $\rho_5(2350)$ WIDTH $\pi^- p \rightarrow \omega \pi^0 n$

VALUE (MeV)	DOCUMENT ID	TECN	COMMENT
400 ± 100	ALDE	95 GAM2	38 $\pi^- p \rightarrow \omega \pi^0 n$

 $\bar{p}p \rightarrow \pi\pi$ or $\bar{K}K$

VALUE (MeV)	DOCUMENT ID	TECN	CHG	COMMENT
~ 169	HASAN	94 RVUE		$\bar{p}p \rightarrow \pi\pi$
~ 250	9 MARTIN	80B RVUE		
~ 300	9 MARTIN	80C RVUE		
~ 150	10 CARTER	78B CNTR 0		0.7-2.4 $\bar{p}p \rightarrow K^- K^+$
~ 210	11 CARTER	77 CNTR 0		0.7-2.4 $\bar{p}p \rightarrow \pi\pi$

S-CHANNEL $\bar{N}N$

VALUE (MeV)	DOCUMENT ID	TECN	CHG	COMMENT
135 ⁺¹⁵⁰ ₋₆₅	12,13 COUPLAND	77 CNTR 0		0.7-2.4 $\bar{p}p \rightarrow \bar{p}p$
165 ⁺¹⁸ ₋₈	13 ALSPECTOR	73 CNTR		$\bar{p}p$ S channel
< 60	14 OH	70B HDIBC -0		$\bar{p}(p\eta)$, $K^*K2\pi$
~ 140	ABRAMS	67C CNTR		S channel $\bar{N}N$

- 9 $I(J^P) = 1(5^-)$ from simultaneous analysis of $p\bar{p} \rightarrow \pi^- \pi^+$ and $\pi^0 \pi^0$.
 10 $I = 0(1)$; $J^P = 5^-$ from Barrelet-zero analysis.
 11 $I(J^P) = 1(5^-)$ from amplitude analysis.
 12 From a fit to the total elastic cross section.
 13 Isospins 0 and 1 not separated.
 14 No evidence for this bump seen in the $\bar{p}p$ data of CHAPMAN 71B. Narrow state not confirmed by OH 73 with more data.

 $\rho_5(2350)$ REFERENCES

ALDE	95	ZPHY C66 379	D.M. Alde et al.	(GAMS Collab.) JP
HASAN	94	PL B334 215	A. Hasan, D.V. Bugg	(LOQM)
MARTIN	80B	NP B176 355	B.R. Martin, D. Morgan	(LOUC, RHEL) JP
MARTIN	80C	NP B169 216	A.D. Martin, M.R. Pennington	(DURH) JP
CARTER	78B	NP B141 467	A.A. Carter	(LOQM)
CUTTS	78B	PR D17 16	D. Cutts et al.	(STON, WISC)
CARTER	77	PL 67B 117	A.A. Carter et al.	(LOQM, RHEL) JP
COUPLAND	77	PL 71B 460	M. Coupland et al.	(LOQM, RHEL)
ALSPECTOR	73	PRL 30 511	J. Alspector et al.	(RUTG, UPNJ)
OH	73	NP B51 57	B.Y. Oh et al.	(MSU)
CHAPMAN	71B	PR D4 1275	J.W. Chapman et al.	(MICH)
ABRAMS	70	PR D1 1917	R.J. Abrams et al.	(BNL)
OH	70B	PRL 24 1257	B.Y. Oh et al.	(MSU)
ABRAMS	67C	PRL 18 1209	R.J. Abrams et al.	(BNL)

OTHER RELATED PAPERS

EISENHAND...	75	NP B96 109	E. Eisenhandler et al.	(LOQM, LIVP, DARE+)
CASO	70	LCN 3 707	C. Caso et al.	(GENO, HAMB, MILA, SACL)
BRICMAN	69	PL 29B 451	C. Bricman et al.	(CERN, CAEN, SACL)

 $a_6(2450)$

$I^G(J^{PC}) = 1^-(6^{++})$

OMITTED FROM SUMMARY TABLE
Needs confirmation. $a_6(2450)$ MASS

VALUE (MeV)	DOCUMENT ID	TECN	CHG	COMMENT
2450 ± 130	1 CLELAND	82B SPEC	±	50 $\pi p \rightarrow K_S^0 K^\pm p$

¹ From an amplitude analysis.

 $a_6(2450)$ WIDTH

VALUE (MeV)	DOCUMENT ID	TECN	CHG	COMMENT
400 ± 250	2 CLELAND	82B SPEC	±	50 $\pi p \rightarrow K_S^0 K^\pm p$

² From an amplitude analysis.

 $a_6(2450)$ DECAY MODES

Mode	Fraction (Γ_i/Γ)
Γ_1 $K\bar{K}$	(6.0 ± 1.0) %

 $a_6(2450)$ REFERENCES

CLELAND	82B	NP B208 228	W.E. Cleland et al.	(DURH, GEVA, LAUS+)
---------	-----	-------------	---------------------	---------------------

 $f_6(2510)$

$I^G(J^{PC}) = 0^+(6^{++})$

OMITTED FROM SUMMARY TABLE
Needs confirmation. $f_6(2510)$ MASS

VALUE (MeV)	DOCUMENT ID	TECN	COMMENT
2465 ± 50 OUR AVERAGE	Error includes scale factor of 2.1.		
2420 ± 30	ALDE	98 GAM4	100 $\pi^- p \rightarrow \pi^0 \pi^0 n$
2510 ± 30	BINON	84B GAM2	38 $\pi^- p \rightarrow n2\pi^0$

 $f_6(2510)$ WIDTH

VALUE (MeV)	DOCUMENT ID	TECN	COMMENT
255 ± 40 OUR AVERAGE			
270 ± 60	ALDE	98 GAM4	100 $\pi^- p \rightarrow \pi^0 \pi^0 n$
240 ± 60	BINON	84B GAM2	38 $\pi^- p \rightarrow n2\pi^0$

 $f_6(2510)$ DECAY MODES

Mode	Fraction (Γ_i/Γ)
Γ_1 $\pi\pi$	(6.0 ± 1.0) %

 $f_6(2510)$ BRANCHING RATIOS

$\Gamma(\pi\pi)/\Gamma_{total}$	DOCUMENT ID	TECN	COMMENT	Γ_1/Γ
0.06 ± 0.01	1 BINON	83C GAM2	38 $\pi^- p \rightarrow n4\gamma$	

¹ Assuming one pion exchange and using data of BOLOTOV 74.

 $f_6(2510)$ REFERENCES

ALDE	98	EPJ A3 361	D. Alde et al.	(GAM4 Collab.)
Also	99	PAN 62 405	D. Alde et al.	(GAMS Collab.)
BINON	84B	LCN 39 41	F.G. Binon et al.	(SERP, BELG, LAPP) JP
BINON	83C	SJNP 38 723	F.G. Binon et al.	(SERP, BRUX+)
BOLOTOV	74	PL 52B 489	V.N. Bolotov et al.	(SERP)

OTHER RELATED PAPERS

PROKOSHKIN	99	FAN 62 356	Yu.D. Prokoshkin et al.	
		Translated from YAF 62 396.		
EISENHAND...	75	NP B96 109	E. Eisenhandler et al.	(LOQM, LIVP, DARE+)

See key on page 239

Meson Particle Listings
X(3250)

X(3250)

$$I^G(J^{PC}) = ?^?(???)$$

OMITTED FROM SUMMARY TABLE

Narrow peak observed in several final states with hidden strangeness ($\Lambda\bar{p}K^+$, $\Lambda\bar{p}K^+\pi^\pm$, $K^0\rho\bar{p}K^\pm$). Needs confirmation.

X(3250) MASS

3-BODY DECAYS

VALUE (MeV)	DOCUMENT ID	TECN	COMMENT
• • • We do not use the following data for averages, fits, limits, etc. • • •			
3250 ± 8 ± 20	ALEEV	93 BIS2	X(3250) → $\Lambda\bar{p}K^+$
3265 ± 7 ± 20	ALEEV	93 BIS2	X(3250) → $\bar{\Lambda}pK^-$

4-BODY DECAYS

VALUE (MeV)	DOCUMENT ID	TECN	COMMENT
• • • We do not use the following data for averages, fits, limits, etc. • • •			
3245 ± 8 ± 20	ALEEV	93 BIS2	X(3250) → $\Lambda\bar{p}K^+\pi^\pm$
3250 ± 9 ± 20	ALEEV	93 BIS2	X(3250) → $\bar{\Lambda}pK^-\pi^\mp$
3270 ± 8 ± 20	ALEEV	93 BIS2	X(3250) → $K_S^0\rho\bar{p}K^\pm$

X(3250) WIDTH

3-BODY DECAYS

VALUE (MeV)	DOCUMENT ID	TECN	COMMENT
• • • We do not use the following data for averages, fits, limits, etc. • • •			
45 ± 18	ALEEV	93 BIS2	X(3250) → $\Lambda\bar{p}K^+$
40 ± 18	ALEEV	93 BIS2	X(3250) → $\bar{\Lambda}pK^-$

4-BODY DECAYS

VALUE (MeV)	DOCUMENT ID	TECN	COMMENT
• • • We do not use the following data for averages, fits, limits, etc. • • •			
25 ± 11	ALEEV	93 BIS2	X(3250) → $\Lambda\bar{p}K^+\pi^\pm$
50 ± 20	ALEEV	93 BIS2	X(3250) → $\bar{\Lambda}pK^-\pi^\mp$
25 ± 11	ALEEV	93 BIS2	X(3250) → $K_S^0\rho\bar{p}K^\pm$

X(3250) DECAY MODES

Mode
Γ_1 $\Lambda\bar{p}K^+$
Γ_2 $\Lambda\bar{p}K^+\pi^\pm$
Γ_3 $K^0\rho\bar{p}K^\pm$

X(3250) REFERENCES

ALEEV	93	PAN 56 1358	A.N. Aleev et al.	(BIS-2 Collab.)
Translated from YAF 56 100.				

Meson Particle Listings

$e^+e^-(1100-2200), \bar{N}N(1100-3600)$

OTHER LIGHT UNFLAVORED MESONS ($S = C = B = 0$)

$e^+e^-(1100-2200)$ $I^G(J^{PC}) = ?^?(1^{--})$

OMITTED FROM SUMMARY TABLE
 This entry contains unflavored vector mesons coupled to e^+e^- (photon) between the ϕ and $J/\psi(1S)$ mass regions. See also $\omega(1420)$, $\rho(1450)$, $\omega(1650)$, $\phi(1680)$, and $\rho(1700)$.

$e^+e^-(1100-2200)$ MASSES AND WIDTHS

We do not use the following data for averages, fits, limits, etc.

VALUE (MeV)	DOCUMENT ID	TECN	CHG	COMMENT
1100 to 2200 OUR LIMIT				
1097.0 ^{+16.0} _{-19.0}	BARTALUCCI 79	OSPK	7	$\gamma\rho \rightarrow e^+e^-\rho$
31.0 ^{+24.0} _{-20.0}	BARTALUCCI 79	OSPK	7	$\gamma\rho \rightarrow e^+e^-\rho$
1266.0 ± 5.0	BARTALUCCI 79	DASP	0	$7\gamma\rho \rightarrow e^+e^-\rho$
110.0 ± 35.0	BARTALUCCI 79	DASP	0	$7\gamma\rho \rightarrow e^+e^-\rho$
~ 1830.0	PETERSON 78	SPEC	7	$\gamma\rho \rightarrow K^+K^-\rho$
~ 120.0	PETERSON 78	SPEC	7	$\gamma\rho \rightarrow K^+K^-\rho$
• • • We do not use the following data for averages, fits, limits, etc. • • •				
1870 ± 10	ANTONELLI 96	SPEC	96	$e^+e^- \rightarrow$ hadrons
10 ± 5	ANTONELLI 96	SPEC	96	$e^+e^- \rightarrow$ hadrons
~ 2130	¹ ESPOSITO 78	FRAM	78	$e^+e^- \rightarrow K^*(892)^+ \dots$
~ 30	¹ ESPOSITO 78	FRAM	78	$e^+e^- \rightarrow K^*(892)^+ \dots$

¹ Not seen by DELCOURT 79.

$e^+e^-(1100-2200)$ REFERENCES

ANTONELLI 96	PL B365 427	A. Antonelli <i>et al.</i>	(FENICE Collab.)
BARTALUCCI 79	NC 49A 207	S. Bartalucci <i>et al.</i>	(DESY, FRAS)
DELCOURT 79	PL 86B 395	B. Delcourt <i>et al.</i>	(LALO)
ESPOSITO 78	LNC 22 305	B. Esposito, F. Felicetti	(FRAS, NAPL, PADO+)
PETERSON 78	PR D18 3955	D. Peterson <i>et al.</i>	(CORN. HARV)

OTHER RELATED PAPERS

BACCI 76	PL 64B 356	C. Bacci <i>et al.</i>	(ROMA, FRAS)
BACCI 75	PL 58B 481	C. Bacci <i>et al.</i>	(ROMA, FRAS)

$\bar{N}N(1100-3600)$

OMITTED FROM SUMMARY TABLE
 This entry contains various high mass, unflavored structures coupled to the baryon-antibaryon system, as well as quasi-nuclear bound states below threshold.

$\bar{N}N(1100-3600)$ MASSES AND WIDTHS

We do not use the following data for averages, fits, limits etc.

VALUE (MeV)	DOCUMENT ID	TECN	CHG	COMMENT
1100 to 3600 OUR LIMIT				
1107 ± 4	DAFTARI 87	DBC	0	$0. \bar{p}n \rightarrow \rho^-\pi^+\pi^-$
111 ± 8 ± 15	DAFTARI 87	DBC	0	$0. \bar{p}n \rightarrow \rho^-\pi^+\pi^-$
1167 ± 7	⁹ CHIBA 91	CNTR	0	$\bar{p}d \rightarrow \gamma X$
1191.0 ± 9.9	⁹ CHIBA 87	CNTR	0	$0. \bar{p}p \rightarrow \gamma X$
1210 ± 5.0	^{9,10,11,12} RICHTER 83	CNTR	0	Stopped \bar{p}
1325 ± 5	⁹ CHIBA 91	CNTR	0	$\bar{p}d \rightarrow \gamma X$
1329.2 ± 7.6	⁹ CHIBA 87	CNTR	0	$0. \bar{p}p \rightarrow \gamma X$

VALUE (MeV)	DOCUMENT ID	TECN	CHG	COMMENT
1390.9 ± 6.3	⁹ CHIBA 87	CNTR	0	$0. \bar{p}p \rightarrow \gamma X$
1395	^{9,11,12,13} PAVLOPO... 78	CNTR	0	Stopped \bar{p}

VALUE (MeV)	DOCUMENT ID	TECN	CHG	COMMENT
~ 1410	BETTINI 66	DBC	0	$0. \bar{p}N \rightarrow 5\pi$
~ 100	BETTINI 66	DBC	0	$0. \bar{p}N \rightarrow 5\pi$

VALUE (MeV)	DOCUMENT ID	TECN	CHG	COMMENT
1468 ± 6	¹⁴ BRIDGES 86B	DBC	0	$0. \bar{p}N \rightarrow 2\pi^-\pi^+\pi^0$
88 ± 18	¹⁴ BRIDGES 86B	DBC	0	$0. \bar{p}N \rightarrow 2\pi^-\pi^+\pi^0$

VALUE (MeV)	DOCUMENT ID	TECN	CHG	COMMENT
1512 ± 7	⁹ CHIBA 91	CNTR	0	$\bar{p}d \rightarrow \gamma X$
1523.8 ± 3.6	⁹ CHIBA 87	CNTR	0	$0. \bar{p}p \rightarrow \gamma X$
1522 ± 7	¹⁴ BRIDGES 86B	DBC	0	$0. \bar{p}N \rightarrow 2\pi^-\pi^+\pi^0$

VALUE (MeV)	DOCUMENT ID	TECN	CHG	COMMENT
59 ± 12	¹⁴ BRIDGES 86B	DBC	0	$0. \bar{p}N \rightarrow 2\pi^-\pi^+\pi^0$

VALUE (MeV)	DOCUMENT ID	TECN	CHG	COMMENT
1577.8 ± 3.4	⁹ CHIBA 87	CNTR	0	$0. \bar{p}p \rightarrow \gamma X$
1594 ± 9	¹⁴ BRIDGES 86B	DBC	-	$0. \bar{p}N \rightarrow 2\pi^-\pi^+\pi^0$
81 ± 12	¹⁴ BRIDGES 86B	DBC	-	$0. \bar{p}N \rightarrow 2\pi^-\pi^+\pi^0$

VALUE (MeV)	DOCUMENT ID	TECN	CHG	COMMENT
1633.6 ± 4.1	⁹ CHIBA 87	CNTR	0	$0. \bar{p}p \rightarrow \gamma X$
1637.1 ^{+5.6} _{-7.3}	ADIELS 84	CNTR	0	$\bar{p}He$

VALUE (MeV)	DOCUMENT ID	TECN	CHG	COMMENT
1638 ± 3.0	^{9,10,11,12} RICHTER 83	CNTR	0	Stopped \bar{p}

VALUE (MeV)	DOCUMENT ID	TECN	CHG	COMMENT
1644.0 ^{+5.6} _{-7.3}	ADIELS 84	CNTR	0	$\bar{p}He$

VALUE (MeV)	DOCUMENT ID	TECN	CHG	COMMENT
1646	^{9,11,12,13} PAVLOPO... 78	CNTR	0	Stopped \bar{p}

VALUE (MeV)	DOCUMENT ID	TECN	CHG	COMMENT
1687.1 ^{+5.0} _{-4.3}	ADIELS 84	CNTR	0	$\bar{p}He$
1684	^{9,11,12,13} PAVLOPO... 78	CNTR	0	Stopped \bar{p}

VALUE (MeV)	DOCUMENT ID	TECN	CHG	COMMENT
1693 ± 2	⁹ CHIBA 91	CNTR	0	$\bar{p}d \rightarrow \gamma X$
1694 ± 2.0	^{9,10,11,12} RICHTER 83	CNTR	0	Stopped \bar{p}

VALUE (MeV)	DOCUMENT ID	TECN	CHG	COMMENT
1713.0 ± 2.6	⁹ CHIBA 87	CNTR	0	$0. \bar{p}p \rightarrow \gamma X$

VALUE (MeV)	DOCUMENT ID	TECN	CHG	COMMENT
1731.0 ± 1.5	⁹ CHIBA 87	CNTR	0	$0. \bar{p}p \rightarrow \gamma X$

VALUE (MeV)	DOCUMENT ID	TECN	CHG	COMMENT
1771 ± 1.0	^{9,11,12,15} RICHTER 83	CNTR	0	Stopped \bar{p}

VALUE (MeV)	DOCUMENT ID	TECN	CHG	COMMENT
1812.3 ± 1.2	CHIBA 97	CNTR	0	$\bar{p}d \rightarrow nX$
3.7 ± 1.3	CHIBA 97	CNTR	0	$\bar{p}d \rightarrow nX$

VALUE (MeV)	DOCUMENT ID	TECN	CHG	COMMENT
1856.6 ± 5	BRIDGES 86D	SPEC	0	$0. \bar{p}d \rightarrow \pi\pi N$
20 ± 5	BRIDGES 86D	SPEC	0	$0. \bar{p}d \rightarrow \pi\pi N$

VALUE (MeV)	DOCUMENT ID	TECN	CHG	COMMENT
1870 ± 10	ANTONELLI 98	SPEC	98	$e^+e^- \rightarrow n\bar{n}, p\bar{p}$
10 ± 5	ANTONELLI 98	SPEC	98	$e^+e^- \rightarrow n\bar{n}, p\bar{p}$
~ 1870	¹⁶ DALKAROV 97	RVUE	-	$0.0 \bar{p}d \rightarrow p3\pi^-2\pi^+$

VALUE (MeV)	DOCUMENT ID	TECN	CHG	COMMENT
~ 10	¹⁶ DALKAROV 97	RVUE	-	$0.0 \bar{p}d \rightarrow p3\pi^-2\pi^+$
1873 ± 2.5	BRIDGES 86D	SPEC	0	$0. \bar{p}d \rightarrow \pi\pi N$
< 5	BRIDGES 86D	SPEC	0	$0. \bar{p}d \rightarrow \pi\pi N$

VALUE (MeV)	DOCUMENT ID	TECN	CHG	COMMENT
1897 ± 17	¹⁷ ABASHIAN 76	STRC	76	$8\pi^-p \rightarrow p3\pi$
110 ± 82	¹⁷ ABASHIAN 76	STRC	76	$8\pi^-p \rightarrow p3\pi$
1897 ± 1	KALOGERO... 75	DBC	75	$\bar{p}n$ annihilation near threshold
25 ± 6	KALOGERO... 75	DBC	75	$\bar{p}n$ annihilation near threshold

See key on page 239

Meson Particle Listings
NN(1100-3600)

Table with columns: VALUE (MeV), DOCUMENT ID, TECN, CHG, COMMENT. Contains entries for ANISOVICH 99J SPEC 0.

¹ From a fit to the $J^G(J^{PC}) = 0^+(2^{++})$.

Table with columns: VALUE (MeV), DOCUMENT ID, TECN, COMMENT. Contains entries for EVANGELISTA 79 OMEG 10,16.

Table with columns: VALUE (MeV), EVTS, DOCUMENT ID, TECN, CHG, COMMENT. Contains a large list of entries with various meson decays and parameters.

Table with columns: VALUE (MeV), DOCUMENT ID, TECN, CHG, COMMENT. Contains entries for ANISOVICH 99C SPEC and DEFOIX 80 HBC.

Table with columns: VALUE (MeV), DOCUMENT ID, TECN, CHG, COMMENT. Contains entries for ANISOVICH 99J SPEC.

² From a fit to the $J^G(J^{PC}) = 1^+(3^{--})$.
³ From a fit to the $J^G(J^{PC}) = 0^+(0^{++})$.
⁴ From a fit to the $J^G(J^{PC}) = 1^+(1^{--})$.

Table with columns: VALUE (MeV), DOCUMENT ID, TECN, COMMENT. Contains entries for ANISOVICH 99E SPEC.

Table with columns: VALUE (MeV), DOCUMENT ID, TECN, COMMENT. Contains a large list of entries with various meson decays and parameters.

Table with columns: VALUE (MeV), DOCUMENT ID, TECN, COMMENT. Contains entries for ANISOVICH 99D SPEC.

Table with columns: VALUE (MeV), DOCUMENT ID, TECN, CHG, COMMENT. Contains entries for ANISOVICH 99J SPEC.

⁵ From a fit to the $J^G(J^{PC}) = 0^+(4^{++})$.

Table with columns: VALUE (MeV), DOCUMENT ID, TECN, CHG, COMMENT. Contains entries for AZOOZ 83 HYBR.

Table with columns: VALUE (MeV), DOCUMENT ID, TECN, CHG, COMMENT. Contains entries for BODENKAMP 83 SPEC.

Table with columns: VALUE (MeV), DOCUMENT ID, TECN, CHG, COMMENT. Contains entries for AZOOZ 83 HYBR.

Table with columns: VALUE (MeV), DOCUMENT ID, TECN, COMMENT. Contains entries for ANISOVICH 99D SPEC.

Table with columns: VALUE (MeV), DOCUMENT ID, TECN, CHG, COMMENT. Contains entries for ANISOVICH 99 SPEC and KREYMER 80 STRC.

Table with columns: VALUE (MeV), DOCUMENT ID, TECN, COMMENT. Contains entries for ANISOVICH 99E SPEC.

Table with columns: VALUE (MeV), DOCUMENT ID, TECN, COMMENT. Contains entries for ANISOVICH 99C SPEC and DEFOIX 80 HBC.

Table with columns: VALUE (MeV), DOCUMENT ID, TECN, COMMENT. Contains entries for EVANGELISTA 79 OMEG.

Table with columns: VALUE (MeV), DOCUMENT ID, TECN, COMMENT. Contains entries for ANISOVICH 99E SPEC.

Table with columns: VALUE (MeV), DOCUMENT ID, TECN, COMMENT. Contains entries for ANISOVICH 99E SPEC.

Table with columns: VALUE (MeV), DOCUMENT ID, TECN, CHG, COMMENT. Contains entries for ANISOVICH 99J SPEC.

Table with columns: VALUE (MeV), DOCUMENT ID, TECN, COMMENT. Contains entries for ROZANSKA 80 SPRK.

Table with columns: VALUE (MeV), DOCUMENT ID, TECN, COMMENT. Contains entries for ANISOVICH 99D SPEC.

Table with columns: VALUE (MeV), DOCUMENT ID, TECN, CHG, COMMENT. Contains entries for DONALD 73 HBC.

Table with columns: VALUE (MeV), DOCUMENT ID, TECN, CHG, COMMENT. Contains entries for ANISOVICH 99J SPEC.

Meson Particle Listings

 $\bar{N}N(1100-3600)$

VALUE (MeV)	DOCUMENT ID	TECN	CHG	COMMENT	VALUE (MeV)	DOCUMENT ID	TECN	CHG	COMMENT
2180 ± 10	46 ROZANSKA	80 SPRK		18 $\pi^- p \rightarrow p \bar{p} n$	2320 ± 30	18,50 ANISOVICH	99D SPEC		0.6-1.94 $p \bar{p} \rightarrow \pi^0 \pi^0 \eta$
270 ± 10	46 ROZANSKA	80 SPRK		18 $\pi^- p \rightarrow p \bar{p} n$	220 ± 30	18,50 ANISOVICH	99D SPEC		0.6-1.94 $p \bar{p} \rightarrow \pi^0 \pi^0 \eta$
					2310 ± 40	18,38 ANISOVICH	99E SPEC		0.6-1.94 $p \bar{p} \rightarrow 3\pi^0$
VALUE (MeV)	DOCUMENT ID	TECN	CHG	COMMENT	180 ⁺¹² ₋₆₀	18,38 ANISOVICH	99E SPEC		0.6-1.94 $p \bar{p} \rightarrow 3\pi^0$
2207 ± 13	47 ALLES-...	67B HBC	0	5.7 $\bar{p} p$	VALUE (MeV)	DOCUMENT ID	TECN	COMMENT	
62 ± 52	47 ALLES-...	67B HBC	0	5.7 $\bar{p} p$	2231.9 ± 0.1	51 BARNES	94 SPEC		0-46 $\bar{p} p \rightarrow \bar{\Lambda} \Lambda$
VALUE (MeV)	DOCUMENT ID	TECN	COMMENT		0.59 ± 0.25	51 BARNES	94 SPEC		0-46 $p \bar{p} \rightarrow \bar{\Lambda} \Lambda$
2210 ⁺⁷⁹ ₋₂₁	EVANGELISTA 79B	OMEG	10	$\pi^- p \rightarrow K^+ K^- n$	VALUE (MeV)	DOCUMENT ID	TECN	COMMENT	
~ 203	EVANGELISTA 79B	OMEG	10	$\pi^- p \rightarrow K^+ K^- n$	2340 ± 40	18,42 ANISOVICH	99E SPEC		0.6-1.94 $p \bar{p} \rightarrow 3\pi^0$
VALUE (MeV)	DOCUMENT ID	TECN	CHG	COMMENT	230 ± 70	18,42 ANISOVICH	99E SPEC		0.6-1.94 $p \bar{p} \rightarrow 3\pi^0$
2210 ± 40	2,18 ANISOVICH	99J SPEC	0	0.6-1.94 $p \bar{p} \rightarrow \pi \pi, \eta \eta, \eta \eta'$	VALUE (MeV)	DOCUMENT ID	TECN	COMMENT	
360 ± 55	2,18 ANISOVICH	99J SPEC	0	0.6-1.94 $p \bar{p} \rightarrow \pi \pi, \eta \eta, \eta \eta'$	2340 ± 40	18,44 ANISOVICH	99D SPEC		0.6-1.94 $p \bar{p} \rightarrow \pi^0 \pi^0 \eta$
VALUE (MeV)	DOCUMENT ID	TECN	COMMENT		340 ± 40	18,44 ANISOVICH	99D SPEC		0.6-1.94 $p \bar{p} \rightarrow \pi^0 \pi^0 \eta$
~ 2229.2	CARBONELL 93	RVUE		$\bar{p} p \rightarrow \bar{\Lambda} \Lambda$	VALUE (MeV)	DOCUMENT ID	TECN	COMMENT	
~ 1.8	CARBONELL 93	RVUE		$\bar{p} p \rightarrow \bar{\Lambda} \Lambda$	2370 ± 50	18,34 ANISOVICH	99D SPEC		0.6-1.94 $p \bar{p} \rightarrow \pi^0 \pi^0 \eta$
VALUE (MeV)	DOCUMENT ID	TECN	CHG	COMMENT	320 ± 50	18,34 ANISOVICH	99D SPEC		0.6-1.94 $p \bar{p} \rightarrow \pi^0 \pi^0 \eta$
2230 ± 30	1,18 ANISOVICH	99J SPEC	0	0.6-1.94 $p \bar{p} \rightarrow \pi \pi, \eta \eta, \eta \eta'$	VALUE (MeV)	DOCUMENT ID	TECN	COMMENT	
245 ± 45	1,18 ANISOVICH	99J SPEC	0	0.6-1.94 $p \bar{p} \rightarrow \pi \pi, \eta \eta, \eta \eta'$	2380 ± 10	52 ROZANSKA	80 SPRK		18 $\pi^- p \rightarrow p \bar{p} n$
VALUE (MeV)	DOCUMENT ID	TECN	COMMENT		380 ± 20	52 ROZANSKA	80 SPRK		18 $\pi^- p \rightarrow p \bar{p} n$
2240 ± 40	18,34 ANISOVICH	99D SPEC		0.6-1.94 $p \bar{p} \rightarrow \pi^0 \pi^0 \eta$	VALUE (MeV)	DOCUMENT ID	TECN	COMMENT	
170 ± 50	18,34 ANISOVICH	99D SPEC		0.6-1.94 $p \bar{p} \rightarrow \pi^0 \pi^0 \eta$	2450 ± 10	53 ROZANSKA	80 SPRK		18 $\pi^- p \rightarrow p \bar{p} n$
VALUE (MeV)	DOCUMENT ID	TECN	COMMENT		280 ± 20	53 ROZANSKA	80 SPRK		18 $\pi^- p \rightarrow p \bar{p} n$
2260 ± 15	18,31 ANISOVICH	99E SPEC		0.6-1.94 $p \bar{p} \rightarrow 3\pi^0$	VALUE (MeV)	DOCUMENT ID	TECN	CHG	COMMENT
180 ± 20	18,31 ANISOVICH	99E SPEC		0.6-1.94 $p \bar{p} \rightarrow 3\pi^0$	2485 ± 40	7,8 ANISOVICH	99J SPEC	0	0.79-2.43 $p \bar{p} \rightarrow \pi \pi$
VALUE (MeV)	DOCUMENT ID	TECN	COMMENT		410 ± 90	7,8 ANISOVICH	99J SPEC	0	0.79-2.43 $p \bar{p} \rightarrow \pi \pi$
2265 ± 20	18 ANISOVICH	99C SPEC		0.6-1.94 $p \bar{p} \rightarrow \pi^0 \eta, \pi^0 \eta'$	~ 2500	6,7 ANISOVICH	99J SPEC	0	0.79-2.43 $p \bar{p} \rightarrow \pi \pi$
235 ⁺⁶⁰ ₋₃₅	18 ANISOVICH	99C SPEC		0.6-1.94 $p \bar{p} \rightarrow \pi^0 \eta, \pi^0 \eta'$	~ 470	6,7 ANISOVICH	99J SPEC	0	0.79-2.43 $p \bar{p} \rightarrow \pi \pi$
~ 2260	48 EVANGELISTA 79	OMEG	10,16	$\pi^- p \rightarrow \bar{p} p$	7 Using data of EISENHANDLER 75 and CARTER 77.				
~ 440	48 EVANGELISTA 79	OMEG	10,16	$\pi^- p \rightarrow \bar{p} p$	8 From a fit to the $J^G(J^{PC}) = 0^+(6^{+-})$.				
VALUE (MeV)	DOCUMENT ID	TECN	COMMENT		VALUE (MeV)	DOCUMENT ID	TECN	CHG	COMMENT
2280 ± 30	18,49 ANISOVICH	99D SPEC		0.6-1.94 $p \bar{p} \rightarrow \pi^0 \pi^0 \eta$	2480 ± 30	54 CARTER	77 CNTR	0	0.7-2.4 $\bar{p} p \rightarrow \pi \pi$
210 ± 30	18,49 ANISOVICH	99D SPEC		0.6-1.94 $p \bar{p} \rightarrow \pi^0 \pi^0 \eta$	210 ± 25	54 CARTER	77 CNTR	0	0.7-2.4 $\bar{p} p \rightarrow \pi \pi$
VALUE (MeV)	DOCUMENT ID	TECN	COMMENT		VALUE (MeV)	DOCUMENT ID	TECN	CHG	COMMENT
2280 ± 30	18,41 ANISOVICH	99E SPEC		0.6-1.94 $p \bar{p} \rightarrow 3\pi^0$	~ 2500	55 CARTER	78B CNTR	0	0.7-2.4 $\bar{p} p \rightarrow K^- K^+$
280 ± 50	18,41 ANISOVICH	99E SPEC		0.6-1.94 $p \bar{p} \rightarrow 3\pi^0$	~ 150	55 CARTER	78B CNTR	0	0.7-2.4 $\bar{p} p \rightarrow K^- K^+$
VALUE (MeV)	DOCUMENT ID	TECN	CHG	COMMENT	VALUE (MeV)	DOCUMENT ID	TECN	CHG	COMMENT
2295 ± 30	6,18 ANISOVICH	99J SPEC	0	0.6-1.94 $p \bar{p} \rightarrow \pi \pi, \eta \eta, \eta \eta'$	~ 2620	1,7 ANISOVICH	99J SPEC	0	0.79-2.43 $p \bar{p} \rightarrow \pi \pi$
235 ⁺⁶⁵ ₋₄₀	6,18 ANISOVICH	99J SPEC	0	0.6-1.94 $p \bar{p} \rightarrow \pi \pi, \eta \eta, \eta \eta'$	~ 430	1,7 ANISOVICH	99J SPEC	0	0.79-2.43 $p \bar{p} \rightarrow \pi \pi$
6 From a fit to the $J^G(J^{PC}) = 1^+(5^{--})$.					VALUE (MeV)	DOCUMENT ID	TECN	COMMENT	
VALUE (MeV)	DOCUMENT ID	TECN	CHG	COMMENT	2710 ± 20	ROZANSKA	80 SPRK		18 $\pi^- p \rightarrow p \bar{p} n$
2300 ± 20	18 ANISOVICH	99C SPEC		0.6-1.94 $p \bar{p} \rightarrow \pi^0 \eta, \pi^0 \eta'$	170 ± 40	ROZANSKA	80 SPRK		18 $\pi^- p \rightarrow p \bar{p} n$
230 ± 40	18 ANISOVICH	99C SPEC		0.6-1.94 $p \bar{p} \rightarrow \pi^0 \eta, \pi^0 \eta'$	VALUE (MeV)	DOCUMENT ID	TECN	CHG	COMMENT
2307 ± 6	ALPER	80 CNTR	0	62 $\pi^- p \rightarrow K^+ K^- n$	2850 ± 5	56 BRAUN	76 DBC	-	5.5 $\bar{p} d \rightarrow N \bar{N} \pi$
245 ± 20	ALPER	80 CNTR	0	62 $\pi^- p \rightarrow K^+ K^- n$	< 39	56 BRAUN	76 DBC	-	5.5 $\bar{p} d \rightarrow N \bar{N} \pi$
VALUE (MeV)	DOCUMENT ID	TECN	COMMENT		VALUE (MeV)	DOCUMENT ID	TECN	CHG	COMMENT
2300 ± 40	18,36 ANISOVICH	99D SPEC		0.6-1.94 $p \bar{p} \rightarrow \pi^0 \pi^0 \eta$	3370 ± 10	57 ALEXANDER	72 HBC	0	6.94 $\bar{p} p$
270 ± 40	18,36 ANISOVICH	99D SPEC		0.6-1.94 $p \bar{p} \rightarrow \pi^0 \pi^0 \eta$	150 ± 40	57 ALEXANDER	72 HBC	0	6.94 $\bar{p} p$
VALUE (MeV)	DOCUMENT ID	TECN	CHG	COMMENT	VALUE (MeV)	DOCUMENT ID	TECN	CHG	COMMENT
2300 ± 35	1,18 ANISOVICH	99J SPEC	0	0.6-1.94 $p \bar{p} \rightarrow \pi \pi, \eta \eta, \eta \eta'$	3600 ± 20	57 ALEXANDER	72 HBC	0	6.94 $\bar{p} p$
290 ± 50	1,18 ANISOVICH	99J SPEC	0	0.6-1.94 $p \bar{p} \rightarrow \pi \pi, \eta \eta, \eta \eta'$	140 ± 20	57 ALEXANDER	72 HBC	0	6.94 $\bar{p} p$
2300 ⁺⁵⁰ ₋₈₀	2,18 ANISOVICH	99J SPEC	0	0.6-1.94 $p \bar{p} \rightarrow \pi \pi, \eta \eta, \eta \eta'$	9 Not seen by GRAF 91.				
340 ± 150	2,18 ANISOVICH	99J SPEC	0	0.6-1.94 $p \bar{p} \rightarrow \pi \pi, \eta \eta, \eta \eta'$	10 Not seen by CHIBA 88, ANGELOPOULOS 86, ADIELS 86.				
2300 ± 25	5,18 ANISOVICH	99J SPEC	0	0.6-1.94 $p \bar{p} \rightarrow \pi \pi, \eta \eta, \eta \eta'$	11 They looked for radiative transitions to bound $p \bar{p}$ states, mono-energetic γ rays detected.				
270 ± 50	5,18 ANISOVICH	99J SPEC	0	0.6-1.94 $p \bar{p} \rightarrow \pi \pi, \eta \eta, \eta \eta'$	12 Observed widths consistent with experimental resolution.				
2320 ± 30	ANISOVICH	99J SPEC	0	0.6-1.94 $p \bar{p} \rightarrow \pi \pi, \eta \eta, \eta \eta'$	13 Not seen by ADIELS 86.				
175 ± 45	ANISOVICH	99J SPEC	0	0.6-1.94 $p \bar{p} \rightarrow \pi \pi, \eta \eta, \eta \eta'$	14 From analysis of difference of π^- and π^+ spectra.				
					15 Not seen by CHIBA 88, ANGELOPOULOS 86.				
					16 From a phenomenological analysis of ASTERIX data.				
					17 Produced backwards.				
					18 Using preliminary Crystal Barrel data.				
					19 $f(J^{PC}) = 1(1^-)$ from a mass dependent partial-wave analysis taking solution A.				
					20 From reanalysis of data from JASTRZEMBSKI 81.				
					21 Not seen by BUSENITZ 89.				
					22 From energy dependence of 5π cross section. $J^G = 1^-$ from observation of $\omega \rho$ decay. $P = +$ and $J > 1$. $\rho_2(1320) \pi \pi$ also seen.				

See key on page 239

Meson Particle Listings

 $\bar{N}N(1100-3600)$, $X(1900-3600)$

- ²³ $I = 0$ favored, $J = 0$ or 1, seen in total $\bar{p}p$ total cross section. Primarily from annihilation reactions. Not seen in $\bar{p}d$ total and annihilation cross sections.
- ²⁴ Narrow bump seen in total $\bar{p}p$, $\bar{p}d$ cross sections. Isospin uncertain. Not seen in $\bar{p}p$ charge exchange by ALSTON-GARNJOST 75, CHALOUPKA 76. Integrated cross section three times larger than BRUCKNER 77.
- ²⁵ Narrow bump seen in total $\bar{p}p$, $\bar{p}d$ cross sections. Isospin uncertain. Not seen in $\bar{p}p$ charge exchange by ALSTON-GARNJOST 75, CHALOUPKA 76. Integrated cross section three times larger than BRUCKNER 77. Not seen by CLOUGH 84.
- ²⁶ From energy dependence of far backward elastic scattering. Some indication of additional structure.
- ²⁷ From energy dependence of far backward elastic scattering. Some indication of additional structure.
- ²⁸ Not seen by ALBERI 79 with comparable statistics.
- ²⁹ Seen as a bump in the $\bar{p}p \rightarrow K_S^0 K_L^0$ cross section with $J^{PC} = 1^-$.
- ³⁰ Isospin 1 favored.
- ³¹ From a fit to the $I^G(J^{PC}) = 1^+(4^+ +) f_2(1270)\pi$ wave.
- ³² From a fit to the $I^G(J^{PC}) = 0^+(3^+ +) \pi^0 \pi^0 \eta$ wave.
- ³³ Not seen by AJALTOUNI 82, ARMSTRONG 79, BUZZO 97.
- ³⁴ From a fit to the $I^G(J^{PC}) = 0^+(2^+ +) \pi^0 \pi^0 \eta$ wave.
- ³⁵ Not seen by BIONTA 80, CARROLL 80, HAMILTON 80, BANKS 81, CHUNG 81, BARNETT 83.
- ³⁶ From a fit to the $I^G(J^{PC}) = 0^+(2^- +) \pi^0 \pi^0 \eta$ wave.
- ³⁷ Neutron spectator. See also $np\bar{p}\pi^-(p)$ channel following.
- ³⁸ From a fit to the $I^G(J^{PC}) = 1^+(3^+ +) f_2(1270)\pi$ wave.
- ³⁹ Proton spectator. See also $p\bar{p}n(n)$ channel above.
- ⁴⁰ $I(J^P) = 1(3^-)$ from a mass dependent partial-wave analysis taking solution A.
- ⁴¹ From a fit to the $I^G(J^{PC}) = 1^+(2^+ +) f_2(1270)\pi$ wave.
- ⁴² From a fit to the $I^G(J^{PC}) = 1^+(1^+ +) f_2(1270)\pi$ wave.
- ⁴³ $I(J^P) = 1(3^-)$ from amplitude analysis assuming one-pion exchange.
- ⁴⁴ From a fit to the $I^G(J^{PC}) = 0^+(1^+ +) \pi^0 \pi^0 \eta$ wave.
- ⁴⁵ Seen in final state $\omega\pi^+\pi^-$.
- ⁴⁶ $I(J^P) = 0(2^+)$ from amplitude analysis assuming one-pion exchange.
- ⁴⁷ ALLES-BORELLI 67b see neutral mode only $\pi^+\pi^-\pi^0$.
- ⁴⁸ $I(J^P) = 0(4^+)$ from a mass dependent partial-wave analysis taking solution A.
- ⁴⁹ From a fit to the $I^G(J^{PC}) = 0^+(3^+ +) \pi^0 \pi^0 \eta$ wave.
- ⁵⁰ From a fit to the $I^G(J^{PC}) = 0^+(4^+ +) \pi^0 \pi^0 \eta$ wave.
- ⁵¹ Supersedes CARBONELL 93.
- ⁵² $I(J^P) = 0(4^+)$ from amplitude analysis assuming one-pion exchange.
- ⁵³ $I(J^P) = 1(5^-)$ from amplitude analysis assuming one-pion exchange.
- ⁵⁴ $I(J^P) = 1(5^-)$ from amplitude analysis of $\bar{p}p \rightarrow \pi\pi$.
- ⁵⁵ $I=0, J^P = 5^-$ from Barrelet-zero analysis.
- ⁵⁶ Decays to $\bar{N}N$ and $\bar{N}N\pi$. Not seen by BARNETT 83.
- ⁵⁷ Decays to $4\pi^+4\pi^-$.

 $\bar{N}N(1100-3600)$ REFERENCES

ANISOVICH	99	PL B449 145	A.V. Anisovich et al.
ANISOVICH	99C	PL B452 173	A.V. Anisovich et al.
ANISOVICH	99D	PL B452 180	A.V. Anisovich et al.
Also	99F	NP A651 253	A.V. Anisovich et al.
ANISOVICH	99E	PL B452 187	A.V. Anisovich et al.
ANISOVICH	99J	PL B471 271	A.V. Anisovich et al.
FERRER	99	EPJ C10 249	A. Ferrer et al.
ANTONELLI	98	NP B517 3	A. Antonelli et al. (FENICE Collab.)
BUZZO	97	ZPHY C76 475	A. Buzzo et al. (JETSET Collab.)
CHIBA	97	PR D55 40	M. Chiba et al. (FUKI, INUS, KEK, SANG+)
DALKAROV	97	PL B392 229	O.D. Dalkarov et al. (LEBD)
BARNES	94	PL B331 203	P.D. Barnes et al. (PS185 Collab.)
CARBONELL	93	PL B306 407	J. Carbonell, K.V. Protasov, O.D. Dalkarov (ISNG+)
FERRER	93	NP A558 191c	A. Ferrer, A.A. Grigorian (WAS6 Collab.)
CHIBA	91	PR D44 1933	M. Chiba et al. (FUKI, KEK, SANG, OSAK+)
GRAF	91	PR D44 1945	N.A. Graf et al. (UCI, PENN, NMSU, KARLK+)
BUSENITZ	89	PR D40 1	J.K. Busenitz et al. (ILL, FNAL)
CHIBA	88	PL B202 447	M. Chiba, K. Doi (FUKI, INUS, KEK, SANG, OSAK+)
CHIBA	87	PR D36 3321	M. Chiba et al. (FUKI, INUS, KEK, SANG+)
DAFTARI	87	PR 58 859	I.K. Daftari et al. (SYRA)
FRANKLIN	87	PL B184 81	J. Franklin
ADIELS	86	PL B182 405	L. Adiels et al. (STOH, BASL, LASL, THES+)
ANGELOPO... BRIDGES BRIDGES	86 86B 86D	PL B178 441 PL 56 215 PL B180 313	A. Angelopoulos et al. (ATHU, UCI, KARLK+) D.L. Bridges et al. (SYRA, CASE) D.L. Bridges et al. (SYRA, BNL, CASE+)
ADIELS	84	PL 138B 235	L. Adiels et al. (BASL, KARLK, KARLE, STOHH+)
CLOUGH	84	PL 146B 299	A.S. Clough et al. (SURR, LOQM, ANIK+)
AZOOZ	83	PL 122B 471	F. Azooz, I. Butterworth (LOIC, RHEL, SACL+)
BARNETT	83	PR D27 493	B. Barnett et al. (JHU)
BODENKAMP	83	PL 133B 275	J. Bodenkamp et al. (KARLK, KARLE, DESY)
RICHTER	83	PL 126B 284	B. Richter, L. Adiels (BASL, KARLK, KARLE, STOHH+)
AJALTOUNI	82	NP B209 301	Z. Ajaltouni et al. (CERN, NEUC+)
BANKS	81	PL 100B 191	A.D. Banks et al. (LIVP, CERN)
CHUNG	81	PRL 46 395	S.U. Chung et al. (BNL, BRAN, CINC+)
JASTRZEM... ALPER	81 80	PR D23 2784 PL 94B 422	E. Jastrzembski et al. (TEMP, UCI, UNM) B. Alper et al. (AMST, CERN, CRAC, MPIM+)
ASTON	80D	PL 93B 517	D. Aston (BONN, CERN, EPOL, GLAS, LANG+)
BIONTA	80	PRL 44 909	R.M. Bionta et al. (BNL, CMU, FNAL+)
CARROLL	80	PRL 44 1572	A.S. Carroll et al. (BNL, PRIN)
DAUM	80E	PL 90B 475	C. Daum et al. (AMST, CERN, CRAC, MPIM+)
DEFOIX	80	NP B162 12	C. Defoix et al. (CDEF, PISA)
HAMILTON	80	PRL 44 1179	R.P. Hamilton et al. (LBL, BNL, MTHO)
HAMILTON	80B	PRL 44 1182	R.P. Hamilton et al. (LBL, BNL, MTHO)
KREYMER	80	PR D22 36	A.E. Kreymer et al. (IND, PURD, SLAC+)
ROZANSKA	80	NP B162 505	M. Rozanska et al. (MPIM, CERN)

ALBERI	79	PL 83B 247	G. Alberi et al. (TRST, CERN, IFRJ)
ARMSTRONG	79	PL 88B 304	T.A. Armstrong et al. (DESY, GLAS)
EVANGELISTA	79	NP B153 253	C. Evangelista et al. (BARI, BONN, CERN+)
EVANGELISTA	79B	NP B154 381	C. Evangelista et al. (BARI, BONN, CERN+)
GIBBARD	79	PRL 42 1593	B.G. Gibbard et al. (CORN)
SAKAMOTO	79	NP B158 410	S. Sakamoto et al. (INUS)
CARTER	78B	NP B141 467	A.A. Carter (LOQM)
PAVLOPO...	78	PL 72B 415	P. Pavlopoulos et al. (KARLK, KARLE, BASL+)
BENKHEIRI	77	PL 68B 483	P. Benkheiri et al. (CERN, CDEF, EPOL+)
BRUCKNER	77	PL 67B 222	W. Bruckner et al. (MPIH, HEIDP, CERN)
CARTER	77	PL 67B 117	A.A. Carter et al. (LOQM, RHEL) JP
ABASHIAN	76	PR D13 5	A. Abashian et al. (ILL, ANL, CIN+)
BRAUN	76	PL 60B 481	H.M. Braun et al. (STRB)
CHALOUPKA	76	PL 61B 487	V. Chaloupka et al. (CERN, LIVP, MONS+)
ALSTON...	75	PRL 35 1685	M. Alston-Garnjost et al. (LBL, MTHO)
D'ANDLAU	75	PL 58B 223	C. d'Andlau et al. (CDEF, PISA)
EISENHAND...	75	NP B96 109	E. Eisenhandler et al. (LOQM, LIVP, DARE+)
KALOGERO...	75	PRL 34 1047	T. Kalogeropoulos, G.S. Tzanakos (SYRA)
CARROLL	74	PRL 32 247	A.S. Carroll et al. (BNL)
DONALD	73	NP B51 333	R.A. Donald et al. (LIVP, PARIS)
ALEXANDER	72	NP B45 29	G. Alexander et al. (TELA)
BENVENUTI	71	PRL 27 283	A.C. Benvenuti et al. (WISC)
ALLES...	67B	NC 50A 776	V. Alles-Borelli et al. (CERN, BONN) G
BETTINI	66	NC 42A 695	A. Bettini et al. (PADO, PISA)

OTHER RELATED PAPERS

ANISOVICH	99F	NP A651 253	A.V. Anisovich et al.
CHIBA	99	PR C60 035204	M. Chiba et al.
BUZZO	97	ZPHY C76 475	A. Buzzo et al. (JETSET Collab.)
TANIMORI	90	PR D41 744	T. Tanimori et al. (KEK, INUS, KYOT+)
LIU	87	PRL 58 2288	K.F. Liu, Kiu, B.A. Li (STON)
ARMSTRONG	86C	PL B175 383	T.A. Armstrong et al. (BNL, HOUS, PENN+)
BRIDGES	86	PRL 56 211	D.L. Bridges et al. (BLSU, BNL, CASE+)
BRIDGES	86C	PRL 57 1534	D.L. Bridges et al. (SYRA)
DOVER	86	PRL 57 1207	C.B. Dover et al. (BNL) JP
ANGELOPO...	85	PL 159B 210	A. Angelopoulos et al. (ATHU, UCI, UNM+)
BODENKAMP	85	NP B255 717	J. Bodenkamp et al. (KARLK, KARLE, DESY)
AZOOZ	84	NP B244 277	F. Azooz, I. Butterworth (LOIC, RHEL, SACL+)

 $X(1900-3600)$ OMITTED FROM SUMMARY TABLE
THE $X(1900-3600)$ REGION

This high-mass region is covered nearly continuously with evidence for peaks of various widths and decay modes. As no satisfactory grouping into particles is yet possible, we list together in order of increasing mass all the $Y=0$ bumps above 1900 MeV that are coupled neither to $\bar{N}N$ nor to e^+e^- .

 $X(1900-3600)$ MASSES AND WIDTHS

We do not use the following data for averages, fits, limits, etc.

VALUE (MeV)	DOCUMENT ID	TECN	CHG	COMMENT
1900 to 3600 OUR LIMIT				
1870 ± 40	¹ ALDE	86D GAM4	0	100 $\pi^- p \rightarrow 2\eta X$
250 ± 30	¹ ALDE	86D GAM4	0	100 $\pi^- p \rightarrow 2\eta X$
1898 ± 18	THOMPSON	74 HBC	+	13 $\pi^+ p \rightarrow 2\rho X$
108 ⁺⁴¹ ₋₂₇	THOMPSON	74 HBC	+	13 $\pi^+ p \rightarrow 2\rho X$
1900 ± 40	BOESEBECK	68 HBC	+	8 $\pi^+ p \rightarrow \pi^+ \pi^0 X$
216 ± 105	BOESEBECK	68 HBC	+	8 $\pi^+ p \rightarrow \pi^+ \pi^0 X$
1929 ± 14	² FOCACCI	66 MMS	-	3-12 $\pi^- p$
22 ± 2	² FOCACCI	66 MMS	-	3-12 $\pi^- p$
1970 ± 10	CHLIAPNIK...	80 HBC	0	32 $K^+ p \rightarrow 2K_S^0 2\pi X$
40 ± 20	CHLIAPNIK...	80 HBC	0	32 $K^+ p \rightarrow 2K_S^0 2\pi X$
1973 ± 15	CASO	70 HBC	-	11.2 $\pi^- p \rightarrow \rho 2\pi$
80	CASO	70 HBC	-	11.2 $\pi^- p \rightarrow \rho 2\pi$
2070	TAKAHASHI	72 HBC	8	$\pi^- p \rightarrow N 2\pi$
160	TAKAHASHI	72 HBC	8	$\pi^- p \rightarrow N 2\pi$

Meson Particle Listings

X(1900–3600)

VALUE (MeV)	EVTs	DOCUMENT ID	TECN	CHG	COMMENT
~ 2104		BUGG	95	MRK3	$J/\psi \rightarrow \gamma \pi^+ \pi^- \pi^+ \pi^-$
2103 ± 50	586	³ BISELLO	89B	DM2	$J/\psi \rightarrow 4\pi\gamma$
187 ± 75	586	³ BISELLO	89B	DM2	$J/\psi \rightarrow 4\pi\gamma$
2100 ± 40		⁴ ALDE	86D	GAM4 0	$100 \pi^- \rho \rightarrow 2\eta X$
250 ± 40		⁴ ALDE	86D	GAM4 0	$100 \pi^- \rho \rightarrow 2\eta X$
VALUE (MeV)	EVTs	DOCUMENT ID	TECN	CHG	COMMENT
2141 ± 12	389	GREEN	86	MPSF	$400 \rho A \rightarrow 4KX$
49 ± 28	389	GREEN	86	MPSF	$400 \rho A \rightarrow 4KX$
VALUE (MeV)	EVTs	DOCUMENT ID	TECN	CHG	COMMENT
2190 ± 10		CLAYTON	67	HBC	$\pm 2.5 \bar{p} p \rightarrow a_2, \omega$
VALUE (MeV)	EVTs	DOCUMENT ID	TECN	CHG	COMMENT
2195 ± 15		² FOCACCI	66	MMS	$- 3-12 \pi^- \rho$
39 ± 14		² FOCACCI	66	MMS	$- 3-12 \pi^- \rho$
VALUE (MeV)	EVTs	DOCUMENT ID	TECN	CHG	COMMENT
2207 ± 22		⁵ CASO	70	HBC	$- 11.2 \pi^- \rho$
130		⁵ CASO	70	HBC	$- 11.2 \pi^- \rho$
VALUE (MeV)	EVTs	DOCUMENT ID	TECN	CHG	COMMENT
2280 ± 50		ATKINSON	85	OMEG	$20-70 \gamma \rho \rightarrow \rho \omega \pi^+ \pi^- \pi^0$
440 ± 110		ATKINSON	85	OMEG	$20-70 \gamma \rho \rightarrow \rho \omega \pi^+ \pi^- \pi^0$
VALUE (MeV)	EVTs	DOCUMENT ID	TECN	CHG	COMMENT
2300 ± 100		ATKINSON	84F	OMEG ± 0	$20-70 \gamma \rho \rightarrow \rho f$
~ 250		ATKINSON	84F	OMEG ± 0	$20-70 \gamma \rho \rightarrow \rho f$
VALUE (MeV)	EVTs	DOCUMENT ID	TECN	CHG	COMMENT
2330 ± 30		ATKINSON	88	OMEG 0	$25-50 \gamma \rho \rightarrow \rho^\pm \rho^0 \pi^\mp$
435 ± 75		ATKINSON	88	OMEG 0	$25-50 \gamma \rho \rightarrow \rho^\pm \rho^0 \pi^\mp$
VALUE (MeV)	EVTs	DOCUMENT ID	TECN	CHG	COMMENT
2340 ± 20	126	⁶ BALTAY	75	HBC	$+ 15 \pi^+ \rho \rightarrow \rho 5\pi$
180 ± 60	126	⁶ BALTAY	75	HBC	$+ 15 \pi^+ \rho \rightarrow \rho 5\pi$
VALUE (MeV)	EVTs	DOCUMENT ID	TECN	CHG	COMMENT
2382 ± 24		² FOCACCI	66	MMS	$- 3-12 \pi^- \rho$
62 ± 6		² FOCACCI	66	MMS	$- 3-12 \pi^- \rho$
VALUE (MeV)	EVTs	DOCUMENT ID	TECN	CHG	COMMENT
2500 ± 32		ANDERSON	69	MMS	$- 16 \pi^- \rho$ backward
87		ANDERSON	69	MMS	$- 16 \pi^- \rho$ backward
VALUE (MeV)	EVTs	DOCUMENT ID	TECN	CHG	COMMENT
2620 ± 20	550	BAUD	69	MMS	$- 8-10 \pi^- \rho$
85 ± 30	550	BAUD	69	MMS	$- 8-10 \pi^- \rho$
VALUE (MeV)	EVTs	DOCUMENT ID	TECN	CHG	COMMENT
2676 ± 27		⁵ CASO	70	HBC	$- 11.2 \pi^- \rho$
150		⁵ CASO	70	HBC	$- 11.2 \pi^- \rho$
VALUE (MeV)	EVTs	DOCUMENT ID	TECN	CHG	COMMENT
2747 ± 32		DENNEY	83	LASS	$10 \pi^+ N$
195 ± 75		DENNEY	83	LASS	$10 \pi^+ N$
VALUE (MeV)	EVTs	DOCUMENT ID	TECN	CHG	COMMENT
2800 ± 20	640	BAUD	69	MMS	$- 8-10 \pi^- \rho$
46 ± 10	640	BAUD	69	MMS	$- 8-10 \pi^- \rho$

VALUE (MeV)	EVTs	DOCUMENT ID	TECN	CHG	COMMENT
2820 ± 10	15	⁷ SABAU	71	HBC	$+ 8 \pi^+ \rho$
50 ± 10	15	⁷ SABAU	71	HBC	$+ 8 \pi^+ \rho$
VALUE (MeV)	EVTs	DOCUMENT ID	TECN	CHG	COMMENT
2880 ± 20	230	BAUD	69	MMS	$- 8-10 \pi^- \rho$
< 15	230	BAUD	69	MMS	$- 8-10 \pi^- \rho$
VALUE (MeV)	EVTs	DOCUMENT ID	TECN	CHG	COMMENT
3025 ± 20		BAUD	70	MMS	$- 10.5-13 \pi^- \rho$
~ 25		BAUD	70	MMS	$- 10.5-13 \pi^- \rho$
VALUE (MeV)	EVTs	DOCUMENT ID	TECN	CHG	COMMENT
3075 ± 20		BAUD	70	MMS	$- 10.5-13 \pi^- \rho$
~ 25		BAUD	70	MMS	$- 10.5-13 \pi^- \rho$
VALUE (MeV)	EVTs	DOCUMENT ID	TECN	CHG	COMMENT
3145 ± 20		BAUD	70	MMS	$- 10.5-15 \pi^- \rho$
< 10		BAUD	70	MMS	$- 10.5-15 \pi^- \rho$
VALUE (MeV)	EVTs	DOCUMENT ID	TECN	CHG	COMMENT
3475 ± 20		BAUD	70	MMS	$- 14-15.5 \pi^- \rho$
~ 30		BAUD	70	MMS	$- 14-15.5 \pi^- \rho$
VALUE (MeV)	EVTs	DOCUMENT ID	TECN	CHG	COMMENT
3535 ± 20		BAUD	70	MMS	$- 14-15.5 \pi^- \rho$
~ 30		BAUD	70	MMS	$- 14-15.5 \pi^- \rho$

¹ Seen in $J = 2$ wave in one of the two ambiguous solutions.

² Not seen by ANTIPOV 72, who performed a similar experiment at 25 and 40 GeV/c.

³ ASTON 81B sees no peak, has 850 events in Ajinenko+Barth bins. ARESTOV 80 sees no peak.

⁴ Seen in $J = 0$ wave in one of the two ambiguous solutions.

⁵ Seen in $\rho^- \pi^+ \pi^-$ (ω and η antiselected in 4π system).

⁶ Dominant decay into $\rho^0 \rho^0 \pi^+$. BALTAY 78 finds confirmation in $2\pi^+ \pi^- 2\pi^0$ events which contain $\rho^+ \rho^0 \pi^0$ and $2\rho^+ \pi^-$.

⁷ Seen in $(K \bar{K} \pi \pi)$ mass distribution.

X(1900–3600) REFERENCES

BUGG	95	PL B353 378	D.V. Bugg <i>et al.</i>	(LOQM, PNPI, WASH)
BISELLO	89B	PR D39 701	G. Busetto <i>et al.</i>	(DM2 Collab.)
ATKINSON	88	ZPHY C38 535	M. Atkinson <i>et al.</i>	(BONN, CERN, GLAS+)
ALDE	86D	NP B269 485	D.M. Alde <i>et al.</i>	(BELG, LAPP, SERP, CERN+)
GREEN	86	PRL 56 1639	D.R. Green <i>et al.</i>	(FNAL, ARIZ, FSU+)
ATKINSON	85	ZPHY C29 333	M. Atkinson <i>et al.</i>	(BONN, CERN, GLAS+)
ATKINSON	84F	NP 5229 1	M. Atkinson <i>et al.</i>	(BONN, CERN, GLAS+)
DENNEY	83	PR D28 2726	D.L. Denney <i>et al.</i>	(IOWA, MICH) J
ASTON	81B	NP B189 205	D. Aston <i>et al.</i>	(BONN, CERN, EPOL, GLAS+)
ARESTOV	80	IHEP 80-165	Y.I. Arestov <i>et al.</i>	(SERP)
CHLIAPNIK...	80	ZPHY C3 285	P.V. Chliapnikov <i>et al.</i>	(SERP, BRUX, MORIS)
BALTAY	78	PR D17 52	C. Baltay <i>et al.</i>	(COLU, BING)
BALTAY	75	PRL 35 891	C. Baltay <i>et al.</i>	(COLU, BING)
THOMPSON	74	NP B69 220	G. Thompson <i>et al.</i>	(PURD)
ANTIPOV	72	PL 40 147	Y.M. Antipov <i>et al.</i>	(SERP)
TAKAHASHI	72	PR D6 1266	K. Takahashi <i>et al.</i>	(TOHOK, PENN, NDAM+)
SABAU	71	LNC 1 514	M. Sabau, J.L. Uretsky	(BUCH, ANL)
BAUD	70	PL 31B 549	R. Baud <i>et al.</i>	
CASO	70	LNC 3 707	C. Caso <i>et al.</i>	(GENO, HAMB, MILA, SACL)
ANDERSON	69	PRL 22 1390	E.W. Anderson <i>et al.</i>	(BNL, CMU)
BAUD	69	PL 30B 129	R. Baud <i>et al.</i>	
BOESEBECK	68	NP B4 501	K. Boesebeck <i>et al.</i>	(AACH, BERL, CERN)
CLAYTON	67	Heidelberg Conf. 57	J.C. Clayton <i>et al.</i>	(LIVP, ATHU)
FOCACCI	66	PRL 17 890	M.N. Focacci <i>et al.</i>	(CERN)

OTHER RELATED PAPERS

ANTIPOV	72	PL 40 147	Y.M. Antipov <i>et al.</i>	(SERP)
CHIKOVANI	66	PL 22 233	G.E. Chikovani <i>et al.</i>	(SERP)

STRANGE MESONS ($S = \pm 1, C = B = 0$)

$K^+ = u\bar{s}, K^0 = d\bar{s}, \bar{K}^0 = \bar{d}s, K^- = \bar{u}s$, similarly for K^{*} 's

K^\pm

$$I(J^P) = \frac{1}{2}(0^-)$$

THE CHARGED KAON MASS

Revised 1994 by T.G. Trippe, (LBNL).

The average of the six charged kaon mass measurements which we use in the Particle Listings is

$$m_{K^\pm} = 493.677 \pm 0.013 \text{ MeV } (S = 2.4), \quad (1)$$

where the error has been increased by the scale factor S . The large scale factor indicates a serious disagreement between different input data. The average before scaling the error is

$$m_{K^\pm} = 493.677 \pm 0.005 \text{ MeV},$$

$$\chi^2 = 22.9 \text{ for } 5 \text{ D.F.}, \text{ Prob.} = 0.04\%, \quad (2)$$

where the high χ^2 and correspondingly low χ^2 probability further quantify the disagreement.

The main disagreement is between the two most recent and precise results,

$$m_{K^\pm} = 493.696 \pm 0.007 \text{ MeV} \quad \text{DENISOV 91}$$

$$m_{K^\pm} = 493.636 \pm 0.011 \text{ MeV } (S = 1.5) \quad \text{GALL 88}$$

$$\text{Average} = 493.679 \pm 0.006 \text{ MeV}$$

$$\chi^2 = 21.2 \text{ for } 1 \text{ D.F.}, \text{ Prob.} = 0.0004\%, \quad (3)$$

both of which are measurements of x-ray energies from kaonic atoms. Comparing the average in Eq. (3) with the overall average in Eq. (2), it is clear that DENISOV 91 and GALL 88 dominate the overall average, and that their disagreement is responsible for most of the high χ^2 .

The GALL 88 measurement was made using four different kaonic atom transitions, $K^- \text{Pb } (9 \rightarrow 8)$, $K^- \text{Pb } (11 \rightarrow 10)$, $K^- \text{W } (9 \rightarrow 8)$, and $K^- \text{W } (11 \rightarrow 10)$. The m_{K^\pm} values they obtain from each of these transitions is shown in the Particle Listings and in Fig. 1. Their $K^- \text{Pb } (9 \rightarrow 8)$ m_{K^\pm} is below and somewhat inconsistent with their other three transitions. The average of their four measurements is

$$m_{K^\pm} = 493.636 \pm 0.007,$$

$$\chi^2 = 7.0 \text{ for } 3 \text{ D.F.}, \text{ Prob.} = 7.2\%. \quad (4)$$

This is a low but acceptable χ^2 probability so, to be conservative, GALL 88 scaled up the error on their average by $S=1.5$ to obtain their published error ± 0.011 shown in Eq. (3) above and used in the Particle Listings average.

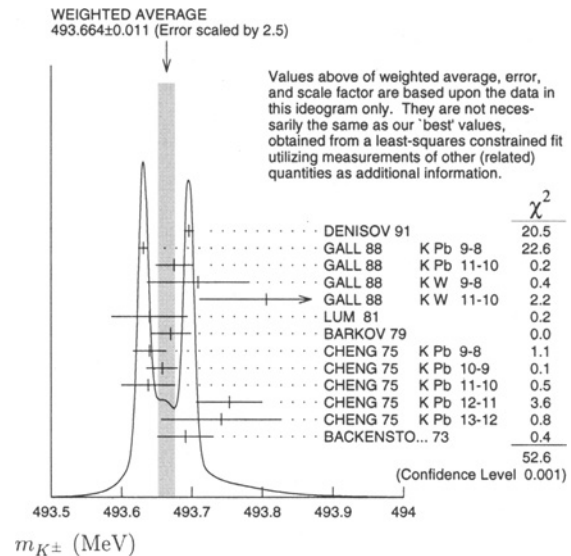


Figure 1: Ideogram of m_{K^\pm} mass measurements. GALL 88 and CHENG 75 measurements are shown separately for each transition they measured.

The ideogram in Fig. 1 shows that the DENISOV 91 measurement and the GALL 88 $K^- \text{Pb } (9 \rightarrow 8)$ measurement yield two well-separated peaks. One might suspect the GALL 88 $K^- \text{Pb } (9 \rightarrow 8)$ measurement since it is responsible both for the internal inconsistency in the GALL 88 measurements and the disagreement with DENISOV 91.

To see if the disagreement could result from a systematic problem with the $K^- \text{Pb } (9 \rightarrow 8)$ transition, we have separated the CHENG 75 data, which also used $K^- \text{Pb}$, into its separate transitions. Figure 1 shows that the CHENG 75 and GALL 88 $K^- \text{Pb } (9 \rightarrow 8)$ values are consistent, suggesting the possibility of a common effect such as contaminant nuclear γ rays near the $K^- \text{Pb } (9 \rightarrow 8)$ transition energy, although the CHENG 75 errors are too large to make a strong conclusion. The average of all 13 measurements has a χ^2 of 52.6 as shown in Fig. 1 and the first line of Table 1, yielding an unacceptable χ^2 probability of 0.00005%. The second line of Table 1 excludes both the GALL 88 and CHENG 75 measurements of the $K^- \text{Pb } (9 \rightarrow 8)$ transition and yields a χ^2 probability of 43%. The third [fourth] line of Table 1 excludes only the GALL 88 $K^- \text{Pb } (9 \rightarrow 8)$ [DENISOV 91] measurement and yields a χ^2 probability of 20% [8.6%]. Table 1 shows that removing both measurements of the $K^- \text{Pb } (9 \rightarrow 8)$ transition produces the most consistent set of data, but that excluding only the GALL 88 $K^- \text{Pb } (9 \rightarrow 8)$ transition or DENISOV 91 also produces acceptable probabilities.

Yu.M. Ivanov, representing DENISOV 91, has estimated corrections needed for the older experiments because of improved ^{192}Ir and ^{198}Au calibration γ -ray energies. He estimates that CHENG 75 and BACKENSTOSS 73 m_{K^\pm} values could be

Meson Particle Listings

K^\pm

Table 1: m_{K^\pm} averages for some combinations of Fig. 1 data.

m_{K^\pm} (MeV)	χ^2	D.F.	Prob. (%)	Measurements used
493.664 ± 0.004	52.6	12	0.00005	all 13 measurements
493.690 ± 0.006	10.1	10	43	no K^- Pb(9→8)
493.687 ± 0.006	14.6	11	20	no GALL 88 K^- Pb(9→8)
493.642 ± 0.006	17.8	11	8.6	no DENISOV 91

raised by about 15 keV and 22 keV, respectively. With these estimated corrections, Table 1 becomes Table 2. The last line of Table 2 shows that if such corrections are assumed, then GALL 88 K^- Pb (9 → 8) is inconsistent with the rest of the data even when DENISOV 91 is excluded. Yu.M. Ivanov warns that these are rough estimates. Accordingly, we do not use Table 2 to reject the GALL 88 K^- Pb (9 → 8) transition, but we note that a future reanalysis of the CHENG 75 data could be useful because it might provide supporting evidence for such a rejection.

Table 2: m_{K^\pm} averages for some combinations of Fig. 1 data after raising CHENG 75 and BACKENSTOSS 73 values by 0.015 and 0.022 MeV respectively.

m_{K^\pm} (MeV)	χ^2	D.F.	Prob. (%)	Measurements used
493.666 ± 0.004	53.9	12	0.00003	all 13 measurements
493.693 ± 0.006	9.0	10	53	no K^- Pb(9→8)
493.690 ± 0.006	11.5	11	40	no GALL 88 K^- Pb(9→8)
493.645 ± 0.006	23.0	11	1.8	no DENISOV 91

The GALL 88 measurement uses a Ge semiconductor spectrometer which has a resolution of about 1 keV, so they run the risk of some contaminant nuclear γ rays. Studies of γ rays following stopped π^- and Σ^- absorption in nuclei (unpublished) do not show any evidence for contaminants according to GALL 88 spokesperson, B.L. Roberts. The DENISOV 91 measurement uses a crystal diffraction spectrometer with a resolution of 6.3 eV for radiation at 22.1 keV to measure the 4f-3d transition in $K^-^{12}\text{C}$. The high resolution and the light nucleus reduce the probability for overlap by contaminant γ rays, compared with the measurement of GALL 88. The DENISOV 91 measurement is supported by their high-precision measurement of the 4d-2p transition energy in $\pi^-^{12}\text{C}$, which is good agreement with the calculated energy.

While we suspect that the GALL 88 K^- Pb (9 → 8) measurements could be the problem, we are unable to find clear grounds for rejecting it. Therefore, we retain their measurement in the average and accept the large scale factor until further information can be obtained from new measurements and/or from reanalysis of GALL 88 and CHENG 75 data.

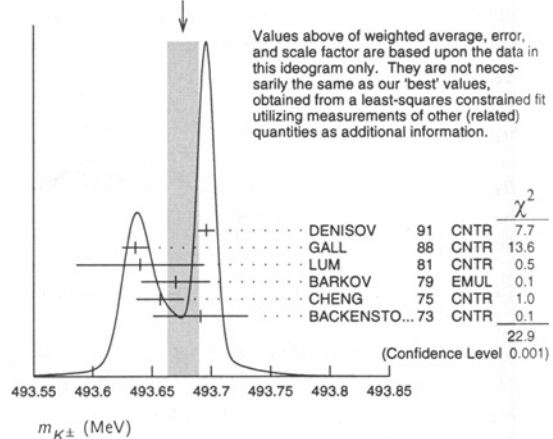
We thank B.L. Roberts (Boston Univ.) and Yu.M. Ivanov (Petersburg Nuclear Physics Inst.) for their extensive help in understanding this problem.

K^\pm MASS

VALUE (MeV)	DOCUMENT ID	TECN	CHG	COMMENT
493.677 ± 0.016 OUR FIT	Error includes scale factor of 2.8.			
493.677 ± 0.013 OUR AVERAGE	Error includes scale factor of 2.4. See the ideogram below.			
493.696 ± 0.007	¹ DENISOV	91	CNTR	- Kaonic atoms
493.636 ± 0.011	² GALL	88	CNTR	- Kaonic atoms
493.640 ± 0.054	LUM	81	CNTR	- Kaonic atoms
493.670 ± 0.029	BARKOV	79	EMUL	$\pm e^+ e^- \rightarrow K^+ K^-$
493.657 ± 0.020	² CHENG	75	CNTR	- Kaonic atoms
493.691 ± 0.040	BACKENSTO...73	CNTR	-	- Kaonic atoms
• • • We do not use the following data for averages, fits, limits, etc. • • •				
493.631 ± 0.007	GALL	88	CNTR	- K^- Pb (9 → 8)
493.675 ± 0.026	GALL	88	CNTR	- K^- Pb (11 → 10)
493.709 ± 0.073	GALL	88	CNTR	- K^- W (9 → 8)
493.806 ± 0.095	GALL	88	CNTR	- K^- W (11 → 10)
$493.640 \pm 0.022 \pm 0.008$	³ CHENG	75	CNTR	- K^- Pb (9 → 8)
$493.658 \pm 0.019 \pm 0.012$	³ CHENG	75	CNTR	- K^- Pb (10 → 9)
$493.638 \pm 0.035 \pm 0.016$	³ CHENG	75	CNTR	- K^- Pb (11 → 10)
$493.753 \pm 0.042 \pm 0.021$	³ CHENG	75	CNTR	- K^- Pb (12 → 11)
$493.742 \pm 0.081 \pm 0.027$	³ CHENG	75	CNTR	- K^- Pb (13 → 12)
493.662 ± 0.19	KUNSELMAN	74	CNTR	- Kaonic atoms
493.78 ± 0.17	GREIMER	65	EMUL	+
493.7 ± 0.3	BARKAS	63	EMUL	-
493.9 ± 0.2	COHEN	57	RVUE	+

- ¹ Error increased from 0.0059 based on the error analysis in IVANOV 92.
- ² This value is the authors' combination of all of the separate transitions listed for this paper.
- ³ The CHENG 75 values for separate transitions were calculated from their Table 7 transition energies. The first error includes a 20% systematic error in the noncircular contaminant shift. The second error is due to a ± 5 eV uncertainty in the theoretical transition energies.

WEIGHTED AVERAGE
 493.677 ± 0.013 (Error scaled by 2.4)



$m_{K^+} - m_{K^-}$

Test of CPT.

VALUE (MeV)	EVTS	DOCUMENT ID	TECN	CHG
-0.032 ± 0.090	1.5M	⁴ FORD	72	ASPK \pm

⁴ FORD 72 uses $m_{\pi^+} - m_{\pi^-} = +28 \pm 70$ keV.

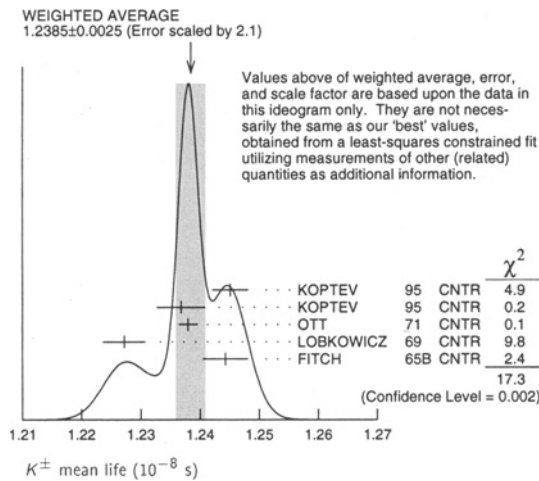
K^\pm MEAN LIFE

VALUE (10^{-8} s)	EVTS	DOCUMENT ID	TECN	CHG	COMMENT
1.2386 ± 0.0024 OUR FIT	Error includes scale factor of 2.0.				
1.2385 ± 0.0025 OUR AVERAGE	Error includes scale factor of 2.1. See the ideogram below.				
1.2451 ± 0.0030	250k	KOPTEV	95	CNTR	K at rest, U target
1.2368 ± 0.0041	150k	KOPTEV	95	CNTR	K at rest, Cu target
1.2380 ± 0.0016	3M	OTT	71	CNTR	+
1.2272 ± 0.0036		LOBKOWICZ	69	CNTR	+
1.2443 ± 0.0038		FITCH	65B	CNTR	+

• • • We do not use the following data for averages, fits, limits, etc. • • •

1.2415 ± 0.0024	400k	⁵ KOPTEV	95	CNTR	K at rest
1.221 ± 0.011		FORD	67	CNTR	±
1.231 ± 0.011		BOYARSKI	62	CNTR	+
1.25 +0.22 -0.17		BARKAS	61	EMUL	
1.27 +0.36 -0.23	51	BHOWMIK	61	EMUL	
1.31 ± 0.08	293	NORDIN	61	HBC	-
1.24 ± 0.07		NORDIN	61	RVUE	-
1.38 ± 0.24	33	FREDEN	60B	EMUL	
1.21 ± 0.06		BURROWES	59	CNTR	
1.60 ± 0.3	52	EISENBERG	58	EMUL	
0.95 +0.36 -0.25		ILOFF	56	EMUL	

⁵KOPTEV 95 report this weighted average of their U-target and Cu-target results, where they have weighted by $1/\sigma$ rather than $1/\sigma^2$.



$$\frac{(\tau_{K^+} - \tau_{K^-})}{\tau_{\text{average}}}$$

This quantity is a measure of CPT invariance in weak interactions.

VALUE (%)	DOCUMENT ID	TECN
0.11 ± 0.09 OUR AVERAGE	Error includes scale factor of 1.2.	
0.090 ± 0.078	LOBKOWICZ	69 CNTR
0.47 ± 0.30	FORD	67 CNTR

RARE KAON DECAYS

(Revised April 2000 by L. Littenberg, BNL and G. Valencia, Iowa State University)

A. Introduction: There are several useful reviews on rare kaon decays and related topics [1–11]. The current activity in rare kaon decays can be divided roughly into four categories:

1. Searches for explicit violations of the Standard Model
2. Measurements of Standard Model parameters
3. Searches for CP violation
4. Studies of strong interactions at low energy.

The paradigm of Category 1 is the lepton flavor violating decay $K_L \rightarrow \mu e$. Category 2 includes processes such as $K^+ \rightarrow \pi^+ \nu \bar{\nu}$, which is sensitive to $|V_{td}|$. Much of the interest in Category 3 is focussed on the decays $K_L \rightarrow \pi^0 \ell \bar{\ell}$, where $\ell \equiv e, \mu, \nu$. Category 4 includes reactions like $K^+ \rightarrow \pi^+ \ell^+ \ell^-$ which constitute a testing ground for the ideas of chiral perturbation theory. Other reactions of this type are $K_L \rightarrow \pi^0 \gamma \gamma$, which also scales a CP -conserving background to CP violation in $K_L \rightarrow \pi^0 \ell^+ \ell^-$ and $K_L \rightarrow \gamma \ell^+ \ell^-$, which could possibly shed light on long distance contributions to $K_L \rightarrow \mu^+ \mu^-$.

B. Explicit violations of the Standard Model: Most of the activity here is in searches for lepton flavor violation (LFV). This is motivated by the fact that many extensions of the minimal Standard Model violate lepton flavor and by the potential to access very high energy scales. For example, the tree-level exchange of a LFV vector boson of mass M_X that couples to left-handed fermions with electroweak strength and without mixing angles yields $B(K_L \rightarrow \mu e) = 4.7 \times 10^{-12} (148 \text{ TeV}/M_X)^4$ [5]. This simple dimensional analysis may be used to read from Table 1 that the reaction $K_L \rightarrow \mu e$ is already probing scales of over 100 TeV. Table 1 summarizes the present experimental situation vis a vis LFV, along with the expected near-future progress. The decays $K_L \rightarrow \mu^\pm e^\mp$ and $K^+ \rightarrow \pi^+ e^\mp \mu^\pm$ (or $K_L \rightarrow \pi^0 e^\mp \mu^\pm$) provide complementary information on potential family number violating interactions since the former is sensitive to parity-odd couplings and the latter is sensitive to parity-even couplings. Related searches in μ and τ process are discussed in our section “Tests of Conservation Laws”.

Table 1: Searches for lepton flavor violation in K decay

Mode	90% CL		Exp't	Yr./Ref.	(Near-)
	upper limit				future aim
$K^+ \rightarrow \pi^+ e \mu$	4.8×10^{-11} *	BNL-865	99/12	9×10^{-12}	(BNL-865)
$K_L \rightarrow \mu e$	4.7×10^{-12}	BNL-871	98/13		
$K_L \rightarrow \pi^0 e \mu$	3.2×10^{-9}	FNAL-799	94/14	5×10^{-11}	(KTeV)

*preliminary

Another forbidden decay currently being pursued is $K^+ \rightarrow \pi^+ X^0$, where X^0 is a very light, noninteracting particle (*e.g.* hyperphoton, axion, familon, *etc.*). The 90% CL upper limit on this process was recently improved to 1.1×10^{-10} [15]. Data already collected by BNL-787 are expected to yield a further factor ~ 2 in sensitivity to this process.

C. Measurements of Standard Model parameters: Until 1997, searches for $K^+ \rightarrow \pi^+ \nu \bar{\nu}$ were motivated by the possibility of observing non-SM physics because the sensitivity attained was far short of the SM prediction for this decay [16] and long-distance contributions were known to be negligible [2]. However, BNL-787 has attained the sensitivity at which the observation of an event can no longer be unambiguously attributed to non-SM physics. In 1997 BNL-787 observed a single candidate event and has recently released the results of further running in which no further events were seen, yielding a branching ratio of $(1.5^{+3.4}_{-1.2}) \times 10^{-10}$ [15]. Further data already collected are expected to increase the sensitivity by approximately a factor 2, and there are plans for an upgrade to the experiment to collect roughly an order of magnitude more sensitivity [17]. This reaction is now interesting from the point of view of constraining SM parameters. The branching ratio can be written in terms of the very well-measured rate of K_{e3} as [2]:

$$B(K^+ \rightarrow \pi^+ \nu \bar{\nu}) = \frac{\alpha^2 B(K^+ \rightarrow \pi^0 e^+ \nu)}{V_{us}^2 2\pi^2 \sin^4 \theta_W} \times \sum_{l=e,\mu,\tau} |V_{cs}^* V_{cd} X_{NL}^l + V_{ts}^* V_{td} X(m_t)|^2 \quad (1)$$

Meson Particle Listings

K^\pm

to eliminate the *a priori* unknown hadronic matrix element. Isospin breaking corrections to the ratio of matrix elements reduce this rate by 10% [18]. In Eq. (1) the Inami-Lim function $X(m_t)$ is of order 1 [19], and X_{NL}^ℓ is several hundred times smaller. This form exhibits the strong dependence of this branching ratio on $|V_{td}|$. QCD corrections, which are contained in X_{NL}^ℓ , are relatively small and now known [10] to $\leq 10\%$. Evaluating the constants in Eq. (1) with $m_t = 175$ GeV, one can cast this result in terms of the CKM parameters A , ρ and η (see our Section on “The Cabibbo-Kobayashi-Maskawa mixing matrix”) [10]

$$B(K^+ \rightarrow \pi^+ \nu \bar{\nu}) \approx 1.0 \times 10^{-10} A^4 [\eta^2 + (\rho_o - \rho)^2] \quad (2)$$

where $\rho_o \equiv 1 + (\frac{2}{3} X_{NL}^e + \frac{1}{3} X_{NL}^\tau) / (A^2 V_{us}^4 X(m_t)) \approx 1.4$. Thus, $B(K^+ \rightarrow \pi^+ \nu \bar{\nu})$ determines a circle in the ρ , η plane with center $(\rho_o, 0)$ and radius $\approx \frac{1}{A^2} \sqrt{\frac{B(K^+ \rightarrow \pi^+ \nu \bar{\nu})}{1.0 \times 10^{-10}}}$.

The decay $K_L \rightarrow \mu^+ \mu^-$ also has a short distance contribution sensitive to the CKM parameter ρ . For $m_t = 175$ GeV it is given by [10]:

$$B_{SD}(K_L \rightarrow \mu^+ \mu^-) \approx 1.7 \times 10^{-9} A^4 (\rho'_o - \rho)^2 \quad (3)$$

where ρ'_o depends on the charm quark mass and is around 1.2. This decay, however, is dominated by a long-distance contribution from a two-photon intermediate state. The absorptive (imaginary) part of the long-distance component is calculated in terms of the measured rate for $K_L \rightarrow \gamma\gamma$ to be $B_{\text{abs}}(K_L \rightarrow \mu^+ \mu^-) = (7.07 \pm 0.18) \times 10^{-9}$; and it almost completely saturates the observed rate $B(K_L \rightarrow \mu^+ \mu^-) = (7.18 \pm 0.17) \times 10^{-9}$ [20]. The difference between the observed rate and the absorptive component can be attributed to the (coherent) sum of the short-distance amplitude and the real part of the long-distance amplitude. In order to use this mode to constrain ρ it is, therefore, necessary to know the real part of the long-distance contribution. Unlike the absorptive part, the real part of the long-distance contribution cannot be derived from the measured rate for $K_L \rightarrow \gamma\gamma$. At present, it is not possible to compute this long-distance component reliably and, therefore, it is not possible to constrain ρ from this mode in a model independent way [21]. Several models exist to estimate this long-distance component [22,23] that are sufficient to place rough bounds on new physics from the measured rate for $K_L \rightarrow \mu^+ \mu^-$ [24]. The decay $K_L \rightarrow e^+ e^-$ is completely dominated by long distance physics and is easier to estimate. The result, $B(K_L \rightarrow e^+ e^-) \sim 9 \times 10^{-12}$ [21,23], is in good agreement with the recent measurement [25]. It is expected that studies of the reactions $K_L \rightarrow \ell^+ \ell^- \gamma$, and $K_L \rightarrow \ell^+ \ell^- \ell'^+ \ell'^-$ for $\ell, \ell' = e$ or μ , currently under active study by the KTeV and NA48 experiments, will improve our understanding of the long distance effects in $K_L \rightarrow \mu^+ \mu^-$ (the current data is parameterized in terms of α_K^* , discussed on page 25 of the K_L^0 Particle Properties Listing in our 1999 WWW update).

D. Searches for direct CP violation: The mode $K_L \rightarrow \pi^0 \nu \bar{\nu}$ is dominantly CP-violating and free of hadronic uncertainties [2,26]. The Standard Model predicts a branching ratio $(3.0 \pm 1.3) \times 10^{-11}$; for $m_t = 175$ GeV it is given approximately by [10]:

$$B(K_L \rightarrow \pi^0 \nu \bar{\nu}) \approx 4.1 \times 10^{-10} A^4 \eta^2. \quad (4)$$

The current upper bound is $B(K_L \rightarrow \pi^0 \nu \bar{\nu}) \leq 5.9 \times 10^{-7}$ [27] and KTeV (FNAL799II) is expected to place a bound of order 10^{-8} [28]. The 90% CL bound on $K^+ \rightarrow \pi^+ \nu \bar{\nu}$ provides a nearly model independent bound $B(K_L \rightarrow \pi^0 \nu \bar{\nu}) < 3 \times 10^{-9}$ [29]. A KEK experiment to reach the 10^{-10} /event level is in preparation [30]. The BNL-926 [31] proposal aims to make a $\sim 15\%$ measurement of $B(K_L \rightarrow \pi^0 \nu \bar{\nu})$. There is also a Fermilab EOI [32] with comparable goals.

There has been much recent theoretical work on possible contributions to ϵ'/ϵ and rare K decays within a generic supersymmetric extension of the Standard Model with R parity conservation and minimal particle content [24,33]. These conclude that contributions to rare decays much larger than those of the Standard Model are possible without violating current phenomenological constraints.

The decay $K_L \rightarrow \pi^0 e^+ e^-$ also has sensitivity to the product $A^4 \eta^2$. It has a direct CP-violating component that for $m_t = 175$ GeV is given by [10]:

$$B_{\text{dir}}(K_L \rightarrow \pi^0 e^+ e^-) \approx 6.7 \times 10^{-11} A^4 \eta^2. \quad (5)$$

However, like $K_L \rightarrow \mu^+ \mu^-$ this mode suffers from large theoretical uncertainties due to long distance strong interaction effects. It has an indirect CP-violating component given by:

$$B_{\text{ind}}(K_L \rightarrow \pi^0 e^+ e^-) = |\epsilon|^2 \frac{\tau_{K_L}}{\tau_{K_S}} B(K_S \rightarrow \pi^0 e^+ e^-), \quad (6)$$

that has been estimated to be less than 10^{-12} [34], but that will not be known precisely until a measurement of $K_S \rightarrow \pi^0 e^+ e^-$ is available [4,35]. There is also a CP-conserving component dominated by a two-photon intermediate state that cannot be computed reliably at present. This component has an absorptive part that can be, in principle, determined from a detailed analysis of $K_L \rightarrow \pi^0 \gamma\gamma$.

To understand the rate and the shape of the distribution $d\Gamma/dm_{\gamma\gamma}$ in $K_L \rightarrow \pi^0 \gamma\gamma$ within chiral perturbation theory it is necessary to go beyond leading order. The measured rate and spectrum can be accommodated naturally, for example, by allowing only one of the free parameters that occur, a_V , to vary [36]. There is new data on this decay from KTeV [37] and a fit to the distribution has given $a_V = -0.72 \pm 0.05 \pm 0.06$. This value suggests that the absorptive part of the CP-conserving contribution to $K_L \rightarrow \pi^0 e^+ e^-$ could be comparable to the direct CP-violating component [37,35]. The related process, $K_L \rightarrow \pi^0 \gamma e^+ e^-$, is potentially an additional background in some region of phase space [38]. This process has recently been

observed with a branching ratio of $(2.42 \pm 0.38_{stat} \pm 0.11_{sys}) \times 10^{-8}$ [39]. Finally, BNL-845 observed a potential background to $K_L \rightarrow \pi^0 e^+ e^-$ from the decay $K_L \rightarrow \gamma \gamma e^+ e^-$ [40]. This has recently been confirmed with a 500-fold larger sample by FNAL-799 [41], which measured additional kinematic quantities. It has been estimated that this background will enter at the level of 10^{-11} [42], comparable to the signal level. Because of this, the observation of $K_L \rightarrow \pi^0 e^+ e^-$ will depend on background subtraction with good statistics.

The current 90% CL preliminary upper bound for the process $K_L \rightarrow \pi^0 e^+ e^-$ is 5.64×10^{-10} [41]. For the closely related muonic process, the corresponding upper bound is $B(K_L \rightarrow \pi^0 \mu^+ \mu^-) \leq 3.8 \times 10^{-10}$ [43]. KTeV expects to reach a sensitivity of roughly 10^{-11} for both reactions [28].

E. Other long distance dominated modes:

The decays $K^+ \rightarrow \pi^+ \ell^+ \ell^-$ ($\ell = e$ or μ) are described by leading order chiral perturbation theory in terms of one parameter, ω^+ [44]. It now appears that this parameterization is not sufficient to account for both the rate and the detailed shape of the spectrum in $K^+ \rightarrow \pi^+ e^+ e^-$ [45]. An analysis beyond leading order in chiral perturbation theory can accommodate both the rate and the spectrum [46], at the cost of introducing at least one new parameter.

References

- D. Bryman, Int. J. Mod. Phys. **A4**, 79 (1989).
- J. Hagelin and L. Littenberg, Prog. in Part. Nucl. Phys. **23**, 1 (1989).
- R. Battiston *et al.*, Phys. Reports **214**, 293 (1992).
- L. Littenberg and G. Valencia, Ann. Rev. Nucl. and Part. Sci. **43**, 729 (1993).
- J. Ritchie and S. Wojcicki, Rev. Mod. Phys. **65**, 1149 (1993).
- B. Winstein and L. Wolfenstein, Rev. Mod. Phys. **65**, 1113 (1993).
- N. Bilic and B. Guberina, Fortsch. Phys. **42**, 209 (1994).
- G. D'Ambrosio, G. Ecker, G. Isidori and H. Neufeld, *Radiative Non-Leptonic Kaon Decays*, in The DAΦNE Physics Handbook (second edition), eds. L. Maiani, G. Pancheri and N. Paver (Frascati), Vol. I, 265 (1995).
- A. Pich, Rept. on Prog. in Phys. **58**, 563 (1995).
- A.J. Buras and R. Fleischer, TUM-HEP-275-97, hep-ph/9704376, *Heavy Flavours II*, World Scientific, eds. A.J. Buras and M. Lindner (1997), 65–238.
- A.J. Buras, TUM-HEP-349-99, Lectures given at Lake Louise Winter Institute: Electroweak Physics, Lake Louise, Alberta, Canada, 14–20 Feb. 1999.
- M. Zeller, KAON-99, June 1999.
- D. Ambrose *et al.*, Phys. Rev. Lett. **81**, 5734 (1998).
- K. Arisaka *et al.*, Phys. Lett. **B432**, 230 (1998).
- S. Adler *et al.*, Phys. Rev. Lett. **84**, 3768 (2000).
- I. Bigi and F. Gabbiani, Nucl. Phys. **B367**, 3 (1991).
- M. Aoki *et al.*, AGS Proposal 949, October 1998.
- W. Marciano and Z. Parsa, Phys. Rev. **D53**, 1 (1996).
- T. Inami and C.S. Lim, Prog. Theor. Phys. **65**, 297 (1981); erratum Prog. Theor. Phys. **65**, 172 (1981).
- D. Ambrose *et al.*, Phys. Rev. Lett. **84**, 1389 (2000).
- G. Valencia, Nucl. Phys. **B517**, 339 (1998).
- G. D'Ambrosio, G. Isidori, and J. Portoles, Phys. Lett. **B423**, 385 (1998).
- D. Gomez-Dumm and A. Pich, Phys. Rev. Lett. **80**, 4633 (1998).
- A.J. Buras and L. Silvestrini Nucl. Phys. **B546**, 299 (1999).
- D. Ambrose *et al.*, Phys. Rev. Lett. **81**, 4309 (1998).
- L. Littenberg, Phys. Rev. **D39**, 3322 (1989).
- A. Alavi-Harati *et al.*, Phys. Rev. **D61**, 072006 (2000).
- S. Schnetzer, *Proceedings of the Workshop on K Physics*, ed. L. Iconomidou-Fayard, 285 (1997).
- Y. Grossman and Y. Nir, Phys. Lett. **B398**, 163 (1997).
- T. Inagaki *et al.*, KEK Internal 96-13, November 1996.
- I-H. Chiang *et al.*, "Measurement of $K_L \rightarrow \pi^0 \nu \bar{\nu}$ ", AGS Proposal 926 (1996).
- E. Cheu *et al.*, "An Expression of Interest to Detect and Measure the Direct CP Violating Decay $K_L \rightarrow \pi^0 \nu \bar{\nu}$ and other Rare Decays at Fermilab Using the Main Injector", FERMILAB-PUB-97-321-E, hep-ex/9709026 (1997).
- F. Gabbiani *et al.*, Nucl. Phys. **B477**, 321 (1996); Y. Nir and M.P. Worah, Phys. Lett. **B423**, 319 (1998); A.J. Buras, A. Romanino, and L. Silvestrini, Nucl. Phys. **B520**, 3 (1998); G. Colangelo and G. Isidori, JHEP 09, 009 (1998); A.J. Buras *et al.*, Nucl. Phys. **B566**, 3 (2000).
- G. Ecker, A. Pich, and E. de Rafael, Nucl. Phys. **B303**, 665 (1988).
- J.F. Donoghue and F. Gabbiani, Phys. Rev. **D51**, 2187 (1995).
- G. Ecker, A. Pich, and E. de Rafael, Phys. Lett. **237B**, 481 (1990); L. Cappiello, G. D'Ambrosio, and M. Miragliuolo, Phys. Lett. **B298**, 423 (1993); A. Cohen, G. Ecker, and A. Pich, Phys. Lett. **B304**, 347 (1993).
- A. Alavi-Harati *et al.*, Phys. Rev. Lett. **83**, 917 (1999).
- J. Donoghue and F. Gabbiani, Phys. Rev. **D56**, 1605 (1997).
- G.E. Graham, "First observation of the rare decay $K_L \rightarrow \pi^0 e^+ e^- \gamma$ ", University of Chicago Ph.D. thesis, (August, 1999).
- W.M. Morse *et al.*, Phys. Rev. **D45**, 36 (1992).
- J. Whitmore, KAON-99 Conference, June 1999.
- H.B. Greenlee, Phys. Rev. **D42**, 3724 (1990).
- A. Alavi-Harati *et al.*, hep-ex/0001006 (2000).
- G. Ecker, A. Pich, and E. de Rafael, Nucl. Phys. **B291**, 692 (1987).
- R. Appel *et al.*, Phys. Rev. Lett. **83**, 4482 (1999).
- G. D'Ambrosio *et al.*, JHEP 9808:004, 1998.

Meson Particle Listings

K^\pm

K⁺ DECAY MODES

K^- modes are charge conjugates of the modes below.

Mode	Fraction (Γ_i/Γ)	Scale factor/ Confidence level
$\Gamma_1 \mu^+ \nu_\mu$	(63.51 ± 0.18) %	S=1.3
$\Gamma_2 e^+ \nu_e$	(1.55 ± 0.07) × 10 ⁻⁵	
$\Gamma_3 \pi^+ \pi^0$	(21.16 ± 0.14) %	S=1.1
$\Gamma_4 \pi^+ \pi^+ \pi^-$	(5.59 ± 0.05) %	S=1.8
$\Gamma_5 \pi^+ \pi^0 \pi^0$	(1.73 ± 0.04) %	S=1.2
$\Gamma_6 \pi^0 \mu^+ \nu_\mu$	(3.18 ± 0.08) %	S=1.5
Called $K_{\mu 3}^+$		
$\Gamma_7 \pi^0 e^+ \nu_e$	(4.82 ± 0.06) %	S=1.3
Called $K_{e 3}^+$		
$\Gamma_8 \pi^0 \pi^0 e^+ \nu_e$	(2.1 ± 0.4) × 10 ⁻⁵	
$\Gamma_9 \pi^+ \pi^- e^+ \nu_e$	(3.91 ± 0.17) × 10 ⁻⁵	
$\Gamma_{10} \pi^+ \pi^- \mu^+ \nu_\mu$	(1.4 ± 0.9) × 10 ⁻⁵	
$\Gamma_{11} \pi^0 \pi^0 \pi^0 e^+ \nu_e$	< 3.5 × 10 ⁻⁶	CL=90%
$\Gamma_{12} \mu^+ \nu_\mu \nu \bar{\nu}$	< 6.0 × 10 ⁻⁶	CL=90%
$\Gamma_{13} e^+ \nu_e \nu \bar{\nu}$	< 6 × 10 ⁻⁵	CL=90%
$\Gamma_{14} \mu^+ \nu_\mu e^+ e^-$	(1.3 ± 0.4) × 10 ⁻⁷	
$\Gamma_{15} e^+ \nu_e e^+ e^-$	(3.0 ^{+3.0} _{-1.5}) × 10 ⁻⁸	
$\Gamma_{16} e^+ \nu_e \mu^+ \mu^-$	< 5 × 10 ⁻⁷	CL=90%
$\Gamma_{17} \mu^+ \nu_\mu \mu^+ \mu^-$	< 4.1 × 10 ⁻⁷	CL=90%
$\Gamma_{18} \mu^+ \nu_\mu \gamma$	[a,b] (5.50 ± 0.28) × 10 ⁻³	
$\Gamma_{19} \pi^+ \pi^0 \gamma$	[a,b] (2.75 ± 0.15) × 10 ⁻⁴	
$\Gamma_{20} \pi^+ \pi^0 \gamma$ (DE)	[b,c] (1.8 ± 0.4) × 10 ⁻⁵	
$\Gamma_{21} \pi^+ \pi^+ \pi^- \gamma$	[a,b] (1.04 ± 0.31) × 10 ⁻⁴	
$\Gamma_{22} \pi^+ \pi^0 \pi^0 \gamma$	[a,b] (7.5 ^{+5.5} _{-3.0}) × 10 ⁻⁶	
$\Gamma_{23} \pi^0 \mu^+ \nu_\mu \gamma$	[a,b] < 6.1 × 10 ⁻⁵	CL=90%
$\Gamma_{24} \pi^0 e^+ \nu_e \gamma$	[a,b] (2.62 ± 0.20) × 10 ⁻⁴	
$\Gamma_{25} \pi^0 e^+ \mu_e \gamma$ (SD)	[d] < 5.3 × 10 ⁻⁵	CL=90%
$\Gamma_{26} \pi^0 \pi^0 e^+ \nu_e \gamma$	< 5 × 10 ⁻⁶	CL=90%
$\Gamma_{27} \pi^+ \gamma \gamma$	[b] (1.10 ± 0.32) × 10 ⁻⁶	
$\Gamma_{28} \pi^+ 3\gamma$	[b] < 1.0 × 10 ⁻⁴	CL=90%

Lepton Family number (LF), Lepton number (L), $\Delta S = \Delta Q$ (SQ) violating modes, or $\Delta S = 1$ weak neutral current (SI) modes

$\Gamma_{29} \pi^+ \pi^+ e^- \bar{\nu}_e$	SQ	< 1.2 × 10 ⁻⁸	CL=90%
$\Gamma_{30} \pi^+ \pi^+ \mu^- \bar{\nu}_\mu$	SQ	< 3.0 × 10 ⁻⁶	CL=95%
$\Gamma_{31} \pi^+ e^+ e^-$	SI	(2.88 ± 0.13) × 10 ⁻⁷	
$\Gamma_{32} \pi^+ \mu^+ \mu^-$	SI	(7.6 ± 2.1) × 10 ⁻⁸	S=3.4
$\Gamma_{33} \pi^+ \nu \bar{\nu}$	SI	(1.5 ^{+3.4} _{-1.2}) × 10 ⁻¹⁰	
$\Gamma_{34} \mu^- \nu e^+ e^+$	LF	< 2.0 × 10 ⁻⁸	CL=90%
$\Gamma_{35} \mu^+ \nu e^- e^-$	LF	[e] < 4 × 10 ⁻³	CL=90%
$\Gamma_{36} \pi^+ \mu^+ e^-$	LF	< 2.1 × 10 ⁻¹⁰	CL=90%
$\Gamma_{37} \pi^+ \mu^- e^+$	LF	< 7 × 10 ⁻⁹	CL=90%
$\Gamma_{38} \pi^- \mu^+ e^+$	L	< 7 × 10 ⁻⁹	CL=90%
$\Gamma_{39} \pi^- e^+ e^+$	L	< 1.0 × 10 ⁻⁸	CL=90%
$\Gamma_{40} \pi^- \mu^+ \mu^+$	L	[e] < 1.5 × 10 ⁻⁴	CL=90%
$\Gamma_{41} \mu^+ \bar{\nu}_e$	L	[e] < 3.3 × 10 ⁻³	CL=90%
$\Gamma_{42} \pi^0 e^+ \bar{\nu}_e$	L	< 3 × 10 ⁻³	CL=90%
$\Gamma_{43} \pi^+ \gamma$	[f]		

[a] Most of this radiative mode, the low-momentum γ part, is also included in the parent mode listed without γ 's.

[b] See the Particle Listings below for the energy limits used in this measurement.

[c] Direct-emission branching fraction.

[d] Structure-dependent part.

[e] Derived from an analysis of neutrino-oscillation experiments.

[f] Violates angular-momentum conservation.

CONSTRAINED FIT INFORMATION

An overall fit to the mean life, 2 decay rate, and 20 branching ratios uses 60 measurements and one constraint to determine 8 parameters. The overall fit has a $\chi^2 = 78.1$ for 53 degrees of freedom.

The following off-diagonal array elements are the correlation coefficients $\langle \delta p_i \delta p_j \rangle / (\delta p_i \delta p_j)$, in percent, from the fit to parameters p_i , including the branching fractions, $x_i \equiv \Gamma_i / \Gamma_{\text{total}}$. The fit constrains the x_i whose labels appear in this array to sum to one.

x_3	-58						
x_4	-41	-12					
x_5	-27	-4	21				
x_6	-48	-17	14	2			
x_7	-50	-16	34	6	39		
x_8	-3	-1	2	0	2	6	
Γ	7	2	-18	-4	-2	-6	0
	x_1	x_3	x_4	x_5	x_6	x_7	x_8

Mode	Rate (10 ⁸ s ⁻¹)	Scale factor
$\Gamma_1 \mu^+ \nu_\mu$	0.5128 ± 0.0018	1.5
$\Gamma_3 \pi^+ \pi^0$	0.1708 ± 0.0012	1.1
$\Gamma_4 \pi^+ \pi^+ \pi^-$	0.0452 ± 0.0004	1.8
$\Gamma_5 \pi^+ \pi^0 \pi^0$	0.01399 ± 0.00032	1.2
$\Gamma_6 \pi^0 \mu^+ \nu_\mu$	0.0257 ± 0.0006	1.5
Called $K_{\mu 3}^+$		
$\Gamma_7 \pi^0 e^+ \nu_e$	0.0389 ± 0.0005	1.3
Called $K_{e 3}^+$		
$\Gamma_8 \pi^0 \pi^0 e^+ \nu_e$	(1.69 ^{+0.34} _{-0.29}) × 10 ⁻⁵	

K[±] DECAY RATES

$\Gamma(\mu^+ \nu_\mu)$	VALUE (10 ⁶ s ⁻¹)	DOCUMENT ID	TECN	CHG
	51.28 ± 0.18 OUR FIT	Error includes scale factor of 1.5.		
	51.2 ± 0.8	FORD	67	CNTR ±

$\Gamma(\pi^+ \pi^+ \pi^-)$	VALUE (10 ⁶ s ⁻¹)	EVTS	DOCUMENT ID	TECN	CHG
	4.52 ± 0.04 OUR FIT	Error includes scale factor of 1.8.			
	4.511 ± 0.024		⁶ FORD	70	ASPK
• • • We do not use the following data for averages, fits, limits, etc. • • •					
	4.529 ± 0.032	3.2M	⁶ FORD	70	ASPK
	4.496 ± 0.030		⁶ FORD	67	CNTR ±
⁶ First FORD 70 value is second FORD 70 combined with FORD 67.					

$$(\Gamma(K^+) - \Gamma(K^-)) / \Gamma(K)$$

$K^\pm \rightarrow \mu^\pm \nu_\mu$ RATE DIFFERENCE/AVERAGE	VALUE (%)	DOCUMENT ID	TECN	CHG
Test of CPT conservation.				
	-0.54 ± 0.41	FORD	67	CNTR

$K^\pm \rightarrow \pi^\pm \pi^+ \pi^-$ RATE DIFFERENCE/AVERAGE	VALUE (%)	EVTS	DOCUMENT ID	TECN	CHG
Test of CP conservation.					
	0.07 ± 0.12 OUR AVERAGE				
	0.08 ± 0.12		⁷ FORD	70	ASPK
	-0.50 ± 0.90		FLETCHER	67	OSPK
• • • We do not use the following data for averages, fits, limits, etc. • • •					
	-0.02 ± 0.16		⁸ SMITH	73	ASPK ±
	0.10 ± 0.14	3.2M	⁷ FORD	70	ASPK
	-0.04 ± 0.21		⁷ FORD	67	CNTR
⁷ First FORD 70 value is second FORD 70 combined with FORD 67.					
⁸ SMITH 73 value of $K^\pm \rightarrow \pi^\pm \pi^+ \pi^-$ rate difference is derived from SMITH 73 value of $K^\pm \rightarrow \pi^\pm 2\pi^0$ rate difference.					

$K^\pm \rightarrow \pi^\pm \pi^0 \pi^0$ RATE DIFFERENCE/AVERAGE	VALUE (%)	EVTS	DOCUMENT ID	TECN	CHG
Test of CP conservation.					
	0.0 ± 0.6 OUR AVERAGE				
	0.08 ± 0.58		SMITH	73	ASPK ±
	-1.1 ± 1.8	1802	HERZO	69	OSPK

$K^\pm \rightarrow \pi^\pm \pi^0$ RATE DIFFERENCE/AVERAGE	VALUE (%)	DOCUMENT ID	TECN	CHG
Test of CPT conservation.				
	0.8 ± 1.2	HERZO	69	OSPK

$K^\pm \rightarrow \pi^\pm \pi^0 \gamma$ RATE DIFFERENCE/AVERAGE

Test of CP conservation.

VALUE (%)	EVTS	DOCUMENT ID	TECN	CHG	COMMENT
0.9 ± 3.3 OUR AVERAGE					
0.8 ± 5.8	2461	SMITH	76	WIRE ±	E_π 55-90 MeV
1.0 ± 4.0	4000	ABRAMS	73b	ASPK ±	E_π 51-100 MeV
0.0 ± 24.0	24	EDWARDS	72	OSPK	E_π 58-90 MeV

K^+ BRANCHING RATIOS

$\Gamma(\mu^+ \nu_\mu) / \Gamma_{total}$ Γ_1 / Γ

VALUE (units 10^{-2})	EVTS	DOCUMENT ID	TECN	CHG	COMMENT
63.51 ± 0.18 OUR FIT					Error includes scale factor of 1.3.
63.24 ± 0.44	62k	CHIANG	72	OSPK +	1.84 GeV/c K^+
56.9 ± 2.6		⁹ ALEXANDER	57	EMUL +	
58.5 ± 3.0		⁹ BIRGE	56	EMUL +	

• • • We do not use the following data for averages, fits, limits, etc. • • •

$\Gamma(\mu^+ \nu_\mu) / \Gamma(\pi^+ \pi^+ \pi^-)$ Γ_1 / Γ_4

VALUE	EVTS	DOCUMENT ID	TECN	CHG	COMMENT
11.35 ± 0.12 OUR FIT					Error includes scale factor of 1.8.
10.38 ± 0.82	427	¹⁰ YOUNG	65	EMUL +	

• • • We do not use the following data for averages, fits, limits, etc. • • •

¹⁰ Deleted from overall fit because YOUNG 65 constrains his results to add up to 1. Only YOUNG 65 measured ($\mu\nu$) directly.

$\Gamma(e^+ \nu_e) / \Gamma_{total}$ Γ_2 / Γ

VALUE (units 10^{-5})	CL%	EVTS	DOCUMENT ID	TECN	CHG
2.1 ^{+1.8} _{-1.3}		4	BOWEN	67b	OSPK +
<160.0	95		BORREANI	64	HBC +

• • • We do not use the following data for averages, fits, limits, etc. • • •

$\Gamma(e^+ \nu_e) / \Gamma(\mu^+ \nu_\mu)$ Γ_2 / Γ_1

VALUE (units 10^{-5})	EVTS	DOCUMENT ID	TECN	CHG	COMMENT
2.45 ± 0.11 OUR AVERAGE					
2.51 ± 0.15	404	HEINTZE	76	SPEC +	
2.37 ± 0.17	534	HEARD	75b	SPEC +	
2.42 ± 0.42	112	CLARK	72	OSPK +	
1.8 ^{+0.8} _{-0.6}	8	MACEK	69	ASPK +	
1.9 ^{+0.7} _{-0.5}	10	BOTTERILL	67	ASPK +	

• • • We do not use the following data for averages, fits, limits, etc. • • •

$\Gamma(\pi^+ \pi^0) / \Gamma_{total}$ Γ_3 / Γ

VALUE (units 10^{-2})	EVTS	DOCUMENT ID	TECN	CHG	COMMENT
21.16 ± 0.14 OUR FIT					Error includes scale factor of 1.1.
21.18 ± 0.28	16k	CHIANG	72	OSPK +	1.84 GeV/c K^+
21.0 ± 0.6		CALLAHAN	65	HLBC	See $\Gamma(\pi^+ \pi^0) / \Gamma(\pi^+ \pi^+ \pi^-)$
21.6 ± 0.6		TRILLING	65b	RVUE	
23.2 ± 2.2		¹¹ ALEXANDER	57	EMUL +	
27.7 ± 2.7		¹¹ BIRGE	56	EMUL +	

• • • We do not use the following data for averages, fits, limits, etc. • • •

¹¹ Earlier experiments not averaged.

$\Gamma(\pi^+ \pi^0) / \Gamma(\mu^+ \nu_\mu)$ Γ_3 / Γ_1

VALUE	EVTS	DOCUMENT ID	TECN	CHG	COMMENT
0.3331 ± 0.0028 OUR FIT					Error includes scale factor of 1.1.
0.3316 ± 0.0032 OUR AVERAGE					
0.3329 ± 0.0047 ± 0.0010	45k	USHER	92	SPEC +	$p\bar{p}$ at rest
0.3355 ± 0.0057		¹² WEISSENBE...	76	SPEC +	
0.305 ± 0.018	1600	ZELLER	69	ASPK +	
0.3277 ± 0.0065	4517	¹³ AUERBACH	67	OSPK +	
0.328 ± 0.005	25k	¹² WEISSENBE...	74	STRC +	

• • • We do not use the following data for averages, fits, limits, etc. • • •

¹² WEISSENBERG 76 revises WEISSENBERG 74.

¹³ AUERBACH 67 changed from 0.3253 ± 0.0065. See comment with ratio $\Gamma(\pi^0 \mu^+ \nu_\mu) / \Gamma(\mu^+ \nu_\mu)$.

$\Gamma(\pi^+ \pi^0) / \Gamma(\pi^+ \pi^+ \pi^-)$ Γ_3 / Γ_4

VALUE	EVTS	DOCUMENT ID	TECN	CHG	COMMENT
3.78 ± 0.04 OUR FIT					Error includes scale factor of 1.5.
3.84 ± 0.27 OUR AVERAGE					Error includes scale factor of 1.9.
3.96 ± 0.15	1045	CALLAHAN	66	FBC +	
3.24 ± 0.34	134	YOUNG	65	EMUL +	

$\Gamma(\pi^+ \pi^+ \pi^-) / \Gamma_{total}$ Γ_4 / Γ

VALUE (units 10^{-2})	EVTS	DOCUMENT ID	TECN	CHG	COMMENT
5.59 ± 0.05 OUR FIT					Error includes scale factor of 1.8.
5.52 ± 0.10 OUR AVERAGE					Error includes scale factor of 1.3. See the ideogram below.
5.34 ± 0.21	693	¹⁴ PANDOULAS	70	EMUL +	
5.71 ± 0.15		DEMARCO	65	HBC	
6.0 ± 0.4	44	YOUNG	65	EMUL +	
5.54 ± 0.12	2332	CALLAHAN	64	HLBC +	
5.1 ± 0.2	540	SHAKLEE	64	HLBC +	
5.7 ± 0.3		ROE	61	HLBC +	
5.56 ± 0.20	2330	¹⁵ CHIANG	72	OSPK +	1.84 GeV/c K^+
5.2 ± 0.3		¹⁶ TAYLOR	59	EMUL +	
6.8 ± 0.4		¹⁶ ALEXANDER	57	EMUL +	
5.6 ± 0.4		¹⁶ BIRGE	56	EMUL +	

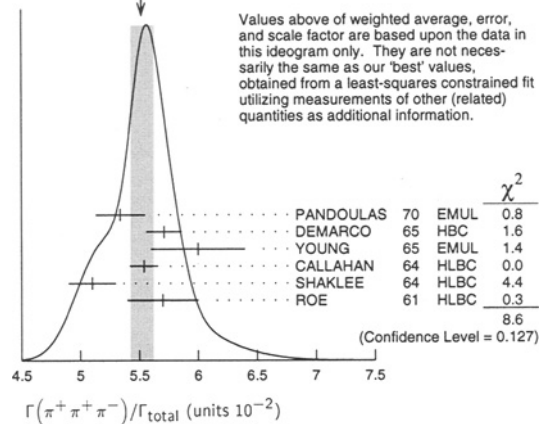
• • • We do not use the following data for averages, fits, limits, etc. • • •

¹⁴ Includes events of TAYLOR 59.

¹⁵ Value is not independent of CHIANG 72 $\Gamma(\mu^+ \nu_\mu) / \Gamma_{total}$, $\Gamma(\pi^+ \pi^0) / \Gamma_{total}$, $\Gamma(\pi^+ \pi^0 \pi^0) / \Gamma_{total}$, $\Gamma(\pi^0 \mu^+ \nu_\mu) / \Gamma_{total}$, and $\Gamma(\pi^0 e^+ \nu_e) / \Gamma_{total}$.

¹⁶ Earlier experiments not averaged.

WEIGHTED AVERAGE
5.52 ± 0.10 (Error scaled by 1.3)



$\Gamma(\pi^+ \pi^0 \pi^0) / \Gamma_{total}$ Γ_5 / Γ

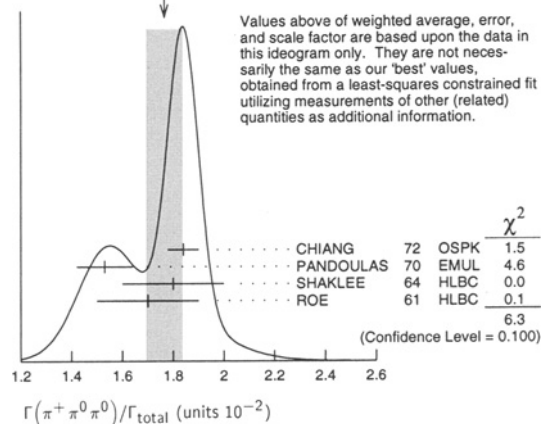
VALUE (units 10^{-2})	EVTS	DOCUMENT ID	TECN	CHG	COMMENT
1.73 ± 0.04 OUR FIT					Error includes scale factor of 1.2.
1.77 ± 0.07 OUR AVERAGE					Error includes scale factor of 1.4. See the ideogram below.
1.84 ± 0.06	1307	CHIANG	72	OSPK +	1.84 GeV/c K^+
1.53 ± 0.11	198	¹⁷ PANDOULAS	70	EMUL +	
1.8 ± 0.2	108	SHAKLEE	64	HLBC +	
1.7 ± 0.2		ROE	61	HLBC +	
1.5 ± 0.2		¹⁸ TAYLOR	59	EMUL +	
2.2 ± 0.4		¹⁸ ALEXANDER	57	EMUL +	
2.1 ± 0.5		¹⁸ BIRGE	56	EMUL +	

• • • We do not use the following data for averages, fits, limits, etc. • • •

¹⁷ Includes events of TAYLOR 59.

¹⁸ Earlier experiments not averaged.

WEIGHTED AVERAGE
1.77 ± 0.07 (Error scaled by 1.4)



Meson Particle Listings

K^\pm

$\Gamma(\pi^+\pi^0\pi^0)/\Gamma(\pi^+\pi^-)$ Γ_5/Γ_3

VALUE	EVTS	DOCUMENT ID	TECN	CHG	COMMENT
0.0819 ± 0.0020 OUR FIT	Error includes scale factor of 1.2.				
0.081 ± 0.005	574	¹⁹ LUCAS	73B	HBC	- Dalitz pairs only

¹⁹LUCAS 73B gives $N(\pi 2\pi^0) = 574 \pm 5.9\%$, $N(2\pi) = 3564 \pm 3.1\%$. We quote $0.5N(\pi 2\pi^0)/N(2\pi)$ where 0.5 is because only Dalitz pair π^0 's were used.

$\Gamma(\pi^+\pi^0\pi^0)/\Gamma(\pi^+\pi^+\pi^-)$ Γ_5/Γ_4

VALUE	EVTS	DOCUMENT ID	TECN	CHG	COMMENT
0.310 ± 0.007 OUR FIT	Error includes scale factor of 1.2.				
0.304 ± 0.009 OUR AVERAGE					
0.303 ± 0.009	2027	BISI	65	BC	+ HBC+HLBC
0.393 ± 0.099	17	YOUNG	65	EMUL	+

$\Gamma(\pi^0\mu^+\nu_\mu)/\Gamma_{total}$ Γ_6/Γ

VALUE (units 10^{-2})	EVTS	DOCUMENT ID	TECN	CHG	COMMENT
3.18 ± 0.08 OUR FIT	Error includes scale factor of 1.5.				
3.33 ± 0.16	2345	CHIANG	72	OSPK	+ 1.84 GeV/c K^+

• • • We do not use the following data for averages, fits, limits, etc. • • •

2.8 ± 0.4	20	TAYLOR	59	EMUL	+
5.9 ± 1.3	20	ALEXANDER	57	EMUL	+
2.8 ± 1.0	20	BIRGE	56	EMUL	+

²⁰ Earlier experiments not averaged.

$\Gamma(\pi^0\mu^+\nu_\mu)/\Gamma(\mu^+\nu_\mu)$ Γ_6/Γ_1

VALUE	EVTS	DOCUMENT ID	TECN	CHG	COMMENT
0.0501 ± 0.0013 OUR FIT	Error includes scale factor of 1.5.				
0.0488 ± 0.0026 OUR AVERAGE					
0.054 ± 0.009	240	ZELLER	69	ASPK	+
0.0480 ± 0.0037	424	²¹ GARLAND	68	OSPK	+
0.0486 ± 0.0040	307	²² AUERBACH	67	OSPK	+

²¹GARLAND 68 changed from 0.055 ± 0.004 in agreement with μ -spectrum calculation of GAILLARD 70 appendix B. L.G.Pondrom, (private communication 73).
²²AUERBACH 67 changed from 0.0602 ± 0.0046 by erratum which brings the μ -spectrum calculation into agreement with GAILLARD 70 appendix B.

$\Gamma(\pi^0\mu^+\nu_\mu)/\Gamma(\pi^+\pi^+\pi^-)$ Γ_6/Γ_4

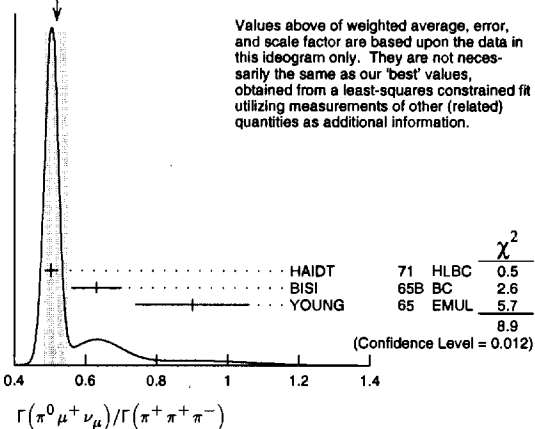
VALUE	EVTS	DOCUMENT ID	TECN	CHG	COMMENT
0.569 ± 0.014 OUR FIT	Error includes scale factor of 1.5.				
0.517 ± 0.032 OUR AVERAGE	Error includes scale factor of 1.8. See the ideogram below.				
0.503 ± 0.019	1505	²³ HAIDT	71	HLBC	+
0.63 ± 0.07	2845	²⁴ BISI	65B	BC	+ HBC+HLBC
0.90 ± 0.16	38	YOUNG	65	EMUL	+

• • • We do not use the following data for averages, fits, limits, etc. • • •

0.510 ± 0.017	1505	²³ EICHTEN	68	HLBC	+
---------------	------	-----------------------	----	------	---

²³HAIDT 71 is a reanalysis of EICHTEN 68.
²⁴Error enlarged for background problems. See GAILLARD 70.

WEIGHTED AVERAGE
 0.517 ± 0.032 (Error scaled by 1.8)



$\Gamma(\pi^0\mu^+\nu_\mu)/\Gamma(\pi^0 e^+\nu_e)$ Γ_6/Γ_7

VALUE	EVTS	DOCUMENT ID	TECN	CHG	COMMENT
0.660 ± 0.015 OUR FIT	Error includes scale factor of 1.5.				
0.680 ± 0.013 OUR AVERAGE					
0.705 ± 0.063	554	²⁵ LUCAS	73B	HBC	- Dalitz pairs only
0.698 ± 0.025	3480	²⁶ CHIANG	72	OSPK	+ 1.84 GeV/c K^+
0.667 ± 0.017	5601	BOTTERILL	68B	ASPK	+
0.703 ± 0.056	1509	²⁷ CALLAHAN	66B	HLBC	

• • • We do not use the following data for averages, fits, limits, etc. • • •

0.670 ± 0.014	²⁸ HEINTZE	77	SPEC	+
0.67 ± 0.12	WEISSENBE...	76	SPEC	+
0.608 ± 0.014	²⁹ BRAUN	75	HLBC	+
0.596 ± 0.025	³⁰ HAIDT	71	HLBC	+
0.604 ± 0.022	³⁰ EICHTEN	68	HLBC	

²⁵LUCAS 73B gives $N(K_{\mu 3}) = 554 \pm 7.6\%$, $N(K_{e 3}) = 786 \pm 3.1\%$. We divide.
²⁶CHIANG 72 $\Gamma(\pi^0\mu^+\nu_\mu)/\Gamma(\pi^0 e^+\nu_e)$ is statistically independent of CHIANG 72 $\Gamma(\pi^0\mu^+\nu_\mu)/\Gamma_{total}$ and $\Gamma(\pi^0 e^+\nu_e)/\Gamma_{total}$.
²⁷From CALLAHAN 66B we use only the $K_{\mu 3}/K_{e 3}$ ratio and do not include in the fit the ratios $K_{\mu 3}/(\pi\pi^+\pi^0)$ and $K_{e 3}/(\pi\pi^+\pi^0)$, since they show large disagreements with the rest of the data.
²⁸HEINTZE 77 value from fit to λ_0 . Assumes μ -e universality.
²⁹BRAUN 75 value is from form factor fit. Assumes μ -e universality.
³⁰HAIDT 71 is a reanalysis of EICHTEN 68. Only individual ratios included in fit (see $\Gamma(\pi^0\mu^+\nu_\mu)/\Gamma(\pi^+\pi^+\pi^-)$ and $\Gamma(\pi^0 e^+\nu_e)/\Gamma(\pi^+\pi^+\pi^-)$).

$[\Gamma(\pi^+\pi^0) + \Gamma(\pi^0\mu^+\nu_\mu)]/\Gamma_{total}$ $(\Gamma_3 + \Gamma_6)/\Gamma$

We combine these two modes for experiments measuring them in xenon bubble chamber because of difficulties of separating them there.

VALUE (units 10^{-2})	EVTS	DOCUMENT ID	TECN	CHG	COMMENT
24.34 ± 0.15 OUR FIT	Error includes scale factor of 1.2.				
24.6 ± 1.0 OUR AVERAGE	Error includes scale factor of 1.4.				
25.4 ± 0.9	886	SHAKLEE	64	HLBC	+
23.4 ± 1.1		ROE	61	HLBC	+

$\Gamma(\pi^0 e^+\nu_e)/\Gamma_{total}$ Γ_7/Γ

VALUE (units 10^{-2})	EVTS	DOCUMENT ID	TECN	CHG	COMMENT
4.82 ± 0.06 OUR FIT	Error includes scale factor of 1.3.				
4.85 ± 0.09 OUR AVERAGE					
4.86 ± 0.10	3516	CHIANG	72	OSPK	+ 1.84 GeV/c K^+
4.7 ± 0.3	429	SHAKLEE	64	HLBC	+
5.0 ± 0.5		ROE	61	HLBC	+

• • • We do not use the following data for averages, fits, limits, etc. • • •

5.1 ± 1.3	³¹ ALEXANDER	57	EMUL	+
3.2 ± 1.3	³¹ BIRGE	56	EMUL	+

³¹ Earlier experiments not averaged.

$\Gamma(\pi^0 e^+\nu_e)/\Gamma(\mu^+\nu_\mu)$ Γ_7/Γ_1

VALUE	EVTS	DOCUMENT ID	TECN	CHG	COMMENT
0.0759 ± 0.0011 OUR FIT	Error includes scale factor of 1.4.				
0.0752 ± 0.0024 OUR AVERAGE					
0.069 ± 0.006	350	ZELLER	69	ASPK	+
0.0775 ± 0.0033	960	BOTTERILL	68C	ASPK	+
0.069 ± 0.006	561	GARLAND	68	OSPK	+
0.0791 ± 0.0054	295	³² AUERBACH	67	OSPK	+

³²AUERBACH 67 changed from 0.0797 ± 0.0054. See comment with ratio $\Gamma(\pi^0\mu^+\nu_\mu)/\Gamma(\mu^+\nu_\mu)$. The value 0.0785 ± 0.0025 given in AUERBACH 67 is an average of AUERBACH 67 $\Gamma(\pi^0 e^+\nu_e)/\Gamma(\mu^+\nu_\mu)$ and CESTER 66 $\Gamma(\pi^0 e^+\nu_e)/[\Gamma(\mu^+\nu_\mu) + \Gamma(\pi^+\pi^0)]$.

$\Gamma(\pi^0 e^+\nu_e)/\Gamma(\pi^+\pi^0)$ Γ_7/Γ_3

VALUE	EVTS	DOCUMENT ID	TECN	CHG	COMMENT
0.2280 ± 0.0035 OUR FIT	Error includes scale factor of 1.3.				
0.221 ± 0.012	786	³³ LUCAS	73B	HBC	- Dalitz pairs only

³³LUCAS 73B gives $N(K_{e 3}) = 786 \pm 3.1\%$, $N(2\pi) = 3564 \pm 3.1\%$. We divide.

$\Gamma(\pi^0 e^+\nu_e)/\Gamma(\pi^+\pi^+\pi^-)$ Γ_7/Γ_4

VALUE	EVTS	DOCUMENT ID	TECN	CHG	COMMENT
0.862 ± 0.011 OUR FIT	Error includes scale factor of 1.3.				
0.860 ± 0.014 OUR AVERAGE					
0.867 ± 0.027	2768	BARMIN	87	XEBC	+
0.856 ± 0.040	2827	BRAUN	75	HLBC	+
0.850 ± 0.019	4385	³⁴ HAIDT	71	HLBC	+
0.94 ± 0.09	854	BELLOTTI	67B	HLBC	
0.90 ± 0.06	230	BORREANI	64	HBC	+

• • • We do not use the following data for averages, fits, limits, etc. • • •

0.846 ± 0.021	4385	³⁴ EICHTEN	68	HLBC	+
0.90 ± 0.16	37	YOUNG	65	EMUL	+

³⁴HAIDT 71 is a reanalysis of EICHTEN 68.

$\Gamma(\pi^0 e^+\nu_e)/[\Gamma(\mu^+\nu_\mu) + \Gamma(\pi^+\pi^0)]$ $\Gamma_7/(\Gamma_1 + \Gamma_3)$

VALUE (units 10^{-2})	EVTS	DOCUMENT ID	TECN	CHG	COMMENT
5.70 ± 0.08 OUR FIT	Error includes scale factor of 1.4.				
6.01 ± 0.15 OUR AVERAGE					
5.92 ± 0.65		³⁵ WEISSENBE...	76	SPEC	+
6.16 ± 0.22	5110	ESCHSTRUTH	68	OSPK	+
5.89 ± 0.21	1679	CESTER	66	OSPK	+

³⁵Value calculated from WEISSENBERG 76 ($\pi^0 e\nu$), ($\mu\nu$), and ($\pi\pi^0$) values to eliminate dependence on our 1974 ($\pi 2\pi^0$) and ($\pi\pi^+\pi^-$) fractions.

Meson Particle Listings

K^\pm

⁴⁶BARMIN 91 quotes branching ratio $\Gamma(K \rightarrow e^0 \nu \gamma)/\Gamma_{\text{all}}$. The measured normalization is $[\Gamma(K \rightarrow e^0 \nu) + \Gamma(K \rightarrow \pi^+ \pi^+ \pi^-)]$. For comparison with other experiments we used $\Gamma(K \rightarrow e^0 \nu)/\Gamma_{\text{all}} = 0.0482$ to calculate the values quoted here.

⁴⁷ $\cos\theta(e\gamma)$ between 0.6 and 0.9.

⁴⁸Both ROMANO 71 values are for $\cos\theta(e\gamma)$ between 0.6 and 0.9. Second value is for comparison with second LJUNG 73 value. We use lowest $E(\gamma)$ cut for Summary Table value. See ROMANO 71 for E_γ dependence.

⁴⁹First LJUNG 73 value is for $\cos\theta(e\gamma) < 0.9$, second value is for $\cos\theta(e\gamma)$ between 0.6 and 0.9 for comparison with ROMANO 71.

$\Gamma(\pi^0 e^+ \nu_e \gamma(\text{SD}))/\Gamma_{\text{total}}$ Γ_{25}/Γ Structure-dependent part. Table with columns: VALUE (units 10⁻⁵), CL%, DOCUMENT ID, TECN, CHG. Row: <5.3, 90, BOLOTOV, 86B, CALO, -

$\Gamma(\pi^0 \pi^0 e^+ \nu_e \gamma)/\Gamma_{\text{total}}$ Γ_{26}/Γ Table with columns: VALUE (units 10⁻⁶), CL%, EVTS, DOCUMENT ID, TECN, CHG, COMMENT. Row: <5, 90, 0, BARMIN, 92, XEBC, +, $E_\gamma > 10 \text{ MeV}$

$\Gamma(\pi^+ \gamma \gamma)/\Gamma_{\text{total}}$ Γ_{27}/Γ All values given here assume a phase space pion energy spectrum. Table with columns: VALUE (units 10⁻⁷), CL%, EVTS, DOCUMENT ID, TECN, CHG, COMMENT. Row: 11 ± 3 ± 1, 31, 50, KITCHING, 97, B787. Includes text: "We do not use the following data for averages, fits, limits, etc. ..."

$\Gamma(\pi^+ 3\gamma)/\Gamma_{\text{total}}$ Γ_{28}/Γ Values given here assume a phase space pion energy spectrum. Table with columns: VALUE (units 10⁻⁴), CL%, DOCUMENT ID, TECN, CHG, COMMENT. Row: <1.0, 90, ASANO, 82, CNTR, +, $T(\pi) 117-127 \text{ MeV}$. Includes text: "We do not use the following data for averages, fits, limits, etc. ..."

$\Gamma(\pi^+ \pi^+ e^- \bar{\nu}_e)/\Gamma_{\text{total}}$ Γ_{29}/Γ Test of $\Delta S = \Delta Q$ rule. Table with columns: VALUE (units 10⁻⁷), CL%, EVTS, DOCUMENT ID, TECN, CHG. Row: < 9.0, 95, 0, SCHWEINB..., 71, HLBC, +

$\Gamma(\pi^+ \pi^+ e^- \bar{\nu}_e)/\Gamma(\pi^+ \pi^- e^+ \nu_e)$ Γ_{29}/Γ_9 Test of $\Delta S = \Delta Q$ rule. Table with columns: VALUE (units 10⁻⁴), CL%, EVTS, DOCUMENT ID, TECN. Row: < 3, 90, 3, 51, BLOCH, 76, SPEC. Includes text: "We do not use the following data for averages, fits, limits, etc. ..."

$\Gamma(\pi^+ \pi^+ \mu^- \bar{\nu}_\mu)/\Gamma_{\text{total}}$ Γ_{30}/Γ Test of $\Delta S = \Delta Q$ rule. Table with columns: VALUE (units 10⁻⁶), CL%, EVTS, DOCUMENT ID, TECN, CHG. Row: <3.0, 95, 0, BIRGE, 65, FBC, +

$\Gamma(\pi^+ e^+ e^-)/\Gamma_{\text{total}}$ Γ_{31}/Γ Test for $\Delta S = 1$ weak neutral current. Allowed by combined first-order weak and electromagnetic interactions. Table with columns: VALUE (units 10⁻⁷), CL%, EVTS, DOCUMENT ID, TECN, CHG, COMMENT. Row: 2.88 ± 0.13 OUR AVERAGE. Includes text: "We do not use the following data for averages, fits, limits, etc. ..."

⁵²APPEL 99 establishes vector nature of this decay and determines form factor $f(Z) = f_0(1+\delta Z)$, $Z = M_e^2/m_K^2$, $\delta = 2.14 \pm 0.13 \pm 0.15$.

⁵³ALLIEGRO 92 assumes a vector interaction with a form factor given by $\lambda = 0.105 \pm 0.035 \pm 0.015$ and a correlation coefficient of -0.82 .

⁵⁴BLOCH 75 assumes a vector interaction.

$\Gamma(\pi^+ \mu^+ \mu^-)/\Gamma_{\text{total}}$ Γ_{32}/Γ Test for $\Delta S = 1$ weak neutral current. Allowed by higher-order electroweak interactions.

Table with columns: VALUE (units 10⁻⁸), CL%, EVTS, DOCUMENT ID, TECN, CHG. Row: 7.6 ± 2.1 OUR AVERAGE. Includes text: "We do not use the following data for averages, fits, limits, etc. ..."

⁵⁵ADLER 97c gives systematic error 0.7×10^{-8} and theoretical uncertainty 0.6×10^{-8} , which we combine in quadrature to obtain our second error.

$\Gamma(\pi^+ \nu \bar{\nu})/\Gamma_{\text{total}}$ Γ_{33}/Γ Test for $\Delta S = 1$ weak neutral current. Allowed by higher-order electroweak interactions.

Table with columns: VALUE (units 10⁻⁹), CL%, EVTS, DOCUMENT ID, TECN, CHG, COMMENT. Row: 0.15^{+0.34}_{-0.12}, 1, ADLER, 00, B787. Includes text: "We do not use the following data for averages, fits, limits, etc. ..."

⁵⁶Combining ATIYA 93 and ATIYA 93B results. Superseded by ADLER 96.

⁵⁷KLEMS 71 and CABLE 73 assume π spectrum same as K_{e3} decay. Second CABLE 73 limit combines CABLE 73 and KLEMS 71 data for vector interaction.

⁵⁸LJUNG 73 assumes vector interaction.

$\Gamma(\mu^- \nu e^+ e^+)/\Gamma(\pi^+ \pi^- e^+ \nu_e)$ Γ_{34}/Γ_9 Test of lepton family number conservation.

Table with columns: VALUE (units 10⁻³), CL%, EVTS, DOCUMENT ID, TECN, CHG. Row: <0.5, 90, 0, 59, DIAMANT-..., 76, SPEC, +. Includes text: "DIAMANT-BERGER 76 quotes this result times our 1975 $\pi^+ \pi^- e \nu$ BR ratio."

$\Gamma(\mu^+ \nu_e)/\Gamma_{\text{total}}$ Γ_{35}/Γ Forbidden by lepton family number conservation.

Table with columns: VALUE, CL%, EVTS, DOCUMENT ID, TECN, CHG, COMMENT. Row: <0.004, 90, 0, 60, LYONS, 81, HLBC, 0, 200 GeV K^+ narrow band ν beam. Includes text: "We do not use the following data for averages, fits, limits, etc. ..."

$\Gamma(\pi^+ \mu^+ e^-)/\Gamma_{\text{total}}$ Γ_{36}/Γ Test of lepton family number conservation.

Table with columns: VALUE (units 10⁻¹⁰), CL%, EVTS, DOCUMENT ID, TECN, CHG, COMMENT. Row: < 2.1, 90, 0, LEE, 90, SPEC, +. Includes text: "We do not use the following data for averages, fits, limits, etc. ..."

$\Gamma(\pi^+ \mu^- e^+)/\Gamma_{\text{total}}$ Γ_{37}/Γ Test of lepton family number conservation.

Table with columns: VALUE (units 10⁻⁹), CL%, EVTS, DOCUMENT ID, TECN, CHG. Row: < 7, 90, 0, 61, DIAMANT-..., 76, SPEC, +. Includes text: "We do not use the following data for averages, fits, limits, etc. ..."

$\Gamma(\pi^- \mu^+ e^+)/\Gamma_{\text{total}}$ Γ_{38}/Γ Test of total lepton number conservation.

Table with columns: VALUE (units 10⁻⁹), CL%, EVTS, DOCUMENT ID, TECN, CHG. Row: < 7, 90, 0, 62, DIAMANT-..., 76, SPEC, +. Includes text: "We do not use the following data for averages, fits, limits, etc. ..."

$\Gamma(\pi^+ \mu^- e^+)/\Gamma_{\text{total}}$ Γ_{37}/Γ

Table with columns: VALUE (units 10⁻⁸), CL%, DOCUMENT ID, TECN, CHG. Row: <1.4, 90, BEIER, 72, OSPK, ±. Includes text: "We do not use the following data for averages, fits, limits, etc. ..."

$\Gamma(\pi^- e^+ e^+)/\Gamma_{\text{total}}$						Γ_{39}/Γ
Test of total lepton number conservation.						
VALUE (units 10^{-5})	CL%	DOCUMENT ID	TECN	CHG		
<1.5		CHANG	68	HBC	-	
••• We do not use the following data for averages, fits, limits, etc. •••						
$\Gamma(\pi^- e^+ e^+)/\Gamma(\pi^+ \pi^- e^+ \nu_e)$						Γ_{39}/Γ_9
Test of total lepton number conservation.						
VALUE (units 10^{-4})	CL%	EVT5	DOCUMENT ID	TECN	CHG	
<2.5	90	0	63	DIAMANT...	76	SPEC +
63 DIAMANT-BERGER 76 quotes this result times our 1975 BR ratio.						
$\Gamma(\pi^- \mu^+ \mu^+)/\Gamma_{\text{total}}$						Γ_{40}/Γ
Forbidden by total lepton number conservation.						
VALUE (units 10^{-4})	CL%	DOCUMENT ID	TECN			
<1.5	90	64	LITTENBERG	92	HBC	
64 LITTENBERG 92 is from retroactive data analysis of CHANG 68 bubble chamber data.						
$\Gamma(\pi^+ \nu_e)/\Gamma_{\text{total}}$						Γ_{41}/Γ
Forbidden by total lepton number conservation.						
VALUE (units 10^{-3})	CL%	DOCUMENT ID	TECN	COMMENT		
<3.3	90	65	COOPER	82	HLBC	Wideband ν beam
65 COOPER 82 limit on $\bar{\nu}_e$ observation is here interpreted as a limit on lepton number violation in the absence of mixing.						
$\Gamma(\pi^0 e^+ \nu_e)/\Gamma_{\text{total}}$						Γ_{42}/Γ
Forbidden by total lepton number conservation.						
VALUE	CL%	DOCUMENT ID	TECN	COMMENT		
<0.003	90	66	COOPER	82	HLBC	Wideband ν beam
66 COOPER 82 limit on $\bar{\nu}_e$ observation is here interpreted as a limit on lepton number violation in the absence of mixing.						
$\Gamma(\pi^+ \gamma)/\Gamma_{\text{total}}$						Γ_{43}/Γ
Violates angular momentum conservation. Not listed in Summary Table.						
VALUE (units 10^{-6})	CL%	DOCUMENT ID	TECN	CHG		
<1.4	90	ASANO	82	CNTR	+	
<4.0	90	67	KLEMS	71	OSPK	+
67 Test of model of Selleri, Nuovo Cimento 60A 291 (1969).						

 K^+ LONGITUDINAL POLARIZATION OF EMITTED μ^+

VALUE	CL%	DOCUMENT ID	TECN	CHG	COMMENT
<-0.990	90	68	AOKI	94	SPEC +
••• We do not use the following data for averages, fits, limits, etc. •••					
<-0.990	90	IMAZATO	92	SPEC +	Repl. by AOKI 94
-0.970 \pm 0.047		69	YAMANAKA	86	SPEC +
-1.0 \pm 0.1		69	CUTTS	69	SPRK +
-0.96 \pm 0.12		69	COOMBES	57	CNTR +
68 AOKI 94 measures $\xi P_\mu = -0.9996 \pm 0.0030 \pm 0.0048$. The above limit is obtained by summing the statistical and systematic errors in quadrature, normalizing to the physically significant region ($ \xi P_\mu < 1$) and assuming that $\xi = 1$, its maximum value.					
69 Assumes $\xi = 1$.					

DALITZ PLOT PARAMETERS FOR $K \rightarrow 3\pi$ DECAYS

Revised 1999 by T.G. Trippe (LBNL).

The Dalitz plot distribution for $K^\pm \rightarrow \pi^\pm \pi^\pm \pi^\mp$, $K^\pm \rightarrow \pi^0 \pi^0 \pi^\pm$, and $K_L^0 \rightarrow \pi^+ \pi^- \pi^0$ can be parameterized by a series expansion such as that introduced by Weinberg [1]. We use the form

$$\begin{aligned}
 |M|^2 \propto & 1 + g \frac{(s_3 - s_0)}{am_{\pi^+}^2} + h \left[\frac{s_3 - s_0}{m_{\pi^+}^2} \right]^2 \\
 & + j \frac{(s_2 - s_1)}{m_{\pi^+}^2} + k \left[\frac{s_2 - s_1}{m_{\pi^+}^2} \right]^2 \\
 & + f \frac{(s_2 - s_1)(s_3 - s_0)}{m_{\pi^+}^2 m_{\pi^+}^2} + \dots, \quad (1)
 \end{aligned}$$

where $m_{\pi^+}^2$ has been introduced to make the coefficients g , h , j , and k dimensionless, and

$$s_i = (P_K - P_i)^2 = (m_K - m_i)^2 - 2m_K T_i, \quad i = 1, 2, 3,$$

$$s_0 = \frac{1}{3} \sum_i s_i = \frac{1}{3} (m_K^2 + m_1^2 + m_2^2 + m_3^2)$$

Here the P_i are four-vectors, m_i and T_i are the mass and kinetic energy of the i^{th} pion, and the index 3 is used for the odd pion.

The coefficient g is a measure of the slope in the variable s_3 (or T_3) of the Dalitz plot, while h and k measure the quadratic dependence on s_3 and $(s_2 - s_1)$, respectively. The coefficient j is related to the asymmetry of the plot and must be zero if CP invariance holds. Note also that if CP is good, g , h , and k must be the same for $K^+ \rightarrow \pi^+ \pi^+ \pi^-$ as for $K^- \rightarrow \pi^- \pi^- \pi^+$.

Since different experiments use different forms for $|M|^2$, in order to compare the experiments we have converted to g , h , j , and k whatever coefficients have been measured. Where such conversions have been done, the measured coefficient a_y , a_t , a_u , or a_v is given in the comment at the right. For definitions of these coefficients, details of this conversion, and discussion of the data, see the April 1982 version of this note [2].

References

- S. Weinberg, Phys. Rev. Lett. **4**, 87 (1960).
- Particle Data Group, Phys. Lett. **111B**, 69 (1982).

ENERGY DEPENDENCE OF K^\pm DALITZ PLOT

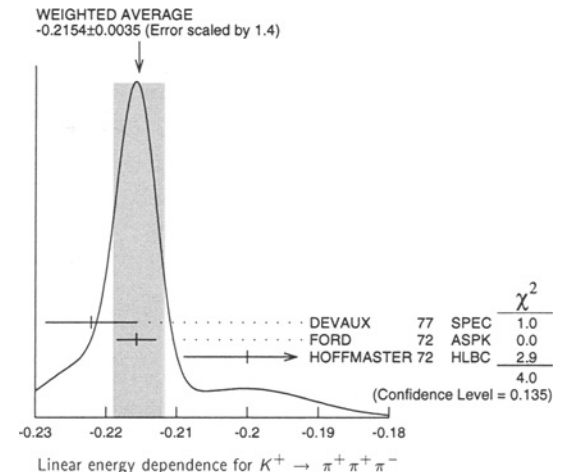
$$\begin{aligned}
 |\text{matrix element}|^2 &= 1 + gu + hv^2 + kv^2 \\
 \text{where } u &= (s_3 - s_0) / m_{\pi^+}^2 \text{ and } v = (s_1 - s_2) / m_{\pi^+}^2
 \end{aligned}$$

LINEAR COEFFICIENT g_{π^+} FOR $K^+ \rightarrow \pi^+ \pi^+ \pi^-$

Some experiments use Dalitz variables x and y . In the comments we give a_y = coefficient of y term. See note above on "Dalitz Plot Parameters for $K \rightarrow 3\pi$ Decays." For discussion of the conversion of a_y to g , see the earlier version of the same note in the Review published in Physics Letters **111B** 70 (1982).

VALUE	EVT5	DOCUMENT ID	TECN	CHG	COMMENT
-0.2154 \pm 0.0035 OUR AVERAGE					Error includes scale factor of 1.4. See the ideogram below.
-0.2221 \pm 0.0065	225k	DEVAUX	77	SPEC +	$a_y = .2814 \pm .0082$
-0.2157 \pm 0.0028	750k	FORD	72	ASPK +	$a_y = .2734 \pm .0035$
-0.200 \pm 0.009	39819	70 HOFFMASTER	72	HLBC +	
••• We do not use the following data for averages, fits, limits, etc. •••					
-0.196 \pm 0.012	17898	71 GRAUMAN	70	HLBC +	$a_y = 0.228 \pm 0.030$
-0.218 \pm 0.016	9994	72 BUTLER	68	HBC +	$a_y = 0.277 \pm 0.020$
-0.22 \pm 0.024	5428	72,73 ZINCHENKO	67	HBC +	$a_y = 0.28 \pm 0.03$

70 HOFFMASTER 72 includes GRAUMAN 70 data.
 71 Emulsion data added — all events included by HOFFMASTER 72.
 72 Experiments with large errors not included in average.
 73 Also includes DBC events.

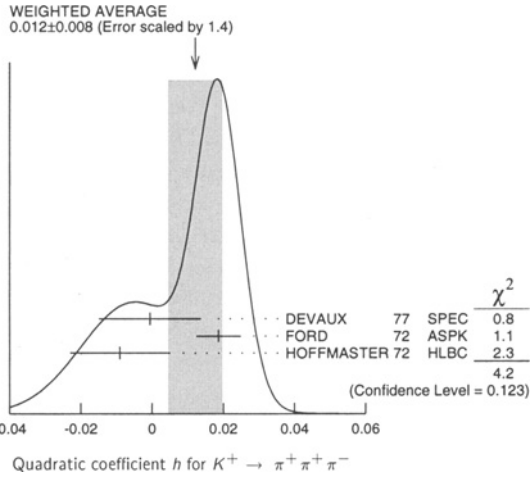


Meson Particle Listings

K^\pm

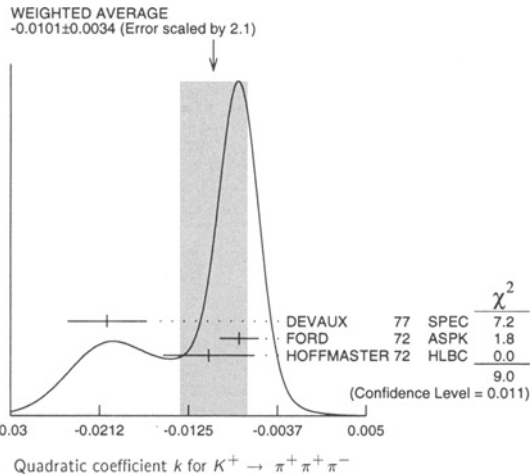
QUADRATIC COEFFICIENT h FOR $K^+ \rightarrow \pi^+ \pi^+ \pi^-$

VALUE	EVTS	DOCUMENT ID	TECN	CHG
0.012 ± 0.008 OUR AVERAGE		Error includes scale factor of 1.4. See the ideogram below.		
-0.0006 ± 0.0143	225k	DEVAUX	77	SPEC +
0.0187 ± 0.0062	750k	FORD	72	ASPK +
-0.009 ± 0.014	39819	HOFFMASTER	72	HLBC +



QUADRATIC COEFFICIENT k FOR $K^+ \rightarrow \pi^+ \pi^+ \pi^-$

VALUE	EVTS	DOCUMENT ID	TECN	CHG
-0.0101 ± 0.0034 OUR AVERAGE		Error includes scale factor of 2.1. See the ideogram below.		
-0.0205 ± 0.0039	225k	DEVAUX	77	SPEC +
-0.0075 ± 0.0019	750k	FORD	72	ASPK +
-0.0105 ± 0.0045	39819	HOFFMASTER	72	HLBC +



LINEAR COEFFICIENT g_{π^-} FOR $K^- \rightarrow \pi^- \pi^- \pi^+$

Some experiments use Dalitz variables x and y . In the comments we give a_y = coefficient of y term. See note above on "Dalitz Plot Parameters for $K^- \rightarrow 3\pi$ Decays." For discussion of the conversion of a_y to g , see the earlier version of the same note in the Review published in Physics Letters **111B** 70 (1982).

VALUE	EVTS	DOCUMENT ID	TECN	CHG	COMMENT
-0.217 ± 0.007 OUR AVERAGE		Error includes scale factor of 2.5.			
-0.2186 ± 0.0028	750k	FORD	72	ASPK -	$a_y = .2770 \pm .0035$
-0.193 ± 0.010	50919	MAST	69	HBC -	$a_y = 0.244 \pm 0.013$
-0.199 ± 0.008	81k	⁷⁴ LUCAS	73	HBC -	$a_y = 0.252 \pm 0.011$
-0.190 ± 0.023	5778	^{75,76} MOSCOSO	68	HBC -	$a_y = 0.242 \pm 0.029$
-0.220 ± 0.035	1347	⁷⁷ FERRO-LUZZI	61	HBC -	$a_y = 0.28 \pm 0.045$

⁷⁴ Quadratic dependence is required by K_L^0 experiments. For comparison we average only those K^\pm experiments which quote quadratic fit values.
⁷⁵ Experiments with large errors not included in average.
⁷⁶ Also includes DBC events.
⁷⁷ No radiative corrections included.

QUADRATIC COEFFICIENT h FOR $K^- \rightarrow \pi^- \pi^- \pi^+$

VALUE	EVTS	DOCUMENT ID	TECN	CHG
0.010 ± 0.006 OUR AVERAGE		Error includes scale factor of 1.4. See the ideogram below.		
0.0125 ± 0.0062	750k	FORD	72	ASPK -
-0.001 ± 0.012	50919	MAST	69	HBC -

QUADRATIC COEFFICIENT k FOR $K^- \rightarrow \pi^- \pi^- \pi^+$

VALUE	EVTS	DOCUMENT ID	TECN	CHG
-0.0084 ± 0.0019 OUR AVERAGE		Error includes scale factor of 2.7. See the ideogram below.		
-0.0083 ± 0.0019	750k	FORD	72	ASPK -
-0.014 ± 0.012	50919	MAST	69	HBC -

$(g_{\pi^+} - g_{\pi^-}) / (g_{\pi^+} + g_{\pi^-})$ FOR $K^\pm \rightarrow \pi^\pm \pi^+ \pi^-$

A nonzero value for this quantity indicates CP violation.

VALUE (%)	EVTS	DOCUMENT ID	TECN
-0.70 ± 0.53	3.2M	FORD	70

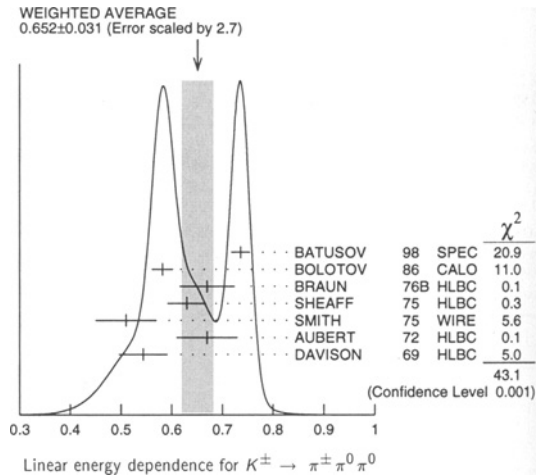
LINEAR COEFFICIENT g FOR $K^\pm \rightarrow \pi^\pm \pi^0 \pi^0$

Unless otherwise stated, all experiments include terms quadratic in $(s_3 - s_0) / m_{\pi^+}^2$. See note above on "Dalitz Plot Parameters for $K^- \rightarrow 3\pi$ Decays."

See BATUSOV 98 for a discussion of the discrepancy between their result and others, especially BOLOTOV 86. At this time we have no way to resolve the discrepancy so we depend on the large scale factor as a warning.

VALUE	EVTS	DOCUMENT ID	TECN	CHG	COMMENT
0.652 ± 0.031 OUR AVERAGE		Error includes scale factor of 2.7. See the ideogram below.			
0.736 ± 0.014 ± 0.012	33k	BATUSOV	98	SPEC	+
0.582 ± 0.021	43k	BOLOTOV	86	CALO	-
0.670 ± 0.054	3263	BRAUN	76B	HLBC	+
0.630 ± 0.038	5635	SHEAFF	75	HLBC	+
0.510 ± 0.060	27k	SMITH	75	WIRE	+
0.67 ± 0.06	1365	AUBERT	72	HLBC	+
0.544 ± 0.048	4048	DAVISON	69	HLBC	+
					Also emulsion
• • • We do not use the following data for averages, fits, limits, etc. • • •					
0.806 ± 0.220	4639	⁷⁸ BERTRAND	76	EMUL	+
0.484 ± 0.084	574	⁷⁹ LUCAS	73B	HBC	-
0.527 ± 0.102	198	⁷⁸ PANDOULAS	70	EMUL	+
0.586 ± 0.098	1874	⁷⁹ BISI	65	HLBC	+
0.48 ± 0.04	1792	⁷⁹ KALMUS	64	HLBC	+

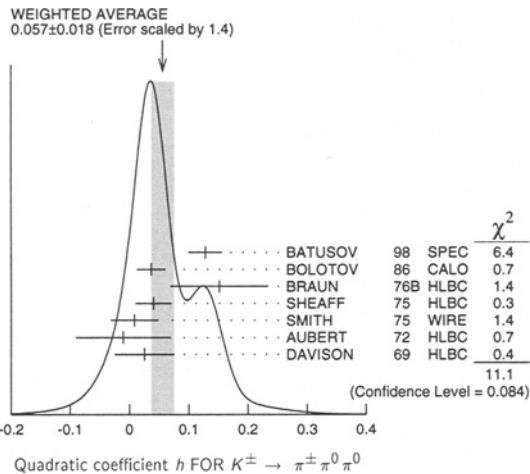
⁷⁸ Experiments with large errors not included in average.
⁷⁹ Authors give linear fit only.



QUADRATIC COEFFICIENT h FOR $K^\pm \rightarrow \pi^\pm \pi^0 \pi^0$

VALUE	EVTS	DOCUMENT ID	TECN	CHG	COMMENT
0.057 ± 0.018 OUR AVERAGE		Error includes scale factor of 1.4. See the ideogram below.			
0.128 ± 0.015 ± 0.024	33k	BATUSOV	98	SPEC	+
0.037 ± 0.024	43k	BOLOTOV	86	CALO	-
0.152 ± 0.082	3263	BRAUN	76B	HLBC	+
0.041 ± 0.030	5635	SHEAFF	75	HLBC	+
0.009 ± 0.040	27k	SMITH	75	WIRE	+
-0.01 ± 0.08	1365	AUBERT	72	HLBC	+
0.026 ± 0.050	4048	DAVISON	69	HLBC	+
					Also emulsion
• • • We do not use the following data for averages, fits, limits, etc. • • •					
0.164 ± 0.121	4639	⁸⁰ BERTRAND	76	EMUL	+
0.018 ± 0.124	198	⁸⁰ PANDOULAS	70	EMUL	+

⁸⁰ Experiments with large errors not included in average.



QUADRATIC COEFFICIENT h FOR $K^\pm \rightarrow \pi^\pm \pi^0 \pi^0$				
VALUE	EVTs	DOCUMENT ID	TECN	CHG
0.0197±0.0045±0.0029	33k	BATISOV	98 SPEC	+

$K_{\ell 3}^\pm$ AND $K_{\ell 3}^0$ FORM FACTORS

Written by T.G. Trippe (LBNL).

Assuming that only the vector current contributes to $K \rightarrow \pi \ell \nu$ decays, we write the matrix element as

$$M \propto f_+(t) [(P_K + P_\pi)_\mu \bar{\ell} \gamma_\mu (1 + \gamma_5) \nu] + f_-(t) [m_\ell \bar{\ell} (1 + \gamma_5) \nu], \quad (1)$$

where P_K and P_π are the four-momenta of the K and π mesons, m_ℓ is the lepton mass, and f_+ and f_- are dimensionless form factors which can depend only on $t = (P_K - P_\pi)^2$, the square of the four-momentum transfer to the leptons. If time-reversal invariance holds, f_+ and f_- are relatively real. $K_{\mu 3}$ experiments measure f_+ and f_- , while $K_{e 3}$ experiments are sensitive only to f_+ because the small electron mass makes the f_- term negligible.

(a) $K_{\mu 3}$ experiments. Analyses of $K_{\mu 3}$ data frequently assume a linear dependence of f_+ and f_- on t , i.e.,

$$f_\pm(t) = f_\pm(0) [1 + \lambda_\pm(t/m_\pi^2)] \quad (2)$$

Most $K_{\mu 3}$ data are adequately described by Eq. (2) for f_+ and a constant f_- (i.e., $\lambda_- = 0$). There are two equivalent parametrizations commonly used in these analyses:

(1) λ_+ , $\xi(0)$ parametrization. Analyses of $K_{\mu 3}$ data often introduce the ratio of the two form factors

$$\xi(t) = f_-(t)/f_+(t). \quad (3)$$

The $K_{\mu 3}$ decay distribution is then described by the two parameters λ_+ and $\xi(0)$ (assuming time reversal invariance and $\lambda_- = 0$). These parameters can be determined by three different methods:

Method A. By studying the Dalitz plot or the pion spectrum of $K_{\mu 3}$ decay. The Dalitz plot density is (see, e.g., Chounet *et al.* [1]):

$$\rho(E_\pi, E_\mu) \propto f_+^2(t) [A + B\xi(t) + C\xi(t)^2],$$

where

$$A = m_K (2E_\mu E_\nu - m_K E'_\pi) + m_\mu^2 \left(\frac{1}{4} E'_\pi - E_\nu \right),$$

$$B = m_\mu^2 \left(E_\nu - \frac{1}{2} E'_\pi \right),$$

$$C = \frac{1}{4} m_\mu^2 E'_\pi,$$

$$E'_\pi = E_\pi^{\max} - E_\pi = (m_K^2 + m_\pi^2 - m_\mu^2) / 2m_K - E_\pi. \quad (4)$$

Here E_π , E_μ , and E_ν are, respectively, the pion, muon, and neutrino energies in the kaon center of mass. The density ρ is fit to the data to determine the values of λ_+ , $\xi(0)$, and their correlation.

Method B. By measuring the $K_{\mu 3}/K_{e 3}$ branching ratio and comparing it with the theoretical ratio (see, e.g., Fearing *et al.* [2]) as given in terms of λ_+ and $\xi(0)$, assuming μ - e universality:

$$\begin{aligned} \Gamma(K_{\mu 3}^\pm)/\Gamma(K_{e 3}^\pm) &= 0.6457 + 1.4115\lambda_+ + 0.1264\xi(0) \\ &\quad + 0.0192\xi(0)^2 + 0.0080\lambda_+\xi(0), \\ \Gamma(K_{\mu 3}^0)/\Gamma(K_{e 3}^0) &= 0.6452 + 1.3162\lambda_+ + 0.1264\xi(0) \\ &\quad + 0.0186\xi(0)^2 + 0.0064\lambda_+\xi(0). \end{aligned} \quad (5)$$

This cannot determine λ_+ and $\xi(0)$ simultaneously but simply fixes a relationship between them.

Method C. By measuring the muon polarization in $K_{\mu 3}$ decay. In the rest frame of the K , the μ is expected to be polarized in the direction \mathbf{A} with $\mathbf{P} = \mathbf{A}/|\mathbf{A}|$, where \mathbf{A} is given (Cabibbo and Maksymowicz [3]) by

$$\begin{aligned} \mathbf{A} &= a_1(\xi) \mathbf{p}_\mu \\ &\quad - a_2(\xi) \left[\frac{\mathbf{p}_\mu}{m_\mu} \left(m_K - E_\pi + \frac{\mathbf{p}_\pi \cdot \mathbf{p}_\mu}{|\mathbf{p}_\mu|^2} (E_\mu - m_\mu) \right) + \mathbf{p}_\pi \right] \\ &\quad + m_K \text{Im}\xi(t) (\mathbf{p}_\pi \times \mathbf{p}_\mu). \end{aligned} \quad (6)$$

If time-reversal invariance holds, ξ is real, and thus there is no polarization perpendicular to the K -decay plane. Polarization experiments measure the weighted average of $\xi(t)$ over the t range of the experiment, where the weighting accounts for the variation with t of the sensitivity to $\xi(t)$.

(2) λ_+ , λ_0 parametrization. Most of the more recent $K_{\mu 3}$ analyses have parameterized in terms of the form factors f_+ and f_0 which are associated with vector and scalar exchange, respectively, to the lepton pair. f_0 is related to f_+ and f_- by

$$f_0(t) = f_+(t) + [t/(m_K^2 - m_\pi^2)] f_-(t). \quad (7)$$

Here $f_0(0)$ must equal $f_+(0)$ unless $f_-(t)$ diverges at $t = 0$. The earlier assumption that f_+ is linear in t and f_- is constant leads to f_0 linear in t :

$$f_0(t) = f_0(0) [1 + \lambda_0(t/m_\pi^2)]. \quad (8)$$

Meson Particle Listings

 K^\pm

With the assumption that $f_0(0) = f_+(0)$, the two parametrizations, $(\lambda_+, \xi(0))$ and (λ_+, λ_0) are equivalent as long as correlation information is retained. (λ_+, λ_0) correlations tend to be less strong than $(\lambda_+, \xi(0))$ correlations.

The experimental results for $\xi(0)$ and its correlation with λ_+ are listed in the K^\pm and K_L^0 sections of the Particle Listings in section ξ_A , ξ_B , or ξ_C depending on whether method A, B, or C discussed above was used. The corresponding values of λ_+ are also listed.

Because recent experiments tend to use the (λ_+, λ_0) parametrization, we include a subsection for λ_0 results. Whenever possible we have converted $\xi(0)$ results into λ_0 results and vice versa.

See the 1982 version of this note [4] for additional discussion of the $K_{\mu 3}^0$ parameters, correlations, and conversion between parametrizations, and also for a comparison of the experimental results.

(b) K_{e3} experiments. Analysis of K_{e3} data is simpler than that of $K_{\mu 3}$ because the second term of the matrix element assuming a pure vector current [Eq. (1) above] can be neglected. Here f_+ is usually assumed to be linear in t , and the linear coefficient λ_+ of Eq. (2) is determined.

If we remove the assumption of a pure vector current, then the matrix element for the decay, in addition to the terms in Eq. (1), would contain

$$+2m_K f_S \bar{\ell}(1 + \gamma_5)\nu + (2f_T/m_K)(P_K)_\lambda (P_\pi)_\mu \bar{\ell} \sigma_{\lambda\mu}(1 + \gamma_5)\nu, \quad (9)$$

where f_S is the scalar form factor, and f_T is the tensor form factor. In the case of the K_{e3} decays where the f_- term can be neglected, experiments have yielded limits on $|f_S/f_+|$ and $|f_T/f_+|$.

References

1. L.M. Chounet, J.M. Gaillard, and M.K. Gaillard, Phys. Reports **4C**, 199 (1972).
2. H.W. Fearing, E. Fischbach, and J. Smith, Phys. Rev. **D2**, 542 (1970).
3. N. Cabibbo and A. Maksymowicz, Phys. Lett. **9**, 352 (1964).
4. Particle Data Group, Phys. Lett. **111B**, 73 (1982).

 K_{e3}^\pm FORM FACTORS

In the form factor comments, the following symbols are used.

f_+ and f_- are form factors for the vector matrix element.

f_S and f_T refer to the scalar and tensor term.

$f_0 = f_+ + f_- t/(m_K^2 - m_\pi^2)$.

λ_+ , λ_- , and λ_0 are the linear expansion coefficients of f_+ , f_- , and f_0 .

λ_+ refers to the $K_{\mu 3}^\pm$ value except in the K_{e3}^\pm sections.

$d\xi(0)/d\lambda_+$ is the correlation between $\xi(0)$ and λ_+ in $K_{\mu 3}^\pm$.

$d\lambda_0/d\lambda_+$ is the correlation between λ_0 and λ_+ in $K_{\mu 3}^\pm$.

$t =$ momentum transfer to the π in units of m_π^2 .

DP = Dalitz plot analysis.

PI = π spectrum analysis.

MU = μ spectrum analysis.

POL = μ polarization analysis.

BR = $K_{\mu 3}^\pm/K_{e3}^\pm$ branching ratio analysis.

E = positron or electron spectrum analysis.

RC = radiative corrections.

 λ_+ (LINEAR ENERGY DEPENDENCE OF f_+ IN K_{e3}^\pm DECAY)

For radiative correction of K_{e3}^\pm Dalitz plot, see GINSBERG 67 and BECHERRAWY 70.

VALUE	EVT5	DOCUMENT ID	TECN	CHG	COMMENT
0.0276 ± 0.0021 OUR AVERAGE					
0.018 ± 0.007	3k	ARTEMOV	97B SPEC	-	DP
0.0284 ± 0.0027 ± 0.0020	32k	⁸¹ AKIMENKO	91 SPEC		PI, no RC
0.029 ± 0.004	62k	⁸² BOLOTOV	88 SPEC		PI, no RC
0.027 ± 0.008		⁸³ BRAUN	73B HLBC	+	DP, no RC
0.029 ± 0.011	4017	CHIANG	72 OSPK	+	DP, RC neglig- ble
0.027 ± 0.010	2707	STEINER	71 HLBC	+	DP, uses RC
0.045 ± 0.015	1458	BOTTERILL	70 OSPK		PI, uses RC
0.08 ± 0.04	960	BOTTERILL	68C ASPK	+	e ⁺ , uses RC
-0.02 ± 0.08 -0.12	90	EISLER	68 HLBC	+	PI, uses RC
0.045 ± 0.017 -0.018	854	BELLOTTI	67B FBC	+	DP, uses RC
+0.016 ± 0.016	1393	IMLAY	67 OSPK	+	DP, no RC
+0.028 ± 0.013 -0.014	515	KALMUS	67 FBC	+	e ⁺ , PI, no RC
-0.04 ± 0.05	230	BORREANI	64 HBC	+	e ⁺ , no RC
-0.010 ± 0.029	407	JENSEN	64 XEBC	+	PI, no RC
+0.036 ± 0.045	217	BROWN	62B XEBC	+	PI, no RC

• • • We do not use the following data for averages, fits, limits, etc. • • •

0.025 ± 0.007		⁸⁴ BRAUN	74 HLBC	+	$K_{\mu 3}/K_{e3}$ vs. t
		⁸¹ AKIMENKO	91		state that radiative corrections would raise λ_+ by 0.0013.
		⁸² BOLOTOV	88		state radiative corrections of GINSBERG 67 would raise λ_+ by 0.002.
		⁸³ BRAUN	73B		states that radiative corrections of GINSBERG 67 would lower λ_+ by 0.002 but that radiative corrections of BECHERRAWY 70 disagrees and would raise λ_+ by 0.005.
		⁸⁴ BRAUN	74		is a combined $K_{\mu 3}$ - K_{e3} result. It is not independent of BRAUN 73C ($K_{\mu 3}$) and BRAUN 73B (K_{e3}) form factor results.

 $\xi_A = f_-/f_+$ (determined from $K_{\mu 3}^\pm$ spectra)

The parameter ξ is redundant with λ_0 below and is not put into the Meson Summary Table.

VALUE	$d\xi(0)/d\lambda_+$	EVT5	DOCUMENT ID	TECN	CHG	COMMENT
-0.31 ± 0.15 OUR EVALUATION						Error includes scale factor of 1.6. Correlation is $d\xi(0)/d\lambda_+ = -14$. From a fit discussed in note on K_{e3} form factors in 1982 edition, PL 111B (April 1982).
-0.27 ± 0.25	-17	3973	WHITMAN	80 SPEC	+	DP
-0.8 ± 0.8	-20	490	⁸⁵ ARNOLD	74 HLBC	+	DP
-0.57 ± 0.24	-9	6527	⁸⁶ MERLAN	74 ASPK	+	DP
-0.36 ± 0.40	-19	1897	⁸⁷ BRAUN	73C HLBC	+	DP
-0.62 ± 0.28	-12	4025	⁸⁸ ANKENBRA...	72 ASPK	+	PI
+0.45 ± 0.28	-15	3480	⁸⁹ CHIANG	72 OSPK	+	DP
-1.1 ± 0.56	-29	3240	⁹⁰ HAIDT	71 HLBC	+	DP
-0.5 ± 0.8	-26	2041	⁹¹ KIJEWski	69 OSPK	+	PI
+0.72 ± 0.93	-17	444	CALLAHAN	66B FBC	+	PI
• • • We do not use the following data for averages, fits, limits, etc. • • •						
-0.5 ± 0.9	none	78	EISLER	68 HLBC	+	PI, $\lambda_+ = 0$
0.0 ± 1.1 -0.9		2648	⁹² CALLAHAN	66B FBC	+	μ , $\lambda_+ = 0$
+0.7 ± 0.5		87	GIACOMELLI	64 EMUL	+	MU+BR, $\lambda_+ = 0$
-0.08 ± 0.7			⁹³ JENSEN	64 XEBC	+	DP+BR
+1.8 ± 0.6		76	BROWN	62B XEBC	+	DP+BR, $\lambda_+ = 0$

⁸⁵ ARNOLD 74 figure 4 was used to obtain ξ_A and $d\xi(0)/d\lambda_+$.

⁸⁶ MERLAN 74 figure 5 was used to obtain $d\xi(0)/d\lambda_+$.

⁸⁷ BRAUN 73C gives $\xi(t) = -0.34 \pm 0.20$, $d\xi(t)/d\lambda_+ = -14$ for $\lambda_+ = 0.027$, $t = 6.6$. We calculate above $\xi(0)$ and $d\xi(0)/d\lambda_+$ for their $\lambda_+ = 0.025 \pm 0.017$.

⁸⁸ ANKENBRANDT 72 figure 3 was used to obtain $d\xi(0)/d\lambda_+$.

⁸⁹ CHIANG 72 figure 10 was used to obtain $d\xi(0)/d\lambda_+$. Fit had $\lambda_- = \lambda_+$ but would not change for $\lambda_- = 0$. L.Pondrom, (private communication 74).

⁹⁰ HAIDT 71 table 8 (Dalitz plot analysis) gives $d\xi(0)/d\lambda_+ = (-1.1 + 0.5)/(0.050 - 0.029) = -29$, error raised from 0.50 to agree with $d\xi(0) = 0.20$ for fixed λ_+ .

⁹¹ KIJEWski 69 figure 17 was used to obtain $d\xi(0)/d\lambda_+$ and errors.

⁹² CALLAHAN 66 table 1 (π analysis) gives $d\xi(0)/d\lambda_+ = (0.72 - 0.05)/(0 - 0.04) = -17$, error raised from 0.80 to agree with $d\xi(0) = 0.37$ for fixed λ_+ . t unknown.

⁹³ JENSEN 64 gives $\lambda_+^\mu = \lambda_+^e = -0.020 \pm 0.027$. $d\xi(0)/d\lambda_+$ unknown. INCLUDE SHAK-LEES 64 $\xi_B(K_{\mu 3}/K_{e3})$.

 $\xi_B = f_-/f_+$ (determined from $K_{\mu 3}^\pm/K_{e3}^\pm$)

The $K_{\mu 3}^\pm/K_{e3}^\pm$ branching ratio fixes a relationship between $\xi(0)$ and λ_+ . We quote the author's $\xi(0)$ and associated λ_+ but do not average because the λ_+ values differ. The fit result and scale factor given below are not obtained from these ξ_B values. Instead they are obtained directly from the fitted $K_{\mu 3}^\pm/K_{e3}^\pm$ ratio $\Gamma(\pi^0 \mu^+ \nu_\mu)/\Gamma(\pi^0 e^+ \nu_e)$, with the exception of HEINTZE 77. The parameter ξ is redundant with λ_0 below and is not put into the Meson Summary Table.

VALUE	EVT5	DOCUMENT ID	TECN	CHG	COMMENT
-0.31 ± 0.15 OUR EVALUATION					Error includes scale factor of 1.6. Correlation is $d\xi(0)/d\lambda_+ = -14$. From a fit discussed in note on K_{e3} form factors in 1982 edition, PL 111B (April 1982).
-0.12 ± 0.12	55k	⁹⁴ HEINTZE	77 CNTR	+	$\lambda_+ = 0.029$

See key on page 239

Meson Particle Listings

K^\pm, K^0

BOTTERILL 67 PRL 19 982	D.R. Botterill <i>et al.</i>	(OXF)
Also 68 PR 171 1402	D.R. Botterill <i>et al.</i>	(OXF)
BOWEN 67B PR 154 1314	D.R. Bowen <i>et al.</i>	(PPA)
CLINE 67B Herceg Novi Tbl. 4	D. Cline	
Proc. International School on Elementary Particle Physics.		
FLETCHER 67 PRL 19 98	C.R. Fletcher <i>et al.</i>	(ILL)
FORD 67 PRL 18 1214	W.T. Ford <i>et al.</i>	(PRIN)
GINSBERG 67 PR 162 1570	E.S. Ginsberg	(MASH)
IMLAY 67 PR 150 1203	R.L. Imlay <i>et al.</i>	(PRIN)
KALMUS 67 PR 159 1187	G.E. Kalmus, A. Kernan	(LRL)
ZINCHENKO 67 Thesis Rutgers	A.I. Zinchenko	(RUTG)
CALLAHAN 66 NC 44A 90	A.C. Callahan	(WISC)
CALLAHAN 66B PR 150 1153	A.C. Callahan <i>et al.</i>	(WISC, LRL, UCR+)
CESTER 66 PL 21 343	R. Cester <i>et al.</i>	(PPA)
See footnote 1 in AUERBACH 67.		
Also 67 PR 155 1505	L.B. Auerbach <i>et al.</i>	(PENN, PRIN)
BIRGE 65 PR 139B 1600	R.W. Birge <i>et al.</i>	(LRL, WISC)
BISI 65 NC 35 766	V. Bisi <i>et al.</i>	(TORI)
BISI 65B PR 139B 1068	V. Bisi <i>et al.</i>	(TORI)
BORREANI 65 PR 140B 1686	G. Borreani <i>et al.</i>	(BARI, TORI)
CALLAHAN 65 PRL 15 129	A. Callahan, D. Cline	(WISC)
CAMERINI 65 NC 37 1795	U. Camerini <i>et al.</i>	(WISC, LRL)
CLINE 65 PL 15 293	D. Cline, W.F. Fry	(WISC)
CUTTS 65 PR 138B 969	D. Cutts, T. Elloff, R. Stiening	(LRL)
DEMARCO 65 PR 140B 1430	A. de Marco, C. Grosso, G. Rinaudo	(TORI, CERN)
FITCH 65B PR 140B 1088	V.L. Fitch, C.A. Quarles, H.C. Wilkins	(PRIN+)
GREINER 65 ARNS 15 67	D. Greiner	(LRL)
STAMER 65 PR 138B 440	P. Stamer <i>et al.</i>	(STEV)
TRILLING 65B UCRL 16473	G.N. Trilling	(LRL)
Updated from 1965 Argonne Conference, page 5.		
YOUNG 65 Thesis UCRL 16362	P.S. Young	(LRL)
Also 67 PR 156 1464	P.S. Young, W.Z. Osborne, W.H. Barkas	(LRL)
BORREANI 64 PL 12 123	G. Borreani, G. Rinaudo, A.E. Werbrouck	(TORI)
CALLAHAN 64 PR 136B 1463	A. Callahan, R. March, R. Stark	(WISC)
CAMERINI 64 PRL 13 318	U. Camerini <i>et al.</i>	(WISC, LRL)
CLINE 64 PRL 13 101	D. Cline, W.F. Fry	(WISC)
GIACOMELLI 64 NC 34 1134	G. Giacomelli <i>et al.</i>	(BGNA, MUNI)
GREINER 64 PRL 13 284	D.E. Greiner, W.Z. Osborne, W.H. Barkas	(LRL)
JENSEN 64 PR 136B 1431	G.L. Jensen <i>et al.</i>	(MICH)
KALMUS 64 PRL 13 99	G.E. Kalmus <i>et al.</i>	(LRL, WISC)
SHAKLEE 64 PR 136B 1423	F.S. Shaklee <i>et al.</i>	(MICH)
BARKAS 63 PRL 11 26	W.H. Barkas, J.N. Dyer, H.H. Heckman	(LRL)
BOYARSKI 62 PR 128 2398	A.M. Boyarski <i>et al.</i>	(MIT)
BROWN 62B PR 138 450	J.L. Brown <i>et al.</i>	(LRL, MICH)
BARKAS 61 PR 124 1209	W.H. Barkas <i>et al.</i>	(LRL)
BHOWMIK 61 NC 20 857	B. Bhowmik, P.C. Jain, P.C. Mathur	(DELH)
FERRO-LUZZI 61 NC 22 1067	M. Ferro-Luzzi <i>et al.</i>	(LRL)
NORDIN 61 PR 123 2166	P. Nordin	(LRL)
ROE 61 PRL 7 346	B.P. Roe <i>et al.</i>	(MICH, LRL)
FREDEN 60B PR 118 564	S.C. Freden, F.C. Gilbert, R.S. White	(LRL)
BURROWES 59 PRL 2 117	H.C. Burrowes <i>et al.</i>	(MIT)
TAYLOR 59 PR 114 359	S. Taylor <i>et al.</i>	(COLU)
EISENBERG 58 NC 9 663	Y. Eisenberg <i>et al.</i>	(BERN)
ALEXANDER 57 NC 6 478	G. Alexander, R.H.W. Johnston, C. O'Ceallaigh	(NAAS+)
COHEN 57 Fund. Cons. Phys.	E.R. Cohen, K.M. Crowe, J.W.M. du Mond	(LRL)
COOMBES 57 PR 108 1348	C.A. Coombes <i>et al.</i>	(LRL)
BIRGE 56 NC 4 834	R.W. Birge <i>et al.</i>	(LRL)
ILOFF 56 PR 102 927	E.L. Iloff <i>et al.</i>	(LRL)

OTHER RELATED PAPERS

LITTENBERG 93 ARNPS 43 729	L.S. Littenberg, G. Valencia	(BNL, FNAL)
Rare and Radiative Kaon Decays		
RITCHIE 93 RMP 65 1149	J.L. Ritchie, S.G. Wojcicki	
"Rare K Decays"		
BATTISTON 92 PRPL 214 293	R. Battiston <i>et al.</i>	(PGIA, CERN, TRSTT)
Status and Perspectives of K Decay Physics		
BRYMAN 89 LMP A4 79	D.A. Bryman	(TRIUM)
"Rare Kaon Decays"		
CHOUNET 72 PRPL 4C 199	L.M. Chounet, J.M. Gaillard, M.K. Gaillard	(ORSAY+)
FEARING 70 PR D2 542	H.W. Fearing, E. Fischbach, J. Smith	(STON, BOHR)
HAIDT 69B PL 29B 636	D. Haidt <i>et al.</i>	(AACH, BARI, CERN, EPOL+)
CRONIN 68B Vienna Conf. 241	J.W. Cronin	(PRIN)
Rapporteur talk.		
WILLIS 67 Heidelberg Conf. 273	W.J. Willis	(YALE)
Rapporteur talk.		
CABIBBO 66 Berkeley Conf. 33	N. Cabibbo	(CERN)
ADAIR 64 PL 12 67	R.K. Adair, L.B. Leipuner	(YALE, BNL)
CABIBBO 64 PL 9 352	N. Cabibbo, Maksymowicz	(CERN)
Also 64B PL 11 360	N. Cabibbo, Maksymowicz	(CERN)
Also 65 PL 14 72	N. Cabibbo, Maksymowicz	(CERN)
BIRGE 63 PRL 11 35	R.W. Birge <i>et al.</i>	(LRL, WISC, BARI)
BLOCK 62B CERN Conf. 371	M.M. Block, L. Lendinara, L. Monari	(NWES, BGNA)
BRENE 61 NP 22 553	N. Brene, L. Egardt, B. Qvist	(NORD)



$$I(J^P) = \frac{1}{2}(0^-)$$

K^0 MASS

VALUE (MeV)	EVTS	DOCUMENT ID	TECN	COMMENT
497.672 ± 0.031 OUR FIT				
497.672 ± 0.031 OUR AVERAGE				
497.661 ± 0.033	3713	BARKOV	87B CMD	$e^+e^- \rightarrow K^0_S K^0_S$
497.742 ± 0.085	780	BARKOV	85B CMD	$e^+e^- \rightarrow K^0_S K^0_S$
• • • We do not use the following data for averages, fits, limits, etc. • • •				
497.44 ± 0.50		FITCH	67 OSPK	
498.9 ± 0.5	4500	BALTAY	66 HBC	K^0 from $\bar{p}p$
497.44 ± 0.33	2223	KIM	65B HBC	K^0 from $\bar{p}p$
498.1 ± 0.4		CHRISTENS...	64 OSPK	

$m_{K^0} - m_{K^\pm}$

VALUE (MeV)	EVTS	DOCUMENT ID	TECN	CHG	COMMENT
3.995 ± 0.034 OUR FIT					Error includes scale factor of 1.1.
• • • We do not use the following data for averages, fits, limits, etc. • • •					
3.95 ± 0.21	417	HILL	68B DBC	+	$K^+d \rightarrow K^0 p p$
3.90 ± 0.25	9	BURNSTEIN	65 HBC	-	
3.71 ± 0.35	7	KIM	65B HBC	-	$K^-p \rightarrow n \bar{K}^0$
5.4 ± 1.1		CRAWFORD	59 HBC	+	
3.9 ± 0.6		ROSENFELD	59 HBC	-	

$$|m_{K^0} - m_{\bar{K}^0}| / m_{\text{average}}$$

A test of CPT invariance.

VALUE	DOCUMENT ID
<10⁻¹⁸ OUR EVALUATION	

T-VIOLATION PARAMETER IN K^0 - \bar{K}^0 MIXING

The asymmetry $A_T = \frac{\Gamma(\bar{K}^0 \rightarrow K^0) - \Gamma(K^0 \rightarrow \bar{K}^0)}{\Gamma(\bar{K}^0 \rightarrow K^0) + \Gamma(K^0 \rightarrow \bar{K}^0)}$ must vanish if T invariance holds.

ASYMMETRY A_T IN K^0 - \bar{K}^0 MIXING

VALUE (units 10 ⁻³)	EVTS	DOCUMENT ID	TECN
6.6 ± 1.3 ± 1.0	640k	¹ ANGELOPO... 98E CPLR	

¹ ANGELOPOULOS 98E measures the asymmetry $A_T = [\Gamma(\bar{K}^0_{t=0} \rightarrow e^+ \pi^- \nu_{t=\tau}) - \Gamma(K^0_{t=0} \rightarrow e^- \pi^+ \bar{\nu}_{t=\tau})] / [\Gamma(\bar{K}^0_{t=0} \rightarrow e^+ \pi^- \nu_{t=\tau}) + \Gamma(K^0_{t=0} \rightarrow e^- \pi^+ \bar{\nu}_{t=\tau})]$ as a function of the neutral-kaon eigentime τ . The initial strangeness of the neutral kaon is tagged by the charge of the accompanying charged kaon in the reactions $\bar{p}p \rightarrow K^- \pi^+ K^0$ and $p\bar{p} \rightarrow K^+ \pi^- \bar{K}^0$. The strangeness at the time of the decay is tagged by the lepton charge. The reported result is the average value of A_T over the interval $1\tau_S < \tau < 20\tau_S$.

CPT INVARIANCE TESTS IN NEUTRAL KAON DECAY

Written September 1999 by P. Bloch, CERN.

The time evolution of a neutral kaon state is described by

$$\frac{d}{dt} \Psi = -i\Lambda \Psi, \quad \Lambda \equiv M - \frac{i}{2}\Gamma \quad (1)$$

where M and Γ are Hermitian 2×2 matrices known as the mass and decay matrices. The corresponding eigenvalues are $\lambda_{L,S} = m_{L,S} - \frac{i}{2}\gamma_{L,S}$. CPT invariance requires the diagonal elements of Λ to be equal. The CPT-violation complex parameter Δ is defined as

$$\Delta = \frac{\Lambda_{\bar{K}^0 K^0} - \Lambda_{K^0 \bar{K}^0}}{2(\lambda_L - \lambda_S)} = \Delta_{\parallel} \exp(i\phi_{SW}) + \Delta_{\perp} \exp(i(\phi_{SW} + \frac{\pi}{2})) \quad (2)$$

where we have introduced the projections Δ_{\parallel} and Δ_{\perp} respectively parallel and perpendicular to the superweak direction $\phi_{SW} = \tan^{-1}(2\Delta m/\Delta\gamma)$. These projections are linked to the mass and width difference between K^0 and \bar{K}^0 :

$$\Delta_{\parallel} = \frac{1}{4} \frac{\gamma_{K^0} - \gamma_{\bar{K}^0}}{\sqrt{\Delta m^2 + \left(\frac{\Delta\gamma}{2}\right)^2}}, \quad \Delta_{\perp} = \frac{1}{2} \frac{m_{K^0} - m_{\bar{K}^0}}{\sqrt{\Delta m^2 + \left(\frac{\Delta\gamma}{2}\right)^2}} \quad (3)$$

Re(Δ) can be directly measured by studying the time evolution of the strangeness content of initially pure K^0 and \bar{K}^0 states, for example through the asymmetry

$$A_{CPT} = \frac{P[\bar{K}^0 \rightarrow \bar{K}^0(t)] - P[K^0 \rightarrow K^0(t)]}{P[\bar{K}^0 \rightarrow \bar{K}^0(t)] + P[K^0 \rightarrow K^0(t)]} = 4\text{Re}(\Delta) \quad (4)$$

Meson Particle Listings

 K^0

where $P[a \rightarrow b(t)]$ is the probability that the pure initial state a is seen as state b at proper time t . This method has been used by tagging the initial strangeness with strong interactions and the final strangeness with the semileptonic decay (a more appropriate combination of semileptonic rates allows to be independent of any direct CPT violation in the decay itself) and yields today's best value of $\text{Re}(\Delta)$, compatible with zero with an error of $\sim 3 \times 10^{-4}$.

As an alternative it has been proposed to compare the semileptonic charge asymmetries for K_L and K_S

$$\delta_{L,S} = \frac{R(K_{L,S} \rightarrow \pi^- \ell^+ \nu) - R(K_{L,S} \rightarrow \pi^+ \ell^- \bar{\nu})}{R(K_{L,S} \rightarrow \pi^- \ell^+ \nu) + R(K_{L,S} \rightarrow \pi^+ \ell^- \bar{\nu})}, \quad (5)$$

$$\delta_S - \delta_L = 4\text{Re}(\Delta).$$

δ_L has been accurately measured and δ_S should be measured in the near future with tagged K_S at ϕ factories. Note however that Eq. (5) assumes CPT invariance in the $\Delta S = -\Delta Q$ semileptonic decay amplitude.

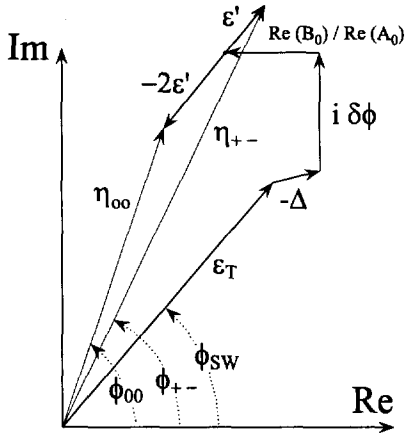


Figure 1: CP - and CPT -violation parameters in 2π decay.

Δ_{\perp} can be obtained from the measurement of the $\pi\pi$ decays CP -violation parameters η_{+-} and η_{00} . Figure 1 shows the various contributions to $\eta_{\pi\pi}$ [1]. The T -violation parameter ϵ_T

$$\epsilon_T = i \frac{|\Lambda_{K^0\bar{K}^0}|^2 - |\Lambda_{\bar{K}^0K^0}|^2}{\Delta\gamma(\lambda_L - \lambda_S)} \quad (6)$$

has been defined in such a way that it is exactly aligned along the superweak direction [4]. A_I (resp. B_I) is the CPT -conserving (resp. violating) decay amplitude for the $\pi\pi$ Isospin I state, ϵ' is the direct CP/CPT -violation parameter [$\epsilon' = 1/3(\eta_{+-} - \eta_{00})$] and $\delta\phi = \frac{1}{2}[\varphi_T - \arg(A_0^*\bar{A}_0)]$ is the phase difference between the $I = 0$ component of the decay amplitude and the matrix element $\Gamma_{K^0\bar{K}^0}$. From Fig. 1 one obtains

$$\Delta_{\perp} = |\eta_{+-}|(\phi_{SW} - \frac{2}{3}\phi_{+-} - \frac{1}{3}\phi_{00}) - \frac{\text{Re}(B_0)}{\text{Re}(A_0)} \sin(\phi_{SW}) + \delta\phi \cos(\phi_{SW}). \quad (7)$$

The present accuracy on the term $|\eta_{+-}|(\phi_{SW} - \frac{2}{3}\phi_{+-} - \frac{1}{3}\phi_{00})$ is 2.6×10^{-5} . $\delta\phi$ gets contributions from CP violation in semileptonic and 3π decays [2,3] and can only be neglected at the present time if one assumes that η_{000} is not significantly larger than η_{+-0} . Furthermore, B_0 is not directly measured, so additional assumptions (for example, CPT conservation in the decay which implies $B_0 = 0$) or a combination with other measurements are necessary to obtain Δ_{\perp} .

If one assumes unitarity, one can measure $\text{Im}(\Delta)$ using the Bell-Steinberger relation which relates K_S and K_L decay amplitudes into all final states f :

$$\text{Re}(\epsilon_T) - i\text{Im}(\Delta) = \frac{1}{2(i\Delta m + \frac{1}{2}(\gamma_L + \gamma_S))} \times \sum A_{fL} A_{fS}^* \quad (8)$$

Since the $\pi\pi$ amplitudes dominate, the result relies also strongly on the $\phi_{\pi\pi}$ phase measurements. The advantage is that B_0 does not enter. Using all available data, one obtains a value of $\text{Im}(\Delta)$ compatible with zero with a precision of 5×10^{-5} . The precision here is also limited by the poor measurement of η_{000} .

The results on $\text{Re}(\Delta)$ and $\text{Im}(\Delta)$ can be combined to obtain Δ_{\parallel} and Δ_{\perp} and therefore the K^0 - \bar{K}^0 mass and width difference shown in Fig. 2. The current accuracy is a few 10^{-18} GeV for both.

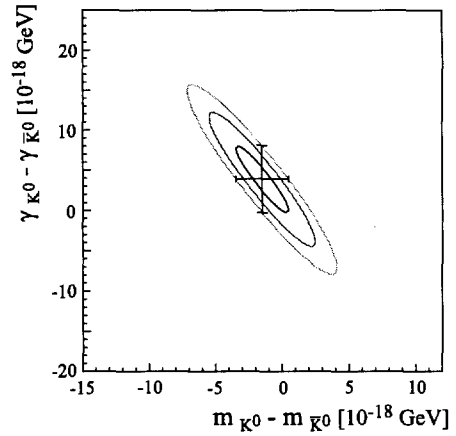


Figure 2: K^0 - \bar{K}^0 mass vs width difference.

If one assumes that CPT is conserved in the decays ($\gamma_{K^0} = \gamma_{\bar{K}^0}$, $\Delta_{\parallel} = 0$, $B_I = 0$), the phase of Δ is known, and the Δ_{\perp} and Bell-Steinberger methods are identical. Assuming in addition $\eta_{+-0} = \eta_{000}$, one in this case obtains a limit for $|m_{K^0} - m_{\bar{K}^0}|$ of 4.4×10^{-19} GeV (90%CL).

Footnotes and References

[4] Many authors have a different definition of the T -violation parameter, $\epsilon = (\Lambda_{\bar{K}^0K^0} - \Lambda_{K^0\bar{K}^0})/(2(\lambda_L - \lambda_S))$. ϵ is not exactly aligned with the superweak direction. The two definitions can be related through $\epsilon = \epsilon_T + i\delta\phi$.

1. See for instance, C.D. Buchanan *et al.*, Phys. Rev. **D45**, 4088 (1992). See also the Second Daphne Handbook, Ed. L.Maiani *et al.*, INFN Frascati (1995).
2. V.V. Barmin *et al.*, Nucl. Phys. **B247**, 293 (1984).
3. L. Lavoura, Mod. Phys. Lett. **A7**, 1367 (1992).

CPT-VIOLATION PARAMETERS IN K^0 - \bar{K}^0 MIXING

If CP-violating interactions include a T conserving part then

$$|K_S\rangle = [|K_1\rangle + (\epsilon + \Delta) |K_2\rangle] / \sqrt{1 + |\epsilon + \Delta|^2}$$

$$|K_L\rangle = [|K_2\rangle + (\epsilon - \Delta) |K_1\rangle] / \sqrt{1 + |\epsilon - \Delta|^2}$$

where

$$|K_1\rangle = [|K^0\rangle + |\bar{K}^0\rangle] / \sqrt{2}$$

$$|K_2\rangle = [|K^0\rangle - |\bar{K}^0\rangle] / \sqrt{2}$$

and

$$|\bar{K}^0\rangle = CP|K^0\rangle.$$

The parameter Δ specifies the CPT-violating part.

Estimates of Δ are given below assuming the validity of the $\Delta S = \Delta Q$ rule. See also THOMSON 95 for a test of CPT-symmetry conservation in K^0 decays using the Bell-Steinberger relation.

REAL PART OF Δ

A nonzero value violates CPT invariance.

VALUE (units 10^{-4})	EVTS	DOCUMENT ID	TECN	COMMENT
2.9 ± 2.7 OUR AVERAGE				
$2.9 \pm 2.6 \pm 0.6$	1.3M	² ANGELOPO... 98F	CPLR	
180 ± 200	6481	³ DEMIDOV 95		K_{L3} reanalysis

² If $\Delta S = \Delta Q$ is not assumed, ANGELOPOULOS 98F finds $\text{Re}\Delta = (3.0 \pm 3.3 \pm 0.6) \times 10^{-4}$.
³ DEMIDOV 95 reanalyzes data from HART 73 and NIEBERGALL 74.

IMAGINARY PART OF Δ

A nonzero value violates CPT invariance.

VALUE (units 10^{-3})	EVTS	DOCUMENT ID	TECN	COMMENT
-0.8 ± 3.1 OUR AVERAGE				
$-0.9 \pm 2.9 \pm 1.0$	1.3M	⁴ ANGELOPO... 98F	CPLR	
21 ± 37	6481	⁵ DEMIDOV 95		K_{L3} reanalysis

⁴ If $\Delta S = \Delta Q$ is not assumed, ANGELOPOULOS 98F finds $\text{Im}\Delta = (-15 \pm 23 \pm 3) \times 10^{-3}$.
⁵ DEMIDOV 95 reanalyzes data from HART 73 and NIEBERGALL 74.

K^0 REFERENCES

ANGELOPO... 98E	PL B444 43	A. Angelopoulos et al.	(CPLEAR Collab.)
ANGELOPO... 98F	PL B444 52	A. Angelopoulos et al.	(CPLEAR Collab.)
DEMIDOV 95	PAN 58 968	V. Demidov, K. Gusev, E. Shabalin	(ITEP)
From YAF 58 1041.			
THOMSON 95	PR D51 1412	G.B. Thomson, Y. Zou	(RUTG)
BARKOV 87B	SJNP 46 530	L.M. Barkov et al.	(NOVO)
	Translated from YAF 46 1008.		
BARKOV 85B	JETPL 42 138	L.M. Barkov et al.	(NOVO)
	Translated from ZETFP 42 113.		
NIEBERGALL 74	PL 49B 103	F. Niebergall et al.	(CERN, ORSAY, VIEN)
HART 73	NP B66 317	J.C. Hart et al.	(CAVE, RHEL)
HILL 68B	PR 158 1534	D.G. Hill et al.	(BNL, CMU)
FITCH 67	PR 154 1711	V.L. Fitch et al.	(PRIN)
BALTAY 66	PR 142 932	C. Baltay et al.	(YALE, BNL)
BURNSTEIN 65	PR 138B 895	R.A. Burnstein, H.A. Rubin	(UMD)
KIM 65B	PR 140B 1334	J.K. Kim, L. Kirsch, D. Miller	(COLU)
CHRISTENS... 64	PRL 13 138	J.H. Christenson et al.	(PRIN)
CRAWFORD 59	PRL 2 112	F.S. Crawford et al.	(LRL)
ROSENFELD 59	PRL 2 110	A.H. Rosenfeld, F.T. Solmitz, R.D. Tripp	(LRL)



$$I(J^P) = \frac{1}{2}(0^-)$$

K_S^0 MEAN LIFE

For earlier measurements, beginning with BOLDT 58B, see our 1986 edition, Physics Letters **170B** 130 (1986).

OUR FIT is described in the note on "Fits for K_L^0 CP-Violation Parameters" in the K_L^0 Particle Listings.

VALUE (10^{-10} s)	EVTS	DOCUMENT ID	TECN	COMMENT
0.8935 ± 0.0008 OUR FIT				
0.8940 ± 0.0009 OUR AVERAGE				
0.8971 ± 0.0021		BERTANZA 97	NA31	
$0.8941 \pm 0.0014 \pm 0.0009$		SCHWINGEN...95	E773	Δm free, $\phi_{+-} = \phi_{SW}$
0.8929 ± 0.0016		GIBBONS 93	E731	
0.8920 ± 0.0044	214k	GROSSMAN 87	SPEC	
0.881 ± 0.009	26k	ARONSON 76	SPEC	
0.8924 ± 0.0032		¹ CARITHERS 75	SPEC	
0.8937 ± 0.0048	6M	GEWENIGER 74B	ASPK	
0.8958 ± 0.0045	50k	² SKJEGGEST... 72	HBC	
• • • We do not use the following data for averages, fits, limits, etc. • • •				
0.905 ± 0.007		³ ARONSON 82B	SPEC	
0.867 ± 0.024	2173	⁴ FACKLER 73	OSPK	
0.856 ± 0.008	19994	⁵ DONALD 68B	HBC	
0.872 ± 0.009	20000	^{5,6} HILL 68	DBC	
0.866 ± 0.016		⁵ ALFF... 66B	OSPK	
0.843 ± 0.013	5000	⁵ KIRSCH 66	HBC	

¹ CARITHERS 75 value is for $m_{K_L^0} - m_{K_S^0} \Delta m = 0.5301 \pm 0.0013$. The Δm dependence of the total decay rate (inverse mean life) is $\Gamma(K_S^0) = [(1.122 \pm 0.004) + 0.16(\Delta m - 0.5348)/\Delta m]10^{10}/s$, or, in terms of meanlife $\tau_S = 0.8913 \pm 0.0032 - 0.238(\Delta m - 0.5348)$ where Δm and τ_S are in units of 10^{10}hs^{-1} and $10^{-10} s$ respectively.

² HILL 68 has been changed by the authors from the published value (0.865 ± 0.009) because of a correction in the shift due to η_{+-} . SKJEGGESTAD 72 and HILL 68 give detailed discussions of systematics encountered in this type of experiment.

³ ARONSON 82 find that K_S^0 mean life may depend on the kaon energy.

⁴ FACKLER 73 does not include systematic errors.

⁵ Pre-1971 experiments are excluded from the average because of disagreement with later more precise experiments.

⁶ HILL 68 has been changed by the authors from the published value (0.865 ± 0.009) because of a correction in the shift due to η_{+-} . SKJEGGESTAD 72 and HILL 68 give detailed discussions of systematics encountered in this type of experiment.

K_S^0 DECAY MODES

Mode	Fraction (Γ_i/Γ)	Scale factor/ Confidence level
$\Gamma_1 \pi^+ \pi^-$	$(68.61 \pm 0.28) \%$	$S=1.2$
$\Gamma_2 \pi^0 \pi^0$	$(31.39 \pm 0.28) \%$	$S=1.2$
$\Gamma_3 \pi^+ \pi^- \gamma$	[a,b] $(1.78 \pm 0.05) \times 10^{-3}$	
$\Gamma_4 \gamma \gamma$	$(2.4 \pm 0.9) \times 10^{-6}$	
$\Gamma_5 \pi^+ \pi^- \pi^0$	$(3.2 \pm 1.2 \pm 1.0) \times 10^{-7}$	
$\Gamma_6 3\pi^0$	$< 1.4 \times 10^{-5}$	CL=90%
$\Gamma_7 \pi^\pm e^\mp \nu_e$	[c] $(7.2 \pm 1.4) \times 10^{-4}$	
$\Gamma_8 \pi^\pm \mu^\mp \nu_\mu$	[c]	
$\Delta S = 1$ weak neutral current (SI) modes		
$\Gamma_9 \mu^+ \mu^-$	SI $< 3.2 \times 10^{-7}$	CL=90%
$\Gamma_{10} e^+ e^-$	SI $< 1.4 \times 10^{-7}$	CL=90%
$\Gamma_{11} \pi^0 e^+ e^-$	SI $< 1.1 \times 10^{-6}$	CL=90%

[a] Most of this radiative mode, the low-momentum γ part, is also included in the parent mode listed without γ 's.

[b] See the Particle Listings below for the energy limits used in this measurement.

[c] The value is for the sum of the charge states or particle/antiparticle states indicated.

CONSTRAINED FIT INFORMATION

An overall fit to 3 branching ratios uses 17 measurements and one constraint to determine 2 parameters. The overall fit has a $\chi^2 = 16.5$ for 16 degrees of freedom.

The following off-diagonal array elements are the correlation coefficients $\langle \delta x_i \delta x_j \rangle / (\delta x_i \delta x_j)$, in percent, from the fit to the branching fractions, $x_i \equiv \Gamma_i / \Gamma_{\text{total}}$. The fit constrains the x_i whose labels appear in this array to sum to one.

$$x_2 \begin{matrix} | & -100 \\ & x_1 \end{matrix}$$

K_S^0 DECAY RATES

VALUE ($10^6 s^{-1}$)	EVTS	DOCUMENT ID	TECN	COMMENT
8.1 ± 1.6	75	⁷ AKHMETSHIN 99	CMD2	Tagged K_S^0 using $\phi \rightarrow K_L^0 K_S^0$
• • • We do not use the following data for averages, fits, limits, etc. • • •				
7.50 ± 0.08		⁸ PDG 98		
seen		BURGUN 72	HBC	$K^+ p \rightarrow K^0 p \pi^+$
9.3 ± 2.5		AUBERT 65	HLBC	$\Delta S = \Delta Q$, CP cons. not assumed
⁷ AKHMETSHIN 99 is from a measured branching ratio $B(K_S^0 \rightarrow \pi e \nu_e) = (7.2 \pm 1.4) \times 10^{-4}$ and $\tau_{K_S^0} = (0.8934 \pm 0.0008) \times 10^{-10} s$.				
⁸ PDG 98 from K_L^0 measurements, assuming that $\Delta S = \Delta Q$ in K^0 decay so that $\Gamma(K_S^0 \rightarrow \pi^\pm e^\mp \nu_e) = \Gamma(K_L^0 \rightarrow \pi^\pm e^\mp \nu_e)$.				
$\Gamma(\pi^\pm \mu^\mp \nu_\mu)$				
VALUE ($10^6 s^{-1}$)		DOCUMENT ID		
• • • We do not use the following data for averages, fits, limits, etc. • • •				
5.25 ± 0.07		⁹ PDG 98		
⁹ PDG 98 from K_L^0 measurements, assuming that $\Delta S = \Delta Q$ in K^0 decay so that $\Gamma(K_S^0 \rightarrow \pi^\pm \mu^\mp \nu_\mu) = \Gamma(K_L^0 \rightarrow \pi^\pm \mu^\mp \nu_\mu)$.				

Meson Particle Listings

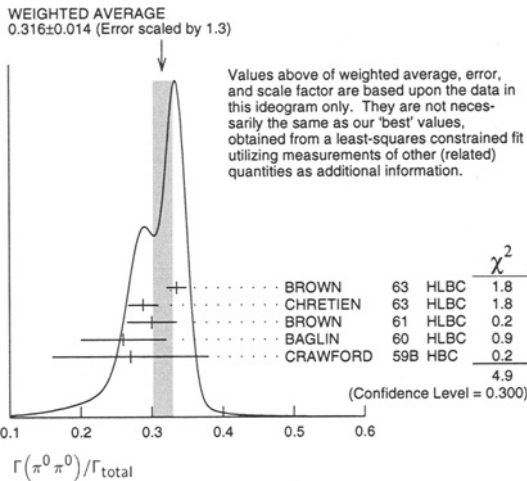
K_S^0

K_S^0 BRANCHING RATIOS

$\Gamma(\pi^+\pi^-)/\Gamma_{total}$					Γ_1/Γ
VALUE	EVTs	DOCUMENT ID	TECN	COMMENT	
0.6861 ± 0.0028 OUR FIT				Error includes scale factor of 1.2.	
0.671 ± 0.010 OUR AVERAGE					
0.670 ± 0.010	3447	¹⁰ DOYLE	69 HBC	$\pi^- \rho \rightarrow \Lambda K^0$	
0.70 ± 0.08		COLUMBIA	60B HBC		
0.68 ± 0.04		CRAWFORD	59B HBC		
• • • We do not use the following data for averages, fits, limits, etc. • • •					
0.740 ± 0.024		¹⁰ ANDERSON	62B HBC		
¹⁰ Anderson result not published, events added to Doyle sample.					

$\Gamma(\pi^+\pi^-)/\Gamma(\pi^0\pi^0)$					Γ_1/Γ_2
VALUE	EVTs	DOCUMENT ID	TECN	COMMENT	
2.186 ± 0.028 OUR FIT				Error includes scale factor of 1.2.	
2.197 ± 0.026 OUR AVERAGE					
2.11 ± 0.09	1315	EVERHART	76 WIRE	$\pi^- \rho \rightarrow \Lambda K^0$	
2.169 ± 0.094	16k	COWELL	74 OSPK	$\pi^- \rho \rightarrow \Lambda K^0$	
2.16 ± 0.08	4799	HILL	73 DBC	$K^+ d \rightarrow K^0 p p$	
2.22 ± 0.10	3068	¹¹ ALITTI	72 HBC	$K^+ \rho \rightarrow \pi^+ \rho K^0$	
2.22 ± 0.08	6380	MORSE	72B DBC	$K^+ n \rightarrow K^0 p$	
2.10 ± 0.11	701	¹² NAGY	72 HLBC	$K^+ n \rightarrow K^0 p$	
2.22 ± 0.095	6150	¹³ BALTAY	71 HBC	$K \rho \rightarrow K^0 \text{ neutrals}$	
2.282 ± 0.043	7944	¹⁴ MOFFETT	70 OSPK	$K^+ n \rightarrow K^0 p$	
2.10 ± 0.06	3700	MORFIN	69 HLBC	$K^+ n \rightarrow K^0 p$	
• • • We do not use the following data for averages, fits, limits, etc. • • •					
2.12 ± 0.17	267	¹² BOZOKI	69 HLBC		
2.285 ± 0.055	3016	¹⁴ GOBBI	69 OSPK	$K^+ n \rightarrow K^0 p$	
¹¹ The directly measured quantity is $K_S^0 \rightarrow \pi^+\pi^-$ / all $K^0 = 0.345 \pm 0.005$.					
¹² NAGY 72 is a final result which includes BOZOKI 69.					
¹³ The directly measured quantity is $K_S^0 \rightarrow \pi^+\pi^-$ / all $K^0 = 0.345 \pm 0.005$.					
¹⁴ MOFFETT 70 is a final result which includes GOBBI 69.					

$\Gamma(\pi^0\pi^0)/\Gamma_{total}$					Γ_2/Γ
VALUE	EVTs	DOCUMENT ID	TECN	COMMENT	
0.3139 ± 0.0028 OUR FIT				Error includes scale factor of 1.2.	
0.316 ± 0.014 OUR AVERAGE				Error includes scale factor of 1.3. See the ideogram below.	
0.335 ± 0.014	1066	BROWN	63 HLBC		
0.288 ± 0.021	198	CHRETIEN	63 HLBC		
0.30 ± 0.035		BROWN	61 HLBC		
0.26 ± 0.06		BAGLIN	60 HLBC		
0.27 ± 0.11		CRAWFORD	59B HBC		



$\Gamma(\pi^+\pi^-\gamma)/\Gamma(\pi^+\pi^-)$					Γ_3/Γ_1
VALUE (units 10 ⁻³)	EVTs	DOCUMENT ID	TECN	COMMENT	
2.60 ± 0.08 OUR AVERAGE					
2.56 ± 0.09	1286	RAMBERG	93 E731	$p_\gamma > 50$ MeV/c	
2.68 ± 0.15		¹⁵ TAUREG	76 SPEC	$p_\gamma > 50$ MeV/c	
2.8 ± 0.6		¹⁶ BURGUN	73 HBC	$p_\gamma > 50$ MeV/c	
3.3 ± 1.2	10	WEBBER	70 HBC	$p_\gamma > 50$ MeV/c	
no ratio given	27	BELLOTTI	66 HBC	$p_\gamma > 50$ MeV/c	
• • • We do not use the following data for averages, fits, limits, etc. • • •					
7.10 ± 0.22	3723	RAMBERG	93 E731	$p_\gamma > 20$ MeV/c	
3.0 ± 0.6	29	¹⁷ BOBISUT	74 HLBC	$p_\gamma > 40$ MeV/c	

¹⁵ TAUREG 76 find direct emission contribution < 0.06, CL = 90%.
¹⁶ BURGUN 73 estimates that direct emission contribution is 0.3 ± 0.6.
¹⁷ BOBISUT 74 not included in average because p_γ cut differs. Estimates direct emission contribution to be 0.5 or less, CL = 95%.

$\Gamma(\gamma\gamma)/\Gamma_{total}$					Γ_4/Γ
VALUE (units 10 ⁻⁶)	CL%	EVTs	DOCUMENT ID	TECN	
2.4 ± 0.9		35	¹⁸ BARR	95B NA31	
• • • We do not use the following data for averages, fits, limits, etc. • • •					
2.2 ± 1.1		16	¹⁹ BARR	95B NA31	
< 13	90		BALATS	89 SPEC	
2.4 ± 1.2		19	BURKHARDT	87 NA31	
< 133	90		BARMIN	86B XEBC	
< 200	90		VASSERMAN	86 CALO	$\phi \rightarrow K_S^0 K_L^0$
< 400	90	0	BARMIN	73B HLBC	
< 710	90	0	²⁰ BANNER	72B OSPK	
< 2000	90	0	MORSE	72B DBC	
< 2200	90	0	²⁰ REPELLIN	71 OSPK	
< 21000	90	0	²⁰ BANNER	69 OSPK	
¹⁸ BARR 95B quotes this as the combined BARR 95B + BURKHARDT 87 result after rescaling BURKHARDT 87 to use same branching ratios and lifetimes as BARR 95B.					
¹⁹ BARR 95B result is calculated using $B(K_L \rightarrow \gamma\gamma) = (5.86 \pm 0.17) \times 10^{-4}$.					
²⁰ These limits are for maximum interference in $K_S^0 - K_L^0$ to 2γ 's.					

$\Gamma(\pi^+\pi^-\pi^0)/\Gamma_{total}$					Γ_5/Γ
VALUE (units 10 ⁻⁷)	CL%	EVTs	DOCUMENT ID	TECN	
3.2 ± 1.2 OUR AVERAGE					
2.5 + 1.3 + 0.5 - 1.9 - 0.6		500k	²¹ ADLER	97B CPLR	
4.8 + 2.2 - 1.6 ± 1.1			²² ZOU	96 E621	
• • • We do not use the following data for averages, fits, limits, etc. • • •					
4.1 + 2.5 + 0.5 - 1.9 - 0.6			²³ ADLER	96E CPLR	Sup. by ADLER 97B
3.9 + 5.4 + 0.9 - 1.8 - 0.7			²⁴ THOMSON	94 E621	Sup. by ZOU 96
< 490	90		²⁵ BARMIN	85 HLBC	
< 850	90		METCALF	72 ASPK	

²¹ ADLER 97B find the CP-conserving parameters $Re(\lambda) = (28 \pm 7 \pm 3) \times 10^{-3}$, $Im(\lambda) = (-10 \pm 8 \pm 2) \times 10^{-3}$. They estimate $B(K_S^0 \rightarrow \pi^+\pi^-\pi^0)$ from $Re(\lambda)$ and the K_L^0 decay parameters. See also ANGELOPOULOS 98C.
²² ZOU 96 is from the the measured quantities $|\rho_{+-}| = 0.039^{+0.009}_{-0.006} \pm 0.005$ and $\phi_\rho = (-9 \pm 18)^\circ$.
²³ ADLER 96E is from the measured quantities $Re(\lambda) = 0.036 \pm 0.010^{+0.002}_{-0.003}$ and $Im(\lambda)$ consistent with zero. Note that the quantity λ is the same as ρ_{+-} used in other footnotes.
²⁴ THOMSON 94 calculates this branching ratio from their measurements $|\rho_{+-}| = 0.035^{+0.019}_{-0.011} \pm 0.004$ and $\phi_\rho = (-59 \pm 48)^\circ$ where $|\rho_{+-}| e^{i\phi_\rho} = A(K_S^0 \rightarrow \pi^+\pi^-\pi^0, I=2)/A(K_L^0 \rightarrow \pi^+\pi^-\pi^0)$.
²⁵ BARMIN 85 assumes that CP-allowed and CP-violating amplitudes are equally suppressed.

$\Gamma(3\pi^0)/\Gamma_{total}$					Γ_6/Γ
VALUE (units 10 ⁻⁵)	CL%	EVTs	DOCUMENT ID	TECN	
< 1.4	90	7M	ACHASOV	99D SND	
• • • We do not use the following data for averages, fits, limits, etc. • • •					
< 1.9	90	17300	²⁶ ANGELOPO...	98B CPLR	
< 3.7	90		BARMIN	83 HLBC	
< 43	90		BARMIN	73 HLBC	
²⁶ ANGELOPOULOS 98B is from $Im(\eta_{000}) = -0.05 \pm 0.12 \pm 0.05$, assuming $Re(\eta_{000}) = Re(\epsilon) = 1.635 \times 10^{-3}$ and using the value $B(K_L^0 \rightarrow \pi^0\pi^0\pi^0) = 0.2112 \pm 0.0027$.					

$\Gamma(\pi^\pm e^\mp \nu_e)/\Gamma_{total}$					Γ_7/Γ
VALUE (units 10 ⁻⁴)	EVTs	DOCUMENT ID	TECN	COMMENT	
7.2 ± 1.4	75	AKHMETSHIN	99 CMD2	Tagged K_S^0 using $\phi \rightarrow K_L^0 K_S^0$	

$\Gamma(\mu^+\mu^-)/\Gamma_{total}$					Γ_9/Γ
VALUE (units 10 ⁻⁵)	CL%	DOCUMENT ID	TECN	COMMENT	
< 0.032	90	GJESDAL	73 ASPK		
• • • We do not use the following data for averages, fits, limits, etc. • • •					
< 14	90	BOHM	69 OSPK		
< 0.7	90	HYAMS	69B OSPK		
< 22	90	STUTZKE	69 OSPK		
< 7	90	BOTT-...	67 OSPK		
²⁷ Value calculated by us, using 2.3 instead of 1 event, 90% CL.					

²⁷ Value calculated by us, using 2.3 instead of 1 event, 90% CL.

$\Gamma(e^+e^-)/\Gamma_{\text{total}}$ Γ_{10}/Γ
 Test for $\Delta S = 1$ weak neutral current. Allowed by first-order weak interaction combined with electromagnetic interaction.

VALUE (units 10^{-7})	CL%	EVTS	DOCUMENT ID	TECN	COMMENT
< 1.4	90		ANGELOPO... 97	CPLR	
• • • We do not use the following data for averages, fits, limits, etc. • • •					
< 28	90	0	BLICK 94	CNTR	Hyperon facility
< 100	90		BARMIN 86	XEBC	
< 1100	90		BITSADZE 86	CALO	
< 3400	90		BOHM 69	OSPK	

$\Gamma(\pi^0 e^+ e^-)/\Gamma_{\text{total}}$ Γ_{11}/Γ
 Test for $\Delta S = 1$ weak neutral current. Allowed by first-order weak interaction combined with electromagnetic interaction.

VALUE (units 10^{-6})	CL%	EVTS	DOCUMENT ID	TECN	COMMENT
< 1.1	90	0	BARR 93B	NA31	
• • • We do not use the following data for averages, fits, limits, etc. • • •					
< 45	90		GIBBONS 88	E731	

CP VIOLATION IN $K_S \rightarrow 3\pi$

Written 1996 by T. Nakada (Paul Scherrer Institute) and L. Wolfenstein (Carnegie-Mellon University).

The possible final states for the decay $K^0 \rightarrow \pi^+\pi^-\pi^0$ have isospin $I = 0, 1, 2$, and 3 . The $I = 0$ and $I = 2$ states have $CP = +1$ and K_S can decay into them without violating CP symmetry, but they are expected to be strongly suppressed by centrifugal barrier effects. The $I = 1$ and $I = 3$ states, which have no centrifugal barrier, have $CP = -1$ so that the K_S decay to these requires CP violation.

In order to see CP violation in $K_S \rightarrow \pi^+\pi^-\pi^0$, it is necessary to observe the interference between K_S and K_L decay, which determines the amplitude ratio

$$\eta_{+-0} = \frac{A(K_S \rightarrow \pi^+\pi^-\pi^0)}{A(K_L \rightarrow \pi^+\pi^-\pi^0)} \quad (1)$$

If η_{+-0} is obtained from an integration over the whole Dalitz plot, there is no contribution from the $I = 0$ and $I = 2$ final states and a nonzero value of η_{+-0} is entirely due to CP violation.

Only $I = 1$ and $I = 3$ states, which are $CP = -1$, are allowed for $K^0 \rightarrow \pi^0\pi^0\pi^0$ decays and the decay of K_S into $3\pi^0$ is an unambiguous sign of CP violation. Similarly to η_{+-0} , η_{000} is defined as

$$\eta_{000} = \frac{A(K_S \rightarrow \pi^0\pi^0\pi^0)}{A(K_L \rightarrow \pi^0\pi^0\pi^0)} \quad (2)$$

If one assumes that CPT invariance holds and that there are no transitions to $I = 3$ (or to nonsymmetric $I = 1$ states), it can be shown that

$$\eta_{+-0} = \eta_{000} = \epsilon + i \frac{\text{Im } a_1}{\text{Re } a_1} \quad (3)$$

With the Wu-Yang phase convention, a_1 is the weak decay amplitude for K^0 into $I = 1$ final states; ϵ is determined from CP violation in $K_L \rightarrow 2\pi$ decays. The real parts of η_{+-0} and η_{000} are equal to $\text{Re}(\epsilon)$. Since currently-known upper limits on $|\eta_{+-0}|$ and $|\eta_{000}|$ are much larger than $|\epsilon|$, they can be interpreted as upper limits on $\text{Im}(\eta_{+-0})$ and $\text{Im}(\eta_{000})$ and so as limits on the CP -violating phase of the decay amplitude a_1 .

CP-VIOLATION PARAMETERS IN K_S^0 DECAY

$\text{Im}(\eta_{+-0})^2 = \Gamma(K_S^0 \rightarrow \pi^+\pi^-\pi^0, CP\text{-violating}) / \Gamma(K_L^0 \rightarrow \pi^+\pi^-\pi^0)$
 CPT assumed valid (i.e. $\text{Re}(\eta_{+-0}) \approx 0$).

VALUE	CL%	EVTS	DOCUMENT ID	TECN	COMMENT
• • • We do not use the following data for averages, fits, limits, etc. • • •					
< 0.23	90	601	28 BARMIN	85	HLBC
< 1.2	90	192	BALDO-...	75	HLBC
< 0.71	90	148	MALLARY 73	OSPK	$\text{Re}(A) = -0.05 \pm 0.17$
< 0.66	90	180	JAMES 72	HBC	
< 1.2	90	99	JONES 72	OSPK	
< 0.12	90	384	METCALF 72	ASPK	
< 1.2	90	99	CHO 71	DBC	
< 1.0	90	98	JAMES 71	HBC	Incl. in JAMES 72
< 1.2	95	50	29 MEISNER 71	HBC	$\text{CL} = 90\%$ not avail.
< 0.8	90	71	WEBBER 70	HBC	
< 0.45	90		BEHR 66	HLBC	
< 3.8	90	18	ANDERSON 65	HBC	Incl. in WEBBER 70

28 BARMIN 85 find $\text{Re}(\eta_{+-0}) = (0.05 \pm 0.17)$ and $\text{Im}(\eta_{+-0}) = (0.15 \pm 0.33)$. Includes events of BALDO-CEOLIN 75.
 29 These authors find $\text{Re}(A) = 2.75 \pm 0.65$, above value at $\text{Re}(A) = 0$.

$\text{Im}(\eta_{+-0}) = \text{Im}(A(K_S^0 \rightarrow \pi^+\pi^-\pi^0, CP\text{-violating}) / A(K_L^0 \rightarrow \pi^+\pi^-\pi^0))$

VALUE	EVTS	DOCUMENT ID	TECN	COMMENT
$-0.002 \pm 0.009 + 0.002 - 0.001$	500k	30 ADLER	97B	CPLR
• • • We do not use the following data for averages, fits, limits, etc. • • •				
$-0.002 \pm 0.018 \pm 0.003$	137k	31 ADLER	96D	CPLR Sup. by ADLER 97B
$-0.015 \pm 0.017 \pm 0.025$	272k	32 ZOU	94	SPEC

30 ADLER 97B also find $\text{Re}(\eta_{+-0}) = -0.002 \pm 0.007 + 0.004 - 0.001$. See also ANGELOPOULOS 98C.

31 The ADLER 96D fit also yields $\text{Re}(\eta_{+-0}) = 0.006 \pm 0.013 \pm 0.001$ with a correlation $+0.66$ between real and imaginary parts. Their results correspond to $|\eta_{+-0}| < 0.037$ with 90% CL.

32 ZOU 94 use theoretical constraint $\text{Re}(\eta_{+-0}) = \text{Re}(\epsilon) = 0.0016$. Without this constraint they find $\text{Im}(\eta_{+-0}) = 0.019 \pm 0.061$ and $\text{Re}(\eta_{+-0}) = 0.019 \pm 0.027$.

$\text{Im}(\eta_{000})^2 = \Gamma(K_S^0 \rightarrow 3\pi^0) / \Gamma(K_L^0 \rightarrow 3\pi^0)$

CPT assumed valid (i.e. $\text{Re}(\eta_{000}) \approx 0$). This limit determines branching ratio $\Gamma(3\pi^0)/\Gamma_{\text{total}}$ above.

VALUE	CL%	EVTS	DOCUMENT ID	TECN	COMMENT
• • • We do not use the following data for averages, fits, limits, etc. • • •					
< 0.1	90	632	33 BARMIN	83	HLBC
< 0.28	90		34 GJESDAL	74B	SPEC Indirect meas.
< 1.2	90	22	BARMIN	73	HLBC

33 BARMIN 83 find $\text{Re}(\eta_{000}) = (-0.08 \pm 0.18)$ and $\text{Im}(\eta_{000}) = (-0.05 \pm 0.27)$. Assuming CPT invariance they obtain the limit quoted above.

34 GJESDAL 74B uses $K_{2\pi}$, $K_{\mu 3}$, and K_{e3} decay results, unitarity, and CPT . Calculates $|\eta_{000}| = 0.26 \pm 0.20$. We convert to upper limit.

$\text{Im}(\eta_{000}) = \text{Im}(A(K_S^0 \rightarrow \pi^0\pi^0\pi^0) / A(K_L^0 \rightarrow \pi^0\pi^0\pi^0))$

$K_S^0 \rightarrow \pi^0\pi^0\pi^0$ violates CP conservation, in contrast to $K_S^0 \rightarrow \pi^+\pi^-\pi^0$ which has a CP -conserving part.

VALUE	EVTS	DOCUMENT ID	TECN
$-0.05 \pm 0.12 \pm 0.05$	17300	35 ANGELOPO... 98B	CPLR

35 ANGELOPOULOS 98B assumes $\text{Re}(\eta_{000}) = \text{Re}(\epsilon) = 1.635 \times 10^{-3}$. Without assuming CPT invariance, they obtain $\text{Re}(\eta_{000}) = 0.18 \pm 0.14 \pm 0.06$ and $\text{Im}(\eta_{000}) = 0.15 \pm 0.20 \pm 0.03$.

K_S^0 REFERENCES

ACHASOV 99D	PL B459 674	M.N. Achasov et al.	
AKHMETSHIN 99	PL B456 90	R.R. Akhmetshin et al.	(CMD-2 Collab.)
ANGELOPO... 98B	PL B425 391	A. Angelopoulos et al.	(CLEAR Collab.)
ANGELOPO... 98C	EPJ C5 389	A. Angelopoulos et al.	(CLEAR Collab.)
PDG 98	EPJ C3 1	C. Caso et al.	
ADLER 97B	PL B407 193	R. Adler et al.	(CLEAR Collab.)
ANGELOPO... 97	PL B413 232	A. Angelopoulos et al.	(CLEAR Collab.)
BERTANZA 97	ZPHY C73 629	L. Bertanza (PISA, CERN, EDIN, MANZ, ORSAY+)	
ADLER 96D	PL B370 167	R. Adler et al.	(CLEAR Collab.)
ADLER 96E	PL B374 313	R. Adler et al.	(CLEAR Collab.)
ZOU 96	PL B369 362	Y. Zou et al.	(RUTG, MINN, MICH)
BARR 95B	PL B351 579	G.D. Barr et al.	(CERN, EDIN, MANZ, LALO+)
SCHWINGEN... 95	PL 74 4376	B. Schwingerheuer et al.	(EFI, CHIC+)
BLICK 94	PL B334 234	A.M. Blick et al.	(SERP, JINR)
THOMSON 94	PL B337 411	G.B. Thomson et al.	(RUTG, MINN, MICH)
ZOU 94	PL B329 519	Y. Zou et al.	(RUTG, MINN, MICH)
BARR 93B	PL B304 381	G.D. Barr et al.	(CERN, EDIN, MANZ, LALO+)
GIBBONS 93	PRL 70 1199	L.K. Gibbons et al.	(FNAL E731 Collab.)
Also 97	PR D55 6225	L.K. Gibbons et al.	(CLEAR Collab.)
RAMBERG 93	PRL 70 2525	E. Ramberg et al.	(FNAL E731 Collab.)
BALATS 89	SJNP 49 828	M.Y. Balats et al.	(FNAL E731 Collab.)
	Translated from YAF 49 1332.		(ITEP)
GIBBONS 88	PRL 61 2661	L.K. Gibbons et al.	(FNAL E731 Collab.)
BURKHARDT 87	PL B199 139	H. Burkhardt et al.	(CERN, EDIN, MANZ+)
GROSSMAN 87	PRL 59 18	N. Grossman et al.	(MINN, MICH, RUTG)
BARMIN 86	SJNP 44 622	V.V. Barmin et al.	(ITEP)
	Translated from YAF 44 365.		
BARMIN 86B	NC 96A 159	V.V. Barmin et al.	(ITEP, PADO)
BITSADZE 86	PL 167B 138	G.S. Bitsadze, Y.A. Budagov	(CMNS, SOFI, SERP+)
PDG 86B	PL 170B 130	M. Aguilar-Benitez et al.	(CERN, CIT+)
VASSERMAN 86	JETPL 43 588	I.B. Vasserma et al.	(NOVO)
	Translated from ZETFP 43 457.		
BARMIN 85	NC 85A 67	V.V. Barmin et al.	(ITEP, PADO)
Also 85B	SJNP 41 759	V.V. Barmin et al.	(ITEP)
	Translated from YAF 41 1187.		

Γ_{28}	$e^+e^-e^+e^-$	SI	(4.1 ± 0.8) × 10 ⁻⁸	S=1.2
Γ_{29}	$\pi^0\mu^+\mu^-$	CP,SI [d]	< 5.1 × 10 ⁻⁹	CL=90%
Γ_{30}	$\pi^0e^+e^-$	CP,SI [d]	< 4.3 × 10 ⁻⁹	CL=90%
Γ_{31}	$\pi^0\nu\bar{\nu}$	CP,SI [e]	< 5.9 × 10 ⁻⁷	CL=90%
Γ_{32}	$e^\pm\mu^\mp$	LF [a]	< 4.7 × 10 ⁻¹²	CL=90%
Γ_{33}	$e^\pm e^\pm\mu^\mp\mu^\mp$	LF [a]	< 6.1 × 10 ⁻⁹	CL=90%
Γ_{34}	$\pi^0\mu^\pm e^\mp$	LF [a]	< 6.2 × 10 ⁻⁹	CL=90%

- [a] The value is for the sum of the charge states or particle/antiparticle states indicated.
- [b] See the Particle Listings below for the energy limits used in this measurement.
- [c] Most of this radiative mode, the low-momentum γ part, is also included in the parent mode listed without γ 's.
- [d] Allowed by higher-order electroweak interactions.
- [e] Violates CP in leading order. Test of direct CP violation since the indirect CP-violating and CP-conserving contributions are expected to be suppressed.

CONSTRAINED FIT INFORMATION

An overall fit to the mean life, 4 decay rate, and 12 branching ratios uses 46 measurements and one constraint to determine 8 parameters. The overall fit has a $\chi^2 = 40.5$ for 39 degrees of freedom.

The following off-diagonal array elements are the correlation coefficients $(\delta\rho_i\delta\rho_j)/(\delta\rho_i\delta\rho_j)$, in percent, from the fit to parameters ρ_i , including the branching fractions, $x_i \equiv \Gamma_i/\Gamma_{total}$. The fit constrains the x_i whose labels appear in this array to sum to one.

x_2	-19						
x_3	-37	-28					
x_6	-49	-28	-36				
x_9	-7	21	-5	-5			
x_{22}	-12	34	-8	-7	63		
x_{23}	-9	26	-6	-6	83	77	
Γ	0	0	0	0	0	0	0
	x_1	x_2	x_3	x_6	x_9	x_{22}	x_{23}

Mode	Rate (10 ⁸ s ⁻¹)	Scale factor
Γ_1 $3\pi^0$	0.0408 ± 0.0006	
Γ_2 $\pi^+\pi^-\pi^0$	0.0243 ± 0.0004	1.5
Γ_3 $\pi^\pm\mu^\mp\nu_\mu$ Called $K_{\mu 3}^0$	[a] 0.0525 ± 0.0007	1.1
Γ_6 $\pi^\pm e^\mp\nu_e$ Called $K_{e 3}^0$	[a] 0.0750 ± 0.0008	1.1
Γ_9 2γ	(1.133 ± 0.030) × 10 ⁻⁴	
Γ_{22} $\pi^+\pi^-$	(3.97 ± 0.07) × 10 ⁻⁴	1.1
Γ_{23} $\pi^0\pi^0$	(1.79 ± 0.04) × 10 ⁻⁴	

K_L^0 DECAY RATES

$\Gamma(3\pi^0)$	$\Gamma(\pi^+\pi^-\pi^0)$																																																																																
<table border="1"> <tr> <th>VALUE (10⁶ s⁻¹)</th> <th>EVTS</th> <th>DOCUMENT ID</th> <th>TECN</th> <th>COMMENT</th> </tr> <tr> <td>4.08 ± 0.06 OUR FIT</td> <td></td> <td></td> <td></td> <td></td> </tr> <tr> <td>5.22^{+1.03}_{-0.84}</td> <td>54</td> <td>BEHR</td> <td>66 HLBC</td> <td>Assumes CP</td> </tr> </table>	VALUE (10 ⁶ s ⁻¹)	EVTS	DOCUMENT ID	TECN	COMMENT	4.08 ± 0.06 OUR FIT					5.22 ^{+1.03} _{-0.84}	54	BEHR	66 HLBC	Assumes CP	<table border="1"> <tr> <th>VALUE (10⁶ s⁻¹)</th> <th>EVTS</th> <th>DOCUMENT ID</th> <th>TECN</th> <th>COMMENT</th> </tr> <tr> <td>2.43 ± 0.04 OUR FIT</td> <td></td> <td></td> <td></td> <td>Error includes scale factor of 1.5.</td> </tr> <tr> <td>2.38 ± 0.09 OUR AVERAGE</td> <td></td> <td></td> <td></td> <td></td> </tr> <tr> <td>2.32^{+0.13}_{-0.15}</td> <td>192</td> <td>BALDO...</td> <td>75 HLBC</td> <td>Assumes CP</td> </tr> <tr> <td>2.35 ± 0.20</td> <td>180</td> <td>⁹JAMES</td> <td>72 HBC</td> <td>Assumes CP</td> </tr> <tr> <td>2.71 ± 0.28</td> <td>99</td> <td>CHO</td> <td>71 DBC</td> <td>Assumes CP</td> </tr> <tr> <td>2.12 ± 0.33</td> <td>50</td> <td>MEISNER</td> <td>71 HBC</td> <td>Assumes CP</td> </tr> <tr> <td>2.20 ± 0.35</td> <td>53</td> <td>WEBBER</td> <td>70 HBC</td> <td>Assumes CP</td> </tr> <tr> <td>2.62^{+0.28}_{-0.27}</td> <td>136</td> <td>BEHR</td> <td>66 HLBC</td> <td>Assumes CP</td> </tr> <tr> <td colspan="5">• • • We do not use the following data for averages, fits, limits, etc. • • •</td> </tr> <tr> <td>2.5 ± 0.3</td> <td>98</td> <td>⁹JAMES</td> <td>71 HBC</td> <td>Assumes CP</td> </tr> <tr> <td>3.26 ± 0.77</td> <td>18</td> <td>ANDERSON</td> <td>65 HBC</td> <td></td> </tr> <tr> <td>1.4 ± 0.4</td> <td>14</td> <td>FRANZINI</td> <td>65 HBC</td> <td></td> </tr> </table>	VALUE (10 ⁶ s ⁻¹)	EVTS	DOCUMENT ID	TECN	COMMENT	2.43 ± 0.04 OUR FIT				Error includes scale factor of 1.5.	2.38 ± 0.09 OUR AVERAGE					2.32 ^{+0.13} _{-0.15}	192	BALDO...	75 HLBC	Assumes CP	2.35 ± 0.20	180	⁹ JAMES	72 HBC	Assumes CP	2.71 ± 0.28	99	CHO	71 DBC	Assumes CP	2.12 ± 0.33	50	MEISNER	71 HBC	Assumes CP	2.20 ± 0.35	53	WEBBER	70 HBC	Assumes CP	2.62 ^{+0.28} _{-0.27}	136	BEHR	66 HLBC	Assumes CP	• • • We do not use the following data for averages, fits, limits, etc. • • •					2.5 ± 0.3	98	⁹ JAMES	71 HBC	Assumes CP	3.26 ± 0.77	18	ANDERSON	65 HBC		1.4 ± 0.4	14	FRANZINI	65 HBC	
VALUE (10 ⁶ s ⁻¹)	EVTS	DOCUMENT ID	TECN	COMMENT																																																																													
4.08 ± 0.06 OUR FIT																																																																																	
5.22 ^{+1.03} _{-0.84}	54	BEHR	66 HLBC	Assumes CP																																																																													
VALUE (10 ⁶ s ⁻¹)	EVTS	DOCUMENT ID	TECN	COMMENT																																																																													
2.43 ± 0.04 OUR FIT				Error includes scale factor of 1.5.																																																																													
2.38 ± 0.09 OUR AVERAGE																																																																																	
2.32 ^{+0.13} _{-0.15}	192	BALDO...	75 HLBC	Assumes CP																																																																													
2.35 ± 0.20	180	⁹ JAMES	72 HBC	Assumes CP																																																																													
2.71 ± 0.28	99	CHO	71 DBC	Assumes CP																																																																													
2.12 ± 0.33	50	MEISNER	71 HBC	Assumes CP																																																																													
2.20 ± 0.35	53	WEBBER	70 HBC	Assumes CP																																																																													
2.62 ^{+0.28} _{-0.27}	136	BEHR	66 HLBC	Assumes CP																																																																													
• • • We do not use the following data for averages, fits, limits, etc. • • •																																																																																	
2.5 ± 0.3	98	⁹ JAMES	71 HBC	Assumes CP																																																																													
3.26 ± 0.77	18	ANDERSON	65 HBC																																																																														
1.4 ± 0.4	14	FRANZINI	65 HBC																																																																														

In the fit this rate is well determined by the mean life and the branching ratio $\Gamma(\pi^+\pi^-\pi^0)/[\Gamma(\pi^+\pi^-\pi^0) + \Gamma(\pi^\pm\mu^\mp\nu_\mu) + \Gamma(\pi^\pm e^\mp\nu_e)]$. For this reason the discrepancy between the $\Gamma(\pi^+\pi^-\pi^0)$ measurements does not affect the scale factor of the overall fit.

⁹JAMES 72 is a final measurement and includes JAMES 71.

$\Gamma(\pi^\pm\mu^\mp\nu_\mu)$	$\Gamma(\pi^\pm e^\mp\nu_e)$																																					
<table border="1"> <tr> <th>VALUE (10⁶ s⁻¹)</th> <th>EVTS</th> <th>DOCUMENT ID</th> <th>TECN</th> </tr> <tr> <td>5.25 ± 0.07 OUR FIT</td> <td></td> <td></td> <td>Error includes scale factor of 1.1.</td> </tr> <tr> <td>4.54^{+1.24}_{-1.08}</td> <td>19</td> <td>LOWYS</td> <td>67 HLBC</td> </tr> </table>	VALUE (10 ⁶ s ⁻¹)	EVTS	DOCUMENT ID	TECN	5.25 ± 0.07 OUR FIT			Error includes scale factor of 1.1.	4.54 ^{+1.24} _{-1.08}	19	LOWYS	67 HLBC	<table border="1"> <tr> <th>VALUE (10⁶ s⁻¹)</th> <th>EVTS</th> <th>DOCUMENT ID</th> <th>TECN</th> <th>COMMENT</th> </tr> <tr> <td>7.50 ± 0.08 OUR FIT</td> <td></td> <td></td> <td></td> <td>Error includes scale factor of 1.1.</td> </tr> <tr> <td>7.7 ± 0.5 OUR AVERAGE</td> <td></td> <td></td> <td></td> <td></td> </tr> <tr> <td>7.81 ± 0.56</td> <td>620</td> <td>CHAN</td> <td>71 HBC</td> <td></td> </tr> <tr> <td>7.52^{+0.85}_{-0.72}</td> <td></td> <td>AUBERT</td> <td>65 HLBC</td> <td>$\Delta S = \Delta Q, CP$ assumed</td> </tr> </table>	VALUE (10 ⁶ s ⁻¹)	EVTS	DOCUMENT ID	TECN	COMMENT	7.50 ± 0.08 OUR FIT				Error includes scale factor of 1.1.	7.7 ± 0.5 OUR AVERAGE					7.81 ± 0.56	620	CHAN	71 HBC		7.52 ^{+0.85} _{-0.72}		AUBERT	65 HLBC	$\Delta S = \Delta Q, CP$ assumed
VALUE (10 ⁶ s ⁻¹)	EVTS	DOCUMENT ID	TECN																																			
5.25 ± 0.07 OUR FIT			Error includes scale factor of 1.1.																																			
4.54 ^{+1.24} _{-1.08}	19	LOWYS	67 HLBC																																			
VALUE (10 ⁶ s ⁻¹)	EVTS	DOCUMENT ID	TECN	COMMENT																																		
7.50 ± 0.08 OUR FIT				Error includes scale factor of 1.1.																																		
7.7 ± 0.5 OUR AVERAGE																																						
7.81 ± 0.56	620	CHAN	71 HBC																																			
7.52 ^{+0.85} _{-0.72}		AUBERT	65 HLBC	$\Delta S = \Delta Q, CP$ assumed																																		

$\Gamma(\pi^+\pi^-\pi^0) + \Gamma(\pi^\pm\mu^\mp\nu_\mu) + \Gamma(\pi^\pm e^\mp\nu_e)$															
<table border="1"> <tr> <th>VALUE (10⁶ s⁻¹)</th> <th>EVTS</th> <th>DOCUMENT ID</th> <th>TECN</th> <th>COMMENT</th> </tr> <tr> <td>15.18 ± 0.14 OUR FIT</td> <td></td> <td></td> <td></td> <td>Error includes scale factor of 1.1.</td> </tr> <tr> <td>15.1 ± 1.9</td> <td>98</td> <td>AUERBACH</td> <td>66B OSPK</td> <td></td> </tr> </table>	VALUE (10 ⁶ s ⁻¹)	EVTS	DOCUMENT ID	TECN	COMMENT	15.18 ± 0.14 OUR FIT				Error includes scale factor of 1.1.	15.1 ± 1.9	98	AUERBACH	66B OSPK	
VALUE (10 ⁶ s ⁻¹)	EVTS	DOCUMENT ID	TECN	COMMENT											
15.18 ± 0.14 OUR FIT				Error includes scale factor of 1.1.											
15.1 ± 1.9	98	AUERBACH	66B OSPK												

$\Gamma(\pi^\pm\mu^\mp\nu_\mu) + \Gamma(\pi^\pm e^\mp\nu_e)$																																																												
<table border="1"> <tr> <th>VALUE (10⁶ s⁻¹)</th> <th>EVTS</th> <th>DOCUMENT ID</th> <th>TECN</th> <th>COMMENT</th> </tr> <tr> <td>12.75 ± 0.12 OUR FIT</td> <td></td> <td></td> <td></td> <td>Error includes scale factor of 1.1.</td> </tr> <tr> <td>11.9 ± 0.6 OUR AVERAGE</td> <td></td> <td></td> <td></td> <td>Error includes scale factor of 1.2.</td> </tr> <tr> <td>12.4 ± 0.7</td> <td>410</td> <td>BURGUN</td> <td>72 HBC</td> <td>$K^+p \rightarrow K^0p\pi^+$</td> </tr> <tr> <td>13.1 ± 1.3</td> <td>252</td> <td>¹⁰WEBBER</td> <td>71 HBC</td> <td>$K^-p \rightarrow n\bar{K}^0$</td> </tr> <tr> <td>11.6 ± 0.9</td> <td>393</td> <td>^{10,11}CHO</td> <td>70 DBC</td> <td>$K^+n \rightarrow K^0p$</td> </tr> <tr> <td>9.85^{+1.15}_{-1.05}</td> <td>109</td> <td>¹⁰FRANZINI</td> <td>65 HBC</td> <td></td> </tr> <tr> <td colspan="5">• • • We do not use the following data for averages, fits, limits, etc. • • •</td> </tr> <tr> <td>8.47 ± 1.69</td> <td>126</td> <td>¹⁰MANN</td> <td>72 HBC</td> <td>$K^-p \rightarrow n\bar{K}^0$</td> </tr> <tr> <td>10.3 ± 0.8</td> <td>335</td> <td>¹¹HILL</td> <td>67 DBC</td> <td>$K^+n \rightarrow K^0p$</td> </tr> <tr> <td colspan="5">¹⁰Assumes $\Delta S = \Delta Q$ rule.</td> </tr> <tr> <td colspan="5">¹¹CHO 70 includes events of HILL 67.</td> </tr> </table>	VALUE (10 ⁶ s ⁻¹)	EVTS	DOCUMENT ID	TECN	COMMENT	12.75 ± 0.12 OUR FIT				Error includes scale factor of 1.1.	11.9 ± 0.6 OUR AVERAGE				Error includes scale factor of 1.2.	12.4 ± 0.7	410	BURGUN	72 HBC	$K^+p \rightarrow K^0p\pi^+$	13.1 ± 1.3	252	¹⁰ WEBBER	71 HBC	$K^-p \rightarrow n\bar{K}^0$	11.6 ± 0.9	393	^{10,11} CHO	70 DBC	$K^+n \rightarrow K^0p$	9.85 ^{+1.15} _{-1.05}	109	¹⁰ FRANZINI	65 HBC		• • • We do not use the following data for averages, fits, limits, etc. • • •					8.47 ± 1.69	126	¹⁰ MANN	72 HBC	$K^-p \rightarrow n\bar{K}^0$	10.3 ± 0.8	335	¹¹ HILL	67 DBC	$K^+n \rightarrow K^0p$	¹⁰ Assumes $\Delta S = \Delta Q$ rule.					¹¹ CHO 70 includes events of HILL 67.				
VALUE (10 ⁶ s ⁻¹)	EVTS	DOCUMENT ID	TECN	COMMENT																																																								
12.75 ± 0.12 OUR FIT				Error includes scale factor of 1.1.																																																								
11.9 ± 0.6 OUR AVERAGE				Error includes scale factor of 1.2.																																																								
12.4 ± 0.7	410	BURGUN	72 HBC	$K^+p \rightarrow K^0p\pi^+$																																																								
13.1 ± 1.3	252	¹⁰ WEBBER	71 HBC	$K^-p \rightarrow n\bar{K}^0$																																																								
11.6 ± 0.9	393	^{10,11} CHO	70 DBC	$K^+n \rightarrow K^0p$																																																								
9.85 ^{+1.15} _{-1.05}	109	¹⁰ FRANZINI	65 HBC																																																									
• • • We do not use the following data for averages, fits, limits, etc. • • •																																																												
8.47 ± 1.69	126	¹⁰ MANN	72 HBC	$K^-p \rightarrow n\bar{K}^0$																																																								
10.3 ± 0.8	335	¹¹ HILL	67 DBC	$K^+n \rightarrow K^0p$																																																								
¹⁰ Assumes $\Delta S = \Delta Q$ rule.																																																												
¹¹ CHO 70 includes events of HILL 67.																																																												

K_L^0 BRANCHING RATIOS

$\Gamma(3\pi^0)/\Gamma_{total}$												
<table border="1"> <tr> <th>VALUE</th> <th>EVTS</th> <th>DOCUMENT ID</th> <th>TECN</th> </tr> <tr> <td>0.2113 ± 0.0027 OUR FIT</td> <td></td> <td></td> <td>Error includes scale factor of 1.1.</td> </tr> <tr> <td>0.2105 ± 0.0028</td> <td>38k</td> <td>¹²KREUTZ</td> <td>95 NA31</td> </tr> </table>	VALUE	EVTS	DOCUMENT ID	TECN	0.2113 ± 0.0027 OUR FIT			Error includes scale factor of 1.1.	0.2105 ± 0.0028	38k	¹² KREUTZ	95 NA31
VALUE	EVTS	DOCUMENT ID	TECN									
0.2113 ± 0.0027 OUR FIT			Error includes scale factor of 1.1.									
0.2105 ± 0.0028	38k	¹² KREUTZ	95 NA31									

¹²KREUTZ 95 measure $3\pi^0, \pi^+\pi^-\pi^0$, and $\pi e\nu_e$ modes. They assume PDG 1992 values for $\pi\mu\nu_\mu, 2\pi$, and 2γ modes.

$\Gamma(3\pi^0)/\Gamma(\pi^+\pi^-\pi^0)$																																													
<table border="1"> <tr> <th>VALUE</th> <th>EVTS</th> <th>DOCUMENT ID</th> <th>TECN</th> <th>COMMENT</th> </tr> <tr> <td>1.68 ± 0.04 OUR FIT</td> <td></td> <td></td> <td></td> <td>Error includes scale factor of 1.3.</td> </tr> <tr> <td>1.63 ± 0.05 OUR AVERAGE</td> <td></td> <td></td> <td></td> <td>Error includes scale factor of 1.4.</td> </tr> <tr> <td>1.611 ± 0.014 ± 0.034</td> <td>38k</td> <td>¹³KREUTZ</td> <td>95 NA31</td> <td></td> </tr> <tr> <td>1.80 ± 0.13</td> <td>1010</td> <td>BUDAGOV</td> <td>68 HLBC</td> <td></td> </tr> <tr> <td>2.0 ± 0.6</td> <td>188</td> <td>ALEKSANYAN</td> <td>64B FBC</td> <td></td> </tr> <tr> <td colspan="5">• • • We do not use the following data for averages, fits, limits, etc. • • •</td> </tr> <tr> <td>1.65 ± 0.07</td> <td>883</td> <td>BARMIN</td> <td>72B HLBC</td> <td>Error statistical only</td> </tr> <tr> <td colspan="5">¹³KREUTZ 95 excluded from fit because it is not independent of their $\Gamma(3\pi^0)/\Gamma_{total}$ measurement, which is in the fit.</td> </tr> </table>	VALUE	EVTS	DOCUMENT ID	TECN	COMMENT	1.68 ± 0.04 OUR FIT				Error includes scale factor of 1.3.	1.63 ± 0.05 OUR AVERAGE				Error includes scale factor of 1.4.	1.611 ± 0.014 ± 0.034	38k	¹³ KREUTZ	95 NA31		1.80 ± 0.13	1010	BUDAGOV	68 HLBC		2.0 ± 0.6	188	ALEKSANYAN	64B FBC		• • • We do not use the following data for averages, fits, limits, etc. • • •					1.65 ± 0.07	883	BARMIN	72B HLBC	Error statistical only	¹³ KREUTZ 95 excluded from fit because it is not independent of their $\Gamma(3\pi^0)/\Gamma_{total}$ measurement, which is in the fit.				
VALUE	EVTS	DOCUMENT ID	TECN	COMMENT																																									
1.68 ± 0.04 OUR FIT				Error includes scale factor of 1.3.																																									
1.63 ± 0.05 OUR AVERAGE				Error includes scale factor of 1.4.																																									
1.611 ± 0.014 ± 0.034	38k	¹³ KREUTZ	95 NA31																																										
1.80 ± 0.13	1010	BUDAGOV	68 HLBC																																										
2.0 ± 0.6	188	ALEKSANYAN	64B FBC																																										
• • • We do not use the following data for averages, fits, limits, etc. • • •																																													
1.65 ± 0.07	883	BARMIN	72B HLBC	Error statistical only																																									
¹³ KREUTZ 95 excluded from fit because it is not independent of their $\Gamma(3\pi^0)/\Gamma_{total}$ measurement, which is in the fit.																																													

$\Gamma(3\pi^0)/\Gamma(\pi^\pm e^\mp\nu_e)$												
<table border="1"> <tr> <th>VALUE</th> <th>EVTS</th> <th>DOCUMENT ID</th> <th>TECN</th> </tr> <tr> <td>0.545 ± 0.009 OUR FIT</td> <td></td> <td></td> <td>Error includes scale factor of 1.1.</td> </tr> <tr> <td>0.545 ± 0.004 ± 0.009</td> <td>38k</td> <td>¹⁴KREUTZ</td> <td>95 NA31</td> </tr> </table>	VALUE	EVTS	DOCUMENT ID	TECN	0.545 ± 0.009 OUR FIT			Error includes scale factor of 1.1.	0.545 ± 0.004 ± 0.009	38k	¹⁴ KREUTZ	95 NA31
VALUE	EVTS	DOCUMENT ID	TECN									
0.545 ± 0.009 OUR FIT			Error includes scale factor of 1.1.									
0.545 ± 0.004 ± 0.009	38k	¹⁴ KREUTZ	95 NA31									

¹⁴KREUTZ 95 measurement excluded from fit because it is not independent of their $\Gamma(3\pi^0)/\Gamma_{total}$ measurement, which is in the fit.

$\Gamma(3\pi^0)/[\Gamma(\pi^+\pi^-\pi^0) + \Gamma(\pi^\pm\mu^\mp\nu_\mu) + \Gamma(\pi^\pm e^\mp\nu_e)]$																																			
<table border="1"> <tr> <th>VALUE</th> <th>EVTS</th> <th>DOCUMENT ID</th> <th>TECN</th> <th>COMMENT</th> </tr> <tr> <td>0.269 ± 0.004 OUR FIT</td> <td></td> <td></td> <td></td> <td>Error includes scale factor of 1.1.</td> </tr> <tr> <td>0.260 ± 0.011 OUR AVERAGE</td> <td></td> <td></td> <td></td> <td></td> </tr> <tr> <td>0.251 ± 0.014</td> <td>549</td> <td>BUDAGOV</td> <td>68 HLBC</td> <td>ORSAY measur.</td> </tr> <tr> <td>0.277 ± 0.021</td> <td>444</td> <td>BUDAGOV</td> <td>68 HLBC</td> <td>Ecole polytec.meas</td> </tr> <tr> <td>0.31 ± 0.07</td> <td>29</td> <td>KULYUKINA</td> <td>68 CC</td> <td></td> </tr> <tr> <td>0.24 ± 0.08</td> <td>24</td> <td>ANIKINA</td> <td>64 CC</td> <td></td> </tr> </table>	VALUE	EVTS	DOCUMENT ID	TECN	COMMENT	0.269 ± 0.004 OUR FIT				Error includes scale factor of 1.1.	0.260 ± 0.011 OUR AVERAGE					0.251 ± 0.014	549	BUDAGOV	68 HLBC	ORSAY measur.	0.277 ± 0.021	444	BUDAGOV	68 HLBC	Ecole polytec.meas	0.31 ± 0.07	29	KULYUKINA	68 CC		0.24 ± 0.08	24	ANIKINA	64 CC	
VALUE	EVTS	DOCUMENT ID	TECN	COMMENT																															
0.269 ± 0.004 OUR FIT				Error includes scale factor of 1.1.																															
0.260 ± 0.011 OUR AVERAGE																																			
0.251 ± 0.014	549	BUDAGOV	68 HLBC	ORSAY measur.																															
0.277 ± 0.021	444	BUDAGOV	68 HLBC	Ecole polytec.meas																															
0.31 ± 0.07	29	KULYUKINA	68 CC																																
0.24 ± 0.08	24	ANIKINA	64 CC																																

$\Gamma(\pi^+\pi^-\pi^0)/\Gamma_{total}$				
<table border="1"> <tr> <th>VALUE</th> <th>DOCUMENT ID</th> </tr> <tr> <td>0.1255 ± 0.0020 OUR FIT</td> <td></td> </tr> </table>	VALUE	DOCUMENT ID	0.1255 ± 0.0020 OUR FIT	
VALUE	DOCUMENT ID			
0.1255 ± 0.0020 OUR FIT				

Error includes scale factor of 1.7.

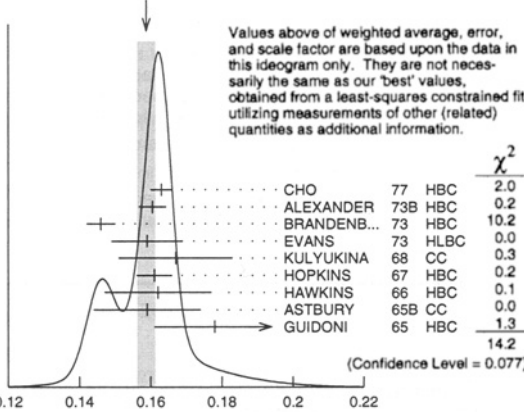
Meson Particle Listings

K_L^0

$\Gamma(\pi^+ \pi^- \pi^0) / [\Gamma(\pi^+ \pi^- \pi^0) + \Gamma(\pi^\pm \mu^\mp \nu_\mu) + \Gamma(\pi^\pm e^\mp \nu_e)] \quad \Gamma_2 / (\Gamma_2 + \Gamma_3 + \Gamma_6)$

Table with columns: VALUE, EVTS, DOCUMENT ID, TECN, COMMENT. Includes 'OUR FIT' and 'OUR AVERAGE' values. Lists various experiments like CHO, ALEXANDER, BRANDENB...

WEIGHTED AVERAGE 0.1588±0.0024 (Error scaled by 1.4)



$\Gamma(\pi^+ \pi^- \pi^0) / \Gamma(\pi^\pm e^\mp \nu_e) \quad \Gamma_2 / \Gamma_6$

Table with columns: VALUE, EVTS, DOCUMENT ID, TECN, COMMENT. Includes 'OUR FIT' and 'OUR AVERAGE' values.

$\Gamma(\pi^\pm \mu^\mp \nu_\mu) / \Gamma(\pi^\pm e^\mp \nu_e) \quad \Gamma_3 / \Gamma_6$

Table with columns: VALUE, EVTS, DOCUMENT ID, TECN, COMMENT. Includes 'OUR FIT' and 'OUR AVERAGE' values. Lists experiments like BASILE, BEILLIERE, EVANS...

Footnote 15: BEILLIERE 69 is a scanning experiment using same exposure as BUDAGOV 68. Footnote 16: KULYUKINA 68 $\Gamma(\pi^\pm \mu^\mp \nu_\mu) / \Gamma(\pi^\pm e^\mp \nu_e)$ is not measured independently from...

$\Gamma(\pi^\pm \mu^\mp \nu_\mu) / [\Gamma(\pi^+ \pi^- \pi^0) + \Gamma(\pi^\pm \mu^\mp \nu_\mu) + \Gamma(\pi^\pm e^\mp \nu_e)] \quad \Gamma_3 / (\Gamma_2 + \Gamma_3 + \Gamma_6)$

Table with columns: VALUE, EVTS, DOCUMENT ID, TECN, COMMENT. Includes 'OUR FIT' and 'OUR AVERAGE' values. Lists experiments like KULYUKINA, ASTBURY, LUERS...

17 This mode not measured independently from $\Gamma(\pi^+ \pi^- \pi^0) / [\Gamma(\pi^+ \pi^- \pi^0) + \Gamma(\pi^\pm \mu^\mp \nu_\mu) + \Gamma(\pi^\pm e^\mp \nu_e)]$ and $\Gamma(\pi^\pm e^\mp \nu_e) / [\Gamma(\pi^+ \pi^- \pi^0) + \Gamma(\pi^\pm \mu^\mp \nu_\mu) + \Gamma(\pi^\pm e^\mp \nu_e)]$.

$\Gamma(\pi^\pm e^\mp \nu_e) / [\Gamma(\pi^+ \pi^- \pi^0) + \Gamma(\pi^\pm \mu^\mp \nu_\mu) + \Gamma(\pi^\pm e^\mp \nu_e)] \quad \Gamma_6 / (\Gamma_2 + \Gamma_3 + \Gamma_6)$

Table with columns: VALUE, EVTS, DOCUMENT ID, TECN, COMMENT. Includes 'OUR FIT' and 'OUR AVERAGE' values. Lists experiments like KULYUKINA, ASTBURY, LUERS...

$\Gamma(\pi^\pm e^\mp \nu_e) / [\Gamma(\pi^\pm \mu^\mp \nu_\mu) + \Gamma(\pi^\pm e^\mp \nu_e)] \quad \Gamma_6 / (\Gamma_3 + \Gamma_6)$

Table with columns: VALUE, EVTS, DOCUMENT ID, TECN, COMMENT. Includes 'OUR FIT' and 'OUR AVERAGE' values. Lists experiments like ASTIER.

$[\Gamma(\pi^\pm \mu^\mp \nu_\mu) + \Gamma(\pi^\pm e^\mp \nu_e)] / \Gamma_{total} \quad (\Gamma_3 + \Gamma_6) / \Gamma$

Table with columns: VALUE, DOCUMENT ID, TECN, COMMENT. Includes 'OUR FIT' and 'OUR AVERAGE' values.

$\Gamma(2\gamma) / \Gamma_{total} \quad \Gamma_9 / \Gamma$

Table with columns: VALUE (units 10^-4), EVTS, DOCUMENT ID, TECN, COMMENT. Includes 'OUR FIT' and 'OUR AVERAGE' values. Lists experiments like BANNER, ENSTROM, REPPELLIN...

18 This value uses $(\eta_{00} / \eta_{+-})^2 = 1.05 \pm 0.14$. In general, $\Gamma(2\gamma) / \Gamma_{total} = [(4.32 \pm 0.55) \times 10^{-4}] [(\eta_{00} / \eta_{+-})^2]$. 19 Assumes regeneration amplitude in copper at 2 GeV is 22 mb. To evaluate for a given regeneration amplitude and error, multiply by (regeneration amplitude/22mb)^2. 20 CRONIN 67 replaced by KUNZ 68. 21 CRIEGEE 66 replaced by TODOROFF 67.

$\Gamma(2\gamma) / \Gamma(3\pi^0) \quad \Gamma_9 / \Gamma_1$

Table with columns: VALUE (units 10^-3), EVTS, DOCUMENT ID, TECN, COMMENT. Includes 'OUR FIT' and 'OUR AVERAGE' values. Lists experiments like BARMIN, BANNER, ARNOLD...

$\Gamma(2\gamma) / \Gamma(\pi^0 \pi^0) \quad \Gamma_9 / \Gamma_{23}$

Table with columns: VALUE, EVTS, DOCUMENT ID, TECN, COMMENT. Includes 'OUR FIT' and 'OUR AVERAGE' values.

$\Gamma(3\gamma) / \Gamma_{total} \quad \Gamma_{10} / \Gamma$

Table with columns: VALUE, CL%, EVTS, DOCUMENT ID, TECN, COMMENT. Includes 'OUR FIT' and 'OUR AVERAGE' values.

$\Gamma(\pi^0 2\gamma) / \Gamma_{total} \quad \Gamma_{11} / \Gamma$

Table with columns: VALUE (units 10^-6), CL%, EVTS, DOCUMENT ID, TECN, COMMENT. Includes 'OUR FIT' and 'OUR AVERAGE' values. Lists experiments like ALAVI-HARATI, BARR, PAPADIMITR...

$\Gamma(\pi^0 \pi^\pm e^\mp \nu) / \Gamma_{total} \quad \Gamma_{12} / \Gamma$

Table with columns: VALUE (units 10^-5), CL%, EVTS, DOCUMENT ID, TECN, COMMENT. Includes 'OUR FIT' and 'OUR AVERAGE' values. Lists experiments like MAKOFF, CARROLL, DONALDSON...

See key on page 239

Meson Particle Listings

K_L^0

$\Gamma((\pi\mu\text{atom})\nu)/\Gamma(\pi^\pm\mu^\mp\nu_\mu)$ Γ_{13}/Γ_3

VALUE (units 10^{-7})	EVTS	DOCUMENT ID	TECN	COMMENT
3.90 ± 0.39	155	26 ARONSON	86 SPEC	
• • • We do not use the following data for averages, fits, limits, etc. • • •				
seen	18	COOMBES	76 WIRE	
26 ARONSON 86 quote theoretical value of $(4.31 \pm 0.08) \times 10^{-7}$.				

$\Gamma(\pi^\pm e^\mp\nu_e\gamma)/\Gamma(\pi^\pm e^\mp\nu_e)$ Γ_{14}/Γ_6

VALUE (units 10^{-2})	EVTS	DOCUMENT ID	TECN	COMMENT
0.934 ± 0.036^{+0.055}_{-0.039}	1384	LEBER	96 NA31	$E_\gamma^* \geq 30$ MeV, $\theta_{e^-\gamma}^* \geq 20^\circ$
• • • We do not use the following data for averages, fits, limits, etc. • • •				
3.3 ± 2.0	10	PEACH	71 HLBC	γ KE > 15 MeV

$\Gamma(\pi^\pm\mu^\mp\nu_\mu\gamma)/\Gamma(\pi^\pm\mu^\mp\nu_\mu)$ Γ_{15}/Γ_3

VALUE (units 10^{-3})	EVTS	DOCUMENT ID	TECN	COMMENT
2.08 ± 0.17^{+0.16}_{-0.21}	4261	BENDER	98 NA48	$E_\gamma^* \geq 30$ MeV

$\Gamma(\pi^+\pi^-\gamma)/\Gamma_{\text{total}}$ Γ_{16}/Γ

For earlier limits see our 1992 edition Physical Review **D45**, 1 June, Part II (1992).

VALUE (units 10^{-5})	EVTS	DOCUMENT ID	TECN	COMMENT
4.61 ± 0.14 OUR AVERAGE				
4.66 ± 0.15	3136	27 RAMBERG	93 E731	$E_\gamma > 20$ MeV
4.41 ± 0.32	1062	28 CARROLL	80B SPEC	$E_\gamma > 20$ MeV
• • • We do not use the following data for averages, fits, limits, etc. • • •				
1.52 ± 0.16	516	29 CARROLL	80B SPEC	$E_\gamma > 20$ MeV
2.89 ± 0.28	546	30 CARROLL	80B SPEC	
6.2 ± 2.1	24	31 DONALDSON	74c SPEC	

27 RAMBERG 93 finds that fraction of Direct Emission (DE) decays with $E_\gamma > 20$ MeV is 0.685 ± 0.041 .
 28 Both components. Uses $K_L^0 \rightarrow \pi^+\pi^-\pi^0$ /(all K_L^0) decays = 0.1239.
 29 Internal Bremsstrahlung component only.
 30 Direct γ emission component only.
 31 Uses $K_L^0 \rightarrow \pi^+\pi^-\pi^0$ /(all K_L^0) decays = 0.126.

$\Gamma(\pi^0\pi^0\gamma)/\Gamma_{\text{total}}$ Γ_{17}/Γ

VALUE (units 10^{-6})	CL%	EVTS	DOCUMENT ID	TECN
< 5.6			BARR	94 NA31
• • • We do not use the following data for averages, fits, limits, etc. • • •				
< 230	90	0	ROBERTS	94 E799

$\Gamma(\mu^+\mu^-\gamma)/\Gamma_{\text{total}}$ Γ_{18}/Γ

VALUE (units 10^{-7})	CL%	EVTS	DOCUMENT ID	TECN
3.25 ± 0.28 OUR AVERAGE				
3.4 ± 0.6 ± 0.4		45	FANTI	97 NA48
3.23 ± 0.23 ± 0.19		197	SPENCER	95 E799
• • • We do not use the following data for averages, fits, limits, etc. • • •				
2.8 ± 2.8		1	32 CARROLL	80B SPEC
< 78.1		90	33 DONALDSON	74 SPEC

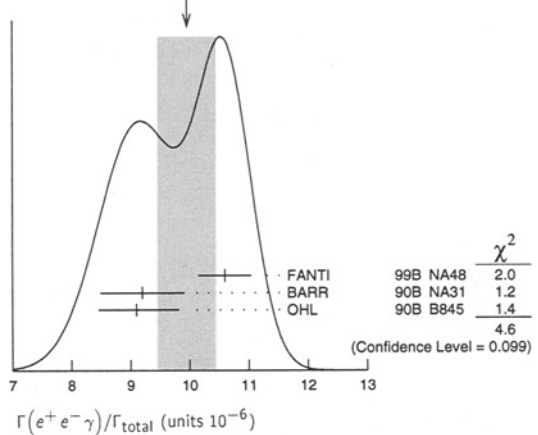
32 Uses $K_L^0 \rightarrow \pi^+\pi^-\pi^0$ /(all K_L^0) decays = 0.1239.
 33 Uses $K_L^0 \rightarrow \pi^+\pi^-\pi^0$ /(all K_L^0) decays = 0.126.

$\Gamma(e^+e^-\gamma)/\Gamma_{\text{total}}$ Γ_{19}/Γ

VALUE (units 10^{-6})	CL%	EVTS	DOCUMENT ID	TECN
10.0 ± 0.5 OUR AVERAGE				
10.6 ± 0.2 ± 0.4		6864	34 FANTI	99B NA48
9.2 ± 0.5 ± 0.5		1053	BARR	90B NA31
9.1 ± 0.4 ^{+0.6} _{-0.5}		919	OHL	90B B845
• • • We do not use the following data for averages, fits, limits, etc. • • •				
17.4 ± 8.7		4	35 CARROLL	80D SPEC
< 27		90	36 BARMIN	72 HLBC

34 For FANTI 99B, the ± 0.4 systematic error includes for uncertainties in the calculation, primarily uncertainties in the $\pi^0 \rightarrow e^+e^-\gamma$ and $K_L^0 \rightarrow \pi^0\pi^0$ branching ratios, evaluated using our 1999 Web edition values.
 35 Uses $K_L^0 \rightarrow \pi^+\pi^-\pi^0$ /(all K_L^0) decays = 0.1239.
 36 Uses $K_L^0 \rightarrow 3\pi^0$ /total = 0.214.

WEIGHTED AVERAGE
 10.0 ± 0.5 (Error scaled by 1.5)



$\Gamma(e^+e^-\gamma\gamma)/\Gamma_{\text{total}}$ Γ_{20}/Γ

VALUE (units 10^{-7})	EVTS	DOCUMENT ID	TECN	COMMENT
6.9 ± 1.0 OUR AVERAGE				
8.0 ± 1.5 ^{+1.4} _{-1.2}	40	SETZU	98 NA31	$E_\gamma > 5$ MeV
6.5 ± 1.2 ± 0.6	58	NAKAYA	94 E799	$E_\gamma > 5$ MeV
6.6 ± 3.2		MORSE	92 B845	$E_\gamma > 5$ MeV

$\Gamma(\pi^0\gamma e^+e^-)/\Gamma_{\text{total}}$ Γ_{21}/Γ

VALUE (units 10^{-7})	CL%	EVTS	DOCUMENT ID	TECN
< 7.1	90	0	MURAKAMI	99 SPEC

$\Gamma(\pi^+\pi^-)/\Gamma_{\text{total}}$ Γ_{22}/Γ

Violates CP conservation.

VALUE (units 10^{-3})	DOCUMENT ID
2.056 ± 0.033 OUR FIT	
2.071 ± 0.049	37 ETAFIT 00

37 This ETAFIT value is computed from fitted values of $|\eta_{+-}|$, the K_L^0 and K_S^0 lifetimes, and the $K_S^0 \rightarrow \pi^+\pi^-$ branching fraction. See the discussion in the note "Fits for K_L^0 CP-Violation Parameters."

$\Gamma(\pi^+\pi^-)/\Gamma(\pi^+\pi^-\pi^0)$ Γ_{22}/Γ_2

Violates CP conservation.

VALUE (units 10^{-2})	EVTS	DOCUMENT ID	TECN	COMMENT
1.637 ± 0.030 OUR FIT				Error includes scale factor of 1.1.
1.64 ± 0.04	4200	MESSNER	73 ASPK	$\eta_{+-} = 2.23$

$\Gamma(\pi^+\pi^-)/[\Gamma(\pi^\pm\mu^\mp\nu_\mu) + \Gamma(\pi^\pm e^\mp\nu_e)]$ $\Gamma_{22}/(\Gamma_3 + \Gamma_6)$

Violates CP conservation.

VALUE (units 10^{-3})	EVTS	DOCUMENT ID	TECN	COMMENT
3.12 ± 0.05 OUR FIT				Error includes scale factor of 1.1.
3.08 ± 0.10 OUR AVERAGE				
3.13 ± 0.14	1687	COUPAL	85 SPEC	$\eta_{+-} = 2.28 \pm 0.06$
3.04 ± 0.14	2703	DEVOE	77 SPEC	$\eta_{+-} = 2.25 \pm 0.05$
• • • We do not use the following data for averages, fits, limits, etc. • • •				
2.51 ± 0.23	309	38 DEBOUARD	67 OSPK	$\eta_{+-} = 2.00 \pm 0.09$
2.35 ± 0.19	525	38 FITCH	67 OSPK	$\eta_{+-} = 1.94 \pm 0.08$

38 Old experiments excluded from fit. See subsection on η_{+-} in section on "PARAMETERS FOR $K_L^0 \rightarrow 2\pi$ DECAY" below for average η_{+-} of these experiments and for note on discrepancy.

$\Gamma(\pi^+\pi^-)/[\Gamma(\pi^+\pi^-\pi^0) + \Gamma(\pi^\pm\mu^\mp\nu_\mu) + \Gamma(\pi^\pm e^\mp\nu_e)]$ $\Gamma_{22}/(\Gamma_2 + \Gamma_3 + \Gamma_6)$

Violates CP conservation.

VALUE (units 10^{-3})	EVTS	DOCUMENT ID	TECN	COMMENT
2.62 ± 0.04 OUR FIT				
• • • We do not use the following data for averages, fits, limits, etc. • • •				
2.60 ± 0.07	4200	39 MESSNER	73 ASPK	$\eta_{+-} = 2.23 \pm 0.05$
1.93 ± 0.26		40 BASILE	66 OSPK	$\eta_{+-} = 1.92 \pm 0.13$
1.993 ± 0.080		40 BOTT...	66 OSPK	$\eta_{+-} = 1.95 \pm 0.04$
2.08 ± 0.35	54	40 GALBRAITH	65 OSPK	$\eta_{+-} = 1.99 \pm 0.16$
2.0 ± 0.4	45	40 CHRISTENS...	64 OSPK	$\eta_{+-} = 1.95 \pm 0.20$

39 From same data as $\Gamma(\pi^+\pi^-)/\Gamma(\pi^+\pi^-\pi^0)$ MESSNER 73, but with different normalization.

40 Old experiments excluded from fit. See subsection on η_{+-} in section on "PARAMETERS FOR $K_L^0 \rightarrow 2\pi$ DECAY" below for average η_{+-} .

Meson Particle Listings

 K_L^0

$\Gamma(\pi^0\pi^0)/\Gamma_{\text{total}}$		Γ_{23}/Γ	
Violates CP conservation.			
VALUE (units 10^{-3})	EVTS	DOCUMENT ID	TECN COMMENT
0.927 ± 0.019 OUR FIT			
• • • We do not use the following data for averages, fits, limits, etc. • • •			
2.5 ± 0.8	189	41 GAILLARD	69 OSPK $\eta_{00}=3.6 \pm 0.6$
1.2 +1.5 -1.2	7	42 CRIEGEE	66 OSPK

⁴¹ Latest result of this experiment given by FAISSNER 70 $\Gamma(\pi^0\pi^0)/\Gamma(3\pi^0)$.
⁴² CRIEGEE 66 experiment not designed to measure $2\pi^0$ decay mode.

$\Gamma(\pi^0\pi^0)/\Gamma(3\pi^0)$		Γ_{23}/Γ_1	
Violates CP conservation.			
VALUE (units 10^{-2})	EVTS	DOCUMENT ID	TECN COMMENT
0.439 ± 0.011 OUR FIT			Error includes scale factor of 1.1.
0.39 ± 0.06 OUR AVERAGE			
0.37 ± 0.08	29	BARMIN	70 HLBC $\eta_{00}=2.02 \pm 0.23$
0.32 ± 0.15	30	BUDAGOV	70 HLBC $\eta_{00}=1.9 \pm 0.5$
0.46 ± 0.11	57	BANNER	69 OSPK $\eta_{00}=2.2 \pm 0.3$
not seen		BARTLETT	68 OSPK See η_{00} below
• • • We do not use the following data for averages, fits, limits, etc. • • •			
1.21 ± 0.30	150	43 REY	76 OSPK $\eta_{00}=3.8 \pm 0.5$
0.90 ± 0.30	172	44 FAISSNER	70 OSPK $\eta_{00}=3.2 \pm 0.5$
1.31 ± 0.31	133	43 CENCE	69 OSPK $\eta_{00}=3.7 \pm 0.5$
1.89 ± 0.31	109	45 CRONIN	67 OSPK $\eta_{00}=4.9 \pm 0.5$
1.36 ± 0.18		45 CRONIN	67B OSPK $\eta_{00}=3.92 \pm 0.3$

⁴³ CENCE 69 events are included in REY 76.
⁴⁴ FAISSNER 70 contains same $2\pi^0$ events as GAILLARD 69 $\Gamma(\pi^0\pi^0)/\Gamma_{\text{total}}$.
⁴⁵ CRONIN 67B is further analysis of CRONIN 67, now both withdrawn.

$\Gamma(\pi^0\pi^0)/\Gamma(\pi^+\pi^-)$		Γ_{23}/Γ_{22}	
Violates CP conservation.			
VALUE	DOCUMENT ID	TECN	COMMENT
0.451 ± 0.006 OUR FIT			
0.4517 ± 0.0060	46 ETAFIT	00	

⁴⁶ This ETAFIT value is computed from fitted values of $|\eta_{00}/\eta_{+-}|$ and the $\Gamma(K_S^0 \rightarrow \pi^+\pi^-)/\Gamma(K_S^0 \rightarrow \pi^0\pi^0)$ branching fraction. See the discussion in the note "Fits for K_L^0 CP-Violation Parameters."

$\Gamma(\mu^+\mu^-)/[\Gamma(\pi^+\pi^-\pi^0) + \Gamma(\pi^\pm\mu^\mp\nu_\mu) + \Gamma(\pi^\pm e^\mp\nu_e)]$		$\Gamma_{24}/(\Gamma_2+\Gamma_3+\Gamma_6)$	
Test for $\Delta S = 1$ weak neutral current. Allowed by higher-order electroweak interaction.			
VALUE (units 10^{-6})	CL%	DOCUMENT ID	TECN
• • • We do not use the following data for averages, fits, limits, etc. • • •			
< 2.0	90	BOTT-...	67 OSPK
< 35.0	90	FITCH	67 OSPK
< 250.0	90	ALFF-...	66B OSPK
< 100.0		ANIKINA	65 CC

$\Gamma(\mu^+\mu^-)/\Gamma(\pi^+\pi^-)$		Γ_{24}/Γ_{22}	
Test for $\Delta S = 1$ weak neutral current. Allowed by higher-order electroweak interaction.			
VALUE (units 10^{-6})	CL%	EVTS	DOCUMENT ID TECN COMMENT
3.48 ± 0.05 OUR AVERAGE			
3.474 ± 0.057		6210	AMBROSE 00 B871
3.87 ± 0.30		179	47 AKAGI 95 SPEC
3.38 ± 0.17		707	HEINSON 95 B791
• • • We do not use the following data for averages, fits, limits, etc. • • •			
3.9 ± 0.3 ± 0.1	178	48 AKAGI	91B SPEC In AKAGI 95
3.45 ± 0.18 ± 0.13	368	49 HEINSON	91 SPEC In HEINSON 95
4.1 ± 0.5	54	INAGAKI	89 SPEC In AKAGI 91B
2.8 ± 0.3 ± 0.2	87	MATHIAZHA...	89B SPEC In HEINSON 91
4.0 +1.4 -0.9	15	SHOCHET	79 SPEC
4.2 +5.1 -2.6	3	50 FUKUSHIMA	76 SPEC
5.8 +2.3 -1.5	9	51 CARITHERS	73 SPEC
< 1.53	90	0 52 CLARK	71 SPEC
< 18.	90	0 DARRIULAT	70 SPEC
< 140.	90	0 FOETH	69 SPEC

⁴⁷ AKAGI 95 gives this number multiplied by the PDG 1992 average for $\Gamma(K_L^0 \rightarrow \pi^+\pi^-)/\Gamma(\text{total})$.

⁴⁸ AKAGI 91B give this number multiplied by the 1990 PDG average for $\Gamma(K_L^0 \rightarrow \pi^+\pi^-)/\Gamma(\text{total})$.

⁴⁹ HEINSON 91 give $\Gamma(K_L^0 \rightarrow \mu\mu)/\Gamma_{\text{total}}$. We divide out the $\Gamma(K_L^0 \rightarrow \pi^+\pi^-)/\Gamma_{\text{total}}$ PDG average which they used.

⁵⁰ FUKUSHIMA 76 errors are at CL = 90%.

⁵¹ CARITHERS 73 errors are at CL = 68%, W.Carithers, (private communication 79).

⁵² CLARK 71 limit raised from 1.2×10^{-6} by FIELD 74 reanalysis. Not in agreement with subsequent experiments. So not averaged.

$\Gamma(e^+e^-)/\Gamma_{\text{total}}$		Γ_{25}/Γ	
Test for $\Delta S = 1$ weak neutral current. Allowed by higher-order electroweak interaction.			
VALUE (units 10^{-10})	CL%	EVTS	DOCUMENT ID TECN COMMENT
0.087 +0.057 -0.041		4	AMBROSE 98 B871
• • • We do not use the following data for averages, fits, limits, etc. • • •			
< 1.6	90	1	AKAGI 95 SPEC
< 0.41	90	0	53 ARISAKA 93B B791
< 1.6	90	1	AKAGI 91 SPEC Sup. by AKAGI 95
< 5.6	90		INAGAKI 89 SPEC In AKAGI 91
< 3.2	90		MATHIAZHA... 89 SPEC In ARISAKA 93B
< 110	90		COUSINS 88 SPEC
< 45	90		GREENLEE 88 SPEC Repl. by JAS-TRZEMBSKI 88
< 12	90		JASTRZEM... 88 SPEC
< 15.7	90	54	CLARK 71 ASPK
< 1500	90	0	FOETH 69 ASPK

⁵³ ARISAKA 93B includes all events with <6 MeV radiated energy.

⁵⁴ Possible (but unknown) systematic errors. See note on CLARK 71 $\Gamma(\mu^+\mu^-)/\Gamma(\pi^+\pi^-)$ entry.

$\Gamma(e^+e^-)/[\Gamma(\pi^+\pi^-\pi^0) + \Gamma(\pi^\pm\mu^\mp\nu_\mu) + \Gamma(\pi^\pm e^\mp\nu_e)]$		$\Gamma_{25}/(\Gamma_2+\Gamma_3+\Gamma_6)$	
Test for $\Delta S = 1$ weak neutral current. Allowed by higher-order electroweak interaction.			
VALUE (units 10^{-6})	CL%	DOCUMENT ID	TECN
• • • We do not use the following data for averages, fits, limits, etc. • • •			
< 23.0	90	BOTT-...	67 OSPK
< 200.0	90	ALFF-...	66B OSPK
< 1000.0		ANIKINA	65 CC

$\Gamma(\pi^+\pi^-e^+e^-)/\Gamma_{\text{total}}$		Γ_{26}/Γ	
Test for $\Delta S = 1$ weak neutral current. Allowed by higher-order electroweak interaction.			
VALUE (units 10^{-7})	CL%	EVTS	DOCUMENT ID TECN COMMENT
3.5 ± 0.6 OUR AVERAGE			
3.2 ± 0.6 ± 0.4		37	ADAMS 98 KTEV
4.4 ± 1.3 ± 0.5		13	TAKEUCHI 98 SPEC
• • • We do not use the following data for averages, fits, limits, etc. • • •			
< 4.6	90		NOMURA 97 SPEC $m_{ee} > 4$ MeV
< 25	90	0	BALATS 83 SPEC
< 88.1	90	55	DONALDSON 76 SPEC
< 300			ANIKINA 73 STRC

⁵⁵ Uses $K_L^0 \rightarrow \pi^+\pi^-\pi^0/(all K_L^0)$ decays = 0.126.

$\Gamma(\mu^+\mu^-e^+e^-)/\Gamma_{\text{total}}$		Γ_{27}/Γ	
Test for $\Delta S = 1$ weak neutral current. Allowed by higher-order electroweak interaction.			
VALUE (units 10^{-9})	CL%	EVTS	DOCUMENT ID TECN
2.9 +6.7 -2.4		1	GU 96 E799
• • • We do not use the following data for averages, fits, limits, etc. • • •			
< 4900	90		BALATS 83 SPEC

$\Gamma(e^+e^-e^+e^-)/\Gamma_{\text{total}}$		Γ_{28}/Γ	
Test for $\Delta S = 1$ weak neutral current. Allowed by higher-order electroweak interaction.			
VALUE (units 10^{-8})	CL%	EVTS	DOCUMENT ID TECN COMMENT
4.1 ± 0.8 OUR AVERAGE			Error includes scale factor of 1.2.
6 ± 2 ± 1		18	56 AKAGI 95 SPEC $m_{ee} > 470$ MeV
10.4 ± 3.7 ± 1.1		8	57 BARR 95 NA31
3.96 ± 0.78 ± 0.32		27	GU 94 E799
3.07 ± 1.25 ± 0.26		6	VAGINS 93 B845
• • • We do not use the following data for averages, fits, limits, etc. • • •			
7 ± 3 ± 2		6	56 AKAGI 95 SPEC $m_{ee} > 470$ MeV
6 ± 2 ± 1		18	AKAGI 93 CNTR Sup. by AKAGI 95
4 ± 3		2	BARR 91 NA31 Sup. by BARR 95
< 260	90		BALATS 83 SPEC

⁵⁶ Values are for the total branching fraction, acceptance-corrected for the m_{ee} cuts shown.
⁵⁷ Distribution of angles between two e^+e^- pair planes favors $CP = -1$ for K_L^0 .

$\Gamma(\pi^0\mu^+\mu^-)/\Gamma_{\text{total}}$		Γ_{29}/Γ	
Violates CP in leading order. Test for $\Delta S = 1$ weak neutral current. Allowed by higher-order electroweak interaction.			
VALUE (units 10^{-9})	CL%	EVTS	DOCUMENT ID TECN
< 5.1	90	0	HARRIS 93 E799
• • • We do not use the following data for averages, fits, limits, etc. • • •			
< 1200	90	0	58 CARROLL 80B SPEC
< 56600	90	59	DONALDSON 74 SPEC

⁵⁸ Uses $K_L^0 \rightarrow \pi^+\pi^-\pi^0/(all K_L^0)$ decays = 0.1239.

⁵⁹ Uses $K_L^0 \rightarrow \pi^+\pi^-\pi^0/(all K_L^0)$ decays = 0.126.

$\Gamma(\pi^0 e^+ e^-)/\Gamma_{total}$ Γ_{30}/Γ
 Violates CP in leading order. Direct and indirect CP-violating contributions are expected to be comparable and to dominate the CP-conserving part. Test for $\Delta S = 1$ weak neutral current. Allowed by higher-order electroweak interaction.

VALUE (units 10^{-9})	CL%	EVTs	DOCUMENT ID	TECN
< 4.3	90	0	HARRIS 93B	E799
< 7.5	90	0	BARKER 90	E731
< 5.5	90	0	OHL 90	B845

• • • We do not use the following data for averages, fits, limits, etc. • • •

< 40	90	0	BARR 88	NA31
< 320	90	0	JASTRZEM... 88	SPEC
< 2300	90	0	CARROLL 80D	SPEC

⁶⁰ Uses $K_L^0 \rightarrow \pi^+ \pi^- \pi^0$ (all K_L^0) decays = 0.1239.

$\Gamma(\pi^0 \nu \bar{\nu})/\Gamma_{total}$ Γ_{31}/Γ
 Violates CP in leading order. Test of direct CP violation since the indirect CP-violating and CP-conserving contributions are expected to be suppressed. Test of $\Delta S = 1$ weak neutral current.

VALUE (units 10^{-5})	CL%	EVTs	DOCUMENT ID	TECN
< 0.059	90	0	ALAVI-HARATI00	KTEV

• • • We do not use the following data for averages, fits, limits, etc. • • •

< 0.16	90	0	ADAMS 99	KTEV
< 5.8	90	0	WEAVER 94	E799
< 22	90	0	GRAHAM 92	CNTR
< 760	90	0	LITTENBERG 89	RVUE

⁶¹ LITTENBERG 89 is from retroactive data analysis of CRONIN 67.

$\Gamma(e^\pm \mu^\mp)/\Gamma_{total}$ Γ_{32}/Γ
 Test of lepton family number conservation.

VALUE (units 10^{-11})	CL%	EVTs	DOCUMENT ID	TECN	COMMENT
< 0.47	90	0	AMBROSE 98B	B871	

• • • We do not use the following data for averages, fits, limits, etc. • • •

< 9.4	90	0	AKAGI 95	SPEC	
< 3.9	90	0	ARISAKA 93	B791	
< 3.3	90	0	ARISAKA 93	B791	
< 9.4	90	0	AKAGI 91	SPEC	Sup. by AKAGI 95
< 43	90	0	INAGAKI 89	SPEC	In AKAGI 91
< 22	90	0	MATHIAZHAGAN...89	SPEC	
< 190	90	0	SCHAFFNER 89	SPEC	
< 1100	90	0	COUSINS 88	SPEC	
< 670	90	0	GREENLEE 88	SPEC	Repl. by SCHAFFNER 89
< 157	90	0	CLARK 71	ASPK	

⁶² This is the combined result of ARISAKA 93 and MATHIAZHAGAN 89.
⁶³ Possible (but unknown) systematic errors. See note on CLARK 71 $\Gamma(\mu^+ \mu^-)/\Gamma(\pi^+ \pi^-)$ entry.

$\Gamma(e^\pm e^\pm \mu^\mp \mu^\mp)/\Gamma_{total}$ Γ_{33}/Γ
 Test of lepton family number conservation.

VALUE (units 10^{-9})	CL%	EVTs	DOCUMENT ID	TECN
< 6.1	90	0	GU 64	E799

⁶⁴ Assuming uniform phase space distribution.

$\Gamma(e^\pm \mu^\mp)/[\Gamma(\pi^+ \pi^- \pi^0) + \Gamma(\pi^\pm \mu^\mp \nu_\mu) + \Gamma(\pi^\pm e^\mp \nu_e)]$ $\Gamma_{32}/(\Gamma_2 + \Gamma_3 + \Gamma_6)$
 Test of lepton family number conservation.

VALUE (units 10^{-4})	CL%	DOCUMENT ID	TECN
< 0.1	90	BOTT... 67	OSPK
< 0.08	90	FITCH 67	OSPK
< 1.0	90	CARPENTER 66	OSPK
< 10.0		ANIKINA 65	CC

• • • We do not use the following data for averages, fits, limits, etc. • • •

$\Gamma(\pi^0 \mu^\pm e^\mp)/\Gamma_{total}$ Γ_{34}/Γ
 Test of lepton family number conservation.

VALUE	CL%	DOCUMENT ID	TECN
< 6.2×10^{-9}	90	ARISAKA 98	E799

ENERGY DEPENDENCE OF K_L^0 DALITZ PLOT

For discussion, see note on Dalitz plot parameters in the K^\pm section of the Particle Listings above. For definitions of a_u, a_t, a_{ll} , and a_y , see the earlier version of the same note in the 1982 edition of this Review published in Physics Letters **111B** 70 (1982).

$|matrix\ element|^2 = 1 + gu + hu^2 + jv + kv^2 + fuv$
 where $u = (s_3 - s_0) / m_\pi^2$ and $v = (s_1 - s_2) / m_\pi^2$

LINEAR COEFFICIENT g FOR $K_L^0 \rightarrow \pi^+ \pi^- \pi^0$

VALUE	EVTs	DOCUMENT ID	TECN	COMMENT
0.678 ± 0.008 OUR AVERAGE				Error includes scale factor of 1.5. See the ideogram below.
0.6823 ± 0.0044 ± 0.0044	500k	ANGELOPO...	98C CPLR	
0.681 ± 0.024	6499	CHO	77 HBC	
0.620 ± 0.023	4709	PEACH	77 HBC	
0.677 ± 0.010	509k	MESSNER	74 ASPK	$a_y = -0.917 \pm 0.013$

• • • We do not use the following data for averages, fits, limits, etc. • • •

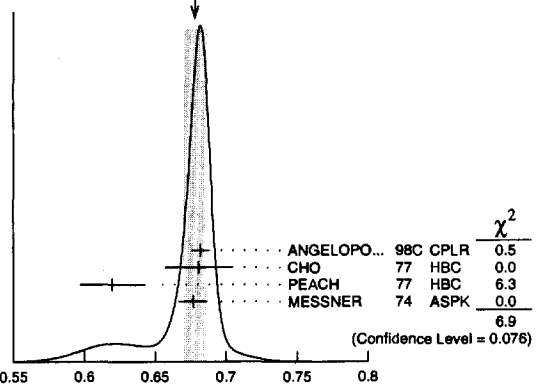
0.69 ± 0.07	192	⁶⁵ BALDO...	75 HIBC	
0.590 ± 0.022	56k	⁶⁵ BUCHANAN	75 SPEC	$a_u = -0.277 \pm 0.010$
0.619 ± 0.027	20k	^{65,66} BISI	74 ASPK	$a_t = -0.282 \pm 0.011$
0.612 ± 0.032		⁶⁵ ALEXANDER	73B HBC	
0.73 ± 0.04	3200	⁶⁵ BRANDENB...	73 HBC	
0.50 ± 0.11	180	⁶⁵ JAMES	72 HBC	
0.608 ± 0.043	1486	⁶⁵ KRENZ	72 HIBC	$a_t = -0.277 \pm 0.018$
0.688 ± 0.074	384	⁶⁵ METCALF	72 ASPK	$a_t = -0.31 \pm 0.03$
0.650 ± 0.012	29k	⁶⁵ ALBROW	70 ASPK	$a_y = -0.858 \pm 0.015$
0.593 ± 0.022	36k	^{65,67} BUCHANAN	70 SPEC	$a_{ll} = -0.278 \pm 0.010$
0.664 ± 0.056	4400	⁶⁵ SMITH	70 OSPK	$a_t = -0.306 \pm 0.024$
0.400 ± 0.045	2446	⁶⁵ BASILE	68B OSPK	$a_t = -0.188 \pm 0.020$
0.649 ± 0.044	1350	⁶⁵ HOPKINS	67 HBC	$a_t = -0.294 \pm 0.018$
0.428 ± 0.055	1198	⁶⁵ NEFKENS	67 OSPK	$a_{ll} = -0.204 \pm 0.025$
0.64 ± 0.17	280	⁶⁵ ANIKINA	66 CC	$a_y = -8.2 \pm 0.9$ -1.3
0.70 ± 0.12	126	⁶⁵ HAWKINS	66 HBC	$a_y = -8.6 \pm 0.7$
0.32 ± 0.13	66	⁶⁵ ASTBURY	65 CC	$a_y = -5.5 \pm 1.5$
0.51 ± 0.09	310	⁶⁵ ASTBURY	65B CC	$a_y = -7.3 \pm 0.6$ -0.8
0.55 ± 0.23	79	⁶⁵ ADAIR	64 HBC	$a_y = -7.6 \pm 1.7$
0.51 ± 0.20	77	⁶⁵ LUERS	64 HBC	$a_y = -7.3 \pm 1.6$

⁶⁵ Quadratic dependence required by some experiments. (See sections on "QUADRATIC COEFFICIENT h " and "QUADRATIC COEFFICIENT k " below.) Correlations prevent us from averaging results of fits not including $g, h,$ and k terms.

⁶⁶ BISI 74 value comes from quadratic fit with quad. term consistent with zero. g error is thus larger than if linear fit were used.

⁶⁷ BUCHANAN 70 result revised by BUCHANAN 75 to include radiative correlations and to use more reliable K_L^0 momentum spectrum of second experiment (had same beam).

WEIGHTED AVERAGE
 0.678±0.008 (Error scaled by 1.5)



Linear coeff. g for $K_L^0 \rightarrow \pi^+ \pi^- \pi^0$ matrix element squared

QUADRATIC COEFFICIENT h FOR $K_L^0 \rightarrow \pi^+ \pi^- \pi^0$

VALUE	EVTs	DOCUMENT ID	TECN
0.076 ± 0.006 OUR AVERAGE			
0.061 ± 0.004 ± 0.015	500k	ANGELOPO...	98C CPLR
0.095 ± 0.032	6499	CHO	77 HBC
0.048 ± 0.036	4709	PEACH	77 HBC
0.079 ± 0.007	509k	MESSNER	74 ASPK

• • • We do not use the following data for averages, fits, limits, etc. • • •

-0.011 ± 0.018	29k	⁶⁸ ALBROW	70 ASPK
0.043 ± 0.052	4400	⁶⁸ SMITH	70 OSPK

See notes in section "LINEAR COEFFICIENT g FOR $K_L^0 \rightarrow \pi^+ \pi^- \pi^0$ |MATRIX ELEMENT|²" above.

⁶⁸ Quadratic coefficients h and k required by some experiments. (See section on "QUADRATIC COEFFICIENT k " below.) Correlations prevent us from averaging results of fits not including $g, h,$ and k terms.

QUADRATIC COEFFICIENT k FOR $K_L^0 \rightarrow \pi^+ \pi^- \pi^0$

VALUE	EVTs	DOCUMENT ID	TECN
0.0099 ± 0.0015 OUR AVERAGE			
0.0104 ± 0.0017 ± 0.0024	500k	ANGELOPO...	98C CPLR
0.024 ± 0.010	6499	CHO	77 HBC
-0.008 ± 0.012	4709	PEACH	77 HBC
0.0097 ± 0.0018	509k	MESSNER	74 ASPK

LINEAR COEFFICIENT j FOR $K_L^0 \rightarrow \pi^+ \pi^- \pi^0$ (CP-VIOLATING TERM)

Listed in CP-violation section below.

QUADRATIC COEFFICIENT f FOR $K_L^0 \rightarrow \pi^+ \pi^- \pi^0$ (CP-VIOLATING TERM)

Listed in CP-violation section below.

Meson Particle Listings

K_L^0

QUADRATIC COEFFICIENT h FOR $K_L^0 \rightarrow \pi^0 \pi^0 \pi^0$

VALUE (units 10^{-3})	EVTs	DOCUMENT ID	TECN
$-3.3 \pm 1.1 \pm 0.7$	5M	69 SOMALWAR 92	E731

⁶⁹SOMALWAR 92 chose m_{π^+} as normalization to make it compatible with the Particle Data Group $K_L^0 \rightarrow \pi^+ \pi^- \pi^0$ definitions.

K_L^0 FORM FACTORS

For discussion, see note on form factors in the K^\pm section of the Particle Listings above.

In the form factor comments, the following symbols are used.

f_+ and f_- are form factors for the vector matrix element.

f_S and f_T refer to the scalar and tensor term.

$$f_0 = f_+ + f_- t / (m_K^2 - m_\pi^2).$$

λ_+ , λ_- , and λ_0 are the linear expansion coefficients of f_+ , f_- , and f_0 .

λ_+ refers to the $K_{\mu 3}^0$ value except in the $K_{e 3}^0$ sections.

$d\xi(0)/d\lambda_+$ is the correlation between $\xi(0)$ and λ_+ in $K_{\mu 3}^0$.

$d\lambda_0/d\lambda_+$ is the correlation between λ_0 and λ_+ in $K_{\mu 3}^0$.

t = momentum transfer to the π in units of m_π^2 .

DP = Dalitz plot analysis.

PI = π spectrum analysis.

MU = μ spectrum analysis.

POL = μ polarization analysis.

BR = $K_{\mu 3}^0/K_{e 3}^0$ branching ratio analysis.

E = positron or electron spectrum analysis.

RC = radiative corrections.

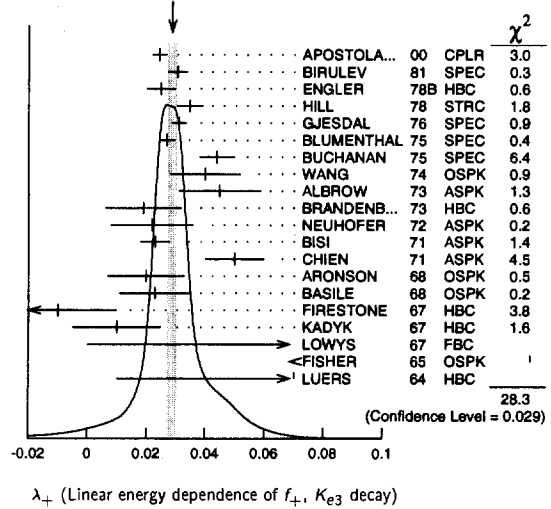
λ_+ (LINEAR ENERGY DEPENDENCE OF f_+ IN $K_{e 3}^0$ DECAY)

For radiative correction of $K_{e 3}^0$ DP, see GINSBERG 67 and BECHERRAWY 70.

VALUE	EVTs	DOCUMENT ID	TECN	COMMENT
0.0288 ± 0.0015 OUR AVERAGE				Error includes scale factor of 1.3. See the ideogram below.
0.0245 ± 0.0012 ± 0.0022	366k	APOSTOLA...	00 CPLR	DP
0.0306 ± 0.0034	74k	BIRULEV	81 SPEC	DP
0.025 ± 0.005	12k	⁷⁰ ENGLER	78B HBC	DP
0.0348 ± 0.0044	18k	HILL	78 STRC	DP
0.0312 ± 0.0025	500k	GJESDAL	76 SPEC	DP
0.0270 ± 0.0028	25k	BLUMENTHAL	75 SPEC	DP
0.044 ± 0.006	24k	BUCHANAN	75 SPEC	DP
0.040 ± 0.012	2171	WANG	74 OSPK	DP
0.045 ± 0.014	5600	ALBROW	73 ASPK	DP
0.019 ± 0.013	1871	BRANDENB...	73 HBC	PI transv.
0.022 ± 0.014	1910	NEUHOFER	72 ASPK	PI
0.023 ± 0.005	42k	BISI	71 ASPK	DP
0.05 ± 0.01	16k	CHIEN	71 ASPK	DP, no RC
0.02 ± 0.013	1000	ARONSON	68 OSPK	PI
+0.023 ± 0.012	4800	BASILE	68 OSPK	DP, no RC
-0.01 ± 0.02	762	FIRESTONE	67 HBC	DP, no RC
+0.01 ± 0.015	531	KADYK	67 HBC	e,PI, no RC
+0.08 ^{+0.10} _{-0.08}	240	LOWYS	67 FBC	PI
+0.15 ± 0.08	577	FISHER	65 OSPK	DP, no RC
+0.07 ± 0.06	153	LUERS	64 HBC	DP, no RC
• • • We do not use the following data for averages, fits, limits, etc. • • •				
0.029 ± 0.005	19k	⁷⁰ CHO	80 HBC	DP
0.0286 ± 0.0049	26k	BIRULEV	79 SPEC	Repl. by BIRULEV 81
0.032 ± 0.0042	48k	BIRULEV	76 SPEC	Repl. by BIRULEV 81

⁷⁰ENGLER 78B uses an unique $K_{e 3}^0$ subset of CHO 80 events and is less subject to systematic effects.

WEIGHTED AVERAGE
0.0288 ± 0.0015 (Error scaled by 1.3)



$\xi_a = f_-/f_+$ (determined from $K_{\mu 3}^0$ spectra)

The parameter ξ is redundant with λ_0 below and is not put into the Meson Summary Table.

VALUE	$d\xi(0)/d\lambda_+$	EVTs	DOCUMENT ID	TECN	COMMENT
-0.11 ± 0.09 OUR EVALUATION					Error includes scale factor of 2.3. Correlation is $d\xi(0)/d\lambda_+ = -14$. From a fit discussed in note on $K_{\mu 3}^0$ form factors in 1982 edition, PL 111B (April 1982).
-0.10 ± 0.09	-12	150k	71 BIRULEV	81 SPEC	DP
+0.26 ± 0.16	-13	14k	72 CHO	80 HBC	DP
+0.13 ± 0.23	-20	16k	72 HILL	79 STRC	DP
-0.25 ± 0.22	-5.9	32k	73 BUCHANAN	75 SPEC	DP
-0.11 ± 0.07	-17	1.6M	74 DONALDSON	74B SPEC	DP
-1.00 ± 0.45	-20	1385	75 PEACH	73 HLBC	DP
-1.5 ± 0.7	-28	9086	76 ALBROW	72 ASPK	DP
+1.2 ± 0.8	-18	1341	77 CARPENTER	66 OSPK	DP
• • • We do not use the following data for averages, fits, limits, etc. • • •					
+0.50 ± 0.61	unknown	16k	78 DALLY	72 ASPK	DP
-3.9 ± 0.4		3140	79 BASILE	70 OSPK	DP, indep of λ_+
-0.68 ^{+0.12} _{-0.20}	-26	16k	78 CHIEN	70 ASPK	DP
⁷¹ BIRULEV 81 error, $d\xi(0)/d\lambda_+$ calculated by us from λ_0 , λ_+ . $d\lambda_0/d\lambda_+ = 0$ used.					
⁷² HILL 79 and CHO 80 calculated by us from λ_0 , λ_+ , and $d\lambda_0/d\lambda_+$.					
⁷³ BUCHANAN 75 is calculated by us from λ_0 , λ_+ , and $d\lambda_0/d\lambda_+$ because their appendix A value -0.20 ± 22 assumes $\xi(t)$ constant, i.e. $\lambda_- = \lambda_+$.					
⁷⁴ DONALDSON 74B gives $\xi = -0.11 \pm 0.02$ not including systematics. Above error and $d\xi(0)/d\lambda_+$ were calculated by us from λ_0 and λ_+ errors (which include systematics) and $d\lambda_0/d\lambda_+$.					
⁷⁵ PEACH 73 gives $\xi(0) = -0.95 \pm 0.45$ for $\lambda_+ = \lambda_- = 0.025$. The above value is for $\lambda_- = 0$. K.Peach, private communication (1974).					
⁷⁶ ALBROW 72 fit has λ_- free, gets $\lambda_- = -0.030 \pm 0.060$ or $\Lambda = +0.15 +0.17-0.11$.					
⁷⁷ CARPENTER 66 $\xi(0)$ is for $\lambda_+ = 0$. $d\xi(0)/d\lambda_+$ is from figure 9.					
⁷⁸ CHIEN 70 errors are statistical only. $d\xi(0)/d\lambda_+$ from figure 4. DALLY 72 is a reanalysis of CHIEN 70. The DALLY 72 result is not compatible with assumption $\lambda_- = 0$ so not included in our fit. The nonzero λ_- value and the relatively large λ_+ value found by DALLY 72 come mainly from a single low t bin (figures 1,2). The (f_+, ξ) correlation was ignored. We estimate from figure 2 that fixing $\lambda_- = 0$ would give $\xi(0) = -1.4 \pm 0.3$ and would add 10 to χ^2 . $d\xi(0)/d\lambda_+$ is not given.					
⁷⁹ BASILE 70 is incompatible with all other results. Authors suggest that efficiency estimates might be responsible.					

$\xi_b = f_-/f_+$ (determined from $K_{\mu 3}^0/K_{e 3}^0$)

The $K_{\mu 3}^0/K_{e 3}^0$ branching ratio fixes a relationship between $\xi(0)$ and λ_+ . We quote the author's $\xi(0)$ and associated λ_+ but do not average because the λ_+ values differ. The fit result and scale factor given below are not obtained from these ξ_b values. Instead they are obtained directly from the authors $K_{\mu 3}^0/K_{e 3}^0$ branching ratio via the fitted $K_{\mu 3}^0/K_{e 3}^0$ ratio ($\Gamma(\pi^\pm \mu^\mp \nu_\mu)/\Gamma(\pi^\pm e^\mp \nu_e)$). The parameter ξ is redundant with λ_0 below and is not put into the Meson Summary Table.

VALUE	EVTs	DOCUMENT ID	TECN	COMMENT
-0.11 ± 0.09 OUR EVALUATION				Error includes scale factor of 2.3. Correlation is $d\xi(0)/d\lambda_+ = -14$. From a fit discussed in note on $K_{e 3}^0$ form factors in 1982 edition, PL 111B (April 1982).

See key on page 239

Meson Particle Listings

K_L^0

• • • We do not use the following data for averages, fits, limits, etc. • • •

0.5 ± 0.4	6700	BRANDENB...	73	HBC	BR, $\lambda_+ = 0.019 \pm 0.013$
-0.08 ± 0.25	1309	80 EVANS	73	HLBC	BR, $\lambda_+ = 0.02$
-0.5 ± 0.5	3548	BASILE	70	OSPK	BR, $\lambda_+ = 0.02$
$+0.45 \pm 0.28$	569	BEILLIERE	69	HLBC	BR, $\lambda_+ = 0$
-0.22 ± 0.30	1309	80 EVANS	69	HLBC	
$+0.2 \begin{smallmatrix} +0.8 \\ -1.2 \end{smallmatrix}$		KULYUKINA	68	CC	BR, $\lambda_+ = 0$
$+1.1 \pm 1.1$	389	ADAIR	64	HBC	BR, $\lambda_+ = 0$
$+0.66 \begin{smallmatrix} +0.9 \\ -1.3 \end{smallmatrix}$		LUERS	64	HBC	BR, $\lambda_+ = 0$

80 EVANS 73 replaces EVANS 69.

$\xi_c = f_-/f_+$ (determined from μ polarization in $K_{\mu 3}^0$)

The μ polarization is a measure of $\xi(t)$. No assumptions on λ_{+-} necessary, t (weighted by sensitivity to $\xi(t)$) should be specified. In λ_{+-} , $\xi(0)$ parametrization this is $\xi(0)$ for $\lambda_{+-} = 0$. $d\xi/d\lambda = \xi t$. For radiative correction to μ polarization in $K_{\mu 3}^0$, see GINSBERG 73. The parameter ξ is redundant with λ_0 below and is not put into the Meson Summary Table.

VALUE	EVTs	DOCUMENT ID	TECN	COMMENT
-0.11 ± 0.09	OUR EVALUATION			Error includes scale factor of 2.3. Correlation is $d\xi(0)/d\lambda_+ = -14$. From a fit discussed in note on $K_{\mu 3}^0$ form factors in 1982 edition, PL 111B (April 1982).
$+0.178 \pm 0.105$	207k	81 CLARK	77	SPEC POL, $d\xi(0)/d\lambda_+ = +0.68$
-0.385 ± 0.105	2.2M	82 SANDWEISS	73	CNTR POL, $d\xi(0)/d\lambda_+ = -6$
$-1.81 \begin{smallmatrix} +0.50 \\ -0.26 \end{smallmatrix}$		83 LONGO	69	CNTR POL, $t = 3.3$

• • • We do not use the following data for averages, fits, limits, etc. • • •

-1.6 ± 0.5	638	84 ABRAMS	68B	OSPK Polarization
-1.2 ± 0.5	2608	84 AUERBACH	66B	OSPK Polarization

81 CLARK 77 $t = +3.80$, $d\xi(0)/d\lambda_+ = \xi(t)t = 0.178 \times 3.80 = +0.68$.
 82 SANDWEISS 73 is for $\lambda_{+-} = 0$ and $t = 0$.
 83 LONGO 69 $t = 3.3$ calculated from $d\xi(0)/d\lambda_+ = -6.0$ (table 1) divided by $\xi = -1.81$.
 84 t value not given.

$Im(\xi)$ in $K_{\mu 3}^0$ DECAY (from transverse μ pol.)

Test of T reversal invariance.

VALUE	EVTs	DOCUMENT ID	TECN	COMMENT
-0.007 ± 0.026	OUR AVERAGE			
0.009 ± 0.030	12M	MORSE	80	CNTR Polarization
0.35 ± 0.30	207k	85 CLARK	77	SPEC POL, $t = 0$
-0.085 ± 0.064	2.2M	86 SANDWEISS	73	CNTR POL, $t = 0$
-0.02 ± 0.08		LONGO	69	CNTR POL, $t = 3.3$
-0.2 ± 0.6		ABRAMS	68B	OSPK Polarization

• • • We do not use the following data for averages, fits, limits, etc. • • •

0.012 ± 0.026		SCHMIDT	79	CNTR Repl. by MORSE 80
-------------------	--	---------	----	------------------------

85 CLARK 77 value has additional $\xi(0)$ dependence $+0.21\text{Re}[\xi(0)]$.
 86 SANDWEISS 73 value corrected from value quoted in their paper due to new value of $\text{Re}(\xi)$. See footnote 4 of SCHMIDT 79.

λ_+ (LINEAR ENERGY DEPENDENCE OF f_+ IN $K_{\mu 3}^0$ DECAY)

See also the corresponding entries and notes in section " $\xi_A = f_-/f_+$ " above and section " λ_0 (LINEAR ENERGY DEPENDENCE OF f_0 IN $K_{\mu 3}^0$ DECAY)" below. For radiative correction of $K_{\mu 3}^0$ Dalitz plot see GINSBERG 70 and BECHERRAWY 70.

VALUE	EVTs	DOCUMENT ID	TECN	COMMENT
0.034 ± 0.005	OUR EVALUATION			From a fit discussed in note on $K_{\mu 3}^0$ form factors in 1982 edition, PL 111B (April 1982).
0.0427 ± 0.0044	150k	BIRULEV	81	SPEC DP
0.028 ± 0.010	14k	CHO	80	HBC DP
0.028 ± 0.011	16k	HILL	79	STRC DP
0.046 ± 0.030	32k	BUCHANAN	75	SPEC DP
0.030 ± 0.003	1.6M	DONALDSON	74B	SPEC DP
0.085 ± 0.015	9086	ALBROW	72	ASPK DP

• • • We do not use the following data for averages, fits, limits, etc. • • •

0.0337 ± 0.0033	129k	DZHORD...	77	SPEC Repl. by BIRULEV 81
0.046 ± 0.008	82k	ALBRECHT	74	WIRE Repl. by BIRULEV 81
0.11 ± 0.04	16k	DALLY	72	ASPK DP
0.07 ± 0.02	16k	CHIEN	70	ASPK Repl. by DALLY 72

λ_0 (LINEAR ENERGY DEPENDENCE OF f_0 IN $K_{\mu 3}^0$ DECAY)

Wherever possible, we have converted the above values of $\xi(0)$ into values of λ_0 using the associated λ_+^H and $d\xi(0)/d\lambda_+$.

VALUE	$d\lambda_0/d\lambda_+$	EVTs	DOCUMENT ID	TECN	COMMENT
0.025 ± 0.006	OUR EVALUATION				Error includes scale factor of 2.3. Correlation is $d\lambda_0/d\lambda_+ = -0.16$. From a fit discussed in note on $K_{\mu 3}^0$ form factors in 1982 edition, PL 111B (April 1982).

0.0341 ± 0.0067	unknown	150k	87 BIRULEV	81	SPEC DP
$+0.050 \pm 0.008$	-0.11	14k	CHO	80	HBC DP
$+0.039 \pm 0.010$	-0.67	16k	HILL	79	STRC DP
$+0.047 \pm 0.009$	1.06	207k	88 CLARK	77	SPEC POL
$+0.025 \pm 0.019$	+0.5	32k	89 BUCHANAN	75	SPEC DP
$+0.019 \pm 0.004$	-0.47	1.6M	90 DONALDSON	74B	SPEC DP
-0.060 ± 0.038	-0.71	1385	91 PEACH	73	HLBC DP
-0.018 ± 0.009	+0.49	2.2M	88 SANDWEISS	73	CNTR POL
-0.043 ± 0.052	-1.39	9086	92 ALBROW	72	ASPK DP
$-0.140 \begin{smallmatrix} +0.043 \\ -0.022 \end{smallmatrix}$	+0.49		88 LONGO	69	CNTR POL
$+0.08 \pm 0.07$	-0.54	1371	88 CARPENTER	66	OSPK DP

• • • We do not use the following data for averages, fits, limits, etc. • • •

0.041 ± 0.008	14k	93 CHO	80	HBC BR, $\lambda_+ = 0.028$
$+0.0485 \pm 0.0076$	47k	DZHORD...	77	SPEC In BIRULEV 81
$+0.024 \pm 0.011$	82k	ALBRECHT	74	WIRE In BIRULEV 81
$+0.06 \pm 0.03$	6700	94 BRANDENB...	73	HBC BR, $\lambda_+ = 0.019 \pm 0.013$

-0.067 ± 0.227	unknown	16k	95 DALLY	72	ASPK DP
-0.333 ± 0.034	+1.	3140	96 BASILE	70	OSPK DP

87 BIRULEV 81 gives $d\lambda_0/d\lambda_+ = -1.5$, giving an unreasonably narrow error ellipse which dominates all other results. We use $d\lambda_0/d\lambda_+ = 0$.
 88 λ_0 value is for $\lambda_{+-} = 0.03$ calculated by us from $\xi(0)$ and $d\xi(0)/d\lambda_+$.
 89 BUCHANAN 75 value is from their appendix A and uses only $K_{\mu 3}$ data. $d\lambda_0/d\lambda_+$ was obtained by private communication, C.Buchanan, 1976.
 90 DONALDSON 74B $d\lambda_0/d\lambda_+$ obtained from figure 18.
 91 PEACH 73 assumes $\lambda_{+-} = 0.025$. Calculated by us from $\xi(0)$ and $d\xi(0)/d\lambda_+$.
 92 ALBROW 72 λ_0 is calculated by us from ξ_A , λ_+ and $d\xi(0)/d\lambda_+$. They give $\lambda_0 = -0.043 \pm 0.039$ for $\lambda_- = 0$. We use our larger calculated error.
 93 CHO 80 BR result not independent of their Dalitz plot result.
 94 Fit for λ_0 does not include this value but instead includes the $K_{\mu 3}/K_{e 3}$ result from this experiment.
 95 DALLY 72 gives $f_0 = 1.20 \pm 0.35$, $\lambda_0 = -0.080 \pm 0.272$, $\lambda_0^f = -0.006 \pm 0.045$, but with a different definition of λ_0 . Our quoted λ_0 is his λ_0/f_0 . We cannot calculate true λ_0 error without his (λ_0, f_0) correlations. See also note on DALLY 72 in section ξ_A .
 96 BASILE 70 λ_0 is for $\lambda_{+-} = 0$. Calculated by us from ξ_A with $d\xi(0)/d\lambda_+ = 0$. BASILE 70 is incompatible with all other results. Authors suggest that efficiency estimates might be responsible.

$|f_0/f_+|$ FOR $K_{e 3}^0$ DECAY

Ratio of scalar to f_+ couplings.

VALUE	CL%	EVTs	DOCUMENT ID	TECN	COMMENT
<0.04	68	25k	BLUMENTHAL75	SPEC	

• • • We do not use the following data for averages, fits, limits, etc. • • •

<0.095	95	18k	HILL	78	STRC
<0.07	68	48k	BIRULEV	76	SPEC See also BIRULEV 81
<0.19	95	5600	ALBROW	73	ASPK
<0.15	68		KULYUKINA	67	CC

$|f_T/f_+|$ FOR $K_{e 3}^0$ DECAY

Ratio of tensor to f_+ couplings.

VALUE	CL%	EVTs	DOCUMENT ID	TECN	COMMENT
<0.23	68	25k	BLUMENTHAL75	SPEC	

• • • We do not use the following data for averages, fits, limits, etc. • • •

<0.40	95	18k	HILL	78	STRC
<0.34	68	48k	BIRULEV	76	SPEC See also BIRULEV 81
<1.0	95	5600	ALBROW	73	ASPK
<1.0	68		KULYUKINA	67	CC

$|f_T/f_+|$ FOR $K_{\mu 3}^0$ DECAY

Ratio of tensor to f_+ couplings.

VALUE	DOCUMENT ID	TECN
0.12 ± 0.12	BIRULEV	81 SPEC

α_{K^*} DECAY FORM FACTOR FOR $K_L \rightarrow e^+ e^- \gamma$

α_{K^*} is the constant in the model of BERGSTROM 83 which measures the relative strength of the vector-vector transition $K_L \rightarrow K^* \gamma$ with $K^* \rightarrow \rho, \omega, \phi \rightarrow \gamma^*$ and the pseudoscalar-pseudoscalar transition $K_L \rightarrow \pi, \eta, \eta' \rightarrow \gamma \gamma^*$.

VALUE	EVTs	DOCUMENT ID	TECN
-0.33 ± 0.05	OUR AVERAGE		
$-0.36 \pm 0.06 \pm 0.02$	6864	FANTI	99B NA48
-0.28 ± 0.13		BARR	90B NA31
$-0.280 \begin{smallmatrix} +0.099 \\ -0.090 \end{smallmatrix}$		OHL	90B B845

DECAY FORM FACTORS FOR $K_L^0 \rightarrow \pi^\pm \pi^0 e^\mp \nu_e$

Given in MAKOFF 93.

FITS FOR K_L^0 CP -VIOLATION PARAMETERS

Revised April 2000 by T.G. Trippe (LBNL).

In recent years, K_L^0 CP -violation experiments have improved our knowledge of CP -violation parameters and their consistency with the expectations of CPT invariance and unitarity. For definitions of K_L^0 CP -violation parameters and a brief discussion of the theory, see the article “ CP Violation” by L. Wolfenstein in Section 12 of this *Review*.

This note describes our two fits for the CP -violation parameters in $K_L^0 \rightarrow \pi^+\pi^-$ and $\pi^0\pi^0$ decay, one for the phases ϕ_{+-} and ϕ_{00} , and another for the amplitudes $|\eta_{+-}|$ and $|\eta_{00}|$.

Fit to ϕ_{+-} , ϕ_{00} , $\Delta\phi$, Δm , and τ_s data: We perform a joint fit to the data on ϕ_{+-} , ϕ_{00} , the phase difference $\Delta\phi = \phi_{00} - \phi_{+-}$, the $K_L^0 - K_S^0$ mass difference Δm , and the K_S^0 mean life τ_s , including the effects of correlations. Measurements of ϕ_{+-} and ϕ_{00} are highly correlated with Δm and τ_s . Some measurements of τ_s are correlated with Δm . The correlations are given in the footnotes of the ϕ_{+-} and ϕ_{00} sections of the K_L^0 Particle Listings and the τ_s section of the K_S^0 Particle Listings. In editions of the Review prior to 1996, we adjusted the experimental values of ϕ_{+-} and ϕ_{00} to account for correlations with Δm and τ_s but did not include the effects of these correlations when evaluating Δm and τ_s . In 1996, we introduced a joint fit including these correlations. In this fit, the ϕ_{+-} measurements have a strong influence on the fitted value of Δm . This is because the CERN NA31 vacuum regeneration experiments (CAROSI 90 [1] and GEWENIGER 74B [2]), the Fermilab E773/E731 regenerator experiments (SCHWINGENHEUER 95 [3] and GIBBONS 93 [4]), and the CPLEAR $K^0 - \bar{K}^0$ asymmetry experiment (APOSTOLAKIS 99C [5]) have very different dependences of ϕ_{+-} on Δm , as can be seen from their diagonal bands in Fig. 1.

The region where the ϕ_{+-} bands from these experiments cross gives a powerful measurement of Δm which decreases the fitted Δm value relative to our pre-1996 average Δm and earlier measurements such as CULLEN 70 [6], GEWENIGER 74C [7], and GJESDAL 74 [8]. This decrease brings the Δm -dependent ϕ_{+-} measurements into good agreement with each other and with $\phi(\text{superweak})$, where

$$\phi(\text{superweak}) = \tan^{-1} \left(\frac{2\Delta m}{\Delta\Gamma} \right) = \tan^{-1} \left(\frac{2\Delta m \tau_s \tau_L}{\hbar(\tau_L - \tau_S)} \right). \quad (1)$$

The (ϕ_{+-}, τ_s) correlations influence the τ_s fit result in a similar manner, as can be seen in Fig. 2. The influence of the ϕ_{+-} experiments is not as great on τ_s as it is on Δm because the indirect measurements of τ_s derived from the diagonal crossing bands in Fig. 2 are not as precise as the direct measurements of τ_s from E773 (SCHWINGENHEUER 95 [3]), E731 (GIBBONS 93 [4]), and NA31 (BERTANZA 97 [9]).

In Fig. 1 [Fig. 2] the slope of the diagonal ϕ_{+-} bands shows the Δm [τ_s] dependence; the unseen τ_s [Δm] dependent term is evaluated using the fitted τ_s [Δm]. The vertical half-width

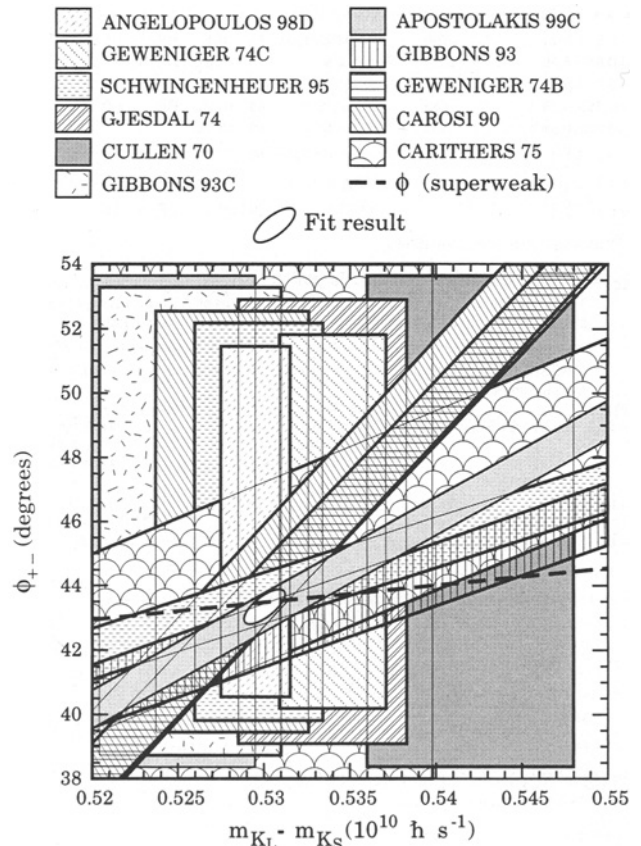


Figure 1: ϕ_{+-} vs Δm . Δm measurements appear as vertical bands spanning $\Delta m \pm 1\sigma$, some of which are cut near the top to aid the eye. The ϕ_{+-} measurements appear as diagonal bands spanning $\phi_{+-} \pm \sigma_\phi$. The dashed line shows $\phi(\text{superweak})$. The ellipse shows the 1σ contour of the fit result. See Table 1 for data references.

σ_ϕ of each band is the ϕ_{+-} error for fixed Δm [τ_s] and includes the systematic error due to the error in the fitted τ_s [Δm].

Table 2 gives the resulting fit values for the parameters and Table 3 gives the correlation matrix. The resulting ϕ_{+-} is in good agreement with $\phi(\text{superweak}) = 43.49 \pm 0.07^\circ$ obtained from Eq. (1) using Δm and τ_s from Table 2.

The χ^2 is 16.0 for 20 degrees of freedom, indicating good agreement of the input data. Nevertheless, there has been criticism that Fermilab E773 (SCHWINGENHEUER 95 [3]) and E731 (GIBBONS 93 [4]) measure $\phi_{+-} - \phi_f$ and calculate the regeneration phase ϕ_f from the power law momentum dependence of the regeneration amplitude using analyticity and dispersion relations. In the E731 result, a systematic error of ± 0.5 degrees for departures from a pure power-law is included. For the E773 result, they modeled a variety of effects that do distort the amplitude from a pure power law and ascribed a $\pm 0.35^\circ$ systematic error from uncertainties in these effects. Even so, the E731 result remains valid within its quoted errors. KLEINKNECHT 94 [16] and KLEINKNECHT 95 [17] argue that these systematic errors should be around 3° , primarily

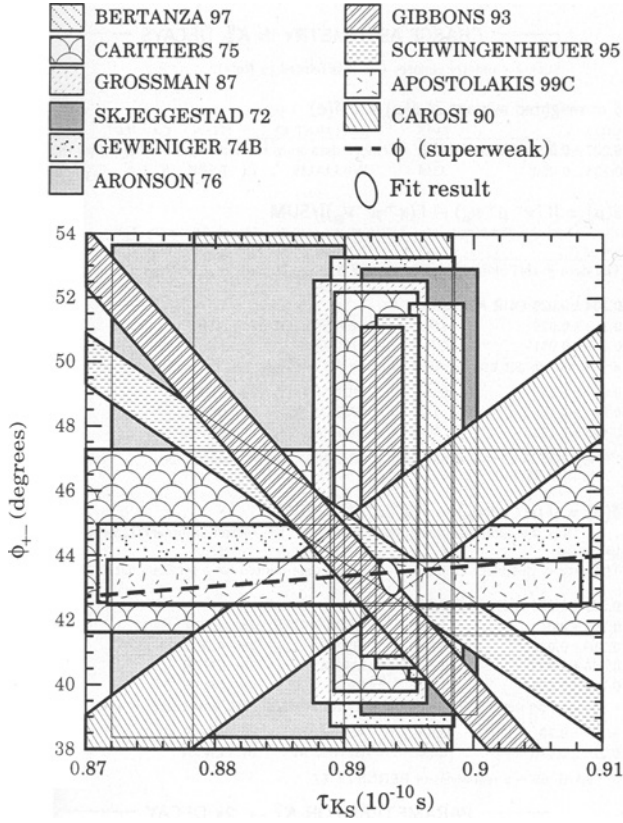


Figure 2: ϕ_{+-} vs τ_S . τ_S measurements appear as vertical bands spanning $\tau_S \pm 1\sigma$, some of which are cut near the top to aid the eye. The ϕ_{+-} measurements appear as diagonal bands spanning $\phi_{+-} \pm \sigma_\phi$. The dashed line shows ϕ (superweak). The ellipse shows the fit result's 1σ contour. See Table 1 for data references.

because of the absence of data on the momentum dependence of the regeneration amplitude above 160 GeV/c. BRIERE 95 [18] and BRIERE 95C [19] reply that the current understanding of regeneration is sufficient to allow a precise and reliable correction for the region above 160 GeV/c. The question is one of judgement about the reliability of the assumptions used. In the absence of any contradictory evidence, we choose to accept the judgement of the E731/E773 experimenters in setting their systematic errors.

Fit for ϵ'/ϵ , $|\eta_{+-}|$, $|\eta_{00}|$, and $B(K_L \rightarrow \pi\pi)$

We list measurements of $|\eta_{+-}|$, $|\eta_{00}|$, $|\eta_{00}/\eta_{+-}|$ and ϵ'/ϵ . Independent information on $|\eta_{+-}|$ and $|\eta_{00}|$ can be obtained from measurements of the K_L^0 and K_S^0 lifetimes (τ_L , τ_S) and branching ratios (B) to $\pi\pi$, using the relations

$$|\eta_{+-}| = \left[\frac{B(K_L^0 \rightarrow \pi^+\pi^-)}{\tau_L} \frac{\tau_S}{B(K_S^0 \rightarrow \pi^+\pi^-)} \right]^{1/2}, \quad (2a)$$

$$|\eta_{00}| = \left[\frac{B(K_L^0 \rightarrow \pi^0\pi^0)}{\tau_L} \frac{\tau_S}{B(K_S^0 \rightarrow \pi^0\pi^0)} \right]^{1/2}. \quad (2b)$$

Table 1: References and location of input data for Fig. 1 and Fig. 2. Unless otherwise indicated by a footnote, a check (\checkmark) indicates that the data can be found in the ϕ_{+-} or Δm sections of the K_L Particle Listings, or the τ_S section of the K_S Particle Listings, according to the column headers.

Location of input data

Fig. 1		Fig. 2		PDG Document ID	Ref.
ϕ_{+-}	Δm	ϕ_{+-}	τ_S		
\checkmark	\checkmark	\checkmark		APOSTOLAKIS 99C	[5]
\checkmark		\checkmark	\checkmark	GIBBONS 93	[4]
\checkmark	\checkmark	\checkmark	\checkmark	SCHWINGENHEUER 95	[3]
\checkmark		\checkmark	\checkmark	GEWENIGER 74B	[2]
\checkmark	\checkmark^*	\checkmark	\checkmark^*	CAROSI 90	[1]
\checkmark	\checkmark^\dagger	\checkmark	\checkmark	CARITHERS 75	[10]
	\checkmark			ANGELOPOULOS 98D	[11]
	\checkmark			GEWENIGER 74C	[7]
	\checkmark			GJESDAL 74	[8]
	\checkmark			CULLEN 70	[6]
	\checkmark			GIBBONS 93C	[12]
			\checkmark	BERTANZA 97	[9]
			\checkmark	GROSSMAN 87	[13]
			\checkmark	SKJEGGESTAD 72	[14]
			\checkmark	ARONSON 76	[15]

* from $\phi_{00}(\Delta m, \tau_S)$ in ϕ_{00} Particle Listings.

† from $\tau_S(\Delta m)$ in τ_S Particle Listings.

Table 2: Results of the fit for ϕ_{+-} , ϕ_{00} , $\phi_{00} - \phi_{+-}$, Δm , and τ_S . The fit has $\chi^2 = 16.0$ for 20 degrees of freedom (24 measurements $- 5$ parameters $+ 1$ constraint).

Quantity	Fit Result
ϕ_{+-}	$43.3 \pm 0.5^\circ$
Δm	$(0.5300 \pm 0.0012) \times 10^{10} \hbar^{-1} \text{s}^{-1}$
τ_S	$(0.8935 \pm 0.0008) \times 10^{-10} \text{s}$
ϕ_{00}	$43.2 \pm 1.0^\circ$
$\Delta\phi$	$-0.1 \pm 0.8^\circ$

Table 3: Correlation matrix for the fitted parameters.

	ϕ_{+-}	Δm	τ_S	ϕ_{00}	$\Delta\phi$
ϕ_{+-}	1.00	0.71	-0.30	0.54	-0.02
Δm	0.71	1.00	-0.19	0.43	0.04
τ_S	-0.30	-0.19	1.00	-0.14	0.04
ϕ_{00}	0.54	0.43	-0.14	1.00	0.83
$\Delta\phi$	-0.02	0.04	0.04	0.83	1.00

Meson Particle Listings

 K_L^0

For historical reasons the branching ratio fits and the CP -violation fits are done separately, but we want to include the influence of $|\eta_{+-}|$, $|\eta_{00}|$, $|\eta_{00}/\eta_{+-}|$, and ϵ'/ϵ measurements on $B(K_L^0 \rightarrow \pi^+\pi^-)$ and $B(K_L^0 \rightarrow \pi^0\pi^0)$ and vice versa. We approximate a global fit to all of these measurements by first performing two independent fits: 1) BRFIT, a fit to the K_L^0 branching ratios, rates, and mean life, and 2) ETAFIT, a fit to the $|\eta_{+-}|$, $|\eta_{00}|$, $|\eta_{+-}/\eta_{00}|$, and ϵ'/ϵ measurements. The results from fit 1, along with the K_S^0 values from this edition are used to compute values of $|\eta_{+-}|$ and $|\eta_{00}|$ which are included as measurements in the $|\eta_{00}|$ and $|\eta_{+-}|$ sections with a document ID of BRFIT 00. Thus the fit values of $|\eta_{+-}|$ and $|\eta_{00}|$ given in this edition include both the direct measurements and the results from the branching ratio fit.

The process is reversed in order to include the direct $|\eta|$ measurements in the branching ratio fit. The results from fit 2 above (before including BRFIT 00 values) are used along with the K_L^0 and K_S^0 mean lives and the $K_S^0 \rightarrow \pi\pi$ branching fractions to compute the K_L^0 branching ratios $\Gamma(K_L^0 \rightarrow \pi^+\pi^-)/\Gamma(\text{total})$ and $\Gamma(K_L^0 \rightarrow \pi^0\pi^0)/\Gamma(K_L^0 \rightarrow \pi^+\pi^-)$. These branching ratio values are included as measurements in the branching ratio section with a document ID of ETAFIT 00. Thus the K_L^0 branching ratio fit values in this edition include the results of direct measurements of $|\eta_{+-}|$, $|\eta_{00}|$, $|\eta_{00}/\eta_{+-}|$, and ϵ'/ϵ . A more detailed discussion of these fits is given in the 1990 edition of this *Review* [20].

References

1. R. Carosi *et al.*, Phys. Lett. **B237**, 303 (1990).
2. C. Geweniger *et al.*, Phys. Lett. **48B**, 487 (1974).
3. B. Schwingenheuer *et al.*, Phys. Rev. Lett. **74**, 4376 (1995).
4. L.K. Gibbons *et al.*, Phys. Rev. Lett. **70**, 1199 (1993) and footnote in Ref. [3].
5. A. Apostolakis *et al.*, Phys. Lett. **B458**, 545 (1999).
6. M. Cullen *et al.*, Phys. Lett. **32B**, 523 (1970).
7. C. Geweniger *et al.*, Phys. Lett. **52B**, 108 (1974).
8. S. Gjesdal *et al.*, Phys. Lett. **52B**, 113 (1974).
9. L. Bertanza *et al.*, Z. Phys. **C73**, 629 (1997).
10. W. Carithers *et al.*, Phys. Rev. Lett. **34**, 1244 (1975).
11. A. Angelopoulos *et al.*, Phys. Lett. **B444**, 38 (1998).
12. L.K. Gibbons, Thesis, RX-1487, Univ. of Chicago, 1993.
13. N. Grossman *et al.*, Phys. Rev. Lett. **59**, 18 (1987).
14. O. Skjeggstad *et al.*, Nucl. Phys. **B48**, 343 (1972).
15. S.H. Aronson *et al.*, Nuovo Cimento **32A**, 236 (1976).
16. K. Kleinknecht and S. Luitz, Phys. Lett. **B336**, 581 (1994).
17. K. Kleinknecht, Phys. Rev. Lett. **75**, 4784 (1995).
18. R. Briere and B. Winstein, Phys. Rev. Lett. **75**, 402 (1995).
19. R. Briere and B. Winstein, Phys. Rev. Lett. **75**, 4785 (1995).
20. J.J. Hernandez *et al.*, Phys. Lett. **B239**, 1 (1990).

CP-VIOLATION PARAMETERS IN K_L^0 DECAYSCHARGE ASYMMETRY IN K_S^0 DECAYS

Such asymmetry violates CP . It is related to $\text{Re}(\epsilon)$.

 $\delta = \text{weighted average of } \delta(\mu) \text{ and } \delta(e)$

VALUE (%)	EVTS	DOCUMENT ID	TECN	COMMENT
0.327 ± 0.012 OUR AVERAGE				Includes data from the 2 datablocks that follow this one.
0.333 ± 0.050	33M	WILLIAMS	73	ASPK $K_{\mu 3} + K_{e 3}$

 $\delta(\mu) = [\Gamma(\pi^- \mu^+ \nu_\mu) - \Gamma(\pi^+ \mu^- \bar{\nu}_\mu)]/\text{SUM}$

Only the combined value below is put into the Meson Summary Table.

VALUE (%)	EVTS	DOCUMENT ID	TECN
The data in this block is included in the average printed for a previous datablock.			

0.304 ± 0.025 OUR AVERAGE

0.313 ± 0.029	15M	GEWENIGER	74	ASPK
0.278 ± 0.051	7.7M	PICCIONI	72	ASPK
• • • We do not use the following data for averages, fits, limits, etc. • • •				
0.60 ± 0.14	4.1M	MCCARTHY	73	CNTR
0.57 ± 0.17	1M	97 PACIOTTI	69	OSPK
0.403 ± 0.134	1M	97 DORFAN	67	OSPK

97 PACIOTTI 69 is a reanalysis of DORFAN 67 and is corrected for $\mu^+\mu^-$ range difference in MCCARTHY 72.

 $\delta(e) = [\Gamma(\pi^- e^+ \nu_e) - \Gamma(\pi^+ e^- \bar{\nu}_e)]/\text{SUM}$

Only the combined value below is put into the Meson Summary Table.

VALUE (%)	EVTS	DOCUMENT ID	TECN
The data in this block is included in the average printed for a previous datablock.			

0.333 ± 0.014 OUR AVERAGE

0.341 ± 0.018	34M	GEWENIGER	74	ASPK
0.318 ± 0.038	40M	FITCH	73	ASPK
0.346 ± 0.033	10M	MARX	70	CNTR
0.246 ± 0.059	10M	98 SAAL	69	CNTR
• • • We do not use the following data for averages, fits, limits, etc. • • •				
0.36 ± 0.18	600k	ASHFORD	72	ASPK
0.224 ± 0.036	10M	98 BENNETT	67	CNTR

98 SAAL 69 is a reanalysis of BENNETT 67.

PARAMETERS FOR $K_L^0 \rightarrow 2\pi$ DECAY

$$\eta_{+-} = A(K_L^0 \rightarrow \pi^+\pi^-) / A(K_S^0 \rightarrow \pi^+\pi^-)$$

$$\eta_{00} = A(K_L^0 \rightarrow \pi^0\pi^0) / A(K_S^0 \rightarrow \pi^0\pi^0)$$

The fitted values of $|\eta_{+-}|$ and $|\eta_{00}|$ given below are the results of a fit to $|\eta_{+-}|$, $|\eta_{00}|$, $|\eta_{00}/\eta_{+-}|$, and $\text{Re}(\epsilon'/\epsilon)$. Independent information on $|\eta_{+-}|$ and $|\eta_{00}|$ can be obtained from the fitted values of the $K_L^0 \rightarrow \pi\pi$ and $K_S^0 \rightarrow \pi\pi$ branching ratios and the K_L^0 and K_S^0 lifetimes. This information is included as data in the $|\eta_{+-}|$ and $|\eta_{00}|$ sections with a Document ID "BRFIT." See the note "Fits for K_L^0 CP-Violation Parameters" above for details.

$$|\eta_{00}| = |A(K_L^0 \rightarrow 2\pi^0) / A(K_S^0 \rightarrow 2\pi^0)|$$

VALUE (units 10^{-3})	DOCUMENT ID	TECN	COMMENT
2.262 ± 0.017 OUR FIT			
2.23 ± 0.11 OUR AVERAGE			
2.12 ± 0.16	99 BRFIT	00	
2.47 ± 0.31 ± 0.24	ANGELOPOU...	98	CPLR
2.33 ± 0.18	CHRISTENS...	79	ASPK
• • • We do not use the following data for averages, fits, limits, etc. • • •			
2.49 ± 0.40	100 ADLER	96b	CPLR Sup. by ANGELOPOU-LOS 98
2.71 ± 0.37	101 WOLFF	71	OSPK Cu reg., 4γ's
2.95 ± 0.63	101 CHOLLET	70	OSPK Cu reg., 4γ's

99 This BRFIT value is computed from fitted values of the K_L^0 and K_S^0 lifetimes and branching fractions to $\pi\pi$. See the discussion in the note "Fits for K_L^0 CP-Violation Parameters."

100 Error is statistical only.

101 CHOLLET 70 gives $|\eta_{00}| = (1.23 \pm 0.24) \times (\text{regeneration amplitude, 2 GeV/c Cu})/10000\text{mb}$. WOLFF 71 gives $|\eta_{00}| = (1.13 \pm 0.12) \times (\text{regeneration amplitude, 2 GeV/c Cu})/10000\text{mb}$. We compute both $|\eta_{00}|$ values for (regeneration amplitude, 2 GeV/c Cu) = $24 \pm 2\text{mb}$. This regeneration amplitude results from averaging over FAISSNER 69, extrapolated using optical-model calculations of Bohm *et al.*, Physics Letters **27B** 594 (1968) and the data of BALATS 71. (From H. Faissner, private communication).

$$|\eta_{+-}| = |A(K_L^0 \rightarrow \pi^+\pi^-) / A(K_S^0 \rightarrow \pi^+\pi^-)|$$

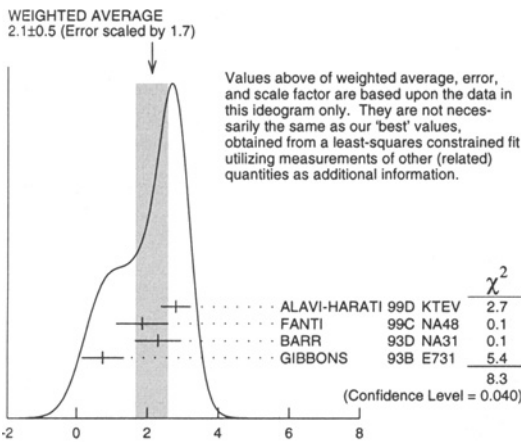
VALUE (units 10^{-3})	EVTS	DOCUMENT ID	TECN	COMMENT
2.276 ± 0.017 OUR FIT				
2.277 ± 0.017 OUR AVERAGE				
2.272 ± 0.024		102 BRFIT	00	
2.264 ± 0.023 ± 0.027	70M	103 APOSTOLA...	99C CPLR	$K^0\bar{K}^0$ asymmetry
2.30 ± 0.035		GEWENIGER	74B ASPK	
• • • We do not use the following data for averages, fits, limits, etc. • • •				
2.310 ± 0.043 ± 0.031		104 ADLER	95B CPLR	$K^0\bar{K}^0$ asymmetry
2.32 ± 0.14 ± 0.03	10 ⁵	ADLER	92B CPLR	$K^0\bar{K}^0$ asymmetry
102 This BRFIT value is computed from fitted values of the K_L^0 and K_S^0 lifetimes and branching fractions to $\pi\pi$. See the discussion in the note "Fits for K_L^0 CP-Violation Parameters."				
103 APOSTOLAKIS 99c report $(2.264 \pm 0.023 \pm 0.026 + 9.1[\tau_S - 0.8934]) \times 10^{-3}$. We evaluate for our 1998 best value $\tau_S = (0.8934 \pm 0.0008) \times 10^{-10}$ s.				
104 ADLER 95b report $(2.312 \pm 0.043 \pm 0.030 - 1[\Delta m - 0.5274] + 9.1[\tau_S - 0.8926]) \times 10^{-3}$. We evaluate for our 1996 best values $\Delta m = (0.5304 \pm 0.0014) \times 10^{-10} \text{ s}^{-1}$ and $\tau_S = (0.8927 \pm 0.0009) \times 10^{-10}$ s. Superseded by APOSTOLAKIS 99c.				

$$|\eta_{00}/\eta_{+-}|$$

VALUE	EVTS	DOCUMENT ID	TECN	COMMENT
0.9936 ± 0.0014 OUR FIT				Error includes scale factor of 1.6.
0.9930 ± 0.0020 OUR AVERAGE				
0.9931 ± 0.0020		105,106 BARR	93D NA31	
0.9904 ± 0.0084 ± 0.0036		107 WOODS	88 E731	
• • • We do not use the following data for averages, fits, limits, etc. • • •				
0.9939 ± 0.0013 ± 0.0015	1M	105 BARR	93D NA31	
0.9899 ± 0.0020 ± 0.0025		105 BURKHARDT	88 NA31	
105 This is the square root of the ratio R given by BURKHARDT 88 and BARR 93D.				
106 This is the combined results from BARR 93D and BURKHARDT 88, taking into account a common systematic uncertainty of 0.0014.				
107 We calculate $ \eta_{00}/\eta_{+-} = 1 - 3(\epsilon'/\epsilon)$ from WOODS 88 (ϵ'/ϵ) value.				

$$\epsilon'/\epsilon \approx \text{Re}(\epsilon'/\epsilon) = (1 - |\eta_{00}/\eta_{+-}|)/3$$

VALUE (units 10^{-3})	DOCUMENT ID	TECN	COMMENT
2.1 ± 0.5 OUR FIT			Error includes scale factor of 1.6.
2.1 ± 0.5 OUR AVERAGE			Error includes scale factor of 1.7. See the ideogram below.
2.80 ± 0.30 ± 0.28	ALAVI-HARATI	99D KTEV	
1.85 ± 0.45 ± 0.58	FANTI	99C NA48	
2.3 ± 0.65	108,109 BARR	93D NA31	
0.74 ± 0.52 ± 0.29	GIBBONS	93B E731	
• • • We do not use the following data for averages, fits, limits, etc. • • •			
2.0 ± 0.7	110 BARR	93D NA31	
-0.4 ± 1.4 ± 0.6	PATTERSON	90 E731	in GIBBONS 93B
3.3 ± 1.1	110 BURKHARDT	88 NA31	
3.2 ± 2.8 ± 1.2	108 WOODS	88 E731	
108 These values are derived from $ \eta_{00}/\eta_{+-} $ measurements. They enter the average in this section but enter the fit via the $ \eta_{00}/\eta_{+-} $ section only.			
109 This is the combined results from BARR 93D and BURKHARDT 88, taking into account their common systematic uncertainty.			
110 These values are derived from $ \eta_{00}/\eta_{+-} $ measurements.			



$$\epsilon'/\epsilon \approx \text{Re}(\epsilon'/\epsilon) = (1 - |\eta_{00}/\eta_{+-}|)/3$$

ϕ_{+-} , PHASE of η_{+-}

The dependence of the phase on Δm and τ_S is given for each experiment in the comments below, where Δm is the $K_L^0 - K_S^0$ mass difference in units 10^{10} s^{-1} and τ_S is the K_S mean life in units 10^{-10} s. For the "used" data, we have evaluated these mass dependences using our 2000 values, $\Delta m = 0.5300 \pm 0.0012$, $\tau_S = 0.8935 \pm 0.0008$ to obtain the values quoted below. We also give the regeneration phase ϕ_f in the comments below.

OUR FIT is described in the note on "Fits for K_L^0 CP-Violation Parameters" in the K_L^0 Particle Listings.

VALUE (°)	EVTS	DOCUMENT ID	TECN	COMMENT
43.3 ± 0.5 OUR FIT				
43.2 ± 0.7	70M	111 APOSTOLA...	99C CPLR	$K^0\bar{K}^0$ asymmetry
43.6 ± 0.8		112,113 SCHWINGEN...	95 E773	$\text{CH}_{1,1}$ regenerator
42.4 ± 1.0		113,114 GIBBONS	93 E731	B_4C regenerator
44.4 ± 1.7		115 CAROSI	90 NA31	Vacuum regen.
44.4 ± 2.8		116 CARITHERS	75 SPEC	C regenerator
43.8 ± 1.2		117 GEWENIGER	74B ASPK	Vacuum regen.
• • • We do not use the following data for averages, fits, limits, etc. • • •				
43.82 ± 0.63		118,119 ADLER	96C RVUE	
43.6 ± 1.2		120 ADLER	95B CPLR	$K^0\bar{K}^0$ asymmetry
42.3 ± 4.4 ± 1.4	10 ⁵	121 ADLER	92B CPLR	$K^0\bar{K}^0$ asymmetry
47.7 ± 2.0 ± 0.9		113,122 KARLSSON	90 E731	
111 APOSTOLAKIS 99c report $(43.19 \pm 0.53 \pm 0.28)^\circ + 300 [\Delta m - 0.5301]^\circ$.				
112 SCHWINGENHEUER 95 reports $\phi_{+-} = 43.53 \pm 0.76 + 173[\Delta m - 0.5282] - 275[\tau_S - 0.8926]$.				
113 These experiments measure $\phi_{+-} - \phi_f$ and calculate the regeneration phase from the power law momentum dependence of the regeneration amplitude using analyticity and dispersion relations. SCHWINGENHEUER 95 [GIBBONS 93] includes a systematic error of 0.35° [0.5°] for uncertainties in their modeling of the regeneration amplitude. See the discussion of these systematic errors, including criticism that they could be underestimated, in the note on "C violation in K_L^0 decay."				
114 GIBBONS 93 measures $\phi_{+-} - \phi_f$ and calculates the regeneration phase ϕ_f from the power law momentum dependence of the regeneration amplitude using analyticity. An error of 0.6° is included for possible uncertainties in the regeneration phase. They find $\phi_{+-} = 42.21 \pm 0.9 + 189 [\Delta m - 0.5257] - 460 [\tau_S - 0.8922]^\circ$, as given in SCHWINGENHEUER 95, footnote 8. GIBBONS 93 reports $\phi_{+-} (42.2 \pm 1.4)^\circ$.				
115 CAROSI 90 $\phi_{+-} = 46.9 \pm 1.4 \pm 0.7 + 579 [\Delta m - 0.5351] + 303 [\tau_S - 0.8922]^\circ$.				
116 CARITHERS 75 $\phi_{+-} = (45.5 \pm 2.8) + 224 [\Delta m - 0.5348]^\circ$, $\phi_f = -40.9 \pm 2.6^\circ$.				
117 GEWENIGER 74B $\phi_{+-} = (49.4 \pm 1.0) + 565 [\Delta m - 0.540]^\circ$.				
118 ADLER 96C fit gives $(43.82 \pm 0.41)^\circ + 339(\Delta m - 0.5307)^\circ - 252(\tau_S - 0.8922)^\circ$.				
119 ADLER 96C is the result of a fit which includes nearly the same data as entered into the "OUR FIT" value in the 1996 edition of this Review (Physical Review D54 1 (1996)).				
120 ADLER 95b report $42.7^\circ \pm 0.9^\circ \pm 0.6^\circ + 316[\Delta m - 0.5274]^\circ + 30[\tau_S - 0.8926]^\circ$.				
121 ADLER 92a quote separately two systematic errors: ± 0.4 from their experiment and ± 1.0 degrees due to the uncertainty in the value of Δm .				
122 KARLSSON 90 systematic error does not include regeneration phase uncertainty.				

ϕ_{00} , PHASE OF η_{00}

See comment in ϕ_{+-} header above for treatment of Δm and τ_S dependence.

OUR FIT is described in the note on "Fits for K_L^0 CP-Violation Parameters" in the K_L^0 Particle Listings.

VALUE (°)	DOCUMENT ID	TECN	COMMENT
43.2 ± 1.0 OUR FIT			
41.9 ± 5.6 ± 1.9	123 ANGELOPOU...	98 CPLR	
44.5 ± 2.5	124 CAROSI	90 NA31	
• • • We do not use the following data for averages, fits, limits, etc. • • •			
50.8 ± 7.1 ± 1.7	125 ADLER	96B CPLR	Sup. by ANGELOPOU-LOS 98
47.4 ± 1.4 ± 0.9	126 KARLSSON	90 E731	
123 ANGELOPOULOS 98 $\phi_{00} = 42.0 \pm 5.6 \pm 1.9 + 240[\Delta m - 0.5307]$ with negligible τ_S dependence.			
124 CAROSI 90 $\phi_{00} = 47.1 \pm 2.1 \pm 1.0 + 579 [\Delta m - 0.5351] + 252 [\tau_S - 0.8922]^\circ$.			
125 ADLER 96b identified initial neutral kaon individually as being a K^0 or a \bar{K}^0 . The systematic uncertainty is $\pm 1.5^\circ$ combined in quadrature with $\pm 0.8^\circ$ due to Δm .			
126 KARLSSON 90 systematic error does not include regeneration phase uncertainty.			

PHASE DIFFERENCE $\phi_{00} - \phi_{+-}$

Test of CPT.

OUR FIT is described in the note on "Fits for K_L^0 CP-Violation Parameters" in the K_L^0 Particle Listings.

VALUE (°)	DOCUMENT ID	TECN	COMMENT
-0.1 ± 0.8 OUR FIT			
-0.3 ± 0.8 OUR AVERAGE			
-0.30 ± 0.88	127 SCHWINGEN...	95	Combined E731, E773
0.2 ± 2.6 ± 1.2	128 CAROSI	90 NA31	
• • • We do not use the following data for averages, fits, limits, etc. • • •			
0.62 ± 0.71 ± 0.75	SCHWINGEN...	95 E773	
-1.6 ± 1.2	129 GIBBONS	93 E731	
-0.3 ± 2.4 ± 1.2	KARLSSON	90 E731	
127 This SCHWINGENHEUER 95 values is the combined result of SCHWINGENHEUER 95 and GIBBONS 93, accounting for correlated systematic errors.			
128 CAROSI 90 is excluded from the fit because it is not independent of ϕ_{+-} and ϕ_{00} values.			
129 GIBBONS 93 give detailed dependence of systematic error on lifetime (see the section on the K_S^0 mean life) and mass difference (see the section on $m_{K_L^0} - m_{K_S^0}$).			

Meson Particle Listings

K_L^0

DECAY-PLANE ASYMMETRY IN $\pi^+\pi^-e^+e^-$ DECAYS

This is the CP-violating asymmetry

$$A = \frac{N_{\sin\phi\cos\phi > 0.0} - N_{\sin\phi\cos\phi < 0.0}}{N_{\sin\phi\cos\phi > 0.0} + N_{\sin\phi\cos\phi < 0.0}}$$

where ϕ is the angle between the e^+e^- and $\pi^+\pi^-$ planes in the K_L^0 rest frame.

CP ASYMMETRY A in $K_L^0 \rightarrow \pi^+\pi^-e^+e^-$

VALUE (%)	DOCUMENT ID	TECN
13.6 ± 2.5 ± 1.2	ALAVI-HARATI00B	KTEV

CHARGE ASYMMETRY IN $\pi^+\pi^-\pi^0$ DECAYS

These are CP-violating charge-asymmetry parameters, defined at beginning of section "LINEAR COEFFICIENT f FOR $K_L^0 \rightarrow \pi^+\pi^-\pi^0$ above. See also note on Dalitz plot parameters in K^\pm section and note on CP violation in K_L^0 decay above.

LINEAR COEFFICIENT f FOR $K_L^0 \rightarrow \pi^+\pi^-\pi^0$

VALUE	EVTS	DOCUMENT ID	TECN
0.0011 ± 0.0008 OUR AVERAGE			
0.0010 ± 0.0024 ± 0.0030	500k	ANGELOPO...	98C CPLR
0.001 ± 0.011	6499	CHO	77
-0.001 ± 0.003	4709	PEACH	77
0.0013 ± 0.0009	3M	SCRIBANO	70
0.0 ± 0.017	4400	SMITH	70 OSPK
0.001 ± 0.004	238k	BLANPIED	68

QUADRATIC COEFFICIENT f FOR $K_L^0 \rightarrow \pi^+\pi^-\pi^0$

VALUE	EVTS	DOCUMENT ID	TECN
0.0045 ± 0.0024 ± 0.0059	500k	ANGELOPO...	98C CPLR

PARAMETERS for $K_L^0 \rightarrow \pi^+\pi^-\gamma$ DECAY

$$|\eta_{+-\gamma}| = |A(K_L^0 \rightarrow \pi^+\pi^-\gamma, CP \text{ violating}) / A(K_S^0 \rightarrow \pi^+\pi^-\gamma)|$$

VALUE (units 10^{-3})	EVTS	DOCUMENT ID	TECN
2.35 ± 0.07 OUR AVERAGE			
2.359 ± 0.062 ± 0.040	9045	MATTHEWS	95 E773
2.15 ± 0.26 ± 0.20	3671	RAMBERG	93B E731

$$\phi_{+-\gamma} = \text{phase of } \eta_{+-\gamma}$$

VALUE (°)	EVTS	DOCUMENT ID	TECN
44 ± 4 OUR AVERAGE			
43.8 ± 3.5 ± 1.9	9045	MATTHEWS	95 E773
72 ± 23 ± 17	3671	RAMBERG	93B E731

$$|\epsilon'_{+-\gamma}| / \epsilon \text{ for } K_L^0 \rightarrow \pi^+\pi^-\gamma$$

VALUE	CL%	EVTS	DOCUMENT ID	TECN
< 0.3	90	3671	130 RAMBERG	93B E731

130 RAMBERG 93B limit on $|\epsilon'_{+-\gamma}| / \epsilon$ assumes than any difference between η_{+-} and $\eta_{+-\gamma}$ is due to direct CP violation.

$\Delta S = \Delta Q$ IN K^0 DECAYS

The relative amount of $\Delta S \neq \Delta Q$ component present is measured by the parameter x , defined as

$$x = A(\bar{K}^0 \rightarrow \pi^-\ell^+\nu) / A(K^0 \rightarrow \pi^-\ell^+\nu)$$

We list $\text{Re}\{x\}$ and $\text{Im}\{x\}$ for K_{e3} and $K_{\mu 3}$ combined.

$$x = A(\bar{K}^0 \rightarrow \pi^-\ell^+\nu) / A(K^0 \rightarrow \pi^-\ell^+\nu) = A(\Delta S = -\Delta Q) / A(\Delta S = \Delta Q)$$

REAL PART OF x

VALUE	EVTS	DOCUMENT ID	TECN	COMMENT
-0.0018 ± 0.0041 ± 0.0045		ANGELOPO...	98D CPLR	K_{e3} from K^0
• • • We do not use the following data for averages, fits, limits, etc. • • •				
0.10 +0.18 -0.19	79	SMITH	75B WIRE	$\pi^-p \rightarrow K^0\Lambda$
0.04 ± 0.03	4724	NIEBERGALL	74 ASPK	$K^+p \rightarrow K^0p\pi^+$
-0.008 ± 0.044	1757	FACKLER	73 OSPK	K_{e3} from K^0
-0.03 ± 0.07	1367	HART	73 OSPK	K_{e3} from $K^0\Lambda$
-0.070 ± 0.036	1079	MALLARY	73 OSPK	K_{e3} from $K^0\Lambda X$
0.03 ± 0.06	410	131 BURGUN	72 HBC	$K^+p \rightarrow K^0p\pi^+$
0.04 +0.10 -0.13	100	132 GRAHAM	72 OSPK	$K_{\mu 3}$ from $K^0\Lambda$
-0.05 ± 0.09	442	132 GRAHAM	72 OSPK	$\pi^-p \rightarrow K^0\Lambda$
0.26 +0.10 -0.14	126	MANN	72 HBC	$K^-p \rightarrow n\bar{K}^0$
-0.13 ± 0.11	342	132 MANTSCH	72 OSPK	K_{e3} from $K^0\Lambda$
0.04 +0.07 -0.08	222	131 BURGUN	71 HBC	$K^+p \rightarrow K^0p\pi^+$

0.25 +0.07 -0.09	252	WEBBER	71 HBC	$K^-p \rightarrow n\bar{K}^0$
0.12 ± 0.09	215	133 CHO	70 DBC	$K^+d \rightarrow K^0pp$
-0.020 ± 0.025	134	BENNETT	69 CNTR	Charge asym + Cu regen.
0.09 +0.14 -0.16	686	LITTENBERG	69 OSPK	$K^+n \rightarrow K^0p$
0.03 ± 0.03	134	BENNETT	68 CNTR	
0.09 +0.07 -0.09	121	JAMES	68 HBC	$\bar{p}p$
0.17 +0.16 -0.35	116	FELDMAN	67B OSPK	$\pi^-p \rightarrow K^0\Lambda$
0.17 ± 0.10	335	133 HILL	67 DBC	$K^+d \rightarrow K^0pp$
0.035 +0.11 -0.13	196	AUBERT	65 HLBC	K^+ charge exchange
0.06 +0.18 -0.44	152	135 BALDO...	65 HLBC	K^+ charge exchange
-0.08 +0.16 -0.28	109	136 FRANZINI	65 HBC	$\bar{p}p$

131 BURGUN 72 is a final result which includes BURGUN 71.
 132 First GRAHAM 72 value is second GRAHAM 72 value combined with MANTSCH 72.
 133 CHO 70 is analysis of unambiguous events in new data and HILL 67.
 134 BENNETT 69 is a reanalysis of BENNETT 68.
 135 BALDO-CEOLIN 65 gives x and θ converted by us to $\text{Re}(x)$ and $\text{Im}(x)$.
 136 FRANZINI 65 gives x and θ for $\text{Re}(x)$ and $\text{Im}(x)$. See SCHMIDT 67.

IMAGINARY PART OF x

Assumes $m_{K_L^0} - m_{K_S^0}$ positive. See Listings above.

VALUE	EVTS	DOCUMENT ID	TECN	COMMENT
0.0012 ± 0.0019	640k	ANGELOPO...	98E CPLR	K_{e3} from K^0
• • • We do not use the following data for averages, fits, limits, etc. • • •				
-0.10 +0.16 -0.19	79	SMITH	75B WIRE	$\pi^-p \rightarrow K^0\Lambda$
-0.06 ± 0.05	4724	NIEBERGALL	74 ASPK	$K^+p \rightarrow K^0p\pi^+$
-0.017 ± 0.060	1757	FACKLER	73 OSPK	K_{e3} from K^0
0.09 ± 0.07	1367	HART	73 OSPK	K_{e3} from $K^0\Lambda$
0.107 +0.092 -0.074	1079	MALLARY	73 OSPK	K_{e3} from $K^0\Lambda X$
0.07 +0.06 -0.07	410	137 BURGUN	72 HBC	$K^+p \rightarrow K^0p\pi^+$
0.12 +0.17 -0.16	100	138 GRAHAM	72 OSPK	$K_{\mu 3}$ from $K^0\Lambda$
0.05 ± 0.13	442	138 GRAHAM	72 OSPK	$\pi^-p \rightarrow K^0\Lambda$
0.21 +0.15 -0.12	126	MANN	72 HBC	$K^-p \rightarrow n\bar{K}^0$
-0.04 ± 0.16	342	138 MANTSCH	72 OSPK	K_{e3} from $K^0\Lambda$
0.12 +0.08 -0.09	222	137 BURGUN	71 HBC	$K^+p \rightarrow K^0p\pi^+$
0.0 ± 0.08	252	WEBBER	71 HBC	$K^-p \rightarrow n\bar{K}^0$
-0.08 ± 0.07	215	139 CHO	70 DBC	$K^+d \rightarrow K^0pp$
-0.11 +0.10 -0.11	686	LITTENBERG	69 OSPK	$K^+n \rightarrow K^0p$
+0.22 +0.37 -0.29	121	JAMES	68 HBC	$\bar{p}p$
0.0 ± 0.25	116	FELDMAN	67B OSPK	$\pi^-p \rightarrow K^0\Lambda$
-0.20 ± 0.10	335	139 HILL	67 DBC	$K^+d \rightarrow K^0pp$
-0.21 +0.11 -0.15	196	AUBERT	65 HLBC	K^+ charge exchange
-0.44 +0.32 -0.19	152	140 BALDO...	65 HLBC	K^+ charge exchange
+0.24 +0.40 -0.30	109	141 FRANZINI	65 HBC	$\bar{p}p$

137 BURGUN 72 is a final result which includes BURGUN 71.
 138 First GRAHAM 72 value is second GRAHAM 72 value combined with MANTSCH 72.
 139 Footnote 10 of HILL 67 should read +0.58, not -0.58 (private communication) CHO 70 is analysis of unambiguous events in new data and HILL 67.
 140 BALDO-CEOLIN 65 gives x and θ converted by us to $\text{Re}(x)$ and $\text{Im}(x)$.
 141 FRANZINI 65 gives x and θ for $\text{Re}(x)$ and $\text{Im}(x)$. See SCHMIDT 67.

K_L^0 REFERENCES

ALAVI-HARATI 00	PR D61 072006	A. Alavi-Harati et al.	(KTeV Collab.)
ALAVI-HARATI 00B	PRL 84 408	A. Alavi-Harati et al.	(KTeV Collab.)
AMBROSE 00	PRL 84 1389	D. Ambrose et al.	(BNL E871 Collab.)
APOSTOLA... 00	PL B473 186	A. Apostolakis et al.	(CLEAR Collab.)
BRFIT 00	RPP		
ETAFIT 00	RPP		
ADAMS 99	PL B447 240	J. Adams et al.	(KTeV Collab.)
ALAVI-HARATI 99B	PRL 83 917	A. Alavi-Harati et al.	(KTeV Collab.)
ALAVI-HARATI 99D	PRL 83 22	A. Alavi-Harati et al.	(KTeV Collab.)
APOSTOLA... 99C	PL B458 545	A. Apostolakis et al.	(CLEAR Collab.)
FANTI 99B	PL B458 553	V. Fanti et al.	(CERN NA48 Collab.)
FANTI 99C	PL B465 335	V. Fanti et al.	(CERN NA48 Collab.)
MURAKAMI 99	PL B463 333	K. Murakami et al.	(KEK E162 Collab.)
ADAMS 98	PRL 80 4123	J. Adams et al.	(KTeV Collab.)
AMBROSE 98	PRL 81 4309	D. Ambrose et al.	(BNL E871 Collab.)
AMBROSE 98B	PRL 81 5734	D. Ambrose et al.	(BNL E871 Collab.)
ANGELOPO... 98	PL B420 191	A. Angelopoulos et al.	(CLEAR Collab.)
ANGELOPO... 98C	PL B420 191	A. Angelopoulos et al.	(CLEAR Collab.)
ANGELOPO... 98D	PL B444 38	A. Angelopoulos et al.	(CLEAR Collab.)
ANGELOPO... 98E	PL B444 43	A. Angelopoulos et al.	(CLEAR Collab.)
ARISAKA 98	PL B432 230	K. Arisaka et al.	(FNAL E799 Collab.)
BENDER 98	PL B418 411	M. Bender et al.	(CERN NA48 Collab.)
SETZU 98	PL B420 205	M.G. Setzu et al.	(KYOT, KEK, HIRO)
TAKEUCHI 98	PL B413 409	Y. Takeuchi et al.	(CERN NA48 Collab.)
FANTI 97	ZPHY C76 453	V. Fanti et al.	(BNL E871 Collab.)
NOMURA 97	PL B408 445	T. Nomura et al.	(KYOT, KEK, HIRO)
ADLER 96B	ZPHY C70 211	R. Adler et al.	(CLEAR Collab.)
ADLER 96C	PL B369 367	R. Adler et al.	(CLEAR Collab.)

See key on page 239

Meson Particle Listings

K⁰_L

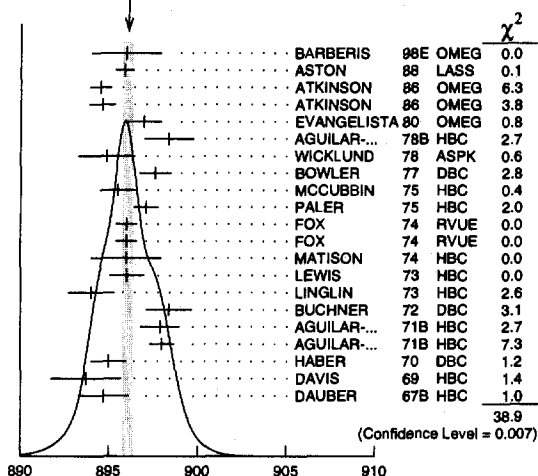
Table listing meson particles with columns for author names, experiment codes (e.g., PRL, PL, NP), and various laboratory or project identifiers (e.g., SLAC, CERN, JHU).

See key on page 239

Meson Particle Listings

$K^*(892)$

WEIGHTED AVERAGE
896.10±0.27 (Error scaled by 1.4)



$K^*(892)^0$ mass (MeV)

- ²Inclusive reaction. Complicated background and phase-space effects.
- ³Mass errors enlarged by us to Γ/\sqrt{N} . See note.
- ⁴Number of events in peak reevaluated by us.
- ⁵From a partial wave amplitude analysis.
- ⁶From pole extrapolation.

$K^*(892)$ MASSES AND MASS DIFFERENCES

Unrealistically small errors have been reported by some experiments. We use simple "realistic" tests for the minimum errors on the determination of a mass and width from a sample of N events:

$$\delta_{\min}(m) = \frac{\Gamma}{\sqrt{N}}, \quad \delta_{\min}(\Gamma) = 4 \frac{\Gamma}{\sqrt{N}} \quad (1)$$

We consistently increase unrealistic errors before averaging. For a detailed discussion, see the 1971 edition of this Note.

$m_{K^*(892)^0} - m_{K^*(892)^\pm}$

VALUE (MeV)	EVTs	DOCUMENT ID	TECN	CHG	COMMENT
6.7±1.2 OUR AVERAGE					
7.7±1.7	2980	AGUILAR...	78B HBC	±0	0.76 $\bar{p}p \rightarrow K^\mp K_S^0 \pi^\pm$
5.7±1.7	7338	AGUILAR...	71B HBC	-0	3.9,4.6 K^-p
6.3±4.1	283	BARASH	67B HBC		0.0 $\bar{p}p$

⁷Number of events in peak reevaluated by us.

$K^*(892)$ RANGE PARAMETER

All from partial wave amplitude analyses.

VALUE (GeV ⁻¹)	DOCUMENT ID	TECN	CHG	COMMENT
3.4±0.7	ASTON 88 LASS 0			11 $K^-p \rightarrow K^- \pi^+ n$
12.1±3.2±3.0	BIRD 89 LASS -			11 $K^-p \rightarrow \bar{K}^0 \pi^- p$

• • • We do not use the following data for averages, fits, limits, etc. • • •

$K^*(892)$ WIDTH

CHARGED ONLY

VALUE (MeV)	EVTs	DOCUMENT ID	TECN	CHG	COMMENT
50.8±0.9 OUR FIT					
50.8±0.9 OUR AVERAGE					
49 ± 2	5840	BAUBILLIER 84B HBC -			8.25 $K^-p \rightarrow \bar{K}^0 \pi^- p$
56 ± 4		NAPIER 84 SPEC -			200 $\pi^- p \rightarrow 2K_S^0 X$
51 ± 2	4100	TOAFF 81 HBC -			6.5 $K^-p \rightarrow \bar{K}^0 \pi^- p$
50.5±5.6		AJINENKO 80 HBC +			32 $K^+p \rightarrow K^0 \pi^+ X$
45.8±3.6	1800	AGUILAR... 78B HBC ±			0.76 $\bar{p}p \rightarrow K^\mp K_S^0 \pi^\pm$
52.0±2.5	6706	⁹ COOPER 78 HBC ±			0.76 $\bar{p}p \rightarrow (K\pi)^\pm X$

52.1±2.2	9000	¹⁰ PALER 75 HBC -			14.3 $K^-p \rightarrow (K\pi)^-$
46.3±6.7	765	⁹ CLARK 73 HBC -			3.13 $K^-p \rightarrow \bar{K}^0 \pi^- p$
48.2±5.7	1150	^{9,11} CLARK 73 HBC -			3.3 $K^-p \rightarrow \bar{K}^0 \pi^- p$
54.3±3.3	4404	⁹ AGUILAR... 71B HBC -			3.9,4.6 $K^-p \rightarrow (K\pi)^- p$
46 ± 5	1700	^{9,11} WOJCICKI 64 HBC -			1.7 $K^-p \rightarrow \bar{K}^0 \pi^- p$
54.8±1.7	27k	⁸ ABELE 99D CBAR ±			0.0 $\bar{p}p \rightarrow K^+ K^- \pi^0$
45.2±1 ± 2	79709± 801	¹² BIRD 89 LASS -			11 $K^-p \rightarrow \bar{K}^0 \pi^- p$
42.8±7.1	3700	BARTH 83 HBC +			70 $K^+p \rightarrow K^0 \pi^+ X$
64.0±9.2	800	^{9,11} CLELAND 82 SPEC +			30 $K^+p \rightarrow K_S^0 \pi^+ p$
62.0±4.4	3200	^{9,11} CLELAND 82 SPEC +			50 $K^+p \rightarrow K_S^0 \pi^+ p$
55 ± 4	3600	^{9,11} CLELAND 82 SPEC -			50 $K^+p \rightarrow K_S^0 \pi^- p$
62.6±3.8	380	DELFOSE 81 SPEC +			50 $K^\pm p \rightarrow K^\pm \pi^0 p$
50.5±3.9	187	DELFOSE 81 SPEC -			50 $K^\pm p \rightarrow K^\pm \pi^0 p$

⁸K-matrix pole.

NEUTRAL ONLY

VALUE (MeV)	EVTs	DOCUMENT ID	TECN	CHG	COMMENT
50.7±0.6 OUR FIT					Error includes scale factor of 1.1.
50.7±0.6 OUR AVERAGE					Error includes scale factor of 1.1.
54 ± 3		BARBERIS 98E OMEG			450 $pp \rightarrow Pf D_S K^* \bar{K}^*$
50.8±0.8±0.9		ASTON 88 LASS 0			11 $K^-p \rightarrow K^- \pi^+ n$
46.5±4.3	5900	BARTH 83 HBC 0			70 $K^+p \rightarrow K^+ \pi^- X$
54 ± 2	28k	EVANGELISTA 80 OMEG 0			10 $\pi^- p \rightarrow K^+ \pi^- (\Lambda, \Sigma)$
45.9±4.8	1180	AGUILAR... 78B HBC 0			0.76 $\bar{p}p \rightarrow K^\mp K_S^0 \pi^\pm$
51.2±1.7		WICKLUND 78 ASPK 0			3.4,6 $K^\pm N \rightarrow (K\pi)^0 N$
48.9±2.5		BOWLER 77 DBC 0			5.4 $K^+ d \rightarrow K^+ \pi^- pp$
48 ⁺³ / ₋₂	3600	MCCUBBIN 75 HBC 0			3.6 $K^-p \rightarrow K^- \pi^+ n$
50.6±2.5	22k	¹⁰ PALER 75 HBC 0			14.3 $K^-p \rightarrow (K\pi)^0 X$
47 ± 2	10k	FOX 74 RVUE 0			2 $K^-p \rightarrow K^- \pi^+ n$
51 ± 2		FOX 74 RVUE 0			2 $K^+n \rightarrow K^+ \pi^- p$
46.0±3.3	3186	⁹ LEWIS 73 HBC 0			2.1-2.7 $K^+p \rightarrow K\pi\pi p$
51.4±5.0	1700	⁹ BUCHNER 72 DBC 0			4.6 $K^+n \rightarrow K^+ \pi^- p$
55.8 ^{+4.2} / _{-3.4}	2934	⁹ AGUILAR... 71B HBC 0			3.9,4.6 $K^-p \rightarrow K^- \pi^+ n$
48.5±2.7	5362	AGUILAR... 71B HBC 0			3.9,4.6 $K^-p \rightarrow K^- \pi^+ \pi^- p$
54.0±3.3	4300	^{9,11} HABER 70 DBC 0			3 $K^-N \rightarrow K^- \pi^+ X$
53.2±2.1	10k	⁹ DAVIS 69 HBC 0			12 $K^+p \rightarrow K^+ \pi^- \pi^+ p$
44 ± 5.5	1040	⁹ DAUBER 67B HBC 0			2.0 $K^-p \rightarrow K^- \pi^+ \pi^- p$

⁹Width errors enlarged by us to $4 \times \Gamma/\sqrt{N}$; see note.

¹⁰Inclusive reaction. Complicated background and phase-space effects.

¹¹Number of events in peak reevaluated by us.

¹²From a partial wave amplitude analysis.

$K^*(892)$ DECAY MODES

Mode	Fraction (Γ_i/Γ)	Confidence level
Γ_1 $K\pi$	~ 100	%
Γ_2 $(K\pi)^\pm$	(99.901±0.009)	%
Γ_3 $(K\pi)^0$	(99.770±0.020)	%
Γ_4 $K^0 \gamma$	(2.30 ± 0.20)	$\times 10^{-3}$
Γ_5 $K^\pm \gamma$	(9.9 ± 0.9)	$\times 10^{-4}$
Γ_6 $K\pi\pi$	< 7	$\times 10^{-4}$ 95%

Meson Particle Listings

 $K^*(892)$, $K_1(1270)$

CONSTRAINED FIT INFORMATION

An overall fit to the total width and a partial width uses 13 measurements and one constraint to determine 3 parameters. The overall fit has a $\chi^2 = 7.8$ for 11 degrees of freedom.

The following off-diagonal array elements are the correlation coefficients $\langle \delta p_i \delta p_j \rangle / (\delta p_i \delta p_j)$, in percent, from the fit to parameters p_i , including the branching fractions, $x_i \equiv \Gamma_i / \Gamma_{\text{total}}$. The fit constrains the x_i whose labels appear in this array to sum to one.

x_5	-100	
Γ	19	-19
	x_2	x_5
Mode	Rate (MeV)	
Γ_2 ($K\pi$) [±]	50.7 ± 0.9	
Γ_5 $K^\pm \gamma$	0.050 ± 0.005	

CONSTRAINED FIT INFORMATION

An overall fit to the total width and a partial width uses 19 measurements and one constraint to determine 3 parameters. The overall fit has a $\chi^2 = 19.7$ for 17 degrees of freedom.

The following off-diagonal array elements are the correlation coefficients $\langle \delta p_i \delta p_j \rangle / (\delta p_i \delta p_j)$, in percent, from the fit to parameters p_i , including the branching fractions, $x_i \equiv \Gamma_i / \Gamma_{\text{total}}$. The fit constrains the x_i whose labels appear in this array to sum to one.

x_4	-100	
Γ	14	-14
	x_3	x_4
Mode	Rate (MeV)	Scale factor
Γ_3 ($K\pi$) ⁰	50.6 ± 0.6	1.1
Γ_4 $K^0 \gamma$	0.117 ± 0.010	

 $K^*(892)$ PARTIAL WIDTHS

$\Gamma(K^0 \gamma)$	EVTS	DOCUMENT ID	TECN	CHG	COMMENT	Γ_4
116 ± 10						
116.5 ± 9.9	584	CARLSMITH 86	SPEC	0	$K_L^0 A \rightarrow K_S^0 \pi^0 A$	

$\Gamma(K^\pm \gamma)$	EVTS	DOCUMENT ID	TECN	CHG	COMMENT	Γ_5
50 ± 5						
50 ± 5 OUR AVERAGE						
48 ± 11		BERG 83	SPEC	-	156 $K^- A \rightarrow \bar{K} \pi A$	
51 ± 5		CHANDLEE 83	SPEC	+	200 $K^+ A \rightarrow K \pi A$	

 $K^*(892)$ BRANCHING RATIOS

$\Gamma(K^0 \gamma) / \Gamma_{\text{total}}$	DOCUMENT ID	TECN	CHG	COMMENT	Γ_4 / Γ
2.30 ± 0.20					
2.30 ± 0.20 OUR FIT					
1.5 ± 0.7	CARITHERS 75B	CNTR	0	8-16 $\bar{K}^0 A$	

$\Gamma(K^\pm \gamma) / \Gamma_{\text{total}}$	DOCUMENT ID	TECN	CHG	COMMENT	Γ_5 / Γ
0.99 ± 0.09					
0.99 ± 0.09 OUR FIT					
< 1.6	95	BEMPORAD 73	CNTR	+	10-16 $K^+ A$

$\Gamma(K\pi\pi) / \Gamma((K\pi)^\pm)$	DOCUMENT ID	TECN	CHG	COMMENT	Γ_6 / Γ_2
< 0.0007	95	JONGEJANS 78	HBC	4 $K^- p \rightarrow p \bar{K}^0 2\pi$	
< 0.002		WOJCICKI 64	HBC	-	1.7 $K^- p \rightarrow \bar{K}^0 \pi^- p$

 $K^*(892)$ REFERENCES

ABELE 99D	PL B468 178	A. Abele et al.	(Crystal Barrel Collab.)
BARBERIS 98E	PL B436 204	D. Barberis et al.	(Omega expt.)
BIRD 89	SLAC-332	P.F. Bird	(SLAC)
ASTON 88	NP B296 493	D. Aston et al.	(SLAC, NAGO, CINC, INUS)
ATKINSON 86	ZPHY C30 521	M. Atkinson et al.	(BONN, CERN, GLAS+)
CARLSMITH 86	PRL 56 18	D. Carlsmith et al.	(EFI, SACL)
BAUBILLIER 04B	ZPHY C26 37	M. Baubillier et al.	(BIRM, CERN, GLAS+)
NAPIER 84	PL 149B 514	A. Napier et al.	(TUFTS, ARIZ, FNAL, FLOR+)
BARTH 83	NP B223 296	M. Barth et al.	(BRUX, CERN, GENO, MONS+)
BERG 83	Thesis UMI 83-21652	D.M. Berg	(ROCH)
CHANDLEE 83	PRL 51 168	C. Chandlee et al.	(ROCH, FNAL, MINN)
CLELAND 82	NP B208 189	W.E. Cleland et al.	(DURH, GEVA, LAUS+)
DELFOSE 81	NP B183 349	A. Delfosse et al.	(GEVA, LAUS)
TOAFF 81	PR D23 1500	S. Toaff et al.	(ANL, KANS)
AJINENKO 80	ZPHY C5 177	I.V. Ajinenko et al.	(SERP, BRUX, MONS+)
EVANGELISTA 80	NP B165 383	C. Evangelista et al.	(CERN, CEN+)
AGUILAR... 78B	NP B141 101	M. Aguilar-Benitez et al.	(MADR, TATA+)
BALAND 78	NP B140 220	J.F. Baland et al.	(MONS, BELG, CERN+)
COOPER 78	NP B136 365	A.M. Cooper et al.	(TATA, CERN, CDEF+)
JONGEJANS 78	NP B139 383	B. Jongejans et al.	(ZEEB, CERN, NIJH+)
WICKLIUND 78	PR D17 1197	A.B. Wicklund et al.	(ANL)
BOWLER 77	NP B126 31	M.G. Bowler et al.	(OXF)
CARITHERS 75B	PRL 35 349	W.C.J. Carithers et al.	(ROCH, MCGI)
MCCUBBIN 75	NP B86 13	N.A. McCubbin, L. Lyons	(OXF)
PALER 75	NP B96 1	K. Paler et al.	(RHEL, SACL, EPOL)
FOX 74	NP B80 403	G.C. Fox, M.L. Griss	(CIT)
MATISON 74	PR D9 1872	M.J. Matison et al.	(LBL)
BEMPORAD 73	NP B51 1	C. Bemporad et al.	(CERN, ETH, LOIC)
CLARK 73	NP B54 432	A.G. Clark, L. Lyons, D. Radojicic	(OXF)
LEWIS 73	NP B60 283	P.H. Lewis et al.	(LOWC, LOIC, CDEF)
LINGLIN 73	NP B55 408	D. Linglin	(CERN)
BUCHNER 72	NP B45 333	K. Buchner et al.	(MPIM, CERN, BRUX)
AGUILAR... 71B	PR D4 2583	M. Aguilar-Benitez, R.L. Eisner, J.B. Kinson	(BNL)
HABER 70	NP B17 289	B. Haber et al.	(REHO, SACL, BGNA, EPOL)
CRENNELL 69D	PRL 22 487	D.J. Crennell et al.	(BNL)
DAVIS 69	PRL 23 1071	P.J. Davis et al.	(LRL)
SCHWEINGRUBER... 68	PR 166 1317	F. Schweingruber et al.	(ANL, NWES)
BARASH 67B	PR 156 1399	N. Barash et al.	(COLU)
BARLOW 67	NC 50A 701	J. Barlow et al.	(CERN, CDEF, IRAD, LIVP)
DAUBER 67B	PR 153 1403	P.M. Dauber et al.	(UCLA)
DEBAERE 67B	NC 51A 401	W. de Baere et al.	(BRUX, CERN)
WOJCICKI 64	PR 135B 484	S.G. Wojcicki	(LRL)

OTHER RELATED PAPERS

BENAYOUN 99B	PR D59 114027	M. Benayoun et al.	
KAMAL 92	PL B284 421	A.N. Kamal, Q.P. Xu	(ALBE)
NAPIER 84	PL 149B 514	A. Napier et al.	(TUFTS, ARIZ, FNAL, FLOR+)
CLELAND 82	NP B208 189	W.E. Cleland et al.	(DURH, GEVA, LAUS+)
ALEXANDER 62	PRL 8 447	G. Alexander et al.	(LRL)
ALSTON 61	PRL 6 300	M.H. Alston et al.	(LRL)

 $K_1(1270)$

$$I(J^P) = \frac{1}{2}(1^+)$$

 $K_1(1270)$ MASS

VALUE (MeV)	DOCUMENT ID
1273 ± 7	OUR AVERAGE

Includes data from the 2 datablocks that follow this one.

PRODUCED BY K^- , BACKWARD SCATTERING, HYPERON EXCHANGE

VALUE (MeV)	EVTS	DOCUMENT ID	TECN	CHG	COMMENT
1275 ± 10	700	GAUILLET 78	HBC	+	4.2 $K^- p \rightarrow \Xi^- (K\pi\pi)^+$

PRODUCED BY K BEAMS

VALUE (MeV)	DOCUMENT ID	TECN	CHG	COMMENT
1270 ± 10	DAUM 81c	CNTR	-	63 $K^- p \rightarrow K^- 2\pi p$

The data in this block is included in the average printed for a previous datablock.

• • • We do not use the following data for averages, fits, limits, etc. • • •					
~ 1276	1	TORNQVIST 82b	RVUE		
~ 1300		VERGEEST 79	HBC	-	4.2 $K^- p \rightarrow (\bar{K}\pi\pi)^- p$
1289 ± 25	2	CARNEGIE 77	ASPK	±	13 $K^\pm p \rightarrow (K\pi\pi)^\pm p$
~ 1300		BRANDENB... 76	ASPK	±	13 $K^\pm p \rightarrow (K\pi\pi)^\pm p$
~ 1270		OTTER 76	HBC	-	10,14,16 $K^- p \rightarrow (\bar{K}\pi\pi)^- p$
1260		DAVIS 72	HBC	+	12 $K^+ p$
1234 ± 12		FIRESTONE 72b	DBC	+	12 $K^+ d$

¹ From a unitarized quark-model calculation.

² From a model-dependent fit with Gaussian background to BRANDENBURG 76 data.

PRODUCED BY BEAMS OTHER THAN K MESONS

VALUE (MeV)	EVTS	DOCUMENT ID	TECN	CHG	COMMENT	
1294 ± 10	310	RODEBACK 81	HBC		4 $\pi^- p \rightarrow \Lambda K 2\pi$	
1300	40	CRENNELL 72	HBC	0	4.5 $\pi^- p \rightarrow \Lambda K 2\pi$	
1242 ⁺⁹ ₋₁₀		3	ASTIER 69	HBC	0	$\bar{p} p$
1300	45	CRENNELL 67	HBC	0	6 $\pi^- p \rightarrow \Lambda K 2\pi$	

³ This was called the C meson.

See key on page 239

Meson Particle Listings

 $K_1(1270)$, $K_1(1400)$ $K_1(1270)$ WIDTH

VALUE (MeV) DOCUMENT ID
90±20 OUR ESTIMATE This is only an educated guess; the error given is larger than the error on the average of the published values.
87± 7 OUR AVERAGE Includes data from the 2 datablocks that follow this one.

PRODUCED BY K^- , BACKWARD SCATTERING, HYPERON EXCHANGE

VALUE (MeV) EVTS DOCUMENT ID TECN CHG COMMENT
 The data in this block is included in the average printed for a previous datablock.

75±15 700 GAVILLET 78 HBC + 4.2 $K^- p \rightarrow \Xi^- K \pi \pi$

PRODUCED BY K BEAMS

VALUE (MeV) DOCUMENT ID TECN CHG COMMENT
 The data in this block is included in the average printed for a previous datablock.

90± 8 DAUM 81C CNTR - 63 $K^- p \rightarrow K^- 2\pi p$
 • • • We do not use the following data for averages, fits, limits, etc. • • •
 ~150 VERGEEST 79 HBC - 4.2 $K^- p \rightarrow (\bar{K} \pi \pi)^- p$
 150±71 4 CARNEGIE 77 ASPK ± 13 $K^\pm p \rightarrow (K \pi \pi)^\pm p$
 ~200 BRANDENB... 76 ASPK ± 13 $K^\pm p \rightarrow (K \pi \pi)^\pm p$
 120 DAVIS 72 HBC + 12 $K^+ p$
 188±21 FIRESTONE 72B DBC + 12 $K^+ d$

⁴ From a model-dependent fit with Gaussian background to BRANDENBURG 76 data.

PRODUCED BY BEAMS OTHER THAN K MESONS

VALUE (MeV) EVTS DOCUMENT ID TECN CHG COMMENT
 • • • We do not use the following data for averages, fits, limits, etc. • • •

66±15 310 RODEBACK 81 HBC 4 $\pi^- p \rightarrow \Lambda K 2\pi$
 60 40 CRENNELL 72 HBC 0 4.5 $\pi^- p \rightarrow \Lambda K 2\pi$
 127⁺₋₂₅ ASTIER 69 HBC 0 $\bar{p} p$
 60 45 CRENNELL 67 HBC 0 6 $\pi^- p \rightarrow \Lambda K 2\pi$

 $K_1(1270)$ DECAY MODES

Mode	Fraction (Γ_i/Γ)
Γ_1 $K \rho$	(42 ± 6) %
Γ_2 $K_0^*(1430)\pi$	(28 ± 4) %
Γ_3 $K^*(892)\pi$	(16 ± 5) %
Γ_4 $K \omega$	(11.0 ± 2.0) %
Γ_5 $K f_0(1370)$	(3.0 ± 2.0) %

 $K_1(1270)$ PARTIAL WIDTHS

$\Gamma(K \rho)$ Γ_1
 VALUE (MeV) DOCUMENT ID TECN CHG COMMENT
 • • • We do not use the following data for averages, fits, limits, etc. • • •
 57±5 MAZZUCATO 79 HBC + 4.2 $K^- p \rightarrow \Xi^- (K \pi \pi)^+$
 75±6 CARNEGIE 77B ASPK ± 13 $K^\pm p \rightarrow (K \pi \pi)^\pm p$

$\Gamma(K_0^*(1430)\pi)$ Γ_2
 VALUE (MeV) DOCUMENT ID TECN CHG COMMENT
 • • • We do not use the following data for averages, fits, limits, etc. • • •
 26±6 CARNEGIE 77B ASPK ± 13 $K^\pm p \rightarrow (K \pi \pi)^\pm p$

$\Gamma(K^*(892)\pi)$ Γ_3
 VALUE (MeV) DOCUMENT ID TECN CHG COMMENT
 • • • We do not use the following data for averages, fits, limits, etc. • • •
 14±11 MAZZUCATO 79 HBC + 4.2 $K^- p \rightarrow \Xi^- (K \pi \pi)^+$
 2±2 CARNEGIE 77B ASPK ± 13 $K^\pm p \rightarrow (K \pi \pi)^\pm p$

$\Gamma(K \omega)$ Γ_4
 VALUE (MeV) DOCUMENT ID TECN CHG COMMENT
 • • • We do not use the following data for averages, fits, limits, etc. • • •
 4±4 MAZZUCATO 79 HBC + 4.2 $K^- p \rightarrow \Xi^- (K \pi \pi)^+$
 24±3 CARNEGIE 77B ASPK ± 13 $K^\pm p \rightarrow (K \pi \pi)^\pm p$

$\Gamma(K f_0(1370))$ Γ_5
 VALUE (MeV) DOCUMENT ID TECN CHG COMMENT
 • • • We do not use the following data for averages, fits, limits, etc. • • •
 22±5 CARNEGIE 77B ASPK ± 13 $K^\pm p \rightarrow (K \pi \pi)^\pm p$

 $K_1(1270)$ BRANCHING RATIOS

$\Gamma(K \rho)/\Gamma_{\text{total}}$ Γ_1/Γ
 VALUE DOCUMENT ID TECN COMMENT
 0.42±0.06 ⁵ DAUM 81C CNTR 63 $K^- p \rightarrow K^- 2\pi p$
 • • • We do not use the following data for averages, fits, limits, etc. • • •
 dominant RODEBACK 81 HBC 4 $\pi^- p \rightarrow \Lambda K 2\pi$

$\Gamma(K_0^*(1430)\pi)/\Gamma_{\text{total}}$ Γ_2/Γ
 VALUE DOCUMENT ID TECN COMMENT
 0.28±0.04 ⁵ DAUM 81C CNTR 63 $K^- p \rightarrow K^- 2\pi p$

$\Gamma(K^*(892)\pi)/\Gamma_{\text{total}}$ Γ_3/Γ
 VALUE DOCUMENT ID TECN COMMENT
 0.16±0.05 ⁵ DAUM 81C CNTR 63 $K^- p \rightarrow K^- 2\pi p$

$\Gamma(K \omega)/\Gamma_{\text{total}}$ Γ_4/Γ
 VALUE DOCUMENT ID TECN COMMENT
 0.11 ± 0.02 ⁵ DAUM 81C CNTR 63 $K^- p \rightarrow K^- 2\pi p$

$\Gamma(K \omega)/\Gamma(K \rho)$ Γ_4/Γ_1
 VALUE CL% DOCUMENT ID TECN COMMENT
 • • • We do not use the following data for averages, fits, limits, etc. • • •
 <0.30 95 RODEBACK 81 HBC 4 $\pi^- p \rightarrow \Lambda K 2\pi$

$\Gamma(K f_0(1370))/\Gamma_{\text{total}}$ Γ_5/Γ
 VALUE DOCUMENT ID TECN COMMENT
 0.03 ± 0.02 ⁵ DAUM 81C CNTR 63 $K^- p \rightarrow K^- 2\pi p$

D-wave/S-wave RATIO FOR $K_1(1270) \rightarrow K^*(892)\pi$

VALUE DOCUMENT ID TECN COMMENT
 1.0±0.7 ⁵ DAUM 81C CNTR 63 $K^- p \rightarrow K^- 2\pi p$
⁵ Average from low and high t data.

 $K_1(1270)$ REFERENCES

TORNQVIST 82B NP B203 268	N.A. Tornqvist	(HELS)
DAUM 81C NP B187 1	C. Daum et al.	(AMST, CERN, CRAC, MPIM+)
RODEBACK 81 ZPHY C9 9	S. Rodeback et al.	(CERN, CDEF, MADR+)
MAZZUCATO 79 NP B156 532	M. Mazzucato et al.	(CERN, ZEEM, NIJM+)
VERGEEST 79 NP B158 265	J.S.M. Vergeest et al.	(NIJM, AMST, CERN+)
GAVILLET 78 PL 76B 517	P. Gavillet et al.	(AMST, CERN, NIJM+)
CARNEGIE 77 NP B127 509	R.K. Carnegie et al.	(SLAC)
CARNEGIE 77B PL 68B 287	R.K. Carnegie et al.	(SLAC)
BRANDENB... 76 PRL 26 703	G.W. Brandenburg et al.	(SLAC) JP
OTTER 76 NP B106 77	G. Otter et al.	(AACH3, BERL, CERN, LOIC+)
CRENNELL 72 PR D6 1220	D.J. Crennell et al.	(BNL)
DAVIS 72 PR D5 2688	P.J. Davis et al.	(BNL)
FIRESTONE 72B PR D5 505	A. Firestone et al.	(BNL)
ASTIER 69 NP B10 65	A. Astier et al.	(CDEF, CERN, IPNP, LIVP) JP
CRENNELL 67 PRL 19 44	D.J. Crennell et al.	(BNL)1

OTHER RELATED PAPERS

SUZUKI 93 PR D47 1252	M. Suzuki	(LBL)
BAUBILLIER 82B NP B202 21	M. Baubillier et al.	(BIRM, CERN, GLAS+)
FERNANDEZ 82 ZPHY C16 95	C. Fernandez et al.	(MADR, CERN, CDEF+)
GAVILLET 82 ZPHY C16 119	P. Gavillet et al.	(CERN, CDEF, PADO+)
SHEN 66 PRL 17 726	B.C. Shen et al.	(LRL)
Also 66 Private Comm.	G. Goldhaber	(LRL)
ALMEIDA 65 PL 16 184	S.P. Almeida et al.	(CAVE)
ARMENTEROS 64 PL 9 207	R. Armenteros et al.	(CERN, CDEF)
Also 66 PR 145 1095	N. Barash et al.	(COLU)

 $K_1(1400)$

$$J(P) = \frac{1}{2}(1^+)$$

 $K_1(1400)$ MASS

VALUE (MeV) DOCUMENT ID TECN CHG COMMENT
1402± 7 OUR AVERAGE
 1373±14±18 ¹ ASTON 87 LASS 0 11 $K^- p \rightarrow \bar{K}^0 \pi^+ \pi^- n$
 1392±18 BAUBILLIER 82B HBC 0 8.25 $K^- p \rightarrow K_0^0 \pi^+ \pi^- n$
 1410±25 DAUM 81C CNTR - 63 $K^- p \rightarrow K^- 2\pi p$
 1415±15 ETKIN 80 MPS 0 6 $K^- p \rightarrow \bar{K}^0 \pi^+ \pi^- n$
 1404±10 ² CARNEGIE 77 ASPK ± 13 $K^\pm p \rightarrow (K \pi \pi)^\pm p$
 • • • We do not use the following data for averages, fits, limits, etc. • • •
 ~1350 ³ TORNQVIST 82B RVUE
 ~1400 VERGEEST 79 HBC - 4.2 $K^- p \rightarrow (\bar{K} \pi \pi)^- p$
 ~1400 BRANDENB... 76 ASPK ± 13 $K^\pm p \rightarrow (K \pi \pi)^\pm p$
 1420 DAVIS 72 HBC + 12 $K^+ p$
 1368±18 FIRESTONE 72B DBC + 12 $K^+ d$

¹ From partial-wave analysis of $K^0 \pi^+ \pi^-$ system.
² From a model-dependent fit with Gaussian background to BRANDENBURG 76 data.
³ From a unitarized quark-model calculation.

 $K_1(1400)$ WIDTH

VALUE (MeV) DOCUMENT ID TECN CHG COMMENT
174±13 OUR AVERAGE Error includes scale factor of 1.6. See the Ideogram below.
 188±54±60 ⁴ ASTON 87 LASS 0 11 $K^- p \rightarrow \bar{K}^0 \pi^+ \pi^- n$
 276±65 BAUBILLIER 82B HBC 0 8.25 $K^- p \rightarrow K_0^0 \pi^+ \pi^- n$
 195±25 DAUM 81C CNTR - 63 $K^- p \rightarrow K^- 2\pi p$
 180±10 ETKIN 80 MPS 0 6 $K^- p \rightarrow \bar{K}^0 \pi^+ \pi^- n$
 142±16 ⁵ CARNEGIE 77 ASPK ± 13 $K^\pm p \rightarrow (K \pi \pi)^\pm p$

Meson Particle Listings

$K_1(1400)$, $K^*(1410)$

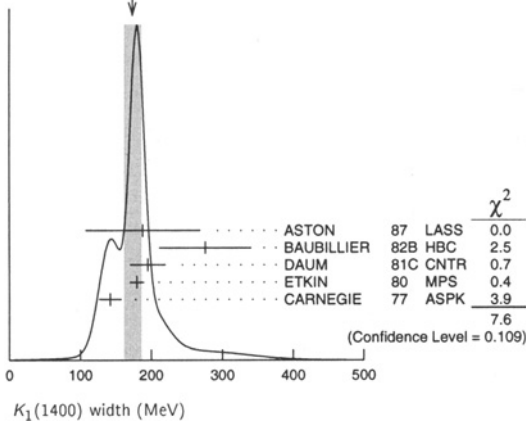
• • • We do not use the following data for averages, fits, limits, etc. • • •

~ 200	VERGEEST	79	HBC	-	$4.2 K^- p \rightarrow (\bar{K}^0 \pi^+) \pi^-$
~ 160	BRANDENB...	76	ASPK	±	$13 K^\pm p \rightarrow (K \pi \pi)^\pm p$
80	DAVIS	72	HBC	+	$12 K^+ p$
241 ± 30	FIRESTONE	72b	DBC	+	$12 K^+ d$

⁴ From partial-wave analysis of $K^0 \pi^+ \pi^-$ system.

⁵ From a model-dependent fit with Gaussian background to BRANDENBURG 76 data.

WEIGHTED AVERAGE
174 ± 13 (Error scaled by 1.6)



$K_1(1400)$ DECAY MODES

Mode	Fraction (Γ_i/Γ)
Γ_1 $K^*(892)\pi$	(94 ± 6) %
Γ_2 $K\rho$	(3.0 ± 3.0) %
Γ_3 $K f_0(1370)$	(2.0 ± 2.0) %
Γ_4 $K\omega$	(1.0 ± 1.0) %
Γ_5 $K_0^*(1430)\pi$	not seen

$K_1(1400)$ PARTIAL WIDTHS

Mode	Fraction (Γ_i/Γ)	Confidence level
Γ_1 $K^*(892)\pi$	> 40 %	95%
Γ_2 $K\pi$	(6.6 ± 1.3) %	
Γ_3 $K\rho$	< 7 %	95%

$K_1(1400)$ BRANCHING RATIOS

Mode	Fraction (Γ_i/Γ)	Confidence level
Γ_1 $K^*(892)\pi$	> 40 %	95%
Γ_2 $K\pi$	(6.6 ± 1.3) %	
Γ_3 $K\rho$	< 7 %	95%

D-wave/S-wave RATIO FOR $K_1(1400) \rightarrow K^*(892)\pi$

Mode	Fraction (Γ_i/Γ)	Confidence level
Γ_1 $K^*(892)\pi$	> 40 %	95%
Γ_2 $K\pi$	(6.6 ± 1.3) %	
Γ_3 $K\rho$	< 7 %	95%

⁶ Average from low and high t data.

$K_1(1400)$ REFERENCES

ASTON 87	NP B292 693	D. Aston et al.	(SLAC, NAGO, CINC, INUS)
BAUBILLIER 82b	NP B202 21	M. Baubillier et al.	(BIRM, CERN, GLAS+)
TORNQVIST 82b	NP B203 268	N.A. Tornqvist	(HELS)
DAUM 81c	NP B187 1	C. Daum et al.	(AMST, CERN, CRAC, MPI4+)
ETKIN 80	PR D22 42	A. Etkin et al.	(BNL, CUNY)JP
VERGEEST 79	NP B158 265	J.S.M. Vergeest et al.	(NIJM, AMST, CERN+)
CARNEGIE 77	NP B127 509	R.K. Carnegie et al.	(SLAC)
BRANDENB... 76	PRL 26 703	G.W. Brandenburg et al.	(SLAC)JP
DAVIS 72	PR D5 2688	P.J. Davis et al.	(LBL)
FIRESTONE 72b	PR D5 505	A. Firestone et al.	(LBL)

OTHER RELATED PAPERS

SUZUKI 93	PR D47 1252	M. Suzuki	(LBL)
FERNANDEZ 82	ZPHY C16 95	C. Fernandez et al.	(MADR, CERN, CDEF+)
SHEN 66	PRL 17 726	B.C. Shen et al.	(LRL)
Also 66	Private Comm.	G. Goldhaber	(LRL)
ALMEIDA 65	PL 16 184	S.P. Almeida et al.	(CAVE)
ARMENTEROS 64	PL 9 207	R. Armenteros et al.	(CERN, CDEF)
Also 66	PR 145 1095	N. Barash et al.	(COLU)

$K^*(1410)$

$$I(J^P) = \frac{1}{2}(1^-)$$

$K^*(1410)$ MASS

VALUE (MeV)	DOCUMENT ID	TECN	CHG	COMMENT
1414 ± 15 OUR AVERAGE	Error includes scale factor of 1.3.			
1380 ± 21 ± 19	ASTON 88	LASS	0	11 $K^- p \rightarrow K^- \pi^+ n$
1420 ± 7 ± 10	ASTON 87	LASS	0	11 $K^- p \rightarrow \bar{K}^0 \pi^+ \pi^- n$
• • • We do not use the following data for averages, fits, limits, etc. • • •				
1367 ± 54	BIRD 89	LASS	-	11 $K^- p \rightarrow \bar{K}^0 \pi^- p$
1474 ± 25	BAUBILLIER 82b	HBC	0	8.25 $K^- p \rightarrow \bar{K}^0 2\pi n$
1500 ± 30	ETKIN 80	MPS	0	6 $K^- p \rightarrow \bar{K}^0 \pi^+ \pi^- n$

$K^*(1410)$ WIDTH

VALUE (MeV)	DOCUMENT ID	TECN	CHG	COMMENT
232 ± 21 OUR AVERAGE	Error includes scale factor of 1.1.			
176 ± 52 ± 22	ASTON 88	LASS	0	11 $K^- p \rightarrow K^- \pi^+ n$
240 ± 18 ± 12	ASTON 87	LASS	0	11 $K^- p \rightarrow \bar{K}^0 \pi^+ \pi^- n$
• • • We do not use the following data for averages, fits, limits, etc. • • •				
114 ± 101	BIRD 89	LASS	-	11 $K^- p \rightarrow \bar{K}^0 \pi^- p$
275 ± 65	BAUBILLIER 82b	HBC	0	8.25 $K^- p \rightarrow \bar{K}^0 2\pi n$
500 ± 100	ETKIN 80	MPS	0	6 $K^- p \rightarrow \bar{K}^0 \pi^+ \pi^- n$

$K^*(1410)$ DECAY MODES

Mode	Fraction (Γ_i/Γ)	Confidence level
Γ_1 $K^*(892)\pi$	> 40 %	95%
Γ_2 $K\pi$	(6.6 ± 1.3) %	
Γ_3 $K\rho$	< 7 %	95%

$K^*(1410)$ BRANCHING RATIOS

Mode	Fraction (Γ_i/Γ)	Confidence level
Γ_1 $K^*(892)\pi$	> 40 %	95%
Γ_2 $K\pi$	(6.6 ± 1.3) %	
Γ_3 $K\rho$	< 7 %	95%

$K^*(1410)$ REFERENCES

BIRD 89	SLAC-332	P.F. Bird	(SLAC)
ASTON 88	NP B296 493	D. Aston et al.	(SLAC, NAGO, CINC, INUS)
ASTON 87	NP B292 693	D. Aston et al.	(SLAC, NAGO, CINC, INUS)
ASTON 84	PL 149B 258	D. Aston et al.	(SLAC, CARL, OTTA)JP
BAUBILLIER 82b	NP B202 21	M. Baubillier et al.	(BIRM, CERN, GLAS+)
ETKIN 80	PR D22 42	A. Etkin et al.	(BNL, CUNY)JP

See key on page 239

Meson Particle Listings

 $K_0^*(1430), K_2^*(1430)$ $K_0^*(1430)$

$$I(J^P) = \frac{1}{2}(0^+)$$

See our minireview in the 1994 edition and in this edition under the $f_0(1370)$. $K_0^*(1430)$ MASS

VALUE (MeV)	DOCUMENT ID	TECN	CHG	COMMENT
1412 ± 6	¹ ASTON	88	LASS	0 11 $K^-p \rightarrow K^- \pi^+ n$
• • • We do not use the following data for averages, fits, limits, etc. • • •				
1436 ± 8	² BARBERIS	98E	OMEG	450 $pp \rightarrow p_f p_s K^+ K^- \pi^+ \pi^-$
1415 ± 25	³ ANISOVICH	97C	RVUE	11 $K^-p \rightarrow K^- \pi^+ n$
~ 1450	⁴ TORNQVIST	96	RVUE	$\pi\pi \rightarrow \pi\pi, K\bar{K}, K\pi$
~ 1430	BAUBILLIER	84B	HBC	- 8.25 $K^-p \rightarrow \bar{K}^0 \pi^- p$
~ 1425	^{5,6} ESTABROOKS	78	ASPK	13 $K^\pm p \rightarrow K^\pm \pi^\pm (n, \Delta)$
~ 1450.0	MARTIN	78	SPEC	10 $K^\pm p \rightarrow K_S^0 \pi p$

¹ Uses a model for the background, without this background they get a mass 1340 MeV, where the phase shift passes 90°.² J^P not determined, could be $K_2^*(1430)$.³ T-matrix pole. Reanalysis of ASTON 88 data.⁴ T-matrix pole.⁵ Mass defined by pole position.⁶ From elastic $K\pi$ partial-wave analysis. $K_0^*(1430)$ WIDTH

VALUE (MeV)	DOCUMENT ID	TECN	CHG	COMMENT
294 ± 23	ASTON	88	LASS	0 11 $K^-p \rightarrow K^- \pi^+ n$
• • • We do not use the following data for averages, fits, limits, etc. • • •				
196 ± 45	⁷ BARBERIS	98E	OMEG	450 $pp \rightarrow p_f p_s K^+ K^- \pi^+ \pi^-$
330 ± 50	⁸ ANISOVICH	97C	RVUE	11 $K^-p \rightarrow K^- \pi^+ n$
~ 320	⁹ TORNQVIST	96	RVUE	$\pi\pi \rightarrow \pi\pi, K\bar{K}, K\pi$
~ 200	BAUBILLIER	84B	HBC	- 8.25 $K^-p \rightarrow \bar{K}^0 \pi^- p$
200 to 300	¹⁰ ESTABROOKS	78	ASPK	13 $K^\pm p \rightarrow K^\pm \pi^\pm (n, \Delta)$

⁷ J^P not determined, could be $K_2^*(1430)$.⁸ T-matrix pole. Reanalysis of ASTON 88 data.⁹ T-matrix pole.¹⁰ From elastic $K\pi$ partial-wave analysis. $K_0^*(1430)$ DECAY MODES

Mode	Fraction (Γ_i/Γ)
Γ_1 $K\pi$	(93±10) %

 $K_0^*(1430)$ BRANCHING RATIOS

$\Gamma(K\pi)/\Gamma_{total}$	DOCUMENT ID	TECN	CHG	COMMENT	Γ_1/Γ
$0.93 \pm 0.04 \pm 0.09$	ASTON	88	LASS	0 11 $K^-p \rightarrow K^- \pi^+ n$	

 $K_0^*(1430)$ REFERENCES

BARBERIS	98E	PL B436 204	D. Barberis et al.	(Omega expt.)
ANISOVICH	97C	PL B413 137	D. Aston et al.	(HEL5)
TORNQVIST	96	PRL 76 1575	N.A. Tornqvist, M. Roos	(SLAC, NAGO, CINC, INUS)
ASTON	88	NP B296 493	D. Aston et al.	(BIRM, CERN, GLAS+)
BAUBILLIER	84B	ZPHY C26 37	M. Baubillier et al.	(MCGI, CARL, DURH+)
ESTABROOKS	78	NP B133 490	P.G. Estabrooks et al.	(MCGI, CARL, DURH+)
MARTIN	78	NP B134 392	A.D. Martin et al.	(DURH, GEVA)

OTHER RELATED PAPERS

BEVEREN	99	EPJ C10 469	E. Van Beveren, G. Rupp	(SABRE Collab.)
OLLER	99	PR D60 099906	J.A. Oller et al.	(UCLA)
OLLER	99C	PR D60 074023	J.A. Oller, E. Oset	(HEL5)
TORNQVIST	82	PRL 49 624	N.A. Tornqvist	(HEL5)
GOLDBERG	69	PL 30B 434	J. Goldberg et al.	(SABRE Collab.)
TRIPPE	68	PL 28B 203	T.G. Trippe et al.	(UCLA)

 $K_2^*(1430)$

$$I(J^P) = \frac{1}{2}(2^+)$$

We consider that phase-shift analyses provide more reliable determinations of the mass and width.

 $K_2^*(1430)$ MASSCHARGED ONLY, WITH FINAL STATE $K\pi$

VALUE (MeV)	EVTS	DOCUMENT ID	TECN	CHG	COMMENT
1425.6 ± 1.5	OUR AVERAGE	Error includes scale factor of 1.1.			
1420 ± 4	1587	BAUBILLIER	84B	HBC	- 8.25 $K^-p \rightarrow \bar{K}^0 \pi^- p$
1436 ± 5.5	400	^{1,2} CLELAND	82	SPEC	+ 30 $K^+p \rightarrow K_S^0 \pi^+ p$
1430 ± 3.2	1500	^{1,2} CLELAND	82	SPEC	+ 50 $K^+p \rightarrow K_S^0 \pi^+ p$
1430 ± 3.2	1200	^{1,2} CLELAND	82	SPEC	- 50 $K^+p \rightarrow K_S^0 \pi^- p$
1423 ± 5	935	TOAFF	81	HBC	- 6.5 $K^-p \rightarrow \bar{K}^0 \pi^- p$
1428.0 ± 4.6		³ MARTIN	78	SPEC	+ 10 $K^\pm p \rightarrow K_S^0 \pi p$
1423.8 ± 4.6		³ MARTIN	78	SPEC	- 10 $K^\pm p \rightarrow K_S^0 \pi p$
1420.0 ± 3.1	1400	AGUILAR...	71B	HBC	- 3.9, 4.6 K^-p
1425 ± 8.0	225	^{1,2} BARNHAM	71C	HBC	+ $K^+p \rightarrow K^0 \pi^+ p$
1416 ± 10	220	CRENNELL	69D	DBC	- 3.9 $K^-p \rightarrow \bar{K}^0 \pi^- p$
1414 ± 13.0	60	¹ LIND	69	HBC	+ 9 $K^+p \rightarrow K^0 \pi^+ p$
1427 ± 12	63	¹ SCHWEING...	68	HBC	- 5.5 $K^-p \rightarrow \bar{K}^0 \pi^- p$
1423 ± 11.0	39	¹ BASSANO	67	HBC	- 4.6-5.0 $K^-p \rightarrow \bar{K}^0 \pi^- p$

• • • We do not use the following data for averages, fits, limits, etc. • • •

 $1423.4 \pm 2 \pm 3$ 24809± 820 ⁴ BIRD 89 LASS - 11 $K^-p \rightarrow \bar{K}^0 \pi^- p$

NEUTRAL ONLY

VALUE (MeV)	EVTS	DOCUMENT ID	TECN	CHG	COMMENT
1432.4 ± 1.3	OUR AVERAGE	Error includes scale factor of 1.1.			
$1431.2 \pm 1.8 \pm 0.7$		⁵ ASTON	88	LASS	0 11 $K^-p \rightarrow K^- \pi^+ n$
$1434 \pm 4 \pm 6$		⁵ ASTON	87	LASS	0 11 $K^-p \rightarrow \bar{K}^0 \pi^+ \pi^- n$
$1433 \pm 6 \pm 10$		⁵ ASTON	84B	LASS	0 11 $K^-p \rightarrow \bar{K}^0 2\pi n$
1471 ± 12		⁵ BAUBILLIER	82B	HBC	0 8.25 $K^-p \rightarrow \bar{K}^0 \pi^- p$
1428 ± 3		⁵ ASTON	81C	LASS	0 11 $K^-p \rightarrow K^- \pi^+ n$
1434 ± 2		⁵ ESTABROOKS	78	ASPK	0 13 $K^\pm p \rightarrow p K\pi$
1440 ± 10		⁵ BOWLER	77	DBC	0 5.5 $K^+d \rightarrow K\pi pp$
• • • We do not use the following data for averages, fits, limits, etc. • • •					
1420 ± 7	300	HENDRICK	76	DBC	8.25 $K^+n \rightarrow K^+ \pi n$
1421.6 ± 4.2	800	MCCUBBIN	75	HBC	0 3.6 $K^-p \rightarrow K^- \pi^+ n$
1420.1 ± 4.2		⁶ LINGLIN	73	HBC	0 2-13 $K^+p \rightarrow K^+ \pi^- X$
1419.1 ± 3.7	1800	AGUILAR...	71B	HBC	0 3.9, 4.6 K^-p
1416 ± 6	600	CORDS	71	DBC	0 9 $K^+n \rightarrow K^+ \pi^- p$
1421.1 ± 2.6	2200	DAVIS	69	HBC	0 12 $K^+p \rightarrow K^+ \pi^- X$

¹ Errors enlarged by us to Γ/\sqrt{N} ; see the note with the $K^*(892)$ mass.² Number of events in peak re-evaluated by us.³ Systematic error added by us.⁴ From a partial wave amplitude analysis.⁵ From phase shift or partial-wave analysis.⁶ From pole extrapolation, using world K^+p data summary tape. $K_2^*(1430)$ WIDTHCHARGED ONLY, WITH FINAL STATE $K\pi$

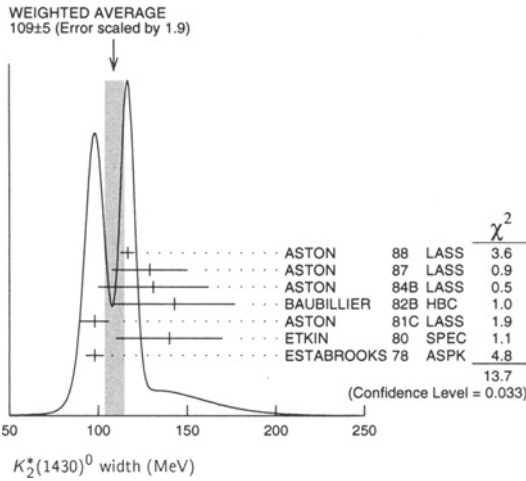
VALUE (MeV)	EVTS	DOCUMENT ID	TECN	CHG	COMMENT
98.5 ± 2.7	OUR FIT	Error includes scale factor of 1.1.			
98.5 ± 2.9	OUR AVERAGE	Error includes scale factor of 1.1.			
109 ± 22	400	^{7,8} CLELAND	82	SPEC	+ 30 $K^+p \rightarrow K_S^0 \pi^+ p$
124 ± 12.8	1500	^{7,8} CLELAND	82	SPEC	+ 50 $K^+p \rightarrow K_S^0 \pi^+ p$
113 ± 12.8	1200	^{7,8} CLELAND	82	SPEC	- 50 $K^+p \rightarrow K_S^0 \pi^- p$
85 ± 16	935	TOAFF	81	HBC	- 6.5 $K^-p \rightarrow \bar{K}^0 \pi^- p$
96.5 ± 3.8		MARTIN	78	SPEC	+ 10 $K^\pm p \rightarrow K_S^0 \pi p$
97.7 ± 4.0		MARTIN	78	SPEC	- 10 $K^\pm p \rightarrow K_S^0 \pi p$
94.7 ± 15.1 -12.5	1400	AGUILAR...	71B	HBC	- 3.9, 4.6 K^-p
• • • We do not use the following data for averages, fits, limits, etc. • • •					
$98 \pm 4 \pm 4$	24809± 820	⁹ BIRD	89	LASS	- 11 $K^-p \rightarrow \bar{K}^0 \pi^- p$

Meson Particle Listings

$K_2^*(1430)$

NEUTRAL ONLY

VALUE (MeV)	EVTS	DOCUMENT ID	TECN	CHG	COMMENT
109 ± 5 OUR AVERAGE		Error includes scale factor of 1.9. See the ideogram below.			
116.5 ± 3.6 ± 1.7	10	ASTON 88	LASS	0	$11 K^- p \rightarrow K^- \pi^+ n$
129 ± 15 ± 15	10	ASTON 87	LASS	0	$11 K^- p \rightarrow \bar{K}^0 \pi^+ \pi^- n$
131 ± 24 ± 20	10	ASTON 84B	LASS	0	$11 K^- p \rightarrow \bar{K}^0 2\pi n$
143 ± 34	10	BAUBILLIER 82B	HBC	0	$8.25 K^- p \rightarrow NK_S^0 \pi \pi$
98 ± 8	10	ASTON 81C	LASS	0	$11 K^- p \rightarrow K^- \pi^+ n$
140 ± 30	10	ETKIN 80	SPEC	0	$6 K^- p \rightarrow \bar{K}^0 \pi^+ \pi^- n$
98 ± 5	10	ESTABROOKS 78	ASPK	0	$13 K^\pm p \rightarrow pK\pi$
• • • We do not use the following data for averages, fits, limits, etc. • • •					
125 ± 29	300	HENDRICK 76	DBC		$8.25 K^+ N \rightarrow K^+ \pi N$
116 ± 18	800	MCCUBBIN 75	HBC	0	$3.6 K^- p \rightarrow K^- \pi^+ n$
61 ± 14	11	LINGLIN 73	HBC	0	$2-13 K^+ p \rightarrow K^+ \pi^- X$
116.6 ^{+10.3} _{-15.5}	1800	AGUILAR... 71B	HBC	0	$3.9, 4.6 K^- p$
144 ± 24.0	600	CORDS 71	DBC	0	$9 K^+ n \rightarrow K^+ \pi^- p$
101 ± 10	2200	DAVIS 69	HBC	0	$12 K^+ p \rightarrow K^+ \pi^- \pi^+ p$



⁷ Errors enlarged by us to $4\Gamma/\sqrt{N}$; see the note with the $K^*(892)$ mass.
⁸ Number of events in peak re-evaluated by us.
⁹ From a partial wave amplitude analysis.
¹⁰ From phase shift or partial-wave analysis.
¹¹ From pole extrapolation, using world $K^+ p$ data summary tape.

$K_2^*(1430)$ DECAY MODES

Mode	Fraction (Γ_i/Γ)	Scale factor/ Confidence level
$\Gamma_1 K\pi$	(49.9 ± 1.2) %	
$\Gamma_2 K^*(892)\pi$	(24.7 ± 1.5) %	
$\Gamma_3 K^*(892)\pi\pi$	(13.4 ± 2.2) %	
$\Gamma_4 K\rho$	(8.7 ± 0.8) %	S=1.2
$\Gamma_5 K\omega$	(2.9 ± 0.8) %	
$\Gamma_6 K^+\gamma$	(2.4 ± 0.5) × 10 ⁻³	S=1.1
$\Gamma_7 K\eta$	(1.5 ^{+3.4} _{-1.0}) × 10 ⁻³	S=1.3
$\Gamma_8 K\omega\pi$	< 7.2 × 10 ⁻⁴	CL=95%
$\Gamma_9 K^0\gamma$	< 9 × 10 ⁻⁴	CL=90%

CONSTRAINED FIT INFORMATION

An overall fit to the total width, a partial width, and 10 branching ratios uses 31 measurements and one constraint to determine 8 parameters. The overall fit has a $\chi^2 = 20.2$ for 24 degrees of freedom.

The following off-diagonal array elements are the correlation coefficients $\langle \delta p_i \delta p_j \rangle / (\delta p_i \delta p_j)$, in percent, from the fit to parameters p_i , including the branching fractions, $x_i \equiv \Gamma_i/\Gamma_{\text{total}}$. The fit constrains the x_i whose labels appear in this array to sum to one.

x_2	-9						
x_3	-40	-73					
x_4	-8	36	-52				
x_5	-11	-3	-26	-7			
x_6	-1	-1	-1	-1	0		
x_7	-4	-7	-5	-5	-2	0	
Γ	0	0	0	0	0	-13	0
	x_1	x_2	x_3	x_4	x_5	x_6	x_7

Mode	Rate (MeV)	Scale factor
$\Gamma_1 K\pi$	49.1 ± 1.8	
$\Gamma_2 K^*(892)\pi$	24.3 ± 1.6	
$\Gamma_3 K^*(892)\pi\pi$	13.2 ± 2.2	
$\Gamma_4 K\rho$	8.5 ± 0.8	1.2
$\Gamma_5 K\omega$	2.9 ± 0.8	
$\Gamma_6 K^+\gamma$	0.24 ± 0.05	1.1
$\Gamma_7 K\eta$	0.15 ^{+0.33} _{-0.10}	1.3

$K_2^*(1430)$ PARTIAL WIDTHS

MODE	VALUE (keV)	DOCUMENT ID	TECN	CHG	COMMENT
$\Gamma(K^+\gamma)$	241 ± 50 OUR FIT	Error includes scale factor of 1.1.			
	240 ± 45	CIHANGIR 82	SPEC	+	$200 K^+ Z \rightarrow ZK^+\pi^0, ZK_S^0\pi^+$
$\Gamma(K^0\gamma)$	< 84	CARLSMITH 87	SPEC	0	$60-200 K_L^0 A \rightarrow K_S^0\pi^0 A$

$K_2^*(1430)$ BRANCHING RATIOS

MODE	VALUE	DOCUMENT ID	TECN	CHG	COMMENT
$\Gamma(K\pi)/\Gamma_{\text{total}}$	0.499 ± 0.012 OUR FIT				
	0.488 ± 0.014 OUR AVERAGE				
	0.485 ± 0.006 ± 0.020	12 ASTON 88	LASS	0	$11 K^- p \rightarrow K^- \pi^+ n$
	0.49 ± 0.02	12 ESTABROOKS 78	ASPK	±	$13 K^\pm p \rightarrow pK\pi$
$\Gamma(K^*(892)\pi)/\Gamma(K\pi)$	0.496 ± 0.034 OUR FIT				
	0.47 ± 0.04 OUR AVERAGE				
	0.44 ± 0.09	ASTON 84B	LASS	0	$11 K^- p \rightarrow \bar{K}^0 2\pi n$
	0.62 ± 0.19	LAUSCHER 75	HBC	0	$10, 16 K^- p \rightarrow K^- \pi^+ n$
	0.54 ± 0.16	DEHM 74	DBC	0	$4.6 K^+ N$
	0.47 ± 0.08	AGUILAR... 71B	HBC		$3.9, 4.6 K^- p$
	0.47 ± 0.10	BASSANO 67	HBC	-0	$4.6, 5.0 K^- p$
	0.45 ± 0.13	BADIER 65c	HBC	-	$3 K^- p$
$\Gamma(K\omega)/\Gamma(K\pi)$	0.059 ± 0.017 OUR FIT				
	0.070 ± 0.035 OUR AVERAGE				
	0.05 ± 0.04	AGUILAR... 71B	HBC		$3.9, 4.6 K^- p$
	0.13 ± 0.07	BASSOMPIE... 69	HBC	0	$5 K^+ p$
$\Gamma(K\rho)/\Gamma(K\pi)$	0.174 ± 0.017 OUR FIT	Error includes scale factor of 1.2.			
	0.150^{+0.029}_{-0.017} OUR AVERAGE				
	0.18 ± 0.05	ASTON 84B	LASS	0	$11 K^- p \rightarrow \bar{K}^0 2\pi n$
	0.02 ^{+0.10} _{-0.02}	DEHM 74	DBC	0	$4.6 K^+ N$
	0.16 ± 0.05	AGUILAR... 71B	HBC		$3.9, 4.6 K^- p$
	0.14 ± 0.10	BASSANO 67	HBC	-0	$4.6, 5.0 K^- p$
	0.14 ± 0.07	BADIER 65c	HBC	-	$3 K^- p$

See key on page 239

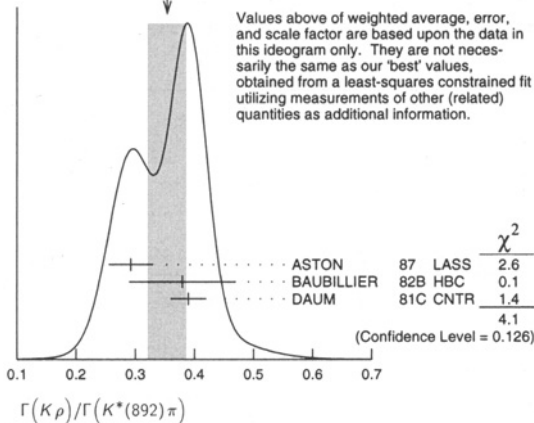
Meson Particle Listings

$K_2^*(1430)$, $K(1460)$

$\Gamma(K\rho)/\Gamma(K^*(892)\pi)$ Γ_4/Γ_2

VALUE	DOCUMENT ID	TECN	CHG	COMMENT
0.354 ± 0.031 OUR FIT	Error includes scale factor of 1.4.			
0.354 ± 0.033 OUR AVERAGE	Error includes scale factor of 1.4. See the ideogram below.			
0.293 ± 0.032 ± 0.020	ASTON	87	LASS	0 11 $K^-p \rightarrow \bar{K}^0 \pi^+ \pi^- n$
0.38 ± 0.09	BAUBILLIER	82b	HBC	0 8.25 $K^-p \rightarrow NK_S^0 \pi \pi$
0.39 ± 0.03	DAUM	81c	CNTR	63 $K^-p \rightarrow K^- 2\pi p$

WEIGHTED AVERAGE
0.354 ± 0.033 (Error scaled by 1.4)



$K_2^*(1430)$ REFERENCES

BIRD	89	SLAC-332	P.F. Bird	(SLAC)
ASTON	88	NP B296 493	D. Aston et al.	(SLAC, NAGO, CINC, INUS)
ASTON	88B	PL B201 169	D. Aston et al.	(SLAC, NAGO, CINC, INUS)
ASTON	87	NP B292 693	D. Aston et al.	(SLAC, NAGO, CINC, INUS)
CARLSMITH	87	PR D36 3502	D. Carlsmith et al.	(EFL, SAFL)
ASTON	84B	NP B247 261	D. Aston et al.	(SLAC, CARL, OTTA)
BAUBILLIER	84B	ZPHY C26 37	M. Baubillier et al.	(BIRM, CERN, GLAS+)
BAUBILLIER	82B	NP B202 21	M. Baubillier et al.	(BIRM, CERN, GLAS+)
CIHANGIR	82	PL 117B 123	S. Cihangir et al.	(FNAL, MINN, ROCH)
CLELAND	82	NP B208 189	W.E. Cleland et al.	(DURH, GEVA, LAUS+)
ASTON	81C	PL 106B 235	D. Aston et al.	(SLAC, CARL, OTTA) JP
DAUM	81C	NP B187 1	C. Daum et al.	(AMST, CERN, CRAC, MFIM+)
TOAFF	81	PR D23 1500	S. Toaff et al.	(ANL, KANS)
ETKIN	80	PR D22 42	A. Etkin et al.	(BNL, CUNY) JP
ESTABROOKS	78	NP B133 490	P.G. Estabrooks et al.	(MCGI, CARL, DURH+)
Also	78B	PR D17 658	P.G. Estabrooks et al.	(MCGI, CARL, DURH+)
JONGEJANS	78	NP B139 383	B. Jongejans et al.	(ZEEM, CERN, NIJUM+)
MARTIN	78	NP B134 392	A.D. Martin et al.	(DURH, GEVA)
BOWLER	77	NP B126 31	M.G. Bowler et al.	(OXF)
GOLDBERG	76	LNC 17 253	J. Goldberg	(HAIF)
HENDRICK	76	NP B112 189	K. Hendrickx et al.	(MONS, SAFL, PARIS+)
LAUSCHER	75	NP B86 189	P. Lauscher et al.	(ABCLV Collab.) JP
MCCUBBIN	75	NP B86 13	N.A. McCubbin, L. Lyons	(OXF)
DEHM	74	NP B75 47	G. Dehm et al.	(MPIM, BRUX, MONS, CERN)
LINGLIN	73	NP B55 408	D. Linglin	(CERN)
AGUILAR...	71B	PR D4 2583	M. Aguilar-Benitez, R.L. Eisner, J.B. Kinson	(BNL)
BARNHAM	71C	NP B28 171	K.W.J. Barnham et al.	(BIRM, GLAS)
CORDS	71	PR D4 1974	D. Cords et al.	(PURD, UCD, IUPU)
BASSOMPIE...	69	NP B13 189	G. Bassompierre et al.	(CERN, BRUX) JP
BISHOP	69	NP B9 403	J.M. Bishop et al.	(WISC)
CRENNELL	69D	PRL 22 487	D.J. Crennell et al.	(BNL)
DAVIS	69	PRL 23 1371	P.J. Davis et al.	(LRL)
LIND	69	NP B14 1	V.G. Lind et al.	(LRL) JP
SCHWEINGRUBER	68	PR 166 1317	F. Schweingruber et al.	(ANL, NWES)
Also	67	Thesis	F.L. Schweingruber	(NWES, NWES)
BASSANO	67	PRL 19 968	D. Bassano et al.	(BNL, SYRA)
FIELD	67	PL 24B 638	J.H. Field et al.	(UCSD)
BADIER	65C	PL 19 612	J. Badier et al.	(EPOL, SAFL, AMST)

OTHER RELATED PAPERS

BARBERIS	98E	PL B436 204	D. Barberis et al.	(Omega expt.)
ATKINSON	86	ZPHY C30 521	M. Atkinson et al.	(BONN, CERN, GLAS+)
BAUBILLIER	82B	NP B202 21	M. Baubillier et al.	(BIRM, CERN, GLAS+)
CHUNG	65	PRL 15 325	S.U. Chung et al.	(LRL)
FOCARDI	65	PL 16 351	S. Focardi et al.	(BGNA, SAFL)
HAGUE	65	PL 14 338	N. Hague et al.	(LRL)
HARDY	65	PRL 14 401	L.M. Hardy et al.	(LRL)

$K(1460)$

$I(J^P) = \frac{1}{2}(0^-)$

OMITTED FROM SUMMARY TABLE
Observed in $K\pi\pi$ partial-wave analysis.

$K(1460)$ MASS

VALUE (MeV)	DOCUMENT ID	TECN	CHG	COMMENT
• • • We do not use the following data for averages, fits, limits, etc. • • •				
~ 1460	DAUM	81c	CNTR	- 63 $K^-p \rightarrow K^- 2\pi p$
~ 1400	¹ BRANDENB...	76b	ASPK	± 13 $K^\pm p \rightarrow K^\pm 2\pi p$
¹ Coupled mainly to $K f_0(1370)$. Decay into $K^*(892)\pi$ seen.				

$K(1460)$ WIDTH

VALUE (MeV)	DOCUMENT ID	TECN	CHG	COMMENT
• • • We do not use the following data for averages, fits, limits, etc. • • •				
~ 260	DAUM	81c	CNTR	- 63 $K^-p \rightarrow K^- 2\pi p$
~ 250	² BRANDENB...	76b	ASPK	± 13 $K^\pm p \rightarrow K^\pm 2\pi p$
² Coupled mainly to $K f_0(1370)$. Decay into $K^*(892)\pi$ seen.				

$K(1460)$ DECAY MODES

Mode	Fraction (Γ_i/Γ)
Γ_1 $K^*(892)\pi$	seen
Γ_2 $K\rho$	seen
Γ_3 $K_0^*(1430)\pi$	seen

$K(1460)$ PARTIAL WIDTHS

$\Gamma(K^*(892)\pi)$	DOCUMENT ID	TECN	COMMENT	Γ_1
VALUE (MeV)				
• • • We do not use the following data for averages, fits, limits, etc. • • •				
~ 109	DAUM	81c	CNTR	63 $K^-p \rightarrow K^- 2\pi p$

$\Gamma(K\rho)$	DOCUMENT ID	TECN	COMMENT	Γ_2
VALUE (MeV)				
• • • We do not use the following data for averages, fits, limits, etc. • • •				
~ 34	DAUM	81c	CNTR	63 $K^-p \rightarrow K^- 2\pi p$

$\Gamma(K\omega)/\Gamma(K^*(892)\pi)$ Γ_5/Γ_2

VALUE	DOCUMENT ID	TECN	CHG	COMMENT
0.118 ± 0.034 OUR FIT	Error includes scale factor of 1.4.			
0.10 ± 0.04	FIELD	67	HBC	- 3.8 K^-p

$\Gamma(K\eta)/\Gamma(K^*(892)\pi)$ Γ_7/Γ_2

VALUE	DOCUMENT ID	TECN	CHG	COMMENT
0.006^{+0.014}_{-0.004} OUR FIT	Error includes scale factor of 1.2.			
0.07 ± 0.04	FIELD	67	HBC	- 3.8 K^-p

$\Gamma(K\eta)/\Gamma(K\pi)$ Γ_7/Γ_1

VALUE	CL%	DOCUMENT ID	TECN	CHG	COMMENT
0.0030^{+0.0068}_{-0.0020} OUR FIT	Error includes scale factor of 1.3.				
0 ± 0.0056	13	ASTON	88B	LASS	- 11 $K^-p \rightarrow K^- \eta p$
• • • We do not use the following data for averages, fits, limits, etc. • • •					
< 0.04	95	AGUILAR...	71B	HBC	3.9, 4.6 K^-p
< 0.065	14	BASSOMPIE...	69	HBC	5.0 $K^+ p$
< 0.02		BISHOP	69	HBC	3.5 $K^+ p$

$\Gamma(K^*(892)\pi\pi)/\Gamma_{total}$ Γ_3/Γ

VALUE	DOCUMENT ID	TECN	CHG	COMMENT
0.134 ± 0.022 OUR FIT				
0.12 ± 0.04	¹⁵ GOLDBERG	76	HBC	- 3 $K^-p \rightarrow \rho \bar{K}^0 \pi \pi \pi$

$\Gamma(K^*(892)\pi\pi)/\Gamma(K\pi)$ Γ_3/Γ_1

VALUE	DOCUMENT ID	TECN	CHG	COMMENT
0.27 ± 0.05 OUR FIT				
0.21 ± 0.08	^{14,15} JONGEJANS	78	HBC	- 4 $K^-p \rightarrow \rho \bar{K}^0 \pi \pi \pi$

$\Gamma(K\omega\pi)/\Gamma_{total}$ Γ_8/Γ

VALUE (units 10 ⁻³)	CL%	EVTS	DOCUMENT ID	TECN	COMMENT
< 0.72	95	0	JONGEJANS	78	HBC 4 $K^-p \rightarrow \rho \bar{K}^0 4\pi$

¹² From phase shift analysis.
¹³ ASTON 88B quote < 0.0092 at CL=95%. We convert this to a central value and 1 sigma error in order to be able to use it in our constrained fit.
¹⁴ Restated by us.
¹⁵ Assuming $\pi\pi$ system has isospin 1, which is supported by the data.

Meson Particle Listings

 $K(1460)$, $K_2(1580)$, $K(1630)$, $K_1(1650)$ $\Gamma(K_2^0(1430)\pi)$

VALUE (MeV)	DOCUMENT ID	TECN	COMMENT	Γ_3
~ 117	DAUM	81C CNTR	63 $K^- p \rightarrow K^- 2\pi p$	

 $K(1460)$ REFERENCES

DAUM	81C	NP B187 1	C. Daum et al.	(AMST, CERN, CRAC, MPIM+)
BRANDENB...	76B	PRL 36 1239	G.W. Brandenburg et al.	(SLAC) JP

OTHER RELATED PAPERS

BARNES	82	PL B116 365	T. Barnes, F.E. Close	(RHEL)
TANIMOTO	82	PL 116B 198	M. Tanimoto	(BIEL)
VERGEEST	79	NP B158 265	J.S.M. Vergeest et al.	(NIJM, AMST, CERN+)

 $K_2(1580)$

$$I(J^P) = \frac{1}{2}(2^-)$$

OMITTED FROM SUMMARY TABLE

Seen in partial-wave analysis of the $K^- \pi^+ \pi^-$ system. Needs confirmation. $K_2(1580)$ MASS

VALUE (MeV)	DOCUMENT ID	CHG	COMMENT
~ 1580	OTTER	79 -	10,14,16 $K^- p$

 $K_2(1580)$ WIDTH

VALUE (MeV)	DOCUMENT ID	CHG	COMMENT
~ 110	OTTER	79 -	10,14,16 $K^- p$

 $K_2(1580)$ DECAY MODES

Mode	Fraction (Γ_i/Γ)
Γ_1 $K^*(892)\pi$	seen
Γ_2 $K_2^*(1430)\pi$	possibly seen

 $K_2(1580)$ BRANCHING RATIOS

$\Gamma(K^*(892)\pi)/\Gamma_{\text{total}}$	VALUE	DOCUMENT ID	TECN	CHG	COMMENT	Γ_1/Γ
seen		OTTER	79	HBC -	10,14,16 $K^- p$	

$\Gamma(K_2^*(1430)\pi)/\Gamma_{\text{total}}$	VALUE	DOCUMENT ID	TECN	CHG	COMMENT	Γ_2/Γ
possibly seen		OTTER	79	HBC -	10,14,16 $K^- p$	

 $K_2(1580)$ REFERENCES

OTTER	79	NP B147 1	G. Otter et al.	(AACH3, BERL, CERN, LOIC+) JP
-------	----	-----------	-----------------	-------------------------------

 $K(1630)$

$$I(J^P) = \frac{1}{2}(2^-)$$

OMITTED FROM SUMMARY TABLE

Seen as a narrow peak, compatible with the experimental resolution, in the invariant mass of the $K_S^0 \pi^+ \pi^-$ system produced in $\pi^- p$ interactions at high momentum transfers. $K(1630)$ MASS

VALUE (MeV)	EVTS	DOCUMENT ID	TECN	COMMENT
1629 ± 7	~ 75	KARNAUKHOV98	BC	16.0 $\pi^- p \rightarrow (K_S^0 \pi^+ \pi^-) \chi^+ \pi^- \chi^0$

 $K(1630)$ WIDTH

VALUE (MeV)	EVTS	DOCUMENT ID	TECN	COMMENT
16_{-16}^{+19}	~ 75	¹ KARNAUKHOV98	BC	16.0 $\pi^- p \rightarrow (K_S^0 \pi^+ \pi^-) \chi^+ \pi^- \chi^0$

¹ Compatible with an experimental resolution of 14 ± 1 MeV. $K(1630)$ DECAY MODES

Mode
Γ_1 $K_S^0 \pi^+ \pi^-$

 $K(1630)$ REFERENCES

KARNAUKHOV 98	PAN 61 203	V.M. Karnaukhov, C. Coca, V.I. Moroz
		Translated from YAF 61 252.

 $K_1(1650)$

$$I(J^P) = \frac{1}{2}(1^+)$$

OMITTED FROM SUMMARY TABLE

This entry contains various peaks in strange meson systems ($K^+ \phi$, $K \pi \pi$) reported in partial-wave analysis in the 1600–1900 mass region. $K_1(1650)$ MASS

VALUE (MeV)	DOCUMENT ID	TECN	CHG	COMMENT
1650 ± 50	FRAME	86	OMEG +	13 $K^+ p \rightarrow \phi K^+ p$
~ 1840	ARMSTRONG	83	OMEG -	18.5 $K^- p \rightarrow 3K p$
~ 1800	DAUM	81C CNTR	-	63 $K^- p \rightarrow K^- 2\pi p$

 $K_1(1650)$ WIDTH

VALUE (MeV)	DOCUMENT ID	TECN	CHG	COMMENT
150 ± 50	FRAME	86	OMEG +	13 $K^+ p \rightarrow \phi K^+ p$
~ 250	DAUM	81C CNTR	-	63 $K^- p \rightarrow K^- 2\pi p$

 $K_1(1650)$ DECAY MODES

Mode
Γ_1 $K \pi \pi$
Γ_2 $K \phi$

 $K_1(1650)$ REFERENCES

FRAME	86	NP B276 667	D. Frame et al.	(GLAS)
ARMSTRONG	83	NP B221 1	T.A. Armstrong et al.	(BARI, BIRM, CERN+)
DAUM	81C	NP B187 1	C. Daum et al.	(AMST, CERN, CRAC, MPIM+)

See key on page 239

Meson Particle Listings

 $K^*(1680)$, $K_2(1770)$ $K^*(1680)$ $I(J^P) = \frac{1}{2}(1^-)$ $K^*(1680)$ MASS

VALUE (MeV)	DOCUMENT ID	TECN	CHG	COMMENT
1717±27 OUR AVERAGE	Error includes scale factor of 1.4.			
1677±10±32	ASTON	88	LASS	0 11 $K^-p \rightarrow K^- \pi^+ n$
1735±10±20	ASTON	87	LASS	0 11 $K^-p \rightarrow \bar{K}^0 \pi^+ \pi^- n$
• • • We do not use the following data for averages, fits, limits, etc. • • •				
1678±64	BIRD	89	LASS	- 11 $K^-p \rightarrow \bar{K}^0 \pi^- p$
1800±70	ETKIN	80	MPS	0 6 $K^-p \rightarrow \bar{K}^0 \pi^+ \pi^- n$
~ 1650	ESTABROOKS	78	ASPK	0 13 $K^\pm p \rightarrow K^\pm \pi^\pm n$

 $K^*(1680)$ WIDTH

VALUE (MeV)	DOCUMENT ID	TECN	CHG	COMMENT
322±110 OUR AVERAGE	Error includes scale factor of 4.2.			
205± 16±34	ASTON	88	LASS	0 11 $K^-p \rightarrow K^- \pi^+ n$
423± 18±30	ASTON	87	LASS	0 11 $K^-p \rightarrow \bar{K}^0 \pi^+ \pi^- n$
• • • We do not use the following data for averages, fits, limits, etc. • • •				
454±270	BIRD	89	LASS	- 11 $K^-p \rightarrow \bar{K}^0 \pi^- p$
170± 30	ETKIN	80	MPS	0 6 $K^-p \rightarrow \bar{K}^0 \pi^+ \pi^- n$
250 to 300	ESTABROOKS	78	ASPK	0 13 $K^\pm p \rightarrow K^\pm \pi^\pm n$

 $K^*(1680)$ DECAY MODES

Mode	Fraction (Γ_i/Γ)
Γ_1 $K\pi$	(38.7±2.5) %
Γ_2 $K\rho$	(31.4 ^{+4.7} _{-2.1}) %
Γ_3 $K^*(892)\pi$	(29.9 ^{+2.2} _{-4.7}) %

CONSTRAINED FIT INFORMATION

An overall fit to 4 branching ratios uses 4 measurements and one constraint to determine 3 parameters. The overall fit has a $\chi^2 = 2.9$ for 2 degrees of freedom.

The following off-diagonal array elements are the correlation coefficients $\langle \delta x_i \delta x_j \rangle / (\delta x_i \delta x_j)$, in percent, from the fit to the branching fractions, $x_i \equiv \Gamma_i/\Gamma_{\text{total}}$. The fit constrains the x_i whose labels appear in this array to sum to one.

x_2	-36	
x_3	-39	-72
x_1		x_2

 $K^*(1680)$ BRANCHING RATIOS

$\Gamma(K\pi)/\Gamma_{\text{total}}$	Γ_1/Γ			
VALUE	DOCUMENT ID	TECN	CHG	COMMENT
0.387±0.026 OUR FIT				
0.388±0.014±0.022	ASTON	88	LASS	0 11 $K^-p \rightarrow K^- \pi^+ n$
$\Gamma(K\pi)/\Gamma(K^*(892)\pi)$	Γ_1/Γ_3			
VALUE	DOCUMENT ID	TECN	CHG	COMMENT
1.30^{+0.23}_{-0.14} OUR FIT				
2.8 ±1.1	ASTON	84	LASS	0 11 $K^-p \rightarrow \bar{K}^0 2\pi n$
$\Gamma(K\rho)/\Gamma(K\pi)$	Γ_2/Γ_1			
VALUE	DOCUMENT ID	TECN	CHG	COMMENT
0.81^{+0.14}_{-0.09} OUR FIT				
1.2 ±0.4	ASTON	84	LASS	0 11 $K^-p \rightarrow \bar{K}^0 2\pi n$
$\Gamma(K\rho)/\Gamma(K^*(892)\pi)$	Γ_2/Γ_3			
VALUE	DOCUMENT ID	TECN	CHG	COMMENT
1.05^{+0.27}_{-0.11} OUR FIT				
0.97±0.09 ^{+0.30} _{-0.10}	ASTON	87	LASS	0 11 $K^-p \rightarrow \bar{K}^0 \pi^+ \pi^- n$

 $K^*(1680)$ REFERENCES

BIRD	89	SLAC-332	P.F. Bird	(SLAC)
ASTON	88	NP B296 493	D. Aston et al.	(SLAC, NAGO, CINC, INUS)
ASTON	87	NP B292 693	D. Aston et al.	(SLAC, NAGO, CINC, INUS)
ASTON	84	PL 149B 258	D. Aston et al.	(SLAC, CARL, OTTA)JP
ETKIN	80	PR D22 42	A. Etkin et al.	(BNL, CUNY)JP
ESTABROOKS	78	NP B133 490	P.G. Estabrooks et al.	(MCGI, CARL, DURH+)JP

 $K_2(1770)$ $I(J^P) = \frac{1}{2}(2^-)$ THE $K_2(1770)$ AND THE $K_2(1820)$

A partial-wave analysis of the $K^- \omega$ system based on about 100,000 $K^- p \rightarrow K^- \omega p$ events (ASTON 93) gives evidence for two $q\bar{q}$ D-wave states near 1.8 GeV. A previous analysis based on about 200,000 diffractively produced $K^- p \rightarrow K^- \pi^+ \pi^- p$ events (DAUM 81) gave evidence for two $J^P = 2^-$ states in this region, with masses ~ 1780 MeV and ~ 1840 MeV and widths ~ 200 MeV, in good agreement with the results of ASTON 93. In contrast, the masses obtained using a single resonance do not agree well: ASTON 93 obtains 1728 ± 7 MeV, while DAUM 81 estimates ~ 1820 MeV. We conclude that there are indeed two K_2 resonances here.

We list under the $K_2(1770)$ other measurements that do not resolve the two-resonance structure of the enhancement.

 $K_2(1770)$ MASS

VALUE (MeV)	EVTS	DOCUMENT ID	TECN	CHG	COMMENT
1773± 8		¹ ASTON	93	LASS	11 $K^-p \rightarrow K^- \omega p$
• • • We do not use the following data for averages, fits, limits, etc. • • •					
1810±20		FRAME	86	OMEG +	13 $K^+p \rightarrow \phi K^+ p$
~ 1730		ARMSTRONG	83	OMEG -	18.5 $K^-p \rightarrow 3Kp$
~ 1780		² DAUM	81c	CNTR -	63 $K^-p \rightarrow K^- 2\pi p$
~ 1710±15	60	CHUNG	74	HBC -	7.3 $K^-p \rightarrow K^- \omega p$
1767± 6		BLIEDEN	72	MMS -	11-16 K^-p
1730±20	306	³ FIRESTONE	72b	DBC +	12 K^+d
1765±40		⁴ COLLEY	71	HBC +	10 $K^+p \rightarrow K_2^+ n$
1740		DENEGRI	71	DBC -	12.6 $K^-d \rightarrow \bar{K} 2\pi d$
1745±20		AGUILAR...	70c	HBC -	4.6 K^-p
1780±15		BARTSCH	70c	HBC -	10.1 K^-p
1760±15		LUDLAM	70	HBC -	12.6 K^-p

¹ From a partial wave analysis of the $K^- \omega$ system.

² From a partial wave analysis of the $K^- 2\pi$ system.

³ Produced in conjunction with excited deuteron.

⁴ Systematic errors added correspond to spread of different fits.

 $K_2(1770)$ WIDTH

VALUE (MeV)	EVTS	DOCUMENT ID	TECN	CHG	COMMENT
186±14		⁵ ASTON	93	LASS	11 $K^-p \rightarrow K^- \omega p$
• • • We do not use the following data for averages, fits, limits, etc. • • •					
140±40		FRAME	86	OMEG +	13 $K^+p \rightarrow \phi K^+ p$
~ 220		ARMSTRONG	83	OMEG -	18.5 $K^-p \rightarrow 3Kp$
~ 210		⁶ DAUM	81c	CNTR -	63 $K^-p \rightarrow K^- 2\pi p$
110±50	60	CHUNG	74	HBC -	7.3 $K^-p \rightarrow K^- \omega p$
100±26		BLIEDEN	72	MMS -	11-16 K^-p
210±30	306	⁷ FIRESTONE	72b	DBC +	12 K^+d
90±70		⁸ COLLEY	71	HBC +	10 $K^+p \rightarrow K_2^+ n$
130		DENEGRI	71	DBC -	12.6 $K^-d \rightarrow \bar{K} 2\pi d$
100±50		AGUILAR...	70c	HBC -	4.6 K^-p
138±40		BARTSCH	70c	HBC -	10.1 K^-p
50 ⁺⁴⁰ ₋₂₀		LUDLAM	70	HBC -	12.6 K^-p

⁵ From a partial wave analysis of the $K^- \omega$ system.

⁶ From a partial wave analysis of the $K^- 2\pi$ system.

⁷ Produced in conjunction with excited deuteron.

⁸ Systematic errors added correspond to spread of different fits.

 $K_2(1770)$ DECAY MODES

Mode	Fraction (Γ_i/Γ)
Γ_1 $K\pi\pi$	
Γ_2 $K_2^*(1430)\pi$	dominant
Γ_3 $K^*(892)\pi$	seen
Γ_4 $K_2^*(1270)$	seen
Γ_5 $K\phi$	seen
Γ_6 $K\omega$	seen

Meson Particle Listings

$K_2(1770)$, $K_3^*(1780)$

$K_2(1770)$ BRANCHING RATIOS

$$\frac{\Gamma(K_2^*(1430)\pi)}{\Gamma(K\pi\pi)} \quad \Gamma_2/\Gamma_1$$

VALUE	DOCUMENT ID	TECN	CHG	COMMENT
0.03	DAUM	81C CNTR		63 $K^-p \rightarrow K^-2\pi p$
~1.0	⁹ FIRESTONE	72B DBC	+	12 K^+d
<1.0	COLLEY	71 HBC		10 K^+p
0.2 ± 0.2	AGUILAR...	70C HBC	-	4.6 K^-p
<1.0	BARTSCH	70C HBC	-	10.1 K^-p
1.0	BARBARO...	69 HBC	+	12.0 K^+p

⁹Produced in conjunction with excited deuteron.

$$\frac{\Gamma(K^*(892)\pi)}{\Gamma(K\pi\pi)} \quad \Gamma_3/\Gamma_1$$

VALUE	DOCUMENT ID	TECN	COMMENT
~0.23	DAUM	81C CNTR	63 $K^-p \rightarrow K^-2\pi p$

$$\frac{\Gamma(K_2^*(1270))}{\Gamma(K_2^*(1270) \rightarrow \pi\pi)} \quad \Gamma_4/\Gamma_1$$

VALUE	DOCUMENT ID	TECN	COMMENT
~0.74	DAUM	81C CNTR	63 $K^-p \rightarrow K^-2\pi p$

$$\frac{\Gamma(K\phi)}{\Gamma_{total}} \quad \Gamma_5/\Gamma$$

VALUE	DOCUMENT ID	TECN	CHG	COMMENT
seen	ARMSTRONG	83	OMEG	- 18.5 $K^-p \rightarrow K^- \phi N$

$$\frac{\Gamma(K\omega)}{\Gamma_{total}} \quad \Gamma_6/\Gamma$$

VALUE	DOCUMENT ID	TECN	CHG	COMMENT
seen	OTTER	81	HBC	± 8.25,10,16 $K^\pm p$
seen	CHUNG	74	HBC	- 7.3 $K^-p \rightarrow K^- \omega p$

$K_2(1770)$ REFERENCES

ASTON	93	PL B308 186	D. Aston et al.	(SLAC, NAGO, CINC, INUS)
FRAME	86	NP B276 667	D. Frame et al.	(GLAS)
ARMSTRONG	83	NP B221 1	T.A. Armstrong et al.	(BARI, BIRM, CERN+)
DAUM	81C	NP B167 1	C. Daum et al.	(AMST, CERN, CRAC, MPIM+)
OTTER	81	NP B181 1	G. Otter	(AACH3, BERL, LOIC, VIEN, BIRM+)
CHUNG	74	PL 51B 413	S.U. Chung et al.	(BNL)
BLIEDEN	72	PL 39B 668	H.R. Blieden et al.	(STON, NEAS)
FIRESTONE	72B	PR D5 505	A. Firestone et al.	(LBL)
COLLEY	71	NP B26 71	D.C. Colley et al.	(BIRM, GLAS)
DENEGRI	71	NP B28 13	D. Denegri et al.	(JHU) JP
AGUILAR...	70C	PRL 25 54	M. Aguilar-Benitez et al.	(BNL)
BARTSCH	70C	PL 33B 186	J. Bartsch et al.	(AACH, BERL, CERN+)
LUDLAM	70	PR D2 1234	T. Ludlam, J. Sandweiss, A.J. Slaughter	(YALE)
BARBARO...	69	PRL 22 1207	A. Barbaro-Galiteri et al.	(LRL)

OTHER RELATED PAPERS

BERLINGHIERI	67	PRL 18 1087	J.C. Berlinghieri et al.	(ROCH) I
CARMONY	67	PRL 18 615	D.D. Carmony, T. Hendricks, R.L. Lander	(UCSD)
JOBES	67	PL 26B 49	M. Jobes et al.	(BIRM, CERN, BRUX)
BARTSCH	66	PL 22 357	J. Bartsch et al.	(AACH, BERL, CERN+)

$K_3^*(1780)$

$$I(J^P) = \frac{1}{2}(3^-)$$

$K_3^*(1780)$ MASS

VALUE (MeV)	EVTS	DOCUMENT ID	TECN	CHG	COMMENT
1776 ± 7 OUR AVERAGE		Error Includes Scale factor of 1.1.			
1781 ± 8 ± 4		¹ ASTON	88	LASS	0 11 $K^-p \rightarrow K^- \pi^+ n$
1740 ± 14 ± 15		¹ ASTON	87	LASS	0 11 $K^-p \rightarrow \bar{K}^0 \pi^+ \pi^- n$
1779 ± 11		² BALDI	76	SPEC	+ 10 $K^+p \rightarrow K^0 \pi^+ p$
1776 ± 26		³ BRANDENB...	76D	ASPK	0 13 $K^\pm p \rightarrow K^\pm \pi^+ n$
1720 ± 10 ± 15	6111	⁴ BIRD	89	LASS	- 11 $K^-p \rightarrow \bar{K}^0 \pi^- p$
1749 ± 10		ASTON	88B	LASS	- 11 $K^-p \rightarrow K^- \eta p$
1780 ± 9	300	BAUBILLIER	84B	HBC	- 8.25 $K^-p \rightarrow \bar{K}^0 \pi^- p$
1790 ± 15		BAUBILLIER	82B	HBC	0 8.25 $K^-p \rightarrow K_S^0 2\pi N$
1784 ± 9	2060	CLELAND	82	SPEC	± 50 $K^+p \rightarrow K_S^0 \pi^\pm p$
1786 ± 15		⁵ ASTON	81D	LASS	0 11 $K^-p \rightarrow K^- \pi^+ n$
1762 ± 9	190	TOAFF	81	HBC	- 6.5 $K^-p \rightarrow \bar{K}^0 \pi^- p$
1850 ± 50		ETKIN	80	MPS	0 6 $K^-p \rightarrow \bar{K}^0 \pi^+ \pi^-$
1812 ± 28		BEUSCH	78	OMEG	10 $K^-p \rightarrow \bar{K}^0 \pi^+ \pi^- n$
1786 ± 8		CHUNG	78	MPS	0 6 $K^-p \rightarrow K^- \pi^+ n$

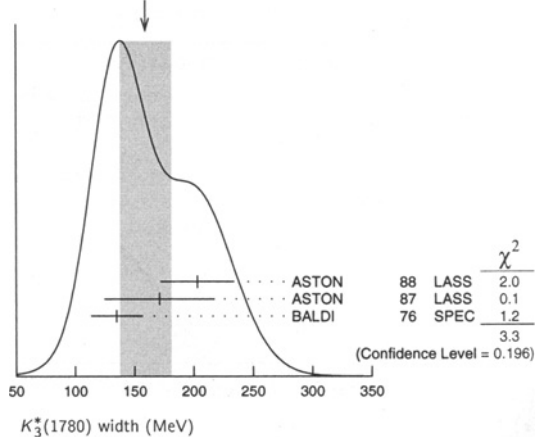
¹ From energy-independent partial-wave analysis.
² From a fit to Y_6^2 moment. $J^P = 3^-$ found.
³ Confirmed by phase shift analysis of ESTABROOKS 78, yields $J^P = 3^-$.
⁴ From a partial wave amplitude analysis.
⁵ From a fit to the Y_6^0 moment.

$K_3^*(1780)$ WIDTH

VALUE (MeV)	EVTS	DOCUMENT ID	TECN	CHG	COMMENT
159 ± 21 OUR AVERAGE		Error includes scale factor of 1.3. See the ideogram below.			
203 ± 30 ± 8		⁶ ASTON	88	LASS	0 11 $K^-p \rightarrow K^- \pi^+ n$
171 ± 42 ± 20		⁶ ASTON	87	LASS	0 11 $K^-p \rightarrow \bar{K}^0 \pi^+ \pi^- n$
135 ± 22		⁷ BALDI	76	SPEC	+ 10 $K^+p \rightarrow K^0 \pi^+ p$
187 ± 31 ± 20	6111	⁸ BIRD	89	LASS	- 11 $K^-p \rightarrow \bar{K}^0 \pi^- p$
193 $\frac{+51}{-37}$		ASTON	88B	LASS	- 11 $K^-p \rightarrow K^- \eta p$
99 ± 30	300	BAUBILLIER	84B	HBC	- 8.25 $K^-p \rightarrow \bar{K}^0 \pi^- p$
~130		BAUBILLIER	82B	HBC	0 8.25 $K^-p \rightarrow K_S^0 2\pi N$
191 ± 24	2060	CLELAND	82	SPEC	± 50 $K^+p \rightarrow K_S^0 \pi^\pm p$
225 ± 60		⁹ ASTON	81D	LASS	0 11 $K^-p \rightarrow K^- \pi^+ n$
~80	190	TOAFF	81	HBC	- 6.5 $K^-p \rightarrow \bar{K}^0 \pi^- p$
240 ± 50		ETKIN	80	MPS	0 6 $K^-p \rightarrow \bar{K}^0 \pi^+ \pi^-$
181 ± 44		¹⁰ BEUSCH	78	OMEG	10 $K^-p \rightarrow \bar{K}^0 \pi^+ \pi^- n$
96 ± 31		CHUNG	78	MPS	0 6 $K^-p \rightarrow K^- \pi^+ n$
270 ± 70		¹¹ BRANDENB...	76D	ASPK	0 13 $K^\pm p \rightarrow K^\pm \pi^+ n$

⁶ From energy-independent partial-wave analysis.
⁷ From a fit to Y_6^2 moment. $J^P = 3^-$ found.
⁸ From a partial wave amplitude analysis.
⁹ From a fit to Y_6^0 moment.
¹⁰ Errors enlarged by us to $4\Gamma/\sqrt{N}$; see the note with the $K^*(892)$ mass.
¹¹ ESTABROOKS 78 find that BRANDENBURG 76D data are consistent with 175 MeV width. Not averaged.

WEIGHTED AVERAGE
159±21 (Error scaled by 1.3)



$K_3^*(1780)$ DECAY MODES

Mode	Fraction (Γ_i/Γ)	Confidence level
Γ_1 $K\rho$	(31 ± 9) %	
Γ_2 $K^*(892)\pi$	(20 ± 5) %	
Γ_3 $K\pi$	(18.8 ± 1.0) %	
Γ_4 $K\eta$	(30 ± 13) %	
Γ_5 $K_2^*(1430)\pi$	< 16 %	95%

CONSTRAINED FIT INFORMATION

An overall fit to 3 branching ratios uses 4 measurements and one constraint to determine 4 parameters. The overall fit has a $\chi^2 = 0.0$ for 1 degrees of freedom.

The following off-diagonal array elements are the correlation coefficients $\langle \delta x_i \delta x_j \rangle / (\delta x_i \delta x_j)$, in percent, from the fit to the branching fractions, $x_i \equiv \Gamma_i/\Gamma_{total}$. The fit constrains the x_i whose labels appear in this array to sum to one.

x_2	85		
x_3	18	21	
x_4	-98	-94	-27
	x_1	x_2	x_3

See key on page 239

Meson Particle Listings

$K_3^*(1780)$, $K_2(1820)$, $K(1830)$

 $K_3^*(1780)$ BRANCHING RATIOS

$\Gamma(K\rho)/\Gamma(K^*(892)\pi)$					Γ_1/Γ_2	
VALUE	DOCUMENT ID	TECN	CHG	COMMENT		
1.52 ± 0.23 OUR FIT						
$1.52 \pm 0.21 \pm 0.10$	ASTON	87	LASS	0	11 $K^-p \rightarrow \bar{K}^0\pi^+\pi^-n$	
$\Gamma(K^*(892)\pi)/\Gamma(K\pi)$					Γ_2/Γ_3	
VALUE	DOCUMENT ID	TECN	CHG	COMMENT		
1.09 ± 0.26 OUR FIT						
1.09 ± 0.26	ASTON	84B	LASS	0	11 $K^-p \rightarrow \bar{K}^0 2\pi n$	
$\Gamma(K\pi)/\Gamma_{\text{total}}$					Γ_3/Γ	
VALUE	DOCUMENT ID	TECN	CHG	COMMENT		
0.188 ± 0.010 OUR FIT						
0.188 ± 0.010 OUR AVERAGE						
$0.187 \pm 0.008 \pm 0.008$	ASTON	88	LASS	0	11 $K^-p \rightarrow K^-\pi^+n$	
0.19 ± 0.02	ESTABROOKS	78	ASPK	0	13 $K^\pm p \rightarrow K\pi N$	
$\Gamma(K\eta)/\Gamma(K\pi)$					Γ_4/Γ_3	
VALUE	DOCUMENT ID	TECN	CHG	COMMENT		
1.6 ± 0.7 OUR FIT						
• • • We do not use the following data for averages, fits, limits, etc. • • •						
0.41 ± 0.050	¹² BIRD	89	LASS	-	11 $K^-p \rightarrow \bar{K}^0\pi^-p$	
0.50 ± 0.18	ASTON	88B	LASS	-	11 $K^-p \rightarrow K^-\eta p$	
¹² This result supersedes ASTON 88B.						
$\Gamma(K_2^*(1430)\pi)/\Gamma(K^*(892)\pi)$					Γ_5/Γ_2	
VALUE	CL%	DOCUMENT ID	TECN	CHG	COMMENT	
<0.78	95	ASTON	87	LASS	0	11 $K^-p \rightarrow \bar{K}^0\pi^+\pi^-n$

 $K_3^*(1780)$ REFERENCES

BIRD	89	SLAC-332	P.F. Bird	(SLAC)
ASTON	88	NP B296 493	D. Aston <i>et al.</i>	(SLAC, NAGO, CINC, INUS)
ASTON	88B	PL B201 169	D. Aston <i>et al.</i>	(SLAC, NAGO, CINC, INUS) JP
ASTON	87	NP B292 693	D. Aston <i>et al.</i>	(SLAC, NAGO, CINC, INUS)
ASTON	84B	NP B247 261	D. Aston <i>et al.</i>	(SLAC, CARL, OTTA)
BAUBILLIER	84B	ZPHY C26 37	M. Baubillier <i>et al.</i>	(BIRM, CERN, GLAS+)
BAUBILLIER	82B	NP B202 21	M. Baubillier <i>et al.</i>	(BIRM, CERN, GLAS+)
CLELAND	82	NP B208 189	W.E. Cleland <i>et al.</i>	(DURH, GEVA, LAUS+)
ASTON	81D	PL 99B 502	D. Aston <i>et al.</i>	(SLAC, CARL, OTTA) JP
TOAFF	81	PR D23 1500	S. Toaff <i>et al.</i>	(ANL, KANS)
ETKIN	80	PR D22 42	A. Etkin <i>et al.</i>	(BNL, CUNY) JP
BEUSCH	78	PL 74B 282	W. Beusch <i>et al.</i>	(CERN, AACH3, ETH) JP
CHUNG	78	PRL 40 355	S.U. Chung <i>et al.</i>	(BNL, BRAN, CUNY+) JP
ESTABROOKS	78	NP B133 490	P.G. Estabrooks <i>et al.</i>	(MCGI, CARL, DURH+) JP
Also	78B	PR D17 658	P.G. Estabrooks <i>et al.</i>	(MCGI, CARL, DURH+)
BALDI	76	PL 63B 344	R. Baldi <i>et al.</i>	(GEVA) JP
BRANDENB...	76D	PL 60B 478	G.W. Brandenburg <i>et al.</i>	(SLAC) JP

OTHER RELATED PAPERS

AGUILAR...	73	PRL 30 672	M. Aguilar-Benitez <i>et al.</i>	(BNL)
WALUCH	73	PR D8 2837	V. Waluch, S.M. Flatte, J.H. Friedman	(LBL)
CARMONY	71	PRL 27 1160	D.D. Carmony <i>et al.</i>	(PURD, UCD, IJFU)
FIRESTONE	71	PL 36B 513	A. Firestone <i>et al.</i>	(LBL)

 $K_2(1820)$

$$I(J^P) = \frac{1}{2}(2^-)$$

Observed by ASTON 93 from a partial wave analysis of the $K^-\omega$ system. See mini-review under $K_2(1770)$.

 $K_2(1820)$ MASS

VALUE (MeV)	DOCUMENT ID	TECN	CHG	COMMENT
1816 ± 13	¹ ASTON	93	LASS	11 $K^-p \rightarrow K^-\omega p$
• • • We do not use the following data for averages, fits, limits, etc. • • •				
~ 1840	² DAUM	81C	CNTR	63 $K^-p \rightarrow K^- 2\pi p$
¹ From a partial wave analysis of the $K^-\omega$ system.				
² From a partial wave analysis of the $K^- 2\pi$ system.				

 $K_2(1820)$ WIDTH

VALUE (MeV)	DOCUMENT ID	TECN	CHG	COMMENT
276 ± 35	³ ASTON	93	LASS	11 $K^-p \rightarrow K^-\omega p$
• • • We do not use the following data for averages, fits, limits, etc. • • •				
~ 230	⁴ DAUM	81C	CNTR	63 $K^-p \rightarrow K^- 2\pi p$
³ From a partial wave analysis of the $K^-\omega$ system.				
⁴ From a partial wave analysis of the $K^- 2\pi$ system.				

 $K_2(1820)$ DECAY MODES

Mode	Fraction (Γ_i/Γ)
Γ_1 $K\pi\pi$	
Γ_2 $K_2^*(1430)\pi$	seen
Γ_3 $K^*(892)\pi$	seen
Γ_4 $K f_2(1270)$	seen
Γ_5 $K\omega$	seen

 $K_2(1820)$ BRANCHING RATIOS

$\Gamma(K_2^*(1430)\pi)/\Gamma(K\pi\pi)$				Γ_2/Γ_1
VALUE	DOCUMENT ID	TECN	COMMENT	
• • • We do not use the following data for averages, fits, limits, etc. • • •				
~ 0.77	DAUM	81C	CNTR	63 $K^-p \rightarrow \bar{K} 2\pi p$
$\Gamma(K^*(892)\pi)/\Gamma(K\pi\pi)$				Γ_3/Γ_1
VALUE	DOCUMENT ID	TECN	COMMENT	
• • • We do not use the following data for averages, fits, limits, etc. • • •				
~ 0.05	DAUM	81C	CNTR	63 $K^-p \rightarrow \bar{K} 2\pi p$
$\Gamma(K f_2(1270))/\Gamma(K\pi\pi)$				Γ_4/Γ_1
VALUE	DOCUMENT ID	TECN	COMMENT	
• • • We do not use the following data for averages, fits, limits, etc. • • •				
~ 0.18	DAUM	81C	CNTR	63 $K^-p \rightarrow \bar{K} 2\pi p$

 $K_2(1820)$ REFERENCES

ASTON	93	PL B308 186	D. Aston <i>et al.</i>	(SLAC, NAGO, CINC, INUS)
DAUM	81C	NP B187 1	C. Daum <i>et al.</i>	(AMST, CERN, CRAC, MPIM+)

 $K(1830)$

$$I(J^P) = \frac{1}{2}(0^-)$$

OMITTED FROM SUMMARY TABLE

Seen in partial-wave analysis of $K^-\phi$ system. Needs confirmation.

 $K(1830)$ MASS

VALUE (MeV)	DOCUMENT ID	TECN	CHG	COMMENT	
• • • We do not use the following data for averages, fits, limits, etc. • • •					
~ 1830	ARMSTRONG	83	OMEG	-	18.5 $K^-p \rightarrow 3Kp$

 $K(1830)$ WIDTH

VALUE (MeV)	DOCUMENT ID	TECN	CHG	COMMENT	
• • • We do not use the following data for averages, fits, limits, etc. • • •					
~ 250	ARMSTRONG	83	OMEG	-	18.5 $K^-p \rightarrow 3Kp$

 $K(1830)$ DECAY MODES

Mode	Fraction (Γ_i/Γ)
Γ_1 $K\phi$	

 $K(1830)$ REFERENCES

ARMSTRONG	83	NP B221 1	T.A. Armstrong <i>et al.</i>	(BARI, BIRM, CERN+) JP
-----------	----	-----------	------------------------------	------------------------

Meson Particle Listings

$K_0^*(1950)$, $K_2^*(1980)$, $K_4^*(2045)$

$K_0^*(1950)$

 $I(J^P) = \frac{1}{2}(0^+)$

OMITTED FROM SUMMARY TABLE
Seen in partial-wave analysis of the $K^- \pi^+$ system. Needs confirmation.

$K_0^*(1950)$ MASS

VALUE (MeV)	DOCUMENT ID	TECN	CHG	COMMENT	
1945 ± 10 ± 20	¹ ASTON	88	LASS	0	11 $K^- p \rightarrow K^- \pi^+ n$
1820 ± 40	² ANISOVICH	97C	RVUE		11 $K^- p \rightarrow K^- \pi^+ n$

• • • We do not use the following data for averages, fits, limits, etc. • • •
¹We take the central value of the two solutions and the larger error given.
²T-matrix pole. Reanalysis of ASTON 88 data.

$K_0^*(1950)$ WIDTH

VALUE (MeV)	DOCUMENT ID	TECN	CHG	COMMENT	
201 ± 34 ± 79	³ ASTON	88	LASS	0	11 $K^- p \rightarrow K^- \pi^+ n$
250 ± 100	⁴ ANISOVICH	97C	RVUE		11 $K^- p \rightarrow K^- \pi^+ n$

• • • We do not use the following data for averages, fits, limits, etc. • • •
³We take the central value of the two solutions and the larger error given.
⁴T-matrix pole. Reanalysis of ASTON 88 data.

$K_0^*(1950)$ DECAY MODES

Mode	Fraction (Γ_i/Γ)
Γ_1 $K \pi$	(52 ± 14) %

$K_0^*(1950)$ BRANCHING RATIOS

$\Gamma(K \pi)/\Gamma_{total}$	DOCUMENT ID	TECN	CHG	COMMENT	Γ_1/Γ	
0.52 ± 0.08 ± 0.12	⁵ ASTON	88	LASS	0	11 $K^- p \rightarrow K^- \pi^+ n$	

⁵We take the central value of the two solutions and the larger error given.

$K_0^*(1950)$ REFERENCES

ANISOVICH 97C PL B413 137
 ASTON 88 NP B296 493
 D. Aston et al. (SLAC, NAGO, CINC, INUS)

$K_2^*(1980)$

 $I(J^P) = \frac{1}{2}(2^+)$

OMITTED FROM SUMMARY TABLE
Needs confirmation.

$K_2^*(1980)$ MASS

VALUE (MeV)	EVTS	DOCUMENT ID	TECN	CHG	COMMENT	
1973 ± 8 ± 25		ASTON	87	LASS	0	11 $K^- p \rightarrow \bar{K}^0 \pi^+ \pi^- n$
1978 ± 40	241 ± 47	BIRD	89	LASS	-	11 $K^- p \rightarrow \bar{K}^0 \pi^- p$

• • • We do not use the following data for averages, fits, limits, etc. • • •

$K_2^*(1980)$ WIDTH

VALUE (MeV)	EVTS	DOCUMENT ID	TECN	CHG	COMMENT	
373 ± 33 ± 60		ASTON	87	LASS	0	11 $K^- p \rightarrow \bar{K}^0 \pi^+ \pi^- n$
398 ± 47	241 ± 47	BIRD	89	LASS	-	11 $K^- p \rightarrow \bar{K}^0 \pi^- p$

• • • We do not use the following data for averages, fits, limits, etc. • • •

$K_2^*(1980)$ DECAY MODES

Mode	Fraction (Γ_i/Γ)
Γ_1 $K^*(892)\pi$	
Γ_2 $K \rho$	

$K_2^*(1980)$ BRANCHING RATIOS

$\Gamma(K \rho)/\Gamma(K^*(892)\pi)$	DOCUMENT ID	TECN	CHG	COMMENT	Γ_2/Γ_1
1.49 ± 0.24 ± 0.09	ASTON	87	LASS	0	11 $K^- p \rightarrow \bar{K}^0 \pi^+ \pi^- n$

$K_2^*(1980)$ REFERENCES

BIRD 89 SLAC-332 P.F. Bird (SLAC)
 ASTON 87 NP B292 693 D. Aston et al. (SLAC, NAGO, CINC, INUS)

$K_4^*(2045)$

 $I(J^P) = \frac{1}{2}(4^+)$

$K_4^*(2045)$ MASS

VALUE (MeV)	EVTS	DOCUMENT ID	TECN	CHG	COMMENT	
2045 ± 9 OUR AVERAGE		Error includes scale factor of 1.1.				
2062 ± 14 ± 13		¹ ASTON	86	LASS	0	11 $K^- p \rightarrow K^- \pi^+ n$
2039 ± 10	400	^{2,3} CLELAND	82	SPEC	±	50 $K^+ p \rightarrow K_S^0 \pi^\pm p$
2070 ⁺¹⁰⁰ ₋₄₀		⁴ ASTON	81C	LASS	0	11 $K^- p \rightarrow K^- \pi^+ n$
2079 ± 7	431	TORRES	86	MPSF		400 $pA \rightarrow 4KX$
2088 ± 20	650	BAUBILLIER	82	HBC	-	8.25 $K^- p \rightarrow K_S^0 \pi^- p$
2115 ± 46	488	CARMONY	77	HBC	0	9 $K^+ d \rightarrow K^+ \pi^+ X$

• • • We do not use the following data for averages, fits, limits, etc. • • •
¹From a fit to all moments.
²From a fit to 8 moments.
³Number of events evaluated by us.
⁴From energy-independent partial-wave analysis.

$K_4^*(2045)$ WIDTH

VALUE (MeV)	EVTS	DOCUMENT ID	TECN	CHG	COMMENT	
198 ± 30 OUR AVERAGE						
221 ± 48 ± 27		⁵ ASTON	86	LASS	0	11 $K^- p \rightarrow K^- \pi^+ n$
189 ± 35	400	^{6,7} CLELAND	82	SPEC	±	50 $K^+ p \rightarrow K_S^0 \pi^\pm p$
61 ± 58	431	TORRES	86	MPSF		400 $pA \rightarrow 4KX$
170 ⁺¹⁰⁰ ₋₅₀	650	BAUBILLIER	82	HBC	-	8.25 $K^- p \rightarrow K_S^0 \pi^- p$
240 ⁺⁵⁰⁰ ₋₁₀₀		⁸ ASTON	81C	LASS	0	11 $K^- p \rightarrow K^- \pi^+ n$
300 ± 200		CARMONY	77	HBC	0	9 $K^+ d \rightarrow K^+ \pi^+ X$

• • • We do not use the following data for averages, fits, limits, etc. • • •
⁵From a fit to all moments.
⁶From a fit to 8 moments.
⁷Number of events evaluated by us.
⁸From energy-independent partial-wave analysis.

$K_4^*(2045)$ DECAY MODES

Mode	Fraction (Γ_i/Γ)
Γ_1 $K \pi$	(9.9 ± 1.2) %
Γ_2 $K^*(892)\pi \pi$	(9 ± 5) %
Γ_3 $K^*(892)\pi \pi \pi$	(7 ± 5) %
Γ_4 $\rho K \pi$	(5.7 ± 3.2) %
Γ_5 $\omega K \pi$	(5.0 ± 3.0) %
Γ_6 $\phi K \pi$	(2.8 ± 1.4) %
Γ_7 $\phi K^*(892)$	(1.4 ± 0.7) %

$K_4^*(2045)$ BRANCHING RATIOS

$\Gamma(K \pi)/\Gamma_{total}$	DOCUMENT ID	TECN	CHG	COMMENT	Γ_1/Γ
0.099 ± 0.012	ASTON	88	LASS	0	11 $K^- p \rightarrow K^- \pi^+ n$
$\Gamma(K^*(892)\pi \pi)/\Gamma(K \pi)$	DOCUMENT ID	TECN	CHG	COMMENT	Γ_2/Γ_1
0.89 ± 0.53	BAUBILLIER	82	HBC	-	8.25 $K^- p \rightarrow p K_S^0 3\pi$
$\Gamma(K^*(892)\pi \pi \pi)/\Gamma(K \pi)$	DOCUMENT ID	TECN	CHG	COMMENT	Γ_3/Γ_1
0.75 ± 0.49	BAUBILLIER	82	HBC	-	8.25 $K^- p \rightarrow p K_S^0 3\pi$
$\Gamma(\rho K \pi)/\Gamma(K \pi)$	DOCUMENT ID	TECN	CHG	COMMENT	Γ_4/Γ_1
0.58 ± 0.32	BAUBILLIER	82	HBC	-	8.25 $K^- p \rightarrow p K_S^0 3\pi$
$\Gamma(\omega K \pi)/\Gamma(K \pi)$	DOCUMENT ID	TECN	CHG	COMMENT	Γ_5/Γ_1
0.50 ± 0.30	BAUBILLIER	82	HBC	-	8.25 $K^- p \rightarrow p K_S^0 3\pi$
$\Gamma(\phi K \pi)/\Gamma_{total}$	DOCUMENT ID	TECN	COMMENT	Γ_6/Γ	
0.028 ± 0.014	⁹ TORRES	86	MPSF	400 $pA \rightarrow 4KX$	
$\Gamma(\phi K^*(892))/\Gamma_{total}$	DOCUMENT ID	TECN	COMMENT	Γ_7/Γ	
0.014 ± 0.007	⁹ TORRES	86	MPSF	400 $pA \rightarrow 4KX$	

⁹ Error determination is model dependent.

See key on page 239

Meson Particle Listings

 $K_4^*(2045)$, $K_2(2250)$, $K_3(2320)$, $K_5^*(2380)$ $K_4^*(2045)$ REFERENCES

ASTON	88	NP B296 493	D. Aston <i>et al.</i>	(SLAC, NAGO, CINC, INUS)
ASTON	86	PL B180 308	D. Aston <i>et al.</i>	(SLAC, NAGO, CINC, INUS)
TORRES	86	PR 34 707	S. Torres <i>et al.</i>	(VPI, ARIZ, FNAL, FSU+)
BAUBILLIER	82	PL 118B 447	M. Baubillier <i>et al.</i>	(BIRM, CERN, GLAS+)
CLELAND	82	NP B208 189	W.E. Cleland <i>et al.</i>	(DURH, GEVA, LAUS+)
ASTON	81C	PL 106B 235	D. Aston <i>et al.</i>	(SLAC, CARL, OTTA) JP
CARMONY	77	PR D16 1251	D.D. Carmony <i>et al.</i>	(PURD, UCD, IUPU)

OTHER RELATED PAPERS

ASTON	87	NP B292 693	D. Aston <i>et al.</i>	(SLAC, NAGO, CINC, INUS)
BROMBERG	80	PR D22 1513	C.M. Bromberg <i>et al.</i>	(CIT, FNAL, ILLC+)
CARMONY	71	PRL 27 1160	D.D. Carmony <i>et al.</i>	(PURD, UCD, IUPU)

 $K_2(2250)$

$$I(J^P) = \frac{1}{2}(2^-)$$

OMITTED FROM SUMMARY TABLE

This entry contains various peaks in strange meson systems reported in the 2150–2260 MeV region, as well as enhancements seen in the antihyperon-nucleon system, either in the mass spectra or in the $J^P = 2^-$ wave.

 $K_2(2250)$ MASS

VALUE (MeV)	EVTS	DOCUMENT ID	TECN	CHG	COMMENT
2247 ± 17 OUR AVERAGE					
2200 ± 40		¹ ARMSTRONG 83c OMEG -	18	$K^- p \rightarrow \Lambda \bar{p} X$	
2235 ± 50		¹ BAUBILLIER 81 HBC -	8	$K^- p \rightarrow \Lambda \bar{p} X$	
2260 ± 20		¹ CLELAND 81 SPEC ±	50	$K^+ p \rightarrow \Lambda \bar{p} X$	
• • • We do not use the following data for averages, fits, limits, etc. • • •					
2147 ± 4	37	CHLIAPNIK... 79 HBC +	32	$K^+ p \rightarrow \bar{\Lambda} p X$	
2240 ± 20	20	LISSAUER 70 HBC	9	$K^+ p$	
¹ $J^P = 2^-$ from moments analysis.					

 $K_2(2250)$ WIDTH

VALUE (MeV)	EVTS	DOCUMENT ID	TECN	CHG	COMMENT
180 ± 30 OUR AVERAGE					Error includes scale factor of 1.4.
150 ± 30		² ARMSTRONG 83c OMEG -	18	$K^- p \rightarrow \Lambda \bar{p} X$	
210 ± 30		² CLELAND 81 SPEC ±	50	$K^+ p \rightarrow \Lambda \bar{p} X$	
• • • We do not use the following data for averages, fits, limits, etc. • • •					
~ 200		² BAUBILLIER 81 HBC -	8	$K^- p \rightarrow \Lambda \bar{p} X$	
~ 40	37	CHLIAPNIK... 79 HBC +	32	$K^+ p \rightarrow \bar{\Lambda} p X$	
80 ± 20	20	LISSAUER 70 HBC	9	$K^+ p$	
² $J^P = 2^-$ from moments analysis.					

 $K_2(2250)$ DECAY MODES

Mode	
Γ_1	$K \pi \pi$
Γ_2	$\rho \bar{\Lambda}$

 $K_2(2250)$ REFERENCES

ARMSTRONG	83C	NP B227 365	T.A. Armstrong <i>et al.</i>	(BARI, BIRM, CERN+)
BAUBILLIER	81	NP B183 1	M. Baubillier <i>et al.</i>	(BIRM, CERN, GLAS+ JP)
CLELAND	81	NP B184 1	W.E. Cleland <i>et al.</i>	(PITT, GEVA, LAUS+ JP)
CHLIAPNIK...	79	NP B158 253	P.V. Chliapnikov <i>et al.</i>	(CERN, BELG, MONS)
LISSAUER	70	NP B18 491	D. Lissauer <i>et al.</i>	(LBL)

OTHER RELATED PAPERS

ALEXANDER	68B	PRL 20 755	G. Alexander <i>et al.</i>	(LRL)
-----------	-----	------------	----------------------------	-------

 $K_3(2320)$

$$I(J^P) = \frac{1}{2}(3^+)$$

OMITTED FROM SUMMARY TABLE

Seen in the $J^P = 3^+$ wave of the antihyperon-nucleon system.
Needs confirmation.

 $K_3(2320)$ MASS

VALUE (MeV)	DOCUMENT ID	TECN	CHG	COMMENT
2324 ± 24 OUR AVERAGE				
2330 ± 40	¹ ARMSTRONG 83c OMEG -	18	$K^- p \rightarrow \Lambda \bar{p} X$	
2320 ± 30	¹ CLELAND 81 SPEC ±	50	$K^+ p \rightarrow \Lambda \bar{p} X$	
¹ $J^P = 3^+$ from moments analysis.				

 $K_3(2320)$ WIDTH

VALUE (MeV)	DOCUMENT ID	TECN	CHG	COMMENT
150 ± 30	² ARMSTRONG 83c OMEG -	18	$K^- p \rightarrow \Lambda \bar{p} X$	
• • • We do not use the following data for averages, fits, limits, etc. • • •				
~ 250	² CLELAND 81 SPEC ±	50	$K^+ p \rightarrow \Lambda \bar{p} X$	
² $J^P = 3^+$ from moments analysis.				

 $K_3(2320)$ DECAY MODES

Mode	
Γ_1	$\rho \bar{\Lambda}$

 $K_3(2320)$ REFERENCES

ARMSTRONG	83C	NP B227 365	T.A. Armstrong <i>et al.</i>	(BARI, BIRM, CERN+)
CLELAND	81	NP B184 1	W.E. Cleland <i>et al.</i>	(PITT, GEVA, LAUS+)

 $K_5^*(2380)$

$$I(J^P) = \frac{1}{2}(5^-)$$

OMITTED FROM SUMMARY TABLE

Needs confirmation.

 $K_5^*(2380)$ MASS

VALUE (MeV)	DOCUMENT ID	TECN	CHG	COMMENT
2382 ± 14 ± 19	¹ ASTON 86 LASS 0	11	$K^- p \rightarrow K^- \pi^+ n$	
¹ From a fit to all the moments.				

 $K_5^*(2380)$ WIDTH

VALUE (MeV)	DOCUMENT ID	TECN	CHG	COMMENT
178 ± 37 ± 32	² ASTON 86 LASS 0	11	$K^- p \rightarrow K^- \pi^+ n$	
² From a fit to all the moments.				

 $K_5^*(2380)$ DECAY MODES

Mode	Fraction (Γ_i/Γ)
Γ_1	$K \pi$ (6.1 ± 1.2) %

 $K_5^*(2380)$ BRANCHING RATIOS

$\Gamma(K \pi)/\Gamma_{\text{total}}$		Γ_1/Γ
0.061 ± 0.012	ASTON 88 LASS 0	11 $K^- p \rightarrow K^- \pi^+ n$

 $K_5^*(2380)$ REFERENCES

ASTON	88	NP B296 493	D. Aston <i>et al.</i>	(SLAC, NAGO, CINC, INUS)
ASTON	86	PL B180 308	D. Aston <i>et al.</i>	(SLAC, NAGO, CINC, INUS)

Meson Particle Listings

$K_4(2500)$, $K(3100)$

$K_4(2500)$ $I(J^P) = \frac{1}{2}(4^-)$
 OMITTED FROM SUMMARY TABLE
 Needs confirmation.

$K_4(2500)$ MASS

VALUE (MeV)	DOCUMENT ID	TECN	CHG	COMMENT
2490 ± 20	¹ CLELAND	81	SPEC ±	50 $K^+ p \rightarrow \Lambda \bar{p}$

¹ $J^P = 4^-$ from moments analysis.

$K_4(2500)$ WIDTH

VALUE (MeV)	DOCUMENT ID	TECN	CHG	COMMENT
~ 250	² CLELAND	81	SPEC ±	50 $K^+ p \rightarrow \Lambda \bar{p}$

• • • We do not use the following data for averages, fits, limits, etc. • • •
² $J^P = 4^-$ from moments analysis.

$K_4(2500)$ DECAY MODES

Mode
$\Gamma_1 \quad \rho \bar{\Lambda}$

$K_4(2500)$ REFERENCES

CLELAND 81 NP B184 1 W.E. Cleland et al. (PITT, GEVA, LAUS+)

$K(3100)$ $I^G(J^{PC}) = ?^?(???)$
 OMITTED FROM SUMMARY TABLE
 Narrow peak observed in several ($\Lambda \bar{p} +$ pions) and ($\bar{\Lambda} p +$ pions) states in Σ^- Be reactions Needs confirmation. by BOURQUIN 86 and in $n p$ and $n A$ reactions by ALEEV 93. Not seen by BOEHNLEIN 91. If due to strong decays, this state has exotic quantum numbers ($B=0, Q=+1, S=-1$ for $\Lambda \bar{p} \pi^+ \pi^+$ and $I \geq 3/2$ for $\Lambda \bar{p} \pi^-$). Needs confirmation.

$K(3100)$ MASS

VALUE (MeV)	DOCUMENT ID
~ 3100 OUR ESTIMATE	

3-BODY DECAYS

VALUE (MeV)	DOCUMENT ID	TECN	COMMENT
3054 ± 11 OUR AVERAGE			
3060 ± 7 ± 20	¹ ALEEV 93 BIS2		$K(3100) \rightarrow \Lambda \bar{p} \pi^+$
3056 ± 7 ± 20	¹ ALEEV 93 BIS2		$K(3100) \rightarrow \bar{\Lambda} \rho \pi^-$
3055 ± 8 ± 20	¹ ALEEV 93 BIS2		$K(3100) \rightarrow \Lambda \bar{p} \pi^-$
3045 ± 8 ± 20	¹ ALEEV 93 BIS2		$K(3100) \rightarrow \bar{\Lambda} \rho \pi^+$

4-BODY DECAYS

VALUE (MeV)	DOCUMENT ID	TECN	COMMENT
3059 ± 11 OUR AVERAGE			
3067 ± 6 ± 20	¹ ALEEV 93 BIS2		$K(3100) \rightarrow \Lambda \bar{p} \pi^+ \pi^+$
3060 ± 8 ± 20	¹ ALEEV 93 BIS2		$K(3100) \rightarrow \Lambda \bar{p} \pi^+ \pi^-$
3055 ± 7 ± 20	¹ ALEEV 93 BIS2		$K(3100) \rightarrow \bar{\Lambda} \rho \pi^- \pi^-$
3052 ± 8 ± 20	¹ ALEEV 93 BIS2		$K(3100) \rightarrow \bar{\Lambda} \rho \pi^- \pi^+$
• • • We do not use the following data for averages, fits, limits, etc. • • •			
3105 ± 30	BOURQUIN 86 SPEC		$K(3100) \rightarrow \Lambda \bar{p} \pi^+ \pi^+$
3115 ± 30	BOURQUIN 86 SPEC		$K(3100) \rightarrow \Lambda \bar{p} \pi^+ \pi^-$

5-BODY DECAYS

VALUE (MeV)	DOCUMENT ID	TECN	COMMENT
• • • We do not use the following data for averages, fits, limits, etc. • • •			
3095 ± 30	BOURQUIN 86 SPEC		$K(3100) \rightarrow \Lambda \bar{p} \pi^+ \pi^+ \pi^-$

¹ Supersedes ALEEV 90.

$K(3100)$ WIDTH

3-BODY DECAYS

VALUE (MeV)	DOCUMENT ID	TECN	COMMENT
• • • We do not use the following data for averages, fits, limits, etc. • • •			
42 ± 16	² ALEEV 93 BIS2		$K(3100) \rightarrow \Lambda \bar{p} \pi^+$
36 ± 15	² ALEEV 93 BIS2		$K(3100) \rightarrow \bar{\Lambda} \rho \pi^-$
50 ± 18	² ALEEV 93 BIS2		$K(3100) \rightarrow \Lambda \bar{p} \pi^-$
30 ± 15	² ALEEV 93 BIS2		$K(3100) \rightarrow \bar{\Lambda} \rho \pi^+$

4-BODY DECAYS

VALUE (MeV)	CL%	DOCUMENT ID	TECN	COMMENT
• • • We do not use the following data for averages, fits, limits, etc. • • •				
22 ± 8		² ALEEV 93 BIS2		$K(3100) \rightarrow \Lambda \bar{p} \pi^+ \pi^+$
28 ± 12		² ALEEV 93 BIS2		$K(3100) \rightarrow \Lambda \bar{p} \pi^+ \pi^-$
32 ± 15		² ALEEV 93 BIS2		$K(3100) \rightarrow \bar{\Lambda} \rho \pi^- \pi^-$
30 ± 15		² ALEEV 93 BIS2		$K(3100) \rightarrow \bar{\Lambda} \rho \pi^- \pi^+$
< 30		BOURQUIN 86 SPEC		$K(3100) \rightarrow \Lambda \bar{p} \pi^+ \pi^+$
< 80		BOURQUIN 86 SPEC		$K(3100) \rightarrow \Lambda \bar{p} \pi^+ \pi^-$

5-BODY DECAYS

VALUE (MeV)	CL%	DOCUMENT ID	TECN	COMMENT
• • • We do not use the following data for averages, fits, limits, etc. • • •				
< 30		BOURQUIN 86 SPEC		$K(3100) \rightarrow \Lambda \bar{p} \pi^+ \pi^+ \pi^-$

² Supersedes ALEEV 90.

$K(3100)$ DECAY MODES

Mode
$\Gamma_1 \quad K(3100)^0 \rightarrow \Lambda \bar{p} \pi^+$
$\Gamma_2 \quad K(3100)^{--} \rightarrow \Lambda \bar{p} \pi^-$
$\Gamma_3 \quad K(3100)^- \rightarrow \Lambda \bar{p} \pi^+ \pi^-$
$\Gamma_4 \quad K(3100)^+ \rightarrow \Lambda \bar{p} \pi^+ \pi^+$
$\Gamma_5 \quad K(3100)^0 \rightarrow \Lambda \bar{p} \pi^+ \pi^+ \pi^-$
$\Gamma_6 \quad K(3100)^0 \rightarrow \Sigma(1385)^+ \bar{p}$

$\Gamma(\Sigma(1385)^+ \bar{p}) / \Gamma(\Lambda \bar{p} \pi^+)$

Γ_6 / Γ_1

VALUE	CL%	DOCUMENT ID	TECN	COMMENT
< 0.04		90 ALEEV 93 BIS2		$K(3100)^0 \rightarrow \Sigma(1385)^+ \bar{p}$

$K(3100)$ REFERENCES

ALEEV 93 PAN 56 1358 A.N. Aleev et al. (BIS-2 Collab.)
 Translated from YAF 56 100.
 BOEHNLEIN 91 NP B21 174 (suppl) A. Boehnlein et al. (FLOR, BNL, IND+)
 ALEEV 90 ZPHY C47 533 A.N. Aleev et al. (BIS-2 Collab.)
 BOURQUIN 86 PL B172 113 M.H. Bourquin et al. (GEVA, RAL, HEIDP+)

See key on page 239

Meson Particle Listings

D MESONS, D^\pm

CHARMED MESONS

(C = ±1)

$$D^+ = c\bar{d}, D^0 = c\bar{u}, \bar{D}^0 = \bar{c}u, D^- = \bar{c}d, \text{ similarly for } D^{*\prime}s$$

D MESONS

Revised January 2000 by P.R. Burchat (Stanford University).

The new experimental results on D mesons reported in this edition are mostly from the CLEO-II experiment at the CESR e^+e^- storage ring and from the fixed-target experiment E791 at Fermilab. The CLEO experiment has measured the D^+ , D^0 , and D_s^+ lifetimes, and E791 has measured the D^0 and D_s^+ lifetimes. The measured ratio of D_s^+ to D^0 lifetimes is now significantly greater than unity: $\tau(D_s^+)/\tau(D^0) = 1.20 \pm 0.02$.

The E791 experiment has obtained the first directly measured limit on the decay-width difference $\Delta\Gamma$ for the mass eigenstates of the neutral D system, looking for a difference in decay rates between the CP -even decay $D^0 \rightarrow K^+K^-$ and the CP -mixed decay $D^0 \rightarrow K^-\pi^+$. The CERN experiment ALEPH and CLEO have made new searches for neutral D mixing in the "wrong-sign" decay $D^0 \rightarrow K^+\pi^-$; no evidence for mixing has been found. CLEO has reduced the uncertainty on the measurement of the doubly Cabibbo-suppressed decay rate $\Gamma(D^0 \rightarrow K^+\pi^-)$ by about a factor of three.

The CERN experiment BEATRICE has measured form factors for the semileptonic decay $D^+ \rightarrow \bar{K}^*(892)^0 \ell^+ \nu_\ell$, and E791 has measured form factors both for this decay and for $D_s^+ \rightarrow \phi \ell^+ \nu_\ell$. The CERN experiment OPAL has measured the semileptonic branching fraction for charm hadrons produced in $Z \rightarrow c\bar{c}$. The Fermilab experiment CDF has set limits on semileptonic decay rates involving K resonances above the $K^*(892)$. The BEPC experiment BES has observed one $D^+ \rightarrow \mu^+ \nu_\mu$ event, and CLEO has improved a measurement of the D_s^+ leptonic decay constant.

CLEO has now measured the important $D^0 \rightarrow K^-\pi^+$ branching fraction using three different methods, and has also measured D^+ and D_s^+ branching fractions involving η and η' mesons. An E791 search for 24 rare or forbidden decays to dilepton final states yielded no evidence for new physics.

D[±]

$$I(J^P) = \frac{1}{2}(0^-)$$

D[±] MASS

The fit includes D^\pm , D^0 , D_s^\pm , $D^{*\pm}$, D^{*0} , and $D_s^{*\pm}$ mass and mass difference measurements.

VALUE (MeV)	EVTS	DOCUMENT ID	TECN	COMMENT
1869.3 ± 0.5 OUR FIT				Error includes scale factor of 1.1.
1869.4 ± 0.5 OUR AVERAGE				
1870.0 ± 0.5 ± 1.0	317	BARLAG	90C ACCM	π^- Cu 230 GeV
1863 ± 4		DERRICK	84 HRS	e^+e^- 29 GeV
1869.4 ± 0.6		¹ TRILLING	81 RVUE	e^+e^- 3.77 GeV

• • • We do not use the following data for averages, fits, limits, etc. • • •

1875 ± 10	9	ADAMOVIICH	87 EMUL	Photoproduction
1860 ± 16	6	ADAMOVIICH	84 EMUL	Photoproduction
1868.4 ± 0.5		¹ SCHINDLER	81 MRK2	e^+e^- 3.77 GeV
1874 ± 5		GOLDHABER	77 MRK1	D^0, D^+ recoil spectra
1868.3 ± 0.9		¹ PERUZZI	77 MRK1	e^+e^- 3.77 GeV
1874 ± 11		PICCOLO	77 MRK1	e^+e^- 4.03, 4.41 GeV
1876 ± 15	50	PERUZZI	76 MRK1	$K^\mp \pi^\pm \pi^\pm$

¹PERUZZI 77 and SCHINDLER 81 errors do not include the 0.13% uncertainty in the absolute SPEAR energy calibration. TRILLING 81 uses the high precision $J/\psi(1S)$ and $\psi(2S)$ measurements of ZHOLENTZ 80 to determine this uncertainty and combines the PERUZZI 77 and SCHINDLER 81 results to obtain the value quoted.

D[±] MEAN LIFE

Measurements with an error $> 0.1 \times 10^{-12}$ s are omitted from the average, and those with an error $> 0.2 \times 10^{-12}$ s have been omitted from the Listings.

VALUE (10^{-12} s)	EVTS	DOCUMENT ID	TECN	COMMENT
1.051 ± 0.013 OUR AVERAGE				
1.0336 ± 0.0221 ^{+0.0099} _{-0.0127}	3777	BONVICINI	99 CLE2	$e^+e^- \approx \tau(4S)$
1.048 ± 0.015 ± 0.011	9K	FRABETTI	94D E687	$D^+ \rightarrow K^-\pi^+\pi^+$
1.075 ± 0.040 ± 0.018	2455	FRABETTI	91 E687	γ Be, $D^+ \rightarrow K^-\pi^+\pi^+$
1.03 ± 0.08 ± 0.06	200	ALVAREZ	90 NA14	$\gamma, D^+ \rightarrow K^-\pi^+\pi^+$
1.05 ^{+0.077} _{-0.072}	317	² BARLAG	90C ACCM	π^- Cu 230 GeV
1.05 ± 0.08 ± 0.07	363	ALBRECHT	88i ARG	e^+e^- 10 GeV
1.090 ± 0.030 ± 0.025	2992	RAAB	88 E691	Photoproduction
• • • We do not use the following data for averages, fits, limits, etc. • • •				
1.12 ^{+0.14} _{-0.11}	149	AGUILAR-...	87D HYBR	$\pi^- p$ and pp
1.09 ^{+0.19} _{-0.15}	59	BARLAG	87B ACCM	K^- and π^- 200 GeV
1.14 ± 0.16 ± 0.07	247	CSORNA	87 CLEO	e^+e^- 10 GeV
1.09 ± 0.14	74	³ PALKA	87B SILI	π Be 200 GeV
0.86 ± 0.13 ^{+0.07} _{-0.03}	48	ABE	86 HYBR	γp 20 GeV

²BARLAG 90C estimates the systematic error to be negligible.

³PALKA 87B observes this in $D^+ \rightarrow \bar{K}^*(892)ev$.

D⁺ DECAY MODES

D^- modes are charge conjugates of the modes below.

Mode	Fraction (Γ_j/Γ)	Scale factor/ Confidence level
Inclusive modes		
Γ_1 e^+ anything	(17.2 ± 1.9) %	
Γ_2 K^- anything	(24.2 ± 2.8) %	S=1.4
Γ_3 \bar{K}^0 anything + K^0 anything	(59 ± 7) %	
Γ_4 K^+ anything	(5.8 ± 1.4) %	
Γ_5 η anything	[a] < 13 %	CL=90%
Γ_6 μ^+ anything		
Leptonic and semileptonic modes		
Γ_7 $\mu^+ \nu_\mu$	(8 ⁺¹⁷ ₋₅) × 10 ⁻⁴	
Γ_8 $\bar{K}^0 \ell^+ \nu_\ell$	[b] (6.8 ± 0.8) %	
Γ_9 $\bar{K}^0 e^+ \nu_e$	(6.7 ± 0.9) %	
Γ_{10} $\bar{K}^0 \mu^+ \nu_\mu$	(7.0 ^{+3.0} _{-2.0}) %	
Γ_{11} $K^-\pi^+ e^+ \nu_e$	(4.1 ^{+0.9} _{-0.7}) %	
Γ_{12} $\bar{K}^*(892)^0 e^+ \nu_e$ × B($\bar{K}^{*0} \rightarrow K^-\pi^+$)	(3.2 ± 0.33) %	
Γ_{13} $K^-\pi^+ e^+ \nu_e$ nonresonant	< 7 × 10 ⁻³	CL=90%
Γ_{14} $K^-\pi^+ \mu^+ \nu_\mu$	(3.2 ± 0.4) %	S=1.1
In the fit as $\frac{2}{3}\Gamma_{26} + \Gamma_{16}$, where $\frac{2}{3}\Gamma_{26} = \Gamma_{15}$.		
Γ_{15} $\bar{K}^*(892)^0 \mu^+ \nu_\mu$ × B($\bar{K}^{*0} \rightarrow K^-\pi^+$)	(2.9 ± 0.4) %	
Γ_{16} $K^-\pi^+ \mu^+ \nu_\mu$ nonresonant	(2.7 ± 1.1) × 10 ⁻³	
Γ_{17} $\bar{K}^0 \pi^+ \pi^- e^+ \nu_e$		
Γ_{18} $K^-\pi^+ \pi^0 e^+ \nu_e$		
Γ_{19} $(\bar{K}^*(892)\pi)^0 e^+ \nu_e$	< 1.2 %	CL=90%
Γ_{20} $(K\pi\pi)^0 e^+ \nu_e$ non- $\bar{K}^*(892)$	< 9 × 10 ⁻³	CL=90%
Γ_{21} $K^-\pi^+ \pi^0 \mu^+ \nu_\mu$	< 1.4 × 10 ⁻³	CL=90%
Γ_{22} $\pi^0 \ell^+ \nu_\ell$	[c] (3.1 ± 1.5) × 10 ⁻³	
Γ_{23} $\pi^+ \pi^- e^+ \nu_e$		

Meson Particle Listings

D[±]

Fractions of some of the following modes with resonances have already appeared above as submodes of particular charged-particle modes.

Γ ₂₄	$\bar{K}^*(892)^0 \ell^+ \nu_\ell$	[b]	(4.7 ± 0.4) %	
Γ ₂₅	$\bar{K}^*(892)^0 e^+ \nu_e$		(4.8 ± 0.5) %	
Γ ₂₆	$\bar{K}^*(892)^0 \mu^+ \nu_\mu$		(4.4 ± 0.6) %	S=1.1
Γ ₂₇	$\bar{K}_1(1270)^0 \mu^+ \nu_\mu$		< 3.5 %	CL=95%
Γ ₂₈	$\bar{K}^*(1410)^0 \mu^+ \nu_\mu$		< 2.7 %	CL=95%
Γ ₂₉	$\bar{K}_2^*(1430)^0 \mu^+ \nu_\mu$		< 8 × 10 ⁻³	CL=95%
Γ ₃₀	$\rho^0 e^+ \nu_e$		(2.2 ± 0.8) × 10 ⁻³	
Γ ₃₁	$\rho^0 \mu^+ \nu_\mu$		(2.7 ± 0.7) × 10 ⁻³	
Γ ₃₂	$\phi e^+ \nu_e$		< 2.09 %	CL=90%
Γ ₃₃	$\phi \mu^+ \nu_\mu$		< 3.72 %	CL=90%
Γ ₃₄	$\eta \ell^+ \nu_\ell$		< 5 × 10 ⁻³	CL=90%
Γ ₃₅	$\eta'(958) \mu^+ \nu_\mu$		< 9 × 10 ⁻³	CL=90%

Hadronic modes with a \bar{K} or $\bar{K}K\bar{K}$

Γ ₃₆	$\bar{K}^0 \pi^+$		(2.89 ± 0.26) %	S=1.1
Γ ₃₇	$K^-\pi^+\pi^+$	[d]	(9.0 ± 0.6) %	
Γ ₃₈	$\bar{K}^*(892)^0 \pi^+$ × B($\bar{K}^{*0} \rightarrow K^-\pi^+$)		(1.27 ± 0.13) %	
Γ ₃₉	$\bar{K}_1^*(1430)^0 \pi^+$ × B($\bar{K}_1^{*0}(1430)^0 \rightarrow K^-\pi^+$)		(2.3 ± 0.3) %	
Γ ₄₀	$\bar{K}^*(1680)^0 \pi^+$ × B($\bar{K}^*(1680)^0 \rightarrow K^-\pi^+$)		(3.7 ± 0.8) × 10 ⁻³	
Γ ₄₁	$K^-\pi^+\pi^+$ nonresonant		(8.5 ± 0.8) %	
Γ ₄₂	$\bar{K}^0 \pi^+ \pi^0$	[d]	(9.7 ± 3.0) %	S=1.1
Γ ₄₃	$\bar{K}^0 \rho^+$		(6.6 ± 2.5) %	
Γ ₄₄	$\bar{K}^*(892)^0 \pi^+$ × B($\bar{K}^{*0} \rightarrow \bar{K}^0 \pi^0$)		(6.3 ± 0.4) × 10 ⁻³	
Γ ₄₅	$\bar{K}^0 \pi^+ \pi^0$ nonresonant		(1.3 ± 1.1) %	
Γ ₄₆	$K^-\pi^+\pi^+\pi^0$	[d]	(6.4 ± 1.1) %	
Γ ₄₇	$\bar{K}^*(892)^0 \rho^+$ total × B($\bar{K}^{*0} \rightarrow K^-\pi^+$)		(1.4 ± 0.9) %	
Γ ₄₈	$\bar{K}_1(1400)^0 \pi^+$ × B($\bar{K}_1(1400)^0 \rightarrow K^-\pi^+\pi^0$)		(2.2 ± 0.6) %	
Γ ₄₉	$K^-\rho^+\pi^+$ total		(3.1 ± 1.1) %	
Γ ₅₀	$K^-\rho^+\pi^+$ 3-body		(1.1 ± 0.4) %	
Γ ₅₁	$\bar{K}^*(892)^0 \pi^+\pi^0$ total × B($\bar{K}^{*0} \rightarrow K^-\pi^+$)		(4.5 ± 0.9) %	
Γ ₅₂	$\bar{K}^*(892)^0 \pi^+\pi^+$ 3-body × B($\bar{K}^{*0} \rightarrow K^-\pi^+$)		(2.8 ± 0.9) %	
Γ ₅₃	$K^*(892)^-\pi^+\pi^+$ 3-body × B($K^{*-} \rightarrow K^-\pi^0$)		(7 ± 3) × 10 ⁻³	
Γ ₅₄	$K^-\pi^+\pi^+\pi^0$ nonresonant	[e]	(1.2 ± 0.6) %	
Γ ₅₅	$\bar{K}^0 \pi^+\pi^+\pi^-$	[d]	(7.0 ± 0.9) %	
Γ ₅₆	$\bar{K}^0 a_1(1260)^+$ × B($a_1(1260)^+ \rightarrow \pi^+\pi^+\pi^-$)		(4.0 ± 0.9) %	
Γ ₅₇	$\bar{K}_1(1400)^0 \pi^+$ × B($\bar{K}_1(1400)^0 \rightarrow \bar{K}^0 \pi^+\pi^-$)		(2.2 ± 0.6) %	
Γ ₅₈	$K^*(892)^-\pi^+\pi^+$ 3-body × B($K^{*-} \rightarrow \bar{K}^0 \pi^-$)		(1.4 ± 0.6) %	
Γ ₅₉	$\bar{K}^0 \rho^0 \pi^+$ total		(4.2 ± 0.9) %	
Γ ₆₀	$\bar{K}^0 \rho^0 \pi^+$ 3-body		(5 ± 5) × 10 ⁻³	
Γ ₆₁	$\bar{K}^0 \pi^+\pi^+\pi^-$ nonresonant		(8 ± 4) × 10 ⁻³	
Γ ₆₂	$K^-\pi^+\pi^+\pi^-$	[d]	(7.2 ± 1.0) × 10 ⁻³	
Γ ₆₃	$\bar{K}^*(892)^0 \pi^+\pi^+\pi^-$ × B($\bar{K}^{*0} \rightarrow K^-\pi^+$)		(5.4 ± 2.3) × 10 ⁻³	
Γ ₆₄	$\bar{K}^*(892)^0 \rho^0 \pi^+$ × B($\bar{K}^{*0} \rightarrow K^-\pi^+$)		(1.9 ± $\frac{1.1}{1.0}$) × 10 ⁻³	
Γ ₆₅	$\bar{K}^*(892)^0 \pi^+\pi^+\pi^-$ no- ρ × B($\bar{K}^{*0} \rightarrow K^-\pi^+$)		(2.9 ± 1.1) × 10 ⁻³	
Γ ₆₆	$K^-\rho^0 \pi^+\pi^+$		(3.1 ± 0.9) × 10 ⁻³	
Γ ₆₇	$K^-\pi^+\pi^+\pi^-$ nonresonant		< 2.3 × 10 ⁻³	CL=90%
Γ ₆₈	$K^-\pi^+\pi^+\pi^0 \pi^0$		(2.2 ± $\frac{5.0}{0.9}$) %	
Γ ₆₉	$\bar{K}^0 \pi^+\pi^+\pi^-\pi^0$		(5.4 ± $\frac{3.0}{1.4}$) %	
Γ ₇₀	$\bar{K}^0 \pi^+\pi^+\pi^+\pi^-\pi^-$		(8 ± 7) × 10 ⁻⁴	
Γ ₇₁	$K^-\pi^+\pi^+\pi^+\pi^-\pi^0$		(2.0 ± 1.8) × 10 ⁻³	
Γ ₇₂	$\bar{K}^0 \bar{K}^0 K^+$		(1.8 ± 0.8) %	

Fractions of some of the following modes with resonances have already appeared above as submodes of particular charged-particle modes.

Γ ₇₃	$\bar{K}^0 \rho^+$		(6.6 ± 2.5) %	
Γ ₇₄	$\bar{K}^0 a_1(1260)^+$		(8.0 ± 1.7) %	
Γ ₇₅	$\bar{K}^0 a_2(1320)^+$		< 3 × 10 ⁻³	CL=90%
Γ ₇₆	$\bar{K}^*(892)^0 \pi^+$		(1.90 ± 0.19) %	
Γ ₇₇	$\bar{K}^*(892)^0 \rho^+$ total	[e]	(2.1 ± 1.3) %	
Γ ₇₈	$\bar{K}^*(892)^0 \rho^+$ S-wave	[e]	(1.6 ± 1.6) %	
Γ ₇₉	$\bar{K}^*(892)^0 \rho^+$ P-wave		< 1 × 10 ⁻³	CL=90%
Γ ₈₀	$\bar{K}^*(892)^0 \rho^+$ D-wave		(10 ± 7) × 10 ⁻³	
Γ ₈₁	$\bar{K}^*(892)^0 \rho^+$ D-wave longitudi- nal		< 7 × 10 ⁻³	CL=90%
Γ ₈₂	$\bar{K}_1(1270)^0 \pi^+$		< 7 × 10 ⁻³	CL=90%
Γ ₈₃	$\bar{K}_1(1400)^0 \pi^+$		(4.9 ± 1.2) %	
Γ ₈₄	$\bar{K}^*(1410)^0 \pi^+$		< 7 × 10 ⁻³	CL=90%
Γ ₈₅	$\bar{K}_0^*(1430)^0 \pi^+$		(3.7 ± 0.4) %	
Γ ₈₆	$\bar{K}^*(1680)^0 \pi^+$		(1.43 ± 0.30) %	
Γ ₈₇	$\bar{K}^*(892)^0 \pi^+\pi^0$ total		(6.7 ± 1.4) %	
Γ ₈₈	$K^*(892)^0 \pi^+\pi^0$ 3-body	[e]	(4.2 ± 1.4) %	
Γ ₈₉	$K^*(892)^-\pi^+\pi^+$ total		(2.0 ± 0.9) %	
Γ ₉₀	$K^-(892)^-\pi^+\pi^+$ 3-body		(3.1 ± 1.1) %	
Γ ₉₁	$K^-\rho^+\pi^+$ total		(3.1 ± 1.1) %	
Γ ₉₂	$K^-\rho^+\pi^+$ 3-body		(1.1 ± 0.4) %	
Γ ₉₃	$\bar{K}^0 \rho^0 \pi^+$ total		(4.2 ± 0.9) %	CL=90%
Γ ₉₄	$\bar{K}^0 \rho^0 \pi^+$ 3-body		(5 ± 5) × 10 ⁻³	
Γ ₉₅	$\bar{K}^0 f_0(980) \pi^+$		< 5 × 10 ⁻³	CL=90%
Γ ₉₆	$\bar{K}^*(892)^0 \pi^+\pi^+\pi^-$		(8.1 ± 3.4) × 10 ⁻³	S=1.7
Γ ₉₇	$\bar{K}^*(892)^0 \rho^0 \pi^+$		(2.9 ± $\frac{1.7}{1.5}$) × 10 ⁻³	S=1.8
Γ ₉₈	$\bar{K}^*(892)^0 \pi^+\pi^+\pi^-\pi^0$		(4.3 ± 1.7) × 10 ⁻³	
Γ ₉₉	$K^-\rho^0 \pi^+\pi^+$		(3.1 ± 0.9) × 10 ⁻³	

Pionic modes

Γ ₁₀₀	$\pi^+\pi^0$		(2.5 ± 0.7) × 10 ⁻³	
Γ ₁₀₁	$\pi^+\pi^+\pi^-$		(3.6 ± 0.4) × 10 ⁻³	
Γ ₁₀₂	$\rho^0 \pi^+$		(1.05 ± 0.31) × 10 ⁻³	
Γ ₁₀₃	$\pi^+\pi^+\pi^-\pi^0$ nonresonant		(2.2 ± 0.4) × 10 ⁻³	
Γ ₁₀₄	$\pi^+\pi^+\pi^-\pi^0$		(1.9 ± $\frac{1.5}{1.2}$) %	
Γ ₁₀₅	$\eta \pi^+ \times B(\eta \rightarrow \pi^+\pi^-\pi^0)$		(6.9 ± 1.4) × 10 ⁻⁴	
Γ ₁₀₆	$\omega \pi^+ \times B(\omega \rightarrow \pi^+\pi^-\pi^0)$		< 6 × 10 ⁻³	CL=90%
Γ ₁₀₇	$\pi^+\pi^+\pi^+\pi^-\pi^-$		(2.1 ± 0.4) × 10 ⁻³	
Γ ₁₀₈	$\pi^+\pi^+\pi^+\pi^-\pi^0$		(2.9 ± $\frac{2.9}{2.0}$) × 10 ⁻³	

Fractions of some of the following modes with resonances have already appeared above as submodes of particular charged-particle modes.

Γ ₁₀₉	$\eta \pi^+$		(3.0 ± 0.6) × 10 ⁻³	
Γ ₁₁₀	$\rho^0 \pi^+$		(1.05 ± 0.31) × 10 ⁻³	
Γ ₁₁₁	$\omega \pi^+$		< 7 × 10 ⁻³	CL=90%
Γ ₁₁₂	$\eta \rho^+$		< 7 × 10 ⁻³	CL=90%
Γ ₁₁₃	$\eta'(958) \pi^+$		(5.0 ± 1.0) × 10 ⁻³	
Γ ₁₁₄	$\eta'(958) \rho^+$		< 5 × 10 ⁻³	CL=90%

Hadronic modes with a $K\bar{K}$ pair

Γ ₁₁₅	$K^+ \bar{K}^0$		(7.4 ± 1.0) × 10 ⁻³	
Γ ₁₁₆	$K^+ K^-\pi^+$	[d]	(8.7 ± 0.7) × 10 ⁻³	
Γ ₁₁₇	$\phi \pi^+ \times B(\phi \rightarrow K^+K^-)$		(3.0 ± 0.3) × 10 ⁻³	
Γ ₁₁₈	$K^+ \bar{K}^*(892)^0$ × B($\bar{K}^{*0} \rightarrow K^-\pi^+$)		(2.8 ± 0.4) × 10 ⁻³	
Γ ₁₁₉	$K^+ K^-\pi^+$ nonresonant		(4.5 ± 0.9) × 10 ⁻³	
Γ ₁₂₀	$K^0 \bar{K}^0 \pi^+$		—	
Γ ₁₂₁	$K^*(892)^+ \bar{K}^0$ × B($K^{*+} \rightarrow K^0 \pi^+$)		(2.1 ± 1.0) %	
Γ ₁₂₂	$K^+ K^-\pi^+\pi^0$		—	
Γ ₁₂₃	$\phi \pi^+ \pi^0 \times B(\phi \rightarrow K^+K^-)$		(1.1 ± 0.5) %	
Γ ₁₂₄	$\phi \rho^+ \times B(\phi \rightarrow K^+K^-)$		< 7 × 10 ⁻³	CL=90%
Γ ₁₂₅	$K^+ K^-\pi^+\pi^0$ non- ϕ		(1.5 ± $\frac{0.7}{0.6}$) %	
Γ ₁₂₆	$K^+ \bar{K}^0 \pi^+\pi^-$		< 2 %	CL=90%
Γ ₁₂₇	$K^0 K^-\pi^+\pi^+$		(1.0 ± 0.6) %	
Γ ₁₂₈	$K^*(892)^+ \bar{K}^*(892)^0$ × B ² ($K^{*+} \rightarrow K^0 \pi^+$)		(1.2 ± 0.5) %	
Γ ₁₂₉	$K^0 K^-\pi^+\pi^+$ non- $K^{*+} \bar{K}^{*0}$		< 7.9 × 10 ⁻³	CL=90%
Γ ₁₃₀	$K^+ K^-\pi^+\pi^+\pi^-$		—	
Γ ₁₃₁	$\phi \pi^+ \pi^+\pi^-$ × B($\phi \rightarrow K^+K^-$)		< 1 × 10 ⁻³	CL=90%
Γ ₁₃₂	$K^+ K^-\pi^+\pi^+\pi^-\pi^0$ nonresonant		< 3 %	CL=90%

Meson Particle Listings

D^\pm

$\Gamma(c \rightarrow \ell^+ \text{ anything}) / \Gamma(c \rightarrow \text{ anything})$

This is an average (not a sum) of e^+ and μ^+ measurements.

VALUE	EVTS	DOCUMENT ID	TECN	COMMENT
$0.095 \pm 0.006 \pm 0.007$ 0.006	854	7 ABBIENDI	99K OPAL	$Z^0 \rightarrow c\bar{c}$

⁷ ABBIENDI 99K uses the excess of right-sign over wrong-sign leptons opposite reconstructed $D^*(2020)^+ \rightarrow D^0 \pi^+$ decays in $Z^0 \rightarrow c\bar{c}$.

Inclusive modes

$\Gamma(e^+ \text{ anything}) / \Gamma_{\text{total}}$

VALUE	EVTS	DOCUMENT ID	TECN	COMMENT	Γ_1/Γ
0.172 ± 0.019 OUR AVERAGE					
0.20 ± 0.09 -0.07		AGUILAR...	87E HYBR	$\pi p, pp$ 360, 400 GeV	
$0.170 \pm 0.019 \pm 0.007$	158	BALTRUSAIT..85B	MRK3	$e^+ e^-$ 3.77 GeV	
0.168 ± 0.064	23	SCHINDLER	81 MRK2	$e^+ e^-$ 3.77 GeV	
• • • We do not use the following data for averages, fits, limits, etc. • • •					
0.220 ± 0.044 -0.022		BACINO	80 DLCO	$e^+ e^-$ 3.77 GeV	

D^+ and $D^0 \rightarrow (e^+ \text{ anything}) / (\text{total } D^+ \text{ and } D^0)$

If measured at the $\psi(3770)$, this quantity is a weighted average of D^+ (44%) and D^0 (56%) branching fractions. Only experiments at $E_{\text{cm}} = 3.77$ GeV are included in the average here. We don't put this result in the Meson Summary Table.

VALUE	EVTS	DOCUMENT ID	TECN	COMMENT
0.110 ± 0.011 OUR AVERAGE				Error includes scale factor of 1.1.
0.117 ± 0.011	295	BALTRUSAIT..85B	MRK3	$e^+ e^-$ 3.77 GeV
0.10 ± 0.032		⁸ SCHINDLER	81 MRK2	$e^+ e^-$ 3.77 GeV
0.072 ± 0.028		FELLER	78 MRK1	$e^+ e^-$ 3.77 GeV
• • • We do not use the following data for averages, fits, limits, etc. • • •				
$0.096 \pm 0.004 \pm 0.011$	2207	⁹ ALBRECHT	96C ARG	$e^+ e^- \approx 10$ GeV
$0.134 \pm 0.015 \pm 0.010$		¹⁰ ABE	93E VNS	$e^+ e^-$ 58 GeV
$0.098 \pm 0.009 \pm 0.006$ 0.005	240	¹¹ ALBRECHT	92F ARG	$e^+ e^- \approx 10$ GeV
$0.096 \pm 0.007 \pm 0.015$		¹² ONG	88 MRK2	$e^+ e^-$ 29 GeV
0.116 ± 0.011 -0.009		¹² PAL	86 DLCO	$e^+ e^-$ 29 GeV
$0.091 \pm 0.009 \pm 0.013$		¹² AIHARA	85 TPC	$e^+ e^-$ 29 GeV
$0.092 \pm 0.022 \pm 0.040$		¹² ALTHOFF	84J TASS	$e^+ e^-$ 34.6 GeV
0.091 ± 0.013		¹² KOOP	84 DLCO	See PAL 86
0.08 ± 0.015		¹³ BACINO	79 DLCO	$e^+ e^-$ 3.77 GeV

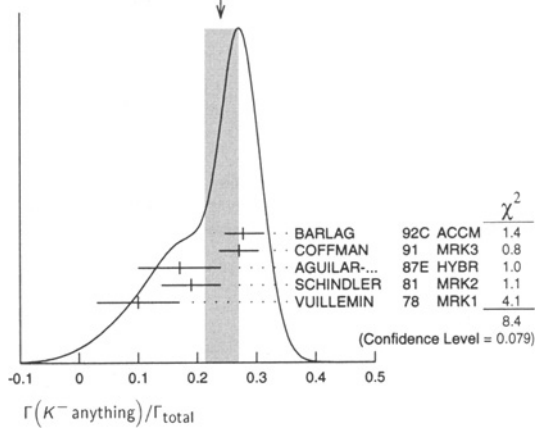
⁸ Isolates D^+ and $D^0 \rightarrow e^+ X$ and weights for relative production (44%–56%).
⁹ ALBRECHT 96C uses e^- in the hemisphere opposite to $D^{*+} \rightarrow D^0 \pi^+$ events.
¹⁰ ABE 93E also measures forward-backward asymmetries and fragmentation functions for c and b quarks.
¹¹ ALBRECHT 92F uses the excess of right-sign over wrong-sign leptons in a sample of events tagged by fully reconstructed $D^*(2010)^+ \rightarrow D^0 \pi^+$ decays.
¹² Average BR for charm $\rightarrow e^+ X$. Unlike at $E_{\text{cm}} = 3.77$ GeV, the admixture of charmed mesons is unknown.
¹³ Not independent of BACINO 80 measurements of $\Gamma(e^+ \text{ anything}) / \Gamma_{\text{total}}$ for the D^+ and D^0 separately.

$\Gamma(K^- \text{ anything}) / \Gamma_{\text{total}}$

VALUE	EVTS	DOCUMENT ID	TECN	COMMENT
0.242 ± 0.028 OUR AVERAGE				Error includes scale factor of 1.4. See the ideogram below.
0.278 ± 0.036 -0.031		¹⁴ BARLAG	92C ACCM	$\pi^- \text{ Cu}$ 230 GeV
$0.271 \pm 0.023 \pm 0.024$		COFFMAN	91 MRK3	$e^+ e^-$ 3.77 GeV
0.17 ± 0.07		AGUILAR...	87E HYBR	$\pi p, pp$ 360, 400 GeV
0.19 ± 0.05	26	SCHINDLER	81 MRK2	$e^+ e^-$ 3.77 GeV
0.10 ± 0.07	3	VUILLEMIN	78 MRK1	$e^+ e^-$ 3.77 GeV
• • • We do not use the following data for averages, fits, limits, etc. • • •				
0.16 ± 0.08 -0.07		AGUILAR...	86B HYBR	See AGUILAR-BENITEZ 87E

¹⁴ BARLAG 92C computes the branching fraction using topological normalization.

WEIGHTED AVERAGE
 0.242 ± 0.028 (Error scaled by 1.4)



$[\Gamma(\bar{K}^0 \text{ anything}) + \Gamma(K^0 \text{ anything})] / \Gamma_{\text{total}}$

VALUE	EVTS	DOCUMENT ID	TECN	COMMENT
0.59 ± 0.07 OUR AVERAGE				
$0.612 \pm 0.065 \pm 0.043$		COFFMAN	91 MRK3	$e^+ e^-$ 3.77 GeV
0.52 ± 0.18	15	SCHINDLER	81 MRK2	$e^+ e^-$ 3.77 GeV
0.39 ± 0.29	3	VUILLEMIN	78 MRK1	$e^+ e^-$ 3.77 GeV

$\Gamma(K^+ \text{ anything}) / \Gamma_{\text{total}}$

VALUE	EVTS	DOCUMENT ID	TECN	COMMENT
0.058 ± 0.014 OUR AVERAGE				
$0.055 \pm 0.013 \pm 0.009$		COFFMAN	91 MRK3	$e^+ e^-$ 3.77 GeV
0.08 ± 0.06 -0.05		AGUILAR...	87E HYBR	$\pi p, pp$ 360, 400 GeV
0.06 ± 0.04	12	SCHINDLER	81 MRK2	$e^+ e^-$ 3.77 GeV
0.06 ± 0.06	2	VUILLEMIN	78 MRK1	$e^+ e^-$ 3.77 GeV

D^+ and $D^0 \rightarrow (\eta \text{ anything}) / (\text{total } D^+ \text{ and } D^0)$

If measured at the $\psi(3770)$, this quantity is a weighted average of D^+ (44%) and D^0 (56%) branching fractions. Only the experiment at $E_{\text{cm}} = 3.77$ GeV is used.

VALUE	DOCUMENT ID	TECN	COMMENT
< 0.13	PARTRIDGE 81	CBAL	$e^+ e^-$ 3.77 GeV
• • • We do not use the following data for averages, fits, limits, etc. • • •			
< 0.02	¹⁵ BRANDELIK 79	DASP	$e^+ e^-$ 4.03 GeV

¹⁵ The BRANDELIK 79 result is based on the absence of an η signal at $E_{\text{cm}} = 4.03$ GeV. PARTRIDGE 81 observes a substantially higher η cross section at 4.03 GeV.

Leptonic and semileptonic modes

$\Gamma(\mu^+ \nu_\mu) / \Gamma_{\text{total}}$

See the "Note on Pseudoscalar-Meson Decay Constants" in the Listings for the π^\pm .

VALUE	CL%	EVTS	DOCUMENT ID	TECN	COMMENT
$0.0008 \pm 0.0016 \pm 0.0005$ -0.0005		1	¹⁶ BAI	98B BES	$e^+ e^- \rightarrow D^{*+} D^-$

• • • We do not use the following data for averages, fits, limits, etc. • • •

< 0.00072	90	ADLER	88B MRK3	$e^+ e^-$ 3.77 GeV
< 0.02	90	0	¹⁷ AUBERT 83	SPEC $\mu^+ \text{ Fe}$, 250 GeV

¹⁶ BAI 98B obtains $f_D = (300 + 180 + 80) / (-150 - 40)$ MeV from this measurement.

¹⁷ AUBERT 83 obtains an upper limit 0.014 assuming the final state contains equal amounts of (D^+, D^-) , (D^+, \bar{D}^0) , (D^-, D^0) , and (D^0, \bar{D}^0) . We quote the limit they get under more general assumptions.

$\Gamma(\bar{K}^0 e^+ \nu_e) / \Gamma_{\text{total}}$

We average our $\bar{K}^0 e^+ \nu_e$ and $\bar{K}^0 \mu^+ \nu_\mu$ branching fractions, after multiplying the latter by a phase-space factor of 1.03 to be able to use it with the $\bar{K}^0 e^+ \nu_e$ fraction. Hence our e^+ here is really an e^+ .

VALUE	DOCUMENT ID	COMMENT
0.067 ± 0.009	PDG	00 Our $\Gamma(\bar{K}^0 e^+ \nu_e) / \Gamma_{\text{total}}$
0.072 ± 0.031 -0.020	PDG	00 $1.03 \times \text{our } \Gamma(\bar{K}^0 \mu^+ \nu_\mu) / \Gamma_{\text{total}}$

$\Gamma(\bar{K}^0 e^+ \nu_e) / \Gamma_{\text{total}}$

VALUE	EVTS	DOCUMENT ID	TECN	COMMENT
0.067 ± 0.009 OUR FIT				
$0.06 \pm 0.022 \pm 0.007$ -0.013	13	BAI	91 MRK3	$e^+ e^- \approx 3.77$ GeV

$\Gamma(\bar{K}^0 e^+ \nu_e) / \Gamma(\bar{K}^0 \pi^+)$

VALUE	EVTS	DOCUMENT ID	TECN	COMMENT
2.32 ± 0.31 OUR FIT				
$2.60 \pm 0.35 \pm 0.26$	186	¹⁸ BEAN	93C CLE2	$e^+ e^- \approx \Upsilon(4S)$

¹⁸ BEAN 93C uses $\bar{K}^0 \mu^+ \nu_\mu$ as well as $\bar{K}^0 e^+ \nu_e$ events and makes a small phase-space adjustment to the number of the μ^+ events to use them as e^+ events.

$\Gamma(\bar{K}^0 e^+ \nu_e)/\Gamma(K^- \pi^+ \pi^+)$		Γ_9/Γ_{37}	
VALUE	DOCUMENT ID	TECN	COMMENT
0.74 ± 0.10 OUR FIT			
0.66 ± 0.09 ± 0.14	ANJOS	91c E691	γ Be 80–240 GeV
$\Gamma(\bar{K}^0 \mu^+ \nu_\mu)/\Gamma_{total}$		Γ_{10}/Γ	
VALUE	EVTs	DOCUMENT ID	TECN COMMENT
0.07 $\begin{smallmatrix} +0.028 \\ -0.016 \end{smallmatrix}$ ± 0.012	14	BAI	91 MRK3 $e^+ e^- \approx 3.77$ GeV
$\Gamma(\bar{K}^0 \mu^+ \nu_\mu)/\Gamma(\mu^+ \text{anything})$		Γ_{10}/Γ_6	
VALUE	EVTs	DOCUMENT ID	COMMENT
0.76 ± 0.06	84	¹⁹ AOKI	88 π^- emulsion
• • • We do not use the following data for averages, fits, limits, etc. • • •			
¹⁹ From topological branching ratios in emulsion with an identified muon.			
$\Gamma(K^- \pi^+ e^+ \nu_e)/\Gamma_{total}$		Γ_{11}/Γ	
VALUE	CL%	EVTs	DOCUMENT ID
0.041 ± 0.009 OUR FIT			
0.035 $\begin{smallmatrix} +0.012 \\ -0.007 \end{smallmatrix}$ ± 0.004	14	²⁰ BAI	91 MRK3 $e^+ e^- \approx 3.77$ GeV
• • • We do not use the following data for averages, fits, limits, etc. • • •			
<0.057	90	²¹ AGUILAR-...	87F HYBR $\pi p, pp$ 360, 400 GeV
²⁰ BAI 91 finds that a fraction $0.79^{+0.15+0.09}_{-0.17-0.03}$ of combined D^+ and D^0 decays to $\bar{K} \pi e^+ \nu_e$ (24 events) are $\bar{K}^*(892)^0 e^+ \nu_e$.			
²¹ AGUILAR-BENITEZ 87F computes the branching fraction using topological normalization.			
$\Gamma(\bar{K}^*(892)^0 \ell^+ \nu_\ell)/\Gamma_{total}$		Γ_{24}/Γ	
We average our $\bar{K}^*(892)^0 e^+ \nu_e$ and $\bar{K}^*(892)^0 \mu^+ \nu_\mu$ branching fractions, after multiplying the latter by a phase-space factor of 1.05 to be able to use it with the $\bar{K}^*(892)^0 e^+ \nu_e$ fraction. Hence our ℓ^+ here is really an e^+ .			
VALUE	DOCUMENT ID	COMMENT	
0.047 ± 0.004 OUR AVERAGE			
0.048 ± 0.005	PDG	00	Our $\Gamma(\bar{K}^*(892)^0 e^+ \nu_e)/\Gamma_{total}$
0.046 ± 0.006	PDG	00	$1.05 \times$ our $\Gamma(\bar{K}^*(892)^0 \mu^+ \nu_\mu)/\Gamma_{total}$
$\Gamma(\bar{K}^*(892)^0 e^+ \nu_e)/\Gamma(K^- \pi^+ e^+ \nu_e)$		Γ_{25}/Γ_{11}	
Unseen decay modes of the $\bar{K}^*(892)^0$ are included.			
VALUE	EVTs	DOCUMENT ID	TECN COMMENT
1.16 $\begin{smallmatrix} +0.21 \\ -0.24 \end{smallmatrix}$ OUR FIT			
1.0 ± 0.3	35	ADAMOVIČH	91 OMEG π^- 340 GeV
$\Gamma(\bar{K}^*(892)^0 e^+ \nu_e)/\Gamma(K^- \pi^+ \pi^+)$		Γ_{25}/Γ_{37}	
Unseen decay modes of the $\bar{K}^*(892)^0$ are included.			
VALUE	EVTs	DOCUMENT ID	TECN COMMENT
0.53 ± 0.05 OUR FIT			
0.54 ± 0.05 OUR AVERAGE			
0.67 ± 0.09 ± 0.07	710	²² BEAN	93c CLE2 $e^+ e^- \approx \tau(45)$
0.62 ± 0.15 ± 0.09	35	ADAMOVIČH	91 OMEG π^- 340 GeV
0.55 ± 0.08 ± 0.10	880	ALBRECHT	91 ARG $e^+ e^- \approx 10.4$ GeV
0.49 ± 0.04 ± 0.05		ANJOS	89b E691 Photoproduction
²² BEAN 93c uses $\bar{K}^*(892)^0 \mu^+ \nu_\mu$ as well as $\bar{K}^*(892)^0 e^+ \nu_e$ events and makes a small phase-space adjustment to the number of the μ^+ events to use them as e^+ events.			
$\Gamma(K^- \pi^+ e^+ \nu_e \text{ nonresonant})/\Gamma_{total}$		Γ_{13}/Γ	
VALUE	CL%	DOCUMENT ID	TECN COMMENT
<0.007	90	²³ ANJOS	89b E691 Photoproduction
²³ ANJOS 89b assumes a $\Gamma(D^+ \rightarrow K^- \pi^+ \pi^+)/\Gamma_{total} = 9.1 \pm 1.3 \pm 0.4\%$.			
$\Gamma(K^- \pi^+ \mu^+ \nu_\mu)/\Gamma_{total}$		$\Gamma_{14}/\Gamma = (\Gamma_{16} + \frac{2}{3}\Gamma_{26})/\Gamma$	
VALUE	DOCUMENT ID	COMMENT	
0.032 ± 0.004 OUR FIT			Error includes scale factor of 1.1.
$\Gamma(\bar{K}^*(892)^0 \mu^+ \nu_\mu)/\Gamma_{total}$		Γ_{26}/Γ	
Unseen decay modes of the $\bar{K}^*(892)^0$ are included.			
VALUE	EVTs	DOCUMENT ID	TECN COMMENT
0.044 ± 0.006 OUR FIT			Error includes scale factor of 1.1.
0.0325 ± 0.0071 ± 0.0075	224	²⁴ KODAMA	92c E653 π^- emulsion 600 GeV
²⁴ KODAMA 92c measures $\Gamma(D^+ \rightarrow \bar{K}^*(892)^0 \mu^+ \nu_\mu)/\Gamma(D^0 \rightarrow K^- \mu^+ \nu_\mu) = 0.43 \pm 0.09 \pm 0.09$ and then uses $\Gamma(D^0 \rightarrow K^- \mu^+ \nu_\mu) = (7.0 \pm 0.7) \times 10^{10} \text{ s}^{-1}$ to get the quoted branching fraction. See also the footnote to KODAMA 92c in the next data block.			
$\Gamma(\bar{K}^*(892)^0 \mu^+ \nu_\mu)/\Gamma(K^- \pi^+ \pi^+)$		Γ_{26}/Γ_{37}	
Unseen decay modes of the $\bar{K}^*(892)^0$ are included.			
VALUE	EVTs	DOCUMENT ID	TECN COMMENT
0.49 ± 0.06 OUR FIT			
0.53 ± 0.06 OUR AVERAGE			
0.56 ± 0.04 ± 0.06	875	FRABETTI	93e E687 γ Be $\bar{E}_\gamma \approx 200$ GeV
0.46 ± 0.07 ± 0.08	224	²⁵ KODAMA	92c E653 π^- emulsion 600 GeV
²⁵ KODAMA 92c uses the same $\bar{K}^*(892)^0 \mu^+ \nu_\mu$ events normalizing instead with $D^0 \rightarrow K^- \mu^+ \nu_\mu$ events, as reported in the preceding data block.			
$\Gamma(K^- \pi^+ \mu^+ \nu_\mu \text{ nonresonant})/\Gamma(K^- \pi^+ \mu^+ \nu_\mu)$		$\Gamma_{16}/\Gamma_{14} = \Gamma_{16}/(\Gamma_{16} + \frac{2}{3}\Gamma_{26})$	
VALUE	DOCUMENT ID	TECN	COMMENT
0.083 ± 0.029 OUR FIT			
0.083 ± 0.029	FRABETTI	93e E687	< 0.12 (90% CL)
$\Gamma(\bar{K}^0 \pi^+ \pi^- e^+ \nu_e)/\Gamma_{total}$		Γ_{17}/Γ	
VALUE	EVTs	DOCUMENT ID	TECN COMMENT
0.022 $\begin{smallmatrix} +0.047 \\ -0.013 \end{smallmatrix}$ ± 0.004	1	²⁶ AGUILAR-...	87F HYBR $\pi p, pp$ 360, 400 GeV
²⁶ AGUILAR-BENITEZ 87F computes the branching fraction using topological normalization.			
$\Gamma(K^- \pi^+ \pi^0 e^+ \nu_e)/\Gamma_{total}$		Γ_{18}/Γ	
VALUE	EVTs	DOCUMENT ID	TECN COMMENT
0.044 $\begin{smallmatrix} +0.052 \\ -0.013 \end{smallmatrix}$ ± 0.007	2	²⁷ AGUILAR-...	87F HYBR $\pi p, pp$ 360, 400 GeV
²⁷ AGUILAR-BENITEZ 87F computes the branching fraction using topological normalization.			
$\Gamma((\bar{K}^*(892)^0 \pi^0 e^+ \nu_e)/\Gamma_{total}$		Γ_{19}/Γ	
Unseen decay modes of the $\bar{K}^*(892)^0$ are included.			
VALUE	CL%	DOCUMENT ID	TECN COMMENT
<0.012	90	ANJOS	92 E691 Photoproduction
$\Gamma((\bar{K} \pi \pi)^0 e^+ \nu_e \text{ non-}\bar{K}^*(892)^0)/\Gamma_{total}$		Γ_{20}/Γ	
VALUE	CL%	DOCUMENT ID	TECN COMMENT
<0.009	90	ANJOS	92 E691 Photoproduction
$\Gamma(K^- \pi^+ \pi^0 \mu^+ \nu_\mu)/\Gamma(K^- \pi^+ \mu^+ \nu_\mu)$		$\Gamma_{21}/\Gamma_{14} = \Gamma_{21}/(\Gamma_{16} + \frac{2}{3}\Gamma_{26})$	
VALUE	CL%	DOCUMENT ID	TECN COMMENT
<0.042	90	FRABETTI	93e E687 γ Be $\bar{E}_\gamma \approx 200$ GeV
$\Gamma(\bar{K}_1(1270)^0 \mu^+ \nu_\mu)/\Gamma(\bar{K}^*(892)^0 \mu^+ \nu_\mu)$		Γ_{27}/Γ_{26}	
VALUE	CL%	DOCUMENT ID	TECN COMMENT
<0.78	95	ABE	99p CDF $p p$ 1.8 TeV
$\Gamma(\bar{K}^*(1410)^0 \mu^+ \nu_\mu)/\Gamma(\bar{K}^*(892)^0 \mu^+ \nu_\mu)$		Γ_{28}/Γ_{26}	
VALUE	CL%	DOCUMENT ID	TECN COMMENT
<0.60	95	ABE	99p CDF $p p$ 1.8 TeV
$\Gamma(\bar{K}_2^*(1430)^0 \mu^+ \nu_\mu)/\Gamma(\bar{K}^*(892)^0 \mu^+ \nu_\mu)$		Γ_{29}/Γ_{26}	
VALUE	CL%	DOCUMENT ID	TECN COMMENT
<0.19	95	ABE	99p CDF $p p$ 1.8 TeV
$\Gamma(\pi^0 \ell^+ \nu_\ell)/\Gamma(\bar{K}^0 \ell^+ \nu_\ell)$		Γ_{22}/Γ_8	
VALUE	EVTs	DOCUMENT ID	TECN COMMENT
0.046 ± 0.014 ± 0.017	100	²⁸ BARTELT	97 CLE2 $e^+ e^- \approx \tau(45)$
• • • We do not use the following data for averages, fits, limits, etc. • • •			
0.085 ± 0.027 ± 0.014	53	²⁹ ALAM	93 CLE2 See BARTELT 97
²⁸ BARTELT 97 thus directly measures the product of ratios squared of CKM matrix elements and form factors at $q^2=0$: $ V_{cd}/V_{cs} ^2 \cdot f_\pi^-(0)/f_K^+(0) ^2 = 0.046 \pm 0.014 \pm 0.017$.			
²⁹ ALAM 93 thus directly measures the product of ratios squared of CKM matrix elements and form factors at $q^2=0$: $ V_{cd}/V_{cs} ^2 \cdot f_\pi^-(0)/f_K^+(0) ^2 = 0.085 \pm 0.027 \pm 0.014$.			
$\Gamma(\pi^+ \pi^- e^+ \nu_e)/\Gamma_{total}$		Γ_{23}/Γ	
VALUE	CL%	DOCUMENT ID	TECN COMMENT
<0.057	90	³⁰ AGUILAR-...	87F HYBR $\pi p, pp$ 360, 400 GeV
³⁰ AGUILAR-BENITEZ 87F computes the branching fraction using topological normalization.			
$\Gamma(\rho^0 e^+ \nu_e)/\Gamma_{total}$		Γ_{30}/Γ	
VALUE	CL%	DOCUMENT ID	TECN COMMENT
<0.0037	90	BAI	91 MRK3 $e^+ e^- \approx 3.77$ GeV
$\Gamma(\rho^0 e^+ \nu_e)/\Gamma(\bar{K}^*(892)^0 e^+ \nu_e)$		Γ_{30}/Γ_{25}	
VALUE	EVTs	DOCUMENT ID	TECN COMMENT
0.045 ± 0.014 ± 0.009	49	³¹ AITALA	97 E791 π^- nucleus, 500 GeV
³¹ AITALA 97 explicitly subtracts $D^+ \rightarrow \eta' e^+ \nu_e$ and other backgrounds to get this result.			

See key on page 239

Meson Particle Listings

 D^\pm

$\Gamma(\bar{K}^*(892)^0 \rho^+ S\text{-wave})/\Gamma(K^-\pi^+\pi^+\pi^0)$ Γ_{78}/Γ_{46}
Unseen decay modes of the $\bar{K}^*(892)^0$ are included. The two experiments here disagree completely.

VALUE	DOCUMENT ID	TECN	COMMENT
0.26 ± 0.25 OUR AVERAGE	Error includes scale factor of 3.1.		
0.15 ± 0.075 ± 0.045	ANJOS	92c E691	γ Be 90-260 GeV
0.833 ± 0.116 ± 0.165	COFFMAN	92b MRK3	e^+e^- 3.77 GeV

$\Gamma(\bar{K}^*(892)^0 \rho^+ P\text{-wave})/\Gamma_{total}$ Γ_{79}/Γ
Unseen decay modes of the $\bar{K}^*(892)^0$ are included.

VALUE	CL%	DOCUMENT ID	TECN	COMMENT
<0.001	90	ANJOS	92c E691	γ Be 90-260 GeV
• • • We do not use the following data for averages, fits, limits, etc. • • •				
<0.005	90	COFFMAN	92b MRK3	e^+e^- 3.77 GeV

$\Gamma(\bar{K}^*(892)^0 \rho^+ D\text{-wave})/\Gamma(K^-\pi^+\pi^+\pi^0)$ Γ_{80}/Γ_{46}
Unseen decay modes of the $\bar{K}^*(892)^0$ are included.

VALUE	DOCUMENT ID	TECN	COMMENT
0.15 ± 0.09 ± 0.045	ANJOS	92c E691	γ Be 90-260 GeV

$\Gamma(\bar{K}^*(892)^0 \rho^+ D\text{-wave longitudinal})/\Gamma_{total}$ Γ_{81}/Γ
Unseen decay modes of the $\bar{K}^*(892)^0$ are included.

VALUE	CL%	DOCUMENT ID	TECN	COMMENT
<0.007	90	COFFMAN	92b MRK3	e^+e^- 3.77 GeV

$\Gamma(\bar{K}_1(1400)^0 \pi^+)/\Gamma(K^-\pi^+\pi^+\pi^0)$ Γ_{83}/Γ_{46}
Unseen decay modes of the $\bar{K}_1(1400)^0$ are included.

VALUE	DOCUMENT ID	TECN	COMMENT
0.77 ± 0.20 OUR FIT			
0.907 ± 0.218 ± 0.180	COFFMAN	92b MRK3	e^+e^- 3.77 GeV

$\Gamma(K^-\rho^+\pi^+ \text{total})/\Gamma(K^-\pi^+\pi^+\pi^0)$ Γ_{91}/Γ_{46}
This includes $\bar{K}^*(892)^0 \rho^+$, etc. The next entry gives the specifically 3-body fraction.

VALUE	DOCUMENT ID	TECN	COMMENT
0.48 ± 0.13 ± 0.09	ANJOS	92c E691	γ Be 90-260 GeV

$\Gamma(K^-\rho^+\pi^+ 3\text{-body})/\Gamma(K^-\pi^+\pi^+\pi^0)$ Γ_{92}/Γ_{46}

VALUE	DOCUMENT ID	TECN	COMMENT
0.17 ± 0.06 OUR AVERAGE			
0.18 ± 0.08 ± 0.04	ANJOS	92c E691	γ Be 90-260 GeV
0.159 ± 0.065 ± 0.060	COFFMAN	92b MRK3	e^+e^- 3.77 GeV

$\Gamma(\bar{K}^*(892)^0 \pi^+\pi^0 \text{total})/\Gamma(K^-\pi^+\pi^+\pi^0)$ Γ_{87}/Γ_{46}
This includes $\bar{K}^*(892)^0 \rho^+$, etc. The next two entries give the specifically 3-body fraction. Unseen decay modes of the $\bar{K}^*(892)^0$ are included.

VALUE	DOCUMENT ID	TECN	COMMENT
1.05 ± 0.11 ± 0.08	ANJOS	92c E691	γ Be 90-260 GeV

$\Gamma(\bar{K}^*(892)^0 \pi^+\pi^0 3\text{-body})/\Gamma_{total}$ Γ_{88}/Γ
Unseen decay modes of the $\bar{K}^*(892)^0$ are included.

VALUE	CL%	DOCUMENT ID	TECN	COMMENT
<0.008	90	45 COFFMAN	92b MRK3	e^+e^- 3.77 GeV

⁴⁵See, however, the next entry: ANJOS 92c sees a large signal in this channel.

$\Gamma(\bar{K}^*(892)^0 \pi^+\pi^0 3\text{-body})/\Gamma(K^-\pi^+\pi^+\pi^0)$ Γ_{88}/Γ_{46}
Unseen decay modes of the $\bar{K}^*(892)^0$ are included.

VALUE	DOCUMENT ID	TECN	COMMENT
0.66 ± 0.09 ± 0.17	ANJOS	92c E691	γ Be 90-260 GeV

$\Gamma(K^*(892)^-\pi^+\pi^+ 3\text{-body})/\Gamma(K^-\pi^+\pi^+\pi^0)$ Γ_{90}/Γ_{46}
Unseen decay modes of the $K^*(892)^-$ are included.

VALUE	DOCUMENT ID	TECN	COMMENT
0.32 ± 0.14 OUR FIT	Error includes scale factor of 1.1.		
0.24 ± 0.12 ± 0.09	ANJOS	92c E691	γ Be 90-260 GeV

$\Gamma(K^-\pi^+\pi^+\pi^0 \text{ nonresonant})/\Gamma_{total}$ Γ_{54}/Γ

VALUE	CL%	DOCUMENT ID	TECN	COMMENT
<0.002	90	46 ANJOS	92c E691	γ Be 90-260 GeV

⁴⁶Whereas ANJOS 92c finds no signal here, COFFMAN 92b finds a fairly large one; see the next entry.

$\Gamma(K^-\pi^+\pi^+\pi^0 \text{ nonresonant})/\Gamma(K^-\pi^+\pi^+\pi^0)$ Γ_{54}/Γ_{46}

VALUE	DOCUMENT ID	TECN	COMMENT
0.184 ± 0.070 ± 0.050	COFFMAN	92b MRK3	e^+e^- 3.77 GeV

$\Gamma(\bar{K}^0 \pi^+\pi^+\pi^-)/\Gamma_{total}$ Γ_{55}/Γ

VALUE	EVTS	DOCUMENT ID	TECN	COMMENT
0.070 ± 0.009 OUR FIT				
0.071 ± 0.016 OUR AVERAGE				
0.066 ± 0.015 ± 0.005	168	ADLER	88c MRK3	e^+e^- 3.77 GeV
0.12 ± 0.05	21	47 SCHINDLER	81 MRK2	e^+e^- 3.771 GeV
• • • We do not use the following data for averages, fits, limits, etc. • • •				
0.042 ^{+0.019} / _{-0.017}		48 BARLAG	92c ACCM	π^- Cu 230 GeV
0.243 ^{+0.064} / _{-0.041} ± 0.041	11	48 AGUILAR...	87f HYBR	$\pi p, p p$ 360, 400 GeV

⁴⁷SCHINDLER 81 (MARK-2) measures $\sigma(e^+e^- \rightarrow \psi(3770)) \times$ branching fraction to be 0.51 ± 0.08 nb. We use the MARK-3 (ADLER 88c) value of $\sigma = 4.2 \pm 0.6 \pm 0.3$ nb.
⁴⁸AGUILAR-BENITEZ 87f and BARLAG 92c compute the branching fraction by topological normalization.

$\Gamma(\bar{K}^0 \pi^+\pi^+\pi^-)/\Gamma(K^-\pi^+\pi^+)$ Γ_{55}/Γ_{37}

VALUE	EVTS	DOCUMENT ID	TECN	COMMENT
0.78 ± 0.10 OUR FIT				
0.77 ± 0.07 ± 0.11	229	ANJOS	92c E691	γ Be 90-260 GeV

$\Gamma(\bar{K}^0 a_1(1260)^+)/\Gamma(\bar{K}^0 \pi^+\pi^+\pi^-)$ Γ_{74}/Γ_{55}
Unseen decay modes of the $a_1(1260)^+$ are included.

VALUE	DOCUMENT ID	TECN	COMMENT
1.15 ± 0.19 OUR AVERAGE	Error includes scale factor of 1.1.		
1.66 ± 0.28 ± 0.40	ANJOS	92c E691	γ Be 90-260 GeV
1.078 ± 0.114 ± 0.140	COFFMAN	92b MRK3	e^+e^- 3.77 GeV

$\Gamma(\bar{K}^0 a_2(1320)^+)/\Gamma_{total}$ Γ_{75}/Γ
Unseen decay modes of the $a_2(1320)^+$ are included.

VALUE	CL%	DOCUMENT ID	TECN	COMMENT
<0.003	90	ANJOS	92c E691	γ Be 90-260 GeV
• • • We do not use the following data for averages, fits, limits, etc. • • •				
<0.008	90	COFFMAN	92b MRK3	e^+e^- 3.77 GeV

$\Gamma(\bar{K}_1(1270)^0 \pi^+)/\Gamma_{total}$ Γ_{82}/Γ
Unseen decay modes of the $\bar{K}_1(1270)^0$ are included.

VALUE	CL%	DOCUMENT ID	TECN	COMMENT
<0.007	90	ANJOS	92c E691	γ Be 90-260 GeV
• • • We do not use the following data for averages, fits, limits, etc. • • •				
<0.011	90	COFFMAN	92b MRK3	e^+e^- 3.77 GeV

$\Gamma(\bar{K}_1(1400)^0 \pi^+)/\Gamma_{total}$ Γ_{83}/Γ
Unseen decay modes of the $\bar{K}_1(1400)^0$ are included.

VALUE	CL%	DOCUMENT ID	TECN	COMMENT
<0.009	90	49 ANJOS	92c E691	γ Be 90-260 GeV

⁴⁹ANJOS 92c sees no evidence for $\bar{K}_1(1400)^0 \pi^+$ in either the $\bar{K}^0 \pi^+\pi^+\pi^-$ or $K^-\pi^+\pi^+\pi^0$ channels, whereas COFFMAN 92b finds the $\bar{K}_1(1400)^0 \pi^+$ branching fraction to be large; see the next entry.

$\Gamma(\bar{K}_1(1400)^0 \pi^+)/\Gamma(\bar{K}^0 \pi^+\pi^+\pi^-)$ Γ_{83}/Γ_{55}
Unseen decay modes of the $\bar{K}_1(1400)^0$ are included.

VALUE	DOCUMENT ID	TECN	COMMENT
0.70 ± 0.17 OUR FIT			
0.623 ± 0.106 ± 0.180	COFFMAN	92b MRK3	e^+e^- 3.77 GeV

$\Gamma(\bar{K}^*(1410)^0 \pi^+)/\Gamma_{total}$ Γ_{84}/Γ
Unseen decay modes of the $\bar{K}^*(1410)^0$ are included.

VALUE	CL%	DOCUMENT ID	TECN	COMMENT
<0.007	90	COFFMAN	92b MRK3	e^+e^- 3.77 GeV

$\Gamma(K^*(892)^-\pi^+\pi^+ \text{total})/\Gamma(\bar{K}^0 \pi^+\pi^+\pi^-)$ Γ_{89}/Γ_{55}
Unseen decay modes of the $K^*(892)^-$ are included.

VALUE	EVTS	DOCUMENT ID	TECN	COMMENT
<0.007				
• • • We do not use the following data for averages, fits, limits, etc. • • •				
0.41 ± 0.14	14	ALEEV	94 B152	$n N$ 20-70 GeV

$\Gamma(K^*(892)^-\pi^+\pi^+ 3\text{-body})/\Gamma_{total}$ Γ_{90}/Γ
Unseen decay modes of the $\bar{K}^*(892)^0$ are included.

VALUE	CL%	DOCUMENT ID	TECN	COMMENT
0.020 ± 0.009 OUR FIT				
• • • We do not use the following data for averages, fits, limits, etc. • • •				
<0.013	90	COFFMAN	92b MRK3	e^+e^- 3.77 GeV

$\Gamma(K^*(892)^-\pi^+\pi^+ 3\text{-body})/\Gamma(\bar{K}^0 \pi^+\pi^+\pi^-)$ Γ_{90}/Γ_{55}
Unseen decay modes of the $K^*(892)^-$ are included.

VALUE	DOCUMENT ID	TECN	COMMENT
0.29 ± 0.13 OUR FIT	Error includes scale factor of 1.1.		
0.50 ± 0.09 ± 0.21	ANJOS	92c E691	γ Be 90-260 GeV

Meson Particle Listings

 D^{\pm}

$\Gamma(K^0 K^- \pi^+ \pi^+ \text{non-} K^{*0} \bar{K}^{*0})/\Gamma_{\text{total}}$ Γ_{129}/Γ
 VALUE CL% EVTS DOCUMENT ID TECN COMMENT
 <0.0079 90 ALBRECHT 92B ARG $e^+ e^- \approx 10.4$ GeV

$\Gamma(\phi \pi^+ \pi^+ \pi^-)/\Gamma_{\text{total}}$ Γ_{136}/Γ
 Unseen decay modes of the ϕ are included.
 VALUE CL% EVTS DOCUMENT ID TECN COMMENT
 <0.002 90 0 ANJOS 88 E691 Photoproduction

$\Gamma(\phi \pi^+ \pi^+ \pi^-)/\Gamma(K^- \pi^+ \pi^+)$ Γ_{136}/Γ_{37}
 Unseen decay modes of the ϕ are included.
 VALUE CL% EVTS DOCUMENT ID TECN COMMENT
 <0.031 90 ALVAREZ 90C NA14 Photoproduction

$\Gamma(\phi \pi^+ \pi^+ \pi^-)/\Gamma(\phi \pi^+)$ $\Gamma_{136}/\Gamma_{133}$
 VALUE CL% EVTS DOCUMENT ID TECN COMMENT
 <0.6 90 FRABETTI 92 E687 γ Be

$\Gamma(K^+ K^- \pi^+ \pi^+ \pi^- \text{nonresonant})/\Gamma_{\text{total}}$ Γ_{132}/Γ
 VALUE CL% EVTS DOCUMENT ID TECN COMMENT
 <0.03 90 12 ANJOS 88 E691 Photoproduction

Rare or forbidden modes

$\Gamma(K^+ \pi^+ \pi^-)/\Gamma(K^- \pi^+ \pi^+)$ Γ_{140}/Γ_{37}
 VALUE EVTS DOCUMENT ID TECN COMMENT
0.0075 ± 0.0016 OUR AVERAGE
 0.0077 ± 0.0017 ± 0.0008 59 AITALA 97C E791 π^- nucleus, 500 GeV
 0.0072 ± 0.0023 ± 0.0017 21 FRABETTI 95E E687 γ Be, $\bar{E}_{\gamma} = 220$ GeV

$\Gamma(K^+ \rho^0)/\Gamma(K^+ \pi^+ \pi^-)$ $\Gamma_{141}/\Gamma_{140}$
 VALUE DOCUMENT ID TECN COMMENT
 0.37 ± 0.14 ± 0.07 AITALA 97C E791 π^- nucleus, 500 GeV

$\Gamma(K^+ \rho^0)/\Gamma(K^- \pi^+ \pi^+)$ Γ_{141}/Γ_{37}
 VALUE CL% EVTS DOCUMENT ID TECN COMMENT
 <0.0067 90 FRABETTI 95E E687 γ Be, $\bar{E}_{\gamma} = 220$ GeV

$\Gamma(K^{*}(892)^0 \pi^+)/\Gamma(K^+ \pi^+ \pi^-)$ $\Gamma_{142}/\Gamma_{140}$
 Unseen decay modes of the $K^{*}(892)^0$ are included.
 VALUE DOCUMENT ID TECN COMMENT
 0.53 ± 0.21 ± 0.02 AITALA 97C E791 π^- nucleus, 500 GeV

$\Gamma(K^{*}(892)^0 \pi^+)/\Gamma(K^- \pi^+ \pi^+)$ Γ_{142}/Γ_{37}
 Unseen decay modes of the $K^{*}(892)^0$ are included.
 VALUE CL% EVTS DOCUMENT ID TECN COMMENT
 <0.0021 90 FRABETTI 95E E687 γ Be, $\bar{E}_{\gamma} = 220$ GeV

$\Gamma(K^+ \pi^+ \pi^- \text{nonresonant})/\Gamma(K^+ \pi^+ \pi^-)$ $\Gamma_{143}/\Gamma_{140}$
 VALUE DOCUMENT ID TECN COMMENT
 0.36 ± 0.14 ± 0.07 AITALA 97C E791 π^- nucleus, 500 GeV

$\Gamma(K^+ K^+ K^-)/\Gamma(K^- \pi^+ \pi^+)$ Γ_{144}/Γ_{37}
 A doubly Cabibbo-suppressed decay with no simple spectator process possible.
 VALUE CL% EVTS DOCUMENT ID TECN COMMENT
 <0.0016 90 66 FRABETTI 95F E687 γ Be, $\bar{E}_{\gamma} \approx 220$ GeV

<0.057 ± 0.020 ± 0.007 13 ADAMOVIĆ 93 WA82 π^- 340 GeV
 66 Using the $\phi \pi^+$ mode to normalize, FRABETTI 95F gets $\Gamma(K^+ K^+ K^-)/\Gamma(\phi \pi^+) < 0.025$.

$\Gamma(\phi K^+)/\Gamma(\phi \pi^+)$ $\Gamma_{145}/\Gamma_{133}$
 A doubly Cabibbo-suppressed decay with no simple spectator process possible.
 VALUE CL% EVTS DOCUMENT ID TECN COMMENT
 <0.021 90 FRABETTI 95F E687 γ Be, $\bar{E}_{\gamma} \approx 220$ GeV
 <0.058 ± 0.032 ± 0.007 4 67 ANJOS 92D E691 γ Be, $\bar{E}_{\gamma} = 145$ GeV

67 The evidence of ANJOS 92D is a small excess of events ($4.5^{+2.4}_{-2.0}$).

$\Gamma(\pi^+ e^+ e^-)/\Gamma_{\text{total}}$ Γ_{146}/Γ
 A test for the $\Delta C = 1$ weak neutral current. Allowed by higher-order electroweak interactions.
 VALUE CL% EVTS DOCUMENT ID TECN COMMENT
 <5.2 × 10⁻⁵ 90 AITALA 99G E791 $\pi^- N$ 500 GeV
 <1.1 × 10⁻⁴ 90 FRABETTI 97B E687 γ Be, $\bar{E}_{\gamma} \approx 220$ GeV
 <6.6 × 10⁻⁵ 90 AITALA 96 E791 $\pi^- N$ 500 GeV
 <2.5 × 10⁻³ 90 WEIR 90B MRK2 $e^+ e^-$ 29 GeV
 <2.6 × 10⁻³ 90 39 HAAS 88 CLEO $e^+ e^-$ 10 GeV

$\Gamma(\pi^+ \mu^+ \mu^-)/\Gamma_{\text{total}}$ Γ_{147}/Γ
 A test for the $\Delta C = 1$ weak neutral current. Allowed by higher-order electroweak interactions.
 VALUE CL% EVTS DOCUMENT ID TECN COMMENT

<1.5 × 10⁻⁵ 90 AITALA 99G E791 $\pi^- N$ 500 GeV
 <8.9 × 10⁻⁵ 90 FRABETTI 97B E687 γ Be, $\bar{E}_{\gamma} \approx 220$ GeV
 <1.8 × 10⁻⁵ 90 AITALA 96 E791 $\pi^- N$ 500 GeV
 <2.2 × 10⁻⁴ 90 0 KODAMA 95 E653 π^- emulsion 600 GeV
 <5.9 × 10⁻³ 90 WEIR 90B MRK2 $e^+ e^-$ 29 GeV
 <2.9 × 10⁻³ 90 36 HAAS 88 CLEO $e^+ e^-$ 10 GeV

$\Gamma(\rho^+ \mu^+ \mu^-)/\Gamma_{\text{total}}$ Γ_{148}/Γ
 A test for the $\Delta C = 1$ weak neutral current. Allowed by higher-order electroweak interactions.

VALUE CL% EVTS DOCUMENT ID TECN COMMENT
 <5.6 × 10⁻⁴ 90 0 KODAMA 95 E653 π^- emulsion 600 GeV

$\Gamma(K^+ e^+ e^-)/\Gamma_{\text{total}}$ Γ_{149}/Γ
 VALUE CL% EVTS DOCUMENT ID TECN COMMENT

<2.0 × 10⁻⁴ 90 AITALA 99G E791 $\pi^- N$ 500 GeV
 <2.0 × 10⁻⁴ 90 FRABETTI 97B E687 γ Be, $\bar{E}_{\gamma} \approx 220$ GeV
 <4.8 × 10⁻³ 90 WEIR 90B MRK2 $e^+ e^-$ 29 GeV

$\Gamma(K^+ \mu^+ \mu^-)/\Gamma_{\text{total}}$ Γ_{150}/Γ
 VALUE CL% EVTS DOCUMENT ID TECN COMMENT

<4.4 × 10⁻⁵ 90 AITALA 99G E791 $\pi^- N$ 500 GeV
 <9.7 × 10⁻⁵ 90 FRABETTI 97B E687 γ Be, $\bar{E}_{\gamma} \approx 220$ GeV
 <3.2 × 10⁻⁴ 90 0 KODAMA 95 E653 π^- emulsion 600 GeV
 <9.2 × 10⁻³ 90 WEIR 90B MRK2 $e^+ e^-$ 29 GeV

$\Gamma(\pi^+ e^{\pm} \mu^{\mp})/\Gamma_{\text{total}}$ Γ_{151}/Γ
 A test of lepton-family-number conservation.
 VALUE CL% EVTS DOCUMENT ID TECN COMMENT

<3.4 × 10⁻⁵ 90 AITALA 99G E791 $\pi^- N$ 500 GeV

$\Gamma(\pi^+ e^+ \mu^-)/\Gamma_{\text{total}}$ Γ_{152}/Γ
 A test of lepton-family-number conservation.
 VALUE CL% EVTS DOCUMENT ID TECN COMMENT

<1.1 × 10⁻⁴ 90 FRABETTI 97B E687 γ Be, $\bar{E}_{\gamma} \approx 220$ GeV
 <3.3 × 10⁻³ 90 WEIR 90B MRK2 $e^+ e^-$ 29 GeV

$\Gamma(\pi^+ e^- \mu^+)/\Gamma_{\text{total}}$ Γ_{153}/Γ
 A test of lepton-family-number conservation.
 VALUE CL% EVTS DOCUMENT ID TECN COMMENT

<1.3 × 10⁻⁴ 90 FRABETTI 97B E687 γ Be, $\bar{E}_{\gamma} \approx 220$ GeV
 <3.3 × 10⁻³ 90 WEIR 90B MRK2 $e^+ e^-$ 29 GeV

$\Gamma(K^+ e^{\pm} \mu^{\mp})/\Gamma_{\text{total}}$ Γ_{154}/Γ
 A test of lepton-family-number conservation.
 VALUE CL% EVTS DOCUMENT ID TECN COMMENT

<6.8 × 10⁻⁵ 90 AITALA 99G E791 $\pi^- N$ 500 GeV

$\Gamma(K^+ e^+ \mu^-)/\Gamma_{\text{total}}$ Γ_{155}/Γ
 A test of lepton-family-number conservation.
 VALUE CL% EVTS DOCUMENT ID TECN COMMENT

<1.3 × 10⁻⁴ 90 FRABETTI 97B E687 γ Be, $\bar{E}_{\gamma} \approx 220$ GeV
 <3.4 × 10⁻³ 90 WEIR 90B MRK2 $e^+ e^-$ 29 GeV

$\Gamma(K^+ e^- \mu^+)/\Gamma_{\text{total}}$ Γ_{156}/Γ
 A test of lepton-family-number conservation.
 VALUE CL% EVTS DOCUMENT ID TECN COMMENT

<1.2 × 10⁻⁴ 90 FRABETTI 97B E687 γ Be, $\bar{E}_{\gamma} \approx 220$ GeV
 <3.4 × 10⁻³ 90 WEIR 90B MRK2 $e^+ e^-$ 29 GeV

$\Gamma(\pi^- e^+ e^-)/\Gamma_{\text{total}}$ Γ_{157}/Γ
 A test of lepton-number conservation.
 VALUE CL% EVTS DOCUMENT ID TECN COMMENT

<9.6 × 10⁻⁵ 90 AITALA 99G E791 $\pi^- N$ 500 GeV
 <1.1 × 10⁻⁴ 90 FRABETTI 97B E687 γ Be, $\bar{E}_{\gamma} \approx 220$ GeV
 <4.8 × 10⁻³ 90 WEIR 90B MRK2 $e^+ e^-$ 29 GeV

See key on page 239

 $\Gamma(\pi^- \mu^+ \mu^+)/\Gamma_{total}$
A test of lepton-number conservation. Γ_{158}/Γ

VALUE	CL%	EVTS	DOCUMENT ID	TECN	COMMENT
$<1.7 \times 10^{-5}$	90		AITALA	99G E791	$\pi^- N$ 500 GeV
• • • We do not use the following data for averages, fits, limits, etc. • • •					
$<8.7 \times 10^{-5}$	90		FRABETTI	97B E687	γ Be, $\bar{E}_\gamma \approx 220$ GeV
$<2.2 \times 10^{-4}$	90	0	KODAMA	95 E653	π^- emulsion 600 GeV
$<6.8 \times 10^{-3}$	90		WEIR	90B MRK2	$e^+ e^-$ 29 GeV

 $\Gamma(\pi^- e^+ \mu^+)/\Gamma_{total}$
A test of lepton-number conservation. Γ_{159}/Γ

VALUE	CL%	EVTS	DOCUMENT ID	TECN	COMMENT
$<5.0 \times 10^{-5}$	90		AITALA	99G E791	$\pi^- N$ 500 GeV
• • • We do not use the following data for averages, fits, limits, etc. • • •					
$<1.1 \times 10^{-4}$	90		FRABETTI	97B E687	γ Be, $\bar{E}_\gamma \approx 220$ GeV
$<3.7 \times 10^{-3}$	90		WEIR	90B MRK2	$e^+ e^-$ 29 GeV

 $\Gamma(\rho^- \mu^+ \mu^+)/\Gamma_{total}$
A test of lepton-number conservation. Γ_{160}/Γ

VALUE	CL%	EVTS	DOCUMENT ID	TECN	COMMENT
$<5.6 \times 10^{-4}$	90	0	KODAMA	95 E653	π^- emulsion 600 GeV

 $\Gamma(K^- e^+ e^+)/\Gamma_{total}$
A test of lepton-number conservation. Γ_{161}/Γ

VALUE	CL%	EVTS	DOCUMENT ID	TECN	COMMENT
$<1.2 \times 10^{-4}$	90		FRABETTI	97B E687	γ Be, $\bar{E}_\gamma \approx 220$ GeV
• • • We do not use the following data for averages, fits, limits, etc. • • •					
$<9.1 \times 10^{-3}$	90		WEIR	90B MRK2	$e^+ e^-$ 29 GeV

 $\Gamma(K^- \mu^+ \mu^+)/\Gamma_{total}$
A test of lepton-number conservation. Γ_{162}/Γ

VALUE	CL%	EVTS	DOCUMENT ID	TECN	COMMENT
$<1.2 \times 10^{-4}$	90		FRABETTI	97B E687	γ Be, $\bar{E}_\gamma \approx 220$ GeV
• • • We do not use the following data for averages, fits, limits, etc. • • •					
$<3.2 \times 10^{-4}$	90	0	KODAMA	95 E653	π^- emulsion 600 GeV
$<4.3 \times 10^{-3}$	90		WEIR	90B MRK2	$e^+ e^-$ 29 GeV

 $\Gamma(K^- e^+ \mu^+)/\Gamma_{total}$
A test of lepton-number conservation. Γ_{163}/Γ

VALUE	CL%	EVTS	DOCUMENT ID	TECN	COMMENT
$<1.3 \times 10^{-4}$	90		FRABETTI	97B E687	γ Be, $\bar{E}_\gamma \approx 220$ GeV
• • • We do not use the following data for averages, fits, limits, etc. • • •					
$<4.0 \times 10^{-3}$	90		WEIR	90B MRK2	$e^+ e^-$ 29 GeV

 $\Gamma(K^*(892)^- \mu^+ \mu^+)/\Gamma_{total}$
A test of lepton-number conservation. Γ_{164}/Γ

VALUE	CL%	EVTS	DOCUMENT ID	TECN	COMMENT
$<8.5 \times 10^{-4}$	90	0	KODAMA	95 E653	π^- emulsion 600 GeV

 D^\pm CP-VIOLATING DECAY-RATE ASYMMETRIES $A_{CP}(K^+ K^- \pi^\pm)$ in $D^\pm \rightarrow K^+ K^- \pi^\pm$ This is the difference between D^+ and D^- partial widths for these modes divided by the sum of the widths.

VALUE	DOCUMENT ID	TECN	COMMENT
-0.017 ± 0.027 OUR AVERAGE			
-0.014 ± 0.029	⁶⁸ AITALA	97B E791	$-0.062 < A_{CP} < +0.034$ (90% CL)
-0.031 ± 0.068	⁶⁸ FRABETTI	94I E687	$-0.14 < A_{CP} < +0.081$ (90% CL)

⁶⁸FRABETTI 94I and AITALA 97B measure $N(D^+ \rightarrow K^- K^+ \pi^+)/N(D^+ \rightarrow K^- \pi^+ \pi^+)$, the ratio of numbers of events observed, and similarly for the D^- . $A_{CP}(K^\pm K^* 0)$ in $D^+ \rightarrow K^+ \bar{K}^{*0}$, $D^- \rightarrow K^- K^{*0}$ This is the difference between D^+ and D^- partial widths for these modes divided by the sum of the widths.

VALUE	DOCUMENT ID	TECN	COMMENT
-0.02 ± 0.05 OUR AVERAGE			
-0.010 ± 0.050	⁶⁹ AITALA	97B E791	$-0.092 < A_{CP} < +0.072$ (90% CL)
-0.12 ± 0.13	⁶⁹ FRABETTI	94I E687	$-0.33 < A_{CP} < +0.094$ (90% CL)

⁶⁹FRABETTI 94I and AITALA 97B measure $N(D^+ \rightarrow K^+ \bar{K}^*(892)^0)/N(D^+ \rightarrow K^- \pi^+ \pi^+)$, the ratio of numbers of events observed, and similarly for the D^- . $A_{CP}(\phi \pi^\pm)$ in $D^\pm \rightarrow \phi \pi^\pm$ This is the difference between D^+ and D^- partial widths for these modes divided by the sum of the widths.

VALUE	DOCUMENT ID	TECN	COMMENT
-0.014 ± 0.033 OUR AVERAGE			
-0.028 ± 0.036	⁷⁰ AITALA	97B E791	$-0.087 < A_{CP} < +0.031$ (90% CL)
$+0.066 \pm 0.086$	⁷⁰ FRABETTI	94I E687	$-0.075 < A_{CP} < +0.21$ (90% CL)

⁷⁰FRABETTI 94I and AITALA 97B measure $N(D^+ \rightarrow \phi \pi^+)/N(D^+ \rightarrow K^- \pi^+ \pi^+)$, the ratio of numbers of events observed, and similarly for the D^- . $A_{CP}(\pi^+ \pi^- \pi^\pm)$ in $D^\pm \rightarrow \pi^+ \pi^- \pi^\pm$ This is the difference between D^+ and D^- partial widths for these modes divided by the sum of the widths.

VALUE	DOCUMENT ID	TECN	COMMENT
-0.017 ± 0.042	⁷¹ AITALA	97B E791	$-0.086 < A_{CP} < +0.052$ (90% CL)

⁷¹AITALA 97B measure $N(D^+ \rightarrow \pi^+ \pi^- \pi^+)/N(D^+ \rightarrow K^- \pi^+ \pi^+)$, the ratio of numbers of events observed, and similarly for the D^- . D^\pm PRODUCTION CROSS SECTION AT $\psi(3770)$ A compilation of the cross sections for the direct production of D^\pm mesons at or near the $\psi(3770)$ peak in $e^+ e^-$ production.

VALUE (nanobarns)	DOCUMENT ID	TECN	COMMENT
• • • We do not use the following data for averages, fits, limits, etc. • • •			
$4.2 \pm 0.6 \pm 0.3$	⁷² ADLER	88C MRK3	$e^+ e^-$ 3.768 GeV
5.5 ± 1.0	⁷³ PARTRIDGE	84 CBAL	$e^+ e^-$ 3.771 GeV
$6.00 \pm 0.72 \pm 1.02$	⁷⁴ SCHINDLER	80 MRK2	$e^+ e^-$ 3.771 GeV
9.1 ± 2.0	⁷⁵ PERUZZI	77 MRK1	$e^+ e^-$ 3.774 GeV

⁷²This measurement compares events with one detected D to those with two detected D mesons, to determine the absolute cross section. ADLER 88C measure the ratio of cross sections (neutral to charged) to be $1.36 \pm 0.23 \pm 0.14$. This measurement does not include the decays of the $\psi(3770)$ not associated with charmed particle production.⁷³This measurement comes from a scan of the $\psi(3770)$ resonance and a fit to the cross section. PARTRIDGE 84 measures 6.4 ± 1.15 nb for the cross section. We take the phase space division of neutral and charged D mesons in $\psi(3770)$ decay to be 1.33, and we assume that the $\psi(3770)$ is an isosinglet to evaluate the cross sections. The noncharm decays (e.g. radiative) of the $\psi(3770)$ are included in this measurement and may amount to a few percent correction.⁷⁴This measurement comes from a scan of the $\psi(3770)$ resonance and a fit to the cross section. SCHINDLER 80 assume the phase space division of neutral and charged D mesons in $\psi(3770)$ decay to be 1.33, and that the $\psi(3770)$ is an isosinglet. The noncharm decays (e.g. radiative) of the $\psi(3770)$ are included in this measurement and may amount to a few percent correction.⁷⁵This measurement comes from a scan of the $\psi(3770)$ resonance and a fit to the cross section. The phase space division of neutral and charged D mesons in $\psi(3770)$ decay is taken to be 1.33, and $\psi(3770)$ is assumed to be an isosinglet. The noncharm decays (e.g. radiative) of the $\psi(3770)$ are included in this measurement and may amount to a few percent correction. We exclude this measurement from the average because of uncertainties in the contamination from τ lepton pairs. Also see RAPIDIS 77. $D^+ \rightarrow \bar{K}^*(892)^0 \ell^+ \nu_\ell$ FORM FACTORS $r_\nu \equiv V(0)/A_1(0)$ in $D^+ \rightarrow \bar{K}^*(892)^0 \ell^+ \nu_\ell$

VALUE	EVTS	DOCUMENT ID	TECN	COMMENT
1.82 ± 0.09 OUR AVERAGE				
$1.45 \pm 0.23 \pm 0.07$	763	ADAMOVICH	99 BEAT	$\bar{K}^*(892)^0 \mu^+ \nu_\mu$
$1.90 \pm 0.11 \pm 0.09$	3000	⁷⁶ AITALA	98B E791	$\bar{K}^*(892)^0 e^+ \nu_e$
$1.84 \pm 0.11 \pm 0.09$	3034	AITALA	98F E791	$\bar{K}^*(892)^0 \mu^+ \nu_\mu$
$1.74 \pm 0.27 \pm 0.28$	874	FRABETTI	93E E687	$\bar{K}^*(892)^0 \mu^+ \nu_\mu$
$2.00^{+0.34}_{-0.32} \pm 0.16$	305	KODAMA	92 E653	$\bar{K}^*(892)^0 \mu^+ \nu_\mu$
$2.0 \pm 0.6 \pm 0.3$	183	ANJOS	90E E691	$\bar{K}^*(892)^0 e^+ \nu_e$

⁷⁶This is slightly different from the AITALA 98B value: see ref. [5] in AITALA 98F. $r_2 \equiv A_2(0)/A_1(0)$ in $D^+ \rightarrow \bar{K}^*(892)^0 \ell^+ \nu_\ell$

VALUE	EVTS	DOCUMENT ID	TECN	COMMENT
0.78 ± 0.07 OUR AVERAGE				
$1.00 \pm 0.15 \pm 0.03$	763	ADAMOVICH	99 BEAT	$\bar{K}^*(892)^0 \mu^+ \nu_\mu$
$0.71 \pm 0.08 \pm 0.09$	3000	AITALA	98B E791	$\bar{K}^*(892)^0 e^+ \nu_e$
$0.75 \pm 0.08 \pm 0.09$	3034	AITALA	98F E791	$\bar{K}^*(892)^0 \mu^+ \nu_\mu$
$0.78 \pm 0.18 \pm 0.10$	874	FRABETTI	93E E687	$\bar{K}^*(892)^0 \mu^+ \nu_\mu$
$0.82^{+0.22}_{-0.23} \pm 0.11$	305	KODAMA	92 E653	$\bar{K}^*(892)^0 \mu^+ \nu_\mu$
$0.0 \pm 0.5 \pm 0.2$	183	ANJOS	90E E691	$\bar{K}^*(892)^0 e^+ \nu_e$

 $r_3 \equiv A_3(0)/A_1(0)$ in $D^+ \rightarrow \bar{K}^*(892)^0 \ell^+ \nu_\ell$

VALUE	EVTS	DOCUMENT ID	TECN	COMMENT
$0.04 \pm 0.33 \pm 0.29$	3034	AITALA	98F E791	$\bar{K}^*(892)^0 \mu^+ \nu_\mu$

 Γ_L/Γ_T in $D^+ \rightarrow \bar{K}^*(892)^0 \ell^+ \nu_\ell$

VALUE	EVTS	DOCUMENT ID	TECN	COMMENT
1.14 ± 0.08 OUR AVERAGE				
$1.09 \pm 0.10 \pm 0.02$	763	ADAMOVICH	99 BEAT	$\bar{K}^*(892)^0 \mu^+ \nu_\mu$
$1.20 \pm 0.13 \pm 0.13$	874	FRABETTI	93E E687	$\bar{K}^*(892)^0 \mu^+ \nu_\mu$
$1.18 \pm 0.18 \pm 0.08$	305	KODAMA	92 E653	$\bar{K}^*(892)^0 \mu^+ \nu_\mu$
$1.8^{+0.6}_{-0.4} \pm 0.3$	183	ANJOS	90E E691	$\bar{K}^*(892)^0 e^+ \nu_e$

See key on page 239

Meson Particle Listings

D^0

$m_{D^\pm} - m_{D^0}$

The fit includes D^\pm , D^0 , D_s^\pm , $D^{*\pm}$, D^{*0} , and $D_s^{*\pm}$ mass and mass difference measurements.

VALUE (MeV)	DOCUMENT ID	TECN	COMMENT
4.79 ± 0.10 OUR FIT	Error includes scale factor of 1.1.		
4.74 ± 0.28 OUR AVERAGE			
4.7 ± 0.3	³ SCHINDLER 81	MRK2	e^+e^- 3.77 GeV
5.0 ± 0.8	³ PERUZZI 77	MRK1	e^+e^- 3.77 GeV

³ See the footnote on TRILLING 81 in the D^0 and D^\pm sections on the mass.

D^0 MEAN LIFE

Measurements with an error $> 0.05 \times 10^{-12}$ s are omitted from the average, and those with an error $> 0.1 \times 10^{-12}$ s or that have been superseded by later results have been removed from the Listings.

VALUE (10^{-12} s)	EVTs	DOCUMENT ID	TECN	COMMENT
0.4126 ± 0.0028 OUR AVERAGE				
0.413 ± 0.003 ± 0.004	35k	AITALA 99E	E791	$K^- \pi^+$
0.4085 ± 0.0041 ^{+0.0035} _{-0.0034}	25k	BONVICINI 99	CLE2	$e^+e^- \approx \gamma(45)$
0.413 ± 0.004 ± 0.003	16k	FRABETTI 94D	E687	$K^- \pi^+$, $K^- \pi^+ \pi^+ \pi^-$
0.424 ± 0.011 ± 0.007	5118	FRABETTI 91	E687	$K^- \pi^+$, $K^- \pi^+ \pi^+ \pi^-$
0.417 ± 0.018 ± 0.015	890	ALVAREZ 90	NA14	$K^- \pi^+$, $K^- \pi^+ \pi^+ \pi^-$
0.388 ^{+0.023} _{-0.021}	641	⁴ BARLAG 90C	ACCM	π^- Cu 230 GeV
0.48 ± 0.04 ± 0.03	776	ALBRECHT 88b	ARG	e^+e^- 10 GeV
0.422 ± 0.008 ± 0.010	4212	RAAB 88	E691	Photoproduction
0.42 ± 0.05	90	BARLAG 87B	ACCM	K^- and π^- 200 GeV

• • • We do not use the following data for averages, fits, limits, etc. • • •

0.34 ^{+0.06} _{-0.05} ± 0.03	58	AMENDOLIA 88	SPEC	Photoproduction
0.46 ^{+0.06} _{-0.05}	145	AGUILAR... 87D	HYBR	$\pi^- p$ and pp
0.50 ± 0.07 ± 0.04	317	CSORNA 87	CLEO	e^+e^- 10 GeV
0.61 ± 0.09 ± 0.03	50	ABE 86	HYBR	γp 20 GeV
0.47 ^{+0.09} _{-0.08} ± 0.05	74	GLADNEY 86	MRK2	e^+e^- 29 GeV
0.43 ^{+0.07} _{-0.05} ^{+0.01} _{-0.02}	58	USHIDA 86B	EMUL	ν wideband
0.37 ^{+0.10} _{-0.07}	26	BAILEY 85	SILI	π^- Be 200 GeV

⁴ BARLAG 90C estimate systematic error to be negligible.

$|m_{D_1^0} - m_{D_2^0}|$

The D_1^0 and D_2^0 are the mass eigenstates of the D^0 meson. To calculate the following limits, we use $\Delta m = [2r/(1-r)]^{1/2} \hbar / 4.126 \times 10^{-13}$ s, where r is the experimental D^0 - \bar{D}^0 mixing ratio.

VALUE (10^{10} h s ⁻¹)	CL%	DOCUMENT ID	TECN	COMMENT
< 7	95	⁵ GODANG 00	CLE2	e^+e^-

• • • We do not use the following data for averages, fits, limits, etc. • • •

<32	90	^{6,7} AITALA 98	E791	π^- nucleus, 500 GeV
<24	90	⁸ AITALA 96C	E791	π^- nucleus, 500 GeV
<21	90	^{7,9} ANJOS 88C	E691	Photoproduction

⁵ This GODANG 00 limit is inferred from the D^0 - \bar{D}^0 mixing ratio $\Gamma(K^+\pi^- / \Gamma(K^-\pi^+))$ given near the end of this D^0 Listings. Decay-time information is used to distinguish DCS decays from D^0 - \bar{D}^0 mixing. The limit allows interference between the DCS and mixing ratios, and also allows CP violation. The strong phase between $D^0 \rightarrow K^+\pi^-$ and $\bar{D}^0 \rightarrow K^-\pi^+$ is assumed to be small.

⁶ AITALA 98 allows interference between the doubly Cabibbo-suppressed and mixing amplitudes, and also allows CP violation in this term.

⁷ This limit is inferred from the D^0 - \bar{D}^0 mixing ratio $\Gamma(K^+\pi^- \text{ or } K^-\pi^+ \text{ or } K^+\pi^+\pi^- \text{ or } K^-\pi^-\pi^+)$ near the end of the D^0 Listings. Decay-time information is used to distinguish doubly Cabibbo-suppressed decays from D^0 - \bar{D}^0 mixing.

⁸ This limit is inferred from the D^0 - \bar{D}^0 mixing ratio $\Gamma(K^+\ell^-\nu_\ell \text{ (via } \bar{D}^0)) / \Gamma(K^-\ell^+\nu_\ell)$ given near the end of the D^0 Listings.

⁹ ANJOS 88C assumes no interference between doubly Cabibbo-suppressed and mixing amplitudes. When interference is allowed, the limit degrades by about a factor of two.

$(\Gamma_{D_1^0} - \Gamma_{D_2^0}) / \Gamma_{D^0}$

The D_1^0 and D_2^0 are the mass eigenstates of the D^0 meson. AITALA 99E uses a difference in directly measured decay rates to obtain its limit. The other experiments infer the limits here from limits on mixing, using $\Delta\Gamma/\Gamma = [8r/(1+r)]^{1/2}$, where r is the experimental D^0 - \bar{D}^0 mixing ratio. See the footnotes to the entries below.

VALUE	CL%	DOCUMENT ID	TECN	COMMENT
-0.116 < $\Delta\Gamma/\Gamma$ < 0.020	95	¹⁰ GODANG 00	CLE2	e^+e^-

• • • We do not use the following data for averages, fits, limits, etc. • • •

-0.08 < $\Delta\Gamma/\Gamma$ < 0.12	90	¹¹ AITALA 99E	E791	$K^- \pi^+$, $K^+ K^-$
$ \Delta\Gamma /\Gamma < 0.26$	90	^{12,13} AITALA 98	E791	π^- nucleus, 500 GeV
$ \Delta\Gamma /\Gamma < 0.20$	90	¹⁴ AITALA 96C	E791	π^- nucleus, 500 GeV
$ \Delta\Gamma /\Gamma < 0.17$	90	^{13,15} ANJOS 88C	E691	Photoproduction

¹⁰ This GODANG 00 limit is inferred from the D^0 - \bar{D}^0 mixing ratio $\Gamma(K^+\pi^- / \Gamma(K^-\pi^+))$ given near the end of this D^0 Listings. Decay-time information is used to distinguish DCS decays from D^0 - \bar{D}^0 mixing. The limit allows interference between the DCS and mixing ratios, and also allows CP violation. The phase between $D^0 \rightarrow K^+\pi^-$ and $\bar{D}^0 \rightarrow K^-\pi^+$ is assumed to be small.

¹¹ AITALA 99E measures $\Delta\Gamma = 2[\Gamma(D^0 \rightarrow K^+K^-) - \Gamma(D^0 \rightarrow K^-\pi^+)] = +0.04 \pm 0.14 \pm 0.05 \text{ ps}^{-1}$ and thus gets 90%-confidence-level limits $-0.20 < \Delta\Gamma < +0.28 \text{ ps}^{-1}$.

¹² AITALA 98 allows interference between the doubly Cabibbo-suppressed and mixing amplitudes, and also allows CP violation in this term.

¹³ This limit is inferred from the D^0 - \bar{D}^0 mixing ratio $\Gamma(K^+\pi^- \text{ or } K^+\pi^-\pi^+\pi^- \text{ (via } \bar{D}^0)) / \Gamma(K^-\pi^+ \text{ or } K^-\pi^+\pi^+\pi^-)$ near the end of the D^0 Listings. Decay-time information is used to distinguish doubly Cabibbo-suppressed decays from D^0 - \bar{D}^0 mixing.

¹⁴ This limit is inferred from the D^0 - \bar{D}^0 mixing ratio $\Gamma(K^+\ell^-\nu_\ell \text{ (via } \bar{D}^0)) / \Gamma(K^-\ell^+\nu_\ell)$ given near the end of the D^0 Listings.

¹⁵ ANJOS 88C assumes no interference between doubly Cabibbo-suppressed and mixing amplitudes. When interference is allowed, the limit degrades by about a factor of two.

D^0 DECAY MODES

\bar{D}^0 modes are charge conjugates of the modes below.

Mode	Fraction (Γ_i/Γ)	Scale factor/ Confidence level
Inclusive modes		
Γ_1 e^+ anything	(6.75 ± 0.29) %	
Γ_2 μ^+ anything	(6.6 ± 0.8) %	
Γ_3 K^- anything	(53 ± 4) %	S=1.3
Γ_4 \bar{K}^0 anything + K^0 anything	(42 ± 5) %	
Γ_5 K^+ anything	(3.4 ^{+0.6} _{-0.4}) %	
Γ_6 η anything	[a] < 13 %	CL=90%
Semileptonic modes		
Γ_7 $K^- \ell^+ \nu_\ell$	[b] (3.47 ± 0.17) %	S=1.3
Γ_8 $K^- e^+ \nu_e$	(3.64 ± 0.18) %	
Γ_9 $K^- \mu^+ \nu_\mu$	(3.22 ± 0.17) %	
Γ_{10} $K^- \pi^0 e^+ \nu_e$	(1.6 ^{+1.3} _{-0.5}) %	
Γ_{11} $\bar{K}^0 \pi^- e^+ \nu_e$	(2.8 ^{+1.7} _{-0.9}) %	
Γ_{12} $\bar{K}^*(892)^- e^+ \nu_e$ $\times B(K^{*-} \rightarrow \bar{K}^0 \pi^-)$	(1.35 ± 0.22) %	
Γ_{13} $K^*(892)^- \ell^+ \nu_\ell$		
Γ_{14} $\bar{K}^*(892)^0 \pi^- e^+ \nu_e$		
Γ_{15} $K^- \pi^+ \pi^- \mu^+ \nu_\mu$	< 1.2 $\times 10^{-3}$	CL=90%
Γ_{16} $(\bar{K}^*(892) \pi)^- \mu^+ \nu_\mu$	< 1.4 $\times 10^{-3}$	CL=90%
Γ_{17} $\pi^- e^+ \nu_e$	(3.7 ± 0.6) $\times 10^{-3}$	
Hadronic modes with a \bar{K} or $\bar{K}K\bar{K}$		
Γ_{18} $K^*(892)^- e^+ \nu_e$	(2.02 ± 0.33) %	
Γ_{19} $K^- \pi^+$	(3.83 ± 0.09) %	
Γ_{20} $\bar{K}^0 \pi^0$	(2.11 ± 0.21) %	S=1.1
Γ_{21} $\bar{K}^0 \pi^+ \pi^-$	[c] (5.4 ± 0.4) %	S=1.2
Γ_{22} $\bar{K}^0 \rho^0$	(1.21 ± 0.17) %	
Γ_{23} $\bar{K}^0 f_0(980)$ $\times B(f_0 \rightarrow \pi^+ \pi^-)$	(3.0 ± 0.8) $\times 10^{-3}$	
Γ_{24} $\bar{K}^0 f_2(1270)$ $\times B(f_2 \rightarrow \pi^+ \pi^-)$	(2.4 ± 0.9) $\times 10^{-3}$	
Γ_{25} $\bar{K}^0 f_0(1370)$ $\times B(f_0 \rightarrow \pi^+ \pi^-)$	(4.3 ± 1.3) $\times 10^{-3}$	
Γ_{26} $K^*(892)^- \pi^+$ $\times B(K^{*-} \rightarrow \bar{K}^0 \pi^-)$	(3.4 ± 0.3) %	
Γ_{27} $K_0^*(1430)^- \pi^+$ $\times B(K_0^*(1430)^- \rightarrow \bar{K}^0 \pi^-)$	(6.4 ± 1.6) $\times 10^{-3}$	
Γ_{28} $\bar{K}^0 \pi^+ \pi^-$ nonresonant	(1.47 ± 0.24) %	
Γ_{29} $K^- \pi^+ \pi^0$	[c] (13.9 ± 0.9) %	S=1.3
Γ_{30} $K^- \rho^+$	(10.8 ± 1.0) %	
Γ_{31} $K^*(892)^- \pi^+$ $\times B(K^{*-} \rightarrow K^- \pi^0)$	(1.7 ± 0.2) %	
Γ_{32} $\bar{K}^*(892)^0 \pi^0$ $\times B(\bar{K}^{*0} \rightarrow K^- \pi^+)$	(2.1 ± 0.3) %	
Γ_{33} $K^- \pi^+ \pi^0$ nonresonant	(6.9 ± 2.5) $\times 10^{-3}$	

A fraction of the following resonance mode has already appeared above as a submode of a charged-particle mode.

[a] $\pi^- \rightarrow \pi^0 \pi^-$

[b] $\pi^- \rightarrow \pi^0 \pi^-$

[c] $\pi^- \rightarrow \pi^0 \pi^-$

Meson Particle Listings

 D^0

Γ_{34}	$\bar{K}^0 \pi^0 \pi^0$	—		
Γ_{35}	$\bar{K}^*(892)^0 \pi^0$ $\times B(\bar{K}^{*0} \rightarrow \bar{K}^0 \pi^0)$	$(1.1 \pm 0.2) \%$		
Γ_{36}	$\bar{K}^0 \pi^0 \pi^0$ nonresonant	$(7.8 \pm 2.0) \times 10^{-3}$		
Γ_{37}	$K^- \pi^+ \pi^+ \pi^-$	$[c]$ $(7.49 \pm 0.31) \%$		
Γ_{38}	$K^- \pi^+ \rho^0$ total	$(6.3 \pm 0.4) \%$		
Γ_{39}	$K^- \pi^+ \rho^0$ 3-body	$(4.7 \pm 2.1) \times 10^{-3}$		
Γ_{40}	$\bar{K}^*(892)^0 \rho^0$ $\times B(\bar{K}^{*0} \rightarrow K^- \pi^+)$	$(9.8 \pm 2.2) \times 10^{-3}$		
Γ_{41}	$K^- a_1(1260)^+$ $\times B(a_1(1260)^+ \rightarrow \pi^+ \pi^+ \pi^-)$	$(3.6 \pm 0.6) \%$		
Γ_{42}	$\bar{K}^*(892)^0 \pi^+ \pi^-$ total $\times B(\bar{K}^{*0} \rightarrow K^- \pi^+)$	$(1.5 \pm 0.4) \%$		
Γ_{43}	$\bar{K}^*(892)^0 \pi^+ \pi^-$ 3-body $\times B(\bar{K}^{*0} \rightarrow K^- \pi^+)$	$(9.5 \pm 2.1) \times 10^{-3}$		
Γ_{44}	$K_1(1270)^- \pi^+$ $\times B(K_1(1270)^- \rightarrow K^- \pi^+ \pi^-)$	$[d]$ $(3.6 \pm 1.0) \times 10^{-3}$		
Γ_{45}	$K^- \pi^+ \pi^+ \pi^-$ nonresonant	$(1.74 \pm 0.25) \%$		
Γ_{46}	$\bar{K}^0 \pi^+ \pi^- \pi^0$	$[c]$ $(10.0 \pm 1.2) \%$		
Γ_{47}	$\bar{K}^0 \eta \times B(\eta \rightarrow \pi^+ \pi^- \pi^0)$	$(1.6 \pm 0.3) \times 10^{-3}$		
Γ_{48}	$\bar{K}^0 \omega \times B(\omega \rightarrow \pi^+ \pi^- \pi^0)$	$(1.9 \pm 0.4) \%$		
Γ_{49}	$K^*(892)^- \rho^+$ $\times B(K^{*-} \rightarrow \bar{K}^0 \pi^-)$	$(4.1 \pm 1.6) \%$		
Γ_{50}	$\bar{K}^*(892)^0 \rho^0$ $\times B(\bar{K}^{*0} \rightarrow \bar{K}^0 \pi^0)$	$(4.9 \pm 1.1) \times 10^{-3}$		
Γ_{51}	$K_1(1270)^- \pi^+$ $\times B(K_1(1270)^- \rightarrow \bar{K}^0 \pi^- \pi^0)$	$[d]$ $(5.1 \pm 1.4) \times 10^{-3}$		
Γ_{52}	$\bar{K}^*(892)^0 \pi^+ \pi^-$ 3-body $\times B(\bar{K}^{*0} \rightarrow \bar{K}^0 \pi^0)$	$(4.8 \pm 1.1) \times 10^{-3}$		
Γ_{53}	$\bar{K}^0 \pi^+ \pi^- \pi^0$ nonresonant	$(2.1 \pm 2.1) \%$		
Γ_{54}	$K^- \pi^+ \pi^0 \pi^0$	$(15 \pm 5) \%$		
Γ_{55}	$K^- \pi^+ \pi^+ \pi^- \pi^0$	$(4.0 \pm 0.4) \%$		
Γ_{56}	$\bar{K}^*(892)^0 \pi^+ \pi^- \pi^0$ $\times B(\bar{K}^{*0} \rightarrow K^- \pi^+)$	$(1.2 \pm 0.6) \%$		
Γ_{57}	$\bar{K}^*(892)^0 \eta$ $\times B(\bar{K}^{*0} \rightarrow K^- \pi^+)$ $\times B(\eta \rightarrow \pi^+ \pi^- \pi^0)$	$(2.9 \pm 0.8) \times 10^{-3}$		
Γ_{58}	$K^- \pi^+ \omega \times B(\omega \rightarrow \pi^+ \pi^- \pi^0)$	$(2.7 \pm 0.5) \%$		
Γ_{59}	$\bar{K}^*(892)^0 \omega$ $\times B(\bar{K}^{*0} \rightarrow K^- \pi^+)$ $\times B(\omega \rightarrow \pi^+ \pi^- \pi^0)$	$(7 \pm 3) \times 10^{-3}$		
Γ_{60}	$\bar{K}^0 \pi^+ \pi^+ \pi^- \pi^-$	$(5.8 \pm 1.6) \times 10^{-3}$		
Γ_{61}	$\bar{K}^0 \pi^+ \pi^- \pi^0 \pi^0 (\pi^0)$	$(10.6 \pm_{-3.0}^{+7.3}) \%$		
Γ_{62}	$\bar{K}^0 K^+ K^-$ In the fit as $\frac{1}{2}\Gamma_{74} + \Gamma_{64}$, where $\frac{1}{2}\Gamma_{74} = \Gamma_{63}$.	$(9.4 \pm 1.0) \times 10^{-3}$		
Γ_{63}	$\bar{K}^0 \phi \times B(\phi \rightarrow K^+ K^-)$	$(4.3 \pm 0.5) \times 10^{-3}$		
Γ_{64}	$\bar{K}^0 K^+ K^-$ non- ϕ	$(5.1 \pm 0.8) \times 10^{-3}$		
Γ_{65}	$K_S^0 K_S^0 K_S^0$	$(8.3 \pm 1.5) \times 10^{-4}$		
Γ_{66}	$K^+ K^- K^- \pi^+$	$(2.1 \pm 0.5) \times 10^{-4}$		
Γ_{67}	$K^+ K^- \bar{K}^0 \pi^0$	$(7.2 \pm_{-3.5}^{+4.8}) \times 10^{-3}$		
Γ_{68} Fractions of many of the following modes with resonances have already appeared above as submodes of particular charged-particle modes. (Modes for which there are only upper limits and $\bar{K}^*(892)^0$ submodes only appear below.)				
Γ_{68}	$\bar{K}^0 \eta$	$(7.0 \pm 1.0) \times 10^{-3}$		
Γ_{69}	$\bar{K}^0 \rho^0$	$(1.21 \pm 0.17) \%$		
Γ_{70}	$K^- \rho^+$	$(10.8 \pm 0.9) \%$	S=1.2	
Γ_{71}	$\bar{K}^0 \omega$	$(2.1 \pm 0.4) \%$		
Γ_{72}	$\bar{K}^0 \eta'(958)$	$(1.71 \pm 0.26) \%$		
Γ_{73}	$\bar{K}^0 f_0(980)$	$(5.7 \pm 1.6) \times 10^{-3}$		
Γ_{74}	$\bar{K}^0 \phi$	$(8.6 \pm 1.0) \times 10^{-3}$		
Γ_{75}	$K^- a_1(1260)^+$	$(7.3 \pm 1.1) \%$		
Γ_{76}	$\bar{K}^0 a_1(1260)^0$	$< 1.9 \%$	CL=90%	
Γ_{77}	$\bar{K}^0 f_2(1270)$	$(4.1 \pm 1.5) \times 10^{-3}$		
Γ_{78}	$K^- a_2(1320)^+$	$< 2 \times 10^{-3}$	CL=90%	
Γ_{79}	$\bar{K}^0 f_0(1370)$	$(6.9 \pm 2.1) \times 10^{-3}$		
Γ_{80}	$K^*(892)^- \pi^+$	$(5.0 \pm 0.4) \%$	S=1.2	
Γ_{81}	$\bar{K}^*(892)^0 \pi^0$	$(3.1 \pm 0.4) \%$		
Γ_{82}	$\bar{K}^*(892)^0 \pi^+ \pi^-$ total	$(2.2 \pm 0.5) \%$		
Γ_{83}	$\bar{K}^*(892)^0 \pi^+ \pi^-$ 3-body	$(1.42 \pm 0.32) \%$		
Γ_{84}	$K^- \pi^+ \rho^0$ total	$(6.3 \pm 0.4) \%$		
Γ_{85}	$K^- \pi^+ \rho^0$ 3-body	$(4.7 \pm 2.1) \times 10^{-3}$		
Γ_{86}	$\bar{K}^*(892)^0 \rho^0$	$(1.46 \pm 0.32) \%$		
Γ_{87}	$\bar{K}^*(892)^0 \rho^0$ transverse	$(1.5 \pm 0.5) \%$		
Γ_{88}	$\bar{K}^*(892)^0 \rho^0$ S-wave	$(2.8 \pm 0.6) \%$		
Γ_{89}	$\bar{K}^*(892)^0 \rho^0$ S-wave long.	$< 3 \times 10^{-3}$	CL=90%	
Γ_{90}	$\bar{K}^*(892)^0 \rho^0$ P-wave	$< 3 \times 10^{-3}$	CL=90%	
Γ_{91}	$\bar{K}^*(892)^0 \rho^0$ D-wave	$(1.9 \pm 0.6) \%$		
Γ_{92}	$K^*(892)^- \rho^+$	$(6.1 \pm 2.4) \%$		
Γ_{93}	$K^*(892)^- \rho^+$ longitudinal	$(2.9 \pm 1.2) \%$		
Γ_{94}	$K^*(892)^- \rho^+$ transverse	$(3.2 \pm 1.8) \%$		
Γ_{95}	$K^*(892)^- \rho^+$ P-wave	$< 1.5 \%$	CL=90%	
Γ_{96}	$K^- \pi^+ f_0(980)$	$< 1.1 \%$	CL=90%	
Γ_{97}	$\bar{K}^*(892)^0 f_0(980)$	$< 7 \times 10^{-3}$	CL=90%	
Γ_{98}	$K_1(1270)^- \pi^+$	$[d]$ $(1.06 \pm 0.29) \%$		
Γ_{99}	$K_1(1400)^- \pi^+$	$< 1.2 \%$	CL=90%	
Γ_{100}	$\bar{K}_1(1400)^0 \pi^0$	$< 3.7 \%$	CL=90%	
Γ_{101}	$K^*(1410)^- \pi^+$	$< 1.2 \%$	CL=90%	
Γ_{102}	$K^*(892)^- \pi^+$	$(1.04 \pm 0.26) \%$		
Γ_{103}	$K_2^0(1430)^- \pi^+$	$< 8 \times 10^{-3}$	CL=90%	
Γ_{104}	$\bar{K}_2^0(1430)^0 \pi^0$	$< 4 \times 10^{-3}$	CL=90%	
Γ_{105}	$\bar{K}^*(892)^0 \pi^+ \pi^- \pi^0$	$(1.8 \pm 0.9) \%$		
Γ_{106}	$\bar{K}^*(892)^0 \eta$	$(1.9 \pm 0.5) \%$		
Γ_{107}	$K^- \pi^+ \omega$	$(3.0 \pm 0.6) \%$		
Γ_{108}	$\bar{K}^*(892)^0 \omega$	$(1.1 \pm 0.4) \%$		
Γ_{109}	$K^- \pi^+ \eta'(958)$	$(7.0 \pm 1.8) \times 10^{-3}$		
Γ_{110}	$\bar{K}^*(892)^0 \eta'(958)$	$< 1.0 \times 10^{-3}$	CL=90%	
Pionic modes				
Γ_{111}	$\pi^+ \pi^-$	$(1.52 \pm 0.09) \times 10^{-3}$		
Γ_{112}	$\pi^0 \pi^0$	$(8.4 \pm 2.2) \times 10^{-4}$		
Γ_{113}	$\pi^+ \pi^- \pi^0$	$(1.6 \pm 1.1) \%$	S=2.7	
Γ_{114}	$\pi^+ \pi^+ \pi^- \pi^-$	$(7.3 \pm 0.5) \times 10^{-3}$		
Γ_{115}	$\pi^+ \pi^+ \pi^- \pi^- \pi^0$	$(1.9 \pm 0.4) \%$		
Γ_{116}	$\pi^+ \pi^+ \pi^+ \pi^- \pi^- \pi^-$	$(4.0 \pm 3.0) \times 10^{-4}$		
Hadronic modes with a $K\bar{K}$ pair				
Γ_{117}	$K^+ K^-$	$(4.25 \pm 0.16) \times 10^{-3}$		
Γ_{118}	$K^0 \bar{K}^0$	$(6.5 \pm 1.8) \times 10^{-4}$	S=1.2	
Γ_{119}	$K^0 K^- \pi^+$	$(6.4 \pm 1.0) \times 10^{-3}$	S=1.1	
Γ_{120}	$\bar{K}^*(892)^0 K^0$ $\times B(\bar{K}^{*0} \rightarrow K^- \pi^+)$	$< 1.1 \times 10^{-3}$	CL=90%	
Γ_{121}	$K^*(892)^+ K^-$ $\times B(K^{*+} \rightarrow K^0 \pi^+)$	$(2.3 \pm 0.5) \times 10^{-3}$		
Γ_{122}	$K^0 K^- \pi^+$ nonresonant	$(2.3 \pm 2.3) \times 10^{-3}$		
Γ_{123}	$\bar{K}^0 K^+ \pi^-$	$(5.0 \pm 1.0) \times 10^{-3}$		
Γ_{124}	$K^*(892)^0 \bar{K}^0$ $\times B(K^{*0} \rightarrow K^+ \pi^-)$	$< 5 \times 10^{-4}$	CL=90%	
Γ_{125}	$K^*(892)^- K^+$ $\times B(K^{*-} \rightarrow \bar{K}^0 \pi^-)$	$(1.2 \pm 0.7) \times 10^{-3}$		
Γ_{126}	$\bar{K}^0 K^+ \pi^-$ nonresonant	$(3.8 \pm_{-1.9}^{+2.3}) \times 10^{-3}$		
Γ_{127}	$K^+ K^- \pi^0$	$(1.3 \pm 0.4) \times 10^{-3}$		
Γ_{128}	$K_S^0 K_S^0 \pi^0$	$< 5.9 \times 10^{-4}$		
Γ_{129}	$K^+ K^- \pi^+ \pi^-$	$[e]$ $(2.50 \pm 0.23) \times 10^{-3}$		
Γ_{130}	$\phi \pi^+ \pi^- \times B(\phi \rightarrow K^+ K^-)$	$(5.3 \pm 1.4) \times 10^{-4}$		
Γ_{131}	$\phi \rho^0 \times B(\phi \rightarrow K^+ K^-)$	$(3.0 \pm 1.6) \times 10^{-4}$		
Γ_{132}	$K^+ K^- \rho^0$ 3-body	$(9.0 \pm 2.3) \times 10^{-4}$		
Γ_{133}	$K^*(892)^0 K^- \pi^+ + c.c.$ $\times B(K^{*0} \rightarrow K^+ \pi^-)$	$[f]$ $< 5 \times 10^{-4}$		
Γ_{134}	$K^*(892)^0 \bar{K}^*(892)^0$ $\times B^2(K^{*0} \rightarrow K^+ \pi^-)$	$(6 \pm 2) \times 10^{-4}$		
Γ_{135}	$K^+ K^- \pi^+ \pi^-$ non- ϕ	—		
Γ_{136}	$K^+ K^- \pi^+ \pi^-$ nonresonant	$< 8 \times 10^{-4}$	CL=90%	
Γ_{137}	$K^0 \bar{K}^0 \pi^+ \pi^-$	$(6.8 \pm 2.7) \times 10^{-3}$		
Γ_{138}	$K^+ K^- \pi^+ \pi^- \pi^0$	$(3.1 \pm 2.0) \times 10^{-3}$		
Fractions of most of the following modes with resonances have already appeared above as submodes of particular charged-particle modes.				
Γ_{139}	$\bar{K}^*(892)^0 K^0$	$< 1.6 \times 10^{-3}$	CL=90%	
Γ_{140}	$K^*(892)^+ K^-$	$(3.5 \pm 0.8) \times 10^{-3}$		
Γ_{141}	$K^*(892)^0 \bar{K}^0$	$< 8 \times 10^{-4}$	CL=90%	
Γ_{142}	$K^*(892)^- K^+$	$(1.8 \pm 1.0) \times 10^{-3}$		
Γ_{143}	$\phi \pi^0$	$< 1.4 \times 10^{-3}$	CL=90%	
Γ_{144}	$\phi \eta$	$< 2.8 \times 10^{-3}$	CL=90%	
Γ_{145}	$\phi \omega$	$< 2.1 \times 10^{-3}$	CL=90%	

Meson Particle Listings

 D^0 D^0 BRANCHING RATIOSSee the "Note on D Mesons" in the D^\pm Listings.

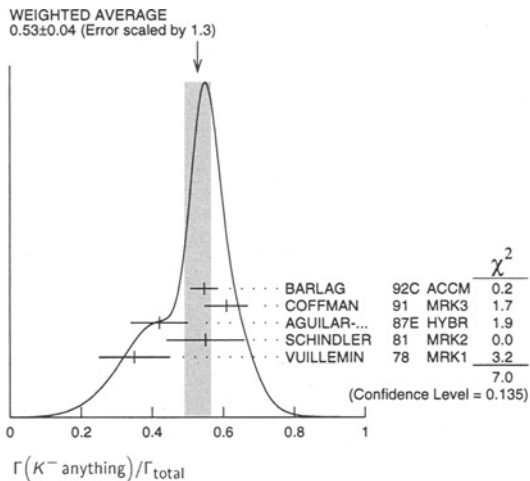
Some older now obsolete results have been omitted from these Listings.

Inclusive modes

$\Gamma(e^+ \text{ anything})/\Gamma_{\text{total}}$					Γ_1/Γ
VALUE	EVTs	DOCUMENT ID	TECN	COMMENT	
0.0675 ± 0.0029 OUR AVERAGE					
0.069 ± 0.003 ± 0.005	1670	ALBRECHT	96C ARG	$e^+ e^- \approx 10$ GeV	
0.0664 ± 0.0018 ± 0.0029	4609	¹⁶ KUBOTA	96B CLE2	$e^+ e^- \approx T(4S)$	
0.075 ± 0.011 ± 0.004	137	BALTRUSAIT..	85B MRK3	$e^+ e^- 3.77$ GeV	
• • • We do not use the following data for averages, fits, limits, etc. • • •					
0.15 ± 0.05		AGUILAR...	87E HYBR	$\pi p, pp$ 360, 400 GeV	
0.055 ± 0.037	12	SCHINDLER	81 MRK2	$e^+ e^- 3.771$ GeV	
¹⁶ KUBOTA 96B uses $D^{*+} \rightarrow D^0 \pi^+$ (and charge conjugate) events in which the D^0 subsequently decays to $X e^+ \nu_e$.					

$\Gamma(\mu^+ \text{ anything})/\Gamma_{\text{total}}$					Γ_2/Γ
VALUE	EVTs	DOCUMENT ID	TECN	COMMENT	
0.066 ± 0.008 OUR FIT					
0.060 ± 0.007 ± 0.012	310	ALBRECHT	96C ARG	$e^+ e^- \approx 10$ GeV	

$\Gamma(K^- \text{ anything})/\Gamma_{\text{total}}$					Γ_3/Γ
VALUE	EVTs	DOCUMENT ID	TECN	COMMENT	
0.53 ± 0.04 OUR AVERAGE					
0.546 ^{+0.039} _{-0.038}		¹⁷ BARLAG	92C ACCM	π^- Cu 230 GeV	
0.609 ± 0.032 ± 0.052		COFFMAN	91 MRK3	$e^+ e^- 3.77$ GeV	
0.42 ± 0.08		AGUILAR...	87E HYBR	$\pi p, pp$ 360, 400 GeV	
0.55 ± 0.11	121	SCHINDLER	81 MRK2	$e^+ e^- 3.771$ GeV	
0.35 ± 0.10	19	VUILLEMIN	78 MRK1	$e^+ e^- 3.772$ GeV	
¹⁷ BARLAG 92C computes the branching fraction using topological normalization.					



$[\Gamma(K^0 \text{ anything}) + \Gamma(K^0 \text{ anything})]/\Gamma_{\text{total}}$					Γ_4/Γ
VALUE	EVTs	DOCUMENT ID	TECN	COMMENT	
0.42 ± 0.05 OUR AVERAGE					
0.455 ± 0.050 ± 0.032		COFFMAN	91 MRK3	$e^+ e^- 3.77$ GeV	
0.29 ± 0.11	13	SCHINDLER	81 MRK2	$e^+ e^- 3.771$ GeV	
0.57 ± 0.26	6	VUILLEMIN	78 MRK1	$e^+ e^- 3.772$ GeV	

$\Gamma(K^+ \text{ anything})/\Gamma_{\text{total}}$					Γ_5/Γ
VALUE	EVTs	DOCUMENT ID	TECN	COMMENT	
0.034 ± 0.006 OUR AVERAGE					
0.034 ^{+0.007} _{-0.005}		¹⁸ BARLAG	92C ACCM	π^- Cu 230 GeV	
0.028 ± 0.009 ± 0.004		COFFMAN	91 MRK3	$e^+ e^- 3.77$ GeV	
0.03 ± 0.05		AGUILAR...	87E HYBR	$\pi p, pp$ 360, 400 GeV	
0.08 ± 0.03	25	SCHINDLER	81 MRK2	$e^+ e^- 3.771$ GeV	
¹⁸ BARLAG 92C computes the branching fraction using topological normalization.					

Semileptonic modes

$\Gamma(K^- \ell^+ \nu_\ell)/\Gamma_{\text{total}}$ Γ_7/Γ
 We average our $K^- e^+ \nu_e$ and $K^- \mu^+ \nu_\mu$ branching fractions, after multiplying the latter by a phase-space factor of 1.03 to be able to use it with the $K^- e^+ \nu_e$ fraction. Hence our ℓ^+ here is really an e^+ .

VALUE	DOCUMENT ID	COMMENT
0.0348 ± 0.0017 OUR AVERAGE		Error includes scale factor of 1.3.
0.0364 ± 0.0018	PDG	00 Our $\Gamma(K^- e^+ \nu_e)/\Gamma_{\text{total}}$
0.0331 ± 0.0018	PDG	00 $1.03 \times \text{our } \Gamma(K^- \mu^+ \nu_\mu)/\Gamma_{\text{total}}$

$\Gamma(K^- e^+ \nu_e)/\Gamma_{\text{total}}$					Γ_8/Γ
VALUE	EVTs	DOCUMENT ID	TECN	COMMENT	
0.0364 ± 0.0018 OUR FIT					
0.034 ± 0.008 ± 0.004	55	ADLER	89 MRK3	$e^+ e^- 3.77$ GeV	

$\Gamma(K^- e^+ \nu_e)/\Gamma(K^- \pi^+)$					Γ_8/Γ_{19}
VALUE	EVTs	DOCUMENT ID	TECN	COMMENT	
0.95 ± 0.04 OUR FIT					
0.95 ± 0.04 OUR AVERAGE					
0.978 ± 0.027 ± 0.044	2510	¹⁹ BEAN	93C CLE2	$e^+ e^- \approx T(4S)$	
0.90 ± 0.06 ± 0.06	584	²⁰ CRAWFORD	91B CLEO	$e^+ e^- \approx 10.5$ GeV	
0.91 ± 0.07 ± 0.11	250	²¹ ANJOS	89F E691	Photoproduction	

¹⁹ BEAN 93C uses $K^- \mu^+ \nu_\mu$ as well as $K^- e^+ \nu_e$ events and makes a small phase-space adjustment to the number of the μ^+ events to use them as e^+ events. A pole mass of $2.00 \pm 0.12 \pm 0.18$ GeV/ c^2 is obtained from the q^2 dependence of the decay rate.
²⁰ CRAWFORD 91B uses $K^- e^+ \nu_e$ and $K^- \mu^+ \nu_\mu$ candidates to measure a pole mass of $2.1^{+0.4+0.3}_{-0.2-0.2}$ GeV/ c^2 from the q^2 dependence of the decay rate.
²¹ ANJOS 89F measures a pole mass of $2.1^{+0.4}_{-0.2} \pm 0.2$ GeV/ c^2 from the q^2 dependence of the decay rate.

$\Gamma(K^- \mu^+ \nu_\mu)/\Gamma(K^- \pi^+)$					Γ_9/Γ_{19}
VALUE	EVTs	DOCUMENT ID	TECN	COMMENT	
0.84 ± 0.04 OUR FIT					
0.84 ± 0.04 OUR AVERAGE					
0.852 ± 0.034 ± 0.028	1897	²² FRABETTI	95G E687	γ Be $\bar{E}_\gamma = 220$ GeV	
0.82 ± 0.13 ± 0.13	338	²³ FRABETTI	93I E687	γ Be $\bar{E}_\gamma = 221$ GeV	
0.79 ± 0.08 ± 0.09	231	²⁴ CRAWFORD	91B CLEO	$e^+ e^- \approx 10.5$ GeV	

²² FRABETTI 95G extracts the ratio of form factors $f_-(0)/f_+(0) = -1.3^{+3.6}_{-3.4} \pm 0.6$, and measures a pole mass of $1.87^{+0.11+0.07}_{-0.08-0.06}$ GeV/ c^2 from the q^2 dependence of the decay rate.
²³ FRABETTI 93I measures a pole mass of $2.1^{+0.7+0.7}_{-0.3-0.3}$ GeV/ c^2 from the q^2 dependence of the decay rate.
²⁴ CRAWFORD 91B measures a pole mass of $2.00 \pm 0.12 \pm 0.18$ GeV/ c^2 from the q^2 dependence of the decay rate.

$\Gamma(K^- \mu^+ \nu_\mu)/\Gamma(\mu^+ \text{ anything})$					Γ_9/Γ_2
VALUE	EVTs	DOCUMENT ID	TECN	COMMENT	
0.49 ± 0.06 OUR FIT					
0.472 ± 0.051 ± 0.040	232	KODAMA	94 E653	π^- emulsion 600 GeV	
• • • We do not use the following data for averages, fits, limits, etc. • • •					
0.32 ± 0.05 ± 0.05	124	KODAMA	91 EMUL	ρA 800 GeV	

$\Gamma(K^- \pi^0 e^+ \nu_e)/\Gamma_{\text{total}}$					Γ_{10}/Γ
VALUE	EVTs	DOCUMENT ID	TECN	COMMENT	
0.016^{+0.013}_{-0.005} ± 0.002	4	²⁵ BAI	91 MRK3	$e^+ e^- \approx 3.77$ GeV	
²⁵ BAI 91 finds that a fraction $0.79^{+0.15+0.09}_{-0.17-0.03}$ of combined D^+ and D^0 decays to $\bar{K} \pi e^+ \nu_e$ (24 events) are $\bar{K}^*(892) e^+ \nu_e$. BAI 91 uses 56 $K^- e^+ \nu_e$ events to measure a pole mass of $1.8 \pm 0.3 \pm 0.2$ GeV/ c^2 from the q^2 dependence of the decay rate.					

$\Gamma(K^0 \pi^- e^+ \nu_e)/\Gamma_{\text{total}}$					Γ_{11}/Γ
VALUE	EVTs	DOCUMENT ID	TECN	COMMENT	
0.028^{+0.017}_{-0.008} ± 0.003	6	²⁶ BAI	91 MRK3	$e^+ e^- \approx 3.77$ GeV	
²⁶ BAI 91 finds that a fraction $0.79^{+0.15+0.09}_{-0.17-0.03}$ of combined D^+ and D^0 decays to $\bar{K} \pi e^+ \nu_e$ (24 events) are $\bar{K}^*(892) e^+ \nu_e$.					

$\Gamma(K^*(892)^- e^+ \nu_e)/\Gamma(K^- e^+ \nu_e)$					Γ_{18}/Γ_8
VALUE	DOCUMENT ID	TECN	COMMENT		
0.55 ± 0.09 OUR FIT					
0.51 ± 0.18 ± 0.06	CRAWFORD	91B CLEO	$e^+ e^- \approx 10.5$ GeV		

$\Gamma(K^*(892)^- e^+ \nu_e)/\Gamma(K^0 \pi^+ \pi^-)$					Γ_{18}/Γ_{21}
VALUE	EVTs	DOCUMENT ID	TECN	COMMENT	
0.37 ± 0.06 OUR FIT					
0.38 ± 0.06 ± 0.03	152	²⁷ BEAN	93C CLE2	$e^+ e^- \approx T(4S)$	
²⁷ BEAN 93C uses $K^* \mu^+ \nu_\mu$ as well as $K^* e^+ \nu_e$ events and makes a small phase-space adjustment to the number of the μ^+ events to use them as e^+ events.					

Meson Particle Listings
 D^0

$\Gamma(K^*(892)^- \ell^+ \nu_\ell) / \Gamma(K^0 \pi^+ \pi^-)$ Γ_{13}/Γ_{21}
This is an average of the $K^*(892)^- e^+ \nu_e$ and $K^*(892)^- \mu^+ \nu_\mu$ ratios. Unseen decay modes of the $K^*(892)^-$ are included.

VALUE	EVTS	DOCUMENT ID	TECN	COMMENT
$0.24 \pm 0.07 \pm 0.06$	137	²⁸ ALEXANDER 90b	CLEO	$e^+ e^-$ 10.5–11 GeV
²⁸ ALEXANDER 90b cannot exclude extra π^0 's in the final state. See nearby data blocks for more detailed results.				

$\Gamma(\bar{K}^*(892)^0 \pi^- e^+ \nu_e) / \Gamma(K^*(892)^- e^+ \nu_e)$ Γ_{14}/Γ_{18}
Unseen decay modes of the $\bar{K}^*(892)^0$ are included.

VALUE	CL%	DOCUMENT ID	TECN	COMMENT
< 0.64	90	²⁹ CRAWFORD 91b	CLEO	$e^+ e^- \approx 10.5$ GeV
²⁹ The limit on $(\bar{K}^*(892)\pi)^- \mu^+ \nu_\mu$ below is much stronger.				

$\Gamma(K^-\pi^+\pi^-\mu^+\nu_\mu) / \Gamma(K^-\mu^+\nu_\mu)$ Γ_{15}/Γ_9

VALUE	CL%	DOCUMENT ID	TECN	COMMENT
< 0.037	90	KODAMA 93b	E653	π^- emulsion 600 GeV

$\Gamma((\bar{K}^*(892)\pi)^- \mu^+ \nu_\mu) / \Gamma(K^-\mu^+\nu_\mu)$ Γ_{16}/Γ_9

VALUE	CL%	DOCUMENT ID	TECN	COMMENT
< 0.043	90	³⁰ KODAMA 93b	E653	π^- emulsion 600 GeV
³⁰ KODAMA 93b searched in $K^-\pi^+\pi^-\mu^+\nu_\mu$, but the limit includes other $(\bar{K}^*(892)\pi)^-$ charge states.				

$\Gamma(\pi^- e^+ \nu_e) / \Gamma_{total}$ Γ_{17}/Γ

VALUE	EVTS	DOCUMENT ID	TECN	COMMENT
0.0037 ± 0.0006	OUR FIT Error includes scale factor of 1.2.			
$0.0039 \pm 0.0023 \pm 0.0004$	7	³¹ ADLER 89	MRK3	$e^+ e^-$ 3.77 GeV

$\Gamma(\pi^- e^+ \nu_e) / \Gamma(K^- e^+ \nu_e)$ Γ_{17}/Γ_8

VALUE	EVTS	DOCUMENT ID	TECN	COMMENT
0.102 ± 0.017	OUR FIT			
0.101 ± 0.018	OUR AVERAGE			
$0.101 \pm 0.020 \pm 0.003$	91	³² FRABETTI 96b	E687	γ Be, $\bar{E}_\gamma \approx 200$ GeV
$0.103 \pm 0.039 \pm 0.013$	87	³³ BUTLER 95	CLE2	< 0.156 (90% CL)

Hadronic modes with a \bar{K} or $\bar{K}KK$

$\Gamma(K^-\pi^+) / \Gamma_{total}$ Γ_{19}/Γ
We list measurements before radiative corrections are made.

VALUE	EVTS	DOCUMENT ID	TECN	COMMENT
0.0383 ± 0.0009	OUR FIT			
0.0385 ± 0.0009	OUR AVERAGE			
$0.0382 \pm 0.0007 \pm 0.0012$				
$0.0390 \pm 0.0009 \pm 0.0012$	5392	³⁴ ARTUSO 98	CLE2	CLEO average
$0.045 \pm 0.006 \pm 0.004$		³⁵ BARATE 97c	ALEP	From Z decays
$0.0341 \pm 0.0012 \pm 0.0028$	1173	³⁶ ALBRECHT 94	ARG	$e^+ e^- \approx \mathcal{T}(45)$
$0.0362 \pm 0.0034 \pm 0.0044$		³⁵ ALBRECHT 94f	ARG	$e^+ e^- \approx \mathcal{T}(45)$
$0.045 \pm 0.008 \pm 0.005$	56	³⁵ DECAMP 91j	ALEP	From Z decays
$0.042 \pm 0.004 \pm 0.004$	930	³⁵ ABACHI 88	HRS	$e^+ e^-$ 29 GeV
0.041 ± 0.006	263	³⁷ ADLER 88c	MRK3	$e^+ e^-$ 3.77 GeV
0.043 ± 0.010	130	³⁷ SCHINDLER 81	MRK2	$e^+ e^-$ 3.771 GeV
		³⁸ PERUZZI 77	MRK1	$e^+ e^-$ 3.77 GeV
• • • We do not use the following data for averages, fits, limits, etc. • • •				
$0.0381 \pm 0.0015 \pm 0.0016$	1165	³⁹ ARTUSO 98	CLE2	$e^+ e^-$ at $\mathcal{T}(45)$
$0.0369 \pm 0.0011 \pm 0.0016$		⁴⁰ COAN 98	CLE2	
$0.0391 \pm 0.0008 \pm 0.0017$	4208	^{35,41} AKERIB 93	CLE2	$e^+ e^- \approx \mathcal{T}(45)$

³⁴This combines the CLEO results of ARTUSO 98, COAN 98, and AKERIB 93.
³⁵ABACHI 88, DECAMP 91j, AKERIB 93, ALBRECHT 94f, and BARATE 97c use $D^*(2010)^+ \rightarrow D^0 \pi^+$ decays. The π^+ is both slow and of low p_T with respect to the event thrust axis or nearest jet ($\approx D^{*+}$ direction). The excess number of such π^+ 's over background gives the number of $D^*(2010)^+ \rightarrow D^0 \pi^+$ events, and the fraction with $D^0 \rightarrow K^-\pi^+$ gives the $D^0 \rightarrow K^-\pi^+$ branching fraction.

³⁶ALBRECHT 94 uses D^0 mesons from $\bar{B}^0 \rightarrow D^{*+} \ell^- \bar{\nu}_\ell$ decays. This is a different set of events than used by ALBRECHT 94f.

³⁷SCHINDLER 81 (MARK-2) measures $\sigma(e^+ e^- \rightarrow \psi(3770)) \times$ branching fraction to be 0.24 ± 0.02 nb. We use the MARK-3 (ADLER 88c) value of $\sigma = 5.8 \pm 0.5 \pm 0.6$ nb.

³⁸PERUZZI 77 (MARK-1) measures $\sigma(e^+ e^- \rightarrow \psi(3770)) \times$ branching fraction to be 0.25 ± 0.05 nb. We use the MARK-3 (ADLER 88c) value of $\sigma = 5.8 \pm 0.5 \pm 0.6$ nb.

³⁹ARTUSO 98, following ALBRECHT 94, uses D^0 mesons from $\bar{B}^0 \rightarrow D^*(2010)^+ X \ell^- \bar{\nu}_\ell$ decays. Our average uses the CLEO average of this value with the values of COAN 98 and AKERIB 93.

⁴⁰COAN 98 assumes that $\Gamma(B \rightarrow D^+ X \ell^+ \nu) / \Gamma(B \rightarrow X \ell^+ \nu) = 1.0 - 3|V_{ub}/V_{cb}|^2 - 0.010 \pm 0.005$, the last term accounting for $\bar{B} \rightarrow D_s^+ K X \ell^- \bar{\nu}$. COAN 98 is included in the CLEO average in ARTUSO 98.

⁴¹This AKERIB 93 value does not include radiative corrections; with them, the value is $0.0395 \pm 0.0008 \pm 0.0017$. AKERIB 93 is included in the CLEO average in ARTUSO 98.

$\Gamma(K^0 \pi^0) / \Gamma(K^- \pi^+)$ Γ_{20}/Γ_{19}

VALUE	EVTS	DOCUMENT ID	TECN	COMMENT
0.55 ± 0.06	OUR FIT Error includes scale factor of 1.1.			
$1.36 \pm 0.23 \pm 0.22$	119	ANJOS 92b	E691	γ Be 80–240 GeV

$\Gamma(K^0 \pi^0) / \Gamma(K^0 \pi^+ \pi^-)$ Γ_{20}/Γ_{21}

VALUE	EVTS	DOCUMENT ID	TECN	COMMENT
0.390 ± 0.031	OUR FIT			
0.378 ± 0.033	OUR AVERAGE			
$0.44 \pm 0.02 \pm 0.05$	1942	PROCARIO 93b	CLE2	$e^+ e^-$ 10.36–10.7 GeV
$0.34 \pm 0.04 \pm 0.02$	92	⁴² ALBRECHT 92p	ARG	$e^+ e^- \approx 10$ GeV
$0.36 \pm 0.04 \pm 0.08$	104	KINOSHITA 91	CLEO	$e^+ e^- \approx 10.7$ GeV

⁴²This value is calculated from numbers in Table 1 of ALBRECHT 92p.

$\Gamma(K^0 \pi^+ \pi^-) / \Gamma_{total}$ Γ_{21}/Γ

VALUE	EVTS	DOCUMENT ID	TECN	COMMENT
0.054 ± 0.004	OUR FIT Error includes scale factor of 1.2.			
0.055 ± 0.006	OUR AVERAGE			
$0.0503 \pm 0.0039 \pm 0.0049$	284	⁴³ ALBRECHT 94f	ARG	$e^+ e^- \approx \mathcal{T}(45)$
$0.064 \pm 0.005 \pm 0.010$		ADLER 87	MRK3	$e^+ e^-$ 3.77 GeV
0.052 ± 0.016	32	⁴⁴ SCHINDLER 81	MRK2	$e^+ e^-$ 3.771 GeV
0.079 ± 0.023	28	⁴⁵ PERUZZI 77	MRK1	$e^+ e^-$ 3.77 GeV

⁴³See the footnote on the ALBRECHT 94f measurement of $\Gamma(K^-\pi^+) / \Gamma_{total}$ for the method used.
⁴⁴SCHINDLER 81 (MARK-2) measures $\sigma(e^+ e^- \rightarrow \psi(3770)) \times$ branching fraction to be 0.30 ± 0.08 nb. We use the MARK-3 (ADLER 88c) value of $\sigma = 5.8 \pm 0.5 \pm 0.6$ nb.
⁴⁵PERUZZI 77 (MARK-1) measures $\sigma(e^+ e^- \rightarrow \psi(3770)) \times$ branching fraction to be 0.46 ± 0.12 nb. We use the MARK-3 (ADLER 88c) value of $\sigma = 5.8 \pm 0.5 \pm 0.6$ nb.

$\Gamma(K^0 \pi^+ \pi^-) / \Gamma(K^- \pi^+)$ Γ_{21}/Γ_{19}

VALUE	EVTS	DOCUMENT ID	TECN	COMMENT
1.42 ± 0.10	OUR FIT Error includes scale factor of 1.2.			
1.65 ± 0.17	OUR AVERAGE			
$1.61 \pm 0.10 \pm 0.15$	856	FRABETTI 94j	E687	γ Be $\bar{E}_\gamma \approx 220$ GeV
1.7 ± 0.8	35	AVERY 80	SPEC	$\gamma N \rightarrow D^{*+}$
2.8 ± 1.0	116	PICCOLO 77	MRK1	$e^+ e^-$ 4.03, 4.41 GeV

$\Gamma(K^0 \rho^0) / \Gamma(K^0 \pi^+ \pi^-)$ Γ_{22}/Γ_{21}

VALUE	EVTS	DOCUMENT ID	TECN	COMMENT
0.223 ± 0.027	OUR AVERAGE Error includes scale factor of 1.2.			
$0.350 \pm 0.028 \pm 0.067$		FRABETTI 94g	E687	γ Be, $\bar{E}_\gamma \approx 220$ GeV
$0.227 \pm 0.032 \pm 0.009$		ALBRECHT 93b	ARG	$e^+ e^- \approx 10$ GeV
$0.215 \pm 0.051 \pm 0.037$		ANJOS 93	E691	γ Be 90–260 GeV
$0.20 \pm 0.06 \pm 0.03$		FRABETTI 92b	E687	γ Be $\bar{E}_\gamma \approx 221$ GeV
$0.12 \pm 0.01 \pm 0.07$		ADLER 87	MRK3	$e^+ e^-$ 3.77 GeV

$\Gamma(K^0 f_0(980)) / \Gamma(K^0 \pi^+ \pi^-)$ Γ_{73}/Γ_{21}
Unseen decay modes of the $f_0(980)$ are included.

VALUE	EVTS	DOCUMENT ID	TECN	COMMENT
0.105 ± 0.029	OUR AVERAGE			
$0.131 \pm 0.031 \pm 0.034$		FRABETTI 94g	E687	γ Be, $\bar{E}_\gamma \approx 220$ GeV
$0.088 \pm 0.035 \pm 0.012$		ALBRECHT 93d	ARG	$e^+ e^- \approx 10$ GeV

$\Gamma(K^0 f_2(1270)) / \Gamma(K^0 \pi^+ \pi^-)$ Γ_{77}/Γ_{21}
Unseen decay modes of the $f_2(1270)$ are included.

VALUE	EVTS	DOCUMENT ID	TECN	COMMENT
0.076 ± 0.028	OUR AVERAGE			
$0.065 \pm 0.025 \pm 0.030$		FRABETTI 94g	E687	γ Be, $\bar{E}_\gamma \approx 220$ GeV
$0.088 \pm 0.037 \pm 0.014$		ALBRECHT 93d	ARG	$e^+ e^- \approx 10$ GeV

$\Gamma(K^0 f_0(1370)) / \Gamma(K^0 \pi^+ \pi^-)$ Γ_{79}/Γ_{21}
Unseen decay modes of the $f_0(1370)$ are included.

VALUE	EVTS	DOCUMENT ID	TECN	COMMENT
0.13 ± 0.04	OUR AVERAGE			
$0.123 \pm 0.035 \pm 0.049$		FRABETTI 94g	E687	γ Be, $\bar{E}_\gamma \approx 220$ GeV
$0.131 \pm 0.045 \pm 0.021$		ALBRECHT 93d	ARG	$e^+ e^- \approx 10$ GeV

$\Gamma(K^*(892)^- \pi^+) / \Gamma(K^0 \pi^+ \pi^-)$ Γ_{80}/Γ_{21}
Unseen decay modes of the $K^*(892)^-$ are included.

VALUE	EVTS	DOCUMENT ID	TECN	COMMENT
0.93 ± 0.04	OUR FIT Error includes scale factor of 1.1.			
0.96 ± 0.04	OUR AVERAGE			
$0.938 \pm 0.054 \pm 0.038$		FRABETTI 94g	E687	γ Be, $\bar{E}_\gamma \approx 220$ GeV
$1.08 \pm 0.063 \pm 0.045$		ALBRECHT 93d	ARG	$e^+ e^- \approx 10$ GeV
$0.720 \pm 0.145 \pm 0.185$		ANJOS 93	E691	γ Be 90–260 GeV
$0.96 \pm 0.12 \pm 0.075$		FRABETTI 92b	E687	γ Be $\bar{E}_\gamma \approx 221$ GeV
$0.84 \pm 0.06 \pm 0.08$		ADLER 87	MRK3	$e^+ e^-$ 3.77 GeV
$1.05 \pm 0.23 \pm 0.07$	25	SCHINDLER 81	MRK2	$e^+ e^-$ 3.771 GeV
-0.26 ± 0.09				

$\Gamma(K_0^*(1430)^- \pi^+) / \Gamma(K^0 \pi^+ \pi^-)$ Γ_{102}/Γ_{21}
Unseen decay modes of the $K_0^*(1430)^-$ are included.

VALUE	EVTS	DOCUMENT ID	TECN	COMMENT
0.19 ± 0.05	OUR AVERAGE			
$0.176 \pm 0.044 \pm 0.047$		FRABETTI 94g	E687	γ Be, $\bar{E}_\gamma \approx 220$ GeV
$0.208 \pm 0.055 \pm 0.034$		ALBRECHT 93d	ARG	$e^+ e^- \approx 10$ GeV

Meson Particle Listings

D^0

$\Gamma(K_2^*(1430)^-\pi^+)/\Gamma(K^0\pi^+\pi^-)$ Γ_{103}/Γ_{21}

Unseen decay modes of the $K_2^*(1430)^-$ are included.

VALUE	CL%	DOCUMENT ID	TECN	COMMENT
<0.15	90	ALBRECHT	93D ARG	$e^+e^- \approx 10$ GeV

$\Gamma(K^0\pi^+\pi^- \text{ nonresonant})/\Gamma(K^0\pi^+\pi^-)$ Γ_{28}/Γ_{21}

VALUE	DOCUMENT ID	TECN	COMMENT
0.27 ± 0.04 OUR AVERAGE			
0.263 ± 0.024 ± 0.041	ANJOS	93 E691	γ Be 90–260 GeV
0.26 ± 0.08 ± 0.05	FRABETTI	92B E687	γ Be $\bar{E}_\gamma = 221$ GeV
0.33 ± 0.05 ± 0.10	ADLER	87 MRK3	e^+e^- 3.77 GeV

$\Gamma(K^-\pi^+\pi^0)/\Gamma_{\text{total}}$ Γ_{29}/Γ

VALUE	EVTs	DOCUMENT ID	TECN	COMMENT
0.199 ± 0.009 OUR FIT				Error includes scale factor of 1.3.
0.131 ± 0.016 OUR AVERAGE				
0.133 ± 0.012 ± 0.013	931	ADLER	88C MRK3	e^+e^- 3.77 GeV
0.117 ± 0.043	37	⁴⁶ SCHINDLER	81 MRK2	e^+e^- 3.771 GeV

⁴⁶SCHINDLER 81 (MARK-2) measures $\sigma(e^+e^- \rightarrow \psi(3770)) \times$ branching fraction to be 0.68 ± 0.23 nb. We use the MARK-3 (ADLER 88C) value of $\sigma = 5.8 \pm 0.5 \pm 0.6$ nb.

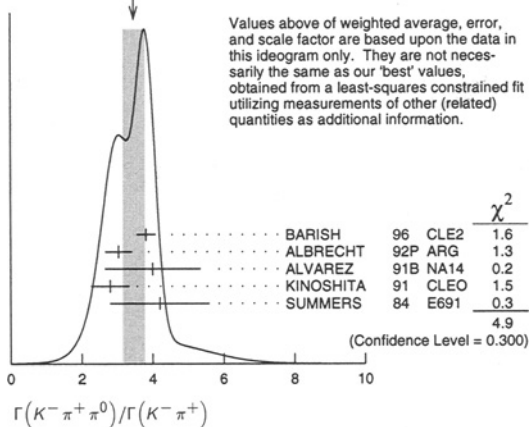
$\Gamma(K^-\pi^+\pi^0)/\Gamma(K^-\pi^+)$ Γ_{29}/Γ_{19}

VALUE	EVTs	DOCUMENT ID	TECN	COMMENT
3.63 ± 0.23 OUR FIT				Error includes scale factor of 1.4.
3.47 ± 0.30 OUR AVERAGE				Error includes scale factor of 1.5. See the ideogram below.

3.81 ± 0.07 ± 0.26	10k	BARISH	96 CLE2	$e^+e^- \approx \Upsilon(4S)$
3.04 ± 0.16 ± 0.34	931	⁴⁷ ALBRECHT	92P ARG	$e^+e^- \approx 10$ GeV
4.0 ± 0.9 ± 1.0	69	ALVAREZ	91B NA14	Photoproduction
2.8 ± 0.14 ± 0.52	1050	KINOSHITA	91 CLEO	$e^+e^- \sim 10.7$ GeV
4.2 ± 1.4	41	SUMMERS	84 E691	Photoproduction

⁴⁷This value is calculated from numbers in Table 1 of ALBRECHT 92P.

WEIGHTED AVERAGE
3.47±0.30 (Error scaled by 1.5)



$\Gamma(K^-\rho^+)/\Gamma(K^-\pi^+\pi^0)$ Γ_{30}/Γ_{29}

VALUE	EVTs	DOCUMENT ID	TECN	COMMENT
0.78 ± 0.05 OUR AVERAGE				
0.765 ± 0.041 ± 0.054		FRABETTI	94G E687	γ Be, $\bar{E}_\gamma \approx 220$ GeV
0.647 ± 0.039 ± 0.150		ANJOS	93 E691	γ Be 90–260 GeV
0.81 ± 0.03 ± 0.06		ADLER	87 MRK3	e^+e^- 3.77 GeV

• • • We do not use the following data for averages, fits, limits, etc. • • •

0.31 +0.20 -0.14	13	SUMMERS	84 E691	Photoproduction
0.85 +0.11 -0.15 +0.09 -0.10	31	SCHINDLER	81 MRK2	e^+e^- 3.771 GeV

$\Gamma(K^*(892)^-\pi^+)/\Gamma(K^-\pi^+\pi^0)$ Γ_{80}/Γ_{29}

Unseen decay modes of the $K^*(892)^-$ are included.

VALUE	DOCUMENT ID	TECN	COMMENT
0.36 ± 0.04 OUR FIT			Error includes scale factor of 1.3.
0.28 ± 0.04 OUR AVERAGE			
0.444 ± 0.084 ± 0.147	FRABETTI	94G E687	γ Be, $\bar{E}_\gamma \approx 220$ GeV
0.252 ± 0.033 ± 0.035	ANJOS	93 E691	γ Be 90–260 GeV
0.36 ± 0.06 ± 0.09	ADLER	87 MRK3	e^+e^- 3.77 GeV

$\Gamma(K^*(892)^0\pi^0)/\Gamma(K^-\pi^+\pi^0)$ Γ_{81}/Γ_{29}

Unseen decay modes of the $K^*(892)^0$ are included.

VALUE	DOCUMENT ID	TECN	COMMENT
0.227 ± 0.027 OUR FIT			
0.221 ± 0.029 OUR AVERAGE			
0.248 ± 0.047 ± 0.023	FRABETTI	94G E687	γ Be, $\bar{E}_\gamma \approx 220$ GeV
0.213 ± 0.027 ± 0.035	ANJOS	93 E691	γ Be 90–260 GeV
0.20 ± 0.03 ± 0.05	ADLER	87 MRK3	e^+e^- 3.77 GeV

$\Gamma(K^-\pi^+\pi^0 \text{ nonresonant})/\Gamma(K^-\pi^+\pi^0)$ Γ_{33}/Γ_{29}

VALUE	EVTs	DOCUMENT ID	TECN	COMMENT
0.049 ± 0.018 OUR AVERAGE				Error includes scale factor of 1.1.
0.101 ± 0.033 ± 0.040		FRABETTI	94G E687	γ Be, $\bar{E}_\gamma \approx 220$ GeV
0.036 ± 0.004 ± 0.018		ANJOS	93 E691	γ Be 90–260 GeV
0.09 ± 0.02 ± 0.04		ADLER	87 MRK3	e^+e^- 3.77 GeV
0.51 ± 0.22	21	SUMMERS	84 E691	Photoproduction

$\Gamma(K^*(892)^0\pi^0)/\Gamma(K^0\pi^0)$ Γ_{81}/Γ_{20}

Unseen decay modes of the $K^*(892)^0$ are included.

VALUE	EVTs	DOCUMENT ID	TECN	COMMENT
1.49 ± 0.23 OUR FIT				Error includes scale factor of 1.1.
1.65 +0.39 -0.31 ± 0.20	122	PROCARIO	93B CLE2	$\bar{K}^0\pi^0\pi^0$ Dalitz plot

$\Gamma(K_2^*(1430)^0\pi^0)/\Gamma(K^*(892)^0\pi^0)$ Γ_{104}/Γ_{81}

Unseen decay modes of the $K_2^*(1430)^0$ and $K^*(892)^0$ are included.

VALUE	CL%	DOCUMENT ID	TECN	COMMENT
<0.12	90	PROCARIO	93B CLE2	$\bar{K}^0\pi^0\pi^0$ Dalitz plot

$\Gamma(K^0\pi^0\pi^0 \text{ nonresonant})/\Gamma(K^0\pi^0)$ Γ_{36}/Γ_{20}

VALUE	EVTs	DOCUMENT ID	TECN	COMMENT
0.37 ± 0.08 ± 0.04	76	PROCARIO	93B CLE2	$\bar{K}^0\pi^0\pi^0$ Dalitz plot

$\Gamma(K^-\pi^+\pi^+\pi^-)/\Gamma_{\text{total}}$ Γ_{37}/Γ

VALUE	EVTs	DOCUMENT ID	TECN	COMMENT
0.0749 ± 0.0031 OUR FIT				Error includes scale factor of 1.3. See the ideogram below.
0.075 ± 0.006 OUR AVERAGE				
0.079 ± 0.015 ± 0.009		48 ALBRECHT	94 ARG	$e^+e^- \approx \Upsilon(4S)$
0.0680 ± 0.0027 ± 0.0057	1430	49 ALBRECHT	94F ARG	$e^+e^- \approx \Upsilon(4S)$
0.091 ± 0.008 ± 0.008	992	ADLER	88C MRK3	e^+e^- 3.77 GeV
0.117 ± 0.025	185	⁵⁰ SCHINDLER	81 MRK2	e^+e^- 3.771 GeV
0.062 ± 0.019	44	⁵¹ PERUZZI	77 MRK1	e^+e^- 3.77 GeV

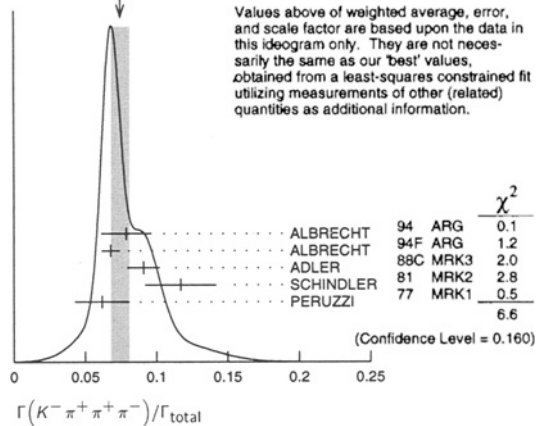
⁴⁸ALBRECHT 94 uses D^0 mesons from $\bar{B}^0 \rightarrow D^{*+} \ell^- \bar{\nu}_\ell$ decays. This is a different set of events than used by ALBRECHT 94F.

⁴⁹See the footnote on the ALBRECHT 94F measurement of $\Gamma(K^-\pi^+)/\Gamma_{\text{total}}$ for the method used.

⁵⁰SCHINDLER 81 (MARK-2) measures $\sigma(e^+e^- \rightarrow \psi(3770)) \times$ branching fraction to be 0.68 ± 0.11 nb. We use the MARK-3 (ADLER 88C) value of $\sigma = 5.8 \pm 0.5 \pm 0.6$ nb.

⁵¹PERUZZI 77 (MARK-1) measures $\sigma(e^+e^- \rightarrow \psi(3770)) \times$ branching fraction to be 0.36 ± 0.10 nb. We use the MARK-3 (ADLER 88C) value of $\sigma = 5.8 \pm 0.5 \pm 0.6$ nb.

WEIGHTED AVERAGE
0.075±0.006 (Error scaled by 1.3)



$\Gamma(K^-\pi^+\pi^+\pi^-)/\Gamma(K^-\pi^+)$ Γ_{37}/Γ_{19}

VALUE	EVTs	DOCUMENT ID	TECN	COMMENT
1.96 ± 0.07 OUR FIT				
1.97 ± 0.09 OUR AVERAGE				
1.94 ± 0.07 +0.09 -0.11		JUN	00 SELX	Σ^- nucleus, 600 GeV
1.7 ± 0.2 ± 0.2	1745	ANJOS	92C E691	γ Be 90–260 GeV
1.90 ± 0.25 ± 0.20	337	ALVAREZ	91B NA14	Photoproduction
2.12 ± 0.16 ± 0.09		BORTOLETTO	88 CLEO	e^+e^- 10.55 GeV
2.0 ± 0.9	48	BAILEY	86 ACCM	π^- Be fixed target
2.17 ± 0.28 ± 0.23		ALBRECHT	85F ARG	e^+e^- 10 GeV
2.0 ± 1.0	10	BAILEY	83B SPEC	π^- Be $\rightarrow D^0$
2.2 ± 0.8	214	PICCOLO	77 MRK1	e^+e^- 4.03, 4.41 GeV

See key on page 239

Meson Particle Listings

 D^0

$\Gamma(K^- \pi^+ \rho^0 \text{ total}) / \Gamma(K^- \pi^+ \pi^+ \pi^-)$ $\Gamma_{38} / \Gamma_{37}$

This includes $K^- a_1(1260)^+$, $\bar{K}^*(892)^0 \rho^0$, etc. The next entry gives the specifically 3-body fraction. We rely on the MARK III and E691 full amplitude analyses of the $K^- \pi^+ \pi^+ \pi^-$ channel for values of the resonant substructure.

VALUE	DOCUMENT ID	TECN	COMMENT
0.835 ± 0.035 OUR AVERAGE			
0.80 ± 0.03 ± 0.05	ANJOS	92C E691	γ Be 90–260 GeV
0.855 ± 0.032 ± 0.030	COFFMAN	92B MRK3	$e^+ e^-$ 3.77 GeV
• • • We do not use the following data for averages, fits, limits, etc. • • •			
0.98 ± 0.12 ± 0.10	ALVAREZ	91B NA14	Photoproduction

$\Gamma(K^- \pi^+ \rho^0 \text{ 3-body}) / \Gamma(K^- \pi^+ \pi^+ \pi^-)$ $\Gamma_{39} / \Gamma_{37}$

We rely on the MARK III and E691 full amplitude analyses of the $K^- \pi^+ \pi^+ \pi^-$ channel for values of the resonant substructure.

VALUE	EVTS	DOCUMENT ID	TECN	COMMENT
0.063 ± 0.028 OUR AVERAGE				
0.05 ± 0.03 ± 0.02		ANJOS	92C E691	γ Be 90–260 GeV
0.084 ± 0.022 ± 0.04		COFFMAN	92B MRK3	$e^+ e^-$ 3.77 GeV
• • • We do not use the following data for averages, fits, limits, etc. • • •				
0.77 ± 0.06 ± 0.06	52	ALVAREZ	91B NA14	Photoproduction
0.85 ^{+0.11} _{-0.22}	180	PICCOLO	77 MRK1	$e^+ e^-$ 4.03, 4.41 GeV

⁵²This value is for ρ^0 ($K^- \pi^+$)-nonresonant. ALVAREZ 91B cannot determine what fraction of this is $K^- a_1(1260)^+$.

$\Gamma(\bar{K}^*(892)^0 \rho^0) / \Gamma(K^- \pi^+ \pi^+ \pi^-)$ $\Gamma_{86} / \Gamma_{37}$

Unseen decay modes of the $\bar{K}^*(892)^0$ are included. We rely on the MARK III and E691 full amplitude analyses of the $K^- \pi^+ \pi^+ \pi^-$ channel for values of the resonant substructure.

VALUE	EVTS	DOCUMENT ID	TECN	COMMENT
0.195 ± 0.03 ± 0.03		ANJOS	92C E691	γ Be 90–260 GeV
• • • We do not use the following data for averages, fits, limits, etc. • • •				
0.34 ± 0.09 ± 0.09		ALVAREZ	91B NA14	Photoproduction
0.75 ± 0.3	5	BAILEY	83B SPEC	π Be $\rightarrow D^0$
0.15 ^{+0.16} _{-0.15}	20	PICCOLO	77 MRK1	$e^+ e^-$ 4.03, 4.41 GeV

$\Gamma(\bar{K}^*(892)^0 \rho^0 \text{ transverse}) / \Gamma(K^- \pi^+ \pi^+ \pi^-)$ $\Gamma_{87} / \Gamma_{37}$

Unseen decay modes of the $\bar{K}^*(892)^0$ are included.

VALUE	DOCUMENT ID	TECN	COMMENT
0.20 ± 0.07 OUR FIT			
0.213 ± 0.024 ± 0.075	COFFMAN	92B MRK3	$e^+ e^-$ 3.77 GeV

$\Gamma(\bar{K}^*(892)^0 \rho^0 \text{ S-wave}) / \Gamma(K^- \pi^+ \pi^+ \pi^-)$ $\Gamma_{88} / \Gamma_{37}$

Unseen decay modes of the $\bar{K}^*(892)^0$ are included.

VALUE	DOCUMENT ID	TECN	COMMENT
0.375 ± 0.045 ± 0.06	ANJOS	92C E691	γ Be 90–260 GeV

$\Gamma(\bar{K}^*(892)^0 \rho^0 \text{ S-wave long.}) / \Gamma_{\text{total}}$ Γ_{89} / Γ

Unseen decay modes of the $\bar{K}^*(892)^0$ are included.

VALUE	CL%	DOCUMENT ID	TECN	COMMENT
<0.003	90	COFFMAN	92B MRK3	$e^+ e^-$ 3.77 GeV

$\Gamma(\bar{K}^*(892)^0 \rho^0 \text{ P-wave}) / \Gamma_{\text{total}}$ Γ_{90} / Γ

Unseen decay modes of the $\bar{K}^*(892)^0$ are included.

VALUE	CL%	DOCUMENT ID	TECN	COMMENT
<0.003	90	COFFMAN	92B MRK3	$e^+ e^-$ 3.77 GeV
• • • We do not use the following data for averages, fits, limits, etc. • • •				
<0.009	90	ANJOS	92C E691	γ Be 90–260 GeV

$\Gamma(\bar{K}^*(892)^0 \rho^0 \text{ D-wave}) / \Gamma(K^- \pi^+ \pi^+ \pi^-)$ $\Gamma_{91} / \Gamma_{37}$

Unseen decay modes of the $\bar{K}^*(892)^0$ are included.

VALUE	DOCUMENT ID	TECN	COMMENT
0.255 ± 0.045 ± 0.06	ANJOS	92C E691	γ Be 90–260 GeV

$\Gamma(K^- \pi^+ f_0(980)) / \Gamma_{\text{total}}$ Γ_{96} / Γ

VALUE	CL%	DOCUMENT ID	TECN	COMMENT
<0.011	90	ANJOS	92C E691	γ Be 90–260 GeV

$\Gamma(\bar{K}^*(892)^0 f_0(980)) / \Gamma_{\text{total}}$ Γ_{97} / Γ

Unseen decay modes of the $\bar{K}^*(892)^0$ and $f_0(980)$ are included.

VALUE	CL%	DOCUMENT ID	TECN	COMMENT
<0.007	90	ANJOS	92C E691	γ Be 90–260 GeV

$\Gamma(K^- a_1(1260)^+) / \Gamma(K^- \pi^+ \pi^+ \pi^-)$ $\Gamma_{75} / \Gamma_{37}$

Unseen decay modes of the $a_1(1260)^+$ are included.

VALUE	DOCUMENT ID	TECN	COMMENT
0.97 ± 0.14 OUR AVERAGE			
0.94 ± 0.13 ± 0.20	ANJOS	92C E691	γ Be 90–260 GeV
0.984 ± 0.048 ± 0.16	COFFMAN	92B MRK3	$e^+ e^-$ 3.77 GeV

$\Gamma(K^- a_2(1320)^+) / \Gamma_{\text{total}}$ Γ_{78} / Γ

Unseen decay modes of the $a_2(1320)^+$ are included.

VALUE	CL%	DOCUMENT ID	TECN	COMMENT
<0.002	90	ANJOS	92C E691	γ Be 90–260 GeV
• • • We do not use the following data for averages, fits, limits, etc. • • •				
<0.006	90	COFFMAN	92B MRK3	$e^+ e^-$ 3.77 GeV

$\Gamma(K_1(1270)^- \pi^+) / \Gamma(K^- \pi^+ \pi^+ \pi^-)$ $\Gamma_{98} / \Gamma_{37}$

Unseen decay modes of the $K_1(1270)^-$ are included. The MARK3 and E691 experiments disagree considerably here.

VALUE	CL%	DOCUMENT ID	TECN	COMMENT
0.14 ± 0.04 OUR FIT				
0.194 ± 0.056 ± 0.088		COFFMAN	92B MRK3	$e^+ e^-$ 3.77 GeV
• • • We do not use the following data for averages, fits, limits, etc. • • •				
<0.013	90	ANJOS	92C E691	γ Be 90–260 GeV

$\Gamma(K_1(1400)^- \pi^+) / \Gamma_{\text{total}}$ Γ_{99} / Γ

VALUE	CL%	DOCUMENT ID	TECN	COMMENT
<0.012	90	COFFMAN	92B MRK3	$e^+ e^-$ 3.77 GeV

$\Gamma(K^*(1410)^- \pi^+) / \Gamma_{\text{total}}$ Γ_{101} / Γ

VALUE	CL%	DOCUMENT ID	TECN	COMMENT
<0.012	90	COFFMAN	92B MRK3	$e^+ e^-$ 3.77 GeV

$\Gamma(\bar{K}^*(892)^0 \pi^+ \pi^- \text{ total}) / \Gamma(K^- \pi^+ \pi^+ \pi^-)$ $\Gamma_{82} / \Gamma_{37}$

This includes $\bar{K}^*(892)^0 \rho^0$, etc. The next entry gives the specifically 3-body fraction. Unseen decay modes of the $\bar{K}^*(892)^0$ are included.

VALUE	DOCUMENT ID	TECN	COMMENT
0.30 ± 0.06 ± 0.03	ANJOS	92C E691	γ Be 90–260 GeV

$\Gamma(\bar{K}^*(892)^0 \pi^+ \pi^- \text{ 3-body}) / \Gamma(K^- \pi^+ \pi^+ \pi^-)$ $\Gamma_{83} / \Gamma_{37}$

Unseen decay modes of the $\bar{K}^*(892)^0$ are included.

VALUE	DOCUMENT ID	TECN	COMMENT
0.19 ± 0.04 OUR FIT			
0.18 ± 0.04 OUR AVERAGE			
0.165 ± 0.03 ± 0.045	ANJOS	92C E691	γ Be 90–260 GeV
0.210 ± 0.027 ± 0.06	COFFMAN	92B MRK3	$e^+ e^-$ 3.77 GeV

$\Gamma(K^- \pi^+ \pi^+ \pi^- \text{ nonresonant}) / \Gamma(K^- \pi^+ \pi^+ \pi^-)$ $\Gamma_{45} / \Gamma_{37}$

VALUE	DOCUMENT ID	TECN	COMMENT
0.233 ± 0.032 OUR AVERAGE			
0.23 ± 0.02 ± 0.03	ANJOS	92C E691	γ Be 90–260 GeV
0.242 ± 0.025 ± 0.06	COFFMAN	92B MRK3	$e^+ e^-$ 3.77 GeV

$\Gamma(\bar{K}^0 \pi^+ \pi^- \pi^0) / \Gamma_{\text{total}}$ Γ_{46} / Γ

VALUE	EVTS	DOCUMENT ID	TECN	COMMENT
0.100 ± 0.012 OUR FIT				
0.103 ± 0.022 ± 0.025	140	COFFMAN	92B MRK3	$e^+ e^-$ 3.77 GeV
• • • We do not use the following data for averages, fits, limits, etc. • • •				
0.134 ^{+0.032} _{-0.033}	53	BARLAG	92C ACCM	π^- Cu 230 GeV

⁵³BARLAG 92C computes the branching fraction using topological normalization.

$\Gamma(\bar{K}^0 \pi^+ \pi^- \pi^0) / \Gamma(\bar{K}^0 \pi^+ \pi^-)$ $\Gamma_{46} / \Gamma_{21}$

VALUE	EVTS	DOCUMENT ID	TECN	COMMENT
1.84 ± 0.20 OUR FIT				
1.86 ± 0.23 OUR AVERAGE				
1.80 ± 0.20 ± 0.21	190	⁵⁴ ALBRECHT	92P ARG	$e^+ e^- \approx 10$ GeV
2.8 ± 0.8 ± 0.8	46	ANJOS	92C E691	γ Be 90–260 GeV
1.85 ± 0.26 ± 0.30	158	KINOSHITA	91 CLEO	$e^+ e^- \sim 10.7$ GeV

⁵⁴This value is calculated from numbers in Table 1 of ALBRECHT 92P.

$\Gamma(\bar{K}^0 \eta) / \Gamma(K^- \pi^+)$ $\Gamma_{68} / \Gamma_{19}$

Unseen decay modes of the η are included.

VALUE	CL%	DOCUMENT ID	TECN	COMMENT
• • • We do not use the following data for averages, fits, limits, etc. • • •				
<0.64	90	ALBRECHT	89D ARG	$e^+ e^- 10$ GeV

$\Gamma(\bar{K}^0 \eta) / \Gamma(\bar{K}^0 \pi^0)$ $\Gamma_{68} / \Gamma_{20}$

Unseen decay modes of the η are included.

VALUE	EVTS	DOCUMENT ID	TECN	COMMENT
0.33 ± 0.04 OUR FIT				
0.32 ± 0.04 ± 0.03	225	PROCARIO	93B CLE2	$\eta \rightarrow \gamma \gamma$

$\Gamma(\bar{K}^0 \eta) / \Gamma(\bar{K}^0 \pi^+ \pi^-)$ $\Gamma_{68} / \Gamma_{21}$

Unseen decay modes of the η are included.

VALUE	EVTS	DOCUMENT ID	TECN	COMMENT
0.130 ± 0.017 OUR FIT				
0.14 ± 0.02 ± 0.02	80	PROCARIO	93B CLE2	$\eta \rightarrow \pi^+ \pi^- \pi^0$

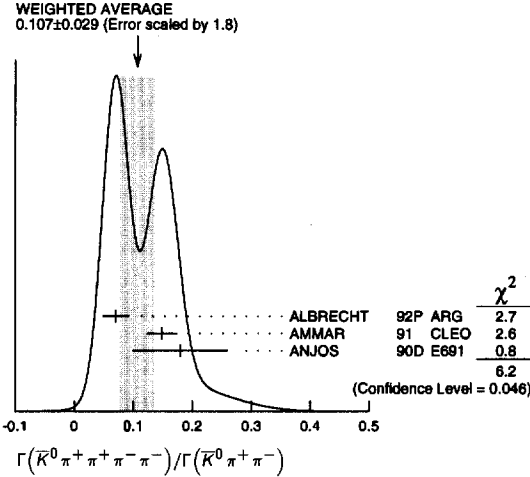
Meson Particle Listings

 D^0

$\Gamma(\bar{K}^0\omega)/\Gamma(K^-\pi^+)$				Γ_{71}/Γ_{19}	
Unseen decay modes of the ω are included.					
VALUE	DOCUMENT ID	TECN	COMMENT		
0.54 ± 0.10 OUR FIT					
1.00 ± 0.36 ± 0.20	ALBRECHT	89D	ARG	e^+e^-	10 GeV
$\Gamma(\bar{K}^0\omega)/\Gamma(\bar{K}^0\pi^+\pi^-)$				Γ_{71}/Γ_{21}	
Unseen decay modes of the ω are included.					
VALUE	EVTs	DOCUMENT ID	TECN	COMMENT	
0.38 ± 0.07 OUR FIT					
0.33 ± 0.09 OUR AVERAGE				Error includes scale factor of 1.1.	
0.29 ± 0.08 ± 0.05	16	55 ALBRECHT	92P	ARG	$e^+e^- \approx 10$ GeV
0.54 ± 0.14 ± 0.16	40	KINOSHITA	91	CLEO	$e^+e^- \sim 10.7$ GeV
55 This value is calculated from numbers in Table 1 of ALBRECHT 92P.					
$\Gamma(\bar{K}^0\omega)/\Gamma(\bar{K}^0\pi^+\pi^-\pi^0)$				Γ_{71}/Γ_{46}	
Unseen decay modes of the ω are included.					
VALUE	DOCUMENT ID	TECN	COMMENT		
0.21 ± 0.04 OUR FIT					
0.220 ± 0.048 ± 0.0116	COFFMAN	92B	MRK3	e^+e^-	3.77 GeV
$\Gamma(\bar{K}^0\eta'(958))/\Gamma(\bar{K}^0\pi^+\pi^-)$				Γ_{72}/Γ_{21}	
Unseen decay modes of the $\eta'(958)$ are included.					
VALUE	EVTs	DOCUMENT ID	TECN	COMMENT	
0.32 ± 0.04 OUR AVERAGE					
0.31 ± 0.02 ± 0.04	594	PROCARIO	93B	CLE2	$\eta' \rightarrow \eta\pi^+\pi^-, \rho^0\gamma$
0.37 ± 0.13 ± 0.06	18	56 ALBRECHT	92P	ARG	$e^+e^- \approx 10$ GeV
56 This value is calculated from numbers in Table 1 of ALBRECHT 92P.					
$\Gamma(K^*(892)^-\rho^+)/\Gamma(\bar{K}^0\pi^+\pi^-)$				Γ_{92}/Γ_{46}	
Unseen decay modes of the $K^*(892)^-$ are included.					
VALUE	DOCUMENT ID	TECN	COMMENT		
0.606 ± 0.188 ± 0.126	COFFMAN	92B	MRK3	e^+e^-	3.77 GeV
$\Gamma(K^*(892)^-\rho^+ \text{longitudinal})/\Gamma(\bar{K}^0\pi^+\pi^-)$				Γ_{93}/Γ_{46}	
Unseen decay modes of the $K^*(892)^-$ are included.					
VALUE	DOCUMENT ID	TECN	COMMENT		
0.290 ± 0.111	COFFMAN	92B	MRK3	e^+e^-	3.77 GeV
$\Gamma(K^*(892)^-\rho^+ \text{transverse})/\Gamma(\bar{K}^0\pi^+\pi^-)$				Γ_{94}/Γ_{46}	
Unseen decay modes of the $K^*(892)^-$ are included.					
VALUE	DOCUMENT ID	TECN	COMMENT		
0.317 ± 0.180	COFFMAN	92B	MRK3	e^+e^-	3.77 GeV
$\Gamma(K^*(892)^-\rho^+ P\text{-wave})/\Gamma_{\text{total}}$				Γ_{95}/Γ	
Unseen decay modes of the $K^*(892)^-$ are included.					
VALUE	CL%	DOCUMENT ID	TECN	COMMENT	
<0.015	90	57 COFFMAN	92B	MRK3	e^+e^- 3.77 GeV
57 Obtained using other $\bar{K}^*(892)^-\rho^+ P\text{-wave}$ limits and isospin relations.					
$\Gamma(\bar{K}^*(892)^0\rho^0 \text{transverse})/\Gamma(\bar{K}^0\pi^+\pi^-)$				Γ_{87}/Γ_{46}	
Unseen decay modes of the $\bar{K}^*(892)^0$ are included.					
VALUE	DOCUMENT ID	TECN	COMMENT		
0.15 ± 0.06 OUR FIT					
0.126 ± 0.111	COFFMAN	92B	MRK3	e^+e^-	3.77 GeV
$\Gamma(\bar{K}^0 a_1(1260)^0)/\Gamma_{\text{total}}$				Γ_{76}/Γ	
Unseen decay modes of the $a_1(1260)^0$ are included.					
VALUE	CL%	DOCUMENT ID	TECN	COMMENT	
<0.019	90	COFFMAN	92B	MRK3	e^+e^- 3.77 GeV
$\Gamma(K_1(1270)^-\pi^+)/\Gamma(\bar{K}^0\pi^+\pi^-)$				Γ_{98}/Γ_{46}	
Unseen decay modes of the $K_1(1270)^-$ are included.					
VALUE	DOCUMENT ID	TECN	COMMENT		
0.106 ± 0.028 OUR FIT					
0.10 ± 0.03	COFFMAN	92B	MRK3	e^+e^-	3.77 GeV
$\Gamma(\bar{K}_1(1400)^0\pi^0)/\Gamma_{\text{total}}$				Γ_{100}/Γ	
Unseen decay modes of the $\bar{K}_1(1400)^0$ are included.					
VALUE	CL%	DOCUMENT ID	TECN	COMMENT	
<0.037	90	COFFMAN	92B	MRK3	e^+e^- 3.77 GeV
$\Gamma(\bar{K}^*(892)^0\pi^+\pi^-\text{-3-body})/\Gamma(\bar{K}^0\pi^+\pi^-)$				Γ_{83}/Γ_{46}	
Unseen decay modes of the $\bar{K}^*(892)^0$ are included.					
VALUE	DOCUMENT ID	TECN	COMMENT		
0.14 ± 0.04 OUR FIT				Error includes scale factor of 1.1.	
0.191 ± 0.105	COFFMAN	92B	MRK3	e^+e^-	3.77 GeV
$\Gamma(\bar{K}^0\pi^+\pi^-\pi^0 \text{nonresonant})/\Gamma(\bar{K}^0\pi^+\pi^-)$				Γ_{53}/Γ_{46}	
Unseen decay modes of the $\bar{K}^0\pi^+\pi^-$ are included.					
VALUE	DOCUMENT ID	TECN	COMMENT		
0.210 ± 0.147 ± 0.150	COFFMAN	92B	MRK3	e^+e^-	3.77 GeV
$\Gamma(K^-\pi^+\pi^0\pi^0)/\Gamma_{\text{total}}$				Γ_{54}/Γ	
Unseen decay modes of the ω are included.					
VALUE	EVTs	DOCUMENT ID	TECN	COMMENT	
0.149 ± 0.037 ± 0.030	24	58 ADLER	88C	MRK3	e^+e^- 3.77 GeV
• • • We do not use the following data for averages, fits, limits, etc. • • •					
0.177 ± 0.029		59 BARLAG	92C	ACCM	π^- Cu 230 GeV
0.209 ^{+0.074} _{-0.043} ± 0.012	9	59 AGUILAR-...	87F	HYBR	$\pi p, pp$ 360, 400 GeV
58 ADLER 88C uses an absolute normalization method finding this decay channel opposite a detected $\bar{D}^0 \rightarrow K^+\pi^-$ in pure $D\bar{D}$ events.					
59 AGUILAR-BENITEZ 87F and BARLAG 92C compute the branching fraction using topological normalization. They do not distinguish the presence of a third π^0 , and thus are not included in the average.					
$\Gamma(K^-\pi^+\pi^-\pi^0)/\Gamma(K^-\pi^+)$				Γ_{55}/Γ_{19}	
Unseen decay modes of the $K^-\pi^+$ are included.					
VALUE	EVTs	DOCUMENT ID	TECN	COMMENT	
1.05 ± 0.10 OUR FIT					
0.98 ± 0.11 ± 0.11	225	60 ALBRECHT	92P	ARG	$e^+e^- \approx 10$ GeV
60 This value is calculated from numbers in Table 1 of ALBRECHT 92P.					
$\Gamma(K^-\pi^+\pi^-\pi^0)/\Gamma(K^-\pi^+\pi^-)$				Γ_{55}/Γ_{37}	
Unseen decay modes of the $K^-\pi^+\pi^-$ are included.					
VALUE	EVTs	DOCUMENT ID	TECN	COMMENT	
0.54 ± 0.05 OUR FIT					
0.56 ± 0.07 OUR AVERAGE					
0.55 ± 0.07 ^{+0.12} _{-0.09}	167	KINOSHITA	91	CLEO	$e^+e^- \sim 10.7$ GeV
0.57 ± 0.06 ± 0.05	180	ANJOS	90D	E691	Photoproduction
$\Gamma(\bar{K}^*(892)^0\pi^+\pi^-)/\Gamma(K^-\pi^+\pi^-)$				Γ_{105}/Γ_{55}	
Unseen decay modes of the $\bar{K}^*(892)^0$ are included.					
VALUE	DOCUMENT ID	TECN	COMMENT		
0.45 ± 0.15 ± 0.15	ANJOS	90D	E691		Photoproduction
$\Gamma(\bar{K}^*(892)^0\eta)/\Gamma(K^-\pi^+)$				Γ_{106}/Γ_{19}	
Unseen decay modes of the $\bar{K}^*(892)^0$ and η are included.					
VALUE	EVTs	DOCUMENT ID	TECN	COMMENT	
0.49 ± 0.12 OUR FIT					
0.58 ± 0.19^{+0.24} _{-0.28}	46	KINOSHITA	91	CLEO	$e^+e^- \sim 10.7$ GeV
$\Gamma(\bar{K}^*(892)^0\eta)/\Gamma(K^-\pi^+\pi^0)$				Γ_{106}/Γ_{29}	
Unseen decay modes of the $\bar{K}^*(892)^0$ and η are included.					
VALUE	EVTs	DOCUMENT ID	TECN	COMMENT	
0.134 ± 0.034 OUR FIT					
0.13 ± 0.02 ± 0.03	214	PROCARIO	93B	CLE2	$\bar{K}^{*0}\eta \rightarrow K^-\pi^+/\gamma\gamma$
$\Gamma(K^-\pi^+\omega)/\Gamma(K^-\pi^+)$				Γ_{107}/Γ_{19}	
Unseen decay modes of the ω are included.					
VALUE	EVTs	DOCUMENT ID	TECN	COMMENT	
0.78 ± 0.12 ± 0.10	99	61 ALBRECHT	92P	ARG	$e^+e^- \approx 10$ GeV
61 This value is calculated from numbers in Table 1 of ALBRECHT 92P.					
$\Gamma(\bar{K}^*(892)^0\omega)/\Gamma(K^-\pi^+)$				Γ_{108}/Γ_{19}	
Unseen decay modes of the $\bar{K}^*(892)^0$ and ω are included.					
VALUE	EVTs	DOCUMENT ID	TECN	COMMENT	
0.28 ± 0.11 ± 0.04	17	62 ALBRECHT	92P	ARG	$e^+e^- \approx 10$ GeV
62 This value is calculated from numbers in Table 1 of ALBRECHT 92P.					
$\Gamma(\bar{K}^*(892)^0\omega)/\Gamma(K^-\pi^+\pi^-\pi^0)$				Γ_{108}/Γ_{55}	
Unseen decay modes of the $\bar{K}^*(892)^0$ and ω are included.					
VALUE	CL%	DOCUMENT ID	TECN	COMMENT	
<0.44	90	63 ANJOS	90D	E691	Photoproduction
63 Recovered from the published limit, $\Gamma(\bar{K}^*(892)^0\omega)/\Gamma_{\text{total}}$, in order to make our normalization consistent.					
$\Gamma(K^-\pi^+\eta(958))/\Gamma(K^-\pi^+\pi^-)$				Γ_{109}/Γ_{37}	
Unseen decay modes of the $\eta(958)$ are included.					
VALUE	EVTs	DOCUMENT ID	TECN	COMMENT	
0.093 ± 0.014 ± 0.019	286	PROCARIO	93B	CLE2	$\eta' \rightarrow \eta\pi^+\pi^-, \rho^0\gamma$
$\Gamma(\bar{K}^*(892)^0\eta(958))/\Gamma(K^-\pi^+\eta(958))$				$\Gamma_{110}/\Gamma_{109}$	
Unseen decay modes of the $\bar{K}^*(892)^0$ are included.					
VALUE	CL%	DOCUMENT ID	TECN	COMMENT	
<0.15	90	PROCARIO	93B	CLE2	

$\Gamma(\bar{K}^0 \pi^+ \pi^+ \pi^- \pi^-)/\Gamma(\bar{K}^0 \pi^+ \pi^-)$		Γ_{60}/Γ_{21}		
VALUE	EVTs	DOCUMENT ID	TECN	COMMENT
0.107 ± 0.029 OUR AVERAGE		Error includes scale factor of 1.8. See the ideogram below.		
0.07 ± 0.02 ± 0.01	11	⁶⁴ ALBRECHT	92P ARG	e ⁺ e ⁻ ≈ 10 GeV
0.149 ± 0.026	56	AMMAR	91 CLEO	e ⁺ e ⁻ ≈ 10.5 GeV
0.18 ± 0.07 ± 0.04	6	ANJOS	90D E691	Photoproduction

⁶⁴ This value is calculated from numbers in Table 1 of ALBRECHT 92P.



$\Gamma(\bar{K}^0 \pi^+ \pi^- \pi^0 \pi^0)/\Gamma_{total}$		Γ_{61}/Γ		
VALUE	EVTs	DOCUMENT ID	TECN	COMMENT
0.106^{+0.073}_{-0.029} ± 0.006	4	⁶⁵ AGUILAR-...	87F HYBR	π p, pp 360, 400 GeV

⁶⁵ AGUILAR-BENITEZ 87F computes the branching fraction using topological normalization, and does not distinguish the presence of a third π⁰.

$\Gamma(\bar{K}^0 K^+ K^-)/\Gamma(\bar{K}^0 \pi^+ \pi^-)$		$\Gamma_{62}/\Gamma_{21} = (\Gamma_{64} + \frac{1}{2}\Gamma_{74})/\Gamma_{21}$		
VALUE	EVTs	DOCUMENT ID	TECN	COMMENT
0.172 ± 0.014 OUR FIT				
0.178 ± 0.019 OUR AVERAGE				
0.20 ± 0.05 ± 0.04	47	FRABETTI	92B E687	γ Be $\bar{E}_\gamma = 221$ GeV
0.170 ± 0.022	136	AMMAR	91 CLEO	e ⁺ e ⁻ ≈ 10.5 GeV
0.24 ± 0.08		BEBEK	86 CLEO	e ⁺ e ⁻ near T(45)
0.185 ± 0.055	52	ALBRECHT	85B ARG	e ⁺ e ⁻ 10 GeV

$\Gamma(\bar{K}^0 \phi)/\Gamma(\bar{K}^0 \pi^+ \pi^-)$		Γ_{74}/Γ_{21}		
VALUE	EVTs	DOCUMENT ID	TECN	COMMENT
0.158 ± 0.016 OUR FIT				
0.156 ± 0.017 OUR AVERAGE				
0.13 ± 0.06 ± 0.02	13	FRABETTI	92B E687	γ Be $\bar{E}_\gamma = 221$ GeV
0.163 ± 0.023	63	AMMAR	91 CLEO	e ⁺ e ⁻ ≈ 10.5 GeV
0.155 ± 0.033	56	ALBRECHT	87E ARG	e ⁺ e ⁻ 10 GeV
0.14 ± 0.05	29	BEBEK	86 CLEO	e ⁺ e ⁻ near T(45)
• • • We do not use the following data for averages, fits, limits, etc. • • •				
0.186 ± 0.052	26	ALBRECHT	85B ARG	See ALBRECHT 87E

$\Gamma(\bar{K}^0 K^+ K^- \text{ non-}\phi)/\Gamma(\bar{K}^0 \pi^+ \pi^-)$		Γ_{64}/Γ_{21}		
VALUE	EVTs	DOCUMENT ID	TECN	COMMENT
0.093 ± 0.014 OUR FIT				
0.088 ± 0.019 OUR AVERAGE				
0.11 ± 0.04 ± 0.03	20	FRABETTI	92B E687	γ Be $\bar{E}_\gamma = 221$ GeV
0.084 ± 0.020		ALBRECHT	87E ARG	e ⁺ e ⁻ 10 GeV

$\Gamma(K_S^0 K_S^0 K_S^0)/\Gamma(\bar{K}^0 \pi^+ \pi^-)$		Γ_{65}/Γ_{21}		
VALUE	EVTs	DOCUMENT ID	TECN	COMMENT
0.0154 ± 0.0025 OUR AVERAGE				
0.0139 ± 0.0019 ± 0.0024	61	ASNER	96B CLE2	e ⁺ e ⁻ ≈ T(45)
0.035 ± 0.012 ± 0.006	10	FRABETTI	94J E687	γ Be $\bar{E}_\gamma = 220$ GeV
0.016 ± 0.005	22	AMMAR	91 CLEO	e ⁺ e ⁻ ≈ 10.5 GeV
0.017 ± 0.007 ± 0.005	5	ALBRECHT	90C ARG	e ⁺ e ⁻ ≈ 10 GeV

$\Gamma(K^+ K^- K^- \pi^+)/\Gamma(K^- \pi^+ \pi^+ \pi^-)$		Γ_{66}/Γ_{37}		
VALUE	EVTs	DOCUMENT ID	TECN	COMMENT
0.0028 ± 0.0007 ± 0.0001	20	FRABETTI	95C E687	γ Be, $\bar{E}_\gamma \approx 200$ GeV

$\Gamma(K^+ K^- \bar{K}^0 \pi^0)/\Gamma_{total}$		Γ_{67}/Γ		
VALUE	EVTs	DOCUMENT ID	TECN	COMMENT
0.0072^{+0.0048}_{-0.0035}				
	66	BARLAG	92C ACCM	π ⁻ Cu 230 GeV

⁶⁶ BARLAG 92C computes the branching fraction using topological normalization.

$\Gamma(\pi^+ \pi^-)/\Gamma(K^- \pi^+)$		Γ_{111}/Γ_{19}		
VALUE	EVTs	DOCUMENT ID	TECN	COMMENT
0.0397 ± 0.0021 OUR AVERAGE				
0.040 ± 0.002 ± 0.003	2043	AITALA	98C E791	π ⁻ nucleus, 500 GeV
0.043 ± 0.007 ± 0.003	177	FRABETTI	94C E687	γ Be $\bar{E}_\gamma = 220$ GeV
0.0348 ± 0.0030 ± 0.0023	227	SELEN	93 CLE2	e ⁺ e ⁻ ≈ T(45)
0.048 ± 0.013 ± 0.008	51	ADAMOVICH	92 OMEG	π ⁻ 340 GeV
0.055 ± 0.008 ± 0.005	120	ANJOS	91D E691	Photoproduction
0.040 ± 0.007 ± 0.006	57	ALBRECHT	90C ARG	e ⁺ e ⁻ ≈ 10 GeV
0.050 ± 0.007 ± 0.005	110	ALEXANDER	90 CLEO	e ⁺ e ⁻ 10.5–11 GeV
0.033 ± 0.010 ± 0.006	39	BALTRUSAITIS..85E	MRK3	e ⁺ e ⁻ 3.77 GeV
0.033 ± 0.015		ABRAMS	79D MRK2	e ⁺ e ⁻ 3.77 GeV

$\Gamma(\pi^0 \pi^0)/\Gamma(K^- \pi^+)$		Γ_{112}/Γ_{19}		
VALUE	EVTs	DOCUMENT ID	TECN	COMMENT
0.022 ± 0.004 ± 0.004	40	SELEN	93 CLE2	e ⁺ e ⁻ ≈ T(45)

$\Gamma(\pi^+ \pi^- \pi^0)/\Gamma_{total}$		Γ_{113}/Γ		
VALUE	EVTs	DOCUMENT ID	TECN	COMMENT
0.016 ± 0.011 OUR AVERAGE		Error includes scale factor of 2.7.		
0.0390 ^{+0.0100} _{-0.0095}	67	BARLAG	92C ACCM	π ⁻ Cu 230 GeV
0.011 ± 0.004 ± 0.002	10	⁶⁸ BALTRUSAITIS..85E	MRK3	e ⁺ e ⁻ 3.77 GeV

⁶⁷ BARLAG 92C computes the branching fraction using topological normalization. Possible contamination by extra π⁰'s may partly explain the unexpectedly large value.
⁶⁸ All the BALTRUSAITIS 85E events are consistent with ρ⁰ π⁰.

$\Gamma(\pi^+ \pi^+ \pi^- \pi^-)/\Gamma(K^- \pi^+ \pi^+ \pi^-)$		Γ_{114}/Γ_{37}		
VALUE	EVTs	DOCUMENT ID	TECN	COMMENT
0.098 ± 0.006 OUR AVERAGE				
0.095 ± 0.007 ± 0.002	814	FRABETTI	95C E687	γ Be, $\bar{E}_\gamma \approx 200$ GeV
0.115 ± 0.023 ± 0.016	64	ADAMOVICH	92 OMEG	π ⁻ 340 GeV
0.108 ± 0.024 ± 0.008	79	FRABETTI	92 E687	γ Be
0.102 ± 0.013	345	⁶⁹ AMMAR	91 CLEO	e ⁺ e ⁻ ≈ 10.5 GeV
0.096 ± 0.018 ± 0.007	66	ANJOS	91 E691	γ Be 80–240 GeV

⁶⁹ AMMAR 91 finds 1.25 ± 0.25 ± 0.25 ρ⁰'s per π⁺ π⁺ π⁻ π⁻ decay, but can't untangle the resonant substructure (ρ⁰ ρ⁰, a₁[±] π[±], ρ⁰ π[±] π⁻).

$\Gamma(\pi^+ \pi^+ \pi^- \pi^0)/\Gamma_{total}$		Γ_{115}/Γ		
VALUE	EVTs	DOCUMENT ID	TECN	COMMENT
0.0192^{+0.0041}_{-0.0038}				
	70	BARLAG	92C ACCM	π ⁻ Cu 230 GeV

⁷⁰ BARLAG 92C computes the branching fraction using topological normalization.

$\Gamma(\pi^+ \pi^+ \pi^+ \pi^- \pi^- \pi^-)/\Gamma_{total}$		Γ_{116}/Γ		
VALUE	EVTs	DOCUMENT ID	TECN	COMMENT
0.0004 ± 0.0003				
	71	BARLAG	92C ACCM	π ⁻ Cu 230 GeV

⁷¹ BARLAG 92C computes the branching fraction using topological normalization.

Hadronic modes with a K \bar{K} pair

$\Gamma(K^+ K^-)/\Gamma(K^- \pi^+)$		Γ_{117}/Γ_{19}		
VALUE	EVTs	DOCUMENT ID	TECN	COMMENT
0.1109 ± 0.0033 OUR FIT				
0.1109 ± 0.0033 OUR AVERAGE				
0.109 ± 0.003 ± 0.003	3317	AITALA	98C E791	π ⁻ nucleus, 500 GeV
0.116 ± 0.007 ± 0.007	1102	ASNER	96B CLE2	e ⁺ e ⁻ ≈ T(45)
0.109 ± 0.007 ± 0.009	581	FRABETTI	94C E687	γ Be $\bar{E}_\gamma = 220$ GeV
0.107 ± 0.029 ± 0.015	103	ADAMOVICH	92 OMEG	π ⁻ 340 GeV
0.138 ± 0.027 ± 0.010	155	FRABETTI	92 E687	γ Be
0.16 ± 0.05	34	ALVAREZ	91B NA14	Photoproduction
0.107 ± 0.010 ± 0.009	193	ANJOS	91D E691	Photoproduction
0.10 ± 0.02 ± 0.001	131	ALBRECHT	90C ARG	e ⁺ e ⁻ ≈ 10 GeV
0.117 ± 0.010 ± 0.007	249	ALEXANDER	90 CLEO	e ⁺ e ⁻ 10.5–11 GeV
0.122 ± 0.018 ± 0.012	118	BALTRUSAITIS..85E	MRK3	e ⁺ e ⁻ 3.77 GeV
0.113 ± 0.030		ABRAMS	79D MRK2	e ⁺ e ⁻ 3.77 GeV

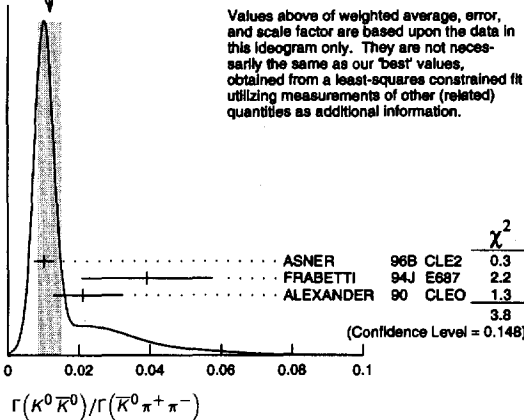
$\Gamma(K^+ K^-)/\Gamma(\pi^+ \pi^-)$		$\Gamma_{117}/\Gamma_{111}$		
VALUE	EVTs	DOCUMENT ID	TECN	COMMENT
The unused results here are redundant with $\Gamma(K^+ K^-)/\Gamma(K^- \pi^+)$ and $\Gamma(\pi^+ \pi^-)/\Gamma(K^- \pi^+)$ measurements by the same experiments.				
		• • • We do not use the following data for averages, fits, limits, etc. • • •		
2.75 ± 0.15 ± 0.16		AITALA	98C E791	π ⁻ nucleus, 500 GeV
2.53 ± 0.46 ± 0.19		FRABETTI	94C E687	γ Be $\bar{E}_\gamma = 220$ GeV
2.23 ± 0.81 ± 0.46		ADAMOVICH	92 OMEG	π ⁻ 340 GeV
1.95 ± 0.34 ± 0.22		ANJOS	91D E691	Photoproduction
2.5 ± 0.7		ALBRECHT	90C ARG	e ⁺ e ⁻ ≈ 10 GeV
2.35 ± 0.37 ± 0.28		ALEXANDER	90 CLEO	e ⁺ e ⁻ 10.5–11 GeV

Meson Particle Listings

D^0

$\Gamma(K^0 \bar{K}^0)/\Gamma(K^0 \pi^+ \pi^-)$					Γ_{118}/Γ_{21}
VALUE	EVTS	DOCUMENT ID	TECN	COMMENT	
0.0120 ± 0.0033	OUR FIT	Error includes scale factor of 1.3.			
0.0117 ± 0.0033	OUR AVERAGE	Error includes scale factor of 1.3. See the ideogram below.			
$0.0101 \pm 0.0022 \pm 0.0016$	26	ASNER	96B CLE2	$e^+ e^- \approx T(4S)$	
$0.039 \pm 0.013 \pm 0.013$	20	FRABETTI	94J E687	$\gamma Be \bar{E}_\gamma = 220 \text{ GeV}$	
$0.021 \pm 0.011 \pm 0.008$	5	ALEXANDER	90 CLEO	$e^+ e^- 10.5-11 \text{ GeV}$	

WEIGHTED AVERAGE
 0.0117 ± 0.0033 (Error scaled by 1.3)



Values above of weighted average, error, and scale factor are based upon the data in this ideogram only. They are not necessarily the same as our 'best' values, obtained from a least-squares constrained fit utilizing measurements of other (related) quantities as additional information.

$\Gamma(K^0 \bar{K}^0)/\Gamma(K^+ K^-)$					$\Gamma_{118}/\Gamma_{117}$
VALUE	EVTS	DOCUMENT ID	TECN	COMMENT	
0.15 ± 0.04	OUR FIT	Error includes scale factor of 1.2.			
0.24 ± 0.16	4	⁷² CUMALAT	88 SPEC	$n N 0-800 \text{ GeV}$	

⁷² Includes a correction communicated to us by the authors of CUMALAT 88.

$\Gamma(K^0 K^- \pi^+)/\Gamma(K^- \pi^+)$					Γ_{119}/Γ_{19}
VALUE	EVTS	DOCUMENT ID	TECN	COMMENT	
0.168 ± 0.026	OUR FIT	Error includes scale factor of 1.1.			
0.15 ± 0.06		⁷³ ANJOS	91 E691	$\gamma Be 80-240 \text{ GeV}$	

⁷³ The factor 100 at the top of column 2 of Table I of ANJOS 91 should be omitted.

$\Gamma(K^0 K^- \pi^+)/\Gamma(K^0 \pi^+ \pi^-)$					Γ_{119}/Γ_{21}
VALUE	EVTS	DOCUMENT ID	TECN	COMMENT	
0.118 ± 0.018	OUR FIT	Error includes scale factor of 1.1.			
0.119 ± 0.021	OUR AVERAGE	Error includes scale factor of 1.3.			
0.108 ± 0.019	61	AMMAR	91 CLEO	$e^+ e^- \approx 10.5 \text{ GeV}$	
$0.16 \pm 0.03 \pm 0.02$	39	ALBRECHT	90C ARG	$e^+ e^- \approx 10 \text{ GeV}$	

$\Gamma(K^*(892)^0 K^0)/\Gamma(K^- \pi^+)$					Γ_{139}/Γ_{19}
VALUE	CL%	DOCUMENT ID	TECN	COMMENT	
Unseen decay modes of the $K^*(892)^0$ are included.					
• • • We do not use the following data for averages, fits, limits, etc. • • •					
0.00 ± 0.03		⁷⁴ ANJOS	91 E691	$\gamma Be 80-240 \text{ GeV}$	

⁷⁴ The factor 100 at the top of column 2 of Table I of ANJOS 91 should be omitted.

$\Gamma(K^*(892)^0 K^0)/\Gamma(K^0 \pi^+ \pi^-)$					Γ_{139}/Γ_{21}
VALUE	CL%	DOCUMENT ID	TECN	COMMENT	
Unseen decay modes of the $K^*(892)^0$ are included.					
• • • We do not use the following data for averages, fits, limits, etc. • • •					
< 0.029		90	AMMAR	91 CLEO $e^+ e^- \approx 10.5 \text{ GeV}$	
< 0.03		90	ALBRECHT	90C ARG $e^+ e^- \approx 10 \text{ GeV}$	

$\Gamma(K^*(892)^+ K^-)/\Gamma(K^- \pi^+)$					Γ_{140}/Γ_{19}
VALUE	CL%	DOCUMENT ID	TECN	COMMENT	
Unseen decay modes of the $K^*(892)^+$ are included.					
• • • We do not use the following data for averages, fits, limits, etc. • • •					
0.090 ± 0.020	OUR FIT				
0.16 ± 0.08		⁷⁵ ANJOS	91 E691	$\gamma Be 80-240 \text{ GeV}$	

⁷⁵ The factor 100 at the top of column 2 of Table I of ANJOS 91 should be omitted.

$\Gamma(K^*(892)^+ K^-)/\Gamma(K^0 \pi^+ \pi^-)$					Γ_{140}/Γ_{21}
VALUE	CL%	DOCUMENT ID	TECN	COMMENT	
Unseen decay modes of the $K^*(892)^+$ are included.					
• • • We do not use the following data for averages, fits, limits, etc. • • •					
0.064 ± 0.014	OUR FIT	Error includes scale factor of 1.1.			
0.058 ± 0.014	OUR AVERAGE				
0.064 ± 0.018		23	AMMAR	91 CLEO $e^+ e^- \approx 10.5 \text{ GeV}$	
$0.05 \pm 0.02 \pm 0.01$		15	ALBRECHT	90C ARG $e^+ e^- \approx 10 \text{ GeV}$	

$\Gamma(K^0 K^- \pi^+ \text{nonresonant})/\Gamma(K^- \pi^+)$					Γ_{122}/Γ_{19}
VALUE	DOCUMENT ID	TECN	COMMENT		
0.06 ± 0.06	⁷⁶ ANJOS	91 E691	$\gamma Be 80-240 \text{ GeV}$		

⁷⁶ The factor 100 at the top of column 2 of Table I of ANJOS 91 should be omitted.

$\Gamma(K^0 K^+ \pi^-)/\Gamma(K^- \pi^+)$					Γ_{123}/Γ_{19}
VALUE	DOCUMENT ID	TECN	COMMENT		
0.129 ± 0.025	OUR FIT				
0.10 ± 0.05		⁷⁷ ANJOS	91 E691	$\gamma Be 80-240 \text{ GeV}$	

⁷⁷ The factor 100 at the top of column 2 of Table I of ANJOS 91 should be omitted.

$\Gamma(K^0 K^+ \pi^-)/\Gamma(K^0 \pi^+ \pi^-)$					Γ_{123}/Γ_{21}
VALUE	EVTS	DOCUMENT ID	TECN	COMMENT	
0.091 ± 0.018	OUR FIT				
0.096 ± 0.020		55	AMMAR	91 CLEO $e^+ e^- \approx 10.5 \text{ GeV}$	

$\Gamma(K^*(892)^0 \bar{K}^0)/\Gamma(K^- \pi^+)$					Γ_{141}/Γ_{19}
VALUE	DOCUMENT ID	TECN	COMMENT		
Unseen decay modes of the $K^*(892)^0$ are included.					
• • • We do not use the following data for averages, fits, limits, etc. • • •					
0.00 ± 0.04		⁷⁸ ANJOS	91 E691	$\gamma Be 80-240 \text{ GeV}$	

⁷⁸ The factor 100 at the top of column 2 of Table I of ANJOS 91 should be omitted.

$\Gamma(K^*(892)^0 \bar{K}^0)/\Gamma(K^0 \pi^+ \pi^-)$					Γ_{141}/Γ_{21}
VALUE	CL%	DOCUMENT ID	TECN	COMMENT	
Unseen decay modes of the $K^*(892)^0$ are included.					
• • • We do not use the following data for averages, fits, limits, etc. • • •					
< 0.015		90	AMMAR	91 CLEO $e^+ e^- \approx 10.5 \text{ GeV}$	

$\Gamma(K^*(892)^- K^+)/\Gamma(K^- \pi^+)$					Γ_{142}/Γ_{19}
VALUE	DOCUMENT ID	TECN	COMMENT		
Unseen decay modes of the $K^*(892)^-$ are included.					
• • • We do not use the following data for averages, fits, limits, etc. • • •					
0.00 ± 0.03		⁷⁹ ANJOS	91 E691	$\gamma Be 80-240 \text{ GeV}$	

⁷⁹ The factor 100 at the top of column 2 of Table I of ANJOS 91 should be omitted.

$\Gamma(K^*(892)^- K^+)/\Gamma(K^0 \pi^+ \pi^-)$					Γ_{142}/Γ_{21}
VALUE	EVTS	DOCUMENT ID	TECN	COMMENT	
Unseen decay modes of the $K^*(892)^-$ are included.					
• • • We do not use the following data for averages, fits, limits, etc. • • •					
0.034 ± 0.019	12	AMMAR	91 CLEO	$e^+ e^- \approx 10.5 \text{ GeV}$	

$\Gamma(K^0 K^+ \pi^- \text{nonresonant})/\Gamma(K^- \pi^+)$					Γ_{126}/Γ_{19}
VALUE	DOCUMENT ID	TECN	COMMENT		
0.10 ± 0.06		⁸⁰ ANJOS	91 E691	$\gamma Be 80-240 \text{ GeV}$	

⁸⁰ The factor 100 at the top of column 2 of Table I of ANJOS 91 should be omitted.

$\Gamma(K^+ K^- \pi^0)/\Gamma(K^- \pi^+ \pi^0)$					Γ_{127}/Γ_{29}
VALUE	EVTS	DOCUMENT ID	TECN	COMMENT	
0.0095 ± 0.0026	151	ASNER	96B CLE2	$e^+ e^- \approx T(4S)$	

$\Gamma(K_S^0 K_S^0 \pi^0)/\Gamma_{\text{total}}$					Γ_{128}/Γ
VALUE	DOCUMENT ID	TECN	COMMENT		
< 0.00059		ASNER	96B CLE2	$e^+ e^- \approx T(4S)$	

$\Gamma(\phi \pi^0)/\Gamma_{\text{total}}$					Γ_{143}/Γ
VALUE	CL%	DOCUMENT ID	TECN	COMMENT	
< 0.0014		90	ALBRECHT	94I ARG $e^+ e^- \approx 10 \text{ GeV}$	

$\Gamma(\phi \eta)/\Gamma_{\text{total}}$					Γ_{144}/Γ
VALUE	CL%	DOCUMENT ID	TECN	COMMENT	
< 0.0028		90	ALBRECHT	94I ARG $e^+ e^- \approx 10 \text{ GeV}$	

$\Gamma(\phi \omega)/\Gamma_{\text{total}}$					Γ_{145}/Γ
VALUE	CL%	DOCUMENT ID	TECN	COMMENT	
< 0.0021		90	ALBRECHT	94I ARG $e^+ e^- \approx 10 \text{ GeV}$	

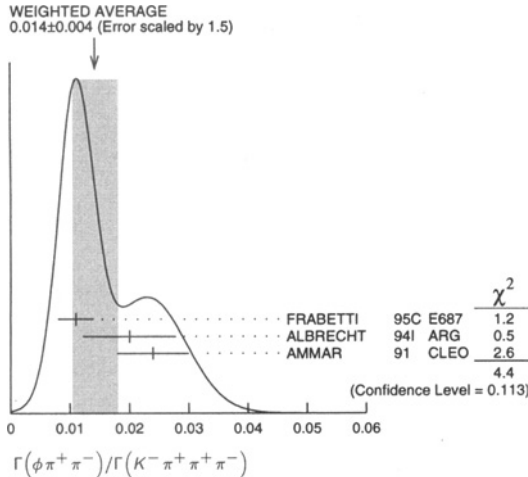
$\Gamma(K^+ K^- \pi^+ \pi^-)/\Gamma(K^- \pi^+ \pi^+ \pi^-)$					Γ_{129}/Γ_{37}
VALUE	EVTS	DOCUMENT ID	TECN	COMMENT	
0.0334 ± 0.0028	OUR AVERAGE				
$0.0313 \pm 0.0037 \pm 0.0036$	136	AITALA	98D E791	π^- nucleus, 500 GeV	
$0.035 \pm 0.004 \pm 0.002$	244	FRABETTI	95C E687	$\gamma Be, \bar{E}_\gamma \approx 200 \text{ GeV}$	
$0.041 \pm 0.007 \pm 0.005$	114	ALBRECHT	94I ARG	$e^+ e^- \approx 10 \text{ GeV}$	
0.0314 ± 0.010	89	AMMAR	91 CLEO	$e^+ e^- \approx 10.5 \text{ GeV}$	
0.028 ± 0.008		ANJOS	91 E691	$\gamma Be 80-240 \text{ GeV}$	

$\Gamma(\phi\pi^+\pi^-)/\Gamma(K^-\pi^+\pi^+\pi^-)$ Γ_{146}/Γ_{37}

Unseen decay modes of the ϕ are included.

VALUE	CL%	EVTS	DOCUMENT ID	TECN	COMMENT
0.014 ± 0.004 OUR AVERAGE					Error includes scale factor of 1.5. See the ideogram below.
0.011 ± 0.003			FRABETTI 95C E687		γ Be, $\bar{E}_\gamma \approx 200$ GeV
0.020 ± 0.006 ± 0.005		28	ALBRECHT 94I ARG		$e^+e^- \approx 10$ GeV
0.024 ± 0.006		34	⁸¹ AMMAR 91 CLEO		$e^+e^- \approx 10.5$ GeV
• • • We do not use the following data for averages, fits, limits, etc. • • •					
0.0076 ^{+0.0066} _{-0.0049}		3	ANJOS 91 E691		γ Be 80–240 GeV

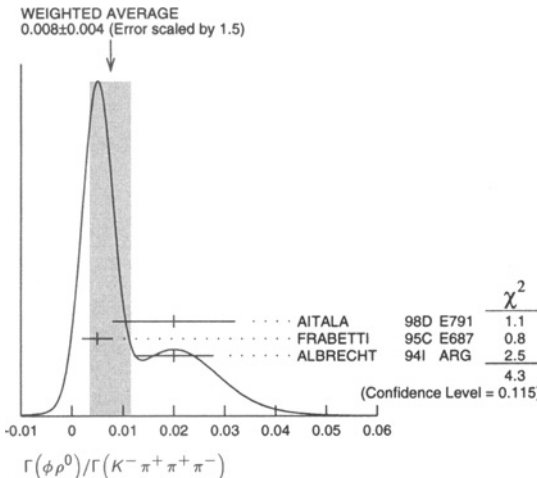
⁸¹AMMAR 91 measures $\phi\rho^0$, but notes that $\phi\rho^0$ dominates $\phi\pi^+\pi^-$. We put the measurement here to keep from having more $\phi\rho^0$ than $\phi\pi^+\pi^-$.



$\Gamma(\phi\rho^0)/\Gamma(K^-\pi^+\pi^+\pi^-)$ Γ_{147}/Γ_{37}

Unseen decay modes of the ϕ are included.

VALUE	CL%	EVTS	DOCUMENT ID	TECN	COMMENT
0.008 ± 0.004 OUR AVERAGE					Error includes scale factor of 1.5. See the ideogram below.
0.02 ± 0.009 ± 0.008			AITALA 98D E791		π^- nucleus, 500 GeV
0.005 ± 0.003			FRABETTI 95C E687		γ Be, $\bar{E}_\gamma \approx 200$ GeV
0.020 ± 0.006 ± 0.005		28	ALBRECHT 94I ARG		$e^+e^- \approx 10$ GeV



$\Gamma(\phi\pi^+\pi^- \text{ 3-body})/\Gamma(K^-\pi^+\pi^+\pi^-)$ Γ_{148}/Γ_{37}

Unseen decay modes of the ϕ are included.

VALUE	CL%	DOCUMENT ID	TECN	COMMENT
0.009 ± 0.004 ± 0.005		AITALA 98D E791		π^- nucleus, 500 GeV
• • • We do not use the following data for averages, fits, limits, etc. • • •				
< 0.006		90 FRABETTI 95C E687		γ Be, $\bar{E}_\gamma \approx 200$ GeV

$\Gamma(K^+K^-\rho^0 \text{ 3-body})/\Gamma(K^-\pi^+\pi^+\pi^-)$ Γ_{132}/Γ_{37}

VALUE	DOCUMENT ID	TECN	COMMENT
0.012 ± 0.003	FRABETTI 95C E687		γ Be, $\bar{E}_\gamma \approx 200$ GeV

$\Gamma(K^*(892)^0 K^-\pi^+ + c.c.)/\Gamma(K^-\pi^+\pi^+\pi^-)$ Γ_{149}/Γ_{37}

Unseen decay modes of the $K^*(892)^0$ are included.

VALUE	CL%	EVTS	DOCUMENT ID	TECN	COMMENT
< 0.01		90	82 AITALA 98D E791		π^- nucleus, 500 GeV
• • • We do not use the following data for averages, fits, limits, etc. • • •					
< 0.017		90	82 FRABETTI 95C E687		γ Be, $\bar{E}_\gamma \approx 200$ GeV
0.010 ^{+0.016} _{-0.010}			ANJOS 91 E691		γ Be 80–240 GeV

⁸²These upper limits are in conflict with values in the next two data blocks.

$\Gamma(K^*(892)^0 K^-\pi^+)/\Gamma(K^-\pi^+\pi^+\pi^-)$ Γ_{150}/Γ_{37}

The $K^{*0}K^-\pi^+$ and $\bar{K}^{*0}K^+\pi^-$ modes are distinguished by the charge of the pion in $D^*(2010)^\pm \rightarrow D^0\pi^\pm$ decays. Unseen decay modes of the $K^*(892)^0$ are included.

VALUE	CL%	EVTS	DOCUMENT ID	TECN	COMMENT
0.043 ± 0.014 ± 0.009		55	⁸³ ALBRECHT 94I ARG		$e^+e^- \approx 10$ GeV
• • • We do not use the following data for averages, fits, limits, etc. • • •					
⁸³ This ALBRECHT 94I value is in conflict with upper limits given above.					

$\Gamma(\bar{K}^*(892)^0 K^+\pi^-)/\Gamma(K^-\pi^+\pi^+\pi^-)$ Γ_{151}/Γ_{37}

The $K^{*0}K^-\pi^+$ and $\bar{K}^{*0}K^+\pi^-$ modes are distinguished by the charge of the pion in $D^*(2010)^\pm \rightarrow D^0\pi^\pm$ decays. Unseen decay modes of the $\bar{K}^*(892)^0$ are included.

VALUE	CL%	EVTS	DOCUMENT ID	TECN	COMMENT
0.023 ± 0.013 ± 0.009		30	⁸⁴ ALBRECHT 94I ARG		$e^+e^- \approx 10$ GeV
• • • We do not use the following data for averages, fits, limits, etc. • • •					
⁸⁴ This ALBRECHT 94I value is in conflict with upper limits given above.					

$\Gamma(K^*(892)^0 \bar{K}^*(892)^0)/\Gamma(K^-\pi^+\pi^+\pi^-)$ Γ_{152}/Γ_{37}

Unseen decay modes of the $K^*(892)^0$ and $\bar{K}^*(892)^0$ are included.

VALUE	CL%	EVTS	DOCUMENT ID	TECN	COMMENT
0.018 ± 0.007 OUR AVERAGE					Error includes scale factor of 1.2.
0.016 ± 0.006			FRABETTI 95C E687		γ Be, $\bar{E}_\gamma \approx 200$ GeV
0.036 ^{+0.020} _{-0.016}		11	ANJOS 91 E691		γ Be 80–240 GeV
• • • We do not use the following data for averages, fits, limits, etc. • • •					
< 0.02		90	AITALA 98D E791		π^- nucleus, 500 GeV
< 0.033		90	⁸⁵ AMMAR 91 CLEO		$e^+e^- \approx 10.5$ GeV

⁸⁵A corrected value (G. Moneti, private communication).

$\Gamma(K^+K^-\pi^+\pi^- \text{ non-}\phi)/\Gamma_{\text{total}}$ Γ_{135}/Γ

VALUE	DOCUMENT ID	TECN	COMMENT
0.0017 ± 0.0005	⁸⁶ BARLAG 92C ACCM		π^- Cu 230 GeV
• • • We do not use the following data for averages, fits, limits, etc. • • •			
⁸⁶ BARLAG 92C computes the branching fraction using topological normalization.			

$\Gamma(K^+K^-\pi^+\pi^- \text{ nonresonant})/\Gamma(K^-\pi^+\pi^+\pi^-)$ Γ_{136}/Γ_{37}

VALUE	CL%	EVTS	DOCUMENT ID	TECN	COMMENT
< 0.011		90	FRABETTI 95C E687		γ Be, $\bar{E}_\gamma \approx 200$ GeV
• • • We do not use the following data for averages, fits, limits, etc. • • •					
0.001 ^{+0.011} _{-0.001}			ANJOS 91 E691		γ Be 80–240 GeV

$\Gamma(K^0\bar{K}^0\pi^+\pi^-)/\Gamma(K^0\pi^+\pi^-)$ Γ_{137}/Γ_{21}

VALUE	CL%	EVTS	DOCUMENT ID	TECN	COMMENT
0.126 ± 0.038 ± 0.030		25	ALBRECHT 94I ARG		$e^+e^- \approx 10$ GeV

$\Gamma(K^+K^-\pi^+\pi^-\pi^0)/\Gamma_{\text{total}}$ Γ_{138}/Γ

VALUE	CL%	DOCUMENT ID	TECN	COMMENT
0.0031 ± 0.0020		⁸⁷ BARLAG 92C ACCM		π^- Cu 230 GeV
• • • We do not use the following data for averages, fits, limits, etc. • • •				
⁸⁷ BARLAG 92C computes the branching fraction using topological normalization.				

Radiative modes

$\Gamma(\rho^0\gamma)/\Gamma_{\text{total}}$ Γ_{153}/Γ

VALUE	CL%	DOCUMENT ID	TECN
< 2.4 × 10⁻⁴		90 ASNER 98 CLE2	

$\Gamma(\omega\gamma)/\Gamma_{\text{total}}$ Γ_{154}/Γ

VALUE	CL%	DOCUMENT ID	TECN
< 2.4 × 10⁻⁴		90 ASNER 98 CLE2	

$\Gamma(\phi\gamma)/\Gamma_{\text{total}}$ Γ_{155}/Γ

VALUE	CL%	DOCUMENT ID	TECN
< 1.9 × 10⁻⁴		90 ASNER 98 CLE2	

$\Gamma(\bar{K}^*(892)^0\gamma)/\Gamma_{\text{total}}$ Γ_{156}/Γ

VALUE	CL%	DOCUMENT ID	TECN
< 7.6 × 10⁻⁴		90 ASNER 98 CLE2	

Rare or forbidden modes

$\Gamma(K^+ \ell^- \bar{\nu}_\ell \text{ (via } \bar{D}^0)) / \Gamma(K^- \ell^+ \nu_\ell)$

 Γ_{157}/Γ_7

This is a D^0 - \bar{D}^0 mixing limit without the complications of possible doubly-Cabibbo-suppressed decays that occur when using hadronic modes. For the limits on $|m_{D_1^0} - m_{D_2^0}|$ and $(\Gamma_{D_1^0} - \Gamma_{D_2^0})/\Gamma_{D_0}$ that come from the best mixing limit, see near the beginning of these D^0 Listings.

VALUE	CL%	EVTs	DOCUMENT ID	TECN	COMMENT
<0.005			88 AITALA	96C E791	π^- nucleus, 500 GeV

88 AITALA 96C uses $D^{*+} \rightarrow D^0 \pi^+$ (and charge conjugate) decays to identify the charm at production and $D^0 \rightarrow K^- \ell^+ \nu_\ell$ (and charge conjugate) decays to identify the charm at decay.

$\Gamma(K^+ \pi^-) / \Gamma(K^- \pi^+)$

 Γ_{158}/Γ_{19}

The $D^0 \rightarrow K^+ \pi^-$ decay can occur directly by doubly Cabibbo-suppressed (DCS) decay, or indirectly by $D^0 \rightarrow \bar{D}^0$ mixing followed by $\bar{D}^0 \rightarrow K^+ \pi^-$ decay. The experiments here use the charge of the pion in $D^*(2010)^\pm \rightarrow (D^0 \text{ or } \bar{D}^0) \pi^\pm$ decay to tell whether a D^0 or a \bar{D}^0 was born. Some of the experiments can use the decay-time information to disentangle the two modes. Here, we list the DCS branching ratio; in the next data block we give the limits on the mixing ratio.

Some early limits have been omitted from this Listing; see our 1998 (EPJ C3 1) edition.

VALUE	CL%	EVTs	DOCUMENT ID	TECN	COMMENT
0.0038 \pm 0.0008 OUR AVERAGE			Error includes scale factor of 1.1.		
0.00332 $^{+0.00063}_{-0.00065} \pm 0.00040$	45		89 GODANG	00 CLE2	$e^+ e^-$
0.0068 $^{+0.0034}_{-0.0033} \pm 0.0007$			90 AITALA	98 E791	π^- nucleus, 500 GeV
0.0184 $\pm 0.0059 \pm 0.0034$	19		91 BARATE	98W ALEP	$e^+ e^-$ at Z^0
0.0077 $\pm 0.0025 \pm 0.0025$	19		92 CINABRO	94 CLE2	$e^+ e^- \approx T(4S)$

• • • We do not use the following data for averages, fits, limits, etc. • • •

<0.011	90		92 AMMAR	91 CLEO	$e^+ e^- \approx 10.5$ GeV
<0.015	90	1 \pm 6	93 ANJOS	88C E691	Photoproduction
<0.014	90		92 ALBRECHT	87K ARG	$e^+ e^-$ 10 GeV

89 This GODANG 00 result assumes no D^0 - \bar{D}^0 mixing; the DCS ratio becomes $0.0048 \pm 0.0012 \pm 0.0004$ when mixing is allowed.

90 This AITALA 98 result assumes no D^0 - \bar{D}^0 mixing; the DCS ratio becomes $0.0090^{+0.0120}_{-0.0109} \pm 0.0044$ when mixing is allowed.

91 BARATE 98W gets $0.0177^{+0.0060}_{-0.0056} \pm 0.0031$ for the DCS ratio when mixing is allowed, assuming no interference between the DCS and mixing amplitudes.

92 CINABRO 94, AMMAR 91, and ALBRECHT 87K cannot distinguish between doubly Cabibbo-suppressed decay and D^0 - \bar{D}^0 mixing.

93 ANJOS 88C allows mixing but assumes no interference between the DCS and mixing amplitudes. When interference is allowed, the limit degrades to 0.049.

$\Gamma(K^+ \pi^- \text{ (via } \bar{D}^0)) / \Gamma(K^- \pi^+)$

 Γ_{159}/Γ_{19}

This is a D^0 - \bar{D}^0 mixing limit. The experiments here (1) use the charge of the pion in $D^*(2010)^\pm \rightarrow (D^0 \text{ or } \bar{D}^0) \pi^\pm$ decay to tell whether a D^0 or a \bar{D}^0 was born; and (2) use the decay-time distribution to disentangle doubly Cabibbo-suppressed decay and mixing. For the limits on $|m_{D_1^0} - m_{D_2^0}|$ and $(\Gamma_{D_1^0} - \Gamma_{D_2^0})/\Gamma_{D_0}$ that come from the best mixing limit, see near the beginning of these D^0 Listings.

VALUE	CL%	EVTs	DOCUMENT ID	TECN	COMMENT
<0.00041	95		94 GODANG	00 CLE2	$e^+ e^-$
<0.0092	95		95 BARATE	98W ALEP	$e^+ e^-$ at Z^0
<0.005	90	1 \pm 4	96 ANJOS	88C E691	Photoproduction

94 This GODANG 00 result assumes that the strong phase between $D^0 \rightarrow K^+ \pi^-$ and $\bar{D}^0 \rightarrow K^+ \pi^-$ is small, and limits only $D^0 \rightarrow \bar{D}^0$ transitions via off-shell intermediate states. The limit on transitions via on-shell intermediate states is 0.0017.

95 This BARATE 98W result assumes no interference between the DCS and mixing amplitudes. When interference is allowed, the limit degrades to 0.036 (95%CL).

96 This ANJOS 88C result assumes no interference between the DCS and mixing amplitudes. When interference is allowed, the limit degrades to 0.019. Combined with results on $K^\pm \pi^+ \pi^+ \pi^-$, the limit is, assuming no interference, 0.0037.

$\Gamma(K^+ \pi^- \pi^+ \pi^-) / \Gamma(K^- \pi^+ \pi^+ \pi^-)$

 Γ_{160}/Γ_{37}

The $D^0 \rightarrow K^+ \pi^- \pi^+ \pi^-$ decay can occur directly by doubly Cabibbo-suppressed (DCS) decay, or indirectly by $D^0 \rightarrow \bar{D}^0$ mixing followed by $\bar{D}^0 \rightarrow K^+ \pi^- \pi^+ \pi^-$ decay. The experiments here use the charge of the pion in $D^*(2010)^\pm \rightarrow (D^0 \text{ or } \bar{D}^0) \pi^\pm$ decay to tell whether a D^0 or a \bar{D}^0 was born. Some of the experiments can use the decay-time information to disentangle the two modes. Here, we list the DCS branching ratio; in the next data block we give the limits on the mixing ratio.

Some early limits have been omitted from this Listing; see our 1998 (EPJ C3 1) edition.

VALUE	CL%	EVTs	DOCUMENT ID	TECN	COMMENT
0.0025 $^{+0.0036}_{-0.0034} \pm 0.0003$			97 AITALA	98 E791	π^- nucleus, 500 GeV
<0.018	90		98 AMMAR	91 CLEO	$e^+ e^- \approx 10.5$ GeV
<0.018	90	5 \pm 12	99 ANJOS	88C E691	Photoproduction

• • • We do not use the following data for averages, fits, limits, etc. • • •

97 AITALA 98 uses the charge of the pion in $D^{*+} \rightarrow (D^0 \text{ or } \bar{D}^0) \pi^\pm$ to tell whether a D^0 or a \bar{D}^0 was born. This result assumes no D^0 - \bar{D}^0 mixing; it becomes $-0.0020^{+0.0117}_{-0.0106} \pm 0.0035$ when mixing is allowed and decay-time information is used to distinguish doubly Cabibbo-suppressed decays from mixing.

98 AMMAR 91 cannot distinguish between doubly Cabibbo-suppressed decay and D^0 - \bar{D}^0 mixing.

99 ANJOS 88C uses decay-time information to distinguish doubly Cabibbo-suppressed (DCS) decays from D^0 - \bar{D}^0 mixing. However, the result assumes no interference between the DCS and mixing amplitudes. When interference is allowed, the limit degrades to 0.033.

$\Gamma(K^+ \pi^- \pi^+ \pi^- \text{ (via } \bar{D}^0)) / \Gamma(K^- \pi^+ \pi^+ \pi^-)$

 Γ_{161}/Γ_{37}

This is a D^0 - \bar{D}^0 mixing limit. The experiments here (1) use the charge of the pion in $D^*(2010)^\pm \rightarrow (D^0 \text{ or } \bar{D}^0) \pi^\pm$ decay to tell whether a D^0 or a \bar{D}^0 was born; and (2) use the decay-time distribution to disentangle doubly Cabibbo-suppressed decay and mixing. For the limits on $|m_{D_1^0} - m_{D_2^0}|$ and $(\Gamma_{D_1^0} - \Gamma_{D_2^0})/\Gamma_{D_0}$ that come from the best mixing limit, see near the beginning of these D^0 Listings.

VALUE	CL%	EVTs	DOCUMENT ID	TECN	COMMENT
<0.005		90 0 ± 4	100 ANJOS	88C E691	Photoproduction

100 ANJOS 88C uses decay-time information to distinguish doubly Cabibbo-suppressed (DCS) decays from D^0 - \bar{D}^0 mixing. However, the result assumes no interference between the DCS and mixing amplitudes. When interference is allowed, the limit degrades to 0.007. Combined with results on $K^\pm \pi^\mp$, the limit is, assuming no interference, 0.0037.

$\Gamma(K^+ \pi^- \text{ or } K^+ \pi^- \pi^+ \pi^- \text{ (via } \bar{D}^0)) / \Gamma(K^- \pi^+ \text{ or } K^- \pi^+ \pi^+ \pi^-)$

 Γ_{162}/Γ_0

This is a D^0 - \bar{D}^0 mixing limit. For the limits on $|m_{D_1^0} - m_{D_2^0}|$ and $(\Gamma_{D_1^0} - \Gamma_{D_2^0})/\Gamma_{D_0}$ that come from the best mixing limit, see near the beginning of these D^0 Listings.

VALUE	CL%	EVTs	DOCUMENT ID	TECN	COMMENT
<0.0085			90	101 AITALA	98 E791 π^- nucleus, 500 GeV

101 AITALA 98 uses decay-time information to distinguish doubly Cabibbo-suppressed decays from D^0 - \bar{D}^0 mixing. The fit allows interference between the two amplitudes, and also allows CP violation in this term. The central value obtained is $0.0039^{+0.0036}_{-0.0032} \pm 0.0016$. When interference is disallowed, the result becomes $0.0021 \pm 0.0009 \pm 0.0002$.

$\Gamma(\mu^- \text{ anything (via } \bar{D}^0)) / \Gamma(\mu^+ \text{ anything})$

 Γ_{163}/Γ_2

This is a D^0 - \bar{D}^0 mixing limit. See the somewhat better limits above.

VALUE	CL%	EVTs	DOCUMENT ID	TECN	COMMENT
<0.0056			90	LOUIS	86 SPEC π^- W 225 GeV
<0.012			90	BENVENUTI	85 CNTR μ C, 200 GeV
<0.044			90	BODEK	82 SPEC π^- , pFe $\rightarrow D^0$

$\Gamma(e^+ e^-) / \Gamma_{\text{total}}$

 Γ_{164}/Γ

A test for the $\Delta C = 1$ weak neutral current. Allowed by first-order weak interaction combined with electromagnetic interaction.

VALUE	CL%	EVTs	DOCUMENT ID	TECN	COMMENT
<6.2 $\times 10^{-6}$	90		AITALA	99G E791	π^- N 500 GeV
<8.19 $\times 10^{-6}$	90		PRIPSTEIN	00 E789	p nucleus, 800 GeV
<1.3 $\times 10^{-5}$	90	0	FREYBERGER	96 CLE2	$e^+ e^- \approx T(4S)$
<1.3 $\times 10^{-4}$	90		ADLER	88 MRK3	$e^+ e^-$ 3.77 GeV
<1.7 $\times 10^{-4}$	90	7	ALBRECHT	88G ARG	$e^+ e^-$ 10 GeV
<2.2 $\times 10^{-4}$	90	8	HAAS	88 CLEO	$e^+ e^-$ 10 GeV

$\Gamma(\mu^+ \mu^-) / \Gamma_{\text{total}}$

 Γ_{165}/Γ

A test for the $\Delta C = 1$ weak neutral current. Allowed by first-order weak interaction combined with electromagnetic interaction.

VALUE	CL%	EVTs	DOCUMENT ID	TECN	COMMENT
<4.1 $\times 10^{-6}$	90		ADAMOVICH	97 BEAT	π^- Cu, W 350 GeV
<1.56 $\times 10^{-5}$	90		PRIPSTEIN	00 E789	p nucleus, 800 GeV
<5.2 $\times 10^{-6}$	90		AITALA	99G E791	π^- N 500 GeV
<4.2 $\times 10^{-6}$	90		ALEXOPOU...	96 E771	p Si, 800 GeV
<3.4 $\times 10^{-5}$	90	1	FREYBERGER	96 CLE2	$e^+ e^- \approx T(4S)$
<7.6 $\times 10^{-6}$	90	0	ADAMOVICH	95 BEAT	See ADAMOVICH 97
<4.4 $\times 10^{-5}$	90	0	KODAMA	95 E653	π^- emulsion 600 GeV
<3.1 $\times 10^{-5}$	90		MISHRA	94 E789	-4.1 \pm 4.8 events
<7.0 $\times 10^{-5}$	90	3	ALBRECHT	88G ARG	$e^+ e^-$ 10 GeV
<1.1 $\times 10^{-5}$	90		LOUIS	86 SPEC	π^- W 225 GeV
<3.4 $\times 10^{-4}$	90		AUBERT	85 EMC	Deep inelast. μ^- N

102 Here MISHRA 94 uses "the statistical approach advocated by the PDG." For an alternate approach, giving a limit of 9×10^{-6} at 90% confidence level, see the paper.

$\Gamma(\pi^0 e^+ e^-) / \Gamma_{\text{total}}$

 Γ_{166}/Γ

A test for the $\Delta C = 1$ weak neutral current. Allowed by higher-order electroweak interactions.

VALUE	CL%	EVTs	DOCUMENT ID	TECN	COMMENT
<4.5 $\times 10^{-5}$	90	0	FREYBERGER	96 CLE2	$e^+ e^- \approx T(4S)$

$\Gamma(\pi^0 \mu^+ \mu^-) / \Gamma_{\text{total}}$

 Γ_{167}/Γ

A test for the $\Delta C = 1$ weak neutral current. Allowed by higher-order electroweak interactions.

VALUE	CL%	EVTs	DOCUMENT ID	TECN	COMMENT
<1.8 $\times 10^{-4}$	90	2	KODAMA	95 E653	π^- emulsion 600 GeV
<5.4 $\times 10^{-4}$	90	3	FREYBERGER	96 CLE2	$e^+ e^- \approx T(4S)$

• • • We do not use the following data for averages, fits, limits, etc. • • •

See key on page 239

Meson Particle Listings

 D^0

$\Gamma(\eta e^+ e^-)/\Gamma_{\text{total}}$ Γ_{168}/Γ
A test for the $\Delta C = 1$ weak neutral current. Allowed by higher-order electroweak interactions.

VALUE	CL%	EVTs	DOCUMENT ID	TECN	COMMENT
$<1.1 \times 10^{-4}$	90	0	FREYBERGER 96	CLE2	$e^+ e^- \approx \Upsilon(4S)$

$\Gamma(\eta \mu^+ \mu^-)/\Gamma_{\text{total}}$ Γ_{169}/Γ
A test for the $\Delta C = 1$ weak neutral current. Allowed by higher-order electroweak interactions.

VALUE	CL%	EVTs	DOCUMENT ID	TECN	COMMENT
$<5.3 \times 10^{-4}$	90	0	FREYBERGER 96	CLE2	$e^+ e^- \approx \Upsilon(4S)$

$\Gamma(\rho^0 e^+ e^-)/\Gamma_{\text{total}}$ Γ_{170}/Γ
A test for the $\Delta C = 1$ weak neutral current. Allowed by higher-order electroweak interactions.

VALUE	CL%	EVTs	DOCUMENT ID	TECN	COMMENT
$<1.0 \times 10^{-4}$	90	2	103 FREYBERGER 96	CLE2	$e^+ e^- \approx \Upsilon(4S)$

• • • We do not use the following data for averages, fits, limits, etc. • • •

$<4.5 \times 10^{-4}$ 90 2 HAAS BB CLEO $e^+ e^-$ 10 GeV

103 This FREYBERGER 96 limit is obtained using a phase-space model. The limit changes to $<1.8 \times 10^{-4}$ using a photon pole amplitude model.

$\Gamma(\rho^0 \mu^+ \mu^-)/\Gamma_{\text{total}}$ Γ_{171}/Γ
A test for the $\Delta C = 1$ weak neutral current. Allowed by higher-order electroweak interactions.

VALUE	CL%	EVTs	DOCUMENT ID	TECN	COMMENT
$<2.3 \times 10^{-4}$	90	0	KODAMA 95	E653	π^- emulsion 600 GeV

• • • We do not use the following data for averages, fits, limits, etc. • • •

$<4.9 \times 10^{-4}$ 90 1 104 FREYBERGER 96 CLE2 $e^+ e^- \approx \Upsilon(4S)$

$<8.1 \times 10^{-4}$ 90 5 HAAS BB CLEO $e^+ e^-$ 10 GeV

104 This FREYBERGER 96 limit is obtained using a phase-space model. The limit changes to $<4.5 \times 10^{-4}$ using a photon pole amplitude model.

$\Gamma(\omega e^+ e^-)/\Gamma_{\text{total}}$ Γ_{172}/Γ
A test for the $\Delta C = 1$ weak neutral current. Allowed by higher-order electroweak interactions.

VALUE	CL%	EVTs	DOCUMENT ID	TECN	COMMENT
$<1.8 \times 10^{-4}$	90	1	105 FREYBERGER 96	CLE2	$e^+ e^- \approx \Upsilon(4S)$

105 This FREYBERGER 96 limit is obtained using a phase-space model. The limit changes to $<2.7 \times 10^{-4}$ using a photon pole amplitude model.

$\Gamma(\omega \mu^+ \mu^-)/\Gamma_{\text{total}}$ Γ_{173}/Γ
A test for the $\Delta C = 1$ weak neutral current. Allowed by higher-order electroweak interactions.

VALUE	CL%	EVTs	DOCUMENT ID	TECN	COMMENT
$<8.3 \times 10^{-4}$	90	0	106 FREYBERGER 96	CLE2	$e^+ e^- \approx \Upsilon(4S)$

106 This FREYBERGER 96 limit is obtained using a phase-space model. The limit changes to $<6.5 \times 10^{-4}$ using a photon pole amplitude model.

$\Gamma(\phi e^+ e^-)/\Gamma_{\text{total}}$ Γ_{174}/Γ
A test for the $\Delta C = 1$ weak neutral current. Allowed by higher-order electroweak interactions.

VALUE	CL%	EVTs	DOCUMENT ID	TECN	COMMENT
$<5.2 \times 10^{-5}$	90	2	107 FREYBERGER 96	CLE2	$e^+ e^- \approx \Upsilon(4S)$

107 This FREYBERGER 96 limit is obtained using a phase-space model. The limit changes to $<7.6 \times 10^{-5}$ using a photon pole amplitude model.

$\Gamma(\phi \mu^+ \mu^-)/\Gamma_{\text{total}}$ Γ_{175}/Γ
A test for the $\Delta C = 1$ weak neutral current. Allowed by higher-order electroweak interactions.

VALUE	CL%	EVTs	DOCUMENT ID	TECN	COMMENT
$<4.1 \times 10^{-4}$	90	0	108 FREYBERGER 96	CLE2	$e^+ e^- \approx \Upsilon(4S)$

108 This FREYBERGER 96 limit is obtained using a phase-space model. The limit changes to $<2.4 \times 10^{-4}$ using a photon pole amplitude model.

$\Gamma(K^0 e^+ e^-)/\Gamma_{\text{total}}$ Γ_{176}/Γ
Allowed by first-order weak interaction combined with electromagnetic interaction.

VALUE	CL%	EVTs	DOCUMENT ID	TECN	COMMENT
$<1.1 \times 10^{-4}$	90	0	FREYBERGER 96	CLE2	$e^+ e^- \approx \Upsilon(4S)$

• • • We do not use the following data for averages, fits, limits, etc. • • •

$<1.7 \times 10^{-3}$ 90 ADLER 89c MRK3 $e^+ e^-$ 3.77 GeV

$\Gamma(K^0 \mu^+ \mu^-)/\Gamma_{\text{total}}$ Γ_{177}/Γ
Allowed by first-order weak interaction combined with electromagnetic interaction.

VALUE	CL%	EVTs	DOCUMENT ID	TECN	COMMENT
$<2.6 \times 10^{-4}$	90	2	KODAMA 95	E653	π^- emulsion 600 GeV

• • • We do not use the following data for averages, fits, limits, etc. • • •

$<6.7 \times 10^{-4}$ 90 1 FREYBERGER 96 CLE2 $e^+ e^- \approx \Upsilon(4S)$

$\Gamma(K^*(892)^0 e^+ e^-)/\Gamma_{\text{total}}$ Γ_{178}/Γ
Allowed by first-order weak interaction combined with electromagnetic interaction.

VALUE	CL%	EVTs	DOCUMENT ID	TECN	COMMENT
$<1.4 \times 10^{-4}$	90	1	109 FREYBERGER 96	CLE2	$e^+ e^- \approx \Upsilon(4S)$

109 This FREYBERGER 96 limit is obtained using a phase-space model. The limit changes to $<2.0 \times 10^{-4}$ using a photon pole amplitude model.

$\Gamma(K^*(892)^0 \mu^+ \mu^-)/\Gamma_{\text{total}}$ Γ_{179}/Γ
Allowed by first-order weak interaction combined with electromagnetic interaction.

VALUE	CL%	EVTs	DOCUMENT ID	TECN	COMMENT
$<1.18 \times 10^{-3}$	90	1	110 FREYBERGER 96	CLE2	$e^+ e^- \approx \Upsilon(4S)$

110 This FREYBERGER 96 limit is obtained using a phase-space model. The limit changes to $<1.0 \times 10^{-3}$ using a photon pole amplitude model.

$\Gamma(\pi^+ \pi^- \pi^0 \mu^+ \mu^-)/\Gamma_{\text{total}}$ Γ_{180}/Γ
A test for the $\Delta C=1$ weak neutral current. Allowed by higher-order electroweak interactions.

VALUE	CL%	EVTs	DOCUMENT ID	TECN	COMMENT
$<8.1 \times 10^{-4}$	90	1	KODAMA 95	E653	π^- emulsion 600 GeV

$\Gamma(\mu^\pm e^\mp)/\Gamma_{\text{total}}$ Γ_{181}/Γ
A test of lepton family number conservation.

VALUE	CL%	EVTs	DOCUMENT ID	TECN	COMMENT
$<8.1 \times 10^{-6}$	90		AITALA 99G	E791	$\pi^- N$ 500 GeV

• • • We do not use the following data for averages, fits, limits, etc. • • •

$<1.72 \times 10^{-5}$ 90 PRIPSTEIN 00 E789 p nucleus, 800 GeV

$<1.9 \times 10^{-5}$ 90 2 111 FREYBERGER 96 CLE2 $e^+ e^- \approx \Upsilon(4S)$

$<1.0 \times 10^{-4}$ 90 4 ALBRECHT 88g ARG $e^+ e^-$ 10 GeV

$<2.7 \times 10^{-4}$ 90 9 HAAS 88 CLEO $e^+ e^-$ 10 GeV

$<1.2 \times 10^{-4}$ 90 BECKER 87c MRK3 $e^+ e^-$ 3.77 GeV

$<9 \times 10^{-4}$ 90 PALKA 87 SILI 200 GeV πp

$<21 \times 10^{-4}$ 90 0 112 RILES 87 MRK2 $e^+ e^-$ 29 GeV

111 This is the corrected result given in the erratum to FREYBERGER 96.

112 RILES 87 assumes $B(D \rightarrow K\pi) = 3.0\%$ and has production model dependency.

$\Gamma(\pi^0 e^\pm \mu^\mp)/\Gamma_{\text{total}}$ Γ_{182}/Γ
A test of lepton family number conservation. The value is for the sum of the two charge states.

VALUE	CL%	EVTs	DOCUMENT ID	TECN	COMMENT
$<8.6 \times 10^{-5}$	90	2	FREYBERGER 96	CLE2	$e^+ e^- \approx \Upsilon(4S)$

$\Gamma(\eta e^\pm \mu^\mp)/\Gamma_{\text{total}}$ Γ_{183}/Γ
A test of lepton family number conservation. The value is for the sum of the two charge states.

VALUE	CL%	EVTs	DOCUMENT ID	TECN	COMMENT
$<1.0 \times 10^{-4}$	90	0	FREYBERGER 96	CLE2	$e^+ e^- \approx \Upsilon(4S)$

$\Gamma(\rho^0 e^\pm \mu^\mp)/\Gamma_{\text{total}}$ Γ_{184}/Γ
A test of lepton family number conservation. The value is for the sum of the two charge states.

VALUE	CL%	EVTs	DOCUMENT ID	TECN	COMMENT
$<4.9 \times 10^{-5}$	90	0	113 FREYBERGER 96	CLE2	$e^+ e^- \approx \Upsilon(4S)$

113 This FREYBERGER 96 limit is obtained using a phase-space model. The limit changes to $<5.0 \times 10^{-5}$ using a photon pole amplitude model.

$\Gamma(\omega e^\pm \mu^\mp)/\Gamma_{\text{total}}$ Γ_{185}/Γ
A test of lepton family number conservation. The value is for the sum of the two charge states.

VALUE	CL%	EVTs	DOCUMENT ID	TECN	COMMENT
$<1.2 \times 10^{-4}$	90	0	114 FREYBERGER 96	CLE2	$e^+ e^- \approx \Upsilon(4S)$

114 This FREYBERGER 96 limit is obtained using a phase-space model. The same limit is obtained using a photon pole amplitude model.

$\Gamma(\phi e^\pm \mu^\mp)/\Gamma_{\text{total}}$ Γ_{186}/Γ
A test of lepton family number conservation. The value is for the sum of the two charge states.

VALUE	CL%	EVTs	DOCUMENT ID	TECN	COMMENT
$<3.4 \times 10^{-5}$	90	0	115 FREYBERGER 96	CLE2	$e^+ e^- \approx \Upsilon(4S)$

115 This FREYBERGER 96 limit is obtained using a phase-space model. The limit changes to $<3.3 \times 10^{-5}$ using a photon pole amplitude model.

$\Gamma(K^0 e^\pm \mu^\mp)/\Gamma_{\text{total}}$ Γ_{187}/Γ
A test of lepton family number conservation. The value is for the sum of the two charge states.

VALUE	CL%	EVTs	DOCUMENT ID	TECN	COMMENT
$<1.0 \times 10^{-4}$	90	0	FREYBERGER 96	CLE2	$e^+ e^- \approx \Upsilon(4S)$

$\Gamma(K^*(892)^0 e^\pm \mu^\mp)/\Gamma_{\text{total}}$ Γ_{188}/Γ
A test of lepton family number conservation. The value is for the sum of the two charge states.

VALUE	CL%	EVTs	DOCUMENT ID	TECN	COMMENT
$<1.0 \times 10^{-4}$	90	0	116 FREYBERGER 96	CLE2	$e^+ e^- \approx \Upsilon(4S)$

116 This FREYBERGER 96 limit is obtained using a phase-space model. The same limit is obtained using a photon pole amplitude model.

Meson Particle Listings

D0

D0 CP-VIOLATING DECAY-RATE ASYMMETRIES

ACP(K+K-) in D0, D0 -> K+K-

This is the difference between D0 and D0 partial widths for these modes divided by the sum of the widths. The D0 and D0 are distinguished by the charge of the parent D+: D+ -> D0 pi+ and D+ -> D0 pi-.

Table with columns: VALUE, EVTS, DOCUMENT ID, TECN, COMMENT. Rows include data for AITALA 98c, BARTELT 95, and FRABETTI 94i.

ACP(pi+pi-) in D0, D0 -> pi+pi-

This is the difference between D0 and D0 partial widths for these modes divided by the sum of the widths. The D0 and D0 are distinguished by the charge of the parent D+: D+ -> D0 pi+ and D+ -> D0 pi-.

Table with columns: VALUE, EVTS, DOCUMENT ID, TECN, COMMENT. Rows include data for AITALA 98c.

ACP(K0S phi) in D0, D0 -> K0S phi

This is the difference between D0 and D0 partial widths for these modes divided by the sum of the widths. The D0 and D0 are distinguished by the charge of the parent D+: D+ -> D0 pi+ and D+ -> D0 pi-.

Table with columns: VALUE, DOCUMENT ID, TECN, COMMENT. Row includes data for BARTELT 95.

ACP(K0S pi0) in D0, D0 -> K0S pi0

This is the difference between D0 and D0 partial widths for these modes divided by the sum of the widths. The D0 and D0 are distinguished by the charge of the parent D+: D+ -> D0 pi+ and D+ -> D0 pi-.

Table with columns: VALUE, DOCUMENT ID, TECN, COMMENT. Row includes data for BARTELT 95.

ACP(K+pi-), D0 -> K+pi-, D0 -> K-pi+

This is the difference between D0 and D0 partial widths for these modes divided by the sum of the widths. The D0 and D0 are distinguished by the charge of the parent D+: D+ -> D0 pi+ and D+ -> D0 pi-.

Table with columns: VALUE, EVTS, DOCUMENT ID, TECN, COMMENT. Row includes data for GODANG 00.

This GODANG 00 result assumes no D0-D0 mixing; it becomes -0.01 +/- 0.16 +/- 0.01 when mixing is allowed.

D0 PRODUCTION CROSS SECTION AT psi(3770)

A compilation of the cross sections for the direct production of D0 mesons at or near the psi(3770) peak in e+e- production.

Table with columns: VALUE (nanobarns), DOCUMENT ID, TECN, COMMENT. Rows list various experiments and their measured cross sections.

D0 REFERENCES

Columnar list of references including authors (e.g., Godang et al., Jun et al., Pripstein et al.), experiment names, and collaborations (e.g., CLEO Collab., FNAL SELEX Collab.).

See key on page 239

Meson Particle Listings

$D^0, D^*(2007)^0, D^*(2010)^\pm$

ALBRECHT	85F	PL 150B 235	H. Albrecht et al.	(ARGUS Collab.)
AUBERT	85	PL 155B 461	J.J. Aubert et al.	(EMC Collab.)
BAILEY	85	ZPHY C28 357	R. Bailey et al.	(ABCCMR Collab.)
BALTRUSAITIS...	85B	PL 54 1976	R.M. Baltrusaitis et al.	(Mark III Collab.)
BALTRUSAITIS...	85E	PRL 55 150	R.M. Baltrusaitis et al.	(Mark III Collab.)
BENVENUTI	85	PL 158B 531	A.C. Benvenuti et al.	(BCDMS Collab.)
ADAMOVICH	84B	PL 140B 123	M.I. Adamovich et al.	(CERN W8B Collab.)
DERRICK	84	PRL 53 1971	M. Derrick et al.	(HRS Collab.)
PARTRIDGE	84	Thesis CALT-68-1150	R.A. Partridge	(Crystal Ball Collab.)
SUMMERS	84	PRL 52 410	D.J. Summers et al.	(UCSB, CARL, COLU+)
BAILEY	83B	PL 132B 237	R. Bailey et al.	(ACCOM Collab.)
BODEK	82	PL 113B 82	A. Bodek et al.	(ROCH, CIT, CHIC, FNAL+)
FIORINO	81	LNC 30 166	A. Fiorino et al.	
SCHINDLER	81	PR D24 78	R.H. Schindler et al.	(Mark II Collab.)
TRILLING	81	PRPL 75 57	G.H. Trilling	(LBL, UCB) J
ASTON	80E	PL 94B 113	D. Aston et al.	(BONN, CERN, EPOL, GLAS+)
AVERY	80	PRL 44 1309	P. Avery et al.	(ILL, FNAL, COLU)
SCHINDLER	80	PR D21 2716	R.H. Schindler et al.	(Mark II Collab.)
ZHOLENTZ	80	PL 95B 214	A.A. Zholents et al.	(NOVO)
Also	81	SJNP 34 814	A.A. Zholents et al.	(NOVO)
Translated from YAF 34 1471.				
ABRAMS	79D	PRL 43 481	G.S. Abrams et al.	(Mark II Collab.)
ATIYA	79	PRL 43 414	M.S. Atiya et al.	(COLU, ILL, FNAL)
BALTAY	78C	PRL 41 73	C. Baltay et al.	(COLU, BNL)
VUILLEMIN	78	PRL 41 1149	V. Vuillemin et al.	(Mark I Collab.)
GOLDHABER	77	PL 69B 503	G. Goldhaber et al.	(Mark I Collab.)
PERUZZI	77	PRL 39 1301	I. Peruzzi et al.	(Mark I Collab.)
PICCOLO	77	PL 70B 260	M. Piccolo et al.	(Mark I Collab.)
RAPIDIS	77	PRL 39 526	P.A. Rapidis et al.	(Mark I Collab.)
GOLDHABER	76	PRL 37 255	G. Goldhaber et al.	(Mark I Collab.)

CONSTRAINED FIT INFORMATION

An overall fit to a branching ratio uses 3 measurements and one constraint to determine 2 parameters. The overall fit has a $\chi^2 = 0.5$ for 2 degrees of freedom.

The following *off-diagonal* array elements are the correlation coefficients $\langle \delta x_i \delta x_j \rangle / (\delta x_i \delta x_j)$, in percent, from the fit to the branching fractions, $x_i \equiv \Gamma_i / \Gamma_{total}$. The fit constrains the x_i whose labels appear in this array to sum to one.

$$x_2 \begin{vmatrix} & -100 \\ & x_1 \end{vmatrix}$$

$D^*(2007)^0$ BRANCHING RATIOS

$\Gamma(D^0 \pi^0) / \Gamma_{total}$	VALUE	EVTS	DOCUMENT ID	TECN	COMMENT	Γ_1 / Γ
0.619 ± 0.029 OUR FIT						
	0.596 ± 0.035 ± 0.028	858	⁴ ALBRECHT	95F ARG	$e^+ e^- \rightarrow$ hadrons	
	0.636 ± 0.023 ± 0.033	1097	⁴ BUTLER	92 CLE2	$e^+ e^- \rightarrow$ hadrons	

$\Gamma(D^0 \gamma) / \Gamma_{total}$	VALUE	EVTS	DOCUMENT ID	TECN	COMMENT	Γ_2 / Γ
0.381 ± 0.029 OUR FIT						
0.381 ± 0.029 OUR AVERAGE						
	0.404 ± 0.035 ± 0.028	456	⁴ ALBRECHT	95F ARG	$e^+ e^- \rightarrow$ hadrons	
	0.364 ± 0.023 ± 0.033	621	⁴ BUTLER	92 CLE2	$e^+ e^- \rightarrow$ hadrons	
	0.37 ± 0.08 ± 0.08		ADLER	88B MRK3	$e^+ e^-$	
	0.47 ± 0.23		LOW	87 HRS	29 GeV $e^+ e^-$	
	0.53 ± 0.13		BARTEL	85G JADE	$e^+ e^-$, hadrons	
	0.47 ± 0.12		COLES	82 MRK2	$e^+ e^-$	
	0.45 ± 0.15		GOLDHABER	77 MRK1	$e^+ e^-$	

⁴The BUTLER 92 and ALBRECHT 95F branching ratios are not independent, they have been constrained by the authors to sum to 100%.

$D^*(2007)^0$ REFERENCES

ALBRECHT	95F	ZPHY C66 63	H. Albrecht et al.	(ARGUS Collab.)
BORTOLETTO	92B	PRL 69 2046	D. Bortoletto et al.	(CLEO Collab.)
BUTLER	92	PRL 69 2041	F. Butler et al.	(CLEO Collab.)
ABACHI	88B	PL B212 533	S. Abachi et al.	(ANL, IND, MICH, PURD+)
ADLER	88D	PL B208 152	J. Adler et al.	(Mark III Collab.)
LOW	87	PL B183 232	E.H. Low et al.	(HRS Collab.)
BARTEL	85G	PL 151B 197	W. Bartel et al.	(JADE Collab.)
COLES	82	PR D25 2190	M.W. Coles et al.	(LBL, SLAC)
SADROZINSKI	80	Madison Conf. 681	H.F.W. Sadroziński et al.	(PRIN, CIT+)
GOLDHABER	77	PL 69B 503	G. Goldhaber et al.	(Mark I Collab.)
NGUYEN	77	PRL 39 262	H.K. Nguyen et al.	(LBL, SLAC) J

OTHER RELATED PAPERS

SEMENOV	99	SPU 42 847	S.V. Semenov	
Translated from UFN 42 937.				
KAMAL	92	PL B284 421	A.N. Kamal, Q.P. Xu	(ALBE)
TRILLING	81	PRPL 75 57	G.H. Trilling	(LBL, UCB)
GOLDHABER	76	PRL 37 255	G. Goldhaber et al.	(Mark I Collab.)

$D^*(2010)^\pm$

$$I(J^P) = \frac{1}{2}(1^-)$$

I, J, P need confirmation.

$D^*(2010)^\pm$ MASS

The fit includes $D^\pm, D^0, D_S^\pm, D^{*\pm}, D^{*0}$, and $D_S^{*\pm}$ mass and mass difference measurements.

VALUE (MeV)	DOCUMENT ID	TECN	CHG	COMMENT
2010.0 ± 0.5 OUR FIT	Error includes scale factor of 1.1.			
				• • • We do not use the following data for averages, fits, limits, etc. • • •
2008 ± 3	¹ GOLDHABER	77 MRK1	±	$e^+ e^-$
2008.6 ± 1.0	² PERUZZI	77 MRK1	±	$e^+ e^-$
¹ From simultaneous fit to $D^*(2010)^+, D^*(2007)^0, D^+$, and D^0 ; not independent of FELDMAN 77b mass difference below.				
² PERUZZI 77 mass not independent of FELDMAN 77b mass difference below and PERUZZI 77 D^0 mass value.				

$m_{D^*(2010)^+ - m_{D^+}}$

The fit includes $D^\pm, D^0, D_S^\pm, D^{*\pm}, D^{*0}$, and $D_S^{*\pm}$ mass and mass difference measurements.

VALUE (MeV)	EVTS	DOCUMENT ID	TECN	COMMENT
140.64 ± 0.10 OUR FIT	Error includes scale factor of 1.1.			
140.64 ± 0.08 ± 0.06	620	BORTOLETTO92b	CLE2	$e^+ e^- \rightarrow$ hadrons

OTHER RELATED PAPERS

RICHMAN	95	RMP 67 893	J.D. Richman, P.R. Burchat	(UCSB, STAN)
ROSNER	95	CNPP 21 369	J. Rosner	(CHIC)

$D^*(2007)^0$

$I(J^P) = \frac{1}{2}(1^-)$
 I, J, P need confirmation.

J consistent with 1, value 0 ruled out (NGUYEN 77).

$D^*(2007)^0$ MASS

The fit includes $D^\pm, D^0, D_S^\pm, D^{*\pm}, D^{*0}$, and $D_S^{*\pm}$ mass and mass difference measurements.

VALUE (MeV)	DOCUMENT ID	TECN	COMMENT
2006.7 ± 0.5 OUR FIT	Error includes scale factor of 1.1.		
			• • • We do not use the following data for averages, fits, limits, etc. • • •
2006 ± 1.5	¹ GOLDHABER	77 MRK1	$e^+ e^-$
¹ From simultaneous fit to $D^*(2010)^+, D^*(2007)^0, D^+$, and D^0 .			

$m_{D^*(2007)^0 - m_{D^0}}$

The fit includes $D^\pm, D^0, D_S^\pm, D^{*\pm}, D^{*0}$, and $D_S^{*\pm}$ mass and mass difference measurements.

VALUE (MeV)	EVTS	DOCUMENT ID	TECN	COMMENT
142.12 ± 0.07 OUR FIT				
142.12 ± 0.07 OUR AVERAGE				
142.2 ± 0.3 ± 0.2	145	ALBRECHT	95F ARG	$e^+ e^- \rightarrow$ hadrons
142.12 ± 0.05 ± 0.05	1176	BORTOLETTO92b	CLE2	$e^+ e^- \rightarrow$ hadrons
				• • • We do not use the following data for averages, fits, limits, etc. • • •
142.2 ± 2.0		SADROZINSKI	80 CBAL	$D^{*0} \rightarrow D^0 \pi^0$
142.7 ± 1.7		² GOLDHABER	77 MRK1	$e^+ e^-$
² From simultaneous fit to $D^*(2010)^+, D^*(2007)^0, D^+$, and D^0 .				

$D^*(2007)^0$ WIDTH

VALUE (MeV)	CL%	DOCUMENT ID	TECN	COMMENT
<2.1	90	³ ABACHI	88B HRS	$D^{*0} \rightarrow D^+ \pi^-$
³ Assuming $m_{D^{*0}} = 2007.2 \pm 2.1$ MeV/ c^2 .				

$D^*(2007)^0$ DECAY MODES

$\bar{D}^*(2007)^0$ modes are charge conjugates of modes below.

Mode	Fraction (Γ_i / Γ)
Γ_1 $D^0 \pi^0$	(61.9 ± 2.9) %
Γ_2 $D^0 \gamma$	(38.1 ± 2.9) %

Meson Particle Listings

$D^*(2010)^\pm$

$m_{D^*(2010)^+} - m_{D^0}$

The fit includes D^\pm , D^0 , D_s^\pm , $D^{*\pm}$, D^{*0} , and $D_s^{*\pm}$ mass and mass difference measurements.

VALUE (MeV)	EVTs	DOCUMENT ID	TECN	COMMENT
145.436 ± 0.016 OUR FIT				
145.436 ± 0.015 OUR AVERAGE				
145.54 ± 0.08	611	ADINOLFI	99 BEAT	$D^{*\pm} \rightarrow D^0 \pi^\pm$
145.45 ± 0.02		BREITWEG	99 ZEUS	$D^{*\pm} \rightarrow D^0 \pi^\pm \rightarrow (K\pi)\pi^\pm$
145.42 ± 0.05		BREITWEG	99 ZEUS	$D^{*\pm} \rightarrow D^0 \pi^\pm \rightarrow (K^- 3\pi^+)\pi^\pm$
145.5 ± 0.15	103	³ ADLOFF	97B H1	$D^{*\pm} \rightarrow D^0 \pi^\pm$
145.44 ± 0.08	152	³ BREITWEG	97 ZEUS	$D^{*\pm} \rightarrow D^0 \pi^\pm, D^0 \rightarrow K^- 3\pi^+$
145.42 ± 0.11	199	³ BREITWEG	97 ZEUS	$D^{*0} \rightarrow K^- 3\pi^+, D^0 \rightarrow K^- \pi^+$
145.4 ± 0.2	48	³ DERRICK	95 ZEUS	$D^{*\pm} \rightarrow D^0 \pi^\pm$
145.39 ± 0.06 ± 0.03		BARLAG	92B ACCM	$\pi^- 230$ GeV
145.5 ± 0.2	115	³ ALEXANDER	91B OPAL	$D^{*\pm} \rightarrow D^0 \pi^\pm$
145.30 ± 0.06		³ DECAMP	91J ALEP	$D^{*\pm} \rightarrow D^0 \pi^\pm$
145.40 ± 0.05 ± 0.10		ABACHI	88B HRS	$D^{*\pm} \rightarrow D^0 \pi^\pm$
145.46 ± 0.07 ± 0.03		ALBRECHT	85F ARG	$D^{*\pm} \rightarrow D^0 \pi^\pm$
145.5 ± 0.3	28	BAILEY	83 SPEC	$D^{*\pm} \rightarrow D^0 \pi^\pm$
145.5 ± 0.3	60	FITCH	81 SPEC	$\pi^- A$
145.3 ± 0.5	30	FELDMAN	77B MRK1	$D^{*+} \rightarrow D^0 \pi^+$
• • • We do not use the following data for averages, fits, limits, etc. • • •				
145.44 ± 0.09	122	³ BREITWEG	97B ZEUS	$D^{*\pm} \rightarrow D^0 \pi^\pm, D^0 \rightarrow K^- \pi^+$
145.8 ± 1.5	16	AHLEN	83 HRS	$D^{*+} \rightarrow D^0 \pi^+$
145.1 ± 1.8	12	BAILEY	83 SPEC	$D^{*\pm} \rightarrow D^0 \pi^\pm$
145.1 ± 0.5	14	BAILEY	83 SPEC	$D^{*+} \rightarrow D^0 \pi^+$
145.5 ± 0.5	14	YELTON	82 MRK2	29 $e^+ e^- \rightarrow K^- \pi^+$
~ 145.5		AVERY	80 SPEC	γA
145.2 ± 0.6	2	BLIETSCHAU	79 BEBC	νp
³ Systematic error not evaluated.				

$m_{D^*(2010)^+} - m_{D^*(2007)^0}$

VALUE (MeV)	DOCUMENT ID	TECN	COMMENT
2.6 ± 1.8	⁴ PERUZZI	77 MRK1	$e^+ e^-$
⁴ Not independent of FELDMAN 77B mass difference above, PERUZZI 77 D^0 mass, and GOLDHABER 77 $D^*(2007)^0$ mass.			

$D^*(2010)^\pm$ WIDTH

VALUE (MeV)	CL%	EVTs	DOCUMENT ID	TECN	COMMENT
<0.131	90	110	BARLAG	92B ACCM	$\pi^- 230$ GeV
• • • We do not use the following data for averages, fits, limits, etc. • • •					
<1.1	90		ABACHI	88B HRS	$D^{*\pm} \rightarrow D^0 \pi^\pm$
<2.2			YELTON	82 MRK2	$e^+ e^- \rightarrow K^- \pi^+ \pi^-$
<2.0	90	30	FELDMAN	77B MRK1	$D^{*+} \rightarrow D^0 \pi^+$

$D^*(2010)^\pm$ DECAY MODES

$D^*(2010)^-$ modes are charge conjugates of the modes below.

Mode	Fraction (Γ_i/Γ)
Γ_1 $D^0 \pi^+$	(67.7 ± 0.5) %
Γ_2 $D^+ \pi^0$	(30.7 ± 0.5) %
Γ_3 $D^+ \gamma$	(1.6 ± 0.4) %

CONSTRAINED FIT INFORMATION

An overall fit to 3 branching ratios uses 6 measurements and one constraint to determine 3 parameters. The overall fit has a $\chi^2 = 0.3$ for 4 degrees of freedom.

The following *off-diagonal* array elements are the correlation coefficients $\langle \delta x_i \delta x_j \rangle / (\delta x_i \delta x_j)$, in percent, from the fit to the branching fractions, $x_i \equiv \Gamma_i/\Gamma_{\text{total}}$. The fit constrains the x_i whose labels appear in this array to sum to one.

x_2	-62	
x_3	-43	-44
	x_1	x_2

$D^*(2010)^+$ BRANCHING RATIOS

$\Gamma(D^0 \pi^+)/\Gamma_{\text{total}}$	VALUE	DOCUMENT ID	TECN	COMMENT	Γ_1/Γ
	0.677 ± 0.005 OUR FIT				
	0.677 ± 0.006 OUR AVERAGE				
	0.6759 ± 0.0029 ± 0.0064	5,6,7	BARTELT	98 CLE2	$e^+ e^-$
	0.688 ± 0.024 ± 0.013		ALBRECHT	95F ARG	$e^+ e^- \rightarrow$ hadrons
	0.681 ± 0.010 ± 0.013	5	BUTLER	92 CLE2	$e^+ e^- \rightarrow$ hadrons
• • • We do not use the following data for averages, fits, limits, etc. • • •					
	0.57 ± 0.04 ± 0.04		ADLER	88D MRK3	$e^+ e^-$
	0.44 ± 0.10		COLES	82 MRK2	$e^+ e^-$
	0.6 ± 0.15	7	GOLDHABER	77 MRK1	$e^+ e^-$

$\Gamma(D^+ \pi^0)/\Gamma_{\text{total}}$	VALUE	EVTs	DOCUMENT ID	TECN	COMMENT	Γ_2/Γ
	0.3073 ± 0.0013 ± 0.0062					
	0.3073 ± 0.0013 ± 0.0062	5,6,7	BARTELT	98 CLE2	$e^+ e^-$	
• • • We do not use the following data for averages, fits, limits, etc. • • •						
	0.312 ± 0.011 ± 0.008	1404	ALBRECHT	95F ARG	$e^+ e^- \rightarrow$ hadrons	
	0.308 ± 0.004 ± 0.008	410	5 BUTLER	92 CLE2	$e^+ e^- \rightarrow$ hadrons	
	0.26 ± 0.02 ± 0.02		ADLER	88D MRK3	$e^+ e^-$	
	0.34 ± 0.07		COLES	82 MRK2	$e^+ e^-$	

$\Gamma(D^+ \gamma)/\Gamma_{\text{total}}$	VALUE	CL%	EVTs	DOCUMENT ID	TECN	COMMENT	Γ_3/Γ
	0.016 ± 0.004 OUR FIT						
	0.016 ± 0.005 OUR AVERAGE						
	0.0168 ± 0.0042 ± 0.0029			5,6	BARTELT	98 CLE2	$e^+ e^-$
	0.011 ± 0.014 ± 0.016		12	5 BUTLER	92 CLE2	$e^+ e^- \rightarrow$ hadrons	
• • • We do not use the following data for averages, fits, limits, etc. • • •							
	<0.052		90	ALBRECHT	95F ARG	$e^+ e^- \rightarrow$ hadrons	
	0.17 ± 0.05 ± 0.05			ADLER	88D MRK3	$e^+ e^-$	
	0.22 ± 0.12			8 COLES	82 MRK2	$e^+ e^-$	

⁵The branching ratios are not independent, they have been constrained by the authors to sum to 100%.
⁶Systematic error includes theoretical error on the prediction of the ratio of hadronic modes.
⁷Assuming that isospin is conserved in the decay.
⁸Not independent of $\Gamma(D^0 \pi^+)/\Gamma_{\text{total}}$ and $\Gamma(D^+ \pi^0)/\Gamma_{\text{total}}$ measurement.

$D^*(2010)^\pm$ REFERENCES

ADINOLFI	99 NP B547 3	M. Adinolfi et al.	(Beatrice Collab.)
BREITWEG	99 EPJ C6 67	J. Breitweg et al.	(ZEUS Collab.)
BARTELT	98 PRL 80 3919	J. Bartelt et al.	(CLEO II Collab.)
ADLOFF	97B ZPHY C72 593	C. Adloff et al.	(H1 Collab.)
BREITWEG	97 PL B401 192	J. Breitweg et al.	(ZEUS Collab.)
BREITWEG	97B PL B407 402	J. Breitweg et al.	(ZEUS Collab.)
ALBRECHT	95F ZPHY C66 63	H. Albrecht et al.	(ARGUS Collab.)
DERRICK	95 PL B349 225	M. Derrick et al.	(ZEUS Collab.)
BARLAG	92B PL B278 480	S. Barlag et al.	(ACCMOR Collab.)
BORTOLETTO	92B PRL 69 2046	D. Bortoletto et al.	(CLEO Collab.)
BUTLER	92 PRL 69 2041	F. Butler et al.	(CLEO Collab.)
ALEXANDER	91B PL B262 341	G. Alexander et al.	(OPAL Collab.)
DECAMP	91J PL B266 218	D. Decamp et al.	(ALEPH Collab.)
ABACHI	88B PL B212 533	S. Abachi et al.	(ANL, IND, MICH, PURD+)
ADLER	88D PL B208 152	J. Adler et al.	(Mark III Collab.)
ALBRECHT	85F PL 150B 235	H. Albrecht et al.	(ARGUS Collab.)
AHLEN	83 PRL 51 1147	S.P. Ahlen et al.	(ANL, IND, LBL+)
BAILEY	83 PL 132B 230	R. Bailey et al.	(AMST, BRIS, CERN, CRAC+)
COLES	82 PR D26 2190	M.W. Coles et al.	(LBL, SLAC)
YELTON	82 PRL 49 430	J.M. Yelton et al.	(SLAC, LBL, UCB+)
FITCH	81 PRL 46 761	V.L. Fitch et al.	(PRIN, SACL, TOR+)
AVERY	80 PRL 44 1309	P. Avery et al.	(ILL, FNAL, COLU)
BLIETSCHAU	79 PL 86B 108	J. Blietschau et al.	(AACHS, BONN, CERN+)
FELDMAN	77B PRL 38 1313	G.J. Feldman et al.	(Mark I Collab.)
GOLDHABER	77 PL 69B 503	G. Goldhaber et al.	(Mark I Collab.)
PERUZZI	77 PRL 39 1301	I. Peruzzi et al.	(Mark I Collab.)

OTHER RELATED PAPERS

SEMENOV	99 SPU 42 847	S.V. Semenov	
	Translated from UFN 42 937.		
NUSSINOV	98 PL B418 383	S. Nussinov	
KAMAL	92 PL B284 421	A.N. Kamal, Q.P. Xu	(ALBE)
ALTHOFF	83C PL 126B 493	M. Althoff et al.	(TASSO Collab.)
BEBEK	82 PRL 49 610	C. Bebek et al.	(HARV, OSU, ROCH, RUTG+)
TRILLING	81 PRL 75 57	G.H. Trilling	(LBL, UCB)
PERUZZI	76 PRL 37 569	I. Peruzzi et al.	(Mark I Collab.)

See key on page 239

Meson Particle Listings
 $D_1(2420)^0, D_1(2420)^\pm, D_2^*(2460)^0$

$D_1(2420)^0$ $I(J^P) = \frac{1}{2}(1^+)$
I, J, P need confirmation.
 Seen in $D^*(2010)^+\pi^-$. $J^P = 1^+$ according to ALBRECHT 89H.

$D_1(2420)^0$ MASS

VALUE (MeV)	EVTS	DOCUMENT ID	TECN	COMMENT
2422.2 ± 1.8 OUR AVERAGE	Error	includes scale factor of 1.2.		
2421 $^{+1}_{-2}$ ± 2	286	AVERY	94c CLE2	$e^+e^- \rightarrow D^{*+}\pi^-X$
2422 ± 2 ± 2	51	FRABETTI	94B E687	$\gamma Be \rightarrow D^{*+}\pi^-X$
2428 ± 3 ± 2	279	AVERY	90 CLEO	$e^+e^- \rightarrow D^{*+}\pi^-X$
2414 ± 2 ± 5	171	ALBRECHT	89H ARG	$e^+e^- \rightarrow D^{*+}\pi^-X$
2428 ± 8 ± 5	171	ANJOS	89c TPS	$\gamma N \rightarrow D^{*+}\pi^-X$
2425 ± 3	235	¹ ABREU	98M DLPH	e^+e^-

• • • We do not use the following data for averages, fits, limits, etc. • • •
¹No systematic error given.

$D_1(2420)^0$ WIDTH

VALUE (MeV)	EVTS	DOCUMENT ID	TECN	COMMENT
18.9 $^{+4.6}_{-3.5}$ OUR AVERAGE				
20 $^{+5}_{-5}$ ± 3	286	AVERY	94c CLE2	$e^+e^- \rightarrow D^{*+}\pi^-X$
15 ± 8 ± 4	51	FRABETTI	94B E687	$\gamma Be \rightarrow D^{*+}\pi^-X$
23 $^{+8}_{-6}$ $^{+10}_{-3}$	279	AVERY	90 CLEO	$e^+e^- \rightarrow D^{*+}\pi^-X$
13 ± 6 $^{+10}_{-5}$	171	ALBRECHT	89H ARG	$e^+e^- \rightarrow D^{*+}\pi^-X$
58 ± 14 ± 10	171	ANJOS	89c TPS	$\gamma N \rightarrow D^{*+}\pi^-X$

• • • We do not use the following data for averages, fits, limits, etc. • • •

$D_1(2420)^0$ DECAY MODES

$\bar{D}_1(2420)^0$ modes are charge conjugates of modes below.

Mode	Fraction (Γ_i/Γ)
Γ_1 $D^*(2010)^+\pi^-$	seen
Γ_2 $D^+\pi^-$	not seen

$D_1(2420)^0$ BRANCHING RATIOS

$\Gamma(D^*(2010)^+\pi^-)/\Gamma_{total}$	Γ_1/Γ
seen	
seen	
seen	

$\Gamma(D^+\pi^-)/\Gamma(D^*(2010)^+\pi^-)$	Γ_2/Γ_1
<0.24	90

$D_1(2420)^0$ REFERENCES

ABREU	98M PL B426 231	P. Abreu et al.	(DELPHI Collab.)
AVERY	94C PL B331 236	P. Avery et al.	(CLEO Collab.)
FRABETTI	94B PRL 72 324	P.L. Frabetti et al.	(FNAL E687 Collab.)
AVERY	90 PR D41 774	P. Avery, D. Besson	(CLEO Collab.)
ALBRECHT	89H PL B232 398	H. Albrecht et al.	(ARGUS Collab.) JP
ANJOS	89C PRL 52 1717	J.C. Anjos et al.	(FNAL E691 Collab.)

OTHER RELATED PAPERS

SEMENOV	99 SPU 42 847	S.V. Semenov	Translated from UFN 42 937.
---------	---------------	--------------	-----------------------------

$D_1(2420)^\pm$ $I(J^P) = \frac{1}{2}(?)^?$
I needs confirmation.
 OMITTED FROM SUMMARY TABLE
 Seen in $D^*(2007)^0\pi^+$. $J^P = 0^+$ ruled out.

$D_1(2420)^\pm$ MASS

VALUE (MeV)	EVTS	DOCUMENT ID	TECN	COMMENT
2427 ± 5 OUR AVERAGE	Error	includes scale factor of 2.0.		
2425 ± 2 ± 2	146	BERGFELD	94B CLE2	$e^+e^- \rightarrow D^{*0}\pi^+X$
2443 ± 7 ± 5	190	ANJOS	89c TPS	$\gamma N \rightarrow D^{*0}\pi^+X^0$

$m_{D_1(2420)^\pm} - m_{D_1(2420)^0}$

VALUE (MeV)	DOCUMENT ID	TECN	COMMENT
4 $^{+2}_{-3}$ ± 3	BERGFELD	94B CLE2	$e^+e^- \rightarrow$ hadrons

$D_1(2420)^\pm$ WIDTH

VALUE (MeV)	EVTS	DOCUMENT ID	TECN	COMMENT
28 ± 8 OUR AVERAGE				
26 $^{+8}_{-7}$ ± 4	146	BERGFELD	94B CLE2	$e^+e^- \rightarrow D^{*0}\pi^+X$
41 ± 19 ± 8	190	ANJOS	89c TPS	$\gamma N \rightarrow D^{*0}\pi^+X^0$

$D_1(2420)^\pm$ DECAY MODES

$D_1^*(2420)^-$ modes are charge conjugates of modes below.

Mode	Fraction (Γ_i/Γ)
Γ_1 $D^*(2007)^0\pi^+$	seen
Γ_2 $D^0\pi^+$	not seen

$D_1(2420)^\pm$ BRANCHING RATIOS

$\Gamma(D^*(2007)^0\pi^+)/\Gamma_{total}$	Γ_1/Γ
seen	
seen	

$\Gamma(D^0\pi^+)/\Gamma(D^*(2007)^0\pi^+)$	Γ_2/Γ_1
<0.18	90

$D_1(2420)^\pm$ REFERENCES

BERGFELD	94B PL B340 194	T. Bergfeld et al.	(CLEO Collab.)
ANJOS	89C PRL 62 1717	J.C. Anjos et al.	(FNAL E691 Collab.)

OTHER RELATED PAPERS

SEMENOV	99 SPU 42 847	S.V. Semenov	Translated from UFN 42 937.
---------	---------------	--------------	-----------------------------

$D_2^*(2460)^0$

$I(J^P) = \frac{1}{2}(2^+)$

$J^P = 2^+$ assignment strongly favored (ALBRECHT 89B).

$D_2^*(2460)^0$ MASS

VALUE (MeV)	EVTS	DOCUMENT ID	TECN	COMMENT
2458.9 ± 2.0 OUR AVERAGE	Error	includes scale factor of 1.2.		
2465 ± 3 ± 3	486	AVERY	94c CLE2	$e^+e^- \rightarrow D^+\pi^-X$
2453 ± 3 ± 2	128	FRABETTI	94B E687	$\gamma Be \rightarrow D^+\pi^-X$
2461 ± 3 ± 1	440	AVERY	90 CLEO	$e^+e^- \rightarrow D^{*+}\pi^-X$
2455 ± 3 ± 5	337	ALBRECHT	89B ARG	$e^+e^- \rightarrow D^+\pi^-X$
2459 ± 3 ± 2	153	ANJOS	89c TPS	$\gamma N \rightarrow D^+\pi^-X$
2461 ± 6	126	¹ ABREU	98M DLPH	e^+e^-
2466 ± 7	1	ASRATYAN	95 BEBC	53,40 $\nu(\bar{\nu}) \rightarrow p + X, d + X$

• • • We do not use the following data for averages, fits, limits, etc. • • •
¹No systematic error given.

$D_2^*(2460)^0$ WIDTH

VALUE (MeV)	EVTS	DOCUMENT ID	TECN	COMMENT
23 ± 5 OUR AVERAGE				
28 $^{+8}_{-7}$ ± 6	486	AVERY	94c CLE2	$e^+e^- \rightarrow D^+\pi^-X$
25 ± 10 ± 5	128	FRABETTI	94B E687	$\gamma Be \rightarrow D^+\pi^-X$
20 $^{+9}_{-12}$ $^{+9}_{-10}$	440	AVERY	90 CLEO	$e^+e^- \rightarrow D^{*+}\pi^-X$
15 $^{+13}_{-10}$ $^{+5}_{-10}$	337	ALBRECHT	89B ARG	$e^+e^- \rightarrow D^+\pi^-X$
20 ± 10 ± 5	153	ANJOS	89c TPS	$\gamma N \rightarrow D^+\pi^-X$

$D_2^*(2460)^0$ DECAY MODES

$\bar{D}_2^*(2460)^0$ modes are charge conjugates of modes below.

Mode	Fraction (Γ_i/Γ)
Γ_1 $D^+\pi^-$	seen
Γ_2 $D^*(2010)^+\pi^-$	seen

Meson Particle Listings

$D_2^*(2460)^0, D_2^*(2460)^+, D^*(2640)^\pm$

$D_2^*(2460)^0$ BRANCHING RATIOS

$\Gamma(D^+\pi^-)/\Gamma_{total}$				Γ_1/Γ
VALUE	EVTS	DOCUMENT ID	TECN	COMMENT
seen	337	ALBRECHT	89B ARG	$e^+e^- \rightarrow D^+\pi^-X$
seen		ANJOS	89C TPS	$\gamma N \rightarrow D^+\pi^-X$

$\Gamma(D^*(2010)^+\pi^-)/\Gamma_{total}$				Γ_2/Γ
VALUE	EVTS	DOCUMENT ID	TECN	COMMENT
seen		AVERY	90 CLEO	$e^+e^- \rightarrow D^{*+}\pi^-X$
seen		ALBRECHT	89H ARG	$e^+e^- \rightarrow D^*\pi^-X$

$\Gamma(D^+\pi^-)/\Gamma(D^*(2010)^+\pi^-)$				Γ_1/Γ_2
VALUE	EVTS	DOCUMENT ID	TECN	COMMENT
2.3 ± 0.6 OUR AVERAGE				
2.2 ± 0.7 ± 0.6		AVERY	94C CLE2	$e^+e^- \rightarrow D^{*+}\pi^-X$
2.3 ± 0.8		AVERY	90 CLEO	e^+e^-
3.0 ± 1.1 ± 1.5		ALBRECHT	89H ARG	$e^+e^- \rightarrow D^*\pi^-X$

$D_2^*(2460)^0$ REFERENCES

ABREU	98M	PL B426 231	P. Abreu <i>et al.</i>	(DELPHI Collab.)
ASRATYAN	95	ZPHY C68 43	A.E. Asratyan <i>et al.</i>	(BIRM, BELG, CERN+)
AVERY	94C	PL B331 236	P. Avery <i>et al.</i>	(CLEO Collab.)
FRABETTI	94B	PRL 72 324	P.L. Frabetti <i>et al.</i>	(FNAL E687 Collab.)
AVERY	90	PR D41 774	P. Avery, D. Besson	(CLEO Collab.)
ALBRECHT	89B	PL B221 422	H. Albrecht <i>et al.</i>	(ARGUS Collab.) JP
ALBRECHT	89H	PL B232 398	H. Albrecht <i>et al.</i>	(ARGUS Collab.) JP
ANJOS	89C	PRL 62 1717	J.C. Anjos <i>et al.</i>	(FNAL E691 Collab.)

OTHER RELATED PAPERS

SEMENOV	99	SPU 42 847	S.V. Semenov	
			Translated from UFN 42 937.	

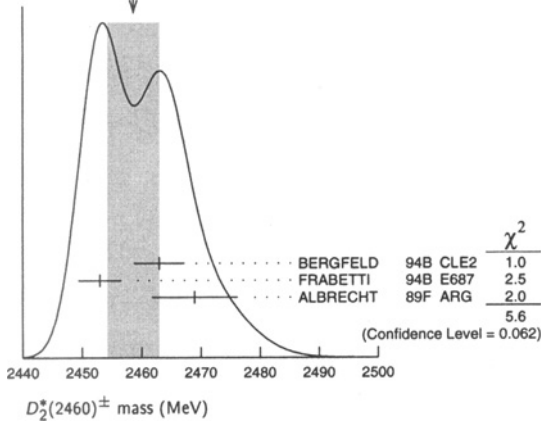
$D_2^*(2460)^\pm$

 $I(J^P) = \frac{1}{2}(2^+)$

$D_2^*(2460)^\pm$ MASS

VALUE (MeV)	EVTS	DOCUMENT ID	TECN	COMMENT
2459 ± 4 OUR AVERAGE Error includes scale factor of 1.7. See the ideogram below.				
2463 ± 3 ± 3	310	BERGFELD	94B CLE2	$e^+e^- \rightarrow D^0\pi^+X$
2453 ± 3 ± 2	185	FRABETTI	94B E687	$\gamma Be \rightarrow D^0\pi^+X$
2469 ± 4 ± 6		ALBRECHT	89F ARG	$e^+e^- \rightarrow D^0\pi^+X$

WEIGHTED AVERAGE
2459 ± 4 (Error scaled by 1.7)



$m_{D_2^*(2460)^\pm} - m_{D_2^*(2460)^0}$

VALUE (MeV)	DOCUMENT ID	TECN	COMMENT
0.9 ± 3.3 OUR AVERAGE Error includes scale factor of 1.1.			
-2 ± 4 ± 4	BERGFELD	94B CLE2	$e^+e^- \rightarrow \text{hadrons}$
0 ± 4	FRABETTI	94B E687	$\gamma Be \rightarrow D\pi X$
14 ± 5 ± 8	ALBRECHT	89F ARG	$e^+e^- \rightarrow D^0\pi^+X$

$D_2^*(2460)^\pm$ WIDTH

VALUE (MeV)	EVTS	DOCUMENT ID	TECN	COMMENT
25 ± 9 OUR AVERAGE				
27 ± 11 ± 5	310	BERGFELD	94B CLE2	$e^+e^- \rightarrow D^0\pi^+X$
23 ± 9 ± 5	185	FRABETTI	94B E687	$\gamma Be \rightarrow D^0\pi^+X$

$D_2^*(2460)^\pm$ DECAY MODES

$D_2^*(2460)^-$ modes are charge conjugates of modes below.

Mode	Fraction (Γ_1/Γ)
Γ_1 $D^0\pi^+$	seen
Γ_2 $D^{*0}\pi^+$	seen

$D_2^*(2460)^\pm$ BRANCHING RATIOS

$\Gamma(D^0\pi^+)/\Gamma_{total}$				Γ_1/Γ
VALUE	EVTS	DOCUMENT ID	TECN	COMMENT
seen		ALBRECHT	89F ARG	$e^+e^- \rightarrow D^0\pi^+X$

$\Gamma(D^{*0}\pi^+)/\Gamma(D^0\pi^+)$				Γ_1/Γ_2
VALUE	EVTS	DOCUMENT ID	TECN	COMMENT
1.9 ± 1.1 ± 0.3				
		BERGFELD	94B CLE2	$e^+e^- \rightarrow \text{hadrons}$

$D_2^*(2460)^\pm$ REFERENCES

BERGFELD	94B	PL B340 194	T. Bergfeld <i>et al.</i>	(CLEO Collab.)
FRABETTI	94B	PRL 72 324	P.L. Frabetti <i>et al.</i>	(FNAL E687 Collab.)
ALBRECHT	89F	PL B231 208	H. Albrecht <i>et al.</i>	(ARGUS Collab.)

$D^*(2640)^\pm$

 $I(J^P) = \frac{1}{2}(?)^?$

OMITTED FROM SUMMARY TABLE
Seen in $D^*(2010)^+\pi^+\pi^-$. Needs confirmation.

$D^*(2640)^\pm$ MASS

VALUE (MeV)	EVTS	DOCUMENT ID	TECN	COMMENT
2637 ± 2 ± 6				
	66 ± 14	ABREU	98M DLPH	$e^+e^- \rightarrow D^{*+}\pi^+\pi^-X$

$D^*(2640)^\pm$ WIDTH

VALUE (MeV)	CL%	DOCUMENT ID	TECN	COMMENT
<15				
	95	ABREU	98M DLPH	$e^+e^- \rightarrow D^{*+}\pi^+\pi^-X$

$D^*(2640)^+$ DECAY MODES

$D^*(2640)^-$ modes are charge conjugates of modes below.

Mode	Fraction (Γ_1/Γ)
Γ_1 $D^*(2010)^+\pi^+\pi^-$	seen

$D^*(2640)^\pm$ REFERENCES

ABREU	98M	PL B426 231	P. Abreu <i>et al.</i>	(DELPHI Collab.)
-------	-----	-------------	------------------------	------------------

CHARMED, STRANGE MESONS (C = S = ±1)

$$D_s^+ = c\bar{s}, D_s^- = \bar{c}s, \text{ similarly for } D_s^{*\pm}$$

D_s^\pm
was F^\pm

$$I(J^P) = 0(0^-)$$

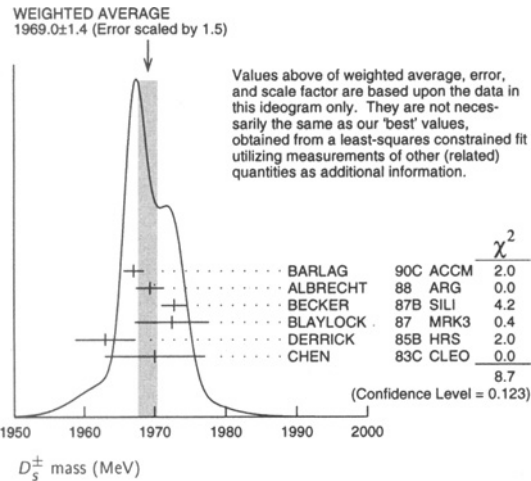
The angular distributions of the decays of the ϕ and $\bar{K}^*(892)^0$ in the $\phi\pi^+$ and $K^+\bar{K}^*(892)^0$ modes strongly indicate that the spin is zero. The parity given is that expected of a $c\bar{s}$ ground state.

D_s^\pm MASS

The fit includes $D^\pm, D^0, D_s^\pm, D^{*\pm}, D^{*0}$, and $D_s^{*\pm}$ mass and mass difference measurements. Measurements of the D_s^\pm mass with an error greater than 10 MeV are omitted from the fit and average. A number of early measurements have been omitted altogether.

VALUE (MeV)	EVTS	DOCUMENT ID	TECN	COMMENT
1968.6 ± 0.6 OUR FIT				Error includes scale factor of 1.1.
1969.0 ± 1.4 OUR AVERAGE				Error includes scale factor of 1.5. See the ideogram below.
1967.0 ± 1.0 ± 1.0	54	BARLAG 90C ACCM	π ⁻ Cu 230 GeV	
1969.3 ± 1.4 ± 1.4		ALBRECHT 88 ARG	e ⁺ e ⁻ 9.4-10.6 GeV	
1972.7 ± 1.5 ± 1.0	21	BECKER 87B SILI	200 GeV π, K, p	
1972.4 ± 3.7 ± 3.7	27	BLAYLOCK 87 MRK3	e ⁺ e ⁻ 4.14 GeV	
1963 ± 3 ± 3	30	DERRICK 85B HRS	e ⁺ e ⁻ 29 GeV	
1970 ± 5 ± 5	104	CHEN 83C CLEO	e ⁺ e ⁻ 10.5 GeV	
• • • We do not use the following data for averages, fits, limits, etc. • • •				
1968.3 ± 0.7 ± 0.7	290	¹ ANJOS 88 E691	Photoproduction	
1980 ± 15	6	USHIDA 86 EMUL	ν wideband	
1973.6 ± 2.6 ± 3.0	163	ALBRECHT 85D ARG	e ⁺ e ⁻ 10 GeV	
1948 ± 28 ± 10	65	AIHARA 84D TPC	e ⁺ e ⁻ 29 GeV	
1975 ± 9 ± 10	49	ALTHOFF 84 TASS	e ⁺ e ⁻ 14-25 GeV	
1975 ± 4	3	BAILEY 84 ACCM	hadron ⁺ Be → φπ ⁺ X	

¹ ANJOS 88 enters the fit via $m_{D_s^\pm} - m_{D^\pm}$ (see below).



$$m_{D_s^\pm} - m_{D^\pm}$$

The fit includes $D^\pm, D^0, D_s^\pm, D^{*\pm}, D^{*0}$, and $D_s^{*\pm}$ mass and mass difference measurements.

VALUE (MeV)	EVTS	DOCUMENT ID	TECN	COMMENT
99.2 ± 0.5 OUR FIT				Error includes scale factor of 1.1.
99.2 ± 0.5 OUR AVERAGE				
99.5 ± 0.6 ± 0.3		BROWN 94 CLE2	e ⁺ e ⁻ ≈ $\Upsilon(4S)$	
98.5 ± 1.5	555	CHEN 89 CLEO	e ⁺ e ⁻ 10.5 GeV	
99.0 ± 0.8	290	ANJOS 88 E691	Photoproduction	

D_s^\pm MEAN LIFE

Measurements with an error greater than 0.2×10^{-12} s or with fewer than 100 events are omitted from the average.

VALUE (10^{-12} s)	EVTS	DOCUMENT ID	TECN	COMMENT
0.496 ± 0.010 -0.009 OUR AVERAGE				
0.518 ± 0.014 ± 0.007	1662	AITALA 99 E791	π ⁻ nucleus, 500 GeV	
0.4863 ± 0.0150 +0.0049 -0.0051	2167	² BONVICINI 99 CLE2	e ⁺ e ⁻ ≈ $\Upsilon(4S)$	
0.475 ± 0.020 ± 0.007	900	FRABETTI 93F E687	γBe, $D_s^+ \rightarrow \phi\pi^+$	
0.50 ± 0.06 ± 0.03	104	FRABETTI 90 E687	γBe, φπ ⁺	
0.56 ± 0.13 -0.12 ± 0.08	144	ALBRECHT 88i ARG	e ⁺ e ⁻ 10 GeV	
0.47 ± 0.04 ± 0.02	228	RAAB 88 E691	Photoproduction	
• • • We do not use the following data for averages, fits, limits, etc. • • •				
0.33 ± 0.12 -0.08 ± 0.03	15	ALVAREZ 90 NA14	γ, $D_s^+ \rightarrow \phi\pi^+$	
0.469 ± 0.102 -0.086 ± 0.05	54	³ BARLAG 90C ACCM	π ⁻ Cu 230 GeV	
0.31 ± 0.24 -0.20 ± 0.05	18	AVERILL 89 HRS	e ⁺ e ⁻ 29 GeV	
0.48 ± 0.06 -0.05 ± 0.02	99	ANJOS 87B E691	See RAAB 88	
0.33 ± 0.10 -0.06 ± 0.09	21	⁴ BECKER 87B SILI	200 GeV π, K, p	
0.57 ± 0.36 -0.26 ± 0.09	9	BRAUNSCH... 87 TASS	e ⁺ e ⁻ 35-44 GeV	
0.47 ± 0.22 ± 0.05	141	CSORNA 87 CLEO	e ⁺ e ⁻ 10 GeV	
0.35 ± 0.24 -0.18 ± 0.09	17	JUNG 86 HRS	See AVERILL 89	
0.26 ± 0.16 -0.09 ± 0.05	6	USHIDA 86 EMUL	ν wideband	
0.32 ± 0.30 -0.13 ± 0.05	3	BAILEY 84 ACCM	hadron ⁺ Be → φπ ⁺ X	
0.19 ± 0.13 -0.07 ± 0.05	4	USHIDA 83 EMUL	See USHIDA 86	

² BONVICINI 99 obtains 1.19 ± 0.04 for the ratio of D_s^+ to D^0 lifetimes.

³ BARLAG 90C estimates the systematic error to be negligible.

⁴ BECKER 87B estimates the systematic error to be negligible.

D_s^\pm DECAY MODES

Branching fractions for modes with a resonance in the final state include all the decay modes of the resonance. D_s^\pm modes are charge conjugates of the modes below.

Mode	Fraction (Γ_i/Γ)	Scale factor/ Confidence level
Inclusive modes		
Γ_1 K ⁻ anything	(13 ± 14 -12) %	
Γ_2 \bar{K}^0 anything + K ⁰ anything	(39 ± 28) %	
Γ_3 K ⁺ anything	(20 ± 18 -14) %	
Γ_4 non-K \bar{K} anything	(64 ± 17) %	
Γ_5 e ⁺ anything	(8 ± 6 -5) %	
Γ_6 φ anything	(18 ± 15 -10) %	
Leptonic and semileptonic modes		
Γ_7 μ ⁺ ν _μ	(4.6 ± 1.9) × 10 ⁻³	S=1.3
Γ_8 τ ⁺ ν _τ	(7 ± 4) %	
Γ_9 φℓ ⁺ ν _ℓ	[a] (2.0 ± 0.5) %	
Γ_{10} ηℓ ⁺ ν _ℓ + η'(958)ℓ ⁺ ν _ℓ	[a] (3.5 ± 1.0) %	
Γ_{11} ηℓ ⁺ ν _ℓ	(2.6 ± 0.7) %	
Γ_{12} η'(958)ℓ ⁺ ν _ℓ	(8.9 ± 3.4) × 10 ⁻³	
Hadronic modes with a K \bar{K} pair (including from a φ)		
Γ_{13} K ⁺ \bar{K}^0	(3.6 ± 1.1) %	
Γ_{14} K ⁺ K ⁻ π ⁺	[b] (4.4 ± 1.2) %	S=1.1
Γ_{15} φπ ⁺	[c] (3.6 ± 0.9) %	
Γ_{16} K ⁺ $\bar{K}^*(892)^0$	[c] (3.3 ± 0.9) %	
Γ_{17} f ₀ (980)π ⁺	[c] (1.8 ± 0.8) %	S=1.3
Γ_{18} K ⁺ $\bar{K}_0^*(1430)^0$	[c] (7 ± 4) × 10 ⁻³	
Γ_{19} f ₀ (1710)π ⁺ → K ⁺ K ⁻ π ⁺	[d] (1.5 ± 1.9) × 10 ⁻³	
Γ_{20} K ⁺ K ⁻ π ⁺ nonresonant	(9 ± 4) × 10 ⁻³	
Γ_{21} K ⁰ \bar{K}^0 π ⁺	—	
Γ_{22} K [*] (892) ⁺ \bar{K}^0	[c] (4.3 ± 1.4) %	

Meson Particle Listings

 D_s^\pm

Γ_{23}	$K^+ K^- \pi^+ \pi^0$	—	
Γ_{24}	$\phi \pi^+ \pi^0$	[c] (9 ± 5) %	
Γ_{25}	$\phi \rho^+$	[c] (6.7 ± 2.3) %	
Γ_{26}	$\phi \pi^+ \pi^0$ 3-body	[c] < 2.6 %	CL=90%
Γ_{27}	$K^+ K^- \pi^+ \pi^0$ non- ϕ	< 9 %	CL=90%
Γ_{28}	$K^+ \bar{K}^0 \pi^+ \pi^-$	< 2.8 %	CL=90%
Γ_{29}	$K^0 K^- \pi^+ \pi^+$	(4.3 ± 1.5) %	
Γ_{30}	$K^*(892)^+ \bar{K}^*(892)^0$	[c] (5.8 ± 2.5) %	
Γ_{31}	$K^0 K^- \pi^+ \pi^+$ non- $K^* \bar{K}^*$	< 2.9 %	CL=90%
Γ_{32}	$K^+ K^- \pi^+ \pi^+ \pi^-$	(8.3 ± 3.3) × 10 ⁻³	
Γ_{33}	$\phi \pi^+ \pi^+ \pi^-$	[c] (1.18 ± 0.35) %	
Γ_{34}	$K^+ K^- \pi^+ \pi^+ \pi^-$ non- ϕ	(3.0 ± 3.0 / 2.0) × 10 ⁻³	

Hadronic modes without K's

Γ_{35}	$\pi^+ \pi^+ \pi^-$	(1.0 ± 0.4) %	S=1.2
Γ_{36}	$\rho^0 \pi^+$	< 8 × 10 ⁻⁴	CL=90%
Γ_{37}	$f_0(980) \pi^+$	[c] (1.8 ± 0.8) %	S=1.7
Γ_{38}	$f_2(1270) \pi^+$	[c] (2.3 ± 1.3) × 10 ⁻³	
Γ_{39}	$f_0(1500) \pi^+ \rightarrow \pi^+ \pi^- \pi^+$	[e] (2.8 ± 1.6) × 10 ⁻³	
Γ_{40}	$\pi^+ \pi^+ \pi^-$ nonresonant	< 2.8 × 10 ⁻³	CL=90%
Γ_{41}	$\pi^+ \pi^+ \pi^- \pi^0$	< 12 %	CL=90%
Γ_{42}	$\eta \pi^+$	[c] (1.7 ± 0.5) %	
Γ_{43}	$\omega \pi^+$	[c] (2.8 ± 1.1) × 10 ⁻³	
Γ_{44}	$\pi^+ \pi^+ \pi^+ \pi^- \pi^-$	(6.9 ± 3.0) × 10 ⁻³	
Γ_{45}	$\pi^+ \pi^+ \pi^- \pi^0 \pi^0$	—	
Γ_{46}	$\eta \rho^+$	[c] (10.8 ± 3.1) %	
Γ_{47}	$\eta \pi^+ \pi^0$ 3-body	[c] < 4 %	CL=90%
Γ_{48}	$\pi^+ \pi^+ \pi^+ \pi^- \pi^- \pi^0$	(4.9 ± 3.2) %	
Γ_{49}	$\eta'(958) \pi^+$	[c] (3.9 ± 1.0) %	
Γ_{50}	$\pi^+ \pi^+ \pi^+ \pi^- \pi^- \pi^0 \pi^0$	—	
Γ_{51}	$\eta'(958) \rho^+$	[c] (10.1 ± 2.8) %	
Γ_{52}	$\eta'(958) \pi^+ \pi^0$ 3-body	[c] < 1.4 %	CL=90%

Modes with one or three K's

Γ_{53}	$K^0 \pi^+$	< 8 × 10 ⁻³	CL=90%
Γ_{54}	$K^+ \pi^+ \pi^-$	(1.0 ± 0.4) %	
Γ_{55}	$K^+ \rho^0$	< 2.9 × 10 ⁻³	CL=90%
Γ_{56}	$K^*(892)^0 \pi^+$	[c] (6.5 ± 2.8) × 10 ⁻³	
Γ_{57}	$K^+ K^+ K^-$	< 6 × 10 ⁻⁴	CL=90%
Γ_{58}	ϕK^+	[c] < 5 × 10 ⁻⁴	CL=90%

 $\Delta C = 1$ weak neutral current (C1) modes, or Lepton number (L) violating modes

Γ_{59}	$\pi^+ e^+ e^-$	[f] < 2.7 × 10 ⁻⁴	CL=90%
Γ_{60}	$\pi^+ \mu^+ \mu^-$	[f] < 1.4 × 10 ⁻⁴	CL=90%
Γ_{61}	$K^+ e^+ e^-$	C1 < 1.6 × 10 ⁻³	CL=90%
Γ_{62}	$K^+ \mu^+ \mu^-$	C1 < 1.4 × 10 ⁻⁴	CL=90%
Γ_{63}	$K^*(892)^+ \mu^+ \mu^-$	C1 < 1.4 × 10 ⁻³	CL=90%
Γ_{64}	$\pi^+ e^\pm \mu^\mp$	LF [g] < 6.1 × 10 ⁻⁴	CL=90%
Γ_{65}	$K^+ e^\pm \mu^\mp$	LF [g] < 6.3 × 10 ⁻⁴	CL=90%
Γ_{66}	$\pi^- e^+ e^+$	L < 6.9 × 10 ⁻⁴	CL=90%
Γ_{67}	$\pi^- \mu^+ \mu^+$	L < 8.2 × 10 ⁻⁵	CL=90%
Γ_{68}	$\pi^- e^+ \mu^+$	L < 7.3 × 10 ⁻⁴	CL=90%
Γ_{69}	$K^- e^+ e^+$	L < 6.3 × 10 ⁻⁴	CL=90%
Γ_{70}	$K^- \mu^+ \mu^+$	L < 1.8 × 10 ⁻⁴	CL=90%
Γ_{71}	$K^- e^+ \mu^+$	L < 6.8 × 10 ⁻⁴	CL=90%
Γ_{72}	$K^*(892)^- \mu^+ \mu^+$	L < 1.4 × 10 ⁻³	CL=90%
Γ_{73}	A dummy mode used by the fit.	(80 ± 5) %	

- [a] For now, we average together measurements of the $X e^+ \nu_e$ and $X \mu^+ \nu_\mu$ branching fractions. This is the *average*, not the *sum*.
- [b] The branching fraction for this mode may differ from the sum of the submodes that contribute to it, due to interference effects. See the relevant papers.
- [c] This branching fraction includes all the decay modes of the final-state resonance.
- [d] This value includes only $K^+ K^-$ decays of the $f_0(1710)$, because branching fractions of this resonance are not known.
- [e] This value includes only $\pi^+ \pi^-$ decays of the $f_0(1500)$, because branching fractions of this resonance are not known.
- [f] This mode is not a useful test for a $\Delta C=1$ weak neutral current because both quarks must change flavor in this decay.
- [g] The value is for the sum of the charge states or particle/antiparticle states indicated.

CONSTRAINED FIT INFORMATION

An overall fit to 15 branching ratios uses 24 measurements and one constraint to determine 10 parameters. The overall fit has a $\chi^2 = 17.5$ for 15 degrees of freedom.

The following *off-diagonal* array elements are the correlation coefficients $\langle \delta x_i \delta x_j \rangle / (\delta x_i \delta x_j)$, in percent, from the fit to the branching fractions, $x_i \equiv \Gamma_i / \Gamma_{\text{total}}$. The fit constrains the x_i whose labels appear in this array to sum to one.

x_9	58								
x_{11}	50	86							
x_{12}	38	65	56						
x_{14}	52	85	73	55					
x_{15}	57	93	79	60	92				
x_{16}	53	86	74	56	92	93			
x_{35}	47	76	65	50	84	82	81		
x_{37}	30	48	42	32	51	52	50	54	
x_{73}	-59	-93	-84	-64	-95	-96	-94	-86	-64
	x_7	x_9	x_{11}	x_{12}	x_{14}	x_{15}	x_{16}	x_{35}	x_{37}

 D_s^\pm BRANCHING RATIOS

A few older, now obsolete results have been omitted. They may be found in earlier editions.

Inclusive modes

$\Gamma(K^- \text{ anything}) / \Gamma_{\text{total}}$								Γ_1 / Γ
VALUE	DOCUMENT ID	TECN	COMMENT					
$0.13^{+0.14}_{-0.12} \pm 0.02$	COFFMAN	91	MRK3	$e^+ e^-$	4.14	GeV		

$[\Gamma(K^0 \text{ anything}) + \Gamma(K^+ \text{ anything})] / \Gamma_{\text{total}}$								Γ_2 / Γ
VALUE	DOCUMENT ID	TECN	COMMENT					
$0.39^{+0.28}_{-0.27} \pm 0.04$	COFFMAN	91	MRK3	$e^+ e^-$	4.14	GeV		

$\Gamma(K^+ \text{ anything}) / \Gamma_{\text{total}}$								Γ_3 / Γ
VALUE	DOCUMENT ID	TECN	COMMENT					
$0.20^{+0.18}_{-0.13} \pm 0.04$	COFFMAN	91	MRK3	$e^+ e^-$	4.14	GeV		

$\Gamma(\text{non-}K\bar{K} \text{ anything}) / \Gamma_{\text{total}}$								Γ_4 / Γ
VALUE	DOCUMENT ID	TECN	COMMENT					
$0.64 \pm 0.17 \pm 0.03$	⁵ COFFMAN	91	MRK3	$e^+ e^-$	4.14	GeV		

⁵ COFFMAN 91 uses the direct measurements of the kaon content to determine this non- $K\bar{K}$ fraction. This number implies that a large fraction of D_s^\pm decays involve η , η' , and/or non-spectator decays.

$\Gamma(e^+ \text{ anything}) / \Gamma_{\text{total}}$								Γ_5 / Γ
VALUE	CL%	DOCUMENT ID	TECN	COMMENT				
$0.077^{+0.057}_{-0.043} + 0.024_{-0.021}$		BAI	97	BES	$e^+ e^- \rightarrow D_s^+ D_s^-$			

• • • We do not use the following data for averages, fits, limits, etc. • • •

<0.20 90 MRK3 $e^+ e^-$ 4.14 GeV

⁶ Expressed as a value, the BAI 90 result is $\Gamma(e^+ \text{ anything}) / \Gamma_{\text{total}} = 0.05 \pm 0.05 \pm 0.02$.

$\Gamma(\phi \text{ anything}) / \Gamma_{\text{total}}$								Γ_6 / Γ
VALUE	EVT5	DOCUMENT ID	TECN	COMMENT				
$0.178^{+0.151}_{-0.072} + 0.006_{-0.063}$	3	BAI	98	BES	$e^+ e^- \rightarrow D_s^+ D_s^-$			

Leptonic and semileptonic modes

$\Gamma(\mu^+ \nu_\mu) / \Gamma_{\text{total}}$								Γ_7 / Γ
VALUE	EVT5	DOCUMENT ID	TECN	COMMENT				

See the "Note on Pseudoscalar-Meson Decay Constants" in the Listings for the π^\pm .

• • • We do not use the following data for averages, fits, limits, etc. • • •

0.015^{+0.013}_{-0.006} + 0.003_{-0.002} 3 ⁷ BAI 95 BES $e^+ e^- \rightarrow D_s^+ D_s^-$

0.004 + 0.0018 + 0.0020
-0.0014 - 0.0019 8 ⁸ AOKI 93 WA75 π^- emulsion 350 GeV

<0.03 0 ⁹ AUBERT 83 SPEC $\mu^+ \text{ Fe}$, 250 GeV

⁷ BAI 95 uses one actual $D_s^+ \rightarrow \mu^+ \nu_\mu$ event together with two $D_s^+ \rightarrow \tau^+ \nu_\tau$ events and assumes μ - τ universality. This value of $\Gamma(\mu^+ \nu_\mu) / \Gamma_{\text{total}}$ gives a pseudoscalar decay constant of $(430^{+150}_{-130} \pm 40)$ MeV.

⁸ AOKI 93 assumes the ratio of production cross sections of the D_s^+ and D^0 is 0.27. The value of $\Gamma(\mu^+ \nu_\mu) / \Gamma_{\text{total}}$ gives a pseudoscalar decay constant $f_{D_s} = (232 \pm 45 \pm 52)$ MeV.

⁹ AUBERT 83 assume that the D_s^\pm production rate is 20% of total charm production rate.

See key on page 239

Meson Particle Listings

D_s^\pm

$\Gamma(\mu^+ \nu_\mu)/\Gamma(\phi\pi^+)$ Γ_7/Γ_{15}

See the "Note on Pseudoscalar-Meson Decay Constants" in the Listings for the π^\pm .
 VALUE EVTS DOCUMENT ID TECN COMMENT
0.13 ± 0.04 OUR FIT Error includes scale factor of 1.5.
0.173 ± 0.023 ± 0.035 182 10 CHADA 98 CLE2 $e^+e^- \approx \mathcal{T}(45)$

• • • We do not use the following data for averages, fits, limits, etc. • • •
 0.245 ± 0.052 ± 0.074 39 11 ACOSTA 94 CLE2 See CHADA 98
 10 CHADA 98 obtains $f_{D_s} = (280 \pm 19 \pm 28 \pm 34)$ MeV from this measurement, using

$\Gamma(D_s^+ \rightarrow \phi\pi^+)/\Gamma(\text{total}) = 0.036 \pm 0.009$.
 11 ACOSTA 94 obtains $f_{D_s} = (344 \pm 37 \pm 52 \pm 42)$ MeV from this measurement, using

$\Gamma(D_s^+ \rightarrow \phi\pi^+)/\Gamma(\text{total}) = 0.037 \pm 0.009$.

$\Gamma(\mu^+ \nu_\mu)/\Gamma(\phi\ell^+ \nu_\ell)$ Γ_7/Γ_9

See the "Note on Pseudoscalar-Meson Decay Constants" in the Listings for the π^\pm .
 VALUE EVTS DOCUMENT ID TECN COMMENT
0.23 ± 0.08 OUR FIT Error includes scale factor of 1.5.
0.16 ± 0.06 ± 0.03 23 12 KODAMA 96 E653 π^- emulsion, 600 GeV

12 KODAMA 96 obtains $f_{D_s} = (194 \pm 35 \pm 20 \pm 14)$ MeV from this measurement, using

$\Gamma(D_s^+ \rightarrow \phi\ell^+ \nu)/\Gamma_{\text{total}} = 0.0188 \pm 0.0029$. The third error is from the uncertainty on $\phi\ell^+ \nu_\ell$ branching fraction.

$\Gamma(\tau^+ \nu_\tau)/\Gamma_{\text{total}}$ Γ_8/Γ

See the "Note on Pseudoscalar-Meson Decay Constants" in the Listings for the π^\pm .
 VALUE EVTS DOCUMENT ID TECN COMMENT
0.074 ± 0.028 ± 0.024 16 13 ACCIARRI 97F L3 $D_s^{*+} \rightarrow \gamma D_s^+$

13 The second ACCIARRI 97F error here combines in quadrature systematic (0.016) and normalization (0.018) errors. The branching fraction gives $f_{D_s} = (309 \pm 58 \pm 33 \pm 38)$ MeV.

$\Gamma(\phi\ell^+ \nu_\ell)/\Gamma(\phi\pi^+)$ Γ_9/Γ_{15}

For now, we average together measurements of the $\Gamma(\phi e^+ \nu_e)/\Gamma(\phi\pi^+)$ and $\Gamma(\phi\mu^+ \nu_\mu)/\Gamma(\phi\pi^+)$ ratios. See the end of the D_s^+ Listings for measurements of $D_s^+ \rightarrow \phi\ell^+ \nu_\ell$ form-factor ratios.

VALUE EVTS DOCUMENT ID TECN COMMENT
0.56 ± 0.05 OUR FIT
0.54 ± 0.05 OUR AVERAGE

0.54 ± 0.05 ± 0.04 367 14 BUTLER 94 CLE2 $e^+e^- \approx \mathcal{T}(45)$
 0.58 ± 0.17 ± 0.07 97 15 FRABETTI 93G E687 $\gamma\text{Be } \bar{E}_\gamma = 220$ GeV
 0.57 ± 0.15 ± 0.15 104 16 ALBRECHT 91 ARG $e^+e^- \approx 10.4$ GeV
 0.49 ± 0.10 ± 0.10
 -0.14 54 17 ALEXANDER 90B CLEO $e^+e^- 10.5\text{--}11$ GeV

14 BUTLER 94 uses both $\phi e^+ \nu_e$ and $\phi\mu^+ \nu_\mu$ events, and makes a phase-space adjustment to the latter to use them as $\phi e^+ \nu_e$ events.

15 FRABETTI 93G measures the $\Gamma(\phi\mu^+ \nu_\mu)/\Gamma(\phi\pi^+)$ ratio.

16 ALBRECHT 91 measures the $\Gamma(\phi e^+ \nu_e)/\Gamma(\phi\pi^+)$ ratio.

17 ALEXANDER 90B measures an average of the $\Gamma(\phi e^+ \nu_e)/\Gamma(\phi\pi^+)$ and $\Gamma(\phi\mu^+ \nu_\mu)/\Gamma(\phi\pi^+)$ ratios.

$\Gamma(\eta\ell^+ \nu_\ell)/\Gamma(\phi\ell^+ \nu_\ell)$ Γ_{11}/Γ_9

Unseen decay modes of the η and the ϕ are included.
 VALUE EVTS DOCUMENT ID TECN COMMENT
1.27 ± 0.19 OUR FIT
1.24 ± 0.12 ± 0.15 440 18 BRANDENB... 95 CLE2 $e^+e^- \approx \mathcal{T}(45)$

18 BRANDENBURG 95 uses both e^+ and μ^+ events and makes a phase-space adjustment to use the μ^+ events as e^+ events.

$\Gamma(\eta'(958)\ell^+ \nu_\ell)/\Gamma(\phi\ell^+ \nu_\ell)$ Γ_{12}/Γ_9

Unseen decay modes of the resonances are included.
 VALUE CL% EVTS DOCUMENT ID TECN COMMENT
0.44 ± 0.13 OUR FIT
0.43 ± 0.11 ± 0.07 29 19 BRANDENB... 95 CLE2 $e^+e^- \approx \mathcal{T}(45)$

• • • We do not use the following data for averages, fits, limits, etc. • • •
 <1.6 90 20 KODAMA 93B E653 π^- emulsion 600 GeV

19 BRANDENBURG 95 uses both e^+ and μ^+ events and makes a phase-space adjustment to use the μ^+ events as e^+ events.

20 KODAMA 93B uses μ^+ events.

$[\Gamma(\eta\ell^+ \nu_\ell) + \Gamma(\eta'(958)\ell^+ \nu_\ell)]/\Gamma(\phi\ell^+ \nu_\ell)$ $\Gamma_{10}/\Gamma_9 = (\Gamma_{11} + \Gamma_{12})/\Gamma_9$

Unseen decay modes of the resonances are included.
 VALUE EVTS DOCUMENT ID TECN COMMENT
1.72 ± 0.23 OUR FIT
3.9 ± 1.6 13 21 KODAMA 93 E653 π^- emulsion 600 GeV

• • • We do not use the following data for averages, fits, limits, etc. • • •
 1.67 ± 0.17 ± 0.17 22 BRANDENB... 95 CLE2 $e^+e^- \approx \mathcal{T}(45)$

21 KODAMA 93 uses μ^+ events.

22 This BRANDENBURG 95 data is redundant with data in previous blocks.

Hadronic modes with a $K\bar{K}$ pair. Γ_{13}/Γ_{15}

$\Gamma(K^+ \bar{K}^0)/\Gamma(\phi\pi^+)$ Γ_{13}/Γ_{15}
 VALUE EVTS DOCUMENT ID TECN COMMENT
1.01 ± 0.16 OUR AVERAGE

1.15 ± 0.31 ± 0.19 68 ANJOS 90C E691 γBe
 0.92 ± 0.32 ± 0.20 89B MRK3 $e^+e^- 4.14$ GeV
 0.99 ± 0.17 ± 0.10 CHEN 89 CLEO $e^+e^- 10$ GeV

$\Gamma(\phi\pi^+)/\Gamma_{\text{total}}$ Γ_{15}/Γ

We now have model-independent measurements of this branching fraction, and so we no longer use the earlier, model-dependent results.

VALUE CL% EVTS DOCUMENT ID TECN COMMENT
0.036 ± 0.009 OUR FIT
0.036 ± 0.009 OUR AVERAGE

0.0359 ± 0.0077 ± 0.0048 23 ARTUSO 96 CLE2 e^+e^- at $\mathcal{T}(45)$
 0.039 + 0.051 + 0.018 24 BAI 95C BES $e^+e^- 4.03$ GeV
 -0.019 -0.011

• • • We do not use the following data for averages, fits, limits, etc. • • •
 0.051 ± 0.004 ± 0.008 25 BUTLER 94 CLE2 $e^+e^- \approx \mathcal{T}(45)$
 <0.048 90 MUHEIM 94

0.046 ± 0.015 26 MUHEIM 94
 0.031 ± 0.009 26 MUHEIM 94
 0.031 ± 0.009 ± 0.006 25 FRABETTI 93G E687 $\gamma\text{Be } \bar{E}_\gamma = 220$ GeV

0.024 ± 0.010 25 ALBRECHT 91 ARG $e^+e^- \approx 10.4$ GeV
 <0.041 90 24 ADLER 90B MRK3 $e^+e^- 35\text{--}44$ GeV

0.031 ± 0.006 + 0.011 - 0.009 25 ALEXANDER 90B CLEO $e^+e^- 10.5\text{--}11$ GeV
 0.048 ± 0.017 ± 0.019 27 ALVAREZ 90C NA14 Photoproduction
 >0.034 90 25 ANJOS 90B E691 $\gamma\text{Be}, \bar{E}_\gamma \approx 145$ GeV

0.02 ± 0.01 405 28 CHEN 89 CLEO $e^+e^- 10$ GeV
 0.033 ± 0.016 ± 0.010 9 28 BRAUNSCH... 87 TASS $e^+e^- 35\text{--}44$ GeV
 0.033 ± 0.011 30 28 DERRICK 85B HRS $e^+e^- 29$ GeV

23 ARTUSO 96 uses partially reconstructed $\bar{B}^0 \rightarrow D^{*+} D_s^{*-}$ decays to get a model-independent value for $\Gamma(D_s^+ \rightarrow \phi\pi^+)/\Gamma(D^0 \rightarrow K^-\pi^+)$ of $0.92 \pm 0.20 \pm 0.11$.

24 BAI 95C uses $e^+e^- \rightarrow D_s^+ D_s^-$ events in which one or both of the D_s^\pm are observed to obtain the first model-independent measurement of the $D_s^+ \rightarrow \phi\pi^+$ branching fraction, without assumptions about $\sigma(D_s^\pm)$. However, with only two "doubly-tagged" events, the statistical error is too large for the result to be competitive with indirect measurements. ADLER 90B used the same method to set a limit.

25 BUTLER 94, FRABETTI 93G, ALBRECHT 91, ALEXANDER 90B, and ANJOS 90B measure the ratio $\Gamma(D_s^+ \rightarrow \phi\ell^+ \nu_\ell)/\Gamma(D_s^+ \rightarrow \phi\pi^+)$, where $\ell = e$ and/or μ , and then use a theoretical calculation of the ratio of widths $\Gamma(D_s^+ \rightarrow \phi\ell^+ \nu_\ell)/\Gamma(D^+ \rightarrow \bar{K}^0 \ell^+ \nu)$. Not everyone uses the same value for this ratio.

26 The two MUHEIM 94 values here are model-dependent calculations based on distinct data sets. The first uses measurements of the $D_2^{*+}(2460)^0$ and $D_{s1}(2536)^+$, the second uses B -decay factorization and $\Gamma(D_s^+ \rightarrow \mu^+ \nu_\mu)/\Gamma(D_s^+ \rightarrow \phi\ell^+ \nu_\ell)$. A third calculation using the semileptonic width of $D_s^+ \rightarrow \phi\ell^+ \nu_\ell$ is not independent of other results listed here. Note also the upper limit, based on the sum of established D_s^+ branching ratios.

27 ALVAREZ 90C relies on the Lund model to estimate the ratio of D_s^+ to D^+ cross sections.

28 Values based on crude estimates of the D_s^\pm production level. DERRICK 85B errors are statistical only.

$\Gamma(\phi\pi^+)/\Gamma(K^+ K^- \pi^+)$ Γ_{15}/Γ_{14}

Unseen decay modes of the ϕ are included.
 VALUE EVTS DOCUMENT ID TECN COMMENT
0.82 ± 0.08 OUR FIT
0.807 ± 0.067 ± 0.096 FRABETTI 95B E687 Dalitz plot analysis

$\Gamma(K^+ \bar{K}^*(892)^0)/\Gamma(K^+ K^- \pi^+)$ Γ_{16}/Γ_{14}

Unseen decay modes of the $\bar{K}^*(892)^0$ are included.
 VALUE EVTS DOCUMENT ID TECN COMMENT
0.75 ± 0.07 OUR FIT
0.717 ± 0.069 ± 0.060 FRABETTI 95B E687 Dalitz plot analysis

$\Gamma(K^+ \bar{K}^*(892)^0)/\Gamma(\phi\pi^+)$ Γ_{16}/Γ_{15}

Unseen decay modes of the resonances are included.
 VALUE EVTS DOCUMENT ID TECN COMMENT
0.92 ± 0.09 OUR FIT
0.95 ± 0.10 OUR AVERAGE

0.85 ± 0.34 ± 0.20 9 ALVAREZ 90C NA14 Photoproduction
 0.84 ± 0.30 ± 0.22 ADLER 89B MRK3 $e^+e^- 4.14$ GeV
 1.05 ± 0.17 ± 0.12 CHEN 89 CLEO $e^+e^- 10$ GeV
 0.87 ± 0.13 ± 0.05 117 ANJOS 88 E691 Photoproduction
 1.44 ± 0.37 87 ALBRECHT 87F ARG $e^+e^- 10$ GeV

$\Gamma(f_0(980)\pi^+)/\Gamma(K^+ K^- \pi^+)$ Γ_{37}/Γ_{14}

Unseen decay modes of the $f_0(980)$ are included.
 VALUE EVTS DOCUMENT ID TECN COMMENT
0.40 ± 0.16 OUR FIT Error includes scale factor of 2.3.
1.00 ± 0.32 ± 0.24 FRABETTI 95B E687 Dalitz plot analysis

See key on page 239

Meson Particle Listings

 D_5^\pm

$\Gamma(\omega\pi^+)/\Gamma(\eta\pi^+)$				Γ_{43}/Γ_{42}
VALUE	DOCUMENT ID	TECN	COMMENT	
$0.16 \pm 0.04 \pm 0.03$	BALEST	97	CLE2	$e^+e^- \approx \Upsilon(4S)$

$\Gamma(\pi^+\pi^+\pi^-\pi^-)/\Gamma(K^+K^-\pi^+)$				Γ_{44}/Γ_{14}
VALUE	EVTs	DOCUMENT ID	TECN	COMMENT
$0.158 \pm 0.042 \pm 0.031$	37	FRABETTI	97C E687	$\gamma\text{Be}, \bar{E}_\gamma \approx 200 \text{ GeV}$

$\Gamma(\pi^+\pi^+\pi^-\pi^-)/\Gamma(\phi\pi^+)$				Γ_{44}/Γ_{15}
VALUE	CL%	DOCUMENT ID	TECN	COMMENT
<0.29	90	ANJOS	89 E691	Photoproduction

• • • We do not use the following data for averages, fits, limits, etc. • • •

$\Gamma(\eta\rho^+)/\Gamma(\phi\pi^+)$				Γ_{46}/Γ_{15}
Unseen decay modes of the resonances are included.				
VALUE	EVTs	DOCUMENT ID	TECN	COMMENT
$2.90 \pm 0.20 \pm 0.39$	447	JESSOP	98 CLE2	$e^+e^- \approx \Upsilon(4S)$
$2.86 \pm 0.38^{+0.36}_{-0.38}$	217	AVERY	92 CLE2	See JESSOP 98

• • • We do not use the following data for averages, fits, limits, etc. • • •

$\Gamma(\eta\pi^+\pi^0\text{-body})/\Gamma(\phi\pi^+)$				Γ_{47}/Γ_{15}
Unseen decay modes of the resonances are included.				
VALUE	CL%	DOCUMENT ID	TECN	COMMENT
<1.1	90	JESSOP	98 CLE2	$e^+e^- \approx \Upsilon(4S)$
<0.82	90	32 DAOUDI	92 CLE2	See JESSOP 98

• • • We do not use the following data for averages, fits, limits, etc. • • •

32 We use the JESSOP 98 limit, even though the DAOUDI 92 limit, from the same experiment but with a much smaller data sample, is more restrictive.

$\Gamma(\pi^+\pi^+\pi^-\pi^-\pi^0)/\Gamma_{\text{total}}$				Γ_{48}/Γ
VALUE	DOCUMENT ID	TECN	COMMENT	
$0.049^{+0.033}_{-0.030}$	BARLAG	92C ACCM	π^-	230 GeV

$\Gamma(\eta'(958)\pi^+)/\Gamma(\phi\pi^+)$				Γ_{49}/Γ_{15}	
Unseen decay modes of the resonances are included.					
VALUE	CL%	EVTs	DOCUMENT ID	TECN	COMMENT
1.00 ± 0.09 OUR AVERAGE					
$1.03 \pm 0.06 \pm 0.07$	537	JESSOP	98 CLE2	$e^+e^- \approx \Upsilon(4S)$	
$2.5 \pm 1.0^{+1.5}_{-0.4}$	22	ALVAREZ	91 NA14	Photoproduction	
$2.5 \pm 0.5 \pm 0.3$	215	ALBRECHT	90D ARG	$e^+e^- \approx 10.4 \text{ GeV}$	
$1.20 \pm 0.15 \pm 0.11$	281	ALEXANDER	92 CLE2	See JESSOP 98	
<1.3	90	ANJOS	91B E691	$\gamma\text{Be}, \bar{E}_\gamma \approx 145 \text{ GeV}$	

• • • We do not use the following data for averages, fits, limits, etc. • • •

$\Gamma(\eta'(958)\rho^+)/\Gamma(\phi\pi^+)$				Γ_{51}/Γ_{15}
Unseen decay modes of the resonances are included.				
VALUE	EVTs	DOCUMENT ID	TECN	COMMENT
$2.78 \pm 0.28 \pm 0.30$	137	JESSOP	98 CLE2	$e^+e^- \approx \Upsilon(4S)$
$3.44 \pm 0.62^{+0.44}_{-0.46}$	68	AVERY	92 CLE2	See JESSOP 98

• • • We do not use the following data for averages, fits, limits, etc. • • •

$\Gamma(\eta'(958)\pi^+\pi^0\text{-body})/\Gamma(\phi\pi^+)$				Γ_{52}/Γ_{15}
Unseen decay modes of the resonances are included.				
VALUE	CL%	DOCUMENT ID	TECN	COMMENT
<0.4	90	JESSOP	98 CLE2	$e^+e^- \approx \Upsilon(4S)$
<0.85	90	DAOUDI	92 CLE2	See JESSOP 98

Modes with one or three K's

$\Gamma(K^0\pi^+)/\Gamma(\phi\pi^+)$				Γ_{53}/Γ_{15}
VALUE	CL%	DOCUMENT ID	TECN	COMMENT
<0.21	90	ADLER	89B MRK3	$e^+e^- 4.14 \text{ GeV}$

$\Gamma(K^0\pi^+)/\Gamma(K^+K^0)$				Γ_{53}/Γ_{13}
VALUE	CL%	DOCUMENT ID	TECN	COMMENT
<0.53	90	FRABETTI	95 E687	$\gamma\text{Be}, \bar{E}_\gamma \approx 200 \text{ GeV}$

• • • We do not use the following data for averages, fits, limits, etc. • • •

$\Gamma(K^+\pi^-\pi^-)/\Gamma(\phi\pi^+)$				Γ_{54}/Γ_{15}
VALUE	EVTs	DOCUMENT ID	TECN	COMMENT
$0.28 \pm 0.06 \pm 0.05$	85	FRABETTI	95E E687	$\gamma\text{Be}, \bar{E}_\gamma \approx 220 \text{ GeV}$

$\Gamma(K^+\rho^0)/\Gamma(\phi\pi^+)$				Γ_{55}/Γ_{15}
VALUE	CL%	DOCUMENT ID	TECN	COMMENT
<0.08	90	FRABETTI	95E E687	$\gamma\text{Be}, \bar{E}_\gamma \approx 220 \text{ GeV}$

$\Gamma(K^*(892)^0\pi^+)/\Gamma(\phi\pi^+)$				Γ_{56}/Γ_{15}
Unseen decay modes of the resonances are included.				
VALUE	EVTs	DOCUMENT ID	TECN	COMMENT
$0.18 \pm 0.05 \pm 0.04$	25	FRABETTI	95E E687	$\gamma\text{Be}, \bar{E}_\gamma \approx 220 \text{ GeV}$

$\Gamma(K^+K^+K^-)/\Gamma(\phi\pi^+)$				Γ_{57}/Γ_{15}
VALUE	CL%	DOCUMENT ID	TECN	COMMENT
<0.016	90	FRABETTI	95F E687	$\gamma\text{Be}, \bar{E}_\gamma \approx 220 \text{ GeV}$

$\Gamma(\phi K^+)/\Gamma(\phi\pi^+)$				Γ_{58}/Γ_{15}
VALUE	CL%	DOCUMENT ID	TECN	COMMENT
<0.013	90	FRABETTI	95F E687	$\gamma\text{Be}, \bar{E}_\gamma \approx 220 \text{ GeV}$
<0.071	90	ANJOS	92D E691	$\gamma\text{Be}, \bar{E}_\gamma \approx 145 \text{ GeV}$

• • • We do not use the following data for averages, fits, limits, etc. • • •

Rare or forbidden modes

$\Gamma(\pi^+e^+e^-)/\Gamma_{\text{total}}$				Γ_{59}/Γ
This mode is not a useful test for a $\Delta C=1$ weak neutral current because both quarks must change flavor in this decay.				
VALUE	CL%	DOCUMENT ID	TECN	COMMENT
$<2.7 \times 10^{-4}$	90	AITALA	99G E791	$\pi^- N 500 \text{ GeV}$

$\Gamma(\pi^+\mu^+\mu^-)/\Gamma_{\text{total}}$				Γ_{60}/Γ	
This mode is not a useful test for a $\Delta C=1$ weak neutral current because both quarks must change flavor in this decay.					
VALUE	CL%	EVTs	DOCUMENT ID	TECN	COMMENT
$<1.4 \times 10^{-4}$	90		AITALA	99G E791	$\pi^- N 500 \text{ GeV}$
$<4.3 \times 10^{-4}$	90	0	KODAMA	95 E653	π^- emulsion 600 GeV

• • • We do not use the following data for averages, fits, limits, etc. • • •

$\Gamma(K^+e^+e^-)/\Gamma_{\text{total}}$				Γ_{61}/Γ
A test for the $\Delta C=1$ weak neutral current. Allowed by higher-order electroweak interactions.				
VALUE	CL%	DOCUMENT ID	TECN	COMMENT
$<1.6 \times 10^{-3}$	90	AITALA	99G E791	$\pi^- N 500 \text{ GeV}$

$\Gamma(K^+\mu^+\mu^-)/\Gamma_{\text{total}}$				Γ_{62}/Γ	
A test for the $\Delta C=1$ weak neutral current. Allowed by higher-order electroweak interactions.					
VALUE	CL%	EVTs	DOCUMENT ID	TECN	COMMENT
$<1.4 \times 10^{-4}$	90		AITALA	99G E791	$\pi^- N 500 \text{ GeV}$
$<5.9 \times 10^{-4}$	90	0	KODAMA	95 E653	π^- emulsion 600 GeV

• • • We do not use the following data for averages, fits, limits, etc. • • •

$\Gamma(K^*(892)^+\mu^+\mu^-)/\Gamma_{\text{total}}$				Γ_{63}/Γ	
A test for the $\Delta C=1$ weak neutral current. Allowed by higher-order electroweak interactions.					
VALUE	CL%	EVTs	DOCUMENT ID	TECN	COMMENT
$<1.4 \times 10^{-3}$	90	0	KODAMA	95 E653	π^- emulsion 600 GeV

$\Gamma(\pi^+e^\pm\mu^\mp)/\Gamma_{\text{total}}$				Γ_{64}/Γ
A test of lepton-family-number conservation.				
VALUE	CL%	DOCUMENT ID	TECN	COMMENT
$<6.1 \times 10^{-4}$	90	AITALA	99G E791	$\pi^- N 500 \text{ GeV}$

$\Gamma(K^+e^\pm\mu^\mp)/\Gamma_{\text{total}}$				Γ_{65}/Γ
A test of lepton-family-number conservation.				
VALUE	CL%	DOCUMENT ID	TECN	COMMENT
$<6.3 \times 10^{-4}$	90	AITALA	99G E791	$\pi^- N 500 \text{ GeV}$

$\Gamma(\pi^-e^+e^+)/\Gamma_{\text{total}}$				Γ_{66}/Γ
A test of lepton-number conservation.				
VALUE	CL%	DOCUMENT ID	TECN	COMMENT
$<6.9 \times 10^{-4}$	90	AITALA	99G E791	$\pi^- N 500 \text{ GeV}$

$\Gamma(\pi^-\mu^+\mu^+)/\Gamma_{\text{total}}$				Γ_{67}/Γ	
A test of lepton-number conservation.					
VALUE	CL%	EVTs	DOCUMENT ID	TECN	COMMENT
$<8.2 \times 10^{-5}$	90		AITALA	99G E791	$\pi^- N 500 \text{ GeV}$
$<4.3 \times 10^{-4}$	90	0	KODAMA	95 E653	π^- emulsion 600 GeV

• • • We do not use the following data for averages, fits, limits, etc. • • •

$\Gamma(\pi^-e^+\mu^+)/\Gamma_{\text{total}}$				Γ_{68}/Γ
A test of lepton-number conservation.				
VALUE	CL%	DOCUMENT ID	TECN	COMMENT
$<7.3 \times 10^{-4}$	90	AITALA	99G E791	$\pi^- N 500 \text{ GeV}$

$\Gamma(K^-e^+e^+)/\Gamma_{\text{total}}$				Γ_{69}/Γ
A test of lepton-number conservation.				
VALUE	CL%	DOCUMENT ID	TECN	COMMENT
$<6.3 \times 10^{-4}$	90	AITALA	99G E791	$\pi^- N 500 \text{ GeV}$

$\Gamma(K^-\mu^+\mu^+)/\Gamma_{\text{total}}$				Γ_{70}/Γ	
A test of lepton-number conservation.					
VALUE	CL%	EVTs	DOCUMENT ID	TECN	COMMENT
$<1.8 \times 10^{-4}$	90		AITALA	99G E791	$\pi^- N 500 \text{ GeV}$
$<5.9 \times 10^{-4}$	90	0	KODAMA	95 E653	π^- emulsion 600 GeV

• • • We do not use the following data for averages, fits, limits, etc. • • •

Meson Particle Listings

$D_s^\pm, D_s^{*\pm}$

$\Gamma(K^- e^+ \mu^+)/\Gamma_{total}$
A test of lepton-number conservation. $\Gamma_{\tau 1}/\Gamma$

VALUE	CL%	DOCUMENT ID	TECN	COMMENT
$< 6.8 \times 10^{-4}$	90	AITALA	99G E791	$\pi^- N 500 \text{ GeV}$

$\Gamma(K^*(892)^- \mu^+ \mu^+)/\Gamma_{total}$
A test of lepton-number conservation. $\Gamma_{\tau 2}/\Gamma$

VALUE	CL%	EVTS	DOCUMENT ID	TECN	COMMENT
$< 1.4 \times 10^{-3}$	90	0	KODAMA	95 E653	$\pi^- \text{ emulsion } 600 \text{ GeV}$

$D_s^+ \rightarrow \phi \ell^+ \nu_\ell$ FORM FACTORS

$f_{\nu_\ell} \equiv A_2(0)/A_1(0)$ in $D_s^+ \rightarrow \phi \ell^+ \nu_\ell$

VALUE	EVTS	DOCUMENT ID	TECN	COMMENT
1.60 ± 0.24 OUR AVERAGE				
1.57 ± 0.25 ± 0.19	271	AITALA	99D E791	$\phi e^+ \nu_e, \phi \mu^+ \nu_\mu$
1.4 ± 0.5 ± 0.3	308	AVERY	94B CLE2	$\phi e^+ \nu_e$
1.1 ± 0.8 ± 0.1	90	FRABETTI	94F E687	$\phi \mu^+ \nu_\mu$
2.1 $\begin{smallmatrix} +0.6 \\ -0.5 \end{smallmatrix}$ ± 0.2	19	KODAMA	93 E653	$\phi \mu^+ \nu_\mu$

$r_\nu \equiv V(0)/A_1(0)$ in $D_s^+ \rightarrow \phi \ell^+ \nu_\ell$

VALUE	EVTS	DOCUMENT ID	TECN	COMMENT
1.92 ± 0.32 OUR AVERAGE				
2.27 ± 0.35 ± 0.22	271	AITALA	99D E791	$\phi e^+ \nu_e, \phi \mu^+ \nu_\mu$
0.9 ± 0.6 ± 0.3	308	AVERY	94B CLE2	$\phi e^+ \nu_e$
1.8 ± 0.9 ± 0.2	90	FRABETTI	94F E687	$\phi \mu^+ \nu_\mu$
2.3 $\begin{smallmatrix} +1.1 \\ -0.9 \end{smallmatrix}$ ± 0.4	19	KODAMA	93 E653	$\phi \mu^+ \nu_\mu$

Γ_L/Γ_T in $D_s^+ \rightarrow \phi \ell^+ \nu_\ell$

VALUE	EVTS	DOCUMENT ID	TECN	COMMENT
0.72 ± 0.18 OUR AVERAGE				
1.0 ± 0.3 ± 0.2	308	AVERY	94B CLE2	$\phi e^+ \nu_e$
1.0 ± 0.5 ± 0.1	90	³³ FRABETTI	94F E687	$\phi \mu^+ \nu_\mu$
0.54 ± 0.21 ± 0.10	19	³³ KODAMA	93 E653	$\phi \mu^+ \nu_\mu$

³³FRABETTI 94F and KODAMA 93 evaluate Γ_L/Γ_T for a lepton mass of zero.

D_s^\pm REFERENCES

AITALA 99 PL B445 449 E.M. Aitala et al. (FNAL E791 Collab.)
 AITALA 99D PL B450 294 E.M. Aitala et al. (FNAL E791 Collab.)
 AITALA 99G PL B462 401 E.M. Aitala et al. (FNAL E791 Collab.)
 BONVICINI 99 PRL 82 4586 G. Bonvicini et al. (CLEO Collab.)
 BAI 98 PR D57 28 J.Z. Bai et al. (BEPAC BES Collab.)
 CHADA 98 PR D58 032002 M. Chada et al. (CLEO Collab.)
 JESSOP 98 PR D58 052002 C.P. Jessop et al. (CLEO Collab.)
 ACCIARRI 97F PL B396 327 M. Acciarri et al. (L3 Collab.)
 BAI 97 PR D56 3779 J.Z. Bai et al. (BEPAC BES Collab.)
 BALEST 97 PRL 79 1436 R. Balest et al. (CLEO Collab.)
 FRABETTI 97C PL B401 131 P.L. Frabetti et al. (FNAL E687 Collab.)
 FRABETTI 97D PL B407 79 P.L. Frabetti et al. (FNAL E687 Collab.)
 ARTUSO 96 PL B378 364 M. Artuso et al. (CLEO Collab.)
 KODAMA 96 PL B382 299 K. Kodama et al. (FNAL E553 Collab.)
 BAI 95C PRL 74 4599 J.Z. Bai et al. (BES Collab.)
 BAI 95C PR D52 3781 J.Z. Bai et al. (BES Collab.)
 BRANDENB... 95 PRL 75 3804 G.W. Brandenburg et al. (CLEO Collab.)
 FRABETTI 95 PL B346 199 P.L. Frabetti et al. (FNAL E687 Collab.)
 FRABETTI 95B PL B351 591 P.L. Frabetti et al. (FNAL E687 Collab.)
 FRABETTI 95E PL B359 403 P.L. Frabetti et al. (FNAL E687 Collab.)
 FRABETTI 95F PL B363 259 P.L. Frabetti et al. (FNAL E687 Collab.)
 KODAMA 95 PL B345 85 K. Kodama et al. (FNAL E553 Collab.)
 ACOSTA 94 PR D49 5690 D. Acosta et al. (CLEO Collab.)
 AVERY 94B PL B337 405 P. Avery et al. (CLEO Collab.)
 BROWN 94 PR D50 1884 D. Brown et al. (CLEO Collab.)
 BUTLER 94 PL B324 255 F. Butler et al. (CLEO Collab.)
 FRABETTI 94F PL B328 187 P.L. Frabetti et al. (FNAL E687 Collab.)
 MUHEIM 94 PR D49 3767 F. Muheim, S. Stone (SYRA)
 ADAMOVI... 93 PL B305 177 M.I. Adamovich et al. (CERN WA82 Collab.)
 AOKI 93 PTP 89 131 S. Aoki et al. (CERN WA75 Collab.)
 FRABETTI 93F PRL 71 827 P.L. Frabetti et al. (FNAL E687 Collab.)
 FRABETTI 93G PL B313 253 P.L. Frabetti et al. (FNAL E687 Collab.)
 KODAMA 93 PL B309 483 K. Kodama et al. (FNAL E553 Collab.)
 KODAMA 93B PL B313 260 K. Kodama et al. (FNAL E553 Collab.)
 ALBRECHT 92B ZPHY C53 361 H. Albrecht et al. (ARGUS Collab.)
 ALEXANDER 92 PRL 68 1275 J. Alexander et al. (CLEO Collab.)
 ANJOS 92D PRL 69 2892 J.C. Anjos et al. (FNAL E691 Collab.)
 AVERY 92 PRL 68 1279 P. Avery et al. (CLEO Collab.)
 BARLAG 92C ZPHY C55 383 S. Barlag et al. (ACCMOR Collab.)
 Also 90D ZPHY C48 29 S. Barlag et al. (ACCMOR Collab.)
 DAUDI 92 PR D45 3965 M. Daouidi et al. (CLEO Collab.)
 FRABETTI 92 PL B281 167 P.L. Frabetti et al. (FNAL E687 Collab.)
 ALBRECHT 91 PL B255 634 H. Albrecht et al. (ARGUS Collab.)
 ALVAREZ 91 PL B255 639 M.P. Alvarez et al. (CERN NA14/2 Collab.)
 ANJOS 91B PR D43 R2063 J.C. Anjos et al. (FNAL E691 Collab.)
 COFFMAN 91 PL B263 135 D.M. Coffman et al. (Mark III Collab.)
 ADLER 90B PRL 64 169 J.C. Adler et al. (Mark III Collab.)
 ALBRECHT 90D PL B245 315 H. Albrecht et al. (ARGUS Collab.)
 ALEXANDER 90B PRL 65 1531 J. Alexander et al. (CLEO Collab.)
 ALVAREZ 90 ZPHY C47 539 M.P. Alvarez et al. (CERN NA14/2 Collab.)
 ALVAREZ 90C PL B246 261 M.P. Alvarez et al. (CERN NA14/2 Collab.)
 ANJOS 90B PRL 64 2885 J.C. Anjos et al. (FNAL E691 Collab.)
 ANJOS 90C PR D41 2705 J.C. Anjos et al. (FNAL E691 Collab.)
 BAI 90 PRL 65 686 Z. Bai et al. (Mark III Collab.)
 BARLAG 90C ZPHY C46 563 S. Barlag et al. (ACCMOR Collab.)

FRABETTI 90 PL B251 639 P.L. Frabetti et al. (FNAL E687 Collab.)
 ADLER 89B PRL 63 1211 J. Adler et al. (Mark III Collab.)
 Also 89D PRL 63 2858 erratum
 ANJOS 89P PRL 62 125 J.C. Anjos et al. (FNAL E691 Collab.)
 ANJOS 89E PL B223 267 J.C. Anjos et al. (FNAL E691 Collab.)
 AVERILL 89 PR D39 123 D.A. Averill et al. (HRS Collab.)
 CHEN 89 PL B226 192 W.Y. Chen et al. (CLEO Collab.)
 ALBRECHT 88 PL B207 349 H. Albrecht et al. (ARGUS Collab.)
 ALBRECHT 88I PL B210 267 H. Albrecht et al. (ARGUS Collab.)
 ANJOS 88 PRL 60 897 J.C. Anjos et al. (FNAL E691 Collab.)
 RAAB 88 PR D37 2391 J.R. Raab et al. (FNAL E691 Collab.)
 ALBRECHT 87F PL B179 398 H. Albrecht et al. (ARGUS Collab.)
 ALBRECHT 87G PL B195 102 H. Albrecht et al. (ARGUS Collab.)
 ANJOS 87B PRL 58 1818 J.C. Anjos et al. (FNAL E691 Collab.)
 BECKER 87B PL B184 277 H. Becker et al. (NA11 and NA32 Collab.)
 BLAYLOCK 87 PRL 58 2171 G.T. Blaylock et al. (Mark III Collab.)
 BRAUNSC... 87 ZPHY C35 317 W. Braunschweig et al. (TASSO Collab.)
 CSORNA 87 PL B191 318 S.E. Csorna et al. (CLEO Collab.)
 JUNG 86 PRL 56 1775 C. Jung et al. (HRS Collab.)
 USHIDA 86 PRL 56 1767 N. Ushida et al. (FNAL E531 Collab.)
 ALBRECHT 85D PL B138 343 H. Albrecht et al. (ARGUS Collab.)
 DERRICK 85B PRL 54 2568 M. Derrick et al. (HRS Collab.)
 AIHARA 84D PRL 53 2465 H. Aihara et al. (TPC Collab.)
 ALTHOFF 84 PL B136B 130 M. Althoff et al. (TASSO Collab.)
 BAILEY 84 PL B139B 320 R. Bailey et al. (ACCMOR Collab.)
 AUBERT 83C NP B213 31 J.J. Aubert et al. (EMC Collab.)
 CHEN 83C PRL 51 634 A. Chen et al. (CLEO Collab.)
 USHIDA 83 PRL 51 2362 N. Ushida et al. (FNAL E53 Collab.)

OTHER RELATED PAPERS

RICHMAN	95	RMP 67 893	J.D. Richman, P.R. Burchat	(UCSB, STAN)
---------	----	------------	----------------------------	--------------

$D_s^{*\pm}$

$I(J^P) = 0(??)$

J^P is natural, width and decay modes consistent with 1^- .

$D_s^{*\pm}$ MASS

The fit includes $D_s^\pm, D_s^0, D_s^{*\pm}, D^{*0}$, and $D_s^{*\pm}$ mass and mass difference measurements.

VALUE (MeV)	EVTS	DOCUMENT ID	TECN	COMMENT
2112.4 ± 0.7 OUR FIT				Error includes scale factor of 1.1.
2106.6 ± 2.1 ± 2.7	¹ 87	BLAYLOCK	MRK3	$e^+ e^- \rightarrow D_s^{*\pm} \gamma X$

¹ Assuming D_s^\pm mass = 1968.7 ± 0.9 MeV.

$m_{D_s^{*\pm}} - m_{D_s^\pm}$

The fit includes $D_s^\pm, D_s^0, D_s^{*\pm}, D^{*0}$, and $D_s^{*\pm}$ mass and mass difference measurements.

VALUE (MeV)	EVTS	DOCUMENT ID	TECN	COMMENT
143.8 ± 0.4 OUR FIT				
143.9 ± 0.4 OUR AVERAGE				
143.76 ± 0.39 ± 0.40	95	GRONBERG	CLE2	$e^+ e^-$
144.22 ± 0.47 ± 0.37	94	BROWN	CLE2	$e^+ e^-$
142.5 ± 0.8 ± 1.5	² 88	ALBRECHT	ARG	$e^+ e^- \rightarrow D_s^{*\pm} \gamma X$
139.5 ± 8.3 ± 9.7	60	AIHARA	84D TPC	$e^+ e^- \rightarrow \text{hadrons}$

• • • We do not use the following data for averages, fits, limits, etc. • • •

143.0 ± 18.0	8	ASRATYAN	85 HLBC	FNAL 15-ft, $\nu^- 2\text{H}$
110 ± 46		BRANDELIK	79 DASP	$e^+ e^- \rightarrow D_s^{*\pm} \gamma X$

² Result includes data of ALBRECHT 84B.

$D_s^{*\pm}$ WIDTH

VALUE (MeV)	CL%	DOCUMENT ID	TECN	COMMENT
< 1.9	90	GRONBERG	95 CLE2	$e^+ e^-$
< 4.5	90	ALBRECHT	88 ARG	$E_{cm}^{eff} = 10.2 \text{ GeV}$

• • • We do not use the following data for averages, fits, limits, etc. • • •

< 4.9	90	BROWN	94 CLE2	$e^+ e^-$
< 22	90	BLAYLOCK	87 MRK3	$e^+ e^- \rightarrow D_s^{*\pm} \gamma X$

$D_s^{*\pm}$ DECAY MODES

$D_s^{*\pm}$ modes are charge conjugates of the modes below.

Mode	Fraction (Γ_i/Γ)
$\Gamma_1 D_s^+ \gamma$	(94.2 ± 2.5) %
$\Gamma_2 D_s^+ \pi^0$	(5.8 ± 2.5) %

See key on page 239

Meson Particle Listings

$D_s^{*\pm}, D_{s1}(2536)^{\pm}$

CONSTRAINED FIT INFORMATION

An overall fit to a branching ratio uses 1 measurements and one constraint to determine 2 parameters. The overall fit has a $\chi^2 = 0.0$ for 0 degrees of freedom.

The following off-diagonal array elements are the correlation coefficients $\langle \delta x_i \delta x_j \rangle / (\delta x_i \delta x_j)$, in percent, from the fit to the branching fractions, $x_i \equiv \Gamma_i / \Gamma_{\text{total}}$. The fit constrains the x_i whose labels appear in this array to sum to one.

$$x_2 \begin{pmatrix} -100 \\ x_1 \end{pmatrix}$$

D_s^{*+} BRANCHING RATIOS

$\Gamma(D_s^{*+} \gamma) / \Gamma_{\text{total}}$	DOCUMENT ID	TECN	COMMENT	Γ_1 / Γ
0.942 ± 0.026 OUR FIT				

• • • We do not use the following data for averages, fits, limits, etc. • • •

seen	DOCUMENT ID	TECN	COMMENT
seen	ASRATYAN 91 HLBC		$\bar{\nu}_\mu \text{ Ne}$
seen	ALBRECHT 88 ARG		$e^+ e^- \rightarrow D_s^{*+} \gamma X$
seen	AIHARA 84D		
seen	ALBRECHT 84B		
seen	BRANDELIK 79		

$\Gamma(D_s^{*+} \pi^0) / \Gamma(D_s^{*+} \gamma)$	DOCUMENT ID	TECN	COMMENT	Γ_2 / Γ_1
0.062 ± 0.029 OUR FIT				

0.062 ± 0.029 ± 0.022 GRONBERG 95 CLE2 $e^+ e^-$

$D_s^{*\pm}$ REFERENCES

GRONBERG 95 PRL 75 3232	J. Gronberg et al.	(CLEO Collab.)
BROWN 94 PR D50 1884	D. Brown et al.	(CLEO Collab.)
ASRATYAN 91 PL B257 525	A.E. Asratyan et al.	(ITEP, BELG, SACL+)
ALBRECHT 88 PL B207 349	H. Albrecht et al.	(ARGUS Collab.)
BLAYLOCK 87 PRL 58 2171	G.T. Blaylock et al.	(Mark III Collab.)
ASRATYAN 85 PL 156B 441	A.E. Asratyan et al.	(ITEP, SERP)
AIHARA 84D PRL 53 2465	H. Aihara et al.	(TPC Collab.)
ALBRECHT 84B PL 146B 111	H. Albrecht et al.	(ARGUS Collab.)
BRANDELIK 79 PL 80B 412	R. Brandelik et al.	(DASP Collab.)

OTHER RELATED PAPERS

KAMAL 92 PL B284 421	A.N. Kamal, Q.P. Xu	(ALBE)
BRANDELIK 78C PL 76B 361	R. Brandelik et al.	(DASP Collab.)
BRANDELIK 77B PL 70B 132	R. Brandelik et al.	(DASP Collab.)

$D_{s1}(2536)^{\pm}$

$I(J^P) = 0(1^+)$
 J, P need confirmation.

Seen in $D^*(2010)^+ K^0$. Not seen in $D^+ K^0$ or $D^0 K^+$. $J^P = 1^+$ assignment strongly favored.

$D_{s1}(2536)^{\pm}$ MASS

VALUE (MeV)	EVTS	DOCUMENT ID	TECN	COMMENT
2535.35 ± 0.34 ± 0.5 OUR EVALUATION				
2535.35 ± 0.34 OUR AVERAGE				

2534.2 ± 1.2	9	ASRATYAN 94 BEBC		$\nu N \rightarrow D^{*+} K^0 X, D^{*0} K^{\pm} X$
2535 ± 0.6 ± 1	75	FRABETTI 94B E687		$\gamma \text{ Be} \rightarrow D^{*+} K^0 X, D^{*0} K^+ X$
2535.3 ± 0.2 ± 0.5	134	ALEXANDER 93 CLE2		$e^+ e^- \rightarrow D^{*0} K^+ X$
2534.8 ± 0.6 ± 0.6	44	ALEXANDER 93 CLE2		$e^+ e^- \rightarrow D^{*+} K^0 X$
2535.2 ± 0.5 ± 1.5	28	ALBRECHT 92R ARG		$10.4 e^+ e^- \rightarrow D^{*0} K^+ X$
2536.6 ± 0.7 ± 0.4		AVERY 90 CLEO		$e^+ e^- \rightarrow D^{*+} K^0 X$
2535.9 ± 0.6 ± 2.0		ALBRECHT 89E ARG		$D_{s1}^* \rightarrow D^*(2010) K^0$

• • • We do not use the following data for averages, fits, limits, etc. • • •

2535 ± 28	1	ASRATYAN 88 HLBC		$\nu N \rightarrow D_{s1} \gamma X$
-----------	---	------------------	--	-------------------------------------

¹ Not seen in $D^* K$.

$m_{D_{s1}(2536)^{\pm}} - m_{D_s^*(2111)}$

VALUE (MeV)	DOCUMENT ID	TECN	COMMENT
424 ± 28	ASRATYAN 88 HLBC		$D_s^{*+} \gamma$

$D_{s1}(2536)^{\pm}$ WIDTH

VALUE (MeV)	CL%	EVTS	DOCUMENT ID	TECN	COMMENT
<2.3	90		ALEXANDER 93 CLEO		$e^+ e^- \rightarrow D^{*0} K^+ X$
<3.2	90	75	FRABETTI 94B E687		$\gamma \text{ Be} \rightarrow D^{*+} K^0 X, D^{*0} K^+ X$
<3.9	90		ALBRECHT 92R ARG		$10.4 e^+ e^- \rightarrow D^{*0} K^+ X$
<5.44	90		AVERY 90 CLEO		$e^+ e^- \rightarrow D^{*+} K^0 X$
<4.6	90		ALBRECHT 89E ARG		$D_{s1}^* \rightarrow D^*(2010) K^0$

• • • We do not use the following data for averages, fits, limits, etc. • • •

$D_{s1}(2536)^+$ DECAY MODES

$D_{s1}(2536)^-$ modes are charge conjugates of the modes below.

Mode	Fraction (Γ_i / Γ)
$\Gamma_1 D^*(2010)^+ K^0$	seen
$\Gamma_2 D^*(2007)^0 K^+$	seen
$\Gamma_3 D^+ K^0$	not seen
$\Gamma_4 D^0 K^+$	not seen
$\Gamma_5 D_s^{*+} \gamma$	possibly seen

$D_{s1}(2536)^+$ BRANCHING RATIOS

$\Gamma(D^+ K^0) / \Gamma(D^*(2010)^+ K^0)$	VALUE	CL%	DOCUMENT ID	TECN	COMMENT	Γ_3 / Γ_1
<0.40	90		ALEXANDER 93 CLEO		$e^+ e^- \rightarrow D^{*+} K^0 X$	
<0.43	90		ALBRECHT 89E ARG		$D_{s1}^* \rightarrow D^*(2010) K^0$	

$\Gamma(D_s^{*+} \gamma) / \Gamma_{\text{total}}$	DOCUMENT ID	TECN	COMMENT	Γ_5 / Γ
possibly seen	ASRATYAN 88 HLBC		$\nu N \rightarrow D_{s1} \gamma X$	

$\Gamma(D^0 K^+) / \Gamma(D^*(2007)^0 K^+)$	VALUE	CL%	DOCUMENT ID	TECN	COMMENT	Γ_4 / Γ_2
<0.12	90		ALEXANDER 93 CLEO		$e^+ e^- \rightarrow D^{*0} K^+ X$	

$\Gamma(D_s^{*+} \gamma) / \Gamma(D^*(2007)^0 K^+)$	VALUE	CL%	DOCUMENT ID	TECN	COMMENT	Γ_5 / Γ_2
<0.42	90		ALEXANDER 93 CLEO		$e^+ e^- \rightarrow D^{*0} K^+ X$	

$\Gamma(D^*(2007)^0 K^+) / \Gamma(D^*(2010)^+ K^0)$	VALUE	DOCUMENT ID	TECN	COMMENT	Γ_2 / Γ_1
1.22 ± 0.23 OUR AVERAGE					

1.1 ± 0.3	ALEXANDER 93 CLEO		$e^+ e^- \rightarrow D^{*0} K^+ X, D^{*+} K^0 X$
1.4 ± 0.3 ± 0.2	2 ALBRECHT 92R ARG		$10.4 e^+ e^- \rightarrow D^{*0} K^+ X, D^{*+} K^0 X$

² Evaluated by us from published inclusive cross-sections.

$D_{s1}(2536)^{\pm}$ REFERENCES

ASRATYAN 94 ZPHY C 61 563	A.E. Asratyan et al.	(BIRM, BELG, CERN+)
FRABETTI 94B PRL 72 324	P.L. Frabetti et al.	(FNAL E687 Collab.)
ALEXANDER 93 PL B303 377	J. Alexander et al.	(CLEO Collab.)
ALBRECHT 92R PL B297 425	H. Albrecht et al.	(ARGUS Collab.)
AVERY 90 PR D41 774	P. Avery, D. Besson	(CLEO Collab.)
ALBRECHT 89E PL B230 162	H. Albrecht et al.	(ARGUS Collab.)
ASRATYAN 88 ZPHY C40 483	A.E. Asratyan et al.	(ITEP, SERP)

OTHER RELATED PAPERS

SEMENOV 99 SPU 42 847	S.V. Semenov
Translated from UFN 42 937.	

Meson Particle Listings

 $D_{sJ}(2573)^\pm$ $D_{sJ}(2573)^\pm$

$I(J^P) = 0(?^?)$

 J^P is natural, width and decay modes consistent with 2^+ . $D_{sJ}(2573)^\pm$ MASS

VALUE (MeV)	EVTs	DOCUMENT ID	TECN	CHG	COMMENT
2573.5 ± 1.7	OUR AVERAGE				
2574.5 ± 3.3 ± 1.6		ALBRECHT 96	ARG		$e^+e^- \rightarrow D^0 K^+ X$
2573.2 ^{+1.7} _{-1.6} ± 0.9	217	KUBOTA 94	CLE2	+	$e^+e^- \sim 10.5$ GeV

 $D_{sJ}(2573)^\pm$ WIDTH

VALUE (MeV)	EVTs	DOCUMENT ID	TECN	CHG	COMMENT
15⁺⁵₋₄	OUR AVERAGE				
10.4 ± 8.3 ± 3.0		ALBRECHT 96	ARG		$e^+e^- \rightarrow D^0 K^+ X$
16 ⁺⁵ ₋₄ ± 3	217	KUBOTA 94	CLE2	+	$e^+e^- \sim 10.5$ GeV

 $D_{sJ}(2573)^\pm$ DECAY MODES $D_{sJ}(2573)^\pm$ modes are charge conjugates of the modes below.

Mode	Fraction (Γ_i/Γ)
Γ_1 $D^0 K^+$	seen
Γ_2 $D^*(2007)^0 K^+$	not seen

 $D_{sJ}(2573)^\pm$ BRANCHING RATIOS

$\Gamma(D^0 K^+)/\Gamma_{total}$	Γ_1/Γ				
VALUE	EVTs	DOCUMENT ID	TECN	CHG	COMMENT
seen	217	KUBOTA 94	CLE2	±	$e^+e^- \sim 10.5$ GeV

$\Gamma(D^*(2007)^0 K^+)/\Gamma(D^0 K^+)$	Γ_2/Γ_1				
VALUE	CL%	DOCUMENT ID	TECN	CHG	COMMENT
<0.33	90	KUBOTA 94	CLE2	+	$e^+e^- \sim 10.5$ GeV

 $D_{sJ}(2573)^\pm$ REFERENCES

ALBRECHT 96	ZPHY C69 405	H. Albrecht <i>et al.</i>	(ARGUS Collab.)
KUBOTA 94	PRL 72 1972	Y. Kubota <i>et al.</i>	(CLEO Collab.)

OTHER RELATED PAPERS

SEMENOV 99	SPU 42 847	S.V. Semenov
		Translated from UFN 42 937.

BOTTOM MESONS

$$(B = \pm 1)$$

$$B^+ = u\bar{b}, B^0 = d\bar{b}, \bar{B}^0 = \bar{d}b, B^- = \bar{u}b, \text{ similarly for } B^{*s}$$

B-particle organization

Many measurements of *B* decays involve admixtures of *B* hadrons. Previously we arbitrarily included such admixtures in the B^\pm section, but because of their importance we have created two new sections: " B^\pm/B^0 Admixture" for $\mathcal{T}(4S)$ results and " $B^\pm/B^0/B_s^0/b$ -baryon Admixture" for results at higher energies. Most inclusive decay branching fractions are found in the Admixture sections. B^0/\bar{B}^0 mixing data are found in the B^0 section, while B_s^0/\bar{B}_s^0 mixing data and $B-\bar{B}$ mixing data for a B^0/B_s^0 admixture are found in the B_s^0 section. *CP*-violation data are found in the B^0 section. *b*-baryons are found near the end of the Baryon section.

The organization of the *B* sections is now as follows, where bullets indicate particle sections and brackets indicate reviews.

[Production and Decay of *b*-flavored Hadrons]

- B^\pm
 - mass, mean life
 - branching fractions
- B^0
 - mass, mean life
 - branching fractions
 - polarization in B^0 decay
 - [$B-\bar{B}$ Mixing]
 - $B^0-\bar{B}^0$ mixing
 - [*CP* Violation in *B* Decay]
 - CP* violation
- B^\pm/B^0 Admixture
 - branching fractions
- $B^\pm/B^0/B_s^0/b$ -baryon Admixture
 - mean life
 - production fractions
 - branching fractions
- B^*
 - mass
- $B_J^*(5732)$
 - mass, width
- B_s^0
 - mass, mean life
 - branching fractions
 - polarization in B_s^0 decay
 - $B_s^0-\bar{B}_s^0$ mixing
 - $B-\bar{B}$ mixing (admixture of B^0, B_s^0)
- B_s^*
 - mass
- $B_{sJ}^*(5850)$
 - mass, width
- B_c^\pm
 - mass, mean life
 - branching fractions

At end of Baryon Listings:

- Λ_b
 - mass, mean life
 - branching fractions
- Ξ_b^0, Ξ_b^-
 - mean life
- *b*-baryon Admixture
 - mean life
 - branching fractions

PRODUCTION AND DECAY OF *b*-FLAVORED HADRONS

Updated March 2000 by L. Gibbons (Cornell University, Ithaca) and K. Honscheid (Ohio State University, Columbus).

This year, we opened a new chapter in *B* physics. A new generation of experiments, BABAR, BELLE, Hera-B, and CLEO III, saw first collisions and started to accumulate *B*-meson decays. The next Fermilab collider run will start soon. The long-awaited B-factory era has begun.

There is great hope these experiments will provide us with precise measurements of fundamental parameters of the Standard Model, in particular the weak-mixing angles and phase of the Cabibbo-Kobayashi-Maskawa matrix, and with it an improved understanding of *CP* violation and maybe even a glimpse at new physics.

While the underlying decay of the heavy quark is governed by the weak interaction, it is the strong force that is responsible for the formation of the hadrons that are observed by experimenters. Although this complicates the extraction of the the Standard Model parameters from the experimental data, it also means that decays of *B* mesons provide an important laboratory to test our understanding of the strong interaction.

Arguably the most exciting development since the last edition of this review is the progress in *b*-quark processes for which amplitudes beyond the tree level play a major role. The long sought after $B^0 \rightarrow \pi^+\pi^-$ decays have finally been observed. Many other $b \rightarrow u$ and gluonic penguin transitions have been measured. In addition to branching fractions, limits on *CP* asymmetries have been measured for several modes. The results on rare hadronic *B* decays have also been used to probe possible values of the angle γ of the CKM triangle. First attempts to measure another CKM angle, $\sin(2\beta)$, have been reported by OPAL, CDF, and ALEPH.

For $b \rightarrow c$ transitions, the CLEO Collaboration used a sample of more than 18 million *B* decays to update branching fractions for many exclusive hadronic decay channels. New results on semileptonic decays have been reported by CLEO and the LEP Collaborations. Lifetime measurements improve steadily and now have reached a precision of a few percent.

Heavy-flavor physics is a very dynamic field, and in this brief review it is impossible to do justice to all recent theoretical and experimental developments. We will highlight a few new results but otherwise refer the interested reader to several excellent reviews [1-3].

Production and spectroscopy: Elementary particles are characterized by their masses, lifetimes, and internal quantum numbers. The bound states with a \bar{b} quark and a *u* or *d* antiquark are referred to as the B_d (\bar{B}^0) and the B_u (B^+) mesons, respectively. The first excitation is called the B^* meson. B^{**} is the generic name for the four orbitally excited ($L = 1$) *B*-meson states that correspond to the *P*-wave mesons in the charm system, D^{**} . Mesons containing an *s* or a *c* quark are denoted B_s and B_c , respectively.

Meson Particle Listings

b -flavored hadrons

Experimental studies of b decay are performed at the $\Upsilon(4S)$ resonance near production threshold, as well as at higher energies in proton-antiproton collisions and Z decays. Most new results from CLEO are based on a sample of $\approx 9.7 \times 10^6$ $B\bar{B}$ events. At the Tevatron, CDF in particular has made significant contributions with 100 pb^{-1} of data. Operating at the Z resonance, each of the four LEP Collaborations recorded slightly under a million $b\bar{b}$ events, while the SLD experiment collected about 0.1 million $b\bar{b}$ events.

For quantitative studies of B decays, the initial composition of the data sample must be known. The $\Upsilon(4S)$ resonance decays only to $B^0\bar{B}^0$ and B^+B^- pairs, while at high-energy collider experiments, heavier states such as B_s or B_c mesons and b -flavored baryons are produced as well. The current experimental limit for non- $B\bar{B}$ decays of the $\Upsilon(4S)$ is less than 4% at the 95% confidence level [4]. CLEO has measured the ratio of charged to neutral $\Upsilon(4S)$ decays using exclusive $B \rightarrow \psi K^{(*)}$ decays. Assuming isospin invariance and $\tau_{B^+}/\tau_{B^0} = 1.066 \pm 0.024$ they found [5]

$$\frac{f_+}{f_0} = \frac{\text{B}(\Upsilon(4S) \rightarrow B^+B^-)}{\text{B}(\Upsilon(4S) \rightarrow B^0\bar{B}^0)} = 1.044 \pm 0.069_{-0.045}^{+0.043}. \quad (1)$$

This is consistent with equal production of B^+B^- and $B^0\bar{B}^0$ pairs, and unless explicitly stated otherwise, we will assume $f_+/f_0 = 1$. This assumption is further supported by the near equality of the B^+ and B^0 masses. Again using exclusive $B \rightarrow J/\psi K^{(*)}$ decays, CLEO determined these masses to $m(B^0) = 5.2791 \pm 0.0007 \pm 0.0003 \text{ GeV}/c^2$ and $m(B^+) = 5.2791 \pm 0.0004 \pm 0.0004 \text{ GeV}/c^2$, respectively [6].

At high-energy collider experiments, b quarks hadronize as \bar{B}^0 , B^- , \bar{B}_s^0 , and B_c^- mesons, or as baryons containing b quarks.

Over the last few years, there have been significant improvements in our understanding of the b -hadron sample composition. Table 1 summarizes the results showing the fractions f_d , f_u , f_s , and f_{baryon} of B^0 , B^+ , B_s^0 , and b baryons in an unbiased sample of weakly decaying b hadrons produced at the Z resonance and in $p\bar{p}$ collisions. A detailed account can be found elsewhere in this Review [7].

Table 1: Fractions of weakly decaying b -hadron species in $Z \rightarrow b\bar{b}$ decay and in $p\bar{p}$ collisions at $\sqrt{s} = 1.8 \text{ TeV}$.

b hadron	Fraction [%]
B^-, \bar{B}^0	38.9 ± 1.3
\bar{B}_s^0	10.7 ± 1.4
b baryons	11.6 ± 2.0

To date, the existence of the b -flavored mesons (B^-, \bar{B}^0 , B_s, B_c , and various excitations), as well as the Λ_b baryon has been established. The current world average of the B^*-B mass difference is $45.78 \pm 0.35 \text{ MeV}/c^2$. Using exclusive hadronic decays such as $B_s^0 \rightarrow J/\psi\phi$ and $\Lambda_b \rightarrow J/\psi\Lambda$, the masses of these states are now known with the precision of a few MeV.

The current world averages of the B_s and the Λ_b mass are $5.3696 \pm 0.0024 \text{ GeV}/c^2$ and $5.624 \pm 0.009 \text{ GeV}/c^2$, respectively. Clear evidence for the B_c , the last weakly decaying bottom meson, has been published by CDF [8]. They reconstruct the semileptonic decay $B_c \rightarrow J/\psi\ell X$, and extract a B_c mass of $6.40 \pm 0.39 \pm 0.13 \text{ GeV}/c^2$.

First indications of Ξ_b production have been presented by the LEP Collaborations [9–10].

Excited B -meson states have been observed by CLEO, CUSB, LEP, and CDF. Evidence for B^{**} production has been presented by CDF and the LEP experiments [11]. Inclusive reconstructing a bottom hadron candidate combined with a charged pion from the primary vertex, they see the B^{**} as a broad resonance around $5.697 \pm 0.009 \text{ GeV}/c^2$ in the $M(B\pi) \equiv M(B)$ mass distribution [12]. Due to the inclusive approach, the mass resolution is limited to about 40 MeV, which makes it very difficult to identify the narrow states, B_1 and B_2^* , separately. The LEP experiments have also provided evidence for excited B_s^{**} states.

Lifetimes: Precise lifetimes are key in extracting the weak parameters that are important for understanding the role of the CKM matrix in CP violation, such as the determination of V_{cb} and $B_s\bar{B}_s$ mixing measurements. In the naive spectator model, the heavy quark can decay only via the external spectator mechanism, and thus the lifetimes of all mesons and baryons containing b quarks would be equal. Nonspectator effects, such as the interference between contributing amplitudes, modify this simple picture and give rise to a lifetime hierarchy for b -flavored hadrons similar to the one in the charm sector. However, since the lifetime differences are expected to scale as $1/m_Q^2$, where m_Q is the mass of the heavy quark, the variation in the b system should be significantly smaller, of order 10% or less [14]. For the b system we expect

$$\tau(B^-) \geq \tau(\bar{B}^0) \approx \tau(B_s) > \tau(\Lambda_b^0) \gg \tau(B_c). \quad (2)$$

In the B_c , both quarks can decay weakly, resulting in its much shorter lifetime. Measurements of lifetimes for the various b -flavored hadrons thus provide a means to determine the importance of non-spectator mechanisms in the b sector.

Over the past years, the field has matured, and advanced algorithms based on impact parameter or decay length measurements exploit the potential of silicon vertex detectors. However, in order to reach the precision necessary to test theoretical predictions, the results from different experiments need to be averaged. This is a challenging task that requires detailed knowledge of common systematic uncertainties, and correlations between the results from different experiments. The average lifetimes for b -flavored hadrons given in this edition have been determined by the LEP B Lifetimes Working Group [15]. The papers used in this calculation are listed in the appropriate sections. A detailed description of the procedures and the treatment of correlated and uncorrelated errors can be found in [16]. The new world average b -hadron lifetimes are summarized in Table 2.

The first measurement of the B_c lifetime comes from the CDF Collaboration [8]. Lifetime measurements have reached a level of precision that the average *b*-hadron lifetime result becomes sensitive to the composition of the data sample. The result listed in Table 2 takes into account correlations between different experiments and analysis techniques, but does not correct for differences due to different admixtures of *b*-flavored hadrons. For inclusive lifetime measurements, the size of this effect can be estimated by dividing the available results into three sets. LEP measurements based on the identification of a lepton from the *b* decay yield $\tau_{b \text{ hadron}} = 1.537 \pm 0.020 \text{ ps}^{-1}$ [17–19]. The average *b*-hadron lifetime based on inclusive secondary vertex techniques is $\tau_{b \text{ hadron}} = 1.577 \pm 0.016 \text{ ps}^{-1}$ [18,20–24]. Finally, CDF [25] used J/ψ mesons to tag the *b* vertex resulting in $\tau_{b \text{ hadron}} = 1.533 \pm 0.015^{+0.035}_{-0.031} \text{ ps}^{-1}$. Contrary to what is observed, the average *b* lifetime determined from a sample of semileptonic decays is expected to be larger than the lifetime extracted from inclusive decays. Given the precision of the measurements, however, the discrepancy is not yet significant. The resulting average *b* lifetime is listed in Table 2.

Table 2: Summary of inclusive and exclusive *b*-hadron lifetime measurements.

Particle	Lifetime [ps]
B^0	1.548 ± 0.032
B^+	1.653 ± 0.028
B_s	1.493 ± 0.062
B_c	$0.46^{+0.18}_{-0.16} \pm 0.03$
<i>b</i> baryon	1.208 ± 0.051
<i>b</i> hadron	1.564 ± 0.014

For comparison with theory, lifetime ratios are preferred. Experimentally we find [15]

$$\frac{\tau_{B^+}}{\tau_{B^0}} = 1.062 \pm 0.029, \quad \frac{\tau_{B_s}}{\tau_{B^0}} = 0.964 \pm 0.045, \quad \frac{\tau_{A_b}}{\tau_{B^0}} = 0.780 \pm 0.037, \quad (3)$$

while theory makes the following predictions [26]

$$\frac{\tau_{B^+}}{\tau_{B^0}} = 1 + 0.05 \left(\frac{f_B}{200 \text{ MeV}} \right)^2, \quad \frac{\tau_{B_s}}{\tau_{B^0}} = 1 \pm 0.01, \quad \frac{\tau_{A_b}}{\tau_{B^0}} = 0.9. \quad (4)$$

In conclusion, the pattern of measured *B*-meson lifetimes follows the theoretical expectations, and non-spectator effects are observed to be small. The short B_c lifetime has been predicted correctly. However, the A_b -baryon lifetime is unexpectedly short. As has been noted by several authors, the observed value of the A_b lifetime is quite difficult to accommodate theoretically [27–33]. This apparent breakdown of the heavy-quark expansion for inclusive, non-leptonic *B* decays could be caused by violations of local quark-hadron duality. Neubert, however, argues that this conclusion is premature because a reliable field-theoretical calculation is still lacking. Exploring a reasonable parameter space for the unknown hadronic matrix elements, he demonstrated that within the experimental errors, theory can

accommodate the measured lifetime ratios [1]. A recent calculation based on QCD sum rules [34] arrives at a similar conclusion allowing $\tau_{A_b}/\tau_{B^0} = 0.79\text{--}0.87$. An initial lattice study [35], on the other hand, finds $\tau_{A_b}/\tau_{B^0} = 0.91\text{--}0.93$.

Similar to the kaon system, neutral *B* mesons contain short- and long-lived components. The lifetime difference is, of course, significantly smaller, and recent experimental limits at 95% C.L. are

$$\frac{\Delta\Gamma_d}{\Gamma_d} < 0.82 \quad \text{and} \quad \frac{\Delta\Gamma_s}{\Gamma_s} < 0.65. \quad (5)$$

These results are based on a comparison of direct δm measurements with χ_d measurements for B_d [36] and a combination [37] of the various B_s proper time measurements. A more restrictive limit for the B_s system can be obtained if one assumes $\Gamma_{B_s} = \Gamma_{B_d}$.

Semileptonic *B* decays: Measurements of semileptonic *B* decays are important to determine the weak couplings $|V_{cb}|$ and $|V_{ub}|$. In addition, these decays can be used to probe the dynamics of heavy quark decay. The leptonic current can be calculated exactly, while corrections due to the strong interaction are restricted to the $b \rightarrow c$ and $b \rightarrow u$ vertices, respectively.

Experimentally, semileptonic decays have the advantage of large branching ratios and the characteristic signature of the energetic charged lepton. The neutrino, however, escapes undetected so a full reconstruction of the decaying *B* meson is impossible. Various techniques which take advantage of production at threshold or the hermiticity of the detector have been developed by the ARGUS, CLEO, and LEP experiments to overcome this difficulty.

Several different approaches have been used to measure the inclusive semileptonic rate $B \rightarrow X\ell\nu_\ell$. These are measurements of the inclusive single lepton momentum spectrum, measurements of dilepton events using charge and angular correlations first pioneered by ARGUS [38], measurements of leptons opposite a *b*-tagged jet at the *Z*, and measurements of the separate B^- and \bar{B}^0 branching ratios by using events which contain a lepton and a reconstructed *B* meson. The double-tagged methods (lepton-lepton) have the smallest model dependence, and only the dilepton results from the $\Upsilon(4S)$ are used. The LEP averages [39] are based primarily on single lepton measurements, which rely on modeling of the semileptonic decays. The uncertainties involved in such modeling are, by their nature, ill-defined and difficult to quantify. The average LEP [39] and the $\Upsilon(4S)$ [40] rates are listed in Table 3. Differences in B_{sl} measured at the $\Upsilon(4S)$ and the *Z* are expected due to the different admixture of *b*-flavored hadrons. Given the short A_b lifetime, the LEP value should be lower than the $\Upsilon(4S)$ result. Previous LEP determinations of $B \rightarrow X\ell\nu_\ell$ have been markedly higher than the $\Upsilon(4S)$ measurements. The current LEP measurements are now in much better agreement with expectations relative to the $\Upsilon(4S)$ rate.

A few new results on the branching fractions of exclusive semileptonic *B* decays have been reported. The current world averages are listed in Table 3. It is interesting to compare

Meson Particle Listings

b-flavored hadrons

the inclusive semileptonic branching fraction to the sum of branching fractions for exclusive modes, which agree at the 1σ level. The exclusive modes measured are consistent with saturating the inclusive rate.

The makeup of the non- D and D^* components of the B semileptonic process is a critical component in the determination of b lifetimes, B mixing, $|V_{cb}|$, and $|V_{ub}|$. It has been known for some time that the D^{**} excited states do not appear to account for the difference between the $D + D^*$ rates and the inclusive rate [41,42]. A recent inclusive $B \rightarrow D^* \pi \ell \nu_\ell X$ study by DELPHI [43] adds information regarding the breakdown into the $D^* \pi$ and $D \pi$ contributions. Unfortunately, we still lack information regarding detailed makeup of, and the hadronic mass spectrum for, this component.

Table 3: Inclusive and exclusive semileptonic branching fractions of B mesons. $B(\bar{B} \rightarrow X_u \ell^- \bar{\nu}_\ell) = 0.15 \pm 0.1\%$ [44] has been included in the sum of the exclusive branching fractions.

Mode	Branching fraction [%]
$\bar{B} \rightarrow X \ell^- \bar{\nu}_\ell (\mathcal{T}(4S))$	$10.49 \pm 0.17 \pm 0.43$
$b \rightarrow X \ell^- \bar{\nu}_\ell (Z)$	$10.58 \pm 0.07 \pm 0.17$
$\bar{B} \rightarrow D \ell^- \bar{\nu}_\ell$	2.13 ± 0.22
$\bar{B} \rightarrow D^* \ell^- \bar{\nu}_\ell$	5.05 ± 0.25
$B \rightarrow D^{(*)} \pi \ell^- \bar{\nu}_\ell$	2.26 ± 0.44
with $\bar{B} \rightarrow D_1^0(2420) \ell^- \bar{\nu}_\ell X$	0.74 ± 0.16
$\bar{B} \rightarrow D_2^{*0}(2460) \ell^- \bar{\nu}_\ell X$	< 0.65 90% CL
$\Sigma B_{\text{exclusive}}$	9.59 ± 0.56

Dynamics of semileptonic B decay and $|V_{cb}|$: Since leptons are not sensitive to the strong interaction, the amplitude for a semileptonic B decay can be factorized into two parts, a leptonic and a hadronic current. The leptonic factor can be calculated exactly, while the hadronic part is parameterized by form factors. A simple example is the transition $B \rightarrow D \ell \nu_\ell$. The differential decay rate in this case is given by

$$\frac{d\Gamma}{dq^2} = \frac{G_F^2}{24\pi^3} |V_{cb}^2| P_D^3 f_+^2(q^2) \quad (6)$$

where q^2 is the mass of the virtual W ($\ell \nu_\ell$), P_D is the D momentum and $f_+(q^2)$ is the single vector form factor which gives the probability that the final state quarks will form a D meson. Since the leptons are very light, the corresponding $f_-(q^2)$ form factor can be neglected. For $B \rightarrow D^* \ell \nu_\ell$ decays, in the limit of zero lepton mass there are three form factors which correspond to the three possible partial waves of the $B \rightarrow D^* \bar{W}$ system (here \bar{W} is the virtual W boson, which becomes the lepton-antineutrino pair). Currently, form factors cannot be predicted by theory and need to be determined experimentally. Over the last years, however, it has been appreciated that there is a symmetry of QCD that is useful in understanding systems containing one heavy quark. This symmetry arises when the

quark becomes sufficiently heavy to make its mass irrelevant to the nonperturbative dynamics of the light quarks. This allows the heavy quark degrees of freedom to be treated in isolation from the light quark degrees of freedom. This is analogous to the canonical treatment of hydrogenic atoms, in which the spin and other properties of the nucleus can be neglected. The behavior and electronic structure of the atom are determined by the light electronic degrees of freedom. Heavy quark effective theory (HQET) was created by Isgur and Wise [45], who define a single universal form factor, $\xi(v \cdot v')$, known as the Isgur-Wise function. In this function, v and v' are the four velocities of the initial and final state heavy mesons. The Isgur-Wise function cannot be calculated from first principles, but unlike the hadronic form factors mentioned above, it is universal to leading order. In the heavy quark limit, it is the same for all heavy meson to heavy meson transitions, and the four form factors parameterizing $B \rightarrow D^* \ell \nu_\ell$ and $B \rightarrow D \ell \nu_\ell$ decays can be related to this single function ξ .

In this framework the differential semileptonic decay rates as functions of $w = v_B \cdot v_{D^{(*)}} = (m_B^2 + m_{D^{(*)}}^2 - q^2)/2m_B m_{D^{(*)}}$ are given by [1]

$$\begin{aligned} \frac{d\Gamma(\bar{B} \rightarrow D^* \ell \bar{\nu}_\ell)}{dw} &= \frac{G_F^2 M_B^5}{48\pi^3} r_*^3 (1 - r_*)^2 \sqrt{w^2 - 1} (w + 1)^2 \\ &\quad \times \left[1 + \frac{4w}{w + 1} \frac{1 - 2wr_* + r_*^2}{(1 - r_*)^2} \right] |V_{cb}|^2 \mathcal{F}^2(w) \\ \frac{d\Gamma(\bar{B} \rightarrow D \ell \bar{\nu}_\ell)}{dw} &= \frac{G_F^2 M_B^5}{48\pi^3} r_*^3 (1 + r_*)^2 (w^2 - 1)^{3/2} |V_{cb}|^2 \mathcal{G}^2(w) \quad (7) \end{aligned}$$

where $r_{(*)} = M_{D^{(*)}}/M_B$ and q^2 is the invariant momentum transfer. For $m_Q \rightarrow \infty$, the two form factors $\mathcal{F}(w)$ and $\mathcal{G}(w)$ coincide with the Isgur-Wise function $\xi(w)$.

Both CLEO [46] and ALEPH [47] have measured the differential decay rate distributions and extracted the ratio $\mathcal{G}(w)/\mathcal{F}(w)$ which is expected to be close to unity. The data are compatible with a universal form factor $\xi(w)$.

CLEO has also performed a direct measurement of the three form factors that are used to parameterize $B \rightarrow D^* \ell \nu_\ell$ decays [48]. These are usually expressed in terms of form factor ratios [49]. $R_1(w) = h_V(w)/h_{A_1}(w)$ and $R_2(w) = h_{A_2}(w)/h_{A_1}(w)$ where $h_V(w)$, $h_{A_1}(w)$ and $h_{A_2}(w)$ are the standard three HQET form factors in the zero lepton mass limit (see Ref. 49 and references therein). At zero recoil, *i.e.* $w = 1$, CLEO finds $R_1(1) = 1.18 \pm 0.30 \pm 0.12$ and $R_2(1) = 0.71 \pm 0.2 \pm 0.07$. While the errors are still large, this is in good agreement with a theoretical prediction of $R_1(1) = 1.3 \pm 0.1$ and $R_2(1) = 0.8 \pm 0.2$ [1].

The universal form factor $\xi(w)$ describes the overlap of wave functions of the light degrees of freedom in the initial and final heavy meson. At zero recoil, *i.e.*, when the two mesons move with the same velocity, the overlap is perfect and the form factor is absolutely normalized, $\xi(1) = 1$. In principle, all that experimentalists have to do to extract a model-independent value for $|V_{cb}|$ is to measure $d\Gamma(B \rightarrow D^{(*)} \ell \nu_\ell)/dw$ for $w \rightarrow 1$. However, in the real, world the b and c quarks are not infinitely heavy, so corrections to the limiting case have to be calculated.

The evaluation of $\mathcal{F}(1)$ and $\mathcal{G}(1)$ remains a topic of some theoretical controversy [1,50–54]. A middle ground could be characterized as

$$\begin{aligned}\mathcal{F}(1) &= 0.92 \pm 0.05, \\ \mathcal{G}(1) &= 1.00 \pm 0.07.\end{aligned}\quad (8)$$

The calculations of $\mathcal{F}(1)$ and $\mathcal{G}(1)$ most commonly accepted have relied upon some of the OPE techniques, and in fact these results are correlated at some level with the inclusive rate calculations. Concerns about duality violation, for example, enter these determinations as well. Other, “exclusive approaches” (see Ref. 54 and references therein) yield results similar to the values quoted and are free from duality uncertainties. However, they rely on modelling to estimate exclusive matrix elements, for which uncertainties are very difficult to quantify. Recently, there has been a prototype lattice determination that obtained an $\mathcal{F}(1)$ value only very slightly higher than the above with a preliminary uncertainty of 3.3%. These results are encouraging, and are free of the intimate correlation with the inclusive calculations. To fully understand the uncertainties, an unquenched calculation is needed.

Measurements of $\mathcal{F}(1)|V_{cb}|$ have been performed by the ALEPH, ARGUS, CLEO, DELPHI, and OPAL experiments. Because the differential decay rate actually vanishes at zero recoil, experimentally the decay rate must be measured as a function of w and extrapolated to zero. This requires a parameterization of the shape of the form factor $\mathcal{F}(w)$. Initial measurements used a linear parameterization and fit the slope and $\mathcal{F}(1)|V_{cb}|$ simultaneously. $\mathcal{F}(w)$ must have a positive curvature, so this linear parameterization results in an intercept that is biased low by about 2.6% [55]. More recent determinations [47,56–58] have used dispersion relation calculations [59,60] that relate the curvature to the slope. In either case, the slope and intercept parameters are highly correlated and require simultaneous averaging [61].

$|V_{cb}|$ from exclusive $D^*\ell\nu_\ell$ determinations and from inclusive determinations (discussed below) are summarized in Table 4. The various averages are in good agreement. Because of the correlations between slope and $\mathcal{F}(1)|V_{cb}|$, and the different meanings of the slopes in the linear and dispersion-relation-based parameterizations, the older CLEO [62] and ARGUS [63] $D^*\ell\nu$ measurements, based on the linear parameterization, have not here been averaged with the LEP results [47,57–58], based on the dispersion-relation parameterization. Determinations of $|V_{cb}|$ based on the $B \rightarrow D\ell\nu_\ell$ process [47,56] give consistent results, but with a factor of two larger uncertainty.

Heavy Quark Symmetry (HQS) has also allowed remarkable precision in the calculation of the semileptonic width $\Gamma(B \rightarrow X_c\ell\nu_\ell)$. The operator product expansion (OPE) of the width in terms of the (inverse) heavy quark mass and in α_s appears free of $1/m_b$ corrections, and at $1/m_b^2$ is given by [66]

Table 4: Current determinations of $|V_{cb}|$. The inclusive branching fractions have been adjusted for a $1.5 \pm 1.0\%$ $b \rightarrow u$ component relative to $b \rightarrow c$ [44]. The uncertainties are experimental followed by theoretical.

Mode	$ V_{cb} $
$\bar{B} \rightarrow D^*\ell^-\bar{\nu}_\ell$ [64]	$0.0367 \pm 0.0023 \pm 0.0018$ (Dispersion relation $\mathcal{F}(w)$ parameterization)
$\bar{B} \rightarrow D^*\ell^-\bar{\nu}_\ell$ [65]	$0.0392 \pm 0.0030 \pm 0.0019$ (Linear $\mathcal{F}(w)$ parameterization (+ bias correction))
$\Gamma(b \rightarrow c\ell\nu_\ell)$	$0.0408 \pm 0.0005 \pm 0.0025$ (B^0, B^+, B_s , and b -baryon admixture at the Z)
$\Gamma(B \rightarrow X_c\ell\nu_\ell)$	$0.0400 \pm 0.0010 \pm 0.0024$ (B^0, B^+ admixture at the $\Upsilon(4S)$)

$$\Gamma_{SL}(B) = \frac{G_F^2 m_b^5 |V_{cb}|^2}{192\pi^3} \times \left[z_0 \left(1 - \frac{\mu_\pi^2 - \mu_G^2}{2m_b^2} \right) - 2 \left(1 - \frac{m_c^2}{m_b^2} \right)^4 \frac{\mu_G^2}{m_b^2} - \frac{2\alpha_S}{3\pi} z_0^{(1)} + \dots \right]. \quad (9)$$

At $1/m_b^2$, three nonperturbative parameters enter the expansion of the differential decay rate: μ_π^2 (or, closely related λ_1), which is related to the average kinetic energy of the b quark in the meson; μ_G^2 (or λ_2), which is related to the hyperfine splitting and can be determined from the B - B^* mass difference; and $\bar{\Lambda}$, which relates the quark mass to the meson mass. This last enters implicitly since the b quark mass, not the B meson mass has been used. The parameters z_0 and $z_0^{(1)}$ are known phase space factors that depend on m_c^2/m_b^2 . Bigi [51] suggests an uncertainty of approximately 6% on $|V_{cb}|$ from such a calculation. Various calculations [67–68] are consistent with a central value

$$|V_{cb}| = 0.0411 \sqrt{\frac{\mathcal{B}(B \rightarrow X_c\ell\nu)}{0.105}} \sqrt{\frac{1.55 \text{ ps}}{\tau_B}} \left(1 - 0.024 \frac{\mu_\pi^2 - 0.5 \text{ GeV}^2}{0.2 \text{ GeV}^2} \right). \quad (10)$$

Combined with the semileptonic branching fractions at the $\Upsilon(4S)$ and the Z quoted above, one obtains the inclusive determinations of $|V_{cb}|$ listed in Table 4. These agree with the exclusive determinations.

The validity of the OPE-based calculation rests upon the assumption of quark-hadron duality. The uncertainty induced from this assumption is unknown. While expected to be small [69–71], there has been a suggestion that the assumption could mask corrections of order $1/m_b$ [72]. A 5% effect, for example, cannot be ruled out at this time.

Moments of the inclusive lepton [73] and hadron mass [74–76] spectra can be used both to determine the nonperturbative parameters and to test the OPE/HQS framework at the $1/m_b^2$ level. A preliminary moment analysis by CLEO [77] suggests that the parameters derived from the leptonic moments may be inconsistent with those from the hadronic moments. A variety of explanations for this exist: an experimental problem, slow convergence of the $1/m$ expansion for the higher moments,

Meson Particle Listings

b-flavored hadrons

or more fundamentally, duality violation. Further investigation is required.

Semileptonic $b \rightarrow u$ transitions: The simplest diagram for a rare B decay is obtained by replacing the $b \rightarrow c$ spectator diagram with a CKM suppressed $b \rightarrow u$ transition. These decays probe the small CKM matrix element V_{ub} , the magnitude of which sets bounds on the combination $\rho^2 + \eta^2$ in the Wolfenstein parameterization of the CKM matrix [78]. As with V_{cb} , extraction of V_{ub} has been attempted using both inclusive and exclusive semileptonic B decays. An accurate method of determining V_{ub} has been somewhat elusive. With exclusive techniques, the heavy-to-light $b \rightarrow u$ transition has no theoretical analogue to the zero recoil ($w = 1$) point in the heavy-to-heavy $b \rightarrow c$ transition of $B \rightarrow D^* \ell \nu$. Rather than calculating a correction of order 10% to the unit form factor expected for a heavy-to-heavy transition at $w = 1$ (in the infinite mass limit), the absolute normalization of the form factors must be predicted. This normalization dominates the uncertainty in exclusive determinations of V_{ub} .

There have been two exclusive V_{ub} analyses by the CLEO Collaboration: a simultaneous measurement of the $B \rightarrow \pi \ell \nu_\ell$ and the $B \rightarrow \rho \ell \nu_\ell$ transitions [79], and a second measurement of the $B \rightarrow \rho \ell \nu_\ell$ rate [80]. The results of the two analyses are largely statistically independent, and their results have been combined, with correlated uncertainties accounted for, to obtain $|V_{ub}| = (3.25 \pm 0.14^{+0.21}_{-0.29} \pm 0.55) \times 10^{-3}$, where the final error is the uncertainty from the form factors. New calculations based on light cone sum rules [81–83] and lattice calculations [84,85,86] promise to result in uncertainties in the 10% to 15% range soon. Uncertainties below 10% will require either unquenched lattice calculations or accurate measurements of the rate for $B \rightarrow K^* \ell^+ \ell^-$, which would allow one to extract $|V_{ub}|/|V_{cb}|$ from a double ratio of B and D decays [87].

In principle, the fully inclusive rate can be calculated reliably enough (barring an unexpectedly large violation of quark-hadron duality) to determine $|V_{ub}|$ with an accuracy under 10% [51]. Realizing this accuracy is extremely difficult in practice because the ferocious background from $b \rightarrow c \ell \nu_\ell$ decays forces experiments to limit measurement to a restricted region of the total phase space. Restriction of the theoretical rate to the restricted region can introduce large uncertainties in the calculation that can be difficult to quantify.

The published inclusive analyses at the $\Upsilon(4S)$ [88] have focused on leptons in the endpoint region of the single lepton spectrum, which are kinematically incompatible with coming from a $b \rightarrow c$ transition. Models were used to estimate the rate into the endpoint, from which $|V_{ub}/V_{cb}| = (0.08 \pm 0.02)$ is obtained. The error is dominated by the theoretical uncertainty, which has been very difficult to quantify. Because the endpoint region extends beyond the partonic endpoint and the size of the endpoint is of order Λ_{QCD} , an infinite series of terms in the OPE rate calculation become equally important [89]. While the leading singularities can be resummed into a structure function [90,91], the structure function is unknown.

Another method for extracting $|V_{ub}|$ from the endpoint has been proposed [92] based on earlier suggestions [90,91] that involve comparison of the endpoint lepton spectrum to the photon spectrum in $b \rightarrow s \gamma$. These decays share the same structure function, and the comparison results in a large cancellation of the theoretical uncertainties. In principle, this technique could lead to a determination of $|V_{ub}|$ with an uncertainty under 10%.

Over the past several years, the ALEPH [93], DELPHI [94], and L3 [95] experiments have attempted inclusive measurements of the $b \rightarrow u \ell \nu_\ell$ rate. The approaches are disparate, but tend to be sensitive to $b \rightarrow u \ell \nu$ primarily when the mass of the hadronic system (m_{X_u}) is in the region $m_{X_u} \lesssim M_D$. They are sensitive to a significantly larger portion of the phase space than the endpoint analyses, but at the cost of very large backgrounds from $b \rightarrow c \ell \nu_\ell$ decays (signal:background ratios of order 1:10). The branching fractions obtained are listed in Table 5. An average by the LEP Heavy Flavour Group [37] results in $|V_{ub}| = 4.04^{+0.41}_{-0.46} (\text{exp})^{+0.43}_{-0.48} (b \rightarrow c)^{+0.24}_{-0.25} (b \rightarrow u) \pm 0.02(\tau_b) \pm 0.19(\text{HQS})$. A note of caution, however. While observation of these decays at LEP is an experimental tour de force, the aggressive systematic errors assigned to unknown aspects of $b \rightarrow c \ell \nu_\ell$ and $b \rightarrow u \ell \nu_\ell$ processes remain a topic of discussion in the community. Among the concerns: the large uncertainties in the makeup of the non- D and D^* components of the background and the need for modeling of the $b \rightarrow u \ell \nu_\ell$ decays to correct for the smearing and nonuniform efficiency over the phase space of the decay.

A new proposal [89] to measure $|V_{ub}|$ inclusively in a restricted region of q^2 has promise. As mentioned above, measurements in the lepton endpoint region suffer from significant theoretical uncertainties from unknown structure functions. Analyses restricted to the hadronic mass range $m_{X_u} < \sqrt{\Lambda m_b}$ are affected by similar uncertainties, so the level appears to be much reduced [96,97], about 10%. The proposed method offers suppression of $b \rightarrow c \ell \nu_\ell$ background without introducing such uncertainties.

So far, the various determinations of $|V_{ub}|$ have produced consistent results. However, with the many theoretical and experimental difficulties with the measurements to date, the authors agree with the conservative assessment of the current uncertainties presented in the CKM review [98].

Table 5: Inclusive semileptonic branching fractions for $b \rightarrow u \ell \nu_\ell$ measured at LEP.

Experiment	Branching Fraction [10^{-3}]
ALEPH [93]	$1.73 \pm 0.55 \pm 0.55$
DELPHI [94]	$1.57 \pm 0.35 \pm 0.55$
L3 [95]	$3.3 \pm 1.0 \pm 1.7$

Hadronic B decays: In hadronic decays of B mesons, the underlying weak transition of the b quark is overshadowed by strong interaction effects caused by the surrounding cloud of light quarks and gluons. While this complicates the extraction of CKM matrix elements from experimental results, it also turns

See key on page 239

the B meson into an excellent laboratory to study perturbative and non-perturbative QCD, hadronization, and Final State Interaction (FSI) effects.

The precision of the experimental data has steadily improved over the past years. In 1997 CLEO updated most branching fractions for exclusive $B \rightarrow (n\pi)^- D^{(*)}$ and $B \rightarrow J/\psi K^{(*)}$ transitions. Tighter limits on color suppressed decays such as $\bar{B} \rightarrow D^0 \pi^0$ have been presented [99]. Updated measurements of the polarization in $B \rightarrow J/\psi K^*$ resolved an outstanding discrepancy between theory and experiment [100]. Angular distributions have been studied for other B decays with two vector mesons in the final state including $B \rightarrow D^* \rho$, $B \rightarrow D^* D^*$, and $B \rightarrow D^* D_s^*$. CLEO found the relative phases of the helicity amplitudes in $B \rightarrow D^* \rho^-$ decays to be non-zero [101], implying that FSI effects may play a role in B decays after all. $B^0 \rightarrow D^{*+} D^{*-}$ decays have been observed with a branching fraction of $(9.9_{-3.3}^{+4.2} \pm 1.2) \times 10^{-4}$, providing unambiguous evidence for Cabibbo-suppressed $b \rightarrow ccd$ transitions [102,103].

Gronau and Wyler [104] first suggested that decays of the type $B \rightarrow DK$ can be used to extract the angle γ of the CKM unitarity triangle, $\gamma \approx \arg(V_{ub})$. The first example of such a Cabibbo-suppressed mode has been observed by CLEO [105]:

$$\frac{\mathcal{B}(B^- \rightarrow D^0 K^-)}{\mathcal{B}(B^- \rightarrow D^0 \pi^-)} = 0.055 \pm 0.014 \pm 0.005. \quad (11)$$

Measurements of exclusive hadronic B decays have reached sufficient precision to challenge our understanding of the dynamics of these decays. It has been suggested that in analogy to semileptonic decays, two-body hadronic decays of B mesons can be expressed as the product of two independent hadronic currents, one describing the formation of a charm meson and the other the hadronization of the remaining $\bar{u}d$ (or $\bar{c}s$) system from the virtual W^- . Qualitatively, for a B decay with a large energy release, the $\bar{u}d$ pair, which is produced as a color singlet, travels fast enough to leave the interaction region without influencing the second hadron formed from the c quark and the spectator antiquark. The assumption that the amplitude can be expressed as the product of two hadronic currents is called “factorization” in this paper. By comparing exclusive hadronic B decays to the corresponding semileptonic modes the factorization hypothesis has been experimentally confirmed for certain $b \rightarrow c$ decays with large energy release [100]. An example is given by the longitudinal polarization of ρ mesons in $B \rightarrow D^* \rho$ decays, which was recently updated by the CLEO Collaboration [101]. Their result of $\Gamma_L/\Gamma = 0.878 \pm 0.034 \pm 0.040$ agrees well with the factorization expectation, 0.85–0.88 [106–109].

For internal spectator decays, the validity of the factorization hypothesis is also questionable and requires experimental verification. The naive color transparency argument used in the previous sections is not applicable to decays such as $B \rightarrow J/\psi K$, and there is no corresponding semileptonic decay for comparison. For internal spectator decays, one can only compare experimental observables to quantities predicted by

models based on factorization. Two such quantities are the production ratio

$$\mathcal{R} = \frac{\mathcal{B}(B \rightarrow J/\psi K^*)}{\mathcal{B}(B \rightarrow J/\psi K)} \quad (12)$$

and the amount of longitudinal polarization Γ_L/Γ in $B \rightarrow J/\psi K^*$ decays. The CLEO Collaboration published new data on $B \rightarrow$ charmonium transitions [110].

$$\mathcal{R} = 1.45 \pm 0.20 \pm 0.17, \quad \Gamma_L/\Gamma = 0.52 \pm 0.07 \pm 0.04, \quad (13)$$

are now consistent with factorization-based models.

In the decays of charm mesons, the effect of color suppression is obscured by the effects of FSI or reduced by nonfactorizable effects. Because of the larger mass of the b quark, a more consistent pattern of color-suppression is expected in the B system, and current experimental results seem to support that color-suppression is operative in hadronic decays of B mesons. Besides $B \rightarrow$ charmonium transitions, no other color-suppressed decay has been observed experimentally [99]. The current upper limit on $\mathcal{B}(\bar{B}^0 \rightarrow D^0 \pi^0)$ is 0.012% at 90% C.L.

By comparing hadronic B^- and \bar{B}^0 decays, the relative contributions from external and internal spectator decays have been disentangled. For all decay modes studied, the B^- branching fraction was found to be larger than the corresponding \bar{B}^0 branching ratio, indicating constructive interference between the external and internal spectator amplitudes. In the BSW model [111], the two amplitudes are proportional to effective coefficients, a_1 and a_2 , respectively. A least squares fit using experimental results and a model by Neubert *et al.* [112] gives

$$a_2/a_1 = 0.22 \pm 0.04 \pm 0.06, \quad (14)$$

where we have ignored uncertainties in the theoretical predictions. The second error is due to the uncertainty in the B -meson production fractions (f_+ , f_0) and lifetimes (τ_+ , τ_0) that enter into the determination of a_2/a_1 in the combination $(f_+ \tau_+ / f_0 \tau_0)$. As this ratio increases, the value of a_2/a_1 decreases. Varying $(f_+ \tau_+ / f_0 \tau_0)$ in the allowed experimental range excludes a negative value of a_2/a_1 . Other uncertainties in the magnitude of the decay constants f_D and f_{D^*} , as well as in the hadronic form factors, can change the magnitude of a_2/a_1 , but not its sign.

The magnitude of a_2 determined from this fit to the ratio of B^- and B^0 branching fractions is consistent with the value of $|a_2|$ determined from the fit to the $B \rightarrow J/\psi X$ decay modes, which only proceed via the color suppressed amplitude. The coefficient a_1 also shows little or no process dependency.

The observation that the coefficients a_1 and a_2 have the same relative sign in B^- decay came as a surprise, since destructive interference was observed in hadronic charm decay. The sign of a_2 disagrees with the theoretical extrapolation from the fit to charm meson decays using the BSW model. It also disagrees with the expectation from the $1/N_c$ rule [113]. The result may be consistent with the expectation of perturbative QCD [114]. B. Stech proposed that the observed interference

Meson Particle Listings

b -flavored hadrons

pattern in charged B and D decay can be understood in terms of the running strong coupling constant α_s [115]. A solution based on PQCD factorization theorems has been suggested by B. Tseng and H.N. Li [116].

Although constructive interference has been observed in all the B^- modes studied so far, these comprise only a small fraction of the total hadronic rate. It is conceivable that higher-multiplicity B^- decays demonstrate a very different behavior.

It is intriguing that $|a_1|$ determined from the $B \rightarrow D^{(*)}\pi$, $D^{(*)}\rho$ modes agrees well with the value of a_1 extracted from $B \rightarrow DD_s$ decays. The observation of color-suppressed decays such as $\bar{B}^0 \rightarrow D^0\pi^0$ would give another measure of $|a_2|$ complementary to that obtained from $B \rightarrow$ charmonium decays.

In summary, experimental results on exclusive B decay match very nicely with theoretical expectations. Unlike charm, the b quark appears to be heavy enough so that corrections due to the strong interaction are small. Factorization and color-suppression are at work. An intriguing pattern of constructive interference in charged B decays has been observed.

Inclusive hadronic decays: Over the last years, inclusive B decays have become an area of intensive studies, experimentally as well as theoretically. Since the hadronization process to specific final state mesons is not involved in inclusive calculations, the theoretical results and predictions are generally believed to be more reliable.

CLEO and the LEP Collaborations presented new measurements of inclusive $b \rightarrow c$ transitions that can be used to extract n_c , the number of charm quarks produced per b decay. Naively we expect $n_c = 115\%$, with the additional 15% coming from the fragmentation of the W boson to $\bar{c}s$. This expectation can be verified experimentally by adding all inclusive $b \rightarrow c$ branching fractions. Using CLEO and DELPHI results, we can perform the calculation shown in Table 6. Modes with 2 charm quarks in the final state are counted twice. For the unobserved $B \rightarrow \eta_c X$ decay, we take the experimental upper limit. B_s mesons and b baryons produced at the Z , but not at the $\Upsilon(4S)$, cause the increase in D_s and A_c production rates seen by LEP. To first order, however, this should not affect the charm yield, as it should be compensated by reduced branching fractions for D mesons. This reduction is not reflected in the current data, but the errors in the D branching fractions are still large. In addition, there are significant uncertainties in the D_s and A_c absolute branching fractions.

New measurements of the multiplicity of charm quarks per b decay have also been reported by ALEPH and OPAL [117]. Combining this with the DELPHI results yields a new correlated average of $n_c = 1.151 \pm 0.022 \pm 0.022 \pm 0.051$, where the errors are statistical, systematic and due to the uncertainties in charm branching fractions [118]. There is now good agreement between the results from the $\Upsilon(4S)$ and the Z^0 .

Table 6: Charm yield per B decay.

Channel	Branching fraction [%]	
	$\Upsilon(4S)$ [100]	LEP (DELPHI) [119]
$B \rightarrow D^0 X$	63.6 ± 3.0	60.05 ± 4.29
+ $B \rightarrow D^+ X$	23.5 ± 2.7	23.01 ± 2.13
+ $B \rightarrow D_s^+ X$	12.1 ± 1.7	16.65 ± 4.50
+ $B \rightarrow A_c^+ X$	2.9 ± 2.0	8.90 ± 3.0
+ $B \rightarrow \bar{E}_c^{+,0} X$	2.0 ± 1.0	4.00 ± 1.60
+ $2 \times B \rightarrow J/\psi_{\text{direct}} X$	0.8 ± 0.08	
+ $2 \times B \rightarrow \psi(2S)_{\text{direct}} X$	0.35 ± 0.05	
+ $2 \times B \rightarrow \chi_{c1} X$	0.37 ± 0.07	
+ $2 \times B \rightarrow \chi_{c2} X$	0.25 ± 0.1	
+ $2 \times B \rightarrow \eta_c X$	< 0.9 (90% C.L.)	
+ $2 \times b \rightarrow (c\bar{c}) X$		2.00 ± 0.65
n_c	110 ± 5	115.1 ± 7.4

The $b \rightarrow c\bar{c}s$ transition: It was previously assumed that the conventional $b \rightarrow c\bar{u}d \rightarrow DX$ and $b \rightarrow c\bar{c}s \rightarrow DD_s X$ mechanisms account for all D -meson production in B decay. Buchalla *et al.* [120] suggested that a significant fraction of D mesons could also arise from $b \rightarrow c\bar{c}s$ transitions with light quark pair production at the upper vertex, *i.e.* $b \rightarrow c\bar{c}s \rightarrow D\bar{D}X_s$. The two mechanisms can be distinguished by the different final states they produce. In the first case the final state includes only D mesons, whereas in the second case two D mesons can be produced, one of which has to be a \bar{D} .

Table 7: CLEO results on $B \rightarrow DDK$ decays.

Mode	Branching fraction
$B(\bar{B}^0 \rightarrow D^{*+}\bar{D}^0 K^-)$	$0.45_{-0.19}^{+0.25} \pm 0.08\%$
$B(B^- \rightarrow D^{*0}\bar{D}^0 K^-)$	$0.54_{-0.24}^{+0.33} \pm 0.12\%$
$B(\bar{B}^0 \rightarrow D^{*+}\bar{D}^{*0} K^-)$	$1.30_{-0.47}^{+0.61} \pm 0.27\%$
$B(B^- \rightarrow D^{*0}\bar{D}^{*0} K^-)$	$1.45_{-0.58}^{+0.78} \pm 0.36\%$

Two routes to search for this addition to $\Gamma(b \rightarrow c\bar{c}s)$ have been pursued experimentally. In an exclusive search for $B \rightarrow D\bar{D}K$ decays, CLEO required the final state to include a D and a \bar{D} meson. Statistically significant signals are observed for several $D^{(*)}\bar{D}^{(*)}$ combinations. The preliminary CLEO results are listed in Table 7 [121]. While the observation of these decays proves the existence of \bar{D} -meson production at the upper vertex, a more inclusive measurement is needed to estimate the overall magnitude of this effect. A recent CLEO analysis exploits the fact that the flavor of the final state D -meson tags the decay mechanism. High momentum leptons ($p_\ell > 1.4$ GeV/ c) are used to classify the flavor of the decaying B meson. $b \rightarrow c\bar{u}d$ transitions lead to $D\ell^+$ combinations, while the observation of $\bar{D}\ell^+$ identifies the new $b \rightarrow c\bar{c}s$ mechanism. Angular correlations are used to remove combinations with both particles coming from the same B meson. CLEO finds [122]

$$\frac{\Gamma(\bar{B} \rightarrow \bar{D}X)}{\Gamma(\bar{B} \rightarrow DX)} = 0.100 \pm 0.026 \pm 0.016, \quad (15)$$

See key on page 239

which implies

$$B(\bar{B} \rightarrow \bar{D}X) = 0.079 \pm 0.022. \quad (16)$$

We can now calculate $n_{cc} = B(b \rightarrow c\bar{c}s)$. n_{cc} is related to n_c , the number of charm quarks produced per b decay

$$n_c = 1 + n_{cc} - n_{B \rightarrow \text{no charm}}. \quad (17)$$

Using the data listed in Table 6 and the above result, we find

$$n_{cc} = (23.9 \pm 3.0)\%. \quad (18)$$

The contribution from $B \rightarrow \Xi_c^0 X$ was reduced by 1/3 to take into account the fraction that is not produced by the $b \rightarrow c\bar{c}s$ subprocess, but by $b \rightarrow c\bar{u}d + s\bar{s}$ quark pair production.

This result is consistent with theoretical predictions, $n_{cc} = 22 \pm 6\%$ [28,123]. $b \rightarrow D\bar{D}X$ decays have also been observed at LEP and at the SLC. ALEPH [102] finds

$$B(B \rightarrow D^0 \bar{D}^0 X + D^0 D^+ X) = 0.078_{-0.018}^{+0.02} \text{ }_{-0.015}^{+0.017+0.005} \text{ }_{-0.004} \text{ ,} \quad (19)$$

where the last error reflects the uncertainty in D meson branching fractions. DELPHI and SLD look for double charm decays of b hadrons by selecting events that are consistent with having two decay vertices. They find $n_{2c} = (13.6 \pm 4.2)\%$ [124] and $n_{2c} = (16.2 \pm 1.9 \pm 4.2)\%$ [125], respectively. n_{2c} does not include $B \rightarrow \text{Charmonium}$ production. Taking this into account we find that these results are consistent with n_{cc} . DELPHI used a b -tagging technique to measure the inclusive charmless B branching fraction to 0.033 ± 0.021 . Subtracting charmonium production allows them to set an upper limit on charmless B decays of 3.7% at 95% CL [124].

Charm Counting and the Semileptonic Branching Fraction: The charm yield per B meson decay is related to an intriguing puzzle in B physics: the experimental value for the semileptonic branching ratio of B mesons, $B(B \rightarrow X\ell\nu) = 10.49 \pm 0.17 \pm 0.43\%$ ($\Upsilon(4S)$), is significantly below the theoretical lower bound $B > 12.5\%$ from QCD calculations within the parton model [126]. Since the semileptonic and hadronic widths are connected via

$$1/\tau = \Gamma = \Gamma_{\text{Semileptonic}} + \Gamma_{\text{Hadronic}}$$

an enhanced hadronic rate is necessary to accommodate the low semileptonic branching fraction. The hadronic width, which can be expressed as

$$\Gamma_{\text{Hadronic}} = \Gamma(b \rightarrow c\bar{c}s) + \Gamma(b \rightarrow c\bar{u}d) + \Gamma(b \rightarrow sg + \text{no charm})$$

is constraint by another experimental quantity, n_c , the average number of charm quarks produced per b decay.

For years it has been difficult to accommodate the experimental results with the theoretical preference for a larger values for B_{sl} , n_c and n_{cc} . Additional confusion has been caused by an apparent discrepancy between LEP (Z^0) and CLEO ($\Upsilon(4S)$) results. The latter issue, however, has been resolved with both the LEP average for B_{sl} and n_c coming down. There is now good agreement between the experiments. Several explanations of this n_c/B_{sl} discrepancy have been proposed:

1. enhancement of $b \rightarrow c\bar{c}s$ due to large QCD corrections or a breakdown of local duality;
2. enhancement of $b \rightarrow c\bar{u}d$ due to non-perturbative effects;
3. enhancement of $b \rightarrow sg$ and/or $b \rightarrow dg$ due to New Physics;
4. systematic problem in the experimental results;

or the problem could be caused by some combination of the above.

Arguably the most intriguing solution to this puzzle would be an enhanced $b \rightarrow sg$ rate but as we will see in the next section, new results from CLEO and LEP show no indication for New Physics and place tight limits on this process.

$B(b \rightarrow c\bar{u}d)$ has been calculated to next-to-leading order. Bagan *et al.* [127] find:

$$\tau_{ud} = \frac{B(b \rightarrow c\bar{u}d)}{B(b \rightarrow c\bar{\nu})} = 4.0 \pm 0.4 \rightarrow B(b \rightarrow c\bar{u}d)_{\text{Theory}} = 41 \pm 4\%$$

which compares well with the experimental value of $43 \pm 6\%$ [100] but the errors are still too large to completely rule out an enhanced $b \rightarrow c\bar{u}d$ rate.

The theoretically preferred solution calls for an enhancement of the $b \rightarrow c\bar{c}s$ channel [127,28]. Increasing the $b \rightarrow c\bar{c}s$ component, however, would increase the average number of c quarks produced per b quark decay as well as n_{cc} , the number of b decays with 2 charm quarks in the final state. This is not supported by the data, in particular the value of n_c appears to be too low at the few σ -level. Systematic problems with D meson branching fractions have been pointed out as potential solution [128] but new results from ALEPH [129] and CLEO [130] on $B(D^0 \rightarrow K^-\pi^+)$ make this less likely.

After years of experimental and theoretical efforts the missing charm/ B_{sl} problem has begun to fade away. The discrepancy between experiments at the $\Upsilon(4S)$ and the Z^0 has been resolved. More data are needed to either resolve this issue or to demonstrate that the problem persists.

Rare B decays: All B -meson decays that do not occur through the usual $b \rightarrow c$ transition are known as rare B decays. These include both tree level semileptonic and hadronic $b \rightarrow u$ decays that are suppressed by the small CKM matrix element V_{ub} , as well as higher order processes such as electromagnetic and gluonic penguin decays. Branching fractions are typically around 10^{-5} , for exclusive channels, and sophisticated background suppression techniques are essential for these analyses.

Arguably the most exciting new experimental results since the last edition of this review are in the field of rare B decays. For many charmless B -decay modes the addition of new data and the refinement of analysis techniques allowed CLEO to observe signals where previously there have been upper limits. For other channels new tighter upper limits have been published.

Hadronic $b \rightarrow u$ transitions: Using almost 20 million charged and neutral B decays, CLEO successfully reconstructed a handful of exclusive hadronic $B^0 \rightarrow \pi^+\pi^-$ decays [131]. As

Meson Particle Listings

b-flavored hadrons

can be seen in Table 8, the branching fraction for this mode is about a factor of 4 smaller than the rate of $B \rightarrow K\pi$ transitions. This is not good news for CP -violation studies. Not only is the branching fraction very small, but in addition the analysis will be complicated by “penguin pollution.”

A theoretically clean method to determine the sum of the angles $\beta + \gamma$ of the unitarity triangle has been proposed by Snyder and Quinn [136]. They suggest that a sample of 10^3 $B \rightarrow \rho\pi$ decays, together with a Dalitz plot analysis, allow a measurement of $\beta + \gamma$ to about 6° . CLEO has recently measured the branching fraction for these modes [132]

$$B(B^+ \rightarrow \rho^0 \pi^+) = (1.5 \pm 0.5 \pm 0.4) \times 10^{-5} \quad (20)$$

$$B(B^0 \rightarrow \rho^\pm \pi^\mp) = (3.5^{+1.1}_{-1.0} \pm 0.5) \times 10^{-5} \quad (21)$$

but it will take a while before a sufficiently large data sample will be available.

Table 8: Summary of CLEO results on $B \rightarrow \pi\pi, K\pi$, and KK branching fractions. The branching fractions and the 90% C.L. upper limits are given in units of 10^{-5} . Using the notation of Gronau *et al.* [137], the third column indicates the dominant amplitudes for each decay (T, C, P, E denote tree, color suppressed, penguin, and exchange amplitudes and the unprimed (primed) amplitudes refer to $\bar{b} \rightarrow \bar{u}u\bar{d}$ ($\bar{b} \rightarrow \bar{u}u\bar{s}$) transitions, respectively.)

Mode ($B \rightarrow$)	B	Amplitude	Theoretical expectation
$\pi^+ \pi^-$	$0.43^{+0.16}_{-0.14} \pm 0.05$	$-(T + P)$	0.8–2.6
$\pi^+ \pi^0$	< 1.3	$-(T + C)/\sqrt{2}$	0.4–2.0
$\pi^0 \pi^0$	< 0.93	$-(C - P)/\sqrt{2}$	0.006–0.1
$K^+ \pi^-$	$1.72^{+0.25}_{-0.24} \pm 0.12$	$-(T' + P')$	0.7–2.4
$K^+ \pi^0$	$1.16^{+0.30+0.14}_{-0.27-0.13}$	$-(T' + C' + P')/\sqrt{2}$	0.3–1.3
$K^0 \pi^-$	$1.82^{+0.46}_{-0.40} \pm 0.16$	P'	0.8–1.5
$K^0 \pi^0$	$1.46^{+0.59+0.24}_{-0.51-0.33}$	$-(C' - P')/\sqrt{2}$	0.3–0.8
$K^+ K^-$	< 0.19	E	—
$K^+ K^0$	< 0.51	P	0.07–0.13
$K^0 K^0$	< 1.7	P	0.07–0.12

Electromagnetic penguin decays: The observation of the decay $B \rightarrow K^*(892)\gamma$, reported in 1993 by the CLEO II experiment, provided first evidence for the one-loop penguin diagram [138]. Using a larger data sample, the analysis was re-done in 1999 [139] yielding a total of 125 events and

$$B(B^0 \rightarrow K^{*0}\gamma) = (4.55^{+0.72}_{-0.68} \pm 0.34) \times 10^{-5}, \quad (22)$$

$$B(B^+ \rightarrow K^{*+}\gamma) = (3.76^{+0.89}_{-0.83} \pm 0.28) \times 10^{-5}. \quad (23)$$

The decay $B \rightarrow K_2^*(1430)\gamma$ was seen with a branching fraction of $(1.66^{+0.59}_{-0.53} \pm 0.13) \times 10^{-5}$. No evidence for the decays $B \rightarrow \rho\gamma$ and $B \rightarrow \omega\gamma$ was found. The current upper limit for the ratio $B(B \rightarrow (\rho/\omega)\gamma)/B(B \rightarrow K^*\gamma)$ is 0.32 at 90% CL. The limit on the ratio of branching fractions implies that $|V_{td}/V_{ts}| < 0.75$ at 90% CL.

The observed branching fractions were used to constrain a large class of Standard Model extensions [140]. However, due to

the uncertainties in the hadronization, only the inclusive $b \rightarrow s\gamma$ rate can be reliably compared with theoretical calculations. This rate can be measured from the endpoint of the inclusive photon spectrum in B decay. CLEO [141] found

$$B(b \rightarrow s\gamma) = (3.15 \pm 0.35 \pm 0.41) \times 10^{-4} \text{ (CLEO)}, \quad (24)$$

to be compared to the Standard Model rate [142–144] of

$$B(b \rightarrow s\gamma)_{SM} = (3.28 \pm 0.33) \times 10^{-4}. \quad (25)$$

ALEPH used a lifetime tagged sample of $Z \rightarrow b\bar{b}$ events to search for high-energy photons in the hemisphere opposite to the tag. This allows them to measure the photon spectrum from B decays which ultimately leads to [145]

$$B(b \rightarrow s\gamma) = (3.11 \pm 0.80 \pm 0.72) \times 10^{-4} \text{ (ALEPH)}. \quad (26)$$

Our theoretical understanding of inclusive $b \rightarrow s\gamma$ transitions has been significantly enhanced by two new calculations that now include all terms to next-to-leading order [142–144]. The expected Standard Model rate, while slightly larger now, is still consistent with both the CLEO and ALEPH results. The substantially reduced uncertainties result in tighter constraints on new physics such as double Higgs models [146].

Gluonic penguin decays: A larger total rate is expected for gluonic penguins, the counterpart of $b \rightarrow s\gamma$ with the photon replaced by a gluon.

Experimentally, it is a major challenge to measure the inclusive $b \rightarrow sg$ rate. The virtual gluon hadronizes as a $q\bar{q}$ pair without leaving a characteristic signature in the detector. CLEO extended D - ℓ correlation measurements described in the section on hadronic B decays to obtain the flavor specific decay rate $\Gamma(\bar{B} \rightarrow DX)_{\text{lower vertex}}/\Gamma_{\text{total}}$. This quantity should be 1 minus corrections for charmonium production, $b \rightarrow u$ transitions, $B \rightarrow$ baryons, and D_s production at the lower vertex. Most importantly, the $b \rightarrow sg$ rate must also be subtracted. To remove uncertainties due to $B(D^0 \rightarrow K^-\pi^+)$, CLEO normalizes to $\Gamma(\bar{B} \rightarrow DX\ell\nu_\ell)/\Gamma(\bar{B} \rightarrow X\ell\nu_\ell)$. Their preliminary result is

$$\frac{\Gamma(\bar{B} \rightarrow DX)_{\text{lower vertex}}/\Gamma_{\text{total}}}{\Gamma(\bar{B} \rightarrow DX\ell\nu_\ell)/\Gamma(\bar{B} \rightarrow X\ell\nu_\ell)} = 0.901 \pm 0.034 \pm 0.014 \quad (27)$$

whereas $0.903 \pm 0.018 - (b \rightarrow sg)$ was expected. This corresponds to an upper limit of $B(b \rightarrow sg) < 6.8\%$ at 90% CL [122]. DELPHI [147] studied the p_T spectrum of charged kaons in B decays and found a model-dependent limit $B(b \rightarrow sg) < 5\%$ (95% C.L.). These results agree well with the Standard Model prediction of $B(\bar{B} \rightarrow \text{no charm}) = (1.6 \pm 0.8)\%$ [148], and there is little experimental support for new physics and an enhanced $b \rightarrow sg$ rate [149]. However, experimental uncertainties are still large, and it is too early to draw final conclusions.

Exclusive decays such as $B \rightarrow K^+\pi^-$ are suppressed at tree level and are expected to proceed via loop processes. CLEO studied these decay modes, and all 4 $K\pi$ combinations have been observed [131]. The results are listed in Table 8.

THIS PAGE IS MISSING

THIS PAGE IS MISSING

THIS PAGE IS MISSING

THIS PAGE IS MISSING

THIS PAGE IS MISSING

THIS PAGE IS MISSING

THIS PAGE IS MISSING

THIS PAGE IS MISSING

THIS PAGE IS MISSING

THIS PAGE IS MISSING

THIS PAGE IS MISSING

THIS PAGE IS MISSING

THIS PAGE IS MISSING

THIS PAGE IS MISSING

THIS PAGE IS MISSING

THIS PAGE IS MISSING

See key on page 239

Meson Particle Listings

 B^0

D, D*, or D _s modes			K or K* modes		
Γ ₈	D ⁻ π ⁺	(3.0 ± 0.4) × 10 ⁻³	Γ ₆₉	K ⁺ π ⁻	(1.5 ^{+0.5} _{-0.4}) × 10 ⁻⁵
Γ ₉	D ⁻ ρ ⁺	(7.9 ± 1.4) × 10 ⁻³	Γ ₇₀	K ⁰ π ⁰	< 4.1 × 10 ⁻⁵
Γ ₁₀	\bar{D}^0 π ⁺ π ⁻	< 1.6 × 10 ⁻³	CL=90%		
Γ ₁₁	D*(2010) ⁻ π ⁺	(2.76 ± 0.21) × 10 ⁻³	Γ ₇₁	η ⁺ K ⁰	(4.7 ^{+2.8} _{-2.2}) × 10 ⁻⁵
Γ ₁₂	D ⁻ π ⁺ π ⁺ π ⁻	(8.0 ± 2.5) × 10 ⁻³	Γ ₇₂	η ⁺ K*(892) ⁰	< 3.9 × 10 ⁻⁵
Γ ₁₃	(D ⁻ π ⁺ π ⁺ π ⁻) nonresonant	(3.9 ± 1.9) × 10 ⁻³	Γ ₇₃	ηK*(892) ⁰	< 3.0 × 10 ⁻⁵
Γ ₁₄	D ⁻ π ⁺ ρ ⁰	(1.1 ± 1.0) × 10 ⁻³	Γ ₇₄	ηK ⁰	< 3.3 × 10 ⁻⁵
Γ ₁₅	D ⁻ a ₁ (1260) ⁺	(6.0 ± 3.3) × 10 ⁻³	Γ ₇₅	ωK ⁰	< 5.7 × 10 ⁻⁵
Γ ₁₆	D*(2010) ⁻ π ⁺ π ⁰	(1.5 ± 0.5) %	Γ ₇₆	ωK*(892) ⁰	< 2.3 × 10 ⁻⁵
Γ ₁₇	D*(2010) ⁻ ρ ⁺	(6.8 ± 3.4) × 10 ⁻³	Γ ₇₇	K ⁺ K ⁻	< 4.3 × 10 ⁻⁶
Γ ₁₈	D*(2010) ⁻ π ⁺ π ⁺ π ⁻	(7.6 ± 1.8) × 10 ⁻³	Γ ₇₈	K ⁰ \bar{K}^0	< 1.7 × 10 ⁻⁵
Γ ₁₉	(D*(2010) ⁻ π ⁺ π ⁺ π ⁻) non-resonant	(0.0 ± 2.5) × 10 ⁻³	Γ ₇₉	K ⁺ ρ ⁻	< 3.5 × 10 ⁻⁵
Γ ₂₀	D*(2010) ⁻ π ⁺ ρ ⁰	(5.7 ± 3.2) × 10 ⁻³	Γ ₈₀	K ⁰ π ⁺ π ⁻	
Γ ₂₁	D*(2010) ⁻ a ₁ (1260) ⁺	(1.30 ± 0.27) %	Γ ₈₁	K ⁰ ρ ⁰	< 3.9 × 10 ⁻⁵
Γ ₂₂	D*(2010) ⁻ π ⁺ π ⁺ π ⁻ π ⁰	(3.5 ± 1.8) %	Γ ₈₂	K ⁰ f ₀ (980)	< 3.6 × 10 ⁻⁴
Γ ₂₃	$\bar{D}_s^*(2460)$ ⁻ π ⁺	< 2.2 × 10 ⁻³	CL=90%		
Γ ₂₄	$\bar{D}_s^*(2460)$ ⁻ ρ ⁺	< 4.9 × 10 ⁻³	CL=90%		
Γ ₂₅	D ⁻ D ⁺	< 1.2 × 10 ⁻³	CL=90%		
Γ ₂₆	D ⁻ D _s ⁺	(8.0 ± 3.0) × 10 ⁻³	Γ ₈₃	K*(892) ⁺ π ⁻	< 7.2 × 10 ⁻⁵
Γ ₂₇	D*(2010) ⁻ D _s ⁺	(9.6 ± 3.4) × 10 ⁻³	Γ ₈₄	K*(892) ⁰ π ⁰	< 2.8 × 10 ⁻⁵
Γ ₂₈	D ⁻ D _s ⁺	(1.0 ± 0.5) %	Γ ₈₅	K ₂ [*] (1430) ⁺ π ⁻	< 2.6 × 10 ⁻³
Γ ₂₉	D*(2010) ⁻ D _s ⁺	(2.0 ± 0.7) %	Γ ₈₆	K ⁰ K ⁺ K ⁻	< 1.3 × 10 ⁻³
Γ ₃₀	D _s ⁺ π ⁻	< 2.8 × 10 ⁻⁴	CL=90%		
Γ ₃₁	D _s ⁺ π ⁰	< 5 × 10 ⁻⁴	CL=90%		
Γ ₃₂	D _s ⁺ ρ ⁻	< 7 × 10 ⁻⁴	CL=90%		
Γ ₃₃	D _s ⁺ ρ ⁰	< 8 × 10 ⁻⁴	CL=90%		
Γ ₃₄	D _s ⁺ a ₁ (1260) ⁻	< 2.6 × 10 ⁻³	CL=90%		
Γ ₃₅	D _s ⁺ a ₁ (1260) ⁰	< 2.2 × 10 ⁻³	CL=90%		
Γ ₃₆	D _s ⁺ K ⁺	< 2.4 × 10 ⁻⁴	CL=90%		
Γ ₃₇	D _s ⁺ K ⁰	< 1.7 × 10 ⁻⁴	CL=90%		
Γ ₃₈	D _s ⁺ K*(892) ⁺	< 9.9 × 10 ⁻⁴	CL=90%		
Γ ₃₉	D _s ⁺ K*(892) ⁰	< 1.1 × 10 ⁻³	CL=90%		
Γ ₄₀	D _s ⁺ π ⁺ K ⁰	< 5 × 10 ⁻³	CL=90%		
Γ ₄₁	D _s ⁺ π ⁺ K ⁺	< 3.1 × 10 ⁻³	CL=90%		
Γ ₄₂	D _s ⁺ π ⁺ K*(892) ⁰	< 4 × 10 ⁻³	CL=90%		
Γ ₄₃	D _s ⁺ π ⁺ K*(892) ⁺	< 2.0 × 10 ⁻³	CL=90%		
Γ ₄₄	\bar{D}^0 π ⁰	< 1.2 × 10 ⁻⁴	CL=90%		
Γ ₄₅	\bar{D}^0 ρ ⁰	< 3.9 × 10 ⁻⁴	CL=90%		
Γ ₄₆	\bar{D}^0 η	< 1.3 × 10 ⁻⁴	CL=90%		
Γ ₄₇	\bar{D}^0 η'	< 9.4 × 10 ⁻⁴	CL=90%		
Γ ₄₈	\bar{D}^0 ω	< 5.1 × 10 ⁻⁴	CL=90%		
Γ ₄₉	$\bar{D}^*(2007)^0$ π ⁰	< 4.4 × 10 ⁻⁴	CL=90%		
Γ ₅₀	$\bar{D}^*(2007)^0$ ρ ⁰	< 5.6 × 10 ⁻⁴	CL=90%		
Γ ₅₁	$\bar{D}^*(2007)^0$ η	< 2.6 × 10 ⁻⁴	CL=90%		
Γ ₅₂	$\bar{D}^*(2007)^0$ η'	< 1.4 × 10 ⁻³	CL=90%		
Γ ₅₃	$\bar{D}^*(2007)^0$ ω	< 7.4 × 10 ⁻⁴	CL=90%		
Γ ₅₄	D*(2010) ⁺ D*(2010) ⁻	(6.2 ^{+4.1} _{-3.1}) × 10 ⁻⁴			
Γ ₅₅	D*(2010) ⁺ D ⁻	< 1.8 × 10 ⁻³	CL=90%		
Γ ₅₆	D*(2010) ⁺ \bar{D}^{*0}	< 2.7 %	CL=90%		
Charmonium modes			Light unflavored meson modes		
Γ ₅₇	J/ψ(1S)K ⁰	(8.9 ± 1.2) × 10 ⁻⁴	Γ ₁₀₇	π ⁺ π ⁻	< 1.5 × 10 ⁻⁵
Γ ₅₈	J/ψ(1S)K ⁺ π ⁻	(1.2 ± 0.6) × 10 ⁻³	Γ ₁₀₈	π ⁰ π ⁰	< 9.3 × 10 ⁻⁶
Γ ₅₉	J/ψ(1S)K*(892) ⁰	(1.50 ± 0.17) × 10 ⁻³	Γ ₁₀₉	ηπ ⁰	< 8 × 10 ⁻⁶
Γ ₆₀	J/ψ(1S)π ⁰	< 5.8 × 10 ⁻⁵	CL=90%		
Γ ₆₁	J/ψ(1S)η	< 1.2 × 10 ⁻³	CL=90%		
Γ ₆₂	J/ψ(1S)ρ ⁰	< 2.5 × 10 ⁻⁴	CL=90%		
Γ ₆₃	J/ψ(1S)ω	< 2.7 × 10 ⁻⁴	CL=90%		
Γ ₆₄	ψ(2S)K ⁰	< 8 × 10 ⁻⁴	CL=90%		
Γ ₆₅	ψ(2S)K ⁺ π ⁻	< 1 × 10 ⁻³	CL=90%		
Γ ₆₆	ψ(2S)K*(892) ⁰	(9.3 ± 2.3) × 10 ⁻⁴			
Γ ₆₇	χ _{c1} (1P)K ⁰	< 2.7 × 10 ⁻³	CL=90%		
Γ ₆₈	χ _{c1} (1P)K*(892) ⁰	< 2.1 × 10 ⁻³	CL=90%		
Γ ₁₁₀	ηη	< 1.8 × 10 ⁻⁵	CL=90%		
Γ ₁₁₁	η'η	< 1.1 × 10 ⁻⁵	CL=90%		
Γ ₁₁₂	η'η'	< 4.7 × 10 ⁻⁵	CL=90%		
Γ ₁₁₃	η'η	< 2.7 × 10 ⁻⁵	CL=90%		
Γ ₁₁₄	η'ρ ⁰	< 2.3 × 10 ⁻⁵	CL=90%		
Γ ₁₁₅	ηρ ⁰	< 1.3 × 10 ⁻⁵	CL=90%		
Γ ₁₁₆	ωη	< 1.2 × 10 ⁻⁵	CL=90%		
Γ ₁₁₇	ωη'	< 6.0 × 10 ⁻⁵	CL=90%		
Γ ₁₁₈	ωρ ⁰	< 1.1 × 10 ⁻⁵	CL=90%		
Γ ₁₁₉	ωω	< 1.9 × 10 ⁻⁵	CL=90%		
Γ ₁₂₀	φπ ⁰	< 5 × 10 ⁻⁶	CL=90%		
Γ ₁₂₁	φη	< 9 × 10 ⁻⁶	CL=90%		
Γ ₁₂₂	φη'	< 3.1 × 10 ⁻⁵	CL=90%		
Γ ₁₂₃	φρ ⁰	< 1.3 × 10 ⁻⁵	CL=90%		
Γ ₁₂₄	φω	< 2.1 × 10 ⁻⁵	CL=90%		
Γ ₁₂₅	φφ	< 1.2 × 10 ⁻⁵	CL=90%		
Γ ₁₂₆	π ⁺ π ⁻ π ⁰	< 7.2 × 10 ⁻⁴	CL=90%		
Γ ₁₂₇	ρ ⁰ π ⁰	< 2.4 × 10 ⁻⁵	CL=90%		
Γ ₁₂₈	ρ [±] π [±]	[c] < 8.8 × 10 ⁻⁵	CL=90%		
Γ ₁₂₉	π ⁺ π ⁻ π ⁺ π ⁻	< 2.3 × 10 ⁻⁴	CL=90%		
Γ ₁₃₀	ρ ⁰ ρ ⁰	< 2.8 × 10 ⁻⁴	CL=90%		
Γ ₁₃₁	a ₁ (1260) [±] π [±]	[c] < 4.9 × 10 ⁻⁴	CL=90%		
Γ ₁₃₂	a ₂ (1320) [±] π [±]	[c] < 3.0 × 10 ⁻⁴	CL=90%		
Γ ₁₃₃	π ⁺ π ⁻ π ⁰ π ⁰	< 3.1 × 10 ⁻³	CL=90%		
Γ ₁₃₄	ρ ⁺ ρ ⁻	< 2.2 × 10 ⁻³	CL=90%		
Γ ₁₃₅	a ₁ (1260) ⁰ π ⁰	< 1.1 × 10 ⁻³	CL=90%		
Γ ₁₃₆	ωπ ⁰	< 1.4 × 10 ⁻⁵	CL=90%		

Meson Particle Listings

B^0

Γ_{137}	$\pi^+\pi^+\pi^-\pi^-\pi^0$	< 9.0	$\times 10^{-3}$	CL=90%
Γ_{138}	$a_1(1260)^+\rho^-$	< 3.4	$\times 10^{-3}$	CL=90%
Γ_{139}	$a_1(1260)^0\rho^0$	< 2.4	$\times 10^{-3}$	CL=90%
Γ_{140}	$\pi^+\pi^+\pi^-\pi^-\pi^0$	< 3.0	$\times 10^{-3}$	CL=90%
Γ_{141}	$a_1(1260)^+a_1(1260)^-$	< 2.8	$\times 10^{-3}$	CL=90%
Γ_{142}	$\pi^+\pi^+\pi^-\pi^-\pi^0$	< 1.1	%	CL=90%

Baryon modes

Γ_{143}	$\rho\bar{p}$	< 7.0	$\times 10^{-6}$	CL=90%
Γ_{144}	$\rho\bar{p}\pi^+\pi^-$	< 2.5	$\times 10^{-4}$	CL=90%
Γ_{145}	$\rho\bar{\Lambda}\pi^-$	< 1.3	$\times 10^{-5}$	CL=90%
Γ_{146}	$\bar{\Lambda}\bar{\Lambda}$	< 3.9	$\times 10^{-6}$	CL=90%
Γ_{147}	$\Delta^0\Delta^0$	< 1.5	$\times 10^{-3}$	CL=90%
Γ_{148}	$\Delta^{++}\Delta^{--}$	< 1.1	$\times 10^{-4}$	CL=90%
Γ_{149}	$\Sigma_c^-\Delta^{++}$	< 1.0	$\times 10^{-3}$	CL=90%
Γ_{150}	$\bar{\Lambda}_c^-\rho\pi^+\pi^-$	$(1.3 \pm 0.6) \times 10^{-3}$		
Γ_{151}	$\bar{\Lambda}_c^-\rho$	< 2.1	$\times 10^{-4}$	CL=90%
Γ_{152}	$\bar{\Lambda}_c^-\rho\pi^0$	< 5.9	$\times 10^{-4}$	CL=90%
Γ_{153}	$\bar{\Lambda}_c^-\rho\pi^+\pi^-\pi^0$	< 5.07	$\times 10^{-3}$	CL=90%
Γ_{154}	$\bar{\Lambda}_c^-\rho\pi^+\pi^-\pi^+\pi^-$	< 2.74	$\times 10^{-3}$	CL=90%

Lepton Family number (LF) violating modes, or $\Delta B = 1$ weak neutral current (BI) modes

Γ_{155}	$\gamma\gamma$	< 3.9	$\times 10^{-5}$	CL=90%
Γ_{156}	e^+e^-	B1 < 5.9	$\times 10^{-6}$	CL=90%
Γ_{157}	$\mu^+\mu^-$	B1 < 6.8	$\times 10^{-7}$	CL=90%
Γ_{158}	$K^0e^+e^-$	B2 < 3.0	$\times 10^{-4}$	CL=90%
Γ_{159}	$K^0\mu^+\mu^-$	B2 < 3.6	$\times 10^{-4}$	CL=90%
Γ_{160}	$K^*(892)^0e^+e^-$	B1 < 2.9	$\times 10^{-4}$	CL=90%
Γ_{161}	$K^*(892)^0\mu^+\mu^-$	B1 < 4.0	$\times 10^{-6}$	CL=90%
Γ_{162}	$K^*(892)^0\nu\bar{\nu}$	B1 < 1.0	$\times 10^{-3}$	CL=90%
Γ_{163}	$e^\pm\tau^\mp$	LF [c] < 3.5	$\times 10^{-6}$	CL=90%
Γ_{164}	$e^\pm\tau^\mp$	LF [c] < 5.3	$\times 10^{-4}$	CL=90%
Γ_{165}	$\mu^\pm\tau^\mp$	LF [c] < 8.3	$\times 10^{-4}$	CL=90%

- [a] An ℓ indicates an e or a μ mode, not a sum over these modes.
- [b] B^0 and B_s^0 contributions not separated. Limit is on weighted average of the two decay rates.
- [c] The value is for the sum of the charge states or particle/antiparticle states indicated.

B^0 BRANCHING RATIOS

For branching ratios in which the charge of the decaying B is not determined, see the B^\pm section.

$\Gamma(\ell^+\nu_\ell \text{ anything})/\Gamma_{\text{total}}$		Γ_1/Γ	
VALUE	DOCUMENT ID	TECN	COMMENT
0.105 ± 0.008 OUR AVERAGE			
$0.1078 \pm 0.0060 \pm 0.0069$	30 ARTUSO 97	CLE2	$e^+e^- \rightarrow \mathcal{T}(4S)$
$0.093 \pm 0.011 \pm 0.015$	ALBRECHT 94	ARG	$e^+e^- \rightarrow \mathcal{T}(4S)$
$0.099 \pm 0.030 \pm 0.009$	HENDERSON 92	CLEO	$e^+e^- \rightarrow \mathcal{T}(4S)$
● ● ● We do not use the following data for averages, fits, limits, etc. ● ● ●			
$0.109 \pm 0.007 \pm 0.011$	ATHANAS 94	CLE2	Sup. by ARTUSO 97

30 ARTUSO 97 uses partial reconstruction of $B \rightarrow D^*\ell\nu_\ell$ and inclusive semileptonic branching ratio from BARISH 96B ($0.1049 \pm 0.0017 \pm 0.0043$).

$\Gamma(D^-\ell^+\nu_\ell)/\Gamma_{\text{total}}$		Γ_2/Γ	
VALUE	DOCUMENT ID	TECN	COMMENT
0.0210 ± 0.0019 OUR AVERAGE			
$0.0209 \pm 0.0013 \pm 0.0018$	31 BARTELT 99	CLE2	$e^+e^- \rightarrow \mathcal{T}(4S)$
$0.0235 \pm 0.0020 \pm 0.0044$	32 BUSKULIC 97	ALEP	$e^+e^- \rightarrow Z$
$0.018 \pm 0.006 \pm 0.003$	33 FULTON 91	CLEO	$e^+e^- \rightarrow \mathcal{T}(4S)$
$0.020 \pm 0.007 \pm 0.006$	34 ALBRECHT 89J	ARG	$e^+e^- \rightarrow \mathcal{T}(4S)$
● ● ● We do not use the following data for averages, fits, limits, etc. ● ● ●			
$0.0187 \pm 0.0015 \pm 0.0032$	35 ATHANAS 97	CLE2	Repl. by BARTELT 99

- 31 Assumes equal production of B^+ and B^0 at the $\mathcal{T}(4S)$.
- 32 BUSKULIC 97 assumes fraction (B^+) = fraction (B^0) = (37.8 ± 2.2)% and PDG 96 values for B lifetime and branching ratio of D^* and D decays.
- 33 FULTON 91 assumes assuming equal production of B^0 and B^+ at the $\mathcal{T}(4S)$ and Mark III D and D^* branching ratios.
- 34 ALBRECHT 89J reports $0.018 \pm 0.006 \pm 0.005$. We rescale using the method described in STONE 94 but with the updated PDG 94 $B(D^0 \rightarrow K^-\pi^+)$.
- 35 ATHANAS 97 uses missing energy and missing momentum to reconstruct neutrino.

$\Gamma(D^*(2010)^-\ell^+\nu_\ell)/\Gamma_{\text{total}}$		Γ_3/Γ	
VALUE	DOCUMENT ID	TECN	COMMENT
0.0460 ± 0.0027 OUR AVERAGE			
$0.0508 \pm 0.0021 \pm 0.0066$	36 ACKERSTAFF 97G	OPAL	$e^+e^- \rightarrow Z$
$0.0553 \pm 0.0026 \pm 0.0052$	37 BUSKULIC 97	ALEP	$e^+e^- \rightarrow Z$
$0.0552 \pm 0.0017 \pm 0.0068$	38 ABREU 96P	DLPH	$e^+e^- \rightarrow Z$
$0.0449 \pm 0.0032 \pm 0.0039$	376 BARISH 95	CLE2	$e^+e^- \rightarrow \mathcal{T}(4S)$
$0.045 \pm 0.003 \pm 0.004$	40 ALBRECHT 94	ARG	$e^+e^- \rightarrow \mathcal{T}(4S)$
$0.047 \pm 0.005 \pm 0.005$	235 41 ALBRECHT 93	ARG	$e^+e^- \rightarrow \mathcal{T}(4S)$
$0.040 \pm 0.004 \pm 0.006$	42 BORTOLETTO89B	CLEO	$e^+e^- \rightarrow \mathcal{T}(4S)$
● ● ● We do not use the following data for averages, fits, limits, etc. ● ● ●			
$0.0518 \pm 0.0030 \pm 0.0062$	410 43 BUSKULIC 95N	ALEP	Sup. by BUSKULIC 97
seen	398 44 SANGHERA 93	CLE2	$e^+e^- \rightarrow \mathcal{T}(4S)$
$0.070 \pm 0.018 \pm 0.014$	45 ANTREASYAN 90B	CBAL	$e^+e^- \rightarrow \mathcal{T}(4S)$
$0.060 \pm 0.010 \pm 0.014$	46 ALBRECHT 89C	ARG	$e^+e^- \rightarrow \mathcal{T}(4S)$
$0.070 \pm 0.012 \pm 0.019$	47 47 ALBRECHT 89J	ARG	$e^+e^- \rightarrow \mathcal{T}(4S)$
	48 48 ALBRECHT 87J	ARG	$e^+e^- \rightarrow \mathcal{T}(4S)$

- 36 ACKERSTAFF 97G assumes fraction (B^+) = fraction (B^0) = (37.8 ± 2.2)% and PDG 96 values for B lifetime and branching ratio of D^* and D decays.
- 37 BUSKULIC 97 assumes fraction (B^+) = fraction (B^0) = (37.8 ± 2.2)% and PDG 96 values for B lifetime and D^* and D branching fractions.
- 38 ABREU 96P result is the average of two methods using exclusive and partial D^* reconstruction.
- 39 BARISH 95 use $B(D^0 \rightarrow K^-\pi^+) = (3.91 \pm 0.08 \pm 0.17)\%$ and $B(D^{*+} \rightarrow D^0\pi^+) = (68.1 \pm 1.0 \pm 1.3)\%$.
- 40 ALBRECHT 94 assumes $B(D^{*+} \rightarrow D^0\pi^+) = 68.1 \pm 1.0 \pm 1.3\%$. Uses partial reconstruction of D^{*+} and is independent of D^0 branching ratios.
- 41 ALBRECHT 93 reports $0.052 \pm 0.005 \pm 0.006$. We rescale using the method described in STONE 94 but with the updated PDG 94 $B(D^0 \rightarrow K^-\pi^+)$. We have taken their average e and μ value. They also obtain $\alpha = 2\Gamma(D^0 \rightarrow \Gamma^-\pi^+)/(\Gamma^-\pi^+ + \Gamma^+\pi^+) - 1 = 1.1 \pm 0.4 \pm 0.2$, $A_{FB} = 3/4*(\Gamma^-\pi^+ - \Gamma^+\pi^+)/\Gamma = 0.2 \pm 0.08 \pm 0.06$ and a value of $|V_{cb}| = 0.036\text{--}0.045$ depending on model assumptions.
- 42 We have taken average of the the BORTOLETTO 89B values for electrons and muons, $0.046 \pm 0.005 \pm 0.007$. We rescale using the method described in STONE 94 but with the updated PDG 94 $B(D^0 \rightarrow K^-\pi^+)$. The measurement suggests a D^* polarization parameter value $\alpha = 0.65 \pm 0.66 \pm 0.25$.
- 43 BUSKULIC 95N assumes fraction (B^+) = fraction (B^0) = $38.2 \pm 1.3 \pm 2.2\%$ and $\tau_{B^0} = 1.58 \pm 0.06$ ps. $\Gamma(D^{*-}\ell^+\nu_\ell)/\text{total} = [5.18 - 0.13(\text{fraction}(B^0) - 38.2) - 1.5(\tau_{B^0} - 1.58)]\%$.
- 44 Combining $\bar{D}^{*0}\ell^+\nu_\ell$ and $\bar{D}^{*-}\ell^+\nu_\ell$ SANGHERA 93 test $V-A$ structure and fit the decay angular distributions to obtain $A_{FB} = 3/4*(\Gamma^-\pi^+ - \Gamma^+\pi^+)/\Gamma = 0.14 \pm 0.06 \pm 0.03$. Assuming a value of V_{cb} , they measure $V, A_1,$ and A_2 , the three form factors for the $D^*\ell\nu_\ell$ decay, where results are slightly dependent on model assumptions.
- 45 ANTREASYAN 90B is average over B and $\bar{D}^*(2010)$ charge states.
- 46 The measurement of ALBRECHT 89C suggests a D^* polarization γ_L/γ_T of 0.85 ± 0.45 or $\alpha = 0.7 \pm 0.9$.
- 47 ALBRECHT 89J is ALBRECHT 87J value rescaled using $B(D^*(2010)^- \rightarrow D^0\pi^-) = 0.57 \pm 0.04 \pm 0.04$. Superseded by ALBRECHT 93.
- 48 ALBRECHT 87J assume μ - e universality, the $B(\mathcal{T}(4S) \rightarrow B^0\bar{B}^0) = 0.45$, the $B(D^0 \rightarrow K^-\pi^+) = (0.042 \pm 0.004 \pm 0.004)$, and the $B(D^*(2010)^- \rightarrow D^0\pi^-) = 0.49 \pm 0.08$. Superseded by ALBRECHT 89J.

$\Gamma(\rho^-\ell^+\nu_\ell)/\Gamma_{\text{total}}$		Γ_4/Γ	
VALUE (units 10^{-4})	DOCUMENT ID	TECN	COMMENT
$2.57 \pm 0.29 \pm 0.53$			
$2.5 \pm 0.4 \pm 0.7$	49 BEHRENS 00	CLE2	$e^+e^- \rightarrow \mathcal{T}(4S)$
-0.9	50 ALEXANDER 96T	CLE2	Repl. by BEHRENS 00
< 4.1	90 51 BEAN 93B	CLE2	$e^+e^- \rightarrow \mathcal{T}(4S)$

- 49 BEHRENS 00 reports systematic errors $+0.33$ -0.46 ± 0.41 , where the second error is theoretical model dependence. We combine these in quadrature.
- 50 ALEXANDER 96T gives systematic errors $+0.5$ -0.7 ± 0.5 where the second error reflects the estimated model dependence. We combine these in quadrature. Assumes isospin symmetry: $\Gamma(B^0 \rightarrow \rho^-\ell^+\nu_\ell) = 2 \times \Gamma(B^+ \rightarrow \rho^0\ell^+\nu_\ell) \sim 2 \times \Gamma(B^+ \rightarrow \omega\ell^+\nu_\ell)$.
- 51 BEAN 93B limit set using ISGW Model. Using isospin and the quark model to combine $\Gamma(\rho^0\ell^+\nu_\ell)$ and $\Gamma(\omega\ell^+\nu_\ell)$ with this result, they obtain a limit $< (1.6\text{--}2.7) \times 10^{-4}$ at 90% CL for $B^+ \rightarrow (\omega \text{ or } \rho^0)\ell^+\nu_\ell$. The range corresponds to the ISGW, WSB, and KS models. An upper limit on $|V_{ub}/V_{cb}| < 0.08\text{--}0.13$ at 90% CL is derived as well.

$\Gamma(\pi^-\ell^+\nu_\ell)/\Gamma_{\text{total}}$		Γ_5/Γ	
VALUE (units 10^{-4})	DOCUMENT ID	TECN	COMMENT
$1.8 \pm 0.4 \pm 0.4$			
$1.8 \pm 0.4 \pm 0.4$	52 ALEXANDER 96T	CLE2	$e^+e^- \rightarrow \mathcal{T}(4S)$

- 52 ALEXANDER 96T gives systematic errors $\pm 0.3 \pm 0.2$ where the second error reflects the estimated model dependence. We combine these in quadrature. Assumes isospin symmetry: $\Gamma(B^0 \rightarrow \pi^-\ell^+\nu_\ell) = 2 \times \Gamma(B^+ \rightarrow \pi^0\ell^+\nu_\ell)$.

$\Gamma(\pi^-\mu^+\nu_\mu)/\Gamma_{\text{total}}$		Γ_6/Γ	
VALUE	DOCUMENT ID	TECN	COMMENT
● ● ● We do not use the following data for averages, fits, limits, etc. ● ● ●			
seen	53 ALBRECHT 91C	ARG	

- 53 In ALBRECHT 91C, one event is fully reconstructed providing evidence for the $b \rightarrow u$ transition.

See key on page 239

Meson Particle Listings

 B^0 $\Gamma(K^+ \text{ anything})/\Gamma_{\text{total}}$

VALUE	DOCUMENT ID	TECN	COMMENT	Γ_7/Γ
0.78 ± 0.08	54 ALBRECHT	96D ARG	$e^+e^- \rightarrow \Upsilon(4S)$	

⁵⁴ Average multiplicity. $\Gamma(D^-\pi^+)/\Gamma_{\text{total}}$

VALUE	EVTS	DOCUMENT ID	TECN	COMMENT	Γ_8/Γ
0.0030 ± 0.0004 OUR AVERAGE					
0.0029 ± 0.0004 ± 0.0002	81	55 ALAM	94 CLE2	$e^+e^- \rightarrow \Upsilon(4S)$	
0.0027 ± 0.0006 ± 0.0005		56 BORTOLETTO92	CLEO	$e^+e^- \rightarrow \Upsilon(4S)$	
0.0048 ± 0.0011 ± 0.0011	22	57 ALBRECHT	90J ARG	$e^+e^- \rightarrow \Upsilon(4S)$	
0.0051 +0.0028 +0.0013 -0.0025 -0.0012	4	58 BEBEK	87 CLEO	$e^+e^- \rightarrow \Upsilon(4S)$	

• • • We do not use the following data for averages, fits, limits, etc. • • •

0.0031 ± 0.0013 ± 0.0010 7 57 ALBRECHT 88K ARG $e^+e^- \rightarrow \Upsilon(4S)$

⁵⁵ ALAM 94 reports $[B(B^0 \rightarrow D^-\pi^+) \times B(D^+ \rightarrow K^-\pi^+\pi^+)] = 0.000265 \pm 0.000032 \pm 0.000023$. We divide by our best value $B(D^+ \rightarrow K^-\pi^+\pi^+) = (9.0 \pm 0.6) \times 10^{-2}$. Our first error is their experiment's error and our second error is the systematic error from using our best value. Assumes equal production of B^+ and B^0 at the $\Upsilon(4S)$.

⁵⁶ BORTOLETTO 92 assumes equal production of B^+ and B^0 at the $\Upsilon(4S)$ and uses Mark III branching fractions for the D .

⁵⁷ ALBRECHT 88K assumes $B^0\bar{B}^0:B^+B^-$ production ratio is 45:55. Superseded by ALBRECHT 90J which assumes 50:50.

⁵⁸ BEBEK 87 value has been updated in BERKELMAN 91 to use same assumptions as noted for BORTOLETTO 92.

 $\Gamma(D^-\rho^+)/\Gamma_{\text{total}}$

VALUE	EVTS	DOCUMENT ID	TECN	COMMENT	Γ_9/Γ
0.0079 ± 0.0014 OUR AVERAGE					
0.0078 ± 0.0013 ± 0.0005	79	59 ALAM	94 CLE2	$e^+e^- \rightarrow \Upsilon(4S)$	
0.009 ± 0.005 ± 0.003	9	60 ALBRECHT	90J ARG	$e^+e^- \rightarrow \Upsilon(4S)$	

• • • We do not use the following data for averages, fits, limits, etc. • • •

0.022 ± 0.012 ± 0.009 6 60 ALBRECHT 88K ARG $e^+e^- \rightarrow \Upsilon(4S)$

⁵⁹ ALAM 94 reports $[B(B^0 \rightarrow D^-\rho^+) \times B(D^+ \rightarrow K^-\pi^+\pi^+)] = 0.000704 \pm 0.000096 \pm 0.000070$. We divide by our best value $B(D^+ \rightarrow K^-\pi^+\pi^+) = (9.0 \pm 0.6) \times 10^{-2}$. Our first error is their experiment's error and our second error is the systematic error from using our best value. Assumes equal production of B^+ and B^0 at the $\Upsilon(4S)$.

⁶⁰ ALBRECHT 88K assumes $B^0\bar{B}^0:B^+B^-$ production ratio is 45:55. Superseded by ALBRECHT 90J which assumes 50:50.

 $\Gamma(D^0\pi^+\pi^-)/\Gamma_{\text{total}}$

VALUE	CL% EVTS	DOCUMENT ID	TECN	COMMENT	Γ_{10}/Γ
<0.0016	90	61 ALAM	94 CLE2	$e^+e^- \rightarrow \Upsilon(4S)$	
<0.007	90	62 BORTOLETTO92	CLEO	$e^+e^- \rightarrow \Upsilon(4S)$	
<0.034	90	63 BEBEK	87 CLEO	$e^+e^- \rightarrow \Upsilon(4S)$	
0.07 ± 0.05	5	64 BEHRENDIS	83 CLEO	$e^+e^- \rightarrow \Upsilon(4S)$	

⁶¹ Assumes equal production of B^+ and B^0 at the $\Upsilon(4S)$.

⁶² BORTOLETTO 92 assumes equal production of B^+ and B^0 at the $\Upsilon(4S)$ and uses Mark III branching fractions for the D . The product branching fraction into $D_0^*(2340)\pi$ followed by $D_0^*(2340) \rightarrow D^0\pi$ is < 0.0001 at 90% CL and into $D_2^*(2460)$ followed by $D_2^*(2460) \rightarrow D^0\pi$ is < 0.0004 at 90% CL.

⁶³ BEBEK 87 assume the $\Upsilon(4S)$ decays 43% to $B^0\bar{B}^0$. We rescale to 50%. $B(D^0 \rightarrow K^-\pi^+) = (4.2 \pm 0.4 \pm 0.4)\%$ and $B(D^0 \rightarrow K^-\pi^+\pi^-\pi^-) = (9.1 \pm 0.8 \pm 0.8)\%$ were used.

⁶⁴ Corrected by us using assumptions: $B(D^0 \rightarrow K^-\pi^+) = (0.042 \pm 0.006)$ and $B(\Upsilon(4S) \rightarrow B^0\bar{B}^0) = 50\%$. The product branching ratio is $B(B^0 \rightarrow \bar{D}^0\pi^+\pi^-)B(\bar{D}^0 \rightarrow K^+\pi^-) = (0.39 \pm 0.26) \times 10^{-2}$.

 $\Gamma(D^*(2010)^-\pi^+)/\Gamma_{\text{total}}$

VALUE	EVTS	DOCUMENT ID	TECN	COMMENT	Γ_{11}/Γ
0.00276 ± 0.00021 OUR AVERAGE					
0.00281 ± 0.00024 ± 0.00005		65 BRANDENBURG...	98 CLE2	$e^+e^- \rightarrow \Upsilon(4S)$	
0.0026 ± 0.0003 ± 0.0004	82	66 ALAM	94 CLE2	$e^+e^- \rightarrow \Upsilon(4S)$	
0.00337 ± 0.00096 ± 0.00002		67 BORTOLETTO92	CLEO	$e^+e^- \rightarrow \Upsilon(4S)$	
0.00236 ± 0.00088 ± 0.00002	12	68 ALBRECHT	90J ARG	$e^+e^- \rightarrow \Upsilon(4S)$	
0.00236 +0.00150 ± 0.00002 -0.00110	5	69 BEBEK	87 CLEO	$e^+e^- \rightarrow \Upsilon(4S)$	

• • • We do not use the following data for averages, fits, limits, etc. • • •

0.010 ± 0.004 ± 0.001 8 70 AKERS 94J OPAL $e^+e^- \rightarrow Z$

0.0027 ± 0.0014 ± 0.0010 5 71 ALBRECHT 87C ARG $e^+e^- \rightarrow \Upsilon(4S)$

0.0035 ± 0.002 ± 0.002 72 ALBRECHT 86F ARG $e^+e^- \rightarrow \Upsilon(4S)$

0.017 ± 0.005 ± 0.005 41 73 GILES 84 CLEO $e^+e^- \rightarrow \Upsilon(4S)$

⁶⁵ BRANDENBURG 98 assume equal production of B^+ and B^0 at $\Upsilon(4S)$ and use the D^* reconstruction technique. The first error is their experiment's error and the second error is the systematic error from the PDG 96 value of $B(D^* \rightarrow D\pi)$.

⁶⁶ ALAM 94 assume equal production of B^+ and B^0 at the $\Upsilon(4S)$ and use the CLEO II $B(D^*(2010)^+ \rightarrow D^0\pi^+)$ and absolute $B(D^0 \rightarrow K^-\pi^+)$ and the PDG 1992 $B(D^0 \rightarrow K^-\pi^+\pi^0)/B(D^0 \rightarrow K^-\pi^+)$ and $B(D^0 \rightarrow K^-\pi^+\pi^-\pi^-)/B(D^0 \rightarrow K^-\pi^+)$.

⁶⁷ BORTOLETTO 92 reports $0.0040 \pm 0.0010 \pm 0.0007$ for $B(D^*(2010)^+ \rightarrow D^0\pi^+) = 0.57 \pm 0.06$. We rescale to our best value $B(D^*(2010)^+ \rightarrow D^0\pi^+) = (67.7 \pm 0.5) \times 10^{-2}$. Our first error is their experiment's error and our second error is the systematic

error from using our best value. Assumes equal production of B^+ and B^0 at the $\Upsilon(4S)$ and uses Mark III branching fractions for the D .

⁶⁸ ALBRECHT 90J reports $0.0028 \pm 0.0009 \pm 0.0006$ for $B(D^*(2010)^+ \rightarrow D^0\pi^+) = 0.57 \pm 0.06$. We rescale to our best value $B(D^*(2010)^+ \rightarrow D^0\pi^+) = (67.7 \pm 0.5) \times 10^{-2}$. Our first error is their experiment's error and our second error is the systematic error from using our best value. Assumes equal production of B^+ and B^0 at the $\Upsilon(4S)$ and uses Mark III branching fractions for the D .

⁶⁹ BEBEK 87 reports $0.0028_{-0.0012}^{+0.0015+0.0010}$ for $B(D^*(2010)^+ \rightarrow D^0\pi^+) = 0.57 \pm 0.06$. We rescale to our best value $B(D^*(2010)^+ \rightarrow D^0\pi^+) = (67.7 \pm 0.5) \times 10^{-2}$. Our first error is their experiment's error and our second error is the systematic error from using our best value. Updated in BERKELMAN 91 to use same assumptions as noted for BORTOLETTO 92 and ALBRECHT 90J.

⁷⁰ Assumes $B(Z \rightarrow b\bar{b}) = 0.217$ and 38% B_J production fraction.

⁷¹ ALBRECHT 87c use PDG 86 branching ratios for D and $D^*(2010)$ and assume $B(\Upsilon(4S) \rightarrow B^+B^-) = 55\%$ and $B(\Upsilon(4S) \rightarrow B^0\bar{B}^0) = 45\%$. Superseded by ALBRECHT 90J.

⁷² ALBRECHT 86F uses pseudomass that is independent of D^0 and D^+ branching ratios.

⁷³ Assumes $B(D^*(2010)^+ \rightarrow D^0\pi^+) = 0.60_{-0.15}^{+0.08}$. Assumes $B(\Upsilon(4S) \rightarrow B^0\bar{B}^0) = 0.40 \pm 0.02$ Does not depend on D branching ratios.

 $\Gamma(D^-\pi^+\pi^-\pi^-)/\Gamma_{\text{total}}$

VALUE	DOCUMENT ID	TECN	COMMENT	Γ_{12}/Γ
0.0080 ± 0.0021 ± 0.0014	74 BORTOLETTO92	CLEO	$e^+e^- \rightarrow \Upsilon(4S)$	

⁷⁴ BORTOLETTO 92 assumes equal production of B^+ and B^0 at the $\Upsilon(4S)$ and uses Mark III branching fractions for the D .

 $\Gamma((D^-\pi^+\pi^-\pi^-) \text{ nonresonant})/\Gamma_{\text{total}}$

VALUE	DOCUMENT ID	TECN	COMMENT	Γ_{13}/Γ
0.0039 ± 0.0014 ± 0.0013	75 BORTOLETTO92	CLEO	$e^+e^- \rightarrow \Upsilon(4S)$	

⁷⁵ BORTOLETTO 92 assumes equal production of B^+ and B^0 at the $\Upsilon(4S)$ and uses Mark III branching fractions for the D .

 $\Gamma(D^-\pi^+\rho^0)/\Gamma_{\text{total}}$

VALUE	DOCUMENT ID	TECN	COMMENT	Γ_{14}/Γ
0.0011 ± 0.0009 ± 0.0004	76 BORTOLETTO92	CLEO	$e^+e^- \rightarrow \Upsilon(4S)$	

⁷⁶ BORTOLETTO 92 assumes equal production of B^+ and B^0 at the $\Upsilon(4S)$ and uses Mark III branching fractions for the D .

 $\Gamma(D^-\rho_1(1260)^+)/\Gamma_{\text{total}}$

VALUE	DOCUMENT ID	TECN	COMMENT	Γ_{15}/Γ
0.0060 ± 0.0022 ± 0.0024	77 BORTOLETTO92	CLEO	$e^+e^- \rightarrow \Upsilon(4S)$	

⁷⁷ BORTOLETTO 92 assumes equal production of B^+ and B^0 at the $\Upsilon(4S)$ and uses Mark III branching fractions for the D .

 $\Gamma(D^*(2010)^-\pi^+\pi^0)/\Gamma_{\text{total}}$

VALUE	EVTS	DOCUMENT ID	TECN	COMMENT	Γ_{16}/Γ
0.0152 ± 0.0052 ± 0.0001	51	78 ALBRECHT	90J ARG	$e^+e^- \rightarrow \Upsilon(4S)$	
<0.015					
0.015 ± 0.008 ± 0.008	8	79 ALBRECHT	87C ARG	$e^+e^- \rightarrow \Upsilon(4S)$	

⁷⁸ ALBRECHT 90J reports $0.018 \pm 0.004 \pm 0.005$ for $B(D^*(2010)^+ \rightarrow D^0\pi^+) = 0.57 \pm 0.06$. We rescale to our best value $B(D^*(2010)^+ \rightarrow D^0\pi^+) = (67.7 \pm 0.5) \times 10^{-2}$. Our first error is their experiment's error and our second error is the systematic error from using our best value. Assumes equal production of B^+ and B^0 at the $\Upsilon(4S)$ and uses Mark III branching fractions for the D .

⁷⁹ ALBRECHT 87c use PDG 86 branching ratios for D and $D^*(2010)$ and assume $B(\Upsilon(4S) \rightarrow B^+B^-) = 55\%$ and $B(\Upsilon(4S) \rightarrow B^0\bar{B}^0) = 45\%$. Superseded by ALBRECHT 90J.

 $\Gamma(D^*(2010)^-\rho^+)/\Gamma_{\text{total}}$

VALUE	EVTS	DOCUMENT ID	TECN	COMMENT	Γ_{17}/Γ
0.0068 ± 0.0034 OUR AVERAGE					
0.0160 ± 0.0113 ± 0.0001		80 BORTOLETTO92	CLEO	$e^+e^- \rightarrow \Upsilon(4S)$	
0.00589 ± 0.00352 ± 0.00004	19	81 ALBRECHT	90J ARG	$e^+e^- \rightarrow \Upsilon(4S)$	
0.0074 ± 0.0010 ± 0.0014	76	82,83 ALAM	94 CLE2	Sup. by JESSOP 97	
0.081 ± 0.029 +0.059 -0.024	19	84 CHEN	85 CLEO	$e^+e^- \rightarrow \Upsilon(4S)$	

⁸⁰ BORTOLETTO 92 reports $0.019 \pm 0.008 \pm 0.011$ for $B(D^*(2010)^+ \rightarrow D^0\pi^+) = 0.57 \pm 0.06$. We rescale to our best value $B(D^*(2010)^+ \rightarrow D^0\pi^+) = (67.7 \pm 0.5) \times 10^{-2}$. Our first error is their experiment's error and our second error is the systematic error from using our best value. Assumes equal production of B^+ and B^0 at the $\Upsilon(4S)$ and uses Mark III branching fractions for the D .

⁸¹ ALBRECHT 90J reports $0.007 \pm 0.003 \pm 0.003$ for $B(D^*(2010)^+ \rightarrow D^0\pi^+) = 0.57 \pm 0.06$. We rescale to our best value $B(D^*(2010)^+ \rightarrow D^0\pi^+) = (67.7 \pm 0.5) \times 10^{-2}$. Our first error is their experiment's error and our second error is the systematic error from using our best value. Assumes equal production of B^+ and B^0 at the $\Upsilon(4S)$ and uses Mark III branching fractions for the D .

⁸² ALAM 94 assume equal production of B^+ and B^0 at the $\Upsilon(4S)$ and use the CLEO II $B(D^*(2010)^+ \rightarrow D^0\pi^+)$ and absolute $B(D^0 \rightarrow K^-\pi^+)$ and the PDG 1992 $B(D^0 \rightarrow K^-\pi^+\pi^0)/B(D^0 \rightarrow K^-\pi^+)$ and $B(D^0 \rightarrow K^-\pi^+\pi^-\pi^-)/B(D^0 \rightarrow K^-\pi^+)$.

⁸³ This decay is nearly completely longitudinally polarized, $\Gamma_L/\Gamma = (93 \pm 5 \pm 5)\%$, as expected from the factorization hypothesis (ROSNER 90). The nonresonant $\pi^+\pi^0$ contribution under the ρ^+ is less than 9% at 90% CL.

⁸⁴ Uses $B(D^* \rightarrow D^0\pi^+) = 0.6 \pm 0.15$ and $B(\Upsilon(4S) \rightarrow B^0\bar{B}^0) = 0.4$. Does not depend on D branching ratios.

Meson Particle Listings

 B^0

$\Gamma(D^*(2010)^- \pi^+ \pi^+ \pi^-) / \Gamma_{\text{total}}$			Γ_{18} / Γ		
VALUE	CL% EVTS	DOCUMENT ID	TECN	COMMENT	
0.0076 ± 0.0018 OUR AVERAGE				Error includes scale factor of 1.4. See the ideogram below.	
0.0063 ± 0.0010 ± 0.0011	49	85,86 ALAM	94 CLE2	$e^+ e^- \rightarrow \Upsilon(4S)$	
0.0134 ± 0.0036 ± 0.0001		87 BORTOLETTO92	CLEO	$e^+ e^- \rightarrow \Upsilon(4S)$	
0.0101 ± 0.0041 ± 0.0001	26	88 ALBRECHT	90J ARG	$e^+ e^- \rightarrow \Upsilon(4S)$	

• • • We do not use the following data for averages, fits, limits, etc. • • •

0.033 ± 0.009 ± 0.016	27	89 ALBRECHT	87c ARG	$e^+ e^- \rightarrow \Upsilon(4S)$	
<0.042	90	90 BEBEK	87 CLEO	$e^+ e^- \rightarrow \Upsilon(4S)$	

85 ALAM 94 assume equal production of B^+ and B^0 at the $\Upsilon(4S)$ and use the CLEO II $B(D^*(2010)^+ \rightarrow D^0 \pi^+)$ and absolute $B(D^0 \rightarrow K^- \pi^+)$ and the PDG 1992 $B(D^0 \rightarrow K^- \pi^+ \pi^0) / B(D^0 \rightarrow K^- \pi^+)$ and $B(D^0 \rightarrow K^- \pi^+ \pi^+ \pi^-) / B(D^0 \rightarrow K^- \pi^+)$.

86 The three pion mass is required to be between 1.0 and 1.6 GeV consistent with an a_1 meson. (If this channel is dominated by a_1^+ , the branching ratio for $\bar{D}^* a_1^+$ is twice that for $\bar{D}^* \pi^+ \pi^+ \pi^-$.)

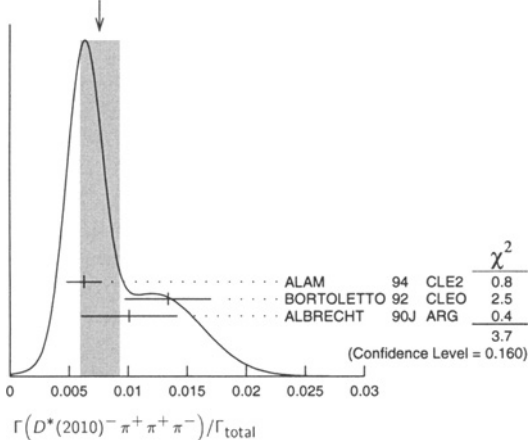
87 BORTOLETTO 92 reports $0.0159 \pm 0.0028 \pm 0.0037$ for $B(D^*(2010)^+ \rightarrow D^0 \pi^+) = 0.57 \pm 0.06$. We rescale to our best value $B(D^*(2010)^+ \rightarrow D^0 \pi^+) = (67.7 \pm 0.5) \times 10^{-2}$. Our first error is their experiment's error and our second error is the systematic error from using our best value. Assumes equal production of B^+ and B^0 at the $\Upsilon(4S)$ and uses Mark III branching fractions for the D .

88 ALBRECHT 90J reports $0.012 \pm 0.003 \pm 0.004$ for $B(D^*(2010)^+ \rightarrow D^0 \pi^+) = 0.57 \pm 0.06$. We rescale to our best value $B(D^*(2010)^+ \rightarrow D^0 \pi^+) = (67.7 \pm 0.5) \times 10^{-2}$. Our first error is their experiment's error and our second error is the systematic error from using our best value. Assumes equal production of B^+ and B^0 at the $\Upsilon(4S)$ and uses Mark III branching fractions for the D .

89 ALBRECHT 87c use PDG 86 branching ratios for D and $D^*(2010)$ and assume $B(\Upsilon(4S) \rightarrow B^+ B^-) = 55\%$ and $B(\Upsilon(4S) \rightarrow B^0 \bar{B}^0) = 45\%$. Superseded by ALBRECHT 90J.

90 BEBEK 87 value has been updated in BERKELMAN 91 to use same assumptions as noted for BORTOLETTO 92.

WEIGHTED AVERAGE
0.0076 ± 0.0018 (Error scaled by 1.4)



$\Gamma((D^*(2010)^- \pi^+ \pi^+ \pi^-) \text{ nonresonant}) / \Gamma_{\text{total}}$			Γ_{19} / Γ		
VALUE	CL% EVTS	DOCUMENT ID	TECN	COMMENT	
0.0000 ± 0.0019 ± 0.0016		91 BORTOLETTO92	CLEO	$e^+ e^- \rightarrow \Upsilon(4S)$	

91 BORTOLETTO 92 assumes equal production of B^+ and B^0 at the $\Upsilon(4S)$ and uses Mark III branching fractions for the D and $D^*(2010)$.

$\Gamma(D^*(2010)^- \pi^+ \rho^0) / \Gamma_{\text{total}}$			Γ_{20} / Γ		
VALUE	CL% EVTS	DOCUMENT ID	TECN	COMMENT	
0.00573 ± 0.00317 ± 0.00004		92 BORTOLETTO92	CLEO	$e^+ e^- \rightarrow \Upsilon(4S)$	

92 BORTOLETTO 92 reports $0.0068 \pm 0.0032 \pm 0.0021$ for $B(D^*(2010)^+ \rightarrow D^0 \pi^+) = 0.57 \pm 0.06$. We rescale to our best value $B(D^*(2010)^+ \rightarrow D^0 \pi^+) = (67.7 \pm 0.5) \times 10^{-2}$. Our first error is their experiment's error and our second error is the systematic error from using our best value. Assumes equal production of B^+ and B^0 at the $\Upsilon(4S)$ and uses Mark III branching fractions for the D .

$\Gamma(D^*(2010)^- a_1(1260)^+) / \Gamma_{\text{total}}$			Γ_{21} / Γ		
VALUE	CL% EVTS	DOCUMENT ID	TECN	COMMENT	
0.0130 ± 0.0027 OUR AVERAGE					
0.0126 ± 0.0020 ± 0.0022		93,94 ALAM	94 CLE2	$e^+ e^- \rightarrow \Upsilon(4S)$	
0.0152 ± 0.0070 ± 0.0001		95 BORTOLETTO92	CLEO	$e^+ e^- \rightarrow \Upsilon(4S)$	

93 ALAM 94 value is twice their $\Gamma(D^*(2010)^- \pi^+ \pi^+ \pi^-) / \Gamma_{\text{total}}$ value based on their observation that the three pions are dominantly in the $a_1(1260)$ mass range 1.0 to 1.6 GeV.

94 ALAM 94 assume equal production of B^+ and B^0 at the $\Upsilon(4S)$ and use the CLEO II $B(D^*(2010)^+ \rightarrow D^0 \pi^+)$ and absolute $B(D^0 \rightarrow K^- \pi^+)$ and the PDG 1992 $B(D^0 \rightarrow K^- \pi^+ \pi^0) / B(D^0 \rightarrow K^- \pi^+)$ and $B(D^0 \rightarrow K^- \pi^+ \pi^+ \pi^-) / B(D^0 \rightarrow K^- \pi^+)$.

95 BORTOLETTO 92 reports $0.018 \pm 0.006 \pm 0.006$ for $B(D^*(2010)^+ \rightarrow D^0 \pi^+) = 0.57 \pm 0.06$. We rescale to our best value $B(D^*(2010)^+ \rightarrow D^0 \pi^+) = (67.7 \pm 0.5) \times 10^{-2}$. Our first error is their experiment's error and our second error is the systematic error from using our best value. Assumes equal production of B^+ and B^0 at the $\Upsilon(4S)$ and uses Mark III branching fractions for the D .

$\Gamma(D^*(2010)^- \pi^+ \pi^+ \pi^0) / \Gamma_{\text{total}}$			Γ_{22} / Γ		
VALUE	CL% EVTS	DOCUMENT ID	TECN	COMMENT	
0.0345 ± 0.0181 ± 0.0003		96 ALBRECHT	90J ARG	$e^+ e^- \rightarrow \Upsilon(4S)$	

96 ALBRECHT 90J reports $0.041 \pm 0.015 \pm 0.016$ for $B(D^*(2010)^+ \rightarrow D^0 \pi^+) = 0.57 \pm 0.06$. We rescale to our best value $B(D^*(2010)^+ \rightarrow D^0 \pi^+) = (67.7 \pm 0.5) \times 10^{-2}$. Our first error is their experiment's error and our second error is the systematic error from using our best value. Assumes equal production of B^+ and B^0 at the $\Upsilon(4S)$ and uses Mark III branching fractions for the D .

$\Gamma(D_2^*(2460)^- \pi^+) / \Gamma_{\text{total}}$			Γ_{23} / Γ		
VALUE	CL% EVTS	DOCUMENT ID	TECN	COMMENT	
<0.0022		97 ALAM	94 CLE2	$e^+ e^- \rightarrow \Upsilon(4S)$	

97 ALAM 94 assumes equal production of B^+ and B^0 at the $\Upsilon(4S)$ and use the CLEO II absolute $B(D^0 \rightarrow K^- \pi^+)$ and $B(D_2^*(2460)^+ \rightarrow D^0 \pi^+) = 30\%$.

$\Gamma(D_2^*(2460)^- \rho^+) / \Gamma_{\text{total}}$			Γ_{24} / Γ		
VALUE	CL% EVTS	DOCUMENT ID	TECN	COMMENT	
<0.0049		98 ALAM	94 CLE2	$e^+ e^- \rightarrow \Upsilon(4S)$	

98 ALAM 94 assumes equal production of B^+ and B^0 at the $\Upsilon(4S)$ and use the CLEO II absolute $B(D^0 \rightarrow K^- \pi^+)$ and $B(D_2^*(2460)^+ \rightarrow D^0 \pi^+) = 30\%$.

$\Gamma(D^- D^+) / \Gamma_{\text{total}}$			Γ_{25} / Γ		
VALUE	CL% EVTS	DOCUMENT ID	TECN	COMMENT	
<5.9 × 10 ⁻³		99 BARATE	98Q ALEP	$e^+ e^- \rightarrow Z$	
<1.2 × 10 ⁻³		90 ASNER	97 CLE2	$e^+ e^- \rightarrow \Upsilon(4S)$	

$\Gamma(D^- D_s^+) / \Gamma_{\text{total}}$			Γ_{26} / Γ		
VALUE	CL% EVTS	DOCUMENT ID	TECN	COMMENT	
0.0080 ± 0.0030 OUR AVERAGE					
0.0084 ± 0.0030 ^{+0.0020} _{-0.0021}		99 GIBAUT	96 CLE2	$e^+ e^- \rightarrow \Upsilon(4S)$	
0.013 ± 0.011 ± 0.003		100 ALBRECHT	92G ARG	$e^+ e^- \rightarrow \Upsilon(4S)$	
0.007 ± 0.004 ± 0.002		101 BORTOLETTO92	CLEO	$e^+ e^- \rightarrow \Upsilon(4S)$	

• • • We do not use the following data for averages, fits, limits, etc. • • •

0.012 ± 0.007	3	102 BORTOLETTO90	CLEO	$e^+ e^- \rightarrow \Upsilon(4S)$	
---------------	---	------------------	------	------------------------------------	--

99 GIBAUT 96 reports $0.0087 \pm 0.0024 \pm 0.0020$ for $B(D_s^+ \rightarrow \phi \pi^+) = 0.035$. We rescale to our best value $B(D_s^+ \rightarrow \phi \pi^+) = (3.6 \pm 0.9) \times 10^{-2}$. Our first error is their experiment's error and our second error is the systematic error from using our best value.

100 ALBRECHT 92G reports $0.017 \pm 0.013 \pm 0.006$ for $B(D_s^+ \rightarrow \phi \pi^+) = 0.027$. We rescale to our best value $B(D_s^+ \rightarrow \phi \pi^+) = (3.6 \pm 0.9) \times 10^{-2}$. Our first error is their experiment's error and our second error is the systematic error from using our best value. Assumes PDG 1990 D^+ branching ratios, e.g., $B(D^+ \rightarrow K^- \pi^+ \pi^+) = 7.7 \pm 1.0\%$.

101 BORTOLETTO 92 reports $0.0080 \pm 0.0045 \pm 0.0030$ for $B(D_s^+ \rightarrow \phi \pi^+) = 0.030 \pm 0.011$. We rescale to our best value $B(D_s^+ \rightarrow \phi \pi^+) = (3.6 \pm 0.9) \times 10^{-2}$. Our first error is their experiment's error and our second error is the systematic error from using our best value. Assumes equal production of B^+ and B^0 at the $\Upsilon(4S)$ and uses Mark III branching fractions for the D .

102 BORTOLETTO 90 assume $B(D_s \rightarrow \phi \pi^+) = 2\%$. Superseded by BORTOLETTO 92.

$\Gamma(D^*(2010)^- D_s^+) / \Gamma_{\text{total}}$			Γ_{27} / Γ		
VALUE	CL% EVTS	DOCUMENT ID	TECN	COMMENT	
0.0096 ± 0.0034 OUR AVERAGE					
0.0090 ± 0.0027 ± 0.0022		103 GIBAUT	96 CLE2	$e^+ e^- \rightarrow \Upsilon(4S)$	
0.010 ± 0.008 ± 0.003		104 ALBRECHT	92G ARG	$e^+ e^- \rightarrow \Upsilon(4S)$	
0.013 ± 0.008 ± 0.003		105 BORTOLETTO92	CLEO	$e^+ e^- \rightarrow \Upsilon(4S)$	

• • • We do not use the following data for averages, fits, limits, etc. • • •

0.024 ± 0.014	3	106 BORTOLETTO90	CLEO	$e^+ e^- \rightarrow \Upsilon(4S)$	
---------------	---	------------------	------	------------------------------------	--

103 GIBAUT 96 reports $0.0093 \pm 0.0023 \pm 0.0016$ for $B(D_s^+ \rightarrow \phi \pi^+) = 0.035$. We rescale to our best value $B(D_s^+ \rightarrow \phi \pi^+) = (3.6 \pm 0.9) \times 10^{-2}$. Our first error is their experiment's error and our second error is the systematic error from using our best value.

104 ALBRECHT 92G reports $0.014 \pm 0.010 \pm 0.003$ for $B(D_s^+ \rightarrow \phi \pi^+) = 0.027$. We rescale to our best value $B(D_s^+ \rightarrow \phi \pi^+) = (3.6 \pm 0.9) \times 10^{-2}$. Our first error is their experiment's error and our second error is the systematic error from using our best value. Assumes PDG 1990 D^+ and $D^*(2010)^+$ branching ratios, e.g., $B(D^0 \rightarrow K^- \pi^+) = 3.71 \pm 0.25\%$, $B(D^+ \rightarrow K^- \pi^+ \pi^+) = 7.1 \pm 1.0\%$, and $B(D^*(2010)^+ \rightarrow D^0 \pi^+) = 55 \pm 4\%$.

105 BORTOLETTO 92 reports $0.016 \pm 0.009 \pm 0.006$ for $B(D_s^+ \rightarrow \phi \pi^+) = 0.030 \pm 0.011$. We rescale to our best value $B(D_s^+ \rightarrow \phi \pi^+) = (3.6 \pm 0.9) \times 10^{-2}$. Our first error is their experiment's error and our second error is the systematic error from using our best value. Assumes equal production of B^+ and B^0 at the $\Upsilon(4S)$ and uses Mark III branching fractions for the D and $D^*(2010)$.

106 BORTOLETTO 90 assume $B(D_s \rightarrow \phi \pi^+) = 2\%$. Superseded by BORTOLETTO 92.

$\Gamma(D^- D_s^{*+})/\Gamma_{total}$ Γ_{28}/Γ

VALUE	DOCUMENT ID	TECN	COMMENT
0.010±0.005 OUR AVERAGE			
0.010±0.004±0.002	107 GIBAUT	96 CLE2	$e^+e^- \rightarrow \Upsilon(4S)$
0.020±0.014±0.005	108 ALBRECHT	92G ARG	$e^+e^- \rightarrow \Upsilon(4S)$

107 GIBAUT 96 reports $0.0100 \pm 0.0035 \pm 0.0022$ for $B(D_s^+ \rightarrow \phi\pi^+) = 0.035$. We rescale to our best value $B(D_s^+ \rightarrow \phi\pi^+) = (3.6 \pm 0.9) \times 10^{-2}$. Our first error is their experiment's error and our second error is the systematic error from using our best value.

108 ALBRECHT 92G reports $0.027 \pm 0.017 \pm 0.009$ for $B(D_s^+ \rightarrow \phi\pi^+) = 0.027$. We rescale to our best value $B(D_s^+ \rightarrow \phi\pi^+) = (3.6 \pm 0.9) \times 10^{-2}$. Our first error is their experiment's error and our second error is the systematic error from using our best value. Assumes PDG 1990 D^+ branching ratios, e.g., $B(D^+ \rightarrow K^-\pi^+\pi^+) = 7.7 \pm 1.0\%$.

 $[\Gamma(D^*(2010)-D_s^+) + \Gamma(D^*(2010)-D_s^{*+})]/\Gamma_{total}$ $(\Gamma_{27}+\Gamma_{29})/\Gamma$

VALUE (units 10^{-2})	EVTS	DOCUMENT ID	TECN	COMMENT
4.15±1.11^{+0.99}_{-1.02}	22	109 BORTOLETTO90	CLEO	$e^+e^- \rightarrow \Upsilon(4S)$

109 BORTOLETTO 90 reports 7.5 ± 2.0 for $B(D_s^+ \rightarrow \phi\pi^+) = 0.02$. We rescale to our best value $B(D_s^+ \rightarrow \phi\pi^+) = (3.6 \pm 0.9) \times 10^{-2}$. Our first error is their experiment's error and our second error is the systematic error from using our best value.

 $\Gamma(D^*(2010)-D_s^{*+})/\Gamma_{total}$ Γ_{29}/Γ

VALUE	DOCUMENT ID	TECN	COMMENT
0.020±0.007 OUR AVERAGE			
0.020±0.006±0.005	110 GIBAUT	96 CLE2	$e^+e^- \rightarrow \Upsilon(4S)$
0.019±0.011±0.005	111 ALBRECHT	92G ARG	$e^+e^- \rightarrow \Upsilon(4S)$

110 GIBAUT 96 reports $0.0203 \pm 0.0050 \pm 0.0036$ for $B(D_s^+ \rightarrow \phi\pi^+) = 0.035$. We rescale to our best value $B(D_s^+ \rightarrow \phi\pi^+) = (3.6 \pm 0.9) \times 10^{-2}$. Our first error is their experiment's error and our second error is the systematic error from using our best value.

111 ALBRECHT 92G reports $0.026 \pm 0.014 \pm 0.006$ for $B(D_s^+ \rightarrow \phi\pi^+) = 0.027$. We rescale to our best value $B(D_s^+ \rightarrow \phi\pi^+) = (3.6 \pm 0.9) \times 10^{-2}$. Our first error is their experiment's error and our second error is the systematic error from using our best value. Assumes PDG 1990 D^+ and $D^*(2010)^+$ branching ratios, e.g., $B(D^0 \rightarrow K^-\pi^+) = 3.71 \pm 0.25\%$, $B(D^+ \rightarrow K^-\pi^+\pi^+) = 7.1 \pm 1.0\%$, and $B(D^*(2010)^+ \rightarrow D^0\pi^+) = 55 \pm 4\%$.

 $\Gamma(D_s^+ \pi^-)/\Gamma_{total}$ Γ_{30}/Γ

VALUE	CL%	DOCUMENT ID	TECN	COMMENT
<0.00028				
<0.0013	90	112 ALEXANDER 93B	CLE2	$e^+e^- \rightarrow \Upsilon(4S)$
		113 BORTOLETTO90	CLEO	$e^+e^- \rightarrow \Upsilon(4S)$

112 ALEXANDER 93B reports $< 2.7 \times 10^{-4}$ for $B(D_s^+ \rightarrow \phi\pi^+) = 0.037$. We rescale to our best value $B(D_s^+ \rightarrow \phi\pi^+) = 0.036$.

113 BORTOLETTO 90 assume $B(D_s \rightarrow \phi\pi^+) = 2\%$.

 $\Gamma(D_s^{*+} \pi^-)/\Gamma_{total}$ Γ_{31}/Γ

VALUE	CL%	DOCUMENT ID	TECN	COMMENT
<0.0005				
<0.0013	90	114 ALEXANDER 93B	CLE2	$e^+e^- \rightarrow \Upsilon(4S)$

114 ALEXANDER 93B reports $< 4.4 \times 10^{-4}$ for $B(D_s^+ \rightarrow \phi\pi^+) = 0.037$. We rescale to our best value $B(D_s^+ \rightarrow \phi\pi^+) = 0.036$.

 $[\Gamma(D_s^+ \pi^-) + \Gamma(D_s^- K^+)]/\Gamma_{total}$ $(\Gamma_{30}+\Gamma_{36})/\Gamma$

VALUE	CL%	DOCUMENT ID	TECN	COMMENT
<0.0013				
<0.0013	90	115 ALBRECHT 93E	ARG	$e^+e^- \rightarrow \Upsilon(4S)$

115 ALBRECHT 93E reports $< 1.7 \times 10^{-3}$ for $B(D_s^+ \rightarrow \phi\pi^+) = 0.027$. We rescale to our best value $B(D_s^+ \rightarrow \phi\pi^+) = 0.036$.

 $[\Gamma(D_s^{*+} \pi^-) + \Gamma(D_s^{*-} K^+)]/\Gamma_{total}$ $(\Gamma_{31}+\Gamma_{37})/\Gamma$

VALUE	CL%	DOCUMENT ID	TECN	COMMENT
<0.0009				
<0.0009	90	116 ALBRECHT 93E	ARG	$e^+e^- \rightarrow \Upsilon(4S)$

116 ALBRECHT 93E reports $< 1.2 \times 10^{-3}$ for $B(D_s^+ \rightarrow \phi\pi^+) = 0.027$. We rescale to our best value $B(D_s^+ \rightarrow \phi\pi^+) = 0.036$.

 $\Gamma(D_s^+ \rho^-)/\Gamma_{total}$ Γ_{32}/Γ

VALUE	CL%	DOCUMENT ID	TECN	COMMENT
<0.0007				
<0.0016	90	117 ALEXANDER 93B	CLE2	$e^+e^- \rightarrow \Upsilon(4S)$
		118 ALBRECHT 93E	ARG	$e^+e^- \rightarrow \Upsilon(4S)$

117 ALEXANDER 93B reports $< 6.6 \times 10^{-4}$ for $B(D_s^+ \rightarrow \phi\pi^+) = 0.037$. We rescale to our best value $B(D_s^+ \rightarrow \phi\pi^+) = 0.036$.

118 ALBRECHT 93E reports $< 2.2 \times 10^{-3}$ for $B(D_s^+ \rightarrow \phi\pi^+) = 0.027$. We rescale to our best value $B(D_s^+ \rightarrow \phi\pi^+) = 0.036$.

 $\Gamma(D_s^{*+} \rho^-)/\Gamma_{total}$ Γ_{33}/Γ

VALUE	CL%	DOCUMENT ID	TECN	COMMENT
<0.0008				
<0.0019	90	119 ALEXANDER 93B	CLE2	$e^+e^- \rightarrow \Upsilon(4S)$
		120 ALBRECHT 93E	ARG	$e^+e^- \rightarrow \Upsilon(4S)$

119 ALEXANDER 93B reports $< 7.4 \times 10^{-4}$ for $B(D_s^+ \rightarrow \phi\pi^+) = 0.037$. We rescale to our best value $B(D_s^+ \rightarrow \phi\pi^+) = 0.036$.

120 ALBRECHT 93E reports $< 2.5 \times 10^{-3}$ for $B(D_s^+ \rightarrow \phi\pi^+) = 0.027$. We rescale to our best value $B(D_s^+ \rightarrow \phi\pi^+) = 0.036$.

 $\Gamma(D_s^+ a_1(1260)^-)/\Gamma_{total}$ Γ_{34}/Γ

VALUE	CL%	DOCUMENT ID	TECN	COMMENT
<0.0026				
<0.0026	90	121 ALBRECHT 93E	ARG	$e^+e^- \rightarrow \Upsilon(4S)$

121 ALBRECHT 93E reports $< 3.5 \times 10^{-3}$ for $B(D_s^+ \rightarrow \phi\pi^+) = 0.027$. We rescale to our best value $B(D_s^+ \rightarrow \phi\pi^+) = 0.036$.

 $\Gamma(D_s^{*+} a_1(1260)^-)/\Gamma_{total}$ Γ_{35}/Γ

VALUE	CL%	DOCUMENT ID	TECN	COMMENT
<0.0022				
<0.0022	90	122 ALBRECHT 93E	ARG	$e^+e^- \rightarrow \Upsilon(4S)$

122 ALBRECHT 93E reports $< 2.9 \times 10^{-3}$ for $B(D_s^+ \rightarrow \phi\pi^+) = 0.027$. We rescale to our best value $B(D_s^+ \rightarrow \phi\pi^+) = 0.036$.

 $\Gamma(D_s^- K^+)/\Gamma_{total}$ Γ_{36}/Γ

VALUE	CL%	DOCUMENT ID	TECN	COMMENT
<0.00024				
<0.0013	90	123 ALEXANDER 93B	CLE2	$e^+e^- \rightarrow \Upsilon(4S)$
		124 BORTOLETTO90	CLEO	$e^+e^- \rightarrow \Upsilon(4S)$

123 ALEXANDER 93B reports $< 2.3 \times 10^{-4}$ for $B(D_s^+ \rightarrow \phi\pi^+) = 0.037$. We rescale to our best value $B(D_s^+ \rightarrow \phi\pi^+) = 0.036$.

124 BORTOLETTO 90 assume $B(D_s \rightarrow \phi\pi^+) = 2\%$.

 $\Gamma(D_s^{*-} K^+)/\Gamma_{total}$ Γ_{37}/Γ

VALUE	CL%	DOCUMENT ID	TECN	COMMENT
<0.00017				
<0.0017	90	125 ALEXANDER 93B	CLE2	$e^+e^- \rightarrow \Upsilon(4S)$

125 ALEXANDER 93B reports $< 1.7 \times 10^{-4}$ for $B(D_s^+ \rightarrow \phi\pi^+) = 0.037$. We rescale to our best value $B(D_s^+ \rightarrow \phi\pi^+) = 0.036$.

 $\Gamma(D_s^- K^*(892)^+)/\Gamma_{total}$ Γ_{38}/Γ

VALUE	CL%	DOCUMENT ID	TECN	COMMENT
<0.0010				
<0.0034	90	126 ALEXANDER 93B	CLE2	$e^+e^- \rightarrow \Upsilon(4S)$
		127 ALBRECHT 93E	ARG	$e^+e^- \rightarrow \Upsilon(4S)$

126 ALEXANDER 93B reports $< 9.7 \times 10^{-4}$ for $B(D_s^+ \rightarrow \phi\pi^+) = 0.037$. We rescale to our best value $B(D_s^+ \rightarrow \phi\pi^+) = 0.036$.

127 ALBRECHT 93E reports $< 4.6 \times 10^{-3}$ for $B(D_s^+ \rightarrow \phi\pi^+) = 0.027$. We rescale to our best value $B(D_s^+ \rightarrow \phi\pi^+) = 0.036$.

 $\Gamma(D_s^{*-} K^*(892)^+)/\Gamma_{total}$ Γ_{39}/Γ

VALUE	CL%	DOCUMENT ID	TECN	COMMENT
<0.0011				
<0.004	90	128 ALEXANDER 93B	CLE2	$e^+e^- \rightarrow \Upsilon(4S)$
		129 ALBRECHT 93E	ARG	$e^+e^- \rightarrow \Upsilon(4S)$

128 ALEXANDER 93B reports $< 11.0 \times 10^{-4}$ for $B(D_s^+ \rightarrow \phi\pi^+) = 0.037$. We rescale to our best value $B(D_s^+ \rightarrow \phi\pi^+) = 0.036$.

129 ALBRECHT 93E reports $< 5.8 \times 10^{-3}$ for $B(D_s^+ \rightarrow \phi\pi^+) = 0.027$. We rescale to our best value $B(D_s^+ \rightarrow \phi\pi^+) = 0.036$.

 $\Gamma(D_s^- \pi^+ K^0)/\Gamma_{total}$ Γ_{40}/Γ

VALUE	CL%	DOCUMENT ID	TECN	COMMENT
<0.0005				
<0.0005	90	130 ALBRECHT 93E	ARG	$e^+e^- \rightarrow \Upsilon(4S)$

130 ALBRECHT 93E reports $< 7.3 \times 10^{-3}$ for $B(D_s^+ \rightarrow \phi\pi^+) = 0.027$. We rescale to our best value $B(D_s^+ \rightarrow \phi\pi^+) = 0.036$.

 $\Gamma(D_s^{*-} \pi^+ K^0)/\Gamma_{total}$ Γ_{41}/Γ

VALUE	CL%	DOCUMENT ID	TECN	COMMENT
<0.0031				
<0.0031	90	131 ALBRECHT 93E	ARG	$e^+e^- \rightarrow \Upsilon(4S)$

131 ALBRECHT 93E reports $< 4.2 \times 10^{-3}$ for $B(D_s^+ \rightarrow \phi\pi^+) = 0.027$. We rescale to our best value $B(D_s^+ \rightarrow \phi\pi^+) = 0.036$.

 $\Gamma(D_s^{*-} \pi^+ K^*(892)^0)/\Gamma_{total}$ Γ_{42}/Γ

VALUE	CL%	DOCUMENT ID	TECN	COMMENT
<0.004				
<0.004	90	132 ALBRECHT 93E	ARG	$e^+e^- \rightarrow \Upsilon(4S)$

132 ALBRECHT 93E reports $< 5.0 \times 10^{-3}$ for $B(D_s^+ \rightarrow \phi\pi^+) = 0.027$. We rescale to our best value $B(D_s^+ \rightarrow \phi\pi^+) = 0.036$.

Meson Particle Listings

 B^0

$\Gamma(D_s^{*-} \pi^+ K^*(892)^0)/\Gamma_{\text{total}}$ Γ_{43}/Γ

VALUE	CL%	DOCUMENT ID	TECN	COMMENT
<0.0020	90	133 ALBRECHT	93E ARG	$e^+e^- \rightarrow \Upsilon(4S)$

133 ALBRECHT 93E reports $< 2.7 \times 10^{-3}$ for $B(D_s^+ \rightarrow \phi \pi^+) = 0.027$. We rescale to our best value $B(D_s^+ \rightarrow \phi \pi^+) = 0.036$.

$\Gamma(D^0 \pi^0)/\Gamma_{\text{total}}$ Γ_{44}/Γ

VALUE	CL%	DOCUMENT ID	TECN	COMMENT
<0.00012	90	134 NEMAT1	98 CLE2	$e^+e^- \rightarrow \Upsilon(4S)$

• • • We do not use the following data for averages, fits, limits, etc. • • •
 <0.00048 90 135 ALAM 94 CLE2 Repl. by NEMAT1 98
 134 NEMAT1 98 assumes equal production of B^+ and B^0 at the $\Upsilon(4S)$ and use the PDG 96 values for D^0 , D^{*0} , η , η' , and ω branching fractions.

135 ALAM 94 assume equal production of B^+ and B^0 at the $\Upsilon(4S)$ and use the CLEO II absolute $B(D^0 \rightarrow K^- \pi^+)$ and the PDG 1992 $B(D^0 \rightarrow K^- \pi^+ \pi^0)/B(D^0 \rightarrow K^- \pi^+)$ and $B(D^0 \rightarrow K^- \pi^+ \pi^- \pi^0)/B(D^0 \rightarrow K^- \pi^+)$.

$\Gamma(D^0 \rho^0)/\Gamma_{\text{total}}$ Γ_{45}/Γ

VALUE	CL%	EVTS	DOCUMENT ID	TECN	COMMENT
<0.00039	90	136	NEMAT1	98 CLE2	$e^+e^- \rightarrow \Upsilon(4S)$

• • • We do not use the following data for averages, fits, limits, etc. • • •
 <0.00055 90 137 ALAM 94 CLE2 Repl. by NEMAT1 98
 <0.0006 90 138 BORTOLETTO92 CLEO $e^+e^- \rightarrow \Upsilon(4S)$
 <0.0027 90 4 139 ALBRECHT 88k ARG $e^+e^- \rightarrow \Upsilon(4S)$

136 NEMAT1 98 assumes equal production of B^+ and B^0 at the $\Upsilon(4S)$ and use the PDG 96 values for D^0 , D^{*0} , η , η' , and ω branching fractions.

137 ALAM 94 assume equal production of B^+ and B^0 at the $\Upsilon(4S)$ and use the CLEO II absolute $B(D^0 \rightarrow K^- \pi^+)$ and the PDG 1992 $B(D^0 \rightarrow K^- \pi^+ \pi^0)/B(D^0 \rightarrow K^- \pi^+)$ and $B(D^0 \rightarrow K^- \pi^+ \pi^- \pi^0)/B(D^0 \rightarrow K^- \pi^+)$.

138 BORTOLETTO 92 assumes equal production of B^+ and B^0 at the $\Upsilon(4S)$ and uses Mark III branching fractions for the D .

139 ALBRECHT 88k reports < 0.003 assuming $B^0 \bar{B}^0 : B^+ B^-$ production ratio is 45:55. We rescale to 50%.

$\Gamma(D^0 \eta)/\Gamma_{\text{total}}$ Γ_{46}/Γ

VALUE	CL%	DOCUMENT ID	TECN	COMMENT
<0.00013	90	140 NEMAT1	98 CLE2	$e^+e^- \rightarrow \Upsilon(4S)$

• • • We do not use the following data for averages, fits, limits, etc. • • •
 <0.00068 90 141 ALAM 94 CLE2 Repl. by NEMAT1 98
 140 NEMAT1 98 assumes equal production of B^+ and B^0 at the $\Upsilon(4S)$ and use the PDG 96 values for D^0 , D^{*0} , η , η' , and ω branching fractions.

141 ALAM 94 assume equal production of B^+ and B^0 at the $\Upsilon(4S)$ and use the CLEO II absolute $B(D^0 \rightarrow K^- \pi^+)$ and the PDG 1992 $B(D^0 \rightarrow K^- \pi^+ \pi^0)/B(D^0 \rightarrow K^- \pi^+)$ and $B(D^0 \rightarrow K^- \pi^+ \pi^- \pi^0)/B(D^0 \rightarrow K^- \pi^+)$.

$\Gamma(D^0 \eta')/\Gamma_{\text{total}}$ Γ_{47}/Γ

VALUE	CL%	DOCUMENT ID	TECN	COMMENT
<0.00094	90	142 NEMAT1	98 CLE2	$e^+e^- \rightarrow \Upsilon(4S)$

• • • We do not use the following data for averages, fits, limits, etc. • • •
 <0.00086 90 143 ALAM 94 CLE2 Repl. by NEMAT1 98
 142 NEMAT1 98 assumes equal production of B^+ and B^0 at the $\Upsilon(4S)$ and use the PDG 96 values for D^0 , D^{*0} , η , η' , and ω branching fractions.

143 ALAM 94 assume equal production of B^+ and B^0 at the $\Upsilon(4S)$ and use the CLEO II absolute $B(D^0 \rightarrow K^- \pi^+)$ and the PDG 1992 $B(D^0 \rightarrow K^- \pi^+ \pi^0)/B(D^0 \rightarrow K^- \pi^+)$ and $B(D^0 \rightarrow K^- \pi^+ \pi^- \pi^0)/B(D^0 \rightarrow K^- \pi^+)$.

$\Gamma(D^0 \omega)/\Gamma_{\text{total}}$ Γ_{48}/Γ

VALUE	CL%	DOCUMENT ID	TECN	COMMENT
<0.00051	90	144 NEMAT1	98 CLE2	$e^+e^- \rightarrow \Upsilon(4S)$

• • • We do not use the following data for averages, fits, limits, etc. • • •
 <0.00063 90 145 ALAM 94 CLE2 Repl. by NEMAT1 98
 144 NEMAT1 98 assumes equal production of B^+ and B^0 at the $\Upsilon(4S)$ and use the PDG 96 values for D^0 , D^{*0} , η , η' , and ω branching fractions.

145 ALAM 94 assume equal production of B^+ and B^0 at the $\Upsilon(4S)$ and use the CLEO II absolute $B(D^0 \rightarrow K^- \pi^+)$ and the PDG 1992 $B(D^0 \rightarrow K^- \pi^+ \pi^0)/B(D^0 \rightarrow K^- \pi^+)$ and $B(D^0 \rightarrow K^- \pi^+ \pi^- \pi^0)/B(D^0 \rightarrow K^- \pi^+)$.

$\Gamma(D^*(2007)^0 \pi^0)/\Gamma_{\text{total}}$ Γ_{49}/Γ

VALUE	CL%	DOCUMENT ID	TECN	COMMENT
<0.00044	90	146 NEMAT1	98 CLE2	$e^+e^- \rightarrow \Upsilon(4S)$

• • • We do not use the following data for averages, fits, limits, etc. • • •
 <0.00097 90 147 ALAM 94 CLE2 Repl. by NEMAT1 98
 146 NEMAT1 98 assumes equal production of B^+ and B^0 at the $\Upsilon(4S)$ and use the PDG 96 values for D^0 , D^{*0} , η , η' , and ω branching fractions.

147 ALAM 94 assume equal production of B^+ and B^0 at the $\Upsilon(4S)$ and use the CLEO II $B(D^*(2007)^0 \rightarrow D^0 \pi^0)$ and absolute $B(D^0 \rightarrow K^- \pi^+)$ and the PDG 1992 $B(D^0 \rightarrow K^- \pi^+ \pi^0)/B(D^0 \rightarrow K^- \pi^+)$ and $B(D^0 \rightarrow K^- \pi^+ \pi^- \pi^0)/B(D^0 \rightarrow K^- \pi^+)$.

$\Gamma(D^*(2007)^0 \rho^0)/\Gamma_{\text{total}}$ Γ_{50}/Γ

VALUE	CL%	DOCUMENT ID	TECN	COMMENT
<0.00056	90	148 NEMAT1	98 CLE2	$e^+e^- \rightarrow \Upsilon(4S)$

• • • We do not use the following data for averages, fits, limits, etc. • • •
 <0.00117 90 149 ALAM 94 CLE2 Repl. by NEMAT1 98
 148 NEMAT1 98 assumes equal production of B^+ and B^0 at the $\Upsilon(4S)$ and use the PDG 96 values for D^0 , D^{*0} , η , η' , and ω branching fractions.

149 ALAM 94 assume equal production of B^+ and B^0 at the $\Upsilon(4S)$ and use the CLEO II $B(D^*(2007)^0 \rightarrow D^0 \pi^0)$ and absolute $B(D^0 \rightarrow K^- \pi^+)$ and the PDG 1992 $B(D^0 \rightarrow K^- \pi^+ \pi^0)/B(D^0 \rightarrow K^- \pi^+)$ and $B(D^0 \rightarrow K^- \pi^+ \pi^- \pi^0)/B(D^0 \rightarrow K^- \pi^+)$.

$\Gamma(D^*(2007)^0 \eta)/\Gamma_{\text{total}}$ Γ_{51}/Γ

VALUE	CL%	DOCUMENT ID	TECN	COMMENT
<0.00026	90	150 NEMAT1	98 CLE2	$e^+e^- \rightarrow \Upsilon(4S)$

• • • We do not use the following data for averages, fits, limits, etc. • • •
 <0.00069 90 151 ALAM 94 CLE2 Repl. by NEMAT1 98
 150 NEMAT1 98 assumes equal production of B^+ and B^0 at the $\Upsilon(4S)$ and use the PDG 96 values for D^0 , D^{*0} , η , η' , and ω branching fractions.

151 ALAM 94 assume equal production of B^+ and B^0 at the $\Upsilon(4S)$ and use the CLEO II $B(D^*(2007)^0 \rightarrow D^0 \pi^0)$ and absolute $B(D^0 \rightarrow K^- \pi^+)$ and the PDG 1992 $B(D^0 \rightarrow K^- \pi^+ \pi^0)/B(D^0 \rightarrow K^- \pi^+)$ and $B(D^0 \rightarrow K^- \pi^+ \pi^- \pi^0)/B(D^0 \rightarrow K^- \pi^+)$.

$\Gamma(D^*(2007)^0 \eta')/\Gamma_{\text{total}}$ Γ_{52}/Γ

VALUE	CL%	DOCUMENT ID	TECN	COMMENT
<0.0014	90	BRANDENB...	98 CLE2	$e^+e^- \rightarrow \Upsilon(4S)$

• • • We do not use the following data for averages, fits, limits, etc. • • •
 <0.0019 90 152 NEMAT1 98 CLE2 $e^+e^- \rightarrow \Upsilon(4S)$
 <0.0027 90 153 ALAM 94 CLE2 Repl. by NEMAT1 98
 152 NEMAT1 98 assumes equal production of B^+ and B^0 at the $\Upsilon(4S)$ and use the PDG 96 values for D^0 , D^{*0} , η , η' , and ω branching fractions.

153 ALAM 94 assume equal production of B^+ and B^0 at the $\Upsilon(4S)$ and use the CLEO II $B(D^*(2007)^0 \rightarrow D^0 \pi^0)$ and absolute $B(D^0 \rightarrow K^- \pi^+)$ and the PDG 1992 $B(D^0 \rightarrow K^- \pi^+ \pi^0)/B(D^0 \rightarrow K^- \pi^+)$ and $B(D^0 \rightarrow K^- \pi^+ \pi^- \pi^0)/B(D^0 \rightarrow K^- \pi^+)$.

$\Gamma(D^*(2007)^0 \omega)/\Gamma_{\text{total}}$ Γ_{53}/Γ

VALUE	CL%	DOCUMENT ID	TECN	COMMENT
<0.00074	90	154 NEMAT1	98 CLE2	$e^+e^- \rightarrow \Upsilon(4S)$

• • • We do not use the following data for averages, fits, limits, etc. • • •
 <0.0021 90 155 ALAM 94 CLE2 Repl. by NEMAT1 98
 154 NEMAT1 98 assumes equal production of B^+ and B^0 at the $\Upsilon(4S)$ and use the PDG 96 values for D^0 , D^{*0} , η , η' , and ω branching fractions.

155 ALAM 94 assume equal production of B^+ and B^0 at the $\Upsilon(4S)$ and use the CLEO II $B(D^*(2007)^0 \rightarrow D^0 \pi^0)$ and absolute $B(D^0 \rightarrow K^- \pi^+)$ and the PDG 1992 $B(D^0 \rightarrow K^- \pi^+ \pi^0)/B(D^0 \rightarrow K^- \pi^+)$ and $B(D^0 \rightarrow K^- \pi^+ \pi^- \pi^0)/B(D^0 \rightarrow K^- \pi^+)$.

$\Gamma(D^*(2010)^+ D^*(2010)^-)/\Gamma_{\text{total}}$ Γ_{54}/Γ

VALUE	CL%	DOCUMENT ID	TECN	COMMENT
$(6.2^{+4.0}_{-2.9} \pm 1.0) \times 10^{-4}$		156 ARTUSO	99 CLE2	$e^+e^- \rightarrow \Upsilon(4S)$

• • • We do not use the following data for averages, fits, limits, etc. • • •
 < 6.1 $\times 10^{-3}$ 90 157 BARATE 98Q ALEP $e^+e^- \rightarrow Z$
 < 2.2 $\times 10^{-3}$ 90 158 ASNER 97 CLE2 Repl. by ARTUSO 99
 156 ARTUSO 99 uses $B(\Upsilon(4S) \rightarrow B^0 \bar{B}^0) = (48 \pm 4)\%$.

157 BARATE 98Q (ALEPH) observes 2 events with an expected background of 0.10 ± 0.03 which corresponds to a branching ratio of $(2.3^{+1.9}_{-1.2} \pm 0.4) \times 10^{-3}$.

158 ASNER 97 at CLEO observes 1 event with an expected background of 0.022 ± 0.011 . This corresponds to a branching ratio of $(5.3^{+7.1}_{-3.7} \pm 1.0) \times 10^{-4}$.

$\Gamma(D^*(2010)^+ D^-)/\Gamma_{\text{total}}$ Γ_{55}/Γ

VALUE	CL%	DOCUMENT ID	TECN	COMMENT
<1.8 $\times 10^{-3}$	90	ASNER	97 CLE2	$e^+e^- \rightarrow \Upsilon(4S)$

• • • We do not use the following data for averages, fits, limits, etc. • • •
 <5.6 $\times 10^{-3}$ 90 BARATE 98Q ALEP $e^+e^- \rightarrow Z$

$\Gamma(D^{(*)0} \bar{D}^{(*)0})/\Gamma_{\text{total}}$ Γ_{56}/Γ

VALUE	CL%	DOCUMENT ID	TECN	COMMENT
<0.027	90	BARATE	98Q ALEP	$e^+e^- \rightarrow Z$

$\Gamma(J/\psi(1S) K^0)/\Gamma_{\text{total}}$ Γ_{57}/Γ

VALUE (units 10^{-4})	CL%	EVTS	DOCUMENT ID	TECN	COMMENT
8.9 ± 1.2 OUR AVERAGE					

8.5^{+1.4}_{-1.2} ± 0.6 159 JESSOP 97 CLE2 $e^+e^- \rightarrow \Upsilon(4S)$
 11.5 ± 2.3 ± 1.7 160 ABE 96H CDF $p\bar{p}$ at 1.8 TeV
 7.0 ± 4.1 ± 0.1 161 BORTOLETTO92 CLEO $e^+e^- \rightarrow \Upsilon(4S)$
 9.3 ± 7.3 ± 0.2 2 162 ALBRECHT 90J ARG $e^+e^- \rightarrow \Upsilon(4S)$

• • • We do not use the following data for averages, fits, limits, etc. • • •
 7.5 ± 2.4 ± 0.8 10 161 ALAM 94 CLE2 Sup. by JESSOP 97
 <50 90 ALAM 86 CLEO $e^+e^- \rightarrow \Upsilon(4S)$

159 Assumes equal production of B^+ and B^0 at the $\Upsilon(4S)$.
 160 ABE 96H assumes that $B(B^+ \rightarrow J/\psi K^+) = (1.02 \pm 0.14) \times 10^{-3}$.

See key on page 239

Meson Particle Listings

 B^0

¹⁶¹BOROLETTO 92 reports $6 \pm 3 \pm 2$ for $B(J/\psi(1S) \rightarrow e^+e^-) = 0.069 \pm 0.009$. We rescale to our best value $B(J/\psi(1S) \rightarrow e^+e^-) = (5.93 \pm 0.10) \times 10^{-2}$. Our first error is their experiment's error and our second error is the systematic error from using our best value. Assumes equal production of B^+ and B^0 at the $\Upsilon(4S)$.

¹⁶²ALBRECHT 90J reports $8 \pm 6 \pm 2$ for $B(J/\psi(1S) \rightarrow e^+e^-) = 0.069 \pm 0.009$. We rescale to our best value $B(J/\psi(1S) \rightarrow e^+e^-) = (5.93 \pm 0.10) \times 10^{-2}$. Our first error is their experiment's error and our second error is the systematic error from using our best value. Assumes equal production of B^+ and B^0 at the $\Upsilon(4S)$.

$\Gamma(J/\psi(1S)K^+\pi^-)/\Gamma_{\text{total}}$			Γ_{58}/Γ		
VALUE	CL%	EVTS	DOCUMENT ID	TECN	COMMENT
$0.00116 \pm 0.00056 \pm 0.00002$			163	BOROLETTO92	CLEO $e^+e^- \rightarrow \Upsilon(4S)$

• • • We do not use the following data for averages, fits, limits, etc. • • •

<0.0013	90		164	ALBRECHT	87D ARG $e^+e^- \rightarrow \Upsilon(4S)$
<0.0063	90	2	GILES	84 CLEO	$e^+e^- \rightarrow \Upsilon(4S)$

¹⁶³BOROLETTO 92 reports $0.0010 \pm 0.0004 \pm 0.0003$ for $B(J/\psi(1S) \rightarrow e^+e^-) = 0.069 \pm 0.009$. We rescale to our best value $B(J/\psi(1S) \rightarrow e^+e^-) = (5.93 \pm 0.10) \times 10^{-2}$. Our first error is their experiment's error and our second error is the systematic error from using our best value. Assumes equal production of B^+ and B^0 at the $\Upsilon(4S)$.

¹⁶⁴ALBRECHT 87D assume $B^+B^-/B^0\bar{B}^0$ ratio is 55/45. $K\pi$ system is specifically selected as nonresonant.

$\Gamma(J/\psi(1S)K^*(892)^0)/\Gamma_{\text{total}}$			Γ_{59}/Γ		
VALUE	CL%	EVTS	DOCUMENT ID	TECN	COMMENT
0.00150 ± 0.00017 OUR AVERAGE					

$0.00174 \pm 0.00020 \pm 0.00018$			165	ABE	98o CDF $p\bar{p}$ 1.8 TeV
$0.00132 \pm 0.00017 \pm 0.00017$			166	JESSOP	97 CLE2 $e^+e^- \rightarrow \Upsilon(4S)$
$0.00128 \pm 0.00066 \pm 0.00002$			167	BOROLETTO92	CLEO $e^+e^- \rightarrow \Upsilon(4S)$
$0.00128 \pm 0.00060 \pm 0.00002$	6		168	ALBRECHT	90J ARG $e^+e^- \rightarrow \Upsilon(4S)$
$0.0041 \pm 0.0018 \pm 0.0001$		5	169	BEBEK	87 CLEO $e^+e^- \rightarrow \Upsilon(4S)$

• • • We do not use the following data for averages, fits, limits, etc. • • •

$0.00136 \pm 0.00027 \pm 0.00022$			170	ABE	96H CDF Sup. by ABE 98o
$0.00169 \pm 0.00031 \pm 0.00018$		29	171	ALAM	94 CLE2 Sup. by JESSOP 97
			172	ALBRECHT	94G ARG $e^+e^- \rightarrow \Upsilon(4S)$
0.0040 ± 0.0030			173	ALBAJAR	91E UAI $E_{\text{cm}}^{\text{pp}} = 630$ GeV
0.0033 ± 0.0018		5	174	ALBRECHT	87D ARG $e^+e^- \rightarrow \Upsilon(4S)$
0.0041 ± 0.0018		5	175	ALAM	86 CLEO Repl. by BEBEK 87

¹⁶⁵ABE 98o reports $[B(B^0 \rightarrow J/\psi(1S)K^*(892)^0)]/[B(B^+ \rightarrow J/\psi(1S)K^+)] = 1.76 \pm 0.14 \pm 0.15$. We multiply by our best value $B(B^+ \rightarrow J/\psi(1S)K^+) = (9.9 \pm 1.0) \times 10^{-4}$. Our first error is their experiment's error and our second error is the systematic error from using our best value.

¹⁶⁶Assumes equal production of B^+ and B^0 at the $\Upsilon(4S)$.

¹⁶⁷BOROLETTO 92 reports $0.0011 \pm 0.0005 \pm 0.0003$ for $B(J/\psi(1S) \rightarrow e^+e^-) = 0.069 \pm 0.009$. We rescale to our best value $B(J/\psi(1S) \rightarrow e^+e^-) = (5.93 \pm 0.10) \times 10^{-2}$. Our first error is their experiment's error and our second error is the systematic error from using our best value. Assumes equal production of B^+ and B^0 at the $\Upsilon(4S)$.

¹⁶⁸ALBRECHT 90J reports $0.0011 \pm 0.0005 \pm 0.0002$ for $B(J/\psi(1S) \rightarrow e^+e^-) = 0.069 \pm 0.009$. We rescale to our best value $B(J/\psi(1S) \rightarrow e^+e^-) = (5.93 \pm 0.10) \times 10^{-2}$. Our first error is their experiment's error and our second error is the systematic error from using our best value. Assumes equal production of B^+ and B^0 at the $\Upsilon(4S)$.

¹⁶⁹BEBEK 87 reports $0.0035 \pm 0.0016 \pm 0.0003$ for $B(J/\psi(1S) \rightarrow e^+e^-) = 0.069 \pm 0.009$. We rescale to our best value $B(J/\psi(1S) \rightarrow e^+e^-) = (5.93 \pm 0.10) \times 10^{-2}$. Our first error is their experiment's error and our second error is the systematic error from using our best value. Updated in BOROLETTO 92 to use the same assumptions.

¹⁷⁰ABE 96H assumes that $B(B^+ \rightarrow J/\psi K^+) = (1.02 \pm 0.14) \times 10^{-3}$.

¹⁷¹The neutral and charged B events together are predominantly longitudinally polarized, $\Gamma_L/\Gamma = 0.080 \pm 0.08 \pm 0.05$. This can be compared with a prediction using HQET, 0.73 (KRAMER 92). This polarization indicates that the $B \rightarrow \psi K^*$ decay is dominated by the $CP = -1$ CP eigenstate. Assumes equal production of B^+ and B^0 at the $\Upsilon(4S)$.

¹⁷²ALBRECHT 94G measures the polarization in the vector-vector decay to be predominantly longitudinal, $\Gamma_T/\Gamma = 0.03 \pm 0.16 \pm 0.15$ making the neutral decay a CP eigenstate when the K^*0 decays through $K_S^0 \pi^0$.

¹⁷³ALBAJAR 91E assumes B_0^0 production fraction of 36%.

¹⁷⁴ALBRECHT 87D assume $B^+B^-/B^0\bar{B}^0$ ratio is 55/45. Superseded by ALBRECHT 90J.

¹⁷⁵ALAM 86 assumes B^\pm/B^0 ratio is 60/40. The observation of the decay $B^+ \rightarrow J/\psi K^*(892)^+$ (HAAS 85) has been retracted in this paper.

$\Gamma(J/\psi(1S)K^*(892)^0)/\Gamma(J/\psi(1S)K^0)$			Γ_{59}/Γ_{57}		
VALUE	CL%	EVTS	DOCUMENT ID	TECN	COMMENT
$1.39 \pm 0.36 \pm 0.10$			ABE	96Q CDF	$p\bar{p}$

$\Gamma(J/\psi(1S)\pi^0)/\Gamma_{\text{total}}$			Γ_{60}/Γ		
VALUE	CL%	EVTS	DOCUMENT ID	TECN	COMMENT
< 5.8×10^{-5}			90	BISHAI	96 CLE2 $e^+e^- \rightarrow \Upsilon(4S)$

• • • We do not use the following data for averages, fits, limits, etc. • • •

< 3.2×10^{-4}	90		176	ACCIARRI	97C L3
< 6.9×10^{-3}	90	1	177	ALEXANDER	95 CLE2 Sup. by BISHAI 96

¹⁷⁶ACCIARRI 97C assumes B^0 production fraction (39.5 ± 4.0%) and B_S (12.0 ± 3.0%).

¹⁷⁷Assumes equal production of B^+B^- and $B^0\bar{B}^0$ on $\Upsilon(4S)$.

$\Gamma(J/\psi(1S)\eta)/\Gamma_{\text{total}}$			Γ_{61}/Γ		
VALUE	CL%	DOCUMENT ID	TECN	COMMENT	
< 1.2×10^{-3}	90	178	ACCIARRI	97C L3	

¹⁷⁸ACCIARRI 97C assumes B^0 production fraction (39.5 ± 4.0%) and B_S (12.0 ± 3.0%).

$\Gamma(J/\psi(1S)\rho^0)/\Gamma_{\text{total}}$			Γ_{62}/Γ		
VALUE	CL%	DOCUMENT ID	TECN	COMMENT	
< 2.5×10^{-4}	90		BISHAI	96 CLE2	$e^+e^- \rightarrow \Upsilon(4S)$

$\Gamma(J/\psi(1S)\omega)/\Gamma_{\text{total}}$			Γ_{63}/Γ		
VALUE	CL%	DOCUMENT ID	TECN	COMMENT	
< 2.7×10^{-4}	90		BISHAI	96 CLE2	$e^+e^- \rightarrow \Upsilon(4S)$

$\Gamma(\psi(2S)K^0)/\Gamma_{\text{total}}$			Γ_{64}/Γ		
VALUE	CL%	DOCUMENT ID	TECN	COMMENT	
<0.0008	90	179	ALAM	94 CLE2	$e^+e^- \rightarrow \Upsilon(4S)$

• • • We do not use the following data for averages, fits, limits, etc. • • •

<0.0015	90	179	BOROLETTO92	CLEO	$e^+e^- \rightarrow \Upsilon(4S)$
<0.0028	90	179	ALBRECHT	90J ARG	$e^+e^- \rightarrow \Upsilon(4S)$

¹⁷⁹Assumes equal production of B^+ and B^0 at the $\Upsilon(4S)$.

$\Gamma(\psi(2S)K^+\pi^-)/\Gamma_{\text{total}}$			Γ_{65}/Γ		
VALUE	CL%	DOCUMENT ID	TECN	COMMENT	
<0.001	90	180	ALBRECHT	90J ARG	$e^+e^- \rightarrow \Upsilon(4S)$

¹⁸⁰Assumes equal production of B^+ and B^0 at the $\Upsilon(4S)$.

$\Gamma(\psi(2S)K^*(892)^0)/\Gamma_{\text{total}}$			Γ_{66}/Γ		
VALUE	CL%	DOCUMENT ID	TECN	COMMENT	
$(9.3 \pm 2.3) \times 10^{-4}$ OUR AVERAGE					
$0.00090 \pm 0.00022 \pm 0.00009$			181	ABE	98o CDF $p\bar{p}$ 1.8 TeV
$0.0014 \pm 0.0008 \pm 0.0004$			182	BOROLETTO92	CLEO $e^+e^- \rightarrow \Upsilon(4S)$

• • • We do not use the following data for averages, fits, limits, etc. • • •

<0.0019	90	182	ALAM	94 CLE2	$e^+e^- \rightarrow \Upsilon(4S)$
<0.0023	90	182	ALBRECHT	90J ARG	$e^+e^- \rightarrow \Upsilon(4S)$

¹⁸¹ABE 98o reports $[B(B^0 \rightarrow \psi(2S)K^*(892)^0)]/[B(B^+ \rightarrow J/\psi(1S)K^+)] = 0.908 \pm 0.194 \pm 0.10$. We multiply by our best value $B(B^+ \rightarrow J/\psi(1S)K^+) = (9.9 \pm 1.0) \times 10^{-4}$. Our first error is their experiment's error and our second error is the systematic error from using our best value.

¹⁸²Assumes equal production of B^+ and B^0 at the $\Upsilon(4S)$.

$\Gamma(\chi_{c1}(1P)K^0)/\Gamma_{\text{total}}$			Γ_{67}/Γ		
VALUE	CL%	DOCUMENT ID	TECN	COMMENT	
<0.0027	90	183	ALAM	94 CLE2	$e^+e^- \rightarrow \Upsilon(4S)$

¹⁸³BOROLETTO 92 assumes equal production of B^+ and B^0 at the $\Upsilon(4S)$.

$\Gamma(\chi_{c1}(1P)K^*(892)^0)/\Gamma_{\text{total}}$			Γ_{68}/Γ		
VALUE	CL%	DOCUMENT ID	TECN	COMMENT	
<0.0021	90	184	ALAM	94 CLE2	$e^+e^- \rightarrow \Upsilon(4S)$

¹⁸⁴BOROLETTO 92 assumes equal production of B^+ and B^0 at the $\Upsilon(4S)$.

$\Gamma(K^+\pi^-)/\Gamma_{\text{total}}$			Γ_{69}/Γ		
VALUE (units 10^{-5})	CL%	DOCUMENT ID	TECN	COMMENT	
$1.5_{-0.4}^{+0.5} \pm 0.14$			GODANG	98 CLE2	$e^+e^- \rightarrow \Upsilon(4S)$

• • • We do not use the following data for averages, fits, limits, etc. • • •

$2.4_{-1.1}^{+1.7} \pm 0.2$			185	ADAM	96D DLPH $e^+e^- \rightarrow Z$
<1.7	90		ASNER	96 CLE2	Sup. by ADAM 96D
<3.0	90		186	BUSKULIC	96V ALEP $e^+e^- \rightarrow Z$
<9	90		187	ABREU	95N DLPH Sup. by ADAM 96D
<8.1	90		188	AKERS	94L OPAL $e^+e^- \rightarrow Z$
<2.6	90		189	BATTLE	93 CLE2 $e^+e^- \rightarrow \Upsilon(4S)$
<18	90		ALBRECHT	91B ARG	$e^+e^- \rightarrow \Upsilon(4S)$
<9	90		190	AVERY	89B CLEO $e^+e^- \rightarrow \Upsilon(4S)$
<32	90		AVERY	87 CLEO	$e^+e^- \rightarrow \Upsilon(4S)$

¹⁸⁵ADAM 96D assumes $f_{B^0} = f_{B^-} = 0.39$ and $f_{B_S} = 0.12$. Contributions from B^0 and B_S decays cannot be separated. Limits are given for the weighted average of the decay rates for the two neutral B mesons.

¹⁸⁶BUSKULIC 96V assumes PDG 96 production fractions for B^0 , B^+ , B_S , b baryons.

¹⁸⁷Assumes a B^0 , B^- production fraction of 0.39 and a B_S production fraction of 0.12. Contributions from B^0 and B_S decays cannot be separated. Limits are given for the weighted average of the decay rates for the two neutral B mesons.

¹⁸⁸Assumes $B(Z \rightarrow b\bar{b}) = 0.217$ and $B_0^0(B_S^0)$ fraction 39.5% (12%).

¹⁸⁹BATTLE 93 assumes equal production of $B^0\bar{B}^0$ and B^+B^- at $\Upsilon(4S)$.

¹⁹⁰Assumes the $\Upsilon(4S)$ decays 43% to $B^0\bar{B}^0$.

$\Gamma(K^0\pi^0)/\Gamma_{\text{total}}$			Γ_{70}/Γ		
VALUE	CL%	DOCUMENT ID	TECN	COMMENT	
< 4.1×10^{-5}	90		GODANG	98 CLE2	$e^+e^- \rightarrow \Upsilon(4S)$

• • • We do not use the following data for averages, fits, limits, etc. • • •

< 4.0×10^{-5}	90		ASNER	96 CLE2	Rep. by GODANG 98
------------------------	----	--	-------	---------	-------------------

Meson Particle Listings

 B^0

$\Gamma(\eta' K^0)/\Gamma_{total}$					Γ_{71}/Γ				
VALUE	CL%	DOCUMENT ID	TECN	COMMENT	VALUE	CL%	DOCUMENT ID	TECN	COMMENT
$(4.7^{+2.7}_{-2.0} \pm 0.9) \times 10^{-5}$		BEHRENS	98	CLE2	$e^+ e^- \rightarrow T(4S)$				
$\Gamma(\eta' K^*(892)^0)/\Gamma_{total}$					Γ_{72}/Γ				
$<3.9 \times 10^{-5}$	90	BEHRENS	98	CLE2	$e^+ e^- \rightarrow T(4S)$				
$\Gamma(\eta K^*(892)^0)/\Gamma_{total}$					Γ_{73}/Γ				
$<3.0 \times 10^{-5}$	90	BEHRENS	98	CLE2	$e^+ e^- \rightarrow T(4S)$				
$\Gamma(\eta K^0)/\Gamma_{total}$					Γ_{74}/Γ				
$<3.3 \times 10^{-5}$	90	BEHRENS	98	CLE2	$e^+ e^- \rightarrow T(4S)$				
$\Gamma(\omega K^0)/\Gamma_{total}$					Γ_{75}/Γ				
$<5.7 \times 10^{-5}$	90	191 BERGFELD	98	CLE2					
191 Assumes equal production of B^+ and B^0 at the $T(4S)$.									
$\Gamma(\omega K^*(892)^0)/\Gamma_{total}$					Γ_{76}/Γ				
$<2.3 \times 10^{-5}$	90	192 BERGFELD	98	CLE2					
192 Assumes equal production of B^+ and B^0 at the $T(4S)$.									
$[\Gamma(K^+ \pi^-) + \Gamma(\pi^+ \pi^-)]/\Gamma_{total}$					$(\Gamma_{69} + \Gamma_{107})/\Gamma$				
$(1.9 \pm 0.6) \times 10^{-5}$		OUR AVERAGE							
$(2.8^{+1.5}_{-1.0} \pm 2.0) \times 10^{-5}$		193 ADAM	96D	DLPH	$e^+ e^- \rightarrow Z$				
$(1.6^{+0.6+0.3}_{-0.5-0.4}) \times 10^{-5}$	17.2	ASNER	96	CLE2	$e^+ e^- \rightarrow T(4S)$				
• • • We do not use the following data for averages, fits, limits, etc. • • •									
$(2.4^{+0.8}_{-0.7} \pm 0.2) \times 10^{-5}$		194 BATTLE	93	CLE2	$e^+ e^- \rightarrow T(4S)$				
193 ADAM 96D assumes $f_{B^0} = f_{B^-} = 0.39$ and $f_{B_s} = 0.12$. Contributions from B^0 and B_s decays cannot be separated. Limits are given for the weighted average of the decay rates for the two neutral B mesons.									
194 BATTLE 93 assumes equal production of $B^0 \bar{B}^0$ and $B^+ B^-$ at $T(4S)$.									
$\Gamma(K^+ K^-)/\Gamma_{total}$					Γ_{77}/Γ				
$<4.3 \times 10^{-6}$	90	GODANG	98	CLE2	$e^+ e^- \rightarrow T(4S)$				
• • • We do not use the following data for averages, fits, limits, etc. • • •									
$<4.6 \times 10^{-5}$		195 ADAM	96D	DLPH	$e^+ e^- \rightarrow Z$				
$<0.4 \times 10^{-5}$	90	ASNER	96	CLE2	Repl. by GODANG 98				
$<1.8 \times 10^{-5}$	90	196 BUSKULIC	96v	ALEP	$e^+ e^- \rightarrow Z$				
$<1.2 \times 10^{-4}$	90	197 ABREU	95N	DLPH	Sup. by ADAM 96D				
$<0.7 \times 10^{-5}$	90	198 BATTLE	93	CLE2	$e^+ e^- \rightarrow T(4S)$				
195 ADAM 96D assumes $f_{B^0} = f_{B^-} = 0.39$ and $f_{B_s} = 0.12$. Contributions from B^0 and B_s decays cannot be separated. Limits are given for the weighted average of the decay rates for the two neutral B mesons.									
196 BUSKULIC 96v assumes PDG 96 production fractions for B^0 , B^+ , B_s , b baryons.									
197 Assumes a B^0 , B^- production fraction of 0.39 and a B_s production fraction of 0.12. Contributions from B^0 and B_s decays cannot be separated. Limits are given for the weighted average of the decay rates for the two neutral B mesons.									
198 BATTLE 93 assumes equal production of $B^0 \bar{B}^0$ and $B^+ B^-$ at $T(4S)$.									
$\Gamma(K^0 \bar{K}^0)/\Gamma_{total}$					Γ_{78}/Γ				
$<1.7 \times 10^{-5}$	90	GODANG	98	CLE2	$e^+ e^- \rightarrow T(4S)$				
$\Gamma(K^+ \rho^-)/\Gamma_{total}$					Γ_{79}/Γ				
$<3.5 \times 10^{-5}$	90	ASNER	96	CLE2	$e^+ e^- \rightarrow T(4S)$				
$\Gamma(K^0 \pi^+ \pi^-)/\Gamma_{total}$					Γ_{80}/Γ				
$<4.4 \times 10^{-4}$	90	ALBRECHT	91E	ARG	$e^+ e^- \rightarrow T(4S)$				
• • • We do not use the following data for averages, fits, limits, etc. • • •									
$\Gamma(K^0 \rho^0)/\Gamma_{total}$					Γ_{81}/Γ				
$<3.9 \times 10^{-5}$	90	ASNER	96	CLE2	$e^+ e^- \rightarrow T(4S)$				
• • • We do not use the following data for averages, fits, limits, etc. • • •									
$<3.2 \times 10^{-4}$	90	ALBRECHT	91B	ARG	$e^+ e^- \rightarrow T(4S)$				
$<5.0 \times 10^{-4}$	90	199 AVERY	89B	CLEO	$e^+ e^- \rightarrow T(4S)$				
<0.064	90	200 AVERY	87	CLEO	$e^+ e^- \rightarrow T(4S)$				
199 AVERY 89B reports $< 5.8 \times 10^{-4}$ assuming the $T(4S)$ decays 43% to $B^0 \bar{B}^0$. We rescale to 50%.									
200 AVERY 87 reports < 0.08 assuming the $T(4S)$ decays 40% to $B^0 \bar{B}^0$. We rescale to 50%.									
$\Gamma(K^0 f_0(980))/\Gamma_{total}$					Γ_{82}/Γ				
$<3.6 \times 10^{-4}$	90	201 AVERY	89B	CLEO	$e^+ e^- \rightarrow T(4S)$				
201 AVERY 89B reports $< 4.2 \times 10^{-4}$ assuming the $T(4S)$ decays 43% to $B^0 \bar{B}^0$. We rescale to 50%.									
$\Gamma(K^*(892)^+ \pi^-)/\Gamma_{total}$					Γ_{83}/Γ				
$<7.2 \times 10^{-5}$	90	ASNER	96	CLE2	$e^+ e^- \rightarrow T(4S)$				
$<3.8 \times 10^{-4}$	90	202 AVERY	89B	CLEO	$e^+ e^- \rightarrow T(4S)$				
• • • We do not use the following data for averages, fits, limits, etc. • • •									
$<6.2 \times 10^{-4}$	90	ALBRECHT	91B	ARG	$e^+ e^- \rightarrow T(4S)$				
$<5.6 \times 10^{-4}$	90	203 AVERY	87	CLEO	$e^+ e^- \rightarrow T(4S)$				
202 AVERY 89B reports $< 4.4 \times 10^{-4}$ assuming the $T(4S)$ decays 43% to $B^0 \bar{B}^0$. We rescale to 50%.									
203 AVERY 87 reports $< 7 \times 10^{-4}$ assuming the $T(4S)$ decays 40% to $B^0 \bar{B}^0$. We rescale to 50%.									
$\Gamma(K^*(892)^0 \pi^0)/\Gamma_{total}$					Γ_{84}/Γ				
$<2.8 \times 10^{-5}$	90	ASNER	96	CLE2	$e^+ e^- \rightarrow T(4S)$				
$\Gamma(K^*_2(1430)^+ \pi^-)/\Gamma_{total}$					Γ_{85}/Γ				
$<2.6 \times 10^{-3}$	90	ALBRECHT	91B	ARG	$e^+ e^- \rightarrow T(4S)$				
$\Gamma(K^0 K^+ K^-)/\Gamma_{total}$					Γ_{86}/Γ				
$<1.3 \times 10^{-3}$	90	ALBRECHT	91E	ARG	$e^+ e^- \rightarrow T(4S)$				
$\Gamma(K^0 \phi)/\Gamma_{total}$					Γ_{87}/Γ				
$<3.1 \times 10^{-5}$	90	204 BERGFELD	98	CLE2					
• • • We do not use the following data for averages, fits, limits, etc. • • •									
$<8.8 \times 10^{-5}$	90	ASNER	96	CLE2	$e^+ e^- \rightarrow T(4S)$				
$<7.2 \times 10^{-4}$	90	ALBRECHT	91B	ARG	$e^+ e^- \rightarrow T(4S)$				
$<4.2 \times 10^{-4}$	90	205 AVERY	89B	CLEO	$e^+ e^- \rightarrow T(4S)$				
$<1.0 \times 10^{-3}$	90	206 AVERY	87	CLEO	$e^+ e^- \rightarrow T(4S)$				
204 Assumes equal production of B^+ and B^0 at the $T(4S)$.									
205 AVERY 89B reports $< 4.9 \times 10^{-4}$ assuming the $T(4S)$ decays 43% to $B^0 \bar{B}^0$. We rescale to 50%.									
206 AVERY 87 reports $< 1.3 \times 10^{-3}$ assuming the $T(4S)$ decays 40% to $B^0 \bar{B}^0$. We rescale to 50%.									
$\Gamma(K^- \pi^+ \pi^+ \pi^-)/\Gamma_{total}$					Γ_{88}/Γ				
$<2.3 \times 10^{-4}$	90	207 ADAM	96D	DLPH	$e^+ e^- \rightarrow Z$				
• • • We do not use the following data for averages, fits, limits, etc. • • •									
$<2.1 \times 10^{-4}$	90	208 ABREU	95N	DLPH	Sup. by ADAM 96D				
207 ADAM 96D assumes $f_{B^0} = f_{B^-} = 0.39$ and $f_{B_s} = 0.12$. Contributions from B^0 and B_s decays cannot be separated. Limits are given for the weighted average of the decay rates for the two neutral B mesons.									
208 Assumes a B^0 , B^- production fraction of 0.39 and a B_s production fraction of 0.12. Contributions from B^0 and B_s decays cannot be separated. Limits are given for the weighted average of the decay rates for the two neutral B mesons.									
$\Gamma(K^*(892)^0 \pi^+ \pi^-)/\Gamma_{total}$					Γ_{89}/Γ				
$<1.4 \times 10^{-3}$	90	ALBRECHT	91E	ARG	$e^+ e^- \rightarrow T(4S)$				
$\Gamma(K^*(892)^0 \rho^0)/\Gamma_{total}$					Γ_{90}/Γ				
$<4.6 \times 10^{-4}$	90	ALBRECHT	91B	ARG	$e^+ e^- \rightarrow T(4S)$				
• • • We do not use the following data for averages, fits, limits, etc. • • •									
$<5.8 \times 10^{-4}$	90	209 AVERY	89B	CLEO	$e^+ e^- \rightarrow T(4S)$				
$<9.6 \times 10^{-4}$	90	210 AVERY	87	CLEO	$e^+ e^- \rightarrow T(4S)$				
209 AVERY 89B reports $< 6.7 \times 10^{-4}$ assuming the $T(4S)$ decays 43% to $B^0 \bar{B}^0$. We rescale to 50%.									
210 AVERY 87 reports $< 1.2 \times 10^{-3}$ assuming the $T(4S)$ decays 40% to $B^0 \bar{B}^0$. We rescale to 50%.									
$\Gamma(K^*(892)^0 f_0(980))/\Gamma_{total}$					Γ_{91}/Γ				
$<1.7 \times 10^{-4}$	90	211 AVERY	89B	CLEO	$e^+ e^- \rightarrow T(4S)$				
211 AVERY 89B reports $< 2.0 \times 10^{-4}$ assuming the $T(4S)$ decays 43% to $B^0 \bar{B}^0$. We rescale to 50%.									
$\Gamma(K^*_1(1400)^+ \pi^-)/\Gamma_{total}$					Γ_{92}/Γ				
$<1.1 \times 10^{-3}$	90	ALBRECHT	91B	ARG	$e^+ e^- \rightarrow T(4S)$				

$\Gamma(K^- a_1(1260)^+)/\Gamma_{\text{total}}$ Γ_{93}/Γ

VALUE	CL%	DOCUMENT ID	TECN	COMMENT
$<2.3 \times 10^{-4}$	90	212 ADAM	96D DLPH	$e^+e^- \rightarrow Z$

• • • We do not use the following data for averages, fits, limits, etc. • • •

$<3.9 \times 10^{-4}$	90	213 ABREU	95N DLPH	Sup. by ADAM 96D
-----------------------	----	-----------	----------	------------------

212 ADAM 96D assumes $f_{B^0} = f_{B^-} = 0.39$ and $f_{B_s} = 0.12$. Contributions from B^0 and B_s decays cannot be separated. Limits are given for the weighted average of the decay rates for the two neutral B mesons.

213 Assumes a B^0 , B^- production fraction of 0.39 and a B_s production fraction of 0.12. Contributions from B^0 and B_s^0 decays cannot be separated. Limits are given for the weighted average of the decay rates for the two neutral B mesons.

 $\Gamma(K^*(892)^0 K^+ K^-)/\Gamma_{\text{total}}$ Γ_{94}/Γ

VALUE	CL%	DOCUMENT ID	TECN	COMMENT
$<6.1 \times 10^{-4}$	90	ALBRECHT	91E ARG	$e^+e^- \rightarrow T(45)$

 $\Gamma(K^*(892)^0 \phi)/\Gamma_{\text{total}}$ Γ_{95}/Γ

VALUE	CL%	DOCUMENT ID	TECN	COMMENT
$<2.1 \times 10^{-5}$	90	214 BERGFELD	98 CLE2	

• • • We do not use the following data for averages, fits, limits, etc. • • •

$<4.3 \times 10^{-5}$	90	ASNER	96 CLE2	$e^+e^- \rightarrow T(45)$
$<3.2 \times 10^{-4}$	90	ALBRECHT	91B ARG	$e^+e^- \rightarrow T(45)$
$<3.8 \times 10^{-4}$	90	215 AVERY	89B CLEO	$e^+e^- \rightarrow T(45)$
$<3.8 \times 10^{-4}$	90	216 AVERY	87 CLEO	$e^+e^- \rightarrow T(45)$

214 Assumes equal production of B^+ and B^0 at the $T(45)$.

215 AVERY 89B reports $<4.4 \times 10^{-4}$ assuming the $T(45)$ decays 43% to $B^0 \bar{B}^0$. We rescale to 50%.

216 AVERY 87 reports $<4.7 \times 10^{-4}$ assuming the $T(45)$ decays 40% to $B^0 \bar{B}^0$. We rescale to 50%.

 $\Gamma(K_1(1400)^0 \rho^0)/\Gamma_{\text{total}}$ Γ_{96}/Γ

VALUE	CL%	DOCUMENT ID	TECN	COMMENT
$<3.0 \times 10^{-3}$	90	ALBRECHT	91B ARG	$e^+e^- \rightarrow T(45)$

 $\Gamma(K_1(1400)^0 \phi)/\Gamma_{\text{total}}$ Γ_{97}/Γ

VALUE	CL%	DOCUMENT ID	TECN	COMMENT
$<5.0 \times 10^{-3}$	90	ALBRECHT	91B ARG	$e^+e^- \rightarrow T(45)$

 $\Gamma(K_2^*(1430)^0 \rho^0)/\Gamma_{\text{total}}$ Γ_{98}/Γ

VALUE	CL%	DOCUMENT ID	TECN	COMMENT
$<1.1 \times 10^{-3}$	90	ALBRECHT	91B ARG	$e^+e^- \rightarrow T(45)$

 $\Gamma(K_2^*(1430)^0 \phi)/\Gamma_{\text{total}}$ Γ_{99}/Γ

VALUE	CL%	DOCUMENT ID	TECN	COMMENT
$<1.4 \times 10^{-3}$	90	ALBRECHT	91B ARG	$e^+e^- \rightarrow T(45)$

 $\Gamma(K^*(892)^0 \gamma)/\Gamma_{\text{total}}$ Γ_{100}/Γ

VALUE (units 10^{-5})	CL%	EVTs	DOCUMENT ID	TECN	COMMENT
$4.0 \pm 1.7 \pm 0.8$		8	217 AMMAR	93 CLE2	$e^+e^- \rightarrow T(45)$

• • • We do not use the following data for averages, fits, limits, etc. • • •

<21	90	218 ADAM	96D DLPH	$e^+e^- \rightarrow Z$
<42	90	ALBRECHT	89G ARG	$e^+e^- \rightarrow T(45)$
<24	90	219 AVERY	89B CLEO	$e^+e^- \rightarrow T(45)$
<210	90	AVERY	87 CLEO	$e^+e^- \rightarrow T(45)$

217 AMMAR 93 observed 6.6 ± 2.8 events above background.

218 ADAM 96D assumes $f_{B^0} = f_{B^-} = 0.39$ and $f_{B_s} = 0.12$.

219 AVERY 89B reports $<2.8 \times 10^{-4}$ assuming the $T(45)$ decays 43% to $B^0 \bar{B}^0$. We rescale to 50%.

 $\Gamma(K_1(1270)^0 \gamma)/\Gamma_{\text{total}}$ Γ_{101}/Γ

VALUE	CL%	DOCUMENT ID	TECN	COMMENT
<0.0070	90	220 ALBRECHT	89G ARG	$e^+e^- \rightarrow T(45)$

220 ALBRECHT 89G reports <0.0078 assuming the $T(45)$ decays 45% to $B^0 \bar{B}^0$. We rescale to 50%.

 $\Gamma(K_1(1400)^0 \gamma)/\Gamma_{\text{total}}$ Γ_{102}/Γ

VALUE	CL%	DOCUMENT ID	TECN	COMMENT
<0.0043	90	221 ALBRECHT	89G ARG	$e^+e^- \rightarrow T(45)$

221 ALBRECHT 89G reports <0.0048 assuming the $T(45)$ decays 45% to $B^0 \bar{B}^0$. We rescale to 50%.

 $\Gamma(K_2^*(1430)^0 \gamma)/\Gamma_{\text{total}}$ Γ_{103}/Γ

VALUE	CL%	DOCUMENT ID	TECN	COMMENT
$<4.0 \times 10^{-4}$	90	222 ALBRECHT	89G ARG	$e^+e^- \rightarrow T(45)$

222 ALBRECHT 89G reports $<4.4 \times 10^{-4}$ assuming the $T(45)$ decays 45% to $B^0 \bar{B}^0$. We rescale to 50%.

 $\Gamma(K^*(1680)^0 \gamma)/\Gamma_{\text{total}}$ Γ_{104}/Γ

VALUE	CL%	DOCUMENT ID	TECN	COMMENT
<0.0020	90	223 ALBRECHT	89G ARG	$e^+e^- \rightarrow T(45)$

223 ALBRECHT 89G reports <0.0022 assuming the $T(45)$ decays 45% to $B^0 \bar{B}^0$. We rescale to 50%.

 $\Gamma(K_2^*(1780)^0 \gamma)/\Gamma_{\text{total}}$ Γ_{105}/Γ

VALUE	CL%	DOCUMENT ID	TECN	COMMENT
<0.010	90	224 ALBRECHT	89G ARG	$e^+e^- \rightarrow T(45)$

224 ALBRECHT 89G reports <0.011 assuming the $T(45)$ decays 45% to $B^0 \bar{B}^0$. We rescale to 50%.

 $\Gamma(K_2^*(2045)^0 \gamma)/\Gamma_{\text{total}}$ Γ_{106}/Γ

VALUE	CL%	DOCUMENT ID	TECN	COMMENT
<0.0043	90	225 ALBRECHT	89G ARG	$e^+e^- \rightarrow T(45)$

225 ALBRECHT 89G reports <0.0048 assuming the $T(45)$ decays 45% to $B^0 \bar{B}^0$. We rescale to 50%.

 $\Gamma(\pi^+ \pi^-)/\Gamma_{\text{total}}$ Γ_{107}/Γ

VALUE	CL%	EVTs	DOCUMENT ID	TECN	COMMENT
$<1.5 \times 10^{-5}$	90		GODANG	98 CLE2	$e^+e^- \rightarrow T(45)$

• • • We do not use the following data for averages, fits, limits, etc. • • •

$<4.5 \times 10^{-5}$	90	226 ADAM	96D DLPH	$e^+e^- \rightarrow Z$
$<2.0 \times 10^{-5}$	90	ASNER	96 CLE2	Repl. by GODANG 98
$<4.1 \times 10^{-5}$	90	227 BUSKULIC	96V ALEP	$e^+e^- \rightarrow Z$
$<5.5 \times 10^{-5}$	90	228 ABREU	95N DLPH	Sup. by ADAM 96D
$<4.7 \times 10^{-5}$	90	229 AKERS	94L OPAL	$e^+e^- \rightarrow Z$
$<2.9 \times 10^{-5}$	90	230 BATTLE	93 CLE2	$e^+e^- \rightarrow T(45)$
$<1.3 \times 10^{-4}$	90	230 ALBRECHT	90B ARG	$e^+e^- \rightarrow T(45)$
$<7.7 \times 10^{-5}$	90	231 BORTOLETTO	089 CLEO	$e^+e^- \rightarrow T(45)$
$<2.6 \times 10^{-4}$	90	231 BEBEK	87 CLEO	$e^+e^- \rightarrow T(45)$
$<5 \times 10^{-4}$	90	4 GILES	84 CLEO	$e^+e^- \rightarrow T(45)$

226 ADAM 96D assumes $f_{B^0} = f_{B^-} = 0.39$ and $f_{B_s} = 0.12$.

227 BUSKULIC 96V assumes PDG 96 production fractions for B^0 , B^+ , B_s , b baryons.

228 Assumes a B^0 , B^- production fraction of 0.39 and a B_s production fraction of 0.12.

229 Assumes $B(Z \rightarrow b\bar{b}) = 0.217$ and B_s^0 (B_s^0) fraction 39.5% (12%).

230 Assumes equal production of $B^0 \bar{B}^0$ and $B^+ B^-$ at $T(45)$.

231 Paper assumes the $T(45)$ decays 43% to $B^0 \bar{B}^0$. We rescale to 50%.

 $\Gamma(\pi^0 \pi^0)/\Gamma_{\text{total}}$ Γ_{108}/Γ

VALUE	CL%	DOCUMENT ID	TECN	COMMENT
$<9.3 \times 10^{-6}$	90	GODANG	98 CLE2	$e^+e^- \rightarrow T(45)$

• • • We do not use the following data for averages, fits, limits, etc. • • •

$<0.91 \times 10^{-5}$	90	ASNER	96 CLE2	Repl. by GODANG 98
$<6.0 \times 10^{-5}$	90	232 ACCIARRI	95H L3	$e^+e^- \rightarrow Z$

232 ACCIARRI 95H assumes $f_{B^0} = 39.5 \pm 4.0$ and $f_{B_s} = 12.0 \pm 3.0\%$.

 $\Gamma(\eta \pi^0)/\Gamma_{\text{total}}$ Γ_{109}/Γ

VALUE	CL%	DOCUMENT ID	TECN	COMMENT
$<8 \times 10^{-6}$	90	BEHRENS	98 CLE2	$e^+e^- \rightarrow T(45)$

• • • We do not use the following data for averages, fits, limits, etc. • • •

$<2.5 \times 10^{-4}$	90	233 ACCIARRI	95H L3	$e^+e^- \rightarrow Z$
$<1.8 \times 10^{-3}$	90	234 ALBRECHT	90B ARG	$e^+e^- \rightarrow T(45)$

233 ACCIARRI 95H assumes $f_{B^0} = 39.5 \pm 4.0$ and $f_{B_s} = 12.0 \pm 3.0\%$.

234 ALBRECHT 90B limit assumes equal production of $B^0 \bar{B}^0$ and $B^+ B^-$ at $T(45)$.

 $\Gamma(\eta \eta)/\Gamma_{\text{total}}$ Γ_{110}/Γ

VALUE	CL%	DOCUMENT ID	TECN	COMMENT
$<1.8 \times 10^{-5}$	90	BEHRENS	98 CLE2	$e^+e^- \rightarrow T(45)$

• • • We do not use the following data for averages, fits, limits, etc. • • •

$<4.1 \times 10^{-4}$	90	235 ACCIARRI	95H L3	$e^+e^- \rightarrow Z$
-----------------------	----	--------------	--------	------------------------

235 ACCIARRI 95H assumes $f_{B^0} = 39.5 \pm 4.0$ and $f_{B_s} = 12.0 \pm 3.0\%$.

 $\Gamma(\eta' \pi^0)/\Gamma_{\text{total}}$ Γ_{111}/Γ

VALUE	CL%	DOCUMENT ID	TECN	COMMENT
$<1.1 \times 10^{-5}$	90	BEHRENS	98 CLE2	$e^+e^- \rightarrow T(45)$

 $\Gamma(\eta' \eta)/\Gamma_{\text{total}}$ Γ_{112}/Γ

VALUE	CL%	DOCUMENT ID	TECN	COMMENT
$<4.7 \times 10^{-5}$	90	BEHRENS	98 CLE2	$e^+e^- \rightarrow T(45)$

 $\Gamma(\eta' \eta)/\Gamma_{\text{total}}$ Γ_{113}/Γ

VALUE	CL%	DOCUMENT ID	TECN	COMMENT
$<2.7 \times 10^{-5}$	90	BEHRENS	98 CLE2	$e^+e^- \rightarrow T(45)$

 $\Gamma(\eta' \rho^0)/\Gamma_{\text{total}}$ Γ_{114}/Γ

VALUE	CL%	DOCUMENT ID	TECN	COMMENT
$<2.3 \times 10^{-5}$	90	BEHRENS	98 CLE2	$e^+e^- \rightarrow T(45)$

Meson Particle Listings

 B^0

$\Gamma(\eta\rho^0)/\Gamma_{\text{total}}$					Γ_{115}/Γ	$\Gamma(\pi^+\pi^-\pi^+\pi^-)/\Gamma_{\text{total}}$					Γ_{129}/Γ
VALUE	CL%	DOCUMENT ID	TECN	COMMENT		VALUE	CL%	DOCUMENT ID	TECN	COMMENT	
$<1.3 \times 10^{-5}$	90	BEHRENS	98 CLE2	$e^+e^- \rightarrow \Upsilon(4S)$		$<2.3 \times 10^{-4}$	90	250 ADAM	96D DLPH	$e^+e^- \rightarrow Z$	
• • • We do not use the following data for averages, fits, limits, etc. • • •						• • • We do not use the following data for averages, fits, limits, etc. • • •					
$<1.2 \times 10^{-5}$	90	236 BERGFELD	98 CLE2			$<2.8 \times 10^{-4}$	90	251 ABREU	95N DLPH	Sup. by ADAM 96D	
236 Assumes equal production of B^+ and B^0 at the $\Upsilon(4S)$.						$<6.7 \times 10^{-4}$	90	252 ALBRECHT	90B ARG	$e^+e^- \rightarrow \Upsilon(4S)$	
$\Gamma(\omega\eta)/\Gamma_{\text{total}}$					Γ_{116}/Γ	250 ADAM 96D assumes $f_{B^0} = f_{B^-} = 0.39$ and $f_{B_s} = 0.12$.					
VALUE	CL%	DOCUMENT ID	TECN			251 Assumes a B^0, B^- production fraction of 0.39 and a B_s production fraction of 0.12.					
$<6.0 \times 10^{-5}$	90	237 BERGFELD	98 CLE2			252 ALBRECHT 90B limit assumes equal production of $B^0\bar{B}^0$ and B^+B^- at $\Upsilon(4S)$.					
237 Assumes equal production of B^+ and B^0 at the $\Upsilon(4S)$.						$\Gamma(\rho^0\rho^0)/\Gamma_{\text{total}}$					Γ_{130}/Γ
VALUE	CL%	DOCUMENT ID	TECN			VALUE	CL%	DOCUMENT ID	TECN	COMMENT	
$<1.1 \times 10^{-5}$	90	238 BERGFELD	98 CLE2			$<2.8 \times 10^{-4}$	90	253 ALBRECHT	90B ARG	$e^+e^- \rightarrow \Upsilon(4S)$	
238 Assumes equal production of B^+ and B^0 at the $\Upsilon(4S)$.						• • • We do not use the following data for averages, fits, limits, etc. • • •					
VALUE	CL%	DOCUMENT ID	TECN			$<2.9 \times 10^{-4}$	90	254 BORTOLETTO	089 CLEO	$e^+e^- \rightarrow \Upsilon(4S)$	
$<1.9 \times 10^{-5}$	90	239 BERGFELD	98 CLE2			$<4.3 \times 10^{-4}$	90	254 BEBEK	87 CLEO	$e^+e^- \rightarrow \Upsilon(4S)$	
239 Assumes equal production of B^+ and B^0 at the $\Upsilon(4S)$.						253 ALBRECHT 90B limit assumes equal production of $B^0\bar{B}^0$ and B^+B^- at $\Upsilon(4S)$.					
VALUE	CL%	DOCUMENT ID	TECN			254 Paper assumes the $\Upsilon(4S)$ decays 43% to $B^0\bar{B}^0$. We rescale to 50%.					
$<1.1 \times 10^{-5}$	90	238 BERGFELD	98 CLE2			$\Gamma(a_1(1260)^{\mp}\pi^{\pm})/\Gamma_{\text{total}}$					Γ_{131}/Γ
238 Assumes equal production of B^+ and B^0 at the $\Upsilon(4S)$.						VALUE	CL%	DOCUMENT ID	TECN	COMMENT	
VALUE	CL%	DOCUMENT ID	TECN			$<4.9 \times 10^{-4}$	90	255 BORTOLETTO	089 CLEO	$e^+e^- \rightarrow \Upsilon(4S)$	
$<1.9 \times 10^{-5}$	90	239 BERGFELD	98 CLE2			• • • We do not use the following data for averages, fits, limits, etc. • • •					
239 Assumes equal production of B^+ and B^0 at the $\Upsilon(4S)$.						$<6.3 \times 10^{-4}$	90	256 ALBRECHT	90B ARG	$e^+e^- \rightarrow \Upsilon(4S)$	
VALUE	CL%	DOCUMENT ID	TECN			$<1.0 \times 10^{-3}$	90	255 BEBEK	87 CLEO	$e^+e^- \rightarrow \Upsilon(4S)$	
$<0.5 \times 10^{-5}$	90	240 BERGFELD	98 CLE2			255 Paper assumes the $\Upsilon(4S)$ decays 43% to $B^0\bar{B}^0$. We rescale to 50%.					
240 Assumes equal production of B^+ and B^0 at the $\Upsilon(4S)$.						256 ALBRECHT 90B limit assumes equal production of $B^0\bar{B}^0$ and B^+B^- at $\Upsilon(4S)$.					
VALUE	CL%	DOCUMENT ID	TECN			$\Gamma(a_2(1320)^{\mp}\pi^{\pm})/\Gamma_{\text{total}}$					Γ_{132}/Γ
$<0.9 \times 10^{-5}$	90	241 BERGFELD	98 CLE2			VALUE	CL%	DOCUMENT ID	TECN	COMMENT	
241 Assumes equal production of B^+ and B^0 at the $\Upsilon(4S)$.						$<3.0 \times 10^{-4}$	90	257 BORTOLETTO	089 CLEO	$e^+e^- \rightarrow \Upsilon(4S)$	
VALUE	CL%	DOCUMENT ID	TECN			• • • We do not use the following data for averages, fits, limits, etc. • • •					
$<0.5 \times 10^{-5}$	90	240 BERGFELD	98 CLE2			$<1.4 \times 10^{-3}$	90	257 BEBEK	87 CLEO	$e^+e^- \rightarrow \Upsilon(4S)$	
240 Assumes equal production of B^+ and B^0 at the $\Upsilon(4S)$.						257 Paper assumes the $\Upsilon(4S)$ decays 43% to $B^0\bar{B}^0$. We rescale to 50%.					
VALUE	CL%	DOCUMENT ID	TECN			$\Gamma(\pi^+\pi^-\pi^0\pi^0)/\Gamma_{\text{total}}$					Γ_{133}/Γ
$<3.1 \times 10^{-5}$	90	242 BERGFELD	98 CLE2			VALUE	CL%	DOCUMENT ID	TECN	COMMENT	
242 Assumes equal production of B^+ and B^0 at the $\Upsilon(4S)$.						$<3.1 \times 10^{-3}$	90	258 ALBRECHT	90B ARG	$e^+e^- \rightarrow \Upsilon(4S)$	
VALUE	CL%	DOCUMENT ID	TECN			258 ALBRECHT 90B limit assumes equal production of $B^0\bar{B}^0$ and B^+B^- at $\Upsilon(4S)$.					
$<1.3 \times 10^{-5}$	90	243 BERGFELD	98 CLE2			$\Gamma(\rho^+\rho^-)/\Gamma_{\text{total}}$					Γ_{134}/Γ
243 Assumes equal production of B^+ and B^0 at the $\Upsilon(4S)$.						VALUE	CL%	DOCUMENT ID	TECN	COMMENT	
VALUE	CL%	DOCUMENT ID	TECN			$<2.2 \times 10^{-3}$	90	259 ALBRECHT	90B ARG	$e^+e^- \rightarrow \Upsilon(4S)$	
$<1.3 \times 10^{-5}$	90	243 BERGFELD	98 CLE2			259 ALBRECHT 90B limit assumes equal production of $B^0\bar{B}^0$ and B^+B^- at $\Upsilon(4S)$.					
243 Assumes equal production of B^+ and B^0 at the $\Upsilon(4S)$.						$\Gamma(a_1(1260)^0\pi^0)/\Gamma_{\text{total}}$					Γ_{135}/Γ
VALUE	CL%	DOCUMENT ID	TECN			VALUE	CL%	DOCUMENT ID	TECN	COMMENT	
$<2.1 \times 10^{-5}$	90	244 BERGFELD	98 CLE2			$<1.1 \times 10^{-3}$	90	260 ALBRECHT	90B ARG	$e^+e^- \rightarrow \Upsilon(4S)$	
244 Assumes equal production of B^+ and B^0 at the $\Upsilon(4S)$.						260 ALBRECHT 90B limit assumes equal production of $B^0\bar{B}^0$ and B^+B^- at $\Upsilon(4S)$.					
VALUE	CL%	DOCUMENT ID	TECN	COMMENT		$\Gamma(\omega\pi^0)/\Gamma_{\text{total}}$					Γ_{136}/Γ
$<1.2 \times 10^{-5}$	90	245 BERGFELD	98 CLE2			VALUE	CL%	DOCUMENT ID	TECN	COMMENT	
• • • We do not use the following data for averages, fits, limits, etc. • • •						$<1.4 \times 10^{-5}$	90	261 BERGFELD	98 CLE2		
$<3.9 \times 10^{-5}$	90	ASNER	96 CLE2	$e^+e^- \rightarrow \Upsilon(4S)$		• • • We do not use the following data for averages, fits, limits, etc. • • •					
245 Assumes equal production of B^+ and B^0 at the $\Upsilon(4S)$.						$<4.6 \times 10^{-4}$	90	262 ALBRECHT	90B ARG	$e^+e^- \rightarrow \Upsilon(4S)$	
VALUE	CL%	DOCUMENT ID	TECN	COMMENT		261 Assumes equal production of B^+ and B^0 at the $\Upsilon(4S)$.					
$<7.2 \times 10^{-4}$	90	246 ALBRECHT	90B ARG	$e^+e^- \rightarrow \Upsilon(4S)$		262 ALBRECHT 90B limit assumes equal production of $B^0\bar{B}^0$ and B^+B^- at $\Upsilon(4S)$.					
246 ALBRECHT 90B limit assumes equal production of $B^0\bar{B}^0$ and B^+B^- at $\Upsilon(4S)$.						$\Gamma(\pi^+\pi^+\pi^-\pi^-\pi^0)/\Gamma_{\text{total}}$					Γ_{137}/Γ
VALUE	CL%	DOCUMENT ID	TECN	COMMENT		VALUE	CL%	DOCUMENT ID	TECN	COMMENT	
$<2.4 \times 10^{-5}$	90	ASNER	96 CLE2	$e^+e^- \rightarrow \Upsilon(4S)$		$<9.0 \times 10^{-3}$	90	263 ALBRECHT	90B ARG	$e^+e^- \rightarrow \Upsilon(4S)$	
• • • We do not use the following data for averages, fits, limits, etc. • • •						263 ALBRECHT 90B limit assumes equal production of $B^0\bar{B}^0$ and B^+B^- at $\Upsilon(4S)$.					
$<4.0 \times 10^{-4}$	90	247 ALBRECHT	90B ARG	$e^+e^- \rightarrow \Upsilon(4S)$		$\Gamma(a_1(1260)^+\rho^-)/\Gamma_{\text{total}}$					Γ_{138}/Γ
247 ALBRECHT 90B limit assumes equal production of $B^0\bar{B}^0$ and B^+B^- at $\Upsilon(4S)$.						VALUE	CL%	DOCUMENT ID	TECN	COMMENT	
VALUE	CL%	DOCUMENT ID	TECN	COMMENT		$<3.4 \times 10^{-3}$	90	264 ALBRECHT	90B ARG	$e^+e^- \rightarrow \Upsilon(4S)$	
$<8.8 \times 10^{-5}$	90	ASNER	96 CLE2	$e^+e^- \rightarrow \Upsilon(4S)$		264 ALBRECHT 90B limit assumes equal production of $B^0\bar{B}^0$ and B^+B^- at $\Upsilon(4S)$.					
• • • We do not use the following data for averages, fits, limits, etc. • • •						$\Gamma(a_1(1260)^0\rho^0)/\Gamma_{\text{total}}$					Γ_{139}/Γ
$<5.2 \times 10^{-4}$	90	248 ALBRECHT	90B ARG	$e^+e^- \rightarrow \Upsilon(4S)$		VALUE	CL%	DOCUMENT ID	TECN	COMMENT	
$<5.2 \times 10^{-3}$	90	249 BEBEK	87 CLEO	$e^+e^- \rightarrow \Upsilon(4S)$		$<2.4 \times 10^{-3}$	90	265 ALBRECHT	90B ARG	$e^+e^- \rightarrow \Upsilon(4S)$	
248 ALBRECHT 90B limit assumes equal production of $B^0\bar{B}^0$ and B^+B^- at $\Upsilon(4S)$.						265 ALBRECHT 90B limit assumes equal production of $B^0\bar{B}^0$ and B^+B^- at $\Upsilon(4S)$.					
249 BEBEK 87 reports $< 6.1 \times 10^{-3}$ assuming the $\Upsilon(4S)$ decays 43% to $B^0\bar{B}^0$. We rescale to 50%.						$\Gamma(\pi^+\pi^+\pi^+\pi^-\pi^-\pi^-)/\Gamma_{\text{total}}$					Γ_{140}/Γ
VALUE	CL%	DOCUMENT ID	TECN	COMMENT		VALUE	CL%	DOCUMENT ID	TECN	COMMENT	
$<3.0 \times 10^{-3}$	90	266 ALBRECHT	90B ARG	$e^+e^- \rightarrow \Upsilon(4S)$		$<3.0 \times 10^{-3}$	90	266 ALBRECHT	90B ARG	$e^+e^- \rightarrow \Upsilon(4S)$	
266 ALBRECHT 90B limit assumes equal production of $B^0\bar{B}^0$ and B^+B^- at $\Upsilon(4S)$.						266 ALBRECHT 90B limit assumes equal production of $B^0\bar{B}^0$ and B^+B^- at $\Upsilon(4S)$.					

See key on page 239

Meson Particle Listings

 B^0 $\Gamma(a_1(1260)^+ a_1(1260)^-)/\Gamma_{total}$ Γ_{141}/Γ

VALUE	CL%	DOCUMENT ID	TECN	COMMENT
$<2.8 \times 10^{-3}$	90	267 BORTOLETTO89	CLEO	$e^+ e^- \rightarrow T(45)$
• • • We do not use the following data for averages, fits, limits, etc. • • •				
$<6.0 \times 10^{-3}$	90	268 ALBRECHT	90B ARG	$e^+ e^- \rightarrow T(45)$
267 BORTOLETTO 89 reports $<3.2 \times 10^{-3}$ assuming the $T(45)$ decays 43% to $B^0 \bar{B}^0$. We rescale to 50%.				
268 ALBRECHT 90B limit assumes equal production of $B^0 \bar{B}^0$ and $B^+ B^-$ at $T(45)$.				

 $\Gamma(\pi^+ \pi^+ \pi^+ \pi^- \pi^- \pi^0)/\Gamma_{total}$ Γ_{142}/Γ

VALUE	CL%	DOCUMENT ID	TECN	COMMENT
$<1.1 \times 10^{-2}$	90	269 ALBRECHT	90B ARG	$e^+ e^- \rightarrow T(45)$
269 ALBRECHT 90B limit assumes equal production of $B^0 \bar{B}^0$ and $B^+ B^-$ at $T(45)$.				

 $\Gamma(p\bar{p})/\Gamma_{total}$ Γ_{143}/Γ

VALUE	CL%	DOCUMENT ID	TECN	COMMENT
$<7.0 \times 10^{-6}$	90	270 COAN	99 CLE2	$e^+ e^- \rightarrow T(45)$
• • • We do not use the following data for averages, fits, limits, etc. • • •				
$<1.8 \times 10^{-5}$	90	271 BUSKULIC	96V ALEP	$e^+ e^- \rightarrow Z$
$<3.5 \times 10^{-4}$	90	272 ABREU	95N DLPH	Sup. by ADAM 96D
$<3.4 \times 10^{-5}$	90	273 BORTOLETTO89	CLEO	$e^+ e^- \rightarrow T(45)$
$<1.2 \times 10^{-4}$	90	274 ALBRECHT	88F ARG	$e^+ e^- \rightarrow T(45)$
$<1.7 \times 10^{-4}$	90	273 BEBEK	87 CLEO	$e^+ e^- \rightarrow T(45)$
270 Assumes equal production of B^+ and B^0 at the $T(45)$.				
271 BUSKULIC 96V assumes PDG 96 production fractions for B^0 , B^+ , B_s^+ , b baryons.				
272 Assumes a B^0 , B^- production fraction of 0.39 and a B_s^- production fraction of 0.12.				
273 Paper assumes the $T(45)$ decays 43% to $B^0 \bar{B}^0$. We rescale to 50%.				
274 ALBRECHT 88F reports $<1.3 \times 10^{-4}$ assuming the $T(45)$ decays 45% to $B^0 \bar{B}^0$. We rescale to 50%.				

 $\Gamma(p\bar{p}\pi^+\pi^-)/\Gamma_{total}$ Γ_{144}/Γ

VALUE (units 10^{-4})	CL%	DOCUMENT ID	TECN	COMMENT
<2.5	90	275 BEBEK	89 CLEO	$e^+ e^- \rightarrow T(45)$
• • • We do not use the following data for averages, fits, limits, etc. • • •				
<9.5	90	276 ABREU	95N DLPH	Sup. by ADAM 96D
$5.4 \pm 1.8 \pm 2.0$		277 ALBRECHT	88F ARG	$e^+ e^- \rightarrow T(45)$
275 BEBEK 89 reports $<2.9 \times 10^{-4}$ assuming the $T(45)$ decays 43% to $B^0 \bar{B}^0$. We rescale to 50%.				
276 Assumes a B^0 , B^- production fraction of 0.39 and a B_s^- production fraction of 0.12.				
277 ALBRECHT 88F reports $6.0 \pm 2.0 \pm 2.2$ assuming the $T(45)$ decays 45% to $B^0 \bar{B}^0$. We rescale to 50%.				

 $\Gamma(p\bar{A}\pi^-)/\Gamma_{total}$ Γ_{145}/Γ

VALUE	CL%	DOCUMENT ID	TECN	COMMENT
$<1.3 \times 10^{-5}$	90	278 COAN	99 CLE2	$e^+ e^- \rightarrow T(45)$
• • • We do not use the following data for averages, fits, limits, etc. • • •				
$<1.8 \times 10^{-4}$	90	279 ALBRECHT	88F ARG	$e^+ e^- \rightarrow T(45)$
278 Assumes equal production of B^+ and B^0 at the $T(45)$.				
279 ALBRECHT 88F reports $<2.0 \times 10^{-4}$ assuming the $T(45)$ decays 45% to $B^0 \bar{B}^0$. We rescale to 50%.				

 $\Gamma(\bar{\Lambda}\Lambda)/\Gamma_{total}$ Γ_{146}/Γ

VALUE	CL%	DOCUMENT ID	TECN	COMMENT
$<3.9 \times 10^{-6}$	90	280 COAN	99 CLE2	$e^+ e^- \rightarrow T(45)$
280 Assumes equal production of B^+ and B^0 at the $T(45)$.				

 $\Gamma(\Delta^0 \bar{\Delta}^0)/\Gamma_{total}$ Γ_{147}/Γ

VALUE	CL%	DOCUMENT ID	TECN	COMMENT
<0.0015	90	281 BORTOLETTO89	CLEO	$e^+ e^- \rightarrow T(45)$
281 BORTOLETTO 89 reports <0.0018 assuming $T(45)$ decays 43% to $B^0 \bar{B}^0$. We rescale to 50%.				

 $\Gamma(\Delta^{++} \Delta^{--})/\Gamma_{total}$ Γ_{148}/Γ

VALUE	CL%	DOCUMENT ID	TECN	COMMENT
$<1.1 \times 10^{-4}$	90	282 BORTOLETTO89	CLEO	$e^+ e^- \rightarrow T(45)$
282 BORTOLETTO 89 reports $<1.3 \times 10^{-4}$ assuming $T(45)$ decays 43% to $B^0 \bar{B}^0$. We rescale to 50%.				

 $\Gamma(\Sigma_c^- \Delta^{++})/\Gamma_{total}$ Γ_{149}/Γ

VALUE	CL%	DOCUMENT ID	TECN	COMMENT
<0.0010	90	283 PROCARIO	94 CLE2	$e^+ e^- \rightarrow T(45)$
283 PROCARIO 94 reports <0.0012 for $B(\Lambda_c^+ \rightarrow pK^- \pi^+) = 0.043$. We rescale to our best value $B(\Lambda_c^+ \rightarrow pK^- \pi^+) = 0.050$.				

 $\Gamma(\bar{\Lambda}_c^- p \pi^+ \pi^-)/\Gamma_{total}$ Γ_{150}/Γ

VALUE (units 10^{-3})	CL%	DOCUMENT ID	TECN	COMMENT
$1.33^{+0.46}_{-0.42} \pm 0.37$		284 FU	97 CLE2	$e^+ e^- \rightarrow T(45)$
284 FU 97 uses PDG 96 values of Λ_c branching fraction.				

 $\Gamma(\bar{\Lambda}_c^- p)/\Gamma_{total}$ Γ_{151}/Γ

VALUE	CL%	DOCUMENT ID	TECN	COMMENT
$<2.1 \times 10^{-4}$	90	285 FU	97 CLE2	$e^+ e^- \rightarrow T(45)$
285 FU 97 uses PDG 96 values of Λ_c branching ratio.				

 $\Gamma(\bar{\Lambda}_c^- p \pi^0)/\Gamma_{total}$ Γ_{152}/Γ

VALUE	CL%	DOCUMENT ID	TECN	COMMENT
$<5.9 \times 10^{-4}$	90	286 FU	97 CLE2	$e^+ e^- \rightarrow T(45)$
286 FU 97 uses PDG 96 values of Λ_c branching ratio.				

 $\Gamma(\bar{\Lambda}_c^- p \pi^+ \pi^- \pi^0)/\Gamma_{total}$ Γ_{153}/Γ

VALUE	CL%	DOCUMENT ID	TECN	COMMENT
$<5.07 \times 10^{-3}$	90	287 FU	97 CLE2	$e^+ e^- \rightarrow T(45)$
287 FU 97 uses PDG 96 values of Λ_c branching ratio.				

 $\Gamma(\bar{\Lambda}_c^- p \pi^+ \pi^- \pi^+ \pi^-)/\Gamma_{total}$ Γ_{154}/Γ

VALUE	CL%	DOCUMENT ID	TECN	COMMENT
$<2.74 \times 10^{-3}$	90	288 FU	97 CLE2	$e^+ e^- \rightarrow T(45)$
288 FU 97 uses PDG 96 values of Λ_c branching ratio.				

 $\Gamma(\gamma\gamma)/\Gamma_{total}$ Γ_{155}/Γ

VALUE	CL%	DOCUMENT ID	TECN	COMMENT
$<3.9 \times 10^{-5}$	90	289 ACCIARRI	95I L3	$e^+ e^- \rightarrow Z$
289 ACCIARRI 95I assumes $f_{B^0} = 39.5 \pm 4.0$ and $f_{B_s} = 12.0 \pm 3.0\%$.				

 $\Gamma(e^+ e^-)/\Gamma_{total}$ Γ_{156}/Γ

VALUE	CL%	DOCUMENT ID	TECN	COMMENT
$<5.9 \times 10^{-6}$	90	AMMAR	94 CLE2	$e^+ e^- \rightarrow T(45)$
• • • We do not use the following data for averages, fits, limits, etc. • • •				
$<1.4 \times 10^{-5}$	90	290 ACCIARRI	97B L3	$e^+ e^- \rightarrow Z$
$<2.6 \times 10^{-5}$	90	291 AVERY	89B CLEO	$e^+ e^- \rightarrow T(45)$
$<7.6 \times 10^{-5}$	90	292 ALBRECHT	87D ARG	$e^+ e^- \rightarrow T(45)$
$<6.4 \times 10^{-5}$	90	293 AVERY	87 CLEO	$e^+ e^- \rightarrow T(45)$
$<3 \times 10^{-4}$	90	GILES	84 CLEO	Repl. by AVERY 87
290 ACCIARRI 97B assume PDG 96 production fractions for B^+ , B^0 , B_s , and Λ_b .				
291 AVERY 89B reports $<3 \times 10^{-5}$ assuming the $T(45)$ decays 43% to $B^0 \bar{B}^0$. We rescale to 50%.				
292 ALBRECHT 87D reports $<8.5 \times 10^{-5}$ assuming the $T(45)$ decays 45% to $B^0 \bar{B}^0$. We rescale to 50%.				
293 AVERY 87 reports $<8 \times 10^{-5}$ assuming the $T(45)$ decays 40% to $B^0 \bar{B}^0$. We rescale to 50%.				

 $\Gamma(\mu^+ \mu^-)/\Gamma_{total}$ Γ_{157}/Γ

VALUE	CL%	DOCUMENT ID	TECN	COMMENT
$<6.8 \times 10^{-7}$	90	294 ABE	98 CDF	$p\bar{p}$ at 1.8 TeV
• • • We do not use the following data for averages, fits, limits, etc. • • •				
$<4.0 \times 10^{-5}$	90	ABBOTT	98B D0	$p\bar{p}$ 1.8 TeV
$<1.0 \times 10^{-5}$	90	295 ACCIARRI	97B L3	$e^+ e^- \rightarrow Z$
$<1.6 \times 10^{-6}$	90	296 ABE	96L CDF	Repl. by ABE 98
$<5.9 \times 10^{-6}$	90	AMMAR	94 CLE2	$e^+ e^- \rightarrow T(45)$
$<8.3 \times 10^{-6}$	90	297 ALBAJAR	91C UA1	$E_{cm}^{pp} = 630$ GeV
$<1.2 \times 10^{-5}$	90	298 ALBAJAR	91C UA1	$E_{cm}^{pp} = 630$ GeV
$<4.3 \times 10^{-5}$	90	299 AVERY	89B CLEO	$e^+ e^- \rightarrow T(45)$
$<4.5 \times 10^{-5}$	90	300 ALBRECHT	87D ARG	$e^+ e^- \rightarrow T(45)$
$<7.7 \times 10^{-5}$	90	301 AVERY	87 CLEO	$e^+ e^- \rightarrow T(45)$
$<2 \times 10^{-4}$	90	GILES	84 CLEO	Repl. by AVERY 87

294 ABE 98 assumes production of $\sigma(B^0) = \sigma(B^+)$ and $\sigma(B_s)/\sigma(B^0) = 1/3$. They normalize to their measured $\sigma(B^0, p_T(B) > 6, |y| < 1.0) = 2.39 \pm 0.32 \pm 0.44 \mu\text{b}$.

295 ACCIARRI 97B assume PDG 96 production fractions for B^+ , B^0 , B_s , and Λ_b .

296 ABE 96L assumes equal B^0 and B^+ production. They normalize to their measured $\sigma(B^+, p_T(B) > 6 \text{ GeV}/c, |y| < 1) = 2.39 \pm 0.54 \mu\text{b}$.

297 B^0 and B_s^0 are not separated.

298 Obtained from unseparated B^0 and B_s^0 measurement by assuming a $B^0: B_s^0$ ratio 2:1.

299 AVERY 89B reports $<5 \times 10^{-3}$ assuming the $T(45)$ decays 43% to $B^0 \bar{B}^0$. We rescale to 50%.

300 ALBRECHT 87D reports $<5 \times 10^{-5}$ assuming the $T(45)$ decays 45% to $B^0 \bar{B}^0$. We rescale to 50%.

301 AVERY 87 reports $<9 \times 10^{-5}$ assuming the $T(45)$ decays 40% to $B^0 \bar{B}^0$. We rescale to 50%.

 $\Gamma(K^0 e^+ e^-)/\Gamma_{total}$ Γ_{158}/Γ

VALUE	CL%	DOCUMENT ID	TECN	COMMENT
$<3.0 \times 10^{-4}$	90	ALBRECHT	91E ARG	$e^+ e^- \rightarrow T(45)$
• • • We do not use the following data for averages, fits, limits, etc. • • •				
$<5.2 \times 10^{-4}$	90	302 AVERY	87 CLEO	$e^+ e^- \rightarrow T(45)$
302 AVERY 87 reports $<6.5 \times 10^{-4}$ assuming the $T(45)$ decays 40% to $B^0 \bar{B}^0$. We rescale to 50%.				

Meson Particle Listings

B^0

$\Gamma(K^0 \mu^+ \mu^-) / \Gamma_{total}$ Γ_{159} / Γ
 Test for $\Delta B = 1$ weak neutral current. Allowed by higher-order electroweak interactions.

VALUE	CL%	DOCUMENT ID	TECN	COMMENT
$< 3.6 \times 10^{-4}$	90	303 AVERY	87 CLEO	$e^+e^- \rightarrow T(4S)$
• • • We do not use the following data for averages, fits, limits, etc. • • •				
$< 5.2 \times 10^{-4}$	90	ALBRECHT	91E ARG	$e^+e^- \rightarrow T(4S)$
303 AVERY 87 reports $< 4.5 \times 10^{-4}$ assuming the $T(4S)$ decays 40% to $B^0 \bar{B}^0$. We rescale to 50%.				

$\Gamma(K^*(892)^0 e^+ e^-) / \Gamma_{total}$ Γ_{160} / Γ
 Test for $\Delta B = 1$ weak neutral current.

VALUE	CL%	DOCUMENT ID	TECN	COMMENT
$< 2.9 \times 10^{-4}$	90	ALBRECHT	91E ARG	$e^+e^- \rightarrow T(4S)$
• • • We do not use the following data for averages, fits, limits, etc. • • •				
$< 4.0 \times 10^{-6}$	90	304 AFFOLDER	99B CDF	$p\bar{p}$ at 1.8 TeV
• • • We do not use the following data for averages, fits, limits, etc. • • •				
$< 2.5 \times 10^{-5}$	90	305 ABE	96L CDF	Repl. by AF-
$< 2.3 \times 10^{-5}$	90	306 ALBAJAR	91C UA1	$E_{CM}^{pp} = 630$ GeV
$< 3.4 \times 10^{-4}$	90	ALBRECHT	91E ARG	$e^+e^- \rightarrow T(4S)$

304 AFFOLDER 99B measured relative to $B^0 \rightarrow J/\psi(1S) K^*(892)^0$.
 305 ABE 96L measured relative to $B^0 \rightarrow J/\psi(1S) K^*(892)^0$ using PDG 94 branching ratios.
 306 ALBAJAR 91C assumes 36% of \bar{b} quarks give B^0 mesons.

$\Gamma(K^*(892)^0 \nu \bar{\nu}) / \Gamma_{total}$ Γ_{162} / Γ
 Test for $\Delta B = 1$ weak neutral current.

VALUE	CL%	DOCUMENT ID	TECN	COMMENT
$< 1.0 \times 10^{-3}$	90	307 ADAM	96D DLPH	$e^+e^- \rightarrow Z$

307 ADAM 96D assumes $f_{B^0} = f_{B^-} = 0.39$ and $f_{B_s} = 0.12$.

$\Gamma(e^\pm \mu^\mp) / \Gamma_{total}$ Γ_{163} / Γ
 Test of lepton family number conservation.

VALUE	CL%	DOCUMENT ID	TECN	COMMENT
$< 3.5 \times 10^{-6}$	90	ABE	98V CDF	$p\bar{p}$ at 1.8 TeV
• • • We do not use the following data for averages, fits, limits, etc. • • •				
$< 1.6 \times 10^{-5}$	90	308 ACCIARRI	97B L3	$e^+e^- \rightarrow Z$
$< 5.9 \times 10^{-6}$	90	AMMAR	94 CLE2	$e^+e^- \rightarrow T(4S)$
$< 3.4 \times 10^{-5}$	90	309 AVERY	89B CLEO	$e^+e^- \rightarrow T(4S)$
$< 4.5 \times 10^{-5}$	90	310 ALBRECHT	87D ARG	$e^+e^- \rightarrow T(4S)$
$< 7.7 \times 10^{-5}$	90	311 AVERY	87 CLEO	$e^+e^- \rightarrow T(4S)$
$< 3 \times 10^{-4}$	90	GILES	84 CLEO	Repl. by AVERY 87

308 ACCIARRI 97B assume PDG 96 production fractions for B^+ , B^0 , B_s , and Λ_b .
 309 Paper assumes the $T(4S)$ decays 43% to $B^0 \bar{B}^0$. We rescale to 50%.
 310 ALBRECHT 87D reports $< 5 \times 10^{-5}$ assuming the $T(4S)$ decays 45% to $B^0 \bar{B}^0$. We rescale to 50%.
 311 AVERY 87 reports $< 9 \times 10^{-5}$ assuming the $T(4S)$ decays 40% to $B^0 \bar{B}^0$. We rescale to 50%.

$\Gamma(e^\pm \tau^\mp) / \Gamma_{total}$ Γ_{164} / Γ
 Test of lepton family number conservation.

VALUE	CL%	DOCUMENT ID	TECN	COMMENT
$< 5.3 \times 10^{-4}$	90	AMMAR	94 CLE2	$e^+e^- \rightarrow T(4S)$

$\Gamma(\mu^\pm \tau^\mp) / \Gamma_{total}$ Γ_{165} / Γ
 Test of lepton family number conservation.

VALUE	CL%	DOCUMENT ID	TECN	COMMENT
$< 8.3 \times 10^{-4}$	90	AMMAR	94 CLE2	$e^+e^- \rightarrow T(4S)$

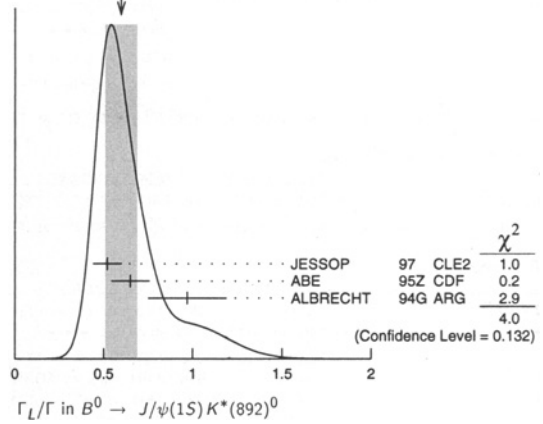
POLARIZATION IN B^0 DECAY

Γ_L / Γ in $B^0 \rightarrow J/\psi(1S) K^*(892)^0$
 $\Gamma_L / \Gamma = 1[0]$ would indicate that $B^0 \rightarrow J/\psi(1S) K^*(892)^0$ followed by $K^*(892)^0 \rightarrow K_S^0 \pi^0$ is a pure CP eigenstate with $CP = -1[+1]$.

VALUE	EVTs	DOCUMENT ID	TECN	COMMENT
0.60 ± 0.09 OUR AVERAGE				Error includes scale factor of 1.4. See the ideogram below.
0.52 ± 0.07 ± 0.04	312	JESSOP	97 CLE2	$e^+e^- \rightarrow T(4S)$
0.65 ± 0.10 ± 0.04	65	ABE	95Z CDF	$p\bar{p}$ at 1.8 TeV
0.97 ± 0.16 ± 0.15	13 313	ALBRECHT	94G ARG	$e^+e^- \rightarrow T(4S)$
• • • We do not use the following data for averages, fits, limits, etc. • • •				
0.80 ± 0.08 ± 0.05	42 313	ALAM	94 CLE2	Sup. by JESSOP 97

312 JESSOP 97 is the average over a mixture of B^0 and B^+ decays. The p -wave fraction is found to be $0.16 \pm 0.08 \pm 0.04$.
 313 Averaged over an admixture of B^0 and B^+ decays.

WEIGHTED AVERAGE
 0.60±0.09 (Error scaled by 1.4)



Γ_L / Γ in $B^0 \rightarrow D^{*-} \rho^+$

VALUE	EVTs	DOCUMENT ID	TECN	COMMENT
0.93 ± 0.05 ± 0.05	76	ALAM	94 CLE2	$e^+e^- \rightarrow T(4S)$

$B^0 - \bar{B}^0$ MIXING

Written March 2000 by O. Schneider (Univ. of Lausanne)

Formalism in quantum mechanics

There are two neutral $B^0 - \bar{B}^0$ meson systems, $B_d - \bar{B}_d$ and $B_s - \bar{B}_s$ (generically denoted $B_q - \bar{B}_q$, $q = s, d$), which exhibit the phenomenon of particle-antiparticle mixing [1]. Such a system is produced in one of its two possible states of well-defined flavor: $|B^0\rangle$ ($\bar{b}q$) or $|\bar{B}^0\rangle$ ($b\bar{q}$). Due to flavor-changing interactions, this initial state evolves into a time-dependent quantum superposition of the two flavor states, $a(t)|B^0\rangle + b(t)|\bar{B}^0\rangle$, satisfying the equation

$$i \frac{\partial}{\partial t} \begin{pmatrix} a(t) \\ b(t) \end{pmatrix} = \left(M - \frac{i}{2} \Gamma \right) \begin{pmatrix} a(t) \\ b(t) \end{pmatrix}, \quad (1)$$

where M and Γ , known as the mass and decay matrices, describe the dispersive and absorptive parts of $B^0 - \bar{B}^0$ mixing. These matrices are hermitian, and CPT invariance requires $M_{11} = M_{22} \equiv M$ and $\Gamma_{11} = \Gamma_{22} \equiv \Gamma$, where M and Γ are the mass and decay width of the B^0 and \bar{B}^0 flavor states.

The two eigenstates of the effective hamiltonian matrix $(M - \frac{i}{2} \Gamma)$ are given by

$$|B_\pm\rangle = p|B^0\rangle \pm q|\bar{B}^0\rangle, \quad (2)$$

and correspond to the eigenvalues

$$\lambda_\pm = \left(M - \frac{i}{2} \Gamma \right) \pm \frac{q}{p} \left(M_{12} - \frac{i}{2} \Gamma_{12} \right), \quad (3)$$

where

$$\frac{q}{p} = \sqrt{\frac{M_{12}^* - \frac{i}{2} \Gamma_{12}^*}{M_{12} - \frac{i}{2} \Gamma_{12}}}. \quad (4)$$

We choose a convention where $\text{Re}(q/p) > 0$ and $CP|B^0\rangle = |\bar{B}^0\rangle$.

An alternative notation is

$$|B_\pm\rangle = \frac{(1 + \epsilon)|B^0\rangle \pm (1 - \epsilon)|\bar{B}^0\rangle}{\sqrt{2(1 + |\epsilon|^2)}} \quad \text{with} \quad \frac{1 - \epsilon}{1 + \epsilon} = \frac{q}{p}. \quad (5)$$

The time dependence of these eigenstates of well-defined masses $M_\pm = \text{Re}(\lambda_\pm)$ and widths $\Gamma_\pm = -2 \text{Im}(\lambda_\pm)$ is given by

the phases $e^{-i\lambda_{\pm}t} = e^{-iM_{\pm}t}e^{-\frac{1}{2}\Gamma_{\pm}t}$: the evolution of a pure $|B^0\rangle$ or $|\bar{B}^0\rangle$ state at $t = 0$ is thus given by

$$|B^0(t)\rangle = g_+(t)|B^0\rangle + \frac{q}{p}g_-(t)|\bar{B}^0\rangle, \quad (6)$$

$$|\bar{B}^0(t)\rangle = g_+(t)|\bar{B}^0\rangle + \frac{p}{q}g_-(t)|B^0\rangle, \quad (7)$$

where

$$g_{\pm}(t) = \frac{1}{2} \left(e^{-i\lambda_+t} \pm e^{-i\lambda_-t} \right). \quad (8)$$

This means that the flavor states oscillate into each other with time-dependent probabilities proportional to

$$|g_{\pm}(t)|^2 = \frac{e^{-\Gamma t}}{2} \left[\cosh\left(\frac{\Delta\Gamma}{2}t\right) \pm \cos(\Delta m t) \right], \quad (9)$$

where

$$\Delta m = |M_+ - M_-|, \quad \Delta\Gamma = |\Gamma_+ - \Gamma_-|. \quad (10)$$

Time-integrated mixing probabilities are only well defined when considering decays to flavor-specific final states, *i.e.* final states f such that the instantaneous decay amplitudes $A_{\bar{f}} = \langle \bar{f} | H | B^0 \rangle$ and $\bar{A}_f = \langle f | H | \bar{B}^0 \rangle$, where H is the weak interaction hamiltonian, are both zero. Due to mixing, a produced B^0 can decay to the final state \bar{f} (mixed event) in addition to the final state f (unmixed event). Restricting the sample to these two decay channels, the time-integrated mixing probability is given by

$$\begin{aligned} \chi_f^{B^0 \rightarrow \bar{B}^0} &= \frac{\int_0^{\infty} |\langle \bar{f} | H | B^0(t) \rangle|^2 dt}{\int_0^{\infty} |\langle \bar{f} | H | B^0(t) \rangle|^2 dt + \int_0^{\infty} |\langle f | H | B^0(t) \rangle|^2 dt} \\ &= \frac{|\xi_f|^2 (x^2 + y^2)}{|\xi_f|^2 (x^2 + y^2) + 2 + x^2 - y^2}, \end{aligned} \quad (11)$$

where we have defined $\xi_f = \frac{q}{p} \frac{\bar{A}_{\bar{f}}}{A_f}$ and

$$x = \frac{\Delta m}{\Gamma}, \quad y = \frac{\Delta\Gamma}{2\Gamma}. \quad (12)$$

The mixing probability $\chi_f^{B^0 \rightarrow \bar{B}^0}$ for the case of a produced \bar{B}^0 is obtained by replacing ξ_f with $1/\xi_f$ in Eq. (11). It is different from $\chi_f^{B^0 \rightarrow \bar{B}^0}$ if $|\xi_f|^2 \neq 1$, a condition reflecting non-invariance under the CP transformation. CP violation in the decay amplitudes is discussed elsewhere [2] and we assume $|\bar{A}_{\bar{f}}| = |A_f|$ from now on. The deviation of $|q/p|^2$ from 1, namely the quantity

$$1 - \left| \frac{q}{p} \right|^2 = \frac{4 \operatorname{Re}(\epsilon)}{1 + |\epsilon|^2} + \mathcal{O} \left(\left(\frac{\operatorname{Re}(\epsilon)}{1 + |\epsilon|^2} \right)^2 \right), \quad (13)$$

describes CP violation in B^0 - \bar{B}^0 mixing. As can be seen from Eq. (4), this can occur only if $M_{12} \neq 0$, $\Gamma_{12} \neq 0$ and if the phase difference between M_{12} and Γ_{12} is different from 0 or π .

In the absence of CP violation, $|q/p|^2 = 1$, $\operatorname{Re}(\epsilon) = 0$, the mass eigenstates are also CP eigenstates,

$$CP |B_{\pm}\rangle = \pm |B_{\pm}\rangle, \quad (14)$$

the phases $\varphi_{M_{12}} = \arg(M_{12})$ and $\varphi_{\Gamma_{12}} = \arg(\Gamma_{12})$ satisfy

$$\sin(\varphi_{M_{12}} - \varphi_{\Gamma_{12}}) = 0, \quad (15)$$

the mass and decay width differences reduce to

$$\Delta m = 2 |M_{12}|, \quad \Delta\Gamma = 2 |\Gamma_{12}|, \quad (16)$$

and the time-integrated mixing probabilities $\chi_f^{B^0 \rightarrow \bar{B}^0}$ and $\chi_f^{\bar{B}^0 \rightarrow B^0}$ become both equal to

$$\chi = \frac{x^2 + y^2}{2(x^2 + 1)}. \quad (17)$$

Standard Model predictions and phenomenology

In the Standard Model, the transitions $B_q^0 \rightarrow \bar{B}_q^0$ and $\bar{B}_q^0 \rightarrow B_q^0$ are due to the weak interaction. They are described, at the lowest order, by the box diagrams involving two W bosons and two up-type quarks, as is the case for K^0 - \bar{K}^0 mixing. However, the long range interactions arising from intermediate virtual states are negligible for the neutral B meson systems, because the large B mass is away from the region of hadronic resonances. The calculation of the dispersive and absorptive parts of the box diagrams yields the following predictions for the off-diagonal element of the mass and decay matrices [3],

$$M_{12} = - \frac{G_F^2 m_W^2 \eta_B m_{B_q} B_{B_q} f_{B_q}^2}{12\pi^2} S_0(m_i^2/m_W^2) (V_{tq}^* V_{tb})^2 \quad (18)$$

$$\begin{aligned} \Gamma_{12} &= \frac{G_F^2 m_b^2 \eta_B' m_{B_q} B_{B_q} f_{B_q}^2}{8\pi} \\ &\times \left[(V_{tq}^* V_{tb})^2 + V_{tq}^* V_{tb} V_{cq}^* V_{cb} \mathcal{O} \left(\frac{m_c^2}{m_b^2} \right) \right. \\ &\quad \left. + (V_{cq}^* V_{cb})^2 \mathcal{O} \left(\frac{m_c^4}{m_b^4} \right) \right] \end{aligned} \quad (19)$$

where G_F is the Fermi constant, m_W the W mass, m_i the mass of quark i , and where $m_{B_q} = M$, f_{B_q} and B_{B_q} are the B_q^0 mass, decay constant and bag parameter. The known function $S_0(x_i)$ can be approximated very well with $0.784 x_i^{0.76}$ [4] and V_{ij} are the elements of the CKM matrix [5]. The QCD corrections η_B and η_B' are of order unity. The only non negligible contributions to M_{12} are from top-top diagrams. The phases of M_{12} and Γ_{12} satisfy

$$\varphi_{M_{12}} - \varphi_{\Gamma_{12}} = \pi + \mathcal{O} \left(\frac{m_c^2}{m_b^2} \right) \quad (20)$$

implying that the mass eigenstates have mass and width differences of opposite signs. This means that, like in the K^0 - \bar{K}^0 system, the ‘‘heavy’’ state with mass $M_{\text{heavy}} = \max(M_+, M_-)$ has a smaller decay width than that of the ‘‘light’’ state with mass $M_{\text{light}} = \min(M_+, M_-)$. We thus redefine

$$\Delta m = M_{\text{heavy}} - M_{\text{light}}, \quad \Delta\Gamma = \Gamma_{\text{light}} - \Gamma_{\text{heavy}}, \quad (21)$$

where Δm is positive by definition and $\Delta\Gamma$ is expected to be positive in the Standard Model.

Furthermore, since Γ_{12} is, like M_{12} , dominated by the top-top diagrams, the quantity

$$\left| \frac{\Gamma_{12}}{M_{12}} \right| \simeq \frac{3\pi m_b^2}{2 m_W^2} \frac{1}{S_0(m_i^2/m_W^2)} \sim \mathcal{O} \left(\frac{m_b^2}{m_i^2} \right) \quad (22)$$

Meson Particle Listings

B^0

is small, and a power expansion of $|q/p|^2$ yields

$$\left|\frac{q}{p}\right|^2 = 1 + \left|\frac{\Gamma_{12}}{M_{12}}\right| \sin(\varphi_{M_{12}} - \varphi_{\Gamma_{12}}) + \mathcal{O}\left(\left|\frac{\Gamma_{12}}{M_{12}}\right|^2\right). \quad (23)$$

Therefore, considering both Eqs. (20) and (22), the CP -violating parameter

$$1 - \left|\frac{q}{p}\right|^2 \simeq \text{Im}\left(\frac{\Gamma_{12}}{M_{12}}\right) \quad (24)$$

is expected to be tiny: $\sim \mathcal{O}(10^{-3})$ for the $B_d-\bar{B}_d$ system and $\lesssim \mathcal{O}(10^{-4})$ for the $B_s-\bar{B}_s$ system [6].

In the approximation of negligible CP violation in the mixing, the ratio $\Delta\Gamma/\Delta m$ is equal to the small quantity $|\Gamma_{12}/M_{12}|$ of Eq. (22); it is hence independent of CKM matrix elements, *i.e.* the same for the $B_d-\bar{B}_d$ and $B_s-\bar{B}_s$ systems. It can be calculated with lattice QCD techniques; typical results are $\sim 5 \times 10^{-3}$ with quoted uncertainties of 30% at least. Given the current experimental knowledge (discussed below) on the mixing parameter x ,

$$\begin{cases} x_d = 0.73 \pm 0.03 & (B_d-\bar{B}_d \text{ system}) \\ x_s \gtrsim 20 \text{ at 95\% CL} & (B_s-\bar{B}_s \text{ system}) \end{cases}, \quad (25)$$

the Standard Model thus predicts that $\Delta\Gamma/\Gamma$ is very small for the $B_d-\bar{B}_d$ system (below 1%), but may be quite large for the $B_s-\bar{B}_s$ system (up to $\sim 20\%$). This width difference is caused by the existence of final states to which both the B_q^0 and \bar{B}_q^0 mesons can decay. Such decays involve $b \rightarrow c\bar{q}$ quark-level transitions, which are Cabibbo-suppressed if $q = d$ and Cabibbo-allowed if $q = s$. If the final states common to B_s^0 and \bar{B}_s^0 are predominantly CP -even as discussed in Ref. 7, then the $B_s-\bar{B}_s$ mass eigenstate with the largest decay width corresponds to the CP -even eigenstate. Taking Eq. (21) into account, one thus expects $\Gamma_{\text{light}} = \Gamma_+$ and

$$\Delta m_s = M_- - M_+ > 0, \quad \Delta\Gamma_s = \Gamma_+ - \Gamma_- > 0. \quad (26)$$

Experimental issues and methods for oscillation analyses

Time-integrated measurements of $B^0-\bar{B}^0$ mixing were published for the first time in 1987 by UA1 [8] and ARGUS [9], and since then by many different experiments. These are typically based on counting same-sign and opposite-sign lepton pairs from the semileptonic decay of the produced $b\bar{b}$ pairs. At high energy colliders, such analyses cannot easily separate the B_d and B_s contributions, therefore experiments at $\Upsilon(4S)$ machines are best suited to measure χ_d .

However, better sensitivity is obtained from time-dependent analyses aimed at the direct measurement of the oscillation frequencies Δm_d and Δm_s , from the proper time distributions of B_d or B_s candidates identified through their decay in (mostly) flavor-specific modes and suitably tagged as mixed or unmixed. This is particularly true for the $B_s-\bar{B}_s$ system where the large value of x_s implies maximal mixing, *i.e.* $\chi_s \simeq 1/2$. In such analyses, performed at high-energy colliders, the neutral B

mesons are either partially reconstructed from a charm meson, or selected from a lepton with high transverse momentum with respect to the b jet, or selected from a reconstructed displaced vertex. The proper time $t = \frac{m_B}{p}L$ is measured from the distance L between the production vertex and the B decay vertex, as measured with a silicon vertex detector, and from an estimate of the B momentum p .

The statistical significance \mathcal{S} of an oscillation signal can be approximated as [10]

$$\mathcal{S} \approx \sqrt{N/2} f_{\text{sig}} (1 - 2\eta) e^{-(\Delta m \sigma_t)^2/2}, \quad (27)$$

where N and f_{sig} are the number of candidates and the fraction of signal in the selected sample, η is the mistag probability, and σ_t is the proper time resolution. The quantity \mathcal{S} decreases very quickly as Δm increases; this dependence is controlled by σ_t , which is therefore a critical parameter for Δm_s analyses. The proper time resolution $\sigma_t \sim \frac{m_B}{\langle p \rangle} \sigma_L \oplus t \frac{\sigma_p}{p}$ includes a constant contribution due to the decay length resolution σ_L (typically 0.1–0.3 ps), and a term due to the relative momentum resolution $\frac{\sigma_p}{p}$ (typically 10–20% for partially reconstructed decays), which increases with proper time.

In order to tag a B candidate as mixed or unmixed, it is necessary to determine its flavor state both at production (initial state) and at decay (final state). The initial and final state mistag probabilities, η_i and η_f , degrade \mathcal{S} by a total factor $(1 - 2\eta) = (1 - 2\eta_i)(1 - 2\eta_f)$. In inclusive lepton analyses, the final state is tagged by the charge of the lepton from $b \rightarrow \ell^-$ decays; the biggest contribution to η_f is then due to $\bar{b} \rightarrow \bar{c} \rightarrow \ell^-$ decays. Alternatively, the charge of a reconstructed charm meson (D^{*-} from B_d^0 or D_s^- from B_s^0), or that of a kaon thought to come from a $b \rightarrow c \rightarrow s$ decay [11], can be used. For fully inclusive analyses based on topological vertexing, final state tagging techniques include jet charge [12] and charge dipole methods [11].

The initial state tags are somewhat less dependent on the procedure used to select B candidates. They can be divided in two groups: the ones that tag the initial charge of the \bar{b} quark contained in the B candidate itself (same-side tag), and the ones that tag the initial charge of the other b quark produced in the event (opposite-side tag). On the same side, the charge of a track from the primary vertex is correlated with the production state of the B if that track is a decay product of a B^{**} state or the first particle in the fragmentation chain [13,14]. Jet charge techniques work on both sides. Finally, the charge of a lepton from $b \rightarrow \ell^-$ or of a kaon from $b \rightarrow c \rightarrow s$ can be used as opposite side tags, keeping in mind that their performance depends on integrated mixing. At SLC, the beam polarization produced a sizeable forward-backward asymmetry in the $Z \rightarrow b\bar{b}$ decays and provided another very interesting and effective initial state tag based on the polar angle of the B candidate [11]. Initial state tags have also been combined to reach $\eta_i \sim 26\%$ at LEP [14,15] or even 16% at SLD [11]

See key on page 239

with full efficiency. The equivalent figure at CDF is currently $\sim 40\%$ [16].

In the absence of experimental evidence for a width difference, and since $\Delta\Gamma/\Delta m$ is predicted to be very small, oscillation analyses typically neglect $\Delta\Gamma$ and describe the data with the physics functions $\Gamma e^{-\Gamma t}(1 \pm \cos \Delta m t)/2$. As can be seen from Eq. (9), a non zero value of $\Delta\Gamma$ would effectively reduce the oscillation amplitude with a small time-dependent factor that would be very difficult to distinguish from time resolution effects. Whereas measurements of Δm_d are usually extracted from the data using a maximum likelihood fit, no significant $B_s-\bar{B}_s$ oscillations have been seen so far, and all B_s analyses set lower limits on Δm_s . The original technique used to set such limits was to study the likelihood as a function of Δm_s . However, these limits turned out to be difficult to combine. A method was therefore developed [10], in which a B_s oscillation amplitude \mathcal{A} is measured at each fixed value of Δm_s , using a maximum likelihood fit based on the functions $\Gamma_s e^{-\Gamma_s t}(1 \pm \mathcal{A} \cos \Delta m_s t)/2$. To a very good approximation, the statistical uncertainty on \mathcal{A} is Gaussian and equal to $1/S$ [10]. Measurements of \mathcal{A} performed at a given value of Δm_s can be averaged easily. If $\Delta m_s = \Delta m_s^{\text{true}}$, one expects $\mathcal{A} = 1$ within the total uncertainty $\sigma_{\mathcal{A}}$; however, if Δm_s is far from its true value, a measurement consistent with $\mathcal{A} = 0$ is expected. A value of Δm_s can be excluded at 95% CL if $\mathcal{A} + 1.645 \sigma_{\mathcal{A}} \leq 1$. If Δm_s^{true} is very large, one expects $\mathcal{A} = 0$, and all values of Δm_s such that $1.645 \sigma_{\mathcal{A}}(\Delta m_s) < 1$ are expected to be excluded at 95% CL. Because of the proper time resolution, the quantity $\sigma_{\mathcal{A}}(\Delta m_s)$ is an increasing function of Δm_s and one therefore expects to be able to exclude individual Δm_s values up to Δm_s^{sens} , where Δm_s^{sens} , called here the sensitivity of the analysis, is defined by $1.645 \sigma_{\mathcal{A}}(\Delta m_s^{\text{sens}}) = 1$.

B_d mixing studies

Many $B_d-\bar{B}_d$ oscillations analyses have been performed by the ALEPH [17,12], CDF [13,18], DELPHI [19], L3 [20], OPAL [21] and SLD [11] collaborations. Although a variety of different techniques have been used, the Δm_d results have remarkably similar precision. The systematic uncertainties are not negligible; they are often dominated by sample composition, mistag probability, or b -hadron lifetime contributions. Before being combined, the measurements are adjusted on the basis of a common set of input values, including the b -hadron lifetimes and fractions published in this *Review*. Some measurements are statistically correlated. Systematic correlations arise both from common physics sources (fragmentation fractions, lifetimes, branching ratios of b hadrons), and from purely experimental or algorithmic effects (efficiency, resolution, tagging, background description). Combining all published measurements [17,13,19,20,21] and accounting for all identified correlations as described in Ref. 22 yields $\Delta m_d = 0.478 \pm 0.012(\text{stat}) \pm 0.013(\text{syst}) \text{ ps}^{-1}$.

On the other hand, ARGUS and CLEO have published time-integrated measurements based on semileptonic decays [23,24],

which average to $\chi_d^{T(4S)} = 0.156 \pm 0.024$. The width difference $\Delta\Gamma_d$ could in principle be extracted from the measured value of Γ_d , and the above averages for Δm_d and χ_d (see Eqs. (12) and (17)). The results are however compatible with $\Delta\Gamma_d = 0$, and their precision is still insufficient to provide an interesting constraint. Neglecting $\Delta\Gamma_d$ and using the measured B_d lifetime, the Δm_d and χ_d results are combined to yield the world average

$$\Delta m_d = 0.472 \pm 0.017 \text{ ps}^{-1} \quad (28)$$

or, equivalently,

$$\chi_d = 0.174 \pm 0.009. \quad (29)$$

Evidence for CP violation in B_d mixing has been searched for, both with semileptonic and inclusive B_d decays, in samples where the initial flavor state is tagged. In the semileptonic case, where the final state tag is also available, the following asymmetry

$$\frac{N(\bar{B}_d^0(t) \rightarrow \ell^+ \nu_\ell X) - N(B_d^0(t) \rightarrow \ell^- \bar{\nu}_\ell X)}{N(\bar{B}_d^0(t) \rightarrow \ell^+ \nu_\ell X) + N(B_d^0(t) \rightarrow \ell^- \bar{\nu}_\ell X)} = a_{CP} \simeq 1 - |q/p|_d^2 \simeq \frac{4\text{Re}(\epsilon_d)}{1 + |\epsilon_d|^2} \quad (30)$$

has been measured, either in time-integrated analyses at CLEO [24] and CDF [25], or in more recent and sensitive time-dependent analyses at LEP [26,27,28]. In the inclusive case, also investigated at LEP [29,27,30], no final state tag is used, and the asymmetry [31]

$$\frac{N(B_d^0(t) \rightarrow \text{all}) - N(\bar{B}_d^0(t) \rightarrow \text{all})}{N(B_d^0(t) \rightarrow \text{all}) + N(\bar{B}_d^0(t) \rightarrow \text{all})} \simeq a_{CP} \left[\frac{x_d}{2} \sin(\Delta m_d t) - \sin^2 \left(\frac{\Delta m_d t}{2} \right) \right] \quad (31)$$

must be measured as a function of the proper time to extract information on CP violation. In all cases asymmetries compatible with zero have been found, with a precision limited by the available statistics. A simple average of all published and preliminary results [24–30] neglecting small possible statistical correlations and assuming half of the systematics to be correlated, is $a_{CP} = -0.017 \pm 0.016$, a result which does not yet constrain the Standard Model.

The Δm_d result of Eq. (28) provides an estimate of $|M_{12}|$ and can be used, together with Eqs. (16) and (18), to extract the modulus of the CKM matrix element V_{td} within the Standard Model [32]. The main experimental uncertainties on the resulting estimate of $|V_{td}|$ come from m_t and Δm_d ; however, these are at present completely dominated by the 15–20% uncertainty usually quoted on the hadronic matrix element $f_{B_d} \sqrt{B_{B_d}} \sim 200 \text{ MeV}$ obtained from lattice QCD calculations [33].

B_s mixing studies

$B_s-\bar{B}_s$ oscillation has been the subject of many recent studies from ALEPH [14], CDF [34], DELPHI [35,15], OPAL [36] and SLD [37]. No oscillation signal has been found so far. The

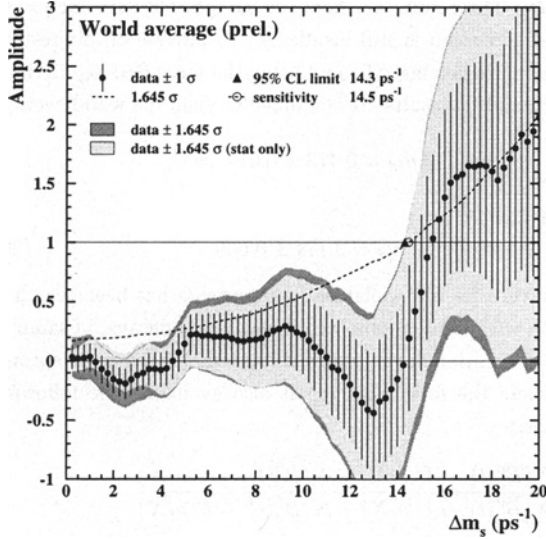


Figure 1: Combined measurements of the B_s oscillation amplitude as a function of Δm_s [22], including all preliminary results available at the end of 1999. The measurements are dominated by statistical uncertainties. Neighboring points are statistically correlated.

most sensitive analyses appear to be the ones based on inclusive lepton samples, and on samples where a lepton and a D_s meson have been reconstructed in the same jet. All results are limited by the available statistics. These are combined to yield the amplitudes \mathcal{A} shown in Fig. 1 as a function of Δm_s [22].

As before, the individual results have been adjusted to common physics inputs, and all known correlations have been accounted for; furthermore, the sensitivities of the inclusive analyses, which depend directly through Eq. (27) on the assumed fraction f_s of B_s mesons in an unbiased sample of weakly-decaying b hadrons, have been rescaled to a common value of $f_s = 0.100 \pm 0.012$ [22]. The combined sensitivity for 95% CL exclusion of Δm_s values is found to be 14.5 ps^{-1} . All values of Δm_s below 14.3 ps^{-1} are excluded at 95% CL, and no deviation from $\mathcal{A} = 0$ is seen in Fig. 1 that would indicate the observation of a signal.

Some Δm_s analyses are still preliminary [15,37]. Using only published results, the combined Δm_s result is

$$\Delta m_s > 10.6 \text{ ps}^{-1} \quad \text{at 95\% CL,} \quad (32)$$

with a sensitivity of 12.1 ps^{-1} .

The information on $|V_{ts}|$ obtained, in the framework of the Standard Model, from the combined limit is hampered by the hadronic uncertainty, as in the B_d case. However, many uncertainties cancel in the frequency ratio

$$\frac{\Delta m_s}{\Delta m_d} = \frac{m_{B_s}}{m_{B_d}} \xi^2 \left| \frac{V_{ts}}{V_{td}} \right|^2, \quad (33)$$

where $\xi = (f_{B_s} \sqrt{B_{B_s}}) / (f_{B_d} \sqrt{B_{B_d}})$, of order unity, is currently estimated from lattice QCD with a 5-6% uncertainty [33]. The CKM matrix can be constrained using the experimental results on Δm_d , Δm_s , $|V_{ub}/V_{cb}|$ and ϵ_K , together with theoretical inputs and unitarity conditions [32]. Given the information available from $|V_{ub}/V_{cb}|$ and ϵ_K measurements, the constraint from our knowledge on the ratio $\Delta m_d/\Delta m_s$ is presently more effective in limiting the position of the apex of the CKM unitarity triangle than the one obtained from the Δm_d measurements alone, due to the reduced hadronic uncertainty in Eq. (33). We note also that the Standard Model would not easily accommodate values of Δm_s above $\sim 25 \text{ ps}^{-1}$.

Information on $\Delta\Gamma_s$ can be obtained by studying the proper time distribution of untagged data samples enriched in B_s mesons [38]. In the case of an inclusive B_s selection [39] or a semileptonic B_s decay selection [40,41], both the short- and long-lived components are present, and the proper time distribution is a superposition of two exponentials with decay constants $\Gamma_s \pm \Delta\Gamma_s/2$. In principle, this provides sensitivity to both Γ_s and $(\Delta\Gamma_s/\Gamma_s)^2$. Ignoring $\Delta\Gamma_s$ and fitting for a single exponential leads to an estimate of Γ_s with a relative bias proportional to $(\Delta\Gamma_s/\Gamma_s)^2$. An alternative approach, which is directly sensitive to first order in $\Delta\Gamma_s/\Gamma_s$, is to determine the lifetime of B_s candidates decaying to CP eigenstates; measurements already exist for $B_s^0 \rightarrow J/\psi\phi$ [42] and $B_s^0 \rightarrow D_s^{(*)+} D_s^{(*)-}$ [43], which are mostly CP -even states [7]. An estimate of $\Delta\Gamma_s/\Gamma_s$ has also been obtained directly from a measurement of the $B_s^0 \rightarrow D_s^{(*)+} D_s^{(*)-}$ branching ratio [43], under the assumption that these decays practically account for all the CP -even final states.

Present data is not precise enough to efficiently constrain both Γ_s and $\Delta\Gamma_s/\Gamma_s$; since the B_s and B_d lifetimes are predicted to be equal within less than a percent [44], an expectation compatible with the current experimental data [45], the constraint $\Gamma_s = \Gamma_d$ can also be used to extract $\Delta\Gamma_s/\Gamma_s$. Applying the combination procedure described in Ref. 22 on the published B_s lifetime results [40,42,46] yields

$$\Delta\Gamma_s/\Gamma_s < 0.65 \quad \text{at 95\% CL} \quad (34)$$

without external constraint, or

$$\Delta\Gamma_s/\Gamma_s < 0.33 \quad \text{at 95\% CL} \quad (35)$$

when constraining $1/\Gamma_s$ to the measured B_d lifetime. These results are not yet precise enough to test Standard Model predictions.

Average b -hadron mixing and b -hadron production fractions

Let f_u , f_d , f_s and f_{baryon} be the B_u , B_d , B_s and b -baryon fractions composing an unbiased sample of weakly-decaying b hadrons produced in high energy colliders. LEP experiments have measured $f_s \times \text{BR}(B_s^0 \rightarrow D_s^- \ell^+ \nu_\ell X)$ [47], $\text{BR}(b \rightarrow A_b^0) \times \text{BR}(A_b^0 \rightarrow A_c^+ \ell^- \bar{\nu}_\ell X)$ [48] and $\text{BR}(b \rightarrow \Xi_b^-) \times \text{BR}(\Xi_b^- \rightarrow \Xi^- \ell^- \bar{\nu}_\ell X)$ [49] from partially reconstructed final

See key on page 239

states including a lepton, f_{baryon} from protons identified in b events [50], and the production rate of charged b hadrons [51]. The various b hadron fractions have also been measured at CDF from electron-charm final states [52]. All the published results have been combined following the procedure and assumptions described in Ref. 22, to yield $f_u = f_d = (38.4 \pm 1.8)\%$, $f_s = (11.7 \pm 3.0)\%$ and $f_{\text{baryon}} = (11.5 \pm 2.0)\%$ under the constraints

$$f_u = f_d \quad \text{and} \quad f_u + f_d + f_s + f_{\text{baryon}} = 1. \quad (36)$$

Time-integrated mixing analyses performed with lepton pairs from $b\bar{b}$ events produced at high energy colliders measure the quantity

$$\bar{\chi} = f'_d \chi_d + f'_s \chi_s, \quad (37)$$

where f'_d and f'_s are the fractions of B_d and B_s hadrons in a sample of semileptonic b -hadron decays. Assuming that all b hadrons have the same semileptonic decay width implies $f'_q = f_q/(\Gamma_q \tau_b)$ ($q = s, d$), where τ_b is the average b -hadron lifetime. Hence $\bar{\chi}$ measurements can be used to improve our knowledge on the fractions f_u , f_d , f_s and f_{baryon} .

Combining the above estimates of these fractions with the average $\bar{\chi} = 0.118 \pm 0.005$ (published in this *Review*), χ_d from Eq. (29) and $\chi_s = \frac{1}{2}$ yields, under the constraints of Eq. (36),

$$f_u = f_d = (38.9 \pm 1.3)\%, \quad (38)$$

$$f_s = (10.7 \pm 1.4)\%, \quad (39)$$

$$f_{\text{baryon}} = (11.6 \pm 2.0)\%, \quad (40)$$

showing that mixing information substantially reduces the uncertainty on f_s . These results and the averages quoted in Eqs. (28) and (29) for χ_d and Δm_d have been obtained in a consistent way by the B oscillations working group [22], taking into account the fact that many individual measurements of Δm_d depend on the assumed values for the b -hadron fractions.

Summary and prospects

B^0 - \bar{B}^0 mixing has been a field of intense study in the last few years. The mass difference in the B_d - \bar{B}_d system is very well measured (with an accuracy of $\sim 3.5\%$) but, despite an impressive theoretical effort, the hadronic uncertainty still limits the precision of the extracted estimate of $|V_{td}|$. The mass difference in the B_s - \bar{B}_s system is much larger and still unmeasured. However, the current experimental lower limit on Δm_s already provides, together with Δm_d , a significant constraint on the CKM matrix within the Standard Model. No strong experimental evidence exists yet for the rather large decay width difference expected in the B_s - \bar{B}_s system. It is interesting to recall that the ratio $\Delta\Gamma_s/\Delta m_s$ does not depend on CKM matrix elements in the Standard Model (see Eq. (22)), and that a measurement of either Δm_s or $\Delta\Gamma_s$ could be turned into a Standard Model prediction of the other one.

The LEP and SLD experiments have still not finalized all their B_s oscillation analyses, but a measurement of Δm_s from data collected at the Z pole becomes unlikely. In the near future, the most promising prospects for B_s mixing are from

Run II at the Tevatron, where both Δm_s and $\Delta\Gamma_s$ are expected to be measured; CDF will be able to observe B_s oscillations for values of Δm_s up to $\sim 40 \text{ ps}^{-1}$ [53], well above the current Standard Model prediction.

CP violation in B mixing, which has not been seen yet, as well as the phases involved in B mixing, will be further investigated with the large statistics that will become available both at the B factories and at the Tevatron.

B mixing may not have delivered all its secrets yet, because it is one of the phenomena where new physics might very well reveal itself (for example new particles involved in the box diagrams). Theoretical calculations in lattice QCD are becoming more reliable and further progress in reducing hadronic uncertainties is expected. In the long term, a stringent check of the consistency, within the Standard Model, of the B_d and B_s mixing measurements with all other measured observables in B physics (including CP asymmetries in B decays) will be possible, allowing to place limits on new physics or, better, discover new physics.

References

1. T.D. Lee and C.S. Wu, *Ann. Rev. Nucl. Sci.* **16**, 511 (1966);
I.I. Bigi and A.I. Sanda, " CP violation," Cambridge, Cambridge Univ. Press, 2000;
G.C. Branco, L. Lavoura, and J.P. Silva, " CP violation," Clarendon Press Oxford, 1999;
see also the review on B^0 - \bar{B}^0 mixing by H. Quinn in C. Caso *et al.*, *Eur. Phys. J.* **C3**, 1 (1998).
2. See the review on CP violation in B decays by H. Quinn and A. Sanda in this publication.
3. A.J. Buras, W. Slominski, and H. Steger, *Nucl. Phys.* **B245**, 369 (1984).
4. A.J. Buras and R. Fleischer, in "Heavy Flavours II," ed. A.J. Buras and M. Lindner, Singapore World Scientific (1998).
5. M. Kobayashi and K. Maskawa, *Prog. Theor. Phys.* **49**, 652 (1973).
6. I.I. Bigi *et al.*, in " CP violation," ed. C. Jarlskog, Singapore World Scientific, 1989.
7. R. Aleksan *et al.*, *Phys. Lett.* **B316**, 567 (1993).
8. C. Albajar *et al.*, *UA1 Collab.*, *Phys. Lett.* **B186**, 247 (1987).
9. H. Albrecht *et al.*, *ARGUS Collab.*, *Phys. Lett.* **B192**, 245 (1987).
10. H.-G. Moser and A. Roussarie, *Nucl. Instrum. Methods* **384**, 491 (1997).
11. *SLD Collab.*, *SLAC-PUB-7228*, *SLAC-PUB-7229*, *SLAC-PUB-7230*, contrib. to 28th Int. Conf. on High Energy Physics, Warsaw, 1996.
12. *ALEPH Collab.*, contrib. 596 to Int. Europhysics Conf. on High Energy Physics, Jerusalem, 1997.
13. F. Abe *et al.*, *CDF Collab.*, *Phys. Rev. Lett.* **80**, 2057 (1998), *Phys. Rev.* **D59**, 032001 (1999) *Phys. Rev.* **D60**, 051101 (1999); *Phys. Rev.* **D60**, 072003 (1999);
T. Affolder *et al.*, *CDF Collab.*, *Phys. Rev.* **D60**, 112004 (1999).
14. R. Barate *et al.*, *ALEPH Collab.*, *Eur. Phys. J.* **C4**, 367 (1998); *Eur. Phys. J.* **C7**, 553 (1999).

Meson Particle Listings

 B^0

-
15. DELPHI Collab., contrib. 4.520 to Int. Europhysics Conf. on High Energy Physics, Tampere, 1999; contrib. 236 to 29th Int. Conf. on High Energy Physics, Vancouver, 1998.
 16. M. Paulini, private communication.
 17. D. Buskalic *et al.*, ALEPH Collab., Z. Phys. **C75**, 397 (1997).
 18. CDF Collab., www-cdf.fnal.gov/physics/new/bottom/bottom.html.
 19. P. Abreu *et al.*, DELPHI Collab., Z. Phys. **C76**, 579 (1997).
 20. M. Acciarri *et al.*, L3 Collab., Eur. Phys. J. **C5**, 195 (1998).
 21. G. Alexander *et al.*, OPAL Collab., Z. Phys. **C72**, 377 (1996); K. Ackerstaff *et al.*, OPAL Collab., Z. Phys. **C76**, 401 (1997); Z. Phys. **C76**, 417 (1997).
 22. ALEPH, CDF, DELPHI, L3, OPAL, and SLD Collab., "Combined results on b -hadron production rates, lifetimes, oscillations, and semileptonic decays," LEPHFS note 99-02, to be subm. as CERN-EP preprint; the combined results on B mixing and b hadron fractions included in the above paper or published in this *Review* have been obtained by the B oscillations working group; see <http://www.cern.ch/LEPBOSC/> for more information.
 23. H. Albrecht *et al.*, ARGUS Collab., Z. Phys. **C55**, 357 (1992); Phys. Lett. **B324**, 249 (1994).
 24. J. Bartelt *et al.*, CLEO Collab., Phys. Rev. Lett. **71**, 1680 (1993).
 25. F. Abe *et al.*, CDF Collab., Phys. Rev. **D55**, 2546 (1997).
 26. K. Ackerstaff *et al.*, OPAL Collab., Z. Phys. **C76**, 401 (1997).
 27. DELPHI Collab., conf. note 97-98, contrib. 449 to Int. Europhysics Conf. on High Energy Physics, Jerusalem, 1997.
 28. ALEPH Collab., conf. note 99-026, contrib. 4.421 to Int. Europhysics Conf. on High Energy Physics, Tampere, 1999.
 29. G. Abbiendi *et al.*, OPAL Collab., Eur. Phys. J. **C12**, 609 (2000).
 30. ALEPH Collab., conf. note 98-032, contrib. 4.396 to Int. Europhysics Conf. on High Energy Physics, Tampere, 1999.
 31. M. Beneke, G. Buchalla, and I. Dunietz, Phys. Lett. **B393**, 132 (1997); I. Dunietz, Eur. Phys. J. **C7**, 197 (1999).
 32. See the review on the CKM quark-mixing matrix by F.J. Gilman, K. Kleinknecht and B. Renk in this publication.
 33. S. Aoki, talk at 19th Int. Symp. on Lepton and Photon Interactions, Stanford, 1999, hep-ph/9912288; P. Ball *et al.*, " B decays at the LHC," hep-ph/0003238 and CERN-TH/2000-101, to appear in the proceedings of the 1999 workshop on Standard Model physics at the LHC, CERN.
 34. F. Abe *et al.*, CDF Collab., Phys. Rev. Lett. **82**, 3576 (1999).
 35. W. Adam *et al.*, DELPHI Collab., Phys. Lett. **B414**, 382 (1997).
 36. G. Abbiendi *et al.*, OPAL Collab., Eur. Phys. J. **C11**, 587 (1999).
 37. SLD Collab., SLAC-PUB-8225, contrib. to 19th Int. Symp. on Lepton and Photon Interactions, Stanford, 1999.
 38. K. Hartkorn and H.-G. Moser, Eur. Phys. J. **C8**, 381 (1999).
 39. M. Acciarri *et al.*, L3 Collab., Phys. Lett. **B438**, 417 (1998).
 40. F. Abe *et al.*, CDF Collab., Phys. Rev. **D59**, 032004 (1999).
 41. DELPHI Collab., contrib. 4.520 to Int. Europhysics Conf. on High Energy Physics, Tampere, 1999.
 42. F. Abe *et al.*, CDF Collab., Phys. Rev. **D57**, 5382 (1998).
 43. R. Barate *et al.*, ALEPH Collab., CERN-EP/2000-036, Feb. 2000, subm. to Phys. Lett. B.
 44. See for example M. Beneke, G. Buchalla, and I. Dunietz, Phys. Rev. **D54**, 4419 (1996).
 45. See the review on production and decay of b -hadrons by L. Gibbons and K. Honscheid in this publication.
 46. D. Buskalic *et al.*, ALEPH Collab., Phys. Lett. **B377**, 205 (1996); P. Abreu *et al.*, DELPHI Collab., Z. Phys. **C71**, 11 (1996); K. Ackerstaff *et al.*, OPAL Collab., Phys. Lett. **B426**, 161 (1998).
 47. P. Abreu *et al.*, DELPHI Collab., Phys. Lett. **B289**, 199 (1992); P.D. Acton *et al.*, OPAL Collab., Phys. Lett. **B295**, 357 (1992); D. Buskalic *et al.*, ALEPH Collab., Phys. Lett. **B361**, 221 (1995).
 48. P. Abreu *et al.*, DELPHI Collab., Z. Phys. **C68**, 375 (1995); R. Barate *et al.*, ALEPH Collab., Eur. Phys. J. **C2**, 197 (1998).
 49. P. Abreu *et al.*, DELPHI Collab., Z. Phys. **C68**, 541 (1995); D. Buskalic *et al.*, ALEPH Collab., Phys. Lett. **B384**, 449 (1996).
 50. R. Barate *et al.*, ALEPH Collab., Eur. Phys. J. **C5**, 205 (1998).
 51. DELPHI Collab., contrib. 5.515 to Int. Europhysics Conf. on High Energy Physics, Tampere, 1999.
 52. F. Abe *et al.*, CDF Collab., Phys. Rev. **D60**, 092005 (1999); T. Affolder *et al.*, CDF Collab., Phys. Rev. Lett. **84**, 1663 (2000).
 53. CDF Collab., "Update to Proposal P-909: physics performance of the CDF II detector with an inner silicon layer and a time-of-flight detector," Jan. 1999; see www-cdf.fnal.gov/upgrades/btb_update_jan99.ps.
-

B^0 - \bar{B}^0 MIXING PARAMETERS

For a discussion of B^0 - \bar{B}^0 mixing see the note on " B^0 - \bar{B}^0 Mixing" in the B^0 Particle Listings above.

χ_d is a measure of the time-integrated B^0 - \bar{B}^0 mixing probability that a produced $B^0(\bar{B}^0)$ decays as a $\bar{B}^0(B^0)$. Mixing violates $\Delta B \neq 2$ rule.

$$\chi_d = \frac{x_d^2}{2(1+x_d^2)}$$

$$x_d = \frac{\Delta m_{B^0}}{\Gamma_{B^0}} = (m_{B_H^0} - m_{B_L^0}) \tau_{B^0}$$

where H, L stand for heavy and light states of two B^0 CP eigenstates and $\tau_{B^0} = \frac{1}{0.5(\Gamma_{B_H^0} + \Gamma_{B_L^0})}$.

χ_d

This B^0 - \bar{B}^0 mixing parameter is the probability (integrated over time) that a produced B^0 (or \bar{B}^0) decays as a \bar{B}^0 (or B^0), e.g. for inclusive lepton decays

$$\chi_d = \frac{\Gamma(B^0 \rightarrow \ell^+ X \text{ (via } \bar{B}^0)}) / \Gamma(B^0 \rightarrow \ell^+ X)}{\Gamma(B^0 \rightarrow \ell^+ X \text{ (via } B^0)) / \Gamma(B^0 \rightarrow \ell^+ X)}$$

Where experiments have measured the parameter $r = \chi/(1-\chi)$, we have converted to χ . Mixing violates the $\Delta B \neq 2$ rule.

Note that the measurement of χ at energies higher than the $T(4S)$ have not separated χ_d from χ_s where the subscripts indicate $B^0(d\bar{d})$ or $B_s^0(b\bar{b})$. They are listed in the B_s^0 - \bar{B}_s^0 MIXING section.

The experiments at $T(4S)$ make an assumption about the $B^0\bar{B}^0$ fraction and about the ratio of the B^\pm and B^0 semileptonic branching ratios (usually that it equals one).

OUR EVALUATION, provided by the LEP B Oscillation Working Group, includes χ_d calculated from Δm_{B^0} and τ_{B^0} .

VALUE	CL%	DOCUMENT ID	TECN	COMMENT
0.174 ± 0.009 OUR EVALUATION				
0.156 ± 0.024 OUR AVERAGE				
0.16 ± 0.04 ± 0.04		314 ALBRECHT	94 ARG	$e^+e^- \rightarrow T(4S)$
0.149 ± 0.023 ± 0.022		315 BARTELT	93 CLE2	$e^+e^- \rightarrow T(4S)$
0.171 ± 0.048		316 ALBRECHT	92L ARG	$e^+e^- \rightarrow T(4S)$
• • • We do not use the following data for averages, fits, limits, etc. • • •				
0.20 ± 0.13 ± 0.12		317 ALBRECHT	96D ARG	$e^+e^- \rightarrow T(4S)$
0.19 ± 0.07 ± 0.09		318 ALBRECHT	96D ARG	$e^+e^- \rightarrow T(4S)$
0.24 ± 0.12		319 ELSEN	90 JADE	e^+e^- 35-44 GeV
0.158 ^{+0.052} _{-0.059}		ARTUSO	89 CLEO	$e^+e^- \rightarrow T(4S)$
0.17 ± 0.05		320 ALBRECHT	87I ARG	$e^+e^- \rightarrow T(4S)$
<0.19	90	321 BEAN	87B CLEO	$e^+e^- \rightarrow T(4S)$
<0.27	90	322 AVERY	84 CLEO	$e^+e^- \rightarrow T(4S)$

- 314 ALBRECHT 94 reports $r=0.194 \pm 0.062 \pm 0.054$. We convert to χ for comparison. Uses tagged events (lepton + pion from D^*).
- 315 BARTELT 93 analysis performed using tagged events (lepton+pion from D^*). Using dilepton events they obtain $0.157 \pm 0.016^{+0.033}_{-0.028}$.
- 316 ALBRECHT 92L is a combined measurement employing several lepton-based techniques. It uses all previous ARGUS data in addition to new data and therefore supersedes ALBRECHT 87I. A value of $r = 20.6 \pm 7.0\%$ is directly measured. The value can be used to measure $x = \Delta M/\Gamma = 0.72 \pm 0.15$ for the B_d meson. Assumes $f_{+,-}/f_0 = 1.0 \pm 0.05$ and uses $\tau_{B^\pm}/\tau_{B^0} \approx (0.95 \pm 0.14) (f_{+,-}/f_0)$.
- 317 Uses $D^{*+}K^\pm$ correlations.
- 318 Uses $(D^{*+}l^-)K^\pm$ correlations.
- 319 These experiments see a combination of B_s and B_d mesons.
- 320 ALBRECHT 87I is inclusive measurement with like-sign dileptons, with tagged B decays plus leptons, and one fully reconstructed event. Measures $r=0.21 \pm 0.08$. We convert to χ for comparison. Superseded by ALBRECHT 92L.
- 321 BEAN 87B measured $r < 0.24$; we converted to χ .
- 322 Same-sign dilepton events. Limit assumes semileptonic BR for B^+ and B^0 equal. If B^0/B^\pm ratio < 0.58 , no limit exists. The limit was corrected in BEAN 87B from $r < 0.30$ to $r < 0.37$. We converted this limit to χ .

$\Delta m_{B^0} = m_{B_H^0} - m_{B_L^0}$

Δm_{B^0} is a measure of 2π times the B^0 - \bar{B}^0 oscillation frequency in time-dependent mixing experiments.

The second "OUR EVALUATION" (0.478 ± 0.018) is an average of the data listed below performed by the LEP B Oscillation Working Group as described in our "Review of B - \bar{B} Mixing" in the B^0 Section of these Listings. The averaging procedure takes into account correlations between the measurements.

The first "OUR EVALUATION" (0.472 ± 0.017), also provided by the LEP B Oscillation Working Group, includes Δm_d calculated from χ_d measured at $T(4S)$.

VALUE ($10^{12} h s^{-1}$)	EVTS	DOCUMENT ID	TECN	COMMENT
0.472 ± 0.017 OUR EVALUATION				
0.478 ± 0.018 OUR EVALUATION				
0.503 ± 0.064 ± 0.071		323 ABE	99K CDF	$p\bar{p}$ at 1.8 TeV
0.500 ± 0.052 ± 0.043		324 ABE	99Q CDF	$p\bar{p}$ at 1.8 TeV

0.516 ± 0.099 ^{+0.029} _{-0.035}		325 AFFOLDER	99C CDF	$p\bar{p}$ at 1.8 TeV
0.471 ^{+0.078} _{-0.068} ± 0.033 ± 0.034		326 ABE	98C CDF	$p\bar{p}$ at 1.8 TeV
0.458 ± 0.046 ± 0.032		327 ACCIARRI	98D L3	$e^+e^- \rightarrow Z$
0.437 ± 0.043 ± 0.044		328 ACCIARRI	98D L3	$e^+e^- \rightarrow Z$
0.472 ± 0.049 ± 0.053		329 ACCIARRI	98D L3	$e^+e^- \rightarrow Z$
0.523 ± 0.072 ± 0.043		330 ABREU	97N DLPH	$e^+e^- \rightarrow Z$
0.493 ± 0.042 ± 0.027		328 ABREU	97N DLPH	$e^+e^- \rightarrow Z$
0.499 ± 0.053 ± 0.015		331 ABREU	97N DLPH	$e^+e^- \rightarrow Z$
0.480 ± 0.040 ± 0.051		327 ABREU	97N DLPH	$e^+e^- \rightarrow Z$
0.444 ± 0.029 ^{+0.020} _{-0.017}		328 ACKERSTAFF	97U OPAL	$e^+e^- \rightarrow Z$
0.430 ± 0.043 ^{+0.028} _{-0.030}		327 ACKERSTAFF	97V OPAL	$e^+e^- \rightarrow Z$
0.482 ± 0.044 ± 0.024		332 BUSKULIC	97D ALEP	$e^+e^- \rightarrow Z$
0.404 ± 0.045 ± 0.027		328 BUSKULIC	97D ALEP	$e^+e^- \rightarrow Z$
0.452 ± 0.039 ± 0.044		327 BUSKULIC	97D ALEP	$e^+e^- \rightarrow Z$
0.539 ± 0.060 ± 0.024		333 ALEXANDER	96V OPAL	$e^+e^- \rightarrow Z$
0.567 ± 0.089 ^{+0.029} _{-0.023}		334 ALEXANDER	96V OPAL	$e^+e^- \rightarrow Z$
• • • We do not use the following data for averages, fits, limits, etc. • • •				
0.444 ± 0.028 ± 0.028		335 ACCIARRI	98D L3	$e^+e^- \rightarrow Z$
0.497 ± 0.035		336 ABREU	97N DLPH	$e^+e^- \rightarrow Z$
0.467 ± 0.022 ^{+0.017} _{-0.015}		337 ACKERSTAFF	97V OPAL	$e^+e^- \rightarrow Z$
0.446 ± 0.032		338 BUSKULIC	97D ALEP	$e^+e^- \rightarrow Z$
0.531 ± 0.050 ± 0.078		339 ABREU	96Q DLPH	Sup. by ABREU 97N
0.496 ^{+0.055} _{-0.051} ± 0.043		327 ACCIARRI	96E L3	Repl. by ACCIARRI 98D
0.548 ± 0.050 ^{+0.023} _{-0.019}		340 ALEXANDER	96V OPAL	$e^+e^- \rightarrow Z$
0.496 ± 0.046		341 AKERS	95J OPAL	Repl. by ACKERSTAFF 97V
0.462 ^{+0.040} _{-0.053} ± 0.052 ± 0.035		327 AKERS	95J OPAL	Repl. by ACKERSTAFF 97V
0.50 ± 0.12 ± 0.06		330 ABREU	94M DLPH	Sup. by ABREU 97N
0.508 ± 0.075 ± 0.025		333 AKERS	94C OPAL	Repl. by ALEXANDER 96V
0.57 ± 0.11 ± 0.02	153	334 AKERS	94H OPAL	Repl. by ALEXANDER 96V
0.50 ^{+0.07} _{-0.06} ± 0.11 ± 0.10		327 BUSKULIC	94B ALEP	Sup. by BUSKULIC 97D
0.52 ^{+0.10} _{-0.11} ± 0.04 ± 0.03		334 BUSKULIC	93K ALEP	Sup. by BUSKULIC 97D
323 Uses di-muon events.				
324 Uses jet-charge and lepton-flavor tagging.				
325 Uses $\ell^-D^{*+}-\ell$ events.				
326 Uses $\pi-B$ in the same side.				
327 Uses $\ell-\ell$.				
328 Uses $\ell-Q_{hem}$.				
329 Uses $\ell-\ell$ with impact parameters.				
330 Uses $D^{*\pm}-Q_{hem}$.				
331 Uses $\pi_s^\pm-\ell-Q_{hem}$.				
332 Uses $D^{*\pm}-\ell/Q_{hem}$.				
333 Uses $D^{*\pm}-\ell-Q_{hem}$.				
334 Uses $D^{*\pm}-\ell$.				
335 ACCIARRI 98D combines results from $\ell-\ell$, $\ell-Q_{hem}$, and $\ell-\ell$ with impact parameters.				
336 ABREU 97N combines results from $D^{*\pm}-Q_{hem}$, $\ell-Q_{hem}$, $\pi_s^\pm-\ell-Q_{hem}$, and $\ell-\ell$.				
337 ACKERSTAFF 97V combines results from $\ell-\ell$, $\ell-Q_{hem}$, $D^{*-}\ell$, and $D^{*+}-Q_{hem}$.				
338 BUSKULIC 97D combines results from $D^{*\pm}-\ell/Q_{hem}$, $\ell-Q_{hem}$, and $\ell-\ell$.				
339 ABREU 96Q analysis performed using lepton, kaon, and jet-charge tags.				
340 ALEXANDER 96V combines results from $D^{*+}-\ell$ and $D^{*+}-\ell-Q_{hem}$.				
341 AKERS 95J combines results from charge measurement, $D^{*\pm}-\ell-Q_{hem}$ and $\ell-\ell$.				

$\chi_d = \Delta m_{B^0}/\Gamma_{B^0}$

The second "OUR EVALUATION" (0.740 ± 0.031) is an average of the data listed in Δm_{B^0} section performed by the LEP B Oscillation Working Group as described in our "Review of B - \bar{B} Mixing" in the B^0 Section of these Listings. The averaging procedure takes into account correlations between the measurements.

The first "OUR EVALUATION" (0.730 ± 0.029), also provided by the LEP B Oscillation Working Group, includes χ_d measured at $T(4S)$.

VALUE	DOCUMENT ID
0.730 ± 0.029 OUR EVALUATION	
0.740 ± 0.031 OUR EVALUATION	

Meson Particle Listings

B^0

CP VIOLATION IN B DECAY – STANDARD MODEL PREDICTIONS

Revised January 2000 by H. Quinn (SLAC) and A.I. Sanda (Nagoya University).

With the commissioning of the asymmetric B Factories at KEKB and PEP II, and of CESR III and with the completion of the main ring injector at Fermilab, we are headed into an exciting time for the study of CP violation in B meson decays. This review outlines the basic ideas of such studies. For the most part, we follow the discussions given in Refs. [1–3].

Time evolution of neutral B meson states

Neutral B mesons, like neutral K mesons, have mass eigenstates which are not flavor eigenstates. This subject is reviewed separately [4]. Here we give some formulae to establish the notation used in this review. The mass eigenstates are given by:

$$\begin{aligned} |B_1\rangle &= p|B^0\rangle + q|\bar{B}^0\rangle, \\ |B_2\rangle &= p|B^0\rangle - q|\bar{B}^0\rangle, \end{aligned} \quad (1)$$

where B^0 and \bar{B}^0 are flavor eigenstates containing the \bar{b} and b quarks respectively. The ratio

$$\frac{q}{p} = + \sqrt{\frac{M_{12}^* - \frac{i}{2}\Gamma_{12}^*}{M_{12} - \frac{i}{2}\Gamma_{12}}}. \quad (2)$$

Here, the CP operator is defined so that $CP|B^0\rangle = |\bar{B}^0\rangle$, and CPT symmetry is assumed. We define $M_{12} = \bar{M}_{12}e^{i\xi}$, where the phase ξ is restricted to $-\frac{1}{2}\pi < \xi < \frac{1}{2}\pi$, and \bar{M}_{12} is taken to be real but not necessarily positive; and similarly (with a different phase) for Γ_{12} . The convention used here is that the real part of q/p is positive.

The differences in the eigenvalues $\Delta M = M_2 - M_1$ and $\Delta\Gamma = \Gamma_1 - \Gamma_2$ are given by

$$\begin{aligned} \Delta M &= -2\text{Re}\left(\frac{q}{p}(M_{12} - \frac{i}{2}\Gamma_{12})\right) \\ &\simeq -2\bar{M}_{12} \\ \Delta\Gamma &= -4\text{Im}\left(\frac{q}{p}(M_{12} - \frac{i}{2}\Gamma_{12})\right) \\ &\simeq 2\bar{\Gamma}_{12} \cos \zeta. \end{aligned} \quad (3)$$

Here we denoted $\frac{\Gamma_{12}}{M_{12}} = re^{i\zeta}$. As we expect $r \sim 10^{-3}$ in the Standard Model for B_d , we kept only the leading order term in r . In the Standard Model, with these conventions and given that all models give a positive value for the parameter B_B , ΔM is positive, so that B_2 is heavier than B_1 ; this is unlikely to be tested soon. (Note that a common alternative convention is to name the two states B_L and B_H for light and heavy respectively; then the sign of q/p becomes the quantity to be tested.)

This review focuses on the B_d system, but also mentions some possibly interesting studies for CP violation in B_s decays, which may be pursued at hadron colliders. Much of the discussion here can be applied directly for B_s decays with the appropriate replacement of the spectator quark type.

The time evolution of states starting out at time $t = 0$ as pure B^0 or \bar{B}^0 is given by:

$$\begin{aligned} |B^0(t)\rangle &= g_+(t)|B^0\rangle + \frac{q}{p}g_-(t)|\bar{B}^0\rangle \\ |\bar{B}^0(t)\rangle &= g_+(t)|\bar{B}^0\rangle + \frac{p}{q}g_-(t)|B^0\rangle, \end{aligned} \quad (4)$$

where

$$g_{\pm}(t) = \frac{1}{2}e^{-iM_1 t}e^{-\frac{1}{2}\Gamma_1 t} \left[1 \pm e^{-i\Delta M t}e^{\frac{1}{2}\Delta\Gamma t} \right]. \quad (5)$$

We define

$$\begin{aligned} A(f) &= \langle f|H|B^0\rangle, \\ \bar{A}(f) &= \langle f|H|\bar{B}^0\rangle, \\ \bar{\rho}(f) &= \frac{\bar{A}(f)}{A(f)} = \rho(f)^{-1}, \end{aligned} \quad (6)$$

where f is a final state that is possible for both B^0 and \bar{B}^0 decays. The time-dependent decay rates are thus given by

$$\begin{aligned} \Gamma(B^0(t) \rightarrow f) &\propto e^{-\Gamma_1 t} |A(f)|^2 \left[K_+(t) + K_-(t) \left| \frac{q}{p} \right|^2 |\bar{\rho}(f)|^2 \right. \\ &\quad \left. + 2\text{Re}\left[L^*(t) \left(\frac{q}{p} \right) \bar{\rho}(f) \right] \right], \end{aligned} \quad (7)$$

$$\begin{aligned} \Gamma(\bar{B}^0(t) \rightarrow f) &\propto e^{-\Gamma_1 t} |\bar{A}(f)|^2 \left[K_+(t) + K_-(t) \left| \frac{p}{q} \right|^2 |\rho(f)|^2 \right. \\ &\quad \left. + 2\text{Re}\left[L^*(t) \left(\frac{p}{q} \right) \rho(f) \right] \right], \end{aligned} \quad (8)$$

where

$$\begin{aligned} |g_{\pm}(t)|^2 &= \frac{1}{4}e^{-\Gamma_1 t} K_{\pm}(t), \\ g_-(t)g_+^*(t) &= \frac{1}{4}e^{-\Gamma_1 t} L^*(t), \\ K_{\pm}(t) &= 1 + e^{\Delta\Gamma t} \pm 2e^{\frac{1}{2}\Delta\Gamma t} \cos \Delta M t, \\ L^*(t) &= 1 - e^{\Delta\Gamma t} + 2ie^{\frac{1}{2}\Delta\Gamma t} \sin \Delta M t. \end{aligned} \quad (9)$$

For the case of B_d decays the quantity $\Delta\Gamma/\Gamma$ is small and is usually dropped, for B_s decays it may be significant [6] and hence is retained in Eqs. 4–8.

See key on page 239

Three classes of CP violation in B decays

When two amplitudes with different phase-structure contribute to a B decay, they may interfere and produce CP -violating effects [5]. There are three distinct types of CP violation: (1) CP violation from nonvanishing relative phase between the mass and the width parts of the mixing matrix which gives $|q/p| \neq 1$, often called “indirect;” (2) Direct CP violation, which is any effect that indicates two decay amplitudes have different weak phases (those arising from Lagrangian couplings), in particular it occurs whenever $|\rho(f)| \neq 1$; (3) Interference between a decays with and without mixing which can occur for decays to CP eigenstates whenever $\text{Arg}((q/p)\bar{\rho}(f)) \neq 0$. This can occur even for modes where both the other types do not, i.e. $|q/p|, |\rho(f)| = 1$.

(1) Indirect CP violation

In the next few years, experiments will accumulate a large number of semileptonic B decays. Any asymmetry in the wrong-sign semileptonic decays (or in any other wrong-flavor decays) is a clean sign of indirect CP violation.

The semileptonic asymmetry for the wrong sign B_q decay, where $q = d$ or s , is given by

$$a_{SL}(B_q) = \frac{\Gamma(\bar{B}_q(t) \rightarrow \ell^+ X) - \Gamma(B_q(t) \rightarrow \ell^- X)}{\Gamma(\bar{B}_q(t) \rightarrow \ell^+ X) + \Gamma(B_q(t) \rightarrow \ell^- X)} = \frac{|p/q|^2 - |q/p|^2}{|p/q|^2 + |q/p|^2} = r_{B_q} \sin \zeta_{B_q}, \quad (10)$$

where we kept only the leading order term in r_{B_q} . Within the context of the Standard Model, if hadronic rescattering effects are small then $\sin \zeta_{B_q}$ is small because M_{12} and Γ_{12} acquire their phases from the same combination of CKM matrix elements. Since this asymmetry is tiny in the Standard Model, this may be a fruitful area to search for physics beyond the Standard Model.

(2) Direct CP violation

Direct CP violation is the name given to CP violation that arises because there is a difference between the weak phases of any two decay amplitudes for a single decay. Weak phases are those that arise because of a complex coupling constant in the Lagrangian. Note that a single weak phase from a complex coupling constant is never physically meaningful because it can generally be removed by redefining some field by a phase. Only the differences between the phases of couplings which cannot be changed by such redefinitions are physically meaningful. The strong and electromagnetic couplings can always be defined to be real but, as Kobayashi and Maskawa first observed, in the three generation Standard Model one cannot remove all the phases from the CKM matrix by any choice of field redefinitions [7].

There are two distinct ways to observe direct CP -violation effects in B decays:

- $|\bar{A}_f/A_f| \neq 1$ leading to rate asymmetries for CP -conjugate decays. Here, two amplitudes with different weak phases must contribute to the same decay; they must also have different

strong phases, that is, the phases that arise because of absorptive parts (often called final-state interaction effects). When the final state f has different flavor content than its CP conjugate, this gives a rate asymmetry that is directly observable. The asymmetry is given by

$$a = \frac{2A_1 A_2 \sin(\xi_1 - \xi_2) \sin(\delta_1 - \delta_2)}{A_1^2 + A_2^2 + 2A_1 A_2 \cos(\xi_1 - \xi_2) \cos(\delta_1 - \delta_2)}, \quad (11)$$

where the A_i are the magnitudes, the ξ_i are the weak phases, and the δ_i are the strong phases of the two amplitudes contributing to A_f . The impact of direct CP violation of this type in decays of neutral B 's to flavor eigenstates is discussed below.

- Any difference (other than an overall sign) between the CP asymmetries for decays of B_d mesons to flavor eigenstates, or between those of neutral B_s mesons, is an evidence of direct CP violation. As is shown below, such asymmetries arise whenever the decay weak phase is not canceled by the mixing weak phase, hence any two different results imply that there is a difference between the weak phases of the amplitudes for the two decays. Only if the asymmetries are the same can one choose a phase convention which ascribes all CP -violating phases to the mixing amplitude. For example, the expected asymmetries for the $B \rightarrow J/\psi K_S$ and $B \rightarrow \pi\pi$ decays are different (whether or not penguin graphs add additional direct CP -violating effects of the type $|\bar{A}_f/A_f| \neq 1$ in the latter channel) because the dominant decay amplitudes have different weak phases in the Standard Model.

(3) Decays of B^0 and \bar{B}^0 to CP eigenstates

In decays to CP eigenstates, the time-dependent asymmetry is given by

$$a_f(t) = \frac{\Gamma(\bar{B}^0(t) \rightarrow f) - \Gamma(B^0(t) \rightarrow f)}{\Gamma(\bar{B}^0(t) \rightarrow f) + \Gamma(B^0(t) \rightarrow f)}. \quad (12)$$

Asymmetry is generated if: (i) both $A(B \rightarrow f)$ and $A(\bar{B} \rightarrow f)$ are nonzero; and (ii) the mixing weak phase in $\frac{q}{p}$ is different from the weak decay phase in $\bar{\rho}(f)$. To the leading order in τ , the Standard Model predicts

$$q/p = \frac{V_{tb}^* V_{td}}{V_{td} V_{tb}^*} = e^{-i2\phi_{\text{mixing}}}. \quad (13)$$

If there is only one amplitude (or two with the same weak phase) contributing to $A(B \rightarrow f)$ and $A(\bar{B} \rightarrow f)$ then $|\bar{\rho}(f)| = 1$ and the relationship between the measured asymmetry and the Kobayashi-Maskawa phases is cleanly predicted by

$$a_f(t) = \text{Im} \left(\frac{q}{p} \bar{\rho}(f) \right) \sin \Delta M t = -\eta_f \sin 2(\phi_{\text{mixing}} + \phi_{\text{decay}}) \sin \Delta M t. \quad (14)$$

Here we have used the fact that in such cases we can write $\bar{\rho}(f) = \eta_f e^{-i2\phi_{\text{decay}}}$ where $\eta_f = \pm 1$ is the CP eigenvalue of the state f . The weak phases ϕ_{mixing} and ϕ_{decay} are parameterization dependent quantities, but the combination $\phi_{\text{mixing}} + \phi_{\text{decay}}$ is parameterization independent. This is CP violation due to the interference between decays with and without mixing. Note

Meson Particle Listings

B^0

that a single measurement of $\sin(2\phi)$ yields four ambiguous solutions for ϕ .

When more than one amplitude with different weak phases contribute to a decay to a CP eigenstate there can also be direct CP violation effects $|\lambda_f = (q/p)\rho(f)| \neq 1$ and the asymmetry takes the more complicated form

$$a_f(t) = \frac{(|\lambda_f|^2 - 1) \cos(\Delta Mt) + 2\text{Im}\lambda_f \sin(\Delta Mt)}{(1 + |\lambda_f|^2)}. \quad (15)$$

The quantity λ_f involves the ratio of the two amplitudes that contribute to A_f as well as their relative strong phases and hence introduces the uncertainties of hadronic physics into the relationship between the measured asymmetry and the K-M phases. However in certain cases such channels can be useful in resolving the ambiguities mentioned above. If $\cos(2\phi)$ can be measured as well as $\sin(\phi)$ only a two-fold ambiguity remains. This can be resolved only by knowledge of the sign of certain strong phase shifts [8].

When a B meson decays to a CP self-conjugate set of quarks the final state is in general a mixture of CP even and CP odd states, which contribute opposite sign and hence partially canceling asymmetries. In two special cases, namely the decay to two spin zero particles, or one spin zero and one non-zero spin particle there is a unique CP eigenvalue because there is only one possible relative angular momentum between the two final state particles. Quasi-two-body modes involving two particles with non-zero spin can sometimes be resolved into contributions of definite CP by angular analysis of the decays of the “final-state” particles [9].

There can also be a direct CP violation in these channels from the interference of two contributions to the same decay amplitude, $|\rho(f)| \neq 1$. This introduces dependence on the relative strengths of the two amplitude contributions and on their relative strong phases. Since these cannot be reliably calculated at present, this complicates the attempt to relate the measured asymmetry to the phases of CKM matrix elements.

Standard Model predictions for CP -violating asymmetries

• Unitarity Triangles

The requirement that the CKM matrix be unitary leads to a number of relationships among its entries. The constraints that the product of row i with the complex conjugate of row j is zero are generically referred to as “unitarity triangles” because they each take the form of a sum of three complex numbers equal to zero and hence can be represented by triangles in the complex plane. There are six such relationships, (see for example Ref. 10); the most commonly studied is that with all angles of the same order of magnitude, given by the relationship

$$V_{ud}V_{ub}^* + V_{cd}V_{cb}^* + V_{td}V_{tb}^* = 0. \quad (16)$$

This relation can be represented as a triangle on the complex plane, as shown in Fig. 1, where the signs of all three angles are also defined. When the sides are scaled by $|V_{cd}V_{cb}^*|$, the apex of

the triangle is the point ρ, η , where these parameters are defined by the Wolfenstein parameterization of the CKM matrix [11]. If $\eta = 0$, the CKM matrix is real and there is no CP violation in the Standard Model.

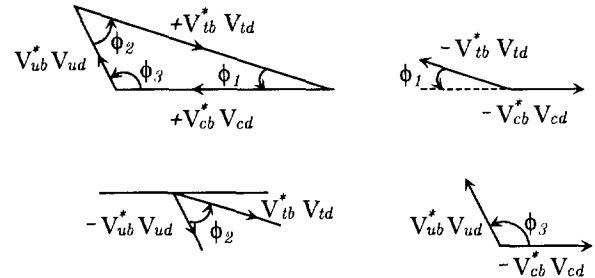


Figure 1: Angles of the unitarity triangle are related to the Kobayashi-Maskawa phases of the CKM matrix. The right-hand rule gives the positive direction of the angle between two vectors. This figure was reproduced from Ref. 1 with permission from Cambridge University Press.

The angles of the triangle are

$$\begin{aligned} \phi_1 &= \pi - \arg\left(\frac{-V_{tb}^* V_{td}}{-V_{cb}^* V_{cd}}\right) = \beta, \\ \phi_2 &= \arg\left(\frac{V_{tb}^* V_{td}}{-V_{ub}^* V_{ud}}\right) = \alpha, \\ \phi_3 &= \arg\left(\frac{V_{ub}^* V_{ud}}{-V_{cb}^* V_{cd}}\right) = \gamma. \end{aligned} \quad (17)$$

Two naming conventions for these angles are commonly used in the literature [12,13]; we provide the translation dictionary in Eq. (17), but use the ϕ_i notation in the remainder of this review, where ϕ_i is the angle opposite the side $V_{ib}^* V_{id}$ of the unitarity triangle and i represents the i -th up-type quark. As defined here, for consistency with the measured value of ϵ_K , these angles are all positive in the Standard Model, thus a determination of the sign of these angles constitutes a test of the Standard Model [14].

There are two other independent angles of the Standard Model which appear in other triangles. These are denoted

$$\begin{aligned} \chi &= \arg\left(\frac{-V_{cs}^* V_{cb}}{V_{ts}^* V_{tb}}\right) = \beta_s, \\ \chi' &= \arg\left(\frac{-V_{ud}^* V_{us}}{V_{cd}^* V_{cs}}\right) = -\beta_K. \end{aligned} \quad (18)$$

Again there are two naming conventions in common usage so we give both. These angles are of order λ^2 and λ^4 respectively [15], where $\lambda = V_{us}$. The first of them is the phase of the B_s mixing and thus is in principle measurable, though it will not be easy to achieve a result significantly different from zero for such a small angle. The angle χ' will be even more difficult to measure. Meaningful standard model tests can be defined which use the measured value of λ coupled with χ and any two of the three ϕ_i [16].

A major aim of CP -violation studies of B decays is to make enough independent measurements of the sides and angles that

this unitarity triangle is overdetermined, and thereby check the validity of the Standard Model predictions that relate various measurements to aspects of this triangle. Constraints can be made on the basis of present data on the B -meson mixing and lifetime, and on the ratio of charmless decays to decays with charm (V_{ub}/V_{cb}), and on ϵ in K decays [17]. These constraints have been discussed in many places in the literature; for a recent summary of the measurements involved, see Ref. [18]. Note, however, that any given “Standard Model allowed range” cannot be interpreted as a statistically-based error range. The ranges of allowed values depend on matrix element estimates. Improved methods to calculate such quantities, and understand the uncertainties in them, are needed to further sharpen tests of the Standard Model. Recent progress in lattice simulation using dynamical fermions seems encouraging [19]. It can be hoped that reliable computations of f_B , B_B , and B_K will be completed in the next few years. This will reduce the theoretical uncertainties in the relationships between measured mixing effects and the magnitudes of CKM parameters.

In the Standard Model there are only two independent phases in this triangle since, by definition, the three angles add up to π . The literature often discusses tests of whether the angles add up to π ; but this really means tests of whether relationships between different measurements, predicted in terms of the two independent parameters in the Standard Model, hold true. For example, many models that go beyond the Standard Model predict an additional contribution to the mixing matrix. Any change in phase of M_{12} will change the measured asymmetries so that $\phi_1(\text{measured}) \rightarrow \phi_1 - \phi_{\text{new}}$ and $\phi_2(\text{measured}) \rightarrow \phi_2 + \phi_{\text{new}}$. Thus the requirement that the sum of the three angles must add up to π is not sensitive to ϕ_{new} [20]. However, the angles as determined from the sides of the triangle would, in general, no longer coincide with those measured from asymmetries. It is equally important to check the asymmetries in channels for which the Standard model predicts very small or vanishing asymmetries. A new mixing contribution which changes the phase of M_{12} will generate significant asymmetries in such channels. In the Standard Model the CKM matrix must be unitary, this leads to relationships among its entries.

• Standard Model decay amplitudes

In the Standard Model, there are two classes of quark-level diagrams that contribute to hadronic B decays, as shown in Fig. 2. Tree diagrams are those where the W produces an additional quark-antiquark pair. Penguin diagrams are loop diagrams where the W reconnects to the same quark line. Penguin diagrams can further be classified by the nature of the particle emitted from the loop: gluonic or QCD penguins if it is a gluon, and electroweak penguins if it is a photon or a Z boson. In addition, one can label penguin diagrams by the flavor of the up-type quark in the loop; for any process all three flavor types contribute. For some processes, there are additional annihilation-type diagrams; these always contribute to the same CKM structure as the corresponding trees. For a

detailed discussion of the status of calculations based on these diagrams, or rather on the more complete operator product approach which also includes higher order QCD corrections see, for example, Ref. 21. Note that the distinction between tree and penguin contributions is a heuristic one, the separation of contributions by the operator that enters is more precise.

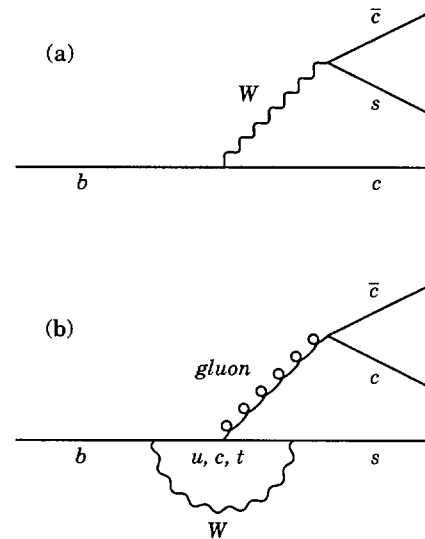


Figure 2: Quark level processes for the example of $b \rightarrow c\bar{c}s$. (a) Tree diagram; (b) Penguin diagram. In the case of electroweak penguin contributions, the gluon is replaced by a Z or a γ .

To explore possible CP violations, it is useful to tabulate all possible decays by the CKM structure of the various amplitudes. Let us first consider decays $b \rightarrow q\bar{q}'s$. The CKM factors for the diagrams for such decays are given in Table 1. Here we have used the fact that, for all such decays, the contribution to the amplitude from penguin graphs has the structure

$$A_P(q\bar{q}s) = V_{tb}V_{ts}^*P_t + V_{cb}V_{cs}^*P_c + V_{ub}V_{us}^*P_u, \quad (19)$$

where the P_i quantities are the amplitudes described by the loop diagram with a flavor i quark apart from the explicitly shown CKM factor (*i.e.*, including strong phases). These are actually divergent quantities, so it is convenient to use a Standard Model unitarity relationship, $V_{tb}V_{ts}^* + V_{cb}V_{cs}^* + V_{ub}V_{us}^* = 0$, to regroup them in the following way

$$A_P(q\bar{q}s) = V_{cb}V_{cs}^*(P_c - P_t) + V_{ub}V_{us}^*(P_u - P_t), \quad (20)$$

or, equivalently,

$$A_P(q\bar{q}s) = V_{tb}V_{ts}^*(P_t - P_c) + V_{ub}V_{us}^*(P_u - P_c). \quad (21)$$

The first term is of order λ^2 , whereas the second is of order λ^4 , and can be ignored in most instances. For modes with $q' \neq q$, there are no penguin contributions. Note also that for the $q\bar{q} = u\bar{u}, d\bar{d}$ cases, the QCD penguin graphs contribute only to the isospin zero combinations, whereas tree graphs contribute

Meson Particle Listings

 B^0

only for $u\bar{u}$ and hence have both $\Delta I = 0$ and $\Delta I = 1$ parts, as do electroweak penguins.

The CKM coefficients for $b \rightarrow q\bar{q}'d$ are listed in Table 2. A similar exercise to that described above for the penguins yields

$$A_P(q\bar{q}d) = V_{tb}V_{td}^*(P_t - P_c) + V_{ub}V_{ud}^*(P_u - P_c). \quad (22)$$

Here the two CKM contributions are of the same order of magnitude λ^3 , so both must be considered. This grouping is generally preferred over the alternative, because the second term here is somewhat smaller than the first term; it has no top-quark contribution and would vanish if the up and charm quarks were degenerate. In early literature it was often dropped, but, particularly for modes where there is no tree contribution, its effect in generating direct CP violation may be important [22]. Here the $q\bar{q} = u\bar{u}, d\bar{d}$ cases in the penguin graph contribute only to the isospin zero combinations, yielding $\Delta I = 1/2$ for the three-quark combination, whereas tree graphs and electroweak penguins have both $\Delta I = 1/2$ and $\Delta I = 3/2$ parts. For $q\bar{q} = c\bar{c}$, isospin does not distinguish between tree and penguin contributions.

Modes with direct CP violation

The largest direct CP violation is expected when there are two comparable magnitude contributions with different weak phases. Modes where the tree graphs are Cabibbo suppressed, compared to the penguins or modes with two comparable penguin contributions, are thus the best candidates. As can be seen from the tables and expressions for penguin contributions above, there are many possible modes to study. Because strong phases cannot usually be predicted, there is no clean prediction as to which modes will show the largest direct CP -violation effects. One interesting suggestion is to study three-body modes with more than one resonance in the same kinematic region. Then the different amplitudes can have very different, possibly known, strong phase structure because of the resonance (Breit-Wigner) phases [23].

Over the past two years, new information has become available from the CLEO Collaboration which suggests that penguin contributions, at least for some modes, are larger than initial estimates suggested. This is seen by using $SU(3)$ and comparing $B \rightarrow K\pi$ and $B \rightarrow \pi\pi$ decays. To get an order of

Table 1: $B \rightarrow q\bar{q}s$ decay modes

Quark process	Leading term	Secondary term	Sample B_d modes	B_d angle	Sample B_s modes	B_s angle
$b \rightarrow c\bar{c}s$	$V_{cb}V_{cs}^* = A\lambda^2$ tree + penguin($c-t$)	$V_{ub}V_{us}^* = A\lambda^4(\rho - i\eta)$ penguin only($u-t$)	$J/\psi K_S$	β	$J/\psi\eta$ $D_s\bar{D}_s$	0
$b \rightarrow s\bar{s}s$	$V_{cb}V_{cs}^* = A\lambda^2$ penguin only($c-t$)	$V_{ub}V_{us}^* = A\lambda^4(\rho - i\eta)$ penguin only($u-t$)	ϕK_S	β	$\phi\eta'$	0
$b \rightarrow u\bar{u}s$	$V_{cb}V_{cs}^* = A\lambda^2$ penguin only($c-t$)	$V_{ub}V_{us}^* = A\lambda^4(\rho - i\eta)$ tree + penguin($u-t$)	$\pi^0 K_S$ ρK_S	competing terms	$\phi\pi^0$ $K_S\bar{K}_S$	competing terms

Table 2: $B \rightarrow q\bar{q}d$ decay modes

Quark process	Leading term	Secondary term	Sample B_d modes	B_d angle	Sample B_s modes	B_s angle
$b \rightarrow c\bar{c}d$	$V_{cb}V_{cd}^* = -A\lambda^3$ tree + penguin($c-u$)	$V_{tb}V_{td}^* = A\lambda^3(1 - \rho + i\eta)$ penguin only($t-u$)	D^+D^-	$*\beta$	$J/\psi K_S$	$*\beta_s$
$b \rightarrow s\bar{s}d$	$V_{tb}V_{td}^* = A\lambda^3(1 - \rho + i\eta)$ penguin only($t-u$)	$V_{cb}V_{cd}^* = A\lambda^3$ penguin only($c-u$)	$\phi\pi$ $K_S\bar{K}_S$	competing terms	ϕK_S	competing terms
$b \rightarrow u\bar{u}d$	$V_{ub}V_{ud}^* = A\lambda^3(\rho - i\eta)$ tree + penguin($u-c$)	$V_{tb}V_{td}^* = A\lambda^3(1 - \rho + i\eta)$ penguin only($t-c$)	$\pi\pi; \pi\rho$ πa_1	$*\alpha$	$\pi^0 K_S$ $\rho^0 K_S$	competing terms
$b \rightarrow c\bar{u}d$	$V_{cb}V_{ud}^* = A\lambda^2$	0	$D^0\pi^0, D^0\rho^0$ └──┬──┘ CP eigenstate	β	$D^0 K_S$ └──┬──┘ CP eigenstate	0

*Leading terms only, large secondary terms shift asymmetry.

magnitude picture, we ignore such details as Clebsch-Gordan coefficients and assume that top penguins dominate the penguin contributions. Thus, we identify the tree and penguin contributions, minus their CKM coefficients, as T and P , the same for both modes. Writing $A_{T,P}(K\pi)$ for the tree and penguin contributions to the $K\pi$ amplitude, and similarly for $\pi\pi$ from the Tables, we see that $|A^T(K\pi)/A^T(\pi\pi)| = \mathcal{O}(\lambda)$. Thus, if the tree graph matrix elements were to dominate both decays, we would expect $\text{Br}(B \rightarrow K\pi)/\text{Br}(B \rightarrow \pi\pi) \sim \mathcal{O}(\lambda^2)$. Naively, this was expected, since the ratio of tree to penguin contribution was estimated to be $\frac{P}{T} = \frac{\alpha_S}{12\pi} \log \frac{m_t^2}{m_b^2} \sim \mathcal{O}(0.02)$. Experimentally, this is not so [24]; in fact, the $K\pi$ branching ratio is larger. This indicates that $A^P(K\pi) \sim A^T(\pi\pi)$, which suggests that $\frac{P}{T} = \mathcal{O}(\lambda)$ or larger, considerably bigger than expected. Note that this is one way that new physics could be hidden in modes with $|\rho(f)| \neq 1$; any new physics contribution can always be written as a sum of two terms with the weak phases of the two Standard Model terms (for example in Eq. (22)), and thus, when added to the Standard Model contributions, appears only as a change in the sizes of P and T from that expected in the Standard Model. However, we cannot calculate these relative sizes well enough to identify such an effect with confidence.

From the point of view of looking for direct CP -violation effects, a large P/T is good news. The largest asymmetry is expected when the interfering amplitudes have comparable magnitudes. This may be so in $B \rightarrow K\pi$ decay (or the penguin contribution may even be larger than the tree). There is no reason for the strong phases to be equal (although they could both be small). Therefore, $B^\pm \rightarrow K^\pm\pi$ is a likely hunting ground for direct CP violation. (Note there is no gluonic penguin contribution to charged $B \rightarrow \pi\pi$, and hence, no significant CP violation expected in the Standard Model.) However, as we will see below, a large P/T complicates the relationship between the measured asymmetry in neutral B decays to $\pi^+\pi^-$ and KM phases.

Studies of CP eigenstates

• $f = J/\psi K_S$

The asymmetry in the Golden Mode $B \rightarrow J/\psi K_S$ [25] will be measured soon. Since, using Eq. (20), the dominant penguin contribution has the same weak phase as the tree graph, and the remaining term is tiny, there is effectively only one weak phase in the decay amplitude. Hence, in the asymmetry, all dependence on the amplitudes cancel. With about 1% uncertainty,

$$\frac{q}{p} \bar{\rho}(J/\psi K_S) \simeq -\frac{V_{tb}^* V_{td}}{V_{tb} V_{td}^*} \cdot \frac{V_{cb} V_{cs}^*}{V_{cb}^* V_{cs}} \cdot \frac{V_{cs} V_{cd}^*}{V_{cs}^* V_{cd}} \equiv -e^{-2i\phi_1}, \quad (23)$$

where the last factor arises from the $K^0-\bar{K}^0$ mixing amplitude and appears because of the K_S in the final state. The asymmetry is thus given by

$$a_{J/\psi K_S} = \sin(2\phi_1) \sin \Delta M t, \quad (24)$$

where the angle ϕ_1 is defined in Fig. 1. Given current constraints a large positive value for $\sin(2\phi_1)$ will be strongly suggestive that the KM ansatz for CP violation is at least one of the sources of this interesting phenomenon.

• $B^0 \rightarrow \pi^+\pi^-$

The tree and penguin terms appear at the same order in λ (see Eq. (22) and Table 2.) If penguin decays were negligible the asymmetry would directly measure $\sin(2\phi_2)$. Given the enhanced penguin contribution seen from comparing $\pi\pi$ and $K\pi$ decays, the penguins cannot be ignored, and a treatment that does not assume $|\rho(f)| = 1$ must be made.

If all six modes of $B^+ \rightarrow \pi^+\pi^0$, $B^0 \rightarrow \pi^+\pi^-$, $B^0 \rightarrow \pi^0\pi^0$ and their charge conjugates can be measured with sufficient accuracy, ϕ_2 can be extracted using an isospin analysis [26], up to small corrections from electroweak penguins. However, the branching ratio for the charged modes is less than 10^{-5} [24], and that for the more difficult to measure $B^0 \rightarrow \pi^0\pi^0$ is expected to be even smaller. Therefore, further ingenuity is needed to get at this angle cleanly. A future possibility is to study the Dalitz plot of $B \rightarrow 3\pi$ decays [27].

Further Measurements

As Tables 1 and 2 suggest there are many more CP -eigenstate modes that are interesting to study, both for B_d and similarly for B_s decays. The latter states are not accessible for the B factories operating at the $\Upsilon(4S)$ resonance, but may be studied at hadronic colliders. The CDF result on the asymmetry in the $J/\psi K_S$ mode is an indication of the capabilities of such facilities for B physics [29]. Upgrades of the Fermilab detectors are in progress and proposals for new detectors with the capability to achieve fast triggers for a larger variety of purely hadronic modes are under development, promising some future improvement in this capability.

In addition to CP -eigenstate modes there are many additional modes for which particular studies have been proposed, in particular those focussed on extracting ϕ_3 (γ). Modes such as DK , DK^* and D^*K where the D mesons decay to CP eigenstates provide theoretically clean extraction of this parameter but have small branching ratios [30]. Other approaches involve the more copious $K\pi$ modes but rely on the use of isospin and $SU(3)$ (U -spin) symmetries, so have larger theoretical uncertainties [31]. This is an active area of current theoretical work.

For a recent review of how predictions for CP -violating effects are affected by Beyond Standard Model effects see Ref. 28. There are also many ways to search for new physics effects in B decays that do not involve just the CP -violation effects. For example searches for isospin breaking effects in $K\pi$ modes have recently been suggested as a likely method to isolate such effects [32].

References

1. Much of what is presented is explained in further detail in I.I. Bigi and A.I. Sanda, *CP Violation*, Cambridge University Press, Cambridge (1999).
2. For a review of CP violation in B decays see: I.I. Bigi, V.A. Khoze, N.G. Uraltsev, and A.I. Sanda, in *CP Violation*, ed. C. Jarlskog (World Scientific, Singapore, 1989).
3. Y. Nir and H.R. Quinn, *Ann. Rev. Nucl. Sci.* **42**, 211 (1992).
4. See our review on " $B^0-\bar{B}^0$ Mixing" by O. Schneider in the B^0 Listings in the full *Review*.
5. A.B. Carter and A.I. Sanda, *Phys. Rev. Lett.* **45**, 952 (1980); *Phys. Rev.* **D23**, 1567 (1981).

Meson Particle Listings

 B^0

6. R. Aleksan *et al.*, Phys. Lett. **B316**, 567 (1993); M. Beneke, G. Buchalla, I. Dunietz, Phys. Rev. **D54**, 4419 (1996).
7. See our review on the CKM mixing matrix by F.J. Gilman, K. Kleinknecht and B. Renk in the full *Review*.
8. Y. Grossman and H. Quinn, Phys. Rev. **D56**, 7259 (1997).
9. J.R. Dell'Aquila and C.A. Nelson, Phys. Rev. **D33**, 101 (1986); B. Kayser *et al.*, Phys. Lett. **B237**, 3339 (1990); I. Dunietz *et al.*, Phys. Rev. **D43**, 2193 (1991).
10. R. Aleksan, B. Kayser, and D. London, Phys. Rev. Lett. **73**, 18 (1994).
11. L. Wolfenstein, Phys. Rev. Lett. **51**, 1945 (1983).
12. The angles of the unitarity triangle ϕ_1 , ϕ_2 , ϕ_3 are those used in J.L. Rosner, A.I. Sanda, and M. Schmidt in *Proc. Fermilab Workshop on High Sensitivity Beauty Physics at Fermilab*, A.J. Slaughter, N. Lockyer and M. Schmidt, eds., 1987.
13. C.O. Dib *et al.*, Phys. Rev. **D41**, 1522 (1990). See also Y. Nir SLAC Report 412 p. 102 (1992) for careful definition of the signs in the α, β, γ notation.
14. Y. Nir and H. Quinn, Phys. Rev. **D42**, 1473 (1990).
15. I.I. Bigi and A.I. Sanda, Nucl. Phys. **B193**, 85 (1981); I.I. Bigi, in *Proceedings of the Tau-Charm Workshop*, SLAC-Report 343, p. 169 (1989).
16. J.P. Silva and L. Wolfenstein Phys. Rev. **D55**, 5331 (1997).
17. See our review on "CP Violation" by L. Wolfenstein in the full *Review*.
18. Adam F. Falk, talk presented at *19th International Symposium on Lepton and Photon Interactions at High-Energies (LP 99)* (Stanford, CA 9-14 Aug 1999) hep-ph/9908520.
19. S. Aoki, talk presented at *19th International Symposium on Lepton and Photon Interactions at High-Energies (LP 99)* (Stanford, CA, 9-14 Aug 1999).
20. See for example Y. Nir and D. Silverman, Nucl. Phys. **B345**, 301 (1990).
21. G. Buchalla, A. J. Buras, M. E. Lautenbacher, Rev. Mod. Phys. **68**, 1125 (1996).
22. J.M. Gérard and W.S. Hou, Phys. Rev. **D43**, 2909 (1991) and Phys. Lett. **B253**, 478 (1991); H. Simma, G. Eilam, and D. Wyler, Nucl. Phys. **B352**, 367 (1991); R. Fleischer, Phys. Lett. **B341**, 205 (1994).
23. D. Atwood and A. Soni, Z. Phys. **C64**, 241 (1994); Phys. Rev. Lett. **74**, 220 (1995).
24. Y. Kwon *et al.*, CLEO-CONF-99-14, Talk given at *19th International Symposium on Lepton and Photon Interactions at High-Energies (LP 99)* (Stanford, CA, 9-14 Aug 1999) hep-ex/9908039.
25. I.I. Bigi and A.I. Sanda, Nucl. Phys. **B193**, 85 (1981); Nucl. Phys. **B281**, 41 (1987).
26. M. Gronau and D. London, Phys. Rev. Lett. **65**, 3381 (1990).
27. H.R. Quinn and A.E. Snyder, Phys. Rev. **48**, 2139 (1993).
28. CP Violation beyond the Standard Model. By Y. Grossman, Y. Nir, R. Rattazzi, SLAC-PUB-7379, Jan 1997. In *Heavy flavours II* p. 755, A.J. Buras, M. Lindner, eds., e-Print Archive: hep-ph/9701231.
29. CDF Collaboration: T. Affolder *et al.*, Phys. Rev. **D61**, 072005 (2000).
30. I. Dunietz, Phys. Lett. **B270**, 75 (1991); M. Gronau and D. Wyler, Phys. Lett. **B265**, 172 (1991); D. Atwood, I. Dunietz, and A. Soni, Phys. Rev. Lett. **78**, 3257 (1997).
31. See for example M. Gronau, J.L. Rosner, and D. London, Phys. Rev. Lett. **73**, 21 (1994); M. Gronau, O.F. Hernandez, D. London, and J.L. Rosner Phys. Rev. **D50**, 4529 (1994); M. Gronau and J.L. Rosner, Phys. Rev. Lett. **76**, 1200 (1996); R. Fleischer and T. Mannel, Phys. Rev. **D57**, 2752 (1998); M. Neubert and J. L. Rosner, Phys. Lett. **B441**, 403 (1998) and Phys. Rev. Lett. **81**, 5076 (1998); M. Neubert, Invited talk at *High Energy Physics International Euroconference on Quantum Chromo Dynamics (QCD '99)* (Montpellier, France, 7-13 July 1999) hep-ph/9909564.
32. Y. Grossman, M. Neubert, and A.L. Kagan (Cincinnati U.). SLAC-PUB-8243, hep-ph/9909297.

CP VIOLATION PARAMETERS

 $\text{Re}(\epsilon_{B^0})/(1+|\epsilon_{B^0}|^2)$

CP Impurity in B_d^0 system. It is obtained from either $a_{\ell\ell}$, the charge asymmetry in like-sign dilepton events or a_{CP} , the time-dependent asymmetry of inclusive B^0 and \bar{B}^0 decays.

VALUE	DOCUMENT ID	TECN	COMMENT
0.002 ± 0.007 OUR AVERAGE			
0.001 ± 0.014 ± 0.003	342	ABBIENDI	99J OPAL $e^+e^- \rightarrow Z$
0.002 ± 0.007 ± 0.003	343	ACKERSTAFF	97U OPAL $e^+e^- \rightarrow Z$
• • • We do not use the following data for averages, fits, limits, etc. • • •			
<0.045	344	BARTELT	93 CLE2 $e^+e^- \rightarrow \Upsilon(4S)$
342 Data analyzed using the time-dependent asymmetry of inclusive B^0 decay. The production flavor of B^0 mesons is determined using both the jet charge and the charge of secondary vertex in the opposite hemisphere.			
343 ACKERSTAFF 97U assumes CPT and is based on measuring the charge asymmetry in a sample of B^0 decays defined by lepton and Q_{hem} tags. If CPT is not invoked, $\text{Re}(\epsilon_B) = -0.006 \pm 0.010 \pm 0.006$ is found. The indirect CPT violation parameter is determined to $\text{Im}(\delta B) = -0.020 \pm 0.016 \pm 0.006$.			
344 BARTELT 93 finds $a_{\ell\ell} = 0.031 \pm 0.096 \pm 0.032$ which corresponds to $ a_{\ell\ell} < 0.18$, which yields the above $ \text{Re}(\epsilon_{B^0})/(1+ \epsilon_{B^0} ^2) $.			

 $\sin(2\beta)$

For a discussion of CP violation, see the note on "CP Violation in B Decay Standard Model Predictions" in the B^0 Particle Listings above. $\sin(2\beta)$ is a measure of the CP-violating amplitude in the $B_d^0 \rightarrow J/\psi(1S)K_S^0$.

VALUE	DOCUMENT ID	TECN	COMMENT
0.9 ± 0.4 OUR AVERAGE			
0.79 ^{+0.41} _{-0.44}	345	AFFOLDER	00c CDF $p\bar{p}$ at 1.8 TeV
3.2 ^{+1.8} _{-2.0} ± 0.5	346	ACKERSTAFF	98z OPAL $e^+e^- \rightarrow Z$
• • • We do not use the following data for averages, fits, limits, etc. • • •			
1.8 ± 1.1 ± 0.3	347	ABE	98u CDF Repl: by AFFOLDER 00c
345 AFFOLDER 00c uses about 400 $B^0 \rightarrow J/\psi(1S)K_S^0$ events. The production flavor of B^0 was determined using three tagging algorithms: a same-side tag, a jet-charge tag, and a soft-lepton tag.			
346 ACKERSTAFF 98z uses 24 candidates for $B_d^0 \rightarrow J/\psi(1S)K_S^0$ decay. A combination of jet-charge and vertex-charge techniques were used to tag the B_d^0 production flavor.			
347 ABE 98u uses 198 ± 17 $B_d^0 \rightarrow J/\psi(1S)K^0$ events. The production flavor of B^0 was determined using the same side tagging technique.			

 $B^0 \rightarrow D^{*-} \ell^+ \nu_\ell$ FORM FACTORS

R_1 (form factor ratio $\sim V/A_1$)			
VALUE	DOCUMENT ID	TECN	COMMENT
1.18 ± 0.30 ± 0.12	DUBOSCQ	96	CLE2 $e^+e^- \rightarrow \Upsilon(4S)$
R_2 (form factor ratio $\sim A_2/A_1$)			
VALUE	DOCUMENT ID	TECN	COMMENT
0.71 ± 0.22 ± 0.07	DUBOSCQ	96	CLE2 $e^+e^- \rightarrow \Upsilon(4S)$
$\rho_{A_1}^2$ (form factor slope)			
VALUE	DOCUMENT ID	TECN	COMMENT
0.91 ± 0.15 ± 0.06	DUBOSCQ	96	CLE2 $e^+e^- \rightarrow \Upsilon(4S)$

Meson Particle Listings

B^\pm/B^0 ADMIXTURE

D, D*, or D _s modes			
Γ ₂₁	$B \rightarrow D^\pm$ anything	(24.1 ± 1.9) %	
Γ ₂₂	$B \rightarrow D^0/\bar{D}^0$ anything	(63.5 ± 2.9) %	S=1.1
Γ ₂₃	$B \rightarrow D^*(2010)^\pm$ anything	(22.7 ± 1.6) %	
Γ ₂₄	$B \rightarrow D^*(2007)^0$ anything	(26.0 ± 2.7) %	
Γ ₂₅	$B \rightarrow D_s^\pm$ anything	[d] (10.0 ± 2.5) %	
Γ ₂₆	$B \rightarrow D^{(*)}\bar{D}^{(*)}K^0 + D^{(*)}\bar{D}^{(*)}K^\pm$	[d,e] (7.1 $\begin{smallmatrix} +2.7 \\ -1.7 \end{smallmatrix}$) %	
Γ ₂₇	$b \rightarrow c\bar{c}s$	(22 ± 4) %	
Γ ₂₈	$B \rightarrow D_s^{(*)}\bar{D}^{(*)}$	[d,e] (4.9 ± 1.3) %	
Γ ₂₉	$B \rightarrow D^*D^*(2010)^\pm$	[d] < 5.9 × 10 ⁻³	CL=90%
Γ ₃₀	$B \rightarrow DD^*(2010)^\pm + D^*D^\pm$	[d] < 5.5 × 10 ⁻³	CL=90%
Γ ₃₁	$B \rightarrow DD^\pm$	[d] < 3.1 × 10 ⁻³	CL=90%
Γ ₃₂	$B \rightarrow D_s^{(*)}\bar{D}^{(*)}X(n\pi^\pm)$	[d,e] (9 $\begin{smallmatrix} +5 \\ -4 \end{smallmatrix}$) %	
Γ ₃₃	$B \rightarrow D^*(2010)\gamma$	< 1.1 × 10 ⁻³	CL=90%
Γ ₃₄	$B \rightarrow D_s^+\pi^-, D_s^{*+}\pi^-, D_s^+\rho^-, D_s^{*+}\rho^-, D_s^+\pi^0, D_s^{*+}\pi^0, D_s^-\eta, D_s^{*-}\eta, D_s^-\rho^0, D_s^{*-}\rho^0, D_s^+\omega, D_s^{*+}\omega$	[d] < 5 × 10 ⁻⁴	CL=90%
Γ ₃₅	$B \rightarrow D_{s1}(2536)^+$ anything	< 9.5 × 10 ⁻³	CL=90%
Charmonium modes			
Γ ₃₆	$B \rightarrow J/\psi(1S)$ anything	(1.15 ± 0.06) %	
Γ ₃₇	$B \rightarrow J/\psi(1S)$ (direct) anything	(8.0 ± 0.8) × 10 ⁻³	
Γ ₃₈	$B \rightarrow \psi(2S)$ anything	(3.5 ± 0.5) × 10 ⁻³	
Γ ₃₉	$B \rightarrow \chi_{c1}(1P)$ anything	(4.2 ± 0.7) × 10 ⁻³	
Γ ₄₀	$B \rightarrow \chi_{c1}(1P)$ (direct) anything	(3.7 ± 0.7) × 10 ⁻³	
Γ ₄₁	$B \rightarrow \chi_{c2}(1P)$ anything	< 3.8 × 10 ⁻³	CL=90%
Γ ₄₂	$B \rightarrow \eta_c(1S)$ anything	< 9 × 10 ⁻³	CL=90%
K or K* modes			
Γ ₄₃	$B \rightarrow K^\pm$ anything	[d] (78.9 ± 2.5) %	
Γ ₄₄	$B \rightarrow K^+$ anything	(66 ± 5) %	
Γ ₄₅	$B \rightarrow K^-$ anything	(13 ± 4) %	
Γ ₄₆	$B \rightarrow K^0/\bar{K}^0$ anything	[d] (64 ± 4) %	
Γ ₄₇	$B \rightarrow K^*(892)^\pm$ anything	(18 ± 6) %	
Γ ₄₈	$B \rightarrow K^*(892)^0/\bar{K}^*(892)^0$ anything	[d] (14.6 ± 2.6) %	
Γ ₄₉	$B \rightarrow K^*(892)\gamma$		
Γ ₅₀	$B \rightarrow K_1(1400)\gamma$	< 4.1 × 10 ⁻⁴	CL=90%
Γ ₅₁	$B \rightarrow K_2^*(1430)\gamma$	< 8.3 × 10 ⁻⁴	CL=90%
Γ ₅₂	$B \rightarrow K_2(1770)\gamma$	< 1.2 × 10 ⁻³	CL=90%
Γ ₅₃	$B \rightarrow K_3^*(1780)\gamma$	< 3.0 × 10 ⁻³	CL=90%
Γ ₅₄	$B \rightarrow K_4^*(2045)\gamma$	< 1.0 × 10 ⁻³	CL=90%
Γ ₅₅	$B \rightarrow \bar{b} \rightarrow \bar{s}\gamma$	(2.3 ± 0.7) × 10 ⁻⁴	
Γ ₅₆	$B \rightarrow \bar{b} \rightarrow \bar{s}\text{gluon}$	< 6.8 %	CL=90%
Γ ₅₇	$B \rightarrow \eta$ anything	< 4.4 × 10 ⁻⁴	CL=90%
Γ ₅₈	$B \rightarrow \eta'$ anything	(6.2 $\begin{smallmatrix} +2.1 \\ -2.6 \end{smallmatrix}$) × 10 ⁻⁴	
Light unflavored meson modes			
Γ ₅₉	$B \rightarrow \pi^\pm$ anything	[d,f] (358 ± 7) %	
Γ ₆₀	$B \rightarrow \eta$ anything	(17.6 ± 1.6) %	
Γ ₆₁	$B \rightarrow \rho^0$ anything	(21 ± 5) %	
Γ ₆₂	$B \rightarrow \omega$ anything	< 81 %	CL=90%
Γ ₆₃	$B \rightarrow \phi$ anything	(3.5 ± 0.7) %	S=1.8
Γ ₆₄	$B \rightarrow \phi K^*(892)$	< 2.2 × 10 ⁻⁵	CL=90%
Baryon modes			
Γ ₆₅	$B \rightarrow \Lambda_c^\pm$ anything	(6.4 ± 1.1) %	
Γ ₆₆	$B \rightarrow \Lambda_c^+$ anything		
Γ ₆₇	$B \rightarrow \bar{\Lambda}_c^-$ anything		
Γ ₆₈	$B \rightarrow \bar{\Lambda}_c^- e^+$ anything	< 3.2 × 10 ⁻³	CL=90%
Γ ₆₉	$B \rightarrow \bar{\Lambda}_c^- p$ anything	(3.6 ± 0.7) %	
Γ ₇₀	$B \rightarrow \bar{\Lambda}_c^- p e^+ \nu_e$	< 1.5 × 10 ⁻³	CL=90%
Γ ₇₁	$B \rightarrow \bar{\Sigma}_c^-$ anything	(4.2 ± 2.4) × 10 ⁻³	
Γ ₇₂	$B \rightarrow \bar{\Sigma}_c^0$ anything	< 9.6 × 10 ⁻³	CL=90%
Γ ₇₃	$B \rightarrow \bar{\Sigma}_c^+$ anything	(4.6 ± 2.4) × 10 ⁻³	
Γ ₇₄	$B \rightarrow \bar{\Sigma}_c^0(N = p \text{ or } n)$	< 1.5 × 10 ⁻³	CL=90%
Γ ₇₅	$B \rightarrow \Xi_c^0$ anything	(1.4 ± 0.5) × 10 ⁻⁴	
	$\times B(\Xi_c^0 \rightarrow \Xi^- \pi^+)$		

Γ ₇₆	$B \rightarrow \Xi_c^+ \text{ anything}$	(4.5 $\begin{smallmatrix} +1.3 \\ -1.2 \end{smallmatrix}$) × 10 ⁻⁴	
	$\times B(\Xi_c^+ \rightarrow \Xi^- \pi^+ \pi^+)$		
Γ ₇₇	$B \rightarrow p/\bar{p}$ anything	[d] (8.0 ± 0.4) %	
Γ ₇₈	$B \rightarrow p/\bar{p}$ (direct) anything	[d] (5.5 ± 0.5) %	
Γ ₇₉	$B \rightarrow \Lambda/\bar{\Lambda}$ anything	[d] (4.0 ± 0.5) %	
Γ ₈₀	$B \rightarrow \Lambda$ anything		
Γ ₈₁	$B \rightarrow \bar{\Lambda}$ anything		
Γ ₈₂	$B \rightarrow \Xi^-/\bar{\Xi}^+$ anything	[d] (2.7 ± 0.6) × 10 ⁻³	
Γ ₈₃	$B \rightarrow$ baryons anything	(6.8 ± 0.6) %	
Γ ₈₄	$B \rightarrow p\bar{p}$ anything	(2.47 ± 0.23) %	
Γ ₈₅	$B \rightarrow \Lambda p/\bar{\Lambda} p$ anything	[d] (2.5 ± 0.4) %	
Γ ₈₆	$B \rightarrow \Lambda\bar{\Lambda}$ anything	< 5 × 10 ⁻³	CL=90%

Lepton Family number (LF) violating modes or $\Delta B = 1$ weak neutral current (BI) modes

Γ ₈₇	$B \rightarrow e^+ e^- s$	BI < 5.7 × 10 ⁻⁵	CL=90%
Γ ₈₈	$B \rightarrow \mu^+ \mu^- s$	BI < 5.8 × 10 ⁻⁵	CL=90%
Γ ₈₉	$B \rightarrow e^\pm \mu^\mp s$	LF < 2.2 × 10 ⁻⁵	CL=90%

[a] These values are model dependent. See 'Note on Semileptonic Decays' in the B^+ Particle Listings.

[b] An ℓ indicates an e or a μ mode, not a sum over these modes.

[c] D^{**} stands for the sum of the $D(1^1P_1)$, $D(1^3P_0)$, $D(1^3P_1)$, $D(1^3P_2)$, $D(2^1S_0)$, and $D(2^1S_1)$ resonances.

[d] The value is for the sum of the charge states or particle/antiparticle states indicated.

[e] $D^{(*)}\bar{D}^{(*)}$ stands for the sum of $D^*\bar{D}^*$, $D^*\bar{D}$, $D\bar{D}^*$, and $D\bar{D}$.

[f] Inclusive branching fractions have a multiplicity definition and can be greater than 100%.

B^\pm/B^0 ADMIXTURE BRANCHING RATIOS

$\Gamma(e^+ \nu_e \text{ anything})/\Gamma_{\text{total}}$ These branching fraction values are model dependent. See the note on "Semileptonic Decays of B Mesons at the beginning of the B^+ Particle Listings.

VALUE	DOCUMENT ID	TECN	COMMENT
0.1045 ± 0.0021 OUR AVERAGE	Includes data from the 2 datablocks that follow this one.		
0.108 ± 0.002 ± 0.0056	¹ HENDERSON 92	CLEO	$e^+ e^- \rightarrow \Upsilon(4S)$

¹ HENDERSON 92 measurement employs e and μ . The systematic error contains 0.004 in quadrature from model dependence. The authors average a variation of the Isgur, Scora, Grinstein, and Wise model with that of the Altarelli-Cabibbo-Corbò-Maiani-Martinelli model for semileptonic decays to correct the acceptance.

$\Gamma(e^+ \nu_e \text{ anything})/\Gamma_{\text{total}}$ These branching fraction values are model dependent. See the note on "Semileptonic Decays of B Mesons at the beginning of the B^+ Particle Listings.

VALUE	DOCUMENT ID	TECN	COMMENT
0.1041 ± 0.0029 OUR AVERAGE	Error includes scale factor of 1.2.		
0.1049 ± 0.0017 ± 0.0043	² BARISH 96b	CLE2	$e^+ e^- \rightarrow \Upsilon(4S)$
0.097 ± 0.005 ± 0.004	³ ALBRECHT 93H	ARG	$e^+ e^- \rightarrow \Upsilon(4S)$
0.100 ± 0.004 ± 0.003	⁴ YANAGISAWA 91	CSB2	$e^+ e^- \rightarrow \Upsilon(4S)$
0.103 ± 0.006 ± 0.002	⁵ ALBRECHT 90H	ARG	$e^+ e^- \rightarrow \Upsilon(4S)$
0.117 ± 0.004 ± 0.010	⁶ WACHS 89	CBAL	Direct e at $\Upsilon(4S)$
0.120 ± 0.007 ± 0.005	CHEN 84	CLEO	Direct e at $\Upsilon(4S)$
• • • We do not use the following data for averages, fits, limits, etc. • • •			
0.132 ± 0.008 ± 0.014	⁷ KLOPFEN...	83b	CUSB Direct e at $\Upsilon(4S)$

² BARISH 96b analysis performed using tagged semileptonic decays of the B . This technique is almost model independent for the lepton branching ratio.

³ ALBRECHT 93H analysis performed using tagged semileptonic decays of the B . This technique is almost model independent for the lepton branching ratio.

⁴ YANAGISAWA 91 also measures an average semileptonic branching ratio at the $\Upsilon(5S)$ of 9.6–10.5% depending on assumptions about the relative production of different B meson species.

⁵ ALBRECHT 90H uses the model of ALTARELLI 82 to correct over all lepton momenta. 0.099 ± 0.006 is obtained using ISGUR 89b.

⁶ Using data above $p(e) = 2.4$ GeV, WACHS 89 determine $\sigma(B \rightarrow e\nu p)/\sigma(B \rightarrow e\nu \text{charm}) < 0.065$ at 90% CL.

⁷ Ratio $\sigma(b \rightarrow e\nu p)/\sigma(b \rightarrow e\nu \text{charm}) < 0.055$ at CL = 90%.

$\Gamma(\mu^+ \nu_\mu \text{ anything})/\Gamma_{\text{total}}$ These branching fraction values are model dependent. See the note on "Semileptonic Decays of B Mesons at the beginning of the B^+ Particle Listings.

VALUE	DOCUMENT ID	TECN	COMMENT
0.103 ± 0.005 OUR AVERAGE			
0.100 ± 0.006 ± 0.002	⁸ ALBRECHT 90H	ARG	$e^+ e^- \rightarrow \Upsilon(4S)$
0.108 ± 0.006 ± 0.01	CHEN 84	CLEO	Direct μ at $\Upsilon(4S)$
0.112 ± 0.009 ± 0.01	LEVMAN 84	CUSB	Direct μ at $\Upsilon(4S)$

⁸ ALBRECHT 90H uses the model of ALTARELLI 82 to correct over all lepton momenta. 0.097 ± 0.006 is obtained using ISGUR 89b.

$\Gamma(\bar{p}e^+\nu_e \text{ anything})/\Gamma_{\text{total}}$					Γ_2/Γ
VALUE	CL%	DOCUMENT ID	TECN	COMMENT	
<0.0016	90	ALBRECHT	90H ARG	$e^+e^- \rightarrow \Upsilon(4S)$	
$\Gamma(D^- \ell^+ \nu_\ell \text{ anything})/\Gamma(\ell^+ \nu_\ell \text{ anything})$					Γ_5/Γ_4
$\ell = e \text{ or } \mu.$					
VALUE	CL%	DOCUMENT ID	TECN	COMMENT	
0.26 ± 0.07 ± 0.04		9 FULTON	91 CLEO	$e^+e^- \rightarrow \Upsilon(4S)$	
9 FULTON 91 uses $B(D^+ \rightarrow K^- \pi^+ \pi^+) = (9.1 \pm 1.3 \pm 0.4)\%$ as measured by MARK III.					
$\Gamma(\bar{D}^0 \ell^+ \nu_\ell \text{ anything})/\Gamma(\ell^+ \nu_\ell \text{ anything})$					Γ_6/Γ_4
$\ell = e \text{ or } \mu.$					
VALUE	CL%	DOCUMENT ID	TECN	COMMENT	
0.67 ± 0.09 ± 0.10		10 FULTON	91 CLEO	$e^+e^- \rightarrow \Upsilon(4S)$	
10 FULTON 91 uses $B(D^0 \rightarrow K^- \pi^+) = (4.2 \pm 0.4 \pm 0.4)\%$ as measured by MARK III.					
$\Gamma(D^{*+} \ell^+ \nu_\ell \text{ anything})/\Gamma_{\text{total}}$					Γ_7/Γ
VALUE (units 10 ⁻²)					
••• We do not use the following data for averages, fits, limits, etc. •••					
0.6 ± 0.3 ± 0.1		11 BARISH	95 CLE2	$e^+e^- \rightarrow \Upsilon(4S)$	
11 BARISH 95 use $B(D^0 \rightarrow K^- \pi^+) = (3.91 \pm 0.08 \pm 0.17)\%$ and $B(D^{*+} \rightarrow D^0 \pi^+) = (68.1 \pm 1.0 \pm 1.3)\%$.					
$\Gamma(D^{*0} \ell^+ \nu_\ell \text{ anything})/\Gamma_{\text{total}}$					Γ_8/Γ
VALUE (units 10 ⁻²)					
••• We do not use the following data for averages, fits, limits, etc. •••					
0.6 ± 0.6 ± 0.1		12 BARISH	95 CLE2	$e^+e^- \rightarrow \Upsilon(4S)$	
12 BARISH 95 use $B(D^0 \rightarrow K^- \pi^+) = (3.91 \pm 0.08 \pm 0.17)\%$, $B(D^{*+} \rightarrow D^0 \pi^+) = (68.1 \pm 1.0 \pm 1.3)\%$, $B(D^{*0} \rightarrow D^0 \pi^0) = (63.6 \pm 2.3 \pm 3.3)\%$.					
$\Gamma(\bar{D}^{*+} \ell^+ \nu_\ell)/\Gamma_{\text{total}}$					Γ_9/Γ
D^{*+} stands for the sum of the $D(1^1 P_1)$, $D(1^3 P_0)$, $D(1^3 P_1)$, $D(1^3 P_2)$, $D(2^1 S_0)$, and $D(2^1 S_1)$ resonances. $\ell = e \text{ or } \mu$, not sum over e and μ modes.					
VALUE	CL%	EVTS	DOCUMENT ID	TECN	COMMENT
0.027 ± 0.005 ± 0.005		63	13 ALBRECHT	93 ARG	$e^+e^- \rightarrow \Upsilon(4S)$
••• We do not use the following data for averages, fits, limits, etc. •••					
<0.028	95		14 BARISH	95 CLE2	$e^+e^- \rightarrow \Upsilon(4S)$
13 ALBRECHT 93 assumes the GISW model to correct for unseen modes. Using the BHKT model, the result becomes $0.023 \pm 0.006 \pm 0.004$. Assumes $B(D^{*+} \rightarrow D^0 \pi^+) = 68.1\%$, $B(D^0 \rightarrow K^- \pi^+) = 3.65\%$, $B(D^0 \rightarrow K^- \pi^+ \pi^+) = 7.5\%$. We have taken their average e and μ value.					
14 BARISH 95 use $B(D^0 \rightarrow K^- \pi^+) = (3.91 \pm 0.08 \pm 0.17)\%$, assume all nonresonant channels are zero, and use GISW model for relative abundances of D^{*+} states.					
$\Gamma(\bar{D}_1(2420) \ell^+ \nu_\ell \text{ anything})/\Gamma_{\text{total}}$					Γ_{10}/Γ
VALUE	CL%	DOCUMENT ID	TECN	COMMENT	
0.0074 ± 0.0016		15 BUSKULIC	97B ALEP	$e^+e^- \rightarrow Z$	
••• We do not use the following data for averages, fits, limits, etc. •••					
seen					
16 BUSKULIC 95B ALEP Repl. by BUSKULIC 97B					
15 BUSKULIC 97B assumes $B(\bar{D}_1(2420) \rightarrow D^* \pi) = 1$, $B(\bar{D}_1(2420) \rightarrow D^* \pi^\pm) = 2/3$, and $B(b \rightarrow B) = 0.378 \pm 0.022$.					
16 BUSKULIC 95B reports $f_B \times B(B \rightarrow \bar{D}_1(2420)^0 \ell^+ \nu_\ell \text{ anything}) \times B(\bar{D}_1(2420)^0 \rightarrow \bar{D}^*(2010)^- \pi^+) = (2.04 \pm 0.58 \pm 0.34)10^{-3}$, where f_B is the production fraction for a single B charge state.					
$[\Gamma(D \pi \ell^+ \nu_\ell \text{ anything}) + \Gamma(D^* \pi \ell^+ \nu_\ell \text{ anything})]/\Gamma_{\text{total}}$					Γ_{11}/Γ
VALUE	CL%	DOCUMENT ID	TECN	COMMENT	
0.0226 ± 0.0029 ± 0.0033		17 BUSKULIC	97B ALEP	$e^+e^- \rightarrow Z$	
17 BUSKULIC 97B assumes $B(b \rightarrow B) = 0.378 \pm 0.022$ and uses isospin invariance by assuming that all observed $D^0 \pi^+$, $D^0 \pi^0$, $D^+ \pi^-$, and $D^{*+} \pi^-$ are from D^{*+} states. A correction has been applied to account for the production of B_S^0 and A_B^0 .					
$\Gamma(\bar{D}_2^*(2460) \ell^+ \nu_\ell \text{ anything})/\Gamma_{\text{total}}$					Γ_{12}/Γ
VALUE	CL%	DOCUMENT ID	TECN	COMMENT	
<0.0065	95	18 BUSKULIC	97B ALEP	$e^+e^- \rightarrow Z$	
••• We do not use the following data for averages, fits, limits, etc. •••					
not seen					
19 BUSKULIC 95B ALEP $e^+e^- \rightarrow Z$					
18 A revised number based on BUSKULIC 97B which assumes $B(\bar{D}_2^*(2460) \rightarrow D^* \pi^\pm) = 0.20$ and $B(b \rightarrow B) = 0.378 \pm 0.022$.					
19 BUSKULIC 95B reports $f_B \times B(B \rightarrow \bar{D}_2^*(2460)^0 \ell^+ \nu_\ell \text{ anything}) \times B(\bar{D}_2^*(2460)^0 \rightarrow \bar{D}^*(2010)^- \pi^+) \leq 0.81 \times 10^{-3}$ at CL=95%, where f_B is the production fraction for a single B charge state.					
$\Gamma(D^{*+} \ell^+ \nu_\ell \text{ anything})/\Gamma_{\text{total}}$					Γ_{13}/Γ
Includes resonant and nonresonant contributions.					
VALUE (units 10 ⁻³)	CL%	DOCUMENT ID	TECN	COMMENT	
10.0 ± 2.7 ± 2.1		20 BUSKULIC	95B ALEP	$e^+e^- \rightarrow Z$	
20 BUSKULIC 95B reports $f_B \times B(B \rightarrow \bar{D}^*(2010)^- \pi^+ \ell^+ \nu_\ell \text{ anything}) = (3.7 \pm 1.0 \pm 0.7)10^{-3}$. Above value assumes $f_B = 0.37 \pm 0.03$.					
$\Gamma(D_s^- \ell^+ \nu_\ell \text{ anything})/\Gamma_{\text{total}}$					Γ_{14}/Γ
VALUE	CL%	DOCUMENT ID	TECN	COMMENT	
<0.009	90	21 ALBRECHT	93E ARG	$e^+e^- \rightarrow \Upsilon(4S)$	
21 ALBRECHT 93E reports < 0.012 for $B(D_s^+ \rightarrow \phi \pi^+) = 0.027$. We rescale to our best value $B(D_s^+ \rightarrow \phi \pi^+) = 0.036$.					
$\Gamma(D_s^- \ell^+ \nu_\ell K^+ \text{ anything})/\Gamma_{\text{total}}$					Γ_{15}/Γ
VALUE	CL%	DOCUMENT ID	TECN	COMMENT	
<0.006	90	22 ALBRECHT	93E ARG	$e^+e^- \rightarrow \Upsilon(4S)$	
22 ALBRECHT 93E reports < 0.008 for $B(D_s^+ \rightarrow \phi \pi^+) = 0.027$. We rescale to our best value $B(D_s^+ \rightarrow \phi \pi^+) = 0.036$.					
$\Gamma(D_s^- \ell^+ \nu_\ell K^0 \text{ anything})/\Gamma_{\text{total}}$					Γ_{16}/Γ
VALUE	CL%	DOCUMENT ID	TECN	COMMENT	
<0.009	90	23 ALBRECHT	93E ARG	$e^+e^- \rightarrow \Upsilon(4S)$	
23 ALBRECHT 93E reports < 0.012 for $B(D_s^+ \rightarrow \phi \pi^+) = 0.027$. We rescale to our best value $B(D_s^+ \rightarrow \phi \pi^+) = 0.036$.					
$\Gamma(\ell^+ \nu_\ell \text{ noncharged})/\Gamma(\ell^+ \nu_\ell \text{ anything})$					Γ_{17}/Γ_4
ℓ denotes e or μ , not the sum. These experiments measure this ratio in very limited momentum intervals.					
VALUE	CL%	EVTS	DOCUMENT ID	TECN	COMMENT
<0.04	90		24 ALBRECHT	94C ARG	$e^+e^- \rightarrow \Upsilon(4S)$
<0.04	90		25 BARTELT	93B CLE2	$e^+e^- \rightarrow \Upsilon(4S)$
<0.055	90		26 ALBRECHT	91C ARG	$e^+e^- \rightarrow \Upsilon(4S)$
			27 FULTON	90 CLEO	$e^+e^- \rightarrow \Upsilon(4S)$
••• We do not use the following data for averages, fits, limits, etc. •••					
<0.04	90		28 ALBRECHT	90 ARG	$e^+e^- \rightarrow \Upsilon(4S)$
<0.04	90		29 BEHRENDIS	87 CLEO	$e^+e^- \rightarrow \Upsilon(4S)$
<0.055	90		CHEN	84 CLEO	Direct e at $\Upsilon(4S)$
			KLOPFEN...	83B CUSB	Direct e at $\Upsilon(4S)$
24 ALBRECHT 94C find $\Gamma(b \rightarrow c)/\Gamma(b \rightarrow \text{all}) = 0.99 \pm 0.02 \pm 0.04$.					
25 BARTELT 93B (CLEO II) measures an excess of $107 \pm 15 \pm 11$ leptons in the lepton momentum interval 2.3–2.6 GeV/c which is attributed to $b \rightarrow u \ell \nu_\ell$. This corresponds to a model-dependent partial branching ratio ΔB_{ub} between $(1.15 \pm 0.16 \pm 0.15) \times 10^{-4}$, as evaluated using the KS model (KOERNER 88), and $(1.54 \pm 0.22 \pm 0.20) \times 10^{-4}$ using the ACCMM model (ARTUSO 93). The corresponding values of $ V_{ub} / V_{cb} $ are 0.056 ± 0.006 and 0.076 ± 0.008 , respectively.					
26 ALBRECHT 91C result supersedes ALBRECHT 90. Two events are fully reconstructed providing evidence for the $b \rightarrow u$ transition. Using the model of ALTARELLI 82, they obtain $ V_{ub} / V_{cb} = 0.11 \pm 0.012$ from 77 leptons in the 2.3–2.6 GeV momentum range.					
27 FULTON 90 observe 76 ± 20 excess e and μ (lepton) events in the momentum interval $p = 2.4$ – 2.6 GeV signaling the presence of the $b \rightarrow u$ transition. The average branching ratio, $(1.8 \pm 0.4 \pm 0.3) \times 10^{-4}$, corresponds to a model-dependent measurement of approximately $ V_{ub} / V_{cb} = 0.1$ using $B(b \rightarrow c \ell \nu) = 10.2 \pm 0.2 \pm 0.7\%$.					
28 ALBRECHT 90 observes 41 ± 10 excess e and μ (lepton) events in the momentum interval $p = 2.3$ – 2.6 GeV signaling the presence of the $b \rightarrow u$ transition. The events correspond to a model-dependent measurement of $ V_{ub} / V_{cb} = 0.10 \pm 0.01$.					
29 The quoted possible limits range from 0.018 to 0.04 for the ratio, depending on which model or momentum range is chosen. We select the most conservative limit they have calculated. This corresponds to a limit on $ V_{ub} / V_{cb} < 0.20$. While the endpoint technique employed is more robust than their previous results in CHEN 84, these results do not provide a numerical improvement in the limit.					
$\Gamma(K^+ \ell^+ \nu_\ell \text{ anything})/\Gamma(\ell^+ \nu_\ell \text{ anything})$					Γ_{18}/Γ_4
ℓ denotes e or μ , not the sum.					
VALUE	CL%	DOCUMENT ID	TECN	COMMENT	
0.58 ± 0.05 OUR AVERAGE					
0.594 ± 0.021 ± 0.056			ALBRECHT	94C ARG	$e^+e^- \rightarrow \Upsilon(4S)$
0.54 ± 0.07 ± 0.06		30 ALAM	87B CLEO	$e^+e^- \rightarrow \Upsilon(4S)$	
30 ALAM 87B measurement relies on lepton-kaon correlations.					
$\Gamma(K^- \ell^+ \nu_\ell \text{ anything})/\Gamma(\ell^+ \nu_\ell \text{ anything})$					Γ_{19}/Γ_4
ℓ denotes e or μ , not the sum.					
VALUE	CL%	DOCUMENT ID	TECN	COMMENT	
0.092 ± 0.035 OUR AVERAGE					
0.086 ± 0.011 ± 0.044			ALBRECHT	94C ARG	$e^+e^- \rightarrow \Upsilon(4S)$
0.10 ± 0.05 ± 0.02		31 ALAM	87B CLEO	$e^+e^- \rightarrow \Upsilon(4S)$	
31 ALAM 87B measurement relies on lepton-kaon correlations.					
$\Gamma(K^0/\bar{K}^0 \ell^+ \nu_\ell \text{ anything})/\Gamma(\ell^+ \nu_\ell \text{ anything})$					Γ_{20}/Γ_4
ℓ denotes e or μ , not the sum. Sum over K^0 and \bar{K}^0 states.					
VALUE	CL%	DOCUMENT ID	TECN	COMMENT	
0.42 ± 0.05 OUR AVERAGE					
0.452 ± 0.038 ± 0.056			32 ALBRECHT	94C ARG	$e^+e^- \rightarrow \Upsilon(4S)$
0.39 ± 0.06 ± 0.04		33 ALAM	87B CLEO	$e^+e^- \rightarrow \Upsilon(4S)$	
32 ALBRECHT 94C assume a K^0/\bar{K}^0 multiplicity twice that of K_S^0 .					
33 ALAM 87B measurement relies on lepton-kaon correlations.					

Meson Particle Listings

 B^\pm/B^0 ADMIXTURE $\langle n_c \rangle$

VALUE	DOCUMENT ID	TECN	COMMENT
1.10 ± 0.05	34 GIBBONS	97B CLE2	$e^+e^- \rightarrow T(45)$
• • • We do not use the following data for averages, fits, limits, etc. • • •			
0.98 ± 0.16 ± 0.12	35 ALAM	87B CLEO	$e^+e^- \rightarrow T(45)$
34 GIBBONS 97B from charm counting using $B(D_s^+ \rightarrow \phi\pi) = 0.036 \pm 0.009$ and $B(A_c^+ \rightarrow \rho K^- \pi^+) = 0.044 \pm 0.006$.			
35 From the difference between K^- and K^+ widths. ALAM 87B measurement relies on lepton-kaon correlations. It does not consider the possibility of $B\bar{B}$ mixing. We have thus removed it from the average.			

$\Gamma(D^\pm \text{ anything})/\Gamma_{\text{total}}$			Γ_{21}/Γ	
VALUE	EVTs	DOCUMENT ID	TECN	COMMENT
0.241 ± 0.019 OUR AVERAGE				
0.240 ± 0.013 ^{+0.015} _{-0.016}		36 GIBBONS	97B CLE2	$e^+e^- \rightarrow T(45)$
0.25 ± 0.04 ± 0.02		37 BORTOLETT092	CLEO	$e^+e^- \rightarrow T(45)$
0.23 ± 0.05 ^{+0.01} _{-0.02}		38 ALBRECHT	91H ARG	$e^+e^- \rightarrow T(45)$
• • • We do not use the following data for averages, fits, limits, etc. • • •				
0.21 ± 0.05 ± 0.01	20k	39 BORTOLETT087	CLEO	Sup. by BORTOLETT092

36 GIBBONS 97B reports $[B(B \rightarrow D^\pm \text{ anything}) \times B(D^+ \rightarrow K^- \pi^+ \pi^+)] = 0.0216 \pm 0.0008 \pm 0.00082$. We divide by our best value $B(D^+ \rightarrow K^- \pi^+ \pi^+) = (9.0 \pm 0.6) \times 10^{-2}$. Our first error is their experiment's error and our second error is the systematic error from using our best value.				
37 BORTOLETT092 reports $[B(B \rightarrow D^\pm \text{ anything}) \times B(D^+ \rightarrow K^- \pi^+ \pi^+)] = 0.0226 \pm 0.0030 \pm 0.0018$. We divide by our best value $B(D^+ \rightarrow K^- \pi^+ \pi^+) = (9.0 \pm 0.6) \times 10^{-2}$. Our first error is their experiment's error and our second error is the systematic error from using our best value.				
38 ALBRECHT 91H reports $[B(B \rightarrow D^\pm \text{ anything}) \times B(D^+ \rightarrow K^- \pi^+ \pi^+)] = 0.0209 \pm 0.0027 \pm 0.0040$. We divide by our best value $B(D^+ \rightarrow K^- \pi^+ \pi^+) = (9.0 \pm 0.6) \times 10^{-2}$. Our first error is their experiment's error and our second error is the systematic error from using our best value.				
39 BORTOLETT087 reports $[B(B \rightarrow D^\pm \text{ anything}) \times B(D^+ \rightarrow K^- \pi^+ \pi^+)] = 0.019 \pm 0.004 \pm 0.002$. We divide by our best value $B(D^+ \rightarrow K^- \pi^+ \pi^+) = (9.0 \pm 0.6) \times 10^{-2}$. Our first error is their experiment's error and our second error is the systematic error from using our best value.				

$\Gamma(D^0/\bar{D}^0 \text{ anything})/\Gamma_{\text{total}}$			Γ_{22}/Γ	
VALUE	EVTs	DOCUMENT ID	TECN	COMMENT
0.635 ± 0.029 OUR AVERAGE				
0.655 ± 0.025 ± 0.015		40 GIBBONS	97B CLE2	$e^+e^- \rightarrow T(45)$
0.61 ± 0.05 ± 0.01		41 BORTOLETT092	CLEO	$e^+e^- \rightarrow T(45)$
0.51 ± 0.08 ± 0.01		42 ALBRECHT	91H ARG	$e^+e^- \rightarrow T(45)$
• • • We do not use the following data for averages, fits, limits, etc. • • •				
0.55 ± 0.07 ± 0.01	21k	43 BORTOLETT087	CLEO	$e^+e^- \rightarrow T(45)$
0.63 ± 0.19 ± 0.01		44 GREEN	83 CLEO	Repl. by BORTOLETT087

40 GIBBONS 97B reports $[B(B \rightarrow D^0/\bar{D}^0 \text{ anything}) \times B(D^0 \rightarrow K^- \pi^+)] = 0.0251 \pm 0.0006 \pm 0.00075$. We divide by our best value $B(D^0 \rightarrow K^- \pi^+) = (3.83 \pm 0.09) \times 10^{-2}$. Our first error is their experiment's error and our second error is the systematic error from using our best value.				
41 BORTOLETT092 reports $[B(B \rightarrow D^0/\bar{D}^0 \text{ anything}) \times B(D^0 \rightarrow K^- \pi^+)] = 0.0233 \pm 0.0012 \pm 0.0014$. We divide by our best value $B(D^0 \rightarrow K^- \pi^+) = (3.83 \pm 0.09) \times 10^{-2}$. Our first error is their experiment's error and our second error is the systematic error from using our best value.				
42 ALBRECHT 91H reports $[B(B \rightarrow D^0/\bar{D}^0 \text{ anything}) \times B(D^0 \rightarrow K^- \pi^+)] = 0.0194 \pm 0.0015 \pm 0.0025$. We divide by our best value $B(D^0 \rightarrow K^- \pi^+) = (3.83 \pm 0.09) \times 10^{-2}$. Our first error is their experiment's error and our second error is the systematic error from using our best value.				
43 BORTOLETT087 reports $[B(B \rightarrow D^0/\bar{D}^0 \text{ anything}) \times B(D^0 \rightarrow K^- \pi^+)] = 0.0210 \pm 0.0015 \pm 0.0021$. We divide by our best value $B(D^0 \rightarrow K^- \pi^+) = (3.83 \pm 0.09) \times 10^{-2}$. Our first error is their experiment's error and our second error is the systematic error from using our best value.				
44 GREEN 83 reports $[B(B \rightarrow D^0/\bar{D}^0 \text{ anything}) \times B(D^0 \rightarrow K^- \pi^+)] = 0.024 \pm 0.006 \pm 0.004$. We divide by our best value $B(D^0 \rightarrow K^- \pi^+) = (3.83 \pm 0.09) \times 10^{-2}$. Our first error is their experiment's error and our second error is the systematic error from using our best value.				

$\Gamma(D^*(2010)^\pm \text{ anything})/\Gamma_{\text{total}}$			Γ_{23}/Γ	
VALUE	EVTs	DOCUMENT ID	TECN	COMMENT
0.227 ± 0.016 OUR AVERAGE				
0.247 ± 0.019 ± 0.01		45 GIBBONS	97B CLE2	$e^+e^- \rightarrow T(45)$
0.205 ± 0.019 ± 0.007		46 ALBRECHT	96D ARG	$e^+e^- \rightarrow T(45)$
0.230 ± 0.028 ± 0.009		47 BORTOLETT092	CLEO	$e^+e^- \rightarrow T(45)$
• • • We do not use the following data for averages, fits, limits, etc. • • •				
0.283 ± 0.053 ± 0.002		48 ALBRECHT	91H ARG	Sup. by ALBRECHT 96D
0.22 ± 0.04 ^{+0.07} _{-0.04}	5200	49 BORTOLETT087	CLEO	$e^+e^- \rightarrow T(45)$
0.27 ± 0.06 ^{+0.08} _{-0.06}	510	50 CSORNA	85 CLEO	Repl. by BORTOLETT087

45 GIBBONS 97B reports $B(B \rightarrow D^*(2010)^\pm \text{ anything}) = 0.239 \pm 0.015 \pm 0.014 \pm 0.009$ using CLEO measured D and D^* branching fractions. We rescale to our PDG 96 values of D and D^* branching ratios. Our first error is their experiment's error and our second error is the systematic error from using our best value.				
--	--	--	--	--

46 ALBRECHT 96D reports $B(B \rightarrow D^*(2010)^\pm \text{ anything}) = 0.196 \pm 0.019$ using CLEO measured $B(D^*(2010)^\pm \rightarrow D^0 \pi^\pm) = 0.681 \pm 0.01 \pm 0.013$, $B(D^0 \rightarrow K^- \pi^+) = 0.0401 \pm 0.0014$, $B(D^0 \rightarrow K^- \pi^+ \pi^0) = 0.081 \pm 0.005$. We rescale to our PDG 96 values of D and D^* branching ratios. Our first error is their experiment's error and our second error is the systematic error from using our best value.				
47 BORTOLETT092 reports $B(B \rightarrow D^*(2010)^\pm \text{ anything}) = 0.25 \pm 0.03 \pm 0.04$ using MARK II $B(D^*(2010)^\pm \rightarrow D^0 \pi^\pm) = 0.57 \pm 0.06$ and $B(D^0 \rightarrow K^- \pi^+) = 0.042 \pm 0.008$. We rescale to our PDG 96 values of D and D^* branching ratios. Our first error is their experiment's error and our second error is the systematic error from using our best value.				
48 ALBRECHT 91H reports $0.348 \pm 0.060 \pm 0.035$ for $B(D^*(2010)^\pm \rightarrow D^0 \pi^\pm) = 0.55 \pm 0.04$. We rescale to our best value $B(D^*(2010)^\pm \rightarrow D^0 \pi^\pm) = (67.7 \pm 0.5) \times 10^{-2}$. Our first error is their experiment's error and our second error is the systematic error from using our best value. Uses the PDG 90 $B(D^0 \rightarrow K^- \pi^+) = 0.0371 \pm 0.0025$.				
49 BORTOLETT087 uses old MARK III (BALTRUSAITIS 86E) branching ratios $B(D^0 \rightarrow K^- \pi^+) = 0.056 \pm 0.004 \pm 0.003$ and also assumes $B(D^*(2010)^\pm \rightarrow D^0 \pi^\pm) = 0.60^{+0.08}_{-0.15}$. The product branching ratio for $B(B \rightarrow D^*(2010)^\pm) B(D^*(2010)^\pm \rightarrow D^0 \pi^\pm)$ is $0.13 \pm 0.02 \pm 0.012$. Superseded by BORTOLETT092.				
50 $V-A$ momentum spectrum used to extrapolate below $p = 1$ GeV. We correct the value assuming $B(D^0 \rightarrow K^- \pi^+) = 0.042 \pm 0.006$ and $B(D^{*+} \rightarrow D^0 \pi^+) = 0.6^{+0.08}_{-0.15}$. The product branching fraction is $B(B \rightarrow D^{*+} X) B(D^{*+} \rightarrow \pi^+ D^0) B(D^0 \rightarrow K^- \pi^+) = (68 \pm 15 \pm 9) \times 10^{-4}$.				

$\Gamma(D^*(2007)^0 \text{ anything})/\Gamma_{\text{total}}$			Γ_{24}/Γ
VALUE	DOCUMENT ID	TECN	COMMENT
0.260 ± 0.023 ± 0.015	51 GIBBONS	97B CLE2	$e^+e^- \rightarrow T(45)$

51 GIBBONS 97B reports $B(B \rightarrow D^*(2007)^0 \text{ anything}) = 0.247 \pm 0.012 \pm 0.018 \pm 0.018$ using CLEO measured D and D^* branching fractions. We rescale to our PDG 96 values of D and D^* branching ratios. Our first error is their experiment's error and our second error is the systematic error from using our best value.				
--	--	--	--	--

$\Gamma(D_s^\pm \text{ anything})/\Gamma_{\text{total}}$			Γ_{25}/Γ	
VALUE	EVTs	DOCUMENT ID	TECN	COMMENT
0.100 ± 0.025 OUR AVERAGE				
0.117 ± 0.009 ^{+0.028} _{-0.029}		52 GIBAUT	96 CLE2	$e^+e^- \rightarrow T(45)$
0.081 ± 0.014 ^{+0.019} _{-0.020}		53 ALBRECHT	92G ARG	$e^+e^- \rightarrow T(45)$
0.085 ± 0.013 ^{+0.020} _{-0.021}	257	54 BORTOLETT090	CLEO	$e^+e^- \rightarrow T(45)$
0.105 ± 0.028 ^{+0.025} _{-0.026}		55 HAAS	86 CLEO	$e^+e^- \rightarrow T(45)$
• • • We do not use the following data for averages, fits, limits, etc. • • •				
0.116 ± 0.030 ± 0.028		56 ALBRECHT	87H ARG	$e^+e^- \rightarrow T(45)$

52 GIBAUT 96 reports $0.1211 \pm 0.0039 \pm 0.0088$ for $B(D_s^\pm \rightarrow \phi\pi^\pm) = 0.035$. We rescale to our best value $B(D_s^\pm \rightarrow \phi\pi^\pm) = (3.6 \pm 0.9) \times 10^{-2}$. Our first error is their experiment's error and our second error is the systematic error from using our best value.				
53 ALBRECHT 92G reports $[B(B \rightarrow D_s^\pm \text{ anything}) \times B(D_s^\pm \rightarrow \phi\pi^\pm)] = 0.00292 \pm 0.00039 \pm 0.00031$. We divide by our best value $B(D_s^\pm \rightarrow \phi\pi^\pm) = (3.6 \pm 0.9) \times 10^{-2}$. Our first error is their experiment's error and our second error is the systematic error from using our best value.				
54 BORTOLETT090 reports $[B(B \rightarrow D_s^\pm \text{ anything}) \times B(D_s^\pm \rightarrow \phi\pi^\pm)] = 0.00306 \pm 0.00047$. We divide by our best value $B(D_s^\pm \rightarrow \phi\pi^\pm) = (3.6 \pm 0.9) \times 10^{-2}$. Our first error is their experiment's error and our second error is the systematic error from using our best value.				
55 HAAS 86 reports $[B(B \rightarrow D_s^\pm \text{ anything}) \times B(D_s^\pm \rightarrow \phi\pi^\pm)] = 0.0038 \pm 0.0010$. We divide by our best value $B(D_s^\pm \rightarrow \phi\pi^\pm) = (3.6 \pm 0.9) \times 10^{-2}$. Our first error is their experiment's error and our second error is the systematic error from using our best value. $64 \pm 22\%$ decays are 2-body.				
56 ALBRECHT 87H reports $[B(B \rightarrow D_s^\pm \text{ anything}) \times B(D_s^\pm \rightarrow \phi\pi^\pm)] = 0.0042 \pm 0.0009 \pm 0.0006$. We divide by our best value $B(D_s^\pm \rightarrow \phi\pi^\pm) = (3.6 \pm 0.9) \times 10^{-2}$. Our first error is their experiment's error and our second error is the systematic error from using our best value. $46 \pm 16\%$ of $B \rightarrow D_s X$ decays are 2-body. Superseded by ALBRECHT 92G.				

$[\Gamma(D^{(*)} \bar{D}^{(*)} K^0) + \Gamma(D^{(*)} \bar{D}^{(*)} K^\pm)]/\Gamma_{\text{total}}$			Γ_{26}/Γ
VALUE	DOCUMENT ID	TECN	COMMENT
0.071 ± 0.025 ± 0.010 -0.015 - 0.009	57 BARATE	98Q ALEP	$e^+e^- \rightarrow Z$

57 The systematic error includes the uncertainties due to the charm branching ratios.				
---	--	--	--	--

$\Gamma(c\bar{c}s)/\Gamma_{\text{total}}$			Γ_{27}/Γ
VALUE	DOCUMENT ID	TECN	COMMENT
0.219 ± 0.037	58 COAN	98 CLE2	$e^+e^- \rightarrow T(45)$

58 COAN 98 uses $D-l$ correlation.				
------------------------------------	--	--	--	--

$\Gamma(D_s^{(*)} \bar{D}^{(*)})/\Gamma(D_s^\pm \text{ anything})$			Γ_{28}/Γ_{25}
VALUE	DOCUMENT ID	TECN	COMMENT
0.49 ± 0.04 OUR AVERAGE			
0.56 ± 0.21 ^{+0.09} _{-0.15 - 0.08}	59 BARATE	98Q ALEP	$e^+e^- \rightarrow Z$
0.457 ± 0.019 ± 0.037	GIBAUT	96 CLE2	$e^+e^- \rightarrow T(45)$
0.58 ± 0.07 ± 0.09	ALBRECHT	92G ARG	$e^+e^- \rightarrow T(45)$
0.56 ± 0.10	BORTOLETT090	CLEO	$e^+e^- \rightarrow T(45)$

Sum over modes.				
-----------------	--	--	--	--

Meson Particle Listings

B^\pm/B^0 ADMIXTURE

⁵⁹ BARATE 98Q measures $B(B \rightarrow D_s^{(*)} \bar{D}^{(*)}) = 0.056^{+0.021+0.009+0.019}_{-0.015-0.008-0.011}$, where the third error results from the uncertainty on the different D branching ratios and is dominated by the uncertainty on $B(D_s^+ \rightarrow \phi\pi^+)$. We divide $B(B \rightarrow D_s^{(*)} \bar{D}^{(*)})$ by our best value of $B(B \rightarrow D_s \text{ anything}) = 0.1 \pm 0.025$.

$\Gamma(D^* D^*(2010)^\pm)/\Gamma_{\text{total}}$				Γ_{29}/Γ
VALUE	CL%	DOCUMENT ID	TECN	COMMENT
$<5.9 \times 10^{-3}$	90	BARATE	98Q ALEP	$e^+ e^- \rightarrow Z$

$[\Gamma(D^* D^*(2010)^\pm) + \Gamma(D^* D^\pm)]/\Gamma_{\text{total}}$				Γ_{30}/Γ
VALUE	CL%	DOCUMENT ID	TECN	COMMENT
$<5.5 \times 10^{-3}$	90	BARATE	98Q ALEP	$e^+ e^- \rightarrow Z$

$\Gamma(D D^\pm)/\Gamma_{\text{total}}$				Γ_{31}/Γ
VALUE	CL%	DOCUMENT ID	TECN	COMMENT
$<3.1 \times 10^{-3}$	90	BARATE	98Q ALEP	$e^+ e^- \rightarrow Z$

$\Gamma(D_s^{(*)} \bar{D}^{(*)} X (n\pi^\pm))/\Gamma_{\text{total}}$				Γ_{32}/Γ
VALUE	CL%	DOCUMENT ID	TECN	COMMENT
$0.094^{+0.040+0.034}_{-0.031-0.024}$	60	BARATE	98Q ALEP	$e^+ e^- \rightarrow Z$

⁶⁰ The systematic error includes the uncertainties due to the charm branching ratios.

$\Gamma(D^*(2010)\gamma)/\Gamma_{\text{total}}$				Γ_{33}/Γ
VALUE	CL%	DOCUMENT ID	TECN	COMMENT
$<1.1 \times 10^{-3}$	90	61 LESIAK	92 CBAL	$e^+ e^- \rightarrow \Upsilon(4S)$

⁶¹ LESIAK 92 set a limit on the inclusive process $B(b \rightarrow s\gamma) < 2.8 \times 10^{-3}$ at 90% CL for the range of masses of 892–2045 MeV, independent of assumptions about s -quark hadronization.

$\Gamma(D_s^+ \pi^-, D_s^{*+} \pi^-, D_s^+ \rho^-, D_s^{*+} \rho^-, D_s^+ \pi^0, D_s^{*+} \pi^0, D_s^+ \eta, D_s^{*+} \eta, D_s^+ \rho^0, D_s^{*+} \rho^0, D_s^+ \omega, D_s^{*+} \omega)/\Gamma_{\text{total}}$				Γ_{34}/Γ
Sum over modes.				
VALUE	CL%	DOCUMENT ID	TECN	COMMENT
<0.0005	90	62 ALEXANDER	93B CLE2	$e^+ e^- \rightarrow \Upsilon(4S)$

⁶² ALEXANDER 93B reports $< 4.8 \times 10^{-4}$ for $B(D_s^+ \rightarrow \phi\pi^+) = 0.037$. We rescale to our best value $B(D_s^+ \rightarrow \phi\pi^+) = 0.036$. This branching ratio limit provides a model-dependent upper limit $|V_{ub}|/|V_{cb}| < 0.16$ at CL=90%.

$\Gamma(D_{s1}(2536)^+ \text{ anything})/\Gamma_{\text{total}}$				Γ_{35}/Γ
$D_{s1}(2536)^+$ is the narrow P -wave D_s^+ meson with $J^P = 1^+$.				
VALUE	CL%	DOCUMENT ID	TECN	COMMENT
<0.0095	90	63 BISHAI	98 CLE2	$e^+ e^- \rightarrow \Upsilon(4S)$

⁶³ Assuming factorization, the decay constant $f_{D_{s1}^+}$ is at least a factor of 2.5 times smaller than $f_{D_s^+}$.

$\Gamma(J/\psi(1S) \text{ anything})/\Gamma_{\text{total}}$				Γ_{36}/Γ
VALUE (units 10^{-2})	EVTS	DOCUMENT ID	TECN	COMMENT
1.15 ± 0.06	OUR AVERAGE			
$1.13 \pm 0.06 \pm 0.02$	1489	64 BALEST	95B CLE2	$e^+ e^- \rightarrow \Upsilon(4S)$
$1.30 \pm 0.45 \pm 0.02$	27	65 MASCHMANN	90 CBAL	$e^+ e^- \rightarrow \Upsilon(4S)$
$1.24 \pm 0.27 \pm 0.02$	120	66 ALBRECHT	87D ARG	$e^+ e^- \rightarrow \Upsilon(4S)$
$1.37 \pm 0.25 \pm 0.02$	52	67 ALAM	86 CLEO	$e^+ e^- \rightarrow \Upsilon(4S)$

• • • We do not use the following data for averages, fits, limits, etc. • • •

$1.4^{+0.6}_{-0.5}$	7	68 ALBRECHT	85H ARG	$e^+ e^- \rightarrow \Upsilon(4S)$
$1.1 \pm 0.21 \pm 0.23$	46	69 HAAS	85 CLEO	Repl. by ALAM 86

⁶⁴ BALEST 95B reports $1.12 \pm 0.04 \pm 0.06$ for $B(J/\psi(1S) \rightarrow e^+ e^-) = 0.0599 \pm 0.0025$. We rescale to our best value $B(J/\psi(1S) \rightarrow e^+ e^-) = (5.93 \pm 0.10) \times 10^{-2}$. Our first error is their experiment's error and our second error is the systematic error from using our best value.. They measure $J/\psi(1S) \rightarrow e^+ e^-$ and $\mu^+ \mu^-$ and use PDG 1994 values for the branching fractions. The rescaling is the same for either mode so we use $e^+ e^-$.

⁶⁵ MASCHMANN 90 reports $1.12 \pm 0.33 \pm 0.25$ for $B(J/\psi(1S) \rightarrow e^+ e^-) = 0.069 \pm 0.009$. We rescale to our best value $B(J/\psi(1S) \rightarrow e^+ e^-) = (5.93 \pm 0.10) \times 10^{-2}$. Our first error is their experiment's error and our second error is the systematic error from using our best value.

⁶⁶ ALBRECHT 87D reports $1.07 \pm 0.16 \pm 0.22$ for $B(J/\psi(1S) \rightarrow e^+ e^-) = 0.069 \pm 0.009$. We rescale to our best value $B(J/\psi(1S) \rightarrow e^+ e^-) = (5.93 \pm 0.10) \times 10^{-2}$. Our first error is their experiment's error and our second error is the systematic error from using our best value. ALBRECHT 87D find the branching ratio for J/ψ not from $\psi(2S)$ to be 0.0081 ± 0.0023 .

⁶⁷ ALAM 86 reports $1.09 \pm 0.16 \pm 0.21$ for $B(J/\psi(1S) \rightarrow \mu^+ \mu^-) = 0.074 \pm 0.012$. We rescale to our best value $B(J/\psi(1S) \rightarrow \mu^+ \mu^-) = (5.88 \pm 0.10) \times 10^{-2}$. Our first error is their experiment's error and our second error is the systematic error from using our best value.

⁶⁸ Statistical and systematic errors were added in quadrature. ALBRECHT 85H also report a CL = 90% limit of 0.007 for $B \rightarrow J/\psi(1S) + X$ where $m_X < 1$ GeV.

⁶⁹ Dimuon and dielectron events used.

$\Gamma(J/\psi(1S) \text{ (direct) anything})/\Gamma_{\text{total}}$				Γ_{37}/Γ
VALUE	CL%	DOCUMENT ID	TECN	COMMENT
0.0080 ± 0.0008	70	BALEST	95B CLE2	$e^+ e^- \rightarrow \Upsilon(4S)$

⁷⁰ BALEST 95B assume PDG 1994 values for sub mode branching ratios. $J/\psi(1S)$ mesons are reconstructed in $J/\psi(1S) \rightarrow e^+ e^-$ and $J/\psi(1S) \rightarrow \mu^+ \mu^-$. The $B \rightarrow J/\psi(1S) X$ branching ratio contains $J/\psi(1S)$ mesons directly from B decays and also from feeddown through $\psi(2S) \rightarrow J/\psi(1S), \chi_{c1}(1P) \rightarrow J/\psi(1S)$, or $\chi_{c2}(1P) \rightarrow J/\psi(1S)$. Using the measured inclusive rates, BALEST 95B corrects for the feeddown and finds the $B \rightarrow J/\psi(1S)$ (direct) X branching ratio.

$\Gamma(\psi(2S) \text{ anything})/\Gamma_{\text{total}}$				Γ_{38}/Γ	
VALUE	CL%	EVTS	DOCUMENT ID	TECN	COMMENT
0.0035 ± 0.0005	OUR AVERAGE				
$0.0034 \pm 0.0004 \pm 0.0003$	240	71 BALEST	95B CLE2	$e^+ e^- \rightarrow \Upsilon(4S)$	
$0.0046 \pm 0.0017 \pm 0.0011$	8	ALBRECHT	87D ARG	$e^+ e^- \rightarrow \Upsilon(4S)$	

⁷¹ BALEST 95B assume PDG 1994 values for sub mode branching ratios. They find $B(B \rightarrow \psi(2S) X, \psi(2S) \rightarrow \ell^+ \ell^-) = 0.30 \pm 0.05 \pm 0.04$ and $B(B \rightarrow \psi(2S) X, \psi(2S) \rightarrow J/\psi(1S) \pi^+ \pi^-) = 0.37 \pm 0.05 \pm 0.05$. Weighted average is quoted for $B(B \rightarrow \psi(2S) X)$.

$\Gamma(\chi_{c1}(1P) \text{ anything})/\Gamma_{\text{total}}$				Γ_{39}/Γ	
VALUE	CL%	EVTS	DOCUMENT ID	TECN	COMMENT
0.0042 ± 0.0007	OUR AVERAGE				
$0.0040 \pm 0.0006 \pm 0.0004$	112	72 BALEST	95B CLE2	$e^+ e^- \rightarrow \Upsilon(4S)$	
$0.0105 \pm 0.0035 \pm 0.0025$	73	ALBRECHT	92E ARG	$e^+ e^- \rightarrow \Upsilon(4S)$	

⁷² BALEST 95B assume $B(\chi_{c1}(1P) \rightarrow J/\psi(1S)\gamma) = (27.3 \pm 1.6) \times 10^{-2}$, the PDG 1994 value. Fit to ψ -photon invariant mass distribution allows for a $\chi_{c1}(1P)$ and a $\chi_{c2}(1P)$ component.

⁷³ ALBRECHT 92E assumes no $\chi_{c2}(1P)$ production.

$\Gamma(\chi_{c1}(1P) \text{ (direct) anything})/\Gamma_{\text{total}}$				Γ_{40}/Γ
VALUE	CL%	DOCUMENT ID	TECN	COMMENT
0.0037 ± 0.0007	74	BALEST	95B CLE2	$e^+ e^- \rightarrow \Upsilon(4S)$

⁷⁴ BALEST 95B assume PDG 1994 values. $J/\psi(1S)$ mesons are reconstructed in the $e^+ e^-$ and $\mu^+ \mu^-$ modes. The $B \rightarrow \chi_{c1}(1P) X$ branching ratio contains $\chi_{c1}(1P)$ mesons directly from B decays and also from feeddown through $\psi(2S) \rightarrow \chi_{c1}(1P)\gamma$. Using the measured inclusive rates, BALEST 95B corrects for the feeddown and finds the $B \rightarrow \chi_{c1}(1P)$ (direct) X branching ratio.

$\Gamma(\chi_{c2}(1P) \text{ anything})/\Gamma_{\text{total}}$				Γ_{41}/Γ	
VALUE	CL%	EVTS	DOCUMENT ID	TECN	COMMENT
<0.0038	90	35	75 BALEST	95B CLE2	$e^+ e^- \rightarrow \Upsilon(4S)$

⁷⁵ BALEST 95B assume $B(\chi_{c2}(1P) \rightarrow J/\psi(1S)\gamma) = (13.5 \pm 1.1) \times 10^{-2}$, the PDG 1994 value. $J/\psi(1S)$ mesons are reconstructed in the $e^+ e^-$ and $\mu^+ \mu^-$ modes, and PDG 1994 branching fractions are used. If interpreted as signal, the 35 ± 13 events correspond to $B(B \rightarrow \chi_{c2}(1P) X) = (0.25 \pm 0.10 \pm 0.03) \times 10^{-2}$.

$\Gamma(\eta_c(1S) \text{ anything})/\Gamma_{\text{total}}$				Γ_{42}/Γ
VALUE	CL%	DOCUMENT ID	TECN	COMMENT
<0.009	90	76 BALEST	95B CLE2	$e^+ e^- \rightarrow \Upsilon(4S)$

⁷⁶ BALEST 95B assume PDG 1994 values for sub mode branching ratios. $J/\psi(1S)$ mesons are reconstructed in $J/\psi(1S) \rightarrow e^+ e^-$ and $J/\psi(1S) \rightarrow \mu^+ \mu^-$. Search region $2960 < m_{\eta_c(1S)} < 3010$ MeV/ c^2 .

$\Gamma(K^\pm \text{ anything})/\Gamma_{\text{total}}$				Γ_{43}/Γ
VALUE	CL%	DOCUMENT ID	TECN	COMMENT
0.789 ± 0.025	OUR AVERAGE			
$0.82 \pm 0.01 \pm 0.05$		ALBRECHT	94C ARG	$e^+ e^- \rightarrow \Upsilon(4S)$
$0.775 \pm 0.015 \pm 0.025$		77 ALBRECHT	93I ARG	$e^+ e^- \rightarrow \Upsilon(4S)$
$0.85 \pm 0.07 \pm 0.09$		ALAM	87B CLEO	$e^+ e^- \rightarrow \Upsilon(4S)$

• • • We do not use the following data for averages, fits, limits, etc. • • •

seen	78	BRODY	82 CLEO	$e^+ e^- \rightarrow \Upsilon(4S)$
seen	79	GIANNINI	82 CUSB	$e^+ e^- \rightarrow \Upsilon(4S)$

⁷⁷ ALBRECHT 93I value is not independent of the sum of $B \rightarrow K^+ \text{ anything}$ and $B \rightarrow K^- \text{ anything}$ ALBRECHT 94C values.

⁷⁸ Assuming $\Upsilon(4S) \rightarrow B\bar{B}$, a total of $3.38 \pm 0.34 \pm 0.68$ kaons per $\Upsilon(4S)$ decay is found (the second error is systematic). In the context of the standard B -decay model, this leads to a value for $(b\text{-quark} \rightarrow c\text{-quark})/(b\text{-quark} \rightarrow \text{all})$ of $1.09 \pm 0.33 \pm 0.13$.

⁷⁹ GIANNINI 82 at CESR-CUSB observed $1.58 \pm 0.35 K^0$ per hadronic event much higher than 0.82 ± 0.10 below threshold. Consistent with predominant $b \rightarrow cX$ decay.

$\Gamma(K^+ \text{ anything})/\Gamma_{\text{total}}$				Γ_{44}/Γ
VALUE	CL%	DOCUMENT ID	TECN	COMMENT
0.66 ± 0.05	80	ALBRECHT	94C ARG	$e^+ e^- \rightarrow \Upsilon(4S)$

• • • We do not use the following data for averages, fits, limits, etc. • • •

$0.620 \pm 0.013 \pm 0.038$	81	ALBRECHT	94C ARG	$e^+ e^- \rightarrow \Upsilon(4S)$
$0.66 \pm 0.05 \pm 0.07$	81	ALAM	87B CLEO	$e^+ e^- \rightarrow \Upsilon(4S)$

⁸⁰ Measurement relies on lepton-kaon correlations. It is for the weak decay vertex and does not include mixing of the neutral B meson. Mixing effects were corrected for by assuming a mixing parameter r of $(18.1 \pm 4.3)\%$.

⁸¹ Measurement relies on lepton-kaon correlations. It includes production through mixing of the neutral B meson.

Meson Particle Listings

 B^\pm/B^0 ADMIXTURE

$\Gamma(K^- \text{ anything})/\Gamma_{\text{total}}$					Γ_{45}/Γ
VALUE		DOCUMENT ID	TECN	COMMENT	
0.13 ± 0.04		82 ALBRECHT	94C ARG	$e^+e^- \rightarrow \Upsilon(4S)$	
• • • We do not use the following data for averages, fits, limits, etc. • • •					
$0.165 \pm 0.011 \pm 0.036$		83 ALBRECHT	94C ARG	$e^+e^- \rightarrow \Upsilon(4S)$	
$0.19 \pm 0.05 \pm 0.02$		83 ALAM	87B CLEO	$e^+e^- \rightarrow \Upsilon(4S)$	
82 Measurement relies on lepton-kaon correlations. It is for the weak decay vertex and does not include mixing of the neutral B meson. Mixing effects were corrected for by assuming a mixing parameter r of $(18.1 \pm 4.3)\%$.					
83 Measurement relies on lepton-kaon correlations. It includes production through mixing of the neutral B meson.					
$\Gamma(K^0/\bar{K}^0 \text{ anything})/\Gamma_{\text{total}}$					Γ_{46}/Γ
VALUE		DOCUMENT ID	TECN	COMMENT	
0.64 ± 0.04	OUR AVERAGE				
$0.642 \pm 0.010 \pm 0.042$		84 ALBRECHT	94C ARG	$e^+e^- \rightarrow \Upsilon(4S)$	
$0.63 \pm 0.06 \pm 0.06$		ALAM	87B CLEO	$e^+e^- \rightarrow \Upsilon(4S)$	
84 ALBRECHT 94C assume a K^0/\bar{K}^0 multiplicity twice that of K_S^0 .					
$\Gamma(K^*(892)^\pm \text{ anything})/\Gamma_{\text{total}}$					Γ_{47}/Γ
VALUE		DOCUMENT ID	TECN	COMMENT	
$0.182 \pm 0.054 \pm 0.024$		ALBRECHT	94J ARG	$e^+e^- \rightarrow \Upsilon(4S)$	
$\Gamma(K^*(892)^0/\bar{K}^*(892)^0 \text{ anything})/\Gamma_{\text{total}}$					Γ_{48}/Γ
VALUE		DOCUMENT ID	TECN	COMMENT	
$0.146 \pm 0.016 \pm 0.020$		ALBRECHT	94J ARG	$e^+e^- \rightarrow \Upsilon(4S)$	
$\Gamma(K^*(892)\gamma)/\Gamma_{\text{total}}$					Γ_{49}/Γ
VALUE	CL%	DOCUMENT ID	TECN	COMMENT	
• • • We do not use the following data for averages, fits, limits, etc. • • •					
$<1.5 \times 10^{-3}$		90	85 LESIAK	92 CBAL $e^+e^- \rightarrow \Upsilon(4S)$	
$<2.4 \times 10^{-4}$		90	ALBRECHT	88H ARG $e^+e^- \rightarrow \Upsilon(4S)$	
85 LESIAK 92 set a limit on the inclusive process $B(b \rightarrow s\gamma) < 2.8 \times 10^{-3}$ at 90% CL for the range of masses of 892–2045 MeV, independent of assumptions about s -quark hadronization.					
$\Gamma(K_1(1400)\gamma)/\Gamma_{\text{total}}$					Γ_{50}/Γ
VALUE	CL%	DOCUMENT ID	TECN	COMMENT	
$<4.1 \times 10^{-4}$		90	ALBRECHT	88H ARG $e^+e^- \rightarrow \Upsilon(4S)$	
• • • We do not use the following data for averages, fits, limits, etc. • • •					
$<1.6 \times 10^{-3}$		90	86 LESIAK	92 CBAL $e^+e^- \rightarrow \Upsilon(4S)$	
86 LESIAK 92 set a limit on the inclusive process $B(b \rightarrow s\gamma) < 2.8 \times 10^{-3}$ at 90% CL for the range of masses of 892–2045 MeV, independent of assumptions about s -quark hadronization.					
$\Gamma(K_2^*(1430)\gamma)/\Gamma_{\text{total}}$					Γ_{51}/Γ
VALUE	CL%	DOCUMENT ID	TECN	COMMENT	
$<8.3 \times 10^{-4}$		90	ALBRECHT	88H ARG $e^+e^- \rightarrow \Upsilon(4S)$	
$\Gamma(K_2(1770)\gamma)/\Gamma_{\text{total}}$					Γ_{52}/Γ
VALUE	CL%	DOCUMENT ID	TECN	COMMENT	
$<1.2 \times 10^{-3}$		90	87 LESIAK	92 CBAL $e^+e^- \rightarrow \Upsilon(4S)$	
87 LESIAK 92 set a limit on the inclusive process $B(b \rightarrow s\gamma) < 2.8 \times 10^{-3}$ at 90% CL for the range of masses of 892–2045 MeV, independent of assumptions about s -quark hadronization.					
$\Gamma(K_3^*(1780)\gamma)/\Gamma_{\text{total}}$					Γ_{53}/Γ
VALUE	CL%	DOCUMENT ID	TECN	COMMENT	
$<3.0 \times 10^{-3}$		90	ALBRECHT	88H ARG $e^+e^- \rightarrow \Upsilon(4S)$	
$\Gamma(K_2^*(2045)\gamma)/\Gamma_{\text{total}}$					Γ_{54}/Γ
VALUE	CL%	DOCUMENT ID	TECN	COMMENT	
$<1.0 \times 10^{-3}$		90	88 LESIAK	92 CBAL $e^+e^- \rightarrow \Upsilon(4S)$	
88 LESIAK 92 set a limit on the inclusive process $B(b \rightarrow s\gamma) < 2.8 \times 10^{-3}$ at 90% CL for the range of masses of 892–2045 MeV, independent of assumptions about s -quark hadronization.					
$\Gamma(\bar{b} \rightarrow \bar{s}\gamma)/\Gamma_{\text{total}}$					Γ_{55}/Γ
VALUE		DOCUMENT ID	TECN	COMMENT	
$(2.32 \pm 0.57 \pm 0.35) \times 10^{-4}$		ALAM	95 CLE2	$e^+e^- \rightarrow \Upsilon(4S)$	
$\Gamma(\bar{b} \rightarrow \bar{s}\text{gluon})/\Gamma_{\text{total}}$					Γ_{56}/Γ
VALUE	CL%	DOCUMENT ID	TECN	COMMENT	
<0.068		90	89 COAN	98 CLE2 $e^+e^- \rightarrow \Upsilon(4S)$	
• • • We do not use the following data for averages, fits, limits, etc. • • •					
<0.08		2	90 ALBRECHT	95D ARG $e^+e^- \rightarrow \Upsilon(4S)$	
89 COAN 98 uses D - ℓ correlation.					
90 ALBRECHT 95D use full reconstruction of one B decay as tag. Two candidate events for charmless B decay can be interpreted as either $b \rightarrow s\text{gluon}$ or $b \rightarrow u$ transition. If interpreted as $b \rightarrow s\text{gluon}$ they find a branching ratio of ~ 0.026 or the upper limit quoted above. Result is highly model dependent.					
$\Gamma(\eta \text{ anything})/\Gamma_{\text{total}}$					Γ_{57}/Γ
VALUE	CL%	DOCUMENT ID	TECN	COMMENT	
$<4.4 \times 10^{-4}$		90	91 BROWDER	98 CLE2 $e^+e^- \rightarrow \Upsilon(4S)$	
91 BROWDER 98 search for high momentum $B \rightarrow \eta X_S$ between 2.1 and 2.7 GeV/c.					
$\Gamma(\eta' \text{ anything})/\Gamma_{\text{total}}$					Γ_{58}/Γ
VALUE		DOCUMENT ID	TECN	COMMENT	
$(6.2 \pm 1.6 \pm 1.3 \pm 2.0) \times 10^{-4}$		92 BROWDER	98 CLE2	$e^+e^- \rightarrow \Upsilon(4S)$	
92 BROWDER 98 observed a signal of 39.0 ± 11.6 events in high momentum $B \rightarrow \eta' X_S$ production between 2.0 and 2.7 GeV/c. The branching fraction is based on the interpretation of $b \rightarrow s\gamma$, where the last error includes additional uncertainties due to the color-suppressed $b \rightarrow \text{backgrounds}$.					
$\Gamma(\pi^\pm \text{ anything})/\Gamma_{\text{total}}$					Γ_{59}/Γ
VALUE		DOCUMENT ID	TECN	COMMENT	
$3.585 \pm 0.025 \pm 0.070$		93 ALBRECHT	93J ARG	$e^+e^- \rightarrow \Upsilon(4S)$	
93 ALBRECHT 93 excludes π^\pm from K_S^0 and Λ decays. If included, they find $4.105 \pm 0.025 \pm 0.080$.					
$\Gamma(\eta \text{ anything})/\Gamma_{\text{total}}$					Γ_{60}/Γ
VALUE		DOCUMENT ID	TECN	COMMENT	
$0.176 \pm 0.011 \pm 0.012$		KUBOTA	96 CLE2	$e^+e^- \rightarrow \Upsilon(4S)$	
$\Gamma(\rho^0 \text{ anything})/\Gamma_{\text{total}}$					Γ_{61}/Γ
VALUE		DOCUMENT ID	TECN	COMMENT	
$0.208 \pm 0.042 \pm 0.032$		ALBRECHT	94J ARG	$e^+e^- \rightarrow \Upsilon(4S)$	
$\Gamma(\omega \text{ anything})/\Gamma_{\text{total}}$					Γ_{62}/Γ
VALUE	CL%	DOCUMENT ID	TECN	COMMENT	
<0.81		90	ALBRECHT	94J ARG $e^+e^- \rightarrow \Upsilon(4S)$	
$\Gamma(\phi \text{ anything})/\Gamma_{\text{total}}$					Γ_{63}/Γ
VALUE		DOCUMENT ID	TECN	COMMENT	
0.035 ± 0.007	OUR AVERAGE				
$0.0390 \pm 0.0030 \pm 0.0035$		ALBRECHT	94J ARG	$e^+e^- \rightarrow \Upsilon(4S)$	
$0.023 \pm 0.006 \pm 0.005$		BORTOLETTO	086 CLEO	$e^+e^- \rightarrow \Upsilon(4S)$	
Error includes scale factor of 1.8.					
$\Gamma(\phi K^*(892))/\Gamma_{\text{total}}$					Γ_{64}/Γ
VALUE	CL%	DOCUMENT ID	TECN	COMMENT	
$<2.2 \times 10^{-5}$		90	94 BERGFELD	98 CLE2	
94 Assumes equal production of B^+ and B^0 at the $\Upsilon(4S)$.					
$\Gamma(\Lambda_c^\pm \text{ anything})/\Gamma_{\text{total}}$					Γ_{65}/Γ
VALUE	CL%	DOCUMENT ID	TECN	COMMENT	
$0.064 \pm 0.008 \pm 0.008$		95 CRAWFORD	92 CLEO	$e^+e^- \rightarrow \Upsilon(4S)$	
• • • We do not use the following data for averages, fits, limits, etc. • • •					
0.14 ± 0.09		96 ALBRECHT	88E ARG	$e^+e^- \rightarrow \Upsilon(4S)$	
<0.112		90	97 ALAM	87 CLEO $e^+e^- \rightarrow \Upsilon(4S)$	
95 CRAWFORD 92 result derived from lepton baryon correlations. Assumes all charmed baryons in B^0 and B^\pm decay are Λ_c .					
96 ALBRECHT 88E measured $B(B \rightarrow \Lambda_c^+ X) \cdot B(\Lambda_c^+ \rightarrow pK^- \pi^+) = (0.30 \pm 0.12 \pm 0.06)\%$ and used $B(\Lambda_c^+ \rightarrow pK^- \pi^+) = (2.2 \pm 1.0)\%$ from ABRAMS 80 to obtain above number.					
97 Assuming all baryons result from charmed baryons, ALAM 86 conclude the branching fraction is $7.4 \pm 2.9\%$. The limit given above is model independent.					
$\Gamma(\Lambda_c^+ \text{ anything})/\Gamma(\bar{\Lambda}_c^- \text{ anything})$					Γ_{66}/Γ_{67}
VALUE		DOCUMENT ID	TECN	COMMENT	
$0.19 \pm 0.13 \pm 0.04$		98 AMMAR	97 CLE2	$e^+e^- \rightarrow \Upsilon(4S)$	
98 AMMAR 97 uses a high-momentum lepton tag ($P_\ell > 1.4 \text{ GeV}/c^2$).					
$\Gamma(\bar{\Lambda}_c^- e^+ \text{ anything})/\Gamma(\Lambda_c^\pm \text{ anything})$					Γ_{68}/Γ_{65}
VALUE	CL%	DOCUMENT ID	TECN	COMMENT	
<0.05		90	99 BONVICINI	98 CLE2 $e^+e^- \rightarrow \Upsilon(4S)$	
99 BONVICINI 98 uses the electron with momentum above 0.6 GeV/c.					
$\Gamma(\bar{\Lambda}_c^- p e^+ \nu_e)/\Gamma(\bar{\Lambda}_c^- p \text{ anything})$					Γ_{70}/Γ_{69}
VALUE	CL%	DOCUMENT ID	TECN	COMMENT	
<0.04		90	100 BONVICINI	98 CLE2 $e^+e^- \rightarrow \Upsilon(4S)$	
100 BONVICINI 98 uses the electron with momentum above 0.6 GeV/c.					
$\Gamma(\bar{\Sigma}_c^{--} \text{ anything})/\Gamma_{\text{total}}$					Γ_{71}/Γ
VALUE	EVTS	DOCUMENT ID	TECN	COMMENT	
$0.0042 \pm 0.0021 \pm 0.0011$		77	101 PROCARIO	94 CLE2 $e^+e^- \rightarrow \Upsilon(4S)$	
101 PROCARIO 94 reports $[B(B \rightarrow \bar{\Sigma}_c^{--} \text{ anything}) \times B(\Lambda_c^+ \rightarrow pK^- \pi^+)] = 0.00021 \pm 0.00008 \pm 0.00007$. We divide by our best value $B(\Lambda_c^+ \rightarrow pK^- \pi^+) = (5.0 \pm 1.3) \times 10^{-2}$. Our first error is their experiment's error and our second error is the systematic error from using our best value.					

See key on page 239

Meson Particle Listings

B^\pm/B^0 ADMIXTURE

$\Gamma(\Sigma_c^- \text{ anything})/\Gamma_{\text{total}}$					Γ_{72}/Γ
VALUE	CL%	DOCUMENT ID	TECN	COMMENT	
<0.010	90	102 PROCARIO	94 CLE2	$e^+e^- \rightarrow \Upsilon(4S)$	

102 PROCARIO 94 reports $[B(B \rightarrow \Sigma_c^- \text{ anything}) \times B(\Lambda_c^+ \rightarrow pK^- \pi^+)] = < 0.00048$. We divide by our best value $B(\Lambda_c^+ \rightarrow pK^- \pi^+) = 0.050$.

$\Gamma(\Sigma_c^0 \text{ anything})/\Gamma_{\text{total}}$					Γ_{73}/Γ
VALUE	EVTS	DOCUMENT ID	TECN	COMMENT	
$0.0046 \pm 0.0021 \pm 0.0012$	76	103 PROCARIO	94 CLE2	$e^+e^- \rightarrow \Upsilon(4S)$	

103 PROCARIO 94 reports $[B(B \rightarrow \Sigma_c^0 \text{ anything}) \times B(\Lambda_c^+ \rightarrow pK^- \pi^+)] = 0.00023 \pm 0.00008 \pm 0.00007$. We divide by our best value $B(\Lambda_c^+ \rightarrow pK^- \pi^+) = (5.0 \pm 1.3) \times 10^{-2}$. Our first error is their experiment's error and our second error is the systematic error from using our best value.

$\Gamma(\Sigma_c^0 N(N=p \text{ or } n))/\Gamma_{\text{total}}$					Γ_{74}/Γ
VALUE	CL%	DOCUMENT ID	TECN	COMMENT	
<0.0015	90	104 PROCARIO	94 CLE2	$e^+e^- \rightarrow \Upsilon(4S)$	

104 PROCARIO 94 reports < 0.0017 for $B(\Lambda_c^+ \rightarrow pK^- \pi^+) = 0.043$. We rescale to our best value $B(\Lambda_c^+ \rightarrow pK^- \pi^+) = 0.050$.

$\Gamma(\Xi_c^0 \text{ anything} \times B(\Xi_c^0 \rightarrow \Xi^- \pi^+))/\Gamma_{\text{total}}$					Γ_{75}/Γ
VALUE (units 10^{-3})	DOCUMENT ID	TECN	COMMENT		
$0.144 \pm 0.048 \pm 0.021$	105 BARISH	97 CLE2	$e^+e^- \rightarrow \Upsilon(4S)$		

105 BARISH 97 find $79 \pm 27 \Xi_c^0$ events.

$\Gamma(\Xi_c^+ \text{ anything} \times B(\Xi_c^+ \rightarrow \Xi^- \pi^+ \pi^+))/\Gamma_{\text{total}}$					Γ_{76}/Γ
VALUE (units 10^{-3})	DOCUMENT ID	TECN	COMMENT		
$0.453 \pm 0.096 \pm 0.085$ -0.065	106 BARISH	97 CLE2	$e^+e^- \rightarrow \Upsilon(4S)$		

106 BARISH 97 find $125 \pm 28 \Xi_c^+$ events.

$\Gamma(p/\bar{p} \text{ anything})/\Gamma_{\text{total}}$					Γ_{77}/Γ
Includes p and \bar{p} from Λ and $\bar{\Lambda}$ decay.					
VALUE	EVTS	DOCUMENT ID	TECN	COMMENT	
0.080 ± 0.004 OUR AVERAGE					
$0.080 \pm 0.005 \pm 0.005$		ALBRECHT 93i	ARG	$e^+e^- \rightarrow \Upsilon(4S)$	
$0.080 \pm 0.005 \pm 0.003$		CRAWFORD 92	CLEO	$e^+e^- \rightarrow \Upsilon(4S)$	
$0.082 \pm 0.005 \pm 0.013$ -0.010	2163	107 ALBRECHT	89k ARG	$e^+e^- \rightarrow \Upsilon(4S)$	

• • • We do not use the following data for averages, fits, limits, etc. • • •
>0.021 108 ALAM 83b CLEO $e^+e^- \rightarrow \Upsilon(4S)$

107 ALBRECHT 89k include direct and nondirect protons.
108 ALAM 83b reported their result as $> 0.036 \pm 0.006 \pm 0.009$. Data are consistent with equal yields of p and \bar{p} . Using assumed yields below cut, $B(B \rightarrow p + X) = 0.03$ not including protons from Λ decays.

$\Gamma(p/\bar{p} \text{ (direct) anything})/\Gamma_{\text{total}}$					Γ_{78}/Γ
VALUE	EVTS	DOCUMENT ID	TECN	COMMENT	
0.055 ± 0.005 OUR AVERAGE					
$0.055 \pm 0.005 \pm 0.0035$		ALBRECHT 93i	ARG	$e^+e^- \rightarrow \Upsilon(4S)$	
$0.056 \pm 0.006 \pm 0.005$		CRAWFORD 92	CLEO	$e^+e^- \rightarrow \Upsilon(4S)$	
0.055 ± 0.016	1220	109 ALBRECHT	89k ARG	$e^+e^- \rightarrow \Upsilon(4S)$	

109 ALBRECHT 89k subtract contribution of Λ decay from the inclusive proton yield.

$\Gamma(\Lambda/\bar{\Lambda} \text{ anything})/\Gamma_{\text{total}}$					Γ_{79}/Γ
VALUE	EVTS	DOCUMENT ID	TECN	COMMENT	
0.040 ± 0.005 OUR AVERAGE					
$0.038 \pm 0.004 \pm 0.006$	2998	CRAWFORD 92	CLEO	$e^+e^- \rightarrow \Upsilon(4S)$	
$0.042 \pm 0.005 \pm 0.006$	943	ALBRECHT 89k	ARG	$e^+e^- \rightarrow \Upsilon(4S)$	

• • • We do not use the following data for averages, fits, limits, etc. • • •
 $0.022 \pm 0.003 \pm 0.0022$ 110 ACKERSTAFF 97n OPAL $e^+e^- \rightarrow Z$
>0.011 111 ALAM 83b CLEO $e^+e^- \rightarrow \Upsilon(4S)$

110 ACKERSTAFF 97n assumes $B(b \rightarrow B) = 0.868 \pm 0.041$, i.e., an admixture of B^0 , B^\pm , and B_s .
111 ALAM 83b reported their result as $> 0.022 \pm 0.007 \pm 0.004$. Values are for $(B(\Lambda X) + B(\bar{\Lambda} X))/2$. Data are consistent with equal yields of p and \bar{p} . Using assumed yields below cut, $B(B \rightarrow \Lambda X) = 0.03$.

$\Gamma(\Lambda \text{ anything})/\Gamma(\bar{\Lambda} \text{ anything})$					Γ_{80}/Γ_{81}
VALUE	DOCUMENT ID	TECN	COMMENT		
$0.43 \pm 0.09 \pm 0.07$	112 AMMAR	97 CLE2	$e^+e^- \rightarrow \Upsilon(4S)$		

112 AMMAR 97 uses a high-momentum lepton tag ($P_\ell > 1.4 \text{ GeV}/c^2$).

$\Gamma(\Xi^-/\Xi^+ \text{ anything})/\Gamma_{\text{total}}$					Γ_{82}/Γ
VALUE	EVTS	DOCUMENT ID	TECN	COMMENT	
0.0027 ± 0.0006 OUR AVERAGE					
$0.0027 \pm 0.0005 \pm 0.0004$	147	CRAWFORD 92	CLEO	$e^+e^- \rightarrow \Upsilon(4S)$	
0.0028 ± 0.0014	54	ALBRECHT 89k	ARG	$e^+e^- \rightarrow \Upsilon(4S)$	

$\Gamma(\text{baryons anything})/\Gamma_{\text{total}}$					Γ_{83}/Γ
VALUE	DOCUMENT ID	TECN	COMMENT		
0.068 ± 0.005 ± 0.003	113 ALBRECHT	92o ARG	$e^+e^- \rightarrow \Upsilon(4S)$		

• • • We do not use the following data for averages, fits, limits, etc. • • •
 0.076 ± 0.014 114 ALBRECHT 89k ARG $e^+e^- \rightarrow \Upsilon(4S)$

113 ALBRECHT 92o result is from simultaneous analysis of p and Λ yields, $p\bar{p}$ and $\Lambda\bar{p}$ correlations, and various lepton-baryon and lepton-baryon-antibaryon correlations. Supersedes ALBRECHT 89k.
114 ALBRECHT 89k obtain this result by adding their their measurements ($5.5 \pm 1.6\%$) for direct protons and ($4.2 \pm 0.5 \pm 0.6\%$) for inclusive Λ production. They then assume ($5.5 \pm 1.6\%$) for neutron production and add it in also. Since each B decay has two baryons, they divide by 2 to obtain ($7.6 \pm 1.4\%$).

$\Gamma(p\bar{p} \text{ anything})/\Gamma_{\text{total}}$					Γ_{84}/Γ
Includes p and \bar{p} from Λ and $\bar{\Lambda}$ decay.					
VALUE	EVTS	DOCUMENT ID	TECN	COMMENT	
0.0247 ± 0.0023 OUR AVERAGE					
$0.024 \pm 0.001 \pm 0.004$		CRAWFORD 92	CLEO	$e^+e^- \rightarrow \Upsilon(4S)$	
$0.025 \pm 0.002 \pm 0.002$	918	ALBRECHT 89k	ARG	$e^+e^- \rightarrow \Upsilon(4S)$	

$\Gamma(p\bar{p} \text{ anything})/\Gamma(p/\bar{p} \text{ anything})$					Γ_{84}/Γ_{77}
Includes p and \bar{p} from Λ and $\bar{\Lambda}$ decay.					
VALUE	DOCUMENT ID	TECN	COMMENT		
$0.30 \pm 0.02 \pm 0.05$	115 CRAWFORD	92 CLEO	$e^+e^- \rightarrow \Upsilon(4S)$		

115 CRAWFORD 92 value is not independent of their $\Gamma(p\bar{p} \text{ anything})/\Gamma_{\text{total}}$ value.

$\Gamma(\Lambda\bar{p}/\bar{\Lambda}p \text{ anything})/\Gamma_{\text{total}}$					Γ_{85}/Γ
Includes p and \bar{p} from Λ and $\bar{\Lambda}$ decay.					
VALUE	EVTS	DOCUMENT ID	TECN	COMMENT	
0.025 ± 0.004 OUR AVERAGE					
$0.029 \pm 0.005 \pm 0.005$		CRAWFORD 92	CLEO	$e^+e^- \rightarrow \Upsilon(4S)$	
$0.023 \pm 0.004 \pm 0.003$	165	ALBRECHT 89k	ARG	$e^+e^- \rightarrow \Upsilon(4S)$	

$\Gamma(\Lambda\bar{p}/\bar{\Lambda}p \text{ anything})/\Gamma(\Lambda/\bar{\Lambda} \text{ anything})$					Γ_{85}/Γ_{79}
Includes p and \bar{p} from Λ and $\bar{\Lambda}$ decay.					
VALUE	DOCUMENT ID	TECN	COMMENT		
$0.76 \pm 0.11 \pm 0.08$	116 CRAWFORD	92 CLEO	$e^+e^- \rightarrow \Upsilon(4S)$		

116 CRAWFORD 92 value is not independent of their $[(\Lambda\bar{p} \text{ anything}) + (\bar{\Lambda}p \text{ anything})]/\Gamma_{\text{total}}$ value.

$\Gamma(\Lambda\bar{\Lambda} \text{ anything})/\Gamma_{\text{total}}$					Γ_{86}/Γ
VALUE	CL%	EVTS	DOCUMENT ID	TECN	COMMENT
<0.005	90		CRAWFORD 92	CLEO	$e^+e^- \rightarrow \Upsilon(4S)$

• • • We do not use the following data for averages, fits, limits, etc. • • •
<0.0088 90 12 ALBRECHT 89k ARG $e^+e^- \rightarrow \Upsilon(4S)$

$\Gamma(\Lambda\bar{\Lambda} \text{ anything})/\Gamma(\Lambda/\bar{\Lambda} \text{ anything})$					Γ_{86}/Γ_{79}
VALUE	CL%	DOCUMENT ID	TECN	COMMENT	
<0.13	90	117 CRAWFORD	92 CLEO	$e^+e^- \rightarrow \Upsilon(4S)$	

117 CRAWFORD 92 value is not independent of their $\Gamma(\Lambda\bar{\Lambda} \text{ anything})/\Gamma_{\text{total}}$ value.

$\Gamma(e^+e^- s)/\Gamma_{\text{total}}$					Γ_{87}/Γ
Test for $\Delta B = 1$ weak neutral current.					
VALUE	CL%	DOCUMENT ID	TECN	COMMENT	
$<5.7 \times 10^{-5}$	90	GLENN 98	CLEO	$e^+e^- \rightarrow \Upsilon(4S)$	

• • • We do not use the following data for averages, fits, limits, etc. • • •
<0.05 90 BEBEK 81 CLEO $e^+e^- \rightarrow \Upsilon(4S)$

$\Gamma(\mu^+ \mu^- s)/\Gamma_{\text{total}}$					Γ_{88}/Γ
Test for $\Delta B = 1$ weak neutral current.					
VALUE	CL%	DOCUMENT ID	TECN	COMMENT	
$<5.8 \times 10^{-5}$	90	GLENN 98	CLEO	$e^+e^- \rightarrow \Upsilon(4S)$	

• • • We do not use the following data for averages, fits, limits, etc. • • •
<0.017 90 CHADWICK 81 CLEO $e^+e^- \rightarrow \Upsilon(4S)$

$[\Gamma(e^+e^- s) + \Gamma(\mu^+ \mu^- s)]/\Gamma_{\text{total}}$					$(\Gamma_{87} + \Gamma_{88})/\Gamma$
Test for $\Delta B = 1$ weak neutral current.					
VALUE	CL%	DOCUMENT ID	TECN	COMMENT	
$<4.2 \times 10^{-5}$	90	GLENN 98	CLEO	$e^+e^- \rightarrow \Upsilon(4S)$	

• • • We do not use the following data for averages, fits, limits, etc. • • •
<0.0024 90 118 BEAN 87 CLEO Repl. by GLENN 98
<0.0062 90 119 AVERY 84 CLEO Repl. by BEAN 87

118 BEAN 87 reports $[(\mu^+ \mu^-) + (e^+ e^-)]/2$ and we converted it.
119 Determine ratio of B^+ to B^0 semileptonic decays to be in the range 0.25–2.9.

$\Gamma(e^\pm \mu^\mp s)/\Gamma_{\text{total}}$					Γ_{89}/Γ
Test for lepton family number conservation.					
VALUE	CL%	DOCUMENT ID	TECN	COMMENT	
$<2.2 \times 10^{-5}$	90	GLENN 98	CLEO	$e^+e^- \rightarrow \Upsilon(4S)$	

Meson Particle Listings

 B^\pm/B^0 ADMIXTURE, $B^\pm/B^0/B_s^0/b$ -baryon ADMIXTURE B^\pm/B^0 ADMIXTURE REFERENCES

BARATE	98Q	EPJ C4 387	R. Barate et al.	(ALEPH Collab.)
BERGFELD	98	PRL 81 272	T. Bergfeld et al.	(CLEO Collab.)
BISHAI	98	PR D57 3847	M. Bishai et al.	(CLEO Collab.)
BONVICINI	98	PR D57 6504	G. Bonvicini et al.	(CLEO Collab.)
BROWDER	98	PRL 81 1785	T.E. Browder et al.	(CLEO Collab.)
CDAN	98	PRL 80 1150	T.E. Coan et al.	(CLEO Collab.)
GLENN	98	PRL 80 2289	S. Glenn et al.	(CLEO Collab.)
ACKERSTAFF	97N	ZPHY C74 423	K. Ackerstaff et al.	(OPAL Collab.)
AMMAR	97	PR D55 13	R. Ammar et al.	(CLEO Collab.)
BARISH	97	PRL 79 3599	B. Barish et al.	(CLEO Collab.)
BUSKULIC	97B	ZPHY C73 601	D. Buskulic et al.	(ALEPH Collab.)
GIBBONS	97B	PR D56 3783	L. Gibbons et al.	(CLEO Collab.)
ALBRECHT	96D	PL B374 256	H. Albrecht et al.	(ARGUS Collab.)
BARISH	96B	PRL 76 1570	B.C. Barish et al.	(CLEO Collab.)
GIBAUT	96	PR D53 4734	D. Gibaut et al.	(CLEO Collab.)
KUBOTA	96	PR D53 6033	Y. Kubota et al.	(CLEO Collab.)
PDG	96	PR D54 1		
ALAM	95	PRL 74 2885	M.S. Alam et al.	(CLEO Collab.)
ALBRECHT	95D	PL B353 554	H. Albrecht et al.	(ARGUS Collab.)
BALEST	95B	PR D52 2661	R. Balest et al.	(CLEO Collab.)
BARISH	95	PR D51 1014	B.C. Barish et al.	(CLEO Collab.)
BUSKULIC	95B	PL B345 103	D. Buskulic et al.	(ALEPH Collab.)
ALBRECHT	94C	ZPHY C62 371	H. Albrecht et al.	(ARGUS Collab.)
ALBRECHT	94J	ZPHY C61 1	H. Albrecht et al.	(ARGUS Collab.)
PROCARIO	94	PRL 73 1306	M. Procario et al.	(CLEO Collab.)
ALBRECHT	93	ZPHY C57 533	H. Albrecht et al.	(ARGUS Collab.)
ALBRECHT	93E	ZPHY C60 11	H. Albrecht et al.	(ARGUS Collab.)
ALBRECHT	93H	PL B318 397	H. Albrecht et al.	(ARGUS Collab.)
ALBRECHT	93I	ZPHY C58 191	H. Albrecht et al.	(ARGUS Collab.)
ALEXANDER	93B	PL B319 365	J. Alexander et al.	(CLEO Collab.)
ARTUSO	93	PL B311 307	M. Artuso	(SYRFA)
BARTELT	93B	PRL 71 4111	J.E. Bartelt et al.	(CLEO Collab.)
ALBRECHT	92E	PL B277 209	H. Albrecht et al.	(ARGUS Collab.)
ALBRECHT	92G	ZPHY C54 1	H. Albrecht et al.	(ARGUS Collab.)
ALBRECHT	92O	ZPHY C56 1	H. Albrecht et al.	(ARGUS Collab.)
BORTOLETTO	92	PR D45 21	D. Bortoletto et al.	(CLEO Collab.)
CRAWFORD	92	PR D45 752	G. Crawford et al.	(CLEO Collab.)
HENDERSON	92	PR D45 2212	S. Henderson et al.	(CLEO Collab.)
LESIAK	92	ZPHY C55 33	T. Lesiak et al.	(Crystal Ball Collab.)
ALBRECHT	91C	ZPHY C52 297	H. Albrecht et al.	(ARGUS Collab.)
ALBRECHT	91H	ZPHY C52 353	H. Albrecht et al.	(ARGUS Collab.)
FULTON	91	PR D43 651	R. Fulton et al.	(CLEO Collab.)
YANAGISAWA	91	PRL 66 2436	C. Yanagisawa et al.	(CUSB II Collab.)
ALBRECHT	90	PL B234 409	H. Albrecht et al.	(ARGUS Collab.)
ALBRECHT	90H	PL B249 359	H. Albrecht et al.	(ARGUS Collab.)
BORTOLETTO	90	PL 64 2117	D. Bortoletto et al.	(CLEO Collab.)
Also	92	PR D45 21	D. Bortoletto et al.	(CLEO Collab.)
FULTON	90	PR D45 16	R. Fulton et al.	(CLEO Collab.)
MASCHIMANN	90	ZPHY C46 555	W.S. Maschmann et al.	(Crystal Ball Collab.)
PDG	90	PL B239	J.J. Hernandez et al.	(IFIC, BOST, CIT+)
ALBRECHT	89K	ZPHY C42 519	H. Albrecht et al.	(ARGUS Collab.)
ISGUR	89B	PR D39 799	N. Isgur et al.	(TNT0, CIT)
WACHS	89	ZPHY C42 33	K. Wachs et al.	(Crystal Ball Collab.)
ALBRECHT	88E	PL B210 263	H. Albrecht et al.	(ARGUS Collab.)
ALBRECHT	88H	PL B210 258	H. Albrecht et al.	(ARGUS Collab.)
KOERNER	88	ZPHY C38 511	J.G. Korner, G.A. Schuler	(MANZ, DESY)
ALAM	87	PRL 59 22	M.S. Alam et al.	(CLEO Collab.)
ALAM	87B	PR 58 1814	M.S. Alam et al.	(CLEO Collab.)
ALBRECHT	87D	PL B199 451	H. Albrecht et al.	(ARGUS Collab.)
ALBRECHT	87H	PL B187 425	H. Albrecht et al.	(ARGUS Collab.)
BEAN	87	PR D35 3533	A. Bean et al.	(CLEO Collab.)
BEHRENDIS	87	PRL 59 407	S. Behrendis et al.	(CLEO Collab.)
BORTOLETTO	87	PR D35 19	D. Bortoletto et al.	(CLEO Collab.)
ALAM	86	PR D34 3279	M.S. Alam et al.	(CLEO Collab.)
BALTUSAITIS...	86E	PRL 56 2140	R.M. Baltusaitis et al.	(Mark III Collab.)
BORTOLETTO	86	PL 56 800	D. Bortoletto et al.	(CLEO Collab.)
HAAS	86	PR 56 2781	J. Haas et al.	(CLEO Collab.)
ALBRECHT	85H	PL 162B 395	H. Albrecht et al.	(ARGUS Collab.)
CSORNA	85	PRL 54 1894	S.E. Csorna et al.	(CLEO Collab.)
HAAS	85	PR 55 1248	J. Haas et al.	(CLEO Collab.)
AVERY	84	PRL 53 1309	P. Avery et al.	(CLEO Collab.)
CHEN	84	PRL 52 1084	A. Chen et al.	(CLEO Collab.)
LEVMAN	84	PL 141B 271	G.M. Levman et al.	(CUSB Collab.)
ALAM	83B	PRL 51 1143	M.S. Alam et al.	(CLEO Collab.)
GREEN	83	PRL 51 347	J. Green et al.	(CLEO Collab.)
KLOPFEN...	83B	PL 130B 444	C. Klopferstein et al.	(CUSB Collab.)
ALTARELLI	82	NP B208 365	G. Altarelli et al.	(ROMA, INFN, FRAS)
BRODY	82	PRL 48 1070	A.D. Brody et al.	(CLEO Collab.)
GIANNINI	82	NP B206 1	G. Giannini et al.	(CUSB Collab.)
BEBEK	81	PRL 46 84	C. Bebek et al.	(CLEO Collab.)
CHADWICK	81	PRL 46 88	K. Chadwick et al.	(CLEO Collab.)
ABRAMS	80	PRL 44 10	G.S. Abrams et al.	(SLAC, LBL)

1.564±0.030±0.036	5	ABE,K	95B SLD	$e^+e^- \rightarrow Z$
1.542±0.021±0.045	6	ABREU	94L DLPH	$e^+e^- \rightarrow Z$
1.523±0.034±0.038	5372	7	ACTON	93L OPAL $e^+e^- \rightarrow Z$
1.511±0.022±0.078	8	BUSKULIC	93O ALEP	$e^+e^- \rightarrow Z$
••• We do not use the following data for averages, fits, limits, etc. •••				
1.575±0.010±0.026	9	ABREU	96E DLPH	$e^+e^- \rightarrow Z$
1.50 ^{+0.24} _{-0.21} ±0.03	10	ABREU	94P DLPH	$e^+e^- \rightarrow Z$
1.46±0.06±0.06	5344	11	ABE	93J CDF Repl. by ABE 98B
1.23 ^{+0.14} _{-0.13} ±0.15	188	12	ABREU	93D DLPH Sup. by ABREU 94L
1.49±0.11±0.12	253	13	ABREU	93G DLPH Sup. by ABREU 94L
1.51 ^{+0.16} _{-0.14} ±0.11	130	14	ACTON	93C OPAL $e^+e^- \rightarrow Z$
1.535±0.035±0.028	7357	7	ADRIANI	93K L3 Repl. by ACCIARRI 98
1.28±0.10	15	ABREU	92 DLPH	Sup. by ABREU 94L
1.37±0.07±0.06	1354	16	ACTON	92 OPAL Sup. by ACTON 93L
1.49±0.03±0.06	17	BUSKULIC	92F ALEP	Sup. by BUSKULIC 96F
1.35 ^{+0.19} _{-0.17} ±0.05	18	BUSKULIC	92G ALEP	$e^+e^- \rightarrow Z$
1.32±0.08±0.09	1386	19	ADEVA	91H L3 Sup. by ADRIANI 93K
1.32 ^{+0.31} _{-0.25} ±0.15	37	20	ALEXANDER	91G OPAL $e^+e^- \rightarrow Z$
1.29±0.06±0.10	2973	21	DECAMP	91C ALEP Sup. by BUSKULIC 92F
1.36 ^{+0.25} _{-0.23}	22	HAGEMANN	90 JADE	$E_{cm}^{90} = 35$ GeV
1.13±0.15	23	LYONS	90 RVUE	
1.35±0.10±0.24		BRAUNSCH...	89B TASS	$E_{cm}^{89} = 35$ GeV
0.98±0.12±0.13		ONG	89 MRK2	$E_{cm}^{89} = 29$ GeV
1.17 ^{+0.27} _{-0.22} ±0.17		KLEM	88 DLCO	$E_{cm}^{88} = 29$ GeV
1.29±0.20±0.21	24	ASH	87 MAC	$E_{cm}^{87} = 29$ GeV
1.02 ^{+0.42} _{-0.39}	301	25	BROM	87 HRS $E_{cm}^{87} = 29$ GeV

- 1 Measured using inclusive $J/\psi(1S) \rightarrow \mu^+\mu^-$ vertex.
- 2 ACCIARRI 98 uses inclusively reconstructed secondary vertex and lepton impact parameter.
- 3 ACKERSTAFF 97F uses inclusively reconstructed secondary vertices.
- 4 BUSKULIC 96F analyzed using 3D impact parameter.
- 5 ABE,K 95B uses an inclusive topological technique.
- 6 ABREU 94L uses charged particle impact parameters. Their result from inclusively reconstructed secondary vertices is superseded by ABREU 96E.
- 7 ACTON 93L and ADRIANI 93K analyzed using lepton (e and μ) impact parameter at Z .
- 8 BUSKULIC 93O analyzed using dipole method.
- 9 Combines ABREU 96E secondary vertex result with ABREU 94L impact parameter result.
- 10 From proper time distribution of $b \rightarrow J/\psi(1S)$ anything.
- 11 ABE 93J analyzed using $J/\psi(1S) \rightarrow \mu\mu$ vertices.
- 12 ABREU 93D data analyzed using $D/D^* \ell$ anything event vertices.
- 13 ABREU 93G data analyzed using charged and neutral vertices.
- 14 ACTON 93C analysed using $D/D^* \ell$ anything event vertices.
- 15 ABREU 92 is combined result of muon and hadron impact parameter analyses. Hadron tracks gave $(12.7 \pm 0.4 \pm 1.2) \times 10^{-13}$ s for an admixture of B species weighted by production fraction and mean charge multiplicity, while muon tracks gave $(13.0 \pm 1.0 \pm 0.8) \times 10^{-13}$ s for an admixture weighted by production fraction and semileptonic branching fraction.
- 16 ACTON 92 is combined result of muon and electron impact parameter analyses.
- 17 BUSKULIC 92F uses the lepton impact parameter distribution for data from the 1991 run.
- 18 BUSKULIC 92G use $J/\psi(1S)$ tags to measure the average b lifetime. This is comparable to other methods only if the $J/\psi(1S)$ branching fractions of the different b -flavored hadrons are in the same ratio.
- 19 Using $Z \rightarrow e^+X$ or μ^+X , ADEVA 91H determined the average lifetime for an admixture of B hadrons from the impact parameter distribution of the lepton.
- 20 Using $Z \rightarrow J/\psi(1S)X$, $J/\psi(1S) \rightarrow \ell^+\ell^-$, ALEXANDER 91G determined the average lifetime for an admixture of B hadrons from the decay point of the $J/\psi(1S)$.
- 21 Using $Z \rightarrow eX$ or μX , DECAMP 91C determines the average lifetime for an admixture of B hadrons from the signed impact parameter distribution of the lepton.
- 22 HAGEMANN 90 uses electrons and muons in an impact parameter analysis.
- 23 LYONS 90 combine the results of the B lifetime measurements of ONG 89, BRAUNSCHWEIG 89B, KLEM 88, and ASH 87, and JADE data by private communication. They use statistical techniques which include variation of the error with the mean life, and possible correlations between the systematic errors. This result is not independent of the measured results used in our average.
- 24 We have combined an overall scale error of 15% in quadrature with the systematic error of ± 0.7 to obtain ± 2.1 systematic error.
- 25 Statistical and systematic errors were combined by BROM 87.

 $B^\pm/B^0/B_s^0/b$ -baryon ADMIXTURE $B^\pm/B^0/B_s^0/b$ -baryon ADMIXTURE MEAN LIFE

Each measurement of the B mean life is an average over an admixture of various bottom mesons and baryons which decay weakly. Different techniques emphasize different admixtures of produced particles, which could result in a different B mean life.

"OUR EVALUATION" is an average of the data listed below performed by the LEP B Lifetime Working Group as described in our review "Production and Decay of b -flavored Hadrons" in the B^\pm Section of these Listings. The averaging procedure takes into account correlations between the measurements and asymmetric lifetime errors, but ignores the small differences due to different techniques.

VALUE (10^{-12} s)	EVTS	DOCUMENT ID	TECN	COMMENT
1.564±0.014 OUR EVALUATION				
1.533±0.015 ^{+0.035} _{-0.031}	1	ABE	98B CDF	$p\bar{p}$ at 1.8 TeV
1.549±0.009±0.015	2	ACCIARRI	98 L3	$e^+e^- \rightarrow Z$
1.611±0.010±0.027	3	ACKERSTAFF	97F OPAL	$e^+e^- \rightarrow Z$
1.582±0.011±0.027	3	ABREU	96E DLPH	$e^+e^- \rightarrow Z$
1.533±0.013±0.022	19.8k	4	BUSKULIC	96F ALEP $e^+e^- \rightarrow Z$

CHARGED b -HADRON ADMIXTURE MEAN LIFE

VALUE (10^{-12} s)	DOCUMENT ID	TECN	COMMENT
1.72±0.08±0.06	26	ADAM	95 DLPH $e^+e^- \rightarrow Z$

26 ADAM 95 data analyzed using vertex-charge technique to tag b -hadron charge.

NEUTRAL b -HADRON ADMIXTURE MEAN LIFE

VALUE (10^{-12} s)	DOCUMENT ID	TECN	COMMENT
1.58±0.11±0.09	27	ADAM	95 DLPH $e^+e^- \rightarrow Z$

27 ADAM 95 data analyzed using vertex-charge technique to tag b -hadron charge.

See key on page 239

Meson Particle Listings

$B^\pm/B^0/B_s^0/b$ -baryon ADMIXTURE

MEAN LIFE RATIO $\tau_{\text{charged } b\text{-hadron}}/\tau_{\text{neutral } b\text{-hadron}}$

VALUE	DOCUMENT ID	TECN	COMMENT
$1.09^{+0.11}_{-0.10} \pm 0.08$	28 ADAM	95 DLPH	$e^+e^- \rightarrow Z$

28 ADAM 95 data analyzed using vertex-charge technique to tag b -hadron charge.

$$|\Delta\tau_b|/\tau_{b,\bar{b}}$$

$\tau_{b,\bar{b}}$ and $|\Delta\tau_b|$ are the mean life average and difference between b and \bar{b} hadrons.

VALUE	DOCUMENT ID	TECN	COMMENT
$-0.001 \pm 0.012 \pm 0.008$	29 ABBIENDI	99J OPAL	$e^+e^- \rightarrow Z$

29 Data analyzed using both the jet charge and the charge of secondary vertex in the opposite hemisphere.

\bar{b} PRODUCTION FRACTIONS AND DECAY MODES

The branching fraction measurements are for an admixture of B mesons and baryons at energies above the $\Upsilon(4S)$. Only the highest energy results (LEP, Tevatron, $Spp\bar{S}$) are used in the branching fraction averages. In the following, we assume that the production fractions are the same at the LEP and at the Tevatron.

For inclusive branching fractions, e.g., $B \rightarrow D^\pm$ anything, the treatment of multiple D 's in the final state must be defined. One possibility would be to count the number of events with one-or-more D 's and divide by the total number of B 's. Another possibility would be to count the total number of D 's and divide by the total number of B 's, which is the definition of average multiplicity. The two definitions are identical when only one of the specified particles is allowed in the final state. Even though the "one-or-more" definition seems sensible, for practical reasons inclusive branching fractions are almost always measured using the multiplicity definition. For heavy final state particles, authors call their results inclusive branching fractions while for light particles some authors call their results multiplicities. In the B sections, we list all results as inclusive branching fractions, adopting a multiplicity definition. This means that inclusive branching fractions can exceed 100% and that inclusive partial widths can exceed total widths, just as inclusive cross sections can exceed total cross sections.

The modes below are listed for a \bar{b} initial state. b modes are their charge conjugates. Reactions indicate the weak decay vertex and do not include mixing.

Mode	Fraction (Γ_i/Γ)	Scale factor/ Confidence level
------	--------------------------------	-----------------------------------

PRODUCTION FRACTIONS

The production fractions for weakly decaying b -hadrons at high energy have been calculated from the best values of mean lives, mixing parameters, and branching fractions in this edition by the LEP B Oscillation Working Group as described in the note "Production and Decay of b -Flavored Hadrons" in the B^\pm Particle Listings. Values assume

$$B(\bar{b} \rightarrow B^+) = B(\bar{b} \rightarrow B^0)$$

$$B(\bar{b} \rightarrow B^+) + B(\bar{b} \rightarrow B^0) + B(\bar{b} \rightarrow B_s^0) + B(b \rightarrow b\text{-baryon}) = 100\%.$$

The notation for production fractions varies in the literature (f_d , d_{B^0} , $f(b \rightarrow \bar{B}^0)$, $\text{Br}(b \rightarrow \bar{B}^0)$). We use our own branching fraction notation here, $B(\bar{b} \rightarrow B^0)$.

Γ_1	B^+	(38.9 \pm 1.3) %
Γ_2	B^0	(38.9 \pm 1.3) %
Γ_3	B_s^0	(10.7 \pm 1.4) %
Γ_4	b -baryon	(11.6 \pm 2.0) %
Γ_5	B_c	—

DECAY MODES

Semileptonic and leptonic modes

Γ_6	ν anything	(23.1 \pm 1.5) %	
Γ_7	$\ell^+ \nu_\ell$ anything	[a] (10.73 \pm 0.18) %	S=1.1
Γ_8	$e^+ \nu_e$ anything	(10.86 \pm 0.35) %	
Γ_9	$\mu^+ \nu_\mu$ anything	(10.95 \pm 0.29) %	
Γ_{10}	$D^- \ell^+ \nu_\ell$ anything	[a] (2.02 \pm 0.29) %	
Γ_{11}	$\bar{D}^0 \ell^+ \nu_\ell$ anything	[a] (6.6 \pm 0.6) %	
Γ_{12}	$D^{*-} \ell^+ \nu_\ell$ anything	[a] (2.76 \pm 0.29) %	
Γ_{13}	$\bar{D}_s^0 \ell^+ \nu_\ell$ anything	[a,b] seen	
Γ_{14}	$D_s^- \ell^+ \nu_\ell$ anything	[a,b] seen	
Γ_{15}	$\bar{D}_s^*(2460)^0 \ell^+ \nu_\ell$ anything	seen	
Γ_{16}	$D_s^*(2460)^- \ell^+ \nu_\ell$ anything	seen	
Γ_{17}	charmless $\ell^+ \bar{\nu}_\ell$	[a] (1.7 \pm 0.6) $\times 10^{-3}$	
Γ_{18}	$\tau^+ \nu_\tau$ anything	(2.6 \pm 0.4) %	
Γ_{19}	$\bar{c} \rightarrow \ell^- \bar{\nu}_\ell$ anything	[a] (8.3 \pm 0.4) %	

Charmed meson and baryon modes

Γ_{20}	\bar{D}^0 anything	(60.5 \pm 3.2) %	
Γ_{21}	$D^0 D_s^\pm$ anything	[c] (9.1 \pm 3.9) %	
Γ_{22}	$D^\mp D_s^\pm$ anything	[c] (4.0 \pm 2.3) %	
Γ_{23}	$\bar{D}^0 D^0$ anything	[c] (5.1 \pm 2.0) %	
Γ_{24}	$D^0 D^\pm$ anything	[c] (2.7 \pm 1.6) %	
Γ_{25}	$D^\pm D^\mp$ anything	[c] < 9 $\times 10^{-3}$	CL=90%
Γ_{26}	D^- anything	(23.7 \pm 2.3) %	
Γ_{27}	$D^*(2010)^+$ anything	(17.3 \pm 2.0) %	
Γ_{28}	$D_1(2420)^0$ anything	(5.0 \pm 1.5) %	
Γ_{29}	$D^*(2010)^\mp D_s^\pm$ anything	[c] (3.3 \pm 1.6) %	
Γ_{30}	$D^0 D^*(2010)^\pm$ anything	[c] (3.0 \pm 1.1) %	
Γ_{31}	$D^*(2010)^\pm D^\mp$ anything	[c] (2.5 \pm 1.2) %	
Γ_{32}	$D^*(2010)^\pm D^*(2010)^\mp$ anything	[c] (1.2 \pm 0.4) %	
Γ_{33}	$D_s^*(2460)^0$ anything	(4.7 \pm 2.7) %	
Γ_{34}	\bar{D}_s^0 anything	(18 \pm 5) %	
Γ_{35}	Λ_c anything	(9.7 \pm 2.9) %	
Γ_{36}	\bar{c}/c anything	[d] (117 \pm 4) %	

Charmonium modes

Γ_{37}	$J/\psi(1S)$ anything	(1.16 \pm 0.10) %
Γ_{38}	$\psi(2S)$ anything	(4.8 \pm 2.4) $\times 10^{-3}$
Γ_{39}	$\chi_{c1}(1P)$ anything	(1.8 \pm 0.5) %

K or K^* modes

Γ_{40}	$\bar{3}\gamma$	(3.1 \pm 1.1) $\times 10^{-4}$
Γ_{41}	K^\pm anything	(74 \pm 6) %
Γ_{42}	K_S^0 anything	(29.0 \pm 2.9) %

Pion modes

Γ_{43}	π^\pm anything	(397 \pm 21) %
Γ_{44}	π^0 anything	[d] (278 \pm 60) %

Baryon modes

Γ_{45}	p/\bar{p} anything	(13.1 \pm 1.1) %
---------------	----------------------	----------------------

Other modes

Γ_{46}	charged anything	[d] (497 \pm 7) %
Γ_{47}	hadron ⁺ hadron ⁻	(1.7 \pm 1.0) $\times 10^{-5}$
Γ_{48}	charmless	(7 \pm 21) $\times 10^{-3}$

Baryon modes

Γ_{49}	$\Lambda/\bar{\Lambda}$ anything	(5.9 \pm 0.6) %
Γ_{50}	b -baryon anything	(10.2 \pm 2.8) %

$\Delta B = 1$ weak neutral current (B_1) modes

Γ_{51}	e^+e^- anything		
Γ_{52}	$\mu^+\mu^-$ anything	B_1	< 3.2 $\times 10^{-4}$ CL=90%
Γ_{53}	$\nu\bar{\nu}$ anything		

[a] An ℓ indicates an e or a μ mode, not a sum over these modes.

[b] D_j represents an unresolved mixture of pseudoscalar and tensor D^{**} (P -wave) states.

[c] The value is for the sum of the charge states or particle/antiparticle states indicated.

[d] Inclusive branching fractions have a multiplicity definition and can be greater than 100%.

$B^\pm/B^0/B_s^0/b$ -baryon ADMIXTURE BRANCHING RATIOS

$\Gamma(B_s^0)/[\Gamma(B^+) + \Gamma(B^0)]$	$\Gamma_3/(\Gamma_1 + \Gamma_2)$		
VALUE	DOCUMENT ID	TECN	COMMENT
0.21 ± 0.04 OUR AVERAGE			
0.213 \pm 0.068	30 AFFOLDER	00E CDF	$p\bar{p}$ at 1.8 TeV
0.21 \pm 0.036 \pm 0.038 \pm 0.030	31 ABE	99P CDF	$\bar{p}p$ at 1.8 TeV
	30 AFFOLDER	00E	uses several electron-charm final states in $b \rightarrow ce^-X$.
	31 ABE	99P	uses the numbers of $K^*(892)^0$, $K^*(892)^+$, and $\phi(1020)$ events produced in association with the double semileptonic decays $b \rightarrow c\mu^-X$ with $c \rightarrow s\mu^+X$.
$\Gamma(b\text{-baryon})/[\Gamma(B^+) + \Gamma(B^0)]$	$\Gamma_4/(\Gamma_1 + \Gamma_2)$		
VALUE	DOCUMENT ID	TECN	COMMENT
0.118 ± 0.042	32 AFFOLDER	00E CDF	$p\bar{p}$ at 1.8 TeV
	32 AFFOLDER	00E	uses several electron-charm final states in $b \rightarrow ce^-X$.

Meson Particle Listings

 $B^\pm/B^0/B_s^0/b$ -baryon ADMIXTURE $\Gamma(\nu\text{ anything})/\Gamma_{\text{total}}$

VALUE	DOCUMENT ID	TECN	COMMENT	Γ_6/Γ
-------	-------------	------	---------	-------------------

$0.2308 \pm 0.0077 \pm 0.0124$ 33,34 ACCIARRI 96c L3 $e^+e^- \rightarrow Z$

³³ ACCIARRI 96c assumes relative b semileptonic decay rates $e:\mu:\tau$ of 1:1:0.25. Based on missing-energy spectrum.

³⁴ Assumes Standard Model value for R_B .

 $\Gamma(\ell^+ \nu_\ell \text{ anything})/\Gamma_{\text{total}}$

VALUE	DOCUMENT ID	TECN	COMMENT	Γ_7/Γ
-------	-------------	------	---------	-------------------

0.1073 ± 0.0018 OUR AVERAGE Error includes scale factor of 1.1.

$0.1083 \pm 0.0010^{+0.0028}_{-0.0024}$ 35 ABBIENDI 00E OPAL $e^+e^- \rightarrow Z$

$0.1016 \pm 0.0013 \pm 0.0030$ 36 ACCIARRI 00 L3 $e^+e^- \rightarrow Z$

$0.1085 \pm 0.0012 \pm 0.0047$ 37,38 ACCIARRI 96c L3 $e^+e^- \rightarrow Z$

$0.1106 \pm 0.0039 \pm 0.0022$ 39 ABREU 95d DLPH $e^+e^- \rightarrow Z$

$0.114 \pm 0.003 \pm 0.004$ 40 BUSKULIC 94g ALEP $e^+e^- \rightarrow Z$

$0.100 \pm 0.007 \pm 0.007$ 41 ABREU 93c DLPH $e^+e^- \rightarrow Z$

• • • We do not use the following data for averages, fits, limits, etc. • • •

$0.105 \pm 0.006 \pm 0.005$ 42 AKERS 93b OPAL Repl. by ABBIENDI 00E

³⁵ ABBIENDI 00E result is determined by comparing the distribution of several kinematic variables of leptonic events in a lifetime tagged $Z \rightarrow b\bar{b}$ sample using artificial neural network techniques. The first error is statistical; the second error is the total systematic error.

³⁶ ACCIARRI 00 result obtained from a combined fit of $R_b = \Gamma(Z \rightarrow b\bar{b})/\Gamma(Z \rightarrow \text{hadrons})$ and $B(b \rightarrow \ell\nu X)$, using double-tagging method.

³⁷ ACCIARRI 96c result obtained by a fit to the single lepton spectrum.

³⁸ Assumes Standard Model value for R_B .

³⁹ ABREU 95d give systematic errors ± 0.0019 (model) and 0.0012 (R_C). We combine these in quadrature.

⁴⁰ BUSKULIC 94g uses e and μ events. This value is from a global fit to the lepton p and p_T (relative to jet) spectra which also determines the b and c production fractions, the fragmentation functions, and the forward-backward asymmetries. This branching ratio depends primarily on the ratio of dileptons to single leptons at high p_T , but the lower p_T portion of the lepton spectrum is included in the global fit to reduce the model dependence. The model dependence is ± 0.0026 and is included in the systematic error.

⁴¹ ABREU 93c event count includes ee events. Combining ee , $\mu\mu$, and $e\mu$ events, they obtain $0.100 \pm 0.007 \pm 0.007$.

⁴² AKERS 93b analysis performed using single and dilepton events.

 $\Gamma(e^+ \nu_e \text{ anything})/\Gamma_{\text{total}}$

VALUE	DOCUMENT ID	TECN	COMMENT	Γ_8/Γ
-------	-------------	------	---------	-------------------

0.1086 ± 0.0035 OUR AVERAGE

$0.1078 \pm 0.0008^{+0.0050}_{-0.0046}$ 43 ABBIENDI 00E OPAL $e^+e^- \rightarrow Z$

$0.1089 \pm 0.0020 \pm 0.0051$ 44,45 ACCIARRI 96c L3 $e^+e^- \rightarrow Z$

$0.107 \pm 0.015 \pm 0.007$ 260 46 ABREU 93c DLPH $e^+e^- \rightarrow Z$

$0.138 \pm 0.032 \pm 0.008$ 47 ADEVA 91c L3 $e^+e^- \rightarrow Z$

• • • We do not use the following data for averages, fits, limits, etc. • • •

$0.086 \pm 0.027 \pm 0.008$ 48 ABE 93E VNS $E_{\text{cm}}^{ee} = 58$ GeV

$0.109 \pm 0.014^{+0.0055}_{-0.013}$ 2719 49 AKERS 93b OPAL Repl. by ABBIENDI 00E

$0.111 \pm 0.028 \pm 0.026$ BEHREND 90d CELL $E_{\text{cm}}^{ee} = 43$ GeV

$0.150 \pm 0.011 \pm 0.022$ BEHREND 90d CELL $E_{\text{cm}}^{ee} = 35$ GeV

$0.112 \pm 0.009 \pm 0.011$ ONG 88 MRK2 $E_{\text{cm}}^{ee} = 29$ GeV

$0.149 \pm 0.022^{+0.019}_{-0.019}$ PAL 86 DLCO $E_{\text{cm}}^{ee} = 29$ GeV

$0.110 \pm 0.018 \pm 0.010$ AIHARA 85 TPC $E_{\text{cm}}^{ee} = 29$ GeV

$0.111 \pm 0.034 \pm 0.040$ ALTHOFF 84J TASS $E_{\text{cm}}^{ee} = 34.6$ GeV

0.146 ± 0.028 KOOP 84 DLCO Repl. by PAL 86

$0.116 \pm 0.021 \pm 0.017$ NELSON 83 MRK2 $E_{\text{cm}}^{ee} = 29$ GeV

⁴³ ABBIENDI 00E result is determined by comparing the distribution of several kinematic variables of leptonic events in a lifetime tagged $Z \rightarrow b\bar{b}$ sample using artificial neural network techniques. The first error is statistical; the second error is the total systematic error.

⁴⁴ ACCIARRI 96c result obtained by a fit to the single lepton spectrum.

⁴⁵ Assumes Standard Model value for R_B .

⁴⁶ ABREU 93c event count includes ee events. Combining ee , $\mu\mu$, and $e\mu$ events, they obtain $0.100 \pm 0.007 \pm 0.007$.

⁴⁷ ADEVA 91c measure the average $B(b \rightarrow eX)$ branching ratio using single and double tagged b enhanced Z events. Combining e and μ results, they obtain $0.113 \pm 0.010 \pm 0.006$. Constraining the initial number of b quarks by the Standard Model prediction (378 ± 3 MeV) for the decay of the Z into $b\bar{b}$, the electron result gives $0.112 \pm 0.004 \pm 0.008$. They obtain $0.119 \pm 0.003 \pm 0.006$ when e and μ results are combined. Used to measure the $b\bar{b}$ width itself, this electron result gives $370 \pm 12 \pm 24$ MeV and combined with the muon result gives $385 \pm 7 \pm 22$ MeV.

⁴⁸ ABE 93E experiment also measures forward-backward asymmetries and fragmentation functions for b and c .

⁴⁹ AKERS 93b analysis performed using single and dilepton events.

 $\Gamma(\mu^+ \nu_\mu \text{ anything})/\Gamma_{\text{total}}$

VALUE	DOCUMENT ID	TECN	COMMENT	Γ_9/Γ
-------	-------------	------	---------	-------------------

0.1095 ± 0.0029 OUR AVERAGE

$0.1096 \pm 0.0008^{+0.0034}_{-0.0027}$ 50 ABBIENDI 00E OPAL $e^+e^- \rightarrow Z$

$0.1082 \pm 0.0015 \pm 0.0059$ 51,52 ACCIARRI 96c L3 $e^+e^- \rightarrow Z$

$0.110 \pm 0.012 \pm 0.007$ 656 53 ABREU 93c DLPH $e^+e^- \rightarrow Z$

$0.113 \pm 0.012 \pm 0.006$ 54 ADEVA 91c L3 $e^+e^- \rightarrow Z$

• • • We do not use the following data for averages, fits, limits, etc. • • •

VALUE	DOCUMENT ID	TECN	COMMENT	Γ_6/Γ
-------	-------------	------	---------	-------------------

$0.122 \pm 0.006 \pm 0.007$ 52 UENO 96 AMY e^+e^- at 57.9 GeV

$0.101 \pm 0.010^{+0.0055}_{-0.009}$ 4248 55 AKERS 93b OPAL Repl. by ABBIENDI 00E

$0.104 \pm 0.023 \pm 0.016$ BEHREND 90d CELL $E_{\text{cm}}^{ee} = 43$ GeV

$0.148 \pm 0.010 \pm 0.016$ BEHREND 90d CELL $E_{\text{cm}}^{ee} = 35$ GeV

$0.118 \pm 0.012 \pm 0.010$ ONG 88 MRK2 $E_{\text{cm}}^{ee} = 29$ GeV

$0.117 \pm 0.016 \pm 0.015$ BARTEL 87 JADE $E_{\text{cm}}^{ee} = 34.6$ GeV

$0.114 \pm 0.018 \pm 0.025$ BARTEL 85J JADE Repl. by BARTEL 87

$0.117 \pm 0.028 \pm 0.010$ ALTHOFF 84G TASS $E_{\text{cm}}^{ee} = 34.5$ GeV

$0.105 \pm 0.015 \pm 0.013$ ADEVA 83b MRKJ $E_{\text{cm}}^{ee} = 33\text{--}38.5$ GeV

$0.155 \pm 0.054^{+0.029}_{-0.029}$ FERNANDEZ 83d MAC $E_{\text{cm}}^{ee} = 29$ GeV

⁵⁰ ABBIENDI 00E result is determined by comparing the distribution of several kinematic variables of leptonic events in a lifetime tagged $Z \rightarrow b\bar{b}$ sample using artificial neural network techniques. The first error is statistical; the second error is the total systematic error.

⁵¹ ACCIARRI 96c result obtained by a fit to the single lepton spectrum.

⁵² Assumes Standard Model value for R_B .

⁵³ ABREU 93c event count includes $\mu\mu$ events. Combining ee , $\mu\mu$, and $e\mu$ events, they obtain $0.100 \pm 0.007 \pm 0.007$.

⁵⁴ ADEVA 91c measure the average $B(b \rightarrow eX)$ branching ratio using single and double tagged b enhanced Z events. Combining e and μ results, they obtain $0.113 \pm 0.010 \pm 0.006$. Constraining the initial number of b quarks by the Standard Model prediction (378 ± 3 MeV) for the decay of the Z into $b\bar{b}$, the muon result gives $0.123 \pm 0.003 \pm 0.006$. They obtain $0.119 \pm 0.003 \pm 0.006$ when e and μ results are combined. Used to measure the $b\bar{b}$ width itself, this muon result gives $394 \pm 9 \pm 22$ MeV and combined with the electron result gives $385 \pm 7 \pm 22$ MeV.

⁵⁵ AKERS 93b analysis performed using single and dilepton events.

 $\Gamma(D^- \ell^+ \nu_\ell \text{ anything})/\Gamma_{\text{total}}$

VALUE	DOCUMENT ID	TECN	COMMENT	Γ_{10}/Γ
-------	-------------	------	---------	----------------------

$0.2020 \pm 0.0026 \pm 0.0013$ 56 AKERS 95Q OPAL $e^+e^- \rightarrow Z$

⁵⁶ AKERS 95Q reports $B(\bar{b} \rightarrow D^- \ell^+ \nu_\ell \text{ anything}) \times B(D^+ \rightarrow K^- \pi^+ \pi^+) = (1.82 \pm 0.20 \pm 0.12) \times 10^{-3}$. We divide by our best value $B(D^+ \rightarrow K^- \pi^+ \pi^+) = (9.0 \pm 0.6) \times 10^{-2}$. Our first error is their experiment's error and our second error is the systematic error from using our best value.

 $\Gamma(D^0 \ell^+ \nu_\ell \text{ anything})/\Gamma_{\text{total}}$

VALUE	DOCUMENT ID	TECN	COMMENT	Γ_{11}/Γ
-------	-------------	------	---------	----------------------

$0.066 \pm 0.006 \pm 0.001$ 57 AKERS 95Q OPAL $e^+e^- \rightarrow Z$

⁵⁷ AKERS 95Q reports $B(\bar{b} \rightarrow D^0 \ell^+ \nu_\ell \text{ anything}) \times B(D^0 \rightarrow K^- \pi^+) = (2.52 \pm 0.14 \pm 0.17) \times 10^{-3}$. We divide by our best value $B(D^0 \rightarrow K^- \pi^+) = (3.83 \pm 0.09) \times 10^{-2}$. Our first error is their experiment's error and our second error is the systematic error from using our best value.

 $\Gamma(D^{*+} \ell^+ \nu_\ell \text{ anything})/\Gamma_{\text{total}}$

VALUE	DOCUMENT ID	TECN	COMMENT	Γ_{12}/Γ
-------	-------------	------	---------	----------------------

$0.0276 \pm 0.0027 \pm 0.0011$ 58 AKERS 95Q OPAL $e^+e^- \rightarrow Z$

⁵⁸ AKERS 95Q reports $B(\bar{b} \rightarrow D^{*+} \ell^+ \nu_\ell X) \times B(D^{*+} \rightarrow D^0 \pi^+) \times B(D^0 \rightarrow K^- \pi^+) = ((7.53 \pm 0.47 \pm 0.56) \times 10^{-4})$ and uses $B(D^{*+} \rightarrow D^0 \pi^+) = 0.681 \pm 0.013$ and $B(D^0 \rightarrow K^- \pi^+) = 0.0401 \pm 0.0014$ to obtain the above result. The first error is the experiments error and the second error is the systematic error from the D^{*+} and D^0 branching ratios.

 $\Gamma(D_j^0 \ell^+ \nu_\ell \text{ anything})/\Gamma_{\text{total}}$

VALUE	DOCUMENT ID	TECN	COMMENT	Γ_{13}/Γ
-------	-------------	------	---------	----------------------

D_j represents an unresolved mixture of pseudoscalar and tensor D^{**} (P -wave) states.

seen 59 AKERS 95Q OPAL $e^+e^- \rightarrow Z$

⁵⁹ AKERS 95Q quotes the product branching ratio $B(\bar{b} \rightarrow D_j^0 \ell^+ \nu_\ell X) B(D_j^0 \rightarrow D^{*+} \pi^-) = ((6.1 \pm 1.3 \pm 1.3) \times 10^{-3})$.

 $\Gamma(D_j^- \ell^+ \nu_\ell \text{ anything})/\Gamma_{\text{total}}$

VALUE	DOCUMENT ID	TECN	COMMENT	Γ_{14}/Γ
-------	-------------	------	---------	----------------------

D_j represents an unresolved mixture of pseudoscalar and tensor D^{**} (P -wave) states.

seen 60 AKERS 95Q OPAL $e^+e^- \rightarrow Z$

⁶⁰ AKERS 95Q quotes the product branching ratio $B(\bar{b} \rightarrow D_j^- \ell^+ \nu_\ell X) B(D_j^- \rightarrow D^0 \pi^-) = ((7.0 \pm 1.9 \pm 1.3) \times 10^{-3})$.

 $\Gamma(D_2^*(2460)^0 \ell^+ \nu_\ell \text{ anything})/\Gamma_{\text{total}}$

VALUE	DOCUMENT ID	TECN	COMMENT	Γ_{15}/Γ
-------	-------------	------	---------	----------------------

seen 61 AKERS 95Q OPAL $e^+e^- \rightarrow Z$

⁶¹ AKERS 95Q quotes the product branching ratio $B(\bar{b} \rightarrow D_2^*(2460)^0 \ell^+ \nu_\ell \text{ anything}) B(D_2^*(2460)^0 \rightarrow D^+ \pi^-) = (1.6 \pm 0.7 \pm 0.3) \times 10^{-3}$.

 $\Gamma(D_2^*(2460)^- \ell^+ \nu_\ell \text{ anything})/\Gamma_{\text{total}}$

VALUE	DOCUMENT ID	TECN	COMMENT	Γ_{16}/Γ
-------	-------------	------	---------	----------------------

seen 62 AKERS 95Q OPAL $e^+e^- \rightarrow Z$

⁶² AKERS 95Q quotes the product branching ratio $B(\bar{b} \rightarrow D_2^*(2460)^- \ell^+ \nu_\ell \text{ anything}) B(D_2^*(2460)^- \rightarrow D^0 \pi^-) = 4.2 \pm 1.3^{+0.7}_{-1.2}$.

See key on page 239

Meson Particle Listings

$B^\pm/B^0/B_s^0/b$ -baryon ADMIXTURE

$\Gamma(\text{charmless } \ell\nu_\ell)/\Gamma_{\text{total}}$ Γ_{17}/Γ
 "OUR EVALUATION" is an average of the data listed below performed by the LEP Heavy Flavour Steering Group. The averaging procedure takes into account correlations between the measurements.

VALUE	DOCUMENT ID	TECN	COMMENT
0.00167 ± 0.00055 OUR EVALUATION			
0.0017 ± 0.0005 OUR AVERAGE			
0.00157 ± 0.00035 ± 0.00055	63 ABREU	00D DLPH	$e^+e^- \rightarrow Z$
0.00173 ± 0.00055 ± 0.00055	64 BARATE	99G ALEP	$e^+e^- \rightarrow Z$
0.0033 ± 0.0010 ± 0.0017	65 ACCIARRI	98K L3	$e^+e^- \rightarrow Z$

63 ABREU 00D result obtained from a fit to the numbers of decays in $b \rightarrow u$ enriched and depleted samples and their lepton spectra, and assuming $|V_{cb}| = 0.0384 \pm 0.0033$ and $\tau_b = 1.564 \pm 0.014$ ps.

64 Uses lifetime tagged $b\bar{d}$ sample.

65 ACCIARRI 98K assumes $R_b = 0.2174 \pm 0.0009$ at Z decay.

$\Gamma(\tau^+ \nu_\tau \text{ anything})/\Gamma_{\text{total}}$ Γ_{18}/Γ
 VALUE (units 10^{-2})

VALUE (units 10^{-2})	DOCUMENT ID	TECN	COMMENT
2.6 ± 0.4 OUR AVERAGE			
1.7 ± 0.5 ± 1.1	66,67 ACCIARRI	96C L3	$e^+e^- \rightarrow Z$
2.75 ± 0.30 ± 0.37	405 68 BUSKULIC	95 ALEP	$e^+e^- \rightarrow Z$
2.4 ± 0.7 ± 0.8	1032 69 ACCIARRI	94C L3	$e^+e^- \rightarrow Z$

• • • We do not use the following data for averages, fits, limits, etc. • • •

4.08 ± 0.76 ± 0.62 BUSKULIC 93B ALEP Repl. by BUSKULIC 95

66 ACCIARRI 96C result obtained from missing energy spectrum.

67 Assumes Standard Model value for R_B .

68 BUSKULIC 95 uses missing-energy technique.

69 This is a direct result using tagged $b\bar{d}$ events at the Z, but species are not separated.

$\Gamma(\bar{b} \rightarrow \bar{c} \rightarrow \ell^+ \nu_\ell \text{ anything})/\Gamma_{\text{total}}$ Γ_{19}/Γ
 VALUE

VALUE	DOCUMENT ID	TECN	COMMENT
0.083 ± 0.004 OUR AVERAGE			
0.0840 ± 0.0016 +0.0039 -0.0036	70 ABBIENDI	00E OPAL	$e^+e^- \rightarrow Z$
0.0770 ± 0.0097 ± 0.0046	71 ABREU	95D DLPH	$e^+e^- \rightarrow Z$
0.082 ± 0.003 ± 0.012	72 BUSKULIC	94G ALEP	$e^+e^- \rightarrow Z$

• • • We do not use the following data for averages, fits, limits, etc. • • •

0.077 ± 0.004 ± 0.007 73 AKERS 93B OPAL Repl. by ABBIENDI 00E

70 ABBIENDI 00E result is determined by comparing the distribution of several kinematic variables of leptonic events in a lifetime tagged $Z \rightarrow b\bar{b}$ sample using artificial neural network techniques. The first error is statistic; the second error is the total systematic error.

71 ABREU 95D give systematic errors ± 0.0033 (model) and 0.0032 (R_C). We combine these in quadrature. This result is from the same global fit as their $\Gamma(\bar{b} \rightarrow \ell^+ \nu_\ell X)$ data.

72 BUSKULIC 94G uses e and μ events. This value is from the same global fit as their $\Gamma(\bar{b} \rightarrow \ell^+ \nu_\ell \text{ anything})/\Gamma_{\text{total}}$ data.

73 AKERS 93B analysis performed using single and dilepton events.

$\Gamma(D^0 \text{ anything})/\Gamma_{\text{total}}$ Γ_{20}/Γ
 VALUE

VALUE	DOCUMENT ID	TECN	COMMENT
0.605 ± 0.029 ± 0.014	74 BUSKULIC	96Y ALEP	$e^+e^- \rightarrow Z$

74 BUSKULIC 96Y reports $0.605 \pm 0.024 \pm 0.016$ for $B(D^0 \rightarrow K^- \pi^+) = 0.0383$. We rescale to our best value $B(D^0 \rightarrow K^- \pi^+) = (3.83 \pm 0.09) \times 10^{-2}$. Our first error is their experiment's error and our second error is the systematic error from using our best value.

$\Gamma(D^0 D_s^\pm \text{ anything})/\Gamma_{\text{total}}$ Γ_{21}/Γ
 VALUE

VALUE	DOCUMENT ID	TECN	COMMENT
0.091 ± 0.020 + 0.034 - 0.018 - 0.022	75 BARATE	98Q ALEP	$e^+e^- \rightarrow Z$

75 The systematic error includes the uncertainties due to the charm branching ratios.

$\Gamma(D^\mp D_s^\pm \text{ anything})/\Gamma_{\text{total}}$ Γ_{22}/Γ
 VALUE

VALUE	DOCUMENT ID	TECN	COMMENT
0.040 ± 0.017 + 0.016 - 0.014 - 0.011	76 BARATE	98Q ALEP	$e^+e^- \rightarrow Z$

76 The systematic error includes the uncertainties due to the charm branching ratios.

$[\Gamma(D^0 D_s^\pm \text{ anything}) + \Gamma(D^\mp D_s^\pm \text{ anything})]/\Gamma_{\text{total}}$ $(\Gamma_{21} + \Gamma_{22})/\Gamma$
 VALUE

VALUE	DOCUMENT ID	TECN	COMMENT
0.131 ± 0.026 + 0.048 - 0.022 - 0.031	77 BARATE	98Q ALEP	$e^+e^- \rightarrow Z$

77 The systematic error includes the uncertainties due to the charm branching ratios.

$\Gamma(D^0 D^0 \text{ anything})/\Gamma_{\text{total}}$ Γ_{23}/Γ
 VALUE

VALUE	DOCUMENT ID	TECN	COMMENT
0.051 ± 0.016 + 0.012 - 0.014 - 0.011	78 BARATE	98Q ALEP	$e^+e^- \rightarrow Z$

78 The systematic error includes the uncertainties due to the charm branching ratios.

$\Gamma(D^0 D^\pm \text{ anything})/\Gamma_{\text{total}}$ Γ_{24}/Γ
 VALUE

VALUE	DOCUMENT ID	TECN	COMMENT
0.027 ± 0.015 + 0.010 - 0.013 - 0.009	79 BARATE	98Q ALEP	$e^+e^- \rightarrow Z$

79 The systematic error includes the uncertainties due to the charm branching ratios.

$[\Gamma(D^0 D^0 \text{ anything}) + \Gamma(D^0 D^\pm \text{ anything})]/\Gamma_{\text{total}}$ $(\Gamma_{23} + \Gamma_{24})/\Gamma$
 VALUE

VALUE	DOCUMENT ID	TECN	COMMENT
0.078 ± 0.020 + 0.018 - 0.018 - 0.016	80 BARATE	98Q ALEP	$e^+e^- \rightarrow Z$

80 The systematic error includes the uncertainties due to the charm branching ratios.

$\Gamma(D^\pm D^\mp \text{ anything})/\Gamma_{\text{total}}$ Γ_{25}/Γ
 VALUE

VALUE	CL%	DOCUMENT ID	TECN	COMMENT
< 0.009	90	BARATE	98Q ALEP	$e^+e^- \rightarrow Z$

$\Gamma(D^- \text{ anything})/\Gamma_{\text{total}}$ Γ_{26}/Γ
 VALUE

VALUE	DOCUMENT ID	TECN	COMMENT
0.237 ± 0.017 ± 0.015	81 BUSKULIC	96Y ALEP	$e^+e^- \rightarrow Z$

81 BUSKULIC 96Y reports $0.234 \pm 0.013 \pm 0.010$ for $B(D^+ \rightarrow K^- \pi^+ \pi^+) = 0.091$. We rescale to our best value $B(D^+ \rightarrow K^- \pi^+ \pi^+) = (9.0 \pm 0.6) \times 10^{-2}$. Our first error is their experiment's error and our second error is the systematic error from using our best value.

$\Gamma(D^*(2010)^+ \text{ anything})/\Gamma_{\text{total}}$ Γ_{27}/Γ
 VALUE

VALUE	DOCUMENT ID	TECN	COMMENT
0.173 ± 0.016 ± 0.012	82 ACKERSTAFF	98E OPAL	$e^+e^- \rightarrow Z$

82 Uses lepton tags to select $Z \rightarrow b\bar{b}$ events.

$\Gamma(D_1(2420)^0 \text{ anything})/\Gamma_{\text{total}}$ Γ_{28}/Γ
 VALUE

VALUE	DOCUMENT ID	TECN	COMMENT
0.050 ± 0.014 ± 0.006	83 ACKERSTAFF	97W OPAL	$e^+e^- \rightarrow Z$

83 ACKERSTAFF 97W assumes $B(D_1^*(2460)^0 \rightarrow D^{*+} \pi^-) = 0.21 \pm 0.04$ and $\Gamma_{b\bar{b}}/\Gamma_{\text{hadrons}} = 0.216$ at Z decay.

$\Gamma(D^*(2010)^\mp D_s^\pm \text{ anything})/\Gamma_{\text{total}}$ Γ_{29}/Γ
 VALUE

VALUE	DOCUMENT ID	TECN	COMMENT
0.033 ± 0.010 + 0.012 - 0.009 - 0.009	84 BARATE	98Q ALEP	$e^+e^- \rightarrow Z$

84 The systematic error includes the uncertainties due to the charm branching ratios.

$\Gamma(D^0 D^*(2010)^\pm \text{ anything})/\Gamma_{\text{total}}$ Γ_{30}/Γ
 VALUE

VALUE	DOCUMENT ID	TECN	COMMENT
0.030 ± 0.009 + 0.007 - 0.006 - 0.005	85 BARATE	98Q ALEP	$e^+e^- \rightarrow Z$

85 The systematic error includes the uncertainties due to the charm branching ratios.

$\Gamma(D^*(2010)^\pm D^\mp \text{ anything})/\Gamma_{\text{total}}$ Γ_{31}/Γ
 VALUE

VALUE	DOCUMENT ID	TECN	COMMENT
0.025 ± 0.010 + 0.006 - 0.009 - 0.005	86 BARATE	98Q ALEP	$e^+e^- \rightarrow Z$

86 The systematic error includes the uncertainties due to the charm branching ratios.

$\Gamma(D^*(2010)^\pm D^*(2010)^\mp \text{ anything})/\Gamma_{\text{total}}$ Γ_{32}/Γ
 VALUE

VALUE	DOCUMENT ID	TECN	COMMENT
0.012 ± 0.004 ± 0.002	87 BARATE	98Q ALEP	$e^+e^- \rightarrow Z$

87 The systematic error includes the uncertainties due to the charm branching ratios.

$\Gamma(D_s^*(2460)^0 \text{ anything})/\Gamma_{\text{total}}$ Γ_{33}/Γ
 VALUE

VALUE	DOCUMENT ID	TECN	COMMENT
0.047 ± 0.024 ± 0.013	88 ACKERSTAFF	97W OPAL	$e^+e^- \rightarrow Z$

88 ACKERSTAFF 97W assumes $B(D_s^*(2460)^0 \rightarrow D^{*+} \pi^-) = 0.21 \pm 0.04$ and $\Gamma_{b\bar{b}}/\Gamma_{\text{hadrons}} = 0.216$ at Z decay.

$\Gamma(D_s^- \text{ anything})/\Gamma_{\text{total}}$ Γ_{34}/Γ
 VALUE

VALUE	DOCUMENT ID	TECN	COMMENT
0.18 ± 0.02 ± 0.04	89 BUSKULIC	96Y ALEP	$e^+e^- \rightarrow Z$

89 BUSKULIC 96Y reports $0.183 \pm 0.019 \pm 0.009$ for $B(D_s^+ \rightarrow \phi \pi^+) = 0.036$. We rescale to our best value $B(D_s^+ \rightarrow \phi \pi^+) = (3.6 \pm 0.9) \times 10^{-2}$. Our first error is their experiment's error and our second error is the systematic error from using our best value.

$\Gamma(b \rightarrow \Lambda_c \text{ anything})/\Gamma_{\text{total}}$ Γ_{35}/Γ
 VALUE

VALUE	DOCUMENT ID	TECN	COMMENT
0.097 ± 0.013 ± 0.025	90 BUSKULIC	96Y ALEP	$e^+e^- \rightarrow Z$

90 BUSKULIC 96Y reports $0.110 \pm 0.014 \pm 0.006$ for $B(\Lambda_c^+ \rightarrow p K^- \pi^+) = 0.044$. We rescale to our best value $B(\Lambda_c^+ \rightarrow p K^- \pi^+) = (5.0 \pm 1.3) \times 10^{-2}$. Our first error is their experiment's error and our second error is the systematic error from using our best value.

$\Gamma(\bar{c} \text{ anything})/\Gamma_{\text{total}}$ Γ_{36}/Γ
 VALUE

VALUE	DOCUMENT ID	TECN	COMMENT
1.17 ± 0.04 OUR AVERAGE			
1.147 ± 0.041	91 ABREU	98D DLPH	$e^+e^- \rightarrow Z$
1.230 ± 0.036 ± 0.065	92 BUSKULIC	96Y ALEP	$e^+e^- \rightarrow Z$

91 ABREU 98D results are extracted from a fit to the b -tagging probability distribution based on the impact parameter.

92 BUSKULIC 96Y assumes PDG 96 production fractions for B^0, B^+, B_s, b baryons, and PDG 96 branching ratios for charm decays. This is sum of their inclusive $D^0, D^-, \bar{D}_s,$ and Λ_c branching ratios, corrected to include inclusive Ξ_c and charmonium.

See key on page 239

Meson Particle Listings

$B^\pm/B^0/B_s^0/b$ -baryon ADMIXTURE, B^* , $B_j^*(5732)$

ABREU	93C	PL B301 145	P. Abreu et al.	(DELPHI Collab.)
ABREU	93D	ZPHY C57 181	P. Abreu et al.	(DELPHI Collab.)
ABREU	93G	PL B312 253	P. Abreu et al.	(DELPHI Collab.)
ACTON	93C	PL B307 247	P.D. Acton et al.	(OPAL Collab.)
ACTON	93L	ZPHY C60 217	P.D. Acton et al.	(OPAL Collab.)
ADRIANI	93J	PL B317 467	O. Adriani et al.	(L3 Collab.)
ADRIANI	93K	PL B317 474	O. Adriani et al.	(L3 Collab.)
ADRIANI	93L	PL B317 637	O. Adriani et al.	(L3 Collab.)
AKERS	93B	ZPHY C60 199	R. Akers et al.	(OPAL Collab.)
BUSKULIC	93B	PL B298 479	D. Buskulic et al.	(ALEPH Collab.)
BUSKULIC	93D	PL B314 459	D. Buskulic et al.	(ALEPH Collab.)
ABREU	92	ZPHY C53 557	P. Abreu et al.	(DELPHI Collab.)
ACTON	92	PL B274 513	D.P. Acton et al.	(OPAL Collab.)
ADRIANI	92	PL B288 412	O. Adriani et al.	(L3 Collab.)
BUSKULIC	92F	PL B295 174	D. Buskulic et al.	(ALEPH Collab.)
BUSKULIC	92G	PL B295 396	D. Buskulic et al.	(ALEPH Collab.)
ADEVA	91C	PL B261 177	B. Adeva et al.	(L3 Collab.)
ADEVA	91H	PL B270 111	B. Adeva et al.	(L3 Collab.)
ALBAJAR	91C	PL B262 163	C. Albajar et al.	(UA1 Collab.)
ALEXANDER	91G	PL B266 485	G. Alexander et al.	(OPAL Collab.)
DECAMP	91C	PL B257 492	D. Decamp et al.	(ALEPH Collab.)
BEHREND	90D	ZPHY C47 333	H.J. Behrend et al.	(CELLO Collab.)
HAGEMANN	90	ZPHY C48 401	J. Hagemann et al.	(JADE Collab.)
LYONS	90	PR D41 982	L. Lyons, A.J. Martin, D.H. Saxon	(OXF, BRIS+)
BRAUNNSCH...	89B	ZPHY C44 1	R. Braunschweig et al.	(TASSO Collab.)
ONG	89	PRL 62 1236	R.A. Ong et al.	(Mark II Collab.)
KLEM	88	PR D37 41	D.E. Klem et al.	(DELCO Collab.)
ONG	88	PRL 60 2587	R.A. Ong et al.	(Mark II Collab.)
ASH	87	PL 59 640	W.W. Ash et al.	(MAC Collab.)
BARTEL	87	ZPHY C33 339	W. Bartel et al.	(JADE Collab.)
BROM	87	PL B195 301	J.M. Brom et al.	(HRS Collab.)
PAL	86	PR D33 2708	T. Pal et al.	(DELCO Collab.)
AIHARA	85	ZPHY C27 39	H. Aihara et al.	(TPC Collab.)
BARTEL	85J	PL 163B 277	W. Bartel et al.	(JADE Collab.)
ALTHOFF	84G	ZPHY C22 219	M. Althoff et al.	(TASSO Collab.)
ALTHOFF	84J	PL 146B 443	M. Althoff et al.	(DELCO Collab.)
KOOP	84	PRL 52 970	D.E. Koop et al.	(DELCO Collab.)
ADEVA	83	PRL 50 799	B. Adeva et al.	(Mark-J Collab.)
ADEVA	83B	PRL 51 443	B. Adeva et al.	(Mark-J Collab.)
BARTEL	83B	PL 132B 241	W. Bartel et al.	(JADE Collab.)
FERNANDEZ	83D	PRL 50 2054	E. Fernandez et al.	(MAC Collab.)
MATTEUZZI	83	PL 129B 141	C. Matteuzzi et al.	(Mark II Collab.)
NELSON	83	PRL 50 1542	M.E. Nelson et al.	(Mark II Collab.)

B* REFERENCES

ACKERSTAFF	97M	ZPHY C74 413	K. Ackerstaff et al.	(OPAL Collab.)
BUSKULIC	96D	ZPHY C69 393	D. Buskulic et al.	(ALEPH Collab.)
ABREU	95R	ZPHY C68 353	P. Abreu et al.	(DELPHI Collab.)
ACCIARRI	95B	PL B345 589	M. Acciari et al.	(L3 Collab.)
AKERIB	91	PRL 67 1692	D.S. Akerib et al.	(CLEO Collab.)
WU	91	PL B273 177	Q.W. Wu et al.	(CUSB II Collab.)
LEE-FRANZINI	90	PRL 65 2947	J. Lee-Franzini et al.	(CUSB II Collab.)
HAN	85	PRL 55 36	K. Han et al.	(COLU, LSU, MPIM, STON)

$B_j^*(5732)$
or B^{**}

$$J(P) = ?(??)$$

I, J, P need confirmation.

OMITTED FROM SUMMARY TABLE

Signal can be interpreted as stemming from several narrow and broad resonances. Needs confirmation.

$B_j^*(5732)$ MASS

VALUE (MeV)	EVTS	DOCUMENT ID	TECN	COMMENT
5697 ± 9	OUR AVERAGE	Error includes scale factor of 1.3. See the ideogram below.		
5695^{+17}_{-19}		¹ BARATE	98L ALEP	$e^+e^- \rightarrow Z$
$5704 \pm 4 \pm 10$	1944	² BUSKULIC	96D ALEP	$E_{cm}^{90} = 88-94$ GeV
$5732 \pm 5 \pm 20$	2157	ABREU	95B DLPH	$E_{cm}^{90} = 88-94$ GeV
5681 ± 11	1738	AKERS	95E OPAL	$E_{cm}^{90} = 88-94$ GeV
5713 ± 2		³ ACCIARRI	99N L3	$e^+e^- \rightarrow Z$

¹ BARATE 98L uses fully reconstructed B mesons to search for B^{**} production in the $B\pi^\pm$ system. In the framework of heavy quark symmetry (HQS), they also measured the mass of B_2^* to be $5739^{+8}_{-11} +^{+6}_{-4}$ MeV/ c^2 and the relative production rate of $B(b \rightarrow B_2^* \rightarrow B^{(*)}\pi)/B(b \rightarrow B_{u,d}) = (31 \pm 9 \pm 5)\%$.

² Using $m_{B\pi} - m_B = 424 \pm 4 \pm 10$ MeV.

³ ACCIARRI 99N uses inclusive reconstructed B mesons to search for B^{**} production in the $B^{(*)}\pi^\pm$ system. In the framework of HQET, they measured the mass of B_1^* and B_2^* to be $5670 \pm 10 \pm 13$ MeV and $5768 \pm 5 \pm 6$ with the $B(b \rightarrow B^{**}) = (32 \pm 3 \pm 6) \times 10^{-2}$. They also reported the evidence for the existence of an excited B -meson state or mixture of states in the region 5.9-6.0 GeV.

B^*

$$J(P) = \frac{1}{2}(1^-)$$

I, J, P need confirmation. Quantum numbers shown are quark-model predictions.

B^* MASS

From mass difference below and the average of our B masses ($m_{B^\pm} + m_{B^0}$)/2.

VALUE (MeV)	DOCUMENT ID
5325.0 ± 0.6	OUR FIT

$m_{B^*} - m_B$

VALUE (MeV)	EVTS	DOCUMENT ID	TECN	COMMENT
45.78 ± 0.35	OUR FIT			
45.78 ± 0.35	OUR AVERAGE			
$46.2 \pm 0.3 \pm 0.8$		¹ ACKERSTAFF	97M OPAL	$e^+e^- \rightarrow Z$
$45.3 \pm 0.35 \pm 0.87$	4227	¹ BUSKULIC	96D ALEP	$E_{cm}^{90} = 88-94$ GeV
$45.5 \pm 0.3 \pm 0.8$		¹ ABREU	95R DLPH	$E_{cm}^{90} = 88-94$ GeV
46.3 ± 1.9	1378	¹ ACCIARRI	95B L3	$E_{cm}^{90} = 88-94$ GeV
$46.4 \pm 0.3 \pm 0.8$		² AKERIB	91 CLE2	$e^+e^- \rightarrow \gamma X$
45.6 ± 0.8		² WU	91 CSB2	$e^+e^- \rightarrow \gamma X, \gamma \ell X$
45.4 ± 1.0		³ LEE-FRANZINI	90 CSB2	$e^+e^- \rightarrow T(5S)$

• • • We do not use the following data for averages, fits, limits, etc. • • •

- ⁴ HAN 85 is for $E_{cm} = 10.6-11.2$ GeV, giving an admixture of $B^0, B^+,$ and B_s .
- ¹ u, d, s flavor averaged.
- ² These papers report E_γ in the B^* center of mass. The $m_{B^*} - m_B$ is 0.2 MeV higher. $E_{cm} = 10.61-10.7$ GeV. Admixture of B^0 and B^+ mesons, but not B_s .
- ³ LEE-FRANZINI 90 value is for an admixture of B^0 and B^+ . They measure $46.7 \pm 0.4 \pm 0.2$ MeV for an admixture of $B^0, B^+,$ and B_s , and use the shape of the photon line to separate the above value.

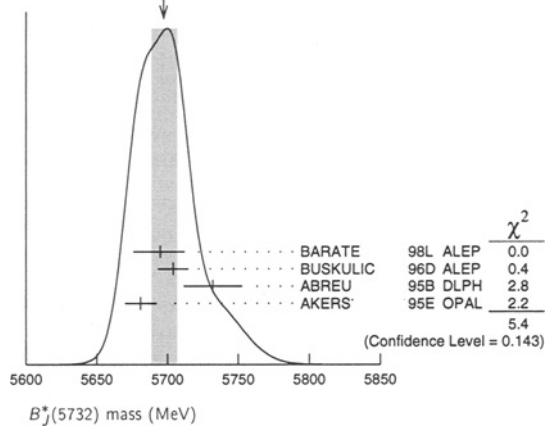
$$|(m_{B^{*+}} - m_{B^+}) - (m_{B^{*0}} - m_{B^0})|$$

VALUE (MeV)	CL%	DOCUMENT ID	TECN	COMMENT
< 6	95	ABREU	95R DLPH	$E_{cm}^{90} = 88-94$ GeV

B^* DECAY MODES

Mode	Fraction (Γ_i/Γ)
$\Gamma_1 B\gamma$	dominant

WEIGHTED AVERAGE
5697±9 (Error scaled by 1.3)



$B_j^*(5732)$ WIDTH

VALUE (MeV)	EVTS	DOCUMENT ID	TECN	COMMENT
128 ± 18	OUR AVERAGE			
145 ± 28	2157	ABREU	95B DLPH	$E_{cm}^{90} = 88-94$ GeV
116 ± 24	1738	AKERS	95E OPAL	$E_{cm}^{90} = 88-94$ GeV

$B_j^*(5732)$ DECAY MODES

Mode	Fraction (Γ_i/Γ)
$\Gamma_1 B^* \pi + B\pi$	dominant

$B_j^*(5732)$ REFERENCES

ACCIARRI	99N	PL B465 323	M. Acciari et al.	(L3 Collab.)
BARATE	98L	PL B425 215	R. Barate et al.	(ALEPH Collab.)
BUSKULIC	96D	ZPHY C69 393	D. Buskulic et al.	(ALEPH Collab.)
ABREU	95B	PL B345 598	P. Abreu et al.	(DELPHI Collab.)
AKERS	95E	ZPHY C66 19	R. Akers et al.	(OPAL Collab.)

Meson Particle Listings

B_s^0

BOTTOM, STRANGE MESONS

$(B = \pm 1, S = \mp 1)$

$B_s^0 = s\bar{b}, \bar{B}_s^0 = \bar{s}b$, similarly for $B_s^{*\prime}$'s

B_s^0

$I(J^P) = 0(0^-)$

I, J, P need confirmation. Quantum numbers shown are quark-model predictions.

B_s^0 MASS

VALUE (MeV)	EVTS	DOCUMENT ID	TECN	COMMENT
5369.6 ± 2.4 OUR FIT				
5369.6 ± 2.4 OUR AVERAGE				
5369.9 ± 2.3 ± 1.3	32	¹ ABE	96B CDF	$p\bar{p}$ at 1.8 TeV
5374 ± 16 ± 2	3	ABREU	94D DLPH	$e^+e^- \rightarrow Z$
5359 ± 19 ± 7	1	¹ AKERS	94J OPAL	$e^+e^- \rightarrow Z$
5368.6 ± 5.6 ± 1.5	2	BUSKULIC	93G ALEP	$e^+e^- \rightarrow Z$
• • • We do not use the following data for averages, fits, limits, etc. • • •				
5370 ± 40	6	² AKERS	94J OPAL	$e^+e^- \rightarrow Z$
5383.3 ± 4.5 ± 5.0	14	ABE	93F CDF	Repl by ABE 96B
¹ From the decay $B_s \rightarrow J/\psi(1S)\phi$.				
² From the decay $B_s \rightarrow D_s^- \pi^+$.				

$m_{B_s^0} - m_B$

m_B is the average of our B masses $(m_{B^\pm} + m_{B^0})/2$.

VALUE (MeV)	CL%	DOCUMENT ID	TECN	COMMENT
90.4 ± 2.4 OUR FIT				
89.7 ± 2.7 ± 1.2		ABE	96B CDF	$p\bar{p}$ at 1.8 TeV
• • • We do not use the following data for averages, fits, limits, etc. • • •				
80 to 130	68	LEE-FRANZINI90	CSB2	$e^+e^- \rightarrow \Upsilon(5S)$

$m_{B_s^0} - m_{B_s^{\pm}}$

See the $B_s^0 - \bar{B}_s^0$ MIXING section near the end of these B_s^0 Listings.

B_s^0 MEAN LIFE

"OUR EVALUATION" is an average of the data listed below performed by the LEP B Lifetimes Working Group as described in our review "Production and Decay of b -flavored Hadrons" in the B^\pm Section of the Listings. The averaging procedure takes into account correlations between the measurements and asymmetric lifetime errors.

VALUE (10^{-12} s)	EVTS	DOCUMENT ID	TECN	COMMENT
1.493 ± 0.062 OUR EVALUATION				
1.36 ± 0.09 +0.06 -0.05	3	ABE	99D CDF	$p\bar{p}$ at 1.8 TeV
1.34 +0.23 -0.19 ± 0.05	4	ABE	98B CDF	$p\bar{p}$ at 1.8 TeV
1.72 +0.20 -0.19 +0.18 -0.17	5	ACKERSTAFF	98F OPAL	$e^+e^- \rightarrow Z$
1.50 +0.16 -0.15 ± 0.04	3	ACKERSTAFF	98G OPAL	$e^+e^- \rightarrow Z$
1.47 ± 0.14 ± 0.08	6	BARATE	98C ALEP	$e^+e^- \rightarrow Z$
1.56 +0.29 -0.26 +0.08 -0.07	3	ABREU	96F DLPH	$e^+e^- \rightarrow Z$
1.65 +0.34 -0.31 ± 0.12	6	ABREU	96F DLPH	$e^+e^- \rightarrow Z$
1.76 ± 0.20 +0.15 -0.10	7	ABREU	96F DLPH	$e^+e^- \rightarrow Z$
1.60 ± 0.26 +0.13 -0.15	8	ABREU	96F DLPH	$e^+e^- \rightarrow Z$
1.54 +0.14 -0.13 ± 0.04	3	BUSKULIC	96M ALEP	$e^+e^- \rightarrow Z$
• • • We do not use the following data for averages, fits, limits, etc. • • •				
1.51 ± 0.11	9	BARATE	98C ALEP	$e^+e^- \rightarrow Z$
1.34 +0.23 -0.19 ± 0.05	10	ABE	96N CDF	Repl. by ABE 98B
1.67 ± 0.14	11	ABREU	96F DLPH	$e^+e^- \rightarrow Z$
1.61 +0.30 -0.29 +0.18 -0.16	90	6	BUSKULIC	96E ALEP Repl. by BARATE 98C
1.42 +0.27 -0.23 ± 0.11	76	3	ABE	95R CDF Repl. by ABE 99D
1.74 +1.08 -0.69 ± 0.07	8	12	ABE	95R CDF Sup. by ABE 96N
1.54 +0.25 -0.21 ± 0.06	79	3	AKERS	95G OPAL Repl. by ACKERSTAFF 98G
1.59 +0.17 -0.15 ± 0.03	134	3	BUSKULIC	95O ALEP Sup. by BUSKULIC 96M
0.96 ± 0.37	41	13	ABREU	94E DLPH Sup. by ABREU 96F
1.92 +0.45 -0.35 ± 0.04	31	3	BUSKULIC	94C ALEP Sup. by BUSKULIC 95O
1.13 +0.35 -0.26 ± 0.09	22	3	ACTON	93H OPAL Sup. by AKERS 95G

- ³ Measured using $D_s^- \ell^+$ vertices.
- ⁴ Measured using fully reconstructed $B_s \rightarrow J/\psi(1S)\phi$ decay.
- ⁵ ACKERSTAFF 98F use fully reconstructed $D_s^- \rightarrow \phi\pi^-$ and $D_s^- \rightarrow K^*0 K^-$ in the inclusive B_s^0 decay.
- ⁶ Measured using D_s hadron vertices.
- ⁷ Measured using $\phi\ell$ vertices.
- ⁸ Measured using inclusive D_s vertices.
- ⁹ Combined results from $D_s^- \ell^+$ and D_s hadron.
- ¹⁰ ABE 96N uses 58 ± 12 exclusive $B_s \rightarrow J/\psi(1S)\phi$ events.
- ¹¹ Combined result for the four ABREU 96F methods.
- ¹² Exclusive reconstruction of $B_s \rightarrow \psi\phi$.
- ¹³ ABREU 94E uses the flight-distance distribution of D_s vertices, ϕ -lepton vertices, and $D_s \mu$ vertices.

$|\Delta\Gamma_{B_s^0}|/\Gamma_{B_s^0}$

$\Gamma_{B_s^0}$ and $|\Delta\Gamma_{B_s^0}|$ are the decay rate average and difference between two B_s^0 CP eigenstates.

The first "OUR EVALUATION," < 0.33 (CL=95%), also provided by the LEP B Oscillation Working Group, including the assumption of $\Gamma_s = \frac{1}{\tau_{B_d}}$.

The second "OUR EVALUATION," < 0.65 (CL=95%), is an average of all available B_s semi-leptonic lifetime measurements with the $\Delta\Gamma_{B_s^0}/\Gamma_s$ analyses performed by the LEP B Oscillation Working Group as described in our "Review on B - \bar{B} Mixing" in the B^0 Section of these Listings.

VALUE	CL%	DOCUMENT ID	TECN	COMMENT
< 0.65 (CL = 95%) OUR EVALUATION				
< 0.33 (CL = 95%) OUR EVALUATION				
• • • We do not use the following data for averages, fits, limits, etc. • • •				
< 0.83	95	¹⁴ ABE	99D CDF	$p\bar{p}$ at 1.8 TeV
< 0.67	95	¹⁵ ACCIARRI	98S L3	$e^+e^- \rightarrow Z$
¹⁴ ABE 99D assumes $\tau_{B_s^0} = 1.55 \pm 0.05$ ps.				
¹⁵ ACCIARRI 98S assumes $\tau_{B_s^0} = 1.49 \pm 0.06$ ps and PDG 98 values of b production fraction.				

B_s^0 DECAY MODES

These branching fractions all scale with $B(\bar{b} \rightarrow B_s^0)$, the LEP B_s^0 production fraction. The first four were evaluated using $B(\bar{b} \rightarrow B_s^0) = (10.7 \pm 1.4)\%$ and the rest assume $B(\bar{b} \rightarrow B_s^0) = 12\%$.

The branching fraction $B(B_s^0 \rightarrow D_s^- \ell^+ \nu_\ell \text{ anything})$ is not a pure measurement since the measured product branching fraction $B(\bar{b} \rightarrow B_s^0) \times B(B_s^0 \rightarrow D_s^- \ell^+ \nu_\ell \text{ anything})$ was used to determine $B(\bar{b} \rightarrow B_s^0)$, as described in the note on "Production and Decay of b -Flavored Hadrons."

Mode	Fraction (Γ_i/Γ)	Confidence level
Γ_1 D_s^- anything	(92 ± 31) %	
Γ_2 $D_s^- \ell^+ \nu_\ell$ anything	[a] (8.1 ± 2.4) %	
Γ_3 $D_s^- \pi^+$	< 13 %	
Γ_4 $D_s^- (*^+) + D_s^- (*^-)$	< 21.8 %	90%
Γ_5 $J/\psi(1S)\phi$	(9.3 ± 3.3) × 10 ⁻⁴	
Γ_6 $J/\psi(1S)\pi^0$	< 1.2 × 10 ⁻³	90%
Γ_7 $J/\psi(1S)\eta$	< 3.8 × 10 ⁻³	90%
Γ_8 $\psi(2S)\phi$	seen	
Γ_9 $\pi^+ \pi^-$	< 1.7 × 10 ⁻⁴	90%
Γ_{10} $\pi^0 \pi^0$	< 2.1 × 10 ⁻⁴	90%
Γ_{11} $\eta \pi^0$	< 1.0 × 10 ⁻³	90%
Γ_{12} $\eta \eta$	< 1.5 × 10 ⁻³	90%
Γ_{13} $\pi^+ K^-$	< 2.1 × 10 ⁻⁴	90%
Γ_{14} $K^+ K^-$	< 5.9 × 10 ⁻⁵	90%
Γ_{15} $\rho \bar{\rho}$	< 5.9 × 10 ⁻⁵	90%
Γ_{16} $\gamma \gamma$	< 1.48 × 10 ⁻⁴	90%
Γ_{17} $\phi \gamma$	< 7 × 10 ⁻⁴	90%
Lepton Family number (LF) violating modes or $\Delta B = 1$ weak neutral current ($B1$) modes		
Γ_{18} $\mu^+ \mu^-$	$B1$ < 2.0 × 10 ⁻⁶	90%
Γ_{19} $e^+ e^-$	$B1$ < 5.4 × 10 ⁻⁵	90%
Γ_{20} $e^\pm \mu^\mp$	LF [b] < 6.1 × 10 ⁻⁶	90%
Γ_{21} $\phi \nu \bar{\nu}$	$B1$ < 5.4 × 10 ⁻³	90%

[a] Not a pure measurement. See note at head of B_s^0 Decay Modes.

[b] The value is for the sum of the charge states or particle/antiparticle states indicated.

B_s^0 BRANCHING RATIOS $\Gamma(D_s^- \text{ anything})/\Gamma_{\text{total}}$ Γ_1/Γ

VALUE	EVTS	DOCUMENT ID	TECN	COMMENT
0.92 ± 0.31 OUR AVERAGE				
0.81 ± 0.24 ± 0.22	90	16 BUSKULIC	96E ALEP	$e^+ e^- \rightarrow Z$
1.56 ± 0.58 ± 0.44	147	17 ACTON	92N OPAL	$e^+ e^- \rightarrow Z$

¹⁶BUSKULIC 96E separate $c\bar{c}$ and $b\bar{b}$ sources of D_s^+ mesons using a lifetime tag, subtract generic $\bar{b} \rightarrow W^+ \rightarrow D_s^+$ events, and obtain $B(\bar{b} \rightarrow B_s^0) \times B(B_s^0 \rightarrow D_s^- \text{ anything}) = 0.088 \pm 0.020 \pm 0.020$ assuming $B(D_s^- \rightarrow \phi\pi) = (3.5 \pm 0.4) \times 10^{-2}$ and PDG 1994 values for the relative partial widths to other D_s channels. We evaluate using our current values $B(\bar{b} \rightarrow B_s^0) = 0.107 \pm 0.014$ and $B(D_s^- \rightarrow \phi\pi) = 0.036 \pm 0.009$. Our first error is their experiment's and our second error is that due to $B(\bar{b} \rightarrow B_s^0)$ and $B(D_s^- \rightarrow \phi\pi)$.

¹⁷ACTON 92N assume that excess of $147 \pm 48 D_s^0$ events over that expected from B^0 , B^+ , and $c\bar{c}$ is all from B_s^0 decay. The product branching fraction is measured to be $B(\bar{b} \rightarrow B_s^0)B(B_s^0 \rightarrow D_s^- \text{ anything}) \times B(D_s^- \rightarrow \phi\pi^-) = (5.9 \pm 1.9 \pm 1.1) \times 10^{-3}$. We evaluate using our current values $B(\bar{b} \rightarrow B_s^0) = 0.107 \pm 0.014$ and $B(D_s^- \rightarrow \phi\pi) = 0.036 \pm 0.009$. Our first error is their experiment's and our second error is that due to $B(\bar{b} \rightarrow B_s^0)$ and $B(D_s^- \rightarrow \phi\pi)$.

 $\Gamma(D_s^- \ell^+ \nu_\ell \text{ anything})/\Gamma_{\text{total}}$ Γ_2/Γ

The values and averages in this section serve only to show what values result if one assumes our $B(\bar{b} \rightarrow B_s^0)$. They cannot be thought of as measurements since the underlying product branching fractions were also used to determine $B(\bar{b} \rightarrow B_s^0)$ as described in the note on "Production and Decay of b -Flavored Hadrons."

VALUE	EVTS	DOCUMENT ID	TECN	COMMENT
0.081 ± 0.024 OUR AVERAGE				
0.076 ± 0.012 ± 0.021	134	18 BUSKULIC	950 ALEP	$e^+ e^- \rightarrow Z$
0.107 ± 0.043 ± 0.029		19 ABREU	92M DLPH	$e^+ e^- \rightarrow Z$
0.103 ± 0.036 ± 0.028	18	20 ACTON	92N OPAL	$e^+ e^- \rightarrow Z$
0.13 ± 0.04 ± 0.04	27	21 BUSKULIC	92E ALEP	$e^+ e^- \rightarrow Z$

¹⁸BUSKULIC 950 use $D_s \ell$ correlations. The measured product branching ratio is $B(\bar{b} \rightarrow B_s) \times B(B_s \rightarrow D_s^- \ell^+ \nu_\ell \text{ anything}) = (0.82 \pm 0.09 \pm 0.13 \pm 0.14)\%$ assuming $B(D_s^- \rightarrow \phi\pi) = (3.5 \pm 0.4) \times 10^{-2}$ and PDG 1994 values for the relative partial widths to the six other D_s channels used in this analysis. Combined with results from $T(4S)$ experiments this can be used to extract $B(\bar{b} \rightarrow B_s) = (11.0 \pm 1.2 \pm 2.5)\%$. We evaluate using our current values $B(\bar{b} \rightarrow B_s^0) = 0.107 \pm 0.014$ and $B(D_s^- \rightarrow \phi\pi) = 0.036 \pm 0.009$. Our first error is their experiment's and our second error is that due to $B(\bar{b} \rightarrow B_s^0)$ and $B(D_s^- \rightarrow \phi\pi)$.

¹⁹ABREU 92M measured muons only and obtained product branching ratio $B(Z \rightarrow b\bar{c}) \times B(\bar{b} \rightarrow B_s) \times B(B_s \rightarrow D_s^- \mu^+ \nu_\mu \text{ anything}) \times B(D_s^- \rightarrow \phi\pi) = (18 \pm 8) \times 10^{-5}$. We evaluate using our current values $B(\bar{b} \rightarrow B_s^0) = 0.107 \pm 0.014$ and $B(D_s^- \rightarrow \phi\pi) = 0.036 \pm 0.009$. Our first error is their experiment's and our second error is that due to $B(\bar{b} \rightarrow B_s^0)$ and $B(D_s^- \rightarrow \phi\pi)$. We use $B(Z \rightarrow b\bar{c}) = 2B(Z \rightarrow b\bar{b}) = 2 \times (0.2212 \pm 0.0019)$.

²⁰ACTON 92N is measured using $D_s \rightarrow \phi\pi^+$ and $K^*(892)^0 K^+$ events. The product branching fraction measured is measured to be $B(\bar{b} \rightarrow B_s^0)B(B_s^0 \rightarrow D_s^- \ell^+ \nu_\ell \text{ anything}) \times B(D_s^- \rightarrow \phi\pi^-) = (3.9 \pm 1.1 \pm 0.8) \times 10^{-4}$. We evaluate using our current values $B(\bar{b} \rightarrow B_s^0) = 0.107 \pm 0.014$ and $B(D_s^- \rightarrow \phi\pi) = 0.036 \pm 0.009$. Our first error is their experiment's and our second error is that due to $B(\bar{b} \rightarrow B_s^0)$ and $B(D_s^- \rightarrow \phi\pi)$.

²¹BUSKULIC 92E is measured using $D_s \rightarrow \phi\pi^+$ and $K^*(892)^0 K^+$ events. They use $2.7 \pm 0.7\%$ for the $\phi\pi^+$ branching fraction. The average product branching fraction is measured to be $B(\bar{b} \rightarrow B_s^0)B(B_s^0 \rightarrow D_s^- \ell^+ \nu_\ell \text{ anything}) = 0.020 \pm 0.0055 \pm 0.005 \pm 0.006$. We evaluate using our current values $B(\bar{b} \rightarrow B_s^0) = 0.107 \pm 0.014$ and $B(D_s^- \rightarrow \phi\pi) = 0.036 \pm 0.009$. Our first error is their experiment's and our second error is that due to $B(\bar{b} \rightarrow B_s^0)$ and $B(D_s^- \rightarrow \phi\pi)$. Superseded by BUSKULIC 950.

 $\Gamma(D_s^- \pi^+)/\Gamma_{\text{total}}$ Γ_3/Γ

VALUE	EVTS	DOCUMENT ID	TECN	COMMENT
<0.13	6	22 AKERS	94J OPAL	$e^+ e^- \rightarrow Z$
seen	1	BUSKULIC	93G ALEP	$e^+ e^- \rightarrow Z$
				$\bullet \bullet \bullet$ We do not use the following data for averages, fits, limits, etc. $\bullet \bullet \bullet$
				²² AKERS 94J sees ≤ 6 events and measures the limit on the product branching fraction $f(\bar{b} \rightarrow B_s^0) \cdot B(B_s^0 \rightarrow D_s^- \pi^+) < 1.3\%$ at CL = 90%. We divide by our current value $B(\bar{b} \rightarrow B_s^0) = 0.105$.

 $\Gamma(D_s^-(*) + D_s^{(*)-})/\Gamma_{\text{total}}$ Γ_4/Γ

VALUE	CL%	DOCUMENT ID	TECN	COMMENT
<0.218	90	BARATE	98Q ALEP	$e^+ e^- \rightarrow Z$

 $\Gamma(J/\psi(1S)\phi)/\Gamma_{\text{total}}$ Γ_5/Γ

VALUE (units 10^{-3})	EVTS	DOCUMENT ID	TECN	COMMENT
0.93 ± 0.28 ± 0.17		23 ABE	96Q CDF	$\rho\bar{\rho}$
<6	1	24 AKERS	94J OPAL	$e^+ e^- \rightarrow Z$
seen	14	25 ABE	93F CDF	$\rho\bar{\rho}$ at 1.8 TeV
seen	1	26 ACTON	92N OPAL	Sup. by AKERS 94J
				$\bullet \bullet \bullet$ We do not use the following data for averages, fits, limits, etc. $\bullet \bullet \bullet$
				²³ ABE 96Q assumes $f_{D^*} = f_D$ and $f_5/f_1 = 0.40 \pm 0.06$. Uses $B \rightarrow J/\psi(1S) K$ and $B \rightarrow J/\psi(1S) K^*$ branching fractions from PDG 94. They quote two systematic errors, ± 0.10 and ± 0.14 where the latter is the uncertainty in f_5 . We combine in quadrature.
				²⁴ AKERS 94J sees one event and measures the limit on the product branching fraction $f(\bar{b} \rightarrow B_s^0) \cdot B(B_s^0 \rightarrow J/\psi(1S)\phi) < 7 \times 10^{-4}$ at CL = 90%. We divide by $B(\bar{b} \rightarrow B_s^0) = 0.112$.
				²⁵ ABE 93F measured using $J/\psi(1S) \rightarrow \mu^+ \mu^-$ and $\phi \rightarrow K^+ K^-$.
				²⁶ In ACTON 92N a limit on the product branching fraction is measured to be $f(\bar{b} \rightarrow B_s^0) \cdot B(B_s^0 \rightarrow J/\psi(1S)\phi) \leq 0.22 \times 10^{-2}$.

 $\Gamma(J/\psi(1S)\pi^0)/\Gamma_{\text{total}}$ Γ_6/Γ

VALUE	CL%	DOCUMENT ID	TECN	
<1.2 × 10⁻³	90	27 ACCIARRI	97C L3	
				²⁷ ACCIARRI 97C assumes B^0 production fraction $(39.5 \pm 4.0\%)$ and B_s $(12.0 \pm 3.0\%)$.

 $\Gamma(J/\psi(1S)\eta)/\Gamma_{\text{total}}$ Γ_7/Γ

VALUE	CL%	DOCUMENT ID	TECN	
<3.8 × 10⁻³	90	28 ACCIARRI	97C L3	
				²⁸ ACCIARRI 97C assumes B^0 production fraction $(39.5 \pm 4.0\%)$ and B_s $(12.0 \pm 3.0\%)$.

 $\Gamma(\psi(2S)\phi)/\Gamma_{\text{total}}$ Γ_8/Γ

VALUE	EVTS	DOCUMENT ID	TECN	COMMENT
seen	1	BUSKULIC	93G ALEP	$e^+ e^- \rightarrow Z$

 $\Gamma(\pi^+ \pi^-)/\Gamma_{\text{total}}$ Γ_9/Γ

VALUE	CL%	DOCUMENT ID	TECN	COMMENT
<1.7 × 10⁻⁴	90	29 BUSKULIC	96V ALEP	$e^+ e^- \rightarrow Z$
				²⁹ BUSKULIC 96V assumes PDG 96 production fractions for B^0 , B^+ , B_s , b baryons.

 $\Gamma(\pi^0 \pi^0)/\Gamma_{\text{total}}$ Γ_{10}/Γ

VALUE	CL%	DOCUMENT ID	TECN	COMMENT
<2.1 × 10⁻⁴	90	30 ACCIARRI	95H L3	$e^+ e^- \rightarrow Z$
				³⁰ ACCIARRI 95H assumes $f_{B^0} = 39.5 \pm 4.0$ and $f_{B_s} = 12.0 \pm 3.0\%$.

 $\Gamma(\eta\pi^0)/\Gamma_{\text{total}}$ Γ_{11}/Γ

VALUE	CL%	DOCUMENT ID	TECN	COMMENT
<1.0 × 10⁻³	90	31 ACCIARRI	95H L3	$e^+ e^- \rightarrow Z$
				³¹ ACCIARRI 95H assumes $f_{B^0} = 39.5 \pm 4.0$ and $f_{B_s} = 12.0 \pm 3.0\%$.

 $\Gamma(\eta\eta)/\Gamma_{\text{total}}$ Γ_{12}/Γ

VALUE	CL%	DOCUMENT ID	TECN	COMMENT
<1.5 × 10⁻³	90	32 ACCIARRI	95H L3	$e^+ e^- \rightarrow Z$
				³² ACCIARRI 95H assumes $f_{B^0} = 39.5 \pm 4.0$ and $f_{B_s} = 12.0 \pm 3.0\%$.

 $\Gamma(\pi^+ K^-)/\Gamma_{\text{total}}$ Γ_{13}/Γ

VALUE	CL%	DOCUMENT ID	TECN	COMMENT
<2.1 × 10⁻⁴	90	33 BUSKULIC	96V ALEP	$e^+ e^- \rightarrow Z$
				$\bullet \bullet \bullet$ We do not use the following data for averages, fits, limits, etc. $\bullet \bullet \bullet$
<2.6 × 10 ⁻⁴	90	34 AKERS	94L OPAL	$e^+ e^- \rightarrow Z$
				³³ BUSKULIC 96V assumes PDG 96 production fractions for B^0 , B^+ , B_s , b baryons.
				³⁴ Assumes $B(Z \rightarrow b\bar{b}) = 0.217$ and $B_D^0(B_s^0)$ fraction 39.5% (12%).

 $\Gamma(K^+ K^-)/\Gamma_{\text{total}}$ Γ_{14}/Γ

VALUE	CL%	DOCUMENT ID	TECN	COMMENT
<5.9 × 10⁻⁵	90	35 BUSKULIC	96V ALEP	$e^+ e^- \rightarrow Z$
				$\bullet \bullet \bullet$ We do not use the following data for averages, fits, limits, etc. $\bullet \bullet \bullet$
<1.4 × 10 ⁻⁴	90	36 AKERS	94L OPAL	$e^+ e^- \rightarrow Z$
				³⁵ BUSKULIC 96V assumes PDG 96 production fractions for B^0 , B^+ , B_s , b baryons.
				³⁶ Assumes $B(Z \rightarrow b\bar{b}) = 0.217$ and $B_D^0(B_s^0)$ fraction 39.5% (12%).

 $\Gamma(\rho\bar{\rho})/\Gamma_{\text{total}}$ Γ_{15}/Γ

VALUE	CL%	DOCUMENT ID	TECN	COMMENT
<5.9 × 10⁻⁵	90	37 BUSKULIC	96V ALEP	$e^+ e^- \rightarrow Z$
				³⁷ BUSKULIC 96V assumes PDG 96 production fractions for B^0 , B^+ , B_s , b baryons.

 $\Gamma(\gamma\gamma)/\Gamma_{\text{total}}$ Γ_{16}/Γ

VALUE	CL%	DOCUMENT ID	TECN	COMMENT
<14.8 × 10⁻⁵	90	38 ACCIARRI	95I L3	$e^+ e^- \rightarrow Z$
				³⁸ ACCIARRI 95I assumes $f_{B^0} = 39.5 \pm 4.0$ and $f_{B_s} = 12.0 \pm 3.0\%$.

Meson Particle Listings

 B_s^0

$\Gamma(\phi\gamma)/\Gamma_{\text{total}}$					Γ_{17}/Γ
VALUE	CL%	DOCUMENT ID	TECN	COMMENT	
$<7 \times 10^{-4}$	90	39 ADAM	96D DLPH	$e^+e^- \rightarrow Z$	
39 ADAM 96D assumes $f_{B^0} = f_{B^-} = 0.39$ and $f_{B_s} = 0.12$.					

$\Gamma(\mu^+\mu^-)/\Gamma_{\text{total}}$					Γ_{18}/Γ
VALUE	CL%	DOCUMENT ID	TECN	COMMENT	
$<2.0 \times 10^{-6}$	90	40 ABE	98 CDF	$p\bar{p}$ at 1.8 TeV	
• • • We do not use the following data for averages, fits, limits, etc. • • •					
$<3.8 \times 10^{-5}$	90	41 ACCIARRI	97B L3	$e^+e^- \rightarrow Z$	
$<8.4 \times 10^{-6}$	90	42 ABE	96L CDF	Repl. by ABE 98	

40 ABE 98 assumes production of $\sigma(B^0) = \sigma(B^+)$ and $\sigma(B_s)/\sigma(B^0) = 1/3$. They normalize to their measured $\sigma(B^0, p_T(B) > 6, |y| < 1.0) = 2.39 \pm 0.32 \pm 0.44 \mu\text{b}$.
 41 ACCIARRI 97B assume PDG 96 production fractions for B^+ , B^0 , B_s , and Λ_b .
 42 ABE 96L assumes B^+/B_s production ratio 3/1. They normalize to their measured $\sigma(B^+, p_T(B) > 6 \text{ GeV}/c, |y| < 1) = 2.39 \pm 0.54 \mu\text{b}$.

$\Gamma(e^+e^-)/\Gamma_{\text{total}}$					Γ_{19}/Γ
VALUE	CL%	DOCUMENT ID	TECN	COMMENT	
$<5.4 \times 10^{-5}$	90	43 ACCIARRI	97B L3	$e^+e^- \rightarrow Z$	
43 ACCIARRI 97B assume PDG 96 production fractions for B^+ , B^0 , B_s , and Λ_b .					

$\Gamma(e^\pm\mu^\mp)/\Gamma_{\text{total}}$					Γ_{20}/Γ
VALUE	CL%	DOCUMENT ID	TECN	COMMENT	
$<6.1 \times 10^{-6}$	90	ABE	98V CDF	$p\bar{p}$ at 1.8 TeV	
• • • We do not use the following data for averages, fits, limits, etc. • • •					
$<4.1 \times 10^{-5}$	90	44 ACCIARRI	97B L3	$e^+e^- \rightarrow Z$	
44 ACCIARRI 97B assume PDG 96 production fractions for B^+ , B^0 , B_s , and Λ_b .					

$\Gamma(\phi\nu\bar{\nu})/\Gamma_{\text{total}}$					Γ_{21}/Γ
VALUE	CL%	DOCUMENT ID	TECN	COMMENT	
$<5.4 \times 10^{-3}$	90	45 ADAM	96D DLPH	$e^+e^- \rightarrow Z$	
45 ADAM 96D assumes $f_{B^0} = f_{B^-} = 0.39$ and $f_{B_s} = 0.12$.					

POLARIZATION IN B_s^0 DECAY

Γ_L/Γ in $B_s^0 \rightarrow J/\psi(1S)\phi$				
VALUE	EVTs	DOCUMENT ID	TECN	COMMENT
$0.56 \pm 0.21^{+0.02}_{-0.04}$	19	ABE	95Z CDF	$p\bar{p}$ at 1.8 TeV

 B_s^0 - \bar{B}_s^0 MIXING

For a discussion of B_s^0 - \bar{B}_s^0 mixing see the note on " B^0 - \bar{B}^0 Mixing" in the B^0 Particle Listings above.

x_s is a measure of the time-integrated B_s^0 - \bar{B}_s^0 mixing probability that produced $B_s^0(\bar{B}_s^0)$ decays as a $\bar{B}_s^0(B_s^0)$. Mixing violates $\Delta B \neq 2$ rule.

$$x_s = \frac{x_s^2}{2(1+x_s^2)}$$

$$x_s = \frac{\Delta m_{B_s}}{\Gamma_{B_s}} = (m_{B_{sH}} - m_{B_{sL}}) \tau_{B_s^0}$$

where H, L stand for heavy and light states of two B_s^0 CP eigenstates and

$$\tau_{B_s^0} = 0.5 \left(\frac{1}{\Gamma_{B_{sH}} + \Gamma_{B_{sL}}} \right)$$

 x_B at high energy

This is a B - \bar{B} mixing measurement for an admixture of B^0 and B_s^0 at high energy.

$$x_B = f_d' x_d + f_s' x_s$$

where f_d' and f_s' are the branching ratio times production fractions of B_d^0 and B_s^0 mesons relative to all b -flavored hadrons which decay weakly. Mixing violates $\Delta B \neq 2$ rule.

VALUE	CL%	EVTs	DOCUMENT ID	TECN	COMMENT
0.118 ± 0.005 OUR AVERAGE					
0.1192 ± 0.0068 ± 0.0051			46 ACCIARRI	99D L3	$e^+e^- \rightarrow Z$
0.131 ± 0.020 ± 0.016			47 ABE	97I CDF	$p\bar{p}$ 1.8 TeV
0.1107 ± 0.0062 ± 0.0055			48 ALEXANDER	96 OPAL	$e^+e^- \rightarrow Z$
0.121 ± 0.016 ± 0.006			49 ABREU	94J DLPH	$e^+e^- \rightarrow Z$
0.114 ± 0.014 ± 0.008			50 BUSKULIC	94G ALEP	$e^+e^- \rightarrow Z$
0.129 ± 0.022			51 BUSKULIC	92B ALEP	$e^+e^- \rightarrow Z$
0.176 ± 0.031 ± 0.032		1112	52 ABE	91G CDF	$p\bar{p}$ 1.8 TeV
0.148 ± 0.029 ± 0.017			53 ALBAJAR	91D UA1	$p\bar{p}$ 630 GeV

• • • We do not use the following data for averages, fits, limits, etc. • • •

0.136 ± 0.037 ± 0.040			54 UENO	96 AMY	e^+e^- at 57.9 GeV
0.144 ± 0.014 $^{+0.017}_{-0.011}$			55 ABREU	94F DLPH	Sup. by ABREU 94J
0.131 ± 0.014			56 ABREU	94J DLPH	$e^+e^- \rightarrow Z$
0.123 ± 0.012 ± 0.008			ACCIARRI	94D L3	Repl. by ACCIARRI 99D
0.157 ± 0.020 ± 0.032			57 ALBAJAR	94 UA1	$\sqrt{s} = 630 \text{ GeV}$
0.121 $^{+0.044}_{-0.040}$ ± 0.017		1665	58 ABREU	93C DLPH	Sup. by ABREU 94J
0.143 $^{+0.022}_{-0.021}$ ± 0.007			59 AKERS	93B OPAL	Sup. by ALEXANDER 96
0.145 $^{+0.041}_{-0.035}$ ± 0.018			60 ACTON	92C OPAL	$e^+e^- \rightarrow Z$
0.121 ± 0.017 ± 0.006			61 ADEVA	92C L3	Sup. by ACCIARRI 94D
0.132 ± 0.22 $^{+0.015}_{-0.012}$		823	62 DECAMP	91 ALEP	$e^+e^- \rightarrow Z$
0.178 $^{+0.049}_{-0.040}$ ± 0.020			63 ADEVA	90P L3	$e^+e^- \rightarrow Z$
0.17 $^{+0.15}_{-0.08}$			64,65 WEIR	90 MRK2	e^+e^- 29 GeV
0.21 $^{+0.29}_{-0.15}$			64 BAND	88 MAC	$E_{\text{cm}}^{\text{ee}} = 29 \text{ GeV}$
>0.02		90	64 BAND	88 MAC	$E_{\text{cm}}^{\text{ee}} = 29 \text{ GeV}$
0.121 ± 0.047			64,66 ALBAJAR	87C UA1	Repl. by ALBAJAR 91D
<0.12		90	64,67 SCHAAD	85 MRK2	$E_{\text{cm}}^{\text{ee}} = 29 \text{ GeV}$

46 ACCIARRI 99D uses maximum-likelihood fits to extract χ_b as well as the A_{FB}^b in $Z \rightarrow b\bar{b}$ events containing prompt leptons.

47 Uses di-muon events.

48 ALEXANDER 96 uses a maximum likelihood fit to simultaneously extract χ as well as the forward-backward asymmetries in $e^+e^- \rightarrow Z \rightarrow b\bar{b}$ and $c\bar{c}$.

49 This ABREU 94J result is from 5182 $\ell\ell$ and 279 $\Lambda\ell$ events. The systematic error includes 0.004 for model dependence.

50 BUSKULIC 94G data analyzed using ee , $e\mu$, and $\mu\mu$ events.

51 BUSKULIC 92B uses a jet charge technique combined with electrons and muons.

52 ABE 91G measurement of χ is done with $e\mu$ and ee events.

53 ALBAJAR 91D measurement of χ is done with dimuons.

54 UENO 96 extracted χ from the energy dependence of the forward-backward asymmetry.

55 ABREU 94F uses the average electric charge sum of the jets recoiling against a b -quark jet tagged by a high p_T muon. The result is for $\bar{\chi} = f_d x_d + 0.9 f_s x_s$.

56 This ABREU 94J result combines $\ell\ell$, $\Lambda\ell$, and jet-charge ℓ (ABREU 94F) analyses. It is for $\bar{\chi} = f_d x_d + 0.96 f_s x_s$.

57 ALBAJAR 94 uses dimuon events. Not independent of ALBAJAR 91D.

58 ABREU 93C data analyzed using ee , $e\mu$, and $\mu\mu$ events.

59 AKERS 93B analysis performed using dilepton events.

60 ACTON 92C uses electrons and muons. Superseded by AKERS 93B.

61 ADEVA 92C uses electrons and muons.

62 DECAMP 91 one with opposite and like-sign dileptons. Superseded by BUSKULIC 92B.

63 ADEVA 90P measurement uses ee , $\mu\mu$, and $e\mu$ events from 118k events at the Z. Superseded by ADEVA 92C.

64 These experiments are not in the average because the combination of B_s and B_d mesons which they see could differ from those at higher energy.

65 The WEIR 90 measurement supersedes the limit obtained in SCHAAD 85. The 90% CL are 0.06 and 0.38.

66 ALBAJAR 87C measured $\chi = (\bar{B}^0 \rightarrow B^0 \rightarrow \mu^+ \chi)$ divided by the average production weighted semileptonic branching fraction for B hadrons at 546 and 630 GeV.

67 Limit is average probability for hadron containing B quark to produce a positive lepton.

$$\Delta m_{B_s^0} = m_{B_{sH}} - m_{B_{sL}}$$

$\Delta m_{B_s^0}$ is a measure of 2π times the B_s^0 - \bar{B}_s^0 oscillation frequency in time-dependent mixing experiments.

"OUR EVALUATION" is an average of the data listed below performed by the LEP B Oscillation Working Group as described in our "Review of B - \bar{B} Mixing" in the B^0 Section of these Listings. The averaging procedure takes into account correlations between the measurements.

VALUE (10^{12} h s^{-1})	CL%	DOCUMENT ID	TECN	COMMENT
>10.6 (CL = 95%) OUR EVALUATION				
> 5.2	95	68 ABBIENDI	99S OPAL	$e^+e^- \rightarrow Z$
> 5.8	95	69 ABE	99J CDF	$p\bar{p}$ at 1.8 TeV
> 6.6	95	70 BARATE	99J ALEP	$e^+e^- \rightarrow Z$
> 9.5	95	71 ADAM	97 DLPH	$e^+e^- \rightarrow Z$
• • • We do not use the following data for averages, fits, limits, etc. • • •				
< 96	95	72 ABE	99D CDF	$p\bar{p}$ at 1.8 TeV
> 7.9	95	73 BARATE	98C ALEP	Repl. by BARATE 99J
> 3.1	95	74 ACKERSTAFF	97U OPAL	Repl. by ABBIENDI 99S
> 2.2	95	75 ACKERSTAFF	97V OPAL	Repl. by ABBIENDI 99S
> 6.6	95	76 BUSKULIC	96M ALEP	Repl. by BARATE 98C
> 2.2	95	75 AKERS	95J OPAL	Sup. by ACKERSTAFF 97V
> 5.7	95	77 BUSKULIC	95J ALEP	$e^+e^- \rightarrow Z$
> 1.8	95	75 BUSKULIC	94B ALEP	$e^+e^- \rightarrow Z$

68 Uses ℓ - Q_{hem} and ℓ - ℓ .

69 ABE 99J uses ϕ ℓ - ℓ correlation.

70 BARATE 99J uses combination of an inclusive lepton and D_s^- -based analyses.

71 ADAM 97 combines results from D_s ℓ - Q_{hem} , ℓ - Q_{hem} , and ℓ - ℓ .

See key on page 239

Meson Particle Listings

$B_s^0, B_s^*, B_{sJ}^*(5850)$

- 72 ABE 99D assumes $\tau_{B_s^0} = 1.55 \pm 0.05$ ps and $\Delta\Gamma/\Delta m = (5.6 \pm 2.6) \times 10^{-3}$.
- 73 BARATE 98C combines results from $D_s h\text{-}l/Q_{\text{hem}}$, $D_s h\text{-}K$ in the same side, $D_s l\text{-}l/Q_{\text{hem}}$ and $D_s l\text{-}K$ in the same side.
- 74 Uses $l\text{-}Q_{\text{hem}}$.
- 75 Uses $l\text{-}l$.
- 76 BUSKULIC 96M uses D_s lepton correlations and lepton, kaon, and jet charge tags.
- 77 BUSKULIC 95J uses $l\text{-}Q_{\text{hem}}$. They find $\Delta m_s > 5.6$ [> 6.1] for $f_s = 10\%$ [12%]. We interpolate to our central value $f_s = 10.5\%$.

$x_s = \Delta m_{B_s^0} / \Gamma_{B_s^0}$

This is derived by the LEP B Oscillation Working Group from the results on $\Delta m_{B_s^0}$ and "OUR EVALUATION" of the B_s^0 mean lifetime.

VALUE	CL%	DOCUMENT ID
>15.7	(CL = 95%)	OUR EVALUATION

X_s

This $B_s^0\text{-}\bar{B}_s^0$ integrated mixing parameter is derived from x_s above.

VALUE	CL%	DOCUMENT ID
>0.4980	(CL = 95%)	OUR EVALUATION

B_s^0 REFERENCES

ABBIENDI 995 EPJ C11 587	G. Abbiendi et al.	(OPAL Collab.)
ABE 99D PR D59 032004	F. Abe et al.	(CDF Collab.)
ABE 99J PRL 82 3575	F. Abe et al.	(CDF Collab.)
ACCIARRI 99D PL B448 152	M. Acciari et al.	(L3 Collab.)
BARATE 99J EPJ C7 553	R. Barate et al.	(ALEPH Collab.)
Also 00 EPJ C12 181 (erratum)		(ALEPH Collab.)
ABE 98 PR D57 R3811	F. Abe et al.	(CDF Collab.)
ABE 98B PR D57 5382	F. Abe et al.	(CDF Collab.)
ABE 98V PRL 81 5742	F. Abe et al.	(CDF Collab.)
ACCIARRI 98S PL B438 417	M. Acciari et al.	(L3 Collab.)
ACKERSTAFF 98F EPJ C2 407	K. Ackerstaff et al.	(OPAL Collab.)
ACKERSTAFF 98G PL B426 161	K. Ackerstaff et al.	(OPAL Collab.)
BARATE 98C EPJ C4 357	R. Barate et al.	(ALEPH Collab.)
BARATE 98Q EPJ C4 387	R. Barate et al.	(ALEPH Collab.)
PDG 98 EPJ C3 1	C. Caso et al.	
ABE 97I PR D55 2546	F. Abe et al.	(CDF Collab.)
ACCIARRI 97B PL B391 474	M. Acciari et al.	(L3 Collab.)
ACCIARRI 97C PL B391 481	M. Acciari et al.	(L3 Collab.)
ACKERSTAFF 97U ZPHY C76 401	K. Ackerstaff et al.	(OPAL Collab.)
ACKERSTAFF 97V ZPHY C76 417	K. Ackerstaff et al.	(OPAL Collab.)
ADAM 97 PL B414 382	W. Adam et al.	(DELPHI Collab.)
ABE 96B PR D53 3496	F. Abe et al.	(CDF Collab.)
ABE 96L PRL 76 4675	F. Abe et al.	(CDF Collab.)
ABE 96N PRL 77 1945	F. Abe et al.	(CDF Collab.)
ABE 96Q PR D54 6596	F. Abe et al.	(CDF Collab.)
ABREU 96F ZPHY C71 11	P. Abreu et al.	(DELPHI Collab.)
ADAM 96D ZPHY C72 207	W. Adam et al.	(DELPHI Collab.)
ALEXANDER 96 ZPHY C70 357	G. Alexander et al.	(OPAL Collab.)
BUSKULIC 96E ZPHY C69 585	D. Buskulic et al.	(ALEPH Collab.)
BUSKULIC 96M PL B377 205	D. Buskulic et al.	(ALEPH Collab.)
BUSKULIC 96V PL B384 471	D. Buskulic et al.	(ALEPH Collab.)
PDG 96 PR D54 1		
UENO 96 PL B381 365	K. Ueno et al.	(AMY Collab.)
ABE 95R PRL 74 4988	F. Abe et al.	(CDF Collab.)
ABE 95Z PRL 75 3068	F. Abe et al.	(CDF Collab.)
ACCIARRI 95H PL B363 127	M. Acciari et al.	(L3 Collab.)
ACCIARRI 95I PL B363 137	M. Acciari et al.	(L3 Collab.)
AKERS 95G PL B350 273	R. Akers et al.	(OPAL Collab.)
AKERS 95J ZPHY C66 555	R. Akers et al.	(OPAL Collab.)
BUSKULIC 95J PL B356 409	D. Buskulic et al.	(ALEPH Collab.)
BUSKULIC 95O PL B361 221	D. Buskulic et al.	(ALEPH Collab.)
ABREU 94D PL B324 500	P. Abreu et al.	(DELPHI Collab.)
ABREU 94E ZPHY C61 407	P. Abreu et al.	(DELPHI Collab.)
Also 92M PL B289 199	P. Abreu et al.	(DELPHI Collab.)
ABREU 94F PL B322 459	P. Abreu et al.	(DELPHI Collab.)
ABREU 94J PL B332 488	P. Abreu et al.	(DELPHI Collab.)
ACCIARRI 94D PL B335 542	M. Acciari et al.	(L3 Collab.)
AKERS 94J PL B337 196	R. Akers et al.	(OPAL Collab.)
AKERS 94L PL B337 393	R. Akers et al.	(OPAL Collab.)
ALBAJAR 94 ZPHY C61 41	C. Albajar et al.	(UA1 Collab.)
BUSKULIC 94B PL B322 441	D. Buskulic et al.	(ALEPH Collab.)
BUSKULIC 94C PL B322 275	D. Buskulic et al.	(ALEPH Collab.)
BUSKULIC 94G ZPHY C62 179	D. Buskulic et al.	(ALEPH Collab.)
PDG 94 PR D50 1173	L. Montanet et al.	(CERN, LBL, BOST+)
ABE 93F PRL 71 1685	F. Abe et al.	(CDF Collab.)
ABREU 93C PL B301 145	P. Abreu et al.	(DELPHI Collab.)
ACTON 93H PL B312 501	P.D. Acton et al.	(OPAL Collab.)
AKERS 93B ZPHY C60 199	R. Akers et al.	(OPAL Collab.)
BUSKULIC 93G PL B311 425	D. Buskulic et al.	(ALEPH Collab.)
ABREU 92M PL B289 199	P. Abreu et al.	(DELPHI Collab.)
ACTON 92C PL B276 379	D.P. Acton et al.	(OPAL Collab.)
ACTON 92N PL B295 357	P.D. Acton et al.	(OPAL Collab.)
ADEVA 92C PL B288 395	B. Adeva et al.	(L3 Collab.)
BUSKULIC 92B PL B284 177	D. Buskulic et al.	(ALEPH Collab.)
BUSKULIC 92E PL B294 145	D. Buskulic et al.	(ALEPH Collab.)
ABE 91G PRL 67 3351	F. Abe et al.	(CDF Collab.)
ALBAJAR 91D PL B262 171	C. Albajar et al.	(UA1 Collab.)
DECAMP 91 PL B258 236	D. Decamp et al.	(ALEPH Collab.)
ADEVA 90P PL B252 703	B. Adeva et al.	(L3 Collab.)
LEE-FRANZINI 90 PRL 65 2947	J. Lee-Franzini et al.	(CUSB II Collab.)
WEIR 90 PL B240 289	A.J. Weir et al.	(Mark II Collab.)
BAND 88 PL B200 221	H.R. Band et al.	(MAC Collab.)
ALBAJAR 87C PL B186 247	C. Albajar et al.	(UA1 Collab.)
SCHAAD 85 PL 160B 188	T. Schaad et al.	(Mark II Collab.)

B_s^*

$I(J^P) = 0(1^-)$

OMITTED FROM SUMMARY TABLE

l, J, P need confirmation. Quantum numbers shown are quark-model predictions.

B_s^* MASS

From mass difference below and the B_s^0 mass.

VALUE (MeV)	DOCUMENT ID
47.0 ± 2.6	OUR FIT

$m_{B_s^*} - m_{B_s}$

VALUE (MeV)	DOCUMENT ID	TECN	COMMENT
47.0 ± 2.6	OUR FIT		

¹ LEE-FRANZINI 90 CSB2 $e^+e^- \rightarrow \Upsilon(5S)$

¹ LEE-FRANZINI 90 measure $46.7 \pm 0.4 \pm 0.2$ MeV for an admixture of $B^0, B^+,$ and B_s . They use the shape of the photon line to separate the above value for B_s .

$|(m_{B_s^*} - m_{B_s}) - (m_{B^*} - m_B)|$

VALUE (MeV)	CL%	DOCUMENT ID	TECN	COMMENT
<6	95	ABREU	95R DLPH	$E_{\text{cm}}^{\text{exp}} = 88\text{-}94$ GeV

B_s^* DECAY MODES

Mode	Fraction (Γ_i/Γ)
$\Gamma_1 B_s \gamma$	dominant

B_s^* REFERENCES

ABREU 95R ZPHY C68 353	P. Abreu et al.	(DELPHI Collab.)
LEE-FRANZINI 90 PRL 65 2947	J. Lee-Franzini et al.	(CUSB II Collab.)

$B_{sJ}^*(5850)$

$I(J^P) = ?(??)$

l, J, P need confirmation.

OMITTED FROM SUMMARY TABLE

Signal can be interpreted as coming from \bar{D}_s states. Needs confirmation.

$B_{sJ}^*(5850)$ MASS

VALUE (MeV)	EVTS	DOCUMENT ID	TECN	COMMENT
5853 ± 15	141	AKERS	95E OPAL	$E_{\text{cm}}^{\text{exp}} = 88\text{-}94$ GeV

$B_{sJ}^*(5850)$ WIDTH

VALUE (MeV)	EVTS	DOCUMENT ID	TECN	COMMENT
47 ± 22	141	AKERS	95E OPAL	$E_{\text{cm}}^{\text{exp}} = 88\text{-}94$ GeV

$B_{sJ}^*(5850)$ REFERENCES

AKERS 95E ZPHY C66 19	R. Akers et al.	(OPAL Collab.)
-----------------------	-----------------	----------------

Meson Particle Listings

 B_c^\pm

BOTTOM, CHARMED MESONS ($B = C = \pm 1$)

$$B_c^+ = c\bar{b}, B_c^- = \bar{c}b, \text{ similarly for } B_c^{*s}$$

 B_c^\pm

$$I(J^P) = 0(0^-)$$

I, J, P need confirmation.

Quantum numbers shown are quark-model predictions.

 B_c^\pm MASS

VALUE (GeV)	DOCUMENT ID	TECN	COMMENT
$6.4 \pm 0.39 \pm 0.13$	¹ ABE	98M CDF	$p\bar{p}$ 1.8 TeV
• • • We do not use the following data for averages, fits, limits, etc. • • •			
6.32 ± 0.06	² ACKERSTAFF	98O OPAL	$e^+e^- \rightarrow Z$
¹ ABE 98M observed $20.4^{+6.2}_{-5.5}$ events in the $B_c^+ \rightarrow J/\psi(1S)\ell\nu_\ell$ with a significance of > 4.8 standard deviations. The mass value is estimated from $m(J/\psi(1S)\ell)$.			
² ACKERSTAFF 98O observed 2 candidate events in the $B_c \rightarrow J/\psi(1S)\pi^+\pi^-$ channel with an estimated background of 0.63 ± 0.20 events.			

 B_c^\pm MEAN LIFE

VALUE (10^{-12} s)	DOCUMENT ID	TECN	COMMENT
$0.46^{+0.18}_{-0.16} \pm 0.03$	³ ABE	98M CDF	$p\bar{p}$ 1.8 TeV
³ The lifetime is measured from the $J/\psi(1S)\ell$ decay vertices.			

 B_c^\pm DECAY MODES $\times B(\bar{b} \rightarrow B_c)$ B_c^- modes are charge conjugates of the modes below.

Mode	Fraction (Γ_i/Γ)	Confidence level	
The following quantities are not pure branching ratios; rather the fraction $\Gamma_i/\Gamma \times B(\bar{b} \rightarrow B_c)$.			
Γ_1	$J/\psi(1S)\ell^+\nu_\ell$ anything	$(5.2^{+2.4}_{-2.1}) \times 10^{-5}$	
Γ_2	$J/\psi(1S)\pi^+$	$< 8.2 \times 10^{-5}$	90%
Γ_3	$J/\psi(1S)\pi^+\pi^+\pi^-$	$< 5.7 \times 10^{-4}$	90%
Γ_4	$J/\psi(1S)a_1(1260)$	$< 1.2 \times 10^{-3}$	90%
Γ_5	$D^*(2010)^+\bar{D}^0$	$< 6.2 \times 10^{-3}$	90%

 B_c^\pm BRANCHING RATIOS

$\Gamma(J/\psi(1S)\ell^+\nu_\ell \text{ anything})/\Gamma_{\text{total}} \times B(\bar{b} \rightarrow B_c)$	$\Gamma_1/\Gamma \times B$			
VALUE	CL%	DOCUMENT ID	TECN	COMMENT
$(5.2^{+2.4}_{-2.1}) \times 10^{-5}$		⁴ ABE	98M CDF	$p\bar{p}$ 1.8 TeV
• • • We do not use the following data for averages, fits, limits, etc. • • •				
$< 1.6 \times 10^{-4}$	90	⁵ ACKERSTAFF	98O OPAL	$e^+e^- \rightarrow Z$
$< 1.9 \times 10^{-4}$	90	⁶ ABREU	97E DLPH	$e^+e^- \rightarrow Z$
$< 1.2 \times 10^{-4}$	90	⁷ BARATE	97H ALEP	$e^+e^- \rightarrow Z$

⁴ ABE 98M result is derived from the measurement of $[\sigma(B_c) \times B(B_c \rightarrow J/\psi(1S)\ell\nu_\ell)] / [\sigma(B^+) \times B(B^+ \rightarrow J/\psi(1S)K^+)] = 0.132^{+0.041}_{-0.037} (\text{stat}) \pm 0.031 (\text{sys})^{+0.032}_{-0.020} (\text{lifetime})$ by using PDG 98 values of $B(b \rightarrow B^+)$ and $B(B^+ \rightarrow J/\psi(1S)K^+)$.

⁵ ACKERSTAFF 98O reports $B(Z \rightarrow B_c X)/B(Z \rightarrow qq) \times B(B_c \rightarrow J/\psi(1S)\ell\nu_\ell) < 6.95 \times 10^{-5}$ at 90%CL. We rescale to our PDG 98 values of $B(Z \rightarrow b\bar{b})$.

⁶ ABREU 97E value listed is for an assumed $\tau_{B_c} = 0.4$ ps and improves to 1.6×10^{-4} for $\tau_{B_c} = 1.4$ ps.

⁷ BARATE 97H reports $B(Z \rightarrow B_c X)/B(Z \rightarrow qq) \times B(B_c \rightarrow J/\psi(1S)\ell\nu_\ell) < 5.2 \times 10^{-5}$ at 90%CL. We rescale to our PDG 96 values of $B(Z \rightarrow b\bar{b})$. A $B_c^+ \rightarrow J/\psi(1S)\mu^+\nu_\mu$ candidate event is found, compared to all the known background sources 2×10^{-3} , which gives $m_{B_c} = 5.96^{+0.25}_{-0.19}$ GeV and $\tau_{B_c} = 1.77 \pm 0.17$ ps.

$\Gamma(J/\psi(1S)\pi^+)/\Gamma_{\text{total}} \times B(\bar{b} \rightarrow B_c)$	$\Gamma_2/\Gamma \times B$			
VALUE	CL%	DOCUMENT ID	TECN	COMMENT
$< 8.2 \times 10^{-5}$	90	⁸ BARATE	97H ALEP	$e^+e^- \rightarrow Z$

• • • We do not use the following data for averages, fits, limits, etc. • • •

$< 2.4 \times 10^{-4}$	90	⁹ ACKERSTAFF	98O OPAL	$e^+e^- \rightarrow Z$
$< 3.4 \times 10^{-4}$	90	¹⁰ ABREU	97E DLPH	$e^+e^- \rightarrow Z$
$< 2.0 \times 10^{-5}$	95	¹¹ ABE	96R CDF	$p\bar{p}$ 1.8 TeV
⁸ BARATE 97H reports $B(Z \rightarrow B_c X)/B(Z \rightarrow qq) \times B(B_c \rightarrow J/\psi(1S)\pi) < 3.6 \times 10^{-5}$ at 90%CL. We rescale to our PDG 96 values of $B(Z \rightarrow b\bar{b})$.				
⁹ ACKERSTAFF 98O reports $B(Z \rightarrow B_c X)/B(Z \rightarrow qq) \times B(B_c \rightarrow J/\psi(1S)\pi^+) < 1.06 \times 10^{-4}$ at 90%CL. We rescale to our PDG 98 values of $B(Z \rightarrow b\bar{b})$.				
¹⁰ ABREU 97E value listed is for an assumed $\tau_{B_c} = 0.4$ ps and improves to 2.7×10^{-4} for $\tau_{B_c} = 1.4$ ps.				
¹¹ ABE 96R reports $B(b \rightarrow B_c X)/B(b \rightarrow B^+ X) \times B(B_c^+ \rightarrow J/\psi(1S)\pi^+)/B(B^+ \rightarrow J/\psi(1S)K^+) < 0.053$ at 95%CL for $\tau_{B_c} = 0.8$ ps. It changes from 0.15 to 0.04 for $0.17 \text{ ps} < \tau_{B_c} < 1.6$ ps. We rescale to our PDG 96 values of $B(b \rightarrow B^+) = 0.378 \pm 0.022$ and $B(B^+ \rightarrow J/\psi(1S)K^+) = 0.00101 \pm 0.00014$.				

$\Gamma(J/\psi(1S)\pi^+\pi^+\pi^-)/\Gamma_{\text{total}} \times B(\bar{b} \rightarrow B_c)$	$\Gamma_3/\Gamma \times B$			
VALUE	CL%	DOCUMENT ID	TECN	COMMENT
$< 5.7 \times 10^{-4}$	90	¹² ABREU	97E DLPH	$e^+e^- \rightarrow Z$
¹² ABREU 97E value listed is independent of $0.4 \text{ ps} < \tau_{B_c} < 1.4$ ps.				

$\Gamma(J/\psi(1S)a_1(1260))/\Gamma_{\text{total}} \times B(\bar{b} \rightarrow B_c)$	$\Gamma_4/\Gamma \times B$			
VALUE	CL%	DOCUMENT ID	TECN	COMMENT
$< 1.2 \times 10^{-3}$	90	¹³ ACKERSTAFF	98O OPAL	$e^+e^- \rightarrow Z$
¹³ ACKERSTAFF 98O reports $B(Z \rightarrow B_c X)/B(Z \rightarrow qq) \times B(B_c \rightarrow J/\psi(1S)a_1(1260)) < 5.29 \times 10^{-4}$ at 90%CL. We rescale to our PDG 98 values of $B(Z \rightarrow b\bar{b})$.				

$\Gamma(D^*(2010)^+\bar{D}^0)/\Gamma_{\text{total}} \times B(\bar{b} \rightarrow B_c)$	$\Gamma_5/\Gamma \times B$			
VALUE	CL%	DOCUMENT ID	TECN	COMMENT
$< 6.2 \times 10^{-3}$	90	¹⁴ BARATE	98Q ALEP	$e^+e^- \rightarrow Z$
¹⁴ BARATE 98Q reports $B(Z \rightarrow B_c X) \times B(B_c \rightarrow D^*(2010)^+\bar{D}^0) < 1.9 \times 10^{-3}$ at 90%CL. We rescale to our PDG 98 values of $B(Z \rightarrow b\bar{b})$.				

 B_c^\pm REFERENCES

ABE	98M PRL 81 2432	F. Abe et al.	(CDF Collab.)
Also	98R PR D58 112004	F. Abe et al.	(CDF Collab.)
ACKERSTAFF	98O PL B420 157	K. Ackerstaff et al.	(OPAL Collab.)
BARATE	98Q EPJ C4 387	R. Barate et al.	(ALEPH Collab.)
PDG	98 EPJ C3 1	C. Caso et al.	
ABREU	97E PL B398 207	P. Abreu et al.	(DELPHI Collab.)
BARATE	97H PL B402 213	R. Barate et al.	(ALEPH Collab.)
ABE	96R PRL 77 5176	F. Abe et al.	(CDF Collab.)
PDG	96 PR D54 1		

See key on page 239

Meson Particle Listings

Charmonium, $\eta_c(1S)$

$c\bar{c}$ MESONS

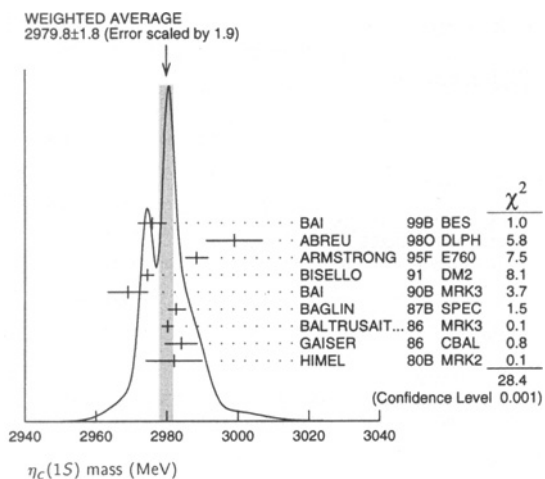
$\eta_c(1S)$

$$I^G(J^{PC}) = 0^+(0^{-+})$$

$\eta_c(1S)$ MASS

VALUE (MeV)	EVTS	DOCUMENT ID	TECN	COMMENT
2979.8 ± 1.8 OUR AVERAGE		Error includes scale factor of 1.9. See the ideogram below.		
2975.8 ± 3.9 ± 1.2		1,2 BAI	99b BES	$\psi(2S) \rightarrow \gamma X$
2999 ± 8	25	ABREU	98o DLPH	$e^+e^- \rightarrow e^+e^- + \text{hadrons}$
2988.3 ⁺ _{-3.1}		ARMSTRONG	95F E760	$\bar{p}p \rightarrow \gamma\gamma$
2974.4 ± 1.9		1 BISELLO	91 DM2	$J/\psi \rightarrow \eta_c\gamma$
2969 ± 4 ± 4	80	BAI	90b MRK3	$J/\psi \rightarrow \gamma X, \psi(2S) \rightarrow \gamma K^+ K^- K^+ K^-$
2982.6 ⁺ _{-2.3}	12	BAGLIN	87b SPEC	$\bar{p}p \rightarrow \gamma\gamma$
2980.2 ± 1.6		1 BALTRUSAIT...86	MRK3	$J/\psi \rightarrow \eta_c\gamma$
2984 ± 2.3 ± 4.0		GAISER	86 CBAL	$J/\psi \rightarrow \gamma X, \psi(2S) \rightarrow \gamma X$
2982 ± 8	18	3 HIMEL	80b MRK2	e^+e^-
2956 ± 12 ± 12		BAI	90b MRK3	$J/\psi \rightarrow \gamma K^+ K^- K_S^0 K_L^0$
2976 ± 8		4 BALTRUSAIT...84	MRK3	$J/\psi \rightarrow 2\phi\gamma$
2980 ± 9		PARTRIDGE	80b CBAL	e^+e^-

- • • We do not use the following data for averages, fits, limits, etc. • • •
- 1 Average of several decay modes.
- 2 Using an η_c width of 13.2 MeV.
- 3 Mass adjusted by us to correspond to $J/\psi(1S)$ mass = 3097 MeV.
- 4 $\eta_c \rightarrow \phi\phi$.



$\eta_c(1S)$ WIDTH

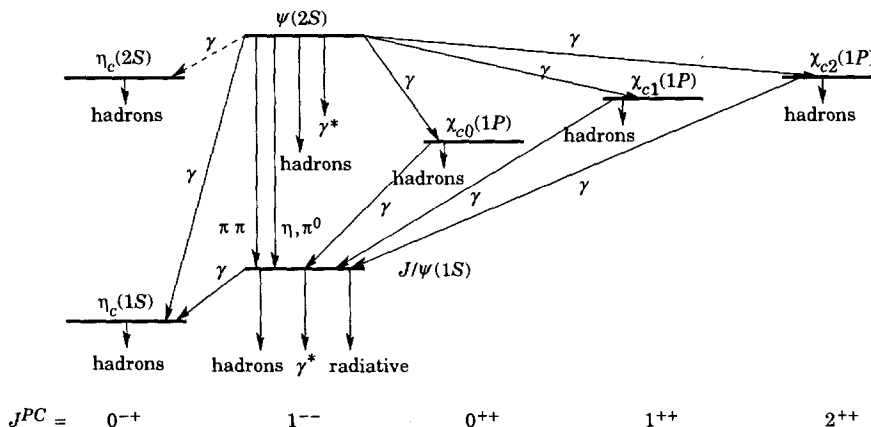
VALUE (MeV)	CL%	EVTS	DOCUMENT ID	TECN	COMMENT
13.2⁺_{-3.2} OUR AVERAGE					
23.9 ⁺ _{-7.1}			ARMSTRONG	95F E760	$\bar{p}p \rightarrow \gamma\gamma$
7.0 ⁺ _{-7.0}		12	BAGLIN	87b SPEC	$\bar{p}p \rightarrow \gamma\gamma$
10.1 ⁺ _{-8.2}		23	5 BALTRUSAIT...86	MRK3	$J/\psi \rightarrow \gamma\rho\bar{\rho}$
11.5 ± 4.5			GAISER	86 CBAL	$J/\psi \rightarrow \gamma X, \psi(2S) \rightarrow \gamma X$
<40	90	18	HIMEL	80b MRK2	e^+e^-
<20	90		PARTRIDGE	80b CBAL	e^+e^-

• • • We do not use the following data for averages, fits, limits, etc. • • •
 5 Positive and negative errors correspond to 90% confidence level.

$\eta_c(1S)$ DECAY MODES

Mode	Fraction (Γ_i/Γ)	Confidence level
Decays involving hadronic resonances		
Γ_1 $\eta'(958)\pi\pi$	(4.1 ± 1.7) %	
Γ_2 $\rho\rho$	(2.6 ± 0.9) %	
Γ_3 $K^*(892)^0 K^- \pi^+ + c.c.$	(2.0 ± 0.7) %	
Γ_4 $K^*(892) \bar{K}^*(892)$	(8.5 ± 3.1) × 10 ⁻³	
Γ_5 $\phi\phi$	(7.1 ± 2.8) × 10 ⁻³	
Γ_6 $a_0(980)\pi$	< 2 %	90%
Γ_7 $a_2(1320)\pi$	< 2 %	90%
Γ_8 $K^*(892) \bar{K} + c.c.$	< 1.28 %	90%
Γ_9 $f_2(1270)\eta$	< 1.1 %	90%
Γ_{10} $\omega\omega$	< 3.1 × 10 ⁻³	90%
Decays into stable hadrons		
Γ_{11} $K\bar{K}\pi$	(5.5 ± 1.7) %	
Γ_{12} $\eta\pi\pi$	(4.9 ± 1.8) %	
Γ_{13} $\pi^+\pi^-K^+K^-$	(2.0 ^{+0.7} _{-0.6}) %	
Γ_{14} $2(K^+K^-)$	(2.1 ± 1.2) %	
Γ_{15} $2(\pi^+\pi^-)$	(1.2 ± 0.4) %	
Γ_{16} $\rho\bar{\rho}$	(1.2 ± 0.4) × 10 ⁻³	
Γ_{17} $K\bar{K}\eta$	< 3.1 %	90%
Γ_{18} $\pi^+\pi^-\rho\bar{\rho}$	< 1.2 %	90%
Γ_{19} $\Lambda\bar{\Lambda}$	< 2 × 10 ⁻³	90%
Radiative decays		
Γ_{20} $\gamma\gamma$	(3.0 ± 1.2) × 10 ⁻⁴	

THE CHARMONIUM SYSTEM



The current state of knowledge of the charmonium system and transitions, as interpreted by the charmonium model. Uncertain states and transitions are indicated by dashed lines. The notation γ^* refers to decay processes involving intermediate virtual photons, including decays to e^+e^- and $\mu^+\mu^-$.

Meson Particle Listings

$\eta_c(1S)$

$\eta_c(1S)$ PARTIAL WIDTHS

$\Gamma(\gamma\gamma)$					Γ_{20}
VALUE (keV)	EVTS	DOCUMENT ID	TECN	COMMENT	
7.4 ± 1.4 OUR AVERAGE					
6.9 ± 1.7 ± 2.1	76 ± 19	ACCIARRI	99T L3	$\gamma\gamma$	
27 ± 16 ± 10	5	SHIRAI	98 AMY	58 e^+e^-	
6.7 ⁺ 2.4 ± 2.3		ARMSTRONG	95F E760	$\bar{p}p \rightarrow \gamma\gamma$	
11.3 ± 4.2		ALBRECHT	94H ARG	$\gamma\gamma$	
5.9 ⁺ 2.1 ± 1.9		CHEN	90B CLEO	$e^+e^- \rightarrow e^+e^-\eta_c$	
6.4 ⁺ 5.0		AIHARA	88D TPC	$e^+e^- \rightarrow e^+e^-X$	
28 ± 15		⁶ BERGER	86 PLUT	$\gamma\gamma \rightarrow K\bar{K}\pi$	
••• We do not use the following data for averages, fits, limits, etc. •••					
8.0 ± 2.3 ± 2.4	17	⁷ ADRIANI	93N L3	$e^+e^- \rightarrow e^+e^-\eta_c$	
⁶ Re-evaluated by AIHARA 88D.					
⁷ Superseded by ACCIARRI 99T.					

$\eta_c(1S)$ $\Gamma(\gamma\gamma)/\Gamma(\text{total})$

$\Gamma(K\bar{K}\pi) \times \Gamma(\gamma\gamma)/\Gamma_{\text{total}}$					$\Gamma_{11}\Gamma_{20}/\Gamma$
VALUE (keV)	CL% EVTS	DOCUMENT ID	TECN	COMMENT	
0.94 ± 0.18 OUR AVERAGE					
0.84 ± 0.21		⁸ ALBRECHT	94H ARG	$\gamma\gamma \rightarrow K^\pm K_S^0 \pi^\mp$	
1.06 ± 0.41 ± 0.27	11	BRAUNSCH...	89 TASS	$\gamma\gamma \rightarrow K\bar{K}\pi$	
1.5 ⁺ 0.60 ± 0.3	7	⁸ BERGER	86 PLUT	$\gamma\gamma \rightarrow K\bar{K}\pi$	
••• We do not use the following data for averages, fits, limits, etc. •••					
<0.63	95	⁸ BEHREND	89 CELL	$\gamma\gamma \rightarrow K_S^0 K^\pm \pi^\mp$	
<4.4	95	ALTHOFF	85B TASS	$\gamma\gamma \rightarrow K\bar{K}\pi$	
⁸ $K^\pm K_S^0 \pi^\mp$ corrected to $K\bar{K}\pi$ by factor 3.					

$\eta_c(1S)$ BRANCHING RATIOS

HADRONIC DECAYS

$\Gamma(\eta'(958)\pi\pi)/\Gamma_{\text{total}}$					Γ_1/Γ
VALUE	EVTS	DOCUMENT ID	TECN	COMMENT	
0.041 ± 0.017	14	⁹ BALTRUSAIT..86	MRK3	$J/\psi \rightarrow \eta_c\gamma$	

$\Gamma(\rho\rho)/\Gamma_{\text{total}}$					Γ_2/Γ
VALUE (units 10 ⁻³)	CL% EVTS	DOCUMENT ID	TECN	COMMENT	
26 ± 9 OUR EVALUATION				(Treating systematic errors as correlated.)	
25 ± 8 OUR AVERAGE					
26.0 ± 2.4 ± 8.8	113	⁹ BISELLO	91 DM2	$J/\psi \rightarrow \gamma\rho^0\rho^0$	
23.6 ± 10.6 ± 8.2	32	⁹ BISELLO	91 DM2	$J/\psi \rightarrow \gamma\rho^+\rho^-$	
••• We do not use the following data for averages, fits, limits, etc. •••					
<140	90	⁹ BALTRUSAIT..86	MRK3	$J/\psi \rightarrow \eta_c\gamma$	

$\Gamma(K^*(892)^0 K^- \pi^+ + \text{c.c.})/\Gamma_{\text{total}}$					Γ_3/Γ
VALUE	EVTS	DOCUMENT ID	TECN	COMMENT	
0.02 ± 0.007	63	⁹ BALTRUSAIT..86	MRK3	$J/\psi \rightarrow \eta_c\gamma$	

$\Gamma(K^*(892)\bar{K}^*(892))/\Gamma_{\text{total}}$					Γ_4/Γ
VALUE (units 10 ⁻⁴)	EVTS	DOCUMENT ID	TECN	COMMENT	
85 ± 31 OUR AVERAGE					
82 ± 28 ± 27	14	⁹ BISELLO	91 DM2	$e^+e^- \rightarrow \gamma K^+ K^- \pi^+ \pi^-$	
90 ± 50	9	⁹ BALTRUSAIT..86	MRK3	$J/\psi \rightarrow \eta_c\gamma$	

$\Gamma(K^*(892)\bar{K} + \text{c.c.})/\Gamma_{\text{total}}$					Γ_8/Γ
VALUE	CL%	DOCUMENT ID	TECN	COMMENT	
<0.0128	90	BISELLO	91 DM2	$J/\psi \rightarrow \gamma K_S^0 K^\pm \pi^\mp$	
<0.0132	90	⁹ BISELLO	91 DM2	$J/\psi \rightarrow \gamma K^+ K^- \pi^0$	

$\Gamma(\phi\phi)/\Gamma_{\text{total}}$					Γ_5/Γ
VALUE (units 10 ⁻⁴)	EVTS	DOCUMENT ID	TECN	COMMENT	
71 ± 28 OUR EVALUATION				(Treating systematic errors as correlated.)	
71 ± 22 OUR AVERAGE					
74 ± 18 ± 24	80	⁹ BAI	90B MRK3	$J/\psi \rightarrow \gamma K^+ K^- K^+ K^-$	
67 ± 21 ± 24		⁹ BAI	90B MRK3	$J/\psi \rightarrow \gamma K^+ K^- K_S^0 K_L^0$	

••• We do not use the following data for averages, fits, limits, etc. •••					
31 ± 7 ± 10	19	⁹ BISELLO	91 DM2	$J/\psi \rightarrow \gamma K^+ K^- K^+ K^-$	
30 ⁺ 18 ± 10	5	⁹ BISELLO	91 DM2	$J/\psi \rightarrow \gamma K^+ K^- K_S^0 K_L^0$	

$\Gamma(a_0(980)\pi)/\Gamma_{\text{total}}$					Γ_6/Γ
VALUE	CL%	DOCUMENT ID	TECN	COMMENT	
<0.02	90	^{9,10} BALTRUSAIT..86	MRK3	$J/\psi \rightarrow \eta_c\gamma$	

$\Gamma(a_2(1320)\pi)/\Gamma_{\text{total}}$					Γ_7/Γ
VALUE	CL%	DOCUMENT ID	TECN	COMMENT	
<0.02	90	⁹ BALTRUSAIT..86	MRK3	$J/\psi \rightarrow \eta_c\gamma$	

$\Gamma(f_2(1270)\eta)/\Gamma_{\text{total}}$					Γ_9/Γ
VALUE	CL%	DOCUMENT ID	TECN	COMMENT	
<0.011	90	⁹ BALTRUSAIT..86	MRK3	$J/\psi \rightarrow \eta_c\gamma$	

$\Gamma(\omega\omega)/\Gamma_{\text{total}}$					Γ_{10}/Γ
VALUE	CL%	DOCUMENT ID	TECN	COMMENT	
<0.0031	90	⁹ BALTRUSAIT..86	MRK3	$J/\psi \rightarrow \eta_c\gamma$	
••• We do not use the following data for averages, fits, limits, etc. •••					
<0.0063		⁹ BISELLO	91 DM2	$J/\psi \rightarrow \gamma\omega$	

$\Gamma(K\bar{K}\pi)/\Gamma_{\text{total}}$					Γ_{11}/Γ
VALUE	CL% EVTS	DOCUMENT ID	TECN	COMMENT	
0.055 ± 0.017 OUR EVALUATION				(Treating systematic errors as correlated.)	
0.055 ± 0.008 OUR AVERAGE					
0.0690 ± 0.0142 ± 0.0132	33	⁹ BISELLO	91 DM2	$J/\psi \rightarrow \gamma K^+ K^- \pi^0$	
0.0543 ± 0.0094 ± 0.0094	68	⁹ BISELLO	91 DM2	$J/\psi \rightarrow \gamma K^\pm \pi^\mp K_S^0$	
0.048 ± 0.011	95	^{9,11} BALTRUSAIT..86	MRK3	$J/\psi \rightarrow \eta_c\gamma$	
0.161 ⁺ 0.092		¹² HIMEL	80B MRK2	$\psi(2S) \rightarrow \eta_c\gamma$	
-0.073					
••• We do not use the following data for averages, fits, limits, etc. •••					
<0.107	90	⁹ PARTRIDGE	80B CBAL	$J/\psi \rightarrow \eta_c\gamma$	

$\Gamma(\eta\pi\pi)/\Gamma_{\text{total}}$					Γ_{12}/Γ
VALUE	EVTS	DOCUMENT ID	TECN	COMMENT	
0.049 ± 0.018 OUR EVALUATION					
0.047 ± 0.015 OUR AVERAGE					
0.054 ± 0.020	75	⁹ BALTRUSAIT..86	MRK3	$J/\psi \rightarrow \eta_c\gamma$	
0.037 ± 0.013 ± 0.020	18	⁹ PARTRIDGE	80B CBAL	$J/\psi \rightarrow \eta\pi^+\pi^-\gamma$	

$\Gamma(\pi^+ \pi^- K^+ K^-)/\Gamma_{\text{total}}$					Γ_{13}/Γ
VALUE	EVTS	DOCUMENT ID	TECN	COMMENT	
0.020 ± 0.007					
0.020 ± 0.006 OUR AVERAGE					
0.021 ± 0.007	110	⁹ BALTRUSAIT..86	MRK3	$J/\psi \rightarrow \eta_c\gamma$	
0.014 ⁺ 0.022		¹² HIMEL	80B MRK2	$\psi(2S) \rightarrow \eta_c\gamma$	
-0.009					

$\Gamma(2(\pi^+ \pi^-))/\Gamma_{\text{total}}$					Γ_{15}/Γ
VALUE	EVTS	DOCUMENT ID	TECN	COMMENT	
0.012 ± 0.004 OUR EVALUATION					
0.0120 ± 0.0031 OUR AVERAGE					
0.0105 ± 0.0017 ± 0.0034	137	⁹ BISELLO	91 DM2	$J/\psi \rightarrow \gamma 2\pi^+ 2\pi^-$	
0.013 ± 0.006	25	⁹ BALTRUSAIT..86	MRK3	$J/\psi \rightarrow \eta_c\gamma$	
0.020 ⁺ 0.015		¹² HIMEL	80B MRK2	$\psi(2S) \rightarrow \eta_c\gamma$	
-0.010					

$\Gamma(2(K^+ K^-))/\Gamma_{\text{total}}$					Γ_{14}/Γ
VALUE	EVTS	DOCUMENT ID	TECN	COMMENT	
0.021 ± 0.010 ± 0.006					
		ALBRECHT	94H ARG	$\gamma\gamma \rightarrow K^+ K^- K^+ K^-$	

$\Gamma(\rho\bar{\rho})/\Gamma_{\text{total}}$					Γ_{16}/Γ
VALUE (units 10 ⁻⁴)	EVTS	DOCUMENT ID	TECN	COMMENT	
12 ± 4 OUR AVERAGE					
10 ± 3 ± 4	18	⁹ BISELLO	91 DM2	$J/\psi \rightarrow \gamma\rho\bar{\rho}$	
11 ± 6	23	⁹ BALTRUSAIT..86	MRK3	$J/\psi \rightarrow \eta_c\gamma$	
29 ⁺ 29		¹² HIMEL	80B MRK2	$\psi(2S) \rightarrow \eta_c\gamma$	
-15					

$\Gamma(K\bar{K}\eta)/\Gamma_{\text{total}}$					Γ_{17}/Γ
VALUE	CL%	DOCUMENT ID	TECN	COMMENT	
<0.031	90	⁹ BALTRUSAIT..86	MRK3	$J/\psi \rightarrow \eta_c\gamma$	

$\Gamma(\pi^+ \pi^- \rho\bar{\rho})/\Gamma_{\text{total}}$					Γ_{18}/Γ
VALUE	CL%	DOCUMENT ID	TECN	COMMENT	
<0.012	90	HIMEL	80B MRK2	$\psi(2S) \rightarrow \eta_c\gamma$	

$\Gamma(\Lambda\bar{\Lambda})/\Gamma_{\text{total}}$					Γ_{19}/Γ
VALUE	CL%	DOCUMENT ID	TECN	COMMENT	
<0.002	90	⁹ BISELLO	91 DM2	$e^+e^- \rightarrow \gamma\Lambda\bar{\Lambda}$	

$\Gamma_f/\Gamma_{\text{total}}^2$ in $\rho\bar{\rho} \rightarrow \eta_c(1S) \rightarrow \phi\phi$					$\Gamma_{16}\Gamma_5/\Gamma^2$
VALUE (units 10 ⁻⁵)	CL%	DOCUMENT ID	TECN	COMMENT	
4.0 ± 3.5					
-3.2		BAGLIN	89 SPEC	$\bar{p}p \rightarrow K^+ K^- K^+ K^-$	

⁹The quoted branching ratios use $B(J/\psi(1S) \rightarrow \gamma\eta_c(1S)) = 0.0127 \pm 0.0036$. Where relevant, the error in this branching ratio is treated as a common systematic in computing averages.

¹⁰We are assuming $B(a_0(980) \rightarrow \eta\pi) > 0.5$.

¹¹Average from $K^+ K^- \pi^0$ and $K^\pm K_S^0 \pi^\mp$ decay channels.

¹²Estimated using $B(\psi(2S) \rightarrow \gamma\eta_c(1S)) = 0.0028 \pm 0.0006$.

RADIATIVE DECAYS

$\Gamma(\gamma\gamma)/\Gamma_{total}$	CL%	DOCUMENT ID	TECN	COMMENT	Γ_{20}/Γ
VALUE (units 10^{-4})					
3.0 ± 1.2 OUR AVERAGE					
2.80 ^{+0.67} _{-0.58} ± 1.0		ARMSTRONG 95F E760		$\bar{p}p \rightarrow \gamma\gamma$	
6 ⁺⁴ ₋₃ ± 4		BAGLIN 87B SPEC		$\bar{p}p \rightarrow \gamma\gamma$	
• • • We do not use the following data for averages, fits, limits, etc. • • •					
< 9	90	⁹ BISELLO 91 DM2		$J/\psi \rightarrow \gamma\gamma\gamma$	
< 18	90	¹³ BLOOM 83 CBAL		$J/\psi \rightarrow \eta_c\gamma$	
¹³ Using $B(J/\psi(1S) \rightarrow \gamma\eta_c(1S)) = 0.0127 \pm 0.0036$.					
$\Gamma_i/\Gamma_{total}^2$ in $\rho\bar{p} \rightarrow \eta_c(1S) \rightarrow \gamma\gamma$					$\Gamma_{16}\Gamma_{20}/\Gamma^2$
VALUE (units 10^{-6})	EVTS	DOCUMENT ID	TECN	COMMENT	
0.36 ± 0.08				Error includes scale factor of 1.1.	
0.36 ± 0.08					
0.336 ^{+0.080} _{-0.070}		ARMSTRONG 95F E760		$\bar{p}p \rightarrow \gamma\gamma$	
0.68 ^{+0.42} _{-0.31}	12	BAGLIN 87B SPEC		$\bar{p}p \rightarrow \gamma\gamma$	

$\eta_c(1S)$ REFERENCES

ACCARI 99T	PL B461 155	M. Acciarri et al.	(L3 Collab.)
BAI 99B	PR D60 072001	J.Z. Bai et al.	(BES Collab.)
ABREU 98O	PL B441 479	P. Abreu et al.	(DELPHI Collab.)
SHIRAI 98	PL B424 405	M. Shirai et al.	(AMY Collab.)
ARMSTRONG 95F	PR D52 4839	T.A. Armstrong et al.	(FNAL, FERR, GENO+)
ALBRECHT 94H	PL B338 390	H. Albrecht et al.	(ARGUS Collab.)
ADRIANI 93N	PL B318 575	O. Adriani et al.	(L3 Collab.)
BISELLO 91	NP B350 1	D. Bisello et al.	(DM2 Collab.)
BAI 90B	PRL 65 1309	Z. Bai et al.	(Mark III Collab.)
CHEN 90B	PL B243 169	W.Y. Chen et al.	(CLEO Collab.)
BAGLIN 89	PL B231 557	C. Baglin, S. Baird, G. Bassompierre	(R704 Collab.)
BEHREND 89	ZPHY C42 367	H.J. Behrend et al.	(CELLO Collab.)
BRAUNSCH... 89	ZPHY C41 533	W. Braunschweig et al.	(TASSO Collab.)
AIHARA 88D	PRL 60 2355	H. Ahara et al.	(TTC Collab.)
BAGLIN 87B	PL B167 191	C. Baglin et al.	(R704 Collab.)
BALTRUSAIT... 86	PR D33 629	R.M. Baltrusaitis et al.	(Mark III Collab.)
BERGER 86	PL 167B 120	C. Berger et al.	(PLUTO Collab.)
GAISER 86	PR D34 711	J. Gaiser et al.	(Crystal Ball Collab.)
ALTHOFF 85B	ZPHY C29 189	M. Althoff et al.	(TASSO Collab.)
BALTRUSAIT... 84	PRL 52 2126	R.M. Baltrusaitis et al.	(CIT, UCSC+) JP
BLOOM 83	ARNS 33 143	E.D. Bloom, C. Peck	(SLAC, CIT)
HIMEL 80B	PRL 45 1146	T.M. Himel et al.	(SLAC, LBL, UCB)
PARTRIDGE 80B	PRL 45 1150	R. Partridge et al.	(CIT, HARV, PRIN+)

OTHER RELATED PAPERS

ARMSTRONG 89	PL B221 216	T.A. Armstrong et al.	(CERN, CDEF, BIRM+)
--------------	-------------	-----------------------	---------------------

$J/\psi(1S)$

$I^G(J^{PC}) = 0^-(1^{--})$

$J/\psi(1S)$ MASS

VALUE (MeV)	EVTS	DOCUMENT ID	TECN	COMMENT
3096.87 ± 0.04 OUR AVERAGE				
3096.89 ± 0.09	502	¹ ARTAMONOV 00 OLYA		$e^+e^- \rightarrow$ hadrons
3096.87 ± 0.03 ± 0.03		ARMSTRONG 93B E760		$\bar{p}p \rightarrow e^+e^-$
3096.95 ± 0.1 ± 0.3	193	BAGLIN 87 SPEC		$\bar{p}p \rightarrow e^+e^-X$
• • • We do not use the following data for averages, fits, limits, etc. • • •				
3097.5 ± 0.3		GRIBUSHIN 96 FMPS	515	$\pi^-Be \rightarrow 2\mu X$
3098.4 ± 2.0	38k	LEMOIGNE 82 GOLI	190	$\pi^-Be \rightarrow 2\mu$
3096.93 ± 0.09	502	² ZHOLENTZ 80 REDE		e^+e^-
3097.0 ± 1		³ BRANDELIK 79C DASP		e^+e^-
¹ Reanalysis of ZHOLENTZ 80 using new electron mass (COHEN 87) and radiative corrections (KURAEV 85).				
² Superseded by ARTAMONOV 00.				
³ From a simultaneous fit to e^+e^- , $\mu^+\mu^-$ and hadronic channels assuming $\Gamma(e^+e^-) = \Gamma(\mu^+\mu^-)$.				

$J/\psi(1S)$ WIDTH

VALUE (keV)	DOCUMENT ID	TECN	COMMENT
87 ± 5 OUR AVERAGE			
84.4 ± 8.9	BAI 95B BES		e^+e^-
99 ± 12 ± 6	ARMSTRONG 93B E760		$\bar{p}p \rightarrow e^+e^-$
85.5 ^{+6.1} _{-5.8}	⁴ HSUEH 92 RVUE		See Υ mini-review
⁴ Using data from COFFMAN 92, BALDINI-CELIO 75, BOYARSKI 75, ESPOSITO 75b, BRANDELIK 79c.			

$J/\psi(1S)$ DECAY MODES

Mode	Fraction (Γ_i/Γ)	Scale factor/ Confidence level
Γ_1 hadrons	(87.7 ± 0.5) %	
Γ_2 virtual $\gamma \rightarrow$ hadrons	(17.0 ± 2.0) %	
Γ_3 e^+e^-	(5.93 ± 0.10) %	
Γ_4 $\mu^+\mu^-$	(5.88 ± 0.10) %	

Decays involving hadronic resonances

Γ_5 $\rho\pi$	(1.27 ± 0.09) %	
Γ_6 $\rho^0\pi^0$	(4.2 ± 0.5) × 10 ⁻³	
Γ_7 $\varrho_2(1320)\rho$	(1.09 ± 0.22) %	
Γ_8 $\omega\pi^+\pi^-\pi^-\pi^-$	(8.5 ± 3.4) × 10 ⁻³	
Γ_9 $\omega\pi^+\pi^-$	(7.2 ± 1.0) × 10 ⁻³	
Γ_{10} $\omega f_2(1270)$	(4.3 ± 0.6) × 10 ⁻³	
Γ_{11} $K^*(892)^0\bar{K}_2^*(1430)^0 + c.c.$	(6.7 ± 2.6) × 10 ⁻³	
Γ_{12} $\omega K^*(892)\bar{K} + c.c.$	(5.3 ± 2.0) × 10 ⁻³	
Γ_{13} $K^+\bar{K}^*(892)^- + c.c.$	(5.0 ± 0.4) × 10 ⁻³	
Γ_{14} $K^0\bar{K}^*(892)^0 + c.c.$	(4.2 ± 0.4) × 10 ⁻³	
Γ_{15} $K_1(1400)\pi^{\pm}K^{\mp}$	(3.8 ± 1.4) × 10 ⁻³	
Γ_{16} $\omega\pi^0\pi^0$	(3.4 ± 0.8) × 10 ⁻³	
Γ_{17} $b_1(1235)\pi^{\mp}$	[a] (3.0 ± 0.5) × 10 ⁻³	
Γ_{18} $\omega K^{\pm}K_S^0\pi^{\mp}$	[a] (2.9 ± 0.7) × 10 ⁻³	
Γ_{19} $b_1(1235)\pi^0$	(2.3 ± 0.6) × 10 ⁻³	
Γ_{20} $\phi K^*(892)\bar{K} + c.c.$	(2.04 ± 0.28) × 10 ⁻³	
Γ_{21} $\omega K\bar{K}$	(1.9 ± 0.4) × 10 ⁻³	
Γ_{22} $\omega f_0(1710) \rightarrow \omega K\bar{K}$	(4.8 ± 1.1) × 10 ⁻⁴	
Γ_{23} $\phi 2(\pi^+\pi^-)$	(1.60 ± 0.32) × 10 ⁻³	
Γ_{24} $\Delta(1232)^{++}\bar{p}\pi^-$	(1.6 ± 0.5) × 10 ⁻³	
Γ_{25} $\omega\eta$	(1.58 ± 0.16) × 10 ⁻³	
Γ_{26} $\phi K\bar{K}$	(1.48 ± 0.22) × 10 ⁻³	
Γ_{27} $\phi f_0(1710) \rightarrow \phi K\bar{K}$	(3.6 ± 0.6) × 10 ⁻⁴	
Γ_{28} $\rho\bar{\rho}\omega$	(1.30 ± 0.25) × 10 ⁻³	S=1.3
Γ_{29} $\Delta(1232)^{++}\bar{\Delta}(1232)^{--}$	(1.10 ± 0.29) × 10 ⁻³	
Γ_{30} $\Sigma(1385)^-\bar{\Sigma}(1385)^+ (or c.c.)$	[a] (1.03 ± 0.13) × 10 ⁻³	
Γ_{31} $\rho\bar{\rho}\eta'(958)$	(9 ± 4) × 10 ⁻⁴	S=1.7
Γ_{32} $\phi f_2'(1525)$	(8 ± 4) × 10 ⁻⁴	S=2.7
Γ_{33} $\phi\pi^+\pi^-$	(8.0 ± 1.2) × 10 ⁻⁴	
Γ_{34} $\phi K^{\pm}K_S^0\pi^{\mp}$	[a] (7.2 ± 0.9) × 10 ⁻⁴	
Γ_{35} $\omega f_1(1420)$	(6.8 ± 2.4) × 10 ⁻⁴	
Γ_{36} $\phi\eta$	(6.5 ± 0.7) × 10 ⁻⁴	
Γ_{37} $\Xi(1530)^-\Xi^+$	(5.9 ± 1.5) × 10 ⁻⁴	
Γ_{38} $\rho K^-\bar{\Sigma}(1385)^0$	(5.1 ± 3.2) × 10 ⁻⁴	
Γ_{39} $\omega\pi^0$	(4.2 ± 0.6) × 10 ⁻⁴	S=1.4
Γ_{40} $\phi\eta'(958)$	(3.3 ± 0.4) × 10 ⁻⁴	
Γ_{41} $\phi f_0(980)$	(3.2 ± 0.9) × 10 ⁻⁴	S=1.9
Γ_{42} $\Xi(1530)^0\Xi^0$	(3.2 ± 1.4) × 10 ⁻⁴	
Γ_{43} $\Sigma(1385)^-\bar{\Sigma}^+ (or c.c.)$	[a] (3.1 ± 0.5) × 10 ⁻⁴	
Γ_{44} $\phi f_1(1285)$	(2.6 ± 0.5) × 10 ⁻⁴	S=1.1
Γ_{45} $\rho\eta$	(1.93 ± 0.23) × 10 ⁻⁴	
Γ_{46} $\omega\eta'(958)$	(1.67 ± 0.25) × 10 ⁻⁴	
Γ_{47} $\omega f_0(980)$	(1.4 ± 0.5) × 10 ⁻⁴	
Γ_{48} $\rho\eta'(958)$	(1.05 ± 0.18) × 10 ⁻⁴	
Γ_{49} $\rho\bar{\rho}\phi$	(4.5 ± 1.5) × 10 ⁻⁵	
Γ_{50} $a_2(1320)\pi^{\mp}$	[a] < 4.3 × 10 ⁻³	CL=90%
Γ_{51} $K\bar{K}_2^*(1430) + c.c.$	< 4.0 × 10 ⁻³	CL=90%
Γ_{52} $K_1(1270)\pi^{\mp}$	< 3.0 × 10 ⁻³	CL=90%
Γ_{53} $K_2^*(1430)^0\bar{K}_2^*(1430)^0$	< 2.9 × 10 ⁻³	CL=90%
Γ_{54} $K^*(892)^0\bar{K}^*(892)^0$	< 5 × 10 ⁻⁴	CL=90%
Γ_{55} $\phi f_2(1270)$	< 3.7 × 10 ⁻⁴	CL=90%
Γ_{56} $\rho\bar{\rho}\rho$	< 3.1 × 10 ⁻⁴	CL=90%
Γ_{57} $\phi\eta(1440) \rightarrow \phi\eta\pi\pi$	< 2.5 × 10 ⁻⁴	CL=90%
Γ_{58} $\omega f_2'(1525)$	< 2.2 × 10 ⁻⁴	CL=90%
Γ_{59} $\Sigma(1385)^0\bar{\Lambda}$	< 2 × 10 ⁻⁴	CL=90%
Γ_{60} $\Delta(1232)^+\bar{p}$	< 1 × 10 ⁻⁴	CL=90%
Γ_{61} $\Sigma^0\bar{\Lambda}$	< 9 × 10 ⁻⁵	CL=90%
Γ_{62} $\phi\pi^0$	< 6.8 × 10 ⁻⁶	CL=90%
Decays into stable hadrons		
Γ_{63} $2(\pi^+\pi^-)\pi^0$	(3.37 ± 0.26) %	
Γ_{64} $3(\pi^+\pi^-)\pi^0$	(2.9 ± 0.6) %	
Γ_{65} $\pi^+\pi^-\pi^0$	(1.50 ± 0.20) %	
Γ_{66} $\pi^+\pi^-\pi^0 K^+K^-$	(1.20 ± 0.30) %	
Γ_{67} $4(\pi^+\pi^-)\pi^0$	(9.0 ± 3.0) × 10 ⁻³	
Γ_{68} $\pi^+\pi^-K^+K^-$	(7.2 ± 2.3) × 10 ⁻³	
Γ_{69} $K\bar{K}\pi$	(6.1 ± 1.0) × 10 ⁻³	
Γ_{70} $\rho\bar{\rho}\pi^+\pi^-$	(6.0 ± 0.5) × 10 ⁻³	S=1.3
Γ_{71} $2(\pi^+\pi^-)$	(4.0 ± 1.0) × 10 ⁻³	
Γ_{72} $3(\pi^+\pi^-)$	(4.0 ± 2.0) × 10 ⁻³	
Γ_{73} $n\bar{n}\pi^+\pi^-$	(4 ± 4) × 10 ⁻³	
Γ_{74} $\Sigma^0\bar{\Sigma}^0$	(1.27 ± 0.17) × 10 ⁻³	
Γ_{75} $2(\pi^+\pi^-)K^+K^-$	(3.1 ± 1.3) × 10 ⁻³	
Γ_{76} $\rho\bar{\rho}\pi^+\pi^-\pi^0$	[b] (2.3 ± 0.9) × 10 ⁻³	S=1.9

Meson Particle Listings

$J/\psi(1S)$

Γ_{77}	$p\bar{p}$	$(2.12 \pm 0.10) \times 10^{-3}$	
Γ_{78}	$p\bar{p}\eta$	$(2.09 \pm 0.18) \times 10^{-3}$	
Γ_{79}	$p\bar{n}\pi^-$	$(2.00 \pm 0.10) \times 10^{-3}$	
Γ_{80}	$n\bar{n}$	$(2.2 \pm 0.4) \times 10^{-3}$	
Γ_{81}	$\Xi\bar{\Xi}$	$(1.8 \pm 0.4) \times 10^{-3}$	S=1.8
Γ_{82}	$\Lambda\bar{\Lambda}$	$(1.30 \pm 0.12) \times 10^{-3}$	S=1.1
Γ_{83}	$p\bar{p}\pi^0$	$(1.09 \pm 0.09) \times 10^{-3}$	
Γ_{84}	$\Lambda\bar{\Sigma}^-\pi^+$ (or c.c.)	[a] $(1.06 \pm 0.12) \times 10^{-3}$	
Γ_{85}	$\rho K^-\bar{\Lambda}$	$(8.9 \pm 1.6) \times 10^{-4}$	
Γ_{86}	$2(K^+K^-)$	$(7.0 \pm 3.0) \times 10^{-4}$	
Γ_{87}	$\rho K^-\bar{\Sigma}^0$	$(2.9 \pm 0.8) \times 10^{-4}$	
Γ_{88}	K^+K^-	$(2.37 \pm 0.31) \times 10^{-4}$	
Γ_{89}	$\Lambda\bar{\Lambda}\pi^0$	$(2.2 \pm 0.6) \times 10^{-4}$	
Γ_{90}	$\pi^+\pi^-$	$(1.47 \pm 0.23) \times 10^{-4}$	
Γ_{91}	$K_S^0 K_L^0$	$(1.08 \pm 0.14) \times 10^{-4}$	
Γ_{92}	$\Lambda\bar{\Sigma}^+ + c.c.$	$< 1.5 \times 10^{-4}$	CL=90%
Γ_{93}	$K_S^0 K_S^0$	$< 5.2 \times 10^{-6}$	CL=90%

Radiative decays

Γ_{94}	$\gamma\eta_c(1S)$	$(1.3 \pm 0.4) \%$	
Γ_{95}	$\gamma\pi^+\pi^-2\pi^0$	$(8.3 \pm 3.1) \times 10^{-3}$	
Γ_{96}	$\gamma\eta\pi\pi$	$(6.1 \pm 1.0) \times 10^{-3}$	
Γ_{97}	$\gamma\eta(1440) \rightarrow \gamma K\bar{K}\pi$	[c] $(9.1 \pm 1.8) \times 10^{-4}$	
Γ_{98}	$\gamma\eta(1440) \rightarrow \gamma\gamma\rho^0$	$(6.4 \pm 1.4) \times 10^{-5}$	
Γ_{99}	$\gamma\eta(1440) \rightarrow \gamma\eta\pi^+\pi^-$	$(3.0 \pm 0.5) \times 10^{-4}$	
Γ_{100}	$\gamma\rho\rho$	$(4.5 \pm 0.8) \times 10^{-3}$	
Γ_{101}	$\gamma\eta_2(1870) \rightarrow \gamma\pi^+\pi^-$	$(6.2 \pm 2.4) \times 10^{-4}$	
Γ_{102}	$\gamma\eta'(958)$	$(4.31 \pm 0.30) \times 10^{-3}$	
Γ_{103}	$\gamma 2\pi^+2\pi^-$	$(2.8 \pm 0.5) \times 10^{-3}$	S=1.9
Γ_{104}	$\gamma K^+K^-\pi^+\pi^-$	$(2.1 \pm 0.6) \times 10^{-3}$	
Γ_{105}	$\gamma f_4(2050)$	$(2.7 \pm 0.7) \times 10^{-3}$	
Γ_{106}	$\gamma\omega\omega$	$(1.59 \pm 0.33) \times 10^{-3}$	
Γ_{107}	$\gamma\eta(1440) \rightarrow \gamma\rho^0\rho^0$	$(1.7 \pm 0.4) \times 10^{-3}$	S=1.3
Γ_{108}	$\gamma f_2(1270)$	$(1.38 \pm 0.14) \times 10^{-3}$	
Γ_{109}	$\gamma f_0(1710) \rightarrow \gamma K\bar{K}$	$(8.5^{+1.2}_{-0.9}) \times 10^{-4}$	S=1.2
Γ_{110}	$\gamma f_0(1710) \rightarrow \gamma\pi\pi$		
Γ_{111}	$\gamma\eta$	$(8.6 \pm 0.8) \times 10^{-4}$	
Γ_{112}	$\gamma f_1(1420) \rightarrow \gamma K\bar{K}\pi$	$(8.3 \pm 1.5) \times 10^{-4}$	
Γ_{113}	$\gamma f_1(1285)$	$(6.1 \pm 0.9) \times 10^{-4}$	
Γ_{114}	$\gamma f_1(1510) \rightarrow \gamma\eta\pi^+\pi^-$	$(4.5 \pm 1.2) \times 10^{-4}$	
Γ_{115}	$\gamma f_2'(1525)$	$(4.7^{+0.7}_{-0.5}) \times 10^{-4}$	
Γ_{116}	$\gamma f_2(1950) \rightarrow \gamma K^*(892)\bar{K}^*(892)$	$(7.0 \pm 2.2) \times 10^{-4}$	
Γ_{117}	$\gamma K^*(892)\bar{K}^*(892)$	$(4.0 \pm 1.3) \times 10^{-3}$	
Γ_{118}	$\gamma\phi\phi$	$(4.0 \pm 1.2) \times 10^{-4}$	S=2.1
Γ_{119}	$\gamma\rho\bar{\rho}$	$(3.8 \pm 1.0) \times 10^{-4}$	
Γ_{120}	$\gamma\eta(2225)$	$(2.9 \pm 0.6) \times 10^{-4}$	
Γ_{121}	$\gamma\eta(1760) \rightarrow \gamma\rho^0\rho^0$	$(1.3 \pm 0.9) \times 10^{-4}$	
Γ_{122}	$\gamma\pi^0$	$(3.9 \pm 1.3) \times 10^{-5}$	
Γ_{123}	$\gamma\rho\bar{\rho}\pi^+\pi^-$	$< 7.9 \times 10^{-4}$	CL=90%
Γ_{124}	$\gamma\gamma$	$< 5 \times 10^{-4}$	CL=90%
Γ_{125}	$\gamma\Lambda\bar{\Lambda}$	$< 1.3 \times 10^{-4}$	CL=90%
Γ_{126}	3γ	$< 5.5 \times 10^{-5}$	CL=90%
Γ_{127}	$\gamma f_0(2200)$		
Γ_{128}	$\gamma f_J(2220)$	$> 2.50 \times 10^{-3}$	CL=99.9%
Γ_{129}	$\gamma f_J(2220) \rightarrow \gamma\pi\pi$	$(8 \pm 4) \times 10^{-5}$	
Γ_{130}	$\gamma f_J(2220) \rightarrow \gamma K\bar{K}$	$(8.1 \pm 3.0) \times 10^{-5}$	
Γ_{131}	$\gamma f_J(2220) \rightarrow \gamma\rho\bar{\rho}$	$(1.5 \pm 0.8) \times 10^{-5}$	
Γ_{132}	$\gamma f_0(1500)$	$< 5.7 \pm 0.8 \times 10^{-4}$	
Γ_{133}	γe^+e^-	$(8.8 \pm 1.4) \times 10^{-3}$	

[a] The value is for the sum of the charge states or particle/antiparticle states indicated.

[b] Includes $p\bar{p}\pi^+\pi^-\gamma$ and excludes $p\bar{p}\eta, p\bar{p}\omega, p\bar{p}\eta'$.

[c] See the "Note on the $\eta(1440)$ " in the $\eta(1440)$ Particle Listings.

$J/\psi(1S)$ PARTIAL WIDTHS

$\Gamma(\text{hadrons})$				Γ_1
VALUE (keV)	DOCUMENT ID	TECN	COMMENT	
● ● ● We do not use the following data for averages, fits, limits, etc. ● ● ●				
74.1 ± 8.1	BAI	95B BES	e^+e^-	
59 ± 24	BALDINI...	75 FRAG	e^+e^-	
59 ± 14	BOYARSKI	75 MRK1	e^+e^-	
50 ± 25	ESPOSITO	75B FRAM	e^+e^-	

$\Gamma(\text{virtual } \gamma \rightarrow \text{hadrons})$				Γ_2
VALUE (keV)	DOCUMENT ID	TECN	COMMENT	
12 ± 2	⁵ BOYARSKI	75 MRK1	e^+e^-	
⁵ Included in $\Gamma(\text{hadrons})$.				

$\Gamma(e^+e^-)$				Γ_3
VALUE (keV)	DOCUMENT ID	TECN	COMMENT	
5.26 ± 0.37 OUR EVALUATION				
● ● ● We do not use the following data for averages, fits, limits, etc. ● ● ●				
5.14 ± 0.39	BAI	95B BES	e^+e^-	
5.36 ^{+0.29} _{-0.28}	⁶ HSUEH	92 RVUE	See Υ mini-review	
4.72 ± 0.35	ALEXANDER	89 RVUE	See Υ mini-review	
4.4 ± 0.6	⁶ BRANDELIK	79C DASP	e^+e^-	
4.6 ± 0.8	⁷ BALDINI...	75 FRAG	e^+e^-	
4.8 ± 0.6	BOYARSKI	75 MRK1	e^+e^-	
4.6 ± 1.0	ESPOSITO	75B FRAM	e^+e^-	
⁶ From a simultaneous fit to e^+e^- , $\mu^+\mu^-$, and hadronic channels assuming $\Gamma(e^+e^-) = \Gamma(\mu^+\mu^-)$.				
⁷ Assuming equal partial widths for e^+e^- and $\mu^+\mu^-$.				

$\Gamma(\mu^+\mu^-)$				Γ_4
VALUE (keV)	DOCUMENT ID	TECN	COMMENT	
● ● ● We do not use the following data for averages, fits, limits, etc. ● ● ●				
5.13 ± 0.52	BAI	95B BES	e^+e^-	
4.8 ± 0.6	BOYARSKI	75 MRK1	e^+e^-	
5 ± 1	ESPOSITO	75B FRAM	e^+e^-	

$\Gamma(\gamma\gamma)$				Γ_{124}
VALUE (eV)	CL%	DOCUMENT ID	TECN	COMMENT
<5.4	90	BRANDELIK	79C DASP	e^+e^-

$J/\psi(1S) \Gamma(I)\Gamma(e^+e^-)/\Gamma(\text{total})$

This combination of a partial width with the partial width into e^+e^- and with the total width is obtained from the integrated cross section into channel I in the e^+e^- annihilation.

$\Gamma(\text{hadrons}) \times \Gamma(e^+e^-)/\Gamma_{\text{total}}$				$\Gamma_1\Gamma_3/\Gamma$
VALUE (keV)	DOCUMENT ID	TECN	COMMENT	
● ● ● We do not use the following data for averages, fits, limits, etc. ● ● ●				
4 ± 0.8	⁸ BALDINI...	75 FRAG	e^+e^-	
3.9 ± 0.8	⁸ ESPOSITO	75B FRAM	e^+e^-	

$\Gamma(e^+e^-) \times \Gamma(e^+e^-)/\Gamma_{\text{total}}$				$\Gamma_3\Gamma_3/\Gamma$
VALUE (keV)	DOCUMENT ID	TECN	COMMENT	
● ● ● We do not use the following data for averages, fits, limits, etc. ● ● ●				
0.35 ± 0.02	BRANDELIK	79C DASP	e^+e^-	
0.32 ± 0.07	⁸ BALDINI...	75 FRAG	e^+e^-	
0.34 ± 0.09	⁸ ESPOSITO	75B FRAM	e^+e^-	
0.36 ± 0.10	⁸ FORD	75 SPEC	e^+e^-	

$\Gamma(\mu^+\mu^-) \times \Gamma(e^+e^-)/\Gamma_{\text{total}}$				$\Gamma_4\Gamma_3/\Gamma$
VALUE (keV)	DOCUMENT ID	TECN	COMMENT	
● ● ● We do not use the following data for averages, fits, limits, etc. ● ● ●				
0.51 ± 0.09	DASP	75 DASP	e^+e^-	
0.38 ± 0.05	⁸ ESPOSITO	75B FRAM	e^+e^-	

$\Gamma(p\bar{p}) \times \Gamma(e^+e^-)/\Gamma_{\text{total}}$				$\Gamma_7\Gamma_3/\Gamma$
VALUE (eV)	DOCUMENT ID	TECN	COMMENT	
9.7 ± 1.7	⁹ ARMSTRONG	93B E760	$p\bar{p} \rightarrow e^+e^-$	
⁸ Data redundant with branching ratios or partial widths above.				
⁹ Using $\Gamma_{\text{total}} = 85.5^{+6.1}_{-5.8}$ MeV.				

$J/\psi(1S)$ BRANCHING RATIOS

For the first four branching ratios, see also the partial widths, and (partial widths) $\times \Gamma(e^+e^-)/\Gamma_{\text{total}}$ above.

$\Gamma(\text{hadrons})/\Gamma_{\text{total}}$				Γ_1/Γ
VALUE	DOCUMENT ID	TECN	COMMENT	
0.877 ± 0.005 OUR AVERAGE				
0.878 ± 0.005	BAI	95B BES	e^+e^-	
0.86 ± 0.02	BOYARSKI	75 MRK1	e^+e^-	

$\Gamma(\text{virtual } \gamma \rightarrow \text{hadrons})/\Gamma_{\text{total}}$				Γ_2/Γ
VALUE	DOCUMENT ID	TECN	COMMENT	
0.17 ± 0.02	¹⁰ BOYARSKI	75 MRK1	e^+e^-	
¹⁰ Included in $\Gamma(\text{hadrons})/\Gamma_{\text{total}}$.				

See key on page 239

Meson Particle Listings

 $J/\psi(1S)$

$\Gamma(e^+e^-)/\Gamma_{total}$				Γ_3/Γ					
VALUE	DOCUMENT ID	TECN	COMMENT	VALUE (units 10^{-3})	EVTS	DOCUMENT ID	TECN	COMMENT	
0.0593 ± 0.0010 OUR AVERAGE				4.3 ± 0.6 OUR AVERAGE					
0.0590 ± 0.0005 ± 0.0010	BAI	98D	BES $\psi(2S) \rightarrow J/\psi \pi^+ \pi^-$	4.3 ± 0.2 ± 0.6	5860	AUGUSTIN	89	DM2 e^+e^-	
0.0609 ± 0.0033	BAI	95B	BES e^+e^-	4.0 ± 1.6	70	BURMESTER	77D	PLUT e^+e^-	
0.0592 ± 0.0015 ± 0.0020	COFFMAN	92	MRK3 $\psi(2S) \rightarrow J/\psi \pi^+ \pi^-$	• • • We do not use the following data for averages, fits, limits, etc. • • •					
0.069 ± 0.009	BOYARSKI	75	MRK1 e^+e^-	1.9 ± 0.8	81	VANNUCCI	77	MRK1 $e^+e^- \rightarrow 2(\pi^+ \pi^-) \pi^0$	
$\Gamma(\mu^+ \mu^-)/\Gamma_{total}$				$\Gamma(K^+ \bar{K}^*(892)^- + c.c.)/\Gamma_{total}$					
VALUE	DOCUMENT ID	TECN	COMMENT	VALUE (units 10^{-3})	EVTS	DOCUMENT ID	TECN	COMMENT	
0.0588 ± 0.0010 OUR AVERAGE				5.0 ± 0.4 OUR AVERAGE					
0.0584 ± 0.0006 ± 0.0010	BAI	98D	BES $\psi(2S) \rightarrow J/\psi \pi^+ \pi^-$	4.57 ± 0.17 ± 0.70	2285	JOUSSET	90	DM2 $J/\psi \rightarrow$ hadrons	
0.0608 ± 0.0033	BAI	95B	BES e^+e^-	5.26 ± 0.13 ± 0.53		COFFMAN	88	MRK3 $J/\psi \rightarrow K^\pm K_S^0 \pi^\mp$, $K^+ K^- \pi^0$	
0.0590 ± 0.0015 ± 0.0019	COFFMAN	92	MRK3 $\psi(2S) \rightarrow J/\psi \pi^+ \pi^-$	• • • We do not use the following data for averages, fits, limits, etc. • • •					
0.069 ± 0.009	BOYARSKI	75	MRK1 e^+e^-	2.6 ± 0.6	24	FRANKLIN	83	MRK2 $J/\psi \rightarrow K^+ K^- \pi^0$	
$\Gamma(e^+e^-)/\Gamma(\mu^+ \mu^-)$				$\Gamma(K^0 \bar{K}^*(892)^0 + c.c.)/\Gamma_{total}$					
VALUE	DOCUMENT ID	TECN	COMMENT	VALUE (units 10^{-3})	EVTS	DOCUMENT ID	TECN	COMMENT	
• • • We do not use the following data for averages, fits, limits, etc. • • •									
1.00 ± 0.07	BAI	95B	BES e^+e^-	4.33 ± 0.12 ± 0.45	1192	JOUSSET	90	DM2 $J/\psi \rightarrow$ hadrons	
1.00 ± 0.05	BOYARSKI	75	MRK1 e^+e^-	4.33 ± 0.12 ± 0.45		COFFMAN	88	MRK3 $J/\psi \rightarrow K^\pm K_S^0 \pi^\mp$	
0.91 ± 0.15	ESPOSITO	75B	FRAM e^+e^-	2.7 ± 0.6	45	VANNUCCI	77	MRK1 $J/\psi \rightarrow K^\pm K_S^0 \pi^\mp$	
0.93 ± 0.10	FORD	75	SPEC e^+e^-	• • • We do not use the following data for averages, fits, limits, etc. • • •					
HADRONIC DECAYS									
$\Gamma(\rho\pi)/\Gamma_{total}$				Γ_5/Γ					
VALUE	DOCUMENT ID	TECN	COMMENT	VALUE (units 10^{-3})	EVTS	DOCUMENT ID	TECN	COMMENT	
0.0127 ± 0.0009 OUR AVERAGE				4.2 ± 0.4 OUR AVERAGE					
0.0121 ± 0.0020	BAI	96D	BES $e^+e^- \rightarrow \rho\pi$	3.96 ± 0.15 ± 0.60	1192	JOUSSET	90	DM2 $J/\psi \rightarrow$ hadrons	
0.0142 ± 0.0001 ± 0.0019	COFFMAN	88	MRK3 e^+e^-	4.33 ± 0.12 ± 0.45		COFFMAN	88	MRK3 $J/\psi \rightarrow K^\pm K_S^0 \pi^\mp$	
0.013 ± 0.003	150	FRANKLIN	83	MRK2 e^+e^-	• • • We do not use the following data for averages, fits, limits, etc. • • •				
0.016 ± 0.004	183	ALEXANDER	78	PLUT e^+e^-	2.7 ± 0.6	45	VANNUCCI	77	MRK1 $J/\psi \rightarrow K^\pm K_S^0 \pi^\mp$
0.0133 ± 0.0021		BRANDELIK	78B	DASP e^+e^-	• • • We do not use the following data for averages, fits, limits, etc. • • •				
0.010 ± 0.002	543	BARTEL	76	CNTR e^+e^-	3.8 ± 0.15 ± 0.2	12	BAI	99C	BES e^+e^-
0.013 ± 0.003	153	JEAN-MARIE	76	MRK1 e^+e^-	12 Assuming $B(K_1(1400) \rightarrow K^* \pi) = 0.94 \pm 0.06$				
$\Gamma(\rho^0 \pi^0)/\Gamma(\rho\pi)$				$\Gamma(K_1(1400)^\pm K^\mp)/\Gamma_{total}$					
VALUE	DOCUMENT ID	TECN	COMMENT	VALUE (units 10^{-3})	EVTS	DOCUMENT ID	TECN	COMMENT	
0.328 ± 0.005 ± 0.027				3.8 ± 0.8 ± 1.2					
• • • We do not use the following data for averages, fits, limits, etc. • • •									
0.35 ± 0.08	ALEXANDER	78	PLUT e^+e^-	3.4 ± 0.3 ± 0.7	509	AUGUSTIN	89	DM2 $J/\psi \rightarrow \pi^+ \pi^- 3\pi^0$	
0.32 ± 0.08	BRANDELIK	78B	DASP e^+e^-	$\Gamma(b_1(1235)^\pm \pi^\mp)/\Gamma_{total}$					
0.39 ± 0.11	BARTEL	76	CNTR e^+e^-	30 ± 5	OUR AVERAGE				
0.37 ± 0.09	JEAN-MARIE	76	MRK1 e^+e^-	31 ± 6	4600	AUGUSTIN	89	DM2 $J/\psi \rightarrow 2(\pi^+ \pi^-) \pi^0$	
$\Gamma(a_2(1320)\rho)/\Gamma_{total}$				$\Gamma(\omega K^\pm K_S^0 \pi^\mp)/\Gamma_{total}$					
VALUE (units 10^{-3})	DOCUMENT ID	TECN	COMMENT	VALUE (units 10^{-4})	EVTS	DOCUMENT ID	TECN	COMMENT	
10.9 ± 2.2 OUR AVERAGE				29.5 ± 1.4 ± 7.0					
11.7 ± 0.7 ± 2.5	7584	AUGUSTIN	89	DM2 $J/\psi \rightarrow \rho^0 \pi^\pm \pi^\mp$	29 ± 7	87	BURMESTER	77D	PLUT e^+e^-
8.4 ± 4.5	36	VANNUCCI	77	MRK1 $e^+e^- \rightarrow 2(\pi^+ \pi^-) \pi^0$	$\Gamma(\phi K^*(892) \bar{K} + c.c.)/\Gamma_{total}$				
$\Gamma(\omega \pi^+ \pi^- \pi^+ \pi^-)/\Gamma_{total}$				$\Gamma(b_1(1235)^0 \pi^0)/\Gamma_{total}$					
VALUE (units 10^{-4})	DOCUMENT ID	TECN	COMMENT	VALUE (units 10^{-4})	EVTS	DOCUMENT ID	TECN	COMMENT	
85 ± 34				23 ± 3 ± 5					
140	VANNUCCI	77	MRK1 $e^+e^- \rightarrow 3(\pi^+ \pi^-) \pi^0$	$\Gamma(\omega K^\pm K_S^0 \pi^\mp)/\Gamma_{total}$					
$\Gamma(\omega \pi^+ \pi^-)/\Gamma_{total}$				$\Gamma(\phi K^*(892) \bar{K} + c.c.)/\Gamma_{total}$					
VALUE (units 10^{-3})	DOCUMENT ID	TECN	COMMENT	VALUE (units 10^{-4})	EVTS	DOCUMENT ID	TECN	COMMENT	
7.2 ± 1.0 OUR AVERAGE				20.4 ± 2.8 OUR AVERAGE					
7.0 ± 1.6	18058	AUGUSTIN	89	DM2 $J/\psi \rightarrow 2(\pi^+ \pi^-) \pi^0$	20.7 ± 2.4 ± 3.0	155 ± 20	FALVARD	88	DM2 $J/\psi \rightarrow$ hadrons
7.8 ± 1.6	215	BURMESTER	77D	PLUT e^+e^-	20 ± 3 ± 3		BECKER	87	MRK3 $e^+e^- \rightarrow$ hadrons
6.8 ± 1.9	348	VANNUCCI	77	MRK1 $e^+e^- \rightarrow 2(\pi^+ \pi^-) \pi^0$	$\Gamma(\omega K \bar{K})/\Gamma_{total}$				
$\Gamma(\omega \pi^+ \pi^-)/\Gamma(2(\pi^+ \pi^-) \pi^0)$				$\Gamma(\omega K \bar{K})/\Gamma_{total}$					
VALUE	DOCUMENT ID	TECN	COMMENT	VALUE (units 10^{-4})	EVTS	DOCUMENT ID	TECN	COMMENT	
• • • We do not use the following data for averages, fits, limits, etc. • • •									
0.3	11	JEAN-MARIE	76	MRK1 e^+e^-	19 ± 4 OUR AVERAGE				
11 Final state $(\pi^+ \pi^-) \pi^0$ under the assumption that $\pi\pi$ is isospin 0.									
$\Gamma(K^*(892)^0 \bar{K}_S^0(1430)^0 + c.c.)/\Gamma_{total}$				$\Gamma(\omega f_0(1710) \rightarrow \omega K \bar{K})/\Gamma_{total}$					
VALUE (units 10^{-4})	DOCUMENT ID	TECN	COMMENT	VALUE (units 10^{-4})	EVTS	DOCUMENT ID	TECN	COMMENT	
67 ± 26				4.8 ± 1.1 ± 0.3					
40	VANNUCCI	77	MRK1 $e^+e^- \rightarrow \pi^+ \pi^- K^+ K^-$	14.8 ± 2.1 ± 3.9	13	FALVARD	88	DM2 $J/\psi \rightarrow$ hadrons	
13 Addition of $\omega K^+ K^-$ and $\omega K^0 \bar{K}^0$ branching ratios.									
$\Gamma(\omega K^*(892) \bar{K} + c.c.)/\Gamma_{total}$				$\Gamma(\phi 2(\pi^+ \pi^-))/\Gamma_{total}$					
VALUE (units 10^{-4})	DOCUMENT ID	TECN	COMMENT	VALUE (units 10^{-4})	EVTS	DOCUMENT ID	TECN	COMMENT	
53 ± 14 ± 14				16.0 ± 1.0 ± 3.0					
140	BECKER	87	MRK3 $e^+e^- \rightarrow$ hadrons	14,15	FALVARD	88	DM2	$J/\psi \rightarrow$ hadrons	
14 Includes unknown branching fraction $f_0(1710) \rightarrow K \bar{K}$.									
15 Addition of $f_0(1710) \rightarrow K^+ K^-$ and $f_0(1710) \rightarrow K^0 \bar{K}^0$ branching ratios.									

Meson Particle Listings

 $J/\psi(1S)$

$\Gamma(\Delta(1232)^{++}\bar{p}\pi^-)/\Gamma_{total}$					Γ_{24}/Γ	$\Gamma(\Xi(1530)^-\Xi^+)/\Gamma_{total}$					Γ_{37}/Γ
VALUE (units 10^{-3})	EVTS	DOCUMENT ID	TECN	COMMENT		VALUE (units 10^{-3})	EVTS	DOCUMENT ID	TECN	COMMENT	
1.58 ± 0.23 ± 0.40	332	EATON	84	MRK2	e^+e^-	0.59 ± 0.09 ± 0.12	75 ± 11	HENRARD	87	DM2	e^+e^-
$\Gamma(\omega\eta)/\Gamma_{total}$					Γ_{25}/Γ	$\Gamma(\rho K^-\bar{\Sigma}(1385)^0)/\Gamma_{total}$					Γ_{38}/Γ
VALUE (units 10^{-3})	EVTS	DOCUMENT ID	TECN	COMMENT		VALUE (units 10^{-3})	EVTS	DOCUMENT ID	TECN	COMMENT	
1.58 ± 0.16 OUR AVERAGE						0.51 ± 0.26 ± 0.18	89	EATON	84	MRK2	e^+e^-
1.43 ± 0.10 ± 0.21	378	JOUSSET	90	DM2	$J/\psi \rightarrow$ hadrons	$\Gamma(\omega\pi^0)/\Gamma_{total}$					Γ_{39}/Γ
1.71 ± 0.08 ± 0.20		COFFMAN	88	MRK3	$e^+e^- \rightarrow 3\pi\eta$	VALUE (units 10^{-3})	EVTS	DOCUMENT ID	TECN	COMMENT	
$\Gamma(\phi K\bar{K})/\Gamma_{total}$					Γ_{26}/Γ	0.42 ± 0.06 OUR AVERAGE	222	JOUSSET	90	DM2	$J/\psi \rightarrow$ hadrons
VALUE (units 10^{-4})	EVTS	DOCUMENT ID	TECN	COMMENT		0.360 ± 0.028 ± 0.054		COFFMAN	88	MRK3	$e^+e^- \rightarrow \pi^0\pi^+\pi^-\pi^0$
14.8 ± 2.2 OUR AVERAGE						0.482 ± 0.019 ± 0.064		Error includes scale factor of 1.4.			
14.6 ± 0.8 ± 2.1		¹⁶ FALVARD	88	DM2	$J/\psi \rightarrow$ hadrons	$\Gamma(\phi\eta'(958))/\Gamma_{total}$					Γ_{40}/Γ
18 ± 8	14	FELDMAN	77	MRK1	e^+e^-	VALUE (units 10^{-3})	CL% EVTS	DOCUMENT ID	TECN	COMMENT	
¹⁶ Addition of ϕK^+K^- and $\phi K^0\bar{K}^0$ branching ratios.						0.33 ± 0.04 OUR AVERAGE	167	JOUSSET	90	DM2	$J/\psi \rightarrow$ hadrons
$\Gamma(\phi f_0(1710) \rightarrow \phi K\bar{K})/\Gamma_{total}$					Γ_{27}/Γ	0.41 ± 0.03 ± 0.08		COFFMAN	88	MRK3	$e^+e^- \rightarrow K^+K^-\eta'$
VALUE (units 10^{-4})	EVTS	DOCUMENT ID	TECN	COMMENT		0.308 ± 0.034 ± 0.036		• • • We do not use the following data for averages, fits, limits, etc. • • •			
3.6 ± 0.2 ± 0.6		^{17,18} FALVARD	88	DM2	$J/\psi \rightarrow$ hadrons	<1.3	90	VANNUCCI	77	MRK1	e^+e^-
¹⁷ Including interference with $f_2'(1525)$.						$\Gamma(\phi f_0(980))/\Gamma_{total}$					Γ_{41}/Γ
¹⁸ Includes unknown branching fraction $f_0(1710) \rightarrow K\bar{K}$.						VALUE (units 10^{-4})	EVTS	DOCUMENT ID	TECN	COMMENT	
$\Gamma(\rho\bar{p}\omega)/\Gamma_{total}$					Γ_{28}/Γ	3.2 ± 0.9 OUR AVERAGE	21	FALVARD	88	DM2	$J/\psi \rightarrow$ hadrons
VALUE (units 10^{-3})	EVTS	DOCUMENT ID	TECN	COMMENT		4.6 ± 0.4 ± 0.8		GIDAL	81	MRK2	$J/\psi \rightarrow$ hadrons
1.30 ± 0.25 OUR AVERAGE						2.6 ± 0.6	50	Error includes scale factor of 1.9.			
1.10 ± 0.17 ± 0.18	486	EATON	84	MRK2	e^+e^-	$\Gamma(\Xi(1530)^0\Xi^0)/\Gamma_{total}$					Γ_{42}/Γ
1.6 ± 0.3	77	PERUZZI	78	MRK1	e^+e^-	VALUE (units 10^{-3})	EVTS	DOCUMENT ID	TECN	COMMENT	
$\Gamma(\Delta(1232)^{++}\bar{\Delta}(1232)^{-})/\Gamma_{total}$					Γ_{29}/Γ	0.32 ± 0.12 ± 0.07	24 ± 9	HENRARD	87	DM2	e^+e^-
VALUE (units 10^{-3})	EVTS	DOCUMENT ID	TECN	COMMENT		$\Gamma(\Sigma(1385)^-\bar{\Sigma}^+(or c.c.))/\Gamma_{total}$					Γ_{43}/Γ
1.10 ± 0.09 ± 0.28	233	EATON	84	MRK2	e^+e^-	VALUE (units 10^{-3})	EVTS	DOCUMENT ID	TECN	COMMENT	
$\Gamma(\Sigma(1385)^-\bar{\Sigma}(1385)^+(or c.c.))/\Gamma_{total}$					Γ_{30}/Γ	0.31 ± 0.05 OUR AVERAGE	74 ± 8	HENRARD	87	DM2	$e^+e^- \rightarrow \Sigma^{*-}$
VALUE (units 10^{-3})	EVTS	DOCUMENT ID	TECN	COMMENT		0.30 ± 0.03 ± 0.07		HENRARD	87	DM2	$e^+e^- \rightarrow \Sigma^{*+}$
1.03 ± 0.13 OUR AVERAGE						0.34 ± 0.04 ± 0.07	77 ± 9	HENRARD	87	DM2	$e^+e^- \rightarrow \Sigma^{*+}$
1.00 ± 0.04 ± 0.21	631 ± 25	HENRARD	87	DM2	$e^+e^- \rightarrow \Sigma^{*-}$	0.29 ± 0.11 ± 0.10	26	EATON	84	MRK2	$e^+e^- \rightarrow \Sigma^{*-}$
1.19 ± 0.04 ± 0.25	754 ± 27	HENRARD	87	DM2	$e^+e^- \rightarrow \Sigma^{*+}$	0.31 ± 0.11 ± 0.11	28	EATON	84	MRK2	$e^+e^- \rightarrow \Sigma^{*+}$
0.86 ± 0.18 ± 0.22	56	EATON	84	MRK2	$e^+e^- \rightarrow \Sigma^{*-}$	$\Gamma(\phi f_1(1285))/\Gamma_{total}$					Γ_{44}/Γ
1.03 ± 0.24 ± 0.25	68	EATON	84	MRK2	$e^+e^- \rightarrow \Sigma^{*+}$	VALUE (units 10^{-4})	EVTS	DOCUMENT ID	TECN	COMMENT	
$\Gamma(\rho\bar{p}\eta'(958))/\Gamma_{total}$					Γ_{31}/Γ	2.6 ± 0.5 OUR AVERAGE	25	JOUSSET	90	DM2	$J/\psi \rightarrow \phi(2\pi^+\pi^-)$
VALUE (units 10^{-3})	EVTS	DOCUMENT ID	TECN	COMMENT		3.2 ± 0.6 ± 0.4		JOUSSET	90	DM2	$J/\psi \rightarrow \phi\eta\pi^+\pi^-$
0.9 ± 0.4 OUR AVERAGE						2.1 ± 0.5 ± 0.4	25	Error includes scale factor of 1.7.			
0.68 ± 0.23 ± 0.17	19	EATON	84	MRK2	e^+e^-	$\Gamma(\phi f_2'(1525))/\Gamma_{total}$					Γ_{32}/Γ
1.8 ± 0.6	19	PERUZZI	78	MRK1	e^+e^-	VALUE (units 10^{-4})	EVTS	DOCUMENT ID	TECN	COMMENT	
$\Gamma(\phi f_2'(1525))/\Gamma_{total}$					Γ_{32}/Γ	8 ± 4 OUR AVERAGE		^{19,20} FALVARD	88	DM2	$J/\psi \rightarrow$ hadrons
VALUE (units 10^{-4})	EVTS	DOCUMENT ID	TECN	COMMENT		12.3 ± 0.6 ± 2.0		¹⁹ GIDAL	81	MRK2	$J/\psi \rightarrow$ hadrons
8 ± 4 OUR AVERAGE						4.8 ± 1.8	46	Error includes scale factor of 2.7.			
8 ± 4						$\Gamma(\phi K^\pm K_S^0 \pi^\mp)/\Gamma_{total}$					Γ_{34}/Γ
12.3 ± 0.6 ± 2.0						VALUE (units 10^{-4})	EVTS	DOCUMENT ID	TECN	COMMENT	
4.8 ± 1.8						7.2 ± 0.9 OUR AVERAGE					
¹⁹ Re-evaluated using $B(f_2'(1525) \rightarrow K\bar{K}) = 0.713$.						7.4 ± 0.9 ± 1.1		FALVARD	88	DM2	$J/\psi \rightarrow$ hadrons
²⁰ Including interference with $f_0(1710)$.						7 ± 0.6 ± 1.0	163 ± 15	BECKER	87	MRK3	$e^+e^- \rightarrow$ hadrons
$\Gamma(\phi\pi^+\pi^-)/\Gamma_{total}$					Γ_{33}/Γ	$\Gamma(\omega\eta'(958))/\Gamma_{total}$					Γ_{46}/Γ
VALUE (units 10^{-3})	EVTS	DOCUMENT ID	TECN	COMMENT		VALUE (units 10^{-3})	EVTS	DOCUMENT ID	TECN	COMMENT	
0.80 ± 0.12 OUR AVERAGE						0.167 ± 0.025 OUR AVERAGE					
0.78 ± 0.03 ± 0.12		FALVARD	88	DM2	$J/\psi \rightarrow$ hadrons	0.18 ^{+0.10} _{-0.08} ± 0.03	6	JOUSSET	90	DM2	$J/\psi \rightarrow$ hadrons
2.1 ± 0.9	23	FELDMAN	77	MRK1	e^+e^-	0.166 ± 0.017 ± 0.019		COFFMAN	88	MRK3	$e^+e^- \rightarrow 3\pi\eta'$
$\Gamma(\phi K^\pm K_S^0 \pi^\mp)/\Gamma_{total}$					Γ_{34}/Γ	$\Gamma(\omega f_0(980))/\Gamma_{total}$					Γ_{47}/Γ
VALUE (units 10^{-4})	EVTS	DOCUMENT ID	TECN	COMMENT		VALUE (units 10^{-4})	EVTS	DOCUMENT ID	TECN	COMMENT	
7.2 ± 0.9 OUR AVERAGE						1.41 ± 0.27 ± 0.47		²³ AUGUSTIN	89	DM2	$J/\psi \rightarrow 2(\pi^+\pi^-)\pi^0$
7.4 ± 0.9 ± 1.1		FALVARD	88	DM2	$J/\psi \rightarrow$ hadrons	$\Gamma(\rho\eta)/\Gamma_{total}$					Γ_{45}/Γ
7 ± 0.6 ± 1.0	163 ± 15	BECKER	87	MRK3	$e^+e^- \rightarrow$ hadrons	VALUE (units 10^{-3})	EVTS	DOCUMENT ID	TECN	COMMENT	
$\Gamma(\omega f_1(1420))/\Gamma_{total}$					Γ_{35}/Γ	0.193 ± 0.023 OUR AVERAGE	299	JOUSSET	90	DM2	$J/\psi \rightarrow$ hadrons
VALUE (units 10^{-4})	EVTS	DOCUMENT ID	TECN	COMMENT		0.194 ± 0.017 ± 0.029		COFFMAN	88	MRK3	$e^+e^- \rightarrow \pi^+\pi^-\eta$
6.8 ^{+1.9} _{-1.8} ± 1.7	111 ± ³¹ ₂₆	BECKER	87	MRK3	$e^+e^- \rightarrow$ hadrons	0.193 ± 0.013 ± 0.029		Error includes scale factor of 1.1.			
$\Gamma(\phi\eta)/\Gamma_{total}$					Γ_{36}/Γ	$\Gamma(\omega\eta'(958))/\Gamma_{total}$					Γ_{46}/Γ
VALUE (units 10^{-3})	EVTS	DOCUMENT ID	TECN	COMMENT		VALUE (units 10^{-3})	EVTS	DOCUMENT ID	TECN	COMMENT	
0.65 ± 0.07 OUR AVERAGE						0.105 ± 0.018 OUR AVERAGE					
0.64 ± 0.04 ± 0.11	346	JOUSSET	90	DM2	$J/\psi \rightarrow$ hadrons	0.083 ± 0.030 ± 0.012	19	JOUSSET	90	DM2	$J/\psi \rightarrow$ hadrons
0.661 ± 0.045 ± 0.078		COFFMAN	88	MRK3	$e^+e^- \rightarrow K^+K^-\eta$	0.114 ± 0.014 ± 0.016		COFFMAN	88	MRK3	$J/\psi \rightarrow \pi^+\pi^-\eta'$

$\Gamma(p\bar{p}\phi)/\Gamma_{total}$	DOCUMENT ID	TECN	COMMENT	Γ_{49}/Γ
VALUE (units 10^{-4})	FALVARD	88	DM2	$J/\psi \rightarrow$ hadrons
$0.45 \pm 0.13 \pm 0.07$				

$\Gamma(a_2(1320)^\pm \pi^\mp)/\Gamma_{total}$	DOCUMENT ID	TECN	COMMENT	Γ_{50}/Γ
VALUE (units 10^{-4})	BRAUNSCH...	76	DASP	$e^+ e^-$
<43				

$\Gamma(K\bar{K}_2^*(1430) + c.c.)/\Gamma_{total}$	DOCUMENT ID	TECN	COMMENT	Γ_{51}/Γ
VALUE (units 10^{-4})	VANNUCCI	77	MRK1	$e^+ e^- \rightarrow K^0 \bar{K}_2^{*0}$
<40				

• • • We do not use the following data for averages, fits, limits, etc. • • •

<66	90	BRAUNSCH...	76	DASP	$e^+ e^- \rightarrow K^\pm \bar{K}_2^{*\mp}$
-----	----	-------------	----	------	--

$\Gamma(K_1(1270)^\pm K^\mp)/\Gamma_{total}$	DOCUMENT ID	TECN	COMMENT	Γ_{52}/Γ	
VALUE (units 10^{-3})	BAI	24	99c	BES	$e^+ e^-$
<3.0					

²⁴ Assuming $B(K_1(1270) \rightarrow K\rho) = 0.42 \pm 0.06$

$\Gamma(K_2^*(1430)^0 \bar{K}_2^*(1430)^0)/\Gamma_{total}$	DOCUMENT ID	TECN	COMMENT	Γ_{53}/Γ
VALUE (units 10^{-4})	VANNUCCI	77	MRK1	$e^+ e^- \rightarrow \pi^+ \pi^- K^+ K^-$
<29				

$\Gamma(K^*(892)^0 \bar{K}^*(892)^0)/\Gamma_{total}$	DOCUMENT ID	TECN	COMMENT	Γ_{54}/Γ
VALUE (units 10^{-4})	VANNUCCI	77	MRK1	$e^+ e^- \rightarrow \pi^+ \pi^- K^+ K^-$
<5				

$\Gamma(\phi f_2(1270))/\Gamma_{total}$	DOCUMENT ID	TECN	COMMENT	Γ_{55}/Γ
VALUE (units 10^{-4})	VANNUCCI	77	MRK1	$e^+ e^- \rightarrow \pi^+ \pi^- K^+ K^-$
<3.7				

• • • We do not use the following data for averages, fits, limits, etc. • • •

<4.5	90	FALVARD	88	DM2	$J/\psi \rightarrow$ hadrons
------	----	---------	----	-----	------------------------------

$\Gamma(p\bar{p}\rho)/\Gamma_{total}$	DOCUMENT ID	TECN	COMMENT	Γ_{56}/Γ
VALUE (units 10^{-3})	EATON	84	MRK2	$e^+ e^- \rightarrow$ hadrons γ
<0.31				

$\Gamma(\phi\eta(1440) \rightarrow \phi\eta\pi\pi)/\Gamma_{total}$	DOCUMENT ID	TECN	COMMENT	Γ_{57}/Γ
VALUE (units 10^{-4})	FALVARD	88	DM2	$J/\psi \rightarrow$ hadrons
<2.5				

²⁵ Includes unknown branching fraction $\eta(1440) \rightarrow \eta\pi\pi$.

$\Gamma(\omega f_2'(1525))/\Gamma_{total}$	DOCUMENT ID	TECN	COMMENT	Γ_{58}/Γ
VALUE (units 10^{-4})	VANNUCCI	77	MRK1	$e^+ e^- \rightarrow \pi^+ \pi^- \pi^0 K^+ K^-$
<2.2				

• • • We do not use the following data for averages, fits, limits, etc. • • •

<2.8	90	FALVARD	88	DM2	$J/\psi \rightarrow$ hadrons
------	----	---------	----	-----	------------------------------

²⁶ Re-evaluated assuming $B(f_2'(1525) \rightarrow K\bar{K}) = 0.713$.

$\Gamma(\Sigma(1385)^0 \Lambda)/\Gamma_{total}$	DOCUMENT ID	TECN	COMMENT	Γ_{59}/Γ
VALUE (units 10^{-3})	HENRARD	87	DM2	$e^+ e^-$
<0.2				

$\Gamma(\Delta(1232)^+ \bar{p})/\Gamma_{total}$	DOCUMENT ID	TECN	COMMENT	Γ_{60}/Γ
VALUE (units 10^{-3})	HENRARD	87	DM2	$e^+ e^-$
<0.1				

$\Gamma(\Sigma^0 \Lambda)/\Gamma_{total}$	DOCUMENT ID	TECN	COMMENT	Γ_{61}/Γ
VALUE (units 10^{-4})	HENRARD	87	DM2	$e^+ e^-$
<0.9				

$\Gamma(\phi\pi^0)/\Gamma_{total}$	DOCUMENT ID	TECN	COMMENT	Γ_{62}/Γ
VALUE (units 10^{-4})	COFFMAN	88	MRK3	$e^+ e^- \rightarrow K^+ K^- \pi^0$
<0.068				

$\Gamma(2(\pi^+ \pi^- \pi^0))/\Gamma_{total}$	DOCUMENT ID	TECN	COMMENT	Γ_{63}/Γ
VALUE				
0.0337 ± 0.0026 OUR AVERAGE				

0.0325 \pm 0.0049	46055	AUGUSTIN	89	DM2	$J/\psi \rightarrow 2(\pi^+ \pi^-) \pi^0$
0.0317 \pm 0.0042	147	FRANKLIN	83	MRK2	$e^+ e^- \rightarrow$ hadrons
0.0364 \pm 0.0052	1500	BURMESTER	77b	PLUT	$e^+ e^-$
0.04 \pm 0.01	675	JEAN-MARIE	76	MRK1	$e^+ e^-$

$\Gamma(3(\pi^+ \pi^- \pi^0))/\Gamma_{total}$	DOCUMENT ID	TECN	COMMENT	Γ_{64}/Γ
VALUE				
0.029 ± 0.006 OUR AVERAGE				

0.028 \pm 0.009	11	FRANKLIN	83	MRK2	$e^+ e^- \rightarrow$ hadrons
0.029 \pm 0.007	181	JEAN-MARIE	76	MRK1	$e^+ e^-$

$\Gamma(\pi^+ \pi^- \pi^0)/\Gamma_{total}$	EVTS	DOCUMENT ID	TECN	COMMENT	Γ_{65}/Γ
VALUE	168	FRANKLIN	83	MRK2	$e^+ e^-$
0.015 ± 0.002					

$\Gamma(\pi^+ \pi^- \pi^0 K^+ K^-)/\Gamma_{total}$	EVTS	DOCUMENT ID	TECN	COMMENT	Γ_{66}/Γ
VALUE	309	VANNUCCI	77	MRK1	$e^+ e^-$
0.012 ± 0.003					

$\Gamma(4(\pi^+ \pi^-) \pi^0)/\Gamma_{total}$	EVTS	DOCUMENT ID	TECN	COMMENT	Γ_{67}/Γ
VALUE (units 10^{-4})	13	JEAN-MARIE	76	MRK1	$e^+ e^-$
90 ± 30					

$\Gamma(\pi^+ \pi^- K^+ K^-)/\Gamma_{total}$	EVTS	DOCUMENT ID	TECN	COMMENT	Γ_{68}/Γ
VALUE (units 10^{-4})	205	VANNUCCI	77	MRK1	$e^+ e^-$
72 ± 23					

$\Gamma(K\bar{K}\pi)/\Gamma_{total}$	EVTS	DOCUMENT ID	TECN	COMMENT	Γ_{69}/Γ
VALUE (units 10^{-4})	25	FRANKLIN	83	MRK2	$e^+ e^- \rightarrow K^+ K^- \pi^0$
61 ± 10 OUR AVERAGE					

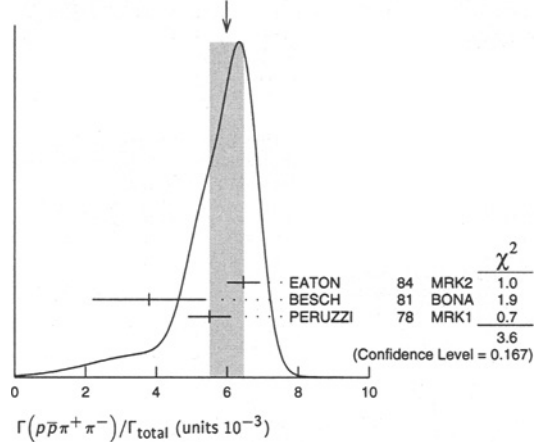
55.2 \pm 12.0	25	FRANKLIN	83	MRK2	$e^+ e^- \rightarrow K^+ K^- \pi^0$
78.0 \pm 21.0	126	VANNUCCI	77	MRK1	$e^+ e^- \rightarrow K_S^0 K^\pm \pi^\mp$

$\Gamma(p\bar{p}\pi^+ \pi^-)/\Gamma_{total}$	EVTS	DOCUMENT ID	TECN	COMMENT	Γ_{70}/Γ
VALUE (units 10^{-3})	1435	EATON	84	MRK2	$e^+ e^-$
6.0 ± 0.5 OUR AVERAGE					

Error includes scale factor of 1.3. See the ideogram below.

6.46 \pm 0.17 \pm 0.43	1435	EATON	84	MRK2	$e^+ e^-$
3.8 \pm 1.6	48	BESCH	81	BONA	$e^+ e^-$
5.5 \pm 0.6	533	PERUZZI	78	MRK1	$e^+ e^-$

WEIGHTED AVERAGE
6.0 \pm 0.5 (Error scaled by 1.3)



$\Gamma(2(\pi^+ \pi^-))/\Gamma_{total}$	EVTS	DOCUMENT ID	TECN	COMMENT	Γ_{71}/Γ
VALUE	76	JEAN-MARIE	76	MRK1	$e^+ e^-$
0.004 ± 0.001					

$\Gamma(3(\pi^+ \pi^-))/\Gamma_{total}$	EVTS	DOCUMENT ID	TECN	COMMENT	Γ_{72}/Γ
VALUE (units 10^{-4})	32	JEAN-MARIE	76	MRK1	$e^+ e^-$
40 ± 20					

$\Gamma(n\bar{n}\pi^+ \pi^-)/\Gamma_{total}$	EVTS	DOCUMENT ID	TECN	COMMENT	Γ_{73}/Γ
VALUE (units 10^{-3})	5	BESCH	81	BONA	$e^+ e^-$
3.8 ± 3.6					

$\Gamma(\Sigma^0 \bar{\Sigma}^0)/\Gamma_{total}$	EVTS	DOCUMENT ID	TECN	COMMENT	Γ_{74}/Γ
VALUE (units 10^{-3})	884 \pm 30	PALLIN	87	DM2	$e^+ e^- \rightarrow \Sigma^0 \bar{\Sigma}^0$
1.27 ± 0.17 OUR AVERAGE					

1.06 \pm 0.04 \pm 0.23	884 \pm 30	PALLIN	87	DM2	$e^+ e^- \rightarrow \Sigma^0 \bar{\Sigma}^0$
1.58 \pm 0.16 \pm 0.25	90	EATON	84	MRK2	$e^+ e^- \rightarrow \Sigma^0 \bar{\Sigma}^0$
1.3 \pm 0.4	52	PERUZZI	78	MRK1	$e^+ e^- \rightarrow \Sigma^0 \bar{\Sigma}^0$

• • • We do not use the following data for averages, fits, limits, etc. • • •

2.4 \pm 2.6	3	BESCH	81	BONA	$e^+ e^- \rightarrow \Sigma^+ \bar{\Sigma}^-$
---------------	---	-------	----	------	---

$\Gamma(2(\pi^+ \pi^-) K^+ K^-)/\Gamma_{total}$	EVTS	DOCUMENT ID	TECN	COMMENT	Γ_{75}/Γ
VALUE (units 10^{-4})	30	VANNUCCI	77	MRK1	$e^+ e^-$
31 ± 13					

Meson Particle Listings

$J/\psi(1S)$

$\Gamma(p\bar{p}\pi^+\pi^-\pi^0)/\Gamma_{total}$
Including $p\bar{p}\pi^+\pi^-\gamma$ and excluding ω, η, η'
Error includes scale factor of 1.9.

VALUE (units 10^{-3})	EVTs	DOCUMENT ID	TECN	COMMENT
2.3 ± 0.9 OUR AVERAGE				
3.36 ± 0.65 ± 0.28	364	EATON	84 MRK2	e^+e^-
1.6 ± 0.6	39	PERUZZI	78 MRK1	e^+e^-

$\Gamma(p\bar{p})/\Gamma_{total}$

VALUE (units 10^{-3})	EVTs	DOCUMENT ID	TECN	COMMENT
2.12 ± 0.10 OUR AVERAGE				
1.97 ± 0.22	99	BALDINI	98 FENI	e^+e^-
1.91 ± 0.04 ± 0.30		PALLIN	87 DM2	e^+e^-
2.16 ± 0.07 ± 0.15	1420	EATON	84 MRK2	e^+e^-
2.5 ± 0.4	133	BRANDELIK	79c DASP	e^+e^-
2.0 ± 0.5		BESCH	78 BONA	e^+e^-
2.2 ± 0.2	331	PERUZZI	78 MRK1	e^+e^-

• • • We do not use the following data for averages, fits, limits, etc. • • •
2.0 ± 0.3 48 ANTONELLI 93 SPEC e^+e^-
27 Assuming angular distribution $(1 + \cos^2\theta)$.

$\Gamma(p\bar{p}\eta)/\Gamma_{total}$

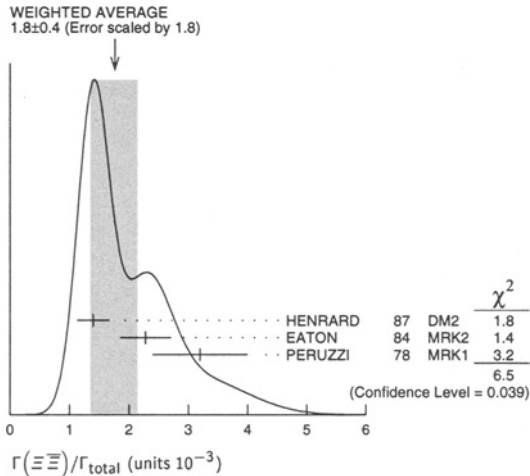
VALUE (units 10^{-3})	EVTs	DOCUMENT ID	TECN	COMMENT
2.09 ± 0.18 OUR AVERAGE				
2.03 ± 0.13 ± 0.15	826	EATON	84 MRK2	e^+e^-
2.5 ± 1.2		BRANDELIK	79c DASP	e^+e^-
2.3 ± 0.4	197	PERUZZI	78 MRK1	e^+e^-

$\Gamma(p\bar{p}\pi^-)/\Gamma_{total}$

VALUE (units 10^{-3})	EVTs	DOCUMENT ID	TECN	COMMENT
2.00 ± 0.10 OUR AVERAGE				
2.02 ± 0.07 ± 0.16	1288	EATON	84 MRK2	$e^+e^- \rightarrow p\pi^-$
1.93 ± 0.07 ± 0.16	1191	EATON	84 MRK2	$e^+e^- \rightarrow \bar{p}\pi^+$
1.7 ± 0.7	32	BESCH	81 BONA	$e^+e^- \rightarrow p\pi^-$
1.6 ± 1.2	5	BESCH	81 BONA	$e^+e^- \rightarrow \bar{p}\pi^+$
2.16 ± 0.29	194	PERUZZI	78 MRK1	$e^+e^- \rightarrow p\pi^-$
2.04 ± 0.27	204	PERUZZI	78 MRK1	$e^+e^- \rightarrow \bar{p}\pi^+$

$\Gamma(\Xi\Xi)/\Gamma_{total}$

VALUE (units 10^{-3})	EVTs	DOCUMENT ID	TECN	COMMENT
1.8 ± 0.4 OUR AVERAGE				Error includes scale factor of 1.8. See the ideogram below.
1.40 ± 0.12 ± 0.24	132 ± 11	HENRRARD	87 DM2	$e^+e^- \rightarrow \Xi^-\Xi^+$
2.28 ± 0.16 ± 0.40	194	EATON	84 MRK2	$e^+e^- \rightarrow \Xi^-\Xi^+$
3.2 ± 0.8	71	PERUZZI	78 MRK1	e^+e^-



$\Gamma(n\bar{n})/\Gamma_{total}$

VALUE (units 10^{-2})	EVTs	DOCUMENT ID	TECN	COMMENT
0.22 ± 0.04 OUR AVERAGE				
0.231 ± 0.049	79	BALDINI	98 FENI	e^+e^-
0.18 ± 0.09		BESCH	78 BONA	e^+e^-

• • • We do not use the following data for averages, fits, limits, etc. • • •
0.190 ± 0.055 40 ANTONELLI 93 SPEC e^+e^-

$\Gamma(\Lambda\bar{\Lambda})/\Gamma_{total}$

VALUE (units 10^{-3})	EVTs	DOCUMENT ID	TECN	COMMENT
1.30 ± 0.12 OUR AVERAGE				Error includes scale factor of 1.1.
1.08 ± 0.06 ± 0.24	631	BAI	98c BES	e^+e^-
1.38 ± 0.05 ± 0.20	1847	PALLIN	87 DM2	e^+e^-
1.58 ± 0.08 ± 0.19	365	EATON	84 MRK2	e^+e^-
2.6 ± 1.6	5	BESCH	81 BONA	e^+e^-
1.1 ± 0.2	196	PERUZZI	78 MRK1	e^+e^-

$\Gamma(p\bar{p}\pi^0)/\Gamma_{total}$

VALUE (units 10^{-3})	EVTs	DOCUMENT ID	TECN	COMMENT
1.09 ± 0.09 OUR AVERAGE				
1.13 ± 0.09 ± 0.09	685	EATON	84 MRK2	e^+e^-
1.4 ± 0.4		BRANDELIK	79c DASP	e^+e^-
1.00 ± 0.15	109	PERUZZI	78 MRK1	e^+e^-

$\Gamma(\Lambda\Sigma^-\pi^+ \text{ (or c.c.)})/\Gamma_{total}$

VALUE (units 10^{-3})	EVTs	DOCUMENT ID	TECN	COMMENT
1.06 ± 0.12 OUR AVERAGE				
0.90 ± 0.06 ± 0.16	225 ± 15	HENRRARD	87 DM2	$e^+e^- \rightarrow \Lambda\Sigma^+\pi^-$
1.11 ± 0.06 ± 0.20	342 ± 18	HENRRARD	87 DM2	$e^+e^- \rightarrow \Lambda\Sigma^-\pi^+$
1.53 ± 0.17 ± 0.38	135	EATON	84 MRK2	$e^+e^- \rightarrow \Lambda\Sigma^+\pi^-$
1.38 ± 0.21 ± 0.35	118	EATON	84 MRK2	$e^+e^- \rightarrow \Lambda\Sigma^-\pi^+$

$\Gamma(\rho K^-\bar{\Lambda})/\Gamma_{total}$

VALUE (units 10^{-3})	EVTs	DOCUMENT ID	TECN	COMMENT
0.89 ± 0.07 ± 0.14	307	EATON	84 MRK2	e^+e^-

$\Gamma(2(K^+K^-))/\Gamma_{total}$

VALUE (units 10^{-4})	DOCUMENT ID	TECN	COMMENT
7 ± 3	VANNUCCI	77 MRK1	e^+e^-

$\Gamma(\rho K^-\Sigma^0)/\Gamma_{total}$

VALUE (units 10^{-3})	EVTs	DOCUMENT ID	TECN	COMMENT
0.29 ± 0.06 ± 0.05	90	EATON	84 MRK2	e^+e^-

$\Gamma(K^+K^-)/\Gamma_{total}$

VALUE (units 10^{-4})	EVTs	DOCUMENT ID	TECN	COMMENT
2.37 ± 0.31 OUR AVERAGE				
2.39 ± 0.24 ± 0.22	107	BALTRUSAIT..85d	MRK3	e^+e^-
2.2 ± 0.9	6	BRANDELIK	79c DASP	e^+e^-

$\Gamma(\Lambda\bar{\Lambda}\pi^0)/\Gamma_{total}$

VALUE (units 10^{-3})	EVTs	DOCUMENT ID	TECN	COMMENT
0.22 ± 0.06 OUR AVERAGE				
0.23 ± 0.07 ± 0.08	11	BAI	98c BES	e^+e^-
0.22 ± 0.05 ± 0.05	19 ± 4	HENRRARD	87 DM2	e^+e^-

$\Gamma(\pi^+\pi^-)/\Gamma_{total}$

VALUE (units 10^{-4})	EVTs	DOCUMENT ID	TECN	COMMENT
1.47 ± 0.23 OUR AVERAGE				
1.58 ± 0.20 ± 0.15	84	BALTRUSAIT..85d	MRK3	e^+e^-
1.0 ± 0.5	5	BRANDELIK	78b DASP	e^+e^-
1.6 ± 1.6	1	VANNUCCI	77 MRK1	e^+e^-

$\Gamma(K_S^0 K_L^0)/\Gamma_{total}$

VALUE (units 10^{-4})	EVTs	DOCUMENT ID	TECN	COMMENT
1.08 ± 0.14 OUR AVERAGE				
1.18 ± 0.12 ± 0.18		JOUSSET	90 DM2	$J/\psi \rightarrow \text{hadrons}$
1.01 ± 0.16 ± 0.09	74	BALTRUSAIT..85d	MRK3	e^+e^-

$\Gamma(\Lambda\Sigma^+ \text{ c.c.})/\Gamma_{total}$

VALUE (units 10^{-3})	CL%	DOCUMENT ID	TECN	COMMENT
< 0.15	90	PERUZZI	78 MRK1	$e^+e^- \rightarrow \Lambda X$

$\Gamma(K_S^0 K_S^0)/\Gamma_{total}$

VALUE (units 10^{-4})	CL%	DOCUMENT ID	TECN	COMMENT
< 0.052	90	28 BALTRUSAIT..85c	MRK3	e^+e^-

28 Forbidden by CP.

RADIATIVE DECAYS

$\Gamma(\gamma\eta_c(1S))/\Gamma_{total}$

VALUE	EVTs	DOCUMENT ID	TECN	COMMENT
0.0127 ± 0.0036		GAISER	86 CBAL	$J/\psi \rightarrow \gamma X$
seen	16	BALTRUSAIT..84	MRK3	$J/\psi \rightarrow 2\phi\gamma$

• • • We do not use the following data for averages, fits, limits, etc. • • •

$\Gamma(\gamma\pi^+\pi^-2\pi^0)/\Gamma_{total}$

VALUE (units 10^{-3})	DOCUMENT ID	TECN	COMMENT	
8.3 ± 0.2 ± 3.1	29	BALTRUSAIT..86b	MRK3	$J/\psi \rightarrow 4\pi\gamma$

29 4π mass less than 2.0 GeV.

$\Gamma(\gamma\eta\pi\pi)/\Gamma_{total}$

VALUE (units 10^{-3})	DOCUMENT ID	TECN	COMMENT	
6.1 ± 1.0 OUR AVERAGE				
5.85 ± 0.3 ± 1.05	30	EDWARDS	83b CBAL	$J/\psi \rightarrow \eta\pi^+\pi^-$
7.8 ± 1.2 ± 2.4	30	EDWARDS	83b CBAL	$J/\psi \rightarrow \eta2\pi^0$

30 Broad enhancement at 1700 MeV.

See key on page 239

Meson Particle Listings

$J/\psi(1S)$

$\Gamma(\gamma\eta(1440) \rightarrow \gamma K \bar{K} \pi) / \Gamma_{total}$ Γ_{97} / Γ

VALUE (units 10^{-3})	DOCUMENT ID	TECN	COMMENT
0.91 ± 0.18 OUR AVERAGE			
0.83 ± 0.13 ± 0.18	31,32	AUGUSTIN 92 DM2	$J/\psi \rightarrow \gamma K \bar{K} \pi$
1.03 ^{-0.21 + 0.26} _{-0.18 - 0.19}	31,33	BAI 90C MRK3	$J/\psi \rightarrow \gamma K_S^0 K^\pm \pi^\mp$
• • • We do not use the following data for averages, fits, limits, etc. • • •			
1.78 ± 0.21 ± 0.33	31,34	AUGUSTIN 92 DM2	$J/\psi \rightarrow \gamma K \bar{K} \pi$
3.8 ± 0.3 ± 0.6	31	AUGUSTIN 90 DM2	$J/\psi \rightarrow \gamma K \bar{K} \pi$
0.66 ^{+0.17 + 0.24} _{-0.16 - 0.15}	31,35	BAI 90C MRK3	$J/\psi \rightarrow \gamma K_S^0 K^\pm \pi^\mp$
4.0 ± 0.7 ± 1.0	31	EDWARDS 82E CBAL	$J/\psi \rightarrow K^+ K^- \pi^0 \gamma$
4.3 ± 1.7	31,36	SCHARRE 80 MRK2	$e^+ e^-$

31 Includes unknown branching fraction $\eta(1440) \rightarrow K \bar{K} \pi$.
 32 From fit to the $K^*(892) K^0$ 0^- partial wave.
 33 From $K^*(890) K$ final state.
 34 From fit to the $a_0(980) \pi^0$ 0^- partial wave.
 35 From $a_0(980) \pi$ final state.
 36 Corrected for spin-zero hypothesis for $\eta(1440)$.

$\Gamma(\gamma\eta(1440) \rightarrow \gamma \gamma \rho^0) / \Gamma_{total}$ Γ_{98} / Γ

VALUE (units 10^{-5})	DOCUMENT ID	TECN	COMMENT
6.4 ± 1.2 ± 0.7	37	COFFMAN 90 MRK3	$J/\psi \rightarrow \gamma \gamma \pi^+ \pi^-$
37 Includes unknown branching fraction $\eta(1440) \rightarrow \gamma \rho^0$.			

$\Gamma(\gamma\eta(1440) \rightarrow \gamma \eta \pi^+ \pi^-) / \Gamma_{total}$ Γ_{99} / Γ

VALUE (units 10^{-4})	EVTS	DOCUMENT ID	TECN	COMMENT
3.0 ± 0.5 OUR AVERAGE				
2.6 ± 0.7 ± 0.4		BAI 99 BES		$J/\psi \rightarrow \gamma \eta \pi^+ \pi^-$
3.38 ± 0.33 ± 0.64		38 BOLTON 92B MRK3		$J/\psi \rightarrow \gamma \eta \pi^+ \pi^-$
• • • We do not use the following data for averages, fits, limits, etc. • • •				
7.0 ± 0.6 ± 1.1	261	39 AUGUSTIN 90 DM2		$J/\psi \rightarrow \gamma \eta \pi^+ \pi^-$
38 Via $a_0(980) \pi$. 39 Includes unknown branching fraction to $\eta \pi^+ \pi^-$.				

$\Gamma(\gamma \rho \rho) / \Gamma_{total}$ Γ_{100} / Γ

VALUE (units 10^{-3})	CL%	DOCUMENT ID	TECN	COMMENT
4.5 ± 0.8 OUR AVERAGE				
4.7 ± 0.3 ± 0.9		40 BALTRUSAIT..86B MRK3		$J/\psi \rightarrow 4\pi \gamma$
3.75 ± 1.05 ± 1.20		41 BURKE 82 MRK2		$J/\psi \rightarrow 4\pi \gamma$
• • • We do not use the following data for averages, fits, limits, etc. • • •				
< 0.09	90	42 BISELLO 89B		$J/\psi \rightarrow 4\pi \gamma$
40 4π mass less than 2.0 GeV. 41 4π mass less than 2.0 GeV, $2\rho^0$ corrected to 2ρ by factor of 3. 42 4π mass in the range 2.0–25 GeV.				

$\Gamma(\gamma \eta_2(1870) \rightarrow \gamma \pi^+ \pi^-) / \Gamma_{total}$ Γ_{101} / Γ

VALUE (units 10^{-4})	DOCUMENT ID	TECN	COMMENT
6.2 ± 2.2 ± 0.9	BAI 99 BES		$J/\psi \rightarrow \gamma \eta \pi^+ \pi^-$

$\Gamma(\gamma \eta'(958)) / \Gamma_{total}$ Γ_{102} / Γ

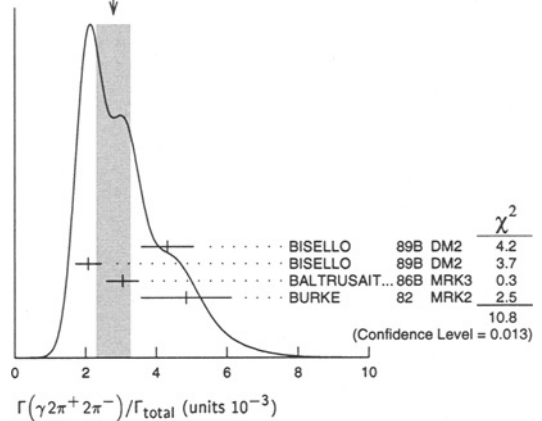
VALUE (units 10^{-3})	EVTS	DOCUMENT ID	TECN	COMMENT
4.31 ± 0.30 OUR AVERAGE				
4.50 ± 0.14 ± 0.53		BOLTON 92B MRK3		$J/\psi \rightarrow \gamma \pi^+ \pi^- \eta, \eta \rightarrow \gamma \gamma$
4.30 ± 0.31 ± 0.71		BOLTON 92B MRK3		$J/\psi \rightarrow \gamma \pi^+ \pi^- \eta, \eta \rightarrow \pi^+ \pi^- \pi^0$
4.04 ± 0.16 ± 0.85	622	AUGUSTIN 90 DM2		$J/\psi \rightarrow \gamma \eta \pi^+ \pi^-$
4.39 ± 0.09 ± 0.66	2420	AUGUSTIN 90 DM2		$J/\psi \rightarrow \gamma \eta \pi^+ \pi^-$
4.1 ± 0.3 ± 0.6		BLOOM 83 CBAL		$e^+ e^- \rightarrow 3\gamma + \text{hadrons}$

• • • We do not use the following data for averages, fits, limits, etc. • • •
 2.9 ± 1.1 6 BRANDELIK 79C DASP $e^+ e^- \rightarrow 3\gamma$
 2.4 ± 0.7 57 BARTEL 76 CNTR $e^+ e^- \rightarrow 2\gamma \rho$

$\Gamma(\gamma 2\pi^+ 2\pi^-) / \Gamma_{total}$ Γ_{103} / Γ

VALUE (units 10^{-3})	DOCUMENT ID	TECN	COMMENT
2.8 ± 0.5 OUR AVERAGE			Error includes scale factor of 1.9. See the ideogram below.
4.32 ± 0.14 ± 0.73	43 BISELLO 89B DM2		$J/\psi \rightarrow 4\pi \gamma$
2.08 ± 0.13 ± 0.35	44 BISELLO 89B DM2		$J/\psi \rightarrow 4\pi \gamma$
3.05 ± 0.08 ± 0.45	44	BALTRUSAIT..86B MRK3	$J/\psi \rightarrow 4\pi \gamma$
4.85 ± 0.45 ± 1.20	45	BURKE 82 MRK2	$e^+ e^-$
43 4π mass less than 3.0 GeV. 44 4π mass less than 2.0 GeV. 45 4π mass less than 2.5 GeV.			

WEIGHTED AVERAGE
 2.8 ± 0.5 (Error scaled by 1.9)



$\Gamma(\gamma K^+ K^- \pi^+ \pi^-) / \Gamma_{total}$ Γ_{104} / Γ

VALUE (units 10^{-3})	EVTS	DOCUMENT ID	TECN	COMMENT
2.1 ± 0.1 ± 0.6	1516	BAI 00B BES		$J/\psi \rightarrow \gamma K^+ K^0 \pi^+ \pi^-$

$\Gamma(\gamma f_4(2050)) / \Gamma_{total}$ Γ_{105} / Γ

VALUE (units 10^{-3})	DOCUMENT ID	TECN	COMMENT
2.7 ± 0.5 ± 0.5	46	BALTRUSAIT..87 MRK3	$J/\psi \rightarrow \gamma \pi^+ \pi^-$
46 Assuming branching fraction $f_4(2050) \rightarrow \pi \pi / \text{total} = 0.167$.			

$\Gamma(\gamma \omega \omega) / \Gamma_{total}$ Γ_{106} / Γ

VALUE (units 10^{-3})	EVTS	DOCUMENT ID	TECN	COMMENT
1.59 ± 0.33 OUR AVERAGE				
1.41 ± 0.2 ± 0.42	120 ± 17	BISELLO 87 SPEC		$e^+ e^-$, hadrons γ
1.76 ± 0.09 ± 0.45		BALTRUSAIT..85C MRK3		$e^+ e^- \rightarrow \text{hadrons} \gamma$

$\Gamma(\gamma \eta(1440) \rightarrow \gamma \rho^0 \rho^0) / \Gamma_{total}$ Γ_{107} / Γ

VALUE (units 10^{-3})	DOCUMENT ID	TECN	COMMENT
1.7 ± 0.4 OUR AVERAGE			Error includes scale factor of 1.3.
2.1 ± 0.4	BUGG 95 MRK3		$J/\psi \rightarrow \gamma \pi^+ \pi^- \pi^+ \pi^-$
1.36 ± 0.38	47,48	BISELLO 89B DM2	$J/\psi \rightarrow 4\pi \gamma$
47 Estimated by us from various fits. 48 Includes unknown branching fraction to $\rho^0 \rho^0$.			

$\Gamma(\gamma f_2(1270)) / \Gamma_{total}$ Γ_{108} / Γ

VALUE (units 10^{-3})	EVTS	DOCUMENT ID	TECN	CHG	COMMENT
1.38 ± 0.14 OUR AVERAGE					
1.33 ± 0.05 ± 0.20		49 AUGUSTIN 87 DM2			$J/\psi \rightarrow \gamma \pi^+ \pi^-$
1.36 ± 0.09 ± 0.23		49	BALTRUSAIT..87 MRK3		$J/\psi \rightarrow \gamma \pi^+ \pi^-$
1.48 ± 0.25 ± 0.30	178	EDWARDS 82B CBAL			$e^+ e^- \rightarrow 2\pi^0 \gamma$
2.0 ± 0.7	35	ALEXANDER 78 PLUT 0			$e^+ e^-$
1.2 ± 0.6	30	50 BRANDELIK 78B DASP			$e^+ e^- \rightarrow \pi^+ \pi^- \gamma$

49 Estimated using $B(f_2(1270) \rightarrow \pi \pi) = 0.843 \pm 0.012$. The errors do not contain the uncertainty in the $f_2(1270)$ decay.
 50 Restated by us to take account of spread of E1, M2, E3 transitions.

$\Gamma(\gamma f_0(1710) \rightarrow \gamma K \bar{K}) / \Gamma_{total}$ Γ_{109} / Γ

VALUE (units 10^{-4})	CL%	DOCUMENT ID	TECN	COMMENT
8.5 ± 1.2 OUR AVERAGE				Error includes scale factor of 1.2.
5.0 ± 0.8 ± 1.8		51,52	BAI 96C BES	$J/\psi \rightarrow \gamma K^+ K^-$
9.2 ± 1.4 ± 1.4		52	AUGUSTIN 88 DM2	$J/\psi \rightarrow \gamma K^+ K^-$
10.4 ± 1.2 ± 1.6		52	AUGUSTIN 88 DM2	$J/\psi \rightarrow \gamma K_S^0 K_S^0$
9.6 ± 1.2 ± 1.8		52	BALTRUSAIT..87 MRK3	$J/\psi \rightarrow \gamma K^+ K^-$
• • • We do not use the following data for averages, fits, limits, etc. • • •				
1.6 ± 0.2 ± 0.6		52,53	BAI 96C BES	$J/\psi \rightarrow \gamma K^+ K^-$
< 0.8	90	54 BISELLO 89B		$J/\psi \rightarrow 4\pi \gamma$
1.6 ± 0.4 ± 0.3		55	BALTRUSAIT..87 MRK3	$J/\psi \rightarrow \gamma \pi^+ \pi^-$
3.8 ± 1.6		56	EDWARDS 82D CBAL	$e^+ e^- \rightarrow \eta \eta \gamma$

51 Assuming $J^P = 2^+$ for $f_0(1710)$.
 52 Includes unknown branching fraction to $K^+ K^-$ or $K_S^0 K_S^0$. We have multiplied $K^+ K^-$ measurement by 2, and $K_S^0 K_S^0$ by 4 to obtain $K \bar{K}$ result.
 53 Assuming $J^P = 0^+$ for $f_0(1710)$.
 54 Includes unknown branching fraction to $\rho^0 \rho^0$.
 55 Includes unknown branching fraction to $\pi^+ \pi^-$.
 56 Includes unknown branching fraction to $\eta \eta$.

Meson Particle Listings

$J/\psi(1S)$

$\Gamma(\gamma f_0(1710) \rightarrow \gamma \pi \pi) / \Gamma_{total}$ Γ_{110}/Γ

VALUE (units 10^{-4})	DOCUMENT ID	TECN	COMMENT
• • • We do not use the following data for averages, fits, limits, etc. • • •			
$2.5 \pm 1.6 \pm 0.8$	BAI	98H BES	$J/\psi \rightarrow \gamma \pi^0 \pi^0$

$\Gamma(\gamma \eta) / \Gamma_{total}$ Γ_{111}/Γ

VALUE (units 10^{-3})	EVTS	DOCUMENT ID	TECN	COMMENT
0.86 ± 0.08 OUR AVERAGE				
$0.88 \pm 0.08 \pm 0.11$		BLOOM	83 CBAL	$e^+ e^-$
0.82 ± 0.10		BRANDELIK	79c DASP	$e^+ e^-$
1.3 ± 0.4	21	BARTEL	77 CNTR	$e^+ e^-$

$\Gamma(\gamma f_1(1420) \rightarrow \gamma K \bar{K} \pi) / \Gamma_{total}$ Γ_{112}/Γ

VALUE (units 10^{-3})	DOCUMENT ID	TECN	COMMENT
0.83 ± 0.15 OUR AVERAGE			
$0.76 \pm 0.15 \pm 0.21$	57,58 AUGUSTIN	92 DM2	$J/\psi \rightarrow \gamma K \bar{K} \pi$
$0.87 \pm 0.14^{+0.14}_{-0.11}$	57 BAI	90c MRK3	$J/\psi \rightarrow \gamma K_S^0 K^\pm \pi^\mp$

57 Included unknown branching fraction $f_1(1420) \rightarrow K \bar{K} \pi$.
58 From fit to the $K^*(892) K 1^+ +$ partial wave.

$\Gamma(\gamma f_1(1285)) / \Gamma_{total}$ Γ_{113}/Γ

VALUE (units 10^{-3})	DOCUMENT ID	TECN	COMMENT
0.61 ± 0.09 OUR AVERAGE			
$0.45 \pm 0.09 \pm 0.17$	59 BAI	99 BES	$J/\psi \rightarrow \gamma \eta \pi^+ \pi^-$
$0.625 \pm 0.063 \pm 0.103$	60 BOLTON	92 MRK3	$J/\psi \rightarrow \gamma f_1(1285)$
$0.70 \pm 0.08 \pm 0.16$	61 BOLTON	92b MRK3	$J/\psi \rightarrow \gamma \eta \pi^+ \pi^-$

59 Assuming $\Gamma(f_1(1285) \rightarrow \eta \pi \pi) / \Gamma_{total} = 0.5 \pm 0.18$.
60 Obtained summing the sequential decay channels
 $B(J/\psi \rightarrow \gamma f_1(1285), f_1(1285) \rightarrow \pi \pi \pi) = (1.44 \pm 0.39 \pm 0.27) \times 10^{-4}$;
 $B(J/\psi \rightarrow \gamma f_1(1285), f_1(1285) \rightarrow a_0(980) \pi, a_0(980) \rightarrow \eta \pi) = (3.90 \pm 0.42 \pm 0.87) \times 10^{-4}$;
 $B(J/\psi \rightarrow \gamma f_1(1285), f_1(1285) \rightarrow a_0(980) \pi, a_0(980) \rightarrow K \bar{K}) = (0.66 \pm 0.26 \pm 0.29) \times 10^{-4}$;
 $B(J/\psi \rightarrow \gamma f_1(1285), f_1(1285) \rightarrow \gamma \rho^0) = (0.25 \pm 0.07 \pm 0.03) \times 10^{-4}$.
61 Using $B(f_1(1285) \rightarrow a_0(980) \pi) = 0.37$, and including unknown branching ratio for $a_0(980) \rightarrow \eta \pi$.

$\Gamma(\gamma f_1(1510) \rightarrow \gamma \eta \pi^+ \pi^-) / \Gamma_{total}$ Γ_{114}/Γ

VALUE (units 10^{-4})	DOCUMENT ID	TECN	COMMENT
$4.5 \pm 1.0 \pm 0.7$	BAI	99 BES	$J/\psi \rightarrow \gamma \eta \pi^+ \pi^-$

$\Gamma(\gamma f_2'(1525)) / \Gamma_{total}$ Γ_{115}/Γ

VALUE (units 10^{-3})	CL%	EVTS	DOCUMENT ID	TECN	COMMENT
$0.47^{+0.07}_{-0.05}$ OUR AVERAGE					
$0.36 \pm 0.04^{+0.14}_{-0.04}$			62 BAI	96c BES	$J/\psi \rightarrow \gamma K^+ K^-$
$0.56 \pm 0.14 \pm 0.09$			62 AUGUSTIN	88 DM2	$J/\psi \rightarrow \gamma K^+ K^-$
$0.45 \pm 0.04 \pm 0.09$			62 AUGUSTIN	88 DM2	$J/\psi \rightarrow \gamma K_S^0 K_S^0$
$0.68 \pm 0.16 \pm 0.14$			62 BALTRUSAIT..87	MRK3	$J/\psi \rightarrow \gamma K^+ K^-$

• • • We do not use the following data for averages, fits, limits, etc. • • •

<0.34	90	4	63 BRANDELIK	79c DASP	$e^+ e^- \rightarrow \pi^+ \pi^- \gamma$
<0.23	90	3	ALEXANDER	78 PLUT	$e^+ e^- \rightarrow K^+ K^- \gamma$

62 Using $B(f_2'(1525) \rightarrow K \bar{K}) = 0.888$.
63 Assuming isotropic production and decay of the $f_2'(1525)$ and isospin.

$\Gamma(\gamma f_2(1950) \rightarrow \gamma K^*(892) \bar{K}^*(892)) / \Gamma_{total}$ Γ_{116}/Γ

VALUE (units 10^{-3})	DOCUMENT ID	TECN	COMMENT
$0.7 \pm 0.1 \pm 0.2$	BAI	00B BES	$J/\psi \rightarrow \gamma K^+ K^0 \pi^+ \pi^-$

$\Gamma(\gamma K^*(892) \bar{K}^*(892)) / \Gamma_{total}$ Γ_{117}/Γ

VALUE (units 10^{-3})	EVTS	DOCUMENT ID	TECN	COMMENT
$4.0 \pm 0.3 \pm 1.3$	320	64 BAI	00B BES	$J/\psi \rightarrow \gamma K^+ K^0 \pi^+ \pi^-$

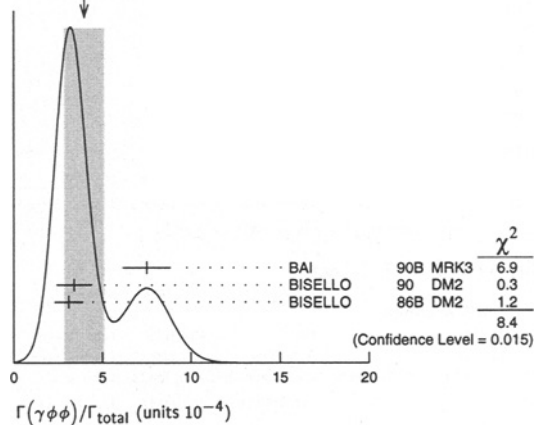
64 Summed over all charges.

$\Gamma(\gamma \phi \phi) / \Gamma_{total}$ Γ_{118}/Γ

VALUE (units 10^{-4})	EVTS	DOCUMENT ID	TECN	COMMENT
4.0 ± 1.2 OUR AVERAGE Error includes scale factor of 2.1. See the ideogram below.				
$7.5 \pm 0.6 \pm 1.2$	168	BAI	90B MRK3	$J/\psi \rightarrow \gamma 4K$
$3.4 \pm 0.8 \pm 0.6$	33 ± 7	65 BISELLO	90 DM2	$J/\psi \rightarrow \gamma K^+ K^- K_S^0 K_L^0$
$3.1 \pm 0.7 \pm 0.4$		65 BISELLO	86B DM2	$J/\psi \rightarrow \gamma K^+ K^- K^+ K^-$

65 $\phi \phi$ mass less than 2.9 GeV, η_c excluded.

WEIGHTED AVERAGE
 4.0 ± 1.2 (Error scaled by 2.1)



$\Gamma(\gamma \rho \bar{\rho}) / \Gamma_{total}$ Γ_{119}/Γ

VALUE (units 10^{-3})	CL%	EVTS	DOCUMENT ID	TECN	COMMENT
$0.38 \pm 0.07 \pm 0.07$		49	EATON	84 MRK2	$e^+ e^-$
• • • We do not use the following data for averages, fits, limits, etc. • • •					
<0.11	90		PERUZZI	78 MRK1	$e^+ e^-$

$\Gamma(\gamma \eta(2225)) / \Gamma_{total}$ Γ_{120}/Γ

VALUE (units 10^{-3})	DOCUMENT ID	TECN	COMMENT
0.29 ± 0.06 OUR AVERAGE			
$0.33 \pm 0.08 \pm 0.05$	66 BAI	90B MRK3	$J/\psi \rightarrow \gamma K^+ K^- K^+ K^-$
$0.27 \pm 0.06 \pm 0.06$	66 BAI	90B MRK3	$J/\psi \rightarrow \gamma K^+ K^- K_S^0 K_L^0$
$0.24^{+0.15}_{-0.10}$	67,68 BISELLO	89B DM2	$J/\psi \rightarrow 4\pi \gamma$

66 Includes unknown branching fraction to $\phi \phi$.

67 Estimated by us from various fits.

68 Includes unknown branching fraction to $\rho^0 \rho^0$.

$\Gamma(\gamma \eta(1760) \rightarrow \gamma \rho^0 \rho^0) / \Gamma_{total}$ Γ_{121}/Γ

VALUE (units 10^{-3})	DOCUMENT ID	TECN	COMMENT
0.13 ± 0.09	69,70 BISELLO	89B DM2	$J/\psi \rightarrow 4\pi \gamma$

69 Estimated by us from various fits.
70 Includes unknown branching fraction to $\rho^0 \rho^0$.

$\Gamma(\gamma \pi^0) / \Gamma_{total}$ Γ_{122}/Γ

VALUE (units 10^{-3})	EVTS	DOCUMENT ID	TECN	COMMENT
0.039 ± 0.013 OUR AVERAGE				
$0.036 \pm 0.011 \pm 0.007$		BLOOM	83 CBAL	$e^+ e^-$
0.073 ± 0.047	10	BRANDELIK	79c DASP	$e^+ e^-$

$\Gamma(\gamma \rho \bar{\rho} \pi^+ \pi^-) / \Gamma_{total}$ Γ_{123}/Γ

VALUE (units 10^{-3})	CL%	DOCUMENT ID	TECN	COMMENT
<0.79	90	EATON	84 MRK2	$e^+ e^-$

$\Gamma(\gamma \gamma) / \Gamma_{total}$ Γ_{124}/Γ

VALUE (units 10^{-3})	CL%	DOCUMENT ID	TECN	COMMENT
<0.5	90	BARTEL	77 CNTR	$e^+ e^-$

$\Gamma(\gamma A \bar{A}) / \Gamma_{total}$ Γ_{125}/Γ

VALUE (units 10^{-3})	CL%	DOCUMENT ID	TECN	COMMENT
<0.13	90	HENRARD	87 DM2	$e^+ e^-$
• • • We do not use the following data for averages, fits, limits, etc. • • •				
<0.16	90	BAI	98G BES	$e^+ e^-$

$\Gamma(3\gamma) / \Gamma_{total}$ Γ_{126}/Γ

VALUE (units 10^{-3})	CL%	DOCUMENT ID	TECN	COMMENT
<0.055	90	PARTRIDGE	80 CBAL	$e^+ e^-$

Meson Particle Listings

$\chi_{c0}(1P)$

$\chi_{c0}(1P)$ DECAY MODES

Mode	Fraction (Γ_i/Γ)	Scale factor/ Confidence level
Hadronic decays		
Γ_1 $2(\pi^+\pi^-)$	(2.0 ± 0.9) %	S=2.7
Γ_2 $\pi^+\pi^-K^+K^-$	(1.8 ± 0.6) %	S=1.9
Γ_3 $\rho^0\pi^+\pi^-$	(1.6 ± 0.5) %	
Γ_4 $3(\pi^+\pi^-)$	(1.24 ± 0.22) %	
Γ_5 $K^+\bar{K}^*(892)^0\pi^- + c.c.$	(1.2 ± 0.4) %	
Γ_6 $\pi^+\pi^-$	(5.0 ± 0.7) × 10 ⁻³	
Γ_7 K^+K^-	(5.9 ± 0.9) × 10 ⁻³	
Γ_8 $\pi^+\pi^-\rho\bar{\rho}$	(1.8 ± 0.9) × 10 ⁻³	S=1.6
Γ_9 $K^+K^-K^+K^-$	(2.1 ± 0.5) × 10 ⁻³	
Γ_{10} $K_S^0 K_S^0$	(2.0 ± 0.6) × 10 ⁻³	
Γ_{11} $\phi\phi$	(9 ± 5) × 10 ⁻⁴	
Γ_{12} $\pi^0\pi^0$		
Γ_{13} $\eta\eta$		
Γ_{14} $K_S^0 K^+\pi^- + c.c.$	< 7.1 × 10 ⁻⁴	CL=90%
Γ_{15} $\rho\bar{\rho}$	(2.2 ± 1.3) × 10 ⁻⁴	S=2.1
Radiative decays		
Γ_{16} $\gamma J/\psi(1S)$	(6.6 ± 1.8) × 10 ⁻³	
Γ_{17} $\gamma\gamma$	(2.7 ± 1.9) × 10 ⁻⁴	

$\chi_{c0}(1P)$ PARTIAL WIDTHS

$\Gamma(\gamma\gamma)$	CL%	DOCUMENT ID	TECN	COMMENT	Γ_{17}
4.0 ± 2.8		LEE	85 CBAL	$\psi' \rightarrow$ photons	
• • • We do not use the following data for averages, fits, limits, etc. • • •					
< 5.5	95	ACCIARRI	99T L3	$\gamma\gamma$	
< 6.2	95	CHEN	90B CLEO	$e^+e^- \rightarrow e^+e^- \chi_{c0}$	
< 17	95	AIHARA	88D TPC	$e^+e^- \rightarrow e^+e^- X$	

$\chi_{c0}(1P)$ BRANCHING RATIOS

HADRONIC DECAYS

$\Gamma(2(\pi^+\pi^-))/\Gamma_{total}$	Γ_1/Γ		
VALUE	DOCUMENT ID	TECN	COMMENT
0.020 ± 0.009 OUR AVERAGE	Error includes scale factor of 2.7.		
0.0154 ± 0.0005 ± 0.0037	³ BAI	99B BES	$\psi(2S) \rightarrow \gamma\chi_{c0}$
0.037 ± 0.007	⁴ TANENBAUM	78 MRK1	$\psi(2S) \rightarrow \gamma\chi_{c0}$
$\Gamma(\pi^+\pi^-K^+K^-)/\Gamma_{total}$	Γ_2/Γ		
VALUE	DOCUMENT ID	TECN	COMMENT
0.018 ± 0.006 OUR AVERAGE	Error includes scale factor of 1.9.		
0.0147 ± 0.0007 ± 0.0038	³ BAI	99B BES	$\psi(2S) \rightarrow \gamma\chi_{c0}$
0.030 ± 0.007	⁴ TANENBAUM	78 MRK1	$\psi(2S) \rightarrow \gamma\chi_{c0}$
$\Gamma(\rho^0\pi^+\pi^-)/\Gamma_{total}$	Γ_3/Γ		
VALUE	DOCUMENT ID	TECN	COMMENT
0.016 ± 0.005	⁴ TANENBAUM	78 MRK1	$\psi(2S) \rightarrow \gamma\chi_{c0}$
$\Gamma(3(\pi^+\pi^-))/\Gamma_{total}$	Γ_4/Γ		
VALUE	DOCUMENT ID	TECN	COMMENT
0.0124 ± 0.0022 OUR AVERAGE			
0.0117 ± 0.0010 ± 0.0023	³ BAI	99B BES	$\psi(2S) \rightarrow \gamma\chi_{c0}$
0.015 ± 0.005	⁴ TANENBAUM	78 MRK1	$\psi(2S) \rightarrow \gamma\chi_{c0}$
$\Gamma(K^+\bar{K}^*(892)^0\pi^- + c.c.)/\Gamma_{total}$	Γ_5/Γ		
VALUE	DOCUMENT ID	TECN	COMMENT
0.012 ± 0.004	⁴ TANENBAUM	78 MRK1	$\psi(2S) \rightarrow \gamma\chi_{c0}$
$\Gamma(\pi^+\pi^-)/\Gamma_{total}$	Γ_6/Γ		
VALUE (units 10 ⁻³)	DOCUMENT ID	TECN	COMMENT
5.0 ± 0.7 OUR AVERAGE			
4.68 ± 0.26 ± 0.65	³ BAI	98I BES	$\psi(2S) \rightarrow \gamma\chi_{c0}$
7 ± 3	⁴ BRANDELIK	79B DASP	$\psi(2S) \rightarrow \gamma\chi_{c0}$
8 ± 3	⁴ TANENBAUM	78 MRK1	$\psi(2S) \rightarrow \gamma\chi_{c0}$
$\Gamma(K^+K^-)/\Gamma_{total}$	Γ_7/Γ		
VALUE (units 10 ⁻³)	DOCUMENT ID	TECN	COMMENT
5.9 ± 0.9 OUR AVERAGE			
5.68 ± 0.35 ± 0.85	³ BAI	98I BES	$\psi(2S) \rightarrow \gamma\chi_{c0}$
6 ± 3	⁴ BRANDELIK	79B DASP	$\psi(2S) \rightarrow \gamma\chi_{c0}$
9 ± 4	⁴ TANENBAUM	78 MRK1	$\psi(2S) \rightarrow \gamma\chi_{c0}$

$\Gamma(\pi^+\pi^-\rho\bar{\rho})/\Gamma_{total}$	Γ_8/Γ		
VALUE (units 10 ⁻³)	DOCUMENT ID	TECN	COMMENT
1.8 ± 0.9 OUR AVERAGE	Error includes scale factor of 1.6.		
1.57 ± 0.21 ± 0.54	³ BAI	99B BES	$\psi(2S) \rightarrow \gamma\chi_{c0}$
5 ± 2	⁴ TANENBAUM	78 MRK1	$\psi(2S) \rightarrow \gamma\chi_{c0}$

$\Gamma(K^+K^-K^+K^-)/\Gamma_{total}$	Γ_9/Γ		
VALUE (units 10 ⁻³)	DOCUMENT ID	TECN	COMMENT
2.14 ± 0.26 ± 0.40	³ BAI	99B BES	$\psi(2S) \rightarrow \gamma\chi_{c0}$

$\Gamma(K_S^0 K_S^0)/\Gamma_{total}$	Γ_{10}/Γ		
VALUE (units 10 ⁻³)	DOCUMENT ID	TECN	COMMENT
1.96 ± 0.28 ± 0.52	³ BAI	99B BES	$\psi(2S) \rightarrow \gamma\chi_{c0}$

$\Gamma(\phi\phi)/\Gamma_{total}$	Γ_{11}/Γ		
VALUE (units 10 ⁻³)	DOCUMENT ID	TECN	COMMENT
0.92 ± 0.34 ± 0.38	³ BAI	99B BES	$\psi(2S) \rightarrow \gamma\chi_{c0}$

$\Gamma(\pi^0\pi^0)/\Gamma_{total}$	Γ_{12}/Γ		
VALUE (units 10 ⁻³)	DOCUMENT ID	TECN	COMMENT
• • • We do not use the following data for averages, fits, limits, etc. • • •			
3.1 ± 0.4 ± 0.5	³ LEE	85 CBAL	$\psi' \rightarrow$ photons

$\Gamma(\eta\eta)/\Gamma_{total}$	Γ_{13}/Γ		
VALUE (units 10 ⁻³)	DOCUMENT ID	TECN	COMMENT
• • • We do not use the following data for averages, fits, limits, etc. • • •			
2.5 ± 0.8 ± 0.8	³ LEE	85 CBAL	$\psi' \rightarrow$ photons

$\Gamma(K_S^0 K^+\pi^- + c.c.)/\Gamma_{total}$	Γ_{14}/Γ		
VALUE (units 10 ⁻³)	DOCUMENT ID	TECN	COMMENT
< 0.71	90	³ BAI	99B BES $\psi(2S) \rightarrow \gamma\chi_{c0}$

$\Gamma(\rho\bar{\rho})/\Gamma_{total}$	Γ_{15}/Γ		
VALUE (units 10 ⁻³)	DOCUMENT ID	TECN	COMMENT
0.22 ± 0.13 OUR AVERAGE	Error includes scale factor of 2.1.		
0.48 +0.09 +0.21	⁵ AMBROGIANI	99B E835	$\bar{p}p \rightarrow e^+e^- \gamma$
-0.08 -0.11			
0.159 ± 0.043 ± 0.053	³ BAI	98I BES	$\psi(2S) \rightarrow \gamma\chi_{c0}$
< 0.9	90	⁴ BRANDELIK	79B DASP $\psi(2S) \rightarrow \gamma\chi_{c0}$
³ Calculated using $B(\psi(2S) \rightarrow \gamma\chi_{c0}(1P)) = 0.093 \pm 0.008$.			
⁴ Calculated using $B(\psi(2S) \rightarrow \gamma\chi_{c0}(1P)) = 0.094$; the errors do not contain the uncertainty in the $\psi(2S)$ decay.			
⁵ Estimated using $B(\chi_{c0} \rightarrow \gamma J/\psi) = (6.0 \pm 1.8) \times 10^{-3}$ and $B(J/\psi \rightarrow e^+e^-) = (6.02 \pm 0.19) \times 10^{-2}$.			

RADIATIVE DECAYS

$\Gamma(\gamma J/\psi(1S))/\Gamma_{total}$	Γ_{16}/Γ		
VALUE (units 10 ⁻⁴)	DOCUMENT ID	TECN	COMMENT
66 ± 18 OUR AVERAGE			
60 ± 18	GAISER	86 CBAL	$\psi(2S) \rightarrow \gamma\chi_{c0}$
320 ± 210	⁶ BRANDELIK	79B DASP	$\psi(2S) \rightarrow \gamma\chi_{c0}$
150 ± 100	⁶ BARTEL	78B CNTR	$\psi(2S) \rightarrow \gamma\chi_{c0}$
210 ± 210	⁶ TANENBAUM	78 MRK1	$\psi(2S) \rightarrow \gamma\chi_{c0}$

$\Gamma(\gamma\gamma)/\Gamma_{total}$	Γ_{17}/Γ		
VALUE (units 10 ⁻⁴)	DOCUMENT ID	TECN	COMMENT
• • • We do not use the following data for averages, fits, limits, etc. • • •			
4.0 ± 2.0 ± 1.1	³ LEE	85 CBAL	$\psi' \rightarrow$ photons
⁶ Calculated using $B(\psi(2S) \rightarrow \gamma\chi_{c0}(1P)) = 0.094$; the errors do not contain the uncertainty in the $\psi(2S)$ decay.			

$\chi_{c0}(1P)$ REFERENCES

ACCIARRI	99T	PL B461 155	M. Acciari et al.	(L3 Collab.)
AMBROGIANI	99B	PRL B3 2902	M. Ambrogiani et al.	(FNAL E835 Collab.)
BAI	99B	PR D60 072001	J.Z. Bai et al.	(BES Collab.)
BAI	98I	PRL B1 3091	J.Z. Bai et al.	(BES Collab.)
CHEN	90B	PL B243 169	W.Y. Chen et al.	(CLEO Collab.)
AIHARA	88D	PRL B0 2355	H. Aihara et al.	(TPC Collab.)
GAISER	86	PR D34 711	J. Gaiser et al.	(Crystal Ball Collab.)
LEE	85	SLAC 282	R.A. Lee	(SLAC)
BRANDELIK	79B	NP B180 426	R. Brandelik et al.	(DASP Collab.)
BARTEL	78B	PL 79B 492	W. Bartel et al.	(DESY, HEIDP)
TANENBAUM	78	PR D17 1731	W.M. Tanenbaum et al.	(SLAC, LBL)
Also	82	Private Comm.	G. Trilling	(LBL, UCB)
BIDDICK	77	PRL B3 1324	C.J. Biddick et al.	(UCSD, UMD, PAVI+)

OTHER RELATED PAPERS

OREGLIA	82	PR D25 2259	M.J. Oreglia et al.	(SLAC, CIT, HARV+)
FELDMAN	78	PRL B3 821	G.J. Feldman et al.	(LBL, SLAC)
Also	75C	PRL B3 1189	G.J. Feldman	
Erratum.				
TANENBAUM	75	PRL B3 1323	W.M. Tanenbaum et al.	(LBL, SLAC)

See key on page 239

Meson Particle Listings

 $\chi_{c1}(1P)$

$$\chi_{c1}(1P) \quad I^G(J^{PC}) = 0^+(1^{++})$$

 $\chi_{c1}(1P)$ MASS

VALUE (MeV)	EVTS	DOCUMENT ID	TECN	COMMENT
3510.51 ± 0.12 OUR AVERAGE				
3509.4 ± 0.9		BAI	99B BES	$\psi(2S) \rightarrow \gamma X$
3510.53 ± 0.04 ± 0.12	513	ARMSTRONG 92 E760		$\bar{p}p \rightarrow e^+e^-\gamma$
3511.3 ± 0.4 ± 0.4	30	BAGLIN	86B SPEC	$\bar{p}p \rightarrow e^+e^-X$
3512.3 ± 0.3 ± 0.4		¹ GAISER	86 CBAL	$\psi(2S) \rightarrow \gamma X$
3507.4 ± 1.7	91	² LEMOIGNE	82 GOL1	$190 \pi^- Be \rightarrow \gamma 2\mu$
3510.4 ± 0.6		OREGLIA	82 CBAL	$e^+e^- \rightarrow J/\psi 2\gamma$
3510.1 ± 1.1	254	³ HIMEL	80 MRK2	$e^+e^- \rightarrow J/\psi 2\gamma$
3509 ± 11	21	BRANDELIK	79B DASP	$e^+e^- \rightarrow J/\psi 2\gamma$
3507 ± 3		³ BARTEL	78B CNTR	$e^+e^- \rightarrow J/\psi 2\gamma$
3505.0 ± 4 ± 4		^{3,4} TANENBAUM	78 MRK1	e^+e^-
3513 ± 7	367	³ BIDDICK	77 CNTR	$\psi(2S) \rightarrow \gamma X$
• • • We do not use the following data for averages, fits, limits, etc. • • •				
3500 ± 10	40	TANENBAUM 75 MRK1		Hadrons γ

¹ Using mass of $\psi(2S) = 3686.0$ MeV.² $J/\psi(1S)$ mass constrained to 3097 MeV.³ Mass value shifted by us by amount appropriate for $\psi(2S)$ mass = 3686 MeV and $J/\psi(1S)$ mass = 3097 MeV.⁴ From a simultaneous fit to radiative and hadronic decay channels. $\chi_{c1}(1P)$ WIDTH

VALUE (MeV)	CL%	EVTS	DOCUMENT ID	TECN	COMMENT
0.88 ± 0.11 ± 0.08		513	ARMSTRONG 92 E760		$\bar{p}p \rightarrow e^+e^-\gamma$
• • • We do not use the following data for averages, fits, limits, etc. • • •					
<1.3	95		BAGLIN	86B SPEC	$\bar{p}p \rightarrow e^+e^-X$
<3.8	90		GAISER	86 CBAL	$\psi(2S) \rightarrow \gamma X$

 $\chi_{c1}(1P)$ DECAY MODES

Mode	Fraction (Γ_i/Γ)	Scale factor
Hadronic decays		
Γ_1 $3(\pi^+\pi^-)$	$(6.3 \pm 1.4) \times 10^{-3}$	
Γ_2 $2(\pi^+\pi^-)$	$(5.6 \pm 2.6) \times 10^{-3}$	2.2
Γ_3 $\pi^+\pi^-K^+K^-$	$(4.9 \pm 1.2) \times 10^{-3}$	1.1
Γ_4 $\rho^0\pi^+\pi^-$	$(3.9 \pm 3.5) \times 10^{-3}$	
Γ_5 $K^+\bar{K}^*(892)^0\pi^- + c.c.$	$(3.2 \pm 2.1) \times 10^{-3}$	
Γ_6 $K_S^0 K^+\pi^-$	$(2.5 \pm 0.8) \times 10^{-3}$	
Γ_7 $\pi^+\pi^-\rho\bar{\rho}$	$(5.4 \pm 2.1) \times 10^{-4}$	
Γ_8 $K^+K^-K^+K^-$	$(4.2 \pm 1.9) \times 10^{-4}$	
Γ_9 $\rho\bar{\rho}$	$(8.2 \pm 1.3) \times 10^{-5}$	1.2
Γ_{10} $\pi^+\pi^- + K^+K^-$	$< 2.1 \times 10^{-3}$	
Radiative decays		
Γ_{11} $\gamma J/\psi(1S)$	$(27.3 \pm 1.6) \%$	
Γ_{12} $\gamma\gamma$		

 $\chi_{c1}(1P)$ PARTIAL WIDTHS

$\Gamma(\rho\bar{\rho})$	EVTS	DOCUMENT ID	TECN	COMMENT
74 ± 9 OUR AVERAGE				
76 ± 10 ± 5	513	⁵ ARMSTRONG 92 E760		$\bar{p}p \rightarrow e^+e^-\gamma$
69 ± 16 ± 4		⁵ BAGLIN	86B SPEC	$\bar{p}p \rightarrow e^+e^-X$
⁵ Restated by us using $B(\chi_{c1}(1P) \rightarrow J/\psi(1S)\gamma)B(J/\psi(1S) \rightarrow e^+e^-) = 0.0171 \pm 0.0011$.				

 $\chi_{c1}(1P)$ BRANCHING RATIOS

HADRONIC DECAYS

$\Gamma(3(\pi^+\pi^-))/\Gamma_{total}$	Γ_1/Γ
6.3 ± 1.4 OUR AVERAGE	
5.8 ± 0.7 ± 1.2	
22 ± 8	
$\Gamma(2(\pi^+\pi^-))/\Gamma_{total}$	Γ_2/Γ
5.6 ± 2.6 OUR AVERAGE Error includes scale factor of 2.2.	
4.9 ± 0.4 ± 1.2	
16 ± 5	

$\Gamma(\pi^+\pi^-K^+K^-)/\Gamma_{total}$	Γ_3/Γ
49 ± 12 OUR AVERAGE Error includes scale factor of 1.1.	
45 ± 4 ± 11	
90 ± 40	

$\Gamma(\rho^0\pi^+\pi^-)/\Gamma_{total}$	Γ_4/Γ
39 ± 35	
7 TANENBAUM 78 MRK1	$\psi(2S) \rightarrow \gamma X_{c1}$

$\Gamma(K^+\bar{K}^*(892)^0\pi^- + c.c.)/\Gamma_{total}$	Γ_5/Γ
32 ± 21	
7 TANENBAUM 78 MRK1	$\psi(2S) \rightarrow \gamma X_{c1}$

$\Gamma(K_S^0 K^+\pi^-)/\Gamma_{total}$	Γ_6/Γ
2.46 ± 0.44 ± 0.65	
6 BAI	99B BES $\psi(2S) \rightarrow \gamma X_{c1}$

$\Gamma(\pi^+\pi^-\rho\bar{\rho})/\Gamma_{total}$	Γ_7/Γ
5.4 ± 2.1 OUR AVERAGE	
4.9 ± 1.3 ± 1.7	
14 ± 9	
6 BAI	99B BES $\psi(2S) \rightarrow \gamma X_{c1}$
7 TANENBAUM 78 MRK1	$\psi(2S) \rightarrow \gamma X_{c1}$

$\Gamma(K^+K^-K^+K^-)/\Gamma_{total}$	Γ_8/Γ
0.42 ± 0.15 ± 0.12	
6 BAI	99B BES $\psi(2S) \rightarrow \gamma X_{c1}$

$\Gamma(\rho\bar{\rho})/\Gamma_{total}$	Γ_9/Γ
0.82 ± 0.13 OUR AVERAGE Error includes scale factor of 1.2.	
0.42 ± 0.22 ± 0.28	
4.2 ± 2.2	
0.86 ± 0.12	
> 0.54	
<12.0	
• • • We do not use the following data for averages, fits, limits, etc. • • •	
95	
90	
6 BAI	98B BES $\psi(2S) \rightarrow \gamma X_{c1}$
8 ARMSTRONG 92 E760	$\bar{p}p \rightarrow e^+e^-\gamma$
7 BRANDELIK 79B DASP	$\psi(2S) \rightarrow \gamma X_{c1}$
7 BRANDELIK 79B DASP	$\psi(2S) \rightarrow \gamma X_{c1}$

$[\Gamma(\pi^+\pi^-) + \Gamma(K^+K^-)]/\Gamma_{total}$	Γ_{10}/Γ
<21	
7 FELDMAN 77 MRK1	$\psi(2S) \rightarrow \gamma X_{c1}$
• • • We do not use the following data for averages, fits, limits, etc. • • •	
<38	
90	
7 BRANDELIK 79B DASP	$\psi(2S) \rightarrow \gamma X_{c1}$

⁶ Using $B(\psi(2S) \rightarrow \gamma X_{c1}(1P)) = 0.087 \pm 0.008$.

⁷ Estimated using $B(\psi(2S) \rightarrow \gamma X_{c1}(1P)) = 0.087$. The errors do not contain the uncertainty in the $\psi(2S)$ decay.

⁸ Restated by us using $B(\chi_{c1}(1P) \rightarrow J/\psi(1S)\gamma)B(J/\psi(1S) \rightarrow e^+e^-) = 0.0171 \pm 0.0011$.

RADIATIVE DECAYS

$\Gamma(\gamma J/\psi(1S))/\Gamma_{total}$	Γ_{11}/Γ
0.273 ± 0.016 OUR AVERAGE	
0.284 ± 0.021	
0.274 ± 0.046	
0.28 ± 0.07	
0.19 ± 0.05	
0.29 ± 0.05	
0.28 ± 0.09	
0.57 ± 0.17	
• • • We do not use the following data for averages, fits, limits, etc. • • •	
77 CNTR	$\psi(2S) \rightarrow \gamma X$

$\Gamma(\gamma\gamma)/\Gamma_{total}$	Γ_{12}/Γ
<0.0015	
90	
⁹ YAMADA 77 DASP	$e^+e^- \rightarrow 3\gamma$
⁹ Estimated using $B(\psi(2S) \rightarrow \gamma X_{c1}(1P)) = 0.087$. The errors do not contain the uncertainty in the $\psi(2S)$ decay.	

 $\chi_{c1}(1P)$ REFERENCES

BAI	99B PR D60 072001	J.Z. Bai et al.	(BES Collab.)
BAI	981 PRL 81 3091	J.Z. Bai et al.	(BES Collab.)
ARMSTRONG	92 NP B373 35	T.A. Armstrong et al.	(FNAL, FERR, GENO+)
Also	92B PRL 68 1468	T.A. Armstrong et al.	(FNAL, FERR, GENO+)
BAGLIN	86B PL B172 455	C. Baglin	(LAPP, CERN, GENO, LYON, OSLO+)
GAISER	86 PR D34 711	J. Gaiser et al.	(Crystal Ball Collab.)
LEMOIGNE	82 PL 113B 509	Y. Lemoigne et al.	(SACL, LOIC, SHMP+)
OREGLIA	82 PR D25 2259	M.J. Oreglia et al.	(SLAC, CIT, HARV+)
Also	82B Private Comm.	M.J. Oreglia	(SLAC, CIT, HARV+)
HIMEL	80 PRL 44 920	T. Himel et al.	(EPI)
Also	82 Private Comm.	G. Trilling	(LBL, SLAC)
BRANDELIK	79B NP B160 426	R. Brandelik et al.	(DASP Collab.)
BARTEL	78B PL 79B 492	W. Bartel et al.	(DESY, HEIDP)
TANENBAUM	78 PR D17 1731	W.M. Tanenbaum et al.	(SLAC, LBL)
Also	82 Private Comm.	G. Trilling	(SLAC, LBL)
BIDDICK	77 PRL 38 1324	C.J. Biddick et al.	(UCSD, UMD, PAWI+)
FELDMAN	77 PRPL 33C 285	G.J. Feldman, M.L. Perl	(LBL, SLAC)
YAMADA	77 Hamburg Conf. 69	S. Yamada	(DASP Collab.)
TANENBAUM	75 PRL 35 1323	W.M. Tanenbaum et al.	(LBL, SLAC)

Meson Particle Listings

$\chi_{c1}(1P), h_c(1P), \chi_{c2}(1P)$

OTHER RELATED PAPERS

BARATE	83	PL 121B 449	R. Barate et al.	(SACL, LOIC, SHMP, IND)
BRAUNSCH...	75B	PL 57B 407	W. Braunschweig et al.	(DASP Collab.)
SIMPSON	75	PRL 35 699	J.W. Simpson et al.	(STAN, PENN)

$h_c(1P)$

$$I^G(J^{PC}) = ?^?(???)$$

OMITTED FROM SUMMARY TABLE
Needs confirmation.

$h_c(1P)$ MASS

VALUE (MeV)	EVTS	DOCUMENT ID	TECN	COMMENT
3526.14 ± 0.24 OUR AVERAGE				
3526.20 ± 0.15 ± 0.20	59	ARMSTRONG 92D E760	E760	$\bar{p}p \rightarrow J/\psi \pi^0$
3525.4 ± 0.8 ± 0.4	5	BAGLIN 86 SPEC	SPEC	$\bar{p}p \rightarrow J/\psi X$
• • • We do not use the following data for averages, fits, limits, etc. • • •				
3527 ± 8	42	ANTONIAZZI 94 E705	E705	300 $\pi^\pm, \rho \text{Li} \rightarrow J/\psi \pi^0 X$

$h_c(1P)$ WIDTH

VALUE (MeV)	CL%	EVTS	DOCUMENT ID	TECN	COMMENT
<1.1	90	59	ARMSTRONG 92D E760	E760	$\bar{p}p \rightarrow J/\psi \pi^0$

$h_c(1P)$ DECAY MODES

Mode	Fraction (Γ_i/Γ)
Γ_1 $J/\psi(1S)\pi^0$	seen
Γ_2 $J/\psi(1S)\pi\pi$	not seen
Γ_3 $\rho\bar{\rho}$	

$\Gamma(J/\psi(1S)\pi\pi)/\Gamma(J/\psi(1S)\pi^0)$		Γ_2/Γ_1	
VALUE	CL%	DOCUMENT ID	TECN
<0.18	90	ARMSTRONG 92D E760	E760

$h_c(1P)$ REFERENCES

ANTONIAZZI 94 PR D50 4258	L. Antoniazzi et al.	(E705 Collab.)
ARMSTRONG 92D PRL 69 2337	T.A. Armstrong et al.	(FNAL, FERR, GENO+)
BAGLIN 86 PL B171 135	C. Baglin et al.	(LAPP, CERN, TORI, STRB+)

$\chi_{c2}(1P)$

$$I^G(J^{PC}) = 0^+(2^{++})$$

$\chi_{c2}(1P)$ MASS

VALUE (MeV)	EVTS	DOCUMENT ID	TECN	COMMENT
3556.18 ± 0.13 OUR AVERAGE				
3556.4 ± 0.7		BAI 99B BES	BES	$\psi(2S) \rightarrow \gamma X$
3556.15 ± 0.07 ± 0.12	585	ARMSTRONG 92 E760	E760	$\bar{p}p \rightarrow e^+e^-\gamma$
3556.9 ± 0.4 ± 0.5	50	BAGLIN 86B SPEC	SPEC	$\bar{p}p \rightarrow e^+e^-X$
3557.8 ± 0.2 ± 0.4		¹ GAISER 86 CBAL	CBAL	$\psi(2S) \rightarrow \gamma X$
3553.4 ± 2.2	66	² LEMOIGNE 82 GOLI	GOLI	190 $\pi^- \text{Be} \rightarrow \gamma 2\mu$
3555.9 ± 0.7		³ ORÈGLIA 82 CBAL	CBAL	$e^+e^- \rightarrow J/\psi 2\gamma$
3557 ± 1.5	69	⁴ HIMEL 80 MRK2	MRK2	$e^+e^- \rightarrow J/\psi 2\gamma$
3551 ± 11	15	BRANDELIK 79B DASP	DASP	$e^+e^- \rightarrow J/\psi 2\gamma$
3553 ± 4		⁴ BARTEL 78B CNTR	CNTR	$e^+e^- \rightarrow J/\psi 2\gamma$
3553 ± 4 ± 4		^{4,5} TANENBAUM 78 MRK1	MRK1	$e^+e^- \rightarrow \gamma X$
3563 ± 7	360	⁴ BIDDICK 77 CNTR	CNTR	$e^+e^- \rightarrow \gamma X$
• • • We do not use the following data for averages, fits, limits, etc. • • •				
3543 ± 10	4	WHITAKER 76 MRK1	MRK1	$e^+e^- \rightarrow J/\psi 2\gamma$

¹ Using mass of $\psi(2S) = 3686.0$ MeV.
² $J/\psi(1S)$ mass constrained to 3097 MeV.
³ Assuming $\psi(2S)$ mass = 3686 MeV and $J/\psi(1S)$ mass = 3097 MeV.
⁴ Mass value shifted by us by amount appropriate for $\psi(2S)$ mass = 3686 MeV and $J/\psi(1S)$ mass = 3097 MeV.
⁵ From a simultaneous fit to radiative and hadronic decay channels.

$\chi_{c2}(1P)$ WIDTH

VALUE (MeV)	EVTS	DOCUMENT ID	TECN	COMMENT
2.00 ± 0.18 OUR AVERAGE				
1.98 ± 0.17 ± 0.07	585	ARMSTRONG 92 E760	E760	$\bar{p}p \rightarrow e^+e^-\gamma$
2.6 $^{+1.4}_{-1.0}$	50	BAGLIN 86B SPEC	SPEC	$\bar{p}p \rightarrow e^+e^-X$
2.8 $^{+2.1}_{-2.0}$		⁶ GAISER 86 CBAL	CBAL	$\psi(2S) \rightarrow \gamma X$

⁶ Errors correspond to 90% confidence level; authors give only width range.

$\chi_{c2}(1P)$ DECAY MODES

Mode	Fraction (Γ_i/Γ)	Scale factor/ Confidence level
Hadronic decays		
Γ_1 $2(\pi^+\pi^-)$	(1.2 ± 0.5) %	S=2.2
Γ_2 $\pi^+\pi^-K^+K^-$	(10 ± 4) × 10 ⁻³	S=2.0
Γ_3 $3(\pi^+\pi^-)$	(9.2 ± 2.2) × 10 ⁻³	
Γ_4 $\rho^0\pi^+\pi^-$	(7 ± 4) × 10 ⁻³	
Γ_5 $K^+K^*(892)^0\pi^- + \text{c.c.}$	(4.8 ± 2.8) × 10 ⁻³	
Γ_6 $\pi^+\pi^-\rho\bar{\rho}$	(1.4 ± 0.6) × 10 ⁻³	S=1.5
Γ_7 $\phi\phi$	(2.0 ± 0.8) × 10 ⁻³	
Γ_8 $\pi^+\pi^-$	(1.52 ± 0.25) × 10 ⁻³	
Γ_9 K^+K^-	(8.1 ± 1.9) × 10 ⁻⁴	
Γ_{10} $K^+K^-K^+K^-$	(1.5 ± 0.4) × 10 ⁻³	
Γ_{11} $K_S^0K_S^0$	(6.1 ± 2.3) × 10 ⁻⁴	
Γ_{12} $\rho\bar{\rho}$	(9.8 ± 1.0) × 10 ⁻⁵	
Γ_{13} $\pi^0\pi^0$		
Γ_{14} $\eta\eta$		
Γ_{15} $J/\psi(1S)\pi^+\pi^-\pi^0$	< 1.5 %	CL=90%
Γ_{16} $K_S^0K^+\pi^- + \text{c.c.}$	< 1.06 × 10 ⁻³	CL=90%
Radiative decays		
Γ_{17} $\gamma J/\psi(1S)$	(13.5 ± 1.1) %	
Γ_{18} $\gamma\gamma$	(1.6 ± 0.5) × 10 ⁻⁴	

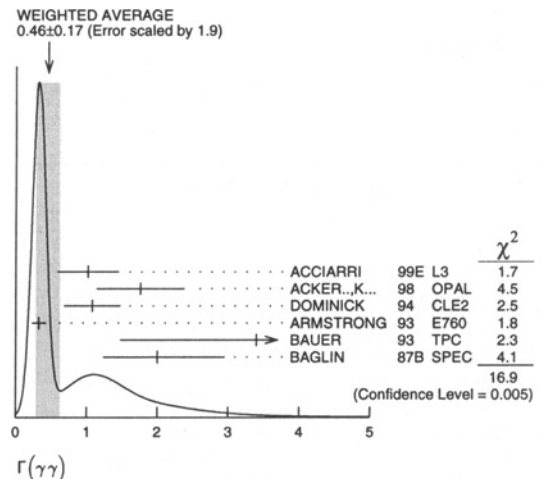
$\chi_{c2}(1P)$ PARTIAL WIDTHS

$\Gamma(\rho\bar{\rho})$		Γ_{12}	
VALUE (eV)	EVTS	DOCUMENT ID	TECN
206 ± 22 OUR AVERAGE			
197 ± 18 ± 16	585	⁷ ARMSTRONG 92 E760	E760
252 $^{+55}_{-48}$ ± 21		⁷ BAGLIN 86B SPEC	SPEC

⁷ Restated by us using $B(\chi_{c2}(1P) \rightarrow J/\psi(1S)\gamma)B(J/\psi(1S) \rightarrow e^+e^-) = 0.0085 \pm 0.0007$.

$\Gamma(\gamma\gamma)$		Γ_{18}	
VALUE (keV)	CL%	DOCUMENT ID	TECN
0.46 ± 0.17 OUR AVERAGE			
Error includes scale factor of 1.9. See the ideogram below.			
1.02 ± 0.40 ± 0.17		⁸ ACCIARRI 99E L3	L3
1.76 ± 0.47 ± 0.40		^{8,9} ACKER...K... 98 OPAL	OPAL
1.08 ± 0.30 ± 0.26		DOMINICK 94 CLE2	CLE2
0.326 ± 0.080 ± 0.055		¹⁰ ARMSTRONG 93 E760	E760
3.4 ± 1.7 ± 0.9		BAUER 93 TPC	TPC
2.0 $^{+0.9}_{-0.7}$ ± 0.3		¹⁰ BAGLIN 87B SPEC	SPEC
• • • We do not use the following data for averages, fits, limits, etc. • • •			
<1.4	95	ACCIARRI 99T L3	L3
<4.2	95	UEHARA 91 VNS	VNS
<1.0	95	CHEN 90B CLEO	CLEO
<4.2	95	AIHARA 88D TPC	TPC

⁸ Systematic error includes, added in quadrature, error due to $B(\chi_{c2} \rightarrow J/\psi\gamma)$ and $B(J/\psi \rightarrow e^+e^-)$ uncertainties.
⁹ Using $B(\chi_{c2} \rightarrow J/\psi\gamma) = 13.5 \pm 1.1\%$ and $B(J/\psi \rightarrow e^+e^-) = 12.03 \pm 0.27\%$.
¹⁰ Using $B(\chi_{c2}(1P) \rightarrow \rho\bar{\rho}) = (0.98 \pm 0.10) \times 10^{-4}$ and $\Gamma_{\text{total}} = 2.00 \pm 0.18$ MeV.



See key on page 239

Meson Particle Listings

 $\chi_{c2}(1P)$ $\chi_{c2}(1P)$ BRANCHING RATIOS

HADRONIC DECAYS

$\Gamma(2(\pi^+\pi^-))/\Gamma_{total}$	Γ_1/Γ
0.012 ± 0.005 OUR AVERAGE	
0.0096 ± 0.0005 ± 0.0024	
0.022 ± 0.005	
DOCUMENT ID	TECN COMMENT
11 BAI	99B BES $\psi(2S) \rightarrow \gamma\chi_{c2}$
12 TANENBAUM	78 MRK1 $\psi(2S) \rightarrow \gamma\chi_{c2}$

$\Gamma(\pi^+\pi^-K^+K^-)/\Gamma_{total}$	Γ_2/Γ
0.010 ± 0.004 OUR AVERAGE	
0.0079 ± 0.0006 ± 0.0021	
0.019 ± 0.005	
DOCUMENT ID	TECN COMMENT
11 BAI	99B BES $\psi(2S) \rightarrow \gamma\chi_{c2}$
12 TANENBAUM	78 MRK1 $\psi(2S) \rightarrow \gamma\chi_{c2}$

$\Gamma(3(\pi^+\pi^-))/\Gamma_{total}$	Γ_3/Γ
0.0092 ± 0.0022 OUR AVERAGE	
0.009 ± 0.001 ± 0.002	
0.012 ± 0.008	
DOCUMENT ID	TECN COMMENT
11 BAI	99B BES $\psi(2S) \rightarrow \gamma\chi_{c2}$
12 TANENBAUM	78 MRK1 $\psi(2S) \rightarrow \gamma\chi_{c2}$

$\Gamma(\rho^0\pi^+\pi^-)/\Gamma_{total}$	Γ_4/Γ
68 ± 40	
DOCUMENT ID	TECN COMMENT
12 TANENBAUM	78 MRK1 $\psi(2S) \rightarrow \gamma\chi_{c2}$

$\Gamma(K^+\bar{K}^*(892)^0\pi^- + c.c.)/\Gamma_{total}$	Γ_5/Γ
48 ± 28	
DOCUMENT ID	TECN COMMENT
12 TANENBAUM	78 MRK1 $\psi(2S) \rightarrow \gamma\chi_{c2}$

$\Gamma(\pi^+\pi^-p\bar{p})/\Gamma_{total}$	Γ_6/Γ
14 ± 6 OUR AVERAGE	
12.3 ± 2.0 ± 3.5	
33 ± 13	
DOCUMENT ID	TECN COMMENT
11 BAI	99B BES $\psi(2S) \rightarrow \gamma\chi_{c2}$
12 TANENBAUM	78 MRK1 $\psi(2S) \rightarrow \gamma\chi_{c2}$

$\Gamma(\phi\phi)/\Gamma_{total}$	Γ_7/Γ
2.00 ± 0.55 ± 0.61	
DOCUMENT ID	TECN COMMENT
11 BAI	99B BES $\psi(2S) \rightarrow \gamma\chi_{c2}$

$\Gamma(\pi^+\pi^-)/\Gamma_{total}$	Γ_8/Γ
1.52 ± 0.25 OUR AVERAGE	
1.49 ± 0.14 ± 0.22	
1.9 ± 1.0	
DOCUMENT ID	TECN COMMENT
11 BAI	98i BES $\psi(2S) \rightarrow \gamma\chi_{c2}$
12 BRANDELIK	79C DASP $\psi(2S) \rightarrow \gamma\chi_{c2}$

$[\Gamma(\pi^+\pi^-) + \Gamma(K^+K^-)]/\Gamma_{total}$	$(\Gamma_8 + \Gamma_9)/\Gamma$
24 ± 10	
DOCUMENT ID	TECN COMMENT
12 TANENBAUM	78 MRK1 $\psi(2S) \rightarrow \gamma\chi_{c2}$

$\Gamma(K^+K^-)/\Gamma_{total}$	Γ_9/Γ
0.81 ± 0.19 OUR AVERAGE	
0.79 ± 0.14 ± 0.13	
1.5 ± 1.1	
DOCUMENT ID	TECN COMMENT
11 BAI	98i BES $\psi(2S) \rightarrow \gamma\chi_{c2}$
12 BRANDELIK	79C DASP $\psi(2S) \rightarrow \gamma\chi_{c2}$

$\Gamma(K^+K^-K^+K^-)/\Gamma_{total}$	Γ_{10}/Γ
1.48 ± 0.26 ± 0.32	
DOCUMENT ID	TECN COMMENT
11 BAI	99B BES $\psi(2S) \rightarrow \gamma\chi_{c2}$

$\Gamma(K_S^0 K_S^0)/\Gamma_{total}$	Γ_{11}/Γ
0.61 ± 0.17 ± 0.16	
DOCUMENT ID	TECN COMMENT
11 BAI	99B BES $\psi(2S) \rightarrow \gamma\chi_{c2}$

$\Gamma(p\bar{p})/\Gamma_{total}$	Γ_{12}/Γ
0.96 ± 0.10 OUR AVERAGE	
0.58 ± 0.31 ± 0.32	
1.00 ± 0.11	
0.97 ^{+0.44} _{-0.28} ± 0.08	
DOCUMENT ID	TECN COMMENT
11 BAI	98i BES $\psi(2S) \rightarrow \gamma\chi_{c2}$
13 ARMSTRONG	92 E760 $\bar{p}p \rightarrow e^+e^- \gamma$
BAGLIN	86B SPEC $\bar{p}p \rightarrow e^+e^- X$

• • • We do not use the following data for averages, fits, limits, etc. • • •

<9.5	90	12 BRANDELIK	79B DASP $\psi(2S) \rightarrow \gamma\chi_{c2}$
------	----	--------------	---

Γ_1/Γ_{total} in $p\bar{p} \rightarrow \chi_{c2}(1P) \rightarrow \gamma\gamma$	$\Gamma_{12}\Gamma_{18}/\Gamma^2$
0.160 ± 0.039 ± 0.016	
0.99 ^{+0.46} _{-0.35}	
DOCUMENT ID	TECN COMMENT
ARMSTRONG	93 E760 $\bar{p}p \rightarrow \gamma\gamma$
14 BAGLIN	87B SPEC $\bar{p}p \rightarrow \gamma\gamma$

$\Gamma(\pi^0\pi^0)/\Gamma_{total}$	Γ_{13}/Γ
1.1 ± 0.2 ± 0.2	
DOCUMENT ID	TECN COMMENT
11 LEE	85 CBAL $\psi' \rightarrow \text{photons}$

$\Gamma(\eta\eta)/\Gamma_{total}$	Γ_{14}/Γ
7.9 ± 4.1 ± 2.4	
DOCUMENT ID	TECN COMMENT
11 LEE	85 CBAL $\psi' \rightarrow \text{photons}$

$\Gamma(J/\psi(1S)\pi^+\pi^-)/\Gamma_{total}$	Γ_{15}/Γ
<0.015	
DOCUMENT ID	TECN COMMENT
90	BARATE 81 SPEC 190 GeV $\pi^- \text{Be} \rightarrow 2\pi 2\mu$

$\Gamma(K_S^0 K^+\pi^- + c.c.)/\Gamma_{total}$	Γ_{16}/Γ
<1.06	
DOCUMENT ID	TECN COMMENT
90	11 BAI 99B BES $\psi(2S) \rightarrow \gamma\chi_{c2}$
11 Calculated using $B(\psi(2S) \rightarrow \gamma\chi_{c2}(1P)) = 0.078 \pm 0.008$.	
12 Estimated using $B(\psi(2S) \rightarrow \gamma\chi_{c2}(1P)) = 0.078$; the errors do not contain the uncertainty in the $\psi(2S)$ decay.	
13 Restated by us using $B(\chi_{c2}(1P) \rightarrow J/\psi(1S)\gamma)B(J/\psi(1S) \rightarrow e^+e^-) = 0.0085 \pm 0.0007$.	
14 Assuming isotropic $\chi_{c2}(1P) \rightarrow \gamma\gamma$ distribution.	

RADIATIVE DECAYS

$\Gamma(\gamma J/\psi(1S))/\Gamma_{total}$	Γ_{17}/Γ
0.135 ± 0.011 OUR AVERAGE	
0.124 ± 0.015	
0.162 ± 0.028	
0.14 ± 0.04	
0.18 ± 0.05	
0.13 ± 0.03	
0.13 ± 0.08	
DOCUMENT ID	TECN COMMENT
GAISER	86 CBAL $\psi(2S) \rightarrow \gamma X$
15 OREGLIA	82 CBAL $\psi(2S) \rightarrow \gamma\chi_{c2}$
15 HIMEL	80 MRK2 $\psi(2S) \rightarrow \gamma\chi_{c2}$
15 BRANDELIK	79B DASP $\psi(2S) \rightarrow \gamma\chi_{c2}$
15 BARTEL	78B CNTR $\psi(2S) \rightarrow \gamma\chi_{c2}$
15 TANENBAUM	78 MRK1 $\psi(2S) \rightarrow \gamma\chi_{c2}$

• • • We do not use the following data for averages, fits, limits, etc. • • •

0.28 ± 0.13	15 BIDDICK	77 CNTR $\psi(2S) \rightarrow \gamma X$
15 Estimated using $B(\psi(2S) \rightarrow \gamma\chi_{c2}(1P)) = 0.078$; the errors do not contain the uncertainty in the $\psi(2S)$ decay.		

$\Gamma(\gamma\gamma)/\Gamma_{total}$	Γ_{18}/Γ
1.60 ± 0.39 ± 0.23	
DOCUMENT ID	TECN COMMENT
16 ARMSTRONG	93 E760 $\bar{p}p \rightarrow \gamma\gamma$
16 Using $B(\chi_{c2}(1P) \rightarrow p\bar{p}) = (1.00 \pm 0.23) \times 10^{-4}$.	

 $\chi_{c2}(1P)$ REFERENCES

ACCIARRI	99E PL B453 73	M. Acciarri et al.	(L3 Collab.)
ACCIARRI	99T PL B461 155	M. Acciarri et al.	(L3 Collab.)
BAI	99B PR D60 072001	J.Z. Bai et al.	(BES Collab.)
ACKER...K...	98 PL B439 197	K. Ackers et al.	(OPAL Collab.)
BAI	98i PRL 81 3091	J.Z. Bai et al.	(BES Collab.)
DOMINICK	94 PR D50 4265	J. Dominick et al.	(CLEO Collab.)
ARMSTRONG	93 PRL 70 2986	T.A. Armstrong et al.	(FNAL E760 Collab.)
BAUER	93 PL B302 345	D.A. Bauer et al.	(TPC Collab.)
ARMSTRONG	92 NP B373 35	T.A. Armstrong et al.	(FNAL, FERR, GENO+)
Also	92B PRL 68 1468	T.A. Armstrong et al.	(FNAL, FERR, GENO+)
UEHARA	91 PL B266 188	S. Uehara et al.	(VENUS Collab.)
CHEN	90B PL B243 169	W.Y. Chen et al.	(CLEO Collab.)
AIHARA	88D PRL 60 2355	H. Aihara et al.	(TPC Collab.)
BAGLIN	87B PL B187 191	C. Baglin et al.	(R704 Collab.)
BAGLIN	86B PL B172 455	C. Baglin et al.	(LAPP, CERN, GENO, LYON, OSLO+)
GAISER	86 PR D34 711	J. Gaiser et al.	(Crystal Ball Collab.)
Also	SLAC 282	R.A. Lee	(SLAC)
LEMOIGNE	82 PL 113B 509	Y. Lemoigne et al.	(SACL, LOIC, SHMP+)
OREGLIA	82 PR D25 2259	M.J. Oreglia et al.	(SLAC, CIT, HARV+)
Also	82B Private Comm.	M.J. Oreglia	(EFI)
BARATE	81 PR D24 2994	R. Barate et al.	(SACL, LOIC, SHMP, CERN+)
HIMEL	80 PRL 44 920	T. Himel et al.	(LBL, SLAC)
Also	82 Private Comm.	G. Trilling	(LBL, UCB)
BRANDELIK	79B NP B160 426	R. Brandelik et al.	(DASP Collab.)
BRANDELIK	79C ZPHY C1 233	R. Brandelik et al.	(DASP Collab.)
BARTEL	78B PL 79B 492	W. Bartel et al.	(DESY, HEIDP)
TANENBAUM	78 PR D17 1731	W.M. Tanenbaum et al.	(SLAC, LBL)
Also	82 Private Comm.	G. Trilling	(LBL, UCB)
BIDDICK	77 PRL 38 1324	C.J. Biddick et al.	(UCSD, UMD, PAVI+)
WHITAKER	76 PRL 37 1596	J.S. Whitaker et al.	(SLAC, LBL)

OTHER RELATED PAPERS

BARATE	83 PL 121B 449	R. Barate et al.	(SACL, LOIC, SHMP, IND)
FELDMAN	75B PRL 35 821	G.J. Feldman et al.	(LBL, SLAC)
Also	75C PRL 35 1189	G.J. Feldman	
Erratum.			
TANENBAUM	75 PRL 35 1323	W.M. Tanenbaum et al.	(LBL, SLAC)

Meson Particle Listings

$\eta_c(2S), \psi(2S)$

$\eta_c(2S)$ $I^G(J^{PC}) = ??(??^+)$

OMITTED FROM SUMMARY TABLE
Needs confirmation.

$\eta_c(2S)$ MASS

VALUE (MeV)	DOCUMENT ID	TECN	COMMENT
3594 ± 5	¹ EDWARDS	82c CBAL	$e^+e^- \rightarrow \gamma X$

¹ Assuming mass of $\psi(2S) = 3686$ MeV.

$\eta_c(2S)$ WIDTH

VALUE (MeV)	CL%	DOCUMENT ID	TECN	COMMENT
<8.0	95	EDWARDS	82c CBAL	$e^+e^- \rightarrow \gamma X$

• • • We do not use the following data for averages, fits, limits, etc. • • •

$\eta_c(2S)$ DECAY MODES

Mode	Fraction (Γ_i/Γ)
Γ_1 hadrons	seen
Γ_2 $\gamma\gamma$	

$\eta_c(2S)$ BRANCHING RATIOS

$\Gamma(\text{hadrons})/\Gamma_{\text{total}}$	DOCUMENT ID	TECN	COMMENT	Γ_1/Γ
seen	EDWARDS	82c CBAL	$e^+e^- \rightarrow \gamma X$	
not seen	ABREU	980 DLPH	$e^+e^- \rightarrow e^+e^- + \text{hadrons}$	

• • • We do not use the following data for averages, fits, limits, etc. • • •

$\Gamma(\gamma\gamma)/\Gamma_{\text{total}}$	DOCUMENT ID	TECN	COMMENT	Γ_2/Γ
<0.01	90	LEE	85 CBAL $\psi' \rightarrow \text{photons}$	

• • • We do not use the following data for averages, fits, limits, etc. • • •

$\eta_c(2S)$ REFERENCES

ABREU	980	PL B441 479	P. Abreu et al.	(DELPHI Collab.)
LEE	85	SLAC 282	R.A. Lee	(SLAC)
EDWARDS	82c	PRL 48 70	C. Edwards et al.	(CIT. HARV. PRIN+)

OTHER RELATED PAPERS

OREGLIA	82	PR D25 2259	M.J. Oreglia et al.	(SLAC, CIT. HARV+)
PORTER	81	SLAC Summer Inst. 355	F.C. Porter et al.	(CIT. HARV, PRIN+)
BARTEL	78B	PL 79B 492	W. Bartel et al.	(DESY, HEIDP)

$\psi(2S)$ $I^G(J^{PC}) = 0^-(1^{--})$

$\psi(2S)$ MASS

VALUE (MeV)	EVTS	DOCUMENT ID	TECN	COMMENT
3685.96 ± 0.09	OUR AVERAGE			
3685.95 ± 0.10	413	¹ ARTAMONOV 00	OLYA	$e^+e^- \rightarrow \text{hadrons}$
3686.02 ± 0.09 ± 0.27		ARMSTRONG 93B	E760	$\bar{p}p \rightarrow e^+e^-$
3684 ± 2		GRIBUSHIN 96	FMP5	515 $\pi^- \text{Be} \rightarrow 2\mu X$
3683 ± 5	77	ANTONIAZZI 94	E705	300 $\pi^\pm, p\text{Li} \rightarrow J/\psi \pi^\pm \pi^- X$
3686.00 ± 0.10	413	² ZHOLENTZ 80	OLYA	e^+e^-

¹ Reanalysis of ZHOLENTZ 80 using new electron mass (COHEN 87) and radiative corrections (KURAEV 85).
² Superseded by ARTAMONOV 00.

$m_{\psi(2S)} - m_{J/\psi(1S)}$

VALUE (MeV)	DOCUMENT ID	TECN	COMMENT
589.07 ± 0.13	OUR AVERAGE		
589.7 ± 1.2	LEMOIGNE 82	GOLI	190 $\pi^- \text{Be} \rightarrow 2\mu$
589.07 ± 0.13	³ ZHOLENTZ 80	OLYA	e^+e^-
588.7 ± 0.8	LUTH 75	MRK1	
588 ± 1	⁴ BAI	98E BES	e^+e^-

• • • We do not use the following data for averages, fits, limits, etc. • • •
³ Redundant with data in mass above.
⁴ Systematic errors not evaluated.

$\psi(2S)$ WIDTH

VALUE (keV)	DOCUMENT ID	TECN	COMMENT
277 ± 31	OUR AVERAGE		Error includes scale factor of 1.1.
306 ± 36 ± 16	ARMSTRONG 93B	E760	$\bar{p}p \rightarrow e^+e^-$
243 ± 43	⁵ PDG	92 RVUE	

⁵ Uses $\Gamma(ee)$ from ALEXANDER 89 and $B(ee) = (88 \pm 13) \times 10^{-4}$ from FELDMAN 77.

$\psi(2S)$ DECAY MODES

Mode	Fraction (Γ_i/Γ)	Scale factor/Confidence level
Γ_1 hadrons	(98.10 ± 0.30) %	
Γ_2 virtual $\gamma \rightarrow \text{hadrons}$	(2.9 ± 0.4) %	
Γ_3 e^+e^-	(8.8 ± 1.3) × 10 ⁻³	
Γ_4 $\mu^+\mu^-$	(1.03 ± 0.35) %	
Decays into $J/\psi(1S)$ and anything		
Γ_5 $J/\psi(1S)$ anything	(55 ± 5) %	
Γ_6 $J/\psi(1S)$ neutrals	(23.1 ± 2.3) %	
Γ_7 $J/\psi(1S)\pi^+\pi^-$	(31.0 ± 2.8) %	
Γ_8 $J/\psi(1S)\pi^0\pi^0$	(18.2 ± 2.3) %	
Γ_9 $J/\psi(1S)\eta$	(2.7 ± 0.4) %	S=1.6
Γ_{10} $J/\psi(1S)\pi^0$	(9.7 ± 2.1) × 10 ⁻⁴	

Hadronic decays

Γ_{11} $3(\pi^+\pi^-)\pi^0$	(3.5 ± 1.6) × 10 ⁻³	
Γ_{12} $2(\pi^+\pi^-)\pi^0$	(3.0 ± 0.8) × 10 ⁻³	
Γ_{13} $\omega f_2(1270)$	< 1.7 × 10 ⁻⁴	CL=90%
Γ_{14} $\rho a_2(1320)$	< 2.3 × 10 ⁻⁴	CL=90%
Γ_{15} $\pi^+\pi^-K^+K^-$	(1.6 ± 0.4) × 10 ⁻³	
Γ_{16} $K^*(892)\bar{K}_2^*(1430)^0$	< 1.2 × 10 ⁻⁴	CL=90%
Γ_{17} $K_1(1270)^\pm K^\mp$	(1.00 ± 0.28) × 10 ⁻³	
Γ_{18} $\pi^+\pi^-p\bar{p}$	(8.0 ± 2.0) × 10 ⁻⁴	
Γ_{19} $K^+K^*(892)^0\pi^- + \text{c.c.}$	(6.7 ± 2.5) × 10 ⁻⁴	
Γ_{20} $b_1^\pm \pi^\mp$	(5.2 ± 1.3) × 10 ⁻⁴	
Γ_{21} $2(\pi^+\pi^-)$	(4.5 ± 1.0) × 10 ⁻⁴	
Γ_{22} $\rho^0\pi^+\pi^-$	(4.2 ± 1.5) × 10 ⁻⁴	
Γ_{23} $\bar{p}p$	(1.9 ± 0.5) × 10 ⁻⁴	
Γ_{24} $3(\pi^+\pi^-)$	(1.5 ± 1.0) × 10 ⁻⁴	
Γ_{25} $\bar{p}p\pi^0$	(1.4 ± 0.5) × 10 ⁻⁴	
Γ_{26} K^+K^-	(1.0 ± 0.7) × 10 ⁻⁴	
Γ_{27} $\pi^+\pi^-\pi^0$	(8 ± 5) × 10 ⁻⁵	
Γ_{28} $\rho\pi$	< 8.3 × 10 ⁻⁵	CL=90%
Γ_{29} $\pi^+\pi^-$	(8 ± 5) × 10 ⁻⁵	
Γ_{30} $\Lambda\bar{\Lambda}$	< 4 × 10 ⁻⁴	CL=90%
Γ_{31} $K_1(1400)^\pm K^\mp$	< 3.1 × 10 ⁻⁴	CL=90%
Γ_{32} $\Xi^-\Xi^+$	< 2 × 10 ⁻⁴	CL=90%
Γ_{33} $K^+K^-\pi^0$	< 2.96 × 10 ⁻⁵	CL=90%
Γ_{34} $K^+K^*(892)^-\pi^0 + \text{c.c.}$	< 5.4 × 10 ⁻⁵	CL=90%
Γ_{35} $\phi f_2'(1525)$	< 4.5 × 10 ⁻⁵	CL=90%

Radiative decays

Γ_{36} $\gamma X_{c0}(1P)$	(9.3 ± 0.9) %	
Γ_{37} $\gamma X_{c1}(1P)$	(8.7 ± 0.8) %	
Γ_{38} $\gamma X_{c2}(1P)$	(7.8 ± 0.8) %	
Γ_{39} $\gamma \eta_c(1S)$	(2.8 ± 0.6) × 10 ⁻³	
Γ_{40} $\gamma \eta_c(2S)$		
Γ_{41} $\gamma \pi^0$		
Γ_{42} $\gamma \eta'(958)$	(1.5 ± 0.4) × 10 ⁻⁴	
Γ_{43} $\gamma \eta$	< 9 × 10 ⁻⁵	CL=90%
Γ_{44} $\gamma \gamma$	< 1.6 × 10 ⁻⁴	CL=90%
Γ_{45} $\gamma \eta(1440) \rightarrow \gamma K\bar{K}\pi$	< 1.2 × 10 ⁻⁴	CL=90%

Mode needed for fitting purposes

Γ_{46} 1. - other fit modes	(21 ± 5) %	
------------------------------------	------------	--

See key on page 239

Meson Particle Listings

 $\psi(2S)$

CONSTRAINED FIT INFORMATION

An overall fit to 10 branching ratios uses 17 measurements and one constraint to determine 8 parameters. The overall fit has a $\chi^2 = 9.0$ for 10 degrees of freedom.

The following off-diagonal array elements are the correlation coefficients $\langle \delta x_i \delta x_j \rangle / (\delta x_i \delta x_j)$, in percent, from the fit to the branching fractions, $x_i \equiv \Gamma_i / \Gamma_{\text{total}}$. The fit constrains the x_i whose labels appear in this array to sum to one.

x_7	27						
x_8	17	63					
x_9	2	9	3				
x_{36}	0	0	0	0			
x_{37}	0	-1	-5	0	0		
x_{38}	0	0	-2	0	0	0	
x_{46}	-30	-89	-83	-15	-17	-13	-15
	x_4	x_7	x_8	x_9	x_{36}	x_{37}	x_{38}

 $\psi(2S)$ PARTIAL WIDTHS

$\Gamma(\text{hadrons})$	VALUE (keV)	DOCUMENT ID	TECN	COMMENT	Γ_1	
• • • We do not use the following data for averages, fits, limits, etc. • • •						
	224 ± 56	LUTH	75	MRK1	e^+e^-	
$\Gamma(e^+e^-)$	VALUE (keV)	DOCUMENT ID	TECN	COMMENT	Γ_3	
2.12 ± 0.18 OUR AVERAGE						
	2.07 ± 0.32	⁶ BAI	98E	BES	e^+e^-	
	2.14 ± 0.21	ALEXANDER	89	RVUE	See γ mini-review	
• • • We do not use the following data for averages, fits, limits, etc. • • •						
	2.0 ± 0.3	BRANDELIK	79C	DASP	e^+e^-	
	2.1 ± 0.3	⁷ LUTH	75	MRK1	e^+e^-	
⁶ Value includes radiative corrections computed by ALEXANDER 89.						
⁷ From a simultaneous fit to e^+e^- , $\mu^+\mu^-$, and hadronic channels assuming $\Gamma(e^+e^-) = \Gamma(\mu^+\mu^-)$.						
$\Gamma(\gamma\gamma)$	VALUE (eV)	CL%	DOCUMENT ID	TECN	COMMENT	Γ_{44}
	<43	90	BRANDELIK	79C	DASP	e^+e^-

 $\psi(2S) \Gamma(i)\Gamma(e^+e^-)/\Gamma(\text{total})$

This combination of a partial width with the partial width into e^+e^- and with the total width is obtained from the integrated cross section into channel i in the e^+e^- annihilation. We list only data that have not been used to determine the partial width $\Gamma(i)$ or the branching ratio $\Gamma(i)/\text{total}$.

$\Gamma(\text{hadrons}) \times \Gamma(e^+e^-)/\Gamma_{\text{total}}$	VALUE (keV)	DOCUMENT ID	TECN	COMMENT	$\Gamma_1\Gamma_3/\Gamma$
• • • We do not use the following data for averages, fits, limits, etc. • • •					
	2.2 ± 0.4	ABRAMS	75	MRK1	e^+e^-

 $\psi(2S)$ BRANCHING RATIOS

$\Gamma(\text{hadrons})/\Gamma_{\text{total}}$	VALUE	DOCUMENT ID	TECN	COMMENT	Γ_1/Γ
	0.981 ± 0.003	⁸ LUTH	75	MRK1	e^+e^-
$\Gamma(\text{virtual } \gamma \rightarrow \text{hadrons})/\Gamma_{\text{total}}$	VALUE	DOCUMENT ID	TECN	COMMENT	Γ_2/Γ
	0.029 ± 0.004	⁹ LUTH	75	MRK1	e^+e^-
$\Gamma(e^+e^-)/\Gamma_{\text{total}}$	VALUE (units 10^{-4})	DOCUMENT ID	TECN	COMMENT	Γ_3/Γ
	88 ± 13	¹⁰ FELDMAN	77	RVUE	e^+e^-
• • • We do not use the following data for averages, fits, limits, etc. • • •					
	83 ± 5 ± 7	¹¹ ARMSTRONG	97	E760	$\bar{p}p \rightarrow \psi(2S)X$
$\Gamma(\mu^+\mu^-)/\Gamma_{\text{total}}$	VALUE (units 10^{-4})	DOCUMENT ID	TECN	COMMENT	Γ_4/Γ
	77 ± 17	¹² HILGER	75	SPEC	e^+e^-

 $\Gamma(\mu^+\mu^-)/\Gamma(e^+e^-)$

VALUE	DOCUMENT ID	TECN	COMMENT	Γ_4/Γ_3
0.89 ± 0.16	BOYARSKI	75C	MRK1	e^+e^-

- ⁸Includes cascade decay into $J/\psi(1S)$.
⁹Included in $\Gamma(\text{hadrons})/\Gamma_{\text{total}}$.
¹⁰From an overall fit assuming equal partial widths for e^+e^- and $\mu^+\mu^-$. For a measurement of the ratio see the entry $\Gamma(\mu^+\mu^-)/\Gamma(e^+e^-)$ below. Includes LUTH 75, HILGER 75, BURMESTER 77.
¹¹Using $B(J/\psi \rightarrow e^+e^-) = 0.0599 \pm 0.0025$ and $B(\psi(2S) \rightarrow J/\psi(1S)\text{anything}) = 0.57 \pm 0.04$. Not an independent measurement, see GU 99.
¹²Restated by us using $B(\psi(2S) \rightarrow J/\psi(1S)\text{anything}) = 0.55$.

DECAYS INTO $J/\psi(1S)$ AND ANYTHING

$\Gamma(J/\psi(1S)\text{anything})/\Gamma_{\text{total}}$	VALUE	DOCUMENT ID	TECN	COMMENT	$\Gamma_5/\Gamma = (\Gamma_7 + \Gamma_8 + \Gamma_9 + 0.273\Gamma_{37} + 0.135\Gamma_{38})/\Gamma$
0.55 ± 0.06 OUR FIT					
0.55 ± 0.07 OUR AVERAGE					
	0.51 ± 0.12	BRANDELIK	79C	DASP	$e^+e^- \rightarrow \mu^+\mu^-X$
	0.57 ± 0.08	ABRAMS	75B	MRK1	$e^+e^- \rightarrow \mu^+\mu^-X$

 $\Gamma(J/\psi(1S)\text{neutrals})/\Gamma_{\text{total}}$

VALUE	DOCUMENT ID	TECN	COMMENT	$\Gamma_6/\Gamma = (0.9761\Gamma_8 + 0.715\Gamma_9 + 0.273\Gamma_{37} + 0.135\Gamma_{38})/\Gamma$
0.231 ± 0.023	OUR FIT			

$\Gamma(J/\psi(1S)\text{neutrals})/\Gamma(J/\psi(1S)\text{anything})$	VALUE	DOCUMENT ID	TECN	COMMENT	$\Gamma_6/\Gamma_5 = (0.9761\Gamma_8 + 0.715\Gamma_9 + 0.273\Gamma_{37} + 0.135\Gamma_{38})/(\Gamma_7 + \Gamma_8 + \Gamma_9 + 0.273\Gamma_{37} + 0.135\Gamma_{38})$
0.418 ± 0.019 OUR FIT					

- • • We do not use the following data for averages, fits, limits, etc. • • •
- | | | | | |
|-------------|----------------------|-----|------|-------------------------------|
| 0.44 ± 0.03 | ¹³ ABRAMS | 75B | MRK1 | $e^+e^- \rightarrow J/\psi X$ |
|-------------|----------------------|-----|------|-------------------------------|

 $\Gamma(J/\psi(1S)\text{neutrals})/\Gamma(J/\psi(1S)\pi^+\pi^-)$

VALUE	DOCUMENT ID	TECN	COMMENT	$\Gamma_6/\Gamma_7 = (0.9761\Gamma_8 + 0.715\Gamma_9 + 0.273\Gamma_{37} + 0.135\Gamma_{38})/\Gamma_7$
0.75 ± 0.06 OUR FIT				
0.73 ± 0.09				
	¹³ TANENBAUM	76	MRK1	e^+e^-

 $\Gamma(J/\psi(1S)\pi^+\pi^-)/\Gamma_{\text{total}}$

VALUE	EVTS	DOCUMENT ID	TECN	COMMENT	Γ_7/Γ
0.310 ± 0.028 OUR FIT					
0.32 ± 0.04					
		ABRAMS	75B	MRK1	$e^+e^- \rightarrow J/\psi\pi^+\pi^-$
• • • We do not use the following data for averages, fits, limits, etc. • • •					
	0.283 ± 0.021 ± 0.020	363	¹⁴ ARMSTRONG	97 E760	$\bar{p}p \rightarrow \psi(2S)X$

 $\Gamma(J/\psi(1S)\pi^0\pi^0)/\Gamma_{\text{total}}$

VALUE	EVTS	DOCUMENT ID	TECN	COMMENT	Γ_8/Γ
0.182 ± 0.023 OUR FIT					
• • • We do not use the following data for averages, fits, limits, etc. • • •					
	0.184 ± 0.019 ± 0.013	157	¹⁴ ARMSTRONG	97 E760	$\bar{p}p \rightarrow \psi(2S)X$

 $\Gamma(J/\psi(1S)\pi^0\pi^0)/\Gamma(J/\psi(1S)\pi^+\pi^-)$

VALUE	DOCUMENT ID	TECN	COMMENT	Γ_8/Γ_7	
0.59 ± 0.06 OUR FIT					
0.609 ± 0.079					
	¹⁵ GU	99	RVUE		
• • • We do not use the following data for averages, fits, limits, etc. • • •					
	0.53 ± 0.06	¹⁶ TANENBAUM	76	MRK1	e^+e^-
	0.64 ± 0.15	¹⁷ HILGER	75	SPEC	e^+e^-

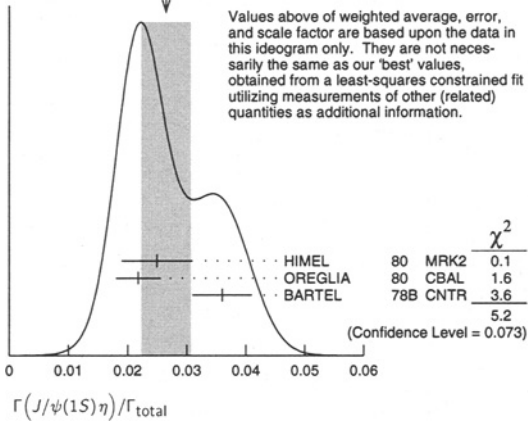
 $\Gamma(J/\psi(1S)\pi^+\pi^-)/\Gamma(\mu^+\mu^-)$

VALUE	DOCUMENT ID	TECN	COMMENT	Γ_7/Γ_4
30 ± 10 OUR FIT				
30.2 ± 7.1 ± 6.8				
	¹⁸ GRIBUSHIN	96	FMPS	515 $\pi^-Be \rightarrow 2\mu X$

 $\Gamma(J/\psi(1S)\eta)/\Gamma_{\text{total}}$

VALUE	EVTS	DOCUMENT ID	TECN	COMMENT	Γ_9/Γ	
0.027 ± 0.004 OUR FIT Error includes scale factor of 1.6.						
0.027 ± 0.004 OUR AVERAGE Error includes scale factor of 1.6. See the ideogram below.						
	0.025 ± 0.006	166	HIMEL	80	MRK2	e^+e^-
	0.0218 ± 0.0014 ± 0.0035	386	OREGLIA	80	CBAL	$e^+e^- \rightarrow J/\psi 2\gamma$
	0.036 ± 0.005	164	BARTEL	78B	CNTR	e^+e^-
• • • We do not use the following data for averages, fits, limits, etc. • • •						
	0.032 ± 0.010 ± 0.002	36	¹⁹ ARMSTRONG	97	E760	$\bar{p}p \rightarrow \psi(2S)X$
	0.035 ± 0.009	17	¹⁹ BRANDELIK	79B	DASP	$e^+e^- \rightarrow J/\psi 2\gamma$
	0.043 ± 0.008	44	¹⁹ TANENBAUM	76	MRK1	e^+e^-

Meson Particle Listings

 $\psi(2S)$ WEIGHTED AVERAGE
0.027±0.004 (Error scaled by 1.6) $\Gamma(J/\psi(1S)\eta)/\Gamma(J/\psi(1S)\text{anything})$ $\Gamma_9/\Gamma_5 = \Gamma_9/(\Gamma_7 + \Gamma_8 + \Gamma_9 + 0.273\Gamma_{37} + 0.135\Gamma_{38})$

VALUE	DOCUMENT ID	TECN
0.049±0.008 OUR FIT		
0.062±0.016	19 GU	99 RVUE

Error includes scale factor of 1.3.

 $\Gamma(J/\psi(1S)\pi^0)/\Gamma_{\text{total}}$

VALUE (units 10^{-4})	EVTs	DOCUMENT ID	TECN	COMMENT	Γ_{10}/Γ
9.7±2.1 OUR AVERAGE					
15 ± 6	7	HIMEL	80 MRK2	e^+e^-	
9 ± 2 ± 1	23	OREGLIA	80 CBAL	$\psi(2S) \rightarrow J/\psi 2\gamma$	

¹³ The ABRAMS 75B measurement of Γ_6/Γ_5 and the TANENBAUM 76 result for Γ_6/Γ_7 are not independent. The TANENBAUM 76 result is used in the fit because it includes more accurate corrections for angular distributions.

¹⁴ Using $B(J/\psi \rightarrow e^+e^-) = 0.0599 \pm 0.0025$ and $B(\psi(2S) \rightarrow J/\psi(1S)\text{anything}) = 0.57 \pm 0.04$.

¹⁵ Using data from ARMSTRONG 97.

¹⁶ Not independent of the TANENBAUM 76 result for Γ_6/Γ_7 .

¹⁷ Ignoring the $J/\psi(1S)\eta$ and $J/\psi(1S)\gamma\gamma$ decays.

¹⁸ Using $B(J/\psi(1S) \rightarrow \mu^+\mu^-) = 0.0597 \pm 0.0025$.

¹⁹ Low statistics data removed from average.

HADRONIC DECAYS

 $\Gamma(3(\pi^+\pi^-\pi^0))/\Gamma_{\text{total}}$

VALUE (units 10^{-4})	EVTs	DOCUMENT ID	TECN	COMMENT	Γ_{11}/Γ
35±16	6	FRANKLIN	83 MRK2	$e^+e^- \rightarrow \text{hadrons}$	

 $\Gamma(2(\pi^+\pi^-\pi^0))/\Gamma_{\text{total}}$

VALUE (units 10^{-4})	EVTs	DOCUMENT ID	TECN	COMMENT	Γ_{12}/Γ
30±8	42	FRANKLIN	83 MRK2	e^+e^-	

 $\Gamma(\pi^+\pi^-K^+K^-)/\Gamma_{\text{total}}$

VALUE (units 10^{-4})	DOCUMENT ID	TECN	COMMENT	Γ_{15}/Γ
16±4	20 TANENBAUM 78	MRK1	e^+e^-	

 $\Gamma(K_1(1270)^\pm K^\mp)/\Gamma_{\text{total}}$

VALUE (units 10^{-4})	DOCUMENT ID	TECN	COMMENT	Γ_{17}/Γ
10.0±1.8±2.1	21 BAI	99c BES	e^+e^-	

 $\Gamma(\pi^+\pi^-p\bar{p})/\Gamma_{\text{total}}$

VALUE (units 10^{-4})	DOCUMENT ID	TECN	COMMENT	Γ_{18}/Γ
8 ± 2	20 TANENBAUM 78	MRK1	e^+e^-	

 $\Gamma(K^+K^*(892)^0\pi^- + \text{c.c.})/\Gamma_{\text{total}}$

VALUE (units 10^{-4})	DOCUMENT ID	TECN	COMMENT	Γ_{19}/Γ
6.7±2.5	TANENBAUM 78	MRK1	e^+e^-	

 $\Gamma(b_1^\pm \pi^\mp)/\Gamma_{\text{total}}$

VALUE (units 10^{-4})	DOCUMENT ID	TECN	COMMENT	Γ_{20}/Γ
5.2±0.8±1.0	22 BAI	99c BES	e^+e^-	

 $\Gamma(2(\pi^+\pi^-))/\Gamma_{\text{total}}$

VALUE (units 10^{-4})	DOCUMENT ID	TECN	COMMENT	Γ_{21}/Γ
4.5±1.0	TANENBAUM 78	MRK1	e^+e^-	

 $\Gamma(\omega f_2(1270))/\Gamma_{\text{total}}$

VALUE (units 10^{-4})	CL%	DOCUMENT ID	TECN	COMMENT	Γ_{13}/Γ
<1.7	90	BAI	98J BES	e^+e^-	

 $\Gamma(\rho^0\pi^+\pi^-)/\Gamma_{\text{total}}$

VALUE (units 10^{-4})	DOCUMENT ID	TECN	COMMENT	Γ_{22}/Γ
4.2±1.5	TANENBAUM 78	MRK1	e^+e^-	

 $\Gamma(\rho\omega(1320))/\Gamma_{\text{total}}$

VALUE (units 10^{-4})	CL%	DOCUMENT ID	TECN	COMMENT	Γ_{14}/Γ
<2.3	90	BAI	98J BES	e^+e^-	

 $\Gamma(\bar{p}\rho)/\Gamma_{\text{total}}$

VALUE (units 10^{-4})	EVTs	DOCUMENT ID	TECN	COMMENT	Γ_{23}/Γ
1.9±0.5 OUR AVERAGE					
1.4±0.8	4	BRANDELIK	79c DASP	e^+e^-	
2.3±0.7		FELDMAN	77 MRK1	e^+e^-	

 $\Gamma(3(\pi^+\pi^-))/\Gamma_{\text{total}}$

VALUE (units 10^{-4})	DOCUMENT ID	TECN	COMMENT	Γ_{24}/Γ
1.5±1.0	20 TANENBAUM 78	MRK1	e^+e^-	

 $\Gamma(\bar{p}\rho\pi^0)/\Gamma_{\text{total}}$

VALUE (units 10^{-4})	EVTs	DOCUMENT ID	TECN	COMMENT	Γ_{25}/Γ
1.4±0.5	9	FRANKLIN	83 MRK2	e^+e^-	

 $\Gamma(K^+K^-)/\Gamma_{\text{total}}$

VALUE (units 10^{-4})	CL%	DOCUMENT ID	TECN	COMMENT	Γ_{26}/Γ
1.0±0.7		BRANDELIK	79c DASP	e^+e^-	

• • • We do not use the following data for averages, fits, limits, etc. • • •

VALUE	CL%	DOCUMENT ID	TECN	COMMENT	Γ_{29}/Γ
<0.5	90	FELDMAN	77 MRK1	e^+e^-	

 $\Gamma(\pi^+\pi^-)/\Gamma_{\text{total}}$

VALUE (units 10^{-4})	CL%	DOCUMENT ID	TECN	COMMENT	Γ_{29}/Γ
0.8±0.5		BRANDELIK	79c DASP	e^+e^-	

• • • We do not use the following data for averages, fits, limits, etc. • • •

VALUE	CL%	DOCUMENT ID	TECN	COMMENT	Γ_{29}/Γ
<0.5	90	FELDMAN	77 MRK1	e^+e^-	

 $\Gamma(\pi^+\pi^-\pi^0)/\Gamma_{\text{total}}$

VALUE (units 10^{-4})	EVTs	DOCUMENT ID	TECN	COMMENT	Γ_{27}/Γ
0.85±0.46	4	FRANKLIN	83 MRK2	$e^+e^- \rightarrow \text{hadrons}$	

 $\Gamma(\Lambda\Lambda)/\Gamma_{\text{total}}$

VALUE (units 10^{-4})	CL%	DOCUMENT ID	TECN	COMMENT	Γ_{30}/Γ
<4	90	FELDMAN	77 MRK1	e^+e^-	

 $\Gamma(K_1(1400)^\pm K^\mp)/\Gamma_{\text{total}}$

VALUE (units 10^{-4})	CL%	DOCUMENT ID	TECN	COMMENT	Γ_{31}/Γ
<3.1	90	23 BAI	99c BES	e^+e^-	

 $\Gamma(\Xi^-\Xi^+)/\Gamma_{\text{total}}$

VALUE (units 10^{-4})	CL%	DOCUMENT ID	TECN	COMMENT	Γ_{32}/Γ
<2	90	FELDMAN	77 MRK1	e^+e^-	

 $\Gamma(\rho\pi)/\Gamma_{\text{total}}$

VALUE (units 10^{-4})	CL%	EVTs	DOCUMENT ID	TECN	COMMENT	Γ_{28}/Γ
< 0.83	90	1	FRANKLIN	83 MRK2	e^+e^-	

• • • We do not use the following data for averages, fits, limits, etc. • • •

VALUE	CL%	DOCUMENT ID	TECN	COMMENT	Γ_{28}/Γ
<10	90	BARTEL	76 CNTR	e^+e^-	
<10	90	24 ABRAMS	75 MRK1	e^+e^-	

 $\Gamma(K^+K^-\pi^0)/\Gamma_{\text{total}}$

VALUE (units 10^{-5})	CL%	EVTs	DOCUMENT ID	TECN	COMMENT	Γ_{33}/Γ
<2.96	90	1	FRANKLIN	83 MRK2	$e^+e^- \rightarrow \text{hadrons}$	

 $\Gamma(K^+K^*(892)^-\pi^0 + \text{c.c.})/\Gamma_{\text{total}}$

VALUE (units 10^{-5})	CL%	DOCUMENT ID	TECN	COMMENT	Γ_{34}/Γ
<5.4	90	FRANKLIN	83 MRK2	$e^+e^- \rightarrow \text{hadrons}$	

 $\Gamma(K^*(892)\bar{K}_2^*(1430)^0)/\Gamma_{\text{total}}$

VALUE (units 10^{-4})	CL%	DOCUMENT ID	TECN	COMMENT	Γ_{16}/Γ
<1.2	90	BAI	98J BES	e^+e^-	

 $\Gamma(\phi f_2(1525))/\Gamma_{\text{total}}$

VALUE (units 10^{-4})	CL%	DOCUMENT ID	TECN	COMMENT	Γ_{35}/Γ
<0.45	90	BAI	98J BES	$e^+e^- \rightarrow 2(K^+K^-)$	

²⁰ Assuming entirely strong decay.

²¹ Assuming $B(K_1(1270) \rightarrow K\rho) = 0.42 \pm 0.06$

²² Assuming $B(b_1 \rightarrow \omega\pi) = 1$.

²³ Assuming $B(K_1(1400) \rightarrow K^*\pi) = 0.94 \pm 0.06$

²⁴ Final state $\rho^0\pi^0$.

See key on page 239

Meson Particle Listings

$\psi(2S), \psi(3770)$

RADIATIVE DECAYS

$\Gamma(\gamma\chi_{c0}(1P))/\Gamma_{total}$ Γ_{36}/Γ
 VALUE (units 10^{-2}) DOCUMENT ID TECN COMMENT

9.3±0.9 OUR FIT
9.3±0.8 OUR AVERAGE

9.9±0.5±0.8
 7.2±2.3
 7.5±2.6

25	GAISER	86	CBAL	$e^+e^- \rightarrow \gamma X$
29	BIDDICK	77	CNTR	$e^+e^- \rightarrow \gamma X$
25	WHITAKER	76	MRK1	e^+e^-

$\Gamma(\gamma\chi_{c1}(1P))/\Gamma_{total}$ Γ_{37}/Γ
 VALUE (units 10^{-2}) DOCUMENT ID TECN COMMENT

8.7±0.8 OUR FIT
8.7±0.8 OUR AVERAGE

9.0±0.5±0.7
 7.1±1.9

26	GAISER	86	CBAL	$e^+e^- \rightarrow \gamma X$
27	BIDDICK	77	CNTR	$e^+e^- \rightarrow \gamma X$

$\Gamma(\gamma\chi_{c2}(1P))/\Gamma_{total}$ Γ_{38}/Γ
 VALUE (units 10^{-2}) DOCUMENT ID TECN COMMENT

7.8±0.8 OUR FIT
7.8±0.8 OUR AVERAGE

8.0±0.5±0.7
 7.0±2.0

28	GAISER	86	CBAL	$e^+e^- \rightarrow \gamma X$
27	BIDDICK	77	CNTR	$e^+e^- \rightarrow \gamma X$

$\Gamma(\gamma\eta_c(1S))/\Gamma_{total}$ Γ_{39}/Γ
 VALUE (units 10^{-2}) DOCUMENT ID TECN COMMENT

0.28±0.06

GAISER	86	CBAL	$e^+e^- \rightarrow \gamma X$
--------	----	------	-------------------------------

$\Gamma(\gamma\eta_c(2S))/\Gamma_{total}$ Γ_{40}/Γ
 VALUE (units 10^{-2}) CL% DOCUMENT ID TECN COMMENT

0.2 to 1.3 95 EDWARDS 82c CBAL $e^+e^- \rightarrow \gamma X$

$\Gamma(\gamma\pi^0)/\Gamma_{total}$ Γ_{41}/Γ
 VALUE (units 10^{-4}) CL% DOCUMENT ID TECN COMMENT

0.0 to 0.1 90 29 LIBERMAN 75 SPEC e^+e^-
 <100 90 WIHK 75 DASP e^+e^-

$\Gamma(\gamma\eta'(958))/\Gamma_{total}$ Γ_{42}/Γ
 VALUE (units 10^{-4}) CL% EVTS DOCUMENT ID TECN COMMENT

1.54±0.31±0.20 ~ 43 BAI 98F BES $\psi(2S) \rightarrow \pi^+\pi^-2\gamma, \pi^+\pi^-3\gamma$

0.0 to 0.1 90 30 BRAUNSCH... 77 DASP e^+e^-
 <11 90 31 BARTEL 76 CNTR e^+e^-

$\Gamma(\gamma\eta)/\Gamma_{total}$ Γ_{43}/Γ
 VALUE (units 10^{-4}) CL% DOCUMENT ID TECN COMMENT

<0.9 90 BAI 98F BES $\psi(2S) \rightarrow \pi^+\pi^-3\gamma$
 <2 90 YAMADA 77 DASP $e^+e^- \rightarrow 3\gamma$

$\Gamma(\gamma\eta(1440) \rightarrow \gamma K \bar{K} \pi)/\Gamma_{total}$ Γ_{45}/Γ
 VALUE (units 10^{-3}) CL% DOCUMENT ID TECN COMMENT

<0.12 90 32 SCHARRE 80 MRK1 e^+e^-

- 25 Angular distribution $(1+\cos^2\theta)$ assumed.
- 26 Angular distribution $(1-0.189\cos^2\theta)$ assumed.
- 27 Valid for isotropic distribution of the photon.
- 28 Angular distribution $(1-0.052\cos^2\theta)$ assumed.
- 29 Restated by us using $B(\psi(2S) \rightarrow \mu^+\mu^-) = 0.0077$.
- 30 Restated by us using total decay width 228 keV.
- 31 The value is normalized to the branching ratio for $\Gamma(J/\psi(1S)\eta)/\Gamma_{total}$.
- 32 Includes unknown branching fraction $\eta(1440) \rightarrow K \bar{K} \pi$.

$\psi(2S)$ REFERENCES

ARTAMONOV	00	PL B474 427	A.S. Artamonov et al.	
BAI	99C	PRL 83 1918	J.Z. Bai et al.	(BES Collab.)
GU	99	PL B449 361	Y.F. Gu, X.H. Li	
BAI	98E	PR D57 3854	J.Z. Bai et al.	(BES Collab.)
BAI	98F	PR D58 097101	J.Z. Bai et al.	(BES Collab.)
BAI	98J	PRL 81 5080	J.Z. Bai et al.	(BES Collab.)
ARMSTRONG	97	PR D55 1153	T.A. Armstrong et al.	(E760 Collab.)
GRIBUSHIN	96	PR D53 4723	A. Gribushin et al.	
ANTONIAZZI	94	PR D50 4258	L. Antoniazzi et al.	(E705 Collab.)
ARMSTRONG	93B	PR D47 772	T.A. Armstrong et al.	(FNAL E760 Collab.)
PDG	92	PR D45, I June, Part II	K. Hikasa et al.	(KEK, LBL, BOST+)
ALEXANDER	89	NP B320 45	J.P. Alexander et al.	(LBL, MICH, SLAC)
COHEN	87	RMP 59 1121	E.R. Cohen, B.N. Taylor	(RISC, NBS)
GAISER	86	PR D34 711	J. Gaiser et al.	(Crystal Ball Collab.)
KURAEV	85	SJNP 41 466	E.A. Kurayev, V.S. Fadin	(NOVO)

Translated from YAF 41 733.

FRANKLIN	83	PRL 51 963	M.E.B. Franklin et al.	(LBL, SLAC)
EDWARDS	82C	PRL 48 79	C. Edwards et al.	(CIT, HARV, PRIN+)
LEMOIGNE	82	PL 1138 509	Y. Lemoigne et al.	(SACL, LOIC, SHMP+)
HIMEL	80	PRL 44 920	T. Himel et al.	(LBL, SLAC)
OREGLIA	80	PRL 45 959	M.J. Oreglia et al.	(SLAC, CIT, HARV+)
SCHARRE	80	PL 97B 329	D.L. Scharre et al.	(SLAC, LBL)
ZHOLENTZ	80	PL 96B 214	A.A. Zholents et al.	(NOVO)
Also	81	SJNP 34 814	A.A. Zholents et al.	(NOVO)
BRANDELK	79B	NP B160 426	R. Brandelik et al.	(DASP Collab.)
BRANDELK	79C	ZPHY C1 233	R. Brandelik et al.	(DASP Collab.)
BARTEL	78B	PL 79B 492	W. Bartel et al.	(DESY, HEIDP)
TANENBAUM	78	PR D17 1731	W.M. Tanenbaum et al.	(SLAC, LBL)
BIDDICK	77	PRL 38 1324	C.J. Biddick et al.	(UCSD, UMD, PAVI+)
BRAUNSCH...	77	PL 67B 249	W. Braunschweig et al.	(DASP Collab.)
BURMESTER	77	PL 66B 395	J. Burmester et al.	(DESY, HAMB, SIEG+)
FELDMAN	77	PRPL 33C 285	G.J. Feldman, M.L. Peri	(LBL, SLAC)
YAMADA	77	Hamburg Conf. 69	S. Yamada	(DASP Collab.)
BARTEL	76	PL 64B 483	W. Bartel et al.	(DESY, HEIDP)
TANENBAUM	76	PRL 36 402	W.M. Tanenbaum et al.	(SLAC, LBL) IG
WHITAKER	76	PRL 37 1596	J.S. Whitaker et al.	(SLAC, LBL)
ABRAMS	75	Stanford Symp. 25	G.S. Abrams	(LBL)
ABRAMS	75B	PRL 34 1181	G.S. Abrams et al.	(LBL, SLAC)
BOYARSKI	75C	Palermo Conf. 54	A.M. Boyarski et al.	(SLAC, LBL)
HILGER	75	PRL 35 625	E. Hilger et al.	(STAN, PENN)
LIBERMAN	75	Stanford Symp. 55	A.D. Liberman	(STAN)
LUTH	75	PRL 35 1124	V. Luth et al.	(SLAC, LBL) JPC
WIHK	75	Stanford Symp. 69	B.H. Wiik	(DESY)

OTHER RELATED PAPERS

CHEN	98	PRL 80 5060	Y.Q. Chen, E. Braaten	
SUZUKI	98	PR D57 5717	M. Suzuki	
HOU	97	PR D55 6952	Wei-Shu Hou	
BARATE	83	PL 121B 449	R. Barate et al.	(SACL, LOIC, SHMP, IND)
AUBERT	75B	PRL 33 1624	J.J. Aubert et al.	(MIT, BNL)
BRAUNSCH...	75B	PL 57B 407	W. Braunschweig et al.	(DASP Collab.)
CAMERINI	75	PRL 35 483	U. Camerini et al.	(WISC, SLAC)
FELDMAN	75B	PRL 35 821	G.J. Feldman et al.	(LBL, SLAC)
GRECO	75	PL 56B 367	M. Greco, G. Pancheri-Srivastava, Y. Srivastava	
JACKSON	75	NIM 128 13	J.D. Jackson, D.L. Scharre	(LBL)
SIMPSON	75	PRL 35 699	J.W. Simpson et al.	(STAN, PENN)
ABRAMS	74	PRL 33 1453	G.S. Abrams et al.	(LBL, SLAC)

$\psi(3770)$

$J^{PC} = 0^{-}(1^{-}-)$

$\psi(3770)$ MASS

VALUE (MeV) DOCUMENT ID TECN COMMENT

3769.9±2.5 OUR EVALUATION Error includes scale factor of 1.8. From $m_{\psi(2S)}$ and mass difference below.

0.0 to 0.1 90 30 BRAUNSCH... 77 DASP e^+e^-
 <100 90 WIHK 75 DASP e^+e^-

3764 ± 5 ¹ SCHINDLER 80 MRK2 e^+e^-
 3770 ± 6 ¹ BACINO 78 DLCO e^+e^-
 3772 ± 6 ¹ RAPIDIS 77 MRK1 e^+e^-

¹ Errors include systematic common to all experiments.

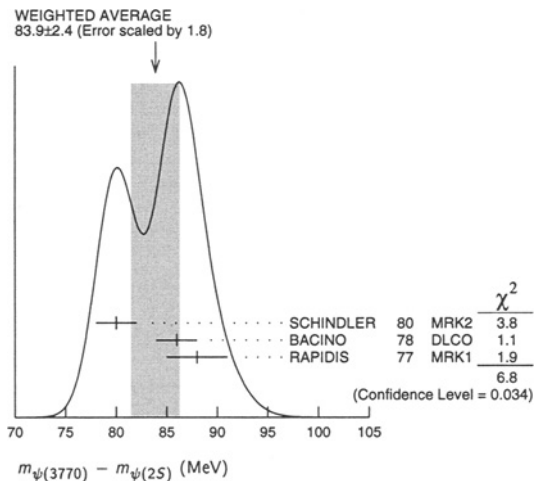
$m_{\psi(3770)} - m_{\psi(2S)}$

VALUE (MeV) DOCUMENT ID TECN COMMENT

83.9±2.4 OUR AVERAGE Error includes scale factor of 1.8. See the ideogram below.

80 ± 2 SCHINDLER 80 MRK2 e^+e^-
 86 ± 2 ² BACINO 78 DLCO e^+e^-
 88 ± 3 RAPIDIS 77 MRK1 e^+e^-

² SPEAR $\psi(2S)$ mass subtracted (see SCHINDLER 80).



Meson Particle Listings

 $\psi(3770)$, $\psi(3836)$, $\psi(4040)$ $\psi(3770)$ WIDTH

VALUE (MeV)	DOCUMENT ID	TECN	COMMENT
23.6 ± 2.7 OUR FIT	Error includes scale factor of 1.1.		
25.3 ± 2.9 OUR AVERAGE			
24 ± 5	SCHINDLER	80 MRK2	e^+e^-
24 ± 5	BACINO	78 DLCO	e^+e^-
28 ± 5	RAPIDIS	77 MRK1	e^+e^-

 $\psi(3770)$ DECAY MODES

Mode	Fraction (Γ_i/Γ)	Scale factor
Γ_1 $D\bar{D}$	dominant	
Γ_2 e^+e^-	$(1.12 \pm 0.17) \times 10^{-5}$	1.2

 $\psi(3770)$ PARTIAL WIDTHS

$\Gamma(e^+e^-)$	DOCUMENT ID	TECN	COMMENT	Γ_2
0.26 ± 0.04 OUR FIT	Error includes scale factor of 1.2.			
0.24 ± 0.05 OUR AVERAGE	Error includes scale factor of 1.2.			
0.276 ± 0.050	SCHINDLER	80 MRK2	e^+e^-	
0.18 ± 0.06	BACINO	78 DLCO	e^+e^-	
• • • We do not use the following data for averages, fits, limits, etc. • • •				
0.37 ± 0.09	³ RAPIDIS	77 MRK1	e^+e^-	
³ See also $\Gamma(e^+e^-)/\Gamma_{\text{total}}$ below.				

 $\psi(3770)$ BRANCHING RATIOS

$\Gamma(D\bar{D})/\Gamma_{\text{total}}$	DOCUMENT ID	TECN	COMMENT	Γ_1/Γ
dominant	PERUZZI	77 MRK1	$e^+e^- \rightarrow D\bar{D}$	

$\Gamma(e^+e^-)/\Gamma_{\text{total}}$	DOCUMENT ID	TECN	COMMENT	Γ_2/Γ
1.12 ± 0.17 OUR FIT	Error includes scale factor of 1.2.			
1.3 ± 0.2	RAPIDIS	77 MRK1	e^+e^-	

 $\psi(3770)$ REFERENCES

SCHINDLER	80	PR D21 2716	R.H. Schindler <i>et al.</i>	(Mark II Collab.)
BACINO	78	PRL 40 671	W.J. Bacino <i>et al.</i>	(SLAC, UCLA, UC)
PERUZZI	77	PRL 39 1301	I. Peruzzi <i>et al.</i>	(Mark I Collab.)
RAPIDIS	77	PRL 39 526	P.A. Rapidis <i>et al.</i>	(Mark I Collab.)

 $\psi(3836)$

$$I^G(J^{PC}) = 0^-(2^{--})$$

OMITTED FROM SUMMARY TABLE
Quantum numbers are not established.

Seen in $\pi^\pm \text{Li}$ interactions by ANTONIAZZI 94 as a peak in the invariant mass of the $J/\psi(1S)\pi^+\pi^-$ system. Possibly seen also in $p\text{Li}$ interactions. Interpretation as a $^3D_2(2^{--})$ charmonium state favored. Not seen by BAI 98E in e^+e^- interactions. Needs confirmation.

 $\psi(3836)$ MASS

VALUE (MeV)	EVTS	DOCUMENT ID	TECN	COMMENT
3836 ± 13	58 ± 21	ANTONIAZZI 94	E705	$\pi^\pm \text{Li} \rightarrow J/\psi \pi^+ \pi^- X$

 $\psi(3836)$ DECAY MODES

Mode	Fraction (Γ_i/Γ)
Γ_1 $J/\psi(1S)\pi^+\pi^-$	seen

 $\psi(3836)$ REFERENCES

BAI	98E	PR D57 3854	J.Z. Bai <i>et al.</i>	(BES Collab.)
ANTONIAZZI	94	PR D50 4258	L. Antoniazzi <i>et al.</i>	(E705 Collab.)

 $\psi(4040)$

$$I^G(J^{PC}) = 0^-(1^{--})$$

 $\psi(4040)$ MASS

VALUE (MeV)	DOCUMENT ID	TECN	COMMENT
4040 ± 10	BRANDELIK	78c DASP	e^+e^-

 $\psi(4040)$ WIDTH

VALUE (MeV)	DOCUMENT ID	TECN	COMMENT
52 ± 10	BRANDELIK	78c DASP	e^+e^-

 $\psi(4040)$ DECAY MODES

Mode	Fraction (Γ_i/Γ)
Γ_1 e^+e^-	$(1.4 \pm 0.4) \times 10^{-5}$
Γ_2 $D^0\bar{D}^0$	seen
Γ_3 $D^*(2007)^0\bar{D}^0 + \text{c.c.}$	seen
Γ_4 $D^*(2007)^0\bar{D}^*(2007)^0$	seen
Γ_5 $J/\psi(1S)$ hadrons	
Γ_6 $\mu^+\mu^-$	

 $\psi(4040)$ PARTIAL WIDTHS

$\Gamma(e^+e^-)$	DOCUMENT ID	TECN	COMMENT	Γ_1
0.75 ± 0.15	BRANDELIK	78c DASP	e^+e^-	

 $\psi(4040)$ BRANCHING RATIOS

$\Gamma(e^+e^-)/\Gamma_{\text{total}}$	DOCUMENT ID	TECN	COMMENT	Γ_1/Γ
1.12 ± 0.17 OUR FIT	Error includes scale factor of 1.2.			
1.3 ± 0.2	RAPIDIS	77 MRK1	e^+e^-	

$\Gamma(D^0\bar{D}^0)/\Gamma(D^*(2007)^0\bar{D}^0 + \text{c.c.})$	DOCUMENT ID	TECN	COMMENT	Γ_2/Γ_3
0.05 ± 0.03	¹ GOLDHABER	77 MRK1	e^+e^-	

$\Gamma(D^*(2007)^0\bar{D}^*(2007)^0)/\Gamma(D^*(2007)^0\bar{D}^0 + \text{c.c.})$	DOCUMENT ID	TECN	COMMENT	Γ_4/Γ_3
32.0 ± 12.0	¹ GOLDHABER	77 MRK1	e^+e^-	

¹Phase-space factor (p^3) explicitly removed.

 $\psi(4040)$ REFERENCES

BRANDELIK	78c	PL 76B 361	R. Brandelik <i>et al.</i>	(DASP Collab.)
Also	79c	ZPHY C1 233	R. Brandelik <i>et al.</i>	(DASP Collab.)
FELDMAN	77	PRPL 33C 285	G.J. Feldman, M.L. Perl	(LBL, SLAC)
GOLDHABER	77	PL 69B 503	G. Goldhaber <i>et al.</i>	(Mark I Collab.)

OTHER RELATED PAPERS

HEIKKILA	84	PR D29 110	K. Heikkila, N.A. Tornqvist, S. Ono	(HELS, AACHT)
ONO	84	ZPHY C26 307	S. Ono	(ORSAY)
SIEGRIST	82	PR D26 969	J.L. Siegrist <i>et al.</i>	(SLAC, LBL)
AUGUSTIN	75	PRL 34 764	J.E. Augustin <i>et al.</i>	(SLAC, LBL)
BACCI	75	PL 58B 481	C. Bacci <i>et al.</i>	(ROMA, FRAS)
BOYARSKI	75B	PRL 34 762	A.M. Boyarski <i>et al.</i>	(SLAC, LBL)
ESPOSITO	75	PL 58B 478	B. Esposito <i>et al.</i>	(FRAS, NAPL, PADO+)

See key on page 239

Meson Particle Listings

 $\psi(4160)$, $\psi(4415)$

$\psi(4160)$		$J^{PC} = 0^{-}(1^{-}-)$	
$\psi(4160)$ MASS			
VALUE (MeV)	DOCUMENT ID	TECN	COMMENT
4159 ± 20	BRANDELIK	78c DASP	e^+e^-
$\psi(4160)$ WIDTH			
VALUE (MeV)	DOCUMENT ID	TECN	COMMENT
78 ± 20	BRANDELIK	78c DASP	e^+e^-
$\psi(4160)$ DECAY MODES			
Mode	Fraction (Γ_i/Γ)		
Γ_1 e^+e^-	$(10 \pm 4) \times 10^{-6}$		
$\psi(4160)$ PARTIAL WIDTHS			
$\Gamma(e^+e^-)$			Γ_1
VALUE (keV)	DOCUMENT ID	TECN	COMMENT
0.77 ± 0.23	BRANDELIK	78c DASP	e^+e^-
$\psi(4160)$ REFERENCES			
BRANDELIK	78c	PL 76B 361	R. Brandelik <i>et al.</i> (DASP Collab.)
OTHER RELATED PAPERS			
IDDIR	98	PL B433 125	F. Iddir <i>et al.</i>
ONO	84	ZPHY C26 307	S. Ono (ORSAY)
BURMESTER	77	PL 66B 395	J. Burmester <i>et al.</i> (DESY, HAMB, SIEG+)

$\psi(4415)$		$J^{PC} = 0^{-}(1^{-}-)$	
$\psi(4415)$ MASS			
VALUE (MeV)	DOCUMENT ID	TECN	COMMENT
4415 ± 6 OUR AVERAGE			
4417 ± 10	BRANDELIK	78c DASP	e^+e^-
4414 ± 7	SIEGRIST	76 MRK1	e^+e^-
$\psi(4415)$ WIDTH			
VALUE (MeV)	DOCUMENT ID	TECN	COMMENT
43 ± 15 OUR AVERAGE	Error includes scale factor of 1.8.		
66 ± 15	BRANDELIK	78c DASP	e^+e^-
33 ± 10	SIEGRIST	76 MRK1	e^+e^-
$\psi(4415)$ DECAY MODES			
Mode	Fraction (Γ_i/Γ)		
Γ_1 hadrons	dominant		
Γ_2 e^+e^-	$(1.1 \pm 0.4) \times 10^{-5}$		
$\psi(4415)$ PARTIAL WIDTHS			
$\Gamma(e^+e^-)$			Γ_2
VALUE (keV)	DOCUMENT ID	TECN	COMMENT
0.47 ± 0.10 OUR AVERAGE			
0.49 ± 0.13	BRANDELIK	78c DASP	e^+e^-
0.44 ± 0.14	SIEGRIST	76 MRK1	e^+e^-
$\psi(4415)$ BRANCHING RATIOS			
$\Gamma(\text{hadrons})/\Gamma_{\text{total}}$			Γ_1/Γ
VALUE	DOCUMENT ID	TECN	COMMENT
dominant	SIEGRIST	76 MRK1	e^+e^-
$\psi(4415)$ REFERENCES			
BRANDELIK	78c	PL 76B 361	R. Brandelik <i>et al.</i> (DASP Collab.)
SIEGRIST	76	PRL 36 700	J.L. Siegrist <i>et al.</i> (LBL, SLAC)
OTHER RELATED PAPERS			
BURMESTER	77	PL 66B 395	J. Burmester <i>et al.</i> (DESY, HAMB, SIEG+)
LUTH	77	PL 70B 120	V. Luth <i>et al.</i> (LBL, SLAC)

Meson Particle Listings

Bottomonium

 $b\bar{b}$ MESONS**WIDTH DETERMINATIONS OF THE Υ STATES**

As is the case for the $J/\psi(1S)$ and $\psi(2S)$, the full widths of the $b\bar{b}$ states $\Upsilon(1S)$, $\Upsilon(2S)$, and $\Upsilon(3S)$ are not directly measurable, since they are much narrower than the energy resolution of the e^+e^- storage rings where these states are produced. The common indirect method to determine Γ starts from

$$\Gamma = \Gamma_{\ell\ell} / B_{\ell\ell}, \quad (1)$$

where $\Gamma_{\ell\ell}$ is one leptonic partial width and $B_{\ell\ell}$ is the corresponding branching fraction ($\ell = e, \mu, \text{ or } \tau$). One then assumes $e\text{-}\mu\text{-}\tau$ universality and uses

$$\begin{aligned} \Gamma_{\ell\ell} &= \Gamma_{ee} \\ B_{\ell\ell} &= \text{average of } B_{ee}, B_{\mu\mu}, \text{ and } B_{\tau\tau}. \end{aligned} \quad (2)$$

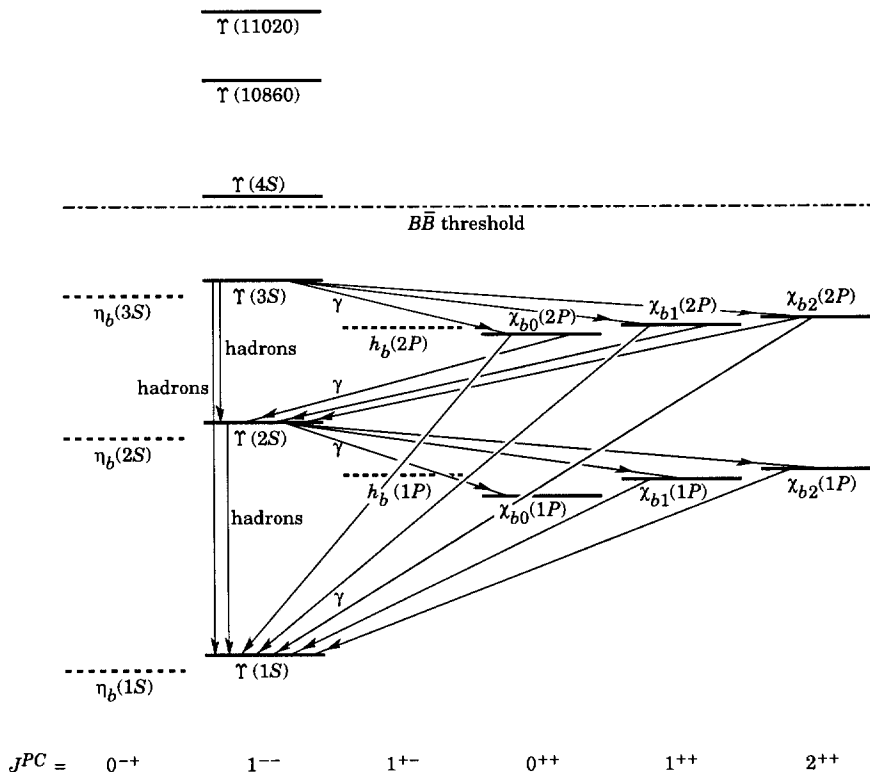
The electronic partial width Γ_{ee} is also not directly measurable at e^+e^- storage rings, only in the combination $\Gamma_{ee}\Gamma_{\text{had}}/\Gamma$, where Γ_{had} is the hadronic partial width and

$$\Gamma_{\text{had}} + 3\Gamma_{ee} = \Gamma. \quad (3)$$

This combination is obtained experimentally from the energy-integrated hadronic cross section

$$\begin{aligned} \int_{\text{resonance}} \sigma(e^+e^- \rightarrow \Upsilon \rightarrow \text{hadrons}) dE \\ = \frac{6\pi^2 \Gamma_{ee}\Gamma_{\text{had}}}{M^2 \Gamma} C_r = \frac{6\pi^2 \Gamma_{ee}^{(0)}\Gamma_{\text{had}}}{M^2 \Gamma} C_r^{(0)}, \end{aligned} \quad (4)$$

where M is the Υ mass, and C_r and $C_r^{(0)}$ are radiative correction factors. C_r is used for obtaining Γ_{ee} as defined in Eq. (1), and contains corrections from all orders of QED for describing $(b\bar{b}) \rightarrow e^+e^-$. The lowest order QED value $\Gamma_{ee}^{(0)}$, relevant for comparison with potential-model calculations, is defined by the lowest order QED graph (Born term) alone, and is about 7% lower than Γ_{ee} .

THE BOTTOMONIUM SYSTEM

The level scheme of the $b\bar{b}$ states showing experimentally established states with solid lines. Singlet states are called η_b and h_b , triplet states Υ and χ_{bJ} . In parentheses it is sufficient to give the radial quantum number and the orbital angular momentum to specify the states with all their quantum numbers. *E.g.*, $h_b(2P)$ means 2^1P_1 with $n = 2, L = 1, S = 0, J = 1, PC = +-.$ If found, D -wave states would be called $\eta_b(nD)$ and $\Upsilon_J(nD)$, with $J = 1, 2, 3$ and $n = 1, 2, 3, 4, \dots$. For the χ_b states, the spins of only the $\chi_{b2}(1P)$ and $\chi_{b1}(1P)$ have been experimentally established. The spins of the other χ_b are given as the preferred values, based on the quarkonium models. The figure also shows the observed hadronic and radiative transitions.

See key on page 239

Meson Particle Listings Bottomonium, $\Upsilon(1S)$

The Listings give experimental results on B_{ee} , $B_{\mu\mu}$, $B_{\tau\tau}$, and $\Gamma_{ee}\Gamma_{had}/\Gamma$. The entries of the last quantity have been re-evaluated consistently using the correction procedure of KURAEV 85. The partial width Γ_{ee} is obtained from the average values for $\Gamma_{ee}\Gamma_{had}/\Gamma$ and $B_{\ell\ell}$ using

$$\Gamma_{ee} = \frac{\Gamma_{ee}\Gamma_{had}}{\Gamma(1-3B_{\ell\ell})} \quad (5)$$

The total width Γ is then obtained from Eq. (1). We do not list Γ_{ee} and Γ values of individual experiments. The Γ_{ee} values in the Meson Summary Table are also those defined in Eq. (1).

$\Upsilon(1S)$			
$I^G(J^{PC}) = 0^-(1^{--})$			
T(1S) MASS			
VALUE (MeV)	DOCUMENT ID	TECN	COMMENT
9460.30 ± 0.26 OUR AVERAGE	Error includes scale factor of 3.3.		
9460.51 ± 0.09 ± 0.05	¹ ARTAMONOV 00	MD1	$e^+e^- \rightarrow$ hadrons
9459.97 ± 0.11 ± 0.07	MACKAY	84	REDE $e^+e^- \rightarrow$ hadrons
• • • We do not use the following data for averages, fits, limits, etc. • • •			
9460.60 ± 0.09 ± 0.05	^{2,3} BARU	92B	REDE $e^+e^- \rightarrow$ hadrons
9460.59 ± 0.12	BARU	86	REDE $e^+e^- \rightarrow$ hadrons
9460.6 ± 0.4	^{3,4} ARTAMONOV 84	REDE	$e^+e^- \rightarrow$ hadrons
¹ Reanalysis of BARU 92B and ARTAMONOV 84 using new electron mass (COHEN 87).			
² Superseding BARU 86.			
³ Superseded by ARTAMONOV 00.			
⁴ Value includes data of ARTAMONOV 82.			

T(1S) WIDTH

VALUE (keV)	DOCUMENT ID	TECN	COMMENT
52.5 ± 1.8 OUR EVALUATION	See the Note on Width Determinations of the Υ states.		

T(1S) DECAY MODES

Mode	Fraction (Γ_i/Γ)	Confidence level
Γ_1 $\tau^+\tau^-$	$(2.67^{+0.14}_{-0.16})\%$	
Γ_2 e^+e^-	$(2.38 \pm 0.11)\%$	
Γ_3 $\mu^+\mu^-$	$(2.48 \pm 0.06)\%$	

Hadronic decays

Γ_4 $J/\psi(1S)$ anything	$(1.1 \pm 0.4) \times 10^{-3}$	
Γ_5 $\rho\pi$	$< 2 \times 10^{-4}$	90%
Γ_6 $\pi^+\pi^-$	$< 5 \times 10^{-4}$	90%
Γ_7 K^+K^-	$< 5 \times 10^{-4}$	90%
Γ_8 $p\bar{p}$	$< 5 \times 10^{-4}$	90%
Γ_9 $\pi^0\pi^+\pi^-$	$< 1.84 \times 10^{-5}$	90%
Γ_{10} $D^*(2010)^\pm$ anything		

Radiative decays

Γ_{11} $\gamma\pi^+\pi^-$	$(6.3 \pm 1.8) \times 10^{-5}$	
Γ_{12} $\gamma\pi^0\pi^0$	$(1.7 \pm 0.7) \times 10^{-5}$	
Γ_{13} $\gamma 2h^+ 2h^-$	$(7.0 \pm 1.5) \times 10^{-4}$	
Γ_{14} $\gamma 3h^+ 3h^-$	$(5.4 \pm 2.0) \times 10^{-4}$	
Γ_{15} $\gamma 4h^+ 4h^-$	$(7.4 \pm 3.5) \times 10^{-4}$	
Γ_{16} $\gamma\pi^+\pi^-K^+K^-$	$(2.9 \pm 0.9) \times 10^{-4}$	
Γ_{17} $\gamma 2\pi^+ 2\pi^-$	$(2.5 \pm 0.9) \times 10^{-4}$	
Γ_{18} $\gamma 3\pi^+ 3\pi^-$	$(2.5 \pm 1.2) \times 10^{-4}$	
Γ_{19} $\gamma 2\pi^+ 2\pi^- K^+ K^-$	$(2.4 \pm 1.2) \times 10^{-4}$	
Γ_{20} $\gamma\pi^+\pi^-\rho\bar{\rho}$	$(1.5 \pm 0.6) \times 10^{-4}$	
Γ_{21} $\gamma 2\pi^+ 2\pi^-\rho\bar{\rho}$	$(4 \pm 6) \times 10^{-5}$	

Γ_{22} $\gamma 2K^+ 2K^-$	$(2.0 \pm 2.0) \times 10^{-5}$	
Γ_{23} $\gamma\eta(958)$	$< 1.3 \times 10^{-3}$	90%
Γ_{24} $\gamma\eta$	$< 3.5 \times 10^{-4}$	90%
Γ_{25} $\gamma f_2(1525)$	$< 1.4 \times 10^{-4}$	90%
Γ_{26} $\gamma f_2(1270)$	$(8 \pm 4) \times 10^{-5}$	
Γ_{27} $\gamma\eta(1440)$	$< 8.2 \times 10^{-5}$	90%
Γ_{28} $\gamma f_0(1710) \rightarrow \gamma K\bar{K}$	$< 2.6 \times 10^{-4}$	90%
Γ_{29} $\gamma f_0(2200) \rightarrow \gamma K^+ K^-$	$< 2 \times 10^{-4}$	90%
Γ_{30} $\gamma f_J(2220) \rightarrow \gamma K^+ K^-$	$< 1.5 \times 10^{-5}$	90%
Γ_{31} $\gamma\eta(2225) \rightarrow \gamma\phi\phi$	$< 3 \times 10^{-3}$	90%
Γ_{32} γX	$< 3 \times 10^{-5}$	90%
$X =$ pseudoscalar with $m < 7.2$ GeV		
Γ_{33} $\gamma X\bar{X}$	$< 1 \times 10^{-3}$	90%
$X\bar{X} =$ vectors with $m < 3.1$ GeV		

T(1S) $\Gamma(I)\Gamma(e^+e^-)/\Gamma(\text{total})$

$\Gamma(e^+e^-) \times \Gamma(\mu^+\mu^-)/\Gamma_{\text{total}}$	DOCUMENT ID	TECN	COMMENT	$\Gamma_2\Gamma_3/\Gamma$
31.2 ± 1.6 ± 1.7	KOBEL	92	CBAL	$e^+e^- \rightarrow \mu^+\mu^-$

$\Gamma(\text{hadrons}) \times \Gamma(e^+e^-)/\Gamma_{\text{total}}$	DOCUMENT ID	TECN	COMMENT	$\Gamma_0\Gamma_2/\Gamma$
1.216 ± 0.027 OUR AVERAGE				

1.187 ± 0.023 ± 0.031	⁵ BARU	92B	MD1	$e^+e^- \rightarrow$ hadrons
1.23 ± 0.02 ± 0.05	⁵ JAKUBOWSKI 88	CBAL		$e^+e^- \rightarrow$ hadrons
1.37 ± 0.06 ± 0.09	⁶ GILES	84B	CLEO	$e^+e^- \rightarrow$ hadrons
1.23 ± 0.08 ± 0.04	⁶ ALBRECHT 82	DASP		$e^+e^- \rightarrow$ hadrons
1.13 ± 0.07 ± 0.11	⁶ NICZYPORUK 82	LENA		$e^+e^- \rightarrow$ hadrons
1.09 ± 0.25	⁶ BOCK	80	CNTR	$e^+e^- \rightarrow$ hadrons
1.35 ± 0.14	⁷ BERGER	79	PLUT	$e^+e^- \rightarrow$ hadrons

⁵ Radiative corrections evaluated following KURAEV 85.

⁶ Radiative corrections reevaluated by BUCHMUELLER 88 following KURAEV 85.

⁷ Radiative corrections reevaluated by ALEXANDER 89 using $B(\mu\mu) = 0.026$.

T(1S) PARTIAL WIDTHS

$\Gamma(e^+e^-)$	DOCUMENT ID	TECN	COMMENT	Γ_2
1.32 ± 0.04 ± 0.03	⁸ ALBRECHT	95E	ARG	$e^+e^- \rightarrow$ hadrons

⁸ Applying the formula of KuraeV and Fadin.

T(1S) BRANCHING RATIOS

$\Gamma(\tau^+\tau^-)/\Gamma_{\text{total}}$	EVTS	DOCUMENT ID	TECN	COMMENT	Γ_1/Γ
0.0267 ± 0.0014					
0.0016					

0.0261 ± 0.0012 ± 0.0009	25k	CINABRO	94B	CLE2	$e^+e^- \rightarrow \tau^+\tau^-$
0.027 ± 0.004 ± 0.002		⁹ ALBRECHT	85c	ARG	$\Upsilon(2S) \rightarrow \pi^+\pi^-\tau^+\tau^-$
0.034 ± 0.004 ± 0.004		GILES	83	CLEO	$e^+e^- \rightarrow \tau^+\tau^-$

⁹ Using $B(\Upsilon(1S) \rightarrow ee) = B(\Upsilon(1S) \rightarrow \mu\mu) = 0.0256$; not used for width evaluations.

$\Gamma(\mu^+\mu^-)/\Gamma_{\text{total}}$	EVTS	DOCUMENT ID	TECN	COMMENT	Γ_3/Γ
0.0248 ± 0.0006 OUR AVERAGE					

0.0249 ± 0.0008 ± 0.0013		ALEXANDER	98	CLE2	$\Upsilon(2S) \rightarrow \pi^+\pi^-\mu^+\mu^-$	
0.0212 ± 0.0020 ± 0.0010		¹⁰ BARU	92	MD1	$e^+e^- \rightarrow \mu^+\mu^-$	
0.0231 ± 0.0012 ± 0.0010		¹⁰ KOBEL	92	CBAL	$e^+e^- \rightarrow \mu^+\mu^-$	
0.0252 ± 0.0007 ± 0.0007		CHEN	89B	CLEO	$e^+e^- \rightarrow \mu^+\mu^-$	
0.0261 ± 0.0009 ± 0.0011		KAARSBERG	89	CSB2	$e^+e^- \rightarrow \mu^+\mu^-$	
0.0230 ± 0.0025 ± 0.0013		86	ALBRECHT	87	ARG	$\Upsilon(2S) \rightarrow \pi^+\pi^-\mu^+\mu^-$
0.029 ± 0.003 ± 0.002	864	BESSON	84	CLEO	$\Upsilon(2S) \rightarrow \pi^+\pi^-\mu^+\mu^-$	
0.027 ± 0.003 ± 0.003		ANDREWS	83	CLEO	$e^+e^- \rightarrow \mu^+\mu^-$	
0.032 ± 0.013 ± 0.003		ALBRECHT	82	DASP	$e^+e^- \rightarrow \mu^+\mu^-$	
0.038 ± 0.015 ± 0.002		NICZYPORUK	82	LENA	$e^+e^- \rightarrow \mu^+\mu^-$	
0.014 ± 0.034		BOCK	80	CNTR	$e^+e^- \rightarrow \mu^+\mu^-$	
-0.014		BERGER	79	PLUT	$e^+e^- \rightarrow \mu^+\mu^-$	
0.022 ± 0.020					$\mu^+\mu^-$	

¹⁰ Taking into account interference between the resonance and continuum.

Meson Particle Listings

 $\Upsilon(1S)$

$\Gamma(e^+e^-)/\Gamma_{total}$					Γ_2/Γ	$\Gamma(\Upsilon 3\pi^+3\pi^-)/\Gamma_{total}$					Γ_{18}/Γ
VALUE	CL%	DOCUMENT ID	TECN	COMMENT		VALUE (units 10^{-4})	CL%	DOCUMENT ID	TECN	COMMENT	
0.0238 ± 0.0011 OUR AVERAGE						2.5 ± 0.9 ± 0.8	17 ± 5	FULTON	90B	CLEO	$e^+e^- \rightarrow$ hadrons
0.0229 ± 0.0008 ± 0.0011		ALEXANDER	98	CLE2	$\Upsilon(2S) \rightarrow \pi^+\pi^-\pi^+e^-e^-$						Γ_{19}/Γ
0.0242 ± 0.0014 ± 0.0014	307	ALBRECHT	87	ARG	$\Upsilon(2S) \rightarrow \pi^+\pi^-\pi^+e^-e^-$	$\Gamma(\Upsilon 2\pi^+2\pi^-K^+K^-)/\Gamma_{total}$					Γ_{19}/Γ
0.028 ± 0.003 ± 0.002	826	BESSON	84	CLEO	$\Upsilon(2S) \rightarrow \pi^+\pi^-\pi^+e^-e^-$	VALUE (units 10^{-4})	EVT%	DOCUMENT ID	TECN	COMMENT	
0.051 ± 0.030		BERGER	80C	PLUT	$e^+e^- \rightarrow \mu^+\mu^-e^+e^-$	2.4 ± 0.9 ± 0.8	18 ± 7	FULTON	90B	CLEO	$e^+e^- \rightarrow$ hadrons
$\Gamma(J/\psi(1S) \text{ anything})/\Gamma_{total}$					Γ_4/Γ	$\Gamma(\Upsilon 2\pi^+2\pi^-\rho\bar{\rho})/\Gamma_{total}$					Γ_{21}/Γ
VALUE (units 10^{-3})	CL%	DOCUMENT ID	TECN	COMMENT		VALUE (units 10^{-4})	EVT%	DOCUMENT ID	TECN	COMMENT	
< 0.68	90	ALBRECHT	92J	ARG	$e^+e^- \rightarrow e^+e^-X$, $e^+e^- \rightarrow \mu^+\mu^-X$	0.4 ± 0.4 ± 0.4	7 ± 6	FULTON	90B	CLEO	$e^+e^- \rightarrow$ hadrons
1.1 ± 0.4 ± 0.2		¹¹ FULTON	89	CLEO	$e^+e^- \rightarrow \mu^+\mu^-X$	$\Gamma(\Upsilon 2h^+2h^-)/\Gamma_{total}$					Γ_{13}/Γ
• • • We do not use the following data for averages, fits, limits, etc. • • •						VALUE (units 10^{-4})	EVT%	DOCUMENT ID	TECN	COMMENT	
< 1.7	90	MASCHMANN	90	CBAL	$e^+e^- \rightarrow$ hadrons	7.0 ± 1.1 ± 1.0	80 ± 12	FULTON	90B	CLEO	$e^+e^- \rightarrow$ hadrons
< 20	90	NICZYPORUK	83	LENA		$\Gamma(\Upsilon 3h^+3h^-)/\Gamma_{total}$					Γ_{14}/Γ
¹¹ Using $B(J/\psi \rightarrow \mu^+\mu^-) = (6.9 \pm 0.9)\%$.						VALUE (units 10^{-4})	EVT%	DOCUMENT ID	TECN	COMMENT	
$\Gamma(\pi^+\pi^-)/\Gamma_{total}$					Γ_6/Γ	$\Gamma(\Upsilon 4h^+4h^-)/\Gamma_{total}$					Γ_{15}/Γ
VALUE (units 10^{-4})	CL%	DOCUMENT ID	TECN	COMMENT		VALUE (units 10^{-4})	EVT%	DOCUMENT ID	TECN	COMMENT	
< 5	90	BARU	92	MD1	$\Upsilon(1S) \rightarrow \pi^+\pi^-$	7.4 ± 2.5 ± 2.5	36 ± 12	FULTON	90B	CLEO	$e^+e^- \rightarrow$ hadrons
$\Gamma(K^+K^-)/\Gamma_{total}$					Γ_7/Γ	$\Gamma(\rho\pi)/\Gamma_{total}$					Γ_5/Γ
VALUE (units 10^{-4})	CL%	DOCUMENT ID	TECN	COMMENT		VALUE (units 10^{-4})	CL%	DOCUMENT ID	TECN	COMMENT	
< 5	90	BARU	92	MD1	$\Upsilon(1S) \rightarrow K^+K^-$	< 2	90	FULTON	90B	$\Upsilon(1S) \rightarrow \rho^0\pi^0$	
$\Gamma(\rho\bar{\rho})/\Gamma_{total}$					Γ_8/Γ	• • • We do not use the following data for averages, fits, limits, etc. • • •					
VALUE (units 10^{-4})	CL%	DOCUMENT ID	TECN	COMMENT		< 10	90	BLINOV	90	MD1	$\Upsilon(1S) \rightarrow \rho^0\pi^0$
< 5	90	¹² BARU	96	MD1	$\Upsilon(1S) \rightarrow \rho\bar{\rho}$	< 21	90	NICZYPORUK	83	LENA	$\Upsilon(1S) \rightarrow \rho^0\pi^0$
¹² Supersedes BARU 92 in this node.						$\Gamma(D^*(2010)^\pm \text{ anything})/\Gamma_{total}$					Γ_{10}/Γ
$\Gamma(\pi^0\pi^+\pi^-)/\Gamma_{total}$					Γ_9/Γ	VALUE (units 10^{-3})	CL%	DOCUMENT ID	TECN	COMMENT	
VALUE (units 10^{-3})	CL%	DOCUMENT ID	TECN	COMMENT		< 19	90	¹⁷ ALBRECHT	92J	ARG	$e^+e^- \rightarrow D^0\pi^\pm X$
< 1.84	90	ANASTASSOV	99	CLE2	$e^+e^- \rightarrow$ hadrons	¹⁷ For $x_p > 0.2$.					
$\Gamma(\Upsilon X)/\Gamma_{total}$					Γ_{32}/Γ	$\Gamma(\Upsilon\eta(1440))/\Gamma_{total}$					Γ_{27}/Γ
(X = pseudoscalar with $m < 7.2$ GeV)						VALUE (units 10^{-3})	CL%	DOCUMENT ID	TECN	COMMENT	
VALUE (units 10^{-5})	CL%	DOCUMENT ID	TECN	COMMENT		< 8.2	90	¹⁸ FULTON	90B	CLEO	$\Upsilon(1S) \rightarrow \gamma K^+\pi^\mp K_S^0$
< 3	90	¹³ BALEST	95	CLEO	$e^+e^- \rightarrow \gamma + X$	• • • We do not use the following data for averages, fits, limits, etc. • • •					
¹³ For a noninteracting pseudoscalar X with mass < 7.2 GeV.						$\Gamma(\Upsilon\eta(958))/\Gamma_{total}$					Γ_{23}/Γ
$\Gamma(\Upsilon X\bar{X})/\Gamma_{total}$					Γ_{33}/Γ	VALUE (units 10^{-3})	CL%	DOCUMENT ID	TECN	COMMENT	
(X \bar{X} = vectors with $m < 3.1$ GeV)						< 1.3	90	SCHMITT	88	CBAL	$\Upsilon(1S) \rightarrow \gamma X$
VALUE (units 10^{-3})	CL%	DOCUMENT ID	TECN	COMMENT		$\Gamma(\Upsilon\eta)/\Gamma_{total}$					Γ_{24}/Γ
< 1	90	¹⁴ BALEST	95	CLEO	$e^+e^- \rightarrow \gamma + X\bar{X}$	VALUE (units 10^{-4})	CL%	DOCUMENT ID	TECN	COMMENT	
¹⁴ For a noninteracting vector X with mass < 3.1 GeV.						< 3.5	90	SCHMITT	88	CBAL	$\Upsilon(1S) \rightarrow \gamma X$
$\Gamma(\Upsilon\pi^+\pi^-)/\Gamma_{total}$					Γ_{11}/Γ	$\Gamma(\Upsilon f_2'(1525))/\Gamma_{total}$					Γ_{25}/Γ
VALUE (units 10^{-5})	CL%	DOCUMENT ID	TECN	COMMENT		VALUE (units 10^{-3})	CL%	DOCUMENT ID	TECN	COMMENT	
6.3 ± 1.2 ± 1.3		¹⁵ ANASTASSOV	99	CLE2	$e^+e^- \rightarrow$ hadrons	< 14	90	¹⁹ FULTON	90B	CLEO	$\Upsilon(1S) \rightarrow \gamma K^+K^-$
¹⁵ For $m_{\pi\pi} > 1$ GeV.						• • • We do not use the following data for averages, fits, limits, etc. • • •					
$\Gamma(\Upsilon\pi^0\pi^0)/\Gamma_{total}$					Γ_{12}/Γ	< 19.4	90	¹⁹ ALBRECHT	89	ARG	$\Upsilon(1S) \rightarrow \gamma K^+K^-$
VALUE (units 10^{-3})	CL%	DOCUMENT ID	TECN	COMMENT		¹⁹ Assuming $B(f_2'(1525) \rightarrow K\bar{K}) = 0.71$.					
1.7 ± 0.6 ± 0.3		¹⁶ ANASTASSOV	99	CLE2	$e^+e^- \rightarrow$ hadrons	$\Gamma(\Upsilon f_0(1710) \rightarrow \gamma K\bar{K})/\Gamma_{total}$					Γ_{28}/Γ
¹⁶ For $m_{\pi\pi} > 1$ GeV.					<th>VALUE (units 10^{-4})</th> <th>CL%</th> <th>DOCUMENT ID</th> <th>TECN</th> <th>COMMENT</th> <th></th>	VALUE (units 10^{-4})	CL%	DOCUMENT ID	TECN	COMMENT	
$\Gamma(\Upsilon 2\pi^+2\pi^-)/\Gamma_{total}$					Γ_{17}/Γ	< 2.6	90	²⁰ ALBRECHT	89	ARG	$\Upsilon(1S) \rightarrow \gamma K^+K^-$
VALUE (units 10^{-4})	EVT%	DOCUMENT ID	TECN	COMMENT		• • • We do not use the following data for averages, fits, limits, etc. • • •					
2.5 ± 0.7 ± 0.5	26 ± 7	FULTON	90B	CLEO	$e^+e^- \rightarrow$ hadrons	< 6.3	90	²⁰ FULTON	90B	CLEO	$\Upsilon(1S) \rightarrow \gamma K^+K^-$
$\Gamma(\Upsilon\pi^+\pi^-K^+K^-)/\Gamma_{total}$					Γ_{16}/Γ	< 19	90	²⁰ FULTON	90B	CLEO	$\Upsilon(1S) \rightarrow \gamma K_S^0 K_S^0$
VALUE (units 10^{-4})	EVT%	DOCUMENT ID	TECN	COMMENT		< 8	90	²¹ ALBRECHT	89	ARG	$\Upsilon(1S) \rightarrow \gamma\pi^+\pi^-$
2.9 ± 0.7 ± 0.6	29 ± 8	FULTON	90B	CLEO	$e^+e^- \rightarrow$ hadrons	< 24	90	²² SCHMITT	88	CBAL	$\Upsilon(1S) \rightarrow \gamma X$
$\Gamma(\Upsilon\pi^+\pi^-\rho\bar{\rho})/\Gamma_{total}$					Γ_{20}/Γ	²⁰ Assuming $B(f_0(1710) \rightarrow K\bar{K}) = 0.38$.					
VALUE (units 10^{-4})	EVT%	DOCUMENT ID	TECN	COMMENT		²¹ Assuming $B(f_0(1710) \rightarrow \pi\pi) = 0.04$.					
1.5 ± 0.5 ± 0.3	22 ± 6	FULTON	90B	CLEO	$e^+e^- \rightarrow$ hadrons	²² Assuming $B(f_0(1710) \rightarrow \eta\eta) = 0.18$.					
$\Gamma(\Upsilon 2K^+2K^-)/\Gamma_{total}$					Γ_{22}/Γ	$\Gamma(\Upsilon f_2(1270))/\Gamma_{total}$					Γ_{26}/Γ
VALUE (units 10^{-4})	EVT%	DOCUMENT ID	TECN	COMMENT		VALUE (units 10^{-3})	CL%	DOCUMENT ID	TECN	COMMENT	
0.2 ± 0.2	2 ± 2	FULTON	90B	CLEO	$e^+e^- \rightarrow$ hadrons	8.1 ± 2.3 ± 2.9 ± 2.7		²³ ANASTASSOV	99	CLE2	$e^+e^- \rightarrow$ hadrons
• • • We do not use the following data for averages, fits, limits, etc. • • •						< 21	90	²³ FULTON	90B	CLEO	$\Upsilon(1S) \rightarrow \gamma\pi^+\pi^-$
< 13	90	²³ ALBRECHT	89	ARG	$\Upsilon(1S) \rightarrow \gamma\pi^+\pi^-$	< 81	90	SCHMITT	88	CBAL	$\Upsilon(1S) \rightarrow \gamma X$
²³ Using $B(f_2(1270) \rightarrow \pi\pi) = 0.84$.											

See key on page 239

Meson Particle Listings

 $\Upsilon(1S), \chi_{b0}(1P), \chi_{b1}(1P)$ $\Gamma(\gamma f_J(2220) \rightarrow \gamma K^+ K^-) / \Gamma_{\text{total}}$

VALUE (units 10^{-5})	CL%	DOCUMENT ID	TECN	COMMENT	Γ_{30}/Γ
< 1.5	90	24 FULTON	90b CLEO	$\Upsilon(1S) \rightarrow \gamma K^+ K^-$	
• • • We do not use the following data for averages, fits, limits, etc. • • •					
< 2.9	90	24 ALBRECHT	89 ARG	$\Upsilon(1S) \rightarrow \gamma K^+ K^-$	
< 20	90	24 BARU	89 MD1	$\Upsilon(1S) \rightarrow \gamma K^+ K^-$	

²⁴Including unknown branching ratio of $f_J(2220) \rightarrow K^+ K^-$. $\Gamma(\gamma \eta(2225) \rightarrow \gamma \phi \phi) / \Gamma_{\text{total}}$

VALUE	CL%	DOCUMENT ID	TECN	COMMENT	Γ_{31}/Γ
< 0.003	90	25 BARU	89 MD1	$\Upsilon(1S) \rightarrow \gamma K^+ K^- K^+ K^-$	

²⁵Assuming that the $\eta(2225)$ decays only into $\phi \phi$. $\Gamma(\gamma f_0(2200) \rightarrow \gamma K^+ K^-) / \Gamma_{\text{total}}$

VALUE	CL%	DOCUMENT ID	TECN	COMMENT	Γ_{29}/Γ
< 0.0002	90	26 BARU	89 MD1	$\Upsilon(1S) \rightarrow \gamma K^+ K^-$	

²⁶Assuming that the $f_0(2200)$ decays only into $K^+ K^-$. $\Upsilon(1S)$ REFERENCES

ARTAMONOV 00	PL B474 427	A.S. Artamonov et al.		
ANASTASSOV 99	PRL 82 286	A. Anastassov et al.	(CLEO Collab.)	
ALEXANDER 98	PR D58 052004	J.P. Alexander et al.	(CLEO Collab.)	
BARU 96	PRPL 267 71	S.E. Baru et al.	(NOVO)	
ALBRECHT 95E	ZPHY C65 619	H. Albrecht et al.	(ARGUS Collab.)	
BALEST 95	PR D51 2053	R. Balest et al.	(CLEO Collab.)	
CINABRO 94B	PL B340 129	D. Cinabro et al.	(CLEO Collab.)	
ALBRECHT 92J	ZPHY C55 25	H. Albrecht et al.	(ARGUS Collab.)	
BARU 92	ZPHY C54 229	S.E. Baru et al.	(NOVO)	
BARU 92B	ZPHY C56 547	S.E. Baru et al.	(NOVO)	
KOBEL 92	ZPHY C53 193	M. Kobel et al.	(Crystal Ball Collab.)	
BLINOV 90	PL B245 311	A.E. Blinov et al.	(NOVO)	
FULTON 90B	PR D41 1401	R. Fulton et al.	(CLEO Collab.)	
MASCHMANN 90	ZPHY C46 555	W.S. Maschmann et al.	(Crystal Ball Collab.)	
ALBRECHT 89	ZPHY C42 349	H. Albrecht et al.	(ARGUS Collab.)	
ALEXANDER 89	NP B320 45	J.P. Alexander et al.	(LBL, MICH, SLAC)	
BARU 89	ZPHY C42 505	S.E. Baru et al.	(NOVO)	
CHEN 89B	PR D39 3529	W.Y. Chen et al.	(CLEO Collab.)	
FULTON 89	PL B224 445	R. Fulton et al.	(CLEO Collab.)	
KAARSBERG 89	PRL 62 2077	T.M. Kaarsberg et al.	(CUSB Collab.)	
BUCHMUELLER... 88	HE e ⁺ e ⁻ Physics 412	W. Buchmueller, S. Cooper	(HANN, DESY, MIT)	
Editors: A. Ali and P. Soeding, World Scientific, Singapore				
JAKUBOWSKI 88	ZPHY C40 49	Z. Jakubowski et al.	(Crystal Ball Collab.)	1GJPC
SCHMITT 88	ZPHY C40 199	P. Schmitt et al.	(Crystal Ball Collab.)	
ALBRECHT 87	ZPHY C35 283	H. Albrecht et al.	(ARGUS Collab.)	
COHEN 87	RMP 59 1121	E.R. Cohen, B.N. Taylor	(RIS, NBS)	
BARU 86	ZPHY C30 551	S.E. Baru et al.	(NOVO)	
ALBRECHT 85C	PL 154B 452	H. Albrecht et al.	(ARGUS Collab.)	
KURAEV 85	SJNP 41 466	E.A. Kurayev, V.S. Fadin	(NOVO)	
Translated from YAF 41 733.				
ARTAMONOV 84	PL 137B 272	A.S. Artamonov et al.	(NOVO)	
BESSON 84	PR D30 1433	D. Besson et al.	(CLEO Collab.)	
GILES 84B	PR D29 1285	R. Giles et al.	(CLEO Collab.)	
MACKEY 84	PR D29 2483	W.W. MacKay et al.	(CUSB Collab.)	
ANDREWS 83	PRL 50 807	D.E. Andrews et al.	(CLEO Collab.)	
GILES 83	PRL 50 877	R. Giles et al.	(HARV, OSU, ROCH, RUTG+)	
NICZYPORUK 83	ZPHY C17 197	B. Niczyporuk et al.	(LENA, Collab.)	
ALBRECHT 82	PL 116B 383	H. Albrecht et al.	(DESY, DORT, HEIDH+)	
ARTAMONOV 82	PL 118B 225	A.S. Artamonov et al.	(NOVO)	
NICZYPORUK 82	ZPHY C15 299	B. Niczyporuk et al.	(LENA Collab.)	
BERGER 80C	PL 93B 497	C. Berger et al.	(PLUTO Collab.)	
BOCK 80	ZPHY C6 125	P. Bock et al.	(HEIDP, MPIM, DESY, HAMB)	
BERGER 79	ZPHY C1 343	C. Berger et al.	(PLUTO Collab.)	

OTHER RELATED PAPERS

KOENIGS... 86	DESY 86/136	K. Koenigsmann	(OESY)	
ALBRECHT 84	PL 134B 137	H. Albrecht et al.	(ARGUS Collab.)	
ARTAMONOV 84	PL 137B 272	A.S. Artamonov et al.	(NOVO)	
ARTAMONOV 82	PL 118B 225	A.S. Artamonov et al.	(NOVO)	
BERGER 78	PL 76B 243	C. Berger et al.	(PLUTO Collab.)	
BIENLEIN 78	PL 78B 360	J.K. Bienlein et al.	(DESY, HAMB, HEIDP+)	
DARDEN 78	PL 76B 246	C.W. Darden et al.	(DESY, DORT, HEIDH+)	
GARELUK 78	PR D18 945	D.A. Garelick et al.	(NEAS, WASH, TUFTS)	
KAPLAN 78	PRL 40 435	D.M. Kaplan et al.	(STON, FNAL, COLU)	
YOH 78	PRL 41 684	J.K. Yoh et al.	(COLU, FNAL, STON)	
COBB 77	PL 72B 273	J.H. Cobb et al.	(BNL, CERN, SYRA, VALE)	
HERB 77	PRL 39 252	S.W. Herb et al.	(COLU, FNAL, STON)	
INNES 77	PRL 39 1240	W.R. Innes et al.	(COLU, FNAL, STON)	

 $\chi_{b0}(1P)$ $I^G(J^{PC}) = 0^+(0^{++})$
J needs confirmation.Observed in radiative decay of the $\Upsilon(2S)$, therefore $C = -$. Branching ratio requires E1 transition, M1 is strongly disfavored, therefore $P = +$. $\chi_{b0}(1P)$ MASS

VALUE (MeV)	DOCUMENT ID	TECN	COMMENT
9859.9 ± 1.0 OUR AVERAGE			
9860.0 ± 0.8 ± 1.2	¹ EDWARDS	99 CLE2	$\Upsilon(2S) \rightarrow \gamma \chi(1P)$
9859.9 ± 0.5 ± 1.4	¹ ALBRECHT	85E ARG	$\Upsilon(2S) \rightarrow \text{conv. } \gamma X$
9858.1 ± 1.6 ± 2.7	¹ NERNST	85 CBAL	$\Upsilon(2S) \rightarrow \gamma X$
9864.0 ± 7 ± 1	¹ HAAS	84 CLEO	$\Upsilon(2S) \rightarrow \text{conv. } \gamma X$
• • • We do not use the following data for averages, fits, limits, etc. • • •			
9872.8 ± 0.7 ± 5.0	¹ KLOPFEN...	83 CUSB	$\Upsilon(2S) \rightarrow \gamma X$

¹From γ energy below, assuming $\Upsilon(2S)$ mass = 10023.3 MeV. γ ENERGY IN $\Upsilon(2S)$ DECAY

VALUE (MeV)	DOCUMENT ID	TECN	COMMENT
162.1 ± 1.0 OUR AVERAGE			
162.0 ± 0.8 ± 1.2	EDWARDS	99 CLE2	$\Upsilon(2S) \rightarrow \gamma \chi(1P)$
162.1 ± 0.5 ± 1.4	ALBRECHT	85E ARG	$\Upsilon(2S) \rightarrow \text{conv. } \gamma X$
163.8 ± 1.6 ± 2.7	NERNST	85 CBAL	$\Upsilon(2S) \rightarrow \gamma X$
158.0 ± 7 ± 1	HAAS	84 CLEO	$\Upsilon(2S) \rightarrow \text{conv. } \gamma X$
• • • We do not use the following data for averages, fits, limits, etc. • • •			
149.4 ± 0.7 ± 5.0	KLOPFEN...	83 CUSB	$\Upsilon(2S) \rightarrow \gamma X$

 $\chi_{b0}(1P)$ DECAY MODES

Mode	Fraction (Γ_i/Γ)	Confidence level
$\Gamma_1 \gamma \Upsilon(1S)$	< 6 %	90%

 $\chi_{b0}(1P)$ BRANCHING RATIOS

$\Gamma(\gamma \Upsilon(1S)) / \Gamma_{\text{total}}$	CL%	DOCUMENT ID	TECN	COMMENT	Γ_1/Γ
< 0.06	90	WALK	86 CBAL	$\Upsilon(2S) \rightarrow \gamma \gamma \ell^+ \ell^-$	
• • • We do not use the following data for averages, fits, limits, etc. • • •					
< 0.11	90	PAUSS	83 CUSB	$\Upsilon(2S) \rightarrow \gamma \gamma \ell^+ \ell^-$	

 $\chi_{b0}(1P)$ REFERENCES

EDWARDS 99	PR D59 032003	K.W. Edwards et al.	(CLEO Collab.)
WALK 86	PR D34 2611	W.S. Walk et al.	(Crystal Ball Collab.)
ALBRECHT 85E	PL 160B 331	H. Albrecht et al.	(ARGUS Collab.)
NERNST 85	PL 54 2195	R. Nernst et al.	(Crystal Ball Collab.)
HAAS 84	PRL 52 799	J. Haas et al.	(CLEO Collab.)
KLOPFEN... 83	PRL 51 160	C. Klopffenstein et al.	(CUSB Collab.)
PAUSS 83	PL 130B 439	F. Pauss et al.	(MPIM, COLU, CORN, LSU+)

 $\chi_{b1}(1P)$ $I^G(J^{PC}) = 0^+(1^{++})$
J needs confirmation.Observed in radiative decay of the $\Upsilon(2S)$, therefore $C = +$. Branching ratio requires E1 transition, M1 is strongly disfavored, therefore $P = +$, $J = 1$ from SKWARNICKI 87. $\chi_{b1}(1P)$ MASS

VALUE (MeV)	DOCUMENT ID	TECN	COMMENT
9892.7 ± 0.6 OUR AVERAGE			Error includes scale factor of 1.1.
9893.7 ± 0.4 ± 0.6	¹ EDWARDS	99 CLE2	$\Upsilon(2S) \rightarrow \gamma \chi(1P)$
9890.7 ± 0.9 ± 1.3	¹ WALK	86 CBAL	$\Upsilon(2S) \rightarrow \gamma \gamma \ell^+ \ell^-$
9890.7 ± 0.3 ± 1.1	¹ ALBRECHT	85E ARG	$\Upsilon(2S) \rightarrow \text{conv. } \gamma X$
9891.8 ± 0.8 ± 2.4	¹ NERNST	85 CBAL	$\Upsilon(2S) \rightarrow \gamma X$
9893.5 ± 0.8 ± 1.0	¹ HAAS	84 CLEO	$\Upsilon(2S) \rightarrow \text{conv. } \gamma X$
9894.4 ± 0.4 ± 3.0	¹ KLOPFEN...	83 CUSB	$\Upsilon(2S) \rightarrow \gamma X$
9892 ± 3	¹ PAUSS	83 CUSB	$\Upsilon(2S) \rightarrow \gamma \gamma \ell^+ \ell^-$

¹From γ energy below, assuming $\Upsilon(2S)$ mass = 10023.3 MeV. γ ENERGY IN $\Upsilon(2S)$ DECAY

VALUE (MeV)	DOCUMENT ID	TECN	COMMENT
129.8 ± 0.5 OUR AVERAGE			Error includes scale factor of 1.1.
128.8 ± 0.4 ± 0.6	EDWARDS	99 CLE2	$\Upsilon(2S) \rightarrow \gamma \chi(1P)$
131.7 ± 0.9 ± 1.3	WALK	86 CBAL	$\Upsilon(2S) \rightarrow \gamma \gamma \ell^+ \ell^-$
131.7 ± 0.3 ± 1.1	ALBRECHT	85E ARG	$\Upsilon(2S) \rightarrow \text{conv. } \gamma X$
130.6 ± 0.8 ± 2.4	NERNST	85 CBAL	$\Upsilon(2S) \rightarrow \gamma X$
129 ± 0.8 ± 1	HAAS	84 CLEO	$\Upsilon(2S) \rightarrow \text{conv. } \gamma X$
128.1 ± 0.4 ± 3.0	KLOPFEN...	83 CUSB	$\Upsilon(2S) \rightarrow \gamma X$
130.6 ± 3.0	PAUSS	83 CUSB	$\Upsilon(2S) \rightarrow \gamma \gamma \ell^+ \ell^-$

Meson Particle Listings

 $\chi_{b1}(1P)$, $\chi_{b2}(1P)$, $\Upsilon(2S)$ $\chi_{b1}(1P)$ DECAY MODES

Mode	Fraction (Γ_i/Γ)
Γ_1 $\gamma \Upsilon(1S)$	(35 ± 8) %

 $\chi_{b1}(1P)$ BRANCHING RATIOS

$\Gamma(\gamma \Upsilon(1S))/\Gamma_{total}$	Γ_1/Γ
0.35 ± 0.08 OUR AVERAGE	
0.32 ± 0.06 ± 0.07	
0.47 ± 0.18	

 $\chi_{b1}(1P)$ REFERENCES

EDWARDS	99	PR D59 032003	K.W. Edwards et al.	(CLEO Collab.)
SKWARNICKI	87	PRL 58 972	T. Skwarnicki et al.	(Crystal Ball Collab.)
WALK	86	PR D34 2611	W.S. Walk et al.	(Crystal Ball Collab.)
ALBRECHT	85E	PL 160B 331	H. Albrecht et al.	(ARGUS Collab.)
NERNST	85	PRL 54 2195	R. Nernst et al.	(Crystal Ball Collab.)
HAAS	84	PRL 52 799	J. Haas et al.	(CLEO Collab.)
KLOPFEN...	83	PRL 51 160	C. Klopfenstein et al.	(CUSB Collab.)
PAUSS	83	PL 130B 439	F. Pauss et al.	(MPIM, COLU, CORN, LSU+)

 $\chi_{b2}(1P)$

$$J^G(J^{PC}) = 0^+(2^{++})$$

J needs confirmation.

Observed in radiative decay of the $\Upsilon(2S)$, therefore $C = +$. Branching ratio requires E1 transition, M1 is strongly disfavored, therefore $P = +$. $J = 2$ from SKWARNICKI 87.

 $\chi_{b2}(1P)$ MASS

VALUE (MeV)	DOCUMENT ID	TECN	COMMENT
9912.6 ± 0.5 OUR AVERAGE	Error includes scale factor of 1.1.		
9911.9 ± 0.3 ± 0.6	¹ EDWARDS	99 CLE2	$\Upsilon(2S) \rightarrow \gamma \chi(1P)$
9915.7 ± 1.1 ± 1.3	¹ WALK	86 CBAL	$\Upsilon(2S) \rightarrow \gamma \gamma \ell^+ \ell^-$
9912.1 ± 0.3 ± 0.9	¹ ALBRECHT	85E ARG	$\Upsilon(2S) \rightarrow \text{conv. } \gamma X$
9912.3 ± 0.8 ± 2.2	¹ NERNST	85 CBAL	$\Upsilon(2S) \rightarrow \gamma X$
9913.2 ± 0.7 ± 1.0	¹ HAAS	84 CLEO	$\Upsilon(2S) \rightarrow \text{conv. } \gamma X$
9914.5 ± 0.3 ± 2.0	¹ KLOPFEN...	83 CUSB	$\Upsilon(2S) \rightarrow \gamma X$
9914 ± 4	¹ PAUSS	83 CUSB	$\Upsilon(2S) \rightarrow \gamma \gamma \ell^+ \ell^-$

¹ From γ energy below, assuming $\Upsilon(2S)$ mass = 10023.3 MeV.

 γ ENERGY IN $\Upsilon(2S)$ DECAY

VALUE (MeV)	DOCUMENT ID	TECN	COMMENT
110.1 ± 0.5 OUR AVERAGE	Error includes scale factor of 1.1.		
110.8 ± 0.3 ± 0.6	EDWARDS	99 CLE2	$\Upsilon(2S) \rightarrow \gamma \chi(1P)$
107.0 ± 1.1 ± 1.3	WALK	86 CBAL	$\Upsilon(2S) \rightarrow \gamma \gamma \ell^+ \ell^-$
110.6 ± 0.3 ± 0.9	ALBRECHT	85E ARG	$\Upsilon(2S) \rightarrow \text{conv. } \gamma X$
110.4 ± 0.8 ± 2.2	NERNST	85 CBAL	$\Upsilon(2S) \rightarrow \gamma X$
109.5 ± 0.7 ± 1.0	HAAS	84 CLEO	$\Upsilon(2S) \rightarrow \text{conv. } \gamma X$
108.2 ± 0.3 ± 2.0	KLOPFEN...	83 CUSB	$\Upsilon(2S) \rightarrow \gamma X$
108.8 ± 4.0	PAUSS	83 CUSB	$\Upsilon(2S) \rightarrow \gamma \gamma \ell^+ \ell^-$

 $\chi_{b2}(1P)$ DECAY MODES

Mode	Fraction (Γ_i/Γ)
Γ_1 $\gamma \Upsilon(1S)$	(22 ± 4) %

 $\chi_{b2}(1P)$ BRANCHING RATIOS

$\Gamma(\gamma \Upsilon(1S))/\Gamma_{total}$	Γ_1/Γ
0.22 ± 0.04 OUR AVERAGE	
0.27 ± 0.06 ± 0.06	
0.20 ± 0.05	

 $\chi_{b2}(1P)$ REFERENCES

EDWARDS	99	PR D59 032003	K.W. Edwards et al.	(CLEO Collab.)
SKWARNICKI	87	PRL 58 972	T. Skwarnicki et al.	(Crystal Ball Collab.)
WALK	86	PR D34 2611	W.S. Walk et al.	(Crystal Ball Collab.)
ALBRECHT	85E	PL 160B 331	H. Albrecht et al.	(ARGUS Collab.)
NERNST	85	PRL 54 2195	R. Nernst et al.	(Crystal Ball Collab.)
HAAS	84	PRL 52 799	J. Haas et al.	(CLEO Collab.)
KLOPFEN...	83	PRL 51 160	C. Klopfenstein et al.	(CUSB Collab.)
PAUSS	83	PL 130B 439	F. Pauss et al.	(MPIM, COLU, CORN, LSU+)

 $\Upsilon(2S)$

$$J^G(J^{PC}) = 0^-(1^{--})$$

 $\Upsilon(2S)$ MASS

VALUE (GeV)	DOCUMENT ID	TECN	COMMENT
10.02326 ± 0.00031 OUR AVERAGE			
10.0235 ± 0.0005	¹ ARTAMONOV 00	MD1	$e^+ e^- \rightarrow \text{hadrons}$
10.0231 ± 0.0004	BARBER	84 REDE	$e^+ e^- \rightarrow \text{hadrons}$
• • • We do not use the following data for averages, fits, limits, etc. • • •			
10.0236 ± 0.0005	^{2,3} BARU	86B REDE	$e^+ e^- \rightarrow \text{hadrons}$

¹ Reanalysis of BARU 86B using new electron mass (COHEN 87).

² Reanalysis of ARTAMONOV 84.

³ Superseded by ARTAMONOV 00.

 $\Upsilon(2S)$ WIDTH

VALUE (keV)	DOCUMENT ID
44 ± 7 OUR EVALUATION	See the Note on Width Determinations of the Υ states

 $\Upsilon(2S)$ DECAY MODES

Mode	Fraction (Γ_i/Γ)	Confidence level
Γ_1 $\Upsilon(1S) \pi^+ \pi^-$	(18.8 ± 0.6) %	
Γ_2 $\Upsilon(1S) \pi^0 \pi^0$	(9.0 ± 0.8) %	
Γ_3 $\tau^+ \tau^-$	(1.7 ± 1.6) %	
Γ_4 $\mu^+ \mu^-$	(1.31 ± 0.21) %	
Γ_5 $e^+ e^-$	(1.18 ± 0.20) %	
Γ_6 $\Upsilon(1S) \pi^0$	< 1.1	× 10 ⁻³ 90%
Γ_7 $\Upsilon(1S) \eta$	< 2	× 10 ⁻³ 90%
Γ_8 $J/\psi(1S)$ anything	< 6	× 10 ⁻³ 90%

Radiative decays

Γ_9 $\gamma \chi_{b1}(1P)$	(6.8 ± 0.7) %	
Γ_{10} $\gamma \chi_{b2}(1P)$	(7.0 ± 0.6) %	
Γ_{11} $\gamma \chi_{b0}(1P)$	(3.8 ± 0.6) %	
Γ_{12} $\gamma f_0(1710)$	< 5.9	× 10 ⁻⁴ 90%
Γ_{13} $\gamma f_2'(1525)$	< 5.3	× 10 ⁻⁴ 90%
Γ_{14} $\gamma f_2(1270)$	< 2.41	× 10 ⁻⁴ 90%
Γ_{15} $\gamma f_3(2220)$		

 $\Upsilon(2S) \Gamma(\ell) \Gamma(e^+ e^-) / \Gamma_{total}$

$\Gamma(e^+ e^-) \times \Gamma(\mu^+ \mu^-) / \Gamma_{total}$	$\Gamma_5 \Gamma_4 / \Gamma$
6.5 ± 1.5 ± 1.0	

VALUE (ev)	DOCUMENT ID	TECN	COMMENT
6.5 ± 1.5 ± 1.0	KOBEL	92 CBAL	$e^+ e^- \rightarrow \mu^+ \mu^-$

$\Gamma(\text{hadrons}) \times \Gamma(e^+ e^-) / \Gamma_{total}$	$\Gamma_0 \Gamma_5 / \Gamma$
0.553 ± 0.023 OUR AVERAGE	

VALUE (keV)	DOCUMENT ID	TECN	COMMENT
0.552 ± 0.031 ± 0.017	⁴ BARU	96 MD1	$e^+ e^- \rightarrow \text{hadrons}$
0.54 ± 0.04 ± 0.02	⁴ JAKUBOWSKI	88 CBAL	$e^+ e^- \rightarrow \text{hadrons}$
0.58 ± 0.03 ± 0.04	⁵ GILES	84B CLEO	$e^+ e^- \rightarrow \text{hadrons}$
0.60 ± 0.12 ± 0.07	⁵ ALBRECHT	82 DASP	$e^+ e^- \rightarrow \text{hadrons}$
0.54 ± 0.07 + 0.09 - 0.05	⁵ NICZYPORUK	81C LENA	$e^+ e^- \rightarrow \text{hadrons}$
0.41 ± 0.18	⁵ BOCK	80 CNTR	$e^+ e^- \rightarrow \text{hadrons}$

⁴ Radiative corrections evaluated following KURAEV 85.

⁵ Radiative corrections reevaluated by BUCHMUELLER 88 following KURAEV 85.

 $\Upsilon(2S)$ PARTIAL WIDTHS

$\Gamma(e^+ e^-)$	Γ_5
0.52 ± 0.03 ± 0.01	

VALUE (keV)	DOCUMENT ID	TECN	COMMENT
0.52 ± 0.03 ± 0.01	⁶ ALBRECHT	95E ARG	$e^+ e^- \rightarrow \text{hadrons}$

⁶ Applying the formula of Kuraev and Fadin.

 $\Upsilon(2S)$ BRANCHING RATIOS

$\Gamma(J/\psi(1S) \text{ anything}) / \Gamma_{total}$	Γ_8 / Γ
< 0.006	

VALUE	CL%	DOCUMENT ID	TECN	COMMENT
< 0.006	90	MASCHMANN 90	CBAL	$e^+ e^- \rightarrow \text{hadrons}$

See key on page 239

Meson Particle Listings
 $\Upsilon(2S)$

$\Gamma(\Upsilon(1S)\pi^+\pi^-)/\Gamma_{total}$		Γ_1/Γ	
VALUE	EVTs	DOCUMENT ID	TECN COMMENT
0.188±0.006 OUR AVERAGE			
0.192±0.002±0.010	52.6k	7 ALEXANDER 98	CLE2 $\pi^+\pi^-\ell^+\ell^-$, $\pi^+\pi^-\text{MM}$
0.181±0.005±0.010	11.6k	ALBRECHT 87	ARG $e^+e^- \rightarrow \pi^+\pi^-\text{MM}$
0.169±0.040		GELPHMAN 85	CBAL $e^+e^- \rightarrow \pi^+\pi^-\text{MM}$
0.191±0.012±0.006		BESSON 84	CLEO $e^+e^- \rightarrow \pi^+\pi^-\text{MM}$
0.189±0.026		FONSECA 84	CUSB $e^+e^- \rightarrow \pi^+\pi^-\text{MM}$
0.21 ± 0.07	7	NICZYPORUK 81b	LENA $e^+e^- \rightarrow \pi^+\pi^-\text{MM}$

⁷ Using $B(\Upsilon(1S) \rightarrow e^+e^-) = (2.52 \pm 0.17)\%$ and $B(\Upsilon(1S) \rightarrow \mu^+\mu^-) = (2.48 \pm 0.07)\%$.

$\Gamma(\Upsilon(1S)\pi^0\pi^0)/\Gamma_{total}$		Γ_2/Γ	
VALUE	EVTs	DOCUMENT ID	TECN COMMENT
0.090±0.008 OUR AVERAGE			
0.092±0.006±0.008	275	8 ALEXANDER 98	CLE2 $e^+e^- \rightarrow \ell^+\ell^-\pi^0\pi^0$
0.095±0.019±0.019	25	ALBRECHT 87	ARG $e^+e^- \rightarrow \pi^0\pi^0\ell^+\ell^-$
0.080±0.015		GELPHMAN 85	CBAL $e^+e^- \rightarrow \ell^+\ell^-\pi^0\pi^0$
0.103±0.023		FONSECA 84	CUSB $e^+e^- \rightarrow \ell^+\ell^-\pi^0\pi^0$

⁸ Using $B(\Upsilon(1S) \rightarrow e^+e^-) = (2.52 \pm 0.17)\%$ and $B(\Upsilon(1S) \rightarrow \mu^+\mu^-) = (2.48 \pm 0.07)\%$.

$\Gamma(\tau^+\tau^-)/\Gamma_{total}$		Γ_3/Γ	
VALUE		DOCUMENT ID	TECN COMMENT
0.017±0.015±0.006			
		HAAS 84b	CLEO $e^+e^- \rightarrow \tau^+\tau^-$

$\Gamma(\mu^+\mu^-)/\Gamma_{total}$		Γ_4/Γ	
VALUE	CL%	DOCUMENT ID	TECN COMMENT
0.0131±0.0021 OUR AVERAGE			
0.0122±0.0028±0.0019		9 KOBEL 92	CBAL $e^+e^- \rightarrow \mu^+\mu^-$
0.0138±0.0025±0.0015		KAARSBERG 89	CSB2 $e^+e^- \rightarrow \mu^+\mu^-$
0.009 ± 0.006 ± 0.006		10 ALBRECHT 85	ARG $e^+e^- \rightarrow \mu^+\mu^-$
0.018 ± 0.008 ± 0.005		HAAS 84b	CLEO $e^+e^- \rightarrow \mu^+\mu^-$

• • • We do not use the following data for averages, fits, limits, etc. • • •

<0.038 90 NICZYPORUK 81c LENA $e^+e^- \rightarrow \mu^+\mu^-$

⁹ Taking into account interference between the resonance and continuum.

¹⁰ Re-evaluated using $B(\Upsilon(1S) \rightarrow \mu^+\mu^-) = 0.026$.

$\Gamma(\Upsilon(1S)\pi^0)/\Gamma_{total}$		Γ_6/Γ	
VALUE	CL%	DOCUMENT ID	TECN COMMENT
<0.0011			
<0.008	90	ALEXANDER 98	CLE2 $e^+e^- \rightarrow \ell^+\ell^-\gamma\gamma$
<0.008	90	LURZ 87	CBAL $e^+e^- \rightarrow \ell^+\ell^-\gamma\gamma$

$\Gamma(\Upsilon(1S)\eta)/\Gamma_{total}$		Γ_7/Γ	
VALUE	CL%	DOCUMENT ID	TECN COMMENT
<0.002			
<0.0028	90	ALEXANDER 98	CLE2 $e^+e^- \rightarrow \ell^+\ell^-\eta$
<0.005	90	ALBRECHT 87	ARG $e^+e^- \rightarrow \ell^+\ell^-\eta$
<0.007	90	LURZ 87	CBAL $e^+e^- \rightarrow \ell^+\ell^-\text{MM}$ $\pi^+\pi^-\ell^+\ell^-\text{MM}$
<0.010	90	BESSON 84	CLEO $e^+e^- \rightarrow \ell^+\ell^-\text{MM}$ $3\pi^0$

$\Gamma(\gamma\chi_{b1}(1P))/\Gamma_{total}$		Γ_9/Γ	
VALUE		DOCUMENT ID	TECN COMMENT
0.068±0.007 OUR AVERAGE			
0.069±0.005±0.009		EDWARDS 99	CLE2 $\Upsilon(2S) \rightarrow \gamma\chi(1P)$
0.091±0.018±0.022		ALBRECHT 85e	ARG $e^+e^- \rightarrow \gamma\text{conv. X}$
0.065±0.007±0.012		NERNST 85	CBAL $e^+e^- \rightarrow \gamma\text{X}$
0.080±0.017±0.016		HAAS 84	CLEO $e^+e^- \rightarrow \gamma\text{conv. X}$
0.059±0.014		KLOPFEN...	83 CUSB $e^+e^- \rightarrow \gamma\text{X}$

$\Gamma(\gamma\chi_{b2}(1P))/\Gamma_{total}$		Γ_{10}/Γ	
VALUE		DOCUMENT ID	TECN COMMENT
0.070±0.006 OUR AVERAGE			
0.074±0.005±0.008		EDWARDS 99	CLE2 $\Upsilon(2S) \rightarrow \gamma\chi(1P)$
0.098±0.021±0.024		ALBRECHT 85e	ARG $e^+e^- \rightarrow \gamma\text{conv. X}$
0.058±0.007±0.010		NERNST 85	CBAL $e^+e^- \rightarrow \gamma\text{X}$
0.102±0.018±0.021		HAAS 84	CLEO $e^+e^- \rightarrow \gamma\text{conv. X}$
0.061±0.014		KLOPFEN...	83 CUSB $e^+e^- \rightarrow \gamma\text{X}$

$\Gamma(\gamma\chi_{b0}(1P))/\Gamma_{total}$		Γ_{11}/Γ	
VALUE		DOCUMENT ID	TECN COMMENT
0.038±0.006 OUR AVERAGE			
0.034±0.005±0.006		EDWARDS 99	CLE2 $\Upsilon(2S) \rightarrow \gamma\chi(1P)$
0.064±0.014±0.016		ALBRECHT 85e	ARG $e^+e^- \rightarrow \gamma\text{conv. X}$
0.036±0.008±0.009		NERNST 85	CBAL $e^+e^- \rightarrow \gamma\text{X}$
0.044±0.023±0.009		HAAS 84	CLEO $e^+e^- \rightarrow \gamma\text{conv. X}$
0.035±0.014		KLOPFEN...	83 CUSB $e^+e^- \rightarrow \gamma\text{X}$

$\Gamma(\gamma f_0(1710))/\Gamma_{total}$		Γ_{12}/Γ	
VALUE (units 10 ⁻⁵)	CL%	DOCUMENT ID	TECN COMMENT
<59			
<5.9	90	11 ALBRECHT 89	ARG $\Upsilon(2S) \rightarrow \gamma K^+ K^-$
<5.9	90	12 ALBRECHT 89	ARG $\Upsilon(2S) \rightarrow \gamma\pi^+\pi^-$

• • • We do not use the following data for averages, fits, limits, etc. • • •

$\Gamma(\gamma f_2'(1525))/\Gamma_{total}$		Γ_{13}/Γ	
VALUE (units 10 ⁻⁵)	CL%	DOCUMENT ID	TECN COMMENT
<53			
<5.9	90	13 ALBRECHT 89	ARG $\Upsilon(2S) \rightarrow \gamma K^+ K^-$

¹¹ Re-evaluated assuming $B(f_0(1710) \rightarrow K^+K^-) = 0.19$.

¹² Includes unknown branching ratio of $f_0(1710) \rightarrow \pi^+\pi^-$.

$\Gamma(\gamma f_2'(1270))/\Gamma_{total}$		Γ_{14}/Γ	
VALUE (units 10 ⁻⁵)	CL%	DOCUMENT ID	TECN COMMENT
<24.1			
<2.4	90	14 ALBRECHT 89	ARG $\Upsilon(2S) \rightarrow \gamma\pi^+\pi^-$

¹⁴ Using $B(f_2'(1270) \rightarrow \pi\pi) = 0.84$.

$\Gamma(\gamma f_J(2220))/\Gamma_{total}$		Γ_{15}/Γ	
VALUE (units 10 ⁻⁵)	CL%	DOCUMENT ID	TECN COMMENT
<6.8			
<0.6	90	15 ALBRECHT 89	ARG $\Upsilon(2S) \rightarrow \gamma K^+ K^-$

¹⁵ Includes unknown branching ratio of $f_J(2220) \rightarrow K^+K^-$.

 $\Upsilon(2S)$ REFERENCES

ARTAMONOV 00	PL B474 427	A.S. Artamonov et al.	(CLEO Collab.)
EDWARDS 99	PR D59 032003	K.W. Edwards et al.	(CLEO Collab.)
ALEXANDER 98	PR D58 052004	J.P. Alexander et al.	(CLEO Collab.)
BARU 96	PR D57 267 71	S.E. Baru et al.	(NOVO)
ALBRECHT 95e	ZPHY C65 619	H. Albrecht et al.	(ARGUS Collab.)
KOBEL 92	ZPHY C53 193	M. Kobel et al.	(Crystal Ball Collab.)
MASCHMANN 90	ZPHY C46 555	W.S. Maschmann et al.	(Crystal Ball Collab.)
ALBRECHT 89	ZPHY C42 349	H. Albrecht et al.	(ARGUS Collab.)
KAARSBERG 89	PRL 62 2077	T.M. Kaarsberg et al.	(CUSB Collab.)
BUCHMUELLER... 88	HE e ⁺ e ⁻ Physics 412	W. Buchmueller, S. Cooper	(HANN, DESY, MIT)
Editors: A. Ali and P. Soeding, World Scientific, Singapore			
JAKUBOWSKI 88	ZPHY C40 49	Z. Jakubowski et al.	(Crystal Ball Collab.)
ALBRECHT 87	ZPHY C35 283	H. Albrecht et al.	(ARGUS Collab.)
COHEN 87	RMP 59 1121	E.R. Cohen, B.N. Taylor	(RISC, NBS)
LURZ 87	ZPHY C36 383	B. Lurz et al.	(Crystal Ball Collab.)
BARU 86b	ZPHY C32 622	S.E. Baru et al.	(NOVO)
ALBRECHT 85	ZPHY C28 445	H. Albrecht et al.	(ARGUS Collab.)
ALBRECHT 85e	PL 1608 231	H. Albrecht et al.	(ARGUS Collab.)
GELPHMAN 85	PR D11 2893	D. Gelphman et al.	(Crystal Ball Collab.)
KURAEV 85	SJNP 41 466	E.A. Kurayev, V.S. Fadin	(NOVO)
Translated from YAF 41 733.			
NERNST 85	PRL 54 2195	R. Nernst et al.	(Crystal Ball Collab.)
ARTAMONOV 84	PL 137B 272	A.S. Artamonov et al.	(NOVO)
BARBER 84	PL 135B 498	D.P. Barber et al.	(CLEO Collab.)
BESSON 84	PR D30 1433	V. Besson et al.	(CUSB Collab.)
FONSECA 84	NP B242 31	F. Fonseca et al.	(CLEO Collab.)
GILES 84b	PR D29 1285	R. Giles et al.	(CLEO Collab.)
HAAS 84	PRL 52 799	J. Haas et al.	(CLEO Collab.)
HAAS 84b	PR D30 1996	J. Haas et al.	(CLEO Collab.)
KLOPFEN... 83	PRL 51 160	C. Klopfenstein et al.	(CUSB Collab.)
ALBRECHT 82	PL 116B 383	H. Albrecht et al.	(DESY, DORT, HEIDH+)
NICZYPORUK 81b	PL 100B 95	B. Niczyporuk et al.	(LENA Collab.)
NICZYPORUK 81c	PL 99B 169	B. Niczyporuk et al.	(LENA Collab.)
BOCK 80	ZPHY C6 125	P. Bock et al.	(HEIDP, MPIM, DESY, HAMB)

OTHER RELATED PAPERS

ALEXANDER 89	NP B320 45	J.P. Alexander et al.	(LBL, MICH, SLAC)
WALK 86	PR D34 2611	W.S. Walk et al.	(Crystal Ball Collab.)
ALBRECHT 84	PL 134B 137	H. Albrecht et al.	(ARGUS Collab.)
ARTAMONOV 84	PL 137B 272	A.S. Artamonov et al.	(NOVO)
ANDREWS 83	PRL 50 807	D.E. Andrews et al.	(CLEO Collab.)
GREEN 82	PRL 49 617	J. Green et al.	(CLEO Collab.)
BIENLEIN 78	PL 78B 360	J.K. Bienlein et al.	(DESY, HAMB, HEIDP+)
DARDEN 78	PL 76B 246	C.W. Darden et al.	(DESY, DORT, HEIDH+)
KAPLAN 78	PRL 40 435	D.M. Kaplan et al.	(STON, FNAL, COLU)
YOH 78	PRL 41 684	J.K. Yoh et al.	(COLU, FNAL, STON)
COBB 77	PL 72B 273	J.H. Cobb et al.	(BNL, CERN, SYRA, YALE)
HERB 77	PRL 39 252	S.W. Herb et al.	(COLU, FNAL, STON)
INNES 77	PRL 39 1240	W.R. Innes et al.	(COLU, FNAL, STON)

Meson Particle Listings

 $\chi_{b0}(2P)$, $\chi_{b1}(2P)$ $\chi_{b0}(2P)$

$$J^G(J^{PC}) = 0^+(0^{++})$$

J needs confirmation.

Observed in radiative decay of the $T(3S)$, therefore $C = +$. Branching ratio requires E1 transition, M1 is strongly disfavored, therefore $P = +$.

 $\chi_{b0}(2P)$ MASS

VALUE (GeV)	DOCUMENT ID	TECN	COMMENT
10.2321 ± 0.0006 OUR AVERAGE			
10.2312 ± 0.0008 ± 0.0012	¹ HEINTZ 92	CSB2	$e^+e^- \rightarrow \gamma X, \ell^+\ell^-\gamma\gamma$
10.2323 ± 0.0007	² MORRISON 91	CLE2	$e^+e^- \rightarrow \gamma X$

¹ From the average photon energy for inclusive and exclusive events and assuming $T(3S)$ mass = 10355.3 ± 0.5 MeV. Supersedes HEINTZ 91 and NARAIN 91.

² From γ energy below assuming $T(3S)$ mass = 10355.3 ± 0.5 MeV. The error on the $T(3S)$ mass is not included in the individual measurements. It is included in the final average.

 γ ENERGY IN $T(3S)$ DECAY

VALUE (MeV)	EVTS	DOCUMENT ID	TECN	COMMENT
122.8 ± 0.5 OUR AVERAGE				Error includes scale factor of 1.1.
123.0 ± 0.8	4959	³ HEINTZ 92	CSB2	$e^+e^- \rightarrow \gamma X$
124.6 ± 1.4	17	⁴ HEINTZ 92	CSB2	$e^+e^- \rightarrow \ell^+\ell^-\gamma\gamma$
122.3 ± 0.3 ± 0.6	9903	MORRISON 91	CLE2	$e^+e^- \rightarrow \gamma X$

³ A systematic uncertainty on the energy scale of 0.9% not included. Supersedes NARAIN 91.

⁴ A systematic uncertainty on the energy scale of 0.9% not included. Supersedes HEINTZ 91.

 $\chi_{b0}(2P)$ DECAY MODES

Mode	Fraction (Γ_i/Γ)
Γ_1 $\gamma T(2S)$	(4.6 ± 2.1) %
Γ_2 $\gamma T(1S)$	(9 ± 6) × 10 ⁻³

 $\chi_{b0}(2P)$ BRANCHING RATIOS

$\Gamma(\gamma T(2S))/\Gamma_{total}$	CL%	DOCUMENT ID	TECN	COMMENT	Γ_1/Γ
< 0.089	90	⁵ CRAWFORD 92B	CLE2	$e^+e^- \rightarrow \ell^+\ell^-\gamma\gamma$	
0.046 ± 0.020 ± 0.007		⁶ HEINTZ 92	CSB2	$e^+e^- \rightarrow \ell^+\ell^-\gamma\gamma$	

⁵ Using $B(T(2S) \rightarrow \mu^+\mu^-) = (1.37 \pm 0.26)\%$, $B(T(3S) \rightarrow \gamma\gamma T(2S)) \times 2 B(T(2S) \rightarrow \mu^+\mu^-) < 1.19 \times 10^{-4}$, and $B(T(3S) \rightarrow \chi_{b0}(2P)\gamma) = 0.049$.

⁶ Using $B(T(2S) \rightarrow \mu^+\mu^-) = (1.44 \pm 0.10)\%$, $B(T(3S) \rightarrow \gamma\chi_{b0}(2P)) = (6.0 \pm 0.4 \pm 0.6)\%$ and assuming $e\mu$ universality. Supersedes HEINTZ 91.

$\Gamma(\gamma T(1S))/\Gamma_{total}$	CL%	DOCUMENT ID	TECN	COMMENT	Γ_2/Γ
< 0.025	90	⁷ CRAWFORD 92B	CLE2	$e^+e^- \rightarrow \ell^+\ell^-\gamma\gamma$	
0.009 ± 0.006 ± 0.001		⁸ HEINTZ 92	CSB2	$e^+e^- \rightarrow \ell^+\ell^-\gamma\gamma$	

⁷ Using $B(T(1S) \rightarrow \mu^+\mu^-) = (2.57 \pm 0.07)\%$, $B(T(3S) \rightarrow \gamma\gamma T(1S)) \times 2 B(T(1S) \rightarrow \mu^+\mu^-) < 0.63 \times 10^{-4}$, and $B(T(3S) \rightarrow \chi_{b0}(2P)\gamma) = 0.049$.

⁸ Using $B(T(1S) \rightarrow \mu^+\mu^-) = (2.57 \pm 0.07)\%$, $B(T(3S) \rightarrow \gamma\chi_{b0}(2P)) = (6.0 \pm 0.4 \pm 0.6)\%$ and assuming $e\mu$ universality. Supersedes HEINTZ 91.

 $\chi_{b0}(2P)$ REFERENCES

CRAWFORD 92B	PL B294 139	G. Crawford, R. Fulton	(CLEO Collab.)
HEINTZ 92	PR D46 1928	U. Heintz et al.	(CUSB II Collab.)
HEINTZ 91	PRL 66 1563	U. Heintz et al.	(CUSB Collab.)
MORRISON 91	PRL 67 1696	R.J. Morrison et al.	(CLEO Collab.)
NARAIN 91	PRL 66 3113	M. Narain et al.	(CUSB Collab.)

OTHER RELATED PAPERS

EIGEN 82	PRL 49 1616	G. Eigen et al.	(CUSB Collab.)
HAN 82	PRL 49 1612	K. Han et al.	(CUSB Collab.)

 $\chi_{b1}(2P)$

$$J^G(J^{PC}) = 0^+(1^{++})$$

J needs confirmation.

Observed in radiative decay of the $T(3S)$, therefore $C = +$. Branching ratio requires E1 transition, M1 is strongly disfavored, therefore $P = +$.

 $\chi_{b1}(2P)$ MASS

VALUE (GeV)	DOCUMENT ID	TECN	COMMENT
10.2552 ± 0.0005 OUR AVERAGE			
10.2547 ± 0.0004 ± 0.0010	¹ HEINTZ 92	CSB2	$e^+e^- \rightarrow \gamma X, \ell^+\ell^-\gamma\gamma$
10.2553 ± 0.0005	² MORRISON 91	CLE2	$e^+e^- \rightarrow \gamma X$

¹ From the average photon energy for inclusive and exclusive events and assuming $T(3S)$ mass = 10355.3 ± 0.5 MeV. Supersedes HEINTZ 91 and NARAIN 91.

² From γ energy below assuming $T(3S)$ mass = 10355.3 ± 0.5 MeV. The error on the $T(3S)$ mass is not included in the individual measurements. It is included in the final evaluation.

 $m_{\chi_{b1}(2P)} - m_{\chi_{b0}(2P)}$

VALUE (MeV)	DOCUMENT ID	TECN	COMMENT
23.5 ± 0.7 ± 0.7	³ HEINTZ 92	CSB2	$e^+e^- \rightarrow \gamma X, \ell^+\ell^-\gamma\gamma$

³ From the average photon energy for inclusive and exclusive events. Supersedes NARAIN 91.

 γ ENERGY IN $T(3S)$ DECAY

VALUE (MeV)	EVTS	DOCUMENT ID	TECN	COMMENT
99.90 ± 0.26 OUR AVERAGE				
99 ± 1	169	CRAWFORD 92B	CLE2	$e^+e^- \rightarrow \ell^+\ell^-\gamma\gamma$
100.1 ± 0.4	11147	⁴ HEINTZ 92	CSB2	$e^+e^- \rightarrow \gamma X$
100.2 ± 0.5	223	⁵ HEINTZ 92	CSB2	$e^+e^- \rightarrow \ell^+\ell^-\gamma\gamma$
99.5 ± 0.1 ± 0.5	25759	MORRISON 91	CLE2	$e^+e^- \rightarrow \gamma X$

⁴ A systematic uncertainty on the energy scale of 0.9% not included. Supersedes NARAIN 91.

⁵ A systematic uncertainty on the energy scale of 0.9% not included. Supersedes HEINTZ 91.

 $\chi_{b1}(2P)$ DECAY MODES

Mode	Fraction (Γ_i/Γ)	Scale factor
Γ_1 $\gamma T(2S)$	(21 ± 4) %	1.5
Γ_2 $\gamma T(1S)$	(8.5 ± 1.3) %	1.3

 $\chi_{b1}(2P)$ BRANCHING RATIOS

$\Gamma(\gamma T(2S))/\Gamma_{total}$	CL%	DOCUMENT ID	TECN	COMMENT	Γ_1/Γ
0.21 ± 0.04 OUR AVERAGE				Error includes scale factor of 1.5.	
0.356 ± 0.042 ± 0.092		⁶ CRAWFORD 92B	CLE2	$e^+e^- \rightarrow \ell^+\ell^-\gamma\gamma$	
0.199 ± 0.020 ± 0.022		⁷ HEINTZ 92	CSB2	$e^+e^- \rightarrow \ell^+\ell^-\gamma\gamma$	

⁶ Using $B(T(2S) \rightarrow \mu^+\mu^-) = (1.37 \pm 0.26)\%$, $B(T(3S) \rightarrow \gamma\gamma T(2S)) \times 2 B(T(2S) \rightarrow \mu^+\mu^-) = (10.23 \pm 1.20 \pm 1.26) \times 10^{-4}$, and $B(T(3S) \rightarrow \gamma\chi_{b1}(2P)) = 0.105^{+0.003}_{-0.002} \pm 0.013$.

⁷ Using $B(T(2S) \rightarrow \mu^+\mu^-) = (1.44 \pm 0.10)\%$, $B(T(3S) \rightarrow \gamma\chi_{b1}(2P)) = (11.5 \pm 0.5 \pm 0.5)\%$ and assuming $e\mu$ universality. Supersedes HEINTZ 91.

$\Gamma(\gamma T(1S))/\Gamma_{total}$	CL%	DOCUMENT ID	TECN	COMMENT	Γ_2/Γ
0.085 ± 0.013 OUR AVERAGE				Error includes scale factor of 1.3.	
0.120 ± 0.021 ± 0.021		⁸ CRAWFORD 92B	CLE2	$e^+e^- \rightarrow \ell^+\ell^-\gamma\gamma$	
0.080 ± 0.009 ± 0.007		⁹ HEINTZ 92	CSB2	$e^+e^- \rightarrow \ell^+\ell^-\gamma\gamma$	

⁸ Using $B(T(1S) \rightarrow \mu^+\mu^-) = (2.57 \pm 0.07)\%$, $B(T(3S) \rightarrow \gamma\gamma T(1S)) \times 2 B(T(1S) \rightarrow \mu^+\mu^-) = (6.47 \pm 1.12 \pm 0.82) \times 10^{-4}$, and $B(T(3S) \rightarrow \gamma\chi_{b1}(2P)) = 0.105^{+0.003}_{-0.002} \pm 0.013$.

⁹ Using $B(T(1S) \rightarrow \mu^+\mu^-) = (2.57 \pm 0.07)\%$, $B(T(3S) \rightarrow \gamma\chi_{b1}(2P)) = (11.5 \pm 0.5 \pm 0.5)\%$ and assuming $e\mu$ universality. Supersedes HEINTZ 91.

 $\chi_{b1}(2P)$ REFERENCES

CRAWFORD 92B	PL B294 139	G. Crawford, R. Fulton	(CLEO Collab.)
HEINTZ 92	PR D46 1928	U. Heintz et al.	(CUSB II Collab.)
HEINTZ 91	PRL 66 1563	U. Heintz et al.	(CUSB Collab.)
MORRISON 91	PRL 67 1696	R.J. Morrison et al.	(CLEO Collab.)
NARAIN 91	PRL 66 3113	M. Narain et al.	(CUSB Collab.)

OTHER RELATED PAPERS

EIGEN 82	PRL 49 1616	G. Eigen et al.	(CUSB Collab.)
HAN 82	PRL 49 1612	K. Han et al.	(CUSB Collab.)

See key on page 239

Meson Particle Listings

 $\chi_{b2}(2P), \Upsilon(3S)$ $\chi_{b2}(2P)$

$$J^{G(J^{PC})} = 0^+(2^{++})$$

J needs confirmation.

Observed in radiative decay of the $\Upsilon(3S)$, therefore $C = +$. Branching ratio requires E1 transition, M1 is strongly disfavored, therefore $P = +$.

 $\chi_{b2}(2P)$ MASS

VALUE (GeV)	DOCUMENT ID	TECN	COMMENT
10.2685 ± 0.0004 OUR AVERAGE			
10.2681 ± 0.0004 ± 0.0010	¹ HEINTZ 92	CSB2	$e^+e^- \rightarrow \gamma X, \ell^+ \ell^- \gamma \gamma$
10.2685 ± 0.0004	² MORRISON 91	CLE2	$e^+e^- \rightarrow \gamma X$

¹ From the average photon energy for inclusive and exclusive events and assuming $\Upsilon(3S)$ mass = 10355.3 ± 0.5 MeV. Supersedes HEINTZ 91 and NARAIN 91.

² From γ energy below, assuming $\Upsilon(3S)$ mass = 10355.3 ± 0.5 MeV. The error on the $\Upsilon(3S)$ mass is not included in the individual measurements. It is included in the final average.

 $m_{\chi_{b2}(2P)} - m_{\chi_{b1}(2P)}$

VALUE (MeV)	DOCUMENT ID	TECN	COMMENT
13.5 ± 0.4 ± 0.5	³ HEINTZ 92	CSB2	$e^+e^- \rightarrow \gamma X, \ell^+ \ell^- \gamma \gamma$

³ From the average photon energy for inclusive and exclusive events. Supersedes NARAIN 91.

 γ ENERGY IN $\Upsilon(3S)$ DECAY

VALUE (MeV)	EVTs	DOCUMENT ID	TECN	COMMENT
86.64 ± 0.23 OUR AVERAGE				
86 ± 1	101	CRAWFORD 92B	CLE2	$e^+e^- \rightarrow \ell^+ \ell^- \gamma \gamma$
86.7 ± 0.4	10319	⁴ HEINTZ 92	CSB2	$e^+e^- \rightarrow \gamma X$
86.9 ± 0.4	157	⁵ HEINTZ 92	CSB2	$e^+e^- \rightarrow \ell^+ \ell^- \gamma \gamma$
86.4 ± 0.1 ± 0.4	30741	MORRISON 91	CLE2	$e^+e^- \rightarrow \gamma X$

⁴ A systematic uncertainty on the energy scale of 0.9% not included. Supersedes NARAIN 91.

⁵ A systematic uncertainty on the energy scale of 0.9% not included. Supersedes HEINTZ 91.

 $\chi_{b2}(2P)$ DECAY MODES

Mode	Fraction (Γ_i/Γ)
$\Gamma_1 \quad \gamma \Upsilon(2S)$	(16.2 ± 2.4) %
$\Gamma_2 \quad \gamma \Upsilon(1S)$	(7.1 ± 1.0) %

 $\chi_{b2}(2P)$ BRANCHING RATIOS

$\Gamma(\gamma \Upsilon(2S))/\Gamma_{total}$	DOCUMENT ID	TECN	COMMENT	Γ_1/Γ
0.162 ± 0.024 OUR AVERAGE				
0.135 ± 0.025 ± 0.035	⁶ CRAWFORD 92B	CLE2	$e^+e^- \rightarrow \ell^+ \ell^- \gamma \gamma$	
0.173 ± 0.021 ± 0.019	⁷ HEINTZ 92	CSB2	$e^+e^- \rightarrow \ell^+ \ell^- \gamma \gamma$	

⁶ Using $B(\Upsilon(2S) \rightarrow \mu^+ \mu^-) = (1.37 \pm 0.26)\%$, $B(\Upsilon(3S) \rightarrow \gamma \gamma \Upsilon(2S)) \times 2 B(\Upsilon(2S) \rightarrow \mu^+ \mu^-) = (4.98 \pm 0.94 \pm 0.62) \times 10^{-4}$, and $B(\Upsilon(3S) \rightarrow \gamma \chi_{b2}(2P)) = 0.135 \pm 0.003 \pm 0.017$.

⁷ Using $B(\Upsilon(2S) \rightarrow \mu^+ \mu^-) = (1.44 \pm 0.10)\%$, $B(\Upsilon(3S) \rightarrow \gamma \chi_{b2}(2P)) = (11.1 \pm 0.5 \pm 0.4)\%$ and assuming $e\mu$ universality. Supersedes HEINTZ 91.

$\Gamma(\gamma \Upsilon(1S))/\Gamma_{total}$	DOCUMENT ID	TECN	COMMENT	Γ_2/Γ
0.071 ± 0.010 OUR AVERAGE				
0.072 ± 0.014 ± 0.013	⁸ CRAWFORD 92B	CLE2	$e^+e^- \rightarrow \ell^+ \ell^- \gamma \gamma$	
0.070 ± 0.010 ± 0.006	⁹ HEINTZ 92	CSB2	$e^+e^- \rightarrow \ell^+ \ell^- \gamma \gamma$	

⁸ Using $B(\Upsilon(1S) \rightarrow \mu^+ \mu^-) = (2.57 \pm 0.07)\%$, $B(\Upsilon(3S) \rightarrow \gamma \gamma \Upsilon(2S)) \times 2 B(\Upsilon(1S) \rightarrow \mu^+ \mu^-) = (5.03 \pm 0.94 \pm 0.63) \times 10^{-4}$, and $B(\Upsilon(3S) \rightarrow \gamma \chi_{b2}(2P)) = 0.135 \pm 0.003 \pm 0.017$.

⁹ Using $B(\Upsilon(1S) \rightarrow \mu^+ \mu^-) = (2.57 \pm 0.07)\%$, $B(\Upsilon(3S) \rightarrow \gamma \chi_{b2}(2P)) = (11.1 \pm 0.5 \pm 0.4)\%$ and assuming $e\mu$ universality. Supersedes HEINTZ 91.

 $\chi_{b2}(2P)$ REFERENCES

CRAWFORD 92B	PL B294 139	G. Crawford, R. Fulton	(CLEO Collab.)
HEINTZ 92	PR D46 1928	U. Heintz et al.	(CUSB II Collab.)
HEINTZ 91	PRL 66 1563	U. Heintz et al.	(CUSB Collab.)
MORRISON 91	PRL 67 1696	R.J. Morrison et al.	(CLEO Collab.)
NARAIN 91	PRL 66 3113	M. Narain et al.	(CUSB Collab.)

OTHER RELATED PAPERS

EIGEN 82	PRL 49 1616	G. Eigen et al.	(CUSB Collab.)
HAN 82	PRL 49 1612	K. Han et al.	(CUSB Collab.)

 $\Upsilon(3S)$

$$J^{G(J^{PC})} = 0^-(1^{--})$$

 $\Upsilon(3S)$ MASS

VALUE (GeV)	DOCUMENT ID	TECN	COMMENT
10.3552 ± 0.0005	¹ ARTAMONOV 00	MD1	$e^+e^- \rightarrow$ hadrons
• • • We do not use the following data for averages, fits, limits, etc. • • •			
10.3553 ± 0.0005	^{2,3} BARU	86B REDE	$e^+e^- \rightarrow$ hadrons

¹ Reanalysis of BARU 86B using new electron mass (COHEN 87).

² Reanalysis of ARTAMONOV 84.

³ Superseded by ARTAMONOV 00.

 $\Upsilon(3S)$ WIDTH

VALUE (keV)	DOCUMENT ID	COMMENT
26.3 ± 3.5 OUR EVALUATION		See the Note on Width Determinations of the Υ states

 $\Upsilon(3S)$ DECAY MODES

Mode	Fraction (Γ_i/Γ)	Scale factor/ Confidence level
$\Gamma_1 \quad \Upsilon(2S)$ anything	(10.6 ± 0.8) %	
$\Gamma_2 \quad \Upsilon(2S) \pi^+ \pi^-$	(2.8 ± 0.6) %	S=2.2
$\Gamma_3 \quad \Upsilon(2S) \pi^0 \pi^0$	(2.00 ± 0.32) %	
$\Gamma_4 \quad \Upsilon(2S) \gamma \gamma$	(5.0 ± 0.7) %	
$\Gamma_5 \quad \Upsilon(1S) \pi^+ \pi^-$	(4.48 ± 0.21) %	
$\Gamma_6 \quad \Upsilon(1S) \pi^0 \pi^0$	(2.06 ± 0.28) %	
$\Gamma_7 \quad \Upsilon(1S) \eta$	< 2.2 × 10 ⁻³	CL=90%
$\Gamma_8 \quad \mu^+ \mu^-$	(1.81 ± 0.17) %	
$\Gamma_9 \quad e^+ e^-$	seen	

Radiative decays

$\Gamma_{10} \quad \gamma \chi_{b2}(2P)$	(11.4 ± 0.8) %	S=1.3
$\Gamma_{11} \quad \gamma \chi_{b1}(2P)$	(11.3 ± 0.6) %	
$\Gamma_{12} \quad \gamma \chi_{b0}(2P)$	(5.4 ± 0.6) %	S=1.1

 $\Upsilon(3S) \Gamma(\ell^+ \ell^- e^+ e^-)/\Gamma_{total}$

$\Gamma(\text{hadrons}) \times \Gamma(e^+ e^-)/\Gamma_{total}$	DOCUMENT ID	TECN	COMMENT	$\Gamma_0 \Gamma_9/\Gamma$
0.45 ± 0.03 ± 0.03	⁴ GILES 84B	CLEO	$e^+e^- \rightarrow$ hadrons	

⁴ Radiative corrections reevaluated by BUCHMUELLER 88 following KURAEV 85.

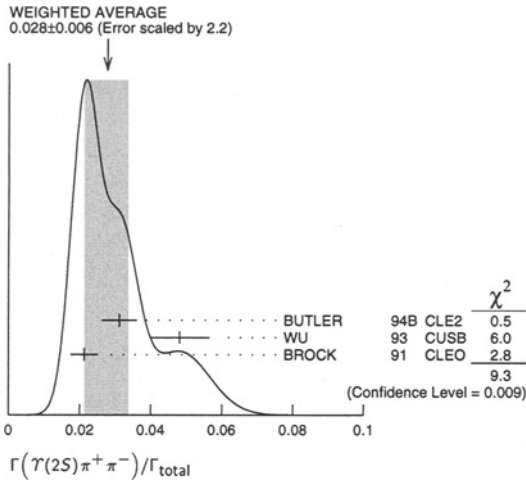
 $\Upsilon(3S)$ BRANCHING RATIOS

$\Gamma(\Upsilon(2S) \text{ anything})/\Gamma_{total}$	EVTs	DOCUMENT ID	TECN	COMMENT	Γ_1/Γ
0.106 ± 0.008 OUR AVERAGE					
0.1023 ± 0.0105	4625	^{5,6,7} BUTLER 94B	CLE2	$e^+e^- \rightarrow \ell^+ \ell^- X$	
0.111 ± 0.012	4891	^{6,7,8} BROCK 91	CLEO	$e^+e^- \rightarrow \pi^+ \pi^- X, \pi^+ \pi^- \ell^+ \ell^-$	

$\Gamma(\Upsilon(2S) \pi^+ \pi^-)/\Gamma_{total}$	EVTs	DOCUMENT ID	TECN	COMMENT	Γ_2/Γ
0.028 ± 0.006 OUR AVERAGE					
0.0312 ± 0.0049	980	^{5,9} BUTLER 94B	CLE2	$e^+e^- \rightarrow \pi^+ \pi^- \ell^+ \ell^-$	
0.0482 ± 0.0065 ± 0.0053	138	⁸ WU 93	CUSB	$\Upsilon(3S) \rightarrow \pi^+ \pi^- \ell^+ \ell^-$	
0.0213 ± 0.0038	974	⁸ BROCK 91	CLEO	$e^+e^- \rightarrow \pi^+ \pi^- X, \pi^+ \pi^- \ell^+ \ell^-$	
• • • We do not use the following data for averages, fits, limits, etc. • • •					
0.031 ± 0.020	5	MAGERAS 82	CUSB	$\Upsilon(3S) \rightarrow \pi^+ \pi^- \ell^+ \ell^-$	

Meson Particle Listings

$\Upsilon(3S), \Upsilon(4S)$



$\Gamma(\Upsilon(2S)\pi^0\pi^0)/\Gamma_{total}$ Γ_3/Γ

VALUE	EVTs	DOCUMENT ID	TECN	COMMENT
0.0200 ± 0.0032 OUR AVERAGE				
0.0216 ± 0.0039	9,10	BUTLER	94B CLE2	$e^+e^- \rightarrow \ell^+\ell^-\pi^0\pi^0$
0.017 ± 0.005 ± 0.002	10	HEINTZ	92 CSB2	$e^+e^- \rightarrow \ell^+\ell^-\pi^0\pi^0$

$\Gamma(\Upsilon(2S)\gamma\gamma)/\Gamma_{total}$ Γ_4/Γ

VALUE	DOCUMENT ID	TECN	COMMENT
0.0502 ± 0.0069	9 BUTLER	94B CLE2	$e^+e^- \rightarrow \ell^+\ell^-2\gamma$

$\Gamma(\Upsilon(1S)\pi^+\pi^-)/\Gamma_{total}$ Γ_5/Γ

VALUE	EVTs	DOCUMENT ID	TECN	COMMENT
0.0448 ± 0.0021 OUR AVERAGE				
0.0452 ± 0.0035	11830	6 BUTLER	94B CLE2	$e^+e^- \rightarrow \pi^+\pi^-X$
0.0446 ± 0.0034 ± 0.0050	451	6 WU	93 CUSB	$\Upsilon(3S) \rightarrow \pi^+\pi^-\ell^+\ell^-$
0.0446 ± 0.0030	11221	6 BROCK	91 CLEO	$e^+e^- \rightarrow \pi^+\pi^-\ell^+\ell^-$

• • • We do not use the following data for averages, fits, limits, etc. • • •

0.049 ± 0.010	22	GREEN	82 CLEO	$\Upsilon(3S) \rightarrow \pi^+\pi^-\ell^+\ell^-$
0.039 ± 0.013	26	MAGERAS	82 CUSB	$\Upsilon(3S) \rightarrow \pi^+\pi^-\ell^+\ell^-$

$\Gamma(\Upsilon(1S)\pi^0\pi^0)/\Gamma_{total}$ Γ_6/Γ

VALUE	EVTs	DOCUMENT ID	TECN	COMMENT
0.0206 ± 0.0028 OUR AVERAGE				
0.0199 ± 0.0034	56	6 BUTLER	94B CLE2	$e^+e^- \rightarrow \ell^+\ell^-\pi^0\pi^0$
0.022 ± 0.004 ± 0.003	33	12 HEINTZ	92 CSB2	$e^+e^- \rightarrow \ell^+\ell^-\pi^0\pi^0$

$\Gamma(\Upsilon(1S)\eta)/\Gamma_{total}$ Γ_7/Γ

VALUE	CL%	DOCUMENT ID	TECN	COMMENT
< 0.0022	90	BROCK	91 CLEO	$e^+e^- \rightarrow \pi^+\pi^-\pi^0\ell^+\ell^-$

$\Gamma(\mu^+\mu^-)/\Gamma_{total}$ Γ_8/Γ

VALUE	EVTs	DOCUMENT ID	TECN	COMMENT
0.0181 ± 0.0017 OUR AVERAGE				
0.0202 ± 0.0019 ± 0.0033		CHEN	89B CLEO	$e^+e^- \rightarrow \mu^+\mu^-$
0.0173 ± 0.0015 ± 0.0011		KAARSBERG	89 CSB2	$e^+e^- \rightarrow \mu^+\mu^-$
0.033 ± 0.013 ± 0.007	1096	ANDREWS	83 CLEO	$e^+e^- \rightarrow \mu^+\mu^-$

$\Gamma(\Upsilon\chi_{b2}(2P))/\Gamma_{total}$ Γ_{10}/Γ

VALUE	EVTs	DOCUMENT ID	TECN	COMMENT
0.114 ± 0.008 OUR AVERAGE				Error includes scale factor of 1.3.
0.111 ± 0.005 ± 0.004	10319	13 HEINTZ	92 CSB2	$e^+e^- \rightarrow \gamma$
0.135 ± 0.003 ± 0.017	30741	MORRISON	91 CLE2	$e^+e^- \rightarrow \gamma X$

$\Gamma(\Upsilon\chi_{b1}(2P))/\Gamma_{total}$ Γ_{11}/Γ

VALUE	EVTs	DOCUMENT ID	TECN	COMMENT
0.113 ± 0.006 OUR AVERAGE				
0.115 ± 0.005 ± 0.005	11147	13 HEINTZ	92 CSB2	$e^+e^- \rightarrow \gamma$
0.105 ± 0.003 ± 0.013	25759	MORRISON	91 CLE2	$e^+e^- \rightarrow \gamma X$

$\Gamma(\Upsilon\chi_{b0}(2P))/\Gamma_{total}$ Γ_{12}/Γ

VALUE	EVTs	DOCUMENT ID	TECN	COMMENT
0.054 ± 0.006 OUR AVERAGE				Error includes scale factor of 1.1.
0.060 ± 0.004 ± 0.006	4959	13 HEINTZ	92 CSB2	$e^+e^- \rightarrow \gamma$
0.049 ± 0.003 ± 0.006	9903	MORRISON	91 CLE2	$e^+e^- \rightarrow \gamma X$

⁵ Using $B(\Upsilon(2S) \rightarrow \Upsilon(1S)\gamma\gamma) = (0.038 \pm 0.007)\%$, and $B(\Upsilon(2S) \rightarrow \Upsilon(1S)\pi^0\pi^0) = (1/2)B(\Upsilon(2S) \rightarrow \Upsilon(1S)\pi^+\pi^-)$.
⁶ Using $B(\Upsilon(1S) \rightarrow \mu^+\mu^-) = (2.48 \pm 0.06)\%$. With the assumption of $e\mu$ universality.
⁷ Using $B(\Upsilon(2S) \rightarrow \Upsilon(1S)\pi^+\pi^-) = (18.5 \pm 0.8)\%$.
⁸ Using $B(\Upsilon(2S) \rightarrow \mu^+\mu^-) = (1.31 \pm 0.21)\%$, $B(\Upsilon(2S) \rightarrow \Upsilon(1S)\gamma\gamma) \times 2B(\Upsilon(1S) \rightarrow \mu^+\mu^-) = (0.188 \pm 0.035)\%$, and $B(\Upsilon(2S) \rightarrow \Upsilon(1S)\pi^0\pi^0) \times 2B(\Upsilon(1S) \rightarrow \mu^+\mu^-) = (0.436 \pm 0.056)\%$. With the assumption of $e\mu$ universality.
⁹ From the exclusive mode.
¹⁰ $B(\Upsilon(2S) \rightarrow \mu^+\mu^-) = (1.31 \pm 0.21)\%$ and assuming $e\mu$ universality.
¹¹ $B(\Upsilon(2S) \rightarrow \mu^+\mu^-) = (1.44 \pm 0.10)\%$ and assuming $e\mu$ universality. Supersedes HEINTZ 91.
¹² Using $B(\Upsilon(1S) \rightarrow \mu^+\mu^-) = (2.57 \pm 0.07)\%$ and assuming $e\mu$ universality. Supersedes HEINTZ 91.
¹³ Supersedes NARAIN 91.

$\Upsilon(3S)$ REFERENCES

ARTAMONOV 00	PL B474 427	A.S. Artamonov et al.	
BUTLER 94B	PR D49 40	F. Butler et al.	(CLEO Collab.)
WU 93	PL B301 307	Q.W. Wu et al.	(CUSB Collab.)
HEINTZ 92	PR D46 1928	U. Heintz et al.	(CUSB II Collab.)
BROCK 91	PR D43 1449	I.C. Brock et al.	(CLEO Collab.)
HEINTZ 91	PRL 66 1563	U. Heintz et al.	(CUSB Collab.)
MORRISON 91	PRL 67 1696	R.J. Morrison et al.	(CLEO Collab.)
NARAIN 91	PRL 66 3113	M. Narain et al.	(CUSB Collab.)
CHEN 89B	PR D39 3528	W.Y. Chen et al.	(CLEO Collab.)
KAARSBERG 89	PRL 62 2077	T.M. Kaarsberg et al.	(CLEO Collab.)
BUCHMUEL... 88	HE e ⁺ e ⁻ Physics 412	W. Buchmueller, S. Cooper	(HANN, DESY, MIT)
Editors: A. Ali and P. Soeding	World Scientific, Singapore		
COHEN 87	RMP 59 1121	E.R. Cohen, B.N. Taylor	(RISC, NBS)
BARU 86B	ZPHY C32 622	S.E. Baru et al.	(NOVO)
KURAEV 85	SJNP 41 466	E.A. Kurayev, V.S. Fadin	(NOVO)
	Translated from YAF 41 733.		
ARTAMONOV 84	PL 137B 272	A.S. Artamonov et al.	(NOVO)
GILES 84B	PR D29 1285	R. Giles et al.	(CLEO Collab.)
ANDREWS 83	PRL 50 807	D.E. Andrews et al.	(CLEO Collab.)
GREEN 82	PRL 49 617	J. Green et al.	(CLEO Collab.)
MAGERAS 82	PL 118B 453	G. Mageras et al.	(COLU, CORN, LSU+)

OTHER RELATED PAPERS

ALEXANDER 89	NP B320 45	J.P. Alexander et al.	(LBL, MICH, SLAC)
ARTAMONOV 84B	PL 137B 272	A.S. Artamonov et al.	(NOVO)
GILES 84B	PR D29 1285	R. Giles et al.	(CLEO Collab.)
HAN 82	PRL 49 1612	K. Han et al.	(CUSB Collab.)
PETERSON 82	PL 114B 277	D. Peterson et al.	(CUSB Collab.)
KAPLAN 78	PRL 40 435	D.M. Kaplan et al.	(STDN, FNAL, COLU)
YOH 78	PRL 41 684	J.K. Yoh et al.	(COLU, FNAL, STON)
COBB 77	PL 72B 273	J.H. Cobb et al.	(BNL, CERN, SYRA, YALE)
HERB 77	PRL 39 252	S.W. Herb et al.	(COLU, FNAL, STON)
INNES 77	PRL 39 1240	W.R. Innes et al.	(COLU, FNAL, STON)

$\Upsilon(4S)$
or $\Upsilon(10580)$

$$I^G(J^{PC}) = 0^-(1^{--})$$

$\Upsilon(4S)$ MASS

VALUE (GeV)	DOCUMENT ID	TECN	COMMENT
10.5800 ± 0.0035	1 BEBEK	87 CLEO	$e^+e^- \rightarrow$ hadrons
• • • We do not use the following data for averages, fits, limits, etc. • • •			
10.5774 ± 0.0010	2 LOVELOCK	85 CUSB	$e^+e^- \rightarrow$ hadrons
	¹ Reanalysis of BESSON 85.		
	² No systematic error given.		

$\Upsilon(4S)$ WIDTH

VALUE (MeV)	DOCUMENT ID	TECN	COMMENT
14 ± 5 OUR AVERAGE			Error includes scale factor of 1.7.
10.0 ± 2.8 ± 2.7	3 ALBRECHT	95E ARG	$e^+e^- \rightarrow$ hadrons
20 ± 2 ± 4	BESSON	85 CLEO	$e^+e^- \rightarrow$ hadrons
• • • We do not use the following data for averages, fits, limits, etc. • • •			
25 ± 2.5	LOVELOCK	85 CUSB	$e^+e^- \rightarrow$ hadrons
	³ Using LEYAOUANC 77 parametrization of $\Gamma(s)$.		

$\Upsilon(4S)$ DECAY MODES

Mode	Fraction (Γ_i/Γ)	Confidence level
Γ_1 $B\bar{B}$	> 96 %	95%
Γ_2 non- $B\bar{B}$	< 4 %	95%
Γ_3 e^+e^-	$(2.8 \pm 0.7) \times 10^{-5}$	
Γ_4 $J/\psi(3097)$ anything	$(2.2 \pm 0.7) \times 10^{-3}$	
Γ_5 D^{*+} anything + c.c.	< 7.4 %	90%
Γ_6 ϕ anything	< 2.3 $\times 10^{-3}$	90%
Γ_7 $\Upsilon(1S)$ anything	< 4 $\times 10^{-3}$	90%
Γ_8 $\Upsilon(1S)\pi^+\pi^-$	< 1.2 $\times 10^{-4}$	90%
Γ_9 $\Upsilon(2S)\pi^+\pi^-$	< 3.9 $\times 10^{-4}$	90%

See key on page 239

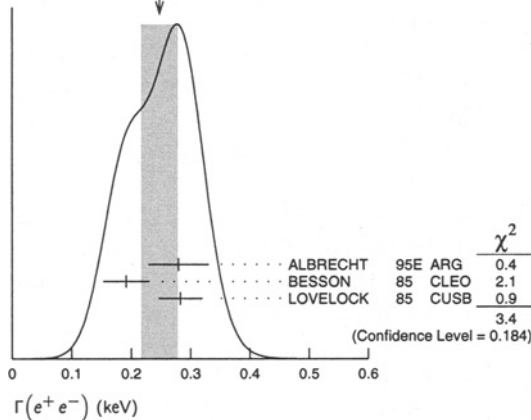
Meson Particle Listings
 $\Upsilon(4S)$, $\Upsilon(10860)$, $\Upsilon(11020)$

$\Upsilon(4S)$ PARTIAL WIDTHS

$\Gamma(e^+e^-)$	DOCUMENT ID	TECN	COMMENT	Γ_3
0.248 ± 0.031 OUR AVERAGE	Error includes scale factor of 1.3. See the ideogram below.			
0.28 ± 0.05 ± 0.01	⁴ ALBRECHT	95E ARG	$e^+e^- \rightarrow$ hadrons	
0.192 ± 0.007 ± 0.038	BESSION	85 CLEO	$e^+e^- \rightarrow$ hadrons	
0.283 ± 0.037	LOVELOCK	85 CUSB	$e^+e^- \rightarrow$ hadrons	

⁴Using LEYAOUANC 77 parametrization of $\Gamma(s)$.

WEIGHTED AVERAGE
 0.248 ± 0.031 (Error scaled by 1.3)



$\Upsilon(4S)$ BRANCHING RATIOS

$\Gamma(e^+e^-)/\Gamma_{total}$	DOCUMENT ID	TECN	COMMENT	Γ_3/Γ
2.77 ± 0.50 ± 0.49	Error includes scale factor of 1.3.			
	⁵ ALBRECHT	95E ARG	$e^+e^- \rightarrow$ hadrons	

⁵Using LEYAOUANC 77 parametrization of $\Gamma(s)$.

$\Gamma(J/\psi(3097)\text{anything})/\Gamma_{total}$	DOCUMENT ID	TECN	COMMENT	Γ_4/Γ
0.0022 ± 0.0006 ± 0.0004	ALEXANDER	90c CLEO	e^+e^-	

$[\Gamma(D^{*+}\text{anything}) + \Gamma(c.c.)]/\Gamma_{total}$	DOCUMENT ID	TECN	COMMENT	Γ_5/Γ
< 0.074	90	⁶ ALEXANDER	90c CLEO e^+e^-	

⁶For $x > 0.473$.

$\Gamma(\phi\text{anything})/\Gamma_{total}$	DOCUMENT ID	TECN	COMMENT	Γ_6/Γ
< 0.0023	90	⁷ ALEXANDER	90c CLEO e^+e^-	

⁷For $x > 0.52$.

$\Gamma(\Upsilon(1S)\text{anything})/\Gamma_{total}$	DOCUMENT ID	TECN	COMMENT	Γ_7/Γ
< 0.004	90	ALEXANDER	90c CLEO e^+e^-	

$\Gamma(\Upsilon(1S)\pi^+\pi^-)/\Gamma_{total}$	DOCUMENT ID	TECN	COMMENT	Γ_8/Γ
< 1.2	90	GLENN	99 CLE2 e^+e^-	

$\Gamma(\Upsilon(2S)\pi^+\pi^-)/\Gamma_{total}$	DOCUMENT ID	TECN	COMMENT	Γ_9/Γ
< 3.9	90	GLENN	99 CLE2 e^+e^-	

$\Gamma(\text{non-}B\bar{B})/\Gamma_{total}$	DOCUMENT ID	TECN	COMMENT	Γ_2/Γ
< 0.04	95	BARISH	96B CLEO e^+e^-	

$\Upsilon(4S)$ REFERENCES

GLENN 99 PR D59 052003	S. Glenn <i>et al.</i>	(CLEO Collab.)
BARISH 96B PRL 76 1570	B.C. Barish <i>et al.</i>	(ARGUS Collab.)
ALBRECHT 95E ZPHY C65 619	H. Albrecht <i>et al.</i>	(CLEO Collab.)
ALEXANDER 90C PRL 64 2226	J. Alexander <i>et al.</i>	(CLEO Collab.)
BEBEK 87 PR D36 1289	C. Bebek <i>et al.</i>	(CLEO Collab.)
BESSION 85 PRL 54 381	D. Besson <i>et al.</i>	(CLEO Collab.)
LOVELOCK 85 PRL 54 377	D.M.J. Lovelock <i>et al.</i>	(CUSB Collab.)
LEYAOUANC 77 PL B71 397	A. Le Yaouanc <i>et al.</i>	(ORSAY)

OTHER RELATED PAPERS

HENDERSON 92 PR D45 2212	S. Henderson <i>et al.</i>	(CLEO Collab.)
ANDREWS 80B PRL 45 219	D. Andrews <i>et al.</i>	(CLEO Collab.)
FINOCCHIARO 80 PRL 45 222	G. Finocchiaro <i>et al.</i>	(CUSB Collab.)

$\Upsilon(10860)$

$J^{PC} = 0^-(1^{--})$

$\Upsilon(10860)$ MASS

VALUE (GeV)	DOCUMENT ID	TECN	COMMENT
10.865 ± 0.008 OUR AVERAGE	Error includes scale factor of 1.1.		
10.868 ± 0.006 ± 0.005	BESSION	85 CLEO	$e^+e^- \rightarrow$ hadrons
10.845 ± 0.020	LOVELOCK	85 CUSB	$e^+e^- \rightarrow$ hadrons

$\Upsilon(10860)$ WIDTH

VALUE (MeV)	DOCUMENT ID	TECN	COMMENT
110 ± 13 OUR AVERAGE			
112 ± 17 ± 23	BESSION	85 CLEO	$e^+e^- \rightarrow$ hadrons
110 ± 15	LOVELOCK	85 CUSB	$e^+e^- \rightarrow$ hadrons

$\Upsilon(10860)$ DECAY MODES

Mode	Fraction (Γ_i/Γ)
$\Gamma_1 e^+e^-$	$(2.8 \pm 0.7) \times 10^{-6}$

$\Upsilon(10860)$ PARTIAL WIDTHS

$\Gamma(e^+e^-)$	DOCUMENT ID	TECN	COMMENT	Γ_1
0.31 ± 0.07 OUR AVERAGE	Error includes scale factor of 1.3.			
0.22 ± 0.05 ± 0.07	BESSION	85 CLEO	$e^+e^- \rightarrow$ hadrons	
0.365 ± 0.070	LOVELOCK	85 CUSB	$e^+e^- \rightarrow$ hadrons	

$\Upsilon(10860)$ REFERENCES

BESSION 85 PRL 54 381	D. Besson <i>et al.</i>	(CLEO Collab.)
LOVELOCK 85 PRL 54 377	D.M.J. Lovelock <i>et al.</i>	(CUSB Collab.)

$\Upsilon(11020)$

$J^{PC} = 0^-(1^{--})$

$\Upsilon(11020)$ MASS

VALUE (GeV)	DOCUMENT ID	TECN	COMMENT
11.019 ± 0.008 OUR AVERAGE			
11.019 ± 0.005 ± 0.007	BESSION	85 CLEO	$e^+e^- \rightarrow$ hadrons
11.020 ± 0.030	LOVELOCK	85 CUSB	$e^+e^- \rightarrow$ hadrons

$\Upsilon(11020)$ WIDTH

VALUE (MeV)	DOCUMENT ID	TECN	COMMENT
79 ± 16 OUR AVERAGE			
61 ± 13 ± 22	BESSION	85 CLEO	$e^+e^- \rightarrow$ hadrons
90 ± 20	LOVELOCK	85 CUSB	$e^+e^- \rightarrow$ hadrons

$\Upsilon(11020)$ DECAY MODES

Mode	Fraction (Γ_i/Γ)
$\Gamma_1 e^+e^-$	$(1.6 \pm 0.5) \times 10^{-6}$

$\Upsilon(11020)$ PARTIAL WIDTHS

$\Gamma(e^+e^-)$	DOCUMENT ID	TECN	COMMENT	Γ_1
0.130 ± 0.030 OUR AVERAGE				
0.095 ± 0.03 ± 0.035	BESSION	85 CLEO	$e^+e^- \rightarrow$ hadrons	
0.156 ± 0.040	LOVELOCK	85 CUSB	$e^+e^- \rightarrow$ hadrons	

$\Upsilon(11020)$ REFERENCES

BESSION 85 PRL 54 381	D. Besson <i>et al.</i>	(CLEO Collab.)
LOVELOCK 85 PRL 54 377	D.M.J. Lovelock <i>et al.</i>	(CUSB Collab.)

Meson Particle Listings

Non- $q\bar{q}$ Candidates

NON- $q\bar{q}$ CANDIDATES

We include here mini-reviews and reference lists on gluonium and other non- $q\bar{q}$ candidates. See also $N\bar{N}$ (1100–3600) for possible bound states.

NON- $q\bar{q}$ MESONS

Written March 2000 by C. Amsler (University of Zürich)

See also $N\bar{N}$ (1100 – 3600) for possible multiquark states.

The constituent quark model describes the observed meson spectrum as bound $q\bar{q}$ states grouped into SU(3) flavor nonets. The self-coupling of gluons in QCD suggests that additional mesons made of bound gluons (glueballs) or $q\bar{q}$ -pairs with an excited gluon (hybrids) may exist. Multi-quark color singlet states like $qq\bar{q}\bar{q}$ or $qqq\bar{q}\bar{q}\bar{q}$ have also been predicted (JAFFE 77). Among the signatures naively expected for glueballs are (i) no place in $q\bar{q}$ nonets, (ii) enhanced production in gluon rich channels such as central production and radiative $J/\psi(1S)$ decay, (iii) decay branching fractions incompatible with SU(3) predictions for $q\bar{q}$ states, and (iv) reduced $\gamma\gamma$ couplings. However, mixing effects with isoscalar $q\bar{q}$ mesons (AMSLER 96, ANISOVICH 97, WEINGARTEN 97, CLOSE 97B) and decay form factors (BARNES 97) may obscure these simple signatures.

Lattice calculations (BALI 93, SEXTON 95, MORNINGSTAR 99), QCD sum rules, flux tube and constituent glue models agree that the lightest glueballs have quantum numbers $J^{PC} = 0^{++}$ and 2^{++} (for a review see SWANSON 97). On the lattice, the scale parameter (estimated from the string tension in heavy quark mesons) gives by extrapolation to zero lattice spacing a mass of 1611 ± 163 MeV for the ground state (0^{++}) glueball, while the first excited state (2^{++}) has a mass of 2232 ± 310 MeV (MICHAEL 97). Hence the low mass glueballs lie in the same mass region as ordinary isoscalar $q\bar{q}$ states, that is in the mass range of the $1^3P_0(0^{++})$, 2^3P_2 , 3^3P_2 , and $1^3F_2(2^{++})$ $q\bar{q}$ states. The 0^{-+} state and exotic glueballs (with non- $q\bar{q}$ quantum numbers like 0^{--} , 0^{+-} , 1^{-+} , 2^{+-} , etc.) are expected above 2 GeV (BALI 93).

The lattice calculations assume that the quark masses are infinite and therefore neglect $q\bar{q}$ loops. However, one expects that glueballs will mix with nearby $q\bar{q}$ states of the same quantum numbers. The effect of $q\bar{q}$ loops on the glueball mass is not clear and the size of the $q\bar{q}$ admixture in the glueball wavefunction is not predicted by lattice calculations. However, the presence of a glueball mixed with $q\bar{q}$ would still lead to a supernumerary isoscalar in the SU(3) classification of $q\bar{q}$ mesons.

For earlier experimental searches we refer to the Notes in the 1996 and 1998 issues of this Review. See also the review on exotic mesons by LANDSBERG 99.

We first deal with non- $q\bar{q}$ candidates in the scalar sector. Five isoscalar resonances are well established: the very broad $f_0(400 - 1200)$ (or σ), the $f_0(980)$, the broad $f_0(1370)$, and the comparatively narrow $f_0(1500)$ and $f_0(1710)$ (see the Note on "Scalar Mesons" and also AMSLER 98). The $f_0(1500)$ was

observed in many experiments, e.g., in pion induced reactions π^-p (BINON 83, AMELIN 96B), in $\bar{p}p$ annihilations (AMSLER 95B, 95C, BERTIN 97C), in central collisions (REYES 98, BARBERIS 99, BELLAZZINI 99), in J/ψ radiative decays (BUGG 95) and in D_s decays (FRABETTI 97D). The $f_0(1710)$, with controversial spin (0 or 2), was recently shown to have spin 0 (DUNWOODIE 97, BARBERIS 99, FRENCH 99) and to decay mainly into $K\bar{K}$ (BARBERIS 99, 99B, 99D). This points to a mostly $s\bar{s}$ structure, although no signal was reported in $K^-p \rightarrow K_S K_S \Lambda$ interactions, but the data sample was rather small (ASTON 88D). In $\gamma\gamma$ collisions leading to $K_S K_S$ (BRACCINI 99) a signal is observed at the $f_0(1710)$ mass (although its spin cannot be determined) but $f_0(1500)$ is absent, while in $\gamma\gamma$ collisions leading to $\pi^+\pi^-$ neither $f_0(1710)$ nor $f_0(1500)$ are observed (BARATE 00E). The production rate for $f_0(1710)$ and the absence of $f_0(1500)$ in both $K\bar{K}$ and $\pi\pi$ favor the former to be mainly $s\bar{s}$ and the latter to have a small coupling to $\gamma\gamma$ at most compatible with an $s\bar{s}$ state (AMSLER 99).

On the other hand, the $K\bar{K}$ decay branching ratio of $f_0(1500)$ is small compared to $\pi\pi$ (ABELE 96B, 98, BARBERIS 99D) indicating that this state cannot be dominantly $s\bar{s}$. Since $f_0(1370)$ does not couple strongly to $s\bar{s}$ either (BARBERIS 99D), $f_0(1370)$ or $f_0(1500)$ appear to be supernumerary. Note that $f_0(1370)$ and $f_0(1500)$ have rather different decay patterns. The former decays to $\sigma\sigma$ and $\rho\rho$, while the latter does not decay to $\rho\rho$ (BUGG 95, THOMA 99). The narrow width of $f_0(1500)$ and its enhanced production at low transverse momentum transfer in central collisions (CLOSE 97, 98B) favor $f_0(1500)$ to be non- $q\bar{q}$. In AMSLER 96 the ground state scalar nonet is made of $a_0(1450)$, $f_0(1370)$, $K_0^*(1430)$ and the at the time missing $s\bar{s}$ state which could now be identified as $f_0(1710)$. The isoscalars $f_0(1370)$ and $f_0(1710)$ contain a small fraction of glue while $f_0(1500)$ is mostly gluonic. Alternative, less straightforward, mixing schemes have been proposed (TORNQVIST 96, ANISOVICH 97, BOGLIONE 97, WEINGARTEN 97, MINKOWSKI 99).

The $a_0(980)$ and $f_0(980)$ could be four-quark states (JAFFE 77) or $K\bar{K}$ molecular states (WEINSTEIN 90, LOCHER 98) due to their strong affinity for $K\bar{K}$, in spite of their masses being very close to threshold. For $q\bar{q}$ states the expected $\gamma\gamma$ widths (OLLER 97B, DELBOURGO 99) are not significantly larger than for molecular states (BARNES 85). A better filter might be radiative $\phi(1020)$ decay to $a_0(980)$ and $f_0(980)$. Recent data (ACHASOV 98B, 98I, AKHMETSHIN 99C) favor these mesons to be four-quark states (ACHASOV 97C), although not everybody agrees (MALTMAN 99B, DELBOURGO 99). Also, the $f_0(980)$ is strongly produced in D_s^+ decay (FRABETTI 97), suggesting a large $s\bar{s}$ component, while hadronic Z^0 decay favors in contrast a large $u\bar{u} + d\bar{d}$ component (ACKERSTAFF 98Q).

We now turn to the 2^{++} sector. The isoscalar $1^3P_2(2^{++})$ $q\bar{q}$ mesons, $f_2(1270)$, and $f_2'(1525)$, are well known. Above the $f_2'(1525)$ none of the reported isoscalars can be definitely

assigned to the 2^3P_2 , 3^3P_2 , or 1^3F_2 nonets and therefore the identification of the 2^{++} glueball is premature. Three states appear to be solid. The $f_2(1565)$ observed in $\bar{p}p$ annihilation at rest (MAY 90, BERTIN 98) is perhaps the same state as $f_2(1640)$ reported to decay into $\omega\omega$ (ALDE 90, BAKER 99) and 4π (ADAMO 92). This could be one of the 2^3P_2 isoscalars or a nucleon-antinucleon resonance. The rather broad $f_2(1950)$ is observed by several experiments, *e.g.*, in central production (BARBERIS 97B) and in $\bar{p}p$ annihilation in flight (ABELE 99B). Finally, a broad structure (of perhaps several states) decaying to $\phi\phi$ was reported around 2300 MeV in π^-N reactions (BOOTH 86, ETKIN 88) in $\bar{p}p$ annihilation in flight (EVANGELISTA 98) and in central collisions (BARBERIS 98).

The evidence for a narrow meson, $f_J(2220)$ (possibly a tensor), is fading with new formation data in $\bar{p}p$ annihilation (KISIEL 99, see the Note under the $f_J(2220)$ section). The measured partial width to $\bar{p}p$ in radiative J/ψ decay (BAI 96B) is too large and inconsistent with the upper limit from $\bar{p}p$ annihilation into $\pi\pi$ (AMSLER 99). However, the suprisingly large $\phi\phi$ cross section in $\bar{p}p$ just above threshold (EVANGELISTA 98) could be due to the production of the 2^{++} glueball. In fact, the broad enhancement was reanalyzed by PALANO 99. The dominating contribution was found to be 2^{++} , resonating at a mass of 2231 MeV with a width of 70 MeV, in accord with earlier observations in π^-N reactions (BOOTH 86, ETKIN 88).

Let us now deal with hybrid states. Hybrids may be viewed as $q\bar{q}$ mesons with a vibrating gluon flux tube. In contrast to glueballs, they can have isospin 0 and 1. The mass spectrum of hybrids with exotic (non- $q\bar{q}$) quantum numbers was predicted by ISGUR 85 while CLOSE 95 also deals with non-exotic quantum numbers. The ground state hybrids with quantum numbers (0^{-+} , 1^{-+} , 1^{--} , and 2^{-+}) are expected around 1.7 to 1.9 GeV. Lattice calculations predict that the hybrid with exotic quantum numbers 1^{-+} lies at a mass of 1.9 ± 0.2 GeV (LACOCK 97, BERNARD 97). Most hybrids are rather broad but some can be as narrow as 100 MeV (PAGE 99). They prefer to decay into a pair of S - and P -wave mesons.

A $J^{PC} = 1^{-+}$ exotic meson with a mass of 1370 MeV and a width of 385 MeV was reported in $\pi^-p \rightarrow \eta\pi^-p$ (THOMPSON 97, CHUNG 99). This state, called $\rho(1405)$ in our previous edition, has now been renamed $\pi_1(1400)$. It was observed as an interference between the angular momentum $L = 1$ and $L = 2$ $\eta\pi$ amplitudes, leading to a forward/backward asymmetry in the $\eta\pi$ angular distribution. This state was reported earlier in π^-p reactions (ALDE 88B) but ambiguous solutions in the partial wave analysis were pointed out by PROKOSHKIN 95B, 95C. A resonating 1^{-+} contribution to the $\eta\pi$ P -wave is also required in the Dalitz plot analysis of $\bar{p}n$ annihilation into $\pi^-\pi^0\eta$ (ABELE 98B) and in $\bar{p}p$ annihilation into $\pi^0\pi^0\eta$ (ABELE 99). The mass of 1400 MeV and the width of 310 MeV (ABELE 98B) are consistent with THOMPSON 97.

Another 1^{-+} state at 1593 MeV with a width of 168 MeV, $\pi_1(1600)$, decaying into $\rho\pi$ was reported in the reaction $\pi^-p \rightarrow \pi^-\rho^0n$ (ADAMS 98B). It was observed earlier in the

decay modes $\rho\pi$, $\eta'\pi$, and $b_1(1235)\pi$, but not $\eta\pi$ (GOUZ 92). A strong enhancement in the 1^{-+} $\eta'\pi$ wave, compared to $\eta\pi$, was reported at this mass by BELADIDZE 93. DONNACHIE 98 suggest that a Deck generated $\eta\pi$ background from final state rescattering in $\pi_1(1600)$ decay could mimick $\pi_1(1400)$. However, this mechanism is absent in $\bar{p}p$ annihilation. The $\eta\pi\pi$ data require $\pi_1(1400)$ and cannot accommodate a state at 1600 MeV (DUENNWEBER 99).

Hence we now have evidence for two 1^{-+} exotics, $\pi_1(1400)$ and $\pi_1(1600)$, while the flux tube model and the lattice concur to predict a mass of about 1.9 GeV, where a signal had been reported earlier (LEE 94). As isovectors, $\pi_1(1400)$ and $\pi_1(1600)$ cannot be glueballs. The coupling to $\eta\pi$ of the former points to a four-quark state while the strong $\eta'\pi$ coupling of the latter is favored for hybrid states (CLOSE 87B). Its mass is not far below the lattice prediction.

Finally, 0^{-+} , 1^{--} , and 2^{-+} hybrids were also reported. The $\pi(1800)$ decays mostly to a pair of S - and P -wave mesons (AMELIN 95B), in line with expectations for a 0^{-+} hybrid meson, although recent data contradict this, indicating a strong $\rho\omega$ decay mode (ZAITSEV 97). This meson is also rather narrow if interpreted as the second radial excitation of the pion. The evidence for 1^{--} hybrids required in e^+e^- annihilation and in τ decays has been discussed by DONNACHIE 99. A candidate for the 2^{-+} hybrid, the $\eta_2(1870)$, was reported in $\gamma\gamma$ interactions (KARCH 92), in $\bar{p}p$ annihilation (ADOMEIT 96) and in central production (BARBERIS 97B). The near degeneracy of $\eta_2(1645)$ and $\pi_2(1670)$ suggests ideal mixing in the 2^{-+} $q\bar{q}$ nonet and hence the second isoscalar should be mainly $s\bar{s}$. However, $\eta_2(1870)$ decays mainly to $a_2(1320)\pi$ and $f_2(1270)\pi$ (ADOMEIT 96) with a relative rate compatible with a hybrid state (CLOSE 95).

Meson Particle Listings

Non- $q\bar{q}$ Candidates,

Non- $q\bar{q}$ Candidates

OMITTED FROM SUMMARY TABLE

NON- $q\bar{q}$ CANDIDATES REFERENCES

BARATE 00E PL B472 189 R. Barate *et al.* (ALEPH Collab.)
 ABLE 99 PL B446 349 A. Abele *et al.* (Crystal Barrel Collab.)
 ABLE 99B EPJ C8 67 A. Abele *et al.* (Crystal Barrel Collab.)
 AKHMETSHIN 99C PL B462 380 R.R. Akhmetshin *et al.* (CMD-2 Collab.)
 AMSLER 99 NP A663 and 664 93C C. Amisler (Uppsala)
 Proceedings XV Particle and Nuclei Int. Conf., Uppsala
 BAKER 99 PL B449 114 C.A. Baker *et al.*
 BARBERIS 99 PL B453 305 D. Barberis *et al.* (Omega expt.)
 BARBERIS 99B PL B453 316 D. Barberis *et al.* (Omega expt.)
 BARBERIS 99D PL B462 462 D. Barberis *et al.* (Omega expt.)
 BELLAZZINI 99 PL B467 296 R. Bellazzini *et al.*
 BRACCINI 99 Hadron Spectroscopy 53 S. Braccini
 Frascati Physics Series XV (1999) 53, Proceedings Workshop on Hadron Spectroscopy
 BUGG 99 PL B458 311 D.V. Bugg *et al.* (BNL E852 Collab.)
 CHUNG 99 PR D60 092001 S.U. Chung *et al.* (BNL E852 Collab.)
 DELBOURGO 99 PL B446 332 R. Delbourgo, D. Liu, M. Scadron
 DONNACHIE 99 PR D60 114011 A. Donnachie, Yu.S. Kalashnikova
 DUENNWEBER 99 NP A 663 + 664, 592C W. Duennweber
 Proc. XV Particles and Nuclei Int. Conf., Uppsala
 FRENCH 99 PL B214 213 B. French *et al.* (WA76 Collab.)
 GODFREY 99 RMP 71 1411 S. Godfrey, J. Napolitano
 KISLEV 99 Proc. Workshop on Hadron Spectroscopy
 Frascati Physics Series XV 357
 LANDSBERG 99 SPU 42 871 L.G. Landsberg
 Translated from UFN 42 361.
 MALTMAN 99B PL B462 14
 MINKOWSKI 99 EPJ C9 283 F. Minkowski, W. Ochs
 MORNINGSTAR 99 PR D60 034509
 PAGE 99 PR D59 034016
 PALANO 99 Hadron Spectroscopy 363 A. Palano
 Frascati Physics Series XV 363, Proceedings Workshop on Hadron Spectroscopy
 THOMA 99 Hadron Spectroscopy 45 U. Thoma
 Frascati Physics Series XV 45, Proceedings Workshop on Hadron Spectroscopy
 TORNVIST 99 EPJ C11 359 N. Tornqvist
 ABLE 98 PR D57 3860 A. Abele *et al.* (Crystal Barrel Collab.)
 ABLE 98B PL B423 175 A. Abele *et al.* (Novosibirsk SND Collab.)
 ACHASOV 98B PL B438 441 M.N. Achasov *et al.* (OPAL Collab.)
 ACHASOV 98L PL B440 442 M.N. Achasov *et al.* (MPS Collab.)
 ACKERSTAFF 98Q EPJ C4 19 K. Ackerstaff *et al.* (MPS Collab.)
 ADAMS 98B PRL 81 5760 G.S. Adams *et al.*
 AMSLER 98 RMP 70 1293 C. Amisler
 BERTIN 98 PR D57 55 A. Bertin *et al.* (OBELIX Collab.)
 CLOSE 98B PL B419 387
 DONNACHIE 98 PR D58 114012 A. Donnachie *et al.*
 EVANGELISTA 98 PR D57 5370 C. Evangelista *et al.* (PSI)
 LOCHER 98 EPJ C4 317 M.P. Locher *et al.*
 REYES 98 PRL 81 4079 M.A. Reyes *et al.*
 ACHASOV 97C PR D56 4084 N.N. Achasov *et al.*
 ACHASOV 97D PR D56 203 N.N. Achasov *et al.*
 ACHASOV 97E IJMP A12 5019 N.N. Achasov *et al.*
 ANISOVICH 97 PL B395 123 A.V. Anisovich, A.V. Sarantsev (PNPI)
 ANISOVICH 97B ZPHY A357 123 A.V. Anisovich *et al.* (PNPI)
 ANISOVICH 97C PL B413 137 A.V. Anisovich *et al.* (PNPI)
 ANISOVICH 97E PAN 60 1892 A.V. Anisovich *et al.* (PNPI)
 Translated from YAF 60 2065
 BARBERIS 97 PL B397 339 D. Barberis *et al.* (WA102 Collab.)
 BARBERIS 97B PL B413 217 D. Barberis *et al.* (WA102 Collab.)
 BARBERIS 97C PL B413 225 D. Barberis *et al.* (WA102 Collab.)
 BARNES 97 PR D55 4157 T. Barnes *et al.* (ORNL, RAL, MCHS)
 BERNARD 97 PR D56 7039 Bernard *et al.*
 BERTIN 97 PL B400 226 A. Bertin *et al.* (OBELIX Collab.)
 BERTIN 97C PL B408 476 A. Bertin *et al.* (OBELIX Collab.)
 BOGLIONE 97 PRL 79 1998 M. Boglione *et al.*
 BUGG 97 PL B396 295 D.V. Bugg *et al.*
 CLOSE 97 PL B397 333 F. Close *et al.* (RAL, BIRM)
 CLOSE 97B PR D55 5749 F. Close *et al.* (RAL, RUTG, BEJUT)
 DUNWOODIE 97 Hadron 97 Conf. W. Dunwoodie (SLAC)
 FRABETTI 97D PL B407 79 P.L. Frabetti *et al.* (FNAL E687 Collab.)
 GERASYUTA 97 ZPHY C74 325 S.M. Gerasyuta *et al.*
 HOU 97 PR D55 6952 Wei-Shu Hou
 KISSLINGER 97 PL B410 1 L.S. Kisslinger *et al.*
 LACOCK 97 PL B401 308 P. Lacock *et al.* (EDIN, LIPP)
 MICHAEL 97 Hadron 97 Conf. C. Michael
 AIP Conf. Proc. 432 657
 OLLER 97B Hadron 97 Conf. J.A. Oller, E. Oset
 AIP Conf. Proc. 432 413
 PAGE 97 PL B402 183 P.R. Page
 PAGE 97B NPB 495 268 P.R. Page
 PAGE 97C PL B415 205 P.R. Page (CEBAF)
 SWANSON 97 Hadron 97 Conf. E.S. Swanson
 AIP Conf. Proc. 432 471
 THOMPSON 97 PRL 79 1630 D.R. Thompson *et al.* (E852 Collab.)
 WEINGARTEN 97 NPPS 53 232 D. Weingarten
 YAN 97 JP G23 L33 Y. Yan *et al.*
 ZAITSEV 97 Hadron 97 Conf. A. Zaitsev
 AIP Conf. Proc. 432 461
 ABLE 96 PL B380 453 A. Abele *et al.* (Crystal Barrel Collab.)
 ABLE 96B PL B385 425 A. Abele *et al.* (Crystal Barrel Collab.)
 ADOMEIT 96 ZPHY C71 227 J. Adomeit *et al.* (Crystal Barrel Collab.)

AMELIN 96B PAN 59 876 D.V. Amelin *et al.* (SERP, T8IL)
 Translated from YAF 59 1021
 AMSLER 96 PR D53 295 C. Amisler, F.E. Close (ZURI, RAL)
 AMSLER 96B ZPHY C70 219 C. Amisler *et al.* (Crystal Barrel Collab.)
 AMSLER 96C Third Paper C. Amisler *et al.* (Crystal Barrel Collab.)
 BAI 96B PRL 76 3502 J.Z. Bai *et al.* (BES Collab.)
 BAI 96C PRL 77 3959 J.Z. Bai *et al.* (BES Collab.)
 BAJC 96 ZPHY A356 187 B. Bajc *et al.* (RAL)
 CLOSE 96 PL B366 323 F.E. Close, P.R. Page (NCARO)
 SZCZEPANIAK 96 PRL 76 2011 A. Szczepaniak *et al.* (HELS)
 TORNVIST 96 PRL 76 1575 N.A. Tornqvist, M. Roos (SERP, T8IL)
 AMELIN 95B PL B356 595 D.V. Amelin *et al.* (Crystal Barrel Collab.)
 AMSLER 95B PL B342 433 C. Amisler *et al.* (Crystal Barrel Collab.)
 AMSLER 95C PL B353 571 C. Amisler *et al.* (Crystal Barrel Collab.)
 AMSLER 95D PL B355 425 C. Amisler *et al.* (ZURI, RAL)
 AMSLER 95E PL B353 385 C. Amisler, F.E. Close (Crystal Barrel Collab.)
 AMSLER 95F PL B358 389 C. Amisler *et al.* (OBELIX Collab.)
 BERTIN 95 PL B361 187 A. Bertin *et al.* (LOQM, PNPI, WASH)
 BUGG 95 PL B353 378 D.V. Bugg *et al.* (RAL)
 CLOSE 95 NP B443 233 F.E. Close, P.R. Page (SERP)
 PROKOSHNIK 95B PAN 58 606 Y.D. Prokoshkin, S.A. Sadovsky
 Translated from YAF 58 662
 PROKOSHNIK 95C PAN 58 853 Y.D. Prokoshkin, S.A. Sadovsky (SERP)
 Translated from YAF 58 921
 SEXTON 95 PRL 75 4563 J. Sexton *et al.* (IBM)
 ALBRECHT 94Z PL B332 451 H. Albrecht *et al.* (ARGUS Collab.)
 AMSLER 94D PL B333 277 C. Amisler *et al.* (Crystal Barrel Collab.)
 ANISOVICH 94 PL B323 233 V.V. Anisovich *et al.*
 BERDNIKOV 94 PL B337 219 E.B. Berdnikov *et al.* (SERP, T8IL)
 LEE 94 PL B323 227 J.H. Lee *et al.* (BNL, IND, KYUN, MASD+)
 TORNVIST 94 ZPHY C61 525 N.A. Tornqvist (HELS)
 KIEHL 93 PAN 56 1358 A.N. Aleev *et al.* (BIS-2 Collab.)
 Translated from YAF 56 100
 AOYAGI 93 PL B314 246 H. Aoyagi *et al.* (BKEI Collab.)
 BALI 93 PL B309 378 G.S. Bali *et al.* (LIPP)
 BARNES 93 PL B309 469 P.D. Barnes, P. Birien, W.H. Breunlich
 BELADIDZE 93 PL 313 276 G.M. Beladidze *et al.* (VES Collab.)
 DONNACHIE 93 ZP C60 187 A. Donnachie, Yu.S. Kalashnikova, A.B. Clegg (BNL)
 ERICSON 93 PL B309 426 T.E.O. Ericson, G. Karl (CERN)
 MANOHAR 93 PR D59 17 A.V. Manohar, M.B. Wise (MIT)
 ADAMO 92 PL B287 368 A. Adamo *et al.* (OBELIX Collab.)
 AMSLER 92 PL B291 347 C. Amisler *et al.* (Crystal Barrel Collab.)
 BARNES 92 PR D46 131 T. Barnes, E.S. Swanson (ORNL)
 DOOLEY 92 PL B275 478 K. Dooley, E.S. Swanson, T. Barnes (ORNL)
 GOUZ 92 Dallas HEP 92, p. 572 Yu.P. Gouz *et al.* (VES Collab.)
 Proceedings XXVI Int. Conf. on High Energy Physics
 KARCH 92 ZPHY C54 33 K. Karch *et al.* (Crystal Ball Collab.)
 ALBRECHT 91F ZPHY C50 1 H. Albrecht *et al.* (ARGUS Collab.)
 DOVER 91 PR C43 379 C.B. Dover, T. Gutsche, A. Faessler (BNL)
 FUKUI 91 PL B257 241 S. Fukui *et al.* (SUGI, NAGO, KEK, KYOT+)
 TORNVIST 91 PRL 67 556 N.A. Tornqvist (HELS)
 ACHASOV 90 TF 20 (178) N.N. Achasov, G.N. Shestakov (NOVM)
 ALDE 90 PL B241 600 D.M. Alde *et al.* (SERP, BELG, LANL, LAPP+)
 BREAKESTONE 90 ZPHY C48 569 A.M. Breakstone *et al.* (ISU, BGNA, CERN+)
 BURNETT 90 ARNP 46 332 T.H. Burnett, S.R. Sharpe (RAL)
 LONGACRE 90 PR D42 874 R.S. Longacre (BNL)
 MAY 90 ZPHY C46 203 J. Weinstein, N. Isgur (TNTO)
 WEINSTEIN 90 PR D41 2226 J. Weinstein, N. Isgur (SERP, BELG, LANL, LAPP+)
 ALDE 89 PL B216 447 D.M. Alde *et al.* (CERN, CDEF, BIRM+)
 ARMSTRONG 89B PL B221 221 T.A. Armstrong *et al.* (ATHU, BARI, BIRM+)
 ARMSTRONG 89D PL B227 186 T.A. Armstrong, M. Benayoun (ATHU, BARI, BIRM+)
 MAY 89 PL B225 450 B. May *et al.* (ASTERIX Collab.)
 ACHASOV 88 PL B207 199 N.N. Achasov, A.A. Kozhevnikov (NOVM)
 AIHARA 88 PR D37 28 H. Aihara *et al.* (TPC-2y Collab.)
 ALDE 88 PL B201 160 D.M. Alde *et al.* (SERP, BELG, LANL, LAPP+)
 ALDE 88B PL B205 397 D.M. Alde *et al.* (SERP, BELG, LANL, LAPP+)
 ASTON 88D NP B301 525 D. Aston *et al.* (SLAC, NAGO, CINC, INUS)
 BERGER 88B ZPHY C38 521 C. Berger *et al.* (PLUTO Collab.)
 BIRMAN 88 PRL 61 1557 A. Birman *et al.* (BNL, FSU, IND, MASD)
 CLEGG 88 ZPHY C40 313 A.B. Clegg, A. Donnachie (MCHS, LANL)
 ETKIN 88 PL B201 568 A. Etkin *et al.* (BNL, CUNY)
 IDDIR 88 PL B205 564 F. Ididir *et al.* (ORSAY, TOKY)
 ACHASOV 87 ZPHY C36 161 N.N. Achasov, V.A. Karnakov, G.N. Shestakov (NOVM)
 ASTON 87 NP B292 693 D. Aston *et al.* (SLAC, NAGO, CINC, INUS)
 BITYUKOV 87 PL B188 383 S.I. Bityukov *et al.* (SERP)
 CLOSE 87 RPP 51 833 (RHEL)
 ANDO 86 PRL 57 1296 A. Ando *et al.* (KEK, KYOT, NIRS, SAGA+)
 BOOTH 86 NP B273 677 P.S.L. Booth *et al.* (LIPP, GLAS, CERN)
 BOURQUIN 86 PL B172 113 M.H. Bourquin *et al.* (GEVA, RAL, HEIDP+)
 LONGACRE 86 PL B177 223 R.S. Longacre *et al.* (BNL, BRAN, CUNY+)
 BARNES 85 PL B165 434
 CHUNG 85 PRL 55 779 S.U. Chung *et al.* (BNL, FLOR, IND+)
 ISGUR 85 PRL 54 869 N. Isgur, R. Kokoski, J. Paton (TNTO)
 LEVAOUANC 85 ZPHY C28 309 A. Le Yaouanc *et al.* (ORSAY)
 BEHREND 84E ZPHY C21 205 H.J. Behrend *et al.* (CELLO Collab.)
 BARNES 83 NP B224 241 T. Barnes *et al.* (RAL, LOUV)
 BINON 83 NC 78A 313 F.G. Binon *et al.* (BELG, LAPP, SERP+)
 WEINSTEIN 83B PR D27 588 J. Weinstein, N. Isgur (TNTO)
 AIHARA 82 PR D37 28 H. Aihara *et al.* (TPC Collab.)
 ALTHOFF 82 ZPHY C16 13 M. Althoff *et al.* (TASSO Collab.)
 BARNES 82 PL B116 365 T. Barnes, F.E. Close (RHEL)
 BURKE 81 PL B103 153 D.L. Burke *et al.* (Mark II Collab.)
 BRANDELIK 80B PL B97 448 R. Brandelik *et al.* (TASSO Collab.)
 GUTBROD 79 ZP C1 391 F. Gutbrod, G. Kramer, C. Rumpf (DESY)
 JAFFE 77 PR D15 267,281 R. Jaffe (MIT)
 VOLOSHIN 75 JETPL 23 333 M.B. Voloshin, L.B. Okun (ITEP)
 Translated from ZETFP 23 369
 BAILLON 67 NC 50A 393 P.H. Bailion *et al.* (CERN, CDEF, IRAD)

N BARYONS (S = 0, I = 1/2)

$$p, N^+ = uud; \quad n, N^0 = udd$$

p

$$I(J^P) = \frac{1}{2}(\frac{1}{2}^+) \text{ Status: } ***$$

p MASS

The mass is known much more precisely in u (atomic mass units) than in MeV; see the footnote. The conversion from u to MeV, $1 \text{ u} = 931.494013 \pm 0.000037 \text{ MeV}/c^2$ (MOHR 99, the 1998 CODATA value), involves the relatively poorly known electronic charge.

VALUE (MeV)	DOCUMENT ID	TECN	COMMENT
938.271998 ± 0.000038	¹ MOHR	99	RVUE 1998 CODATA value
• • • We do not use the following data for averages, fits, limits, etc. • • •			
938.27231 ± 0.00028	² COHEN	87	RVUE 1986 CODATA value
938.2796 ± 0.0027	COHEN	73	RVUE 1973 CODATA value

¹ The mass is known much more precisely in u: $m = 1.00727646688 \pm 0.0000000013 \text{ u}$.

² The mass is known much more precisely in u: $m = 1.007276470 \pm 0.000000012 \text{ u}$.

$$|m_p - m_{\bar{p}}|/m_p$$

A test of CPT invariance. Note that the \bar{p}/p charge-to-mass ratio, given below, is much better determined.

VALUE	DOCUMENT ID	TECN	COMMENT
< 5 × 10⁻⁷	³ TORII	99	SPEC $\bar{p}e^-$ He atom

³ TORII 99 uses the more-precisely-known constraint on the \bar{p} charge-to-mass ratio of GABRIELSE 95 (see below) to get this result. This is not independent of the TORII 99 value for $|q_p + q_{\bar{p}}|/e$, below.

\bar{p}/p CHARGE-TO-MASS RATIO, $|\frac{q_{\bar{p}}}{m_{\bar{p}}}|/(\frac{q_p}{m_p})$

A test of CPT invariance. Listed here are measurements involving the inertial masses. For a discussion of what may be inferred about the ratio of \bar{p} and p gravitational masses, see ERICSON 90; they obtain an upper bound of $10^{-6}-10^{-7}$ for violation of the equivalence principle for \bar{p} 's.

VALUE	DOCUMENT ID	TECN	COMMENT
0.9999999991 ± 0.0000000009	GABRIELSE	99	TRAP Penning trap
• • • We do not use the following data for averages, fits, limits, etc. • • •			
1.0000000015 ± 0.0000000011	⁴ GABRIELSE	95	TRAP Penning trap
1.0000000023 ± 0.0000000042	⁵ GABRIELSE	90	TRAP Penning trap

⁴ Equation (2) of GABRIELSE 95 should read $M(\bar{p})/M(p) = 0.999999985$ (11) (G. Gabrielse, private communication).

⁵ GABRIELSE 90 also measures $m_{\bar{p}}/m_{e^-} = 1836.152660 \pm 0.000083$ and $m_p/m_{e^-} = 1836.152680 \pm 0.000088$. Both are completely consistent with the 1986 CODATA (COHEN 87) value for m_p/m_{e^-} of 1836.152701 ± 0.000037 .

$$(|\frac{q_{\bar{p}}}{m_{\bar{p}}}| - \frac{q_p}{m_p})/\frac{q_p}{m_p}$$

A test of CPT invariance. Taken from the \bar{p}/p charge-to-mass ratio, above.

VALUE	DOCUMENT ID
(-9 ± 9) × 10⁻¹¹ OUR EVALUATION	

$$|q_p + q_{\bar{p}}|/e$$

A test of CPT invariance. Note that the \bar{p}/p charge-to-mass ratio, given above, is much better determined. See also a similar test involving the electron.

VALUE	DOCUMENT ID	TECN	COMMENT
< 5 × 10⁻⁷	⁶ TORII	99	SPEC $\bar{p}e^-$ He atom
• • • We do not use the following data for averages, fits, limits, etc. • • •			
< 2 × 10 ⁻⁵	⁷ HUGHES	92	RVUE

⁶ TORII 99 uses the more-precisely-known constraint on the \bar{p} charge-to-mass ratio of GABRIELSE 95 (see above) to get this result. This is not independent of the TORII 99 value for $|m_p - m_{\bar{p}}|/m_p$, above.

⁷ HUGHES 92 uses recent measurements of Rydberg-energy and cyclotron-frequency ratios.

$$|q_p + q_e|/e$$

See DYLLA 73 for a summary of experiments on the neutrality of matter. See also "n CHARGE" in the neutron Listings.

VALUE	DOCUMENT ID	COMMENT
< 1.0 × 10⁻²¹	⁸ DYLLA	73 Neutrality of SF ₆
• • • We do not use the following data for averages, fits, limits, etc. • • •		
< 0.8 × 10 ⁻²¹	MARINELLI	84 Magnetic levitation

⁸ Assumes that $q_n = q_p + q_e$.

p MAGNETIC MOMENT

See the "Note on Baryon Magnetic Moments" in the A Listings.

VALUE (μ_N)	DOCUMENT ID	TECN	COMMENT
2.792847337 ± 0.000000029	MOHR	99	RVUE 1998 CODATA value
• • • We do not use the following data for averages, fits, limits, etc. • • •			
2.792847386 ± 0.000000063	COHEN	87	RVUE 1986 CODATA value
2.7928456 ± 0.0000011	COHEN	73	RVUE 1973 CODATA value

\bar{p} MAGNETIC MOMENT

A few early results have been omitted.

VALUE (μ_N)	DOCUMENT ID	TECN	COMMENT
-2.800 ± 0.008 OUR AVERAGE			
-2.8005 ± 0.0090	KREISSL	88	CNTR $\bar{p}^{208}\text{Pb} 11 \rightarrow 10 \text{ X-ray}$
-2.817 ± 0.048	ROBERTS	78	CNTR
-2.791 ± 0.021	HU	75	CNTR Exotic atoms

$$(\mu_p + \mu_{\bar{p}})/\mu_p$$

A test of CPT invariance. Calculated from the p and \bar{p} magnetic moments, above.

VALUE	DOCUMENT ID
(-2.6 ± 2.9) × 10⁻³ OUR EVALUATION	

p ELECTRIC DIPOLE MOMENT

A nonzero value is forbidden by both T invariance and P invariance.

VALUE (10 ⁻²³ ecm)	EVTS	DOCUMENT ID	TECN	COMMENT
- 3.7 ± 6.3		CHO	89	NMR Tl F molecules
• • • We do not use the following data for averages, fits, limits, etc. • • •				
< 400		DZUBA	85	THEO Uses ¹²⁹ Xe moment
130 ± 200		⁹ WILKENING	84	
900 ± 1400		¹⁰ WILKENING	84	
700 ± 900	1G	HARRISON	69	MBR Molecular beam

⁹ This WILKENING 84 value includes a finite-size effect and a magnetic effect.

¹⁰ This WILKENING 84 value is more cautious than the other and excludes the finite-size effect, which relies on uncertain nuclear integrals.

p ELECTRIC POLARIZABILITY $\bar{\alpha}_p$

VALUE (10 ⁻⁴ fm ³)	DOCUMENT ID	TECN	COMMENT
12.1 ± 0.8 ± 0.5	¹¹ MACGIBBON	95	RVUE global average
• • • We do not use the following data for averages, fits, limits, etc. • • •			
12.5 ± 0.6 ± 0.9	MACGIBBON	95	CNTR γp Compton scattering
9.8 ± 0.4 ± 1.1	HALLIN	93	CNTR γp Compton scattering
10.62 ^{+1.25+1.07} _{-1.19-1.03}	ZIEGER	92	CNTR γp Compton scattering
10.9 ± 2.2 ± 1.3	¹² FEDERSPIEL	91	CNTR γp Compton scattering
¹¹ MACGIBBON 95 combine the results of ZIEGER 92, FEDERSPIEL 91, and their own experiment to get a "global average" in which model errors and systematic errors are treated in a consistent way. See MACGIBBON 95 for a discussion.			
¹² FEDERSPIEL 91 obtains for the (static) electric polarizability α_p , defined in terms of the induced electric dipole moment by $\mathbf{D} = 4\pi\epsilon_0\alpha_p\mathbf{E}$, the value $(7.0 \pm 2.2 \pm 1.3) \times 10^{-4} \text{ fm}^3$.			

p MAGNETIC POLARIZABILITY $\bar{\beta}_p$

The electric and magnetic polarizabilities are subject to a dispersion sum-rule constraint $\bar{\alpha} + \bar{\beta} = (14.2 \pm 0.5) \times 10^{-4} \text{ fm}^3$. Errors here are anticorrelated with those on $\bar{\alpha}_p$ due to this constraint.

VALUE (10 ⁻⁴ fm ³)	DOCUMENT ID	TECN	COMMENT
2.1 ± 0.8 ± 0.5	¹³ MACGIBBON	95	RVUE global average
• • • We do not use the following data for averages, fits, limits, etc. • • •			
1.7 ± 0.6 ± 0.9	MACGIBBON	95	CNTR γp Compton scattering
4.4 ± 0.4 ± 1.1	HALLIN	93	CNTR γp Compton scattering
3.58 ^{+1.19+1.03} _{-1.25-1.07}	ZIEGER	92	CNTR γp Compton scattering
3.3 ± 2.2 ± 1.3	FEDERSPIEL	91	CNTR γp Compton scattering
¹³ MACGIBBON 95 combine the results of ZIEGER 92, FEDERSPIEL 91, and their own experiment to get a "global average" in which model errors and systematic errors are treated in a consistent way. See MACGIBBON 95 for a discussion.			

Baryon Particle Listings

p

p MEAN LIFE

A test of baryon conservation. See the "p Partial Mean Lives" section below for limits that depend on decay modes. p = proton, n = bound neutron.

LIMIT (years)	PARTICLE	DOCUMENT ID	TECN
$>1.6 \times 10^{25}$	p, n	14,15 EVANS	77
$>3 \times 10^{23}$	p	15 DIX	70 CNTR
$>3 \times 10^{23}$	p, n	15,16 FLEROV	58

• • • We do not use the following data for averages, fits, limits, etc. • • •

¹⁴ Mean lifetime of nucleons in ¹³⁰Te nuclei.
¹⁵ Converted to mean life by dividing half-life by $\ln(2) = 0.693$.
¹⁶ Mean lifetime of nucleons in ²³²Th nuclei.

\bar{p} MEAN LIFE

The best limit by far, that of GOLDEN 79, relies, however, on a number of astrophysical assumptions. The other limits come from direct observations of stored antiprotons. See also "p Partial Mean Lives" after "p Partial Mean Lives," below.

LIMIT (years)	CL%	EVTS	DOCUMENT ID	TECN	COMMENT
>0.28			GABRIELSE 90	TRAP	Penning trap
>0.08	90	1	BELL 79	CNTR	Storage ring
$>1 \times 10^7$			GOLDEN 79	SPEC	\bar{p}/p , cosmic rays
$>3.7 \times 10^{-3}$			BREGMAN 78	CNTR	Storage ring

p DECAY MODES

Below, for N decays, p and n distinguish proton and neutron partial lifetimes. See also the "Note on Nucleon Decay" in our 1994 edition (Phys. Rev. D50, 1673) for a short review.

The "partial mean life" limits tabulated here are the limits on τ/B_i , where τ is the total mean life and B_i is the branching fraction for the mode in question.

Mode	Partial mean life (10^{30} years)	Confidence level
Antilepton + meson		
$T_1 N \rightarrow e^+ \pi$	$> 158 (n), > 1600 (p)$	90%
$T_2 N \rightarrow \mu^+ \pi$	$> 100 (n), > 473 (p)$	90%
$T_3 N \rightarrow \nu \pi$	$> 112 (n), > 25 (p)$	90%
$T_4 p \rightarrow e^+ \eta$	> 313	90%
$T_5 p \rightarrow \mu^+ \eta$	> 126	90%
$T_6 n \rightarrow \nu \eta$	> 158	90%
$T_7 N \rightarrow e^+ \rho$	$> 217 (n), > 75 (p)$	90%
$T_8 N \rightarrow \mu^+ \rho$	$> 228 (n), > 110 (p)$	90%
$T_9 N \rightarrow \nu \rho$	$> 19 (n), > 162 (p)$	90%
$T_{10} p \rightarrow e^+ \omega$	> 107	90%
$T_{11} p \rightarrow \mu^+ \omega$	> 117	90%
$T_{12} n \rightarrow \nu \omega$	> 108	90%
$T_{13} N \rightarrow e^+ K$	$> 17 (n), > 150 (p)$	90%
$T_{14} p \rightarrow e^+ K_S^0$	> 76	90%
$T_{15} p \rightarrow e^+ K_L^0$	> 44	90%
$T_{16} N \rightarrow \mu^+ K$	$> 26 (n), > 120 (p)$	90%
$T_{17} p \rightarrow \mu^+ K_S^0$	> 64	90%
$T_{18} p \rightarrow \mu^+ K_L^0$	> 44	90%
$T_{19} N \rightarrow \nu K$	$> 86 (n), > 670 (p)$	90%
$T_{20} p \rightarrow e^+ K^*(892)^0$	> 84	90%
$T_{21} N \rightarrow \nu K^*(892)$	$> 78 (n), > 51 (p)$	90%
Antilepton + mesons		
$T_{22} p \rightarrow e^+ \pi^+ \pi^-$	> 82	90%
$T_{23} p \rightarrow e^+ \pi^0 \pi^0$	> 147	90%
$T_{24} n \rightarrow e^+ \pi^- \pi^0$	> 52	90%
$T_{25} p \rightarrow \mu^+ \pi^+ \pi^-$	> 133	90%
$T_{26} p \rightarrow \mu^+ \pi^0 \pi^0$	> 101	90%
$T_{27} n \rightarrow \mu^+ \pi^- \pi^0$	> 74	90%
$T_{28} n \rightarrow e^+ K^0 \pi^-$	> 18	90%
Lepton + meson		
$T_{29} n \rightarrow e^- \pi^+$	> 65	90%
$T_{30} n \rightarrow \mu^- \pi^+$	> 49	90%
$T_{31} n \rightarrow e^- \rho^+$	> 62	90%
$T_{32} n \rightarrow \mu^- \rho^+$	> 7	90%
$T_{33} n \rightarrow e^- K^+$	> 32	90%
$T_{34} n \rightarrow \mu^- K^+$	> 57	90%

Lepton + mesons

$T_{35} p \rightarrow e^- \pi^+ \pi^+$	> 30	90%
$T_{36} n \rightarrow e^- \pi^+ \pi^0$	> 29	90%
$T_{37} p \rightarrow \mu^- \pi^+ \pi^+$	> 17	90%
$T_{38} n \rightarrow \mu^- \pi^+ \pi^0$	> 34	90%
$T_{39} p \rightarrow e^- \pi^+ K^+$	> 75	90%
$T_{40} p \rightarrow \mu^- \pi^+ K^+$	> 245	90%

Antilepton + photon(s)

$T_{41} p \rightarrow e^+ \gamma$	> 670	90%
$T_{42} p \rightarrow \mu^+ \gamma$	> 478	90%
$T_{43} n \rightarrow \nu \gamma$	> 28	90%
$T_{44} p \rightarrow e^+ \gamma \gamma$	> 100	90%
$T_{45} n \rightarrow \nu \gamma \gamma$	> 219	90%

Three (or more) leptons

$T_{46} p \rightarrow e^+ e^+ e^-$	> 793	90%
$T_{47} p \rightarrow e^+ \mu^+ \mu^-$	> 359	90%
$T_{48} p \rightarrow e^+ \nu \nu$	> 17	90%
$T_{49} n \rightarrow e^+ e^- \nu$	> 257	90%
$T_{50} n \rightarrow \mu^+ e^- \nu$	> 83	90%
$T_{51} n \rightarrow \mu^+ \mu^- \nu$	> 79	90%
$T_{52} p \rightarrow \mu^+ e^+ e^-$	> 529	90%
$T_{53} p \rightarrow \mu^+ \mu^+ \mu^-$	> 675	90%
$T_{54} p \rightarrow \mu^+ \nu \nu$	> 21	90%
$T_{55} p \rightarrow e^- \mu^+ \mu^+$	> 6	90%
$T_{56} n \rightarrow 3\nu$	> 0.0005	90%
$T_{57} n \rightarrow 5\nu$		

Inclusive modes

$T_{58} N \rightarrow e^+ \text{anything}$	$> 0.6 (n, p)$	90%
$T_{59} N \rightarrow \mu^+ \text{anything}$	$> 12 (n, p)$	90%
$T_{60} N \rightarrow \nu \text{anything}$		
$T_{61} N \rightarrow e^+ \pi^0 \text{anything}$	$> 0.6 (n, p)$	90%
$T_{62} N \rightarrow 2 \text{ bodies, } \nu\text{-free}$		

$\Delta B = 2$ dinucleon modes

The following are lifetime limits per iron nucleus.

$T_{63} pp \rightarrow \pi^+ \pi^+$	> 0.7	90%
$T_{64} pn \rightarrow \pi^+ \pi^0$	> 2	90%
$T_{65} nn \rightarrow \pi^+ \pi^-$	> 0.7	90%
$T_{66} nn \rightarrow \pi^0 \pi^0$	> 3.4	90%
$T_{67} pp \rightarrow e^+ e^+$	> 5.8	90%
$T_{68} pp \rightarrow e^+ \mu^+$	> 3.6	90%
$T_{69} pp \rightarrow \mu^+ \mu^+$	> 1.7	90%
$T_{70} pn \rightarrow e^+ \bar{\nu}$	> 2.8	90%
$T_{71} pn \rightarrow \mu^+ \bar{\nu}$	> 1.6	90%
$T_{72} nn \rightarrow \nu_e \bar{\nu}_e$	> 0.000012	90%
$T_{73} nn \rightarrow \nu_\mu \bar{\nu}_\mu$	> 0.000006	90%

\bar{p} DECAY MODES

Mode	Partial mean life (years)	Confidence level
$T_{74} \bar{p} \rightarrow e^- \gamma$	$> 7 \times 10^5$	90%
$T_{75} \bar{p} \rightarrow \mu^- \gamma$	$> 5 \times 10^4$	90%
$T_{76} \bar{p} \rightarrow e^- \pi^0$	$> 4 \times 10^5$	90%
$T_{77} \bar{p} \rightarrow \mu^- \pi^0$	$> 5 \times 10^4$	90%
$T_{78} \bar{p} \rightarrow e^- \eta$	$> 2 \times 10^4$	90%
$T_{79} \bar{p} \rightarrow \mu^- \eta$	$> 8 \times 10^3$	90%
$T_{80} \bar{p} \rightarrow e^- K_S^0$	> 900	90%
$T_{81} \bar{p} \rightarrow \mu^- K_S^0$	$> 4 \times 10^3$	90%
$T_{82} \bar{p} \rightarrow e^- K_L^0$	$> 9 \times 10^3$	90%
$T_{83} \bar{p} \rightarrow \mu^- K_L^0$	$> 7 \times 10^3$	90%
$T_{84} \bar{p} \rightarrow e^- \gamma \gamma$	$> 2 \times 10^4$	90%
$T_{85} \bar{p} \rightarrow \mu^- \gamma \gamma$	$> 2 \times 10^4$	90%
$T_{86} \bar{p} \rightarrow e^- \rho$	> 200	90%
$T_{87} \bar{p} \rightarrow e^- \omega$	> 200	90%
$T_{88} \bar{p} \rightarrow e^- K^*(892)^0$	$> 1 \times 10^3$	90%

ρ

ρ PARTIAL MEAN LIVES

The "partial mean life" limits tabulated here are the limits on τ/B_j , where τ is the total mean life for the proton and B_j is the branching fraction for the mode in question.

Decaying particle: p = proton, n = bound neutron. The same event may appear under more than one partial decay mode. Background estimates may be accurate to a factor of two.

Antilepton + meson

$\tau(N \rightarrow e^+\pi)$

LIMIT (10 ³⁰ years)	PARTICLE	CL%	EVTS	BKGD EST	DOCUMENT ID	TECN
> 158	n	90	3	5	MCGREW	99 IMB3
> 1600	p	90	0	0.1	SHIOZAWA	98 SKAM
• • • We do not use the following data for averages, fits, limits, etc. • • •						
> 540	p	90	0	0.2	MCGREW	99 IMB3
> 70	p	90	0	0.5	BERGER	91 FREJ
> 70	n	90	0	<0.1	BERGER	91 FREJ
> 550	p	90	0	0.7	17 BECKER-SZ...	90 IMB3
> 260	p	90	0	<0.04	HIRATA	89C KAMI
> 130	n	90	0	<0.2	HIRATA	89C KAMI
> 310	p	90	0	0.6	SEIDEL	88 IMB
> 100	n	90	0	1.6	SEIDEL	88 IMB
> 1.3	n	90	0		BARTELT	87 SOUD
> 1.3	p	90	0		BARTELT	87 SOUD
> 250	p	90	0	0.3	HAINES	86 IMB
> 31	n	90	8	9	HAINES	86 IMB
> 64	p	90	0	<0.4	ARISAKA	85 KAMI
> 26	n	90	0	<0.7	ARISAKA	85 KAMI
> 82	p (free)	90	0	0.2	BLEWITT	85 IMB
> 250	p	90	0	0.2	BLEWITT	85 IMB
> 25	n	90	4	4	PARK	85 IMB
> 15	p, n	90	0		BATTISTONI	84 NUSX
> 0.5	p	90	1	0.3	18 BARTELT	83 SOUD
> 0.5	n	90	1	0.3	18 BARTELT	83 SOUD
> 5.8	p	90	2		19 KRISHNA...	82 KOLR
> 5.8	n	90	2		19 KRISHNA...	82 KOLR
> 0.1	n	90			20 GURR	67 CNTR

17 This BECKER-SZENDY 90 result includes data from SEIDEL 88.

18 Limit based on zero events.

19 We have calculated 90% CL limit from 1 confined event.

20 We have converted half-life to 90% CL mean life.

$\tau(N \rightarrow \mu^+\pi)$

LIMIT (10 ³⁰ years)	PARTICLE	CL%	EVTS	BKGD EST	DOCUMENT ID	TECN
> 473	p	90	0	0.6	MCGREW	99 IMB3
> 100	n	90	0	<0.2	HIRATA	89C KAMI
• • • We do not use the following data for averages, fits, limits, etc. • • •						
> 90	n	90	1	1.9	MCGREW	99 IMB3
> 81	p	90	0	0.2	BERGER	91 FREJ
> 35	n	90	1	1.0	BERGER	91 FREJ
> 230	p	90	0	<0.07	HIRATA	89C KAMI
> 270	p	90	0	0.5	SEIDEL	88 IMB
> 63	n	90	0	0.5	SEIDEL	88 IMB
> 76	p	90	2	1	HAINES	86 IMB
> 23	n	90	8	7	HAINES	86 IMB
> 46	p	90	0	<0.7	ARISAKA	85 KAMI
> 20	n	90	0	<0.4	ARISAKA	85 KAMI
> 59	p (free)	90	0	0.2	BLEWITT	85 IMB
> 100	p	90	1	0.4	BLEWITT	85 IMB
> 38	n	90	1	4	PARK	85 IMB
> 10	p, n	90	0		BATTISTONI	84 NUSX
> 1.3	p, n	90	0		ALEKSEEV	81 BASK

$\tau(N \rightarrow \nu\pi)$

LIMIT (10 ³⁰ years)	PARTICLE	CL%	EVTS	BKGD EST	DOCUMENT ID	TECN
> 112	n	90	6	6.6	MCGREW	99 IMB3
> 25	p	90	32	32.8	HIRATA	89C KAMI
• • • We do not use the following data for averages, fits, limits, etc. • • •						
> 10	p	90	15	20.3	MCGREW	99 IMB3
> 13	n	90	1	1.2	BERGER	89 FREJ
> 10	p	90	11	14	BERGER	89 FREJ
> 100	n	90	1	3	HIRATA	89C KAMI
> 6	n	90	73	60	HAINES	86 IMB
> 2	p	90	16	13	KAJITA	86 KAMI
> 40	n	90	0	1	KAJITA	86 KAMI
> 7	n	90	28	19	PARK	85 IMB
> 7	n	90	0		BATTISTONI	84 NUSX
> 2	p	90	≤ 3		BATTISTONI	84 NUSX
> 5.8	p	90	1		21 KRISHNA...	82 KOLR
> 0.3	p	90	2		22 CHERRY	81 HOME
> 0.1	p	90			23 GURR	67 CNTR

21 We have calculated 90% CL limit from 1 confined event.

22 We have converted 2 possible events to 90% CL limit.

23 We have converted half-life to 90% CL mean life.

$\tau(\rho \rightarrow e^+\eta)$

LIMIT (10 ³⁰ years)	PARTICLE	CL%	EVTS	BKGD EST	DOCUMENT ID	TECN
> 313	p	90	0	0.2	MCGREW	99 IMB3
• • • We do not use the following data for averages, fits, limits, etc. • • •						
> 44	p	90	0	0.1	BERGER	91 FREJ
> 140	p	90	0	<0.04	HIRATA	89C KAMI
> 100	p	90	0	0.6	SEIDEL	88 IMB
> 200	p	90	5	3.3	HAINES	86 IMB
> 64	p	90	0	<0.8	ARISAKA	85 KAMI
> 64	p (free)	90	5	6.5	BLEWITT	85 IMB
> 200	p	90	5	4.7	BLEWITT	85 IMB
> 1.2	p	90	2		24 CHERRY	81 HOME

24 We have converted 2 possible events to 90% CL limit.

$\tau(\rho \rightarrow \mu^+\eta)$

LIMIT (10 ³⁰ years)	PARTICLE	CL%	EVTS	BKGD EST	DOCUMENT ID	TECN
> 126	p	90	3	2.8	MCGREW	99 IMB3
• • • We do not use the following data for averages, fits, limits, etc. • • •						
> 26	p	90	1	0.8	BERGER	91 FREJ
> 69	p	90	1	<0.08	HIRATA	89C KAMI
> 1.3	p	90	0	0.7	PHILLIPS	89 HPW
> 34	p	90	1	1.5	SEIDEL	88 IMB
> 46	p	90	7	6	HAINES	86 IMB
> 26	p	90	1	<0.8	ARISAKA	85 KAMI
> 17	p (free)	90	6	6	BLEWITT	85 IMB
> 46	p	90	7	8	BLEWITT	85 IMB

$\tau(n \rightarrow \nu\eta)$

LIMIT (10 ³⁰ years)	PARTICLE	CL%	EVTS	BKGD EST	DOCUMENT ID	TECN
> 158	n	90	0	1.2	MCGREW	99 IMB3
• • • We do not use the following data for averages, fits, limits, etc. • • •						
> 29	n	90	0	0.9	BERGER	89 FREJ
> 54	n	90	2	0.9	HIRATA	89C KAMI
> 16	n	90	3	2.1	SEIDEL	88 IMB
> 25	n	90	7	6	HAINES	86 IMB
> 30	n	90	0	0.4	KAJITA	86 KAMI
> 18	n	90	4	3	PARK	85 IMB
> 0.6	n	90	2		25 CHERRY	81 HOME

25 We have converted 2 possible events to 90% CL limit.

$\tau(N \rightarrow e^+\rho)$

LIMIT (10 ³⁰ years)	PARTICLE	CL%	EVTS	BKGD EST	DOCUMENT ID	TECN
> 217	n	90	4	4.8	MCGREW	99 IMB3
> 75	p	90	2	2.7	HIRATA	89C KAMI
• • • We do not use the following data for averages, fits, limits, etc. • • •						
> 29	p	90	0	2.2	BERGER	91 FREJ
> 41	n	90	0	1.4	BERGER	91 FREJ
> 58	n	90	0	1.9	HIRATA	89C KAMI
> 38	n	90	2	4.1	SEIDEL	88 IMB
> 1.2	p	90	0		BARTELT	87 SOUD
> 1.5	n	90	0		BARTELT	87 SOUD
> 17	p	90	7	7	HAINES	86 IMB
> 14	n	90	9	4	HAINES	86 IMB
> 12	p	90	0	<1.2	ARISAKA	85 KAMI
> 6	n	90	2	<1	ARISAKA	85 KAMI
> 6.7	p (free)	90	6	6	BLEWITT	85 IMB
> 17	p	90	7	7	BLEWITT	85 IMB
> 12	n	90	4	2	PARK	85 IMB
> 0.6	n	90	1	0.3	26 BARTELT	83 SOUD
> 0.5	p	90	1	0.3	26 BARTELT	83 SOUD
> 9.8	p	90	1		27 KRISHNA...	82 KOLR
> 0.8	p	90	2		28 CHERRY	81 HOME

26 Limit based on zero events.

27 We have calculated 90% CL limit from 0 confined events.

28 We have converted 2 possible events to 90% CL limit.

$\tau(N \rightarrow \mu^+\rho)$

LIMIT (10 ³⁰ years)	PARTICLE	CL%	EVTS	BKGD EST	DOCUMENT ID	TECN
> 228	n	90	3	9.5	MCGREW	99 IMB3
> 110	p	90	0	1.7	HIRATA	89C KAMI
• • • We do not use the following data for averages, fits, limits, etc. • • •						
> 12	p	90	0	0.5	BERGER	91 FREJ
> 22	n	90	0	1.1	BERGER	91 FREJ
> 23	n	90	1	1.8	HIRATA	89C KAMI
> 4.3	p	90	0	0.7	PHILLIPS	89 HPW
> 30	p	90	0	0.5	SEIDEL	88 IMB
> 11	n	90	1	1.1	SEIDEL	88 IMB
> 16	p	90	4	4.5	HAINES	86 IMB
> 7	n	90	6	5	HAINES	86 IMB
> 12	p	90	0	<0.7	ARISAKA	85 KAMI
> 5	n	90	1	<1.2	ARISAKA	85 KAMI
> 5.5	p (free)	90	4	5	BLEWITT	85 IMB
> 16	p	90	4	5	BLEWITT	85 IMB
> 9	n	90	1	2	PARK	85 IMB

Baryon Particle Listings

 p $\tau(N \rightarrow \nu \rho)$

LIMIT (10^{30} years)	PARTICLE	CL%	EVTS	BKGD EST	DOCUMENT ID	TECN
>162	p	90	18	21.7	MCGREW 99	IMB3
>19	n	90	0	0.5	SEIDEL 88	IMB
••• We do not use the following data for averages, fits, limits, etc. •••						
>9	n	90	4	2.4	BERGER 89	FREJ
>24	p	90	0	0.9	BERGER 89	FREJ
>27	p	90	5	1.5	HIRATA 89c	KAMI
>13	n	90	4	3.6	HIRATA 89c	KAMI
>13	p	90	1	1.1	SEIDEL 88	IMB
>8	p	90	6	5	HAINES 86	IMB
>2	n	90	15	10	HAINES 86	IMB
>11	p	90	2	1	KAJITA 86	KAMI
>4	n	90	2	2	KAJITA 86	KAMI
>4.1	p (free)	90	6	7	BLEWITT 85	IMB
>8.4	p	90	6	5	BLEWITT 85	IMB
>2	n	90	7	3	PARK 85	IMB
>0.9	p	90	2		²⁹ CHERRY 81	HOME
>0.6	n	90	2		²⁹ CHERRY 81	HOME

²⁹We have converted 2 possible events to 90% CL limit. $\tau(p \rightarrow e^+ \omega)$

LIMIT (10^{30} years)	PARTICLE	CL%	EVTS	BKGD EST	DOCUMENT ID	TECN
>107	p	90	7	10.8	MCGREW 99	IMB3
••• We do not use the following data for averages, fits, limits, etc. •••						
>17	p	90	0	1.1	BERGER 91	FREJ
>45	p	90	2	1.45	HIRATA 89c	KAMI
>26	p	90	1	1.0	SEIDEL 88	IMB
>1.5	p	90	0		BARTELT 87	SOUD
>37	p	90	6	5.3	HAINES 86	IMB
>25	p	90	1	<1.4	ARISAKA 85	KAMI
>12	p (free)	90	6	7.5	BLEWITT 85	IMB
>37	p	90	6	5.7	BLEWITT 85	IMB
>0.6	p	90	1	0.3	³⁰ BARTELT 83	SOUD
>9.8	p	90	1		³¹ KRISHNA... 82	KOLR
>2.8	p	90	2		³² CHERRY 81	HOME

³⁰Limit based on zero events.³¹We have calculated 90% CL limit from 0 confined events.³²We have converted 2 possible events to 90% CL limit. $\tau(p \rightarrow \mu^+ \omega)$

LIMIT (10^{30} years)	PARTICLE	CL%	EVTS	BKGD EST	DOCUMENT ID	TECN
>117	p	90	11	12.1	MCGREW 99	IMB3
••• We do not use the following data for averages, fits, limits, etc. •••						
>11	p	90	0	1.0	BERGER 91	FREJ
>57	p	90	2	1.9	HIRATA 89c	KAMI
>4.4	p	90	0	0.7	PHILLIPS 89	HPW
>10	p	90	2	1.3	SEIDEL 88	IMB
>23	p	90	2	1	HAINES 86	IMB
>6.5	p (free)	90	9	8.7	BLEWITT 85	IMB
>23	p	90	8	7	BLEWITT 85	IMB

 $\tau(n \rightarrow \nu \omega)$

LIMIT (10^{30} years)	PARTICLE	CL%	EVTS	BKGD EST	DOCUMENT ID	TECN
>108	n	90	12	22.5	MCGREW 99	IMB3
••• We do not use the following data for averages, fits, limits, etc. •••						
>17	n	90	1	0.7	BERGER 89	FREJ
>43	n	90	3	2.7	HIRATA 89c	KAMI
>6	n	90	2	1.3	SEIDEL 88	IMB
>12	n	90	6	6	HAINES 86	IMB
>18	n	90	2	2	KAJITA 86	KAMI
>16	n	90	1	2	PARK 85	IMB
>2.0	n	90	2		³³ CHERRY 81	HOME

³³We have converted 2 possible events to 90% CL limit. $\tau(N \rightarrow e^+ K)$

LIMIT (10^{30} years)	PARTICLE	CL%	EVTS	BKGD EST	DOCUMENT ID	TECN
>17	n	90	35	29.4	MCGREW 99	IMB3
>150	p	90	0	<0.27	HIRATA 89c	KAMI
••• We do not use the following data for averages, fits, limits, etc. •••						
>31	p	90	23	25.2	MCGREW 99	IMB3
>60	p	90	0		BERGER 91	FREJ
>70	p	90	0	1.8	SEIDEL 88	IMB
>77	p	90	5	4.5	HAINES 86	IMB
>38	p	90	0	<0.8	ARISAKA 85	KAMI
>24	p (free)	90	7	8.5	BLEWITT 85	IMB
>77	p	90	5	4	BLEWITT 85	IMB
>1.3	p	90	0		ALEKSEEV 81	BAKS
>1.3	n	90	0		ALEKSEEV 81	BAKS

 $\tau(p \rightarrow e^+ K_S^0)$

LIMIT (10^{30} years)	PARTICLE	CL%	EVTS	BKGD EST	DOCUMENT ID	TECN
>76	p	90	0	0.5	BERGER 91	FREJ

 $\tau(p \rightarrow e^+ K_L^0)$

LIMIT (10^{30} years)	PARTICLE	CL%	EVTS	BKGD EST	DOCUMENT ID	TECN
>44	p	90	0	≤ 0.1	BERGER 91	FREJ

 $\tau(N \rightarrow \mu^+ K)$

LIMIT (10^{30} years)	PARTICLE	CL%	EVTS	BKGD EST	DOCUMENT ID	TECN
>120	p	90	4	7.2	MCGREW 99	IMB3
>26	n	90	20	28.4	MCGREW 99	IMB3
>120	p	90	1	0.4	HIRATA 89c	KAMI
••• We do not use the following data for averages, fits, limits, etc. •••						
>54	p	90	0		BERGER 91	FREJ
>3.0	p	90	0	0.7	PHILLIPS 89	HPW
>19	p	90	3	2.5	SEIDEL 88	IMB
>1.5	p	90	0		³⁴ BARTELT 87	SOUD
>1.1	n	90	0		BARTELT 87	SOUD
>40	p	90	7	6	HAINES 86	IMB
>19	p	90	1	<1.1	ARISAKA 85	KAMI
>6.7	p (free)	90	11	13	BLEWITT 85	IMB
>40	p	90	7	8	BLEWITT 85	IMB
>6	p	90	1		BATTISTONI 84	NUSX
>0.6	p	90	0		³⁵ BARTELT 83	SOUD
>0.4	n	90	0		³⁵ BARTELT 83	SOUD
>5.8	p	90	2		³⁶ KRISHNA... 82	KOLR
>2.0	p	90	0		CHERRY 81	HOME
>0.2	n	90	0		³⁷ GURR 67	CNTR

³⁴BARTELT 87 limit applies to $p \rightarrow \mu^+ K_S^0$.³⁵Limit based on zero events.³⁶We have calculated 90% CL limit from 1 confined event.³⁷We have converted half-life to 90% CL mean life. $\tau(p \rightarrow \mu^+ K_S^0)$

LIMIT (10^{30} years)	PARTICLE	CL%	EVTS	BKGD EST	DOCUMENT ID	TECN
>64	p	90	0	1.2	BERGER 91	FREJ

 $\tau(p \rightarrow \mu^+ K_L^0)$

LIMIT (10^{30} years)	PARTICLE	CL%	EVTS	BKGD EST	DOCUMENT ID	TECN
>44	p	90	0	≤ 0.1	BERGER 91	FREJ

 $\tau(N \rightarrow \nu K)$

LIMIT (10^{30} years)	PARTICLE	CL%	EVTS	BKGD EST	DOCUMENT ID	TECN
>670	p	90	15	21.4	MCGREW 99	IMB3
>86	n	90	0	2.4	HIRATA 89c	KAMI
••• We do not use the following data for averages, fits, limits, etc. •••						
>151	p	90	15	21.4	MCGREW 99	IMB3
>30	n	90	34	34.1	MCGREW 99	IMB3
>43	p	90	1	1.54	³⁸ ALLISON 98	SOU2
>15	n	90	1	1.8	BERGER 89	FREJ
>15	p	90	1	1.8	BERGER 89	FREJ
>100	p	90	9	7.3	HIRATA 89c	KAMI
>0.28	p	90	0	0.7	PHILLIPS 89	HPW
>0.3	p	90	0		BARTELT 87	SOUD
>0.75	n	90	0		³⁹ BARTELT 87	SOUD
>10	p	90	6	5	HAINES 86	IMB
>15	n	90	3	5	HAINES 86	IMB
>28	p	90	3	3	KAJITA 86	KAMI
>32	n	90	0	1.4	KAJITA 86	KAMI
>1.8	p (free)	90	6	11	BLEWITT 85	IMB
>9.6	p	90	6	5	BLEWITT 85	IMB
>10	n	90	2	2	PARK 85	IMB
>5	n	90	0		BATTISTONI 84	NUSX
>2	p	90	0		BATTISTONI 84	NUSX
>0.3	n	90	0		⁴⁰ BARTELT 83	SOUD
>0.1	p	90	0		⁴⁰ BARTELT 83	SOUD
>5.8	p	90	1		⁴¹ KRISHNA... 82	KOLR
>0.3	n	90	2		⁴² CHERRY 81	HOME

³⁸This ALLISON 98 limit is with no background subtraction; with subtraction the limit becomes $>46 \times 10^{30}$ years.³⁹BARTELT 87 limit applies to $n \rightarrow \nu K_S^0$.⁴⁰Limit based on zero events.⁴¹We have calculated 90% CL limit from 1 confined event.⁴²We have converted 2 possible events to 90% CL limit.

See key on page 239

Baryon Particle Listings

 p $\tau(p \rightarrow e^+ K^*(892)^0)$

720

LIMIT (10 ³⁰ years)	PARTICLE	CL%	EVTS	BKGD EST	DOCUMENT ID	TECN
>84	p	90	38	52.0	MCGREW 99	IMB3
••• We do not use the following data for averages, fits, limits, etc. •••						
>10	p	90	0	0.8	BERGER 91	FREJ
>52	p	90	2	1.55	HIRATA 89C	KAMI
>10	p	90	1	<1	ARISAKA 85	KAMI

 $\tau(N \rightarrow \nu K^*(892))$

721

LIMIT (10 ³⁰ years)	PARTICLE	CL%	EVTS	BKGD EST	DOCUMENT ID	TECN
>51	p	90	7	9.1	MCGREW 99	IMB3
>78	n	90	40	50	MCGREW 99	IMB3
••• We do not use the following data for averages, fits, limits, etc. •••						
>22	n	90	0	2.1	BERGER 89	FREJ
>17	p	90	0	2.4	BERGER 89	FREJ
>20	p	90	5	2.1	HIRATA 89C	KAMI
>21	n	90	4	2.4	HIRATA 89C	KAMI
>10	p	90	7	6	HAINES 86	IMB
> 5	n	90	8	7	HAINES 86	IMB
> 8	p	90	3	2	KAJITA 86	KAMI
> 6	n	90	2	1.6	KAJITA 86	KAMI
> 5.8	p (free)	90	10	16	BLEWITT 85	IMB
> 9.6	p	90	7	6	BLEWITT 85	IMB
> 7	n	90	1	4	PARK 85	IMB
> 2.1	p	90	1		43 BATTISTONI 82	NUSX

43 We have converted 1 possible event to 90% CL limit.

Antilepton + mesons

 $\tau(p \rightarrow e^+ \pi^+ \pi^-)$

722

LIMIT (10 ³⁰ years)	PARTICLE	CL%	EVTS	BKGD EST	DOCUMENT ID	TECN
>82	p	90	16	23.1	MCGREW 99	IMB3
••• We do not use the following data for averages, fits, limits, etc. •••						
>21	p	90	0	2.2	BERGER 91	FREJ

 $\tau(p \rightarrow e^+ \pi^0 \pi^0)$

723

LIMIT (10 ³⁰ years)	PARTICLE	CL%	EVTS	BKGD EST	DOCUMENT ID	TECN
>147	p	90	2	0.8	MCGREW 99	IMB3
••• We do not use the following data for averages, fits, limits, etc. •••						
> 38	p	90	1	0.5	BERGER 91	FREJ

 $\tau(n \rightarrow e^+ \pi^- \pi^0)$

724

LIMIT (10 ³⁰ years)	PARTICLE	CL%	EVTS	BKGD EST	DOCUMENT ID	TECN
>52	n	90	38	34.2	MCGREW 99	IMB3
••• We do not use the following data for averages, fits, limits, etc. •••						
>32	n	90	1	0.8	BERGER 91	FREJ

 $\tau(p \rightarrow \mu^+ \pi^+ \pi^-)$

725

LIMIT (10 ³⁰ years)	PARTICLE	CL%	EVTS	BKGD EST	DOCUMENT ID	TECN
>133	p	90	25	38.0	MCGREW 99	IMB3
••• We do not use the following data for averages, fits, limits, etc. •••						
> 17	p	90	1	2.6	BERGER 91	FREJ
> 3.3	p	90	0	0.7	PHILLIPS 89	HPW

 $\tau(p \rightarrow \mu^+ \pi^0 \pi^0)$

726

LIMIT (10 ³⁰ years)	PARTICLE	CL%	EVTS	BKGD EST	DOCUMENT ID	TECN
>101	p	90	3	1.6	MCGREW 99	IMB3
••• We do not use the following data for averages, fits, limits, etc. •••						
> 33	p	90	1	0.9	BERGER 91	FREJ

 $\tau(n \rightarrow \mu^+ \pi^- \pi^0)$

727

LIMIT (10 ³⁰ years)	PARTICLE	CL%	EVTS	BKGD EST	DOCUMENT ID	TECN
>74	n	90	17	20.8	MCGREW 99	IMB3
••• We do not use the following data for averages, fits, limits, etc. •••						
>33	n	90	0	1.1	BERGER 91	FREJ

 $\tau(n \rightarrow e^+ K^0 \pi^-)$

728

LIMIT (10 ³⁰ years)	PARTICLE	CL%	EVTS	BKGD EST	DOCUMENT ID	TECN
>18	n	90	1	0.2	BERGER 91	FREJ

Lepton + meson

 $\tau(n \rightarrow e^- \pi^+)$

729

LIMIT (10 ³⁰ years)	PARTICLE	CL%	EVTS	BKGD EST	DOCUMENT ID	TECN
>65	n	90	0	1.6	SEIDEL 88	IMB
••• We do not use the following data for averages, fits, limits, etc. •••						
>55	n	90	0	1.09	BERGER 91B	FREJ
>16	n	90	9	7	HAINES 86	IMB
>25	n	90	2	4	PARK 85	IMB

 $\tau(n \rightarrow \mu^- \pi^+)$

730

LIMIT (10 ³⁰ years)	PARTICLE	CL%	EVTS	BKGD EST	DOCUMENT ID	TECN
>49	n	90	0	0.5	SEIDEL 88	IMB
••• We do not use the following data for averages, fits, limits, etc. •••						
>33	n	90	0	1.40	BERGER 91B	FREJ
> 2.7	n	90	0	0.7	PHILLIPS 89	HPW
>25	n	90	7	6	HAINES 86	IMB
>27	n	90	2	3	PARK 85	IMB

 $\tau(n \rightarrow e^- \rho^+)$

731

LIMIT (10 ³⁰ years)	PARTICLE	CL%	EVTS	BKGD EST	DOCUMENT ID	TECN
>62	n	90	2	4.1	SEIDEL 88	IMB
••• We do not use the following data for averages, fits, limits, etc. •••						
>12	n	90	13	6	HAINES 86	IMB
>12	n	90	5	3	PARK 85	IMB

 $\tau(n \rightarrow \mu^- \rho^+)$

732

LIMIT (10 ³⁰ years)	PARTICLE	CL%	EVTS	BKGD EST	DOCUMENT ID	TECN
>7	n	90	1	1.1	SEIDEL 88	IMB
••• We do not use the following data for averages, fits, limits, etc. •••						
>2.6	n	90	0	0.7	PHILLIPS 89	HPW
>9	n	90	7	5	HAINES 86	IMB
>9	n	90	2	2	PARK 85	IMB

 $\tau(n \rightarrow e^- K^+)$

733

LIMIT (10 ³⁰ years)	PARTICLE	CL%	EVTS	BKGD EST	DOCUMENT ID	TECN
>32	n	90	3	2.96	BERGER 91B	FREJ
••• We do not use the following data for averages, fits, limits, etc. •••						
> 0.23	n	90	0	0.7	PHILLIPS 89	HPW

 $\tau(n \rightarrow \mu^- K^+)$

734

LIMIT (10 ³⁰ years)	PARTICLE	CL%	EVTS	BKGD EST	DOCUMENT ID	TECN
>57	n	90	0	2.18	BERGER 91B	FREJ
••• We do not use the following data for averages, fits, limits, etc. •••						
> 4.7	n	90	0	0.7	PHILLIPS 89	HPW

Lepton + mesons

 $\tau(p \rightarrow e^- \pi^+ \pi^+)$

735

LIMIT (10 ³⁰ years)	PARTICLE	CL%	EVTS	BKGD EST	DOCUMENT ID	TECN
>30	p	90	1	2.50	BERGER 91B	FREJ
••• We do not use the following data for averages, fits, limits, etc. •••						
> 2.0	p	90	0	0.7	PHILLIPS 89	HPW

 $\tau(n \rightarrow e^- \pi^+ \pi^0)$

736

LIMIT (10 ³⁰ years)	PARTICLE	CL%	EVTS	BKGD EST	DOCUMENT ID	TECN
>29	n	90	1	0.78	BERGER 91B	FREJ

 $\tau(p \rightarrow \mu^- \pi^+ \pi^+)$

737

LIMIT (10 ³⁰ years)	PARTICLE	CL%	EVTS	BKGD EST	DOCUMENT ID	TECN
>17	p	90	1	1.72	BERGER 91B	FREJ
••• We do not use the following data for averages, fits, limits, etc. •••						
> 7.8	p	90	0	0.7	PHILLIPS 89	HPW

 $\tau(n \rightarrow \mu^- \pi^+ \pi^0)$

738

LIMIT (10 ³⁰ years)	PARTICLE	CL%	EVTS	BKGD EST	DOCUMENT ID	TECN
>34	n	90	0	0.78	BERGER 91B	FREJ

 $\tau(p \rightarrow e^- \pi^+ K^+)$

739

LIMIT (10 ³⁰ years)	PARTICLE	CL%	EVTS	BKGD EST	DOCUMENT ID	TECN
>75	p	90	81	127.2	MCGREW 99	IMB3
••• We do not use the following data for averages, fits, limits, etc. •••						
>20	p	90	3	2.50	BERGER 91B	FREJ

 $\tau(p \rightarrow \mu^- \pi^+ K^+)$

740

LIMIT (10 ³⁰ years)	PARTICLE	CL%	EVTS	BKGD EST	DOCUMENT ID	TECN
>245	p	90	3	4.0	MCGREW 99	IMB3
••• We do not use the following data for averages, fits, limits, etc. •••						
> 5	p	90	2	0.78	BERGER 91B	FREJ

Baryon Particle Listings

p

Antilepton + photon(s)

$\tau(p \rightarrow e^+\gamma)$ 741

LIMIT (10^{30} years)	PARTICLE	CL%	EVTS	BKGD EST	DOCUMENT ID	TECN
>670	p	90	0	0.1	MCGREW	99 IMB3
••• We do not use the following data for averages, fits, limits, etc. •••						
>133	p	90	0	0.3	BERGER	91 FREJ
>460	p	90	0	0.6	SEIDEL	88 IMB
>360	p	90	0	0.3	HAINES	86 IMB
> 87	p (free)	90	0	0.2	BLEWITT	85 IMB
>360	p	90	0	0.2	BLEWITT	85 IMB
> 0.1	p	90			44 GURR	67 CNTR

44 We have converted half-life to 90% CL mean life.

$\tau(p \rightarrow \mu^+\gamma)$ 742

LIMIT (10^{30} years)	PARTICLE	CL%	EVTS	BKGD EST	DOCUMENT ID	TECN
>478	p	90	0	0.1	MCGREW	99 IMB3
••• We do not use the following data for averages, fits, limits, etc. •••						
>155	p	90	0	0.1	BERGER	91 FREJ
>380	p	90	0	0.5	SEIDEL	88 IMB
> 97	p	90	3	2	HAINES	86 IMB
> 61	p (free)	90	0	0.2	BLEWITT	85 IMB
>280	p	90	0	0.6	BLEWITT	85 IMB
> 0.3	p	90			45 GURR	67 CNTR

45 We have converted half-life to 90% CL mean life.

$\tau(n \rightarrow \nu\gamma)$ 743

LIMIT (10^{30} years)	PARTICLE	CL%	EVTS	BKGD EST	DOCUMENT ID	TECN
>28	n	90	163	144.7	MCGREW	99 IMB3
••• We do not use the following data for averages, fits, limits, etc. •••						
>24	n	90	10	6.86	BERGER	91B FREJ
> 9	n	90	73	60	HAINES	86 IMB
>11	n	90	28	19	PARK	85 IMB

$\tau(p \rightarrow e^+\gamma\gamma)$ 744

LIMIT (10^{30} years)	PARTICLE	CL%	EVTS	BKGD EST	DOCUMENT ID	TECN
>100	p	90	1	0.8	BERGER	91 FREJ

$\tau(n \rightarrow \nu\gamma\gamma)$ 745

LIMIT (10^{30} years)	PARTICLE	CL%	EVTS	BKGD EST	DOCUMENT ID	TECN
>219	n	90	5	7.5	MCGREW	99 IMB3

Three (or more) leptons

$\tau(p \rightarrow e^+e^+e^-)$ 746

LIMIT (10^{30} years)	PARTICLE	CL%	EVTS	BKGD EST	DOCUMENT ID	TECN
>793	p	90	0	0.5	MCGREW	99 IMB3
••• We do not use the following data for averages, fits, limits, etc. •••						
>147	p	90	0	0.1	BERGER	91 FREJ
>510	p	90	0	0.3	HAINES	86 IMB
> 89	p (free)	90	0	0.5	BLEWITT	85 IMB
>510	p	90	0	0.7	BLEWITT	85 IMB

$\tau(p \rightarrow e^+\mu^+\mu^-)$ 747

LIMIT (10^{30} years)	PARTICLE	CL%	EVTS	BKGD EST	DOCUMENT ID	TECN
>359	p	90	1	0.9	MCGREW	99 IMB3
••• We do not use the following data for averages, fits, limits, etc. •••						
> 81	p	90	0	0.16	BERGER	91 FREJ
> 5.0	p	90	0	0.7	PHILLIPS	89 HPW

$\tau(p \rightarrow e^+\nu\nu)$ 748

LIMIT (10^{30} years)	PARTICLE	CL%	EVTS	BKGD EST	DOCUMENT ID	TECN
>17	p	90	152	153.7	MCGREW	99 IMB3
••• We do not use the following data for averages, fits, limits, etc. •••						
>11	p	90	11	6.08	BERGER	91B FREJ

$\tau(n \rightarrow e^+e^-\nu)$ 749

LIMIT (10^{30} years)	PARTICLE	CL%	EVTS	BKGD EST	DOCUMENT ID	TECN
>257	n	90	5	7.5	MCGREW	99 IMB3
••• We do not use the following data for averages, fits, limits, etc. •••						
> 74	n	90	0	< 0.1	BERGER	91B FREJ
> 45	n	90	5	5	HAINES	86 IMB
> 26	n	90	4	3	PARK	85 IMB

$\tau(n \rightarrow \mu^+e^-\nu)$ 750

LIMIT (10^{30} years)	PARTICLE	CL%	EVTS	BKGD EST	DOCUMENT ID	TECN
>83	n	90	25	29.4	MCGREW	99 IMB3
••• We do not use the following data for averages, fits, limits, etc. •••						
>47	n	90	0	< 0.1	BERGER	91B FREJ

$\tau(n \rightarrow \mu^+\mu^-\nu)$ 751

LIMIT (10^{30} years)	PARTICLE	CL%	EVTS	BKGD EST	DOCUMENT ID	TECN
>79	n	90	100	145	MCGREW	99 IMB3
••• We do not use the following data for averages, fits, limits, etc. •••						
>42	n	90	0	1.4	BERGER	91B FREJ
> 5.1	n	90	0	0.7	PHILLIPS	89 HPW
>16	n	90	14	7	HAINES	86 IMB
>19	n	90	4	7	PARK	85 IMB

$\tau(p \rightarrow \mu^+e^+e^-)$ 752

LIMIT (10^{30} years)	PARTICLE	CL%	EVTS	BKGD EST	DOCUMENT ID	TECN
>529	p	90	0	1.0	MCGREW	99 IMB3
••• We do not use the following data for averages, fits, limits, etc. •••						
> 91	p	90	0	≤ 0.1	BERGER	91 FREJ

$\tau(p \rightarrow \mu^+\mu^+\mu^-)$ 753

LIMIT (10^{30} years)	PARTICLE	CL%	EVTS	BKGD EST	DOCUMENT ID	TECN
>675	p	90	0	0.3	MCGREW	99 IMB3
••• We do not use the following data for averages, fits, limits, etc. •••						
>119	p	90	0	0.2	BERGER	91 FREJ
> 10.5	p	90	0	0.7	PHILLIPS	89 HPW
>190	p	90	1	0.1	HAINES	86 IMB
> 44	p (free)	90	1	0.7	BLEWITT	85 IMB
>190	p	90	1	0.9	BLEWITT	85 IMB
> 2.1	p	90	1		46 BATTISTONI	82 NUSX

46 We have converted 1 possible event to 90% CL limit.

$\tau(p \rightarrow \mu^+\nu\nu)$ 754

LIMIT (10^{30} years)	PARTICLE	CL%	EVTS	BKGD EST	DOCUMENT ID	TECN
>21	p	90	7	11.23	BERGER	91B FREJ

$\tau(p \rightarrow e^-\mu^+\mu^+)$ 755

LIMIT (10^{30} years)	PARTICLE	CL%	EVTS	BKGD EST	DOCUMENT ID	TECN
>6.0	p	90	0	0.7	PHILLIPS	89 HPW

$\tau(n \rightarrow 3\nu)$ 756

LIMIT (10^{30} years)	PARTICLE	CL%	EVTS	BKGD EST	DOCUMENT ID	TECN
>0.00049	n	90	2	2	47 SUZUKI	93B KAMI
••• We do not use the following data for averages, fits, limits, etc. •••						
>0.0023	n	90			48 GLICENSTEIN	97 KAMI
>0.00003	n	90	11	6.1	49 BERGER	91B FREJ
>0.00012	n	90	7	11.2	49 BERGER	91B FREJ
>0.0005	n	90	0		LEARNED	79 RVUE

47 The SUZUKI 93B limit applies to any of $\nu_e\nu_e\bar{\nu}_e$, $\nu_\mu\nu_\mu\bar{\nu}_\mu$, or $\nu_\tau\nu_\tau\bar{\nu}_\tau$.

48 GLICENSTEIN 97 uses Kamioka data and the idea that the disappearance of the neutron's magnetic moment should produce radiation.

49 The first BERGER 91B limit is for $n \rightarrow \nu_e\nu_e\bar{\nu}_e$, the second is for $n \rightarrow \nu_\mu\nu_\mu\bar{\nu}_\mu$.

$\tau(n \rightarrow 5\nu)$ 757

LIMIT (10^{30} years)	PARTICLE	CL%	EVTS	BKGD EST	DOCUMENT ID	TECN
>0.0017	n	90			50 GLICENSTEIN	97 KAMI
••• We do not use the following data for averages, fits, limits, etc. •••						

50 GLICENSTEIN 97 uses Kamioka data and the idea that the disappearance of the neutron's magnetic moment should produce radiation.

Inclusive modes

$\tau(N \rightarrow e^+$ anything) 758

LIMIT (10^{30} years)	PARTICLE	CL%	EVTS	BKGD EST	DOCUMENT ID	TECN
>0.6	p, n	90			51 LEARNED	79 RVUE
••• We do not use the following data for averages, fits, limits, etc. •••						
51 The electron may be primary or secondary.						

$\tau(N \rightarrow \mu^+$ anything) 759

LIMIT (10^{30} years)	PARTICLE	CL%	EVTS	BKGD EST	DOCUMENT ID	TECN
>12	p, n	90	2		52,53 CHERRY	81 HOME
••• We do not use the following data for averages, fits, limits, etc. •••						
> 1.8	p, n	90			53 COWSIK	80 CNTR
> 6	p, n	90			53 LEARNED	79 RVUE

52 We have converted 2 possible events to 90% CL limit.

53 The muon may be primary or secondary.

$\tau(N \rightarrow \nu \text{ anything})$ 760
 Anything = π, ρ, K , etc.

LIMIT (10^{30} years)	PARTICLE	CL%	EVTs	BKGD EST	DOCUMENT ID	TECN	COMMENT
>0.0002	ρ, n	90	0		LEARNED	79	RVUE

$\tau(N \rightarrow e^+ \pi^0 \text{ anything})$ 761

LIMIT (10^{30} years)	PARTICLE	CL%	EVTs	BKGD EST	DOCUMENT ID	TECN	COMMENT
>0.6	ρ, n	90	0		LEARNED	79	RVUE

$\tau(N \rightarrow 2 \text{ bodies, } \nu\text{-free})$ 762

LIMIT (10^{30} years)	PARTICLE	CL%	EVTs	BKGD EST	DOCUMENT ID	TECN	COMMENT
>1.3	ρ, n	90	0		ALEKSEEV	81	BAKS

———— $\Delta B = 2$ dinucleon modes ————

$\tau(pp \rightarrow \pi^+ \pi^+)$ 763

LIMIT (10^{30} years)	CL%	EVTs	BKGD EST	DOCUMENT ID	TECN	COMMENT
>0.7	90	4	2.34	BERGER	91B FREJ	τ per iron nucleus

$\tau(pn \rightarrow \pi^+ \pi^0)$ 764

LIMIT (10^{30} years)	CL%	EVTs	BKGD EST	DOCUMENT ID	TECN	COMMENT
>2.0	90	0	0.31	BERGER	91B FREJ	τ per iron nucleus

$\tau(nn \rightarrow \pi^+ \pi^-)$ 765

LIMIT (10^{30} years)	CL%	EVTs	BKGD EST	DOCUMENT ID	TECN	COMMENT
>0.7	90	4	2.18	BERGER	91B FREJ	τ per iron nucleus

$\tau(nn \rightarrow \pi^0 \pi^0)$ 766

LIMIT (10^{30} years)	CL%	EVTs	BKGD EST	DOCUMENT ID	TECN	COMMENT
>3.4	90	0	0.78	BERGER	91B FREJ	τ per iron nucleus

$\tau(pp \rightarrow e^+ e^+)$ 767

LIMIT (10^{30} years)	CL%	EVTs	BKGD EST	DOCUMENT ID	TECN	COMMENT
>5.8	90	0	<0.1	BERGER	91B FREJ	τ per iron nucleus

$\tau(pp \rightarrow e^+ \mu^+)$ 768

LIMIT (10^{30} years)	CL%	EVTs	BKGD EST	DOCUMENT ID	TECN	COMMENT
>3.6	90	0	<0.1	BERGER	91B FREJ	τ per iron nucleus

$\tau(pp \rightarrow \mu^+ \mu^+)$ 769

LIMIT (10^{30} years)	CL%	EVTs	BKGD EST	DOCUMENT ID	TECN	COMMENT
>1.7	90	0	0.62	BERGER	91B FREJ	τ per iron nucleus

$\tau(pn \rightarrow e^+ \bar{\nu})$ 770

LIMIT (10^{30} years)	CL%	EVTs	BKGD EST	DOCUMENT ID	TECN	COMMENT
>2.8	90	5	9.67	BERGER	91B FREJ	τ per iron nucleus

$\tau(pn \rightarrow \mu^+ \bar{\nu})$ 771

LIMIT (10^{30} years)	CL%	EVTs	BKGD EST	DOCUMENT ID	TECN	COMMENT
>1.6	90	4	4.37	BERGER	91B FREJ	τ per iron nucleus

$\tau(nn \rightarrow \nu_e \bar{\nu}_e)$ 772

LIMIT (10^{30} years)	CL%	EVTs	BKGD EST	DOCUMENT ID	TECN	COMMENT
>0.000012	90	5	9.7	BERGER	91B FREJ	τ per iron nucleus

$\tau(nn \rightarrow \nu_\mu \bar{\nu}_\mu)$ 773

LIMIT (10^{30} years)	CL%	EVTs	BKGD EST	DOCUMENT ID	TECN	COMMENT
>0.000006	90	4	4.4	BERGER	91B FREJ	τ per iron nucleus

\bar{p} PARTIAL MEAN LIVES

The "partial mean life" limits tabulated here are the limits on $\bar{\tau}/B_j$, where $\bar{\tau}$ is the total mean life for the antiproton and B_j is the branching fraction for the mode in question.

$\tau(\bar{p} \rightarrow e^- \gamma)$ 774

VALUE (years)	CL%	DOCUMENT ID	TECN	COMMENT
> 7×10^5	90	GEER 00 APEX	8.9 GeV/c \bar{p} beam	••• We do not use the following data for averages, fits, limits, etc. •••
>1848	95	GEER 94 CALO	8.9 GeV/c \bar{p} beam	

$\tau(\bar{p} \rightarrow \mu^- \gamma)$ 775

VALUE (years)	CL%	DOCUMENT ID	TECN	COMMENT
> 5×10^4	90	GEER 00 APEX	8.9 GeV/c \bar{p} beam	••• We do not use the following data for averages, fits, limits, etc. •••
> 5.0×10^4	90	HU 98B APEX	8.9 GeV/c \bar{p} beam	

$\tau(\bar{p} \rightarrow e^- \pi^0)$ 776

VALUE (years)	CL%	DOCUMENT ID	TECN	COMMENT
> 4×10^5	90	GEER 00 APEX	8.9 GeV/c \bar{p} beam	••• We do not use the following data for averages, fits, limits, etc. •••
>554	95	GEER 94 CALO	8.9 GeV/c \bar{p} beam	

$\tau(\bar{p} \rightarrow \mu^- \pi^0)$ 777

VALUE (years)	CL%	DOCUMENT ID	TECN	COMMENT
> 5×10^4	90	GEER 00 APEX	8.9 GeV/c \bar{p} beam	••• We do not use the following data for averages, fits, limits, etc. •••
> 4.8×10^4	90	HU 98B APEX	8.9 GeV/c \bar{p} beam	

$\tau(\bar{p} \rightarrow e^- \eta)$ 778

VALUE (years)	CL%	DOCUMENT ID	TECN	COMMENT
> 2×10^4	90	GEER 00 APEX	8.9 GeV/c \bar{p} beam	••• We do not use the following data for averages, fits, limits, etc. •••
>171	95	GEER 94 CALO	8.9 GeV/c \bar{p} beam	

$\tau(\bar{p} \rightarrow \mu^- \eta)$ 779

VALUE (years)	CL%	DOCUMENT ID	TECN	COMMENT
> 8×10^3	90	GEER 00 APEX	8.9 GeV/c \bar{p} beam	••• We do not use the following data for averages, fits, limits, etc. •••
> 7.9×10^3	90	HU 98B APEX	8.9 GeV/c \bar{p} beam	

$\tau(\bar{p} \rightarrow e^- K_S^0)$ 780

VALUE (years)	CL%	DOCUMENT ID	TECN	COMMENT
>900	90	GEER 00 APEX	8.9 GeV/c \bar{p} beam	••• We do not use the following data for averages, fits, limits, etc. •••
> 29	95	GEER 94 CALO	8.9 GeV/c \bar{p} beam	

$\tau(\bar{p} \rightarrow \mu^- K_S^0)$ 781

VALUE (years)	CL%	DOCUMENT ID	TECN	COMMENT
> 4×10^3	90	GEER 00 APEX	8.9 GeV/c \bar{p} beam	••• We do not use the following data for averages, fits, limits, etc. •••
> 4.3×10^3	90	HU 98B APEX	8.9 GeV/c \bar{p} beam	

$\tau(\bar{p} \rightarrow e^- K_L^0)$ 782

VALUE (years)	CL%	DOCUMENT ID	TECN	COMMENT
> 9×10^3	90	GEER 00 APEX	8.9 GeV/c \bar{p} beam	••• We do not use the following data for averages, fits, limits, etc. •••
>9	95	GEER 94 CALO	8.9 GeV/c \bar{p} beam	

$\tau(\bar{p} \rightarrow \mu^- K_L^0)$ 783

VALUE (years)	CL%	DOCUMENT ID	TECN	COMMENT
> 7×10^3	90	GEER 00 APEX	8.9 GeV/c \bar{p} beam	••• We do not use the following data for averages, fits, limits, etc. •••
> 6.5×10^3	90	HU 98B APEX	8.9 GeV/c \bar{p} beam	

$\tau(\bar{p} \rightarrow e^- \gamma \gamma)$ 784

VALUE (years)	CL%	DOCUMENT ID	TECN	COMMENT
> 2×10^4	90	GEER 00 APEX	8.9 GeV/c \bar{p} beam	

$\tau(\bar{p} \rightarrow \mu^- \gamma \gamma)$ 785

VALUE (years)	CL%	DOCUMENT ID	TECN	COMMENT
> 2×10^4	90	GEER 00 APEX	8.9 GeV/c \bar{p} beam	••• We do not use the following data for averages, fits, limits, etc. •••
> 2.3×10^4	90	HU 98B APEX	8.9 GeV/c \bar{p} beam	

$\tau(\bar{p} \rightarrow e^- \rho)$ 786

VALUE (years)	CL%	DOCUMENT ID	TECN	COMMENT
>200	90	⁵⁴ GEER 00 APEX	8.9 GeV/c \bar{p} beam	••• We do not use the following data for averages, fits, limits, etc. •••
⁵⁴ This GEER 00 measurement has been withdrawn (APEX Collaboration, private communication).				

$\tau(\bar{p} \rightarrow e^- \omega)$ 787

VALUE (years)	CL%	DOCUMENT ID	TECN	COMMENT
>200	90	GEER 00 APEX	8.9 GeV/c \bar{p} beam	

$\tau(\bar{p} \rightarrow e^- K^*(892)^0)$ 788

VALUE (years)	CL%	DOCUMENT ID	TECN	COMMENT
> 1×10^3	90	⁵⁵ GEER 00 APEX	8.9 GeV/c \bar{p} beam	••• We do not use the following data for averages, fits, limits, etc. •••
⁵⁵ This GEER 00 measurement has been withdrawn (APEX Collaboration, private communication).				

Baryon Particle Listings

p, n

p REFERENCES

GEER	00	PRL 84 590	S. Geer et al.	(FNAL APEX Collab.)
GABRIELSE	99	PR 82 3198	G. Gabrielse et al.	
HAYATO	99	PRL 83 1529	Y. Hayato et al.	(Super-Kamiokande Collab.)
MCGREW	99	PR D59 052004	C. McGrew et al.	(IMB-3 Collab.)
MOHR	99	JPCRD 28 1713	F.J. Mohr, B.N. Taylor	(NIST)
Also	00	RMP 72 351	F.J. Mohr, B.N. Taylor	(NIST)
TORII	99	PR A59 223	H.A. Torii et al.	(CERN-PS-205 Collab.)
ALLISON	98	PL B427 217	W.W.M. Allison et al.	(Soudan-2 Collab.)
HU	98B	PR D58 111101	M. Hu et al.	(FNAL APEX Collab.)
SHIOZAWA	99	PRL 81 3319	M. Shiozawa et al.	(Super-Kamiokande Collab.)
GLICKENSTEIN	97	PL B411 326	J.R. Glickenstein	(SACL)
GABRIELSE	95	PRL 74 3544	G. Gabrielse et al.	(HARV, MANZ, SEOUL)
MACGIBBON	95	PR C52 2097	B.E. MacGibbon et al.	(ILL, SASK, INRM)
GEER	94	PRL 72 1596	S. Geer et al.	(FNAL, UCLA, PSU)
HALLIN	93	PR C48 1497	E.L. Hallin et al.	(SASK, BOST, ILL)
SUZUKI	93B	PL B311 357	Y. Suzuki et al.	(KAMIOKANDE Collab.)
HUGHES	92	PRL 69 578	R.J. Hughes, B.I. Deutch	(LANL, AARH)
ZIEGER	92	PL B278 34	A. Zieger et al.	(MPCM)
Also	92B	PL B281 417 (erratum)	A. Zieger et al.	(FREJUS Collab.)
BERGER	91	ZPHY C50 385	C. Berger et al.	(FREJUS Collab.)
BERGER	91B	PL B269 227	C. Berger et al.	(FREJUS Collab.)
FEDERSPIEL	91	PRL 67 1511	F.J. Federspiel et al.	(ILL)
BECKER-SZ...	90	PR D42 2974	R.A. Becker-Szendy et al.	(IMB-3 Collab.)
ERICSON	90	EPL 11 295	T.E.O. Ericson, A. Richter	(CERN, DARM)
GABRIELSE	90	PR 65 1317	G. Gabrielse et al.	(HARV, MANZ, WASH+)
BERGER	89	NP B313 509	C. Berger et al.	(FREJUS Collab.)
CHO	89	PR 63 2959	D. Cho, K. Sangster, E.A. Hinds	(YALE)
HIRATA	89C	PL B220 308	K.S. Hirata et al.	(Kamiokande Collab.)
PHILLIPS	89	PL B224 348	T.J. Phillips et al.	(HPW Collab.)
KREISSL	88	ZPHY C37 557	A. Kreissl et al.	(CERN PS176 Collab.)
SEIDEL	88	PRL 61 2522	S. Seidel et al.	(IMB Collab.)
BARTELT	87	PR D36 1990	J.E. Bartelt et al.	(Soudan Collab.)
Also	89	PR D40 1701 (erratum)	J.E. Bartelt et al.	(Soudan Collab.)
COHEN	87	RMP 59 1121	E.R. Cohen, B.N. Taylor	(RISC, NBS)
HAINES	86	PRL 57 1986	T.J. Haines et al.	(IMB Collab.)
KAJITA	86	JPSJ 55 711	T. Kajita et al.	(Kamiokande Collab.)
ARISAKA	85	JPSJ 54 3213	K. Arisaka et al.	(Kamiokande Collab.)
BLEWITT	85	PRL 55 2114	G.B. Blewitt et al.	(IMB Collab.)
DZUBA	85	PL 154B 93	V.A. Dzuba, V.V. Flambaum, P.G. Silvestrov	(NOVO)
PARK	85	PRL 54 22	H.S. Park et al.	(IMB Collab.)
BATTISTONI	84	PL 133B 454	G. Battistoni et al.	(NUSEX Collab.)
MARINELLI	84	PL 137B 439	M. Marinelli, G. Morpurgo	(GENO)
WILKENING	84	PR A29 425	Wilkening, Ramsey, Larson	(HARV, VIRG)
BARTELT	83	PRL 50 651	J.E. Bartelt et al.	(MINN, ANL)
BATTISTONI	82	PL 118B 461	G. Battistoni et al.	(NUSEX Collab.)
KRISHNA...	82	PL 115B 349	M.R. Krishnaswamy et al.	(TATA, OSKC+)
ALEKSEEV	81	JETPL 33 651	E.N. Alekseev et al.	(PNPI)
Translated from ZETP	33	664.		
CHERRY	81	PRL 47 1507	M.L. Cherry et al.	(PENN, BNL)
COWSIK	80	PR D22 2204	R. Cowsik, V.S. Narasimham	(TATA)
BELL	79	PL 86B 215	M. Bell et al.	(CERN)
GOLDEN	79	PRL 43 1196	R.L. Golden et al.	(NASA, PSSL)
LEARNED	79	PR 43 907	J.G. Learned, F. Reines, A. Soni	(UCI)
BREGMAN	78	PL 78B 174	M. Bregman et al.	(CERN)
ROBERTS	78	PR D17 358	B.L. Roberts	(WILL, RHSL)
EVANS	77	Science 197 989	J.C. Evans Jr., R.I. Steinberg	(BNL, PENN)
HU	75	NP A254 403	E. Hu et al.	(COLL, YALE)
COHEN	73	JPCRD 2 563	E.R. Cohen, B.N. Taylor	(RISC, NBS)
DYLLA	73	PR A7 1224	H.F. Dylla, J.G. King	(MIT)
DIX	70	Thesis Case	F.W. Dix	(CASE)
HARRISON	69	PR 22 1263	G.E. Harrison, P.G.H. Sandars, S.J. Wright	(OXF)
GURR	67	PR 158 1321	H.S. Gurr et al.	(CASE, WITW)
FLEROV	58	DOKL 3 79	Flerov et al.	(ASCI)

$(m_n - m_p) / m_n$

A test of CPT invariance. Calculated from the *n* and *p* masses, above.

VALUE (9±5) × 10⁻⁵ OUR EVALUATION DOCUMENT ID

$m_n - m_p$

VALUE (MeV)	DOCUMENT ID	TECN	COMMENT
1.2933318 ± 0.0000005	⁸ MOHR	99 RVUE	1998 CODATA value
● ● ● We do not use the following data for averages, fits, limits, etc. ● ● ●			
1.293318 ± 0.000009	⁹ COHEN	87 RVUE	1986 CODATA value
1.2933328 ± 0.0000072	GREENE	86 SPEC	<i>np</i> → <i>dγ</i>
1.293429 ± 0.0000036	COHEN	73 RVUE	1973 CODATA value
⁸ Calculated by us from the MOHR 99 ratio $m_n/m_p = 1.00137841887 \pm 0.00000000058$.			
In u, $m_n - m_p = (1.3884489 \pm 0.0000006) \times 10^{-3}$ u.			
⁹ Calculated by us from the COHEN 87 ratio $m_n/m_p = 1.001378404 \pm 0.000000009$. In u, $m_n - m_p = 0.001388434 \pm 0.000000009$ u.			

n MEAN LIFE

We now compile only direct measurements of the lifetime, not those inferred from decay correlation measurements. (Limits on lifetimes for bound neutrons are given in the section "p PARTIAL MEAN LIVES.")

For a review, see EROZOLIMSKI 89 and papers that follow it in an issue of NIM devoted to the "Proceedings of the International Workshop on Fundamental Physics with Slow Neutrons" (Grenoble 1989). For later reviews and/or commentary, see FREEDMAN 90, SCHRECKENBACH 92, and PENDLEBURY 93.

VALUE (s)	DOCUMENT ID	TECN	COMMENT
886.7 ± 1.9 OUR AVERAGE	Error includes scale factor of 1.2.		
889.2 ± 3.0 ± 3.8	BYRNE	96 CNTR	Penning trap
882.6 ± 2.7	¹⁰ MAMPE	93 CNTR	Gravitational trap
888.4 ± 3.1 ± 1.1	NESVIZHEV...	92 CNTR	Gravitational trap
878 ± 27 ± 14	KOSSAKOV...	89 TPC	Pulsed beam
887.6 ± 3.0	MAMPE	89 CNTR	Gravitational trap
877 ± 10	PAUL	89 CNTR	Storage ring
876 ± 10 ± 19	LAST	88 SPEC	Pulsed beam
891 ± 9	SPIVAK	88 CNTR	Beam
903 ± 13	KOSVINTSEV	86 CNTR	Gravitational trap
918 ± 14	CHRISTENSEN72		CNTR
● ● ● We do not use the following data for averages, fits, limits, etc. ● ● ●			
888.4 ± 2.9	ALFIMENKOV	90 CNTR	See NESVIZHEVSKII 92
893.6 ± 3.8 ± 3.7	BYRNE	90 CNTR	See BYRNE 96
937 ± 18	¹¹ BYRNE	80 CNTR	
875 ± 95	KOSVINTSEV	80 CNTR	
881 ± 8	BONDAREN...	78 CNTR	See SPIVAK 88

¹⁰IGNATOVICH 95 calls into question some of the corrections and averaging procedures used by MAMPE 93. The response, BONDARENKO 96, denies the validity of the criticisms.

¹¹This measurement has been withdrawn (J. Byrne, private communication, 1990).

n MAGNETIC MOMENT

See the "Note on Baryon Magnetic Moments" in the *Λ* Listings.

VALUE (μ _N)	DOCUMENT ID	TECN	COMMENT
-1.91304272 ± 0.00000045	MOHR	99 RVUE	1998 CODATA value
● ● ● We do not use the following data for averages, fits, limits, etc. ● ● ●			
-1.91304275 ± 0.00000045	COHEN	87 RVUE	1986 CODATA value
-1.91304277 ± 0.00000048	¹² GREENE	82 MRS	
¹² GREENE 82 measures the moment to be $(1.04187564 \pm 0.000000026) \times 10^{-3}$ Bohr magnetons. The value above is obtained by multiplying this by $m_p/m_e = 1836.152701 \pm 0.000037$ (the 1986 CODATA value from COHEN 87).			

n ELECTRIC DIPOLE MOMENT d_n

A nonzero value is forbidden by both *T* invariance and *P* invariance. A number of early results have been omitted. See RAMSEY 90 and GOLUB 94 for reviews.

VALUE (10 ⁻²⁵ ecm)	CL%	DOCUMENT ID	TECN	COMMENT
< 0.63	90	¹³ HARRIS	99 MRS	$d = (-0.1 \pm 0.36) \times 10^{-25}$
● ● ● We do not use the following data for averages, fits, limits, etc. ● ● ●				
< 0.97	90	ALTAREV	96 MRS	$(-0.26 \pm 0.40 \pm 0.16) \times 10^{-25}$
< 1.1	95	ALTAREV	92 MRS	See ALTAREV 96
< 1.2	95	SMITH	90 MRS	See HARRIS 99
< 2.6	95	ALTAREV	86 MRS	$d = (-1.4 \pm 0.6) \times 10^{-25}$
0.3 ± 4.8		PENDLEBURY	84 MRS	Ultracold neutrons
< 6	90	ALTAREV	81 MRS	$d = (2.1 \pm 2.4) \times 10^{-25}$
< 16	90	ALTAREV	79 MRS	$d = (4.0 \pm 7.5) \times 10^{-25}$

¹³This HARRIS 99 result includes the result of SMITH 90. However, the averaging of the results of these two experiments has been criticized by LAMOREAUX 00.

n

$I(J^P) = \frac{1}{2}(\frac{1}{2}^+)$ Status: * * * *

We have omitted some results that have been superseded by later experiments. See our earlier editions.

n MASS

The mass is known much more precisely in u (atomic mass units) than in MeV; see the footnotes. The conversion from u to MeV, 1 u = 931.494013 ± 0.000037 MeV/c² (MOHR 99, the 1998 CODATA value), involves the relatively poorly known electronic charge.

VALUE (MeV)	DOCUMENT ID	TECN	COMMENT
939.565330 ± 0.000038	¹ MOHR	99 RVUE	1998 CODATA value
● ● ● We do not use the following data for averages, fits, limits, etc. ● ● ●			
939.565331 ± 0.000037	² KESSLER	99 SPEC	<i>np</i> → <i>dγ</i>
939.56565 ± 0.00028	^{3,4} DIFILIPPO	94 TRAP	Penning trap
939.56563 ± 0.00028	⁵ COHEN	87 RVUE	1986 CODATA value
939.56564 ± 0.00028	^{4,6} GREENE	86 SPEC	<i>np</i> → <i>dγ</i>
939.5731 ± 0.0027	⁴ COHEN	73 RVUE	1973 CODATA value

- ¹ The mass is known much more precisely in u: $m = 1.00866491578 \pm 0.00000000055$ u.
- ² We use the 1998 CODATA u-to-MeV conversion factor (see the heading above) to get this mass in MeV from the much more precisely measured KESSLER 99 value of $1.00866491637 \pm 0.00000000082$ u.
- ³ The mass is known much more precisely in u: $m = 1.0086649235 \pm 0.0000000023$ u. We use the 1986 CODATA conversion factor to get the mass in MeV.
- ⁴ These determinations are not independent of the $m_n - m_p$ measurements below.
- ⁵ The mass is known much more precisely in u: $m = 1.008664904 \pm 0.000000014$ u.
- ⁶ The mass is known much more precisely in u: $m = 1.008664919 \pm 0.000000014$ u.

n MASS

VALUE (MeV)	EVTS	DOCUMENT ID	TECN	COMMENT
939.485 ± 0.051	59	⁷ CRESTI	86 HBC	$\bar{p}p \rightarrow \bar{n}n$

⁷This is a corrected result (see the erratum). The error is statistical. The maximum systematic error is 0.029 MeV.

n ELECTRIC POLARIZABILITY α_n

Following is the electric polarizability α_n defined in terms of the induced electric dipole moment by $\mathbf{D} = 4\pi\epsilon_0\alpha_n\mathbf{E}$. For a review, see SCHMIED-MAYER 89.

VALUE (10^{-3}fm^3)	DOCUMENT ID	TECN	COMMENT
0.90^{+0.19}_{-0.23} OUR AVERAGE			Error includes scale factor of 1.1.
0.0 ± 0.5	14 KOESTER	95 CNTR	n Pb, n Bi transmission
1.20 ± 0.15 ± 0.20	SCHMIEDM...	91 CNTR	n Pb transmission
1.07 ^{+0.33} _{-1.07}	ROSE	90B CNTR	$\gamma d \rightarrow \gamma np$
0.8 ± 1.0	KOESTER	88 CNTR	n Pb, n Bi transmission
1.2 ± 1.0	SCHMIEDM...	88 CNTR	n Pb, n C transmission
• • • We do not use the following data for averages, fits, limits, etc. • • •			
1.17 ^{+0.43} _{-1.17}	ROSE	90 CNTR	See ROSE 90B

¹⁴KOESTER 95 uses natural Pb and the isotopes 208, 207, and 206. See this paper for a discussion of methods used by various groups to extract α_n from data.

n CHARGE

See also " $|q_p + q_e|/e$ " in the proton Listings.

VALUE ($10^{-21} e$)	DOCUMENT ID	TECN	COMMENT
-0.4 ± 1.1	15 BAUMANN	88	Cold n deflection
• • • We do not use the following data for averages, fits, limits, etc. • • •			
-15 ± 22	16 GAEHLER	82 CNTR	Reactor neutrons
¹⁵ The BAUMANN 88 error ± 1.1 gives the 68% CL limits about the the value -0.4.			
¹⁶ The GAEHLER 82 error ± 22 gives the 90% CL limits about the the value -15.			

LIMIT ON $n\bar{n}$ OSCILLATIONS**Mean Time for $n\bar{n}$ Transition in Vacuum**

A test of $\Delta B=2$ baryon number nonconservation. MOHAPATRA 80 and MOHAPATRA 89 discuss the theoretical motivations for looking for $n\bar{n}$ oscillations. DOVER 83 and DOVER 85 give phenomenological analyses. The best limits come from looking for the decay of neutrons bound in nuclei. However, these analyses require model-dependent corrections for nuclear effects. See KABIR 83, DOVER 89, and ALBERICO 91 for discussions. Direct searches for $n \rightarrow \bar{n}$ transitions using reactor neutrons are cleaner but give somewhat poorer limits. We include limits for both free and bound neutrons in the Summary Table.

VALUE (s)	CL%	DOCUMENT ID	TECN	COMMENT
>8.6 × 10 ⁷	90	BALDO-...	94 CNTR	Reactor (free) neutrons
>1.2 × 10 ⁸	90	BERGER	90 FREJ	n bound in iron
>1.2 × 10 ⁸	90	TAKITA	86 CNTR	Kamiokande
• • • We do not use the following data for averages, fits, limits, etc. • • •				
>1 × 10 ⁷	90	BALDO-...	90 CNTR	See BALDO-CEOLIN 94
>4.9 × 10 ⁵	90	BRESSI	90 CNTR	Reactor neutrons
>4.7 × 10 ⁵	90	BRESSI	89 CNTR	See BRESSI 90
>1 × 10 ⁶	90	FIDECARO	85 CNTR	Reactor neutrons
>8.8 × 10 ⁷	90	PARK	85B CNTR	
>3 × 10 ⁷		BATTISTONI	84 NUSX	
>2.7 × 10 ⁷ -1.1 × 10 ⁸		JONES	84 CNTR	
>2 × 10 ⁷		CHERRY	83 CNTR	

n DECAY MODES

Mode	Fraction (Γ_i/Γ)	Confidence level
Γ_1 $p e^- \bar{\nu}_e$	100 %	
Γ_2 hydrogen-atom $\bar{\nu}_e$		
Charge conservation (Q) violating mode		
Γ_3 $p \nu_e \bar{\nu}_e$	Q < 8 × 10 ⁻²⁷	68%

n BRANCHING RATIOS

$\Gamma(\text{hydrogen-atom } \bar{\nu}_e)/\Gamma_{\text{total}}$	Γ_2/Γ		
VALUE	CL%	DOCUMENT ID	TECN
• • • We do not use the following data for averages, fits, limits, etc. • • •			
<3 × 10 ⁻²	95	17 GREEN	90 RVUE

¹⁷GREEN 90 infers that $\tau(\text{hydrogen-atom } \bar{\nu}_e) > 3 \times 10^4 \text{ s}$ by comparing neutron lifetime measurements made in storage experiments with those made in β -decay experiments. However, the result depends sensitively on the lifetime measurements, and does not of course take into account more recent measurements of same.

 $\Gamma(p\nu_e\bar{\nu}_e)/\Gamma_{\text{total}}$

Forbidden by charge conservation.

VALUE	CL%	DOCUMENT ID	TECN	COMMENT
<8 × 10 ⁻²⁷	68	18 NORMAN	96 RVUE	⁷¹ Ga → ⁷¹ Ge neutrals
• • • We do not use the following data for averages, fits, limits, etc. • • •				
<9.7 × 10 ⁻¹⁸	90	ROY	83 CNTR	¹¹³ Cd → ^{113m} Inneut.
<7.9 × 10 ⁻²¹		VAIDYA	83 CNTR	⁸⁷ Rb → ^{87m} Srneut.
<9 × 10 ⁻²⁴	90	BARABANOV	80 CNTR	⁷¹ Ga → ⁷¹ GeX
<3 × 10 ⁻¹⁹		NORMAN	79 CNTR	⁸⁷ Rb → ^{87m} Srneut.

¹⁸NORMAN 96 gets this limit by attributing SAGE and GALLEX counting rates to the charge-nonconserving transition ⁷¹Ga → ⁷¹Ge+neutrals rather than to solar-neutrino reactions.

BARYON DECAY PARAMETERS

Written 1996 by E.D. Commins (University of California, Berkeley).

Baryon semileptonic decays

The typical spin-1/2 baryon semileptonic decay is described by a matrix element, the hadronic part of which may be written as:

$$\bar{B}_f [f_1(q^2)\gamma_\lambda + i f_2(q^2)\sigma_{\lambda\mu}q^\mu + g_1(q^2)\gamma_\lambda\gamma_5 + g_3(q^2)\gamma_5q_\lambda] B_i \quad (1)$$

Here B_i and \bar{B}_f are spinors describing the initial and final baryons, and $q = p_i - p_f$, while the terms in f_1 , f_2 , g_1 , and g_3 account for vector, induced tensor ("weak magnetism"), axial vector, and induced pseudoscalar contributions [1]. Second-class current contributions are ignored here. In the limit of zero momentum transfer, f_1 reduces to the vector coupling constant g_V , and g_1 reduces to the axial-vector coupling constant g_A . The latter coefficients are related by Cabibbo's theory [2], generalized to six quarks (and three mixing angles) by Kobayashi and Maskawa [3]. The g_3 term is negligible for transitions in which an e^\pm is emitted, and gives a very small correction, which can be estimated by PCAC [4], for μ^\pm modes. Recoil effects include weak magnetism, and are taken into account adequately by considering terms of first order in

$$\delta = \frac{m_i - m_f}{m_i + m_f}, \quad (2)$$

where m_i and m_f are the masses of the initial and final baryons.

The experimental quantities of interest are the total decay rate, the lepton-neutrino angular correlation, the asymmetry coefficients in the decay of a polarized initial baryon, and the polarization of the decay baryon in its own rest frame for an unpolarized initial baryon. Formulae for these quantities are derived by standard means [5] and are analogous to formulae for nuclear beta decay [6]. We use the notation of Ref. 6 in the Listings for neutron beta decay. For comparison with experiments at higher q^2 , it is necessary to modify the form factors at $q^2 = 0$ by a "dipole" q^2 dependence, and for high-precision comparisons to apply appropriate radiative corrections [7].

The ratio g_A/g_V may be written as

$$g_A/g_V = |g_A/g_V| e^{i\phi_{AV}} \quad (3)$$

The presence of a "triple correlation" term in the transition probability, proportional to $\text{Im}(g_A/g_V)$ and of the form

$$\sigma_i \cdot (\mathbf{p}_\ell \times \mathbf{p}_\nu) \quad (4)$$

Baryon Particle Listings

n

for initial baryon polarization or

$$\sigma_f \cdot (\mathbf{p}_\ell \times \mathbf{p}_\nu) \quad (5)$$

for final baryon polarization, would indicate failure of time-reversal invariance. The phase angle ϕ has been measured precisely only in neutron decay (and in ^{19}Ne nuclear beta decay), and the results are consistent with T invariance.

Hyperon nonleptonic decays

The amplitude for a spin-1/2 hyperon decaying into a spin-1/2 baryon and a spin-0 meson may be written in the form

$$M = G_F m_\pi^2 \cdot \bar{B}_f (A - B\gamma_5) B_i, \quad (6)$$

where A and B are constants [1]. The transition rate is proportional to

$$R = 1 + \gamma \hat{\omega}_f \cdot \hat{\omega}_i + (1 - \gamma)(\hat{\omega}_f \cdot \hat{\mathbf{n}})(\hat{\omega}_i \cdot \hat{\mathbf{n}}) + \alpha(\hat{\omega}_f \cdot \hat{\mathbf{n}} + \hat{\omega}_i \cdot \hat{\mathbf{n}}) + \beta \hat{\mathbf{n}} \cdot (\hat{\omega}_f \times \hat{\omega}_i), \quad (7)$$

where $\hat{\mathbf{n}}$ is a unit vector in the direction of the final baryon momentum, and $\hat{\omega}_i$ and $\hat{\omega}_f$ are unit vectors in the directions of the initial and final baryon spins. (The sign of the last term in the above equation was incorrect in our 1988 and 1990 editions.) The parameters α , β , and γ are defined as

$$\begin{aligned} \alpha &= 2 \operatorname{Re}(s^* p) / (|s|^2 + |p|^2), \\ \beta &= 2 \operatorname{Im}(s^* p) / (|s|^2 + |p|^2), \\ \gamma &= (|s|^2 - |p|^2) / (|s|^2 + |p|^2), \end{aligned} \quad (8)$$

where $s = A$ and $p = |\mathbf{p}_f| B / (E_f + m_f)$; here E_f and \mathbf{p}_f are the energy and momentum of the final baryon. The parameters α , β , and γ satisfy

$$\alpha^2 + \beta^2 + \gamma^2 = 1. \quad (9)$$

If the hyperon polarization is \mathbf{P}_Y , the polarization \mathbf{P}_B of the decay baryons is

$$\mathbf{P}_B = \frac{(\alpha + \mathbf{P}_Y \cdot \hat{\mathbf{n}})\hat{\mathbf{n}} + \beta(\mathbf{P}_Y \times \hat{\mathbf{n}}) + \gamma\hat{\mathbf{n}} \times (\mathbf{P}_Y \times \hat{\mathbf{n}})}{1 + \alpha\mathbf{P}_Y \cdot \hat{\mathbf{n}}}. \quad (10)$$

Here \mathbf{P}_B is defined in the rest system of the baryon, obtained by a Lorentz transformation along $\hat{\mathbf{n}}$ from the hyperon rest frame, in which $\hat{\mathbf{n}}$ and \mathbf{P}_Y are defined.

An additional useful parameter ϕ is defined by

$$\beta = (1 - \alpha^2)^{1/2} \sin\phi. \quad (11)$$

In the Listings, we compile α and ϕ for each decay, since these quantities are most closely related to experiment and are essentially uncorrelated. When necessary, we have changed the signs of reported values to agree with our sign conventions. In the Baryon Summary Table, we give α , ϕ , and Δ (defined below) with errors, and also give the value of γ without error.

Time-reversal invariance requires, in the absence of final-state interactions, that s and p be relatively real, and therefore

that $\beta = 0$. However, for the decays discussed here, the final-state interaction is strong. Thus

$$s = |s| e^{i\delta_s} \text{ and } p = |p| e^{i\delta_p}, \quad (12)$$

where δ_s and δ_p are the pion-baryon s - and p -wave strong interaction phase shifts. We then have

$$\beta = \frac{-2|s||p|}{|s|^2 + |p|^2} \sin(\delta_s - \delta_p). \quad (13)$$

One also defines $\Delta = -\tan^{-1}(\beta/\alpha)$. If T invariance holds, $\Delta = \delta_s - \delta_p$. For $\Lambda \rightarrow p\pi^-$ decay, the value of Δ may be compared with the s - and p -wave phase shifts in low-energy $\pi^- p$ scattering, and the results are consistent with T invariance.

Radiative hyperon decays

For the radiative decay of a polarized spin-1/2 hyperon, $B_i \rightarrow B_f \gamma$, the angular distribution of the direction \hat{p} of the final spin-1/2 baryon in the hyperon rest frame is

$$\frac{d\Gamma_\gamma}{d\Omega} = \frac{\Gamma_\gamma}{4\pi} (1 + \alpha_\gamma \hat{p} \cdot \mathbf{P}_i), \quad (14)$$

where \mathbf{P}_i is the hyperon polarization and the asymmetry parameter α_γ is

$$\alpha_\gamma = \frac{2 \operatorname{Re} [g_1^*(0) f_M^*(0)]}{|g_1^*(0)|^2 + |f_M^*(0)|^2}. \quad (15)$$

Here $f_M = \frac{(m_i - m_f)}{(m_i + m_f)} [(m_i + m_f) f_2' - f_1']$, where $f_1'(q^2)$, $f_2'(q^2)$, and $g_1'(q^2)$ are the $\Delta Q = 0$ analogs of the $|\Delta Q| = 1$ form factors defined above.

References

1. E.D. Commins and P.H. Bucksbaum, *Weak Interactions of Leptons and Quarks* (Cambridge University Press, Cambridge, England, 1983).
2. N. Cabibbo, *Phys. Rev. Lett.* **10**, 531 (1963).
3. M. Kobayashi and T. Maskawa, *Prog. Theor. Phys.* **49**, 652 (1973).
4. M.L. Goldberger and S.B. Treiman, *Phys. Rev.* **111**, 354 (1958).
5. P.H. Frampton and W.K. Tung, *Phys. Rev.* **D3**, 1114 (1971).
6. J.D. Jackson, S.B. Treiman, and H.W. Wyld, Jr., *Phys. Rev.* **106**, 517 (1957), and *Nucl. Phys.* **4**, 206 (1957).
7. Y. Yokoo, S. Suzuki, and M. Morita, *Prog. Theor. Phys.* **50**, 1894 (1973).

Baryon Particle Listings

 n , N 's and Δ 's

KOESTER	95	PR C51 3363	L. Koester et al.	(MUNT, JINR, LATV)
KUZNETSOV	95	PRL 75 794	I.A. Kuznetsov et al.	(PNPI, KIAE, HARV+)
SCHRECK...	95	PL B349 427	K. Schreckenbach et al.	(MUNT, ILLG, LAPP)
BALDO...	94	ZPHY C63 409	M. Baldo-Ceolin et al.	(HEID, ILLG, PADO+)
DIFILIPPO	94	PRL 73 1481	F. DiFilippo et al.	(MIT)
Also	93	PRL 71 1998	V. Natarajan et al.	(MIT)
GOLUB	94	PRPL 237C 1	R. Golub, K. Lamoreaux	(HAHN, WASH)
MAMPE	93	JETPL 57 82	B. Mampe et al.	(KIAE)
PENDLEBURY	93	ARNPS 43 687	J.M. Pendlebury	(ILLG)
ALTAREV	92	PL B276 242	I.S. Altarev et al.	(PNPI)
NEVZIVZHEV...	92	JETP 75 405	V.V. Nevzhevsky et al.	(PNPI, JINR)
Translated from ZETFP 57 77				
SCHRECK...	92	JPG 18 1	K. Schreckenbach, W. Mampe	(ILLG)
ALBERICO	91	NP A523 488	W.M. Alberico, A. de Pace, M. Pignone	(TORI)
DUBBERS	91	NP A527 239C	D. Dubbers	(ILLG)
Also	90	EPL 11 195	D. Dubbers, W. Mampe, J. Oohner	(ILLG, HEID)
EROZOLIM...	91	PL B263 33	B.G. Eroozolimsky et al.	(PNPI, KIAE)
Also	90	SJNP 52 999	B.G. Eroozolimsky et al.	(PNPI, KIAE)
Translated from YAF 52 1583				
EROZOLIM...	91B	SJNP 53 260	B.G. Eroozolimsky, Y.A. Mostovoy	(KIAE)
Translated from YAF 53 419				
SCHMIEDM...	91	PRL 66 1215	J. Schmiedmayer et al.	(TUW, ORNL)
WOOLCOCK	91	MPL A6 2579	W.S. Woolcock	(CANB)
ALFIMENKOV	90	JETPL 52 373	V.P. Alfimenkov et al.	(PNPI, JINR)
Translated from ZETFP 52 984				
BALDO...	90	PL B236 95	M. Baldo-Ceolin et al.	(PADO, PAVI, HEIOP+)
BERGER	90	PL B240 237	C. Berger et al.	(FREJUS Collab.)
BRESSI	90	NC 103A 731	G. Bressi et al.	(PAVI, ROMA, MILA)
BYRNE	90	PRL 65 289	J. Byrne et al.	(SUSS, NBS, SCOT, CBM)
FREEDMAN	90	CNPP 19 209	S.J. Freedman	(ANL)
GREEN	90	JPG 16 L75	M.G. Green, Thompson	(RAL)
RAMSEY	90	ARNPS 40 1	N.F. Ramsey	(HARV)
ROSE	90	PL B234 460	K.W. Rose et al.	(GOET, MPCM, MANZ)
ROSE	90B	NP A514 621	K.W. Rose et al.	(GOET, MPCM)
SMITH	90	PL B234 191	K.F. Smith et al.	(SUSS, RAL, HARV+)
BRESSI	89	ZPHY C43 175	G. Bressi et al.	(INFN, MILA, PAVI, ROMA)
DOVER	89	NC A284 13	C.B. Dover, A. Gal, J.M. Richard	(BNL, HEBR+)
EROZOLIM...	89	NIM A284 89	B.G. Eroozolimsky	(PNPI)
KOSSAKOW...	89	NP A503 473	R. Kossakowski et al.	(LAPP, SAVO, ISNG+)
MAMPE	89	PRL 63 593	W. Mampe et al.	(ILLG, RISL, SUSS, URI)
MOHAPATRA	89	NIM A284 1	R.N. Mohapatra	(UMD)
PAUL	89	ZPHY C45 25	W. Paul et al.	(BDNN, WUPP, MPH, ILLG)
SCHMIEDM...	89	NIM A284 137	J. Schmiedmayer, H. Rauch, P. Rieths	(WIEN)
BAUMANN	88	PRL D37 3107	J. Baumann et al.	(BAYR, MUNI, ILLG)
KOESTER	88	ZPHY A329 229	L. Koester, W. Waschkowski, Meier	(MUNI, MUNT)
LAST	88	PRL 60 995	I. Last et al.	(HEIDP, ILLG, ANL)
SCHMIEDM...	88	PRL 61 1065	J. Schmiedmayer, H. Rauch, P. Rieths	(TUW)
Also	88B	PRL 61 2509 erratum	J. Schmiedmayer, H. Rauch, P. Rieths	(TUW)
SPIVAK	88	JETP 67 1735	P.E. Spivak	(KIAE)
Translated from ZETFP 94 1				
COHEN	87	RMP 59 1121	E.R. Cohen, B.N. Taylor	(RISC, NBS)
ALTAREV	86	JETPL 44 460	I.S. Altarev et al.	(PNPI)
Translated from ZETFP 44 360				
BOPP	86	PRL 56 919	P. Bopp et al.	(HEIDP, ANL, ILLG)
Also	86	ZPHY C37 179	E. Klempf et al.	(HEIDP, ANL, ILLG)
CRESTI	86	PL B177 206	M. Cresti et al.	(PADO)
Also	88	PL B200 587 erratum	M. Cresti et al.	(PADO)
GREENE	86	PRL 56 819	G.L. Greene et al.	(NBS, ILLG)
KOSVINTSEV	86	JETPL 44 571	Y.Y. Kosvintsev, V.I. Morozov, G.I. Terekhov	(KIAE)
Translated from ZETFP 44 444				
TAKITA	86	PRL D34 902	M. Takita et al.	(KEK, TOKY+)
DOVER	85	PR C31 1423	C.B. Dover, A. Gal, J.M. Richard	(BNL)
FIDECARO	85	PL 156B 122	G. Fidencaro et al.	(CERN, ILLG, PADO+)
PARK	85B	NP B252 261	H.S. Park et al.	(IMB Collab.)
BATTISTONI	84	PL 133B 454	G. Battistoni et al.	(NUSEX Collab.)
JONES	84	PRL 52 720	T.W. Jones et al.	(IMB Collab.)
PENDLEBURY	84	PL 136B 327	J.M. Pendlebury et al.	(SUSS, HARV, RAL+)
CHERRY	83	PRL 50 1354	M.L. Cherry et al.	(PENN, BNL)
DOVER	83	PR D27 1090	C.B. Dover, A. Gal, J.M. Richard	(BNL)
KABIR	83	PRL 51 231	P.K. Kabir	(HARV)
MOSTOVOY	83	JETPL 37 196	Y.A. Mostovoy	(KIAE)
Translated from ZETFP 37 162				
ROY	83	PR D28 1770	A. Roy et al.	(TATA)
VAIDYA	83	PR D27 486	S.C. Vaidya et al.	(TATA)
GAEHLER	82	PR D25 2887	R. Gahler, J. Kalus, W. Mampe	(BAYR, ILLG)
GREENE	82	Metrologia 18 93	G.L. Greene et al.	(YALE, HARV, ILLG+)
ALTAREV	81	PL 102B 13	I.S. Altarev et al.	(PNPI)
BARABANOV	80	JETPL 32 359	I.R. Barabanov et al.	(PNPI)
Translated from ZETFP 32 384				
BYRNE	80	PL 92B 274	J. Byrne et al.	(SUSS, RL)
KOSVINTSEV	80	JETPL 31 235	Y.Y. Kosvintsev et al.	(JINR)
Translated from ZETFP 31 257				
MOHAPATRA	80	PRL 44 1316	R.N. Mohapatra, R.E. Marshak	(CUNY, VPI)
ALTAREV	79	JETPL 29 730	I.S. Altarev et al.	(PNPI)
Translated from ZETFP 29 794				
EROZOLIM...	79	SJNP 30 355	B.G. Eroozolimsky et al.	(KIAE)
Translated from YAF 30 692				
NORMAN	79	PRL 43 1225	E.B. Norman, A.G. Seanster	(WASH)
BONDAREN...	78	JETPL 28 303	L.N. Bondarenko et al.	(KIAE)
Translated from ZETFP 28 328				
Also	82	Smolenice Conf.	P.G. Bondarenko	(KIAE)
EROZOLIM...	78	SJNP 28 48	B.G. Eroozolimsky et al.	(KIAE)
Translated from YAF 28 38				
STRATOWA	78	PR D18 3970	C. Stratowa, R. Dobrozemsky, P. Weinzierl	(SEIB)
EROZOLIM...	77	JETPL 23 663	B.G. Eroozolimsky et al.	(KIAE)
Translated from ZETFP 23 745				
STEINBERG	76	PR D13 2469	R.I. Steinberg et al.	(YALE, ISNG)
DOBROZE...	75	PR D11 510	R. Dobrozemsky et al.	(SEIB)
KROHN	75	PL 55B 175	V.E. Krohn, G.R. Ringo	(ANL)
EROZOLIM...	74	JETPL 20 345	B.G. Eroozolimsky et al.	(KIAE)
Translated from ZETFP 20 745				
KROPP	74	ZPHY 267 129	H. Kropp, E. Paul	(LINZ)
Also	70	NP A154 160	H. Paul	(WIEN)
STEINBERG	74	PRL 33 41	R.I. Steinberg et al.	(YALE, ISNG)
COHEN	73	JPCRD 2 6623	E.R. Cohen, B.N. Taylor	(RISC, NBS)
CHRISTENSEN	72	PR D5 1628	C.J. Christensen et al.	(RISO)
CHRISTENSEN	70	PR C1 1693	C.J. Christensen, V.E. Krohn, G.R. Ringo	(ANL)
EROZOLIM...	70C	PL 33B 351	B.G. Eroozolimsky et al.	(KIAE)
GRIGOREV	68	SJNP 6 239	V.K. Grigoriev et al.	(ITEP)
Translated from YAF 6 329				

 N AND Δ RESONANCES

Revised January 2000 by R.L. Workman (George Washington University, Virginia Campus).

I. Introduction

The excited states of the nucleon have been studied in a large number of formation and production experiments. The conventional (*i.e.*, Breit-Wigner) masses, pole positions, widths, and elasticities of the N and Δ resonances in the Baryon Summary Table come largely from partial-wave analyses of πN total, elastic, and charge-exchange scattering data. Partial-wave analyses have also been performed on much smaller data sets to get $N\eta$, AK , and EK branching fractions. Other branching fractions come from isobar-model analyses of $\pi N \rightarrow N\pi\pi$ data. Finally, many $N\gamma$ branching fractions have been determined from photoproduction experiments (see Sec. III).

Table 1 lists all the N and Δ entries in the Baryon Listings and gives our evaluation of the status of each, both overall and channel by channel. Only the "established" resonances (overall status 3 or 4 stars) appear in the Baryon Summary Table. We generally consider a resonance to be established only if it has been seen in at least two independent analyses of elastic scattering and if the relevant partial-wave amplitudes do not behave erratically or have large errors.

No new elastic partial-wave analyses have been published since our last edition. Preliminary new results from the Virginia Tech group were reported at MENU 99 [1]; this reference also reports recent studies of the πN sigma term, scattering lengths, and possible isospin-breaking effects. Two extensions of an earlier [2] multi-channel analysis have appeared since our last edition. The first [3] extracted pole positions and residues for the $N(1535)$ and $N(1650)$. The second [4] added $\gamma N \rightarrow N\pi$ multipoles to the previous set of $\pi N \rightarrow N\pi$, $\pi N \rightarrow N\eta$ and $\gamma N \rightarrow N\eta$ data and amplitudes.

The interested reader will find further discussions in the proceedings of three recent conferences [1,5,6], and in two older reviews [7,8].

II. Against Breit-Wigner parameters — a pole-emic

Written December 1997 by G. Höhler (University of Karlsruhe).

(1) All theoretical approaches to the resonance phenomenon have in common that the variation of a partial-wave amplitude $T(W)$, where W is the total c.m. energy, is related to a nearly bound state of the projectile-target system (see *e.g.*, Refs. [9–13]). In πN scattering, this state is an excited state of the nucleon (= isobar). The nearly bound state is described in the framework of S-matrix theory by a pole of the S-matrix element at $W_p = M - i\Gamma/2$ in the lower half of the complex W -plane, close to the real axis; M and Γ are called the mass and width of the resonance. The location of the resonance pole is the same for all reactions to which the resonance couples.

Table 1. The status of the N and Δ resonances. Only those with an overall status of *** or **** are included in the main Baryon Summary Table.

Particle	L_{2I-2J}	Overall status	Status as seen in —						
			$N\pi$	$N\eta$	ΛK	ΣK	$\Delta\pi$	$N\rho$	$N\gamma$
$N(939)$	P_{11}	****							
$N(1440)$	P_{11}	****	**** *				*** *	***	
$N(1520)$	D_{13}	****	**** *				**** ****	****	
$N(1535)$	S_{11}	****	**** ****				* **	***	
$N(1650)$	S_{11}	****	**** *	*** **			*** **	***	
$N(1675)$	D_{15}	****	**** *	*			**** *	****	
$N(1680)$	F_{15}	****	****				**** ****	****	
$N(1700)$	D_{13}	***	*** *	** *			** *	**	
$N(1710)$	P_{11}	***	*** **	** *			** *	***	
$N(1720)$	P_{13}	****	**** *	** *			* **	**	
$N(1900)$	P_{13}	**	**				*		
$N(1990)$	F_{17}	**	** *	*	*			*	
$N(2000)$	F_{15}	**	** *	*	*	*	**		
$N(2080)$	D_{13}	**	** *	*				*	
$N(2090)$	S_{11}	*	*						
$N(2100)$	P_{11}	*	*	*					
$N(2190)$	G_{17}	****	**** *	*	*		*	*	
$N(2200)$	D_{15}	**	** *	*					
$N(2220)$	H_{19}	****	**** *						
$N(2250)$	G_{19}	****	**** *						
$N(2600)$	I_{111}	***	***						
$N(2700)$	K_{113}	**	**						
$\Delta(1232)$	P_{33}	****	****	F				****	
$\Delta(1600)$	P_{33}	***	***	o			*** *	**	
$\Delta(1620)$	S_{31}	****	****	r			**** ****	***	
$\Delta(1700)$	D_{33}	****	****	b	*		*** **	***	
$\Delta(1750)$	P_{31}	*	*	i					
$\Delta(1900)$	S_{31}	**	**	d	*	*	** *	*	
$\Delta(1905)$	F_{35}	****	****	d	*	**	** **	***	
$\Delta(1910)$	P_{31}	****	****	e	*	*	*	*	
$\Delta(1920)$	P_{33}	***	***	n	*	**		*	
$\Delta(1930)$	D_{35}	***	***		*			**	
$\Delta(1940)$	D_{33}	*	*	F					
$\Delta(1950)$	F_{37}	****	****	o	*	****	*	****	
$\Delta(2000)$	F_{35}	**	**	r			**		
$\Delta(2150)$	S_{31}	*	*	b					
$\Delta(2200)$	G_{37}	*	*	i					
$\Delta(2300)$	H_{39}	**	**	d					
$\Delta(2350)$	D_{35}	*	*	d					
$\Delta(2390)$	F_{37}	*	*	e					
$\Delta(2400)$	G_{39}	**	**	n					
$\Delta(2420)$	H_{311}	****	****					*	
$\Delta(2750)$	I_{313}	**	**						
$\Delta(2950)$	K_{315}	**	**						

**** Existence is certain, and properties are at least fairly well explored.
*** Existence ranges from very likely to certain, but further confirmation is desirable and/or quantum numbers, branching fractions, etc. are not well determined.
** Evidence of existence is only fair.
* Evidence of existence is poor.

In the inelastic region, a resonance is associated with a cluster of poles on different Riemann sheets. If one of these poles is located near the real axis and sufficiently far from branch points, it will be strongly dominant. If one of the final-state particles itself has a strong decay, one also has to consider branch points in the lower half plane that belong to thresholds for two-particle final states (see *e.g.*, Refs. [14,15]).

(2) If the formation of an unstable intermediate particle occurs in a scattering process, one expects a *time-delay between the arrival of the incident wave packet and its departure from the collision region*. Goldberger and Watson [16], starting from

earlier work by Wigner, derived for elastic scattering the time-delay Q . Expressed in terms of the amplitude $T(W)$, it is $Q = 2 Sp(W)$, where $Sp(W) = |dT/dW|$ is the *speed* with which the complex vector T traverses the Argand diagram. If the background can be neglected, a resonance pole leads to a peak of $Sp(W)$ at $W = M$ (see the cited books and Refs. [17–19]).

(3) It is an old tradition that authors of partial-wave analyses determine *conventional resonance parameters* from fits to generalized Breit-Wigner formulas. Each group has its own prescription for the treatment of analyticity, the choice of the background, and other details, so the model-dependence is much larger than in the determination of pole parameters. A serious shortcoming is the poor or missing information on inelastic channels. The conventional parameters are the “mass” m , the “width” $\Gamma(W)$ at $W = m$, and the branching ratios. Following are some problems with these parametrizations.

(a) The conventional $\Delta(1232)$ parameters come from a fit to the P_{33} partial wave. It is well known from the Chew-Low plot and dispersion relations [20] that this partial wave has a *large background from the nucleon pole term*. The pole position, $1210 - 50i$ MeV, belongs to the Δ -resonance, whereas the conventional parameters, $m = 1232$ MeV and $\Gamma(m) = 120$ MeV, belong to the Δ *together with the large background in πN scattering*.

(b) The $N(1535) S_{11}$ is the *only 4-star resonance that does not show a signal in the speed plot*. The signal is probably part of the large peak due to the threshold for η production [21]. In this case, poles in other Riemann sheets are expected to give contributions of comparable magnitude. One of these poles produces the threshold cusp [14]. In the 1960's, this problem was treated in many papers (see Ref. 21). In calculations that rely on the conventional mass of 1535 MeV, one cannot see that one has to study a combined resonance plus threshold-cusp phenomenon.

A similar situation of poles in different sheets arises in $\pi\pi$ scattering near the $K\bar{K}$ threshold. See remarks in footnotes to our $f_0(980)$ Listing.

(c) Around 1440 MeV, the VPI group found *two poles in the P_{11} amplitude in different Riemann sheets* [22]. This was interpreted, by other authors, as evidence for the existence of two nearly degenerate P_{11} resonances, in conflict with the constituent quark model. Cutkosky pointed out that the branch point for $\Delta\pi$ decay is located near the poles, so the poles belong to the same resonance. This was confirmed by a new calculation [23], which also led to conventional parameters of $m = 1471$ MeV and $\Gamma(m) = 545$ MeV, which are *much different from the pole parameters*, $1370 - 114i$ and $1360 - 120i$ MeV. The speed plot confirms that the formation of the unstable particle $N(1440) P_{11}$ occurs at a considerably lower energy than expected from the conventional parameters.

Conclusion: In contrast to the conventional parameters, the pole positions and speed plots have a well-defined relation

Baryon Particle Listings

N 's and Δ 's

to S-matrix theory. They also give more information on the resonances and thresholds and can be used for predictions on other reactions that couple to the excited states.

III. Electromagnetic interactions

Revised January 2000 by R.L. Workman (George Washington University, Virginia Campus).

Nearly all the entries in the Listings concerning electromagnetic properties of the N and Δ resonances are $N\gamma$ couplings. These couplings, the helicity amplitudes $A_{1/2}$ and $A_{3/2}$, have been obtained in partial-wave analyses of single-pion photoproduction, η photoproduction, and Compton scattering. Most photoproduction analyses have taken the existence, masses, and widths of the resonances from the $\pi N \rightarrow \pi N$ analyses, and have only determined the $N\gamma$ couplings. This approach is only applicable to resonances with a significant $N\pi$ coupling. A brief description of the various methods of analysis of photoproduction data may be found in our 1992 edition [24].

Our Listings omit a number of analyses that are now obsolete. Most of the older results may be found in our 1982 edition [25]. The errors quoted for the couplings in the Listings are calculated in different ways in different analyses and therefore should be used with care. In general, the systematic differences between the analyses caused by using different parameterization schemes are probably more indicative of the true uncertainties than are the quoted errors.

Probably the most reliable analyses, for most resonances, are ARAI 80, CRAWFORD 80, AWAJI 81, FUJII 81, CRAWFORD 83, and ARNDT 96. Several special cases are discussed separately below. The errors we give are a combination of the stated statistical errors on the analyses and the systematic differences between them. The analyses are given equal weight, except ARNDT 96 is weighted, rather arbitrarily, by a factor of two because its data set is at least 50% larger than those of the other analyses and contains many new high-quality measurements. The $\Delta(1232)$ and $N(1535)$ are special cases, discussed below.

The Baryon Summary Table gives $N\gamma$ branching fractions for those resonances whose couplings are considered to be reasonably well established. The $N\gamma$ partial width Γ_γ is given in terms of the helicity amplitudes $A_{1/2}$ and $A_{3/2}$ by

$$\Gamma_\gamma = \frac{k^2}{\pi} \frac{2M_N}{(2J+1)M_R} [|A_{1/2}|^2 + |A_{3/2}|^2] . \quad (1)$$

Here M_N and M_R are the nucleon and resonance masses, J is the resonance spin, and k is the photon c.m. decay momentum.

New results for $\Delta(1232) \rightarrow p\gamma$: Recent studies of the $\Delta(1232)$ have focussed on the problem of separating background from resonance, and on the $E2/M1$ ratio at nonzero values of Q^2 . The electric quadrupole ($E2$) and magnetic dipole ($M1$) amplitudes are related to our helicity amplitudes by

$$A_{1/2} = -\frac{1}{2}(M1 + 3E2) \quad \text{and} \quad A_{3/2} = -\frac{\sqrt{3}}{2}(M1 - E2) . \quad (2)$$

Problems associated with the $E2/M1$ ratio at $Q^2 = 0$ [26] were discussed in our 1998 Review [27].

The $E2/M1$ ratio has been given at $Q^2 = 2.8$ and 4.0 (GeV/c)², based on analyses of Jefferson Lab $p(e, e'p)\pi^0$ data [28], and at 3.2 (GeV/c)², based on a re-analysis of older DESY measurements [29]. Results are not yet stable, and depend upon the method employed. This is particularly evident in analyses of the DESY measurements, which have resulted in $E2/M1$ ratios differing in both sign and magnitude [28,30,31].

Results for the $E2/M1$ ratio at $Q^2 = 2.8$ and 4.0 (GeV/c)² are 0.039 ± 0.029 and 0.04 ± 0.031 from Ref. 30, compared to $-0.020 \pm 0.012 \pm 0.005$ and $-0.031 \pm 0.012 \pm 0.005$ from Ref. 28. Notice the difference in sign. There is general agreement that the ratio remains small relative to the perturbative QCD expectation that $E2/M1$ should approach unity.

The method [32] used in Ref. 30 gives values for the $Q^2 = 0$ $N\gamma$ amplitudes, $A_{1/2}$ and $A_{3/2}$, that are about 30% smaller (in magnitude) than our previous estimates. While this shift improves agreement with quark models, there is no consensus on its validity [26].

The ratio of scalar quadrupole and magnetic dipole amplitudes (S_{1+}/M_{1+}) is also problematic. A previous fit [33] to the DESY measurements gave $0.07 \pm 0.02 \pm 0.03$ at $Q^2 = 3.2$ (GeV/c)². This disagrees with a recent fit [28] to the Jefferson Lab data, $-0.112 \pm 0.013 \pm 0.01$ and $-0.148 \pm 0.013 \pm 0.01$ at $Q^2 = 2.8$ and 4.0 (GeV/c)², and with a fit [30] to both DESY and Jefferson Lab data sets, -0.049 ± 0.029 , -0.099 ± 0.041 , and -0.085 ± 0.021 at $Q^2 = 2.8, 3.2,$ and 4.0 (GeV/c)².

New results for $p\eta$: Fits to η -photoproduction data have given $N\gamma$ amplitudes for the $N(1535)$ that are substantially larger than those extracted from fits to π -photoproduction data (see the 1998 Review [27] for details). More recent analyses [34,35] have considered the sensitivity of this reaction to contributions from the $N(1520)$. The ratio of $N(1520) \rightarrow N\gamma$ amplitudes, $A_{3/2}/A_{1/2}$, was found to be $-2.5 \pm 0.5 \pm 0.4$ in Ref. 34 and -2.1 ± 0.2 in Ref. 35. Results inferred from π -photoproduction are about a factor of three larger in magnitude (see the Particle Listings). The η -photoproduction result is particularly surprising, as the $N(1520)$ has a very clean resonance signature in π photoproduction.

Recent $p(e, e'p)\eta$ cross-section measurements [36] have been fitted to extract the $N(1535)$ transition amplitude. Values for $A_{1/2}$ are 0.050 ± 0.007 $\text{GeV}^{-1/2}$ at 2.4 (GeV/c)² and 0.035 ± 0.005 $\text{GeV}^{-1/2}$ at 3.6 (GeV/c)². These are in qualitative agreement with the results of Ref. 37.

New results for $p\eta'$: A fit to SAPHIR total and differential cross sections has been made [38], assuming resonance dominance and taking only S - and P -wave multipoles. The extracted resonance parameters are $S_{11}(M, \Gamma) = (1897 \pm 50_{-2}^{+30}, 396 \pm 115_{-45}^{+35})$ MeV and $P_{11}(M, \Gamma) = (1986 \pm 26_{-30}^{+10}, 296 \pm 100_{-10}^{+60})$ MeV. Other reaction mechanisms have been proposed [39], and more definitive statements will require the measurement of polarization observables.

New results for ΛK^+ : Recent measurements of $\gamma p \rightarrow \Lambda K^+$ total cross sections from SAPHIR [40] suggest a broad structure around 1900 MeV. An analysis [41] of these and associated differential cross-section and recoil-polarization data suggests the influence of a broad D_{13} state. The fitted resonance parameters are $D_{13}(M, \Gamma) = (1895, 372)$ MeV. The choice of a D_{13} state was based on agreement with quark-model predictions, and further polarization measurements are needed to support this claim.

IV. Non- qqq baryon candidates

Revised January 2000 by R.L. Workman (George Washington University, Virginia Campus).

The standard quark-model assignments for baryons are outlined in Sec. 13.3, "Baryons: qqq states." Just as with mesons (see the "Note on Non- $q\bar{q}$ mesons"), there have been suggestions that non- qqq baryons might exist, such as hybrid ($qqqg$) baryons and unstable meson-nucleon bound states [42] (see the "Note on the $\Lambda(1405)$ ").

If non- qqq states exist, they will be more difficult to verify than hybrid mesons: Hybrid baryons would not have the clean signature of exotic quantum numbers. They should also mix with ordinary qqq states. Their identification will be based on (a) characteristics of their formation and decay, and (b) an over-population of expected qqq states.

Most investigations have focused on the properties of the lightest predicted hybrids. If the first hybrid state lies below 2 GeV, as is suggested by bag-model calculations [43,44,45], it may already exist in our Listings. (However, some estimates put the lightest state well above 2 GeV [46].) At present, there are actually not enough known resonances to fill the known multiplets. If an existing resonance is identified as a hybrid, yet another ordinary qqq state must be found.

The Roper resonance, the $N(1440) P_{11}$, has been a hybrid candidate based upon its quantum numbers [43,47] and difficulties with its mass and electromagnetic couplings. If so, this would alter our interpretation of the low-lying P_{11} , P_{13} , P_{31} , and P_{33} resonances [43,48]. In Ref. 48, both the $N(1440) P_{11}$ and $\Delta(1600) P_{33}$ are hybrid candidates, and $N(1540) P_{13}$ and $\Delta(1550) P_{31}$ states are predicted. One-star P_{13} and P_{31} states were listed in our 1990 Review [49] but were then removed.

Both photoproduction [48,50,51] and electroproduction [51,52] have been considered in the search for a unique hybrid signature. In Ref. 53, QCD counting rules were used to reveal a characteristic of hybrid electroproduction at high Q^2 . If the $N(1440)$ is a hybrid, its transverse form factor is expected to fall asymptotically $O(1/Q^2)$ faster than for a pure qqq state. However, mixing between qqq and $qqqg$ states will make this identification difficult.

A number of recent experiments have searched for pentaquark ($qqqq\bar{q}$) resonances and H dibaryons ($uuddss$ states). Narrow structures found in proton-nucleus scattering [54] have been attributed to $qqqs\bar{s}$ states, an association based on anomalously large branching fractions to strange-particle channels.

The H-dibaryon experiments, while finding possible candidates [55], have generally quoted upper limits [56] for exotic resonance production. Searches for narrow dibaryons in the nucleon-nucleon interactions are also continuing [57].

Finally, there has been a report [58] of resonances lying below the $\Delta(1232)$. A very weak signal was found using the reaction $pp \rightarrow \pi^+ p X^0$. An earlier search [59] for isospin-3/2 states, using $pp \rightarrow n X^{++}$, found a null result in the mass range between M_N and $M_N + M_\pi$. At present, there appears to be no evidence for such low-mass states from other reactions.

References

1. *Proceedings of the 8th International Symposium on Meson-Nucleon Physics and the Structure of the Nucleon (MENU 99)*, (Zuoz, August 1999), πN Newsletter No. 15 (1999).
2. A.M. Green and S. Wycech, Phys. Rev. **C55**, R2167 (1997).
3. R.A. Arndt, A.M. Green, R.L. Workman, and S. Wycech, Phys. Rev. **C58**, 3636 (1998).
4. A.M. Green and S. Wycech, Phys. Rev. **C60**, 035208 (1999).
5. *Proceedings of the 8th International Conference on the Structure of Baryons (Baryons '98)*, ed. D.W. Menze and B.Ch. Metsch, World Scientific (1999).
6. *Proceedings of the Joint ECT* / JLAB Workshop*, ed. S. Simula, B. Saghai, N.C. Mukhopadhyay, and V.D. Burkert, Few Body Systems Suppl. 11 (1999).
7. G. Höhler, *Pion-Nucleon Scattering*, Landolt-Börnstein Vol. I/b2 (1983), ed. H. Schopper (Springer Verlag).
8. A.J.G. Hey and R.L. Kelly, Phys. Reports **96**, 71 (1983).
9. R.J. Eden, P.V. Landshoff, D.I. Olive, J.C. Polkinghorne, *The Analytic S-Matrix* (Cambridge Univ. Press, 1966).
10. R.G. Newton, *Scattering Theory of Waves and Particles* (McGraw Hill, 1966).
11. A.D. Martin, T.D. Spearman, *Elementary Particle Theory* (North Holland, 1970).
12. J.R. Taylor, *Scattering Theory* (John Wiley, 1972).
13. B.H. Bransden, R.G. Moorhouse, *The Pion-Nucleon System* (Princeton Univ. Press, 1973).
14. W.R. Frazer, A.W. Hendry, Phys. Rev. **134**, B1307 (1964).
15. R.E. Cutkosky, Phys. Rev. **D20**, 2839 (1979).
16. M.L. Goldberger, K.M. Watson, *Collision Theory* (John Wiley, 1964).
17. R.H. Dalitz, R.G. Moorhouse, Proc. Roy. Soc. London **A318** 279 (1970).
18. A. Bohm, *Quantum Mechanics*, 3rd ed. (Springer Verlag, 1993).
19. G. Höhler, πN Newsletter 9, 1 (1993).
20. J. Hamilton, Pion-Nucleon Scattering in High Energy Physics, Vol. I, p. 193, ed. E. Burhop, (Academic Press, 1967).
21. G. Höhler, contribution to the 4th Workshop on N^* Physics, held at George Washington University, Oct. 30 - Nov. 1 (1997), πN Newsletter 14 (1998).
22. R.A. Arndt *et al.*, Phys. Rev. **D43**, 2131 (1991); **C52**, 2120 (1995).
23. R.E. Cutkosky, S. Wang, Phys. Rev. **D42**, 235 (1990).
24. K. Hikasa *et al.*, Phys. Rev. **D45**, S1 (1992).

Baryon Particle Listings

 N 's and Δ 's, $N(1440)$

25. Particle Data Group, Phys. Lett. **B111** (1982).
26. This topic is well reviewed in Baryons '98, Ref. 5 above.
27. C. Caso *et al.*, Eur. Phys. J. **C3**, 1 (1998).
28. V.V. Frolov *et al.*, Phys. Rev. Lett. **82**, 45 (1999).
29. R. Haiden, Report No. DESY-F21-79-03 (1979, unpublished).
30. I.G. Aznauryan and S.G. Stepanyan, Phys. Rev. **D59**, 054009 (1999).
31. G.A. Warren and C.E. Carlson, Phys. Rev. **D42**, 3020 (1990).
32. I.G. Aznauryan, Phys. Rev. **D57**, 2727 (1998); see also A. Jurewicz, Phys. Rev. **D26**, 1171 (1982).
33. V.D. Burkert and L. Elouadrhiri, Phys. Rev. Lett. **75**, 3614 (1995).
34. N.C. Mukhopadhyay and N. Mathur, Phys. Lett. **B444**, 7 (1998).
35. L. Tiator, D. Drechsel, G. Knöchlein, and C. Bennhold, Phys. Rev. **C60**, 035210 (1999).
36. C.S. Armstrong *et al.*, Phys. Rev. **D60**, 052004 (1999).
37. F. Brasse *et al.*, Z. Phys. **C22**, 33 (1984).
38. R. Plötzke *et al.*, Phys. Lett. **B444**, 555 (1998).
39. N.C. Mukhopadhyay *et al.*, Phys. Lett. **B410**, 73 (1997); Z. Li, J. Phys. **G23**, 1127 (1997).
40. M.Q. Tran *et al.*, Phys. Lett. **B445**, 20 (1998).
41. T. Mart and C. Bennhold, Phys. Rev. **C61**, 012201 (1999).
42. S. Pakvasa and S.F. Tuan, Phys. Lett. **B459**, 301 (1999); N. Kaiser, T. Waas, and W. Weise, Nucl. Phys. **A612**, 297 (1997); N. Kaiser, P.B. Siegel, and W. Weise, Phys. Lett. **B362**, 23 (1995).
43. T. Barnes and F.E. Close, Phys. Lett. **123B**, 89 (1983).
44. E. Golowich, E. Haqq, and G. Karl, Phys. Rev. **D28**, 160 (1983).
45. I. Duck and E. Umland, Phys. Lett. **128B**, 221 (1983).
46. N. Isgur and J. Paton, Phys. Rev. **D31**, 2910 (1985).
47. There also have been suggestions that the observed Roper "resonance" is a purely dynamical effect, or possibly a combination of two different structures. See, for example, H.P. Morsch and P. Zupranski, Phys. Rev. **C61**, 024002 (1999) and C. Schütz, J. Haidenbauer, J. Speth, and J.W. Durso, Phys. Rev. **C57**, 1464 (1998).
48. Z. Li, Phys. Rev. **D44**, 2841 (1991).
49. Review of Particle Properties, Phys. Lett. **B239**, 1 (1990).
50. T. Barnes and F.E. Close, Phys. Lett. **128B**, 277 (1983).
51. S. Capstick and B.D. Keister, Phys. Rev. **D51**, 3598 (1995).
52. Zhenping Li, V. Burkert, and Zhujun Li, Phys. Rev. **D46**, 70 (1992).
53. C.E. Carlson and N.C. Mukhopadhyay, Phys. Rev. Lett. **67**, 3745 (1991).
54. S.V. Golovkin *et al.*, Eur. Phys. J. **A5**, 409 (1999); V.A. Bezzubov *et al.*, PAN **59**, 2117 (1996); S.V. Golovkin *et al.*, Z. Phys. **C68**, 585 (1995).
55. B.A. Shahbazian, T.A. Volokhovskaya, V.N. Yemelyanenko, and A.S. Martynov, JINRRC **1**, 61 (1995).
56. E.M. Aitala *et al.*, Phys. Lett. **B448**, 303 (1999); Phys. Rev. Lett. **81**, 44 (1998); R.W. Stotzer *et al.*, Phys. Rev. Lett. **78**, 3646 (1997); B. Bassalleck *et al.*, πN Newsletter No. 11, p. 59 (1995).
57. B. Tatischeff *et al.*, Phys. Rev. **C59**, 1878 (1999); L.S. Vorobyev *et al.*, Phys. Atomic Nuclei **61**, 771 (1998); H. Calén *et al.*, Phys. Lett. **B427**, 248 (1998); A. Deloff and T. Siemiarzczuk, Z. Phys. **A353**, 121 (1995); R. Bilger, M. Schepkin *et al.*, A.J. Buchmann *et al.*, and A.S. Khrykin, πN Newsletter No. 10, p. 47 (1995).
58. B. Tatischeff *et al.*, Phys. Rev. Lett. **79**, 601 (1997); see also A.I. L'vov and R.L. Workman, Phys. Rev. Lett. **81**, 1346 (1998); B. Tatischeff *et al.*, Phys. Rev. Lett. **81**, 1347 (1998).
59. S. Ram *et al.*, Phys. Rev. **D49**, 3120 (1994).

 $N(1440) P_{11}$

$$I(J^P) = \frac{1}{2}(\frac{1}{2}^+) \text{ Status: } ***$$

Most of the results published before 1975 are now obsolete and have been omitted. They may be found in our 1982 edition, Physics Letters **111B** (1982).

 $N(1440)$ BREIT-WIGNER MASS

VALUE (MeV)	DOCUMENT ID	TECN	COMMENT
1430 to 1470 (≈ 1440) OUR ESTIMATE			
1462 \pm 10	MANLEY 92	IPWA	$\pi N \rightarrow \pi N \& N\pi\pi$
1440 \pm 30	CUTKOSKY 80	IPWA	$\pi N \rightarrow \pi N$
1410 \pm 12	HOEHLER 79	IPWA	$\pi N \rightarrow \pi N$
• • • We do not use the following data for averages, fits, limits, etc. • • •			
1463 \pm 7	ARNDT 96	IPWA	$\gamma N \rightarrow \pi N$
1467	ARNDT 95	DPWA	$\pi N \rightarrow N\pi$
1421 \pm 18	BATINIC 95	DPWA	$\pi N \rightarrow N\pi, N\eta$
1465	LI 93	IPWA	$\gamma N \rightarrow \pi N$
1471	CUTKOSKY 90	IPWA	$\pi N \rightarrow \pi N$
1411	CRAWFORD 80	DPWA	$\gamma N \rightarrow \pi N$
1472	¹ BAKER 79	DPWA	$\pi^- p \rightarrow n\eta$
1417	BARBOUR 78	DPWA	$\gamma N \rightarrow \pi N$
1460	BERENDS 77	IPWA	$\gamma N \rightarrow \pi N$
1380	² LONGACRE 77	IPWA	$\pi N \rightarrow N\pi\pi$
1390	³ LONGACRE 75	IPWA	$\pi N \rightarrow N\pi\pi$

 $N(1440)$ BREIT-WIGNER WIDTH

VALUE (MeV)	DOCUMENT ID	TECN	COMMENT
250 to 450 (≈ 350) OUR ESTIMATE			
391 \pm 34	MANLEY 92	IPWA	$\pi N \rightarrow \pi N \& N\pi\pi$
545 \pm 170	CUTKOSKY 90	IPWA	$\pi N \rightarrow \pi N$
340 \pm 70	CUTKOSKY 80	IPWA	$\pi N \rightarrow \pi N$
135 \pm 10	HOEHLER 79	IPWA	$\pi N \rightarrow \pi N$
• • • We do not use the following data for averages, fits, limits, etc. • • •			
360 \pm 20	ARNDT 96	IPWA	$\gamma N \rightarrow \pi N$
440	ARNDT 95	DPWA	$\pi N \rightarrow N\pi$
250 \pm 63	BATINIC 95	DPWA	$\pi N \rightarrow N\pi, N\eta$
315	LI 93	IPWA	$\gamma N \rightarrow \pi N$
334	CRAWFORD 80	DPWA	$\gamma N \rightarrow \pi N$
113	¹ BAKER 79	DPWA	$\pi^- p \rightarrow n\eta$
331	BARBOUR 78	DPWA	$\gamma N \rightarrow \pi N$
279	BERENDS 77	IPWA	$\gamma N \rightarrow \pi N$
200	² LONGACRE 77	IPWA	$\pi N \rightarrow N\pi\pi$
200	³ LONGACRE 75	IPWA	$\pi N \rightarrow N\pi\pi$

 $N(1440)$ POLE POSITION

REAL PART			
VALUE (MeV)	DOCUMENT ID	TECN	COMMENT
1345 to 1385 (≈ 1365) OUR ESTIMATE			
1346	⁴ ARNDT 95	DPWA	$\pi N \rightarrow N\pi$
1385	⁵ HOEHLER 93	SPED	$\pi N \rightarrow \pi N$
1370	CUTKOSKY 90	IPWA	$\pi N \rightarrow \pi N$
1375 \pm 30	CUTKOSKY 80	IPWA	$\pi N \rightarrow \pi N$
• • • We do not use the following data for averages, fits, limits, etc. • • •			
1360	⁶ ARNDT 91	DPWA	$\pi N \rightarrow \pi N$ Soln SM90
1381 or 1379	⁷ LONGACRE 78	IPWA	$\pi N \rightarrow N\pi\pi$
1360 or 1333	² LONGACRE 77	IPWA	$\pi N \rightarrow N\pi\pi$

See key on page 239

Baryon Particle Listings

N(1440)

 $-2 \times \text{IMAGINARY PART}$

VALUE (MeV)	DOCUMENT ID	TECN	COMMENT
160 to 260 (≈ 210) OUR ESTIMATE			
176	⁴ ARNDT 95	DPWA	$\pi N \rightarrow N\pi$
164	⁵ HOEHLER 93	SPED	$\pi N \rightarrow \pi N$
228	CUTKOSKY 90	IPWA	$\pi N \rightarrow \pi N$
180 \pm 40	CUTKOSKY 80	IPWA	$\pi N \rightarrow \pi N$
• • • We do not use the following data for averages, fits, limits, etc. • • •			
252	⁶ ARNDT 91	DPWA	$\pi N \rightarrow \pi N$ Soln SM90
209 or 210	⁷ LONGACRE 78	IPWA	$\pi N \rightarrow N\pi\pi$
167 or 234	² LONGACRE 77	IPWA	$\pi N \rightarrow N\pi\pi$

N(1440) ELASTIC POLE RESIDUE

MODULUS $|r|$

VALUE (MeV)	DOCUMENT ID	TECN	COMMENT
42	⁴ ARNDT 95	DPWA	$\pi N \rightarrow N\pi$
40	HOEHLER 93	SPED	$\pi N \rightarrow \pi N$
74	CUTKOSKY 90	IPWA	$\pi N \rightarrow \pi N$
52 \pm 5	CUTKOSKY 80	IPWA	$\pi N \rightarrow \pi N$
• • • We do not use the following data for averages, fits, limits, etc. • • •			
109	⁶ ARNDT 91	DPWA	$\pi N \rightarrow \pi N$ Soln SM90

PHASE θ

VALUE ($^\circ$)	DOCUMENT ID	TECN	COMMENT
-101	⁴ ARNDT 95	DPWA	$\pi N \rightarrow N\pi$
-84	CUTKOSKY 90	IPWA	$\pi N \rightarrow \pi N$
-100 \pm 35	CUTKOSKY 80	IPWA	$\pi N \rightarrow \pi N$
• • • We do not use the following data for averages, fits, limits, etc. • • •			
-93	⁶ ARNDT 91	DPWA	$\pi N \rightarrow \pi N$ Soln SM90

N(1440) DECAY MODES

The following branching fractions are our estimates, not fits or averages.

Mode	Fraction (Γ_i/Γ)
Γ_1 $N\pi$	60-70 %
Γ_2 $N\eta$	
Γ_3 $N\pi\pi$	30-40 %
Γ_4 $\Delta\pi$	20-30 %
Γ_5 $\Delta(1232)\pi$, P-wave	
Γ_6 $N\rho$	<8 %
Γ_7 $N\rho$, $S=1/2$, P-wave	
Γ_8 $N\rho$, $S=3/2$, P-wave	
Γ_9 $N(\pi\pi)_{S\text{-wave}}^{I=0}$	5-10 %
Γ_{10} $\rho\gamma$	0.035-0.048 %
Γ_{11} $\rho\gamma$, helicity=1/2	0.035-0.048 %
Γ_{12} $n\gamma$	0.009-0.032 %
Γ_{13} $n\gamma$, helicity=1/2	0.009-0.032 %

N(1440) BRANCHING RATIOS

$\Gamma(N\pi)/\Gamma_{\text{total}}$	DOCUMENT ID	TECN	COMMENT	Γ_1/Γ
0.6 to 0.7 OUR ESTIMATE				
0.69 \pm 0.03	MANLEY 92	IPWA	$\pi N \rightarrow \pi N$ & $N\pi\pi$	
0.68 \pm 0.04	CUTKOSKY 80	IPWA	$\pi N \rightarrow \pi N$	
0.51 \pm 0.05	HOEHLER 79	IPWA	$\pi N \rightarrow \pi N$	
• • • We do not use the following data for averages, fits, limits, etc. • • •				
0.68	ARNDT 95	DPWA	$\pi N \rightarrow N\pi$	
0.56 \pm 0.08	BATINIC 95	DPWA	$\pi N \rightarrow N\pi$, $N\eta$	

$(\Gamma_1/\Gamma_2)^{1/2}/\Gamma_{\text{total}}$ in $N\pi \rightarrow N(1440) \rightarrow N\eta$	DOCUMENT ID	TECN	COMMENT	$(\Gamma_1/\Gamma_2)^{1/2}/\Gamma$
0.6 to 0.7 OUR ESTIMATE				
seen	¹ BAKER 79	DPWA	$\pi^- \rho \rightarrow n\eta$	
+0.328	⁸ FELTESSE 75	DPWA	1488-1745 MeV	

Note: Signs of couplings from $\pi N \rightarrow N\pi\pi$ analyses were changed in the 1986 edition to agree with the baryon-first convention; the overall phase ambiguity is resolved by choosing a negative sign for the $\Delta(1620) S_{31}$ coupling to $\Delta(1232)\pi$.

$(\Gamma_1/\Gamma_2)^{1/2}/\Gamma_{\text{total}}$ in $N\pi \rightarrow N(1440) \rightarrow \Delta(1232)\pi$, P-wave	DOCUMENT ID	TECN	COMMENT	$(\Gamma_1/\Gamma_2)^{1/2}/\Gamma$
+0.37 to +0.41 OUR ESTIMATE				
+0.39 \pm 0.02	MANLEY 92	IPWA	$\pi N \rightarrow \pi N$ & $N\pi\pi$	
+0.41	^{2,9} LONGACRE 77	IPWA	$\pi N \rightarrow N\pi\pi$	
+0.37	³ LONGACRE 75	IPWA	$\pi N \rightarrow N\pi\pi$	

$(\Gamma_1/\Gamma_2)^{1/2}/\Gamma_{\text{total}}$ in $N\pi \rightarrow N(1440) \rightarrow N\rho$, $S=1/2$, P-wave	DOCUMENT ID	TECN	COMMENT	$(\Gamma_1/\Gamma_2)^{1/2}/\Gamma$
± 0.07 to ± 0.25 OUR ESTIMATE				
-0.11	^{2,9} LONGACRE 77	IPWA	$\pi N \rightarrow N\pi\pi$	
+0.23	³ LONGACRE 75	IPWA	$\pi N \rightarrow N\pi\pi$	

$(\Gamma_1/\Gamma_2)^{1/2}/\Gamma_{\text{total}}$ in $N\pi \rightarrow N(1440) \rightarrow N\rho$, $S=3/2$, P-wave	DOCUMENT ID	TECN	COMMENT	$(\Gamma_1/\Gamma_2)^{1/2}/\Gamma$
± 0.17 to ± 0.25 OUR ESTIMATE				
+0.18	^{2,9} LONGACRE 77	IPWA	$\pi N \rightarrow N\pi\pi$	

$(\Gamma_1/\Gamma_2)^{1/2}/\Gamma_{\text{total}}$ in $N\pi \rightarrow N(1440) \rightarrow N(\pi\pi)_{S\text{-wave}}^{I=0}$	DOCUMENT ID	TECN	COMMENT	$(\Gamma_1/\Gamma_2)^{1/2}/\Gamma$
± 0.17 to ± 0.25 OUR ESTIMATE				
+0.24 \pm 0.03	MANLEY 92	IPWA	$\pi N \rightarrow \pi N$ & $N\pi\pi$	
-0.18	^{2,9} LONGACRE 77	IPWA	$\pi N \rightarrow N\pi\pi$	
-0.23	³ LONGACRE 75	IPWA	$\pi N \rightarrow N\pi\pi$	

N(1440) PHOTON DECAY AMPLITUDES

N(1440) $\rightarrow \rho\gamma$, helicity-1/2 amplitude $A_{1/2}$

VALUE (GeV $^{-1/2}$)	DOCUMENT ID	TECN	COMMENT
-0.065 \pm 0.004 OUR ESTIMATE			
-0.063 \pm 0.005	ARNDT 96	IPWA	$\gamma N \rightarrow \pi N$
-0.069 \pm 0.018	CRAWFORD 83	IPWA	$\gamma N \rightarrow \pi N$
-0.063 \pm 0.008	AWAJI 81	DPWA	$\gamma N \rightarrow \pi N$
-0.069 \pm 0.004	ARAI 80	DPWA	$\gamma N \rightarrow \pi N$ (fit 1)
-0.066 \pm 0.004	ARAI 80	DPWA	$\gamma N \rightarrow \pi N$ (fit 2)
-0.079 \pm 0.009	BRATASHEV... 80	DPWA	$\gamma N \rightarrow \pi N$
-0.068 \pm 0.015	CRAWFORD 80	DPWA	$\gamma N \rightarrow \pi N$
-0.0584 \pm 0.0148	ISHII 80	DPWA	Compton scattering
• • • We do not use the following data for averages, fits, limits, etc. • • •			
-0.085 \pm 0.003	LI 93	IPWA	$\gamma N \rightarrow \pi N$
-0.129	¹⁰ WADA 84	DPWA	Compton scattering
-0.075 \pm 0.015	BARBOUR 78	DPWA	$\gamma N \rightarrow \pi N$
-0.125	¹¹ NOELLE 78		$\gamma N \rightarrow \pi N$
-0.076	BERRENDS 77	IPWA	$\gamma N \rightarrow \pi N$
-0.087 \pm 0.006	FELLER 76	DPWA	$\gamma N \rightarrow \pi N$

N(1440) $\rightarrow n\gamma$, helicity-1/2 amplitude $A_{1/2}$

VALUE (GeV $^{-1/2}$)	DOCUMENT ID	TECN	COMMENT
+0.040 \pm 0.010 OUR ESTIMATE			
0.045 \pm 0.015	ARNDT 96	IPWA	$\gamma N \rightarrow \pi N$
0.037 \pm 0.010	AWAJI 81	DPWA	$\gamma N \rightarrow \pi N$
0.030 \pm 0.003	FUJII 81	DPWA	$\gamma N \rightarrow \pi N$
0.023 \pm 0.009	ARAI 80	DPWA	$\gamma N \rightarrow \pi N$ (fit 1)
0.019 \pm 0.012	ARAI 80	DPWA	$\gamma N \rightarrow \pi N$ (fit 2)
0.056 \pm 0.015	CRAWFORD 80	DPWA	$\gamma N \rightarrow \pi N$
-0.029 \pm 0.035	TAKEDA 80	DPWA	$\gamma N \rightarrow \pi N$
• • • We do not use the following data for averages, fits, limits, etc. • • •			
0.085 \pm 0.006	LI 93	IPWA	$\gamma N \rightarrow \pi N$
+0.059 \pm 0.016	BARBOUR 78	DPWA	$\gamma N \rightarrow \pi N$
0.062	¹¹ NOELLE 78		$\gamma N \rightarrow \pi N$

N(1440) FOOTNOTES

- ¹ BAKER 79 finds a coupling of the N(1440) to the $N\eta$ channel near (but slightly below) threshold.
- ² LONGACRE 77 pole positions are from a search for poles in the unitarized T-matrix; the first (second) value uses, in addition to $\pi N \rightarrow N\pi\pi$ data, elastic amplitudes from a Saclay (CERN) partial-wave analysis. The other LONGACRE 77 values are from eyeball fits with Breit-Wigner circles to the T-matrix amplitudes.
- ³ From method II of LONGACRE 75: eyeball fits with Breit-Wigner circles to the T-matrix amplitudes.
- ⁴ ARNDT 95 also finds a second-sheet pole with real part = 1383 MeV, $-2 \times$ imaginary part = 210 MeV, and residue with modulus 92 MeV and phase = -54° .
- ⁵ See HOEHLER 93 for a detailed discussion of the evidence for and the pole parameters of N and Δ resonances as determined from Argand diagrams of πN elastic partial-wave amplitudes and from plots of the speeds with which the amplitudes traverse the diagrams.
- ⁶ ARNDT 91 (Soln SM90) also finds a second-sheet pole with real part = 1413 MeV, $-2 \times$ imaginary part = 256 MeV, and residue = (78-153) MeV.
- ⁷ LONGACRE 78 values are from a search for poles in the unitarized T-matrix. The first (second) value uses, in addition to $\pi N \rightarrow N\pi\pi$ data, elastic amplitudes from a Saclay (CERN) partial-wave analysis.
- ⁸ An alternative which cannot be distinguished from this is to have a P_{13} resonance with $M = 1530$ MeV, $\Gamma = 79$ MeV, and elasticity = +0.271.
- ⁹ LONGACRE 77 considers this coupling to be well determined.
- ¹⁰ WADA 84 is inconsistent with other analyses; see the Note on N and Δ Resonances.
- ¹¹ Converted to our conventions using $M = 1486$ MeV, $\Gamma = 613$ MeV from NOELLE 78.

Baryon Particle Listings

$N(1440)$, $N(1520)$

$N(1440)$ REFERENCES

For early references, see Physics Letters **111B** 70 (1982).

Author	Year	Ref	Author	Year	Ref	Author	Year	Ref
ARNDT	96	PR C53 430	R.A. Arndt, I.I. Strakovsky, R.L. Workman		(VPI)			
ARNDT	95	PR C52 2120	R.A. Arndt et al.		(VPI, BRCD)			
BATINIC	95	PR C51 2310	M. Batinic et al.		(BOSK, UCLA)			
Also	98	PR C57 1004 (erratum)	M. Batinic et al.					
HOEHLER	93	πN Newsletter 9 1	G. Hoehler		(KARL)			
LI	93	PR C47 2759	Z.J. Li et al.		(VPI)			
MANLEY	92	PR D45 4002	D.M. Manley, E.M. Saleski		(KENT) IJP			
Also	84	PR D30 904	D.M. Manley et al.		(VPI)			
ARNDT	91	PR D43 2131	R.A. Arndt et al.		(VPI, TELE) IJP			
CUTKOSKY	90	PR D42 235	R.E. Cutkosky, S. Wang		(CMU)			
WADA	84	NP B247 313	Y. Wada et al.		(INUS)			
CRAWFORD	83	NP B211 1	R.L. Crawford, W.T. Morton		(GLAS)			
PDG	82	PL 111B	M. Roos et al.		(HELS, CIT, CERN)			
AWAJI	81	Bonn Conf. 352	N. Awaji, R. Kajikawa		(NAGO)			
Also	82	NP B197 365	K. Fujii et al.		(NAGO)			
FUJII	81	NP B187 53	K. Fujii et al.		(NAGO, OSAK)			
ARAI	80	Toronto Conf. 93	I. Arai		(INUS)			
Also	82	NP B194 251	I. Arai, H. Fujii		(INUS)			
BRATASHEV...	80	NP B166 525	A.S. Bratashchev et al.		(KFTI)			
CRAWFORD	80	Toronto Conf. 107	R.L. Crawford		(GLAS)			
CUTKOSKY	80	Toronto Conf. 19	R.E. Cutkosky et al.		(CMU, LBL) IJP			
Also	79	PR D20 2839	R.E. Cutkosky et al.		(CMU, LBL) IJP			
ISHII	80	NP B165 189	T. Ishii et al.		(KYOT, INUS)			
TAKEDA	80	NP B168 17	H. Takeda et al.		(TOKY, INUS)			
BAKER	79	NP B156 93	R.D. Baker et al.		(RHEL) IJP			
HOEHLER	79	PDAT 12-1	G. Hoehler et al.		(KARLT) IJP			
Also	80	Toronto Conf. 3	R. Koch		(KARLT) IJP			
BARBOUR	78	NP B141 253	I.M. Barbour, R.L. Crawford, N.H. Parsons		(GLAS)			
LONGACRE	78	PR D17 1795	R.S. Longacre et al.		(LBL, SLAC)			
NOELLE	78	PTP 60 778	P. Noelle		(NAGO)			
BERENDS	77	NP B136 317	F.A. Berends, A. Donnachie		(LEID, MCHS) IJP			
LONGACRE	77	NP B322 493	R.S. Longacre, J. Dolbeau		(SACL) IJP			
Also	75	NP B108 355	J. Dolbeau et al.		(SACL) IJP			
FELLER	76	NP B104 219	P. Feller et al.		(NAGO, OSAK) IJP			
FELTESSE	75	NP B93 242	J. Feltesse et al.		(SACL) IJP			
LONGACRE	75	PL 59B 415	R.S. Longacre et al.		(LBL, SLAC) IJP			

$N(1520) D_{13}$

$$I(J^P) = \frac{1}{2}(3_2^-) \text{ Status: } ***$$

Most of the results published before 1975 are now obsolete and have been omitted. They may be found in our 1982 edition, Physics Letters **111B** (1982).

$N(1520)$ BREIT-WIGNER MASS

VALUE (MeV)	DOCUMENT ID	TECN	COMMENT
1515 to 1530 (≈ 1520) OUR ESTIMATE			
1524 \pm 4	MANLEY 92	IPWA	$\pi N \rightarrow \pi N$ & $N\pi\pi$
1525 \pm 10	CUTKOSKY 80	IPWA	$\pi N \rightarrow \pi N$
1519 \pm 4	HOEHLER 79	IPWA	$\pi N \rightarrow \pi N$
• • • We do not use the following data for averages, fits, limits, etc. • • •			
1516 \pm 10	ARNDT 96	IPWA	$\gamma N \rightarrow \pi N$
1515	ARNDT 95	DPWA	$\pi N \rightarrow N\pi$
1526 \pm 18	BATINIC 95	DPWA	$\pi N \rightarrow N\pi, N\eta$
1510	LI 93	IPWA	$\gamma N \rightarrow \pi N$
1504	CRAWFORD 80	DPWA	$\gamma N \rightarrow \pi N$
1503	BARBOUR 78	DPWA	$\gamma N \rightarrow \pi N$
1510	BERENDS 77	IPWA	$\gamma N \rightarrow \pi N$
1510	¹ LONGACRE 77	IPWA	$\pi N \rightarrow N\pi\pi$
1520	² LONGACRE 75	IPWA	$\pi N \rightarrow N\pi\pi$

$N(1520)$ BREIT-WIGNER WIDTH

VALUE (MeV)	DOCUMENT ID	TECN	COMMENT
110 to 135 (≈ 120) OUR ESTIMATE			
124 \pm 8	MANLEY 92	IPWA	$\pi N \rightarrow \pi N$ & $N\pi\pi$
120 \pm 15	CUTKOSKY 80	IPWA	$\pi N \rightarrow \pi N$
114 \pm 7	HOEHLER 79	IPWA	$\pi N \rightarrow \pi N$
• • • We do not use the following data for averages, fits, limits, etc. • • •			
106 \pm 4	ARNDT 96	IPWA	$\gamma N \rightarrow \pi N$
106	ARNDT 95	DPWA	$\pi N \rightarrow N\pi$
143 \pm 32	BATINIC 95	DPWA	$\pi N \rightarrow N\pi, N\eta$
120	LI 93	IPWA	$\gamma N \rightarrow \pi N$
124	CRAWFORD 80	DPWA	$\gamma N \rightarrow \pi N$
183	BAKER 79	DPWA	$\pi^- p \rightarrow n\eta$
135	BARBOUR 78	DPWA	$\gamma N \rightarrow \pi N$
105	BERENDS 77	IPWA	$\gamma N \rightarrow \pi N$
110	¹ LONGACRE 77	IPWA	$\pi N \rightarrow N\pi\pi$
150	² LONGACRE 75	IPWA	$\pi N \rightarrow N\pi\pi$

$N(1520)$ POLE POSITION

REAL PART

VALUE (MeV)	DOCUMENT ID	TECN	COMMENT
1505 to 1515 (≈ 1510) OUR ESTIMATE			
1515	ARNDT 95	DPWA	$\pi N \rightarrow N\pi$
1510	³ HOEHLER 93	ARGD	$\pi N \rightarrow \pi N$
1510 \pm 5	CUTKOSKY 80	IPWA	$\pi N \rightarrow \pi N$
• • • We do not use the following data for averages, fits, limits, etc. • • •			
1511	ARNDT 91	DPWA	$\pi N \rightarrow \pi N$ Soln SM90
1514 or 1511	⁴ LONGACRE 78	IPWA	$\pi N \rightarrow N\pi\pi$
1508 or 1505	¹ LONGACRE 77	IPWA	$\pi N \rightarrow N\pi\pi$

-2xIMAGINARY PART

VALUE (MeV)	DOCUMENT ID	TECN	COMMENT
110 to 120 (≈ 115) OUR ESTIMATE			
110	ARNDT 95	DPWA	$\pi N \rightarrow N\pi$
120	³ HOEHLER 93	ARGD	$\pi N \rightarrow \pi N$
114 \pm 10	CUTKOSKY 80	IPWA	$\pi N \rightarrow \pi N$
• • • We do not use the following data for averages, fits, limits, etc. • • •			
108	ARNDT 91	DPWA	$\pi N \rightarrow \pi N$ Soln SM90
146 or 137	⁴ LONGACRE 78	IPWA	$\pi N \rightarrow N\pi\pi$
109 or 107	¹ LONGACRE 77	IPWA	$\pi N \rightarrow N\pi\pi$

$N(1520)$ ELASTIC POLE RESIDUE

MODULUS $|r|$

VALUE (MeV)	DOCUMENT ID	TECN	COMMENT
34	ARNDT 95	DPWA	$\pi N \rightarrow N\pi$
32	HOEHLER 93	ARGD	$\pi N \rightarrow \pi N$
35 \pm 2	CUTKOSKY 80	IPWA	$\pi N \rightarrow \pi N$
• • • We do not use the following data for averages, fits, limits, etc. • • •			
33	ARNDT 91	DPWA	$\pi N \rightarrow \pi N$ Soln SM90

PHASE θ

VALUE ($^\circ$)	DOCUMENT ID	TECN	COMMENT
7	ARNDT 95	DPWA	$\pi N \rightarrow N\pi$
-8	HOEHLER 93	ARGD	$\pi N \rightarrow \pi N$
-12 \pm 5	CUTKOSKY 80	IPWA	$\pi N \rightarrow \pi N$
• • • We do not use the following data for averages, fits, limits, etc. • • •			
-10	ARNDT 91	DPWA	$\pi N \rightarrow \pi N$ Soln SM90

$N(1520)$ DECAY MODES

The following branching fractions are our estimates, not fits or averages.

Mode	Fraction (Γ_i/Γ)
Γ_1 $N\pi$	50-60 %
Γ_2 $N\eta$	
Γ_3 $N\pi\pi$	40-50 %
Γ_4 $\Delta\pi$	15-25 %
Γ_5 $\Delta(1232)\pi$, S-wave	5-12 %
Γ_6 $\Delta(1232)\pi$, D-wave	10-14 %
Γ_7 $N\rho$	15-25 %
Γ_8 $N\rho$, S=1/2, D-wave	
Γ_9 $N\rho$, S=3/2, S-wave	
Γ_{10} $N\rho$, S=3/2, D-wave	
Γ_{11} $N(\pi\pi)_{S=0}^{L=0}$	<8 %
Γ_{12} $p\gamma$	0.46-0.56 %
Γ_{13} $p\gamma$, helicity=1/2	0.001-0.034 %
Γ_{14} $p\gamma$, helicity=3/2	0.44-0.53 %
Γ_{15} $n\gamma$	0.30-0.53 %
Γ_{16} $n\gamma$, helicity=1/2	0.04-0.10 %
Γ_{17} $n\gamma$, helicity=3/2	0.25-0.45 %

$N(1520)$ BRANCHING RATIOS

$\Gamma(N\pi)/\Gamma_{total}$	DOCUMENT ID	TECN	COMMENT	Γ_1/Γ
0.5 to 0.6 OUR ESTIMATE				
0.59 \pm 0.03	MANLEY 92	IPWA	$\pi N \rightarrow \pi N$ & $N\pi\pi$	
0.58 \pm 0.03	CUTKOSKY 80	IPWA	$\pi N \rightarrow \pi N$	
0.54 \pm 0.03	HOEHLER 79	IPWA	$\pi N \rightarrow \pi N$	
• • • We do not use the following data for averages, fits, limits, etc. • • •				
0.61	ARNDT 95	DPWA	$\pi N \rightarrow N\pi$	
0.46 \pm 0.06	BATINIC 95	DPWA	$\pi N \rightarrow N\pi, N\eta$	

$\Gamma(N\eta)/\Gamma_{total}$	DOCUMENT ID	TECN	COMMENT	Γ_2/Γ
• • • We do not use the following data for averages, fits, limits, etc. • • •				
0.0008 \pm 0.0001	TIATOR 99	DPWA	$\gamma p \rightarrow \rho\eta$	
0.001 \pm 0.002	BATINIC 95	DPWA	$\pi N \rightarrow N\pi, N\eta$	

See key on page 239

Baryon Particle Listings

N(1520)

$(\Gamma_1\Gamma_f)^{1/2}/\Gamma_{total}$ in $N\pi \rightarrow N(1520) \rightarrow N\eta$ $(\Gamma_1\Gamma_2)^{1/2}/\Gamma$

VALUE	DOCUMENT ID	TECN	COMMENT
••• We do not use the following data for averages, fits, limits, etc. •••			
0.02	BAKER 79	DPWA	$\pi^- \rho \rightarrow n\eta$
+0.011	FELTESSE 75	DPWA	Soin A; see BAKER 79

Note: Signs of couplings from $\pi N \rightarrow N\pi\pi$ analyses were changed in the 1986 edition to agree with the baryon-first convention; the overall phase ambiguity is resolved by choosing a negative sign for the $\Delta(1620) S_{31}$ coupling to $\Delta(1232)\pi$.

$(\Gamma_1\Gamma_f)^{1/2}/\Gamma_{total}$ in $N\pi \rightarrow N(1520) \rightarrow \Delta(1232)\pi$, S-wave $(\Gamma_1\Gamma_5)^{1/2}/\Gamma$

VALUE	DOCUMENT ID	TECN	COMMENT
-0.26 to -0.20 OUR ESTIMATE			
-0.18 ± 0.05	MANLEY 92	IPWA	$\pi N \rightarrow \pi N$ & $N\pi\pi$
-0.26	1,5 LONGACRE 77	IPWA	$\pi N \rightarrow N\pi\pi$
-0.24	2 LONGACRE 75	IPWA	$\pi N \rightarrow N\pi\pi$

$(\Gamma_1\Gamma_f)^{1/2}/\Gamma_{total}$ in $N\pi \rightarrow N(1520) \rightarrow \Delta(1232)\pi$, D-wave $(\Gamma_1\Gamma_6)^{1/2}/\Gamma$

VALUE	DOCUMENT ID	TECN	COMMENT
-0.28 to -0.24 OUR ESTIMATE			
-0.29 ± 0.03	MANLEY 92	IPWA	$\pi N \rightarrow \pi N$ & $N\pi\pi$
-0.21	1,5 LONGACRE 77	IPWA	$\pi N \rightarrow N\pi\pi$
-0.30	2 LONGACRE 75	IPWA	$\pi N \rightarrow N\pi\pi$

$(\Gamma_1\Gamma_f)^{1/2}/\Gamma_{total}$ in $N\pi \rightarrow N(1520) \rightarrow N\rho$, S=3/2, S-wave $(\Gamma_1\Gamma_9)^{1/2}/\Gamma$

VALUE	DOCUMENT ID	TECN	COMMENT
-0.35 to -0.31 OUR ESTIMATE			
-0.35 ± 0.03	MANLEY 92	IPWA	$\pi N \rightarrow \pi N$ & $N\pi\pi$
-0.35	1,5 LONGACRE 77	IPWA	$\pi N \rightarrow N\pi\pi$
-0.24	2 LONGACRE 75	IPWA	$\pi N \rightarrow N\pi\pi$

$(\Gamma_1\Gamma_f)^{1/2}/\Gamma_{total}$ in $N\pi \rightarrow N(1520) \rightarrow N(\pi\pi)^{J=0}_{S-wave}$ $(\Gamma_1\Gamma_{11})^{1/2}/\Gamma$

VALUE	DOCUMENT ID	TECN	COMMENT
-0.22 to -0.06 OUR ESTIMATE			
-0.13	1,5 LONGACRE 77	IPWA	$\pi N \rightarrow N\pi\pi$
-0.17	2 LONGACRE 75	IPWA	$\pi N \rightarrow N\pi\pi$

N(1520) PHOTON DECAY AMPLITUDES

$N(1520) \rightarrow p\gamma$, helicity-1/2 amplitude $A_{1/2}$

VALUE (GeV ^{-1/2})	DOCUMENT ID	TECN	COMMENT
-0.024 ± 0.009 OUR ESTIMATE			
-0.020 ± 0.007	ARNDT 96	IPWA	$\gamma N \rightarrow \pi N$
-0.028 ± 0.014	CRAWFORD 83	IPWA	$\gamma N \rightarrow \pi N$
-0.007 ± 0.004	AWAJI 81	DPWA	$\gamma N \rightarrow \pi N$
-0.032 ± 0.005	ARAI 80	DPWA	$\gamma N \rightarrow \pi N$ (fit 1)
-0.032 ± 0.004	ARAI 80	DPWA	$\gamma N \rightarrow \pi N$ (fit 2)
-0.031 ± 0.009	BRATASHEV... 80	DPWA	$\gamma N \rightarrow \pi N$
-0.019 ± 0.007	CRAWFORD 80	DPWA	$\gamma N \rightarrow \pi N$
-0.0430 ± 0.0063	ISHII 80	DPWA	Compton scattering
••• We do not use the following data for averages, fits, limits, etc. •••			
-0.052 ± 0.010 ± 0.007	6 MUKHOPAD... 98		$\gamma p \rightarrow \eta p$
-0.020 ± 0.002	LI 93	IPWA	$\gamma N \rightarrow \pi N$
-0.012	WADA 84	DPWA	Compton scattering
-0.016 ± 0.008	BARBOUR 78	DPWA	$\gamma N \rightarrow \pi N$
-0.008	7 NOELLE 78		$\gamma N \rightarrow \pi N$
-0.021	BERENDS 77	IPWA	$\gamma N \rightarrow \pi N$
-0.005 ± 0.005	FELLER 76	DPWA	$\gamma N \rightarrow \pi N$

$N(1520) \rightarrow p\gamma$, helicity-3/2 amplitude $A_{3/2}$

VALUE (GeV ^{-1/2})	DOCUMENT ID	TECN	COMMENT
+0.166 ± 0.005 OUR ESTIMATE			
0.167 ± 0.005	ARNDT 96	IPWA	$\gamma N \rightarrow \pi N$
0.156 ± 0.022	CRAWFORD 83	IPWA	$\gamma N \rightarrow \pi N$
0.168 ± 0.013	AWAJI 81	DPWA	$\gamma N \rightarrow \pi N$
0.178 ± 0.003	ARAI 80	DPWA	$\gamma N \rightarrow \pi N$ (fit 1)
0.162 ± 0.003	ARAI 80	DPWA	$\gamma N \rightarrow \pi N$ (fit 2)
0.166 ± 0.005	BRATASHEV... 80	DPWA	$\gamma N \rightarrow \pi N$
0.167 ± 0.010	CRAWFORD 80	DPWA	$\gamma N \rightarrow \pi N$
0.1695 ± 0.0014	ISHII 80	DPWA	Compton scattering
••• We do not use the following data for averages, fits, limits, etc. •••			
0.130 ± 0.020 ± 0.015	6 MUKHOPAD... 98		$\gamma p \rightarrow \eta p$
0.167 ± 0.002	LI 93	IPWA	$\gamma N \rightarrow \pi N$
0.168	WADA 84	DPWA	Compton scattering
+0.157 ± 0.007	BARBOUR 78	DPWA	$\gamma N \rightarrow \pi N$
0.206	7 NOELLE 78		$\gamma N \rightarrow \pi N$
+0.075	BERENDS 77	IPWA	$\gamma N \rightarrow \pi N$
+0.164 ± 0.008	FELLER 76	DPWA	$\gamma N \rightarrow \pi N$

$N(1520) \rightarrow n\gamma$, helicity-1/2 amplitude $A_{1/2}$

VALUE (GeV ^{-1/2})	DOCUMENT ID	TECN	COMMENT
-0.059 ± 0.009 OUR ESTIMATE			
-0.048 ± 0.008	ARNDT 96	IPWA	$\gamma N \rightarrow \pi N$
-0.066 ± 0.013	AWAJI 81	DPWA	$\gamma N \rightarrow \pi N$
-0.067 ± 0.004	FUJII 81	DPWA	$\gamma N \rightarrow \pi N$
-0.076 ± 0.006	ARAI 80	DPWA	$\gamma N \rightarrow \pi N$ (fit 1)
-0.071 ± 0.011	ARAI 80	DPWA	$\gamma N \rightarrow \pi N$ (fit 2)
-0.056 ± 0.011	CRAWFORD 80	DPWA	$\gamma N \rightarrow \pi N$
-0.050 ± 0.014	TAKEDA 80	DPWA	$\gamma N \rightarrow \pi N$
••• We do not use the following data for averages, fits, limits, etc. •••			
-0.058 ± 0.003	LI 93	IPWA	$\gamma N \rightarrow \pi N$
-0.055 ± 0.014	BARBOUR 78	DPWA	$\gamma N \rightarrow \pi N$
-0.060	7 NOELLE 78		$\gamma N \rightarrow \pi N$

$N(1520) \rightarrow n\gamma$, helicity-3/2 amplitude $A_{3/2}$

VALUE (GeV ^{-1/2})	DOCUMENT ID	TECN	COMMENT
-0.139 ± 0.011 OUR ESTIMATE			
-0.140 ± 0.010	ARNDT 96	IPWA	$\gamma N \rightarrow \pi N$
-0.124 ± 0.009	AWAJI 81	DPWA	$\gamma N \rightarrow \pi N$
-0.158 ± 0.003	FUJII 81	DPWA	$\gamma N \rightarrow \pi N$
-0.147 ± 0.008	ARAI 80	DPWA	$\gamma N \rightarrow \pi N$ (fit 1)
-0.148 ± 0.009	ARAI 80	DPWA	$\gamma N \rightarrow \pi N$ (fit 2)
-0.144 ± 0.015	CRAWFORD 80	DPWA	$\gamma N \rightarrow \pi N$
-0.118 ± 0.011	TAKEDA 80	DPWA	$\gamma N \rightarrow \pi N$
••• We do not use the following data for averages, fits, limits, etc. •••			
-0.131 ± 0.003	LI 93	IPWA	$\gamma N \rightarrow \pi N$
-0.141 ± 0.015	BARBOUR 78	DPWA	$\gamma N \rightarrow \pi N$
-0.127	7 NOELLE 78		$\gamma N \rightarrow \pi N$

N(1520) FOOTNOTES

- LONGACRE 77 pole positions are from a search for poles in the unitarized T-matrix; the first (second) value uses, in addition to $\pi N \rightarrow N\pi\pi$ data, elastic amplitudes from a Saclay (CERN) partial-wave analysis. The other LONGACRE 77 values are from eyeball fits with Breit-Wigner circles to the T-matrix amplitudes.
- From method II of LONGACRE 75: eyeball fits with Breit-Wigner circles to the T-matrix amplitudes.
- See HOEHLER 93 for a detailed discussion of the evidence for and the pole parameters of N and Δ resonances as determined from Argand diagrams of πN elastic partial-wave amplitudes and from plots of the speeds with which the amplitudes traverse the diagrams.
- LONGACRE 78 values are from a search for poles in the unitarized T-matrix. The first (second) value uses, in addition to πN → Nππ data, elastic amplitudes from a Saclay (CERN) partial-wave analysis.
- LONGACRE 77 considers this coupling to be well determined.
- MUKHOPADHYAY 98 uses an effective Lagrangian approach to analyze η photoproduction data. The ratio of the A_{3/2} and A_{1/2} amplitudes is determined, with less model dependence than the amplitudes themselves, to be A_{3/2}/A_{1/2} = -2.5 ± 0.5 ± 0.4.
- Converted to our conventions using M = 1528 MeV, Γ = 187 MeV from NOELLE 78.

N(1520) REFERENCES

For early references, see Physics Letters **111B** 70 (1982). For very early references, see Reviews of Modern Physics **37** 633 (1965).

TIATOR 99	PR C60 035210	L. Tiator et al.	
MUKHOPAD... 98	PL B444 7	N.C. Mukhopadhyay, N. MATHUR	(VPI)
ARNDT 96	PR C53 430	R.A. Arndt, I.I. Strakovsky, R.L. Workman	(VPI, BRCO)
ARNDT 95	PR C52 2120	R.A. Arndt et al.	(VPI, BRCO)
BATINIC 95	PR C51 2310	M. Batinic et al.	(BOSK, UCLA)
Also 98	PR C57 1004 (erratum)	M. Batinic et al.	
HOEHLER 93	π N Newsletter 9 1	G. Hoehler	(KARL)
LI 93	PR C47 2759	Z.J. Li et al.	(VPI)
MANLEY 92	PR D45 4002	D.M. Manley, E.M. Saleski	(KENT) IJP
Also 84	PR D30 904	D.M. Manley et al.	(VPI)
ARNDT 91	PR D43 2131	R.A. Arndt et al.	(VPI, TELE) IJP
WADA 84	NP B247 313	Y. Wada et al.	(INUS)
CRAWFORD 83	NP B211 1	R.L. Crawford, W.T. Morton	(GLAS)
PDG 82	PL 111B	M. Roos et al.	(HELS, CIT, CERN)
AWAJI 81	Bonn Conf. 352	N. Awaji, R. Kajikawa	(NAGO)
Also 82	NP B197 365	K. Fujii et al.	(NAGO)
FUJII 81	NP B187 53	K. Fujii et al.	(NAGO, OSAK)
ARAI 80	Toronto Conf. 93	I. Arai	(INUS)
Also 82	NP B194 251	I. Arai, H. Fujii	(INUS)
BRATASHEV... 80	NP B166 525	A.S. Bratashvsky et al.	(KFTI)
CRAWFORD 80	Toronto Conf. 107	R.L. Crawford	(GLAS)
CUTKOSKY 80	Toronto Conf. 19	R.E. Cutkosky et al.	(CMU, LBL) IJP
Also 79	PR D20 2839	R.E. Cutkosky et al.	(CMU, LBL) IJP
ISHII 80	NP B165 189	T. Ishii et al.	(KYOT, INUS)
TAKEDA 80	NP B168 17	H. Takeda et al.	(TOKY, INUS)
BAKER 79	NP B156 93	R.D. Baker et al.	(RHEL) IJP
HOEHLER 79	PDAT 12-1	G. Hoehler et al.	(KARLT) IJP
Also 80	Toronto Conf. 3	R. Koch	(KARLT) IJP
BARBOUR 78	NP B141 253	I.M. Barbour, R.L. Crawford, N.H. Parsons	(GLAS)
LONGACRE 78	PR D17 1795	R.S. Longacre et al.	(LBL, SLAC)
NOELLE 78	PTP 60 778	P. Noelle	(NAGO)
BERENDS 77	NP B136 317	F.A. Berends, A. Donnachie	(LEID, MCHS) IJP
LONGACRE 77	NP B122 493	R.S. Longacre, J. Dolbeau	(SACL) IJP
Also 76	NP B108 365	J. Dolbeau et al.	(SACL) IJP
FELLER 76	NP B104 219	P. Feller et al.	(NAGO, OSAK) IJP
FELTESSE 75	NP B93 242	J. Feltesse et al.	(SACL) IJP
LONGACRE 75	PL 55B 415	R.S. Longacre et al.	(LBL, SLAC) IJP

Baryon Particle Listings

$N(1535)$

$N(1535) S_{11}$

$I(J^P) = \frac{1}{2}(\frac{1}{2}^-)$ Status: * * * *

Most of the results published before 1975 are now obsolete and have been omitted. They may be found in our 1982 edition, Physics Letters 111B (1982).

$N(1535)$ BREIT-WIGNER MASS

VALUE (MeV)	DOCUMENT ID	TECN	COMMENT
1520 to 1556 (≈ 1535) OUR ESTIMATE			
1534 \pm 7	MANLEY 92	IPWA	$\pi N \rightarrow \pi N & N\pi\pi$
1550 \pm 40	CUTKOSKY 80	IPWA	$\pi N \rightarrow \pi N$
1526 \pm 7	HOEHLER 79	IPWA	$\pi N \rightarrow \pi N$
• • • We do not use the following data for averages, fits, limits, etc. • • •			
1532 \pm 5	ARMSTRONG 99b	DPWA	$\gamma^* p \rightarrow p\eta$
1549 \pm 2	ABAEV 96	DPWA	$\pi^- p \rightarrow \eta n$
1525 \pm 10	ARNDT 96	IPWA	$\gamma N \rightarrow \pi N$
1535	ARNDT 95	DPWA	$\pi N \rightarrow N\pi$
1542 \pm 6	BATINIC 95	DPWA	$\pi N \rightarrow N\pi, N\eta$
1537	BATINIC 95b	DPWA	$\pi N \rightarrow N\pi, N\eta$
1544 \pm 13	KRUSCHE 95	DPWA	$\gamma p \rightarrow p\eta$
1518	LI 93	IPWA	$\gamma N \rightarrow \pi N$
1513	CRAWFORD 80	DPWA	$\gamma N \rightarrow \pi N$
1511	BARBOUR 78	DPWA	$\gamma N \rightarrow \pi N$
1500	BERENDS 77	IPWA	$\gamma N \rightarrow \pi N$
1547 \pm 6	BHANDARI 77	DPWA	Uses $N\eta$ cusp
1520	¹ LONGACRE 77	IPWA	$\pi N \rightarrow N\pi\pi$
1510	² LONGACRE 75	IPWA	$\pi N \rightarrow N\pi\pi$

$N(1535)$ BREIT-WIGNER WIDTH

VALUE (MeV)	DOCUMENT ID	TECN	COMMENT
100 to 250 (≈ 150) OUR ESTIMATE			
148.2 \pm 8.1	GREEN 97	DPWA	$\pi N \rightarrow \pi N, \eta N$
151 \pm 27	MANLEY 92	IPWA	$\pi N \rightarrow \pi N & N\pi\pi$
240 \pm 80	CUTKOSKY 80	IPWA	$\pi N \rightarrow \pi N$
120 \pm 20	HOEHLER 79	IPWA	$\pi N \rightarrow \pi N$
• • • We do not use the following data for averages, fits, limits, etc. • • •			
154 \pm 20	ARMSTRONG 99b	DPWA	$\gamma^* p \rightarrow p\eta$
212 \pm 20	³ KRUSCHE 97	DPWA	$\gamma N \rightarrow \eta N$
169 \pm 12	ABAEV 96	DPWA	$\pi^- p \rightarrow \eta n$
103 \pm 5	ARNDT 96	IPWA	$\gamma N \rightarrow \pi N$
66	ARNDT 95	DPWA	$\pi N \rightarrow N\pi$
150 \pm 15	BATINIC 95	DPWA	$\pi N \rightarrow N\pi, N\eta$
145	BATINIC 95b	DPWA	$\pi N \rightarrow N\pi, N\eta$
200 \pm 40	KRUSCHE 95	DPWA	$\gamma p \rightarrow p\eta$
84	LI 93	IPWA	$\gamma N \rightarrow \pi N$
136	CRAWFORD 80	DPWA	$\gamma N \rightarrow \pi N$
180	BAKER 79	DPWA	$\pi^- p \rightarrow n\eta$
132	BARBOUR 78	DPWA	$\gamma N \rightarrow \pi N$
57	BERENDS 77	IPWA	$\gamma N \rightarrow \pi N$
139 \pm 33	BHANDARI 77	DPWA	Uses $N\eta$ cusp
135	¹ LONGACRE 77	IPWA	$\pi N \rightarrow N\pi\pi$
100	² LONGACRE 75	IPWA	$\pi N \rightarrow N\pi\pi$

$N(1535)$ POLE POSITION

REAL PART			
VALUE (MeV)	DOCUMENT ID	TECN	COMMENT
1495 to 1515 (≈ 1505) OUR ESTIMATE			
1510 \pm 10	⁴ ARNDT 98	DPWA	$\pi N \rightarrow \pi N, \eta N$
1501	ARNDT 95	DPWA	$\pi N \rightarrow N\pi$
1487	⁵ HOEHLER 93	SPED	$\pi N \rightarrow \pi N$
1510 \pm 50	CUTKOSKY 80	IPWA	$\pi N \rightarrow \pi N$
• • • We do not use the following data for averages, fits, limits, etc. • • •			
1499	ARNDT 91	DPWA	$\pi N \rightarrow \pi N$ Soln SM90
1496 or 1499	⁶ LONGACRE 78	IPWA	$\pi N \rightarrow N\pi\pi$
1519 \pm 4	BHANDARI 77	DPWA	Uses $N\eta$ cusp
1525 or 1527	¹ LONGACRE 77	IPWA	$\pi N \rightarrow N\pi\pi$
-2xIMAGINARY PART			
VALUE (MeV)	DOCUMENT ID	TECN	COMMENT
90 to 250 (≈ 170) OUR ESTIMATE			
170 \pm 30	⁴ ARNDT 98	DPWA	$\pi N \rightarrow \pi N, \eta N$
124	ARNDT 95	DPWA	$\pi N \rightarrow N\pi$
260 \pm 80	CUTKOSKY 80	IPWA	$\pi N \rightarrow \pi N$
• • • We do not use the following data for averages, fits, limits, etc. • • •			
110	ARNDT 91	DPWA	$\pi N \rightarrow \pi N$ Soln SM90
103 or 105	⁶ LONGACRE 78	IPWA	$\pi N \rightarrow N\pi\pi$
140 \pm 32	BHANDARI 77	DPWA	Uses $N\eta$ cusp
135 or 123	¹ LONGACRE 77	IPWA	$\pi N \rightarrow N\pi\pi$

$N(1535)$ ELASTIC POLE RESIDUE

MODULUS $ r $			
VALUE (MeV)	DOCUMENT ID	TECN	COMMENT
31	ARNDT 95	DPWA	$\pi N \rightarrow N\pi$
120 \pm 40	CUTKOSKY 80	IPWA	$\pi N \rightarrow \pi N$
• • • We do not use the following data for averages, fits, limits, etc. • • •			
23	ARNDT 91	DPWA	$\pi N \rightarrow \pi N$ Soln SM90
PHASE θ			
VALUE ($^\circ$)	DOCUMENT ID	TECN	COMMENT
-12	ARNDT 95	DPWA	$\pi N \rightarrow N\pi$
+15 \pm 45	CUTKOSKY 80	IPWA	$\pi N \rightarrow \pi N$
• • • We do not use the following data for averages, fits, limits, etc. • • •			
-13	ARNDT 91	DPWA	$\pi N \rightarrow \pi N$ Soln SM90

$N(1535)$ DECAY MODES

The following branching fractions are our estimates, not fits or averages.

Mode	Fraction (Γ_i/Γ)
Γ_1 $N\pi$	35-55 %
Γ_2 $N\eta$	30-55 %
Γ_3 $N\pi\pi$	1-10 %
Γ_4 $\Delta\pi$	<1 %
Γ_5 $\Delta(1232)\pi, D$ -wave	
Γ_6 $N\rho$	<4 %
Γ_7 $N\rho, S=1/2, S$ -wave	
Γ_8 $N\rho, S=3/2, D$ -wave	
Γ_9 $N(\pi\pi)_{S=0}^{I=0}$	<3 %
Γ_{10} $N(1440)\pi$	<7 %
Γ_{11} $p\gamma$	0.15-0.35 %
Γ_{12} $p\gamma, \text{helicity}=1/2$	0.15-0.35 %
Γ_{13} $n\gamma$	0.004-0.29 %
Γ_{14} $n\gamma, \text{helicity}=1/2$	0.004-0.29 %

$N(1535)$ BRANCHING RATIOS

$\Gamma(N\pi)/\Gamma_{\text{total}}$				Γ_1/Γ	
VALUE	DOCUMENT ID	TECN	COMMENT		
0.35 to 0.55 OUR ESTIMATE					
0.394 \pm 0.009	GREEN 97	DPWA	$\pi N \rightarrow \pi N, \eta N$		
0.51 \pm 0.05	MANLEY 92	IPWA	$\pi N \rightarrow \pi N & N\pi\pi$		
0.50 \pm 0.10	CUTKOSKY 80	IPWA	$\pi N \rightarrow \pi N$		
0.38 \pm 0.04	HOEHLER 79	IPWA	$\pi N \rightarrow \pi N$		
• • • We do not use the following data for averages, fits, limits, etc. • • •					
0.31	ARNDT 95	DPWA	$\pi N \rightarrow N\pi$		
0.34 \pm 0.09	BATINIC 95	DPWA	$\pi N \rightarrow N\pi, N\eta$		
0.297 \pm 0.026	BHANDARI 77	DPWA	Uses $N\eta$ cusp		
$\Gamma(N\eta)/\Gamma_{\text{total}}$				Γ_2/Γ	
VALUE	CL%	DOCUMENT ID	TECN	COMMENT	
+0.30 to 0.55 OUR ESTIMATE					
• • • We do not use the following data for averages, fits, limits, etc. • • •					
> 0.45	95	⁷ ARMSTRONG 99b	DPWA	$p(e, e' p)\eta$	
0.568 \pm 0.011		GREEN 97	DPWA	$\pi N \rightarrow \pi N, \eta N$	
0.59 \pm 0.02		ABAEV 96	DPWA	$\pi^- p \rightarrow \eta n$	
0.63 \pm 0.07		BATINIC 95	DPWA	$\pi N \rightarrow N\pi, N\eta$	

$(\Gamma_1\Gamma_2)^{1/2}/\Gamma_{\text{total}} \ln N\pi \rightarrow N(1535) \rightarrow N\eta$				$(\Gamma_1\Gamma_2)^{1/2}/\Gamma$
VALUE	DOCUMENT ID	TECN	COMMENT	
+0.44 to +0.50 OUR ESTIMATE				
+0.47 \pm 0.02	MANLEY 92	IPWA	$\pi N \rightarrow \pi N & N\pi\pi$	
• • • We do not use the following data for averages, fits, limits, etc. • • •				
+0.33	BAKER 79	DPWA	$\pi^- p \rightarrow n\eta$	
+0.48	FELTESSE 75	DPWA	1488-1745 MeV	

Note: Signs of couplings from $\pi N \rightarrow N\pi\pi$ analyses were changed in the 1986 edition to agree with the baryon-first convention; the overall phase ambiguity is resolved by choosing a negative sign for the $\Delta(1620) S_{31}$ coupling to $\Delta(1232)\pi$.

$(\Gamma_1\Gamma_5)^{1/2}/\Gamma_{\text{total}} \ln N\pi \rightarrow N(1535) \rightarrow \Delta(1232)\pi, D$ -wave				$(\Gamma_1\Gamma_5)^{1/2}/\Gamma$
VALUE	DOCUMENT ID	TECN	COMMENT	
-0.04 to +0.06 OUR ESTIMATE				
+0.00 \pm 0.04	MANLEY 92	IPWA	$\pi N \rightarrow \pi N & N\pi\pi$	
0.00	¹ LONGACRE 77	IPWA	$\pi N \rightarrow N\pi\pi$	
+0.06	² LONGACRE 75	IPWA	$\pi N \rightarrow N\pi\pi$	

See key on page 239

Baryon Particle Listings
 $N(1535)$, $N(1650)$
 $(\Gamma_1\Gamma_2)^{1/2}/\Gamma_{\text{total}}$ in $N\pi \rightarrow N(1535) \rightarrow N\rho, S=1/2, S\text{-wave}$ $(\Gamma_1\Gamma_2)^{1/2}/\Gamma$

VALUE	DOCUMENT ID	TECN	COMMENT
-0.14 to -0.06 OUR ESTIMATE			
-0.10 ± 0.03	MANLEY 92	IPWA	$\pi N \rightarrow \pi N & N\pi\pi$
-0.10	¹ LONGACRE 77	IPWA	$\pi N \rightarrow N\pi\pi$
-0.09	² LONGACRE 75	IPWA	$\pi N \rightarrow N\pi\pi$

 $(\Gamma_1\Gamma_2)^{1/2}/\Gamma_{\text{total}}$ in $N\pi \rightarrow N(1535) \rightarrow N(\pi\pi)_{S\text{-wave}}^{I=0}$ $(\Gamma_1\Gamma_2)^{1/2}/\Gamma$

VALUE	DOCUMENT ID	TECN	COMMENT
+0.03 to +0.13 OUR ESTIMATE			
+0.07 ± 0.04	MANLEY 92	IPWA	$\pi N \rightarrow \pi N & N\pi\pi$
+0.08	¹ LONGACRE 77	IPWA	$\pi N \rightarrow N\pi\pi$
+0.09	² LONGACRE 75	IPWA	$\pi N \rightarrow N\pi\pi$

 $(\Gamma_1\Gamma_2)^{1/2}/\Gamma_{\text{total}}$ in $N\pi \rightarrow N(1535) \rightarrow N(1440)\pi$ $(\Gamma_1\Gamma_2)^{1/2}/\Gamma$

VALUE	DOCUMENT ID	TECN	COMMENT
+0.10 ± 0.05	MANLEY 92	IPWA	$\pi N \rightarrow \pi N & N\pi\pi$

N(1535) PHOTON DECAY AMPLITUDES

 $N(1535) \rightarrow p\gamma$, helicity-1/2 amplitude $A_{1/2}$

VALUE (GeV ^{-1/2})	DOCUMENT ID	TECN	COMMENT
+0.090 ± 0.030 OUR ESTIMATE			
0.120 ± 0.011 ± 0.015	³ KRUSCHE 97	DPWA	$\gamma N \rightarrow \eta N$
0.060 ± 0.015	ARNDT 96	IPWA	$\gamma N \rightarrow \pi N$
0.097 ± 0.006	BENMERROU...95	DPWA	$\gamma N \rightarrow N\eta$
0.095 ± 0.011	⁸ BENMERROU...91		$\gamma p \rightarrow p\eta$
0.053 ± 0.015	CRAWFORD 83	IPWA	$\gamma N \rightarrow \pi N$
0.077 ± 0.021	AWAJI 81	DPWA	$\gamma N \rightarrow \pi N$
0.083 ± 0.007	ARAI 80	DPWA	$\gamma N \rightarrow \pi N$ (fit 1)
0.080 ± 0.007	ARAI 80	DPWA	$\gamma N \rightarrow \pi N$ (fit 2)
0.029 ± 0.007	BRATASHEV...80	DPWA	$\gamma N \rightarrow \pi N$
0.065 ± 0.016	CRAWFORD 80	DPWA	$\gamma N \rightarrow \pi N$
0.0704 ± 0.0091	ISHII 80	DPWA	Compton scattering
• • • We do not use the following data for averages, fits, limits, etc. • • •			
0.110 to 0.140	KRUSCHE 95	DPWA	$\gamma p \rightarrow p\eta$
0.125 ± 0.025	KRUSCHE 95C	IPWA	$\gamma d \rightarrow \eta N(N)$
0.061 ± 0.003	LI 93	IPWA	$\gamma N \rightarrow \pi N$
0.055	WADA 84	DPWA	Compton scattering
+0.082 ± 0.019	BARBOUR 78	DPWA	$\gamma N \rightarrow \pi N$
0.046	⁹ NOELLE 78		$\gamma N \rightarrow \pi N$
+0.034	BERENDS 77	IPWA	$\gamma N \rightarrow \pi N$
+0.070 ± 0.004	FELLER 76	DPWA	$\gamma N \rightarrow \pi N$

 $N(1535) \rightarrow n\gamma$, helicity-1/2 amplitude $A_{1/2}$

VALUE (GeV ^{-1/2})	DOCUMENT ID	TECN	COMMENT
-0.046 ± 0.027 OUR ESTIMATE			
-0.020 ± 0.035	ARNDT 96	IPWA	$\gamma N \rightarrow \pi N$
0.035 ± 0.014	AWAJI 81	DPWA	$\gamma N \rightarrow \pi N$
-0.062 ± 0.003	FUJII 81	DPWA	$\gamma N \rightarrow \pi N$
-0.075 ± 0.019	ARAI 80	DPWA	$\gamma N \rightarrow \pi N$ (fit 1)
-0.075 ± 0.018	ARAI 80	DPWA	$\gamma N \rightarrow \pi N$ (fit 2)
-0.098 ± 0.026	CRAWFORD 80	DPWA	$\gamma N \rightarrow \pi N$
-0.011 ± 0.017	TAKEDA 80	DPWA	$\gamma N \rightarrow \pi N$
• • • We do not use the following data for averages, fits, limits, etc. • • •			
-0.100 ± 0.030	KRUSCHE 95C	IPWA	$\gamma d \rightarrow \eta N(N)$
-0.046 ± 0.005	LI 93	IPWA	$\gamma N \rightarrow \pi N$
-0.112 ± 0.034	BARBOUR 78	DPWA	$\gamma N \rightarrow \pi N$
-0.048	⁹ NOELLE 78		$\gamma N \rightarrow \pi N$

 $N(1535) \rightarrow N\gamma$, ratio $A_{1/2}^p/A_{1/2}^n$

VALUE (GeV ^{-1/2})	DOCUMENT ID	TECN	COMMENT
-0.84 ± 0.15	MUKHOPAD... 95b	IPWA	

N(1535) FOOTNOTES

- LONGACRE 77 pole positions are from a search for poles in the unitarized T-matrix; the first (second) value uses, in addition to $\pi N \rightarrow N\pi\pi$ data, elastic amplitudes from a Saclay (CERN) partial-wave analysis. The other LONGACRE 77 values are from eyeball fits with Breit-Wigner circles to the T-matrix amplitudes.
- From method II of LONGACRE 75: eyeball fits with Breit-Wigner circles to the T-matrix amplitudes.
- KRUSCHE 97 fits with the mass fixed at 1544 MeV.
- ARNDT 98 also lists pole residues, which display more model dependence than do the associated pole positions.
- See HOEHLER 93 for a detailed discussion of the evidence for and the pole parameters of N and Δ resonances as determined from Argand diagrams of πN elastic partial-wave amplitudes and from plots of the speeds with which the amplitudes traverse the diagrams.
- LONGACRE 78 values are from a search for poles in the unitarized T-matrix. The first (second) value uses, in addition to $\pi N \rightarrow N\pi\pi$ data, elastic amplitudes from a Saclay (CERN) partial-wave analysis.
- The best value ARMSTRONG 99b obtains is ≈ 0.55 ; this assumes S_{11} dominance in the reaction $p(e, e'\gamma)\eta$ at $Q^2 = 4$ (GeV/c)².
- BENMERROUCHE 91 uses an effective Lagrangian approach to analyze η photoproduction data.
- Converted to our conventions using $M = 1548$ MeV, $\Gamma = 73$ MeV from NOELLE 78.

N(1535) REFERENCES

For early references, see Physics Letters 111B 70 (1982).

ARMSTRONG 99b	PR D60 052004	C.S. Armstrong et al.
ARNDT 98	PR C58 3636	R.A. Arndt et al.
GREEN 97	PR C55 R2167	A.M. Green, S. Wycech (HELs, WINR)
KRUSCHE 97	PL B397 171	B. Krusche et al. (GIES, RPI, SASK)
ABAEV 98	PR C53 325	V.V. Abaev, B.M.K. Nefkens (UCLA)
ARNDT 96	PR C53 430	R.A. Arndt, I.I. Strakovsky, R.L. Workman (VPI)
ARNDT 95	PR C52 2120	R.A. Arndt et al. (VPI, BRCO)
BATINIC 95	PR C51 2310	M. Batinic et al. (BOSK, UCLA)
Also 98	PR C57 1004 (erratum)	M. Batinic et al.
BATINIC 95b	PR C52 2188	M. Batinic, I. Slaus, A. Svarc (BOSK)
BENMERROU...95	PR D51 3237	M. Benmerrouche, N.C. Mukhopadhyay, J.F. Zhang
KRUSCHE 95	PRL 74 3736	B. Krusche et al. (GIES, MANZ, GLAS+)
KRUSCHE 95C	PL B358 40	B. Krusche et al. (GIES, MANZ, GLAS+)
MUKHOPAD...95b	PL B364 1	N.C. Mukhopadhyay, J.F. Zhang, M. Benmerrouche
HOEHLER 93	πN Newsletter 9 1	G. Hoehler (KARL)
LI 93	PR C47 2759	Z.J. Li et al. (RPI)
MANLEY 92	PR D45 4002	D.M. Manley, E.M. Saleski (KENT) IJP
Also 84	PR D30 904	D.M. Manley et al. (VPI)
ARNDT 91	PR D43 2131	R.A. Arndt et al. (VPI, TELE) IJP
BENMERROU...91	PRL 67 1070	M. Benmerrouche, N.C. Mukhopadhyay
WADA 84	NP B247 313	Y. Wada et al. (INUS)
CRAWFORD 83	NP B211 1	R.L. Crawford, W.T. Morton (GLAS)
PDS 82	PL 111B	M. Roos et al. (HELs, CIT, CERN)
AWAJI 81	Bonn Conf. 352	N. Awaji, R. Kajikawa (NAGO)
Also 82	NP B197 365	K. Fujii et al. (NAGO)
FUJII 81	NP B187 53	K. Fujii et al. (NAGO, OSAK)
ARAI 80	Toronto Conf. 93	I. Arai (INUS)
Also 82	NP B194 251	I. Arai, H. Fujii (INUS)
BRATASHEV...80	NP B166 525	A.S. Bratashovsky et al. (KFTI)
CRAWFORD 80	Toronto Conf. 107	R.L. Crawford (GLAS)
CUTKOSKY 80	Toronto Conf. 19	R.E. Cutkosky et al. (CMU, LBL) IJP
Also 79	PR D20 2839	R.E. Cutkosky et al. (CMU, LBL) IJP
ISHII 80	NP B165 189	T. Ishii et al. (KYOT, INUS)
TAKEDA 80	NP B168 17	H. Takeda et al. (TOKY, INUS)
BAKER 79	NP B156 93	R.D. Baker et al. (RHEL) IJP
HOEHLER 79	PDAT 12-1	G. Hoehler et al. (KARLT) IJP
Also 80	Toronto Conf. 3	R. Koch (KARLT) IJP
BARBOUR 78	NP B141 253	I.M. Barbour, R.L. Crawford, N.H. Parsons (GLAS)
LONGACRE 78	PR D17 1795	R.S. Longacre et al. (LBL, SLAC)
NOELLE 78	PTP 60 779	P. Noelle (NAGO)
BERENDS 77	NP B136 317	F.A. Berends, A. Donnachie (LEID, MCHS) IJP
BHANDARI 77	PR D15 192	R. Bhandari, Y.A. Chao (CMU) IJP
LONGACRE 77	NP B122 493	R.S. Longacre, J. Dolbeau (SACL) IJP
Also 76	NP B108 365	J. Dolbeau et al. (SACL) IJP
FELLER 76	NP B104 219	P. Feller et al. (NAGO, OSAK) IJP
FELTESSE 75	NP B93 242	J. Feltesse et al. (SACL) IJP
LONGACRE 75	PL 95B 415	R.S. Longacre et al. (LBL, SLAC) IJP

N(1650) S₁₁ $i(J^P) = \frac{1}{2}(\frac{1}{2}^-)$ Status: * * * *

Most of the results published before 1975 are now obsolete and have been omitted. They may be found in our 1982 edition, Physics Letters 111B (1982).

N(1650) BREIT-WIGNER MASS

VALUE (MeV)	DOCUMENT ID	TECN	COMMENT
1640 to 1680 (≈ 1650) OUR ESTIMATE			
1659 ± 9	MANLEY 92	IPWA	$\pi N \rightarrow \pi N & N\pi\pi$
1650 ± 30	CUTKOSKY 80	IPWA	$\pi N \rightarrow \pi N$
1670 ± 8	HOEHLER 79	IPWA	$\pi N \rightarrow \pi N$
• • • We do not use the following data for averages, fits, limits, etc. • • •			
1677 ± 8	ARNDT 96	IPWA	$\gamma N \rightarrow \pi N$
1667	ARNDT 95	DPWA	$\pi N \rightarrow N\pi$
1712	¹ ARNDT 95	DPWA	$\pi N \rightarrow N\pi$
1669 ± 17	BATINIC 95	DPWA	$\pi N \rightarrow N\pi, N\eta$
1713 ± 27	² BATINIC 95	DPWA	$\pi N \rightarrow N\pi, N\eta$
1674	LI 93	IPWA	$\gamma N \rightarrow \pi N$
1688	CRAWFORD 80	DPWA	$\gamma N \rightarrow \pi N$
1672	MUSETTE 80	IPWA	$\pi^- p \rightarrow \Lambda K^0$
1680	SAXON 80	DPWA	$\pi^- p \rightarrow \Lambda K^0$
1680	BAKER 78	DPWA	$\pi^- p \rightarrow \Lambda K^0$
1694	BARBOUR 78	DPWA	$\gamma N \rightarrow \pi N$
1700 ± 5	³ BAKER 77	IPWA	$\pi^- p \rightarrow \Lambda K^0$
1680	³ BAKER 77	DPWA	$\pi^- p \rightarrow \Lambda K^0$
1700	⁴ LONGACRE 77	IPWA	$\pi N \rightarrow N\pi\pi$
1675	KNASEL 75	DPWA	$\pi^- p \rightarrow \Lambda K^0$
1660	⁵ LONGACRE 75	IPWA	$\pi N \rightarrow N\pi\pi$

N(1650) BREIT-WIGNER WIDTH

VALUE (MeV)	DOCUMENT ID	TECN	COMMENT
145 to 190 (≈ 150) OUR ESTIMATE			
167.9 ± 9.4	GREEN 97	DPWA	$\pi N \rightarrow \pi N, \eta N$
173 ± 12	MANLEY 92	IPWA	$\pi N \rightarrow \pi N & N\pi\pi$
150 ± 40	CUTKOSKY 80	IPWA	$\pi N \rightarrow \pi N$
180 ± 20	HOEHLER 79	IPWA	$\pi N \rightarrow \pi N$

Baryon Particle Listings

N(1650)

• • • We do not use the following data for averages, fits, limits, etc. • • •

160 ± 12	ARNDT	96	IPWA	$\gamma N \rightarrow \pi N$
90	ARNDT	95	DPWA	$\pi N \rightarrow N\pi$
184	¹ ARNDT	95	DPWA	$\pi N \rightarrow N\pi$
215 ± 32	BATINIC	95	DPWA	$\pi N \rightarrow N\pi, N\eta$
279 ± 54	² BATINIC	95	DPWA	$\pi N \rightarrow N\pi, N\eta$
225	LI	93	IPWA	$\gamma N \rightarrow \pi N$
183	CRAWFORD	80	DPWA	$\gamma N \rightarrow \pi N$
179	MUSETTE	80	IPWA	$\pi^- p \rightarrow \Lambda K^0$
120	SAXON	80	DPWA	$\pi^- p \rightarrow \Lambda K^0$
90	BAKER	78	DPWA	$\pi^- p \rightarrow \Lambda K^0$
193	BARBOUR	78	DPWA	$\gamma N \rightarrow \pi N$
130 ± 10	³ BAKER	77	IPWA	$\pi^- p \rightarrow \Lambda K^0$
90	³ BAKER	77	DPWA	$\pi^- p \rightarrow \Lambda K^0$
170	⁴ LONGACRE	77	IPWA	$\pi N \rightarrow N\pi\pi$
170	KNASEL	75	DPWA	$\pi^- p \rightarrow \Lambda K^0$
130	⁵ LONGACRE	75	IPWA	$\pi N \rightarrow N\pi\pi$

N(1650) POLE POSITION

REAL PART

VALUE (MeV)	DOCUMENT ID	TECN	COMMENT
1640 to 1680 (≈ 1660) OUR ESTIMATE			
1660 ± 10	⁶ ARNDT	98	DPWA $\pi N \rightarrow \pi N, \eta N$
1673	ARNDT	95	DPWA $\pi N \rightarrow N\pi$
1689	¹ ARNDT	95	DPWA $\pi N \rightarrow N\pi$
1670	⁷ HOEHLER	93	ARGD $\pi N \rightarrow \pi N$
1640 ± 20	CUTKOSKY	80	IPWA $\pi N \rightarrow \pi N$
• • • We do not use the following data for averages, fits, limits, etc. • • •			
1657	ARNDT	91	DPWA $\pi N \rightarrow \pi N$ Soln SM90
1648 or 1651	⁸ LONGACRE	78	IPWA $\pi N \rightarrow N\pi\pi$
1699 or 1698	⁴ LONGACRE	77	IPWA $\pi N \rightarrow N\pi\pi$

-2×IMAGINARY PART

VALUE (MeV)	DOCUMENT ID	TECN	COMMENT
150 to 170 (≈ 160) OUR ESTIMATE			
140 ± 20	⁶ ARNDT	98	DPWA $\pi N \rightarrow \pi N, \eta N$
82	ARNDT	95	DPWA $\pi N \rightarrow N\pi$
192	¹ ARNDT	95	DPWA $\pi N \rightarrow N\pi$
163	⁷ HOEHLER	93	ARGD $\pi N \rightarrow \pi N$
150 ± 30	CUTKOSKY	80	IPWA $\pi N \rightarrow \pi N$
• • • We do not use the following data for averages, fits, limits, etc. • • •			
160	ARNDT	91	DPWA $\pi N \rightarrow \pi N$ Soln SM90
117 or 119	⁸ LONGACRE	78	IPWA $\pi N \rightarrow N\pi\pi$
174 or 173	⁴ LONGACRE	77	IPWA $\pi N \rightarrow N\pi\pi$

N(1650) ELASTIC POLE RESIDUE

MODULUS |r|

VALUE (MeV)	DOCUMENT ID	TECN	COMMENT
22	ARNDT	95	DPWA $\pi N \rightarrow N\pi$
72	¹ ARNDT	95	DPWA $\pi N \rightarrow N\pi$
39	HOEHLER	93	ARGD $\pi N \rightarrow \pi N$
60 ± 10	CUTKOSKY	80	IPWA $\pi N \rightarrow \pi N$
• • • We do not use the following data for averages, fits, limits, etc. • • •			
54	ARNDT	91	DPWA $\pi N \rightarrow \pi N$ Soln SM90

PHASE θ

VALUE (°)	DOCUMENT ID	TECN	COMMENT
29	ARNDT	95	DPWA $\pi N \rightarrow N\pi$
-85	¹ ARNDT	95	DPWA $\pi N \rightarrow N\pi$
-37	HOEHLER	93	ARGD $\pi N \rightarrow \pi N$
-75 ± 25	CUTKOSKY	80	IPWA $\pi N \rightarrow \pi N$
• • • We do not use the following data for averages, fits, limits, etc. • • •			
-38	ARNDT	91	DPWA $\pi N \rightarrow \pi N$ Soln SM90

N(1650) DECAY MODES

The following branching fractions are our estimates, not fits or averages.

Mode	Fraction (Γ_i/Γ)
Γ_1 $N\pi$	55-90 %
Γ_2 $N\eta$	3-10 %
Γ_3 ΛK	3-11 %
Γ_4 ΣK	
Γ_5 $N\pi\pi$	10-20 %
Γ_6 $\Delta\pi$	1-7 %
Γ_7 $\Delta(1232)\pi, D\text{-wave}$	
Γ_8 $N\rho$	4-12 %
Γ_9 $N\rho, S=1/2, S\text{-wave}$	
Γ_{10} $N\rho, S=3/2, D\text{-wave}$	
Γ_{11} $N(\pi\pi)_{S=0}^{J=0}$	<4 %
Γ_{12} $N(1440)\pi$	<5 %

Γ_{13} $\rho\gamma$	0.04-0.18 %
Γ_{14} $\rho\gamma, \text{helicity}=1/2$	0.04-0.18 %
Γ_{15} $n\gamma$	0.003-0.17 %
Γ_{16} $n\gamma, \text{helicity}=1/2$	0.003-0.17 %

N(1650) BRANCHING RATIOS

$\Gamma(N\pi)/\Gamma_{\text{total}}$	DOCUMENT ID	TECN	COMMENT	Γ_1/Γ
0.55 to 0.90 OUR ESTIMATE				
0.735 ± 0.011	GREEN	97	DPWA $\pi N \rightarrow \pi N, \eta N$	
0.89 ± 0.07	MANLEY	92	IPWA $\pi N \rightarrow \pi N \& N\pi\pi$	
0.65 ± 0.10	CUTKOSKY	80	IPWA $\pi N \rightarrow \pi N$	
0.61 ± 0.04	HOEHLER	79	IPWA $\pi N \rightarrow \pi N$	
• • • We do not use the following data for averages, fits, limits, etc. • • •				
0.99	ARNDT	95	DPWA $\pi N \rightarrow N\pi$	
0.27	¹ ARNDT	95	DPWA $\pi N \rightarrow N\pi$	
0.94 ± 0.07	BATINIC	95	DPWA $\pi N \rightarrow N\pi, N\eta$	
0.49 ± 0.21	² BATINIC	95	DPWA $\pi N \rightarrow N\pi, N\eta$	

$\Gamma(N\eta)/\Gamma_{\text{total}}$	DOCUMENT ID	TECN	COMMENT	Γ_2/Γ
• • • We do not use the following data for averages, fits, limits, etc. • • •				
0.06 ± 0.05	BATINIC	95	DPWA $\pi N \rightarrow N\pi, N\eta$	
0.02 ± 0.03	² BATINIC	95	DPWA $\pi N \rightarrow N\pi, N\eta$	

$(\Gamma_1\Gamma_f)^{1/2}/\Gamma_{\text{total}}$ in $N\pi \rightarrow N(1650) \rightarrow N\eta$	DOCUMENT ID	TECN	COMMENT	$(\Gamma_1\Gamma_2)^{1/2}/\Gamma$
• • • We do not use the following data for averages, fits, limits, etc. • • •				
-0.09	⁹ BAKER	79	DPWA $\pi^- p \rightarrow n\eta$	

$(\Gamma_1\Gamma_f)^{1/2}/\Gamma_{\text{total}}$ in $N\pi \rightarrow N(1650) \rightarrow \Lambda K$	DOCUMENT ID	TECN	COMMENT	$(\Gamma_1\Gamma_3)^{1/2}/\Gamma$
-0.27 to -0.17 OUR ESTIMATE				
-0.22	BELL	83	DPWA $\pi^- p \rightarrow \Lambda K^0$	
-0.22	SAXON	80	DPWA $\pi^- p \rightarrow \Lambda K^0$	
• • • We do not use the following data for averages, fits, limits, etc. • • •				
-0.25	¹⁰ BAKER	-78	DPWA See SAXON 80	
-0.23 ± 0.01	³ BAKER	77	IPWA $\pi^- p \rightarrow \Lambda K^0$	
-0.25	³ BAKER	77	DPWA $\pi^- p \rightarrow \Lambda K^0$	
0.12	KNASEL	75	DPWA $\pi^- p \rightarrow \Lambda K^0$	

$(\Gamma_1\Gamma_f)^{1/2}/\Gamma_{\text{total}}$ in $N\pi \rightarrow N(1650) \rightarrow \Sigma K$	DOCUMENT ID	TECN	COMMENT	$(\Gamma_1\Gamma_4)^{1/2}/\Gamma$
• • • We do not use the following data for averages, fits, limits, etc. • • •				
-0.254	LIVANOS	80	DPWA $\pi p \rightarrow \Sigma K$	
0.066 to 0.137	¹¹ DEANS	75	DPWA $\pi N \rightarrow \Sigma K$	
0.20	KNASEL	75	DPWA	

Note: Signs of couplings from $\pi N \rightarrow N\pi\pi$ analyses were changed in the 1986 edition to agree with the baryon-first convention; the overall phase ambiguity is resolved by choosing a negative sign for the $\Delta(1620)S_{31}$ coupling to $\Delta(1232)\pi$.

$(\Gamma_1\Gamma_f)^{1/2}/\Gamma_{\text{total}}$ in $N\pi \rightarrow N(1650) \rightarrow \Delta(1232)\pi, D\text{-wave}$	DOCUMENT ID	TECN	COMMENT	$(\Gamma_1\Gamma_7)^{1/2}/\Gamma$
+0.15 to 0.23 OUR ESTIMATE				
+0.12 ± 0.04	MANLEY	92	IPWA $\pi N \rightarrow \pi N \& N\pi\pi$	
+0.29	^{4,12} LONGACRE	77	IPWA $\pi N \rightarrow N\pi\pi$	
+0.15	⁵ LONGACRE	75	IPWA $\pi N \rightarrow N\pi\pi$	

$(\Gamma_1\Gamma_f)^{1/2}/\Gamma_{\text{total}}$ in $N\pi \rightarrow N(1650) \rightarrow N\rho, S=1/2, S\text{-wave}$	DOCUMENT ID	TECN	COMMENT	$(\Gamma_1\Gamma_9)^{1/2}/\Gamma$
±0.03 to ±0.19 OUR ESTIMATE				
-0.01 ± 0.09	MANLEY	92	IPWA $\pi N \rightarrow \pi N \& N\pi\pi$	
+0.17	^{4,12} LONGACRE	77	IPWA $\pi N \rightarrow N\pi\pi$	
-0.16	⁵ LONGACRE	75	IPWA $\pi N \rightarrow N\pi\pi$	

$(\Gamma_1\Gamma_f)^{1/2}/\Gamma_{\text{total}}$ in $N\pi \rightarrow N(1650) \rightarrow N\rho, S=3/2, D\text{-wave}$	DOCUMENT ID	TECN	COMMENT	$(\Gamma_1\Gamma_{10})^{1/2}/\Gamma$
+0.17 to +0.29 OUR ESTIMATE				
+0.16 ± 0.06	MANLEY	92	IPWA $\pi N \rightarrow \pi N \& N\pi\pi$	
+0.29	^{4,12} LONGACRE	77	IPWA $\pi N \rightarrow N\pi\pi$	

$(\Gamma_1\Gamma_f)^{1/2}/\Gamma_{\text{total}}$ in $N\pi \rightarrow N(1650) \rightarrow N(\pi\pi)_{S=0}^{J=0}$	DOCUMENT ID	TECN	COMMENT	$(\Gamma_1\Gamma_{11})^{1/2}/\Gamma$
+0.04 to +0.18 OUR ESTIMATE				
+0.12 ± 0.08	MANLEY	92	IPWA $\pi N \rightarrow \pi N \& N\pi\pi$	
0.00	^{4,12} LONGACRE	77	IPWA $\pi N \rightarrow N\pi\pi$	
+0.25	⁵ LONGACRE	75	IPWA $\pi N \rightarrow N\pi\pi$	

See key on page 239

Baryon Particle Listings
N(1650), N(1675)

(\Gamma_1/\Gamma_f)^{1/2}/\Gamma_{total} ln N\pi \to N(1650) \to N(1440)\pi (\Gamma_1/\Gamma_{12})^{1/2}/\Gamma

N(1650) REFERENCES

For early references, see Physics Letters 111B 70 (1982).

N(1650) PHOTON DECAY AMPLITUDES

N(1650) \to p\gamma, helicity-1/2 amplitude A_{1/2}

Table with columns: VALUE (GeV^{-1/2}), DOCUMENT ID, TECN, COMMENT. Includes rows for ARNDT, CRAWFORD, AWAJI, ARAI, BELL, CRAWFORD, PDG, AWAJI, ARAI, BARBOUR, FELLER.

N(1650) \to n\gamma, helicity-1/2 amplitude A_{1/2}

Table with columns: VALUE (GeV^{-1/2}), DOCUMENT ID, TECN, COMMENT. Includes rows for ARNDT, AWAJI, FUJII, ARAI, CRAWFORD, TAKEDA, LI, BARBOUR.

N(1650) \gamma p \to \Lambda K^+ AMPLITUDES

(\Gamma_1/\Gamma_f)^{1/2}/\Gamma_{total} ln p\gamma \to N(1650) \to \Lambda K^+ (E_{0+} amplitude)

Table with columns: VALUE (units 10^{-3}), DOCUMENT ID, TECN, COMMENT. Includes rows for WORKMAN, TANABE.

p\gamma \to N(1650) \to \Lambda K^+ phase angle \theta (E_{0+} amplitude)

Table with columns: VALUE (degrees), DOCUMENT ID, TECN, COMMENT. Includes rows for WORKMAN, TANABE.

N(1650) FOOTNOTES

- 1 ARNDT 95 finds two distinct states.
2 BATINIC 95 finds two distinct states. This second resonance was associated with the N(2090) S_{11}.
3 The two BAKER 77 entries are from an IPWA using the Barrelet-zero method and from a conventional energy-dependent analysis.
4 LONGACRE 77 pole positions are from a search for poles in the unitarized T-matrix; the first (second) value uses, in addition to \pi N \to N\pi\pi data, elastic amplitudes from a Saclay (CERN) partial-wave analysis. The other LONGACRE 77 values are from eyeball fits with Breit-Wigner circles to the T-matrix amplitudes.
5 From method II of LONGACRE 75: eyeball fits with Breit-Wigner circles to the T-matrix amplitudes.
6 ARNDT 98 also lists pole residues, which display more model dependence than do the associated pole positions.
7 See HOEHLER 93 for a detailed discussion of the evidence for and the pole parameters of N and \Delta resonances as determined from Argand diagrams of \pi N elastic partial-wave amplitudes and from plots of the speeds with which the amplitudes traverse the diagrams.
8 LONGACRE 78 values are from a search for poles in the unitarized T-matrix. The first (second) value uses, in addition to \pi N \to N\pi\pi data, elastic amplitudes from a Saclay (CERN) partial-wave analysis.
9 BAKER 79 fixed this coupling during fitting, but the negative sign relative to the N(1535) is well determined.
10 The overall phase of BAKER 78 couplings has been changed to agree with previous conventions. Superseded by SAXON 80.
11 The range given for DEANS 75 is from the four best solutions.
12 LONGACRE 77 considers this coupling to be well determined.

Large table of references for N(1650) with columns: AUTHOR, DOCUMENT ID, TECN, COMMENT. Includes authors like R.A. Arndt, A.M. Green, R.A. Arndt, M. Batinic, G. Hoehler, Z.J. Li, D.M. Manley, R.A. Arndt, R.L. Workman, H. Tanabe, M. Kohno, Y. Wada, K.W. Bell, R.L. Crawford, M. Roos, N. Awaji, K. Fuji, R. Kuch, R.L. Crawford, R.E. Cutkosky, P. Livanos, M. Musette, D.H. Saxon, H. Takeda, R.D. Baker, G. Hoehler, R. Koch, R.D. Baker, I.M. Barbour, R.S. Longacre, R.D. Baker, J. Dolbeau, P. Feller, S.R. Deans, T.M. Knaese, R.S. Longacre.

N(1675) D_{15}

I(J^P) = \frac{1}{2}(5^-) Status: ***

Most of the results published before 1975 are now obsolete and have been omitted. They may be found in our 1982 edition, Physics Letters 111B (1982).

N(1675) BREIT-WIGNER MASS

Table with columns: VALUE (MeV), DOCUMENT ID, TECN, COMMENT. Includes rows for 1676 \pm 2, 1675 \pm 10, 1679 \pm 8, 1673 \pm 5, 1683 \pm 19, 1666, 1685, 1670, 1680, 1650, 1660.

N(1675) BREIT-WIGNER WIDTH

Table with columns: VALUE (MeV), DOCUMENT ID, TECN, COMMENT. Includes rows for 140 to 180 OUR ESTIMATE, 159 \pm 7, 160 \pm 20, 120 \pm 15, 154 \pm 7, 154, 142 \pm 23, 136, 191, 40, 88, 192, 130, 150.

Baryon Particle Listings

N(1675)

N(1675) POLE POSITION

REAL PART			
VALUE (MeV)	DOCUMENT ID	TECN	COMMENT
1655 to 1665 (\approx 1660) OUR ESTIMATE			
1663	ARNDT 95	DPWA	$\pi N \rightarrow N\pi$
1656	³ HOEHLER 93	ARGD	$\pi N \rightarrow \pi N$
1660 \pm 10	CUTKOSKY 80	IPWA	$\pi N \rightarrow \pi N$
• • • We do not use the following data for averages, fits, limits, etc. • • •			
1655	ARNDT 91	DPWA	$\pi N \rightarrow \pi N$ Soln SM90
1663 or 1668	⁴ LONGACRE 78	IPWA	$\pi N \rightarrow N\pi\pi$
1649 or 1650	¹ LONGACRE 77	IPWA	$\pi N \rightarrow N\pi\pi$
-2<i>x</i>IMAGINARY PART			
VALUE (MeV)	DOCUMENT ID	TECN	COMMENT
125 to 155 (\approx 140) OUR ESTIMATE			
152	ARNDT 95	DPWA	$\pi N \rightarrow N\pi$
126	³ HOEHLER 93	ARGD	$\pi N \rightarrow \pi N$
140 \pm 10	CUTKOSKY 80	IPWA	$\pi N \rightarrow \pi N$
• • • We do not use the following data for averages, fits, limits, etc. • • •			
124	ARNDT 91	DPWA	$\pi N \rightarrow \pi N$ Soln SM90
146 or 171	⁴ LONGACRE 78	IPWA	$\pi N \rightarrow N\pi\pi$
127 or 127	¹ LONGACRE 77	IPWA	$\pi N \rightarrow N\pi\pi$

N(1675) ELASTIC POLE RESIDUE

MODULUS $ r $			
VALUE (MeV)	DOCUMENT ID	TECN	COMMENT
29	ARNDT 95	DPWA	$\pi N \rightarrow N\pi$
23	HOEHLER 93	ARGD	$\pi N \rightarrow \pi N$
31 \pm 5	CUTKOSKY 80	IPWA	$\pi N \rightarrow \pi N$
• • • We do not use the following data for averages, fits, limits, etc. • • •			
28	ARNDT 91	DPWA	$\pi N \rightarrow \pi N$ Soln SM90
PHASE θ			
VALUE ($^\circ$)	DOCUMENT ID	TECN	COMMENT
-6	ARNDT 95	DPWA	$\pi N \rightarrow N\pi$
-22	HOEHLER 93	ARGD	$\pi N \rightarrow \pi N$
-30 \pm 10	CUTKOSKY 80	IPWA	$\pi N \rightarrow \pi N$
• • • We do not use the following data for averages, fits, limits, etc. • • •			
-17	ARNDT 91	DPWA	$\pi N \rightarrow \pi N$ Soln SM90

N(1675) DECAY MODES

The following branching fractions are our estimates, not fits or averages.

Mode	Fraction (Γ_i/Γ)
Γ_1 $N\pi$	40-50 %
Γ_2 $N\eta$	
Γ_3 ΛK	<1 %
Γ_4 ΣK	
Γ_5 $N\pi\pi$	50-60 %
Γ_6 $\Delta\pi$	50-60 %
Γ_7 $\Delta(1232)\pi, D$ -wave	
Γ_8 $\Delta(1232)\pi, G$ -wave	
Γ_9 $N\rho$	<1-3 %
Γ_{10} $N\rho, S=1/2, D$ -wave	
Γ_{11} $N\rho, S=3/2, D$ -wave	
Γ_{12} $N\rho, S=3/2, G$ -wave	
Γ_{13} $N(\pi\pi)_{S=0}^0$	
Γ_{14} $p\gamma$	0.004-0.023 %
Γ_{15} $p\gamma, \text{helicity}=1/2$	0.0-0.015 %
Γ_{16} $p\gamma, \text{helicity}=3/2$	0.0-0.011 %
Γ_{17} $n\gamma$	0.02-0.12 %
Γ_{18} $n\gamma, \text{helicity}=1/2$	0.006-0.046 %
Γ_{19} $n\gamma, \text{helicity}=3/2$	0.01-0.08 %

N(1675) BRANCHING RATIOS

$\Gamma(N\pi)/\Gamma_{\text{total}}$			
VALUE	DOCUMENT ID	TECN	COMMENT
0.4 to 0.5 OUR ESTIMATE			
0.47 \pm 0.02	MANLEY 92	IPWA	$\pi N \rightarrow \pi N$ & $N\pi\pi$
0.38 \pm 0.05	CUTKOSKY 80	IPWA	$\pi N \rightarrow \pi N$
0.38 \pm 0.03	HOEHLER 79	IPWA	$\pi N \rightarrow \pi N$
• • • We do not use the following data for averages, fits, limits, etc. • • •			
0.38	ARNDT 95	DPWA	$\pi N \rightarrow N\pi$
0.31 \pm 0.06	BATINIC 95	DPWA	$\pi N \rightarrow N\pi, N\eta$

$\Gamma(N\eta)/\Gamma_{\text{total}}$			
VALUE	DOCUMENT ID	TECN	COMMENT
• • • We do not use the following data for averages, fits, limits, etc. • • •			
0.001 \pm 0.001	BATINIC 95	DPWA	$\pi N \rightarrow N\pi, N\eta$
$(\Gamma_1\Gamma_2)^{1/2}/\Gamma_{\text{total}}$ in $N\pi \rightarrow N(1675) \rightarrow N\eta$			
VALUE	DOCUMENT ID	TECN	COMMENT
• • • We do not use the following data for averages, fits, limits, etc. • • •			
-0.07	BAKER 79	DPWA	$\pi^- p \rightarrow n\eta$
+0.009	FELTESSE 75	DPWA	Soln A; see BAKER 79
$(\Gamma_1\Gamma_3)^{1/2}/\Gamma_{\text{total}}$ in $N\pi \rightarrow N(1675) \rightarrow \Lambda K$			
VALUE	DOCUMENT ID	TECN	COMMENT
± 0.04 to ± 0.08 OUR ESTIMATE			
-0.01	BELL 83	DPWA	$\pi^- p \rightarrow \Lambda K^0$
+0.036	⁵ SAXON 80	DPWA	$\pi^- p \rightarrow \Lambda K^0$
• • • We do not use the following data for averages, fits, limits, etc. • • •			
-0.034 \pm 0.006	DEVENISH 74B		Fixed- t dispersion rel.
$(\Gamma_1\Gamma_4)^{1/2}/\Gamma_{\text{total}}$ in $N\pi \rightarrow N(1675) \rightarrow \Sigma K$			
VALUE	DOCUMENT ID	TECN	COMMENT
• • • We do not use the following data for averages, fits, limits, etc. • • •			
<0.003	⁶ DEANS 75	DPWA	$\pi N \rightarrow \Sigma K$

Note: Signs of couplings from $\pi N \rightarrow N\pi\pi$ analyses were changed in the 1986 edition to agree with the baryon-first convention; the overall phase ambiguity is resolved by choosing a negative sign for the $\Delta(1620) S_{31}$ coupling to $\Delta(1232)\pi$.

$(\Gamma_1\Gamma_7)^{1/2}/\Gamma_{\text{total}}$ in $N\pi \rightarrow N(1675) \rightarrow \Delta(1232)\pi, D$ -wave			
VALUE	DOCUMENT ID	TECN	COMMENT
+0.46 to +0.50 OUR ESTIMATE			
+0.496 \pm 0.003	MANLEY 92	IPWA	$\pi N \rightarrow \pi N$ & $N\pi\pi$
+0.46	^{1,7} LONGACRE 77	IPWA	$\pi N \rightarrow N\pi\pi$
+0.50	² LONGACRE 75	IPWA	$\pi N \rightarrow N\pi\pi$
• • • We do not use the following data for averages, fits, limits, etc. • • •			
+0.5	⁸ NOVOSELLER 78	IPWA	$\pi N \rightarrow N\pi\pi$
$(\Gamma_1\Gamma_{10})^{1/2}/\Gamma_{\text{total}}$ in $N\pi \rightarrow N(1675) \rightarrow N\rho, S=1/2, D$ -wave			
VALUE	DOCUMENT ID	TECN	COMMENT
+0.04 \pm 0.02	MANLEY 92	IPWA	$\pi N \rightarrow \pi N$ & $N\pi\pi$
$(\Gamma_1\Gamma_{11})^{1/2}/\Gamma_{\text{total}}$ in $N\pi \rightarrow N(1675) \rightarrow N\rho, S=3/2, D$ -wave			
VALUE	DOCUMENT ID	TECN	COMMENT
-0.12 to -0.06 OUR ESTIMATE			
-0.03 \pm 0.02	MANLEY 92	IPWA	$\pi N \rightarrow \pi N$ & $N\pi\pi$
-0.15	^{1,7} LONGACRE 77	IPWA	$\pi N \rightarrow N\pi\pi$
$(\Gamma_1\Gamma_{13})^{1/2}/\Gamma_{\text{total}}$ in $N\pi \rightarrow N(1675) \rightarrow N(\pi\pi)_{S=0}^0$			
VALUE	DOCUMENT ID	TECN	COMMENT
+0.03	^{1,7} LONGACRE 77	IPWA	$\pi N \rightarrow N\pi\pi$

N(1675) PHOTON DECAY AMPLITUDES

$N(1675) \rightarrow p\gamma, \text{helicity}=1/2$ amplitude $A_{1/2}$			
VALUE (GeV ^{-1/2})	DOCUMENT ID	TECN	COMMENT
+0.019\pm0.008 OUR ESTIMATE			
0.015 \pm 0.010	ARNDT 96	IPWA	$\gamma N \rightarrow \pi N$
0.021 \pm 0.011	CRAWFORD 83	IPWA	$\gamma N \rightarrow \pi N$
0.034 \pm 0.005	AWAJI 81	DPWA	$\gamma N \rightarrow \pi N$
0.006 \pm 0.005	ARAI 80	DPWA	$\gamma N \rightarrow \pi N$ (fit 1)
0.006 \pm 0.004	ARAI 80	DPWA	$\gamma N \rightarrow \pi N$ (fit 2)
0.023 \pm 0.015	CRAWFORD 80	DPWA	$\gamma N \rightarrow \pi N$
• • • We do not use the following data for averages, fits, limits, etc. • • •			
0.012 \pm 0.002	LI 93	IPWA	$\gamma N \rightarrow \pi N$
+0.022 \pm 0.010	BARBOUR 78	DPWA	$\gamma N \rightarrow \pi N$
+0.034 \pm 0.004	FELLER 76	DPWA	$\gamma N \rightarrow \pi N$
$N(1675) \rightarrow p\gamma, \text{helicity}=3/2$ amplitude $A_{3/2}$			
VALUE (GeV ^{-1/2})	DOCUMENT ID	TECN	COMMENT
+0.015\pm0.009 OUR ESTIMATE			
0.010 \pm 0.007	ARNDT 96	IPWA	$\gamma N \rightarrow \pi N$
0.015 \pm 0.009	CRAWFORD 83	IPWA	$\gamma N \rightarrow \pi N$
0.024 \pm 0.008	AWAJI 81	DPWA	$\gamma N \rightarrow \pi N$
0.030 \pm 0.004	ARAI 80	DPWA	$\gamma N \rightarrow \pi N$ (fit 1)
0.029 \pm 0.004	ARAI 80	DPWA	$\gamma N \rightarrow \pi N$ (fit 2)
0.003 \pm 0.012	CRAWFORD 80	DPWA	$\gamma N \rightarrow \pi N$
• • • We do not use the following data for averages, fits, limits, etc. • • •			
0.021 \pm 0.002	LI 93	IPWA	$\gamma N \rightarrow \pi N$
+0.015 \pm 0.006	BARBOUR 78	DPWA	$\gamma N \rightarrow \pi N$
+0.019 \pm 0.009	FELLER 76	DPWA	$\gamma N \rightarrow \pi N$

See key on page 239

Baryon Particle Listings

N(1680), N(1700)

N(1680) → nγ, helicity-3/2 amplitude A_{3/2}

VALUE (GeV ^{-1/2})	DOCUMENT ID	TECN	COMMENT
-0.033 ± 0.009 OUR ESTIMATE			
-0.040 ± 0.015	ARNDT 96	IPWA	γN → πN
-0.033 ± 0.013	AWAJI 81	DPWA	γN → πN
-0.023 ± 0.005	FUJII 81	DPWA	γN → πN
-0.024 ± 0.009	ARAI 80	DPWA	γN → πN (fit 1)
-0.029 ± 0.017	ARAI 80	DPWA	γN → πN (fit 2)
-0.033 ± 0.015	CRAWFORD 80	DPWA	γN → πN
-0.035 ± 0.012	TAKEDA 80	DPWA	γN → πN
• • • We do not use the following data for averages, fits, limits, etc. • • •			
-0.048 ± 0.002	LI 93	IPWA	γN → πN
-0.038 ± 0.018	BARBOUR 78	DPWA	γN → πN

N(1680) FOOTNOTES

- LONGACRE 77 pole positions are from a search for poles in the unitarized T-matrix; the first (second) value uses, in addition to πN → Nππ data, elastic amplitudes from a Saclay (CERN) partial-wave analysis. The other LONGACRE 77 values are from eyeball fits with Breit-Wigner circles to the T-matrix amplitudes.
- From method II of LONGACRE 75: eyeball fits with Breit-Wigner circles to the T-matrix amplitudes.
- See HOEHLER 93 for a detailed discussion of the evidence for and the pole parameters of N and Δ resonances as determined from Argand diagrams of πN elastic partial-wave amplitudes and from plots of the speeds with which the amplitudes traverse the diagrams.
- LONGACRE 78 values are from a search for poles in the unitarized T-matrix. The first (second) value uses, in addition to πN → Nππ data, elastic amplitudes from a Saclay (CERN) partial-wave analysis.
- The parametrization used may be double counting.
- The range given is from 3 of 4 best solutions; not present in solution 1. DEANS 75 disagrees with π⁺p → Σ⁺K⁺ data of WINNIK 77 around 1920 MeV.
- LONGACRE 77 considers this coupling to be well determined.
- A Breit-Wigner fit to the HERNDON 75 IPWA.

N(1680) REFERENCES

For early references, see Physics Letters **111B** 70 (1982). For very early references, see Reviews of Modern Physics **37** 633 (1965).

TIATOR 99	PR C60 035210	L. Tiator et al.	
ARNDT 96	PR C53 430	R.A. Arndt, I.I. Strakovsky, R.L. Workman	(VPI)
ARNDT 95	PR C52 2120	R.A. Arndt et al.	(VPI, BRCO)
BATINIC 95	PR C51 2310	M. Batinic et al.	(BOSK, UCLA)
Also	98 PR C57 1004 (erratum)	M. Batinic et al.	
HOEHLER 93	πN Newsletter 9 1	G. Hoehler	(KARL)
LI 93	PR C47 2759	Z.J. Li et al.	(VPI)
MANLEY 92	PR D45 4002	D.M. Manley, E.M. Saleski	(KENT) IJP
Also	84 PR D30 904	D.M. Manley et al.	(VPI)
ARNDT 91	PR D43 2131	R.A. Arndt et al.	(VPI, TELE) IJP
BELL 83	NP B222 389	K.W. Bell et al.	(RL) IJP
CRAWFORD 83	NP B211 1	R.L. Crawford, W.T. Morton	(GLAS)
PDG 82	PL 111B	M. Roos et al.	(HELSE, CIT, CERN)
AWAJI 81	Bonn Conf. 352	N. Awaji, R. Kajikawa	(NAGO)
Also	82 NP B137 365	K. Fujii et al.	(NAGO)
FUJII 81	NP B187 53	K. Fujii et al.	(NAGO, OSAK)
ARAI 80	Toronto Conf. 93	I. Arai	(INUS)
Also	82 NP B194 251	I. Arai, H. Fujii	(INUS)
CRAWFORD 80	Toronto Conf. 107	R.L. Crawford	(GLAS)
CUTKOSKY 80	Toronto Conf. 19	R.E. Cutkosky et al.	(CMU, LBL) IJP
Also	79 PR D20 2839	R.E. Cutkosky et al.	(CMU, LBL) IJP
SAXON 80	NP B162 522	D.H. Saxon et al.	(RHEL, BRIS) IJP
TAKEDA 80	NP B158 17	H. Takeda et al.	(TOKY, INUS)
BAKER 79	NP B156 93	R.D. Baker et al.	(RHEL) IJP
HOEHLER 79	PDAT 12-1	G. Hoehler et al.	(KARLT) IJP
Also	80 Toronto Conf. 3	R. Koch	(KARLT) IJP
BARBOUR 78	NP B141 253	I.M. Barbour, R.L. Crawford, N.H. Parsons	(GLAS)
LONGACRE 78	PR D17 1795	R.S. Longacre et al.	(LBL, SLAC)
NOVOSELLER 78	NP B137 509	D.E. Novoseller	(CIT) IJP
Also	78B NP B137 445	D.E. Novoseller	(CIT) IJP
BAKER 77	NP B126 365	R.D. Baker et al.	(RHEL) IJP
LONGACRE 77	NP B122 493	R.S. Longacre, J. Dolbeau	(SACL) IJP
Also	76 NP B108 365	J. Dolbeau et al.	(SACL) IJP
WINNIK 77	NP B128 66	M. Winnik et al.	(HAIF) I
FELLER 76	NP B104 219	P. Feller et al.	(NAGO, OSAK) IJP
DEANS 75	NP B96 90	S.R. Deans et al.	(SFLA, ALAH) IJP
HERNDON 75	PR D11 3183	D. Herndon et al.	(LBL, SLAC)
KNASEL 75	PR D11 1	T.M. Knasel et al.	(CHIC, WUSL, OSU+) IJP
LONGACRE 75	PL 55B 415	R.S. Longacre et al.	(LBL, SLAC) IJP
DEVENISH 74B	NP B81 330	R.C.E. Devenish, C.D. Froggatt, B.R. Martin	(DESY+) IJP
CARRERAS 70	NP B16 35	B. Carreras, A. Donnachie	(DARE, MCHIS)
BOTKE 69	PR 180 1417	J.C. Botke	(UCSB)
DEANS 69	PR 185 1797	S.R. Deans, J.W. Wooten	(SFLA)
HEUSCH 66	PRL 17 1019	C.A. Heusch, C.Y. Prescott, R.F. Dashen	(CIT)

N(1700) D₁₃

$$I(J^P) = \frac{1}{2}(\frac{3}{2}^-) \text{ Status: } ***$$

Most of the results published before 1975 are now obsolete and have been omitted. They may be found in our 1982 edition, Physics Letters **111B** (1982).

The various partial-wave analyses do not agree very well.

N(1700) BREIT-WIGNER MASS

VALUE (MeV)	DOCUMENT ID	TECN	COMMENT
1650 to 1750 (≈ 1700) OUR ESTIMATE			
1737 ± 44	MANLEY 92	IPWA	πN → πN & Nππ
1675 ± 25	CUTKOSKY 80	IPWA	πN → πN
1731 ± 15	HOEHLER 79	IPWA	πN → πN
• • • We do not use the following data for averages, fits, limits, etc. • • •			
1791 ± 46	BATINIC 95	DPWA	πN → Nπ, Nη
1709	CRAWFORD 80	DPWA	γN → πN
1650	SAXON 80	DPWA	π ⁻ p → ΛK ⁰
1690 to 1710	BAKER 78	DPWA	π ⁻ p → ΛK ⁰
1719	BARBOUR 78	DPWA	γN → πN
1670 ± 10	¹ BAKER 77	IPWA	π ⁻ p → ΛK ⁰
1690	¹ BAKER 77	DPWA	π ⁻ p → ΛK ⁰
1660	² LONGACRE 77	IPWA	πN → Nππ
1710	³ LONGACRE 75	IPWA	πN → Nππ

N(1700) BREIT-WIGNER WIDTH

VALUE (MeV)	DOCUMENT ID	TECN	COMMENT
50 to 150 (≈ 100) OUR ESTIMATE			
250 ± 220	MANLEY 92	IPWA	πN → πN & Nππ
90 ± 40	CUTKOSKY 80	IPWA	πN → πN
110 ± 30	HOEHLER 79	IPWA	πN → πN
• • • We do not use the following data for averages, fits, limits, etc. • • •			
215 ± 60	BATINIC 95	DPWA	πN → Nπ, Nη
166	CRAWFORD 80	DPWA	γN → πN
70	SAXON 80	DPWA	π ⁻ p → ΛK ⁰
70 to 100	BAKER 78	DPWA	π ⁻ p → ΛK ⁰
126	BARBOUR 78	DPWA	γN → πN
90 ± 25	¹ BAKER 77	IPWA	π ⁻ p → ΛK ⁰
100	¹ BAKER 77	DPWA	π ⁻ p → ΛK ⁰
300	² LONGACRE 77	IPWA	πN → Nππ
600	³ LONGACRE 75	IPWA	πN → Nππ

N(1700) POLE POSITION

REAL PART			
VALUE (MeV)	DOCUMENT ID	TECN	COMMENT
1630 to 1730 (≈ 1680) OUR ESTIMATE			
1700	⁴ HOEHLER 93	SPED	πN → πN
1660 ± 30	CUTKOSKY 80	IPWA	πN → πN
• • • We do not use the following data for averages, fits, limits, etc. • • •			
not seen	ARNDT 91	DPWA	πN → πN Soln SM90
1710 or 1678	⁵ LONGACRE 78	IPWA	πN → Nππ
1616 or 1613	² LONGACRE 77	IPWA	πN → Nππ

-2×IMAGINARY PART

VALUE (MeV)	DOCUMENT ID	TECN	COMMENT
50 to 150 (≈ 100) OUR ESTIMATE			
120	⁴ HOEHLER 93	SPED	πN → πN
90 ± 40	CUTKOSKY 80	IPWA	πN → πN
• • • We do not use the following data for averages, fits, limits, etc. • • •			
not seen	ARNDT 91	DPWA	πN → πN Soln SM90
607 or 567	⁵ LONGACRE 78	IPWA	πN → Nππ
577 or 575	² LONGACRE 77	IPWA	πN → Nππ

N(1700) ELASTIC POLE RESIDUE

MODULUS r			
VALUE (MeV)	DOCUMENT ID	TECN	COMMENT
5	HOEHLER 93	SPED	πN → πN
6 ± 3	CUTKOSKY 80	IPWA	πN → πN
PHASE θ			
VALUE (°)	DOCUMENT ID	TECN	COMMENT
0 ± 50	CUTKOSKY 80	IPWA	πN → πN

See key on page 239

Baryon Particle Listings

N(1720)

N(1720) P₁₃

$$I(J^P) = \frac{1}{2}(3^+) \text{ Status: } ****$$

Most of the results published before 1975 are now obsolete and have been omitted. They may be found in our 1982 edition, Physics Letters **111B** (1982).

N(1720) BREIT-WIGNER MASS

VALUE (MeV)	DOCUMENT ID	TECN	COMMENT
1650 to 1750 (≈ 1720) OUR ESTIMATE			
1717 ± 31	MANLEY 92	IPWA	$\pi N \rightarrow \pi N \& N\pi\pi$
1700 ± 50	CUTKOSKY 80	IPWA	$\pi N \rightarrow \pi N$
1710 ± 20	HOEHLER 79	IPWA	$\pi N \rightarrow \pi N$
• • • We do not use the following data for averages, fits, limits, etc. • • •			
1713 ± 10	ARNDT 96	IPWA	$\gamma N \rightarrow \pi N$
1820	ARNDT 95	DPWA	$\pi N \rightarrow N\pi$
1711 ± 26	BATINIC 95	DPWA	$\pi N \rightarrow N\pi, N\eta$
1720	LI 93	IPWA	$\gamma N \rightarrow \pi N$
1785	CRAWFORD 80	DPWA	$\gamma N \rightarrow \pi N$
1690	SAXON 80	DPWA	$\pi^- \rho \rightarrow \Lambda K^0$
1710 to 1790	BAKER 78	DPWA	$\pi^- \rho \rightarrow \Lambda K^0$
1809	BARBOUR 78	DPWA	$\gamma N \rightarrow \pi N$
1640 ± 10	¹ BAKER 77	IPWA	$\pi^- \rho \rightarrow \Lambda K^0$
1710	¹ BAKER 77	DPWA	$\pi^- \rho \rightarrow \Lambda K^0$
1750	² LONGACRE 77	IPWA	$\pi N \rightarrow N\pi\pi$
1850	KNASEL 75	DPWA	$\pi^- \rho \rightarrow \Lambda K^0$
1720	³ LONGACRE 75	IPWA	$\pi N \rightarrow N\pi\pi$

N(1720) BREIT-WIGNER WIDTH

VALUE (MeV)	DOCUMENT ID	TECN	COMMENT
100 to 200 (≈ 150) OUR ESTIMATE			
380 ± 180	MANLEY 92	IPWA	$\pi N \rightarrow \pi N \& N\pi\pi$
125 ± 70	CUTKOSKY 80	IPWA	$\pi N \rightarrow \pi N$
190 ± 30	HOEHLER 79	IPWA	$\pi N \rightarrow \pi N$
• • • We do not use the following data for averages, fits, limits, etc. • • •			
153 ± 15	ARNDT 96	IPWA	$\gamma N \rightarrow \pi N$
354	ARNDT 95	DPWA	$\pi N \rightarrow N\pi$
235 ± 51	BATINIC 95	DPWA	$\pi N \rightarrow N\pi, N\eta$
200	LI 93	IPWA	$\gamma N \rightarrow \pi N$
308	CRAWFORD 80	DPWA	$\gamma N \rightarrow \pi N$
120	SAXON 80	DPWA	$\pi^- \rho \rightarrow \Lambda K^0$
447	BAKER 79	DPWA	$\pi^- \rho \rightarrow \eta$
300 to 400	BAKER 78	DPWA	$\pi^- \rho \rightarrow \Lambda K^0$
285	BARBOUR 78	DPWA	$\gamma N \rightarrow \pi N$
200 ± 50	¹ BAKER 77	IPWA	$\pi^- \rho \rightarrow \Lambda K^0$
500	¹ BAKER 77	DPWA	$\pi^- \rho \rightarrow \Lambda K^0$
130	² LONGACRE 77	IPWA	$\pi N \rightarrow N\pi\pi$
327	KNASEL 75	DPWA	$\pi^- \rho \rightarrow \Lambda K^0$
150	³ LONGACRE 75	IPWA	$\pi N \rightarrow N\pi\pi$

N(1720) POLE POSITION

REAL PART			
VALUE (MeV)	DOCUMENT ID	TECN	COMMENT
1650 to 1750 (≈ 1700) OUR ESTIMATE			
1717	ARNDT 95	DPWA	$\pi N \rightarrow N\pi$
1686	⁴ HOEHLER 93	SPED	$\pi N \rightarrow \pi N$
1680 ± 30	CUTKOSKY 80	IPWA	$\pi N \rightarrow \pi N$
• • • We do not use the following data for averages, fits, limits, etc. • • •			
1675	ARNDT 91	DPWA	$\pi N \rightarrow \pi N$ Soln SM90
1716 or 1716	⁵ LONGACRE 78	IPWA	$\pi N \rightarrow N\pi\pi$
1745 or 1748	² LONGACRE 77	IPWA	$\pi N \rightarrow N\pi\pi$
-2×IMAGINARY PART			
VALUE (MeV)	DOCUMENT ID	TECN	COMMENT
110 to 390 (≈ 250) OUR ESTIMATE			
388	ARNDT 95	DPWA	$\pi N \rightarrow N\pi$
187	⁴ HOEHLER 93	SPED	$\pi N \rightarrow \pi N$
120 ± 40	CUTKOSKY 80	IPWA	$\pi N \rightarrow \pi N$
• • • We do not use the following data for averages, fits, limits, etc. • • •			
114	ARNDT 91	DPWA	$\pi N \rightarrow \pi N$ Soln SM90
124 or 126	⁵ LONGACRE 78	IPWA	$\pi N \rightarrow N\pi\pi$
135 or 123	² LONGACRE 77	IPWA	$\pi N \rightarrow N\pi\pi$

N(1720) ELASTIC POLE RESIDUE

MODULUS r 			
VALUE (MeV)	DOCUMENT ID	TECN	COMMENT
39	ARNDT 95	DPWA	$\pi N \rightarrow N\pi$
15	HOEHLER 93	SPED	$\pi N \rightarrow \pi N$
8 ± 2	CUTKOSKY 80	IPWA	$\pi N \rightarrow \pi N$
• • • We do not use the following data for averages, fits, limits, etc. • • •			
11	ARNDT 91	DPWA	$\pi N \rightarrow \pi N$ Soln SM90

PHASE θ

VALUE (°)	DOCUMENT ID	TECN	COMMENT
-70	ARNDT 95	DPWA	$\pi N \rightarrow N\pi$
-160 ± 30	CUTKOSKY 80	IPWA	$\pi N \rightarrow \pi N$
• • • We do not use the following data for averages, fits, limits, etc. • • •			
-130	ARNDT 91	DPWA	$\pi N \rightarrow \pi N$ Soln SM90

N(1720) DECAY MODES

The following branching fractions are our estimates, not fits or averages.

Mode	Fraction (Γ_i/Γ)
Γ_1 $N\pi$	10-20 %
Γ_2 $N\eta$	
Γ_3 ΛK	1-15 %
Γ_4 ΣK	
Γ_5 $N\pi\pi$	>70 %
Γ_6 $\Delta\pi$	
Γ_7 $\Delta(1232)\pi, P\text{-wave}$	
Γ_8 $N\rho$	70-85 %
Γ_9 $N\rho, S=1/2, P\text{-wave}$	
Γ_{10} $N\rho, S=3/2, P\text{-wave}$	
Γ_{11} $N(\pi\pi)_{S\text{-wave}}^{J=0}$	
Γ_{12} $\rho\gamma$	0.003-0.10 %
Γ_{13} $\rho\gamma, \text{helicity}=1/2$	0.003-0.08 %
Γ_{14} $\rho\gamma, \text{helicity}=3/2$	0.001-0.03 %
Γ_{15} $n\gamma$	0.002-0.39 %
Γ_{16} $n\gamma, \text{helicity}=1/2$	0.0-0.002 %
Γ_{17} $n\gamma, \text{helicity}=3/2$	0.001-0.39 %

N(1720) BRANCHING RATIOS

$\Gamma(N\pi)/\Gamma_{\text{total}}$				Γ_1/Γ
VALUE	DOCUMENT ID	TECN	COMMENT	
0.10 to 0.20 OUR ESTIMATE				
0.13 ± 0.05	MANLEY 92	IPWA	$\pi N \rightarrow \pi N \& N\pi\pi$	
0.10 ± 0.04	CUTKOSKY 80	IPWA	$\pi N \rightarrow \pi N$	
0.14 ± 0.03	HOEHLER 79	IPWA	$\pi N \rightarrow \pi N$	
• • • We do not use the following data for averages, fits, limits, etc. • • •				
0.16	ARNDT 95	DPWA	$\pi N \rightarrow N\pi$	
0.18 ± 0.04	BATINIC 95	DPWA	$\pi N \rightarrow N\pi, N\eta$	
$\Gamma(N\eta)/\Gamma_{\text{total}}$				Γ_2/Γ
VALUE	DOCUMENT ID	TECN	COMMENT	
• • • We do not use the following data for averages, fits, limits, etc. • • •				
0.002 ± 0.01	BATINIC 95	DPWA	$\pi N \rightarrow N\pi, N\eta$	
$(\Gamma_1\Gamma_2)^{1/2}/\Gamma_{\text{total}}$ in $N\pi \rightarrow N(1720) \rightarrow N\eta$				$(\Gamma_1\Gamma_2)^{1/2}/\Gamma$
VALUE	DOCUMENT ID	TECN	COMMENT	
• • • We do not use the following data for averages, fits, limits, etc. • • •				
-0.08	BAKER 79	DPWA	$\pi^- \rho \rightarrow \eta$	
$(\Gamma_1\Gamma_3)^{1/2}/\Gamma_{\text{total}}$ in $N\pi \rightarrow N(1720) \rightarrow \Lambda K$				$(\Gamma_1\Gamma_3)^{1/2}/\Gamma$
VALUE	DOCUMENT ID	TECN	COMMENT	
-0.14 to -0.06 OUR ESTIMATE				
-0.09	BELL 83	DPWA	$\pi^- \rho \rightarrow \Lambda K^0$	
-0.11	SAXON 80	DPWA	$\pi^- \rho \rightarrow \Lambda K^0$	
• • • We do not use the following data for averages, fits, limits, etc. • • •				
-0.09	⁶ BAKER 78	DPWA	See SAXON 80	
-0.06 ± 0.02	¹ BAKER 77	IPWA	$\pi^- \rho \rightarrow \Lambda K^0$	
-0.09	¹ BAKER 77	DPWA	$\pi^- \rho \rightarrow \Lambda K^0$	
$(\Gamma_1\Gamma_4)^{1/2}/\Gamma_{\text{total}}$ in $N\pi \rightarrow N(1720) \rightarrow \Sigma K$				$(\Gamma_1\Gamma_4)^{1/2}/\Gamma$
VALUE	DOCUMENT ID	TECN	COMMENT	
• • • We do not use the following data for averages, fits, limits, etc. • • •				
0.051 to 0.087	⁷ DEANS 75	DPWA	$\pi N \rightarrow \Sigma K$	

Note: Signs of couplings from $\pi N \rightarrow N\pi\pi$ analyses were changed in the 1986 edition to agree with the baryon-first convention; the overall phase ambiguity is resolved by choosing a negative sign for the $\Delta(1620) S_{31}$ coupling to $\Delta(1232)\pi$.

$(\Gamma_1\Gamma_7)^{1/2}/\Gamma_{\text{total}}$ in $N\pi \rightarrow N(1720) \rightarrow \Delta(1232)\pi, P\text{-wave}$				$(\Gamma_1\Gamma_7)^{1/2}/\Gamma$
VALUE	DOCUMENT ID	TECN	COMMENT	
±0.27 to ±0.37 OUR ESTIMATE				
-0.17	² LONGACRE 77	IPWA	$\pi N \rightarrow N\pi\pi$	

Baryon Particle Listings

$N(1720)$, $N(1900)$

$(\Gamma_1 \Gamma_f)^{1/2} / \Gamma_{\text{total}}$ in $N\pi \rightarrow N(1720) \rightarrow N\rho, S=1/2, P\text{-wave}$ $(\Gamma_1 \Gamma_g)^{1/2} / \Gamma$

VALUE	DOCUMENT ID	TECN	COMMENT
+0.34 ± 0.05	MANLEY 92	IPWA	$\pi N \rightarrow \pi N$ & $N\pi\pi$
-0.26	2 LONGACRE 77	IPWA	$\pi N \rightarrow N\pi\pi$
+0.40	3 LONGACRE 75	IPWA	$\pi N \rightarrow N\pi\pi$

$(\Gamma_1 \Gamma_f)^{1/2} / \Gamma_{\text{total}}$ in $N\pi \rightarrow N(1720) \rightarrow N\rho, S=3/2, P\text{-wave}$ $(\Gamma_1 \Gamma_{10})^{1/2} / \Gamma$

VALUE	DOCUMENT ID	TECN	COMMENT
+0.15	2 LONGACRE 77	IPWA	$\pi N \rightarrow N\pi\pi$

$(\Gamma_1 \Gamma_f)^{1/2} / \Gamma_{\text{total}}$ in $N\pi \rightarrow N(1720) \rightarrow N(\pi\pi)_{S=0}^{J=0}$ $(\Gamma_1 \Gamma_{11})^{1/2} / \Gamma$

VALUE	DOCUMENT ID	TECN	COMMENT
-0.19	2 LONGACRE 77	IPWA	$\pi N \rightarrow N\pi\pi$

$N(1720)$ PHOTON DECAY AMPLITUDES

$N(1720) \rightarrow p\gamma$, helicity-1/2 amplitude $A_{1/2}$

VALUE (GeV ^{-1/2})	DOCUMENT ID	TECN	COMMENT
+0.018 ± 0.030 OUR ESTIMATE			
-0.015 ± 0.015	ARNDT 96	IPWA	$\gamma N \rightarrow \pi N$
0.044 ± 0.066	CRAWFORD 83	IPWA	$\gamma N \rightarrow \pi N$
-0.004 ± 0.007	AWAJI 81	DPWA	$\gamma N \rightarrow \pi N$
0.051 ± 0.009	ARAI 80	DPWA	$\gamma N \rightarrow \pi N$ (fit 1)
0.071 ± 0.010	ARAI 80	DPWA	$\gamma N \rightarrow \pi N$ (fit 2)
0.038 ± 0.050	CRAWFORD 80	DPWA	$\gamma N \rightarrow \pi N$
• • • We do not use the following data for averages, fits, limits, etc. • • •			
0.012 ± 0.003	LI 93	IPWA	$\gamma N \rightarrow \pi N$
+0.111 ± 0.047	BARBOUR 78	DPWA	$\gamma N \rightarrow \pi N$

$N(1720) \rightarrow p\gamma$, helicity-3/2 amplitude $A_{3/2}$

VALUE (GeV ^{-1/2})	DOCUMENT ID	TECN	COMMENT
-0.019 ± 0.020 OUR ESTIMATE			
0.007 ± 0.010	ARNDT 96	IPWA	$\gamma N \rightarrow \pi N$
-0.024 ± 0.006	CRAWFORD 83	IPWA	$\gamma N \rightarrow \pi N$
-0.040 ± 0.016	AWAJI 81	DPWA	$\gamma N \rightarrow \pi N$
-0.058 ± 0.010	ARAI 80	DPWA	$\gamma N \rightarrow \pi N$ (fit 1)
-0.011 ± 0.011	ARAI 80	DPWA	$\gamma N \rightarrow \pi N$ (fit 2)
-0.014 ± 0.040	CRAWFORD 80	DPWA	$\gamma N \rightarrow \pi N$
• • • We do not use the following data for averages, fits, limits, etc. • • •			
-0.022 ± 0.003	LI 93	IPWA	$\gamma N \rightarrow \pi N$
-0.063 ± 0.032	BARBOUR 78	DPWA	$\gamma N \rightarrow \pi N$

$N(1720) \rightarrow n\gamma$, helicity-1/2 amplitude $A_{1/2}$

VALUE (GeV ^{-1/2})	DOCUMENT ID	TECN	COMMENT
+0.001 ± 0.015 OUR ESTIMATE			
0.007 ± 0.015	ARNDT 96	IPWA	$\gamma N \rightarrow \pi N$
0.002 ± 0.005	AWAJI 81	DPWA	$\gamma N \rightarrow \pi N$
-0.019 ± 0.033	ARAI 80	DPWA	$\gamma N \rightarrow \pi N$ (fit 1)
0.001 ± 0.038	ARAI 80	DPWA	$\gamma N \rightarrow \pi N$ (fit 2)
-0.003 ± 0.034	CRAWFORD 80	DPWA	$\gamma N \rightarrow \pi N$
• • • We do not use the following data for averages, fits, limits, etc. • • •			
0.050 ± 0.004	LI 93	IPWA	$\gamma N \rightarrow \pi N$
+0.007 ± 0.020	BARBOUR 78	DPWA	$\gamma N \rightarrow \pi N$

$N(1720) \rightarrow n\gamma$, helicity-3/2 amplitude $A_{3/2}$

VALUE (GeV ^{-1/2})	DOCUMENT ID	TECN	COMMENT
-0.029 ± 0.061 OUR ESTIMATE			
-0.005 ± 0.025	ARNDT 96	IPWA	$\gamma N \rightarrow \pi N$
-0.015 ± 0.019	AWAJI 81	DPWA	$\gamma N \rightarrow \pi N$
-0.139 ± 0.039	ARAI 80	DPWA	$\gamma N \rightarrow \pi N$ (fit 1)
-0.134 ± 0.044	ARAI 80	DPWA	$\gamma N \rightarrow \pi N$ (fit 2)
0.018 ± 0.028	CRAWFORD 80	DPWA	$\gamma N \rightarrow \pi N$
• • • We do not use the following data for averages, fits, limits, etc. • • •			
-0.017 ± 0.004	LI 93	IPWA	$\gamma N \rightarrow \pi N$
+0.051 ± 0.051	BARBOUR 78	DPWA	$\gamma N \rightarrow \pi N$

$N(1720) \gamma\rho \rightarrow \Lambda K^+$ AMPLITUDES

$(\Gamma_1 \Gamma_f)^{1/2} / \Gamma_{\text{total}}$ in $p\gamma \rightarrow N(1720) \rightarrow \Lambda K^+$ $(E_{1+}$ amplitude)

VALUE (units 10 ⁻³)	DOCUMENT ID	TECN	COMMENT
• • • We do not use the following data for averages, fits, limits, etc. • • •			
10.2 ± 0.2	WORKMAN 90	DPWA	
9.52	TANABE 89	DPWA	

$p\gamma \rightarrow N(1720) \rightarrow \Lambda K^+$ phase angle θ $(E_{1+}$ amplitude)

VALUE (degrees)	DOCUMENT ID	TECN	COMMENT
• • • We do not use the following data for averages, fits, limits, etc. • • •			
-124 ± 2	WORKMAN 90	DPWA	
-103.4	TANABE 89	DPWA	

$(\Gamma_1 \Gamma_f)^{1/2} / \Gamma_{\text{total}}$ in $p\gamma \rightarrow N(1720) \rightarrow \Lambda K^+$ $(M_{1+}$ amplitude)

VALUE (units 10 ⁻³)	DOCUMENT ID	TECN	COMMENT
• • • We do not use the following data for averages, fits, limits, etc. • • •			
-4.5 ± 0.2	WORKMAN 90	DPWA	
3.18	TANABE 89	DPWA	

$N(1720)$ FOOTNOTES

- The two BAKER 77 entries are from an IPWA using the Barrelet-zero method and from a conventional energy-dependent analysis.
- LONGACRE 77 pole positions are from a search for poles in the unitarized T-matrix; the first (second) value uses, in addition to $\pi N \rightarrow N\pi\pi$ data, elastic amplitudes from a Saclay (CERN) partial-wave analysis. The other LONGACRE 77 values are from eyeball fits with Breit-Wigner circles to the T-matrix amplitudes.
- From method II of LONGACRE 75: eyeball fits with Breit-Wigner circles to the T-matrix amplitudes.
- See HOEHLER 93 for a detailed discussion of the evidence for and the pole parameters of N and Δ resonances as determined from Argand diagrams of πN elastic partial-wave amplitudes and from plots of the speeds with which the amplitudes traverse the diagrams.
- LONGACRE 78 values are from a search for poles in the unitarized T-matrix. The first (second) value uses, in addition to $\pi N \rightarrow N\pi\pi$ data, elastic amplitudes from a Saclay (CERN) partial-wave analysis.
- The overall phase of BAKER 78 couplings has been changed to agree with previous conventions.
- The range given is from the four best solutions. DEANS 75 disagrees with $\pi^+ p \rightarrow \Sigma^+ K^+$ data of WINNIK 77 around 1920 MeV.

$N(1720)$ REFERENCES

For early references, see Physics Letters **111B** 70 (1982).

ARNDT 96	PR C53 430	R.A. Arndt, I.I. Strakovsky, R.L. Workman	(VPI)
ARNDT 95	PR C52 2120	R.A. Arndt et al.	(VPI, BRCC)
BATINIC 95	PR C51 2310	M. Batinic et al.	(BOSK, UCLA)
Also	PR C57 1004 (erratum)	M. Batinic et al.	
HOEHLER 93	πN Newsletter 9 1	G. Hoehler	(KARL)
LI 93	PR C47 2759	Z.J. Li et al.	(VPI)
MANLEY 92	PR D45 4002	D.M. Manley, E.M. Saleski	(KENT) IJP
Also	PR D30 904	D.M. Manley et al.	(VPI)
ARNDT 91	PR D43 2131	R.A. Arndt et al.	(VPI, TELE) IJP
WORKMAN 90	PR C42 781	R.L. Workman	(VPI)
TANABE 89	PR C39 741	H. Tanabe, M. Kohno, C. Bennhold	(MANZ)
Also	NC 102A 193	M. Kohno, H. Tanabe, C. Bennhold	(MANZ)
BELL 83	NP B222 389	K.W. Bell et al.	(RL) IJP
CRAWFORD 83	NP B211 1	R.L. Crawford, W.T. Morton	(GLAS)
PDG 82	PL 111B	M. Roos et al.	(HELS, CIT, CERN)
AWAJI 81	Bonn Conf. 352	N. Awaji, R. Kajikawa	(NAGO)
Also	NP B197 365	K. Fujii et al.	(NAGO)
ARAI 80	Toronto Conf. 93	I. Arai	(INUS)
Also	NP B194 251	I. Arai, H. Fujii	(INUS)
CRAWFORD 80	Toronto Conf. 107	R.L. Crawford	(GLAS)
CUTKOSKY 80	Toronto Conf. 19	R.E. Cutkosky et al.	(CMU, LBL) IJP
Also	PR D20 2859	R.E. Cutkosky et al.	(CMU, LBL) IJP
SAXON 80	NP B162 522	D.H. Saxon et al.	(RHEL, BRIS) IJP
BAKER 79	NP B156 93	R.D. Baker et al.	(RHEL) IJP
HOEHLER 79	PDAT 12-1	G. Hoehler et al.	(KARL) IJP
Also	Toronto Conf. 3	R. Koch	(KARLT) IJP
BAKER 78	NP B141 29	R.D. Baker et al.	(RL, CAVE) IJP
BARBOUR 78	NP B141 253	I.M. Barbour, R.L. Crawford, N.H. Parsons	(GLAS)
LONGACRE 78	PR D17 1795	R.S. Longacre et al.	(LBL, SLAC)
BAKER 77	NP B126 365	R.D. Baker et al.	(RHEL) IJP
LONGACRE 77	NP B122 493	R.S. Longacre, J. Dolbeau	(SACL) IJP
Also	NP B108 365	J. Dolbeau et al.	(SACL) IJP
WINNIK 77	NP B128 66	M. Winnik et al.	(HAIF) I
DEANS 75	NP B96 90	S.R. Deans et al.	(SFLA, ALAH) IJP
KNASEL 75	PR D11 1	T.M. Knasel et al.	(CHIC, WUSL, OSU+) IJP
LONGACRE 75	PL 55B 415	R.S. Longacre et al.	(LBL, SLAC) IJP

$N(1900) P_{13}$

$$J(P) = \frac{1}{2}(\frac{3}{2}^+)$$
 Status: **

OMITTED FROM SUMMARY TABLE

$N(1900)$ BREIT-WIGNER MASS

VALUE (MeV)	DOCUMENT ID	TECN	COMMENT
≈ 1900 OUR ESTIMATE			
1879 ± 17	MANLEY 92	IPWA	$\pi N \rightarrow \pi N$ & $N\pi\pi$

$N(1900)$ BREIT-WIGNER WIDTH

VALUE (MeV)	DOCUMENT ID	TECN	COMMENT
498 ± 78	MANLEY 92	IPWA	$\pi N \rightarrow \pi N$ & $N\pi\pi$

$N(1900)$ DECAY MODES

Mode	TECN	COMMENT
Γ_1	$N\pi$	
Γ_2	$N\pi\pi$	
Γ_3	$N\rho, S = 1/2, P\text{-wave}$	

See key on page 239

Baryon Particle Listings
N(1900), N(1990)

N(1900) BRANCHING RATIOS

$\Gamma(N\pi)/\Gamma_{\text{total}}$	DOCUMENT ID	TECN	COMMENT	Γ_1/Γ
0.26 ± 0.06	MANLEY	92	IPWA $\pi N \rightarrow \pi N \& N\pi\pi$	
$(\Gamma_1\Gamma_2)^{1/2}/\Gamma_{\text{total}}$ in $N\pi \rightarrow N(1900) \rightarrow N\rho, S=1/2, P\text{-wave}$				$(\Gamma_1\Gamma_3)^{1/2}/\Gamma$
-0.34 ± 0.03	MANLEY	92	IPWA $\pi N \rightarrow \pi N \& N\pi\pi$	

N(1900) REFERENCES

MANLEY	92	PR D45 4002	D.M. Manley, E.M. Saleski	(KENT)
Also	84	PR D30 904	D.M. Manley et al.	(VPI)

N(1990) F₁₇

$$I(J^P) = \frac{1}{2}(7^+) \text{ Status: } **$$

OMITTED FROM SUMMARY TABLE

Most of the results published before 1975 are now obsolete and have been omitted. They may be found in our 1982 edition, Physics Letters **111B** (1982).

The various analyses do not agree very well with one another.

N(1990) BREIT-WIGNER MASS

VALUE (MeV)	DOCUMENT ID	TECN	COMMENT
≈ 1990 OUR ESTIMATE			
2086 ± 28	MANLEY	92	IPWA $\pi N \rightarrow \pi N \& N\pi\pi$
2018	CRAWFORD	80	DPWA $\gamma N \rightarrow \pi N$
1970 ± 50	CUTKOSKY	80	IPWA $\pi N \rightarrow \pi N$
2005 ± 150	HOEHLER	79	IPWA $\pi N \rightarrow \pi N$
1999	BARBOUR	78	DPWA $\gamma N \rightarrow \pi N$

N(1990) BREIT-WIGNER WIDTH

VALUE (MeV)	DOCUMENT ID	TECN	COMMENT
535 ± 120	MANLEY	92	IPWA $\pi N \rightarrow \pi N \& N\pi\pi$
295	CRAWFORD	80	DPWA $\gamma N \rightarrow \pi N$
350 ± 120	CUTKOSKY	80	IPWA $\pi N \rightarrow \pi N$
350 ± 100	HOEHLER	79	IPWA $\pi N \rightarrow \pi N$
216	BARBOUR	78	DPWA $\gamma N \rightarrow \pi N$

N(1990) POLE POSITION

REAL PART

VALUE (MeV)	DOCUMENT ID	TECN	COMMENT
1900 ± 30	CUTKOSKY	80	IPWA $\pi N \rightarrow \pi N$
• • • We do not use the following data for averages, fits, limits, etc. • • •			
not seen	ARNDT	91	DPWA $\pi N \rightarrow \pi N$ Soln SM90

-2×IMAGINARY PART

VALUE (MeV)	DOCUMENT ID	TECN	COMMENT
260 ± 60	CUTKOSKY	80	IPWA $\pi N \rightarrow \pi N$
• • • We do not use the following data for averages, fits, limits, etc. • • •			
not seen	ARNDT	91	DPWA $\pi N \rightarrow \pi N$ Soln SM90

N(1990) ELASTIC POLE RESIDUE

MODULUS |r|

VALUE (MeV)	DOCUMENT ID	TECN	COMMENT
9 ± 3	CUTKOSKY	80	IPWA $\pi N \rightarrow \pi N$

PHASE θ

VALUE (°)	DOCUMENT ID	TECN	COMMENT
-60 ± 30	CUTKOSKY	80	IPWA $\pi N \rightarrow \pi N$

N(1990) DECAY MODES

Mode	Γ_1	Γ_2	Γ_3	Γ_4	Γ_5	Γ_6	Γ_7	Γ_8	Γ_9
$N\pi$									
$N\eta$									
ΛK									
ΣK									
$N\pi\pi$									
$p\gamma, \text{ helicity}=1/2$									
$p\gamma, \text{ helicity}=3/2$									
$n\gamma, \text{ helicity}=1/2$									
$n\gamma, \text{ helicity}=3/2$									

N(1990) BRANCHING RATIOS

$\Gamma(N\pi)/\Gamma_{\text{total}}$	DOCUMENT ID	TECN	COMMENT	Γ_1/Γ
0.06 ± 0.02	MANLEY	92	IPWA $\pi N \rightarrow \pi N \& N\pi\pi$	
0.06 ± 0.02	CUTKOSKY	80	IPWA $\pi N \rightarrow \pi N$	
0.04 ± 0.02	HOEHLER	79	IPWA $\pi N \rightarrow \pi N$	
$(\Gamma_1\Gamma_2)^{1/2}/\Gamma_{\text{total}}$ in $N\pi \rightarrow N(1990) \rightarrow N\eta$				$(\Gamma_1\Gamma_2)^{1/2}/\Gamma$
-0.043	BAKER	79	DPWA $\pi^- p \rightarrow n\eta$	

$(\Gamma_1\Gamma_2)^{1/2}/\Gamma_{\text{total}}$ in $N\pi \rightarrow N(1990) \rightarrow \Lambda K$	DOCUMENT ID	TECN	COMMENT	$(\Gamma_1\Gamma_3)^{1/2}/\Gamma$
+0.01	BELL	83	DPWA $\pi^- p \rightarrow \Lambda K^0$	
not seen	SAXON	80	DPWA $\pi^- p \rightarrow \Lambda K^0$	
-0.021 ± 0.033	DEVENISH	74B	Fixed-t dispersion rel.	

$(\Gamma_1\Gamma_2)^{1/2}/\Gamma_{\text{total}}$ in $N\pi \rightarrow N(1990) \rightarrow \Sigma K$	DOCUMENT ID	TECN	COMMENT	$(\Gamma_1\Gamma_4)^{1/2}/\Gamma$
0.010 to 0.023	DEANS	75	DPWA $\pi N \rightarrow \Sigma K$	
0.06	LANGBEIN	73	IPWA $\pi N \rightarrow \Sigma K$ (sol. 1)	

$(\Gamma_1\Gamma_2)^{1/2}/\Gamma_{\text{total}}$ in $N\pi \rightarrow N(1990) \rightarrow N\pi\pi$	DOCUMENT ID	TECN	COMMENT	$(\Gamma_1\Gamma_5)^{1/2}/\Gamma$
not seen	LONGACRE	75	IPWA $\pi N \rightarrow N\pi\pi$	

N(1990) PHOTON DECAY AMPLITUDES

N(1990) → pγ, helicity-1/2 amplitude A_{1/2}

VALUE (GeV ^{-1/2})	DOCUMENT ID	TECN	COMMENT
0.030 ± 0.029	AWAJI	81	DPWA $\gamma N \rightarrow \pi N$
0.001 ± 0.040	CRAWFORD	80	DPWA $\gamma N \rightarrow \pi N$
• • • We do not use the following data for averages, fits, limits, etc. • • •			
0.040	BARBOUR	78	DPWA $\gamma N \rightarrow \pi N$

N(1990) → pγ, helicity-3/2 amplitude A_{3/2}

VALUE (GeV ^{-1/2})	DOCUMENT ID	TECN	COMMENT
0.086 ± 0.060	AWAJI	81	DPWA $\gamma N \rightarrow \pi N$
0.004 ± 0.025	CRAWFORD	80	DPWA $\gamma N \rightarrow \pi N$
• • • We do not use the following data for averages, fits, limits, etc. • • •			
+0.004	BARBOUR	78	DPWA $\gamma N \rightarrow \pi N$

N(1990) → nγ, helicity-1/2 amplitude A_{1/2}

VALUE (GeV ^{-1/2})	DOCUMENT ID	TECN	COMMENT
-0.001	AWAJI	81	DPWA $\gamma N \rightarrow \pi N$
-0.078 ± 0.030	CRAWFORD	80	DPWA $\gamma N \rightarrow \pi N$
• • • We do not use the following data for averages, fits, limits, etc. • • •			
-0.069	BARBOUR	78	DPWA $\gamma N \rightarrow \pi N$

N(1990) → nγ, helicity-3/2 amplitude A_{3/2}

VALUE (GeV ^{-1/2})	DOCUMENT ID	TECN	COMMENT
-0.178	AWAJI	81	DPWA $\gamma N \rightarrow \pi N$
-0.116 ± 0.045	CRAWFORD	80	DPWA $\gamma N \rightarrow \pi N$
• • • We do not use the following data for averages, fits, limits, etc. • • •			
-0.072	BARBOUR	78	DPWA $\gamma N \rightarrow \pi N$

N(1990) FOOTNOTES

¹ The range given for DEANS 75 is from the four best solutions.

N(1990) REFERENCES

For early references, see Physics Letters **111B** 70 (1982).

MANLEY	92	PR D45 4002	D.M. Manley, E.M. Saleski	(KENT) IJP
Also	84	PR D30 904	D.M. Manley et al.	(VPI)
ARNDT	91	PR D43 2131	R.A. Arndt et al.	(VPI, TELE) IJP
BELL	83	NP B222 389	K.W. Bell et al.	(RL) IJP
PDG	82	PL 111B	M. Roos et al.	(HELS, CIT, CERN)
AWAJI	81	Bonn Conf. 352	N. Awaji, R. Kajikawa	(NAGO)
Also	82	NP B197 365	K. Fujii et al.	(NAGO)
CRAWFORD	80	Toronto Conf. 107	R.L. Crawford	(GLAS)
CUTKOSKY	80	Toronto Conf. 19	R.E. Cutkosky et al.	(CMU, LBL) IJP
Also	79	PR D20 2839	R.E. Cutkosky et al.	(CMU, LBL) IJP
SAXON	80	NP B162 522	D.H. Saxon et al.	(RIHEL, BRIS) IJP
BAKER	79	NP B156 93	R.D. Baker et al.	(RIHEL) IJP
HOEHLER	79	PDAT 12-1	G. Hoehler et al.	(KARLT) IJP
Also	80	Toronto Conf. 3	R. Koch	(KARLT) IJP
BARBOUR	78	NP B141 253	I.M. Barbour, R.L. Crawford, N.H. Parsons	(GLAS)
OEANS	75	NP B96 90	S.R. Deans et al.	(SFLA, ALAH) IJP
LONGACRE	75	PL 55B 415	R.S. Longacre et al.	(LBL, SLAC) IJP
DEVENISH	74B	NP B81 330	R.C.E. Devenish, C.D. Froggatt, B.R. Martin	(DESY+) IJP
LANGBEIN	73	NP B53 251	W. Langbein, F. Wagner	(MUNI) IJP

Baryon Particle Listings

 $N(2000)$, $N(2080)$ $N(2000) F_{15}$

$$I(J^P) = \frac{1}{2}(\frac{5}{2}^+) \text{ Status: } **$$

OMITTED FROM SUMMARY TABLE

Older results have been retained simply because there is little information at all about this possible state.

 $N(2000)$ BREIT-WIGNER MASS

VALUE (MeV)	DOCUMENT ID	TECN	COMMENT
≈ 2000 OUR ESTIMATE			
1903±87	MANLEY 92	IPWA	$\pi N \rightarrow \pi N \& N\pi\pi$
1882±10	HOEHLER 79	IPWA	$\pi N \rightarrow \pi N$
2025	AYED 76	IPWA	$\pi N \rightarrow \pi N$
1970	¹ LANGBEIN 73	IPWA	$\pi N \rightarrow \Sigma K$ (sol. 2)
2175	ALMEHED 72	IPWA	$\pi N \rightarrow \pi N$
1930	DEANS 72	MPWA	$\gamma p \rightarrow \Lambda K$ (sol. D)
• • • We do not use the following data for averages, fits, limits, etc. • • •			
1814	ARNDT 95	DPWA	$\pi N \rightarrow N\pi$

 $N(2000)$ BREIT-WIGNER WIDTH

VALUE (MeV)	DOCUMENT ID	TECN	COMMENT
490±310	MANLEY 92	IPWA	$\pi N \rightarrow \pi N \& N\pi\pi$
95±20	HOEHLER 79	IPWA	$\pi N \rightarrow \pi N$
157	AYED 76	IPWA	$\pi N \rightarrow \pi N$
170	¹ LANGBEIN 73	IPWA	$\pi N \rightarrow \Sigma K$ (sol. 2)
150	ALMEHED 72	IPWA	$\pi N \rightarrow \pi N$
112	DEANS 72	MPWA	$\gamma p \rightarrow \Lambda K$ (sol. D)
• • • We do not use the following data for averages, fits, limits, etc. • • •			
176	ARNDT 95	DPWA	$\pi N \rightarrow N\pi$

 $N(2000)$ DECAY MODES

Mode	
Γ_1	$N\pi$
Γ_2	$N\eta$
Γ_3	ΛK
Γ_4	ΣK
Γ_5	$N\pi\pi$
Γ_6	$\Delta(1232)\pi$, P-wave
Γ_7	$N\rho$, $S=3/2$, P-wave
Γ_8	$N\rho$, $S=3/2$, F-wave
Γ_9	$\rho\gamma$

 $N(2000)$ BRANCHING RATIOS

$\Gamma(N\pi)/\Gamma_{\text{total}}$	DOCUMENT ID	TECN	COMMENT	Γ_1/Γ
0.08±0.05	MANLEY 92	IPWA	$\pi N \rightarrow \pi N \& N\pi\pi$	
0.04±0.02	HOEHLER 79	IPWA	$\pi N \rightarrow \pi N$	
0.08	AYED 76	IPWA	$\pi N \rightarrow \pi N$	
0.25	ALMEHED 72	IPWA	$\pi N \rightarrow \pi N$	
• • • We do not use the following data for averages, fits, limits, etc. • • •				
0.10	ARNDT 95	DPWA	$\pi N \rightarrow N\pi$	

$(\Gamma_1\Gamma_2)^{1/2}/\Gamma_{\text{total}}$ in $N\pi \rightarrow N(2000) \rightarrow N\eta$	DOCUMENT ID	TECN	COMMENT	$(\Gamma_1\Gamma_2)^{1/2}/\Gamma$
+0.03	BAKER 79	DPWA	$\pi^- p \rightarrow n\eta$	

$(\Gamma_1\Gamma_3)^{1/2}/\Gamma_{\text{total}}$ in $N\pi \rightarrow N(2000) \rightarrow \Lambda K$	DOCUMENT ID	TECN	COMMENT	$(\Gamma_1\Gamma_3)^{1/2}/\Gamma$
not seen	SAXON 80	DPWA	$\pi^- p \rightarrow \Lambda K^0$	

$(\Gamma_1\Gamma_4)^{1/2}/\Gamma_{\text{total}}$ in $N\pi \rightarrow N(2000) \rightarrow \Sigma K$	DOCUMENT ID	TECN	COMMENT	$(\Gamma_1\Gamma_4)^{1/2}/\Gamma$
0.022	² DEANS 75	DPWA	$\pi N \rightarrow \Sigma K$	
0.05	¹ LANGBEIN 73	IPWA	$\pi N \rightarrow \Sigma K$ (sol. 2)	

$(\Gamma_1\Gamma_6)^{1/2}/\Gamma_{\text{total}}$ in $N\pi \rightarrow N(2000) \rightarrow \Delta(1232)\pi$, P-wave	DOCUMENT ID	TECN	COMMENT	$(\Gamma_1\Gamma_6)^{1/2}/\Gamma$
+0.10±0.06	MANLEY 92	IPWA	$\pi N \rightarrow \pi N \& N\pi\pi$	

$(\Gamma_1\Gamma_7)^{1/2}/\Gamma_{\text{total}}$ in $N\pi \rightarrow N(2000) \rightarrow N\rho$, $S=3/2$, P-wave	DOCUMENT ID	TECN	COMMENT	$(\Gamma_1\Gamma_7)^{1/2}/\Gamma$
-0.22±0.08	MANLEY 92	IPWA	$\pi N \rightarrow \pi N \& N\pi\pi$	

$(\Gamma_1\Gamma_8)^{1/2}/\Gamma_{\text{total}}$ in $N\pi \rightarrow N(2000) \rightarrow N\rho$, $S=3/2$, F-wave	DOCUMENT ID	TECN	COMMENT	$(\Gamma_1\Gamma_8)^{1/2}/\Gamma$
+0.11±0.06	MANLEY 92	IPWA	$\pi N \rightarrow \pi N \& N\pi\pi$	

$(\Gamma_1\Gamma_9)^{1/2}/\Gamma_{\text{total}}$ in $p\gamma \rightarrow N(2000) \rightarrow \Lambda K$	DOCUMENT ID	TECN	COMMENT	$(\Gamma_9\Gamma_3)^{1/2}/\Gamma$
0.0022	DEANS 72	MPWA	$\gamma p \rightarrow \Lambda K$ (sol. D)	

 $N(2000)$ FOOTNOTES¹ Not seen in solution 1 of LANGBEIN 73.² Value given is from solution 1 of DEANS 75; not present in solutions 2, 3, or 4. $N(2000)$ REFERENCES

ARNDT 95	PR C52 2120	R.A. Arndt et al.	(VPI, BRCC)
MANLEY 92	PR D45 4002	D.M. Manley, E.M. Saleski	(KENT) IJP
Also	84 PR D30 904	D.M. Manley et al.	(VPI)
SAXON 80	NP B162 522	D.H. Saxon et al.	(RHEL, BRIS) IJP
BAKER 79	NP B156 93	R.D. Baker et al.	(RHEL) IJP
HOEHLER 79	PDAT 12-1	G. Hoehler et al.	(KARLT) IJP
Also	80 Toronto Conf. 3	R. Koch	(KARLT) IJP
AYED 76	Thesis CEA-N-1921	R. Ayed	(SACL) IJP
DEANS 75	NP B96 90	S.R. Deans et al.	(SFLA, ALAH) IJP
LANGBEIN 73	NP B53 251	W. Langbein, F. Wagner	(MUNI) IJP
ALMEHED 72	NP B40 157	S. Almehed, C. Lovelace	(LUND, RUTG) IJP
DEANS 72	PR D6 1906	S.R. Deans et al.	(SFLA) IJP

 $N(2080) D_{13}$

$$I(J^P) = \frac{1}{2}(\frac{3}{2}^-) \text{ Status: } **$$

OMITTED FROM SUMMARY TABLE

There is some evidence for two resonances in this wave between 1800 and 2200 MeV (see CUTKOSKY 80). However, the solution of HOEHLER 79 is quite different.

Most of the results published before 1975 are now obsolete and have been omitted. They may be found in our 1982 edition, Physics Letters **111B** (1982). $N(2080)$ BREIT-WIGNER MASS

VALUE (MeV)	DOCUMENT ID	TECN	COMMENT
≈ 2080 OUR ESTIMATE			
1804±55	MANLEY 92	IPWA	$\pi N \rightarrow \pi N \& N\pi\pi$
1920	BELL 83	DPWA	$\pi^- p \rightarrow \Lambda K^0$
1880±100	¹ CUTKOSKY 80	IPWA	$\pi N \rightarrow \pi N$
2060±80	¹ CUTKOSKY 80	IPWA	$\pi N \rightarrow \pi N$
1900	SAXON 80	DPWA	$\pi^- p \rightarrow \Lambda K^0$
2081±20	HOEHLER 79	IPWA	$\pi N \rightarrow \pi N$
• • • We do not use the following data for averages, fits, limits, etc. • • •			
1986±75	BATINIC 95	DPWA	$\pi N \rightarrow N\pi, N\eta$
1880	BAKER 79	DPWA	$\pi^- p \rightarrow n\eta$

 $N(2080)$ BREIT-WIGNER WIDTH

VALUE (MeV)	DOCUMENT ID	TECN	COMMENT
450±185	MANLEY 92	IPWA	$\pi N \rightarrow \pi N \& N\pi\pi$
320	BELL 83	DPWA	$\pi^- p \rightarrow \Lambda K^0$
180±60	¹ CUTKOSKY 80	IPWA	$\pi N \rightarrow \pi N$ (lower m)
300±100	¹ CUTKOSKY 80	IPWA	$\pi N \rightarrow \pi N$ (higher m)
240	SAXON 80	DPWA	$\pi^- p \rightarrow \Lambda K^0$
265±40	HOEHLER 79	IPWA	$\pi N \rightarrow \pi N$
• • • We do not use the following data for averages, fits, limits, etc. • • •			
1050±225	BATINIC 95	DPWA	$\pi N \rightarrow N\pi, N\eta$
87	BAKER 79	DPWA	$\pi^- p \rightarrow n\eta$

 $N(2080)$ POLE POSITION

REAL PART	DOCUMENT ID	TECN	COMMENT
1880±100	¹ CUTKOSKY 80	IPWA	$\pi N \rightarrow \pi N$ (lower m)
2050±70	¹ CUTKOSKY 80	IPWA	$\pi N \rightarrow \pi N$ (higher m)
• • • We do not use the following data for averages, fits, limits, etc. • • •			
not seen	ARNDT 91	DPWA	$\pi N \rightarrow \pi N$ Soln SM90

-2×IMAGINARY PART

VALUE (MeV)	DOCUMENT ID	TECN	COMMENT
160±80	¹ CUTKOSKY 80	IPWA	$\pi N \rightarrow \pi N$ (lower m)
200±80	¹ CUTKOSKY 80	IPWA	$\pi N \rightarrow \pi N$ (higher m)
• • • We do not use the following data for averages, fits, limits, etc. • • •			
not seen	ARNDT 91	DPWA	$\pi N \rightarrow \pi N$ Soln SM90

 $N(2080)$ ELASTIC POLE RESIDUE

MODULUS r	DOCUMENT ID	TECN	COMMENT
10±5	¹ CUTKOSKY 80	IPWA	$\pi N \rightarrow \pi N$ (lower m)
30±20	¹ CUTKOSKY 80	IPWA	$\pi N \rightarrow \pi N$ (higher m)

See key on page 239

Baryon Particle Listings
N(2080), N(2090)

PHASE θ
VALUE (°)

VALUE (°)	DOCUMENT ID	TECN	COMMENT
100 ± 80	1 CUTKOSKY 80	IPWA	$\pi N \rightarrow \pi N$ (lower m)
0 ± 100	1 CUTKOSKY 80	IPWA	$\pi N \rightarrow \pi N$ (higher m)

N(2080) DECAY MODES

Mode

Γ_1	$N\pi$
Γ_2	$N\eta$
Γ_3	ΛK
Γ_4	ΣK
Γ_5	$N\pi\pi$
Γ_6	$\Delta(1232)\pi$, S-wave
Γ_7	$\Delta(1232)\pi$, D-wave
Γ_8	$N\rho$, $S=3/2$, S-wave
Γ_9	$N(\pi\pi)_{S=0}^0$ -wave
Γ_{10}	$\rho\gamma$, helicity=1/2
Γ_{11}	$\rho\gamma$, helicity=3/2
Γ_{12}	$n\gamma$, helicity=1/2
Γ_{13}	$n\gamma$, helicity=3/2
Γ_{14}	$\rho\gamma$

N(2080) BRANCHING RATIOS

$\Gamma(N\pi)/\Gamma_{total}$

VALUE	DOCUMENT ID	TECN	COMMENT	Γ_1/Γ
0.23 ± 0.03	MANLEY 92	IPWA	$\pi N \rightarrow \pi N$ & $N\pi\pi$	
0.10 ± 0.04	1 CUTKOSKY 80	IPWA	$\pi N \rightarrow \pi N$ (lower m)	
0.14 ± 0.07	1 CUTKOSKY 80	IPWA	$\pi N \rightarrow \pi N$ (higher m)	
0.06 ± 0.02	HOEHLER 79	IPWA	$\pi N \rightarrow \pi N$	
• • • We do not use the following data for averages, fits, limits, etc. • • •				
0.09 ± 0.02	BATINIC 95	DPWA	$\pi N \rightarrow N\pi, N\eta$	

$\Gamma(N\eta)/\Gamma_{total}$

VALUE	DOCUMENT ID	TECN	COMMENT	Γ_2/Γ
• • • We do not use the following data for averages, fits, limits, etc. • • •				
0.07 ± 0.04	BATINIC 95	DPWA	$\pi N \rightarrow N\pi, N\eta$	

$(\Gamma_1\Gamma_7)^{1/2}/\Gamma_{total}$ in $N\pi \rightarrow N(2080) \rightarrow N\eta$

VALUE	DOCUMENT ID	TECN	COMMENT	$(\Gamma_1\Gamma_2)^{1/2}/\Gamma$
0.065	BAKER 79	DPWA	$\pi^- \rho \rightarrow n\eta$	

$(\Gamma_1\Gamma_7)^{1/2}/\Gamma_{total}$ in $N\pi \rightarrow N(2080) \rightarrow \Lambda K$

VALUE	DOCUMENT ID	TECN	COMMENT	$(\Gamma_1\Gamma_3)^{1/2}/\Gamma$
+0.04	BELL 83	DPWA	$\pi^- \rho \rightarrow \Lambda K^0$	
+0.03	SAXON 80	DPWA	$\pi^- \rho \rightarrow \Lambda K^0$	

$(\Gamma_1\Gamma_7)^{1/2}/\Gamma_{total}$ in $N\pi \rightarrow N(2080) \rightarrow \Sigma K$

VALUE	DOCUMENT ID	TECN	COMMENT	$(\Gamma_1\Gamma_4)^{1/2}/\Gamma$
0.014 to 0.037	2 DEANS 75	DPWA	$\pi N \rightarrow \Sigma K$	

$(\Gamma_1\Gamma_7)^{1/2}/\Gamma_{total}$ in $N\pi \rightarrow N(2080) \rightarrow \Delta(1232)\pi$, S-wave

VALUE	DOCUMENT ID	TECN	COMMENT	$(\Gamma_1\Gamma_6)^{1/2}/\Gamma$
-0.09 ± 0.09	MANLEY 92	IPWA	$\pi N \rightarrow \pi N$ & $N\pi\pi$	

$(\Gamma_1\Gamma_7)^{1/2}/\Gamma_{total}$ in $N\pi \rightarrow N(2080) \rightarrow \Delta(1232)\pi$, D-wave

VALUE	DOCUMENT ID	TECN	COMMENT	$(\Gamma_1\Gamma_7)^{1/2}/\Gamma$
+0.22 ± 0.07	MANLEY 92	IPWA	$\pi N \rightarrow \pi N$ & $N\pi\pi$	

$(\Gamma_1\Gamma_7)^{1/2}/\Gamma_{total}$ in $N\pi \rightarrow N(2080) \rightarrow N\rho$, $S=3/2$, S-wave

VALUE	DOCUMENT ID	TECN	COMMENT	$(\Gamma_1\Gamma_8)^{1/2}/\Gamma$
-0.24 ± 0.06	MANLEY 92	IPWA	$\pi N \rightarrow \pi N$ & $N\pi\pi$	

$(\Gamma_1\Gamma_7)^{1/2}/\Gamma_{total}$ in $N\pi \rightarrow N(2080) \rightarrow N(\pi\pi)_{S=0}^0$ -wave

VALUE	DOCUMENT ID	TECN	COMMENT	$(\Gamma_1\Gamma_9)^{1/2}/\Gamma$
+0.25 ± 0.06	MANLEY 92	IPWA	$\pi N \rightarrow \pi N$ & $N\pi\pi$	

$(\Gamma_1\Gamma_7)^{1/2}/\Gamma_{total}$ in $\rho\gamma \rightarrow N(2080) \rightarrow N\eta$

VALUE	DOCUMENT ID	TECN	COMMENT	$(\Gamma_{14}\Gamma_2)^{1/2}/\Gamma$
0.0037	HICKS 73	MPWA	$\gamma\rho \rightarrow \rho\eta$	

N(2080) PHOTON DECAY AMPLITUDES

N(2080) $\rightarrow \rho\gamma$, helicity-1/2 amplitude $A_{1/2}$
VALUE (GeV^{-1/2})

VALUE (GeV ^{-1/2})	DOCUMENT ID	TECN	COMMENT
-0.020 ± 0.008	AWAJI 81	DPWA	$\gamma N \rightarrow \pi N$
• • • We do not use the following data for averages, fits, limits, etc. • • •			
0.026 ± 0.052	DEVENISH 74	DPWA	$\gamma N \rightarrow \pi N$

N(2080) $\rightarrow \rho\gamma$, helicity-3/2 amplitude $A_{3/2}$
VALUE (GeV^{-1/2})

VALUE (GeV ^{-1/2})	DOCUMENT ID	TECN	COMMENT
0.017 ± 0.011	AWAJI 81	DPWA	$\gamma N \rightarrow \pi N$
• • • We do not use the following data for averages, fits, limits, etc. • • •			
0.128 ± 0.057	DEVENISH 74	DPWA	$\gamma N \rightarrow \pi N$

N(2080) $\rightarrow n\gamma$, helicity-1/2 amplitude $A_{1/2}$
VALUE (GeV^{-1/2})

VALUE (GeV ^{-1/2})	DOCUMENT ID	TECN	COMMENT
0.007 ± 0.013	AWAJI 81	DPWA	$\gamma N \rightarrow \pi N$
• • • We do not use the following data for averages, fits, limits, etc. • • •			
0.053 ± 0.083	DEVENISH 74	DPWA	$\gamma N \rightarrow \pi N$

N(2080) $\rightarrow n\gamma$, helicity-3/2 amplitude $A_{3/2}$
VALUE (GeV^{-1/2})

VALUE (GeV ^{-1/2})	DOCUMENT ID	TECN	COMMENT
-0.053 ± 0.034	AWAJI 81	DPWA	$\gamma N \rightarrow \pi N$
• • • We do not use the following data for averages, fits, limits, etc. • • •			
0.100 ± 0.141	DEVENISH 74	DPWA	$\gamma N \rightarrow \pi N$

N(2080) $\gamma\rho \rightarrow \Lambda K^+$ AMPLITUDES

$(\Gamma_1\Gamma_7)^{1/2}/\Gamma_{total}$ in $\rho\gamma \rightarrow N(2080) \rightarrow \Lambda K^+$ (E_{2-} amplitude)
VALUE (units 10⁻³)

VALUE (units 10 ⁻³)	DOCUMENT ID	TECN
• • • We do not use the following data for averages, fits, limits, etc. • • •		
5.5 ± 0.3	WORKMAN 90	DPWA
4.09	TANABE 89	DPWA

$\rho\gamma \rightarrow N(2080) \rightarrow \Lambda K^+$ phase angle θ (E_{2-} amplitude)
VALUE (degrees)

VALUE (degrees)	DOCUMENT ID	TECN
• • • We do not use the following data for averages, fits, limits, etc. • • •		
-48 ± 5	WORKMAN 90	DPWA
-35.9	TANABE 89	DPWA

$(\Gamma_1\Gamma_7)^{1/2}/\Gamma_{total}$ in $\rho\gamma \rightarrow N(2080) \rightarrow \Lambda K^+$ (M_{2-} amplitude)
VALUE (units 10⁻³)

VALUE (units 10 ⁻³)	DOCUMENT ID	TECN
• • • We do not use the following data for averages, fits, limits, etc. • • •		
-6.7 ± 0.2	WORKMAN 90	DPWA
-4.09	TANABE 89	DPWA

N(2080) FOOTNOTES

- ¹ CUTKOSKY 80 finds a lower mass D_{13} resonance, as well as one in this region. Both are listed here.
- ² The range given for DEANS 75 is from the four best solutions. Disagrees with $\pi^+ p \rightarrow \Sigma^+ K^+$ data of WINNIK 77 around 1920 MeV.

N(2080) REFERENCES

For early references, see Physics Letters **111B** 70 (1982).

BATINIC 95	PR C51 2310	M. Batinic et al.	(BOSK, UCLA)
Also	PR C57 1004 (erratum)	M. Batinic et al.	
MANLEY 92	PR D45 4002	D.M. Manley, E.M. Saleski	(KENT) IJP
Also	PR D30 904	D.M. Manley et al.	(VPI)
ARNDT 91	PR D43 2131	R.A. Arndt et al.	(VPI, TELE) IJP
WORKMAN 90	PR C42 781	R.L. Workman et al.	(VPI)
TANABE 89	PR C39 741	H. Tanabe, M. Kohno, C. Bennhold	(MANZ)
Also	NC 102A 193	M. Kohno, H. Tanabe, C. Bennhold	(MANZ)
BELL 83	NP B222 389	K.W. Bell et al.	(RL) IJP
PDG 82	PL 111B	M. Roos et al.	(HELS, CIT, CERN)
AWAJI 81	Bonn Conf. 352	N. Awaji, R. Kajikawa	(NAGO)
Also	NP B197 365	K. Fujii et al.	(NAGO)
CUTKOSKY 80	Toronto Conf. 19	R.E. Cutkosky et al.	(CMU, LBL) IJP
Also	PR D20 2839	R.E. Cutkosky et al.	(CMU, LBL) IJP
SAXON 80	NP B162 522	D.H. Saxon et al.	(RIHEL, BRIS) IJP
BAKER 79	NP B156 93	R.D. Baker et al.	(RIHEL) IJP
HOEHLER 79	PDAT 12-1	G. Hoehler et al.	(KARLT) IJP
Also	Toronto Conf. 3	R. Koch	(KARLT) IJP
WINNIK 77	NP B128 66	M. Winnik et al.	(HAIF) I
DEANS 75	NP B96 90	S.R. Deans et al.	(SFLA, ALAH) IJP
DEVENISH 74	PL 52B 227	R.C.C. Devenish, D.H. Lyth, W.A. Rankin	(DESY+) IJP
HICKS 73	PR D7 2614	H.R. Hicks et al.	(CMU, ORNL, SFLA) IJP

N(2090) S_{11}

$I(J^P) = \frac{1}{2}(\frac{1}{2}^-)$ Status: *

OMITTED FROM SUMMARY TABLE
Any structure in the S_{11} wave above 1800 MeV is listed here. A few early results that are now obsolete have been omitted.

N(2090) BREIT-WIGNER MASS

VALUE (MeV)

VALUE (MeV)	DOCUMENT ID	TECN	COMMENT
≈ 2090 OUR ESTIMATE			
1928 ± 59	MANLEY 92	IPWA	$\pi N \rightarrow \pi N$ & $N\pi\pi$
2180 ± 80	CUTKOSKY 80	IPWA	$\pi N \rightarrow \pi N$
1880 ± 20	HOEHLER 79	IPWA	$\pi N \rightarrow \pi N$
• • • We do not use the following data for averages, fits, limits, etc. • • •			
1897 ± 50 ⁺³⁰ ₋₂	PLOETZKE 98	SPEC	$\gamma\rho \rightarrow p\eta'(958)$

Baryon Particle Listings

 $N(2090)$, $N(2100)$ $N(2090)$ BREIT-WIGNER WIDTH

VALUE (MeV)	DOCUMENT ID	TECN	COMMENT
414 ± 157	MANLEY 92	IPWA	$\pi N \rightarrow \pi N$ & $N\pi\pi$
350 ± 100	CUTKOSKY 80	IPWA	$\pi N \rightarrow \pi N$
95 ± 30	HOEHLER 79	IPWA	$\pi N \rightarrow \pi N$
• • • We do not use the following data for averages, fits, limits, etc. • • •			
396 ± 155 ⁺³⁵ ₋₄₅	PLOETZKE 98	SPEC	$\gamma p \rightarrow p\eta'$ (958)

 $N(2090)$ POLE POSITION

REAL PART

VALUE (MeV)	DOCUMENT ID	TECN	COMMENT
2150 ± 70	CUTKOSKY 80	IPWA	$\pi N \rightarrow \pi N$
1937 or 1949	¹ LONGACRE 78	IPWA	$\pi N \rightarrow N\pi\pi$

-2xIMAGINARY PART

VALUE (MeV)	DOCUMENT ID	TECN	COMMENT
350 ± 100	CUTKOSKY 80	IPWA	$\pi N \rightarrow \pi N$
139 or 131	¹ LONGACRE 78	IPWA	$\pi N \rightarrow N\pi\pi$

 $N(2090)$ ELASTIC POLE RESIDUEMODULUS $|r|$

VALUE (MeV)	DOCUMENT ID	TECN	COMMENT
40 ± 20	CUTKOSKY 80	IPWA	$\pi N \rightarrow \pi N$

PHASE θ

VALUE (°)	DOCUMENT ID	TECN	COMMENT
0 ± 90	CUTKOSKY 80	IPWA	$\pi N \rightarrow \pi N$

 $N(2090)$ DECAY MODES

Mode

Γ_1	$N\pi$
Γ_2	ΛK
Γ_3	$N\pi\pi$

 $N(2090)$ BRANCHING RATIOS

$\Gamma(N\pi)/\Gamma_{\text{total}}$	DOCUMENT ID	TECN	COMMENT	Γ_1/Γ
0.10 ± 0.10	MANLEY 92	IPWA	$\pi N \rightarrow \pi N$ & $N\pi\pi$	
0.18 ± 0.08	CUTKOSKY 80	IPWA	$\pi N \rightarrow \pi N$	
0.09 ± 0.05	HOEHLER 79	IPWA	$\pi N \rightarrow \pi N$	

$(\Gamma_1\Gamma_2)^{1/2}/\Gamma_{\text{total}}$ in $N\pi \rightarrow N(2090) \rightarrow \Lambda K$	DOCUMENT ID	TECN	COMMENT	$(\Gamma_1\Gamma_2)^{1/2}/\Gamma$
not seen	SAXON 80	DPWA	$\pi^- p \rightarrow \Lambda K^0$	

 $N(2090)$ FOOTNOTES

¹ LONGACRE 78 values are from a search for poles in the unitarized T-matrix. The first (second) value uses, in addition to $\pi N \rightarrow N\pi\pi$ data, elastic amplitudes from a Saclay (CERN) partial-wave analysis.

 $N(2090)$ REFERENCES

PLOETZKE 98	PL B444 555	R. Ploetzke et al.	(Bonn SAPHIR Collab.)
MANLEY 92	PR D45 4002	D.M. Manley, E.M. Saleski	(KENT) IJP
Also 84	PR D30 904	D.M. Manley et al.	(VPI)
CUTKOSKY 80	Toronto Conf. 19	R.E. Cutkosky et al.	(CMU, LBL) IJP
Also 79	FR D20 2839	R.E. Cutkosky et al.	(CMU, LBL)
SAXON 80	NP B162 522	D.H. Saxon et al.	(RHEL, BRIS) IJP
HOEHLER 79	PDAT 12-1	G. Hohler et al.	(KARLT) IJP
Also 80	Toronto Conf. 3	R. Koch	(KARLT) IJP
LONGACRE 78	PR D17 1795	R.S. Longacre et al.	(LBL, SLAC)

 $N(2100) P_{11}$

$$I(J^P) = \frac{1}{2}(\frac{1}{2}^+) \text{ Status: } *$$

OMITTED FROM SUMMARY TABLE

 $N(2100)$ BREIT-WIGNER MASS

VALUE (MeV)	DOCUMENT ID	TECN	COMMENT
≈ 2100 OUR ESTIMATE			
1885 ± 30	MANLEY 92	IPWA	$\pi N \rightarrow \pi N$ & $N\pi\pi$
2125 ± 75	CUTKOSKY 80	IPWA	$\pi N \rightarrow \pi N$
2050 ± 20	HOEHLER 79	IPWA	$\pi N \rightarrow \pi N$
• • • We do not use the following data for averages, fits, limits, etc. • • •			
1986 ± 26 ⁺¹⁰ ₋₃₀	PLOETZKE 98	SPEC	$\gamma p \rightarrow p\eta'$ (958)
2203 ± 70	BATINIC 95	DPWA	$\pi N \rightarrow N\pi, N\eta$

 $N(2100)$ BREIT-WIGNER WIDTH

VALUE (MeV)	DOCUMENT ID	TECN	COMMENT
113 ± 44	MANLEY 92	IPWA	$\pi N \rightarrow \pi N$ & $N\pi\pi$
260 ± 100	CUTKOSKY 80	IPWA	$\pi N \rightarrow \pi N$
200 ± 30	HOEHLER 79	IPWA	$\pi N \rightarrow \pi N$
• • • We do not use the following data for averages, fits, limits, etc. • • •			
296 ± 100 ⁺⁶⁰ ₋₁₀	PLOETZKE 98	SPEC	$\gamma p \rightarrow p\eta'$ (958)
418 ± 171	BATINIC 95	DPWA	$\pi N \rightarrow N\pi, N\eta$

 $N(2100)$ POLE POSITION

REAL PART

VALUE (MeV)	DOCUMENT ID	TECN	COMMENT
2120 ± 40	CUTKOSKY 80	IPWA	$\pi N \rightarrow \pi N$

• • • We do not use the following data for averages, fits, limits, etc. • • •

not seen

ARNDT 91 DPWA $\pi N \rightarrow \pi N$ Soln SM90

-2xIMAGINARY PART

VALUE (MeV)	DOCUMENT ID	TECN	COMMENT
240 ± 80	CUTKOSKY 80	IPWA	$\pi N \rightarrow \pi N$

• • • We do not use the following data for averages, fits, limits, etc. • • •

not seen

ARNDT 91 DPWA $\pi N \rightarrow \pi N$ Soln SM90 $N(2100)$ ELASTIC POLE RESIDUEMODULUS $|r|$

VALUE (MeV)	DOCUMENT ID	TECN	COMMENT
14 ± 7	CUTKOSKY 80	IPWA	$\pi N \rightarrow \pi N$

PHASE θ

VALUE (°)	DOCUMENT ID	TECN	COMMENT
35 ± 25	CUTKOSKY 80	IPWA	$\pi N \rightarrow \pi N$

 $N(2100)$ DECAY MODES

Mode

Γ_1	$N\pi$
Γ_2	$N\eta$
Γ_3	$N\pi\pi$
Γ_4	$\Delta(1232)\pi, P\text{-wave}$

 $N(2100)$ BRANCHING RATIOS

$\Gamma(N\pi)/\Gamma_{\text{total}}$	DOCUMENT ID	TECN	COMMENT	Γ_1/Γ
0.15 ± 0.06	MANLEY 92	IPWA	$\pi N \rightarrow \pi N$ & $N\pi\pi$	
0.12 ± 0.03	CUTKOSKY 80	IPWA	$\pi N \rightarrow \pi N$	
0.10 ± 0.04	HOEHLER 79	IPWA	$\pi N \rightarrow \pi N$	
• • • We do not use the following data for averages, fits, limits, etc. • • •				
0.11 ± 0.07	BATINIC 95	DPWA	$\pi N \rightarrow N\pi, N\eta$	

$\Gamma(N\eta)/\Gamma_{\text{total}}$	DOCUMENT ID	TECN	COMMENT	Γ_2/Γ
0.86 ± 0.07	BATINIC 95	DPWA	$\pi N \rightarrow N\pi, N\eta$	

$(\Gamma_1\Gamma_2)^{1/2}/\Gamma_{\text{total}}$ in $N\pi \rightarrow N(2100) \rightarrow \Delta(1232)\pi, P\text{-wave}$	DOCUMENT ID	TECN	COMMENT	$(\Gamma_1\Gamma_2)^{1/2}/\Gamma$
-0.19 ± 0.08	MANLEY 92	IPWA	$\pi N \rightarrow \pi N$ & $N\pi\pi$	

 $N(2100)$ REFERENCES

PLOETZKE 98	PL B444 555	R. Ploetzke et al.	(Bonn SAPHIR Collab.)
BATINIC 95	PR C51 2310	M. Batinic et al.	(BOSK, UCLA)
Also 98	PR C57 1004 (erratum)	M. Batinic et al.	
MANLEY 92	PR D45 4002	D.M. Manley, E.M. Saleski	(KENT) IJP
Also 84	PR D30 904	D.M. Manley et al.	(VPI)
ARNDT 91	PR D43 2131	R.A. Arndt et al.	(VPI, TELE) IJP
CUTKOSKY 80	Toronto Conf. 19	R.E. Cutkosky et al.	(CMU, LBL) IJP
Also 79	PR D20 2839	R.E. Cutkosky et al.	(CMU, LBL)
HOEHLER 79	PDAT 12-1	G. Hohler et al.	(KARLT) IJP
Also 80	Toronto Conf. 3	R. Koch	(KARLT) IJP

See key on page 239

Baryon Particle Listings

$N(2190)$

 $N(2190) G_{17}$

$$I(J^P) = \frac{1}{2}(\frac{7}{2}^-) \text{ Status: } ****$$

Most of the results published before 1975 are now obsolete and have been omitted. They may be found in our 1982 edition, Physics Letters **111B** (1982).

 $N(2190)$ BREIT-WIGNER MASS

VALUE (MeV)	DOCUMENT ID	TECN	COMMENT
2190 to 2200 (\approx 2190) OUR ESTIMATE			
2127 \pm 9	MANLEY 92	IPWA	$\pi N \rightarrow \pi N \& N\pi\pi$
2200 \pm 70	CUTKOSKY 80	IPWA	$\pi N \rightarrow \pi N$
2140 \pm 12	HOEHLER 79	IPWA	$\pi N \rightarrow \pi N$
2140 \pm 40	HENDRY 78	MPWA	$\pi N \rightarrow \pi N$
• • • We do not use the following data for averages, fits, limits, etc. • • •			
2131	ARNDT 95	DPWA	$\pi N \rightarrow N\pi$
2198 \pm 68	BATINIC 95	DPWA	$\pi N \rightarrow N\pi, N\eta$
2098	CRAWFORD 80	DPWA	$\gamma N \rightarrow \pi N$
2180	SAXON 80	DPWA	$\pi^- \rho \rightarrow \Lambda K^0$
2140	BAKER 79	DPWA	$\pi^- \rho \rightarrow n\eta$
2117	BARBOUR 78	DPWA	$\gamma N \rightarrow \pi N$

 $N(2190)$ BREIT-WIGNER WIDTH

VALUE (MeV)	DOCUMENT ID	TECN	COMMENT
350 to 550 (\approx 450) OUR ESTIMATE			
550 \pm 50	MANLEY 92	IPWA	$\pi N \rightarrow \pi N \& N\pi\pi$
500 \pm 150	CUTKOSKY 80	IPWA	$\pi N \rightarrow \pi N$
390 \pm 30	HOEHLER 79	IPWA	$\pi N \rightarrow \pi N$
270 \pm 50	HENDRY 78	MPWA	$\pi N \rightarrow \pi N$
• • • We do not use the following data for averages, fits, limits, etc. • • •			
476	ARNDT 95	DPWA	$\pi N \rightarrow N\pi$
805 \pm 140	BATINIC 95	DPWA	$\pi N \rightarrow N\pi, N\eta$
238	CRAWFORD 80	DPWA	$\gamma N \rightarrow \pi N$
80	SAXON 80	DPWA	$\pi^- \rho \rightarrow \Lambda K^0$
319	BAKER 79	DPWA	$\pi^- \rho \rightarrow n\eta$
220	BARBOUR 78	DPWA	$\gamma N \rightarrow \pi N$

 $N(2190)$ POLE POSITION

REAL PART VALUE (MeV)	DOCUMENT ID	TECN	COMMENT
1950 to 2150 (\approx 2050) OUR ESTIMATE			
2030	ARNDT 95	DPWA	$\pi N \rightarrow N\pi$
2042	¹ HOEHLER 93	SPED	$\pi N \rightarrow \pi N$
2100 \pm 50	CUTKOSKY 80	IPWA	$\pi N \rightarrow \pi N$
• • • We do not use the following data for averages, fits, limits, etc. • • •			
2060	ARNDT 91	DPWA	$\pi N \rightarrow \pi N$ Soln SM90
-2xIMAGINARY PART VALUE (MeV)			
350 to 550 (\approx 450) OUR ESTIMATE			
460	ARNDT 95	DPWA	$\pi N \rightarrow N\pi$
482	¹ HOEHLER 93	SPED	$\pi N \rightarrow \pi N$
400 \pm 160	CUTKOSKY 80	IPWA	$\pi N \rightarrow \pi N$
• • • We do not use the following data for averages, fits, limits, etc. • • •			
464	ARNDT 91	DPWA	$\pi N \rightarrow \pi N$ Soln SM90

 $N(2190)$ ELASTIC POLE RESIDUE

MODULUS $ r $ VALUE (MeV)	DOCUMENT ID	TECN	COMMENT
46	ARNDT 95	DPWA	$\pi N \rightarrow N\pi$
45	HOEHLER 93	SPED	$\pi N \rightarrow \pi N$
25 \pm 10	CUTKOSKY 80	IPWA	$\pi N \rightarrow \pi N$
• • • We do not use the following data for averages, fits, limits, etc. • • •			
54	ARNDT 91	DPWA	$\pi N \rightarrow \pi N$ Soln SM90
PHASE θ VALUE ($^\circ$)			
-23	ARNDT 95	DPWA	$\pi N \rightarrow N\pi$
-30 \pm 50	CUTKOSKY 80	IPWA	$\pi N \rightarrow \pi N$
• • • We do not use the following data for averages, fits, limits, etc. • • •			
-44	ARNDT 91	DPWA	$\pi N \rightarrow \pi N$ Soln SM90

 $N(2190)$ DECAY MODES

The following branching fractions are our estimates, not fits or averages.

Mode	Fraction (Γ_i/Γ)
Γ_1 $N\pi$	10-20 %
Γ_2 $N\eta$	
Γ_3 ΛK	
Γ_4 ΣK	
Γ_5 $N\pi\pi$	
Γ_6 $N\rho$	
Γ_7 $N\rho, S=3/2, D\text{-wave}$	
Γ_8 $p\gamma, \text{ helicity}=1/2$	
Γ_9 $p\gamma, \text{ helicity}=3/2$	
Γ_{10} $n\gamma, \text{ helicity}=1/2$	
Γ_{11} $n\gamma, \text{ helicity}=3/2$	

 $N(2190)$ BRANCHING RATIOS

$\Gamma(N\pi)/\Gamma_{\text{total}}$ VALUE	DOCUMENT ID	TECN	COMMENT	Γ_1/Γ
0.1 to 0.2 OUR ESTIMATE				
0.22 \pm 0.01	MANLEY 92	IPWA	$\pi N \rightarrow \pi N \& N\pi\pi$	
0.12 \pm 0.06	CUTKOSKY 80	IPWA	$\pi N \rightarrow \pi N$	
0.14 \pm 0.02	HOEHLER 79	IPWA	$\pi N \rightarrow \pi N$	
0.16 \pm 0.04	HENDRY 78	MPWA	$\pi N \rightarrow \pi N$	
• • • We do not use the following data for averages, fits, limits, etc. • • •				
0.23	ARNDT 95	DPWA	$\pi N \rightarrow N\pi$	
0.19 \pm 0.05	BATINIC 95	DPWA	$\pi N \rightarrow N\pi, N\eta$	
$\Gamma(N\eta)/\Gamma_{\text{total}}$ Γ_2/Γ				
VALUE DOCUMENT ID TECN COMMENT				
• • • We do not use the following data for averages, fits, limits, etc. • • •				
0.001 \pm 0.003	BATINIC 95	DPWA	$\pi N \rightarrow N\pi, N\eta$	
$(\Gamma_1\Gamma_7)^{1/2}/\Gamma_{\text{total}}$ in $N\pi \rightarrow N(2190) \rightarrow N\eta$ $(\Gamma_1\Gamma_2)^{1/2}/\Gamma$				
VALUE DOCUMENT ID TECN COMMENT				
• • • We do not use the following data for averages, fits, limits, etc. • • •				
+0.052	BAKER 79	DPWA	$\pi^- \rho \rightarrow n\eta$	
$(\Gamma_1\Gamma_3)^{1/2}/\Gamma_{\text{total}}$ in $N\pi \rightarrow N(2190) \rightarrow \Lambda K$ $(\Gamma_1\Gamma_3)^{1/2}/\Gamma$				
VALUE DOCUMENT ID TECN COMMENT				
-0.02	BELL 83	DPWA	$\pi^- \rho \rightarrow \Lambda K^0$	
-0.02	SAXON 80	DPWA	$\pi^- \rho \rightarrow \Lambda K^0$	
$(\Gamma_1\Gamma_4)^{1/2}/\Gamma_{\text{total}}$ in $N\pi \rightarrow N(2190) \rightarrow \Sigma K$ $(\Gamma_1\Gamma_4)^{1/2}/\Gamma$				
VALUE DOCUMENT ID TECN COMMENT				
• • • We do not use the following data for averages, fits, limits, etc. • • •				
0.014 to 0.019	² DEANS 75	DPWA	$\pi N \rightarrow \Sigma K$	
$(\Gamma_1\Gamma_7)^{1/2}/\Gamma_{\text{total}}$ in $N\pi \rightarrow N(2190) \rightarrow N\rho, S=3/2, D\text{-wave}$ $(\Gamma_1\Gamma_7)^{1/2}/\Gamma$				
VALUE DOCUMENT ID TECN COMMENT				
-0.25 \pm 0.03	MANLEY 92	IPWA	$\pi N \rightarrow \pi N \& N\pi\pi$	

 $N(2190)$ PHOTON DECAY AMPLITUDES

$N(2190) \rightarrow p\gamma, \text{ helicity-1/2}$ amplitude $A_{1/2}$ VALUE (GeV $^{-1/2}$)	DOCUMENT ID	TECN	COMMENT
• • • We do not use the following data for averages, fits, limits, etc. • • •			
-0.055	CRAWFORD 80	DPWA	$\gamma N \rightarrow \pi N$
-0.030	BARBOUR 78	DPWA	$\gamma N \rightarrow \pi N$
$N(2190) \rightarrow p\gamma, \text{ helicity-3/2}$ amplitude $A_{3/2}$			
VALUE (GeV $^{-1/2}$) DOCUMENT ID TECN COMMENT			
• • • We do not use the following data for averages, fits, limits, etc. • • •			
0.081	CRAWFORD 80	DPWA	$\gamma N \rightarrow \pi N$
+0.180	BARBOUR 78	DPWA	$\gamma N \rightarrow \pi N$
$N(2190) \rightarrow n\gamma, \text{ helicity-1/2}$ amplitude $A_{1/2}$			
VALUE (GeV $^{-1/2}$) DOCUMENT ID TECN COMMENT			
• • • We do not use the following data for averages, fits, limits, etc. • • •			
-0.042	CRAWFORD 80	DPWA	$\gamma N \rightarrow \pi N$
-0.085	BARBOUR 78	DPWA	$\gamma N \rightarrow \pi N$
$N(2190) \rightarrow n\gamma, \text{ helicity-3/2}$ amplitude $A_{3/2}$			
VALUE (GeV $^{-1/2}$) DOCUMENT ID TECN COMMENT			
• • • We do not use the following data for averages, fits, limits, etc. • • •			
-0.126	CRAWFORD 80	DPWA	$\gamma N \rightarrow \pi N$
+0.007	BARBOUR 78	DPWA	$\gamma N \rightarrow \pi N$

Baryon Particle Listings

$N(2190)$, $N(2200)$, $N(2220)$

$N(2190) \quad \gamma p \rightarrow \Lambda K^+$ AMPLITUDES

$(\Gamma_1 \Gamma_2)^{1/2} / \Gamma_{\text{total}}$ in $p\gamma \rightarrow N(2190) \rightarrow \Lambda K^+$ (E_4 amplitude)

VALUE (units 10^{-3})	DOCUMENT ID	TECN
2.5 \pm 1.0	WORKMAN 90	DPWA
2.04	TANABE 89	DPWA

$p\gamma \rightarrow N(2190) \rightarrow \Lambda K^+$ phase angle θ (E_4 amplitude)

VALUE (degrees)	DOCUMENT ID	TECN
-4 \pm 9	WORKMAN 90	DPWA
-27.5	TANABE 89	DPWA

$(\Gamma_1 \Gamma_2)^{1/2} / \Gamma_{\text{total}}$ in $p\gamma \rightarrow N(2190) \rightarrow \Lambda K^+$ (M_4 amplitude)

VALUE (units 10^{-3})	DOCUMENT ID	TECN
-7.0 \pm 0.7	WORKMAN 90	DPWA
-5.78	TANABE 89	DPWA

$N(2190)$ FOOTNOTES

- See HOEHLER 93 for a detailed discussion of the evidence for and the pole parameters of N and Δ resonances as determined from Argand diagrams of πN elastic partial-wave amplitudes and from plots of the speeds with which the amplitudes traverse the diagrams.
- The range given for DEANS 75 is from the four best solutions. Disagrees with $\pi^+ p \rightarrow \Sigma^+ K^+$ data of WINNIK 77 around 1920 MeV.

$N(2190)$ REFERENCES

For early references, see Physics Letters 111B 70 (1982).

ARNDT 95	PR C52 2120	R.A. Arndt <i>et al.</i>	(VPI, BRCO)
BATINIC 95	PR C51 2310	M. Batinic <i>et al.</i>	(BOSK, UCLA)
Also 98	PR C57 1004 (erratum)	M. Batinic <i>et al.</i>	
HOEHLER 93	πN Newsletter 9 1	G. Hoehler	(KARL)
MANLEY 92	PR D45 4002	D.M. Manley, E.M. Saleski	(KENT) IJP
Also 84	PR D30 904	D.M. Manley <i>et al.</i>	(VPI)
ARNDT 91	PR D43 2131	R.A. Arndt <i>et al.</i>	(VPI, TELE) IJP
WORKMAN 90	PR C42 781	R.L. Workman	(VPI)
TANABE 89	PR C39 741	H. Tanabe, M. Kohno, C. Bennhold	(MANZ)
Also 89	NC 102A 193	M. Kohno, H. Tanabe, C. Bennhold	(MANZ)
BELL 83	NP B222 389	K.W. Bell <i>et al.</i>	(RL) IJP
PDG 82	PL-111B	M. Roos <i>et al.</i>	(HEL5, CIT, CERN)
CRAWFORD 80	Toronto Conf. 107	R.L. Crawford	(GLAS)
CUTKOSKY 80	Toronto Conf. 19	R.E. Cutkosky <i>et al.</i>	(CMU, LBL) IJP
Also 79	PR D20 2839	R.E. Cutkosky <i>et al.</i>	(CMU, LBL) IJP
SAXON 80	NP B162 522	D.H. Saxon <i>et al.</i>	(RHEL, BRIS) IJP
BAKER 79	NP B156 93	R.D. Baker <i>et al.</i>	(RHEL) IJP
HOEHLER 79	PDAT 12-1	G. Hoehler <i>et al.</i>	(KARLT) IJP
Also 80	Toronto Conf. 3	R. Koch	(KARLT) IJP
BARBOUR 78	NP B141 253	I.M. Barbour, R.L. Crawford, N.H. Parsons	(GLAS)
HENDRY 78	PRL 41 222	A.W. Hendry	(IND, LBL) IJP
Also 81	ANP 136 1	A.W. Hendry	(IND)
WINNIK 77	NP B128 66	M. Winnik <i>et al.</i>	(HAIF) I
DEANS 75	NP B96 90	S.R. Deans <i>et al.</i>	(SFLA, ALAH) IJP

$N(2200) D_{15}$ $I(J^P) = \frac{1}{2}(\frac{5}{2}^-)$ Status: **

OMITTED FROM SUMMARY TABLE
The mass is not well determined. A few early results have been omitted.

$N(2200)$ BREIT-WIGNER MASS

VALUE (MeV)	DOCUMENT ID	TECN	COMMENT
\approx 2200 OUR ESTIMATE			
1900	BELL 83	DPWA	$\pi^- p \rightarrow \Lambda K^0$
2180 \pm 80	CUTKOSKY 80	IPWA	$\pi N \rightarrow \pi N$
1920	SAXON 80	DPWA	$\pi^- p \rightarrow \Lambda K^0$
2228 \pm 30	HOEHLER 79	IPWA	$\pi N \rightarrow \pi N$
• • • We do not use the following data for averages, fits, limits, etc. • • •			
2240 \pm 65	BATINIC 95	DPWA	$\pi N \rightarrow N\pi, N\eta$

$N(2200)$ BREIT-WIGNER WIDTH

VALUE (MeV)	DOCUMENT ID	TECN	COMMENT
130	BELL 83	DPWA	$\pi^- p \rightarrow \Lambda K^0$
400 \pm 100	CUTKOSKY 80	IPWA	$\pi N \rightarrow \pi N$
220	SAXON 80	DPWA	$\pi^- p \rightarrow \Lambda K^0$
310 \pm 50	HOEHLER 79	IPWA	$\pi N \rightarrow \pi N$
• • • We do not use the following data for averages, fits, limits, etc. • • •			
761 \pm 139	BATINIC 95	DPWA	$\pi N \rightarrow N\pi, N\eta$

$N(2200)$ POLE POSITION

REAL PART	DOCUMENT ID	TECN	COMMENT
2100 \pm 60	CUTKOSKY 80	IPWA	$\pi N \rightarrow \pi N$

-2xIMAGINARY PART

VALUE (MeV)	DOCUMENT ID	TECN	COMMENT
360 \pm 80	CUTKOSKY 80	IPWA	$\pi N \rightarrow \pi N$

$N(2200)$ ELASTIC POLE RESIDUE

MODULUS $ r $	DOCUMENT ID	TECN	COMMENT
20 \pm 10	CUTKOSKY 80	IPWA	$\pi N \rightarrow \pi N$

PHASE θ	DOCUMENT ID	TECN	COMMENT
VALUE ($^\circ$)			
-90 \pm 50	CUTKOSKY 80	IPWA	$\pi N \rightarrow \pi N$

$N(2200)$ DECAY MODES

Mode	
Γ_1	$N\pi$
Γ_2	$N\eta$
Γ_3	ΛK

$N(2200)$ BRANCHING RATIOS

$\Gamma(N\pi) / \Gamma_{\text{total}}$	DOCUMENT ID	TECN	COMMENT	Γ_1 / Γ
0.10 \pm 0.03	CUTKOSKY 80	IPWA	$\pi N \rightarrow \pi N$	
0.07 \pm 0.02	HOEHLER 79	IPWA	$\pi N \rightarrow \pi N$	
• • • We do not use the following data for averages, fits, limits, etc. • • •				
0.08 \pm 0.04	BATINIC 95	DPWA	$\pi N \rightarrow N\pi, N\eta$	

$\Gamma(N\eta) / \Gamma_{\text{total}}$	DOCUMENT ID	TECN	COMMENT	Γ_2 / Γ
0.001 \pm 0.01	BATINIC 95	DPWA	$\pi N \rightarrow N\pi, N\eta$	

$(\Gamma_1 \Gamma_2)^{1/2} / \Gamma_{\text{total}}$ in $N\pi \rightarrow N(2200) \rightarrow N\eta$	DOCUMENT ID	TECN	COMMENT	$(\Gamma_1 \Gamma_2)^{1/2} / \Gamma$
0.066	BAKER 79	DPWA	$\pi^- p \rightarrow n\eta$	

$(\Gamma_1 \Gamma_3)^{1/2} / \Gamma_{\text{total}}$ in $N\pi \rightarrow N(2200) \rightarrow \Lambda K$	DOCUMENT ID	TECN	COMMENT	$(\Gamma_1 \Gamma_3)^{1/2} / \Gamma$
-0.03	BELL 83	DPWA	$\pi^- p \rightarrow \Lambda K^0$	
-0.05	SAXON 80	DPWA	$\pi^- p \rightarrow \Lambda K^0$	

$N(2200)$ REFERENCES

BATINIC 95	PR C51 2310	M. Batinic <i>et al.</i>	(BOSK, UCLA)
Also 98	PR C57 1004 (erratum)	M. Batinic <i>et al.</i>	
BELL 83	NP B222 389	K.W. Bell <i>et al.</i>	(RL) IJP
CUTKOSKY 80	Toronto Conf. 19	R.E. Cutkosky <i>et al.</i>	(CMU, LBL) IJP
Also 79	PR D20 2839	R.E. Cutkosky <i>et al.</i>	(CMU, LBL)
SAXON 80	NP B162 522	D.H. Saxon <i>et al.</i>	(RHEL, BRIS) IJP
BAKER 79	NP B156 93	R.D. Baker <i>et al.</i>	(RHEL) IJP
HOEHLER 79	PDAT 12-1	G. Hoehler <i>et al.</i>	(KARLT) IJP
Also 80	Toronto Conf. 3	R. Koch	(KARLT) IJP

$N(2220) H_{19}$

$I(J^P) = \frac{1}{2}(\frac{9}{2}^+)$ Status: ***

Most of the results published before 1975 are now obsolete and have been omitted. They may be found in our 1982 edition, Physics Letters 111B (1982).

$N(2220)$ BREIT-WIGNER MASS

VALUE (MeV)	DOCUMENT ID	TECN	COMMENT
2180 to 2310 (\approx 2220) OUR ESTIMATE			
2230 \pm 80	CUTKOSKY 80	IPWA	$\pi N \rightarrow \pi N$
2205 \pm 10	HOEHLER 79	IPWA	$\pi N \rightarrow \pi N$
2300 \pm 100	HENDRY 78	MPWA	$\pi N \rightarrow \pi N$
• • • We do not use the following data for averages, fits, limits, etc. • • •			
2258	ARNDT 95	DPWA	$\pi N \rightarrow N\pi$
2050	BAKER 79	DPWA	$\pi^- p \rightarrow n\eta$

$N(2220)$ BREIT-WIGNER WIDTH

VALUE (MeV)	DOCUMENT ID	TECN	COMMENT
320 to 550 (\approx 400) OUR ESTIMATE			
500 \pm 150	CUTKOSKY 80	IPWA	$\pi N \rightarrow \pi N$
365 \pm 30	HOEHLER 79	IPWA	$\pi N \rightarrow \pi N$
450 \pm 150	HENDRY 78	MPWA	$\pi N \rightarrow \pi N$
• • • We do not use the following data for averages, fits, limits, etc. • • •			
334	ARNDT 95	DPWA	$\pi N \rightarrow N\pi$

See key on page 239

Baryon Particle Listings
 $N(2220)$, $N(2250)$ $N(2220)$ POLE POSITION

REAL PART

VALUE (MeV)	DOCUMENT ID	TECN	COMMENT
2100 to 2240 (\approx 2170) OUR ESTIMATE			
2203	ARNDT 95	DPWA	$\pi N \rightarrow N\pi$
2135	¹ HOEHLER 93	ARGD	$\pi N \rightarrow \pi N$
2160 \pm 80	CUTKOSKY 80	IPWA	$\pi N \rightarrow \pi N$
• • • We do not use the following data for averages, fits, limits, etc. • • •			
2253	ARNDT 91	DPWA	$\pi N \rightarrow \pi N$ Soln SM90

-2xIMAGINARY PART

VALUE (MeV)	DOCUMENT ID	TECN	COMMENT
370 to 570 (\approx 470) OUR ESTIMATE			
536	ARNDT 95	DPWA	$\pi N \rightarrow N\pi$
400	¹ HOEHLER 93	ARGD	$\pi N \rightarrow \pi N$
480 \pm 100	CUTKOSKY 80	IPWA	$\pi N \rightarrow \pi N$
• • • We do not use the following data for averages, fits, limits, etc. • • •			
640	ARNDT 91	DPWA	$\pi N \rightarrow \pi N$ Soln SM90

 $N(2220)$ ELASTIC POLE RESIDUE

VALUE (MeV)	DOCUMENT ID	TECN	COMMENT
68	ARNDT 95	DPWA	$\pi N \rightarrow N\pi$
40	HOEHLER 93	ARGD	$\pi N \rightarrow \pi N$
45 \pm 20	CUTKOSKY 80	IPWA	$\pi N \rightarrow \pi N$
• • • We do not use the following data for averages, fits, limits, etc. • • •			
85	ARNDT 91	DPWA	$\pi N \rightarrow \pi N$ Soln SM90

PHASE θ

VALUE (°)	DOCUMENT ID	TECN	COMMENT
-43	ARNDT 95	DPWA	$\pi N \rightarrow N\pi$
-50	HOEHLER 93	ARGD	$\pi N \rightarrow \pi N$
-45 \pm 25	CUTKOSKY 80	IPWA	$\pi N \rightarrow \pi N$
• • • We do not use the following data for averages, fits, limits, etc. • • •			
-62	ARNDT 91	DPWA	$\pi N \rightarrow \pi N$ Soln SM90

 $N(2220)$ DECAY MODES

The following branching fractions are our estimates, not fits or averages.

Mode	Fraction (Γ_i/Γ)
Γ_1 $N\pi$	10-20 %
Γ_2 $N\eta$	
Γ_3 ΛK	

 $N(2220)$ BRANCHING RATIOS

$\Gamma(N\pi)/\Gamma_{total}$	DOCUMENT ID	TECN	COMMENT	Γ_1/Γ
0.1 to 0.2 OUR ESTIMATE				
0.15 \pm 0.03	CUTKOSKY 80	IPWA	$\pi N \rightarrow \pi N$	
0.18 \pm 0.015	HOEHLER 79	IPWA	$\pi N \rightarrow \pi N$	
0.12 \pm 0.04	HENDRY 78	MPWA	$\pi N \rightarrow \pi N$	
• • • We do not use the following data for averages, fits, limits, etc. • • •				
0.26	ARNDT 95	DPWA	$\pi N \rightarrow N\pi$	

$(\Gamma_1\Gamma_2)^{1/2}/\Gamma_{total}$ in $N\pi \rightarrow N(2220) \rightarrow N\eta$	DOCUMENT ID	TECN	COMMENT	$(\Gamma_1\Gamma_2)^{1/2}/\Gamma$
• • • We do not use the following data for averages, fits, limits, etc. • • •				
0.034	BAKER 79	DPWA	$\pi^- p \rightarrow n\eta$	

$(\Gamma_1\Gamma_3)^{1/2}/\Gamma_{total}$ in $N\pi \rightarrow N(2220) \rightarrow \Lambda K$	DOCUMENT ID	TECN	COMMENT	$(\Gamma_1\Gamma_3)^{1/2}/\Gamma$
not required	BELL 83	DPWA	$\pi^- p \rightarrow \Lambda K^0$	
not seen	SAXON 80	DPWA	$\pi^- p \rightarrow \Lambda K^0$	

 $N(2220)$ FOOTNOTES¹ See HOEHLER 93 for a detailed discussion of the evidence for and the pole parameters of N and Δ resonances as determined from Argand diagrams of πN elastic partial-wave amplitudes and from plots of the speeds with which the amplitudes traverse the diagrams. $N(2220)$ REFERENCES

For early references, see Physics Letters 111B 70 (1982).

ARNDT 95	PR C52 2120	R.A. Arndt et al.	(VPI, BRCO)
HOEHLER 93	πN Newsletter 9 1	G. Hohler	(KARL)
ARNDT 91	PR D43 2131	R.A. Arndt et al.	(VPI, TELE) IJP
BELL 83	NP B222 389	K.W. Bell et al.	(RL) IJP
PDG 82	PL 111B	M. Roos et al.	(HELS, CIT, CERN)
CUTKOSKY 80	Toronto Conf. 19	R.E. Cutkosky et al.	(CMU, LBL) IJP
Also 79	PR D20 2839	R.E. Cutkosky et al.	(CMU, LBL) IJP
SAXON 80	NP B162 522	D.H. Saxon et al.	(RHEL, BRIS) IJP
BAKER 79	NP B156 93	R.D. Baker et al.	(RHEL) IJP
HOEHLER 79	PDAT 12-1	G. Hohler et al.	(KARLT) IJP
Also 80	Toronto Conf. 3	R. Koch	(KARLT) IJP
HENDRY 78	PRL 41 222	A.W. Hendry	(IND, LBL) IJP
Also 81	ANP 136 1	A.W. Hendry	(IND)

 $N(2250) G_{19}$

$$I(J^P) = \frac{1}{2}(\frac{9}{2}^-) \text{ Status: } ***$$

 $N(2250)$ BREIT-WIGNER MASS

VALUE (MeV)	DOCUMENT ID	TECN	COMMENT
2170 to 2310 (\approx 2250) OUR ESTIMATE			
2250 \pm 80	CUTKOSKY 80	IPWA	$\pi N \rightarrow \pi N$
2268 \pm 15	HOEHLER 79	IPWA	$\pi N \rightarrow \pi N$
2200 \pm 100	HENDRY 78	MPWA	$\pi N \rightarrow \pi N$
• • • We do not use the following data for averages, fits, limits, etc. • • •			
2291	ARNDT 95	DPWA	$\pi N \rightarrow N\pi$

 $N(2250)$ BREIT-WIGNER WIDTH

VALUE (MeV)	DOCUMENT ID	TECN	COMMENT
290 to 470 (\approx 400) OUR ESTIMATE			
480 \pm 120	CUTKOSKY 80	IPWA	$\pi N \rightarrow \pi N$
300 \pm 40	HOEHLER 79	IPWA	$\pi N \rightarrow \pi N$
350 \pm 100	HENDRY 78	MPWA	$\pi N \rightarrow \pi N$
• • • We do not use the following data for averages, fits, limits, etc. • • •			
772	ARNDT 95	DPWA	$\pi N \rightarrow N\pi$

 $N(2250)$ POLE POSITION

REAL PART

VALUE (MeV)	DOCUMENT ID	TECN	COMMENT
2080 to 2200 (\approx 2140) OUR ESTIMATE			
2087	ARNDT 95	DPWA	$\pi N \rightarrow N\pi$
2187	¹ HOEHLER 93	SPED	$\pi N \rightarrow \pi N$
2150 \pm 50	CUTKOSKY 80	IPWA	$\pi N \rightarrow \pi N$
• • • We do not use the following data for averages, fits, limits, etc. • • •			
2243	ARNDT 91	DPWA	$\pi N \rightarrow \pi N$ Soln SM90

-2xIMAGINARY PART

VALUE (MeV)	DOCUMENT ID	TECN	COMMENT
280 to 680 (\approx 480) OUR ESTIMATE			
680	ARNDT 95	DPWA	$\pi N \rightarrow N\pi$
388	¹ HOEHLER 93	SPED	$\pi N \rightarrow \pi N$
360 \pm 100	CUTKOSKY 80	IPWA	$\pi N \rightarrow \pi N$
• • • We do not use the following data for averages, fits, limits, etc. • • •			
650	ARNDT 91	DPWA	$\pi N \rightarrow \pi N$ Soln SM90

 $N(2250)$ ELASTIC POLE RESIDUE

VALUE (MeV)	DOCUMENT ID	TECN	COMMENT
24	ARNDT 95	DPWA	$\pi N \rightarrow N\pi$
21	HOEHLER 93	SPED	$\pi N \rightarrow \pi N$
20 \pm 6	CUTKOSKY 80	IPWA	$\pi N \rightarrow \pi N$
• • • We do not use the following data for averages, fits, limits, etc. • • •			
47	ARNDT 91	DPWA	$\pi N \rightarrow \pi N$ Soln SM90

PHASE θ

VALUE (°)	DOCUMENT ID	TECN	COMMENT
-44	ARNDT 95	DPWA	$\pi N \rightarrow N\pi$
-50 \pm 20	CUTKOSKY 80	IPWA	$\pi N \rightarrow \pi N$
• • • We do not use the following data for averages, fits, limits, etc. • • •			
-37	ARNDT 91	DPWA	$\pi N \rightarrow \pi N$ Soln SM90

 $N(2250)$ DECAY MODES

The following branching fractions are our estimates, not fits or averages.

Mode	Fraction (Γ_i/Γ)
Γ_1 $N\pi$	5-15 %
Γ_2 $N\eta$	
Γ_3 ΛK	

 $N(2250)$ BRANCHING RATIOS

$\Gamma(N\pi)/\Gamma_{total}$	DOCUMENT ID	TECN	COMMENT	Γ_1/Γ
0.05 to 0.15 OUR ESTIMATE				
0.10 \pm 0.02	CUTKOSKY 80	IPWA	$\pi N \rightarrow \pi N$	
0.10 \pm 0.02	HOEHLER 79	IPWA	$\pi N \rightarrow \pi N$	
0.09 \pm 0.02	HENDRY 78	MPWA	$\pi N \rightarrow \pi N$	
• • • We do not use the following data for averages, fits, limits, etc. • • •				
0.10	ARNDT 95	DPWA	$\pi N \rightarrow N\pi$	

Baryon Particle Listings

 $N(2250)$, $N(2600)$, $N(2700)$, $N(\sim 3000)$

$(\Gamma_1 \Gamma_2)^{1/2} / \Gamma_{\text{total}}$ in $N\pi \rightarrow N(2250) \rightarrow N\eta$ $(\Gamma_1 \Gamma_2)^{1/2} / \Gamma$
 VALUE DOCUMENT ID TECN COMMENT

• • • We do not use the following data for averages, fits, limits, etc. • • •
 -0.043 BAKER 79 DPWA $\pi^- p \rightarrow n\eta$

$(\Gamma_1 \Gamma_3)^{1/2} / \Gamma_{\text{total}}$ in $N\pi \rightarrow N(2250) \rightarrow \Lambda K$ $(\Gamma_1 \Gamma_3)^{1/2} / \Gamma$
 VALUE DOCUMENT ID TECN COMMENT

-0.02 BELL 83 DPWA $\pi^- p \rightarrow \Lambda K^0$
 not seen SAXON 80 DPWA $\pi^- p \rightarrow \Lambda K^0$

 $N(2250)$ FOOTNOTES

¹ See HOEHLER 93 for a detailed discussion of the evidence for and the pole parameters of N and Δ resonances as determined from Argand diagrams of πN elastic partial-wave amplitudes and from plots of the speeds with which the amplitudes traverse the diagrams.

 $N(2250)$ REFERENCES

ARNDT 95 PR C52 2120	R.A. Arndt et al.	(VPI, BRCO)
HOEHLER 93 πN Newsletter 9 1	G. Hohler et al.	(KARLT) IJP
ARNDT 91 PR D43 2131	R.A. Arndt et al.	(VPI, TELE) IJP
BELL 83 NP B222 389	K.W. Bell et al.	(RL) IJP
CUTKOSKY 80 Toronto Conf. 19	R.E. Cutkosky et al.	(CMU, LBL) IJP
Also 79 PR D20 2839	R.E. Cutkosky et al.	(CMU, LBL) IJP
SAXON 80 NP B162 522	D.H. Saxon et al.	(RHEL, BRIS) IJP
BAKER 79 NP B156 93	R.D. Baker et al.	(RHEL) IJP
HOEHLER 79 PDAT 12-1	G. Hohler et al.	(KARLT) IJP
Also 80 Toronto Conf. 3	R. Koch	(KARLT) IJP
HENDRY 78 PRL 41 222	A.W. Hendry	(IND, LBL) IJP
Also 81 ANP 136 1	A.W. Hendry	(IND)

 $N(2600) I_{1,11}$ $I(J^P) = \frac{1}{2}(\frac{1}{2}^-)$ Status: * * * **$N(2600)$ BREIT-WIGNER MASS**

VALUE (MeV)	DOCUMENT ID	TECN	COMMENT
2550 to 2750 (≈ 2600) OUR ESTIMATE			
2577 \pm 50	HOEHLER 79	IPWA	$\pi N \rightarrow \pi N$
2700 \pm 100	HENDRY 78	MPWA	$\pi N \rightarrow \pi N$

 $N(2600)$ BREIT-WIGNER WIDTH

VALUE (MeV)	DOCUMENT ID	TECN	COMMENT
500 to 800 (≈ 650) OUR ESTIMATE			
400 \pm 100	HOEHLER 79	IPWA	$\pi N \rightarrow \pi N$
900 \pm 100	HENDRY 78	MPWA	$\pi N \rightarrow \pi N$

 $N(2600)$ DECAY MODES

Mode	Fraction (Γ_i / Γ)
$\Gamma_1 N\pi$	5-10 %

 $N(2600)$ BRANCHING RATIOS

$\Gamma(N\pi) / \Gamma_{\text{total}}$	DOCUMENT ID	TECN	COMMENT	Γ_1 / Γ
0.05 to 0.1 OUR ESTIMATE				
0.05 \pm 0.01	HOEHLER 79	IPWA	$\pi N \rightarrow \pi N$	
0.08 \pm 0.02	HENDRY 78	MPWA	$\pi N \rightarrow \pi N$	

 $N(2600)$ REFERENCES

HOEHLER 79 PDAT 12-1	G. Hohler et al.	(KARLT) IJP
Also 80 Toronto Conf. 3	R. Koch	(KARLT) IJP
HENDRY 78 PRL 41 222	A.W. Hendry	(IND, LBL) IJP
Also 81 ANP 136 1	A.W. Hendry	(IND)

 $N(2700) K_{1,13}$ $I(J^P) = \frac{1}{2}(\frac{1}{2}^+)$ Status: * * *

OMITTED FROM SUMMARY TABLE

 $N(2700)$ BREIT-WIGNER MASS

VALUE (MeV)	DOCUMENT ID	TECN	COMMENT
≈ 2700 OUR ESTIMATE			
2612 \pm 45	HOEHLER 79	IPWA	$\pi N \rightarrow \pi N$
3000 \pm 100	HENDRY 78	MPWA	$\pi N \rightarrow \pi N$

 $N(2700)$ BREIT-WIGNER WIDTH

VALUE (MeV)	DOCUMENT ID	TECN	COMMENT
350 \pm 50	HOEHLER 79	IPWA	$\pi N \rightarrow \pi N$
900 \pm 150	HENDRY 78	MPWA	$\pi N \rightarrow \pi N$

 $N(2700)$ DECAY MODES

Mode
$\Gamma_1 N\pi$

 $N(2700)$ BRANCHING RATIOS

$\Gamma(N\pi) / \Gamma_{\text{total}}$	DOCUMENT ID	TECN	COMMENT	Γ_1 / Γ
0.04 \pm 0.01				
0.07 \pm 0.02				
	HOEHLER 79	IPWA	$\pi N \rightarrow \pi N$	
	HENDRY 78	MPWA	$\pi N \rightarrow \pi N$	

 $N(2700)$ REFERENCES

HOEHLER 79 PDAT 12-1	G. Hohler et al.	(KARLT) IJP
Also 80 Toronto Conf. 3	R. Koch	(KARLT) IJP
HENDRY 78 PRL 41 222	A.W. Hendry	(IND, LBL) IJP
Also 81 ANP 136 1	A.W. Hendry	(IND)

 **$N(\sim 3000)$ Region
Partial-Wave Analyses****OMITTED FROM SUMMARY TABLE**

We list here miscellaneous high-mass candidates for isospin-1/2 resonances found in partial-wave analyses.

Our 1982 edition had an $N(3245)$, an $N(3690)$, and an $N(3755)$, each a narrow peak seen in a production experiment. Since nothing has been heard from them since the 1960's, we declare them to be dead. There was also an $N(3030)$, deduced from total cross-section and 180° elastic cross-section measurements; it is the KOCH 80 $L_{1,15}$ state below.

 $N(\sim 3000)$ BREIT-WIGNER MASS

VALUE (MeV)	DOCUMENT ID	TECN	COMMENT
≈ 3000 OUR ESTIMATE			
2600	KOCH 80	IPWA	$\pi N \rightarrow \pi N D_{13}$
3100	KOCH 80	IPWA	$\pi N \rightarrow \pi N L_{1,15}$ wave
3500	KOCH 80	IPWA	$\pi N \rightarrow \pi N M_{1,17}$ wave
3500 to 4000	KOCH 80	IPWA	$\pi N \rightarrow \pi N N_{1,19}$ wave
3500 \pm 200	HENDRY 78	MPWA	$\pi N \rightarrow \pi N L_{1,15}$ wave
3800 \pm 200	HENDRY 78	MPWA	$\pi N \rightarrow \pi N M_{1,17}$ wave
4100 \pm 200	HENDRY 78	MPWA	$\pi N \rightarrow \pi N N_{1,19}$ wave

 $N(\sim 3000)$ BREIT-WIGNER WIDTH

VALUE (MeV)	DOCUMENT ID	TECN	COMMENT
1300 \pm 200	HENDRY 78	MPWA	$\pi N \rightarrow \pi N L_{1,15}$ wave
1600 \pm 200	HENDRY 78	MPWA	$\pi N \rightarrow \pi N M_{1,17}$ wave
1900 \pm 300	HENDRY 78	MPWA	$\pi N \rightarrow \pi N N_{1,19}$ wave

 $N(\sim 3000)$ DECAY MODES

Mode
$\Gamma_1 N\pi$

 $N(\sim 3000)$ BRANCHING RATIOS

$\Gamma(N\pi) / \Gamma_{\text{total}}$	DOCUMENT ID	TECN	COMMENT	Γ_1 / Γ
0.055 \pm 0.02				
0.040 \pm 0.015				
0.030 \pm 0.015				
	HENDRY 78	MPWA	$\pi N \rightarrow \pi N L_{1,15}$ wave	
	HENDRY 78	MPWA	$\pi N \rightarrow \pi N M_{1,17}$ wave	
	HENDRY 78	MPWA	$\pi N \rightarrow \pi N N_{1,19}$ wave	

 $N(\sim 3000)$ REFERENCES

KOCH 80 Toronto Conf. 3	R. Koch	(KARLT) IJP
HENDRY 78 PRL 41 222	A.W. Hendry	(IND, LBL) IJP
Also 81 ANP 136 1	A.W. Hendry	(IND) IJP

See key on page 239

Baryon Particle Listings

 $\Delta(1232)$ **Δ BARYONS**
($S = 0, I = 3/2$)

$$\Delta^{++} = uuu, \Delta^+ = uud, \Delta^0 = udd, \Delta^- = ddd$$

 $\Delta(1232) P_{33}$

$$I(J^P) = \frac{3}{2}(\frac{3}{2}^+) \text{ Status: } ****$$

Most of the results published before 1977 are now obsolete and have been omitted. They may be found in our 1982 edition, Physics Letters **111B** (1982).

 $\Delta(1232)$ BREIT-WIGNER MASSES**MIXED CHARGES**

VALUE (MeV)	DOCUMENT ID	TECN	COMMENT
1230 to 1234 (≈ 1232) OUR ESTIMATE			
1231 ± 1	MANLEY 92	IPWA	$\pi N \rightarrow \pi N$ & $N\pi\pi$
1232 ± 3	CUTKOSKY 80	IPWA	$\pi N \rightarrow \pi N$
1233 ± 2	HOEHLER 79	IPWA	$\pi N \rightarrow \pi N$
• • • We do not use the following data for averages, fits, limits, etc. • • •			
1233	ARNDT 95	DPWA	$\pi N \rightarrow N\pi$

 $\Delta(1232)^{++}$ MASS

VALUE (MeV)	DOCUMENT ID	TECN	COMMENT
1230.5 ± 0.2	ABAEV 95	IPWA	$\pi N \rightarrow \pi N$
1230.9 ± 0.3	KOCH 80b	IPWA	$\pi N \rightarrow \pi N$
1231.1 ± 0.2	PEDRONI 78		$\pi N \rightarrow \pi N$ 70-370 MeV

 $\Delta(1232)^+$ MASS

VALUE (MeV)	DOCUMENT ID	TECN	COMMENT
• • • We do not use the following data for averages, fits, limits, etc. • • •			
1231.6	CRAWFORD 80	DPWA	$\gamma N \rightarrow \pi N$
1234.9 ± 1.4	MIROSHNIC... 79		Fit photoproduction
1231.2	BARBOUR 78	DPWA	$\gamma N \rightarrow \pi N$
1231.8	BERENDS 75	IPWA	$\gamma p \rightarrow \pi N$

 $\Delta(1232)^0$ MASS

VALUE (MeV)	DOCUMENT ID	TECN	COMMENT
1233.1 ± 0.3	ABAEV 95	IPWA	$\pi N \rightarrow \pi N$
1233.6 ± 0.5	KOCH 80b	IPWA	$\pi N \rightarrow \pi N$
1233.8 ± 0.2	PEDRONI 78		$\pi N \rightarrow \pi N$ 70-370 MeV

 $m_{\Delta^0} - m_{\Delta^{++}}$

VALUE (MeV)	DOCUMENT ID	TECN	COMMENT
• • • We do not use the following data for averages, fits, limits, etc. • • •			
2.25 ± 0.68	BERNICHIA 96		Fit to PEDRONI 78
2.6 ± 0.4	ABAEV 95	IPWA	$\pi N \rightarrow \pi N$
2.7 ± 0.3	¹ PEDRONI 78		See the masses

 $\Delta(1232)$ BREIT-WIGNER WIDTHS**MIXED CHARGES**

VALUE (MeV)	DOCUMENT ID	TECN	COMMENT
115 to 125 (≈ 120) OUR ESTIMATE			
118 ± 4	MANLEY 92	IPWA	$\pi N \rightarrow \pi N$ & $N\pi\pi$
120 ± 5	CUTKOSKY 80	IPWA	$\pi N \rightarrow \pi N$
116 ± 5	HOEHLER 79	IPWA	$\pi N \rightarrow \pi N$
• • • We do not use the following data for averages, fits, limits, etc. • • •			
114	ARNDT 95	DPWA	$\pi N \rightarrow \pi N$

 $\Delta(1232)^{++}$ WIDTH

VALUE (MeV)	DOCUMENT ID	TECN	COMMENT
111.0 ± 1.0	KOCH 80b	IPWA	$\pi N \rightarrow \pi N$
111.3 ± 0.5	PEDRONI 78		$\pi N \rightarrow \pi N$ 70-370 MeV

 $\Delta(1232)^+$ WIDTH

VALUE (MeV)	DOCUMENT ID	TECN	COMMENT
• • • We do not use the following data for averages, fits, limits, etc. • • •			
111.2	CRAWFORD 80	DPWA	$\gamma N \rightarrow \pi N$
131.1 ± 2.4	MIROSHNIC... 79		Fit photoproduction
111.0	BARBOUR 78	DPWA	$\gamma N \rightarrow \pi N$

 $\Delta(1232)^0$ WIDTH

VALUE (MeV)	DOCUMENT ID	TECN	COMMENT
113.0 ± 1.5	KOCH 80b	IPWA	$\pi N \rightarrow \pi N$
117.9 ± 0.9	PEDRONI 78		$\pi N \rightarrow \pi N$ 70-370 MeV

 $\Delta^0 - \Delta^{++}$ WIDTH DIFFERENCE

VALUE (MeV)	DOCUMENT ID	TECN	COMMENT
• • • We do not use the following data for averages, fits, limits, etc. • • •			
8.45 ± 1.11	BERNICHIA 96		Fit to PEDRONI 78
5.1 ± 1.0	ABAEV 95	IPWA	$\pi N \rightarrow \pi N$
6.6 ± 1.0	PEDRONI 78		See the widths

 $\Delta(1232)$ POLE POSITIONS**REAL PART, MIXED CHARGES**

VALUE (MeV)	DOCUMENT ID	TECN	COMMENT
1209 to 1211 (≈ 1210) OUR ESTIMATE			
1211	ARNDT 95	DPWA	$\pi N \rightarrow N\pi$
1209	² HOEHLER 93	ARGD	$\pi N \rightarrow \pi N$
1210 ± 1	CUTKOSKY 80	IPWA	$\pi N \rightarrow \pi N$
• • • We do not use the following data for averages, fits, limits, etc. • • •			
1210	ARNDT 91	DPWA	$\pi N \rightarrow \pi N$ Soln SM90

-2xIMAGINARY PART, MIXED CHARGES

VALUE (MeV)	DOCUMENT ID	TECN	COMMENT
98 to 102 (≈ 100) OUR ESTIMATE			
100	ARNDT 95	DPWA	$\pi N \rightarrow N\pi$
100	² HOEHLER 93	ARGD	$\pi N \rightarrow \pi N$
100 ± 2	CUTKOSKY 80	IPWA	$\pi N \rightarrow \pi N$
• • • We do not use the following data for averages, fits, limits, etc. • • •			
100	ARNDT 91	DPWA	$\pi N \rightarrow \pi N$ Soln SM90

REAL PART, $\Delta(1232)^{++}$

VALUE (MeV)	DOCUMENT ID	COMMENT
1209.6 ± 0.5	³ VASAN 76b	Fit to CARTER 73
• • • We do not use the following data for averages, fits, limits, etc. • • •		
1210.5 to 1210.8	⁴ VASAN 76b	Fit to CARTER 73

-2xIMAGINARY PART, $\Delta(1232)^{++}$

VALUE (MeV)	DOCUMENT ID	COMMENT
100.8 ± 1.0	³ VASAN 76b	Fit to CARTER 73
• • • We do not use the following data for averages, fits, limits, etc. • • •		
99.8 to 100	⁴ VASAN 76b	Fit to CARTER 73

REAL PART, $\Delta(1232)^+$

VALUE (MeV)	DOCUMENT ID	TECN	COMMENT
1208.0 ± 2.0	CAMPBELL 76		Fit photoproduction
• • • We do not use the following data for averages, fits, limits, etc. • • •			
1211 ± 1 to 1212 ± 1	HANSTEIN 96	DPWA	$\gamma N \rightarrow \pi N$
1206.9 ± 0.9 to 1210.5 ± 1.8	MIROSHNIC... 79		Fit photoproduction

-2xIMAGINARY PART, $\Delta(1232)^+$

VALUE (MeV)	DOCUMENT ID	TECN	COMMENT
106 ± 4	CAMPBELL 76		Fit photoproduction
• • • We do not use the following data for averages, fits, limits, etc. • • •			
102 ± 2 to 99 ± 2	HANSTEIN 96	DPWA	$\gamma N \rightarrow \pi N$
111.2 ± 2.0 to 116.6 ± 2.2	MIROSHNIC... 79		Fit photoproduction

REAL PART, $\Delta(1232)^0$

VALUE (MeV)	DOCUMENT ID	COMMENT
1210.75 ± 0.6	³ VASAN 76b	Fit to CARTER 73
• • • We do not use the following data for averages, fits, limits, etc. • • •		
1210.2	⁴ VASAN 76b	Fit to CARTER 73

-2xIMAGINARY PART, $\Delta(1232)^0$

VALUE (MeV)	DOCUMENT ID	COMMENT
105.6 ± 1.2	³ VASAN 76b	Fit to CARTER 73
• • • We do not use the following data for averages, fits, limits, etc. • • •		
105.8 to 106.2	⁴ VASAN 76b	Fit to CARTER 73

 $\Delta(1232)$ ELASTIC POLE RESIDUES**ABSOLUTE VALUE, MIXED CHARGES**

VALUE (MeV)	DOCUMENT ID	TECN	COMMENT
38	ARNDT 95	DPWA	$\pi N \rightarrow N\pi$
50	HOEHLER 93	ARGD	$\pi N \rightarrow \pi N$
53 ± 2	CUTKOSKY 80	IPWA	$\pi N \rightarrow \pi N$
• • • We do not use the following data for averages, fits, limits, etc. • • •			
52	ARNDT 91	DPWA	$\pi N \rightarrow \pi N$ Soln SM90

PHASE, MIXED CHARGES

VALUE ($^\circ$)	DOCUMENT ID	TECN	COMMENT
-22	ARNDT 95	DPWA	$\pi N \rightarrow N\pi$
-48	HOEHLER 93	ARGD	$\pi N \rightarrow \pi N$
-47 ± 1	CUTKOSKY 80	IPWA	$\pi N \rightarrow \pi N$
• • • We do not use the following data for averages, fits, limits, etc. • • •			
-31	ARNDT 91	DPWA	$\pi N \rightarrow \pi N$ Soln SM90

Baryon Particle Listings

 $\Delta(1232)$ ABSOLUTE VALUE, $\Delta(1232)^{++}$

VALUE (MeV)	DOCUMENT ID	COMMENT
• • • We do not use the following data for averages, fits, limits, etc. • • •		
52.4 to 53.2	³ VASAN	76b Fit to CARTER 73
52.1 to 52.4	⁴ VASAN	76b Fit to CARTER 73

PHASE, $\Delta(1232)^{++}$

VALUE (rad)	DOCUMENT ID	COMMENT
• • • We do not use the following data for averages, fits, limits, etc. • • •		
-0.822 to -0.833	³ VASAN	76b Fit to CARTER 73
-0.823 to -0.830	⁴ VASAN	76b Fit to CARTER 73

ABSOLUTE VALUE, $\Delta(1232)^0$

VALUE (MeV)	DOCUMENT ID	COMMENT
• • • We do not use the following data for averages, fits, limits, etc. • • •		
54.8 to 55.0	³ VASAN	76b Fit to CARTER 73
55.2 to 55.3	⁴ VASAN	76b Fit to CARTER 73

PHASE, $\Delta(1232)^0$

VALUE (rad)	DOCUMENT ID	COMMENT
• • • We do not use the following data for averages, fits, limits, etc. • • •		
-0.840 to -0.847	³ VASAN	76b Fit to CARTER 73
-0.848 to -0.856	⁴ VASAN	76b Fit to CARTER 73

 $\Delta(1232)$ DECAY MODES

The following branching fractions are our estimates, not fits or averages.

Mode	Fraction (Γ_i/Γ)
Γ_1 $N\pi$	>99 %
Γ_2 $N\gamma$	0.52-0.60 %
Γ_3 $N\gamma$, helicity=1/2	0.11-0.13 %
Γ_4 $N\gamma$, helicity=3/2	0.41-0.47 %

 $\Delta(1232)$ BRANCHING RATIOS

$\Gamma(N\pi)/\Gamma_{total}$	DOCUMENT ID	TECN	COMMENT	Γ_i/Γ
0.993 to 0.995 OUR ESTIMATE				
1.0	MANLEY	92	IPWA $\pi N \rightarrow \pi N$ & $N\pi\pi$	
1.0	CUTKOSKY	80	IPWA $\pi N \rightarrow \pi N$	
1.0	HOEHLER	79	IPWA $\pi N \rightarrow \pi N$	
• • • We do not use the following data for averages, fits, limits, etc. • • •				
1.0	ARNDT	95	DPWA $\pi N \rightarrow N\pi$	

 $\Delta(1232)$ PHOTON DECAY AMPLITUDES $\Delta(1232) \rightarrow N\gamma$, helicity-1/2 amplitude $A_{1/2}$

VALUE (GeV ^{-1/2})	DOCUMENT ID	TECN	COMMENT
-0.135 ± 0.006 OUR ESTIMATE			
-0.1294 ± 0.0013	HANSTEIN	98	IPWA $\gamma N \rightarrow \pi N$
-0.135 ± 0.005	ARNDT	97	IPWA $\gamma N \rightarrow \pi N$
-0.1278 ± 0.0012	DAVIDSON	97	DPWA $\gamma N \rightarrow \pi N$
-0.141 ± 0.005	ARNDT	96	IPWA $\gamma N \rightarrow \pi N$
-0.135 ± 0.016	DAVIDSON	91b	FIT $\gamma N \rightarrow \pi N$
-0.145 ± 0.015	CRAWFORD	83	IPWA $\gamma N \rightarrow \pi N$
-0.138 ± 0.004	AWAJI	81	DPWA $\gamma N \rightarrow \pi N$
-0.147 ± 0.001	ARAI	80	DPWA $\gamma N \rightarrow \pi N$ (fit 1)
-0.145 ± 0.001	ARAI	80	DPWA $\gamma N \rightarrow \pi N$ (fit 2)
-0.136 ± 0.006	CRAWFORD	80	DPWA $\gamma N \rightarrow \pi N$
• • • We do not use the following data for averages, fits, limits, etc. • • •			
-0.1312	HANSTEIN	98	DPWA $\gamma N \rightarrow \pi N$
-0.143 ± 0.004	LI	93	IPWA $\gamma N \rightarrow \pi N$
-0.140 ± 0.007	DAVIDSON	90	FIT See DAVIDSON 91b
-0.142 ± 0.007	BARBOUR	78	DPWA $\gamma N \rightarrow \pi N$
-0.140	NOELLE	78	$\gamma N \rightarrow \pi N$
-0.141 ± 0.004	FELLER	76	DPWA $\gamma N \rightarrow \pi N$

 $\Delta(1232) \rightarrow N\gamma$, helicity-3/2 amplitude $A_{3/2}$

VALUE (GeV ^{-1/2})	DOCUMENT ID	TECN	COMMENT
-0.255 ± 0.008 OUR ESTIMATE			
-0.2466 ± 0.0013	HANSTEIN	98	IPWA $\gamma N \rightarrow \pi N$
-0.250 ± 0.008	ARNDT	97	IPWA $\gamma N \rightarrow \pi N$
-0.2524 ± 0.0013	DAVIDSON	97	DPWA $\gamma N \rightarrow \pi N$
-0.261 ± 0.005	ARNDT	96	IPWA $\gamma N \rightarrow \pi N$
-0.251 ± 0.033	DAVIDSON	91b	FIT $\gamma N \rightarrow \pi N$
-0.263 ± 0.026	CRAWFORD	83	IPWA $\gamma N \rightarrow \pi N$
-0.259 ± 0.006	AWAJI	81	DPWA $\gamma N \rightarrow \pi N$
-0.264 ± 0.002	ARAI	80	DPWA $\gamma N \rightarrow \pi N$ (fit 1)
-0.261 ± 0.002	ARAI	80	DPWA $\gamma N \rightarrow \pi N$ (fit 2)
-0.247 ± 0.010	CRAWFORD	80	DPWA $\gamma N \rightarrow \pi N$

• • • We do not use the following data for averages, fits, limits, etc. • • •

-0.2522	HANSTEIN	98	DPWA $\gamma N \rightarrow \pi N$
-0.262 ± 0.004	LI	93	IPWA $\gamma N \rightarrow \pi N$
-0.254 ± 0.011	DAVIDSON	90	FIT See DAVIDSON 91b
-0.271 ± 0.010	BARBOUR	78	DPWA $\gamma N \rightarrow \pi N$
-0.247	NOELLE	78	$\gamma N \rightarrow \pi N$
-0.256 ± 0.003	FELLER	76	DPWA $\gamma N \rightarrow \pi N$

 $\Delta(1232) \rightarrow N\gamma$, E_2/M_1 ratio

VALUE	DOCUMENT ID	TECN	COMMENT
-0.025 ± 0.005 OUR ESTIMATE			
-0.0254 ± 0.0010	HANSTEIN	98	DPWA $\gamma N \rightarrow \pi N$
-0.015 ± 0.005	ARNDT	97	IPWA $\gamma N \rightarrow \pi N$
-0.025 ± 0.002 ± 0.002	BECK	97	IPWA $\gamma N \rightarrow \pi N$
-0.030 ± 0.003 ± 0.002	BLANPIED	97	DPWA $\gamma N \rightarrow \pi N, \gamma N$
-0.0319 ± 0.0024	DAVIDSON	97	DPWA $\gamma N \rightarrow \pi N$
-0.015 ± 0.005	WORKMAN	92	IPWA $\gamma N \rightarrow \pi N$
-0.0157 ± 0.0072	DAVIDSON	91b	FIT $\gamma N \rightarrow \pi N$
• • • We do not use the following data for averages, fits, limits, etc. • • •			
-0.0233 ± 0.0017	HANSTEIN	98	IPWA $\gamma N \rightarrow \pi N$
-0.027 ± 0.003 ± 0.001	KHANDAKER	95	DPWA $\gamma N \rightarrow \pi N$
-0.0107 ± 0.0037	DAVIDSON	90	FIT $\gamma N \rightarrow \pi N$
-0.015 ± 0.002	DAVIDSON	86	FIT $\gamma N \rightarrow \pi N$
+0.037 ± 0.004	TANABE	85	FIT $\gamma N \rightarrow \pi N$

 $\Delta(1232) \rightarrow N\gamma$, absolute value of E_2/M_1 ratio at pole

VALUE	DOCUMENT ID	TECN	COMMENT
• • • We do not use the following data for averages, fits, limits, etc. • • •			
0.065 ± 0.007	ARNDT	97	DPWA $\gamma N \rightarrow \pi N$
0.058	HANSTEIN	96	DPWA $\gamma N \rightarrow \pi N$

 $\Delta(1232) \rightarrow N\gamma$, phase of E_2/M_1 ratio at pole

VALUE	DOCUMENT ID	TECN	COMMENT
• • • We do not use the following data for averages, fits, limits, etc. • • •			
-122 ± 5	ARNDT	97	DPWA $\gamma N \rightarrow \pi N$
-127.2	HANSTEIN	96	DPWA $\gamma N \rightarrow \pi N$

 $\Delta(1232)^{++}$ MAGNETIC MOMENT

The values are extracted from UCLA and SIN data on π^+p bremsstrahlung using a variety of different theoretical approximations and methods. Our estimate is only a rough guess of the range we expect the moment to lie within.

VALUE (μ_N)	DOCUMENT ID	COMMENT
3.7 to 7.5 OUR ESTIMATE		
• • • We do not use the following data for averages, fits, limits, etc. • • •		
4.52 ± 0.50 ± 0.45	BOSSHARD	91 $\pi^+p \rightarrow \pi^+p\gamma$ (SIN data)
3.7 to 4.2	LIN	91b $\pi^+p \rightarrow \pi^+p\gamma$ (from UCLA data)
4.6 to 4.9	LIN	91b $\pi^+p \rightarrow \pi^+p\gamma$ (from SIN data)
5.6 to 7.5	WITTMAN	88 $\pi^+p \rightarrow \pi^+p\gamma$ (from UCLA data)
6.9 to 9.8	HELLER	87 $\pi^+p \rightarrow \pi^+p\gamma$ (from UCLA data)
4.7 to 6.7	NEFKENS	78 $\pi^+p \rightarrow \pi^+p\gamma$ (UCLA data)

 $\Delta(1232)$ FOOTNOTES

- Using $\pi^\pm d$ as well, PEDRONI 78 determine $(M^- - M^{++}) + (M^0 - M^+)/3 = 4.6 \pm 0.2$ MeV.
- See HOEHLER 93 for a detailed discussion of the evidence for and the pole parameters of N and Δ resonances as determined from Argand diagrams of πN elastic partial-wave amplitudes and from plots of the speeds with which the amplitudes traverse the diagrams.
- This VASAN 76b value is from fits to the coulomb-barrier-corrected CARTER 73 phase shift.
- This VASAN 76b value is from fits to the CARTER 73 nuclear phase shift without coulomb barrier corrections.
- Converted to our conventions using $M = 1232$ MeV, $\Gamma = 110$ MeV from NOELLE 78.
- This ARNDT 97 value is very sensitive to the database being fitted. The result is from a fit to the full pion photoproduction database, apart from the BLANPIED 97 cross-section measurements.

 $\Delta(1232)$ REFERENCES

For early references, see Physics Letters 111B 70 (1982).

HANSTEIN	98	NP A632 561	O. Hanstein, D. Drechsel, L. Tiator
ARNDT	97	PR C56 577	R.A. Arndt, I.I. Strakovsky, R.L. Workman (VPI)
BECK	97	PRL 78 606	R. Beck et al. (MANZ, SACL, PAVL, GLAS)
Also	97b	PRL 79 4510	R.L. Beck, H.P. Krahn (MANZ)
Also	97c	PRL 79 4512	R.L. Beck, H.P. Krahn (MANZ)
Also	97d	PRL 79 4515 (erratum)	R.L. Beck et al. (MANZ, SACL, PAVL, GLAS)
BLANPIED	97	PRL 79 4337	G.S. Blani Pied et al. (LEGS Collab.)
DAVIDSON	97	PRL 79 4509	R.M. Davidson, N.C.A. Mukhopadhyay (RI)
ARNDT	96	PR C53 430	R.A. Arndt, I.I. Strakovsky, R.L. Workman (VPI)
BERNICHIA	96	NP A597 623	A. Bernichia, G. Lopez Castro, J. Pestieau (LOUV+)
HANSTEIN	96	PL B385 45	O. Hanstein, D. Drechsel, L. Tiator (MANZ)
ABAEV	95	ZPHY A352 85	V.V. Abaev, S.P. Kruglov (PNPI)
ARNDT	95	PR C52 2120	R.A. Arndt et al. (VPI, BRCO)
KHANDAKER	95	PR D51 3966	M. Khandaker, A.M. Sandoz (BNL, VPI)
HOEHLER	93	πN Newsletter 9 1	G. Honler (KARL)
LI	93	PR C47 2759	Z.J. Li et al. (VPI)
MANLEY	92	PR D45 4002	D.M. Manley, E.M. Saleski (KENT) IJP
Also	84	PR D30 904	D.M. Manley et al. (VPI)
WORKMAN	92	PR C46 1546	R.L. Workman, R.A. Arndt, Z.J. Li (VPI)
ARNDT	91	PR D43 2131	R.A. Arndt et al. (VPI, TELLE) IJP
BOSSHARD	91	PR D44 1962	A. Bosshard et al. (ZURI, LBL, VILL+)
Also	90	PRL 64 2619	A. Bosshard et al. (CATH, LAUS, LBL+)
DAVIDSON	91b	PR D43 71	R.M. Davidson, N.C. Mukhopadhyay, R.S. Wittman

See key on page 239

Baryon Particle Listings
 $\Delta(1232)$, $\Delta(1600)$

LIN	91B	PR C44 1819	D.H. Lin, M.K. Liou, Z.M. Ding	(CUNY, C50K)
Also	31	PR C43 R930	D. Lin, M.K. Liou	(CUNY)
DAVIDSON	90	PR D42 20	R.M. Davidson, N.C. Mukhopadhyay	(RPI)
WITTMAN	88	PR C37 2075	R. Wittman	(TRIUMF)
HELLER	87	PR C35 718	L. Heller et al.	(LANL, MIT, ILL)
DAVIDSON	86	PR 56 804	R.M. Davidson, N.C. Mukhopadhyay, R. Wittman	(RPI)
TANABE	85	PR C31 1876	H. Tanabe, K. Ohta	(KOMAB)
CRAWFORD	83	NP B211 1	R.L. Crawford, W.T. Morton	(GLAS)
PDG	82	PL 111B	M. Roos et al.	(HELS, CIT, CERN)
AWAJI	81	Bonn Conf. 352	N. Awaji, R. Kajikawa	(NAGO)
Also	82	NP B157 365	K. Fujii et al.	(NAGO)
ARAI	80	Toronto Conf. 93	I. Arai	(INUS)
Also	82	NP B194 251	I. Arai, H. Fujii	(INUS)
CRAWFORD	80	Toronto Conf. 107	R.L. Crawford	(GLAS)
CUTKOSKY	80	Toronto Conf. 19	R.E. Cutkosky et al.	(CMU, LBL) IJP
Also	79	PR D20 2839	R.E. Cutkosky et al.	(CMU, LBL)
KOCH	80B	NP A336 331	R. Koch, E. Pietarinen	(KARLT) IJP
HOEHLER	79	PDAT 12-1	G. Hoehler et al.	(KARLT) IJP
Also	80	Toronto Conf. 3	R. Koch	(KARLT) IJP
MIROSHNIC...	79	SJNP 29 94	I.I. Miroshnichenko et al.	(KFTI) IJP
Translated from YAF 29 188.				
BARBOUR	78	NP B141 253	I.M. Barbour, R.L. Crawford, N.H. Parsons	(GLAS)
NEFKENS	78	PR D18 3911	B.M.K. Nefkens et al.	(UCLA, CATH) IJP
NOELLE	78	PTP 60 778	P. Noelle	(NAGO)
PEDRONI	78	NP A300 321	E. Pedroni et al.	(SIN, ISNG, KARLE+) IJP
CAMPBELL	76	PR D14 2431	R.R. Campbell, G.L. Shaw, J.S. Ball	(BOIS, UCI+) IJP
FELLER	76	NP B104 219	P. Feller et al.	(NAGO, OSAK) IJP
VASAN	76B	NP B106 535	S.S. Vasan	(CMU) IJP
Also	76	NP B106 526	S.S. Vasan	(CMU) IJP
BERENDS	75	NP B84 342	F.A. Berends, A. Donnachie	(LEID, MCHS)
CARTER	73	NP B58 378	J.R. Carter, D.V. Bugg, J.R. Carter	(CAVE, LOQM) IJP

 $\Delta(1600) P_{33}$

$$I(J^P) = \frac{3}{2}(\frac{3}{2}^+) \text{ Status: } ***$$

Most of the results published before 1975 are now obsolete and have been omitted. They may be found in our 1982 edition, Physics Letters **111B** (1982).

The various analyses are not in good agreement.

 $\Delta(1600)$ BREIT-WIGNER MASS

VALUE (MeV)	DOCUMENT ID	TECN	COMMENT
1550 to 1700 (\approx 1600) OUR ESTIMATE			
1706 \pm 10	MANLEY 92	IPWA	$\pi N \rightarrow \pi N$ & $N\pi\pi$
1600 \pm 50	CUTKOSKY 80	IPWA	$\pi N \rightarrow \pi N$
1522 \pm 13	HOEHLER 79	IPWA	$\pi N \rightarrow \pi N$
● ● ● We do not use the following data for averages, fits, limits, etc. ● ● ●			
1672 \pm 15	ARNDT 96	IPWA	$\gamma N \rightarrow \pi N$
1706	LI 93	IPWA	$\gamma N \rightarrow \pi N$
1690	BARNHAM 80	IPWA	$\pi N \rightarrow N\pi\pi$
1560	¹ LONGACRE 77	IPWA	$\pi N \rightarrow N\pi\pi$
1640	² LONGACRE 75	IPWA	$\pi N \rightarrow N\pi\pi$

 $\Delta(1600)$ BREIT-WIGNER WIDTH

VALUE (MeV)	DOCUMENT ID	TECN	COMMENT
250 to 450 (\approx 350) OUR ESTIMATE			
430 \pm 73	MANLEY 92	IPWA	$\pi N \rightarrow \pi N$ & $N\pi\pi$
300 \pm 100	CUTKOSKY 80	IPWA	$\pi N \rightarrow \pi N$
220 \pm 40	HOEHLER 79	IPWA	$\pi N \rightarrow \pi N$
● ● ● We do not use the following data for averages, fits, limits, etc. ● ● ●			
315 \pm 20	ARNDT 96	IPWA	$\gamma N \rightarrow \pi N$
215	LI 93	IPWA	$\gamma N \rightarrow \pi N$
250	BARNHAM 80	IPWA	$\pi N \rightarrow N\pi\pi$
180	¹ LONGACRE 77	IPWA	$\pi N \rightarrow N\pi\pi$
300	² LONGACRE 75	IPWA	$\pi N \rightarrow N\pi\pi$

 $\Delta(1600)$ POLE POSITION

REAL PART			
VALUE (MeV)	DOCUMENT ID	TECN	COMMENT
1500 to 1700 (\approx 1600) OUR ESTIMATE			
1675	ARNDT 95	DPWA	$\pi N \rightarrow \pi N$
1550	³ HOEHLER 93	SPEL	$\pi N \rightarrow \pi N$
1550 \pm 40	CUTKOSKY 80	IPWA	$\pi N \rightarrow \pi N$
● ● ● We do not use the following data for averages, fits, limits, etc. ● ● ●			
1612	ARNDT 91	DPWA	$\pi N \rightarrow \pi N$ Soln SM90
1609 or 1610	⁴ LONGACRE 78	IPWA	$\pi N \rightarrow N\pi\pi$
1541 or 1542	¹ LONGACRE 77	IPWA	$\pi N \rightarrow N\pi\pi$
-2xIMAGINARY PART			
VALUE (MeV)	DOCUMENT ID	TECN	COMMENT
200 to 400 (\approx 300) OUR ESTIMATE			
386	ARNDT 95	DPWA	$\pi N \rightarrow \pi N$
200 \pm 60	CUTKOSKY 80	IPWA	$\pi N \rightarrow \pi N$
● ● ● We do not use the following data for averages, fits, limits, etc. ● ● ●			
230	ARNDT 91	DPWA	$\pi N \rightarrow \pi N$ Soln SM90
323 or 325	⁴ LONGACRE 78	IPWA	$\pi N \rightarrow N\pi\pi$
178 or 178	¹ LONGACRE 77	IPWA	$\pi N \rightarrow N\pi\pi$

 $\Delta(1600)$ ELASTIC POLE RESIDUE

MODULUS $ r $			
VALUE (MeV)	DOCUMENT ID	TECN	COMMENT
52	ARNDT 95	DPWA	$\pi N \rightarrow \pi N$
17 \pm 4	CUTKOSKY 80	IPWA	$\pi N \rightarrow \pi N$
● ● ● We do not use the following data for averages, fits, limits, etc. ● ● ●			
16	ARNDT 91	DPWA	$\pi N \rightarrow \pi N$ Soln SM90
PHASE θ			
VALUE ($^\circ$)	DOCUMENT ID	TECN	COMMENT
+ 14	ARNDT 95	DPWA	$\pi N \rightarrow \pi N$
-150 \pm 30	CUTKOSKY 80	IPWA	$\pi N \rightarrow \pi N$
● ● ● We do not use the following data for averages, fits, limits, etc. ● ● ●			
- 73	ARNDT 91	DPWA	$\pi N \rightarrow \pi N$ Soln SM90

 $\Delta(1600)$ DECAY MODES

The following branching fractions are our estimates, not fits or averages.

Mode	Fraction (Γ_i/Γ)
Γ_1 $N\pi$	10-25 %
Γ_2 ΣK	
Γ_3 $N\pi\pi$	75-90 %
Γ_4 $\Delta\pi$	40-70 %
Γ_5 $\Delta(1232)\pi$, P-wave	
Γ_6 $\Delta(1232)\pi$, F-wave	
Γ_7 $N\rho$	<25 %
Γ_8 $N\rho$, S=1/2, P-wave	
Γ_9 $N\rho$, S=3/2, P-wave	
Γ_{10} $N\rho$, S=3/2, F-wave	
Γ_{11} $N(1440)\pi$	10-35 %
Γ_{12} $N(1440)\pi$, P-wave	
Γ_{13} $N\gamma$	0.001-0.02 %
Γ_{14} $N\gamma$, helicity=1/2	0.0-0.02 %
Γ_{15} $N\gamma$, helicity=3/2	0.001-0.005 %

 $\Delta(1600)$ BRANCHING RATIOS

$\Gamma(N\pi)/\Gamma_{\text{total}}$				Γ_1/Γ
VALUE	DOCUMENT ID	TECN	COMMENT	
0.10 to 0.25 OUR ESTIMATE				
0.12 \pm 0.02	MANLEY 92	IPWA	$\pi N \rightarrow \pi N$ & $N\pi\pi$	
0.18 \pm 0.04	CUTKOSKY 80	IPWA	$\pi N \rightarrow \pi N$	
0.21 \pm 0.06	HOEHLER 79	IPWA	$\pi N \rightarrow \pi N$	
$(\Gamma_7/\Gamma)^{1/2}/\Gamma_{\text{total}}$ in $N\pi \rightarrow \Delta(1600) \rightarrow \Sigma K$				$(\Gamma_1/\Gamma)^{1/2}/\Gamma$
VALUE	DOCUMENT ID	TECN	COMMENT	
-0.36 to -0.28 OUR ESTIMATE				
● ● ● We do not use the following data for averages, fits, limits, etc. ● ● ●				
0.006 to 0.042	⁵ DEANS 75	DPWA	$\pi N \rightarrow \Sigma K$	

Note: Signs of couplings from $\pi N \rightarrow N\pi\pi$ analyses were changed in the 1986 edition to agree with the baryon-first convention; the overall phase ambiguity is resolved by choosing a negative sign for the $\Delta(1620) S_{31}$ coupling to $\Delta(1232)\pi$.

$(\Gamma_7/\Gamma)^{1/2}/\Gamma_{\text{total}}$ in $N\pi \rightarrow \Delta(1600) \rightarrow \Delta(1232)\pi$, P-wave				$(\Gamma_1/\Gamma)^{1/2}/\Gamma$
VALUE	DOCUMENT ID	TECN	COMMENT	
+0.27 to +0.33 OUR ESTIMATE				
+0.29 \pm 0.02	MANLEY 92	IPWA	$\pi N \rightarrow \pi N$ & $N\pi\pi$	
+0.24 \pm 0.05	BARNHAM 80	IPWA	$\pi N \rightarrow N\pi\pi$	
+0.34	^{1,6} LONGACRE 77	IPWA	$\pi N \rightarrow N\pi\pi$	
-0.30	² LONGACRE 75	IPWA	$\pi N \rightarrow N\pi\pi$	
$(\Gamma_7/\Gamma)^{1/2}/\Gamma_{\text{total}}$ in $N\pi \rightarrow \Delta(1600) \rightarrow \Delta(1232)\pi$, F-wave				$(\Gamma_1/\Gamma)^{1/2}/\Gamma$
VALUE	DOCUMENT ID	TECN	COMMENT	
-0.15 to -0.03 OUR ESTIMATE				
-0.07	^{1,6} LONGACRE 77	IPWA	$\pi N \rightarrow N\pi\pi$	
$(\Gamma_7/\Gamma)^{1/2}/\Gamma_{\text{total}}$ in $N\pi \rightarrow \Delta(1600) \rightarrow N\rho$, S=1/2, P-wave				$(\Gamma_1/\Gamma)^{1/2}/\Gamma$
VALUE	DOCUMENT ID	TECN	COMMENT	
+0.10				
+0.10	^{1,6} LONGACRE 77	IPWA	$\pi N \rightarrow N\pi\pi$	
$(\Gamma_7/\Gamma)^{1/2}/\Gamma_{\text{total}}$ in $N\pi \rightarrow \Delta(1600) \rightarrow N\rho$, S=3/2, P-wave				$(\Gamma_1/\Gamma)^{1/2}/\Gamma$
VALUE	DOCUMENT ID	TECN	COMMENT	
+0.10				
+0.10	^{1,6} LONGACRE 77	IPWA	$\pi N \rightarrow N\pi\pi$	

Baryon Particle Listings

 $\Delta(1600)$, $\Delta(1620)$

$(\Gamma_1 \Gamma_2)^{1/2} / \Gamma_{\text{total}}$ in $N\pi \rightarrow \Delta(1600) \rightarrow N(1440)\pi$, P-wave	$(\Gamma_1 \Gamma_2)^{1/2} / \Gamma$		
VALUE	DOCUMENT ID	TECN	COMMENT
+0.15 to +0.23 OUR ESTIMATE			
+0.16 ± 0.02	MANLEY	92	IPWA $\pi N \rightarrow \pi N$ & $N\pi\pi$
+0.23 ± 0.04	BARNHAM	80	IPWA $\pi N \rightarrow N\pi\pi$

 $\Delta(1620) S_{31}$

$$I(J^P) = \frac{3}{2}(\frac{1}{2}^-) \text{ Status: } ***$$

Most of the results published before 1975 are now obsolete and have been omitted. They may be found in our 1982 edition, Physics Letters 111B (1982).

 $\Delta(1600)$ PHOTON DECAY AMPLITUDES $\Delta(1600) \rightarrow N\gamma$, helicity-1/2 amplitude $A_{1/2}$

VALUE (GeV ^{-1/2})	DOCUMENT ID	TECN	COMMENT
-0.023 ± 0.020 OUR ESTIMATE			
-0.018 ± 0.015	ARNDT	96	IPWA $\gamma N \rightarrow \pi N$
-0.039 ± 0.030	CRAWFORD	83	IPWA $\gamma N \rightarrow \pi N$
-0.046 ± 0.013	AWAJI	81	DPWA $\gamma N \rightarrow \pi N$
0.005 ± 0.020	CRAWFORD	80	DPWA $\gamma N \rightarrow \pi N$
• • • We do not use the following data for averages, fits, limits, etc. • • •			
-0.026 ± 0.002	LI	93	IPWA $\gamma N \rightarrow \pi N$
-0.200	7 WADA	84	DPWA Compton scattering
0.000 ± 0.030	BARBOUR	78	DPWA $\gamma N \rightarrow \pi N$
0.0 ± 0.020	FELLER	76	DPWA $\gamma N \rightarrow \pi N$

 $\Delta(1600) \rightarrow N\gamma$, helicity-3/2 amplitude $A_{3/2}$

VALUE (GeV ^{-1/2})	DOCUMENT ID	TECN	COMMENT
-0.009 ± 0.021 OUR ESTIMATE			
-0.025 ± 0.015	ARNDT	96	IPWA $\gamma N \rightarrow \pi N$
-0.013 ± 0.014	CRAWFORD	83	IPWA $\gamma N \rightarrow \pi N$
0.025 ± 0.031	AWAJI	81	DPWA $\gamma N \rightarrow \pi N$
-0.009 ± 0.020	CRAWFORD	80	DPWA $\gamma N \rightarrow \pi N$
• • • We do not use the following data for averages, fits, limits, etc. • • •			
-0.016 ± 0.002	LI	93	IPWA $\gamma N \rightarrow \pi N$
0.023	WADA	84	DPWA Compton scattering
0.000 ± 0.045	BARBOUR	78	DPWA $\gamma N \rightarrow \pi N$
0.0 ± 0.015	FELLER	76	DPWA $\gamma N \rightarrow \pi N$

 $\Delta(1600)$ FOOTNOTES

- LONGACRE 77 pole positions are from a search for poles in the unitarized T-matrix; the first (second) value uses, in addition to $\pi N \rightarrow N\pi\pi$ data, elastic amplitudes from a Saclay (CERN) partial-wave analysis. The other LONGACRE 77 values are from eyeball fits with Breit-Wigner circles to the T-matrix amplitudes.
- From method II of LONGACRE 75: eyeball fits with Breit-Wigner circles to the T-matrix amplitudes.
- See HOEHLER 93 for a detailed discussion of the evidence for and the pole parameters of N and Δ resonances as determined from Argand diagrams of πN elastic partial-wave amplitudes and from plots of the speeds with which the amplitudes traverse the diagrams.
- LONGACRE 78 values are from a search for poles in the unitarized T-matrix. The first (second) value uses, in addition to $\pi N \rightarrow N\pi\pi$ data, elastic amplitudes from a Saclay (CERN) partial-wave analysis.
- The range given is from the four best solutions. DEANS 75 disagrees with $\pi^+ p \rightarrow \Sigma^+ K^+$ data of WINNIK 77 around 1920 MeV.
- LONGACRE 77 considers this coupling to be well determined.
- WADA 84 is inconsistent with other analyses — see the Note on N and Δ Resonances.

 $\Delta(1600)$ REFERENCES

For early references, see Physics Letters 111B 70 (1982).

ARNDT 96	PR C53 430	R.A. Arndt, I.I. Strakovsky, R.L. Workman	(VPI)
ARNDT 95	PR C52 2120	R.A. Arndt et al.	(VPI, BRCO)
HOEHLER 93	πN Newsletter 9 1	G. Hohler	(KARL)
LI 93	PR C47 2759	Z.J. Li et al.	(VPI)
MANLEY 92	PR D45 4002	D.M. Manley, E.M. Saleski	(KENT) IUP
Also 84	PR D30 904	D.M. Manley et al.	(VPI)
ARNDT 91	PR D43 2131	R.A. Arndt et al.	(VPI, TELE) IUP
WADA 84	NP B247 313	Y. Wada et al.	(INUS)
CRAWFORD 83	NP B211 1	R.L. Crawford, W.T. Morton	(GLAS)
PDG 82	PL 111B	M. Roos et al.	(HELS, CIT, CERN)
AWAJI 81	Bonn Conf. 352	N. Awaji, R. Kajikawa	(NAGO)
Also 82	NP B197 365	K. Fujii et al.	(NAGO)
BARNHAM 80	NP B168 243	K.W.J. Barnham et al.	(LOIC)
CRAWFORD 80	Toronto Conf. 107	R.L. Crawford	(GLAS)
CUTKOSKY 80	Toronto Conf. 19	R.E. Cutkosky et al.	(CMU, LBL) IUP
Also 79	PR D20 2839	R.E. Cutkosky et al.	(CMU, LBL) IUP
HOEHLER 79	PDAT 12-1	G. Hohler et al.	(KARLT) IUP
Also 80	Toronto Conf. 3	R. Koch	(KARLT) IUP
BARBOUR 78	NP B141 253	I.M. Barbour, R.L. Crawford, N.H. Parsons	(GLAS)
LONGACRE 78	PR D17 1795	R.S. Longacre et al.	(LBL, SLAC)
LONGACRE 77	NP B122 493	R.S. Longacre, J. Dolbeau	(SACL) IUP
Also 76	NP B108 365	J. Dolbeau et al.	(SACL) IUP
WINNIK 77	NP B128 56	M. Winnik et al.	(HAIF) I
FELLER 76	NP B104 219	P. Feller et al.	(NAGO, OSAK) IUP
DEANS 75	NP B96 90	S.R. Deans et al.	(SFLA, ALAH) IUP
LONGACRE 75	PL 55B 415	R.S. Longacre et al.	(LBL, SLAC) IUP

 $\Delta(1620)$ BREIT-WIGNER MASS

VALUE (MeV)	DOCUMENT ID	TECN	COMMENT
1615 to 1675 (≈ 1620) OUR ESTIMATE			
1672 ± 7	MANLEY	92	IPWA $\pi N \rightarrow \pi N$ & $N\pi\pi$
1620 ± 20	CUTKOSKY	80	IPWA $\pi N \rightarrow \pi N$
1610 ± 7	HOEHLER	79	IPWA $\pi N \rightarrow \pi N$
• • • We do not use the following data for averages, fits, limits, etc. • • •			
1672 ± 5	ARNDT	96	IPWA $\gamma N \rightarrow \pi N$
1617	ARNDT	95	DPWA $\pi N \rightarrow N\pi$
1669	LI	93	IPWA $\gamma N \rightarrow \pi N$
1620	BARNHAM	80	IPWA $\pi N \rightarrow N\pi\pi$
1712.8 ± 6.0	1 CHEW	80	BPWA $\pi^+ p \rightarrow \pi^+ p$
1786.7 ± 2.0	1 CHEW	80	BPWA $\pi^+ p \rightarrow \pi^+ p$
1657	CRAWFORD	80	DPWA $\gamma N \rightarrow \pi N$
1662	BARBOUR	78	DPWA $\gamma N \rightarrow \pi N$
1580	2 LONGACRE	77	IPWA $\pi N \rightarrow N\pi\pi$
1600	3 LONGACRE	75	IPWA $\pi N \rightarrow N\pi\pi$

 $\Delta(1620)$ BREIT-WIGNER WIDTH

VALUE (MeV)	DOCUMENT ID	TECN	COMMENT
120 to 180 (≈ 150) OUR ESTIMATE			
154 ± 37	MANLEY	92	IPWA $\pi N \rightarrow \pi N$ & $N\pi\pi$
140 ± 20	CUTKOSKY	80	IPWA $\pi N \rightarrow \pi N$
139 ± 18	HOEHLER	79	IPWA $\pi N \rightarrow \pi N$
• • • We do not use the following data for averages, fits, limits, etc. • • •			
147 ± 8	ARNDT	96	IPWA $\gamma N \rightarrow \pi N$
108	ARNDT	95	DPWA $\pi N \rightarrow N\pi$
184	LI	93	IPWA $\gamma N \rightarrow \pi N$
120	BARNHAM	80	IPWA $\pi N \rightarrow N\pi\pi$
228.3 ± 18.0	1 CHEW	80	BPWA $\pi^+ p \rightarrow \pi^+ p$ (lower mass)
30.0 ± 6.4	1 CHEW	80	BPWA $\pi^+ p \rightarrow \pi^+ p$ (higher mass)
161	CRAWFORD	80	DPWA $\gamma N \rightarrow \pi N$
180	BARBOUR	78	DPWA $\gamma N \rightarrow \pi N$
120	2 LONGACRE	77	IPWA $\pi N \rightarrow N\pi\pi$
150	3 LONGACRE	75	IPWA $\pi N \rightarrow N\pi\pi$

 $\Delta(1620)$ POLE POSITION

REAL PART	DOCUMENT ID	TECN	COMMENT
VALUE (MeV)			
1580 to 1620 (≈ 1600) OUR ESTIMATE			
1585	ARNDT	95	DPWA $\pi N \rightarrow N\pi$
1608	4 HOEHLER	93	SPED $\pi N \rightarrow \pi N$
1600 ± 15	CUTKOSKY	80	IPWA $\pi N \rightarrow \pi N$
• • • We do not use the following data for averages, fits, limits, etc. • • •			
1587	ARNDT	91	DPWA $\pi N \rightarrow \pi N$ Soln SM90
1583 or 1583	5 LONGACRE	78	IPWA $\pi N \rightarrow N\pi\pi$
1575 or 1572	2 LONGACRE	77	IPWA $\pi N \rightarrow N\pi\pi$

-2xIMAGINARY PART

VALUE (MeV)	DOCUMENT ID	TECN	COMMENT
100 to 130 (≈ 115) OUR ESTIMATE			
104	ARNDT	95	DPWA $\pi N \rightarrow N\pi$
116	4 HOEHLER	93	SPED $\pi N \rightarrow \pi N$
120 ± 20	CUTKOSKY	80	IPWA $\pi N \rightarrow \pi N$
• • • We do not use the following data for averages, fits, limits, etc. • • •			
120	ARNDT	91	DPWA $\pi N \rightarrow \pi N$ Soln SM90
143 or 149	5 LONGACRE	78	IPWA $\pi N \rightarrow N\pi\pi$
119 or 128	2 LONGACRE	77	IPWA $\pi N \rightarrow N\pi\pi$

 $\Delta(1620)$ ELASTIC POLE RESIDUE

MODULUS r	DOCUMENT ID	TECN	COMMENT
VALUE (MeV)			
14	ARNDT	95	DPWA $\pi N \rightarrow N\pi$
19	HOEHLER	93	SPED $\pi N \rightarrow \pi N$
15 ± 2	CUTKOSKY	80	IPWA $\pi N \rightarrow \pi N$
• • • We do not use the following data for averages, fits, limits, etc. • • •			
15	ARNDT	91	DPWA $\pi N \rightarrow \pi N$ Soln SM90

See key on page 239

Baryon Particle Listings

 $\Delta(1620)$, $\Delta(1700)$ PHASE θ

VALUE ($^\circ$)	DOCUMENT ID	TECN	COMMENT
-121	ARNDT 95	DPWA	$\pi N \rightarrow N\pi$
-95	HOEHLER 93	SPED	$\pi N \rightarrow \pi N$
-110 \pm 20	CUTKOSKY 80	IPWA	$\pi N \rightarrow \pi N$
••• We do not use the following data for averages, fits, limits, etc. •••			
-125	ARNDT 91	DPWA	$\pi N \rightarrow \pi N$ Soln SM90

 $\Delta(1620)$ DECAY MODES

The following branching fractions are our estimates, not fits or averages.

Mode	Fraction (Γ_i/Γ)
Γ_1 $N\pi$	20-30 %
Γ_2 $N\pi\pi$	70-80 %
Γ_3 $\Delta\pi$	30-60 %
Γ_4 $\Delta(1232)\pi$, D-wave	
Γ_5 $N\rho$	7-25 %
Γ_6 $N\rho$, $S=1/2$, S-wave	
Γ_7 $N\rho$, $S=3/2$, D-wave	
Γ_8 $N(1440)\pi$	
Γ_9 $N\gamma$	0.004-0.044 %
Γ_{10} $N\gamma$, helicity=1/2	0.004-0.044 %

 $\Delta(1620)$ BRANCHING RATIOS

$\Gamma(N\pi)/\Gamma_{total}$	DOCUMENT ID	TECN	COMMENT	Γ_1/Γ
0.2 to 0.3 OUR ESTIMATE				
0.09 \pm 0.02	MANLEY 92	IPWA	$\pi N \rightarrow \pi N$ & $N\pi\pi$	
0.25 \pm 0.03	CUTKOSKY 80	IPWA	$\pi N \rightarrow \pi N$	
0.35 \pm 0.06	HOEHLER 79	IPWA	$\pi N \rightarrow \pi N$	
••• We do not use the following data for averages, fits, limits, etc. •••				
0.29	ARNDT 95	DPWA	$\pi N \rightarrow N\pi$	
0.60	¹ CHEW 80	BPWA	$\pi^+ p \rightarrow \pi^+ p$ (lower mass)	
0.36	¹ CHEW 80	BPWA	$\pi^+ p \rightarrow \pi^+ p$ (higher mass)	

Note: Signs of couplings from $\pi N \rightarrow N\pi\pi$ analyses were changed in the 1986 edition to agree with the baryon-first convention; the overall phase ambiguity is resolved by choosing a negative sign for the $\Delta(1620)$ S_{31} coupling to $\Delta(1232)\pi$.

$(\Gamma_1/\Gamma_2)^{1/2}/\Gamma_{total}$ in $N\pi \rightarrow \Delta(1620) \rightarrow \Delta(1232)\pi$, D-wave	DOCUMENT ID	TECN	COMMENT	$(\Gamma_1/\Gamma_4)^{1/2}/\Gamma$
-0.36 to -0.28 OUR ESTIMATE				
-0.24 \pm 0.03	MANLEY 92	IPWA	$\pi N \rightarrow \pi N$ & $N\pi\pi$	
-0.33 \pm 0.06	BARNHAM 80	IPWA	$\pi N \rightarrow N\pi\pi$	
-0.39	^{2,6} LONGACRE 77	IPWA	$\pi N \rightarrow N\pi\pi$	
-0.40	³ LONGACRE 75	IPWA	$\pi N \rightarrow N\pi\pi$	

$(\Gamma_1/\Gamma_5)^{1/2}/\Gamma_{total}$ in $N\pi \rightarrow \Delta(1620) \rightarrow N\rho$, $S=1/2$, S-wave	DOCUMENT ID	TECN	COMMENT	$(\Gamma_1/\Gamma_6)^{1/2}/\Gamma$
+0.12 to +0.22 OUR ESTIMATE				
+0.15 \pm 0.02	MANLEY 92	IPWA	$\pi N \rightarrow \pi N$ & $N\pi\pi$	
+0.40 \pm 0.10	BARNHAM 80	IPWA	$\pi N \rightarrow N\pi\pi$	
+0.08	^{2,6} LONGACRE 77	IPWA	$\pi N \rightarrow N\pi\pi$	
+0.28	³ LONGACRE 75	IPWA	$\pi N \rightarrow N\pi\pi$	

$(\Gamma_1/\Gamma_7)^{1/2}/\Gamma_{total}$ in $N\pi \rightarrow \Delta(1620) \rightarrow N\rho$, $S=3/2$, D-wave	DOCUMENT ID	TECN	COMMENT	$(\Gamma_1/\Gamma_7)^{1/2}/\Gamma$
-0.15 to -0.03 OUR ESTIMATE				
-0.06 \pm 0.02	MANLEY 92	IPWA	$\pi N \rightarrow \pi N$ & $N\pi\pi$	
-0.13	^{2,6} LONGACRE 77	IPWA	$\pi N \rightarrow N\pi\pi$	

$(\Gamma_1/\Gamma_8)^{1/2}/\Gamma_{total}$ in $N\pi \rightarrow \Delta(1620) \rightarrow N(1440)\pi$	DOCUMENT ID	TECN	COMMENT	$(\Gamma_1/\Gamma_8)^{1/2}/\Gamma$
0.11 \pm 0.05	BARNHAM 80	IPWA	$\pi N \rightarrow N\pi\pi$	

 $\Delta(1620)$ PHOTON DECAY AMPLITUDES $\Delta(1620) \rightarrow N\gamma$, helicity-1/2 amplitude $A_{1/2}$

VALUE (GeV $^{-1/2}$)	DOCUMENT ID	TECN	COMMENT
+0.027 \pm 0.011 OUR ESTIMATE			
0.035 \pm 0.020	ARNDT 96	IPWA	$\gamma N \rightarrow \pi N$
0.035 \pm 0.010	CRAWFORD 83	IPWA	$\gamma N \rightarrow \pi N$
0.010 \pm 0.015	AWAJI 81	DPWA	$\gamma N \rightarrow \pi N$
-0.022 \pm 0.007	ARAI 80	DPWA	$\gamma N \rightarrow \pi N$ (fit 1)
-0.026 \pm 0.008	ARAI 80	DPWA	$\gamma N \rightarrow \pi N$ (fit 2)
0.021 \pm 0.020	CRAWFORD 80	DPWA	$\gamma N \rightarrow \pi N$
0.126 \pm 0.021	TAKEDA 80	DPWA	$\gamma N \rightarrow \pi N$

••• We do not use the following data for averages, fits, limits, etc. •••

0.042 \pm 0.003	LI 93	IPWA	$\gamma N \rightarrow \pi N$
0.066	WADA 84	DPWA	Compton scattering
+0.034 \pm 0.028	BARBOUR 78	DPWA	$\gamma N \rightarrow \pi N$
-0.005 \pm 0.016	FELLER 76	DPWA	$\gamma N \rightarrow \pi N$

 $\Delta(1620)$ FOOTNOTES

- CHEW 80 reports two S_{31} resonances at somewhat higher masses than other analyses. Problems with this analysis are discussed in section 2.1.11 of HOEHLER 83.
- LONGACRE 77 pole positions are from a search for poles in the unitarized T-matrix; the first (second) value uses, in addition to $\pi N \rightarrow N\pi\pi$ data, elastic amplitudes from a Saclay (CERN) partial-wave analysis. The other LONGACRE 77 values are from eyeball fits with Breit-Wigner circles to the T-matrix amplitudes.
- From method II of LONGACRE 75: eyeball fits with Breit-Wigner circles to the T-matrix amplitudes.
- See HOEHLER 93 for a detailed discussion of the evidence for and the pole parameters of N and Δ resonances as determined from Argand diagrams of πN elastic partial-wave amplitudes and from plots of the speeds with which the amplitudes traverse the diagrams.
- LONGACRE 78 values are from a search for poles in the unitarized T-matrix. The first (second) value uses, in addition to $\pi N \rightarrow N\pi\pi$ data, elastic amplitudes from a Saclay (CERN) partial-wave analysis.
- LONGACRE 77 considers this coupling to be well determined.

 $\Delta(1620)$ REFERENCESFor early references, see Physics Letters **111B** 70 (1982).

ARNDT 96	PR C53 430	R.A. Arndt, I.I. Strakovsky, R.L. Workman	(VPI)
ARNDT 95	PR C52 2120	R.A. Arndt et al.	(VPI, BRCO)
HOEHLER 93	πN Newsletter 9 1	G. Hoehler	(KARL)
LI 93	PR C47 2759	Z.J. Li et al.	(VPI)
MANLEY 92	PR D45 4002	D.M. Manley, E.M. Saleski	(KENT) IJP
Also 84	PR D30 904	D.M. Manley et al.	(VPI)
ARNDT 91	PR D43 2131	R.A. Arndt et al.	(VPI, TELE) IJP
WADA 84	NP B247 313	Y. Wada et al.	(INUS)
CRAWFORD 83	NP B211 1	R.L. Crawford, W.T. Morton	(GLAS)
HOEHLER 83	Landolt-Boernstein 1/9B2	G. Hoehler	(KARL)
FDG 82	PL 111B	M. Roos et al.	(HELS. CIT. CERN)
AWAJI 81	Bonn Conf. 352	N. Awaji, R. Kajikawa	(NAGO)
Also 82	NP B197 365	K. Fujii et al.	(NAGO)
ARAI 80	Toronto Conf. 93	I. Arai	(INUS)
Also 82	NP B194 251	I. Arai, H. Fujii	(INUS)
BARNHAM 80	NP B168 243	K.W.J. Barnham et al.	(LOIC)
CHEW 80	Toronto Conf. 123	D.M. Chew	(LBL) IJP
CRAWFORD 80	Toronto Conf. 107	R.L. Crawford	(GLAS)
CUTKOSKY 80	Toronto Conf. 19	R.E. Cutkosky et al.	(CMU, LBL) IJP
Also 79	PR D20 2839	R.E. Cutkosky et al.	(CMU, LBL) IJP
TAKEDA 80	NP B168 17	H. Takeda et al.	(TOKY, INUS)
HOEHLER 79	PDAT 12-1	G. Hoehler et al.	(KARL) IJP
Also 80	Toronto Conf. 3	R. Koch	(KARL) IJP
BARBOUR 78	NP B141 253	I.M. Barbour, R.L. Crawford, N.H. Parsons	(GLAS)
LONGACRE 78	PR D17 1795	R.S. Longacre et al.	(LBL, SLAC)
LONGACRE 77	NP B122 493	R.S. Longacre, J. Dolbeau	(SACL) IJP
Also 76	NP B108 365	J. Dolbeau et al.	(SACL) IJP
FELLER 76	NP B104 219	P. Feller et al.	(NAGO, OSAK) IJP
LONGACRE 75	PL 55B 415	R.S. Longacre et al.	(LBL, SLAC) IJP

 $\Delta(1700)$ D_{33}

$$I(J^P) = \frac{3}{2}(\frac{3}{2}^-) \text{ Status: } ***$$

Most of the results published before 1975 are now obsolete and have been omitted. They may be found in our 1982 edition, Physics Letters **111B** (1982).

 $\Delta(1700)$ BREIT-WIGNER MASS

VALUE (MeV)	DOCUMENT ID	TECN	COMMENT
1670 to 1770 (\approx 1700) OUR ESTIMATE			
1762 \pm 44	MANLEY 92	IPWA	$\pi N \rightarrow \pi N$ & $N\pi\pi$
1710 \pm 30	CUTKOSKY 80	IPWA	$\pi N \rightarrow \pi N$
1680 \pm 70	HOEHLER 79	IPWA	$\pi N \rightarrow \pi N$
••• We do not use the following data for averages, fits, limits, etc. •••			
1690 \pm 15	ARNDT 96	IPWA	$\gamma N \rightarrow \pi N$
1680	ARNDT 95	DPWA	$\pi N \rightarrow N\pi$
1655	LI 93	IPWA	$\gamma N \rightarrow \pi N$
1650	BARNHAM 80	IPWA	$\pi N \rightarrow N\pi\pi$
1718.4 $^{+13.1}_{-13.0}$	¹ CHEW 80	BPWA	$\pi^+ p \rightarrow \pi^+ p$
1622	CRAWFORD 80	DPWA	$\gamma N \rightarrow \pi N$
1629	BARBOUR 78	DPWA	$\gamma N \rightarrow \pi N$
1600	² LONGACRE 77	IPWA	$\pi N \rightarrow N\pi\pi$
1680	³ LONGACRE 75	IPWA	$\pi N \rightarrow N\pi\pi$

 $\Delta(1700)$ BREIT-WIGNER WIDTH

VALUE (MeV)	DOCUMENT ID	TECN	COMMENT
200 to 400 (\approx 300) OUR ESTIMATE			
600 \pm 250	MANLEY 92	IPWA	$\pi N \rightarrow \pi N$ & $N\pi\pi$
280 \pm 80	CUTKOSKY 80	IPWA	$\pi N \rightarrow \pi N$
230 \pm 80	HOEHLER 79	IPWA	$\pi N \rightarrow \pi N$

Baryon Particle Listings

 $\Delta(1700)$

• • • We do not use the following data for averages, fits, limits, etc. • • •

285 ± 20	ARNDT	96	IPWA	$\gamma N \rightarrow \pi N$
272	ARNDT	95	DPWA	$\pi N \rightarrow N\pi$
348	LI	93	IPWA	$\gamma N \rightarrow \pi N$
160	BARNHAM	80	IPWA	$\pi N \rightarrow N\pi\pi$
193.3 ± 26.0	¹ CHEW	80	BPWA	$\pi^+ p \rightarrow \pi^+ p$
209	CRAWFORD	80	DPWA	$\gamma N \rightarrow \pi N$
216	BARBOUR	78	DPWA	$\gamma N \rightarrow \pi N$
200	² LONGACRE	77	IPWA	$\pi N \rightarrow N\pi\pi$
240	³ LONGACRE	75	IPWA	$\pi N \rightarrow N\pi\pi$

 $\Delta(1700)$ POLE POSITION

REAL PART

VALUE (MeV)	DOCUMENT ID	TECN	COMMENT
1620 to 1700 (≈ 1660) OUR ESTIMATE			
1655	ARNDT	95	DPWA $\pi N \rightarrow N\pi$
1651	⁴ HOEHLER	93	SPED $\pi N \rightarrow \pi N$
1675 ± 25	CUTKOSKY	80	IPWA $\pi N \rightarrow \pi N$

• • • We do not use the following data for averages, fits, limits, etc. • • •

1646	ARNDT	91	DPWA $\pi N \rightarrow \pi N$ Soln SM90
1681 or 1672	⁵ LONGACRE	78	IPWA $\pi N \rightarrow N\pi\pi$
1600 or 1594	² LONGACRE	77	IPWA $\pi N \rightarrow N\pi\pi$

-2xIMAGINARY PART

VALUE (MeV)	DOCUMENT ID	TECN	COMMENT
150 to 250 (≈ 200) OUR ESTIMATE			
242	ARNDT	95	DPWA $\pi N \rightarrow N\pi$
159	⁴ HOEHLER	93	SPED $\pi N \rightarrow \pi N$
220 ± 40	CUTKOSKY	80	IPWA $\pi N \rightarrow \pi N$

• • • We do not use the following data for averages, fits, limits, etc. • • •

208	ARNDT	91	DPWA $\pi N \rightarrow \pi N$ Soln SM90
245 or 241	⁵ LONGACRE	78	IPWA $\pi N \rightarrow N\pi\pi$
208 or 201	² LONGACRE	77	IPWA $\pi N \rightarrow N\pi\pi$

 $\Delta(1700)$ ELASTIC POLE RESIDUEMODULUS $|r|$

VALUE (MeV)	DOCUMENT ID	TECN	COMMENT
16	ARNDT	95	DPWA $\pi N \rightarrow N\pi$
10	HOEHLER	93	SPED $\pi N \rightarrow \pi N$
13 ± 3	CUTKOSKY	80	IPWA $\pi N \rightarrow \pi N$

• • • We do not use the following data for averages, fits, limits, etc. • • •

13	ARNDT	91	DPWA $\pi N \rightarrow \pi N$ Soln SM90
----	-------	----	--

PHASE θ

VALUE (°)	DOCUMENT ID	TECN	COMMENT
-12	ARNDT	95	DPWA $\pi N \rightarrow N\pi$
-20 ± 25	CUTKOSKY	80	IPWA $\pi N \rightarrow \pi N$

• • • We do not use the following data for averages, fits, limits, etc. • • •

-22	ARNDT	91	DPWA $\pi N \rightarrow \pi N$ Soln SM90
-----	-------	----	--

 $\Delta(1700)$ DECAY MODES

The following branching fractions are our estimates, not fits or averages.

Mode	Fraction (Γ_i/Γ)
Γ_1 $N\pi$	10-20 %
Γ_2 ΣK	
Γ_3 $N\pi\pi$	80-90 %
Γ_4 $\Delta\pi$	30-60 %
Γ_5 $\Delta(1232)\pi$, S-wave	25-50 %
Γ_6 $\Delta(1232)\pi$, D-wave	1-7 %
Γ_7 $N\rho$	30-55 %
Γ_8 $N\rho$, S=1/2, D-wave	
Γ_9 $N\rho$, S=3/2, S-wave	5-20 %
Γ_{10} $N\rho$, S=3/2, D-wave	
Γ_{11} $N\gamma$	0.12-0.26 %
Γ_{12} $N\gamma$, helicity=1/2	0.08-0.16 %
Γ_{13} $N\gamma$, helicity=3/2	0.025-0.12 %

 $\Delta(1700)$ BRANCHING RATIOS

$\Gamma(N\pi)/\Gamma_{\text{total}}$	DOCUMENT ID	TECN	COMMENT	Γ_1/Γ
0.10 to 0.20 OUR ESTIMATE				
0.14 ± 0.06	MANLEY	92	IPWA $\pi N \rightarrow \pi N$ & $N\pi\pi$	
0.12 ± 0.03	CUTKOSKY	80	IPWA $\pi N \rightarrow \pi N$	
0.20 ± 0.03	HOEHLER	79	IPWA $\pi N \rightarrow \pi N$	

• • • We do not use the following data for averages, fits, limits, etc. • • •

0.16	ARNDT	95	DPWA $\pi N \rightarrow N\pi$	
0.16	¹ CHEW	80	BPWA $\pi^+ p \rightarrow \pi^+ p$	

 $(\Gamma_1\Gamma_7)^{1/2}/\Gamma_{\text{total}}$ in $N\pi \rightarrow \Delta(1700) \rightarrow \Sigma K$

VALUE	DOCUMENT ID	TECN	COMMENT
• • • We do not use the following data for averages, fits, limits, etc. • • •			
0.002	LIVANOS	80	DPWA $\pi p \rightarrow \Sigma K$
0.001 to 0.011	⁶ DEANS	75	DPWA $\pi N \rightarrow \Sigma K$

Note: Signs of couplings from $\pi N \rightarrow N\pi\pi$ analyses were changed in the 1986 edition to agree with the baryon-first convention; the overall phase ambiguity is resolved by choosing a negative sign for the $\Delta(1620)$ S_{31} coupling to $\Delta(1232)\pi$.

 $(\Gamma_1\Gamma_7)^{1/2}/\Gamma_{\text{total}}$ in $N\pi \rightarrow \Delta(1700) \rightarrow \Delta(1232)\pi$, S-wave

VALUE	DOCUMENT ID	TECN	COMMENT
+0.21 to +0.29 OUR ESTIMATE			
+0.32 ± 0.06	MANLEY	92	IPWA $\pi N \rightarrow \pi N$ & $N\pi\pi$
+0.16 ± 0.04	BARNHAM	80	IPWA $\pi N \rightarrow N\pi\pi$
+0.30	^{2,7} LONGACRE	77	IPWA $\pi N \rightarrow N\pi\pi$
+0.24	³ LONGACRE	75	IPWA $\pi N \rightarrow N\pi\pi$

 $(\Gamma_1\Gamma_7)^{1/2}/\Gamma_{\text{total}}$ in $N\pi \rightarrow \Delta(1700) \rightarrow \Delta(1232)\pi$, D-wave

VALUE	DOCUMENT ID	TECN	COMMENT
+0.05 to +0.11 OUR ESTIMATE			
+0.08 ± 0.03	MANLEY	92	IPWA $\pi N \rightarrow \pi N$ & $N\pi\pi$
0.14 ± 0.04	BARNHAM	80	IPWA $\pi N \rightarrow N\pi\pi$
+0.05	^{2,7} LONGACRE	77	IPWA $\pi N \rightarrow N\pi\pi$
+0.10	³ LONGACRE	75	IPWA $\pi N \rightarrow N\pi\pi$

 $(\Gamma_1\Gamma_7)^{1/2}/\Gamma_{\text{total}}$ in $N\pi \rightarrow \Delta(1700) \rightarrow N\rho$, S=1/2, D-wave

VALUE	DOCUMENT ID	TECN	COMMENT
+0.17 ± 0.05	BARNHAM	80	IPWA $\pi N \rightarrow N\pi\pi$

 $(\Gamma_1\Gamma_7)^{1/2}/\Gamma_{\text{total}}$ in $N\pi \rightarrow \Delta(1700) \rightarrow N\rho$, S=3/2, S-wave

VALUE	DOCUMENT ID	TECN	COMMENT
±0.11 to ±0.19 OUR ESTIMATE			
+0.10 ± 0.03	MANLEY	92	IPWA $\pi N \rightarrow \pi N$ & $N\pi\pi$
+0.04	^{2,7} LONGACRE	77	IPWA $\pi N \rightarrow N\pi\pi$
-0.30	³ LONGACRE	75	IPWA $\pi N \rightarrow N\pi\pi$

 $(\Gamma_1\Gamma_7)^{1/2}/\Gamma_{\text{total}}$ in $N\pi \rightarrow \Delta(1700) \rightarrow N\rho$, S=3/2, D-wave

VALUE	DOCUMENT ID	TECN	COMMENT
0.18 ± 0.07	BARNHAM	80	IPWA $\pi N \rightarrow N\pi\pi$

 $\Delta(1700)$ PHOTON DECAY AMPLITUDES $\Delta(1700) \rightarrow N\gamma$, helicity-1/2 amplitude $A_{1/2}$

VALUE (GeV ^{-1/2})	DOCUMENT ID	TECN	COMMENT
+0.104 ± 0.015 OUR ESTIMATE			
0.090 ± 0.025	ARNDT	96	IPWA $\gamma N \rightarrow \pi N$
0.111 ± 0.017	CRAWFORD	83	IPWA $\gamma N \rightarrow \pi N$
0.089 ± 0.033	AWAJI	81	DPWA $\gamma N \rightarrow \pi N$
0.112 ± 0.006	ARAI	80	DPWA $\gamma N \rightarrow \pi N$ (fit 1)
0.130 ± 0.006	ARAI	80	DPWA $\gamma N \rightarrow \pi N$ (fit 2)
0.123 ± 0.022	CRAWFORD	80	DPWA $\gamma N \rightarrow \pi N$

• • • We do not use the following data for averages, fits, limits, etc. • • •

0.121 ± 0.004	LI	93	IPWA $\gamma N \rightarrow \pi N$
+0.130 ± 0.037	BARBOUR	78	DPWA $\gamma N \rightarrow \pi N$
+0.072 ± 0.033	FELLER	76	DPWA $\gamma N \rightarrow \pi N$

 $\Delta(1700) \rightarrow N\gamma$, helicity-3/2 amplitude $A_{3/2}$

VALUE (GeV ^{-1/2})	DOCUMENT ID	TECN	COMMENT
+0.085 ± 0.022 OUR ESTIMATE			
0.097 ± 0.020	ARNDT	96	IPWA $\gamma N \rightarrow \pi N$
0.107 ± 0.015	CRAWFORD	83	IPWA $\gamma N \rightarrow \pi N$
0.060 ± 0.015	AWAJI	81	DPWA $\gamma N \rightarrow \pi N$
0.047 ± 0.007	ARAI	80	DPWA $\gamma N \rightarrow \pi N$ (fit 1)
0.050 ± 0.007	ARAI	80	DPWA $\gamma N \rightarrow \pi N$ (fit 2)
0.102 ± 0.015	CRAWFORD	80	DPWA $\gamma N \rightarrow \pi N$

• • • We do not use the following data for averages, fits, limits, etc. • • •

0.115 ± 0.004	LI	93	IPWA $\gamma N \rightarrow \pi N$
+0.098 ± 0.036	BARBOUR	78	DPWA $\gamma N \rightarrow \pi N$
+0.087 ± 0.023	FELLER	76	DPWA $\gamma N \rightarrow \pi N$

 $\Delta(1700)$ FOOTNOTES

- Problems with CHEW 80 are discussed in section 2.1.11 of HOEHLER 83.
- LONGACRE 77 pole positions are from a search for poles in the unitarized T-matrix; the first (second) value uses, in addition to $\pi N \rightarrow N\pi\pi$ data, elastic amplitudes from a Saclay (CERN) partial-wave analysis. The other LONGACRE 77 values are from eyeball fits with Breit-Wigner circles to the T-matrix amplitudes.
- From method II of LONGACRE 75: eyeball fits with Breit-Wigner circles to the T-matrix amplitudes.
- See HOEHLER 93 for a detailed discussion of the evidence for and the pole parameters of N and Δ resonances as determined from Argand diagrams of πN elastic partial-wave amplitudes and from plots of the speeds with which the amplitudes traverse the diagrams.

See key on page 239

Baryon Particle Listings

$\Delta(1700)$, $\Delta(1750)$, $\Delta(1900)$

⁵ LONGACRE 78 values are from a search for poles in the unitarized T-matrix. The first (second) value uses, in addition to $\pi N \rightarrow N\pi\pi$ data, elastic amplitudes from a Saclay (CERN) partial-wave analysis.
⁶ The range given is from the four best solutions. DEANS 75 disagrees with $\pi^+ p \rightarrow \Sigma^+ K^+$ data of WINNIK 77 around 1920 MeV.
⁷ LONGACRE 77 considers this coupling to be well determined.

$\Delta(1900) S_{31}$

$$I(J^P) = \frac{3}{2}(\frac{1}{2}^-) \text{ Status: } **$$

OMITTED FROM SUMMARY TABLE

$\Delta(1700)$ REFERENCES

For early references, see Physics Letters 111B 70 (1982).

Author	Year	Reference	Method	Comment
ARNDT	96	PR C53 430	R.A. Arndt, I.I. Strakovsky, R.L. Workman	(VPI)
ARNDT	95	PR C52 2120	R.A. Arndt et al.	(VPI, BRCO)
HOEHLER	93	πN Newsletter 9 1	G. Hohler	(KARL)
LI	93	PR C47 2759	Z.J. Li et al.	(VPI)
MANLEY	92	PR D45 4002	D.M. Manley, E.M. Saleski	(KENT) IJP
Also	84	PR D39 904	D.M. Manley et al.	(VPI)
ARNDT	91	PR D43 2131	R.A. Arndt et al.	(VPI, TELE) IJP
CRAWFORD	83	NP B211 1	R.L. Crawford, W.T. Morton	(GLAS)
HOEHLER	83	Landolt-Boernstein 1/9B2	G. Hohler	(KARLT)
PDG	82	PL 111B	M. Roos et al.	(HEL5, CIT, CERN)
AWAJI	81	Bonn Conf. 352	N. Awaji, R. Kajikawa	(NAGO)
Also	82	NP B197 365	K. Fujii et al.	(NAGO)
ARAI	80	Toronto Conf. 93	I. Arai	(INUS)
Also	82	NP B194 251	I. Arai, H. Fujii	(INUS)
BARNHAM	80	NP B168 243	K.W.J. Barnham et al.	(LOIC)
CHEW	80	Toronto Conf. 123	D.M. Chew	(LBL) IJP
CRAWFORD	80	Toronto Conf. 107	R.L. Crawford	(GLAS)
CUTKOSKY	80	Toronto Conf. 19	R.E. Cutkosky et al.	(CMU, LBL) IJP
Also	79	PR D20 2839	R.E. Cutkosky et al.	(CMU, LBL) IJP
LIVANOS	80	Toronto Conf. 35	P. Livanos et al.	(SACL) IJP
HOEHLER	79	PDAT 12-1	G. Hohler et al.	(KARLT) IJP
Also	80	Toronto Conf. 3	R. Koch	(KARLT) IJP
BARBOUR	78	NP B141 253	I.M. Barbour, R.L. Crawford, N.H. Parsons	(GLAS)
LONGACRE	78	PR D17 1795	R.S. Longacre et al.	(LBL, SLAC)
LONGACRE	77	NP B122 493	R.S. Longacre, J. Dolbeau	(SACL) IJP
Also	76	NP B108 365	J. Dolbeau et al.	(SACL) IJP
WINNIK	77	NP B128 66	M. Winnik et al.	(HAIF) I
FELLER	76	NP B104 219	P. Feller et al.	(NAGO, OSAK) IJP
DEANS	75	NP B96 90	S.R. Deans et al.	(SFLA, ALAH) IJP
LONGACRE	75	PL 55B 415	R.S. Longacre et al.	(LBL, SLAC) IJP

$\Delta(1750) P_{31}$

$$I(J^P) = \frac{3}{2}(\frac{1}{2}^+) \text{ Status: } *$$

OMITTED FROM SUMMARY TABLE

$\Delta(1750)$ BREIT-WIGNER MASS

VALUE (MeV)	DOCUMENT ID	TECN	COMMENT
≈ 1750 OUR ESTIMATE			
1744 \pm 36	MANLEY 92	IPWA	$\pi N \rightarrow \pi N \& N\pi\pi$
• • • We do not use the following data for averages, fits, limits, etc. • • •			
1715.2 \pm 21.0	¹ CHEW 80	BPWA	$\pi^+ p \rightarrow \pi^+ p$
1778.4 \pm 9.0	¹ CHEW 80	BPWA	$\pi^+ p \rightarrow \pi^+ p$

$\Delta(1750)$ BREIT-WIGNER WIDTH

VALUE (MeV)	DOCUMENT ID	TECN	COMMENT
300 \pm 120	MANLEY 92	IPWA	$\pi N \rightarrow \pi N \& N\pi\pi$
• • • We do not use the following data for averages, fits, limits, etc. • • •			
93.3 \pm 55.0	¹ CHEW 80	BPWA	$\pi^+ p \rightarrow \pi^+ p$
23.0 \pm 29.0	¹ CHEW 80	BPWA	$\pi^+ p \rightarrow \pi^+ p$

$\Delta(1750)$ DECAY MODES

Mode	Fraction (Γ_i/Γ)
Γ_1 $N\pi$	
Γ_2 $N\pi\pi$	
Γ_3 $N(1440)\pi$	

$\Gamma(N\pi)/\Gamma_{total}$	DOCUMENT ID	TECN	COMMENT	Γ_1/Γ
0.08 \pm 0.03	MANLEY 92	IPWA	$\pi N \rightarrow \pi N \& N\pi\pi$	
• • • We do not use the following data for averages, fits, limits, etc. • • •				
0.18	¹ CHEW 80	BPWA	$\pi^+ p \rightarrow \pi^+ p$	
0.20	¹ CHEW 80	BPWA	$\pi^+ p \rightarrow \pi^+ p$	
$(\Gamma_i \Gamma_j)^{1/2} / \Gamma_{total}$ in $N\pi \rightarrow \Delta(1700) \rightarrow N(1440)\pi$				$(\Gamma_1 \Gamma_3)^{1/2} / \Gamma$
0.15 \pm 0.03	MANLEY 92	IPWA	$\pi N \rightarrow \pi N \& N\pi\pi$	

$\Delta(1750)$ FOOTNOTES

¹ CHEW 80 reports four resonances in the P_{31} wave — see also the $\Delta(1910)$. Problems with this analysis are discussed in section 2.1.11 of HOEHLER 83.

$\Delta(1750)$ REFERENCES

Author	Year	Reference	Method	Comment
MANLEY	92	PR D45 4002	D.M. Manley, E.M. Saleski	(KENT)
Also	84	PR D30 904	D.M. Manley et al.	(VPI)
HOEHLER	83	Landolt-Boernstein 1/9B2	G. Hohler	(KARLT)
CHEW	80	Toronto Conf. 123	D.M. Chew	(LBL)

$\Delta(1900)$ BREIT-WIGNER MASS

VALUE (MeV)	DOCUMENT ID	TECN	COMMENT
1850 to 1950 (\approx 1900) OUR ESTIMATE			
1920 \pm 24	MANLEY 92	IPWA	$\pi N \rightarrow \pi N \& N\pi\pi$
1890 \pm 50	CUTKOSKY 80	IPWA	$\pi N \rightarrow \pi N$
1908 \pm 30	HOEHLER 79	IPWA	$\pi N \rightarrow \pi N$
• • • We do not use the following data for averages, fits, limits, etc. • • •			
1918.5 \pm 23.0	CHEW 80	BPWA	$\pi^+ p \rightarrow \pi^+ p$
1803	CRAWFORD 80	DPWA	$\gamma N \rightarrow \pi N$

$\Delta(1900)$ BREIT-WIGNER WIDTH

VALUE (MeV)	DOCUMENT ID	TECN	COMMENT
140 to 240 (\approx 200) OUR ESTIMATE			
263 \pm 39	MANLEY 92	IPWA	$\pi N \rightarrow \pi N \& N\pi\pi$
170 \pm 50	CUTKOSKY 80	IPWA	$\pi N \rightarrow \pi N$
140 \pm 40	HOEHLER 79	IPWA	$\pi N \rightarrow \pi N$
• • • We do not use the following data for averages, fits, limits, etc. • • •			
93.5 \pm 54.0	CHEW 80	BPWA	$\pi^+ p \rightarrow \pi^+ p$
137	CRAWFORD 80	DPWA	$\gamma N \rightarrow \pi N$

$\Delta(1900)$ POLE POSITION

VALUE (MeV)	DOCUMENT ID	TECN	COMMENT
1780	¹ HOEHLER 93	SPED	$\pi N \rightarrow \pi N$
1870 \pm 40	CUTKOSKY 80	IPWA	$\pi N \rightarrow \pi N$
• • • We do not use the following data for averages, fits, limits, etc. • • •			
not seen	ARNDT 91	DPWA	$\pi N \rightarrow \pi N$ Soln SM90
2029 or 2025	² LONGACRE 78	IPWA	$\pi N \rightarrow N\pi\pi$

-2xIMAGINARY PART

VALUE (MeV)	DOCUMENT ID	TECN	COMMENT
180 \pm 50	CUTKOSKY 80	IPWA	$\pi N \rightarrow \pi N$
• • • We do not use the following data for averages, fits, limits, etc. • • •			
not seen	ARNDT 91	DPWA	$\pi N \rightarrow \pi N$ Soln SM90
164 or 163	² LONGACRE 78	IPWA	$\pi N \rightarrow N\pi\pi$

$\Delta(1900)$ ELASTIC POLE RESIDUE

MODULUS $ r $	DOCUMENT ID	TECN	COMMENT
10 \pm 3	CUTKOSKY 80	IPWA	$\pi N \rightarrow \pi N$

PHASE θ

VALUE ($^\circ$)	DOCUMENT ID	TECN	COMMENT
+20 \pm 40	CUTKOSKY 80	IPWA	$\pi N \rightarrow \pi N$

$\Delta(1900)$ DECAY MODES

The following branching fractions are our estimates, not fits or averages.

Mode	Fraction (Γ_i/Γ)
Γ_1 $N\pi$	
Γ_2 ΣK	10-30 %
Γ_3 $N\pi\pi$	
Γ_4 $\Delta\pi$	
Γ_5 $\Delta(1232)\pi, D$ -wave	
Γ_6 $N\rho$	
Γ_7 $N\rho, S=1/2, S$ -wave	
Γ_8 $N\rho, S=3/2, D$ -wave	
Γ_9 $N(1440)\pi, S$ -wave	
Γ_{10} $N\gamma, \text{helicity}=1/2$	

$\Delta(1900)$ BRANCHING RATIOS

$\Gamma(N\pi)/\Gamma_{total}$	DOCUMENT ID	TECN	COMMENT	Γ_1/Γ
0.1 to 0.3 OUR ESTIMATE				
0.41 \pm 0.04	MANLEY 92	IPWA	$\pi N \rightarrow \pi N \& N\pi\pi$	
0.10 \pm 0.03	CUTKOSKY 80	IPWA	$\pi N \rightarrow \pi N$	
0.08 \pm 0.04	HOEHLER 79	IPWA	$\pi N \rightarrow \pi N$	
• • • We do not use the following data for averages, fits, limits, etc. • • •				
0.28	CHEW 80	BPWA	$\pi^+ p \rightarrow \pi^+ p$	

Baryon Particle Listings

 $\Delta(1900)$, $\Delta(1905)$

$(\Gamma_1 \Gamma_2)^{1/2} / \Gamma_{\text{total}}$ in $N\pi \rightarrow \Delta(1900) \rightarrow \Sigma K$	DOCUMENT ID	TECN	COMMENT	$(\Gamma_1 \Gamma_2)^{1/2} / \Gamma$
VALUE				
<0.03	CANDLIN 84	DPWA	$\pi^+ p \rightarrow \Sigma^+ K^+$	
• • • We do not use the following data for averages, fits, limits, etc. • • •				
0.076	³ DEANS 75	DPWA	$\pi N \rightarrow \Sigma K$	
0.11	LANGBEIN 73	IPWA	$\pi N \rightarrow \Sigma K$ (sol. 1)	
0.12	LANGBEIN 73	IPWA	$\pi N \rightarrow \Sigma K$ (sol. 2)	

$(\Gamma_1 \Gamma_2)^{1/2} / \Gamma_{\text{total}}$ in $N\pi \rightarrow \Delta(1900) \rightarrow \Delta(1232)\pi$, D-wave	DOCUMENT ID	TECN	COMMENT	$(\Gamma_1 \Gamma_2)^{1/2} / \Gamma$
VALUE				
+0.25 ± 0.07	MANLEY 92	IPWA	$\pi N \rightarrow \pi N$ & $N\pi\pi$	

$(\Gamma_1 \Gamma_2)^{1/2} / \Gamma_{\text{total}}$ in $N\pi \rightarrow \Delta(1900) \rightarrow N\rho$, S=1/2, S-wave	DOCUMENT ID	TECN	COMMENT	$(\Gamma_1 \Gamma_2)^{1/2} / \Gamma$
VALUE				
-0.14 ± 0.11	MANLEY 92	IPWA	$\pi N \rightarrow \pi N$ & $N\pi\pi$	

$(\Gamma_1 \Gamma_2)^{1/2} / \Gamma_{\text{total}}$ in $N\pi \rightarrow \Delta(1900) \rightarrow N\rho$, S=3/2, D-wave	DOCUMENT ID	TECN	COMMENT	$(\Gamma_1 \Gamma_2)^{1/2} / \Gamma$
VALUE				
-0.37 ± 0.07	MANLEY 92	IPWA	$\pi N \rightarrow \pi N$ & $N\pi\pi$	

$(\Gamma_1 \Gamma_2)^{1/2} / \Gamma_{\text{total}}$ in $N\pi \rightarrow \Delta(1900) \rightarrow N(1440)\pi$, S-wave	DOCUMENT ID	TECN	COMMENT	$(\Gamma_1 \Gamma_2)^{1/2} / \Gamma$
VALUE				
-0.16 ± 0.11	MANLEY 92	IPWA	$\pi N \rightarrow \pi N$ & $N\pi\pi$	

 $\Delta(1900)$ PHOTON DECAY AMPLITUDES $\Delta(1900) \rightarrow N\gamma$, helicity-1/2 amplitude $A_{1/2}$

VALUE (GeV ^{-1/2})	DOCUMENT ID	TECN	COMMENT
-0.004 ± 0.016	CRAWFORD 83	IPWA	$\gamma N \rightarrow \pi N$
0.029 ± 0.008	AWAJI 81	DPWA	$\gamma N \rightarrow \pi N$
• • • We do not use the following data for averages, fits, limits, etc. • • •			
-0.006 to -0.025	CRAWFORD 80	DPWA	$\gamma N \rightarrow \pi N$

 $\Delta(1900)$ FOOTNOTES

- ¹ See HOEHLER 93 for a detailed discussion of the evidence for and the pole parameters of N and Δ resonances as determined from Argand diagrams of πN elastic partial-wave amplitudes and from plots of the speeds with which the amplitudes traverse the diagrams.
- ² LONGACRE 78 values are from a search for poles in the unitarized T-matrix. The first (second) value uses, in addition to $\pi N \rightarrow N\pi\pi$ data, elastic amplitudes from a Saclay (CERN) partial-wave analysis.
- ³ The value given is from solution 1; the resonance is not present in solutions 2, 3, or 4.

 $\Delta(1900)$ REFERENCES

For early references, see Physics Letters **111B** 70 (1982).

HOEHLER 93	πN Newsletter 9 1	G. Hohler	(KARL)
MANLEY 92	PR D45 4002	D.M. Manley, E.M. Saleski	(KENT) IJP
Also	PR D30 904	D.M. Manley et al.	(VPI)
ARNDT 91	PR D43 2131	R.A. Arndt et al.	(VPI, TELE) IJP
CANDLIN 84	NP B238 477	D.J. Candlin et al.	(EDIN, RAL, LOWC)
CRAWFORD 83	NP B211 1	R.L. Crawford, W.T. Morton	(GLAS)
AWAJI 81	Bonn Conf. 352	N. Awaji, R. Kajikawa	(NAGO)
Also	NP B197 365	K. Fujii et al.	(NAGO)
CHEW 80	Toronto Conf. 123	D.M. Chew	(LBL) IJP
CRAWFORD 80	Toronto Conf. 107	R.L. Crawford	(GLAS)
CUTKOSKY 80	Toronto Conf. 19	R.E. Cutkosky et al.	(CMU, LBL) IJP
Also	PR D20 2839	R.E. Cutkosky et al.	(CMU, LBL) IJP
HOEHLER 79	PDAT 12-1	G. Hohler et al.	(KARLT) IJP
Also	Toronto Conf. 3	R. Koch	(KARLT) IJP
LONGACRE 78	PR D17 1795	R.S. Longacre et al.	(LBL, SLAC)
DEANS 75	NP B96 90	S.R. Deans et al.	(SFLA, ALAH) IJP
LANGBEIN 73	NP B53 251	W. Langbein, F. Wagner	(MUNI) IJP

 $\Delta(1905) F_{35}$

$$I(J^P) = \frac{3}{2}(\frac{5}{2}^+) \text{ Status: } ***$$

Most of the results published before 1975 are now obsolete and have been omitted. They may be found in our 1982 edition, Physics Letters **111B** (1982).

 $\Delta(1905)$ BREIT-WIGNER MASS

VALUE (MeV)	DOCUMENT ID	TECN	COMMENT
1870 to 1920 (\approx 1905) OUR ESTIMATE			
1881 ± 18	MANLEY 92	IPWA	$\pi N \rightarrow \pi N$ & $N\pi\pi$
1910 ± 30	CUTKOSKY 80	IPWA	$\pi N \rightarrow \pi N$
1905 ± 20	HOEHLER 79	IPWA	$\pi N \rightarrow \pi N$
• • • We do not use the following data for averages, fits, limits, etc. • • •			
1895 ± 8	ARNDT 96	IPWA	$\gamma N \rightarrow \pi N$
1850	ARNDT 95	DPWA	$\pi N \rightarrow N\pi$
1960 ± 40	CANDLIN 84	DPWA	$\pi^+ p \rightarrow \Sigma^+ K^+$
1787.0 ⁺ ± 6.0 - 5.7	CHEW 80	BPWA	$\pi^+ p \rightarrow \pi^+ p$
1880	CRAWFORD 80	DPWA	$\gamma N \rightarrow \pi N$
1892	BARBOUR 78	DPWA	$\gamma N \rightarrow \pi N$
1830	¹ LONGACRE 75	IPWA	$\pi N \rightarrow N\pi\pi$

 $\Delta(1905)$ BREIT-WIGNER WIDTH

VALUE (MeV)	DOCUMENT ID	TECN	COMMENT
280 to 440 (\approx 350) OUR ESTIMATE			
327 ± 51	MANLEY 92	IPWA	$\pi N \rightarrow \pi N$ & $N\pi\pi$
400 ± 100	CUTKOSKY 80	IPWA	$\pi N \rightarrow \pi N$
260 ± 20	HOEHLER 79	IPWA	$\pi N \rightarrow \pi N$
• • • We do not use the following data for averages, fits, limits, etc. • • •			
354 ± 10	ARNDT 96	IPWA	$\gamma N \rightarrow \pi N$
294	ARNDT 95	DPWA	$\pi N \rightarrow N\pi$
270 ± 40	CANDLIN 84	DPWA	$\pi^+ p \rightarrow \Sigma^+ K^+$
66.0 ⁺ ± 24.0 - 16.0	CHEW 80	BPWA	$\pi^+ p \rightarrow \pi^+ p$
193	CRAWFORD 80	DPWA	$\gamma N \rightarrow \pi N$
159	BARBOUR 78	DPWA	$\gamma N \rightarrow \pi N$
220	¹ LONGACRE 75	IPWA	$\pi N \rightarrow N\pi\pi$

 $\Delta(1905)$ POLE POSITION

REAL PART

VALUE (MeV)	DOCUMENT ID	TECN	COMMENT
1800 to 1860 (\approx 1830) OUR ESTIMATE			
1832	ARNDT 95	DPWA	$\pi N \rightarrow N\pi$
1829	² HOEHLER 93	SPED	$\pi N \rightarrow \pi N$
1830 ± 40	CUTKOSKY 80	IPWA	$\pi N \rightarrow \pi N$
• • • We do not use the following data for averages, fits, limits, etc. • • •			
1794	ARNDT 91	DPWA	$\pi N \rightarrow \pi N$ Soln SM90
1813 or 1808	³ LONGACRE 78	IPWA	$\pi N \rightarrow N\pi\pi$

-2xIMAGINARY PART

VALUE (MeV)	DOCUMENT ID	TECN	COMMENT
230 to 330 (\approx 280) OUR ESTIMATE			
254	ARNDT 95	DPWA	$\pi N \rightarrow N\pi$
303	² HOEHLER 93	SPED	$\pi N \rightarrow \pi N$
280 ± 60	CUTKOSKY 80	IPWA	$\pi N \rightarrow \pi N$
• • • We do not use the following data for averages, fits, limits, etc. • • •			
230	ARNDT 91	DPWA	$\pi N \rightarrow \pi N$ Soln SM90
193 or 187	³ LONGACRE 78	IPWA	$\pi N \rightarrow N\pi\pi$

 $\Delta(1905)$ ELASTIC POLE RESIDUEMODULUS $|r|$

VALUE (MeV)	DOCUMENT ID	TECN	COMMENT
12	ARNDT 95	DPWA	$\pi N \rightarrow N\pi$
25	HOEHLER 93	SPED	$\pi N \rightarrow \pi N$
25 ± 8	CUTKOSKY 80	IPWA	$\pi N \rightarrow \pi N$
• • • We do not use the following data for averages, fits, limits, etc. • • •			
14	ARNDT 91	DPWA	$\pi N \rightarrow \pi N$ Soln SM90

PHASE θ

VALUE (°)	DOCUMENT ID	TECN	COMMENT
- 4	ARNDT 95	DPWA	$\pi N \rightarrow N\pi$
-50 ± 20	CUTKOSKY 80	IPWA	$\pi N \rightarrow \pi N$
• • • We do not use the following data for averages, fits, limits, etc. • • •			
-40	ARNDT 91	DPWA	$\pi N \rightarrow \pi N$ Soln SM90

See key on page 239

Baryon Particle Listings
 $\Delta(1905)$, $\Delta(1910)$ $\Delta(1905)$ DECAY MODES

The following branching fractions are our estimates, not fits or averages.

Mode	Fraction (Γ_i/Γ)
Γ_1 $N\pi$	5-15 %
Γ_2 ΣK	
Γ_3 $N\pi\pi$	85-95 %
Γ_4 $\Delta\pi$	<25 %
Γ_5 $\Delta(1232)\pi$, P-wave	
Γ_6 $\Delta(1232)\pi$, F-wave	
Γ_7 $N\rho$	>60 %
Γ_8 $N\rho$, S=3/2, P-wave	
Γ_9 $N\rho$, S=3/2, F-wave	
Γ_{10} $N\rho$, S=1/2, F-wave	
Γ_{11} $N\gamma$	0.01-0.03 %
Γ_{12} $N\gamma$, helicity=1/2	0.0-0.1 %
Γ_{13} $N\gamma$, helicity=3/2	0.004-0.03 %

 $\Delta(1905)$ BRANCHING RATIOS

$\Gamma(N\pi)/\Gamma_{total}$	DOCUMENT ID	TECN	COMMENT	Γ_1/Γ
0.05 to 0.15 OUR ESTIMATE				
0.12 ± 0.03	MANLEY 92	IPWA	$\pi N \rightarrow \pi N$ & $N\pi\pi$	
0.08 ± 0.03	CUTKOSKY 80	IPWA	$\pi N \rightarrow \pi N$	
0.15 ± 0.02	HOEHLER 79	IPWA	$\pi N \rightarrow \pi N$	
• • • We do not use the following data for averages, fits, limits, etc. • • •				
0.12	ARNDT 95	DPWA	$\pi N \rightarrow N\pi$	
0.11	CHEW 80	BPWA	$\pi^+\rho \rightarrow \pi^+\rho$	

$(\Gamma_1\Gamma_7)^{1/2}/\Gamma_{total}$ in $N\pi \rightarrow \Delta(1905) \rightarrow \Sigma K$	DOCUMENT ID	TECN	COMMENT	$(\Gamma_1\Gamma_2)^{1/2}/\Gamma$
0.015 ± 0.003	CANDLIN 84	DPWA	$\pi^+\rho \rightarrow \Sigma^+ K^+$	
• • • We do not use the following data for averages, fits, limits, etc. • • •				
-0.013	LIVANOS 80	DPWA	$\pi\rho \rightarrow \Sigma K$	
0.021 to 0.054	⁴ DEANS 75	DPWA	$\pi N \rightarrow \Sigma K$	

Note: Signs of couplings from $\pi N \rightarrow N\pi\pi$ analyses were changed in the 1986 edition to agree with the baryon-first convention; the overall phase ambiguity is resolved by choosing a negative sign for the $\Delta(1620)$ S_{31} coupling to $\Delta(1232)\pi$.

$(\Gamma_1\Gamma_7)^{1/2}/\Gamma_{total}$ in $N\pi \rightarrow \Delta(1905) \rightarrow \Delta(1232)\pi$, P-wave	DOCUMENT ID	TECN	COMMENT	$(\Gamma_1\Gamma_5)^{1/2}/\Gamma$
-0.04 ± 0.05	MANLEY 92	IPWA	$\pi N \rightarrow \pi N$ & $N\pi\pi$	

$(\Gamma_1\Gamma_7)^{1/2}/\Gamma_{total}$ in $N\pi \rightarrow \Delta(1905) \rightarrow \Delta(1232)\pi$, F-wave	DOCUMENT ID	TECN	COMMENT	$(\Gamma_1\Gamma_6)^{1/2}/\Gamma$
+0.02 ± 0.03	MANLEY 92	IPWA	$\pi N \rightarrow \pi N$ & $N\pi\pi$	
+0.20	¹ LONGACRE 75	IPWA	$\pi N \rightarrow N\pi\pi$	
• • • We do not use the following data for averages, fits, limits, etc. • • •				
+0.17	⁵ NOVOSELLER 78	IPWA	$\pi N \rightarrow N\pi\pi$	
+0.06	⁶ NOVOSELLER 78	IPWA	$\pi N \rightarrow N\pi\pi$	

$(\Gamma_1\Gamma_7)^{1/2}/\Gamma_{total}$ in $N\pi \rightarrow \Delta(1905) \rightarrow N\rho$, S=3/2, P-wave	DOCUMENT ID	TECN	COMMENT	$(\Gamma_1\Gamma_8)^{1/2}/\Gamma$
+0.030 to +0.36 OUR ESTIMATE				
+0.33 ± 0.03	MANLEY 92	IPWA	$\pi N \rightarrow \pi N$ & $N\pi\pi$	
+0.33	¹ LONGACRE 75	IPWA	$\pi N \rightarrow N\pi\pi$	
• • • We do not use the following data for averages, fits, limits, etc. • • •				
+0.26	⁵ NOVOSELLER 78	IPWA	$\pi N \rightarrow N\pi\pi$	
+0.11 to +0.33	⁷ NOVOSELLER 78	IPWA	$\pi N \rightarrow N\pi\pi$	

 $\Delta(1905)$ PHOTON DECAY AMPLITUDES $\Delta(1905) \rightarrow N\gamma$, helicity-1/2 amplitude $A_{1/2}$

VALUE (GeV ^{-1/2})	DOCUMENT ID	TECN	COMMENT
+0.026 ± 0.011 OUR ESTIMATE			
0.022 ± 0.005	ARNDT 96	IPWA	$\gamma N \rightarrow \pi N$
0.021 ± 0.010	CRAWFORD 83	IPWA	$\gamma N \rightarrow \pi N$
0.043 ± 0.020	AWAJI 81	DPWA	$\gamma N \rightarrow \pi N$
0.022 ± 0.010	ARAI 80	DPWA	$\gamma N \rightarrow \pi N$ (fit 1)
0.031 ± 0.009	ARAI 80	DPWA	$\gamma N \rightarrow \pi N$ (fit 2)
0.024 ± 0.014	CRAWFORD 80	DPWA	$\gamma N \rightarrow \pi N$
• • • We do not use the following data for averages, fits, limits, etc. • • •			
0.055 ± 0.004	LI 93	IPWA	$\gamma N \rightarrow \pi N$
+0.033 ± 0.018	BARBOUR 78	DPWA	$\gamma N \rightarrow \pi N$

 $\Delta(1905) \rightarrow N\gamma$, helicity-3/2 amplitude $A_{3/2}$

VALUE (GeV ^{-1/2})	DOCUMENT ID	TECN	COMMENT
-0.045 ± 0.020 OUR ESTIMATE			
-0.045 ± 0.005	ARNDT 96	IPWA	$\gamma N \rightarrow \pi N$
-0.056 ± 0.028	CRAWFORD 83	IPWA	$\gamma N \rightarrow \pi N$
-0.025 ± 0.023	AWAJI 81	DPWA	$\gamma N \rightarrow \pi N$
-0.029 ± 0.007	ARAI 80	DPWA	$\gamma N \rightarrow \pi N$ (fit 1)
-0.045 ± 0.006	ARAI 80	DPWA	$\gamma N \rightarrow \pi N$ (fit 2)
-0.072 ± 0.035	CRAWFORD 80	DPWA	$\gamma N \rightarrow \pi N$
• • • We do not use the following data for averages, fits, limits, etc. • • •			
0.002 ± 0.003	LI 93	IPWA	$\gamma N \rightarrow \pi N$
-0.055 ± 0.019	BARBOUR 78	DPWA	$\gamma N \rightarrow \pi N$

 $\Delta(1905)$ FOOTNOTES

- From method II of LONGACRE 75: eyeball fits with Breit-Wigner circles to the T-matrix amplitudes.
- See HOEHLER 93 for a detailed discussion of the evidence for and the pole parameters of N and Δ resonances as determined from Argand diagrams of πN elastic partial-wave amplitudes and from plots of the speeds with which the amplitudes traverse the diagrams.
- LONGACRE 78 values are from a search for poles in the unitarized T-matrix. The first (second) value uses, in addition to $\pi N \rightarrow N\pi\pi$ data, elastic amplitudes from a Saclay (CERN) partial-wave analysis.
- The range given for DEANS 75 is from the four best solutions.
- A Breit-Wigner fit to the HERNDON 75 IPWA.
- A Breit-Wigner fit to the NOVOSELLER 78B IPWA.
- A Breit-Wigner fit to the NOVOSELLER 78B IPWA; the phase is near 90°.

 $\Delta(1905)$ REFERENCESFor early references, see Physics Letters **111B** 70 (1982).

ARNDT 96	PR C53 430	R.A. Arndt, I.I. Strakovsky, R.L. Workman	(VPI)
ARNDT 95	PR C52 2120	R.A. Arndt et al.	(VPI, BRCO)
HOEHLER 93	πN Newsletter 9 1	G. Hohler et al.	(KARL)
LI 93	PR C47 2759	Z.J. Li et al.	(VPI)
MANLEY 92	PR D45 4002	D.M. Manley, E.M. Saleski	(KENT) IJP
Also	PR D30 904	D.M. Manley et al.	(VPI)
ARNDT 91	PR D43 2131	R.A. Arndt et al.	(VPI, TELE) IJP
CANDLIN 84	NP B238 477	D.J. Candlin et al.	(EDIN, RAL, LOWC)
CRAWFORD 83	NP B211 1	R.L. Crawford, W.T. Morton	(GLAS)
PDG 82	PL 111B	M. Roos et al.	(HELS, CIT, CERN)
AWAJI 81	Bonn Conf. 352	N. Awaji, R. Kajikawa	(NAGO)
Also	NP B197 365	K. Fuji et al.	(NAGO)
ARAI 80	Toronto Conf. 93	I. Arai	(INUS)
Also	NP B194 251	I. Arai, H. Fuji	(INUS)
CHEW 80	Toronto Conf. 123	D.M. Chew	(LBL) IJP
CRAWFORD 80	Toronto Conf. 107	R.L. Crawford	(GLAS)
CUTKOSKY 80	Toronto Conf. 19	R.E. Cutkosky et al.	(CMU, LBL) IJP
Also	PR D20 2839	R.E. Cutkosky et al.	(CMU, LBL) IJP
LIVANOS 80	Toronto Conf. 35	P. Livanos et al.	(SACL) IJP
HOEHLER 79	PDAT 12-1	G. Hohler et al.	(KARLT) IJP
Also	Toronto Conf. 3	R. Koch	(KARLT) IJP
BARBOUR 78	NP B141 253	I.M. Barbour, R.L. Crawford, N.H. Parsons	(LBL, SLAC)
LONGACRE 78	PR D17 1795	R.S. Longacre et al.	(LBL, SLAC)
NOVOSELLER 78B	NP B137 509	D.E. Novoseller	(CIT) IJP
NOVOSELLER 78B	NP B137 445	D.E. Novoseller	(CIT) IJP
DEANS 75	NP B96 90	S.R. Deans et al.	(SFLA, ALAH) IJP
HERNDON 75	PR D11 3183	D. Herndon et al.	(LBL, SLAC)
LONGACRE 75	PL 55B 415	R.S. Longacre et al.	(LBL, SLAC) IJP

 $\Delta(1910) P_{31}$

$$I(J^P) = \frac{3}{2}(1^+) \text{ Status: } ***$$

Most of the results published before 1975 are now obsolete and have been omitted. They may be found in our 1982 edition, Physics Letters **111B** (1982).

 $\Delta(1910)$ BREIT-WIGNER MASS

VALUE (MeV)	DOCUMENT ID	TECN	COMMENT
1870 ± 120 (≈ 1910) OUR ESTIMATE			
1882 ± 10	MANLEY 92	IPWA	$\pi N \rightarrow \pi N$ & $N\pi\pi$
1910 ± 40	CUTKOSKY 80	IPWA	$\pi N \rightarrow \pi N$
1888 ± 20	HOEHLER 79	IPWA	$\pi N \rightarrow \pi N$
• • • We do not use the following data for averages, fits, limits, etc. • • •			
2152	ARNDT 95	DPWA	$\pi N \rightarrow N\pi$
1960.1 ± 21.0	¹ CHEW 80	BPWA	$\pi^+\rho \rightarrow \pi^+\rho$
2121.4 ^{+13.0} _{-14.3}	¹ CHEW 80	BPWA	$\pi^+\rho \rightarrow \pi^+\rho$
1921	CRAWFORD 80	DPWA	$\gamma N \rightarrow \pi N$
1899	BARBOUR 78	DPWA	$\gamma N \rightarrow \pi N$
1790	² LONGACRE 77	IPWA	$\pi N \rightarrow N\pi\pi$

 $\Delta(1910)$ BREIT-WIGNER WIDTH

VALUE (MeV)	DOCUMENT ID	TECN	COMMENT
190 to 270 (≈ 250) OUR ESTIMATE			
239 ± 25	MANLEY 92	IPWA	$\pi N \rightarrow \pi N$ & $N\pi\pi$
225 ± 50	CUTKOSKY 80	IPWA	$\pi N \rightarrow \pi N$
280 ± 50	HOEHLER 79	IPWA	$\pi N \rightarrow \pi N$

Baryon Particle Listings

 $\Delta(1910)$

• • • We do not use the following data for averages, fits, limits, etc. • • •

760	ARNDT	95	DPWA	$\pi N \rightarrow N\pi$
152.9 ± 60.0	¹ CHEW	80	BPWA	$\pi^+ p \rightarrow \pi^+ p$
172.2 ± 37.0	¹ CHEW	80	BPWA	$\pi^+ p \rightarrow \pi^+ p$
351	CRAWFORD	80	DPWA	$\gamma N \rightarrow \pi N$
230	BARBOUR	78	DPWA	$\gamma N \rightarrow \pi N$
170	² LONGACRE	77	IPWA	$\pi N \rightarrow N\pi\pi$

 $\Delta(1910)$ POLE POSITION

REAL PART

VALUE (MeV)	DOCUMENT ID	TECN	COMMENT
1830 to 1880 (≈ 1855) OUR ESTIMATE			
1810	ARNDT	95	DPWA $\pi N \rightarrow N\pi$
1874	³ HOEHLER	93	SPED $\pi N \rightarrow \pi N$
1880 ± 30	CUTKOSKY	80	IPWA $\pi N \rightarrow \pi N$

• • • We do not use the following data for averages, fits, limits, etc. • • •

1950	ARNDT	91	DPWA	$\pi N \rightarrow \pi N$ Soln SM90
1792 or 1801	² LONGACRE	77	IPWA	$\pi N \rightarrow N\pi\pi$

-2xIMAGINARY PART

VALUE (MeV)	DOCUMENT ID	TECN	COMMENT
200 to 500 (≈ 350) OUR ESTIMATE			
494	ARNDT	95	DPWA $\pi N \rightarrow N\pi$
283	³ HOEHLER	93	SPED $\pi N \rightarrow \pi N$
200 ± 40	CUTKOSKY	80	IPWA $\pi N \rightarrow \pi N$

• • • We do not use the following data for averages, fits, limits, etc. • • •

398	ARNDT	91	DPWA	$\pi N \rightarrow \pi N$ Soln SM90
172 or 165	² LONGACRE	77	IPWA	$\pi N \rightarrow N\pi\pi$

 $\Delta(1910)$ ELASTIC POLE RESIDUEMODULUS $|r|$

VALUE (MeV)	DOCUMENT ID	TECN	COMMENT
53	ARNDT	95	DPWA $\pi N \rightarrow N\pi$
38	HOEHLER	93	SPED $\pi N \rightarrow \pi N$
20 ± 4	CUTKOSKY	80	IPWA $\pi N \rightarrow \pi N$

• • • We do not use the following data for averages, fits, limits, etc. • • •

37	ARNDT	91	DPWA	$\pi N \rightarrow \pi N$ Soln SM90
----	-------	----	------	-------------------------------------

PHASE θ

VALUE (°)	DOCUMENT ID	TECN	COMMENT
-176	ARNDT	95	DPWA $\pi N \rightarrow N\pi$
-90 ± 30	CUTKOSKY	80	IPWA $\pi N \rightarrow \pi N$

• • • We do not use the following data for averages, fits, limits, etc. • • •

-91	ARNDT	91	DPWA	$\pi N \rightarrow \pi N$ Soln SM90
-----	-------	----	------	-------------------------------------

 $\Delta(1910)$ DECAY MODES

The following branching fractions are our estimates, not fits or averages.

Mode	Fraction (Γ_i/Γ)
Γ_1 $N\pi$	15-30 %
Γ_2 ΣK	
Γ_3 $N\pi\pi$	
Γ_4 $\Delta\pi$	
Γ_5 $\Delta(1232)\pi$, P-wave	
Γ_6 $N\rho$	
Γ_7 $N\rho$, $S=3/2$, P-wave	
Γ_8 $N(1440)\pi$	
Γ_9 $N(1440)\pi$, P-wave	
Γ_{10} $N\gamma$	0.0-0.2 %
Γ_{11} $N\gamma$, helicity=1/2	0.0-0.2 %

 $\Delta(1910)$ BRANCHING RATIOS

$\Gamma(N\pi)/\Gamma_{total}$ Γ_1/Γ

VALUE	DOCUMENT ID	TECN	COMMENT
0.15 to 0.3 OUR ESTIMATE			
0.23 ± 0.08	MANLEY	92	IPWA $\pi N \rightarrow \pi N$ & $N\pi\pi$
0.19 ± 0.03	CUTKOSKY	80	IPWA $\pi N \rightarrow \pi N$
0.24 ± 0.06	HOEHLER	79	IPWA $\pi N \rightarrow \pi N$

• • • We do not use the following data for averages, fits, limits, etc. • • •

0.26	ARNDT	95	DPWA	$\pi N \rightarrow N\pi$
0.17	¹ CHEW	80	BPWA	$\pi^+ p \rightarrow \pi^+ p$
0.40	¹ CHEW	80	BPWA	$\pi^+ p \rightarrow \pi^+ p$

$(\Gamma_1\Gamma_7)^{1/2}/\Gamma_{total}$ in $N\pi \rightarrow \Delta(1910) \rightarrow \Sigma K$ $(\Gamma_1\Gamma_2)^{1/2}/\Gamma$

VALUE	DOCUMENT ID	TECN	COMMENT
< 0.03	CANDLIN	84	DPWA $\pi^+ p \rightarrow \Sigma^+ K^+$

• • • We do not use the following data for averages, fits, limits, etc. • • •

-0.019	LIVANOS	80	DPWA	$\pi p \rightarrow \Sigma K$
+0.082 to 0.184	⁴ DEANS	75	DPWA	$\pi N \rightarrow \Sigma K$

Note: Signs of couplings from $\pi N \rightarrow N\pi\pi$ analyses were changed in the 1986 edition to agree with the baryon-first convention; the overall phase ambiguity is resolved by choosing a negative sign for the $\Delta(1620) S_{31}$ coupling to $\Delta(1232)\pi$.

$(\Gamma_1\Gamma_7)^{1/2}/\Gamma_{total}$ in $N\pi \rightarrow \Delta(1910) \rightarrow \Delta(1232)\pi$, P-wave $(\Gamma_1\Gamma_5)^{1/2}/\Gamma$

VALUE	DOCUMENT ID	TECN	COMMENT
+0.06	² LONGACRE	77	IPWA $\pi N \rightarrow N\pi\pi$

$(\Gamma_1\Gamma_7)^{1/2}/\Gamma_{total}$ in $N\pi \rightarrow \Delta(1910) \rightarrow N\rho$, $S=3/2$, P-wave $(\Gamma_1\Gamma_7)^{1/2}/\Gamma$

VALUE	DOCUMENT ID	TECN	COMMENT
+0.29	² LONGACRE	77	IPWA $\pi N \rightarrow N\pi\pi$

• • • We do not use the following data for averages, fits, limits, etc. • • •

+0.17	⁵ NOVOSELLER	78	IPWA	$\pi N \rightarrow N\pi\pi$
-------	-------------------------	----	------	-----------------------------

$(\Gamma_1\Gamma_7)^{1/2}/\Gamma_{total}$ in $N\pi \rightarrow \Delta(1910) \rightarrow N(1440)\pi$, P-wave $(\Gamma_1\Gamma_9)^{1/2}/\Gamma$

VALUE	DOCUMENT ID	TECN	COMMENT
-0.39 ± 0.04	MANLEY	92	IPWA $\pi N \rightarrow \pi N$ & $N\pi\pi$

 $\Delta(1910)$ PHOTON DECAY AMPLITUDES

$\Delta(1910) \rightarrow N\gamma$, helicity-1/2 amplitude $A_{1/2}$

VALUE (GeV ^{-1/2})	DOCUMENT ID	TECN	COMMENT
+0.003 ± 0.014 OUR ESTIMATE			
-0.002 ± 0.008	ARNDT	96	IPWA $\gamma N \rightarrow \pi N$
0.014 ± 0.030	CRAWFORD	83	IPWA $\gamma N \rightarrow \pi N$
0.025 ± 0.011	AWAJI	81	DPWA $\gamma N \rightarrow \pi N$
-0.012 ± 0.005	ARAI	80	DPWA $\gamma N \rightarrow \pi N$ (fit 1)
-0.031 ± 0.004	ARAI	80	DPWA $\gamma N \rightarrow \pi N$ (fit 2)
-0.005 ± 0.030	CRAWFORD	80	DPWA $\gamma N \rightarrow \pi N$

• • • We do not use the following data for averages, fits, limits, etc. • • •

0.032 ± 0.003	LI	93	IPWA	$\gamma N \rightarrow \pi N$
-0.035 ± 0.021	BARBOUR	78	DPWA	$\gamma N \rightarrow \pi N$

 $\Delta(1910)$ FOOTNOTES

- ¹ CHEW 80 reports four resonances in the P_{31} wave — see also the $\Delta(1750)$. Problems with this analysis are discussed in section 2.1.11 of HOEHLER 83.
- ² LONGACRE 77 pole positions are from a search for poles in the unitarized T-matrix; the first (second) value uses, in addition to $\pi N \rightarrow N\pi\pi$ data, elastic amplitudes from a Saclay (CERN) partial-wave analysis. The other LONGACRE 77 values are from eyeball fits with Breit-Wigner circles to the T-matrix amplitudes.
- ³ See HOEHLER 93 for a detailed discussion of the evidence for and the pole parameters of N and Δ resonances as determined from Argand diagrams of πN elastic partial-wave amplitudes and from plots of the speeds with which the amplitudes traverse the diagrams.
- ⁴ The range given for DEANS 75 is from the four best solutions.
- ⁵ Evidence for this coupling is weak; see NOVOSELLER 78. This coupling assumes the mass is near 1820 MeV.

 $\Delta(1910)$ REFERENCES

For early references, see Physics Letters **111B** 70 (1982).

ARNDT	96	PR C53 430	R.A. Arndt, I.I. Strakovsky, R.L. Workman	(VPI)	
ARNDT	95	PR C52 2120	R.A. Arndt et al.	(VPI, BRCC)	
HOEHLER	93	πN Newsletter 9 1	G. Hohler	(KARL)	
LI	93	PR C47 2759	Z.J. Li et al.	(VPI)	
MANLEY	92	PR D45 4002	D.M. Manley, E.M. Saleski	(KENT) IJP	
	84	PR D30 904	D.M. Manley et al.	(VPI)	
ARNDT	91	PR D43 2131	R.A. Arndt et al.	(VPI, TELE) IJP	
CANDLIN	84	NP B238 477	D.J. Candlin et al.	(EDIN, RAL, LOWC)	
CRAWFORD	83	NP B211 1	R.L. Crawford, W.T. Morton	(GLAS)	
HOEHLER	83	Landolt-Boernstein 1/9B2	G. Hohler	(KARLT)	
FDC	82	PL 111B	M. Roos et al.	(HELS, CIT, CERN)	
AWAJI	81	Bonn Conf. 352	N. Awaji, R. Kajikawa	(NAGO)	
	82	NP B197 365	K. Fujii et al.	(NAGO)	
ARAI	80	Toronto Conf. 93	I. Arai	(INUS)	
	82	NP B194 251	I. Arai, H. Fujii	(INUS)	
CHEW	80	Toronto Conf. 123	D.M. Chew	(LBL) IJP	
CRAWFORD	80	Toronto Conf. 107	R.L. Crawford	(GLAS)	
CUTKOSKY	80	Toronto Conf. 19	R.E. Cutkosky et al.	(CMU, LBL) IJP	
	Also	PR G20 2839	R.E. Cutkosky et al.	(CMU, LBL) IJP	
LIVANOS	80	Toronto Conf. 35	P. Livanos et al.	(SACL) IJP	
HOEHLER	79	PDAT 12-1	G. Hohler et al.	(KARLT) IJP	
	80	Toronto Conf. 3	R. Koch	(KARLT) IJP	
BARBOUR	78	NP B141 253	I.M. Barbour, R.L. Crawford, N.H. Parsons	(GLAS)	
NOVOSELLER	78	NP B137 509	D.E. Novoseller	(CIT) IJP	
	78B	NP B137 445	D.E. Novoseller	(CIT) IJP	
LONGACRE	77	NP B122 493	R.S. Longacre, J. Dolbeau	(SACL) IJP	
	Also	76	NP B108 365	J. Dolbeau et al.	(SACL) IJP
DEANS	75	NP B96 90	S.R. Deans et al.	(SFLA, ALAH) IJP	

See key on page 239

Baryon Particle Listings
 $\Delta(1920), \Delta(1930)$

$\Delta(1920) P_{33}$

$I(J^P) = \frac{3}{2}(\frac{3}{2}^+)$ Status: ***

Most of the results published before 1975 are now obsolete and have been omitted. They may be found in our 1982 edition, Physics Letters 111B (1982).

$\Delta(1920)$ BREIT-WIGNER MASS

VALUE (MeV)	DOCUMENT ID	TECN	COMMENT
1900 to 1970 (≈ 1920) OUR ESTIMATE			
2014 ± 16	MANLEY 92	IPWA	$\pi N \rightarrow \pi N \& N\pi\pi$
1920 ± 80	CUTKOSKY 80	IPWA	$\pi N \rightarrow \pi N$
1866 ± 10	HOEHLER 79	IPWA	$\pi N \rightarrow \pi N$
• • • We do not use the following data for averages, fits, limits, etc. • • •			
1840 ± 40	CANDLIN 84	DPWA	$\pi^+ p \rightarrow \Sigma^+ K^+$
1955.0 ± 13.0	¹ CHEW 80	BPWA	$\pi^+ p \rightarrow \pi^+ p$
2065.0 $^{+13.6}_{-12.9}$	¹ CHEW 80	BPWA	$\pi^+ p \rightarrow \pi^+ p$

$\Delta(1920)$ BREIT-WIGNER WIDTH

VALUE (MeV)	DOCUMENT ID	TECN	COMMENT
150 to 300 (≈ 200) OUR ESTIMATE			
152 ± 55	MANLEY 92	IPWA	$\pi N \rightarrow \pi N \& N\pi\pi$
300 ± 100	CUTKOSKY 80	IPWA	$\pi N \rightarrow \pi N$
220 ± 80	HOEHLER 79	IPWA	$\pi N \rightarrow \pi N$
• • • We do not use the following data for averages, fits, limits, etc. • • •			
200 ± 40	CANDLIN 84	DPWA	$\pi^+ p \rightarrow \Sigma^+ K^+$
88.3 ± 35.0	¹ CHEW 80	BPWA	$\pi^+ p \rightarrow \pi^+ p$
62.0 ± 44.0	¹ CHEW 80	BPWA	$\pi^+ p \rightarrow \pi^+ p$

$\Delta(1920)$ POLE POSITION

REAL PART VALUE (MeV)	DOCUMENT ID	TECN	COMMENT
1950 to 1950 (≈ 1900) OUR ESTIMATE			
1900	² HOEHLER 93	SPED	$\pi N \rightarrow \pi N$
1900 ± 80	CUTKOSKY 80	IPWA	$\pi N \rightarrow \pi N$
• • • We do not use the following data for averages, fits, limits, etc. • • •			
not seen	ARNDT 91	DPWA	$\pi N \rightarrow \pi N$ Soln SM90

-2xIMAGINARY PART

VALUE (MeV)	DOCUMENT ID	TECN	COMMENT
200 to 400 (≈ 300) OUR ESTIMATE			
300 ± 100	CUTKOSKY 80	IPWA	$\pi N \rightarrow \pi N$
• • • We do not use the following data for averages, fits, limits, etc. • • •			
not seen	ARNDT 91	DPWA	$\pi N \rightarrow \pi N$ Soln SM90

$\Delta(1920)$ ELASTIC POLE RESIDUE

MODULUS $ r $ VALUE (MeV)	DOCUMENT ID	TECN	COMMENT
24 ± 4	CUTKOSKY 80	IPWA	$\pi N \rightarrow \pi N$

PHASE θ

VALUE ($^\circ$)	DOCUMENT ID	TECN	COMMENT
-150 ± 30	CUTKOSKY 80	IPWA	$\pi N \rightarrow \pi N$

$\Delta(1920)$ DECAY MODES

The following branching fractions are our estimates, not fits or averages.

Mode	Fraction (Γ_i/Γ)
Γ_1 $N\pi$	5-20 %
Γ_2 ΣK	
Γ_3 $N\pi\pi$	
Γ_4 $\Delta(1232)\pi, P$ -wave	
Γ_5 $N(1440)\pi, P$ -wave	
Γ_6 $N\gamma, \text{helicity}=1/2$	
Γ_7 $N\gamma, \text{helicity}=3/2$	

$\Delta(1920)$ BRANCHING RATIOS

$\Gamma(N\pi)/\Gamma_{\text{total}}$ VALUE	DOCUMENT ID	TECN	COMMENT
0.05 to 0.2 OUR ESTIMATE			
0.02 ± 0.02	MANLEY 92	IPWA	$\pi N \rightarrow \pi N \& N\pi\pi$
0.20 ± 0.05	CUTKOSKY 80	IPWA	$\pi N \rightarrow \pi N$
0.14 ± 0.04	HOEHLER 79	IPWA	$\pi N \rightarrow \pi N$
• • • We do not use the following data for averages, fits, limits, etc. • • •			
0.24	¹ CHEW 80	BPWA	$\pi^+ p \rightarrow \pi^+ p$
0.18	¹ CHEW 80	BPWA	$\pi^+ p \rightarrow \pi^+ p$

$(\Gamma_1/\Gamma_2)^{1/2}/\Gamma_{\text{total}}$ in $N\pi \rightarrow \Delta(1920) \rightarrow \Sigma K$ $(\Gamma_1/\Gamma_2)^{1/2}/\Gamma$

VALUE	DOCUMENT ID	TECN	COMMENT
-0.052 ± 0.015	CANDLIN 84	DPWA	$\pi^+ p \rightarrow \Sigma^+ K^+$
• • • We do not use the following data for averages, fits, limits, etc. • • •			
-0.049	LIVANOS 80	DPWA	$\pi p \rightarrow \Sigma K$
0.046 to 0.120	³ DEANS 75	DPWA	$\pi N \rightarrow \Sigma K$

$(\Gamma_1/\Gamma_2)^{1/2}/\Gamma_{\text{total}}$ in $N\pi \rightarrow \Delta(1920) \rightarrow \Delta(1232)\pi, P$ -wave $(\Gamma_1/\Gamma_4)^{1/2}/\Gamma$

VALUE	DOCUMENT ID	TECN	COMMENT
-0.13 ± 0.04	MANLEY 92	IPWA	$\pi N \rightarrow \pi N \& N\pi\pi$
0.3	⁴ NOVOSELLER 78	IPWA	$\pi N \rightarrow N\pi\pi$
0.27	⁵ NOVOSELLER 78	IPWA	$\pi N \rightarrow N\pi\pi$

$(\Gamma_1/\Gamma_2)^{1/2}/\Gamma_{\text{total}}$ in $N\pi \rightarrow \Delta(1920) \rightarrow N(1440)\pi, P$ -wave $(\Gamma_1/\Gamma_5)^{1/2}/\Gamma$

VALUE	DOCUMENT ID	TECN	COMMENT
+0.06 ± 0.07	MANLEY 92	IPWA	$\pi N \rightarrow \pi N \& N\pi\pi$

$\Delta(1920)$ PHOTON DECAY AMPLITUDES

$\Delta(1920) \rightarrow N\gamma, \text{helicity}=1/2$ amplitude $A_{1/2}$

VALUE (GeV $^{-1/2}$)	DOCUMENT ID	TECN	COMMENT
0.040 ± 0.014	AWAJI 81	DPWA	$\gamma N \rightarrow \pi N$

$\Delta(1920) \rightarrow N\gamma, \text{helicity}=3/2$ amplitude $A_{3/2}$

VALUE (GeV $^{-1/2}$)	DOCUMENT ID	TECN	COMMENT
0.023 ± 0.017	AWAJI 81	DPWA	$\gamma N \rightarrow \pi N$

$\Delta(1920)$ FOOTNOTES

- ¹ CHEW 80 reports two P_{33} resonances in this mass region. Problems with this analysis are discussed in section 2.1.11 of HOEHLER 83.
- ² See HOEHLER 93 for a detailed discussion of the evidence for and the pole parameters of N and Δ resonances as determined from Argand diagrams of πN elastic partial-wave amplitudes and from plots of the speeds with which the amplitudes traverse the diagrams.
- ³ The range given for DEANS 75 is from the four best solutions.
- ⁴ A Breit-Wigner fit to the HERNDON 75 IPWA; the phase is near -90° .
- ⁵ A Breit-Wigner fit to the NOVOSELLER 78B IPWA; the phase is near -90° .

$\Delta(1920)$ REFERENCES

For early references, see Physics Letters 111B 70 (1982).

HOEHLER 93	πN Newsletter 9 1	G. Hohlner	(KARL)
MANLEY 92	PR D45 4002	D.M. Manley, E.M. Saleski	(KENT) IJP
Also	PR D30 904	D.M. Manley et al.	(VPI)
ARNDT 91	PR D43 2131	R.A. Arnot et al.	(VPI, TELE) IJP
CANDLIN 84	NP B238 477	D.J. Candlin et al.	(EDIN, RAL, LOWC)
HOEHLER 83	Landolt-Boernstein 1/982	G. Hohlner	(KARLT)
PDG 82	PL 111B	M. Roos et al.	(HELS, CIT, CERN)
AWAJI 81	Bonn Conf. 352	N. Awaji, R. Kajikawa	(NAGO)
Also	NP B197 365	K. Fujii et al.	(NAGO)
CHEW 80	Toronto Conf. 123	D.M. Chew	(LBL) IJP
CUTKOSKY 80	Toronto Conf. 19	R.E. Cutkosky et al.	(CMU, LBL) IJP
Also	PR D20 2839	R.E. Cutkosky et al.	(CMU, LBL) IJP
LIVANOS 80	Toronto Conf. 35	P. Livanos et al.	(SACL) IJP
HOEHLER 79	PDAT 12-1	G. Hohlner et al.	(KARLT) IJP
Also	Toronto Conf. 3	R. Koch	(KARLT) IJP
NOVOSELLER 78	NP B137 509	D.E. Novoseller	(CIT)
NOVOSELLER 78B	NP B137 445	D.E. Novoseller	(CIT)
DEANS 75	NP B96 90	S.R. Deans et al.	(SFLA, ALAH) IJP
HERNDON 75	PR D11 3183	D. Herndon et al.	(LBL, SLAC)

$\Delta(1930) D_{35}$

$I(J^P) = \frac{3}{2}(\frac{5}{2}^-)$ Status: ***

Most of the results published before 1975 are now obsolete and have been omitted. They may be found in our 1982 edition, Physics Letters 111B (1982).

The various analyses are not in good agreement.

$\Delta(1930)$ BREIT-WIGNER MASS

VALUE (MeV)	DOCUMENT ID	TECN	COMMENT
1920 to 1970 (≈ 1930) OUR ESTIMATE			
1956 ± 22	MANLEY 92	IPWA	$\pi N \rightarrow \pi N \& N\pi\pi$
1940 ± 30	CUTKOSKY 80	IPWA	$\pi N \rightarrow \pi N$
1901 ± 15	HOEHLER 79	IPWA	$\pi N \rightarrow \pi N$
• • • We do not use the following data for averages, fits, limits, etc. • • •			
1955 ± 15	ARNDT 96	IPWA	$\gamma N \rightarrow \pi N$
2056	ARNDT 95	DPWA	$\pi N \rightarrow N\pi$
1963	LI 93	IPWA	$\gamma N \rightarrow \pi N$
1910.0 $^{+15.0}_{-17.2}$	CHEW 80	BPWA	$\pi^+ p \rightarrow \pi^+ p$
2000	CRAWFORD 80	DPWA	$\gamma N \rightarrow \pi N$
2024	BARBOUR 78	DPWA	$\gamma N \rightarrow \pi N$

Baryon Particle Listings

$\Delta(1930), \Delta(1940)$

$\Delta(1930)$ BREIT-WIGNER WIDTH

VALUE (MeV)	DOCUMENT ID	TECN	COMMENT
250 to 450 (≈ 350) OUR ESTIMATE			
530 \pm 140	MANLEY 92	IPWA	$\pi N \rightarrow \pi N$ & $N\pi\pi$
320 \pm 60	CUTKOSKY 80	IPWA	$\pi N \rightarrow \pi N$
195 \pm 60	HOEHLER 79	IPWA	$\pi N \rightarrow \pi N$
• • • We do not use the following data for averages, fits, limits, etc. • • •			
350 \pm 20	ARNDT 96	IPWA	$\gamma N \rightarrow \pi N$
590	ARNDT 95	DPWA	$\pi N \rightarrow N\pi$
260	LI 93	IPWA	$\gamma N \rightarrow \pi N$
74.8 ⁺ 17.0 - 16.0	CHEW 80	BPWA	$\pi^+ p \rightarrow \pi^+ p$
442	CRAWFORD 80	DPWA	$\gamma N \rightarrow \pi N$
462	BARBOUR 78	DPWA	$\gamma N \rightarrow \pi N$

$\Delta(1930)$ POLE POSITION

REAL PART

VALUE (MeV)	DOCUMENT ID	TECN	COMMENT
1840 to 1940 (≈ 1890) OUR ESTIMATE			
1913	ARNDT 95	DPWA	$\pi N \rightarrow N\pi$
1850	¹ HOEHLER 93	SPED	$\pi N \rightarrow \pi N$
1890 \pm 50	CUTKOSKY 80	IPWA	$\pi N \rightarrow \pi N$
• • • We do not use the following data for averages, fits, limits, etc. • • •			
2018	ARNDT 91	DPWA	$\pi N \rightarrow \pi N$ Soln SM90

-2xIMAGINARY PART

VALUE (MeV)	DOCUMENT ID	TECN	COMMENT
200 to 300 (≈ 250) OUR ESTIMATE			
246	ARNDT 95	DPWA	$\pi N \rightarrow N\pi$
180	¹ HOEHLER 93	SPED	$\pi N \rightarrow \pi N$
260 \pm 60	CUTKOSKY 80	IPWA	$\pi N \rightarrow \pi N$
• • • We do not use the following data for averages, fits, limits, etc. • • •			
398	ARNDT 91	DPWA	$\pi N \rightarrow \pi N$ Soln SM90

$\Delta(1930)$ ELASTIC POLE RESIDUE

MODULUS $|r|$

VALUE (MeV)	DOCUMENT ID	TECN	COMMENT
8	ARNDT 95	DPWA	$\pi N \rightarrow N\pi$
20	HOEHLER 93	SPED	$\pi N \rightarrow \pi N$
18 \pm 6	CUTKOSKY 80	IPWA	$\pi N \rightarrow \pi N$
• • • We do not use the following data for averages, fits, limits, etc. • • •			
15	ARNDT 91	DPWA	$\pi N \rightarrow \pi N$ Soln SM90

PHASE θ

VALUE ($^\circ$)	DOCUMENT ID	TECN	COMMENT
-47	ARNDT 95	DPWA	$\pi N \rightarrow N\pi$
-20 \pm 40	CUTKOSKY 80	IPWA	$\pi N \rightarrow \pi N$
• • • We do not use the following data for averages, fits, limits, etc. • • •			
-24	ARNDT 91	DPWA	$\pi N \rightarrow \pi N$ Soln SM90

$\Delta(1930)$ DECAY MODES

The following branching fractions are our estimates, not fits or averages.

Mode	Fraction (Γ_i/Γ)
Γ_1 $N\pi$	10-20 %
Γ_2 ΣK	
Γ_3 $N\pi\pi$	
Γ_4 $N\gamma$	0.0-0.02 %
Γ_5 $N\gamma$, helicity=1/2	0.0-0.01 %
Γ_6 $N\gamma$, helicity=3/2	0.0-0.01 %

$\Delta(1930)$ BRANCHING RATIOS

$\Gamma(N\pi)/\Gamma_{total}$	DOCUMENT ID	TECN	COMMENT	Γ_1/Γ
0.1 to 0.2 OUR ESTIMATE				
0.18 \pm 0.02	MANLEY 92	IPWA	$\pi N \rightarrow \pi N$ & $N\pi\pi$	
0.14 \pm 0.04	CUTKOSKY 80	IPWA	$\pi N \rightarrow \pi N$	
0.04 \pm 0.03	HOEHLER 79	IPWA	$\pi N \rightarrow \pi N$	
• • • We do not use the following data for averages, fits, limits, etc. • • •				
0.11	ARNDT 95	DPWA	$\pi N \rightarrow N\pi$	
0.11	CHEW 80	BPWA	$\pi^+ p \rightarrow \pi^+ p$	

$(\Gamma_1\Gamma_2)^{1/2}/\Gamma_{total}$ in $N\pi \rightarrow \Delta(1930) \rightarrow \Sigma K$	DOCUMENT ID	TECN	COMMENT	$(\Gamma_1\Gamma_2)^{1/2}/\Gamma$
< 0.015				
< 0.015	CANCLIN 84	DPWA	$\pi^+ p \rightarrow \Sigma^+ K^+$	
• • • We do not use the following data for averages, fits, limits, etc. • • •				
-0.031	LIVANOS 80	DPWA	$\pi p \rightarrow \Sigma K$	
0.018 to 0.035	² DEANS 75	DPWA	$\pi N \rightarrow \Sigma K$	

$(\Gamma_1\Gamma_2)^{1/2}/\Gamma_{total}$ in $N\pi \rightarrow \Delta(1930) \rightarrow N\pi\pi$	DOCUMENT ID	TECN	COMMENT	$(\Gamma_1\Gamma_3)^{1/2}/\Gamma$
not seen	LONGACRE 75	IPWA	$\pi N \rightarrow N\pi\pi$	

$\Delta(1930)$ PHOTON DECAY AMPLITUDES

$\Delta(1930) \rightarrow N\gamma$, helicity-1/2 amplitude $A_{1/2}$

VALUE ($\text{GeV}^{-1/2}$)	DOCUMENT ID	TECN	COMMENT
-0.009 \pm 0.028 OUR ESTIMATE			
-0.007 \pm 0.010	ARNDT 96	IPWA	$\gamma N \rightarrow \pi N$
0.009 \pm 0.009	AWAJI 81	DPWA	$\gamma N \rightarrow \pi N$
-0.030 \pm 0.047	CRAWFORD 80	DPWA	$\gamma N \rightarrow \pi N$
• • • We do not use the following data for averages, fits, limits, etc. • • •			
-0.019 \pm 0.001	LI 93	IPWA	$\gamma N \rightarrow \pi N$
-0.062 \pm 0.064	BARBOUR 78	DPWA	$\gamma N \rightarrow \pi N$

$\Delta(1930) \rightarrow N\gamma$, helicity-3/2 amplitude $A_{3/2}$

VALUE ($\text{GeV}^{-1/2}$)	DOCUMENT ID	TECN	COMMENT
-0.018 \pm 0.028 OUR ESTIMATE			
0.005 \pm 0.010	ARNDT 96	IPWA	$\gamma N \rightarrow \pi N$
-0.025 \pm 0.011	AWAJI 81	DPWA	$\gamma N \rightarrow \pi N$
-0.033 \pm 0.060	CRAWFORD 80	DPWA	$\gamma N \rightarrow \pi N$
• • • We do not use the following data for averages, fits, limits, etc. • • •			
0.009 \pm 0.001	LI 93	IPWA	$\gamma N \rightarrow \pi N$
+0.019 \pm 0.054	BARBOUR 78	DPWA	$\gamma N \rightarrow \pi N$

$\Delta(1930)$ FOOTNOTES

- See HOEHLER 93 for a detailed discussion of the evidence for and the pole parameters of N and Δ resonances as determined from Argand diagrams of πN elastic partial-wave amplitudes and from plots of the speeds with which the amplitudes traverse the diagrams.
- The range given for DEANS 75 is from the four best solutions.

$\Delta(1930)$ REFERENCES

For early references, see Physics Letters 111B 70 (1982).

ARNDT 96	PR C53 430	R.A. Arndt, I.I. Strakovsky, R.L. Workman	(VPI)
ARNDT 95	PR C52 2120	R.A. Arndt <i>et al.</i>	(VPI, BRCO)
HOEHLER 93	πN Newsletter 9 1	G. Hohler	(KARL)
LI 93	PR C47 2759	Z.J. Li <i>et al.</i>	(VPI)
MANLEY 92	PR D45 4002	D.M. Manley, E.M. Saleski	(KENT) IJF
Also	PR D30 904	D.M. Manley <i>et al.</i>	(VPI)
ARNDT 91	PR D43 2131	R.A. Arndt <i>et al.</i>	(VPI, TELE) IJF
CANCLIN 84	NP B238 477	D.J. Candlin <i>et al.</i>	(EDIN, RAL, LOWC)
PDG 82	PL 111B	M. Roos <i>et al.</i>	(HELS, CIT, CERN)
AWAJI 81	Bonn Conf. 352	N. Awaji, R. Kajikawa	(NAGO)
Also	NP B197 365	K. Fujii <i>et al.</i>	(NAGO)
CHEW 80	Toronto Conf. 123	D.M. Chew	(LBL) IJF
CRAWFORD 80	Toronto Conf. 107	R.L. Crawford	(GLAS)
CUTKOSKY 80	Toronto Conf. 19	R.E. Cutkosky <i>et al.</i>	(CMU, LBL) IJF
Also	PR D20 2839	R.E. Cutkosky <i>et al.</i>	(CMU, LBL) IJF
LIVANOS 80	Toronto Conf. 35	P. Livanos <i>et al.</i>	(SACL) IJF
HOEHLER 79	PDAT 12-1	G. Hohler <i>et al.</i>	(KARLT) IJF
Also	Toronto Conf. 3	R. Koch	(KARLT) IJF
BARBOUR 78	NP B141 253	I.M. Barbour, R.L. Crawford, N.H. Parsons	(GLAS)
DEANS 75	NP B96 90	S.R. Deans <i>et al.</i>	(SFLA, ALAH) IJF
LONGACRE 75	PL 55B 415	R.S. Longacre <i>et al.</i>	(LBL, SLAC) IJF

$\Delta(1940) D_{33}$

$I(J^P) = \frac{3}{2}(3^-)$ Status: *

OMITTED FROM SUMMARY TABLE

$\Delta(1940)$ BREIT-WIGNER MASS

VALUE (MeV)	DOCUMENT ID	TECN	COMMENT
≈ 1940 OUR ESTIMATE			
2057 \pm 110	MANLEY 92	IPWA	$\pi N \rightarrow \pi N$ & $N\pi\pi$
2058.1 \pm 34.5	CHEW 80	BPWA	$\pi^+ p \rightarrow \pi^+ p$
1940 \pm 100	CUTKOSKY 80	IPWA	$\pi N \rightarrow \pi N$

$\Delta(1940)$ BREIT-WIGNER WIDTH

VALUE (MeV)	DOCUMENT ID	TECN	COMMENT
460 \pm 320	MANLEY 92	IPWA	$\pi N \rightarrow \pi N$ & $N\pi\pi$
198.4 \pm 45.5	CHEW 80	BPWA	$\pi^+ p \rightarrow \pi^+ p$
200 \pm 100	CUTKOSKY 80	IPWA	$\pi N \rightarrow \pi N$

$\Delta(1940)$ POLE POSITION

REAL PART

VALUE (MeV)	DOCUMENT ID	TECN	COMMENT
1900 \pm 100	CUTKOSKY 80	IPWA	$\pi N \rightarrow \pi N$
1915 or 1926	¹ LONGACRE 78	IPWA	$\pi N \rightarrow N\pi\pi$

-2xIMAGINARY PART

VALUE (MeV)	DOCUMENT ID	TECN	COMMENT
200 \pm 60	CUTKOSKY 80	IPWA	$\pi N \rightarrow \pi N$
190 or 186	¹ LONGACRE 78	IPWA	$\pi N \rightarrow N\pi\pi$

See key on page 239

Baryon Particle Listings

 $\Delta(1940)$, $\Delta(1950)$ $\Delta(1940)$ ELASTIC POLE RESIDUEMODULUS $|r|$

VALUE (MeV)	DOCUMENT ID	TECN	COMMENT
8 ± 3	CUTKOSKY 80	IPWA	$\pi N \rightarrow \pi N$

PHASE θ

VALUE ($^\circ$)	DOCUMENT ID	TECN	COMMENT
135 ± 45	CUTKOSKY 80	IPWA	$\pi N \rightarrow \pi N$

 $\Delta(1940)$ DECAY MODES

Mode	
Γ_1	$N\pi$
Γ_2	ΣK
Γ_3	$N\pi\pi$
Γ_4	$\Delta(1232)\pi$, S-wave
Γ_5	$\Delta(1232)\pi$, D-wave
Γ_6	$N\rho$, $S=3/2$, S-wave
Γ_7	$N\gamma$, helicity=1/2
Γ_8	$N\gamma$, helicity=3/2

 $\Delta(1940)$ BRANCHING RATIOS

$\Gamma(N\pi)/\Gamma_{\text{total}}$	DOCUMENT ID	TECN	COMMENT	Γ_1/Γ
0.18 ± 0.12	MANLEY 92	IPWA	$\pi N \rightarrow \pi N$ & $N\pi\pi$	
0.18	CHEW 80	BPWA	$\pi^+\rho \rightarrow \pi^+\rho$	
0.05 ± 0.02	CUTKOSKY 80	IPWA	$\pi N \rightarrow \pi N$	

$(\Gamma_1\Gamma_2)^{1/2}/\Gamma_{\text{total}}$ in $N\pi \rightarrow \Delta(1940) \rightarrow \Sigma K$	DOCUMENT ID	TECN	COMMENT	$(\Gamma_1\Gamma_2)^{1/2}/\Gamma$
<0.015	CANDLIN 84	DPWA	$\pi^+\rho \rightarrow \Sigma^+K^+$	

$(\Gamma_1\Gamma_4)^{1/2}/\Gamma_{\text{total}}$ in $N\pi \rightarrow \Delta(1940) \rightarrow \Delta(1232)\pi$, S-wave	DOCUMENT ID	TECN	COMMENT	$(\Gamma_1\Gamma_4)^{1/2}/\Gamma$
$+0.11 \pm 0.10$	MANLEY 92	IPWA	$\pi N \rightarrow \pi N$ & $N\pi\pi$	

$(\Gamma_1\Gamma_5)^{1/2}/\Gamma_{\text{total}}$ in $N\pi \rightarrow \Delta(1940) \rightarrow \Delta(1232)\pi$, D-wave	DOCUMENT ID	TECN	COMMENT	$(\Gamma_1\Gamma_5)^{1/2}/\Gamma$
$+0.27 \pm 0.16$	MANLEY 92	IPWA	$\pi N \rightarrow \pi N$ & $N\pi\pi$	

$(\Gamma_1\Gamma_6)^{1/2}/\Gamma_{\text{total}}$ in $N\pi \rightarrow \Delta(1940) \rightarrow N\rho$, $S=3/2$, S-wave	DOCUMENT ID	TECN	COMMENT	$(\Gamma_1\Gamma_6)^{1/2}/\Gamma$
$+0.25 \pm 0.10$	MANLEY 92	IPWA	$\pi N \rightarrow \pi N$ & $N\pi\pi$	

 $\Delta(1940)$ PHOTON DECAY AMPLITUDES $\Delta(1940) \rightarrow N\gamma$, helicity-1/2 amplitude $A_{1/2}$

VALUE ($\text{GeV}^{-1/2}$)	DOCUMENT ID	TECN	COMMENT
-0.036 ± 0.058	AWAJI 81	DPWA	$\gamma N \rightarrow \pi N$

 $\Delta(1940) \rightarrow N\gamma$, helicity-3/2 amplitude $A_{3/2}$

VALUE ($\text{GeV}^{-1/2}$)	DOCUMENT ID	TECN	COMMENT
-0.031 ± 0.012	AWAJI 81	DPWA	$\gamma N \rightarrow \pi N$

 $\Delta(1940)$ FOOTNOTES

¹ LONGACRE 78 values are from a search for poles in the unitarized T-matrix. The first (second) value uses, in addition to $\pi N \rightarrow N\pi\pi$ data, elastic amplitudes from a Saclay (CERN) partial-wave analysis.

 $\Delta(1940)$ REFERENCES

MANLEY 92	PR D45 4002	D.M. Manley, E.M. Saleski	(KENT) IJP
Also	84 PR D30 904	D.M. Manley et al.	(VPI)
CANDLIN 84	NP B238 477	D.J. Candlin et al.	(EDIN, RAL, LOWC)
AWAJI 81	Bonn Conf. 352	N. Awaji, R. Kajikawa	(NAGO)
Also	82 NP B197 365	K. Fujii et al.	(NAGO)
CHEW 80	Toronto Conf. 123	D.M. Chew	(LBL) IJP
CUTKOSKY 80	Toronto Conf. 19	R.E. Cutkosky et al.	(CMU, LBL) IJP
Also	79 PR D20 2839	R.E. Cutkosky et al.	(CMU, LBL)
LONGACRE 78	PR D17 1795	R.S. Longacre et al.	(LBL, SLAC)

 $\Delta(1950) F_{37}$ $I(J^P) = \frac{3}{2}(\frac{7}{2}^+)$ Status: * * * *

Most of the results published before 1975 are now obsolete and have been omitted. They may be found in our 1982 edition, Physics Letters **111B** (1982).

 $\Delta(1950)$ BREIT-WIGNER MASS

VALUE (MeV)	DOCUMENT ID	TECN	COMMENT
1940 to 1960 (≈ 1950) OUR ESTIMATE			
1945 ± 2	MANLEY 92	IPWA	$\pi N \rightarrow \pi N$ & $N\pi\pi$
1950 ± 15	CUTKOSKY 80	IPWA	$\pi N \rightarrow \pi N$
1913 ± 8	HOEHLER 79	IPWA	$\pi N \rightarrow \pi N$
• • • We do not use the following data for averages, fits, limits, etc. • • •			
1947 ± 9	ARNDT 96	IPWA	$\gamma N \rightarrow \pi N$
1921	ARNDT 95	DPWA	$\pi N \rightarrow N\pi$
1940	LI 93	IPWA	$\gamma N \rightarrow \pi N$
1925 ± 20	CANDLIN 84	DPWA	$\pi^+\rho \rightarrow \Sigma^+K^+$
$1855.0^{+11.0}_{-10.0}$	CHEW 80	BPWA	$\pi^+\rho \rightarrow \pi^+\rho$
1902	CRAWFORD 80	DPWA	$\gamma N \rightarrow \pi N$
1912	BARBOUR 78	DPWA	$\gamma N \rightarrow \pi N$
1925	¹ LONGACRE 75	IPWA	$\pi N \rightarrow N\pi\pi$

 $\Delta(1950)$ BREIT-WIGNER WIDTH

VALUE (MeV)	DOCUMENT ID	TECN	COMMENT
290 to 350 (≈ 300) OUR ESTIMATE			
300 ± 7	MANLEY 92	IPWA	$\pi N \rightarrow \pi N$ & $N\pi\pi$
340 ± 50	CUTKOSKY 80	IPWA	$\pi N \rightarrow \pi N$
224 ± 10	HOEHLER 79	IPWA	$\pi N \rightarrow \pi N$
• • • We do not use the following data for averages, fits, limits, etc. • • •			
302 ± 9	ARNDT 96	IPWA	$\gamma N \rightarrow \pi N$
232	ARNDT 95	DPWA	$\pi N \rightarrow N\pi$
306	LI 93	IPWA	$\gamma N \rightarrow \pi N$
330 ± 40	CANDLIN 84	DPWA	$\pi^+\rho \rightarrow \Sigma^+K^+$
$157.2^{+22.0}_{-19.0}$	CHEW 80	BPWA	$\pi^+\rho \rightarrow \pi^+\rho$
225	CRAWFORD 80	DPWA	$\gamma N \rightarrow \pi N$
198	BARBOUR 78	DPWA	$\gamma N \rightarrow \pi N$
240	¹ LONGACRE 75	IPWA	$\pi N \rightarrow N\pi\pi$

 $\Delta(1950)$ POLE POSITION

REAL PART

VALUE (MeV)	DOCUMENT ID	TECN	COMMENT
1880 to 1890 (≈ 1885) OUR ESTIMATE			
1880	ARNDT 95	DPWA	$\pi N \rightarrow \pi N$
1878	² HOEHLER 93	ARGD	$\pi N \rightarrow \pi N$
1890 ± 15	CUTKOSKY 80	IPWA	$\pi N \rightarrow \pi N$
• • • We do not use the following data for averages, fits, limits, etc. • • •			
1884	ARNDT 91	DPWA	$\pi N \rightarrow \pi N$ Soln SM90
1924 or 1924	³ LONGACRE 78	IPWA	$\pi N \rightarrow N\pi\pi$

-2xIMAGINARY PART

VALUE (MeV)	DOCUMENT ID	TECN	COMMENT
210 to 270 (≈ 240) OUR ESTIMATE			
236	ARNDT 95	DPWA	$\pi N \rightarrow \pi N$
230	² HOEHLER 93	ARGD	$\pi N \rightarrow \pi N$
260 ± 40	CUTKOSKY 80	IPWA	$\pi N \rightarrow \pi N$
• • • We do not use the following data for averages, fits, limits, etc. • • •			
238	ARNDT 91	DPWA	$\pi N \rightarrow \pi N$ Soln SM90
258 or 258	³ LONGACRE 78	IPWA	$\pi N \rightarrow N\pi\pi$

 $\Delta(1950)$ ELASTIC POLE RESIDUEMODULUS $|r|$

VALUE (MeV)	DOCUMENT ID	TECN	COMMENT
54	ARNDT 95	DPWA	$\pi N \rightarrow N\pi$
47	HOEHLER 93	ARGD	$\pi N \rightarrow \pi N$
50 ± 7	CUTKOSKY 80	IPWA	$\pi N \rightarrow \pi N$
• • • We do not use the following data for averages, fits, limits, etc. • • •			
61	ARNDT 91	DPWA	$\pi N \rightarrow \pi N$ Soln SM90

PHASE θ

VALUE ($^\circ$)	DOCUMENT ID	TECN	COMMENT
-17	ARNDT 95	DPWA	$\pi N \rightarrow N\pi$
-32	HOEHLER 93	ARGD	$\pi N \rightarrow \pi N$
-33 ± 8	CUTKOSKY 80	IPWA	$\pi N \rightarrow \pi N$
• • • We do not use the following data for averages, fits, limits, etc. • • •			
-23	ARNDT 91	DPWA	$\pi N \rightarrow \pi N$ Soln SM90

Baryon Particle Listings

 $\Delta(1950), \Delta(2000)$ $\Delta(1950)$ DECAY MODES

The following branching fractions are our estimates, not fits or averages.

Mode	Fraction (Γ_i/Γ)
Γ_1 $N\pi$	35-40 %
Γ_2 ΣK	
Γ_3 $N\pi\pi$	
Γ_4 $\Delta\pi$	20-30 %
Γ_5 $\Delta(1232)\pi$, F-wave	
Γ_6 $\Delta(1232)\pi$, H-wave	
Γ_7 $N\rho$	<10 %
Γ_8 $N\rho$, S=1/2, F-wave	
Γ_9 $N\rho$, S=3/2, F-wave	
Γ_{10} $N\gamma$	0.08-0.13 %
Γ_{11} $N\gamma$, helicity=1/2	0.03-0.055 %
Γ_{12} $N\gamma$, helicity=3/2	0.05-0.075 %

 $\Delta(1950)$ BRANCHING RATIOS

$\Gamma(N\pi)/\Gamma_{total}$	DOCUMENT ID	TECN	COMMENT	Γ_1/Γ
0.35 to 0.4 OUR ESTIMATE				
0.38 ± 0.01	MANLEY 92	IPWA	$\pi N \rightarrow \pi N$ & $N\pi\pi$	
0.39 ± 0.04	CUTKOSKY 80	IPWA	$\pi N \rightarrow \pi N$	
0.38 ± 0.02	HOEHLER 79	IPWA	$\pi N \rightarrow \pi N$	
• • • We do not use the following data for averages, fits, limits, etc. • • •				
0.49	ARNDT 95	DPWA	$\pi N \rightarrow N\pi$	
0.44	CHEW 80	BPWA	$\pi^+ p \rightarrow \pi^+ p$	
$(\Gamma_1\Gamma_2)^{1/2}/\Gamma_{total}$ in $N\pi \rightarrow \Delta(1950) \rightarrow \Sigma K$				$(\Gamma_1\Gamma_2)^{1/2}/\Gamma$
0.022 to 0.040				
-0.053 ± 0.005	CANDLIN 84	DPWA	$\pi^+ p \rightarrow \Sigma^+ K^+$	
• • • We do not use the following data for averages, fits, limits, etc. • • •				
0.022 to 0.040	4 DEANS 75	DPWA	$\pi N \rightarrow \Sigma K$	

Note: Signs of couplings from $\pi N \rightarrow N\pi\pi$ analyses were changed in the 1986 edition to agree with the baryon-first convention; the overall phase ambiguity is resolved by choosing a negative sign for the $\Delta(1620) S_{31}$ coupling to $\Delta(1232)\pi$.

$(\Gamma_1\Gamma_2)^{1/2}/\Gamma_{total}$ in $N\pi \rightarrow \Delta(1950) \rightarrow \Delta(1232)\pi$, F-wave	DOCUMENT ID	TECN	COMMENT	$(\Gamma_1\Gamma_2)^{1/2}/\Gamma$
+0.28 to +0.32 OUR ESTIMATE				
+0.27 ± 0.02	MANLEY 92	IPWA	$\pi N \rightarrow \pi N$ & $N\pi\pi$	
+0.32	1 LONGACRE 75	IPWA	$\pi N \rightarrow N\pi\pi$	
• • • We do not use the following data for averages, fits, limits, etc. • • •				
0.21	5 NOVOSELLER 78	IPWA	$\pi N \rightarrow N\pi\pi$	
0.38	6 NOVOSELLER 78	IPWA	$\pi N \rightarrow N\pi\pi$	

$(\Gamma_1\Gamma_2)^{1/2}/\Gamma_{total}$ in $N\pi \rightarrow \Delta(1950) \rightarrow N\rho$, S=3/2, F-wave	DOCUMENT ID	TECN	COMMENT	$(\Gamma_1\Gamma_2)^{1/2}/\Gamma$
0.24	1 LONGACRE 75	IPWA	$\pi N \rightarrow N\pi\pi$	
• • • We do not use the following data for averages, fits, limits, etc. • • •				
0.24	7 NOVOSELLER 78	IPWA	$\pi N \rightarrow N\pi\pi$	
0.43	8 NOVOSELLER 78	IPWA	$\pi N \rightarrow N\pi\pi$	

 $\Delta(1950)$ PHOTON DECAY AMPLITUDES

$\Delta(1950) \rightarrow N\gamma$, helicity-1/2 amplitude $A_{1/2}$	DOCUMENT ID	TECN	COMMENT
-0.076 ± 0.012 OUR ESTIMATE			
-0.079 ± 0.006	ARNDT 96	IPWA	$\gamma N \rightarrow \pi N$
-0.068 ± 0.007	AWAJI 81	DPWA	$\gamma N \rightarrow \pi N$
-0.091 ± 0.005	ARAI 80	DPWA	$\gamma N \rightarrow \pi N$ (fit 1)
-0.083 ± 0.005	ARAI 80	DPWA	$\gamma N \rightarrow \pi N$ (fit 2)
-0.067 ± 0.014	CRAWFORD 80	DPWA	$\gamma N \rightarrow \pi N$
• • • We do not use the following data for averages, fits, limits, etc. • • •			
-0.102 ± 0.003	LI 93	IPWA	$\gamma N \rightarrow \pi N$
-0.058 ± 0.013	BARBOUR 78	DPWA	$\gamma N \rightarrow \pi N$
$\Delta(1950) \rightarrow N\gamma$, helicity-3/2 amplitude $A_{3/2}$			
-0.097 ± 0.010 OUR ESTIMATE			
-0.103 ± 0.006	ARNDT 96	IPWA	$\gamma N \rightarrow \pi N$
-0.094 ± 0.016	AWAJI 81	DPWA	$\gamma N \rightarrow \pi N$
-0.101 ± 0.005	ARAI 80	DPWA	$\gamma N \rightarrow \pi N$ (fit 1)
-0.100 ± 0.005	ARAI 80	DPWA	$\gamma N \rightarrow \pi N$ (fit 2)
-0.082 ± 0.017	CRAWFORD 80	DPWA	$\gamma N \rightarrow \pi N$
• • • We do not use the following data for averages, fits, limits, etc. • • •			
-0.115 ± 0.003	LI 93	IPWA	$\gamma N \rightarrow \pi N$
-0.075 ± 0.020	BARBOUR 78	DPWA	$\gamma N \rightarrow \pi N$

 $\Delta(1950)$ FOOTNOTES

- From method II of LONGACRE 75: eyeball fits with Breit-Wigner circles to the T-matrix amplitudes.
- See HOEHLER 93 for a detailed discussion of the evidence for and the pole parameters of N and Δ resonances as determined from Argand diagrams of πN elastic partial-wave amplitudes and from plots of the speeds with which the amplitudes traverse the diagrams.
- LONGACRE 78 values are from a search for poles in the unitarized T-matrix. The first (second) value uses, in addition to $\pi N \rightarrow N\pi\pi$ data, elastic amplitudes from a Saclay (CERN) partial-wave analysis.
- The range given is from the four best solutions. DEANS 75 disagrees with $\pi^+ p \rightarrow \Sigma^+ K^+$ data of WINNIK 77 around 1920 MeV.
- A Breit-Wigner fit to the HERNDON 75 IPWA; the phase is near -60° .
- A Breit-Wigner fit to the NOVOSELLER 78B IPWA; the phase is near -60° .
- A Breit-Wigner fit to the HERNDON 75 IPWA; the phase is near 120° .
- A Breit-Wigner fit to the NOVOSELLER 78B IPWA; the phase is near 120° .

 $\Delta(1950)$ REFERENCES

ARNDT 96	PR C53 430	R.A. Arndt, I.I. Strakovsky, R.L. Workman	(VPI)
ARNDT 95	PR C52 2120	R.A. Arndt et al.	(VPI, BRCC)
HOEHLER 93	πN Newsletter 9 1	G. Hoehler	(KARL)
LI 93	PR C47 2759	Z.J. Li et al.	(VPI)
MANLEY 92	PR D45 4002	D.M. Manley, E.M. Saleski	(KENT) IJP
Also	84 PR D30 904	D.M. Manley et al.	(VPI)
ARNDT 91	PR D43 2131	R.A. Arndt et al.	(VPI, TEL) IJP
CANDLIN 84	NP B738 477	D.J. Candlin et al.	(EDIN, RAL, LOWC)
PDG	82 PL 111B	M. Roos et al.	(HELS, CIT, CERN)
AWAJI 81	Bonn Conf. 352	N. Awaji, R. Kajikawa	(NAGO)
Also	82 NP B197 365	K. Fujii et al.	(NAGO)
ARAI 80	Toronto Conf. 93	I. Arai	(INUS)
Also	82 NP B194 251	I. Arai, H. Fujii	(INUS)
CHEW 80	Toronto Conf. 123	D.M. Chew	(LBL) IJP
CRAWFORD 80	Toronto Conf. 107	R.L. Crawford	(GLAS)
CUTKOSKY 80	Toronto Conf. 19	R.E. Cutkosky et al.	(CMU, LBL) IJP
Also	79 PR D20 2839	R.E. Cutkosky et al.	(CMU, LBL) IJP
HOEHLER 79	PDAT 12-1	G. Hoehler et al.	(KARLT) IJP
Also	80 Toronto Conf. 3	R. Koch	(KARLT) IJP
BARBOUR 78	NP B141 253	I.M. Barbour, R.L. Crawford, N.H. Parsons	(GLAS)
LONGACRE 78	PR D17 1795	R.S. Longacre et al.	(LBL, SLAC)
NOVOSELLER 78	NP B137 509	D.E. Novoseller	(CIT) IJP
NOVOSELLER 78B	NP B137 445	D.E. Novoseller	(CIT) IJP
WINNIK 77	NP B128 66	M. Winnik et al.	(HAIF) I
DEANS 75	NP B96 90	S.R. Deans et al.	(SFLA, ALAB) IJP
HERNDON 75	PR D11 3183	D. Herndon et al.	(LBL, SLAC)
LONGACRE 75	PL 55B 415	R.S. Longacre et al.	(LBL, SLAC) IJP

 $\Delta(2000) F_{35}$

$$I(J^P) = \frac{3}{2}(5^+) \text{ Status: } **$$

OMITTED FROM SUMMARY TABLE

 $\Delta(2000)$ BREIT-WIGNER MASS

VALUE (MeV)	DOCUMENT ID	TECN	COMMENT
≈ 2000 OUR ESTIMATE			
1752 ± 32	MANLEY 92	IPWA	$\pi N \rightarrow \pi N$ & $N\pi\pi$
2200 ± 125	CUTKOSKY 80	IPWA	$\pi N \rightarrow \pi N$

 $\Delta(2000)$ BREIT-WIGNER WIDTH

VALUE (MeV)	DOCUMENT ID	TECN	COMMENT
251 ± 93	MANLEY 92	IPWA	$\pi N \rightarrow \pi N$ & $N\pi\pi$
400 ± 125	CUTKOSKY 80	IPWA	$\pi N \rightarrow \pi N$

 $\Delta(2000)$ POLE POSITION

REAL PART	DOCUMENT ID	TECN	COMMENT
2150 ± 100	CUTKOSKY 80	IPWA	$\pi N \rightarrow \pi N$
-2xIMAGINARY PART			
350 ± 100	CUTKOSKY 80	IPWA	$\pi N \rightarrow \pi N$

 $\Delta(2000)$ ELASTIC POLE RESIDUE

MODULUS $ r $	DOCUMENT ID	TECN	COMMENT
16 ± 5	CUTKOSKY 80	IPWA	$\pi N \rightarrow \pi N$
PHASE θ			
150 ± 90	CUTKOSKY 80	IPWA	$\pi N \rightarrow \pi N$

 $\Delta(2000)$ DECAY MODES

Mode	Fraction (Γ_i/Γ)
Γ_1 $N\pi$	
Γ_2 $N\pi\pi$	
Γ_3 $\Delta(1232)\pi$, P-wave	
Γ_4 $\Delta(1232)\pi$, F-wave	
Γ_5 $N\rho$, S=3/2, P-wave	

See key on page 239

Baryon Particle Listings

$\Delta(2000)$, $\Delta(2150)$, $\Delta(2200)$

 $\Delta(2000)$ BRANCHING RATIOS

$\Gamma(N\pi)/\Gamma_{\text{total}}$	DOCUMENT ID	TECN	COMMENT	Γ_1/Γ
0.02 ± 0.01	MANLEY 92	IPWA	$\pi N \rightarrow \pi N$ & $N\pi\pi$	
0.07 ± 0.04	CUTKOSKY 80	IPWA	$\pi N \rightarrow \pi N$	

$(\Gamma_1\Gamma_2)^{1/2}/\Gamma_{\text{total}}$ in $N\pi \rightarrow \Delta(2000) \rightarrow \Delta(1232)\pi$, P-wave	DOCUMENT ID	TECN	COMMENT	$(\Gamma_1\Gamma_2)^{1/2}/\Gamma$
+0.07 ± 0.03	MANLEY 92	IPWA	$\pi N \rightarrow \pi N$ & $N\pi\pi$	

$(\Gamma_1\Gamma_2)^{1/2}/\Gamma_{\text{total}}$ in $N\pi \rightarrow \Delta(2000) \rightarrow \Delta(1232)\pi$, F-wave	DOCUMENT ID	TECN	COMMENT	$(\Gamma_1\Gamma_2)^{1/2}/\Gamma$
+0.09 ± 0.04	MANLEY 92	IPWA	$\pi N \rightarrow \pi N$ & $N\pi\pi$	

$(\Gamma_1\Gamma_2)^{1/2}/\Gamma_{\text{total}}$ in $N\pi \rightarrow \Delta(2000) \rightarrow N\rho$, S=3/2, P-wave	DOCUMENT ID	TECN	COMMENT	$(\Gamma_1\Gamma_2)^{1/2}/\Gamma$
-0.06 ± 0.01	MANLEY 92	IPWA	$\pi N \rightarrow \pi N$ & $N\pi\pi$	

 $\Delta(2000)$ REFERENCES

MANLEY 92	PR D45 4002	D.M. Manley, E.M. Saleski	(KENT) IJP
Also 84	PR D30 904	D.M. Manley et al.	(VPI)
CUTKOSKY 80	Toronto Conf. 19	R.E. Cutkosky et al.	(CMU, LBL)
Also 79	PR D20 2839	R.E. Cutkosky et al.	(CMU, LBL)

 $\Delta(2150)$ S_{31}

$$I(J^P) = \frac{3}{2}(\frac{1}{2}^-) \text{ Status: } *$$

OMITTED FROM SUMMARY TABLE

 $\Delta(2150)$ BREIT-WIGNER MASS

VALUE (MeV)	DOCUMENT ID	TECN	COMMENT
≈ 2150 OUR ESTIMATE			
2047.4 ± 27.0	¹ CHEW 80	BPWA	$\pi^+ p \rightarrow \pi^+ p$
2203.2 ± 8.4	¹ CHEW 80	BPWA	$\pi^+ p \rightarrow \pi^+ p$
2150 ± 100	CUTKOSKY 80	IPWA	$\pi N \rightarrow \pi N$

 $\Delta(2150)$ BREIT-WIGNER WIDTH

VALUE (MeV)	DOCUMENT ID	TECN	COMMENT
121.6 ± 62.0	¹ CHEW 80	BPWA	$\pi^+ p \rightarrow \pi^+ p$
120.5 ± 45.0	¹ CHEW 80	BPWA	$\pi^+ p \rightarrow \pi^+ p$
200 ± 100	CUTKOSKY 80	IPWA	$\pi N \rightarrow \pi N$

 $\Delta(2150)$ POLE POSITION

REAL PART	DOCUMENT ID	TECN	COMMENT
2140 ± 80	CUTKOSKY 80	IPWA	$\pi N \rightarrow \pi N$

-2×IMAGINARY PART	DOCUMENT ID	TECN	COMMENT
200 ± 80	CUTKOSKY 80	IPWA	$\pi N \rightarrow \pi N$

 $\Delta(2150)$ ELASTIC POLE RESIDUE

MODULUS r	DOCUMENT ID	TECN	COMMENT
7 ± 2	CUTKOSKY 80	IPWA	$\pi N \rightarrow \pi N$

PHASE θ	DOCUMENT ID	TECN	COMMENT
-60 ± 90	CUTKOSKY 80	IPWA	$\pi N \rightarrow \pi N$

 $\Delta(2150)$ DECAY MODES

Mode
Γ_1 $N\pi$
Γ_2 ΣK

 $\Delta(2150)$ BRANCHING RATIOS

$\Gamma(N\pi)/\Gamma_{\text{total}}$	DOCUMENT ID	TECN	COMMENT	Γ_1/Γ
0.41	¹ CHEW 80	BPWA	$\pi^+ p \rightarrow \pi^+ p$	
0.37	¹ CHEW 80	BPWA	$\pi^+ p \rightarrow \pi^+ p$	
0.08 ± 0.02	CUTKOSKY 80	IPWA	$\pi N \rightarrow \pi N$	

$(\Gamma_1\Gamma_2)^{1/2}/\Gamma_{\text{total}}$ in $N\pi \rightarrow \Delta(2150) \rightarrow \Sigma K$	DOCUMENT ID	TECN	COMMENT	$(\Gamma_1\Gamma_2)^{1/2}/\Gamma$
<0.03	CANDLIN 84	DPWA	$\pi^+ p \rightarrow \Sigma^+ K^+$	

 $\Delta(2150)$ FOOTNOTES

¹ CHEW 80 reports two S_{31} resonances in this mass region. Problems with this analysis are discussed in section 2.1.11 of HOEHLER 83.

 $\Delta(2150)$ REFERENCES

CANDLIN 84	NP B238 477	D.J. Candlin et al.	(EDIN, RAL, LOWC)
HOEHLER 83	Landolt-Boernstein 1/9B2	G. Hohler	(KARLT)
CHEW 80	Toronto Conf. 123	D.M. Chew	(LBL) IJP
CUTKOSKY 80	Toronto Conf. 19	R.E. Cutkosky et al.	(CMU, LBL) IJP
Also 79	PR D20 2839	R.E. Cutkosky et al.	(CMU, LBL)

 $\Delta(2200)$ G_{37}

$$I(J^P) = \frac{3}{2}(\frac{1}{2}^-) \text{ Status: } *$$

OMITTED FROM SUMMARY TABLE

The various analyses are not in good agreement.

 $\Delta(2200)$ BREIT-WIGNER MASS

VALUE (MeV)	DOCUMENT ID	TECN	COMMENT
≈ 2200 OUR ESTIMATE			
2200 ± 80	CUTKOSKY 80	IPWA	$\pi N \rightarrow \pi N$
2215 ± 60	HOEHLER 79	IPWA	$\pi N \rightarrow \pi N$
2280 ± 60	HENDRY 78	MPWA	$\pi N \rightarrow \pi N$
• • • We do not use the following data for averages, fits, limits, etc. • • •			
2280 ± 40	CANDLIN 84	DPWA	$\pi^+ p \rightarrow \Sigma^+ K^+$

 $\Delta(2200)$ BREIT-WIGNER WIDTH

VALUE (MeV)	DOCUMENT ID	TECN	COMMENT
450 ± 100	CUTKOSKY 80	IPWA	$\pi N \rightarrow \pi N$
400 ± 100	HOEHLER 79	IPWA	$\pi N \rightarrow \pi N$
400 ± 150	HENDRY 78	MPWA	$\pi N \rightarrow \pi N$
• • • We do not use the following data for averages, fits, limits, etc. • • •			
400 ± 50	CANDLIN 84	DPWA	$\pi^+ p \rightarrow \Sigma^+ K^+$

 $\Delta(2200)$ POLE POSITION

REAL PART	DOCUMENT ID	TECN	COMMENT
2100 ± 50	CUTKOSKY 80	IPWA	$\pi N \rightarrow \pi N$

-2×IMAGINARY PART	DOCUMENT ID	TECN	COMMENT
340 ± 80	CUTKOSKY 80	IPWA	$\pi N \rightarrow \pi N$

 $\Delta(2200)$ ELASTIC POLE RESIDUE

MODULUS r	DOCUMENT ID	TECN	COMMENT
8 ± 3	CUTKOSKY 80	IPWA	$\pi N \rightarrow \pi N$

PHASE θ	DOCUMENT ID	TECN	COMMENT
-70 ± 40	CUTKOSKY 80	IPWA	$\pi N \rightarrow \pi N$

 $\Delta(2200)$ DECAY MODES

Mode
Γ_1 $N\pi$
Γ_2 ΣK

 $\Delta(2200)$ BRANCHING RATIOS

$\Gamma(N\pi)/\Gamma_{\text{total}}$	DOCUMENT ID	TECN	COMMENT	Γ_1/Γ
0.06 ± 0.02	CUTKOSKY 80	IPWA	$\pi N \rightarrow \pi N$	
0.05 ± 0.02	HOEHLER 79	IPWA	$\pi N \rightarrow \pi N$	
0.09 ± 0.02	HENDRY 78	MPWA	$\pi N \rightarrow \pi N$	

$(\Gamma_1\Gamma_2)^{1/2}/\Gamma_{\text{total}}$ in $N\pi \rightarrow \Delta(2200) \rightarrow \Sigma K$	DOCUMENT ID	TECN	COMMENT	$(\Gamma_1\Gamma_2)^{1/2}/\Gamma$
-0.014 ± 0.005	CANDLIN 84	DPWA	$\pi^+ p \rightarrow \Sigma^+ K^+$	

 $\Delta(2200)$ REFERENCES

CANDLIN 84	NP B238 477	D.J. Candlin et al.	(EDIN, RAL, LOWC)
CUTKOSKY 80	Toronto Conf. 19	R.E. Cutkosky et al.	(CMU, LBL) IJP
Also 79	PR D20 2839	R.E. Cutkosky et al.	(CMU, LBL) IJP
HOEHLER 79	PDAT 12-1	G. Hohler et al.	(KARLT) IJP
Also 80	Toronto Conf. 3	R. Koch	(KARLT) IJP
HENDRY 78	PRL 41 222	A.W. Hendry	(IND, LBL) IJP
Also 81	ANP 136 1	A.W. Hendry	(IND)

Baryon Particle Listings

 $\Delta(2300)$, $\Delta(2350)$ $\Delta(2300) H_{39}$ $I(J^P) = \frac{3}{2}(\frac{9}{2}^+)$ Status: **

OMITTED FROM SUMMARY TABLE

 $\Delta(2300)$ BREIT-WIGNER MASS

VALUE (MeV)	DOCUMENT ID	TECN	COMMENT
≈ 2300 OUR ESTIMATE			
2204.5 \pm 3.4	CHEW	80	BPWA $\pi^+ p \rightarrow \pi^+ p$
2400 \pm 125	CUTKOSKY	80	IPWA $\pi N \rightarrow \pi N$
2217 \pm 80	HOEHLER	79	IPWA $\pi N \rightarrow \pi N$
2450 \pm 100	HENDRY	78	MPWA $\pi N \rightarrow \pi N$
• • • We do not use the following data for averages, fits, limits, etc. • • •			
2400	CANDLIN	84	DPWA $\pi^+ p \rightarrow \Sigma^+ K^+$

 $\Delta(2300)$ BREIT-WIGNER WIDTH

VALUE (MeV)	DOCUMENT ID	TECN	COMMENT
32.3 \pm 1.0	CHEW	80	BPWA $\pi^+ p \rightarrow \pi^+ p$
425 \pm 150	CUTKOSKY	80	IPWA $\pi N \rightarrow \pi N$
300 \pm 100	HOEHLER	79	IPWA $\pi N \rightarrow \pi N$
500 \pm 200	HENDRY	78	MPWA $\pi N \rightarrow \pi N$
• • • We do not use the following data for averages, fits, limits, etc. • • •			
200	CANDLIN	84	DPWA $\pi^+ p \rightarrow \Sigma^+ K^+$

 $\Delta(2300)$ POLE POSITION

REAL PART VALUE (MeV)	DOCUMENT ID	TECN	COMMENT
2370 \pm 80	CUTKOSKY	80	IPWA $\pi N \rightarrow \pi N$

-2xIMAGINARY PART VALUE (MeV)	DOCUMENT ID	TECN	COMMENT
420 \pm 160	CUTKOSKY	80	IPWA $\pi N \rightarrow \pi N$

 $\Delta(2300)$ ELASTIC POLE RESIDUE

MODULUS $ r $ VALUE (MeV)	DOCUMENT ID	TECN	COMMENT
10 \pm 4	CUTKOSKY	80	IPWA $\pi N \rightarrow \pi N$

PHASE θ VALUE ($^\circ$)	DOCUMENT ID	TECN	COMMENT
-20 \pm 30	CUTKOSKY	80	IPWA $\pi N \rightarrow \pi N$

 $\Delta(2300)$ DECAY MODES

Mode
Γ_1 $N\pi$
Γ_2 ΣK

 $\Delta(2300)$ BRANCHING RATIOS

$\Gamma(N\pi)/\Gamma_{total}$ VALUE	DOCUMENT ID	TECN	COMMENT	Γ_1/Γ_2
0.05	CHEW	80	BPWA $\pi^+ p \rightarrow \pi^+ p$	
0.06 \pm 0.02	CUTKOSKY	80	IPWA $\pi N \rightarrow \pi N$	
0.03 \pm 0.02	HOEHLER	79	IPWA $\pi N \rightarrow \pi N$	
0.08 \pm 0.02	HENDRY	78	MPWA $\pi N \rightarrow \pi N$	

$(\Gamma_1\Gamma_2)^{1/2}/\Gamma_{total}$ in $N\pi \rightarrow \Delta(2300) \rightarrow \Sigma K$ VALUE	DOCUMENT ID	TECN	COMMENT	$(\Gamma_1\Gamma_2)^{1/2}/\Gamma$
-0.017	CANDLIN	84	DPWA $\pi^+ p \rightarrow \Sigma^+ K^+$	

 $\Delta(2300)$ REFERENCES

CANDLIN 84 NP B238 477	D.J. Candlin <i>et al.</i>	(EDIN, RAL, LOWC)
CHEW 80 Toronto Conf. 123	D.M. Chew	(LBL) IJP
CUTKOSKY 80 Toronto Conf. 19	R.E. Cutkosky <i>et al.</i>	(CMU, LBL) IJP
Also 79 PR D20 2839	R.E. Cutkosky <i>et al.</i>	(CMU, LBL)
HOEHLER 79 PDAT 12-1	G. Hoehler <i>et al.</i>	(KARLT) IJP
Also 80 Toronto Conf. 3	R. Koch	(KARLT) IJP
HENDRY 78 PRL 41 222	A.W. Hendry	(IND, LBL) IJP
Also 81 ANP 136 1	A.W. Hendry	(IND)

 $\Delta(2350) D_{35}$ $I(J^P) = \frac{3}{2}(\frac{5}{2}^-)$ Status: *

OMITTED FROM SUMMARY TABLE

 $\Delta(2350)$ BREIT-WIGNER MASS

VALUE (MeV)	DOCUMENT ID	TECN	COMMENT
≈ 2350 OUR ESTIMATE			
2171 \pm 18	MANLEY	92	IPWA $\pi N \rightarrow \pi N$ & $N\pi\pi$
2400 \pm 125	CUTKOSKY	80	IPWA $\pi N \rightarrow \pi N$
2305 \pm 26	HOEHLER	79	IPWA $\pi N \rightarrow \pi N$

 $\Delta(2350)$ BREIT-WIGNER WIDTH

VALUE (MeV)	DOCUMENT ID	TECN	COMMENT
264 \pm 51	MANLEY	92	IPWA $\pi N \rightarrow \pi N$ & $N\pi\pi$
400 \pm 150	CUTKOSKY	80	IPWA $\pi N \rightarrow \pi N$
300 \pm 70	HOEHLER	79	IPWA $\pi N \rightarrow \pi N$

 $\Delta(2350)$ POLE POSITION

REAL PART VALUE (MeV)	DOCUMENT ID	TECN	COMMENT
2400 \pm 125	CUTKOSKY	80	IPWA $\pi N \rightarrow \pi N$

-2xIMAGINARY PART VALUE (MeV)	DOCUMENT ID	TECN	COMMENT
400 \pm 150	CUTKOSKY	80	IPWA $\pi N \rightarrow \pi N$

 $\Delta(2350)$ ELASTIC POLE RESIDUE

MODULUS $ r $ VALUE (MeV)	DOCUMENT ID	TECN	COMMENT
15 \pm 8	CUTKOSKY	80	IPWA $\pi N \rightarrow \pi N$

PHASE θ VALUE ($^\circ$)	DOCUMENT ID	TECN	COMMENT
-70 \pm 70	CUTKOSKY	80	IPWA $\pi N \rightarrow \pi N$

 $\Delta(2350)$ DECAY MODES

Mode
Γ_1 $N\pi$
Γ_2 ΣK

 $\Delta(2350)$ BRANCHING RATIOS

$\Gamma(N\pi)/\Gamma_{total}$ VALUE	DOCUMENT ID	TECN	COMMENT	Γ_1/Γ_2
0.020 \pm 0.003	MANLEY	92	IPWA $\pi N \rightarrow \pi N$ & $N\pi\pi$	
0.20 \pm 0.10	CUTKOSKY	80	IPWA $\pi N \rightarrow \pi N$	
0.04 \pm 0.02	HOEHLER	79	IPWA $\pi N \rightarrow \pi N$	

$(\Gamma_1\Gamma_2)^{1/2}/\Gamma_{total}$ in $N\pi \rightarrow \Delta(2350) \rightarrow \Sigma K$ VALUE	DOCUMENT ID	TECN	COMMENT	$(\Gamma_1\Gamma_2)^{1/2}/\Gamma$
<0.015	CANDLIN	84	DPWA $\pi^+ p \rightarrow \Sigma^+ K^+$	

 $\Delta(2350)$ REFERENCES

MANLEY 92 PR D45 4002	D.M. Manley, E.M. Saleski	(KENT) IJP
Also 84 PR D30 904	D.M. Manley <i>et al.</i>	(VPI)
CANDLIN 84 NP B238 477	D.J. Candlin <i>et al.</i>	(EDIN, RAL, LOWC)
CUTKOSKY 80 Toronto Conf. 19	R.E. Cutkosky <i>et al.</i>	(CMU, LBL) IJP
Also 79 PR D20 2839	R.E. Cutkosky <i>et al.</i>	(CMU, LBL)
HOEHLER 79 PDAT 12-1	G. Hoehler <i>et al.</i>	(KARLT) IJP
Also 80 Toronto Conf. 3	R. Koch	(KARLT) IJP

See key on page 239

Baryon Particle Listings
 $\Delta(2390)$, $\Delta(2400)$ $\Delta(2390) F_{37}$ $I(J^P) = \frac{3}{2}(\frac{7}{2}^+)$ Status: *

OMITTED FROM SUMMARY TABLE

 $\Delta(2390)$ BREIT-WIGNER MASS

VALUE (MeV)	DOCUMENT ID	TECN	COMMENT
≈ 2390 OUR ESTIMATE			
2350 \pm 100	CUTKOSKY 80	IPWA	$\pi N \rightarrow \pi N$
2425 \pm 60	HOEHLER 79	IPWA	$\pi N \rightarrow \pi N$

 $\Delta(2390)$ BREIT-WIGNER WIDTH

VALUE (MeV)	DOCUMENT ID	TECN	COMMENT
300 \pm 100	CUTKOSKY 80	IPWA	$\pi N \rightarrow \pi N$
300 \pm 80	HOEHLER 79	IPWA	$\pi N \rightarrow \pi N$

 $\Delta(2390)$ POLE POSITION

REAL PART VALUE (MeV)	DOCUMENT ID	TECN	COMMENT
2350 \pm 100	CUTKOSKY 80	IPWA	$\pi N \rightarrow \pi N$

-2xIMAGINARY PART VALUE (MeV)	DOCUMENT ID	TECN	COMMENT
260 \pm 100	CUTKOSKY 80	IPWA	$\pi N \rightarrow \pi N$

 $\Delta(2390)$ ELASTIC POLE RESIDUE

MODULUS $ r $ VALUE (MeV)	DOCUMENT ID	TECN	COMMENT
12 \pm 6	CUTKOSKY 80	IPWA	$\pi N \rightarrow \pi N$

PHASE θ VALUE ($^\circ$)	DOCUMENT ID	TECN	COMMENT
-90 \pm 60	CUTKOSKY 80	IPWA	$\pi N \rightarrow \pi N$

 $\Delta(2390)$ DECAY MODES

Mode

Γ_1	$N\pi$
Γ_2	ΣK

 $\Delta(2390)$ BRANCHING RATIOS

$\Gamma(N\pi)/\Gamma_{total}$ VALUE	DOCUMENT ID	TECN	COMMENT	Γ_1/Γ_2
0.08 \pm 0.04	CUTKOSKY 80	IPWA	$\pi N \rightarrow \pi N$	
0.07 \pm 0.04	HOEHLER 79	IPWA	$\pi N \rightarrow \pi N$	

$(\Gamma_1\Gamma_2)^{1/2}/\Gamma_{total}$ in $N\pi \rightarrow \Delta(2390) \rightarrow \Sigma K$ VALUE	DOCUMENT ID	TECN	COMMENT	$(\Gamma_1\Gamma_2)^{1/2}/\Gamma$
<0.015	CANDLIN 84	DPWA	$\pi^+ p \rightarrow \Sigma^+ K^+$	

 $\Delta(2390)$ REFERENCES

CANDLIN 84	NP B238 477	D.J. Candlin <i>et al.</i>	(EDIN, RAL, LOWC)
CUTKOSKY 80	Toronto Conf. 19	R.E. Cutkosky <i>et al.</i>	(CMU, LBL) IJP
Also 79	PR D20 2839	R.E. Cutkosky <i>et al.</i>	(CMU, LBL)
HOEHLER 79	PDAT 12-1	G. Hohler <i>et al.</i>	(KARLT) IJP
Also 80	Toronto Conf. 3	R. Koch	(KARLT) IJP

 $\Delta(2400) G_{39}$ $I(J^P) = \frac{3}{2}(\frac{9}{2}^-)$ Status: **

OMITTED FROM SUMMARY TABLE

 $\Delta(2400)$ BREIT-WIGNER MASS

VALUE (MeV)	DOCUMENT ID	TECN	COMMENT
≈ 2400 OUR ESTIMATE			
2300 \pm 100	CUTKOSKY 80	IPWA	$\pi N \rightarrow \pi N$
2468 \pm 50	HOEHLER 79	IPWA	$\pi N \rightarrow \pi N$
2200 \pm 100	HENDRY 78	MPWA	$\pi N \rightarrow \pi N$

 $\Delta(2400)$ BREIT-WIGNER WIDTH

VALUE (MeV)	DOCUMENT ID	TECN	COMMENT
330 \pm 100	CUTKOSKY 80	IPWA	$\pi N \rightarrow \pi N$
480 \pm 100	HOEHLER 79	IPWA	$\pi N \rightarrow \pi N$
450 \pm 200	HENDRY 78	MPWA	$\pi N \rightarrow \pi N$

 $\Delta(2400)$ POLE POSITION

REAL PART VALUE (MeV)	DOCUMENT ID	TECN	COMMENT
2260 \pm 60	CUTKOSKY 80	IPWA	$\pi N \rightarrow \pi N$

-2xIMAGINARY PART VALUE (MeV)	DOCUMENT ID	TECN	COMMENT
320 \pm 160	CUTKOSKY 80	IPWA	$\pi N \rightarrow \pi N$

 $\Delta(2400)$ ELASTIC POLE RESIDUE

MODULUS $ r $ VALUE (MeV)	DOCUMENT ID	TECN	COMMENT
8 \pm 4	CUTKOSKY 80	IPWA	$\pi N \rightarrow \pi N$

PHASE θ VALUE ($^\circ$)	DOCUMENT ID	TECN	COMMENT
-25 \pm 15	CUTKOSKY 80	IPWA	$\pi N \rightarrow \pi N$

 $\Delta(2400)$ DECAY MODES

Mode

Γ_1	$N\pi$
Γ_2	ΣK

 $\Delta(2400)$ BRANCHING RATIOS

$\Gamma(N\pi)/\Gamma_{total}$ VALUE	DOCUMENT ID	TECN	COMMENT	Γ_1/Γ_2
0.05 \pm 0.02	CUTKOSKY 80	IPWA	$\pi N \rightarrow \pi N$	
0.06 \pm 0.03	HOEHLER 79	IPWA	$\pi N \rightarrow \pi N$	
0.10 \pm 0.03	HENDRY 78	MPWA	$\pi N \rightarrow \pi N$	

$(\Gamma_1\Gamma_2)^{1/2}/\Gamma_{total}$ in $N\pi \rightarrow \Delta(2400) \rightarrow \Sigma K$ VALUE	DOCUMENT ID	TECN	COMMENT	$(\Gamma_1\Gamma_2)^{1/2}/\Gamma$
<0.015	CANDLIN 84	DPWA	$\pi^+ p \rightarrow \Sigma^+ K^+$	

 $\Delta(2400)$ REFERENCES

CANDLIN 84	NP B238 477	D.J. Candlin <i>et al.</i>	(EDIN, RAL, LOWC)
CUTKOSKY 80	Toronto Conf. 19	R.E. Cutkosky <i>et al.</i>	(CMU, LBL) IJP
Also 79	PR D20 2839	R.E. Cutkosky <i>et al.</i>	(CMU, LBL)
HOEHLER 79	PDAT 12-1	G. Hohler <i>et al.</i>	(KARLT) IJP
Also 80	Toronto Conf. 3	R. Koch	(KARLT) IJP
HENDRY 78	PRL 41 222	A.W. Hendry	(IND, LBL) IJP
Also 81	ANP 136 1	A.W. Hendry	(IND)

Baryon Particle Listings

$\Delta(2420), \Delta(2750), \Delta(2950)$

$\Delta(2420) H_{3,11}$

$$I(J^P) = \frac{3}{2}(\frac{11}{2}^+) \text{Status: } ***$$

Most of the results published before 1975 are now obsolete and have been omitted. They may be found in our 1982 edition, Physics Letters 111B (1982).

$\Delta(2420)$ BREIT-WIGNER MASS

VALUE (MeV)	DOCUMENT ID	TECN	COMMENT
2300 to 2500 (≈ 2420) OUR ESTIMATE			
2400 ± 125	CUTKOSKY 80	IPWA	$\pi N \rightarrow \pi N$
2416 ± 17	HOEHLER 79	IPWA	$\pi N \rightarrow \pi N$
2400 ± 60	HENDRY 78	MPWA	$\pi N \rightarrow \pi N$
• • • We do not use the following data for averages, fits, limits, etc. • • •			
2400	CANDLIN 84	DPWA	$\pi^+ p \rightarrow \Sigma^+ K^+$
2358.0 ± 9.0	CHEW 80	BPWA	$\pi^+ p \rightarrow \pi^+ p$

$\Delta(2420)$ BREIT-WIGNER WIDTH

VALUE (MeV)	DOCUMENT ID	TECN	COMMENT
300 to 500 (≈ 400) OUR ESTIMATE			
450 ± 150	CUTKOSKY 80	IPWA	$\pi N \rightarrow \pi N$
340 ± 28	HOEHLER 79	IPWA	$\pi N \rightarrow \pi N$
460 ± 100	HENDRY 78	MPWA	$\pi N \rightarrow \pi N$
• • • We do not use the following data for averages, fits, limits, etc. • • •			
400	CANDLIN 84	DPWA	$\pi^+ p \rightarrow \Sigma^+ K^+$
202.2 ± 45.0	CHEW 80	BPWA	$\pi^+ p \rightarrow \pi^+ p$

$\Delta(2420)$ POLE POSITION

REAL PART			
VALUE (MeV)	DOCUMENT ID	TECN	COMMENT
2260 to 2400 (≈ 2330) OUR ESTIMATE			
2300	¹ HOEHLER 93	ARGD	$\pi N \rightarrow \pi N$
2360 ± 100	CUTKOSKY 80	IPWA	$\pi N \rightarrow \pi N$
-2xIMAGINARY PART			
VALUE (MeV)	DOCUMENT ID	TECN	COMMENT
350 to 750 (≈ 550) OUR ESTIMATE			
620	¹ HOEHLER 93	ARGD	$\pi N \rightarrow \pi N$
420 ± 100	CUTKOSKY 80	IPWA	$\pi N \rightarrow \pi N$

$\Delta(2420)$ ELASTIC POLE RESIDUE

MODULUS $ r $			
VALUE (MeV)	DOCUMENT ID	TECN	COMMENT
39	HOEHLER 93	ARGD	$\pi N \rightarrow \pi N$
18 ± 6	CUTKOSKY 80	IPWA	$\pi N \rightarrow \pi N$
PHASE θ			
VALUE ($^\circ$)	DOCUMENT ID	TECN	COMMENT
-60	HOEHLER 93	ARGD	$\pi N \rightarrow \pi N$
-30 ± 40	CUTKOSKY 80	IPWA	$\pi N \rightarrow \pi N$

$\Delta(2420)$ DECAY MODES

The following branching fractions are our estimates, not fits or averages.

Mode	Fraction (Γ_i/Γ)
$\Gamma_1 N\pi$	5-15 %
$\Gamma_2 \Sigma K$	

$\Delta(2420)$ BRANCHING RATIOS

$\Gamma(N\pi)/\Gamma_{total}$	VALUE	DOCUMENT ID	TECN	COMMENT	Γ_1/Γ
0.05 to 0.15 OUR ESTIMATE					
0.08 ± 0.03	CUTKOSKY 80	IPWA	$\pi N \rightarrow \pi N$		
0.08 ± 0.015	HOEHLER 79	IPWA	$\pi N \rightarrow \pi N$		
0.11 ± 0.02	HENDRY 78	MPWA	$\pi N \rightarrow \pi N$		
• • • We do not use the following data for averages, fits, limits, etc. • • •					
0.22	CHEW 80	BPWA	$\pi^+ p \rightarrow \pi^+ p$		
$(\Gamma_1\Gamma_2)^{1/2}/\Gamma_{total}$ in $N\pi \rightarrow \Delta(2420) \rightarrow \Sigma K$	VALUE	DOCUMENT ID	TECN	COMMENT	$(\Gamma_1\Gamma_2)^{1/2}/\Gamma$
-0.016	CANDLIN 84	DPWA	$\pi^+ p \rightarrow \Sigma^+ K^+$		

$\Delta(2420)$ FOOTNOTES

¹ See HOEHLER 93 for a detailed discussion of the evidence for and the pole parameters of N and Δ resonances as determined from Argand diagrams of πN elastic partial-wave amplitudes and from plots of the speeds with which the amplitudes traverse the diagrams.

$\Delta(2420)$ REFERENCES

HOEHLER 93	πN Newsletter 9 1	G. Hohler	(KARL)
CANDLIN 84	NP B238 477	D.J. Candlin et al.	(EDIN, RAL, LOWC)
PDG 82	PL 111B	M. Roos et al.	(HELS, CIT, CERN)
CHEW 80	Toronto Conf. 123	D.M. Chew	(LBL) IJP
CUTKOSKY 80	Toronto Conf. 19	R.E. Cutkosky et al.	(CMU, LBL) IJP
Also 79	PR D20 2839	R.E. Cutkosky et al.	(CMU, LBL)
HOEHLER 79	PDAT 12-1	G. Hohler et al.	(KARLT) IJP
Also 80	Toronto Conf. 3	R. Koch	(KARLT) IJP
HENDRY 78	PRL 41 222	A.W. Hendry	(IND, LBL) IJP
Also 81	ANP 136 1	A.W. Hendry	(IND)

$\Delta(2750) I_{3,13}$

$$I(J^P) = \frac{3}{2}(\frac{13}{2}^-) \text{Status: } **$$

OMITTED FROM SUMMARY TABLE

$\Delta(2750)$ BREIT-WIGNER MASS

VALUE (MeV)	DOCUMENT ID	TECN	COMMENT
≈ 2750 OUR ESTIMATE			
2794 ± 80	HOEHLER 79	IPWA	$\pi N \rightarrow \pi N$
2650 ± 100	HENDRY 78	MPWA	$\pi N \rightarrow \pi N$

$\Delta(2750)$ BREIT-WIGNER WIDTH

VALUE (MeV)	DOCUMENT ID	TECN	COMMENT
350 ± 100	HOEHLER 79	IPWA	$\pi N \rightarrow \pi N$
500 ± 100	HENDRY 78	MPWA	$\pi N \rightarrow \pi N$

$\Delta(2750)$ DECAY MODES

Mode	Fraction (Γ_i/Γ)
$\Gamma_1 N\pi$	

$\Delta(2750)$ BRANCHING RATIOS

$\Gamma(N\pi)/\Gamma_{total}$	VALUE	DOCUMENT ID	TECN	COMMENT	Γ_1/Γ
0.04 ± 0.015	HOEHLER 79	IPWA	$\pi N \rightarrow \pi N$		
0.05 ± 0.01	HENDRY 78	MPWA	$\pi N \rightarrow \pi N$		

$\Delta(2750)$ REFERENCES

HOEHLER 79	PDAT 12-1	G. Hohler et al.	(KARLT) IJP
Also 80	Toronto Conf. 3	R. Koch	(KARLT) IJP
HENDRY 78	PRL 41 222	A.W. Hendry	(IND, LBL) IJP
Also 81	ANP 136 1	A.W. Hendry	(IND)

$\Delta(2950) K_{3,15}$

$$I(J^P) = \frac{3}{2}(\frac{15}{2}^+) \text{Status: } **$$

OMITTED FROM SUMMARY TABLE

$\Delta(2950)$ BREIT-WIGNER MASS

VALUE (MeV)	DOCUMENT ID	TECN	COMMENT
≈ 2950 OUR ESTIMATE			
2990 ± 100	HOEHLER 79	IPWA	$\pi N \rightarrow \pi N$
2850 ± 100	HENDRY 78	MPWA	$\pi N \rightarrow \pi N$

$\Delta(2950)$ BREIT-WIGNER WIDTH

VALUE (MeV)	DOCUMENT ID	TECN	COMMENT
330 ± 100	HOEHLER 79	IPWA	$\pi N \rightarrow \pi N$
700 ± 200	HENDRY 78	MPWA	$\pi N \rightarrow \pi N$

$\Delta(2950)$ DECAY MODES

Mode	Fraction (Γ_i/Γ)
$\Gamma_1 N\pi$	

$\Delta(2950)$ BRANCHING RATIOS

$\Gamma(N\pi)/\Gamma_{total}$	VALUE	DOCUMENT ID	TECN	COMMENT	Γ_1/Γ
0.04 ± 0.02	HOEHLER 79	IPWA	$\pi N \rightarrow \pi N$		
0.03 ± 0.01	HENDRY 78	MPWA	$\pi N \rightarrow \pi N$		

$\Delta(2950)$ REFERENCES

HOEHLER 79	PDAT 12-1	G. Hohler et al.	(KARLT) IJP
Also 80	Toronto Conf. 3	R. Koch	(KARLT) IJP
HENDRY 78	PRL 41 222	A.W. Hendry	(IND, LBL) IJP
Also 81	ANP 136 1	A.W. Hendry	(IND)

See key on page 239

Baryon Particle Listings

 $\Delta(\sim 3000)$ **$\Delta(\sim 3000)$ Region
Partial-Wave Analyses**

OMITTED FROM SUMMARY TABLE

We list here miscellaneous high-mass candidates for isospin-3/2 resonances found in partial-wave analyses.

Our 1982 edition also had a $\Delta(2850)$ and a $\Delta(3230)$. The evidence for them was deduced from total cross-section and 180° elastic cross-section measurements. The $\Delta(2850)$ has been resolved into the $\Delta(2750) I_{3,13}$ and $\Delta(2950) K_{3,15}$. The $\Delta(3230)$ is perhaps related to the $K_{3,13}$ of HENDRY 78 and to the $L_{3,17}$ of KOCH 80. **$\Delta(\sim 3000)$ BREIT-WIGNER MASS**

VALUE (MeV)	DOCUMENT ID	TECN	COMMENT
≈ 3000 OUR ESTIMATE			
3300	¹ KOCH	80	IPWA $\pi N \rightarrow \pi N L_{3,17}$ wave
3500	¹ KOCH	80	IPWA $\pi N \rightarrow \pi N M_{3,19}$ wave
2850 \pm 150	HENDRY	78	MPWA $\pi N \rightarrow \pi N I_{3,11}$ wave
3200 \pm 200	HENDRY	78	MPWA $\pi N \rightarrow \pi N K_{3,13}$ wave
3300 \pm 200	HENDRY	78	MPWA $\pi N \rightarrow \pi N L_{3,17}$ wave
3700 \pm 200	HENDRY	78	MPWA $\pi N \rightarrow \pi N M_{3,19}$ wave
4100 \pm 300	HENDRY	78	MPWA $\pi N \rightarrow \pi N N_{3,21}$ wave

 $\Delta(\sim 3000)$ BREIT-WIGNER WIDTH

VALUE (MeV)	DOCUMENT ID	TECN	COMMENT
700 \pm 200	HENDRY	78	MPWA $\pi N \rightarrow \pi N I_{3,11}$ wave
1000 \pm 300	HENDRY	78	MPWA $\pi N \rightarrow \pi N K_{3,13}$ wave
1100 \pm 300	HENDRY	78	MPWA $\pi N \rightarrow \pi N L_{3,17}$ wave
1300 \pm 400	HENDRY	78	MPWA $\pi N \rightarrow \pi N M_{3,19}$ wave
1600 \pm 500	HENDRY	78	MPWA $\pi N \rightarrow \pi N N_{3,21}$ wave

 $\Delta(\sim 3000)$ DECAY MODES

Mode
Γ_1 $N\pi$

 $\Delta(\sim 3000)$ BRANCHING RATIOS

$\Gamma(N\pi)/\Gamma_{\text{total}}$	DOCUMENT ID	TECN	COMMENT	Γ_1/Γ
0.06 \pm 0.02	HENDRY	78	MPWA $\pi N \rightarrow \pi N I_{3,11}$ wave	
0.045 \pm 0.02	HENDRY	78	MPWA $\pi N \rightarrow \pi N K_{3,13}$ wave	
0.03 \pm 0.01	HENDRY	78	MPWA $\pi N \rightarrow \pi N L_{3,17}$ wave	
0.025 \pm 0.01	HENDRY	78	MPWA $\pi N \rightarrow \pi N M_{3,19}$ wave	
0.018 \pm 0.01	HENDRY	78	MPWA $\pi N \rightarrow \pi N N_{3,21}$ wave	

 $\Delta(\sim 3000)$ FOOTNOTES¹ In addition, KOCH 80 reports some evidence for an S_{31} $\Delta(2700)$ and a P_{33} $\Delta(2800)$. **$\Delta(\sim 3000)$ REFERENCES**

KOCH	80	Toronto Conf. 3	R. Koch	(KARLT) IJP
HENDRY	78	PRL 41 222	A.W. Hendry	(IND, LBL) IJP
Also	81	ANP 136 1	A.W. Hendry	(IND)

Baryon Particle Listings

Λ

Λ BARYONS

($S = -1, I = 0$)

$\Lambda^0 = uds$

Λ

$I(J^P) = 0(\frac{1}{2}^+)$ Status: * * * *

We have omitted some results that have been superseded by later experiments. See our earlier editions.

Λ MASS

The fit uses $\Lambda, \Sigma^+, \Sigma^0, \Sigma^-$ mass and mass-difference measurements.

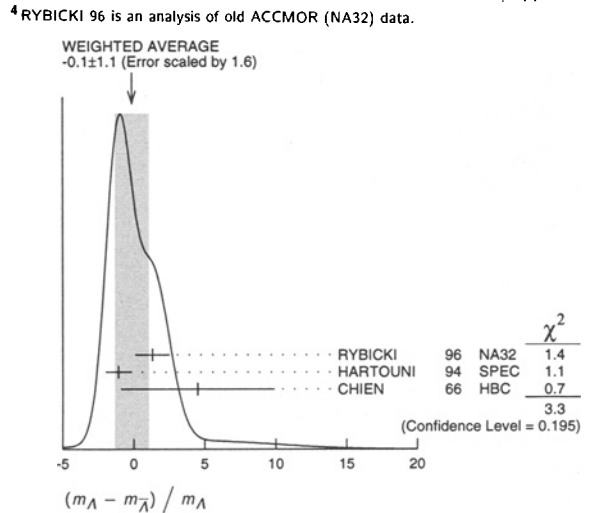
VALUE (MeV)	EVTS	DOCUMENT ID	TECN	COMMENT
1115.683 ± 0.006	OUR FIT			
1115.683 ± 0.006	OUR AVERAGE			
1115.678 ± 0.006 ± 0.006	20k	HARTOUNI	94	SPEC pp 27.5 GeV/c
1115.690 ± 0.008 ± 0.006	18k	¹ HARTOUNI	94	SPEC pp 27.5 GeV/c
* * * We do not use the following data for averages, fits, limits, etc. * * *				
1115.59 ± 0.08	935	HYMAN	72	HEBC
1115.39 ± 0.12	195	MAYEUR	67	EMUL
1115.6 ± 0.4		LONDON	66	HBC
1115.65 ± 0.07	488	² SCHMIDT	65	HBC
1115.44 ± 0.12		³ BHOWMIK	63	RVUE

¹We assume CPT invariance: this is the $\bar{\Lambda}$ mass as measured by HARTOUNI 94. See below for the fractional mass difference, testing CPT.
²The SCHMIDT 65 masses have been reevaluated using our April 1973 proton and K^\pm and π^\pm masses. P. Schmidt, private communication (1974).
³The mass has been raised 35 keV to take into account a 46 keV increase in the proton mass and an 11 keV decrease in the π^\pm mass (note added Reviews of Modern Physics 39 1 (1967)).

$(m_\Lambda - m_{\bar{\Lambda}}) / m_\Lambda$

A test of CPT invariance.

VALUE (units 10^{-5})	EVTS	DOCUMENT ID	TECN	COMMENT
-0.1 ± 1.1	OUR AVERAGE			Error includes scale factor of 1.6. See the ideogram below.
+ 1.3 ± 1.2	31k	⁴ RYBICKI	96	NA32 π^- Cu, 230 GeV
- 1.08 ± 0.90		HARTOUNI	94	SPEC pp 27.5 GeV/c
- 4.5 ± 5.4		CHIEN	66	HBC 6.9 GeV/c $\bar{p}p$
* * * We do not use the following data for averages, fits, limits, etc. * * *				
-26 ± 13		BADIER	67	HBC 2.4 GeV/c $\bar{p}p$



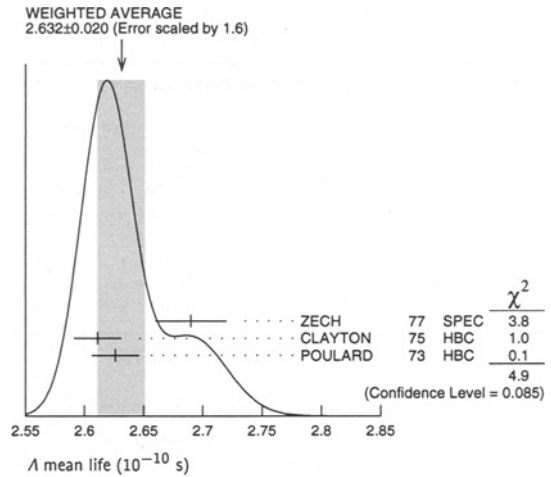
Λ MEAN LIFE

Measurements with an error $\geq 0.1 \times 10^{-10}$ s have been omitted altogether, and only the latest high-statistics measurements are used for the average.

VALUE (10^{-10} s)	EVTS	DOCUMENT ID	TECN	COMMENT
2.632 ± 0.020	OUR AVERAGE			Error includes scale factor of 1.6. See the ideogram below.
2.69 ± 0.03	53k	ZECH	77	SPEC Neutral hyperon beam
2.611 ± 0.020	34k	CLAYTON	75	HBC 0.96-1.4 GeV/c $K^- p$
2.626 ± 0.020	36k	POULARD	73	HBC 0.4-2.3 GeV/c $K^- p$

* * * We do not use the following data for averages, fits, limits, etc. * * *

2.69 ± 0.05	6582	ALTHOFF	73B	OSPK $\pi^+ n \rightarrow \Lambda K^+$
2.54 ± 0.04	4572	BALTAY	71B	HBC $K^- p$ at rest
2.535 ± 0.035	8342	GRIMM	68	HBC
2.47 ± 0.08	2600	HEPP	68	HBC
2.35 ± 0.09	916	BURAN	66	HLBC
2.452 ⁺ _{-0.054}	2213	ENGELMANN	66	HBC
2.59 ± 0.09	794	HUBBARD	64	HBC
2.59 ± 0.07	1378	SCHWARTZ	64	HBC
2.36 ± 0.06	2239	BLOCK	63	HEBC



$(\tau_\Lambda - \tau_{\bar{\Lambda}}) / \tau_\Lambda$

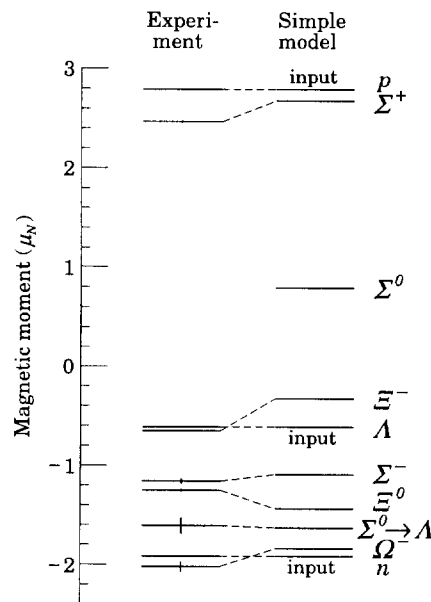
A test of CPT invariance.

VALUE	DOCUMENT ID	TECN	COMMENT
0.044 ± 0.085	BADIER	67	HBC 2.4 GeV/c $\bar{p}p$

BARYON MAGNETIC MOMENTS

Written 1994 by C.G. Wohl (LBNL).

The figure shows the measured magnetic moments of the stable baryons. It also shows the predictions of the simplest quark model, using the measured $p, n,$ and Λ moments as input. In this model, the moments are [1]



$$\begin{aligned} \mu_p &= (4\mu_u - \mu_d)/3 & \mu_n &= (4\mu_d - \mu_u)/3 \\ \mu_{\Sigma^+} &= (4\mu_u - \mu_s)/3 & \mu_{\Sigma^-} &= (4\mu_d - \mu_s)/3 \\ \mu_{\Sigma^0} &= (4\mu_s - \mu_u)/3 & \mu_{\Xi^-} &= (4\mu_s - \mu_d)/3 \\ \mu_\Lambda &= \mu_s & \mu_{\Sigma^0} &= (2\mu_u + 2\mu_d - \mu_s)/3 \\ & & \mu_{\Omega^-} &= 3\mu_s \end{aligned}$$

and the $\Sigma^0 \rightarrow \Lambda$ transition moment is

$$\mu_{\Sigma^0\Lambda} = (\mu_d - \mu_u)/\sqrt{3}.$$

The quark moments that result from this model are $\mu_u = +1.852 \mu_N$, $\mu_d = -0.972 \mu_N$, and $\mu_s = -0.613 \mu_N$. The corresponding effective quark masses, taking the quarks to be Dirac point particles, where $\mu = q\hbar/2m$, are 338, 322, and 510 MeV. As the figure shows, the model gives a good first approximation to the experimental moments. For efforts to make a better model, we refer to the literature [2].

References

- See, for example, D.H. Perkins, *Introduction to High Energy Physics* (Addison-Wesley, Reading, MA, 1987), or D. Griffiths, *Introduction to Elementary Particles* (Harper & Row, New York, 1987).
- See, for example, J. Franklin, *Phys. Rev.* **D29**, 2648 (1984); H.J. Lipkin, *Nucl. Phys.* **B241**, 477 (1984); K. Suzuki, H. Kumagai, and Y. Tanaka, *Europhys. Lett.* **2**, 109 (1986); S.K. Gupta and S.B. Khadkikar, *Phys. Rev.* **D36**, 307 (1987); M.I. Krivoruchenko, *Sov. J. Nucl. Phys.* **45**, 109 (1987); L. Brekke and J.L. Rosner, *Comm. Nucl. Part. Phys.* **18**, 83 (1988); K.-T. Chao, *Phys. Rev.* **D41**, 920 (1990) and references cited therein. Also, see references cited in discussions of results in the experimental papers.

Λ MAGNETIC MOMENT

See the "Note on Baryon Magnetic Moments" above. Measurements with an error $\geq 0.15 \mu_N$ have been omitted.

VALUE (μ_N)	EVTS	DOCUMENT ID	TECN	COMMENT
-0.613 ± 0.004 OUR AVERAGE				
-0.606 ± 0.015	200k	COX	81 SPEC	
-0.6138 ± 0.0047	3M	SCHACHIN...	78 SPEC	
-0.59 ± 0.07	350k	HELLER	77 SPEC	
-0.57 ± 0.05	1.2M	BUNCE	76 SPEC	
-0.66 ± 0.07	1300	DAHL-JENSEN 71	EMUL	200 kG field

Λ ELECTRIC DIPOLE MOMENT

A nonzero value is forbidden by both T invariance and P invariance.

VALUE (10^{-16} e-cm)	CL%	DOCUMENT ID	TECN	COMMENT
< 1.5	95	⁵ PONDROM 81	SPEC	
• • • We do not use the following data for averages, fits, limits, etc. • • •				
<100	95	⁶ BARONI 71	EMUL	
<500	95	GIBSON 66	EMUL	
⁵ PONDROM 81 measures $(-3.0 \pm 7.4) \times 10^{-17}$ e-cm.				
⁶ BARONI 71 measures $(-5.9 \pm 2.9) \times 10^{-15}$ e-cm.				

Λ DECAY MODES

Mode	Fraction (Γ_i/Γ)
Γ_1 $p\pi^-$	(63.9 ± 0.5) %
Γ_2 $n\pi^0$	(35.8 ± 0.5) %
Γ_3 $n\gamma$	(1.75 ± 0.15) × 10 ⁻³
Γ_4 $p\pi^-\gamma$	[a] (8.4 ± 1.4) × 10 ⁻⁴
Γ_5 $p e^- \bar{\nu}_e$	(8.32 ± 0.14) × 10 ⁻⁴
Γ_6 $p \mu^- \bar{\nu}_\mu$	(1.57 ± 0.35) × 10 ⁻⁴

[a] See the Listings below for the pion momentum range used in this measurement.

CONSTRAINED FIT INFORMATION

An overall fit to 5 branching ratios uses 20 measurements and one constraint to determine 5 parameters. The overall fit has a $\chi^2 = 10.5$ for 16 degrees of freedom.

The following off-diagonal array elements are the correlation coefficients $\langle \delta x_i \delta x_j \rangle / (\delta x_i \delta x_j)$, in percent, from the fit to the branching fractions, $x_i \equiv \Gamma_i/\Gamma_{\text{total}}$. The fit constrains the x_i whose labels appear in this array to sum to one.

x_2	-100			
x_3	-2	-1		
x_5	46	-46	-1	
x_6	0	0	0	0
	x_1	x_2	x_3	x_5

Λ BRANCHING RATIOS

$\Gamma(p\pi^-)/\Gamma(N\pi)$	VALUE	EVTS	DOCUMENT ID	TECN	COMMENT	$\Gamma_1/(\Gamma_1+\Gamma_2)$
	0.641 ± 0.005 OUR FIT					
	0.640 ± 0.005 OUR AVERAGE					
	0.646 ± 0.008	4572	BALTAY	71B HBC	$K^- p$ at rest	
	0.635 ± 0.007	6736	DOYLE	69 HBC	$\pi^- p \rightarrow \Lambda K^0$	
	0.643 ± 0.016	903	HUMPHREY	62 HBC		
	0.624 ± 0.030		CRAWFORD	59B HBC	$\pi^- p \rightarrow \Lambda K^0$	

$\Gamma(n\pi^0)/\Gamma(N\pi)$	VALUE	EVTS	DOCUMENT ID	TECN	COMMENT	$\Gamma_2/(\Gamma_1+\Gamma_2)$
	0.359 ± 0.005 OUR FIT					
	0.310 ± 0.028 OUR AVERAGE					
	0.35 ± 0.05		BROWN	63 HLBC		
	0.291 ± 0.034	75	CHRETIEN	63 HLBC		

$\Gamma(n\gamma)/\Gamma_{\text{total}}$	VALUE (units 10^{-3})	EVTS	DOCUMENT ID	TECN	COMMENT	Γ_3/Γ
	1.75 ± 0.15 OUR FIT					
	1.75 ± 0.15	1816	LARSON	93 SPEC	$K^- p$ at rest	
• • • We do not use the following data for averages, fits, limits, etc. • • •						
	1.78 ± 0.24 ^{+0.14} _{-0.16}	287	NOBLE	92 SPEC	See LARSON 93	

$\Gamma(n\gamma)/\Gamma(n\pi^0)$	VALUE (units 10^{-3})	EVTS	DOCUMENT ID	TECN	COMMENT	Γ_3/Γ_2
• • • We do not use the following data for averages, fits, limits, etc. • • •						
	2.86 ± 0.74 ± 0.57	24	BIAGI	86 SPEC	SPS hyperon beam	

$\Gamma(p\pi^-\gamma)/\Gamma(p\pi^-)$	VALUE (units 10^{-3})	EVTS	DOCUMENT ID	TECN	COMMENT	Γ_4/Γ_1
	1.32 ± 0.22	72	BAGGETT	72c HBC	$\pi^- < 95$ MeV/c	

$\Gamma(p e^- \bar{\nu}_e)/\Gamma(p\pi^-)$	VALUE (units 10^{-3})	EVTS	DOCUMENT ID	TECN	COMMENT	Γ_5/Γ_1
	1.301 ± 0.019 OUR FIT					
	1.301 ± 0.019 OUR AVERAGE					
	1.335 ± 0.056	7111	BOURQUIN	83 SPEC	SPS hyperon beam	
	1.313 ± 0.024	10k	WISE	80 SPEC		
	1.23 ± 0.11	544	LINDQUIST	77 SPEC	$\pi^- p \rightarrow K^0 \Lambda$	
	1.27 ± 0.07	1089	KATZ	73 HBC		
	1.31 ± 0.06	1078	ALTHOFF	71 OSPK		
	1.17 ± 0.13	86	⁷ CANTER	71 HBC	$K^- p$ at rest	
	1.20 ± 0.12	143	⁸ MALONEY	69 HBC		
	1.17 ± 0.18	120	⁸ BAGLIN	64 FBC	K^- freon 1.45 GeV/c	
	1.23 ± 0.20	150	⁸ ELY	63 FBC		
• • • We do not use the following data for averages, fits, limits, etc. • • •						
	1.32 ± 0.15	218	⁷ LINDQUIST	71 OSPK	See LINDQUIST 77	

⁷ Changed by us from $\Gamma(p e^- \bar{\nu}_e)/\Gamma(N\pi)$ assuming the authors used $\Gamma(p\pi^-)/\Gamma_{\text{total}} = 2/3$.

⁸ Changed by us from $\Gamma(p e^- \bar{\nu}_e)/\Gamma(N\pi)$ because $\Gamma(p e^- \nu)/\Gamma(p\pi^-)$ is the directly measured quantity.

$\Gamma(p\mu^- \bar{\nu}_\mu)/\Gamma(N\pi)$	VALUE (units 10^{-4})	EVTS	DOCUMENT ID	TECN	COMMENT	$\Gamma_6/(\Gamma_1+\Gamma_2)$
	1.57 ± 0.35 OUR FIT					
	1.57 ± 0.35 OUR AVERAGE					
	1.4 ± 0.5	14	BAGGETT	72b HBC	$K^- p$ at rest	
	2.4 ± 0.8	9	CANTER	71B HBC	$K^- p$ at rest	
	1.3 ± 0.7	3	LIND	64 RVUE		
	1.5 ± 1.2	2	RONNE	64 FBC		

Baryon Particle Listings

Λ

Λ DECAY PARAMETERS

See the "Note on Baryon Decay Parameters" in the neutron Listings. Some early results have been omitted.

 α_- FOR $\Lambda \rightarrow p\pi^-$

VALUE	EVTs	DOCUMENT ID	TECN	COMMENT
0.642 ± 0.013 OUR AVERAGE				
0.584 ± 0.046	8500	ASTBURY	75	SPEC
0.649 ± 0.023	10325	CLELAND	72	OSPK
0.67 ± 0.06	3520	DAUBER	69	HBC From Ξ decay
0.645 ± 0.017	10130	OVERSETH	67	OSPK Λ from $\pi^- p$
0.62 ± 0.07	1156	CRONIN	63	CNTR Λ from $\pi^- p$

 ϕ ANGLE FOR $\Lambda \rightarrow p\pi^-$

VALUE (°)	EVTs	DOCUMENT ID	TECN	COMMENT
-6.5 ± 3.5 OUR AVERAGE				
-7.0 ± 4.5	10325	CLELAND	72	OSPK Λ from $\pi^- p$
-8.0 ± 6.0	10130	OVERSETH	67	OSPK Λ from $\pi^- p$
13.0 ± 17.0	1156	CRONIN	63	OSPK Λ from $\pi^- p$

 $\alpha_0 / \alpha_- = \alpha(\Lambda \rightarrow n\pi^0) / \alpha(\Lambda \rightarrow p\pi^-)$

VALUE	EVTs	DOCUMENT ID	TECN	COMMENT
1.01 ± 0.07 OUR AVERAGE				
1.000 ± 0.068	4760	⁹ OLSEN	70	OSPK $\pi^+ n \rightarrow \Lambda K^+$
1.10 ± 0.27		CORK	60	CNTR

⁹OLSEN 70 compares proton and neutron distributions from Λ decay.

 $[\alpha_-(\Lambda) + \alpha_+(\bar{\Lambda})] / [\alpha_-(\Lambda) - \alpha_+(\bar{\Lambda})]$

Zero if CP is conserved; α_- and α_+ are the asymmetry parameters for $\Lambda \rightarrow p\pi^-$ and $\bar{\Lambda} \rightarrow \bar{p}\pi^+$ decay.

VALUE	EVTs	DOCUMENT ID	TECN	COMMENT
-0.03 ± 0.06 OUR AVERAGE				
$+0.01 \pm 0.10$	770	TIXIER	88	DM2 $J/\psi \rightarrow \Lambda \bar{\Lambda}$
-0.07 ± 0.09	4063	BARNES	87	CNTR $\bar{p}p \rightarrow \bar{\Lambda} \Lambda$ LEAR
-0.02 ± 0.14	10k	¹⁰ CHAUVAT	85	CNTR $pp, \bar{p}p$ ISR

¹⁰CHAUVAT 85 actually gives $\alpha_+(\bar{\Lambda})/\alpha_-(\Lambda) = -1.04 \pm 0.29$. Assumes polarization is same in $\bar{p}p \rightarrow \bar{\Lambda} \Lambda$ and $pp \rightarrow \Lambda X$. Tests of this assumption, based on C-invariance and fragmentation, are satisfied by the data.

 g_A / g_V FOR $\Lambda \rightarrow p e^- \bar{\nu}_e$

Measurements with fewer than 500 events have been omitted. Where necessary, signs have been changed to agree with our conventions, which are given in the "Note on Baryon Decay Parameters" in the neutron Listings. The measurements all assume that the form factor $g_2 = 0$. See also the footnote on DWORKIN 90.

VALUE	EVTs	DOCUMENT ID	TECN	COMMENT
-0.718 ± 0.015 OUR AVERAGE				
$-0.719 \pm 0.016 \pm 0.012$	37k	¹¹ DWORKIN	90	SPEC $e\nu$ angular corr.
-0.70 ± 0.03	7111	BOURQUIN	83	SPEC $\Xi \rightarrow \Lambda \pi^-$
-0.734 ± 0.031	10k	¹² WISE	81	SPEC $e\nu$ angular correl.
-0.63 ± 0.06	817	ALTHOFF	73	OSPK Polarized Λ

• • • We do not use the following data for averages, fits, limits, etc. • • •

¹¹The tabulated result assumes the weak-magnetism coupling $w \equiv g_W(0)/g_V(0)$ to be 0.97, as given by the CVC hypothesis and as assumed by the other listed measurements. However, DWORKIN 90 measures w to be 0.15 ± 0.30 , and then $g_A/g_V = -0.731 \pm 0.016$.

¹²This experiment measures only the absolute value of g_A/g_V .

Λ REFERENCES

We have omitted some papers that have been superseded by later experiments. See our earlier editions.

RYBICKI	96	APP B27 2155	K. Rybicki	
HARTOUNI	94	PRL 72 1322	E.P. Hartouni <i>et al.</i>	(BNL E766 Collab.)
Also	94B	PRL 72 2021 (erratum)	E.P. Hartouni <i>et al.</i>	(BNL E766 Collab.)
LARSON	93	PR D47 799	K.D. Larson <i>et al.</i>	(BNL-811 Collab.)
NOBLE	92	PRL 69 414	A.J. Noble <i>et al.</i>	(BIRM, BOST, BRCO+)
DWORKIN	90	PR D41 790	J. Dworkin <i>et al.</i>	(MICH, WISC, RUTG+)
TIXIER	88	PL B212 523	M.H. Tixier <i>et al.</i>	(DM2 Collab.)
BARNES	87	PL B199 147	P.D. Barnes <i>et al.</i>	(CMU, SACL, LANL+)
BIAGI	86	ZPHY C30 201	S.F. Biagi <i>et al.</i>	(BRIS, CERN, GEVA+)
CHAUVAT	85	PL 163B 273	P. Chauvat <i>et al.</i>	(CERN, CLER, UCLA+)
BOURQUIN	83	ZPHY C21 1	M.H. Bourquin <i>et al.</i>	(BRIS, GEVA, HEIDP+)
COX	81	PRL 46 877	P.T. Cox <i>et al.</i>	(MICH, WISC, RUTG, MINN+)
PONDROM	81	PR D23 814	L. Pondrom <i>et al.</i>	(WISC, MICH, RUTG+)
WISE	81	PL 98B 123	J.E. Wise <i>et al.</i>	(MASA, BNL)
WISE	80	PL 91B 165	J.E. Wise <i>et al.</i>	(MASA, BNL)
SCHACHIN...	78	PRL 41 1348	L. Schachinger <i>et al.</i>	(MICH, RUTG, WISC)
HELLER	77	PL 68B 480	K. Heller <i>et al.</i>	(MICH, WISC, HEIDH)
LINDQUIST	77	PR D16 2104	J. Lindquist <i>et al.</i>	(EFI, OSU, ANL)
Also	76	JPG 2 L211	J. Lindquist <i>et al.</i>	(EFI, WUSL, OSU+)
ZECH	77	NP B124 413	G. Zech <i>et al.</i>	(SIEG, CERN, DORT, HEIDH)
BUNCE	76	PRL 36 1113	G.R.M. Bunce <i>et al.</i>	(WISC, MICH, RUTG)
ASTBURY	75	NP B99 30	P. Astbury <i>et al.</i>	(LOIC, CERN, ETH+)
CLAYTON	75	NP B95 130	E.F. Clayton <i>et al.</i>	(LOIC, RHEL)
ALTHOFF	73	PL 43B 237	K.H. Althoff <i>et al.</i>	(CERN, HEID)
ALTHOFF	73B	NP B66 29	K.H. Althoff <i>et al.</i>	(CERN, HEID)
KATZ	73	Thesis MDDP-TR-74-044	C.N. Katz	(UMD)
POULARD	73	PL 46B 135	G. Poulard, A. Givernaud, A.C. Borg	(SACL)
BAGGETT	72B	ZPHY 252 362	M.J. Baggett <i>et al.</i>	(HEID)
BAGGETT	72C	PL 42B 379	M.J. Baggett <i>et al.</i>	(HEID)
CLELAND	72	NP B40 221	W.E. Cleland <i>et al.</i>	(CERN, GEVA, LUND)
HYMAN	72	PR D5 1063	L.G. Hyman <i>et al.</i>	(ANL, CMU)
ALTHOFF	71	PL 37B 531	K.H. Althoff <i>et al.</i>	(CERN, HEID)
BALTAY	71B	PR D4 670	C. Baltay <i>et al.</i>	(COLL, BING)
BARONI	71	LCN 2 1256	G. Baroni, S. Pettrera, G. Romano	(ROMA)
CANTER	71	PRL 26 868	J. Canter <i>et al.</i>	(STON, COLU)
CANTER	71B	PRL 27 59	J. Canter <i>et al.</i>	(STON, COLU)
DAHL-JENSEN	71	NC 3A 1	E. Dahl-Jensen <i>et al.</i>	(CERN, ANKA, LAUS+)
LINDQUIST	71	PRL 27 612	J. Lindquist <i>et al.</i>	(EFI, WUSL, OSU+)
OLSEN	70	PRL 24 843	S.L. Olsen <i>et al.</i>	(WISC, MICH)
DAUBER	69	PR 179 1262	P.M. Dauber <i>et al.</i>	(LRL)
DOYLE	69	Thesis UCRL 18139	J.C. Doyle	(LRL)
MALONEY	69	PRL 23 425	J.E. Maloney, B. Sechi-Zorn	(UMD)
GRIMM	68	NC 54A 187	H.J. Grimm	(HEID)
HEPP	68	ZPHY 214 71	V. Hepp, H. Schleich	(HEID)
BADIER	67	PL 25B 152	J. Badier <i>et al.</i>	(EPOL)
MAYEUR	67	U.Libr.Brux.Bul. 32	C. Mayeur, E. Tompa, J.H. Wickens	(BELG, LOUC)
OVERSETH	67	PRL 19 391	O.E. Overseth, R.F. Roth	(MICH, PRIN)
PDG	67	RMP 39 1	A.R. Rosenfeld <i>et al.</i>	(LRL, CERN, YALE)
BURAN	66	PL 20 318	T. Buran <i>et al.</i>	(OSLO)
CHIEN	66	PR 152 1171	C.Y. Chien <i>et al.</i>	(YALE, BNL)
ENGELMANN	66	NC 45A 1038	R. Engelmann <i>et al.</i>	(HEID, REHO)
GIBSON	66	NC 45A 882	W.M. Gibson, K. Green	(BRIS)
LONDON	66	PR 143 1034	G.W. London <i>et al.</i>	(BNL, SYRA)
SCHMIDT	65	PR 140B 1328	P. Schmidt	(COLU)
BAGLIN	64	NC 35 977	C. Baglin <i>et al.</i>	(EPOL, CERN, LOUC, RHEL+)
HUBBARD	64	PR 135B 183	J.R. Hubbard <i>et al.</i>	(LRL)
LIND	64	PR 135B 1483	V.G. Lind <i>et al.</i>	(WISC)
RONNE	64	PL 11 357	B.E. Ronne <i>et al.</i>	(CERN, EPOL, LOUC+)
SCHWARTZ	64	Thesis UCRL 11360	Schwartz	(LRL)
BHOWMIK	63	NC 28 1494	B. Bhowmik, D.P. Goyal	(DELH)
BLOCK	63	PR 130 766	M.M. Block <i>et al.</i>	(NWES, BGNA, SYRA+)
BROWN	63	PR 130 769	J.L. Brown <i>et al.</i>	(LRL, MICH)
CHRETIEN	63	PR 131 2208	M. Chretien <i>et al.</i>	(BRAN, BROW, HARV+)
CRONIN	63	PR 129 1795	J.W. Cronin, O.E. Overseth	(PRIN)
ELY	63	PR 131 868	R.P. Ely <i>et al.</i>	(LRL)
HUMPHREY	62	PR 127 1305	W.E. Humphrey, R.R. Ross	(LRL)
CORK	60	PR 120 1000	B. Cork <i>et al.</i>	(LRL, PRIN, BNL)
CRAWFORD	59B	PRL 2 266	F.S. Crawford <i>et al.</i>	(LRL)

Λ AND Σ RESONANCES

Introduction: There are no new results at all on Λ and Σ resonances. The field remains at a standstill and will only be revived if a kaon factory is built. What follows is a much abbreviated version of the note on Λ and Σ Resonances from our 1990 edition. In particular, see that edition for some representative Argand plots from partial-wave analyses.

Table 1 is an attempt to evaluate the status, both overall and channel by channel, of each Λ and Σ resonance in the Particle Listings. The evaluations are of course partly subjective. A blank indicates there is no evidence at all: either the relevant couplings are small or the resonance does not really exist. The main Baryon Summary Table includes only the established resonances (overall status 3 or 4 stars). A number of the 1- and 2-star entries may eventually disappear, but there are certainly many resonances yet to be discovered underlying the established ones.

Sign conventions for resonance couplings: In terms of the isospin-0 and -1 elastic scattering amplitudes A_0 and A_1 , the amplitude for $K^-p \rightarrow \bar{K}^0 n$ scattering is $\pm(A_1 - A_0)/2$, where the sign depends on conventions used in conjunction with the Clebsch-Gordan coefficients (such as, is the baryon or the meson the "first" particle). If this reaction is partial-wave analyzed and if the overall phase is chosen so that, say, the $\Sigma(1775)D_{15}$ amplitude at resonance points along the positive imaginary axis (points "up"), then any Σ at resonance will point "up" and any Λ at resonance will point "down" (along the negative imaginary axis). Thus the phase at resonance determines the isospin. The above ignores background amplitudes in the resonating partial waves.

That is the basic idea. In a similar but somewhat more complicated way, the phases of the $\bar{K}N \rightarrow \Lambda\pi$ and $\bar{K}N \rightarrow \Sigma\pi$ amplitudes for a resonating wave help determine the SU(3) multiplet to which the resonance belongs. Again, a convention

has to be adopted for some overall arbitrary phases: which way is "up"? Our convention is that of Levi-Setti [1] and is shown in Fig. 1, which also compares experimental results with theoretical predictions for the signs of several resonances. In the Listings, a + or - sign in front of a measurement of an inelastic resonance coupling indicates the sign (the *absence* of a sign means that the sign is not determined, *not* that it is positive). For more details, see Appendix II of our 1982 edition [2].

Errors on masses and widths: The errors quoted on resonance parameters from partial-wave analyses are often only statistical, and the parameters can change by more than these errors when a different parametrization of the waves is used. Furthermore, the different analyses use more or less the same data, so it is not really appropriate to treat the different determinations of the resonance parameters as independent or to average them together. In any case, the spread of the masses, widths, and branching fractions from the different analyses is certainly a better indication of the uncertainties than are the quoted errors. In the Baryon Summary Table, we usually give a range reflecting the spread of the values rather than a particular value with error.

For three states, the $\Lambda(1520)$, the $\Lambda(1820)$, and the $\Sigma(1775)$, there is enough information to make an overall fit to the various branching fractions. It is then necessary to use the quoted errors, but the errors obtained from the fit should not be taken seriously.

Production experiments: Partial-wave analyses of course separate partial waves, whereas a peak in a cross section or an invariant mass distribution usually cannot be disentangled from background and analyzed for its quantum numbers; and more than one resonance may be contributing to the peak. Results from partial-wave analyses and from production experiments are generally kept separate in the Listings, and in the Baryon Summary Table results from production experiments

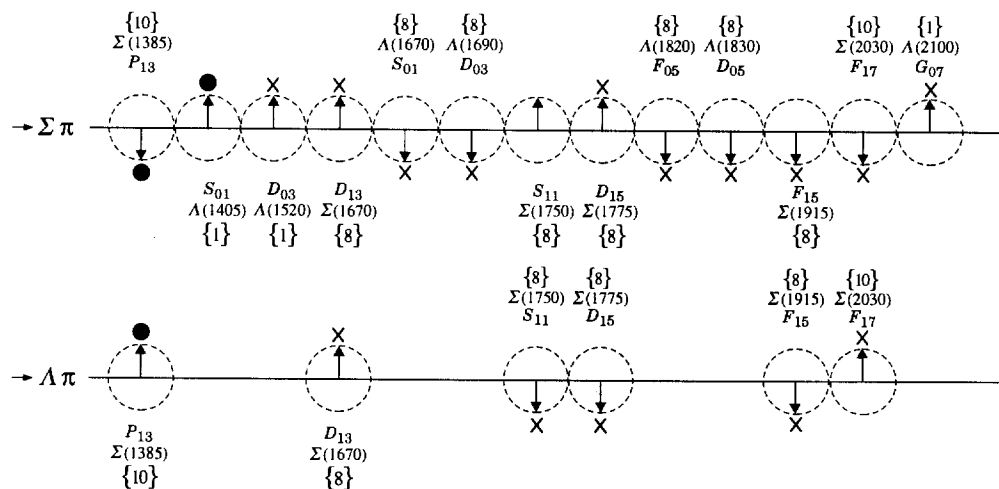


Figure 1. The signs of the imaginary parts of resonating amplitudes in the $\bar{K}N \rightarrow \Lambda\pi$ and $\Sigma\pi$ channels. The signs of the $\Sigma(1385)$ and $\Lambda(1405)$, marked with a \bullet , are set by convention, and then the others are determined relative to them. The signs required by the SU(3) assignments of the resonances are shown with an arrow, and the experimentally determined signs are shown with an \times .

Baryon Particle Listings

 Λ 's and Σ 's, $\Lambda(1405)$ Table 1. The status of the Λ and Σ resonances. Only those with an overall status of *** or **** are included in the main Baryon Summary Table.

Particle	$L_{I,2J}$	Overall status	Status as seen in --			
			$N\bar{K}$	$\Lambda\pi$	$\Sigma\pi$	Other channels
$\Lambda(1116)$	P_{01}	****		F		$N\pi$ (weakly)
$\Lambda(1405)$	S_{01}	****	****	o	****	
$\Lambda(1520)$	D_{03}	****	****	r	****	$\Lambda\pi\pi, \Lambda\gamma$
$\Lambda(1600)$	F_{01}	***	***	b	**	
$\Lambda(1670)$	S_{01}	****	****	i	****	$\Lambda\eta$
$\Lambda(1690)$	D_{03}	****	****	d	****	$\Lambda\pi\pi, \Sigma\pi\pi$
$\Lambda(1800)$	S_{01}	***	***	d	**	$N\bar{K}^*, \Sigma(1385)\pi$
$\Lambda(1810)$	F_{01}	***	***	e	**	$N\bar{K}^*$
$\Lambda(1820)$	F_{05}	****	****	n	****	$\Sigma(1385)\pi$
$\Lambda(1830)$	D_{05}	****	***	F	****	$\Sigma(1385)\pi$
$\Lambda(1890)$	P_{03}	****	****	o	**	$N\bar{K}^*, \Sigma(1385)\pi$
$\Lambda(2000)$	*	*	*	r	*	$\Lambda\omega, N\bar{K}^*$
$\Lambda(2020)$	F_{07}	*	*	b	*	
$\Lambda(2100)$	G_{07}	****	****	i	***	$\Lambda\omega, N\bar{K}^*$
$\Lambda(2110)$	F_{05}	***	**	d	*	$\Lambda\omega, N\bar{K}^*$
$\Lambda(2325)$	D_{03}	*	*	d	*	$\Lambda\omega$
$\Lambda(2350)$		***	***	e	*	
$\Lambda(2585)$		**	**	n		
$\Sigma(1193)$	P_{11}	****				$N\pi$ (weakly)
$\Sigma(1385)$	P_{13}	****		****	****	
$\Sigma(1480)$		*	*	*	*	
$\Sigma(1560)$		**	**	**	**	
$\Sigma(1580)$	D_{13}	**	*	*	*	
$\Sigma(1620)$	S_{11}	**	**	*	*	
$\Sigma(1660)$	P_{11}	***	***	*	**	
$\Sigma(1670)$	D_{13}	****	****	****	****	several others
$\Sigma(1690)$		**	*	**	*	$\Lambda\pi\pi$
$\Sigma(1750)$	S_{11}	***	***	**	*	$\Sigma\eta$
$\Sigma(1770)$	P_{11}	*				
$\Sigma(1775)$	D_{15}	****	****	****	***	several others
$\Sigma(1840)$	P_{13}	*	*	**	*	
$\Sigma(1880)$	P_{11}	**	**	**	**	$N\bar{K}^*$
$\Sigma(1915)$	F_{15}	****	***	****	***	$\Sigma(1385)\pi$
$\Sigma(1940)$	D_{13}	***	*	***	**	quasi-2-body
$\Sigma(2000)$	S_{11}	*		*		$N\bar{K}^*, \Lambda(1520)\pi$
$\Sigma(2030)$	F_{17}	****	****	****	**	several others
$\Sigma(2070)$	F_{15}	*	*		*	
$\Sigma(2080)$	P_{13}	**		**		
$\Sigma(2100)$	G_{17}	*		*	*	
$\Sigma(2250)$		***	***	*	*	
$\Sigma(2455)$		**	*			
$\Sigma(2620)$		**	*			
$\Sigma(3000)$		*	*	*		
$\Sigma(3170)$		*				multi-body

**** Existence is certain, and properties are at least fairly well explored.
 *** Existence ranges from very likely to certain, but further confirmation is desirable and/or quantum numbers, branching fractions, etc. are not well determined.
 ** Evidence of existence is only fair.
 * Evidence of existence is poor.

are used only for the low-mass states. The $\Sigma(1385)$ and $\Lambda(1405)$ of course lie below the $\bar{K}N$ threshold and nearly everything about them is learned from production experiments; and production and formation experiments agree quite well in the case of $\Lambda(1520)$ and results have been combined. There is some disagreement between production and formation experiments in the 1600–1700 MeV region: see the note on the $\Sigma(1670)$.

References

1. R. Levi-Setti, in *Proceedings of the Lund International Conference on Elementary Particles* (Lund, 1969), p. 339.
2. Particle Data Group, Phys. Lett. **111B** (1982).

 $\Lambda(1405) S_{01}$ $I(J^P) = 0(\frac{1}{2}^-)$ Status: ****THE $\Lambda(1405)$

Revised March 1998 by R.H. Dalitz (Oxford University).

It is generally accepted that the $\Lambda(1405)$ is a well-established $J^P = 1/2^-$ resonance. It is assigned to the lowest $L = 1$ supermultiplet of the 3-quark system and paired with the $J^P = 3/2^-$ $\Lambda(1520)$. Lying about 30 MeV below the $N\bar{K}$ threshold, the $\Lambda(1405)$ can be observed directly only as a resonance bump in the $(\Sigma\pi)^0$ subsystem in final states of production experiments. It was first reported by ALSTON 61B in the reaction $K^-p \rightarrow \Sigma\pi\pi$ at 1.15 GeV/c and has since been seen in at least eight other experiments. However, only two of them had enough events for a detailed analysis: THOMAS 73, with about 400 $\Sigma^\pm\pi^\mp$ events from $\pi^-p \rightarrow K^0(\Sigma\pi)^0$ at 1.69 GeV/c; and HEMINGWAY 85, with 766 $\Sigma^+\pi^-$ and 1106 $\Sigma^-\pi^+$ events from $K^-p \rightarrow (\Sigma\pi\pi)^+\pi^-$ at 4.2 GeV/c, after the selections $1600 \leq M(\Sigma\pi\pi)^+ \leq 1720$ MeV and momentum transfer ≤ 1.0 (GeV/c)² to purify the $\Lambda(1405) \rightarrow (\Sigma\pi)^0$ sample. These experiments agree on a mass of about 1395–1400 MeV and a width of about 60 MeV. (Hemingway's mass of 1391 ± 1 MeV is from his best, but unacceptably poor, Breit-Wigner fit.)

The Byers-Fenster tests on these data allow any spin and either parity: neither J nor P has yet been determined *directly*. The early indications for $J^P = 1/2^-$ came from finding $\text{Re } A_{I=0}$ to be large and negative in a constant-scattering-length analysis of low-energy $N\bar{K}$ reaction data (see KIM 65, SAKITT 65, and earlier references cited therein). The first multichannel energy-dependent K-matrix analysis (KIM 67) strengthened the case for a resonance around 1400–1420 MeV strongly coupled to the $I = 0$ S -wave $N\bar{K}$ system.

THOMAS 73 and HEMINGWAY 85 both found the $\Lambda(1405)$ bump to be asymmetric and not well fitted by a Breit-Wigner resonance function with constant parameters. The asymmetry involves a rapid fall in intensity as the $N\bar{K}$ threshold energy is approached from below. This is readily understood as due to a strong coupling of the $\Lambda(1405)$ to the S -wave $N\bar{K}$ channel (see DALITZ 81). This striking S -shaped cusp behavior at a new threshold is characteristic of S -wave coupling; the other below-threshold hyperon, the $\Sigma(1385)$, has no such threshold distortion because its $N\bar{K}$ coupling is P -wave. For the $\Lambda(1405)$, this asymmetry is the *sole direct evidence* that $J^P = 1/2^-$.

Following the early work cited above, a considerable literature has developed on proper procedures for phenomenological extrapolation below the $N\bar{K}$ threshold, partly in order to strengthen the evidence for the spin-parity of the $\Lambda(1405)$, and partly to provide an estimate for the amplitude $f(N\bar{K})$ in the unphysical domain below the $N\bar{K}$ threshold; the latter is needed for the evaluation of the dispersion relation for $N\bar{K}$ and NK forward scattering amplitudes. For recent reviews, see MILLER 84 and BARRETT 89. In most recent work, the $(\Sigma\pi)^0$ production spectrum is included in the data fitted (see, e.g., CHAO 73, MARTIN 81).

It is now accepted that the data can be fitted only with an S -wave pole in the reaction amplitudes below $N\bar{K}$ threshold (see, however, FINK 90), but there is still controversy about the physical origin of this pole (for a review, see DALITZ 81 and DALITZ 82). Two extreme possibilities are: (a) an $L = 1$ $SU(3)$ -singlet uds state coupled with the S -wave meson-baryon systems; or (b) an unstable $N\bar{K}$ bound state, analogous to the (stable) deuteron in the NN system. The problem with (a) is that the $\Lambda(1405)$ mass is so much lower than that of its partner, the $\Lambda(1520)$. This requires, in the QCD-inspired quark model, rather large spin-orbit couplings, whether or not one uses relativistic kinetic energies. CAPSTICK 86 and CAPSTICK 89 conclude that a proper QCD calculation leads only to small energy splittings, whereas LEINWEBER 90, using QCD sum rules, obtains a good fit to this splitting.

On the other hand, the problem with (b) is that then another $J^P = 1/2^- A$ is needed to replace the $\Lambda(1405)$ in the $L = 1$ supermultiplet, and it would have to lie close to the $\Lambda(1520)$, a region already well explored by $N\bar{K}$ experiments without result. Intermediate structures are possible; for example, the cloudy bag model allows the configurations (a) and (b) to mix and finds the intensity of (a) in the $\Lambda(1405)$ to be only 14% (VEIT 84, VEIT 85, JENNINGS 86). Such models naturally predict a second $1/2^- A$ close to the $\Lambda(1520)$.

The determination of the mass and width of the resonance from $(\Sigma\pi)^0$ data is usually based on the "Watson approximation," which states that the production rate $R(\Sigma\pi)$ of the $(\Sigma\pi)^0$ state has a mass dependence proportional to $(\sin^2\delta_{\Sigma\pi})/q$, q being the $\Sigma\pi$ c.m. momentum, in a $\Sigma\pi$ mass range where $\delta_{\Sigma\pi}$ is not far from $\pi/2$ and only the $\Sigma\pi$ channel is open, *i.e.*, between the $\Sigma\pi$ and the $N\bar{K}$ thresholds. Then $qR(\Sigma\pi)$ is proportional to $\sin^2\delta_{\Sigma\pi}$, and the mass M may be defined as the energy at which $\sin^2\delta_{\Sigma\pi} = 1$. The width Γ may be determined from the rate at which $\delta_{\Sigma\pi}$ goes through $\pi/2$, or from the FWHM; this is a matter of convention.

This determination of M and Γ from the data suffers from the following defects:

(i) The determination of $\sin^2\delta_{\Sigma\pi}$ requires that $R(\Sigma\pi)$ be scaled to give $\sin^2\delta_{\Sigma\pi} = 1$ at the peak for the best fit to the data; *i.e.*, the bump must be *assumed* to arise from a resonance. However, this assumption is supported by the analysis of the low-energy $N\bar{K}$ data and its extrapolation below threshold.

(ii) Owing to the nearby $N\bar{K}$ threshold, the shape of the best fit to the $M(\Sigma\pi)$ bump is uncertain. For energies below this threshold at $E_{N\bar{K}}$, the general form for $\delta_{\Sigma\pi}$ is

$$q \cot \delta_{\Sigma\pi} = \frac{1 + \kappa\alpha}{\gamma + \kappa(\alpha\gamma - \beta^2)}. \quad (1)$$

Here α, β , and γ are the (generally energy-dependent) NN , $N\Sigma$, and $\Sigma\Sigma$ elements of the $I = 0$ S -wave K -matrix for the $(\Sigma\pi, N\bar{K})$ system, and κ is the magnitude of the (imaginary) c.m. momentum k_K for the $N\bar{K}$ system below threshold. The elements α, β, γ are real functions of E ; they have no branch cuts at the $\Sigma\pi$ and $N\bar{K}$ thresholds, but they are permitted

to have poles in E along the real E axis. The resonance asymmetry arises from the effect of κ on $\delta_{\Sigma\pi}$. We note that $\delta_{\Sigma\pi} = \pi/2$ when $\kappa = -1/\alpha$.

Accepting this close connection of $\delta_{\Sigma\pi}$ with the low-energy $N\bar{K}$ data, it is natural to analyze the two sets of data together (*e.g.*, MARTIN 81), and there is now a large body of accurate $N\bar{K}$ data for laboratory momenta between 100 and 300 MeV/ c (see MILLER 84). The two sets of data span c.m. energies from 1370 MeV to 1490 MeV, and the K -matrix elements will not be energy independent over such a broad range. For the $I = 0$ channels, a linear energy dependence for K^{-1} has been adopted routinely ever since the work of KIM 67, and it is essential when fitting the $qR(\Sigma\pi)$ and $N\bar{K}$ data together. However, $qR(\Sigma\pi)$ is not always well fitted in this procedure; the value obtained for the $\Lambda(1405)$ mass M varies a good deal with the type of fit, not a surprising result when the $\Sigma\pi$ mass spectrum below the pK^- threshold contributes only nine data points in a total of about 200. The value of M obtained from an overall fit is not necessarily much better than from one using only the $qR(\Sigma\pi)$ data; and M may be a function of the representation— K -matrix, K^{-1} -matrix, relativistic-separable or nonseparable potentials, *etc.*—used in fitting over the full energy range. DALITZ 91 fitted the $qR(\Sigma^+\pi^-)$ Hemingway data with each of the first three representations just mentioned, constrained to the $I = 0$ $N\bar{K}$ threshold scattering length from low-energy $N\bar{K}$ data. The (nonseparable) meson-exchange potentials of MÜLLER-GROELING 90, fitted to the low-energy $N\bar{K}$ (and NK) data, predicted an unstable $N\bar{K}$ bound state with mass and width compatible with the $\Lambda(1405)$.

From the measurement of $2p \rightarrow 1s$ x rays from kaonic-hydrogen, the energy-level shift ΔE and width Γ of its $1s$ state can give us two further constraints on the $(\Sigma\pi, N\bar{K})$ system, at an energy roughly midway between those from the low-energy hydrogen bubble chamber studies and those from $qR(\Sigma\pi)$ observations below the pK^- threshold. IWASAKI 97 have reported the first convincing observation of this x ray, with a good initial estimate:

$$\Delta E - i\Gamma/2 = (-323 \pm 63 \pm 11) - i(204 \pm 104 \pm 50) \text{ eV}. \quad (2)$$

The errors here encompass about half of the predictions made following the various analyses and/or models for the in-flight K^-p and sub-threshold $qR(\Sigma\pi)$ data. Better measurements will be needed to discriminate between the analyses and predictions. Now that ΔE is known with some certainty, we can anticipate much-improved data on kaonic-hydrogen, perhaps from the DAΦNE storage ring at Frascati, information vital for our quantitative understanding of the $(\Sigma\pi, N\bar{K})$ system in this region. This will lead to better knowledge of kaonic coupling strengths and to more reliable dispersion-theoretic arguments concerning strange-particle processes.

The present status of the $\Lambda(1405)$ thus depends heavily on theoretical arguments, a somewhat unsatisfactory basis for a four-star rating. Nevertheless, there is no known reason to doubt its existence or quantum numbers. The 3-quark model

Baryon Particle Listings

 $\Lambda(1405)$

for baryons has been broadly successful in accounting for all of the $L^P = 1^-$ excited baryonic states (CAPSTICK 89), apart from the relatively large mass separation between the $\Lambda(1405)$ and $\Lambda(1520)$. Quark model builders have no reservations about accepting the $\Lambda(1405)$ as a 3-quark state. However, calculations with broken-chiral-symmetric models, which combine internal 3-quark configurations with external meson-baryon states (e.g., VEIT 85, KAISER 95) end up with descriptions of the $\Lambda(1405)$ dominated by the meson-baryon terms in the wavefunctions. Models using meson-baryon potentials readily fit its mass, and give ΔE negative, as is found empirically. The problem is not so much one of "either (a) or (b)," but rather how to achieve "both (a) and (b)." Theoreticians have not yet been able to deal with the full coupled-channels system, with qqq and $qqq\bar{q}$ configurations (at the least) being treated on the same footing. On the experimental side, better statistics are needed, both above and below the pK^- threshold. To disentangle the physics, the $I = 1$ channels also need more attention. For example, low-energy pK_L^0 interactions have not been studied at all in the last 25 years.

 $\Lambda(1405)$ MASS

PRODUCTION EXPERIMENTS

VALUE (MeV)	EVTS	DOCUMENT ID	TECN	COMMENT
1406.5 ± 4.0		¹ DALITZ 91		M-matrix fit
• • • We do not use the following data for averages, fits, limits, etc. • • •				
1391 ± 1	700	¹ HEMINGWAY 85	HBC	$K^- p$ 4.2 GeV/c
~ 1405	400	² THOMAS 73	HBC	$\pi^- p$ 1.69 GeV/c
1405	120	BARBARO... 68B	DBC	$K^- d$ 2.1-2.7 GeV/c
1400 ± 5	67	BIRMINGHAM 66	HBC	$K^- p$ 3.5 GeV/c
1382 ± 8		ENGLER 65	HDBC	$\pi^- p, \pi^+ d$ 1.68 GeV/c
1400 ± 24		MUSGRAVE 65	HBC	$\bar{p} p$ 3-4 GeV/c
1410		ALEXANDER 62	HBC	$\pi^- p$ 2.1 GeV/c
1405		ALSTON 62	HBC	$K^- p$ 1.2-0.5 GeV/c
1405		ALSTON 61B	HBC	$K^- p$ 1.15 GeV/c

EXTRAPOLATIONS BELOW $N\bar{K}$ THRESHOLD

VALUE (MeV)	DOCUMENT ID	TECN	COMMENT
• • • We do not use the following data for averages, fits, limits, etc. • • •			
1411	³ MARTIN 81		K-matrix fit
1406	⁴ CHAO 73	DPWA	0-range fit (sol. B)
1421	MARTIN 70	RVUE	Constant K-matrix
1416 ± 4	MARTIN 69	HBC	Constant K-matrix
1403 ± 3	KIM 67	HBC	K-matrix fit
1407.5 ± 1.2	⁵ KITTEL 66	HBC	0-effective-range fit
1410.7 ± 1.0	KIM 65	HBC	0-effective-range fit
1409.6 ± 1.7	⁵ SAKITT 65	HBC	0-effective-range fit

 $\Lambda(1405)$ WIDTH

PRODUCTION EXPERIMENTS

VALUE (MeV)	EVTS	DOCUMENT ID	TECN	COMMENT
50 ± 2		¹ DALITZ 91		M-matrix fit
• • • We do not use the following data for averages, fits, limits, etc. • • •				
32 ± 1	700	¹ HEMINGWAY 85	HBC	$K^- p$ 4.2 GeV/c
45 to 55	400	² THOMAS 73	HBC	$\pi^- p$ 1.69 GeV/c
35	120	BARBARO... 68B	DBC	$K^- d$ 2.1-2.7 GeV/c
50 ± 10	67	BIRMINGHAM 66	HBC	$K^- p$ 3.5 GeV/c
89 ± 20		ENGLER 65	HDBC	
60 ± 20		MUSGRAVE 65	HBC	
35 ± 5		ALEXANDER 62	HBC	
50		ALSTON 62	HBC	
20		ALSTON 61B	HBC	

EXTRAPOLATIONS BELOW $N\bar{K}$ THRESHOLD

VALUE (MeV)	DOCUMENT ID	TECN	COMMENT
• • • We do not use the following data for averages, fits, limits, etc. • • •			
30	³ MARTIN 81		K-matrix fit
55	^{4,6} CHAO 73	DPWA	0-range fit (sol. B)
20	MARTIN 70	RVUE	Constant K-matrix
29 ± 6	MARTIN 69	HBC	Constant K-matrix
50 ± 5	KIM 67	HBC	K-matrix fit
34.1 ± 4.1	⁵ KITTEL 66	HBC	
37.0 ± 3.2	KIM 65	HBC	
28.2 ± 4.1	⁵ SAKITT 65	HBC	

 $\Lambda(1405)$ DECAY MODES

Mode	Fraction (Γ_i/Γ)
Γ_1 $\Sigma \pi$	100 %
Γ_2 $\Lambda \gamma$	
Γ_3 $\Sigma^0 \gamma$	
Γ_4 $N\bar{K}$	

 $\Lambda(1405)$ PARTIAL WIDTHS

$\Gamma(\Lambda \gamma)$	DOCUMENT ID	COMMENT	Γ_2
• • • We do not use the following data for averages, fits, limits, etc. • • •			
27 ± 8	BURKHARDT 91	Isobar model fit	
$\Gamma(\Sigma^0 \gamma)$	DOCUMENT ID	COMMENT	Γ_3
• • • We do not use the following data for averages, fits, limits, etc. • • •			
10 ± 4 or 23 ± 7	BURKHARDT 91	Isobar model fit	

 $\Lambda(1405)$ BRANCHING RATIOS

$\Gamma(N\bar{K})/\Gamma(\Sigma \pi)$	CL%	DOCUMENT ID	TECN	COMMENT	Γ_4/Γ_1
• • • We do not use the following data for averages, fits, limits, etc. • • •					
< 3	95	HEMINGWAY 85	HBC	$K^- p$ 4.2 GeV/c	

 $\Lambda(1405)$ FOOTNOTES

- ¹DALITZ 91 fits the HEMINGWAY 85 data.
- ²THOMAS 73 data is fit by CHAO 73 (see next section).
- ³The MARTIN 81 fit includes the $K^\pm p$ forward scattering amplitudes and the dispersion relations they must satisfy.
- ⁴See also the accompanying paper of THOMAS 73.
- ⁵Data of SAKITT 65 are used in the fit by KITTEL 66.
- ⁶An asymmetric shape, with $\Gamma/2 = 41$ MeV below resonance, 14 MeV above.

 $\Lambda(1405)$ REFERENCES

BURKHARDT 91	PR C44 607	H. Burkhardt, J. Lowe	(NOTT, UNM, BIRM)
DALITZ 91	JPG 17 289	R.H. Dalitz, A. Deloff	(OXFTF, WINR)
HEMINGWAY 85	NP B253 742	R.J. Hemingway	(CERN) J
MARTIN 81	NP B179 33	A.D. Martin	(DURH)
CHAO 73	NP B56 46	Y.A. Chao et al.	(RHEL, CMU, LOUC)
THOMAS 73	NP B56 15	D.W. Thomas et al.	(CMU) J
MARTIN 70	NP B16 479	A.D. Martin, G.G. Ross	(DURH)
MARTIN 69	PR 183 1352	B.R. Martin, M. Sakitt	(LOUC, BNL)
Also 69B	PR 183 1345	B.R. Martin, M. Sakitt	(LOUC, BNL)
BARBARO... 68B	PRL 21 573	A. Barbaro-Galsteri et al.	(LRL, SLAC)
KIM 67	PRL 19 1074	J.K. Kim	(YALE)
BIRMINGHAM 66	PR 152 1148	Birmingham	(BIRM, GLAS, LOIC, OXF, RHEL)
KITTEL 66	PL 21 349	W. Kittel, G. Otter, I. Wacek	(VIEN)
ENGLER 65	PRL 15 224	A. Engler et al.	(CMU, BNL) J
KIM 65	PRL 14 29	Kim	(COLU)
MUSGRAVE 65	NC 35 735	B. Musgrave et al.	(BIRM, CERN, EPOL+)
SAKITT 65	PR 139B 719	M. Sakitt et al.	(UMO, LRL)
ALEXANDER 62	PRL 8 447	G. Alexander et al.	(LRL) J
ALSTON 62	CERN Conf. 311	M.H. Alston et al.	(LRL) J
ALSTON 61B	PRL 6 698	M.H. Alston et al.	(LRL) J

OTHER RELATED PAPERS

IWASAKI 97	PRL 78 3067	M. Iwasaki et al.	(KEK-228 Collab)
FINK 90	PR C41 2720	P.J. Fink et al.	(IBMY, ORST, ANSM)
LEINWEBER 90	ANP 138 203	D.B. Leinweber	(MCSM)
MUELLER-GR... 90	NP A513 557	A. Mueller-Groeling, K. Holinde, J. Speth	(JULI)
BARRETT 89	NC 102A 179	R.C. Barrett	(SURR)
BATTY 89	NC 102A 255	C.J. Batty, A. Gal	(RAL, HEBR)
CAPSTICK 89	Excited Baryons 88, p.32	S. Capstick	(GUEL)
LOWE 89	NC 102A 167	J. Lowe	(BIRM)

See key on page 239

Baryon Particle Listings

$\Lambda(1405), \Lambda(1520)$

WHITEHOUSE 89	PRL 63 1352	O.A. Whitehouse <i>et al.</i>	(BIRM, BOST, BRCO+)
SIEGEL 88	PR C39 2221	F.B. Siegel, W. Weise	(REG)
WORKMAN 83	PR D37 3117	R.L. Workman, H.W. Fearing	(TRIU)
SCHNICK 87	PR 58 1719	J. Schnick, R.H. Landau	(ORST)
CAPSTICK 86	PR D34 2809	S. Capstick, N. Isgur	(TNT)
JENNINGS 86	PL B176 229	B.K. Jennings	(TRIU)
MALTMAN 86	PR D34 1372	K. Maltman, N. Isgur	(LANL, TNT)
ZHONG 86	PL B171 471	Y.S. Zhong <i>et al.</i>	(ADLD, TRIU, SURR)
BURKHARDT 85	NP A440 653	H. Burkhardt, J. Lowe, A.S. Rosenthal	(NOTT+)
DAREWYCH 85	PR D32 1765	J.W. Darewych, R. Koniuk, N. Isgur	(YORK, TNT)
VEIT 85	PR D31 1033	E.A. Veit <i>et al.</i>	(TRIU, ADLD, SURR)
KIANG 84	PR C30 1638	D. Kiang <i>et al.</i>	(DALH, MCMS)
MILLER 84		Miller	(LOUC)
Conf. Intersections between Particle and Nuclear Physics, p. 783			
VANDUJ 84	PR D30 937	W. van Dijk	(MCMS)
VEIT 84	PL 137B 415	E.A. Veit <i>et al.</i>	(TRIU, SURR, CERN)
DALITZ 82		Dalitz <i>et al.</i>	(OXFTP)
Heidelberg Conf., p. 201			
DALITZ 81		Dalitz, McGinley	(OXFTP)
Low and Intermediate Energy Kaon-Nucleon Physics, p.381			
MARTIN 81B	L.I.E. K-N Phys., p. 97	A.D. Martin	(DURH)
OADES 77	NC 42A 462	G.C. Oades, G. Rasche	(AARH, ZURI)
SHAW 73	Purdue Conf. 417	G.L. Shaw	(UCI)
BARBARO... 72	LBL-555	A. Barbaro-Galleri	(LBL)
DOBSON 72	PR D6 3256	P.N. Dobson, R. McElhaney	(HAWA)
RAJASEKA... 72	PR D5 610	G. Rajasekaran	(TATA)
Earlier papers also cited in RAJASEKARAN 72.			
CLINE 71	PRL 26 1194	D. Cline, R. Laumann, J. Mapp	(WISC)
MARTIN 71	PL 35B 62	A.D. Martin, A.D. Martin, G.G. Ross	(DURH, LOUC+)
DALITZ 67	PR 153 1617	R.H. Dalitz, T.C. Wong, G. Rajasekaran	(OXFTP+)
DONALD 66	PL 22 711	R.A. Donald <i>et al.</i>	(LIVP)
KADYK 66	PRL 17 599	J.A. Kadyk <i>et al.</i>	(LRL)
ABRAMS 65	PR 139B 454	G.S. Abrams, B. Sechi-Zorn	(UMD)

CONSTRAINED FIT INFORMATION

An overall fit to 9 branching ratios uses 24 measurements and one constraint to determine 6 parameters. The overall fit has a $\chi^2 = 16.5$ for 19 degrees of freedom.

The following *off-diagonal* array elements are the correlation coefficients $\langle \delta x_i \delta x_j \rangle / (\delta x_i \delta x_j)$, in percent, from the fit to the branching fractions, $x_i \equiv \Gamma_i / \Gamma_{total}$. The fit constrains the x_i whose labels appear in this array to sum to one.

x_2	-63				
x_3	-32	-33			
x_7	-4	-3	-1		
x_8	-9	-8	-4	0	
x_9	-24	-21	-10	-1	-2
	x_1	x_2	x_3	x_7	x_8

$\Lambda(1520)$ BRANCHING RATIOS

See "Sign conventions for resonance couplings" in the Note on Λ and Σ Resonances.

$\Gamma(N\bar{K})/\Gamma_{total}$	VALUE	DOCUMENT ID	TECN	COMMENT	Γ_1/Γ
0.45 ± 0.01 OUR ESTIMATE					
0.448 ± 0.007 OUR FIT				Error includes scale factor of 1.2.	
0.455 ± 0.011 OUR AVERAGE					
0.47 ± 0.02		GOPAL	80	DPWA $\bar{K}N \rightarrow \bar{K}N$	
0.45 ± 0.03		ALSTON-...	78	DPWA $\bar{K}N \rightarrow \bar{K}N$	
0.448 ± 0.014		CORDEN	75	DBC $K^- d$ 1.4-1.8 GeV/c	
• • • We do not use the following data for averages, fits, limits, etc. • • •					
0.47 ± 0.01		GOPAL	77	DPWA See GOPAL 80	
0.42		MAST	76	HBC $K^- p \rightarrow \bar{K}^0 n$	

$\Gamma(\Sigma\pi)/\Gamma_{total}$	VALUE	DOCUMENT ID	TECN	COMMENT	Γ_2/Γ
0.42 ± 0.01 OUR ESTIMATE					
0.421 ± 0.007 OUR FIT				Error includes scale factor of 1.2.	
0.423 ± 0.011 OUR AVERAGE					
0.426 ± 0.014		CORDEN	75	DBC $K^- d$ 1.4-1.8 GeV/c	
0.418 ± 0.017		BARBARO-...	69B	HBC $K^- p$ 0.28-0.45 GeV/c	
• • • We do not use the following data for averages, fits, limits, etc. • • •					
0.46		KIM	71	DPWA K-matrix analysis	

$\Gamma(\Sigma\pi)/\Gamma(N\bar{K})$	VALUE	DOCUMENT ID	TECN	COMMENT	Γ_2/Γ_1
0.940 ± 0.026 OUR FIT				Error includes scale factor of 1.3.	
0.95 ± 0.04 OUR AVERAGE				Error includes scale factor of 1.7. See the ideogram below.	
0.98 ± 0.03		GOPAL	77	DPWA $\bar{K}N$ multichannel	
0.82 ± 0.08		BURKHARDT	69	HBC $K^- p$ 0.8-1.2 GeV/c	
1.06 ± 0.14		SCHEUER	68	DBC $K^- N$ 3 GeV/c	
0.96 ± 0.20		DAHL	67	HBC $\pi^- p$ 1.6-4 GeV/c	
0.73 ± 0.11		DAUBER	67	HBC $K^- p$ 2 GeV/c	
• • • We do not use the following data for averages, fits, limits, etc. • • •					
1.06 ± 0.12		BERTHON	74	HBC Quasi-2-body σ	
1.72 ± 0.78		MUSGRAVE	65	HBC	

$\Lambda(1520) D_{03}$

$I(J^P) = 0(\frac{3}{2}^-)$ Status: * * * *

Discovered by FERRO-LUZZI 62; the elaboration in WATSON 63 is the classic paper on the Breit-Wigner analysis of a multichannel resonance.

The measurements of the mass, width, and elasticity published before 1975 are now obsolete and have been omitted. They were last listed in our 1982 edition Physics Letters **111B** (1982).

Production and formation experiments agree quite well, so they are listed together here.

$\Lambda(1520)$ MASS

VALUE (MeV)	EVTS	DOCUMENT ID	TECN	COMMENT
1519.5 ± 1.0 OUR ESTIMATE				
1519.50 ± 0.18 OUR AVERAGE				
1517.3 ± 1.5	300	BARBER	80D	SPEC $\gamma p \rightarrow \Lambda(1520) K^+$
1519 ± 1		GOPAL	80	DPWA $\bar{K}N \rightarrow \bar{K}N$
1517.8 ± 1.2	5k	BARLAG	79	HBC $K^- p$ 4.2 GeV/c
1520.0 ± 0.5		ALSTON-...	78	DPWA $\bar{K}N \rightarrow \bar{K}N$
1519.7 ± 0.3	4k	CAMERON	77	HBC $K^- p$ 0.96-1.36 GeV/c
1519 ± 1		GOPAL	77	DPWA $\bar{K}N$ multichannel
1519.4 ± 0.3	2000	CORDEN	75	DBC $K^- d$ 1.4-1.8 GeV/c

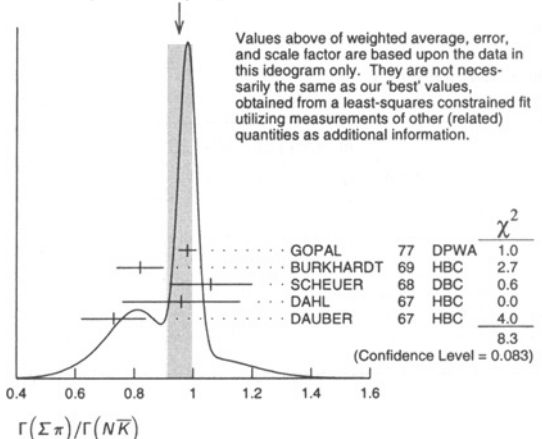
$\Lambda(1520)$ WIDTH

VALUE (MeV)	EVTS	DOCUMENT ID	TECN	COMMENT
15.6 ± 1.0 OUR ESTIMATE				
15.59 ± 0.27 OUR AVERAGE				
16.3 ± 3.3	300	BARBER	80D	SPEC $\gamma p \rightarrow \Lambda(1520) K^+$
16 ± 1		GOPAL	80	DPWA $\bar{K}N \rightarrow \bar{K}N$
14 ± 3	677	BARLAG	79	HBC $K^- p$ 4.2 GeV/c
15.4 ± 0.5		ALSTON-...	78	DPWA $\bar{K}N \rightarrow \bar{K}N$
16.3 ± 0.5	4k	CAMERON	77	HBC $K^- p$ 0.96-1.36 GeV/c
15.0 ± 0.5		GOPAL	77	DPWA $\bar{K}N$ multichannel
15.5 ± 1.6	2000	CORDEN	75	DBC $K^- d$ 1.4-1.8 GeV/c

$\Lambda(1520)$ DECAY MODES

Mode	Fraction (Γ_i/Γ)
Γ_1 $N\bar{K}$	45 ± 1%
Γ_2 $\Sigma\pi$	42 ± 1%
Γ_3 $\Lambda\pi\pi$	10 ± 1%
Γ_4 $\Sigma(1385)\pi$	
Γ_5 $\Sigma(1385)\pi(\rightarrow \Lambda\pi\pi)$	
Γ_6 $\Lambda(\pi\pi)$ -s-wave	
Γ_7 $\Sigma\pi\pi$	0.9 ± 0.1%
Γ_8 $\Lambda\gamma$	0.8 ± 0.2%
Γ_9 $\Sigma^0\gamma$	

WEIGHTED AVERAGE
0.95±0.04 (Error scaled by 1.7)



Baryon Particle Listings

 $\Lambda(1520), \Lambda(1600)$ $\Gamma(\Lambda\pi\pi)/\Gamma_{total}$

VALUE	DOCUMENT ID	TECN	COMMENT
0.10 ± 0.01 OUR ESTIMATE			
0.095 ± 0.005 OUR FIT			Error includes scale factor of 1.2.
0.096 ± 0.008 OUR AVERAGE			Error includes scale factor of 1.6.
0.091 ± 0.006	CORDEN	75 DBC	$K^- d$ 1.4-1.8 GeV/c
0.11 ± 0.01	³ MAST	73b IPWA	$K^- p \rightarrow \Lambda\pi\pi$

 $\Gamma(\Lambda\pi\pi)/\Gamma(N\bar{K})$

VALUE	DOCUMENT ID	TECN	COMMENT
0.213 ± 0.012 OUR FIT			Error includes scale factor of 1.2.
0.202 ± 0.021 OUR AVERAGE			
0.22 ± 0.03	BURKHARDT	69 HBC	$K^- p$ 0.8-1.2 GeV/c
0.19 ± 0.04	SCHEUER	68 DBC	$K^- N$ 3 GeV/c
0.17 ± 0.05	DAHL	67 HBC	$\pi^- p$ 1.6-4 GeV/c
0.21 ± 0.18	DAUBER	67 HBC	$K^- p$ 2 GeV/c
• • • We do not use the following data for averages, fits, limits, etc. • • •			
0.27 ± 0.13	BERTHON	74 HBC	Quasi-2-body σ
0.2	KIM	71 DPWA	K-matrix analysis

 $\Gamma(\Sigma\pi)/\Gamma(\Lambda\pi\pi)$

VALUE	DOCUMENT ID	TECN	COMMENT
4.42 ± 0.25 OUR FIT			Error includes scale factor of 1.2.
3.9 ± 0.6 OUR AVERAGE			
3.9 ± 1.0	UHLIG	67 HBC	$K^- p$ 0.9-1.0 GeV/c
3.3 ± 1.1	BIRMINGHAM	66 HBC	$K^- p$ 3.5 GeV/c
4.5 ± 1.0	ARMENTEROS565c	HBC	

 $\Gamma(\Sigma(1385)\pi)/\Gamma_{total}$

VALUE	DOCUMENT ID	TECN	COMMENT
0.041 ± 0.005	CHAN	72 HBC	$K^- p \rightarrow \Lambda\pi\pi$

 $\Gamma(\Sigma(1385)\pi(\rightarrow \Lambda\pi\pi))/\Gamma(\Lambda\pi\pi)$

The $\Lambda\pi\pi$ mode is largely due to $\Sigma(1385)\pi$. Only the values of $(\Sigma(1385)\pi)/(\Lambda\pi\pi)$ given by MAST 73b and CORDEN 75 are based on real 3-body partial-wave analyses. The discrepancy between the two results is essentially due to the different hypotheses made concerning the shape of the $(\pi\pi)_{S\text{-wave}}$ state.

VALUE	DOCUMENT ID	TECN	COMMENT
0.58 ± 0.22	CORDEN	75 DBC	$K^- d$ 1.4-1.8 GeV/c
0.82 ± 0.10	⁴ MAST	73b IPWA	$K^- p \rightarrow \Lambda\pi\pi$
• • • We do not use the following data for averages, fits, limits, etc. • • •			
0.39 ± 0.10	⁵ BURKHARDT	71 HBC	$K^- p \rightarrow (\Lambda\pi\pi)\pi$

 $\Gamma(\Lambda(\pi\pi)_{S\text{-wave}})/\Gamma(\Lambda\pi\pi)$

VALUE	DOCUMENT ID	TECN	COMMENT
0.20 ± 0.08	CORDEN	75 DBC	$K^- d$ 1.4-1.8 GeV/c

 $\Gamma(\Sigma\pi\pi)/\Gamma_{total}$

VALUE	DOCUMENT ID	TECN	COMMENT
0.009 ± 0.001 OUR ESTIMATE			
0.0086 ± 0.0005 OUR FIT			
0.0086 ± 0.0005 OUR AVERAGE			
0.007 ± 0.002	⁶ CORDEN	75 DBC	$K^- d$ 1.4-1.8 GeV/c
0.0085 ± 0.0006	⁷ MAST	73 MPWA	$K^- p \rightarrow \Sigma\pi\pi$
0.010 ± 0.0015	BARBARO...	69b HBC	$K^- p$ 0.28-0.45 GeV/c

 $\Gamma(\Lambda\gamma)/\Gamma_{total}$

VALUE	EVTS	DOCUMENT ID	TECN	COMMENT
0.008 ± 0.002 OUR ESTIMATE				
0.0079 ± 0.0014 OUR FIT				
0.0080 ± 0.0014	238	MAST	68b HBC	Using $\Gamma(N\bar{K})/\Gamma_{total} = 0.45$

 $\Gamma(\Sigma^0\gamma)/\Gamma_{total}$

VALUE	DOCUMENT ID	TECN	COMMENT
0.0195 ± 0.0034 OUR FIT			
0.02 ± 0.0035	⁸ MAST	68b HBC	Not measured; see note

 $\Lambda(1520)$ FOOTNOTES

- From the best-resolution sample of $\Lambda\pi\pi$ events only.
- The $\bar{K}N \rightarrow \Sigma\pi$ amplitude at resonance is $+0.46 \pm 0.01$.
- Assumes $\Gamma(N\bar{K})/\Gamma_{total} = 0.46 \pm 0.02$.
- Both $\Sigma(1385)\pi$ DS_{03} and $\Sigma(\pi\pi)$ DP_{03} contribute.
- The central bin (1514-1524 MeV) gives 0.74 ± 0.10 ; other bins are lower by 2-to-5 standard deviations.
- Much of the $\Sigma\pi\pi$ decay proceeds via $\Sigma(1385)\pi$.
- Assumes $\Gamma(N\bar{K})/\Gamma_{total} = 0.46$.
- Calculated from $\Gamma(\Lambda\gamma)/\Gamma_{total}$, assuming SU(3). Needed to constrain the sum of all the branching ratios to be unity.

 $\Lambda(1520)$ REFERENCES

PDG	82	PL 111B	M. Roos et al.	(HEL5, CIT, CERN)
BARBER	80D	ZPHY C7 17	D.P. Barber et al.	(DARE, LANC, SHEF)
GOPAL	80	Toronto Conf. 159	G.P. Gopal	(RHEL) IJP
BARLAG	79	NP B149 220	S.J.M. Barlag et al.	(AMST, CERN, NIJM+)
ALSTON...	78	PR D18 182	M. Alston-Garnjost et al.	(LBL, MTHO+) IJP
Also	77	PRL 38 1007	M. Alston-Garnjost et al.	(LBL, MTHO+) IJP
CAMERON	77	NP B131 399	W. Cameron et al.	(RHEL, LOIC) IJP
GOPAL	77	NP B119 362	G.P. Gopal et al.	(LOIC, RHEL) IJP
MAST	76	PR D14 13	T.S. Mast et al.	(LBL)
CORDEN	75	NP B84 306	M.J. Corden et al.	(BIRM)
BERTHON	74	NC 21A 146	A. Berthon et al.	(CDEF, RHEL, SACL+)
MAST	73	PR D7 3212	T.S. Mast et al.	(LBL) IJP
MAST	73B	PR D7 5	T.S. Mast et al.	(LBL) IJP
CHAN	72	PRL 28 256	S.B. Chan et al.	(MASA, YALE)
BURKHARDT	71	NP B27 64	E. Burkhardt et al.	(HEID, CERN, SACL)
KIM	71	PRL 27 356	J.K. Kim	(HARV) IJP
Also	70	Duke Conf. 161	J.K. Kim	(HARV) IJP
BARBARO...	69B	Lund Conf. 352	A. Barbaro-Galiteri et al.	(LRL)
Also	70	Duke Conf. 95	Tripp	(LRL)
BURKHARDT	69	NP B14 106	E. Burkhardt et al.	(HEID, EFI, CERN+)
MAST	68B	PRL 21 1715	T.S. Mast et al.	(LRL)
SCHUEER	68	NP B8 503	J.C. Schueer et al.	(SABRE Collab.)
DAHL	67	PR 163 1377	O.I. Dahl et al.	(LRL)
DAUBER	67	PL 24B 525	P.M. Dauber et al.	(UCLA)
UHLIG	67	PR 155 1448	R.P. Uhlig et al.	(UMD, NRL)
BIRMINGHAM	66	PR 152 1148	Birmingham	(BIRM, GLAS, LOIC, OXF, RHEL)
ARMENTEROS 65C	PL 19 338		R. Armenteros et al.	(CERN, HEID, SACL)
MUSGRAVE	65	NC 35 735	B. Musgrave et al.	(BIRM, CERN, EPOL+)
WATSON	63	PR 131 2248	M.B. Watson, M. Ferro-Luzzi, R.D. Tripp	(LRL) IJP
FERRO-LUZZI	62	PRL 8 28	M. Ferro-Luzzi, R.D. Tripp, M.B. Watson	(LRL) IJP

 $\Lambda(1600) P_{01}$

$$J(P) = 0(\frac{1}{2}^+) \text{ Status: } ***$$

See also the $\Lambda(1810) P_{01}$. There are quite possibly two P_{01} states in this region.

 $\Lambda(1600)$ MASS

VALUE (MeV)	DOCUMENT ID	TECN	COMMENT
1560 to 1700 (≈ 1600) OUR ESTIMATE			
1568 ± 20	GOPAL	80	DPWA $\bar{K}N \rightarrow \bar{K}N$
1703 ± 100	ALSTON...	78	DPWA $\bar{K}N \rightarrow \bar{K}N$
1573 ± 25	GOPAL	77	DPWA $\bar{K}N$ multichannel
1596 ± 6	KANE	74	DPWA $K^- p \rightarrow \Sigma\pi$
1620 ± 10	LANGBEIN	72	IPWA $\bar{K}N$ multichannel
• • • We do not use the following data for averages, fits, limits, etc. • • •			
1572 or 1617	¹ MARTIN	77	DPWA $\bar{K}N$ multichannel
1646 ± 7	² CARROLL	76	DPWA Isospin-0 total σ
1570	KIM	71	DPWA K-matrix analysis

 $\Lambda(1600)$ WIDTH

VALUE (MeV)	DOCUMENT ID	TECN	COMMENT
50 to 250 (≈ 150) OUR ESTIMATE			
116 ± 20	GOPAL	80	DPWA $\bar{K}N \rightarrow \bar{K}N$
593 ± 200	ALSTON...	78	DPWA $\bar{K}N \rightarrow \bar{K}N$
147 ± 50	GOPAL	77	DPWA $\bar{K}N$ multichannel
175 ± 20	KANE	74	DPWA $K^- p \rightarrow \Sigma\pi$
60 ± 10	LANGBEIN	72	IPWA $\bar{K}N$ multichannel
• • • We do not use the following data for averages, fits, limits, etc. • • •			
247 or 271	¹ MARTIN	77	DPWA $\bar{K}N$ multichannel
20	² CARROLL	76	DPWA Isospin-0 total σ
50	KIM	71	DPWA K-matrix analysis

 $\Lambda(1600)$ DECAY MODES

Mode	Fraction (Γ_i/Γ)
Γ_1 $N\bar{K}$	15-30 %
Γ_2 $\Sigma\pi$	10-60 %

The above branching fractions are our estimates, not fits or averages.

 $\Lambda(1600)$ BRANCHING RATIOS

See "Sign conventions for resonance couplings" in the Note on Λ and Σ Resonances.

 $\Gamma(N\bar{K})/\Gamma_{total}$

VALUE	DOCUMENT ID	TECN	COMMENT
0.15 to 0.30 OUR ESTIMATE			
0.23 ± 0.04	GOPAL	80	DPWA $\bar{K}N \rightarrow \bar{K}N$
0.14 ± 0.05	ALSTON...	78	DPWA $\bar{K}N \rightarrow \bar{K}N$
0.25 ± 0.15	LANGBEIN	72	IPWA $\bar{K}N$ multichannel
• • • We do not use the following data for averages, fits, limits, etc. • • •			
0.24 ± 0.04	GOPAL	77	DPWA See GOPAL 80
0.30 or 0.29	¹ MARTIN	77	DPWA $\bar{K}N$ multichannel

See key on page 239

Baryon Particle Listings

$\Lambda(1600)$, $\Lambda(1670)$, $\Lambda(1690)$

$(\Gamma_1 \Gamma_2)^{1/2} / \Gamma_{\text{total}}$ in $N\bar{K} \rightarrow \Lambda(1600) \rightarrow \Sigma \pi$		$(\Gamma_1 \Gamma_2)^{1/2} / \Gamma$	
VALUE	DOCUMENT ID	TECN	COMMENT
-0.16 ± 0.04	GOPAL 77	DPWA	$\bar{K}N$ multichannel
-0.33 ± 0.11	KANE 74	DPWA	$K^- p \rightarrow \Sigma \pi$
0.28 ± 0.09	LANGBEIN 72	IPWA	$\bar{K}N$ multichannel
• • • We do not use the following data for averages, fits, limits, etc. • • •			
-0.39 or -0.39	¹ MARTIN 77	DPWA	$\bar{K}N$ multichannel
not seen	HEPP 76B	DPWA	$K^- N \rightarrow \Sigma \pi$

$\Lambda(1600)$ FOOTNOTES

- ¹ The two MARTIN 77 values are from a T-matrix pole and from a Breit-Wigner fit.
² A total cross-section bump with $(J+1/2) \Gamma_{\text{el}} / \Gamma_{\text{total}} = 0.04$.

$\Lambda(1600)$ REFERENCES

GOPAL 80	Toronto Conf. 159	G.P. Gopal	(RHEL) IJP
ALSTON... 78	PR D18 182	M. Alston-Garnjost et al.	(LBL, MTHO+) IJP
Also 77	PRL 38 1007	M. Alston-Garnjost et al.	(LBL, MTHO+) IJP
GOPAL 77	NP B119 362	G.P. Gopal et al.	(LOIC, RHEL) IJP
MARTIN 77	NP B127 349	B.R. Martin, M.K. Pidcock, R.G. Moorhouse	(LOUC+) IJP
Also 77B	NP B126 266	B.R. Martin, M.K. Pidcock	(LOUC)
Also 77C	NP B126 285	B.R. Martin, M.K. Pidcock	(LOUC) IJP
CARROLL 76	PRL 37 806	A.S. Carroll et al.	(BNL) I
HEPP 76B	PL 65B 487	V. Hepp et al.	(CERN, HEIDH, MPIM) IJP
KANE 74	LBL-2452	D.F. Kane	(LBL) IJP
LANGBEIN 72	NP B47 477	W. Langbein, F. Wagner	(MPIM) IJP
KIM 71	PRL 27 356	J.K. Kim	(HARV) IJP

$\Lambda(1670) S_{01}$

$$I(J^P) = 0(\frac{1}{2}^-) \text{ Status: } ***$$

The measurements of the mass, width, and elasticity published before 1974 are now obsolete and have been omitted. They were last listed in our 1982 edition Physics Letters **111B** (1982).

$\Lambda(1670)$ MASS

VALUE (MeV)	DOCUMENT ID	TECN	COMMENT
1660 to 1680 (≈ 1670) OUR ESTIMATE			
1670.8 ± 1.7	KOISO 85	DPWA	$K^- p \rightarrow \Sigma \pi$
1667 ± 5	GOPAL 80	DPWA	$\bar{K}N \rightarrow \bar{K}N$
1671 ± 3	ALSTON... 78	DPWA	$\bar{K}N \rightarrow \bar{K}N$
1670 ± 5	GOPAL 77	DPWA	$\bar{K}N$ multichannel
1675 ± 2	HEPP 76B	DPWA	$K^- N \rightarrow \Sigma \pi$
1679 ± 1	KANE 74	DPWA	$K^- p \rightarrow \Sigma \pi$
1665 ± 5	PREVOST 74	DPWA	$K^- N \rightarrow \Sigma(1385) \pi$
• • • We do not use the following data for averages, fits, limits, etc. • • •			
1669 ± 2	ABAEV 96	DPWA	$\pi^- p \rightarrow \eta n$
1664	¹ MARTIN 77	DPWA	$\bar{K}N$ multichannel

$\Lambda(1670)$ WIDTH

VALUE (MeV)	DOCUMENT ID	TECN	COMMENT
25 to 50 (≈ 35) OUR ESTIMATE			
34.1 ± 3.7	KOISO 85	DPWA	$K^- p \rightarrow \Sigma \pi$
29 ± 5	GOPAL 80	DPWA	$\bar{K}N \rightarrow \bar{K}N$
29 ± 5	ALSTON... 78	DPWA	$\bar{K}N \rightarrow \bar{K}N$
45 ± 10	GOPAL 77	DPWA	$\bar{K}N$ multichannel
46 ± 5	HEPP 76B	DPWA	$K^- N \rightarrow \Sigma \pi$
40 ± 3	KANE 74	DPWA	$K^- p \rightarrow \Sigma \pi$
19 ± 5	PREVOST 74	DPWA	$K^- N \rightarrow \Sigma(1385) \pi$
• • • We do not use the following data for averages, fits, limits, etc. • • •			
21 ± 4	ABAEV 96	DPWA	$\pi^- p \rightarrow \eta n$
12	¹ MARTIN 77	DPWA	$\bar{K}N$ multichannel

$\Lambda(1670)$ DECAY MODES

Mode	Fraction (Γ_i / Γ)
Γ_1 $N\bar{K}$	15–25 %
Γ_2 $\Sigma \pi$	20–60 %
Γ_3 $\Lambda \eta$	15–35 %
Γ_4 $\Sigma(1385) \pi$	

The above branching fractions are our estimates, not fits or averages.

$\Lambda(1670)$ BRANCHING RATIOS

See "Sign conventions for resonance couplings" in the Note on Λ and Σ Resonances.

$\Gamma(N\bar{K}) / \Gamma_{\text{total}}$		Γ_1 / Γ	
VALUE	DOCUMENT ID	TECN	COMMENT
0.15 to 0.25 OUR ESTIMATE			
0.18 ± 0.03	GOPAL 80	DPWA	$\bar{K}N \rightarrow \bar{K}N$
0.17 ± 0.03	ALSTON... 78	DPWA	$\bar{K}N \rightarrow \bar{K}N$
• • • We do not use the following data for averages, fits, limits, etc. • • •			
0.20 ± 0.03	GOPAL 77	DPWA	See GOPAL 80
0.15	¹ MARTIN 77	DPWA	$\bar{K}N$ multichannel

$(\Gamma_1 \Gamma_2)^{1/2} / \Gamma_{\text{total}}$ in $N\bar{K} \rightarrow \Lambda(1670) \rightarrow \Sigma \pi$		$(\Gamma_1 \Gamma_2)^{1/2} / \Gamma$	
VALUE	DOCUMENT ID	TECN	COMMENT
-0.26 ± 0.02	KOISO 85	DPWA	$K^- p \rightarrow \Sigma \pi$
-0.31 ± 0.03	GOPAL 77	DPWA	$\bar{K}N$ multichannel
-0.29 ± 0.03	HEPP 76B	DPWA	$K^- N \rightarrow \Sigma \pi$
-0.23 ± 0.03	LONDON 75	HLBC	$K^- p \rightarrow \Sigma^0 \pi^0$
-0.27 ± 0.02	KANE 74	DPWA	$K^- p \rightarrow \Sigma \pi$
• • • We do not use the following data for averages, fits, limits, etc. • • •			
-0.13	¹ MARTIN 77	DPWA	$\bar{K}N$ multichannel

$(\Gamma_1 \Gamma_2)^{1/2} / \Gamma_{\text{total}}$ in $N\bar{K} \rightarrow \Lambda(1670) \rightarrow \Lambda \eta$		$(\Gamma_1 \Gamma_2)^{1/2} / \Gamma$	
VALUE	DOCUMENT ID	TECN	COMMENT
+0.20 ± 0.05	BAXTER 73	DPWA	$K^- p \rightarrow$ neutrals
• • • We do not use the following data for averages, fits, limits, etc. • • •			
0.06	ABAEV 96	DPWA	$\pi^- p \rightarrow \eta n$
0.24	KIM 71	DPWA	K-matrix analysis
0.26	ARMENTEROS69C	HBC	
0.20 or 0.23	BERLEY 65	HBC	

$(\Gamma_1 \Gamma_2)^{1/2} / \Gamma_{\text{total}}$ in $N\bar{K} \rightarrow \Lambda(1670) \rightarrow \Sigma(1385) \pi$		$(\Gamma_1 \Gamma_2)^{1/2} / \Gamma$	
VALUE	DOCUMENT ID	TECN	COMMENT
-0.18 ± 0.05	PREVOST 74	DPWA	$K^- N \rightarrow \Sigma(1385) \pi$

$\Lambda(1670)$ FOOTNOTES

- ¹ MARTIN 77 obtains identical resonance parameters from a T-matrix pole and from a Breit-Wigner fit.

$\Lambda(1670)$ REFERENCES

ABAEV 96	PR C53 385	V.V. Aboev, B.M.K. Nefkens	(UCLA)
KOISO 85	NP A433 619	H. Koiso et al.	(TOKY, MASA)
PDG 82	PL 111B	M. Roos et al.	(HELS, CIT, CERN)
GOPAL 80	Toronto Conf. 159	G.P. Gopal	(RHEL) IJP
ALSTON... 78	PR D18 182	M. Alston-Garnjost et al.	(LBL, MTHO+) IJP
Also 77	PRL 38 1007	M. Alston-Garnjost et al.	(LBL, MTHO+) IJP
GOPAL 77	NP B119 362	G.P. Gopal et al.	(LOIC, RHEL) IJP
MARTIN 77	NP B127 349	B.R. Martin, M.K. Pidcock, R.G. Moorhouse	(LOUC+) IJP
Also 77B	NP B126 266	B.R. Martin, M.K. Pidcock	(LOUC)
Also 77C	NP B126 285	B.R. Martin, M.K. Pidcock	(LOUC) IJP
HEPP 76B	PL 65B 487	V. Hepp et al.	(CERN, HEIDH, MPIM) IJP
LONDON 75	NP B85 289	G.W. London et al.	(BNL, CERN, EPOL+)
KANE 74	LBL-2452	D.F. Kane	(LBL) IJP
PREVOST 74	NP B69 246	J. Prevost et al.	(SACL, CERN, HEIO)
BAXTER 73	NP B67 125	D.F. Baxter et al.	(OXF) IJP
KIM 71	PRL 27 356	J.K. Kim	(HARV) IJP
Also 70	Duke Conf. 161	J.K. Kim	(HARV) IJP
ARMENTEROS 69C	Lund Paper 229	R. Armenteros et al.	(CERN, HEIO, SACL) IJP
Values are quoted in LEVI-SETTI 69.			
BERLEY 65	PRL 15 641	D. Berley et al.	(BNL) IJP

$\Lambda(1690) D_{03}$

$$I(J^P) = 0(\frac{3}{2}^-) \text{ Status: } ***$$

The measurements of the mass, width, and elasticity published before 1974 are now obsolete and have been omitted. They were last listed in our 1982 edition Physics Letters **111B** (1982).

$\Lambda(1690)$ MASS

VALUE (MeV)	DOCUMENT ID	TECN	COMMENT
1685 to 1695 (≈ 1690) OUR ESTIMATE			
1695.7 ± 2.6	KOISO 85	DPWA	$K^- p \rightarrow \Sigma \pi$
1690 ± 5	GOPAL 80	DPWA	$\bar{K}N \rightarrow \bar{K}N$
1692 ± 5	ALSTON... 78	DPWA	$\bar{K}N \rightarrow \bar{K}N$
1690 ± 5	GOPAL 77	DPWA	$\bar{K}N$ multichannel
1690 ± 3	HEPP 76B	DPWA	$K^- N \rightarrow \Sigma \pi$
1689 ± 1	KANE 74	DPWA	$K^- p \rightarrow \Sigma \pi$
• • • We do not use the following data for averages, fits, limits, etc. • • •			
1687 or 1689	¹ MARTIN 77	DPWA	$\bar{K}N$ multichannel
1692 ± 4	CARROLL 76	DPWA	Isospin-0 total σ

$\Lambda(1690)$ WIDTH

VALUE (MeV)	DOCUMENT ID	TECN	COMMENT
50 to 70 (≈ 60) OUR ESTIMATE			
67.2 ± 5.6	KOISO 85	DPWA	$K^- p \rightarrow \Sigma \pi$
61 ± 5	GOPAL 80	DPWA	$\bar{K}N \rightarrow \bar{K}N$
64 ± 10	ALSTON... 78	DPWA	$\bar{K}N \rightarrow \bar{K}N$
60 ± 5	GOPAL 77	DPWA	$\bar{K}N$ multichannel
82 ± 8	HEPP 76B	DPWA	$K^- N \rightarrow \Sigma \pi$
60 ± 4	KANE 74	DPWA	$K^- p \rightarrow \Sigma \pi$
• • • We do not use the following data for averages, fits, limits, etc. • • •			
62 or 62	¹ MARTIN 77	DPWA	$\bar{K}N$ multichannel
38	CARROLL 76	DPWA	Isospin-0 total σ

Baryon Particle Listings

 $\Lambda(1690)$, $\Lambda(1800)$ $\Lambda(1690)$ DECAY MODES

Mode	Fraction (Γ_i/Γ)
Γ_1 $N\bar{K}$	20-30 %
Γ_2 $\Sigma\pi$	20-40 %
Γ_3 $\Lambda\pi\pi$	~ 25 %
Γ_4 $\Sigma\pi\pi$	~ 20 %
Γ_5 $\Lambda\eta$	
Γ_6 $\Sigma(1385)\pi$, S-wave	

The above branching fractions are our estimates, not fits or averages.

 $\Lambda(1690)$ BRANCHING RATIOS

The sum of all the quoted branching ratios is more than 1.0. The two-body ratios are from partial-wave analyses, and thus probably are more reliable than the three-body ratios, which are determined from bumps in cross sections. Of the latter, the $\Sigma\pi\pi$ bump looks more significant. (The error given for the $\Lambda\pi\pi$ ratio looks unreasonably small.) Hardly any of the $\Sigma\pi\pi$ decay can be via $\Sigma(1385)$, for then seven times as much $\Lambda\pi\pi$ decay would be required. See "Sign conventions for resonance couplings" in the Note on Λ and Σ Resonances.

$\Gamma(N\bar{K})/\Gamma_{\text{total}}$	VALUE	DOCUMENT ID	TECN	COMMENT	Γ_1/Γ
0.2 to 0.3 OUR ESTIMATE					
0.23 ± 0.03		GOPAL	80	DPWA $\bar{K}N \rightarrow \bar{K}N$	
0.22 ± 0.03		ALSTON-...	78	DPWA $\bar{K}N \rightarrow \bar{K}N$	
• • • We do not use the following data for averages, fits, limits, etc. • • •					
0.24 ± 0.03		GOPAL	77	DPWA See GOPAL 80	
0.28 or 0.26		¹ MARTIN	77	DPWA $\bar{K}N$ multichannel	

$(\Gamma_1\Gamma_2)^{1/2}/\Gamma_{\text{total}}$ in $N\bar{K} \rightarrow \Lambda(1690) \rightarrow \Sigma\pi$	VALUE	DOCUMENT ID	TECN	COMMENT	$(\Gamma_1\Gamma_2)^{1/2}/\Gamma$
-0.34 ± 0.02		KOISO	85	DPWA $K^-p \rightarrow \Sigma\pi$	
-0.25 ± 0.03		GOPAL	77	DPWA $\bar{K}N$ multichannel	
-0.29 ± 0.03		HEPP	76b	DPWA $K^-N \rightarrow \Sigma\pi$	
-0.28 ± 0.03		LONDON	75	HLBC $K^-p \rightarrow \Sigma^0\pi^0$	
-0.28 ± 0.02		KANE	74	DPWA $K^-p \rightarrow \Sigma\pi$	
• • • We do not use the following data for averages, fits, limits, etc. • • •					
-0.30 or -0.28		¹ MARTIN	77	DPWA $\bar{K}N$ multichannel	

$(\Gamma_1\Gamma_5)^{1/2}/\Gamma_{\text{total}}$ in $N\bar{K} \rightarrow \Lambda(1690) \rightarrow \Lambda\eta$	VALUE	DOCUMENT ID	TECN	COMMENT	$(\Gamma_1\Gamma_5)^{1/2}/\Gamma$
0.00 ± 0.03		BAXTER	73	DPWA $K^-p \rightarrow$ neutrals	

$(\Gamma_1\Gamma_3)^{1/2}/\Gamma_{\text{total}}$ in $N\bar{K} \rightarrow \Lambda(1690) \rightarrow \Lambda\pi\pi$	VALUE	DOCUMENT ID	TECN	COMMENT	$(\Gamma_1\Gamma_3)^{1/2}/\Gamma$
0.25 ± 0.02		² BARTLEY	68	HDBC $K^-p \rightarrow \Lambda\pi\pi$	

$(\Gamma_1\Gamma_7)^{1/2}/\Gamma_{\text{total}}$ in $N\bar{K} \rightarrow \Lambda(1690) \rightarrow \Sigma\pi\pi$	VALUE	DOCUMENT ID	TECN	COMMENT	$(\Gamma_1\Gamma_7)^{1/2}/\Gamma$
0.21		ARMENTEROS68c	HDBC	$K^-N \rightarrow \Sigma\pi\pi$	

$(\Gamma_1\Gamma_6)^{1/2}/\Gamma_{\text{total}}$ in $N\bar{K} \rightarrow \Lambda(1690) \rightarrow \Sigma(1385)\pi$, S-wave	VALUE	DOCUMENT ID	TECN	COMMENT	$(\Gamma_1\Gamma_6)^{1/2}/\Gamma$
+0.27 ± 0.04		PREVOST	74	DPWA $K^-N \rightarrow \Sigma(1385)\pi$	

 $\Lambda(1690)$ FOOTNOTES

- ¹ The two MARTIN 77 values are from a T-matrix pole and from a Breit-Wigner fit. Another D_{03} Λ at 1966 MeV is also suggested by MARTIN 77, but is very uncertain.
² BARTLEY 68 uses only cross-section data. The enhancement is not seen by PREVOST 71.

 $\Lambda(1690)$ REFERENCES

KOISO 85	NP A433 619	H. Koiso et al.	(TOKY, MASA)
FDG 82	PL 111B	M. Roos et al.	(HELS. CIT., CERN)
GOPAL 80	Toronto Conf. 159	G.P. Gopal	(RHEL) IJP
ALSTON-... 78	PR D18 182	M. Alston-Garnjost et al.	(LBL, MTHO+) IJP
Also 77	PRL 38 1007	M. Alston-Garnjost et al.	(LBL, MTHO+) IJP
GOPAL 77	NP B119 362	G.P. Gopal et al.	(LOIC, RHEL) IJP
MARTIN 77	NP B127 349	B.R. Martin, M.K. Pidcock, R.G. Moorhouse	(LOUC+) IJP
Also 77b	NP B126 266	B.R. Martin, M.K. Pidcock	(LOUC) IJP
Also 77c	NP B126 285	B.R. Martin, M.K. Pidcock	(LOUC) IJP
CARROLL 76b	PRL 37 806	A.S. Carroll et al.	(BNL) I
HEPP 76b	PL 65B 487	V. Hepp et al.	(CERN, HEIDH, MPH) IJP
LONDON 75	NP B85 289	G.W. London et al.	(BNL, CERN, EPOL+) IJP
KANE 74	LBL-2452	D.F. Kane	(LBL) IJP
PREVOST 74	NP B69 245	J. Prevost et al.	(SACL, CERN, HEID)
BAXTER 73	NP B67 125	D.F. Baxter et al.	(OXF) IJP
PREVOST 71	Amsterdam Conf.	J. Prevost	(CERN, HEID, SACL)
ARMENTEROS 68c	NP B8 216	R. Armenteros et al.	(CERN, HEID, SACL) I
BARTLEY 68	PRL 21 1111	J.H. Bartley et al.	(TUFTS, FSU, BRAN) I

 $\Lambda(1800) S_{01}$

$$I(J^P) = 0(\frac{1}{2}^-) \text{ Status: } ***$$

This is the second resonance in the S_{01} wave, the first being the $\Lambda(1670)$.

 $\Lambda(1800)$ MASS

VALUE (MeV)	DOCUMENT ID	TECN	COMMENT
1720 to 1850 (≈ 1800) OUR ESTIMATE			
1841 ± 10	GOPAL	80	DPWA $\bar{K}N \rightarrow \bar{K}N$
1725 ± 20	ALSTON-...	78	DPWA $\bar{K}N \rightarrow \bar{K}N$
1825 ± 20	GOPAL	77	DPWA $\bar{K}N$ multichannel
1830 ± 20	LANGBEIN	72	IPWA $\bar{K}N$ multichannel
• • • We do not use the following data for averages, fits, limits, etc. • • •			
1767 or 1842	¹ MARTIN	77	DPWA $\bar{K}N$ multichannel
1780	KIM	71	DPWA K-matrix analysis
1872 ± 10	BRICMAN	70b	DPWA $\bar{K}N \rightarrow \bar{K}N$

 $\Lambda(1800)$ WIDTH

VALUE (MeV)	DOCUMENT ID	TECN	COMMENT
200 to 400 (≈ 300) OUR ESTIMATE			
228 ± 20	GOPAL	80	DPWA $\bar{K}N \rightarrow \bar{K}N$
185 ± 20	ALSTON-...	78	DPWA $\bar{K}N \rightarrow \bar{K}N$
230 ± 20	GOPAL	77	DPWA $\bar{K}N$ multichannel
70 ± 15	LANGBEIN	72	IPWA $\bar{K}N$ multichannel
• • • We do not use the following data for averages, fits, limits, etc. • • •			
435 or 473	¹ MARTIN	77	DPWA $\bar{K}N$ multichannel
40	KIM	71	DPWA K-matrix analysis
100 ± 20	BRICMAN	70b	DPWA $\bar{K}N \rightarrow \bar{K}N$

 $\Lambda(1800)$ DECAY MODES

Mode	Fraction (Γ_i/Γ)
Γ_1 $N\bar{K}$	25-40 %
Γ_2 $\Sigma\pi$	seen
Γ_3 $\Sigma(1385)\pi$	seen
Γ_4 $N\bar{K}^*(892)$	seen
Γ_5 $N\bar{K}^*(892)$, S=1/2, S-wave	
Γ_6 $N\bar{K}^*(892)$, S=3/2, D-wave	

The above branching fractions are our estimates, not fits or averages.

 $\Lambda(1800)$ BRANCHING RATIOS

See "Sign conventions for resonance couplings" in the Note on Λ and Σ Resonances.

$\Gamma(N\bar{K})/\Gamma_{\text{total}}$	VALUE	DOCUMENT ID	TECN	COMMENT	Γ_1/Γ
0.25 to 0.40 OUR ESTIMATE					
0.36 ± 0.04		GOPAL	80	DPWA $\bar{K}N \rightarrow \bar{K}N$	
0.28 ± 0.05		ALSTON-...	78	DPWA $\bar{K}N \rightarrow \bar{K}N$	
0.35 ± 0.15		LANGBEIN	72	IPWA $\bar{K}N$ multichannel	
• • • We do not use the following data for averages, fits, limits, etc. • • •					
0.37 ± 0.05		GOPAL	77	DPWA See GOPAL 80	
1.21 or 0.70		¹ MARTIN	77	DPWA $\bar{K}N$ multichannel	
0.80		KIM	71	DPWA K-matrix analysis	
0.18 ± 0.02		BRICMAN	70b	DPWA $\bar{K}N \rightarrow \bar{K}N$	

$(\Gamma_1\Gamma_2)^{1/2}/\Gamma_{\text{total}}$ in $N\bar{K} \rightarrow \Lambda(1800) \rightarrow \Sigma\pi$	VALUE	DOCUMENT ID	TECN	COMMENT	$(\Gamma_1\Gamma_2)^{1/2}/\Gamma$
-0.08 ± 0.05		GOPAL	77	DPWA $\bar{K}N$ multichannel	
• • • We do not use the following data for averages, fits, limits, etc. • • •					
-0.74 or -0.43		¹ MARTIN	77	DPWA $\bar{K}N$ multichannel	
0.24		KIM	71	DPWA K-matrix analysis	

$(\Gamma_1\Gamma_3)^{1/2}/\Gamma_{\text{total}}$ in $N\bar{K} \rightarrow \Lambda(1800) \rightarrow \Sigma(1385)\pi$	VALUE	DOCUMENT ID	TECN	COMMENT	$(\Gamma_1\Gamma_3)^{1/2}/\Gamma$
+0.056 ± 0.028		² CAMERON	78	DPWA $K^-p \rightarrow \Sigma(1385)\pi$	

$(\Gamma_1\Gamma_5)^{1/2}/\Gamma_{\text{total}}$ in $N\bar{K} \rightarrow \Lambda(1800) \rightarrow N\bar{K}^*(892)$, S=1/2, S-wave	VALUE	DOCUMENT ID	TECN	COMMENT	$(\Gamma_1\Gamma_5)^{1/2}/\Gamma$
-0.17 ± 0.03		² CAMERON	78b	DPWA $K^-p \rightarrow N\bar{K}^*$	

$(\Gamma_1\Gamma_6)^{1/2}/\Gamma_{\text{total}}$ in $N\bar{K} \rightarrow \Lambda(1800) \rightarrow N\bar{K}^*(892)$, S=3/2, D-wave	VALUE	DOCUMENT ID	TECN	COMMENT	$(\Gamma_1\Gamma_6)^{1/2}/\Gamma$
-0.13 ± 0.04		CAMERON	78b	DPWA $K^-p \rightarrow N\bar{K}^*$	

See key on page 239

Baryon Particle Listings

$\Lambda(1800)$, $\Lambda(1810)$, $\Lambda(1820)$

 $\Lambda(1800)$ FOOTNOTES

- ¹ The two MARTIN 77 values are from a T-matrix pole and from a Breit-Wigner fit.
² The published sign has been changed to be in accord with the baryon-first convention.

 $\Lambda(1800)$ REFERENCES

NAME	REF	CONF	TECH	COMMENT
GOPAL	80	Toronto Conf. 159	DPWA	$\bar{K}N \rightarrow \bar{K}N$ (RHEL) IJP
ALSTON...	78	PR D18 182	IPWA	$\bar{K}N \rightarrow \bar{K}N$ (LBL, MTHIO+) IJP
Also	77	PRL 38 1007	IPWA	$\bar{K}N \rightarrow \bar{K}N$ (LBL, MTHIO+) IJP
CAMERON	78	NP B143 189	DPWA	$\bar{K}N \rightarrow \bar{K}N$ (RHEL, LOIC) IJP
CAMERON	78B	NP B146 327	DPWA	$\bar{K}N \rightarrow \bar{K}N$ (RHEL, LOIC) IJP
GOPAL	77	NP B119 362	DPWA	$\bar{K}N \rightarrow \bar{K}N$ (LOIC, RHEL) IJP
MARTIN	77	NP B127 349	DPWA	$\bar{K}N \rightarrow \bar{K}N$ (LOUC+) IJP
Also	77B	NP B126 266	DPWA	$\bar{K}N \rightarrow \bar{K}N$ (LOUC) IJP
Also	77C	NP B126 285	DPWA	$\bar{K}N \rightarrow \bar{K}N$ (LOUC) IJP
LANGBEIN	72	NP B47 477	IPWA	$\bar{K}N \rightarrow \bar{K}N$ (MPHM) IJP
KIM	71	PRL 27 356	IPWA	$\bar{K}N \rightarrow \bar{K}N$ (HARV) IJP
Also	70	Duke Conf. 161	IPWA	$\bar{K}N \rightarrow \bar{K}N$ (HARV) IJP
BRICMAN	70B	PL 33B 511	IPWA	$\bar{K}N \rightarrow \bar{K}N$ (CERN) IJP

 $\Lambda(1810) P_{01}$

$$I(J^P) = 0(\frac{1}{2}^+)$$
 Status: ***

Almost all the recent analyses contain a P_{01} state, and sometimes two of them, but the masses, widths, and branching ratios vary greatly. See also the $\Lambda(1600) P_{01}$.

 $\Lambda(1810)$ MASS

VALUE (MeV)	DOCUMENT ID	TECN	COMMENT
1750 to 1850 (≈ 1810) OUR ESTIMATE			
1841 \pm 20	GOPAL 80	DPWA	$\bar{K}N \rightarrow \bar{K}N$
1853 \pm 20	GOPAL 77	DPWA	$\bar{K}N$ multichannel
1735 \pm 5	CARROLL 76	DPWA	Isospin-0 total σ
1746 \pm 10	PREVOST 74	DPWA	$K^-N \rightarrow \Sigma(1385)\pi$
1780 \pm 20	LANGBEIN 72	IPWA	$\bar{K}N$ multichannel
• • • We do not use the following data for averages, fits, limits, etc. • • •			
1861 or 1953	¹ MARTIN 77	DPWA	$\bar{K}N$ multichannel
1755	KIM 71	DPWA	K-matrix analysis
1800	ARMENTEROS70	HBC	$\bar{K}N \rightarrow \bar{K}N$
1750	ARMENTEROS70	HBC	$\bar{K}N \rightarrow \Sigma\pi$
1690 \pm 10	BARBARO... 70	HBC	$\bar{K}N \rightarrow \Sigma\pi$
1740	BAILEY 69	DPWA	$\bar{K}N \rightarrow \bar{K}N$
1745	ARMENTEROS68B	HBC	$\bar{K}N \rightarrow \bar{K}N$

 $\Lambda(1810)$ WIDTH

VALUE (MeV)	DOCUMENT ID	TECN	COMMENT
50 to 250 (≈ 150) OUR ESTIMATE			
164 \pm 20	GOPAL 80	DPWA	$\bar{K}N \rightarrow \bar{K}N$
90 \pm 20	CAMERON 78B	DPWA	$K^-p \rightarrow N\bar{K}^*$
166 \pm 20	GOPAL 77	DPWA	$\bar{K}N$ multichannel
46 \pm 20	PREVOST 74	DPWA	$K^-N \rightarrow \Sigma(1385)\pi$
120 \pm 10	LANGBEIN 72	IPWA	$\bar{K}N$ multichannel
• • • We do not use the following data for averages, fits, limits, etc. • • •			
535 or 585	¹ MARTIN 77	DPWA	$\bar{K}N$ multichannel
28	CARROLL 76	DPWA	Isospin-0 total σ
35	KIM 71	DPWA	K-matrix analysis
30	ARMENTEROS70	HBC	$\bar{K}N \rightarrow \bar{K}N$
70	ARMENTEROS70	HBC	$\bar{K}N \rightarrow \Sigma\pi$
22	BARBARO... 70	HBC	$\bar{K}N \rightarrow \Sigma\pi$
300	BAILEY 69	DPWA	$\bar{K}N \rightarrow \bar{K}N$
147	ARMENTEROS68B	HBC	

 $\Lambda(1810)$ DECAY MODES

Mode	Fraction (Γ_i/Γ)
Γ_1 $N\bar{K}$	20–50 %
Γ_2 $\Sigma\pi$	10–40 %
Γ_3 $\Sigma(1385)\pi$	seen
Γ_4 $N\bar{K}^*(892)$	30–60 %
Γ_5 $N\bar{K}^*(892), S=1/2, P\text{-wave}$	
Γ_6 $N\bar{K}^*(892), S=3/2, P\text{-wave}$	

The above branching fractions are our estimates, not fits or averages.

 $\Lambda(1810)$ BRANCHING RATIOS

See "Sign conventions for resonance couplings" in the Note on Λ and Σ Resonances.

$\Gamma(N\bar{K})/\Gamma_{\text{total}}$	DOCUMENT ID	TECN	COMMENT	Γ_1/Γ
0.24 to 0.5 OUR ESTIMATE				
0.24 \pm 0.04	GOPAL 80	DPWA	$\bar{K}N \rightarrow \bar{K}N$	
0.36 \pm 0.05	LANGBEIN 72	IPWA	$\bar{K}N$ multichannel	
• • • We do not use the following data for averages, fits, limits, etc. • • •				
0.21 \pm 0.04	GOPAL 77	DPWA	See GOPAL 80	
0.52 or 0.49	¹ MARTIN 77	DPWA	$\bar{K}N$ multichannel	
0.30	KIM 71	DPWA	K-matrix analysis	
0.15	ARMENTEROS70	DPWA	$\bar{K}N \rightarrow \bar{K}N$	
0.55	BAILEY 69	DPWA	$\bar{K}N \rightarrow \bar{K}N$	
0.4	ARMENTEROS68B	DPWA	$\bar{K}N \rightarrow \bar{K}N$	

$(\Gamma_1\Gamma_2)^{1/2}/\Gamma_{\text{total}}$ in $N\bar{K} \rightarrow \Lambda(1810) \rightarrow \Sigma\pi$	DOCUMENT ID	TECN	COMMENT	$(\Gamma_1\Gamma_2)^{1/2}/\Gamma$
-0.24 \pm 0.04	GOPAL 77	DPWA	$\bar{K}N$ multichannel	
• • • We do not use the following data for averages, fits, limits, etc. • • •				
+0.25 or +0.23	¹ MARTIN 77	DPWA	$\bar{K}N$ multichannel	
< 0.01	LANGBEIN 72	IPWA	$\bar{K}N$ multichannel	
0.17	KIM 71	DPWA	K-matrix analysis	
+0.20	² ARMENTEROS70	DPWA	$\bar{K}N \rightarrow \Sigma\pi$	
-0.13 \pm 0.03	BARBARO... 70	DPWA	$\bar{K}N \rightarrow \Sigma\pi$	

$(\Gamma_1\Gamma_2)^{1/2}/\Gamma_{\text{total}}$ in $N\bar{K} \rightarrow \Lambda(1810) \rightarrow \Sigma(1385)\pi$	DOCUMENT ID	TECN	COMMENT	$(\Gamma_1\Gamma_3)^{1/2}/\Gamma$
-0.18 \pm 0.10	PREVOST 74	DPWA	$K^-N \rightarrow \Sigma(1385)\pi$	

$(\Gamma_1\Gamma_2)^{1/2}/\Gamma_{\text{total}}$ in $N\bar{K} \rightarrow \Lambda(1810) \rightarrow N\bar{K}^*(892), S=1/2, P\text{-wave}$	DOCUMENT ID	TECN	COMMENT	$(\Gamma_1\Gamma_5)^{1/2}/\Gamma$
-0.14 \pm 0.03	² CAMERON 78B	DPWA	$K^-p \rightarrow N\bar{K}^*$	

$(\Gamma_1\Gamma_2)^{1/2}/\Gamma_{\text{total}}$ in $N\bar{K} \rightarrow \Lambda(1810) \rightarrow N\bar{K}^*(892), S=3/2, P\text{-wave}$	DOCUMENT ID	TECN	COMMENT	$(\Gamma_1\Gamma_6)^{1/2}/\Gamma$
+0.35 \pm 0.06	CAMERON 78B	DPWA	$K^-p \rightarrow N\bar{K}^*$	

 $\Lambda(1810)$ FOOTNOTES

- ¹ The two MARTIN 77 values are from a T-matrix pole and from a Breit-Wigner fit.
² The published sign has been changed to be in accord with the baryon-first convention.

 $\Lambda(1810)$ REFERENCES

NAME	REF	CONF	TECH	COMMENT
GOPAL	80	Toronto Conf. 159	DPWA	$\bar{K}N \rightarrow \bar{K}N$ (RHEL) IJP
CAMERON	78B	NP B146 327	DPWA	$\bar{K}N \rightarrow \bar{K}N$ (RHEL, LOIC) IJP
GOPAL	77	NP B119 362	DPWA	$\bar{K}N \rightarrow \bar{K}N$ (LOIC, RHEL) IJP
MARTIN	77	NP B127 349	DPWA	$\bar{K}N \rightarrow \bar{K}N$ (LOUC+) IJP
Also	77B	NP B126 266	DPWA	$\bar{K}N \rightarrow \bar{K}N$ (LOUC) IJP
Also	77C	NP B126 285	DPWA	$\bar{K}N \rightarrow \bar{K}N$ (LOUC) IJP
CARROLL	76	PRL 37 806	DPWA	$\bar{K}N \rightarrow \bar{K}N$ (BNL) IJP
PREVOST	74	NP B59 246	DPWA	$\bar{K}N \rightarrow \bar{K}N$ (SACL, CERN, HEID) IJP
LANGBEIN	72	NP B47 477	IPWA	$\bar{K}N \rightarrow \bar{K}N$ (MPHM) IJP
KIM	71	PRL 27 356	IPWA	$\bar{K}N \rightarrow \bar{K}N$ (HARV) IJP
Also	70	Duke Conf. 161	IPWA	$\bar{K}N \rightarrow \bar{K}N$ (HARV) IJP
ARMENTEROS 70	Duke Conf. 123	IPWA	$\bar{K}N \rightarrow \bar{K}N$ (CERN, HEID, SACL) IJP	
BARBARO... 70	Duke Conf. 173	IPWA	$\bar{K}N \rightarrow \bar{K}N$ (LRL) IJP	
BAILEY 69	Thesis UCRL 50617	IPWA	$\bar{K}N \rightarrow \bar{K}N$ (LLL) IJP	
ARMENTEROS 68B	NP B8 195	IPWA	$\bar{K}N \rightarrow \bar{K}N$ (CERN, HEID, SACL) IJP	

 $\Lambda(1820) F_{05}$

$$I(J^P) = 0(\frac{3}{2}^+)$$
 Status: ***

This resonance is the cornerstone for all partial-wave analyses in this region. Most of the results published before 1973 are now obsolete and have been omitted. They may be found in our 1982 edition Physics Letters **111B** (1982).

Most of the quoted errors are statistical only; the systematic errors due to the particular parametrizations used in the partial-wave analyses are not included. For this reason we do not calculate weighted averages for the mass and width.

 $\Lambda(1820)$ MASS

VALUE (MeV)	DOCUMENT ID	TECN	COMMENT
1815 to 1825 (≈ 1820) OUR ESTIMATE			
1823 \pm 3	GOPAL 80	DPWA	$\bar{K}N \rightarrow \bar{K}N$
1819 \pm 2	ALSTON... 78	DPWA	$\bar{K}N \rightarrow \bar{K}N$
1822 \pm 2	GOPAL 77	DPWA	$\bar{K}N$ multichannel
1821 \pm 2	KANE 74	DPWA	$K^-p \rightarrow \Sigma\pi$
• • • We do not use the following data for averages, fits, limits, etc. • • •			
1830	DECLAIS 77	DPWA	$\bar{K}N \rightarrow \bar{K}N$
1817 or 1819	¹ MARTIN 77	DPWA	$\bar{K}N$ multichannel

Baryon Particle Listings

 $\Lambda(1820)$, $\Lambda(1830)$ $\Lambda(1820)$ WIDTH

VALUE (MeV)	DOCUMENT ID	TECN	COMMENT
70 to 90 (≈ 80) OUR ESTIMATE			
77 \pm 5	GOPAL	80	DPWA $\bar{K}N \rightarrow \bar{K}N$
72 \pm 5	ALSTON...	78	DPWA $\bar{K}N \rightarrow \bar{K}N$
81 \pm 5	GOPAL	77	DPWA $\bar{K}N$ multichannel
87 \pm 3	KANE	74	DPWA $K^- p \rightarrow \Sigma\pi$
••• We do not use the following data for averages, fits, limits, etc. •••			
82	DECLAIS	77	DPWA $\bar{K}N \rightarrow \bar{K}N$
76 or 76	¹ MARTIN	77	DPWA $\bar{K}N$ multichannel

 $\Lambda(1820)$ DECAY MODES

Mode	Fraction (Γ_j/Γ)
Γ_1 $N\bar{K}$	55–65 %
Γ_2 $\Sigma\pi$	8–14 %
Γ_3 $\Sigma(1385)\pi$	5–10 %
Γ_4 $\Sigma(1385)\pi$, P-wave	
Γ_5 $\Sigma(1385)\pi$, F-wave	
Γ_6 $\Lambda\eta$	
Γ_7 $\Sigma\pi\pi$	

The above branching fractions are our estimates, not fits or averages.

 $\Lambda(1820)$ BRANCHING RATIOS

Errors quoted do not include uncertainties in the parametrizations used in the partial-wave analyses and are thus too small. See also "Sign conventions for resonance couplings" in the Note on Λ and Σ Resonances.

$\Gamma(N\bar{K})/\Gamma_{\text{total}}$	DOCUMENT ID	TECN	COMMENT	Γ_1/Γ
0.55 to 0.65 OUR ESTIMATE				
0.58 \pm 0.02	GOPAL	80	DPWA $\bar{K}N \rightarrow \bar{K}N$	
0.60 \pm 0.03	ALSTON...	78	DPWA $\bar{K}N \rightarrow \bar{K}N$	
••• We do not use the following data for averages, fits, limits, etc. •••				
0.51	DECLAIS	77	DPWA $\bar{K}N \rightarrow \bar{K}N$	
0.57 \pm 0.02	GOPAL	77	DPWA See GOPAL 80	
0.59 or 0.58	¹ MARTIN	77	DPWA $\bar{K}N$ multichannel	

$(\Gamma_1\Gamma_2)^{1/2}/\Gamma_{\text{total}}$ in $N\bar{K} \rightarrow \Lambda(1820) \rightarrow \Sigma\pi$	DOCUMENT ID	TECN	COMMENT	$(\Gamma_1\Gamma_2)^{1/2}/\Gamma$
-0.28 \pm 0.03	GOPAL	77	DPWA $\bar{K}N$ multichannel	
-0.28 \pm 0.01	KANE	74	DPWA $K^- p \rightarrow \Sigma\pi$	
••• We do not use the following data for averages, fits, limits, etc. •••				
-0.25 or -0.25	¹ MARTIN	77	DPWA $\bar{K}N$ multichannel	

$(\Gamma_1\Gamma_7)^{1/2}/\Gamma_{\text{total}}$ in $N\bar{K} \rightarrow \Lambda(1820) \rightarrow \Lambda\eta$	DOCUMENT ID	TECN	COMMENT	$(\Gamma_1\Gamma_6)^{1/2}/\Gamma$
-0.096 \pm 0.040	RADER	73	MPWA	
-0.020				

$\Gamma(\Sigma\pi\pi)/\Gamma_{\text{total}}$	DOCUMENT ID	TECN	COMMENT	Γ_7/Γ
no clear signal	² ARMENTEROS68C	HDBC	$K^- N \rightarrow \Sigma\pi\pi$	

$(\Gamma_1\Gamma_4)^{1/2}/\Gamma_{\text{total}}$ in $N\bar{K} \rightarrow \Lambda(1820) \rightarrow \Sigma(1385)\pi$, P-wave	DOCUMENT ID	TECN	COMMENT	$(\Gamma_1\Gamma_4)^{1/2}/\Gamma$
-0.167 \pm 0.054	³ CAMERON	78	DPWA $K^- p \rightarrow \Sigma(1385)\pi$	
+0.27 \pm 0.03	PREVOST	74	DPWA $K^- N \rightarrow \Sigma(1385)\pi$	

$(\Gamma_1\Gamma_5)^{1/2}/\Gamma_{\text{total}}$ in $N\bar{K} \rightarrow \Lambda(1820) \rightarrow \Sigma(1385)\pi$, F-wave	DOCUMENT ID	TECN	COMMENT	$(\Gamma_1\Gamma_5)^{1/2}/\Gamma$
+0.065 \pm 0.029	³ CAMERON	78	DPWA $K^- p \rightarrow \Sigma(1385)\pi$	

 $\Lambda(1820)$ FOOTNOTES

- ¹ The two MARTIN 77 values are from a T-matrix pole and from a Breit-Wigner fit.
² There is a suggestion of a bump, enough to be consistent with what is expected from $\Sigma(1385) \rightarrow \Sigma\pi$ decay.
³ The published sign has been changed to be in accord with the baryon-first convention.

 $\Lambda(1820)$ REFERENCES

PDG	82	PL 111B	M. Roos <i>et al.</i>	(HEL5, CIT, CERN)
GOPAL	80	Toronto Conf. 159	G.P. Gopal	(RHEL) IJP
ALSTON...	78	PR D18 182	M. Alston-Garnjost <i>et al.</i>	(LBL, MTHO+) IJP
Also	77	PRL 38 1007	M. Alston-Garnjost <i>et al.</i>	(LBL, MTHO+) IJP
CAMERON	78	NP B143 189	W. Cameron <i>et al.</i>	(RHEL, LOIC) IJP
DECLAIS	77	CERN 77-16	Y. Declais <i>et al.</i>	(CAEN, CERN) IJP
GOPAL	77	NP B119 362	G.P. Gopal <i>et al.</i>	(LOIC, RHEL) IJP
MARTIN	77	NP B127 349	B.R. Martin, M.K. Pidcock, R.G. Moorhouse	(LOUC+) IJP
Also	77B	NP B126 266	B.R. Martin, M.K. Pidcock	(LOUC) IJP
Also	77C	NP B126 285	B.R. Martin, M.K. Pidcock	(LOUC) IJP
KANE	74	LBL-2452	D.F. Kane	(LBL) IJP
PREVOST	74	NP B69 246	J. Prevost <i>et al.</i>	(SACL, CERN, HEID)
RADER	73	NC 16A 178	R.K. Rader <i>et al.</i>	(SACL, HEID, CERN+)
ARMENTEROS 68C	NP B8 216		R. Armenteros <i>et al.</i>	(CERN, HEID, SACL) I

 $\Lambda(1830)$ D_{05}

$$I(J^P) = 0(\frac{5}{2}^-) \text{ Status: } ***$$

For results published before 1973 (they are now obsolete), see our 1982 edition Physics Letters 111B (1982).

The best evidence for this resonance is in the $\Sigma\pi$ channel.

 $\Lambda(1830)$ MASS

VALUE (MeV)	DOCUMENT ID	TECN	COMMENT
1810 to 1830 (≈ 1830) OUR ESTIMATE			
1831 \pm 10	GOPAL	80	DPWA $\bar{K}N \rightarrow \bar{K}N$
1825 \pm 10	GOPAL	77	DPWA $\bar{K}N$ multichannel
1825 \pm 1	KANE	74	DPWA $K^- p \rightarrow \Sigma\pi$
••• We do not use the following data for averages, fits, limits, etc. •••			
1817 or 1818	¹ MARTIN	77	DPWA $\bar{K}N$ multichannel

 $\Lambda(1830)$ WIDTH

VALUE (MeV)	DOCUMENT ID	TECN	COMMENT
60 to 110 (≈ 95) OUR ESTIMATE			
100 \pm 10	GOPAL	80	DPWA $\bar{K}N \rightarrow \bar{K}N$
94 \pm 10	GOPAL	77	DPWA $\bar{K}N$ multichannel
119 \pm 3	KANE	74	DPWA $K^- p \rightarrow \Sigma\pi$
••• We do not use the following data for averages, fits, limits, etc. •••			
56 or 56	¹ MARTIN	77	DPWA $\bar{K}N$ multichannel

 $\Lambda(1830)$ DECAY MODES

Mode	Fraction (Γ_j/Γ)
Γ_1 $N\bar{K}$	3–10 %
Γ_2 $\Sigma\pi$	35–75 %
Γ_3 $\Sigma(1385)\pi$	>15 %
Γ_4 $\Sigma(1385)\pi$, D-wave	
Γ_5 $\Lambda\eta$	

The above branching fractions are our estimates, not fits or averages.

 $\Lambda(1830)$ BRANCHING RATIOS

See "Sign conventions for resonance couplings" in the Note on Λ and Σ Resonances.

$\Gamma(N\bar{K})/\Gamma_{\text{total}}$	DOCUMENT ID	TECN	COMMENT	Γ_1/Γ
0.03 to 0.10 OUR ESTIMATE				
0.08 \pm 0.03	GOPAL	80	DPWA $\bar{K}N \rightarrow \bar{K}N$	
0.02 \pm 0.02	ALSTON...	78	DPWA $\bar{K}N \rightarrow \bar{K}N$	
••• We do not use the following data for averages, fits, limits, etc. •••				
0.04 \pm 0.03	GOPAL	77	DPWA See GOPAL 80	
0.04 or 0.04	¹ MARTIN	77	DPWA $\bar{K}N$ multichannel	

$(\Gamma_1\Gamma_7)^{1/2}/\Gamma_{\text{total}}$ in $N\bar{K} \rightarrow \Lambda(1830) \rightarrow \Sigma\pi$	DOCUMENT ID	TECN	COMMENT	$(\Gamma_1\Gamma_2)^{1/2}/\Gamma$
-0.17 \pm 0.03	GOPAL	77	DPWA $\bar{K}N$ multichannel	
-0.15 \pm 0.01	KANE	74	DPWA $K^- p \rightarrow \Sigma\pi$	
••• We do not use the following data for averages, fits, limits, etc. •••				
-0.17 or -0.17	¹ MARTIN	77	DPWA $\bar{K}N$ multichannel	

$(\Gamma_1\Gamma_7)^{1/2}/\Gamma_{\text{total}}$ in $N\bar{K} \rightarrow \Lambda(1830) \rightarrow \Lambda\eta$	DOCUMENT ID	TECN	COMMENT	$(\Gamma_1\Gamma_5)^{1/2}/\Gamma$
-0.044 \pm 0.020	RADER	73	MPWA	

$(\Gamma_1\Gamma_3)^{1/2}/\Gamma_{\text{total}}$ in $N\bar{K} \rightarrow \Lambda(1830) \rightarrow \Sigma(1385)\pi$	DOCUMENT ID	TECN	COMMENT	$(\Gamma_1\Gamma_3)^{1/2}/\Gamma$
+0.141 \pm 0.014	² CAMERON	78	DPWA $K^- p \rightarrow \Sigma(1385)\pi$	
+0.13 \pm 0.03	PREVOST	74	DPWA $K^- N \rightarrow \Sigma(1385)\pi$	

 $\Lambda(1830)$ FOOTNOTES

- ¹ The two MARTIN 77 values are from a T-matrix pole and from a Breit-Wigner fit.
² The CAMERON 78 upper limit on G-wave decay is 0.03. The published sign has been changed to be in accord with the baryon-first convention.

 $\Lambda(1830)$ REFERENCES

PDG	82	PL 111B	M. Roos <i>et al.</i>	(HEL5, CIT, CERN)
GOPAL	80	Toronto Conf. 159	G.P. Gopal	(RHEL) IJP
ALSTON...	78	PR D18 182	M. Alston-Garnjost <i>et al.</i>	(LBL, MTHO+) IJP
Also	77	PRL 38 1007	M. Alston-Garnjost <i>et al.</i>	(LBL, MTHO+) IJP
CAMERON	78	NP B143 189	W. Cameron <i>et al.</i>	(RHEL, LOIC) IJP
GOPAL	77	NP B119 362	G.P. Gopal <i>et al.</i>	(LOIC, RHEL) IJP
MARTIN	77	NP B127 349	B.R. Martin, M.K. Pidcock, R.G. Moorhouse	(LOUC+) IJP
Also	77B	NP B126 266	B.R. Martin, M.K. Pidcock	(LOUC) IJP
Also	77C	NP B126 285	B.R. Martin, M.K. Pidcock	(LOUC) IJP
KANE	74	LBL-2452	D.F. Kane	(LBL) IJP
PREVOST	74	NP B69 246	J. Prevost <i>et al.</i>	(SACL, CERN, HEID)
RADER	73	NC 16A 178	R.K. Rader <i>et al.</i>	(SACL, HEID, CERN+)

See key on page 239

Baryon Particle Listings
 $\Lambda(1890), \Lambda(2000)$ $\Lambda(1890) P_{03}$

$$I(J^P) = 0(\frac{3}{2}^+) \text{ Status: } ****$$

For results published before 1974 (they are now obsolete), see our 1982 edition Physics Letters **111B** (1982).The $J^P = 3/2^+$ assignment is consistent with all available data (including polarization) and recent partial-wave analyses. The dominant inelastic modes remain unknown. $\Lambda(1890)$ MASS

VALUE (MeV)	DOCUMENT ID	TECN	COMMENT
1850 to 1910 (≈ 1890) OUR ESTIMATE			
1897 \pm 5	GOPAL 80	DPWA	$\bar{K}N \rightarrow \bar{K}N$
1908 \pm 10	ALSTON.... 78	DPWA	$\bar{K}N \rightarrow \bar{K}N$
1900 \pm 5	GOPAL 77	DPWA	$\bar{K}N$ multichannel
1894 \pm 10	HEMINGWAY 75	DPWA	$K^- p \rightarrow \bar{K}N$
• • • We do not use the following data for averages, fits, limits, etc. • • •			
1856 or 1868	¹ MARTIN 77	DPWA	$\bar{K}N$ multichannel
1900	² NAKKASYAN 75	DPWA	$K^- p \rightarrow \Lambda w$

 $\Lambda(1890)$ WIDTH

VALUE (MeV)	DOCUMENT ID	TECN	COMMENT
60 to 200 (≈ 100) OUR ESTIMATE			
74 \pm 10	GOPAL 80	DPWA	$\bar{K}N \rightarrow \bar{K}N$
119 \pm 20	ALSTON.... 78	DPWA	$\bar{K}N \rightarrow \bar{K}N$
72 \pm 10	GOPAL 77	DPWA	$\bar{K}N$ multichannel
107 \pm 10	HEMINGWAY 75	DPWA	$K^- p \rightarrow \bar{K}N$
• • • We do not use the following data for averages, fits, limits, etc. • • •			
191 or 193	¹ MARTIN 77	DPWA	$\bar{K}N$ multichannel
100	² NAKKASYAN 75	DPWA	$K^- p \rightarrow \Lambda w$

 $\Lambda(1890)$ DECAY MODES

Mode	Fraction (Γ_i/Γ)
Γ_1 $\bar{N}\bar{K}$	20–35 %
Γ_2 $\Sigma \pi$	3–10 %
Γ_3 $\Sigma(1385)\pi$	seen
Γ_4 $\Sigma(1385)\pi, P$ -wave	
Γ_5 $\Sigma(1385)\pi, F$ -wave	
Γ_6 $N\bar{K}^*(892)$	seen
Γ_7 $N\bar{K}^*(892), S=1/2, P$ -wave	
Γ_8 Λw	

The above branching fractions are our estimates, not fits or averages.

 $\Lambda(1890)$ BRANCHING RATIOSSee "Sign conventions for resonance couplings" in the Note on Λ and Σ Resonances.

$\Gamma(N\bar{K})/\Gamma_{\text{total}}$	DOCUMENT ID	TECN	COMMENT	Γ_1/Γ
OUR ESTIMATE				
0.20 \pm 0.02	GOPAL 80	DPWA	$\bar{K}N \rightarrow \bar{K}N$	
0.34 \pm 0.05	ALSTON.... 78	DPWA	$\bar{K}N \rightarrow \bar{K}N$	
0.24 \pm 0.04	HEMINGWAY 75	DPWA	$K^- p \rightarrow \bar{K}N$	
• • • We do not use the following data for averages, fits, limits, etc. • • •				
0.18 \pm 0.02	GOPAL 77	DPWA	See GOPAL 80	
0.36 or 0.34	¹ MARTIN 77	DPWA	$\bar{K}N$ multichannel	

$(\Gamma_1\Gamma_2)^{1/2}/\Gamma_{\text{total}}$ in $N\bar{K} \rightarrow \Lambda(1890) \rightarrow \Sigma \pi$	DOCUMENT ID	TECN	COMMENT	$(\Gamma_1\Gamma_2)^{1/2}/\Gamma$
OUR ESTIMATE				
-0.09 \pm 0.03	GOPAL 77	DPWA	$\bar{K}N$ multichannel	
• • • We do not use the following data for averages, fits, limits, etc. • • •				
+0.15 or +0.14	¹ MARTIN 77	DPWA	$\bar{K}N$ multichannel	

$(\Gamma_1\Gamma_3)^{1/2}/\Gamma_{\text{total}}$ in $N\bar{K} \rightarrow \Lambda(1890) \rightarrow \Lambda w$	DOCUMENT ID	TECN	COMMENT	$(\Gamma_1\Gamma_3)^{1/2}/\Gamma$
OUR ESTIMATE				
seen	BACCARI 77	IPWA	$K^- p \rightarrow \Lambda w$	
0.032	² NAKKASYAN 75	DPWA	$K^- p \rightarrow \Lambda w$	

$(\Gamma_1\Gamma_4)^{1/2}/\Gamma_{\text{total}}$ in $N\bar{K} \rightarrow \Lambda(1890) \rightarrow \Sigma(1385)\pi, P$ -wave	DOCUMENT ID	TECN	COMMENT	$(\Gamma_1\Gamma_4)^{1/2}/\Gamma$
OUR ESTIMATE				
<0.03	CAMERON 78	DPWA	$K^- p \rightarrow \Sigma(1385)\pi$	

$(\Gamma_1\Gamma_5)^{1/2}/\Gamma_{\text{total}}$ in $N\bar{K} \rightarrow \Lambda(1890) \rightarrow \Sigma(1385)\pi, F$ -wave	DOCUMENT ID	TECN	COMMENT	$(\Gamma_1\Gamma_5)^{1/2}/\Gamma$
OUR ESTIMATE				
-0.126 \pm 0.055	³ CAMERON 78	DPWA	$K^- p \rightarrow \Sigma(1385)\pi$	

$(\Gamma_1\Gamma_7)^{1/2}/\Gamma_{\text{total}}$ in $N\bar{K} \rightarrow \Lambda(1890) \rightarrow N\bar{K}^*(892)$	DOCUMENT ID	TECN	COMMENT	$(\Gamma_1\Gamma_6)^{1/2}/\Gamma$
OUR ESTIMATE				
-0.07 \pm 0.03	^{3,4} CAMERON 78B	DPWA	$K^- p \rightarrow N\bar{K}^*$	

 $\Lambda(1890)$ FOOTNOTES

- The two MARTIN 77 values are from a T-matrix pole and from a Breit-Wigner fit.
- Found in one of two best solutions.
- The published sign has been changed to be in accord with the baryon-first convention.
- Upper limits on the P_3 and F_3 waves are each 0.03.

 $\Lambda(1890)$ REFERENCES

PDG 82	PL 111B	M. Roos <i>et al.</i>	(HELS, CIT, CERN)
GOPAL 80	Toronto Conf. 159	G.P. Gopal	(RHEL) IJP
ALSTON.... 78	PR D18 182	M. Alston-Garnjost <i>et al.</i>	(LBL, MTHO+) IJP
Also 77	PR 38 1007	M. Alston-Garnjost <i>et al.</i>	(LBL, MTHO+) IJP
CAMERON 78	NP B143 189	W. Cameron <i>et al.</i>	(RHEL, LOIC) IJP
CAMERON 78B	NP B146 327	W. Cameron <i>et al.</i>	(RHEL, LOIC) IJP
BACCARI 77	NC 41A 96	B. Baccari <i>et al.</i>	(SACL, CDEF) IJP
GOPAL 77	NP B119 362	G.P. Gopal <i>et al.</i>	(LOIC, RHEL) IJP
MARTIN 77	NP B127 349	B.R. Martin, M.K. Pidcock, R.G. Moorhouse	(LOUC+) IJP
Also 77B	NP B126 266	B.R. Martin, M.K. Pidcock	(LOUC)
Also 77C	NP B126 285	B.R. Martin, M.K. Pidcock	(LOUC) IJP
HEMINGWAY 75	NP B91 12	R.J. Hemingway <i>et al.</i>	(CERN, HEIDH, MPIIM) IJP
NAKKASYAN 75	NP B93 85	A. Nakkasyan	(CERN) IJP

 $\Lambda(2000)$

$$I(J^P) = 0(?^?) \text{ Status: } *$$

OMITTED FROM SUMMARY TABLE

We list here all the ambiguous resonance possibilities with a mass around 2 GeV. The proposed quantum numbers are D_3 (BARBARO-GALTIERI 70 in $\Sigma \pi$), $D_3 + F_5$, $P_3 + D_5$, or $P_1 + D_3$ (BRANDSTETTER 72 in Λw), and S_1 (CAMERON 78B in $N\bar{K}^*$). The first two of the above analyses should now be considered obsolete. See also NAKKASYAN 75. $\Lambda(2000)$ MASS

VALUE (MeV)	DOCUMENT ID	TECN	COMMENT
≈ 2000 OUR ESTIMATE			
2030 \pm 30	CAMERON 78B	DPWA	$K^- p \rightarrow N\bar{K}^*$
1935 to 1971	¹ BRANDSTET...72	DPWA	$K^- p \rightarrow \Lambda w$
1951 to 2034	¹ BRANDSTET...72	DPWA	$K^- p \rightarrow \Lambda w$
2010 \pm 30	BARBARO.... 70	DPWA	$K^- p \rightarrow \Sigma \pi$

 $\Lambda(2000)$ WIDTH

VALUE (MeV)	DOCUMENT ID	TECN	COMMENT
125 \pm 25	CAMERON 78B	DPWA	$K^- p \rightarrow N\bar{K}^*$
180 to 240	¹ BRANDSTET...72	DPWA	(lower mass)
73 to 154	¹ BRANDSTET...72	DPWA	(higher mass)
130 \pm 50	BARBARO.... 70	DPWA	$K^- p \rightarrow \Sigma \pi$

 $\Lambda(2000)$ DECAY MODES

Mode
Γ_1 $N\bar{K}$
Γ_2 $\Sigma \pi$
Γ_3 Λw
Γ_4 $N\bar{K}^*(892), S=1/2, S$ -wave
Γ_5 $N\bar{K}^*(892), S=3/2, D$ -wave

 $\Lambda(2000)$ BRANCHING RATIOSSee "Sign conventions for resonance couplings" in the Note on Λ and Σ Resonances.

$(\Gamma_1\Gamma_2)^{1/2}/\Gamma_{\text{total}}$ in $N\bar{K} \rightarrow \Lambda(2000) \rightarrow \Sigma \pi$	DOCUMENT ID	TECN	COMMENT	$(\Gamma_1\Gamma_2)^{1/2}/\Gamma$
OUR ESTIMATE				
-0.20 \pm 0.04	BARBARO.... 70	DPWA	$K^- p \rightarrow \Sigma \pi$	

$(\Gamma_1\Gamma_3)^{1/2}/\Gamma_{\text{total}}$ in $N\bar{K} \rightarrow \Lambda(2000) \rightarrow \Lambda w$	DOCUMENT ID	TECN	COMMENT	$(\Gamma_1\Gamma_3)^{1/2}/\Gamma$
OUR ESTIMATE				
0.17 to 0.25	¹ BRANDSTET...72	DPWA	(lower mass)	
0.04 to 0.15	¹ BRANDSTET...72	DPWA	(higher mass)	

$(\Gamma_1\Gamma_4)^{1/2}/\Gamma_{\text{total}}$ in $N\bar{K} \rightarrow \Lambda(2000) \rightarrow N\bar{K}^*(892), S=1/2, S$ -wave	DOCUMENT ID	TECN	COMMENT	$(\Gamma_1\Gamma_4)^{1/2}/\Gamma$
OUR ESTIMATE				
-0.12 \pm 0.03	² CAMERON 78B	DPWA	$K^- p \rightarrow N\bar{K}^*$	

$(\Gamma_1\Gamma_5)^{1/2}/\Gamma_{\text{total}}$ in $N\bar{K} \rightarrow \Lambda(2000) \rightarrow N\bar{K}^*(892), S=3/2, D$ -wave	DOCUMENT ID	TECN	COMMENT	$(\Gamma_1\Gamma_5)^{1/2}/\Gamma$
OUR ESTIMATE				
+0.09 \pm 0.03	CAMERON 78B	DPWA	$K^- p \rightarrow N\bar{K}^*$	

Baryon Particle Listings

 $\Lambda(2000)$, $\Lambda(2020)$, $\Lambda(2100)$ $\Lambda(2000)$ FOOTNOTES

- ¹The parameters quoted here are ranges from the three best fits; the lower state probably has $J \leq 3/2$, and the higher one probably has $J \leq 5/2$.
²The published sign has been changed to be in accord with the baryon-first convention.

 $\Lambda(2000)$ REFERENCES

CAMERON 78B	NP B146 327	W. Cameron <i>et al.</i>	(RHEL, LOIC) IJP
NAKKASYAN 75	NP B93 85	A. Nakkasyan	(CERN) IJP
BRANDSTETTER... 72	NP B39 13	A.A. Brandstetter <i>et al.</i>	(RHEL, CDEF+)
BARBARO... 70	Duke Conf. 173	A. Barbaro-Galtrieri	(LRL) IJP

 $\Lambda(2020)$ F_{07}

$$I(J^P) = 0(\frac{1}{2}^+) \text{ Status: } *$$

OMITTED FROM SUMMARY TABLE

In LITCHFIELD 71, need for the state rests solely on a possibly inconsistent polarization measurement at 1.784 GeV/c. HEMINGWAY 75 does not require this state. GOPAL 77 does not need it in either $N\bar{K}$ or $\Sigma\pi$. With new K^-n angular distributions included, DECLAIS 77 sees it. However, this and other new data are included in GOPAL 80 and the state is not required. BACCARI 77 weakly supports it.

 $\Lambda(2020)$ MASS

VALUE (MeV)	DOCUMENT ID	TECN	COMMENT
≈ 2020 OUR ESTIMATE			
2140	BACCARI 77	DPWA	$K^-p \rightarrow \Lambda\omega$
2117	DECLAIS 77	DPWA	$\bar{K}N \rightarrow \bar{K}N$
2100 \pm 30	LITCHFIELD 71	DPWA	$K^-p \rightarrow \bar{K}N$
2020 \pm 20	BARBARO... 70	DPWA	$K^-p \rightarrow \Sigma\pi$

 $\Lambda(2020)$ WIDTH

VALUE (MeV)	DOCUMENT ID	TECN	COMMENT
128	BACCARI 77	DPWA	$K^-p \rightarrow \Lambda\omega$
167	DECLAIS 77	DPWA	$\bar{K}N \rightarrow \bar{K}N$
120 \pm 30	LITCHFIELD 71	DPWA	$K^-p \rightarrow \bar{K}N$
160 \pm 30	BARBARO... 70	DPWA	$K^-p \rightarrow \Sigma\pi$

 $\Lambda(2020)$ DECAY MODES

Mode	Fraction (Γ_i/Γ)
Γ_1 $N\bar{K}$	25-35 %
Γ_2 $\Sigma\pi$	\sim 5 %
Γ_3 $\Lambda\eta$	< 3 %
Γ_4 ΞK	< 3 %
Γ_5 $\Lambda\omega$	< 8 %
Γ_6 $N\bar{K}^*(892)$	10-20 %
Γ_7 $N\bar{K}^*(892)$, $S=1/2$, G-wave	
Γ_8 $N\bar{K}^*(892)$, $S=3/2$, D-wave	

 $\Lambda(2020)$ BRANCHING RATIOS

See "Sign conventions for resonance couplings" in the Note on Λ and Σ Resonances.

$\Gamma(N\bar{K})/\Gamma_{\text{total}}$	DOCUMENT ID	TECN	COMMENT	Γ_1/Γ
0.05	DECLAIS 77	DPWA	$\bar{K}N \rightarrow \bar{K}N$	
0.05 \pm 0.02	LITCHFIELD 71	DPWA	$K^-p \rightarrow \bar{K}N$	

$(\Gamma_1\Gamma_2)^{1/2}/\Gamma_{\text{total}}$ in $N\bar{K} \rightarrow \Lambda(2020) \rightarrow \Sigma\pi$	DOCUMENT ID	TECN	COMMENT	$(\Gamma_1\Gamma_2)^{1/2}/\Gamma$
-0.15 \pm 0.02	BARBARO... 70	DPWA	$K^-p \rightarrow \Sigma\pi$	

$(\Gamma_1\Gamma_3)^{1/2}/\Gamma_{\text{total}}$ in $N\bar{K} \rightarrow \Lambda(2020) \rightarrow \Lambda\omega$	DOCUMENT ID	TECN	COMMENT	$(\Gamma_1\Gamma_3)^{1/2}/\Gamma$
< 0.05	BACCARI 77	DPWA	$K^-p \rightarrow \Lambda\omega$	

 $\Lambda(2020)$ REFERENCES

GOPAL 80	Toronto Conf. 159	G.P. Gopal	(RHEL)
BACCARI 77	NC 41A 96	B. Baccari <i>et al.</i>	(SACL, CDEF) IJP
DECLAIS 77	CERN 77-16	Y. Declais <i>et al.</i>	(CAEN, CERN) IJP
GOPAL 77	NP B119 362	G.P. Gopal <i>et al.</i>	(LOIC, RHEL)
HEMINGWAY 75	NP B91 12	R.J. Hemingway <i>et al.</i>	(CERN, HEIDH, MPIM) IJP
LITCHFIELD 71	NP B30 125	P.J. Litchfield <i>et al.</i>	(RHEL, CDEF, SACL) IJP
BARBARO... 70	Duke Conf. 173	A. Barbaro-Galtrieri	(LRL) IJP

 $\Lambda(2100)$ G_{07}

$$I(J^P) = 0(\frac{1}{2}^-) \text{ Status: } ***$$

Discovered by COOL 66 and by WOHL 66. Most of the results published before 1973 are now obsolete and have been omitted. They may be found in our 1982 edition Physics Letters **111B** (1982).

This entry only includes results from partial-wave analyses. Parameters of peaks seen in cross sections and in invariant-mass distributions around 2100 MeV used to be listed in a separate entry immediately following. It may be found in our 1986 edition Physics Letters **170B** (1986).

 $\Lambda(2100)$ MASS

VALUE (MeV)	DOCUMENT ID	TECN	COMMENT
2090 to 2110 (\approx 2100) OUR ESTIMATE			
2104 \pm 10	GOPAL 80	DPWA	$\bar{K}N \rightarrow \bar{K}N$
2106 \pm 30	DEBELLEFON 78	DPWA	$\bar{K}N \rightarrow \bar{K}N$
2110 \pm 10	GOPAL 77	DPWA	$\bar{K}N$ multichannel
2105 \pm 10	HEMINGWAY 75	DPWA	$K^-p \rightarrow \bar{K}N$
2115 \pm 10	KANE 74	DPWA	$K^-p \rightarrow \Sigma\pi$
• • • We do not use the following data for averages, fits, limits, etc. • • •			
2094	BACCARI 77	DPWA	$K^-p \rightarrow \Lambda\omega$
2094	DECLAIS 77	DPWA	$\bar{K}N \rightarrow \bar{K}N$
2110 or 2089	¹ NAKKASYAN 75	DPWA	$K^-p \rightarrow \Lambda\omega$

 $\Lambda(2100)$ WIDTH

VALUE (MeV)	DOCUMENT ID	TECN	COMMENT
100 to 250 (\approx 200) OUR ESTIMATE			
157 \pm 40	DEBELLEFON 78	DPWA	$\bar{K}N \rightarrow \bar{K}N$
250 \pm 30	GOPAL 77	DPWA	$\bar{K}N$ multichannel
241 \pm 30	HEMINGWAY 75	DPWA	$K^-p \rightarrow \bar{K}N$
152 \pm 15	KANE 74	DPWA	$K^-p \rightarrow \Sigma\pi$
• • • We do not use the following data for averages, fits, limits, etc. • • •			
98	BACCARI 77	DPWA	$K^-p \rightarrow \Lambda\omega$
250	DECLAIS 77	DPWA	$\bar{K}N \rightarrow \bar{K}N$
244 or 302	¹ NAKKASYAN 75	DPWA	$K^-p \rightarrow \Lambda\omega$

 $\Lambda(2100)$ DECAY MODES

Mode	Fraction (Γ_i/Γ)
Γ_1 $N\bar{K}$	25-35 %
Γ_2 $\Sigma\pi$	\sim 5 %
Γ_3 $\Lambda\eta$	< 3 %
Γ_4 ΞK	< 3 %
Γ_5 $\Lambda\omega$	< 8 %
Γ_6 $N\bar{K}^*(892)$	10-20 %
Γ_7 $N\bar{K}^*(892)$, $S=1/2$, G-wave	
Γ_8 $N\bar{K}^*(892)$, $S=3/2$, D-wave	

The above branching fractions are our estimates, not fits or averages.

 $\Lambda(2100)$ BRANCHING RATIOS

See "Sign conventions for resonance couplings" in the Note on Λ and Σ Resonances.

$\Gamma(N\bar{K})/\Gamma_{\text{total}}$	DOCUMENT ID	TECN	COMMENT	Γ_1/Γ
0.25 to 0.35 OUR ESTIMATE				
0.34 \pm 0.03	GOPAL 80	DPWA	$\bar{K}N \rightarrow \bar{K}N$	
0.24 \pm 0.06	DEBELLEFON 78	DPWA	$\bar{K}N \rightarrow \bar{K}N$	
0.31 \pm 0.03	HEMINGWAY 75	DPWA	$K^-p \rightarrow \bar{K}N$	
• • • We do not use the following data for averages, fits, limits, etc. • • •				
0.29	DECLAIS 77	DPWA	$\bar{K}N \rightarrow \bar{K}N$	
0.30 \pm 0.03	GOPAL 77	DPWA	See GOPAL 80	

$(\Gamma_1\Gamma_2)^{1/2}/\Gamma_{\text{total}}$ in $N\bar{K} \rightarrow \Lambda(2100) \rightarrow \Sigma\pi$	DOCUMENT ID	TECN	COMMENT	$(\Gamma_1\Gamma_2)^{1/2}/\Gamma$
+0.12 \pm 0.04	GOPAL 77	DPWA	$\bar{K}N$ multichannel	
+0.11 \pm 0.01	KANE 74	DPWA	$K^-p \rightarrow \Sigma\pi$	

$(\Gamma_1\Gamma_3)^{1/2}/\Gamma_{\text{total}}$ in $N\bar{K} \rightarrow \Lambda(2100) \rightarrow \Lambda\eta$	DOCUMENT ID	TECN	COMMENT	$(\Gamma_1\Gamma_3)^{1/2}/\Gamma$
-0.050 \pm 0.020	RADER 73	MPWA	$K^-p \rightarrow \Lambda\eta$	

See key on page 239

Baryon Particle Listings

 $\Lambda(2100)$, $\Lambda(2110)$, $\Lambda(2325)$

$(\Gamma_1\Gamma_2)^{1/2}/\Gamma_{\text{total}}$ in $N\bar{K} \rightarrow \Lambda(2100) \rightarrow \Xi K$	DOCUMENT ID	TECN	COMMENT	$(\Gamma_1\Gamma_4)^{1/2}/\Gamma$
0.035 ± 0.018	LITCHFIELD 71	DPWA	$K^- p \rightarrow \Xi K$	
• • • We do not use the following data for averages, fits, limits, etc. • • •				
0.003	MULLER 69B	DPWA	$K^- p \rightarrow \Xi K$	
0.05	TRIPP 67	RVUE	$K^- p \rightarrow \Xi K$	

$(\Gamma_1\Gamma_2)^{1/2}/\Gamma_{\text{total}}$ in $N\bar{K} \rightarrow \Lambda(2100) \rightarrow \Lambda\omega$	DOCUMENT ID	TECN	COMMENT	$(\Gamma_1\Gamma_5)^{1/2}/\Gamma$
-0.070	² BACCARI 77	DPWA	GD_{37} wave	
+0.011	² BACCARI 77	DPWA	GG_{17} wave	
+0.008	² BACCARI 77	DPWA	GG_{37} wave	
0.122 or 0.154	¹ NAKKASYAN 75	DPWA	$K^- p \rightarrow \Lambda\omega$	

$(\Gamma_1\Gamma_2)^{1/2}/\Gamma_{\text{total}}$ in $N\bar{K} \rightarrow \Lambda(2100) \rightarrow N\bar{K}^*(892), S=3/2, D\text{-wave}$	DOCUMENT ID	TECN	COMMENT	$(\Gamma_1\Gamma_8)^{1/2}/\Gamma$
+0.21 ± 0.04	CAMERON 78B	DPWA	$K^- p \rightarrow N\bar{K}^*$	

$(\Gamma_1\Gamma_2)^{1/2}/\Gamma_{\text{total}}$ in $N\bar{K} \rightarrow \Lambda(2100) \rightarrow N\bar{K}^*(892), S=1/2, G\text{-wave}$	DOCUMENT ID	TECN	COMMENT	$(\Gamma_1\Gamma_7)^{1/2}/\Gamma$
-0.04 ± 0.03	³ CAMERON 78B	DPWA	$K^- p \rightarrow N\bar{K}^*$	

 $\Lambda(2100)$ FOOTNOTES

¹ The NAKKASYAN 75 values are from the two best solutions found. Each has the $\Lambda(2100)$ and one additional resonance (P_3 or F_5).

² Note that the three for BACCARI 77 entries are for three different waves.

³ The published sign has been changed to be in accord with the baryon-first convention. The upper limit on the G_3 wave is 0.03.

 $\Lambda(2100)$ REFERENCES

PDG 86	PL 170B	M. Aguilar-Benitez et al.	(CERN, CIT+)
PDG 82	PL 111B	M. Roos et al.	(HELS, CIT, CERN)
GOPAL 80	Toronto Conf. 159	G.P. Gopal	(RHEL) IJP
CAMERON 78B	NP B146 327	W. Cameron et al.	(RHEL, LOIC) IJP
DEBELLEFON 78	NC 42A 403	A. de Bellefon et al.	(CDEF, SACL) IJP
BACCARI 77	NC 41A 96	B. Baccari et al.	(SACL, CDEF) IJP
DECLAIS 77	CERN 77-16	Y. Declais et al.	(CAEN, CERN) IJP
GOPAL 77	NP B119 362	G.P. Gopal et al.	(LOIC, RHEL) IJP
HEMINGWAY 75	NP B91 12	R.J. Hemingway et al.	(CERN, HEIDH, MPIM) IJP
NAKKASYAN 75	NP B93 85	A. Nakkasyan	(CERN) IJP
KANE 74	LBL-2452	D.F. Kane	(LBL) IJP
RADER 73	NC 16A 178	R.K. Rader et al.	(SACL, HEID, CERN+) IJP
LITCHFIELD 71	NP B30 125	P.J. Litchfield et al.	(RHEL, CDEF, SACL) IJP
MULLER 69B	Thesis UCL 19372	R.A. Muller	(LRL)
TRIPP 67	NP B3 10	R.D. Tripp et al.	(LRL, SLAC, CERN+) IJP
COOL 66	PRL 16 1228	R.L. Cool et al.	(BNL)
WOHL 66	PRL 17 107	C.G. Wohl, F.T. Solmitz, M.L. Stevenson	(LRL) IJP

 $\Lambda(2110) F_{05}$ $I(J^P) = 0(\frac{5}{2}^+)$ Status: ***

For results published before 1974 (they are now obsolete), see our 1982 edition Physics Letters **111B** (1982). All the references have been retained.

This resonance is in the Baryon Summary Table, but the evidence for it could be better.

 $\Lambda(2110)$ MASS

VALUE (MeV)	DOCUMENT ID	TECN	COMMENT
2090 to 2140 (≈ 2110) OUR ESTIMATE			
2092 ± 25	GOPAL 80	DPWA	$\bar{K}N \rightarrow \bar{K}N$
2125 ± 25	CAMERON 78B	DPWA	$K^- p \rightarrow N\bar{K}^*$
2106 ± 50	DEBELLEFON 78	DPWA	$\bar{K}N \rightarrow \bar{K}N$
2140 ± 20	DEBELLEFON 77	DPWA	$K^- p \rightarrow \Sigma\pi$
2100 ± 50	GOPAL 77	DPWA	$\bar{K}N$ multichannel
2112 ± 7	KANE 74	DPWA	$K^- p \rightarrow \Sigma\pi$
• • • We do not use the following data for averages, fits, limits, etc. • • •			
2137	BACCARI 77	DPWA	$K^- p \rightarrow \Lambda\omega$
2103	¹ NAKKASYAN 75	DPWA	$K^- p \rightarrow \Lambda\omega$

 $\Lambda(2110)$ WIDTH

VALUE (MeV)	DOCUMENT ID	TECN	COMMENT
150 to 250 (≈ 200) OUR ESTIMATE			
245 ± 25	GOPAL 80	DPWA	$\bar{K}N \rightarrow \bar{K}N$
160 ± 30	CAMERON 78B	DPWA	$K^- p \rightarrow N\bar{K}^*$
251 ± 50	DEBELLEFON 78	DPWA	$\bar{K}N \rightarrow \bar{K}N$
140 ± 20	DEBELLEFON 77	DPWA	$K^- p \rightarrow \Sigma\pi$
200 ± 50	GOPAL 77	DPWA	$\bar{K}N$ multichannel
190 ± 30	KANE 74	DPWA	$K^- p \rightarrow \Sigma\pi$
• • • We do not use the following data for averages, fits, limits, etc. • • •			
132	BACCARI 77	DPWA	$K^- p \rightarrow \Lambda\omega$
391	¹ NAKKASYAN 75	DPWA	$K^- p \rightarrow \Lambda\omega$

 $\Lambda(2110)$ DECAY MODES

Mode	Fraction (Γ_i/Γ)
Γ_1 $N\bar{K}$	5–25 %
Γ_2 $\Sigma\pi$	10–40 %
Γ_3 $\Lambda\omega$	seen
Γ_4 $\Sigma(1385)\pi$	seen
Γ_5 $\Sigma(1385)\pi, P\text{-wave}$	
Γ_6 $N\bar{K}^*(892)$	10–60 %
Γ_7 $N\bar{K}^*(892), S=1/2, F\text{-wave}$	

The above branching fractions are our estimates, not fits or averages.

 $\Lambda(2110)$ BRANCHING RATIOS

See "Sign conventions for resonance couplings" in the Note on Λ and Σ Resonances.

$\Gamma(N\bar{K})/\Gamma_{\text{total}}$	DOCUMENT ID	TECN	COMMENT	Γ_1/Γ
0.05 to 0.25 OUR ESTIMATE				
0.07 ± 0.03	GOPAL 80	DPWA	$\bar{K}N \rightarrow \bar{K}N$	
0.27 ± 0.06	² DEBELLEFON 78	DPWA	$\bar{K}N \rightarrow \bar{K}N$	
• • • We do not use the following data for averages, fits, limits, etc. • • •				
0.07 ± 0.03	GOPAL 77	DPWA	See GOPAL 80	

$(\Gamma_1\Gamma_2)^{1/2}/\Gamma_{\text{total}}$ in $N\bar{K} \rightarrow \Lambda(2110) \rightarrow \Sigma\pi$	DOCUMENT ID	TECN	COMMENT	$(\Gamma_1\Gamma_2)^{1/2}/\Gamma$
+0.14 ± 0.01	DEBELLEFON 77	DPWA	$K^- p \rightarrow \Sigma\pi$	
+0.20 ± 0.03	KANE 74	DPWA	$K^- p \rightarrow \Sigma\pi$	
• • • We do not use the following data for averages, fits, limits, etc. • • •				
+0.10 ± 0.03	GOPAL 77	DPWA	$\bar{K}N$ multichannel	

$(\Gamma_1\Gamma_2)^{1/2}/\Gamma_{\text{total}}$ in $N\bar{K} \rightarrow \Lambda(2110) \rightarrow \Lambda\omega$	DOCUMENT ID	TECN	COMMENT	$(\Gamma_1\Gamma_3)^{1/2}/\Gamma$
<0.05	BACCARI 77	DPWA	$K^- p \rightarrow \Lambda\omega$	
0.112	¹ NAKKASYAN 75	DPWA	$K^- p \rightarrow \Lambda\omega$	

$(\Gamma_1\Gamma_2)^{1/2}/\Gamma_{\text{total}}$ in $N\bar{K} \rightarrow \Lambda(2110) \rightarrow \Sigma(1385)\pi$	DOCUMENT ID	TECN	COMMENT	$(\Gamma_1\Gamma_4)^{1/2}/\Gamma$
+0.071 ± 0.025	³ CAMERON 78	DPWA	$K^- p \rightarrow \Sigma(1385)\pi$	

$(\Gamma_1\Gamma_2)^{1/2}/\Gamma_{\text{total}}$ in $N\bar{K} \rightarrow \Lambda(2110) \rightarrow N\bar{K}^*(892)$	DOCUMENT ID	TECN	COMMENT	$(\Gamma_1\Gamma_6)^{1/2}/\Gamma$
-0.17 ± 0.04	⁴ CAMERON 78B	DPWA	$K^- p \rightarrow N\bar{K}^*$	

 $\Lambda(2110)$ FOOTNOTES

¹ Found in one of two best solutions.

² The published error of 0.6 was a misprint.

³ The CAMERON 78 upper limit on F -wave decay is 0.03. The sign here has been changed to be in accord with the baryon-first convention.

⁴ The published sign has been changed to be in accord with the baryon-first convention. The CAMERON 78B upper limits on the P_3 and F_3 waves are each 0.03.

 $\Lambda(2110)$ REFERENCES

PDG 82	PL 111B	M. Roos et al.	(HELS, CIT, CERN)
GOPAL 80	Toronto Conf. 159	G.P. Gopal	(RHEL) IJP
CAMERON 78	NP B143 189	W. Cameron et al.	(RHEL, LOIC) IJP
CAMERON 78B	NP B146 327	W. Cameron et al.	(RHEL, LOIC) IJP
DEBELLEFON 78	NC 42A 403	A. de Bellefon et al.	(CDEF, SACL) IJP
BACCARI 77	NC 41A 96	B. Baccari et al.	(SACL, CDEF) IJP
DEBELLEFON 77	NC 37A 175	A. de Bellefon et al.	(CDEF, SACL) IJP
GOPAL 77	NP B119 362	G.P. Gopal et al.	(LOIC, RHEL) IJP
NAKKASYAN 75	NP B93 85	A. Nakkasyan	(CERN) IJP
KANE 74	LBL-2452	D.F. Kane	(LBL) IJP

 $\Lambda(2325) D_{03}$ $I(J^P) = 0(\frac{3}{2}^-)$ Status: *

OMITTED FROM SUMMARY TABLE

BACCARI 77 finds this state with either $J^P = 3/2^-$ or $3/2^+$ in a energy-dependent partial-wave analyses of $K^- p \rightarrow \Lambda\omega$ from 2070 to 2436 MeV. A subsequent semi-energy-independent analysis from threshold to 2436 MeV selects $3/2^-$. DEBELLEFON 78 (same group) also sees this state in an energy-dependent partial-wave analysis of $K^- p \rightarrow \bar{K}N$ data, and finds $J^P = 3/2^-$ or $3/2^+$. They again prefer $J^P = 3/2^-$, but only on the basis of model-dependent considerations.

Baryon Particle Listings

$\Lambda(2325)$, $\Lambda(2350)$, $\Lambda(2585)$ Bumps

$\Lambda(2325)$ MASS

VALUE (MeV)	DOCUMENT ID	TECN	COMMENT
≈ 2325 OUR ESTIMATE			
2342 \pm 30	DEBELLEFON 78	DPWA	$\bar{K}N \rightarrow \bar{K}N$
2327 \pm 20	BACCARI 77	DPWA	$K^-p \rightarrow \Lambda\omega$

$\Lambda(2325)$ WIDTH

VALUE (MeV)	DOCUMENT ID	TECN	COMMENT
177 \pm 40	DEBELLEFON 78	DPWA	$\bar{K}N \rightarrow \bar{K}N$
160 \pm 40	BACCARI 77	IPWA	$K^-p \rightarrow \Lambda\omega$

$\Lambda(2325)$ DECAY MODES

Mode	DOCUMENT ID	TECN	COMMENT
Γ_1 $N\bar{K}$			
Γ_2 $\Lambda\omega$			

$\Lambda(2325)$ BRANCHING RATIOS

$\Gamma(N\bar{K})/\Gamma_{total}$	DOCUMENT ID	TECN	COMMENT	Γ_1/Γ
0.19 \pm 0.06	DEBELLEFON 78	DPWA	$\bar{K}N \rightarrow \bar{K}N$	

$(\Gamma_1\Gamma_2)^{1/2}/\Gamma_{total}$ in $N\bar{K} \rightarrow \Lambda(2325) \rightarrow \Lambda\omega$	DOCUMENT ID	TECN	COMMENT	$(\Gamma_1\Gamma_2)^{1/2}/\Gamma$
0.06 \pm 0.02	¹ BACCARI 77	IPWA	DS_{33} wave	
0.05 \pm 0.02	¹ BACCARI 77	DPWA	DD_{13} wave	
0.08 \pm 0.03	¹ BACCARI 77	DPWA	DD_{33} wave	

$\Lambda(2325)$ FOOTNOTES

¹ Note that the three BACCARI 77 entries are for three different waves.

$\Lambda(2325)$ REFERENCES

DEBELLEFON 78	NC 42A 403	A. de Bellefon et al.	(CDEF, SACL) IJP
BACCARI 77	NC 41A 96	B. Baccari et al.	(SACL, COEF) IJP

$\Lambda(2350)$ H_{09} $I(J^P) = 0(\frac{9}{2}^+)$ Status: * * *

DAUM 68 favors $J^P = 7/2^-$ or $9/2^+$. BRICMAN 70 favors $9/2^+$. LASINSKI 71 suggests three states in this region using a Pomeron + resonances model. There are now also three formation experiments from the College de France-Saclay group, DEBELLEFON 77, BACCARI 77, and DEBELLEFON 78, which find $9/2^+$ in energy-dependent partial-wave analyses of $\bar{K}N \rightarrow \Sigma\pi, \Lambda\omega$, and $N\bar{K}$.

$\Lambda(2350)$ MASS

VALUE (MeV)	DOCUMENT ID	TECN	COMMENT
2340 to 2370 (≈ 2350) OUR ESTIMATE			
2370 \pm 50	DEBELLEFON 78	DPWA	$\bar{K}N \rightarrow \bar{K}N$
2365 \pm 20	DEBELLEFON 77	DPWA	$K^-p \rightarrow \Sigma\pi$
2358 \pm 6	BRICMAN 70	CNTR	Total, charge exchange
• • • We do not use the following data for averages, fits, limits, etc. • • •			
2372	BACCARI 77	DPWA	$K^-p \rightarrow \Lambda\omega$
2344 \pm 15	COOL 70	CNTR	K^-p, K^-d total
2360 \pm 20	LU 70	CNTR	$\gamma p \rightarrow K^+\gamma^*$
2340 \pm 7	BUGG 68	CNTR	K^-p, K^-d total

$\Lambda(2350)$ WIDTH

VALUE (MeV)	DOCUMENT ID	TECN	COMMENT
100 to 250 (≈ 150) OUR ESTIMATE			
204 \pm 50	DEBELLEFON 78	DPWA	$\bar{K}N \rightarrow \bar{K}N$
110 \pm 20	DEBELLEFON 77	DPWA	$K^-p \rightarrow \Sigma\pi$
324 \pm 30	BRICMAN 70	CNTR	Total, charge exchange
• • • We do not use the following data for averages, fits, limits, etc. • • •			
257	BACCARI 77	DPWA	$K^-p \rightarrow \Lambda\omega$
190	COOL 70	CNTR	K^-p, K^-d total
55	LU 70	CNTR	$\gamma p \rightarrow K^+\gamma^*$
140 \pm 20	BUGG 68	CNTR	K^-p, K^-d total

$\Lambda(2350)$ DECAY MODES

Mode	Fraction (Γ_j/Γ)
Γ_1 $N\bar{K}$	$\sim 12\%$
Γ_2 $\Sigma\pi$	$\sim 10\%$
Γ_3 $\Lambda\omega$	

The above branching fractions are our estimates, not fits or averages.

$\Lambda(2350)$ BRANCHING RATIOS

See "Sign conventions for resonance couplings" in the Note on Λ and Σ Resonances.

$\Gamma(N\bar{K})/\Gamma_{total}$	DOCUMENT ID	TECN	COMMENT	Γ_1/Γ
~ 0.12 OUR ESTIMATE				
0.12 \pm 0.04	DEBELLEFON 78	DPWA	$\bar{K}N \rightarrow \bar{K}N$	

$(\Gamma_1\Gamma_2)^{1/2}/\Gamma_{total}$ in $N\bar{K} \rightarrow \Lambda(2350) \rightarrow \Sigma\pi$	DOCUMENT ID	TECN	COMMENT	$(\Gamma_1\Gamma_2)^{1/2}/\Gamma$
-0.11 \pm 0.02	DEBELLEFON 77	DPWA	$K^-p \rightarrow \Sigma\pi$	

$(\Gamma_1\Gamma_2)^{1/2}/\Gamma_{total}$ in $N\bar{K} \rightarrow \Lambda(2350) \rightarrow \Lambda\omega$	DOCUMENT ID	TECN	COMMENT	$(\Gamma_1\Gamma_2)^{1/2}/\Gamma$
<0.05	BACCARI 77	DPWA	$K^-p \rightarrow \Lambda\omega$	

$\Lambda(2350)$ REFERENCES

DEBELLEFON 78	NC 42A 403	A. de Bellefon et al.	(CDEF, SACL) IJP
BACCARI 77	NC 41A 96	B. Baccari et al.	(SACL, CDEF) IJP
DEBELLEFON 77	NC 37A 175	A. de Bellefon et al.	(CDEF, SACL) IJP
LASINSKI 71	NP B29 125	T.A. Lasinski	(EFI) IJP
BRICMAN 70	PL 31B 152	C. Bricman et al.	(CERN, CAEN, SACL)
COOL 70	PR D1 1887	R.L. Cool et al.	(BNL) I
Also	66	PRL 16 1228	(BNL) I
LU 70	PR D2 1846	D.C. Lu et al.	(YALE)
BUGG 68	PR 168 1466	D.V. Bugg et al.	(RHEL, BIRM, CAVE) I
DAUM 68	NP B7 19	C. Daum et al.	(CERN) JP

$\Lambda(2585)$ Bumps $I(J^P) = 0(?^?)$ Status: * *

OMITTED FROM SUMMARY TABLE

$\Lambda(2585)$ MASS (BUMPS)

VALUE (MeV)	DOCUMENT ID	TECN	COMMENT
≈ 2585 OUR ESTIMATE			
2585 \pm 45	ABRAMS 70	CNTR	K^-p, K^-d total
2530 \pm 25	LU 70	CNTR	$\gamma p \rightarrow K^+\gamma^*$

$\Lambda(2585)$ WIDTH (BUMPS)

VALUE (MeV)	DOCUMENT ID	TECN	COMMENT
300	ABRAMS 70	CNTR	K^-p, K^-d total
150	LU 70	CNTR	$\gamma p \rightarrow K^+\gamma^*$

$\Lambda(2585)$ DECAY MODES (BUMPS)

Mode	DOCUMENT ID	TECN	COMMENT
Γ_1 $N\bar{K}$			

$\Lambda(2585)$ BRANCHING RATIOS (BUMPS)

$(J+\frac{1}{2}) \times \Gamma(N\bar{K})/\Gamma_{total}$	DOCUMENT ID	TECN	COMMENT	Γ_1/Γ
J is not known, so only $(J+\frac{1}{2}) \times \Gamma(N\bar{K})/\Gamma_{total}$ can be given.				
0.12 \pm 0.12	ABRAMS 70	CNTR	K^-p, K^-d total	
	¹ BRICMAN 70	CNTR	Total, charge exchange	

$\Lambda(2585)$ FOOTNOTES (BUMPS)

¹ The resonance is at the end of the region analyzed — no clear signal.

$\Lambda(2585)$ REFERENCES (BUMPS)

ABRAMS 70	PR D1 1917	R.J. Abrams et al.	(BNL) I
Also	66	PRL 16 1228	(BNL) I
BRICMAN 70	PL 31B 152	C. Bricman et al.	(CERN, CAEN, SACL)
LU 70	PR D2 1846	D.C. Lu et al.	(YALE)

See key on page 239

Baryon Particle Listings

Σ^+

Σ BARYONS ($S = -1, I = 1$)

$$\Sigma^+ = uus, \Sigma^0 = uds, \Sigma^- = dds$$

Σ^+

$$I(J^P) = 1(\frac{1}{2}^+)$$
 Status: * * * *

We have omitted some results that have been superseded by later experiments. See our earlier editions.

Σ^+ MASS

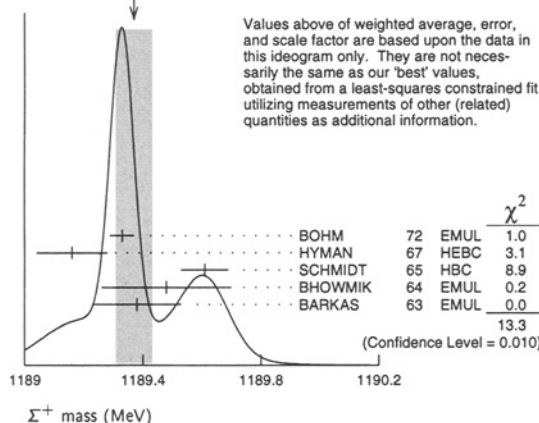
The fit uses $\Sigma^+, \Sigma^0, \Sigma^-$, and Λ mass and mass-difference measurements.

VALUE (MeV)	EVTS	DOCUMENT ID	TECN	COMMENT
1189.37 ± 0.07 OUR FIT				Error includes scale factor of 2.2.
1189.37 ± 0.06 OUR AVERAGE				Error includes scale factor of 1.8. See the ideogram below.
1189.33 ± 0.04	607	¹ BOHM 72	EMUL	
1189.16 ± 0.12		HYMAN 67	HEBC	
1189.61 ± 0.08	4205	SCHMIDT 65	HBC	See note with Λ mass
1189.48 ± 0.22	58	² BHOWMIK 64	EMUL	
1189.38 ± 0.15	144	² BARKAS 63	EMUL	

¹ BOHM 72 is updated with our 1973 $K^-, \pi^-,$ and π^0 masses (Reviews of Modern Physics 45 No. 2 Pt. II (1973)).

² These masses have been raised 30 keV to take into account a 46 keV increase in the proton mass and a 21 keV decrease in the π^0 mass (note added 1967 edition, Reviews of Modern Physics 39 1 (1967)).

WEIGHTED AVERAGE
1189.37 ± 0.06 (Error scaled by 1.8)



Values above of weighted average, error, and scale factor are based upon the data in this ideogram only. They are not necessarily the same as our 'best' values, obtained from a least-squares constrained fit utilizing measurements of other (related) quantities as additional information.

				χ^2
BOHM	72	EMUL	1.0	
HYMAN	67	HEBC	3.1	
SCHMIDT	65	HBC	8.9	
BHOWMIK	64	EMUL	0.2	
BARKAS	63	EMUL	0.0	
			13.3	

(Confidence Level = 0.010)

Σ^+ MEAN LIFE

Measurements with fewer than 1000 events have been omitted.

VALUE (10^{-10} s)	EVTS	DOCUMENT ID	TECN	COMMENT
0.8018 ± 0.0026 OUR AVERAGE				
0.8038 ± 0.0040 ± 0.0014		BARBOSA 00	E761	hyperons, 375 GeV
0.8043 ± 0.0080 ± 0.0014		³ BARBOSA 00	E761	hyperons, 375 GeV
0.798 ± 0.005	30k	MARRAFFINO 80	HBC	$K^- p$ 0.42-0.5 GeV/c
0.807 ± 0.013	5719	CONFORTO 76	HBC	$K^- p$ 1-1.4 GeV/c
0.795 ± 0.010	20k	EISELE 70	HBC	$K^- p$ at rest
0.803 ± 0.008	10664	BARLOUTAUD 69	HBC	$K^- p$ 0.4-1.2 GeV/c
0.83 ± 0.032	1300	⁴ CHANG 66	HBC	

³ This is a measurement of the Σ^- lifetime. Here we assume CPT invariance; see below for the fractional $\Sigma^+ - \Sigma^-$ lifetime difference obtained by BARBOSA 00.

⁴ We have increased the CHANG 66 error of 0.018; see our 1970 edition, Reviews of Modern Physics 42 No. 1 (1970).

$$(\tau_{\Sigma^+} - \tau_{\Sigma^-}) / \tau_{\Sigma^+}$$

A test of CPT invariance.

VALUE	DOCUMENT ID	TECN	COMMENT
(-6 ± 12) × 10⁻⁴	BARBOSA 00	E761	hyperons, 375 GeV

Σ^+ MAGNETIC MOMENT

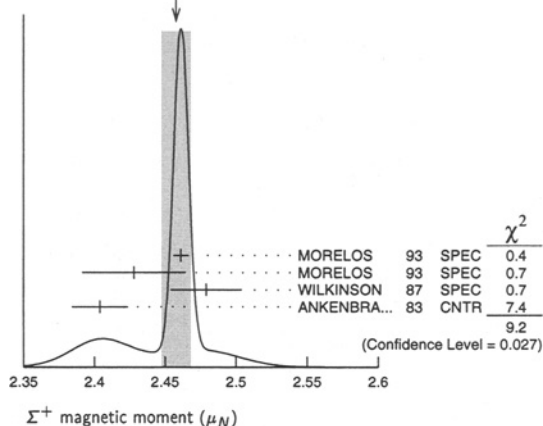
See the "Note on Baryon Magnetic Moments" in the Λ Listings. Measurements with an error $\geq 0.1 \mu_N$ have been omitted.

VALUE (μ_N)	EVTS	DOCUMENT ID	TECN	COMMENT
2.458 ± 0.010 OUR AVERAGE				Error includes scale factor of 2.1. See the ideogram below.
2.4613 ± 0.0034 ± 0.0040	250k	MORELOS 93	SPEC	pCu 800 GeV
2.428 ± 0.036 ± 0.007	12k	⁵ MORELOS 93	SPEC	pCu 800 GeV
2.479 ± 0.012 ± 0.022	137k	WILKINSON 87	SPEC	pBe 400 GeV
2.4040 ± 0.0198	44k	⁶ ANKENBRA... 83	CNTR	pCu 400 GeV

⁵ We assume CPT invariance: this is (minus) the Σ^- magnetic moment as measured by MORELOS 93. See below for the moment difference testing CPT.

⁶ ANKENBRANDT 83 gives the value $2.38 \pm 0.02 \mu_N$. MORELOS 93 uses the same hyperon magnet and channel and claims to determine the field integral better, leading to the revised value given here.

WEIGHTED AVERAGE
2.458 ± 0.010 (Error scaled by 2.1)



				χ^2
MORELOS	93	SPEC	0.4	
MORELOS	93	SPEC	0.7	
WILKINSON	87	SPEC	0.7	
ANKENBRA...	83	CNTR	7.4	
			9.2	

(Confidence Level = 0.027)

$$(\mu_{\Sigma^+} + \mu_{\Sigma^-}) / \mu_{\Sigma^+}$$

A test of CPT invariance.

VALUE	DOCUMENT ID	TECN	COMMENT
0.014 ± 0.015	⁷ MORELOS 93	SPEC	pCu 800 GeV

⁷ This is our calculation from the MORELOS 93 measurements of the Σ^+ and Σ^- magnetic moments given above. The statistical error on μ_{Σ^-} dominates the error here.

Σ^+ DECAY MODES

Mode	Fraction (Γ_i/Γ)	Confidence level
Γ_1 $p\pi^0$	(51.57 ± 0.30) %	
Γ_2 $n\pi^+$	(48.31 ± 0.30) %	
Γ_3 $p\gamma$	(1.23 ± 0.05) × 10 ⁻³	
Γ_4 $n\pi^+\gamma$	[a] (4.5 ± 0.5) × 10 ⁻⁴	
Γ_5 $\Lambda e^+\nu_e$	(2.0 ± 0.5) × 10 ⁻⁵	

$\Delta S = \Delta Q$ (SQ) violating modes or

$\Delta S = 1$ weak neutral current (SI) modes

Γ_6	$n e^+ \nu_e$	SQ	< 5	× 10 ⁻⁶ 90%
Γ_7	$n \mu^+ \nu_\mu$	SQ	< 3.0	× 10 ⁻⁵ 90%
Γ_8	$p e^+ e^-$	SI	< 7	× 10 ⁻⁶

[a] See the Listings below for the pion momentum range used in this measurement.

CONSTRAINED FIT INFORMATION

An overall fit to 2 branching ratios uses 14 measurements and one constraint to determine 3 parameters. The overall fit has a $\chi^2 = 7.7$ for 12 degrees of freedom.

The following off-diagonal array elements are the correlation coefficients $\langle \delta x_i \delta x_j \rangle / (\delta x_i \delta x_j)$, in percent, from the fit to the branching fractions, $x_i \equiv \Gamma_i / \Gamma_{\text{total}}$. The fit constrains the x_i whose labels appear in this array to sum to one.

x_2	-100	
x_3	12	-14
	x_1	x_2

Baryon Particle Listings

 Σ^+ Σ^+ BRANCHING RATIOS

$\Gamma(n\pi^+)/\Gamma(N\pi)$		$\Gamma_2/(\Gamma_1+\Gamma_2)$		
VALUE	EVTs	DOCUMENT ID	TECN	COMMENT
0.4836 ± 0.0030 OUR FIT				
0.4836 ± 0.0030 OUR AVERAGE				
0.4828 ± 0.0036	10k	⁸ MARRAFFINO 80	HBC	$K^- p$ 0.42–0.5 GeV/c
0.488 ± 0.008	1861	NOWAK 78	HBC	
0.484 ± 0.015	537	TOVEE 71	EMUL	
0.488 ± 0.010	1331	BARLOUTAUD 69	HBC	$K^- p$ 0.4–1.2 GeV/c
0.46 ± 0.02	534	CHANG 66	HBC	
0.490 ± 0.024	308	HUMPHREY 62	HBC	

⁸ MARRAFFINO 80 actually gives $\Gamma(p\pi^0)/\Gamma(\text{total}) = 0.5172 \pm 0.0036$.

$\Gamma(p\gamma)/\Gamma(p\pi^0)$		Γ_3/Γ_1		
VALUE (units 10^{-3})	EVTs	DOCUMENT ID	TECN	COMMENT
2.38 ± 0.10 OUR FIT				
2.38 ± 0.10 OUR AVERAGE				
2.32 ± 0.11 ± 0.10	32k	TIMM 95	E761	Σ^+ 375 GeV
2.81 ± 0.39 ^{+0.21} _{-0.43}	408	HESSEY 89	CNTR	$K^- p \rightarrow \Sigma^+ \pi^-$ at rest
2.52 ± 0.28	190	⁹ KOBAYASHI 87	CNTR	$\pi^+ p \rightarrow \Sigma^+ K^+$
2.46 ^{+0.30} _{-0.35}	155	BIAGI 85	CNTR	CERN hyperon beam
2.11 ± 0.38	46	MANZ 80	HBC	$K^- p \rightarrow \Sigma^+ \pi^-$
2.1 ± 0.3	45	ANG 69b	HBC	$K^- p$ at rest
2.76 ± 0.51	31	GERSHWIN 69b	HBC	$K^- p \rightarrow \Sigma^+ \pi^-$
3.7 ± 0.8	24	BAZIN 65	HBC	$K^- p$ at rest

⁹ KOBAYASHI 87 actually gives $\Gamma(p\gamma)/\Gamma(\text{total}) = (1.30 \pm 0.15) \times 10^{-3}$.

$\Gamma(n\pi^+\gamma)/\Gamma(n\pi^+)$		Γ_4/Γ_2		
VALUE (units 10^{-3})	EVTs	DOCUMENT ID	TECN	COMMENT
0.93 ± 0.10	180	EBENHOH 73	HBC	$\pi^+ < 150$ MeV/c
• • • We do not use the following data for averages, fits, limits, etc. • • •				
0.27 ± 0.05	29	ANG 69b	HBC	$\pi^+ < 110$ MeV/c
~ 1.8		BAZIN 65b	HBC	$\pi^+ < 116$ MeV/c

The π^+ momentum cuts differ, so we do not average the results but simply use the latest value in the Summary Table.

$\Gamma(\Lambda e^+ \nu_e)/\Gamma_{\text{total}}$		Γ_5/Γ		
VALUE (units 10^{-5})	EVTs	DOCUMENT ID	TECN	COMMENT
2.0 ± 0.5 OUR AVERAGE				
1.6 ± 0.7	5	BALTAY 69	HBC	$K^- p$ at rest
2.9 ± 1.0	10	EISELE 69	HBC	$K^- p$ at rest
2.0 ± 0.8	6	BARASH 67	HBC	$K^- p$ at rest

$\Gamma(ne^+ \nu_e)/\Gamma(n\pi^+)$		Γ_6/Γ_2		
EFFECTIVE DENOM.	EVTs	DOCUMENT ID	TECN	COMMENT
< 1.1 × 10⁻⁵ OUR LIMIT				Our 90% CL limit = (2.3 events)/(effective denominator sum). [Number of events increased to 2.3 for a 90% confidence level.]
111000	0	¹⁰ EBENHOH 74	HBC	$K^- p$ at rest
105000	0	¹⁰ SECHI-ZORN 73	HBC	$K^- p$ at rest

¹⁰ Effective denominator calculated by us.

$\Gamma(n\mu^+ \nu_\mu)/\Gamma(n\pi^+)$		Γ_7/Γ_2		
EFFECTIVE DENOM.	EVTs	DOCUMENT ID	TECN	COMMENT
< 6.2 × 10⁻⁵ OUR LIMIT				Our 90% CL limit = (6.7 events)/(effective denominator sum). [Number of events increased to 6.7 for a 90% confidence level.]
33800	0	BAGGETT 69b	HBC	
62000	2	¹¹ EISELE 69b	HBC	
10150	0	¹² COURANT 64	HBC	
1710	0	¹² NAUENBERG 64	HBC	
120	1	GALTIERI 62	EMUL	

¹¹ Effective denominator calculated by us.
¹² Effective denominator taken from EISELE 67.

$\Gamma(pe^+ e^-)/\Gamma_{\text{total}}$		Γ_8/Γ		
VALUE (units 10^{-6})		DOCUMENT ID	TECN	COMMENT
< 7		¹³ ANG 69b	HBC	$K^- p$ at rest

¹³ ANG 69b found three $pe^+ e^-$ events in agreement with $\gamma \rightarrow e^+ e^-$ conversion from $\Sigma^+ \rightarrow p\gamma$. The limit given here is for neutral currents.

$\Gamma(\Sigma^+ \rightarrow ne^+ \nu_e)/\Gamma(\Sigma^- \rightarrow ne^- \nu_e)$				
VALUE	CL%	EVTs	DOCUMENT ID	TECN
< 0.009 OUR LIMIT				Our 90% CL limit, using $\Gamma(ne^+ \nu_e)/\Gamma(n\pi^+)$ above.
• • • We do not use the following data for averages, fits, limits, etc. • • •				
< 0.019	90	0	EBENHOH 74	HBC $K^- p$ at rest
< 0.018	90	0	SECHI-ZORN 73	HBC $K^- p$ at rest
< 0.12	95	0	COLE 71	HBC $K^- p$ at rest
< 0.03	90	0	EISELE 69b	HBC See EBENHOH 74

 $\Gamma(\Sigma^+ \rightarrow n\mu^+ \nu_\mu)/\Gamma(\Sigma^- \rightarrow n\mu^- \nu_\mu)$

VALUE	EVTs	DOCUMENT ID	TECN	COMMENT
< 0.12 OUR LIMIT				Our 90% CL limit, using $\Gamma(n\mu^+ \nu_\mu)/\Gamma(n\pi^+)$ above.
• • • We do not use the following data for averages, fits, limits, etc. • • •				
0.06 ^{+0.045} _{-0.03}	2	EISELE 69b	HBC	$K^- p$ at rest

 $\Gamma(\Sigma^+ \rightarrow n\ell^+ \nu)/\Gamma(\Sigma^- \rightarrow n\ell^- \nu)$

$\Gamma(\Sigma^+ \rightarrow n\ell^+ \nu)/\Gamma(\Sigma^- \rightarrow n\ell^- \nu)$				
VALUE	EVTs	DOCUMENT ID	TECN	COMMENT
< 0.043 OUR LIMIT				Our 90% CL limit, using $[\Gamma(ne^+ \nu_e) + \Gamma(n\mu^+ \nu_\mu)]/\Gamma(n\pi^+)$.
• • • We do not use the following data for averages, fits, limits, etc. • • •				
< 0.08	1	NORTON 69	HBC	
< 0.034	0	BAGGETT 67	HBC	

 Σ^+ DECAY PARAMETERS

See the "Note on Baryon Decay Parameters" in the neutron Listings. A few early results have been omitted.

 α_0 FOR $\Sigma^+ \rightarrow p\pi^0$

VALUE	EVTs	DOCUMENT ID	TECN	COMMENT
-0.960 ± 0.017 OUR FIT				
-0.960 ± 0.017 OUR AVERAGE				
-0.945 ± 0.055 _{-0.042}	1259	¹⁴ LIPMAN 73	OSPK	$\pi^+ p \rightarrow \Sigma^+$
-0.940 ± 0.045	16k	BELLAMY 72	ASPK	$\pi^+ p \rightarrow \Sigma^+ K^+$
-0.98 ± 0.05 _{-0.02}	1335	¹⁵ HARRIS 70	OSPK	$\pi^+ p \rightarrow \Sigma^+ K^+$
-0.999 ± 0.022	32k	BANGERTER 69	HBC	$K^- p$ 0.4 GeV/c

¹⁴ Decay protons scattered off aluminum.
¹⁵ Decay protons scattered off carbon.

 ϕ_0 ANGLE FOR $\Sigma^+ \rightarrow p\pi^0$

VALUE (°)	EVTs	DOCUMENT ID	TECN	COMMENT
36 ± 34 OUR AVERAGE				($\tan \phi_0 = \beta/\gamma$)
38.1 ^{+35.7} _{-37.1}	1259	¹⁶ LIPMAN 73	OSPK	$\pi^+ p \rightarrow \Sigma^+ K^+$
22 ± 90		¹⁷ HARRIS 70	OSPK	$\pi^+ p \rightarrow \Sigma^+ K^+$

¹⁶ Decay proton scattered off aluminum.
¹⁷ Decay protons scattered off carbon.

 α_+ / α_0

VALUE	EVTs	DOCUMENT ID	TECN	COMMENT
-0.069 ± 0.013 OUR FIT				Older results have been omitted.
-0.073 ± 0.021	23k	MARRAFFINO 80	HBC	$K^- p$ 0.42–0.5 GeV/c

 α_+ FOR $\Sigma^+ \rightarrow n\pi^+$

VALUE	EVTs	DOCUMENT ID	TECN	COMMENT
0.068 ± 0.013 OUR FIT				
0.066 ± 0.016 OUR AVERAGE				
0.037 ± 0.049	4101	BERLEY 70b	HBC	
0.069 ± 0.017	35k	BANGERTER 69	HBC	$K^- p$ 0.4 GeV/c

 ϕ_+ ANGLE FOR $\Sigma^+ \rightarrow n\pi^+$

VALUE (°)	EVTs	DOCUMENT ID	TECN	COMMENT
167 ± 20 OUR AVERAGE				($\tan \phi_+ = \beta/\gamma$)
184 ± 24	1054	¹⁸ BERLEY 70b	HBC	Error includes scale factor of 1.1.
143 ± 29	560	BANGERTER 69b	HBC	$K^- p$ 0.4 GeV/c

¹⁸ Changed from 176 to 184° to agree with our sign convention.

 α_γ FOR $\Sigma^+ \rightarrow p\gamma$

VALUE	EVTs	DOCUMENT ID	TECN	COMMENT
-0.76 ± 0.08 OUR AVERAGE				
-0.720 ± 0.086 ± 0.045	35k	¹⁹ FOUCHER 92	SPEC	Σ^+ 375 GeV
-0.86 ± 0.13 ± 0.04	190	KOBAYASHI 87	CNTR	$\pi^+ p \rightarrow \Sigma^+ K^+$
-0.53 ^{+0.38} _{-0.36}	46	MANZ 80	HBC	$K^- p \rightarrow \Sigma^+ \pi^-$
-1.03 ^{+0.52} _{-0.42}	61	GERSHWIN 69b	HBC	$K^- p \rightarrow \Sigma^+ \pi^-$

¹⁹ See TIMM 95 for a detailed description of the analysis.

Σ^+ REFERENCES

We have omitted some papers that have been superseded by later experiments. See our earlier editions.

BARBOSA	00	PR D61 031101R	R.F. Barbosa <i>et al.</i>	(FNAL E761 Collab.)
TIMM	95	PR D51 4638	S. Timm <i>et al.</i>	(FNAL E761 Collab.)
MORELOS	93	PRL 71 3417	A. Morelos <i>et al.</i>	(FNAL E761 Collab.)
FOUCHER	92	PRL 68 3004	M. Foucher <i>et al.</i>	(FNAL E761 Collab.)
HESSEY	89	ZPHY C42 175	N.P. Hessey <i>et al.</i>	(BNL-811 Collab.)
KOBAYASHI	87	PRL 59 868	M. Kobayashi <i>et al.</i>	(KYOT)
WILKINSON	87	PRL 58 855	C.A. Wilkinson <i>et al.</i>	(WISC, MICH, RUTG+)
BIAGI	85	ZPHY C28 495	S.F. Biagi <i>et al.</i>	(CERN WA62 Collab.)
ANKENBRANDT	83	PRL 51 863	C.M. Ankenbrandt <i>et al.</i>	(FNAL, IOWA, ISU+)
MANZ	80	PL 96B 217	A. Manz <i>et al.</i>	(MPIW, VAND)
MARRAFFINO	80	PR D21 2501	J. Marraffino <i>et al.</i>	(VAND, MPIM)
NOWAK	78	NP B139 61	R.J. Nowak <i>et al.</i>	(LOUC, BELG, DURH+)
CONFORTO	76	NP B105 189	B. Conforto <i>et al.</i>	(RHEI, LOIC)
EBENHOH	74	ZPHY 266 367	H. Ebenhoh <i>et al.</i>	(HEIDT)
EBENHOH	73	ZPHY 264 413	W. Ebenhoh <i>et al.</i>	(HEIDT)
LIPMAN	73	PL 43B 89	N.H. Lipman <i>et al.</i>	(RHEL, SUSS, LOWC)
PDC	73	RMP 45 No. 2 Pt. II	T.A. Lasinski <i>et al.</i>	(LBL, BRAN, CERN+)
SECHI-ZORN	73	PR D8 12	B. Sechi-Zorn, G.A. Snow	(UMD)
BELLAMY	72	PL 39B 299	E.H. Bellamy <i>et al.</i>	(LOWC, RHEI, SUSS)
BOHM	72	NP B48 1	G. Bohm <i>et al.</i>	(BERL, KIDR, BRUX, IASD+)
Also	73	IIHE-73.2 Nov	G. Bohm	(BERL, KIDR, BRUX, DUUC+)
COLE	71	PR D4 631	J. Cole <i>et al.</i>	(STON, COLU)
TOVEE	71	NP B33 493	D.N. Tovee <i>et al.</i>	(LOUC, KIDR, BERL+)
BERLEY	70B	PR D1 2015	D. Berley <i>et al.</i>	(BNL, MASA, YALE)
EISELE	70	ZPHY 238 372	F. Eisele <i>et al.</i>	(HEID)
HARRIS	70	PRL 24 165	F. Harris <i>et al.</i>	(MICH, WISC)
PDC	70	RMP 42 No. 1	A. Barbaro-Gallieri <i>et al.</i>	(LRL, BRAN+)
ANG	69B	ZPHY 228 151	G. Ang <i>et al.</i>	(HEID)
BAGGETT	69B	Thesis MDDP-TR-973	N.V. Baggett	(UMD)
BALTAY	69	PRL 22 615	C. Baltay <i>et al.</i>	(COLU, STON)
BANGERTER	69	Thesis UCLR 19244	R.O. Bangertter	(LRL)
BANGERTER	69B	PR 187 1821	R.O. Bangertter <i>et al.</i>	(LRL)
BARLOUTAUD	69	NP B14 153	R. Barloutaud <i>et al.</i>	(SACL, CERN, HEID)
EISELE	69	ZPHY 221 1	F. Eisele <i>et al.</i>	(HEID)
Also	64	PRL 13 291	W. Willis <i>et al.</i>	(BNL, CERN, HEID, UMD)
EISELE	69B	ZPHY 221 401	F. Eisele <i>et al.</i>	(HEID)
GERSHWIN	69B	PR 188 2077	L.K. Gershwin <i>et al.</i>	(LRL)
Also	69	Thesis UCLR 19245	L.K. Gershwin	(COLU)
NORTON	69	Thesis Nevis 175	H. Norton	(COLU)
BAGGETT	67	PRL 19 1458	N. Baggett <i>et al.</i>	(UMD)
Also	68	Vienna Abs. 374	N.V. Baggett, B. Kehoe	(UMD)
Also	68B	Private Comm.	N.V. Baggett	(UMD)
BARASH	67	PRL 19 181	N. Barash <i>et al.</i>	(UMD)
EISELE	67	ZPHY 205 409	F. Eisele <i>et al.</i>	(HEID)
HYMAN	67	PL 25B 376	L.G. Hyman <i>et al.</i>	(ANL, CMU, NWES)
PDC	67	RMP 39 1	A.H. Rosenfeld <i>et al.</i>	(LRL, CERN, YALE)
CHANG	66	PR 151 1081	C.Y. Chang	(COLU)
Also	65	Thesis Nevis 145	Chang	(COLU)
BAZIN	65	PRL 14 154	M. Bazin <i>et al.</i>	(PRIN, COLU)
BAZIN	65B	PR 140B 1358	M. Bazin <i>et al.</i>	(PRIN, RUTG, COLU)
SCHMIDT	65	PR 140B 1328	P. Schmidt	(COLU)
BHOWMIK	64	NP 53 22	B. Bhowmik <i>et al.</i>	(DELH)
COURANT	64	PR 136B 1791	H. Courant <i>et al.</i>	(CERN, HEID, UMD+)
NAUENBERG	64	PRL 12 679	U. Nauenberg <i>et al.</i>	(COLU, RUTG, PRIN)
BARKAS	63	PRL 11 26	W.H. Barkas, J.N. Dyer, H.H. Heckman	(LRL)
Also	61	Thesis UCLR 9450	J.N. Dyer	(LRL)
GALTIERI	62	PRL 9 26	A. Barbaro-Gallieri <i>et al.</i>	(LRL)
HUMPHREY	62	PR 127 1305	W.E. Humphrey, R.R. Ross	(LRL)

Σ^0 MEAN LIFE

These lifetimes are deduced from measurements of the cross sections for the Primakoff process $\Lambda \rightarrow \Sigma^0$ in nuclear Coulomb fields. An alternative expression of the same information is the Σ^0 - Λ transition magnetic moment given in the following section. The relation is $(\mu_{\Sigma^0 \Lambda} / \mu_N)^2 \tau = 1.92951 \times 10^{-19}$ s (see DEVLIN 86).

VALUE (10^{-20} s)	DOCUMENT ID	TECN	COMMENT
7.4 ± 0.7 OUR EVALUATION	Using $\mu_{\Sigma^0 \Lambda}$ (see the above note).		
6.5 +1.7 -1.1	² DEVLIN	86	SPEC Primakoff effect
7.6 ± 0.5 ± 0.7	³ PETERSEN	86	SPEC Primakoff effect
• • • We do not use the following data for averages, fits, limits, etc. • • •			
5.8 ± 1.3	² DYDAK	77	SPEC See DEVLIN 86
² DEVLIN 86 is a recalculation of the results of DYDAK 77 removing a numerical approximation made in that work.			
³ An additional uncertainty of the Primakoff formalism is estimated to be < 5%.			

$|\mu(\Sigma^0 \rightarrow \Lambda)|$ TRANSITION MAGNETIC MOMENT

See the note in the Σ^0 mean-life section above. Also, see the "Note on Baryon Magnetic Moments" in the Λ Listings.

VALUE (μ_N)	DOCUMENT ID	TECN	COMMENT
1.61 ± 0.08 OUR AVERAGE			
1.72 ± 0.17 -0.19	⁴ DEVLIN	86	SPEC Primakoff effect
1.59 ± 0.05 ± 0.07	⁵ PETERSEN	86	SPEC Primakoff effect
• • • We do not use the following data for averages, fits, limits, etc. • • •			
1.82 ± 0.25 -0.18	⁴ DYDAK	77	SPEC See DEVLIN 86
⁴ DEVLIN 86 is a recalculation of the results of DYDAK 77 removing a numerical approximation made in that work.			
⁵ An additional uncertainty of the Primakoff formalism is estimated to be < 2.5%.			

Σ^0 DECAY MODES

Mode	Fraction (Γ_i/Γ)	Confidence level
$\Gamma_1 \Lambda\gamma$	100 %	
$\Gamma_2 \Lambda\gamma\gamma$	< 3 %	90%
$\Gamma_3 \Lambda e^+ e^-$	[a] 5×10^{-3}	

[a] A theoretical value using QED.

Σ^0 BRANCHING RATIOS

$\Gamma(\Lambda\gamma\gamma)/\Gamma_{total}$	CL%	DOCUMENT ID	TECN	Γ_2/Γ
<0.03	90	COLAS	75	HLBC
$\Gamma(\Lambda e^+ e^-)/\Gamma_{total}$		DOCUMENT ID	COMMENT	Γ_3/Γ
0.00545		FEINBERG	58	Theoretical QED calculation

See COURANT 63 and ALFF-STEINBERGER 65 for measurements of the invariant-mass spectrum of the Dalitz pairs.

Σ^0 REFERENCES

WANG	97	PR D56 2544	M.H.L.S. Wang <i>et al.</i>	(BNL-E766 Collab.)
DEVLIN	86	PR D34 1626	T. Devlin, P.C. Petersen, A. Baretvas	(RUTG)
PETERSEN	86	PRL 57 949	P.C. Petersen <i>et al.</i>	(RUTG, WISC, MICH+)
DYDAK	77	NP B118 1	F. Dydak <i>et al.</i>	(CERN, DORT, HEID)
COLAS	75	NP B91 253	J. Colas <i>et al.</i>	(ORSAY)
ALFF...	65	PR 137B 1105	C. Alff-Steinberger <i>et al.</i>	(COLU, RUTG+) P
DOSCH	65	PL 14 239	H.C. Dosch <i>et al.</i>	(HEID)
SCHMIDT	65	PR 140B 1328	P. Schmidt	(COLU)
BURNSTEIN	64	PRL 13 66	R.A. Burnstein <i>et al.</i>	(UMD)
COURANT	63	PRL 10 409	H. Courant <i>et al.</i>	(CERN, UMD) P
FEINBERG	58	PR 109 1019	G. Feinberg	(BNL)

Σ^0

$I(J^P) = 1(\frac{1}{2}^+)$ Status: * * * *

COURANT 63 and ALFF-STEINBERGER 65, using $\Sigma^0 \rightarrow \Lambda e^+ e^-$ decays (Dalitz decays), determined the Σ^0 parity to be positive, given that $J = 1/2$ and that certain very reasonable assumptions about form factors are true. The results of experiments involving the Primakoff effect, from which the Σ^0 mean life and $\Sigma^0 \rightarrow \Lambda$ transition magnetic moment come (see below), strongly support $J = 1/2$.

Σ^0 MASS

The fit uses Σ^+ , Σ^0 , Σ^- , and Λ mass and mass-difference measurements.

VALUE (MeV)	EVTS	DOCUMENT ID	TECN	COMMENT
1192.642 ± 0.024 OUR FIT				
• • • We do not use the following data for averages, fits, limits, etc. • • •				
1192.65 ± 0.020 ± 0.014	3327	¹ WANG	97	SPEC $\Sigma^0 \rightarrow \Lambda\gamma \rightarrow (\rho\pi^-)(e^+e^-)$
¹ This WANG 97 result is redundant with the Σ^0 - Λ mass-difference measurement below.				

$m_{\Sigma^-} - m_{\Sigma^0}$

VALUE (MeV)	EVTS	DOCUMENT ID	TECN	COMMENT
4.607 ± 0.035 OUR FIT				Error includes scale factor of 1.1.
4.66 ± 0.08 OUR AVERAGE				Error includes scale factor of 1.2.
4.87 ± 0.12	37	DOSCH	65	HBC
5.01 ± 0.12	12	SCHMIDT	65	HBC See note with Λ mass
4.75 ± 0.1	18	BURNSTEIN	64	HBC

$m_{\Sigma^0} - m_{\Lambda}$

VALUE (MeV)	EVTS	DOCUMENT ID	TECN	COMMENT
76.959 ± 0.023 OUR FIT				
76.966 ± 0.020 ± 0.013	3327	WANG	97	SPEC $\Sigma^0 \rightarrow \Lambda\gamma \rightarrow (\rho\pi^-)(e^+e^-)$
• • • We do not use the following data for averages, fits, limits, etc. • • •				
76.23 ± 0.55	109	COLAS	75	HLBC $\Sigma^0 \rightarrow \Lambda\gamma$
76.63 ± 0.28	208	SCHMIDT	65	HBC See note with Λ mass

See key on page 239

Baryon Particle Listings

≡⁰

≡ BARYONS
(S = -2, I = 1/2)
 $\Xi^0 = uss, \Xi^- = dss$

≡⁰

$I(J^P) = \frac{1}{2}(\frac{1}{2}^+)$ Status: ****

The parity has not actually been measured, but + is of course expected.

≡⁰ MASS

The fit uses the $\Xi^0, \Xi^-,$ and Ξ^+ mass and mass difference measurements.

VALUE (MeV)	EVTS	DOCUMENT ID	TECN	COMMENT
1314.83 ± 0.20 OUR FIT				
1314.82 ± 0.20 OUR AVERAGE				
1314.82 ± 0.06 ± 0.20	3120	FANTI	00 NA48	p Be, 450 GeV
1315.2 ± 0.92	49	WILQUET	72 HLBC	
1313.4 ± 1.8	1	PALMER	68 HBC	

$m_{\Xi^-} - m_{\Xi^0}$

The fit uses the $\Xi^0, \Xi^-,$ and Ξ^+ mass and mass difference measurements.

VALUE (MeV)	EVTS	DOCUMENT ID	TECN	COMMENT
6.48 ± 0.24 OUR FIT				
6.3 ± 0.7 OUR AVERAGE				
6.9 ± 2.2	29	LONDON	66 HBC	
6.1 ± 0.9	88	PJERROU	65b HBC	
6.8 ± 1.6	23	JAUNEAU	63 FBC	
6.1 ± 1.6	45	CARMONY	64b HBC	See PJERROU 65b

≡⁰ MEAN LIFE

VALUE (10 ⁻¹⁰ s)	EVTS	DOCUMENT ID	TECN	COMMENT
2.90 ± 0.09 OUR AVERAGE				
2.83 ± 0.16	6300	¹ ZECH	77 SPEC	Neutral hyperon beam
2.88 ^{+0.21} _{-0.19}	652	BALTAY	74 HBC	1.75 GeV/c K ⁻ p
2.90 ^{+0.32} _{-0.27}	157	² MAYEUR	72 HLBC	2.1 GeV/c K ⁻
3.07 ^{+0.22} _{-0.20}	340	DAUBER	69 HBC	
3.0 ± 0.5	80	PJERROU	65b HBC	
2.5 ^{+0.4} _{-0.3}	101	HUBBARD	64 HBC	
3.9 ^{+1.4} _{-0.8}	24	JAUNEAU	63 FBC	
3.5 ^{+1.0} _{-0.8}	45	CARMONY	64b HBC	See PJERROU 65b

¹ The ZECH 77 result is $\tau_{\Xi^0} = [2.77 - (\tau_A - 2.69)] \times 10^{-10}$ s, in which we use $\tau_A = 2.63 \times 10^{-10}$ s.
² The MAYEUR 72 value is modified by the erratum.

≡⁰ MAGNETIC MOMENT

See the "Note on Baryon Magnetic Moments" in the Λ Listings.

VALUE (μ_N)	EVTS	DOCUMENT ID	TECN	COMMENT
-1.250 ± 0.014 OUR AVERAGE				
-1.253 ± 0.014	270k	COX	81 SPEC	
-1.20 ± 0.06	42k	BUNCE	79 SPEC	

≡⁰ DECAY MODES

Mode	Fraction (Γ_i/Γ)	Scale factor/Confidence level
$\Gamma_1 \Lambda\pi^0$	(99.51 ± 0.05) %	S=1.2
$\Gamma_2 \Lambda\gamma$	(1.18 ± 0.30) × 10 ⁻³	S=2.0
$\Gamma_3 \Sigma^0\gamma$	(3.5 ± 0.4) × 10 ⁻³	
$\Gamma_4 \Sigma^+ e^- \bar{\nu}_e$	(2.7 ± 0.4) × 10 ⁻⁴	
$\Gamma_5 \Sigma^+ \mu^- \bar{\nu}_\mu$	< 1.1 × 10 ⁻³	CL=90%

ΔS = ΔQ (S_Q) violating modes or ΔS = 2 forbidden (S₂) modes

$\Gamma_6 \Sigma^- e^+ \nu_e$	S _Q < 9	× 10 ⁻⁴	CL=90%
$\Gamma_7 \Sigma^- \mu^+ \nu_\mu$	S _Q < 9	× 10 ⁻⁴	CL=90%
$\Gamma_8 p\pi^-$	S ₂ < 4	× 10 ⁻⁵	CL=90%
$\Gamma_9 p e^- \bar{\nu}_e$	S ₂ < 1.3	× 10 ⁻³	
$\Gamma_{10} p \mu^- \bar{\nu}_\mu$	S ₂ < 1.3	× 10 ⁻³	

CONSTRAINED FIT INFORMATION

An overall fit to 3 branching ratios uses 5 measurements and one constraint to determine 4 parameters. The overall fit has a $\chi^2 = 4.2$ for 2 degrees of freedom.

The following off-diagonal array elements are the correlation coefficients $\langle \delta x_i \delta x_j \rangle / (\delta x_i \delta x_j)$, in percent, from the fit to the branching fractions, $x_i \equiv \Gamma_i/\Gamma_{\text{total}}$. The fit constrains the x_i whose labels appear in this array to sum to one.

x_2	-62		
x_3	-78	0	
x_4	-8	0	0
	x_1	x_2	x_3

≡⁰ BRANCHING RATIOS

$\Gamma(\Lambda\gamma)/\Gamma(\Lambda\pi^0)$ Γ_2/Γ_1

VALUE (units 10 ⁻³)	EVTS	DOCUMENT ID	TECN	COMMENT
1.19 ± 0.30 OUR FIT				Error includes scale factor of 2.0.
1.19 ± 0.30 OUR AVERAGE				Error includes scale factor of 2.0.
1.91 ± 0.34 ± 0.19	31	³ FANTI	00 NA48	p Be, 450 GeV
1.06 ± 0.12 ± 0.11	116	JAMES	90 SPEC	FNAL hyperons

³ FANTI 00 used our 1998 value of 99.5% for the $\Xi^0 \rightarrow \Lambda\pi^0$ branching fraction to get $\Gamma(\Xi^0 \rightarrow \Lambda\gamma)/\Gamma_{\text{total}} = (1.90 \pm 0.34 \pm 0.19) \times 10^{-3}$. We adjust slightly to go back to what was directly measured.

$\Gamma(\Sigma^0\gamma)/\Gamma(\Lambda\pi^0)$ Γ_3/Γ_1

VALUE (units 10 ⁻³)	EVTS	DOCUMENT ID	TECN	COMMENT
3.5 ± 0.4 OUR FIT				
3.5 ± 0.4 OUR AVERAGE				
3.16 ± 0.76 ± 0.32	17	⁴ FANTI	00 NA48	p Be, 450 GeV
3.56 ± 0.42 ± 0.10	85	TEIGE	89 SPEC	FNAL hyperons

⁴ FANTI 00 used our 1998 value of 99.5% for the $\Xi^0 \rightarrow \Lambda\pi^0$ branching fraction to get $\Gamma(\Xi^0 \rightarrow \Sigma^0\gamma)/\Gamma_{\text{total}} = (3.14 \pm 0.76 \pm 0.32) \times 10^{-3}$. We adjust slightly to go back to what was directly measured.

$\Gamma(\Sigma^+ e^- \bar{\nu}_e)/\Gamma_{\text{total}}$ Γ_4/Γ

VALUE (units 10 ⁻⁴)	EVTS	DOCUMENT ID	TECN	COMMENT
2.7 ± 0.4 OUR FIT				
2.71 ± 0.22 ± 0.31	176	AFFOLDER	99 KTEV	p nucleus 800 GeV

$\Gamma(\Sigma^+ \mu^- \bar{\nu}_\mu)/\Gamma(\Lambda\pi^0)$ Γ_5/Γ_1

VALUE (units 10 ⁻³)	CL%	EVTS	DOCUMENT ID	TECN	COMMENT
<1.1	90	0	YEH	74 HBC	Effective denom.=2100
<1.5			DAUBER	69 HBC	
<7			HUBBARD	66 HBC	

$\Gamma(\Sigma^- e^+ \nu_e)/\Gamma(\Lambda\pi^0)$ Γ_6/Γ_1

Test of $\Delta S = \Delta Q$ rule.

VALUE (units 10 ⁻³)	CL%	EVTS	DOCUMENT ID	TECN	COMMENT
<0.9	90	0	YEH	74 HBC	Effective denom.=2500
<1.5			DAUBER	69 HBC	
<6			HUBBARD	66 HBC	

$\Gamma(\Sigma^- \mu^+ \nu_\mu)/\Gamma(\Lambda\pi^0)$ Γ_7/Γ_1

Test of $\Delta S = \Delta Q$ rule.

VALUE (units 10 ⁻³)	CL%	EVTS	DOCUMENT ID	TECN	COMMENT
<0.9	90	0	YEH	74 HBC	Effective denom.=2500
<1.5			DAUBER	69 HBC	
<6			HUBBARD	66 HBC	

$\Gamma(p\pi^-)/\Gamma(\Lambda\pi^0)$ Γ_8/Γ_1

ΔS=2. Forbidden in first-order weak interaction.

VALUE (units 10 ⁻⁵)	CL%	EVTS	DOCUMENT ID	TECN	COMMENT
< 3.6	90		GEWENIGER	75 SPEC	
<180	90	0	YEH	74 HBC	Effective denom.=1300
< 90			DAUBER	69 HBC	
<500			HUBBARD	66 HBC	

CHARMED BARYONS ($C = +1$)

$$\Lambda_c^+ = udc, \quad \Sigma_c^{++} = uuc, \quad \Sigma_c^+ = udc, \quad \Sigma_c^0 = ddc,$$

$$\Xi_c^+ = usc, \quad \Xi_c^0 = dsc, \quad \Omega_c^0 = ssc$$

CHARMED BARYONS

Revised April 2000 by C.G. Wohl (LBNL).

There are now ten (!) known charmed baryons, each with one c quark. Figure 1(a) shows the mass spectrum, and for comparison Fig. 1(b) shows the spectrum of the lightest strange baryons. The Λ_c and Σ_c spectra ought to look much like the Λ and Σ spectra, since a Λ_c or a Σ_c is obtained from a Λ or a Σ by changing the s quark to a c quark. However, a Ξ or an Ω has more than one s quark, only *one* of which is changed to a c quark to make a Ξ_c or an Ω_c . Thus the Ξ_c and Ω_c spectra ought to be richer than the Ξ or Ω spectra.

Before discussing the observed spectra, we review the theory of SU(4) multiplets, which tells us what charmed baryons we should expect to find; this is essential, because the spin-parity assignments given in Fig. 1(a) have not been measured but have been assigned in accord with expectations of the theory.

SU(4) multiplets—Baryons made from u , d , s , and c quarks belong to SU(4) multiplets. The multiplet numerology, analogous to $3 \times 3 \times 3 = 10 + 8_1 + 8_2 + 1$ for the subset of baryons made from just u , d , and s quarks, is $4 \times 4 \times 4 = 20 + 20'_1 + 20'_2 + \bar{4}$. Figure 2(a) shows the $20'$ -plet whose bottom level is an SU(3) octet, such as the octet that includes the nucleon. Figure 2(b) shows the 20 -plet whose bottom level is an SU(3) decuplet, such as the decuplet that includes the $\Delta(1232)$. One level up in each multiplet are the baryons with one c quark. The $\bar{4}$ multiplet (not shown), an inverted tetrahedron, contains a Λ , a Λ_c^+ , a Ξ_c^+ , and a Ξ_c^0 (states at the centers of the four faces of the $20'$ -plet). All the baryons in a given multiplet have the same spin and parity. Each N or Δ or SU(3)-singlet- Λ resonance calls for another $20'$ - or 20 - or $\bar{4}$ -plet, respectively.

The flavor symmetries shown in Fig. 2 are of course very badly broken, but the figure is the simplest way to see what charmed baryons should exist. For example, from Fig. 2(a), we expect to find, in the same $J^P = 1/2^+$ $20'$ -plet as the nucleon, a Λ_c , a Σ_c , *two* Ξ_c 's, and an Ω_c . Note that this Ω_c is not in the same SU(4) multiplet as the famous $J^P = 3/2^+$ Ω^- .

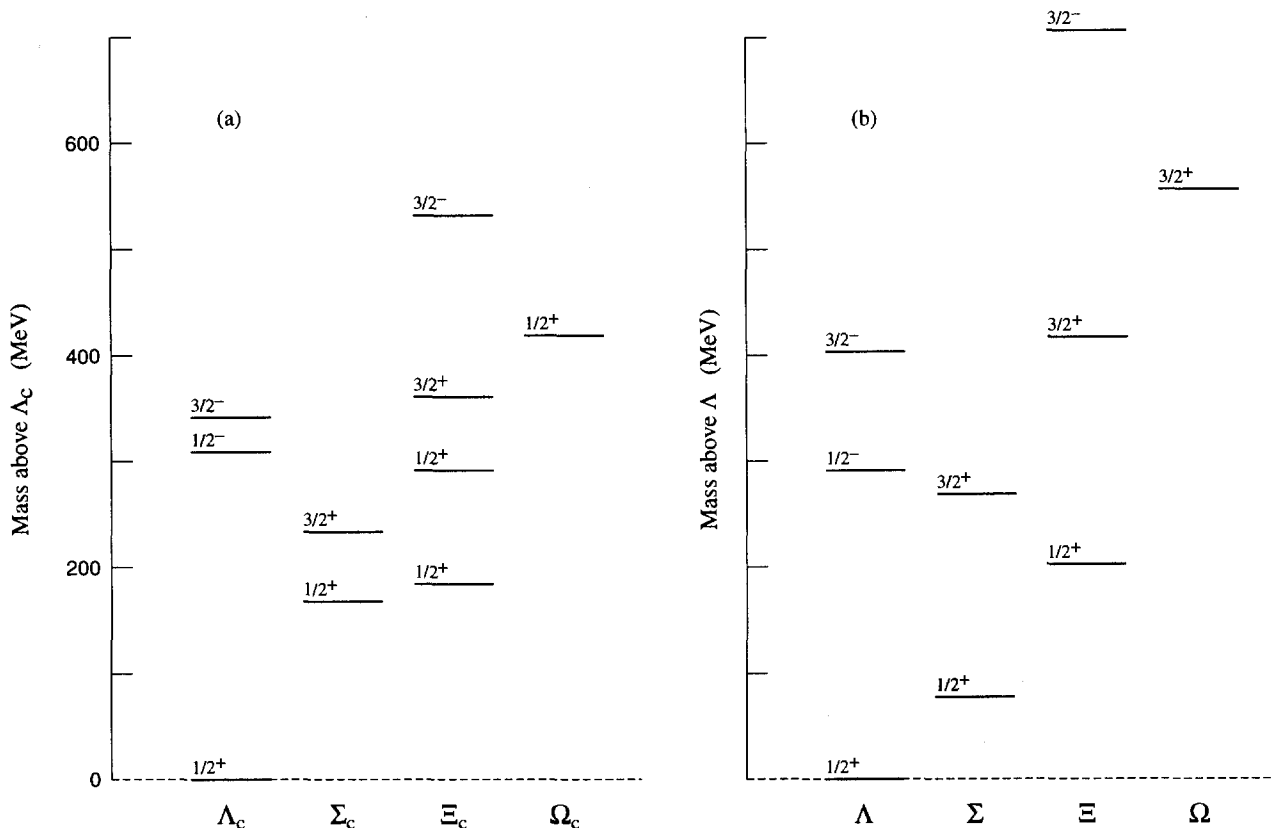


Figure 1. (a) The known charmed baryons, and (b) the lightest strange baryons. The baseline masses are $m(\Lambda_c) = 2284.9$ MeV and $m(\Lambda) = 1115.7$ MeV. Isospin splittings are not shown. Note that there are two $J^P = 1/2^+$ Ξ_c states, and that the Ω_c does not have $J = 3/2$. In fact, none of the J^P values of the charmed baryons has been measured (except perhaps for the $1/2^+ \Lambda_c$), but they are all very likely as shown—see the discussion.

CHARMED BARYONS ($C = +1$)

$$\Lambda_c^+ = udc, \quad \Sigma_c^{++} = uuc, \quad \Sigma_c^+ = udc, \quad \Sigma_c^0 = ddc,$$

$$\Xi_c^+ = usc, \quad \Xi_c^0 = dsc, \quad \Omega_c^0 = ssc$$

CHARMED BARYONS

Revised April 2000 by C.G. Wohl (LBNL).

There are now ten (!) known charmed baryons, each with one c quark. Figure 1(a) shows the mass spectrum, and for comparison Fig. 1(b) shows the spectrum of the lightest strange baryons. The Λ_c and Σ_c spectra ought to look much like the Λ and Σ spectra, since a Λ_c or a Σ_c is obtained from a Λ or a Σ by changing the s quark to a c quark. However, a Ξ or an Ω has more than one s quark, only *one* of which is changed to a c quark to make a Ξ_c or an Ω_c . Thus the Ξ_c and Ω_c spectra ought to be richer than the Ξ or Ω spectra.

Before discussing the observed spectra, we review the theory of SU(4) multiplets, which tells us what charmed baryons we should expect to find; this is essential, because the spin-parity assignments given in Fig. 1(a) have not been measured but have been assigned in accord with expectations of the theory.

SU(4) multiplets—Baryons made from u , d , s , and c quarks belong to SU(4) multiplets. The multiplet numerology, analogous to $3 \times 3 \times 3 = 10 + 8_1 + 8_2 + 1$ for the subset of baryons made from just u , d , and s quarks, is $4 \times 4 \times 4 = 20 + 20'_1 + 20'_2 + \bar{4}$. Figure 2(a) shows the $20'$ -plet whose bottom level is an SU(3) octet, such as the octet that includes the nucleon. Figure 2(b) shows the 20 -plet whose bottom level is an SU(3) decuplet, such as the decuplet that includes the $\Delta(1232)$. One level up in each multiplet are the baryons with one c quark. The $\bar{4}$ multiplet (not shown), an inverted tetrahedron, contains a Λ , a Λ_c^+ , a Ξ_c^+ , and a Ξ_c^0 (states at the centers of the four faces of the $20'$ -plet). All the baryons in a given multiplet have the same spin and parity. Each N or Δ or SU(3)-singlet- Λ resonance calls for another $20'$ - or 20 - or $\bar{4}$ -plet, respectively.

The flavor symmetries shown in Fig. 2 are of course very badly broken, but the figure is the simplest way to see what charmed baryons should exist. For example, from Fig. 2(a), we expect to find, in the same $J^P = 1/2^+$ $20'$ -plet as the nucleon, a Λ_c , a Σ_c , *two* Ξ_c 's, and an Ω_c . Note that this Ω_c is not in the same SU(4) multiplet as the famous $J^P = 3/2^+$ Ω^- .

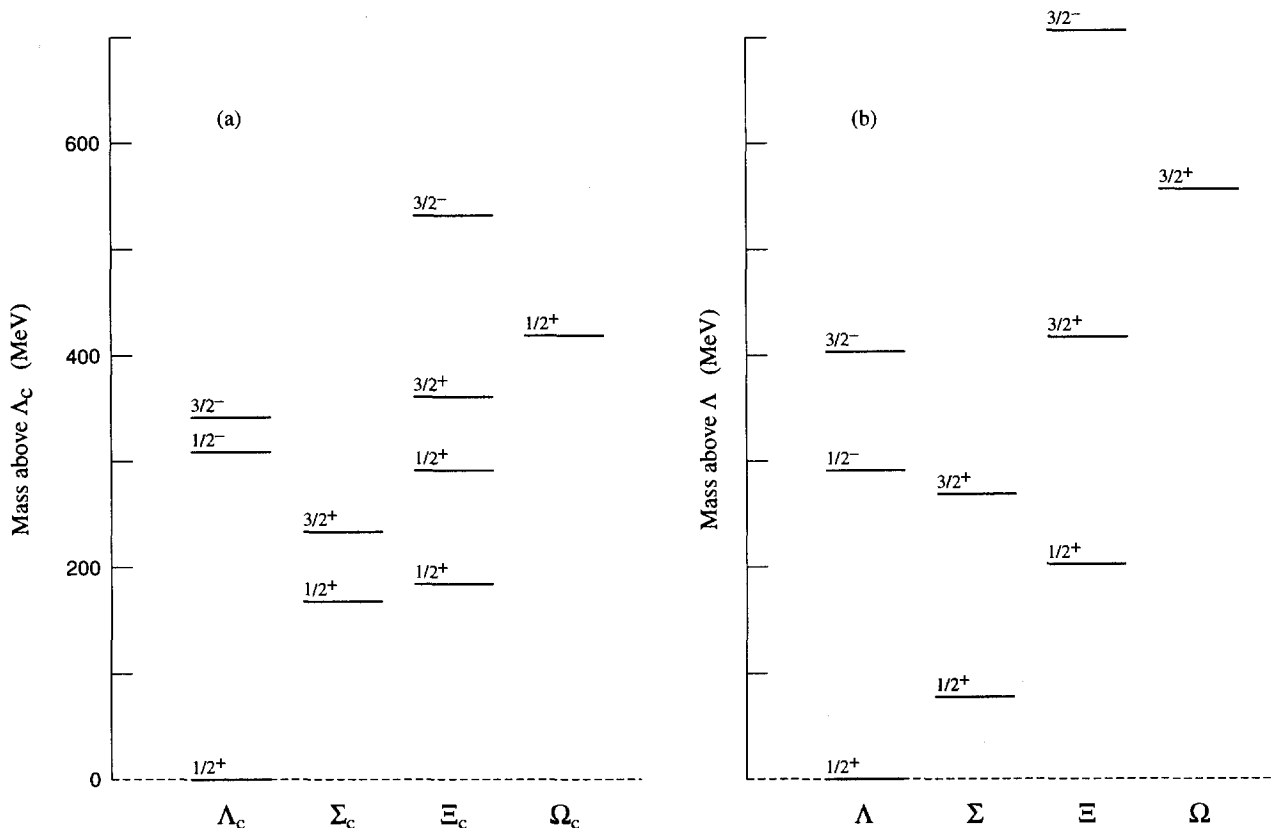


Figure 1. (a) The known charmed baryons, and (b) the lightest strange baryons. The baseline masses are $m(\Lambda_c) = 2284.9$ MeV and $m(\Lambda) = 1115.7$ MeV. Isospin splittings are not shown. Note that there are two $J^P = 1/2^+$ Ξ_c states, and that the Ω_c does not have $J = 3/2$. In fact, none of the J^P values of the charmed baryons has been measured (except perhaps for the $1/2^+ \Lambda_c$), but they are all very likely as shown—see the discussion.

Baryon Particle Listings

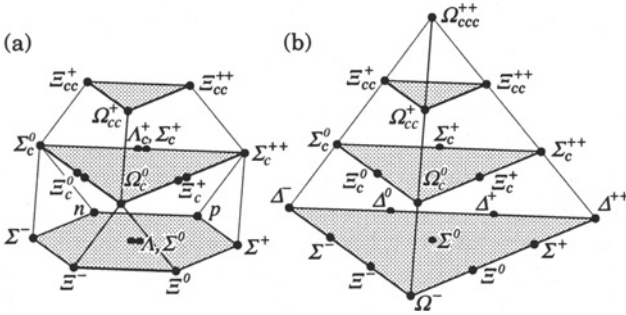
Charmed Baryons, Λ_c^+ 

Figure 2: SU(4) multiplets of baryons made of u , d , s , and c quarks. (a) The 20-plet with an SU(3) octet on the lowest level. (b) The 20-plet with an SU(3) decuplet on the lowest level.

Figure 3 shows in more detail the middle level of the 20'-plet of Fig. 2(a); it splits apart into two SU(3) multiplets, a $\bar{3}$ and a 6. The states of the $\bar{3}$ are antisymmetric under the interchange of the two light quarks (the u , d , and s quarks), whereas the states of the 6 are symmetric under this interchange. We use a prime to distinguish the Ξ_c in the 6 from the one in the $\bar{3}$.

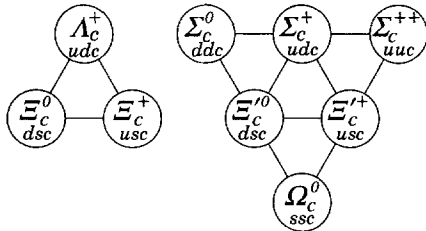


Figure 3: The SU(3) multiplets on the second level of the SU(4) multiplet of Fig. 2(a).

The observed spectra—(1) The parity of the lowest Λ_c is defined to be positive (as are the parities of the p , n , and Λ); and the limited evidence about its spin is consistent with $J = 1/2$. Otherwise, however, none of the J^P quantum numbers in Fig. 1(a) has been measured. Models using spin-spin and spin-orbit interactions between the quarks, with parameters determined using a few of the masses as input, lead to the J^P assignments shown.[†] There are no surprises: the $J^P = 1/2^+$ states come first, then the $J^P = 3/2^+$ states ...

(2) There is, however, strong evidence that at least some of the J^P assignments in Fig. 1(a) are correct. As is well known, the successive mass differences between the $J^P = 3/2^+$ $\Delta(1232)^-$, $\Sigma(1385)^-$, $\Xi(1535)^-$, and Ω^- , those particles along the lower left edge of the 20-plet in Fig. 2(b), should be, according to SU(3), and nearly are equal; see the $J^P = 3/2^+$

states in Fig. 1(b). Similarly, the mass differences between the $J^P = 1/2^+$ $\Sigma_c(2455)^0$, $\Xi_c^{\prime 0}$, and $\Omega_c^{\prime 0}$,[†] the particles along the left edge of Fig. 3(b), should be equal—assuming, of course, that they *do* all have the same J^P . And the observed differences are 126.6 ± 3.3 MeV and 125.2 ± 5.1 MeV—perfect, within errors. In fact, the mass difference between the presumed $J^P = 3/2^+$ $\Sigma_c(2520)^0$ and $\Xi_c(2645)^0$ is the same, 127.0 ± 2.3 MeV, which would put the $3/2^+$ Ω_c^0 at about 2772 MeV (= 487 MeV on Fig. 1(a)).

(3) Other evidence comes from the decay of the $\Lambda_c(2593)$. The only allowed strong decay is $\Lambda_c(2593)^+ \rightarrow \Lambda_c^+ \pi \pi$, and this appears to be dominated by the submode $\Sigma_c(2455)\pi$, despite little available phase space for the latter (the ‘ Q ’ is about 2 MeV, the c.m. decay momentum about 20 MeV/ c). Thus the decay is almost certainly s -wave, which, assuming that the $\Sigma_c(2455)$ does indeed have $J^P = 1/2^+$, makes $J^P = 1/2^-$ for the $\Lambda_c(2593)$.

(4) The heavier c baryons, such as the $J^P = 1/2^-$ and $3/2^-$ Λ_c 's, have much narrower widths than do their strange counterparts, such as the $\Lambda(1405)$ and $\Lambda(1520)$. The clean Λ_c spectrum has in fact been taken to settle the decades-long discussion about the nature of the $\Lambda(1405)$ —true 3-quark state or mere $\bar{K}N$ threshold effect?—unambiguously in favor of the first interpretation; which is not to say that the proximity of the $\bar{K}N$ threshold has no effect on the $\Lambda(1405)$.

Footnotes:

[†] This is not the place to discuss the details of the models, nor to attempt a guide to the literature. See the discovery papers of the various charmed baryons for references to the models that lead to the quantum-number assignments.

[‡] A reminder about the Particle Data Group naming scheme: A particle that decays strongly has its mass as part of its name; otherwise it doesn't. Thus $\Sigma(1385)$ and $\Sigma_c(2455)$ but Ω^- and Ξ_c' .

Λ_c^+

$I(J^P) = 0(\frac{1}{2}^+)$ Status: * * * *

The parity of the Λ_c^+ is defined to be positive (as are the parities of the proton, neutron, and Λ). The spin J has not actually been measured yet. Results of an analysis of $\rho K^- \pi^+$ decays (JEZABEK 92) are consistent with the expected $J = 1/2$. The quark content is udc .

We have omitted some results that have been superseded by later experiments. The omitted results may be found in earlier editions.

 Λ_c^+ MASS

Measurements with an error greater than 5 MeV or that are otherwise obsolete have been omitted.

The fit also includes $\Sigma_c - \Lambda_c^+$ and $\Lambda_c^{*+} - \Lambda_c^+$ mass-difference measurements.

VALUE (MeV)	EVTS	DOCUMENT ID	TECN	COMMENT
2284.9 ± 0.6 OUR FIT				
2284.9 ± 0.6 OUR AVERAGE				
2284.7 ± 0.6 ± 0.7	1134	AVERY	91 CLEO	Six modes
2281.7 ± 2.7 ± 2.6	29	ALVAREZ	90B NA14	$\rho K^- \pi^+$
2285.8 ± 0.6 ± 1.2	101	BARLAG	89 NA32	$\rho K^- \pi^+$
2284.7 ± 2.3 ± 0.5	5	AGUILAR...	88B LEBE	$\rho K^- \pi^+$
2283.1 ± 1.7 ± 2.0	628	ALBRECHT	88C ARG	$\rho K^- \pi^+$, ρK^0 , $\Lambda 3\pi$
2286.2 ± 1.7 ± 0.7	97	ANJOS	88B E691	$\rho K^- \pi^+$
2281 ± 3	2	JONES	87 HBC	$\rho K^- \pi^+$
2283 ± 3	3	BOSETTI	82 HBC	$\rho K^- \pi^+$
2290 ± 3	1	CALICCHIO	80 HYBR	$\rho K^- \pi^+$

Λ_c^+ MEAN LIFE

Measurements with an error $\geq 0.1 \times 10^{-12}$ s or with fewer than 20 events have been omitted.

VALUE (10^{-12} s)	EVTS	DOCUMENT ID	TECN	COMMENT
0.206 ± 0.012 OUR AVERAGE				
0.215 ± 0.016 ± 0.008	1340	FRABETTI	93D E687	γ Be, $\Lambda_c^+ \rightarrow pK^- \pi^+$
0.18 ± 0.03 ± 0.03	29	ALVAREZ	90 NA14	γ , $\Lambda_c^+ \rightarrow pK^- \pi^+$
0.20 ± 0.03 ± 0.03	90	FRABETTI	90 E687	γ Be, $\Lambda_c^+ \rightarrow pK^- \pi^+$
0.196 ^{+0.023} _{-0.020}	101	BARLAG	89 NA32	$pK^- \pi^+ + c.c.$
0.22 ± 0.03 ± 0.02	97	ANJOS	88B E691	$pK^- \pi^+ + c.c.$

Λ_c^+ DECAY MODES

Nearly all branching fractions of the Λ_c^+ are measured relative to the $pK^- \pi^+$ mode, but there are no model-independent measurements of this branching fraction. We explain how we arrive at our value of $B(\Lambda_c^+ \rightarrow pK^- \pi^+)$ in a Note at the beginning of the branching-ratio measurements, below. When this branching fraction is eventually well determined, all the other branching fractions will slide up or down proportionally as the true value differs from the value we use here.

Mode	Fraction (Γ_i/Γ)	Scale factor/ Confidence level
Hadronic modes with a p and one \bar{K}		
Γ_1 $p\bar{K}^0$	(2.3 ± 0.6) %	
Γ_2 $pK^- \pi^+$	[a] (5.0 ± 1.3) %	
Γ_3 $p\bar{K}^*(892)^0$	[b] (1.6 ± 0.5) %	
Γ_4 $\Delta(1232)^{++} K^-$	(8.6 ± 3.0) × 10 ⁻³	
Γ_5 $\Lambda(1520)\pi^+$	[b] (5.9 ± 2.1) × 10 ⁻³	
Γ_6 $pK^- \pi^+$ nonresonant	(2.8 ± 0.8) %	
Γ_7 $p\bar{K}^0 \pi^0$	(3.3 ± 1.0) %	
Γ_8 $p\bar{K}^0 \eta$	(1.2 ± 0.4) %	
Γ_9 $p\bar{K}^0 \pi^+ \pi^-$	(2.6 ± 0.7) %	
Γ_{10} $pK^- \pi^+ \pi^0$	(3.4 ± 1.0) %	
Γ_{11} $p\bar{K}^*(892)^- \pi^+$	[b] (1.1 ± 0.5) %	
Γ_{12} $p(K^- \pi^+)$ nonresonant π^0	(3.6 ± 1.2) %	
Γ_{13} $\Delta(1232)\bar{K}^*(892)$	seen	
Γ_{14} $pK^- \pi^+ \pi^+ \pi^-$	(1.1 ± 0.8) × 10 ⁻³	
Γ_{15} $pK^- \pi^+ \pi^0 \pi^0$	(8 ± 4) × 10 ⁻³	
Γ_{16} $pK^- \pi^+ \pi^0 \pi^0 \pi^0$	(5.0 ± 3.4) × 10 ⁻³	
Hadronic modes with a p and zero or two K's		
Γ_{17} $p\pi^+ \pi^-$	(3.5 ± 2.0) × 10 ⁻³	
Γ_{18} $p\bar{K}^0(980)$	[b] (2.8 ± 1.9) × 10 ⁻³	
Γ_{19} $p\pi^+ \pi^+ \pi^- \pi^-$	(1.8 ± 1.2) × 10 ⁻³	
Γ_{20} $pK^+ K^-$	(2.3 ± 0.9) × 10 ⁻³	
Γ_{21} $p\phi$	[b] (1.2 ± 0.5) × 10 ⁻³	
Hadronic modes with a hyperon		
Γ_{22} $\Lambda\pi^+$	(9.0 ± 2.8) × 10 ⁻³	
Γ_{23} $\Lambda\pi^+ \pi^0$	(3.6 ± 1.3) %	
Γ_{24} $\Lambda\rho^+$	< 5 %	CL=95%
Γ_{25} $\Lambda\pi^+ \pi^+ \pi^-$	(3.3 ± 1.0) %	
Γ_{26} $\Lambda\pi^+ \eta$	(1.8 ± 0.6) %	
Γ_{27} $\Sigma(1385)^+ \eta$	[b] (8.5 ± 3.3) × 10 ⁻³	
Γ_{28} $\Lambda K^+ \bar{K}^0$	(6.0 ± 2.1) × 10 ⁻³	
Γ_{29} $\Sigma^0 \pi^+$	(9.9 ± 3.2) × 10 ⁻³	
Γ_{30} $\Sigma^+ \pi^0$	(1.00 ± 0.34) %	
Γ_{31} $\Sigma^+ \eta$	(5.5 ± 2.3) × 10 ⁻³	
Γ_{32} $\Sigma^+ \pi^+ \pi^-$	(3.4 ± 1.0) %	
Γ_{33} $\Sigma^+ \rho^0$	< 1.4 %	CL=95%
Γ_{34} $\Sigma^- \pi^+ \pi^+$	(1.8 ± 0.8) %	
Γ_{35} $\Sigma^0 \pi^+ \pi^0$	(1.8 ± 0.8) %	
Γ_{36} $\Sigma^0 \pi^+ \pi^+ \pi^-$	(1.1 ± 0.4) %	
Γ_{37} $\Sigma^+ \pi^+ \pi^- \pi^0$	—	
Γ_{38} $\Sigma^+ \omega$	[b] (2.7 ± 1.0) %	
Γ_{39} $\Sigma^+ \pi^+ \pi^+ \pi^- \pi^-$	(3.0 ± 4.1) × 10 ⁻³	
Γ_{40} $\Sigma^+ K^+ K^-$	(3.5 ± 1.2) × 10 ⁻³	
Γ_{41} $\Sigma^+ \phi$	[b] (3.5 ± 1.7) × 10 ⁻³	
Γ_{42} $\Sigma^+ K^+ \pi^-$	(7 ± 6) × 10 ⁻³	
Γ_{43} $\Xi^0 K^+$	(3.9 ± 1.4) × 10 ⁻³	
Γ_{44} $\Xi^- K^+ \pi^+$	(4.9 ± 1.7) × 10 ⁻³	
Γ_{45} $\Xi(1530)^0 K^+$	[b] (2.6 ± 1.0) × 10 ⁻³	

Semileptonic modes

Γ_{46} $\Lambda\ell^+ \nu_\ell$	[c] (2.0 ± 0.6) %
Γ_{47} $\Lambda e^+ \nu_e$	(2.1 ± 0.6) %
Γ_{48} $\Lambda\mu^+ \nu_\mu$	(2.0 ± 0.7) %

Inclusive modes

Γ_{49} e^+ anything	(4.5 ± 1.7) %
Γ_{50} $p e^+$ anything	(1.8 ± 0.9) %
Γ_{51} Λe^+ anything	
Γ_{52} p anything	(50 ± 16) %
Γ_{53} p anything (no Λ)	(12 ± 19) %
Γ_{54} p hadrons	
Γ_{55} n anything	(50 ± 16) %
Γ_{56} n anything (no Λ)	(29 ± 17) %
Γ_{57} Λ anything	(35 ± 11) %
Γ_{58} Σ^\pm anything	[d] (10 ± 5) %

$\Delta C = 1$ weak neutral current (CI) modes, or Lepton number (L) violating modes

Γ_{59} $p\mu^+ \mu^-$	CI < 3.4	× 10 ⁻⁴	CL=90%
Γ_{60} $\Sigma^- \mu^+ \mu^+$	L < 7.0	× 10 ⁻⁴	CL=90%

[a] See the "Note on Λ_c^+ Branching Fractions" below.

[b] This branching fraction includes all the decay modes of the final-state resonance.

[c] An ℓ indicates an e or a μ mode, not a sum over these modes.

[d] The value is for the sum of the charge states or particle/antiparticle states indicated.

Λ_c^+ BRANCHING FRACTIONS

Revised 2000 by P.R. Burchat (Stanford University).

Most Λ_c^+ branching fractions are measured relative to the decay mode $\Lambda_c^+ \rightarrow pK^- \pi^+$. However, there are no model-independent measurements of the absolute branching fraction for $\Lambda_c^+ \rightarrow pK^- \pi^+$. Here we describe the measurements that have been used to extract $B(\Lambda_c^+ \rightarrow pK^- \pi^+)$, the model-dependence of the results, and the method we have used to average the results.

ARGUS (ALBRECHT 88C) and CLEO (CRAWFORD 92) measure $B(\bar{B} \rightarrow \Lambda_c^+ X) \times B(\Lambda_c^+ \rightarrow pK^- \pi^+)$ to be $(0.30 \pm 0.12 \pm 0.06)\%$ and $(0.273 \pm 0.051 \pm 0.039)\%$. Under the assumptions that decays of \bar{B} mesons to baryons are dominated by $\bar{B} \rightarrow \Lambda_c^+ X$ and that $\Lambda_c^+ X$ final states other than $\Lambda_c^+ \bar{N} X$ can be neglected, they also measure $B(\bar{B} \rightarrow \Lambda_c^+ X)$ to be $(6.8 \pm 0.5 \pm 0.3)\%$ (ALBRECHT 92O) and $(6.4 \pm 0.8 \pm 0.8)\%$ (CRAWFORD 92). Combining these results, we get $B(\Lambda_c^+ \rightarrow pK^- \pi^+) = (4.14 \pm 0.91)\%$. However, the assumption that \bar{B} decay modes to baryons other than $\Lambda_c^+ \bar{N} X$ are negligible is not on solid ground experimentally or theoretically [1]. Therefore, the branching fraction for $\Lambda_c^+ \rightarrow pK^- \pi^+$ given above may be low by some undetermined amount.

The second type of model-dependent determination of $B(\Lambda_c^+ \rightarrow pK^- \pi^+)$ is based on measurements by ARGUS (ALBRECHT 91G) and CLEO (BERGFELD 94) of $\sigma(e^+e^- \rightarrow \Lambda_c^+ X) \cdot B(\Lambda_c^+ \rightarrow \Lambda\ell^+ \nu_\ell) = (4.15 \pm 1.03 \pm 1.18)$ pb and $(4.77 \pm 0.25 \pm 0.66)$ pb. ARGUS (ALBRECHT 96E) and CLEO (AVERY 91) have also measured $\sigma(e^+e^- \rightarrow \Lambda_c^+ X) \cdot B(\Lambda_c^+ \rightarrow pK^- \pi^+)$. The weighted average is (11.2 ± 1.3) pb.

From these measurements, we extract $R \equiv B(\Lambda_c^+ \rightarrow pK^- \pi^+)/B(\Lambda_c^+ \rightarrow \Lambda\ell^+ \nu_\ell) = 2.40 \pm 0.43$. We estimate the $\Lambda_c^+ \rightarrow pK^- \pi^+$ branching fraction from the equation

Baryon Particle Listings

 Λ_c^+

$$B(\Lambda_c^+ \rightarrow pK^-\pi^+) = R f F \frac{\Gamma(D \rightarrow X\ell^+\nu_\ell)}{1 + |V_{cd}/V_{cs}|^2} \cdot \tau(\Lambda_c^+), \quad (1)$$

where $f = B(\Lambda_c^+ \rightarrow \Lambda\ell^+\nu_\ell)/B(\Lambda_c^+ \rightarrow X_s\ell^+\nu_\ell)$ and $F = \Gamma(\Lambda_c^+ \rightarrow X_s\ell^+\nu_\ell)/\Gamma(D^0 \rightarrow X_s\ell^+\nu_\ell)$. When we use $1 + |V_{cd}/V_{cs}|^2 = 1.05$ and the world averages $\Gamma(D \rightarrow X\ell^+\nu_\ell) = (0.163 \pm 0.006) \times 10^{-12} \text{ s}^{-1}$ and $\tau(\Lambda_c^+) = (0.206 \pm 0.012) \times 10^{-12} \text{ s}$, we calculate $B(\Lambda_c^+ \rightarrow pK^-\pi^+) = (7.7 \pm 1.5)\% \cdot f F$. Theoretical estimates for f and F are near 1.0 with significant uncertainties.

So, we have two results with significant model-dependence: $B(\Lambda_c^+ \rightarrow pK^-\pi^+) = (4.14 \pm 0.91)\%$ from \bar{B} decays, and $B(\Lambda_c^+ \rightarrow pK^-\pi^+) = (7.7 \pm 1.5)\% \cdot f F$ from semileptonic Λ_c^+ decays. If we set $f F = 1.0$ in the second result, and assign an uncertainty of 30% to each result to account for the unknown model-dependence, we get the consistent results $B(\Lambda_c^+ \rightarrow pK^-\pi^+) = (4.14 \pm 0.91 \pm 1.24)\%$ and $B(\Lambda_c^+ \rightarrow pK^-\pi^+) = (7.7 \pm 1.5 \pm 2.3)\%$. The weighted average of these two results is $B(\Lambda_c^+ \rightarrow pK^-\pi^+) = (5.0 \pm 1.3)\%$, where the uncertainty contains both the experimental uncertainty and the 30% estimate of model dependence in each result.

This procedure is clearly rather arbitrary, but so is any other procedure until good measurements of the absolute branching fraction are made. Therefore, we have assigned the value $(5.0 \pm 1.3)\%$ to the $\Lambda_c^+ \rightarrow pK^-\pi^+$ branching fraction (given as PDG 00 below). As was noted earlier, most of the other modes are measured relative to this mode.

New methods for measuring the Λ_c^+ absolute branching fractions have been proposed [1,2].

References

1. I. Dunietz, Phys. Rev. D **58**, 094010 (1998).
2. P. Migliozi *et al.*, Phys. Lett. **B462**, 217 (1999).

 Λ_c^+ BRANCHING RATIOS

————— Hadronic modes with a p and one \bar{K} —————

$\Gamma(p\bar{K}^0)/\Gamma(pK^-\pi^+)$				Γ_1/Γ_2
VALUE	EVTs	DOCUMENT ID	TECN	COMMENT
0.47 ± 0.04 OUR AVERAGE				
0.46 ± 0.02 ± 0.04	1025	ALAM	98 CLE2	$e^+e^- \approx \gamma(45)$
0.44 ± 0.07 ± 0.05	133	AVERY	91 CLEO	e^+e^- 10.5 GeV
0.55 ± 0.17 ± 0.14	45	ANJOS	90 E691	γ Be 70–260 GeV
0.62 ± 0.15 ± 0.03	73	ALBRECHT	88c ARG	e^+e^- 10 GeV

$\Gamma(pK^-\pi^+)/\Gamma_{\text{total}}$				Γ_2/Γ
See the "Note on Λ_c^+ Branching Fractions" above.				

VALUE	DOCUMENT ID	TECN	COMMENT
0.050 ± 0.013	PDG	00	See note at top of ratios
• • • We do not use the following data for averages, fits, limits, etc. • • •			
0.041 ± 0.010	1,2 ALBRECHT	92a ARG	$e^+e^- \approx \gamma(45)$
0.044 ± 0.012	1,3 CRAWFORD	92 CLEO	e^+e^- 10.5 GeV

¹ To extract $\Gamma(pK^-\pi^+)/\Gamma_{\text{total}}$, we use $B(\bar{B} \rightarrow \Lambda_c^+ X) \cdot B(\Lambda_c^+ \rightarrow pK^-\pi^+) = (0.28 \pm 0.06)\%$, which is the average of measurements from ARGUS (ALBRECHT 88c) and CLEO (CRAWFORD 92).

² ALBRECHT 92a measures $B(\bar{B} \rightarrow \Lambda_c^+ X) = (6.8 \pm 0.5 \pm 0.3)\%$.

³ CRAWFORD 92 measures $B(\bar{B} \rightarrow \Lambda_c^+ X) = (6.4 \pm 0.8 \pm 0.8)\%$.

 $\Gamma(p\bar{K}^*(892)^0)/\Gamma(pK^-\pi^+)$ Γ_3/Γ_2

$\Gamma(p\bar{K}^*(892)^0)/\Gamma(pK^-\pi^+)$				Γ_3/Γ_2
VALUE	EVTs	DOCUMENT ID	TECN	COMMENT
0.31 ± 0.04 OUR AVERAGE				
0.29 ± 0.04 ± 0.03		⁴ AITALA	00 E791	$\pi^- N$, 500 GeV
0.35 ^{+0.06} _{-0.07} ± 0.03	39	BOZEK	93 NA32	π^- Cu 230 GeV
0.42 ± 0.24	12	BASILE	81B CNTR	$pp \rightarrow \Lambda_c^+ e^- X$
• • • We do not use the following data for averages, fits, limits, etc. • • •				
0.35 ± 0.11		BARLAG	90d NA32	See BOZEK 93
⁴ AITALA 00 makes a coherent 5-dimensional amplitude analysis of $946 \pm 38 \Lambda_c^+ \rightarrow pK^-\pi^+$ decays.				

 $\Gamma(\Delta(1232)^{++}K^-)/\Gamma(pK^-\pi^+)$ Γ_4/Γ_2

$\Gamma(\Delta(1232)^{++}K^-)/\Gamma(pK^-\pi^+)$				Γ_4/Γ_2
VALUE	EVTs	DOCUMENT ID	TECN	COMMENT
0.17 ± 0.04 OUR AVERAGE				Error includes scale factor of 1.1.
0.18 ± 0.03 ± 0.03		⁵ AITALA	00 E791	$\pi^- N$, 500 GeV
0.12 ^{+0.04} _{-0.05} ± 0.05	14	BOZEK	93 NA32	π^- Cu 230 GeV
0.40 ± 0.17	17	BASILE	81B CNTR	$pp \rightarrow \Lambda_c^+ e^- X$
⁵ AITALA 00 makes a coherent 5-dimensional amplitude analysis of $946 \pm 38 \Lambda_c^+ \rightarrow pK^-\pi^+$ decays.				

 $\Gamma(\Lambda(1520)\pi^+)/\Gamma(pK^-\pi^+)$ Γ_5/Γ_2

$\Gamma(\Lambda(1520)\pi^+)/\Gamma(pK^-\pi^+)$				Γ_5/Γ_2
VALUE	EVTs	DOCUMENT ID	TECN	COMMENT
0.119 ± 0.032				Unseen decay modes of the $\Lambda(1520)$ are included.
0.17 ± 0.04 OUR AVERAGE				Error includes scale factor of 1.1.
0.15 ± 0.04 ± 0.02		⁶ AITALA	00 E791	$\pi^- N$, 500 GeV
0.09 ^{+0.04} _{-0.03} ± 0.02	12	BOZEK	93 NA32	π^- Cu 230 GeV
⁶ AITALA 00 makes a coherent 5-dimensional amplitude analysis of $946 \pm 38 \Lambda_c^+ \rightarrow pK^-\pi^+$ decays.				

 $\Gamma(pK^-\pi^+\text{nonresonant})/\Gamma(pK^-\pi^+)$ Γ_6/Γ_2

$\Gamma(pK^-\pi^+\text{nonresonant})/\Gamma(pK^-\pi^+)$				Γ_6/Γ_2
VALUE	EVTs	DOCUMENT ID	TECN	COMMENT
0.55 ± 0.06 OUR AVERAGE				
0.55 ± 0.06 ± 0.04		⁷ AITALA	00 E791	$\pi^- N$, 500 GeV
0.56 ^{+0.07} _{-0.09} ± 0.05	71	BOZEK	93 NA32	π^- Cu 230 GeV
⁷ AITALA 00 makes a coherent 5-dimensional amplitude analysis of $946 \pm 38 \Lambda_c^+ \rightarrow pK^-\pi^+$ decays.				

 $\Gamma(p\bar{K}^0\pi^0)/\Gamma(pK^-\pi^+)$ Γ_7/Γ_2

$\Gamma(p\bar{K}^0\pi^0)/\Gamma(pK^-\pi^+)$				Γ_7/Γ_2
VALUE	EVTs	DOCUMENT ID	TECN	COMMENT
0.66 ± 0.05 ± 0.07	774	ALAM	98 CLE2	$e^+e^- \approx \gamma(45)$

 $\Gamma(p\bar{K}^0\eta)/\Gamma(pK^-\pi^+)$ Γ_8/Γ_2

$\Gamma(p\bar{K}^0\eta)/\Gamma(pK^-\pi^+)$				Γ_8/Γ_2
VALUE	EVTs	DOCUMENT ID	TECN	COMMENT
0.25 ± 0.04 ± 0.04	57	AMMAR	95 CLE2	$e^+e^- \approx \gamma(45)$

 $\Gamma(p\bar{K}^0\pi^+\pi^-)/\Gamma(pK^-\pi^+)$ Γ_9/Γ_2

$\Gamma(p\bar{K}^0\pi^+\pi^-)/\Gamma(pK^-\pi^+)$				Γ_9/Γ_2
VALUE	EVTs	DOCUMENT ID	TECN	COMMENT
0.51 ± 0.06 OUR AVERAGE				
0.52 ± 0.04 ± 0.05	985	ALAM	98 CLE2	$e^+e^- \approx \gamma(45)$
0.43 ± 0.12 ± 0.04	83	AVERY	91 CLEO	e^+e^- 10.5 GeV
0.98 ± 0.36 ± 0.08	12	BARLAG	90d NA32	π^- 230 GeV

 $\Gamma(pK^-\pi^+\pi^0)/\Gamma(pK^-\pi^+)$ Γ_{10}/Γ_2

$\Gamma(pK^-\pi^+\pi^0)/\Gamma(pK^-\pi^+)$				Γ_{10}/Γ_2
VALUE	EVTs	DOCUMENT ID	TECN	COMMENT
0.67 ± 0.04 ± 0.11	2606	ALAM	98 CLE2	$e^+e^- \approx \gamma(45)$

 $\Gamma(pK^*(892)^-\pi^+)/\Gamma(p\bar{K}^0\pi^+\pi^-)$ Γ_{11}/Γ_9

$\Gamma(pK^*(892)^-\pi^+)/\Gamma(p\bar{K}^0\pi^+\pi^-)$				Γ_{11}/Γ_9
VALUE	EVTs	DOCUMENT ID	TECN	COMMENT
0.44 ± 0.14	17	ALEEV	94 B152	nN 20–70 GeV

 $\Gamma(p(K^-\pi^+)\text{nonresonant}\pi^0)/\Gamma(pK^-\pi^+)$ Γ_{12}/Γ_2

$\Gamma(p(K^-\pi^+)\text{nonresonant}\pi^0)/\Gamma(pK^-\pi^+)$				Γ_{12}/Γ_2
VALUE	EVTs	DOCUMENT ID	TECN	COMMENT
0.73 ± 0.12 ± 0.05	67	BOZEK	93 NA32	π^- Cu 230 GeV

 $\Gamma(\Delta(1232)\bar{K}^*(892))/\Gamma_{\text{total}}$ Γ_{13}/Γ

$\Gamma(\Delta(1232)\bar{K}^*(892))/\Gamma_{\text{total}}$				Γ_{13}/Γ
VALUE	EVTs	DOCUMENT ID	TECN	COMMENT
seen	35	AMENDOLIA	87 SPEC	γ Ge-Si

 $\Gamma(pK^-\pi^+\pi^+\pi^-)/\Gamma(pK^-\pi^+)$ Γ_{14}/Γ_2

$\Gamma(pK^-\pi^+\pi^+\pi^-)/\Gamma(pK^-\pi^+)$				Γ_{14}/Γ_2
VALUE	EVTs	DOCUMENT ID	TECN	COMMENT
0.022 ± 0.015		BARLAG	90d NA32	π^- 230 GeV

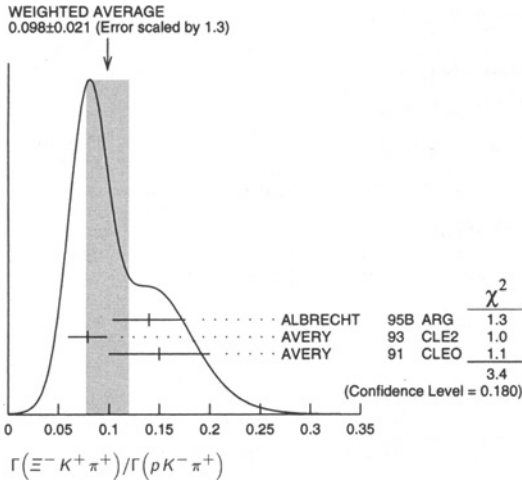
 $\Gamma(pK^-\pi^+\pi^0\pi^0)/\Gamma(pK^-\pi^+)$ Γ_{15}/Γ_2

$\Gamma(pK^-\pi^+\pi^0\pi^0)/\Gamma(pK^-\pi^+)$				Γ_{15}/Γ_2
VALUE	EVTs	DOCUMENT ID	TECN	COMMENT
0.16 ± 0.07 ± 0.03	15	BOZEK	93 NA32	π^- Cu 230 GeV

$\Gamma(\rho K^- \pi^+ \pi^0 \pi^0)/\Gamma(\rho K^- \pi^+)$					Γ_{16}/Γ_2	$\Gamma(\Lambda K^+ \bar{K}^0)/\Gamma(\rho K^- \pi^+)$					Γ_{28}/Γ_2
VALUE	EVTs	DOCUMENT ID	TECN	COMMENT		VALUE	EVTs	DOCUMENT ID	TECN	COMMENT	
$0.10 \pm 0.06 \pm 0.02$	8	BOZEK	93 NA32	π^- Cu 230 GeV		$0.12 \pm 0.02 \pm 0.02$	59	AMMAR	95 CLE2	$e^+ e^- \approx \Upsilon(4S)$	
----- Hadronic modes with a ρ and 0 or 2 K 's -----											
$\Gamma(\rho \pi^+ \pi^-)/\Gamma(\rho K^- \pi^+)$					Γ_{17}/Γ_2	$\Gamma(\Sigma^0 \pi^+)/\Gamma(\rho K^- \pi^+)$					Γ_{29}/Γ_2
VALUE		DOCUMENT ID	TECN	COMMENT		VALUE	EVTs	DOCUMENT ID	TECN	COMMENT	
0.069 ± 0.036		BARLAG	90D NA32	π^- 230 GeV		0.20 ± 0.04 OUR AVERAGE					
						$0.21 \pm 0.02 \pm 0.04$	196	AVERY	94 CLE2	$e^+ e^- \approx \Upsilon(3S), \Upsilon(4S)$	
						$0.17 \pm 0.06 \pm 0.04$		ALBRECHT	92 ARG	$e^+ e^- \approx 10.4$ GeV	
$\Gamma(\rho f_0(980))/\Gamma(\rho K^- \pi^+)$					Γ_{18}/Γ_2	$\Gamma(\Sigma^+ \pi^0)/\Gamma(\rho K^- \pi^+)$					Γ_{30}/Γ_2
Unseen decay modes of the $f_0(980)$ are included.						VALUE	EVTs	DOCUMENT ID	TECN	COMMENT	
0.055 ± 0.036		BARLAG	90D NA32	π^- 230 GeV		$0.20 \pm 0.03 \pm 0.03$	93	KUBOTA	93 CLE2	$e^+ e^- \approx \Upsilon(4S)$	
$\Gamma(\rho \pi^+ \pi^+ \pi^- \pi^-)/\Gamma(\rho K^- \pi^+)$					Γ_{19}/Γ_2	$\Gamma(\Sigma^+ \eta)/\Gamma(\rho K^- \pi^+)$					Γ_{31}/Γ_2
VALUE		DOCUMENT ID	TECN	COMMENT		VALUE	EVTs	DOCUMENT ID	TECN	COMMENT	
0.036 ± 0.023		BARLAG	90D NA32	π^- 230 GeV		$0.11 \pm 0.03 \pm 0.02$	26	AMMAR	95 CLE2	$e^+ e^- \approx \Upsilon(4S)$	
$\Gamma(\rho K^+ K^-)/\Gamma(\rho K^- \pi^+)$					Γ_{20}/Γ_2	$\Gamma(\Sigma^+ \pi^+ \pi^-)/\Gamma(\rho K^- \pi^+)$					Γ_{32}/Γ_2
VALUE	EVTs	DOCUMENT ID	TECN	COMMENT		VALUE	EVTs	DOCUMENT ID	TECN	COMMENT	
0.046 ± 0.012 OUR AVERAGE		Error includes scale factor of 1.2.				0.68 ± 0.09 OUR AVERAGE					
$0.039 \pm 0.009 \pm 0.007$	214	ALEXANDER	96C CLE2	$e^+ e^- \approx \Upsilon(4S)$		$0.74 \pm 0.07 \pm 0.09$	487	KUBOTA	93 CLE2	$e^+ e^- \approx \Upsilon(4S)$	
$0.096 \pm 0.029 \pm 0.010$	30	FRABETTI	93H E687	γ Be, \bar{E}_γ 220 GeV		$0.54^{+0.18}_{-0.15}$	11	BARLAG	92 NA32	π^- Cu 230 GeV	
0.048 ± 0.027		BARLAG	90D NA32	π^- 230 GeV							
$\Gamma(\rho \phi)/\Gamma(\rho K^- \pi^+)$					Γ_{21}/Γ_2	$\Gamma(\Sigma^+ \rho^0)/\Gamma(\rho K^- \pi^+)$					Γ_{33}/Γ_2
Unseen decay modes of the ϕ are included.						VALUE	CL%	DOCUMENT ID	TECN	COMMENT	
$0.024 \pm 0.006 \pm 0.003$	54	ALEXANDER	96C CLE2	$e^+ e^- \approx \Upsilon(4S)$		< 0.27	95	KUBOTA	93 CLE2	$e^+ e^- \approx \Upsilon(4S)$	
• • • We do not use the following data for averages, fits, limits, etc. • • •											
0.040 ± 0.027		BARLAG	90D NA32	π^- 230 GeV							
$\Gamma(\rho \phi)/\Gamma(\rho K^+ K^-)$					Γ_{21}/Γ_{20}	$\Gamma(\Sigma^- \pi^+ \pi^+)/\Gamma(\Sigma^+ \pi^+ \pi^-)$					Γ_{34}/Γ_{32}
Unseen decay modes of the ϕ are included.						VALUE	EVTs	DOCUMENT ID	TECN	COMMENT	
< 0.58	90	FRABETTI	93H E687	γ Be, \bar{E}_γ 220 GeV		$0.53 \pm 0.15 \pm 0.07$	56	FRABETTI	94E E687	γ Be, \bar{E}_γ 220 GeV	
• • • We do not use the following data for averages, fits, limits, etc. • • •											
----- Hadronic modes with a hyperon -----											
$\Gamma(\Lambda \pi^+)/\Gamma(\rho K^- \pi^+)$					Γ_{22}/Γ_2	$\Gamma(\Sigma^0 \pi^+ \pi^0)/\Gamma(\rho K^- \pi^+)$					Γ_{35}/Γ_2
VALUE	CL%	EVTs	DOCUMENT ID	TECN	COMMENT	VALUE	EVTs	DOCUMENT ID	TECN	COMMENT	
0.180 ± 0.032 OUR AVERAGE						$0.36 \pm 0.09 \pm 0.10$	117	AVERY	94 CLE2	$e^+ e^- \approx \Upsilon(3S), \Upsilon(4S)$	
$0.18 \pm 0.03 \pm 0.04$			ALBRECHT	92 ARG	$e^+ e^- \approx 10.4$ GeV						
$0.18 \pm 0.03 \pm 0.03$		87	AVERY	91 CLEO	$e^+ e^- \approx 10.5$ GeV						
• • • We do not use the following data for averages, fits, limits, etc. • • •											
< 0.33	90		ANJOS	90 E691	γ Be 70–260 GeV						
< 0.16	90		ALBRECHT	88C ARG	$e^+ e^-$ 10 GeV						
$\Gamma(\Lambda \pi^+ \pi^0)/\Gamma(\rho K^- \pi^+)$					Γ_{23}/Γ_2	$\Gamma(\Sigma^+ \omega)/\Gamma(\rho K^- \pi^+)$					Γ_{38}/Γ_2
VALUE	EVTs	DOCUMENT ID	TECN	COMMENT		Unseen decay modes of the ω are included.					
$0.73 \pm 0.09 \pm 0.16$	464	AVERY	94 CLE2	$e^+ e^- \approx \Upsilon(3S), \Upsilon(4S)$		$0.54 \pm 0.13 \pm 0.06$	107	KUBOTA	93 CLE2	$e^+ e^- \approx \Upsilon(4S)$	
$\Gamma(\Lambda \rho^+)/\Gamma(\rho K^- \pi^+)$					Γ_{24}/Γ_2	$\Gamma(\Sigma^+ \pi^+ \pi^+ \pi^- \pi^-)/\Gamma(\rho K^- \pi^+)$					Γ_{39}/Γ_2
VALUE	CL%	DOCUMENT ID	TECN	COMMENT		VALUE	EVTs	DOCUMENT ID	TECN	COMMENT	
< 0.95	95	AVERY	94 CLE2	$e^+ e^- \approx \Upsilon(3S), \Upsilon(4S)$		$0.06^{+0.08}_{-0.04}$	1	BARLAG	92 NA32	π^- Cu 230 GeV	
$\Gamma(\Lambda \pi^+ \pi^+ \pi^-)/\Gamma(\rho K^- \pi^+)$					Γ_{25}/Γ_2	$\Gamma(\Sigma^+ K^+ K^-)/\Gamma(\rho K^- \pi^+)$					Γ_{40}/Γ_2
VALUE	EVTs	DOCUMENT ID	TECN	COMMENT		VALUE	EVTs	DOCUMENT ID	TECN	COMMENT	
0.66 ± 0.11 OUR AVERAGE						$0.070 \pm 0.011 \pm 0.011$	59	AVERY	93 CLE2	$e^+ e^- \approx 10.5$ GeV	
$0.65 \pm 0.11 \pm 0.12$	289	AVERY	91 CLEO	$e^+ e^-$ 10.5 GeV							
$0.82 \pm 0.29 \pm 0.27$	44	ANJOS	90 E691	γ Be 70–260 GeV							
$0.94 \pm 0.41 \pm 0.13$	10	BARLAG	90D NA32	π^- 230 GeV							
$0.61 \pm 0.16 \pm 0.04$	105	ALBRECHT	88C ARG	$e^+ e^-$ 10 GeV							
$\Gamma(\rho \bar{K}^0 \pi^+ \pi^-)/\Gamma(\Lambda \pi^+ \pi^+ \pi^-)$					Γ_9/Γ_{25}	$\Gamma(\Sigma^+ \phi)/\Gamma(\rho K^- \pi^+)$					Γ_{41}/Γ_2
VALUE	EVTs	DOCUMENT ID	TECN	COMMENT		Unseen decay modes of the ϕ are included.					
2.6 ± 1.2		ALEEV	96 SPEC	n nucleus, 50 GeV/c		$0.069 \pm 0.023 \pm 0.016$	26	AVERY	93 CLE2	$e^+ e^- \approx 10.5$ GeV	
4.3 ± 1.2	130	ALEEV	84 BIS2	n C 40–70 GeV							
• • • We do not use the following data for averages, fits, limits, etc. • • •						$\Gamma(\Sigma^+ K^+ \pi^-)/\Gamma(\rho K^- \pi^+)$					Γ_{42}/Γ_2
VALUE	EVTs	DOCUMENT ID	TECN	COMMENT		VALUE	EVTs	DOCUMENT ID	TECN	COMMENT	
$0.35 \pm 0.05 \pm 0.06$	116	AMMAR	95 CLE2	$e^+ e^- \approx \Upsilon(4S)$		$0.13^{+0.12}_{-0.07}$	2	BARLAG	92 NA32	π^- Cu 230 GeV	
$\Gamma(\Sigma(1385)^+ \eta)/\Gamma(\rho K^- \pi^+)$					Γ_{27}/Γ_2	$\Gamma(\Xi^0 K^+)/\Gamma(\rho K^- \pi^+)$					Γ_{43}/Γ_2
Unseen decay modes of the $\Sigma(1385)^+$ are included.						VALUE	EVTs	DOCUMENT ID	TECN	COMMENT	
$0.17 \pm 0.04 \pm 0.03$	54	AMMAR	95 CLE2	$e^+ e^- \approx \Upsilon(4S)$		$0.078 \pm 0.013 \pm 0.013$	56	AVERY	93 CLE2	$e^+ e^- \approx 10.5$ GeV	
$\Gamma(\Sigma(1385)^+ \eta)/\Gamma(\rho K^- \pi^+)$					Γ_{27}/Γ_2	$\Gamma(\Xi^- K^+ \pi^+)/\Gamma(\rho K^- \pi^+)$					Γ_{44}/Γ_2
VALUE	EVTs	DOCUMENT ID	TECN	COMMENT		VALUE	EVTs	DOCUMENT ID	TECN	COMMENT	
$0.14 \pm 0.03 \pm 0.02$	34	ALBRECHT	95B ARG	$e^+ e^- \approx 10.4$ GeV		0.098 ± 0.021 OUR AVERAGE		Error includes scale factor of 1.3. See the Ideogram below.			
$0.079 \pm 0.013 \pm 0.014$	60	AVERY	93 CLE2	$e^+ e^- \approx 10.5$ GeV		$0.14 \pm 0.03 \pm 0.02$	34	ALBRECHT	95B ARG	$e^+ e^- \approx 10.4$ GeV	
$0.15 \pm 0.04 \pm 0.03$	30	AVERY	91 CLEO	$e^+ e^-$ 10.5 GeV		$0.079 \pm 0.013 \pm 0.014$	60	AVERY	93 CLE2	$e^+ e^- \approx 10.5$ GeV	

Baryon Particle Listings

Λ_c^+



$\Gamma(\Xi(1530)^0 K^+)/\Gamma(\rho K^- \pi^+)$ Γ₄₅/Γ₂

Unseen decay modes of the $\Xi(1530)^0$ are included.

VALUE	EVTS	DOCUMENT ID	TECN	COMMENT
0.052±0.014 OUR AVERAGE				
0.05 ± 0.02 ± 0.01	11	ALBRECHT 95B ARG		$e^+e^- \approx 10.4$ GeV
0.053 ± 0.016 ± 0.010	24	AVERY 93 CLE2		$e^+e^- \approx 10.5$ GeV

Semileptonic modes

$\Gamma(\Lambda e^+ \nu_e)/\Gamma(\rho K^- \pi^+)$ Γ₄₆/Γ₂

We average here the averages of the next two data blocks.

VALUE	DOCUMENT ID	TECN	COMMENT
0.41 ± 0.05 OUR AVERAGE			
0.42 ± 0.07	PDG 00		Our $\Gamma(\Lambda e^+ \nu_e)/\Gamma(\rho K^- \pi^+)$
0.39 ± 0.08	PDG 00		Our $\Gamma(\Lambda \mu^+ \nu_\mu)/\Gamma(\rho K^- \pi^+)$

$\Gamma(\Lambda e^+ \nu_e)/\Gamma(\rho K^- \pi^+)$ Γ₄₇/Γ₂

VALUE	DOCUMENT ID	TECN	COMMENT
0.42 ± 0.07 OUR AVERAGE			
0.43 ± 0.08	8,9 BERGFELD 94 CLE2		$e^+e^- \approx \Upsilon(4S)$
0.38 ± 0.14	9,10 ALBRECHT 91G ARG		$e^+e^- \approx 10.4$ GeV

⁸ BERGFELD 94 measures $\sigma(e^+e^- \rightarrow \Lambda_c^+ X) \cdot B(\Lambda_c^+ \rightarrow \Lambda e^+ \nu_e) = (4.87 \pm 0.28 \pm 0.69)$ pb.

⁹ To extract $\Gamma(\Lambda_c^+ \rightarrow \Lambda e^+ \nu_e)/\Gamma(\Lambda_c^+ \rightarrow \rho K^- \pi^+)$, we use $\sigma(e^+e^- \rightarrow \Lambda_c^+ X) \cdot B(\Lambda_c^+ \rightarrow \rho K^- \pi^+) = (11.2 \pm 1.3)$ pb, which is the weighted average of measurements from ARGUS (ALBRECHT 96E) and CLEO (AVERY 91).

¹⁰ ALBRECHT 91G measures $\sigma(e^+e^- \rightarrow \Lambda_c^+ X) \cdot B(\Lambda_c^+ \rightarrow \Lambda e^+ \nu_e) = (4.20 \pm 1.28 \pm 0.71)$ pb.

$\Gamma(\Lambda \mu^+ \nu_\mu)/\Gamma(\rho K^- \pi^+)$ Γ₄₈/Γ₂

VALUE	DOCUMENT ID	TECN	COMMENT
0.39 ± 0.06 OUR AVERAGE			
0.40 ± 0.09	11,12 BERGFELD 94 CLE2		$e^+e^- \approx \Upsilon(4S)$
0.35 ± 0.20	12,13 ALBRECHT 91G ARG		$e^+e^- \approx 10.4$ GeV

¹¹ BERGFELD 94 measures $\sigma(e^+e^- \rightarrow \Lambda_c^+ X) \cdot B(\Lambda_c^+ \rightarrow \Lambda \mu^+ \nu_\mu) = (4.43 \pm 0.51 \pm 0.64)$ pb.

¹² To extract $\Gamma(\Lambda_c^+ \rightarrow \Lambda \mu^+ \nu_\mu)/\Gamma(\Lambda_c^+ \rightarrow \rho K^- \pi^+)$, we use $\sigma(e^+e^- \rightarrow \Lambda_c^+ X) \cdot B(\Lambda_c^+ \rightarrow \rho K^- \pi^+) = (11.2 \pm 1.3)$ pb, which is the weighted average of measurements from ARGUS (ALBRECHT 96E) and CLEO (AVERY 91).

¹³ ALBRECHT 91G measures $\sigma(e^+e^- \rightarrow \Lambda_c^+ X) \cdot B(\Lambda_c^+ \rightarrow \Lambda \mu^+ \nu_\mu) = (3.91 \pm 2.02 \pm 0.90)$ pb.

Inclusive modes

$\Gamma(e^+ \text{ anything})/\Gamma_{\text{total}}$ Γ₄₉/Γ

VALUE	DOCUMENT ID	TECN	COMMENT
0.045 ± 0.017	VELLA 82 MRK2		e^+e^- 4.5–6.8 GeV

$\Gamma(\rho e^+ \text{ anything})/\Gamma_{\text{total}}$ Γ₅₀/Γ

VALUE	DOCUMENT ID	TECN	COMMENT
0.018 ± 0.009	14 VELLA 82 MRK2		e^+e^- 4.5–6.8 GeV

¹⁴ VELLA 82 includes protons from Λ decay.

$\Gamma(\Lambda e^+ \text{ anything})/\Gamma_{\text{total}}$ Γ₅₁/Γ

VALUE	DOCUMENT ID	TECN	COMMENT
0.011 ± 0.008	15 VELLA 82 MRK2		e^+e^- 4.5–6.8 GeV

¹⁵ VELLA 82 includes Λ 's from Σ^0 decay.

$\Gamma(\rho \text{ anything})/\Gamma_{\text{total}}$ Γ₅₂/Γ

VALUE	DOCUMENT ID	TECN	COMMENT
0.50 ± 0.08 ± 0.14	16 CRAWFORD 92 CLEO		e^+e^- 10.5 GeV

¹⁶ This CRAWFORD 92 value includes protons from Λ decay. The value is model dependent, but account is taken of this in the systematic error.

$\Gamma(\rho \text{ anything (no } \Lambda))/\Gamma_{\text{total}}$ Γ₅₃/Γ

VALUE	DOCUMENT ID	TECN	COMMENT
0.12 ± 0.10 ± 0.16	CRAWFORD 92 CLEO		e^+e^- 10.5 GeV

$\Gamma(n \text{ anything})/\Gamma_{\text{total}}$ Γ₅₅/Γ

VALUE	DOCUMENT ID	TECN	COMMENT
0.50 ± 0.08 ± 0.14	17 CRAWFORD 92 CLEO		e^+e^- 10.5 GeV

¹⁷ This CRAWFORD 92 value includes neutrons from Λ decay. The value is model dependent, but account is taken of this in the systematic error.

$\Gamma(n \text{ anything (no } \Lambda))/\Gamma_{\text{total}}$ Γ₅₆/Γ

VALUE	DOCUMENT ID	TECN	COMMENT
0.29 ± 0.09 ± 0.15	CRAWFORD 92 CLEO		e^+e^- 10.5 GeV

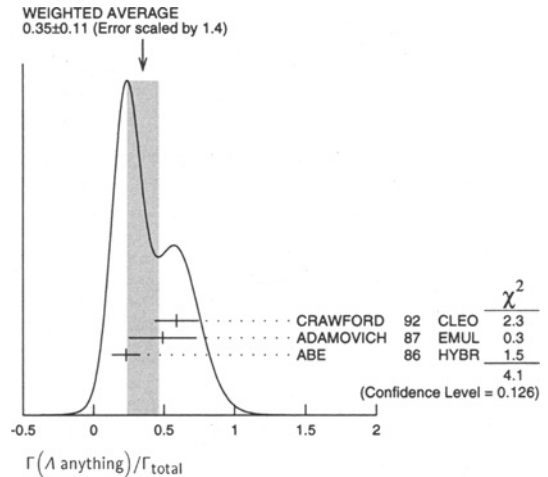
$\Gamma(\rho \text{ hadrons})/\Gamma_{\text{total}}$ Γ₅₄/Γ

VALUE	DOCUMENT ID	TECN	COMMENT
0.41 ± 0.24	ADAMOVIICH 87 EMUL		γA 20–70 GeV/c

$\Gamma(\Lambda \text{ anything})/\Gamma_{\text{total}}$ Γ₅₇/Γ

VALUE	EVTS	DOCUMENT ID	TECN	COMMENT
0.35 ± 0.11 OUR AVERAGE				Error includes scale factor of 1.4. See the ideogram below.
0.59 ± 0.10 ± 0.12		CRAWFORD 92 CLEO		e^+e^- 10.5 GeV
0.49 ± 0.24		ADAMOVIICH 87 EMUL		γA 20–70 GeV/c
0.23 ± 0.10	8	18 ABE 86 HYBR		20 GeV γp

¹⁸ ABE 86 includes Λ 's from Σ^0 decay.



$\Gamma(\Sigma^\pm \text{ anything})/\Gamma_{\text{total}}$ Γ₅₈/Γ

VALUE	EVTS	DOCUMENT ID	TECN	COMMENT
0.1 ± 0.05	5	ABE 86 HYBR		20 GeV γp

Rare or forbidden modes

$\Gamma(\rho \mu^+ \mu^-)/\Gamma_{\text{total}}$ Γ₅₉/Γ

A test for the $\Delta C=1$ weak neutral current. Allowed by higher-order electroweak interactions.

VALUE	CL%	EVTS	DOCUMENT ID	TECN	COMMENT
<3.4 × 10⁻⁴	90	0	KODAMA 95 E653		π^- emulsion 600 GeV

$\Gamma(\Sigma^- \mu^+ \mu^-)/\Gamma_{\text{total}}$ Γ₆₀/Γ

A test of lepton-number conservation.

VALUE	CL%	EVTS	DOCUMENT ID	TECN	COMMENT
<7.0 × 10⁻⁴	90	0	KODAMA 95 E653		π^- emulsion 600 GeV

Λ_c^+ DECAY PARAMETERS

See the "Note on Baryon Decay Parameters" in the neutron Listings.

α FOR $\Lambda_c^+ \rightarrow \Lambda \pi^+$

VALUE	EVTS	DOCUMENT ID	TECN	COMMENT
-0.90 ± 0.19 OUR AVERAGE				
-0.94 ± 0.21 ± 0.12	414	19 BISHAI 95 CLE2		$e^+e^- \approx \Upsilon(4S)$
-0.96 ± 0.42		ALBRECHT 92 ARG		$e^+e^- \approx 10.4$ GeV
-1.1 ± 0.4	86	AVERY 90B CLEO		$e^+e^- \approx 10.6$ GeV

¹⁹ BISHAI 95 actually gives $\alpha = -0.94^{+0.21+0.12}_{-0.06-0.06}$, chopping the errors at the physical limit -1.0. However, for $\alpha \approx -1.0$, some experiments should get unphysical values ($\alpha < -1.0$), and for averaging with other measurements such values (or errors that extend below -1.0) should not be chopped.

See key on page 239

Baryon Particle Listings

Λ_c^+ , $\Lambda_c(2593)^+$

α FOR $\Lambda_c^+ \rightarrow \Sigma^+ \pi^0$

VALUE	EVTS	DOCUMENT ID	TECN	COMMENT
$-0.45 \pm 0.31 \pm 0.06$	89	BISHAI	95 CLE2	$e^+ e^- \approx T(45)$

α FOR $\Lambda_c^+ \rightarrow \Lambda e^+ \nu_e$

The experiments don't cover the complete (or same incomplete) $M(\Lambda e^+)$ range, but we average them together anyway.

VALUE	EVTS	DOCUMENT ID	TECN	COMMENT
-0.82 ± 0.11 -0.07				OUR AVERAGE
$-0.82 \pm 0.09 \pm 0.06$ $-0.06 - 0.03$	700	²⁰ CRAWFORD	95 CLE2	$e^+ e^- \approx T(45)$
$-0.91 \pm 0.42 \pm 0.25$		²¹ ALBRECHT	94B ARG	$e^+ e^- \approx 10$ GeV
$-0.89 \pm 0.17 \pm 0.09$ $-0.11 - 0.05$	350	²² BERGFELD	94 CLE2	See CRAWFORD 95

²⁰ CRAWFORD 95 measures the form-factor ratio $R \equiv f_2/f_1$ for $\Lambda_c^+ \rightarrow \Lambda e^+ \nu_e$ events to be $-0.25 \pm 0.14 \pm 0.08$ and from this calculates α , averaged over q^2 , to be the above.
²¹ ALBRECHT 94B uses Λe^+ and $\Lambda \mu^+$ events in the mass range $1.85 < M(\Lambda e^+) < 2.20$ GeV.
²² BERGFELD 94 uses Λe^+ events.

Λ_c^+ REFERENCES

We have omitted some papers that have been superseded by later experiments. The omitted papers may be found in our 1992 edition (Physical Review D45, 1 June, Part II) or in earlier editions.

AITALA	00	PL B471 449	E.M. Aitala et al.	(FNAL E791 Collab.)
PDG	00	EPJ C15 1		
ALAM	98	PR D57 4467	M.S. Alam et al.	(CLEO Collab.)
ALBRECHT	96E	PR L 276 223	H. Albrecht et al.	(ARGUS Collab.)
ALEEV	96	JINRRC 3 31	A.N. Aleev et al.	(Serpukhov EXCHARM Collab.)
ALEXANDER	96C	PR D53 R1013	J.P. Alexander et al.	(CLEO Collab.)
ALBRECHT	95B	PL B342 397	H. Albrecht et al.	(ARGUS Collab.)
AMMAR	95	PRL 74 3534	R. Ammar et al.	(CLEO Collab.)
BISHAI	95	PL B350 256	M. Bishai et al.	(CLEO Collab.)
CRAWFORD	95	PRL 75 624	G. Crawford et al.	(CLEO Collab.)
KODAMA	95	PL B345 85	K. Kodama et al.	(FNAL E653 Collab.)
ALBRECHT	94B	PL B326 320	H. Albrecht et al.	(ARGUS Collab.)
ALEEV	94	PAN 57 1370	A.N. Aleev et al.	(Serpukhov BIS-2 Collab.)
		Translated from YF 57 1443		
AVERY	94	PL B325 257	P. Avery et al.	(CLEO Collab.)
BERGFELD	94	PL B323 219	T. Bergfeld et al.	(CLEO Collab.)
FRABETTI	94E	PL B328 193	P.L. Frabetti et al.	(FNAL E687 Collab.)
AVERY	93	PRL 71 2391	P. Avery et al.	(CLEO Collab.)
BOZEK	93	PL B312 247	A. Bozek et al.	(CERN NA32 Collab.)
FRABETTI	93D	PRL 70 1755	P.L. Frabetti et al.	(FNAL E687 Collab.)
FRABETTI	93H	PL B314 4777	P.L. Frabetti et al.	(FNAL E687 Collab.)
KUBOTA	93	PRL 71 3255	Y. Kubota et al.	(CLEO Collab.)
ALBRECHT	92	PL B274 239	H. Albrecht et al.	(ARGUS Collab.)
ALBRECHT	92O	ZPHY C56 1	H. Albrecht et al.	(ARGUS Collab.)
BARLAG	92	PL B283 465	S. Barlag et al.	(ACCMOR Collab.)
CRAWFORD	92	PR D45 752	G. Crawford et al.	(CLEO Collab.)
JEZABEK	92	PL B286 175	M. Jezabek, K. Rybicki, R. Rylko	(CRAC)
ALBRECHT	91G	PL B269 234	H. Albrecht et al.	(ARGUS Collab.)
AVERY	91	PR D43 3599	P. Avery et al.	(CLEO Collab.)
ALVAREZ	90	ZPHY C47 539	M.P. Alvarez et al.	(CERN NA14/2 Collab.)
ALVAREZ	90B	PL B246 256	M.P. Alvarez et al.	(CERN NA14/2 Collab.)
ANJOS	90	PR D41 801	J.C. Anjos et al.	(FNAL E691 Collab.)
AVERY	90B	PRL 65 2842	P. Avery et al.	(CLEO Collab.)
BARLAG	90D	ZPHY C48 29	S. Barlag et al.	(ACCMOR Collab.)
FRABETTI	90	PL B251 639	P.L. Frabetti et al.	(FNAL E687 Collab.)
BARLAG	89	PL B218 374	S. Barlag et al.	(ACCMOR Collab.)
AGUILAR...	88B	ZPHY C40 321	M. Aguilar-Benitez et al.	(LEBC-EHS Collab.)
Also	87	PL B189 254	M. Aguilar-Benitez et al.	(LEBC-EHS Collab.)
Also	87B	PL B199 462	M. Aguilar-Benitez et al.	(LEBC-EHS Collab.)
Also	88	SJNP 48 833	M. Begalli et al.	(LEBC-EHS Collab.)
		Translated from YAF 48 1310.		
ALBRECHT	88C	PL B207 109	H. Albrecht et al.	(ARGUS Collab.)
ANJOS	88B	PRL 60 1379	J.C. Anjos et al.	(FNAL E691 Collab.)
ADAMOVICH	87	EPL 4 887	M.I. Adamovich et al.	
Also	87	SJNP 46 447	F. Viaggi et al.	(Photon Emulsion Collab.)
		Translated from YAF 46 799.		
AMENDOLIA	87	ZPHY C36 513	S.R. Amendolia et al.	(CERN NA1 Collab.)
JONES	87	ZPHY C36 593	G.T. Jones et al.	(CERN WA21 Collab.)
ABE	86	PR D33 1	K. Abe et al.	
ALEEV	84	ZPHY C23 333	A.N. Aleev et al.	(BIS-2 Collab.)
BOSETTI	82	PRL 109B 234	P.C. Bosetti et al.	(AACH3, BONN, CERN+)
VELLA	82	PRL 48 1515	E. Vella et al.	(SLAC, LBL, UCBL)
BASILE	81B	NC 02A 14	M. Basile et al.	(CERN, BGNA, PGIA, FRAS)
CALICCHIO	80	PL 93B 521	M. Calicchio et al.	(BARI, BIRM, BRUX+)

OTHER RELATED PAPERS

MIGLIOZZI	99	PL B462 217	P. Migliozi et al.
DUNNETZ	98	PR D58 094010	I. Dunietz

$\Lambda_c(2593)^+$

$I(J^P) = 0(\frac{1}{2}^-)$ Status: ***

Seen in $\Lambda_c^+ \pi^+ \pi^-$ but not in $\Lambda_c^+ \pi^0$, so this is indeed an excited Λ_c^+ rather than a Σ_c^+ . The $\Lambda_c^+ \pi^+ \pi^-$ mode is largely, and perhaps entirely, $\Sigma_c \pi$, which is just at threshold; thus (assuming, as has not yet been proven, that the Σ_c has $J^P = 1/2^+$) the J^P here is almost certainly $1/2^-$. This result is in accord with the theoretical expectation that this is the charm counterpart of the strange $\Lambda(1405)$.

$\Lambda_c(2593)^+$ MASS

The mass is obtained from the $\Lambda_c(2593)^+ - \Lambda_c^+$ mass-difference measurements below.

VALUE (MeV)	DOCUMENT ID
2593.9 ± 0.8 OUR FIT	

$\Lambda_c(2593)^+ - \Lambda_c^+$ MASS DIFFERENCE

VALUE (MeV)	EVTS	DOCUMENT ID	TECN	COMMENT
308.9 ± 0.6 OUR FIT				Error includes scale factor of 1.1.
308.9 ± 0.6 OUR AVERAGE				Error includes scale factor of 1.1.
$309.7 \pm 0.9 \pm 0.4$	19	ALBRECHT	97 ARG	$e^+ e^- \approx 10$ GeV
$309.2 \pm 0.7 \pm 0.3$	14	¹ FRABETTI	96 E687	γ Be, $\bar{E}_\gamma \approx 220$ GeV
$307.5 \pm 0.4 \pm 1.0$	112	² EDWARDS	95 CLE2	$e^+ e^- \approx 10.5$ GeV

¹ FRABETTI 96 claims a signal of 13.9 ± 4.5 events.
² EDWARDS 95 claims a signal of 112.5 ± 16.5 events in $\Lambda_c^+ \pi^+ \pi^-$.

$\Lambda_c(2593)^+$ WIDTH

VALUE (MeV)	EVTS	DOCUMENT ID	TECN	COMMENT
3.6 ± 2.0 -1.3 OUR AVERAGE				
$2.9 \pm 2.9 \pm 1.8$ $-2.1 - 1.4$	19	ALBRECHT	97 ARG	$e^+ e^- \approx 10$ GeV
$3.9 \pm 1.4 \pm 2.0$ $-1.2 - 1.0$	112	EDWARDS	95 CLE2	$e^+ e^- \approx 10.5$ GeV

$\Lambda_c(2593)^+$ DECAY MODES

$\Lambda_c^+ \pi \pi$ and its submode $\Sigma_c(2455)\pi$ — the latter just barely — are the only strong decays allowed to an excited Λ_c^+ having this mass; and the submode seems to dominate.

Mode	Fraction (Γ_i/Γ)
$\Gamma_1 \Lambda_c^+ \pi^+ \pi^-$	$[a] \approx 67\%$
$\Gamma_2 \Sigma_c(2455)^{++} \pi^-$	$24 \pm 7\%$
$\Gamma_3 \Sigma_c(2455)^0 \pi^+$	$24 \pm 7\%$
$\Gamma_4 \Lambda_c^+ \pi^+ \pi^-$ 3-body	$18 \pm 10\%$
$\Gamma_5 \Lambda_c^+ \pi^0$	not seen
$\Gamma_6 \Lambda_c^+ \gamma$	not seen

[a] Assuming isospin conservation, so that the other third is $\Lambda_c^+ \pi^0 \pi^0$.

$\Lambda_c(2593)^+$ BRANCHING RATIOS

$\Gamma(\Sigma_c(2455)^{++} \pi^-) / \Gamma(\Lambda_c^+ \pi^+ \pi^-)$	TECN	COMMENT	Γ_2/Γ_1
---	------	---------	---------------------

0.36 ± 0.10 OUR AVERAGE			
$0.37 \pm 0.12 \pm 0.13$	ALBRECHT	97 ARG	$e^+ e^- \approx 10$ GeV
$0.36 \pm 0.09 \pm 0.09$	EDWARDS	95 CLE2	$e^+ e^- \approx 10.5$ GeV

$\Gamma(\Sigma_c(2455)^0 \pi^+) / \Gamma(\Lambda_c^+ \pi^+ \pi^-)$	TECN	COMMENT	Γ_3/Γ_1
--	------	---------	---------------------

0.37 ± 0.10 OUR AVERAGE			
$0.29 \pm 0.10 \pm 0.11$	ALBRECHT	97 ARG	$e^+ e^- \approx 10$ GeV
$0.42 \pm 0.09 \pm 0.09$	EDWARDS	95 CLE2	$e^+ e^- \approx 10.5$ GeV

$[\Gamma(\Sigma_c(2455)^{++} \pi^-) + \Gamma(\Sigma_c(2455)^0 \pi^+)] / \Gamma(\Lambda_c^+ \pi^+ \pi^-)$	TECN	COMMENT	$(\Gamma_2 + \Gamma_3)/\Gamma_1$
--	------	---------	----------------------------------

0.66 ± 0.13 -0.16 OUR AVERAGE			
$0.66 \pm 0.13 \pm 0.07$	ALBRECHT	97 ARG	$e^+ e^- \approx 10$ GeV
>0.51	90	³ FRABETTI	96 E687 γ Be, $\bar{E}_\gamma \approx 220$ GeV

• • • We do not use the following data for averages, fits, limits, etc. • • •

³ The results of FRABETTI 96 are consistent with this ratio being 100%.

Baryon Particle Listings

 $\Lambda_c(2593)^+$, $\Lambda_c(2625)^+$, $\Sigma_c(2455)$

$\Gamma(\Lambda_c^+ \pi^0)/\Gamma(\Lambda_c^+ \pi^+ \pi^-)$ Γ_5/Γ_1
 $\Lambda_c^+ \pi^0$ decay is forbidden by isospin conservation if this state is in fact a Λ_c .

VALUE	CL%	DOCUMENT ID	TECN	COMMENT
<3.53	90	EDWARDS 95	CLE2	$e^+ e^- \approx 10.5$ GeV

$\Gamma(\Lambda_c^+ \gamma)/\Gamma(\Lambda_c^+ \pi^+ \pi^-)$ Γ_6/Γ_1
 $e^+ e^- \approx 10.5$ GeV

 $\Lambda_c(2593)^+$ REFERENCES

ALBRECHT 97	PL B402 207	H. Albrecht et al.	(ARGUS Collab.)
FRABETTI 96	PL B365 461	P.L. Frabetti et al.	(FNAL E687 Collab.)
EDWARDS 95	PRL 74 3331	K.W. Edwards et al.	(CLEO Collab.)

$\Lambda_c(2625)^+$ $I(J^P) = 0(\frac{3}{2}^-)$ Status: * * *

Seen in $\Lambda_c^+ \pi^+ \pi^-$ but not in $\Lambda_c^+ \pi^0$ so this is indeed an excited Λ_c^+ rather than a Σ_c^+ . The spin-parity has not been measured but is expected to be $3/2^-$: this is presumably the charm counterpart of the strange $\Lambda(1520)$.

 $\Lambda_c(2625)^+$ MASS

The mass is obtained from the $\Lambda_c(2625)^+ - \Lambda_c^+$ mass-difference measurements below.

VALUE (MeV)	EVTs	DOCUMENT ID	TECN	COMMENT
2626.6 ± 0.8 OUR FIT				Error includes scale factor of 1.2.
• • • We do not use the following data for averages, fits, limits, etc. • • •				
2626.6 ± 0.5 ± 1.5	42	¹ ALBRECHT 93f	ARG	See ALBRECHT 97

¹ ALBRECHT 93f claims a signal of 42.4 ± 8.8 events.

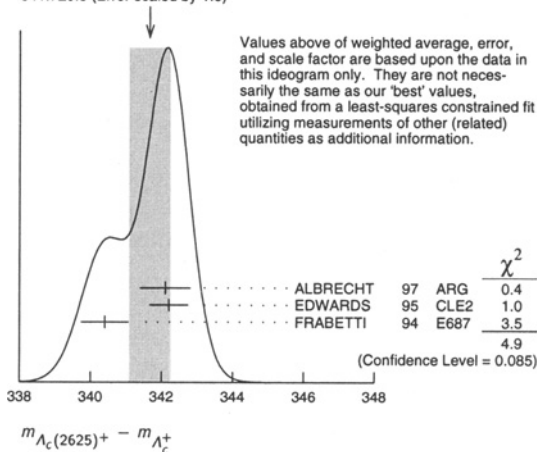
 $\Lambda_c(2625)^+ - \Lambda_c^+$ MASS DIFFERENCE

VALUE (MeV)	EVTs	DOCUMENT ID	TECN	COMMENT
341.7 ± 0.6 OUR FIT				Error includes scale factor of 1.6.
341.7 ± 0.6 OUR AVERAGE				Error includes scale factor of 1.6. See the Ideogram below.
342.1 ± 0.5 ± 0.5	51	ALBRECHT 97	ARG	$e^+ e^- \approx 10$ GeV
342.2 ± 0.2 ± 0.5	245	² EDWARDS 95	CLE2	$e^+ e^- \approx 10.5$ GeV
340.4 ± 0.6 ± 0.3	40	³ FRABETTI 94	E687	γ Be, $\bar{E}_\gamma = 220$ GeV

² EDWARDS 95 claims a signal of 244.6 ± 19.0 events in $\Lambda_c^+ \pi^+ \pi^-$.

³ FRABETTI 94 claims a signal of 39.7 ± 8.7 events.

WEIGHTED AVERAGE
 341.7 ± 0.6 (Error scaled by 1.6)

 $\Lambda_c(2625)^+$ WIDTH

VALUE (MeV)	CL%	EVTs	DOCUMENT ID	TECN	COMMENT
<1.9	90	245	EDWARDS 95	CLE2	$e^+ e^- \approx 10.5$ GeV
• • • We do not use the following data for averages, fits, limits, etc. • • •					
<3.2	90		ALBRECHT 93f	ARG	$e^+ e^- \approx \gamma(45)$

 $\Lambda_c(2625)^+$ DECAY MODES

$\Lambda_c^+ \pi \pi$ and its submode $\Sigma(2455)\pi$ are the only strong decays allowed to an excited Λ_c^+ having this mass.

Mode	Fraction (Γ_i/Γ)	Confidence level
Γ_1 $\Lambda_c^+ \pi^+ \pi^-$	[a] $\approx 67\%$	
Γ_2 $\Sigma_c(2455)^{++} \pi^-$	<5	90%
Γ_3 $\Sigma_c(2455)^0 \pi^+$	<5	90%
Γ_4 $\Lambda_c^+ \pi^+ \pi^-$ 3-body	large	
Γ_5 $\Lambda_c^+ \pi^0$	not seen	
Γ_6 $\Lambda_c^+ \gamma$	not seen	

[a] Assuming isospin conservation, so that the other third is $\Lambda_c^+ \pi^0 \pi^0$.

 $\Lambda_c(2625)^+$ BRANCHING RATIOS

$\Gamma(\Sigma_c(2455)^{++} \pi^-)/\Gamma(\Lambda_c^+ \pi^+ \pi^-)$ Γ_2/Γ_1
 $e^+ e^- \approx 10.5$ GeV

$\Gamma(\Sigma_c(2455)^0 \pi^+)/\Gamma(\Lambda_c^+ \pi^+ \pi^-)$ Γ_3/Γ_1
 $e^+ e^- \approx 10.5$ GeV

$[\Gamma(\Sigma_c(2455)^{++} \pi^-) + \Gamma(\Sigma_c(2455)^0 \pi^+)]/\Gamma(\Lambda_c^+ \pi^+ \pi^-)$ $(\Gamma_2 + \Gamma_3)/\Gamma_1$
 • • • We do not use the following data for averages, fits, limits, etc. • • •
 <0.36 90 FRABETTI 94 E687 γ Be, $\bar{E}_\gamma = 220$ GeV
 0.46 ± 0.14 21 ALBRECHT 93f ARG $e^+ e^- \approx \gamma(45)$

$\Gamma(\Lambda_c^+ \pi^+ \pi^- \text{ 3-body})/\Gamma(\Lambda_c^+ \pi^+ \pi^-)$ Γ_4/Γ_1
 • • • We do not use the following data for averages, fits, limits, etc. • • •
 0.54 ± 0.14 16 ALBRECHT 93f ARG $e^+ e^- \approx \gamma(45)$

$\Gamma(\Lambda_c^+ \pi^0)/\Gamma(\Lambda_c^+ \pi^+ \pi^-)$ Γ_5/Γ_1
 $\Lambda_c^+ \pi^0$ decay is forbidden by isospin conservation if this state is in fact a Λ_c .

$\Gamma(\Lambda_c^+ \gamma)/\Gamma(\Lambda_c^+ \pi^+ \pi^-)$ Γ_6/Γ_1
 $e^+ e^- \approx 10.5$ GeV

 $\Lambda_c(2625)^+$ REFERENCES

ALBRECHT 97	PL B402 207	H. Albrecht et al.	(ARGUS Collab.)
EDWARDS 95	PRL 74 3331	K.W. Edwards et al.	(CLEO Collab.)
FRABETTI 94	PRL 72 961	P.L. Frabetti et al.	(FNAL E687 Collab.)
ALBRECHT 93f	PL B317 227	H. Albrecht et al.	(ARGUS Collab.)

$\Sigma_c(2455)$ $I(J^P) = 1(\frac{1}{2}^+)$ Status: * * * *

Neither J nor P has been measured; $1/2^+$ is the quark model prediction.

 $\Sigma_c(2455)$ MASSES

The masses are obtained from the mass-difference measurements that follow.

 $\Sigma_c(2455)^{++}$ MASS

VALUE (MeV)	DOCUMENT ID
2452.8 ± 0.6 OUR FIT	

 $\Sigma_c(2455)^+$ MASS

VALUE (MeV)	DOCUMENT ID
2453.6 ± 0.9 OUR FIT	

 $\Sigma_c(2455)^0$ MASS

VALUE (MeV)	DOCUMENT ID
2452.2 ± 0.6 OUR FIT	

See key on page 239

Baryon Particle Listings

 $\Sigma_c(2455), \Sigma_c(2520)$ $\Sigma_c(2455) - \Lambda_c^+$ MASS DIFFERENCES

$m_{\Sigma_c^{++}} - m_{\Lambda_c^+}$				
VALUE (MeV)	EVTS	DOCUMENT ID	TECN	COMMENT
167.87 ± 0.19 OUR FIT				
167.87 ± 0.20 OUR AVERAGE				
167.76 ± 0.29 ± 0.15	122	AITALA 96B E791	$\pi^- N$, 500 GeV	
167.6 ± 0.6 ± 0.6	56	FRABETTI 96 E687	$\gamma Be, \bar{E}_\gamma \approx 220$ GeV	
168.2 ± 0.3 ± 0.2	126	CRAWFORD 93 CLE2	$e^+ e^- \approx \Upsilon(4S)$	
167.8 ± 0.4 ± 0.3	54	BOWCOCK 89 CLEO	$e^+ e^-$ 10 GeV	
168.2 ± 0.5 ± 1.6	92	ALBRECHT 88D ARG	$e^+ e^-$ 10 GeV	
167.4 ± 0.5 ± 2.0	46	DIESBURG 87 SPEC	$nA \sim 600$ GeV	
167 ± 1	2	JONES 87 HBC	νp in BEBC	
168 ± 3	6	BALTAY 79 HLBC	$\nu Ne-H$ in 15-ft	
• • • We do not use the following data for averages, fits, limits, etc. • • •				
166 ± 1	1	BOSETTI 82 HBC	See JONES 87	
166 ± 15	1	CAZZOLI 75 HBC	νp in BNL 7-ft	

$m_{\Sigma_c^+} - m_{\Lambda_c^+}$				
VALUE (MeV)	EVTS	DOCUMENT ID	TECN	COMMENT
168.7 ± 0.6 OUR FIT				
168 ± 3	1	CALICCHIO 80 HBC	νp in BEBC-TST	
• • • We do not use the following data for averages, fits, limits, etc. • • •				
168.5 ± 0.4 ± 0.2	111	¹ CRAWFORD 93 CLE2	$e^+ e^- \approx \Upsilon(4S)$	
¹ This result enters the fit through $m_{\Sigma_c^+} - m_{\Sigma_c^0}$ below.				

$m_{\Sigma_c^0} - m_{\Lambda_c^+}$				
VALUE (MeV)	EVTS	DOCUMENT ID	TECN	COMMENT
167.30 ± 0.20 OUR FIT				
167.31 ± 0.21 OUR AVERAGE				
167.38 ± 0.29 ± 0.15	143	AITALA 96B E791	$\pi^- N$, 500 GeV	
167.8 ± 0.6 ± 0.2		ALEEV 96 SPEC	n nucleus, 50 GeV/c	
166.6 ± 0.5 ± 0.6	69	FRABETTI 96 E687	$\gamma Be, \bar{E}_\gamma \approx 220$ GeV	
167.1 ± 0.3 ± 0.2	124	CRAWFORD 93 CLE2	$e^+ e^- \approx \Upsilon(4S)$	
168.4 ± 1.0 ± 0.3	14	ANJOS 89D E691	γBe 90–260 GeV	
• • • We do not use the following data for averages, fits, limits, etc. • • •				
167.9 ± 0.5 ± 0.3	48	² BOWCOCK 89 CLEO	$e^+ e^-$ 10 GeV	
167.0 ± 0.5 ± 1.6	70	² ALBRECHT 88D ARG	$e^+ e^-$ 10 GeV	
178.2 ± 0.4 ± 2.0	85	³ DIESBURG 87 SPEC	$nA \sim 600$ GeV	
163 ± 2	1	AMMAR 86 EMUL	νA	
² This result enters the fit through $m_{\Sigma_c^{++}} - m_{\Sigma_c^0}$ given below.				
³ See the note on DIESBURG 87 in the $m_{\Sigma_c^{++}} - m_{\Sigma_c^0}$ section below.				

 $\Sigma_c(2455)$ MASS DIFFERENCES

$m_{\Sigma_c^{++}} - m_{\Sigma_c^0}$				
VALUE (MeV)	EVTS	DOCUMENT ID	TECN	COMMENT
0.57 ± 0.23 OUR FIT				
0.66 ± 0.28 OUR AVERAGE Error includes scale factor of 1.1.				
+ 0.38 ± 0.40 ± 0.15		AITALA 96B E791	$\pi^- N$, 500 GeV	
1.1 ± 0.4 ± 0.1		CRAWFORD 93 CLE2	$e^+ e^- \approx \Upsilon(4S)$	
- 0.1 ± 0.6 ± 0.1		BOWCOCK 89 CLEO	$e^+ e^-$ 10 GeV	
+ 1.2 ± 0.7 ± 0.3		ALBRECHT 88D ARG	$e^+ e^- \sim 10$ GeV	
• • • We do not use the following data for averages, fits, limits, etc. • • •				
- 10.8 ± 2.9		⁴ DIESBURG 87 SPEC	$nA \sim 600$ GeV	
⁴ DIESBURG 87 is completely incompatible with the other experiments, which is surprising since it agrees with them about $m_{\Sigma_c(2455)^{++}} - m_{\Lambda_c^+}$. We go with the majority here.				

$m_{\Sigma_c^+} - m_{\Sigma_c^0}$				
VALUE (MeV)	EVTS	DOCUMENT ID	TECN	COMMENT
1.4 ± 0.6 OUR FIT				
1.4 ± 0.5 ± 0.3		CRAWFORD 93 CLE2	$e^+ e^- \approx \Upsilon(4S)$	

 $\Sigma_c(2455)$ DECAY MODES $\Lambda_c^+ \pi$ is the only strong decay allowed to a Σ_c having this mass.

Mode	Fraction (Γ_i/Γ)
$\Gamma_1 \Lambda_c^+ \pi$	$\approx 100\%$

 $\Sigma_c(2455)$ REFERENCES

AITALA 96B	PL B379 292	E.M. Aitala <i>et al.</i>	(FNAL E751 Collab.)
ALEEV 96	JINRRC 3 31	A.N. Aleev <i>et al.</i>	(Serpukhov EXCHARM Collab.)
FRABETTI 96	PL B365 461	P.L. Frabetti <i>et al.</i>	(FNAL E687 Collab.)
CRAWFORD 93	PRL 71 3259	G. Crawford <i>et al.</i>	(CLEO Collab.)
ANJOS 89D	PRL 62 1721	J.C. Anjos <i>et al.</i>	(FNAL E691 Collab.)
BOWCOCK 89	PRL 62 1240	T.J.V. Bowcock <i>et al.</i>	(CLEO Collab.)
ALBRECHT 88D	PL B211 489	H. Albrecht <i>et al.</i>	(ARGUS Collab.)
DIESBURG 87	PRL 59 2711	M. Diesburg <i>et al.</i>	(FNAL E400 Collab.)
JONES 87	ZPHY C36 593	G.T. Jones <i>et al.</i>	(CERN WA21 Collab.)
AMMAR 86	JETPL 43 515	R. Ammar <i>et al.</i>	(ITEP)
BOSETTI 82	Translated from ZETFP 43 401	P.C. Bosetti <i>et al.</i>	(AACH3, BONN, CERN++)
CALICCHIO 80	PL 93B 521	M. Calicchio <i>et al.</i>	(BARI, BIRM, BRUX++)
BALTAY 79	PRL 42 1721	C. Baltay <i>et al.</i>	(COLU, BNL I)
CAZZOLI 75	PRL 34 1125	E.G. Cazzoli <i>et al.</i>	(BNL)

 $\Sigma_c(2520)$

$$1(J^P) = 1(\frac{3}{2}^+) \text{ Status: } ***$$

Seen in the $\Lambda_c^+ \pi^\pm$ mass spectrum. The natural assignment is that this is the $J^P = 3/2^+$ excitation of the $\Sigma_c(2455)$, the charm counterpart of the $\Sigma(1385)$, but neither J nor P has been measured.

 $\Sigma_c(2520)$ MASSES

The masses are obtained from the mass-difference measurements that follow.

 $\Sigma_c(2520)^{++}$ MASS

VALUE (MeV)	EVTS	DOCUMENT ID	TECN	COMMENT
2519.4 ± 1.5 OUR FIT				
• • • We do not use the following data for averages, fits, limits, etc. • • •				
2530 ± 5 ± 5	6	¹ AMMOSOV 93 HLBC	$\nu p \rightarrow \mu^- \Sigma_c(2530)^{++}$	
¹ AMMOSOV 93 sees a cluster of 6 events and estimates the background to be 1 event.				

 $\Sigma_c(2520)^0$ MASS

VALUE (MeV)	DOCUMENT ID
2517.5 ± 1.4 OUR FIT	

 $\Sigma_c(2520)$ MASS DIFFERENCES

$m_{\Sigma_c(2520)^{++}} - m_{\Lambda_c^+}$				
VALUE (MeV)	EVTS	DOCUMENT ID	TECN	COMMENT
234.5 ± 1.4 OUR FIT				
234.5 ± 1.1 ± 0.8	677	BRANDENB... 97	CLE2	$e^+ e^- \approx \Upsilon(4S)$
$m_{\Sigma_c(2520)^0} - m_{\Lambda_c^+}$				
VALUE (MeV)	EVTS	DOCUMENT ID	TECN	COMMENT
232.6 ± 1.3 OUR FIT				
232.6 ± 1.0 ± 0.8	504	BRANDENB... 97	CLE2	$e^+ e^- \approx \Upsilon(4S)$
$m_{\Sigma_c(2520)^{++}} - m_{\Sigma_c(2520)^0}$				
VALUE (MeV)	EVTS	DOCUMENT ID	TECN	COMMENT
1.9 ± 1.7 OUR FIT				
1.9 ± 1.4 ± 1.0		² BRANDENB... 97	CLE2	$e^+ e^- \approx \Upsilon(4S)$
² This BRANDENBURG 97 result is redundant with measurements in earlier entries.				

 $\Sigma_c(2520)$ WIDTHS $\Sigma_c(2520)^{++}$ WIDTH

VALUE (MeV)	EVTS	DOCUMENT ID	TECN	COMMENT
17.9^{+3.8}_{-3.2} ± 4.0	677	BRANDENB... 97	CLE2	$e^+ e^- \approx \Upsilon(4S)$

 $\Sigma_c(2520)^0$ WIDTH

VALUE (MeV)	EVTS	DOCUMENT ID	TECN	COMMENT
13.0^{+3.7}_{-3.0} ± 4.0	504	BRANDENB... 97	CLE2	$e^+ e^- \approx \Upsilon(4S)$

 $\Sigma_c(2520)$ DECAY MODES $\Lambda_c^+ \pi$ is the only strong decay allowed to a Σ_c having this mass.

Mode	Fraction (Γ_i/Γ)
$\Gamma_1 \Lambda_c^+ \pi$	$\approx 100\%$

 $\Sigma_c(2520)$ REFERENCES

BRANDENB... 97	PRL 78 2304	G. Brandenburg <i>et al.</i>	(CLEO Collab.)
AMMOSOV 93	JETPL 58 247	V.V. Ammosov <i>et al.</i>	(SERP)
Translated from ZETFP 58 241.			

Baryon Particle Listings

 Ξ_c^+ Ξ_c^+

$$I(J^P) = \frac{1}{2}(\frac{1}{2}^+) \text{ Status: } ***$$

According to the quark model, the Ξ_c^+ (quark content usc) and Ξ_c^0 form an isospin doublet, and the spin-parity ought to be $J^P = 1/2^+$. None of I , J , or P has actually been measured.

 Ξ_c^+ MASS

The fit uses the Ξ_c^+ and Ξ_c^0 mass and mass-difference measurements.

VALUE (MeV)	EVTs	DOCUMENT ID	TECN	COMMENT
2466.3 ± 1.4 OUR FIT				
2466.4 ± 1.5 OUR AVERAGE				
2465.8 ± 1.9 ± 2.5	90	FRABETTI	98 E687	γ Be, $\bar{E}_\gamma = 220$ GeV
2467.0 ± 1.6 ± 2.0	147	EDWARDS	96 CLE2	$e^+e^- \approx \Upsilon(4S)$
2465.1 ± 3.6 ± 1.9	30	ALBRECHT	90f ARG	e^+e^- at $\Upsilon(4S)$
2467 ± 3 ± 4	23	ALAM	89 CLEO	e^+e^- 10.6 GeV
2466.5 ± 2.7 ± 1.2	5	BARLAG	89c ACCM	π^- Cu 230 GeV
• • • We do not use the following data for averages, fits, limits, etc. • • •				
2464.4 ± 2.0 ± 1.4	30	FRABETTI	93b E687	See FRABETTI 98
2459 ± 5 ± 30	56	¹ COTEUS	87 SPEC	$nA \approx 600$ GeV
2460 ± 25	82	BIAGI	83 SPEC	Σ^- Be 135 GeV

¹Although COTEUS 87 claims to agree well with BIAGI 83 on the mass and width, there appears to be a discrepancy between the two experiments. BIAGI 83 sees a single peak (stated significance about 6 standard deviations) in the $\Lambda K^- \pi^+ \pi^+$ mass spectrum. COTEUS 87 sees two peaks in the same spectrum, one at the Ξ_c^+ mass, the other 75 MeV lower. The latter is attributed to $\Xi_c^+ \rightarrow \Sigma^0 K^- \pi^+ \pi^+ \rightarrow (\Lambda \gamma) K^- \pi^+ \pi^+$, with the γ unseen. The combined significance of the double peak is stated to be 5.5 standard deviations. But the absence of any trace of a lower peak in BIAGI 83 seems to us to throw into question the interpretation of the lower peak of COTEUS 87.

 Ξ_c^+ MEAN LIFE

VALUE (10^{-12} s)	EVTs	DOCUMENT ID	TECN	COMMENT
0.33^{+0.06}_{-0.04} OUR AVERAGE				
0.34 ^{+0.07} _{-0.05} ± 0.02	56	FRABETTI	98 E687	γ Be, $\bar{E}_\gamma = 220$ GeV
0.20 ^{+0.11} _{-0.06}	6	BARLAG	89c ACCM	π^- (K^-) Cu 230 GeV
0.40 ^{+0.18} _{-0.12} ± 0.10	102	COTEUS	87 SPEC	$nA \approx 600$ GeV
0.48 ^{+0.21+0.20} _{-0.15-0.10}	53	BIAGI	85c SPEC	Σ^- Be 135 GeV
• • • We do not use the following data for averages, fits, limits, etc. • • •				
0.41 ^{+0.11} _{-0.08} ± 0.02	30	FRABETTI	93b E687	See FRABETTI 98

 Ξ_c^+ DECAY MODES

No absolute branching fractions have been measured. The following are branching ratios relative to $\Xi^- \pi^+ \pi^+$.

Mode	Fraction (Γ_i/Γ)	Confidence level
Γ_1 $\Lambda K^- \pi^+ \pi^+$	[a] 0.58 ± 0.18	
Γ_2 $\Lambda \bar{K}^*(892)^0 \pi^+$	[a,b] <0.29	90%
Γ_3 $\Sigma(1385)^+ K^- \pi^+$	[a,b] <0.41	90%
Γ_4 $\Sigma^+ K^- \pi^+$	[a] 1.18 ± 0.31	
Γ_5 $\Sigma^+ \bar{K}^*(892)^0$	[a,b] 0.92 ± 0.30	
Γ_6 $\Sigma^0 K^- \pi^+ \pi^+$	[a] 0.49 ± 0.26	
Γ_7 $\Xi^0 \pi^+$	[a] 0.55 ± 0.16	
Γ_8 $\Xi^- \pi^+ \pi^+$	[a] $\equiv 1.0$	
Γ_9 $\Xi(1530)^0 \pi^+$	[a,b] <0.2	90%
Γ_{10} $\Xi^0 \pi^+ \pi^0$	[a] 2.34 ± 0.68	
Γ_{11} $\Xi^0 \pi^+ \pi^+ \pi^-$	[a] 1.74 ± 0.50	
Γ_{12} $\Xi^0 e^+ \nu_e$	[a] 2.3 ^{+0.7} _{-0.9}	
Γ_{13} $\rho K^- \pi^+$	[a] 0.20 ± 0.05	

[a] No absolute branching fractions have been measured. The following are branching ratios relative to $\Xi^- \pi^+ \pi^+$.

[b] This branching fraction includes all the decay modes of the final-state resonance.

 Ξ_c^+ BRANCHING RATIOS

$$\Gamma(\Lambda K^- \pi^+ \pi^+)/\Gamma_{\text{total}} \quad \Gamma_1/\Gamma$$

VALUE	EVTs	DOCUMENT ID	TECN	COMMENT
seen	56	COTEUS	87 SPEC	$nA \approx 600$ GeV
seen	82	² BIAGI	83 SPEC	Σ^- Be 135 GeV

²BIAGI 85b looks for but does not see the Ξ_c^+ in $\rho K^- \bar{K}^0 \pi^+$ ($\Gamma(\rho K^- \bar{K}^0 \pi^+)/\Gamma(\Lambda K^- \pi^+ \pi^+) < 0.08$ with 90% CL), $\rho 2K^- 2\pi^+$ ($\Gamma(\rho 2K^- 2\pi^+)/\Gamma(\Lambda K^- \pi^+ \pi^+) < 0.03$, 90% CL), $\Omega^- K^+ \pi^+$, $\Lambda K^* 0 \pi^+$, and $\Sigma(1385)^+ K^- \pi^+$.

$$\Gamma(\Lambda K^- \pi^+ \pi^+)/\Gamma(\Xi^- \pi^+ \pi^+) \quad \Gamma_1/\Gamma_8$$

VALUE	EVTs	DOCUMENT ID	TECN	COMMENT
0.58 ± 0.16 ± 0.07	61	BERGFELD	96 CLE2	$e^+e^- \approx \Upsilon(4S)$

$$\Gamma(\Lambda \bar{K}^*(892)^0 \pi^+)/\Gamma(\Lambda K^- \pi^+ \pi^+) \quad \Gamma_2/\Gamma_1$$

Unseen decay modes of the $\bar{K}^*(892)^0$ are included.

VALUE	CL%	DOCUMENT ID	TECN	COMMENT
<0.5	90	BERGFELD	96 CLE2	$e^+e^- \approx \Upsilon(4S)$

$$\Gamma(\Sigma(1385)^+ K^- \pi^+)/\Gamma(\Lambda K^- \pi^+ \pi^+) \quad \Gamma_3/\Gamma_1$$

Unseen decay modes of the $\Sigma(1385)^+$ are included.

VALUE	CL%	DOCUMENT ID	TECN	COMMENT
<0.7	90	BERGFELD	96 CLE2	$e^+e^- \approx \Upsilon(4S)$

$$\Gamma(\Sigma^+ K^- \pi^+)/\Gamma(\Xi^- \pi^+ \pi^+) \quad \Gamma_4/\Gamma_8$$

VALUE	EVTs	DOCUMENT ID	TECN	COMMENT
1.18 ± 0.26 ± 0.17	119	BERGFELD	96 CLE2	$e^+e^- \approx \Upsilon(4S)$

• • • We do not use the following data for averages, fits, limits, etc. • • •

VALUE	EVTs	DOCUMENT ID	TECN	COMMENT
0.92 ± 0.20 ± 0.07		³ JUN	00 SELX	Σ^- nucleus, 600 GeV
0.09 ^{+0.13+0.03} _{-0.06-0.02}	5	BARLAG	89c ACCM	2 $\Sigma^+ K^- \pi^+$, 3 $\Xi^- \pi^+ \pi^+$

³This JUN 00 result is redundant with other results given below.

$$\Gamma(\Sigma^+ \bar{K}^*(892)^0 \pi^+)/\Gamma(\Xi^- \pi^+ \pi^+) \quad \Gamma_5/\Gamma_8$$

Unseen decay modes of the $\bar{K}^*(892)^0$ are included.

VALUE	EVTs	DOCUMENT ID	TECN	COMMENT
0.92 ± 0.27 ± 0.14	61	BERGFELD	96 CLE2	$e^+e^- \approx \Upsilon(4S)$

• • • We do not use the following data for averages, fits, limits, etc. • • •

VALUE	EVTs	DOCUMENT ID	TECN	COMMENT
seen	59	AVERY	95 CLE2	$e^+e^- \approx \Upsilon(4S)$

$$\Gamma(\Sigma^0 K^- \pi^+ \pi^+)/\Gamma(\Lambda K^- \pi^+ \pi^+) \quad \Gamma_6/\Gamma_1$$

VALUE	EVTs	DOCUMENT ID	TECN	COMMENT
0.84 ± 0.36	47	⁴ COTEUS	87 SPEC	$nA \approx 600$ GeV

⁴See, however, the note on the COTEUS 87 Ξ_c^+ mass measurement.

$$\Gamma(\Xi^0 \pi^+)/\Gamma(\Xi^- \pi^+ \pi^+) \quad \Gamma_7/\Gamma_8$$

VALUE	EVTs	DOCUMENT ID	TECN	COMMENT
0.55 ± 0.13 ± 0.09	39	EDWARDS	96 CLE2	$e^+e^- \approx \Upsilon(4S)$

$$\Gamma(\Xi^- \pi^+ \pi^+)/\Gamma_{\text{total}} \quad \Gamma_8/\Gamma$$

VALUE	EVTs	DOCUMENT ID	TECN	COMMENT
seen	131	BERGFELD	96 CLE2	$e^+e^- \approx \Upsilon(4S)$
seen	160	AVERY	95 CLE2	$e^+e^- \approx \Upsilon(4S)$
seen	30	FRABETTI	93b E687	γ Be, $\bar{E}_\gamma = 220$ GeV
seen	30	ALBRECHT	90f ARG	e^+e^- at $\Upsilon(4S)$
seen	23	ALAM	89 CLEO	e^+e^- 10.6 GeV

$$\Gamma(\Xi(1530)^0 \pi^+)/\Gamma(\Xi^- \pi^+ \pi^+) \quad \Gamma_9/\Gamma_8$$

Unseen decay modes of the $\Xi(1530)^0$ are included.

VALUE	CL%	DOCUMENT ID	TECN	COMMENT
<0.2	90	BERGFELD	96 CLE2	$e^+e^- \approx \Upsilon(4S)$

$$\Gamma(\Xi^0 \pi^+ \pi^0)/\Gamma(\Xi^- \pi^+ \pi^+) \quad \Gamma_{10}/\Gamma_8$$

VALUE	EVTs	DOCUMENT ID	TECN	COMMENT
2.34 ± 0.57 ± 0.37	81	EDWARDS	96 CLE2	$e^+e^- \approx \Upsilon(4S)$

$$\Gamma(\Xi(1530)^0 \pi^+)/\Gamma(\Xi^0 \pi^+ \pi^0) \quad \Gamma_9/\Gamma_{10}$$

• • • We do not use the following data for averages, fits, limits, etc. • • •

VALUE	CL%	DOCUMENT ID	TECN	COMMENT
<0.3	90	EDWARDS	96 CLE2	$e^+e^- \approx \Upsilon(4S)$

$$\Gamma(\Xi^0 \pi^+ \pi^+ \pi^-)/\Gamma(\Xi^- \pi^+ \pi^+) \quad \Gamma_{11}/\Gamma_8$$

VALUE	EVTs	DOCUMENT ID	TECN	COMMENT
1.74 ± 0.42 ± 0.27	57	EDWARDS	96 CLE2	$e^+e^- \approx \Upsilon(4S)$

$$\Gamma(\Xi^0 e^+ \nu_e)/\Gamma(\Xi^- \pi^+ \pi^+) \quad \Gamma_{12}/\Gamma_8$$

VALUE	EVTs	DOCUMENT ID	TECN	COMMENT
2.3 ± 0.6^{+0.3}_{-0.6}	41	ALEXANDER	95b CLE2	$e^+e^- \approx \Upsilon(4S)$

See key on page 239

Baryon Particle Listings

$$\Xi_c^+, \Xi_c^0, \Xi_c^-$$

$\Gamma(\rho K^- \pi^+)/\Gamma(\Sigma^+ K^- \pi^+)$		Γ_{13}/Γ_4	
VALUE	EVTs	DOCUMENT ID	TECN COMMENT
$0.22 \pm 0.06 \pm 0.03$	76	JUN	00 SELX Σ^- nucleus, 600 GeV

$\Gamma(\rho K^- \pi^+)/\Gamma(\Xi^- \pi^+ \pi^+)$		Γ_{13}/Γ_8	
VALUE	EVTs	DOCUMENT ID	TECN COMMENT
$0.20 \pm 0.04 \pm 0.02$	76	JUN	00 SELX Σ^- nucleus, 600 GeV

Ξ_c^+ REFERENCES

Author	Year	Pub	Collab	Comment
JUN	00	PRL 84 1857	S.Y. Jun et al.	(FNAL SELEX Collab.)
FRABETTI	98	PL B427 211	P.L. Frabetti et al.	(FNAL E687 Collab.)
BERGFELD	96	PL B365 431	T. Bergfeld et al.	(CLEO Collab.)
EDWARDS	96	PL B373 261	K.W. Edwards et al.	(CLEO Collab.)
ALEXANDER	95B	PRL 74 3113	J. Alexander et al.	(CLEO Collab.)
Also	95E	PRL 75 4155 (erratum)		
EVERY	95	PRL 75 4364	P. Avery et al.	(CLEO Collab.)
FRABETTI	93B	PRL 70 1381	P.L. Frabetti et al.	(FNAL E687 Collab.)
ALBRECHT	90F	PL B247 121	H. Albrecht et al.	(ARGUS Collab.)
ALAM	89	PL B226 401	M.S. Alam et al.	(CLEO Collab.)
BARLAG	89C	PL B233 522	S. Barlag et al.	(ACCMOR Collab.)
COTEUS	87	PRL 59 1530	P. Coteus et al.	(FNAL E400 Collab.)
BIAGI	85B	ZPHY C28 175	S.F. Biagi et al.	(CERN WA62 Collab.)
BIAGI	85C	PL 150B 230	S.F. Biagi et al.	(CERN WA62 Collab.)
BIAGI	83	PL 122B 455	S.F. Biagi et al.	(CERN WA62 Collab.)

$$\Xi_c^0$$

$$I(J^P) = \frac{1}{2}(\frac{1}{2}^+) \text{ Status: } ***$$

According to the quark model, the Ξ_c^0 (quark content dsc) and Ξ_c^+ form an isospin doublet, and the spin-parity ought to be $J^P = 1/2^+$. None of I, J , or P has actually been measured.

Ξ_c^0 MASS

The fit uses the Ξ_c^0 and Ξ_c^+ mass and mass-difference measurements.

VALUE (MeV)	EVTs	DOCUMENT ID	TECN COMMENT
2471.8 ± 1.4 OUR FIT			
2471.8 ± 1.4 OUR AVERAGE			
2470.0 ± 2.8 ± 2.6	85	FRABETTI 98B E687	γ Be, $\bar{E}_\gamma = 220$ GeV
2469 ± 2 ± 3	9	HENDERSON 92B CLEO	$\Omega^- K^+$
2472.1 ± 2.7 ± 1.6	54	ALBRECHT 90F ARG	$e^+ e^-$ at $T(4S)$
2473.3 ± 1.9 ± 1.2	4	BARLAG 90 ACCM	$\pi^- (K^-)$ Cu 230 GeV
2472 ± 3 ± 4	19	ALAM 89 CLEO	$e^+ e^- 10.6$ GeV
• • • We do not use the following data for averages, fits, limits, etc. • • •			
2462.1 ± 3.1 ± 1.4	42	¹ FRABETTI 93C E687	See FRABETTI 98B
2471 ± 3 ± 4	14	EVERY 89 CLEO	See ALAM 89

¹ The FRABETTI 93C mass is well below the other measurements.

$\Xi_c^0 - \Xi_c^+$ MASS DIFFERENCE

VALUE (MeV)	DOCUMENT ID	TECN COMMENT
5.5 ± 1.8 OUR FIT		
6.3 ± 2.3 OUR AVERAGE		
+7.0 ± 4.5 ± 2.2	ALBRECHT 90F ARG	$e^+ e^-$ at $T(4S)$
+6.8 ± 3.3 ± 0.5	BARLAG 90 ACCM	$\pi^- (K^-)$ Cu 230 GeV
+5 ± 4 ± 1	ALAM 89 CLEO	$\Xi_c^0 \rightarrow \Xi^- \pi^+, \Xi_c^+ \rightarrow \Xi^- \pi^+ \pi^+$

Ξ_c^0 MEAN LIFE

VALUE (10^{-12} s)	EVTs	DOCUMENT ID	TECN COMMENT
0.098 ± 0.023 - 0.015 OUR AVERAGE			
0.101 ± 0.025 - 0.017 ± 0.005	42	FRABETTI 93C E687	γ Be, $\bar{E}_\gamma = 220$ GeV
0.082 ± 0.059 - 0.030	4	BARLAG 90 ACCM	$\pi^- (K^-)$ Cu 230 GeV

Ξ_c^0 DECAY MODES

Mode	Fraction (Γ_i/Γ)
$\Gamma_1 \Lambda \bar{K}^0$	seen
$\Gamma_2 \Lambda \bar{K}^0 \pi^+ \pi^-$	seen
$\Gamma_3 \Lambda K^- \pi^+ \pi^+ \pi^-$	seen
$\Gamma_4 \Xi^- \pi^+$	seen
$\Gamma_5 \Xi^- \pi^+ \pi^+ \pi^-$	seen
$\Gamma_6 \rho K^- \bar{K}^*(892)^0$	seen
$\Gamma_7 \Omega^- K^+$	seen
$\Gamma_8 \Xi^- e^+ \nu_e$	seen
$\Gamma_9 \Xi^- \ell^+ \text{ anything}$	seen

Ξ_c^0 BRANCHING RATIOS

$\Gamma(\Lambda \bar{K}^0)/\Gamma_{total}$		Γ_1/Γ	
VALUE	EVTs	DOCUMENT ID	TECN COMMENT
seen	7	ALBRECHT 95B ARG	$e^+ e^- \approx 10.4$ GeV
$\Gamma(\Lambda \bar{K}^0 \pi^+ \pi^-)/\Gamma_{total}$		Γ_2/Γ	
VALUE	EVTs	DOCUMENT ID	TECN COMMENT
seen		FRABETTI 98B E687	γ Be, $\bar{E}_\gamma = 220$ GeV
$\Gamma(\Lambda K^- \pi^+ \pi^+ \pi^-)/\Gamma_{total}$		Γ_3/Γ	
VALUE	EVTs	DOCUMENT ID	TECN COMMENT
seen		FRABETTI 98B E687	γ Be, $\bar{E}_\gamma = 220$ GeV
$\Gamma(\Xi^- \pi^+)/\Gamma(\Xi^- \pi^+ \pi^+ \pi^-)$		Γ_4/Γ_5	
VALUE	EVTs	DOCUMENT ID	TECN COMMENT
$0.30 \pm 0.12 \pm 0.05$		ALBRECHT 90F ARG	$e^+ e^-$ at $T(4S)$
$\Gamma(\rho K^- \bar{K}^*(892)^0)/\Gamma_{total}$		Γ_6/Γ	
VALUE	EVTs	DOCUMENT ID	TECN COMMENT
seen		BARLAG 90 ACCM	$\pi^- (K^-)$ Cu 230 GeV
$\Gamma(\Omega^- K^+)/\Gamma(\Xi^- \pi^+)$		Γ_7/Γ_4	
VALUE	EVTs	DOCUMENT ID	TECN COMMENT
$0.50 \pm 0.21 \pm 0.05$	9	HENDERSON 92B CLEO	$e^+ e^- \approx 10.6$ GeV
$\Gamma(\Xi^- e^+ \nu_e)/\Gamma(\Xi^- \pi^+)$		Γ_8/Γ_4	
VALUE	EVTs	DOCUMENT ID	TECN COMMENT
$3.1 \pm 1.0_{-0.5}^{+0.3}$	54	ALEXANDER 95B CLE2	$e^+ e^- \approx T(4S)$
$\Gamma(\Xi^- \ell^+ \text{ anything})/\Gamma(\Xi^- \pi^+)$		Γ_9/Γ_4	
VALUE	EVTs	DOCUMENT ID	TECN COMMENT
$0.96 \pm 0.43 \pm 0.18$	18	ALBRECHT 93B ARG	$e^+ e^- \approx 10.4$ GeV
$\Gamma(\Xi^- \ell^+ \text{ anything})/\Gamma(\Xi^- \pi^+ \pi^+ \pi^-)$		Γ_9/Γ_5	
VALUE	EVTs	DOCUMENT ID	TECN COMMENT
$0.29 \pm 0.12 \pm 0.04$	18	ALBRECHT 93B ARG	$e^+ e^- \approx 10.4$ GeV

Ξ_c^0 REFERENCES

Author	Year	Pub	Collab	Comment
FRABETTI	98B	PL B426 403	P.L. Frabetti et al.	(FNAL E687 Collab.)
ALBRECHT	95B	PL B342 397	H. Albrecht et al.	(ARGUS Collab.)
ALEXANDER	95B	PRL 74 3113	J. Alexander et al.	(CLEO Collab.)
Also	95E	PRL 75 4155 (erratum)		
ALBRECHT	93B	PL B303 368	H. Albrecht et al.	(ARGUS Collab.)
FRABETTI	93C	PRL 70 2058	P.L. Frabetti et al.	(FNAL E687 Collab.)
HENDERSON	92B	PL B283 161	S. Henderson et al.	(CLEO Collab.)
ALBRECHT	90F	PL B247 121	H. Albrecht et al.	(ARGUS Collab.)
BARLAG	90	PL B236 495	S. Barlag et al.	(ACCMOR Collab.)
ALAM	89	PL B226 401	M.S. Alam et al.	(CLEO Collab.)
EVERY	89	PRL 62 863	P. Avery et al.	(CLEO Collab.)

$$\Xi_c^{'+}$$

$$I(J^P) = \frac{1}{2}(\frac{1}{2}^+) \text{ Status: } ***$$

The $\Xi_c^{'+}$ and Ξ_c^0 presumably complete the SU(3) sextet whose other members are the $\Sigma_c^{'+}, \Sigma_c^+, \Sigma_c^0$, and Ω_c^0 : see Fig. 3 in the Note on Charmed Baryons just before the the Λ_c^+ Listings. The quantum numbers given above come from this presumption but have not been measured.

$\Xi_c^{'+}$ MASS

The mass is obtained from the mass-difference measurement that follows.

VALUE (MeV)	DOCUMENT ID
2574.1 ± 3.3 OUR FIT	

$\Xi_c^{'+} - \Xi_c^+$ MASS DIFFERENCE	
VALUE (MeV)	EVTs
107.8 ± 3.0 OUR FIT	
107.8 ± 1.7 ± 2.5	25

$\Xi_c^{'+}$ DECAY MODES

The $\Xi_c^{'+} - \Xi_c^+$ mass difference is too small for any strong decay to occur.

Mode	Fraction (Γ_i/Γ)
$\Gamma_1 \Xi_c^+ \gamma$	seen

Baryon Particle Listings

 $\Xi_c^{\prime+}$, $\Xi_c^{\prime0}$, $\Xi_c(2645)$, $\Xi_c(2815)$ $\Xi_c^{\prime+}$ REFERENCES

JESSOP 99 PRL 82 492 C.P. Jessop et al. (CLEO Collab.)

 $\Xi_c^{\prime0}$

$$I(J^P) = \frac{1}{2}(\frac{1}{2}^+) \text{ Status: } ***$$

See the note in the Listing for the $\Xi_c^{\prime+}$, above. $\Xi_c^{\prime0}$ MASS

The mass is obtained from the mass-difference measurement that follows.

VALUE (MeV)	DOCUMENT ID
2578.8 ± 3.2 OUR FIT	

 $\Xi_c^{\prime0} - \Xi_c^0$ MASS DIFFERENCE

VALUE (MeV)	EVTs	DOCUMENT ID	TECN	COMMENT
107.0 ± 2.9 OUR FIT				
107.0 ± 1.4 ± 2.5	28	JESSOP	99 CLE2	$e^+e^- \approx \Upsilon(4S)$

 $\Xi_c^{\prime0}$ DECAY MODESThe $\Xi_c^{\prime0} - \Xi_c^0$ mass difference is too small for any strong decay to occur.

Mode	Fraction (Γ_i/Γ)
$\Gamma_1 \Xi_c^0 \gamma$	seen

 $\Xi_c^{\prime0}$ REFERENCES

JESSOP 99 PRL 82 492 C.P. Jessop et al. (CLEO Collab.)

 $\Xi_c(2645)$

$$I(J^P) = \frac{1}{2}(\frac{3}{2}^+) \text{ Status: } ***$$

A narrow peak seen in the $\Xi_c \pi$ mass spectrum. The natural assignment is that this is the $J^P = 3/2^+$ excitation of the Ξ_c in the same SU(4) multiplet as the $\Delta(1232)$, but the quantum numbers have not been measured. $\Xi_c(2645)$ MASSES

The masses are obtained from the mass-difference measurements that follow.

$\Xi_c(2645)^+$ MASS	VALUE (MeV)	DOCUMENT ID
2647.4 ± 2.0 OUR FIT		Error includes scale factor of 1.2.

$\Xi_c(2645)^0$ MASS	VALUE (MeV)	DOCUMENT ID
2644.5 ± 1.8 OUR FIT		

 $\Xi_c(2645) - \Xi_c$ MASS DIFFERENCES

$m_{\Xi_c(2645)^+} - m_{\Xi_c^+}$	VALUE (MeV)	EVTs	DOCUMENT ID	TECN	COMMENT
175.6 ± 1.4 OUR FIT					Error includes scale factor of 1.7.
175.6 ± 1.4 OUR AVERAGE					Error includes scale factor of 1.7.
	177.1 ± 0.5 ± 1.1	47	FRABETTI 98B E687	γ Be, $\bar{E}_\gamma = 220$ GeV	
	174.3 ± 0.5 ± 1.0	34	GIBBONS 96 CLE2	$e^+e^- \approx \Upsilon(4S)$	

$m_{\Xi_c(2645)^0} - m_{\Xi_c^0}$	VALUE (MeV)	EVTs	DOCUMENT ID	TECN	COMMENT
178.2 ± 1.1 OUR FIT					
178.2 ± 0.5 ± 1.0	55	AVERY 95 CLE2	$e^+e^- \approx \Upsilon(4S)$		

 $\Xi_c(2645)$ WIDTHS

$\Xi_c(2645)^+$ WIDTH	VALUE (MeV)	CL%	DOCUMENT ID	TECN	COMMENT
<3.1	90		GIBBONS 96 CLE2	$e^+e^- \approx \Upsilon(4S)$	

$\Xi_c(2645)^0$ WIDTH	VALUE (MeV)	CL%	EVTs	DOCUMENT ID	TECN	COMMENT
<5.5	90	55		AVERY 95 CLE2	$e^+e^- \approx \Upsilon(4S)$	

 $\Xi_c(2645)$ DECAY MODES $\Xi_c \pi$ is the only strong decay allowed to a Ξ_c resonance having this mass.

Mode	Fraction (Γ_i/Γ)
$\Gamma_1 \Xi_c^0 \pi^+$	seen
$\Gamma_2 \Xi_c^+ \pi^-$	seen

 $\Xi_c(2645)$ REFERENCES

FRABETTI 98B PL B426 403	P.L. Frabetti et al.	(FNAL E687 Collab.)
GIBBONS 96 PRL 77 810	L.K. Gibbons et al.	(CLEO Collab.)
AVERY 95 PRL 75 4364	P. Avery et al.	(CLEO Collab.)

 $\Xi_c(2815)$

$$I(J^P) = \frac{1}{2}(\frac{3}{2}^-) \text{ Status: } ***$$

A narrow peak seen in the $\Xi_c \pi \pi$ mass spectrum. The simplest assignment is that this belongs to the same SU(4) multiplet as the $\Lambda(1520)$ and the $\Lambda_c(2625)$, but the spin and parity have not been measured. $\Xi_c(2815)$ MASSES

The masses are obtained from the mass-difference measurements that follow.

$\Xi_c(2815)^+$ MASS	VALUE (MeV)	DOCUMENT ID
2814.9 ± 1.8 OUR FIT		

$\Xi_c(2815)^0$ MASS	VALUE (MeV)	DOCUMENT ID
2819.0 ± 2.5 OUR FIT		

 $\Xi_c(2815) - \Xi_c$ MASS DIFFERENCES

$m_{\Xi_c(2815)^+} - m_{\Xi_c^+}$	VALUE (MeV)	EVTs	DOCUMENT ID	TECN	COMMENT
348.6 ± 1.2 OUR FIT					
348.6 ± 0.6 ± 1.0	20	ALEXANDER 99B CLE2	$e^+e^- \approx \Upsilon(4S)$		

$m_{\Xi_c(2815)^0} - m_{\Xi_c^0}$	VALUE (MeV)	EVTs	DOCUMENT ID	TECN	COMMENT
347.2 ± 2.1 OUR FIT					
347.2 ± 0.7 ± 2.0	9	ALEXANDER 99B CLE2	$e^+e^- \approx \Upsilon(4S)$		

 $\Xi_c(2815)$ WIDTHS

$\Xi_c(2815)^+$ WIDTH	VALUE (MeV)	CL%	DOCUMENT ID	TECN	COMMENT
<3.5	90		ALEXANDER 99B CLE2	$e^+e^- \approx \Upsilon(4S)$	

$\Xi_c(2815)^0$ WIDTH	VALUE (MeV)	CL%	DOCUMENT ID	TECN	COMMENT
<6.5	90		ALEXANDER 99B CLE2	$e^+e^- \approx \Upsilon(4S)$	

 $\Xi_c(2815)$ DECAY MODESThe $\Xi_c \pi \pi$ modes are consistent with being entirely via $\Xi_c(2645) \pi$.

Mode	Fraction (Γ_i/Γ)
$\Gamma_1 \Xi_c^+ \pi^+ \pi^-$	seen
$\Gamma_2 \Xi_c^0 \pi^+ \pi^-$	seen

 $\Xi_c(2815)$ REFERENCES

ALEXANDER 99B PRL 83 3390 J.P. Alexander et al. (CLEO Collab.)

See key on page 239

Baryon Particle Listings

Ω_c^0

Ω_c^0

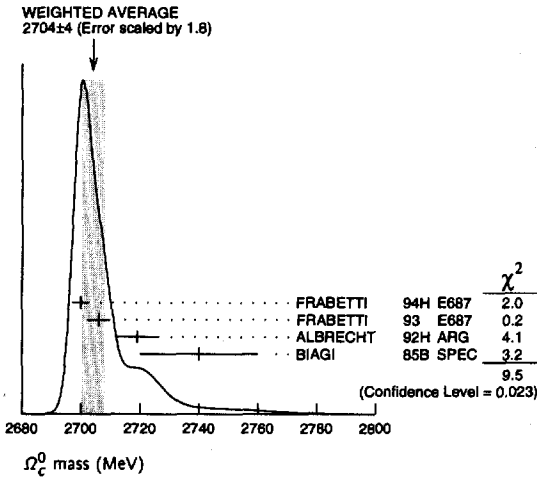
$I(J^P) = 0(\frac{1}{2}^+)$ Status: ***

The quantum numbers have not been measured, but are simply assigned in accord with the quark model, in which the Ω_c^0 is the ssc ground state.

Ω_c^0 MASS

VALUE (MeV)	EVTS	DOCUMENT ID	TECN	COMMENT
2704 ± 4 OUR AVERAGE		Error includes scale factor of 1.8. See the ideogram below.		
2699.9 ± 1.5 ± 2.5	42	¹ FRABETTI 94H E687		γ Be, $\bar{E}_\gamma = 221$ GeV
2705.9 ± 3.3 ± 2.0	10	² FRABETTI 93 E687		γ Be, $\bar{E}_\gamma = 221$ GeV
2719.0 ± 7.0 ± 2.5	11	³ ALBRECHT 92H ARG		$e^+e^- \approx 10.6$ GeV
2740 ± 20	3	BIAGI 85B SPEC		Σ^- Be 135 GeV/c

- ¹ FRABETTI 94H claims a signal of $42.5 \pm 8.8 \Sigma^+ K^- K^- \pi^+$ events. The background is about 24 events.
- ² FRABETTI 93 claims a signal of $10.3 \pm 3.9 \Omega^- \pi^+$ events above a background of 5.8 events.
- ³ ALBRECHT 92H claims a signal of $11.5 \pm 4.3 \Xi^- K^- \pi^+ \pi^+$ events. The background is about 5 events.



Ω_c^0 MEAN LIFE

VALUE (10^{-12} s)	EVTS	DOCUMENT ID	TECN	COMMENT
0.064 ± 0.020 OUR AVERAGE				
0.055 ^{+0.013} _{-0.011} ± 0.018 _{-0.023}	86	ADAMOVIICH 95B WA89		$\Omega^- \pi^- \pi^+ \pi^+$, $\Xi^- K^- \pi^+ \pi^+$
0.086 ^{+0.027} _{-0.020} ± 0.028	25	FRABETTI 95D E687		$\Sigma^+ K^- K^- \pi^+$

Ω_c^0 DECAY MODES

Mode	Fraction (Γ_i/Γ)
$\Gamma_1 \Sigma^+ K^- K^- \pi^+$	seen
$\Gamma_2 \Xi^- K^- \pi^+ \pi^+$	seen
$\Gamma_3 \Omega^- \pi^+$	seen
$\Gamma_4 \Omega^- \pi^- \pi^+ \pi^+$	seen

Ω_c^0 BRANCHING RATIOS

$\Gamma(\Sigma^+ K^- K^- \pi^+)/\Gamma_{total}$					Γ_1/Γ
VALUE	EVTS	DOCUMENT ID	TECN	COMMENT	
seen	42	FRABETTI 94H E687		γ Be, $\bar{E}_\gamma = 221$ GeV	
$\Gamma(\Xi^- K^- \pi^+ \pi^+)/\Gamma_{total}$					Γ_2/Γ
VALUE	EVTS	DOCUMENT ID	TECN	COMMENT	
seen	11	ALBRECHT 92H ARG		$e^+e^- \approx 10.6$ GeV	
seen	3	BIAGI 85B SPEC		Σ^- Be 135 GeV/c	
$\Gamma(\Omega^- \pi^+)/\Gamma_{total}$					Γ_3/Γ
VALUE	EVTS	DOCUMENT ID	TECN	COMMENT	
seen	10	FRABETTI 93 E687		γ Be, $\bar{E}_\gamma = 221$ GeV	
$\Gamma(\Xi^- K^- \pi^+ \pi^+)/\Gamma(\Omega^- \pi^+)$					Γ_2/Γ_3
VALUE	CL%	DOCUMENT ID	TECN	COMMENT	
<2.8	90	FRABETTI 93 E687		γ Be, $\bar{E}_\gamma = 221$ GeV	
$\Gamma(\Omega^- \pi^- \pi^+ \pi^+)/\Gamma(\Omega^- \pi^+)$					Γ_4/Γ_3
VALUE	CL%	DOCUMENT ID	TECN	COMMENT	
seen		ADAMOVIICH 95B WA89		Σ^- 340 GeV	
<1.6	90	FRABETTI 93 E687		γ Be, $\bar{E}_\gamma = 221$ GeV	

Ω_c^0 REFERENCES

ADAMOVIICH 95B PL B358 151	M.I. Adamovich et al.	(CERN WA89 Collab.)
FRABETTI 95D PL B357 678	P.L. Frabetti et al.	(FNAL E687 Collab.)
FRABETTI 94H PL B338 106	P.L. Frabetti et al.	(FNAL E687 Collab.)
FRABETTI 93 PL B300 190	P.L. Frabetti et al.	(FNAL E687 Collab.)
ALBRECHT 92H PL B288 367	H. Albrecht et al.	(ARGUS Collab.)
BIAGI 85B ZPHY C28 175	S.F. Biagi et al.	(CERN WA62 Collab.)

Baryon Particle Listings

Λ_b^0

BOTTOM BARYONS ($B = -1$)

$$\Lambda_b^0 = udb, \Xi_b^0 = usb, \Xi_b^- = dsb$$

Λ_b^0

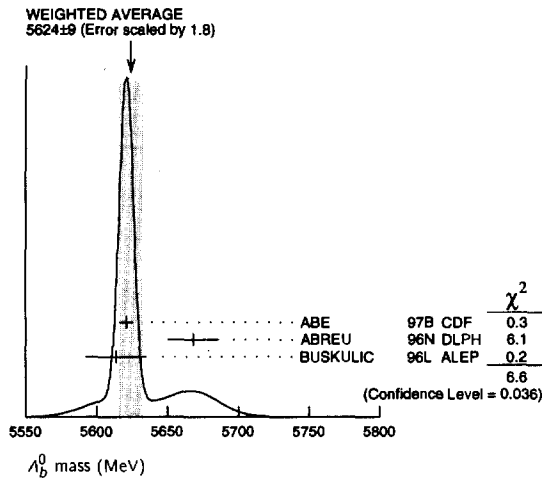
$$I(J^P) = 0(\frac{1}{2}^+)$$
 Status: ***

In the quark model, a Λ_b^0 is an isospin-0 udb state. The lowest Λ_b^0 ought to have $J^P = 1/2^+$. None of $I, J,$ or P have actually been measured.

Λ_b^0 MASS

VALUE (MeV)	EVTs	DOCUMENT ID	TECN	COMMENT
5624 ± 9 OUR AVERAGE		Error includes scale factor of 1.8. See the ideogram below.		
5621 ± 4 ± 3	1	ABE	97B CDF	$p\bar{p}$ at 1.8 TeV
5668 ± 16 ± 8	4	ABREU	96N DLPH	$e^+e^- \rightarrow Z$
5614 ± 21 ± 4	4	BUSKULIC	96L ALEP	$e^+e^- \rightarrow Z$
not seen	3	ABE	93B CDF	Sup. by ABE 97B
5640 ± 50 ± 30	16	ALBAJAR	91E UA1	$p\bar{p}$ 630 GeV
5640 +100 -210	52	BARI	91 SFM	$\Lambda_b^0 \rightarrow \rho D^0 \pi^-$
5650 +150 -200	90	BARI	91 SFM	$\Lambda_b^0 \rightarrow \Lambda_c^+ \pi^+ \pi^- \pi^-$

- • • We do not use the following data for averages, fits, limits, etc. • • •
- 1 ABE 97B observed 38 events above a background 18 ± 1.6 events in the mass range 5.60–5.65 GeV/ c^2 , a significance of > 3.4 standard deviations.
- 2 Uses 4 fully reconstructed Λ_b events.
- 3 ABE 93B states that, based on the signal claimed by ALBAJAR 91E, CDF should have found $30 \pm 23 \Lambda_b^0 \rightarrow J/\psi(1S) \Lambda$ events. Instead, CDF found not more than 2 events.
- 4 ALBAJAR 91E claims 16 ± 5 events above a background of 9 ± 1 events, a significance of about 5 standard deviations.



Λ_b^0 MEAN LIFE

These are actually measurements of the average lifetime of weakly decaying b baryons weighted by generally unknown production rates, branching fractions, and detection efficiencies. Presumably, the mix is mainly Λ_b^0 , with some Ξ_b^0 and Ξ_b^- .

See b -baryon Admixture section for data on b -baryon mean life average over species of b -baryon particles.

"OUR EVALUATION" is an average of the data listed below performed by the LEP B Lifetimes Working Group as described in our review "Production and Decay of b -flavored Hadrons" in the B^\pm Section of the Listings. The averaging procedure takes into account correlations between the measurements and asymmetric lifetime errors.

VALUE (10^{-12} s)	EVTs	DOCUMENT ID	TECN	COMMENT
1.229 ± 0.080 OUR EVALUATION				
1.11 +0.19 -0.18 ± 0.05	5	ABREU	99W DLPH	$e^+e^- \rightarrow Z$
1.29 +0.24 -0.22 ± 0.06	5	ACKERSTAFF	98G OPAL	$e^+e^- \rightarrow Z$
1.21 ± 0.11	5	BARATE	98D ALEP	$e^+e^- \rightarrow Z$
1.32 ± 0.15 ± 0.07		ABE	96M CDF	Excess $\Lambda_c \ell^-$, decay lengths

• • • We do not use the following data for averages, fits, limits, etc. • • •

1.19 +0.21 -0.18 ± 0.06		ABREU	96D DLPH	Repl. by ABREU 99W
1.14 +0.22 -0.19 ± 0.07	69	AKERS	95K OPAL	Repl. by ACKER-STAFF 98G
1.02 +0.23 -0.18 ± 0.06	44	BUSKULIC	95L ALEP	Repl. by BARATE 98D

⁵ Measured using $\Lambda_c \ell^-$ and $\Lambda \ell^+ \ell^-$.

Λ_b^0 DECAY MODES

These branching fractions are actually an average over weakly decaying b -baryons weighted by their production rates in Z decay (or high-energy $p\bar{p}$), branching ratios, and detection efficiencies. They scale with the LEP b -baryon production fraction $B(b \rightarrow b\text{-baryon})$ and are evaluated for our value $B(b \rightarrow b\text{-baryon}) = (11.6 \pm 2.0)\%$.

The branching fractions $B(b\text{-baryon} \rightarrow \Lambda \ell^- \bar{\nu}_\ell \text{ anything})$ and $B(\Lambda_b^0 \rightarrow \Lambda_c^+ \ell^- \bar{\nu}_\ell \text{ anything})$ are not pure measurements because the underlying measured products of these with $B(b \rightarrow b\text{-baryon})$ were used to determine $B(b \rightarrow b\text{-baryon})$, as described in the note "Production and Decay of b -Flavored Hadrons."

Mode	Fraction (Γ_j/Γ)	Confidence level
Γ_1 $J/\psi(1S) \Lambda$	$(4.7 \pm 2.8) \times 10^{-4}$	
Γ_2 $\rho D^0 \pi^-$		
Γ_3 $\Lambda_c^+ \pi^-$	seen	
Γ_4 $\Lambda_c^+ a_1(1260)^-$	seen	
Γ_5 $\Lambda_c^+ \pi^+ \pi^- \pi^-$		
Γ_6 $\Lambda K^0 2\pi^+ 2\pi^-$		
Γ_7 $\Lambda_c^+ \ell^- \bar{\nu}_\ell \text{ anything}$	[a] $(7.9 \pm 1.9)\%$	
Γ_8 $\rho \pi^-$	$< 5.0 \times 10^{-5}$	90%
Γ_9 ρK^-	$< 5.0 \times 10^{-5}$	90%

[a] Not a pure measurement. See note at head of Λ_b^0 Decay Modes.

Λ_b^0 BRANCHING RATIOS

$\Gamma(J/\psi(1S) \Lambda)/\Gamma_{\text{total}}$ Γ_1/Γ

VALUE (units 10^{-4})	EVTs	DOCUMENT ID	TECN	COMMENT
4.7 ± 2.1 ± 1.9	6	ABE	97B CDF	$p\bar{p}$ at 1.8 TeV

• • • We do not use the following data for averages, fits, limits, etc. • • •

- 155.2 ± 94.8 ± 26.8
- 16 ALBAJAR 91E UA1 $J/\psi(1S) \rightarrow \mu^+ \mu^-$
- 6 ABE 97B reports $(0.037 \pm 0.017(\text{stat}) \pm 0.007(\text{sys}))\%$ for $B(b \rightarrow b\text{-baryon}) = 0.1$ and for $B(B^0 \rightarrow J/\psi(1S) K_S^0) = 0.037\%$. We rescale to our PDG 97 best value $B(b \rightarrow b\text{-baryon}) = (10.1 \pm 3.9)\%$ and $B(B^0 \rightarrow J/\psi(1S) K_S^0) = (0.044 \pm 0.006)\%$. Our first error is their experiment's error and our second error is the systematic error from using our best value.
- 7 ALBAJAR 91E reports 180 ± 110 for $B(\bar{b} \rightarrow b\text{-baryon}) = 0.10$. We rescale to our best value $B(\bar{b} \rightarrow b\text{-baryon}) = (11.6 \pm 2.0) \times 10^{-2}$. Our first error is their experiment's error and our second error is the systematic error from using our best value.

$\Gamma(\rho D^0 \pi^-)/\Gamma_{\text{total}}$ Γ_2/Γ

VALUE	EVTs	DOCUMENT ID	TECN	COMMENT
seen	52	BARI	91 SFM	$D^0 \rightarrow K^- \pi^+$
seen		BASILE	81 SFM	$D^0 \rightarrow K^- \pi^+$

• • • We do not use the following data for averages, fits, limits, etc. • • •

$\Gamma(\Lambda_c^+ \pi^-)/\Gamma_{\text{total}}$ Γ_3/Γ

VALUE	EVTs	DOCUMENT ID	TECN	COMMENT
seen	3	ABREU	96N DLPH	$\Lambda_c^+ \rightarrow \rho K^- \pi^+$

seen 4 BUSKULIC 96L ALEP $\Lambda_c^+ \rightarrow \rho K^- \pi^+, \rho \bar{K}^0, \Lambda \pi^+ \pi^+ \pi^-$

$\Gamma(\Lambda_c^+ a_1(1260)^-)/\Gamma_{\text{total}}$ Γ_4/Γ

VALUE	EVTs	DOCUMENT ID	TECN	COMMENT
seen	1	ABREU	96N DLPH	$\Lambda_c^+ \rightarrow \rho K^- \pi^+, a_1^- \rightarrow \rho^0 \pi^- \rightarrow \pi^+ \pi^- \pi^-$

seen 90 BARI 91 SFM $\Lambda_c^+ \rightarrow \rho K^- \pi^+$

$\Gamma(\Lambda_c^+ \pi^+ \pi^- \pi^-)/\Gamma_{\text{total}}$ Γ_5/Γ

VALUE	EVTs	DOCUMENT ID	TECN	COMMENT
seen	90	BARI	91 SFM	$\Lambda_c^+ \rightarrow \rho K^- \pi^+$

• • • We do not use the following data for averages, fits, limits, etc. • • •

$\Gamma(\Lambda K^0 2\pi^+ 2\pi^-)/\Gamma_{\text{total}}$ Γ_6/Γ

VALUE	EVTs	DOCUMENT ID	TECN	COMMENT
seen	4	ARENTON	86 FMPS	$\Lambda K_S^0 2\pi^+ 2\pi^-$

• • • We do not use the following data for averages, fits, limits, etc. • • •

⁸ See the footnote to the ARENTON 86 mass value.

See key on page 239

Baryon Particle Listings

 $\Lambda_b^0, \Xi_b^0, \Xi_b^-, b$ -baryon ADMIXTURE ($\Lambda_b, \Xi_b, \Sigma_b, \Omega_b$) $\Gamma(\Lambda_c^+ \ell^- \bar{\nu}_\ell \text{ anything})/\Gamma_{\text{total}}$

The values and averages in this section serve only to show what values result if one assumes our $B(b \rightarrow b\text{-baryon})$. They cannot be thought of as measurements since the underlying product branching fractions were also used to determine $B(b \rightarrow b\text{-baryon})$ as described in the note on "Production and Decay of b -Flavored Hadrons."

VALUE	EVTS	DOCUMENT ID	TECN	COMMENT
0.079 ± 0.019 OUR AVERAGE				
0.074 ± 0.013 ± 0.013		⁹ BARATE	98D ALEP	$e^+ e^- \rightarrow Z$
0.102 ^{+0.035} _{-0.029} ± 0.018	29	¹⁰ ABREU	95S DLPH	$e^+ e^- \rightarrow Z$
• • • We do not use the following data for averages, fits, limits, etc. • • •				
0.065 ± 0.016 ± 0.011	55	¹¹ BUSKULIC	95L ALEP	Repl. by BARATE 98D
0.13 ± 0.05 ± 0.02	21	¹² BUSKULIC	92E ALEP	$\Lambda_c^+ \rightarrow p K^- \pi^+$

⁹ BARATE 98D reports $[B(\Lambda_b^0 \rightarrow \Lambda_c^+ \ell^- \bar{\nu}_\ell \text{ anything}) \times B(\bar{b} \rightarrow b\text{-baryon})] = 0.0086 \pm 0.0007 \pm 0.0014$. We divide by our best value $B(\bar{b} \rightarrow b\text{-baryon}) = (11.6 \pm 2.0) \times 10^{-2}$. Our first error is their experiment's error and our second error is the systematic error from using our best value. Measured using $\Lambda_c \ell^-$ and $\Lambda \ell^+ \ell^-$.

¹⁰ ABREU 95S reports $[B(\Lambda_b^0 \rightarrow \Lambda_c^+ \ell^- \bar{\nu}_\ell \text{ anything}) \times B(\bar{b} \rightarrow b\text{-baryon})] = 0.0118 \pm 0.0026 \pm 0.0021$. We divide by our best value $B(\bar{b} \rightarrow b\text{-baryon}) = (11.6 \pm 2.0) \times 10^{-2}$. Our first error is their experiment's error and our second error is the systematic error from using our best value.

¹¹ BUSKULIC 95L reports $[B(\Lambda_b^0 \rightarrow \Lambda_c^+ \ell^- \bar{\nu}_\ell \text{ anything}) \times B(\bar{b} \rightarrow b\text{-baryon})] = 0.00755 \pm 0.0014 \pm 0.0012$. We divide by our best value $B(\bar{b} \rightarrow b\text{-baryon}) = (11.6 \pm 2.0) \times 10^{-2}$. Our first error is their experiment's error and our second error is the systematic error from using our best value.

¹² BUSKULIC 92E reports $[B(\Lambda_b^0 \rightarrow \Lambda_c^+ \ell^- \bar{\nu}_\ell \text{ anything}) \times B(\bar{b} \rightarrow b\text{-baryon})] = 0.015 \pm 0.0035 \pm 0.0045$. We divide by our best value $B(\bar{b} \rightarrow b\text{-baryon}) = (11.6 \pm 2.0) \times 10^{-2}$. Our first error is their experiment's error and our second error is the systematic error from using our best value. Superseded by BUSKULIC 95L.

 $\Gamma(p\pi^-)/\Gamma_{\text{total}}$

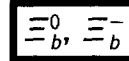
VALUE	CL%	DOCUMENT ID	TECN	COMMENT
< 5.0 × 10⁻⁵	90	¹³ BUSKULIC	96V ALEP	$e^+ e^- \rightarrow Z$
¹³ BUSKULIC 96V assumes PDG 96 production fractions for B^0, B^+, B_s, b baryons.				

 $\Gamma(pK^-)/\Gamma_{\text{total}}$

VALUE	CL%	DOCUMENT ID	TECN	COMMENT
< 5.0 × 10⁻⁵	90	¹⁴ BUSKULIC	96V ALEP	$e^+ e^- \rightarrow Z$
• • • We do not use the following data for averages, fits, limits, etc. • • •				
< 3.6 × 10 ⁻⁴	90	¹⁵ ADAM	96D DLPH	$e^+ e^- \rightarrow Z$
¹⁴ BUSKULIC 96V assumes PDG 96 production fractions for B^0, B^+, B_s, b baryons.				
¹⁵ ADAM 96D assumes $f_{B^0} = f_{B^-} = 0.39$ and $f_{B_s} = 0.12$.				

 Λ_b^0 REFERENCES

ABREU 99W EPJ C10 185	P. Abreu et al.	(DELPHI Collab.)
ACKERSTAFF 98G PL B426 161	K. Ackerstaff et al.	(OPAL Collab.)
BARATE 98D EPJ C2 197	R. Barate et al.	(ALEPH Collab.)
ABE 97B PR D55 1142	F. Abe et al.	(CDF Collab.)
PDG 97 Unofficial 1997 WWW edition		(CDF Collab.)
ABE 96M PRL 77 1439	F. Abe et al.	(CDF Collab.)
ABREU 96D ZPHY C71 199	P. Abreu et al.	(DELPHI Collab.)
ABREU 96N PL B374 351	P. Abreu et al.	(DELPHI Collab.)
ADAM 96D ZPHY C72 207	W. Adam et al.	(DELPHI Collab.)
BUSKULIC 96L PL B380 442	D. Buskulic et al.	(ALEPH Collab.)
BUSKULIC 96V PL B384 471	D. Buskulic et al.	(ALEPH Collab.)
PDG 96 PR D54 1		
ABREU 95S ZPHY C68 375	P. Abreu et al.	(DELPHI Collab.)
AKERS 95K PL B353 402	R. Akers et al.	(OPAL Collab.)
BUSKULIC 95L PL B357 685	D. Buskulic et al.	(ALEPH Collab.)
ABE 93B PR D47 R2639	F. Abe et al.	(CDF Collab.)
BUSKULIC 92E PL B294 145	D. Buskulic et al.	(ALEPH Collab.)
ALBAJAR 91E PL B273 540	C. Albajar et al.	(UA1 Collab.)
BARI 91 NC 104A 1787	G. Bari et al.	(CERN R422 Collab.)
ARENTON 86 NP B274 707	M.W. Arenton et al.	(ARIZ, NDAM, VAND)
BASILE 81 LNC 31 97	M. Basile et al.	(CERN R415 Collab.)



$$I(J^P) = 0(\frac{1}{2}^+) \text{ Status: } *$$

OMITTED FROM SUMMARY TABLE

ABREU 95V observe an excess of same-sign $\Xi^{\mp} \ell^{\mp}$ events in jets, which they interpret as $\Xi_b \rightarrow \Xi^- \ell^- \bar{\nu}_\ell X$. They find that the probability for these events to come from non- b -baryon decays is less than 5×10^{-4} and that Λ_b decays can account for less than 10% of these events.

In the quark model, Ξ_b^0 and Ξ_b^- are an isodoublet ($u s b, d s b$) state; the lowest Ξ_b^0 and Ξ_b^- ought to have $J^P = 1/2^+$. None of I, J , or P have actually been measured.

 Ξ_b MEAN LIFE

This is actually a measurement of the average lifetime of b -baryons that decay to a jet containing a same-sign $\Xi^{\mp} \ell^{\mp}$ pair. Presumably the mix is mainly Ξ_b , with some Λ_b .

"OUR EVALUATION" is an average of the data listed below performed by the LEP B Lifetimes Working Group as described in our review "Production and Decay of b -flavored Hadrons" in the B^{\pm} Section of the Listings. The averaging procedure takes into account correlations between the measurements and asymmetric lifetime errors.

VALUE (10 ⁻¹² s)	EVTS	DOCUMENT ID	TECN	COMMENT
1.39 ± 0.30 OUR EVALUATION				
1.35 ^{+0.37+0.15} _{-0.28-0.17}		BUSKULIC	96T ALEP	Excess $\Xi^- \ell^-$, impact parameters
1.5 ^{+0.7} _{-0.4} ± 0.3	8	ABREU	95V DLPH	Excess $\Xi^- \ell^-$, decay lengths

 Ξ_b DECAY MODES

Mode	Fraction (Γ_i/Γ)
$\Xi^- \ell^- \bar{\nu}_\ell \text{ anything}$	seen

 Ξ_b BRANCHING RATIOS

$\Gamma(\Xi^- \ell^- \bar{\nu}_\ell \text{ anything})/\Gamma_{\text{total}}$	Γ_1/Γ
seen	¹ BUSKULIC 96T ALEP
seen	ABREU 95V DLPH

¹ BUSKULIC 96T measures $[B(b \rightarrow \Xi_b) \times B(\Xi_b \rightarrow \Xi^- \ell^- \bar{\nu}_\ell \text{ anything})] = (5.4 \pm 1.1 \pm 0.8) \times 10^{-4}$ per lepton species, averaged over e and μ .

 Ξ_b REFERENCES

BUSKULIC 96T PL B384 449	D. Buskulic et al.	(ALEPH Collab.)
ABREU 95V ZPHY C68 541	P. Abreu et al.	(DELPHI Collab.)

 b -baryon ADMIXTURE ($\Lambda_b, \Xi_b, \Sigma_b, \Omega_b$) b -baryon ADMIXTURE MEAN LIFE

Each measurement of the b -baryon mean life is an average over an admixture of various b baryons which decay weakly. Different techniques emphasize different admixtures of produced particles, which could result in a different b -baryon mean life. More b -baryon flavor specific channels are not included in the measurement.

"OUR EVALUATION" is an average of the data listed below performed by the LEP B Lifetimes Working Group as described in our review "Production and Decay of b -flavored Hadrons" in the B^{\pm} Section of these Listings. The averaging procedure takes into account correlations between the measurements and asymmetric lifetime errors.

VALUE (10 ⁻¹² s)	EVTS	DOCUMENT ID	TECN	COMMENT
1.208 ± 0.051 OUR EVALUATION				
1.16 ± 0.20 ± 0.08	¹ ABREU	99W DLPH	$e^+ e^- \rightarrow Z$	
1.19 ± 0.14 ± 0.07	² ABREU	99W DLPH	$e^+ e^- \rightarrow Z$	
1.20 ± 0.08 ± 0.06	³ BARATE	98D ALEP	$e^+ e^- \rightarrow Z$	
1.10 ^{+0.19} _{-0.17} ± 0.09	ABREU	96D DLPH	Excess $\Lambda \mu^-$ impact parameters	
1.16 ± 0.11 ± 0.06	AKERS	96 OPAL	Excess $\Lambda \ell^-$, decay lengths and impact parameters	

Baryon Particle Listings

 b -baryon ADMIXTURE ($\Lambda_b, \Xi_b, \Sigma_b, \Omega_b$)

• • • We do not use the following data for averages, fits, limits, etc. • • •

1.14 ± 0.08 ± 0.04	4	ABREU	99w DLPH	$e^+e^- \rightarrow Z$
1.46 +0.22 +0.07 -0.21 -0.09		ABREU	96d DLPH	Repl. by ABREU 99w
1.27 +0.35 ± 0.09 -0.29		ABREU	95s DLPH	Repl. by ABREU 99w
1.05 +0.12 ± 0.09 -0.11	290	BUSKULIC	95L ALEP	Repl. by BARATE 98D
1.04 +0.48 ± 0.10 -0.38	11	5	ABREU	93F DLPH Excess $\Lambda\mu^-$, decay lengths
1.05 +0.23 ± 0.08 -0.20	157	6	AKERS	93 OPAL Excess $\Lambda\ell^-$, decay lengths
1.12 +0.32 ± 0.16 -0.29	101	7	BUSKULIC	92i ALEP Excess $\Lambda\ell^-$, impact parameters

¹ Measured using $\Lambda\ell^-$ decay length.

² Measured using $\rho\ell^-$ decay length.

³ Measured using the excess of $\Lambda\ell^-$, lepton impact parameter.

⁴ This ABREU 99w result is the combined result of the $\Lambda\ell^-$, $\rho\ell^-$, and excess $\Lambda\mu^-$ impact parameter measurements.

⁵ ABREU 93F superseded by ABREU 96d.

⁶ AKERS 93 superseded by AKERS 96.

⁷ BUSKULIC 92i superseded by BUSKULIC 95L.

 b -baryon ADMIXTURE ($\Lambda_b, \Xi_b, \Sigma_b, \Omega_b$)

These branching fractions are actually an average over weakly decaying b -baryons weighted by their production rates in Z decay (or high-energy $p\bar{p}$), branching ratios, and detection efficiencies. They scale with the LEP b -baryon production fraction $B(b \rightarrow b\text{-baryon})$ and are evaluated for our value $B(b \rightarrow b\text{-baryon}) = (11.6 \pm 2.0)\%$.

The branching fractions $B(b\text{-baryon} \rightarrow \Lambda\ell^- \bar{\nu}_\ell \text{ anything})$ and $B(\Lambda_b^0 \rightarrow \Lambda_C^+ \ell^- \bar{\nu}_\ell \text{ anything})$ are not pure measurements because the underlying measured products of these with $B(b \rightarrow b\text{-baryon})$ were used to determine $B(b \rightarrow b\text{-baryon})$, as described in the note "Production and Decay of b -Flavored Hadrons."

Mode	Fraction (Γ_i/Γ)
Γ_1 $\rho\mu^- \bar{\nu}$ anything	(4.2 ± 1.8) %
Γ_2 $\rho\ell^- \bar{\nu}_\ell$ anything	(4.1 ± 1.0) %
Γ_3 ρ anything	(51 ± 17) %
Γ_4 $\Lambda\ell^- \bar{\nu}_\ell$ anything	(2.7 ± 0.8) %
Γ_5 $\Lambda\ell^+ \nu_\ell$ anything	
Γ_6 Λ anything	
Γ_7 $\Lambda_C^+ \ell^- \bar{\nu}_\ell$ anything	
Γ_8 $\Lambda/\bar{\Lambda}$ anything	(28 ± 7) %
Γ_9 $\Xi^- \ell^- \bar{\nu}_\ell$ anything	(4.8 ± 1.3) × 10 ⁻³

 b -baryon ADMIXTURE ($\Lambda_b, \Xi_b, \Sigma_b, \Omega_b$) BRANCHING RATIOS

$\Gamma(\rho\mu^- \bar{\nu} \text{ anything})/\Gamma_{\text{total}}$	Γ_1/Γ			
VALUE	EVTS	DOCUMENT ID	TECN	COMMENT
0.042 +0.016 ± 0.007 -0.013 ± 0.007	125	8	ABREU	95s DLPH $e^+e^- \rightarrow Z$

⁸ ABREU 95s reports $[B(b\text{-baryon} \rightarrow \rho\mu^- \bar{\nu} \text{ anything}) \times B(\bar{b} \rightarrow b\text{-baryon})] = 0.0049 \pm 0.0011 \pm 0.0015$. We divide by our best value $B(\bar{b} \rightarrow b\text{-baryon}) = (11.6 \pm 2.0) \times 10^{-2}$. Our first error is their experiment's error and our second error is the systematic error from using our best value.

$\Gamma(\rho\ell^- \bar{\nu}_\ell \text{ anything})/\Gamma_{\text{total}}$	Γ_2/Γ		
VALUE	DOCUMENT ID	TECN	COMMENT
0.041 ± 0.007 ± 0.007	9	BARATE	98v ALEP $e^+e^- \rightarrow Z$

⁹ BARATE 98v reports $[B(b\text{-baryon} \rightarrow \rho\ell^- \bar{\nu}_\ell \text{ anything}) \times B(\bar{b} \rightarrow b\text{-baryon})] = (4.72 \pm 0.66 \pm 0.44) \times 10^{-3}$. We divide by our best value $B(\bar{b} \rightarrow b\text{-baryon}) = (11.6 \pm 2.0) \times 10^{-2}$. Our first error is their experiment's error and our second error is the systematic error from using our best value.

$\Gamma(\rho\ell^- \bar{\nu}_\ell \text{ anything})/\Gamma(\rho \text{ anything})$	Γ_2/Γ_3		
VALUE	DOCUMENT ID	TECN	COMMENT
0.080 ± 0.012 ± 0.014		BARATE	98v ALEP $e^+e^- \rightarrow Z$

$\Gamma(\Lambda\ell^- \bar{\nu}_\ell \text{ anything})/\Gamma_{\text{total}}$	Γ_4/Γ
---	-------------------

The values and averages in this section serve only to show what values result if one assumes our $B(b \rightarrow b\text{-baryon})$. They cannot be thought of as measurements since the underlying product branching fractions were also used to determine $B(b \rightarrow b\text{-baryon})$ as described in the note on "Production and Decay of b -Flavored Hadrons."

VALUE	EVTS	DOCUMENT ID	TECN	COMMENT
0.027 ± 0.008 OUR AVERAGE				
0.028 ± 0.004 ± 0.005		10	BARATE	98D ALEP $e^+e^- \rightarrow Z$
0.025 ± 0.003 ± 0.004		11	AKERS	96 OPAL Excess of $\Lambda\ell^-$ over $\Lambda\ell^+$
0.026 ± 0.006 ± 0.004	262	12	ABREU	95s DLPH Excess of $\Lambda\ell^-$ over $\Lambda\ell^+$
0.053 ± 0.010 ± 0.009	290	13	BUSKULIC	95L ALEP Excess of $\Lambda\ell^-$ over $\Lambda\ell^+$

• • • We do not use the following data for averages, fits, limits, etc. • • •

seen	157	14	AKERS	93 OPAL Excess of $\Lambda\ell^-$ over $\Lambda\ell^+$
0.060 ± 0.018 ± 0.010	101	15	BUSKULIC	92i ALEP Excess of $\Lambda\ell^-$ over $\Lambda\ell^+$
¹⁰ BARATE 98D reports $[B(b\text{-baryon} \rightarrow \Lambda\ell^- \bar{\nu}_\ell \text{ anything}) \times B(\bar{b} \rightarrow b\text{-baryon})] = 0.00326 \pm 0.00016 \pm 0.00039$. We divide by our best value $B(\bar{b} \rightarrow b\text{-baryon}) = (11.6 \pm 2.0) \times 10^{-2}$. Our first error is their experiment's error and our second error is the systematic error from using our best value. Measured using the excess of $\Lambda\ell^-$, lepton impact parameter.				
¹¹ AKERS 96 reports $[B(b\text{-baryon} \rightarrow \Lambda\ell^- \bar{\nu}_\ell \text{ anything}) \times B(\bar{b} \rightarrow b\text{-baryon})] = 0.00291 \pm 0.00023 \pm 0.00025$. We divide by our best value $B(\bar{b} \rightarrow b\text{-baryon}) = (11.6 \pm 2.0) \times 10^{-2}$. Our first error is their experiment's error and our second error is the systematic error from using our best value.				
¹² ABREU 95s reports $[B(b\text{-baryon} \rightarrow \Lambda\ell^- \bar{\nu}_\ell \text{ anything}) \times B(\bar{b} \rightarrow b\text{-baryon})] = 0.0030 \pm 0.0006 \pm 0.0004$. We divide by our best value $B(\bar{b} \rightarrow b\text{-baryon}) = (11.6 \pm 2.0) \times 10^{-2}$. Our first error is their experiment's error and our second error is the systematic error from using our best value.				
¹³ BUSKULIC 95L reports $[B(b\text{-baryon} \rightarrow \Lambda\ell^- \bar{\nu}_\ell \text{ anything}) \times B(\bar{b} \rightarrow b\text{-baryon})] = 0.0061 \pm 0.0006 \pm 0.0010$. We divide by our best value $B(\bar{b} \rightarrow b\text{-baryon}) = (11.6 \pm 2.0) \times 10^{-2}$. Our first error is their experiment's error and our second error is the systematic error from using our best value.				
¹⁴ AKERS 93 superseded by AKERS 96.				
¹⁵ BUSKULIC 92i reports $[B(b\text{-baryon} \rightarrow \Lambda\ell^- \bar{\nu}_\ell \text{ anything}) \times B(\bar{b} \rightarrow b\text{-baryon})] = 0.0070 \pm 0.0010 \pm 0.0018$. We divide by our best value $B(\bar{b} \rightarrow b\text{-baryon}) = (11.6 \pm 2.0) \times 10^{-2}$. Our first error is their experiment's error and our second error is the systematic error from using our best value. Superseded by BUSKULIC 95L.				

 $\Gamma(\Lambda\ell^\pm \nu_\ell \text{ anything})/\Gamma(\Lambda \text{ anything})$ Γ_5/Γ_6

VALUE	DOCUMENT ID	TECN	COMMENT
0.080 ± 0.012 ± 0.008	ABBIENDI	99L OPAL	$e^+e^- \rightarrow Z$
• • • We do not use the following data for averages, fits, limits, etc. • • •			
0.070 ± 0.012 ± 0.007	ACKERSTAFF	97N OPAL	Repl. by ABBIENDI 99L

 $\Gamma(\Lambda/\bar{\Lambda} \text{ anything})/\Gamma_{\text{total}}$ Γ_8/Γ

VALUE	DOCUMENT ID	TECN	COMMENT
0.28 ± 0.07 OUR AVERAGE			
0.30 ± 0.04 ± 0.05	16	ABBIENDI	99L OPAL $e^+e^- \rightarrow Z$
0.19 +0.11 ± 0.03 -0.07	17	ABREU	95c DLPH $e^+e^- \rightarrow Z$
• • • We do not use the following data for averages, fits, limits, etc. • • •			
0.34 ± 0.05 ± 0.06	18	ACKERSTAFF	97N OPAL Repl. by ABBIENDI 99L

¹⁶ ABBIENDI 99L reports $[B(b\text{-baryon} \rightarrow \Lambda/\bar{\Lambda} \text{ anything}) \times B(\bar{b} \rightarrow b\text{-baryon})] = 0.035 \pm 0.0032 \pm 0.0035$. We divide by our best value $B(\bar{b} \rightarrow b\text{-baryon}) = (11.6 \pm 2.0) \times 10^{-2}$. Our first error is their experiment's error and our second error is the systematic error from using our best value.

¹⁷ ABREU 95c reports 0.28 ± 0.17 for $B(\bar{b} \rightarrow b\text{-baryon}) = 0.08 \pm 0.02$. We rescale to our best value $B(\bar{b} \rightarrow b\text{-baryon}) = (11.6 \pm 2.0) \times 10^{-2}$. Our first error is their experiment's error and our second error is the systematic error from using our best value.

¹⁸ ACKERSTAFF 97N reports $[B(b\text{-baryon} \rightarrow \Lambda/\bar{\Lambda} \text{ anything}) \times B(\bar{b} \rightarrow b\text{-baryon})] = 0.0393 \pm 0.0046 \pm 0.0037$. We divide by our best value $B(\bar{b} \rightarrow b\text{-baryon}) = (11.6 \pm 2.0) \times 10^{-2}$. Our first error is their experiment's error and our second error is the systematic error from using our best value.

 $\Gamma(\Xi^- \ell^- \bar{\nu}_\ell \text{ anything})/\Gamma_{\text{total}}$ Γ_9/Γ

VALUE	DOCUMENT ID	TECN	COMMENT
0.0048 ± 0.0013 OUR AVERAGE			
0.0047 ± 0.0012 ± 0.0008	19	BUSKULIC	96T ALEP Excess $\Xi^- \ell^-$ over $\Xi^- \ell^+$
0.0051 ± 0.0020 ± 0.0009	20	ABREU	95v DLPH Excess $\Xi^- \ell^-$ over $\Xi^- \ell^+$

¹⁹ BUSKULIC 96T reports $[B(b\text{-baryon} \rightarrow \Xi^- \ell^- \bar{\nu}_\ell \text{ anything}) \times B(\bar{b} \rightarrow b\text{-baryon})] = 0.00054 \pm 0.00011 \pm 0.00008$. We divide by our best value $B(\bar{b} \rightarrow b\text{-baryon}) = (11.6 \pm 2.0) \times 10^{-2}$. Our first error is their experiment's error and our second error is the systematic error from using our best value.

²⁰ ABREU 95v reports $[B(b\text{-baryon} \rightarrow \Xi^- \ell^- \bar{\nu}_\ell \text{ anything}) \times B(\bar{b} \rightarrow b\text{-baryon})] = 0.00059 \pm 0.00021 \pm 0.0001$. We divide by our best value $B(\bar{b} \rightarrow b\text{-baryon}) = (11.6 \pm 2.0) \times 10^{-2}$. Our first error is their experiment's error and our second error is the systematic error from using our best value.

 b -baryon ADMIXTURE ($\Lambda_b, \Xi_b, \Sigma_b, \Omega_b$) REFERENCES

ABBIENDI	99L	EPJ C9 1	G. Abbiendi et al.	(OPAL Collab.)
ABREU	99w	EPJ C10 185	P. Abreu et al.	(DELPHI Collab.)
BARATE	98D	EPJ C2 197	R. Barate et al.	(ALEPH Collab.)
BARATE	98V	EPJ C5 205	R. Barate et al.	(ALEPH Collab.)
ACKERSTAFF	97N	ZPHY C74 423	K. Ackerstaff et al.	(OPAL Collab.)
ABREU	96D	ZPHY C71 199	P. Abreu et al.	(DELPHI Collab.)
AKERS	96	ZPHY C69 195	R. Akers et al.	(OPAL Collab.)
BUSKULIC	96T	PL B384 449	D. Buskulic et al.	(ALEPH Collab.)
ABREU	95C	PL B347 447	P. Abreu et al.	(DELPHI Collab.)
ABREU	95S	ZPHY C68 375	P. Abreu et al.	(DELPHI Collab.)
ABREU	95V	ZPHY C68 541	P. Abreu et al.	(DELPHI Collab.)
BUSKULIC	95L	PL B357 685	D. Buskulic et al.	(ALEPH Collab.)
ABREU	93F	PL B311 379	P. Abreu et al.	(DELPHI Collab.)
AKERS	93	PL B316 435	R. Akers et al.	(OPAL Collab.)
BUSKULIC	92i	PL B297 449	D. Buskulic et al.	(ALEPH Collab.)

See key on page 239

Searches Particle Listings

Magnetic Monopole Searches

SEARCHES FOR MONOPOLES, SUPERSYMMETRY, TECHNICOLOR, COMPOSITENESS, etc.

Magnetic Monopole Searches

MAGNETIC MONOPOLE SEARCHES

Revised December 1997 by D.E. Groom (LBNL).

"At the present time (1975) there is no experimental evidence for the existence of magnetic charges or monopoles, but chiefly because of an early, brilliant theoretical argument by Dirac, the search for monopoles is renewed whenever a new energy region is opened up in high energy physics or a new source of matter, such as rocks from the moon, becomes available [1]." Dirac argued that a monopole anywhere in the universe results in electric charge quantization everywhere, and leads to the prediction of a least magnetic charge $g = e/2\alpha$, the Dirac charge [2]. Recently monopoles have become indispensable in many gauge theories, which endow them with a variety of extraordinarily large masses. The discovery by a candidate event in a single superconducting loop in 1982 [6] stimulated an enormous experimental effort to search for supermassive magnetic monopoles [3,4,5].

Monopole detectors have predominantly used either induction or ionization. Induction experiments measure the monopole magnetic charge and are independent of monopole electric charge, mass, and velocity. Monopole candidate events in single semiconductor loops [6,7] have been detected by this method, but no two-loop coincidence has been observed. Ionization experiments rely on a magnetic charge producing more ionization than an electrical charge with the same velocity. In the case of supermassive monopoles, time-of-flight measurements indicating $v \ll c$ has also been a frequently sought signature.

Cosmic rays are the most likely source of massive monopoles, since accelerator energies are insufficient to produce them. Evidence for such monopoles may also be obtained from astrophysical observations.

Jackson's 1975 assessment remains true. The search is somewhat abated by the lack of success in the 1980's and the decrease of interest in grand unified gauge theories.

References

1. J. D. Jackson, *Classical Electrodynamics*, 2nd edition (John Wiley & Sons, New York, 1975).
2. P.A.M. Dirac, Proc. Royal Soc. London **A133**, 60 (1931).
3. J. Preskill, Ann. Rev. Nucl. and Part. Sci. **34**, 461 (1984).
4. G. Giacomelli, La Rivista del Nuovo Cimento **7**, N. 12, 1 (1984).
5. Phys. Rep. **140**, 323 (1986).
6. B. Cabrera, Phys. Rev. Lett. **48**, 1378 (1982).
7. A.D. Caplin *et al.*, Nature **321**, 402 (1986).

Monopole Production Cross Section — Accelerator Searches

X-SECT (cm ²)	MASS (GeV)	CHG (g)	ENERGY (GeV)	BEAM	EVTS	DOCUMENT ID	TECN
<0.65E-33	<3.3	≥ 2	11A	197Au	0	¹ HE	97
<1.90E-33	<8.1	≥ 2	160A	208Pb	0	¹ HE	97
<3.E-37	<45.0	1.0	88-94	e ⁺ e ⁻	0	PINFOLD	93 PLAS
<3.E-37	<41.6	2.0	88-94	e ⁺ e ⁻	0	PINFOLD	93 PLAS
<7.E-35	<44.9	0.2-1.0	89-93	e ⁺ e ⁻	0	KINOSHITA	92 PLAS
<2.E-34	<850	≥ 0.5	1800	p \bar{p}	0	BERTANI	90 PLAS
<1.2E-33	<800	≥ 1	1800	p \bar{p}	0	PRICE	90 PLAS
<1.E-37	<29	1	50-61	e ⁺ e ⁻	0	KINOSHITA	89 PLAS
<1.E-37	<18	2	50-61	e ⁺ e ⁻	0	KINOSHITA	89 PLAS
<1.E-38	<17	<1	35	e ⁺ e ⁻	0	BRAUNSCH...	88B CNTR
<8.E-37	<24	1	50-52	e ⁺ e ⁻	0	KINOSHITA	88 PLAS
<1.3E-35	<22	2	50-52	e ⁺ e ⁻	0	KINOSHITA	88 PLAS
<9.E-37	<4	<0.15	10.6	e ⁺ e ⁻	0	GENTILE	87 CLEO
<3.E-32	<800	≥ 1	1800	p \bar{p}	0	PRICE	87 PLAS
<3.E-38		<3	29	e ⁺ e ⁻	0	FRYBERGER	84 PLAS
<1.E-31		1.3	540	p \bar{p}	0	AUBERT	83B PLAS
<4.E-38	<10	<6	34	e ⁺ e ⁻	0	MUSSET	83 PLAS
<8.E-36	<20		52	p \bar{p}	0	² DELL	82 CNTR
<9.E-37	<30	<3	29	e ⁺ e ⁻	0	KINOSHITA	82 PLAS
<1.E-37	<20	<24	63	p \bar{p}	0	CARRIGAN	78 CNTR
<1.E-37	<30	<3	56	p \bar{p}	0	HOFFMANN	78 PLAS
			62	p \bar{p}	0	² DELL	76 SPRK
<4.E-33			300	p	0	² STEVENS	76B SPRK
<1.E-40	<5	<2	70	p	0	³ ZRELOV	76 CNTR
<2.E-30			300	n	0	² BURKE	75 OSPK
<1.E-38			8	v	0	⁴ CARRIGAN	75 HLBC
<5.E-43	<12	<10	400	p	0	EBERHARD	75B INDU
<2.E-36	<30	<3	60	p \bar{p}	0	GIACOMELLI	75 PLAS
<5.E-42	<13	<24	400	p	0	CARRIGAN	74 CNTR
<6.E-42	<12	<24	300	p	0	CARRIGAN	73 CNTR
<2.E-36		1	0.001	γ	0	³ BARTLETT	72 CNTR
<1.E-41	<5		70	p	0	GUREVICH	72 EMUL
<1.E-40	<3	<2	28	p	0	AMALDI	63 EMUL
<2.E-40	<3	<2	30	p	0	PURCELL	63 CNTR
<1.E-35	<3	<4	28	p	0	FIDECARO	61 CNTR
<2.E-35	<1	1	6	p	0	BRADNER	59 EMUL

¹ HE 97 used a lead target and barium phosphate glass detectors. Cross-section limits are well below those predicted via the Drell-Yan mechanism.

² Multiphoton events.

³ Cherenkov radiation polarization.

⁴ Re-examines CERN neutrino experiments.

Monopole Production — Other Accelerator Searches

MASS (GeV)	CHG (g)	SPIN	ENERGY (GeV)	BEAM	DOCUMENT ID	TECN
> 610	≥ 1	0	1800	p \bar{p}	⁵ ABBOTT	98K D0
> 870	≥ 1	1/2	1800	p \bar{p}	⁵ ABBOTT	98K D0
>1580	≥ 1	1	1800	p \bar{p}	⁵ ABBOTT	98K D0
> 510			88-94	e ⁺ e ⁻	⁶ ACCIARRI	95C L3

⁵ ABBOTT 98K search for heavy pointlike Dirac monopoles via central production of a pair of photons with high transverse energies.

⁶ ACCIARRI 95C finds a limit $B(Z \rightarrow \gamma\gamma) < 0.8 \times 10^{-5}$ (which is possible via a monopole loop) at 95% CL and sets the mass limit via a cross section model.

Monopole Flux — Cosmic Ray Searches

FLUX (cm ⁻² sr ⁻¹ s ⁻¹)	MASS (GeV)	CHG (g)	COMMENTS ($\beta = v/c$)	EVTS	DOCUMENT ID	TECN
<1E-15		1	1.1×10^{-4} -0.1	0	⁷ AMBROSIO	97 MCRO
<4.1E-15		1	(0.18-2.7)E-3	0	⁸ AMBROSIO	97 MCRO
<1.0E-15		1	0.0012-0.1	0	⁹ AMBROSIO	97 MCRO
<0.87E-15			(0.11-5)E-3	0	¹⁰ AMBROSIO	97 MCRO
<6.8E-15		1	4.0E-5	0	¹¹ AMBROSIO	97 MCRO
<2.8E-15		1	0.1-1	0	¹² AMBROSIO	97 MCRO
<4.4E-15		1	0.1-1	0	¹³ AMBROSIO	97 MCRO
<5.6E-15		1	(0.18-3.0)E-3	0	¹⁴ AHLEN	94 MCRO
<2.7E-15		1	$\beta \sim 1 \times 10^{-3}$	0	¹⁵ BECKER-SZ...	94 IMB
<8.7E-15		1	>2.E-3	0	THRON	92 SOUD
<4.4E-12		1	all β	0	GARDNER	91 INDU
<7.2E-13		1	all β	0	HUBER	91 INDU
<3.7E-15	>E12	1	$\beta = 1.E-4$	0	¹⁶ ORITO	91 PLAS
<3.2E-16	>E10	1	$\beta > 0.05$	0	¹⁶ ORITO	91 PLAS
<3.2E-16	>E10-E12	2,3		0	¹⁶ ORITO	91 PLAS
<3.8E-13		1	all β	0	BERMON	90 INDU
<5.E-16		1	$\beta < 1.E-3$	0	¹⁵ BEZRUKOV	90 CHER
<1.8E-14		1	$\beta > 1.1E-4$	0	¹⁷ BUCKLAND	90 HEPT
<1E-18			3.E-4 < β < 1.5E-3	0	¹⁸ GHOSH	90 MICA
<7.2E-13		1	all β	0	HUBER	90 INDU
<5.E-12	>E7	1	3.E-4 < β < 5.E-3	0	BARISH	87 CNTR
<1.E-13			1.E-5 < β < 1	0	¹⁵ BARTELT	87 SOUD
<1.E-10		1	all β	0	EBISU	87 INDU
<2.E-13			1.E-4 < β < 6.E-4	0	MASEK	87 HEPT
<2.E-14			4.E-5 < β < 2.E-4	0	NAKAMURA	87 PLAS
<2.E-14			1.E-3 < β < 1	0	NAKAMURA	87 PLAS

Searches Particle Listings

Magnetic Monopole Searches

<5.E-14	9.E-4 < β < 1.E-2	0	SHEPKO	87	CNTR
<2.E-13	4.E-4 < β < 1	0	TSUKAMOTO	87	CNTR
<5.E-14	1 all β	1	19 CAPLIN	86	INDU
<5.E-12	1	0	CROMAR	86	INDU
<1.E-13	1 7.E-4 < β	0	HARA	86	CNTR
<7.E-11	1 all β	0	INCANDELA	86	INDU
<1.E-18	1 4.E-4 < β < 1.E-3	0	18 PRICE	86	MICA
<5.E-12	1	0	BERMON	85	INDU
<6.E-12	1	0	CAPLIN	85	INDU
<6.E-10	1	0	EBISU	85	INDU
<3.E-15	1 5.E-5 $\leq \beta \leq$ 1.E-3	0	15 KAJITA	85	KAMI
<2.E-21	1 β < 1.E-3	0	15,20 KAJITA	85	KAMI
<3.E-15	1 1.E-3 < β < 1.E-1	0	15 PARK	85B	CNTR
<5.E-12	1 1.E-4 < β < 1	0	BATTISTONI	84	NUSX
<7.E-12	1	0	INCANDELA	84	INDU
<7.E-13	1 3.E-4 < β	0	17 KAJINO	84	CNTR
<2.E-12	1 3.E-4 < β < 1.E-1	0	KAJINO	84B	CNTR
<6.E-13	1 5.E-4 < β < 1	0	KAWAGOE	84	CNTR
<2.E-14	1 1.E-3 < β	0	15 KRISHNA...	84	CNTR
<4.E-13	1 6.E-4 < β < 2.E-3	0	LISS	84	CNTR
<1.E-16	1 3.E-4 < β < 1.E-3	0	18 PRICE	84	MICA
<1.E-13	1 1.E-4 < β	0	PRICE	84B	PLAS
<4.E-13	1 6.E-4 < β < 2.E-3	0	TARLE	84	CNTR
		7	21 ANDERSON	83	EMUL
<4.E-13	1 1.E-2 < β < 1.E-3	0	BARTELT	83B	CNTR
<1.E-12	1 7.E-3 < β < 1	0	BARWICK	83	PLAS
<3.E-13	1 1.E-3 < β < 4.E-1	0	BONARELLI	83	CNTR
<3.E-12	1 5.E-4 < β < 5.E-2	0	15 BOSETTI	83	CNTR
<4.E-11	1	0	CABRERA	83	INDU
<5.E-15	1 1.E-2 < β < 1	0	DOKE	83	PLAS
<8.E-15	1 1.E-4 < β < 1.E-1	0	15 ERREDE	83	IMB
<5.E-12	1 1.E-4 < β < 3.E-2	0	GROOM	83	CNTR
<2.E-12	1 6.E-4 < β < 1	0	MASHIMO	83	CNTR
<1.E-13	1 β = 3.E-3	0	ALEXEYEV	82	CNTR
<2.E-12	1 7.E-3 < β < 6.E-1	0	BONARELLI	82	CNTR
6.E-10	1 all β	1	22 CABRERA	82	INDU
<2.E-11	1 1.E-2 < β < 1.E-1	0	MASHIMO	82	CNTR
<2.E-15	concentrator	0	BARTLETT	81	PLAS
<1.E-13	>1 1.E-3 < β	0	KINOSHITA	81B	PLAS
<5.E-11	<E17 3.E-4 < β < 1.E-3	0	ULLMAN	81	CNTR
<2.E-11	concentrator	0	BARTLETT	78	PLAS
1.E-1	>200 2	1	23 PRICE	75	PLAS
<2.E-13	>2	0	FLEISCHER	71	PLAS
<1.E-19	>2 obsidian, mica	0	FLEISCHER	69C	PLAS
<5.E-15	<15 <3 concentrator	0	CARITHERS	66	ELEC
<2.E-11	<1-3 concentrator	0	MALKUS	51	EMUL

7 AMBROSIO 97 global MACRO 90%CL is 0.78×10^{-15} at $\beta=1.1 \times 10^{-4}$, goes through a minimum at 0.61×10^{-15} near $\beta=(1.1-2.7) \times 10^{-3}$, then rises to 0.84×10^{-15} at $\beta=0.1$. The global limit in this region is below the Parker bound at 10^{-15} . Less stringent limits are established for $4 \times 10^{-5} < \beta < 1$. Limits set by various triggers in the detector are listed below. All limits assume a catalysis cross section smaller than 10 mb.

8 AMBROSIO 97 "Scintillator D" (low velocity) 90%CL increases from 4.1×10^{-15} at $\beta=2.7 \times 10^{-3}$ to 14.6×10^{-15} at $\beta=0.006$.

9 AMBROSIO 97 "Scintillator B" 90%CL (single medium-velocity trigger with two analysis criteria).

10 AMBROSIO 97 streamer tube 90%CL. Tubes contain helium, and hence trigger is sensitive via the atomic induction mechanism.

11 AMBROSIO 97 CR39 90%CL improves to 4.3×10^{-15} at $\beta=1.0 \times 10^{-4}$. CR39 is sensitive for $4 \times 10^{-5} < \beta < 1$ except for a window at $0.25 \times 10^{-3} < \beta < 2.1 \times 10^{-3}$. In the middle region other triggers set better limits.

12 AMBROSIO 97 CR39 90%CL falls to 2.7×10^{-15} at $\beta=1$ and increases at lower velocities. Provides better limit than "Scintillator C" for $0.1 < \beta < 1.0$.

13 AMBROSIO 97 "Scintillator C" 90%CL, based on high absolute energy loss in two scintillator layers.

14 AHLEN 94 limit for dyons extends down to $\beta=0.9E-4$ and a limit of $1.3E-14$ extends to $\beta = 0.8E-4$. Also see comment by PRICE 94 and reply of BARISH 94. One loophole in the AHLEN 94 result is that in the case of monopoles catalyzing nucleon decay, relativistic particles could veto the events. See AMBROSIO 97 for additional results.

15 ALVAREZ 75, FLEISCHER 75, and FRIEDLANDER 75 explain as fragmenting nucleus. EBERHARD 75 and ROSS 76 discuss conflict with other experiments. HAGSTROM 77 reinterprets as antinucleus. PRICE 78 reassesses.

Monopole Flux — Astrophysics

FLUX ($\text{cm}^{-2}\text{sr}^{-1}\text{s}^{-1}$)	MASS (GeV)	CHG (g)	COMMENTS ($\beta = v/c$)	EVTs	DOCUMENT ID	TECN
<1.3E-20			faint white dwarf		24 FREESE	99 ASTR
<1.E-16	E17	1	galactic field	0	25 ADAMS	93 COSM
<1.E-23			Jovian planets		24 ARAFUNE	85 ASTR
<1.E-16	E15	0	solar trapping	0	BRACCI	85B ASTR
<1.E-18		1		0	24 HARVEY	84 COSM
<3.E-23			neutron stars		KOLB	84 ASTR
<7.E-22			pulsars	0	24 FREESE	83B ASTR
<1.E-18	<E18	1	intergalactic field	0	24 REPHAELI	83 COSM
<1.E-23			neutron stars	0	24 DIMOPOUL...	82 COSM
<5.E-22			neutron stars	0	24 KOLB	82 COSM
<5.E-15	>E21		galactic halo		SALPETER	82 COSM
<1.E-12	E19	1	$\beta=3.E-3$	0	26 TURNER	82 COSM
<1.E-16		1	galactic field	0	PARKER	70 COSM

24 Catalysis of nucleon decay.

25 ADAMS 93 limit based on "survival and growth of a small galactic seed field" is $10^{-16} (m/10^{17} \text{ GeV}) \text{ cm}^{-2} \text{ s}^{-1} \text{ sr}^{-1}$. Above 10^{17} GeV , limit $10^{-16} (10^{17} \text{ GeV}/m) \text{ cm}^{-2} \text{ s}^{-1} \text{ sr}^{-1}$ (from requirement that monopole density does not overclose the universe) is more stringent.

26 Re-evaluates PARKER 70 limit for GUT monopoles.

Monopole Density — Matter Searches

DENSITY	CHG (g)	MATERIAL	EVTs	DOCUMENT ID	TECN
<6.9E-6/gram	>1/3	Meteorites and other	0	JEON	95 INDU
<2.E-7/gram	>0.6	Fe ore	0	27 EBISU	87 INDU
<4.6E-6/gram	>0.5	deep schist	0	KOVALIK	86 INDU
<1.6E-6/gram	>0.5	manganese nodules	0	28 KOVALIK	86 INDU
<1.3E-6/gram	>0.5	seawater	0	KOVALIK	86 INDU
>1.E+14/gram	>1/3	iron aerosols	>1	MIKHAILOV	83 SPEC
<6.E-4/gram		air, seawater	0	CARRIGAN	76 CNTR
<5.E-1/gram	>0.04	11 materials	0	CABRERA	75 INDU
<2.E-4/gram	>0.05	moon rock	0	ROSS	73 INDU
<6.E-7/gram	<140	seawater	0	KOLM	71 CNTR
<1.E-2/gram	<120	manganese nodules	0	FLEISCHER	69 PLAS
<1.E-4/gram	>0	manganese	0	FLEISCHER	69B PLAS
<2.E-3/gram	<1-3	magnetite, meteor	0	GOTO	63 EMUL
<2.E-2/gram		meteorite	0	PETUKHOV	63 CNTR

27 Mass $1 \times 10^{14} - 1 \times 10^{17} \text{ GeV}$.

28 KOVALIK 86 examined 498 kg of schist from two sites which exhibited clear mineralogical evidence of having been buried at least 20 km deep and held below the Curie temperature.

Monopole Density — Astrophysics

DENSITY	CHG (g)	MATERIAL	EVTs	DOCUMENT ID	TECN
<1.E-9/gram	1	sun, catalysis	0	29 ARAFUNE	83 COSM
<6.E-33/nucl	1	moon wake	0	SCHATTEN	83 ELEC
<2.E-28/nucl		earth heat	0	CARRIGAN	80 COSM
<2.E-4/prot		42cm absorpton	0	BRODERICK	79 COSM
<2.E-13/m ³		moon wake	0	SCHATTEN	70 ELEC

29 Catalysis of nucleon decay.

REFERENCES FOR Magnetic Monopole Searches

FREESE	99	PR D59 063007	K. Freese, E. Kravtsova
ABBOTT	98K	PRL 81 524	B. Abbott et al.
AMBROSIO	97	PL B406 249	M. Ambrosio et al.
HE	97	PRL 79 3134	Y.D. He
ACCIARRI	95C	PL B345 609	M. Acciarri et al.
JEON	95	PRL 75 1443	H. Jeon, M.J. Longo
Also	96	PRL 76 159 (errata)	
AHLEN	94	PRL 72 608	S.P. Ahlen et al.
BARISH	94	PRL 73 1306	B.C. Barish, G. Giacomelli, J.T. Hong
BECKER-SZ...	94	PR D49 2169	R.A. Becker-Szendy et al.
PRICE	94	PRL 73 1305	P.B. Price
ADAMS	93	PRL 70 2511	F.C. Adams et al.
PINFOLD	93	PL B316 407	J.L. Pinfold et al.
KINOSHITA	92	PR D46 R881	K. Kinoshita et al.
THRON	92	PR D46 4845	J.L. Thron et al.
GARDNER	91	PR D44 622	R.D. Gardner et al.
HUBER	91	PR D44 636	M.E. Huber et al.
ORITO	91	PR 66 1951	S. Orito et al.
BERMON	90	PR 64 839	S. Bermon et al.
BERTANI	90	EPL 12 613	M. Bertani et al.
BEZRUKOV	90	SJNP 52 54	L.B. Bezrukov et al.
Also	90	Translated from YAF 52 86	
BUCKLAND	90	PR D41 2726	K.N. Buckland et al.
GHOSH	90	EPL 12 25	D.C. Ghosh, S. Chatterjee
HUBER	90	PRL 64 835	M.E. Huber et al.
PRICE	90	PRL 65 149	P.B. Price, J. Guiru, K. Kinoshita
KINOSHITA	89	PL B228 543	K. Kinoshita et al.
BRAUNSCH...	88B	ZPHY C38 543	R. Braunschweig et al.
KINOSHITA	88	PRL 60 1610	K. Kinoshita et al.
BARISH	87	PR D36 2641	B.C. Barish, G. Liu, C. Lane
BARTELT	87	PR D36 1990	J.E. Bartelt et al.
Also	89	PR D40 1701 erratum	J.E. Bartelt et al.
EBISU	87	PR D36 3359	T. Ebisu, T. Watanabe
Also	85	JPG 11 883	T. Ebisu, T. Watanabe
GENTILE	87	PR D35 1081	T. Gentile et al.
GUY	87	Nature 325 463	J. Guy

(DO Collab.)
(MACRO Collab.)
(UCB)
(L3 Collab.)
(MICH)
(MACRO Collab.)
(CIT+)
(IMB Collab.)
(UCB)
(MICH, FNAL)
(ALBE, HARV, MONT+)
(HARV, BGNA, REHO)
(SOUDAN-2 Collab.)
(STAN)
(STAN)
(ICEPF, WASC, NIHO, ICRR)
(IBM, BNL)
(BGNA, INFN)
(INRM)
(UCSD)
(JADA)
(STAN)
(HARV, TISA, KEK+)
(TASSO Collab.)
(CIT)
(Soudan Collab.)
(KOBE)
(KOBE)
(CLEO Collab.)
(LOIC)

Supersymmetric Particle Searches

SUPERSYMMETRY

Revised October 1999 by Howard E. Haber (Univ. of California, Santa Cruz) Part I, and by M. Schmitt (Harvard Univ.) Part II

This review is divided into two parts:

Supersymmetry, Part I (Theory)

- I.1. Introduction
- I.2. Structure of the MSSM
- I.3. Parameters of the MSSM
- I.4. The supersymmetric-particle sector
- I.5. The Higgs sector of the MSSM
- I.6. Reducing the MSSM parameter freedom
- I.7. The constrained MSSMs: mSUGRA, GMSB, and SGUTs
- I.8. Beyond the MSSM

Supersymmetry, Part II (Experiment)

- II.1. Introduction
- II.2. Common supersymmetry scenarios
- II.3. Experimental issues
- II.4. Supersymmetry searches in e^+e^- colliders
- II.5. Supersymmetry searches at proton machines
- II.6. Supersymmetry searches at HERA and fixed-target experiments
- II.7. Conclusions

SUPERSYMMETRY, PART I (THEORY)

(by H.E. Haber)

I.1. Introduction: Supersymmetry (SUSY) is a generalization of the space-time symmetries of quantum field theory that transforms fermions into bosons and vice versa. It also provides a framework for the unification of particle physics and gravity [1–3], which is governed by the Planck scale, $M_P \approx 10^{19}$ GeV (defined to be the energy scale where the gravitational interactions of elementary particles become comparable to their gauge interactions). If supersymmetry were an exact symmetry of nature, then particles and their superpartners (which differ in spin by half a unit) would be degenerate in mass. Thus, supersymmetry cannot be an exact symmetry of nature, and must be broken. In theories of “low-energy” supersymmetry, the effective scale of supersymmetry breaking is tied to the electroweak scale [4–6], which is characterized by the Standard Model Higgs vacuum expectation value $v = 246$ GeV. It is thus possible that supersymmetry will ultimately explain the origin of the large hierarchy of energy scales from the W and Z masses to the Planck scale.

At present, there are no unambiguous experimental results that require the existence of low-energy supersymmetry. However, if experimentation at future colliders uncovers evidence for supersymmetry, this would have a profound effect on the study of TeV-scale physics and the development of a more fundamental theory of mass and symmetry-breaking phenomena in particle physics.

MASEK	87	PR D35 2758	G.E. Masek et al.	(UCSD)
NAKAMURA	87	PL B183 395	S. Nakamura et al.	(INUS, WASCR, NIHO)
PRICE	87	PRL 59 2523	P.B. Price, R. Guoxiao, K. Kinoshita	(HARV)
SCHOUTEN	87	JPE 20 850	J.C. Schouten et al.	(LOIC)
SHEPKO	87	PR D35 2917	M.J. Shepko et al.	(TAMU)
TSUKAMOTO	87	EPL 3 39	T. Tsukamoto et al.	(ICRR)
CAPLIN	86	Nature 321 402	A.D. Caplin et al.	(LOIC)
Also	87	JPE 20 850	J.C. Schouten et al.	(LOIC)
Also	87	Nature 325 463	T. Gay	(RIKEN)
CROMAR	86	PRL 56 2561	M.W. Cromar, A.F. Clark, F.R. Fickett	(NBSB)
HARA	86	PRL 56 553	T. Hara et al.	(ICRR, KYOT, KEK, KOBE+)
INCANDELA	86	PR D34 2637	J. Incandela et al.	(CHIC, FNAL, MICH)
KOVALIK	86	PR A33 1183	J.M. Kovalik, J.L. Kirschvink	(CIT)
PRICE	86	PRL 56 1226	P.B. Price, M.H. Saimon	(UCB)
ARAFUNE	85	PR D32 2586	J. Arafune, M. Fukugita, S. Yanagita	(ICRR, KYOTU+)
BERMON	85	PR 55 1650	S. Berman et al.	(IBM)
BRACCI	85B	NP B258 726	L. Bracci, G. Fiorentini, G. Mezzorani	(PISA+)
Also	85	LNC 42 123	L. Bracci, G. Fiorentini	(PISA)
CAPLIN	85	Nature 317 234	A.D. Caplin et al.	(LOIC)
EBISU	85	JPG 11 883	T. Ebisu, T. Watanabe	(KOBE)
KAJITA	85	JPSJ 54 4065	T. Kajita et al.	(ICRR, KEK, NIIG)
PARK	85B	NP B252 261	H.S. Park et al.	(IMB Collab.)
BATTISTONI	84	PL 133B 454	G. Battistoni et al.	(NUSEX Collab.)
FRYBERGER	84	PR D29 1524	D. Fryberger et al.	(SLAC, UCB)
HARVEY	84	NP B236 255	J.A. Harvey et al.	(PRIN)
INCANDELA	84	PRL 53 2067	J. Incandela et al.	(CHIC, FNAL, MICH)
KAJINO	84	PRL 52 1373	F. Kajino et al.	(ICRR)
KAJINO	84B	JPG 10 447	F. Kajino et al.	(ICRR)
KAWAGOE	84	LNC 41 315	K. Kawagoe et al.	(TOKY)
KOLB	84	APJ 286 702	E.W. Kolb, M.S. Turner	(FNAL, CHIC)
KRISHNA...	84	PL 142B 99	M.R. Krishnaswamy et al.	(TATA, OSMK+)
LISS	84	PR D30 884	T.M. Liss, S.P. Ahlen, G. Tarle	(UCB, IND+)
PRICE	84	PRL 52 1265	P.B. Price et al.	(ROMA, UCB, IND+)
PRICE	84B	PL 140B 112	P.B. Price et al.	(CERN)
TARLE	84	PRL 52 90	G. Tarle, S.P. Ahlen, T.M. Liss	(UCB, MICH+)
ANDERSON	83	PR D28 2308	S.N. Anderson et al.	(WASH)
ARAFUNE	83	PL 133B 380	J. Arafune, M. Fukugita	(ICRR, KYOTU)
AUBERT	83B	PL 120B 465	B. Aubert et al.	(CERN, LAPP)
BARTELT	83B	PRL 50 655	J.E. Bartelt et al.	(MINN, ANL)
BARWICK	83	PR D28 2338	S.W. Barwick, K. Kinoshita, P.B. Price	(UCB)
BONARELLI	83	PL 126B 137	R. Bonarelli, P. Capiluppi, I. d'Antone	(BGNA)
BOSETTI	83	PL 133B 265	P.C. Bosetti et al.	(AACH3, HAWA, TOKY)
CABRERA	83	PRL 51 1933	B. Cabrera et al.	(STAN)
DOKE	83	PR D28 3700	T. Doke et al.	(WASU, RIKK, TTAM, RIKEN)
ERREDE	83	PRL 51 245	S.M. Errede et al.	(IMB Collab.)
FREESE	83B	PRL 51 1625	K. Freese, M.S. Turner, D.N. Schramm	(CHIC)
GROOM	83	PRL 50 573	D.E. Groom et al.	(UTAH, STAN)
MASHIMO	83	PL 128B 327	T. Mashimo et al.	(ICEPP)
MIKHAILOV	83	PL 130B 331	V.F. Mikhailov	(KAZA)
MUSSET	83	PL 128B 333	P. Musset, M. Price, E. Lohrmann	(CERN, HAMB)
REPHEL	83	PL 121B 115	Y. Rephaeli, M.S. Turner	(CHIC)
SCHATTEN	83	PR D27 1525	K.H. Schatten	(NASA)
ALEXEYEV	82	LNC 35 413	E.N. Alekseev et al.	(IBR)
BONARELLI	82	PL 112B 100	R. Bonarelli et al.	(BGNA)
CABRERA	82	PRL 48 1378	B. Cabrera	(STAN)
DELL	82	NP B209 45	G.F. Dell et al.	(BNL, ADEL, ROMA)
DIMOPOUL...	82	PL 119B 320	S. Dimopoulos, J. Preskill, F. Wilczek	(HARV+)
KINOSHITA	82	PRL 48 77	K. Kinoshita, P.B. Price, D. Fryberger	(UCB+)
KOLB	82	PRL 49 1373	E.W. Kolb, S.A. Colgate, J.A. Harvey	(LASL, PRIN)
MASHIMO	82	JPSJ 51 3067	T. Mashimo, K. Kawagoe, M. Koshiba	(INUS)
SALPETER	82	PRL 48 1124	M.S. Salpeter, S.L. Shapiro, I. Wasserman	(CORN)
TURNER	82	PR D26 1299	M.S. Turner, E.N. Parker, T.J. Bogdan	(CHIC)
BARTLETT	81	PR D24 612	D.F. Bartlett et al.	(COLO, GESC)
KINOSHITA	81B	PR D24 1707	K. Kinoshita, P.B. Price	(UCB)
ULLMAN	81	PRL 47 289	J.D. Ullman	(LEHM, BNL)
CARRIGAN	80	Nature 288 348	R.A. Carrigan	(FNAL)
BRODERICK	79	PR D19 1046	J.J. Broderick et al.	(VPI)
BARTLETT	78	PR D18 2253	D.F. Bartlett, D. Soo, M.G. White	(COLO, PRIN)
CARRIGAN	78	PR D17 1754	R.A. Carrigan, B.P. Strauss, G. Giacomelli	(FNAL+)
HOFFMANN	78	PR D17 357	H. Hoffmann et al.	(CERN, ROMA)
PRICE	78	PR D18 1382	P.B. Price et al.	(UCB, HOUS)
HAGSTROM	77	PRL 38 729	R. Hagstrom	(LBL)
CARRIGAN	76	PR D13 1823	R.A. Carrigan, F.A. Nezrick, B.P. Strauss	(FNAL)
DELL	76	LNC 15 269	G.F. Dell et al.	(CERN, BNL, ROMA, ADEL)
ROSS	76	LBL-4665	R.R. Ross	(LBL)
STEVENS	76B	PR D14 2207	D.M. Stevens et al.	(VPI, BNL)
ZRELOV	76	CZJP B26 1306	V.P. Zrelov et al.	(JINR)
ALVAREZ	75	LBL-4260	L.W. Alvarez	(LBL)
BURKE	75	PL 60B 113	D.L. Burke et al.	(MICH)
CABRERA	75	Thesis	B. Cabrera	(STAN)
CARRIGAN	75	NP B91 279	R.A. Carrigan, F.A. Nezrick	(FNAL)
Also	71	PR D3 56	R.A. Carrigan, F.A. Nezrick	(FNAL)
EBERHARD	75	PR D11 3099	P.H. Eberhard et al.	(LBL, MPIM)
EBERHARD	75B	LBL-4289	P.H. Eberhard	(LBL)
FLEISCHER	75	PRL 35 1412	R.L. Fleischer, R.N.F. Walker	(GESC, WUSL)
FRIEDLANDER	75	PRL 35 1167	M.W. Friedlander	(WUSL)
GIACOMELLI	75	NC 28A 21	G. Giacomelli et al.	(BGNA, CERN, SAFL+)
PRICE	75	PRL 35 487	P.B. Price et al.	(UCB, HOUS)
CARRIGAN	74	PR D10 3867	R.A. Carrigan, F.A. Nezrick, B.P. Strauss	(FNAL)
CARRIGAN	73	PR D8 3717	R.A. Carrigan, F.A. Nezrick, B.P. Strauss	(FNAL)
ROSS	73	PR D8 698	R.R. Ross et al.	(LBL, SLAC)
Also	71	PR D4 3260	P.H. Eberhard et al.	(LBL, SLAC)
Also	70	Science 167 701	L.W. Alvarez et al.	(LBL, SLAC)
BARTLETT	72	PR D6 1817	D.F. Bartlett, M.D. Lahana	(COLO)
GUREVICH	72	PL 38B 549	I.I. Gurevich et al.	(KIAE, NOVO, SERP)
Also	72B	JETP 34 917	L.M. Barkov, I.I. Gurevich, M.S. Zlotorev	(KIAE+)
Also	72B	Translated from ZETF 61 1721		
Also	70	PL 31B 394	I.I. Gurevich et al.	(KIAE, NOVO, SERP)
FLEISCHER	71	PR D4 24	R.L. Fleischer et al.	(GESC)
KOLM	71	PR D4 1285	H.H. Kolm, F. Villa, A. Odian	(MIT, SLAC)
PARKER	70	APJ 160 383	E.N. Parker	(CHIC)
SCHATTEN	70	PR D1 2245	K.H. Schatten	(NASA)
FLEISCHER	69	PR 177 2029	R.L. Fleischer et al.	(GESC, FSU)
FLEISCHER	69B	PR 184 1393	R.L. Fleischer et al.	(GESC, UNCS, GSCO)
FLEISCHER	69C	PR 184 1398	R.L. Fleischer, P.B. Price, R.T. Woods	(GESC)
Also	70C	JAP 41 958	R.L. Fleischer et al.	(GESC)
CARITHERS	66	PR 149 1070	W.C.J. Carithers, R.J. Stefanski, R.K. Adair	(CERN)
AMALDI	63	NC 28 773	E. Amaldi et al.	(ROMA, UCSD, CERN)
GOTO	63	PR 132 387	E. Goto, H.H. Kolm, K.W. Ford	(TOKY, MIT, BRAN)
PETUKHOV	63	NP 49 87	V.A. Petukhov, M.N. Yakimenko	(LEBD)
PURCELL	63	PR 129 2326	E.M. Purcell et al.	(HARV, BNL)
FIDECARO	61	NC 22 657	M. Fidecaro, G. Finocchiaro, G. Giacomelli	(CERN)
BRADNER	59	PR 124 603	H. Bradner, W.M. Isbell	(LBL)
MALKUS	51	PR 83 899	W.V.R. Malkus	(CHIC)

OTHER RELATED PAPERS

GROOM	86	PRPL 140 323	D.E. Groom	(UTAH)
Review				

Searches Particle Listings

Supersymmetric Particle Searches

I.2. Structure of the MSSM: The minimal supersymmetric extension of the Standard Model (MSSM) consists of taking the Standard Model and adding the corresponding supersymmetric partners [2,7]. In addition, the MSSM contains two hypercharge $Y = \pm 1$ Higgs doublets, which is the minimal structure for the Higgs sector of an anomaly-free supersymmetric extension of the Standard Model. The supersymmetric structure of the theory also requires (at least) two Higgs doublets to generate mass for both “up”-type and “down”-type quarks (and charged leptons) [8,9]. All renormalizable supersymmetric interactions consistent with (global) $B-L$ conservation (B = baryon number and L = lepton number) are included. Finally, the most general soft-supersymmetry-breaking terms are added [10].

If supersymmetry is associated with the origin of the scale of electroweak interactions, then the mass parameters introduced by the soft-supersymmetry-breaking terms must in general be of order 1 TeV or below [11] (although models have been proposed in which some supersymmetric particle masses can be larger, in the range of 1–10 TeV [12]). Some lower bounds on these parameters exist due to the absence of supersymmetric-particle production at current accelerators [13]. Additional constraints arise from limits on the contributions of virtual supersymmetric particle exchange to a variety of Standard Model processes [14,15]. In particular, the Standard Model fit (without supersymmetry) to precision electroweak data is quite good [16]. If all supersymmetric particle masses are significantly heavier than m_Z (in practice, masses greater than 300 GeV are sufficient [17]), then the effects of the supersymmetric particles decouple in loop-corrections to electroweak observables [18]. In this case the Standard Model global fit to precision data and the corresponding MSSM fit yield similar results. On the other hand, regions of parameter space with light supersymmetric particle masses can generate significant one-loop corrections, resulting in a poorer overall fit to the data [19]. Thus, the precision electroweak data provide some constraints on the magnitude of the soft-supersymmetry-breaking terms.

As a consequence of $B-L$ invariance, the MSSM possesses a multiplicative R -parity invariance, where $R = (-1)^{3(B-L)+2S}$ for a particle of spin S [20]. Note that this formula implies that all the ordinary Standard Model particles have even R -parity, whereas the corresponding supersymmetric partners have odd R -parity. The conservation of R -parity in scattering and decay processes has a crucial impact on supersymmetric phenomenology. For example, starting from an initial state involving ordinary (R -even) particles, it follows that supersymmetric particles must be produced in pairs. In general, these particles are highly unstable and decay quickly into lighter states. However, R -parity invariance also implies that the lightest supersymmetric particle (LSP) is absolutely stable, and must eventually be produced at the end of a decay chain initiated by the decay of a heavy unstable supersymmetric particle.

In order to be consistent with cosmological constraints, a stable LSP is almost certainly electrically and color neutral [21]. Consequently, the LSP in a R -parity-conserving theory is weakly-interacting in ordinary matter, *i.e.* it behaves like a stable heavy neutrino and will escape detectors without being directly observed. Thus, the canonical signature for conventional R -parity-conserving supersymmetric theories is missing (transverse) energy, due to the escape of the LSP. Moreover, the LSP is a prime candidate for “cold dark matter” [22], a potentially important component of the non-baryonic dark matter that is required in many models of cosmology and galaxy formation [23].

In the MSSM, supersymmetry breaking is accomplished by including the most general renormalizable soft-supersymmetry-breaking terms consistent with the $SU(3) \times SU(2) \times U(1)$ gauge symmetry and R -parity invariance. These terms parameterize our ignorance of the fundamental mechanism of supersymmetry breaking. If supersymmetry breaking occurs spontaneously, then a massless Goldstone fermion called the *goldstino* (\tilde{G}) must exist. The goldstino would then be the LSP and could play an important role in supersymmetric phenomenology [24]. However, the goldstino is a physical degree of freedom only in models of spontaneously broken global supersymmetry. If the supersymmetry is a local symmetry, then the theory must incorporate gravity; the resulting theory is called supergravity. In models of spontaneously broken supergravity, the goldstino is “absorbed” by the *gravitino* ($\tilde{g}_{3/2}$), the spin-3/2 partner of the graviton [25]. By this super-Higgs mechanism, the goldstino is removed from the physical spectrum and the gravitino acquires a mass ($m_{3/2}$).

It is very difficult (perhaps impossible) to construct a model of spontaneously-broken low-energy supersymmetry where the supersymmetry breaking arises solely as a consequence of the interactions of the particles of the MSSM. A more viable scheme posits a theory consisting of at least two distinct sectors: a “hidden” sector consisting of particles that are completely neutral with respect to the Standard Model gauge group, and a “visible” sector consisting of the particles of the MSSM. There are no renormalizable tree-level interactions between particles of the visible and hidden sectors. Supersymmetry breaking is assumed to occur in the hidden sector, and then transmitted to the MSSM by some mechanism. Two theoretical scenarios have been examined in detail: gravity-mediated and gauge-mediated supersymmetry breaking.

Supergravity models provide a natural mechanism for transmitting the supersymmetry breaking of the hidden sector to the particle spectrum of the MSSM. In models of *gravity-mediated* supersymmetry breaking, gravity is the messenger of supersymmetry breaking [26,27]. More precisely, supersymmetry breaking is mediated by effects of gravitational strength (suppressed by an inverse power of the Planck mass). In this

scenario, the gravitino mass is of order the electroweak-symmetry-breaking scale, while its couplings are roughly gravitational in strength [1,28]. Such a gravitino would play no role in supersymmetric phenomenology at colliders.

In *gauge-mediated* supersymmetry breaking, supersymmetry breaking is transmitted to the MSSM via gauge forces. A typical structure of such models involves a hidden sector where supersymmetry is broken, a “messenger sector” consisting of particles (messengers) with $SU(3) \times SU(2) \times U(1)$ quantum numbers, and the visible sector consisting of the fields of the MSSM [29,30]. The direct coupling of the messengers to the hidden sector generates a supersymmetry breaking spectrum in the messenger sector. Finally, supersymmetry breaking is transmitted to the MSSM via the virtual exchange of the messengers. If this approach is extended to incorporate gravitational phenomena, then supergravity effects will also contribute to supersymmetry breaking. However, in models of gauge-mediated supersymmetry breaking, one usually chooses the model parameters in such a way that the virtual exchange of the messengers dominates the effects of the direct gravitational interactions between the hidden and visible sectors. In this scenario, the gravitino mass is typically in the eV to keV range, and is therefore the LSP. The helicity $\pm \frac{1}{2}$ components of $\tilde{g}_{3/2}$ behave approximately like the goldstino; its coupling to the particles of the MSSM is significantly stronger than a coupling of gravitational strength.

I.3. Parameters of the MSSM: The parameters of the MSSM are conveniently described by considering separately the supersymmetry-conserving sector and the supersymmetry-breaking sector. A careful discussion of the conventions used in defining the MSSM parameters can be found in Ref. 31. For simplicity, consider the case of one generation of quarks, leptons, and their scalar superpartners. The parameters of the supersymmetry-conserving sector consist of: (i) gauge couplings: g_s , g , and g' , corresponding to the Standard Model gauge group $SU(3) \times SU(2) \times U(1)$ respectively; (ii) a supersymmetry-conserving Higgs mass parameter μ ; and (iii) Higgs-fermion Yukawa coupling constants: λ_u , λ_d , and λ_e (corresponding to the coupling of one generation of quarks, leptons, and their superpartners to the Higgs bosons and higgsinos).

The supersymmetry-breaking sector contains the following set of parameters: (i) gaugino Majorana masses M_3 , M_2 and M_1 associated with the $SU(3)$, $SU(2)$, and $U(1)$ subgroups of the Standard Model; (ii) five scalar squared-mass parameters for the squarks and sleptons, $M_{\tilde{Q}}^2$, $M_{\tilde{U}}^2$, $M_{\tilde{D}}^2$, $M_{\tilde{L}}^2$, and $M_{\tilde{E}}^2$ [corresponding to the five electroweak gauge multiplets, *i.e.*, superpartners of $(u, d)_L$, u_L^c , d_L^c , $(\nu, e^-)_L$, and e_L^c]; (iii) Higgs-squark-squark and Higgs-slepton-slepton trilinear interaction terms, with coefficients A_u , A_d , and A_e (these are the so-called “A-parameters”); and (iv) three scalar Higgs squared-mass parameters—two of which contribute to the diagonal Higgs squared-masses, given by $m_1^2 + |\mu|^2$ and $m_2^2 + |\mu|^2$, and one off-diagonal Higgs squared-mass term, $m_{12}^2 \equiv B\mu$ (which defines

the “B-parameter”). These three squared-mass parameters can be re-expressed in terms of the two Higgs vacuum expectation values, v_d and v_u , and one physical Higgs mass. Here, v_d (v_u) is the vacuum expectation value of the Higgs field which couples exclusively to down-type (up-type) quarks and leptons. (Another notation often employed in the literature is $v_1 \equiv v_d$ and $v_2 \equiv v_u$.) Note that $v_d^2 + v_u^2 = (246 \text{ GeV})^2$ is fixed by the W mass, while the ratio

$$\tan \beta = v_u/v_d \quad (1)$$

is a free parameter of the model.

The total number of degrees of freedom of the MSSM is quite large, primarily due to the parameters of the soft-supersymmetry-breaking sector. In particular, in the case of three generations of quarks, leptons, and their superpartners, $M_{\tilde{Q}}^2$, $M_{\tilde{U}}^2$, $M_{\tilde{D}}^2$, $M_{\tilde{L}}^2$, and $M_{\tilde{E}}^2$ are hermitian 3×3 matrices, and the A-parameters are complex 3×3 matrices. In addition, M_1 , M_2 , M_3 , B and μ are in general complex. Finally, as in the Standard Model, the Higgs-fermion Yukawa couplings, λ_f ($f = u, d$, and e), are complex 3×3 matrices which are related to the quark and lepton mass matrices via: $M_f = \lambda_f v_f / \sqrt{2}$, where $v_e \equiv v_d$ (with v_u and v_d as defined above). However, not all these parameters are physical. Some of the MSSM parameters can be eliminated by expressing interaction eigenstates in terms of the mass eigenstates, with an appropriate redefinition of the MSSM fields to remove unphysical degrees of freedom. The analysis of Ref. 32 shows that the MSSM possesses 124 truly independent parameters. Of these, 18 parameters correspond to Standard Model parameters (including the QCD vacuum angle θ_{QCD}), one corresponds to a Higgs sector parameter (the analogue of the Standard Model Higgs mass), and 105 are genuinely new parameters of the model. The latter include: five real parameters and three CP -violating phases in the gaugino/higgsino sector, 21 squark and slepton masses, 36 new real mixing angles to define the squark and slepton mass eigenstates and 40 new CP -violating phases that can appear in squark and slepton interactions. The most general R -parity-conserving minimal supersymmetric extension of the Standard Model (without additional theoretical assumptions) will be denoted henceforth as MSSM-124 [33].

I.4. The supersymmetric-particle sector: Consider the sector of supersymmetric particles (*sparticles*) in the MSSM. The supersymmetric partners of the gauge and Higgs bosons are fermions, whose names are obtained by appending “ino” at the end of the corresponding Standard Model particle name. The *gluino* is the color octet Majorana fermion partner of the gluon with mass $M_{\tilde{g}} = |M_3|$. The supersymmetric partners of the electroweak gauge and Higgs bosons (the *gauginos* and *higgsinos*) can mix. As a result, the physical mass eigenstates are model-dependent linear combinations of these states, called *charginos* and *neutralinos*, which are obtained by diagonalizing the corresponding mass matrices. The chargino-mass matrix depends on M_2 , μ , $\tan \beta$ and m_W [34].

Searches Particle Listings

Supersymmetric Particle Searches

The corresponding chargino-mass eigenstates are denoted by $\tilde{\chi}_1^+$ and $\tilde{\chi}_2^+$, with masses

$$M_{\tilde{\chi}_1^+, \tilde{\chi}_2^+}^2 = \frac{1}{2} \left\{ |\mu|^2 + |M_2|^2 + 2m_W^2 \mp \left[(|\mu|^2 + |M_2|^2 + 2m_W^2)^2 - 4|\mu|^2|M_2|^2 - 4m_W^4 \sin^2 2\beta + 8m_W^2 \sin 2\beta \operatorname{Re}(\mu M_2) \right]^{1/2} \right\}, \quad (2)$$

where the states are ordered such that $M_{\tilde{\chi}_1^+} \leq M_{\tilde{\chi}_2^+}$. If CP -violating effects are neglected (in which case, M_2 and μ are real parameters), then one can choose a convention where $\tan \beta$ and M_2 are positive. (Note that the relative sign of M_2 and μ is meaningful. The sign of μ is convention-dependent; the reader is warned that both sign conventions appear in the literature.) The sign convention for μ implicit in Eq. (2) is used by the LEP collaborations [13] in their plots of exclusion contours in the M_2 vs. μ plane derived from the non-observation of $e^+e^- \rightarrow \tilde{\chi}_1^+ \tilde{\chi}_1^-$.

The neutralino mass matrix depends on M_1 , M_2 , μ , $\tan \beta$, m_Z , and the weak mixing angle θ_W [34]. The corresponding neutralino eigenstates are usually denoted by $\tilde{\chi}_i^0$ ($i = 1, \dots, 4$), according to the convention that $M_{\tilde{\chi}_1^0} \leq M_{\tilde{\chi}_2^0} \leq M_{\tilde{\chi}_3^0} \leq M_{\tilde{\chi}_4^0}$. If a chargino or neutralino eigenstate approximates a particular gaugino or higgsino state, it is convenient to employ the corresponding nomenclature. Specifically, if M_1 and M_2 are small compared to m_Z and $|\mu|$, then the lightest neutralino $\tilde{\chi}_1^0$ would be nearly a pure *photino*, $\tilde{\gamma}$, the supersymmetric partner of the photon. If M_1 and m_Z are small compared to M_2 and $|\mu|$, then the lightest neutralino would be nearly a pure *bin*o, \tilde{B} , the supersymmetric partner of the weak hypercharge gauge boson. If M_2 and m_Z are small compared to M_1 and $|\mu|$, then the lightest chargino pair and neutralino would constitute a triplet of roughly mass-degenerate pure *winos*, \tilde{W}^\pm and \tilde{W}_3^0 , the supersymmetric partners of the weak $SU(2)$ gauge bosons. Finally, if $|\mu|$ and m_Z are small compared to M_1 and M_2 , then the lightest neutralino would be nearly a pure *higgsino*. Each of the above cases leads to a strikingly different phenomenology.

The supersymmetric partners of the quarks and leptons are spin-zero bosons: the *squarks*, charged *sleptons*, and *sneutrinos*. For simplicity, only the one-generation case is illustrated below (using first-generation notation). For a given fermion f , there are two supersymmetric partners \tilde{f}_L and \tilde{f}_R which are scalar partners of the corresponding left and right-handed fermion. (There is no $\tilde{\nu}_R$ in the MSSM.) However, in general, \tilde{f}_L and \tilde{f}_R are not mass-eigenstates since there is \tilde{f}_L - \tilde{f}_R mixing which is proportional in strength to the corresponding element of the scalar squared-mass matrix [35]

$$M_{LR}^2 = \begin{cases} m_d(A_d - \mu \tan \beta), & \text{for "down"-type } f \\ m_u(A_u - \mu \cot \beta), & \text{for "up"-type } f, \end{cases} \quad (3)$$

where m_d (m_u) is the mass of the appropriate "down" ("up") type quark or lepton. The signs of the A -parameters are also convention-dependent; see Ref. 31. Due to the appearance of the *fermion* mass in Eq. (3), one expects M_{LR} to be small compared to the diagonal squark and slepton masses, with the

possible exception of the top-squark, since m_t is large, and the bottom-squark and tau-slepton if $\tan \beta \gg 1$.

The (diagonal) L - and R -type squark and slepton squared-masses are given by

$$\begin{aligned} M_{fL}^2 &= M_F^2 + m_f^2 + (T_{3f} - e_f \sin^2 \theta_W) m_Z^2 \cos 2\beta, \\ M_{fR}^2 &= M_R^2 + m_f^2 + e_f \sin^2 \theta_W m_Z^2 \cos 2\beta, \end{aligned} \quad (4)$$

where $M_F^2 \equiv M_Q^2$ [M_L^2] for \tilde{u}_L and \tilde{d}_L [$\tilde{\nu}_L$ and \tilde{e}_L], and $M_R^2 \equiv M_U^2$, M_D^2 and M_E^2 for \tilde{u}_R , \tilde{d}_R , and \tilde{e}_R , respectively. In addition, $e_f = \frac{2}{3}, -\frac{1}{3}, 0, -1$ for $f = u, d, \nu$, and e , respectively, $T_{3f} = \frac{1}{2}$ [$-\frac{1}{2}$] for up-type [down-type] squarks and sleptons, and m_f is the corresponding quark or lepton mass. Squark and slepton mass eigenstates, generically called \tilde{f}_1 and \tilde{f}_2 (these are linear combinations of \tilde{f}_L and \tilde{f}_R), are obtained by diagonalizing the corresponding 2×2 squared-mass matrices.

In the case of three generations, the general analysis is more complicated. The scalar squared-masses [M_F^2 and M_R^2 in Eq. (4)], the fermion masses m_f and the A -parameters are now 3×3 matrices as noted in Section I.3. Thus, to obtain the squark and slepton mass eigenstates, one must diagonalize 6×6 mass matrices. As a result, intergenerational mixing is possible, although there are some constraints from the nonobservation of FCNC's [14,15]. In practice, because off-diagonal scalar mixing is appreciable only for the third generation, this additional complication can usually be neglected.

It should be noted that all mass formulae quoted in this section are tree-level results. One-loop corrections will modify all these results, and eventually must be included in any precision study of supersymmetric phenomenology [36].

I.5. The Higgs sector of the MSSM: Next, consider the Higgs sector of the MSSM [8,9,37]. Despite the large number of potential CP -violating phases among the MSSM-124 parameters, one can show that the tree-level MSSM Higgs sector is automatically CP -conserving. That is, unphysical phases can be absorbed into the definition of the Higgs fields such that $\tan \beta$ is a real parameter (conventionally chosen to be positive). Moreover, the physical neutral Higgs scalars are CP eigenstates. There are five physical Higgs particles in this model: a charged Higgs boson pair (H^\pm), two CP -even neutral Higgs bosons (denoted by H_1^0 and H_2^0 where $m_{H_1^0} \leq m_{H_2^0}$) and one CP -odd neutral Higgs boson (A^0).

The properties of the Higgs sector are determined by the Higgs potential, which is made up of quadratic terms [whose squared-mass coefficients were mentioned above Eq. (1)] and quartic interaction terms. The strengths of the interaction terms are directly related to the gauge couplings by supersymmetry (and are not affected at tree-level by supersymmetry breaking). As a result, $\tan \beta$ [defined in Eq. (1)] and one Higgs mass determine the tree-level Higgs-sector parameters. These include the Higgs masses, an angle α [which measures the component of the original $Y = \pm 1$ Higgs doublet states

in the physical CP -even neutral scalars], and the Higgs boson couplings.

When one-loop radiative corrections are incorporated, additional parameters of the supersymmetric model enter via virtual loops. The impact of these corrections can be significant [38]. For example, at tree-level, MSSM-124 predicts $m_{H^0} \leq m_Z |\cos 2\beta| \leq m_Z$ [8,9]. If this prediction were unmodified, it would imply that H_1^0 must be discovered at the LEP collider (running at its maximum energy and luminosity); otherwise MSSM-124 would be ruled out. However, when radiative corrections are included, the light Higgs-mass upper bound may be significantly increased. The qualitative behavior of the radiative corrections can be most easily seen in the large top-squark mass limit, where in addition, both the splitting of the two diagonal entries [Eq. (4)] and the two off-diagonal entries [Eq. (3)] of the top-squark squared-mass matrix are small in comparison to the average of the two top-squark squared-masses, $M_S^2 \equiv \frac{1}{2}(M_{t_1}^2 + M_{t_2}^2)$. In this case (assuming $m_{A^0} > m_Z$), the upper bound on the lightest CP -even Higgs mass at one-loop is approximately given by

$$m_{H_1^0}^2 \lesssim m_Z^2 + \frac{3g^2 m_t^4}{8\pi^2 m_W^2} \left\{ \ln(M_S^2/m_t^2) + \frac{X_t^2}{M_S^2} \left(1 - \frac{X_t^2}{12M_S^2} \right) \right\}, \quad (5)$$

where $X_t \equiv A_t - \mu \cot \beta$ is the top-squark mixing factor [see Eq. (3)]. A more complete treatment of the radiative corrections [39] shows that Eq. (5) somewhat overestimates the true upper bound of $m_{H_1^0}$. These more refined computations, which incorporate renormalization group improvement and the leading two-loop contributions, yield $m_{H_1^0} \lesssim 130$ GeV (with an accuracy of a few GeV) for $m_t = 175$ GeV and $M_S \lesssim 1$ TeV [39].

In addition, one-loop radiative corrections can also introduce CP -violating effects in the Higgs sector, which depend on some of the CP -violating phases among the MSSM-124 parameters [40]. Although these effects are more model-dependent, they can have a non-trivial impact on the Higgs searches at LEP and future colliders.

I.6. Reducing the MSSM parameter freedom: Even in the absence of a fundamental theory of supersymmetry breaking, one is hard-pressed to regard MSSM-124 as a fundamental theory. For example, no fundamental explanation is provided for the origin of electroweak symmetry breaking. Moreover, MSSM-124 is not a phenomenologically viable theory over most of its parameter space. Among the phenomenologically deficiencies are: (i) no conservation of the separate lepton numbers L_e , L_μ , and L_τ ; (ii) unsuppressed FCNC's; and (iii) new sources of CP -violation that are inconsistent with the experimental bounds. As a result, almost the entire MSSM-124 parameter space is ruled out! This theory is viable only at very special "exceptional" points of the full parameter space.

MSSM-124 is also theoretically deficient since it provides no explanation for the origin of the supersymmetry-breaking parameters (and in particular, why these parameters should conform to the exceptional points of the parameter space mentioned above). Moreover, the MSSM contains many new

sources of CP violation. For example, some combination of the complex phases of the gaugino-mass parameters, the A -parameters, and μ must be less than of order 10^{-2} – 10^{-3} (for a supersymmetry-breaking scale of 100 GeV) to avoid generating electric dipole moments for the neutron, electron, and atoms in conflict with observed data [41,42].

There are two general approaches for reducing the parameter freedom of MSSM-124. In the low-energy approach, an attempt is made to elucidate the nature of the exceptional points in the MSSM-124 parameter space that are phenomenologically viable. Consider the following two possible choices. First, one can assume that M_Q^2 , M_U^2 , M_D^2 , M_L^2 , M_E^2 and the matrix A -parameters are generation-independent (horizontal universality [5,32,43]). Alternatively, one can simply require that all the aforementioned matrices are flavor diagonal in a basis where the quark and lepton mass matrices are diagonal (flavor alignment [44]). In either case, L_e , L_μ , and L_τ are separately conserved, while tree-level FCNC's are automatically absent. In both cases, the number of free parameters characterizing the MSSM is substantially less than 124. Both scenarios are phenomenologically viable, although there is no strong theoretical basis for either scenario.

In the high-energy approach, one treats the parameters of the MSSM as running parameters and imposes a particular structure on the soft-supersymmetry-breaking terms at a common high-energy scale [such as the Planck scale (M_P)]. Using the renormalization group equations, one can then derive the low-energy MSSM parameters. The initial conditions (at the appropriate high-energy scale) for the renormalization group equations depend on the mechanism by which supersymmetry breaking is communicated to the effective low energy theory. Examples of this scenario are provided by models of gravity-mediated and gauge-mediated supersymmetry breaking (see Section I.2). One bonus of such an approach is that one of the diagonal Higgs squared-mass parameters is typically driven negative by renormalization group evolution. Thus, electroweak symmetry breaking is generated radiatively, and the resulting electroweak symmetry-breaking scale is intimately tied to the scale of low-energy supersymmetry breaking.

One prediction of the high-energy approach that arises in most grand unified supergravity models and gauge-mediated supersymmetry-breaking models is the unification of gaugino mass parameters at some high-energy scale M_X , *i.e.*,

$$M_1(M_X) = M_2(M_X) = M_3(M_X) = m_{1/2}. \quad (6)$$

Consequently, the effective low-energy gaugino mass parameters (at the electroweak scale) are related:

$$M_3 = (g_s^2/g^2)M_2, \quad M_1 = (5g'^2/3g^2)M_2 \simeq 0.5M_2. \quad (7)$$

In this case, the chargino and neutralino masses and mixing angles depend only on three unknown parameters: the gluino mass, μ , and $\tan \beta$. If in addition $|\mu| \gg M_1, m_Z$, then the

Searches Particle Listings

Supersymmetric Particle Searches

lightest neutralino is nearly a pure bino, an assumption often made in supersymmetric particle searches at colliders.

Recently, attention has been given to a class of supergravity models in which Eq. (7) does not hold. In models where no tree-level gaugino masses are generated, one finds a model-independent contribution to the gaugino mass whose origin can be traced to the super-conformal (super-Weyl) anomaly which is common to all supergravity models [45]. This approach has been called *anomaly-mediated* supersymmetry breaking. Eq. (7) is then replaced (in the one-loop approximation) by:

$$M_i \simeq \frac{b_i g_i^2}{16\pi^2} m_{3/2}, \quad (8)$$

where $m_{3/2}$ is the gravitino mass (assumed to be of order 1 TeV), and b_i are the coefficients of the MSSM gauge beta-functions corresponding to the corresponding U(1), SU(2) and SU(3) gauge groups: $(b_1, b_2, b_3) = (\frac{33}{5}, 1, -3)$. Eq. (8) yields $M_1 \simeq 2.8M_2$ and $M_3 \simeq -8.3M_2$, which implies that the lightest chargino pair and neutralino make up a nearly-mass degenerate triplet of winos. The corresponding supersymmetric phenomenology differs significantly from the standard phenomenology based on Eq. (7), and is explored in detail in Ref. [46]. Anomaly-mediated supersymmetry breaking also generates (approximate) flavor-diagonal squark and slepton mass matrices. However, in the MSSM this cannot be the sole source of supersymmetry-breaking in the slepton sector (which yields negative squared-mass contributions for the sleptons).

1.7. The constrained MSSMs: mSUGRA, GMSB, and SGUTs: One way to guarantee the absence of significant FCNC's mediated by virtual supersymmetric-particle exchange is to posit that the diagonal soft-supersymmetry-breaking scalar squared-masses are universal at some energy scale. In models of gauge-mediated supersymmetry breaking, scalar squared-masses are expected to be flavor independent since gauge forces are flavor-blind. In the *minimal* supergravity (mSUGRA) framework [1–3], the soft-supersymmetry-breaking parameters at the Planck scale take a particularly simple form in which the scalar squared-masses and the A -parameters are flavor diagonal and universal [26]:

$$\begin{aligned} M_Q^2(M_P) &= M_U^2(M_P) = M_D^2(M_P) = m_0^2 \mathbf{1}, \\ M_L^2(M_P) &= M_E^2(M_P) = m_0^2 \mathbf{1}, \\ m_{11}^2(M_P) &= m_2^2(M_P) = m_0^2, \\ A_U(M_P) &= A_D(M_P) = A_L(M_P) = A_0 \mathbf{1}, \end{aligned} \quad (9)$$

where $\mathbf{1}$ is a 3×3 identity matrix in generation space. Renormalization group evolution is then used to derive the values of the supersymmetric parameters at the low-energy (electroweak) scale. For example, to compute squark and slepton masses, one must use the *low-energy* values for M_F^2 and M_R^2 in Eq. (4). Through the renormalization group running with boundary conditions specified in Eq. (7) and Eq. (9), one can show that the

low-energy values of M_F^2 and M_R^2 depend primarily on m_0^2 and $m_{1/2}^2$. A number of useful approximate analytic expressions for superpartner masses in terms of the mSUGRA parameters can be found in Ref. 47.

Clearly, in the mSUGRA approach, the MSSM-124 parameter freedom has been sharply reduced. For example, typical mSUGRA models give low-energy values for the scalar mass parameters that satisfy $M_L^- \approx M_E^- < M_Q^- \approx M_U^- \approx M_D^-$ with the squark mass parameters somewhere between a factor of 1–3 larger than the slepton mass parameters (*e.g.*, see Ref. 47). More precisely, the low-energy values of the squark mass parameters of the first two generations are roughly degenerate, while $M_{Q_3}^-$ and $M_{U_3}^-$ are typically reduced by a factor of 1–3 from the values of the first and second generation squark mass parameters because of renormalization effects due to the heavy top quark mass.

As a result, one typically finds that four flavors of squarks (with two squark eigenstates per flavor) and \tilde{b}_R are nearly mass-degenerate. The \tilde{b}_L mass and the diagonal \tilde{t}_L and \tilde{t}_R masses are reduced compared to the common squark mass of the first two generations. (If $\tan\beta \gg 1$, then the pattern of third generation squark masses is somewhat altered; *e.g.*, see Ref. 48.) In addition, there are six flavors of nearly mass-degenerate sleptons (with two slepton eigenstates per flavor for the charged sleptons and one per flavor for the sneutrinos); the sleptons are expected to be somewhat lighter than the mass-degenerate squarks. Finally, third generation squark masses and tau-slepton masses are sensitive to the strength of the respective \tilde{f}_L - \tilde{f}_R mixing as discussed below Eq. (3).

Due to the implicit $m_{1/2}$ dependence in the low-energy values of M_Q^2 , M_U^2 and M_D^2 , there is a tendency for the gluino in mSUGRA models to be lighter than the first and second generation squarks. Moreover, the LSP is typically the lightest neutralino, $\tilde{\chi}_1^0$, which is dominated by its bino component. However, there are some regions of mSUGRA parameter space where the above conclusions do not hold. For example, one can reject those mSUGRA parameter regimes in which the LSP is a chargino.

One can count the number of independent parameters in the mSUGRA framework. In addition to 18 Standard Model parameters (excluding the Higgs mass), one must specify m_0 , $m_{1/2}$, A_0 , and Planck-scale values for μ and B -parameters (denoted by μ_0 and B_0). In principle, A_0 , B_0 and μ_0 can be complex, although in the mSUGRA approach, these parameters are taken (arbitrarily) to be real. As previously noted, renormalization group evolution is used to compute the low-energy values of the mSUGRA parameters, which then fixes all the parameters of the low-energy MSSM. In particular, the two Higgs vacuum expectation values (or equivalently, m_Z and $\tan\beta$) can be expressed as a function of the Planck-scale supergravity parameters. The simplest procedure is to remove μ_0 and B_0 in favor of m_Z and $\tan\beta$ (the sign of μ_0 is not fixed in this process). In this case, the MSSM spectrum and its interaction strengths are determined by five parameters: m_0 , A_0 , $m_{1/2}$, $\tan\beta$, and

the sign of μ_0 , in addition to the 18 parameters of the Standard Model. However, the mSUGRA approach is probably too simplistic. Theoretical considerations suggest that the universality of Planck-scale soft-supersymmetry-breaking parameters is not generic [49].

In the minimal gauge-mediated supersymmetry-breaking (GMSB) approach, there is one effective mass scale, A , that determines all low-energy scalar and gaugino mass parameters through loop-effects (while the resulting A -parameters are suppressed). In order that the resulting superpartner masses be of order 1 TeV or less, one must have $A \sim 100$ TeV. The origin of the μ and B -parameters is quite model dependent and lies somewhat outside the ansatz of gauge-mediated supersymmetry breaking. The simplest models of this type are even more restrictive than mSUGRA, with two fewer degrees of freedom. However, minimal GMSB is not a fully realized model. The sector of supersymmetry-breaking dynamics can be very complex, and no complete model of gauge-mediated supersymmetry yet exists that is both simple and compelling.

It was noted in Section I.2 that the gravitino is the LSP in GMSB models. Thus, in such models, the next-to-lightest supersymmetric particle (NLSP) plays a crucial role in the phenomenology of supersymmetric particle production and decay. Note that unlike the LSP, the NLSP can be charged. In GMSB models, the most likely candidates for the NLSP are $\tilde{\chi}_1^0$ and $\tilde{\tau}_R^\pm$. The NLSP will decay into its superpartner plus a gravitino (*e.g.*, $\tilde{\chi}_1^0 \rightarrow \gamma \tilde{g}_{3/2}$, $\tilde{\chi}_1^0 \rightarrow Z \tilde{g}_{3/2}$ or $\tilde{\tau}_R^\pm \rightarrow \tau^\pm \tilde{g}_{3/2}$), with lifetimes and branching ratios that depend on the model parameters.

Different choices for the identity of the NLSP and its decay rate lead to a variety of distinctive supersymmetric phenomenologies [30,50]. For example, a long-lived $\tilde{\chi}_1^0$ -NLSP that decays outside collider detectors leads to supersymmetric decay chains with missing energy in association with leptons and/or hadronic jets (this case is indistinguishable from the canonical phenomenology of the $\tilde{\chi}_1^0$ -LSP). On the other hand, if $\tilde{\chi}_1^0 \rightarrow \gamma \tilde{g}_{3/2}$ is the dominant decay mode, and the decay occurs inside the detector, then nearly *all* supersymmetric particle decay chains would contain a photon. In contrast, the case of a $\tilde{\tau}_R^\pm$ -NLSP would lead either to a new long-lived charged particle (*i.e.*, the $\tilde{\tau}_R^\pm$) or to supersymmetric particle decay chains with τ -leptons.

Finally, grand unification can impose additional constraints on the MSSM parameters. Perhaps one of the most compelling hints for low-energy supersymmetry is the unification of $SU(3) \times SU(2) \times U(1)$ gauge couplings predicted by models of supersymmetric grand unified theories (SGUTs) [5,51] (with the supersymmetry-breaking scale of order 1 TeV or below). Gauge coupling unification, which takes place at an energy scale of order 10^{16} GeV, is quite robust (*i.e.*, the unification depends weakly on the details of the theory at the unification scale). In particular, given the low-energy values of the electroweak couplings $g(m_Z)$ and $g'(m_Z)$, one can predict $\alpha_s(m_Z)$ by using the MSSM renormalization group equations to extrapolate to higher energies and imposing the unification condition on the

three gauge couplings at some high-energy scale, M_X . This procedure (which fixes M_X) can be successful (*i.e.*, three running couplings will meet at a single point) only for a unique value of $\alpha_s(m_Z)$. The extrapolation depends somewhat on the low-energy supersymmetric spectrum (so-called low-energy “threshold effects”) and on the SGUT spectrum (high-energy threshold effects), which can somewhat alter the evolution of couplings. Ref. [52] summarizes the comparison of present data with the expectations of SGUTs, and shows that the measured value of $\alpha_s(m_Z)$ is in good agreement with the predictions of supersymmetric grand unification for a reasonable choice of supersymmetric threshold corrections.

Additional SGUT predictions arise through the unification of the Higgs-fermion Yukawa couplings (λ_f). There is some evidence that $\lambda_b = \lambda_\tau$ leads to good low-energy phenomenology [53], and an intriguing possibility that $\lambda_b = \lambda_\tau = \lambda_t$ may be phenomenologically viable [54,48] in the parameter regime where $\tan \beta \simeq m_t/m_b$. Finally, grand unification imposes constraints on the soft-supersymmetry-breaking parameters. For example, gaugino-mass unification leads to the relations given in Eq. (7). Diagonal squark and slepton soft-supersymmetry-breaking scalar masses may also be unified, which is analogous to the unification of Higgs-fermion Yukawa couplings.

In the absence of a fundamental theory of supersymmetry breaking, further progress will require a detailed knowledge of the supersymmetric-particle spectrum in order to determine the nature of the high-energy parameters. Of course, any of the theoretical assumptions described in this section could be wrong and must eventually be tested experimentally.

I.8. Beyond the MSSM: Non-minimal models of low-energy supersymmetry can also be constructed. One approach is to add new structure beyond the Standard Model at the TeV scale or below. The supersymmetric extension of such a theory would be a non-minimal extension of the MSSM. Possible new structures include: (i) the supersymmetric generalization of the see-saw model of neutrino masses [55,56]; (ii) an enlarged electroweak gauge group beyond $SU(2) \times U(1)$ [57]; (iii) the addition of new, possibly exotic, matter multiplets [*e.g.*, a vector-like color triplet with electric charge $\frac{1}{3}e$; such states sometimes occur as low-energy remnants in E_6 grand unification models]; and/or (iv) the addition of low-energy $SU(3) \times SU(2) \times U(1)$ singlets [58]. A possible theoretical motivation for such new structure arises from the study of phenomenologically viable string theory ground states [59].

A second approach is to retain the minimal particle content of the MSSM but remove the assumption of R -parity invariance. The most general R -parity-violating (RPV) theory involving the MSSM spectrum introduces many new parameters to both the supersymmetry-conserving and the supersymmetry-breaking sectors. Each new interaction term violates either B or L conservation. For example, consider new scalar-fermion Yukawa couplings derived from the following interactions:

$$(\lambda_L)_{pmn} \hat{L}_p \hat{L}_m \hat{E}_n^c + (\lambda'_L)_{pmn} \hat{L}_p \hat{Q}_m \hat{D}_n^c + (\lambda_B)_{pmn} \hat{U}_p^c \hat{D}_m^c \hat{D}_n^c, \quad (10)$$

Searches Particle Listings

Supersymmetric Particle Searches

where p , m , and n are generation indices, and gauge group indices are suppressed. In the notation above, \hat{Q} , \hat{U}^c , \hat{D}^c , \hat{L} , and \hat{E}^c respectively represent $(u, d)_L$, u_L^c , d_L^c , $(\nu, e^-)_L$, and e_L^c and the corresponding superpartners. The Yukawa interactions are obtained from Eq. (10) by taking all possible combinations involving two fermions and one scalar superpartner. Note that the term in Eq. (10) proportional to λ_B violates B , while the other two terms violate L .

Phenomenological constraints on various low-energy B - and L -violating processes yield limits on each of the coefficients $(\lambda_L)_{pmn}$, $(\lambda'_L)_{pmn}$ and $(\lambda_B)_{pmn}$ taken one at a time [60]. If more than one coefficient is simultaneously non-zero, then the limits are in general more complicated. All possible RPV terms cannot be simultaneously present and unsuppressed; otherwise the proton decay rate would be many orders of magnitude larger than the present experimental bound. One way to avoid proton decay is to impose B - or L -invariance (either one alone would suffice). Otherwise, one must accept the requirement that certain RPV coefficients must be extremely suppressed.

If R -parity is not conserved, supersymmetric phenomenology exhibits features that are quite distinct from that of the MSSM. The LSP is no longer stable, which implies that not all supersymmetric decay chains must yield missing-energy events at colliders. Both $\Delta L=1$ and $\Delta L=2$ phenomena are allowed (if L is violated), leading to neutrino masses and mixing [61], neutrinoless double beta decay [62], sneutrino-antisneutrino mixing [56,63,64]; and s -channel resonant production of the sneutrino in e^+e^- collisions [65]. Since the distinction between the Higgs and matter multiplets is lost, R -parity violation permits the mixing of sleptons and Higgs bosons, the mixing of neutrinos and neutralinos, and the mixing of charged leptons and charginos, leading to more complicated mass matrices and mass eigenstates than in the MSSM. Note that if $\lambda'_L \neq 0$, then squarks can behave as leptoquarks since the following processes are allowed: $e^+\bar{u}_m \rightarrow \bar{d}_n \rightarrow e^+\bar{u}_m$, $\bar{\nu}\bar{d}_m$ and $e^+d_m \rightarrow \bar{u}_n \rightarrow e^+d_m$. (As above, m and n are generation labels, so that $d_2 = s$, $d_3 = b$, etc.)

The theory and phenomenology of alternative low-energy supersymmetric models and its consequences for collider physics have recently begun to attract significant attention. In particular, experimental and theoretical constraints place some non-trivial restrictions on R -parity-violating alternatives to the MSSM (see, e.g., Refs. [60,66] for further details).

References

1. H.P. Nilles, Phys. Reports **110**, 1 (1984).
2. S.P. Martin, in *Perspectives on Supersymmetry*, edited by G.L. Kane (World Scientific, Singapore, 1998) pp. 1–98.
3. R. Arnowitt and P. Nath, in *Perspectives on Supersymmetry*, edited by G.L. Kane (World Scientific, Singapore, 1998) pp. 442–461.
4. E. Witten, Nucl. Phys. **B188**, 513 (1981).
5. S. Dimopoulos and H. Georgi, Nucl. Phys. **B193**, 150 (1981).
6. L. Susskind, Phys. Reports **104**, 181 (1984); N. Sakai, Z. Phys. **C11**, 153 (1981); R.K. Kaul, Phys. Lett. **109B**, 19 (1982).
7. H.E. Haber and G.L. Kane, Phys. Reports **117**, 75 (1985).
8. K. Inoue, A. Kakuto, H. Komatsu, and S. Takeshita, Prog. Theor. Phys. **68**, 927 (1982) [E: **70**, 330 (1983)]; **71**, 413 (1984); R. Flores and M. Sher, Ann. Phys. (NY) **148**, 95 (1983).
9. J.F. Gunion and H.E. Haber, Nucl. Phys. **B272**, 1 (1986) [E: **B402**, 567 (1993)].
10. L. Girardello and M. Grisaru, Nucl. Phys. **B194**, 65 (1982).
11. See, e.g., R. Barbieri and G.F. Giudice, Nucl. Phys. **B305**, 63 (1988); G.W. Anderson and D.J. Castano, Phys. Lett. **B347**, 300 (1995); Phys. Rev. **D52**, 1693 (1995); Phys. Rev. **D53**, 2403 (1996); J.L. Feng, K.T. Matchev and T. Moroi, IASSNS-HEP-99-81 (1999) [hep-ph/9909334].
12. S. Dimopoulos and G.F. Giudice, Phys. Lett. **B357**, 573 (1995); A. Pomarol and D. Tommasini, Nucl. Phys. **B466**, 3 (1996); A.G. Cohen, D.B. Kaplan and A.E. Nelson, Phys. Lett. **B388**, 588 (1996); J.L. Feng, K.T. Matchev and T. Moroi, IASSNS-HEP-99-78 (1999) [hep-ph/9908309].
13. M. Schmitt, “Supersymmetry Part II (Experiment),” immediately following, in the printed version of the *Review of Particle Physics* (see also the Particle Listings immediately following).
14. See, e.g., F. Gabbiani, E. Gabrielli A. Masiero and L. Silvestrini, Nucl. Phys. **B477**, 321 (1996).
15. For a recent review and references to the original literature, see: A. Masiero and L. Silvestrini, hep-ph/9711401 (1997).
16. J. Erler and P. Langacker, “Electroweak Model and Constraints on New Physics,” in the section on Reviews, Tables, and Plots in this *Review*.
17. P.H. Chankowski and S. Pokorski, in *Perspectives on Supersymmetry*, edited by G.L. Kane (World Scientific, Singapore, 1998) pp. 402–422.
18. A. Dobado, M.J. Herrero and S. Penaranda, Eur. Phys. J. **C7**, 313 (1999); hep-ph/9903211 (Eur. Phys. J. C, in press).
19. J. Erler and D.M. Pierce, Nucl. Phys. **B526**, 53 (1998).
20. P. Fayet, Phys. Lett. **69B**, 489 (1977); G. Farrar and P. Fayet, Phys. Lett. **76B**, 575 (1978).
21. J. Ellis, J.S. Hagelin, D.V. Nanopoulos, K. Olive, and M. Srednicki, Nucl. Phys. **B238**, 453 (1984).
22. G. Jungman, M. Kamionkowski, and K. Griest, Phys. Reports **267**, 195 (1996).
23. M. Srednicki, in the section on “Dark Matter” in the full *Review of Particle Physics*.
24. P. Fayet, Phys. Lett. **84B**, 421 (1979); Phys. Lett. **86B**, 272 (1979).
25. S. Deser and B. Zumino, Phys. Rev. Lett. **38**, 1433 (1977).
26. L.J. Hall, J. Lykken, and S. Weinberg, Phys. Rev. **D27**, 2359 (1983).
27. S.K. Soni and H.A. Weldon Phys. Lett. **126B**, 215 (1983); Y. Kawamura, H. Murayama, and M. Yamaguchi, Phys. Rev. **D51**, 1337 (1995).

28. A.B. Lahanas and D.V. Nanopoulos, *Phys. Reports* **145**, 1 (1987).
29. M. Dine and A.E. Nelson, *Phys. Rev.* **D48**, 1277 (1993); M. Dine, A.E. Nelson, and Y. Shirman, *Phys. Rev.* **D51**, 1362 (1995); M. Dine, A.E. Nelson, Y. Nir, and Y. Shirman, *Phys. Rev.* **D53**, 2658 (1996).
30. G.F. Giudice, and R. Rattazzi, hep-ph/9801271 (to appear in *Phys. Reports*), and in *Perspectives on Supersymmetry*, edited by G.L. Kane (World Scientific, Singapore, 1998) pp. 355–377.
31. H.E. Haber, in *Recent Directions in Particle Theory*, Proceedings of the 1992 Theoretical Advanced Study Institute in Particle Physics, edited by J. Harvey and J. Polchinski (World Scientific, Singapore, 1993) pp. 589–686.
32. S. Dimopoulos and D. Sutter, *Nucl. Phys.* **B452**, 496 (1995); D.W. Sutter, Stanford Ph. D. thesis, hep-ph/9704390.
33. H.E. Haber, *Nucl. Phys. B (Proc. Suppl.)* **62A-C**, 469 (1998).
34. Explicit forms for the chargino and neutralino mass matrices can be found in Appendix A of Ref. 9; see also Ref. 31.
35. J. Ellis and S. Rudaz, *Phys. Lett.* **128B**, 248 (1983).
36. D.M. Pierce, J.A. Bagger, K. Matchev and R.J. Zhang, *Nucl. Phys.* **B491**, 3 (1997).
37. J.F. Gunion, H.E. Haber, G. Kane, and S. Dawson, *The Higgs Hunter's Guide* (Addison-Wesley Publishing Company, Redwood City, CA, 1990).
38. H.E. Haber and R. Hempfling, *Phys. Rev. Lett.* **66**, 1815 (1991); Y. Okada, M. Yamaguchi, and T. Yanagida, *Prog. Theor. Phys.* **85**, 1 (1991); J. Ellis, G. Ridolfi, and F. Zwirner, *Phys. Lett.* **B257**, 83 (1991).
39. M. Carena, J.R. Espinosa, M. Quiros, and C.E.M. Wagner, *Phys. Lett.* **B335**, 209 (1995); M. Carena, M. Quiros, and C.E.M. Wagner, *Nucl. Phys.* **B461**, 407 (1996); H.E. Haber, R. Hempfling, and A.H. Hoang, *Z. Phys.* **C75**, 539 (1997); S. Heinemeyer, W. Hollik and G. Weiglein, *Phys. Lett.* **B440**, 296 (1998); **B455**, 179 (1999); *Eur. Phys. J* **C9**, 343 (1999); R.-J. Zhang, *Phys. Lett.* **B447**, 89 (1999).
40. A. Pilaftsis and C.E.M. Wagner, *Nucl. Phys.* **B553**, 3 (1999).
41. W. Fischler, S. Paban, and S. Thomas, *Phys. Lett.* **B289**, 373 (1992); S.M. Barr, *Int. J. Mod. Phys.* **A8**, 209 (1993); T. Ibrahim and P. Nath, *Phys. Rev.* **D58**, 111301 (1998) [E: **D60**, 099902 (1999)]; M. Brhlik, G.J. Good and G.L. Kane, *Phys. Rev.* **D59**, 115004 (1999).
42. A. Masiero and L. Silvestrini, in *Perspectives on Supersymmetry*, edited by G.L. Kane (World Scientific, Singapore, 1998) pp. 423–441.
43. H. Georgi, *Phys. Lett.* **B169B**, 231 (1986); L.J. Hall, V.A. Kostelecky, and S. Raby *Nucl. Phys.* **B267**, 415 (1986).
44. Y. Nir and N. Seiberg, *Phys. Lett.* **B309**, 337 (1993); S. Dimopoulos, G.F. Giudice, and N. Tetradis, *Nucl. Phys.* **B454**, 59 (1995).
45. L. Randall and R. Sundrum, *Nucl. Phys.* **B557**, 79 (1999); G.F. Giudice, R. Rattazzi, M.A. Luty and H. Murayama, *JHEP* **12**, 027 (1998); J.L. Feng and T. Moroi, IASSNS-HEP-99-65 [hep-ph/9907319].
46. J.L. Feng, T. Moroi, L. Randall, M. Strassler and S.-F. Su, *Phys. Rev. Lett.* **83**, 1731 (1999); T. Gherghetta, G.F. Giudice and J.D. Wells, CERN-TH-99-104 [hep-ph/9904378]; J.F. Gunion and S. Mrenna, UCD-99-11 [hep-ph/9906270].
47. M. Drees and S.P. Martin, in *Electroweak Symmetry Breaking and New Physics at the TeV Scale*, edited by T. Barklow, S. Dawson, H.E. Haber, and J. Siegrist (World Scientific, Singapore, 1996) pp. 146–215.
48. M. Carena, M. Olechowski, S. Pokorski, and C.E.M. Wagner, *Nucl. Phys.* **B426**, 269 (1994).
49. L.E. Ibáñez and D. Lüst, *Nucl. Phys.* **B382**, 305 (1992); B. de Carlos, J.A. Casas and C. Muñoz, *Phys. Lett.* **B299**, 234 (1993); V. Kaplunovsky and J. Louis, *Phys. Lett.* **B306**, 269 (1993); A. Brignole, L.E. Ibáñez, and C. Muñoz, *Nucl. Phys.* **B422**, 125 (1994) [E: **B436**, 747 (1995)].
50. For a brief review and guide to the original literature, see J.F. Gunion and H.E. Haber, in *Perspectives on Supersymmetry*, edited by G.L. Kane (World Scientific, Singapore, 1998) pp. 235–255.
51. M.B. Einhorn and D.R.T. Jones, *Nucl. Phys.* **B196**, 475 (1982); W.J. Marciano and G. Senjanovic, *Phys. Rev.* **D25**, 3092 (1982).
52. S. Pokorski, *Acta Phys. Polon.* **B30**, 1759 (1999).
53. H. Arason *et al.*, *Phys. Rev. Lett.* **67**, 2933 (1991); *Phys. Rev.* **D46**, 3945 (1992); V. Barger, M.S. Berger, and P. Ohmann, *Phys. Rev.* **D47**, 1093 (1993); M. Carena, S. Pokorski, and C.E.M. Wagner, *Nucl. Phys.* **B406**, 59 (1993); P. Langacker and N. Polonsky, *Phys. Rev.* **D49**, 1454 (1994).
54. M. Olechowski and S. Pokorski, *Phys. Lett.* **B214**, 393 (1988); B. Ananthanarayan, G. Lazarides, and Q. Shafi, *Phys. Rev.* **D44**, 1613 (1991); S. Dimopoulos, L.J. Hall, and S. Raby, *Phys. Rev. Lett.* **68**, 1984 (1992); L.J. Hall, R. Rattazzi, and U. Sarid, *Phys. Rev.* **D50**, 7048 (1994); R. Rattazzi and U. Sarid, *Phys. Rev.* **D53**, 1553 (1996).
55. J. Hisano, T. Moroi, K. Tobe, M. Yamaguchi, and T. Yanagida, *Phys. Lett.* **B357**, 579 (1995); J. Hisano, T. Moroi, K. Tobe, and M. Yamaguchi, *Phys. Rev.* **D53**, 2442 (1996).
56. Y. Grossman and H.E. Haber, *Phys. Rev. Lett.* **78**, 3438 (1997).
57. J.L. Hewett and T.G. Rizzo, *Phys. Reports* **183**, 193 (1989).
58. See, *e.g.*, U. Ellwanger, M. Rausch de Traubenberg, and C.A. Savoy, *Nucl. Phys.* **B492**, 21 (1997), and references therein.
59. K.R. Dienes, *Phys. Reports* **287**, 447 (1997).

Searches Particle Listings

Supersymmetric Particle Searches

60. H. Dreiner, in *Perspectives on Supersymmetry*, edited by G.L. Kane (World Scientific, Singapore, 1998) pp. 462–479.
61. F.M. Borzumati, Y. Grossman, E. Nardi, and Y. Nir, *Phys. Lett.* **B384**, 123 (1996).
62. R.N. Mohapatra, *Phys. Rev.* **D34**, 3457 (1986); K.S. Babu and R.N. Mohapatra, *Phys. Rev. Lett.* **75**, 2276 (1995); M. Hirsch, H.V. Klapdor-Kleingrothaus, and S.G. Kovalenko, *Phys. Rev. Lett.* **75**, 17 (1995); *Phys. Rev.* **D53**, 1329 (1996).
63. M. Hirsch, H.V. Klapdor-Kleingrothaus, and S.G. Kovalenko, *Phys. Lett.* **B398**, 311 (1997).
64. Y. Grossman and H.E. Haber, *Phys. Rev.* **D59**, 093008 (1999).
65. S. Dimopoulos and L.J. Hall, *Phys. Lett.* **B207**, 210 (1988); J. Kalinowski, R. Ruckl, H. Spiesberger, and P.M. Zerwas, *Phys. Lett.* **B406**, 314 (1997); J. Erler, J.L. Feng, and N. Polonsky, *Phys. Rev. Lett.* **78**, 3063 (1997).
66. M. Bisset, O.C.W. Kong, C. Macesanu and L.H. Orr, UR-1524 (1998) [hep-ph/9811498]; R. Barbier *et al.*, Report of the group on the R parity violation, hep-ph/9810232 (1998).

SUPERSYMMETRY, PART II (EXPERIMENT)

Revised October 1999 by M. Schmitt (Harvard University)

II.1. Introduction: The theoretical strong points of supersymmetry (SUSY) have motivated many searches for supersymmetric particles. Most of these have been guided by the MSSM and are based on the canonical missing-energy signature caused by the escape of the LSP's ('lightest supersymmetric particles'). More recently, other scenarios have received considerable attention from experimenters, widening the range of topologies in which new physics might be found.

Unfortunately, no convincing evidence for the production of supersymmetric particles has been found. The most far reaching laboratory searches have been performed at the Tevatron and at LEP, and these are the main topic of this review. In addition, there are a few special opportunities exploited by HERA and certain fixed-target experiments.

Theoretical aspects of supersymmetry have been covered in Part I of this review by H.E. Haber (see also Ref. 1, 2); we use his notations and terminology.

II.2. Common supersymmetry scenarios: In the 'canonical' scenario [1], supersymmetric particles are pair-produced and decay directly or via cascades to the LSP. For most typical choices of model parameters, the lightest neutralino is the LSP. If R -parity is conserved, the LSP is stable. Since the neutralino is neutral and colorless, interacting only weakly with matter, it can be a candidate for cold dark matter, and in fact for a wide range of theoretical parameters, an appropriate density of relic neutralinos is expected. (See the Listings for current limits and constraints.) Assuming the conservation of R -parity, the LSP's will escape detection, giving signal events the appearance of "missing energy." In proton colliders, the

momentum component along the beam direction is not useful, so one works with the so-called "missing transverse energy" (\cancel{E}_T), which is the vector sum of the transverse components of all visible momenta. In e^+e^- machines, both the missing transverse momentum, p_T^{miss} (essentially the same quantity as \cancel{E}_T), and the missing energy, E^{miss} , which is the difference between twice the beam energy and the total visible energy, are utilized. There are always at least two LSP's per event. Collimated jets, isolated leptons or photons, and appropriate kinematic cuts provide additional handles to reduce backgrounds.

The conservation of R -parity is not required in supersymmetry, however, and in some searches it is assumed that supersymmetric particles decay via interactions which violate R -parity (RPV), and hence, lepton and/or baryon number. For the most part the production of superpartners is unchanged, but in general the missing-energy signature is lost. Depending on the choice of the R -parity-breaking interaction, SUSY events are characterized by an excess of leptons or hadronic jets, and in many cases it is relatively easy to suppress SM backgrounds [3]. A distinction is made between "indirect" RPV, in which the LSP decays close to the interaction point but no other decays are modified, and "direct" RPV, in which the supersymmetric particles decay to SM particles, producing no LSP's. In either case the pair-production of LSP's, which need not be $\tilde{\chi}_1^0$'s or $\tilde{\nu}$'s, is a significant SUSY signal.

In models assuming gauge-mediated supersymmetry breaking (GMSB) [4], the gravitino $\tilde{g}_{3/2}$ is a weakly-interacting fermion with a mass so small that it can be neglected when considering the event kinematics. It is the LSP, and the lightest neutralino decays to it radiatively, possibly with a very long lifetime. With few exceptions the decays and production of other superpartners are the same as in the canonical scenario, so when the $\tilde{\chi}_1^0$ lifetime is not too long, the event topologies are augmented by the presence of photons which can be energetic and isolated. If the $\tilde{\chi}_1^0$ lifetime is so long that it decays outside of the detector, the event topologies are the same as in the canonical scenario. In some variants of this theory the right-sleptons are lighter than the lightest neutralino, and they decay to a lepton and a gravitino. This decay might occur after the slepton exits the apparatus, depending on model parameters.

Finally, in another scenario the gluino \tilde{g} is assumed to be light ($M_{\tilde{g}} < 5 \text{ GeV}/c^2$) [5]. Its decay to the lightest neutralino is kinematically suppressed, so long-lived supersymmetric hadrons ($\tilde{g} + g$ bound states called R^0 's) are formed [6]. While the sensitivity of most searches at LEP and the Tevatron would be lost, specific searches at fixed target experiments seem to have closed this gap definitively. (See the review article by H. Murayama.)

II.3. Experimental issues: Before describing the results of the searches, a few words about experimental issues are in order.

Given no signal for supersymmetric particles, experimenters are forced to derive limits on their production. The most general formulation of supersymmetry is so flexible that few universal bounds can be obtained. Often more restricted forms of the

theory are evoked for which predictions are more definite—and exclusions more constraining. The most popular of these is minimal supergravity ('mSUGRA'). As explained in the Part I of this review, parameter freedom is drastically reduced by requiring related parameters to be equal at the unification scale. Thus, the gaugino masses are equal with value $m_{1/2}$, and the slepton, squark, and Higgs masses depend on a *common* scalar mass parameter, m_0 . In the individual experimental analyses, only some of these assumptions are necessary. For example, the gluon and squark searches at proton machines constrain mainly M_3 and a scalar mass parameter m_0 for the squark masses, while the chargino, neutralino, and slepton searches at e^+e^- colliders constrain M_2 and a scalar mass parameter m_0 for the slepton masses. In addition, results from the Higgs searches can be used to constrain $m_{1/2}$ and m_0 as a function of $\tan\beta$. (The full analysis involves large radiative corrections coming from squark mixing, which is where the dependence on $m_{1/2}$ and m_0 enter.) In the mSUGRA framework, all the scalar mass parameters m_0 are the same and the three gaugino mass parameters are proportional to $m_{1/2}$, so limits from squarks, sleptons, charginos, gluinos, and Higgs all can be used to constrain the parameter space.

While the mSUGRA framework is convenient, it is based on several highly specific theoretical assumptions, so limits presented in this framework cannot easily be applied to other supersymmetric models. Serious attempts to reduce the model dependence of experimental exclusions have been made. When model-independent results are impossible, the underlying assumptions and their consequences are carefully delineated. This is easier to achieve at e^+e^- colliders than at proton machines.

The least model-dependent result from any experiment is the upper limit on the cross section. It requires only the number N of candidate events, the integrated luminosity \mathcal{L} , the total expected background b , and the acceptance ϵ for a given signal. The upper limit on the number of signal events for a given confidence level N^{upper} is computed from N and b (see review of Statistics). The experimental bound is simply

$$\epsilon \cdot \sigma < N^{\text{upper}}/\mathcal{L}. \quad (1)$$

This information is nearly always reported, but some care is needed to understand how the acceptance was estimated, since it can be quite sensitive to assumptions about masses and branching ratios. Also, in the more complicated analyses, N^{upper} also changes as a result of the optimization for a variety of possible signals.

The theoretical parameter space is constrained by computing $\epsilon \cdot \sigma$ of Eq. (1) in terms of the relevant parameters while $N^{\text{upper}}/\mathcal{L}$ is fixed by experiment. Even after the theoretical scenario and assumptions have been specified, some choice remains about how to present the constraints. The quantity $\epsilon \cdot \sigma$ may depend on three or more parameters, yet in a printed page one usually can display limits only in a two-dimensional space. Three rather different tactics are employed by experimenters:

- Select "typical" values for the parameters not shown. These may be suggested by theory, or values giving more conservative—or more powerful—results may be selected. Although the values are usually specified, one sometimes has to work to understand the possible 'loopholes.'
- Scan the parameters not shown. The lowest value for $\epsilon \cdot \sigma$ is used in Eq. (1), thereby giving the weakest limit for the parameters shown. As a consequence, the limit applies for all values of the parameters *not* shown.
- Scan parameters to find the lowest acceptance ϵ and use it as a constant in Eq. (1). The limits are then safe from theoretical uncertainties but may be over-conservative, hiding powerful constraints existing in more typical cases.

Judgment is exercised: the second option is the most correct but may be impractical or uninteresting; most often representative cases are presented. These latter become standard, allowing a direct comparison of experiments, and also the opportunity to combine results.

Limits reported here are derived for 95% C.L. unless noted otherwise.

II.4. Supersymmetry searches in e^+e^- colliders: The large electron-positron collider (LEP) at CERN has been running at center-of-mass energies more than twice the mass of the Z boson. After collecting approximately 150 pb^{-1} at LEP 1 (collider energy at the Z peak), each experiment (ALEPH, DELPHI, L3, OPAL) has accumulated large data sets at LEP 2: about 5.7 pb^{-1} at $\sqrt{s} \sim 133 \text{ GeV}$ (1995), 10 pb^{-1} at 161 GeV and 11 pb^{-1} at 172 GeV (1996), 57 pb^{-1} near 183 GeV (1997), and most recently, 180 pb^{-1} at 189 GeV (1998). This review emphasizes the most recent LEP 2 results.

The LEP experiments and SLD at SLAC excluded essentially all visible supersymmetric particles up to about half the Z mass (see the Listings for details). These limits come mainly from the comparison of the measured Z widths to SM expectations, and are relatively insensitive to the details of SUSY particle decays [7]. The data taken at higher energies allow much stronger limits to be set, although the complex interplay of masses, cross sections, and branching ratios makes simple general limits impossible to specify.

The main signals come from SUSY particles with charge, weak isospin, or large Yukawa couplings. The gauge fermions (charginos and neutralinos) generally are produced with large cross sections, while the scalar particles (sleptons and squarks) are suppressed near threshold by kinematic factors.

Charginos are produced via γ^* , Z^* , and $\tilde{\nu}_e$ exchange. Cross sections are in the 1–10 pb range, but can be an order of magnitude smaller when $M_{\tilde{\nu}_e}$ is less than $100 \text{ GeV}/c^2$ due to the destructive interference between s - and t -channel amplitudes. Under the same circumstances, neutralino production is enhanced, as the t -channel \tilde{e} exchange completely dominates the

Searches Particle Listings

Supersymmetric Particle Searches

s -channel Z^* exchange. When Higgsino components dominate the field content of charginos and neutralinos, cross sections are large and insensitive to slepton masses.

Sleptons and squarks are produced via γ^* and Z^* exchange; for selectrons there is an important additional contribution from t -channel neutralino exchange which generally increases the cross section substantially. Although the Tevatron experiments have placed general limits on squark masses far beyond the reach of LEP, a light top squark (stop) could still be found since the flavor eigenstates can mix to give a large splitting between the mass eigenstates. The coupling of the lightest stop to the Z^* will vary with the mixing angle, however, and for certain values, even vanish, so the limits on squarks from LEP depend on the mixing angle assumed.

The various SUSY particles considered at LEP typically would decay directly to SM particles and LSP's, so signatures consist of some combination of jets, leptons, possibly photons, and missing energy. Consequently the search criteria are geared toward a few distinct topologies. Although they may be optimized for one specific signal, they are often efficient for others. For example, acoplanar jets are expected in both $\tilde{l}_1\tilde{l}_1$ and $\tilde{\chi}_1^0\tilde{\chi}_2^0$ production, and acoplanar leptons for both $\tilde{\ell}^+\tilde{\ell}^-$ and $\tilde{\chi}^+\tilde{\chi}^-$.

The major backgrounds come from three sources. First, there are the so-called 'two-photon interactions,' in which the beam electrons emit photons which combine to produce a low mass hadronic or leptonic system leaving little visible energy in the detector. Since the electrons are seldom deflected through large angles, p_T^{miss} is low. Second, there is difermion production, usually accompanied by large initial-state radiation induced by the Z pole, which gives events that are well balanced with respect to the beam direction. Finally, there is four-fermion production through states with one or two resonating bosons (W^+W^- , ZZ , $W\nu\nu$, Ze^+e^- , etc.) which can give events with large E^{miss} and p_T^{miss} due to neutrinos and electrons lost down the beam pipe.

In the canonical case, E^{miss} and p_T^{miss} are large enough to eliminate most of these backgrounds. The e^+e^- initial state is well defined so searches utilize both transverse and longitudinal momentum components. It is possible to measure the missing mass ($M_{\text{miss}} = \{(\sqrt{s} - E_{\text{vis}})^2 - \vec{p}_{\text{vis}}^2\}^{1/2}$) which is small if p_T^{miss} is caused by a single neutrino or undetected electron or photon, and can be large when there are two massive LSP's. The four-fermion processes cannot be entirely eliminated, however, and a non-negligible irreducible background is expected. Fortunately, the uncertainties for these backgrounds are not large.

High efficiencies are easily achieved when the mass of the LSP is lighter than the parent particle by at least 10 GeV/ c^2 and greater than about 10 GeV/ c^2 . Difficulties arise when the mass difference ΔM between the produced particle and the LSP is smaller than 10 GeV/ c^2 as the signal resembles background from two-photon interactions. A very light LSP is challenging also since, kinematically speaking, it plays a role similar to a neutrino, so that, for example, a signal for charginos of mass 85 GeV/ c^2 is difficult to distinguish from the production of

W^+W^- pairs. The lower signal efficiency obtained in these two extreme cases has been offset by the large integrated luminosities delivered over the last two years, so mass limits are not degraded very much.

Since the start of LEP 2, experimenters have made special efforts to cover a wide range of mass differences. Also, since virtual superpartners exchanged in decays can heavily influence branching ratios to SM particles, care has been taken to ensure that the search efficiencies are not strongly dependent on the final state. This ability to cover a wide range of topologies has driven the push for bounds with a minimum of model dependence.

Charginos have been excluded up to 94 GeV/ c^2 [8,9] except in cases of very low acceptance ($\Delta M = M_{\tilde{\chi}^\pm} - M_{\tilde{\chi}_1^0} \lesssim 3$ GeV/ c^2) or low cross section ($M_{\tilde{\nu}_e} \lesssim 120$ GeV/ c^2). When $|\mu| \ll M_2$, the Higgsino components are large for charginos and neutralinos. In this case the associated production of neutralino pairs $\tilde{\chi}_1^0\tilde{\chi}_2^0$ is large and the problem of small mass differences ($M_{\tilde{\chi}_2^0} - M_{\tilde{\chi}_1^0}$) less severe. Experimental sensitivity now extends down to mass differences of 3 GeV/ c^2 , corresponding to M_2 above 2 TeV/ c^2 .

The possibility of extremely small mass differences has been raised in several theoretical papers, and the DELPHI Collaboration has engineered several searches to cover this scenario [10]. For $\Delta M \sim 1$ GeV/ c^2 , they distinguish signal from two-photon background on the basis of photons radiated in the initial state, which have different kinematic characteristics. For $\Delta M \sim 0.4$ GeV/ c^2 , the chargino acquires a non-negligible lifetime, so they look for displaced vertices and tracks which do not originate from the interaction point. The modeling of lifetime and chargino decays required special care. When $\Delta M < m_\pi$, the lifetime is so long that the chargino appears as a heavily ionizing particle which exits the apparatus before decaying. The bounds on the chargino mass are weaker than in the canonical case with larger ΔM , but still are well above the bounds from LEP 1 (Fig. 1).

The limits from chargino and neutralino production are most often used to constrain M_2 and μ for fixed $\tan\beta$. For large $|\mu|$ (the gaugino case), chargino bounds limit M_2 , and vice versa (the Higgsino case). When $\tan\beta$ is not large, the region of parameter space with $\mu < 0$ and $|\mu| \sim M_2$ corresponds to 'mixed' field content, and the limits on M_2 and $|\mu|$ are relatively modest, numerically. This is especially true when electron sneutrinos are light, leading to a degradation of the indirect limits on the LSP mass, as discussed below.

When the sleptons are light, two important effects must be considered for charginos: the cross section is significantly reduced and the branching ratio to leptons is enhanced, especially to τ 's via $\tilde{\tau}$'s which can have non-negligible mixing. These effects are greatest when the chargino has a large gaugino component. The weakest bounds are found for small negative μ and small $\tan\beta$, as the cross section is reduced with respect to larger $|\mu|$, the impact of $\tilde{\tau}$ mixing can be large, and the efficiency is not optimal because ΔM is large.

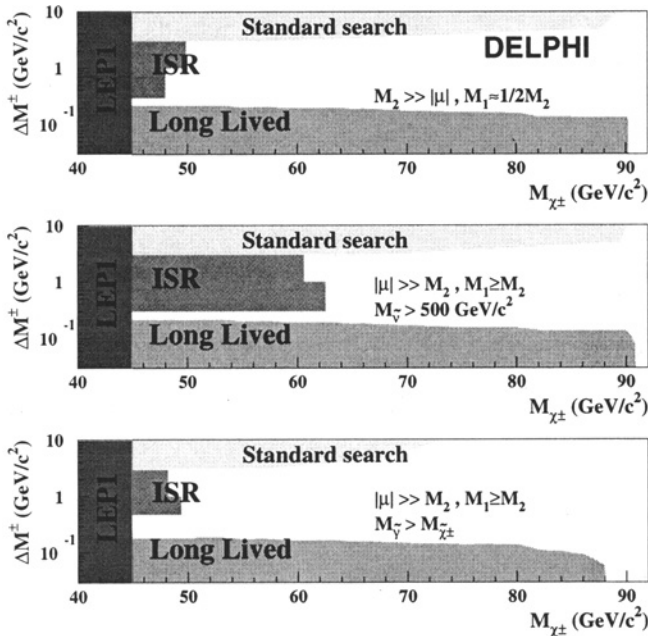


Figure 1: Ranges of excluded chargino and neutralino masses, for very small ΔM , from DELPHI [10].

If the sneutrino is lighter than the chargino, then two-body decays $\tilde{\chi}^+ \rightarrow \ell^+ \tilde{\nu}$ dominate, and in the ‘corridor’ $0 < M_{\tilde{\chi}^\pm} - M_{\tilde{\nu}} \lesssim 3 \text{ GeV}/c^2$ the acceptance is so low that no exclusion is possible [11,9].

The limits on slepton masses [12] fall a bit below the kinematic limit due to a phase space suppression near threshold. The simplest topology results from $\tilde{\ell} \rightarrow \ell \tilde{\chi}_1^0$. Considering the production of $\tilde{\ell}_R$ only, the 189 GeV data from OPAL gives $89 \text{ GeV}/c^2$ for \tilde{e}_R , $82 \text{ GeV}/c^2$ for $\tilde{\mu}_R$, and $81 \text{ GeV}/c^2$ for $\tilde{\tau}_1$. For selectrons and smuons there is a small improvement from the preliminary combination of the four LEP experiments [13], and one sees that the dependence on $\Delta M = M_{\tilde{\ell}} - M_{\tilde{\chi}_1^0}$ is weak for $\Delta M \gtrsim 5 \text{ GeV}/c^2$. Assuming a common scalar mass term m_0 , the masses of the left- and right-sleptons can be related as a function of $\tan\beta$, and one finds $m_{\tilde{\ell}_L} > m_{\tilde{\ell}_R}$ by a few GeV/c^2 . Consequently, in associated $\tilde{e}_L \tilde{e}_R$ production, the special case $M_{\tilde{\chi}} \lesssim M_{\tilde{e}_R}$ still results in a viable signature: a single energetic electron. ALEPH have used this to close the gap $M_{\tilde{e}_R} - M_{\tilde{\chi}} \rightarrow 0$. In this same framework, bounds on the parameters $m_{1/2}$ and m_0 have been derived.

In some GMSB models, photons from the decay $\tilde{\chi}_1^0 \rightarrow \gamma \tilde{g}_{3/2}$ accompany the leptons. The resulting limits are similar to the canonical case. In other GMSB models, sleptons may decay to $\ell^\pm \tilde{g}_{3/2}$ outside the detector, so the experimental signature is a pair of collinear, heavily ionizing tracks [14]. Combined search limits are $86 \text{ GeV}/c^2$ for $\tilde{\mu}_R$ and $\tilde{\tau}_R$ [15]. Shorter lifetimes are possible, however, so searches have been performed for displaced vertices, tracks with kinks, and tracks with large impact parameters. Combining these together, slepton mass

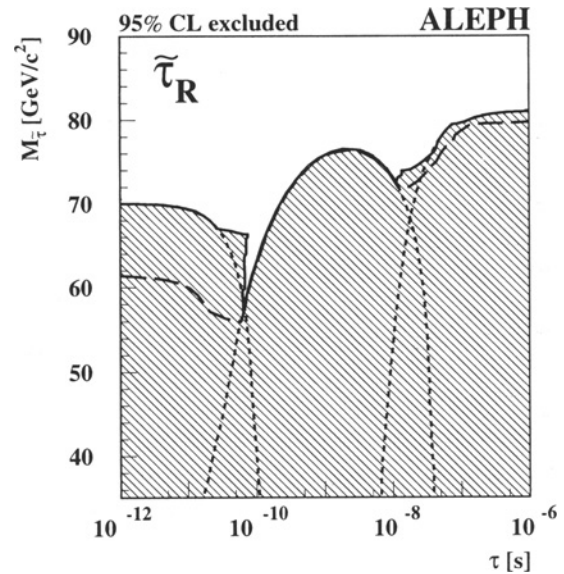


Figure 2: Lower limit on the mass of $\tilde{\tau}_R$ as a function of its lifetime, from the ALEPH 183 GeV data [12]. The full line shows the actual mass limit obtained, while the long dashed line shows the limit expected from Monte Carlo studies. The short dashed lines indicate the limits from the three types of searches: acoplanar leptons ($\tau < 10^{-9} \text{ s}$), tracks with large impact parameters and kinks ($10^{-11} \text{ s} < \tau < 10^{-7} \text{ s}$); and, heavily ionizing tracks ($\tau > 10^{-8} \text{ s}$).

limits independent of lifetime have been derived. The result from ALEPH for $\tilde{\tau}_R$ is shown in Fig. 2 [12].

For these same GMSB models, it is possible that the lightest stau is significantly lighter than the other sleptons. If so, then special topologies may result, such as 4τ final states from neutralino pair production. DELPHI has searched in this and related channels, finding no evidence for a signal [16].

Limits on stop and sbottom masses [17,18], vary with the mixing angle because the cross section does: for $\theta_{\tilde{t}} = 56^\circ$ and $\theta_{\tilde{b}} = 67^\circ$ the contribution from Z exchange is ‘‘turned off.’’ The stop decay $\tilde{t}_1 \rightarrow c \tilde{\chi}_1^0$ proceeds through loops, giving a lifetime long enough to allow the top squark to form supersymmetric hadrons which provide a pair of jets and missing energy. If sneutrinos are light, the decay $\tilde{t}_1 \rightarrow b \tilde{\nu}$ dominates, giving two leptons in addition to the jets. Access to small ΔM is possible due to the visibility of the decay products of the c and b quarks. Limits vary from $91 \text{ GeV}/c^2$ for an unrealistic pure \tilde{t}_L state to $89 \text{ GeV}/c^2$ if the coupling of \tilde{t}_1 to the Z vanishes. The electric charge of the sbottoms is smaller than that of stops, leading to weaker limits, but the use of b -jet tagging helps retain sensitivity: the bounds range between 75 and $90 \text{ GeV}/c^2$ depending on $\theta_{\tilde{b}}$. Limits from the Tevatron reach much higher masses, but only when the neutralino is much lighter than the stop or sbottom. ALEPH has interpreted the

Searches Particle Listings

Supersymmetric Particle Searches

results of their search in terms of generic squarks, excluding a rather small region not covered at the Tevatron [17].

In canonical SUSY scenarios the lightest neutralino leaves no signal in the detector. Nonetheless, the tight correspondences among the neutralino and chargino masses allow an indirect limit on $M_{\tilde{\chi}_1^0}$ to be derived [9,11]. The key assumption is that the gaugino mass parameters M_1 and M_2 unify at the GUT scale, which leads to a definite relation between them at the electroweak scale: $M_1 = \frac{5}{3} \tan^2 \theta_W M_2$. Assuming slepton masses to be at least $200 \text{ GeV}/c^2$, the bound on $M_{\tilde{\chi}_1^0}$ is derived from the results of chargino and neutralino searches and certain bounds from LEP 1.

When sleptons are lighter than $120 \text{ GeV}/c^2$, all the effects of light sneutrinos on both the production and decay of charginos and heavier neutralinos must be taken into account. Although the bounds from charginos are weakened, useful additional constraints from slepton and higher-mass neutralino searches rule out the possibility of a massless neutralino. The current OPAL limit [8], shown in Fig. 3, is $M_{\tilde{\chi}_1^0} > 32.8 \text{ GeV}/c^2$ for $\tan \beta > 1$ and $m_0 \gtrsim 500 \text{ GeV}/c^2$ (effectively, $M_{\tilde{\nu}} > 500 \text{ GeV}/c^2$). Allowing the universal scalar mass parameter m_0 to have any value, the limit is $M_{\tilde{\chi}_1^0} > 31.6 \text{ GeV}/c^2$.

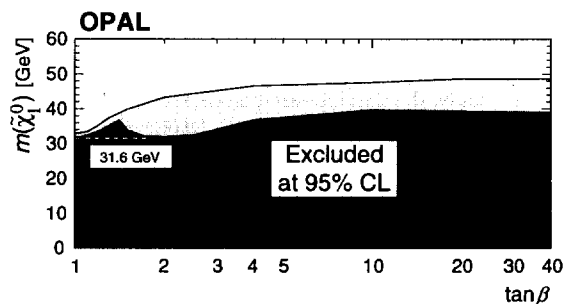


Figure 3: Lower limit on the mass of the lightest neutralino, derived by the OPAL Collaboration using constraints from chargino, neutralino, and slepton searches [8]. The light shaded region is obtained assuming $m_0 \gtrsim 500 \text{ GeV}/c^2$; the dark region, for any m_0 .

The ALEPH Collaboration has explored the constraints coming from the negative results of Higgs searches [9]. These are depicted as excluded regions in the $(m_0, m_{1/2})$ plane and can be translated into bounds on $M_{\tilde{\chi}_1^0}$; they do not, however, substantially strengthen bounds coming from less complicated analyses. This work has also been performed by the LEP SUSY Working Group [19].

If R -parity is not conserved, searches based on missing energy are not viable. The three possible RPV interaction terms ($LL\bar{E}$, $LQ\bar{D}$, $\bar{U}D\bar{D}$) violate lepton or baryon number, consequently precisely measured SM processes constrain products of dissimilar terms. Collider searches assume only one of the many possible terms dominates; given this assumption, searches for charginos and neutralinos, sleptons and squarks

have been performed. All sets of generational indices (λ_{ijk} , λ'_{ijk} , λ''_{ijk}) have been considered, allowing for both *direct* and *indirect* RPV processes. Rather exotic topologies can occur, such as six-lepton final states in slepton production with $LL\bar{E}$ dominating, or ten-jet final states in chargino production with $\bar{U}D\bar{D}$ dominating; entirely new search criteria keyed to an excess of leptons and/or jets have been devised [20]. Searches with a wide scope have found no evidence for supersymmetry with R -parity violation, and limits are as constraining as in the canonical scenario. In fact, the direct exclusion of pair-produced $\tilde{\chi}_1^0$'s rules out some parameter space not accessible in the canonical case.

Visible signals from the lightest neutralino are also realized in special cases of GMSB which predict $\tilde{\chi}_1^0 \rightarrow \gamma \tilde{g}_{3/2}$ with a lifetime short enough for the decay to occur inside the detector [21]. The most promising topology consists of two energetic photons and missing energy resulting from $e^+e^- \rightarrow \tilde{\chi}_1^0 \tilde{\chi}_1^0$. For the DELPHI search, a technique was developed to identify photons which do not originate from the primary vertex. No excess was observed over the expected number of background events [21], leading to a bound on the neutralino mass of about $84 \text{ GeV}/c^2$. When the results are combined [22], the limit is $M_{\tilde{\chi}_1^0} > 89 \text{ GeV}/c^2$. Single-photon production has been used to constrain the process $e^+e^- \rightarrow \tilde{g}_{3/2} \tilde{\chi}_1^0$.

II.5. Supersymmetry searches at proton machines: Although the LEP experiments can investigate a wide range of scenarios and cover obscure corners of parameter space, they cannot match the mass reach of the Tevatron experiments (CDF and DØ). Each experiment has logged approximately 110 pb^{-1} of data at $\sqrt{s} = 1.8 \text{ TeV}$. Although the full energy is never available for annihilation, the cross sections for supersymmetric particle production are large due to color factors and the strong coupling.

The main source of signals for supersymmetry are squarks (scalar partners of quarks) and gluinos (fermionic partners of gluons), in contradistinction to LEP. Pairs of squarks or gluinos are produced in s , t and u -channel processes, which decay directly or via cascades to at least two LSP's. The number of jets depends on whether the gluino or the squark is heavier, with the latter occurring naturally in mSUGRA models. The possibility of cascade decays through charginos or heavier neutralinos also complicates the search. The u , d , s , c , and b squarks are assumed to have similar masses; the search results are reported in terms of their average mass $M_{\tilde{q}}$ and the gluino mass $M_{\tilde{g}}$.

The classic searches [23] rely on large missing transverse energy \cancel{E}_T caused by the escaping neutralinos. Jets with high transverse energy are also required as evidence of a hard interaction; care is taken to distinguish genuine \cancel{E}_T from fluctuations in the jet energy measurement. Backgrounds from W , Z and top production are reduced by rejecting events with identified leptons. Uncertainties in the rates of these processes are minimized by normalizing related samples, such as events with two

jets and one or more leptons. The tails of more ordinary hard-scattering processes accompanied by multiple gluon emission are estimated directly from the data.

The bounds are derived for the $(M_{\tilde{g}}, M_{\tilde{q}})$ plane and have steadily improved with the integrated luminosity. If the squarks are heavier than the gluino, then $M_{\tilde{g}} \gtrsim 180 \text{ GeV}/c^2$. If they all have the same mass, then that mass is at least $260 \text{ GeV}/c^2$, according to the $D\emptyset$ analysis. If the squarks are much lighter than the gluino (in which case they decay via $\tilde{q} \rightarrow q\tilde{\chi}_1^0$), the bounds from UA1 and UA2 [24] play a role giving $M_{\tilde{g}} \gtrsim 300 \text{ GeV}/c^2$. All of these bounds assume there is no gluino lighter than $5 \text{ GeV}/c^2$.

Since these results are expressed in terms of the physical masses relevant to the production process and experimental signature, the excluded region depends primarily on the assumption of nearly equal squark masses with only a small dependence on other parameters such as μ and $\tan\beta$. Direct constraints on the theoretical parameters m_0 and $m_{1/2} \approx 0.34 M_3$ have been obtained by the $D\emptyset$ Collaboration assuming the mass relations of the mSUGRA model [23]. In particular, m_0 is keyed to the squark mass and $m_{1/2}$ to the gluino mass, while for the LEP results these parameters usually relate to slepton and chargino masses.

Charginos and neutralinos may be produced directly by annihilation ($q\bar{q} \rightarrow \tilde{\chi}_i^\pm \tilde{\chi}_j^0$) or in the decays of heavier squarks ($\tilde{q} \rightarrow q' \tilde{\chi}_i^\pm, q \tilde{\chi}_j^0$). They decay to energetic leptons (for example, $\tilde{\chi}_i^\pm \rightarrow \ell \nu \tilde{\chi}_1^0$ and $\tilde{\chi}_2^0 \rightarrow \ell^+ \ell^- \tilde{\chi}_1^0$) and the branching ratio can be high for some parameter choices. The presence of energetic leptons has been exploited in two ways: the 'trilepton' signature and the 'dilepton' signature.

The search for trileptons is most effective for the associated production of $\tilde{\chi}_1^\pm \tilde{\chi}_2^0$ [25]. The requirement of three energetic leptons reduces backgrounds to a very small level, but is efficient for the signal only in special cases. The results reported to date are not competitive with the LEP bounds.

The dilepton signal is geared more for the production of charginos in gluino and squark cascades [26]. Jets are required as expected from the rest of the decay chain; the leptons should be well separated from the jets in order to avoid backgrounds from heavy quark decays. Drell-Yan events are rejected with simple cuts on the relative azimuthal angles of the leptons and their transverse momentum. In some analyses the Majorana nature of the gluino is exploited by requiring two leptons with the same charge, thereby greatly reducing the background. In this scenario limits on squarks and gluinos are almost as stringent as in the classic jets+ \cancel{E}_T case.

It should be noted that the dilepton search complements the multijet+ \cancel{E}_T search in that the acceptance for the latter is reduced when charginos and neutralinos are produced in the decay cascades—exactly the situation in which the dilepton signature is most effective.

The top squark is different from the other squarks because its SM partner is so massive: large off-diagonal terms in the squared-mass matrix lead to large mixing effects and a possible

light mass eigenstate, $M_{\tilde{t}_1} \ll M_{\tilde{q}}$. When the parameters A , μ and $\tan\beta$ are suitably tuned, light bottom squarks can also be expected. Analyses designed to find light stops and sbottoms have been performed [27]. The first of these was based on the jets+ \cancel{E}_T signature expected when the the stop is lighter than the chargino. The search was improved by employing heavy-flavor tagging, which made the selection effective for sbottoms, too. A powerful limit $M_{\tilde{t}} \gtrsim 115 \text{ GeV}/c^2$ was obtained for a neutralino mass around $40 \text{ GeV}/c^2$, shown in Fig. 4.

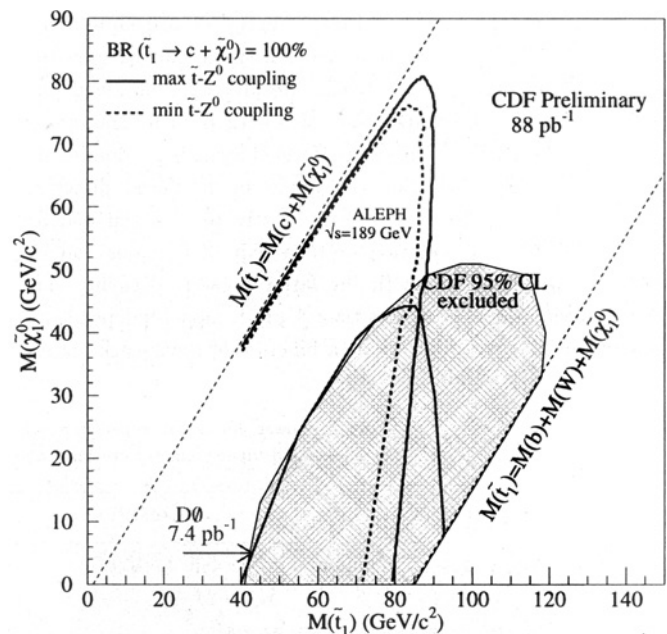


Figure 4: Excluded stop and sneutrino masses, for the $c\tilde{\chi}_1^0$ decay mode, from the CDF Collaboration [27].

A search for the pair-production of light stops decaying to $b\tilde{\chi}_1^\pm$ has been performed by $D\emptyset$ [27]. The presence of two energetic electrons was required; backgrounds from W 's were greatly reduced. Regrettably this experimental bound does not yet improve existing bounds on stop masses.

The CDF and $D\emptyset$ collaborations have searched for supersymmetry in certain RPV scenarios [28]. $D\emptyset$ employs their search for events with two energetic electrons and jets, which is appropriate to decays $\tilde{\chi}_1^0 \rightarrow e q \bar{q}$. Within the mSUGRA framework they sum contributions from all processes predicted as a function of m_0 , $m_{1/2}$ and $\tan\beta$, thereby obtaining exclusions in parameter space. CDF uses the same-sign dielectron and jets topology to look for gluino and squark production and obtain general upper limits on cross sections. They also consider a special case of $\tilde{g} \rightarrow c \tilde{c}_L$ followed by $\tilde{c}_L \rightarrow e d$, motivated by an excess of rare events reported by the HERA collaborations.

Interest in GMSB models was generated by an anomalous event observed by the CDF Collaboration [29]. These models predict large inclusive signals for $p\bar{p} \rightarrow \gamma\gamma + X$ given kinematic constraints derived from the properties of the CDF event.

Searches Particle Listings

Supersymmetric Particle Searches

DØ reported a result from events with two energetic photons and large \cancel{E}_T resulting in the limit $M_{\tilde{\chi}_1^0} > 75 \text{ GeV}/c^2$ [30]. DØ also looked specifically for squarks and gluinos in the scenario, which would give two photons and two or more jets, and obtained squark and gluino mass limits of $320 \text{ GeV}/c^2$. An analysis reported by CDF looks for virtually all thinkable topologies involving two energetic photons [30]. The neutralino mass limit is the same.

II.6. Supersymmetry searches at HERA and fixed-target experiments: The electron-proton collider (HERA) at DESY runs at a center-of-mass energy of 310 GeV and, due to its unique combination of beam types, can be used to probe certain channels effectively. Results were obtained on associated selectron-squark production with R -parity conservation [31]. An RPV search was performed assuming a dominant $LQ\bar{D}$ interaction [32]. Squarks would be produced directly in the s -channel, decaying either directly to a lepton and a quark via R -parity violation or to a pair of fermions and a chargino or neutralino, with the latter possibly decaying via R -parity violation. From less than 3 pb^{-1} , model-independent bounds on λ'_{111} were derived as a function of the squark mass.

The special case of a light \tilde{t}_1 was also considered, and limits derived on λ'_{131} as a function of $M_{\tilde{t}}$.

It is difficult to conduct direct searches for light gluinos ($M_{\tilde{g}} \lesssim 5 \text{ GeV}/c^2$) at colliders because they would form light, long-lived hadrons (R^0 's, a $g\tilde{g}$ bound state) which would be difficult to identify. Certain fixed-target experiments, however, are well suited to the task. The most sensitive searches have been conducted by KTeV at Fermilab and NA48 at CERN, both designed to study very large samples of neutral kaons. KTeV looked for $R^0 \rightarrow \rho^0 \tilde{\gamma}$ with $\rho^0 \rightarrow \pi^+ \pi^-$ and also $R^0 \rightarrow \pi^0 \tilde{\gamma}$, important below the 2π threshold [33]. NA48 searched for $R^0 \rightarrow \eta \tilde{\gamma}$ with $\eta \rightarrow 3\pi^0$ [34]. The searches required decay vertices far downstream of the target and enough missing transverse momentum to eliminate K_L^0 decays. Backgrounds were estimated directly from data and fluxes measured using known K_L^0 decay modes; the R^0 flux is related to the K_L^0 flux theoretically. No evidence for R^0 's was found, and a wide range of R^0 lifetimes was ruled out for $0.9 \text{ GeV}/c^2 < M_{R^0} \lesssim 5 \text{ GeV}/c^2$. These results definitively excludes the possibility of light gluinos with very light photinos (from light gluino decay) solving the cold dark matter problem.

Table 1: Lower limits on supersymmetric particle masses. 'GMSB' refers to models with gauge-mediated supersymmetry breaking, and 'RPV' refers to models allowing R -parity violation.

particle		Condition	Lower limit (GeV/c^2)	Source
$\tilde{\chi}_1^\pm$	gaugino	$M_{\tilde{\nu}} > 500 \text{ GeV}/c^2$	94	LEP 2
		$M_{\tilde{\nu}} > M_{\tilde{\chi}_1^\pm}$	75	LEP 2
		any $M_{\tilde{\nu}}$	45	Z width
	Higgsino	$M_2 < 1 \text{ TeV}/c^2$	89	LEP 2
	GMSB		150	DØ isolated photons
	RPV	$LL\bar{E}$ worst case	87	LEP 2
$LQ\bar{D}$ $m_0 > 500 \text{ GeV}/c^2$		88	LEP 2	
$\tilde{\chi}_1^0$	indirect	any $\tan \beta$, $M_{\tilde{\nu}} > 500 \text{ GeV}/c^2$	33	LEP 2
		any $\tan \beta$, any m_0	32	LEP 2
	GMSB		83	DØ and LEP 2
	RPV	$LL\bar{E}$ worst case	23	LEP 2
\tilde{e}_R	$e\tilde{\chi}_1^0$	$\Delta M > 10 \text{ GeV}/c^2$	89	LEP 2 combined
$\tilde{\mu}_R$	$\mu\tilde{\chi}_1^0$	$\Delta M > 10 \text{ GeV}/c^2$	84	LEP 2 combined
$\tilde{\tau}_R$	$\tau\tilde{\chi}_1^0$	$M_{\tilde{\chi}_1^0} < 20 \text{ GeV}/c^2$	71	LEP 2
$\tilde{\nu}$			43	Z width
$\tilde{\mu}_R, \tilde{\tau}_R$		stable	71	LEP 2 combined
\tilde{t}_1	$c\tilde{\chi}_1^0$	any θ_{mix} , $\Delta M > 10 \text{ GeV}/c^2$	87	LEP 2 combined
		any θ_{mix} , $M_{\tilde{\chi}_1^0} < \frac{1}{2}M_{\tilde{t}}$	88	DØ
	$b\ell\tilde{\nu}$	any θ_{mix} , $\Delta M > 7 \text{ GeV}/c^2$	90	LEP 2 combined
\tilde{g}	any $M_{\tilde{g}}$		190	DØ jets+ \cancel{E}_T
			180	CDF dileptons
\tilde{q}	$M_{\tilde{q}} = M_{\tilde{g}}$		260	DØ jets+ \cancel{E}_T
			230	CDF dileptons

II.7. Conclusions: A huge variety of searches for supersymmetry have been carried out at LEP, the Tevatron, and in fixed-target experiments. Despite all the effort, no signal has been found, forcing the experimenters to derive limits. We have tried to summarize the interesting cases in Table 1. At the present time there is little room for SUSY particles lighter than M_Z . The LEP collaborations will analyze more data taken at a center-of-mass energy of 200 GeV, and the Tevatron collaborations will begin a high luminosity run towards the end of the year 2000. If still no sign of supersymmetry appears, definitive tests will be made at the LHC.

References

- H.E. Haber and G. Kane, Phys. Reports **117**, 75 (1985); H.P. Nilles, Phys. Reports **110**, 1 (1984); M. Chen, C. Dionisi, M. Martinez, and X. Tata, Phys. Reports **159**, 201 (1988).
- H.E. Haber, Nucl. Phys. (Proc. Supp.) **B62**, 469 (1998); S. Dawson, *SUSY and Such*, hep-ph/9612229.
- H. Dreiner, *An Introduction to Explicit R-parity Violation*, in *Perspectives on Supersymmetry*, ed. by G.L. Kane, World Scientific, 1997, p.462; G. Bhattacharyya, Nucl. Phys. Proc. Suppl. **A52**, 83 (1997); V. Barger, W.-Y. Keung, and R.J.N. Phillips, Phys. Lett. **B364**, 27 (1995); R.M. Godbole, P. Roy, and T. Tata, Nucl. Phys. **B401**, 67 (1993); J. Butterworth and H. Dreiner, Nucl. Phys. **B397**, 3 (1993); V. Barger, G.F. Giudice, and T. Han, Phys. Rev. **D40**, 1987 (1989); S. Dawson, Nucl. Phys. **B261**, 297 (1985).
- J. Bagger *et al.*, Phys. Rev. Lett. **78**, 1002 (1997) and Phys. Rev. Lett. **78**, 2497 (1997); M. Dine, Nucl. Phys. Proc. Suppl. **52A**, 201(1997); K.S. Babu, C. Kolda, and F. Wilczek, Phys. Rev. Lett. **77**, 3070 (1996); S. Dimopoulos *et al.*, Phys. Rev. Lett. **76**, 3494 (1996); S. Dimopoulos, S. Thomas, J.D. Wells, Phys. Rev. **D54**, 3283 (1996), and Nucl. Phys. **B488**, 39 (1997); D.R. Stump, M. Wiest, C.P. Yuan, Phys. Rev. **D54**, 1936 (1996); M. Dine, A. Nelson, and Y. Shirman Phys. Rev. **D51**, 1362 (1995); D.A. Dicus, S. Nandi, and J. Woodside, Phys. Rev. **D41**, 2347 (1990) and Phys. Rev. **D43**, 2951 (1990); P. Fayet, Phys. Lett. **B175**, 471 (1986); J. Ellis, K. Enqvist, and D.V. Nanopoulos, Phys. Lett. **B151**, 357 (1985), and Phys. Lett. **B147**, 99 (1984); P. Fayet, Phys. Lett. **B69**, 489 (1977) and Phys. Lett. **B70**, 461 (1977).
- R. Barbieri *et al.*, Nucl. Phys. **B243**, 429 (1984) and Phys. Lett. **B127**, 429 (1983); G. Altarelli, B. Mele, and R. Petronzio, Phys. Lett. **B129**, 456 (1983); G. Farrar and P. Fayet, Phys. Lett. **79B**, 442 (1978) and Phys. Lett. **76B**, 575 (1978).
- G. Farrar, Phys. Rev. Lett. **76**, 4111 (1996), Phys. Rev. Lett. **76**, 4115 (1996), Phys. Rev. **D51**, 3904 (1995), and Phys. Lett. **B265**, 395 (1991); V. Barger *et al.*, Phys. Rev. **D33**, 57 (1986); J. Ellis and H. Kowalski, Nucl. Phys. **B259**, 109 (1985); H.E. Haber and G.L. Kane, Nucl. Phys. **B232**, 333 (1984); M. Chanowitz and S. Sharpe, Phys. Lett. **B126**, 225 (1983).
- J.-F. Grivaz, *Supersymmetric Particle Searches at LEP*, in *Perspectives on Supersymmetry*, *ibid.*, p.179; M. Drees and X. Tata, Phys. Rev. **D43**, 2971 (1991).
- OPAL: CERN-EP/99-XXX (Sept 3, 1999).
- OPAL: Eur. Phys. J. **C8**, 255 (1999); ALEPH: CERN-EP/99-014 and Eur. Phys. J. **C2**, 417 (1998); L3: Eur. Phys. J. **C4**, 207 (1998).
- DELPHI: CERN-EP/99-037.
- ALEPH: Z. Phys. **C72**, 549 (1996).
- OPAL: CERN-EP/99-XXX (Sept 2, 1999) and CERN-EP/98-122; ALEPH: Phys. Lett. **B433**, 176 (1998); DELPHI: Eur. Phys. J. **C6**, 385 (1999); L3: Phys. Lett. **B456**, 283 (1999).
- Preliminary results from the combination of LEP experiments, prepared by the LEP SUSY Working Group. LEPSUSYWG/99-01.1; See also <http://www.cern.ch/lepsusy/>.
- DELPHI: Phys. Lett. **B444**, 491 (1998); OPAL: Phys. Lett. **B433**, 195 (1998); ALEPH: Phys. Lett. **B405**, 379 (1997) and Phys. Lett. **B433**, 176 (1998); L3: CERN-EP/99-075.
- LEP SUSY Working Group, LEPSUSYWG/98-07.1.
- DELPHI: Eur. Phys. J. **C7**, 595 (1999).
- OPAL: Phys. Lett. **B456**, 95 (1999) and Eur. Phys. J. **C6**, 225 (1999); ALEPH: Phys. Lett. **B434**, 189 (1998); L3: Phys. Lett. **B445**, 428 (1999).
- LEP SUSY Working Group, LEPSUSYWG/99-02.1.
- LEPSUSYWG/99-03.1.
- ALEPH: CERN-EP/99-093 and Eur. Phys. J. **C7**, 383 (1999) and Eur. Phys. J. **C4**, 433 (1998); OPAL: CERN-EP/99-043 and CERN-EP/98-203; DELPHI: CERN-EP/99-049; L3: Phys. Lett. **B459**, 354 (1999).
- DELPHI: Eur. Phys. J. **C6**, 371 (1999); OPAL: CERN-EP/99-088 and Eur. Phys. J. **C8**, 23 (1999); ALEPH: Phys. Lett. **B429**, 201 (1998); L3: Phys. Lett. **B444**, 503 (1998).
- LEP SUSY Working Group, LEPSUSYWG/99-05.1.
- DØ: Fermilab Pub-98-402-E and Phys. Rev. Lett. **75**, 618 (1995); CDF: Phys. Rev. **D56**, R1357 (1997) and Phys. Rev. Lett. **76**, 2006 (1996).
- UA2: Phys. Lett. **B235**, 363 (1990); UA1: Phys. Lett. **B198**, 261 (1987).
- DØ: Phys. Rev. Lett. **80**, 1591 (1998); CDF: Phys. Rev. Lett. **80**, 5275 (1998).
- DØ: Fermilab Conf-96/389-E and Fermilab Conf-96/254-E; CDF: Phys. Rev. Lett. **76**, 2006 (1996).
- DØ: Phys. Rev. **D60**, 031101 (1999) and Phys. Rev. **D57**, 589 (1998) and Phys. Rev. Lett. **76**, 2222 (1996); CDF: Fermilab Conf-99/117-E.

Searches Particle Listings

Supersymmetric Particle Searches

28. **CDF**: Fermilab Pub-98-374-E;
DØ: Fermilab Pub-99-200-E.
29. S. Park, in *Proceedings of the 10th Topical Workshop on Proton-Antiproton Collider Physics*, Fermilab, 1995, ed. by R. Raja and J. Yoh (AIP, New York, 1995) 62.
30. **DØ**: Phys. Rev. Lett. **82**, 29 (1999), Phys. Rev. Lett. **80**, 442 (1998) and Phys. Rev. Lett. **78**, 2070 (1997);
CDF: Phys. Rev. **D59**, 092002 (1999) and Phys. Rev. Lett. **81**, 1791 (1998).
31. **ZEUS**: Phys. Lett. **B434**, 214 (1998);
H1: Phys. Lett. **B380**, 461 (1996).
32. **H1**: Z. Phys. **C71**, 211 (1996).
33. **KTeV**: preprint Rutgers-99-12; hep-ex/9903048 and Phys. Rev. Lett. **70**, 4083 (1997).
34. **NA48**: Phys. Lett. **B446**, 117 (1999).

SUPERSYMMETRIC MODEL ASSUMPTIONS

Most of the results shown below, unless stated otherwise, are based on the Minimal Supersymmetric Standard Model (MSSM), as described in the Note on Supersymmetry. Unless otherwise indicated, this includes the assumption of common gaugino and scalar masses at the scale of Grand Unification (GUT), and use of the resulting relations in the spectrum and decay branching ratios. It is also assumed that R -parity (R) is conserved. Unless otherwise indicated, the results also assume that:

- 1) The $\tilde{\chi}_1^0$ is the lightest supersymmetric particle (LSP)
- 2) $m_{\tilde{f}_L} = m_{\tilde{f}_R}$, where $\tilde{f}_{L,R}$ refer to the scalar partners of left- and right-handed fermions.

Limits involving different assumptions are identified in the Comments or in the Footnotes. We summarize here the notations used in this Chapter to characterize some of the most common deviations from the MSSM (for further details, see the Note on Supersymmetry).

Theories with R -parity violation (\mathcal{R}) are characterised by a superpotential of the form: $\lambda_{ijk} L_i L_j e_k^c + \lambda'_{ijk} L_i Q_j d_k^c + \lambda''_{ijk} u_i^c d_j^c d_k^c$, where i, j, k are generation indices. The presence of any of these couplings is often identified in the following by the symbols $L\bar{L}\bar{E}$, $LQ\bar{D}$, and $\bar{U}\bar{D}\bar{D}$. Mass limits in the presence of \mathcal{R} will often refer to "direct" and "indirect" decays. Direct refers to \mathcal{R} decays of the particle in consideration. Indirect refers to cases where \mathcal{R} appears in the decays of the LSP.

In several models, most notably in theories with so-called Gauge Mediated Supersymmetry Breaking (GMSB), the gravitino (\tilde{G}) is the LSP. It is usually much lighter than any other massive particle in the spectrum, and $m_{\tilde{G}}$ is then neglected in all decay processes involving gravitinos. In these scenarios, particles other than the neutralino are sometimes considered as the next-to-lightest supersymmetric particle (NLSP), and are assumed to decay to their even- R partner plus \tilde{G} . If the lifetime is short enough for the decay to take place within the detector, \tilde{G} is assumed to be undetected and to give rise to missing energy (\cancel{E}) or missing transverse energy (\cancel{E}_T) signatures.

When needed, specific assumptions on the eigenstate content of $\tilde{\chi}^0$ and $\tilde{\chi}^\pm$ states are indicated, using the notation $\tilde{\gamma}$

(photino), \tilde{H} (higgsino), \tilde{W} (wino), and \tilde{Z} (zino) to signal that the limit of pure states was used. The terms gaugino is also used, to generically indicate wino-like charginos and zino-like neutralinos.

 $\tilde{\chi}_1^0$ (Lightest Neutralino) MASS LIMIT

$\tilde{\chi}_1^0$ is often assumed to be the lightest supersymmetric particle (LSP). See also the $\tilde{\chi}_2^0, \tilde{\chi}_3^0, \tilde{\chi}_4^0$ section below.

We have divided the $\tilde{\chi}_1^0$ listings below into four sections:

- 1) Accelerator limits for stable $\tilde{\chi}_1^0$,
- 2) Bounds on $\tilde{\chi}_1^0$ from dark matter searches,
- 3) Other bounds on $\tilde{\chi}_1^0$ from astrophysics and cosmology, and
- 4) Bounds on unstable $\tilde{\chi}_1^0$.

Accelerator limits for stable $\tilde{\chi}_1^0$

Unless otherwise stated, results in this section assume spectra, production rates, decay modes, and branching ratios as evaluated in the MSSM, with gaugino and sfermion mass unification at the GUT scale. These papers generally study production of $\tilde{\chi}_i^0 \tilde{\chi}_j^0$ ($i \geq 1, j \geq 2$), $\tilde{\chi}_1^+ \tilde{\chi}_1^-$, and (in the case of hadronic collisions) $\tilde{\chi}_1^+ \tilde{\chi}_2^0$ pairs. The mass limits on $\tilde{\chi}_1^0$ are either direct, or follow indirectly from the constraints set by the non-observation of $\tilde{\chi}_1^\pm$ and $\tilde{\chi}_2^0$ states on the gaugino and higgsino MSSM parameters M_2 and μ .

Obsolete limits obtained from e^+e^- collisions up to $\sqrt{s}=136$ GeV have been removed from this compilation and can be found in the 1998 Edition (The European Physical Journal **C3** 1 (1998)) of this Review. $\Delta m_0 = m_{\tilde{\chi}_2^0} - m_{\tilde{\chi}_1^0}$.

VALUE (GeV)	CL%	DOCUMENT ID	TECN	COMMENT
>31.6	95	1 ABBIENDI	00H OPAL	all $\tan\beta$, all $\Delta m_0 > 5$ GeV, all $m_0 > 31.0$
>31.0	95	2 ABREU	00J DLPH	$\tan\beta \geq 1$, $m_{\tilde{g}} > 300$ GeV
>32.5	95	3 ACCIARRI	00D L3	$\tan\beta > 0.7$, $\Delta m_0 > 3$ GeV, all $m_0 > 27$
>27	95	4 BARATE	99P ALEP	all $\tan\beta$, all m_0
• • • We do not use the following data for averages, fits, limits, etc. • • •				
>30.1	95	5 ABBIENDI	99G OPAL	$\tan\beta=1$, all $\Delta m_0, m_0=500$ GeV
>24.2	95	5 ABBIENDI	99G OPAL	$\tan\beta=1$, all Δm_0 , all m_0
>29.1	95	6 ABREU	99E DLPH	$\tan\beta \geq 1$, all $\Delta m_0, m_0=1$ TeV
		2 ABBOTT	98C DØ	$p\bar{p} \rightarrow \tilde{\chi}_1^\pm \tilde{\chi}_2^0$
>41	95	7 ABE	98J CDF	$p\bar{p} \rightarrow \tilde{\chi}_1^\pm \tilde{\chi}_2^0$
>24.9	95	8 ABREU	98 DLPH	$\tan\beta > 1$, $m_0=1$ TeV
>10.9	95	9 ACCIARRI	98F L3	$\tan\beta > 1$
>13.3	95	10 ACKERSTAFF	98L OPAL	$\tan\beta > 1$
>17	95	11 ELLIS	97C RVUE	All $\tan\beta$

¹ ABBIENDI 00H data collected at $\sqrt{s}=189$ GeV. The results hold over the full parameter space defined by $0 \leq M_2 \leq 2$ TeV, $|\mu| \leq 500$ GeV, $m_0 \leq 500$ GeV, $A = \pm M_2, \pm m_0$, and 0. The minimum mass limit is reached for $\tan\beta=1$. The results of ABBIENDI 99F are used to constrain regions of parameter space dominated by radiative $\tilde{\chi}_2^0 \rightarrow \tilde{\chi}_1^0 \gamma$ decays. The limit improves to 48.5 GeV for $m_0=500$ GeV and $\tan\beta=35$. See their Table and Figs 4-5 for the $\tan\beta$ and m_0 dependence of the limits.

² ABREU 00J data collected at $\sqrt{s}=189$ GeV. The parameter space is scanned in the domain $0 < M_2 < 3000$ GeV, $|\mu| < 200$ GeV, $1 < \tan\beta < 35$. The analysis includes the effects of gaugino cascade decays. In the case of radiative neutralino decays, the limits from $Z \rightarrow \tilde{\chi}_1^0 \tilde{\chi}_2^0$ decays in ABREU 97J are assumed.

³ ACCIARRI 00D data collected at $\sqrt{s}=189$ GeV. The results hold over the full parameter space defined by $0.7 \leq \tan\beta \leq 60$, $0 \leq M_2 \leq 2$ TeV, $m_0 \leq 500$ GeV, $|\mu| \leq 2$ TeV. The minimum mass limit is reached for $\tan\beta=1$ and large m_0 . The results of slepton searches from ACCIARRI 99W are used to help set constraints in the region of small m_0 . The limit improves to 48 GeV for $m_0 \gtrsim 200$ GeV and $\tan\beta \gtrsim 10$. See their Figs. 6-8 for the $\tan\beta$ and m_0 dependence of the limits.

⁴ BARATE 99P data collected at $\sqrt{s}=183$ GeV. The limit is also based on the constraints from the total and invisible Z^0 width from ABBANEO 97, on direct searches for neutralinos at LEP1 from DECAMP 92 and on the slepton limits from BARATE 98K. The limit improves to 29 GeV if the unification of Higgs and sfermion masses is also assumed, and direct constraints on the Higgs mass are used.

⁵ ABBIENDI 99G data collected at $\sqrt{s} \leq 184$ GeV. The parameter space is scanned in the domain $0 < M_2 < 2000$ GeV, $|\mu| < 500$ GeV, and for various values of A . No dependence of the limits on A is found. The analysis includes the effects of gaugino cascade decays. In the case of radiative neutralino decays, the limits from ACKERSTAFF 98J are assumed. The limit for all values of m_0 assumes $m_{\tilde{g}} > 43$ GeV and direct limits on charged sleptons. See Table 5 for limits under different assumptions on Δm_0 and $\tan\beta$.

⁶ ABREU 99E data collected at $\sqrt{s}=183$ GeV. These results include and update the limits from ABREU 98. The parameter space is scanned in the domain $0 < M_2 < 3000$ GeV, $|\mu| < 400$ GeV, $1 < \tan\beta < 35$. The analysis includes the effects of gaugino cascade decays. In the case of radiative neutralino decays, the limits from ABREU 97J are assumed.

⁷ ABE 98J searches for trilepton final states ($\ell=e,\mu$). See footnote to ABE 98J in the Chargino Section for details on the assumptions. The quoted result corresponds to the best limit within the selected range of parameters, obtained for $m_{\tilde{g}} > m_{\tilde{g}}, \tan\beta=2$, and $\mu = -600$ GeV.

⁸ ABREU 98 bound combines the chargino and neutralino searches at $\sqrt{s}=161, 172$ GeV with single-photon-production results at LEP-1 from ABREU 97J.

See key on page 239

Searches Particle Listings Supersymmetric Particle Searches

- ⁹ ACCIARRI 98f limit is obtained for $0 < M_2 < 2000$, $|\mu| < 500$, and $1 < \tan\beta < 40$, but remains valid outside this domain. No dependence on the trilinear-coupling parameter A is found. The limit holds for all values of m_0 consistent with scalar lepton constraints. It improves to 24.6 GeV for $m_{\tilde{\nu}} > 200$ GeV. Data taken at $\sqrt{s} = 130\text{--}172$ GeV.
- ¹⁰ ACKERSTAFF 98L limit is obtained for $0 < M_2 < 1500$, $|\mu| < 500$ and $\tan\beta > 1$, but remains valid outside this domain. The limit holds for the smallest value of m_0 consistent with scalar lepton constraints (ACKERSTAFF 97H). It improves to 24.7 GeV for $m_0 = 1$ TeV. Data taken at $\sqrt{s} = 130\text{--}172$ GeV.
- ¹¹ ELLIS 97c uses constraints on χ^\pm , χ^0 , and \tilde{l} production obtained by the LEP experiments from e^+e^- collisions at $\sqrt{s} = 130\text{--}172$ GeV. It assumes a universal mass m_0 for scalar leptons at the grand unification scale.

Bounds on $\tilde{\chi}_1^0$ from dark matter searches

These papers generally exclude regions in the $M_2 - \mu$ parameter plane assuming that $\tilde{\chi}_1^0$ is the dominant form of dark matter in the galactic halo. These limits are based on the lack of detection in laboratory experiments or by the absence of a signal in underground neutrino detectors. The latter signal is expected if $\tilde{\chi}_1^0$ accumulates in the Sun or the Earth and annihilates into high-energy ν 's.

VALUE	DOCUMENT ID	TECN
• • • We do not use the following data for averages, fits, limits, etc. • • •		
	12 AMBROSIO 99 MCRO	
	13 BOTTINO 97 DAMA	
	14 LOSECCO 95 RVUE	
	15 MORI 93 KAMI	
	16 BOTTINO 92 COSM	
	17 BOTTINO 91 RVUE	
	18 GELMINI 91 COSM	
	19 KAMIONKOW.91 RVUE	
	20 MORI 91B KAMI	
none 4-15 GeV	21 OLIVE 88 COSM	

- ¹² AMBROSIO 99 set new neutrino flux limits which can be used to limit the parameter space in supersymmetric models based on neutralino annihilation in the Sun and the Earth.
- ¹³ BOTTINO 97 points out that the current data from the dark-matter detection experiment DAMA are sensitive to neutralinos in domains of parameter space not excluded by terrestrial laboratory searches.
- ¹⁴ LOSECCO 95 reanalyzed the IMB data and places lower limit on $m_{\tilde{\chi}_1^0}$ of 18 GeV if the LSP is a photino and 10 GeV if the LSP is a higgsino based on LSP annihilation in the sun producing high-energy neutrinos and the limits on neutrino fluxes from the IMB detector.
- ¹⁵ MORI 93 excludes some region in $M_2 - \mu$ parameter space depending on $\tan\beta$ and lightest scalar Higgs mass for neutralino dark matter $m_{\tilde{\chi}_1^0} > m_W$, using limits on upgoing muons produced by energetic neutrinos from neutralino annihilation in the Sun and the Earth.
- ¹⁶ BOTTINO 92 excludes some region $M_2 - \mu$ parameter space assuming that the lightest neutralino is the dark matter, using upgoing muons at Kamiokande, direct searches by Ge detectors, and by LEP experiments. The analysis includes top radiative corrections on Higgs parameters and employs two different hypotheses for nucleon-Higgs coupling. Effects of rescaling in the local neutralino density according to the neutralino relic abundance are taken into account.
- ¹⁷ BOTTINO 91 excluded a region in $M_2 - \mu$ plane using upgoing muon data from Kamioka experiment, assuming that the dark matter surrounding us is composed of neutralinos and that the Higgs boson is not too heavy.
- ¹⁸ GELMINI 91 exclude a region in $M_2 - \mu$ plane using dark matter searches.
- ¹⁹ KAMIONKOWSKI 91 excludes a region in the $M_2 - \mu$ plane using IMB limit on upgoing muons originated by energetic neutrinos from neutralino annihilation in the sun, assuming that the dark matter is composed of neutralinos and that $m_{H_1} \lesssim 50$ GeV. See Fig. 8 in the paper.
- ²⁰ MORI 91B exclude a part of the region in the $M_2 - \mu$ plane with $m_{\tilde{\chi}_1^0} \lesssim 80$ GeV using a limit on upgoing muons originated by energetic neutrinos from neutralino annihilation in the earth, assuming that the dark matter surrounding us is composed of neutralinos and that $m_{H_1} \lesssim 80$ GeV.
- ²¹ OLIVE 88 result assumes that photinos make up the dark matter in the galactic halo. Limit is based on annihilations in the sun and is due to an absence of high energy neutrinos detected in underground experiments. The limit is model dependent.

Other bounds on $\tilde{\chi}_1^0$ from astrophysics and cosmology

Most of these papers generally exclude regions in the $M_2 - \mu$ parameter plane by requiring that the $\tilde{\chi}_1^0$ contribution to the overall cosmological density is less than some maximal value to avoid overclosure of the Universe. Those not based on the cosmological density are indicated. Many of these papers also include LEP and/or other bounds.

VALUE	CL%	DOCUMENT ID	TECN	COMMENT
> 42	95	22 ELLIS 98 RVUE		
• • • We do not use the following data for averages, fits, limits, etc. • • •				
< 600		23 ELLIS 98B COSM		
		EDSJO 97 COSM	Co-annihilation	
> 40		24 ELLIS 97C RVUE		
> 21.4	95	25 ELLIS 96B RVUE	$\tan\beta > 1.2$, $\mu < 0$	
		26 FALK 95 COSM	CP-violating phases	
		DREES 93 COSM	Minimal supergravity	
		FALK 93 COSM	Sfermion mixing	
		KELLEY 93 COSM	Minimal supergravity	
		MIZUTA 93 COSM	Co-annihilation	
		ELLIS 92F COSM	Minimal supergravity	
		KAWASAKI 92 COSM	Minimal supergravity, $m_0 = A = 0$	
		LOPEZ 92 COSM	Minimal supergravity, $m_0 = A = 0$	
		MCDONALD 92 COSM		
		NOJIRI 91 COSM	Minimal supergravity	

	27 OLIVE 91 COSM	
	ROSZKOWSKI 91 COSM	
	ELLIS 90 COSM	
	28 GRIEST 90 COSM	
	29 GRIFOLS 90 ASTR $\tilde{\nu}$; SN 1987A	
	KRAUSS 90 COSM	
	27 OLIVE 89 COSM	
	30 ELLIS 88B ASTR $\tilde{\nu}$; SN 1987A	
> 100 eV	SREDNICKI 88 COSM $\tilde{\nu}$; $m_{\tilde{f}} = 60$ GeV	
none 100 eV - (5-7) GeV	SREDNICKI 88 COSM $\tilde{\nu}$; $m_{\tilde{f}} = 100$ GeV	
none 100 eV - 15 GeV	SREDNICKI 88 COSM $\tilde{\nu}$; for $m_{\tilde{f}} = 100$ GeV	
none 100 eV-5 GeV	ELLIS 84 COSM $\tilde{\nu}$	
	GOLDBERG 83 COSM $\tilde{\nu}$	
	31 KRAUSS 83 COSM $\tilde{\nu}$	
	VYSOTSKII 83 COSM $\tilde{\nu}$	

- ²² ELLIS 98 updates ELLIS 97c (see relative footnote). Use is made of one-loop mass and coupling relations, as well as of chargino limits from e^+e^- data at $\sqrt{s} = 183$ GeV. The limits on $\tan\beta$ from ELLIS 97c improve to: $\tan\beta > 2$ ($\mu < 0$) and $\tan\beta > 1.65$ ($\mu > 0$).
- ²³ ELLIS 98B assumes a universal scalar mass and radiative supersymmetry breaking with universal gaugino masses. The upper limit to the LSP mass is increased due to the inclusion of $\chi - \tilde{\tau}_R$ coannihilations.
- ²⁴ ELLIS 97c uses in addition to cosmological constraints, data from e^+e^- collisions at 170-172 GeV. It assumes a universal scalar mass for both the Higgs and scalar leptons, as well as radiative supersymmetry breaking with universal gaugino masses. ELLIS 97c also uses the absence of Higgs detection (with the assumptions listed above) to set a limit on $\tan\beta > 1.7$ for $\mu < 0$ and $\tan\beta > 1.4$ for $\mu > 0$. This paper updates ELLIS 96b.
- ²⁵ ELLIS 96b uses, in addition to cosmological constraints, data from BUSKULIC 96K and SUGIMOTO 96. It assumes a universal scalar mass m_0 and radiative Supersymmetry breaking, with universal gaugino masses.
- ²⁶ Mass of the bino (=LSP) is limited to $m_{\tilde{B}} \lesssim 350$ GeV for $m_t = 174$ GeV.
- ²⁷ Mass of the bino (=LSP) is limited to $m_{\tilde{B}} \lesssim 350$ GeV for $m_t \leq 200$ GeV. Mass of the higgsino (=LSP) is limited to $m_{\tilde{H}} \lesssim 1$ TeV for $m_t \leq 200$ GeV.
- ²⁸ Mass of the bino (=LSP) is limited to $m_{\tilde{B}} \lesssim 550$ GeV. Mass of the higgsino (=LSP) is limited to $m_{\tilde{H}} \lesssim 3.2$ TeV.
- ²⁹ GRIFOLS 90 argues that SN1987A data exclude a light photino ($\lesssim 1$ MeV) if $m_{\tilde{q}} < 1.1$ TeV, $m_{\tilde{e}} < 0.83$ TeV.
- ³⁰ ELLIS 88B argues that the observed neutrino flux from SN1987A is inconsistent with a light photino if 60 GeV $\lesssim m_{\tilde{q}} \lesssim 2.5$ TeV. If $m(\text{higgsino})$ is $O(100$ eV) the same argument leads to limits on the ratio of the two Higgs v.e.v.'s. LAU 93 discusses possible relations of ELLIS 88B bounds.
- ³¹ KRAUSS 83 finds $m_{\tilde{z}}$ not 30 eV to 2.5 GeV. KRAUSS 83 takes into account the gravitino decay. Find that limits depend strongly on reheated temperature. For example a new allowed region $m_{\tilde{z}} = 4\text{--}20$ MeV exists if $m_{\text{gravitino}} < 40$ TeV. See figure 2.

Unstable $\tilde{\chi}_1^0$ (Lightest Neutralino) MASS LIMIT

Unless otherwise stated, results in this section assume spectra and production rates as evaluated in the MSSM. Unless otherwise stated, the goldstino or gravitino mass $m_{\tilde{G}}$ is assumed to be negligible relative to all other masses. In the following, \tilde{G} is assumed to be undetected and to give rise to a missing energy (\cancel{E}) signature.

VALUE (GeV)	CL%	DOCUMENT ID	TECN	COMMENT
• • • We do not use the following data for averages, fits, limits, etc. • • •				
> 27	95	32 ABREU 00I DLPH	$R(LL\bar{E})$, any $\Delta m_0, 1 \leq \tan\beta \leq$	
> 86	95	33 BARATE 00G ALEP	$e^+e^- \rightarrow \tilde{\chi}_1^0 \tilde{\chi}_1^0 (\tilde{\chi}_1^0 \rightarrow \gamma \tilde{G})$	
		34 ABBIENDI 99F OPAL	$e^+e^- \rightarrow \tilde{G} \tilde{\chi}_1^0 (\tilde{\chi}_1^0 \rightarrow \gamma \tilde{G})$	
none 45-83	95	35 ABBIENDI 99F OPAL	$e^+e^- \rightarrow \tilde{B} \tilde{B} (\tilde{B} \rightarrow \gamma \tilde{G})$	
> 29	95	36 ABBIENDI 99T OPAL	$e^+e^- \rightarrow \tilde{\chi}_1^0 \tilde{\chi}_1^0, R, m_0 = 500$ GeV, $\tan\beta > 1.2$	
> 65	95	37 ABE 99I CDF	$p\bar{p} \rightarrow \tilde{\chi} \tilde{\chi}, \tilde{\chi} = \tilde{\chi}_{1,2}^\pm, \tilde{\chi}_1^0 \rightarrow \gamma \tilde{G}$	
> 83	95	38 ABREU 99D DLPH	$e^+e^- \rightarrow \tilde{B} \tilde{B} (\tilde{B} \rightarrow \gamma \tilde{G})$	
		39 ABREU 99F DLPH	$e^+e^- \rightarrow \tilde{\chi}_1^0 \tilde{\chi}_1^0$, with $\tilde{\chi}_1^0 \rightarrow \tau \tilde{\tau}$ ($\tilde{\tau} \rightarrow \tau \tilde{G}$)	
> 26.8	95	40 ACCIARRI 99I L3	$\tilde{\chi}_1^0 \tilde{\chi}_1^0, R$	
		41 ACCIARRI 99R L3	$e^+e^- \rightarrow \tilde{G} \tilde{\chi}_1^0, \tilde{\chi}_1^0 \rightarrow \tilde{G} \gamma$	
> 88.2	95	42 ACCIARRI 99R L3	$e^+e^- \rightarrow \tilde{\chi}_1^0 \tilde{\chi}_1^0, \tilde{\chi}_1^0 \rightarrow \tilde{G} \gamma$	
> 29	95	43 BARATE 99E ALEP	$R, LQ\bar{D}, \tan\beta = 1.41, m_0 = 500$ GeV	
> 77	95	44 ABBOTT 98 D0	$p\bar{p} \rightarrow \tilde{\chi} \tilde{\chi}, \tilde{\chi} = \tilde{\chi}_{1,2}^\pm, \tilde{\chi}_1^0 \rightarrow \gamma \tilde{G}$	
		45 ABREU 98 DLPH	$e^+e^- \rightarrow \tilde{\chi}_1^0 \tilde{\chi}_1^0 (\tilde{\chi}_1^0 \rightarrow \gamma \tilde{G})$	
		46 ACCIARRI 98V L3	$e^+e^- \rightarrow \tilde{G} \tilde{\chi}_1^0 (\tilde{\chi}_1^0 \rightarrow \gamma \tilde{G})$	
> 79	95	47 ACCIARRI 98V L3	$e^+e^- \rightarrow \tilde{B} \tilde{B} (\tilde{B} \rightarrow \gamma \tilde{G})$	
		48 ACKERSTAFF 98J OPAL	$e^+e^- \rightarrow \tilde{\chi}_1^0 \tilde{\chi}_1^0 (\tilde{\chi}_1^0 \rightarrow \gamma \tilde{G})$	
		49 BARATE 98H ALEP	$e^+e^- \rightarrow \tilde{G} \tilde{\chi}_1^0 (\tilde{\chi}_1^0 \rightarrow \gamma \tilde{G})$	
> 71	95	50 BARATE 98H ALEP	$e^+e^- \rightarrow \tilde{B} \tilde{B} (\tilde{B} \rightarrow \gamma \tilde{G})$	
		51 BARATE 98J ALEP	$e^+e^- \rightarrow \tilde{G} \tilde{\chi}_1^0 (\tilde{\chi}_1^0 \rightarrow \gamma \tilde{G})$	
		52 BARATE 98J ALEP	$e^+e^- \rightarrow \tilde{B} \tilde{B} (\tilde{B} \rightarrow \gamma \tilde{G})$	
> 84	95	53 BARATE 98S ALEP	$R, LL\bar{E}$	
> 23	95	54 ACCIARRI 97V L3	$e^+e^- \rightarrow \tilde{\chi}_1^0 \tilde{\chi}_1^0 (\tilde{\chi}_1^0 \rightarrow \gamma \tilde{G})$	
		55 ELLIS 97 THEO	$e^+e^- \rightarrow \tilde{\chi}_1^0 \tilde{\chi}_1^0, \tilde{\chi}_1^0 \rightarrow \gamma \tilde{G}$	
		56 CABIBBO 81 COSM		

Searches Particle Listings

Supersymmetric Particle Searches

- 32 ABREU 00I searches for the production of charginos and neutralinos in the case of R -parity violation with $LL\bar{E}$ couplings, using data from $\sqrt{s}=183$ GeV. They investigate topologies with multiple leptons or jets plus leptons, assuming one coupling at the time to be non-zero and giving rise to direct or indirect decays. Limits are obtained in the M_2 versus μ plane and a limit on the neutralino mass is derived from a scan over the parameters m_0 and $\tan\beta$.
- 33 BARATE 00G search for diphoton + \bar{B} topologies using data collected at $\sqrt{s}=189$ GeV. Limits are obtained from a scan of GMSB parameter space, under the assumption of a short-lived $\tilde{\chi}_1^0$ NLSP. The limit is reduced to 45 GeV for long-lived neutralinos.
- 34 ABBIENDI 99F obtained an upper bound on the cross section for the process $e^+e^- \rightarrow \tilde{G}\tilde{\chi}_1^0$ followed by the prompt decay $\tilde{\chi}_1^0 \rightarrow \tilde{G}\gamma$ of 0.46–0.075 pb for $m_{\tilde{\chi}_1^0}=91$ –183 GeV. See Fig. 8 for the detailed dependence of $m_{\tilde{\chi}_1^0}$. Data taken at $\sqrt{s}=183$ GeV.
- 35 ABBIENDI 99F looked for $\gamma\gamma\bar{B}$ final states at $\sqrt{s}=183$ GeV. The limit is for pure bino \tilde{B} and assumes $m_{\tilde{e}_R}=1.35m_{\tilde{B}}$ and $m_{\tilde{e}_L}=2m_{\tilde{e}_R}$. See Fig. 13 for the cross-section limits as a function of $m_{\tilde{\chi}_1^0}$.
- 36 ABBIENDI 99T searches for the production of neutralinos in the case of R -parity violation with $LL\bar{E}$, LQD , or UDD couplings using data from $\sqrt{s}=183$ GeV. They investigate topologies with multiple leptons, jets plus leptons, or multiple jets, assuming one coupling at the time to be non-zero and giving rise to direct or indirect decays. Mixed decays (where one particle has a direct, the other an indirect decay) are also considered for the UDD couplings. Upper limits on the cross section are derived which, combined with the constraint from the Z^0 width, allow to exclude regions in the M_2 versus μ plane for any coupling. Limits on the neutralino mass are obtained for non-zero $LL\bar{E}$ couplings $>10^{-5}$. The limit disappears for $\tan\beta < 1.2$ and it improves to 50 GeV for $\tan\beta > 20$.
- 37 ABE 99I looked for chargino and neutralino production, where the lightest neutralino in their decay products further decays into $\gamma\tilde{G}$. The limit assumes the gaugino mass unification, and holds for $1 < \tan\beta < 25$, $M_2 < 200$ GeV, and all μ . ABE 99I is an expanded version of ABE 98L.
- 38 ABREU 99D looked for $\gamma\gamma\bar{B}$ final states at $\sqrt{s}=130$ –183 GeV. The limit is for prompt decay of pure bino \tilde{B} and assumes $m_{\tilde{e}_R}=1.1m_{\tilde{B}}$ GeV. The limit reduces to 76 GeV for $m_{\tilde{e}_R}=150$ GeV. See Fig. 14 for the limits as a function of $m_{\tilde{e}_R}$. Model-independent cross-section limits in the range 0.10–0.13 pb are shown in Fig. 9, for neutralino masses in the range 45–81.5 GeV. Cross section limits were also derived, see Fig. 13, as function of the decay length, including non-pointing single photon final states.
- 39 ABREU 99F looked for acoplanar ditau, taus with large impact parameters, kinks, and stable heavy-charged tracks at $\sqrt{s}=130$ –183 GeV. See Table 5 for explicit $m_{\tilde{\chi}_1^0}$ limits under different model assumptions.
- 40 ACCIARRI 99I looked for multi-lepton and/or multi-jet final states from \bar{R} prompt decays with $LL\bar{E}$ or UDD couplings at $\sqrt{s}=130$ –183 GeV. The situations where the $\tilde{\chi}_1^0$ is the LSP (indirect decays) and where a $\tilde{\ell}$ is the LSP (direct decays) were both considered and both yield the same mass limit.
- 41 ACCIARRI 99R searches for $\gamma\bar{B}$ final states using data from $\sqrt{s}=189$ GeV. From limits on cross section times branching ratio, mass limits are derived in a no-scale SUGRA model, see their Fig. 5. Supersedes the results of ACCIARRI 98V.
- 42 ACCIARRI 99R searches for $\gamma\bar{B}$ final states using data from $\sqrt{s}=189$ GeV. From a scan over the GMSB parameter space, a limit on the mass is derived under the assumption that the neutralino is the NLSP. Supersedes the results of ACCIARRI 98V.
- 43 BARATE 99E looked for the decay of gauginos via R -violating couplings $LQ\bar{D}$. The bound is significantly reduced for smaller values of m_0 . Data collected at $\sqrt{s}=130$ –172 GeV.
- 44 ABBOTT 98 studied the chargino and neutralino production, where the lightest neutralino in their decay products further decays into $\gamma\tilde{G}$. The limit assumes the gaugino mass unification.
- 45 ABREU 98 uses data at $\sqrt{s}=161$ and 172 GeV. Upper bounds on $\gamma\gamma\bar{B}$ cross section are obtained. Similar limits on $\gamma\bar{B}$ are also given, relevant for $e^+e^- \rightarrow \tilde{\chi}_1^0\tilde{G}$ production.
- 46 ACCIARRI 98V obtained an upper bound on the cross section for the process $e^+e^- \rightarrow \tilde{G}\tilde{\chi}_1^0$ followed by the prompt decay $\tilde{\chi}_1^0 \rightarrow \tilde{G}\gamma$ of 0.28–0.07 pb for $m_{\tilde{\chi}_1^0}=0$ –183 GeV. See Fig. 4b for the detailed dependence on $m_{\tilde{\chi}_1^0}$. Data taken at $\sqrt{s}=183$ GeV.
- 47 ACCIARRI 98V looked for $\gamma\gamma\bar{B}$ final states at $\sqrt{s}=183$ GeV. The limit is for pure bino \tilde{B} and assumes $m_{\tilde{e}_{R,L}}=150$ GeV. The limit improves to 84 GeV for $m_{\tilde{e}_{R,L}}=100$ GeV. See Fig. 7 for the cross-section limits as a function of $m_{\tilde{\chi}_1^0}$, for different cases of neutralino composition.
- 48 ACKERSTAFF 98J looked for $\gamma\gamma\bar{B}$ final states at $\sqrt{s}=161$ –172 GeV. They set limits on $\sigma(e^+e^- \rightarrow \tilde{\chi}_1^0\tilde{\chi}_1^0)$ in the range 0.22–0.50 pb for $m_{\tilde{\chi}_1^0}$ in the range 45–86 GeV. Mass limits for explicit models from the literature are given in Fig. 19 of their paper. Similar limits on γ +missing energy are also given, relevant for $\tilde{\chi}_1^0\tilde{G}$ production.
- 49 BARATE 98H obtained an upper bound on the cross section for the process $e^+e^- \rightarrow \tilde{G}\tilde{\chi}_1^0$ followed by the prompt decay $\tilde{\chi}_1^0 \rightarrow \tilde{G}\gamma$ of 0.4–0.75 pb for $m_{\tilde{\chi}_1^0}=40$ –170 GeV. Data taken at $\sqrt{s}=161,172$ GeV.
- 50 BARATE 98H looked for $\gamma\gamma\bar{B}$ final states at $\sqrt{s}=161,172$ GeV. The limit is for pure bino \tilde{B} with $\tau(\tilde{B}) < 3$ ns and assumes $m_{\tilde{e}_R}=1.5m_{\tilde{B}}$. See Fig. 5 for the dependence of the limit on $m_{\tilde{e}_R}$.
- 51 BARATE 98J looked for $\gamma\bar{B}$ final states at $\sqrt{s}=161$ –183 GeV. They obtained an upper bound on the cross section of about 0.2 pb for the process $e^+e^- \rightarrow XY$ followed by the prompt decay $X \rightarrow Y\gamma$ ($\tau(X) < 0.1$ ns) if $m_Y = 0$. The bound applies for $\tilde{G}\tilde{\chi}_1^0$.
- 52 BARATE 98J looked for $\gamma\gamma\bar{B}$ final states at $\sqrt{s}=161$ –183 GeV. The limit is for pure bino \tilde{B} with $\tau(\tilde{B}) < 3$ ns and assumes $m_{\tilde{e}_R}=1.1m_{\tilde{B}}$. See Fig. 5 for the dependence of the limit on $m_{\tilde{e}_R}$.
- 53 BARATE 98S looked for the decay of gauginos via R -violating coupling $LL\bar{E}$. The bound improves to 25 GeV if the chargino decays into neutralino which further decays into lepton pairs. Data collected at $\sqrt{s}=130$ –172 GeV.

- 54 ACCIARRI 97V looked for $\gamma\gamma\bar{B}$ final states at $\sqrt{s}=161$ and 172 GeV. They set limits on $\sigma(e^+e^- \rightarrow \tilde{\chi}_1^0\tilde{\chi}_1^0)$ in the range 0.25–0.50 pb for masses in the range 45–85 GeV. The lower limits on $m_{\tilde{\chi}_1^0}$ vary in the range of 64.8 GeV (pure bino with 90 GeV slepton) to 75.3 GeV (pure higgsino). There is no limit for pure zino case.
- 55 ELLIS 97 reanalyzed the LEP2 ($\sqrt{s}=161$ GeV) limits of $\sigma(\gamma\gamma+E_{\text{miss}}) < 0.2$ pb to exclude $m_{\tilde{\chi}_1^0} < 63$ GeV if $m_{\tilde{e}_L}=m_{\tilde{e}_R} < 150$ GeV and $\tilde{\chi}_1^0$ decays to $\gamma\tilde{G}$ inside detector.
- 56 CABIBBO 81 consider $\tilde{\gamma} \rightarrow \gamma$ goldstino. Photino must be either light enough (<30 eV) to satisfy cosmology bound, or heavy enough (>0.3 MeV) to have disappeared at early universe.

$\tilde{\chi}_2^0, \tilde{\chi}_3^0, \tilde{\chi}_4^0$ (Neutralinos) MASS LIMITS

Neutralinos are unknown mixtures of photinos, z -inos, and neutral higgsinos (the supersymmetric partners of photons and of Z and Higgs bosons). The limits here apply only to $\tilde{\chi}_2^0, \tilde{\chi}_3^0$, and $\tilde{\chi}_4^0$. $\tilde{\chi}_1^0$ is the lightest supersymmetric particle (LSP); see $\tilde{\chi}_1^0$ Mass Limits. It is not possible to quote rigorous mass limits because they are extremely model dependent; i.e. they depend on branching ratios of various $\tilde{\chi}_i^0$ decay modes, on the masses of decay products ($\tilde{e}, \tilde{\gamma}, \tilde{q}, \tilde{g}$), and on the \tilde{e} mass exchanged in $e^+e^- \rightarrow \tilde{\chi}_i^0\tilde{\chi}_j^0$. Limits arise either from direct searches, or from the MSSM constraints set on the gaugino and higgsino mass parameters M_2 and μ through searches for lighter charginos and neutralinos. Often limits are given as contour plots in the $m_{\tilde{\chi}_i^0} - m_{\tilde{e}}$ plane vs other parameters. When specific assumptions are made, e.g. the neutralino is a pure photino ($\tilde{\gamma}$), pure z -ino (\tilde{Z}), or pure neutral higgsino (\tilde{H}^0), the neutralinos will be labelled as such.

Limits obtained from e^+e^- collisions at energies up to 136 GeV, as well as other limits from different techniques, are now superseded and have not been included in this compilation. They can be found in the 1998 Edition (The European Physical Journal C 3 1 (1998)) of this Review.

VALUE (GeV)	CL%	DOCUMENT ID	TECN	COMMENT
> 55.9	95	57 ABBIENDI	00H OPAL	$\tilde{\chi}_2^0, \tan\beta=1.5, \Delta m > 10$ GeV, all m_0
> 106.6	95	57 ABBIENDI	00H OPAL	$\tilde{\chi}_3^0, \tan\beta=1.5, \Delta m > 10$ GeV, all m_0
• • • We do not use the following data for averages, fits, limits, etc. • • •				
> 44	95	58 ABBIENDI	99F OPAL	$e^+e^- \rightarrow \tilde{\chi}_2^0\tilde{\chi}_1^0 (\tilde{\chi}_2^0 \rightarrow \gamma\tilde{\chi}_1^0)$
> 102	95	59 ABBIENDI	99F OPAL	$e^+e^- \rightarrow \tilde{\chi}_2^0\tilde{\chi}_2^0 (\tilde{\chi}_2^0 \rightarrow \gamma\tilde{\chi}_1^0)$
> 34.8	95	60 ABBIENDI	99G OPAL	$\tilde{\chi}_2^0, \tan\beta > 1, \Delta m_0 > 10$ GeV
> 102	95	60 ABBIENDI	99G OPAL	$\tilde{\chi}_3^0, \tan\beta=1.5, \Delta m_0 > 10$ GeV
> 34.8	95	61 ABREU	99D DLPH	$e^+e^- \rightarrow \tilde{\chi}_2^0\tilde{\chi}_2^0 (\tilde{\chi}_2^0 \rightarrow \gamma\tilde{\chi}_1^0)$
> 45.3	95	62 ACCIARRI	99I L3	$\tilde{\chi}_2^0, \bar{R}$
> 75.8	95	63 ACCIARRI	99R L3	$e^+e^- \rightarrow \tilde{\chi}_2^0\tilde{\chi}_2^0, \tilde{\chi}_2^0 \rightarrow \tilde{\chi}_1^0\gamma$
> 53	95	64 ABBOTT	98C D0	$p\bar{p} \rightarrow \tilde{\chi}_1^\pm\tilde{\chi}_2^0$
> 74	95	65 ABE	98J CDF	$p\bar{p} \rightarrow \tilde{\chi}_1^\pm\tilde{\chi}_2^0$
> 86.3	95	66 ACCIARRI	98F L3	$\tilde{H}^0, \tan\beta=1.41, M_2 < 500$ GeV
> 86.3	95	67 ACCIARRI	98V L3	$e^+e^- \rightarrow \tilde{\chi}_2^0\tilde{\chi}_{1,2}^0 (\tilde{\chi}_2^0 \rightarrow \gamma\tilde{\chi}_1^0)$
> 45.3	95	68 ACKERSTAFF	98L OPAL	$\tilde{\chi}_2^0, \tan\beta > 1$
> 75.8	95	68 ACKERSTAFF	98L OPAL	$\tilde{\chi}_3^0, \tan\beta > 1$
> 53	95	69 BARATE	98H ALEP	$e^+e^- \rightarrow \tilde{\gamma}\tilde{\gamma} (\tilde{\gamma} \rightarrow \gamma\tilde{H}^0)$
> 74	95	70 BARATE	98J ALEP	$e^+e^- \rightarrow \tilde{\gamma}\tilde{\gamma} (\tilde{\gamma} \rightarrow \gamma\tilde{H}^0)$
> 86.3	95	71 ABACHI	96 D0	$p\bar{p} \rightarrow \tilde{\chi}_1^\pm\tilde{\chi}_2^0$
> 86.3	95	72 ABE	96K CDF	$p\bar{p} \rightarrow \tilde{\chi}_1^\pm\tilde{\chi}_2^0$
> 86.3	95	73 ACKERSTAFF	96c OPAL	$\tilde{\chi}_3^0$
57 ABBIENDI 00H used the results of direct searches in the $e^+e^- \rightarrow \tilde{\chi}_1^0\tilde{\chi}_{2,3}^0$ channels, as well as the indirect limits from $\tilde{\chi}_1^0$ and $\tilde{\chi}_1^\pm$ searches, in the framework of the MSSM with gaugino and sfermion mass unification at the GUT scale. See the footnote to ABBIENDI 00H in the chargino Section for further details on the assumptions. Data collected at $\sqrt{s}=189$ GeV. The limits improve to 86.2 GeV ($\tilde{\chi}_2^0$) and 124 GeV ($\tilde{\chi}_3^0$) for $\tan\beta=35$. See their Table 6 for more details on the $\tan\beta$ and m_0 dependence of the limits.				
58 ABBIENDI 99F looked for $\gamma\bar{B}$ final states at $\sqrt{s}=183$ GeV. They obtained an upper bound on the cross section for the production $e^+e^- \rightarrow \tilde{\chi}_2^0\tilde{\chi}_1^0$ followed by the prompt decay $\tilde{\chi}_2^0 \rightarrow \gamma\tilde{\chi}_1^0$ of 0.075–0.80 pb in the region $m_{\tilde{\chi}_2^0}, m_{\tilde{\chi}_1^0} > m_Z, m_{\tilde{\chi}_2^0}=91$ –183 GeV, and $\Delta m_0 > 5$ GeV. See Fig. 7 for explicit limits in the $(m_{\tilde{\chi}_2^0}, m_{\tilde{\chi}_1^0})$ plane.				
59 ABBIENDI 99F looked for $\gamma\gamma\bar{B}$ final states at $\sqrt{s}=183$ GeV. They obtained an upper bound on the cross section for the production $e^+e^- \rightarrow \tilde{\chi}_2^0\tilde{\chi}_2^0$ followed by the prompt decay $\tilde{\chi}_2^0 \rightarrow \gamma\tilde{\chi}_1^0$ of 0.08–0.37 pb for $m_{\tilde{\chi}_2^0}=45$ –81.5 GeV, and $\Delta m_0 > 5$ GeV. See Fig. 11 for explicit limits in the $(m_{\tilde{\chi}_2^0}, m_{\tilde{\chi}_1^0})$ plane.				
60 ABBIENDI 99G uses the results of direct searches in the $e^+e^- \rightarrow \tilde{\chi}_1^0\tilde{\chi}_{2,3}^0$ channels, as well as the indirect limits from $\tilde{\chi}_1^0\tilde{\chi}_i^\pm$ searches within the MSSM. See the footnote to ABBIENDI 99G in the Chargino Section for further details on the assumptions. Data collected at $\sqrt{s}=181$ –184 GeV.				
61 ABREU 99D looked for $\gamma\gamma\bar{B}$ final states at $\sqrt{s}=183$ GeV. They obtained upper bounds in the range 0.10–0.25 pb on the cross section for the production $e^+e^- \rightarrow \tilde{\chi}_2^0\tilde{\chi}_2^0$ followed by the prompt decay $\tilde{\chi}_2^0 \rightarrow \gamma\tilde{\chi}_1^0$ with $\Delta m_0 > 6$ GeV. See Fig. 12 for explicit limits in the $(m_{\tilde{\chi}_2^0}, m_{\tilde{\chi}_1^0})$ plane.				

- ⁶² ACCIARRI 99I looked for multi-lepton and/or multi-jet final states from R prompt decays with $LL\bar{E}$ or UDD couplings at $\sqrt{s}=130$ –183 GeV. The situations where the $\tilde{\chi}_1^0$ is the LSP (indirect decays) and where a $\tilde{\ell}$ is the LSP (direct decays) were both considered. The weakest limit, quoted above, comes from direct decays with UDD couplings; indirect decays lead to a limit of 44.3 GeV.
- ⁶³ ACCIARRI 99R searches for $\gamma\tilde{B}$ and $\gamma\tilde{W}$ final states using data from $\sqrt{s}=189$ GeV. Limits on the cross section for the processes $e^+e^- \rightarrow \tilde{\chi}_2^0\tilde{\chi}_{2,1}^0$ with the decay $\tilde{\chi}_2^0 \rightarrow \tilde{\chi}_1^0\gamma$ are derived, as shown in their Figs. 4 and 7. Supersedes the results of ACCIARRI 98V.
- ⁶⁴ ABBOTT 98C searches for trilepton final states ($\ell=e,\mu$). See footnote to ABBOTT 98C in the Chargino Section for details on the assumptions. Assuming a negligible decay rate of $\tilde{\chi}_1^\pm$ to quarks, they obtain $m_{\tilde{\chi}_2^0} \gtrsim 103$ GeV.
- ⁶⁵ ABE 98J searches for trilepton final states ($\ell=e,\mu$). See footnote to ABE 98J in the Chargino Section for details on the assumptions. The quoted result for $m_{\tilde{\chi}_2^0}$ corresponds to the best limit within the selected range of parameters, obtained for $m_{\tilde{g}} > m_{\tilde{g}}$, $\tan\beta=2$, and $\mu=-600$ GeV.
- ⁶⁶ ACCIARRI 98F is obtained from direct searches in the $e^+e^- \rightarrow \tilde{\chi}_1^0\tilde{\chi}_2^0$ production channels, and indirectly from $\tilde{\chi}_1^\pm$ and $\tilde{\chi}_1^0$ searches within the MSSM. See footnote to ACCIARRI 98F in the chargino Section for further details on the assumptions. Data taken at $\sqrt{s}=130$ –172 GeV.
- ⁶⁷ ACCIARRI 98V looked for $\gamma(\gamma)\tilde{B}$ final states at $\sqrt{s}=183$ GeV. They obtained an upper bound on the cross section for the production $e^+e^- \rightarrow \tilde{\chi}_2^0\tilde{\chi}_{1,2}^0$ followed by the prompt decay $\tilde{\chi}_2^0 \rightarrow \gamma\tilde{\chi}_1^0$. See Figs. 4a and 6a for explicit limits in the $(m_{\tilde{\chi}_2^0}, m_{\tilde{\chi}_1^0})$ plane.
- ⁶⁸ ACKERSTAFF 98L is obtained from direct searches in the $e^+e^- \rightarrow \tilde{\chi}_1^0\tilde{\chi}_{2,3}^0$ production channels, and indirectly from $\tilde{\chi}_1^\pm$ and $\tilde{\chi}_1^0$ searches within the MSSM. See footnote to ACKERSTAFF 98L in the chargino Section for further details on the assumptions. Data taken at $\sqrt{s}=130$ –172 GeV.
- ⁶⁹ BARATE 98H looked for $\gamma\gamma\tilde{B}$ final states at $\sqrt{s}=161,172$ GeV. They obtained an upper bound on the cross section for the production $e^+e^- \rightarrow \tilde{\chi}_2^0\tilde{\chi}_2^0$ followed by the prompt decay $\tilde{\chi}_2^0 \rightarrow \gamma\tilde{\chi}_1^0$ of 0.4–0.8 pb for $m_{\tilde{\chi}_2^0} = 10$ –80 GeV. The bound above is for the specific case of $\tilde{\chi}_1^0 = \tilde{H}^0$ and $\tilde{\chi}_2^0 = \tilde{\gamma}$ and $m_{\tilde{e}_R} = 100$ GeV. See Fig. 6 and 7 for explicit limits in the $(\tilde{\chi}_2^0, \tilde{\chi}_1^0)$ plane and in the $(\tilde{\chi}_2^0, \tilde{e}_R)$ plane.
- ⁷⁰ BARATE 98J looked for $\gamma\gamma\tilde{B}$ final states at $\sqrt{s}=161$ –183 GeV. They obtained an upper bound on the cross section for the production $e^+e^- \rightarrow \tilde{\chi}_2^0\tilde{\chi}_2^0$ followed by the prompt decay $\tilde{\chi}_2^0 \rightarrow \gamma\tilde{\chi}_1^0$ of 0.08–0.24 pb for $m_{\tilde{\chi}_2^0} < 91$ GeV. The bound above is for the specific case of $\tilde{\chi}_1^0 = \tilde{H}^0$ and $\tilde{\chi}_2^0 = \tilde{\gamma}$ and $m_{\tilde{e}_R} = 100$ GeV.
- ⁷¹ ABACHI 96 searches for 3-lepton final states. Efficiencies are calculated using mass relations and branching ratios in the Minimal Supergravity scenario. Results are presented as lower bounds on $\sigma(\tilde{\chi}_1^\pm\tilde{\chi}_2^0) \times B(\tilde{\chi}_1^\pm \rightarrow \ell\nu_\ell\tilde{\chi}_1^0) \times B(\tilde{\chi}_2^0 \rightarrow \ell^+\ell^-\tilde{\chi}_1^0)$ as a function of $m_{\tilde{\chi}_2^0}$. Limits range from 3.1 pb ($m_{\tilde{\chi}_1^0} = 45$ GeV) to 0.6 pb ($m_{\tilde{\chi}_1^0} = 100$ GeV).
- ⁷² ABE 96k looked for tripleton events from chargino-neutralino production. They obtained lower bounds on $m_{\tilde{\chi}_2^0}$ as a function of μ . The lower bounds are in the 45–50 GeV range for gaugino-dominant $\tilde{\chi}_2^0$ with negative μ , if $\tan\beta < 10$. See paper for more details of the assumptions.
- ⁷³ ACKERSTAFF 96C is obtained from direct searches in the $e^+e^- \rightarrow \tilde{\chi}_1^0\tilde{\chi}_{2,3}^0$ production channel, and indirectly from $\tilde{\chi}_1^\pm$ searches within MSSM. Data from $\sqrt{s}=130, 136$, and 161 GeV are combined. The same assumptions and constraints of ALEXANDER 96J apply. The limit improves to 94.3 GeV for $m_0 = 1$ TeV.

$\tilde{\chi}_1^\pm, \tilde{\chi}_2^0$ (Charginos) MASS LIMITS

Charginos are unknown mixtures of w -inos and charged higgsinos (the supersymmetric partners of W and Higgs bosons). A lower mass limit for the lightest chargino ($\tilde{\chi}_1^\pm$) of approximately 45 GeV, independent of the field composition and of the decay mode, has been obtained by the LEP experiments from the analysis of the Z width and decays. These results, as well as other now superseded limits from e^+e^- collisions at energies below 136 GeV, and from hadronic collisions, can be found in the 1998 Edition (The European Physical Journal **C3** 1 (1998)) of this Review.

Unless otherwise stated, results in this section assume spectra, production rates, decay modes and branching ratios as evaluated in the MSSM, with gaugino and stfermion mass unification at the GUT scale. These papers generally study production of $\tilde{\chi}_1^0\tilde{\chi}_2^0$, $\tilde{\chi}_1^+\tilde{\chi}_1^-$ and (in the case of hadronic collisions) $\tilde{\chi}_1^+\tilde{\chi}_2^0$ pairs, including the effects of cascade decays. The mass limits on $\tilde{\chi}_1^\pm$ are either direct, or follow indirectly from the constraints set by the non-observation of $\tilde{\chi}_2^0$ states on the gaugino and higgsino MSSM parameters M_2 and μ . For generic values of the MSSM parameters, limits from high-energy e^+e^- collisions coincide with the highest value of the mass allowed by phase-space, namely $m_{\tilde{\chi}_1^\pm} \gtrsim \sqrt{s}/2$. At the time of this writing, preliminary and unpublished results from the 1999 run of LEP2 at \sqrt{s} up to 202 GeV give therefore a lower mass limit of approximately 101 GeV valid for general MSSM models. The limits become however weaker in special regions of the MSSM parameter space where the detection efficiencies or production cross sections are suppressed. For example, this may happen when: (i) the mass differences $\Delta m_\pm = m_{\tilde{\chi}_1^\pm} - m_{\tilde{\chi}_2^0}$ or $\Delta m_\nu = m_{\tilde{\chi}_1^\pm} - m_{\tilde{\nu}}$ are very small, and the detection efficiency is reduced; (ii) the electron sneutrino mass is small, and the $\tilde{\chi}_1^\pm$ production rate is suppressed due to a destructive interference between s and t channel exchange diagrams. The regions of MSSM parameter space where the following limits are valid are indicated in the comment lines or in the footnotes.

VALUE (GeV)	CL%	DOCUMENT ID	TECN	COMMENT
> 71.7	95	74 ABBIENDI	00H OPAL	$\tan\beta=35, \Delta m_\pm > 5$ GeV, all m_0
> 88.4	95	75 ABREU	00J DLPH	$\Delta m_\pm \geq 3$ GeV, $m_{\tilde{\nu}} > m_{\tilde{\chi}_1^\pm}$, $\tan\beta > 1$
> 67.7	95	76 ACCIARRI	00D L3	$\tan\beta > 0.7, \Delta m_\pm > 3$ GeV, all m_0
> 68	95	77 BARATE	98X ALEP	$\tan\beta=1.41$, all m_0
• • • We do not use the following data for averages, fits, limits, etc. • • •				
> 89	95	78 ABREU	00I DLPH	$R(LL\bar{E})$, any $\Delta m_0, 1 \leq \tan\beta \leq 30$
> 94.1	95	79 ABREU	00J DLPH	$e^+e^- \rightarrow \tilde{\chi}_1^\pm\tilde{\chi}_1^\mp (\tilde{\chi}^0 \rightarrow \gamma\tilde{G})$, $\tan\beta \geq 1$
> 91	95	80 BARATE	00H ALEP	$R(LL\bar{E}, LQ\bar{D}, UDD)$, $m_0 > 500$ GeV
> 90.0	95	81 ABBIENDI	99G OPAL	$\tan\beta=1.5, \Delta m_\pm > 5$ GeV, $m_0=500$ GeV
> 69.1	95	81 ABBIENDI	99G OPAL	$\tan\beta=1.5, \Delta m_\pm > 5$ GeV, all m_0
> 76	95	82 ABBIENDI	99T OPAL	$R, m_0=500$ GeV
> 120	95	83 ABE	99I CDF	$p\bar{p} \rightarrow \tilde{\chi}\tilde{\chi}, \tilde{\chi}=\tilde{\chi}_{1,2}^0, \tilde{\chi}_1^\pm, \tilde{\chi}_1^0 \rightarrow \gamma\tilde{G}$
> 89.4	95	84 ABREU	99E DLPH	$\Delta m_\pm > 10$ GeV, $m_{\tilde{\nu}} > 300$ GeV
> 88.8	95	84 ABREU	99E DLPH	$\Delta m_\pm > 5$ GeV, $m_{\tilde{\nu}} > 41$ GeV
> 90.5	95	85 ABREU	99E DLPH	$e^+e^- \rightarrow \tilde{\chi}_1^\pm\tilde{\chi}_1^0, \tilde{\chi}_1^0 \rightarrow \gamma\tilde{G}$
> 85.5	95	86 ABREU	99V DLPH	$e^+e^- \rightarrow \tilde{\chi}^+\tilde{\chi}^-, \tilde{\chi} \rightarrow \tilde{\tau}\nu, \tilde{\tau} \rightarrow \gamma\tilde{G}$
> 76.9	95	87 ABREU	99Z DLPH	$e^+e^- \rightarrow \tilde{\chi}^+\tilde{\chi}^-, \Delta m_\pm < 3$ GeV
> 82	95	88 ACCIARRI	99I L3	$R, LL\bar{E}$ or UDD
> 51	95	89 BARATE	99E ALEP	$R, LQ\bar{D}$
> 150	95	90 MALTONI	99B THEO	EW analysis, $\Delta m_\pm \sim 1$ GeV
> 81.5	95	91 ABBOTT	98 D0	$p\bar{p} \rightarrow \tilde{\chi}\tilde{\chi}, \tilde{\chi}=\tilde{\chi}_{1,2}^0, \tilde{\chi}_1^\pm, \tilde{\chi}_1^0 \rightarrow \gamma\tilde{G}$
> 67.6	95	92 ABBOTT	98C D0	$p\bar{p} \rightarrow \tilde{\chi}_1^\pm\tilde{\chi}_2^0$
> 67.6	95	93 ABE	98J CDF	$p\bar{p} \rightarrow \tilde{\chi}_1^\pm\tilde{\chi}_2^0$
> 71.8	95	94 ABREU	98 DLPH	$\Delta m > 10$ GeV
> 69.2	95	95 ABREU	98 DLPH	$e^+e^- \rightarrow \tilde{\chi}^+\tilde{\chi}^-, \tilde{\chi}_1^0 \rightarrow \tilde{G}\gamma$
> 65.7	95	96 ACCIARRI	98F L3	$\tan\beta < 1.41$, all m_0
> 73	95	97 ACKERSTAFF	98K OPAL	$\tilde{\chi}^+ \rightarrow \ell^+\tilde{B}$
		98 ACKERSTAFF	98L OPAL	$\Delta m_\pm > 3$ GeV, $\Delta m_\nu > 2$ GeV
		99 ACKERSTAFF	98V OPAL	light gluino
		100 BARATE	98S ALEP	$R, LL\bar{E}$
		101 CARENA	97 THEO	$g_\mu - 2$
		102 KALINOWSKI	97 THEO	$W \rightarrow \tilde{\chi}_1^\pm\tilde{\chi}_1^0$
		103 ABE	96K CDF	$p\bar{p} \rightarrow \tilde{\chi}_1^\pm\tilde{\chi}_2^0$
> 62	95	104 ACKERSTAFF	96C OPAL	$e^+e^- \rightarrow \tilde{\chi}^+\tilde{\chi}^-$
⁷⁴ ABBIENDI 00H data collected at $\sqrt{s}=189$ GeV. The results hold over the full parameter space defined by $0 \leq M_2 \leq 2$ TeV, $ \mu \leq 500$ GeV, $m_0 \leq 500$ GeV, $A=\pm M_2, \pm m_0$, and 0. The results of slepton searches from ABBIENDI 00G were used to help set constraints in the region of small m_0 . The limit improves to 78 GeV for $\tan\beta=1.5$. See their Table 5 and Fig. 4 for the $\tan\beta$ and M_2 dependence of the limits.				
⁷⁵ ABREU 00J data collected at $\sqrt{s}=189$ GeV. They investigate topologies with multiple leptons, jets plus leptons, multi-jets, or isolated photons. The parameter space is scanned in the domain $0 < M_2 < 3000$ GeV, $ \mu < 200$ GeV, $1 < \tan\beta < 35$. The analysis includes the effects of gaugino cascade decays.				
⁷⁶ ACCIARRI 00D data collected at $\sqrt{s}=189$ GeV. The results hold over the full parameter space defined by $0.7 \leq \tan\beta \leq 60, 0 \leq M_2 \leq 2$ TeV, $ \mu \leq 2$ TeV, $m_0 \leq 500$ GeV. The results of slepton searches from ACCIARRI 99W are used to help set constraints in the region of small m_0 . See their Figs. 5 for the $\tan\beta$ and M_2 dependence on the limits. See the text for the impact of a large $B(\tilde{\chi}^\pm \rightarrow \tilde{\tau}\nu)$ on the result.				
⁷⁷ BARATE 98X limit holds for all values of m_0 consistent with the slepton mass limits of BARATE 97N. The limit improves to 79 GeV for a mostly higgsino $\tilde{\chi}_1^\pm$ (with $\Delta m > 5$ GeV) and to 85.5 GeV for a mostly gaugino $\tilde{\chi}_1^\pm$ ($\mu=-500$ GeV and $m_{\tilde{\nu}} > 200$ GeV). The cases of $m_{\tilde{\chi}_1^\pm} > m_{\tilde{\nu}}$ or nonuniversal scalar mass or nonuniversal gaugino mass are also studied in the paper. Data collected at $\sqrt{s}=161$ –172 GeV.				
⁷⁸ ABREU 00I searches for the production of charginos and neutralinos in the case of R -parity violation with $LL\bar{E}$ couplings, using data from $\sqrt{s}=183$ GeV. They investigate topologies with multiple leptons or jets plus leptons, assuming one coupling at the time to be non-zero and giving rise to direct or indirect decays. Limits are obtained in the M_2 versus m_0 plane and a limit on the neutralino mass is derived from a scan over the parameters m_0 and $\tan\beta$.				
⁷⁹ This ABREU 00J limit holds for $\Delta m_\pm > 10$ GeV and $m_{\tilde{\nu}} > 300$ GeV. For the other assumptions, see previous footnote to ABREU 00J in this Section. A limit of 94.2 GeV is obtained for $\Delta m_\pm=1$ GeV and $m_{\tilde{\nu}} > m_{\tilde{\chi}_1^\pm}$.				
⁸⁰ BARATE 00H data collected at $\sqrt{s}=183$ GeV. The limit holds for any possible R -parity violating coupling.				
⁸¹ ABBIENDI 99G data collected at $\sqrt{s} \leq 184$ GeV. The parameter space is scanned in the domain $0 < M_2 < 2000$ GeV, $ \mu < 500$ GeV, and for various values of A . No dependence of the limits on A is found. The analysis includes the effects of gaugino cascade decays. In the case of radiative neutralino decays, the limits from ACKERSTAFF 98I are assumed. The limit for all values of m_0 assumes $m_{\tilde{\nu}} > 43$ GeV and direct limits on charged sleptons. See Table 5 for limits under different assumptions on Δm_\pm and $\tan\beta$.				
⁸² ABBIENDI 99T searches for the production of neutralinos in the case of R -parity violation with $LL\bar{E}, LQ\bar{D}$, or UDD couplings using data from $\sqrt{s}=183$ GeV. They investigate topologies with multiple leptons, jets plus leptons, or multiple jets, assuming one coupling at the time to be non-zero and giving rise to direct or indirect decays. Mixed decays (where one particle has a direct, the other an indirect decay) are also considered for the UDD couplings. Upper limits on the cross section are derived which, combined with the				

Searches Particle Listings

Supersymmetric Particle Searches

- constraint from the Z^0 width, allow to exclude regions in the M_2 versus μ plane for any coupling. Limits on the chargino mass are obtained for non-zero $LL\bar{E}$ couplings $> 10^{-5}$ and assuming decays via a W^* .
- 83 ABE 99i looked for chargino and neutralino production, where the lightest neutralino in their decay products further decays into $\gamma\tilde{G}$. The limit assumes the gaugino mass unification, and holds for $1 < \tan\beta < 25$, $M_2 < 200$ GeV, and all μ . ABE 99i is an expanded version of ABE 98L.
- 84 ABREU 99E data collected at $\sqrt{s} \leq 183$ GeV. These results include and update the limits from ABREU 98. The parameter space is scanned in the domain $0 < M_2 < 3000$ GeV, $|\mu| < 400$ GeV, $1 < \tan\beta < 35$. The analysis includes the effects of gaugino cascade decays. In the case of radiative neutralino decays, the limits from ABREU 97j are assumed.
- 85 This ABREU 99E limit holds for $\Delta m_0 > 10$ GeV and $m_{\tilde{\nu}_\tau} > 300$ GeV. For the other assumptions, see previous footnote to ABREU 99E in this Section. A limit of 90.6 GeV is obtained for $\Delta m_{\pm} = 1$ GeV and $m_{\tilde{\nu}_\tau} > 41$ GeV.
- 86 ABREU 99v reinterprets search results at 183 GeV on $\tilde{\tau}$ decays at the interaction vertex (ABREU 99E), visible decay vertices in the tracking devices or large impact parameters (ABREU 99F) and stable charged heavy particles (ABREU 98P). Limits are computed by scanning the GMSB parameter space where $\tilde{\tau}_1$ is the NLSF, with the constraints that electroweak symmetry is broken radiatively and that trilinear couplings are zero at the messenger scale. All branching ratios in the above decay chain are taken equal to 1. The limit holds for $m_{\tilde{\chi}_1^\pm} - m_{\tilde{\tau}_1} > 0.3$ GeV, and any gravitino mass, in the domain $m_{\tilde{\tau}_1} > 68$ GeV, not excluded by the direct $\tilde{\tau}$ production searches of ABREU 99F. The limit is reached for $m_{\tilde{G}} \leq 1$ eV and improves to 89 GeV for $m_{\tilde{G}} > 100$ eV. See Fig. 4 for the dependence of the limit on $m_{\tilde{\tau}_1}$.
- 87 ABREU 99z searches for the production of charginos degenerate with $\tilde{\chi}_1^0$, using data from $\sqrt{s} = 130$ to 183 GeV. The range $\Delta m_{\pm} < 200$ MeV is covered by a search for decays visible in the detector or for heavy stable particles identified by their ionization or Cherenkov radiation. The region $300 \text{ MeV} < \Delta m_{\pm} < 3$ GeV is explored by searching events with initial state radiation and few low energy particles. For $200 \text{ MeV} < \Delta m_{\pm} < 300$ MeV, no limits are obtained. For limits in various scenarios, see Fig. 12 and Table 3.
- 88 ACCIARRI 99i looked for multi-lepton and/or multi-jet final states from \tilde{R} prompt decays with $LL\bar{E}$ or UDD couplings at $\sqrt{s} = 130$ –183 GeV. The situations where the $\tilde{\chi}_1^0$ is the LSP (indirect decays) and where a $\tilde{\ell}$ is the LSP (direct decays) were both considered. The weakest limit, quoted above, comes from direct decays with UDD couplings; indirect decays lead to a limit of 91.1 GeV for $LL\bar{E}$ and 90.9 GeV for UDD couplings.
- 89 BARATE 99E looked for the decay of charginos via R -violating couplings $LQ\bar{D}$. The bound is reduced to 56 GeV for $m_0 = 80$ GeV (in the case of decays via a neutralino), and to 51 GeV for $m_0 = 70$ GeV (in the case of direct R -violating decays). Data collected at $\sqrt{s} = 130$ –172 GeV.
- 90 MALTONI 99b studied the effect of light chargino-neutralino to the electroweak precision data with a particular focus on the case where they are nearly degenerate ($\Delta m_{\pm} \sim 1$ GeV) which is difficult to exclude from direct collider searches. The quoted limit is for higgsino-like case while the bound improves to 56 GeV for wino-like case. The values of the limits presented here are obtained in an update to MALTONI 99b, as described in MALTONI 00.
- 91 ABBOTT 98 studied the chargino and neutralino production, where the lightest neutralino in their decay products further decays into $\gamma\tilde{G}$. The limit assumes the gaugino mass unification.
- 92 ABBOTT 98c searches for trilepton final states ($\ell = e, \mu$). Efficiencies are calculated using mass relations in the Minimal Supergravity scenario, exploring the domain of parameter space defined by $m_{\tilde{\chi}_1^\pm} = m_{\tilde{\chi}_2^0}$ and $m_{\tilde{\chi}_1^\pm} = 2m_{\tilde{\chi}_1^0}$. Results are presented in Fig. 1 as upper bounds on $\sigma(p\bar{p} \rightarrow \tilde{\chi}_1^\pm \tilde{\chi}_2^0) \times B(3\ell)$. Assuming equal branching ratio for all possible leptonic decays, limits range from 2.6 pb ($m_{\tilde{\chi}_1^\pm} = 45$ GeV) to 0.4 pb ($m_{\tilde{\chi}_1^\pm} = 124$ GeV) at 95%CL. Assuming a negligible decay rate of $\tilde{\chi}_1^\pm$ and $\tilde{\chi}_2^0$ to quarks, this corresponds to $m_{\tilde{\chi}_1^\pm} > 103$ GeV.
- 93 ABE 98j searches for trilepton final states ($\ell = e, \mu$). Efficiencies are calculated using mass relations in the Minimal Supergravity scenario, exploring the domain of parameter space defined by $1.1 < \tan\beta < 8$, $-1000 < \mu$ (GeV) < -200 , and $m_{\tilde{G}}/m_{\tilde{g}} = 1-2$. In this region $m_{\tilde{\chi}_1^\pm} \sim m_{\tilde{\chi}_2^0}$ and $m_{\tilde{\chi}_1^\pm} \sim 2m_{\tilde{\chi}_1^0}$. Results are presented in Fig. 1 as upper bounds on $\sigma(p\bar{p} \rightarrow \tilde{\chi}_1^\pm \tilde{\chi}_2^0) \times B(3\ell)$. Limits range from 0.8 pb ($m_{\tilde{\chi}_1^\pm} = 50$ GeV) to 0.23 pb ($m_{\tilde{\chi}_1^\pm} = 100$ GeV) at 95%CL. The gaugino mass unification hypothesis and the assumed mass relation between squarks and gluinos define the value of the leptonic branching ratios. The quoted result corresponds to the best limit within the selected range of parameters, obtained for $m_{\tilde{g}} > m_{\tilde{g}}$, $\tan\beta = 2$, and $\mu = -600$ GeV. Mass limits for different values of $\tan\beta$ and μ are given in Fig. 2.
- 94 ABREU 98 uses data at $\sqrt{s} = 161$ and 172 GeV. The limit is for $41 < m_{\tilde{\nu}_\tau} < 100$ GeV, and $\tan\beta = 1-35$. The limit improves to 84.3 GeV for $m_{\tilde{\nu}_\tau} > 300$ GeV. For Δm_{\pm} below 10 GeV, the limit is independent of $m_{\tilde{\nu}_\tau}$, and is given by 80.3 GeV for $\Delta m_{\pm} = 5$ GeV, and by 52.4 GeV for $\Delta m_{\pm} = 3$ GeV.
- 95 ABREU 98 uses data at $\sqrt{s} = 161$ and 172 GeV. The radiative decay of the lightest neutralino into gravitino is assumed. The limit is for $\Delta m > 10$ GeV, $41 < m_{\tilde{\nu}_\tau} < 100$ GeV, and $\tan\beta = 1-35$. The limit improves to 84.5 GeV if either $m_{\tilde{\nu}_\tau} > 300$ GeV, or $\Delta m_{\pm} = 1$ GeV independently of $m_{\tilde{\nu}_\tau}$.
- 96 ACCIARRI 98F limit is obtained for $0 < M_2 < 2000$, $\tan\beta < 1.41$, and $\mu = -200$ GeV, and holds for all values of m_0 . No dependence on the trilinear-coupling parameter A is found. It improves to 84 GeV for large sneutrino mass, at $\mu = -200$ GeV. See the paper for limits obtained with specific assumptions on the gaugino/higgsino composition of the state. Data taken at $\sqrt{s} = 130$ –172 GeV.
- 97 ACKERSTAFF 98k looked for dilepton+ \tilde{Z} final states at $\sqrt{s} = 130$ –172 GeV. Limits on $\sigma(e^+e^- \rightarrow \tilde{\chi}_1^\pm \tilde{\chi}_1^0) \times B^2(\ell)$, with $B(\ell) = B(\chi^+ \rightarrow \ell^+ \nu_\ell \tilde{\chi}_1^0)$ ($B(\ell) = B(\chi^+ \rightarrow \ell^+ \tilde{\nu}_\ell)$), are given in Fig. 16 (Fig. 17).
- 98 ACKERSTAFF 98L limit is obtained for $0 < M_2 < 1500$, $|\mu| < 500$ and $\tan\beta > 1$, but remains valid outside this domain. The dependence on the trilinear-coupling parameter A is studied, and found negligible. The limit holds for the smallest value of m_0 consistent with scalar lepton constraints (ACKERSTAFF 97H) and for all values of m_0 where the

condition $\Delta m_{\tilde{\nu}_\tau} > 2.0$ GeV is satisfied. $\Delta m_{\tilde{\nu}_\tau} > 10$ GeV if $\tilde{\chi}_1^\pm \rightarrow \ell \tilde{\nu}_\ell$. The limit improves to 84.5 GeV for $m_0 = 1$ TeV. Data taken at $\sqrt{s} = 130$ –172 GeV.

- 99 ACKERSTAFF 98v excludes the light gluino with universal gaugino mass where charginos, neutralinos decay as $\tilde{\chi}_1^\pm, \tilde{\chi}_2^0 \rightarrow q\bar{q}\tilde{g}$ from total hadronic cross sections at $\sqrt{s} = 130$ –172 GeV. See paper for the case of nonuniversal gaugino mass.
- 100 BARATE 98s looked for the decay of charginos via R -violating coupling $LL\bar{E}$. The bound improves to 78 GeV if the chargino decays into neutralino which further decays into lepton pairs. Data collected at $\sqrt{s} = 130$ –172 GeV.
- 101 CARENA 97 studied the constraints on chargino and sneutrino masses from muon $g-2$. The bound can be important for large $\tan\beta$.
- 102 KALINOWSKI 97 studies the constraints on the chargino-neutralino parameter space from limits on $\Gamma(W \rightarrow \tilde{\chi}_1^\pm \tilde{\chi}_1^0)$ achievable at LEP2. This is relevant when $\tilde{\chi}_1^\pm$ is "invisible," i.e., if $\tilde{\chi}_1^\pm$ dominantly decays into $\tilde{\nu}_\ell \ell^\pm$ with little energy for the lepton. Small otherwise allowed regions could be excluded.
- 103 ABREU 96k looked for triplet events from chargino-neutralino production. The bound on $m_{\tilde{\chi}_1^\pm}$ can reach up to 47 GeV for specific choices of parameters. The limits on the combined production cross section times 3-lepton branching ratios range between 1.4 and 0.4 pb, for $45 < m_{\tilde{\chi}_1^\pm}$ (GeV) < 100 . See the paper for more details on the parameter dependence of the results.
- 104 ACKERSTAFF 96c assumes the dominance of off-shell W -exchange in the chargino decay and applies for $\Delta m > 10$ GeV in the region of parameter space defined by: $M_2 < 1500$ GeV, $|\mu| < 500$ GeV and $\tan\beta > 1.5$. The bound is for the smallest $\tilde{\ell}, \tilde{\nu}$ mass allowed by LEP, with the efficiency for $\tilde{\chi}_1^\pm \rightarrow \tilde{\nu}_\ell \ell^\pm$ decays set to zero. The limit improves to 78.5 GeV for $m_0 = 1$ TeV. Data taken at $\sqrt{s} = 130, 136$, and 161 GeV.

Long-lived $\tilde{\chi}_1^\pm$ (Chargino) MASS LIMITS

Limits on charginos which leave the detector before decaying.

VALUE (GeV)	CL%	DOCUMENT ID	TECN	COMMENT
none 2-87.5	95	105 ABREU	98P DLPH	$m_{\tilde{\nu}_\tau} > 41$ GeV
>89.5	95	106 ACKERSTAFF	98P OPAL	
• • • We do not use the following data for averages, fits, limits, etc. • • •				
>80	95	107 ABREU	97D DLPH	
>83	95	108 BARATE	97K ALEP	
>45	95	ABREU	90G DLPH	
>28.2	95	ADACHI	90C TOPZ	
105 ABREU 98P searches for production of pairs of heavy, charged particles in e^+e^- annihilation at $\sqrt{s} = 130$ –183 GeV. The upper bound improves to 89.5 GeV for $m_{\tilde{\nu}_\tau} > 200$ GeV. These limits include and update the results of ABREU 97D.				
106 ACKERSTAFF 98P bound assumes a heavy sneutrino $m_{\tilde{\nu}_\tau} > 500$ GeV. Data collected at $\sqrt{s} = 130$ –183 GeV.				
107 ABREU 97D bound applies only to masses above 45 GeV. Data collected in e^+e^- collisions at $\sqrt{s} = 130$ –172 GeV. The limit improves to 84 GeV for $m_{\tilde{\nu}_\tau} > 200$ GeV.				
108 BARATE 97K uses e^+e^- data collected at $\sqrt{s} = 130$ –172 GeV. Limit valid for $\tan\beta = \sqrt{2}$ and $m_{\tilde{\nu}_\tau} > 100$ GeV. The limit improves to 86 GeV for $m_{\tilde{\nu}_\tau} > 250$ GeV.				

$\tilde{\nu}$ (Sneutrino) MASS LIMIT

The limit depends on the number, $N(\tilde{\nu})$, of sneutrinos assumed to be degenerate in mass. Only $\tilde{\nu}_L$ (not $\tilde{\nu}_R$) is assumed to exist. It is possible that $\tilde{\nu}$ could be the lightest supersymmetric particle (LSP).

We report here, but do not include in the Listings, the limits obtained from preliminary, unpublished constraints by the LEP Collaborations on the invisible width of the Z boson ($\Delta\Gamma_{\text{inv.}} < 2.0$ MeV, LEP 00): $m_{\tilde{\nu}} > 43.7$ GeV ($N(\tilde{\nu}) = 1$) and $m_{\tilde{\nu}} > 44.7$ GeV ($N(\tilde{\nu}) = 3$).

VALUE (GeV)	CL%	DOCUMENT ID	TECN	COMMENT
> 37.1	95	109 ADRIANI	93M L3	$\Gamma(Z \rightarrow \text{invisible}); N(\tilde{\nu}) = 1$
> 41	95	110 DECAMP	92 ALEP	$\Gamma(Z \rightarrow \text{invisible}); N(\tilde{\nu}) = 3$
> 36	95	ABREU	91F DLPH	$\Gamma(Z \rightarrow \text{invisible}); N(\tilde{\nu}) = 1$
> 31.2	95	111 ALEXANDER	91F OPAL	$\Gamma(Z \rightarrow \text{invisible}); N(\tilde{\nu}) = 1$
• • • We do not use the following data for averages, fits, limits, etc. • • •				
> 62	95	112 ABBIENDI	00 OPAL	$\tilde{\nu}_{e,\mu}, \tilde{R}, LL\bar{E}$ or $LQ\bar{D}$ decays
> 62	95	113 ABREU	00I DLPH	$\tilde{\nu}_\ell, \tilde{R}, LL\bar{E}$ decays
none 100-215	95	114 BARATE	00H ALEP	$\tilde{\nu}_\ell, \tilde{R}, LL\bar{E}$ decays
> 51	95	115 ABBIENDI	99 OPAL	$\tilde{\nu}_{\mu,\tau}, \tilde{R}, (s+t)$ -channel
> 49	95	116 ABBIENDI	99 OPAL	$\tilde{\nu}_\tau, \tilde{R}, s$ -channel
none 100-195	95	117 ABBIENDI	99 OPAL	$\tilde{\nu}_e, \tilde{R}, t$ -channel
none 100-160	95	118 ABREU	99A DLPH	$\tilde{\nu}_{e,\mu,\tau}, \tilde{R}, (s+t)$ -channel
> 51	95	119 BARATE	99E ALEP	$\tilde{R}, \tilde{\nu}_\mu \rightarrow jj$
> 49	95	120 BARATE	98S ALEP	$\tilde{\nu}_{\mu,\tau}, \tilde{R}, LL\bar{E}$ decays
> 58	95	121 BARATE	98S ALEP	$\tilde{\nu}_e, \tilde{R}, LL\bar{E}$ decays
$\neq m_Z$	95	122 ACCIARRI	97U L3	$\tilde{\nu}_\tau, \tilde{R}, s$ -channel
none 125-180	95	123 ACCIARRI	97U L3	$\tilde{\nu}_\tau, \tilde{R}, s$ -channel
> 46.0	95	124 CARENA	97 THEO	$\tilde{g}_\mu - 2$
none 20-25000	95	125 BUSKULIC	95E ALEP	$N(\tilde{\nu}) = 1, \tilde{\nu} \rightarrow \nu\nu\ell\ell'$
< 600	95	126 BECK	94 COSM	Stable $\tilde{\nu}$, dark matter
none 3-90	90	127 FALK	94 COSM	$\tilde{\nu}$ LSP, cosmic abundance
none 4-90	90	128 SATO	91 KAMI	Stable $\tilde{\nu}_e$ or $\tilde{\nu}_\mu$, dark matter
none 4-90	90	129 SATO	91 KAMI	Stable $\tilde{\nu}_\tau$, dark matter
109 ADRIANI 93M limit from $\Delta\Gamma(Z)(\text{invisible}) < 16.2$ MeV.				
110 DECAMP 92 limit is from $\Gamma(\text{invisible})/\Gamma(\ell\ell) = 5.91 \pm 0.15$ ($N_\nu = 2.97 \pm 0.07$).				
111 ALEXANDER 91F limit is for one species of $\tilde{\nu}$ and is derived from $\Gamma(\text{invisible, new})/\Gamma(\ell\ell) < 0.38$.				

- 112 **ABBIENDI 00** searches for the production of sneutrinos in the case of R -parity violation with $LL\bar{E}$ or $LQ\bar{D}$ couplings, using data from $\sqrt{s}=183$ GeV. They investigate topologies with multiple leptons, jets plus leptons, or multiple jets, assuming one coupling at the time to be non-zero and giving rise to direct or indirect decays. For non-zero $LL\bar{E}$ couplings, they obtain limits on the electron sneutrino mass of 88 GeV for direct decays and of 87 GeV for indirect decays with a low mass $\tilde{\chi}_1^0$. For non-zero $LQ\bar{D}$ couplings, the limits are 86 GeV for indirect decays of $\tilde{\nu}_e$ with a low mass $\tilde{\chi}_1^0$ and 80 GeV for direct decays of $\tilde{\nu}_e$. There exists a region of small Δm , of varying size, for which no limit is obtained, see Fig. 20. It is assumed that $\tan\beta=1.5$ and $\mu=-200$ GeV. For muon sneutrinos, direct decays via $LL\bar{E}$ couplings lead to a 66 GeV mass limit and via $LQ\bar{D}$ couplings to a 58 GeV limit.
- 113 **ABREU 00i** studies decays induced by R -parity-violating $LL\bar{E}$ couplings, using data from $\sqrt{s}=183$ GeV. They investigate topologies with multiple leptons or jets plus leptons, assuming one coupling at the time to be non-zero and giving rise to direct or indirect decays. The limits, valid for each individual flavor, are determined by the indirect decays and assume a neutralino mass limit of 27 GeV, also derived in **ABREU 00i**. Better limits for specific flavors and for specific \tilde{R} couplings can be obtained and are discussed in the paper.
- 114 **BARATE 00h** data collected at $\sqrt{s}=183$ GeV. The limit holds for indirect $\tilde{\nu}$ decays mediated by $\tilde{R} LL\bar{E}$ couplings, and improves to 66 GeV for direct decays. Better limits are obtained for specific flavors, or couplings. Limits are also given for direct decays via $LQ\bar{D}$ couplings ($m_{\mu,\tau} > 59$ GeV) and for indirect decays via $U\bar{D}\bar{D}$ couplings ($m_{\nu_e} > 70$ GeV with $\mu=-200$ GeV and $\tan\beta=2$). For $LL\bar{E}$ indirect decays, use is made of neutralino mass limits from **BARATE 98s**.
- 115 **ABBIENDI 99** studied the effect of s - and t -channel τ or μ sneutrino exchange in $e^+e^- \rightarrow e^+e^-$ at $\sqrt{s}=130-183$ GeV, via the R -parity violating coupling $\lambda_{1j1} L_1 L_j e_1^c$ ($j=2$ or 3). The limits quoted here hold for $\lambda_{1j1} > 0.13$. The effect of t -channel electron-sneutrino exchange on rate and asymmetries of $e^+e^- \rightarrow \tau^+\tau^-$ leads to weaker limits on the electron sneutrino mass.
- 116 **ABBIENDI 99** studied the effect of s -channel τ sneutrino exchange in $e^+e^- \rightarrow \mu^+\mu^-$ at $\sqrt{s}=130-183$ GeV, in presence of the R -parity violating couplings $\lambda_{131} L_1 L_3 e_1^c$ ($j=1$ and 2), with $\lambda_{131}=\lambda_{232}$. The limits quoted here hold for $\lambda_{131} > 0.09$.
- 117 **ABBIENDI 99** studied the effect of t -channel electron sneutrino exchange in $e^+e^- \rightarrow \tau^+\tau^-$ at $\sqrt{s}=130-183$ GeV, in presence of the R -parity violating couplings $\lambda_{131} L_1 L_3 e_1^c$. The limits quoted here hold for $\lambda_{131} > 0.6$.
- 118 **ABREU 99a** searches for anomalies in the production cross sections and forward-backward asymmetries of the $\ell^+\ell^- (\gamma)$ final states ($\ell=e,\mu,\tau$) from e^+e^- collisions at $\sqrt{s}=130-172$ GeV. Limits are set on the s - and t -channel exchange of sneutrinos in the presence of \tilde{R} with $\lambda LL\bar{e}^c$ couplings. For points between the energies at which data were taken, information is obtained from events in which a photon was radiated. Exclusion limits in the $(\lambda, m_{\tilde{\nu}_j})$ plane are given in Fig. 13.
- 119 **BARATE 99E** looked for $\tilde{\nu}_\mu$ pairs with decay $\tilde{\nu}_\mu \rightarrow jj$ via R -violating coupling $LQ\bar{D}$. Data collected at $\sqrt{s}=130-172$ GeV.
- 120 **BARATE 98s** looked for $\tilde{\nu}_\tau$ pairs with decay $\tilde{\nu}_\tau \rightarrow \ell\tilde{\chi}_1^0$, where $\tilde{\chi}_1^0$ further decays to $\ell^+ \ell^- \nu$ via R -violating coupling $LL\bar{E}$. The limit assumes $\tan\beta=2$. The bound on $\tilde{\nu}_e$ is for the higgsino region. It improves to 72 GeV for the gaugino region. Data collected at $\sqrt{s}=130-172$ GeV.
- 121 **ACCIARRI 97u** studied the effect of the s -channel tau-sneutrino exchange in $e^+e^- \rightarrow e^+e^-$ at $\sqrt{s}=m_Z$ and $\sqrt{s}=130-172$ GeV, via the R -parity violating coupling $\lambda_{131} L_1 L_3 e_1^c$. The limits quoted here hold for $\lambda_{131} > 0.05$. Similar limits were studied in $e^+e^- \rightarrow \mu^+\mu^-$ together with $\lambda_{232} L_2 L_3 e_2^c$ coupling.
- 122 **CARENA 97** studied the constraints on chargino and sneutrino masses from muon $g-2$. The bound can be important for large $\tan\beta$.
- 123 **BUSKULIC 95e** looked for $Z \rightarrow \tilde{\nu}\tilde{\nu}$, where $\tilde{\nu} \rightarrow \nu\tilde{\chi}_1^0$ and $\tilde{\chi}_1^0$ decays via R -parity violating interactions into two leptons and a neutrino.
- 124 **BECK 94** limit can be inferred from limit on Dirac neutrino using $\sigma(\tilde{\nu}) = 4\sigma(\nu)$. Also private communication with H.V. Klapdor-Kleingrothaus.
- 125 **FALK 94** puts an upper bound on $m_{\tilde{\nu}_j}$ when $\tilde{\nu}$ is LSP by requiring its relic density does not overclose the Universe.
- 126 **SATO 91** search for high-energy neutrinos from the sun produced by annihilation of sneutrinos in the sun. Sneutrinos are assumed to be stable and to constitute dark matter in our galaxy. **SATO 91** follow the analysis of **NG 87**, **OLIVE 88**, and **GAISSER 86**.

CHARGED SLEPTONS

This section contains limits on charged scalar leptons ($\tilde{\ell}$, with $\ell=e,\mu,\tau$). Studies of width and decays of the Z boson (use is made here of $\Delta\Gamma_{\text{inv}} < 2.0$ MeV, **LEP 00**) conclusively rule out $m_{\tilde{\ell}_R} < 40$ GeV (41 GeV for $\tilde{\ell}_L$), independently of decay modes, for each individual slepton. The limits improve to 43 GeV (43.5 GeV for $\tilde{\ell}_L$) assuming all 3 flavors to be degenerate. Limits on higher mass sleptons depend on model assumptions and on the mass splitting $\Delta m = m_{\tilde{\ell}_L} - m_{\tilde{\ell}_R}$. The mass and composition of $\tilde{\chi}_1^0$ may affect the slepton production rate in e^+e^- collisions through t -channel exchange diagrams. Production rates are also affected by the potentially large mixing angle of the lightest mass eigenstate $\tilde{\ell}_1 = \tilde{\ell}_R \sin\theta_\ell + \tilde{\ell}_L \cos\theta_\ell$. It is generally assumed that only $\tilde{\tau}$ may have significant mixing. The coupling to the Z vanishes for $\theta_\ell=0.82$. In the high-energy limit of e^+e^- collisions the interference between γ and Z exchange leads to a minimal cross section for $\theta_\ell=0.91$, a value which is sometimes used in the following entries relative to data taken at LEP2. When limits on $m_{\tilde{\ell}_R}$ are quoted, it is understood that limits on $m_{\tilde{\ell}_L}$ are usually at least as strong.

Possibly open decays involving gauginos other than $\tilde{\chi}_1^0$ will affect the detection efficiencies. Unless otherwise stated, the limits presented here result from the study of $\tilde{\ell}^+\tilde{\ell}^-$ production, with production rates and decay properties derived from the MSSM. Limits made obsolete by the recent analyses of e^+e^- collisions at energies above 161 GeV have been

removed from this compilation, and can be found in the 1998 Edition (The European Physical Journal **C** 1 (1998)) of this Review.

For decays with final state gravitinos (\tilde{G}), $m_{\tilde{G}}$ is assumed to be negligible relative to all other masses.

\tilde{e} (Selectron) MASS LIMIT

VALUE (GeV)	CL%	DOCUMENT ID	TECN	COMMENT
>87.1	95	127 ABBIENDI	00G OPAL	$\Delta m > 5$ GeV, $\tilde{e}_R^+ \tilde{e}_R^-$
none 45-73.7	95	128 ABREU	99C DLPH	$m_{\tilde{\chi}_1^0} < 40$ GeV, $\tilde{e}_R^+ \tilde{e}_R^-$
>85.0	95	129 ACCIARRI	99W L3	$\Delta m > 7$ GeV, $\tilde{e}_R^+ \tilde{e}_R^-$
>88	95	130 BARATE	99Q ALEP	$\Delta m > 8$ GeV, $\tilde{e}_R^+ \tilde{e}_R^-$
• • • We do not use the following data for averages, fits, limits, etc. • • •				
>72	95	131 ABBIENDI	00 OPAL	$\tilde{e}_R^+ \tilde{e}_R^-$, \tilde{R} , light $\tilde{\chi}_1^0$
>61	95	132 ABREU	00i DLPH	\tilde{e}_R , \tilde{R} ($LL\bar{E}$)
>85	95	133 BARATE	00G ALEP	$\tilde{\ell}_R \rightarrow \ell\tilde{G}$, any $\tau(\tilde{\ell}_R)$
>76	95	134 BARATE	00h ALEP	\tilde{e}_R , \tilde{R} ($LL\bar{E}$)
>80	95	135 ACCIARRI	99H L3	$\tilde{e}_R^+ \tilde{e}_R^-$, $\Delta m > 20$ GeV
>29.5	95	136 ACCIARRI	99I L3	\tilde{e}_R , \tilde{R} , $\tan\beta \geq 2$
>57	95	137 BARATE	99E ALEP	\tilde{e}_R , \tilde{R} ($LQ\bar{D}$), $\Delta m > 10$ GeV
>56	95	138 ACCIARRI	98F L3	$\Delta m > 5$ GeV, $\tilde{e}_R^+ \tilde{e}_R^-$, $\tan\beta \geq 1.41$
>58.0	95	139 ACKERSTAFF	98k OPAL	$\Delta m > 5$ GeV, $\tilde{e}_R^+ \tilde{e}_R^-$
>78	95	140 BARATE	98k ALEP	$\Delta m > 5$ GeV, $\tilde{e}_R^+ \tilde{e}_R^-$
>77	95	141 BARATE	98k ALEP	Any Δm , $\tilde{e}_R^+ \tilde{e}_R^-$, $\tilde{e}_R \rightarrow e\gamma\tilde{G}$
>71	95	142 BARATE	98k ALEP	$\tilde{e}_R^+ \tilde{e}_R^-$, $\tilde{e}_R \rightarrow e\tilde{G}$, any $\tau(\tilde{e}_R)$
>65	95	143 BARATE	98k ALEP	$\tilde{e}_R^+ \tilde{e}_R^-$, $\tilde{e}_R \rightarrow e\tilde{G}$, universal scalar mass
>64	95	144 BARATE	98s ALEP	\tilde{e}_R , \tilde{R} ($LL\bar{E}$)
>77	95	145 BREITWEG	98 ZEUS	$m_{\tilde{q}}=m_{\tilde{e}}$, $m(\tilde{\chi}_1^0)=40$ GeV
>58	95	146 BARATE	97N ALEP	$\Delta m > 3$ GeV, $\tilde{e}_R^+ \tilde{e}_R^-$
>63	95	147 AID	96C H1	$m_{\tilde{q}}=m_{\tilde{e}}$, $m_{\tilde{\chi}_1^0}=35$ GeV
>45.6	95	148 BUSKULIC	95E ALEP	$\tilde{e} \rightarrow e\nu\tilde{\ell}$

- 127 **ABBIENDI 00g** looked for acoplanar dielectron + $\tilde{B}\tilde{T}$ final states at $\sqrt{s}=183-189$ GeV. The limit assumes $\mu < -100$ GeV and $\tan\beta=1.5$ for the production cross section and decay branching ratios, evaluated within the MSSM, and zero efficiency for decays other than $\tilde{e} \rightarrow e\tilde{\chi}_1^0$. See their Fig. 14 for the dependence of the limit on Δm and $\tan\beta$.
- 128 **ABREU 99c** looked for acoplanar dielectron + \tilde{B} final states at $\sqrt{s}=130-172$ GeV. The limit assumes $\mu=-200$ GeV and $\tan\beta=1.5$ in the calculation of the production cross section, and $B(\tilde{e} \rightarrow e\tilde{\chi}_1^0)=100\%$. See Fig. 8a for limits on the $(m_{\tilde{e}_R}, m_{\tilde{\chi}_1^0})$ plane and for different $\tan\beta$ values. These results include and update limits from **ABREU 96o**.
- 129 **ACCIARRI 99w** looked for acoplanar dielectron $\tilde{B}\tilde{T}$ final states at $\sqrt{s}=130-189$ GeV. The limit assumes $\mu=-200$ GeV and $\tan\beta=\sqrt{2}$ for the production cross section and decay branching ratios, evaluated within the MSSM, and zero efficiency for decays other than $\tilde{e} \rightarrow e\tilde{\chi}_1^0$. The scan of parameter space, covering the region $1 < \tan\beta < 60$, $M_2 < 2$ TeV, $|\mu| < 2$ TeV, $m_0 < 500$ GeV, leads to an absolute lower limit of 65.5 GeV. See their Figs. 5-6 for the dependence of the limit on Δm and $\tan\beta$.
- 130 **BARATE 99Q** looked for acoplanar dielectron + $\tilde{B}\tilde{T}$ final states at $\sqrt{s}=189$ GeV. The limit assumes $\mu=-200$ GeV and $\tan\beta=2$ for the production cross section and decay branching ratios, and zero efficiency for decays other than $\tilde{e} \rightarrow e\tilde{\chi}_1^0$. Assuming a common scalar mass at the GUT scale, and extending the search to $\tilde{e}_R^+ \tilde{e}_L^+$ final states, a Δm independent limit of 68 GeV is obtained. See their Fig. 3 for the dependence of the limit on Δm . The limits presented here make use of, and supersede, the results of **BARATE 98k**.
- 131 **ABBIENDI 00** searches for the production of selectrons in the case of R -parity violation with $LL\bar{E}$ or $LQ\bar{D}$ couplings, using data from $\sqrt{s}=183$ GeV. They investigate topologies with multiple leptons, jets plus leptons, or multiple jets, assuming one coupling at the time to be non-zero and giving rise to direct or indirect decays. For non-zero $LL\bar{E}$ couplings, they obtain limits on the selectron mass of 84 GeV both for direct decays and for indirect decays with a low mass $\tilde{\chi}_1^0$. For non-zero $LQ\bar{D}$ couplings, the limits are 72 GeV for indirect decays of \tilde{e}_R with a low mass $\tilde{\chi}_1^0$ and 76 GeV for direct decays of \tilde{e}_L . It is assumed that $\tan\beta=1.5$ and $\mu=-200$ GeV.
- 132 **ABREU 00i** studies decays induced by R -parity-violating $LL\bar{E}$ couplings, using data from $\sqrt{s}=183$ GeV. They investigate topologies with multiple leptons or jets plus leptons, assuming one coupling at the time to be non-zero and giving rise to direct or indirect decays. The limits, valid for each individual flavor, are determined by the indirect decays and assume a neutralino mass limit of 27 GeV, also derived in **ABREU 00i**. Better limits for specific flavors and for specific \tilde{R} couplings can be obtained and are discussed in the paper.
- 133 **BARATE 00G** combines the search for acoplanar dileptons, leptons with large impact parameters, kinks, and stable heavy-charged tracks, assuming 3 flavors of degenerate sleptons, produced in the s channel. Data collected at $\sqrt{s}=189$ GeV.
- 134 **BARATE 00h** data collected at $\sqrt{s}=183$ GeV. The limit holds for indirect decays mediated by $\tilde{R} LL\bar{E}$ couplings, and improves to 82 GeV for direct decays with $\mu=-200$ GeV and $\tan\beta=2$. Limits are also given for indirect decays via $U\bar{D}\bar{D}$ couplings ($m_{\tilde{e}_R} > 81$ and $m_{\tilde{e}_L} > 70$ GeV, with $\Delta m > 10$ GeV). For $LL\bar{E}$ indirect decays, use is made of neutralino mass limits from **BARATE 98s**.
- 135 **ACCIARRI 99h** looked for acoplanar dilepton + $\tilde{B}\tilde{T}$ final states at $\sqrt{s}=130-183$ GeV. The limit assumes $\mu=-200$ GeV and $\tan\beta=\sqrt{2}$ for the production cross section and zero efficiency for decays other than $\tilde{e} \rightarrow e\tilde{\chi}_1^0$. See Fig. 6 for the dependence of the limit on Δm .
- 136 **ACCIARRI 99i** establish indirect limits on $m_{\tilde{e}_R}$ from the regions excluded in the M_2 versus m_0 plane by their chargino and neutralino searches at $\sqrt{s}=130-183$ GeV. The situations where the $\tilde{\chi}_1^0$ is the LSP (indirect decays) and where a $\tilde{\ell}$ is the LSP (direct

Searches Particle Listings

Supersymmetric Particle Searches

- decays) were both considered. The weakest limit, quoted above, comes from direct decays with UDD couplings; $LL\bar{E}$ couplings or indirect decays lead to a stronger limit.
- 137 BARATE 99E looked for \tilde{e}_R pairs with decay $\tilde{e}_R \rightarrow e\tilde{\chi}_1^0$, where $\tilde{\chi}_1^0$ further decays via R -violating coupling $LQ\bar{D}$. The limit assumes gaugino-like $\tilde{\chi}_1^0$. The limit is 52 GeV for the case of \tilde{e}_L pair production with $\tilde{e}_L \rightarrow jj$ decay. Data collected at $\sqrt{s}=130$ –172 GeV.
- 138 ACCIARRI 98F looked for acoplanar dilepton+ \tilde{B} final states at $\sqrt{s}=130$ –172 GeV. The limit assumes $\mu=200$ GeV, and zero efficiency for decays other than $\tilde{e}_R \rightarrow e\tilde{\chi}_1^0$. See their Fig. 6 for the dependence of the limit on Δm .
- 139 ACKERSTAFF 98K looked for dielectron+ \tilde{B} final states at $\sqrt{s}=130$ –172 GeV. The limit assumes $\mu < 100$ GeV, $\tan\beta=35$, and zero efficiency for decays other than $\tilde{e}_R \rightarrow e\tilde{\chi}_1^0$. The limit improves to 66.5 GeV for $\tan\beta=1.5$.
- 140 BARATE 98K looked for acoplanar dielectron + \tilde{B} final states at $\sqrt{s}=161$ –184 GeV. The limit assumes $\mu=200$ GeV and $\tan\beta=2$ in the calculation of the production cross section, and $B(\tilde{e} \rightarrow e\tilde{\chi}_1^0)=100\%$. See Fig. 3 for limits on the $(m_{\tilde{e}_R}, m_{\tilde{\chi}_1^0})$ plane and for the effect of cascade decays.
- 141 BARATE 98K looked for $e^+e^-\gamma\gamma + \tilde{B}$ final states at $\sqrt{s}=161$ –184 GeV. The limit assumes $\mu=200$ GeV and $\tan\beta=2$ for the evaluation of the production cross section. See Fig. 4 for limits on the $(m_{\tilde{e}_R}, m_{\tilde{\chi}_1^0})$ plane and for the effect of cascade decays.
- 142 BARATE 98K combines the search for acoplanar dielectrons, electrons with large impact parameters, kinks, and stable heavy charged tracks at $\sqrt{s}=161$ –184 GeV. The limit assumes no t -channel neutralino exchange diagram which can make the bound weaker. See Fig. 5 for limits as a function of the lifetime $\tau(\tilde{e}_R)$.
- 143 BARATE 98K combines the search for acoplanar dileptons and single electrons with universal scalar mass assumption at the GUT scale. The limit holds for all Δm , and assumes $\mu=200$ GeV and $\tan\beta=2$ for the evaluation of the \tilde{e} production cross section.
- 144 BARATE 98S looked for \tilde{e}_R pairs with decay $\tilde{e}_R \rightarrow e\tilde{\chi}_1^0$, where $\tilde{\chi}_1^0$ further decays to $\ell^+\ell^-\nu$ via R -violating coupling $LL\bar{E}$. The limit assumes $\tan\beta=2$ and gaugino-like $\tilde{\chi}_1^0$. Data collected at $\sqrt{s}=130$ –172 GeV.
- 145 BREITWEG 98 used positron+jet events with missing energy and momentum to look for $e^+q \rightarrow \tilde{e}q$ via gaugino-like neutralino exchange with decays into $(e\tilde{\chi}_1^0)(q\tilde{\chi}_1^0)$. See paper for dependences in $m(\tilde{q})$, $m(\tilde{\chi}_1^0)$.
- 146 BARATE 97N uses e^+e^- data collected at $\sqrt{s}=161$ and 172 GeV. The limit is for $\tan\beta=2$. It improves to 75 GeV if $\Delta m > 35$ GeV.
- 147 AID 96C used positron+jet events with missing energy and momentum to look for $e^+q \rightarrow \tilde{e}q$ via neutralino exchange with decays into $(e\tilde{\chi}_1^0)(q\tilde{\chi}_1^0)$. See the paper for dependences on $m_{\tilde{q}}$, $m_{\tilde{\chi}_1^0}$.
- 148 BUSKULIC 95E looked for $Z \rightarrow \tilde{e}_R^+\tilde{e}_R^-$ where $\tilde{e}_R \rightarrow e\tilde{\chi}_1^0$ and $\tilde{\chi}_1^0$ decays via R -parity violating interactions into two leptons and a neutrino.

$\tilde{\mu}$ (Smuon) MASS LIMIT

VALUE (GeV)	CL%	DOCUMENT ID	TECN	COMMENT
>82.3	95	149 ABBIENDI	00G OPAL	$\Delta m > 3$ GeV, $\tilde{\mu}_R^+\tilde{\mu}_R^-$
none 45–58.6	95	150 ABREU	99C DLPH	$\Delta m > 5$ GeV, $\tilde{\mu}_R^+\tilde{\mu}_R^-$
>76.6	95	151 ACCIARRI	99W L3	$\Delta m > 5$ GeV, $\tilde{\mu}_R^+\tilde{\mu}_R^-$
>80	95	152 BARATE	99Q ALEP	$\Delta m > 5$ GeV, $\tilde{\mu}_R^+\tilde{\mu}_R^-$
• • • We do not use the following data for averages, fits, limits, etc. • • •				
>50	95	153 ABBIENDI	00 OPAL	$\tilde{\mu}_R^+\tilde{\mu}_R^-$, R , $\Delta m > 5$ GeV
>61	95	154 ABREU	00I DLPH	$\tilde{\mu}_R$, R ($LL\bar{E}$)
>85	95	155 BARATE	00G ALEP	$\tilde{\ell}_R \rightarrow \tilde{\ell}\tilde{G}$, any $\tau(\tilde{\ell}_R)$
>61	95	156 BARATE	00H ALEP	$\tilde{\mu}_R$, R ($LL\bar{E}$)
>66	95	157 ACCIARRI	99H L3	$\Delta m > 6$ GeV, $\tilde{\mu}_R^+\tilde{\mu}_R^-$
>45	95	158 BARATE	99E ALEP	$\tilde{\mu}_R$, R ($LQ\bar{D}$), $\Delta m > 10$ GeV
>55	95	159 ACCIARRI	98F L3	$\Delta m > 5$ GeV, $\tilde{\mu}_R^+\tilde{\mu}_R^-$
>55.6	95	160 ACKERSTAFF	98K OPAL	$\Delta m > 4$ GeV, $\tilde{\mu}_R^+\tilde{\mu}_R^-$
>71	95	161 BARATE	98K ALEP	$\Delta m > 5$ GeV, $\tilde{\mu}_R^+\tilde{\mu}_R^-$
>77	95	162 BARATE	98K ALEP	Any Δm , $\tilde{\mu}_R^+\tilde{\mu}_R^-$, $\tilde{\mu}_R \rightarrow \mu\gamma\tilde{G}$
>71	95	163 BARATE	98K ALEP	$\tilde{\mu}_R^+\tilde{\mu}_R^-$, $\tilde{\mu}_R \rightarrow \mu\gamma\tilde{G}$, any $\tau(\tilde{\mu}_R)$
>62	95	164 BARATE	98S ALEP	$\tilde{\mu}_R$, R ($LL\bar{E}$)
>51	95	165 ACKERSTAFF	97H OPAL	$\Delta m > 5$ GeV, $\tilde{\mu}_R^+\tilde{\mu}_R^-$
>59	95	166 BARATE	97N ALEP	$\Delta m > 10$ GeV, $\tilde{\mu}_R^+\tilde{\mu}_R^-$
>45.6	95	167 BUSKULIC	95E ALEP	$\tilde{\mu} \rightarrow \mu\nu\tilde{\ell}$
>45	95	ADRIANI	93M L3	$m_{\tilde{\chi}_1^0} < 40$ GeV, $\tilde{\mu}_R^+\tilde{\mu}_R^-$
>45	95	DECAMP	92 ALEP	$m_{\tilde{\chi}_1^0} < 41$ GeV, $\tilde{\mu}_R^+\tilde{\mu}_R^-$

- 149 ABBIENDI 00G looked for acoplanar dimuon + \tilde{B} final states at $\sqrt{s}=183$ –189 GeV. The limit assumes $B(\tilde{\mu} \rightarrow \mu\tilde{\chi}_1^0)=1$. Using decay branching ratios derived from the MSSM, a lower limit of 81.7 GeV is obtained for $\mu < 100$ GeV and $\tan\beta=1.5$. See their Figs. 12 and 15 for the dependence of the limits on the branching ratio and on Δm .
- 150 ABREU 99C looked for acoplanar dimuon + \tilde{B} final states at $\sqrt{s}=130$ –172 GeV. The limit assumes $B(\tilde{\mu} \rightarrow \mu\tilde{\chi}_1^0)=100\%$. See Fig. 8b for limits on the $(m_{\tilde{\mu}_R}, m_{\tilde{\chi}_1^0})$ plane. These results include update limits from ABREU 960.
- 151 ACCIARRI 99W looked for acoplanar dimuon + \tilde{B} final states at $\sqrt{s}=189$ GeV. The limit assumes $\mu=200$ GeV and $\tan\beta=\sqrt{2}$ and zero efficiency for decays other than $\tilde{\mu} \rightarrow \mu\tilde{\chi}_1^0$. See their Fig. 5 for the dependence of the limit on Δm and $\tan\beta$.
- 152 BARATE 99Q looked for acoplanar dimuon + \tilde{B} final states at $\sqrt{s}=189$ GeV. The limit assumes $\mu=200$ GeV and $\tan\beta=2$ for the decay branching ratios, evaluated within the MSSM, and zero efficiency for decays other than $\tilde{\mu} \rightarrow \mu\tilde{\chi}_1^0$. See their Fig. 3 for the dependence of the limit on Δm . The limits presented here make use of, and supersede, the results of BARATE 98K.

- 153 ABBIENDI 00 searches for the production of smuons in the case of R -parity violation with $LL\bar{E}$ or $LQ\bar{D}$ couplings, using data from $\sqrt{s}=183$ GeV. They investigate topologies with multiple leptons, jets plus leptons, or multiple jets, assuming one coupling at the time to be non-zero and giving rise to direct or indirect decays. For non-zero $LL\bar{E}$ couplings, they obtain limits on the smuon mass of 66 GeV for direct decays and of 74 GeV for indirect decays with a low mass $\tilde{\chi}_1^0$. For non-zero $LQ\bar{D}$ couplings, the limits are 50 GeV for indirect decays of $\tilde{\mu}_R$ with a low mass $\tilde{\chi}_1^0$ and 64 GeV for direct decays of $\tilde{\mu}_L$. It is assumed that $\tan\beta=1.5$ and $\mu=200$ GeV.
- 154 ABREU 00I studies decays induced by R -parity-violating $LL\bar{E}$ couplings, using data from $\sqrt{s}=183$ GeV. They investigate topologies with multiple leptons or jets plus leptons, assuming one coupling at the time to be non-zero and giving rise to direct or indirect decays. The limits, valid for each individual flavor, are determined by the indirect decays and assume a neutralino mass limit of 27 GeV, also derived in ABREU 00I. Better limits for specific flavors and for specific R couplings can be obtained and are discussed in the paper.
- 155 BARATE 00G combines the search for acoplanar dileptons, leptons with large impact parameters, kinks, and stable heavy-charged tracks, assuming 3 flavors of degenerate sleptons, produced in the s channel. Data collected at $\sqrt{s}=189$ GeV.
- 156 BARATE 00H data collected at $\sqrt{s}=183$ GeV. The limit holds for direct decays mediated by R $LL\bar{E}$ couplings, and improves to 74 GeV for indirect decays. Limits are also given for direct decays via $LQ\bar{D}$ couplings ($m_{\tilde{\mu}_L} > 61$ GeV) for indirect decays via UDD couplings ($m_{\tilde{\mu}_R} > 67$ GeV and $m_{\tilde{\mu}_L} > 70$ GeV, with $\Delta m > 10$ GeV). For $LL\bar{E}$ indirect decays, use is made of neutralino mass limits from BARATE 98S.
- 157 ACCIARRI 99H looked for acoplanar dimuon + \tilde{B} final states at $\sqrt{s}=130$ –183 GeV. The limit assumes $\mu=200$ GeV and $\tan\beta=\sqrt{2}$ and zero efficiency for decays other than $\tilde{\mu} \rightarrow \mu\tilde{\chi}_1^0$. See Fig. 6 for the dependence of the limit on Δm .
- 158 BARATE 99E looked for $\tilde{\mu}_R$ pairs with decay $\tilde{\mu}_R \rightarrow \mu\tilde{\chi}_1^0$, where $\tilde{\chi}_1^0$ further decays via R -violating coupling $LQ\bar{D}$. The limit is 52 GeV for the case of $\tilde{\mu}_L$ pair production with $\tilde{\mu}_L \rightarrow jj$ decay. Data collected at $\sqrt{s}=130$ –172 GeV.
- 159 ACCIARRI 98F looked for dimuon+ \tilde{B} final states at $\sqrt{s}=130$ –172 GeV. The limit assumes $\mu=200$ GeV, and zero efficiency for decays other than $\tilde{\mu}_R \rightarrow \mu\tilde{\chi}_1^0$. See their Fig. 6 for the dependence of the limit on Δm .
- 160 ACKERSTAFF 98K looked for dimuon+ \tilde{B} final states at $\sqrt{s}=130$ –172 GeV. The limit assumes $\mu < 100$ GeV, $\tan\beta=1.5$, and zero efficiency for decays other than $\tilde{\mu}_R \rightarrow \mu\tilde{\chi}_1^0$. The limit improves to 62.7 GeV for $B(\tilde{\mu}_R \rightarrow \mu\tilde{\chi}_1^0)=1$.
- 161 BARATE 98K looked for acoplanar dimuon + \tilde{B} final states at $\sqrt{s}=161$ –184 GeV. The limit assumes $B(\tilde{\mu}_R \rightarrow \mu\tilde{\chi}_1^0)=1$. See Fig. 3 for limits on the $(m_{\tilde{\mu}_R}, m_{\tilde{\chi}_1^0})$ plane and for the effect of cascade decays.
- 162 BARATE 98K looked for $\mu^+\mu^-\gamma\gamma + \tilde{B}$ final states at $\sqrt{s}=161$ –184 GeV. See Fig. 4 for limits on the $(m_{\tilde{\mu}_R}, m_{\tilde{\chi}_1^0})$ plane and for the effect of cascade decays.
- 163 BARATE 98K combines the search for acoplanar dimuons, muons with large impact parameters, kinks, and stable heavy charged tracks at $\sqrt{s}=161$ –184 GeV. See Fig. 5 for limits as a function of the lifetime $\tau(\tilde{\mu}_R)$.
- 164 BARATE 98S looked for $\tilde{\mu}_R$ pairs with decay $\tilde{\mu}_R \rightarrow \mu\tilde{\chi}_1^0$, where $\tilde{\chi}_1^0$ further decays to $\ell^+\ell^-\nu$ via R -violating coupling $LL\bar{E}$. The limit assumes $\tan\beta=2$. Data collected at $\sqrt{s}=130$ –172 GeV.
- 165 ACKERSTAFF 97H limit is for $m_{\tilde{\chi}_1^0} > 12$ GeV allowed by their chargino, neutralino search, and for $\tan\beta \geq 1.5$ and $|\mu| > 200$ GeV. The study includes data from e^+e^- collisions at $\sqrt{s}=161$ GeV, as well as at 130–136 GeV (ALEXANDER 97B).
- 166 BARATE 97N uses e^+e^- data collected at $\sqrt{s}=161$ and 172 GeV. The limit assumes $B(\tilde{\mu} \rightarrow \mu\tilde{\chi}_1^0)=1$.
- 167 BUSKULIC 95E looked for $Z \rightarrow \tilde{\mu}_R^+\tilde{\mu}_R^-$, where $\tilde{\mu}_R \rightarrow \mu\tilde{\chi}_1^0$ and $\tilde{\chi}_1^0$ decays via R -parity violating interactions into two leptons and a neutrino.

$\tilde{\tau}$ (Stau) MASS LIMIT

VALUE (GeV)	CL%	DOCUMENT ID	TECN	COMMENT
>81.0	95	168 ABBIENDI	00G OPAL	$\Delta m > 8$ GeV, $\theta_\tau=\pi/2$
none 45–55	95	169 ABREU	99C DLPH	$m_{\tilde{\chi}_1^0} < 34$ GeV, $\theta_\tau=\pi/2$
none 45–52	95	169 ABREU	99C DLPH	$m_{\tilde{\chi}_1^0} < 35$ GeV, $\theta_\tau=0.82$
>71.5	95	170 ACCIARRI	99W L3	$\Delta m > 12$ GeV, $\theta_\tau=\pi/2$
>60	95	170 ACCIARRI	99W L3	$8 < \Delta m < 42$ GeV, $\theta_\tau=0.91$
>71	95	171 BARATE	99Q ALEP	$\Delta m > 13$ GeV, $\theta_\tau=\pi/2$
>66	95	171 BARATE	99Q ALEP	$\theta_\tau=0.91$
• • • We do not use the following data for averages, fits, limits, etc. • • •				
>66	95	172 ABBIENDI	00 OPAL	$\tilde{\tau}_R^+\tilde{\tau}_R^-$, R , light $\tilde{\chi}_1^0$
>61	95	173 ABREU	00I DLPH	$\tilde{\tau}_R$, R ($LL\bar{E}$)
>85	95	174 BARATE	00G ALEP	$\tilde{\ell}_R \rightarrow \tilde{\ell}\tilde{G}$, any $\tau(\tilde{\ell}_R)$
>67	95	175 BARATE	00G ALEP	$\tilde{\tau}_R \rightarrow \tau\tilde{G}$, any $\tau(\tilde{\tau}_R)$
>61	95	176 BARATE	00H ALEP	$\tilde{\tau}_R$, R ($LL\bar{E}$)
>55	95	177 ABREU	99C DLPH	$\tilde{\tau}_R^+\tilde{\tau}_R^-$, $\tilde{\tau}_R \rightarrow \tau\tilde{G}$, any $\tau(\tilde{\tau}_R)$
>68.5	95	178 ABREU	99F DLPH	$\tilde{\tau}_R^+\tilde{\tau}_R^-$, $\tilde{\tau}_R \rightarrow \tau\tilde{G}$, any $\tau(\tilde{\tau}_R)$
>53	95	179 ACCIARRI	99H L3	$\Delta m > 10$ GeV, $\theta_\tau=0.91$
>45	95	180 BARATE	99E ALEP	$\tilde{\tau}_R$, R ($LQ\bar{D}$), $\Delta m > 10$ GeV
>65	95	181 BARATE	98K ALEP	$\Delta m > 10$ GeV, $\theta_\tau=\pi/2$
>62	95	181 BARATE	98K ALEP	$\Delta m > 10$ GeV, $\theta_\tau=0.82$
>52	95	182 BARATE	98K ALEP	Any Δm , $\theta_\tau=\pi/2$, $\tilde{\tau}_R \rightarrow \tau\gamma\tilde{G}$
none 2–35	95	183 BARATE	98K ALEP	$\Delta m > 2$, $\theta_\tau=0.82$
>56	95	184 BARATE	98S ALEP	$\tilde{\tau}_R$, R ($LL\bar{E}$)

- 168 ABBIENDI 00G looked for acoplanar ditau + \tilde{B} final states at $\sqrt{s}=183$ –189 GeV. The limit assumes $B(\tilde{\tau} \rightarrow \tau\tilde{\chi}_1^0)=1$. Using decay branching ratios derived from the MSSM, a lower limit of 75.9 GeV is obtained for $\mu < 100$ GeV and $\tan\beta=1.5$. See their Figs. 13 and 16 for the dependence of the limits on the branching ratio and on Δm .

- 169 ABREU 99c looked for acoplanar ditau + \cancel{B} final states at $\sqrt{s}=130\text{--}172$ GeV. The limit assumes $B(\tilde{\tau}_R \rightarrow \tau \tilde{\chi}_1^0)=1$. See Figs. 4c and 4d for limits on the $(m_{\tilde{\tau}_R}, m_{\tilde{\chi}_1^0})$ plane and as a function of the mixing angle.
- 170 ACCIARRI 99w looked for acoplanar ditau + \cancel{B} final states at $\sqrt{s}=189$ GeV. See their Fig. 5 for the dependence of the limit on Δm and $\tan\beta$.
- 171 BARATE 99Q looked for acoplanar ditau + \cancel{B} final states at $\sqrt{s}=189$ GeV. The limit assumes $B(\tilde{\tau} \rightarrow \tau \tilde{\chi}_1^0)=1$. See their Fig. 3 for the dependence of the limit on Δm . The limits presented here make use of, and supersede, the results of BARATE 98k.
- 172 ABBIENDI 00 searches for the production of staus in the case of R -parity violation with $LL\bar{E}$ or $LQ\bar{D}$ couplings, using data from $\sqrt{s}=183$ GeV. They investigate topologies with multiple leptons, jets plus leptons, or multiple jets, assuming one coupling at the time to be non-zero and giving rise to direct or indirect decays. For non-zero $LL\bar{E}$ couplings, they obtain limits on the stau mass of 66 GeV both for direct decays and for indirect decays with a low mass $\tilde{\chi}_1^0$. For non-zero $LQ\bar{D}$ couplings, the limits are 66 GeV for indirect decays of $\tilde{\tau}_R$ with a low mass $\tilde{\chi}_1^0$ and 63 GeV for direct decays of $\tilde{\tau}_L$. It is assumed that $\tan\beta=1.5$ and $\mu=-200$ GeV.
- 173 ABREU 00i studies decays induced by R -parity-violating $LL\bar{E}$ couplings, using data from $\sqrt{s}=183$ GeV. They investigate topologies with multiple leptons or jets plus leptons, assuming one coupling at the time to be non-zero and giving rise to direct or indirect decays. The limits, valid for each individual flavor, are determined by the indirect decays and assume a neutralino mass limit of 27 GeV, also derived in ABREU 00i. Better limits for specific flavors and for specific \cancel{R} couplings can be obtained and are discussed in the paper.
- 174 BARATE 00g combines the search for acoplanar dileptons, leptons with large impact parameters, kinks, and stable heavy-charged tracks, assuming 3 flavors of degenerate sleptons, produced in the s channel. Data collected at $\sqrt{s}=189$ GeV.
- 175 BARATE 00g combines the search for acoplanar ditau, taus with large impact parameters, kinks, and stable heavy-charged tracks. Staus are also looked for in the decay chain $\tilde{\chi}_1^0 \rightarrow \tilde{\tau} \tau \rightarrow \tau \tau G$; see paper for results. Data collected at $\sqrt{s}=189$ GeV.
- 176 BARATE 00h data collected at $\sqrt{s}=183$ GeV. The limit holds for direct decays mediated by \cancel{R} $LL\bar{E}$ couplings, and improves up to 70 GeV for indirect decays, using the neutralino mass limits from BARATE 98s.
- 177 ABREU 99c combines the search for acoplanar ditau, taus with large impact parameters, kinks, and stable heavy-charged tracks at $\sqrt{s}=130\text{--}172$ GeV. See Fig. 11 for limits under different lifetime hypothesis.
- 178 ABREU 99f combines the search for acoplanar ditau, taus with large impact parameters, kinks, and stable heavy-charged tracks at $\sqrt{s}=130\text{--}183$ GeV. See Fig. 13 for limits under various lifetime scenarios.
- 179 ACCIARRI 99h looked for acoplanar ditau + \cancel{B} final states at $\sqrt{s}=130\text{--}183$ GeV. The limit assumes $\mu=-200$ GeV and $\tan\beta=\sqrt{2}$ and zero efficiency for decays other than $\tilde{\tau} \rightarrow \tau \tilde{\chi}_1^0$. See Fig. 6 for the dependence on the limit on Δm .
- 180 BARATE 99e looked for $\tilde{\tau}_R$ pairs with decay $\tilde{\tau}_R \rightarrow \tau \tilde{\chi}_1^0$, where $\tilde{\chi}_1^0$ further decays via R -violating coupling $LQ\bar{D}$. Data collected at $\sqrt{s}=130\text{--}172$ GeV.
- 181 BARATE 98k looked for acoplanar ditau + \cancel{B} at $\sqrt{s}=161\text{--}184$ GeV. The limit assumes zero efficiency for decays other than $\tilde{\tau}_R \rightarrow \tau \tilde{\chi}_1^0$. See Fig. 3 for limits on the $(m_{\tilde{\tau}_R}, m_{\tilde{\chi}_1^0})$ plane and for the effect of cascade decays.
- 182 BARATE 98k looked for $\tau^+ \tau^- \gamma \gamma + \cancel{B}$ final states at $\sqrt{s}=161\text{--}184$ GeV. See Fig. 4 for limits on the $(m_{\tilde{\tau}_R}, m_{\tilde{\chi}_1^0})$ plane and for the effect of cascade decays.
- 183 This limit also uses BARATE 97n to extend limit to low $m_{\tilde{\tau}}$.
- 184 BARATE 98s looked for $\tilde{\tau}_R$ pairs with decay $\tilde{\tau}_R \rightarrow \tau \tilde{\chi}_1^0$, where $\tilde{\chi}_1^0$ further decays to $\ell^+ \ell^- \nu$ via R -violating coupling $LL\bar{E}$. The limit assumes $\tan\beta=2$. Data collected at $\sqrt{s}=130\text{--}172$ GeV.

Long-lived $\tilde{\tau}$ (Slepton) MASS LIMIT

Limits on scalar leptons which leave detector before decaying. Limits from Z decays are independent of lepton flavor. Limits from continuum $e^+ e^-$ annihilation are also independent of flavor for smuons and staus. However, selectron limits from continuum $e^+ e^-$ annihilation depend on flavor because there is an additional contribution from neutralino exchange that in general yields stronger limits.

VALUE (GeV)	CL%	DOCUMENT ID	TECN	COMMENT
>81.2	95	185 ACCIARRI	99H L3	$\tilde{\mu}_R, \tilde{\tau}_R$
none 2–80	95	186 ABREU	98P DLPH	$\tilde{\mu}_R, \tilde{\tau}_R$
>82.5	95	187 ACKERSTAFF	98P OPAL	$\tilde{\mu}_R, \tilde{\tau}_R$
>81	95	188 BARATE	98K ALEP	$\tilde{\mu}_R, \tilde{\tau}_R$
185 ACCIARRI 99H searched for production of pairs of back-to-back heavy charged particles at $\sqrt{s}=130\text{--}183$ GeV. The upper bound improves to 82.2 GeV for $\tilde{\mu}_L, \tilde{\tau}_L$.				
186 ABREU 98P searches for production of pairs of heavy, charged particles in $e^+ e^-$ annihilation at $\sqrt{s}=130\text{--}183$ GeV. The upper bound improves to 81 GeV for $\tilde{\mu}_L, \tilde{\tau}_L$. These limits include and update the results of ABREU 97D.				
187 ACKERSTAFF 98P bound improves to 83.5 GeV for $\tilde{\mu}_L, \tilde{\tau}_L$. Data collected at $\sqrt{s}=130\text{--}183$ GeV.				
188 The BARATE 98k mass limit improves to 82 GeV for $\tilde{\mu}_L, \tilde{\tau}_L$. Data collected at $\sqrt{s}=161\text{--}184$ GeV.				

\tilde{q} (Squark) MASS LIMIT

For $m_{\tilde{q}} > 60\text{--}70$ GeV, it is expected that squarks would undergo a cascade decay via a number of neutralinos and/or charginos rather than undergo a direct decay to photinos as assumed by some papers. Limits obtained when direct decay is assumed are usually higher than limits when cascade decays are included.

Limits from $e^+ e^-$ collisions depend on the mixing angle of the lightest mass eigenstate $\tilde{q}_1 = \tilde{q}_R \sin\theta_{\tilde{q}} + \tilde{q}_L \cos\theta_{\tilde{q}}$. It is usually assumed that only the sbottom and stop squarks have non-trivial mixing angles (see the stop and sbottom sections). Here, unless otherwise noted, squarks are always taken to be either left/right degenerate, or purely of left or right type. Data from Z decays have set squark mass limits above 40 GeV, in the case of $\tilde{q} \rightarrow q \tilde{\chi}_1^0$ decays if $\Delta m = m_{\tilde{q}} - m_{\tilde{\chi}_1^0} \geq 5$ GeV. For smaller values of Δm , current constraints on the invisible width of the Z ($\Delta\Gamma_{\text{inv}} < 2.0$ MeV, LEP 00)

exclude $m_{\tilde{u}_{L,R}} < 44$ GeV, $m_{\tilde{d}_R} < 33$ GeV, $m_{\tilde{d}_L} < 44$ GeV and, assuming all squarks degenerate, $m_{\tilde{q}} < 45$ GeV.

Limits which are obsolete relative to the current results are not included in this compilation, and can be found in the 1998 Edition (The European Physical Journal C3 1 (1998)) of this Review.

VALUE (GeV)	CL%	DOCUMENT ID	TECN	COMMENT
>250	95	189 ABBOTT	99L D0	$\tan\beta=2, \mu < 0, A=0$
> 91.5	95	190 ACCIARRI	99v L3	$\Delta m > 10$ GeV, $e^+ e^- \rightarrow \tilde{q} \tilde{q}$
> 92	95	191 BARATE	99Q ALEP	$e^+ e^- \rightarrow \tilde{q} \tilde{q}, \Delta m > 10$ GeV
>224	95	192 ABE	96D CDF	$m_{\tilde{g}} \leq m_{\tilde{q}}$; with cascade decays
• • • We do not use the following data for averages, fits, limits, etc. • • •				
> 69	95	193 BARATE	00H ALEP	\tilde{u}_R, \cancel{R} UDD
> 49	95	193 BARATE	00H ALEP	\tilde{d}_R, \cancel{R} UDD
>240	95	194 ABBOTT	99 D0	$\tilde{q} \rightarrow \tilde{\chi}_2^0 X \rightarrow \tilde{\chi}_1^0 \gamma X, m_{\tilde{\chi}_2^0} - m_{\tilde{\chi}_1^0} > 20$ GeV
>320	95	194 ABBOTT	99 D0	$\tilde{q} \rightarrow \tilde{\chi}_1^0 X \rightarrow \tilde{G} \gamma X$
>243	95	195 ABBOTT	99K D0	any $m_{\tilde{g}}, \cancel{R}, \tan\beta=2, \mu < 0$
>200	95	196 ABE	99M CDF	$p\bar{p} \rightarrow \tilde{q} \tilde{q}, \cancel{R}$
>140	95	197 ACCIARRI	98J L3	$e^+ e^- \rightarrow q\tilde{q}, \cancel{R}, \lambda=0.3$
>140	95	197 ACKERSTAFF	98V OPAL	$e^+ e^- \rightarrow q\tilde{q}, \cancel{R}, \lambda=0.3$
> 87	95	198 BARATE	98N ALEP	$e^+ e^- \rightarrow \tilde{q} \tilde{q}, \Delta m > 5$ GeV
> 77	95	199 BREITWEG	98 ZEUS	$m_{\tilde{q}}=m_{\tilde{g}}, m(\tilde{\chi}_1^0)=40$ GeV
		200 DATTA	97 THEO	$\tilde{\nu}$'s lighter than $\tilde{\chi}_1^{\pm}, \tilde{\chi}_2^0$
>216	95	201 DERRICK	97 ZEUS	$e p \rightarrow \tilde{q}, \tilde{q} \rightarrow \mu^j \text{ or } \tau^j, \cancel{R}$
none 130–573	95	202 HEWETT	97 THEO	$q\tilde{g} \rightarrow \tilde{q}, \tilde{q} \rightarrow q\tilde{g}$, with a light gluino
none 190–650	95	203 TEREKHOV	97 THEO	$q\tilde{g} \rightarrow \tilde{q}\tilde{g}, \tilde{q} \rightarrow q\tilde{g}$, with a light gluino
>215	95	204 AID	96 H1	$e^+ p \rightarrow \tilde{q}, \cancel{R}, \lambda=0.3$
>150	95	204 AID	96 H1	$e^+ p \rightarrow \tilde{q}; \cancel{R}, \lambda=0.3$
> 63	95	205 AID	96C H1	$m_{\tilde{q}}=m_{\tilde{g}}, m_{\tilde{\chi}_1^0}=35$ GeV
none 330–400	95	206 TEREKHOV	96 THEO	$u\tilde{g} \rightarrow \tilde{u}\tilde{g}, \tilde{u} \rightarrow u\tilde{g}$ with a light gluino
>176	95	207 ABACHI	95C D0	Any $m_{\tilde{g}} < 300$ GeV; with cascade decays
		208 ABE	95T CDF	$\tilde{q} \rightarrow \tilde{\chi}_2^0 \rightarrow \tilde{\chi}_1^0 \gamma$
> 45.3	95	209 BUSKULIC	95E ALEP	$\cancel{R}, (LL\bar{E})$
> 90	90	210 ABE	92L CDF	Any $m_{\tilde{g}} < 410$ GeV; with cascade decay
>100		211 ROY	92 RVUE	$p\bar{p} \rightarrow \tilde{q}\tilde{q}; \cancel{R}$
		212 NOJIRI	91 COSM	

- 189 ABBOTT 99L consider events with three or more jets and large \cancel{E}_T . Spectra and decay rates are evaluated in the framework of minimal Supergravity, assuming five flavors of degenerate squarks, and scanning the space of the universal gaugino ($m_{1/2}$) and scalar (m_0) masses. See their Figs. 2–3 for the dependence of the limit on the relative value of $m_{\tilde{q}}$ and $m_{\tilde{g}}$.

- 190 ACCIARRI 99v assumes four degenerate flavors and $B(\tilde{q} \rightarrow q \tilde{\chi}_1^0)=1$, with $\Delta m = m_{\tilde{q}} - m_{\tilde{\chi}_1^0}$. The bound is reduced to 90 GeV if production of only \tilde{q}_R states is considered. See their Fig. 7 for limits in the $(m_{\tilde{q}}, m_{\tilde{\chi}_1^0})$ plane. Data collected at $\sqrt{s}=189$ GeV.

- 191 BARATE 99Q assumes five degenerate flavors and $B(\tilde{q} \rightarrow q \tilde{\chi}_1^0)=1$, with $\Delta m = m_{\tilde{q}} - m_{\tilde{\chi}_1^0}$. Data collected at $\sqrt{s}=189$ GeV. The limits presented here make use of, and update, the results of BARATE 98n.

- 192 ABE 96D searched for production of gluinos and five degenerate squarks in final states containing a pair of leptons, two jets, and missing E_T . The two leptons arise from the semileptonic decays of charginos produced in the cascade decays. The limit is derived for fixed $\tan\beta = 4.0, \mu = -400$ GeV, and $m_{H^\pm} = 500$ GeV, and with the cascade decays of the squarks and gluinos calculated within the framework of the Minimal Supergravity scenario.

- 193 BARATE 00h data collected at $\sqrt{s}=183$ GeV. The limits hold for direct decays of u -type and d -type squarks, mediated by \cancel{R} UDD couplings.

- 194 ABBOTT 99 searched for $\gamma \cancel{B} \tau + \geq 2$ jet final states, and set limits on $\sigma(p\bar{p} \rightarrow \tilde{q} X) \cdot B(\tilde{q} \rightarrow \gamma \cancel{B} X)$. The quoted limits correspond to $m_{\tilde{g}} \geq m_{\tilde{q}}$, with $B(\tilde{\chi}_2^0 \rightarrow \tilde{\chi}_1^0 \gamma)=1$ and $B(\tilde{\chi}_1^0 \rightarrow \tilde{G} \gamma)=1$, respectively. They improve to 310 GeV (360 GeV in the case of $\gamma \tilde{G}$ decay) for $m_{\tilde{g}}=m_{\tilde{q}}$.

- 195 ABBOTT 99k uses events with an electron pair and four jets to search for the decay of the $\tilde{\chi}_1^0$ LSP via \cancel{R} $LQ\bar{D}$ couplings. The particle spectrum and decay branching ratios are taken in the framework of minimal supergravity. An excluded region at 95% CL is obtained in the $(m_0, m_{1/2})$ plane under the assumption that $A_0=0, \mu < 0, \tan\beta=2$ and any one of the couplings $\lambda_{ijk} > 10^{-3}$ ($j=1,2$ and $k=1,2,3$) and from which the above limit is computed. For equal mass squarks and gluinos, the corresponding limit is 277 GeV. The results are essentially independent of A_0 , but the limit deteriorates rapidly with increasing $\tan\beta$ or $\mu > 0$.

- 196 ABE 99m looked in 107 pb^{-1} of $p\bar{p}$ collisions at $\sqrt{s}=1.8$ TeV for events with like sign dielectrons and two or more jets from the sequential decays $\tilde{q} \rightarrow q \tilde{\chi}_1^0$ and $\tilde{\chi}_1^0 \rightarrow e q \tilde{q}'$, assuming \cancel{R} coupling $L_1 Q_j D_k^c$, with $j=2,3$ and $k=1,2,3$. They assume five degenerate squark flavors, $B(\tilde{q} \rightarrow q \tilde{\chi}_1^0)=1, B(\tilde{\chi}_1^0 \rightarrow e q \tilde{q}')=0.25$ for both e^+ and e^- , and $m_{\tilde{g}} \geq 200$ GeV. The limit is obtained for $m_{\tilde{\chi}_1^0} \geq m_{\tilde{q}}/2$ and improves for heavier gluinos or heavier $\tilde{\chi}_1^0$.

Searches Particle Listings

Supersymmetric Particle Searches

- 197 ACKERSTAFF 98V and ACCIARRI 98J studied the interference of t -channel squark (\tilde{d}_R) exchange via R -parity violating $\lambda'_{ijk} L_i Q_j \tilde{d}_k^c$ coupling in $e^+ e^- \rightarrow q \bar{q}$. The limit is for $\lambda'_{ijk} = 0.3$. See paper for related limits on \tilde{u}_L exchange. Data collected at $\sqrt{s}=130-172$ GeV.
- 198 BARATE 98N assumes five degenerate flavors $\tilde{u}_{L,R}, \tilde{d}_{L,R}, \tilde{c}_{L,R}, \tilde{s}_{L,R}, \tilde{b}_{L,R}$, and their direct decay $\tilde{q} \rightarrow q \tilde{\chi}_1^0$. The bound applies for $\Delta m > 5$ GeV. See Fig. 5 for limits in the $(m_{\tilde{q}}, m_{\tilde{\chi}_1^0})$ plane. Data collected at $\sqrt{s}=181-184$ GeV.
- 199 BREITWEG 98 used positron+jets events with missing energy and momentum to look for $e^+ q \rightarrow \tilde{e} \tilde{q}$ via gaugino-like neutralino exchange with decays into $(e \tilde{\chi}_1^0)(q \tilde{\chi}_1^0)$. See paper for dependences in $m_{\tilde{e}}, m_{\tilde{\chi}_1^0}$.
- 200 DATTA 97 argues that the squark mass bound by ABACHI 95C can be weakened by 10-20 GeV if one relaxes the assumption of the universal scalar mass at the GUT-scale so that the $\tilde{\chi}_1^{\pm}, \tilde{\chi}_2^0$ in the squark cascade decays have dominant and invisible decays to $\tilde{\nu}$.
- 201 DERRICK 97 looked for lepton-number violating final states via R -parity violating couplings $\lambda'_{ijk} L_i Q_j \tilde{d}_k$. When $\lambda'_{11k} \lambda'_{ijk} \neq 0$, the process $e u \rightarrow \tilde{d}_k^+ \rightarrow \ell_j u_j$ is possible. When $\lambda'_{1j1} \lambda'_{ijk} \neq 0$, the process $e \bar{d} \rightarrow \tilde{u}_j^+ \rightarrow \ell_j \bar{d}_k$ is possible. 100% branching fraction $\tilde{q} \rightarrow \ell j$ is assumed. The limit quoted here corresponds to $\tilde{t} \rightarrow \tau q$ decay, with $\lambda'=0.3$. For different channels, limits are slightly better. See Table 6 in their paper.
- 202 HEWETT 97 reanalyzed the limits on possible resonances in di-jet mode ($\tilde{q} \rightarrow q \tilde{g}$) from ALITTI 93 quoted in "Limits for Excited q (q^*) from Single Production," ABE 96 in "SCALE LIMITS for Contact Interactions: $A(qqqq)$," and unpublished CDF, $D\Phi$ bounds. The bound applies to the gluino mass of 5 GeV, and improves for lighter gluino. The analysis has gluinos in parton distribution function.
- 203 TEREKHOV 97 improved the analysis of TEREKHOV 96 by including di-jet angular distributions in the analysis.
- 204 AID 96 looked for first-generation squarks as s -channel resonances singly produced in $e^+ p$ collision via the R -parity violating coupling in the superpotential $W=\lambda' L_1 Q_1 \tilde{d}_1^c$. The degeneracy of squarks \tilde{Q}_1 and \tilde{d}_1 is assumed. Eight different channels of possible squark decays are considered.
- 205 AID 96C used positron+jets events with missing energy and momentum to look for $e^+ q \rightarrow \tilde{e} \tilde{q}$ via neutralino exchange with decays into $(e \tilde{\chi}_1^0)(q \tilde{\chi}_1^0)$. See the paper for dependences on $m_{\tilde{e}}, m_{\tilde{\chi}_1^0}$.
- 206 TEREKHOV 96 reanalyzed the limits on possible resonances in di-jet mode ($\tilde{u} \rightarrow u \tilde{g}$) from ABE 95N quoted in "MASS LIMITS for g_A (axigluon)." The bound applies only to the case with a light gluino.
- 207 ABACHI 95C assume five degenerate squark flavors with $m_{\tilde{q}_L} = m_{\tilde{q}_R}$. Sleptons are assumed to be heavier than squarks. The limits are derived for fixed $\tan\beta = 2.0$, $\mu = -250$ GeV, and $m_{H^\pm} = 500$ GeV, and with the cascade decays of the squarks and gluinos calculated within the framework of the Minimal Supergravity scenario. The bounds are weakly sensitive to the three fixed parameters for a large fraction of parameter space. No limit is given for $m_{\text{gluino}} > 547$ GeV.
- 208 ABE 95T looked for a cascade decay of five degenerate squarks into $\tilde{\chi}_2^0$ which further decays into $\tilde{\chi}_1^0$ and a photon. No signal is observed. Limits vary widely depending on the choice of parameters. For $\mu = -40$ GeV, $\tan\beta = 1.5$, and heavy gluinos, the range $50 < m_{\tilde{q}} \text{ (GeV)} < 110$ is excluded at 90% CL. See the paper for details.
- 209 BUSKULIC 95E looked for $Z \rightarrow q \tilde{q}$, where $\tilde{q} \rightarrow q \tilde{\chi}_1^0$ and $\tilde{\chi}_1^0$ decays via R -parity violating interactions into two leptons and a neutrino.
- 210 ABE 92L assume five degenerate squark flavors and $m_{\tilde{q}_L} = m_{\tilde{q}_R}$. ABE 92L includes the effect of cascade decay, for a particular choice of parameters, $\mu = -250$ GeV, $\tan\beta = 2$. Results are weakly sensitive to these parameters over much of parameter space. No limit for $m_{\tilde{q}} \leq 50$ GeV (but other experiments rule out that region). Limits are 10-20 GeV higher if $B(\tilde{q} \rightarrow q \tilde{\gamma}) = 1$. Limit assumes GUT relations between gaugino masses and the gauge coupling; in particular that for $|\mu|$ not small, $m_{\tilde{\chi}_1^0} \approx m_{\tilde{g}}/6$. This last relation implies that as $m_{\tilde{g}}$ increases, the mass of $\tilde{\chi}_1^0$ will eventually exceed $m_{\tilde{q}}$ so that no decay is possible. Even before that occurs, the signal will disappear; in particular no bounds can be obtained for $m_{\tilde{q}} > 410$ GeV. $m_{H^\pm} = 500$ GeV.
- 211 ROY 92 reanalyzed CDF limits on di-lepton events to obtain limits on squark production in R -parity violating models. The 100% decay $\tilde{q} \rightarrow q \tilde{\chi}$ where $\tilde{\chi}$ is the LSP, and the LSP decays either into $\ell q \tilde{d}$ or $\ell \ell \tilde{e}$ is assumed.
- 212 NOJIRI 91 argues that a heavy squark should be nearly degenerate with the gluino in minimal supergravity not to overclose the universe.

Long-lived \tilde{q} (Squark) MASS LIMIT

The following are bounds on long-lived scalar quarks, assumed to hadronise into hadrons with lifetime long enough to escape the detector prior to a possible decay. Limits may depend on the mixing angle of mass eigenstates: $\tilde{q}_1 = \tilde{q}_L \cos\theta_q + \tilde{q}_R \sin\theta_q$. The coupling to the Z^0 boson vanishes for up-type squarks when $\theta_u = 0.98$, and for down type squarks when $\theta_d = 1.17$.

VALUE (GeV)	CL%	DOCUMENT ID	TECN	COMMENT
• • • We do not use the following data for averages, fits, limits, etc. • • •				
none 2-85	95	213 ABREU	98P DLPH	\tilde{u}_L
none 2-81	95	213 ABREU	98P DLPH	\tilde{u}_R
none 2-80	95	213 ABREU	98P DLPH	$\tilde{u}, \theta_u = 0.98$
none 2-83	95	213 ABREU	98P DLPH	\tilde{d}_L
none 5-40	95	213 ABREU	98P DLPH	\tilde{d}_R
none 5-38	95	213 ABREU	98P DLPH	$\tilde{d}, \theta_d = 1.17$
213 ABREU 98P	assumes that 40% of the squarks will hadronise into a charged hadron, and 60% into a neutral hadron which deposits most of its energy in hadron calorimeter. Data collected at $\sqrt{s}=130-183$ GeV.			

\tilde{b} (Sbottom) MASS LIMIT

Limits in $e^+ e^-$ depend on the mixing angle of the mass eigenstate $\tilde{b}_1 = \tilde{b}_L \cos\theta_b + \tilde{b}_R \sin\theta_b$. Coupling to the Z vanishes for $\theta_b \sim 1.17$. As a consequence, no absolute constraint in the mass region $\lesssim 40$ GeV is available in the literature at this time from $e^+ e^-$ collisions. In the Listings below, we use $\Delta m = m_{\tilde{b}_1} - m_{\tilde{\chi}_1^0}$.

VALUE (GeV)	CL%	DOCUMENT ID	TECN	COMMENT
none 80-145		214 AFFOLDER	00D CDF	$\tilde{b} \rightarrow b \tilde{\chi}_1^0, m_{\tilde{\chi}_1^0} < 50$ GeV
>89.8	95	215 ABBIENDI	99M OPAL	$\tilde{b} \rightarrow b \tilde{\chi}_1^0, \theta_b = 0, \Delta m > 10$ GeV
>74.9	95	215 ABBIENDI	99M OPAL	$\tilde{b} \rightarrow b \tilde{\chi}_1^0, \theta_b = 1.17, \Delta m > 10$ GeV
>84	95	216 ACCIARRI	99V L3	$\tilde{b} \rightarrow b \tilde{\chi}_1^0, \theta_b = 0, \Delta m > 15$ GeV
>61	95	216 ACCIARRI	99V L3	$\tilde{b} \rightarrow b \tilde{\chi}_1^0, \theta_b = 1.17, \Delta m > 15$ GeV
>86	95	217 BARATE	99Q ALEP	$\tilde{b} \rightarrow b \tilde{\chi}_1^0, \theta_b = 0, \Delta m > 10$ GeV
>75	95	217 BARATE	99Q ALEP	$\tilde{b} \rightarrow b \tilde{\chi}_1^0, \theta_b = 1.18, \Delta m > 10$ GeV
• • • We do not use the following data for averages, fits, limits, etc. • • •				
none 52-115	95	218 ABBOTT	99F D0	$\tilde{b} \rightarrow b \tilde{\chi}_1^0, m_{\tilde{\chi}_1^0} < 20$ GeV
>73	95	219 ABREU	99C DLPH	$\tilde{b} \rightarrow b \tilde{\chi}_1^0, \theta_b = 0, \Delta m > 10$ GeV
>44	95	219 ABREU	99C DLPH	$\tilde{b} \rightarrow b \tilde{\chi}_1^0, \theta_b = \pi/2, \Delta m > 10$ GeV
>57	95	220 ACCIARRI	99C L3	$\tilde{b} \rightarrow b \tilde{\chi}_1^0, \theta_b = 1.17, \Delta m > 35$ GeV
none 40-54.495		221 ACKERSTAFF	99 OPAL	$\tilde{b} \rightarrow b \tilde{\chi}_1^0, \theta_b = 1.17, \Delta m > 7$ GeV
>54	95	222 BARATE	99E ALEP	$\tilde{b}, \theta_b = 0$
>73	95	223 BARATE	98N ALEP	$\tilde{b} \rightarrow b \tilde{\chi}_1^0, \theta_b = 0, \Delta m > 6$ GeV
>58	95	224 BARATE	98S ALEP	$\tilde{b}, \theta_b = 0$
214 AFFOLDER 00D	search for final states with 2 or 3 jets and \cancel{E}_T , one jet with a b tag. See their Fig. 3 for the mass exclusion in the $m_{\tilde{t}}, m_{\tilde{\chi}_1^0}$ plane.			
215 ABBIENDI 99M	looked for events with two acoplanar jets and \cancel{E}_T . See Fig. 4 and Table 5 for the dependence on the limit on Δm and θ_b . Data taken at $\sqrt{s}=161-189$ GeV. These results supersede ACKERSTAFF 99.			
216 ACCIARRI 99V	looked for events with two acoplanar b -tagged jets and \cancel{E}_T at $\sqrt{s}=189$ GeV. See their Figs. 4 and 6 for the more general dependence of the limits on Δm and θ_b .			
217 BARATE 99Q	looked for events with two acoplanar b -tagged jets and \cancel{E}_T . The limit assumes $B(\tilde{b} \rightarrow b \tilde{\chi}_1^0) = 1$. See their Fig. 2 for the dependence of the limit on Δm and θ_b . Data taken at $\sqrt{s}=189$ GeV.			
218 ABBOTT 99F	looked for events with two jets, with or without an associated muon from b decay, and \cancel{E}_T . See Fig. 2 for the dependence of the limit on $m_{\tilde{\chi}_1^0}$. No limit for $m_{\tilde{\chi}_1^0} > 47$ GeV.			
219 ABREU 99C	looked for \tilde{b} pair production at $\sqrt{s}=130-172$ GeV. See Fig. 4 for other choices of Δm . These results include and update limits from ABREU 960.			
220 ACCIARRI 99C	looked for \tilde{b} pair production at $\sqrt{s}=161-183$ GeV. See Figs. 4-5 for other choices of θ_b and Δm .			
221 ACKERSTAFF 99	looked for \tilde{b} pair production at $\sqrt{s}=130-183$ GeV. The analysis includes and updates the results of ACKERSTAFF 97Q. See Table 11 and Fig. 12 for other choices of θ_b and Δm .			
222 BARATE 99E	looked for \tilde{b}_L pairs with decay $\tilde{b}_L \rightarrow b \tilde{\chi}_1^0$, where $\tilde{\chi}_1^0$ further decays via R -violating coupling $LQ\tilde{D}$. $m_{\tilde{\chi}_1^0} > 30$ GeV. The limit is 73 GeV for the case of \tilde{b}_L pair production with $\tilde{b}_L \rightarrow j\nu$ decay. The limits for \tilde{b}_R pairs with $\tilde{b}_R \rightarrow b\nu j\tau$ are much weaker. Data collected at $\sqrt{s}=130-172$ GeV.			
223 BARATE 98N	data taken at $\sqrt{s}=181-184$ GeV. The limit is significantly reduced for $\theta_b \approx 1.17$.			
224 BARATE 98S	looked for \tilde{b}_L pairs with decay $\tilde{b}_L \rightarrow b \tilde{\chi}_1^0$, where $\tilde{\chi}_1^0$ further decays to $\ell^+ \ell^- \nu$ via R -violating coupling $LL\tilde{E}$. The limit assumes $\tan\beta=2$. Data collected at $\sqrt{s}=130-172$ GeV.			

\tilde{t} (Stop) MASS LIMIT

Limits depend on the decay mode. In $e^+ e^-$ collisions they also depend on the mixing angle of the mass eigenstate $\tilde{t}_1 = \tilde{t}_L \cos\theta_t + \tilde{t}_R \sin\theta_t$. The coupling to the Z vanishes when $\theta_t = 0.98$. In the Listings below, we use $\Delta m \equiv m_{\tilde{t}_1} - m_{\tilde{\chi}_1^0}$ or $\Delta m \equiv m_{\tilde{t}_1} - m_{\tilde{\nu}}$, depending on relevant decay mode. See also bounds in "q (Squark) MASS LIMIT." Previous obsolete limits are not included in this compilation, and can be found in the 1998 Edition (The European Physical Journal C 3 1 (1998)) of this Review.

VALUE (GeV)	CL%	DOCUMENT ID	TECN	COMMENT
> 86.4	95	225 ABBIENDI	99M OPAL	$\tilde{t} \rightarrow c \tilde{\chi}_1^0, \theta_t = 0.98, \Delta m > 5$ GeV
> 88.0	95	225 ABBIENDI	99M OPAL	$\tilde{t} \rightarrow b \ell \nu, \theta_t = 0.98, \Delta m > 10$ GeV
> 87.5	95	225 ABBIENDI	99M OPAL	$\tilde{t} \rightarrow b \tau \tilde{\nu}_\tau, \theta_t = 0.98, \Delta m > 10$ GeV
> 63	95	226 ABREU	99C DLPH	$\tilde{t} \rightarrow c \tilde{\chi}_1^0, \theta_t = 0.98, \Delta m > 10$ GeV
> 81	95	227 ACCIARRI	99V L3	$\tilde{t} \rightarrow c \tilde{\chi}_1^0, \theta_t = 0.96, \Delta m > 15$ GeV
> 86	95	227 ACCIARRI	99V L3	$\tilde{t} \rightarrow b \ell \nu, \theta_t = 0.96, \Delta m > 15$ GeV
> 83	95	227 ACCIARRI	99V L3	$\tilde{t} \rightarrow b \tau \tilde{\nu}_\tau, \theta_t = 0.96, \Delta m > 15$ GeV
> 84	95	228 BARATE	99Q ALEP	$\tilde{t} \rightarrow c \tilde{\chi}_1^0, \text{all } \theta_t, 10 < \Delta m < 40$ GeV
> 86	95	228 BARATE	99Q ALEP	$\tilde{t} \rightarrow b \ell \nu, \text{all } \theta_t, \Delta m > 10$ GeV

• • • We do not use the following data for averages, fits, limits, etc. • • •

> 76	95	229	ABBIENDI	00	OPAL	\mathcal{R} , ($U\bar{D}\bar{D}$), all θ_t
> 61	95	230	ABREU	00i	DLPH	\mathcal{R} ($LL\bar{E}$), $\theta_t=0.98$, $\Delta m > 4$ GeV
none 68–119	95	231	AFFOLDER	00D	CDF	$\tilde{t} \rightarrow c\tilde{\chi}_1^0$, $m_{\tilde{\chi}_1^0} < 40$ GeV
> 58	95	232	BARATE	00H	ALEP	\tilde{t}_L , \mathcal{R} ($U\bar{D}\bar{D}$)
>120	95	233	ABE	99M	CDF	$\rho\bar{\rho} \rightarrow \tilde{t}_1\tilde{t}_1^*$, \mathcal{R}
> 72.5	95	234	ACCIARRI	99C	L3	$\tilde{t} \rightarrow c\tilde{\chi}_1^0$, $\theta_t=0.98$, $\Delta m > 10$ GeV
> 75.8	95	235	ACKERSTAFF	99	OPAL	$\tilde{t} \rightarrow c\tilde{\chi}_1^0$, $\theta_t=0.98$, $\Delta m > 5$ GeV
> 79.2	95	235	ACKERSTAFF	99	OPAL	$\tilde{t} \rightarrow b\tilde{t}\nu$, $\theta_t=0.98$, $\Delta m > 10$ GeV
> 75.0	95	235	ACKERSTAFF	99	OPAL	$\tilde{t} \rightarrow b\tau\tilde{\nu}_\tau$, $\theta_t=0.98$, $\Delta m > 10$ GeV
> 48	95	236	BARATE	99E	ALEP	\mathcal{R} ($LQ\bar{D}$), $\theta_t=0$
> 65	95	237	BARATE	98N	ALEP	$\tilde{t} \rightarrow c\tilde{\chi}_1^0$, $\theta_t=0.98$, $\Delta m > 5$ GeV
> 82	95	237	BARATE	98N	ALEP	$\tilde{t} \rightarrow b\tilde{t}\nu$, any θ_t , $\Delta m > 10$ GeV
> 44	95	238	BARATE	98S	ALEP	\mathcal{R} ($LL\bar{E}$), $\theta_t=0.98$
none 61–91	95	239	ABACHI	96B	D0	$\tilde{t} \rightarrow c\tilde{\chi}_1^0$, $m_{\tilde{\chi}_1^0} < 30$ GeV
none 9–24.4	95	240	AID	96	H1	$e\rho \rightarrow \tilde{t}\tilde{t}^*$, \mathcal{R} decays
>138	95	241	AID	96	H1	$e\rho \rightarrow \tilde{t}, \mathcal{R}$, $\lambda\cos\theta_t > 0.03$
> 45	95	242	CHO	96	RVUE	$B^0\text{-}\bar{B}^0$ and ϵ , $\theta_t = 0.98$, $\tan\beta < 2$
none 11–41	95	243	BUSKULIC	95E	ALEP	\mathcal{R} ($LL\bar{E}$), $\theta_t=0.98$
none 6.0–41.2	95	AKERS	94K	OPAL	$\tilde{t} \rightarrow c\tilde{\chi}_1^0$, $\theta_t=0$, $\Delta m > 2$ GeV	
none 5.0–46.0	95	AKERS	94K	OPAL	$\tilde{t} \rightarrow c\tilde{\chi}_1^0$, $\theta_t=0$, $\Delta m > 5$ GeV	
none 11.2–25.5	95	AKERS	94K	OPAL	$\tilde{t} \rightarrow c\tilde{\chi}_1^0$, $\theta_t=0.98$, $\Delta m > 2$ GeV	
none 7.9–41.2	95	AKERS	94K	OPAL	$\tilde{t} \rightarrow c\tilde{\chi}_1^0$, $\theta_t=0.98$, $\Delta m > 5$ GeV	
none 7.6–28.0	95	244	SHIRAI	94	VNS	$\tilde{t} \rightarrow c\tilde{\chi}_1^0$, any θ_t , $\Delta m > 10$ GeV
none 10–20	95	244	SHIRAI	94	VNS	$\tilde{t} \rightarrow c\tilde{\chi}_1^0$, any θ_t , $\Delta m > 2.5$ GeV
225	ABBIENDI	99M	looked for events with two acoplanar jets, \mathcal{P}_T and, in the case of $b\tilde{t}\nu$ ($b\tau\tilde{\nu}$) final states, two leptons (taus). Limits for θ_t are ~ 2.5 GeV stronger. In the case of $c\tilde{\chi}_1^0$ decays, the limits with $\Delta m > 10$ GeV improve to 90.3 for $\theta_t=0$ and 87.2 for $\theta_t=0.98$. See Figs. 2–3 and Table 4 for the more general dependence of the limits on Δm . Data taken at $\sqrt{s}=161\text{--}189$ GeV. All limits assume 100% branching ratio for the respective decay modes. These results supersede ACKERSTAFF 99.			
226	ABREU	99C	looked for \tilde{t} pair production at $\sqrt{s}=130\text{--}172$ GeV. The limit for θ_t is 72 GeV. See Fig. 4 for other choices of Δm . These results include and update limits from ABREU 96c.			
227	ACCIARRI	99V	looked for events with two acoplanar jets, \mathcal{P}_T and, in the case of $b\tilde{t}\nu$ ($b\tau\tilde{\nu}$) final states, two leptons (taus). The limits for $\theta_t=0$ improve to 88, 89, and 88 GeV, respectively. See their Figs. 4–6 for the more general dependence of the limits on Δm and θ_t . Data taken at $\sqrt{s}=189$ GeV. All limits assume 100% branching ratio for the respective decay modes.			
228	BARATE	99Q	looked for events with two acoplanar jets, \mathcal{P}_T and, in the case of $b\tilde{t}\nu$ final states, two leptons. All limits assume 100% branching ratio for the respective decay modes, with flavor-independent rates in the case of semileptonic decays. See their Fig. 1 for the dependence of the limit on Δm and θ_t . Data taken at $\sqrt{s}=189$ GeV. The limits presented here make use of, and supersede, the results of BARATE 98N.			
229	ABBIENDI	00	searches for the production of stop in the case of R -parity violation with $U\bar{D}\bar{D}$ or $LQ\bar{D}$ couplings, using data from $\sqrt{s}=183$ GeV. They investigate topologies with multiple leptons, jets plus leptons, or multiple jets, assuming one coupling at the time to be non-zero. For mass exclusion limits relative to $LQ\bar{D}$ -induced decays, see their Table 5.			
230	ABREU	00i	searches for the production of stop in the case of R -parity violation with $LL\bar{E}$ couplings, for which only indirect decays are allowed. They investigate topologies with jets plus leptons in data from $\sqrt{s}=183$ GeV. The lower bound on the stop mass assumes a neutralino mass limit of 27 GeV, also derived in ABREU 00i.			
231	AFFOLDER	00D	search for final states with 2 or 3 jets and \mathcal{E}_T , one jet with a c tag. See their Fig. 2 for the mass exclusion in the $(m_{\tilde{t}}, m_{\tilde{\chi}_1^0})$ plane. The maximum excluded $m_{\tilde{t}}$ value is 119 GeV, for $m_{\tilde{\chi}_1^0} = 40$ GeV.			
232	BARATE	00H	data collected at $\sqrt{s}=183$ GeV. The limit holds for indirect decays mediated by \mathcal{R} $U\bar{D}\bar{D}$ couplings, and $m_{\tilde{\chi}_1^0} > 20$ GeV. It improves to 61 GeV for indirect decays mediated by \mathcal{R} $LL\bar{E}$ couplings, with neutralino mass limits from BARATE 98S. For direct decays, the limits from BARATE 00H in the squark section apply.			
233	ABE	99M	looked in 107 pb^{-1} of $p\bar{p}$ collisions at $\sqrt{s}=1.8$ TeV for events with like sign dielectrons and two or more jets from the sequential decays $\tilde{q} \rightarrow q\tilde{\chi}_1^0$ and $\tilde{\chi}_1^0 \rightarrow e q\bar{q}'$, assuming \mathcal{R} coupling $L_1 Q_j D_k^c$, with $j=2,3$ and $k=1,2,3$. They assume $B(\tilde{t}_1 \rightarrow c\tilde{\chi}_1^0)=1$, $B(\tilde{\chi}_1^0 \rightarrow e q\bar{q}')=0.25$ for both e^+ and e^- , and $m_{\tilde{\chi}_1^0} \geq m_{\tilde{t}_1}/2$. The limit improves for heavier $\tilde{\chi}_1^0$.			
234	ACCIARRI	99C	looked for \tilde{t} pair production at $\sqrt{s}=161\text{--}183$ GeV. See Figs. 4–5 for other choices of θ_t and Δm . These results update ACCIARRI 96F.			
235	ACKERSTAFF	99	looked for \tilde{t} pair production. The analysis considers data taken at $\sqrt{s}=130\text{--}183$ GeV, and includes the results of ACKERSTAFF 97Q. Unless the $\ell=\tau$ decay mode is explicitly indicated, the same branching fractions to $\ell=e, \mu$, and τ are assumed for $b\tilde{t}\nu$ modes. See Table 10 and Figs. 9–11 for other choices of θ_t and Δm .			
236	BARATE	99E	looked for \tilde{t}_L pairs with decay $\tilde{t}_L \rightarrow c\tilde{\chi}_1^0$, where $\tilde{\chi}_1^0$ further decays via R -violating coupling $LQ\bar{D}$. $m_{\tilde{\chi}_1^0} > 30$ GeV. The limit is 62 GeV for the case of \tilde{t}_L pair production with $\tilde{t}_L \rightarrow q\tau$ decays. Data collected at $\sqrt{s}=130\text{--}172$ GeV.			
237	BARATE	98N	assumes the lepton universality for the case of $\tilde{t} \rightarrow b\tilde{t}\nu$ and the lower bound on $m_{\tilde{t}}$ from Z decay is used. See Figs. 2 and 3 for limits as a function of Δm . Data collected at $\sqrt{s}=181\text{--}184$ GeV.			

238 BARATE 98s looked for \tilde{t} pairs with decay $\tilde{t} \rightarrow c\tilde{\chi}_1^0$, where $\tilde{\chi}_1^0$ further decays to $\ell^+\ell^-\nu$ via R -violating coupling $LL\bar{E}$. The limit assumes $\tan\beta=2$. Data collected at $\sqrt{s}=130\text{--}172$ GeV.

239 ABACHI 96b searches for final states with 2 jets and missing E_T . Limits on $m_{\tilde{t}}$ are given as a function of $m_{\tilde{\chi}_1^0}$. See Fig. 4 for details.

240 AID 96 considers photoproduction of $\tilde{t}\tilde{t}^*$ pairs, with 100% R -parity violating decays of \tilde{t} to $e q$, with $q=d, s$, or b quarks.

241 AID 96 considers production and decay of \tilde{t} via the R -parity violating coupling $\lambda^i L_1 Q_3 D_3^c$.

242 CHO 96 studied the consistency among the $B^0\text{-}\bar{B}^0$ mixing, ϵ in $K^0\text{-}\bar{K}^0$ mixing, and the measurements of V_{cb} , V_{ub}/V_{cb} . For the range $25.5\text{ GeV} < m_{\tilde{t}_1} < m_Z/2$ left by AKERS 94k for $\theta_t = 0.98$, and within the allowed range in $M_2\text{-}\mu$ parameter space from chargino, neutralino searches by ACCIARRI 95E, they found the scalar top contribution to $B^0\text{-}\bar{B}^0$ mixing and ϵ to be too large if $\tan\beta < 2$. For more on their assumptions, see the paper and their reference 10.

243 BUSKULIC 95E looked for $Z \rightarrow \tilde{t}\tilde{t}^*$, where $\tilde{t} \rightarrow c\tilde{\chi}_1^0$ and $\tilde{\chi}_1^0$ decays via R -parity violating interactions into two leptons and a neutrino.

244 SHIRAI 94 bound assumes the cross section without the s -channel Z -exchange and the QCD correction, underestimating the cross section up to 20% and 30%, respectively. They assume $m_c=1.5$ GeV.

Heavy \tilde{g} (Gluino) MASS LIMIT

For $m_{\tilde{g}} > 60\text{--}70$ GeV, it is expected that gluinos would undergo a cascade decay via a number of neutralinos and/or charginos rather than undergo a direct decay to photinos as assumed by some papers. Limits obtained when direct decay is assumed are usually higher than limits when cascade decays are included.

VALUE (GeV)	CL%	DOCUMENT ID	TECN	COMMENT	
>190	95	245	ABBOTT	99L D0	$\tan\beta=2$, $\mu < 0$, $A=0$
>260	95	245	ABBOTT	99L D0	$m_{\tilde{g}}=m_{\tilde{q}}$
>173	95	246	ABE	97K CDF	Any $m_{\tilde{q}}$; with cascade decays
>216	95	246	ABE	97K CDF	$m_{\tilde{q}}=m_{\tilde{g}}$; with cascade decays
>224	95	247	ABE	96D CDF	$m_{\tilde{q}}=m_{\tilde{g}}$; with cascade decays
>154	95	247	ABE	96D CDF	$m_{\tilde{q}} < m_{\tilde{g}}$; with cascade decays
• • • We do not use the following data for averages, fits, limits, etc. • • •					
>240	95	248	ABBOTT	99 D0	$\tilde{g} \rightarrow \tilde{\chi}_2^0 X \rightarrow \tilde{\chi}_1^0 \gamma X$, $m_{\tilde{\chi}_2^0} - m_{\tilde{\chi}_1^0} > 20$ GeV
>320	95	248	ABBOTT	99 D0	$\tilde{g} \rightarrow \tilde{\chi}_1^0 X \rightarrow \tilde{G} \gamma X$
>227	95	249	ABBOTT	99K D0	any $m_{\tilde{q}}$, \mathcal{R} , $\tan\beta=2$, $\mu < 0$
>212	95	250	ABACHI	95C D0	$m_{\tilde{g}} \geq m_{\tilde{q}}$; with cascade decays
>144	95	250	ABACHI	95C D0	Any $m_{\tilde{q}}$; with cascade decays
		251	ABE	95T CDF	$\tilde{g} \rightarrow \tilde{\chi}_2^0 \rightarrow \tilde{\chi}_1^0 \gamma$
		252	HEBBEKER	93 RVUE	e^+e^- jet analyses
>218	90	253	ABE	92L CDF	$m_{\tilde{q}} \leq m_{\tilde{g}}$; with cascade decay
>100		254	ROY	92 RVUE	$\rho\bar{\rho} \rightarrow \tilde{g}\tilde{g}, \mathcal{R}$
		255	NOJIRI	91 COSM	
none 4–53	90	256	ALBAJAR	87D UA1	Any $m_{\tilde{q}} > m_{\tilde{g}}$
none 4–75	90	256	ALBAJAR	87D UA1	$m_{\tilde{q}} = m_{\tilde{g}}$
none 16–58	90	257	ANSARI	87D UA2	$m_{\tilde{q}} \lesssim 100$ GeV

245 ABBOTT 99L consider events with three or more jets and large \mathcal{E}_T . Spectra and decay rates are evaluated in the framework of minimal Supergravity, assuming five flavors of degenerate squarks, and scanning the space of the universal gaugino ($m_{1/2}$) and scalar (m_0) masses. See their Figs. 2–3 for the dependence of the limit on the relative value of $m_{\tilde{q}}$ and $m_{\tilde{g}}$.

246 ABE 97k searched for production of gluinos and five degenerate squarks in events with three or more jets but no electrons or muons and missing transverse energy $\mathcal{E}_T > 60$ GeV. The limit for any $m_{\tilde{q}}$ is for $\mu=-200$ GeV and $\tan\beta=2$, and that for $m_{\tilde{q}}=m_{\tilde{g}}$ is for $\mu=-400$ GeV and $\tan\beta=4$. Different choices for $\tan\beta$ and μ lead to changes of the order of ± 10 GeV in the limits. See Footnote [16] of the paper for more details on the assumptions.

247 ABE 96D searched for production of gluinos and five degenerate squarks in final states containing a pair of leptons, two jets, and missing E_T . The two leptons arise from the semileptonic decays of charginos produced in the cascade decays. The limits are derived for fixed $\tan\beta=4.0$, $\mu=-400$ GeV, and $m_{H^\pm}=500$ GeV, and with the cascade decays of the squarks and gluinos calculated within the framework of the Minimal Supergravity scenario. The bounds are weakly sensitive to the values of the three fixed parameters for a large fraction of parameter space. See Fig. 2 for the limits corresponding to different parameter choices.

248 ABBOTT 99 searched for $\gamma\mathcal{E}_T + \geq 2$ jet final states, and set limits on $\sigma(\rho\bar{\rho} \rightarrow \tilde{g}X)\text{-}B(\tilde{g} \rightarrow \gamma\mathcal{E}_T X)$. The quoted limits correspond to $m_{\tilde{q}} \geq m_{\tilde{g}}$, with $B(\tilde{\chi}_2^0 \rightarrow \tilde{\chi}_1^0 \gamma)=1$ and $B(\tilde{\chi}_1^0 \rightarrow \tilde{G}\gamma)=1$, respectively. They improve to 310 GeV (360 GeV in the case of $\gamma\tilde{G}$ decay) for $m_{\tilde{g}}=m_{\tilde{q}}$.

249 ABBOTT 99k uses events with an electron pair and four jets to search for the decay of the $\tilde{\chi}_1^0$ LSP via \mathcal{R} $LQ\bar{D}$ couplings. The particle spectrum and decay branching ratios are taken in the framework of minimal supergravity. An excluded region at 95% CL is obtained in the $(m_0, m_{1/2})$ plane under the assumption that $A_0=0$, $\mu < 0$, $\tan\beta=2$ and any one of the couplings $\lambda_{1jk}^i > 10^{-3}$ ($j=1,2$ and $k=1,2,3$) and from which the above limit is computed. For equal mass squarks and gluinos, the corresponding limit is 277 GeV. The results are essentially independent of A_0 , but the limit deteriorates rapidly with increasing $\tan\beta$ or $\mu > 0$.

- 250 ABACHI 95c assume five degenerate squark flavors with $m_{\tilde{q}_L} = m_{\tilde{q}_R}$. Sleptons are assumed to be heavier than squarks. The limits are derived for fixed $\tan\beta = 2.0$, $\mu = -250$ GeV, and $m_{H^\pm} = 500$ GeV, and with the cascade decays of the squarks and gluinos calculated within the framework of the Minimal Supergravity scenario. The bounds are weakly sensitive to the three fixed parameters for a large fraction of parameter space.
- 251 ABE 95T looked for a cascade decay of gluino into $\tilde{\chi}_2^0$ which further decays into $\tilde{\chi}_1^0$ and a photon. No signal is observed. Limits vary widely depending on the choice of parameters. For $\mu = -40$ GeV, $\tan\beta = 1.5$, and heavy squarks, the range $50 < m_{\tilde{g}} \text{ (GeV)} < 140$ is excluded at 90% CL. See the paper for details.
- 252 HEBBEKER 93 combined jet analyses at various e^+e^- colliders. The 4-jet analyses at TRISTAN/LEP and the measured α_s at PEP/PETRA/TRISTAN/LEP are used. A constraint on effective number of quarks $N=6.3 \pm 1.1$ is obtained, which is compared to that with a light gluino, $N=8$.
- 253 ABE 92L bounds are based on similar assumptions as ABACHI 95c. Not sensitive to $m_{\text{gluino}} < 40$ GeV (but other experiments rule out that region).
- 254 ROY 92 reanalyzed CDF limits on di-lepton events to obtain limits on gluino production in R -parity violating models. The 100% decay $\tilde{g} \rightarrow q\bar{q}\tilde{\chi}$ where $\tilde{\chi}$ is the LSP, and the LSP decays either into $\ell q\bar{d}$ or $\ell\ell\bar{e}$ is assumed.
- 255 NOJIRI 91 argues that a heavy gluino should be nearly degenerate with squarks in minimal supergravity not to overclose the universe.
- 256 The limits of ALBAJAR 87D are from $p\bar{p} \rightarrow \tilde{g}\tilde{g}X$ ($\tilde{g} \rightarrow q\bar{q}\tilde{\gamma}$) and assume $m_{\tilde{q}} > m_{\tilde{g}}$. These limits apply for $m_{\tilde{\gamma}} \lesssim 20$ GeV and $\tau(\tilde{g}) < 10^{-10}$ s.
- 257 The limit of ANSARI 87D assumes $m_{\tilde{q}} > m_{\tilde{g}}$ and $m_{\tilde{\gamma}} \approx 0$.

LIGHT GLUINO

Written March 1998 by H. Murayama (UC Berkeley).

It is controversial if a light gluino of mass below 5 GeV is phenomenologically allowed. Below we list some of the most important and least controversial constraints which need to be met for a light gluino to be viable. For reviews on the subject, see, e.g., Ref. 1.

1. Either $m_{\tilde{g}} \lesssim 1.5$ GeV or $m_{\tilde{g}} \gtrsim 3.5$ GeV to avoid the CAKIR 94 limit. See also Ref. 2 for similar quarkonium constraints on lighter masses.
2. The lifetime of the gluino or the ground state gluino-containing hadron (typically, $g\tilde{g}$) must be $\gtrsim 10^{-10}$ s in order to evade beam-dump and missing energy limits [1,2].
3. Charged gluino-containing hadrons (e.g. $\tilde{g}u\bar{d}$) must decay into neutral ones (e.g. $R^0(\tilde{g}g)\pi^+$ or $(\tilde{g}u\bar{u})e^-\bar{\nu}_e$) with a lifetime shorter than about 10^{-7} s to avoid the AKERS 95R limit. Older limits for lower masses and shorter lifetimes are summarized in Ref. 1.
4. The lifetime of R^0 should be outside the ranges excluded by ALAVI-HARATI 99E ($R^0 \rightarrow \pi^+\pi^0\tilde{\gamma}$, $\pi^0\tilde{\gamma}$) and FANTI 99 ($\eta\tilde{\gamma}$). The $R_p^+(\tilde{g}uud)$ state, which is believed to decay weakly into $S^0(\tilde{g}uds)\pi^\pm$ (FARRAR 96), must be heavier than 2 GeV or have lifetime $\tau_{R_p} \gtrsim 1$ ns or $\tau_{R_p} \lesssim 50$ ps (e.g. if the strong decay into S^0K^\pm is allowed), or its production cross sections must be at least a factor of 5 smaller than those of hyperons, to avoid ALBUQUERQUE 97 limit.
5. $m_{\tilde{g}} \geq 6.8$ GeV (95% CL) if the "experimental optimization" method of fixing the renormalization scale is valid and if the hadronization and resummation uncertainties are as estimated in BARATE 97L, from the D_2 event shape observable in Z^0 decay. The 4-jet angular distribution is less sensitive to renormalization scale ambiguities and yields

a 90%CL exclusion of a light gluino (DEGOUVEA 97). A combined LEP analysis based on all the Z^0 data and using the recent NLO calculations [3] is warranted.

6. Constraints from the effect of light gluinos on the running of α_s apply independently of the gluino lifetime and are insensitive to renormalization scale. They disfavor a light gluino at 70% CL (CSIKOR 97), which improves to more than 99% with jet analysis.

References

1. G.R. Farrar, Phys. Rev. **D51**, 3904 (1995); in SUSY 97, Proceedings of the Fifth International Conference on Supersymmetries in Physics, 27-31 May 1997, Philadelphia, USA, edited by M. Cvetič and P. Langacker (Nuc. Phys. B (Proc. Suppl.) 62 (1998)) p. 485. hep-ph/9710277.
2. R.M. Barnett, in SUSY 95, Proceedings of the International Workshop on Supersymmetry and Unification of Fundamental Interactions, Palaiseau, France, 15-19 May 1995, edited by I. Antoniadis and H. Videau (Editions Frontieres, Gif-sur-Yvette, France, 1996) p. 69.
3. L. Dixon and A. Signer, Phys. Rev. **D56**, 4031 (1997); J.M. Campbell, E.W.N. Glover, and D.J. Miller, Phys. Lett. **B409**, 503 (1997).

Long-lived/light \tilde{g} (Gluino) MASS LIMIT

Limits on light gluinos ($m_{\tilde{g}} < 5$ GeV), or gluinos which leave the detector before decaying.

VALUE (GeV)	CL%	DOCUMENT ID	TECN	COMMENT
• • • We do not use the following data for averages, fits, limits, etc. • • •				
		258 ALAVI-HARATI 99E	KTEV	$pN \rightarrow R^0$, with $R^0 \rightarrow \rho^0\tilde{\gamma}$ and $R^0 \rightarrow \pi^0\tilde{\gamma}$
		259 BAER	99 RVUE	Stable \tilde{g} hadrons
		260 FANTI	99 NA48	$pBe \rightarrow R^0 \rightarrow \eta\tilde{\gamma}$
		261 ACKERSTAFF	98V OPAL	$e^+e^- \rightarrow \tilde{\chi}_1^+\tilde{\chi}_1^-$
		262 ADAMS	97B KTEV	$pN \rightarrow R^0 \rightarrow \rho^0\tilde{\gamma}$
		263 ALBUQUERQUE..97	E761	$R^+(uud\tilde{g}) \rightarrow S^0(uds\tilde{g})\pi^+$, $X^-(ssd\tilde{g}) \rightarrow S^0\pi^-$
>6.3	95	264 BARATE	97L ALEP	Color factors
>5	99	265 CSIKOR	97 RVUE	β function, $Z \rightarrow$ jets
>1.5	90	266 DEGOUVEA	97 THEO	$Z \rightarrow jjjj$
		267 FARRAR	96 RVUE	$R^0 \rightarrow \pi^0\tilde{\gamma}$
none	1.9-13.6	268 AKERS	95R OPAL	Z decay into a long-lived $(\tilde{g}q\bar{q})^\pm$ quarkonia
<0.7		269 CLAVELLI	95 RVUE	quarkonia
none 1.5-3.5		270 CAKIR	94 RVUE	$\Upsilon(1S) \rightarrow \gamma +$ gluonium
not 3-5		271 LOPEZ	93C RVUE	LEP
≈ 4		272 CLAVELLI	92 RVUE	α_s running
		273 ANTONIADIS	91 RVUE	α_s running
		274 ANTONIADIS	91 RVUE	$\rho N \rightarrow$ missing energy
		275 NAKAMURA	89 SPEC	$R-\Delta^{++}$
>3.8	90	276 ARNOLD	87 EMUL	π^- (350 GeV). $\sigma \approx A^4$
>3.2	90	276 ARNOLD	87 EMUL	π^- (350 GeV). $\sigma \approx A^{0.72}$
none 0.6-2.2	90	277 TUTS	87 CUSB	$\Upsilon(1S) \rightarrow \gamma +$ gluonium
none 1-4.5	90	278 ALBRECHT	86C ARG	$1 \times 10^{-11} \lesssim \tau \lesssim 1 \times 10^{-9}$ s
none 1-4	90	279 BADIER	86 BDMP	$1 \times 10^{-10} < \tau < 1 \times 10^{-7}$ s
none 3-5		280 BARNETT	86 RVUE	$p\bar{p} \rightarrow$ gluino gluino gluon
none		281 VOLOSHIN	86 RVUE	If (quasi) stable; $\tilde{g}uud$
none 0.5-2		282 COOPER-...	85B BDMP	For $m_{\tilde{g}}=300$ GeV
none 0.5-4		282 COOPER-...	85B BDMP	For $m_{\tilde{g}} < 65$ GeV
none 0.5-3		282 COOPER-...	85B BDMP	For $m_{\tilde{g}}=150$ GeV
none 2-4		283 DAWSON	85 RVUE	$\tau > 10^{-7}$ s
none 1-2.5		283 DAWSON	85 RVUE	For $m_{\tilde{g}}=100$ GeV
none 0.5-4.1	90	284 FARRAR	85 RVUE	FNAL beam dump
>1		285 GOLDMAN	85 RVUE	Gluonium
>1-2		286 HABER	85 RVUE	
		287 BALL	84 CALO	
		288 BRICK	84 RVUE	
		289 FARRAR	84 RVUE	
>2		290 BERGSMA	83C RVUE	For $m_{\tilde{g}} < 100$ GeV
>2-3		291 CHANOWITZ	83 RVUE	$\tilde{g}u\bar{d}, \tilde{g}uud$
>1.5-2		292 KANE	82 RVUE	Beam dump
		FARRAR	78 RVUE	R -hadron

- 250 ABACHI 95c assume five degenerate squark flavors with $m_{\tilde{q}_L} = m_{\tilde{q}_R}$. Sleptons are assumed to be heavier than squarks. The limits are derived for fixed $\tan\beta = 2.0$, $\mu = -250$ GeV, and $m_{H^\pm} = 500$ GeV, and with the cascade decays of the squarks and gluinos calculated within the framework of the Minimal Supergravity scenario. The bounds are weakly sensitive to the three fixed parameters for a large fraction of parameter space.
- 251 ABE 95T looked for a cascade decay of gluino into $\tilde{\chi}_2^0$ which further decays into $\tilde{\chi}_1^0$ and a photon. No signal is observed. Limits vary widely depending on the choice of parameters. For $\mu = -40$ GeV, $\tan\beta = 1.5$, and heavy squarks, the range $50 < m_{\tilde{g}} \text{ (GeV)} < 140$ is excluded at 90% CL. See the paper for details.
- 252 HEBBEKER 93 combined jet analyses at various e^+e^- colliders. The 4-jet analyses at TRISTAN/LEP and the measured α_s at PEP/PETRA/TRISTAN/LEP are used. A constraint on effective number of quarks $N=6.3 \pm 1.1$ is obtained, which is compared to that with a light gluino, $N=8$.
- 253 ABE 92L bounds are based on similar assumptions as ABACHI 95c. Not sensitive to $m_{\text{gluino}} < 40$ GeV (but other experiments rule out that region).
- 254 ROY 92 reanalyzed CDF limits on di-lepton events to obtain limits on gluino production in R -parity violating models. The 100% decay $\tilde{g} \rightarrow q\bar{q}\tilde{\chi}$ where $\tilde{\chi}$ is the LSP, and the LSP decays either into $\ell q\bar{d}$ or $\ell\ell\bar{e}$ is assumed.
- 255 NOJIRI 91 argues that a heavy gluino should be nearly degenerate with squarks in minimal supergravity not to overclose the universe.
- 256 The limits of ALBAJAR 87D are from $p\bar{p} \rightarrow \tilde{g}\tilde{g}X$ ($\tilde{g} \rightarrow q\bar{q}\tilde{\gamma}$) and assume $m_{\tilde{q}} > m_{\tilde{g}}$. These limits apply for $m_{\tilde{\gamma}} \lesssim 20$ GeV and $\tau(\tilde{g}) < 10^{-10}$ s.
- 257 The limit of ANSARI 87D assumes $m_{\tilde{q}} > m_{\tilde{g}}$ and $m_{\tilde{\gamma}} \approx 0$.

LIGHT GLUINO

Written March 1998 by H. Murayama (UC Berkeley).

It is controversial if a light gluino of mass below 5 GeV is phenomenologically allowed. Below we list some of the most important and least controversial constraints which need to be met for a light gluino to be viable. For reviews on the subject, see, *e.g.*, Ref. 1.

1. Either $m_{\tilde{g}} \lesssim 1.5$ GeV or $m_{\tilde{g}} \gtrsim 3.5$ GeV to avoid the CAKIR 94 limit. See also Ref. 2 for similar quarkonium constraints on lighter masses.
2. The lifetime of the gluino or the ground state gluino-containing hadron (typically, $g\tilde{g}$) must be $\gtrsim 10^{-10}$ s in order to evade beam-dump and missing energy limits [1,2].
3. Charged gluino-containing hadrons (*e.g.* $\tilde{g}u\bar{d}$) must decay into neutral ones (*e.g.* $R^0(\tilde{g}g)\pi^+$ or $(\tilde{g}u\bar{u})e^-\bar{\nu}_e$) with a lifetime shorter than about 10^{-7} s to avoid the AKERS 95R limit. Older limits for lower masses and shorter lifetimes are summarized in Ref. 1.
4. The lifetime of R^0 should be outside the ranges excluded by ALAVI-HARATI 99E ($R^0 \rightarrow \pi^+\pi^0\tilde{\gamma}$, $\pi^0\tilde{\gamma}$) and FANTI 99 ($\eta\tilde{\gamma}$). The $R_p^+(\tilde{g}uud)$ state, which is believed to decay weakly into $S^0(\tilde{g}uds)\pi^\pm$ (FARRAR 96), must be heavier than 2 GeV or have lifetime $\tau_{R_p} \gtrsim 1$ ns or $\tau_{R_p} \lesssim 50$ ps (*e.g.* if the strong decay into S^0K^\pm is allowed), or its production cross sections must be at least a factor of 5 smaller than those of hyperons, to avoid ALBUQUERQUE 97 limit.
5. $m_{\tilde{g}} \geq 6.8$ GeV (95% CL) if the "experimental optimization" method of fixing the renormalization scale is valid and if the hadronization and resummation uncertainties are as estimated in BARATE 97L, from the D_2 event shape observable in Z^0 decay. The 4-jet angular distribution is less sensitive to renormalization scale ambiguities and yields

a 90%CL exclusion of a light gluino (DEGOUVEA 97). A combined LEP analysis based on all the Z^0 data and using the recent NLO calculations [3] is warranted.

6. Constraints from the effect of light gluinos on the running of α_s apply independently of the gluino lifetime and are insensitive to renormalization scale. They disfavor a light gluino at 70% CL (CSIKOR 97), which improves to more than 99% with jet analysis.

References

1. G.R. Farrar, Phys. Rev. **D51**, 3904 (1995); in SUSY 97, Proceedings of the Fifth International Conference on Supersymmetries in Physics, 27-31 May 1997, Philadelphia, USA, edited by M. Cvetič and P. Langacker (Nuc. Phys. B (Proc. Suppl.) 62 (1998)) p. 485. hep-ph/9710277.
2. R.M. Barnett, in SUSY 95, Proceedings of the International Workshop on Supersymmetry and Unification of Fundamental Interactions, Palaiseau, France, 15-19 May 1995, edited by I. Antoniadis and H. Videau (Editions Frontieres, Gif-sur-Yvette, France, 1996) p. 69.
3. L. Dixon and A. Signer, Phys. Rev. **D56**, 4031 (1997); J.M. Campbell, E.W.N. Glover, and D.J. Miller, Phys. Lett. **B409**, 503 (1997).

Long-lived/light \tilde{g} (Gluino) MASS LIMIT

Limits on light gluinos ($m_{\tilde{g}} < 5$ GeV), or gluinos which leave the detector before decaying.

VALUE (GeV)	CL%	DOCUMENT ID	TECN	COMMENT
• • • We do not use the following data for averages, fits, limits, etc. • • •				
		258 ALAVI-HARATI 99E	KTEV	$pN \rightarrow R^0$, with $R^0 \rightarrow \rho^0\tilde{\gamma}$ and $R^0 \rightarrow \pi^0\tilde{\gamma}$
		259 BAER	99 RVUE	Stable \tilde{g} hadrons
		260 FANTI	99 NA48	$pBe \rightarrow R^0 \rightarrow \eta\tilde{\gamma}$
		261 ACKERSTAFF	98V OPAL	$e^+e^- \rightarrow \tilde{\chi}_1^+\tilde{\chi}_1^-$
		262 ADAMS	97B KTEV	$pN \rightarrow R^0 \rightarrow \rho^0\tilde{\gamma}$
		263 ALBUQUERQUE..97	E761	$R^+(uud\tilde{g}) \rightarrow S^0(uds\tilde{g})\pi^+$, $X^-(ssd\tilde{g}) \rightarrow S^0\pi^-$
>6.3	95	264 BARATE	97L ALEP	Color factors
>5	99	265 CSIKOR	97 RVUE	β function, $Z \rightarrow$ jets
>1.5	90	266 DEGOUVEA	97 THEO	$Z \rightarrow jjjj$
		267 FARRAR	96 RVUE	$R^0 \rightarrow \pi^0\tilde{\gamma}$
none	1.9-13.6	268 AKERS	95R OPAL	Z decay into a long-lived ($\tilde{g}q\bar{q}$) $^\pm$
<0.7		269 CLAVELLI	95 RVUE	quarkonia
none 1.5-3.5		270 CAKIR	94 RVUE	$\Upsilon(1S) \rightarrow \gamma$ + gluonium
not 3-5		271 LOPEZ	93C RVUE	LEP
≈ 4		272 CLAVELLI	92 RVUE	α_s running
		273 ANTONIADIS	91 RVUE	α_s running
		274 ANTONIADIS	91 RVUE	$\rho N \rightarrow$ missing energy
		275 NAKAMURA	89 SPEC	$R\text{-}\Delta^{++}$
>3.8	90	276 ARNOLD	87 EMUL	π^- (350 GeV). $\sigma \approx A^4$
>3.2	90	276 ARNOLD	87 EMUL	π^- (350 GeV). $\sigma \approx A^{0.72}$
none 0.6-2.2	90	277 TUTS	87 CUSB	$\Upsilon(1S) \rightarrow \gamma$ + gluonium
none 1-4.5	90	278 ALBRECHT	86C ARG	$1 \times 10^{-11} \lesssim \tau \lesssim 1 \times 10^{-9}$ s
none 1-4	90	279 BADIER	86 BDMP	$1 \times 10^{-10} < \tau < 1 \times 10^{-7}$ s
none 3-5		280 BARNETT	86 RVUE	$p\bar{p} \rightarrow$ gluino gluino gluon
none		281 VOLOSHIN	86 RVUE	If (quasi) stable; $\tilde{g}uud$
none 0.5-2		282 COOPER...	85B BDMP	For $m_{\tilde{g}}=300$ GeV
none 0.5-4		282 COOPER...	85B BDMP	For $m_{\tilde{g}} < 65$ GeV
none 0.5-3		282 COOPER...	85B BDMP	For $m_{\tilde{g}}=150$ GeV
none 2-4		283 DAWSON	85 RVUE	$\tau > 10^{-7}$ s
none 1-2.5		283 DAWSON	85 RVUE	For $m_{\tilde{g}}=100$ GeV
none 0.5-4.1	90	284 FARRAR	85 RVUE	FNAL beam dump
>1		285 GOLDMAN	85 RVUE	Gluonium
>1-2		286 HABER	85 RVUE	
		287 BALL	84 CALO	
		288 BRICK	84 RVUE	
		289 FARRAR	84 RVUE	
>2		290 BERGSMA	83C RVUE	For $m_{\tilde{g}} < 100$ GeV
>2-3		291 CHANOWITZ	83 RVUE	$\tilde{g}u\bar{d}$, $\tilde{g}uud$
>1.5-2		292 KANE	82 RVUE	Beam dump
		FARRAR	78 RVUE	R -hadron

Technicolor**DYNAMICAL ELECTROWEAK SYMMETRY BREAKING**

Written October 1999 by R.S. Chivukula (Boston Univ.) and J. Womersley (Fermilab).

In theories of dynamical electroweak symmetry breaking, the electroweak interactions are broken to electromagnetism by the vacuum expectation value of a fermion bilinear. These theories may thereby avoid the introduction of fundamental scalar particles, of which we have no examples in nature. In this note, we review the status of experimental searches for the particles predicted in technicolor, topcolor, and related models.

I. Technicolor

The earliest models [1,2] of dynamical electroweak symmetry breaking [3] include a new non-abelian gauge theory (“technicolor”) and additional massless fermions (“technifermions”) which feel this new force. The global chiral symmetry of the fermions is spontaneously broken by the formation of a technifermion condensate, just as the chiral symmetries in QCD are broken to isospin by the formation of a quark condensate. If the quantum numbers of the technifermions are chosen correctly (*e.g.* by choosing technifermions in the fundamental representation of an $SU(N)$ technicolor gauge group, with the left-handed technifermions being weak doublets and the right-handed ones weak singlets) this condensate can break the electroweak interactions down to electromagnetism.

The breaking of the global chiral symmetries implies the existence of Goldstone bosons, the “technipions” (π_T). Through the Higgs mechanism, three of the Goldstone bosons become the longitudinal components of the W and Z , and the weak gauge bosons acquire a mass proportional to the technipion decay constant (the analog of f_π in QCD). The quantum numbers and masses of any remaining technipions are model dependent. There may be technipions which are colored (octets and triplets) as well as those carrying electroweak quantum numbers, and some technipions could be dangerously light [4,5]. The lightest technicolor resonances are expected to be the analogs of the vector mesons in QCD. The technivector mesons can also have color and electroweak quantum numbers and, for a theory with a small number of technifermions, are expected to have a mass in the TeV range [6].

While technicolor chiral symmetry breaking can give mass to the W and Z particles, additional interactions must be introduced to produce the masses of the standard model fermions. The most thoroughly studied mechanism for this invokes “extended technicolor” (ETC) gauge interactions [4,7]. In ETC, technicolor, color and flavor are embedded into a larger gauge group which is broken to technicolor and color at an energy scale of 100–500 TeV. The massive gauge bosons associated with this breaking mediate transitions between quarks/leptons and technifermions, giving rise to the couplings necessary to produce fermion masses. The ETC gauge bosons also mediate transitions among technifermions themselves, leading to

interactions which can explicitly break unwanted chiral symmetries and raise the masses of any light technipions. The ETC interactions connecting technifermions to quarks/leptons also mediate technipion decays to ordinary fermion pairs. Since these interactions are responsible for fermion masses, one generally expects technipions to decay to the heaviest fermions kinematically allowed (though this need not hold in all models).

In addition to quark masses, ETC interactions must also give rise to quark mixing. One expects, therefore, that there are ETC interactions coupling quarks of the same flavor from different generations. A stringent limit on these flavor-changing neutral current interactions comes from $K^0-\bar{K}^0$ mixing [4]. These force the scale of ETC breaking and the corresponding ETC gauge boson masses to be in the multi-hundred TeV range (at least insofar as ETC interactions of first two generations are concerned). To obtain quark and technipion masses that are large enough then requires an enhancement of the technifermion condensate over that expected naively by scaling from QCD. Such an enhancement can occur if the technicolor gauge coupling runs very slowly, or “walks” [8]. Many technifermions typically are needed to make the TC coupling walk, implying that the technicolor scale and, in particular, the technivector mesons may be much lighter than 1 TeV [3,9]. It should also be noted that there is no reliable calculation of electroweak parameters in a walking technicolor theory, and the values of precisely measured electroweak quantities [10] cannot directly be used to constrain the models.

In existing colliders, technivector mesons are dominantly produced when an off-shell standard model gauge-boson “resonates” into a technivector meson with the same quantum numbers [11]. The technivector mesons may then decay, in analogy with $\rho \rightarrow \pi\pi$, to pairs of technipions. However, in walking technicolor the technipion masses may be increased to the point that the decay of a technirho to pairs of technipions is kinematically forbidden [9]. In this case the decay to a technipion and a longitudinally polarized weak boson (an “eaten” Goldstone boson) may be preferred, and the technivector meson would be very narrow. Alternatively, the technivector may also decay, in analogy with the decay $\rho \rightarrow \pi\gamma$, to a technipion plus a photon, gluon, or transversely polarized weak gauge boson. Finally, in analogy with the decay $\rho \rightarrow e^+e^-$, the technivector meson may resonate back to an off-shell gluon or electroweak gauge boson, leading to a decay into a pair of leptons, quarks, or gluons.

If the dominant decay mode of the technirho is $W_T\pi_T$, promising signal channels [12] are $\rho_T^\pm \rightarrow W^\pm\pi_T^0$ and $\rho_T^0 \rightarrow W^\pm\pi_T^\mp$. Both channels yield a signal of $W(\ell\nu) + 2$ jets, with one or more heavy flavor tags. Recently, the CDF collaboration has carried out a search in this final state [13] based on Run I data and using PYTHIA [14] version 6.1 for the signal simulation. The results are shown in Fig. 1. We see that the search is sensitive to $\sigma \cdot B \gtrsim 10$ pb and that roughly $170 < m_{\rho_T} < 190$ GeV is excluded at the 95% confidence level, for $m_{\pi_T} \approx m_{\rho_T}/2$.

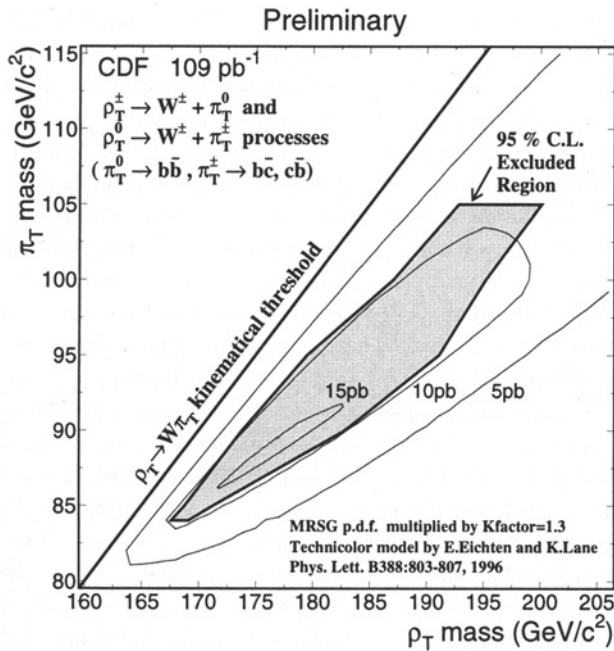


Figure 1: 95% CL exclusion region [13] for light technirho's decaying to W^\pm and a π_T , and in which the π_T decays to two jets including at least one b quark.

CDF has also searched [15] for the process $\omega_T^0 \rightarrow \gamma\pi_T^0$, yielding a signal of a hard photon plus two jets, with one or more heavy flavor tags. The sensitivity to $\sigma \cdot B$ is of order 1 pb. The excluded region is shown in Fig. 2 and is roughly $140 < m_{\omega_T} < 290$ GeV at the 95% level, for $m_{\pi_T} \approx m_{\omega_T}/3$. The analysis assumes four technicolors, $Q_D = Q_U - 1 = \frac{1}{3}$ and $M_T = 100$ GeV/ c^2 . Here Q_U and Q_D are the charges of the lightest technifermion doublet and M_T is a dimensionful parameter, of order 100 GeV/ c^2 , which controls the rate of $\rho_T, \omega_T \rightarrow \gamma\pi_T$.

Both $D\bar{O}$ [16] and CDF [17] have searched for low-scale technicolor resonances ρ_T and ω_T decaying to dileptons, using inclusive e^+e^- (both experiments) and $\mu^+\mu^-$ (CDF) samples from Run I. In the search, the ρ_T and ω_T are assumed to be degenerate in mass. The absence of structure in the dilepton invariant mass distribution is then used to set limits. Those from $D\bar{O}$ are slightly more restrictive. Masses $m_{\rho_T} = m_{\omega_T} < 250$ GeV are excluded, provided $m_{\rho_T} < m_{\pi_T} + m_W$, or provided $M_T > 300$ GeV. The latter case is shown in Fig. 3. With 2 fb^{-1} of data in Run II, the sensitivity will extend to $m_{\rho_T} = m_{\omega_T} \approx 500$ GeV.

L3 [18] has reported a search for four topologies: $e^+e^- \rightarrow W^+W^-$; $e^+e^- \rightarrow W^\pm\pi_T^\mp \rightarrow \ell\nu bc$; $e^+e^- \rightarrow \pi_T\pi_T \rightarrow b\bar{c}b\bar{c}$; $e^+e^- \rightarrow \gamma\pi_T \rightarrow \gamma b\bar{b}$. All processes proceed through an intermediate ρ_T or ω_T resonance, which are assumed to be degenerate in mass. No excess is seen in any channel, based

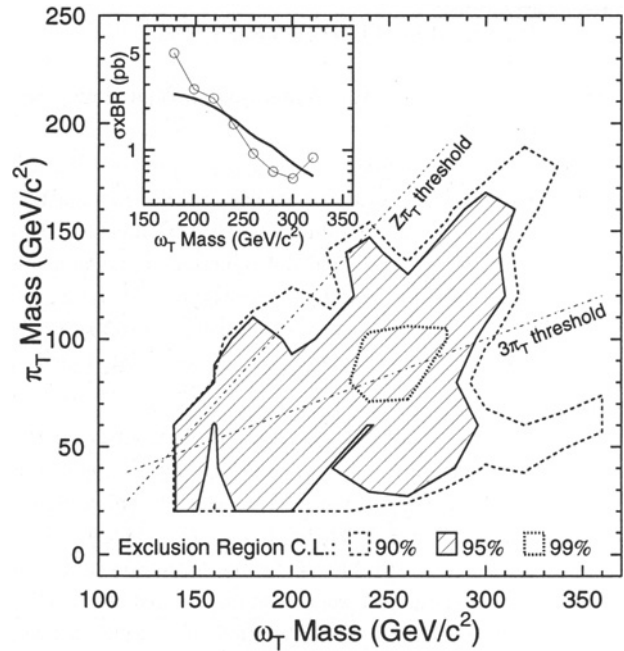


Figure 2: 95% CL exclusion region [15] for light techniomega's decaying to γ and a π_T , and in which the π_T decays to two jets including at least one b quark. (Inset: cross section limit for $m_{\pi_T} = 120$ GeV.)

on 176 pb^{-1} of data taken at an average center of mass energy of 189 GeV. The excluded region in m_{ρ_T}, m_{π_T} parameter space is shown in Fig. 4 and rules out $m_{\rho_T} < 190$ GeV, for all values of m_{π_T} , for the range of parameters considered. This L3 analysis is the only one so far to make use of the latest calculations [19] of technihadron production and decay, as implemented in PYTHIA version 6.126 and higher [20]. All the other analyses described in this review used older versions of PYTHIA and the limits are not directly comparable.

Searches have also been carried out at the Tevatron for colored technihadron resonances [21,22]. CDF has used a search for structure in the dijet invariant mass spectrum to set limits on a color-octet technirho ρ_{T8} produced by an off-shell gluon and decaying to two real quarks or gluons. As shown in Fig. 5 masses $260 < m_{\rho_{T8}} < 480$ GeV are excluded; in Run II the limits will improve to cover the whole mass range up to about 0.8 TeV [23].

The CDF third-generation leptoquark search [24] has also been interpreted in terms of the complementary ρ_{T8} decay mode: $p\bar{p} \rightarrow \rho_{T8} \rightarrow \pi_{LQ}\pi_{LQ} \rightarrow \tau q\tau q$. Here π_{LQ} denotes a color-triplet technipion carrying both color and lepton number, assumed to decay to τ plus quark. Fig. 6 shows that technirho masses $m_{\rho_{T8}} < 465$ GeV and technipion masses up to $m_{\rho_{T8}}/2$ are excluded in this picture ($m_{\pi_{LQ}} < 99$ GeV already having been ruled out by the standard continuum-production leptoquark searches).

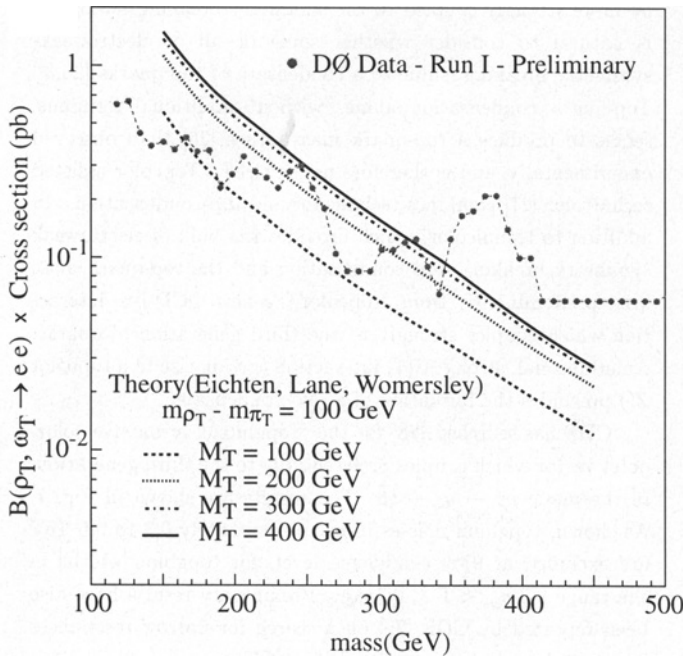


Figure 3: 95% CL cross section limit [16] for light techniomega's and technirho's decaying to l^+l^- .

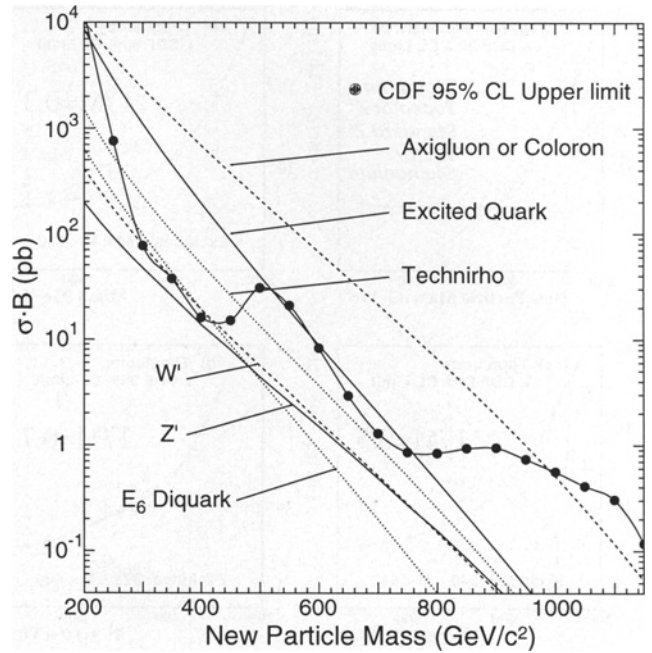


Figure 5: 95% CL cross section limits [22] for technirho's decaying to two jets at the Tevatron.

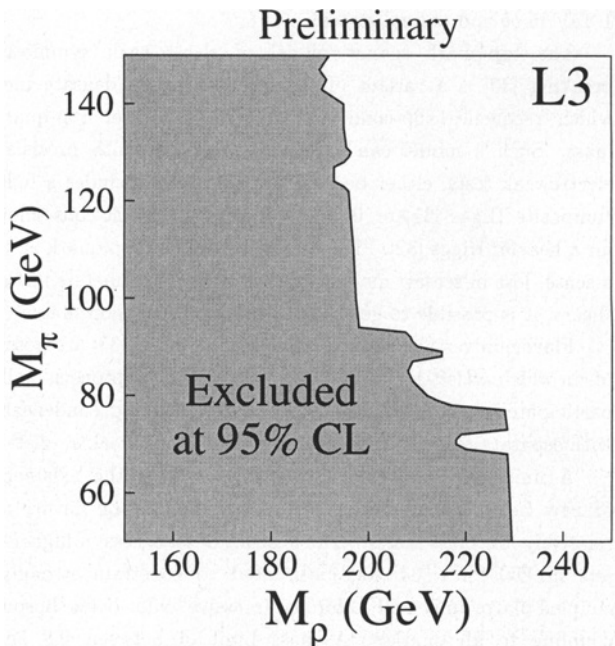


Figure 4: 95% CL exclusion region [18] in the technirho-technipion mass plane obtained from searches by the L3 collaboration at LEP 2.

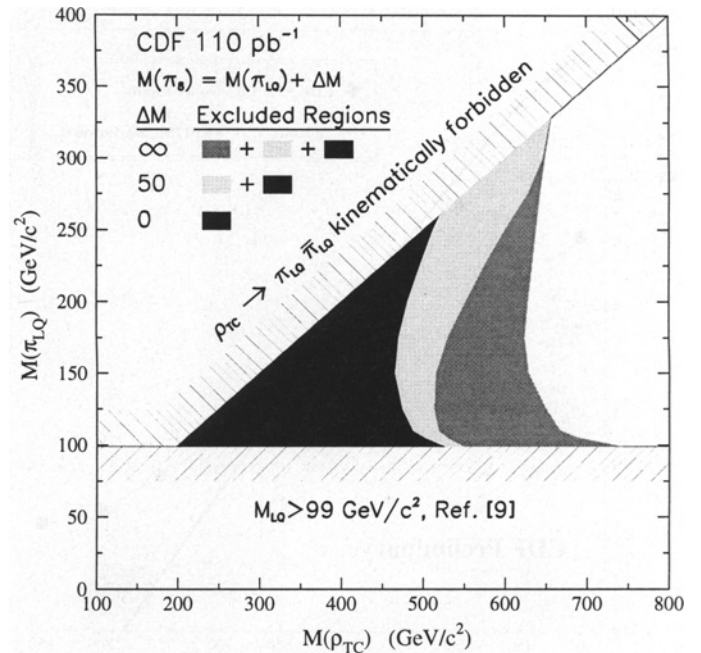


Figure 6: 95% CL exclusion region [24] in the technirho-technipion mass plane for pair produced technipions, with leptoquark couplings, decaying to τq .

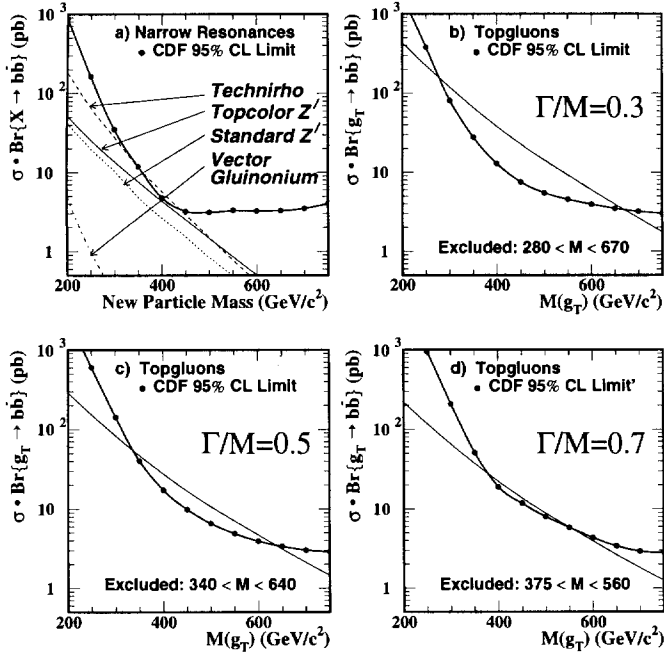


Figure 7: Tevatron limits [28] on new particles decaying to $b\bar{b}$: narrow resonances and topgluons for various widths.

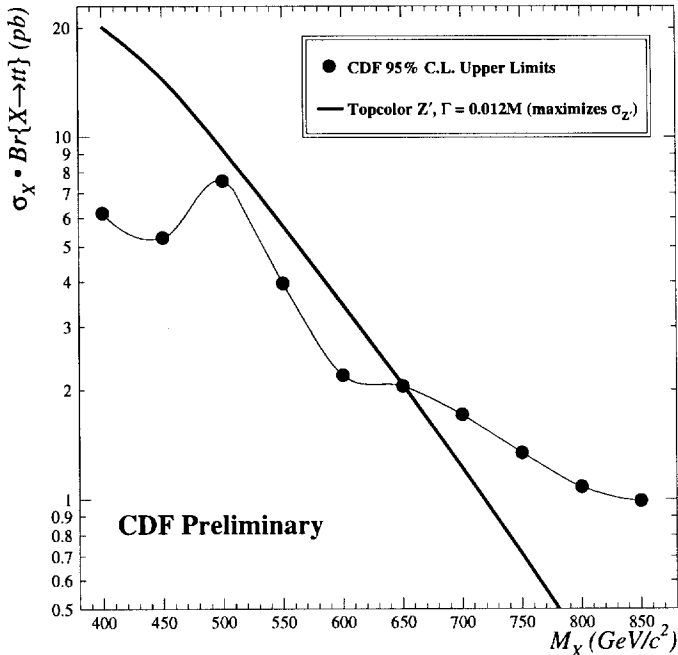


Figure 8: Cross section limits for a narrow resonance decaying to $t\bar{t}$ [29] and expected cross section for a topcolor Z' boson.

II. Top Condensate and Related Models

The top quark is much heavier than other fermions and must be more strongly coupled to the symmetry-breaking sector. It is natural to consider whether some or all of electroweak-symmetry breaking is due to a condensate of top quarks [25,3]. Top-quark condensation alone, without additional fermions, seems to produce a top-quark mass larger [26] than observed experimentally, and is therefore not favored. Topcolor assisted technicolor [27] combines technicolor and top-condensation. In addition to technicolor, which provides the bulk of electroweak symmetry breaking, top condensation and the top-quark mass arise predominantly from “topcolor,” a new QCD-like interaction which couples strongly to the third generation of quarks. An additional, strong, $U(1)$ interaction (giving rise to a topcolor Z') precludes the formation of a $\langle b\bar{b} \rangle$ condensate.

CDF has searched [28] for the “topgluon,” a massive color-octet vector which couples preferentially to the third generation, in the mode $p\bar{p} \rightarrow g_t \rightarrow b\bar{b}$. The results are shown in Fig. 7. As shown, topgluon masses from approximately 0.3 to 0.6 TeV are excluded at 95% confidence level, for topgluon widths in the range $0.3m_{g_t} < \Gamma < 0.7m_{g_t}$. Preliminary results have also been reported by CDF [29] on a search for narrow resonances in the $t\bar{t}$ invariant mass distribution. The cross section limit is shown in Fig. 8 and excludes a topcolor Z' with masses less than 650 GeV/c^2 , for the case where its width $\Gamma = 0.012m_{Z'}$. This choice of width maximizes the cross section. A broad topgluon could also be detected in the same final state, though no results are yet available. In Run II, the Tevatron [23] should be sensitive to topgluon and topcolor Z' masses up to of order 1 TeV in $b\bar{b}$ and $t\bar{t}$ final states.

The top-quark seesaw model of electroweak symmetry breaking [30] is a variant of the original top-condensate idea which reconciles top-condensation with a lighter top-quark mass. Such a model can easily be consistent with precision electroweak tests, either because the spectrum includes a light composite Higgs [31] or because additional interactions allow for a heavier Higgs [32]. The unique role of the top quark is, in a sense, lost in seesaw models. By adjusting parameters in the theory, it is possible to generate *any* required fermion mass.

Flavor-universal versions of the seesaw model [33] are possible in which *all* left-handed quarks (and possibly leptons as well) participate in the electroweak symmetry-breaking condensate with separate (one for each flavor) right-handed weak singlets.

A universal prediction of these models, is the existence of new heavy gauge bosons, coupling to color or flavor, at relatively low mass scales. The absence of an excess of high- E_T jets in $D\bar{O}$ data [34] has been used to constrain strongly-coupled flavor-universal colorons (massive color-octet bosons coupling to all quarks). A mass limit of between 0.8 and 3.5 TeV is set [35] depending on the coloron-gluon mixing angle. Precision electroweak measurements constrain [36] the masses of these new gauge bosons to be greater than 1–3 TeV in a variety of models, for strong couplings. These limits are all summarized in Table 1.

Table 1: Summary of the mass limits. Symbols are defined in the text.

Process	Excluded mass range	Decay channels	Ref.
$p\bar{p} \rightarrow \rho_T \rightarrow W\pi_T$	$170 < m_{\rho_T} < 190$ GeV for $m_{\pi_T} \approx m_{\rho_T}/2$	$\rho_T \rightarrow W\pi_T$ $\pi_T^0 \rightarrow b\bar{b}$ $\pi_T^\pm \rightarrow b\bar{c}$	[13]*
$p\bar{p} \rightarrow \omega_T \rightarrow \gamma\pi_T$	$140 < m_{\omega_T} < 290$ GeV for $m_{\pi_T} \approx m_{\omega_T}/3$ and $M_T = 100$ GeV	$\omega_T \rightarrow \gamma\pi_T$ $\pi_T^0 \rightarrow b\bar{b}$ $\pi_T^\pm \rightarrow b\bar{c}$	[15]
$p\bar{p} \rightarrow \omega_T/\rho_T$	$m_{\omega_T} = m_{\rho_T} < 250$ GeV for $m_{\omega_T} < m_{\pi_T} + m_W$ or $M_T > 300$ GeV	$\omega_T/\rho_T \rightarrow \ell^+\ell^-$	[16]*
$e^+e^- \rightarrow \omega_T/\rho_T$	$m_{\omega_T} = m_{\rho_T} < 190$ GeV	$\rho_T \rightarrow WW,$ $W\pi_T, \pi_T\pi_T$ $\omega_T \rightarrow \gamma\pi_T$ $\pi_T^0 \rightarrow b\bar{b}$ $\pi_T^\pm \rightarrow b\bar{c}$	[18]*
$p\bar{p} \rightarrow \rho_{T8}$	$260 < m_{\rho_{T8}} < 480$ GeV	$\rho_{T8} \rightarrow q\bar{q}, gg$	[22]
$p\bar{p} \rightarrow \rho_{T8}$	$m_{\rho_{T8}} < 465$ GeV	$\rho_{T8} \rightarrow \pi_{LQ}\pi_{LQ}$ $\pi_{LQ} \rightarrow \tau q$	[24]
$p\bar{p} \rightarrow g_t$	$0.3 < m_{g_t} < 0.6$ TeV for $0.3m_{g_t} < \Gamma < 0.7m_{g_t}$	$g_t \rightarrow b\bar{b}$	[28]
$p\bar{p} \rightarrow Z'$	$m_{Z'} < 650$ GeV for $\Gamma = 0.012m_{Z'}$	$Z' \rightarrow t\bar{t}$	[29]*

*Preliminary, not yet published.

Acknowledgments

We thank Tom Appelquist, Robert Harris, Chris Hill, Greg Landsberg, Kenneth Lane, and Elizabeth Simmons for help in the preparation of this article. *This work was supported in part by the Department of Energy under grant DE-FG02-91ER40676.*

References

- S. Weinberg, Phys. Rev. **D19**, 1277 (1979).
- L. Susskind, Phys. Rev. **D20**, 2619 (1979).
- For a recent review, see R.S. Chivukula, hep-ph/9803219.
- E. Eichten and K. Lane, Phys. Lett. **90B**, 125 (1980).
- For reviews, see E. Farhi and L. Susskind, Phys. Reports **74**, 277 (1981);
R.K. Kaul, Rev. Mod. Phys. **55**, 449 (1983);
R.S. Chivukula *et al.*, hep-ph/9503202.
- S. Dimopoulos, S. Raby, and G. L. Kane, Nucl. Phys. **B182**, 77 (1981).
- S. Dimopoulos and L. Susskind, Nucl. Phys. **B155**, 237 (1979).
- B. Holdom, Phys. Rev. **D24**, 1441 (1981) and Phys. Lett. **150B**, 301 (1985);
K. Yamawaki, M. Bando, and K. Matumoto, Phys. Rev. Lett. **56**, 1335 (1986);
T.W. Appelquist, D. Karabali, and L.C.R. Wijewardhana, Phys. Rev. Lett. **57**, 957 (1986);
T. Appelquist and L.C.R. Wijewardhana, Phys. Rev. **D35**, 774 (1987) and Phys. Rev. **D36**, 586 (1987).
- E. Eichten and K. Lane, Phys. Lett. **B388**, 803 (1996).
- See the review on "Electroweak Model and Constraints on New Physics" by Langacker and Erler in this *Review*.
- E. Eichten *et al.*, Rev. Mod. Phys. **56**, 579 (1984) and Phys. Rev. **D34**, 1547 (1986).
- E. Eichten, K. Lane, and J. Womersley, Phys. Lett. **B405**, 305 (1997).
- F. Abe *et al.*, FERMILAB-PUB-99/141-E.
- T. Sjostrand, Comp. Phys. Commun. **82**,74 (1994).
- F. Abe *et al.*, Phys. Rev. Lett. **83**, 3124 (1999).
- DØ: M. Narain, presented at the Workshop on New Strong Dynamics at Run II (Fermilab, October 1998).
- CDF: K. Maeshima, presented at the Workshop on New Strong Dynamics at Run II (Fermilab, October 1998).
- L3: Search for technicolour production at lep, L3 Note 2428, June 1999, submitted to the International Europhysics Conference on High Energy Physics (Tampere, Finland, July 1999).
- K. Lane, Phys. Rev. **D60**, 075007 (1999), hep-ph/9903372.
- S. Mrenna, Phys. Lett. **B461**, 352 (1999).
- K. Lane and M. V. Ramana, Phys. Rev. **D44**, 2678 (1991).
- CDF: F. Abe *et al.*, Phys. Rev. **D55**, R5263 (1997).
- K. Cheung and R.M.Harris, hep-ph/9610382.
- CDF: F. Abe *et al.*, Phys. Rev. Lett. **82**, 3206 (1999).
- V.A. Miransky, M. Tanabashi, and K. Yamawaki, Phys. Lett. **221B**, 177 (1989) and Mod. Phys. Lett. **4**, 1043 (1989);
Y. Nambu, EFI-89-08 (1989);
W.J. Marciano, Phys. Rev. Lett. **62**, 2793 (1989).
- W.A. Bardeen, C.T. Hill, and M. Lindner, Phys. Rev. **D41**, 1647 (1990).
- C.T. Hill, Phys. Lett. **B345**, 483 (1995); see also Phys. Lett. **266B**, 419 (1991).
- CDF: F. Abe *et al.*, Phys. Rev. Lett. **82**, 2038 (1999).
- CDF Collaboration, presented by P. Koehn at the International Europhysics Conference on High Energy Physics (Tampere, Finland, July 1999).
- B.A. Dobrescu and C.T. Hill, Phys. Rev. Lett. **81**, 2634 (1998).
- R.S. Chivukula *et al.*, Phys. Rev. **D59**, 075003 (1999).
- H. Collins, A. Grant, and H. Georgi, Phys. Rev. **D61**, 055002 (2000).
- G. Burdman and N. Evans, Phys. Rev. **D59**, 115005 (1999);
E.H. Simmons, Nucl. Phys. **B324**, 315 (1989).
- DØ: B. Abbott *et al.*, Phys. Rev. Lett. **82**, 2457 (1999).
- I. Bertram and E.H. Simmons, Phys. Lett. **B443**, 347 (1998).
- G. Burdman, R.S. Chivukula, and N. Evans, Phys. Rev. **D61**, 035009 (2000).

Searches Particle Listings

Technicolor, Quark and Lepton Compositeness

MASS LIMITS for Resonances in Models of Dynamical Electroweak Symmetry Breaking

VALUE (GeV)	CL%	DOCUMENT ID	TECN	COMMENT
• • • We do not use the following data for averages, fits, limits, etc. • • •				
none 350-440	95	¹ ABE	99F CDF	color-octet techni- ρ , $\rho_T \rightarrow b\bar{b}$
>465	95	² ABE	99H CDF	color-octet techni- ρ , $\rho_T \rightarrow 2\pi_T$
		³ ABE	99N CDF	color-octet techni- ω , $\omega_T \rightarrow \gamma b\bar{b}$
none 260-480	95	⁴ ABE	97G CDF	color-octet techni- ρ , $\rho_T \rightarrow 2$ jets
none 320-480	95	⁵ ABE	95N CDF	color-octet techni- ρ , $\rho_T \rightarrow 2$ jets

¹ ABE 99F search for a new particle X decaying into $b\bar{b}$ in $p\bar{p}$ collisions at $E_{cm} = 1.8$ TeV. See Fig. 7 in the above Note on "Dynamical Electroweak Symmetry Breaking" for the upper limit on $\sigma(p\bar{p} \rightarrow X) \times B(X \rightarrow b\bar{b})$. ABE 99F also exclude top gluons of width $\Gamma = 0.3M$ in the mass interval $280 < M < 670$ GeV, of width $\Gamma = 0.5M$ in the mass interval $340 < M < 640$ GeV, and of width $\Gamma = 0.7M$ in the mass interval $375 < M < 560$ GeV.

² ABE 99H search for the color-octet techni- ρ decaying into a pair of color-triplet technipions which subsequently decay into $\tau + \text{jet}$. See Fig. 6 in the above Note on "Dynamical Electroweak Symmetry Breaking" for the exclusion plot in the $M_{\rho_T} - M_{\pi_T}$ plane.

³ ABE 99H search for the techni- ω decaying into $\gamma\pi_T$. The technipion is assumed to decay $\pi_T \rightarrow b\bar{b}$. See Fig. 2 in the above Note on "Dynamical Electroweak Symmetry Breaking" for the exclusion plot in the $M_{\rho_T} - M_{\pi_T}$ plane.

⁴ ABE 97G search for a new particle X decaying into dijets in $p\bar{p}$ collisions at $E_{cm} = 1.8$ TeV. See Fig. 5 in the above Note on "Dynamical Electroweak Symmetry Breaking" for the upper limit on $\sigma(p\bar{p} \rightarrow X) \times B(X \rightarrow 2j)$.

⁵ ABE 95N search for a new particle decaying into dijets in $p\bar{p}$ collisions at $E_{cm} = 1.8$ TeV.

REFERENCES FOR Technicolor

ABE	99F	PRL 82 2038	F. Abe et al.	(CDF Collab.)
ABE	99H	PRL 82 3206	F. Abe et al.	(CDF Collab.)
ABE	99N	PRL 83 3124	F. Abe et al.	(CDF Collab.)
ABE	97G	PR D55 R5263	F. Abe et al.	(CDF Collab.)
ABE	95N	PRL 74 3538	F. Abe et al.	(CDF Collab.)

Quark and Lepton Compositeness, Searches for

SEARCHES FOR QUARK AND LEPTON COMPOSITENESS

Revised 1999 by K. Hagiwara (KEK) and K. Hikasa (Tohoku Univ.).

If quarks and leptons are made of constituents, then at the scale of constituent binding energies, there should appear new interactions among quarks and leptons. At energies much below the compositeness scale (Λ), these interactions are suppressed by inverse powers of Λ . The dominant effect should come from the lowest dimensional interactions with four fermions (contact terms), whose most general chirally invariant form reads [1]

$$L = \frac{g^2}{2\Lambda^2} \left[\eta_{LL} \bar{\psi}_L \gamma_\mu \psi_L \bar{\psi}_L \gamma^\mu \psi_L + \eta_{RR} \bar{\psi}_R \gamma_\mu \psi_R \bar{\psi}_R \gamma^\mu \psi_R + 2\eta_{LR} \bar{\psi}_L \gamma_\mu \psi_L \bar{\psi}_R \gamma^\mu \psi_R \right]. \quad (1)$$

Chiral invariance provides a natural explanation why quark and lepton masses are much smaller than their inverse size Λ . We may determine the scale Λ unambiguously by using the above form of the effective interactions; the conventional method [1] is to fix its scale by setting $g^2/4\pi = g^2(\Lambda)/4\pi = 1$ for the new strong interaction coupling and by setting the largest magnitude of the coefficients $\eta_{\alpha\beta}$ to be unity. In the following, we denote

$$\begin{aligned} \Lambda &= \Lambda_{LL}^\pm \text{ for } (\eta_{LL}, \eta_{RR}, \eta_{LR}) = (\pm 1, 0, 0), \\ \Lambda &= \Lambda_{RR}^\pm \text{ for } (\eta_{LL}, \eta_{RR}, \eta_{LR}) = (0, \pm 1, 0), \\ \Lambda &= \Lambda_{VV}^\pm \text{ for } (\eta_{LL}, \eta_{RR}, \eta_{LR}) = (\pm 1, \pm 1, \pm 1), \\ \Lambda &= \Lambda_{AA}^\pm \text{ for } (\eta_{LL}, \eta_{RR}, \eta_{LR}) = (\pm 1, \pm 1, \mp 1), \end{aligned} \quad (2)$$

as typical examples. Such interactions can arise by constituent interchange (when the fermions have common constituents, e.g., for $ee \rightarrow ee$) and/or by exchange of the binding quanta (when- ever binding quanta couple to constituents of both particles).

Another typical consequence of compositeness is the appearance of excited leptons and quarks (ℓ^* and q^*). Phenomenologically, an excited lepton is defined to be a heavy lepton which shares leptonic quantum number with one of the existing leptons (an excited quark is defined similarly). For example, an excited electron e^* is characterized by a nonzero transition-magnetic coupling with electrons. Smallness of the lepton mass and the success of QED prediction for $g-2$ suggest chirality conservation, i.e., an excited lepton should not couple to both left- and right-handed components of the corresponding lepton.

Excited leptons may be classified by $SU(2) \times U(1)$ quantum numbers. Typical examples are:

1. Sequential type

$$\begin{pmatrix} \nu^* \\ \ell^* \end{pmatrix}_L, \quad [\nu_R^*], \quad \ell_R^*.$$

ν_R^* is necessary unless ν^* has a Majorana mass.

2. Mirror type

$$[\nu_L^*], \quad \ell_L^*, \quad \begin{pmatrix} \nu^* \\ \ell^* \end{pmatrix}_R.$$

3. Homodoublet type

$$\begin{pmatrix} \nu^* \\ \ell^* \end{pmatrix}_L, \quad \begin{pmatrix} \nu^* \\ \ell^* \end{pmatrix}_R.$$

Similar classification can be made for excited quarks.

Excited fermions can be pair produced via their gauge couplings. The couplings of excited leptons with Z are listed in the following table (for notation see Eq. (1) in "Standard Model of Electroweak Interactions"):

	Sequential type	Mirror type	Homodoublet type
$V\ell^*$	$-\frac{1}{2} + 2\sin^2\theta_W$	$-\frac{1}{2} + 2\sin^2\theta_W$	$-1 + 2\sin^2\theta_W$
$A\ell^*$	$-\frac{1}{2}$	$+\frac{1}{2}$	0
$V\nu_D^*$	$+\frac{1}{2}$	$+\frac{1}{2}$	+1
$A\nu_D^*$	$+\frac{1}{2}$	$-\frac{1}{2}$	0
$V\nu_M^*$	0	0	—
$A\nu_M^*$	+1	-1	—

Here ν_D^* (ν_M^*) stands for Dirac (Majorana) excited neutrino. The corresponding couplings of excited quarks can be easily obtained. Although form factor effects can be present for the gauge couplings at $q^2 \neq 0$, they are usually neglected.

In addition, transition magnetic type couplings with a gauge boson are expected. These couplings can be generally parametrized as follows:

$$\begin{aligned} \mathcal{L} = & \frac{\lambda_\gamma^{(f^*)}}{2m_{f^*}} \bar{f}^* \sigma^{\mu\nu} (\eta_L \frac{1-\gamma_5}{2} + \eta_R \frac{1+\gamma_5}{2}) f F_{\mu\nu} \\ & + \frac{\lambda_Z^{(f^*)}}{2m_{f^*}} \bar{f}^* \sigma^{\mu\nu} (\eta_L \frac{1-\gamma_5}{2} + \eta_R \frac{1+\gamma_5}{2}) f Z_{\mu\nu} \\ & + \frac{\lambda_W^{(\ell^*)}}{2m_{\ell^*}} \bar{\ell}^* \sigma^{\mu\nu} \frac{1-\gamma_5}{2} \nu W_{\mu\nu} \\ & + \frac{\lambda_W^{(\nu^*)}}{2m_{\nu^*}} \bar{\nu}^* \sigma^{\mu\nu} (\eta_L \frac{1-\gamma_5}{2} + \eta_R \frac{1+\gamma_5}{2}) \ell W_{\mu\nu}^\dagger \\ & + \text{h.c.} , \end{aligned} \quad (3)$$

where $g = e/\sin\theta_W$, $F_{\mu\nu} = \partial_\mu A_\nu - \partial_\nu A_\mu$ is the photon field strength, $Z_{\mu\nu} = \partial_\mu Z_\nu - \partial_\nu Z_\mu$, etc. The normalization of the coupling is chosen such that

$$\max(|\eta_L|, |\eta_R|) = 1 .$$

Chirality conservation requires

$$\eta_L \eta_R = 0 . \quad (4)$$

These couplings can arise from $SU(2) \times U(1)$ -invariant higher-dimensional interactions. A well-studied model is the interaction of homodoublet type ℓ^* with the Lagrangian [2,3]

$$\mathcal{L} = \frac{1}{2\Lambda} \bar{L}^* \sigma^{\mu\nu} (g f \frac{\tau^a}{2} W_{\mu\nu}^a + g' f' Y B_{\mu\nu}) \frac{1-\gamma_5}{2} L + \text{h.c.} , \quad (5)$$

where L denotes the lepton doublet (ν, ℓ) , Λ is the compositeness scale, g, g' are $SU(2)$ and $U(1)_Y$ gauge couplings, and $W_{\mu\nu}^a$ and $B_{\mu\nu}$ are the field strengths for $SU(2)$ and $U(1)_Y$ gauge fields. The same interaction occurs for mirror-type excited leptons. For sequential-type excited leptons, the ℓ^* and ν^* couplings become unrelated, and the couplings receive the extra suppression of $(250 \text{ GeV})/\Lambda$ or m_{L^*}/Λ . In any case, these couplings satisfy the relation

$$\lambda_W = -\sqrt{2} \sin^2 \theta_W (\lambda_Z \cot \theta_W + \lambda_\gamma) . \quad (6)$$

Additional coupling with gluons is possible for excited quarks:

$$\begin{aligned} \mathcal{L} = & \frac{1}{2\Lambda} \bar{Q}^* \sigma^{\mu\nu} \left(g_s f_s \frac{\lambda^a}{2} G_{\mu\nu}^a + g' f' \frac{\tau^a}{2} W_{\mu\nu}^a + g' f' Y B_{\mu\nu} \right) \\ & \times \frac{1-\gamma_5}{2} Q + \text{h.c.} , \end{aligned} \quad (7)$$

where Q denotes a quark doublet, g_s is the QCD gauge coupling, and $G_{\mu\nu}^a$ the gluon field strength.

Some experimental analyses assume the relation $\eta_L = \eta_R = 1$, which violates chiral symmetry. We encode the results of such analyses if the crucial part of the cross section is proportional to the factor $\eta_L^2 + \eta_R^2$ and the limits can be reinterpreted as those for chirality conserving cases $(\eta_L, \eta_R) = (1, 0)$ or $(0, 1)$ after rescaling λ .

Several different conventions are used by LEP experiments to express the transition magnetic couplings. To facilitate comparison, we reexpress these in terms of λ_Z and λ_γ using the following relations and taking $\sin^2 \theta_W = 0.23$. We assume chiral couplings, i.e., $|c| = |d|$ in the notation of Ref. 2.

1. ALEPH (charged lepton and neutrino)

$$\lambda_Z^{\text{ALEPH}} = \frac{1}{2} \lambda_Z \quad (1990 \text{ papers}) \quad (8a)$$

$$\frac{2c}{\Lambda} = \frac{\lambda_Z}{m_{\ell^*} [\text{or } m_{\nu^*}]} \quad (\text{for } |c| = |d|) \quad (8b)$$

2. ALEPH (quark)

$$\lambda_u^{\text{ALEPH}} = \frac{\sin \theta_W \cos \theta_W}{\sqrt{\frac{1}{4} - \frac{2}{3} \sin^2 \theta_W + \frac{8}{9} \sin^4 \theta_W}} \lambda_Z = 1.11 \lambda_Z \quad (9)$$

3. L3 and DELPHI (charged lepton)

$$\lambda^{L3} = \lambda_Z^{\text{DELPHI}} = -\frac{\sqrt{2}}{\cot \theta_W - \tan \theta_W} \lambda_Z = -1.10 \lambda_Z \quad (10)$$

4. L3 (neutrino)

$$f_Z^{L3} = \sqrt{2} \lambda_Z \quad (11)$$

5. OPAL (charged lepton)

$$\frac{f^{\text{OPAL}}}{\Lambda} = -\frac{2}{\cot \theta_W - \tan \theta_W} \frac{\lambda_Z}{m_{\ell^*}} = -1.56 \frac{\lambda_Z}{m_{\ell^*}} \quad (12)$$

6. OPAL (quark)

$$\frac{f^{\text{OPAL}c}}{\Lambda} = \frac{\lambda_Z}{2m_{q^*}} \quad (\text{for } |c| = |d|) \quad (13)$$

7. DELPHI (charged lepton)

$$\lambda_\gamma^{\text{DELPHI}} = -\frac{1}{\sqrt{2}} \lambda_\gamma \quad (14)$$

If leptons are made of color triplet and antitriplet constituents, we may expect their color-octet partners. Transitions between the octet leptons (ℓ_8) and the ordinary lepton (ℓ) may take place via the dimension-five interactions

$$\mathcal{L} = \frac{1}{2\Lambda} \sum_{\ell} \left\{ \bar{\ell}_8^\alpha g_S F_{\mu\nu}^\alpha \sigma^{\mu\nu} (\eta_L \ell_L + \eta_R \ell_R) + \text{h.c.} \right\} \quad (15)$$

where the summation is over charged leptons and neutrinos. The leptonic chiral invariance implies $\eta_L \eta_R = 0$ as before.

References

1. E.J. Eichten, K.D. Lane, and M.E. Peskin, Phys. Rev. Lett. **50**, 811 (1983).
2. K. Hagiwara, S. Komamiya, and D. Zeppenfeld, Z. Phys. **C29**, 115 (1985).
3. N. Cabibbo, L. Maiani, and Y. Srivastava, Phys. Lett. **139B**, 459 (1984).

Searches Particle Listings

Quark and Lepton Compositeness

SCALE LIMITS for Contact Interactions: $\Lambda(eeee)$

Limits are for Λ_{LL}^{\pm} only. For other cases, see each reference.

$\Lambda_{LL}^+(TeV)$	$\Lambda_{LL}^-(TeV)$	CL%	DOCUMENT ID	TECN	COMMENT
> 3.5	> 3.2	95	¹ BARATE 00i	ALEP	$E_{cm} = 130-183$ GeV
> 3.1	> 3.0	95	ABBIENDI 99	OPAL	$E_{cm} = 130-136, 161-172, 183$ GeV
• • • We do not use the following data for averages, fits, limits, etc. • • •					
> 2.2	> 2.8	95	ABREU 99a	DLPH	$E_{cm} = 130-172$ GeV
> 2.7	> 2.4	95	ACCIARRI 98j	L3	$E_{cm} = 130-172$ GeV
> 3.0	> 2.5	95	ACKERSTAFF 98v	OPAL	$E_{cm} = 130-172$ GeV
> 2.4	> 2.2	95	ACKERSTAFF 97c	OPAL	$E_{cm} = 130-136, 161$ GeV
> 1.7	> 2.3	95	² ARIMA 97	VNS	$E_{cm} = 57.77$ GeV
> 1.6	> 2.0	95	³ BUSKULIC 93q	ALEP	$E_{cm} = 88.25-94.25$ GeV
> 1.6		95	^{3,4} BUSKULIC 93q	RVUE	
	> 2.2	95	BUSKULIC 93q	RVUE	
	> 3.6	95	⁵ KROHA 92	RVUE	
		95	⁵ KROHA 92	RVUE	
> 1.3		95			
> 0.7	> 2.8	95	BEHREND 91c	CELL	$E_{cm} = 35$ GeV
> 1.3	> 1.3	95	KIM 89	AMY	$E_{cm} = 50-57$ GeV
> 1.4	> 3.3	95	⁶ BRAUNSCH... 88	TASS	$E_{cm} = 12-46.8$ GeV
> 1.0	> 0.7	95	⁷ FERNANDEZ 87b	MAC	$E_{cm} = 29$ GeV
> 1.1	> 1.4	95	⁸ BARTEL 86c	JADE	$E_{cm} = 12-46.8$ GeV
> 1.17	> 0.87	95	⁹ DERRICK 86	HRS	$E_{cm} = 29$ GeV
> 1.1	> 0.76	95	¹⁰ BERGER 85b	PLUT	$E_{cm} = 34.7$ GeV

- ¹ BARATE 00i limits are from $e^+e^- \rightarrow q\bar{q}$ cross section and jet-charge asymmetry at 130-183 GeV.
- ² $Z-Z'$ mixing is assumed to be zero.
- ³ BUSKULIC 93q uses the following prescription to obtain the limit: when the naive 95%CL limit is better than the statistically expected sensitivity for the limit, the latter is adopted for the limit.
- ⁴ This BUSKULIC 93q value is from ALEPH data plus PEP/PETRA/TRISTAN data re-analyzed by KROHA 92.
- ⁵ KROHA 92 limit is from fit to BERGER 85b, BARTEL 86c, DERRICK 86b, FERNANDEZ 87b, BRAUNSCHWEIG 88, BEHREND 91b, and BEHREND 91c. The fit gives $\eta/\Lambda_{LL}^2 = +0.230 \pm 0.206$ TeV⁻².
- ⁶ BRAUNSCHWEIG 88 assumed $m_Z = 92$ GeV and $\sin^2\theta_W = 0.23$.
- ⁷ FERNANDEZ 87b assumed $\sin^2\theta_W = 0.22$.
- ⁸ BARTEL 86c assumed $m_Z = 93$ GeV and $\sin^2\theta_W = 0.217$.
- ⁹ DERRICK 86 assumed $m_Z = 93$ GeV and $g_V^2 = (-1/2 + 2\sin^2\theta_W)^2 = 0.004$.
- ¹⁰ BERGER 85b assumed $m_Z = 93$ GeV and $\sin^2\theta_W = 0.217$.

SCALE LIMITS for Contact Interactions: $\Lambda(e\mu\mu)$

Limits are for Λ_{LL}^{\pm} only. For other cases, see each reference.

$\Lambda_{LL}^+(TeV)$	$\Lambda_{LL}^-(TeV)$	CL%	DOCUMENT ID	TECN	COMMENT
> 4.0	> 4.7	95	¹¹ BARATE 00i	ALEP	$E_{cm} = 130-183$ GeV
> 4.5	> 4.3	95	ABBIENDI 99	OPAL	$E_{cm} = 130-136, 161-172, 183$ GeV
• • • We do not use the following data for averages, fits, limits, etc. • • •					
> 3.4	> 2.7	95	ABREU 99a	DLPH	$E_{cm} = 130-172$ GeV
> 3.6	> 2.4	95	ACCIARRI 98j	L3	$E_{cm} = 130-172$ GeV
> 2.9	> 3.4	95	ACKERSTAFF 98v	OPAL	$E_{cm} = 130-172$ GeV
> 3.1	> 2.0	95	MIURA 98	VNS	$E_{cm} = 57.77$ GeV
> 2.4	> 2.9	95	ACKERSTAFF 97c	OPAL	$E_{cm} = 130-136, 161$ GeV
> 1.7	> 2.2	95	¹² VELISSARIS 94	AMY	$E_{cm} = 57.8$ GeV
> 1.3	> 1.5	95	¹² BUSKULIC 93q	ALEP	$E_{cm} = 88.25-94.25$ GeV
> 2.6	> 1.9	95	^{12,13} BUSKULIC 93q	RVUE	
> 2.3	> 2.0	95	HOWELL 92	TOPZ	$E_{cm} = 52-61.4$ GeV
	> 1.7	95	¹⁴ KROHA 92	RVUE	
> 2.5	> 1.5	95	BEHREND 91c	CELL	$E_{cm} = 35-43$ GeV
> 1.6	> 2.0	95	ABE 90i	VNS	$E_{cm} = 50-60.8$ GeV
> 1.9	> 1.0	95	KIM 89	AMY	$E_{cm} = 50-57$ GeV
> 2.3	> 1.3	95	⁶ BRAUNSCH... 88d	TASS	$E_{cm} = 30-46.8$ GeV
> 4.4	> 2.1	95	¹⁶ BARTEL 86c	JADE	$E_{cm} = 12-46.8$ GeV
> 2.9	> 0.86	95	¹⁷ BERGER 85	PLUT	$E_{cm} = 34.7$ GeV

- ¹¹ BARATE 00i limits are from $e^+e^- \rightarrow q\bar{q}$ cross section and jet-charge asymmetry at 130-183 GeV.
- ¹² BUSKULIC 93q and VELISSARIS 94 use the following prescription to obtain the limit: when the naive 95%CL limit is better than the statistically expected sensitivity for the limit, the latter is adopted for the limit.
- ¹³ This BUSKULIC 93q value is from ALEPH data plus PEP/PETRA/TRISTAN data re-analyzed by KROHA 92.
- ¹⁴ KROHA 92 limit is from fit to BARTEL 86c, BEHREND 87c, BRAUNSCHWEIG 88d, BRAUNSCHWEIG 89c, ABE 90i, and BEHREND 91c. The fit gives $\eta/\Lambda_{LL}^2 = -0.155 \pm 0.095$ TeV⁻².
- ¹⁵ ABE 90i assumed $m_Z = 91.163$ GeV and $\sin^2\theta_W = 0.231$.
- ¹⁶ BARTEL 86c assumed $m_Z = 93$ GeV and $\sin^2\theta_W = 0.217$.
- ¹⁷ BERGER 85 assumed $m_Z = 93$ GeV and $\sin^2\theta_W = 0.217$.

SCALE LIMITS for Contact Interactions: $\Lambda(eerr)$

Limits are for Λ_{LL}^{\pm} only. For other cases, see each reference.

$\Lambda_{LL}^+(TeV)$	$\Lambda_{LL}^-(TeV)$	CL%	DOCUMENT ID	TECN	COMMENT
> 3.9	> 3.7	95	¹⁸ BARATE 00i	ALEP	$E_{cm} = 130-183$ GeV
> 3.8	> 4.0	95	ABBIENDI 99	OPAL	$E_{cm} = 130-136, 161-172, 183$ GeV

• • • We do not use the following data for averages, fits, limits, etc. • • •

> 2.8	> 2.6	95	ABREU 99a	DLPH	$E_{cm} = 130-172$ GeV
> 2.4	> 2.8	95	ACCIARRI 98j	L3	$E_{cm} = 130-172$ GeV
> 2.3	> 3.7	95	ACKERSTAFF 98v	OPAL	$E_{cm} = 130-172$ GeV
> 1.9	> 3.0	95	ACKERSTAFF 97c	OPAL	$E_{cm} = 130-136, 161$ GeV
> 1.4	> 2.0	95	¹⁹ VELISSARIS 94	AMY	$E_{cm} = 57.8$ GeV
> 1.0	> 1.5	95	¹⁹ BUSKULIC 93q	ALEP	$E_{cm} = 88.25-94.25$ GeV
> 1.8	> 2.3	95	^{19,20} BUSKULIC 93q	RVUE	
> 1.9	> 1.7	95	HOWELL 92	TOPZ	$E_{cm} = 52-61.4$ GeV
> 1.9	> 2.9	95	²¹ KROHA 92	RVUE	
> 1.6	> 2.3	95	BEHREND 91c	CELL	$E_{cm} = 35-43$ GeV
> 1.8	> 1.3	95	²² ABE 90i	VNS	$E_{cm} = 50-60.8$ GeV
> 2.2	> 3.2	95	²³ BARTEL 86	JADE	$E_{cm} = 12-46.8$ GeV

- ¹⁸ BARATE 00i limits are from $e^+e^- \rightarrow q\bar{q}$ cross section and jet-charge asymmetry at 130-183 GeV.
- ¹⁹ BUSKULIC 93q and VELISSARIS 94 use the following prescription to obtain the limit: when the naive 95%CL limit is better than the statistically expected sensitivity for the limit, the latter is adopted for the limit.
- ²⁰ This BUSKULIC 93q value is from ALEPH data plus PEP/PETRA/TRISTAN data re-analyzed by KROHA 92.
- ²¹ KROHA 92 limit is from fit to BARTEL 86c, BEHREND 89b, BRAUNSCHWEIG 89c, ABE 90i, and BEHREND 91c. The fit gives $\eta/\Lambda_{LL}^2 = +0.095 \pm 0.120$ TeV⁻².
- ²² ABE 90i assumed $m_Z = 91.163$ GeV and $\sin^2\theta_W = 0.231$.
- ²³ BARTEL 86 assumed $m_Z = 93$ GeV and $\sin^2\theta_W = 0.217$.

SCALE LIMITS for Contact Interactions: $\Lambda(eeee)$

Lepton universality assumed. Limits are for Λ_{LL}^{\pm} only. For other cases, see each reference.

$\Lambda_{LL}^+(TeV)$	$\Lambda_{LL}^-(TeV)$	CL%	DOCUMENT ID	TECN	COMMENT
> 5.3	> 5.5	95	²⁴ BARATE 00i	ALEP	$E_{cm} = 130-183$ GeV
• • • We do not use the following data for averages, fits, limits, etc. • • •					
> 5.2	> 5.3	95	ABBIENDI 99	OPAL	$E_{cm} = 130-136, 161-172, 183$ GeV
> 4.4	> 4.2	95	ABREU 99a	DLPH	$E_{cm} = 130-172$ GeV
> 4.0	> 3.1	95	ACCIARRI 98j	L3	$E_{cm} = 130-172$ GeV
> 3.4	> 4.4	95	ACKERSTAFF 98v	OPAL	$E_{cm} = 130-172$ GeV
> 2.7	> 3.8	95	ACKERSTAFF 97c	OPAL	$E_{cm} = 130-136, 161$ GeV
> 3.0	> 2.3	95	^{25,26} BUSKULIC 93q	ALEP	$E_{cm} = 88.25-94.25$ GeV
> 3.5	> 2.8	95	^{26,27} BUSKULIC 93q	RVUE	
> 2.5	> 2.2	95	²⁸ HOWELL 92	TOPZ	$E_{cm} = 52-61.4$ GeV
> 3.4	> 2.7	95	²⁹ KROHA 92	RVUE	

- ²⁴ BARATE 00i limits are from $e^+e^- \rightarrow q\bar{q}$ cross section and jet-charge asymmetry at 130-183 GeV.
- ²⁵ From $e^+e^- \rightarrow e^+e^-, \mu^+\mu^-,$ and $\tau^+\tau^-$.
- ²⁶ BUSKULIC 93q uses the following prescription to obtain the limit: when the naive 95%CL limit is better than the statistically expected sensitivity for the limit, the latter is adopted for the limit.
- ²⁷ This BUSKULIC 93q value is from ALEPH data plus PEP/PETRA/TRISTAN data re-analyzed by KROHA 92.
- ²⁸ HOWELL 92 limit is from $e^+e^- \rightarrow \mu^+\mu^-$ and $\tau^+\tau^-$.
- ²⁹ KROHA 92 limit is from fit to most PEP/PETRA/TRISTAN data. The fit gives $\eta/\Lambda_{LL}^2 = -0.0200 \pm 0.0666$ TeV⁻².

SCALE LIMITS for Contact Interactions: $\Lambda(eeqq)$

Limits are for Λ_{LL}^{\pm} only. For other cases, see each reference.

$\Lambda_{LL}^+(TeV)$	$\Lambda_{LL}^-(TeV)$	CL%	DOCUMENT ID	TECN	COMMENT
> 5.4	> 6.2	95	³⁰ BARATE 00i	ALEP	($eeqq$)
> 5.6	> 4.9	95	³¹ BARATE 00i	ALEP	($eabb$)
• • • We do not use the following data for averages, fits, limits, etc. • • •					
> 4.4	> 2.8	95	³² ABBIENDI 99	OPAL	($eeqq$)
> 4.0	> 4.8	95	³³ ABBIENDI 99	OPAL	($eabb$)
> 3.3	> 4.2	95	³⁴ ABBOTT 99d	D0	($eeqq$)
> 2.4	> 2.8	95	³⁵ ABREU 99a	DLPH	($eeqq$) (d or s quark)
> 4.4	> 3.9	95	³⁵ ABREU 99a	DLPH	($eabb$)
> 1.0	> 2.4	95	³⁵ ABREU 99a	DLPH	($eeuu$)
> 1.0	> 2.1	95	³⁵ ABREU 99a	DLPH	($eecc$)
> 4.0	> 3.4	95	³⁶ ZARNECKI 99	RVUE	($eedd$)
> 4.3	> 5.6	95	³⁶ ZARNECKI 99	RVUE	($eeuu$)
> 3.0	> 2.1	95	³⁷ ACCIARRI 98j	L3	($eeuu$)
> 3.4	> 2.2	95	³⁸ ACKERSTAFF 98v	OPAL	($eeqq$)
> 4.0	> 2.8	95	³⁹ ACKERSTAFF 98v	OPAL	($eabb$)
> 2.5	> 3.7	95	⁴⁰ ABE 97t	CDF	($eeqq$) (isosinglet)
> 2.5	> 2.1	95	⁴¹ ACKERSTAFF 97c	OPAL	($eeqq$)
> 3.1	> 2.9	95	⁴² ACKERSTAFF 97c	OPAL	($eabb$)
> 7.4	> 11.7	95	⁴³ DEANDREA 97	RVUE	$eeuu$, atomic parity violation
> 2.3	> 1.0	95	⁴⁴ AID 95	H1	($eeqq$) (u, d quarks)
1.7	> 2.2	95	⁴⁵ ABE 91d	CDF	($eeqq$) (u, d quarks)
> 1.2		95	⁴⁶ ADACHI 91	TOPZ	($eeqq$) (flavor-universal)
	> 1.6	95	⁴⁶ ADACHI 91	TOPZ	($eeqq$) (flavor-universal)
> 0.6	> 1.7	95	⁴⁷ BEHREND 91c	CELL	($eecc$)
> 1.1	> 1.0	95	⁴⁷ BEHREND 91c	CELL	($eabb$)
> 0.9		95	⁴⁸ ABE 89l	VNS	($eeqq$) (flavor-universal)
	> 1.7	95	⁴⁸ ABE 89l	VNS	($eeqq$) (flavor-universal)
> 1.05	> 1.61	95	⁴⁹ HAGIWARA 89	RVUE	($eecc$)
> 1.21	> 0.53	95	⁵⁰ HAGIWARA 89	RVUE	($eabb$)

- 30 BARATE 00i limits are from $e^+e^- \rightarrow q\bar{q}$ cross section and jet-charge asymmetry at 130–183 GeV.
- 31 BARATE 00i limits are from R_b and jet-charge asymmetry at 130–183 GeV.
- 32 ABBIENDI 99 limits are from $e^+e^- \rightarrow q\bar{q}$ cross section at 130–136, 161–172, 183 GeV.
- 33 ABBIENDI 99 limits are from R_b at 130–136, 161–172, 183 GeV.
- 34 ABBOTT 99d limits are from e^+e^- mass distribution in $p\bar{p} \rightarrow e^+e^-X$ at $E_{cm}=1.8$ TeV.
- 35 ABREU 99A limits are from flavor-tagged $e^+e^- \rightarrow q\bar{q}$ cross section at 130–172 GeV.
- 36 ZARNECKI 99 use data from HERA, LEP, Tevatron, and various low-energy experiments.
- 37 ACCIARRI 98J limits are from $e^+e^- \rightarrow q\bar{q}$ cross section at $E_{cm}=130$ –172 GeV.
- 38 ACKERSTAFF 98v limits are from $e^+e^- \rightarrow q\bar{q}$ at $E_{cm}=130$ –172 GeV.
- 39 ACKERSTAFF 98v limits are from R_b measurements at $E_{cm}=130$ –172 GeV.
- 40 ABE 97T limits are from e^+e^- mass distribution in $p\bar{p} \rightarrow e^+e^-X$ at $E_{cm}=1.8$ TeV.
- 41 ACKERSTAFF 97C limits are from $e^+e^- \rightarrow q\bar{q}$ cross section at $E_{cm}=130$ –136 GeV and 161 GeV.
- 42 ACKERSTAFF 97C limits are R_b measurements at $E_{cm}=133$ GeV and 161 GeV.
- 43 DEANDREA 97 limit is from atomic parity violation of cesium. The limit is eluded if the contact interactions are parity conserving.
- 44 AID 95 limits are from the Q^2 spectrum measurement of $ep \rightarrow eX$.
- 45 ABE 91D limits are from e^+e^- mass distribution in $p\bar{p} \rightarrow e^+e^-X$ at $E_{cm}=1.8$ TeV.
- 46 ADACHI 91 limits are from differential jet cross section. Universality of $\Lambda(eeqq)$ for five flavors is assumed.
- 47 BEHREND 91C is from data at $E_{cm}=35$ –43 GeV.
- 48 ABE 89L limits are from jet charge asymmetry. Universality of $\Lambda(eqqq)$ for five flavors is assumed.
- 49 The HAGIWARA 89 limit is derived from forward-backward asymmetry measurements of D/D^* mesons by ALTHOFF 83C, BARTEL 84E, and BARINGER 88.
- 50 The HAGIWARA 89 limit is derived from forward-backward asymmetry measurement of b hadrons by BARTEL 84D.

SCALE LIMITS for Contact Interactions: $\Lambda(\mu\mu qq)$

$\Lambda_{LL}^+(TeV)$	$\Lambda_{LL}^-(TeV)$	CL%	DOCUMENT ID	TECN	COMMENT
> 2.9	> 4.2	95	51 ABE	97T CDF	$(\mu\mu qq)$ (isosinglet)
• • • We do not use the following data for averages, fits, limits, etc. • • •					
> 1.4	> 1.6	95	ABE	92B CDF	$(\mu\mu qq)$ (isosinglet)
51 ABE 97T limits are from $\mu^+\mu^-$ mass distribution in $p\bar{p} \rightarrow \mu^+\mu^-X$ at $E_{cm}=1.8$ TeV.					

SCALE LIMITS for Contact Interactions: $\Lambda(\ell\nu\ell\nu)$

VALUE (TeV)	CL%	DOCUMENT ID	TECN	COMMENT
> 3.10	90	52 JODIDIO	86 SPEC	$\Lambda_{LR}^+(\nu_\mu\nu_e\mu^e)$
• • • We do not use the following data for averages, fits, limits, etc. • • •				
> 3.8		53 DIAZCRUZ	94 RVUE	$\Lambda_{LL}^+(\tau\nu_\tau\nu_e\nu_e)$
> 8.1		53 DIAZCRUZ	94 RVUE	$\Lambda_{LL}^-(\tau\nu_\tau\nu_e\nu_e)$
> 4.1		54 DIAZCRUZ	94 RVUE	$\Lambda_{LL}^+(\tau\nu_\tau\nu_\mu\nu_\mu)$
> 6.5		54 DIAZCRUZ	94 RVUE	$\Lambda_{LL}^-(\tau\nu_\tau\nu_\mu\nu_\mu)$
52 JODIDIO 86 limit is from $\mu^+ \rightarrow \bar{\nu}_\mu e^+ \nu_e$. Chirality invariant interactions $L = (g^2/\Lambda^2)$ [$\eta_{LL}(\bar{\nu}_\mu L \gamma^\alpha \mu_L)(\bar{e} L \gamma^\alpha \nu_e L) + \eta_{LR}(\bar{\nu}_\mu L \gamma^\alpha \nu_e L)(\bar{e} R \gamma^\alpha \mu_R)$] with $g^2/4\pi = 1$ and $(\eta_{LL}, \eta_{LR}) = (0, \pm 1)$ are taken. No limits are given for Λ_{LL}^\pm with $(\eta_{LL}, \eta_{LR}) = (\pm 1, 0)$. For more general constraints with right-handed neutrinos and chirality nonconserving contact interactions, see their text.				
53 DIAZCRUZ 94 limits are from $\Gamma(\tau \rightarrow e\nu\nu)$ and assume flavor-dependent contact interactions with $\Lambda(\tau\nu_\tau\nu_e\nu_e) \ll \Lambda(\mu\nu_\mu\nu_e\nu_e)$.				
54 DIAZCRUZ 94 limits are from $\Gamma(\tau \rightarrow \mu\nu\nu)$ and assume flavor-dependent contact interactions with $\Lambda(\tau\nu_\tau\nu_\mu\nu_\mu) \ll \Lambda(\mu\nu_\mu\nu_e\nu_e)$.				

SCALE LIMITS for Contact Interactions: $\Lambda(qqqq)$

Limits are for Λ_{LL}^\pm with color-singlet isoscalar exchanges among u_L 's and d_L 's only, unless otherwise noted. See EICHTEN 84 for details.

VALUE (TeV)	CL%	DOCUMENT ID	TECN	COMMENT
> 2.7	95	55 ABBOTT	99C D0	$p\bar{p} \rightarrow$ dijet mass. Λ_{LL}^+
• • • We do not use the following data for averages, fits, limits, etc. • • •				
> 2.1	95	56 ABBOTT	98G D0	$p\bar{p} \rightarrow$ dijet angl. Λ_{LL}^+
		57 BERTRAM	98 RVUE	$p\bar{p} \rightarrow$ dijet mass
		58 ABE	96 CDF	$p\bar{p} \rightarrow$ jets inclusive
> 1.6	95	59 ABE	96S CDF	$p\bar{p} \rightarrow$ dijet angl.; Λ_{LL}^+
> 1.3	95	60 ABE	93G CDF	$p\bar{p} \rightarrow$ dijet mass
> 1.4	95	61 ABE	92D CDF	$p\bar{p} \rightarrow$ jets inclusive
> 1.0	95	62 ABE	92M CDF	$p\bar{p} \rightarrow$ dijet angl.
> 0.825	95	63 ALITTI	91B UA2	$p\bar{p} \rightarrow$ jets inclusive
> 0.700	95	61 ABE	89 CDF	$p\bar{p} \rightarrow$ jets inclusive
> 0.330	95	64 ABE	89H CDF	$p\bar{p} \rightarrow$ dijet angl.
> 0.400	95	65 ARNISON	86C UA1	$p\bar{p} \rightarrow$ jets inclusive
> 0.415	95	66 ARNISON	86D UA1	$p\bar{p} \rightarrow$ dijet angl.
> 0.370	95	67 APPEL	85 UA2	$p\bar{p} \rightarrow$ jets inclusive
> 0.275	95	68 BAGNAIA	84C UA2	Repl. by APPEL 85

- 55 The quoted limit is from inclusive dijet mass spectrum in $p\bar{p}$ collisions at $E_{cm}=1.8$ TeV. ABBOTT 99C also obtain $\Lambda_{LL}^- > 2.4$ TeV. All quarks are assumed composite.
- 56 ABBOTT 98G limit is from dijet angular distribution in $p\bar{p}$ collisions at $E_{cm}=1.8$ TeV. All quarks are assumed composite.
- 57 BERTRAM 98 obtain limit on the scale of color-octet axial-vector flavor-universal contact interactions: $\Lambda_{AB} > 2.1$ TeV. They also obtain a limit $\Lambda_{VB} > 2.4$ TeV on a color-octet flavor-universal vectorial contact interaction.
- 58 ABE 96 finds that the inclusive jet cross section for $E_T > 200$ GeV is significantly higher than the $O(\alpha_s^3)$ perturbative QCD prediction. This could be interpreted as the effect of a contact interaction with $\Lambda_{LL} \sim 1.6$ TeV. However, ABE 96 state that uncertainty in the parton distribution functions, higher-order QCD corrections, and the detector calibration may possibly account for the effect.
- 59 ABE 96S limit is from dijet angular distribution in $p\bar{p}$ collisions at $E_{cm}=1.8$ TeV. The limit for Λ_{LL}^- is > 1.4 TeV. ABE 96S also obtain limits for flavor symmetric contact interactions among all quark flavors: $\Lambda_{LL}^+ > 1.8$ TeV and $\Lambda_{LL}^- > 1.6$ TeV.
- 60 ABE 93G limit is from dijet mass distribution in $p\bar{p}$ collisions at $E_{cm}=1.8$ TeV. The limit is the weakest from several choices of structure functions and renormalization scale.
- 61 Limit is from inclusive jet cross-section data in $p\bar{p}$ collisions at $E_{cm}=1.8$ TeV. The limit takes into account uncertainties in choice of structure functions and in choice of process scale.
- 62 ABE 92M limit is from dijet angular distribution for $m_{dijet} > 550$ GeV in $p\bar{p}$ collisions at $E_{cm}=1.8$ TeV.
- 63 ALITTI 91B limit is from inclusive jet cross section in $p\bar{p}$ collisions at $E_{cm}=630$ GeV. The limit takes into account uncertainties in choice of structure functions and in choice of process scale.
- 64 ABE 89H limit is from dijet angular distribution for $m_{dijet} > 200$ GeV at the Fermilab Tevatron Collider with $E_{cm}=1.8$ TeV. The QCD prediction is quite insensitive to choice of structure functions and choice of process scale.
- 65 ARNISON 86C limit is from the study of inclusive high- p_T jet distributions at the CERN $p\bar{p}$ collider ($E_{cm}=546$ and 630 GeV). The QCD prediction renormalized to the low- p_T region gives a good fit to the data.
- 66 ARNISON 86D limit is from the study of dijet angular distribution in the range 240 < m_{dijet} < 300 GeV at the CERN $p\bar{p}$ collider ($E_{cm}=630$ GeV). QCD prediction using EHLQ structure function (EICHTEN 84) with $\Lambda_{QCD}=0.2$ GeV for the choice of $Q^2 = p_T^2$ gives the best fit to the data.
- 67 APPEL 85 limit is from the study of inclusive high- p_T jet distributions at the CERN $p\bar{p}$ collider ($E_{cm}=630$ GeV). The QCD prediction renormalized to the low- p_T region gives a good description of the data.
- 68 BAGNAIA 84C limit is from the study of jet p_T and dijet mass distributions at the CERN $p\bar{p}$ collider ($E_{cm}=540$ GeV). The limit suffers from the uncertainties in comparing the data with the QCD prediction.

SCALE LIMITS for Contact Interactions: $\Lambda(\nu\nu qq)$

Limits are for Λ_{LL}^\pm only. For other cases, see each reference.

$\Lambda_{LL}^+(TeV)$	$\Lambda_{LL}^-(TeV)$	CL%	DOCUMENT ID	TECN	COMMENT
> 5.0	> 5.4	95	69 MCFARLAND 98	CCFR	νN scattering
69 MCFARLAND 98 assumed a flavor universal interaction. Neutrinos were mostly of muon type.					

MASS LIMITS for Excited e^*

Most e^+e^- experiments assume one-photon or Z exchange. The limits from some e^+e^- experiments which depend on λ have assumed transition couplings which are chirality violating ($\eta_L = \eta_R$). However they can be interpreted as limits for chirality-conserving interactions after multiplying the coupling value λ by $\sqrt{2}$; see Note.

Excited leptons have the same quantum numbers as other ortholeptons. See also the searches for ortholeptons in the "Searches for Heavy Leptons" section.

Limits for Excited e^* from Pair Production

These limits are obtained from $e^+e^- \rightarrow e^{*+}e^{*-}$ and thus rely only on the (electroweak) charge of e^* . Form factor effects are ignored unless noted. For the case of limits from Z decay, the e^* coupling is assumed to be of sequential type. Possible t channel contribution from transition magnetic coupling is neglected. All limits assume $e^* \rightarrow e\gamma$ decay except the limits from $\Gamma(Z)$.

For limits prior to 1987, see our 1992 edition (Physical Review D45, 1 June, Part II (1992)).

VALUE (GeV)	CL%	DOCUMENT ID	TECN	COMMENT
> 90.7	95	70 ABREU	990 DLPH	Homodoublet type
• • • We do not use the following data for averages, fits, limits, etc. • • •				
> 85.0	95	71 ACKERSTAFF	98C OPAL	$e^+e^- \rightarrow e^*e^*$ Homodoublet type
		72 BARATE	98U ALEP	$Z \rightarrow e^*e^*$
> 79.6	95	73,74 ABREU	97B DLPH	$e^+e^- \rightarrow e^*e^*$ Homodoublet type
> 77.9	95	73,75 ABREU	97B DLPH	$e^+e^- \rightarrow e^*e^*$ Sequential type
> 79.7	95	73 ACCIARRI	97G L3	$e^+e^- \rightarrow e^*e^*$ Sequential type
> 79.9	95	73,76 ACKERSTAFF	97 OPAL	$e^+e^- \rightarrow e^*e^*$ Homodoublet type
> 62.5	95	77 ABREU	96K DLPH	$e^+e^- \rightarrow e^*e^*$ Homodoublet type
> 64.7	95	78 ACCIARRI	96O L3	$e^+e^- \rightarrow e^*e^*$ Sequential type
> 66.5	95	78 ALEXANDER	96O OPAL	$e^+e^- \rightarrow e^*e^*$ Homodoublet type
> 65.2	95	78 BUSKULIC	96W ALEP	$e^+e^- \rightarrow e^*e^*$ Sequential type
> 45.6	95	ADRIANI	93M L3	$Z \rightarrow e^*e^*$

Searches Particle Listings

Quark and Lepton Compositeness

>45.6	95	ABREU	92C DLPH	$Z \rightarrow e^* e^*$
>29.8	95	79 BARDADIN...	92 RVUE	$\Gamma(Z)$
>26.1	95	80 DECAMP	92 ALEP	$Z \rightarrow e^* e^*; \Gamma(Z)$
>46.1	95	DECAMP	92 ALEP	$Z \rightarrow e^* e^*$
>33	95	80 ABREU	91F DLPH	$Z \rightarrow e^* e^*; \Gamma(Z)$
>45.0	95	81 ADEVA	90F L3	$Z \rightarrow e^* e^*$
>44.9	95	AKRAWY	90I OPAL	$Z \rightarrow e^* e^*$
>44.6	95	82 DECAMP	90G ALEP	$e^+ e^- \rightarrow e^* e^*$
>30.2	95	ADACHI	89B TOPZ	$e^+ e^- \rightarrow e^* e^*$
>28.3	95	KIM	89 AMY	$e^+ e^- \rightarrow e^* e^*$
>27.9	95	83 ABE	88B VNS	$e^+ e^- \rightarrow e^* e^*$

70 From $e^+ e^-$ collisions at $\sqrt{s} = 183$ GeV. $f=f'$ is assumed. ABREU 990 also obtain limit for $f=f'$ ($e^* \rightarrow \nu W$): $m_{e^*} > 81.3$ GeV.

71 From $e^+ e^-$ collisions at $\sqrt{s} = 170-172$ GeV. ACKERSTAFF 98c also obtain limit from $e^* \rightarrow \nu W$ decay mode: $m_{e^*} > 81.3$ GeV.

72 BARATE 98u obtain limits on the form factor. See their Fig. 14 for limits in mass-form factor plane.

73 From $e^+ e^-$ collisions at $\sqrt{s} = 161$ GeV.

74 ABREU 97b also obtain limit from charged current decay mode $e^* \rightarrow \nu W$, $m_{e^*} > 70.9$ GeV.

75 ABREU 97b also obtain limit from charged current decay mode $e^* \rightarrow \nu W$, $m_{e^*} > 44.6$ GeV.

76 ACKERSTAFF 97 also obtain limit from charged current decay mode $e^* \rightarrow \nu W$, $m_{e^*} > 77.1$ GeV.

77 From $e^+ e^-$ collisions at $\sqrt{s} = 130-136$ GeV.

78 From $e^+ e^-$ collisions at $\sqrt{s} = 130-140$ GeV.

79 BARDADIN-OTWINOWSKA 92 limit is independent of decay modes. Based on $\Delta\Gamma(Z) < 36$ MeV.

80 Limit is independent of e^* decay mode.

81 ADEVA 90F is superseded by ADRIANI 93M.

82 Superseded by DECAMP 92.

83 ABE 88b limits assume $e^+ e^- \rightarrow e^+ e^* e^-$ with one photon exchange only and $e^* \rightarrow e\gamma$ giving $e\gamma\gamma$.

Limits for Excited e (e^*) from Single Production

These limits are from $e^+ e^- \rightarrow e^* e, W \rightarrow e^* \nu, \text{ or } e p \rightarrow e^* X$ and depend on transition magnetic coupling between e and e^* . All limits assume $e^* \rightarrow e\gamma$ decay except as noted. Limits from LEP, UA2, and H1 are for chiral coupling, whereas all other limits are for nonchiral coupling, $\eta_L = \eta_R = 1$. In most papers, the limit is expressed in the form of an excluded region in the $\lambda-m_{e^*}$ plane. See the original papers.

For limits prior to 1987, see our 1992 edition (Physical Review D45, 1 June, Part II (1992)).

VALUE (GeV)	CL%	DOCUMENT ID	TECN	COMMENT
none 20-170	95	84 ACCIARRI	98T L3	$e\gamma \rightarrow e^* \rightarrow e\gamma$
none 30-200	95	85 BREITWEG	97C ZEUS	$e p \rightarrow e^* X$
>89	95	ADRIANI	93M L3	$Z \rightarrow ee^*, \lambda_Z > 0.5$
>88	95	ABREU	92C DLPH	$Z \rightarrow ee^*, \lambda_Z > 0.5$
>91	95	DECAMP	92 ALEP	$Z \rightarrow ee^*, \lambda_Z > 1$
>87	95	AKRAWY	90I OPAL	$Z \rightarrow ee^*, \lambda_Z > 0.5$
• • • We do not use the following data for averages, fits, limits, etc. • • •				
		86 ABREU	990 DLPH	$e^+ e^- \rightarrow ee^*$
		87 ACKERSTAFF	98C OPAL	$e^+ e^- \rightarrow ee^*$
		88 BARATE	98U ALEP	$e^+ e^- \rightarrow ee^*$
89,90		ABREU	97B DLPH	$e^+ e^- \rightarrow ee^*$
89,91		ACCIARRI	97G L3	$e^+ e^- \rightarrow ee^*$
		92 ACKERSTAFF	97 OPAL	$e^+ e^- \rightarrow ee^*$
93		ADLOFF	97 H1	Lepton-flavor violation
94		ABREU	96K DLPH	$e^+ e^- \rightarrow ee^*$
95		ACCIARRI	96D L3	$e^+ e^- \rightarrow ee^*$
96		ALEXANDER	96Q OPAL	$e^+ e^- \rightarrow ee^*$
97		BUSKULIC	96W ALEP	$e^+ e^- \rightarrow ee^*$
98		DERRICK	95B ZEUS	$e p \rightarrow e^* X$
99		ABT	93 H1	$e p \rightarrow e^* X$
>86	95	ADRIANI	93M L3	$\lambda_\gamma > 0.04$
		100 DERRICK	93B ZEUS	Superseded by DERRICK 95B
>86	95	ABREU	92C DLPH	$e^+ e^- \rightarrow ee^*, \lambda_\gamma > 0.1$
>88	95	101 ADEVA	90F L3	$Z \rightarrow ee^*, \lambda_Z > 0.5$
>86	95	101 ADEVA	90F L3	$Z \rightarrow ee^*, \lambda_Z > 0.04$
>81	95	102 DECAMP	90G ALEP	$Z \rightarrow ee^*, \lambda_Z > 1$
>50	95	ADACHI	89B TOPZ	$e^+ e^- \rightarrow ee^*, \lambda_\gamma > 0.04$
>56	95	KIM	89 AMY	$e^+ e^- \rightarrow ee^*, \lambda_\gamma > 0.03$
none 23-54	95	103 ABE	88B VNS	$e^+ e^- \rightarrow ee^*, \lambda_\gamma > 0.04$
>75	95	104 ANSARI	87D UA2	$W \rightarrow e^* \nu; \lambda_{WW} > 0.7$
>63	95	104 ANSARI	87D UA2	$W \rightarrow e^* \nu; \lambda_{WW} > 0.2$
>40	95	104 ANSARI	87D UA2	$W \rightarrow e^* \nu; \lambda_{WW} > 0.09$

84 ACCIARRI 98T search for single e^* production in quasi-real Compton scattering. The limit is for $|\lambda| > 1.0 \times 10^{-1}$ and non-chiral coupling of e^* . See their Fig. 7 for the exclusion plot in the mass-coupling plane.

85 BREITWEG 97c search for single e^* production in $e p$ collisions with the decays $e^* \rightarrow e\gamma, eZ, \nu W$. $f=f'=2A/m_{e^*}$ is assumed for the e^* coupling. See their Fig. 9 for the exclusion plot in the mass-coupling plane.

86 ABREU 990 result is from $e^+ e^-$ collisions at $\sqrt{s} = 183$ GeV. See their Figs. 4 and 5 for the exclusion limit in the mass-coupling plane.

87 ACKERSTAFF 98c from $e^+ e^-$ collisions at $\sqrt{s} = 170-172$ GeV. See their Fig. 11 for the exclusion limit in the mass-coupling plane.

88 BARATE 98u is from $e^+ e^-$ collision at $\sqrt{s} = M_Z$. See their Fig. 12 for limits in mass-coupling plane.

89 From $e^+ e^-$ collisions at $\sqrt{s} = 161$ GeV.

90 See Fig. 4a and Fig. 5a of ABREU 97b for the exclusion limit in the mass-coupling plane.

91 See Fig. 2 and Fig. 3 of ACCIARRI 97G for the exclusion limit in the mass-coupling plane.

92 ACKERSTAFF 97 result is from $e^+ e^-$ collisions at $\sqrt{s} = 161$ GeV. See their Fig. 3 for the exclusion limit in the mass-coupling plane.

93 ADLOFF 97 search for single e^* production in $e p$ collisions with the decays $e^* \rightarrow e\gamma, eZ, \nu W$. See their Fig. 4 for the rejection limits on the product of the production cross section and the branching ratio into a specific decay channel.

94 ABREU 96k result is from $e^+ e^-$ collisions at $\sqrt{s} = 130-136$ GeV. See their Fig. 4 for the exclusion limit in the mass-coupling plane.

95 ACCIARRI 96d result is from $e^+ e^-$ collisions at $\sqrt{s} = 130-140$ GeV. See their Fig. 2 for the exclusion limit in the mass-coupling plane.

96 ALEXANDER 96Q result is from $e^+ e^-$ collisions at $\sqrt{s} = 130-140$ GeV. See their Fig. 3a for the exclusion limit in the mass-coupling plane.

97 BUSKULIC 96w result is from $e^+ e^-$ collisions at $\sqrt{s} = 130-140$ GeV. See their Fig. 3 for the exclusion limit in the mass-coupling plane.

98 DERRICK 95b search for single e^* production via $e^* e\gamma$ coupling in $e p$ collisions with the decays $e^* \rightarrow e\gamma, eZ, \nu W$. See their Fig. 13 for the exclusion plot in the $m_{e^*} - \lambda_\gamma$ plane.

99 ABT 93 search for single e^* production via $e^* e\gamma$ coupling in $e p$ collisions with the decays $e^* \rightarrow e\gamma, eZ, \nu W$. See their Fig. 4 for exclusion plot in the $m_{e^*} - \lambda_\gamma$ plane.

100 DERRICK 93b search for single e^* production via $e^* e\gamma$ coupling in $e p$ collisions with the decays $e^* \rightarrow e\gamma, eZ, \nu W$. See their Fig. 3 for exclusion plot in the $m_{e^*} - \lambda_\gamma$ plane.

101 Superseded by ADRIANI 93M.

102 Superseded by DECAMP 92.

103 ABE 88b limits use $e^+ e^- \rightarrow ee^*$ where t-channel photon exchange dominates giving $e\gamma(e)$ (quasi-real compton scattering).

104 ANSARI 87D is at $E_{cm} = 546-630$ GeV.

Limits for Excited e (e^*) from $e^+ e^- \rightarrow \gamma\gamma$

These limits are derived from indirect effects due to e^* exchange in the t channel and depend on transition magnetic coupling between e and e^* . All limits are for $\lambda_\gamma = 1$. All limits except ABE 89j are for nonchiral coupling with $\eta_L = \eta_R = 1$.

For limits prior to 1987, see our 1992 edition (Physical Review D45, 1 June, Part II (1992)).

VALUE (GeV)	CL%	DOCUMENT ID	TECN	COMMENT
>306	95	ABBIENDI	99P OPAL	$\sqrt{s} = 189$ GeV
• • • We do not use the following data for averages, fits, limits, etc. • • •				
>231	95	ABREU	98J DLPH	$\sqrt{s} = 130-183$ GeV
>194	95	ACKERSTAFF	98 OPAL	$\sqrt{s} = 130-172$ GeV
>227	95	ACKER...K...	98B OPAL	$\sqrt{s} = 183$ GeV
>250	95	BARATE	98J ALEP	$\sqrt{s} = 183$ GeV
>160	95	BARATE	98U ALEP	
>210	95	106 ACCIARRI	97W L3	$\sqrt{s} = 161, 172$ GeV
>129	95	ACCIARRI	96L L3	$\sqrt{s} = 133$ GeV
>147	95	ALEXANDER	96K OPAL	
>136	95	BUSKULIC	96Z ALEP	$\sqrt{s} = 130, 136$ GeV
>146	95	ACCIARRI	95G L3	
		107 BUSKULIC	93Q ALEP	
>127	95	108 ADRIANI	92B L3	
>114	95	109 BARDADIN...	92 RVUE	
>99	95	DECAMP	92 ALEP	
		110 SHIMOZAWA	92 TOPZ	
>100	95	ABREU	91E DLPH	
>116	95	AKRAWY	91F OPAL	
>83	95	ADEVA	90K L3	
>82	95	AKRAWY	90F OPAL	
>68	95	111 ABE	89J VNS	$\eta_L = 1, \eta_R = 0$
>90.2	95	ADACHI	89B TOPZ	
>65	95	KIM	89 AMY	
105		BARATE 98u		is from $e^+ e^-$ collision at $\sqrt{s} = M_Z$. See their Fig. 5 for limits in mass-coupling plane
106		ACCIARRI 97w		also obtain a limit on e^* with chiral coupling, $m_{e^*} > 157$ GeV (95%CL).
107		BUSKULIC 93q		obtain $\Lambda^+ > 121$ GeV (95%CL) from ALEPH experiment and $\Lambda^+ > 135$ GeV from combined TRISTAN and ALEPH data. These limits roughly correspond to limits on m_{e^*} .
108		ADRIANI 92b		superseded by ACCIARRI 95G.
109		BARDADIN-OTWINOWSKA 92		limit from fit to the combined data of DECAMP 92, ABREU 91E, ADEVA 90K, AKRAWY 91F.
110		SHIMOZAWA 92		fit the data to the limiting form of the cross section with $m_{e^*} \gg E_{cm}$ and obtain $m_{e^*} > 168$ GeV at 95%CL. Use of the full form would reduce this limit by a few GeV. The statistically unexpected large value is due to fluctuation in the data.
111		THE ABE 89j		limit assumes chiral coupling. This corresponds to $\lambda_\gamma = 0.7$ for nonchiral coupling.

Indirect Limits for Excited e^*

These limits make use of loop effects involving e^* and are therefore subject to theoretical uncertainty.

VALUE (GeV)	DOCUMENT ID	TECN	COMMENT
• • • We do not use the following data for averages, fits, limits, etc. • • •			
112	DORENBOS... 89	CHRM	$\bar{\nu}_\mu e \rightarrow \bar{\nu}_\mu e$ and $\nu_\mu e \rightarrow \nu_\mu e$
113	GRIFOLS 86	THEO	$\nu_\mu e \rightarrow \nu_\mu e$
114	RENARD 82	THEO	$g-2$ of electron
112	DORENBOSCH 89		obtain the limit $\lambda_{\gamma}^2 \Lambda_{\text{cut}}^2 / m_{e^*}^2 < 2.6$ (95% CL), where Λ_{cut} is the cutoff scale, based on the one-loop calculation by GRIFOLS 86. If one assumes that $\Lambda_{\text{cut}} = 1$ TeV and $\lambda_\gamma = 1$, one obtains $m_{e^*} > 620$ GeV. However, one generally expects $\lambda_\gamma \approx m_{e^*} / \Lambda_{\text{cut}}$ in composite models.
113	GRIFOLS 86		uses $\nu_\mu e \rightarrow \nu_\mu e$ and $\bar{\nu}_\mu e \rightarrow \bar{\nu}_\mu e$ data from CHARM Collaboration to derive mass limits which depend on the scale of compositeness.
114	RENARD 82		derived from $g-2$ data limits on mass and couplings of e^* and μ^* . See figures 2 and 3 of the paper.

MASS LIMITS for Excited μ^* **Limits for Excited μ^* from Pair Production**

These limits are obtained from $e^+e^- \rightarrow \mu^+\mu^-$ and thus rely only on the (electroweak) charge of μ^* . Form factor effects are ignored unless noted. For the case of limits from Z decay, the μ^* coupling is assumed to be of sequential type. All limits assume $\mu^* \rightarrow \mu\gamma$ decay except for the limits from $\Gamma(Z)$.

For limits prior to 1987, see our 1992 edition (Physical Review D45, 1 June, Part II (1992)).

VALUE (GeV)	CL%	DOCUMENT ID	TECN	COMMENT
>90.7	95	115 ABREU 990	DLPH	Homodoublet type
• • • We do not use the following data for averages, fits, limits, etc. • • •				
>85.3	95	116 ACKERSTAFF 98C	OPAL	$e^+e^- \rightarrow \mu^*\mu^*$ Homodoublet type
		117 BARATE 98U	ALEP	$Z \rightarrow \mu^*\mu^*$
>79.6	95	118,119 ABREU 97B	DLPH	$e^+e^- \rightarrow \mu^*\mu^*$ Homodoublet type
>78.4	95	118,120 ABREU 97B	DLPH	$e^+e^- \rightarrow \mu^*\mu^*$ Sequential type
>79.9	95	118 ACCIARRI 97G	L3	$e^+e^- \rightarrow \mu^*\mu^*$ Sequential type
>80.0	95	118,121 ACKERSTAFF 97	OPAL	$e^+e^- \rightarrow \mu^*\mu^*$ Homodoublet type
>62.6	95	122 ABREU 96K	DLPH	$e^+e^- \rightarrow \mu^*\mu^*$ Homodoublet type
>64.9	95	123 ACCIARRI 96D	L3	$e^+e^- \rightarrow \mu^*\mu^*$ Sequential type
>66.8	95	123 ALEXANDER 96Q	OPAL	$e^+e^- \rightarrow \mu^*\mu^*$ Homodoublet type
>65.4	95	123 BUSKULIC 96W	ALEP	$e^+e^- \rightarrow \mu^*\mu^*$ Sequential type
>45.6	95	ADRIANI 93M	L3	$Z \rightarrow \mu^*\mu^*$
>45.6	95	ABREU 92C	DLPH	$Z \rightarrow \mu^*\mu^*$
>29.8	95	124 BARDADIN... 92	RVUE	$\Gamma(Z)$
>26.1	95	125 DECAMP 92	ALEP	$Z \rightarrow \mu^*\mu^*$; $\Gamma(Z)$
>46.1	95	DECAMP 92	ALEP	$Z \rightarrow \mu^*\mu^*$
>33	95	125 ABREU 91F	DLPH	$Z \rightarrow \mu^*\mu^*$; $\Gamma(Z)$
>45.3	95	126 ADEVA 90F	L3	$Z \rightarrow \mu^*\mu^*$
>44.9	95	AKRAWY 90I	OPAL	$Z \rightarrow \mu^*\mu^*$
>44.6	95	127 DECAMP 90G	ALEP	$e^+e^- \rightarrow \mu^*\mu^*$
>29.9	95	ADACHI 89B	TOPZ	$e^+e^- \rightarrow \mu^*\mu^*$
>28.3	95	KIM 89	AMY	$e^+e^- \rightarrow \mu^*\mu^*$

115 From e^+e^- collisions at $\sqrt{s} = 183$ GeV. $f=f'$ is assumed. ABREU 990 also obtain limit for $f=-f'$ ($\mu^* \rightarrow \nu W$): $m_{\mu^*} > 81.3$ GeV.

116 From e^+e^- collisions at $\sqrt{s} = 170-172$ GeV. ACKERSTAFF 98C also obtain limit from $\mu^* \rightarrow \nu W$ decay mode: $m_{\mu^*} > 81.3$ GeV.

117 BARATE 98U obtain limits on the form factor. See their Fig. 14 for limits in mass-form factor plane.

118 From e^+e^- collisions at $\sqrt{s} = 161$ GeV.

119 ABREU 97B also obtain limit from charged current decay mode $\mu^* \rightarrow \nu W$, $m_{\mu^*} > 70.9$ GeV.

120 ABREU 97B also obtain limit from charged current decay mode $\mu^* \rightarrow \nu W$, $m_{\mu^*} > 44.6$ GeV.

121 ACKERSTAFF 97 also obtain limit from charged current decay mode $\mu^* \rightarrow \nu W$, $m_{\mu^*} > 77.1$ GeV.

122 From e^+e^- collisions at $\sqrt{s} = 130-136$ GeV.

123 From e^+e^- collisions at $\sqrt{s} = 130-140$ GeV.

124 BARDADIN-OTWINOWSKA 92 limit is independent of decay modes. Based on $\Delta\Gamma(Z) < 36$ MeV.

125 Limit is independent of μ^* decay mode.

126 Superseded by ADRIANI 93M.

127 Superseded by DECAMP 92.

Limits for Excited μ^* from Single Production

These limits are from $e^+e^- \rightarrow \mu^*\mu$ and depend on transition magnetic coupling between μ and μ^* . All limits assume $\mu^* \rightarrow \mu\gamma$ decay. Limits from LEP are for chiral coupling, whereas all other limits are for nonchiral coupling, $\eta_L = \eta_R = 1$. In most papers, the limit is expressed in the form of an excluded region in the $\lambda-m_{\mu^*}$ plane. See the original papers.

For limits prior to 1987, see our 1992 edition (Physical Review D45, 1 June, Part II (1992)).

VALUE (GeV)	CL%	DOCUMENT ID	TECN	COMMENT
>89	95	ADRIANI 93M	L3	$Z \rightarrow \mu\mu^*$, $\lambda_Z > 0.5$
>88	95	ABREU 92C	DLPH	$Z \rightarrow \mu\mu^*$, $\lambda_Z > 0.5$
>91	95	DECAMP 92	ALEP	$Z \rightarrow \mu\mu^*$, $\lambda_Z > 1$
>87	95	AKRAWY 90I	OPAL	$Z \rightarrow \mu\mu^*$, $\lambda_Z > 1$
• • • We do not use the following data for averages, fits, limits, etc. • • •				
128		ABREU 990	DLPH	$e^+e^- \rightarrow \mu\mu^*$
129		ACKERSTAFF 98C	OPAL	$e^+e^- \rightarrow \mu\mu^*$
130		BARATE 98U	ALEP	$Z \rightarrow \mu\mu^*$
131,132		ABREU 97B	DLPH	$e^+e^- \rightarrow \mu\mu^*$
131,133		ACCIARRI 97G	L3	$e^+e^- \rightarrow \mu\mu^*$
134		ACKERSTAFF 97	OPAL	$e^+e^- \rightarrow \mu\mu^*$
135		ABREU 96K	DLPH	$e^+e^- \rightarrow \mu\mu^*$
136		ACCIARRI 96D	L3	$e^+e^- \rightarrow \mu\mu^*$
137		ALEXANDER 96Q	OPAL	$e^+e^- \rightarrow \mu\mu^*$
138		BUSKULIC 96W	ALEP	$e^+e^- \rightarrow \mu\mu^*$
>85	95	139 ADEVA 90F	L3	$Z \rightarrow \mu\mu^*$, $\lambda_Z > 1$
>75	95	139 ADEVA 90F	L3	$Z \rightarrow \mu\mu^*$, $\lambda_Z > 0.1$
>80	95	140 DECAMP 90G	ALEP	$e^+e^- \rightarrow \mu\mu^*$, $\lambda_Z = 1$
>50	95	ADACHI 89B	TOPZ	$e^+e^- \rightarrow \mu\mu^*$, $\lambda_\gamma = 0.7$
>46	95	KIM 89	AMY	$e^+e^- \rightarrow \mu\mu^*$, $\lambda_\gamma = 0.2$

128 ABREU 990 result is from e^+e^- collisions at $\sqrt{s} = 183$ GeV. See their Figs. 4 and 5 for the exclusion limit in the mass-coupling plane.

129 ACKERSTAFF 98C from e^+e^- collisions at $\sqrt{s} = 170-172$ GeV. See their Fig. 11 for the exclusion limit in the mass-coupling plane.

130 BARATE 98U obtain limits on the $Z\mu\mu^*$ coupling. See their Fig. 12 for limits in mass-coupling plane.

131 From e^+e^- collisions at $\sqrt{s} = 161$ GeV.

132 See Fig. 4a and Fig. 5a of ABREU 97B for the exclusion limit in the mass-coupling plane.

133 See Fig. 2 and Fig. 3 of ACCIARRI 97G for the exclusion limit in the mass-coupling plane.

134 ACKERSTAFF 97 result is from e^+e^- collisions at $\sqrt{s} = 161$ GeV. See their Fig. 3 for the exclusion limit in the mass-coupling plane.

135 ABREU 96K result is from e^+e^- collisions at $\sqrt{s} = 130-136$ GeV. See their Fig. 4 for the exclusion limit in the mass-coupling plane.

136 ACCIARRI 96D result is from e^+e^- collisions at $\sqrt{s} = 130-140$ GeV. See their Fig. 2 for the exclusion limit in the mass-coupling plane.

137 ALEXANDER 96Q result is from e^+e^- collisions at $\sqrt{s} = 130-140$ GeV. See their Fig. 3a for the exclusion limit in the mass-coupling plane.

138 BUSKULIC 96W result is from e^+e^- collisions at $\sqrt{s} = 130-140$ GeV. See their Fig. 3 for the exclusion limit in the mass-coupling plane.

139 Superseded by ADRIANI 93M.

140 Superseded by DECAMP 92.

Indirect Limits for Excited μ^*

These limits make use of loop effects involving μ^* and are therefore subject to theoretical uncertainty.

VALUE (GeV)	DOCUMENT ID	TECN	COMMENT
• • • We do not use the following data for averages, fits, limits, etc. • • •			
141	RENARD 82	THEO	$g-2$ of muon

141 RENARD 82 derived from $g-2$ data limits on mass and couplings of e^* and μ^* . See figures 2 and 3 of the paper.

MASS LIMITS for Excited τ^* **Limits for Excited τ^* from Pair Production**

These limits are obtained from $e^+e^- \rightarrow \tau^*\tau^*$ and thus rely only on the (electroweak) charge of τ^* . Form factor effects are ignored unless noted. For the case of limits from Z decay, the τ^* coupling is assumed to be of sequential type. All limits assume $\tau^* \rightarrow \tau\gamma$ decay except for the limits from $\Gamma(Z)$.

For limits prior to 1987, see our 1992 edition (Physical Review D45, 1 June, Part II (1992)).

VALUE (GeV)	CL%	DOCUMENT ID	TECN	COMMENT
>89.7	95	142 ABREU 990	DLPH	Homodoublet type
• • • We do not use the following data for averages, fits, limits, etc. • • •				
>84.6	95	143 ACKERSTAFF 98C	OPAL	$e^+e^- \rightarrow \tau^*\tau^*$ Homodoublet type
		144 BARATE 98U	ALEP	$Z \rightarrow \tau^*\tau^*$
>79.4	95	145,146 ABREU 97B	DLPH	$e^+e^- \rightarrow \tau^*\tau^*$ Homodoublet type
>77.4	95	145,147 ABREU 97B	DLPH	$e^+e^- \rightarrow \tau^*\tau^*$ Sequential type
>79.3	95	145 ACCIARRI 97G	L3	$e^+e^- \rightarrow \tau^*\tau^*$ Sequential type
>79.1	95	145,148 ACKERSTAFF 97	OPAL	$e^+e^- \rightarrow \tau^*\tau^*$ Homodoublet type

Searches Particle Listings

Quark and Lepton Compositeness

>62.2	95	149	ABREU	96K DLPH	$e^+e^- \rightarrow \tau^*\tau^*$ Homodoublet type
>64.2	95	150	ACCIARRI	96D L3	$e^+e^- \rightarrow \tau^*\tau^*$ Sequential type
>65.3	95	150	ALEXANDER	96Q OPAL	$e^+e^- \rightarrow \tau^*\tau^*$ Homodoublet type
>64.8	95	150	BUSKULIC	96W ALEP	$e^+e^- \rightarrow \tau^*\tau^*$ Sequential type
>45.6	95		ADRIANI	93M L3	$Z \rightarrow \tau^*\tau^*$
>45.3	95		ABREU	92C DLPH	$Z \rightarrow \tau^*\tau^*$
>29.8	95	151	BARDADIN...	92 RVUE	$\Gamma(Z)$
>26.1	95	152	DECAMP	92 ALEP	$Z \rightarrow \tau^*\tau^*$; $\Gamma(Z)$
>46.0	95		DECAMP	92 ALEP	$Z \rightarrow \tau^*\tau^*$
>33	95	152	ABREU	91F DLPH	$Z \rightarrow \tau^*\tau^*$; $\Gamma(Z)$
>45.5	95	153	ADEVA	90L L3	$Z \rightarrow \tau^*\tau^*$
>44.9	95		AKRAWY	90I OPAL	$Z \rightarrow \tau^*\tau^*$
>41.2	95	154	DECAMP	90G ALEP	$e^+e^- \rightarrow \tau^*\tau^*$
>29.0	95		ADACHI	89B TOPZ	$e^+e^- \rightarrow \tau^*\tau^*$

- 142 From e^+e^- collisions at $\sqrt{s}=183$ GeV. $f=f'$ is assumed. ABREU 990 also obtain limit for $f=-f'$ ($\tau^* \rightarrow \nu W$): $m_{\tau^*} > 81.3$ GeV.
- 143 From e^+e^- collisions at $\sqrt{s}=170-172$ GeV. ACKERSTAFF 98c also obtain limit from $\tau^* \rightarrow \nu W$ decay mode: $m_{\tau^*} > 81.3$ GeV.
- 144 BARATE 98u obtain limits on the form factor. See their Fig. 14 for limits in mass-form factor plane.
- 145 From e^+e^- collisions at $\sqrt{s}=161$ GeV.
- 146 ABREU 97b also obtain limit from charged current decay mode $\tau^* \rightarrow \nu W$, $m_{\tau^*} > 70.9$ GeV.
- 147 ABREU 97a also obtain limit from charged current decay mode $\tau^* \rightarrow \nu W$, $m_{\tau^*} > 44.6$ GeV.
- 148 ACKERSTAFF 97 also obtain limit from charged current decay mode $\tau^* \rightarrow \nu W$, $m_{\tau^*} > 77.1$ GeV.
- 149 From e^+e^- collisions at $\sqrt{s}=130-136$ GeV.
- 150 From e^+e^- collisions at $\sqrt{s}=130-140$ GeV.
- 151 BARDADIN-OTWINOWSKA 92 limit is independent of decay modes. Based on $\Delta\Gamma(Z)<36$ MeV.
- 152 Limit is independent of τ^* decay mode.
- 153 Superseded by ADRIANI 93M.
- 154 Superseded by DECAMP 92.

Limits for Excited τ (τ^*) from Single Production

These limits are from $e^+e^- \rightarrow \tau^*\tau$ and depend on transition magnetic coupling between τ and τ^* . All limits assume $\tau^* \rightarrow \tau\gamma$ decay. Limits from LEP are for chiral coupling, whereas all other limits are for nonchiral coupling, $\eta_L = \eta_R = 1$. In most papers, the limit is expressed in the form of an excluded region in the $\lambda-m_{\tau^*}$ plane. See the original papers.

VALUE (GeV)	CL%	DOCUMENT ID	TECN	COMMENT
>88	95	ADRIANI	93M L3	$Z \rightarrow \tau\tau^*$, $\lambda_Z > 0.5$
>87	95	ABREU	92C DLPH	$Z \rightarrow \tau\tau^*$, $\lambda_Z > 0.5$
>90	95	DECAMP	92 ALEP	$Z \rightarrow \tau\tau^*$, $\lambda_Z > 0.18$
>86.5	95	AKRAWY	90I OPAL	$Z \rightarrow \tau\tau^*$, $\lambda_Z > 1$
• • • We do not use the following data for averages, fits, limits, etc. • • •				
		155 ABREU	990 DLPH	$e^+e^- \rightarrow \tau\tau^*$
		156 ACKERSTAFF	98C OPAL	$e^+e^- \rightarrow \tau\tau^*$
		157 BARATE	98U ALEP	$Z \rightarrow \tau\tau^*$
		158,159 ABREU	97B DLPH	$e^+e^- \rightarrow \tau\tau^*$
		158,160 ACCIARRI	97G L3	$e^+e^- \rightarrow \tau\tau^*$
		161 ACKERSTAFF	97 OPAL	$e^+e^- \rightarrow \tau\tau^*$
		162 ABREU	96K DLPH	$e^+e^- \rightarrow \tau\tau^*$
		163 ACCIARRI	96D L3	$e^+e^- \rightarrow \tau\tau^*$
		164 ALEXANDER	96Q OPAL	$e^+e^- \rightarrow \tau\tau^*$
		165 BUSKULIC	96W ALEP	$e^+e^- \rightarrow \tau\tau^*$
>88	95	166 ADEVA	90L L3	$Z \rightarrow \tau\tau^*$, $\lambda_Z > 1$
>59	95	167 DECAMP	90G ALEP	$Z \rightarrow \tau\tau^*$, $\lambda_Z=1$
>40	95	168 BARTEL	86 JADE	$e^+e^- \rightarrow \tau\tau^*$, $\lambda_\gamma=1$
>41.4	95	169 BEHREND	86 CELL	$e^+e^- \rightarrow \tau\tau^*$, $\lambda_\gamma=1$
>40.8	95	169 BEHREND	86 CELL	$e^+e^- \rightarrow \tau\tau^*$, $\lambda_\gamma=0.7$

- 155 ABREU 990 result is from e^+e^- collisions at $\sqrt{s}=183$ GeV. See their Figs. 4 and 5 for the exclusion limit in the mass-coupling plane.
- 156 ACKERSTAFF 98c from e^+e^- collisions at $\sqrt{s}=170-172$ GeV. See their Fig. 11 for the exclusion limit in the mass-coupling plane.
- 157 BARATE 98u obtain limits on the $Z\tau\tau^*$ coupling. See their Fig. 12 for limits in mass-coupling plane.
- 158 From e^+e^- collisions at $\sqrt{s}=161$ GeV.
- 159 See Fig. 4a and Fig. 5a of ABREU 97b for the exclusion limit in the mass-coupling plane.
- 160 See Fig. 2 and Fig. 3 of ACCIARRI 97G for the exclusion limit in the mass-coupling plane.
- 161 ACKERSTAFF 97 result is from e^+e^- collisions at $\sqrt{s}=161$ GeV. See their Fig. 3 for the exclusion limit in the mass-coupling plane.
- 162 ABREU 96k result is from e^+e^- collisions at $\sqrt{s}=130-136$ GeV. See their Fig. 4 for the exclusion limit in the mass-coupling plane.
- 163 ACCIARRI 96d result is from e^+e^- collisions at $\sqrt{s}=130-140$ GeV. See their Fig. 2 for the exclusion limit in the mass-coupling plane.
- 164 ALEXANDER 96Q result is from e^+e^- collisions at $\sqrt{s}=130-140$ GeV. See their Fig. 3a for the exclusion limit in the mass-coupling plane.
- 165 BUSKULIC 96w result is from e^+e^- collisions at $\sqrt{s}=130-140$ GeV. See their Fig. 3 for the exclusion limit in the mass-coupling plane.
- 166 Superseded by ADRIANI 93M.
- 167 Superseded by DECAMP 92.
- 168 BARTEL 86 is at $E_{cm} = 30-46.78$ GeV.
- 169 BEHREND 86 limit is at $E_{cm} = 33-46.8$ GeV.

MASS LIMITS for Excited Neutrino (ν^*)

Limits for Excited ν (ν^*) from Pair Production

These limits are obtained from $e^+e^- \rightarrow \nu^*\nu^*$ and thus rely only on the (electroweak) charge of ν^* . Form factor effects are ignored unless noted. The ν^* coupling is assumed to be of sequential type unless otherwise noted. Limits assume $\nu^* \rightarrow \nu\gamma$ except for the $\Gamma(Z)$ measurement which makes no assumption about decay mode.

VALUE (GeV)	CL%	DOCUMENT ID	TECN	COMMENT
>90.0	95	170 ABREU	990 DLPH	Homodoublet type
• • • We do not use the following data for averages, fits, limits, etc. • • •				
		171 ABBIENDI	99F OPAL	
>84.9	95	172 ACKERSTAFF	98C OPAL	$e^+e^- \rightarrow \nu^*\nu^*$ Homodoublet type
		173 BARATE	98U ALEP	$Z \rightarrow \nu^*\nu^*$
>77.6	95	174,175 ABREU	97B DLPH	$e^+e^- \rightarrow \nu^*\nu^*$ Homodoublet type
>64.4	95	174,176 ABREU	97B DLPH	$e^+e^- \rightarrow \nu^*\nu^*$ Sequential type
>71.2	95	174,177 ACCIARRI	97G L3	$e^+e^- \rightarrow \nu^*\nu^*$ Sequential type
>77.8	95	174,178 ACKERSTAFF	97 OPAL	$e^+e^- \rightarrow \nu^*\nu^*$ Homodoublet type
>61.4	95	179,180 ACCIARRI	96D L3	$e^+e^- \rightarrow \nu^*\nu^*$ Sequential type
>65.0	95	181,182 ALEXANDER	96Q OPAL	$e^+e^- \rightarrow \nu^*\nu^*$ Homodoublet type
>63.6	95	179 BUSKULIC	96W ALEP	$e^+e^- \rightarrow \nu^*\nu^*$ Sequential type
>43.7	95	183 BARDADIN...	92 RVUE	$\Gamma(Z)$
>47	95	184 DECAMP	92 ALEP	
>42.6	95	185 DECAMP	92 ALEP	$\Gamma(Z)$
>35.4	95	186,187 DECAMP	900 ALEP	$\Gamma(Z)$
>46	95	187,188 DECAMP	900 ALEP	

- 170 From e^+e^- collisions at $\sqrt{s}=183$ GeV. $f=f'$ is assumed. ABREU 990 also obtain limit for $f=-f'$: $m_{\nu^*} > 87.3$ GeV, $m_{\nu^*} > 88.0$ GeV, $m_{\nu^*} > 81.0$ GeV.
- 171 From e^+e^- collisions at $\sqrt{s}=130-183$ GeV, ABBIENDI 99F obtain limit on $\sigma(e^+e^- \rightarrow \nu^*\nu^*) B(\nu^* \rightarrow \nu\gamma)^2$. See their Fig. 13. The limit ranges from 0.094 to 0.14 pb for $\sqrt{s}/2 > m_{\nu^*} > 45$ GeV.
- 172 From e^+e^- collisions at $\sqrt{s}=170-172$ GeV. ACKERSTAFF 98c also obtain limit from charged decay modes: $m_{\nu^*} > 84.1$ GeV, $m_{\nu^*} > 83.9$ GeV, and $m_{\nu^*} > 79.4$ GeV.
- 173 BARATE 98u obtain limits on the form factor. See their Fig. 14 for limits in mass-form factor plane.
- 174 From e^+e^- collisions at $\sqrt{s}=161$ GeV.
- 175 ABREU 97b also obtain limits from charged current decay modes, $m_{\nu^*} > 56.4$ GeV.
- 176 ABREU 97a also obtain limits from charged current decay modes, $m_{\nu^*} > 44.9$ GeV.
- 177 ACCIARRI 97G also obtain limits from charged current decay mode $e^*_e \rightarrow eW$, $m_{\nu^*} > 64.5$ GeV.
- 178 ACKERSTAFF 97 also obtain limits from charged current decay modes $m_{\nu^*} > 78.3$ GeV, $m_{\nu^*} > 78.9$ GeV, $m_{\nu^*} > 76.2$ GeV.
- 179 From e^+e^- collisions at $\sqrt{s}=130-140$ GeV.
- 180 ACCIARRI 96d also obtain limit from $\nu^* \rightarrow eW$ decay mode: $m_{\nu^*} > 57.3$ GeV.
- 181 From e^+e^- collisions at $\sqrt{s}=130-136$ GeV.
- 182 ALEXANDER 96Q also obtain limits from charged current decay modes: $m_{\nu^*} > 66.2$ GeV, $m_{\nu^*} > 66.5$ GeV, $m_{\nu^*} > 64.7$ GeV.
- 183 BARDADIN-OTWINOWSKA 92 limit is for Dirac ν^* . Based on $\Delta\Gamma(Z)<36$ MeV. The limit is 36.4 GeV for Majorana ν^* , 45.4 GeV for homodoublet ν^* .
- 184 Limit is based on $B(Z \rightarrow \nu^*\nu^*) \times B(\nu^* \rightarrow \nu\gamma)^2 < 5 \times 10^{-5}$ (95%CL) assuming Dirac ν^* , $B(\nu^* \rightarrow \nu\gamma) = 1$.
- 185 Limit is for Dirac ν^* . The limit is 34.6 GeV for Majorana ν^* , 45.4 GeV for homodoublet ν^* .
- 186 DECAMP 900 limit is from excess $\Delta\Gamma(Z) < 89$ MeV. The above value is for Dirac ν^* ; 26.6 GeV for Majorana ν^* ; 44.8 GeV for homodoublet ν^* .
- 187 Superseded by DECAMP 92.
- 188 DECAMP 900 limit based on $B(Z \rightarrow \nu^*\nu^*) \times B(\nu^* \rightarrow \nu\gamma)^2 < 7 \times 10^{-5}$ (95%CL), assuming Dirac ν^* , $B(\nu^* \rightarrow \nu\gamma) = 1$.

Limits for Excited ν (ν^*) from Single Production

These limits are from $Z \rightarrow \nu\nu^*$ or $e\mu \rightarrow \nu^*X$ and depend on transition magnetic coupling between ν/e and ν^* . Assumptions about ν^* decay mode are given in footnotes.

VALUE (GeV)	CL%	DOCUMENT ID	TECN	COMMENT
none	40-96	189 BREITWEG	97C ZEUS	$e\mu \rightarrow \nu^*X$
>91	95	ADRIANI	93M L3	$\lambda_Z > 1$, $\nu^* \rightarrow \nu\gamma$
>89	95	ADRIANI	93M L3	$\lambda_Z > 1$, $\nu^*_e \rightarrow eW$
>91	95	190 DECAMP	92 ALEP	$\lambda_Z > 1$
• • • We do not use the following data for averages, fits, limits, etc. • • •				
		191 ABBIENDI	99F OPAL	
		192 ABREU	990 DLPH	$e^+e^- \rightarrow \nu\nu^*$
		193 ACKERSTAFF	98C OPAL	$e^+e^- \rightarrow \nu^*\nu^*$ Homodoublet type
		194 BARATE	98U ALEP	$Z \rightarrow \nu\nu^*$
		195,196 ABREU	97B DLPH	$e^+e^- \rightarrow \nu\nu^*$
		197 ABREU	97I DLPH	$\nu^* \rightarrow lW, \nu Z$
		198 ABREU	97J DLPH	$\nu^* \rightarrow \nu\gamma$
		195,199 ACCIARRI	97G L3	$e^+e^- \rightarrow \nu\nu^*$
		200 ACKERSTAFF	97 OPAL	$e^+e^- \rightarrow \nu\nu^*$

	201	ADLOFF	97 H1	Lepton-flavor violation
	202	ACCIARRI	96D L3	$e^+e^- \rightarrow \nu\nu^*$
	203	ALEXANDER	96Q OPAL	$e^+e^- \rightarrow \nu\nu^*$
	204	BUSKULIC	96W ALEP	$e^+e^- \rightarrow \nu\nu^*$
	205	DERRICK	95B ZEUS	$e\rho \rightarrow \nu^*X$
	206	ABT	93 H1	$e\rho \rightarrow \nu^*X$
>87	95	ADRIANI	93M L3	$\lambda_Z > 0.1, \nu^* \rightarrow \nu\gamma$
>74	95	ADRIANI	93M L3	$\lambda_Z > 0.1, \nu_e^* \rightarrow eW$
	207	BARDADIN...	92 RVUE	
>74	95	190 DECAMP	92 ALEP	$\lambda_Z > 0.034$
>91	95	208,209 ADEVA	90O L3	$\lambda_Z > 1$
>83	95	209 ADEVA	90O L3	$\lambda_Z > 0.1, \nu^* \rightarrow \nu\gamma$
>74	95	209 ADEVA	90O L3	$\lambda_Z > 0.1, \nu_e^* \rightarrow eW$
>90	95	210,211 DECAMP	90O ALEP	$\lambda_Z > 1$
>74.7	95	210,211 DECAMP	90O ALEP	$\lambda_Z > 0.06$

189 BREITWEG 97c search for single ν^* production in $e\rho$ collisions with the decay $\nu^* \rightarrow \nu\gamma$. $f=-f'=2\Lambda/m_{\nu^*}$ is assumed for the ν^* coupling. See their Fig.10 for the exclusion plot in the mass-coupling plane.

190 DECAMP 92 limit is based on $B(Z \rightarrow \nu^*\bar{\nu})\times B(\nu^* \rightarrow \nu\gamma) < 2.7 \times 10^{-5}$ (95%CL) assuming Dirac ν^* , $B(\nu^* \rightarrow \nu\gamma) = 1$.

191 From e^+e^- collisions at $\sqrt{s}=130-183$ GeV, ABBIENDI 99F obtain limit on $\sigma(e^+e^- \rightarrow \nu\nu^*) B(\nu^* \rightarrow \nu\gamma)$. See their Fig. 8.

192 ABREU 99o result is from e^+e^- collisions at $\sqrt{s}=183$ GeV. See their Figs. 4 and 5 for the exclusion limit in the mass-coupling plane.

193 ACKERSTAFF 98c from e^+e^- collisions at $\sqrt{s}=170-172$ GeV. See their Fig. 11 for the exclusion limit in the mass-coupling plane.

194 BARATE 98u obtain limits on the $Z\nu\nu^*$ coupling. See their Fig. 13 for limits in mass-coupling plane

195 From e^+e^- collisions at $\sqrt{s}=161$ GeV.

196 See Fig. 4b and Fig. 5b of ABREU 97b for the exclusion limit in the mass-coupling plane.

197 ABREU 97i limit is from $Z \rightarrow \nu\nu^*$. See their Fig.12 for the exclusion limit in the mass-coupling plane.

198 ABREU 97j limit is from $Z \rightarrow \nu\nu^*$. See their Fig. 5 for the exclusion limit in the mass-coupling plane.

199 See Fig. 2 and Fig. 3 of ACCIARRI 97c for the exclusion limit in the mass-coupling plane.

200 ACKERSTAFF 97 result is from e^+e^- collisions at $\sqrt{s}=161$ GeV, for homodoublet ν^* . See their Fig. 3 for the exclusion limit in the mass-coupling plane.

201 ADLOFF 97 search for single e^* production in $e\rho$ collisions with the decays $e^* \rightarrow e\gamma, eZ, \nu W$. See their Fig. 4 for the rejection limits on the product of the production cross section and the branching ratio.

202 ACCIARRI 96D result is from e^+e^- collisions at $\sqrt{s}=130-140$ GeV. See their Fig. 2 for the exclusion limit in the mass-coupling plane.

203 ALEXANDER 96Q result is from e^+e^- collisions at $\sqrt{s}=130-140$ GeV for homodoublet ν^* . See their Fig. 3b and Fig. 3c for the exclusion limit in the mass-coupling plane.

204 BUSKULIC 96w result is from e^+e^- collisions at $\sqrt{s}=130-140$ GeV. See their Fig. 4 for the exclusion limit in the mass-coupling plane.

205 DERRICK 95B search for single ν^* production via ν^*eW coupling in $e\rho$ collisions with the decays $\nu^* \rightarrow \nu\gamma, \nu Z, eW$. See their Fig. 14 for the exclusion plot in the $m_{\nu^*}-\lambda\gamma$ plane.

206 ABT 93 search for single ν^* production via ν^*eW coupling in $e\rho$ collisions with the decays $\nu^* \rightarrow \nu\gamma, \nu Z, eW$. See their Fig. 4 for exclusion plot in the $m_{\nu^*}-\lambda\gamma$ plane.

207 See Fig. 5 of BARDADIN-OTWINOWSKA 92 for combined limit of ADEVA 90O, DE-CAMP 90O, and DECAMP 92.

208 Limit is either for $\nu^* \rightarrow \nu\gamma$ or $\nu^* \rightarrow eW$.

209 Superseded by ADRIANI 93M.

210 DECAMP 90O limit based on $B(Z \rightarrow \nu\nu^*)\times B(\nu^* \rightarrow \nu\gamma) < 6 \times 10^{-5}$ (95%CL), assuming $B(\nu^* \rightarrow \nu\gamma) = 1$.

211 Superseded by DECAMP 92.

MASS LIMITS for Excited $q (q^*)$

Limits for Excited $q (q^*)$ from Pair Production

These limits are obtained from $e^+e^- \rightarrow q^*\bar{q}^*$ and thus rely only on the (electroweak) charge of the q^* . Form factor effects are ignored unless noted. Assumptions about the q^* decay are given in the comments and footnotes.

VALUE (GeV)	CL%	DOCUMENT ID	TECN	COMMENT
>45.6	95	212 ADRIANI	93M L3	u or d type, $Z \rightarrow q^*q^*$
• • • We do not use the following data for averages, fits, limits, etc. • • •				
>41.7		213 BARATE	98U ALEP	$Z \rightarrow q^*q^*$
>44.7		214 ADRIANI	92F L3	$Z \rightarrow q^*q^*$
>40.6	95	215 BARDADIN...	92 RVUE	u -type, $\Gamma(Z)$
>44.2	95	215 BARDADIN...	92 RVUE	d -type, $\Gamma(Z)$
>45	95	216 DECAMP	92 ALEP	u -type, $\Gamma(Z)$
	95	216 DECAMP	92 ALEP	d -type, $\Gamma(Z)$
	95	217 DECAMP	92 ALEP	u or d type, $Z \rightarrow q^*q^*$
>45	95	216 ABREU	91F DLPH	u -type, $\Gamma(Z)$
>45	95	216 ABREU	91F DLPH	d -type, $\Gamma(Z)$
>21.1	95	218 BEHREND	86C CELL	$\alpha(q^*) = -1/3, q^* \rightarrow qg$
>22.3	95	218 BEHREND	86C CELL	$\alpha(q^*) = 2/3, q^* \rightarrow qg$
>22.5	95	218 BEHREND	86C CELL	$\alpha(q^*) = -1/3, q^* \rightarrow q\gamma$
>23.2	95	218 BEHREND	86C CELL	$\alpha(q^*) = 2/3, q^* \rightarrow q\gamma$

- 212 ADRIANI 93M limit is valid for $B(q^* \rightarrow qg) > 0.25$ (0.17) for up (down) type.
- 213 BARATE 98U obtain limits on the form factor. See their Fig. 16 for limits in mass-form factor plane.
- 214 ADRIANI 92F search for $Z \rightarrow q^*\bar{q}^*$ followed with $q^* \rightarrow q\gamma$ decays and give the limit $\sigma_Z \cdot B(Z \rightarrow q^*\bar{q}^*) \cdot B^2(q^* \rightarrow q\gamma) < 2$ pb at 95%CL. Assuming five flavors of degenerate q^* of homodoublet type, $B(q^* \rightarrow q\gamma) < 4\%$ is obtained for $m_{q^*} < 45$ GeV.
- 215 BARDADIN-OTWINOWSKA 92 limit based on $\Delta\Gamma(Z) < 36$ MeV.
- 216 These limits are independent of decay modes.
- 217 Limit is for $B(q^* \rightarrow qg)+B(q^* \rightarrow q\gamma)=1$.
- 218 BEHREND 86c search for $e^+e^- \rightarrow q^*\bar{q}^*$ for $m_{q^*} > 5$ GeV. But $m < 5$ GeV excluded by total hadronic cross section. The limits are for point-like photon couplings of excited quarks.

Limits for Excited $q (q^*)$ from Single Production

These limits are from $e^+e^- \rightarrow q^*\bar{q}$ or $p\bar{p} \rightarrow q^*X$ and depend on transition magnetic couplings between q and q^* . Assumptions about q^* decay mode are given in the footnotes and comments.

VALUE (GeV)	CL%	DOCUMENT ID	TECN	COMMENT
>570 (CL = 95%) OUR EVALUATION				
none 200-520 and 580-760	95	219 ABE	97G CDF	$p\bar{p} \rightarrow q^*X, q^* \rightarrow 2$ jets
none 40-169	95	220 BREITWEG	97C ZEUS	$e\rho \rightarrow q^*X$
none 80-570	95	221 ABE	95N CDF	$p\bar{p} \rightarrow q^*X, q^* \rightarrow qg, q\gamma, qW$
>288	90	222 ALITTI	93 UA2	$p\bar{p} \rightarrow q^*X, q^* \rightarrow qg$
> 88	95	223 DECAMP	92 ALEP	$Z \rightarrow qq^*, \lambda_Z > 1$
> 86	95	223 AKRAWY	90J OPAL	$Z \rightarrow qq^*, \lambda_Z > 1.2$
• • • We do not use the following data for averages, fits, limits, etc. • • •				
		224 ABREU	99O DLPH	$e^+e^- \rightarrow qq^*$
		225 BARATE	98U ALEP	$Z \rightarrow qq^*$
		226 ADLOFF	97 H1	Lepton-flavor violation
		227 DERRICK	95B ZEUS	$e\rho \rightarrow q^*X$
none 80-540	95	228 ABE	94 CDF	$p\bar{p} \rightarrow q^*X, q^* \rightarrow q\gamma, qW$
> 79	95	229 ADRIANI	93M L3	$\lambda_Z(L3) > 0.06$
		230 ABREU	92D DLPH	$Z \rightarrow qq^*$
		231 ADRIANI	92F L3	$Z \rightarrow qq^*$
> 75	95	229 DECAMP	92 ALEP	$Z \rightarrow qq^*, \lambda_Z > 1$
		232 ALBAJAR	89 UA1	$p\bar{p} \rightarrow q^*X, q^* \rightarrow qW$
> 39	95	233 BEHREND	86C CELL	$e^+e^- \rightarrow q^*\bar{q} (q^* \rightarrow qg, q\gamma), \lambda_{\gamma}=1$

- 219 ABE 97g search for new particle decaying to dijets.
- 220 BREITWEG 97c search for single q^* production in $e\rho$ collisions with the decays $q^* \rightarrow q\gamma, qW$. $f_s=0$, and $f=-f'=2\Lambda/m_{q^*}$ is assumed for the q^* coupling. See their Fig. 11 for the exclusion plot in the mass-coupling plane.
- 221 ABE 95n assume a degenerate u^* and d^* with $f_s=f=f'/\Lambda/m_{q^*}$. See their Fig. 4 for the excluded region in $m_{q^*}-f$ plane.
- 222 ALITTI 93 search for resonances in the two-jet invariant mass. The limit is for $f_s = f = f' = \Lambda/m_{q^*}$. u^* and d^* are assumed to be degenerate. If not, the limit for u^* (d^*) is 277 (247) GeV if $m_{d^*} \gg m_{u^*}$ ($m_{u^*} \gg m_{d^*}$).
- 223 Assumes $B(q^* \rightarrow q\gamma) = 0.1$.
- 224 ABREU 99o result is from e^+e^- collisions at $\sqrt{s}=183$ GeV. See their Fig. 6 for the exclusion limit in the mass-coupling plane.
- 225 BARATE 98u obtain limits on the Zqq^* coupling. See their Fig. 16 for limits in mass-coupling plane
- 226 ADLOFF 97 search for single q^* production in $e\rho$ collisions with the decay $q^* \rightarrow q\gamma$. See their Fig. 6 for the rejection limits on the product of the production cross section and the branching ratio.
- 227 DERRICK 95B search for single q^* production via $q^*q\gamma$ coupling in $e\rho$ collisions with the decays $q^* \rightarrow qW, qZ, qg, q\gamma$. See their Fig. 15 for the exclusion plot in the $m_{q^*}-\lambda\gamma$ plane.
- 228 ABE 94 search for resonances in jet- γ and jet- W invariant mass in $p\bar{p}$ collisions at $E_{cm} = 1.8$ TeV. The limit is for $f_s = f = f' = \Lambda/m_{q^*}$, and u^* and d^* are assumed to be degenerate. See their Fig. 4 for the excluded region in $m_{q^*}-f$ plane.
- 229 Assumes $B(q^* \rightarrow qg) = 1$.
- 230 ABREU 92D give $\sigma(e^+e^- \rightarrow Z \rightarrow q^*\bar{q} \text{ or } q\bar{q}^*)\times B(q^* \rightarrow q\gamma) < 15$ pb (95% CL) for $m_{q^*} < 80$ GeV.
- 231 ADRIANI 92F search for $Z \rightarrow qq^*$ with $q^* \rightarrow q\gamma$ and give the limit $\sigma_Z \cdot B(Z \rightarrow qq^*) \cdot B(q^* \rightarrow q\gamma) < (2-10)$ pb (95%CL) for $m_{q^*} = (46-82)$ GeV.
- 232 ALBAJAR 89 give $\sigma(q^* \rightarrow W + \text{jet})/\sigma(W) < 0.019$ (90% CL) for $m_{q^*} > 220$ GeV.
- 233 BEHREND 86c has $E_{cm} = 42.5-46.8$ GeV. See their Fig. 3 for excluded region in the $m_{q^*}-(\lambda_{\gamma}/m_{q^*})^2$ plane. The limit is for $\lambda_{\gamma} = 1$ with $\eta_L = \eta_R = 1$.

MASS LIMITS for Color Sextet Quarks (q_6)

VALUE (GeV)	CL%	DOCUMENT ID	TECN	COMMENT
>84	95	234 ABE	89D CDF	$p\bar{p} \rightarrow q_6\bar{q}_6$

234 ABE 89D look for pair production of unit-charged particles which leave the detector before decaying. In the above limit the color sextet quark is assumed to fragment into a unit-charged or neutral hadron with equal probability and to have long enough lifetime not to decay within the detector. A limit of 121 GeV is obtained for a color decuplet.

Searches Particle Listings

Quark and Lepton Compositeness

MASS LIMITS for Color Octet Charged Leptons (Lg)

Table with columns: VALUE (GeV), CL%, DOCUMENT ID, TECN, COMMENT. Includes entries for >86, none 3.0-30.3, none 3.5-30.3, >19.8, none 5-23.2, and 235 ABE 89D look for pair production...

MASS LIMITS for Color Octet Neutrinos (nuB)

Table with columns: VALUE (GeV), CL%, DOCUMENT ID, TECN, COMMENT. Includes entries for >110, none 3.8-29.8, none 9-21.9, 241 BARGER 89 RVUE, 242 KIM 90, 243 BARTEL 87B...

MASS LIMITS for Wg (Color Octet W Boson)

Table with columns: VALUE (GeV), DOCUMENT ID, TECN, COMMENT. Includes entry for 244 ALBAJAR 89 UA1 p-pbar to Wg X...

Limits on ZZ gamma Coupling

Limits are for the electric dipole transition form factor for Z -> gamma Z* parametrized as f(s') = beta(s'/mz^2 - 1), where s' is the virtual Z mass...

Table with columns: VALUE, CL%, DOCUMENT ID, TECN, COMMENT. Includes entry for <0.80, 95 ADRIANI 92J L3 Z -> gamma nu nu-bar.

REFERENCES FOR Searches for Quark and Lepton Compositeness

List of references for quark and lepton compositeness searches, including authors like Barate, Abbiendi, Abbott, etc., and experiments like ALEPH, OPAL, DELPHI, etc.

Continuation of references from the previous section, listing authors like Barate, Bertram, McFarland, Miura, etc., and experiments like CDF, LEP, etc.

See key on page 239

Searches Particle Listings

WIMPs and Other Particle Searches

WIMPs and Other Particle Searches

OMITTED FROM SUMMARY TABLE

WIMPS AND OTHER PARTICLE SEARCHES

Revised March 2000 by K. Hikasa (Tohoku University).

We collect here those searches which do not appear in any of the above search categories. These are listed in the following order:

1. Galactic WIMP (weakly-interacting massive particle) searches
2. Concentration of stable particles in matter
3. Limits on neutral particle production at accelerators
4. Limits on jet-jet resonance in hadron collisions
5. Limits on charged particles in e^+e^- collisions
6. Limits on charged particles in hadron reactions
7. Limits on charged particles in cosmic rays
8. Search for low-scale gravity effects

Note that searches appear in separate sections elsewhere for Higgs bosons (and technipions), other heavy bosons (including W_R , W' , Z' , leptiquarks, axiguons), axions (including pseudo-Goldstone bosons, Majorons, familons), heavy leptons, heavy neutrinos, free quarks, monopoles, supersymmetric particles, and compositeness. We include specific WIMP searches in the appropriate sections when they yield limits on hypothetical particles such as supersymmetric particles, axions, massive neutrinos, monopoles, etc.

We omit papers on CHAMP's, millicharged particles, and other exotic particles. We no longer list for limits on tachyons and centauros. See our 1994 edition for these limits.

GALACTIC WIMP SEARCHES

Cross-Section Limits for Dark Matter Particles (χ^0) on Nuclei

These limits are for weakly-interacting stable particles that may constitute the invisible mass in the galaxy. Unless otherwise noted, a local mass density of $0.3 \text{ GeV}/\text{cm}^3$ is assumed; see each paper for velocity distribution assumptions. In the papers the limit is given as a function of the χ^0 mass. Here we list limits only for typical mass values of 20 GeV, 100 GeV, and 1 TeV. Specific limits on supersymmetric dark matter particles may be found in the Supersymmetry section.

For $m_{\chi^0} = 20 \text{ GeV}$

VALUE (nb)	CL%	DOCUMENT ID	TECN	COMMENT
• • • We do not use the following data for averages, fits, limits, etc. • • •				
	90	1 BAUDIS	99 CNTR	^{76}Ge
		2 BELLI	99C CNTR	F
		3 BERNABEI	99 CNTR	NaI
		4 OOTANI	99 BOLO	LIF
		5 BERNABEI	98 CNTR	NaI
		6 BERNABEI	98C CNTR	^{129}Xe
< 0.04	95	5 KLIMENKO	98 CNTR	^{73}Ge , incl.
		7 BERNABEI	97 CNTR	F
< 0.8		ALESSAND...	96 CNTR	O
< 6		ALESSAND...	96 CNTR	Te
< 0.02	90	8 BELLI	96 CNTR	^{129}Xe , incl.
		9 BELLI	96C CNTR	^{129}Xe
< 0.004	90	10 BERNABEI	96 CNTR	Na
< 0.3	90	10 BERNABEI	96 CNTR	I
< 0.2	95	11 SARSA	96 CNTR	Na
< 0.015	90	12 SMITH	96 CNTR	Na
< 0.05	95	13 GARCIA	95 CNTR	Natural Ge
< 0.1	95	QUENBY	95 CNTR	Na
< 90	90	14 SNOWDEN...	95 MICA	^{16}O
< 4 $\times 10^3$	90	14 SNOWDEN...	95 MICA	^{39}K
< 0.7	90	BACCI	92 CNTR	Na
< 0.12	90	15 REUSSER	91 CNTR	Natural Ge
< 0.06	95	CALDWELL	88 CNTR	Natural Ge

¹ BAUDIS 99 give the limit $\sigma < 1 \times 10^{-4}$ pb for scalar χ^0 -nucleon cross section.

² BELLI 99c give $\sigma < 10$ pb for the spin-dependent χ^0 -proton cross section.

³ See the following subsection for claim of a possible signal.

⁴ OOTANI 99 give $\sigma < 40$ pb for the spin-dependent neutralino-proton cross section. The cross-section limit extends to lower masses compared to other experiments.

⁵ BERNABEI 98c use pulse shape discrimination to enhance a possible signal. The limits $\sigma < 3 \times 10^{-4}$ pb (90%CL) for spin-independent χ^0 -nucleon cross section (assuming isoscalar), and $\sigma < 20$ pb (90%CL) for spin-dependent (assuming Z^0 exchange) are given.

⁶ KLIMENKO 98 limit is for inelastic scattering $\chi^0 \ ^{73}\text{Ge} \rightarrow \chi^0 \ ^{73}\text{Ge}^*$ (13.26 keV).

⁷ BERNABEI 97 give $\sigma < 12$ pb (90%CL) for the spin-dependent χ^0 -proton cross section.

⁸ BELLI 96 limit for inelastic scattering $\chi^0 \ ^{129}\text{Xe} \rightarrow \chi^0 \ ^{129}\text{Xe}^*$ (39.58 keV).

⁹ BELLI 96c use background subtraction and obtain $\sigma < 150$ pb (< 1.5 fb) (90%CL) for spin-dependent (independent) χ^0 -proton cross section. The confidence level is from R. Bernabei, private communication, May 20, 1999.

¹⁰ BERNABEI 96 use pulse shape discrimination to enhance the possible signal. The limit here is from R. Bernabei, private communication, September 19, 1997.

¹¹ SARSA 96 search for annual modulation of WIMP signal. See SARSA 97 for details of the analysis. The limit here is from M.L. Sarsa, private communication, May 26, 1997.

¹² SMITH 96 use pulse shape discrimination to enhance the possible signal. A dark matter density of 0.4 GeV cm^{-3} is assumed.

¹³ GARCIA 95 limit is from the event rate. A weaker limit is obtained from searches for diurnal and annual modulation.

¹⁴ SNOWDEN-IFFT 95 look for recoil tracks in an ancient mica crystal. Similar limits are also given for ^{27}Al and ^{28}Si . See COLLAR 96 and SNOWDEN-IFFT 96 for discussion on potential backgrounds.

¹⁵ REUSSER 91 limit here is changed from published (0.04) after reanalysis by authors. J.L. Vuilleumier, private communication, March 29, 1996.

For $m_{\chi^0} = 100 \text{ GeV}$

VALUE (nb)	CL%	DOCUMENT ID	TECN	COMMENT
• • • We do not use the following data for averages, fits, limits, etc. • • •				
		16 BELLI	00 RVUE	
		17 AMBROSIO	99 MCRO	
		18 BAUDIS	99 CNTR	^{76}Ge
	90	19 BELLI	99C CNTR	F
		20 BERNABEI	99 CNTR	NaI
		21 BRHLIK	99 RVUE	
		22 OOTANI	99 BOLO	LIF
		23 BERNABEI	98 CNTR	NaI
		24 BERNABEI	98C CNTR	^{129}Xe
< 0.008	95	25 KLIMENKO	98 CNTR	^{73}Ge , incl.
< 0.08	95	26 KLIMENKO	98 CNTR	^{73}Ge , incl.
		27 BERNABEI	97 CNTR	F
< 4		ALESSAND...	96 CNTR	O
< 25		ALESSAND...	96 CNTR	Te
< 0.006	90	28 BELLI	96 CNTR	^{129}Xe , incl.
		29 BELLI	96C CNTR	^{129}Xe
< 0.001	90	30 BERNABEI	96 CNTR	Na
< 0.3	90	30 BERNABEI	96 CNTR	I
< 0.7	95	31 SARSA	96 CNTR	Na
< 0.03	90	32 SMITH	96 CNTR	Na
< 0.8	90	32 SMITH	96 CNTR	I
< 0.35	95	33 GARCIA	95 CNTR	Natural Ge
< 0.6	95	QUENBY	95 CNTR	Na
< 3	95	QUENBY	95 CNTR	I
< 1.5 $\times 10^2$	90	34 SNOWDEN...	95 MICA	^{16}O
< 4 $\times 10^2$	90	34 SNOWDEN...	95 MICA	^{39}K
< 0.08	90	35 BECK	94 CNTR	^{76}Ge
< 2.5	90	BACCI	92 CNTR	Na
< 3	90	BACCI	92 CNTR	I
< 0.9	90	36 REUSSER	91 CNTR	Natural Ge
< 0.7	95	CALDWELL	88 CNTR	Natural Ge
		16 BELLI 00		discuss the effect of astrophysical uncertainties on the WIMP interpretation of the BERNABEI 99 signal.
		17 AMBROSIO 99		search for upgoing muon events induced by neutrinos originating from WIMP annihilations in the Sun and Earth.
		18 BAUDIS 99		give the limit $\sigma < 7 \times 10^{-6}$ pb for scalar χ^0 -nucleon cross section.
		19 BELLI 99c		give $\sigma < 4.8$ pb for the spin-dependent χ^0 -proton cross section.
		20 BERNABEI 99		search for annual modulation of the WIMP signal. The data favor the hypothesis of annual modulation at 99.6%CL and are consistent with $m_{\chi^0} = 59_{-14}^{+17}$ GeV and spin-independent χ^0 -proton cross section of $(7.0_{-1.2}^{+0.4}) \times 10^{-6}$ pb (1 σ errors).
		21 BRHLIK 99		discuss the effect of astrophysical uncertainties on the WIMP interpretation of the BERNABEI 99 signal.
		22 OOTANI 99		give $\sigma < 0.1$ nb for the spin-dependent neutralino-proton cross section.
		23 BERNABEI 98		search for annual modulation of the WIMP signal. The data is consistent with $m_{\chi^0} = 59_{-19}^{+36}$ GeV and spin-independent χ^0 -proton cross section of $(1.0_{-0.4}^{+0.1}) \times 10^{-5}$ pb (1 σ errors).
		24 BERNABEI 98c		use pulse shape discrimination to enhance a possible signal. The limits $\sigma < 7 \times 10^{-6}$ pb (90%CL) for spin-independent χ^0 -nucleon cross section (assuming isoscalar), and $\sigma < 0.6$ pb (90%CL) for spin-dependent (assuming Z^0 exchange) are given.
		25 KLIMENKO 98		limit is for inelastic scattering $\chi^0 \ ^{73}\text{Ge} \rightarrow \chi^0 \ ^{73}\text{Ge}^*$ (13.26 keV).
		26 KLIMENKO 98		limit is for inelastic scattering $\chi^0 \ ^{73}\text{Ge} \rightarrow \chi^0 \ ^{73}\text{Ge}^*$ (66.73 keV).
		27 BERNABEI 97		give $\sigma < 5$ pb (90%CL) for the spin-dependent χ^0 -proton cross section.
		28 BELLI 96		limit for inelastic scattering $\chi^0 \ ^{129}\text{Xe} \rightarrow \chi^0 \ ^{129}\text{Xe}^*$ (39.58 keV).

Searches Particle Listings

WIMPs and Other Particle Searches

- 29 BELLI 96c use background subtraction and obtain $\sigma < 0.35$ pb (< 0.15 fb) (90%CL) for spin-dependent (independent) X^0 -proton cross section. The confidence level is from R. Bernabei, private communication, May 20, 1999.
- 30 BERNABEI 96 use pulse shape discrimination to enhance the possible signal. The limit here is from R. Bernabei, private communication, September 19, 1997.
- 31 SARSA 96 search for annual modulation of WIMP signal. See SARSA 97 for details of the analysis. The limit here is from M.L. Sarsa, private communication, May 26, 1997.
- 32 SMITH 96 use pulse shape discrimination to enhance the possible signal. A dark matter density of 0.4 GeV cm^{-3} is assumed.
- 33 GARCIA 95 limit is from the event rate. A weaker limit is obtained from searches for diurnal and annual modulation.
- 34 SNOWDEN-IFFT 95 look for recoil tracks in an ancient mica crystal. Similar limits are also given for ^{27}Al and ^{28}Si . See COLLAR 96 and SNOWDEN-IFFT 96 for discussion on potential backgrounds.
- 35 BECK 94 uses enriched ^{76}Ge (86% purity).
- 36 REUSSER 91 limit here is changed from published (0.3) after reanalysis by authors. J.L. Vuilleumier, private communication, March 29, 1996.

For $m_{\chi^0} = 1 \text{ TeV}$

VALUE (nb)	CL%	DOCUMENT ID	TECN	COMMENT
• • • We do not use the following data for averages, fits, limits, etc. • • •				
	90	37 BELLI	99c CNTR	F
		38 BERNABEI	99 CNTR	NaI
		39 BERNABEI	99D CNTR	SIMP
		40 DERBIN	99 CNTR	SIMP
		41 OOTANI	99 BOLO	LIF
		38 BERNABEI	98 CNTR	NaI
		42 BERNABEI	98c CNTR	^{129}Xe
< 0.06	95	43 KLIMENKO	98 CNTR	^{73}Ge , incl.
< 0.4	95	44 KLIMENKO	98 CNTR	^{73}Ge , incl.
		45 BERNABEI	97 CNTR	F
< 40		ALESSAND...	96 CNTR	O
< 700		ALESSAND...	96 CNTR	Te
< 0.05	90	46 BELLI	96 CNTR	^{129}Xe , incl.
< 1.5	90	47 BELLI	96 CNTR	^{129}Xe , incl.
		48 BELLI	96c CNTR	^{129}Xe
< 0.01	90	49 BERNABEI	96 CNTR	Na
< 9	90	49 BERNABEI	96 CNTR	I
< 7	95	50 SARSA	96 CNTR	Na
< 0.3	90	51 SMITH	96 CNTR	Na
< 6	90	51 SMITH	96 CNTR	I
< 6	95	52 GARCIA	95 CNTR	Natural Ge
< 8	95	QUENBY	95 CNTR	Na
< 50	95	QUENBY	95 CNTR	I
< 7×10^2	90	53 SNOWDEN....	95 MICA	^{16}O
< 1×10^3	90	53 SNOWDEN....	95 MICA	^{39}K
< 0.8	90	54 BECK	94 CNTR	^{76}Ge
< 30	90	BACCI	92 CNTR	Na
< 30	90	BACCI	92 CNTR	I
< 15	90	55 REUSSER	91 CNTR	Natural Ge
< 6	95	CALDWELL	88 CNTR	Natural Ge

- 37 BELLI 99c give $\sigma < 28$ pb for the spin-dependent X^0 -proton cross section.
- 38 See the previous subsection for claim of a possible signal.
- 39 BERNABEI 99D search for SIMPs (Strongly Interacting Massive Particles) in the mass range 10^3 – 10^{16} GeV. See their Fig. 3 for cross-section limits.
- 40 DERBIN 99 search for SIMPs (Strongly Interacting Massive Particles) in the mass range 10^2 – 10^{14} GeV. See their Fig. 3 for cross-section limits.
- 41 OOTANI 99 give $\sigma < 1$ nb for the spin-dependent neutralino-proton cross section.
- 42 BERNABEI 98c use pulse shape discrimination to enhance a possible signal. The limits $\sigma < 4 \times 10^{-5}$ pb (90%CL) for spin-independent X^0 -nucleon cross section (assuming isoscalar), and $\sigma < 4$ pb (90%CL) for spin-dependent (assuming Z^0 exchange) are given.
- 43 KLIMENKO 98 limit is for inelastic scattering $X^0 \ ^{73}\text{Ge} \rightarrow X^0 \ ^{73}\text{Ge}^*$ (13.26 keV).
- 44 KLIMENKO 98 limit is for inelastic scattering $X^0 \ ^{73}\text{Ge} \rightarrow X^0 \ ^{73}\text{Ge}^*$ (66.73 keV).
- 45 BERNABEI 97 give $\sigma < 32$ pb (90%CL) for the spin-dependent X^0 -proton cross section.
- 46 BELLI 96 limit for inelastic scattering $X^0 \ ^{129}\text{Xe} \rightarrow X^0 \ ^{129}\text{Xe}^*$ (39.58 keV).
- 47 BELLI 96 limit for inelastic scattering $X^0 \ ^{129}\text{Xe} \rightarrow X^0 \ ^{129}\text{Xe}^*$ (236.14 keV).
- 48 BELLI 96c use background subtraction and obtain $\sigma < 0.7$ pb (< 0.7 fb) (90%CL) for spin-dependent (independent) X^0 -proton cross section. The confidence level is from R. Bernabei, private communication, May 20, 1999.
- 49 BERNABEI 96 use pulse shape discrimination to enhance the possible signal. The limit here is from R. Bernabei, private communication, September 19, 1997.
- 50 SARSA 96 search for annual modulation of WIMP signal. See SARSA 97 for details of the analysis. The limit here is from M.L. Sarsa, private communication, May 26, 1997.
- 51 SMITH 96 use pulse shape discrimination to enhance the possible signal. A dark matter density of 0.4 GeV cm^{-3} is assumed.
- 52 GARCIA 95 limit is from the event rate. A weaker limit is obtained from searches for diurnal and annual modulation.
- 53 SNOWDEN-IFFT 95 look for recoil tracks in an ancient mica crystal. Similar limits are also given for ^{27}Al and ^{28}Si . See COLLAR 96 and SNOWDEN-IFFT 96 for discussion on potential backgrounds.
- 54 BECK 94 uses enriched ^{76}Ge (86% purity).
- 55 REUSSER 91 limit here is changed from published (5) after reanalysis by authors. J.L. Vuilleumier, private communication, March 29, 1996.

CONCENTRATION OF STABLE PARTICLES IN MATTER

Concentration of Heavy (Charge +1) Stable Particles in Matter

VALUE	CL%	DOCUMENT ID	TECN	COMMENT
• • • We do not use the following data for averages, fits, limits, etc. • • •				
$< 4 \times 10^{-17}$	95	56 YAMAGATA	93 SPEC	Deep sea water, $m=5$ – $1600 m_p$
$< 6 \times 10^{-15}$	95	57 VERKERK	92 SPEC	Water, $m=10^5$ to $3 \times 10^7 \text{ GeV}$
$< 7 \times 10^{-15}$	95	57 VERKERK	92 SPEC	Water, $m=10^4$, $6 \times 10^7 \text{ GeV}$
$< 9 \times 10^{-15}$	95	57 VERKERK	92 SPEC	Water, $m=10^8 \text{ GeV}$
$< 3 \times 10^{-23}$	90	58 HEMMICK	90 SPEC	Water, $m=1000 m_p$
$< 2 \times 10^{-21}$	90	58 HEMMICK	90 SPEC	Water, $m=5000 m_p$
$< 3 \times 10^{-20}$	90	58 HEMMICK	90 SPEC	Water, $m=10000 m_p$
$< 1. \times 10^{-29}$		SMITH	82B SPEC	Water, $m=30$ – $400 m_p$
$< 2. \times 10^{-28}$		SMITH	82B SPEC	Water, $m=12$ – $1000 m_p$
$< 1. \times 10^{-14}$		SMITH	82B SPEC	Water, $m=1000 m_p$
$< (0.2-1.) \times 10^{-21}$		SMITH	79 SPEC	Water, $m=6$ – $350 m_p$

- 56 YAMAGATA 93 used deep sea water at 4000 m since the concentration is enhanced in deep sea due to gravity.
- 57 VERKERK 92 looked for heavy isotopes in sea water and put a bound on concentration of stable charged massive particle in sea water. The above bound can be translated into a bound on charged dark matter particle ($5 \times 10^6 \text{ GeV}$), assuming the local density, $\rho=0.3 \text{ GeV/cm}^3$, and the mean velocity (v)= 300 km/s .
- 58 See HEMMICK 90 Fig. 7 for other masses 100 – $10000 m_p$.

Concentration of Heavy (Charge -1) Stable Particles

VALUE	CL%	DOCUMENT ID	TECN	COMMENT
• • • We do not use the following data for averages, fits, limits, etc. • • •				
$< 4 \times 10^{-20}$	90	59 HEMMICK	90 SPEC	C, $M=100 m_p$
$< 8 \times 10^{-20}$	90	59 HEMMICK	90 SPEC	C, $M=1000 m_p$
$< 2 \times 10^{-16}$	90	59 HEMMICK	90 SPEC	C, $M=10000 m_p$
$< 6 \times 10^{-13}$	90	59 HEMMICK	90 SPEC	Li, $M=1000 m_p$
$< 1 \times 10^{-11}$	90	59 HEMMICK	90 SPEC	Be, $M=1000 m_p$
$< 6 \times 10^{-14}$	90	59 HEMMICK	90 SPEC	B, $M=1000 m_p$
$< 4 \times 10^{-17}$	90	59 HEMMICK	90 SPEC	O, $M=1000 m_p$
$< 4 \times 10^{-15}$	90	59 HEMMICK	90 SPEC	F, $M=1000 m_p$
$< 1.5 \times 10^{-13}/\text{nucleon}$	68	60 NORMAN	89 SPEC	$206\text{pb} X^-$
$< 1.2 \times 10^{-12}/\text{nucleon}$	68	60 NORMAN	87 SPEC	$56,58\text{Fe} X^-$

- 59 See HEMMICK 90 Fig. 7 for other masses 100 – $10000 m_p$.
- 60 Bound valid up to $m_{X^-} \sim 100 \text{ TeV}$.

LIMITS ON NEUTRAL PARTICLE PRODUCTION

Production Cross Section of Radiatively-Decaying Neutral Particle

VALUE (pb)	CL%	DOCUMENT ID	TECN	COMMENT
• • • We do not use the following data for averages, fits, limits, etc. • • •				
$< (2.5-0.5)$	95	61 ACKERSTAFF	97B OPAL	$e^+e^- \rightarrow X^0 \gamma^0$, $X^0 \rightarrow \gamma^0 \gamma$
$< (1.6-0.9)$	95	62 ACKERSTAFF	97B OPAL	$e^+e^- \rightarrow X^0 X^0$, $X^0 \rightarrow \gamma^0 \gamma$

- 61 ACKERSTAFF 97B associated production limit is for $m_{\chi^0} = 80$ – 160 GeV , $m_{\gamma^0}=0$ from 10.0 pb^{-1} at $\sqrt{s} = 161 \text{ GeV}$. See their Fig. 3(a).
- 62 ACKERSTAFF 97B pair production limit is for $m_{\chi^0} = 40$ – 80 GeV , $m_{\gamma^0}=0$ from 10.0 pb^{-1} at $\sqrt{s} = 161 \text{ GeV}$. See their Fig. 3(b).

Heavy Particle Production Cross Section

VALUE (cm ² /N)	CL%	EVTs	DOCUMENT ID	TECN	COMMENT
• • • We do not use the following data for averages, fits, limits, etc. • • •					
$< 10^{-36}$ – 10^{-33}	90		63 ADAMS	97B KTEV	$m=1.2$ – 5 GeV
$< (4-0.3) \times 10^{-31}$	95		64 GALLAS	95 TOF	$m=0.5$ – 20 GeV
$< 2 \times 10^{-36}$	90	0	66 BADIER	86 BDMP	$\tau = (0.05-1.) \times 10^{-8} \text{ s}$
$< 2.5 \times 10^{-35}$		0	67 GUSTAFSON	76 CNTR	$\tau > 10^{-7} \text{ s}$

- 63 ADAMS 97B search for a hadron-like neutral particle produced in pN interactions, which decays into a p^0 and a weakly interacting massive particle. Upper limits are given for the ratio to K_L production for the mass range 1.2 – 5 GeV and lifetime 10^{-9} – 10^{-4} s . See also our Light Gluino Section.
- 64 GALLAS 95 limit is for a weakly interacting neutral particle produced in $800 \text{ GeV}/c$ pN interactions decaying with a lifetime of 10^{-4} – 10^{-8} s . See their Figs. 8 and 9. Similar limits are obtained for a stable particle with interaction cross section 10^{-29} – 10^{-33} cm^2 . See Fig. 10.
- 65 AKESSON 91 limit is from weakly interacting neutral long-lived particles produced in pN reaction at $450 \text{ GeV}/c$ performed at CERN SPS. Bourquin-Gaillard formula is used as the production model. The above limit is for $\tau > 10^{-7} \text{ s}$. For $\tau > 10^{-9} \text{ s}$, $\sigma < 10^{-30} \text{ cm}^2/\text{nucleon}$ is obtained.
- 66 BADIER 86 looked for long-lived particles at 300 GeV π^- beam dump. The limit applies for nonstrongly interacting neutral or charged particles with mass $> 2 \text{ GeV}$. The limit applies for particle modes, $\mu^+ \pi^-$, $\mu^+ \mu^-$, $\pi^+ \pi^- X$, $\pi^+ \pi^- \pi^\pm$ etc. See their figure 5 for the contours of limits in the mass- τ plane for each mode.
- 67 GUSTAFSON 76 is a 300 GeV FNAL experiment looking for heavy ($m > 2 \text{ GeV}$) long-lived neutral hadrons in the M4 neutral beam. The above typical value is for $M = 3 \text{ GeV}$ and assumes an interaction cross section of 1 mb . Values as a function of mass and interaction cross section are given in figure 2.

See key on page 239

Searches Particle Listings

WIMPs and Other Particle Searches

Production of New Penetrating Non- ν Like States in Beam Dump

VALUE	DOCUMENT ID	TECN	COMMENT
• • • We do not use the following data for averages, fits, limits, etc. • • •			
	68 LOSECCO	81 CALO	28 GeV protons
68	No excess neutral-current events leads to $\sigma(\text{production}) \times \sigma(\text{interaction}) \times \text{acceptance} < 2.26 \times 10^{-71} \text{ cm}^2/\text{nucleon}^2$ (CL = 90%) for light neutrals. Acceptance depends on models (0.1 to $4. \times 10^{-4}$).		

LIMITS ON JET-JET RESONANCES

Heavy Particle Production Cross Section in $p\bar{p}$

Limits are for a particle decaying to two hadronic jets.

Units(pb)	CL%	Mass(GeV)	DOCUMENT ID	TECN	COMMENT
• • • We do not use the following data for averages, fits, limits, etc. • • •					
			69 ABE	99F CDF	1.8 TeV $p\bar{p} \rightarrow b\bar{b} + \text{anything}$
			70 ABE	97G CDF	1.8 TeV $p\bar{p} \rightarrow 2 \text{ jets}$
<2603	95	200	71 ABE	93G CDF	1.8 TeV $p\bar{p} \rightarrow 2 \text{ jets}$
< 44	95	400	71 ABE	93G CDF	1.8 TeV $p\bar{p} \rightarrow 2 \text{ jets}$
< 7	95	600	71 ABE	93G CDF	1.8 TeV $p\bar{p} \rightarrow 2 \text{ jets}$
69	ABE 99F search for narrow $b\bar{b}$ resonances in $p\bar{p}$ collisions at $E_{\text{cm}}=1.8$ TeV. Limits on $\sigma(p\bar{p} \rightarrow X + \text{anything}) \times B(X \rightarrow b\bar{b})$ in the range $3-10^3$ pb (95%CL) are given for $m_X=200-750$ GeV. See their Table I.				
70	ABE 97G search for narrow dijet resonances in $p\bar{p}$ collisions with 106 pb^{-1} of data at $E_{\text{cm}} = 1.8$ TeV. Limits on $\sigma(p\bar{p} \rightarrow X + \text{anything}) \times B(X \rightarrow jj)$ in the range 10^4-10^{-1} pb (95%CL) are given for dijet mass $m=200-1150$ GeV with both jets having $ \eta < 2.0$ and the dijet system having $ \cos\theta^* < 0.67$. See their Table I for the list of limits. Supersedes ABE 93G.				
71	ABE 93G gives cross section times branching ratio into light (d, u, s, c, b) quarks for $\Gamma = 0.02 M$. Their Table II gives limits for $M = 200-900$ GeV and $\Gamma = (0.02-0.2) M$.				

LIMITS ON CHARGED PARTICLES IN e^+e^-

Heavy Particle Production Cross Section in e^+e^-

Ratio to $\sigma(e^+e^- \rightarrow \mu^+\mu^-)$ unless noted. See also entries in Free Quark Search and Magnetic Monopole Searches.

VALUE	CL%	EVTS	DOCUMENT ID	TECN	COMMENT
• • • We do not use the following data for averages, fits, limits, etc. • • •					
			72 ACKERSTAFF	98P OPAL	$Q=1, 2/3, m=45-89.5$ GeV
			73 ABREU	97D DLPH	$Q=1, 2/3, m=45-84$ GeV
			74 BARATE	97K ALEP	$Q=1, m=45-85$ GeV
<2 $\times 10^{-5}$	95		75 AKERS	95R OPAL	$Q=1, m=5-45$ GeV
<1 $\times 10^{-5}$	95		75 AKERS	95R OPAL	$Q=2, m=5-45$ GeV
<2 $\times 10^{-3}$	90		76 BUSKULIC	93C ALEP	$Q=1, m=32-72$ GeV
<(10 ⁻² -1)	95		77 ADACHI	90C TOPZ	$Q=1, m=1-16, 18-27$ GeV
<7 $\times 10^{-2}$	90		78 ADACHI	90E TOPZ	$Q=1, m=5-25$ GeV
<1.6 $\times 10^{-2}$	95	0	79 KINOSHITA	82 PLAS	$Q=3-180, m < 14.5$ GeV
<5.0 $\times 10^{-2}$	90	0	80 BARTEL	80 JADE	$Q=(3,4,5)/3, 2-12$ GeV
72	ACKERSTAFF 98P search for pair production of long-lived charged particles at \sqrt{s} between 130 and 183 GeV and give limits $\sigma < (0.05-0.2)$ pb (95%CL) for spin-0 and spin-1/2 particles with $m=45-89.5$ GeV, charge 1 and 2/3. The limit is translated to the cross section at $\sqrt{s}=183$ GeV with the s dependence described in the paper. See their Figs. 2-4.				
73	ABREU 97D search for pair production of long-lived particles and give limits $\sigma < (0.4-2.3)$ pb (95%CL) for various center-of-mass energies $\sqrt{s}=130-136, 161,$ and 172 GeV, assuming an almost flat production distribution in $\cos\theta$.				
74	BARATE 97K search for pair production of long-lived charged particles at $\sqrt{s} = 130, 136, 161,$ and 172 GeV and give limits $\sigma < (0.2-0.4)$ pb (95%CL) for spin-0 and spin-1/2 particles with $m=45-85$ GeV. The limit is translated to the cross section at $\sqrt{s}=172$ GeV with the \sqrt{s} dependence described in the paper. See their Figs. 2 and 3 for limits on $J = 1/2$ and $J = 0$ cases.				
75	AKERS 95R is a CERN-LEP experiment with $W_{\text{cm}} \sim m_Z$. The limit is for the production of a stable particle in multihadron events normalized to $\sigma(e^+e^- \rightarrow \text{hadrons})$. Constant phase space distribution is assumed. See their Fig. 3 for bounds for $Q = \pm 2/3, \pm 4/3$.				
76	BUSKULIC 93C is a CERN-LEP experiment with $W_{\text{cm}} = m_Z$. The limit is for a pair or single production of heavy particles with unusual ionization loss in TPC. See their Fig. 5 and Table 1.				
77	ADACHI 90C is a KEK-TRISTAN experiment with $W_{\text{cm}} = 52-60$ GeV. The limit is for pair production of a scalar or spin-1/2 particle. See Figs. 3 and 4.				
78	ADACHI 90E is KEK-TRISTAN experiment with $W_{\text{cm}} = 52-61.4$ GeV. The above limit is for inclusive production cross section normalized to $\sigma(e^+e^- \rightarrow \mu^+\mu^-) \cdot \beta(3-\beta^2)/2$, where $\beta = (1 - 4m^2/W_{\text{cm}}^2)^{1/2}$. See the paper for the assumption about the production mechanism.				
79	KINOSHITA 82 is SLAC PEP experiment at $W_{\text{cm}} = 29$ GeV using lexan and ^{39}Cr plastic sheets sensitive to highly ionizing particles.				
80	BARTEL 80 is DESY-PETRA experiment with $W_{\text{cm}} = 27-35$ GeV. Above limit is for inclusive pair production and ranges between $1. \times 10^{-1}$ and $1. \times 10^{-2}$ depending on mass and production momentum distributions. (See their figures 9, 10, 11).				

Branching Fraction of Z^0 to a Pair of Stable Charged Heavy Fermions

VALUE	CL%	DOCUMENT ID	TECN	COMMENT
• • • We do not use the following data for averages, fits, limits, etc. • • •				
<5 $\times 10^{-6}$	95	81 AKERS	95R OPAL	$m=40.4-45.6$ GeV
<1 $\times 10^{-3}$	95	AKRAWY	90O OPAL	$m=29-40$ GeV
81	AKERS 95R give the 95% CL limit $\sigma(X\bar{X})/\sigma(\mu\mu) < 1.8 \times 10^{-4}$ for the pair production of singly- or doubly-charged stable particles. The limit applies for the mass range 40.4-45.6 GeV for X^\pm and < 45.6 GeV for $X^{\pm\pm}$. See the paper for bounds for $Q = \pm 2/3, \pm 4/3$.			

LIMITS ON CHARGED PARTICLES IN HADRONIC REACTIONS

Heavy Particle Production Cross Section

VALUE (nb)	CL%	EVTS	DOCUMENT ID	TECN	COMMENT
• • • We do not use the following data for averages, fits, limits, etc. • • •					
<0.05	95		82 ABE	92J CDF	$m=50-200$ GeV
<30-130			83 CARROLL	78 SPEC	$m=2-2.5$ GeV
<100	0		84 LEIPUNER	73 CNTR	$m=3-11$ GeV
82	ABE 92J look for pair production of unit-charged particles which leave detector before decaying. Limit shown here is for $m=50$ GeV. See their Fig. 5 for different charges and stronger limits for higher mass.				
83	CARROLL 78 look for neutral, $S = -2$ dihyperon resonance in $pp \rightarrow 2K^+X$. Cross section varies within above limits over mass range and $p_{\text{lab}} = 5.1-5.9$ GeV/c.				
84	LEIPUNER 73 is an NAL 300 GeV p experiment. Would have detected particles with lifetime greater than 200 ns.				

Heavy Particle Production Differential Cross Section

VALUE (cm ² s ⁻¹ GeV ⁻¹)	CL%	EVTS	DOCUMENT ID	TECN	CHG	COMMENT
• • • We do not use the following data for averages, fits, limits, etc. • • •						
<2.6 $\times 10^{-36}$	90	0	85 BALDIN	76 CNTR	-	$Q=1, m=2.1-9.4$ GeV
<2.2 $\times 10^{-33}$	90	0	86 ALBROW	75 SPEC	\pm	$Q=\pm 1, m=4-15$ GeV
<1.1 $\times 10^{-33}$	90	0	86 ALBROW	75 SPEC	\pm	$Q=\pm 2, m=6-27$ GeV
<8. $\times 10^{-35}$	90	0	87 JOVANOVOV...	75 CNTR	\pm	$m=15-26$ GeV
<1.5 $\times 10^{-34}$	90	0	87 JOVANOVOV...	75 CNTR	\pm	$Q=\pm 2, m=3-10$ GeV
<6. $\times 10^{-35}$	90	0	87 JOVANOVOV...	75 CNTR	\pm	$Q=\pm 2, m=10-26$ GeV
<1. $\times 10^{-31}$	90	0	88 APPEL	74 CNTR	\pm	$m=3.2-7.2$ GeV
<5.8 $\times 10^{-34}$	90	0	89 ALPER	73 SPEC	\pm	$m=1.5-24$ GeV
<1.2 $\times 10^{-35}$	90	0	90 ANTIPOV	71B CNTR	-	$Q=-, m=2.2-2.8$ GeV
<2.4 $\times 10^{-35}$	90	0	91 ANTIPOV	71C CNTR	-	$Q=-, m=1.2-1.7, 2.1-4$ GeV
<2.4 $\times 10^{-35}$	90	0	BINON	69 CNTR	-	$Q=-, m=1-1.8$ GeV
<1.5 $\times 10^{-36}$	0		92 DORFAN	65 CNTR		Be target $m=3-7$ GeV
<3.0 $\times 10^{-36}$	0		92 DORFAN	65 CNTR		Fe target $m=3-7$ GeV
85	BALDIN 76 is a 70 GeV Serpukhov experiment. Value is per Al nucleus at $\theta = 0$. For other charges in range -0.5 to -3.0 , CL = 90% limit is $(2.6 \times 10^{-36})/ (\text{charge}) $ for mass range $(2.1-9.4 \text{ GeV}) \times (\text{charge}) $. Assumes stable particle interacting with matter as do antiprotons.					
86	ALBROW 75 is a CERN ISR experiment with $E_{\text{cm}} = 53$ GeV. $\theta = 40$ mr. See figure 5 for mass ranges up to 35 GeV.					
87	JOVANOVOVICH 75 is a CERN ISR 26+26 and 15+15 GeV pp experiment. Figure 4 covers ranges $Q = 1/3$ to 2 and $m = 3$ to 26 GeV. Value is per GeV momentum.					
88	APPEL 74 is NAL 300 GeV pW experiment. Studies forward production of heavy (up to 24 GeV) charged particles with momenta 24-200 GeV ($-$ charge) and 40-150 GeV ($+$ charge). Above typical value is for 75 GeV and is per GeV momentum per nucleon.					
89	ALPER 73 is CERN ISR 26+26 GeV pp experiment. $p > 0.9$ GeV, $0.2 < \beta < 0.65$.					
90	ANTIPOV 71B is from same 70 GeV p experiment as ANTIPOV 71C and BINON 69.					
91	ANTIPOV 71C limit inferred from flux ratio. 70 GeV p experiment.					
92	DORFAN 65 is a 30 GeV/c p experiment at BNL. Units are per GeV momentum per nucleus.					

Long-Lived Heavy Particle Invariant Cross Section

VALUE (cm ² /GeV ² /N)	CL%	EVTS	DOCUMENT ID	TECN	CHG	COMMENT
• • • We do not use the following data for averages, fits, limits, etc. • • •						
< 5 $\times 10^{-35}-7 \times 10^{-33}$	90	0	93 BERNSTEIN	88 CNTR		
< 5 $\times 10^{-37}-7 \times 10^{-35}$	90	0	93 BERNSTEIN	88 CNTR		
<2.5 $\times 10^{-36}$	90	0	94 THRON	85 CNTR	-	$Q=1, m=4-12$ GeV
<1. $\times 10^{-35}$	90	1	94 THRON	85 CNTR	+	$Q=1, m=4-12$ GeV
<6. $\times 10^{-33}$	90	0	95 ARMITAGE	79 SPEC		$m=1.87$ GeV
<1.5 $\times 10^{-33}$	90	0	95 ARMITAGE	79 SPEC		$m=1.5-3.0$ GeV
			96 BOZZOLI	79 CNTR	\pm	$Q = (2/3, 1, 4/3, 2)$
<1.1 $\times 10^{-37}$	90	0	97 CUTTS	78 CNTR		$m=4-10$ GeV
<3.0 $\times 10^{-37}$	90	0	98 VIDAL	78 CNTR		$m=4.5-6$ GeV
93	BERNSTEIN 88 limits apply at $x = 0.2$ and $p_T = 0$. Mass and lifetime dependence of limits are shown in the regions: $m = 1.5-7.5$ GeV and $\tau = 10^{-8}-2 \times 10^{-6}$ s. First number is for hadrons; second is for weakly interacting particles.					

Searches Particle Listings

WIMPs and Other Particle Searches

⁹⁴ THRON 85 is FNAL 400 GeV proton experiment. Mass determined from measured velocity and momentum. Limits are for $\tau > 3 \times 10^{-9}$ s.

⁹⁵ ARMITAGE 79 is CERN-ISR experiment at $E_{cm} = 53$ GeV. Value is for $x = 0.1$ and $p_T = 0.15$. Observed particles at $m = 1.87$ GeV are found all consistent with being antideuterons.

⁹⁶ BOZZOLI 79 is CERN-SPS 200 GeV pN experiment. Looks for particle with τ larger than 10^{-8} s. See their figure 11–18 for production cross-section upper limits vs mass.

⁹⁷ CUTTS 78 is pBe experiment at FNAL sensitive to particles of $\tau > 5 \times 10^{-8}$ s. Value is for $-0.3 < x < 0$ and $p_T = 0.175$.

⁹⁸ VIDAL 78 is FNAL 400 GeV proton experiment. Value is for $x = 0$ and $p_T = 0$. Puts lifetime limit of $< 5 \times 10^{-8}$ s on particle in this mass range.

Long-Lived Heavy Particle Production

 $(\sigma(\text{Heavy Particle}) / \sigma(\pi))$

VALUE	EVTs	DOCUMENT ID	TECN	CHG	COMMENT
-------	------	-------------	------	-----	---------

• • • We do not use the following data for averages, fits, limits, etc. • • •

$< 10^{-8}$		99 NAKAMURA 89	SPEC	±	$Q = (-5/3, \pm 2)$
	0	100 BUSSIÈRE 80	CNTR	±	$Q = (2/3, 1, 4/3, 2)$

⁹⁹ NAKAMURA 89 is KEK experiment with 12 GeV protons on Pt target. The limit applies for mass $\lesssim 1.6$ GeV and lifetime $\gtrsim 10^{-7}$ s.

¹⁰⁰ BUSSIÈRE 80 is CERN-SPS experiment with 200–240 GeV protons on Be and Al target. See their figures 6 and 7 for cross-section ratio vs mass.

Production and Capture of Long-Lived Massive Particles

VALUE (10^{-36} cm ²)	EVTs	DOCUMENT ID	TECN	COMMENT
--------------------------------------	------	-------------	------	---------

• • • We do not use the following data for averages, fits, limits, etc. • • •

< 20 to 800	0	101 ALEKSEEV 76	ELEC	$\tau = 5$ ms to 1 day
< 200 to 2000	0	101 ALEKSEEV 76b	ELEC	$\tau = 100$ ms to 1 day
< 1.4 to 9	0	102 FRANKEL 75	CNTR	$\tau = 50$ ms to 10 hours
< 0.1 to 9	0	103 FRANKEL 74	CNTR	$\tau = 1$ to 1000 hours

¹⁰¹ ALEKSEEV 76 and ALEKSEEV 76b are 61–70 GeV p Serpukhov experiment. Cross section is per Pb nucleus.

¹⁰² FRANKEL 75 is extension of FRANKEL 74.

¹⁰³ FRANKEL 74 looks for particles produced in thick Al targets by 300–400 GeV/c protons.

Long-Lived Particle Search at Hadron Collisions

Limits are for cross section times branching ratio.

VALUE (pb/nucleon)	CL%	EVTs	DOCUMENT ID	TECN	COMMENT
--------------------	-----	------	-------------	------	---------

• • • We do not use the following data for averages, fits, limits, etc. • • •

< 2	90	0	104 BADIER 86	BDMP	$\tau = (0.05-1.) \times 10^{-8}$ s
-------	----	---	---------------	------	-------------------------------------

¹⁰⁴ BADIER 86 looked for long-lived particles at 300 GeV π^- beam dump. The limit applies for nonstrongly interacting neutral or charged particles with mass > 2 GeV. The limit applies for particle modes, $\mu^+ \pi^-$, $\mu^+ \mu^-$, $\pi^+ \pi^- X$, $\pi^+ \pi^- \pi^\pm$ etc. See their figure 5 for the contours of limits in the mass- τ plane for each mode.

Long-Lived Heavy Particle Cross Section

VALUE (pb/sr)	CL%	DOCUMENT ID	TECN	COMMENT
---------------	-----	-------------	------	---------

• • • We do not use the following data for averages, fits, limits, etc. • • •

< 34	95	105 RAM	94	SPEC 1015 $< m_{X^{++}} < 1085$ MeV
< 75	95	105 RAM	94	SPEC 920 $< m_{X^{++}} < 1025$ MeV

¹⁰⁵ RAM 94 search for a long-lived doubly-charged fermion X^{++} with mass between m_N and $m_N + m_\pi$ and baryon number +1 in the reaction $pp \rightarrow X^{++} n$. No candidate is found. The limit is for the cross section at 15° scattering angle at 460 MeV incident energy and applies for $\tau(X^{++}) \gg 0.1$ μ s.

LIMITS ON CHARGED PARTICLES IN COSMIC RAYS

Heavy Particle Flux in Cosmic Rays

VALUE ($\text{cm}^{-2}\text{sr}^{-1}\text{s}^{-1}$)	CL%	EVTs	DOCUMENT ID	TECN	CHG	COMMENT
---	-----	------	-------------	------	-----	---------

• • • We do not use the following data for averages, fits, limits, etc. • • •

~ 6	$\times 10^{-9}$	2	106 SAITO 90			$Q \sim 14, m \sim 370 m_p$
< 1.4	$\times 10^{-12}$	90	0	107 MINCER 85	CALO	$m \geq 1$ TeV
				108 SAKUYAMA 83b	PLAS	$m \sim 1$ TeV
< 1.7	$\times 10^{-11}$	99	0	109 BHAT 82	CC	
$< 1.$	$\times 10^{-9}$	90	0	110 MARINI 82	CNTR	± $Q = 1, m \sim 4.5 m_p$
				111 YOCK 81	SPRK	± $Q = 1, m \sim 4.5 m_p$
				111 YOCK 81	SPRK	Fractionally charged
				112 YOCK 80	SPRK	$m \sim 4.5 m_p$
				113 GOODMAN 79	ELEC	$m \geq 5$ GeV
< 1.3	$\times 10^{-9}$	90	0	113 BHAT 78	CNTR	± $m > 1$ GeV
< 1.0	$\times 10^{-9}$		0	BRIATORE 76	ELEC	
$< 7.$	$\times 10^{-10}$	90	0	YOCK 75	ELEC	± $Q > 7e$ or $< -7e$
$> 6.$	$\times 10^{-9}$	5	114 YOCK 74	CNTR		$m > 6$ GeV
< 3.0	$\times 10^{-8}$	0	DARDO 72	CNTR		
< 1.5	$\times 10^{-9}$	0	TONWAR 72	CNTR		$m > 10$ GeV
< 3.0	$\times 10^{-10}$	0	BJORNBOE 68	CNTR		$m > 5$ GeV
< 5.0	$\times 10^{-11}$	90	0	JONES 67	ELEC	$m = 5-15$ GeV

¹⁰⁶ SAITO 90 candidates carry about 450 MeV/nucleon. Cannot be accounted for by conventional backgrounds. Consistent with strange quark matter hypothesis.

¹⁰⁷ MINCER 85 is high statistics study of calorimeter signals delayed by 20–200 ns. Calibration with AGS beam shows they can be accounted for by rare fluctuations in signals from low-energy hadrons in the shower. Claim that previous delayed signals including BJORNBOE 68, DARDO 72, BHAT 82, SAKUYAMA 83b below may be due to this fake effect.

¹⁰⁸ SAKUYAMA 83b analyzed 6000 extended air shower events. Increase of delayed particles and change of lateral distribution above 10^{17} eV may indicate production of very heavy parent at top of atmosphere.

¹⁰⁹ BHAT 82 observed 12 events with delay $> 2. \times 10^{-8}$ s and with more than 40 particles. 1 eV has good hadron shower. However all events are delayed in only one of two detectors in cloud chamber, and could not be due to strongly interacting massive particle.

¹¹⁰ MARINI 82 applied PEP-counter for TOF. Above limit is for velocity = 0.54 of light. Limit is inconsistent with YOCK 80 YOCK 81 events if isotropic dependence on zenith angle is assumed.

¹¹¹ YOCK 81 saw another 3 events with $Q = \pm 1$ and m about $4.5 m_p$ as well as 2 events with $m > 5.3 m_p$, $Q = \pm 0.75 \pm 0.05$ and $m > 2.8 m_p$, $Q = \pm 0.70 \pm 0.05$ and 1 event with $m = (9.3 \pm 3.) m_p$, $Q = \pm 0.89 \pm 0.06$ as possible heavy candidates.

¹¹² YOCK 80 events are with charge exactly or approximately equal to unity.

¹¹³ BHAT 78 is at Kolar gold fields. Limit is for $\tau > 10^{-6}$ s.

¹¹⁴ YOCK 74 events could be tritons.

Superheavy Particle (Quark Matter) Flux in Cosmic Rays

VALUE ($\text{cm}^{-2}\text{sr}^{-1}\text{s}^{-1}$)	CL%	EVTs	DOCUMENT ID	TECN	COMMENT
---	-----	------	-------------	------	---------

• • • We do not use the following data for averages, fits, limits, etc. • • •

$< 1.8 \times 10^{-12}$	90		115 ASTONE 93	CNTR	$m \geq 1.5 \times 10^{-13}$ gram
$< 1.1 \times 10^{-14}$	90		116 AHLEN 92	MCRO	$10^{-10} < m < 0.1$ gram
$< 3.2 \times 10^{-11}$	90	0	117 NAKAMURA 85	CNTR	$m > 1.5 \times 10^{-13}$ gram
$< 3.5 \times 10^{-11}$	90	0	118 ULLMAN 81	CNTR	Planck-mass 10^{19} GeV
$< 7. \times 10^{-11}$	90	0	118 ULLMAN 81	CNTR	$m \leq 10^{16}$ GeV

¹¹⁵ ASTONE 93 searched for quark matter ("nuclearites") in the velocity/c range = $10^{-3}-1$. Their Table 1 gives a compilation of searches for nuclearites.

¹¹⁶ AHLEN 92 searched for quark matter ("nuclearites"). The bound applies to velocity/c $< 2.5 \times 10^{-3}$. See their Fig. 3 for other velocity/c and heavier mass range.

¹¹⁷ NAKAMURA 85 at KEK searched for quark-matter. These might be lumps of strange quark matter with roughly equal numbers of u, d, s quarks. These lumps or nuclearites were assumed to have velocity/c of $10^{-4}-10^{-3}$.

¹¹⁸ ULLMAN 81 is sensitive for heavy slow singly charge particle reaching earth with vertical velocity 100–350 km/s.

Highly Ionizing Particle Flux

VALUE ($\text{m}^{-2}\text{yr}^{-1}$)	CL%	EVTs	DOCUMENT ID	TECN	COMMENT
---	-----	------	-------------	------	---------

• • • We do not use the following data for averages, fits, limits, etc. • • •

< 0.4	95	0	KINOSHITA 81b	PLAS	Z/ β 30–100
---------	----	---	---------------	------	-------------------

SEARCH FOR LOW-SCALE GRAVITY EFFECTS

This section contains experimental papers searching for effects of real or virtual gravitons (massless and massive, denoted by G) with observable coupling strength. This is expected if there are extra spacetime dimensions with a size larger than the electroweak scale, in which case the fundamental gravity scale can be around TeV, not 10^{19} GeV.

VALUE	DOCUMENT ID	TECN
-------	-------------	------

• • • We do not use the following data for averages, fits, limits, etc. • • •

119	ABBIENDI 99p	OPAL
120	ACCIARRI 99m	L3
121	ACCIARRI 99r	L3
122	ACCIARRI 99s	L3

¹¹⁹ ABBIENDI 99p search for s-channel graviton exchange effects in $e^+e^- \rightarrow \gamma\gamma$ at $E_{cm} = 189$ GeV. The limits $G_\pm > 660$ and $G_- > 634$ are obtained from combined $E_{cm} = 183$ and 189 GeV data, where G_\pm is a scale related to the fundamental gravity scale.

¹²⁰ ACCIARRI 99m search for the reaction $e^+e^- \rightarrow \gamma G$ and s-channel graviton exchange effects in $e^+e^- \rightarrow \gamma\gamma, W^+W^-, ZZ, e^+e^-, \mu^+\mu^-, \tau^+\tau^-, q\bar{q}$ at $E_{cm} = 183$ GeV. Limits on the gravity scale are listed in their Tables 1 and 2.

¹²¹ ACCIARRI 99r search for the reaction $e^+e^- \rightarrow \gamma G$ at $E_{cm} = 189$ GeV. Limits on the gravity scale are listed in their Table 4.

¹²² ACCIARRI 99s search for the reaction $e^+e^- \rightarrow ZG$ and s-channel graviton exchange effects in $e^+e^- \rightarrow \gamma\gamma, W^+W^-, ZZ, e^+e^-, \mu^+\mu^-, \tau^+\tau^-, q\bar{q}$ at $E_{cm} = 189$ GeV. Limits on the gravity scale are listed in their Tables 1 and 2.

See key on page 239

Searches Particle Listings
WIMPs and Other Particle Searches

REFERENCES FOR WIMPs and Other Particle Searches

BELLI	00	PR D61 023512	P. Belli <i>et al.</i>	(DAMA Collab.)	AKRAWY	900	PL B252 290	M.Z. Akrawy <i>et al.</i>	(OPAL Collab.)
ABBIENDI	99P	PL B465 303	G. Abbiendi <i>et al.</i>	(OPAL Collab.)	HEMMICK	90	PR D41 2074	T.K. Hemmick <i>et al.</i>	(ROCH, MICH, OHIO+)
ABE	99F	PRL 82 2038	F. Abe <i>et al.</i>	(CDF Collab.)	SAITO	90	PRL 65 2094	T. Saito <i>et al.</i>	(ICRR, KOBE)
ACCIARRI	99M	PL B464 135	M. Acciari <i>et al.</i>	(L3 Collab.)	NAKAMURA	89	PR D39 1261	T.T. Nakamura <i>et al.</i>	(KYOT, TMTC)
ACCIARRI	99R	PL B470 268	M. Acciari <i>et al.</i>	(L3 Collab.)	NORMAN	89	PR D39 2499	E.B. Norman <i>et al.</i>	(LBL)
ACCIARRI	99S	PL B470 281	M. Acciari <i>et al.</i>	(L3 Collab.)	BERNSTEIN	88	PR D37 3103	R.M. Bernstein <i>et al.</i>	(STAN, WISC)
AMBROSIO	99	FR D60 082902	M. Ambrosio <i>et al.</i>	(Macro Collab.)	CALDWELL	88	PRL 61 510	D.O. Caldwell <i>et al.</i>	(UCSB, UCB, LBL)
BAUDIS	99	PR D59 022001	L. Baudis <i>et al.</i>	(Heidelberg-Moscow Collab.)	NORMAN	87	ZPHY 58 1403	E.B. Norman, S.B. Gazes, D.A. Bennett	(LBL)
BELLI	99C	NP B563 97	P. Belli <i>et al.</i>	(DAMA Collab.)	BADIER	86	ZPHY C31 21	J. Badier <i>et al.</i>	(NA3 Collab.)
BERNABEI	99	PL B450 448	R. Bernabei <i>et al.</i>	(DAMA Collab.)	MINCER	85	PR D32 591	A. Mincer <i>et al.</i>	(UMD, GMAS, NSF)
BERNABEI	99D	PRL 83 4918	R. Bernabei <i>et al.</i>	(DAMA Collab.)	NAKAMURA	85	PL 161B 417	K. Nakamura <i>et al.</i>	(KEK, INUS)
BRHLIK	99	PL B464 303	M. Brhlik, L. Roszkowski	(DAMA Collab.)	THRON	85	PR D31 451	J.L. Thron <i>et al.</i>	(YALE, FNAL, IOWA)
DERBIN	99	PAN 62 1886	A.V. Derbin <i>et al.</i>		SAKUYAMA	83B	LNC 37 17	H. Sakuyama, N. Suzuki	(MEIS)
		Translated from YAF 62 2034			Also	83	LNC 36 389	H. Sakuyama, K. Watanabe	(MEIS)
OOTANI	99	PL B461 371	W. Ootani <i>et al.</i>		Also	83D	NC 76A 147	H. Sakuyama, K. Watanabe	(MEIS)
ACKERSTAFF	98P	PL B433 195	K. Akerstaff <i>et al.</i>	(OPAL Collab.)	Also	83C	NC 6C 371	H. Sakuyama, K. Watanabe	(MEIS)
BERNABEI	98	PL B424 195	R. Bernabei <i>et al.</i>	(DAMA Collab.)	BHAT	82	PR D25 2820	P.N. Bhat <i>et al.</i>	(TATA)
BERNABEI	98C	PL B436 379	R. Bernabei <i>et al.</i>	(DAMA Collab.)	KINOSHITA	82	PRL 48 77	K. Kinoshita, P.B. Price, D. Fryberger	(UCB+)
KLIMENKO	98	JETPL 67 875	A.A. Klimenko <i>et al.</i>		MARINI	82	PR D26 1777	A. Marini <i>et al.</i>	(FRAS, LBL, NWES, STAN+)
		Translated from ZETFP 67 835			SMITH	82B	NP B206 333	P.F. Smith <i>et al.</i>	(RAL)
ABE	97G	PR D55 R5263	F. Abe <i>et al.</i>	(CDF Collab.)	KINOSHITA	81B	PR D24 1707	K. Kinoshita, P.B. Price	(UCB)
ABREU	97D	PL B395 315	P. Abreu <i>et al.</i>	(DELPHI Collab.)	LOSECCO	81	PL 102B 209	J.M. Losecco <i>et al.</i>	(MICH, PENN, BNL)
ACKERSTAFF	97B	PL B391 210	K. Akerstaff <i>et al.</i>	(OPAL Collab.)	ULLMAN	81	PRL 47 289	J.D. Ullman	(LEHM, BNL)
ADAMS	97B	PRL 79 4083	J. Adams <i>et al.</i>	(KTeV Collab.)	YOCK	81	PR D23 1207	P.C.M. Yock	(AUCK)
BARATE	97K	PL B405 379	R. Barate <i>et al.</i>	(ALEPH Collab.)	BARTEL	80	ZPHY C6 295	W. Bartel <i>et al.</i>	(JADE Collab.)
BERNABEI	97	ASP 7 73	R. Bernabei <i>et al.</i>	(DAMA Collab.)	BUSSIERE	80	NP B174 1	A. Bussiere <i>et al.</i>	(BGNA, SACL, LAPP)
SARSA	97	PR D56 1856	M.L. Sarsa <i>et al.</i>	(ZARA)	YOCK	80	PR D22 61	P.C.M. Yock	(AUCK)
ALESSAND...	96	PL B384 316	A. Alessandrello <i>et al.</i>	(MILA, MILA, SASSO)	ARMITAGE	79	NP B150 87	J.C.M. Armitage <i>et al.</i>	(CERN, DARE, FOM+)
BELLI	96	PL B387 222	P. Belli <i>et al.</i>	(DAMA Collab.)	BOZZOLI	79	NP B159 363	W. Bozzoli <i>et al.</i>	(BGNA, LAPP, SACL+)
Also		PL B389 783 (erratum)	P. Belli <i>et al.</i>	(DAMA Collab.)	GOODMAN	79	PR D19 2572	J.A. Goodman <i>et al.</i>	(UMD)
BELLI	96C	NC 19C 537	P. Belli <i>et al.</i>	(DAMA Collab.)	SMITH	79	NP B149 525	P.F. Smith, J.R.J. Bennett	(RHUL)
BERNABEI	96	PL B389 757	R. Bernabei <i>et al.</i>	(DAMA Collab.)	BHAT	78	Pramana 10 115	P.N. Bhat, P.V. Ramana Murthy	(TATA)
COLLAR	96	PRL 76 331	J.J. Collar	(DAMA Collab.)	CARROLL	78	PRL 41 777	A.S. Carroll <i>et al.</i>	(BNL, PRIN)
SARSA	96	PL B386 458	M.L. Sarsa <i>et al.</i>	(ZARA)	CUTTS	78	PRL 41 363	D. Cutts <i>et al.</i>	(BROW, FNAL, ILL, BARI+)
Also		PR D56 1856	M.L. Sarsa <i>et al.</i>	(ZARA)	VIDAL	78	PL 77B 344	R.A. Vidal <i>et al.</i>	(COLU, FNAL, STON+)
SMITH	96	PL B379 299	P.F. Smith <i>et al.</i>	(RAL, SHEF, LOIC+)	ALEKSEEV	76	SJNP 22 531	G.D. Alekseev <i>et al.</i>	(JINR)
SNOWDEN...	96	PRL 76 332	D.P. Snowden-III, E.S. Freeman, P.B. Price	(UCB)	ALEKSEEV	76B	SJNP 23 633	G.D. Alekseev <i>et al.</i>	(JINR)
AKERS	95R	ZPHY C67 203	R. Akers <i>et al.</i>	(OPAL Collab.)	BALDIN	76	SJNP 22 264	B.Y. Baldin <i>et al.</i>	(JINR)
GALLAS	95	PR D52 6	E. Gallas <i>et al.</i>	(MSU, FNAL, MIT, FLOR)			Translated from YAF 22 512		
GARCIA	95	PR D51 1458	E. Garcia <i>et al.</i>	(ZARA, SCUC, PNL)	BRIATORE	75	NC 31A 553	L. Briatore <i>et al.</i>	(LCGT, FRAS, FREIB)
QUENBY	95	PL B351 70	J.J. Quenby <i>et al.</i>	(LOIC, RAL, SHEF+)	GUSTAFSON	75	PRL 37 474	H.R. Gustafson <i>et al.</i>	(MICH)
SNOWDEN...	95	PRL 74 4133	D.P. Snowden-III, E.S. Freeman, P.B. Price	(UCB)	ALBROW	75	NP B97 189	M.G. Albrow <i>et al.</i>	(CERN, DARE, FOM+)
Also		PRL 76 331	J.J. Collar	(SCUC)	FRANKEL	75	PR D12 2561	S. Frankel <i>et al.</i>	(PENN, FNAL)
Also		PRL 76 332	D.P. Snowden-III, E.S. Freeman, P.B. Price	(UCB)	JOVANOV...	75	PL 56B 105	J.V. Jovanovich <i>et al.</i>	(MANI, AACH, CERN+)
BECK	94	PL B336 141	M. Beck <i>et al.</i>	(MPIH, KIAE, SASSO)	YOCK	75	NP B86 216	P.C.M. Yock	(AUCK, SLAC)
RAM	94	PR D49 3120	S. Ram <i>et al.</i>	(TELA, TRIU)	APPEL	74	PR 32 428	J.A. Appel <i>et al.</i>	(COLU, FNAL)
ABE	93G	PRL 71 2542	F. Abe <i>et al.</i>	(CDF Collab.)	FRANKEL	74	PR D9 1932	S. Frankel <i>et al.</i>	(PENN, FNAL)
ASTONE	93	PR D47 4770	P. Astone <i>et al.</i>	(ROMA, ROMAI, CATA, FRAS)	YOCK	74	NP B76 175	P.C.M. Yock	(AUCK)
BUSKULIC	93C	PL B303 195	D. Buskulic <i>et al.</i>	(ALEPH Collab.)	ALPER	73	PL 46B 265	B. Alper <i>et al.</i>	(CERN, LIVP, LUND, BOHR+)
YAMAGATA	93	PR D47 1231	T. Yamagata, Y. Takamori, H. Utsunomiya	(ALEPH Collab.)	LEIPUNER	73	PRL 31 1226	L.B. Leipuner <i>et al.</i>	(BNL, YALE)
ABE	92J	PR D46 R1889	F. Abe <i>et al.</i>	(CDF Collab.)	DARDO	72	NC 9A 319	M. Dardo <i>et al.</i>	(TORI)
AHLEN	92	PRL 69 1860	S.P. Ahlen <i>et al.</i>	(MACRO Collab.)	TONWAR	72	JPA 5 569	S.C. Tonwar, S. Naranan, B.V. Sreekantan	(TATA)
BACCI	92	PL B293 460	C. Bacci <i>et al.</i>	(Beijing-Roma-Saclay Collab.)	ANTIPOV	71B	NP B31 235	Y.M. Antipov <i>et al.</i>	(SERP)
VERKERK	92	PRL 68 1116	P. Verkerk <i>et al.</i>	(ENSP, SACL, PAST)	ANTIPOV	71C	PL 34B 164	Y.M. Antipov <i>et al.</i>	(SERP)
AKESSON	91	ZPHY C52 219	T. Akesson <i>et al.</i>	(HELIOS Collab.)	BINON	69	PL 30B 510	F.G. Binon <i>et al.</i>	(SERP)
REUSSER	91	PL B255 143	D. Reusser <i>et al.</i>	(NEUC, CIT, PSI)	BJORNBOE	68	NC B53 241	J. Bjornboe <i>et al.</i>	(BOHR, TATA, BERN+)
ADACHI	90C	PL B244 352	I. Adachi <i>et al.</i>	(TOPAZ Collab.)	JONES	67	PR 164 1584	L.W. Jones	(MICH, WISC, LBL, UCL, MINN+)
ADACHI	90E	PL B249 336	I. Adachi <i>et al.</i>	(TOPAZ Collab.)	DORFAN	65	PRL 14 999	D.E. Dorfan <i>et al.</i>	(COLU)